Scientific Programming

Artificial Intelligence for Evaluation Decision-making in Modern Product Design

Lead Guest Editor: Lianhui Li
Guest Editors: Jie Liu and Rémy Houssin

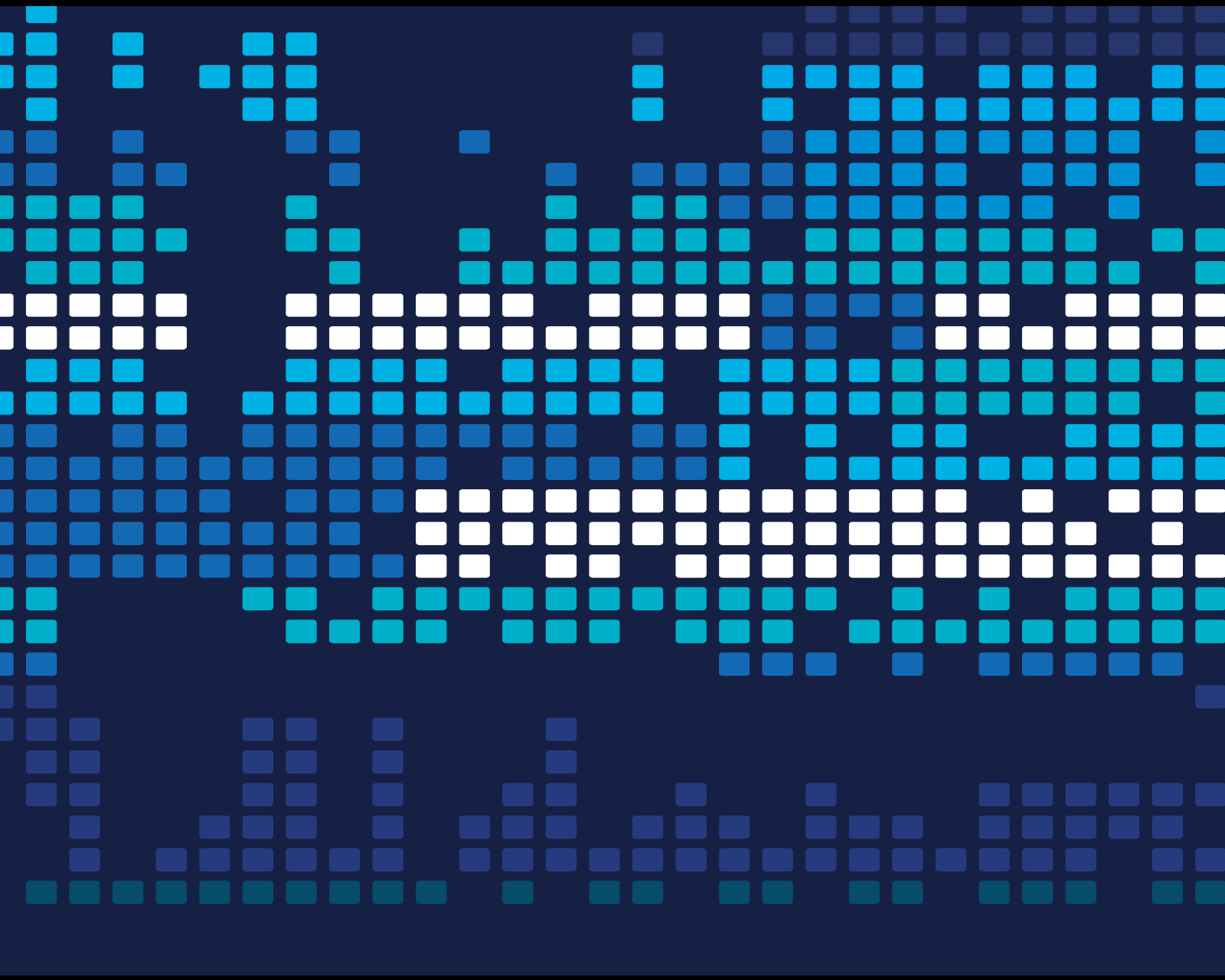

Artificial Intelligence for Evaluation Decision-making in Modern Product Design

Scientific Programming

Artificial Intelligence for Evaluation Decision-making in Modern Product Design

Lead Guest Editor: Lianhui Li
Guest Editors: Jie Liu and Rémy Houssin

Contents

Retracted: Innovation and Practical Methods of Music Education Path in Colleges and Universities under the Popularization of the 5G Network
Scientific Programming
Retraction (1 page), Article ID 9847362, Volume 2023 (2023)

Retracted: System Analysis of the Learning Behavior Recognition System for Students in a Law Classroom: Based on the Improved SSD Behavior Recognition Algorithm
Scientific Programming
Retraction (1 page), Article ID 9837098, Volume 2023 (2023)

Retracted: Intelligent Detection of Foreign Matter in Coal Mine Transportation Belt Based on Convolution Neural Network
Scientific Programming
Retraction (1 page), Article ID 9831951, Volume 2023 (2023)

Retracted: Feasibility Analysis of Intelligent Piano in Piano Teaching
Scientific Programming
Retraction (1 page), Article ID 9829648, Volume 2023 (2023)

Retracted: Tobacco Leaves Disease Identification and Spot Segmentation Based on the Improved ORB Algorithm
Scientific Programming
Retraction (1 page), Article ID 9803061, Volume 2023 (2023)

Retracted: The Method of Graphic Design Using 3D Virtual Vision Technology
Scientific Programming
Retraction (1 page), Article ID 9793108, Volume 2023 (2023)

Retracted: Impact of Carbon Information on Enterprise Value: Analysis Model Design Based on Big Data
Scientific Programming
Retraction (1 page), Article ID 9787612, Volume 2023 (2023)

Retracted: Emotion Analysis of Literary Works Based on Attentional Mechanisms and the Fusion of Two-Channel Features
Scientific Programming
Retraction (1 page), Article ID 9783528, Volume 2023 (2023)

Retracted: An Auxiliary Teaching System for Spoken English Based on Speech Recognition Technology
Scientific Programming
Retraction (1 page), Article ID 9783524, Volume 2023 (2023)

Retracted: A Method of Extracting and Identifying College Students' Music Psychological Features Based on EEG Signals
Scientific Programming
Retraction (1 page), Article ID 9767390, Volume 2023 (2023)

Contents

Contents

Contents

Contents

Contents

Contents

Contents

Contents

Contents

Contents

Hindawi
Scientific Programming
Volume 2023, Article ID 9816825, 1 page
https://doi.org/10.1155/2023/9816825

Retraction

Retracted: Application of Three-Dimensional Image Reconstruction Technology in Neurogenic Intestinal Nursing Tasks

Scientific Programming

Received 26 September 2023; Accepted 26 September 2023; Published 27 September 2023

This article has been retracted by Hindawi following an investigation undertaken by the publisher [1]. This investigation has uncovered evidence of one or more of the following indicators of systematic manipulation of the publication process:

(1) Discrepancies in scope
(2) Discrepancies in the description of the research reported
(3) Discrepancies between the availability of data and the research described
(4) Inappropriate citations
(5) Incoherent, meaningless and/or irrelevant content included in the article
(6) Peer-review manipulation

The presence of these indicators undermines our confidence in the integrity of the article's content and we cannot, therefore, vouch for its reliability. Please note that this notice is intended solely to alert readers that the content of this article is unreliable. We have not investigated whether authors were aware of or involved in the systematic manipulation of the publication process.

Wiley and Hindawi regrets that the usual quality checks did not identify these issues before publication and have since put additional measures in place to safeguard research integrity.

We wish to credit our own Research Integrity and Research Publishing teams and anonymous and named external researchers and research integrity experts for contributing to this investigation.

The corresponding author, as the representative of all authors, has been given the opportunity to register their agreement or disagreement to this retraction. We have kept a record of any response received.

References

[1] Y. Shen, X. Huang, Y. Zhang, J. Pan, Y. Liu, and Y. Jiang, "Application of Three-Dimensional Image Reconstruction Technology in Neurogenic Intestinal Nursing Tasks," *Scientific Programming*, vol. 2022, Article ID 4840189, 10 pages, 2022.

Hindawi
Scientific Programming
Volume 2023, Article ID 9815350, 1 page
https://doi.org/10.1155/2023/9815350

Retraction

Retracted: Deep Learning Analysis of English Education Blended Teaching in Virtual Reality Environment

Scientific Programming

Received 26 September 2023; Accepted 26 September 2023; Published 27 September 2023

This article has been retracted by Hindawi following an investigation undertaken by the publisher [1]. This investigation has uncovered evidence of one or more of the following indicators of systematic manipulation of the publication process:

(1) Discrepancies in scope
(2) Discrepancies in the description of the research reported
(3) Discrepancies between the availability of data and the research described
(4) Inappropriate citations
(5) Incoherent, meaningless and/or irrelevant content included in the article
(6) Peer-review manipulation

The presence of these indicators undermines our confidence in the integrity of the article's content and we cannot, therefore, vouch for its reliability. Please note that this notice is intended solely to alert readers that the content of this article is unreliable. We have not investigated whether authors were aware of or involved in the systematic manipulation of the publication process.

In addition, our investigation has also shown that one or more of the following human-subject reporting requirements has not been met in this article: ethical approval by an Institutional Review Board (IRB) committee or equivalent, patient/participant consent to participate, and/or agreement to publish patient/participant details (where relevant).

Wiley and Hindawi regrets that the usual quality checks did not identify these issues before publication and have since put additional measures in place to safeguard research integrity.

We wish to credit our own Research Integrity and Research Publishing teams and anonymous and named external researchers and research integrity experts for contributing to this investigation.

The corresponding author, as the representative of all authors, has been given the opportunity to register their agreement or disagreement to this retraction. We have kept a record of any response received.

References

[1] W. Wu and C. Qiu, "Deep Learning Analysis of English Education Blended Teaching in Virtual Reality Environment," *Scientific Programming*, vol. 2022, Article ID 8218672, 11 pages, 2022.

Hindawi
Scientific Programming
Volume 2023, Article ID 9891427, 1 page
https://doi.org/10.1155/2023/9891427

Retraction

Retracted: Analysis on the Artistic Presentation Effect of 3D Rendering Ink Painting Based on the Evaluation of Deep Learning Model

Scientific Programming

Received 18 July 2023; Accepted 18 July 2023; Published 19 July 2023

This article has been retracted by Hindawi following an investigation undertaken by the publisher [1]. This investigation has uncovered evidence of one or more of the following indicators of systematic manipulation of the publication process:

(1) Discrepancies in scope
(2) Discrepancies in the description of the research reported
(3) Discrepancies between the availability of data and the research described
(4) Inappropriate citations
(5) Incoherent, meaningless and/or irrelevant content included in the article
(6) Peer-review manipulation

The presence of these indicators undermines our confidence in the integrity of the article's content and we cannot, therefore, vouch for its reliability. Please note that this notice is intended solely to alert readers that the content of this article is unreliable. We have not investigated whether authors were aware of or involved in the systematic manipulation of the publication process.

Wiley and Hindawi regrets that the usual quality checks did not identify these issues before publication and have since put additional measures in place to safeguard research integrity.

We wish to credit our own Research Integrity and Research Publishing teams and anonymous and named external researchers and research integrity experts for contributing to this investigation.

The corresponding author, as the representative of all authors, has been given the opportunity to register their agreement or disagreement to this retraction. We have kept a record of any response received.

References

[1] Y. Pan, "Analysis on the Artistic Presentation Effect of 3D Rendering Ink Painting Based on the Evaluation of Deep Learning Model," *Scientific Programming*, vol. 2022, Article ID 9259389, 12 pages, 2022.

Hindawi
Scientific Programming
Volume 2023, Article ID 9890860, 1 page
https://doi.org/10.1155/2023/9890860

Retraction

Retracted: Construction and Application of College Smart Party-Building Platform Integrating Artificial Intelligence and Internet Technology

Scientific Programming

Received 18 July 2023; Accepted 18 July 2023; Published 19 July 2023

This article has been retracted by Hindawi following an investigation undertaken by the publisher [1]. This investigation has uncovered evidence of one or more of the following indicators of systematic manipulation of the publication process:

(1) Discrepancies in scope
(2) Discrepancies in the description of the research reported
(3) Discrepancies between the availability of data and the research described
(4) Inappropriate citations
(5) Incoherent, meaningless and/or irrelevant content included in the article
(6) Peer-review manipulation

The presence of these indicators undermines our confidence in the integrity of the article's content and we cannot, therefore, vouch for its reliability. Please note that this notice is intended solely to alert readers that the content of this article is unreliable. We have not investigated whether authors were aware of or involved in the systematic manipulation of the publication process.

Wiley and Hindawi regrets that the usual quality checks did not identify these issues before publication and have since put additional measures in place to safeguard research integrity.

We wish to credit our own Research Integrity and Research Publishing teams and anonymous and named external researchers and research integrity experts for contributing to this investigation.

The corresponding author, as the representative of all authors, has been given the opportunity to register their agreement or disagreement to this retraction. We have kept a record of any response received.

References

[1] H. Chen and J. Su, "Construction and Application of College Smart Party-Building Platform Integrating Artificial Intelligence and Internet Technology," *Scientific Programming*, vol. 2022, Article ID 8569301, 9 pages, 2022.

Hindawi
Scientific Programming
Volume 2023, Article ID 9878574, 1 page
https://doi.org/10.1155/2023/9878574

Retraction

Retracted: Optimization Method of Urban Square Public Space from the Perspective of Contextualism

Scientific Programming

Received 18 July 2023; Accepted 18 July 2023; Published 19 July 2023

This article has been retracted by Hindawi following an investigation undertaken by the publisher [1]. This investigation has uncovered evidence of one or more of the following indicators of systematic manipulation of the publication process:

(1) Discrepancies in scope
(2) Discrepancies in the description of the research reported
(3) Discrepancies between the availability of data and the research described
(4) Inappropriate citations
(5) Incoherent, meaningless and/or irrelevant content included in the article
(6) Peer-review manipulation

The presence of these indicators undermines our confidence in the integrity of the article's content and we cannot, therefore, vouch for its reliability. Please note that this notice is intended solely to alert readers that the content of this article is unreliable. We have not investigated whether authors were aware of or involved in the systematic manipulation of the publication process.

Wiley and Hindawi regrets that the usual quality checks did not identify these issues before publication and have since put additional measures in place to safeguard research integrity.

We wish to credit our own Research Integrity and Research Publishing teams and anonymous and named external researchers and research integrity experts for contributing to this investigation.

The corresponding author, as the representative of all authors, has been given the opportunity to register their agreement or disagreement to this retraction. We have kept a record of any response received.

References

[1] M. Zhang and M. Lee, "Optimization Method of Urban Square Public Space from the Perspective of Contextualism," *Scientific Programming*, vol. 2022, Article ID 3811260, 8 pages, 2022.

Hindawi
Scientific Programming
Volume 2023, Article ID 9878425, 1 page
https://doi.org/10.1155/2023/9878425

Retraction

Retracted: Application Research and Case Analysis of Landscape Design in Artificial Intelligence Platform

Scientific Programming

Received 18 July 2023; Accepted 18 July 2023; Published 19 July 2023

This article has been retracted by Hindawi following an investigation undertaken by the publisher [1]. This investigation has uncovered evidence of one or more of the following indicators of systematic manipulation of the publication process:

(1) Discrepancies in scope
(2) Discrepancies in the description of the research reported
(3) Discrepancies between the availability of data and the research described
(4) Inappropriate citations
(5) Incoherent, meaningless and/or irrelevant content included in the article
(6) Peer-review manipulation

The presence of these indicators undermines our confidence in the integrity of the article's content and we cannot, therefore, vouch for its reliability. Please note that this notice is intended solely to alert readers that the content of this article is unreliable. We have not investigated whether authors were aware of or involved in the systematic manipulation of the publication process.

Wiley and Hindawi regrets that the usual quality checks did not identify these issues before publication and have since put additional measures in place to safeguard research integrity.

We wish to credit our own Research Integrity and Research Publishing teams and anonymous and named external researchers and research integrity experts for contributing to this investigation.

The corresponding author, as the representative of all authors, has been given the opportunity to register their agreement or disagreement to this retraction. We have kept a record of any response received.

References

[1] Y. Cao, "Application Research and Case Analysis of Landscape Design in Artificial Intelligence Platform," *Scientific Programming*, vol. 2022, Article ID 7122276, 10 pages, 2022.

Hindawi
Scientific Programming
Volume 2023, Article ID 9873894, 1 page
https://doi.org/10.1155/2023/9873894

Retraction

Retracted: Rapid Identification of Tobacco Mildew Based on Random Forest Algorithm

Scientific Programming

Received 18 July 2023; Accepted 18 July 2023; Published 19 July 2023

This article has been retracted by Hindawi following an investigation undertaken by the publisher [1]. This investigation has uncovered evidence of one or more of the following indicators of systematic manipulation of the publication process:

(1) Discrepancies in scope
(2) Discrepancies in the description of the research reported
(3) Discrepancies between the availability of data and the research described
(4) Inappropriate citations
(5) Incoherent, meaningless and/or irrelevant content included in the article
(6) Peer-review manipulation

The presence of these indicators undermines our confidence in the integrity of the article's content and we cannot, therefore, vouch for its reliability. Please note that this notice is intended solely to alert readers that the content of this article is unreliable. We have not investigated whether authors were aware of or involved in the systematic manipulation of the publication process.

Wiley and Hindawi regrets that the usual quality checks did not identify these issues before publication and have since put additional measures in place to safeguard research integrity.

We wish to credit our own Research Integrity and Research Publishing teams and anonymous and named external researchers and research integrity experts for contributing to this investigation.

The corresponding author, as the representative of all authors, has been given the opportunity to register their agreement or disagreement to this retraction. We have kept a record of any response received.

References

[1] Z. Jiang, W. Zhang, H. Huang et al., "Rapid Identification of Tobacco Mildew Based on Random Forest Algorithm," *Scientific Programming*, vol. 2022, Article ID 1818398, 10 pages, 2022.

Hindawi
Scientific Programming
Volume 2023, Article ID 9857605, 1 page
https://doi.org/10.1155/2023/9857605

Retraction

Retracted: Design and Implementation of Music Teaching System Based on J2EE

Scientific Programming

Received 18 July 2023; Accepted 18 July 2023; Published 19 July 2023

This article has been retracted by Hindawi following an investigation undertaken by the publisher [1]. This investigation has uncovered evidence of one or more of the following indicators of systematic manipulation of the publication process:

(1) Discrepancies in scope
(2) Discrepancies in the description of the research reported
(3) Discrepancies between the availability of data and the research described
(4) Inappropriate citations
(5) Incoherent, meaningless and/or irrelevant content included in the article
(6) Peer-review manipulation

The presence of these indicators undermines our confidence in the integrity of the article's content and we cannot, therefore, vouch for its reliability. Please note that this notice is intended solely to alert readers that the content of this article is unreliable. We have not investigated whether authors were aware of or involved in the systematic manipulation of the publication process.

Wiley and Hindawi regrets that the usual quality checks did not identify these issues before publication and have since put additional measures in place to safeguard research integrity.

We wish to credit our own Research Integrity and Research Publishing teams and anonymous and named external researchers and research integrity experts for contributing to this investigation.

The corresponding author, as the representative of all authors, has been given the opportunity to register their agreement or disagreement to this retraction. We have kept a record of any response received.

References

[1] Y. Zhu and S. Liang, "Design and Implementation of Music Teaching System Based on J2EE," *Scientific Programming*, vol. 2022, Article ID 2179882, 10 pages, 2022.

Hindawi
Scientific Programming
Volume 2023, Article ID 9857484, 1 page
https://doi.org/10.1155/2023/9857484

Retraction

Retracted: College Students' Ideological and Political In-Depth Teaching Community Based on Core Literacy Model

Scientific Programming

Received 18 July 2023; Accepted 18 July 2023; Published 19 July 2023

This article has been retracted by Hindawi following an investigation undertaken by the publisher [1]. This investigation has uncovered evidence of one or more of the following indicators of systematic manipulation of the publication process:

(1) Discrepancies in scope
(2) Discrepancies in the description of the research reported
(3) Discrepancies between the availability of data and the research described
(4) Inappropriate citations
(5) Incoherent, meaningless and/or irrelevant content included in the article
(6) Peer-review manipulation

The presence of these indicators undermines our confidence in the integrity of the article's content and we cannot, therefore, vouch for its reliability. Please note that this notice is intended solely to alert readers that the content of this article is unreliable. We have not investigated whether authors were aware of or involved in the systematic manipulation of the publication process.

Wiley and Hindawi regrets that the usual quality checks did not identify these issues before publication and have since put additional measures in place to safeguard research integrity.

We wish to credit our own Research Integrity and Research Publishing teams and anonymous and named external researchers and research integrity experts for contributing to this investigation.

The corresponding author, as the representative of all authors, has been given the opportunity to register their agreement or disagreement to this retraction. We have kept a record of any response received.

References

[1] F. Yanju, D. Chao, and L. Man, "College Students' Ideological and Political In-Depth Teaching Community Based on Core Literacy Model," *Scientific Programming*, vol. 2022, Article ID 5481853, 9 pages, 2022.

Hindawi
Scientific Programming
Volume 2023, Article ID 9851726, 1 page
https://doi.org/10.1155/2023/9851726

Retraction

Retracted: Study on the Influence of Wuthering Heights Characters Based on Web Analysis and Text Mining

Scientific Programming

Received 18 July 2023; Accepted 18 July 2023; Published 19 July 2023

This article has been retracted by Hindawi following an investigation undertaken by the publisher [1]. This investigation has uncovered evidence of one or more of the following indicators of systematic manipulation of the publication process:

(1) Discrepancies in scope
(2) Discrepancies in the description of the research reported
(3) Discrepancies between the availability of data and the research described
(4) Inappropriate citations
(5) Incoherent, meaningless and/or irrelevant content included in the article
(6) Peer-review manipulation

The presence of these indicators undermines our confidence in the integrity of the article's content and we cannot, therefore, vouch for its reliability. Please note that this notice is intended solely to alert readers that the content of this article is unreliable. We have not investigated whether authors were aware of or involved in the systematic manipulation of the publication process.

Wiley and Hindawi regrets that the usual quality checks did not identify these issues before publication and have since put additional measures in place to safeguard research integrity.

We wish to credit our own Research Integrity and Research Publishing teams and anonymous and named external researchers and research integrity experts for contributing to this investigation.

The corresponding author, as the representative of all authors, has been given the opportunity to register their agreement or disagreement to this retraction. We have kept a record of any response received.

References

[1] R. Wang and L. Deng, "Study on the Influence of Wuthering Heights Characters Based on Web Analysis and Text Mining," *Scientific Programming*, vol. 2022, Article ID 4326551, 11 pages, 2022.

Hindawi
Scientific Programming
Volume 2023, Article ID 9847362, 1 page
https://doi.org/10.1155/2023/9847362

Retraction

Retracted: Innovation and Practical Methods of Music Education Path in Colleges and Universities under the Popularization of the 5G Network

Scientific Programming

Received 18 July 2023; Accepted 18 July 2023; Published 19 July 2023

This article has been retracted by Hindawi following an investigation undertaken by the publisher [1]. This investigation has uncovered evidence of one or more of the following indicators of systematic manipulation of the publication process:

(1) Discrepancies in scope
(2) Discrepancies in the description of the research reported
(3) Discrepancies between the availability of data and the research described
(4) Inappropriate citations
(5) Incoherent, meaningless and/or irrelevant content included in the article
(6) Peer-review manipulation

The presence of these indicators undermines our confidence in the integrity of the article's content and we cannot, therefore, vouch for its reliability. Please note that this notice is intended solely to alert readers that the content of this article is unreliable. We have not investigated whether authors were aware of or involved in the systematic manipulation of the publication process.

Wiley and Hindawi regrets that the usual quality checks did not identify these issues before publication and have since put additional measures in place to safeguard research integrity.

We wish to credit our own Research Integrity and Research Publishing teams and anonymous and named external researchers and research integrity experts for contributing to this investigation.

The corresponding author, as the representative of all authors, has been given the opportunity to register their agreement or disagreement to this retraction. We have kept a record of any response received.

References

[1] Y. Sun and H. Jin, "Innovation and Practical Methods of Music Education Path in Colleges and Universities under the Popularization of the 5G Network," *Scientific Programming*, vol. 2022, Article ID 1536911, 7 pages, 2022.

Hindawi
Scientific Programming
Volume 2023, Article ID 9837098, 1 page
https://doi.org/10.1155/2023/9837098

Retraction

Retracted: System Analysis of the Learning Behavior Recognition System for Students in a Law Classroom: Based on the Improved SSD Behavior Recognition Algorithm

Scientific Programming

Received 18 July 2023; Accepted 18 July 2023; Published 19 July 2023

This article has been retracted by Hindawi following an investigation undertaken by the publisher [1]. This investigation has uncovered evidence of one or more of the following indicators of systematic manipulation of the publication process:

(1) Discrepancies in scope
(2) Discrepancies in the description of the research reported
(3) Discrepancies between the availability of data and the research described
(4) Inappropriate citations
(5) Incoherent, meaningless and/or irrelevant content included in the article
(6) Peer-review manipulation

The presence of these indicators undermines our confidence in the integrity of the article's content and we cannot, therefore, vouch for its reliability. Please note that this notice is intended solely to alert readers that the content of this article is unreliable. We have not investigated whether authors were aware of or involved in the systematic manipulation of the publication process.

Wiley and Hindawi regrets that the usual quality checks did not identify these issues before publication and have since put additional measures in place to safeguard research integrity.

We wish to credit our own Research Integrity and Research Publishing teams and anonymous and named external researchers and research integrity experts for contributing to this investigation.

The corresponding author, as the representative of all authors, has been given the opportunity to register their agreement or disagreement to this retraction. We have kept a record of any response received.

References

[1] Q. Guo, "System Analysis of the Learning Behavior Recognition System for Students in a Law Classroom: Based on the Improved SSD Behavior Recognition Algorithm," *Scientific Programming*, vol. 2022, Article ID 3525266, 11 pages, 2022.

Hindawi
Scientific Programming
Volume 2023, Article ID 9831951, 1 page
https://doi.org/10.1155/2023/9831951

Retraction

Retracted: Intelligent Detection of Foreign Matter in Coal Mine Transportation Belt Based on Convolution Neural Network

Scientific Programming

Received 18 July 2023; Accepted 18 July 2023; Published 19 July 2023

This article has been retracted by Hindawi following an investigation undertaken by the publisher [1]. This investigation has uncovered evidence of one or more of the following indicators of systematic manipulation of the publication process:

(1) Discrepancies in scope
(2) Discrepancies in the description of the research reported
(3) Discrepancies between the availability of data and the research described
(4) Inappropriate citations
(5) Incoherent, meaningless and/or irrelevant content included in the article
(6) Peer-review manipulation

The presence of these indicators undermines our confidence in the integrity of the article's content and we cannot, therefore, vouch for its reliability. Please note that this notice is intended solely to alert readers that the content of this article is unreliable. We have not investigated whether authors were aware of or involved in the systematic manipulation of the publication process.

Wiley and Hindawi regrets that the usual quality checks did not identify these issues before publication and have since put additional measures in place to safeguard research integrity.

We wish to credit our own Research Integrity and Research Publishing teams and anonymous and named external researchers and research integrity experts for contributing to this investigation.

The corresponding author, as the representative of all authors, has been given the opportunity to register their agreement or disagreement to this retraction. We have kept a record of any response received.

References

[1] G. Ma, X. Wang, J. Liu et al., "Intelligent Detection of Foreign Matter in Coal Mine Transportation Belt Based on Convolution Neural Network," *Scientific Programming*, vol. 2022, Article ID 9740622, 10 pages, 2022.

Hindawi
Scientific Programming
Volume 2023, Article ID 9829648, 1 page
https://doi.org/10.1155/2023/9829648

Retraction

Retracted: Feasibility Analysis of Intelligent Piano in Piano Teaching

Scientific Programming

Received 18 July 2023; Accepted 18 July 2023; Published 19 July 2023

This article has been retracted by Hindawi following an investigation undertaken by the publisher [1]. This investigation has uncovered evidence of one or more of the following indicators of systematic manipulation of the publication process:

(1) Discrepancies in scope
(2) Discrepancies in the description of the research reported
(3) Discrepancies between the availability of data and the research described
(4) Inappropriate citations
(5) Incoherent, meaningless and/or irrelevant content included in the article
(6) Peer-review manipulation

The presence of these indicators undermines our confidence in the integrity of the article's content and we cannot, therefore, vouch for its reliability. Please note that this notice is intended solely to alert readers that the content of this article is unreliable. We have not investigated whether authors were aware of or involved in the systematic manipulation of the publication process.

In addition, our investigation has also shown that one or more of the following human-subject reporting requirements has not been met in this article: ethical approval by an Institutional Review Board (IRB) committee or equivalent, patient/participant consent to participate, and/or agreement to publish patient/participant details (where relevant).

Wiley and Hindawi regrets that the usual quality checks did not identify these issues before publication and have since put additional measures in place to safeguard research integrity.

We wish to credit our own Research Integrity and Research Publishing teams and anonymous and named external researchers and research integrity experts for contributing to this investigation.

The corresponding author, as the representative of all authors, has been given the opportunity to register their agreement or disagreement to this retraction. We have kept a record of any response received.

References

[1] Y. Ma, "Feasibility Analysis of Intelligent Piano in Piano Teaching," *Scientific Programming*, vol. 2022, Article ID 5010428, 8 pages, 2022.

Hindawi
Scientific Programming
Volume 2023, Article ID 9803061, 1 page
https://doi.org/10.1155/2023/9803061

Retraction

Retracted: Tobacco Leaves Disease Identification and Spot Segmentation Based on the Improved ORB Algorithm

Scientific Programming

Received 18 July 2023; Accepted 18 July 2023; Published 19 July 2023

This article has been retracted by Hindawi following an investigation undertaken by the publisher [1]. This investigation has uncovered evidence of one or more of the following indicators of systematic manipulation of the publication process:

(1) Discrepancies in scope
(2) Discrepancies in the description of the research reported
(3) Discrepancies between the availability of data and the research described
(4) Inappropriate citations
(5) Incoherent, meaningless and/or irrelevant content included in the article
(6) Peer-review manipulation

The presence of these indicators undermines our confidence in the integrity of the article's content and we cannot, therefore, vouch for its reliability. Please note that this notice is intended solely to alert readers that the content of this article is unreliable. We have not investigated whether authors were aware of or involved in the systematic manipulation of the publication process.

Wiley and Hindawi regrets that the usual quality checks did not identify these issues before publication and have since put additional measures in place to safeguard research integrity.

We wish to credit our own Research Integrity and Research Publishing teams and anonymous and named external researchers and research integrity experts for contributing to this investigation.

The corresponding author, as the representative of all authors, has been given the opportunity to register their agreement or disagreement to this retraction. We have kept a record of any response received.

References

[1] M. Xu, L. Li, L. Cheng et al., "Tobacco Leaves Disease Identification and Spot Segmentation Based on the Improved ORB Algorithm," *Scientific Programming*, vol. 2022, Article ID 4285045, 12 pages, 2022.

Hindawi
Scientific Programming
Volume 2023, Article ID 9793108, 1 page
https://doi.org/10.1155/2023/9793108

Retraction

Retracted: The Method of Graphic Design Using 3D Virtual Vision Technology

Scientific Programming

Received 18 July 2023; Accepted 18 July 2023; Published 19 July 2023

This article has been retracted by Hindawi following an investigation undertaken by the publisher [1]. This investigation has uncovered evidence of one or more of the following indicators of systematic manipulation of the publication process:

(1) Discrepancies in scope
(2) Discrepancies in the description of the research reported
(3) Discrepancies between the availability of data and the research described
(4) Inappropriate citations
(5) Incoherent, meaningless and/or irrelevant content included in the article
(6) Peer-review manipulation

The presence of these indicators undermines our confidence in the integrity of the article's content and we cannot, therefore, vouch for its reliability. Please note that this notice is intended solely to alert readers that the content of this article is unreliable. We have not investigated whether authors were aware of or involved in the systematic manipulation of the publication process.

Wiley and Hindawi regrets that the usual quality checks did not identify these issues before publication and have since put additional measures in place to safeguard research integrity.

We wish to credit our own Research Integrity and Research Publishing teams and anonymous and named external researchers and research integrity experts for contributing to this investigation.

The corresponding author, as the representative of all authors, has been given the opportunity to register their agreement or disagreement to this retraction. We have kept a record of any response received.

References

[1] L. Li, "The Method of Graphic Design Using 3D Virtual Vision Technology," *Scientific Programming*, vol. 2022, Article ID 4135519, 9 pages, 2022.

Hindawi
Scientific Programming
Volume 2023, Article ID 9787612, 1 page
https://doi.org/10.1155/2023/9787612

Retraction

Retracted: Impact of Carbon Information on Enterprise Value: Analysis Model Design Based on Big Data

Scientific Programming

Received 18 July 2023; Accepted 18 July 2023; Published 19 July 2023

This article has been retracted by Hindawi following an investigation undertaken by the publisher [1]. This investigation has uncovered evidence of one or more of the following indicators of systematic manipulation of the publication process:

(1) Discrepancies in scope
(2) Discrepancies in the description of the research reported
(3) Discrepancies between the availability of data and the research described
(4) Inappropriate citations
(5) Incoherent, meaningless and/or irrelevant content included in the article
(6) Peer-review manipulation

The presence of these indicators undermines our confidence in the integrity of the article's content and we cannot, therefore, vouch for its reliability. Please note that this notice is intended solely to alert readers that the content of this article is unreliable. We have not investigated whether authors were aware of or involved in the systematic manipulation of the publication process.

Wiley and Hindawi regrets that the usual quality checks did not identify these issues before publication and have since put additional measures in place to safeguard research integrity.

We wish to credit our own Research Integrity and Research Publishing teams and anonymous and named external researchers and research integrity experts for contributing to this investigation.

The corresponding author, as the representative of all authors, has been given the opportunity to register their agreement or disagreement to this retraction. We have kept a record of any response received.

References

[1] C. Kong and Y. Zhao, "Impact of Carbon Information on Enterprise Value: Analysis Model Design Based on Big Data," *Scientific Programming*, vol. 2022, Article ID 6180988, 8 pages, 2022.

Hindawi
Scientific Programming
Volume 2023, Article ID 9783528, 1 page
https://doi.org/10.1155/2023/9783528

Retraction

Retracted: Emotion Analysis of Literary Works Based on Attentional Mechanisms and the Fusion of Two-Channel Features

Scientific Programming

Received 18 July 2023; Accepted 18 July 2023; Published 19 July 2023

This article has been retracted by Hindawi following an investigation undertaken by the publisher [1]. This investigation has uncovered evidence of one or more of the following indicators of systematic manipulation of the publication process:

(1) Discrepancies in scope
(2) Discrepancies in the description of the research reported
(3) Discrepancies between the availability of data and the research described
(4) Inappropriate citations
(5) Incoherent, meaningless and/or irrelevant content included in the article
(6) Peer-review manipulation

The presence of these indicators undermines our confidence in the integrity of the article's content and we cannot, therefore, vouch for its reliability. Please note that this notice is intended solely to alert readers that the content of this article is unreliable. We have not investigated whether authors were aware of or involved in the systematic manipulation of the publication process.

Wiley and Hindawi regrets that the usual quality checks did not identify these issues before publication and have since put additional measures in place to safeguard research integrity.

We wish to credit our own Research Integrity and Research Publishing teams and anonymous and named external researchers and research integrity experts for contributing to this investigation.

The corresponding author, as the representative of all authors, has been given the opportunity to register their agreement or disagreement to this retraction. We have kept a record of any response received.

References

[1] Y. Han, "Emotion Analysis of Literary Works Based on Attentional Mechanisms and the Fusion of Two-Channel Features," *Scientific Programming*, vol. 2022, Article ID 8237466, 9 pages, 2022.

Hindawi
Scientific Programming
Volume 2023, Article ID 9783524, 1 page
https://doi.org/10.1155/2023/9783524

Retraction

Retracted: An Auxiliary Teaching System for Spoken English Based on Speech Recognition Technology

Scientific Programming

Received 18 July 2023; Accepted 18 July 2023; Published 19 July 2023

This article has been retracted by Hindawi following an investigation undertaken by the publisher [1]. This investigation has uncovered evidence of one or more of the following indicators of systematic manipulation of the publication process:

(1) Discrepancies in scope
(2) Discrepancies in the description of the research reported
(3) Discrepancies between the availability of data and the research described
(4) Inappropriate citations
(5) Incoherent, meaningless and/or irrelevant content included in the article
(6) Peer-review manipulation

The presence of these indicators undermines our confidence in the integrity of the article's content and we cannot, therefore, vouch for its reliability. Please note that this notice is intended solely to alert readers that the content of this article is unreliable. We have not investigated whether authors were aware of or involved in the systematic manipulation of the publication process.

Wiley and Hindawi regrets that the usual quality checks did not identify these issues before publication and have since put additional measures in place to safeguard research integrity.

We wish to credit our own Research Integrity and Research Publishing teams and anonymous and named external researchers and research integrity experts for contributing to this investigation.

The corresponding author, as the representative of all authors, has been given the opportunity to register their agreement or disagreement to this retraction. We have kept a record of any response received.

References

[1] L. Bao and J. Lv, "An Auxiliary Teaching System for Spoken English Based on Speech Recognition Technology," *Scientific Programming*, vol. 2022, Article ID 6519228, 11 pages, 2022.

Hindawi
Scientific Programming
Volume 2023, Article ID 9767390, 1 page
https://doi.org/10.1155/2023/9767390

Retraction

Retracted: A Method of Extracting and Identifying College Students' Music Psychological Features Based on EEG Signals

Scientific Programming

Received 18 July 2023; Accepted 18 July 2023; Published 19 July 2023

This article has been retracted by Hindawi following an investigation undertaken by the publisher [1]. This investigation has uncovered evidence of one or more of the following indicators of systematic manipulation of the publication process:

(1) Discrepancies in scope
(2) Discrepancies in the description of the research reported
(3) Discrepancies between the availability of data and the research described
(4) Inappropriate citations
(5) Incoherent, meaningless and/or irrelevant content included in the article
(6) Peer-review manipulation

The presence of these indicators undermines our confidence in the integrity of the article's content and we cannot, therefore, vouch for its reliability. Please note that this notice is intended solely to alert readers that the content of this article is unreliable. We have not investigated whether authors were aware of or involved in the systematic manipulation of the publication process.

In addition, our investigation has also shown that one or more of the following human-subject reporting requirements has not been met in this article: ethical approval by an Institutional Review Board (IRB) committee or equivalent, patient/participant consent to participate, and/or agreement to publish patient/participant details (where relevant).

Wiley and Hindawi regrets that the usual quality checks did not identify these issues before publication and have since put additional measures in place to safeguard research integrity.

We wish to credit our own Research Integrity and Research Publishing teams and anonymous and named external researchers and research integrity experts for contributing to this investigation.

The corresponding author, as the representative of all authors, has been given the opportunity to register their agreement or disagreement to this retraction. We have kept a record of any response received.

References

[1] L. Liang, "A Method of Extracting and Identifying College Students' Music Psychological Features Based on EEG Signals," *Scientific Programming*, vol. 2022, Article ID 1503757, 10 pages, 2022.

Hindawi
Scientific Programming
Volume 2023, Article ID 9761635, 1 page
https://doi.org/10.1155/2023/9761635

Retraction

Retracted: Redistribution of Resources: Sustainable System Mechanisms for Enterprise Migration

Scientific Programming

Received 18 July 2023; Accepted 18 July 2023; Published 19 July 2023

This article has been retracted by Hindawi following an investigation undertaken by the publisher [1]. This investigation has uncovered evidence of one or more of the following indicators of systematic manipulation of the publication process:

(1) Discrepancies in scope
(2) Discrepancies in the description of the research reported
(3) Discrepancies between the availability of data and the research described
(4) Inappropriate citations
(5) Incoherent, meaningless and/or irrelevant content included in the article
(6) Peer-review manipulation

The presence of these indicators undermines our confidence in the integrity of the article's content and we cannot, therefore, vouch for its reliability. Please note that this notice is intended solely to alert readers that the content of this article is unreliable. We have not investigated whether authors were aware of or involved in the systematic manipulation of the publication process.

Wiley and Hindawi regrets that the usual quality checks did not identify these issues before publication and have since put additional measures in place to safeguard research integrity.

We wish to credit our own Research Integrity and Research Publishing teams and anonymous and named external researchers and research integrity experts for contributing to this investigation.

The corresponding author, as the representative of all authors, has been given the opportunity to register their agreement or disagreement to this retraction. We have kept a record of any response received.

References

[1] Y. Wang, Y. Liang, Y. Wang, Z. Li, and C. Guo, "Redistribution of Resources: Sustainable System Mechanisms for Enterprise Migration," *Scientific Programming*, vol. 2022, Article ID 2898460, 17 pages, 2022.

Hindawi
Scientific Programming
Volume 2023, Article ID 9760437, 1 page
https://doi.org/10.1155/2023/9760437

Retraction

Retracted: The Integrated Development of Furniture Design and Children's Characteristics Based on Artificial Intelligence

Scientific Programming

Received 18 July 2023; Accepted 18 July 2023; Published 19 July 2023

This article has been retracted by Hindawi following an investigation undertaken by the publisher [1]. This investigation has uncovered evidence of one or more of the following indicators of systematic manipulation of the publication process:

(1) Discrepancies in scope
(2) Discrepancies in the description of the research reported
(3) Discrepancies between the availability of data and the research described
(4) Inappropriate citations
(5) Incoherent, meaningless and/or irrelevant content included in the article
(6) Peer-review manipulation

The presence of these indicators undermines our confidence in the integrity of the article's content and we cannot, therefore, vouch for its reliability. Please note that this notice is intended solely to alert readers that the content of this article is unreliable. We have not investigated whether authors were aware of or involved in the systematic manipulation of the publication process.

Wiley and Hindawi regrets that the usual quality checks did not identify these issues before publication and have since put additional measures in place to safeguard research integrity.

We wish to credit our own Research Integrity and Research Publishing teams and anonymous and named external researchers and research integrity experts for contributing to this investigation.

The corresponding author, as the representative of all authors, has been given the opportunity to register their agreement or disagreement to this retraction. We have kept a record of any response received.

References

[1] W. Zhang and S. Li, "The Integrated Development of Furniture Design and Children's Characteristics Based on Artificial Intelligence," *Scientific Programming*, vol. 2022, Article ID 6036160, 9 pages, 2022.

Hindawi
Scientific Programming
Volume 2023, Article ID 9756367, 1 page
https://doi.org/10.1155/2023/9756367

Retraction

Retracted: Analysis of the Impact of Moral Education in Colleges and Universities Based on Short Video Technology

Scientific Programming

Received 18 July 2023; Accepted 18 July 2023; Published 19 July 2023

This article has been retracted by Hindawi following an investigation undertaken by the publisher [1]. This investigation has uncovered evidence of one or more of the following indicators of systematic manipulation of the publication process:

(1) Discrepancies in scope
(2) Discrepancies in the description of the research reported
(3) Discrepancies between the availability of data and the research described
(4) Inappropriate citations
(5) Incoherent, meaningless and/or irrelevant content included in the article
(6) Peer-review manipulation

The presence of these indicators undermines our confidence in the integrity of the article's content and we cannot, therefore, vouch for its reliability. Please note that this notice is intended solely to alert readers that the content of this article is unreliable. We have not investigated whether authors were aware of or involved in the systematic manipulation of the publication process.

Wiley and Hindawi regrets that the usual quality checks did not identify these issues before publication and have since put additional measures in place to safeguard research integrity.

We wish to credit our own Research Integrity and Research Publishing teams and anonymous and named external researchers and research integrity experts for contributing to this investigation.

The corresponding author, as the representative of all authors, has been given the opportunity to register their agreement or disagreement to this retraction. We have kept a record of any response received.

References

[1] Y. Jiang, "Analysis of the Impact of Moral Education in Colleges and Universities Based on Short Video Technology," *Scientific Programming*, vol. 2022, Article ID 3337606, 7 pages, 2022.

Hindawi
Scientific Programming
Volume 2023, Article ID 9885859, 10 pages
https://doi.org/10.1155/2023/9885859

Research Article

Automatic Annotation of Functional Semantics for 3D Product Model Based on Latent Functional Semantics

Zhoupeng Han, Hua Zhang, Weirong He, Li Ba, and Qilong Yuan

Key Laboratory of NC Machine Tools and Integrated Manufacturing Equipment of the Education Ministry, Xi'an University of Technology, Xi'an 70048, China

Correspondence should be addressed to Zhoupeng Han; hanzp@xaut.edu.cn

Received 6 October 2022; Revised 21 October 2022; Accepted 24 November 2022; Published 4 February 2023

Academic Editor: Lianhui Li

To support effectively function-driven 3D model retrieval in the phase of mechanical product conceptual design and improve the efficiency of functional semantics annotation for 3D models, an approach for functional semantics automatic annotation for mechanical 3D product model based on latent functional semantics is presented. First, the design knowledge and function knowledge of mechanical product model are analyzed, and the ontology-based functional semantics for assembly product is constructed. Then, some concept about functional region is defined, and the 3D product model is decomposed into functional regions with different levels of granularity. The similarity of the functional region is evaluated considering multisource attribute information and geometric shape. Subsequently, the similarity based on latent functional semantics annotation model for functional regions is established, which is employed for annotating automatic latent functional semantics in the 3D product model structure. Finally, mechanical 3D models in the model library are used to verify the effectiveness and feasibility of the proposed approach.

1. Introduction

More and more 3D models have been accumulated with 3D CAD software applied widely in enterprises, which are important knowledge resources and can be employed for reference and reuse during developing new products. When 3D CAD model is reused, it is very difficult for meeting the practical needs of engineering designers by retrieving the CAD model only considering the topological and geometric information. Especially, in the process of product conceptual design, engineers pay more attention to searching for 3D CAD model structures with specific functions by making use of product function requirements' information. The existing 3D model structures embodying plenty of design/assembly intent can achieve specific function requirements. However, there is no explicit and clear correlation mapping relationship between structure and function. The functional semantics tagging correspondingly to the model structure is becoming a hot issue in the 3D model reuse field.

In the process of design and development for mechanical products utilizing computer-aided design systems, designers mostly design the structure/geometry of 3D product model in terms of the product's functional requirements, parameters, and performance. The functional requirements' information and the 3D model structure are independent. In this case, there is a gap between functions and structures for the 3D product CAD model [1]. It means that there is no explicit and clear structure-function correlation for an isolated 3D CAD model, lacking of functional information that the structure can accomplish. It will have an impact on the level of 3D model reuse.

Currently, the research on the 3D CAD model retrieval is mainly grouped into two classification: geometry-based [2, 3] retrieval and topology-based [4, 5] retrieval. But these query information is uncertain and vague; at the stage of product conceptual design, it is difficult to support the reuse of 3D CAD model knowledge. With the emergence of semantic modeling tools, some researchers are concerned for visualization and semantic expression for resolving the

semantics gap between the high-level design semantics and the bottom-level geometric shape of the 3D model. To simplify the process of semantic-based 3D model retrieval, Attene et al. [6] presented a semantic description of the local shape of the 3D model, where the 3D model is segmented into regions and the segmented region is labeled with marking semantics by using ontology-based concept instance semantics. Cheng et al. [7] proposed a complex surface shape design method for the CAD model based on semantic features, where the different geometric constraints and geometric surface types are defined as corresponding semantic features, and the semantic features are used for modeling complex surfaces of the CAD model. To capture the design intent of the 3D model, Abdul-Ghafour et al. [8] integrated semantic web into the CAD system and built a common design feature ontology for feature modeling of the CAD model, where the semantics is used for modeling and reasoning, and the association relationship between the product data can be effectively managed and discovered.

The existing semantics annotation methods for 3D models mainly considered the geometric shape and topological structure information. On the basis of semantic labeled sample 3D models, machine learning algorithm is employed for automatic semantics annotation [9]. However, there are fewer researchers on functional semantics annotation of 3D models. In fact, functional semantics as a special class of semantics is not only an abstraction of geometric shapes, but also a high-level semantic description for potential information such as design or assembly intent, usage, and efficacy of the 3D model. The functional semantics annotation of the 3D model is much more difficult and complex than the shape or structure semantics annotation; it still faces many challenges for functional semantics-based retrieval of the 3D model. To meet the requirements of the CAD model retrieval at the stage of mechanical product conceptual design, Wang et al. [10] constructed function semantic ontology of 3D CAD models, where the overall functional semantics of 3D models are annotated, and the functional semantics-based retrieval of 3D models is realized. It is concerned about functional semantics annotation of the 3D part model, lacking functional analysis and annotation of the 3D assembly model at different granularity structure. Han et al. [11] proposed an approach for structure-function semantic correlation analysis and annotation of the 3D assembly model, where the 3D assembly model is divided into different functional regions for structure-function semantic correlation analysis, and the polychromatic sets is used to describe correlations of structure-function semantics. This method is concerned with the structure-function analysis of the 3D parts/assembly model, and functional semantics is labeled by the human-computer interaction mode so that the annotation efficiency is not high. Hao et al. [12] took key parts in the assembly model as the object and evaluated the similarity of the participated shape structure key parts. The functional semantics is annotated based on the shape and structure similarity, without consideration attribute information of the 3D model structure. The accuracy of the functional semantic annotation is affected to some extent. The function is not only related to the geometric shape of the 3D model, but also related to the geometric parameters, type of kinematic pair, and so on. Therefore, a reasonable and feasible solution for structure-function semantic correlation analysis and automatic annotation of the 3D product model can be provided by comprehensively considering geometric structure and attribute information of the 3D model.

Functions can reflect the specific requirement, objective, and purpose that the product needs to achieve, which exists throughout the life of the product design. In the stage of the product conceptual design, it is usually on the premise that the product function requirements have been determined to find correspondingly the structural design scheme, that is, the product function-structure mapping. Function-structure mapping is the key process of the top-down product design, which is an approach of transforming the product function model to parametric structure model [13]. The function is the abstraction of the product structure and the purpose of structure realization, and the structure is the shape and composition structure that is shown to achieve certain functions. The mapping relation of function-structure is a many-to-many relationship, where a certain function may be completed by one structure or multiple structures, and a structure may also implement one or more functions. The current more typical design process model about function-structure mapping relation include function-structure (Function-Structure, FS) [14] and function-behavior-structure [15]. To realize the relationship between the function and structure, a behavioral layer is introduced to describe the action and principle which are performed to complete the function, and explain "how the structure realizes the function." Based on that, the models including function-behavior-state model [16] is proposed. The issue about function-structure mapping can be effectively solved by using the abovementioned approaches in the product conceptual design.

To improve the efficiency and accuracy of the structure-function semantic annotation for the 3D CAD product model, and support 3D CAD model retrieval by means of functional semantics, an approach for structure-function semantic automatic annotation of the 3D product CAD model is presented. The structure of the 3D product model is decomposed into functional regions (i.e. assembly region and flow-activity region) with different levels of granularity. Multisource attributes information and structural similarity are considered for evaluating the similarity between any two functional regions. Based on that, an approach for automatic annotation of latent functional semantics for 3D model structure based on semi-supervised learning is built for improving the accuracy and efficiency of functional semantics annotation of the 3D model structure.

This rest of the paper is organized as follows: ontology-based functional semantics is constructed for providing standard and formal terms for functional semantic annotation in the 3D product model is discussed in Section 2. In Section 3, similarity evaluation of the 3D product model structure is given by taking advantage of multisource information. A latent functional semantic annotation model of

functional regions is presented in Section 4. Cases are designed and tested in Section 5. In Section 6, the paper is concluded and further works are provided.

2. Function Ontology of the 3D Product Model

2.1. Product Function Classification. Design knowledge is mainly related to the product conceptual and detailed design phase, which contains design document, domain expert experience, and so on. The design knowledge can help capture design and assemble intent of the 3D CAD model, which can provide basis and support for design thinking analysis for the correlation between the structure and function of the 3D model. It can be obtained from design documents, PDM, BoM, machining, assembly process documents, and so on.

The function is viewed as an abstract description of the task that a system or product can accomplish, and the parameters or state changing when the system or subsystem is input/output. It is an understanding for the system from the perspective of technical realization, as explanatory description and behavior abstraction of the structure, which is the main goal and core of the product design. Product function is generally determined in the stage of the product conceptual design and has an essential role in the life of the product design.

The concept of function basis, classification of function, and flow is proposed [17]. On this basis, the function is described as "verb + object," where the function is expressed through the verb and noun form. In this paper, the basic classifications of the function are further summarized and refined for covering the function's description of the mechanical product as far as possible. Based on that, function ontology is constructed for providing functional semantic specification and expression of the 3D product model structure in the mechanical field. The functional classification and common terms of the mechanical product are shown in Table 1.

2.2. Function Ontology. Ontology, as explicit and formal specification of conceptualization, can offer a formal description and defining common terms, classification, and relationship for conceptualization, which can be employed to represent, storage, share, and integrate knowledge [18]. To reduce and avoid the randomness and ambiguity of functional description and ensure standardization of the definition of functional vocabulary, a function ontology should be constructed to standardize the functional vocabulary of the product, so that functional terms of the 3D product model structure have a unified and standard expression form. According to the classification of the function and flow of mechanical products, the function ontology was constructed by Protégé through the analysis of function and flow concepts and their logical relationships. Parts of function ontology are shown in Figure 1, where the solid blue line represents parent-child relationship of concepts and the dashed red line represents object attribute relationship between concepts [11].The function ontology provides standard terms of functional semantic annotation of the 3D product model.

3. Similarity Evaluation of the 3D Product Model Structure Considering Multisource Information

3.1. Functional Region. To analyze convenient assembly constraints of the product model, assembled parts are grouped into two categories: functional part and connector [19]. The connected relationships between assembled parts are classified into soft connection and hard connection in terms of corresponding connection relationship [20]. Connectors contain a type of part used for sealing or fastening, such as gaskets, screws, bolts, nuts, pins, keys, and other standard parts. The functional part is viewed as some function characteristics apart from connectors.

Functional Region: For a 3D product model, the function mainly reflects in the structure at different granularity level. The structure unit with certain function characteristics is considered as a functional region. Functional region may be a subassembly structure composed of multiple parts or shape structure of the part. To annotate easily functional semantics' indifferent granularity structure for the 3D assembly model, functional regions are grouped into assembly region and flow-activity region. The functional structure of the 3D product model can be considered comprehensively by the assembly region and flow-activity region from the aspects of assembly structure and part shape. The correlation relationships between the function and structure is analyzed comprehensively from the coarse and fine-granularity structure of the 3D product model.

3.2. Functional Region Similarity Considering Multisource Information. The similarity for functional regions of the 3D product model is evaluated by considering multiple attributes and geometric shapes.

3.2.1. Multisource Information Similarity of the Assembled Part. Multisource information is mainly grouped into qualitative attribute, quantitative attribute, text attribute [21], and geometric shape. The similarity calculation rule and method of each classification information of the assembled part are given as follows [22]:

(1) Quantitative attribute: The attributes are quantitative including size, surface area, volume, and so on. It can be expressed by a numeric value. The similarity of the quantitative attribute can be expressed as follows:

$$\text{sim\_attribute}\left(q_k^i, p_k^j\right) = 1 - \left|\frac{q_k^i - p_k^j}{\max\left(q_k^i, p_k^j\right)}\right|, \quad (1)$$

where q_k^i denotes the kth quantitative attribute of part i for the product model Q and p_k^i denotes the kth quantitative attribute of part j for the product model P.

Table 1: Functional classification and common terms of the mechanical product.

Functional classification	Functional basis	Verb vocabulary
Branch	Separate	Isolate, disconnect, cut, and detach
	Remove	Cut, lathe, mill, drill, grind, polish, bore, and remove
	Divide	Disassembly, isolate, release, classify, group, and divide
	Refine	Extract, filter, purify, permeate, wash, clean, and refine
	Distribute	Disperse, spread, dissipate, disperse, and distribute
Channel	Import	Entry, accept, permit, capture, and import
	Export	Discharge, eject, jet, release, destroy, eliminate, and export
	Transfer	Convey, handle, carry, move, lift, conduct, communicate, and transmit
	Guide	Guide, drive, switch, move, transfer, migrate, rotate, turn, flip, limit, release, and oriented
Connect	Couple	Connect, assemble, install, tie, and couple
	Mix	Merge, merge, package, mix, add, and mix
Control	Actuate	Begin, start, launch, initiate, and actuate
	Regulate	Control, balance, limit, block, interrupt, delay, close, forbid, and allow
	Change	Adapt, correct, reverse, adjust, modify, increase, enlarge, magnify, enhance, enlarge, expand, strengthen, reduce, weaken, shrink, reduce, compress, transform, construct, form, and change
	Stop	Inhibit, protect, seal, insulate, isolate, shield, end, close, terminate, stop, interrupt, and prevent
Convert	Convert	Conversion, transform, concentrate, melt, liquefy, solidify, evaporate, fusion, integrate, and process
Supply	Store	Store, contain, include, encapsulate, enclose, accumulate, gather, collect, reserve, occupy, and retain
	Supply	Supply, furnish, fill, supplement, and expose
Signal	Sense	Sense, identify, distinguish, and confirm
	Display	Display, show, indicate, register, record, expose, choose, and select
	Measure	Measure, calculate, process, estimate, check, proofread, examine, and compare
Support	Stabilize	Stabilize, firm, and prop
	Secure	Secure, place, arrange, press, clamp, and tighten
	Position	Position, orient, limit, and guide

(2) Qualitative attribute: The attributes are not quantified, such as face type of the part, design/assembled feature type, and so on. The similarity of the qualitative attribute is expressed as follows:

$$\text{sim\_attribute}\left(q_k^i, p_k^j\right) = \begin{cases} 1, & q_k^i = p_k^j, \\ 0, & \text{else}, \end{cases} \tag{2}$$

where q_k^i denotes the kth qualitative attribute of part i for the product model Q and p_k^i denotes the kth qualitative attribute of part j for the product model P.

(3) Text attribute: The attributes are expressed mostly by string/text set for assembled constraints [23]. The set theory is employed to the similarity of the text attribute, which is expressed as follows:

$$\text{sim\_attribute}\left(q_k^i, p_k^j\right) = \frac{q_k^i \cap p_k^j}{q_k^i \cup p_k^j}, \tag{3}$$

where q_k^i denotes the kth text attribute of part i for the product model Q and p_k^i denotes the kth text attribute of part j for the product model P.

(4) Geometric shape: The geometric shape of assembled parts is taken into account during the similarity of the functional region. The similarity calculation about the geometric shape is mainly referred to the literature [24]. Here, it can be expressed as $\text{sim\_shape}\,(q_k^i, p_k^j)$.

(5) Multisource information similarity of parts: Based on similarity evaluation of assembled parts considering multisource information, the weight coefficient α is introduced for describing the importance degree of each factor in terms of requirements of engineering designer. The similarity of parts considering multisource attributes $sim\_part\,(q^i, p^j)$ can be expressed as follows:

$$\begin{cases} \text{sim\_part}\left(q^i, p^j\right) = \omega_1 \bullet \sum_{t=1}^{T} \text{sim\_attribute}\left(q_k^i, p_k^j\right) \bullet \alpha_k + \omega_2 \bullet \text{sim\_shape}\left(q_k^i, p_k^j\right), \\ \sum_{t=1}^{T} \alpha_t = 1, \end{cases} \tag{4}$$

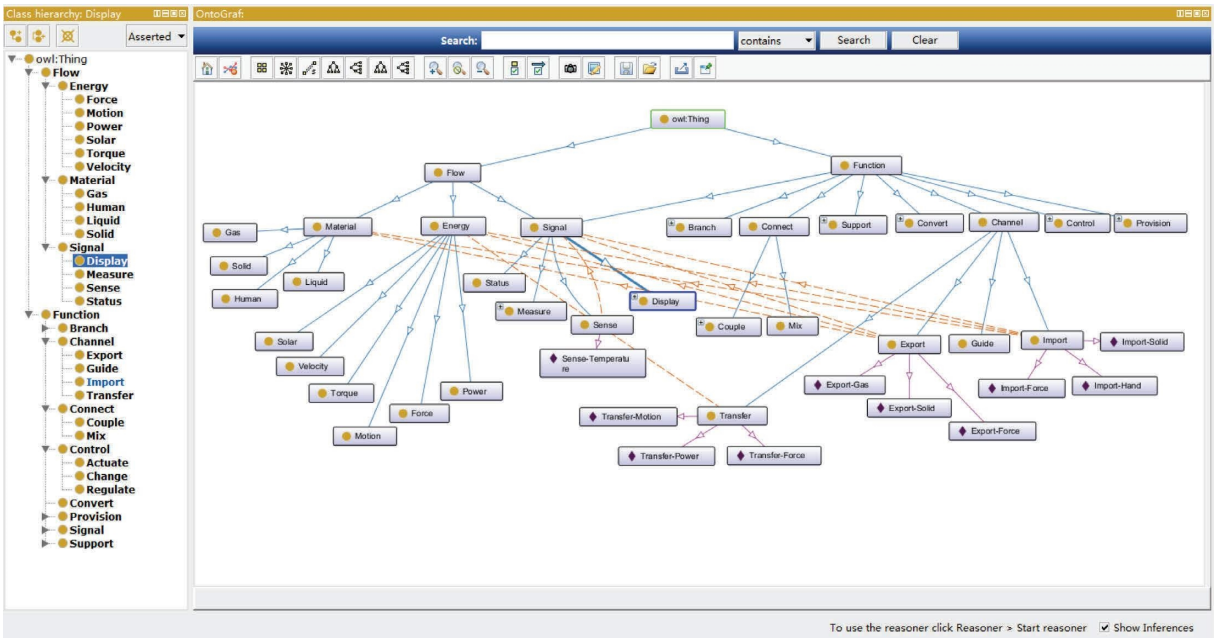

Figure 1: Parts of function ontology for the CAD product model.

where $\text{sim\_attribute}(q^i, p^j)$ denotes the similarity of part i for the assembly region Q and part j for the assembly region P considering multisource attributes, T denotes the total number of attributes, α_t denotes the weight of the tth attribute, w_1 denotes the weight of the similarity of attribute information, and w_2 denotes the weight of the similarity of the geometric shape.

3.2.2. Similarity Measure of the Functional Region. The similarity of the functional region mainly contains the similarity of the assembly region and the flow- activity region.

(1) Similarity measure of the assembly region: Similarity of assembly region should not only consider the shape structure and attribute information of assembled parts, but also take into account the information of assembly relation, such as connection form, contact form, degree of freedom, assembly feature pair and so on. By using the above similarity evaluation through multisource attribute, the similarity for assembly relationship could be expressed as follows:

$$\begin{cases} \text{sim\_relationship}\left(q^i, p^j\right) = \sum_{h=1}^{H} \text{sim\_attribute}\left(q_k^i, p_k^j\right) \bullet \beta_h, \\ \sum_{h=1}^{H} \beta_h = 1, \end{cases} \tag{5}$$

where $\text{sim\_relationship}(q^i, p^j)$ denotes the similarity for assembly relationships between assembled parts i and j for the product models Q and P, H denotes the number of attributes for assembly relationships, and β_h denotes the weight of the hth attribute.

Considering the attributes about the assembly relationship and assembled part comprehensively, the similarity of the assembly region can be expressed as follows:

$$\text{sim\_assem}\left(q^i, p^j\right) = \text{sim\_part}\left(q^i, p^j\right) \bullet w_1 + \text{sim\_relationship}\left(q^i, p^j\right) \bullet w_2, \tag{6}$$

where w_1 denotes the weight of similarity of the assembled part and w_2 denotes the corresponding assembly relationship similarity.

The assembly region may consist of different assembled parts. It is necessary that the assembled parts should be considered as matching problem between regions while calculating the similarity of assembly region. In fact, it has found the best assembled parts pair among two part-sets from corresponding functional regions when the total sum value of the similarity between functional region pairs is maximal. The matching problem can be solved by using maximum matching in the weighted bipartite graph. The Kuhn–Munkres algorithm [25] adopted the similarity $sim_{ass}(Q, P)$ between the assembly regions Q and P can be expressed as follows:

$$\mathrm{sim}_{\mathrm{ass}}(Q,P) = \frac{\sum_{l(q_i,p_j)\in L_0} \mathrm{sim\_assem}(q_i, p_j)}{\max(m,n)}, \tag{7}$$

where M denotes the maximal matching, L_0 denotes the set of corresponding edges, $l(q_i^i, p_j^j) \in L_0$ denotes the best matching between assembled parts q^i and p^j, and m, n denote respectively the number of assembled parts in assembly regions Q and P.

(2) Similarity measure of the flow-activity region: Flow-activity area mainly refers to the shape structure of the part that does not participate in the assembly region. In fact, it specifically refers to the similarity evaluation of the part model. Similarity of the flow-activity region q' and the flow-activity region p', $sim_{part}(q', p')$ can be expressed as follows:

$$\mathrm{sim}_{\mathrm{part}}(q', p') = \mathrm{sim\_part}(q', p'), \tag{8}$$

during the similarity evaluation, the weight values can be determined by domain expert and experience generally. Moreover, to avoid subjective interference, the weight values can be determined by using AHP and TOPSIS [26].

4. Latent Function Semantic Annotation of the Functional Region

Functional region as a structure with certain functions in the 3D product model, functional semantic annotation of the functional region is viewed as essentially functional semantic annotation of the model structure. Through analysis of the function region, the function that the corresponding structure of the function region can achieve will be obtained. Based on that, the corresponding latent functional semantics can be annotated. The process of latent functional semantic annotation of the functional region consists of two steps: ① functional semantic annotation of sample CAD models, that is, the structure-function is analyzed for 3D CAD product sample models, and corresponding functional semantics is annotated interactively. ② Latent functional semantic annotation based on the similarity. A latent functional semantic prediction model is built for automatically annotating latent functional semantics in the 3D assembly model structure. The process of latent functional semantic annotation of the functional region is shown in Figure 2.

4.1. Functional Semantic Annotation of the Sample Model. For mechanical product, functions are mainly reflected in assembly regions and flow-activity regions. Through analyzing the structure-function of the product model from the two aspects of the assembly region and the flow-activity region.

(1) Functional semantic interactive annotation of the assembly region: The assembly region can be expressed by assembled parts, assembly feature, and corresponding attribute information involved in the assembled structure. By analyzing the part attributes, connection types, matching types, degrees of freedom, and other information in the assembly region, together with the mechanical design theory and design experience, designers can capture the assembly intent, function, and degree of freedom, which is contained in the features of the assembly region. According to the function ontology, functional semantics of the assembled structure are labeled, thereby absorbing and understanding the assembly structure knowledge.

(2) Functional semantics interactive annotation of Flow-activity region: Flow-activity region is a description of the geometric shape with some functions in the functional parts, except for participating fit or assembled structure. The structure represented by a flow-activity region is considered as a carrier in the process of function flow from input to output. Therefore, when analyzing the flow-activity region, it is needful to consider the input and output of flow during the working process of the assembled structure. The key integral/local structures and corresponding functions in the assembled function part represented by the flow-activity region is acquired. The flow-activity region can be described by the design feature, attribute, and other information of the part, for example, the shape feature, geometric shape surface, and other attribute descriptions of the part model.

4.2. Latent Function Semantic Annotation of the Function Region. There are many-to-many mapping relationships between structures and functions, that is, the same structure will perform different functions in different products, and different structures will also achieve the same function. In most cases, structures with the same attributes may achieve the same functions for different assembly models. It is a probability event that the same structure is provided with the same function. As the similarity of the structure increases, the probability having the same function also increases. Based on that, a prediction model for latent functional

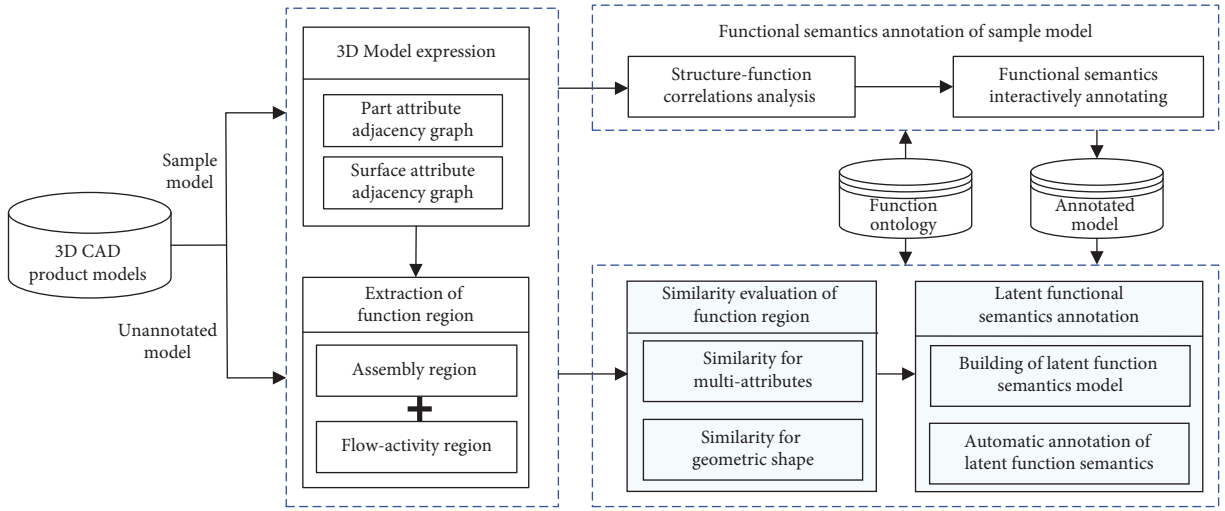

Figure 2: The process of latent functional semantic annotation of the functional region.

semantic annotation of the 3D CAD product model is given using sample models annotated functional semantics. Drawing on the historical information of the structure-function semantic annotation, the probability that the product model structure can achieve certain functions is inferred. Finally, combining with the participation of artificial knowledge, the functional semantics that can be realized is determined. It enhances the efficiency of functional semantics annotating to some extent.

Assuming that the annotated functional semantic model library is M, the unannotated structure (functional region) is $Stru$. The structure in the model library M that has the maximum similarity with the structure $Stru$ is $Stru_{\max}$, and the latent functional semantic annotation model based on the similarity can be expressed as follows:

$$p\left(f_i \mid \mathrm{Stru}\right) = \mathrm{Sim}\left(\mathrm{Stru}, \mathrm{Stru}_{\max}\right) * \frac{\mathrm{count}\left(f_i \mid \mathrm{Stru}_{\max}\right)}{\mathrm{sum}\left(\mathrm{Stru}_{\max}\right)}, \tag{9}$$

where $p(f_i|Stru)$ denotes the probability that the structure $Stru$ can achieve the function f_i. $Stru$ represents the unannotated structure (functional region). $Stru_{\max}$ represents the structure (functional region) in the model library M that has the greatest similarity with the structure to the unannotated structure $Stru$. $Sim(Stru, Stru_{\max})$ represents the similarity between $Stru_{\max}$ and $Stru$, equations (7) and (8) are used for similarity measurement of functional regions. $Sum(Stru_{\max})$ denotes the number of the structure $Stru_{\max}$ in the model library M. $Count(f_i|Stru_{max})$ denotes the number of the structure $Stru_{\max}$ that has the function f_i in the model library M.

5. Case Study

5.1. Function Semantic Annotation of the Sample Model. The 3D CAD model of gear oil pump is used as an example for analyzing and annotating functions in the 3D product model. The correlation relationship among the structure, function, and attribute of the 3D model is expressed by using the polychromatic set, and corresponding functional semantics is annotated interactively. The 3D CAD product model of gear oil pump and parts information is shown in Figure 3.

The 3D model structure of gear oil pump is divided into several independent and stable assembly regions AR1~AR8. The parts and assembly feature pairs attribute information contained in the assembly region are analyzed for determining the functions that can be realized in each assembly region. The function analysis of the flow-activity region is mainly about the function analysis of the local shape structure that can transmit the flow in the 3D part model. The flow-activity region of the functional part that can transmit flow is analyzed from the perspective of the material flow, signal flow, and energy flow. Through the structure function analysis and functional semantic annotation of the flow-activity region, the key structure in the parts can be discovered and the design intent can be captured. It improves the efficiency of complex parts and key structures reuse. The functional region and functional semantic annotation in the 3D CAD model of gear oil pump is shown in Table 2.

5.2. Latent Functional Semantic Annotation Based on Similarity. Some 3D CAD product models with annotated functional semantics can be obtained through the structure-function correlation analysis and functional semantics labeling for 3D CAD product sample models. Based on that, the latent functional semantic prediction model based on the similarity can be used to automatically annotate the functional semantics in 3D CAD product models in the model library. Through equation (9), the latent functional semantics can be predicted and annotated probabilistically.

Several typical 3D models are taken as example, which is given with latent functional semantics corresponding probability, as shown in Table 3. Among them, the maximum similarity structure is the annotated model structure in the model library, and the probability of latent functional

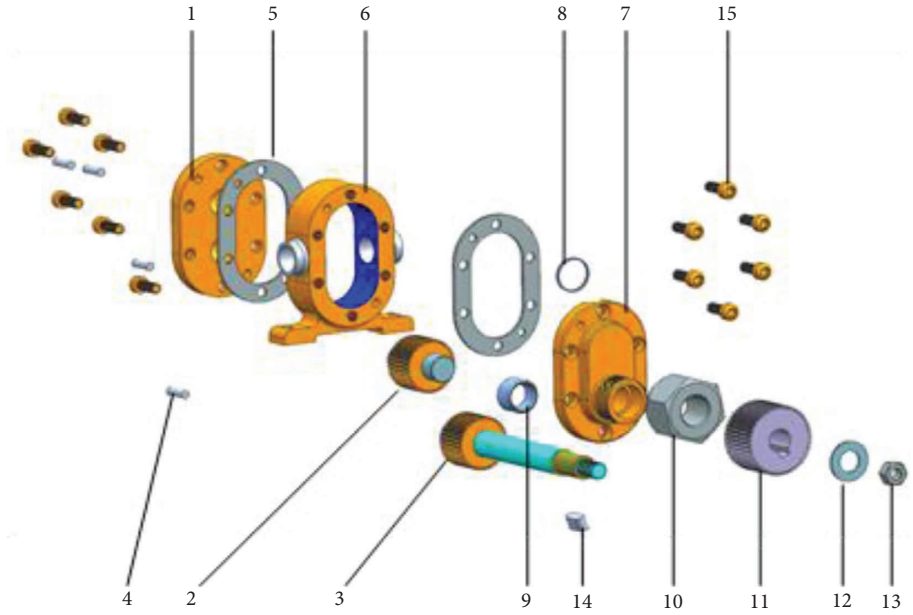

Figure 3: 3D CAD model of gear oil pump.

Table 2: Functional regions and their functional semantics.

Category	*FR*	Assembled part	Functional semantics
Assembly regions	AR_1	$\{p_1, p_4, p_5, p_6, p_7\}$	F_1: sealing liquid F_2: position pump cover F_3: stabilize pump cover
	AR_2	$\{p_1, p_2, p_3, p_7\}$	F_4: position-driven gear shaft F_5: support-driven gear shaft F_6: transform motion F_7: supply liquid
	AR_3	$\{p_3, p_7, p_8, p_9\}$	F_8: prevent liquid
	AR_4	$\{p_1, p_5, p_6, p_7, p_{15}\}$	F_9: fasten-pump cover
	AR_5	$\{p_3, p_{11}, p_{14}\}$	F_{10}: position driving gear F_{11}: stabilize driving gear
	AR_6	$\{p_3, p_{11}, p_{12}, p_{13}\}$	F_{11}: stabilize driving gear F_{12}: fasten driving gear
	AR_7	$\{p_3, p_7, p_9, p_{10}\}$	F_9: fasten pump cover F_{13}: stabilize bush
Flow-activity regions	FAR_1	p_3: gear structure	F_7: supply liquid
	FAR_2	p_2: gear structure	F_7: supply liquid
	FAR_3	p_6: boss structure 2	F_{14}: export liquid
	FAR_4	p_6: boss structure 1	F_{15}: import liquid F_{16}: transfer torque
	FAR_5	p_{11}: gear structure	F_{17}: export liquid F_{18}: transfer power
	FAR_6	p_6: cavity structure	F_{17}: export liquid

Table 3: Latent functional semantic annotation of the 3D model.

No.	Unannotated model	Maximum similarity structure	Latent functional semantics and probability
1			F1: transfer-torque (0.856) F2: transfer-power (0.856) F3: change-speed (0.762)
2		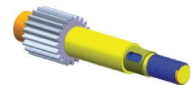	F1: transfer-torque (0.758) F2: convert-motion (0.758) F3: transform-motion (0.758) F4: change-speed (0.652)
3	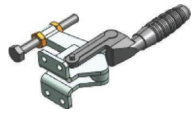	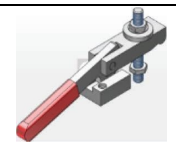	F1: position-part (0.755) F2: fasten-part (0.755)
4		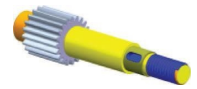	F1: transfer-torque (0.763) F2: convert-motion (0.763) F3: transform-motion (0.763) F4: change-speed (0.672)
5			F1: position-part (0.765)

semantics is calculated by equation (9). Since the calculation of probability is related to the annotated sample model library, if sample models are fewer, the accuracy of latent functional semantic annotation will be low. In this case, the designer's design history knowledge and experience should be considered for determining the final functional semantics to be annotated.

6. Conclusion

In this paper, an approach for functional semantic annotation of the mechanical 3D product model is proposed. 3D product model-oriented function ontology is constructed to provide standard, unified feature and function vocabulary for functional semantic annotation. The 3D CAD product models break up into functional regions at different granularity. Functional region is used as semantic structure unit, together with product design experience, working principle, and so on; the functional semantics of sample models is annotated interactively. The similarity of functional regions is evaluated comprehensively considering multisource information. Similarity-based latent functional semantic annotation model is given for automatic annotation of functional semantics in CAD models.

The proposed approach improves efficiency and accuracy of functional semantic annotation to a certain extent, which can assist designers accelerating the speed of the functional semantic annotation. It provides support for searching 3D CAD model using product function requirement, promotes the understanding, absorbs and reuses the complex 3D product model knowledge structure, and inspires the product design innovation. Further research will focus on functional semantics-driven retrieval and product structure optimization of the 3D CAD model.

Data Availability

The data used to support the findings of this study are available from the corresponding author upon request.

Conflicts of Interest

The authors declare that there are no conflicts of interest regarding the publication of this article.

Acknowledgments

This work is supported by National Natural Science Foundation of China (Grant No. 52005404), Key Research and Development Program of Shaanxi (Program No. 2023-YBGY-328), Scientific Research Program Funded by Shaanxi Provincial Education Department (No. 20JS114), and China Postdoctoral Science Foundation (Grant No. 2020M673612XB).

References

[1] P. Wang, Y. Li, J. Zhang, and J. Yu, *Probabilistic Description of the Function-Structure Relationship in Products*, American Society of Mechanical Engineers (ASME), Phoenix, AZ, United states, 2016.

[2] R. Osada, T. Funkhouser, B. Chazelle, and D. Dobkin, "Shape distributions," *ACM Transactions on Graphics*, vol. 21, no. 4, pp. 807–832, 2002.

[3] M. Novotni and R. Klein, "Shape retrieval using 3D Zernike descriptors," *Computer-Aided Design*, vol. 36, no. 11, pp. 1047–1062, 2004.

[4] M. Hilaga, Y. Shinagawa, T. Kohmura, and T. L. Kunii, "Topology matching for fully automatic similarity estimation of 3d shapes," in *Proceedings of the 28th annual conference on Computer graphics and interactive techniques*, Los Angeles, CA, USA, August 2001.

[5] M. Li, Y. F. Zhang, J. Y. H. Fuh, and Z. M. Qiu, "Toward effective mechanical design reuse: CAD model retrieval based on general and partial shapes," *Journal of Mechanical Design*, vol. 131, no. 12, Article ID 124501, 2009.

[6] M. Attene, F. Robbiano, M. Spagnuolo, and B. Falcidieno, "Characterization of 3D shape parts for semantic annotation," *Computer-Aided Design*, vol. 41, no. 10, pp. 756–763, 2009.

[7] F. Cheng, Z. Liu, G. Duan, C. Qiu, B. Yi, and J. Tan, "Complex CAD surface shape design using semantic features," *Journal of Mechanical Science and Technology*, vol. 28, no. 7, pp. 2715–2722, 2014.

[8] S. Abdul-Ghafour, P. Ghodous, B. Shariat, E. Perna, and F. Khosrowshahi, "Semantic interoperability of knowledge in feature-based CAD models," *Computer-Aided Design*, vol. 56, pp. 45–57, 2014.

[9] S. Ma and L. Tian, "Ontology-based semantic retrieval for mechanical design knowledge," *International Journal of Computer Integrated Manufacturing*, vol. 28, no. 2, pp. 226–238, 2015.

[10] Z. Wang, L. Tian, and W. Duan, "Annotation and retrieval system of CAD models based on functional semantics," *Chinese Journal of Mechanical Engineering*, vol. 27, no. 6, pp. 1112–1124, 2014.

[11] Z. Han, R. Mo, H. Yang, and L. Hao, "Structure-function correlations analysis and functional semantic annotation of mechanical CAD assembly model," *Assembly Automation*, vol. 39, no. 4, pp. 636–647, 2019.

[12] L. Hao, R. Mo, Z. Han, and B. Wei, "Functional semantics annotation of assembly model using the fusion of bag of relationships model and spectral technology," *Journal of Advanced Mechanical Design, Systems, and Manufacturing*, vol. 13, no. 4, 2019.

[13] X. Chen, S. Gao, Y. Yang, and S. Zhang, "Multi-level assembly model for top-down design of mechanical products," *Computer-Aided Design*, vol. 44, no. 10, pp. 1033–1048, 2012.

[14] S. J. Chiou and K. Sridhar, "Automated conceptual design of mechanisms," *Mechanism and Machine Theory*, vol. 34, no. 3, pp. 467–495, 1999.

[15] J. S. Gero and U. Kannengiesser, "The situated function–behaviour–structure framework," *Design Studies*, vol. 25, no. 4, pp. 373–391, 2004.

[16] Y. Umeda, M. Ishii, M. Yoshioka, Y. Shimomura, and T. Tomiyama, "Supporting conceptual design based on the function-behavior-state modeler," *Artificial Intelligence for Engineering Design, Analysis and Manufacturing*, vol. 10, no. 4, pp. 275–288, 1996.

[17] C. F. Kirschman, G. M. Fadel, and C. C. Jara-Almonte, "Classifying functions for mechanical design," *Journal of Mechanical Design*, vol. 120, 1998.

[18] R. Studer, V. R. Benjamins, and D. Fensel, "Knowledge engineering: p," *Data and Knowledge Engineering*, vol. 25, no. 1-2, pp. 161–197, 1998.

[19] Z. Han, R. Mo, Z. Chang, L. Hao, and W. Niu, "Key assembly structure identification in complex mechanical assembly based on multi-source information," *Assembly Automation*, vol. 37, no. 2, pp. 208–218, 2017.

[20] C. Pan, S. S. Smith, and G. C. Smith, "Automatic assembly sequence planning from STEP CAD files," *International Journal of Computer Integrated Manufacturing*, vol. 19, no. 8, pp. 775–783, 2006.

[21] J. Zhang, M. Zuo, P. Wang, J. F. Yu, and Y. Li, "A method for common design structure discovery in assembly models using information from multiple sources," *Assembly Automation*, vol. 36, no. 3, pp. 274–294, 2016.

[22] Z. Han, R. Mo, and L. Hao, "Clustering and retrieval of mechanical CAD assembly models based on multi-source attributes information," *Robotics and Computer-Integrated Manufacturing*, vol. 58, pp. 220–229, 2019.

[23] F. Pech, A. Martinez, H. Estrada, and Y. Hernandez, "Semantic annotation of unstructured documents using concepts similarity," *Scientific Programming*, vol. 2017, pp. 1–10, Article ID 7831897, 2017.

[24] J. Zhang, Z. Xu, Y. Li, S. Jiang, and N. Wei, "Generic face adjacency graph for automatic common design structure discovery in assembly models," *Computer-Aided Design*, vol. 45, no. 8-9, pp. 1138–1151, 2013.

[25] Y. Gao, Q. Dai, M. Wang, and N. Zhang, "3D model retrieval using weighted bipartite graph matching," *Signal Processing: Image Communication*, vol. 26, no. 1, pp. 39–47, 2011.

[26] Z. Han, C. Tian, Z. Zhou, and Q. Yuan, "Discovery of key function module in complex mechanical 3D CAD assembly model for design reuse," *Assembly Automation*, vol. 42, no. 1, pp. 54–66, 2022.

Hindawi
Scientific Programming
Volume 2022, Article ID 2062791, 8 pages
https://doi.org/10.1155/2022/2062791

Research Article

Research on Dance Motion Capture Technology for Visualization Requirements

Kaiqiang Sun

Weifang University, Shandong, Weifang 261000, China

Correspondence should be addressed to Kaiqiang Sun; 20111919@wfu.edu.cn

Received 25 July 2022; Revised 5 September 2022; Accepted 20 September 2022; Published 17 November 2022

Academic Editor: Lianhui Li

"Motion capture technology" refers to the use of optical sensing equipment to record the dancer's movement trajectory during dance and then convert this movement trajectory into applicable data information in animation software. In the 3D animation software, the corresponding dancer model can be constructed, and the matching costumes can also be designed. After combining it with the motion capture data, animation and dance data can be generated. In this way, virtual simulation software can create some virtual visualization scenes and present more diverse and complex demonstration effects. This article focuses on three aspects: "an overview of the connotation of motion capture technology," "design of virtual dance visualization scene based on motion capture technology," and "application of virtual dance visualization scene based on motion capture technology."

1. Introduction

"Motion capture technology" was initially applied in a very narrow field, mainly in the field of animation films. With the maturity of motion capture technology, its application fields are becoming more and more extensive, such as motion analysis and sports training. A complete motion capture system usually includes multiple parts such as signal acquisition equipment, data processing, data transmission, and sensors [1]. At present, motion capture systems mainly include optical motion capture systems, electromagnetic motion capture systems, and mechanical motion capture systems. What we call motion capture today usually refers to the use of sensors and software to transcribe the movements of real actors into the movements of digital models in 3D games or animations. As we all know, characters (including characters and animals) in animation and games must have actions, such as running, jumping, and fighting. The "optical motion capture system" has better stability and higher precision. The dance data is presented through an optical motion capture system, and the effect will be better [2].

Regarding the connotation of motion capture technology, it can be understood as a computer recognition technology, which is mainly used to recognize data information during motion. Through motion capture technology, various real actions of people in three-dimensional space can be collected, and the collected data information can be entered into the virtual model, thereby generating a series of motion data records [3]. Mechanical motion capture relies on mechanical devices to track and measure motion trajectories. A typical system consists of multiple joints and rigid links, and angle sensors are installed in the rotatable joints, which can measure the changes in the rotation angle of the joints. When the device moves, according to the angle change measured by the angle sensor and the length of the connecting rod, the position and movement trajectory of the endpoint of the rod in space can be obtained. In fact, the motion trajectory of any point on the device can be obtained, and the rigid link can also be replaced with a telescopic rod with a variable length, and the change in its length can be measured with a displacement sensor. An early mechanical motion capture device uses joints and links with angle sensors to form an "adjustable digital model" whose shape can simulate the human body or other animals or objects. The user can adjust the posture of the model according to the needs of the plot and then lock it. The angle sensor measures and records the rotation angles of the joints. According to these angles and the mechanical dimensions of the model,

the pose of the model can be calculated, and these pose data are transmitted to the animation software so that the character model in it can also make the same pose. This is an early motion capture device, but there is still a certain market until now. Foreign countries have given this device a very vivid name: "Monkey." An application form of mechanical motion capture is to connect the moving object to be captured with the mechanical structure, and the motion of the object drives the mechanical device, which is recorded by the sensor in real time. The advantages of this method are low cost, high accuracy, real-time measurement, and simultaneous performance of multiple characters. But its shortcomings are also very obvious, mainly because it is very inconvenient to use, and the mechanical structure greatly hinders and restricts the movements of performers. The "monkey" is more difficult to use for real-time capture of continuous actions. It requires the operator to continuously adjust the posture of the "monkey" according to the requirements of the plot, which is very troublesome. It is mainly used for static modeling capture and key frame determination. Moreover, this motion data information can be well recognized by the computer. After the relevant personnel put this motion data information into the 3D animation software, they can build a "3D human body model" in the 3D animation software. The three-dimensional mannequin is both virtual and vivid and can depict the dancer's facial features according to the dancer's physical fitness. Society is progressing, science and technology are developing, and computer hardware and software equipment is becoming more and more perfect. Many researchers choose to conduct scientific research and auxiliary teaching training through computers. Motion capture technology is the latest scientific and technological research project that has been developing and growing in recent years. Through the motion capture system, the animation production of film and television entertainment, the rehabilitation of patients in the medical field, the field of sports training, and the analysis of digital human motion posture assisted by college teaching are realized, and the guidance of rigorous scientific theory is provided [4]. This paper analyzes the motion posture of the human body, proposes a posture analysis method based on eigenvector matching, and analyzes the characteristics of the motion posture of the human body based on the real-time characteristics of the optical motion capture system,. This paper analyzes the development prospects and research significance of motion capture technology in sports dance teaching, provides an effective theoretical basis for scientific training, promotes the efficiency of students' learning, and effectively improves the scientific research level of education and teaching. The main research work of this paper is as follows: (1) A dance posture analysis method based on feature vector matching is proposed, which can accurately analyze the dance movement posture of the human body, obtain the difference in effective human movement, and provide theoretical support for the scientific training of dance. (2) Applying motion capture technology to the research of dance teaching in colleges and universities, by tracking, capturing, checking, recording, etc. of human movement, the dance movements are demonstrated in sections, which solves the traditional problem of repeated demonstrations when teachers teach, get rid of the interference of students or teachers due to individual differences, psychological, physical, and other factors, and, through the effective analysis of computer data, timely find problems and correct them, which greatly improves the efficiency of education and teaching. The advantages of this study are mainly connected with the dance teaching through the optical motion capture system, which improves the intuitiveness of the learning effect. The collection and analysis of real-time data provide timely feedback for teaching. From the technical level, teaching form, and student acceptance level, it provides scientific theoretical support in terms of innovation and other aspects, gets rid of other interference factors of the traditional teaching mode, provides a reliable basis for the improvement of the teaching mode, and helps the system to improve the personalized teaching system. The next main research work is to complete the real-time analysis of human motion posture with the assistance of the optical motion capture system.

In addition, the technology can also build a variety of clothing models. Due to the large number of ethnic minorities in our country, there are also many dances with ethnic characteristics. When building costume models, you can refer to the styles of different ethnic groups and different dances. After the construction of these models is completed, they will enter the next step of construction, that is, "three-dimensional bones" [5]. In this process, the 3D skeleton is meant to correspond to the model. Only when the correspondence is good, can we lay a good foundation for "skinning" [6]. The main function of skinning is to make the bones and the model closely connected to form a whole, making it look more harmonious and unified. At the same time, the relevant personnel must match the corresponding costumes and match the costumes, bones, and models into a set. At this time, the data information transmitted by the motion capture system can make the 3D model move and become various animations that people see. According to the needs of the market and people, these animations can be placed on the virtual platform, which is mainly used to save dance information, demonstrate dance content, and create new dance materials [7].

The advent of motion capture technology dates back to the 1970s. With the rapid development of computer software and hardware technology and the improvement of animation production requirements, its application fields cover many aspects, such as film and television production, virtual reality, games, ergonomic research, simulation training, and biomechanical research [8]. In principle, the commonly used motion capture technologies can be divided into four types: mechanical, acoustic, electromagnetic, and optical. Optical motion capture is currently the most commonly used motion capture technology. It accomplishes the task of motion capture by tracking specific light points on the target [9]. At present, common optical motion capture is mostly based on the principle of computer vision. When the camera continuously shoots at a high enough rate, the movement trajectory of the point can be obtained from the image sequence, as shown in Figure 1.

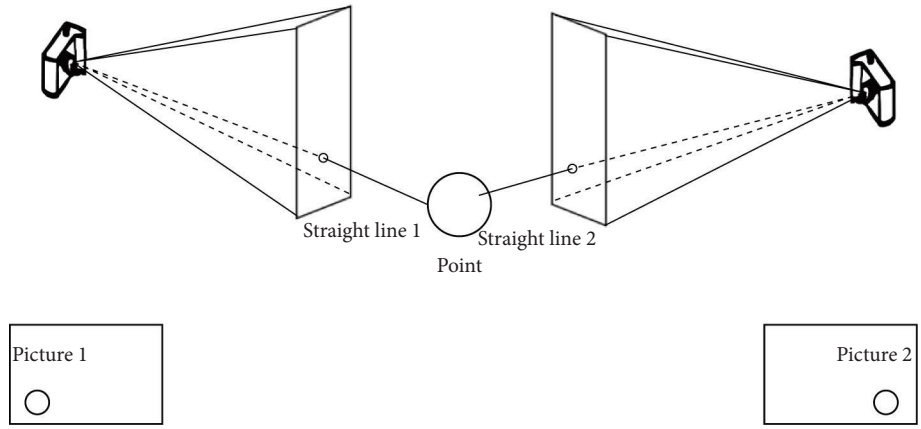

Figure 1: Optical motion capture system.

The advantage of optical motion capture is that the performer has a large range of motion, no cables, and the limitation of mechanical devices. The performer can perform freely and it is very convenient to use. Its high sampling rate can meet the needs of most high-speed motion measurements [10]. The disadvantage is that the system is expensive, and although it can capture real-time motion, the postprocessing (including Marker recognition, tracking, and calculation of spatial coordinates) takes long time. At present, it cannot achieve real-time driving of the character model and real-time viewing effects. Such systems are sensitive to lighting and reflections in the performance venue. The device calibration is also more complicated [11]. Especially when the motion is complex, the markers in different parts are easily confused, and the occlusion produces wrong results, which often requires manual intervention in the postprocessing process [12].

2. Related Technologies

2.1. Design of Dance Virtual Visualization Scene Based on Motion Capture Technology

2.1.1. Dance Data Collection. "Dance data acquisition" is the first step in the dance virtual visualization scene design of motion capture technology. Data acquisition is a prerequisite and foundation in the process of dance digitization. In the process of dance digitization, data acquisition is a prerequisite and foundation. Only after the data information has been collected, the data information can be presented through the subsequent virtual display platform [13]. At present, dance data collection mainly includes three parts: first, "collecting dance materials." There are many dance materials in our country, and there are many channels for collection, such as individual performances, stage performances, and folk visits. The relevant personnel should prepare the collection equipment in advance and choose more advanced digital cameras, digital cameras, etc. Second, "digitize the material." After the dance materials are collected, they should be systematically organized. During this process, the relevant personnel should actively listen to the suggestions of professional dancers, make reasonable use of the dance materials, and then perform dance demonstrations based on the dance materials finally sorted out. Through the motion capture system, capture those classic dance moments and realize the digitalization of dance. Third, "Building 3D Models." The three-dimensional model is constructed in 3 ds Max. The reference is based on the general body proportions of most men and women, and the corresponding costume models are established in combination with dance characteristics. It should be noted that the models are mainly divided into two types: one is the "fine model," which is generally not displayed on the virtual platform and is mainly saved as a kind of data which saves 360-degree video files; the other is the "fine model." One is the "simple model," which is mainly used for virtual platform display. There are many classifications of dance, and combined with the characteristics of different dances, it is also possible to carry out "key binding," that is, to systematically evaluate the bound skeletal model and set relevant weights [14].

2.1.2. Dance Animation. Dance animation can be understood as the combination of "3D animation" and "motion capture data." 3 ds Max, MotionBuilder, and other software can well link 3D animation and motion capture data [15]. At this point, the work of data acquisition and dance animation is basically completed. After that, export the model file, motion data, etc. through 3 ds Max, and save it in FBX format.

2.1.3. Display System. At present, the "display system" mainly uses the three-dimensional game engine UNITY 3D. This display system includes the following modules:in the opening session, just like film and television dramas, basically every three-dimensional animation video will introduce some basic information, such as production unit, content introduction, system name, which has become a conventional general title module; dress-up module - In short, this module is mainly used to change clothes, according to different regions, different dance style, and switch between different clothing animation models; camera control module: - unity 3D is a very popular 3D game engine

because it has a very powerful control ability, through the dance movements presented by the 3D model. The viewer can observe from various angles, and can basically achieve a 360-degree panorama. At this time, the viewer will feel very wonderful. The presentation of the dance and the change of perspective can be controlled by a small mouse in the hand. At present, the camera control module can be programmed independently, or the default control system can be used: the dance selection module—the classification of dance can be measured from different dimensions. The dance selection module is mainly used to select the type of dance. At present, the main types of dances are dances performed on a large scale and in a standardized manner on major holidays, some minority dances circulated in the folk, some collective dances created by people spontaneously, and some dances composed and performed by dancers with special talents, used for dances on some special occasions, with certain funny elements and commemorative meanings in Children's Day, weddings, and corporate annual meetings; gender selection module - the role of this module is well understood, which is to distinguish male dancers and female dancers. In the three-dimensional game engine U-NITY 3D display system, through the coordinated operation of these five modules, the effect of virtual demonstration is finally presented [16].This system can now be used not only on computers but also on mobile phones.

2.2. Application of Virtual Dance Visualization Scene Based on Motion Capture Technology. By first collecting text records, taking pictures and videos, obtaining relevant text, pictures, and video-related materials of Lusheng Dance, performing dance choreography, and using motion capture equipment to record dance movements to obtain dance movement data. At the same time, 3D StudioMax is used to preliminarily establish dancer characters model. After having motion data and a dancer model, digital postproduction can be performed to realize animation display [17]. The production process is shown in Figure 2.

At this stage, the application of dance virtual visualization scene based on motion capture technology is mainly reflected in the following aspects:

2.2.1. Teaching Field. When teaching dance classes, art teachers can use the virtual display platform to digitally present dance, bring students more abundant teaching content, facilitate students to learn "dance movement decomposition," and facilitate teachers to carry out dance-related activities. research [18].

2.2.2. Multimedia Display Field. In the field of multimedia display, the application of dance virtual visualization scene based on motion capture technology can combine traditional dance teaching content with modern technology, such as three-dimensional dynamic imaging technology, human scene synthesis technology, phantom imaging technology, and laser technology. This gives viewers a new impact. From the perspective of dance research, this is an efficient research method, that is conducive to improving the accuracy and standardization of dance research.

2.2.3. Internet Field. The application of dance virtual visualization scene based on motion capture technology can well adapt to the Internet environment and compile and generate some dance content that can be disseminated and displayed in the Internet environment. With the increasing number of mobile phone users, the Unity 3D game engine can also compile and generate mobile apps, so that more people can enjoy this convenient service anytime, anywhere, and feel the popular educational atmosphere of dance in the new era. The dance of the public has broadened the path of inheritance and development.

3. Dance Motion Capture Technology Based on Visualization Requirements

To meet the needs of efficient and high-precision human gesture recognition methods, an efficient gesture analysis method based on similarity matching between feature planes is proposed. The human motion data is collected in real time through the optical motion capture system, and the skeleton and its human feature plane are effectively extracted. Furthermore, an efficient matching mechanism is established by taking the plane feature vector and its included angle as the judgment basis for attitude analysis. This method is combined with dance teaching. After experimental verification, it not only provides a stable and accurate analysis of human posture but can also effectively obtain the difference between human movements, thus providing good theoretical support for dancers to carry out scientific dance training [19].

3.1. Acquisition of 3D Data from Motion Capture. In this paper, an optical motion capture system is used to obtain motion data, thereby establishing a database of the human motion pose models and skeleton model. The basic process is as follows, as shown in Figure 3.

3.1.1. Real-Time Acquisition of 3D Human Motion Data. In the data collection, the performers first put on monochrome clothing with 21 markers on key parts, stand within the preset motion space, start the high-precision 3D motion capture software, set the specified time, and press. It is required to shoot the specified dance movements and use the camera to capture and track the movement of the 21 marker points. Match the captured and edited human motion data of 21 marker identification points with the actor model, activate the 21 identification points to complete the data matching with the actor, so as to complete the establishment of the database of human motion posture.

3.1.2. Establish Motion Model Database. Applying the motion capture system to analyze the motion posture of the human body is to estimate the motion posture characteristics of the human body from different perspectives. In this paper, the key points of the motion feature are used to mark

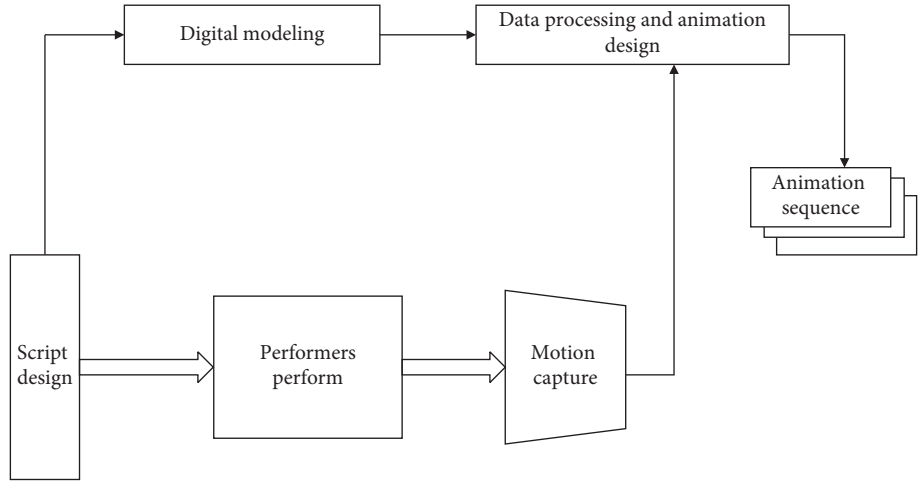

Figure 2: Production process.

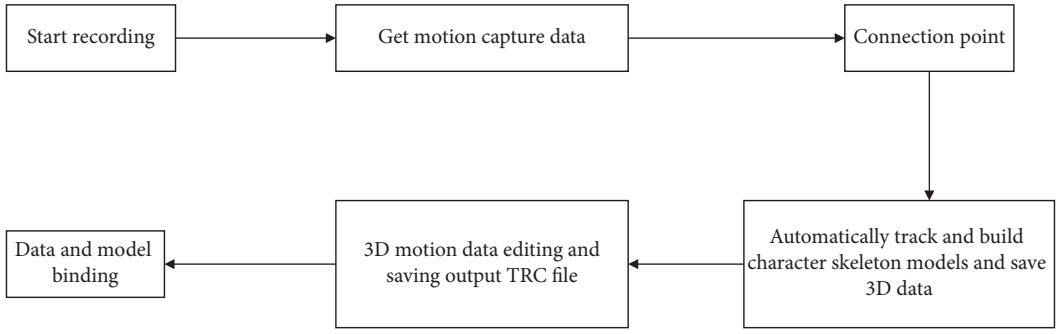

Figure 3: 3D data acquisition flow chart.

the key parts of the human body. The connection between the key points represents the rigid body. When they are "shape unchanged," the connections between key points represent rigid bodies [20]. The main research on movement posture is to build a database of human movement postures based on the head, body, hips, and limbs.

3.1.3. Human Motion Pose Analysis Based on Feature Vector Matching. Movement posture analysis is the process of tracking, capturing, acquiring, and analyzing human body posture characteristics so as to obtain relevant movement posture parameters. Through the effective combination of motion analysis and teaching, the teaching system can be more personalized and featured, and the performers' performances can be decomposed in detail, and each dance movement can be demonstrated step by step. The parameters obtained are conducive to quantitative analysis of the movement posture, providing good help for more scientific and intelligent dance teaching [21].

In order to better analyze the motion state of dance performers, a method for analyzing human motion posture using the principle of feature plane similarity matching is proposed. This method simplifies the traditional calculation of Euclidean distance based on multiple identification points to the calculation of a feature plane feature vector and its included angle [22]. In this paper, the identification points of 21 key parts are simplified into 7 feature planes to calculate the motion difference and correlation. Through verification, this method can quickly and effectively analyze the motion posture of the human body and can be applied to dance teaching to improve the efficiency of dance teaching. The specific process is as follows, as shown in Figure 4. The main steps of the analysis process include the following:

Step 1 Real-time acquisition of skeleton data: in the form of optical motion capture, real-time acquisition of dance action sequences, and storage of the coordinates of each identification point of the human body model in the space coordinate system.

Step 2 Posture analysis: determine 7 feature planes according to the feature points, extract the angle between the feature vector and the posture feature vector, and calculate the feature correlation coefficient of the human body posture according to the motion characteristics of the key parts of the dance movement.

Step 3: Analysis of the difference degree of characteristic posture: through the correlation coefficient of the characteristic vector and its included angle, analyze the difference and accuracy between the dance movements and standard movements of the students.

The motion of the human body is a complex process. Without considering conditions such as muscles and

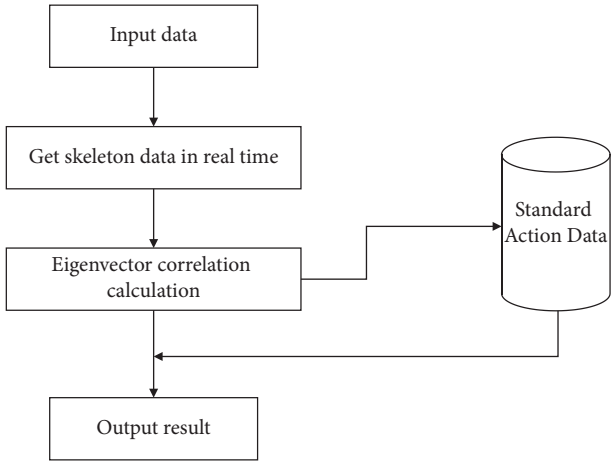

Figure 4: Method flow chart.

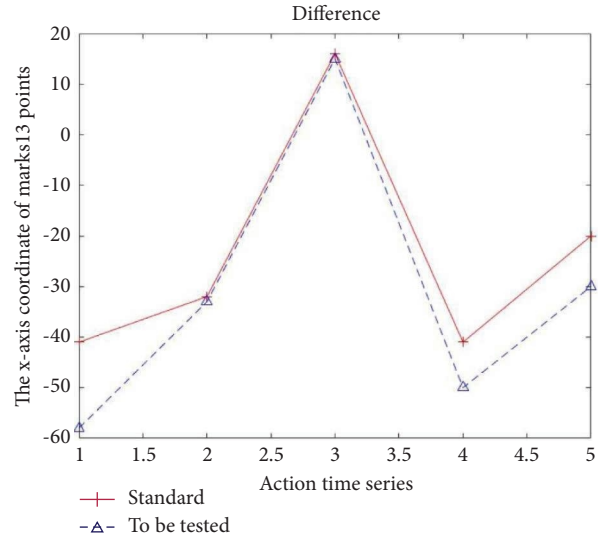

Figure 5: Comparison of motion trajectories in one direction between single identification points.

nervous systems, the motion of the human body can be abstracted into a simple chain system connected by some rigid bodies [23]. The upper limb is composed of two rigid bodies connected by the elbow joint, the upper arm, and the forearm; the lower limb is composed of the two rigid bodies of the thigh and the calf connected by the hip joint, and the thigh and the calf are connected by the knee joint. The body and hip are also represented as a rigid body by a line connecting the joint points [24].

3.2. Traditional 3D Model Similarity Matching. The similarity matching of human body poses is to realize the measure of the difference or similarity of the poses between different human bodies. The most commonly used method is the traditional Euclidean distance metric.

The traditional 3D model similarity matching is based on the Euclidean distance, and the calculation methods are as follows:

$$D = \text{sqrt}\left((x_1 - x_2)^2 + (y_1 - y_2)^2\right),$$
$$D = \text{sqrt}\left((x_1 - x_2)^2 + (y_1 - y_2)^2 + (z_1 - z_2)^2\right). \quad (1)$$

With two identification points, the difference between the two identification points can be obtained through the calculation formula based on the Euclidean distance. If the obtained difference is less than the threshold, the threshold is set by the coach, and the two identification points are considered to be similar. If the difference is greater than this threshold, the two identification points are considered dissimilar. The standard action is compared with the trajectory of the same identification point of the action to be tested, as shown in Figure 5.

The direct comparison method based on the traditional Euclidean distance is to compare the activity trajectories of two moving targets, and the corresponding distance difference will be obtained during the comparison of each action sequence, and the data matching degree will be calculated according to the preset threshold. However, this method not only requires too much calculation but also depends on the inherent characteristics of the object to be measured. When the body ratio of the object changes, such as height, short, fat, and thin, the distance between the marking points also changes accordingly, and it must be repeated. Therefore, due to the strict requirements for moving objects, the use of traditional methods is limited, which not only greatly reduces the computational efficiency but also lacks universality [25].

The traditional form of dance teaching is generally taught by the teacher's oral and deeds, through oral movement essentials and personal demonstration of dance movements to students, so that students can understand the essentials of movements in class. However, in traditional sports teaching, the internal reasons such as high difficulty, fast speed, difficult memory, and the instantaneousness and complexity of movements lead to increased teaching difficulty. Teachers cannot standardize each movement due to psychological, physical and other factors. It is shown meticulously that due to individual differences and different observation angles, students cannot master the essentials of movements in this class, which has an impact on the understanding of the key and difficult points of dance movements, so that teachers have to repeatedly demonstrate and explain, which affects teaching efficiency. The teacher's oral and deed teaching method has a single teaching form, and the students only focus on movement practice and lack the ability to think actively.

The combination of motion capture technology and teaching will make up for the deficiencies of traditional teaching forms and has advantages that traditional teaching does not have in the acquisition and transmission of motor skills. According to the students' own state, they can purposefully learn and demonstrate the movements, and then compare them with the standard movement postures according to the analysis results of the three-dimensional movement data and correct the standard movements in time, which is beneficial to the students' learning and performance. Teachers' teaching efficiency has been greatly improved.

The teacher's standard dance movements are made into three-dimensional teaching animations through motion capture technology. Before class, students learn the dance movements in the teaching animations by themselves, and draw gestures and movements in their minds while watching the animation. Repeated demonstrations are performed in multiangle segments, and then students perform real demonstrations. The high-precision 3D camera of the motion capture device captures the movements demonstrated by the students and compares them with the teacher's standard movements. The teacher can give students specific goals through the comparison of 3D data. The guidance helps students master the essentials of standard dance movements, and students can make self-correction according to the analysis results. Throughout the development of computer-assisted teaching, computer science, educational technology, cognitive psychology, etc have had an important impact on the development of motion capture technology-assisted dance teaching. The kinds of enlightenment that can be obtained are as follows:

(1) From the technical application point of view, motion capture technology establishes a teaching model database and generates teaching animation videos, which makes the computing technology-assisted dance teaching more concise, easy to understand, vivid, and so on, gives full play to the role of virtual reality technology, and analyzes students' mastery. It provides learning navigation and suggestions for students' dance movement learning; students realize independent learning and inquiry learning, and teachers can assist students' learning process from the side, so that students' "learning" and teachers' "teaching" are more in line with the concept of digital teaching; it is also more feasible at the technical level.

(2) From the perspective of teaching form, due to the innovation of teaching methods, teachers are guided to fully realize the teaching advantages of motion capture technology - 33 -, play the leading role of teachers, get rid of the shackles of traditional teaching methods, and create indoor training classrooms for different dance forms, such as ballet, Latin dance, folk, dance, can use motion capture technology to quickly, and effectively help students discover the completion of their own movements through detailed demonstrations and real-time effects feedback, thereby making up for irregular movements. Students learn the essence of the movements to be mastered in the form of self-learning, which is conducive to giving full play to the initiative of students in learning, fully realizing the main body of students' learning, enhancing the pertinence and timeliness of teaching effects, and improving the attractiveness and effectiveness of classroom education models. Infectious is conducive to enhancing the level of students' reform and innovation.

(3) The dance teaching form based on motion capture technology is the intersection of computer science, educational science, and teaching psychology. This technology can improve teaching quality, enhance teaching appeal, and make motion capture technology make creative progress and development in the scope of computer-aided instruction.

4. Conclusion

The virtual visual scene design of dance based on motion capture technology is of great significance for the diversified presentation and inheritance of dance, especially for some relatively classic and small minority dances, because fewer people learn these dances, these dance forms are facing a crisis of inheritance. The virtual visual scene design of dance based on motion capture technology can better protect these minority ethnic dances, so that more people can see the charm of this dance and are willing to inherit and develop it.

Data Availability

The dataset can be accessed upon request.

Conflicts of Interest

The authors declare that they have no conflicts of interest.

References

[1] V. T. Keller, J. B. Outerleys, R. M. Kanko, E. K. Laende, and K. J. Deluzio, "Clothing condition does not affect meaningful clinical interpretation in markerless motion capture," *Journal of Biomechanics*, vol. 141, Article ID 111182, 2022.

[2] M. Kukla and W. Maliga, "Symmetry analysis of manual wheelchair propulsion using motion capture techniques," *Symmetry*, vol. 14, no. 6, p. 1164, 2022.

[3] J. Thomas, J. B. Hall, R. Bliss, and T. M. Guess, "Comparison of Azure Kinect and optical retroreflective motion capture for kinematic and spatiotemporal evaluation of the sit-to-stand test," *Gait & Posture*, vol. 94, pp. 153–159, 2022.

[4] T. Gao, F. Meng, X. Zhang, W. Chen, and H. Song, "Operational kinematic parameter identification of industrial robots based on a motion capture system through the recurrence way," *Mechanism and Machine Theory*, vol. 172, Article ID 104795, 2022.

[5] K. P. Veirs, A. H. Fagg, A. M. Haleem et al., "Applications of biomechanical foot models to evaluate dance movements using three -dimensional motion capture: a review of the literature," *Journal of Dance Medicine and Science*, vol. 26, no. 2, pp. 69–86, 2022.

[6] S. Vafadar, W. Skalli, A. Bonnet-Lebrun, A. Assi, and L. Gajny, "Assessment of a novel deep learning-based markerless motion capture system for gait study," *Gait & Posture*, vol. 94, pp. 138–143, 2022.

[7] J. Dong, Q. Shuai, J. Sun, Y. Zhang, H. Bao, and X. Zhou, "iMoCap: motion capture from internet videos," *International Journal of Computer Vision*, vol. 130, no. 5, pp. 1165–1180, 2022, (prepublish).

[8] C. D. Johnson, J. Outerleys, and I. S. Davis, "Agreement between sagittal foot and tibia angles during running derived from an open-source markerless motion capture platform and

manual digitization," *Journal of Applied Biomechanics*, vol. 38, no. 2, pp. 111–116, 2022.

[9] W. Hu, Y. Lu, and J. Ren, "A fixed-point proximity algorithm for recovering low-rank components from incomplete observation data with application to motion capture data refinement," *Journal of Computational and Applied Mathematics*, vol. 410, Article ID 114224, 2022 (prepublish).

[10] C. Park, Y. An, H. Yoon et al., "Comparative accuracy of a shoulder range motion measurement sensor and Vicon 3D motion capture for shoulder abduction in frozen shoulder," *Technology and Health Care*, vol. 30, no. S1, pp. 251–257, 2022.

[11] J. Yao and Y. Chen, "A motion capture data-driven automatic labanotation generation model using the convolutional neural network algorithm," *Wireless Communications and Mobile Computing*, vol. 2022, Article ID 2618940, 9 pages, 2022.

[12] T. Zhao, Y. Fu, C. Sun et al., "Wearable biosensors for real-time sweat analysis and body motion capture based on stretchable fiber-based triboelectric nanogenerators," *Biosensors and Bioelectronics*, vol. 2022, Article ID 114115, 2022.

[13] I. Kačerová, J. Kubr, P. Hořejší, and J. Kleinová, "Ergonomic design of a workplace using virtual reality and a motion capture suit," *Applied Sciences*, vol. 12, no. 4, p. 2150, 2022.

[14] Y. Wei, "Deep-learning-based motion capture technology in film and television animation production," *Security and Communication Networks*, vol. 2022, Article ID 6040371, 9 pages, 2022.

[15] Y. Liu, K. Iwata, S. Sanda, and M. Nishiyama, "Utilization of motion capture systems for low cycle fatigue tests on induction-hardened steel," *Journal of Constructional Steel Research*, vol. 190, Article ID 107166, 2022.

[16] C. Armitano-Lago, D. Willoughby, and A. W. Kiefer, "A SWOT analysis of portable and low-cost markerless motion capture systems to assess lower-limb musculoskeletal kinematics in sport," *Frontiers in Sports and Active Living*, vol. 3, Article ID 809898, 2021.

[17] K. Armstrong and K. Armstrong, "Novel clinical applications of marker-less motion capture as a low-cost humanmotion analysis method in the detection and treatment of knee osteoarthritis," *Journal of Arthritis*, vol. 11, no. 1, 2022.

[18] A. Thierfelder, J. Seemann, N. John et al., "Real-life turning movements capture subtle longitudinal and preataxic changes in cerebellar ataxia," *Movement Disorders*, vol. 37, no. 5, pp. 1047–1058, 2022.

[19] R. J. Aughey, K. Ball, S. J. Robertson et al., "Comparison of a computer vision system against three-dimensional motion capture for tracking football movements in a stadium environment," *Sports Engineering*, vol. 25, no. 1, p. 2, 2022.

[20] X. Yin, C. C. Vignesh, and T. Vadivel, "Motion capture and evaluation system of football special teaching in colleges and universities based on deep learning," *International Journal of System Assurance Engineering and Management*, 2022, (prepublish).

[21] G. Zhang, G. Huang, H. Chen, C. M. Pun, Z. Yu, and W. K. Ling, "Video action recognition with Key-detail Motion Capturing based on motion spectrum analysis and multiscale feature fusion," *The Visual Computer*, 2022, (prepublish).

[22] H. Maezawa, M. Fujimoto, Y. Hata et al., "Functional cortical localization of tongue movements using corticokinematic coherence with a deep learning-assisted motion capture system," *Scientific Reports*, vol. 12, no. 1, p. 388, 2022.

[23] V. Girbés-Juan, V. Schettino, L. Gracia, J. E. Solanes, Y. Demiris, and J. Tornero, "Combining haptics and inertial motion capture to enhance remote control of a dual-arm robot," *Journal on Multimodal User Interfaces*, vol. 16, no. 2, pp. 219–238, 2022, (prepublish).

[24] N. Boroda, S. Pradhan, C. W. Forsthoefel, S. M. Mardjetko, J. Bou Monsef, and F. Amirouche, "Motion capture evaluation of sagittal spino-pelvic biomechanics after lumbar spinal fusion," *Spine Deformity*, vol. 10, no. 3, pp. 473–478, 2022, (prepublish).

[25] L. Wade, L. Needham, P. McGuigan, and J. Bilzon, "Applications and limitations of current markerless motion capture methods for clinical gait biomechanics," *PeerJ*, vol. 10, Article ID e12995, 2022.

Hindawi
Scientific Programming
Volume 2022, Article ID 3644525, 10 pages
https://doi.org/10.1155/2022/3644525

Research Article

On the Willingness of Fujian Farmers to Sell Agricultural Products by Means of New Media from the Perspective of Rural Revitalization: Analysis Model Design Based on Programmed Grounded Theory

Li Lin, Xiong Zhou, Shenghua Zhang, and Jinwang Fan

Fujian Vocational College of Agriculture, Fuzhou, Fujian 350007, China

Correspondence should be addressed to Shenghua Zhang; 805376262@qq.com

Received 1 August 2022; Revised 8 September 2022; Accepted 12 September 2022; Published 12 October 2022

Academic Editor: Lianhui Li

In the post-epidemic era, it is difficult for farmers to sell agricultural products offline due to their characteristics, and farmers once again fall into the situation of "difficult sales." New media marketing of agricultural products, as an emerging form conforming to the trend of the times, not only increases farmers' income but also promotes industrial integration and development. However, as this model is still in the early stage of development, a large number of farmers are not willing to transform the traditional sales channels into new media marketing for agricultural product sales. In this study, the interview data of 76 new-type professional farmers in Fujian were analyzed by three-level coding based on programmed grounded theory. It is found that core factors, and macro- and microfactors such as farmers' characteristics and sales situation will affect farmers' willingness to sell agricultural products through new media. Therefore, this study deeply explores the relationship between farmers' willingness and various factors and puts forward three suggestions for solving the actual problems of agricultural product sales.

1. Introduction

In the era of mobile Internet, agricultural products are difficult to sell due to the lack of good sales channels. Moreover, affected by the epidemic, offline sales of agricultural products have become increasingly difficult, and farmers are trapped in the predicament of "difficult sales." The new media marketing of agricultural products is accelerating its development by virtue of its low marketing cost, rapid information dissemination, and other advantages. Under the new media, the new business form, live streaming e-commerce of agricultural products, has emerged, which not only improves farmers' income but also promotes industrial integration and speeds up the development of the agricultural economy. In 2022, the No. 1 Central Document proposed the implementation of the project of "Revitalizing agriculture by developing digital commerce" to enable the development of rural e-commerce through digital elements and data elements and jointly open up a new era of new media marketing of agricultural products.

At present, this new mode is still in the preliminary stage of development under the new media. With the increasingly fierce competition in agricultural product sales in the new track, the means of live streaming e-commerce and short video marketing of agricultural products are flexible and changeable. Due to the particularity of agricultural products and the lack of new media marketing talents, as well as the immaturity of operating basis, platform rules and regulations, and industry norms, a large number of farmers are unwilling to change the traditional sales channels and explore new media means for sales. In this context, it is of great significance to deeply explore the willingness and mechanism of farmers to promote the sale of agricultural products

by means of live streaming e-commerce and short video marketing from the perspective of new media, so as to solve the problem of farmers' "difficulty in selling" and realize rural revitalization through industrial revitalization.

2. Overview of Related Research

2.1. UTAUT Theory. UTAUT theory [1] holds that there are four core dimensions of factors affecting users' willingness and behaviors to adopt new information technologies. (1) PE (performance expectancy) means the degree to which an individual feels from the inside to be helpful to his or her job by using an advanced technology. The greater the degree of help is, the stronger the willingness of users to adopt. (2) EE (effort expectancy) refers to how much time and energy an individual has to invest in learning to use the technology. (3) SI (social influence) appertains to the degree to which the perception of the people around the adoption of certain information technology affects an individual. (4) FC (facilitating conditions) signifies the degree to which an individual perceives that the external environment is sufficient for the adoption of new information technology (Figure 1).

2.2. Research Studies on the Development Model of Farmers' E-Commerce. Jalali AA et al. studied the development of rural e-commerce in Iran and proposed a new practice model for its effective development. Xie et al. summarized development models of farmers' e-commerce from the perspective of regional collaborative development as A2A, A2B, and B2A. Among them, the A2B mode refers to the establishment of a relevant website with complete and timely information or an effective management platform for suppliers and purchasers to integrate resources and carry out online transactions with the help of third-party logistics [2].

Domestic scholar Lyu proposed an e-commerce model of fresh agricultural products based on supply chain integration and basic social network to deal with the unsalable products caused by excessive supply chain links of fresh agricultural products [3]. Huang and Wang conducted a study on Anhui Province's characteristic agricultural products' e-commerce based on e-commerce models such as "origin + platform + consumer" and "platform + self-support + consumer" [4].

2.3. Research Studies on Factors Affecting Farmers' E-Commerce Entrepreneurial Behaviors

2.3.1. Subjective Cognition. Berglund believed that "Entrepreneurship for survival" and "Entrepreneurship for an opportunity" are two motivations of modern farmers. According to Liu, there is a positive correlation between the willingness of e-commerce operators to sell agricultural products in virtue of e-commerce and the perceived usefulness, ease of use, and profits [5]. Social trust proposed by Wenetal and individual innovation proposed by Mao have a positive effect on the willingness to use e-commerce for sales [6].

2.3.2. Individual Traits. Yao and Zhu research showed that, with the growth of age, farmers tend to be conservative in their ideas, and farmers of different genders also have different behavioral choices [7]. Korgaonkar et al. considered that age has a negative impact on farmers' willingness to engage in e-commerce sales. In addition, Li pointed out that people with higher education are better at using emerging Internet means and computer technology to participate in the e-commerce of agricultural products [8].

2.3.3. External Environment. Arayesh [9] stated that social economy, privacy and security, infrastructure, and national policies are the main factors affecting farmers' adoption of agricultural product e-commerce. Mao said that external conditions such as the market environment, national economic policies, and related services have a greater impact on farmers' willingness to use e-commerce for sales than operators' own factors [10]. In terms of government policies, Huang believes that national policies such as e-commerce subsidies have little impact on farmers' willingness to choose e-commerce [11]. According to Su et al., external factors such as network facilities, traffic conditions, and government support at the current stage have little influence on the use of new media for marketing [12].

Studies by scholars at home and abroad mostly focus on farmers' use of marketing behavior, but rarely discuss farmers' willingness to use e-commerce, especially new media to sell agricultural products. With reference to the research of domestic and foreign scholars, this study, on the strength of the programmed grounded theory, analyzes the willingness of farmers to sell agricultural products through new media, including live streaming and short video sales to determine the corresponding relationship between key influencing factors and farmers' willingness and to explore the formation mechanism, so as to better play the role of new media marketing in solving farmers' "difficulty in selling" and helping rural revitalization.

3. Research Contents

3.1. Research Methods. Grounded theory is an exploratory qualitative research method proposed by American scholars Strauss and Glaser that obtains the original data through in-depth interviews and abstracts and condenses the original data through three-level coding, with social phenomena and problems as the research object, so that a scientific and reasonable theory and model and a bottom-up systematic theory are established to deeply analyze the existing problems.

In this study, in-depth interviews with new professional farmers in Fujian Province are conducted, and the willingness of farmers in Fujian Province to sell agricultural products through new media marketing is studied using the research paradigm of Straus' programmed grounded theory [13–16]. Nvivo12plus software is used as an auxiliary coding tool to reduce, screen, and extract the original data in the form of open coding, spindle coding, and selective coding,

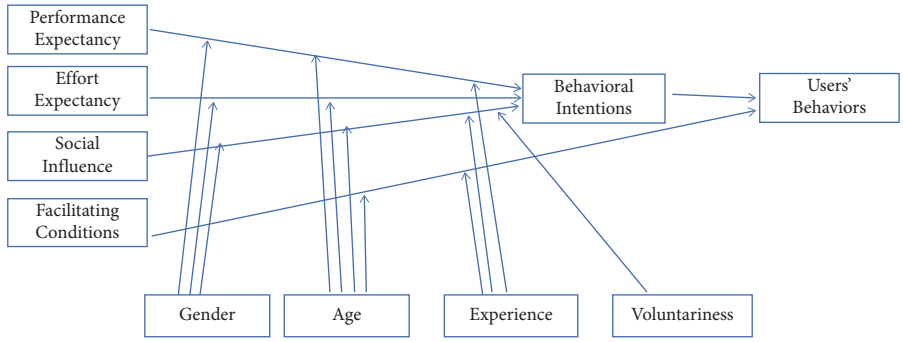

Figure 1: Model of UTAUT theory.

determine the concept and category, and finally establish the theoretical framework model [17–20].

3.2. Data Collection. In this study, a total of 76 new-type professional farmers are selected as the interview objects, including 40 males and 36 females, aged between 31 and 50 years, more than 90% of whom have a high school or junior college education. After obtaining the consent of the interviewees, a face-to-face semistructured interview is conducted, and the interview content is recorded by mobile phone. The average interview time is 45 minutes, the longest is 75 minutes, and the shortest is 40 minutes. The whole interview process strictly follows the research paradigm of grounded theory. Thirty five copies of text information were organized according to the recorded information, of which, 30 are randomly selected for coding analysis combined with the details such as tone and expression of interviewees marked by on-site observation, and the remaining 5 are used for the theoretical saturation test.

The interview outline and specific contents are set around the investigation of farmers' willingness to use new media for agricultural product marketing. From the four dimensions of PE, EE, SI, and FC, 26 related interview questions are designed based on the UTAUT model of "integration theory of technology adoption and utilization," involving the personal situation of farmers, application of agricultural products e-commerce to product sales, and personal attitudes towards new media marketing of agricultural products. Then, in strict accordance with the theme of new media marketing intention, these data are screened, processed, and numbered for and coding.

4. Coding Analysis and Model Building

4.1. Open Coding. In grounded theory, the first is to conduct an open coding analysis on all interview data texts; that is, the interviewer will code, conceptualize, and categorize the data in the original text records of interviewees, so as to form the original data statements, as well as initial concepts and categories. In this study, Nvivo12plus software [21–25] is used to sort out the interview materials, and more than 300 original sentences are obtained. Then, 37 initial concepts and 17 effective initial categories are generated by categorizing the initial concepts with word frequency greater than 2 times. Specific information is shown in Table 1.

4.2. Axial Coding. Axial coding is carried out after open coding. In this process, the initial concepts formed should be first analyzed and refined through cluster analysis and then put into the local social and cultural background for practical analysis to refine the main categories and merge the secondary categories. In the second round of coding, this study extracts eight main categories: natural conditions, characteristics of agricultural products, financial costs, social culture, population structure, the government environment, and the characteristics of farmers and sales. Specific information is shown in Table 2.

4.3. Selective Coding. In this study, eight main categories [26–30] of natural conditions, the characteristics of agricultural products, financial costs, social culture, population structure, the government environment, and the characteristics of farmers and sales are first determined by axial coding to form and develop the story line of "farmers' willingness to engage in new media marketing." Then, the logical relations among the factors of each category are integrated to construct the theoretical model framework of the research problem.

4.4. Model Building. After refining 35 original texts, 17 initial categories, and 8 main categories and sorting out the "story line" through selective coding, the research model of farmers' willingness to sell agricultural products by means of new media marketing is finally constructed. The results show that farmers' willingness to sell is influenced by eight factors, including natural conditions, characteristics of agricultural products, financial costs, social culture, population structure, government environment, characteristics of farmers, and sales. The model is shown in Figure 2.

4.5. Theoretical Saturation Test. Nvivo12plus software is used here to import the five unanalyzed interview text materials into the coding verification. The results show that no new concepts and categories are found in the theoretical saturation test, and the sample data can no longer generate

Table 1: Open coding results of Fujian farmers' willingness to sell agricultural products by new media marketing.

Initial categories	Initial concepts	Original data statements
Growing climate of agricultural products	Status of cash crops	The climate of Wuyi mountain is suitable for growing tea, so we are planting Wuyi mountain rock tea; we mainly grow Mandarin oranges, which are greatly affected by the weather
	Status of food crops	We usually grow sweet potatoes in a small area of three or four mu
	Climate for agricultural production	The weather has been bad these years and drought led to a sharp decline in tea production; fruit production is affected by the weather
Growing temperature of agricultural products	Temperature for agricultural production	The weather is hot these two years and our planting is affected by high temperatures
	Weather for agricultural production	The sweetness of the oranges will be affected by rain, too much of which will cause oranges not to be as sweet as they used to be
Growing environment of agricultural products	Producing areas of agricultural products	We live in Zhengyan mountain farm, where the tea is sold so well for its quality that you do not even need to sell it online; our tea is in Tianxing village in Wuyi mountain, but there are fewer tourists here these years
Qualification of agricultural products	Quality certification of agricultural products	"San pin yi biao" agricultural products can get government subsidies; consumers are more inclined to have agricultural products of certification, such as pollution-free agricultural products, and green food; we can sell our own produce; however, if they are to be strictly examined, it may be difficult to guarantee their quality
	System certification of agricultural products	Food industry certification requires ISO22000, HACCP system, which is also a large amount of expenditure
Standardization of production	Branding of fresh products	The same produce, once branded, costs a lot more; slightly better packaged tea sells well in douyin studios
	Construction of standardized production system	From these years of operation, I also realize that the standardized production of agricultural products is very important
Advanced production technology	Production technology of agricultural products	Nowadays, the management of agricultural products is also very particular about production technology; technology is now necessary for everything, such as how to store produce, and how to process it
	Scientific packaging, storage, and transportation of agricultural products	Online sales challenge the supply chain; although live-streaming can bring orders, but how to deliver, how to pack, etc., must be considered clearly before live-streaming; now, a large part of the operating cost is spent on packaging, storage, and transportation
Production costs of agricultural products	Production of agricultural products	The product volume is relatively small, so it is not easy to sell; our own Mandarin oranges usually come to market around winter; our tea farmers pay special attention to the growth of tea leaves and dare not to use pesticides
	Expiration date	Because fruit has a very short shelf life, it is usually picked and sent out before it is fully ripe; otherwise, the fruit will easily rot in transit
Logistics costs	Product packaging costs	We do not sell our own products online because of the high cost of packaging; the packaging alone costs a lot of money, but in fact, the product itself is not expensive
	Logistics and delivery	The epidemic has increased the difficulty and cost of logistics operations; the epidemic has made national distribution difficult
Marketing and promotion costs	Costs of the operating team	I am too old to know much about Internet; a small amount of product is not worth paying someone to live stream; I cannot afford to have people conduct live streaming; typically, the cost of operation teams and platforms is high
	Advertising expense	It is not worth the cost; if there is no advertising, there is no traffic; without money, there would be no traffic and no consumers to buy our products

Table 1: Continued.

Initial categories	Initial concepts	Original data statements
Local traditions and customs	Behavioral modes	With a low level of education, we can only play on mobile phones, but do not know how to run live streaming and short videos; we watch live streams and short videos, but we cannot operate; I will use e-commerce only after many of my peers have adopted it
	Living habits	After dinner, young people watch Douyin or play cards; usually, when we are not working outside, we get together to chat and play cards
	Social experience	In our village, people who go out to start businesses have experienced many things; now, the outside world is changing a lot; we really need to learn more
Social cognition	Reflections on social activities	The women here generally do not like to talk in front of others and feel very uncomfortable; I get so nervous in front of the camera that I cannot run live streaming, and I do not know what to say; I do not feel comfortable exposing myself to cameras or interacting with fans in the studio;
	Local customs	People in our village are conservative and do not like live streaming, and we feel the same as the host; Minnan people are quite bold and willing to try new ways
Population structure	Family structure	We have a larger family and the children will come back to help when they grow up; we only have two kids, and the whole business is dependent on us, so we do not have the energy to do anything else
	Cultural structure	My own education level is low, but my kids know a little bit about it, and they will make live streaming on Douyin when they have time; I went on to a junior college later; with more communication with my classmates, I am much braver
Policy and technology development	National policy	In recent years, the government has issued a lot of e-commerce policies to benefit farmers and provided a lot of training; our cooperative runs special e-commerce training courses, which we attend whenever we have time; thanks to good policies, times, and technology, we can sell things at home; mobile phones and the Internet are developing rapidly; Ii you do not learn, you will be left behind
	Scientific and technological development	
Characteristics of farmers	Level of education	The county's agricultural machinery station provides farmers with e-commerce training; there are many college students in our village now
	Scale of incomes	I opened a taobao shop a few years ago and made a little money; I was an early e-commerce entrepreneur in my village, so relatively speaking, I earn more than others
	Personalities	I have a quick temper, and I do what I decide to do; in retrospect, I made the right decision; I like making friends, more friends and more opportunities; I am ordinary and conservative
	Interpersonal connections	We should get to know more people and learn their advantages; most of the time, judgment is important, and the correct judgment comes from experience; I am used to rely on my experience
Product price	Product price	Fruit prices have not changed much in the past two years; tea prices have been heavily affected by the pandemic
	Differences in different sales channels	Products are purchased by customers at a low price but sold online at a high price; live streaming can lead to better prices for produce

Table 1: Continued.

Initial categories	Initial concepts	Original data statements
Sales risk	Differences in sales	If products are sold to buyers, we can quickly sell out the products, but the profit is low; selling products by live streaming is a matter of luck; sometimes products sell well, sometimes they do not
	Differences in channel risk	The buyer can take all the products at once; I just wait at home; online sales take a long time; customer source depends on accumulation; the product will be easy to sell on some accounts that run for a long time
	Risk of damage	Online sales require seven days of gratuitous compensation service for bad fruit, which makes online sales more risky and in debt; what we fear most is that the fruit will spoil in transit; poor logistics will make us lose money
Investment costs	Pre-investment restriction	I Know e-commerce will be profitable, but it will take a big investment to start with; what we farmers need most is money

Table 2: Axial coding results of Fujian farmers' willingness to sell agricultural products by new media marketing.

Main categories	Independent categories	Initial concepts
Natural conditions	Growing climate of agricultural products	Status of cash crops; status of food crops; climate for agricultural production
	Growing temperature of agricultural products	Temperature for agricultural production
	Growing environment of agricultural products	Weather for agricultural production; producing areas of agricultural products
Characteristics of agricultural products	Qualification of agricultural products	Quality certification of agricultural products; system certification of agricultural products
	Standardization of production	Branding of fresh products; construction of standardized production system
	Advanced production technology	Production technology of agricultural products; scientific packaging, storage, and transportation of agricultural products
Financial costs	Production costs of agricultural products	Production of agricultural products; expiration date
	Logistics costs	Product packaging costs; logistics and delivery
	Marketing and promotion costs	Costs of the operating team; advertising expense
	Investment costs	Pre-investment restrictions
Social culture	Local traditions and customs	Behavioral modes; living habits
	Social cognition	Social experience; reflections on social activities; local customs
Population structure	Family structure	Number of family members; family relationship
	Cultural structure	Regional culture; folk customs and family traditions
Policy environment	Policy and technology development	National policy; scientific and technological development
Characteristics of farmers	Characteristics of farmers	Level of education; scale of incomes; personalities; interpersonal connections
Sales	Product price	Product price; differences in different sales channels; risk of damage
	Sales risk	Differences in sales; differences in channel risk

new theories. It can be seen that the research model of farmers' willingness to sell agricultural products through new media marketing based on the programmed grounded theory has reached theoretical saturation and thus has certain realistic explanatory power.

5. Discussion and Analysis

5.1. Impact of Macrofactors on Farmers' Willingness to Sell Agricultural Products through New Media. With the wide use of new media, agricultural product marketing also ushered in a rare opportunity for development. However, due to the late start and a weak development base of new media in China, the majority of farmers, restricted by geographical location and the overall low-level of economic development, as well as the influence of long-term traditional culture, are relatively conservative and slow to accept new things. In addition, affected by such problems as poor infrastructure and unstable Internet speed in the outward environment, new media marketing is still in its infancy with a relatively low penetration rate, although the national government has strongly supported farmers to participate in rural

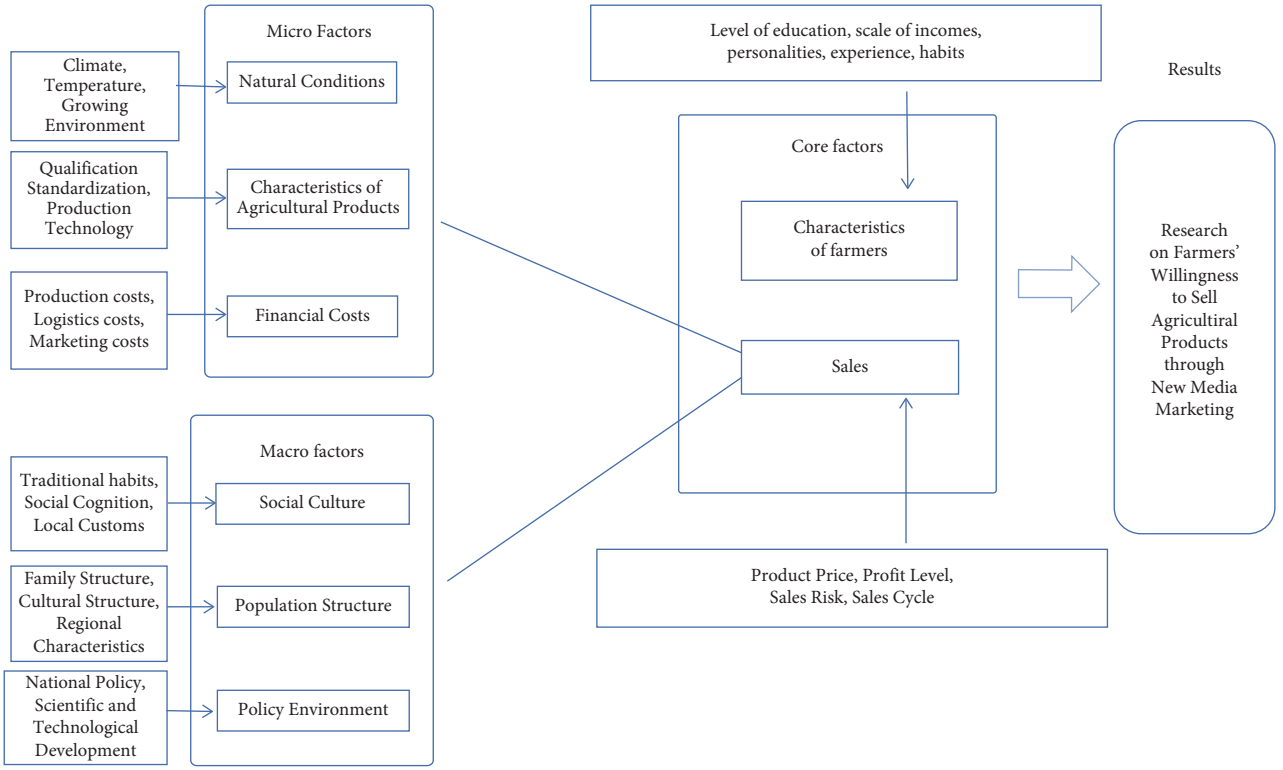

Figure 2: Model of factors influencing Fujian farmers' willingness to sell agricultural products by new media marketing.

e-commerce in recent years. Hence, farmers' willingness to sell agricultural products using new media is influenced by social culture, population structure, and policy environments. Moreover, in the use of new media, most farmers show a herd mentality. According to the interview data, some interviewees think that "Being an ordinary person, I am conservative and used to rely on my own experience." And when asked about "the influence of the external environment on my willingness to use new agricultural products marketing methods," some interviewees say "I will use e-commerce only after many peers around me have adopted it." Also, some interviewees express visceral resistance, saying, "Especially when it comes to 'showing up' on camera and interacting with fans in the studio, I am reluctant."

5.2. Impact of Microfactors on Farmers' Willingness to Sell Agricultural Products through New Media. Microfactors mainly refer to the natural conditions, characteristics of agricultural products, financial costs, and other key links closely related to the production and management of agricultural products.

Natural conditions include climate, temperature, and environment suitable for the production or processing of agricultural products. For a long time, the cultivation, processing, and production of agricultural products have been highly dispersed and small in size due to the influence of multiple factors, and too little sales result in the failure to form the influence of products. In the interview, when asked about "factors affecting the sale of agricultural products," 17.81% of the farmers said that their products were small in quantity and difficult to sell. Scale and concentrated production are the premise of building agricultural products brand. The lack of a certain scale makes it costly to build information platforms, trading platforms, and circulation channels, which leads to the difficulty of unified processing and marketing of agricultural products. In the interview, nearly 60% of the interviewees think that there is no good sales channel, and 30% consider that the cost of trading on the platform is high.

Quality is the premise of building a brand and selling well. In new media marketing, when consumers can only indirectly perceive products through short videos and live streaming rooms, farmers are more needed to check the quality of agricultural products. Whether to have qualification, certification, and standardization is an indispensable "inspection rule" of high-quality agricultural products, which directly determines the quality of agricultural products. In the interview, when it came to "factors affecting the sale of agricultural products," 15.07% of farmers believe that it is difficult to guarantee the quality of their products, which affects their willingness.

Financial costs are mainly reflected as product packaging, logistics, and advertising costs to attract fans on new media platforms. In the new media marketing, it is necessary to attract consumers' "eyes" more from the sensory experience of consumers and to maximize the safety and undamaged arrival of agricultural products to consumers from the perspective of storage and transportation. Therefore, in new media marketing, farmers need to consider the cost of physical packaging and storage and transportation

packaging. In addition, new anchors and vloggers need to spend a certain amount of money to attract fans. These marketing costs are also factors influencing farmers' use of new media to sell their produce.

5.3. Impact of Farmers' Characteristics on Their Willingness to Sell Agricultural Products through New Media. The characteristics of farmers, such as personalities, long-formed habits, education level, and personal and family income level, are core factors affecting their willingness to use new media marketing. In the interview of farmers who have adopted new media marketing to sell agricultural products and obtained better income compared with the previous year, it is found that 91.78% of the farmers have a high school or college degree or above. Furthermore, 62.12% of farmers say that "I don't want to be too conservative, and I like to break through the present," and 35.17% of farmers think "I am a person who dares to think and do. I am willing to try electronic products and new things and get started quickly." In terms of "attitude towards new media marketing in rural areas," 45.21% of farmers express great interest and 41.1% express interest. Meanwhile, farmers' income status will affect their willingness since the level of income affects their personal cognition to a certain extent. Benefiting from their good economic basis, farmers with high income are more willing to explore new ways to expand sales channels of agricultural products.

5.4. Impact of Sales Status on Farmers' Willingness to Sell Agricultural Products through New Media. The sales status herein refers to the unit price, profit level, sales risk, and sales cycle of agricultural products provided by farmers for the third parties.

When the unit price of agricultural products is high, it is difficult for farmers to sell them through short videos or live broadcast rooms, and vice versa. In the interview, interviewees say that 40% of the tea produced by them that has higher price than other agricultural products are sold through offline wholesale markets, distributors, or agents, and 25% is sold online. Farmers who choose new media marketing say that "as the source producer, they can get more profits by choosing new media for sales." On the contrary, farmers who grow less profitable agricultural products are less willing to choose new media for sales.

Farmers generally believe that merchants' acquisition in traditional offline sales channels is the most stable, rapid, and convenient, but the price and sales volume of products brought by online new media marketing are unstable. Also, there is a popular belief among them that, under the background of new media marketing, the product sales cycle is affected by the individual's knowledge of new media technology, live streaming sales technology, and short video production technology. Therefore, farmers, who lack professional new media marketing technology, generally express their concern about the use of new media marketing. Nearly half of the interviewees say that they only understand the basic use of new media tools, but have some difficulty in applying them to marketing or they cannot use new media tools. In the interview with the theme of "The most important problems to be solved in participating in rural e-commerce," most of the interviewees indicate that they are in urgent need of training and technical guidance of professional e-commerce talents or in urgent need of being trained as professional new media operation talents.

6. Strategies and Suggestions

6.1. Strengthening the Training of Farmers on New Media Marketing Techniques. Strengthening the training of farmers on new media marketing techniques of agricultural products can improve their cognition of e-commerce, psychologically shorten their distance from new sales methods, and enhance their willingness to use new media. First of all, to strengthen the training support of new media marketing, a combination of horizontal and horizontal training can be adopted to make full use of the advantages of new media marketing related majors in agricultural colleges and universities under the coordination of "government, school, industry, and enterprise" for rural revitalization. The practical operation skills of farmers should be strengthened by improving new professional farmers' educational background and training them on rural live streaming e-commerce and new media operation so that farmers can get familiar with the operation process of new media operation. Secondly, the opportunities for cooperation with large e-commerce platforms can be increased to train farmers on the production quality of agricultural products and e-commerce transactions and improve their skills in product production and network information technology processing, so as to enable them to better resist future risks and enhance their willingness to use new media to sell agricultural products.

6.2. The Government Issue a "Package" of New Media Marketing Support Policies. Governments at all levels should encourage farmers to their agricultural products using new media and promote rural revitalization through industrial revitalization. In terms of top-level design, better service and support policies should be introduced in various aspects such as industrial development planning, new media talent training, and follow-up service guarantee. First, build the brand of agricultural products. New media cloud support is provided for agricultural products with strong regional representation, a large number of employees and considerable market potential, so as to shape local characteristic brands. Secondly, prepare training materials for farmers' new media marketing, as well as supporting teaching plans, courseware and microclass short videos. To highlight the main line of selling agricultural products through new media, the electronic textbook package can adopt methods of navigation-style bookmarks, "nanny level" companionship, and the way of accessing knowledge at any time through "clicking." Thirdly, the professional new media operation team develops the operation package of "live streaming e-commerce of agricultural products" at a suitable price for farmers who are willing to buy it. By simplifying the

process of new media, this operation package enables farmers to experience the use of new media marketing methods with "low cost and zero distance," accumulating operation experience, such as setting character and attracting fans and learning efficient output, so that farmers can become local talents of live streaming e-commerce of agricultural products with their own characteristics and the gold spokesperson of local agricultural products.

6.3. Build the Brand of High-Quality Agricultural Products by Giving Full Play to the Value of Producing Area. Brand building is a crucial link for farmers to open the market with agricultural products. In the investigation of farmers' willingness to sell agricultural products through new media, it is found that most farmers are reluctant to sell their products through new media because of the sales difficulties caused by the lack of brand promotion. In response to the proposal to take action to improve varieties, enhance qualities, build brands, and promote standardized production of agricultural products in *No. 1 Central Document* for agricultural product branding construction, the government should enhance the brand construction of agricultural products. First is brand empowerment. The tourism Bureau, agriculture Bureau, and other forces and resources are integrated to form a new media marketing force to boost agriculture. The professional team will select 1-2 single agricultural products with local characteristics according to regional resource advantages and market thinking and carry out brand construction through packaging design, trademark registration, relevant certification, and other ways. The second is content distribution. A series of promotional videos, brand promotion activities, and food selection activities are launched by making full use of news media and video websites on the basis of their own media to accelerate the development of leisure agriculture and rural tourism, and other industries. The power of new media platform is used to help rural areas promote featured products and tourism resources and explore the historical and cultural deposits, so as to continuously expand the brand influence.

Data Availability

The dataset can be obtained from the corresponding author upon request.

Conflicts of Interest

The authors declare that they have no conflicts of interest.

Authors' Contributions

Li Lin and Xiong Zhou contributed equally to this work.

Acknowledgments

This study was supported by The Commerce Economy Association 2022 Special Research Project on Vocational Education "On the dilemmas of Fujian farmers' e-commerce entrepreneurship and their solutions from the perspective of rural revitalization," Project no. 2022ZSZJYB38.

References

[1] Y. Zheng and R. Li, "Research on mobile learning based on UTAUT model: a case study of international journals from 2017 to 2021," *Advances in Education*, vol. 11, no. 4, pp. 1136–1145, 2021.

[2] L. Xie, P. Liu, and D. Liu, "Research on the development of rural e-commerce in Guizhou under the background of rural revitalization," *Advances in Social Sciences*, vol. 10, no. 12, pp. 3376–3381, 2021.

[3] X. Lyu, "On the operation mode of fresh agricultural products e-commerce," *Industrial & Science Tribune*, vol. 16, no. 9, pp. 14-15, 2017.

[4] S. Huang and B. Wang, "Study on e-commerce model of local agricultural products under the background of "Internet +": a case study of Wuhu," *Think Tank Era*, vol. 2, no. 40, pp. 69–73, 2018.

[5] Q. Liu, *Research on the Willingness to Use Rural E-Commerce under the Background of New Urbanization*, China National Conditions and Strength, China, 2016.

[6] Y. Mao, "Analysis of factors affecting consumption intention in cross-border retail e-commerce platform," *Modern Marketing*, vol. 12, no. 5, p. 6, 2016.

[7] L. Yao and H. Zhu, "Analysis on factors influencing farmers' choice of entrepreneurial location: based on a questionnaire survey of 1080 entrepreneurial farmers in Jiangxi Province," *Journal of Hunan Agricultural University*, vol. 16, no. 5, pp. 18–24, 2015.

[8] G. Li, L. Kong, Z. He, and R. Jiang, "Analysis on factors influencing farmers' participation in e-commerce sales: a case study of fresh fruits and vegetables e-commerce," *Finance and Economics*, vol. 37, no. 12, pp. 42–45, 2018.

[9] M. B. Arayesh, "Investigating the financial and legal - security infrastructure affecting the electronic marketing of agricultural products in ilam Province," *Procedia-social and Behavioral Sciences*, vol. 205, no. 9, pp. 542–549, 2015.

[10] Y. Mao, "An empirical study on the willingness of agricultural operators to develop E-commerce: a case study of Longquan City, Zhejiang Province," *China Journal of Commerce*, no. 19, pp. 26–28, 2018.

[11] Y. Huang, "Research on Farmers' Behavior of Adopting E-Commerce Sales," *Journal of Fujian Agriculture and Forestry University*, 2017.

[12] L. Su, L. Zhou, Q. Wang, and S. Zhang, "Research on factors influencing farmers' e-commerce response based on AHP," *E-commerce*, vol. 25, no. 10, pp. 42–44, 2018.

[13] J. M. Cobin and A. L. Strauss, *Basis of Qualitative Research: Procedure and Method of Forming Grounded Theory*, pp. 48–96, Chongqing University Press, Chongqing, China, 2015.

[14] Y. Han, X. Li, Z. Feng, R. Jin, J. Kangwa, and O. J. Ebohon, "Grounded theory and social psychology approach to investigating the formation of construction workers' unsafe behaviour," *Computational Intelligence and Neuroscience*, vol. 2022, Article ID 3581563, 16 pages, 2022.

[15] L. Li, C. Mao, H. Sun, Y. Yuan, and B. Lei, "Digital twin driven green performance evaluation methodology of intelligent manufacturing: hybrid model based on fuzzy rough-sets AHP, multistage weight synthesis, and PROMETHEE II," *Complexity*, vol. 2020, no. 6, 24 pages, Article ID 3853925, 2020.

[16] X. Tang, M. Wang, Q. Wang, J. Zhang, H. Li, and J. Tang, "Exploring technical decision-making risks in construction megaprojects using grounded theory and system dynamics," *Computational Intelligence and Neuroscience*, vol. 2022, Article ID 9598781, 22 pages, 2022.

[17] L. Li and C. Mao, "Big data supported PSS evaluation decision in service-oriented manufacturing," *IEEE Access*, vol. 8, Article ID 154663, 2020.

[18] H. Yang, H. Wei, X. He, Y. Yan, and X. Liu, "User experience evaluation of cross-channel consumption: based on grounded theory and neural network," *Wireless Communications and Mobile Computing*, vol. 2021, Article ID 1133414, 12 pages, 2021.

[19] R. Harald Baayen, Y.-Y. Chuang, E. Shafaei-Bajestan, and J. P. Blevins, "The discriminative lexicon: a unified computational model for the lexicon and lexical processing in comprehension and production grounded not in (De)Composition but in linear discriminative learning," *Complexity*, vol. 2019, Article ID 4895891, 39 pages, 2019.

[20] L. Li, T. Qu, Y. Liu et al., "Sustainability assessment of intelligent manufacturing supported by digital twin," *IEEE Access*, vol. 8, Article ID 174988, 2020.

[21] N. S. Aldahwan and M. S. Ramzan, "Descriptive literature review and classification of community cloud computing research," *Scientific Programming*, vol. 2022, Article ID 8194140, 12 pages, 2022.

[22] Y. Chen and Y. Xu, "The influencing factors and improvement paths of the manufacturing industry innovation system of products for the elderly," *Mathematical Problems in Engineering*, vol. 2022, Article ID 1174622, 18 pages, 2022.

[23] L. H. Li, J. C. Hang, Y. Gao, and C. Y. Mu, "Using an integrated group decision method based on SVM, TFN-RS-AHP, and TOPSIS-CD for cloud service supplier selection," *Mathematical Problems in Engineering*, vol. 2017, 14 pages, 2017.

[24] M. d C. Machado, R. L. R. Ferreira, and L. Ishitani, "Heuristics and recommendations for the design of mobile serious games for older adults," *International Journal of Computer Games Technology*, vol. 2018, 15 pages, 2018.

[25] L. H. Li, J. C. Hang, H. X. Sun, and L. Wang, "A conjunctive multiple-criteria decision-making approach for cloud service supplier selection of manufacturing enterprise," *Advances in Mechanical Engineering*, vol. 9, no. 3, Article ID 168781401668626, 2017.

[26] Z. Zou, J. Yang, Z. Wang, and H. Liu, "The plastic zone of tunnel surrounding rock under unequal stress in two directions based on the unified strength theory," *Mathematical Problems in Engineering*, vol. 2021, Article ID 8842153, 11 pages, 2021.

[27] W.-M. Chen, S.-Y. Wang, and X.-L. Wu, "Concept refinement, factor symbiosis, and innovation activity efficiency analysis of innovation ecosystem," *Mathematical Problems in Engineering*, vol. 2022, Article ID 1942026, 15 pages, 2022.

[28] L. Li, B. Lei, and C. Mao, "Digital twin in smart manufacturing," *Journal of Industrial Information Integration*, vol. 26, no. 9, Article ID 100289, 2022.

[29] G. Chen, X. Zhou, Y. Jin, and Y. Liu, "A study on parents' willingness to pay for online learning of middle school students based on perceived value," *Mobile Information Systems*, vol. 2021, Article ID 4300434, 15 pages, 2021.

[30] L. Khatibzadeh, Z. Bornaee, and G. Bafghi, "Applying catastrophe theory for network anomaly detection in cloud computing traffic," *Security and Communication Networks*, vol. 2019, Article ID 5306395, 11 pages, 2019.

Hindawi
Scientific Programming
Volume 2023, Article ID 9816825, 1 page
https://doi.org/10.1155/2023/9816825

Retraction

Retracted: Application of Three-Dimensional Image Reconstruction Technology in Neurogenic Intestinal Nursing Tasks

Scientific Programming

Received 26 September 2023; Accepted 26 September 2023; Published 27 September 2023

This article has been retracted by Hindawi following an investigation undertaken by the publisher [1]. This investigation has uncovered evidence of one or more of the following indicators of systematic manipulation of the publication process:

(1) Discrepancies in scope
(2) Discrepancies in the description of the research reported
(3) Discrepancies between the availability of data and the research described
(4) Inappropriate citations
(5) Incoherent, meaningless and/or irrelevant content included in the article
(6) Peer-review manipulation

The presence of these indicators undermines our confidence in the integrity of the article's content and we cannot, therefore, vouch for its reliability. Please note that this notice is intended solely to alert readers that the content of this article is unreliable. We have not investigated whether authors were aware of or involved in the systematic manipulation of the publication process.

Wiley and Hindawi regrets that the usual quality checks did not identify these issues before publication and have since put additional measures in place to safeguard research integrity.

We wish to credit our own Research Integrity and Research Publishing teams and anonymous and named external researchers and research integrity experts for contributing to this investigation.

The corresponding author, as the representative of all authors, has been given the opportunity to register their agreement or disagreement to this retraction. We have kept a record of any response received.

References

[1] Y. Shen, X. Huang, Y. Zhang, J. Pan, Y. Liu, and Y. Jiang, "Application of Three-Dimensional Image Reconstruction Technology in Neurogenic Intestinal Nursing Tasks," *Scientific Programming*, vol. 2022, Article ID 4840189, 10 pages, 2022.

Hindawi
Scientific Programming
Volume 2022, Article ID 4840189, 10 pages
https://doi.org/10.1155/2022/4840189

Research Article

Application of Three-Dimensional Image Reconstruction Technology in Neurogenic Intestinal Nursing Tasks

Yinli Shen,[1,2] Xiaoxing Huang,[1] Yue Zhang,[1] Jing Pan,[1] Yaxin Liu,[1] and Yunlan Jiang [1,2]

[1]*Chengdu University of Traditional Chinese Medicine, Sichuan, Chengdu 610075, China*
[2]*Hospital of Chengdu University of Traditional Chinese Medicine, Sichuan, Chengdu 610072, China*

Correspondence should be addressed to Yunlan Jiang; b20161001418@stu.ccsu.edu.cn

Received 25 August 2022; Revised 19 September 2022; Accepted 24 September 2022; Published 11 October 2022

Academic Editor: Lianhui Li

Neurogenic intestinal care is currently a major research topic in the medical field. In order to improve the accuracy of neurogenic intestinal care and simplify the process of neurogenic intestinal care, this paper adopts a three-dimensional analysis theory to extract the key indicators in neurogenic intestinal care. Through the analysis and calculation of the test data, the calculation results of neurogenic intestinal care under the effect of three-dimensional reconstruction technology were obtained. Through the analysis of the results, the calculation law under the action of the optimization model can be obtained. Based on the three-dimensional reconstruction theory, the contents of neurogenic intestinal care were analyzed by the three-dimensional reconstruction dehighlighting algorithm. The three-dimensional curve was used to screen the key indicators of neurogenic intestinal care, so as to obtain the optimized heavy weight model, and the three-dimensional reconstruction model can analyze the indicators of neurogenic intestinal care. It can be seen from relevant studies that different indicators have different trends in their range of change in the curve projection diagram of the 3D curve screening method. Among them, the curve shadow and curve point have obvious downward changes, while the curve deviation has *U*-shaped changes. The range of curve weights is relatively large. The variation rule between different data in the 3D curve segment can be obtained through the cost function. Among them, the cost function index and the cost model parameter have the same change trend, and the overall fluctuation range is relatively small through the space index. In the calculation results of neurogenic intestinal care, different factors will have a great influence on the calculation results. Neurons and intestinal peristalsis have the same change trend, while the linear characteristics of nerve endings are relatively obvious, and the fluctuation characteristics of gastrointestinal digestion are good. The health standard decreases linearly with the increase of the sample, and the dynamic reconstruction has a positive effect on the data. This study can provide research ideas for the analysis of neurogenic gut.

1. Introduction

The 3D reconstruction theory was based on the image analysis of relevant data and feature values by using 3D technology. By using the method of image analysis, the relevant indicators can be reconstructed in three dimensions, so as to obtain the original state and change process of the sample. Using this method, the original process of the sample can be analyzed, and the corresponding change characteristics and indexes can be obtained. The 3D image reconstruction theory plays a typical role in different professional fields. Related fields mainly include medical surgery [1], model reconstruction [2], ultrasound propagation [3], three-dimensional pixels [4], etc. In the field of medical donor image reconstruction, the existing medical donor image reconstruction needs a large amount of data, and the data cannot better reflect the original shape of the medical donor, there were some problems such as poor accuracy. Based on the three-dimensional reconstruction theory [5], the data analysis method was used to describe the medical donor image, and the description was combined from the local and the whole, so as to obtain the accurate model calculation results. The results of the model can reflect the real situation of the medical donor image to a certain extent, which can provide accurate guidance for the research in the field of medical workers.

Facial contour reconstruction was very important to improve facial recognition. The existing facial contour reconstruction techniques still remain in the qualitative research, and the research on the real situation of the face was relatively poor. Based on the 3D model reconstruction technology [6], the method of data iterative analysis was used to calculate the facial contour iteratively. This method can not only show the variation characteristics of facial contour but also reflect the volatility of specific data to a certain extent, which can better reflect the technical characteristics of facial contour reconstruction. Facial contour reconstruction technology was very important to improve the recognition of facial contour. In order to verify the accuracy of the model, the experimental data and facial contour recognition parameters were compared to illustrate the accuracy of the experimental results, which reflects the broad application prospect of facial contour recognition technology. In the field of visual communication, the existing visual communication efficiency was low, which cannot reflect the real visual communication characteristics of samples. Based on the three-dimensional reconstruction technology [7], the method of neural network iterative calculation was used to optimize the existing visual transmission model. The optimization model mainly iterates on specific parameters, so as to find the optimal parameters and bring the parameters into the model, so as to obtain the visual communication optimization model based on three-dimensional reconstruction technology. The experimental verification can better illustrate the accuracy of the experimental model, which can provide a theoretical basis for the study of visual communication. The low resolution of the model grid was the main factor that disturbs the model grid, and also restricts the popularization of the model grid. Based on the 3D reconstruction technology [8], the data feature simulation method was used to optimize the mesh resolution. The optimization method mainly performs iterative analysis on the corresponding data, so as to find the optimal iterative data. The iterative data were brought back to the grid resolution model to obtain the corresponding optimized grid resolution model. The model can well and accurately explain the changing process of mesh resolution, so as to carry out targeted analysis. The research can provide guidance for mesh resolution.

The abovementioned studies mainly analyzed the application of 3D reconstruction technology from the fields of grid and visual communication, but there were few studies on the existing problems in neurogenic intestinal care. In this paper, based on three-dimensional reconstruction technology, the de-highlighting algorithm and three-dimensional curve screening analysis method were used to analyze the indicators of neurogenic intestinal care. Through the analysis, the corresponding targeted index can be obtained. Using this targeted index, the change process of divine intestinal care can be better explained, so the corresponding optimization model can be obtained. Through calculation, it can be seen that the optimization model can better reflect the change process of key indicators in neurogenic intestinal care. Finally, the corresponding experimental data can be used to verify the accuracy of the model, which can provide support for neurogenic intestinal care.

2. Three-Dimensional Reconstruction Theory

Image quality is the basis of image algorithm, and the quality of image directly affects the effect of the algorithm [9, 10]. Before the implementation of image correlation algorithm, it is necessary to preprocess the image to suppress the useless information in the image and enhance the relevant information of the tested object [11, 12]. First, the number and initial position of the key points of the 3D model were determined according to the segmented 3D point cloud of the catheter center line. Second, the least square method is used to iteratively fit the 3D point cloud model and the initial key point line segment. Finally, the key converges to the stable optimal value to obtain the most accurate coordinate of the key point.

The 3D image reconstruction system plays an important role in many fields [13, 14]. To successfully apply it to neurogenic intestinal care, the flowchart of 3D reconstruction system as shown in Figure 1 was obtained through summary analysis. It can be seen from the figure that the 3D reconstruction system can be divided into three parts: image sequence import, image region segmentation and data processing, which can be shown as follows: In the image sequence processing module, the basic 3D image is linearized first; then, the illumination data of the corresponding image are extracted. Through the corresponding de-highlight processing, the corresponding optimized image is obtained; then, it is imported into the image region segmentation module. In the image region segmentation module, the image should be first segmented regionally, and then further refined to obtain the corresponding center line branch line through image refinement. The corresponding optimization data are obtained by segmentation and then imported into the data architecture module. In the data processing module, the center line of the space should be reconstructed first. Through the reconstruction of the center line of the space, the corresponding center line data can be obtained, and the data can be spliced. The fitting equation of 3D image data is obtained by data stitching, and the final calculation and measurement are carried out; then, the corresponding processing data are exported. First, the polar lines in adjacent images are calculated for a set of 2D curve segments of each data, and the matching points are found through the polar line geometry to generate the candidate 3D curve segments of each set of 2D curve segments. Second, the global selection problem is solved to select the most correct set of 3D curve segments from the candidate set.

2.1. 3D Image De-Highlighting Algorithm. First, the centerline coordinates of the catheter plane image were extracted, and the candidate three-dimensional curve segment set was generated according to the stereo vision principle. Second, the global selection problem is solved to select a 3D curve from the candidate set. Finally, the optimal path

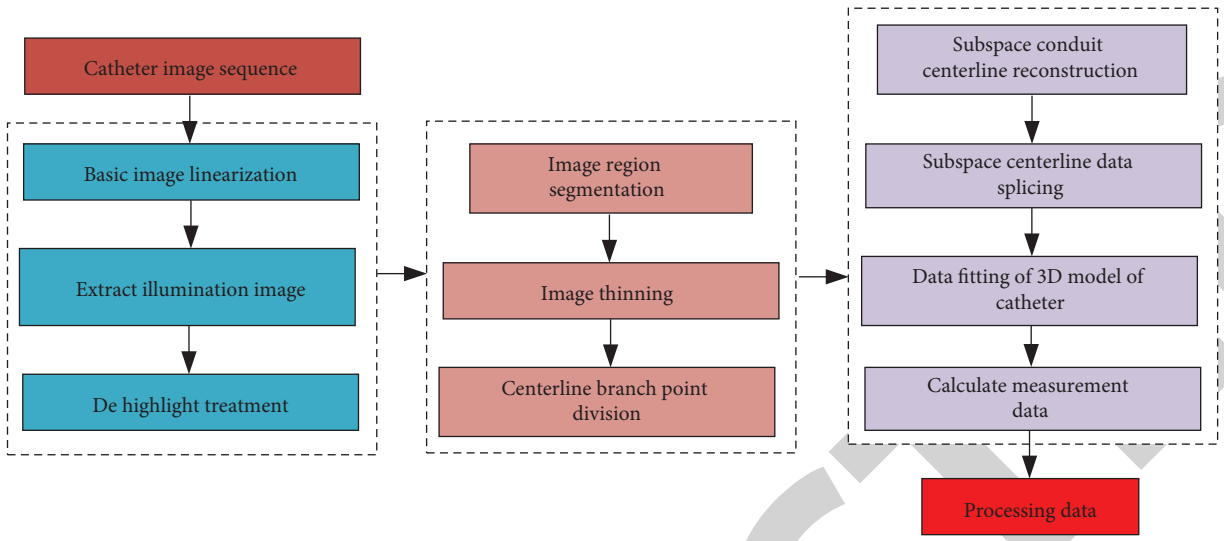

Figure 1: Technical route of the 3D image reconstruction system.

reconstruction catheter 3D model is found. Aiming at the phenomenon of surface highlight reflection produced by 3D reconstruction technology under intestinal care, this section adopts a highlight removal algorithm based on 2D gamma function image [15, 16]. First, the luminance component v in the channel of neurogenic intestine was extracted, and the illumination component was extracted by multiscale Gaussian blur. Second, the 2D gamma function is used to adjust the brightness component of the original image, and the highlight image is corrected on the premise of effectively retaining the effective information of the original image [17, 18]. By recovering the global topological structure of the three-dimensional curve segment, the subspace three-dimensional curve segment of the binocular system was data concatenated to find the optimal path to reconstruct the complete three-dimensional model of the catheter centerline. To solve the problem of weak texture and difficult matching of feature points on the surface of the model, the polar geometry method is used for space matching. The specific implementation steps are as follows:

(1) The multiscale Gaussian function is used to extract the illumination component in the image of neurogenic intestine. The Gaussian function form is as follows:

$$G(x, y) = \lambda \exp\left(-\frac{x^2+y^2}{c^2}\right), \tag{1}$$

where c represents the scale proportion and λ represents the normalization constant. By applying Gaussian blur to the original image, multiscale illumination components of the image in the neurogenic intestinal channel were extracted, and the results were as follows:

$$F(x, y) = I(x, y)G(x, y),$$
$$F(x, y) = I(x, y)\lambda \exp\left(-\frac{x^2+y^2}{c^2}\right), \tag{2}$$

where $F(x, y)$ represents the estimated model component, and $I(x, y)$ represents the input original graph.

The corresponding 3D image de-highlighting algorithm can be obtained by 3D reconstruction theory, and the specific image data in intestinal care can be extracted by the multiscale Gaussian function [19, 20]. The corresponding Gaussian change curve can be obtained through analysis, as shown in Figure 2. It can be seen from the curve in the figure that the factors affecting the change of Gaussian mainly include as follows: input original graph, Gaussian function, and corresponding model components. The output results under the action of these three factors have different changing trends, as can be seen in detail: It can be seen from the input curve corresponding to the original figure that with the increase of independent variables, the curve first slowly increases to the local maximum value, and then gradually tends to be flat. With the further improvement of independent variables, the curve gradually fluctuates, and the fluctuation range is relatively small. Then, when the independent variable is at a higher level, the curve gradually decreases and finally tends to be stable. The change trend of the overall input original graph basically fluctuates within a small range, indicating that its influence on the output result is relatively small. With the increase of independent variables, the corresponding curve of Gaussian function decreases first and then gradually tends to be gentle, and then, the curve fluctuates further. When the independent variables are higher, the curve gradually tends to be stable. The overall variation range and variation trend are exactly opposite to the corresponding curve variation trend under the action of factors in the input original graph. This shows that the two have opposite effects on the output results, and it can be seen from the model component change curve that with the

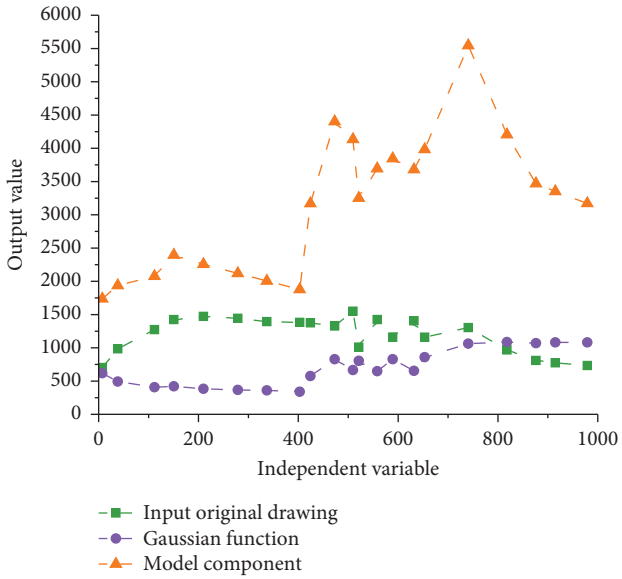

Figure 2: Gaussian change curve.

increase of independent variables, the curve first gradually increases to the local maximum value and then gradually decreases. The amount of decrease in the descending stage of the curve is basically the same, indicating that its linear feature is relatively obvious. Then, when the independent variable is further improved, the curve increases rapidly. Then it is shown that there is a certain jump in the data at this stage, resulting in a large fluctuation of the corresponding output results in a certain range. Then, with the further increase of independent variables, the corresponding output curve shows a trend of greater volatility. The overall fluctuation range of the curve is relatively wide, indicating that it has a great influence on the output result.

(2) Construct the two-dimensional gamma function as shown below and use the two-dimensional gamma function to correct the image of the highlight component and reduce the brightness value of the image of the highlight part.

$$Q(x, y) = 255\left(\frac{F(x, y)}{255}\right)^{\gamma},$$
$$\gamma = (1/2)^{P}, \tag{3}$$
$$P = \frac{I(x, y) - m}{m},$$

where $I(x, y)$ is the input image, $F(x, y)$ is the model component image, $O(x, y)$ is the corrected output image, γ is the index value of image brightness enhancement, and m is the luminance mean value of the illumination component.

By using the multiscale Gaussian function in the theory of 3D image de-highlighting, the corresponding trend map of neurogenic intestinal image processing can be obtained [21, 22]. By constructing a two-dimensional gamma function curve, you can analyze the different parameters in it. Through analysis, it can be seen that the influencing factors of two-dimensional gamma function mainly include input image, model component, output image, incremental index, and corresponding mean function. To illustrate the quantitative analysis of the two-dimensional gamma function curve by these five factors, the variation curve of the two-dimensional gamma function as shown in Figure 3 was obtained by calculation. It can be seen from the curve that the output results under the action of five different factors have different change trends, and their specific data have different change forms. As can be seen from the curve corresponding to the input function, with the increase of samples, the curve firstly linearly increases to the local maximum value and then gradually tends to be gentle and then slowly decreases. The decrease amount is relatively small compared with the first stage. Then, with the further increase of the sample, the curve gradually decreases and then increases again, showing a U-shaped change trend, and the overall range of change is relatively large. It shows that this factor can have a great influence on the calculation result of dependent variable. According to the corresponding curve of the graph component, it can be seen that the curve decreases linearly with the increase of the sample. When it reached the lowest value, the curve showed a trend of gradual improvement with the increase of samples. It can be seen from the change trend that the change range of the first stage is larger than that of the second stage, indicating that the first stage of the curve has a higher impact on the dependent variable. According to the corresponding curve of the output function, when the sample is low, the curve gradually tends to be gentle; when the sample is high, the curve first decreases and then increases and finally gradually tends to be stable. The overall stability of the curve is obvious. This indicates that it has little influence on the dependent variable. According to the curve corresponding to the incremental index, it can be seen that with the increase of samples, the curve first increases rapidly to the highest value. Then the sample increase will lead to the corresponding dependent variable data showing a linear decline, with a relatively small range of decline. When the number of samples is 30, the curve reaches the lowest value, indicating that the corresponding calculation result at this point has the minimum value. Then, with the further increase of samples, the output results of the corresponding dependent variable gradually tend to be stable. The curve has an obvious effect on the dependent variable sample of 12. As can be seen from the mean function, the increase of samples will lead to the linear increase of the corresponding dependent variable. Then, when

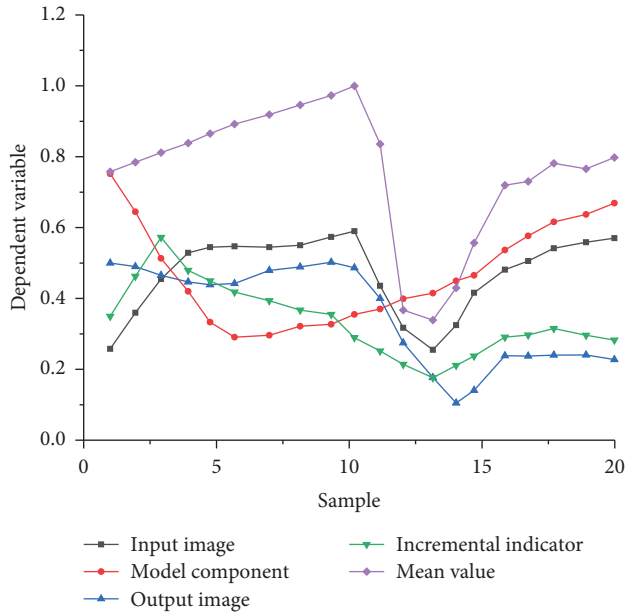

Figure 3: Two-dimensional gamma function graph.

the corresponding sample is gradually improved, the curve decreases first and then increases, showing a *U*-shaped characteristic. The curve shows typical linear characteristics in the first stage, and obvious nonlinear characteristics in the second stage, indicating that the curve corresponding to the mean value function has linear and nonlinear characteristics of common change.

2.2. Three-Dimensional Curve Screening. In the ideal case, there is only one candidate 3D curve segment corresponding to the 2D curve segment of the reference image [23, 24]. If there are multiple candidate 3D curve segments, it is necessary to select a correct curve segment from a set of candidate 3D curve segments by calculating the confidence degree and pairwise cost [25]. The confidence measure measures the matching degree between the 3D candidate curve segment and the curve in the third image, projects each 3D candidate curve segment onto the third image and finds the 2D curve segment in the third image with the smallest projection difference with the candidate curve segment. For the point set, u is the projection on the 3D curve segment, and v is its corresponding point closest to u on the 2D curve segment. The confidence can be calculated as follows:

$$S = \frac{\sum(u, v) + \eta(1 - t)}{s}, \tag{4}$$

where S is confidence degree, s is the sampling point, u is the curve projection, v is the curve point, t is curve deviation, and η is the weight. First, the factors affecting image processing are analyzed, and then, the method of removing highlight of image is introduced in detail, and the light source method used in the measurement system is explained. The influence of light source on image processing quality is also pointed out. Finally, the image is refined and segmented, and the center line of each image is extracted to prepare for 3D reconstruction.

Through the theory of 3D image de-highlighting, the corresponding law of image subdivision calculation can be obtained. To illustrate the role of 3D image reconstruction technology in neurogenic intestinal care, the corresponding curves of 3D images need to be screened to some extent. The curve variation law under the action of different factors was obtained by calculation. To explore the influence of different factors on the projection results in the process of curve projection, the curve projection diagram shown in Figure 4 was obtained through calculation. The influence of different factors on the curve is mainly reflected in the changing shape of the curve. Specifically, it can be seen that: With the increase of the sample points, the curve corresponding to the projection factor shows a gradual decreasing trend. The decline range of the curve in the first stage is relatively small, while the decline range in the second stage is relatively large, indicating that the sampling point has a great impact on the confidence of the data when it is high. As can be seen from the variation law of data points, the curve first increases, then decreases rapidly, and finally gradually tends to be stable, indicating that the curve will gradually tend to be stable under the action of higher sampling points. According to the curve deviation data, it can be seen that with the increase of sampling points, the curve as a whole shows a U-shaped change law. The curve first gradually increases to the highest value, and when the sampling point is about 35, the curve reaches the highest value, and then with the further increase of the sampling point, the corresponding confidence gradually decreases. The overall change in the curve is large in the first period and relatively small in the second period. According to the weight factor of the curve, it can be seen that it shows a typical two-stage change: the inverted U-shaped change range of the curve is relatively small in the first stage. When the corresponding sampling point of the curve is high in the second stage, the curve shows an inverted U-shaped change with a relatively large variation range. The overall variation range of the curve indicates that it has a relatively large impact on the confidence degree. Because of the disparity in the field of view, confidence alone is not enough to describe the matching degree of curve segments to resolve all ambiguities. Therefore, pairwise costs need to be calculated for further screening. Pairwise relation describes the relation between two adjacent three-dimensional candidate curve segments.

Since only one 3D curve segment needs to be selected from each candidate set, a linear constraint for each given is as follows:

$$\sum_{A \in C} X(j) = 1. \tag{5}$$

Next, we define a pairwise relation cost function d to evaluate the pairwise relation between 3D curve segments:

$$\mathrm{dA}A = eA1 + mA2, \tag{6}$$

where e is the space distance; m is the model parameter. The correct 3D curve segment is reconstructed from a curved, continuous conduit object, along which the continuous curve segment is smoothly connected. Therefore, adjacent

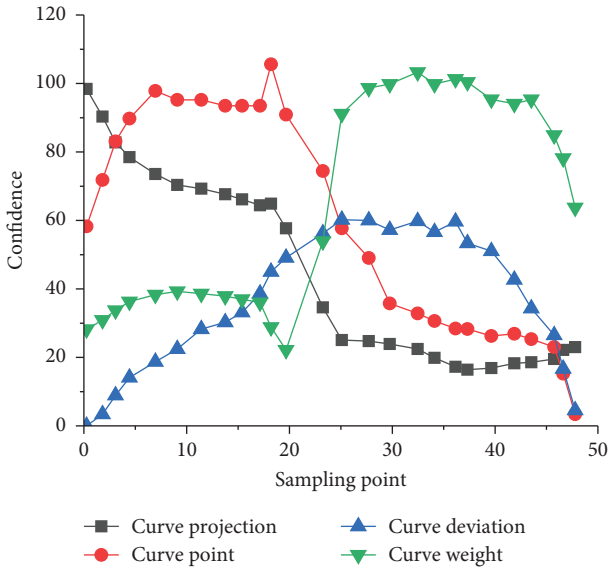

Figure 4: Curve projection diagram.

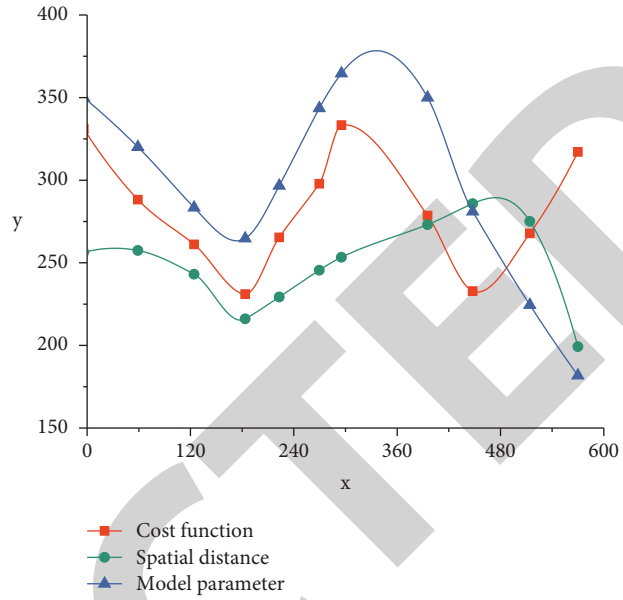

Figure 5: Change of cost function.

3D curve segments with similar angles are more likely to be the correct 3D curve segment, which provides a more effective matching cue to formalize these cues in the optimization problem.

The corresponding linear constraint law can be obtained by selecting 3D curves from different sets. The linear constraint law can reflect the change trend under the action of different cost functions, so as to explain the influence of different factors in the change law of cost functions, and then reflect the corresponding curve screening process and corresponding accurate results. The change trend of the cost function as shown in Figure 5 is obtained through calculation. It can be seen from the figure that the overall fluency of the curve is relatively good. The corresponding output results of the cost function are shown as W-shaped fluctuation changes which first decrease and then increase and then decrease and then increase. The corresponding model parameters also show the same change trend with the increase of independent variables, but under the action of higher independent variables, the curve gradually decreases, contrary to the change trend of the corresponding cost function. However, the corresponding modular space distance decreases first and then increases gradually with the change of the cost function, and the overall change range of the curve is relatively small, indicating that its influence on the output result of the cost function is relatively small.

Finally, the vector U is used to represent the combined confidence scores of all 3D curve segments, and V is the pairwise cost variable, giving U and V, minimizing X as follows:

$$\begin{aligned} X &= \operatorname{argmin}\left(U^T X + X^T \mathrm{VX}\right), \\ \forall C_i^r &= \sum_{A_j = C_i^r} X(j)1, \\ \{\mathrm{xij}\} &= \underset{\{k,\mathrm{xij}\}}{\operatorname{argmin}} \sum_{i,j} \mathrm{xijwij} + \xi k. \end{aligned} \tag{7}$$

Through the above calculation, the quantitative change rule of the cost function under the action of different factors can be obtained. To research the specific changes of confidence in the three-dimensional curve, the direct line parameter analysis diagram shown in Figure 6 is obtained through calculation. It can be seen from the analysis figure that the three factors will have an impact on the output result of the dependent variable of confidence, and the curve under the action of the three factors can be seen that the overall fluctuation range is relatively large. As can be seen from the changes in the figure, with the increase of independent variables, the curve first gradually increases to the highest value and then gradually decreases to the lowest value. However, it can be seen from the cost that the curve is contrary to the confidence degree, that is, the curve gradually decreases to the highest value first and then increases gradually. As can be seen from the minimization factor curve, the curve decreases first and then increases with the increase of the independent variable. The three curves as a whole show fluctuations, and the variation range of the minimization curve is relatively small.

3. Application of Three-Dimensional Image Reconstruction Technology in Neurogenic Intestinal Care

3.1. The Main Content of Neurogenic Intestinal Care. The 3D reconstruction theory can be used to de-highlight the 3D image, so as to obtain the corresponding 3D image screening results. Through the screening results of 3D images, the application model of 3D images in neurogenic intestinal care was obtained by further analysis. First of all, we need to conduct qualitative analysis of neurogenic gut, and the

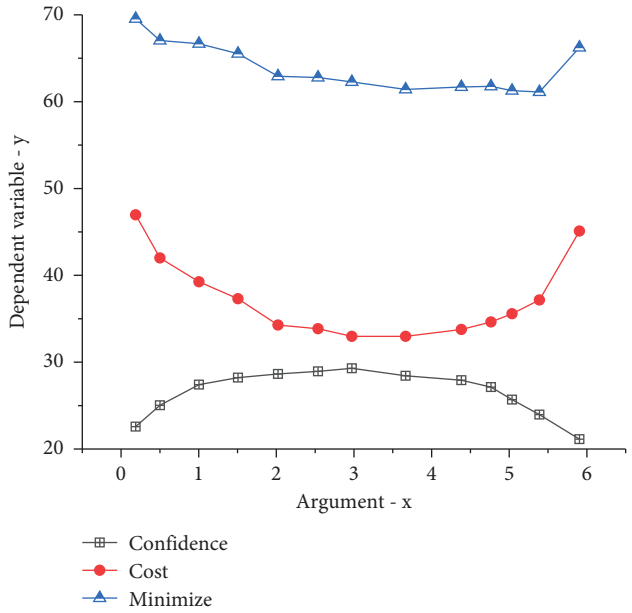

Figure 6: Confidence parameter analysis diagram.

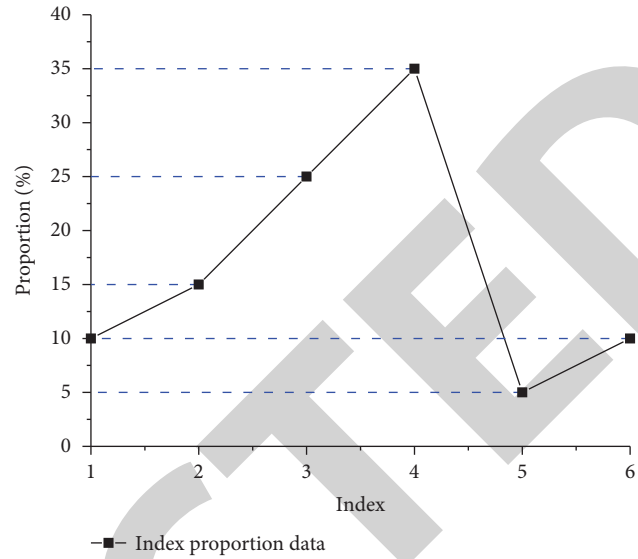

Figure 7: Neurogenic bowel analysis diagram.

corresponding neurogenic gut analysis chart shown in Figure 7 can be obtained by summarizing relevant data. As can be seen from the figure, the proportion of neurons under the action of different factors is different, so it is necessary to carry out targeted analysis. Among them, the proportion of neurons is only 10%, while the proportion of intestinal peristalsis is about 15%. The corresponding nerve terminal factors accounted for about 25%, while the corresponding intestinal digestion accounted for the highest proportion (about 35%), the health standard accounted for the lowest proportion (only 5%), and the dynamic remodeling accounted for about 10%.

3.2. Calculation and Analysis of Three-Dimensional Image Reconstruction Technology in Neurogenic Intestinal Care. There are many problems in the nursing of neurogenic intestines. To better solve the problem of low accuracy in the nursing of neurogenic intestines. In this paper, the 3D reconstruction technology is used to de-highlight the related images and screen the curves, so as to get the corresponding 3D image reconstruction model. This model can quantitatively analyze neurogenic intestines. To better illustrate the analysis process of 3D image reconstruction technology, the 3D image reconstruction analysis flowchart shown in Figure 8 is obtained by summarizing. Through the model analysis process, it can be seen that: first, graphic modeling should be carried out for 3D reconstruction technology, and the corresponding cloud generated graph should be obtained through graphic modeling. The corresponding gastrointestinal model was obtained by correcting the model. The gastrointestinal model can be calculated in the process of model cloud import, and then, the corresponding neurogenic intestinal model can be obtained. The neuronal model is mainly completed by 3D modeling in the aspect of intestinal data collection, and then, the model needs to be adjusted on the basis of this model. The adjustment of 3D neurogenic intestinal model mainly includes model angle, model position, model data, and model indicators. Finally, it is visualized, and the final output result is obtained through model effect rendering. To solve the accuracy problem in 3D reconstruction, the 3D curve segments were divided by the number of intersection points of the polar lines and several candidate 3D curve segments were reconstructed. By reprojecting the candidate 3D curve segments, the 3D curve segment with the minimum projection difference was selected to improve the accuracy of catheter centerline reconstruction.

The abovementioned calculation process can be used to de-highlight the 3D image model and screen the 3D curve, so as to obtain the application of 3D image reconstruction technology in neurogenic intestinal care. The calculation results of neurogenic intestinal care were obtained as shown in Figure 9. Through the calculation results, we can see the overall change trend of different factors under the action of neurogenesis. Specifically, it can be seen that with the increase of samples, neurons show a change of first decreasing, then increasing, and then decreasing. The overall fluctuation range of the curve is relatively obvious, but the fluctuation range is relatively small. As can be seen from the curve of intestinal peristalsis, it is basically consistent with the overall change trend of neurons, that is, the curve decreases first and then increases. However, it is worth noting that the data of the intestinal peristalsis curve are larger than that of the neuron curve, indicating that its influence on intestinal care is relatively extensive. According to the corresponding curve of nerve endings, it can be seen that the curve increases first and then decreases, and the overall decline is relatively obvious, indicating that it has a negative impact on data output. According to the gastrointestinal digestion curve, it can be seen that the curve will fluctuate to a certain extent under the action of small samples, and then gradually tends to be stable under the action of high samples, indicating that different samples will have different effects on the data

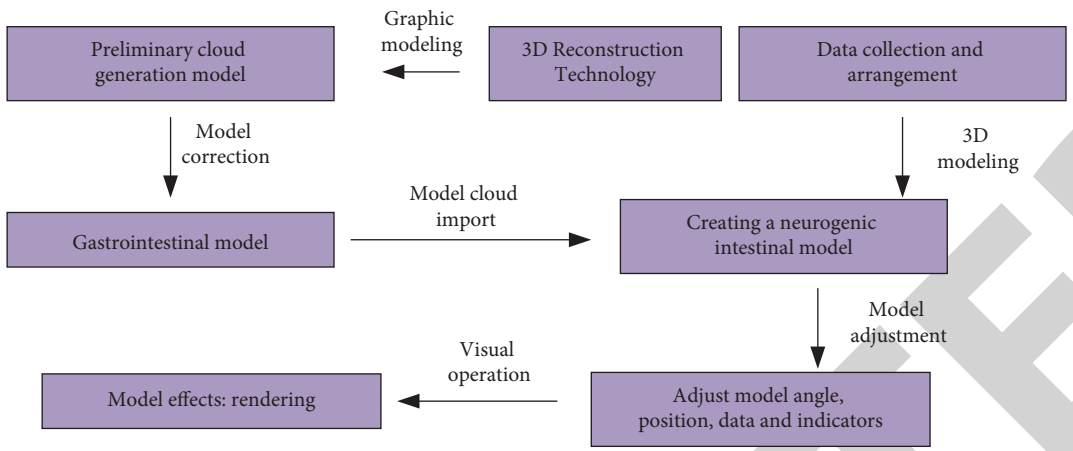

Figure 8: Analysis flowchart of 3D image reconstruction technology.

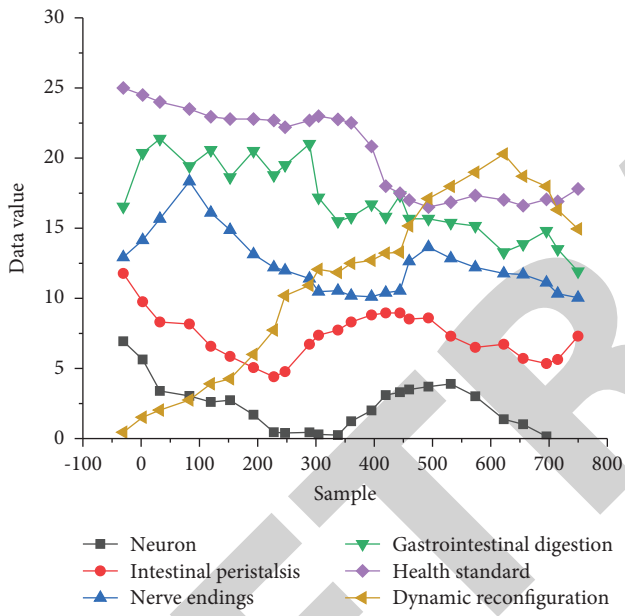

Figure 9: Calculation results of neurogenic intestinal care.

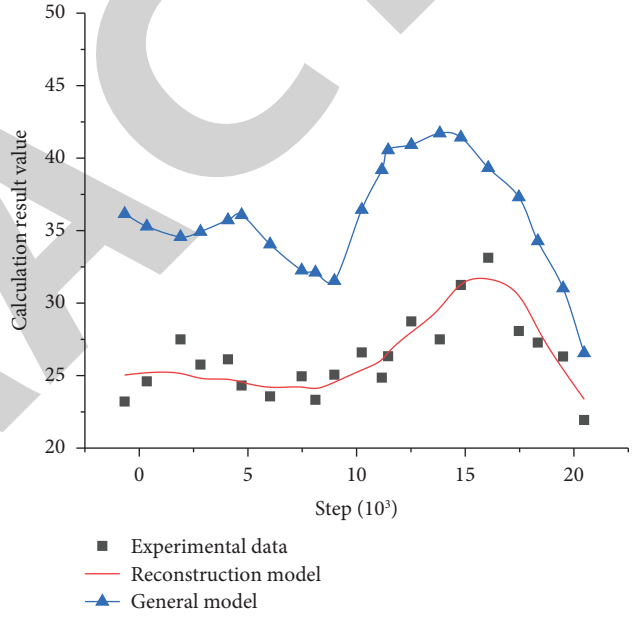

Figure 10: Model validation curve.

results of gastrointestinal digestion. It can be seen from the health standard that the curve corresponding to the health index gradually tends to be stable with the increase of the sample and then decreases rapidly when the sample is about 400, and then gradually tends to be stable. The overall range of change is relatively small, and the curve has good stability. Through dynamic reconstruction, it can be seen that the curve shows a gradual improvement trend under the action of small samples, and the overall linear range is relatively obvious. When it reaches the highest level, the curve gradually decreases with the increase of samples. It shows that it has a certain volatility to the sample data, and the overall linear characteristics are relatively obvious, indicating that it has a positive impact on the data value. The goal is to find multiple different paths that start and end with constant lengths such that each data is contained in exactly one path. Each of these paths corresponds to a continuous 3D line of the conduit model, and each path is uniquely determined by the edges it is composed of. The path finding problem is solved by minimizing the objective function.

4. Discussion

Based on the 3D reconstruction theory, the 3D image dehighlighting algorithm and 3D curve screening method were used to obtain the application of 3D image reconstruction technology in neurogenic intestinal care, and the corresponding optimization model was obtained through calculation. This optimization model can calculate the data of neurogenic intestine at different moments for accurate analysis. To quantitatively illustrate the accuracy of the model curve, the curve calculation results under the action of different models are obtained through calculation, as shown in Figure 10. It can be seen from the results that the corresponding test data gradually increases with a small number of iterations and then gradually decreases. The overall

volatility of the curve is relatively model. Through the conventional model curve, it can be seen that the curve decreases first and then increases with the increase of the number of iteration steps. The overall trend of change can well explain the experimental data, but there are great differences in specific values. Through the reconstruction curve, it can be seen that the curve can not only well illustrate the trend of the data at lower iterations but also the trend of the data and the trend of the curve at higher iterations. It shows that the reconstructed model has good accuracy. At the same time, it also shows that three-dimensional reconstruction technology has a good application in neurogenic intestinal care.

5. Conclusion

(1) According to the Gaussian change curve in the 3D image de-highlighting algorithm, it can be seen that the input original image and Gaussian function have the opposite change trend. On the other hand, the component curve of the model changes significantly with the increase of independent variables, indicating that it has a high impact on the output results.

(2) Five different factors will have different effects on the two-dimensional gamma function, among which the input function model component and the output function have the same changing trend. The corresponding incremental index fluctuates within a small range of change, and the overall linear and nonlinear characteristics are obvious through the mean value.

(3) In the confidence analysis curve, the confidence parameter shows an inverted *U*-shaped change, and the curve corresponding to the cost index shows an opposite *U*-shaped change. The trend of the minimum value shows that its influence on the dependent variable is relatively small, and the stability of the curve is relatively good.

Data Availability

The data used to support the findings of this study are available from the corresponding author upon request.

Conflicts of Interest

The author declare that they have no known conflicts financial interests or personal relationships that could have appeared to influence the work reported in this paper.

References

[1] M. Chen, N. Xia, and Q. Dong, "The application of 3D technology combined with image navigation in nasal skull base surgery," *Journal of Craniofacial Surgery*, vol. 125, no. 60, pp. 630–652, 2020.

[2] D. Jeong, Y. Li, H. J. Lee et al., "Efficient 3D volume reconstruction from a point cloud using a phase-field method," *Mathematical Problems in Engineering*, vol. 28, no. 10, pp. 1–9, 2018.

[3] J. Dong, W. Cong, D. Ai et al., "Multi-resolution cube propagation for 3D ultrasound image reconstruction," *IEEE Transactions on Computational Imaging*, vol. 12, no. 2, pp. 1–15, 2019.

[4] M. Li, A. Mathai, L. Yandi, Q. Chen, X. Wang, and X. Xu, "A brief review on 2D and 3D image reconstruction using single-pixel imaging," *Laser Physics*, vol. 30, no. 9, pp. 095204–095267, 2020.

[5] I. Maamoun and M. M. Khalil,"Assessment of iterative image reconstruction on kidney and liver donors: potential role of adaptive iterative dose reduction 3D (AIDR 3D) technology," *European Journal of Radiology*, vol. 109, no. 110, pp. 120–145, 2018.

[6] Y. Wang, N. Deng, and B. Xin, "Investigation of 3D surface profile reconstruction technology for automatic evaluation of fabric smoothness appearance," *Measurement*, vol. 166, no. 23, pp. 108264–109124, 2020.

[7] J. Yin and J. H. Yang, "Virtual reconstruction method of regional 3D image based on visual transmission effect," *Complexity*, vol. 20, no. 12, pp. 20–30, 2021.

[8] H. Zhang, Y. Shinomiya, and S. Yoshida, "3D MRI reconstruction based on 2D generative adversarial network super-resolution," *Sensors*, vol. 21, no. 9, pp. 536–549, 2021.

[9] A. D. Speers, B. Ma, W. R. Jarnagin, S. Himidan, A. L. Simpson, and R. P. Wildes, "Fast and accurate vision-based stereo reconstruction and motion estimation for image-guided liver surgery," *Healthcare Technology Letters*, vol. 5, no. 20, pp. 208–214, 2018.

[10] F. Chen, K. Muhammad, and S. H. Wang, "Three-dimensional reconstruction of CT image features based on multi-threaded deep learning calculation," *Pattern Recognition Letters*, vol. 136, no. 52, pp. 756–782, 2020.

[11] L. Deng and Y. Pu, "Analysis of college martial arts teaching posture based on 3D image reconstruction and wavelet transform," *Displays*, vol. 69, no. 20, pp. 1064–1086, 2021.

[12] X. Deng, Y. Liu, and H. Chen, "Three-dimensional image reconstruction based on improved U-net network for anatomy of pulmonary segmentectomy," *Mathematical Biosciences and Engineering*, vol. 18, no. 4, pp. 3313–3322, 2021.

[13] J. Han, J. Zhang, and Y. Zhao, "Non-textured objects visual SLAM using pola-rization 3D reconstruction," *Array*, vol. 10, no. 2, pp. 100–126, 2021.

[14] J. Huo and X. Yu, "Three-dimensional mechanical parts reconstruction technology based on two-dimensional image," *International Journal of Advanced Robotic Systems*, vol. 17, no. 2, pp. 36–46, 2020.

[15] S. Jiang and K. Wang, "Image Processing and Splicing Method For 3D optical scanning surface reconstruction of wood grain," *International Journal of Pattern Recognition and Artificial Intelligence*, vol. 34, no. 6, pp. 55–69, 2019.

[16] C. Liu, C. A. Shaheed, C. G. Maher, A. J. McLachlan, J. Latimer, and C. C. Lin, "Response to comment by b," *European Journal of Pain*, vol. 24, no. 6, pp. 1209-1210, 2020.

[17] J. Peng, K. Fu, Q. Wei, Y. Qin, and Q. He, "Improved multiview decomposition for single-image high-resolution 3D object reconstruction," *Wireless Communications and Mobile Computing*, vol. 30, no. 20, pp. 102–123, 2020.

[18] F. M. Shah, T. Gaggero, M. Gaiotti, and C. M. Rizzo, "Condition assessment of ship structure using robot assisted 3D-reconstruction," *Ship Technology Research*, vol. 20, no. 9, pp. 1–18, 2021.

[19] J. Shen, S. Meng, M. Ye, W. Yang, and Z. Liu, "3D image reconstruction using an ECT sensor with a single layer of

Hindawi
Scientific Programming
Volume 2022, Article ID 9273429, 13 pages
https://doi.org/10.1155/2022/9273429

Research Article

Research on Customer Perceived Value Evaluation of New Chinese-Style Clothing Based on PSO-BP Neural Network

Yunfeng Shu

Institutes of Physical Science and Information Technology, Anhui University, Hefei 230601, China

Correspondence should be addressed to Yunfeng Shu; q20301311@stu.ahu.edu.cn

Received 4 August 2022; Accepted 21 September 2022; Published 11 October 2022

Academic Editor: Lianhui Li

In the current era that consumers pursue personalized experience, in order to optimize the customer experience of new Chinese-style clothing products and improve the evaluation procedures of new Chinese-style clothing products, based on the theory of customer perceived value, this paper constructs the evaluation index and evaluation model of new Chinese-style clothing customer perceived value. This study is divided into three stages: firstly, through literature research and interview, thirty-seven elements of the evaluation index of customer perceived value of new Chinese-style clothing are defined; secondly, through questionnaire survey and exploratory factor analysis, seven dimensions of the evaluation index of the customer perceived value of new Chinese-style clothing were extracted, which were cultural and educational value, aesthetic value, creative value, green value, engineering value, social value, and quality value, respectively; thirdly, we propose a PSO-BP neural network to evaluate the customer perceived value of new Chinese-style clothing, and we choose twenty-two and eight new Chinese-style clothing as training samples and test samples, respectively. The experimental results show that the PSO-BP neural network can accurately evaluate the customer perceived value of new Chinese-style clothing, and its error is controlled by 2.5% compared with the traditional BP neural network. The research results show that enterprises can improve the quality of product design through the new Chinese-style clothing customer perceived value evaluation indicators and models, and then improve their sustainable competitive advantage, so as to achieve the sustainable development of the new Chinese-style clothing industry ultimately.

1. Introduction

With the rapid development of China's cultural and creative industries, under the influence of policy guidance, financial support, technology iteration, talent innovation, and other factors, cultural industries represented by new Chinese-style clothing, animation, etc. have gradually become the pillar industries of the national economy, and they play an important role in improving the country's cultural soft power [1]. As far as the new Chinese-style clothing (a design style that grasps the ideological connotation of Chinese style, refines Chinese design elements, and innovates in combination with current materials and technologies) industry is concerned, enterprises continue to strengthen the cultural uniqueness, fashion, and innovation of new Chinese-style clothing products through design, giving product value soul and vitality, and then promoting the sustainable development of the new Chinese-style clothing industry [2]. But from the current market situation, the problem of "misalignment of supply and demand" of products is still a bottleneck that plagues the sustained and healthy development of the new Chinese-style clothing industry. Therefore, from the perspective of consumers, accurately grasping the changing consumer needs and consumption concepts of customers is of great significance for the development of the new Chinese-style clothing industry [3].

Modern product design is a process of a series of activities that seek design solutions to consumer demand [4]. In this activity, a crucial link in the product system analysis and evaluation is an essential basis for product design decisions. The so-called evaluation generally refers to the behavior of determining the attribute of an object according to a clear goal and turning it into the subjective utility (the degree of satisfying the requirements of the subject), that is,

the process of defining the value. In this process, we should compare the evaluated object with a particular object to determine the value of the object [5]. However, looking at the new Chinese-style clothing industry, it is found that there is no unified product evaluation index and method for China. Most of the enterprises determine the final design of products based on the subjective empirical assessment of the products from the designer's perspective, and the evaluation process often has a certain degree of one-sidedness and uncertainty. Therefore, when faced with the market reality that the personalized demand is prominent and the competition is becoming more and more fierce, in order to achieve the sustainable development of new Chinese-style clothing enterprises and industries, it has become an urgent problem for relevant enterprises and academia to build new Chinese-style clothing product value evaluation indicators guided by customer expectations, and to find scientific and reasonable product value evaluation methods, improve the design quality of new Chinese-style clothing products, and alleviate the contradiction between supply and demand.

Given this, this paper firstly introduces the customer perceived value theory. It combines the characteristics of the new Chinese-style clothing products with in-depth interviews and questionnaires with relevant consumers to build a system of measuring indicators of customer perceived value of new Chinese-style clothing products. The customer perceived value theory has received much attention since its inception and is often used to explain customers' subjective preferences and consumption behavior in specific situations. Based on this, this paper further incorporates the BP neural network method for evaluating natural case products. As an interactive evaluation method, the BP neural network can avoid the imprecision of artificially determined evaluation index weights and make the results more realistic. However, the traditional BP neural network also suffers from poor fault tolerance, the algorithm tends to fall into local minima, slow convergence, and instability in learning. To solve the above problems, this paper constructs a BP neural network evaluation model based on the particle swarm optimization algorithm. It uses the particle swarm optimization algorithm to obtain the optimal weights and thresholds for each layer of the BP neural network to further evaluate the consumer perceived value of the new Chinese-style clothing. Combined with the customer perceived value measurement index together, it will provide a more comprehensive, objective, and accurate reflection of the level of customer perceived value of the new Chinese-style clothing products, which will support the optimization of product design and the sustainable development of the company.

2. Literature Review

2.1. Sustainable Competitive Advantage and Customer Perceived Value. As an important part of the sustainable development strategy of enterprises, the sustainable competitiveness of enterprises is not only a strong support for the development of enterprises, but also the only way for the sustainable development of enterprises. Therefore, sustainable competitive advantage has always been the topic of concern of enterprise strategy theory [6, 7]. Porter [8] first mentioned sustainable competitive advantage when discussing the company's long-term competitive advantage to obtain low cost or differentiation, and pointed out that the sustainable competitive advantage of an enterprise comes from the value it creates for customers that exceeds its cost, which ultimately depends on the value it can create for customers. Barney [9] proposed that one of the necessary conditions for obtaining the unique strategic resources of sustainable competitive advantage is that the resources are valuable; that is, they can enable enterprises to increase customer value and improve their business performance. Woodruff [10] also clearly pointed out that customer perceived value is the source of competitive advantage. Although there are great differences in the theoretical assumptions about sustainable competitive advantage and the various theoretical schools of its origin, there is a consistent understanding of the premise of obtaining sustainable competitive advantage: the degree of customer recognition of the value of enterprise products or services, and the customer perceived value determines the sustainable competitive advantage of enterprises.

The recognition and research of value from the perspective of customers began in the 1990s. For the dimensional measurement of customer cognitive value, it has also changed from the initial single dimensional measurement to multidimensional measurement. In the early days of the theory, Zeithaml [11] referred to perceived value as the subjective value that the user has in mind after measuring the gain or loss. Simultaneously, Monroe [12] defined perceived value as the perceived quality or benefit that the customer gets from the product, as opposed to the sacrifice made by the price paid, etc. The above definitions of value in trade-offs between the "get" and "give" items are seen in marketing applications due to trade-offs between quality and price and are one-dimensional value judgments. In subsequent theoretical studies, Bolton and Drew [13] argued that viewing value as a trade-off between quality and price was too simplistic. Sheth et al. [14] argued that measuring perceived value as a single construct would lack validity and therefore proposed five dimensions of customer perceived value: functional value, social value, emotional value, epistemic value, and conditional value.

With the shift in the consumer market in recent years, many clothing companies have shifted from the traditional external competitors or internal resource conditions to the customer, which is fundamental to business survival and development. Under this background, the theory of customer perceived value is widely used in the research field of clothing product design. For example, Yan et al. [15], Yu et al. [16], and Li et al. [17], based on the theory of customer perceived value and combined with the characteristics of Internet distribution, built a measurement model of customer perceived value of online clothing customization; Chen et al. [18] took the value perception of children's clothing safety as the research object and developed a set of children's clothing safety perception measurement scale including 3 dimensions and 27 measurement items; Chi [19] used a multidimensional consumer perceived value model to

explore the characteristics of consumer expected value of environment-friendly clothing, including social value, emotional value, quality value, and price value; Zhou et al. [20] took men's suits as the product object and discussed the design optimization scheme of men's suits by establishing a model between users' perceived image, suit design features, and user preferences. Through the above literature collection and analysis, the customer perceived value theory has been applied to different clothing situations, including clothing customization, green clothing products, and men's clothing. However, there is still a lack of research on new Chinese-style clothing products. The constituent elements of customer perceived value differ for different clothing products. In particular, the new Chinese-style clothing products have distinctive characteristics such as spiritual and cultural categories, aesthetic forms, and cultural symbols, which are different from the general clothing products. Therefore, it is of practical significance to study the connotation of customer perceived value of new Chinese-style clothing.

Based on the above analysis, as a subjective feeling in the customer's heart, the customer's definition of perceived value is subjective, complex, and multidimensional. Therefore, this paper will refer to the functional value, social value, emotional value, epistemic value, and conditional value proposed by Sheth et al. [14] as the basis of the new Chinese-style clothing customer perception value evaluation study.

2.2. BP Neural Network and Particle Swarm Optimization. BP neural network (back-propagation neural network), also known as error back-propagation neural network, is one of the most representative and commonly used artificial neural networks, especially in nonlinear problem-solving. The structure of the BP neural network is divided into input layer, hidden layer, and output layer. Its structure is shown in Figure 1. The process of the BP neural network can be divided into two stages: forward propagation and backward propagation. In forward propagation, the input signal is processed from the input layer through the hidden layer and then passed to the output layer, with the nodes in the previous layer only affecting the nodes in the next layer. Suppose the output layer does not get the desired output. In that case, it is transferred to the error back-propagation process by adjusting the weights and thresholds of the prediction errors to achieve a BP neural network prediction output with a good fit [21]. In Figure 1, x represents the input and y represents the output. $f1$ is the activation function from the input layer to the hidden layer, and $f2$ is the activation function from the hidden layer to the output layer. w_{ij} and w_{jk} represent the weights of the neural network.

From the above analysis, it can be seen that customer perceived value has the characteristics of subjectivity and complexity, and its actual evaluation belongs to a typical nonlinear problem. If traditional product evaluation methods such as AHP and fuzzy comprehensive evaluation are used, it is easy to cause distortion and bias of evaluation results by setting the premise for the operation of the linear

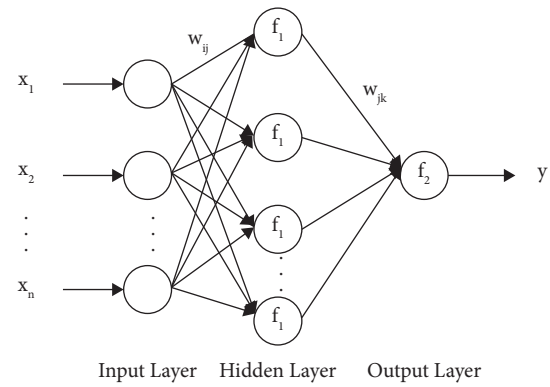

Figure 1: Structure of the BP neural network.

relationship between evaluation indexes. Therefore, it provides a certain theoretical basis for this paper to apply the BP neural network to evaluate the customer perceived value of new Chinese-style clothing. However, before starting training, the BP neural network randomly initializes the weights and thresholds of each layer to the value between [0, 1]. This kind of random initialization without optimization often slows the convergence speed of the BP neural network and easily makes the result nonoptimal [22]. As a swarm intelligence optimization algorithm, the particle swarm optimization (PSO) algorithm can map the weights and thresholds in the BP neural network to particles in the PSO algorithm, and update the speed and position of particles through iteration, so that individuals can find the optimal solution in the solution space [23]. The specific principle of PSO algorithm has been described in detail in Ref. [24], so it will not be repeated here. Therefore, this paper introduces the PSO algorithm to optimize the initial value and threshold, so as to significantly improve the training and modeling speed, stability, and solution accuracy of the BP neural network.

3. Construction and Validation of the Evaluation Index of Customer Perceived Value in the New Chinese-Style Clothing

In the analysis of this section, this paper aims at constructing the evaluation index of new Chinese-style clothing customer perceived value, and verifying the reliability and validity of the evaluation index. The specific research steps are divided into three stages: the first stage is to collect data by means of literature analysis and consumer questionnaire interview, and then sort out and code the interview contents through the research team to define the evaluation element factors; in the second stage, a large-scale questionnaire survey was conducted based on different gender, age, and educational background. Using the exploratory factor analysis method, the main aspects of the new Chinese-style clothing customer perceived value evaluation index are extracted, and based on this, the new Chinese-style clothing customer perceived value evaluation index scale is developed; in the third stage, reliability and validity analysis is used to verify the stability

and predictability of the new Chinese-style clothing customer perceived value evaluation index.

3.1. Exploring the Element Factors for Evaluating the Customer Perceived Value of New Chinese-Style Clothing. To determine the element factors that can be used to establish the evaluation index of new Chinese-style clothing customer perceived value, this paper uses literature analysis and interview method sequentially and gives the interview results to the research group for coding and screening to determine the element factors.

First of all, this paper collects and refers to the research results of Yen et al. [25]'s cultural fashion design measurement index, Liu et al. [3]'s new Chinese-style clothing purchase intention scale based on the product quality theory, Kim et al. [26]'s clothing design evaluation standard scale based on consumer perspective, Yu et al. [16]'s men's shirt custom customer perceived value evaluation scale, Chi et al. [19]'s environment-friendly clothing consumer perceived value scale, and Ahn et al. [27]'s 6-dimensional clothing product quality measurement scale oriented to customer demand. According to the above research results, an interview questionnaire was designed. The interview questionnaire is combined with the context of new Chinese-style clothing products and focuses on referring to various cases listed in the collected literature.

Secondly, this paper uses the interview method to investigate the current situation. To obtain more practical consumption demand and value preference for new Chinese-style clothing products, the author obtained a group of interviewees through a random survey, online forum invitation, and snowball recommendation. After thoroughly considering factors such as age, gender, occupation, education level, and user experience with new Chinese-style clothing products, the author finally selected 41 interviewees from different situations. The selected subjects are between 20 and 59 years old, covering the old, middle-aged, and young generations; the number of men and women in gender tends to be half (22 women and 19 men) to reduce the impact of gender factors. They have more than 3 years of experience in using new Chinese-style clothing products, and the longest is as long as 10 years. Their occupations include college students and those who have participated in the work.

The questionnaire's content is divided into three parts, with four questions in each part, making 12 questions. The first part is an interview with the basic information content of the respondent, in which the respondent explains the content of the case, the reason for purchase, and the occasion of wearing. The second part is an in-depth interview with the respondent. The respondents are encouraged to deepen further their thinking regarding the five dimensions of consumer perceived value: functional value, emotional value, social value, epistemic value, and conditional value. In the third part, in order to obtain valid interview results, we use some consumption cases (choice between well-known and ordinary brand products, different preferences between green and ordinary products, etc.) to stimulate the respondents to reflect on whether they have additional feelings beyond the previous interview. Given the impact of the current epidemic, this paper uses a combination of online and offline interview formats.

In the sorting and analysis of qualitative data, the primary focus is on coding. Coding is a systematic method of extracting data. In the process, data are analyzed and combined according to themes, concepts, or categories. The main procedures include three steps: open coding, axial coding, and selective coding [28]. After the interview and data collection, this paper commissioned a research group composed of experts and academics (a total of five people, including two professors and three associate professors) to conduct open coding first; that is, the research group extracted important information according to the interview content and integrated the obtained information into a unified category. Secondly, based on the understanding of the research topic, the research group linked all categories according to their internal organic associations (i.e., axes), found out the spindle code and named it, and finally obtained the element factors that may affect the evaluation of the perceived value of new Chinese-style clothing. Since the coding in this paper is mainly for inductive results, it is not within the scope of discussion to pay attention to the selective coding of text storylines, so this part is omitted [29]. In the end, the analysis yielded 37 factors such as Convey cultural meaning, Show the charm of regional culture, and Traditional natural fabrics (as shown in Table 1).

3.2. Extracting the Dimension of Customer Perceived Value Evaluation Indicators for New Chinese-Style Clothing. After the first stage of the paper, 37 customer perceived value evaluation factors were coded and calculated. In the second stage, the structures and links between the 37 evaluation factors were identified through exploratory factor analysis. The constructs of the new Chinese-style clothing customer perceived value evaluation indicators were extracted.

Firstly, the 37 element factors from the pretest questionnaire were re-ranked randomly, and each element factor was converted into an item in the questionnaire. Secondly, participants were asked to select the level of agreement with the purchase of the product from a 7-step Liker scale ranging from "strongly disagree" to "strongly agree" on a scale of 1 to 7. The positive sentiments for each item increased as the scores increased. The positive sentiment for each item gradually increases as the score increases, so that the scores can be added up for subsequent analysis. Finally, through exploratory factor analysis, the element factors were analyzed, deleted, or modified to find common factors to be named to extract a suitable index profile for evaluating the customer perceived value of new Chinese-style clothing.

In this paper, the data were collected mainly through online questionnaires, and 253 valid questionnaires were obtained, meeting the sample size requirement suggested by scholars [30]. Among the 253 questionnaires, 132 were completed by women and 121 by men; in terms of age distribution, 27 respondents were aged between 18 and 25 years, 90 were aged between 25 and 32 years, 75 were aged between 33 and 39 years, 40 were aged between 39 and 46

Table 1: List of evaluation element factors.

No.	Evaluation element factor
1	Convey cultural meaning
2	Show the charm of regional culture
3	Positive cultural enlightenment significance
4	Long-lasting and durable performance
5	Comfortable and breathable to wear
6	Convenient for daily cleaning and maintenance
7	Easy to move after wearing
8	Excellent manufacturing technology
9	An overall sense of refinement
10	Exquisite structure
11	Highly textured crafts such as prints and embroideries
12	Compact and beautiful accessories
13	Have an attractive story or moral
14	Have practical functions
15	Bring back fond memories of life
16	Have a sense of glamour
17	Physiotherapy and healthcare fabrics
18	Green textiles
19	Traditional natural fabrics
20	Promote a sense of personal confidence
21	Become more popular
22	Enhance personal image
23	Show personal social status
24	Show professional image
25	Make people feel special
26	Originality or creativity
27	A unique way of dressing
28	Versatility
29	Partial creative design details
30	Variety of matching features
31	Good styling proportions
32	Modern and stylish
33	Harmonious and beautiful color matching
34	Exquisite decoration
35	Exquisite design details
36	Product recyclability
37	Natural dyed fabric

years, and 21 were aged 46 years or above; in terms of education distribution, 32 were with high school education or below, 53 with secondary school or college education, 113 with bachelor's degree, and 55 with postgraduate education.

In statistical analysis, data conforming to normal distribution is the basic assumption and premise of many continuous data comparison and analysis, among which skewness and kurtosis are important normality test indicators [31]. After the collection and collation of the questionnaire, first of all, through descriptive statistical analysis, we can find that the skewness values of 37 element factors are between −0.919 (Product recyclability) and −0.030 (An overall sense of refinement), and the kurtosis values are between −0.543 (An overall sense of refinement) and 0.591 (Convey cultural meaning). The absolute values of skewness and kurtosis meet the verification standards proposed by Kline [32] that the absolute value of skewness is within 2 and the absolute value of kurtosis is within 7. It indicates that the data are normally distributed, which is suitable for exploratory factor analysis and reliability and validity analysis.

Then, in exploratory factor analysis, through the first factor analysis, it was found that the five variable factor loads of Have a sense of glamour, Originality or creativity, Compact and beautiful accessories, Show personal social status, and An overall sense of refinement were not higher than 0.50, so they were eliminated. Then, the data were subjected to a second factor analysis. After the KMO and Bartlett tests, the KMO sampling fitness measure was 0.935 and the Bartlett sphericity test approximate chi-square value was 5456.231, with a significance level of 0.000, indicating that the data were valid and suitable for factor analysis [33, 34]. After passing the check, principal component analysis in factor analysis was continued to extract common constructs, with eigenvalues greater than one as the principle for selecting the number of common factors, resulting in a total of seven major constructs that explained 72.539% of the cumulative variance. Immediately afterwards, the selected conformations were pivoted by the maximum variance pivoting method, resulting in a rotated component matrix (as shown in Table 2).

Finally, the reliability and validity analysis revealed that Cronbach's alpha values of all seven dimensions were higher than 0.7, the average variance extracted (AVE) values of each dimension were greater than 0.5, and the square root values of the average variance extracted were also greater than the correlations with other factors (as shown in Table 3), which verifies that the seven dimensions have good reliability at the same time [35], and it also indicates that the dimensions have good validity [36].

Dimension 1 is mainly composed of five element factors: Convey cultural meaning, Bring back fond memories of life, Show the charm of regional culture, Have an attractive story or moral, and Positive cultural enlightenment. The factor load is between 0.819 and 0.742, and the explained variance is 11.585%. This dimension reflects consumers' pursuit of the emotional cognitive value of new Chinese-style clothing products, but different from the aesthetic value of using product modeling elements as emotional transmission media, dimension 1 emphasizes the attraction of an internal cultural gene of new Chinese-style clothing products, which provides consumers with a unique product impression and cultural attribution through the emotional association of the brain. It also edifies and promotes the spiritual level of consumers, so this dimension is named as the cultural and educational value of the product.

Dimension 2 is made up of five factors: Exquisite design details, Modern and stylish, Exquisite decoration, Good styling proportions, and Harmonious and beautiful color matching. The factor load ranges from 0.787 to 0.705, with an explained variance of 11.449%. This dimension also reflects consumers' pursuit of the emotional perception value of new Chinese-style clothing products, that is, the product shape is used as a medium to convey information through the product shape elements, allowing consumers to form a visual perception of beauty, which in turn gives them a sense of inner pleasure. As the main expression of the product's visual aesthetic features on the consumer's emotions, this dimension is named the aesthetic value of the product.

Table 2: Rotated component matrix.

Dimension	Index	Dimension 1	Dimension 2	Dimension 3	Dimension 4	Dimension 5	Dimension 6	Dimension 7
Cultural and educational value	Convey cultural meaning	**0.819**	0.154	0.201	0.105	0.179	0.145	0.114
	Bring back fond memories of life	**0.777**	0.179	0.084	0.127	0.183	0.184	0.044
	Show the charm of regional culture	**0.771**	0.065	0.203	0.172	0.163	0.083	0.096
	Have an attractive story or moral	**0.766**	0.034	0.099	0.124	0.140	0.103	0.106
	Positive cultural enlightenment significance	**0.742**	0.126	0.141	0.134	0.158	0.198	0.149
Aesthetic value	Exquisite design details	0.145	**0.787**	0.102	0.163	0.134	0.099	0.119
	Modern and stylish	0.140	**0.767**	0.248	0.196	0.231	0.189	0.098
	Exquisite decoration	0.115	**0.764**	0.171	0.088	0.240	0.151	0.061
	Good styling proportions	0.053	**0.754**	0.163	0.170	0.145	0.140	0.068
	Harmonious and beautiful color matching	0.119	**0.705**	0.204	0.129	0.104	0.208	0.222
Creative value	Make people feel special	0.195	0.193	**0.814**	0.199	0.138	0.056	0.099
	A unique way of dressing	0.169	0.197	**0.803**	0.114	0.179	0.178	0.141
	Variety of matching features	0.180	0.171	**0.762**	0.151	0.175	0.238	0.084
	Versatility	0.176	0.175	**0.724**	0.172	0.105	0.022	0.073
	Partial creative design details	0.046	0.124	**0.696**	0.224	0.137	0.128	0.161
Green value	Product recyclability	0.157	0.146	0.208	**0.837**	0.168	0.136	0.119
	Physiotherapy and healthcare fabrics	0.135	0.180	0.154	**0.784**	0.132	0.164	0.082
	Green textiles	0.132	0.279	0.159	**0.781**	0.059	0.091	0.138
	Natural dyed fabric	0.170	0.214	0.185	**0.728**	0.221	0.172	0.121
	Traditional natural fabrics	0.106	-0.013	0.145	**0.641**	0.229	0.047	0.004
Engineering value	Long-lasting and durable performance	0.230	0.242	0.190	0.216	**0.728**	0.219	0.201
	Easy to move after wearing	0.170	0.244	0.223	0.188	**0.717**	0.137	0.123
	Comfortable and breathable to wear	0.215	0.187	0.089	0.129	**0.705**	0.136	0.220
	Have practical functions	0.187	0.149	0.216	0.270	**0.697**	0.146	0.104
	Convenient for daily cleaning and maintenance	0.227	0.176	0.148	0.178	**0.692**	0.237	0.129
Social value	Promote a sense of personal confidence	0.216	0.144	0.115	0.133	0.068	**0.795**	0.078
	Enhance personal image	0.194	0.205	0.177	0.127	0.233	**0.764**	0.094
	Become more popular	0.138	0.221	0.209	0.167	0.165	**0.761**	0.083
	Show professional image	0.144	0.156	0.050	0.124	0.257	**0.693**	0.197

Table 2: Continued.

Dimension	Index	Dimension 1	Dimension 2	Dimension 3	Dimension 4	Dimension 5	Dimension 6	Dimension 7
Quality value	Exquisite structure	0.135	0.128	0.108	0.105	0.173	0.196	**0.827**
	Highly textured crafts such as prints and embroideries	0.146	0.146	0.155	0.119	0.149	0.124	**0.825**
	Excellent manufacturing technology	0.139	0.151	0.178	0.115	0.199	0.054	**0.763**
Explained variance (%)		11.585	11.449	11.419	11.084	10.343	9.156	7.503
Cumulative explained variance (%)		11.585	23.034	34.452	45.537	55.880	65.036	72.539

Table 3: Reliability and validity analysis.

	Cronbach's alpha	AVE	Cultural and educational value	Aesthetic value	Creative value	Green value	Engineering value	Social value	Quality value
Cultural and educational value	0.892	0.601	**0.775***						
Aesthetic value	0.896	0.571	0.396	**0.756***					
Creative value	0.896	0.579	0.456	0.516	**0.761***				
Green value	0.892	0.573	0.434	0.488	0.508	**0.757***			
Engineering value	0.897	0.501	0.549	0.564	0.529	0.551	**0.708***		
Social value	0.867	0.569	0.478	0.513	0.456	0.447	0.563	**0.754***	
Quality value	0.854	0.649	0.390	0.415	0.414	0.374	0.503	0.408	**0.806***

Note. Diagonal bold characters (marked with*) are the open root of mean variance extraction (AVE), and the lower triangle is the Pearson correlation coefficient.

Dimension 3 is made up of five factors: Make people feel special, A unique way of dressing, Variety of matching features, Versatility, and Partial creative design details. The factor load ranges from 0.814 to 0.696, with an explained variance of 11.419%. This dimension reflects consumers' quest for knowledge of new Chinese-style clothing products, that is, to satisfy their curiosity, novelty, and desire for knowledge by enhancing the newness of product details in design, matching, function, and wearing style. The elements of the dimension focus on expressing the uniqueness and novelty of the product, hence the name of the dimension as the creative value of the product.

Dimension 4 is composed of five factors: Product recyclability, Physiotherapy and Health Care, Fabrics, Green textiles, Natural dyed fabric, and Traditional natural fabrics. The factor load ranges from 0.837 to 0.641, with an explained variance of 11.084%. This dimension has an interactive value characteristic, reflecting the contextual value of the product. This dimension reflects the desire of consumers who are influenced by the concept of green to satisfy their pursuit of a green and healthy life through products, and is therefore named the green value of the product.

Dimension 5 is mainly composed of five highly relevant element factors, namely, Long-lasting and durable, Performance, Easy to move after wearing, Comfortable and breathable to wear, Have practical functions, and Convenient for daily cleaning and maintenance. The factor load ranges from 0.728 to 0.692, and the explained variance was 10.343%. This dimension reflects the consumers' pursuit of the functional cognitive value of new Chinese-style clothing products and is related to the basic engineering performance of the products. Therefore, this dimension is named the engineering value of the products.

Dimension 6 is composed of the four elemental factors of Promote a sense of personal confidence, Enhance personal image, Become more popular, and Show professional image. The factor load ranges from 0.795 to 0.693, with an explained variance of 9.156%. This dimension reflects consumers' pursuit of the social perception value of new Chinese-style clothing products; that is, it emphasizes the positive role played by the products in consumers' interpersonal and social interactions, and is therefore named the social value of the products.

Dimension 7 is mainly composed of three element factors: Exquisite structure, Highly textured crafts such as prints and embroideries, and Excellent manufacturing technology. The factor load is between 0.827 and 0.763, and the explained variance is 7.503%. This dimension also reflects the consumers' pursuit of the cognitive value of the new Chinese-style clothing product function. However, different from the basic engineering performance of the product, this dimension focuses on the integrity of the product and the functional details, which can enable consumers to produce high-quality images. It needs to be highlighted through detailed design and high-level technology. Therefore, this dimension is named as the quality value of the product.

Through the above analysis, we have obtained seven dimensions containing cultural and educational value,

aesthetic value, creative value, green value, engineering value, social value, and quality value, and 32 element factors to build an evaluation index of the customers perceived value of new Chinese-style clothing.

4. Customer Perceived Value Evaluation Model of New Chinese-Style Clothing Based on PSO-BP Neural Network

This paper uses the PSO algorithm to find the optimal initial weight and threshold in BP neural network, and obtains a better neural network model to evaluate the customer perceived value of new Chinese-style clothing.

The specific steps of the experiment are as follows:

(1) Obtain sample data of customer perceived value of new Chinese-style clothing, and preprocess and normalize the data.

(2) Determine the number of nodes in each layer of BP neural network.

(3) Initialize the position and velocity of particles.

(4) Calculate the fitness value of each particle, and find the global extremum.

(5) Update the velocity and position of particles to generate a new particle swarm.

(6) Stop iteration if one of the following conditions is met: the number of iterations reaches the preset value; the error accuracy meets the set value. Otherwise, skip to step 5.

(7) After the iteration stops, the optimal weights and thresholds are put into the BP neural network for training. The BP neural network is trained iteratively until the termination condition is met.

(8) Obtain the BP neural network model optimized by the PSO algorithm.

The construction process of the model in this paper follows as shown in Figure 2.

This section designs a questionnaire based on the new Chinese-style clothing customer perceived value evaluation index constructed in Section 3 and collects the evaluation index data of new Chinese-style clothing products. A BP neural network based on the particle swarm optimization algorithm for the new Chinese-style clothing customer perceived value evaluation model was established. Twenty-two new Chinese-style clothing was selected as training samples and eight new Chinese-style clothing as testing samples, and MATLAB software was used to train and test the neural network examples.

4.1. Data Collection and Preprocessing. The main targets of this questionnaire were undergraduates and postgraduates and their families. College students and their families are potential consumers of new Chinese-style clothing. A total of 50 respondents were selected for the survey.

In this paper, a selection of new Chinese-style clothing products that are currently on the market was selected as the tested products. There are two main processes for their selection:

(1) Selection of new Chinese-style clothing brands: Regarding a combination of indicators such as brand awareness, brand style, the status of the brand's published online performance, and the opinions of experts in the field, the new Chinese-style clothing brands selected for this paper are as follows: ICY, INXX, Bosie Agender, HUSENJI, Hua Mu Shen, BYTEHARE, Nengmao Store, CLOT, LI-NING, ANTA, HLA, PEACEBIRD, SHIATZY CHEN, Mi Shan, and Houxu.

(2) Selection of new Chinese-style clothing products: 1–3 products were selected from the official websites or shopping platforms of the above 15 brands according to their sales index and brand representativeness, and finally, 30 new Chinese-style clothing products were selected as experimental products for this paper.

After determining the new Chinese-style clothing customer perceived value evaluation indexes in Table 3, 30 new Chinese-style clothing products were selected. Through the online survey, 50 subjects were asked to rate the customer perceived value evaluation indexes and the overall design of 30 new Chinese-style clothes. The data of the new Chinese-style clothing products No. 1–22 were used for the training of the neural network, and the new Chinese-style clothing products No. 23–30 were used for testing the neural network. The subjects were shown the front and back pictures and pattern designs of the 30 new Chinese-style clothing products during the survey. In addition to the presentation of the picture information of the garments, the design inspiration, fabric, and accessories were presented.

When comes to statistical data, chance errors, human errors, and sampling errors can lead to outliers. To avoid a minimal number of people with solid subjective emotions or recording errors during the research process, an outlier test needs to be conducted on the scores obtained for each evaluation index and the overall design score for each new Chinese-style clothing product. To prevent outliers in the scoring from influencing the final results, this paper uses Grubbs' test (two-tailed test) to eliminate outliers [37]. The statistic for Grubbs' test (equation (1)) is shown in the following:

$$G = \frac{\left|x_i - \overline{x}\right|}{S}, \tag{1}$$

where x_i is the score of a certain indicator of a new Chinese-style clothing product, $\overline{x}$ is the mean score of the corresponding indicator of the corresponding clothing, and S is the corresponding standard deviation.

After testing, 124 outliers, generally extreme data caused by some subjects' strong subjective emotions on some clothing's indicators, were removed. Appendix A lists the scores of some sample clothing evaluation indicators after removing outliers. The data of the input layer of the BP neural network model are the average of the scores of 50 subjects.

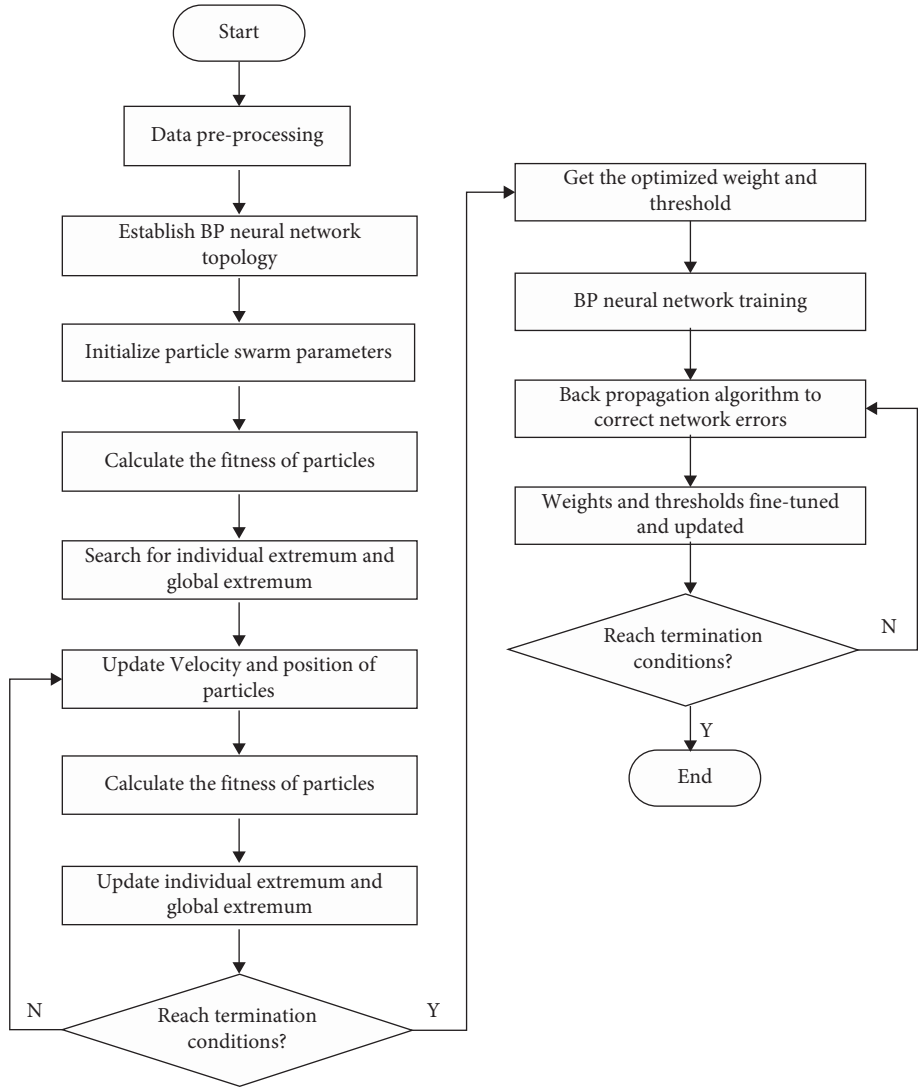

Figure 2: Flowchart of the PSO-BP neural network.

The 32 customer perceived value evaluation indexes data and overall design scores of 30 new Chinese-style clothing are taken as the original data. In order to improve the convergence speed of the BP neural network and the consistency of the results, it is also necessary to normalize the original data. In this paper, the min-max standardization method is adopted, called 0–1 standardization. That is, the original data were linearly transformed. To make the results distributed between 0 and 1, the function is used to process the original data linearly. The transformation function (equation (2)) is as follows:

$$y^* = \frac{y - y_{\min}}{y_{\max} - y_{\min}}, \tag{2}$$

where y^* is the standardization result, y is the sample score, $y_{\max}$ is the maximum score of the sample, and $y_{\min}$ is the minimum score of the sample. After the above processing of the original sample data, the scores of the new Chinese-style clothing customer perceived evaluation index are the input data of the neural network, and the scores of the overall design of the new Chinese-style clothing are the output data of the neural network.

The raw data and normalized data of the overall design scores of samples 1–22 used for training are shown in Table 4, which is the output layer data of the neural network model.

4.2. The Selection of BP Neural Network Parameters. Feature selection is crucial to machine learning, selecting features from all features to introduce into the model that are helpful and reduce the consumption of computational resources. The main role of feature selection is to reduce the number of features to prevent dimensional disasters, reduce training time, enhance generalization, and reduce overfitting. The random forest algorithm is chosen to filter features in this paper. The random forest algorithm is one of the most widely used supervised learning algorithms to solve regression and classification problems. The random forest algorithm provides two methods of feature selection: mean

Table 4: Raw data and normalized data of the overall design score of the training sample.

No.	Original value	Normalized value
1	83.793	0.7028
2	89.487	1
3	81.026	0.5584
4	83.897	0.7083
5	85.538	0.7939
6	84.846	0.7578
7	88.027	0.9238
8	81.676	0.5923
9	86.649	0.8518
10	88.703	0.9591
11	78.703	0.4371
12	80.324	0.5218
13	72.224	0.0990
14	71.810	0.0774
15	75.431	0.2664
16	70.328	0
17	78.724	0.4382
18	79.379	0.4724
19	77.628	0.3810
20	85.070	0.7694
21	81.488	0.5825
22	87.395	0.8908

decrease impurity and mean decrease accuracy. This paper chooses the mean decrease impurity method, which can easily measure the relative importance of each feature to prediction. The higher the feature importance value, the more important the feature is to the model. After screening 32 features, the top 15 features with high feature importance values were finally selected, which are Become more popular, Exquisite structure, Exquisite design details, Promote a sense of personal confidence, Partial creative design details, Make people feel special, Good styling proportions, Exquisite decoration, Enhance personal image, Excellent manufacturing technology, Highly textured crafts such as prints and embroideries, Physiotherapy and Health Care Fabrics, Variety of matching features, A unique way of dressing, and Have an attractive story or moral. Therefore, the number of nodes in the input layer of the BP neural network is 15.

The number of hidden layer nodes is determined by trial-and-error method. When the number of hidden layer nodes is 9, the training error of the BP neural network is the smallest. The selection of the BP neural network parameters is shown in Table 5.

4.3. Particle Swam Optimization Algorithm. The selection of relevant parameters in the PSO algorithm is shown in Table 6. Figure 3 shows the change in the fitness value of the particles, that is, the MSE of the BP neural network training. The fitness value gradually decreases with the increase in the number of iterations.

4.4. Experiments. The established structure has 15 nodes in the input layer, 9 nodes in the hidden layer, and 1 node in the output layer of the three-layer BP neural network. The MATLAB model is shown in Figure 4.

Table 5: Selection of BP neural network parameters.

Parameter	Value
Number of input layer nodes	15
Number of hidden layer nodes	9
Number of output layer nodes	1
Activation function of input layer	Log-sigmoid
Activation function of hidden layer	Purelin
Learning step	0.01
The maximum number of training sessions	2000
Training error	1×10^{-3}
Error function	Mean square error (MSE)

Table 6: Selection of PSO algorithm parameters.

Parameter	Value
Number of particles	20
The maximum number of iterations	70
Individual learning factor	2
Population learning factor	2
Inertia weight	0.9
The maximum restricted velocity	3

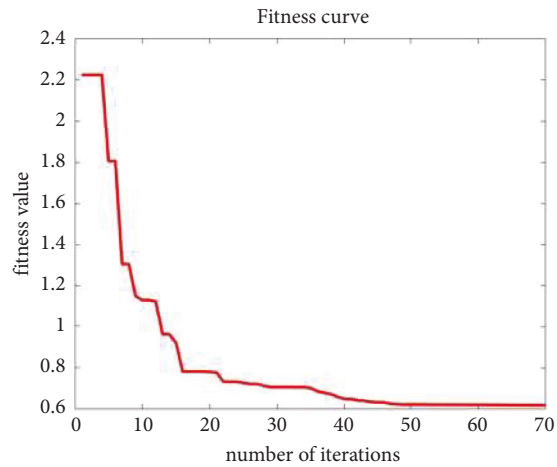

Figure 3: Plot of changes in particle swarm fitness values.

4.4.1. Training Experiment of PSO-BP Neural Network. The data of No. 1–22 new Chinese-style clothing are input into the PSO-BP neural network for training. The following "PSO-BP neural network model" will be referred to as "the model" for short. After 4 iterations, the termination conditions are met and the training is completed. As shown in Table 7, the actual value is the overall design score of No. 1–22 new Chinese-style clothing, and the predicted value is the output of the model after training with these 22 groups of data. The relative error is the relative error between the predicted value of the model and the actual value of 22 new Chinese-style clothing data. The relative error can reflect the

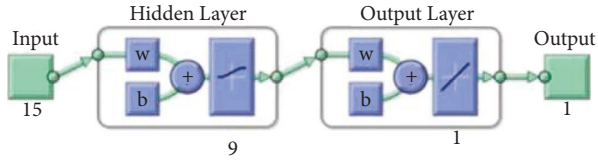

Figure 4: MATLAB model of the BP neural network.

Table 7: Training results of the PSO-BP neural network.

No.	Actual value	Predicted value	Relative error (%)
1	79.941	79.432	0.637
2	85.091	84.661	0.505
3	71.143	71.274	0.184
4	73.857	73.917	0.081
5	82.030	82.151	0.148
6	78.041	78.225	0.236
7	86.576	86.046	0.612
8	87.406	87.183	0.255
9	81.879	81.807	0.088
10	76.742	76.798	0.073
11	74.448	74.189	0.348
12	78.971	79.008	0.047
13	80.682	80.685	0.004
14	76.571	76.650	0.103
15	74.863	75.561	0.932
16	84.833	84.732	0.119
17	81.077	81.363	0.353
18	83.132	82.462	0.806
19	76.226	75.314	1.196
20	84.027	84.460	0.515
21	74.897	75.292	0.527
22	86.839	86.827	0.014

reliability of model prediction. The formula of relative error η is

$$\eta = \frac{|R - R'|}{R} \times 100\%, \tag{3}$$

where R is the actual value and R' is the predicted value of the model.

The overall design score of No. 19 new Chinese-style clothing is 76.226. The predicted value trained by the model is 75.314, and the relative error is 1.196%, which is the largest error in 22 groups of new Chinese-style clothing data. The relative error of No. 13 new Chinese-style clothing is the smallest, 0.004%. The average relative error of 22 groups of new Chinese-style clothing data is 0.354%, and the prediction results are accurate, so it can be concluded that the model has good learning ability and reliability.

4.4.2. Prediction Experiment of PSO-BP Neural Network. In order to test the prediction ability of the PSO-BP neural network model, No. 23–30 new Chinese-style clothing data were selected for testing. The following "PSO-BP neural network model" will be referred to as "the model" for short.

Table 8: Testing results of the PSO-BP neural network.

No.	Actual value	Predicted value	Relative error (%)
23	79.294	77.645	2.080
24	85.351	85.211	0.164
25	75.971	76.261	0.382
26	83.500	84.332	0.996
27	80.367	81.531	1.448
28	74.628	75.191	0.754
29	81.765	80.814	1.163
30	72.143	73.779	2.268

As shown in Table 8, the actual value is the overall design score of 8 new Chinese-style clothing from No. 22 to No. 30, and the predicted value is the predicted score of the trained model for the overall design of these 8 new Chinese-style clothing. The overall design score of No. 30 new Chinese-style clothing is 72.143, the predicted value trained by the model is 73.779, and the relative error is 2.268%, which is the largest relative error among the 8 groups of data. The average relative error of 8 groups of data is 1.157%, less than 5%, which indicates that the model is reliable and has good generalization ability. This shows that the model has certain reference significance for the evaluation of customer perceived value of new Chinese-style clothing and provides a relatively objective method for the evaluation of new Chinese-style clothing design.

4.5. Comparison between PSO-BP Neural Network Model and Traditional BP Neural Network Model. To compare the prediction accuracy of the PSO-BP neural network model and the traditional BP neural network model, the data of No. 22–30 new Chinese-style clothing were input into these two models, and the output results are compared as shown in Table 9. The following "PSO-BP neural network model" will be referred to as "the model" for short. The overall design score of No. 24 new Chinese-style clothing was 85.351, and the predicted score of the model was 85.211 with a relative error of 0.164%; the predicted score of the traditional BP neural network was 82.538 with a relative error of 3.296%. From Table 9, it is easy to find that the traditional BP neural network error fluctuates wildly, and the maximum relative error reaches 11.815%. The traditional BP neural network has the defect that it is easy to fall into the local minimum. For example, the predicted result of the customer perceived

Table 9: Comparison of traditional BP neural network and PSO-BP neural network prediction values.

No.	Actual value	PSO-BP neural network		Traditional BP neural network	
		Predicted value	Relative error (%)	Predicted value	Relative error (%)
23	79.294	77.645	2.080	79.472	0.224
24	85.351	85.211	0.164	82.538	3.296
25	75.971	76.261	0.382	78.592	3.450
26	83.500	84.332	0.996	84.084	0.699
27	80.367	81.531	1.448	82.601	2.780
28	74.628	75.191	0.754	72.849	2.384
29	81.765	80.814	1.163	81.816	0.062
30	72.143	73.779	2.268	63.619	11.815

value of No. 30 new Chinese-style clothing is quite different from the predicted result of the model. However, the relative error fluctuation of the model is small, and its error is controlled within 2.5%. The prediction accuracy of the model is obviously higher than that of traditional BP neural network, indicating that the model has better generalization ability and fault tolerance.

5. Conclusions

In the new Chinese-style clothing industry, sustainable development not only refers to the organic unity of industrial economic growth and ecological environmental protection, or the inheritance and development of traditional culture through products and modern fashion, but also includes the sustainable consumption of turning to the demand side and pursuing the harmony of supply and demand. In order to improve the evaluation level of the customer perceived value of new Chinese-style clothing and help enterprises more accurately grasp the consumer demand of products, this paper uses interview method, questionnaire survey method, exploratory factor analysis method, BP neural network, and particle swarm optimization algorithm to build new Chinese-style clothing customer perceived value measurement indicators and evaluation model, and obtains the following main conclusions.

Based on the results of open-ended questionnaire interviews, this paper summarizes 37 element factors of new Chinese-style clothing customer perceived value measurement indicators through coding procedures. Then, through exploratory factor analysis and reliability and validity analysis, the evaluation index dimensions of the customer perceived value of new Chinese-style clothing are extracted. The results show that after the dimensionality reduction of 37 element factors through factor analysis, seven dimensions can be summarized: engineering value, aesthetic value, green value, creative value, cultural and educational value, social value, and quality value.

This paper uses the ability of BP neural network to solve nonlinear problems and establishes a new Chinese-style clothing customer perceived value evaluation model based on the BP neural network. However, the BP neural network falls into local optimization and its convergence speed is slow. A new Chinese-style clothing customer perceived value evaluation model based on the particle swarm optimization algorithm is proposed. The experimental results show that the PSO-BP neural network has a very good learning and predictability in the evaluation of the customer perceived value of new Chinese-style clothing. It can evaluate the customer perceived value of new Chinese-style clothing well and provide an objective evaluation model for future new Chinese-style clothing design ideas.

The use of the new Chinese-style clothing customer perceived value measurement index allows designers to design products according to the characteristics of the target customer, avoiding the misalignment between design and demand, product homogenization, and other issues, so as to enhance the sustainable competitive advantage of enterprises. Similarly, new Chinese-style clothing enterprises can also use this measurement index to classify products, and the design plan or product can be found out in advance through the new Chinese-style clothing customer perceived value measurement index to find out its unique product personality (such as focusing on cultural and educational products, aesthetic products, green products, or creative products), which will be more conducive to market planners to carry out market classification and competitor analysis as a reference. In addition, consumers can also use this measurement index in their daily lives to improve the quality of their purchase decisions, etc. and ultimately achieve the sustainable development of the new Chinese-style clothing industry.

Data Availability

The dataset can be obtained from the author upon request.

Conflicts of Interest

The author declares that there are no conflicts of interest.

Acknowledgments

This research was supported by the National Social Science Fund of China (no. 20BG119) and Anhui Province Key Laboratory of Advanced Numerical Control and Servo Technology (no. XJSK202103), China.

Supplementary Materials

Table A. Neural network input layer data (partial). (*Supplementary Materials*)

References

[1] K. K. Fan and T. T. Feng, "Sustainable development strategy of Chinese animation industry," *Sustainability*, vol. 13, pp. 7235–7320, 2021.

[2] C. Tsui, "From symbols to spirit: changing conceptions of national identity in Chinese fashion," *Fashion Theory*, vol. 17, no. 5, pp. 579–604, 2013.

[3] H. W. Liu, X. H. Li, and N. H. Romainoor, "New Chinese style clothing product qualia, consumer product attitude and purchase intention," *J. Silk*, vol. 57, no. 11, pp. 58–65, 2020.

[4] C. Homburg, M. Schwemmle, and C. Kuehnl, "New product design: concept, measurement, and consequences," *Journal of Marketing*, vol. 79, no. 3, pp. 41–56, 2015.

[5] Y. Zuo and Z. Wang, "Subjective product evaluation system based on kansei engineering and analytic hierarchy process," *Symmetry*, vol. 12, no. 8, p. 1340, 2020.

[6] M. A. Rodriguez, J. E. Ricart, and P. Sanchez, "Sustainable development and the sustainability of competitive advantage: a dynamic and sustainable view of the firm," *Creativity and Innovation Management*, vol. 11, no. 3, pp. 135–146, 2002.

[7] N. Bari, R. Chimhundu, and K.-C. Chan, "Dynamic capabilities to achieve corporate sustainability: a roadmap to sustained competitive advantage," *Sustainability*, vol. 14, no. 3, p. 1531, 2022.

[8] M. E. Porter, *Competitive Advantage: Creating and Sustaining Superior Performance*, Free Press, New York, NY, USA, 1985.

[9] J. Barney, "Firm resources and sustained competitive advantage," *Journal of Management*, vol. 17, no. 1, pp. 99–120, 1991.

[10] R. B. Woodruff, "Customer value: the next source for competitive advantage," *Journal of the Academy of Marketing Science*, vol. 25, no. 2, pp. 139–153, 1997.

[11] V. A. Zeithaml, "Consumer perceptions of price, quality and value: a means-end model and synthesis of evidence," *Journal of Marketing*, vol. 52, no. 3, pp. 2–22, 1988.

[12] K. B. Monroe, *Pricing: Making Profitable Decisions*, McGraw-Hill, New York, NY, USA, 1990.

[13] R. N. Bolton and J. H. Drew, "A multistage model of customers' assessments of service quality and value," *Journal of Consumer Research*, vol. 17, no. 4, pp. 375–384, 1991.

[14] J. N. Sheth, B. I. Newman, and B. L. Gross, "Why we buy what we buy: a theory of consumption values," *Journal of Business Research*, vol. 22, no. 2, pp. 159–170, 1991.

[15] W. J. Yan and S. C. Chiou, "Dimensions of customer value for the development of digital customization in the clothing industry," *Sustainability*, vol. 12, no. 11, p. 4639, 2020.

[16] X. H. Yu and J. P. Wang, "Customer perceived value evaluation method of men's shirts customization under internet environment," *Journal of Textile Research*, vol. 41, no. 3, pp. 136–142, 2020.

[17] H. Li, L. W. Gu, W. Gu, and X. G. Liu, "Research on online-to-offline clothing customization mode based on consumer perceived value," *Journal of Textile Research*, vol. 41, no. 9, pp. 128–135, 2020.

[18] L. Chen, X. Ding, and H. Yu, "A measure of consumer perception on children's apparel safety following the customer perceived value paradigm," *Journal of the Textile Institute*, vol. 111, no. 8, pp. 1106–1115, 2020.

[19] T. Chi, "Consumer perceived value of environmentally friendly apparel: an empirical study of Chinese consumers," *Journal of the Textile Institute*, vol. 106, no. 10, pp. 1038–1050, 2015.

[20] X. Zhou, Y. Xu, and T. Chen, "Research on optimization design of men's suit considering users' perception," *International Journal of Clothing Science & Technology*, vol. 34, no. 3, pp. 379–390, 2021.

[21] S. Ding, C. Su, and J. Yu, "An optimizing BP neural network algorithm based on genetic algorithm," *Artificial Intelligence Review*, vol. 36, no. 2, pp. 153–162, 2011.

[22] M. A. Otair and W. A. Salameh, "Speeding up back-propagation neural networks," in *Proceedings of the 2005 Informing Science and IT Education Joint Conference*, pp. 167–173, Arizona, AZ, USA, June 2005.

[23] J. Kennedy and R. Eberhart, "Particle swarm optimization," in *Proceedings of the 1995 ICNN'95 - International Conference on Neural Networks*, vol. 4, Perth, Australia, November 1995.

[24] S. Huang and X. Zhang, "Biologically inspired planning and optimization of foot trajectory of a quadruped robot," in *Proceedings of the 2021 Intelligent Robotics and Applications*, pp. 192–203, Yantai, China, October 2021.

[25] H. Y. Yen and C. I. Hsu, "College student perceptions about the incorporation of cultural elements in fashion design," *Fash Text*, vol. 4, no. 1, p. 20, 2017.

[26] S. Kim, "An exploratory study on apparel design evaluation criteria with consumers' perspectives-focusing on female college students majoring in apparel-fashion design in their 20s," *Journal of the Korean Society of Clothing and Textiles*, vol. 43, no. 3, pp. 384–404, 2019.

[27] M. Y. Ahn and J. O. Park, "A study on classification of apparel product quality characteristics based on customer satisfaction," *Journal of the Korean Society of Clothing and Textiles*, vol. 31, no. 5, pp. 765–776, 2007.

[28] M. Kenny and R. Fourie, "Contrasting classic, Straussian, and constructivist grounded theory: methodological and philosophical conflicts," *Qualitative Report*, vol. 20, no. 8, pp. 1270–1289, 2015.

[29] A. Moghaddam, "Coding issues in grounded theory," *Issues in Educational Research*, vol. 16, no. 1, pp. 52–66, 2006.

[30] J. W. Osborne and A. B. Costello, "Best practices in exploratory factor analysis: four recommendations for getting the most from your analysis," *Pan-pacific management review*, vol. 12, no. 2, pp. 131–146, 2009.

[31] K. D. Hopkins and D. L. Weeks, "Tests for normality and measures of skewness and kurtosis: their place in research reporting," *Educational and Psychological Measurement*, vol. 50, no. 4, pp. 717–729, 1990.

[32] R. B. Kline, *Principles and Practice of Structural Equation Modeling*, Guilford, New York, NY, USA, 2005.

[33] M. S. Bartlett, "A note on the multiplying factors for various x^2 a," *Journal of the Royal Statistical Society: Series B*, vol. 16, no. 2, pp. 296–298, 1954.

[34] H. F. Kaiser, "An index of factorial simplicity," *Psychometrika*, vol. 39, no. 1, pp. 31–36, 1974.

[35] D. G. Bonett and T. A. Wright, "Cronbach's Alpha reliability: interval estimation, hypothesis testing, and sample size planning," *Journal of Organizational Behavior*, vol. 36, no. 1, pp. 3–15, 2015.

[36] C. Fornell and D. F. Larcker, "Evaluating structural equation models with unobservable variables and measurement error," *Journal of Marketing Research*, vol. 18, no. 1, pp. 39–50, 1981.

[37] E. D. Dan and O. A. Ijeoma, "Statistical analysis/methods of detecting outliers in a univariate data in a regression analysis model," *International journal of education and research*, vol. 1, no. 5, pp. 1–24, 2013.

Hindawi
Scientific Programming
Volume 2022, Article ID 4633128, 8 pages
https://doi.org/10.1155/2022/4633128

Research Article

Finite Element Analysis Model Design on the Mechanical Properties of Prefabricated Shear Wall Structure

Yuan Zhang

Faculty of Architecture and Civil Engineering, Huaiyin Institute of Technology, Huai'an 223001, Jiangsu, China

Correspondence should be addressed to Yuan Zhang; zhyuang111@hyit.edu.cn

Received 31 July 2022; Revised 14 August 2022; Accepted 23 August 2022; Published 10 October 2022

Academic Editor: Lianhui Li

At present, the mechanical properties analysis method of prefabricated shear wall structure based on static test is low overall simulation precision. In this paper, the finite element method is used to analyze the force performance of the prefabricated shear wall structure. Based on the shear of concrete material, elastic modulus, Poisson ratio, open fracture, the transfer coefficients of open and closed fracture, and tensile strength parameters, the finite element model is established by ANSYS. The vertical load and the horizontal load of the prefabricated shear wall structure are calculated, and the limit load value is obtained. The maximum stress change of the connector, the energy dissipation of the shear wall structure, and the change of the equivalent viscous damping coefficient are obtained by the way of loading and displacement change. The experimental results show that the simulated values of stiffness degradation, maximum displacement, maximum strain, and stress distribution obtained by this method are in good agreement with the actual values and are reliable.

1. Introduction

Along with city development scale in China more and more big, the requirements of the government for environmental protection are higher, the requirements of real estate developers for time, cost, and quality are more strict, and the requirements of owners for the building product safety and comfort performance gradually increase, which have become the bottleneck restricting the development of the construction industry [1, 2]. The prefabricated shear wall structure has come into being. The fabricated building is a building constructed by precast components at the site. It has the advantages of short construction period, high construction quality, and environmental protection. It is catering to the national policies and development requirements of housing industrialization and building energy conservation and emission reduction. With the continuous development of prefabricated shear wall structure, the stress analysis has become a hot issue in structural engineering [3, 4].

Zhang et al. [5] put forward an assembly scheme for the external wall panel for steel structure. In order to study the lateral resistance and seismic performance of steel frames with such wall panels, the ABAQUS finite element software was used to establish the overall model and comparison model of steel frames, and the finite element analysis of uniaxial loading and low cycle reciprocating loading was carried out. The results showed that the connection of the outer wall panel could guarantee the connection between the outer wall plate and the steel frame. When the structure had large deformation under lateral load, it could limit the transfer force between the wall panels and the frames, ensured that the wall panels were in an elastic state, and avoided wall panels from falling down. The enclosure system consisting of the external wall panel and the connection node significantly improved the mechanical performance of the steel frame, the initial stiffness of the structure was increased by 1.18 times, and the bearing capacity was increased by more than 30%. The scheme could enhance the seismic performance of the structure. When simulating the low cycle reciprocating loading, the total energy dissipation of the external wall panel's steel frame model was increased by more than 90% compared with the pure frame model, but the overall simulation result was quite different from the actual value.

In view of the large discrepancy between the simulation results in the literature and the actual values, a new finite element analysis method of prefabricated shear wall structure is put forward to improve the accuracy of mechanical properties of shear wall structure analysis.

2. Finite Element Analysis of the Mechanical Properties of Prefabricated Shear Wall Structure

The prefabricated shear wall structure is a new type of wallboard. The width of a single plate with a binding body part is selected as an analysis unit. Its size is the length of 3000 mm, the width of 600 mm, the thickness of 200 mm, and the concrete grade is C30. Because the integral modeling of ANSYS is used, the reinforcement ratio of the vertical bar in the plate is 1%, and the reinforcement ratio of the horizontal bar is 0.25%.

The material parameters in finite element analysis are as follows: concrete C30, elastic modulus 3.0 GPa, Poisson's ratio 0.2, steel bar HRB335, opening crack's shear transfer coefficient 0.35, closed crack's shear transfer coefficient 0.95, and the tensile strength 1.43 MPa.

2.1. The Model is Established

2.1.1. Defining the Element Properties. The concrete is defined, the distribution unit type is SOLID65 unit, and the proper real constant and material model are selected. In considering the reinforced modeling, the internal structure of the structure is defined by the reinforcement ratio of the longitudinal reinforcement and the distribution of reinforcement in the real constant [6].

2.1.2. The Division of Grid. The grid division is divided by swept grid and the source surface grid is divided by the mapped grid. The grid precision is controlled within 100 mm [7].

2.1.3. Applying Constraint and Loads. This model is loaded by force mode. The rigid pad is added to the local compression position. The shell 63 element is adopted to prevent the stress concentration to cause that the calculation does not converge.

A fixed end is applied at the bottom of the wallboard, and the top is the free end.

2.2. Solving and Postprocessing. The nonlinear analysis of the wall panel is carried out, and the mechanical properties of the components in the force process are obtained through the general postprocessing and the time postprocessing.

In addition, the prefabricated shear wall model structure is shown in Figure 1.

The single axis strain-stress relation diagram of the concrete in Figure 1 is shown in Figure 2(a), and the stress-strain curve of steel bar is shown in Figure 2(b).

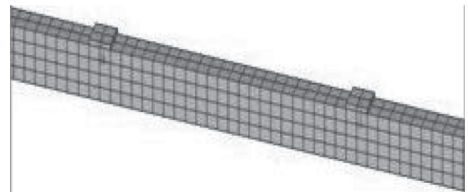

Figure 1: Finite element model of prefabricated shear wall structure.

According to the provisions of the "Technical specification for concrete structure of high rise buildings," under the action of representative value of neutral load, the axial pressure of the one, two, and three grade shear wall limbs is not suitable for the following restrictions: first class (9°): the limit of corresponding axial-compression ratio is 0.4, another level (6°, 7°, and 8°) the limit of corresponding axial-compression ratio is 0.5, and the limit of the axial compression ratio of second or third level is 0.6.

In this paper, the axial compression ratio is 0.4, 0.5, and 0.6 [8], and the vertical load of the prefabricated shear wall structure is calculated according to formula (1).

$$\mu = \frac{N}{(f_c * A)}, \tag{1}$$

where A represents the area of the full section of the shear wall, N represents the axial pressure value of the section of shear wall, and μ represents the load value.

According to the formula (1), there are

$$\begin{aligned} N_1 &= 0.4 * f_c * A = 686\text{kN}, \\ N_2 &= 0.5 * f_c * A = 859\text{kN}, \\ N_3 &= 0.6 * f_c * A = 1030\text{kN}. \end{aligned} \tag{2}$$

Through the above calculation, the maximum bearing capacity of the vertical load of the prefabricated shear wall structure is 1030 kN. According to the provisions of the "Technical specification for concrete structure of high rise buildings," the maximum horizontal displacement and height ratio $\Delta\mu/h$ of the floor layer between the floor layers under the stress load calculated by the elastic method conform to Table 1 [9, 10].

According to Table 1, the calculated maximum displacement of the wall panel is 3 mm. When the vertex displacement of 3 mm can be obtained by using the formula (3), the horizontal load of the prefabricated shear wall structure is 36 kN, that is, the horizontal load under normal serviceability limit state.

$$w_{\max} = \frac{Fl}{EI}, \tag{3}$$

where F represents the load on the model, l represents the length of the model after the deformation, E represents the modulus of elasticity of the model, and I represents the I shaped section of the model.

According to "The technical regulations of high building concrete structure," there are as follows:

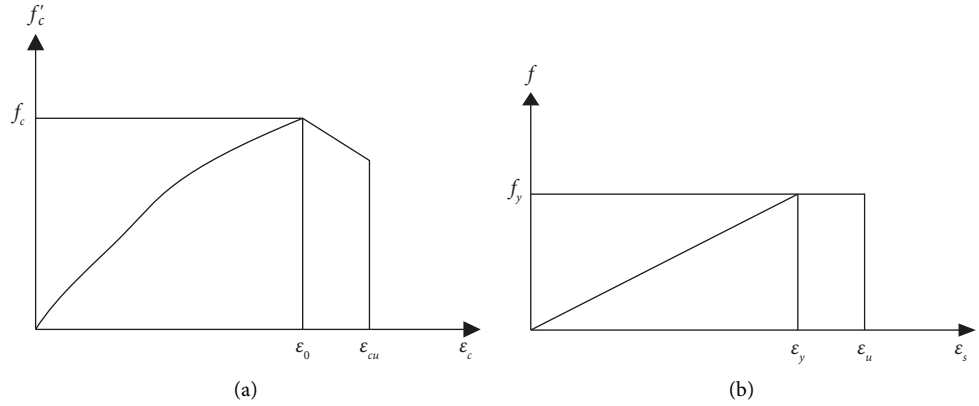

Figure 2: The stress-strain curve of material. (a)Single axis stress-strain relation diagram of concrete and (b) stress-strain curve of steel bar.

Table 1: Ratio of maximum horizontal displacement to height.

Structural system	$\Delta\mu/h$ limit
Frame	1/550
Frame-shear wall, frame-core tube, and flat plate-column-shear wall	1/800
Tube in tube, shear wall	1/1000
The transformation layer other than the frame structure	1/1000

$$V \leq \frac{1}{\lambda - 1}\left(0.5 f_y * b * h + 0.13N\frac{A_w}{s}h\right), \tag{4}$$

where V represents displacement, A_w represents the area of I shaped or T shaped cross-section shear wall, λ represents the shear span ratio of section, s represents the horizontal distribution of reinforcement spacing of shear wall, b represents the section width, and h represents the effective height of the model.

According to formula (4), the shear capacity of the prefabricated shear wall structure is 123.8 kN; that is, the horizontal load under the ultimate bearing capacity of the prefabricated shear wall structure.

Figure 3 is the maximum stress change of the perforated rebar in the prefabricated shear wall structure, and Figure 4 is the maximum stress change of the connecting steel plate.

According to Figures 3 and 4, it is known that at the initial stage of loading displacement, the connections are in the elastic deformation stage. When the displacement is loaded to 25 mm, the maximum stress of the connecting steel plate is 227 Mpa and enters the yield stage. Then, when the displacement is loaded to 45 mm, the perforated rebar enters the yield stage, and the maximum stress is 380 Mpa. When the displacement is loaded to 52 mm, the maximum stress of the steel plate begins to increase and enters the stage of plastic hardening. When the displacement is loaded to 55 mm, the perforated rebar enters the plastic hardening stage. When the displacement is loaded to 75 mm, the connecting steel plate reaches the limit stress 310 Mpa and enters the necking deformation stage. When the specimen is completely destroyed, the connecting steel plate is completely broken, but the reinforcing bar does not destroy.

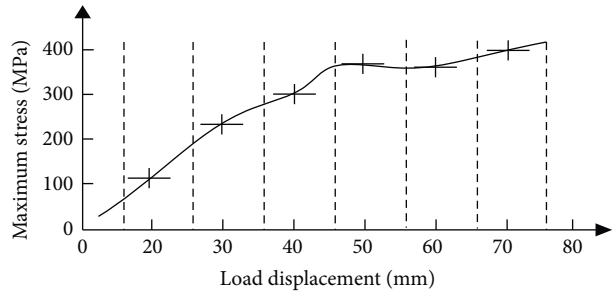

Figure 3: The maximum stress change of perforated rebar.

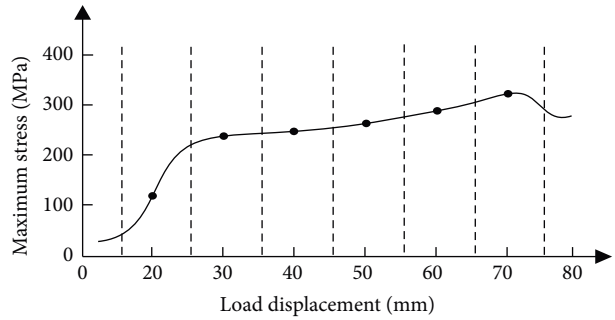

Figure 4: Maximum stress change of connecting steel plate.

There are two main reasons for structural vibration energy dissipation: structural damping energy dissipation and elastoplastic energy dissipation.

Damping and elasticity are one of the most important properties of the structure. When the structure is in the case of elastic vibration, the damping causes the dissipation of the structure energy. When the deformation of the structure exceeds the elastic limit, the structure will undergo plastic

deformation. After unloading, the deformation of the structure cannot be completely recovered and there will be residual deformation and energy dissipation. According to "The technical specification for concrete structures of tall buildings," the energy dissipation capacity of specimens should be measured by the area enclosed by the load-displacement curve [11–14]. Figure 5 is a schematic diagram for calculating the energy dissipation and equivalent viscous damping coefficients of specimens.

The energy dissipation factor is the ratio of the energy consumed by a hysteresis loop to load and unload for a circle to the total energy of loading and unloading. The energy dissipation factor E' of the specimen [15–18] can be calculated by formula (5).

$$E' = \frac{S_{A'BC} + S_{CDA'}}{S_{\Delta BOE'} + S_{\Delta DOF'}}. \tag{5}$$

In the force response analysis of prefabricated shear wall structure [19–21], the equivalent viscous damping coefficient h_e is often used to carry out the pressure analysis. The equivalent viscous damping coefficient h_e can be calculated by using the formula (6).

$$h_e = \frac{E'}{2\pi}. \tag{6}$$

Figure 6 is the energy dissipation diagram for each specimen of prefabricated shear wall structure:

According to Figure 6, it can see that with the increase of the displacement, the hysteretic curve of the specimen tends to be full and the energy consumption increases gradually. The energy dissipation capacity of the specimens under high axial compression ratio is relatively large, whether it is the connecting steel or the connecting steel plate in the prefabricated shear wall structure [22–24].

Figure 7 is the diagram of equivalent viscous damping coefficient of each specimen in a prefabricated shear wall structure.

As can be seen from Figure 7, with the increase of displacement, the hysteresis loops of all the specimens in the prefabricated shear wall structure are gradually full, and the equivalent damping coefficient is increasing.

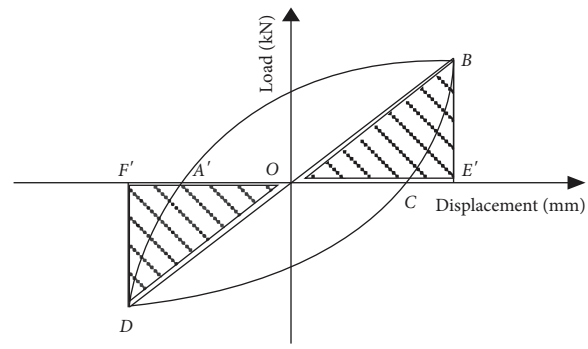

Figure 5: Diagram for calculating energy dissipation and equivalent viscous damping coefficient for prefabricated shear wall structure.

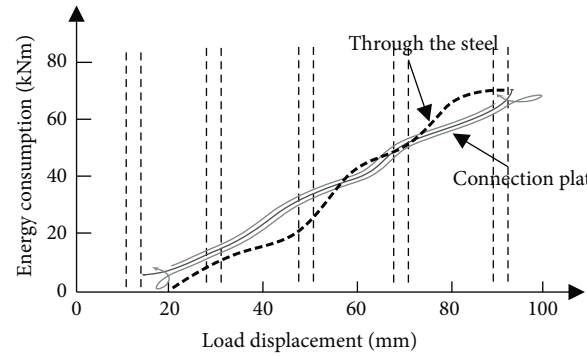

Figure 6: Energy dissipation diagram for each specimen of prefabricated shear wall structure.

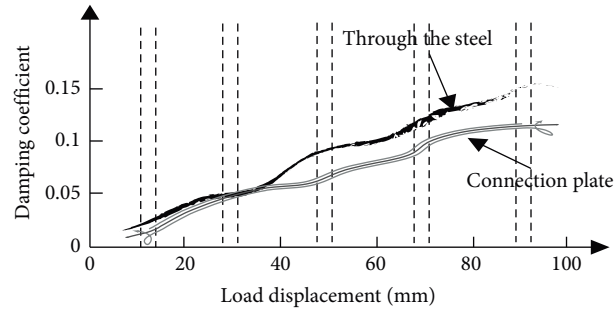

Figure 7: Equivalent viscous damping coefficient diagram of each specimen in prefabricated shear wall structure.

3. Experimental Results and Analysis

In order to verify the correctness of finite element analysis results of prefabricated shear wall structures [25–27], an experiment is needed to verify the above results. The experimental platform is built on MATLAB.

The prefabricated shear wall structure is taken as the experimental object, and the pressure is applied to record and track its bearing changes. The overall experimental results are as follows.

From Figure 8, we can see that the ultimate load of the shear wall finite element simulation is higher than the actual result, because the concrete vibration is not enough, and the specimen maintenance process is not up to standard, but the material in finite element simulation is not defective.

However, the hysteretic curve of the finite element simulation of prefabricated shear wall is quite different from the actual result, and it can be found that the modeling of the finite element is correct.

As shown in Figure 9, the stiffness degradation values in the initial stage of the literature method and the proposed method are in high agreement with the actual values and are in a state of basic level. But with the changing value of displacement, the simulated value of the literature methods gradually deviated from the actual value curve. In the process of small displacement loading, the stiffness of all the specimens in the structure degenerates greatly and the loading continues to continue. The proposed method

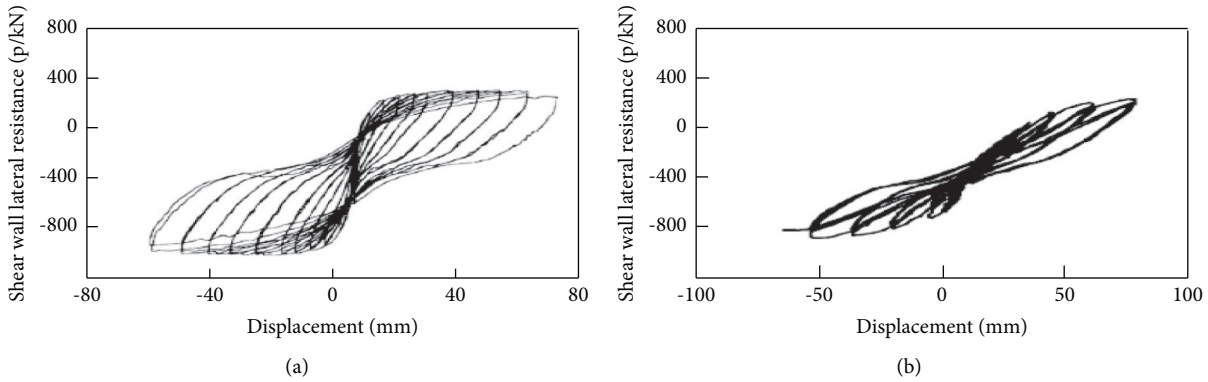

Figure 8: Agreement between hysteretic curve of the shear wall structure by using the proposed method with the actual value. (a) Hysteretic curve of simulated prefabricated shear wall structure and (b) hysteretic curve of actual prefabricated shear wall structure.

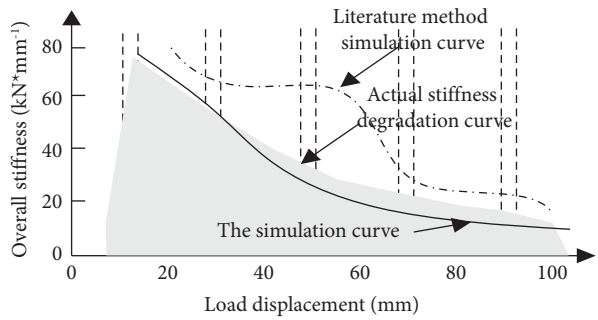

Figure 9: Agreement between simulated values of the overall stiffness degradation of prefabricated shear walls by different methods and actual values.

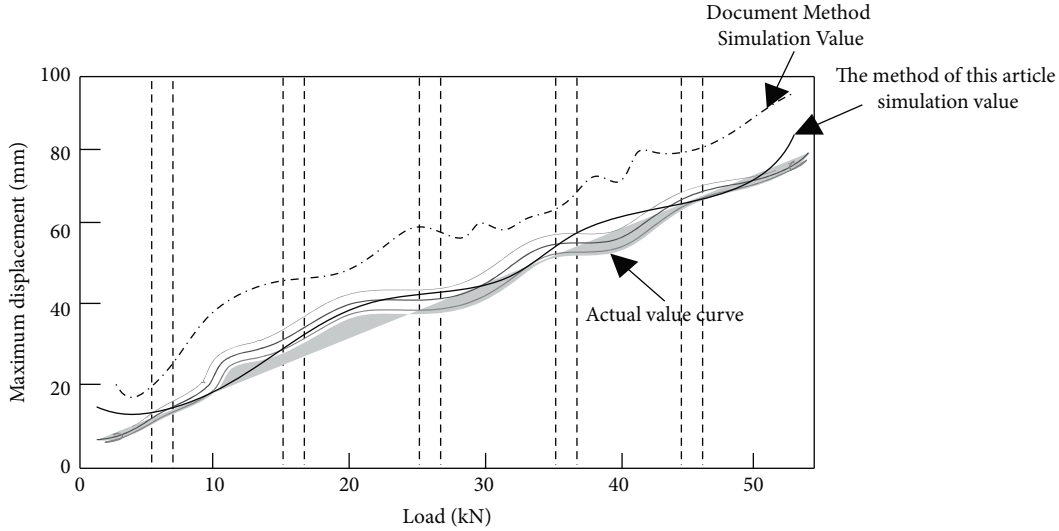

Figure 10: The fitting degree of the maximum displacement and load relation between the simulated value of the different methods and the actual value.

presents the advantages and is in a relatively consistent state with the actual stiffness degradation curve.

Figures 10–13show the fitting degree of the maximum displacement and load relation between simulated values of different methods and actual values; the fitting degree of the maximum strain and displacement relationship between the simulated value of different methods and the actual value; the fitting degree of the simulated values of different methods and the actual values between the stress distribution and the load relation; the fitting degree of the displacement changes of different methods and the actual value under the different friction coefficients.

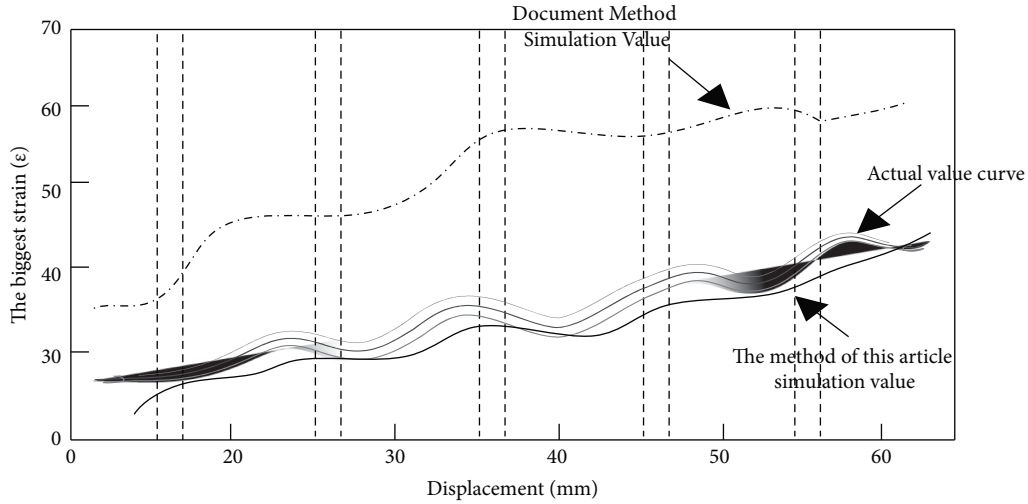

Figure 11: The fitting degree of the maximum strain and displacement relation between the simulated values of different methods and the actual values.

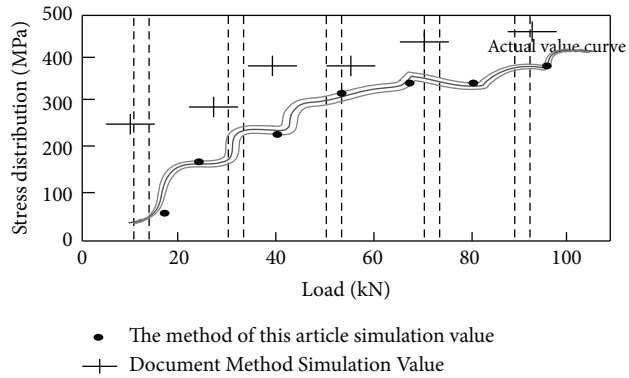

Figure 12: The fitting degree of stress distribution and load relation between the simulated values of different methods and the actual values.

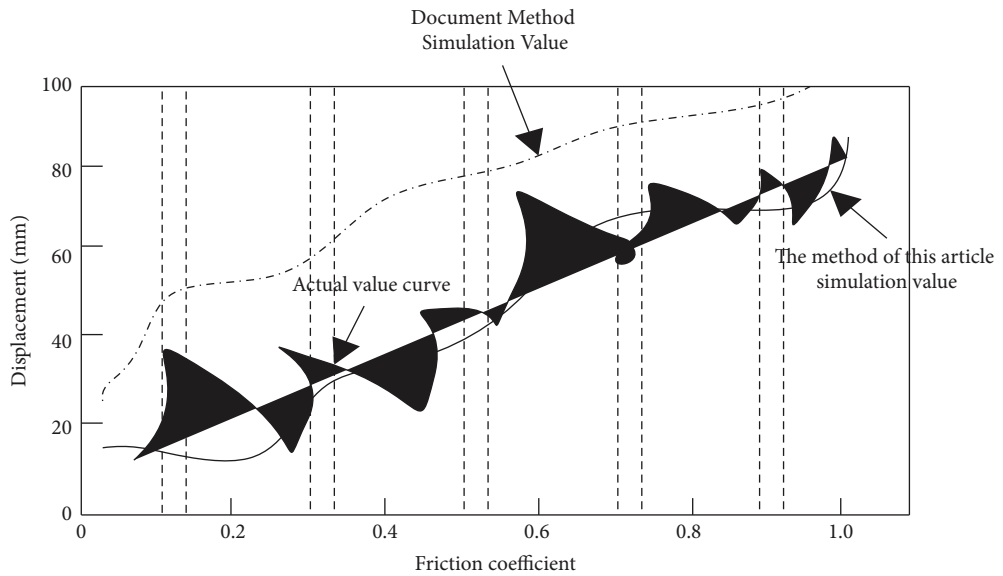

Figure 13: The fitting degree of the displacement changes of different methods and the actual value under the different friction coefficients.

The analysis of Figures 10–13 shows that the simulated value of the maximum displacement and load relation of the proposed method are fitted to the actual value. The maximum strain and displacement relation between the simulated value and the actual value is fitted, and the relationship between stress distribution and load relation of the simulated value and the actual value is fitted. The fitting degree of the displacement changes of different methods and the actual value under the different friction coefficients is better than that of the literature method. This is because in the establishment of finite element model of prefabricated shear wall structure, the grid is divided by using sweep grid division, the control of grid precision is within 100 mm, and the force analysis of the model is always carried out according to "The technical specification for concrete structure of high rise buildings." Moreover, the energy dissipation of shear wall structure and the equivalent viscous damping coefficient are analyzed in detail, and the overall analysis accuracy of the method is improved.

4. Conclusions

Prefabricated shear wall structure is a highly applied energy-saving building material. Its stress performance analysis is the key to promote the development of technology in this field. At present, there are various problems in the analysis of the force performance. Aiming at these problems, this paper puts forward a new research method, to construct the finite element model of prefabricated shear wall structure by using the ANSYS and prove the feasibility of the proposed method through experiments, which can provide a scientific basis for the development of this field.

Data Availability

The dataset can be accessed upon request.

Conflicts of Interest

The author declares that there are no conflicts of interest.

References

[1] W. J. Li and Q. Zheng, "Analysis of dynamic response for concrete wall under blast load," *Computer Simulation*, vol. 33, pp. 27–31, 2016.

[2] M. Heidari, M. A. Nikolinakou, P. B. Flemings, and M. R. Hudec, "A simplified stress analysis of rising salt domes," *Basin Research*, vol. 29, no. 3, pp. 363–376, 2016.

[3] A. F. Liu and J. J. Gurbach, "Application of a p-version finite element code to analysis of cracks," *AIAA Journal*, vol. 32, no. 4, pp. 828–835, 1994.

[4] M. Essuri, B. Maatug, and K. Kurmaji, "Stress analysis of delta fin structure and determination of deformation," *Physics of Plasmas*, vol. 21, pp. 122–143, 2015.

[5] A. L. Zhang, L. Ma, X. C. Liu, and Z. Q. Jiang, "Finite element analysis on mechanical performance of steel frame structure with prefabricated external wall panel," *Journal of Building Structures*, vol. 37, pp. 152–157, 2016.

[6] T. Giesa, C. C. Perry, and M. J. Buehler, "Secondary structure transition and critical stress for a model of spider silk assembly," *Biomacromolecules*, vol. 17, no. 2, pp. 427–436, 2016.

[7] M. Ohsaki, T. Miyamura, M. Kohiyama, T. Yamashita, M. Yamamoto, and N. Nakamura, "Finite-element analysis of laminated rubber bearing of building frame under seismic excitation," *Earthquake Engineering & Structural Dynamics*, vol. 44, no. 11, pp. 1881–1898, 2015.

[8] O. Salomón, S. Oller, and A. Barbat, "Finite element analysis of base isolated buildings subjected to earthquake loads," *International Journal for Numerical Methods in Engineering*, vol. 46, pp. 1741–1761, 2015.

[9] G. Wang, "J integral finite element analysis for three-dimensional cracks," *Journal of Aircraft*, vol. 21, no. 11, pp. 899–905, 1984.

[10] C. García, G. N. Gatica, and S. Meddahi, "Finite element semidiscretization of a pressure-stress formulation for the time-domain fluid-structure interaction problem," *IMA Journal of Numerical Analysis*, vol. 37, pp. 1772–1799, 2017.

[11] H. Xu, J. Song, D. An, Y. Song, and X. Lv, "Local thickening and friction reducing to constant resistance in a prefolded energy absorption device," *Shock and Vibration*, vol. 2020, Article ID 8532534, 11 pages, 2020.

[12] L. H. Li, J. C. Hang, Y. Gao, and C. Y. Mu, "Using an integrated group decision method based on SVM, TFN-RS-AHP, and TOPSIS-CD for cloud service supplier selection," *Mathematical Problems in Engineering*, vol. 2017, Article ID 3143502, 14 pages, 2017.

[13] N. Li, Z. Ma, P. Gong, F. Qi, T. Wang, and S. Cheng, "Simulation research on the load transfer mechanism of anchoring system in soft and hard composite rock strata under tensile loading conditions," *Advances in Materials Science and Engineering*, vol. 2020, Article ID 9097426, 20 pages, 2020.

[14] L. Li, T. Qu, Y. Liu et al., "Sustainability assessment of intelligent manufacturing supported by digital twin," *IEEE Access*, vol. 8, pp. 174988–175008, 2020.

[15] L. Yan, J. Liang, and W. Li, "Axial compression behavior of rubberized concrete-filled square steel tubular columns after exposed to high temperatures," *Advances in Materials Science and Engineering*, vol. 2022, Article ID 1506483, 7 pages, 2022.

[16] L. Li, B. Lei, and C. Mao, "Digital twin in smart manufacturing," *Journal of Industrial Information Integration*, vol. 26, no. 9, Article ID 100289, 2022.

[17] J. X. Li, J. T. Wang, Q. Sun, Y. R. Wu, S. M. Zhou, and F. C. Wang, "Axial compression behavior of circular concrete-filled high-strength thin-walled steel tubular columns with out-of-code D/t ratios," *Advances in Materials Science and Engineering*, vol. 2021, Article ID 9081566, 16 pages, 2021.

[18] Z. Ding, J. Fu, X. Li, and X. Ji, "Mechanical behavior and its influencing factors on engineered cementitious composite linings," *Advances in Materials Science and Engineering*, vol. 201915 pages, Article ID 3979741, 2019.

[19] L. Li and C. Mao, "Big data supported PSS evaluation decision in service-oriented manufacturing," *IEEE Access*, vol. 8, pp. 154663–154670, 2020.

[20] X. Li, C. Ji, Z. Zhang, S. Zhang, H. Liu, and S. Wang, "Shulin.Prediction of adhesively bonded polyurethane-to-steel double butt joint failure using uncertainty analysis," *Advances in Materials Science and Engineering*, vol. 202013 pages, Article ID 3196345, 2020.

[21] L. Li, C. Mao, H. Sun, Y. Yuan, and B. Lei, "Digital twin driven green performance evaluation methodology of intelligent manufacturing: hybrid model based on fuzzy rough-sets AHP,

multistage weight synthesis, and PROMETHEE II," *Complexity*, vol. 2020, no. 6, pp. 1–24, Article ID 3853925, 2020.

[22] S. Zhang, Z. Ren, Z. Ding, J. Wen, and Z. Yan, "Influence of existing defects on mechanical properties of NC lining," *Advances in Materials Science and Engineering*, vol. 2019, Article ID 8571297, 15 pages, 2019.

[23] S. Nie, T. Zhou, Y. Zhang, B. Zhang, and S. Wang, "Shuo.Investigation on the design method of shear strength and lateral stiffness of the cold-formed steel shear wall," *Mathematical Problems in Engineering*, vol. 2020, Article ID 8959712, 13 pages, 2020.

[24] J. Wang and Q. Sun, "Experimental study on improving the compressive strength of UHPC turntable," *Advances in Materials Science and Engineering*, vol. 2020, Article ID 3820756, 21 pages, 2020.

[25] L. H. Li, J. C. Hang, H. X. Sun, and L. Wang, "A conjunctive multiple-criteria decision-making approach for cloud service supplier selection of manufacturing enterprise," *Advances in Mechanical Engineering*, vol. 9, no. 3, Article ID 168781401668626, 2017.

[26] A. Tessler, R. Roy, M. Esposito, C. Surace, and M. Gherlone, "Shape sensing of plate and shell structures undergoing large displacements using the inverse finite element method," *Shock and Vibration*, vol. 2018, Article ID 8076085, 8 pages, 2018.

[27] L. W. Zhang, J. Wu, and D. L. Zhang, "Shape optimization and stability analysis for kiewitt spherical reticulated shell of triangular pyramid system," *Mathematical Problems in Engineering*, vol. 2019, Article ID 2723082, 11 pages, 2019.

Hindawi
Scientific Programming
Volume 2022, Article ID 6544282, 9 pages
https://doi.org/10.1155/2022/6544282

Research Article

3D Face Recognition Neural Network for Digital Human Resource Management

Yiming Dong

Chengxi Management Consulting (Beijing) Co. Ltd., Beijing 100123, China

Correspondence should be addressed to Yiming Dong; ym.dong@tjfsu.edu.cn

Received 25 July 2022; Revised 19 September 2022; Accepted 23 September 2022; Published 10 October 2022

Academic Editor: Lianhui Li

Digital human resource management can improve the organizational and operational efficiency of enterprises.In order to improve the efficiency of enterprise digital management and solve the problems of low security level and insufficient stability of 2D face recognition, we introduce 3D face recognition into the digital human resource management system. We propose a face recognition method based on a multistream convolutional neural network and local binary pattern and build a digital face recognition management system. We first build the system computer vision scene. Then a local binary mode facial expression feature extraction scheme is designed according to the depth camera image extraction method. Considering that face 3D features are easy to be missed, we build a multistream convolutional neural network to learn facial 3D features. Finally, we validate the effectiveness of the method in selecting a public face dataset. Experiments prove that our method can reach 98% face recognition accuracy, which is significantly better than other methods.

1. Introduction

An efficient human resource management (HRM) approach is necessary to maintain organizational efficiency and helps to enhance efficient iterations of organizational change at the company level. Most HRM teams are currently introducing intelligent management systems into their company's personnel management work, reducing workload and lowering HRM costs. Many researchers have proposed many research methods in intelligent HRM, and a large number of research results have been achieved. The intelligent HR management system is a system with a huge system [1, 2]. Considering the multifunctionality and complexity of the HR system, combined with our recent research, we will start the research around the HR punch card assist system. The one that has been applied more in the clock-in aid system is the face recognition clock-in system [3–5].

The human face is a unique biological feature, and each person's face contains features such as expressions, facial features, and contours. The rational use of facial biology in an ethical scope can create great economic benefits, but facial expression feature extraction and analysis is a difficult task. How to correctly extract facial expression features is a major research hotspot, and after extracting facial features, how to efficiently utilize them and incorporate them into automatic feature learning networks is also a major challenge. Initially, in facial recognition research, researchers favored machine learning methods. Initially, facial recognition was only at the 2-dimensional level [6–9]. Commonly used machine learning methods include principal component analysis and support vector machines. However, traditional machine learning methods require a high level of manual feature design and cannot automate the feature labeling process. In addition, it is difficult for traditional machine learning methods to maintain the stability of the model in the irregular changes of an unstructured environment, as a result, machine learning methods are gradually replaced by deep learning methods in the subsequent research. Deep learning methods require a large database as the training set, and the number of training sets determines the accuracy of deep learning models for face recognition. The initial deep learning-like face recognition methods also started from the 2-dimensional level and were mainly based on pixel features. The 2-D facial features always have the problems of

information occlusion and missing information, which cannot complete the high precision facial biometric feature learning. Three-dimensional facial feature analysis based on deep learning is more accurate, and intelligent systems of three-dimensional facial recognition are chosen in some places or companies with high-security level requirements. For a three-dimensional facial recognition algorithm, the requirements for computer vision scene construction are relatively high. Ordinary RGB camera intelligently captures two-dimensional pixel features. If you want to capture three-dimensional facial biometric features, you need to use depth cameras to obtain depth information of the visual scene, and then through depth information data reduction, three-dimensional scene reconstruction, and other operations. The same depth camera is configured in the equivalent 3D facial recognition system for scanning face information [10–14].

To enhance the security of digital management of enterprises. We introduce 3D face recognition into the digital human resource management system. We propose a face recognition method based on a multistream convolutional neural network and local binary pattern and build a digital face recognition management system. We first build the system computer vision scene. Then we designed a local binary mode facial expression feature extraction scheme based on the depth camera image extraction method. We also constructed a multistream convolutional neural network to learn facial 3D features.

The rest of this paper is arranged as follows. Section 2 describes the research related to face recognition. Section 3 details the principles and implementation process associated with improved local binary patterns and multistream neural networks. Section 4 presents the relevant experimental datasets and an analysis of the results. Finally, Section 5 reviews our findings and reveals some additional research.

2. Related Work

The literature [15] was one of the first studies to propose a face recognition system, where the authors built a face pixel autocorrelation matrix to fit the pixel computation model around a feature neural network. Face images require manual production of datasets and each face label needs to be preprocessed and labeled with its data source. The face database requires pixel-level normalization and coordinated positioning for training set and test set classification. However, the method does not perform well enough in the experiments. Researchers in the literature [16] upgraded on previous face recognition studies and the authors proposed the face algebraic database replacement method. The face pixel data is directly converted into a computable feature matrix during the face data collection preprocessing process, which optimizes the substitutability of face data. Researchers in the literature [17] proposed a face feature residual coding structure to determine the three-point pixel localization of the eyes and nose, which solves the undesirable problem of the least constrained environment such as insufficient light.

Considering that face recognition is strongly influenced by unstructured environmental factors, researchers in the literature [18] experimentally analyzed the efficiency of principal component analysis methods and also compared the range of action of fisher faces and local binary patterns. It was found that for the pixel computation of grayscale maps, the monotonic transformation matrix and the face pixel features cannot be converted with a uniform rotation matrix. However, the pixel features obtained from the face pixel texture are more accurate in distinguishing the features of the five senses. The researchers of the literature [19] explained the shortcomings of the local binary pattern approach through experimental data and presented the superiority of the viola-jones approach. Considering the effects of nonstructural environmental factors, the authors also analyzed various optimization methods proposed in the literature [20, 21], detailing the best solutions in various situations such as occlusion, background differences, and noise effects, providing stable technical support for subsequent studies.

Researchers in the literature [22] developed experiments around the effect of light changes on face recognition. In the paper, the authors present common solutions to face recognition lighting variations and point out the drawbacks of each method. In a later experiment, the authors proposed a face facial light transformation balancing method based on distance transformation and kernel feature extraction. The method is based on facial texture features, and for the problem of robust illumination normalization, the authors explain how the method maintains stable extraction of facial features in facial illumination transformations, using facial pixel noise as an example. Researchers in the literature [23] also took a noise treatment approach between face recognition and balancing of illumination. To address the problem that high-level noise has a high impact on facial Lupin features and facial edge detection is weakened, the authors take inspiration from the backpropagation shear wavelet operation. The authors first divide the face into different regions uniformly at the pixel level, each region corresponds to an independent classifier, and the high-level noise can be eliminated by fitting facial features with the same characteristics by similarity at the terminals of the combined face regions, and finally by reorganization. The method achieves a noise elimination rate of 86% in experimental validation, which improves the robustness of the face recognition model.

To improve the accuracy of face recognition, the local binary pattern method is the first approach of most researchers. Optimization and fusion based on local binary patterns can improve the overall model efficiency. With the emergence of deep learning methods, researchers have tried to incorporate convolutional neural networks into face recognition models, while the literature [24] presents a real-time multiplayer face recognition method, which is an embedded system developed in a GPU system and also configured with computer vision scenes that can achieve functions such as face tracking and fast recognition. The method is an example of the successful application of a neural network in a face recognition model, and this face recognition system provides great reference value to the subsequent face system construction. The researchers in the literature [25] introduced and affirmed the former research

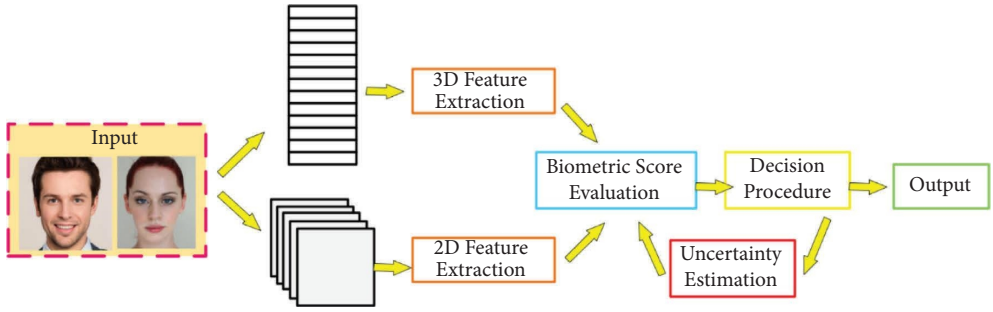

Figure 1: The composition of the face recognition system.

results in their article, and the authors elaborated their research ideas and methodological sources from a new perspective. Starting from a binary histogram algorithm, the article decomposes facial expressions of human faces between low-level and high-level pixels and extracts high-level and low-level features of expressions by pixel enhancement. The experimental results demonstrate that the method can enable face recognition models to obtain generalizability. The literature [26] analyzes in detail the differences and efficiency of local binary models and support vector machines and incorporates a particle swarm algorithm based on support vector machines. The recognition accuracy of this model was improved by 10 percentage points in the test of the public database of faces. Researchers in the literature [27] focused more on the random forest law, and the authors chose facial texture features as a measure of the fusion of symbolic and magnitude features. In the face public dataset supplement experiments, the authors compared the method with the local binary pattern method. The experimental results show that the method is more efficient in the classification of facial expressions.

3. Method

3.1. Face Recognition Pipeline Overview. We have reconstructed the face recognition method and designed a three-dimensional space-based face recognition network. First, we build a digital computer vision scene with three depth cameras REALSENSE, each depth camera's RGB image sensor and depth infrared sensor are in linkage, sharing frame rate to avoid frame loss. The facial RGB image information and depth information are simultaneously input to the face recognition model, and firstly, the physical feature calculation unit is used to fuse the depth information and RGB information to generate 3D facial information. The 3D facial information contains two sets of 3D facial contour features and data stream face classification theme scores. The weight in the estimated score of RGB image information is relatively large, and the features are extracted by a specific face estimation algorithm. The different levels of features in the database are generated by iterative iterations and are used to correct the weight parameters for the score estimation. For uncertain estimates, they will be directly input to the decision layer within the range of small probability events. Finally, all the features will be input to the decision layer and the decision algorithm will make a feature response to the face based on the subject category, and confidence level. The feature response will be directly connected to the human biological database and can be associated with the real company employee information through a mapping matching relationship, thus achieving the function of face recognition. The composition of the face recognition system is shown in Figure 1.

3.2. Local Binary Pattern Network Reconstruction. Most researchers have demonstrated that local binary pattern neural networks have good results in the field of face recognition. We have also experimentally verified the efficiency of the local binary pattern framework, considering the shortcomings of the method in terms of accuracy and network structure. In our work, we will use the local binary pattern as the basis of the framework and focus on improving the recognition accuracy and speed of face recognition systems in unstructured environments. We also optimize feature details at the pixel level and generate facial attribute feature points adaptively.

In the first layer of the face recognition network, we first set up the image information preprocessing layer, assuming that α represents the face image contrast adjustment parameter and β represents the face contour size scale value. During the experimental test, we measure the α and β values in infinite approximation, and we find that the image preprocessing effect is best when $\alpha = 1.5$ and $\beta = 0.3$. The preprocessing layer function relationship is shown below.

$$g(x, y) = \alpha * f(x, y) + \beta. \quad (1)$$

In our previous experiments, we found that when the convolutional neural network filter processed the face RGB image, each convolutional operation was performed, then the specific curve was biased with higher pixel values in the region around the specified pixel. As the filter passes through each region of the image, it changes depending on the type of filter. Considering this problem, we have borrowed filter design rules from other studies, and most of them collectively show that the more similar the filter features are to the convolutional computed image features, the higher the probability of filter activation and more accurate filtering results. To this end, we set up independent experiments to verify the feature similarity of the Gaussian fuzzy filter [28], median filter [29], and bilateral filter [30] in the face recognition framework, respectively. The experimental results

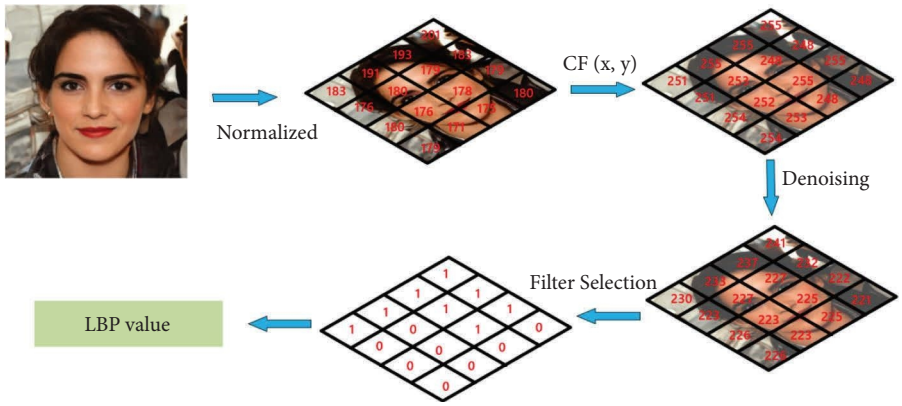

Figure 2: The modified local binary pattern operator.

show that the bilateral filter can obtain filtering results that are more similar to the facial image features. Therefore, we place the bilateral filter in the second layer of the face recognition network, and the bilateral filter mathematical equation is shown in the following formula.

$$F(x,y) = \frac{\sum_{x=-N}^{N}\sum_{y=-N}^{N} I(x,y)W(x,y)}{\sum_{x=-N}^{N}\sum_{y=-N}^{N} W(x,y)}, \tag{2}$$

where $W(x,y)$ represents the weighting function of the facial RGB input in the convolution calculation, $I(x,y)$represents the pixels in the neighborhood of the filtered image area, respectively, and $F(x,y)$ represents the linear summation of the filtering weighting function, and it also represents the result of the bilateral filter applied onn a $2N+1$ neighborhood. Assuming that $\mathrm{CF}(x,y)$represents the fusion result of the input facial image with the noise reduction algorithm, the mathematical equation is shown in the following formula.

$$\mathrm{CF}(x,y) = g(x,y) * F(x,y). \tag{3}$$

We regard it as the image noise control contrast weighting. Where $g(x,y)$represents the facial image contrast and $F(x,y)$represents the type of filter used in the convolution calculation. In the experiments of pixel equalization operation for facial images, we found that facial images are prone to the problem of global low noise. To avoid this problem, we adopt the image histogram method and perform parameter weighting operation based on this method, and the mathematical equation expression is shown in the following equation. Experiments prove that the method can effectively solve the problem of global low noise.

$$\mathrm{Eq} = H'(\mathrm{CF}(x,y)), \tag{4}$$

where H' represents the linear normalization operation, and the optimization of the researchers' line linear normalization in the literature [31] suggested that the local binary pattern behaves more stably in a fixed neighborhood window, and its principle of action is shown in Figure 2.

We also used the local duality mode operator as a basis, and the expression of its underlying mathematical equation is as follows.

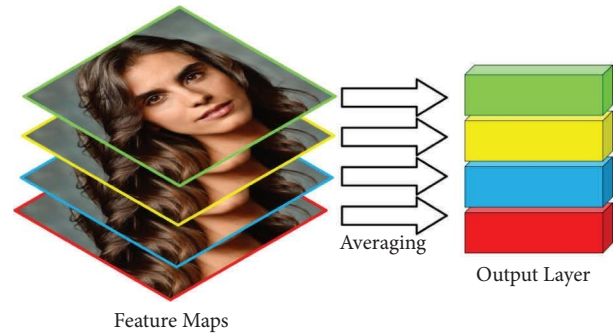

Figure 3: The global average pooling layer.

$$\mathrm{LBP}p,r(X_c,X_c) = \sum_{p=0}^{p-1} 2^p S\left(i_p - i_c\right), \tag{5}$$

where (X_c, Y_c)represents the threshold of the center of the face pixel, $i_p$and $i_c$represent the intensity of the neighboring pixels with the center pixel of the face as the dispersion point, and p represents the computed range of the center dispersion pixel with radius r.

3.3. Multistream Convolutional Neural Networks. Convolutional neural networks have high generalizability and robustness in image processing. In a face recognition system, the neural network model can give full play to its advantages of weight sharing and local connectivity. In the process of facial contour feature extraction and reorganization learning, the reconstruction of facial appearance pixel features can be avoided and the computational cost is reduced. As mentioned in the computer vision reconstruction, we used three depth cameras to reconstruct the computer vision scene and visually capture face features from different angles of the same horizontal plane. To echo the computer vision scene, the multistream convolutional neural network we adopted processes the facial features from different angles separately. All integrated features are separated according to biological categories, and the local detail features of the face are learned by convolution, then the number of feature map network parameters is reduced by connecting pooling layers, and the global average pooling is shown in Figure 3. Finally,

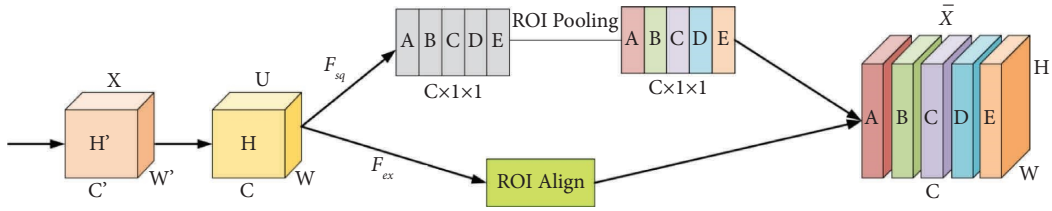

Figure 4: The reconstructed convolutional neural network architecture.

the global information is generated by connecting fully connected layers. We chose a nonlinear activation function to classify the output biological category feature mapping values.

The disadvantage of multistream convolutional neural networks is that the networks are too cumbersome when optimizing the spatial layout of a multistream convolutional neural network. Considering the fusion of local face features and channel features, referring to the SE architecture methods in the literature [32, 33], we compressed the multistream neural network by setting the excitation function in the mid network and resetting the parameters of all neural network layers at the end. Such a network architecture approach helps to establish inter-channel dependencies, improve the perceptual field, and suppress the facial features with low weight coefficients. Our convolutional neural network architecture is shown in Figure 4.

For multistream convolutional neural network compression, the face space depth features are the first input, and the face features are reset and encoded using global average pooling, which is represented in the mathematical equation as follows.

$$z_c = F_{\mathrm{sq}}(u_c) = \frac{1}{H \times wW} \sum_{i=1}^{H} \sum_{j=1}^{W} u_c(i, j) z \in R^C, \tag{6}$$

where C represents its output feature map size, and H and W denote the height and width of the feature map at the pixel level. After the convolutional layer compression, the excitation function is added in the middle of the network, and we choose the sigmoid function as the excitation function. A gating mechanism is also added to the network to balance the mapping rate between channels.

$$S = F_{\mathrm{ex}}(z, W) = \sigma(g(z, W)) = \sigma(W_2 ReLU(W_1, z)), \tag{7}$$

where $W_1 \in R^{C/r \times C}$,$W_2 \in R^{C/r \times C}$. In order to improve the robustness and generalization of the model, the following output can be obtained by matching the feature activation values with the original biometric feature library.

$$\overline{x}c = F_{\mathrm{scale}}(u_c, s_c) = u_c \times s_c. \tag{8}$$

We also added two layers of bottleneck structure at the tail of the network, the first layer is composed of a fully connected layer, and we set the dimensionality reduction parameter as r. The second layer is composed of a ReLU activation layer, and each face RGB channel has the corresponding position and original input activation value. The multistream convolutional neural network face recognition process is shown in Figure 5.

4. Experiment

4.1. Setting. According to the project requirements, the digital face recognition system contains a computer vision unit, a deep convolutional neural network algorithm unit, a GPU accelerated computing unit, a data storage unit, and a PC control unit. In the computer vision unit construction, we use the stereo system architecture platform AVT Pike to assist face image and depth information acquisition, with cameras placed at 45 degrees and kept at the same level. Camera No. 1 is facing the face, and cameras No. 2 and No. 3 are spaced 45 degrees apart from camera No. 1. The interval between the cameras and the face is 1000 mm. The effective range of the three cameras acting together is 500 mm. We use IEEE_1394 firewire to connect the lenses of the three cameras to the central console. The details of the computer vision system build are shown in Figure 6. One of the deep convolutional neural network units uses TensorFlow as the base network framework, and the algorithm editing language is python. The face recognition model training platform is a NVIDIA Quadro P6000 graphics card, the computer memory is 64 GB, and the processor is Intel(R) CoreTM i9-9900 K CPU@3.6 GHz x8. The network training process uses a hierarchical training model with layer-by-layer update iterations to optimize the training parameters.

4.2. Analysis of Face Area Weighting. To divide the face from a 3D level, we split the five senses in terms of facial region division, and we analyze the degree of biometric matching of the five senses of the face. According to the facial region association, in the experiment, we strictly control the light angle to obtain the facial five senses shading. Since multistream convolutional neural network feature learning is more biased toward light reflection and motion blur, the facial images are divided into three angles for shooting. To ensure the uncertainty caused by unstructured environmental factors in the image acquisition, we adopt iterative iterations to update the facial five senses feedback features during the training process.

From the experimental results in the above Table 1, it can be seen that in the facial recognition facial five senses partitioning experiments, the eyes occupy a larger proportion of the weight, and the recognition accuracy of the eyes is higher. The weight proportion of the mouth is second only to the eyes because the change of mouth shape will affect the overall configuration of the face contour. The other five senses occupy a smaller proportion and have little influence on facial recognition. In summary, it can be seen that face recognition accuracy is more closely related to the

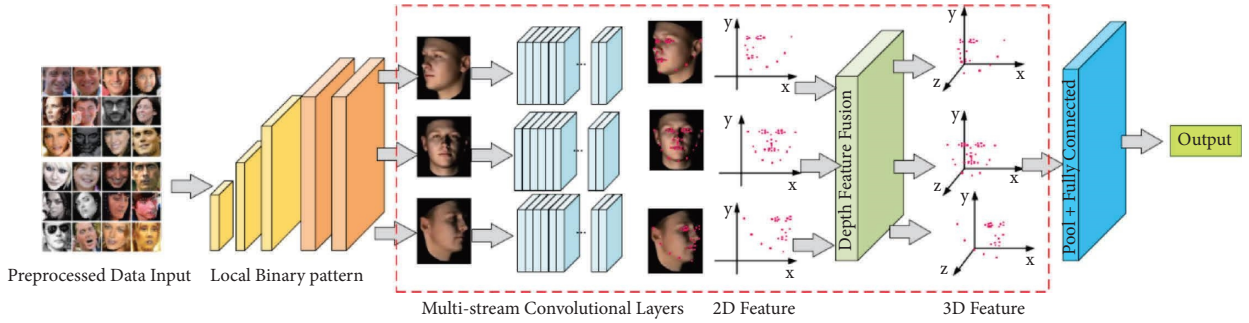

Figure 5: The multistream convolutional neural network face recognition process.

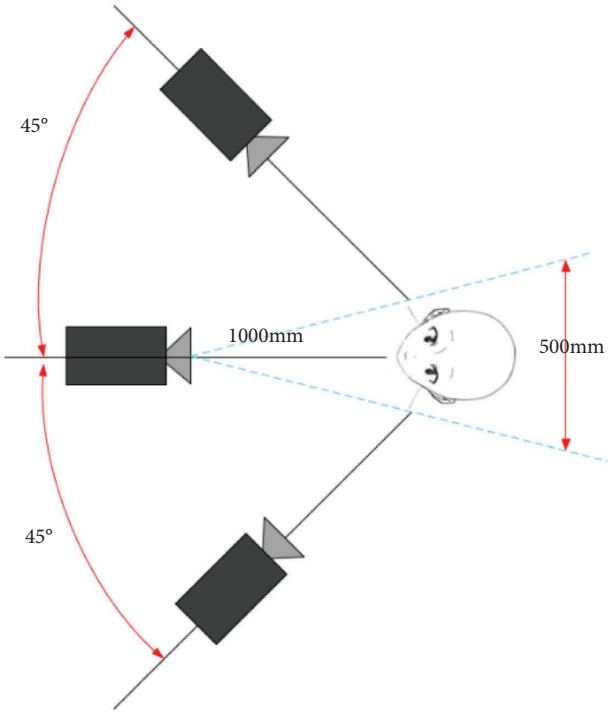

Figure 6: The computer vision system.

Table 1: The weighting of the five facial regions.

Area	Weight	Precision (%)
Eyebrow	0.89	98
Eyes	1.98	96
Nose	1.06	96
Mouth	1.61	95
Jaw	0.21	92

biological features of the eyes and mouth, and the post-training parameter adjustment of the neural network should take the five features with higher weights as the main reference factors.

4.3. Face Recognition Experiment Results. To verify the validity of the method, we first selected public datasets as the experimental validation set, and we chose PubFig: Public Figures Face Database, Large-scale CelebFaces Attributes (CelebA) Dataset, and Colorferet as the base datasets. To maintain the suitability of the datasets to the face recognition model, we adopted the same preprocessing means for all the datasets. The preprocessing process is shown in Figure 7.

All datasets are grayscale images of 384×286 pixels at the input side for testing positive face angle correction. For RGB correction, all datasets were set to 384×286 pixel channel controllable images. The preprocessed output is stored in the format "FACE_XXXX.pgm." Details of the datasets are shown in Table 2.

In concurrent experiments, we conducted independent experimental tests on support vector machines (SVM) [34], local binary patterns (LBP) [35], and convolutional neural networks (CNN) [36]. To balance the variability between each method, we use a closed-form parameter adaptive correction method for each method and migrate to face recognition model training when the parameters reach the optimal state. The comparative experimental results of the various methods are shown in Table 3.

where A_{TP} denotes the recognition efficiency per 100 face samples. p denotes precision and R denotes recall. From the experimental results in Table 3 above, it can be seen that the SVM method produces a large number of misidentified samples in the face recognition dataset test, and the precision is only 77%. Compared with machine learning methods, deep learning methods perform better in face recognition, and convolutional neural network methods are more advantageous in the field of image recognition, with 92% accuracy. Our method incorporates a deep learning network and LBP algorithm framework and achieves 98% accuracy, which is better than other algorithms, thus showing that our method performs best in face recognition. To restore the influence of interaction between network layers, we also added independent network layer performance test experiments, and the experimental results are shown in Table 4.

From the experimental results in the above table, we can see that the multistream convolutional neural network we use has outstanding advantages in the layer-by-layer stacking experiments, and the best face recognition results are obtained when the multistream branch value is 4. After the multistream branch exceeds 4, the accuracy rate starts to decrease. In the final experiments, we also adopt the training scheme with a multistream branch of 4.

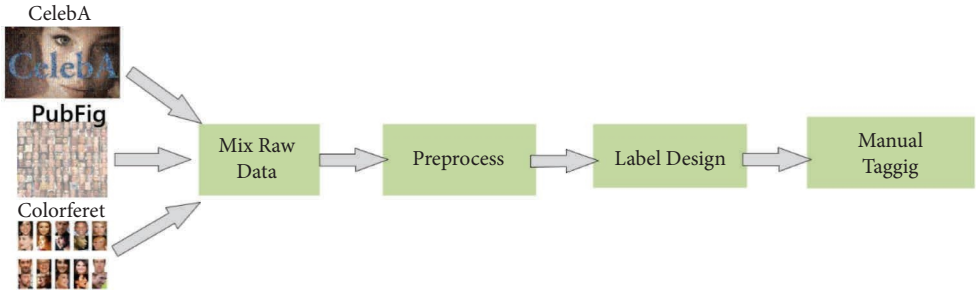

Figure 7: The preprocessing processes.

Table 2: Face recognition dataset details.

	Train	Test	Total
PubFig	14731	2642	17373
CelebA	15214	2946	18160
Colorferet	13541	2503	16044

Table 3: Comparison of face recognition experiments by different methods.

Method	A_{TP}	R (%)	P (%)
SVM	294	64	77
LBP	364	87	84
CNN	382	91	92
Ours	465	97	98

Table 4: Multistream convolutional network layer performance test analysis.

Multistream	Branch	Residual block	Global pool	Parameter (M)	Accuracy		
					PubFig (%)	CelebA (%)	Colorferet (%)
1	ADD	DEL	DEL	1.5	94	93	94
2	ADD	ADD	ADD	2.4	95	95	94
3	DEL	DEL	ADD	0.9	97	97	96
4	ADD	ADD	ADD	3.6	99	98	99
5	ADD	ADD	Add	4.3	92	93	90

5. Conclusion

In this paper, to reduce the cost of human resource management and improve the efficiency of enterprise digital management, we propose a face recognition method based on multistream convolutional neural networks and local binary patterns and build a digital face recognition management system. We first build the system computer vision scene. Then a local binary mode facial expression feature extraction scheme is designed according to the depth camera image extraction method. Considering that face 3D features are easy to be missed, we build a multistream convolutional neural network to learn facial 3D features. Finally, we validate the effectiveness of the method in selecting a public face dataset. Experiments prove that our method can reach 98% face recognition accuracy, which is significantly better than other methods. Also, we proved the scientific efficient of multistream convolutional neural networks by ablation experiments.

Although our method performs well in terms of accuracy, the face recognition system is input to the embedded standalone system. The model implemented by our method requires high hardware facilities for the standalone system, which leads to the low stability of model fusion with the standalone system. In our later research, we will work on reducing the algorithm parameters, reducing the computational cost, and improving the compatibility of the algorithm with the standalone system.

Data Availability

∗The dataset can be accessed upon request.

Conflicts of Interest

The authors declare that they have no conflicts of interest.

References

[1] A. Boragule, H. Akram, J. Kim, and M. Jeona, "Learning to Resolve Uncertainties for Large-Scale Face Recognition," *Pattern Recognition Letters*, vol. 160, pp. 58–65, 2022.

[2] T. Bagchi, A. Mahapatra, D. Yadav, and D. Mishra, "Intelligent security system based on face recognition and IoT," *Materials Today Proceedings*, vol. 62, no. 11, 2022.

[3] M. Billah, X. Wang, J. Yu, and Y. Jiang, "Real-time goat face recognition using convolutional neural network," *Computers and Electronics in Agriculture*, vol. 194, Article ID 106730, 2022.

[4] F. Sellal, "Anatomical and Neurophysiological Basis of Face recognition," *Revue Neurologique*, vol. 178, no. 7, pp. 649–653, 2021.

[5] Y. H. Huang and H. H. Chen, "Deep face recognition for dim images," *Pattern Recognition*, vol. 126, Article ID 108580, 2022.

[6] Y. Yu, X. Han, and L. Du, "Target part detection based on improved SSD algorithm," *Journal of Physics: Conference Series*, vol. 1486, no. 3, Article ID 032024, 2020.

[7] F. Boutros, N. Damer, F. Kirchbuchner, and A Kuijper, "Self-restrained triplet loss for accurate masked face recognition," *Pattern Recognition*, vol. 124, Article ID 108473, 2022.

[8] G. Lokku, G. H. Reddy, and M. G. Prasad, "OPFaceNet: OPtimized Face Recognition Network for noise and occlusion affected face images using Hyperparameters tuned Convolutional Neural Network," *Applied Soft Computing*, vol. 117, Article ID 108365, 2022.

[9] K. Alhanaee, M. Alhammadi, N. Almenhali, and M. Shatnawi, "Face recognition smart attendance system using deep transfer learning," *Procedia Computer Science*, vol. 192, pp. 4093–4102, 2021.

[10] G. Revathy, K. B. Raj, A. Kumar, and T. M. Lathae, "Investigation of E-Voting System Using Face Recognition Using Convolutional Neural Network (CNN)," *Theoretical Computer Science*, vol. 925, pp. 61–67, 2022.

[11] F. Marcolin, E. Vezzetti, and M. G. Monaci, "Face perception foundations for pattern recognition algorithms," *Neurocomputing*, vol. 443, pp. 302–319, 2021.

[12] G. Kaur, R. Sinha, P. K. Tiwari, and M. Rakhra, "Face mask recognition system using CNN model," *Neuroscience Informatics*, vol. 2, no. 3, Article ID 100035, 2021.

[13] S. M. Bah and F. Ming, "An improved face recognition algorithm and its application in attendance management system," *Array*, vol. 5, Article ID 100014, 2020.

[14] W. Wang, J. Qin, Y. Zhang et al., "TNNL: a novel image dimensionality reduction method for face image recognition," *Digital Signal Processing*, vol. 115, Article ID 103082, 2021.

[15] P. Tavan, H. Grubmüller, and H. Kühnel, "Self-organization of associative memory and pattern classification: recurrent signal processing on topological feature maps," *Biological Cybernetics*, vol. 64, no. 2, pp. 95–105, 1990.

[16] M. Kirby and L. Sirovich, "Application of the Karhunen-Loeve procedure for the characterization of human faces," *IEEE Transactions on Pattern Analysis and Machine Intelligence*, vol. 12, no. 1, pp. 103–108, 1990.

[17] M. Turk and A. Pentland, "Eigenfaces for recognition," *Journal of Cognitive Neuroscience*, vol. 3, no. 1, pp. 71–86, 1991.

[18] D. Huang, C. Shan, M. Ardabilian, Y. Wang, and L Chen, "Local binary patterns and its application to facial image analysis: a survey," *IEEE Transactions on Systems, Man, and Cybernetics, Part C (Applications and Reviews)*, vol. 41, no. 6, pp. 765–781, 2011.

[19] A. Chehrehgosha and M. Emadi, "Face detection using fusion of LBP and AdaBoost," *Journal of Soft Computing and Applications*, vol. 2016, no. 1, pp. 1–10, 2016.

[20] A. K. Chanchal and M. Dutta, "Face detection and recognition using local binary patterns[J]," *International Journal of Advanced Research in Electrical, Electronics and Instrumentation Engineering*, vol. 5, no. 10, pp. 7923–7929, 2016.

[21] O. Bilaniuk, E. Fazl-Ersi, R. Laganiere, and C. Moulder, "Fast LBP face detection on low-power SIMD architectures," in *Proceedings of the IEEE Conference on Computer Vision and Pattern Recognition Workshops*, Columbus, OH, USA, June 2014.

[22] P. Kalaiselvi and S. Nithya, "Face recognition system under varying lighting conditions," *IOSR Journal of Computer Engineering*, vol. 14, no. 3, pp. 79–88, 2013.

[23] J. Chen, V. M. Patel, L. Liu et al., "Robust local features for remote face recognition," *Image and Vision Computing*, vol. 64, pp. 34–46, 2017.

[24] S. Saypadith and S. Aramvith, "Real-time Multiple Face Recognition Using Deep Learning on Embedded GPU system," in *Proceedings of the 2018 Asia-Pacific Signal and Information Processing Association Annual Summit and Conference (APSIPA ASC)*, IEEE, Honolulu, HI, USA, November 2018.

[25] F. Deeba, H. Memon, F. Ali, A. Ahmed, and A. Ghaffar, "LBPH-Based enhanced real-time face recognition," *International Journal of Advanced Computer Science and Applications*, vol. 10, no. 5, 2019.

[26] M. D. Nisha, "Improving the recognition of faces using LBP and SVM optimized by PSO technique," *International Journal of Experimental Diabetes Research*, vol. 5, no. 4, pp. 297–303, 2017.

[27] B. O'Connor and K. Roy, "Facial recognition using modified local binary pattern and random forest," *International Journal of Artificial Intelligence & Applications*, vol. 4, no. 6, pp. 25–33, 2013.

[28] D. Van De Ville, M. Nachtegael, D. Van der Weken, and W. R. Philips, "New fuzzy filter for Gaussian noise reduction," *Proceedings of the Visual Communications and Image Processing 2001 SPIEL*, vol. 4310, pp. 1–9, 2000.

[29] D. R. K. Brownrigg, "The weighted median filter," *Communications of the ACM*, vol. 27, no. 8, pp. 807–818, 1984.

[30] M. Elad, "On the origin of the bilateral filter and ways to improve it," *IEEE Transactions on Image Processing*, vol. 11, no. 10, pp. 1141–1151, 2002.

[31] R. Szeliski, *Computer Vision: Algorithms and applications*, Springer Science & Business Media, Berlin, Germany, 2010.

[32] J. Hu, L. Shen, and G. Sun, "Squeeze-and-excitation networks," in *Proceedings of the IEEE Conference on Computer Vision and Pattern Recognition*, Salt Lake City, UT, USA, June 2018.

[33] X. Liu, L. Yiqian, L. Liu, Z. Wang, and Y. Liu, "Improved YOLOV3 Target Recognition Algorithm Embedded in SENet Structure [J/OL]," *Computer Engineering*, vol. 440, pp. 1–6, 2018.

[34] S. Suthaharan, "Support vector machine," *Machine learning Models and Algorithms for Big Data Classification*, pp. 207–235, Springer, Boston, MA, 2016.

[35] T. Ahonen, A. Hadid, and M. Pietikäinen, "Face Recognition with Local Binary patterns," in *Computer Vision - ECCV 2004. ECCV 2004. Lecture Notes in Computer Science*, T. Pajdla and J. Matas, Eds., vol. 3021, pp. 469–481, Springer, Berlin, Heidelberg, 2004.

[36] J. Gu, Z. Wang, J. Kuen et al., "Recent advances in convolutional neural networks," *Pattern Recognition*, vol. 77, pp. 354–377, 2018.

Hindawi
Scientific Programming
Volume 2023, Article ID 9829648, 1 page
https://doi.org/10.1155/2023/9829648

Retraction

Retracted: Feasibility Analysis of Intelligent Piano in Piano Teaching

Scientific Programming

Received 18 July 2023; Accepted 18 July 2023; Published 19 July 2023

This article has been retracted by Hindawi following an investigation undertaken by the publisher [1]. This investigation has uncovered evidence of one or more of the following indicators of systematic manipulation of the publication process:

(1) Discrepancies in scope
(2) Discrepancies in the description of the research reported
(3) Discrepancies between the availability of data and the research described
(4) Inappropriate citations
(5) Incoherent, meaningless and/or irrelevant content included in the article
(6) Peer-review manipulation

The presence of these indicators undermines our confidence in the integrity of the article's content and we cannot, therefore, vouch for its reliability. Please note that this notice is intended solely to alert readers that the content of this article is unreliable. We have not investigated whether authors were aware of or involved in the systematic manipulation of the publication process.

In addition, our investigation has also shown that one or more of the following human-subject reporting requirements has not been met in this article: ethical approval by an Institutional Review Board (IRB) committee or equivalent, patient/participant consent to participate, and/or agreement to publish patient/participant details (where relevant).

Wiley and Hindawi regrets that the usual quality checks did not identify these issues before publication and have since put additional measures in place to safeguard research integrity.

We wish to credit our own Research Integrity and Research Publishing teams and anonymous and named external researchers and research integrity experts for contributing to this investigation.

The corresponding author, as the representative of all authors, has been given the opportunity to register their agreement or disagreement to this retraction. We have kept a record of any response received.

References

[1] Y. Ma, "Feasibility Analysis of Intelligent Piano in Piano Teaching," *Scientific Programming*, vol. 2022, Article ID 5010428, 8 pages, 2022.

Hindawi
Scientific Programming
Volume 2022, Article ID 5010428, 8 pages
https://doi.org/10.1155/2022/5010428

Research Article

Feasibility Analysis of Intelligent Piano in Piano Teaching

Yao Ma

College of Music, Guizhou Normal University, Guizhou, Guiyang 550000, China

Correspondence should be addressed to Yao Ma; 460098906@gznu.edu.cn

Received 25 July 2022; Revised 4 September 2022; Accepted 19 September 2022; Published 10 October 2022

Academic Editor: Lianhui Li

With the rapid development of artificial intelligence, big data, blockchain, and other technologies, the impact of intelligent environment on the development of education has become more and more profound. Other developed countries have realized that education reform is urgent in the intelligent environment. So as to seize the major strategic opportunity of artificial intelligence development, my country has optimized the teaching content, teaching methods, and teaching methods of traditional piano teaching on the basis of respecting the traditional piano teaching concept. Upgrade to achieve the innovation of the relationship between teaching and learning in piano education in normal schools, and create a new situation for piano teaching in normal schools. Based on the current situation of piano education for musicology majors in normal schools, this paper takes the intelligent piano as the research object, compares the advantages and disadvantages of the application of smart pianos and traditional pianos in the environment of normal schools, combines the intelligent technology provided by smart pianos, and explores the application of technology to pianos in normal normal schools. The path of teaching reflects the value and use value of intelligent piano in piano teaching in normal schools and explores the value of intelligent piano teaching.

1. Introduction

The rapid development of information technology has promoted the development handle of educational informatization and the modernization of educational means. Taking the rapid development of the Internet as the horizontal axis, artificial intelligence, personal customization, and network communication as the vertical axis, the high and steady upward curve has been recognized by more researchers, and even mentioned the "fourth industrial revolution," which is the "smart age." Emerging technologies have penetrated all aspects of life, and have gradually occupied an irreplaceable position in the field of learning. Relying on the benefits brought by new science and technology and the Internet, whether teaching or receiving education will reduce the constraints brought by tradition and gradually become an intelligent education system. In the field of music education, intelligent teaching has also become the general trend [1–3]. In the traditional "one-to-one" teaching, teachers mainly impart knowledge to students in an oral way, and a good teacher-student relationship is built between students and teachers. Normal school students' piano learning is mainly based on repertoire skills and is relatively lacking in autonomous learning and classified learning. At the same time, the demonstrations in the piano classes in normal schools are mainly based on the teacher's personal demonstration, and the students learn the repertoire by imitating the teacher as the main learning method. In this way, although students can learn more intuitively about the teacher's playing skills, they lack their own creativity. After graduation, the students trained under the piano education in normal schools are mainly faced with primary and secondary schools, which requires that the piano education and training in normal schools should meet the requirements of normal schools and meet the actual job needs of students. The rapid development of information technology in the 21st century has promoted the development of educational informatization and the modernization of educational means. With the gradual deepening of education reform, the piano education in normal schools has gradually shifted from "examination-oriented education" to "quality education," which requires piano teaching in normal schools to reposition the teaching according to the new needs of cultivating compound music education talents

[4–6]. Therefore, the intelligent piano teaching in colleges and universities under the information technology came into being. It is a new type of teaching with more integration, interaction and creativity. It allows students to form a more comprehensive understanding of music art in the process of piano learning, the systematic acquisition of professional skills adapted to actual work needs [7].

How to speed up the strength and progress of the integration of piano teaching and information technology in normal schools has become an important research topic. Therefore, this paper will focus on the application of intelligent piano in colleges and universities supported by information technology, through in-depth analysis of the evolution of intelligent piano, comparison with traditional piano teaching, and its unique intelligent technology, so as to explore a new type of piano. The new piano course teaching mode provides a certain reference for the future intelligent piano teaching [8–10]. This paper mainly conducts a practical and theoretical exploration of the application of intelligent pianos supported by information technology in the piano classrooms of musicology majors and piano performances in normal high schools, hoping to arouse more musicians, learners, and researchers to the intelligent for the emphasis on the piano. It provides a reference for improving the autonomy, creativity, and practicality of piano learning in normal teachers. And by carrying out piano course teaching research, adding modern technology to the process of piano course teaching, optimizing the resources and teaching process of piano teaching in normal schools, providing a new idea and method for the reform of normal school education, and providing theories for the innovation research of piano education in normal schools' support.

2. Research Status of Intelligent Piano in Piano Teaching Methods at Home and abroad

In the foreign literature, I have only found two descriptions and researches on smart pianos, and there is no relevant research on the combination of smart pianos and music teaching in normal colleges. Among them, "IntelligentPianoAndSystem" analyzes the piano keyboard from the keys, the indicator module, the first data communication module, the key detection module, the MIDI data processing module, the MIDI synthesizer, the audio encoder, the audio amplifier, and the speaker, to show that the smart piano can be realized for the functions of personnel identification, correction, scoring, sound quality replacement, composition, etc., and heighten the efficiency of piano learning. Another article "Intelligent Tutor System For Piano Learning" introduces the invention of the "Piano Learning" intelligent tutor system, which is designed for the piano learners, especially for piano practice after class, and guides piano teachers to effectively teach through intelligent operation methods and processes, guide students how to heighten their piano skills more effectively through this system.

There has been some research on the application of smart pianos in piano education in Chinese normal schools. Relatively large part scholars have thought about the feasibility of combining smart pianos with music education in normal schools from multitudinous perspectives and put forward some ideas at the same time. Chen pointed out that the emergence of smart pianos is caused by various aspects such as science and technology, human needs, and the market, and it is an inevitable combination of old and new. Whether its practicality, its own performance, or its influence and acceptance, it provides an important foundation for research and development. However, the emergence of new things must have a process that is well known to the public, as well as its own selling point compared with traditional pianos, and problems such as the inability of propaganda to accurately locate the target group make smart pianos unable to accurately impress consumers and market sentiment [11]. Yu and Peng believes that the smart piano is now a very important part of the learning field, and its proportion in the market is increasing year by year, which is attributed to him and his influence. Its own characteristic is to use new science and technology on the existing performance of traditional piano, reorganize some internal structures, update use functions, and at the same time integrate some successful scientific research results into it; rational use is a powerful addition to modern music education. One way [12]: Lian integration of science and technology into music teaching itself is a way to heighten autonomy, interactivity, and points of interest, which invisibly reduces a lot of resistance for students in the process of learning music again in a passive position. For him to break through the traditional teaching mode and adopt this kind of teaching mode with more resource integration ability, interaction ability with students, and individualized creativity ability, it is a reform plan for cultivating personalized, innovative, and technological talents in the 21st century music department. It is also the development direction of music education in the future [13]. Zhan and Wu are using questionnaires to conduct sampling surveys to understand the situation of piano teaching based on the quality development of college students in multitudinous regions. The piano teaching method has become an important part of the new quality education. The data shows that it has certain reference for future education and is worth further exploration. The research shows the current development direction of quality education in colleges and universities through this set of data, so as to view the problem in an all-round way and solve the problem in the rapidly advancing education [14].

In the related research on the implementation of children's music education using emerging technology as an investigation method, Mo and Li talked about the comparison between modern and past teaching models, and shortcomings such as knowledge structure lines no longer exist. Nonlinear network structure, diversification of presentation forms has become the characteristic of education in this era [15]. Wei pointed out that modern society is in the environment of the Internet and emerging technologies. The influence of technological development has penetrated into all aspects of study and life, and intelligent communication equipment has also made a significant contribution to this. The development of the smart piano and its introduction

into the market is also due to its own performance, which can bring more teaching benefits and more scientifically formulate a more suitable knowledge system for multitudinous student groups and higher practicability. It has been continuously studied as a direction, and explore Rauscher et al. [16]. In the related research on the use of emerging technologies as an investigation approach, Zhang proposed to make good use of the advantages and characteristics of Internet music software, and integrate it into the teaching of harmony in normal schools. This method makes better use of the accuracy of computers, is more convenient for students to learn, and maximizes the characteristics of harmony. At the same time, it integrates theory and teaching into teaching, and the teaching efficiency is significantly improved compared to before. It also broadens the thinking of students, increases creativity, makes teaching more intelligent and modern, and has a significant impact on my country's music education [17]. In the age of the Internet, Yan et al. have also combined piano teaching with it, using multitudinous educational cloud, database, and other approaches to research and explore the application scheme of cloud computing in the curriculum and constantly develop a form more suitable for modern education. Courses that are more suitable for students' age and comprehension ability enable educated people to better grasp knowledge, and the drawbacks of traditional teaching have been significantly improved [18]. Tubo is a piano concerto digital performance training system based on a set of computer music production tools and the ROM function of digital pianos. It is an orchestra software that develops and produces ten piano concertos. The live performance of the piano and the orchestra is an old performance mode, while the digital orchestra is to make the orchestra part of the piano concerto into audio through music production software and use it in students' daily practice, so as to strengthen the students' understanding of the piano concerto. The ability to perform in this genre helps students gain a more comprehensive understanding of the essence of Western music culture. The smart piano can be applied to the music education of the normal school with reference to the digital orchestra model of the concerto, as an auxiliary tool for the music learning of the normal school [19, 20].

To sum up, from the data I collected, there has been some research on the application of smart pianos in piano education in Chinese normal schools, but there is a lack of attempts to explore specific measures to achieve innovation in piano teaching in normal schools. Theory cannot be connected with practice and cannot really heighten the current situation of piano teaching in normal colleges. Therefore, the intelligent technology of intelligent piano is added, the teaching and learning modules are developed according to the characteristics of piano teaching in normal schools, the intelligent piano teaching in normal schools supported by information technology is established, and the implementation is carried out to improve the current situation of slack in music education in normal schools; make full use of the school. The existing intelligent piano equipment and the hardware facilities to be improved will provide theoretical support for building a modern platform for piano teaching innovation in normal colleges, which is the important research purpose and significance of this paper.

3. Research on Functional Modules of "Smart Piano"

The "smart piano" system has rich learning resources, and its huge resource library provides a reliable guarantee for the "smart piano" teaching activities. The resource library can provide information technology support for teachers to formulate teaching plans and teaching plans. At the same time, students need to use the information in the resource library for after-class preview, practice, review, and assessment [21, 22]. As shown in Figure 1, the resource library expands on the basis of traditional piano teaching materials, digitizes music scores, teaching materials, and articles, and provides information retrieval functions for students and teachers to facilitate teachers and students to access resources.

3.1. Recognition of Playing, Practice with Lights, Intelligent Error Correction. In the existing teaching system, intelligence and multimedia have become very common. Not only has multimedia teaching been widely used in primary and secondary school classrooms, but also in music colleges, teaching and information technology are generally integrated, which is a kind of sublimation from blackboard to whiteboard for the development of education [23–25]. Teachers need to improve the traditional teaching methods in piano courses, keep pace with the times, and make full use of the Internet and "smart piano" terminals to make up for relatively large part defects in traditional teaching. In the past, the piano course was one-on-one teaching with teachers and students, and then students practiced for a week after class. This handle was repeated until the work was completed. For students in higher normal schools, this method is inefficient, and there are not enough teacher resources to realize the whole handle of traditional teaching. Therefore, using the "smart piano" system can solve the problem of teachers, and at the same time improve the fun and efficiency of learning, reduce the learning pressure of piano courses, free up more time for the learning of other courses, and effectively improve the comprehensive quality of students. The core of the "smart piano" is the teaching guidance module, which is divided into two parts: computer guidance and teacher guidance. Among them, computer guidance is the advantage of "smart piano" over traditional teaching methods. The "intelligent piano" connects teachers and students with the network, completes human-computer interaction at the same time, and completes teaching and learning under the dual action of computer and network.

The "smart piano" presents the electronic music score to the students through the display screen. In the initial learning stage, the students can play the audio of the work first, and mark the progress of the audio on the music score in real time, so that students with weak notation ability can follow the music mentally. By listening to the music scores, students have a preliminary and overall understanding of the

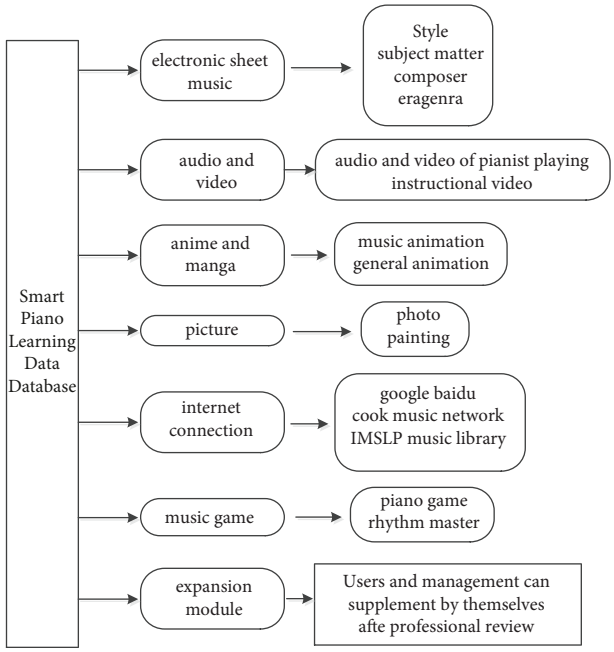

Figure 1: Expansion diagram of intelligent piano learning data.

work. Students can adjust the playback speed according to their own abilities and habits, and listen to the individual stages of the work repeatedly.

3.2. Gradient Teaching Method. The gradient teaching module is designed to evaluate students' learning progress and performance level, then provide guidance for the formulation of learning plans, match students data with individual models, and provide students with appropriate learning content based on their learning needs, as shown in Figure 2 shown.

3.2.1. Primary Assessment. When students use the "smart piano" for the first time to learn, they need to test and evaluate their actual performance ability and music knowledge. Students with a good foundation can directly choose the difficulty of the test, judge the performance level through the computer's evaluation of speed, accuracy, and artistic processing, and finally formulate a corresponding learning plan according to the performance level. Students with poor or zero foundation can skip the test and just fill in the questionnaire, input their preferences and expected learning progress to the computer, and then the computer will directly formulate a learning plan based on the data model.

3.2.2. Intermediate Assessment. The purpose of the intermediate assessment is to investigate the students' learning status and to test the students' learning progress and learning stage achievements, so as to fill in the gaps and prepare for future learning. The intermediate assessment consists of three parts, one of which is self-assessment. The self-evaluation system aims to improve students' self-

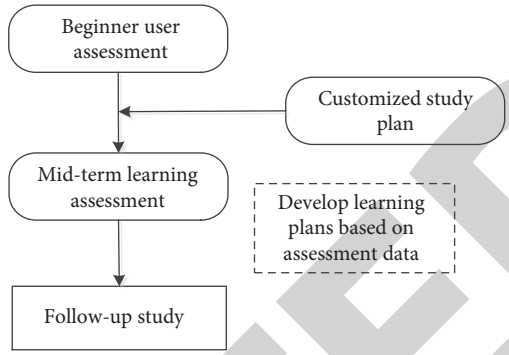

Figure 2: Gradient teaching flow chart.

learning ability, so that they can have a clear understanding of their own level, and can accurately guide their students when they go to teaching positions in the future. Self-evaluation includes self-satisfaction, scores, and learning difficulties. The second is computer evaluation. The computer scores the basic elements of performance according to the sensor data and makes a preliminary judgment on the students' performance level. The third is teacher evaluation and student mutual evaluation. Students upload their performance videos to the Smart Piano cloud platform, and teachers and classmates will score and fill in relevant comments. Finally, the computer comprehensively evaluates the three parts to give concrete results.

3.2.3. Study Schedule. The computer formulates a corresponding learning progress table according to the data filled in by the individual and the test results, which mainly includes two elements, one is the student's performance level, and the other is the student's artistic accomplishment and repertoire preference. The performance level data is obtained from the combination of the computer's primary assessment and the teacher's assessment. According to the final score, the difficulty matching repertoire is selected as the learning target. Learn step by step towards deeper levels of difficulty. The data on artistic accomplishment and repertoire preferences are obtained from questionnaires filled out by the students, and corresponding questions will be arranged in the questionnaires. At the same time, according to the data mining of the search engine, the computer will summarize the students' preferences. Finally, based on the above information, a learning schedule is formulated.

4. Analysis of the Functional Modules of Intelligent Piano in Piano Teaching in Normal Schools

4.1. Intelligent Piano Solo Teaching. The teaching process using the smart piano as a platform is mainly divided into three stages, namely, self-study, online guidance, and face-to-face teaching. The sixth week is face-to-face with teachers. The computer adjusts the teaching progress in real time according to the learning situation and detection data and gives full play to the teaching advantages of the intelligent piano.

4.1.1. Learning Points and Difficulties. Preliminarily master the style and characteristics of the work, understand the writing background of the work, accurately play the notes and musical terms in the work, and complete the basic elements of music, especially pitch, dynamics, and fingering. At the same time, combining network and multimedia means in piano teaching to assist students in learning music-related knowledge, improve students' artistic accomplishment in an all-round way, deepen their understanding of music works, and cultivate more sensitive hearing. Solo works are often difficult to perform, and works of different composers and styles need to be played with relative skills. Therefore, mastering scientific and reasonable practice methods and overcoming difficulties in performance skills is the top priority.

4.1.2. Self-Study Stage. After the teacher assigns the task, the students first watch the relevant performance videos and asynchronous online classes, and read the relevant text materials. In this way, we can understand the relevant background information of the work and have a preliminary understanding of the overall overview of the work. Then, under the guidance of electronic scores and computers, students will be familiar with the fingerings and notes of the works by performing reading and primary exercises. For the more difficult skills in the works, such as fast running, interval jumping, and two-tone running, first try to practice at a slow speed by yourself to explore the tricks of playing. If it cannot be solved, the online class or face-to-face class will be guided by the teacher. When it can be played completely, the qualification rate of basic musical elements such as pitch and rhythm is detected by the computer. Then adjust the study plan and guide students to practice in a targeted manner.

4.1.3. Online and Face-to-Face Teaching. In online classes and face-to-face classes, teachers first listen to students' complete performances of the whole piece, and explain the performance methods and practice methods of difficult skills in the class, and at the same time teach students how to understand music and process works. After the teacher's guidance, the students perform the whole song completely, and the computer and the teacher jointly give a comprehensive score to test the learning results. The computer stores the comprehensive score in a database for use in subsequent study planning.

4.2. Analysis of Intelligent Piano Teaching Design. The teaching handle using the smart piano as a platform is mainly divided into three stages, namely, self-study, online guidance, and face-to-face teaching. The sixth week is face-to-face with teachers. The computer adjusts the teaching progress in real time according to the learning situation and detection data and gives full play to the teaching advantages of the intelligent piano. As a graduate student of a normal university, I have been allowed to carry out teaching practice in the school, and the practice object is the first-year undergraduate students of the school. I have verified whether it is feasible to apply the intelligent piano to the piano teaching of the normal school.

Design 1: The traditional piano is integrated into the teaching of intelligent piano, and the piano solo is used as a teaching case. According to the comparison between the intelligent feedback of the smart piano and the feedback of the artificial teacher as the experimental data, the experiment is a six-week system teaching cycle of the smart piano, and the feedback of the artificial teacher to make a summary and analysis of the progress and quality of the course. The first and second weeks take the form of intelligent piano group lessons, the third and fourth weeks take the form of intelligent piano individual lessons, and the fifth and sixth weeks take the form of traditional piano individual lessons. The teaching selects "Chopin's Ballade in G Minor" as the case repertoire. Starting from the first week, various aspects of teaching are gradually carried out. Based on the students' adaptability, basic piano skills, and the playing complexity of "Chopin's Ballade in G Minor" as the premise, the teaching will be carried out. The process adopts the normal step-by-step and complementary teaching methods, analyzes the students' weekly feedback and draws conclusions, and finally evaluates the students' completion, thus reflecting the advantages of the new intelligent teaching model, as shown in Table 1.

Design 2: Taking piano solo teaching as an example, the religion arrangement is carried out in the form of traditional piano individual lessons. Six weeks are used as a systematic religion cycle. Based on the combination of the artificial teacher feedback and the intelligent feedback of the smart piano in the sixth week as the experimental tracking data, the weekly class situation is summarized and analyzed. Weeks 1 to 6 take traditional piano individual lessons. Taking the example of "Chopin's Ballade in G Minor" as a case, the religion is carried out from the first week to the sixth week, and the combination of students' acceptance ability, basic piano ability, and the difficulty level of "Chopin's Ballade in G Minor" is as follows: in the light of the data obtained from students' feedback every week, the students' completion degree is finally checked, as shown in Table 2.

Through design analysis and comparison with the same religion content, different class forms and religion methods, from the data of teaching practice and the data and feedback of the summary table, a new teaching mode was adopted in the six-week class schedule. This is a piano religion mode of "main + assistant," "human + instrument," and "complementary." This approach further mobilizes the enthusiasm of students and increases their participation in the classroom. It combines the religion advantages of artificial intelligence and intelligence to make up for the shortcomings of traditional piano religion. This "human + device," "complementary," and "remote" piano religion mode is more able to

Table 1: The combination of intelligent piano and traditional piano teaching-take Chopin's Ballade in G Minor as an example.

Teaching time (week)	Class form	Teaching content	Teaching method	Student recognition	Teaching feedback	Student completion
First	Intelligent piano group class	Creative background	(1) Play the original audio (2) Introduce the creative background (3) Introduce the content of the track	Excellent	Have an intuitive perception of the work	85%
Second	Intelligent piano group class	Music analysis	(1) Form analysis (2) Thematic analysis (3) Harmonic gaps to familiarize students with	Generally	Raise awareness and performance with smart media	75%
Third	Intelligent piano individual lessons	Melody and rhythm	(1) Play recording intelligent error correction melody (2) Intelligent error correction rhythm (3) Analyze the cause of the problem	Excellent	Novel teaching methods improved melody and rhythm problems	90%
Fourth	Intelligent piano individual lessons	Emoticons	(1) Play the recording, (2) Add emoji to playing	Generally	More mechanized and Constrains musical performance	65%
Fifth	Intelligent piano individual lessons	Performance skills	(1) Point out repertoire skills (2) Preliminary practice	Excellent	Into the teaching of performance skills is more efficient	90%
Sixth	Traditional piano individual lessons	Performance skills	(1) Point out repertoire skills (2) Track summary	Excellent	Improves the ability of works and the delicacy of performance	90%

Table 2: Traditional piano solo teaching-take Chopin's Ballade in G Minor as an example.

Teaching time (week)	Class form	Teaching content	Teaching method	Student recognition	Teaching feedback	Student completion
First	Traditional piano individual lessons	Creative Background	(1) The teacher plays the selected excerpts (2) Oral introduction of the creative background and the connotation of the repertoire	Bad	The impression of the work is limited and forgotten quickly	55%
Second	Traditional piano individual lessons	Music analysis	(1) Form analysis (2) Thematic analysis (3) Harmonic gaps to familiarize students with	Bad	Inconvenient in instructional media	55%
Third	Traditional piano individual lessons	Melody and rhythm	(1) Play the recorded manual error correction melody (2) Manual error correction rhythm (3) Analyze the cause of the problem	Good	Novel teaching methods improved melody and rhythm problems	80%
Fourth	Traditional piano individual lessons	Emoticons	(1) Play the recording, (2) Add emoji to playing	Generally	Constrains students' imagination and expressiveness of music	65%
Fifth	Traditional piano individual lessons	Performance skills	(1) Point out repertoire skills (2) Preliminary practice	Generally	Playing skills are less affected by preteaching	70%
Sixth	Traditional piano individual lessons	Performance skills	(1) Point out repertoire skills (2) Track summary	Generally	Playing skills are less affected by preteaching	70%

mobilize the enthusiasm of students. The percentage of students' completion in this religion mode reaches 90%, while the traditional religion method reaches only 70%. The emergence of this model is an attempt to update the religion concept in the light of the inheritance of the traditional religion model, combined with the intelligent technology of the smart piano.

5. Conclusion and Outlook

5.1. Summary. Comparing different class forms and teaching methods, it can be seen that the teaching mode combining intelligent piano and traditional piano teaching has certain feasibility and promotion. Existing piano teaching can try to add "smart piano" teaching into it. The piano lessons under the "smart piano" application adopt two types of lessons: individual lessons and group lessons, and the combination of traditional individual lessons is no longer mechanized and simplified. This new teaching form mainly relies on intelligent technology. Through intelligent technology, the knowledge that needs to be taught to students in the form of oral and text can be taught to students with pictures and audio. This mode is more intuitive and can mobilize students. The facial features meet the students' auditory and visual requirements. Compared with the traditional teaching mode, this has stricter requirements on students' learning quality, broadens the path for students to acquire knowledge, and improves teaching efficiency and quality.

5.2. Prospect. The piano teaching mode of "human-+instrument." The "person" here refers specifically to the teachers and students participating in the music class. Since the piano major itself has its own particularity, it is an active output and an active acceptance of such a teaching method. In the classroom, teachers need to use methods such as playing demonstrations, music appreciation, and verbal communication to help students heighten their professional abilities from the perspective of creative background, music analysis, and performance skills. "Device" refers to the use of smart pianos in the classroom. It has functions such as intelligent recognition of rhythm and pitch, switching between multiple versions of smart scores, audio, and video, etc., which undoubtedly provides practical teaching for the improvement of teaching quality.

Data Availability

The dataset can be accessed upon request.

Conflicts of Interest

The authors declare that they have no conflicts of interest.

References

[1] X. Zhang, "The intelligent + development of piano guides the new direction of piano education in the future," *Popular Literature Academic Edition*, vol. 1, no. 12, pp. 1-2, 2017.

[2] X. H. Cao, "Development prospect of piano and intelligent piano," *Musical Instrument*, vol. 1, no. 7, pp. 4-5, 2012.

[3] Z. X. Chen, *New Ideas for Piano Teaching*, Shanghai Music Publishing House, Shanghai, China Mainland, 2011.

[4] Y. H. Wang, "The theory of multiple intelligences and the teaching reform of piano collective lessons in normal colleges," *Chinese Music Journal*, vol. 1, no. 4, pp. 3-4, 2006.

[5] X. K. Wang, "Research on the reform of piano teaching in colleges and universities under the background of multicultural education," *Journal of Henan Normal University (Philosophy and Social Sciences Edition, Bimonthly)*, vol. 1, no. 5, pp. 1-2, 2010.

[6] J. Liu, "The enlightenment of multiple intelligences theory to the practice of piano teaching in teachers colleges," *The Big Stage Journal*, vol. 1, no. 12, pp. 2-3, 2012.

[7] J. Gao, "Piano education and the cultivation of creative thinking ability," *Journal of Wuhan Conservatory of Music*, vol. 1, no. 1, pp. 4-5, 2003.

[8] H. X. Li, "The value orientation of piano teaching from the perspective of multiple intelligences theory," *Journal of Xinzhou Normal University*, vol. 1, no. 4, pp. 129–131, 2011.

[9] G. Q. Chen, "Research on the diversified teaching mode of piano in teachers colleges," *Music Exploration*, vol. 1, no. 2, pp. 5-6, 2002.

[10] J. F. Gao, "A music teaching mode created with modern educational technology," *China's Modern Educational Equipment*, vol. 1, no. 10, pp. 98-99, 2010.

[11] R. Chen, "Research on the universality of the development, evolution and practice of intelligent piano," *Music Creation*, vol. 1, no. 10, pp. 2-3, 2017.

[12] B. Yu and Z. Z. Peng, "Feasibility study of smart piano learning form in the era of Internet +," *Piano Artistry*, vol. 1, no. 1, pp. 7-8, 2018.

[13] P. Lian, "The new driving force of China's piano music education reform——a new model of digital piano music teaching," *Journal of Xinghai Conservatory of Music*, vol. 1, no. 3, pp. 4-5, 2005.

[14] Y. H. Zhan and X. N. Wu, "Investigation and analysis on the piano teaching mode that promotes the development of students' innovative quality," *Arthritis Research: Art Journal of Harbin Normal University*, vol. 1, no. 2, pp. 2-3, 2010.

[15] T. Mo and H. Li, "On the rise and application of intelligent technology assisting children's piano teaching," *Journal of Zunyi Normal University*, vol. 6, no. 9, pp. 4-5, 2017.

[16] F. H. Rauscher and S. C. Hinton, "Music instruction and its diverse extra-musical benefits," *Music Perception*, vol. 29, no. 2, pp. 215–226, 2011.

[17] R. Zhang, *On the Application of Computer Music Software in Harmony Teaching in Normal University*, Northeast Normal University, Changchun, China, 2007.

[18] D. W. Yan, B. Xu, and X. L. Huang, "Research on interactive music teaching mode based on education cloud——take piano teaching as an example," *Journal of Wuhan Conservatory of Music*, vol. 1, no. 3, pp. 135–143, 2014.

[19] B. Xu, D. Tan, X. Yang et al., "Fluorometric titration assay of affinity of tight-binding nonfluorescent inhibitor of glutathione S-transferase," *Journal of Fluorescence*, vol. 25, no. 1, pp. 1–8, 2015.

[20] B. Xu, *Research and Practice of Piano Teaching under the Environment of Information Technology*, Wuhan University Press, Wuhan, Hubei, China, 2017.

[21] Y. Y. Li, "Information technology and piano teaching," *The Voice of the Yellow River*, vol. 1, no. 10, pp. 2-3, 2007.

Hindawi
Scientific Programming
Volume 2022, Article ID 9607755, 15 pages
https://doi.org/10.1155/2022/9607755

Research Article

Construction of a Smart Supply Chain for Sand Factory Using the Edge-Computing-Based Deep Learning Algorithm

Bin Li,[1] **Xuejun Zhang**,[1,2,3] **Yanjiao Ban**,[1] **Xianfu Xu**,[1] **Wenjun Su**,[1] **Jingxian Chen**,[1] **Shan Zhang**,[1] **Feng Li**,[1] **Zuopeng Liang**,[3] **and Shengkai Zhou**[4]

[1]*School of Computer, Electronics and Information, Guangxi University, Nanning, China*
[2]*Guangxi Key Laboratory of Multimedia Communications and Network Technology, Guangxi, China*
[3]*Guangxi Xinhao Construction Engineering Co., Ltd, Guangxi, Nanning, China*
[4]*Yongkai Construction Group Co., Ltd, Guangxi, Nanning, China*

Correspondence should be addressed to Xuejun Zhang; xjzhang@gxu.edu.cn

Received 11 August 2022; Accepted 19 September 2022; Published 7 October 2022

Academic Editor: Lianhui Li

The diminishing natural sand has facilitated the booming of the sand manufacturing industry, and intelligent management of sand factories, in a time- and cost-efficient way, has become a growing tendency for the future. A role has been played in achieving intelligent management by constructing a smart supply chain. However, the smart sand factories are hardly involved in previously reported studies, which is inconsistent with related studies on smart factories and the Industrial Internet of Things (IIoT). In this paper, a smart supply chain management system (SSCMS) is constructed to realize the intelligence and automatization of the management of sand factories, using edge-computing and deep learning techniques. Along the supply chain, the deep learning model is used to realize the automatic identification of sand, avoiding the disadvantages of human identification, while improving the quality of sand factory operations. In order to relieve the pressure of network bandwidth, reduce system delay, and improve system operation efficiency, we use edge-computing technology to process data at the edge. To verify the performance of the constructed system, a sand factory simulation platform is established. Experiments show that the most critical indicator in the system, the accuracy rate of sand type identification, is above 98%, and the sand type identification time is only 0.022 s. In general, compared with traditional supply chain management, the constructed smart supply chain improves the quality and efficiency of sand factory operations, and all indicators of the designed system have achieved satisfactory results.

1. Introduction

Sand and aggregate are the largest, irreplaceable, and indispensable material for infrastructure construction, and it is closely related to the survival and development of human. Sand and aggregate account for 60% to 75% of the volume of concrete, and it is the main component of concrete. Therefore, human needs to consume tens of billions of sand and aggregate to build and transform the world every year. Sand commonly can be divided into natural sand and machine-made sand. Natural sand refers to naturally occurring sand, artificially mined with a particle size of less than 5 mm. Machine-made sand is the finished product processed through multiple processes using the sand-making machine. The characteristics of machine-made sand are that the finished product has good granularity. Moreover, various specifications of sand can be produced according to different material requirements during the manufacturing process. As the exploitation of natural sand resources continues, the natural sand resources that can be exploited are gradually decreasing. The reduction of exploitable natural sand resources has promoted the vigorous development of the sand-making industry, and therefore the number of sand-making factories has gradually increased.

The Internet of Things (IoT) is an intelligent network. It makes all devices connected to the network, and related communication is carried out through the network [1]. After the concept of IoT was proposed, scholars started to use IoT

technology in different fields. Concepts such as smart medical healthcare [2, 3], smart buildings [4, 5], smart grid [6, 7], and smart transportation [8, 9] have begun to be proposed. The Industrial Internet of Things (IIoT) means the use of IoT technology in the industry, which makes industrial manufacturing intelligent [10, 11]. The development of IoT technology will undoubtedly make life smarter in the future.

With the improvement of computer computing power, deep learning has become popular. Deep learning is the process by which computers learn associations between known data and eventually process unknown data as intelligently as humans do [12]. Recently, more and more research has introduced deep learning technology to the IoT [13, 14]. Generally, the use of deep learning to process data requires computers with high-performance computing capabilities. Therefore, many researchers transfer data collected by edge devices to cloud servers with large computation power for processing [15]. However, this method has certain drawbacks. On the one hand, the increasing number of IoT devices will lead to an increasing amount of data being generated. If all the data generated by IoT devices at the edge were to be transmitted to cloud servers for processing, this would be a huge challenge for network bandwidth. On the other hand, the transmission of data will inevitably cause some delay, which is very unfriendly to applications that need to react in real-time.

Edge computing is defined as the processing of data on the side close to the source of generation [16]. The inclusion of edge computing in the IoT can solve the problem of network congestion caused by massive data transmission [17]. Edge computing becomes especially important when deep learning models are used in IoT devices to process data [18].

Field Programmable Gate Array (FPGA) is a typical parallel computing chip featured by the fast celerity, high stability, robust flexibility of computing properties. In contrast to the traditional algorithm, the computing speed of FPGA has increased by dozens, even hundreds of times while with power dissipation and economic cost declined comparatively [19]. FPGA has become popular in the field of deep learning due to its fast parallel computing characteristics [20]. Recently, it has become common to deploy FPGA in data centers [21], but it is an innovative research direction to use FPGA to accelerate programs in IoT. And there is no relevant research involved in deploying FPGA to the edge. But this is an exciting study because deploying FPGA to the edge can achieve more ideal real-time performance, which is good news for applications that require real-time response.

The supply chain is a functional network chain structure, which takes the enterprise as the core, uses raw materials to make final products, and finally delivers the products to consumers through the sales network [22]. Sand-making factories play the roles of suppliers, manufacturers, warehouses, and distribution centers in the supply chain. Building an intelligent supply chain is the key to achieving intelligent management of sand factory. At present, the management of the sand factory is still in the artificial management stage, and traditional supply chain technology is still used in the management process, which inevitably has the following problems:

(1) Most sand factories are still in the traditional mode of operation. Mechanical processing of sand, sand weighing, sand type identification, vehicle access management, and charging management all require a lot of human resources. Therefore, the labor cost of the sand factory accounts for a large proportion of the operating cost of the sand factory.

(2) Scattered distribution of sand resources and long distances between different sand factories. Managers need to spend a huge amount of time and effort to manage multiple sand factories.

(3) The sale of sand is the direct economic income source of the sand factory, and the unit price of different sand types is different. At present, when the sand factory sells the sand, the identification of the sand type is carried out by manual identification, which will inevitably cause problems such as errors in the identification of the sand type and corruption. These problems will directly lead to the loss of the benefits of the sand factory.

(4) The sand factory has a large number of large-heavy industrial vehicles and equipment operating in the sand factory. Therefore, there are potential mechanical hazards that may cause construction accidents. It will increase the risk of personnel disputes and accidents.

As Industry 4.0 evolves [23], IoT technologies are commonly used in the industry. And the proposed concept of Industry 4.0 has driven the development of smart supply chains [24]. Smart supply chain is an intelligent technology and management system built within the enterprise, integrating IoT technology with modern supply chain management theories, methods, and technologies [25]. How to construct the smart supply chain is a hot topic [26, 27], and the introduction of smart supply chain technology in sand factories can promote the realization of intelligent management of sand factories.

Aiming at the existing problems in the sand factory, we used edge-computing and deep learning technology to construct a smart supply chain management system (SSCMS) for the sand factory to realize the intelligence and automation of the sand factory management. In the system, we use the deep learning model to realize the automatic identification of sand types and use edge computing to deploy the model to the edge. At the edge, we have also innovatively added the FPGA to accelerate deep learning models. The use of edge servers and the FPGA can effectively alleviate network congestion, reduce communication delay, and decrease the burden on the cloud server. The overall performance of the system has been significantly improved.

The proposed work has the following contributions:

(1) Combining cloud computing, IoT, edge computing, deep learning, FPGA technology, and modern supply chain management theories and methods to

design a SSCMS for sand factories. The system can realize the intelligence and automation of sand factory management. It is specifically manifested in intelligent identification of sand loading vehicles, intelligent identification of sand types, automatic weighing of sand weight, cloud deduction of fees, and cloud management of sand factories.

(2) Identifying sand by deep learning approach relies on several dataset, but there are no publicly available relevant data sets. To achieve accurate sand identification, we collected a large number of pictures of different sand types and created our data set for sand identification.

(3) To deploy the sand recognition model to the edge, we propose an edge-based convolutional neural networks (CNN) model. Since the computation power of edge-computing nodes is far inferior to cloud servers, we optimized the parameters of the CNN model. The models deployed to the edge can reduce the amount of required computation while maintaining high recognition accuracy.

(4) We innovatively propose deploying FPGA at the edge to accelerate deep learning models. The use of FPGA reduces the processing delay of the system. And this study is innovative and there are no related studies on this subject.

(5) A microsand factory simulation platform is designed. The platform is used to simulate the operation process of a real-life sand factory. This simulation platform allows us to verify the performance of our designed SSCMS. We evaluate our method by experiments. The results show that our designed system realizes the intelligent management of the sand factory, and all indicators have achieved satisfactory results.

The rest of this paper is presented below. In Section 2, we describe in detail the basic architecture of the system being constructed. In Section 3, we present the design of the proposed edge-based CNN model for sand identification and analyze the model. In Section 4, we introduce the setup of the simulation platform and conduct experiments. Finally, we conclude in Section 5.

2. System Design

In this section, we mainly present the system architecture and workflow of the SSCMS. The architecture is mainly consisted of five parts, that is, sand factory gate system, license plate recognition system, weighing system, sand recognition system, and cloud platform management system, as shown in Figure 1.

Since sand resources are scattered, sand factories will have divisions in different locations. There are several IoT devices in each division. If the data generated by IoT devices in the factory of all divisions are transmitted to the cloud server for processing, the processing procedure will require a very large network bandwidth and cloud computation ability. The transmission of large amounts of data also impacts the transmission of control signals in the system.

Edge computing allows the processing of data on the side closer to data sources. We have deployed edge servers in each division of the sand factory, and the edge servers in different divisions process the data generated by IoT devices in their respective divisions. The edge server only needs to send the processed results back to the cloud server. Thus, it greatly reduces data transmission and improves system performance.

A complete sand purchase process is shown in Figure 2.

First, when the sand-purchasing vehicle enters the sand factory, the license plate recognition system activates the camera to capture the license plate picture and transmits the recognized license plate number as the user's ID to the edge server.

The gate system is opened, and then the sand-purchasing vehicle enters the sand identification weighing area, the system will count the weight of the empty vehicle and transmit the weight information back to the edge server. After obtaining the weight information, the edge server will associate the empty vehicle weight with the user information. After the weighing is completed, the sand-purchasing vehicle drives to the sand loading area. Then, the sand is loaded through the automatic device.

Then the sand identification weighing area is entered again, and at this time, the sand recognition system, weighing system, and license plate identification system will operate simultaneously. The sand recognition system identifies and uploads the type of sand purchased. The weighing system measures and uploads the weight information of the sand-purchasing vehicle. The license plate recognition system identifies and uploads the vehicle's identity information. The edge server will associate the uploaded sand type information, sand weight information, and user information.

Finally, by using the empty weight of the sand-purchasing vehicle, the loaded weight of the sand-purchasing vehicle and the type of sand, the cost of this sand purchase is calculated. If the user's balance of the account is sufficient, the edge server can automatically deduct the fee for the corresponding user. After the deduction is successful, the gate system opens and the sand-purchasing vehicle can leave the sand factory.

2.1. Cloud Platform Management System. The web interface of the cloud platform is developed by XOJO software. XOJO is a cross-platform programming language and visual development interface development tool. Compared with other tools, it supports cross-platform development and can develop multiplatform applications. Through cross-compilation, you can develop Linux system and Mac OS X system applications on Windows system. In addition, you can also develop multiple types of platform programs on the same system, such as desktop applications, network programs, console programs, and iOS mobile platforms. The web interfaces development of the cloud platform uses the development function of its network program. The cloud

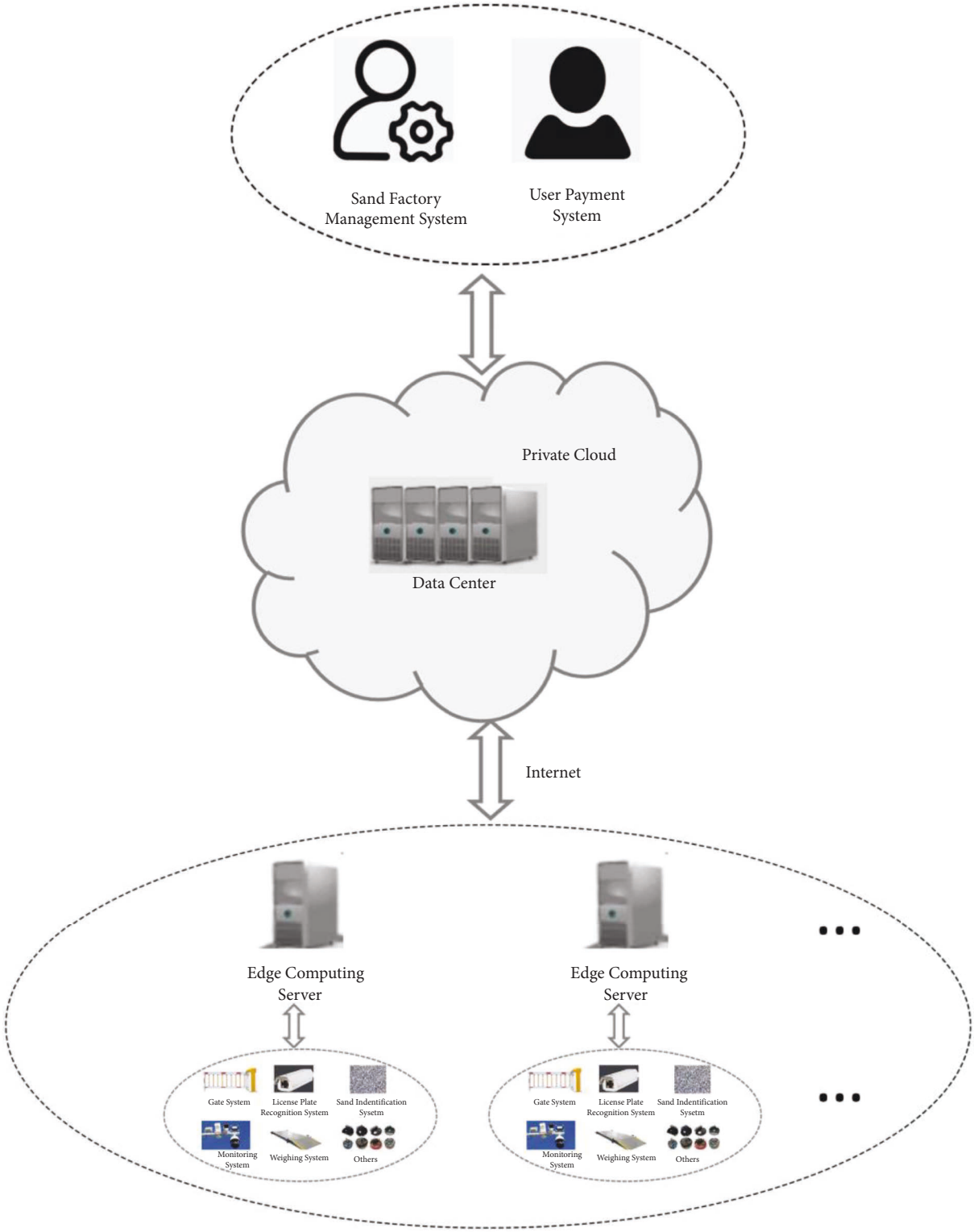

Figure 1: The system architecture of SSCMS.

platform is developed using the B/S architecture, with the client browser as the main application. This approach avoids the need for various applications on the client-side and concentrates on the core part of the system functionality implementation on the server. This approach simplifies the development, maintenance, and use of the system.

Only one browser is required to be installed on the client of this system. The edge server installs the MYSQL database and the executable program used on the edge side. They communicate with XOJO and are finally deployed on the web page and pushed to the client. This design makes the client application not restricted by the user's system

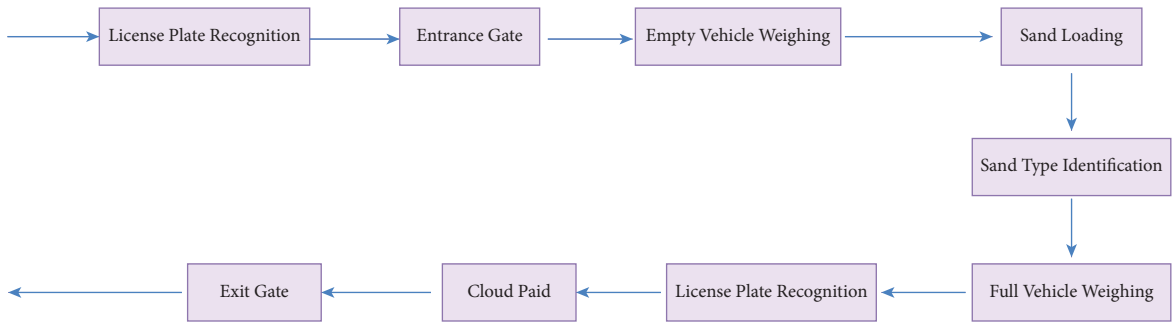

Figure 2: Sand purchase process.

platform and can be expanded on the mobile platform. Some algorithms with a relatively small amount of calculation and some database operation management can be implemented on the XOJO platform, but for algorithms with a relatively large amount of calculation, such as deep learning programs, it is necessary to use the program on the edge side to accelerate the network, that is, the program is placed in the server and it runs in the background. The cloud platform framework is shown in Figure 3.

Different from XOJO's network program, the edge-side program is not executed on the network channel but resides on the server-side in the form of an executable program group. The user sends a message through the browser, parses it through the XOJO web platform, and transmits it to the corresponding executable program. Once the program responds to this command, the client receives the corresponding result via the Internet. The platform is heterogeneity because the executable program on the edge side can be generated by any programming language, such as VS.net, Python, and MATLAB. At the same time, we designed to provide unified standard interface parameters to form an Algorithms Kernel module. Using this method, multiple developers can use different development tools to simultaneously develop programs in different programming languages, and the executable program group only needs to interact with XOJO in the end. This approach greatly shortens the development cycle of the entire cloud platform.

For some time-consuming algorithms, such as deep learning models, to ensure that the entire IoT system achieves an instant response, we use a combination of GPU + FPGA to accelerate the algorithm. FPGA is directly connected to the edge server and interacts with XOJO.

The cloud platform web interface includes the sand factory management interface and the user payment interface.

The web interface of sand factory management is designed to facilitate sand factory administrators to monitor the data of the sand factory at any time. It contains site operation, entering and exiting vehicles, the amount of sand sold on that day, the total amount of sand resources remaining on that day, the turnover of the sand factory, etc. The cloud platform web interface is shown in Figure 4 (the content in the colored area is for supplementary explanation). The administrator interface mainly includes four aspects: IoT system management, private cloud database management, user information management, and sand factory resource management. Among them, the IoT management system can manage all the IoT modules and also can view the operation of each module in real-time to achieve real-time monitoring. The database management systems can be used to check data in real-time. The user information management system can add or delete users and recharge the corresponding one. The sand factory resource management system can set the unit price of different sands, query the flow records of the sand factory, and export relevant data for verification.

The web interface of the user payment cloud platform is to provide sand factory clients with a convenient and fast way to purchase. The user payment cloud platform provides users with the option to reserve in advance the type of sand they need to purchase, the weight of the sand, and the time for arriving at the sand factory to load the sand. After the reservation is completed, the sand-purchasing vehicle can enter the sand factory for sand loading within the corresponding time. Moreover, users can also check their purchase records as well as their bill history.

2.2. License Plate Recognition System. The role of the license plate recognition system is to obtain the identification information of the sand-purchasing vehicle. In a complete sand purchase process, the sand-purchasing vehicle needs to be identified twice. The first plate recognition is to record the vehicle information of the sand-purchasing vehicle when it enters the sand factory. A second plate recognition and a second vehicle weighing are carried out when the sand-purchasing vehicle is loaded with sand. The purpose of this license plate recognition is to correlate the sand-purchasing vehicle information, the sand purchase type, and the sand-purchasing vehicle load information.

License plate recognition system mainly adopts the technology of image processing and deep learning. The procedure can be divided into three steps, namely, image preprocessing, license plate detection, and license plate recognition. The first step is to preprocess the captured images, followed by license plate localization, and character segmentation. The license plate recognition system is directly deployed on the edge server-side with reference to existing research [28].

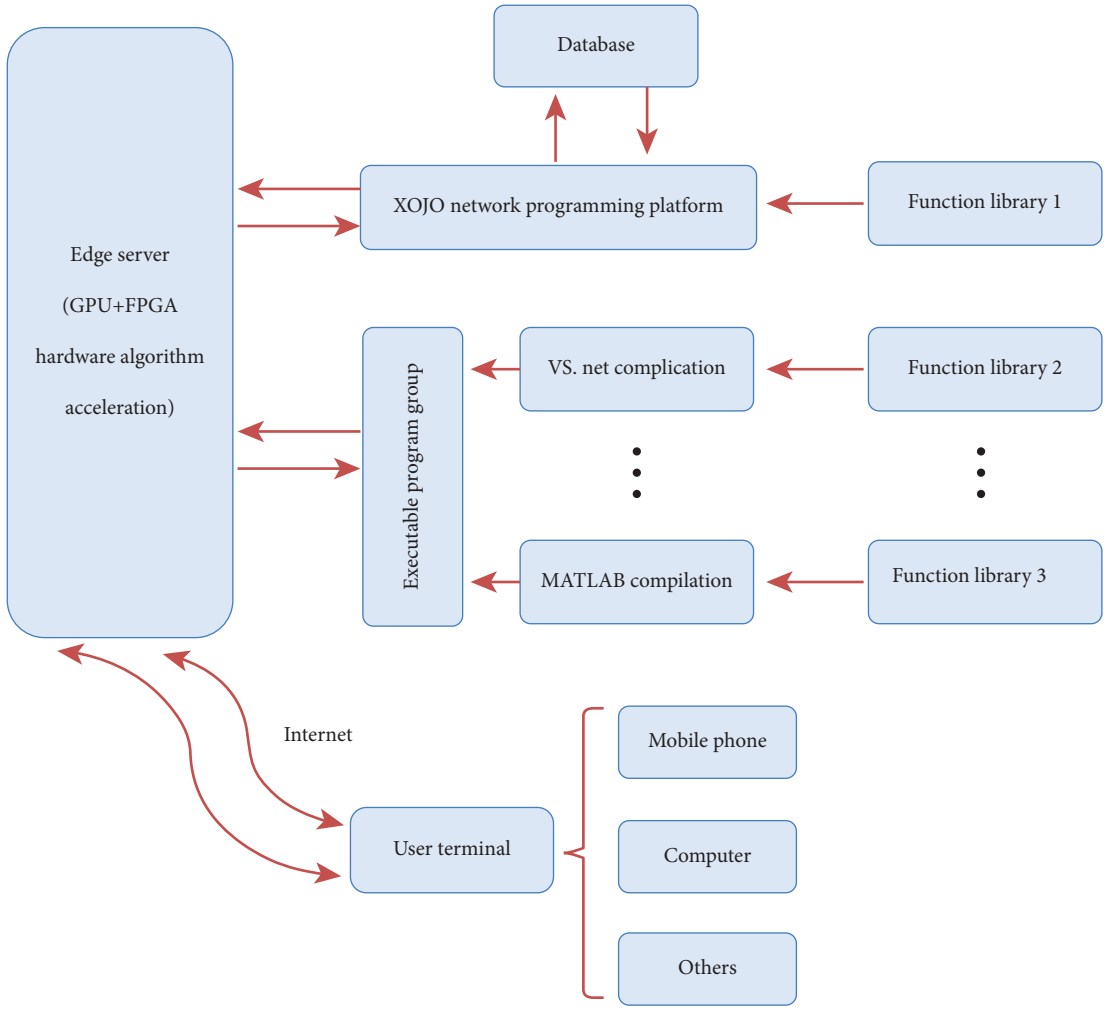

Figure 3: Cloud platform system framework.

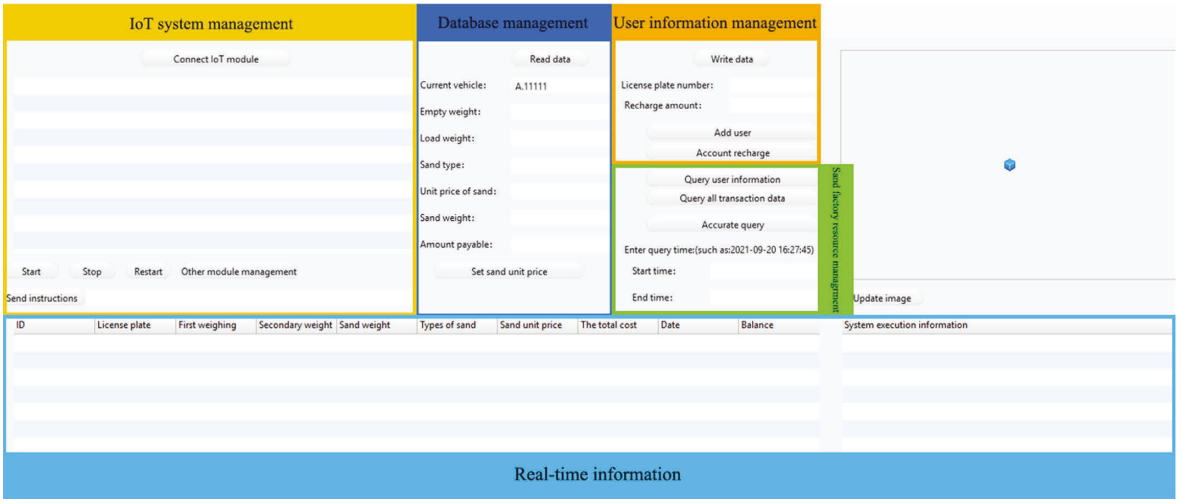

Figure 4: Web interface of sand factory management cloud platform.

2.3. Sand Weighing System. The sand weighing system mainly includes the weighbridge system and the IoT module. In a complete sand purchase process, the vehicle needs to be weighed twice. The weight when the vehicle is empty is recorded as W_0, the weight after loading with sand is recorded as W_1, and the weight of sand W is calculated as follows:

$$W = W_1 - W_0. \tag{1}$$

After the weighbridge system obtains the vehicle weight information, the relevant information needs to be transmitted to the edge server using the IoT module.

The unit prices of different sand types are saved in the cloud, and let the unit price of sand be calculated as P. The unit price of sand can be set on the server. Then the total cost of this sand purchase C is as follows:

$$C = P * W. \tag{2}$$

2.4. Sand Recognition System. Sand recognition system is to identify the type of sand. We use the CNN model to identify the type of sand. The identification of sand involves the processing of high-resolution images. If the images are transmitted to the cloud server for processing, it will be a severe challenge to the network bandwidth and will inevitably cause communication delays. The transmission of large amounts of data will affect the transmission of cloud server control signals, which will directly weaken the performance of the IoT system. Therefore, we propose an edge-based CNN model to identify the type of sand. Because the computing power of the edge server is far inferior to the cloud server, the parameters of the model are optimized. This enables us to reduce the amount of computation without losing recognition accuracy. And we put the recognition of sand in the FPGA at the edge to accelerate.

The workflow of the sand recognition system is as follows: the camera collects the sand pictures in the sand-purchasing vehicle, then transmits the pictures to the nearest edge server for picture preprocessing, and finally the pictures are preprocessed and transmitted to the FPGA for sand recognition. After the sand type is successfully identified, the FPGA will send the result back to the edge server.

2.5. Gate System. Gate system is to control the entry and exit of vehicles. For the sand-purchasing vehicles, before entering the sand factory, the vehicle information is recorded through the license plate recognition system. After that, the gate system opens the gate and releases the vehicle. When the sand-purchasing vehicle is loaded and the corresponding user's deduction is completed in the cloud, the gate system opens the gates to allow sand-purchasing vehicles to leave. At this point, the entire sand purchase process is completed. Besides, we can preload the corresponding license plate in the cloud and then automatically release the vehicles of the staff inside the factory.

3. CNN Model Design

This section mainly introduces the deep learning model design for sand recognition.

3.1. Data Collection and Preprocessing. The sand type recognition method based on deep learning has extremely high requirements for data sets. It is generally believed that the larger the dataset, the higher the recognition accuracy. However, there is no relevant available public sand dataset, so we collect sand pictures to make the dataset by ourselves.

At present, the sand factory mainly includes three types of sand. They are fine sand, coarse sand, and natural sand, respectively. Among them, natural sand is produced by natural forces, mainly rock particles, interspersed with a small amount of rock debris and mud debris sediment of rivers, lakes, and seas, and the grain size of rock particles is below 5 mm. Machine-made sand is the artificial mechanical crushing of hard and unweathered rock. The specifications of the machine-made sand are divided into three types: coarse, fine, and natural, according to the average particle size. The average particle size of coarse sand is 0.5 mm or more. The average particle size of fine sand is 0.25 mm to 0.35 mm. We collected pictures of three kinds of sand: fine sand, coarse sand, and natural sand. The representative pictures of different sands are shown in Figure 5. Figure 5(a) shows the fine sand, and the average particle size of the sand is 0.35 mm–0.25 mm, which is smaller than coarse sand and has less mud than natural sand. Figure 5(b) shows coarse sand, with an average particle size of 0.5 mm–0.35 mm. Compared with fine sand, the particle size of coarse sand is larger, and compared with natural sand, there is only a small amount of mud. Figure 5(c) shows the natural sand, the particle size is between fine sand and coarse sand and contains more mud.

The acquisition process is as follows: first, we spread the sand in the container. Second, we fixed the camera at 1.5 meters directly above the container. A different type of sand was used each time for the photographs. The final collection were 990 pictures for each type of sand.

The deep learning model used for sand recognition is deployed in the edge server, but the computation power of the edge server is far inferior to the cloud server. Therefore, we compressed the collected sand pictures to reduce the computational pressure on the edge server. Each compressed picture of sand is 256×256 pixels.

3.2. Optimal Convolutional Neural Network Structure. Deep Learning is currently the most popular machine learning method. CNN is the most common and stable technology for image classification and recognition. CNN enables images to be used as input to the network model and can automatically learn the training data. It overcomes the accumulation of errors generated by traditional manual feature extraction and achieves the extraction of higher-level features [29]. Combining the traditional CNN model with edge deployment, we propose an optimized CNN model suitable for sand classification.

(a) (b) (c)

Figure 5: Representative images of different types of sand: (a) fine sand; (b) coarse sand; (c) natural sand.

The dataset for each type of sand is 990, for a total of 2970. In the initial experiment, we randomly divided all sampled data into training, validation, and test sets in the ratio of 0.7 : 0.15 : 0.15. We set the learning rate to 0.01. With the training method of momentum stochastic gradient descent, we set the momentum parameter to 0.9, MiniBatch to 64. First of all, the number of layers of convolutional layers needs to be determined by a quantitative experiment, as it is the most important parameter that directly affects the performance of the CNN model. Generally, convolutional layers (Conv) are used in combination with rectified linear unit (ReLU) layers and batch normalization (BN) layers. Therefore, we combine them. The performance of different Conv_ReLU_BN layers is shown in Figure 6.

Figure 6 shows the effect of the number of layers of Conv_ReLU_BN on the classification accuracy and training speed of the CNN model, where ч axis represents the number of Conv_ReLU_BN layers, and y axis represents the values of classification accuracy and training speed. From the figure, it can be obtained that when the number of layers of Conv_ReLU_BN is greater than 4, the accuracy no longer fluctuates substantially; when the number of layers of Conv_ReLU_BN increases, the training time increases. Therefore, we have chosen to keep 4 convolutional layers for feature extraction, and Table 1 shows the detailed parameters.

Secondly, the number of fully connected layers (FC) needs to be determined. FC is one of the key factors affecting the performance of the CNN model. Based on 4 Conv_ReLU_BN layers, we find the optimal number of FC layers by testing the effect of different numbers of FC layers on the CNN classification results. Figure 7 shows the effect of adding 1 to 5 FC layers on the classification results of the CNN model. In the figure, the ч axis represents the number of FC layers, and the y axis represents the value of accuracy and training speed. It can be seen from the figure that when the number of FC layers is greater than 2, the accuracy rate tends to be stable and less time-consuming at this point. Therefore, 2 FC layers were selected for classification, and the detailed parameters are shown in Table 2.

In addition, learning rate tuning is also an indispensable step to establishing a CNN model. The size of the learning rate will directly affect the convergence speed of the model. To make the 6-layer CNN model (4 Conv + 2 FC) converge faster with a higher accuracy rate, we choose different learning rates for experiments to find the best learning rate.

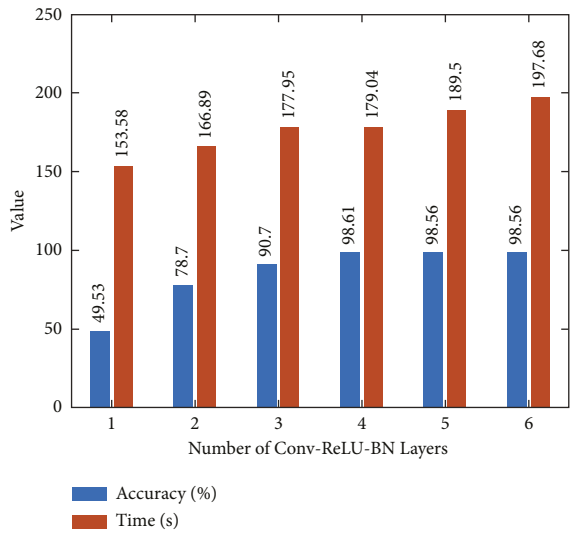

Figure 6: Optimal number of Conv_ReLU_BN layers.

Table 1: Feature extraction layers in proposed CNN structure.

Index	Layer name	Filter/pool size	No. of filters	Stride	Padding
1	Conv_ReLU_BN	5	16	1	2
	Maxpool	2		2	0
2	Conv_ReLU_BN	5	32	1	2
	Maxpool	2		2	0
3	Conv_ReLU_BN	5	64	1	2
	Maxpool	2		2	0
4	Conv_ReLU_BN	5	128	1	2
	Maxpool	2		2	0

Figure 8 shows the average result of 10 runs on the dataset. In the figure, the ч axis represents the learning rate, and the y axis represents the value of accuracy and training speed. As can be seen in Figure 8, the accuracy is maximum and the time consumed is relatively short when the learning rate is 0.01. Therefore, the optimal learning rate is determined to be 0.01.

Finally, in the experiment, we use the momentum stochastic gradient descent method. Thus, we need to determine the optimal MiniBatch. Other parameters were set as mentioned in the previous text, and we conducted ten experiments by changing the size of MiniBatch. Figure 9 shows

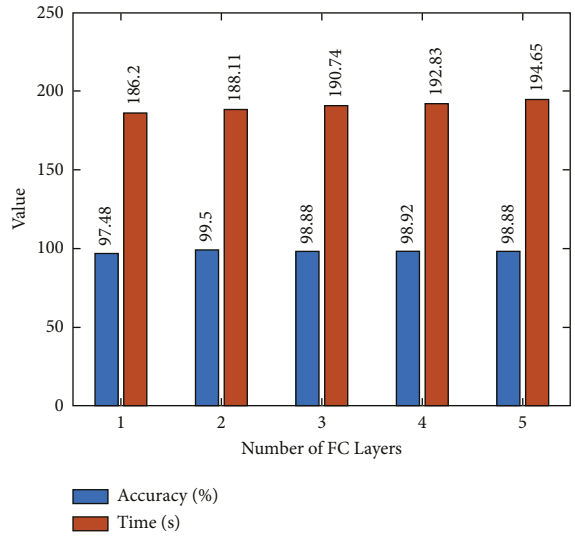

Figure 7: Optimal number of FC layers.

Table 2: Classification layers in proposed CNN structure.

Index	Layer name	Weights	Bias
5	FC_1	256×8192	256×1
6	FC_2	3×256	3×1
	Softmax		

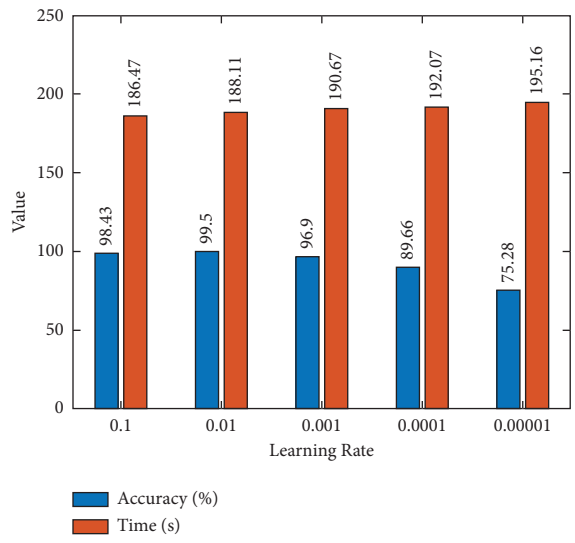

Figure 8: Optimal value of learning rate.

the average value after 10 experiments. In the figure, the ч axis represents the size of MiniBatch, and the y axis represents the value of accuracy and training speed. As we can observe from the figure, the highest accuracy and shorter time is achieved when MiniBatch is set to 64. Therefore, we determined the optimal MiniBatch size to be 64.

In summary, the optimal structure and hyperparameters of the CNN model are determined. The optimal structure is 4 Conv_ReLU_BN layers, 2 FC layers, and softmax layer; the learning rate and MiniBatch are 0.01 and 64, respectively.

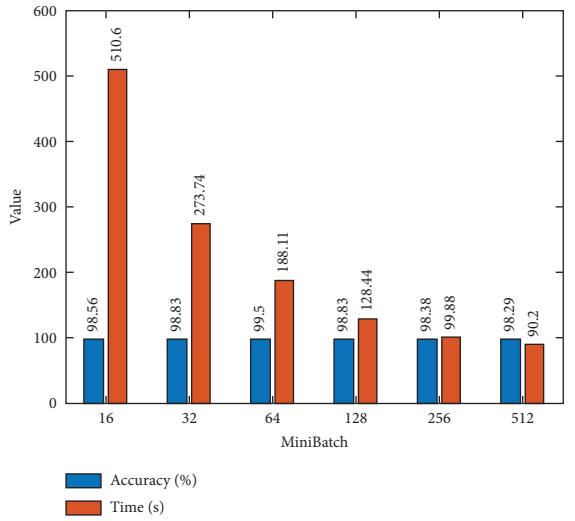

Figure 9: Optimal value of MiniBatch.

The training results of the optimal CNN model are shown in Figure 10.

As shown in Figure 10(a), the training accuracy of our CNN model increases with the number of iterations. Moreover, since 64 data are randomly selected at each update time, the curve fluctuates significantly before leveling off. In Figure 10(b), the training loss of the proposed CNN model decreases as the number of iterations increases and finally tends to zero. Figure 10 shows that the hyperparameters we have chosen are effective and they ensure the convergence of CNN.

3.3. Model Analysis. Generally, the number of convolutional layers will directly affect the model complexity. Then, the model complexity will directly affect the computational requirements in the model training process. And usually, the convolutional layer is followed deployed with the corresponding pooling layer. The total calculation time of the model can be calculated according to the number of convolutional layers and pooling layers, that is

$$T = \sum_{i=1}^{n} \left[N_c \left(L_{K_i}^2 + 1 \right) L_{I_i}^2 + \left(\frac{L_{I_{i+1}}}{L_{P_i}} \right)^2 \right] N_{F_i}, \tag{3}$$

where T represents the total calculation time, i represents the number of inputs, N_c represents the input image's number of channels, L_{K_i} represents the length of the convolution kernel, L_{I_i} represents the length of the input feature, L_{P_i} represents the size of the pooling layer, and N_{F_i} represents the number of convolution filters.

From (3), the time complexity of the model can be obtained as follows:

$$O\left(\sum_{i=1}^{n} L_{K_i}^2 L_{I_i}^2 N_{F_i} \right). \tag{4}$$

We compare the designed model with the popular LeNet-5 model [30] and the VGG-16 model [31]. The convolutional layers of the LeNet-5 model and VGG-16

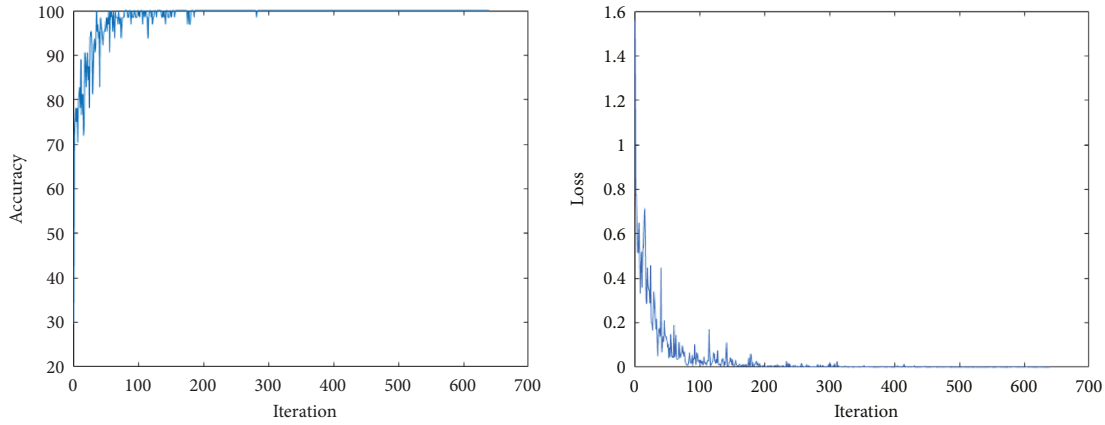

(a) (b)

Figure 10: Training results of the optimal CNN model: (a) training accuracy; (b) training loss.

model are 6 and 16, respectively, while the model proposed in this paper uses only 4 convolutional layers. According to formula 3, the larger the number of convolutional layers, the greater the computational requirements of the model, so the model we propose requires the lowest computational requirements.

3.4. FPGA Design. After the model is determined, we use the FPGA to accelerate the designed deep learning model. The FPGA we used in the experiment was the Zynq UltraScale + MPSoC series board from Xilinx. The development process using the FPGA acceleration is shown in Figure 11.

After obtaining the model parameter file, we need to use Vitis AI Optimizer to trim the redundant connections in the neural network and reduce the overall required operations. Of course, this step is not necessary. After the model is simplified, the Vitis AI Quantizer tool needs to be used to quantify the model parameters, that is, floating-point to fixed-point. Vitis AI Quantizer can reduce computational complexity without loss of prediction accuracy. After the floating-point number is fixed-point, the network model requires less memory bandwidth, so it will provide faster speed and higher power efficiency than the floating-point model. Vitis AI Compiler compiles the quantized model into an efficient instruction set and data stream and can also perform complex optimizations, such as layer fusion, instruction scheduling, and reuse on-chip memory as much as possible. Vitis AI Profiler can conduct in-depth analysis on the efficiency and utilization of AI inference implementation. It can track function calls and running time and can also collect hardware information, including CPU, deep learning processing unit (DPU), and memory utilization. Vitis AI Library is a set of high-level libraries and APIs, which are built for efficient AI inference using the DPU. Vitis AI Library provides an easy-to-use and unified interface by encapsulating many efficient and high-quality neural networks. The Xilinx Runtime library enables applications to use a unified high-level running API at the edge, making edge deployments seamless and efficient.

4. Results

This section describes the relevant experiments and evaluates and analyzes the experimental results.

4.1. Experiment Platform. \We designed a microsand factory for simulating a real-life sand factory, as shown in Figure 12. In addition, we verified the functionality of the system using the designed SSCMS simulation platform.

In the simulation platform, we used the smart sand car to simulate the sand-purchasing vehicle in practical operation. As we discussed previously in Section 2, the red dotted areas in Figure 12 are the corresponding system modules for the simulation. In addition, all our subsystems use Wi-Fi wireless communication modules for communication with the server. The appearance of the wireless communication module used is shown in Figure 13.

4.2. System Verification. In this section, we perform functional tests of the SSCMS deployed in a microsand factory simulation platform. The configuration of the edge server is 2.5 GHz, 24-core CPU frequency, 32 G memory, and NVIDIA GeForce GTX 1650, with 8 T storage. Conducting the first step of the experiment, we connect the FPGA to the edge server, open the web interface of the sand factory management cloud platform on the edge server, run the executable program group, and connect the relevant IoT modules. When the smart sand car drives to the license plate recognition area, the license plate recognition system will capture the license plate information and verify the vehicle identity. The empty vehicle will be weighed after successful identity verification. The relevant data of the weighing will be associated with the license plate information on the server. At this time, the web interface of the sand factory management cloud platform is shown in Figure 14.

Next, after the smart sand car is loaded with sand, it will go to the sand identification weighing area to identify the type of sand. Then the edge server preprocesses the acquired

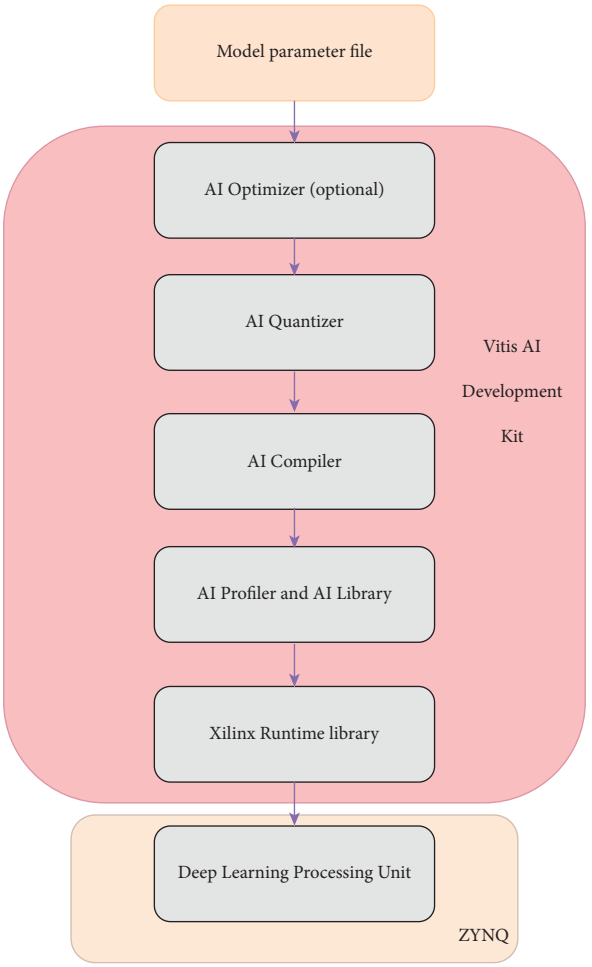

Figure 11: FPGA development process.

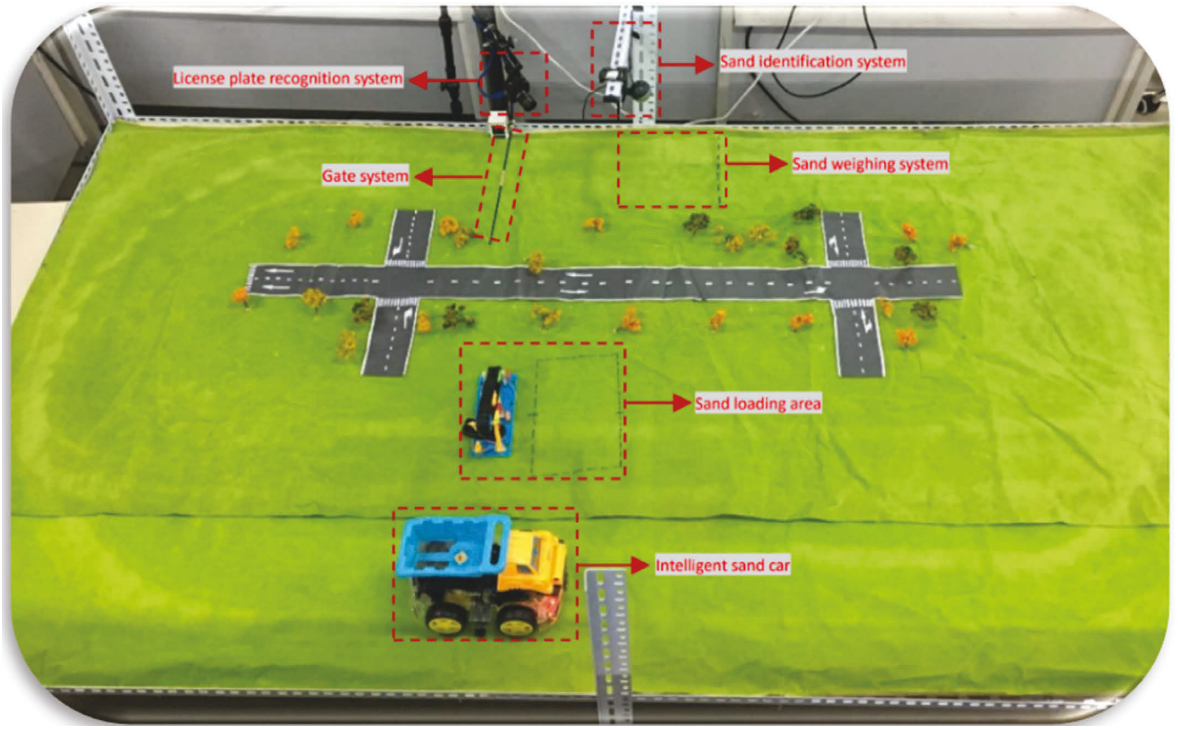

Figure 12: Microsand factory simulation platform.

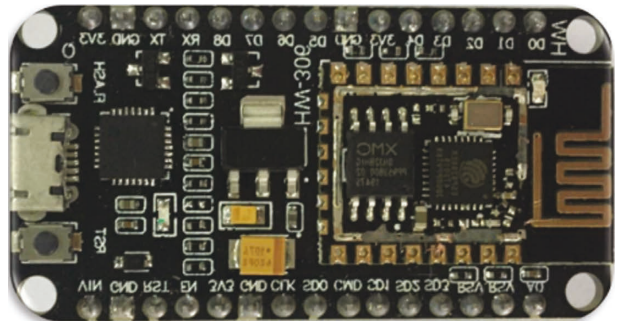

Figure 13: Wi-Fi wireless communication module.

Figure 14: The web interface of empty vehicle status.

sand image, and the preprocessed image will be transferred to the FPGA, and the FPGA will use the designed CNN model to accelerate the identification of the sand type. At this time, the edge server will recognize the license plate and weigh the sand. Finally, vehicle information, sand type, and sand weight will be associated on the edge server-side. The unit price of sand can be set on the edge server-side, and different unit prices can be set for edge servers located in different locations. Using (1) and (2), we calculate the cost of this purchase and display it in the web-side interface of the cloud platform.

We set the unit price for three different types of sand. The unit prices of coarse sand, fine sand, and natural sand were set in the sever to 80, 100, 70, respectively. The operating results are shown in Figures 15–17 respectively. The edge server will calculate the cost of this purchase and then deduct the fee for the corresponding user. After the fee is successfully deducted, the gate will open to let the smart sand car drive out.

In the web-side interface of the sand factory management cloud platform, we can access the user's identity information. Including license plate number, the weight of empty vehicle, weight of loaded vehicle, the weight of sand, type of sand, and the cost of this purchasing. We can obtain a picture of the captured sand from the right of the interface. From the figure, the system can accurately identify different types of sand and their weight information. Eventually, the system will calculate the total cost accurately based on the set unit price of sand.

To test the performance of the built system, we run the system 100 times. Moreover, we have conducted statistic accuracy on sand recognition, license plate recognition, and sand weighing. In these 100 experiments, the type of sand, the license plate number, and the weight of the sand were changed for each experiment. After 100 experiments, the results are shown in Table 3.

In Table 3, the accuracy rate of sand recognition, license plate recognition, and sand weighing of our system is all up to 98 and above.

In our paper, the use of edge servers makes it possible to process data in each division, and the use of the FPGA relieves the computing pressure of the edge server and reduces the system latency. After the data is processed at the edge, it is only necessary to transmit the processing results back to the cloud server. The sand recognition system and the license plate recognition system use deep learning models. The time consumed by model inference is a key metric for evaluating a system. The use of edge servers can significantly reduce data transfer, thereby reducing the time consumed by data transfer. Therefore, we deploy the models to the edge server to avoid unnecessary image transmission. Similar to the recognition accuracy experiments in the previous section, we run the deep learning model system deployed to the edge 100 times. We count the running time of the sand recognition and license plate recognition system. The average value of the results are shown in Table 4.

Table 4 illustrates the very short recognition time of this deep learning model deployed to the edge. Compared to the model deployed to the cloud server, this method reduces the

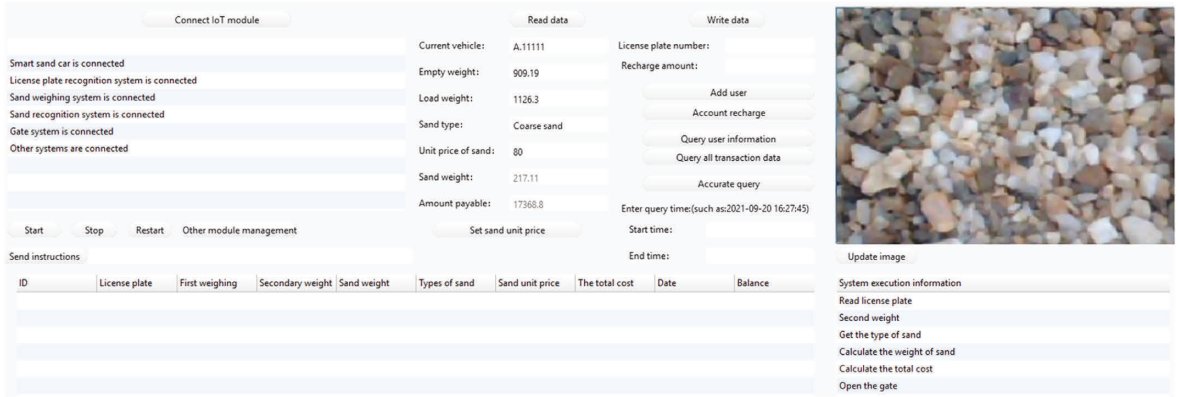

Figure 15: Web interface for coarse sand recognition.

Figure 16: Web interface of fine sand recognition.

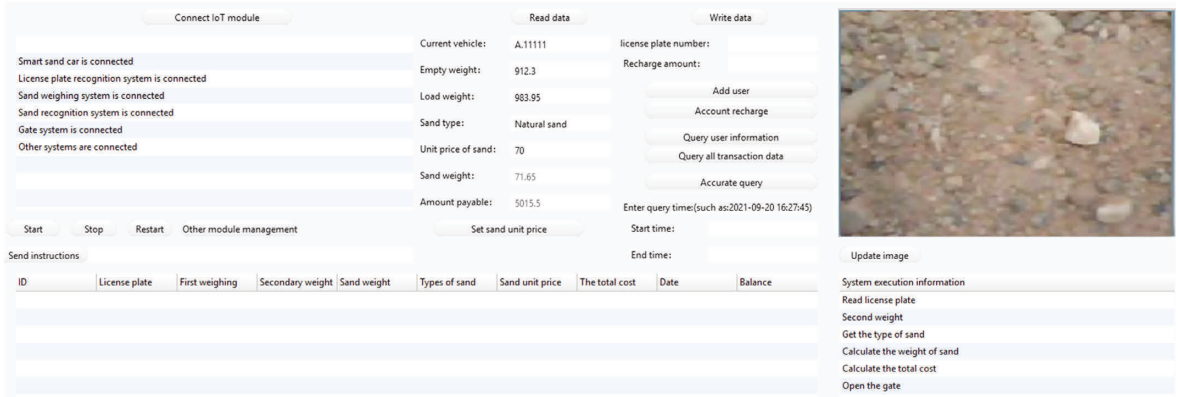

Figure 17: Web interface of natural sand recognition.

Table 3: System recognition accuracy.

Function	Accuracy (%)
Sand recognition	98
License plate ecognition	98
Sand weight	99.3

Table 4: System recognition time.

Function	Time (s)
Sand recognition	0.022
License plate recognition	0.073

time consumed by the image transfer. The recognition of sand is accelerated in the FPGA, and the license plate recognition is performed in the edge server. In the table, the sand type recognition time is significantly lower than the license plate recognition time because we use the edge server combined with FPGA to accelerate the sand type recognition, while the license plate recognition only uses the edge server for inference. The experimental results show that the use of FPGA can greatly reduce the computing pressure of edge servers and improve computing performance.

In summary, the SSCMS we have constructed has enabled intelligent and automated management of the sand factory, with satisfactory results in all indicators. Different from the cloud server–based model, our designed edge-based model avoids the time consumed by a large amount of data transmission, thus improving the performance of the entire system. Compared with traditional supply chain management, the constructed smart supply chain improves the operation quality and efficiency of the sand factory. Compared with the traditional supply chain, the constructed smart supply chain has the following advantages: stronger technology penetration, stronger visualization, stronger information integration, stronger extensibility, stronger collaboration, and stronger agility.

5. Conclusion

This paper addresses the drawbacks of the traditional supply chain and constructs a SSCMS to realize the intelligent management of sand factories. It is specifically manifested in intelligent identification of sand loading vehicles, intelligent identification of sand types, automatic weighing of sand weight, cloud deduction of fees, and cloud management of sand factories. Along the supply chain, we build the optimal deep learning model, which achieves automatic sand identification, avoiding the drawbacks of manual identification and improving the quality of sand factory operations. In addition, considering that edge-computing technology can reduce the transmission of a large amount of data, thus serving to relieve the pressure on network bandwidth and reduce system latency, we make full use of the superiority of edge-computing technology to effectively improve the operational efficiency of the sand factory. A sand factory simulation platform was established to verify the performance of the system. Experiments show that all indicators of the designed system have achieved satisfactory results. In general, compared with traditional supply chain management, the constructed smart supply chain improves the quality and efficiency of sand factory operations.

Recently, we have also deployed the designed system to the actual sand factory for testing. In reality, the applicability of our model has also been verified and we achieved a satisfactory result both in accuracy and speed. In the next research, we will make more efforts in promoting the practical application of the system and continue to improve the system for new problems.

Data Availability

The data are derived from Guangxi Xinhao Construction Engineering Co., Ltd, Nanning, Guangxi, China, and Yongkai Construction Group Co., Ltd, Nanning, Guangxi, China.

Conflicts of Interest

The authors declare that they have no conflicts of interest.

Acknowledgments

This work is supported by the Science and Technology Key Projects of Guangxi Province (Grants no. 2020AA21077007 and Z20210069) and the Innovation Project of Guangxi Graduate Education YCSW2022042.

References

[1] D. Silva, A. Heideker, I. D. Zyrianoff et al., "A management architecture for IoT smart solutions: design and implementation," *J NetwSyst Manage*, vol. 30, no. 2, p. 35, 2022.

[2] T. Lo'ai, M. Fadi, T. Mais, Q. Muhannad, and A. A. E.-L. Ahmed, "Edge enabled IoT system model for secure healthcare," *Measurement*, vol. 192, Article ID 110792, 2022.

[3] H. B. Mahajan, A. S. Rashid, A. A. Junnarkar et al., "Integration of healthcare 4.0 and blockchain into secure cloud-based electronic health records systems," *ApplNanosci*, Springer, Berlin/Heidelberg, Germany, 2022.

[4] A. A. Ahmed, A. C. Mihaela, A. J. Brimicombe, S. A. Ghorashi, A. Baravalle, and P. Falcarin, "Data quality challenges in large-scale cyber-physical systems: A systematic review," *Information Systems*, vol. 105, Article ID 101951, 2022.

[5] W. Zhang, W. Z. Hu, and Y. G. Wen, "Thermal comfort modeling for smart buildings: a fine-grained deep learning approach," *IEEE Internet of Things Journal*, vol. 6, no. 2, pp. 2540–2549, 2019.

[6] J. Gao, X. G. Wang, and W. M. Yang, "SPSO-DBN based compensation algorithm for lackness of electric energy metering in micro-grid," *Alexandria Engineering Journal*, vol. 61, no. 6, pp. 4585–4594, 2022.

[7] H. Wang, X. Wen, Y. Xu, B. Zhou, J. Peng, and W. Liu, "Operating state reconstruction in cyber physical smart grid for automatic attack filtering," *IEEE Transactions on Industrial Informatics*, vol. 18, no. 5, pp. 2909–2922, 2022.

[8] C. Celes, A. Boukerche, and A. A. F. Loureiro, "Mobility trace analysis for intelligent vehicular networks: Methods, models, and applications," *ACM Computing Surveys*, vol. 54, no. 3, pp. 1–38, 2022.

[9] T. Baker, M. Asim, H. Samwini, N. Shamim, M. M. Alani, and R. Buyya, "A blockchain-based Fog-oriented lightweight framework for smart public vehicular transportation systems," *Computer Networks*, vol. 203, Article ID 108676, 2022.

[10] F. Zhou, L. Feng, M. Kadoch, P. Yu, W. Li, and Z. Wang, "Multiagent RL aided task offloading and resource management in wi-fi 6 and 5G coexisting industrial wireless environment," *IEEE Transactions on Industrial Informatics*, vol. 18, no. 5, pp. 2923–2933, 2022.

[11] T. Li, Y. Ma, K. Yoshikawa, O. Nomura, and T. Endoh, "Energy-efficient convolution module with flexible bit-adjustment method and ADC multiplier architecture for industrial IoT," *IEEE Transactions on Industrial Informatics*, vol. 18, no. 5, pp. 3055–3065, 2022.

[12] C. W. Tian, L. K. Fei, W. Zheng, Y. Xu, W. Zuo, and C. W. Lin, "Deep learning on image denoising: an overview," *Neural Networks*, vol. 131, pp. 251–275, 2020.

[13] M. Esmail Karar, A. H. Abdel-Aty, F. Algarni, M. Fadzil Hassan, M. Abdou, and O. Reyad, "Smart IoT-based system for detecting RPW larvae in date palms using mixed depthwise convolutional networks," *Alexandria Engineering Journal*, vol. 61, no. 7, pp. 5309–5319, 2022.

[14] Q. Liu, T. Xia, L. Cheng, M. van Eijk, T. Ozcelebi, and Y. Mao, "Deep reinforcement learning for load-balancing aware network control in IoT edge systems," *IEEE Transactions on Parallel and Distributed Systems*, vol. 33, no. 6, pp. 1491–1502, 2022.

[15] N. Krishnaraj, M. Elhoseny, M. Thenmozhi, M. M. Selim, and K. Shankar, "Deep learning model for real-time image compression in Internet of Underwater Things (IoUT),"

Journal of Real-Time Image Processing, vol. 17, no. 6, pp. 2097–2111, 2020.

[16] X. Wang, Z. Ning, L. Guo, S. Guo, X. Gao, and G. Wang, "Online learning for distributed computation offloading in wireless powered mobile edge computing networks," *IEEE Transactions on Parallel and Distributed Systems*, vol. 33, no. 8, pp. 1841–1855, 2022.

[17] G. Premsankar, M. Di Francesco, and T. Taleb, "Edge computing for the Internet of Things: A case study," *IEEE Internet of Things Journal*, vol. 5, no. 2, pp. 1275–1284, 2018.

[18] H. Li, K. Ota, and M. X. Dong, "Learning IoT in edge: Deep learning for the Internet of Things with edge computing," *IEEE Network*, vol. 32, no. 1, pp. 96–101, 2018.

[19] L. Bustio-Martínez, R. Cumplido, M. Letras, R. Hernandez-Leon, C. Feregrino-Uribe, and J. Hernandez-Palancar, "FPGA/GPU-based acceleration for frequent itemsets mining: A comprehensive review," *ACM Computing Surveys*, vol. 54, no. 9, pp. 1–35, 2022.

[20] H. Cho, J. Lee, and J. Lee, "FARNN: FPGA-GPU hybrid acceleration platform for recurrent neural networks," *IEEE Transactions on Parallel and Distributed Systems*, vol. 33, no. 7, pp. 1725–1738, 2022.

[21] Z. Zhu, A. X. Liu, F. Zhang, and F. Chen, "FPGA resource pooling in cloud computing," *IEEE Transactions on Cloud Computing*, vol. 9, no. 2, pp. 610–626, 2021.

[22] X. L. Wang, Y. Y. Qiu, J. Chen, and X. Hu, "Evaluating natural gas supply security in China: An exhaustible resource market equilibrium model," *Resources Policy*, vol. 76, Article ID 102562, 2022.

[23] F. Siqueira and J. G. Davis, "Service computing for industry 4.0: State of the art, challenges, and research opportunities," *ACM Computing Surveys*, vol. 54, no. 9, pp. 1–38, 2022.

[24] N. Kazantsev, G. Pishchulov, N. Mehandjiev, P. Sampaio, and J. Zolkiewski, "Investigating barriers to demand-driven SME collaboration in low-volume high-variability manufacturing," *Supply Chain Management: International Journal*, vol. 27, no. 2, pp. 265–282, 2022.

[25] S. K. Sardar, B. Sarkar, and B. Kim, "Integrating machine learning, radio frequency identification, and consignment policy for reducing unreliability in smart supply chain management," *Processes*, vol. 9, no. 2, p. 247, 2021.

[26] N. Azizi, H. Malekzadeh, P. Akhavan, O. Haass, S. Saremi, and S. Mirjalili, "IoT-Blockchain: Harnessing the power of Internet of thing and blockchain for smart supply chain," *Sensors*, vol. 21, no. 18, p. 6048, 2021.

[27] S. E. Chen, S. Brahma, J. Mackay, C. Cao, and B. Aliakbarian, "The role of smart packaging system in food supply chain," *Journal of Food Science*, vol. 85, no. 3, pp. 517–525, 2020.

[28] H. Wang, Y. Li, L. M. Dang, and H. Moon, "Robust Korean license plate recognition based on deep neural networks," *Sensors*, vol. 21, no. 12, p. 4140, 2021.

[29] X. L. Zhang, M. L. Shen, X. Li, and F. Feng, "A deformable CNN-based triplet model for fine-grained sketch-based image retrieval," *Pattern Recognition*, vol. 125, Article ID 108508, 2022.

[30] W. Imen, M. Amna, B. Fatma, S. Fatma Ezahra, and N. Masmoudi, "Fast Hevc intra-CU decision partition algorithm with modified Lenet-5 and alexnet," *Signal, Image and Video Processing*, vol. 16, 2022.

[31] D. Tiwari, M. Dixit, and K. Gupta, "Deep multi-view breast cancer detection: A multi-view concatenated infrared thermal images based breast cancer detection system using deep transfer learning," *Traitement du Signal*, vol. 38, no. 6, pp. 1699–1711, 2021.

Hindawi
Scientific Programming
Volume 2022, Article ID 4794073, 10 pages
https://doi.org/10.1155/2022/4794073

Research Article

Corresponding Intelligent Calculation of the Whole Process of Building Civil Engineering Structure Based on Deep Learning

Qian Liu,[1] Tao Liu,[2] Weikang Zhang,[3] and Fang Zhang [4]

[1]*Anhui Vocational and Technical College, Hefei 230061, Anhui, China*
[2]*Qing Jian Group Co., Ltd, Qingdao 266000, Shandong, China*
[3]*Wanjiang University of Technology, Ma'anshan 243000, Anhui, China*
[4]*College of Civil Engineering, Shaoxing University, Shaoxing 312000, Zhejiang, China*

Correspondence should be addressed to Fang Zhang; zhangfang@usx.edu.cn

Received 18 July 2022; Revised 8 August 2022; Accepted 16 August 2022; Published 6 October 2022

Academic Editor: Lianhui Li

This study proposes the first fully deep learning-based structural response intelligent computing framework for civil engineering. For the first time, from the data side to the model side, the structural information of the structure itself and any loading system is comprehensively considered, which can be applied to materials, components, and even structures, system and other multi-level mechanical response prediction problems. First, according to the characteristics of structural calculation scenarios, a unified data interface mode for structural static characteristics is formulated, which preserves the original structural information input and effectively reduces manual intervention. On this basis, an attention mechanism and a deep cross network are introduced, and a structural static feature representation learning model PADCN is proposed, which can take into account the memory and generalization of structural static features, and mine the coupling relationship of different structural information. Then, the PADCN model is integrated with the dynamic feature prediction model Mechformer and connected with the designed general data interface to form an end-to-end data-driven structural response intelligent computing framework. In order to verify the validity of the framework, numerical experiments were carried out with the steel plate shear wall structure as the carrier, in which a data augmentation algorithm suitable for the field of structural calculation was proposed to alleviate the problem of lack of structural engineering data. The results show that the deep learning model based on this framework successfully predicts the whole-process nonlinear response of specimens with different structures, the simulation accuracy is better than that of the fine finite element model, and the computational efficiency exceeds the traditional numerical method by more than 1000 times, achieving a qualitative improvement. It is proven that the intelligent computing framework has excellent accuracy and efficiency.

1. Introduction

Deep learning is the product of a new round of scientific and technological revolution and industrial transformation. It permeates all aspects of human social activities and production activities. Intelligent machines and equipment will definitely replace human large-scale manual labor and work in extremely harsh environments. In the field of civil engineering, artificial intelligence technology is deeply integrated into the entire life cycle process of architectural planning, design, construction, and operation, profoundly changing the development of civil engineering, and comprehensively improving the level of mechanization, automation, informatization, and intelligence [1]. The use of machine learning in the architectural planning phase is a new approach. Machine learning is at the heart of artificial intelligence, improving optimization algorithms based on data and previous experience through machine learning of the existing surrounding environment, geological conditions, objective factors, and needs of big data such as human and traffic behavior, combined with virtual reality situation reproduction technology, to create a new model of planning and design, and to avoid possible errors in reality, providing a greener building environment to achieve intelligent planning [2].

The whole world is working hard on the industrial transformation of the new generation of information

technology, modern manufacturing, and producer services. Internationally, in 2012, Germany launched the "Industry 4.0 Plan" focusing on "smart factories." In December 2016, the United Kingdom published "Artificial Intelligence: Opportunities and Implications for Future Decision Designation" [3]. France released its Artificial Intelligence Strategy in March 2017. Japan has designated 2017 as the first year of artificial intelligence to promote the construction of a "super-intelligent society 5.0." In 2018, the United States released a national strategy for artificial intelligence. China is one of the countries with the earliest and fastest AI action in the world. In July 2015, the State Council issued the "Guiding Opinions on Actively Promoting the "Internet" Action," which clearly listed "Internet + AI" as a key action. On July 20, 2017, the State Council issued the "New Generation Artificial Intelligence Development Plan," which clearly pointed out that artificial intelligence is the core technology of a new round of scientific and technological revolution and industrial transformation. Compared with other industries, although both steel (steel structure) and concrete (concrete engineering) are products of industrialization, the degree of mechanization, automation, intelligence, and informatization of infrastructure is still relatively low. Artificial intelligence technology will permeate all aspects of human social activities and production activities, and human large-scale manual labor and work in harsh environments will be replaced by machines or robots. In the field of civil infrastructure, artificial intelligence technology deeply integrates the whole life cycle of civil infrastructure planning, design, construction, and maintenance, and profoundly changes the development of civil engineering [4].

Building Information Modeling plays an extremely important role in the design phase. BIM technology is a data-based tool for engineering design, construction, and management. By applying BIM technology, virtual reality, cloud computing, and other technologies, it can eliminate design problems such as mistakes, omissions, and defects, reduce the cost of simulation analysis and optimization calculation of design schemes, and effectively to shorten the construction period, improve the visualization level of the design results, and significantly improve the design efficiency and quality [5]. For example, the data from the Shanghai Center project survey show that the use of BIM technology can eliminate 40% of engineering changes, eliminate 90% of drawing errors, reduce rework by 60%, and shorten the construction period by 10%, greatly improving project benefits.

2. Basic Research Fields of Artificial Intelligence

Four basic research areas: natural language processing, computer vision, speech recognition, and cross-cutting areas.

2.1. Natural Language Processing. Natural Language Processing (NLP) is the processing of human-specific natural language by a computer as a medium, so that computers can "process" and "understand" natural language like humans [6]. In the field of civil engineering, NLP has shown great application prospects from basic semantic similarity, and dependency syntax analysis to applied human-computer interaction, report analysis, etc. It can be transformed into unstructured risk information using NLP. The construction organization plan information is transformed into structured information, so as to mine the tacit knowledge (such as dangerous objects, dangerous locations, accident causes, and accident types) of the daily documents of civil engineering construction projects [7].

In 2016, Tixier et al. proved that the use of NLP can eliminate reporting errors caused by manual information analysis. Using the NLP system can automatically scan and quickly analyze a large number of unstructured reports with an accuracy rate of over 95%. We obtained a large number of reliable structured data sets from the information report database, so as to extract new safety information and improve project safety management; in 2018, Wang Fei et al. reviewed the development of natural language processing driven by deep learning and believed that deep learning promoted natural language advances in processing and natural language processing to provide broader application prospects for deep learning; in 2019, Kim et al. proposed an NLP-based knowledge management system for construction accident cases, as shown in Figure 1. In this system, the information retrieval model can be used to query accident cases that are more than 97% related to user intentions, and the information extraction model can be used to automatically analyze tacit knowledge in accident cases to achieve efficient risk management; in 2020, Li Zhoujun et al. proved that static and dynamic pretraining technology combs new pretraining methods including BERT and XLNet and gives the future development direction.

Based on the current research status, the research depth and application scope of NLP are still relatively low [8]. First of all, it is manifested in the poor generality of the thesaurus in the construction field, which leads to the low quality of file preprocessing, which will affect the text data segmentation and part-of-speech tagging in the NLP process. Procedures adversely affect; then there is a limited formulation of information extraction rules, that is, in the field of civil engineering; it is difficult to obtain all project data (such as project contracts, etc.), making it difficult to develop all possible rules for information extraction; In addition, NLP, the deep learning training model, is related to local languages. The same model cannot process text information in different languages, so effective transfer learning cannot be carried out. Finally, the current NLP is mostly used in the construction stage, while the application in the design, maintenance, and other phases is carried out in the subsequent phases. It leads to low efficiency and quality of document management in the whole life cycle of civil engineering [9].

2.2. Computer Vision. Computer vision uses an imaging system instead of the visual organ as an input sensing means, and an intelligent algorithm instead of the human brain as a

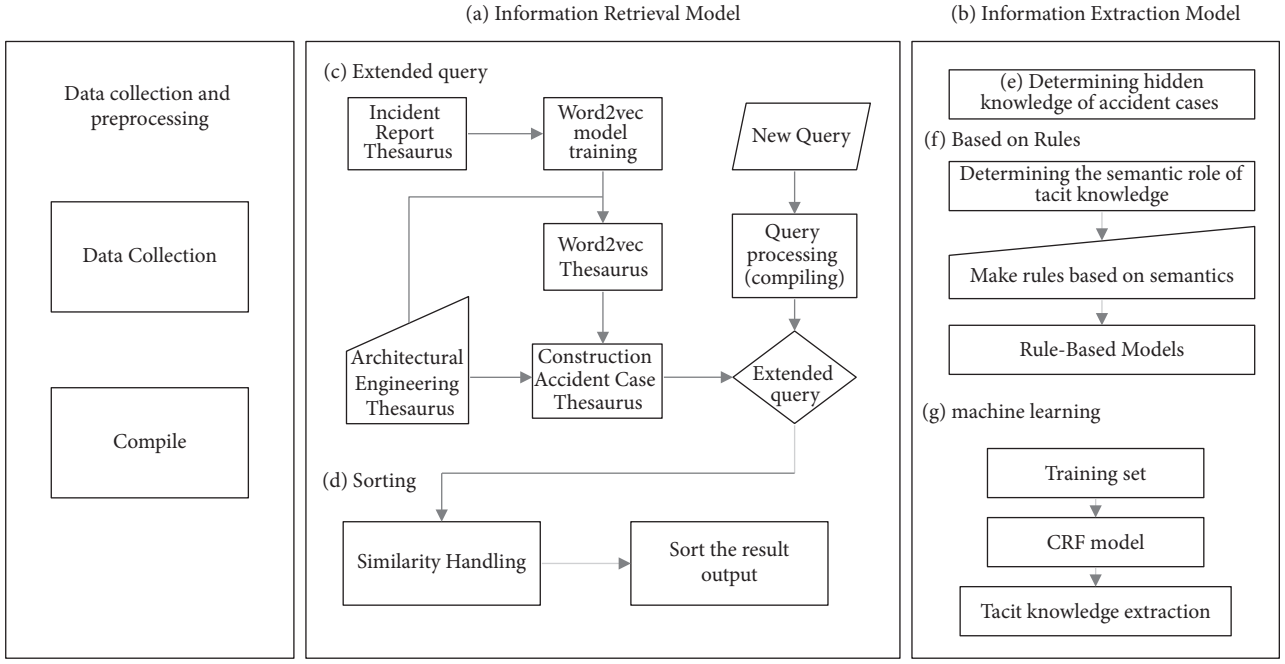

Figure 1: Construction accident case knowledge management system.

processing and analysis hub, extracting symbolic and digital information from images and videos for target recognition, detection, and tracking, and finally. It enables computers to "observe" and "understand" the world through vision like humans [10]. Computer vision has received a lot of research in the field of civil engineering in concrete crack detection, structural damage identification, construction site safety monitoring, etc. and has a very broad application prospect [11].

In 2011, Zaurin et al. proposed the use of computer vision for health monitoring of bridge structures, combining images and videos with computer vision technology to detect, classify and track different vehicles, and use sensor data to determine the standardized response of bridge structures; in 2015, Seo summarized the computer vision-based construction site safety and health monitoring methods, divided the previous computer vision research into three categories: target monitoring, target tracking, and action recognition, and proposed a general framework for computer vision-based safety and health monitoring; in 2018, Han Xiaojian et al. used computer vision technology to conduct research on crack detection on concrete surfaces and established a deep convolutional neural network crack recognition model that can automatically locate cracks and obtain crack widths from images, with a recognition accuracy of over 98%; in 2020, Zhou et al. proposed that a noncontact automatic identification method of vehicle load based on computer vision technology and deep learning algorithm is proposed, and 8624 vehicle image data sets are established and deep convolutional neural network training is carried out. Finally, transfer learning is combined with the general features extracted by ImageNet, and the recognition degree under the reinforcement learning strategy can reach up to 98.17%; in 2020, Song Yanfei and others proposed a three-dimensional model reconstruction method of the space grid structure using binocular stereo vision technology and image recognition technology, and passed the actual test of the grid model to verify the feasibility of the method [12].

With the development of software and hardware technologies such as parallel computing, cloud computing, big data, and deep learning, computer vision technology has been continuously improved, but there are still many technical challenges and application problems at this stage [13]. For example, the research of computer vision in structural health monitoring is still in its infancy. How to reduce errors caused by hardware factors, algorithm factors, environmental factors, etc. is an important research direction in the future. How to improve the application efficiency and reliability of computer vision is a follow-up research focus; in addition, computer vision has achieved good results in detecting whether construction workers wear safety helmets, but how to trigger the alarm system and human-machine coupling in later applications needs further research.

2.3. Speech Recognition. Speech recognition is a process in which the computer recognizes and understands the input speech signal and converts it into text output, so that the computer can have the "hearing" function like a human being.

In the building environment, voice recognition can be used for garage switches and voice password locks; in the home environment, voice recognition can be used for remote sensing of home appliances; in addition, voice recognition can also be used for keyword retrieval, number voice query, etc. In future application research, speech recognition can provide assistance for building intelligent installation, such as building route voice navigation and robot human–computer interaction, and can also provide assistance for the effective identification of life after disasters [14].

In the field of civil engineering, there are few related researches and applications of speech recognition at present, and the research difficulties mainly focus on noise processing, robustness, and speech model. First, various noises often appear when inputting speech signals, and improving the noise processing is an important part of improving the accuracy of speech signal recognition; second, the existing speech signal recognition systems generally relies on the environment. High, different environments will lead to large differences in the recognition accuracy of speech signals, and enhancing the robustness of the speech recognition system will help to achieve the practical application of the system; finally, during speech interaction, semantics, speech rate, and emotion will all be affected. It affects the real meaning of speech, so the optimization of the speech model is also a difficult research point.

2.4. Cross-Domain. Interdisciplinary fields refer to numerous interdisciplinary subject groups, reflecting the trend of scientific research toward comprehensive development, with high complexity, breadth, and diversity. The intersection of artificial intelligence and civil engineering can greatly improve the engineering quality and work efficiency of infrastructure projects.

In 2015, Tang Hesheng et al. established a model for predicting the yield strength of rectangular concrete columns based on artificial neural networks, analyzed the key factors affecting the yield performance of concrete columns, and used Garson sensitivity analysis to prove the rationality of the model; in 2019, Ding Yang proposed that taking the process of mass concrete pouring as an example, a prediction model for the internal temperature of concrete hydration and heat release was established to provide a basis for monitoring, prediction, and early warning of subsequent maintenance. A fire monitoring method based on YOLO-BP neural network is proposed. The accuracy rate of using this method to monitor the fire in the repair stage of ancient buildings is 93.9%. In 2021, Zhao Yannan et al. proposed a tree structure intelligent form-finding based on BP neural network. The method can be used to intelligently locate the lower-level hierarchical nodes, so as to realize the intelligent form-finding of the overall geometric shape of the tree structure [15].

With the deep integration of industrialization, informatization, and intelligence, the traditional civil engineering industry is facing profound changes. The key to promoting the intelligent development of the entire life cycle of civil engineering is to comprehensively carry out the technology research and development and practice of intelligent design, intelligent construction, and intelligent maintenance, and strengthen the construction of the interdisciplinary system of artificial intelligence and civil engineering. In addition, in the construction of the interdisciplinary system of artificial intelligence and civil engineering, civil engineering should be adhered to as the main body, artificial intelligence as the auxiliary, and artificial intelligence technology should be used to support and promote the intelligent development of civil engineering throughout the life cycle.

3. An Intelligent Computing Framework for the Whole-Process Response of Civil Engineering Structures Based on Deep Learning

3.1. Structural Static Characteristics Unified Data Interface Mode. The structure is complex and diverse. In order to establish an end-to-end general computing framework, it is first necessary to solve the problem of how to organize multiple types of structures in an orderly manner, so as to facilitate the unified processing of subsequent deep learning programs. In order to meet the requirement of fidelity structure construction of original information, this study introduces the concept of a feature module, which can decompose, organize, and classify the static features of the structure by referring to the assembly idea of "from part to whole" of fine finite element technology [16].

A feature module corresponds to a certain structural property of a structure and contains many aspects of the structure. Taking the steel plate shear wall structure as an example, an embedded steel plate feature module can be set, and the feature information such as the width, height, and thickness of the steel plate can be recorded in the module. In order to consider the repeatability of construction, define two types of static feature modules: variable-length static feature model and fixed-length static feature model, and specify that any feature module is only one of the two [17]. For example, the opening feature of the steel plate embedded in the steel plate shear wall structure is a typical variable-length static feature module, because one or more openings may be set, and each hole can have its own geometric information. Frame top beams are usually a fixed-length static feature module because there is usually only one top beam. Further, the sub-features in the feature module are divided into dense features and sparse features: dense features mean that the feature value type is a continuous real number (or integer), the value size is comparable, and algebraic operations can be performed. The sparse feature means that the feature value type is discrete, and it represents the category or dummy feature. For example, whether the steel plate shear wall structure has out-of-plane constraints can be 0 to indicate no, 1 to indicate yes; the shape feature under the opening feature module Use 0 for a circle, 1 for a square, and so on. These numbers are not comparable in size and have no operational meaning. In the deep learning model, they will be converted into one-hot representation to avoid the ambiguity of discrete features under the Euclidean space distance metric, and ensure that the distances between discrete features are the same and equal [18].

3.2. PADCN Model. According to the definition of variable-length and fixed-length feature modules, combined with the characteristics of actual structural calculation and analysis, two functions that need to be realized by the structural static feature learning model can be summarized: (1) the internal sub-feature sequence of the variable-length feature module can be reasonably integrated; (2) the coupling relationship between each feature module and each other can be mined. Because of the influence of various factors such as material

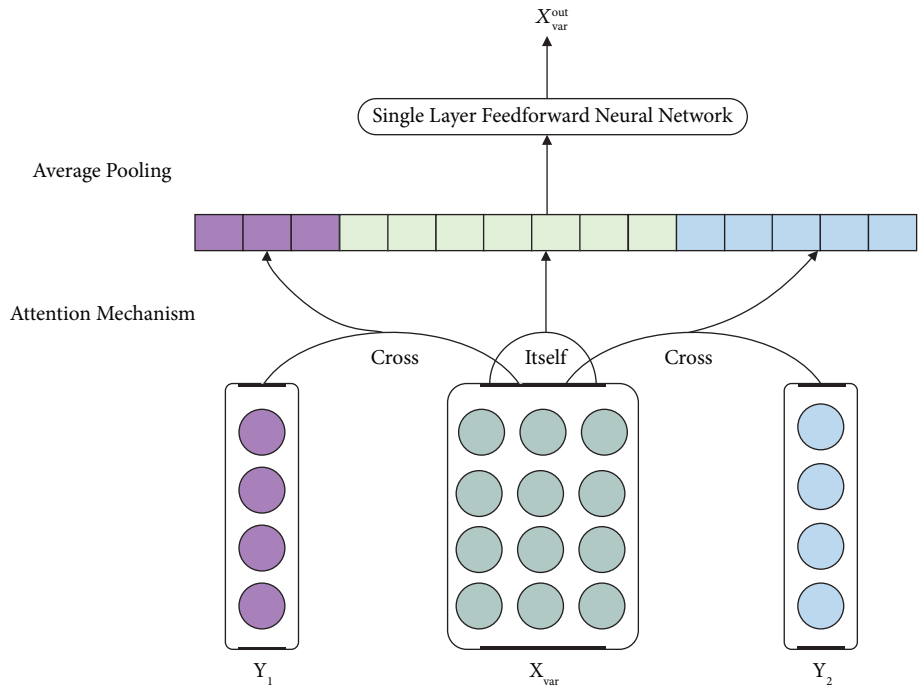

Figure 2: Attention mechanism preprocessing layer.

and geometric nonlinearity, each structure usually does not satisfy the simple superposition principle. Therefore, structural static feature learning is a complex feature processing scenario: there are both sequence features and general fixed-length features, and there is an interactive relationship between the two [19].

The joint feature problem is rare in computer vision and natural language processing, the two main research fields of artificial intelligence, but it is very similar to the recommendation system scenario, one of the core businesses of the Internet industry. In order to recommend a product to a user, the following three categories of information are generally collected and processed: user portrait, product information, and user behavior sequence. Among them, user portraits and product information can be regarded as fixed-length feature modules, and user behavior sequences correspond to variable-length feature modules, and it is also necessary to mine the deep interaction between the user side, the product side, and the user behavior sequence. In this way, the deep learning model of the recommender system can be used to process the static features of the structure [20].

First, we consider the sub-feature sequence integration problem of variable-length feature modules. The purpose of the integration is to form a fixed-length vector, similar to the embedding vector in the recommender system, which contains the main information of the feature module. We adopt the standard multi-head attention mechanism to preprocess the sequence features, including the self-attention mechanism and cross-attention mechanism, as shown in Figure 2. Taking the steel plate shear wall stiffener feature module as an example, the self-attention mechanism can explore the interaction between the stiffeners, because the staggered stiffeners work together rather than independently to delay the buckling of the plate; the cross-attention mechanism is in order to introduce the interaction between the structures in advance, such as the intersection of the feature module of the embedded steel plate and the feature module of the stiffener, it can be expected to integrate the information of the plate into the stiffener expression in advance, which is more helpful for the subsequent extensive cross-learning. After the attention mechanism is implemented, the representation vector of the variable-length feature module is obtained using average pooling and dimensional transformation through a single-layer feed-forward neural network [21].

After the variable-length feature module completes the preprocessing, all feature modules are converted into feature vectors of certain dimensions, which facilitates the mining of coupling relationships. One of the mainstream deep learning models in the recommender system field is introduced into the deep and cross-network, which is connected with the attention mechanism preprocessing layer to form the PADCN model, which realizes the complete structural static feature representation learning, as shown in Figure 3. The structure of the DCN model is derived from thinking about the effectiveness of traditional recommendation system algorithms (such as SVD and FM): first, the memory of user habits, that is, a user must have fixed preferences for a long time. For example, if user A likes electronic products, then as long as the recommendation model can provide popular and latest products such as computers and mobile phones, the possibility of A's positive feedback on the recommendation results is definitely not low; the second is the generalized exploration of user preferences. There are no related products in the browsing footprint, and it is also very likely that you like digital peripherals, such as game figures. In

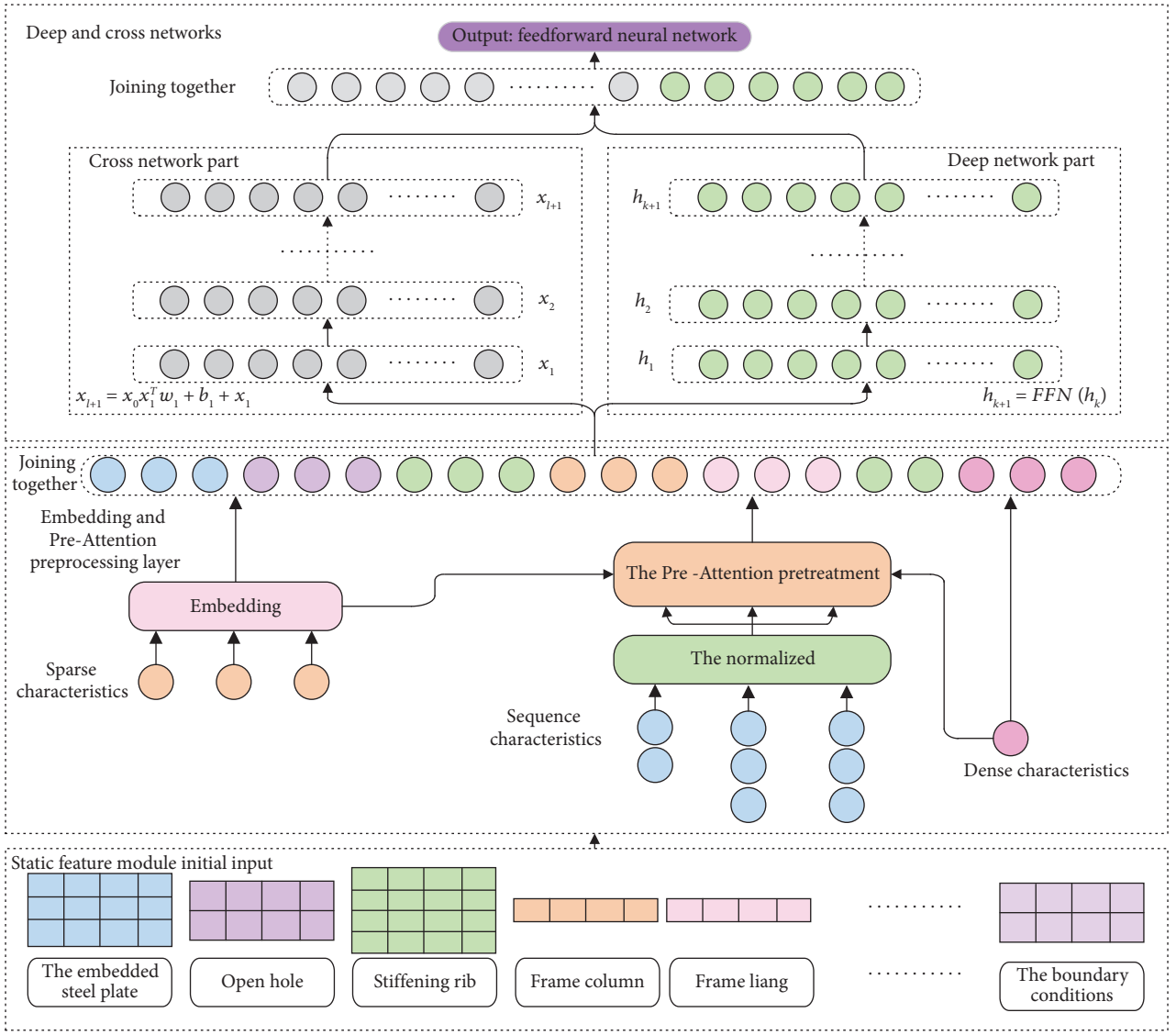

Figure 3: Structural static feature representation learning model PADCN.

conclusion, a high-quality model needs to take into account the two attributes of memory and generalization at the same time. This is also applicable to structural response simulation: the hysteretic responses of structurally similar components are usually not much different, which belongs to memory; and if the model training set contains artificially developed central circular openings. For specimens with holes and central rectangular openings, after learning, it is expected that the model can simulate the mechanical response of a uniform matrix with multiple openings, which belongs to generalization [22].

The method of DCN to take both into consideration is to divide the model into two parts, as the name suggests, one is the cross-network part, which is used to memorize historical patterns. Finally, the two are spliced together for output [23]. The deep network part is a common feedforward neural network, which will not be described in detail. In the intersecting network part, the features themselves are constantly intersected, and then the higher-order interactions are mined; at the same time, the residual connection structure is used to ensure the complete transmission of the initial information.

$$x_{i+1} = x_0 x_l^T w_l + b_l + x_l. \tag{1}$$

Expanding and analyzing the above formula, it can be found that what the first l layer learns is the polynomial of the input feature itself $l + 1$, and the polynomial contains all terms less than or equal to $l + 1$ the order, and there is no information loss of any order [24]. In addition, the complexity of each layer of the cross-network part $O(d)$ realizes the automatic upgrade of the coupling relationship, which effectively avoids the common combination explosion problem in pairwise cross-action learning.

So far, the unified data interface formulation and representation learning of structural static features have been completed. Then, by splicing the representation vector learned by the PADCN model with the input of the

Mechformer model, an end-to-end structural intelligent computing framework based on deep learning can be formed, which comprehensively covers the data side and the model side, and can fully consider the static and dynamic characteristics of the structure, so as to realize the whole-process mechanical response prediction of different structures.

3.3. Numerical Test. This section will use the steel plate shear wall structure as the carrier to verify the effectiveness of the structural intelligence computing framework based on the PADCN-Mechformer model.

3.3.1. Data Preparation. The initial training data are mainly derived from experimental reports in historical documents and generated by means of high-precision and precise finite element technical parameter analysis. However, in practical applications, the initial data volume may not be able to support the training requirements of large-scale deep learning models due to limitations such as high experiment costs and low computational efficiency of finite element models [25]. Therefore, data augmentation algorithms need to be considered.

In the field of computer vision, operations such as rotating, cutting, scaling, and coloring the input image are performed to increase the amount of data. These methods are obviously not suitable for real-valued sequence fitting problems in structural calculations. With the richness of language meaning, the field of natural language processing can use synonym interchange, back translation (that is, translating a sample to another language with an existing model, and then translate it back), based on mask replacement, random deletion, and insertion. Methods such as language noise, in which back-translation can be analogized to the use of fine finite element models for data generation, and the addition of noise can provide inspiration for structural response data augmentation algorithms.

Noise addition methods based on random deletion and insertion cannot be directly applied, because unlike the flexibility and robustness of language (many sentences can be understood by humans even with a large number of typos), the structural response curve once the amplitude points are randomly deleted, etc. data, or randomly interpolating a point that deviates significantly from the loading trajectory, may cause a noticeable change in the shape of the hysteresis curve, impairing the model training process [26].

Corresponding to the random deletion method, a piecewise proportional downsampling algorithm based on amplitude points is proposed for the structural response curve. The flowchart is shown in Figure 4, and the schematic diagram of the results is given on the right side by taking Lubell's SPSW2 test song as an example. The principle of the algorithm is that the test curve usually contains a large number of data points due to the high sampling frequency of the equipment, and the step size between two adjacent points is very small, so reasonable downsampling will not change the overall shape of the response curve and the key mechanics it reflects. At the same time, samples of different step lengths can be obtained to enhance the robustness of the deep learning model. The reason for the segmentation is that the hysteresis curve is highly nonlinear. Generally, the plastic segment is longer, the elastic–plastic transition segment is the second, and the elastic segment is the shortest. The plastic transition is the most prominent and is the key region to control the shape of the curve. If the entire half-ring is directly sampled uniformly, most of the sampling points fall in the plastic segment, and the elastoplastic transition segment is not fully described, resulting in serious curve distortion. Therefore, it is necessary to set the segmentation ratio, roughly frame the range of each segment, and give each segment a reasonable sampling ratio. After testing, the more suitable subsection ratio is {0.1, 0.15, 0.25, 0.5} (the elastic-plastic transition section is further divided into two parts: elastic transition and plastic transition), and the sampling ratio of each section is {0.05, 0.4, 0.25, 0.3 }. After the preliminary sampling is completed, it is recommended to refine the sampling curve. Some segments may have a small amount of data, repeated sampling occurs, and the data needs to be deduplicated. In addition, due to test measurements and other reasons, the maximum point of the displacement amplitude of the hysteretic half-ring of some test curves may not correspond to the point of the maximum load amplitude. The previously extracted displacement time history amplitude data and load time history amplitude data are corrected for relevant points.

Using the above algorithm flow, multiple new hysteresis response curves can be generated by setting different sampling points and trying to change the segmentation ratio and sampling ratio. The parametric analysis results show that for most of the response curves with more than 3000 data points, only 20% of the data points can reproduce the original curve with a high degree of coincidence. Therefore, the sub-scale downsampling algorithm based on amplitude points can generate a considerable number of new samples.

3.4. Simulation Accuracy Metrics. At present, the evaluation of the accuracy of the structural response curve simulation is usually based on the qualitative observation of the researchers, and most of the literature will claim to be "good fit." In order to more reliably compare the accuracy of simulation results with experimental curves, it is necessary to establish relevant quantitative indicators. In structural performance analysis, mechanical indicators such as ultimate bearing capacity and overall (or average) energy consumption are generally used. Both of these two indicators have important physical meanings, but they also have certain limitations: the former is a single-point indicator, suitable for the design stage, and obviously not explanatory for the accuracy of the whole process simulation; the latter can be regarded as a certain sense. For the mean value index, since the number of hysteresis loops experienced by the simulation and the test is the same, the overall energy consumption is determined by the average energy consumption of each cycle. Therefore, this index lacks the control of the variance index and is also not comprehensive. For example, there may be a situation where the final average energy consumption of the hysteresis curve is similar because some segments consume too much energy and some segments consume less

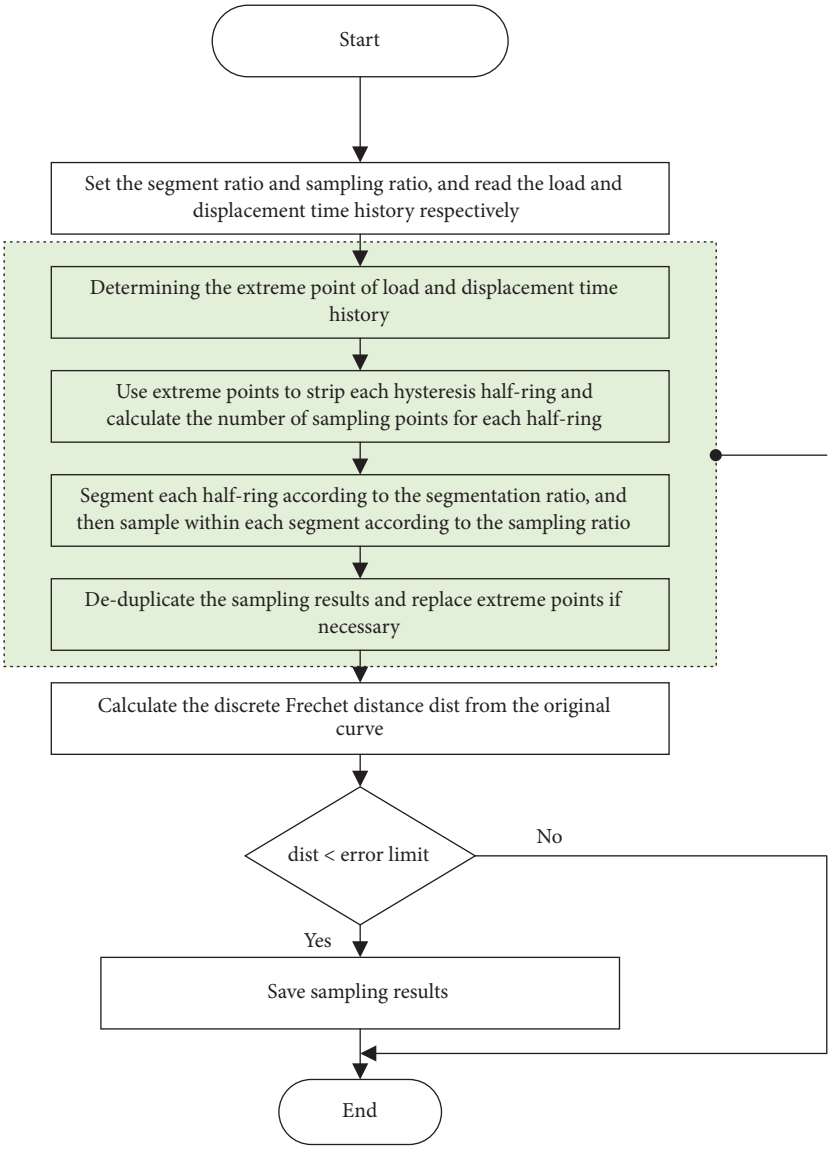

Figure 4: Segmented proportional downsampling algorithm based on amplitude points.

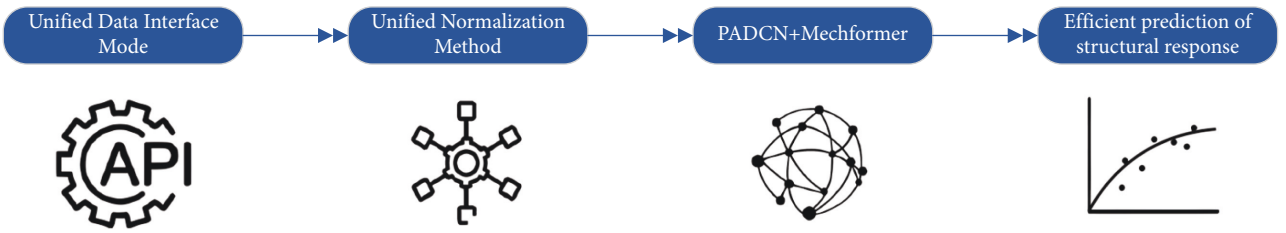

Figure 5: Framework diagram of structural intelligence computing based on deep learning.

energy, but the simulation accuracy is actually low. Therefore, a more comprehensive metric needs to be explored.

3.5. Framework Verification. Through experimental data collection, fine finite element generation, and the expansion of a series of data augmentation algorithms in Section 3.1, the length of the loading regime sequence was controlled between 200 and 3000 data points. We divide 512 samples as a training set, 256 samples as a validation set, and 256 samples as a test set, of which test samples and their data augmentation in the training set account for 58.3%.

The deep learning-based structural whole-process response intelligent computing framework proposed in this

study is universal in the whole process and is suitable for any structural computing and analysis tasks: as shown in Figure 5 (1) First, we establish a database according to the data interface mode specified in Section 1. This step can digitize the inherent properties of the target object "what you see is what you get," almost without manual experience preprocessing; (2) the user specifies the reference value of each physical feature, and the program automatically adopts the reference value scaling method proposed by the author to carry out unified de-dimensioning and normalization; (3) the program uses the PADCN-Mechformer model for training and testing; (4) a deep learning model that can be used for actual structural response prediction is obtained, with high accuracy and far superior to traditional numerical methods computational efficiency.

4. Conclusion

This study proposes an end-to-end structural response intelligent computing framework based on deep learning, including structural static feature data interface mode, data augmentation algorithm, and core deep learning model. It is suitable for multi-level mechanical response prediction problems such as materials, components, and even structural systems.

Data Availability

The dataset can be accessed upon request.

Conflicts of Interest

The authors declare that there are no conflicts of interest.

Acknowledgments

The authors thank the Key Project of Natural Science Research in Anhui Province, Study on Water Restoration Technology of Microbial Filter Bed (No. KJ2016A389).

References

[1] P. Aditya, M. Doron, and C. Caicedo Juan, "Image-based cell phenotyping with deep learning[J]," *Current Opinion in Chemical Biology*, vol. 65, 2021.

[2] Y. Ding, J. Chen, and J. Shen, "Prediction of spectral accelerations of aftershock ground motion with deep learning method[J]," *Soil Dynamics and Earthquake Engineering*, vol. 150, 2021.

[3] M. W. Wang, Y. Y. Zhang, and J. Xu, "A deep learning method based on multi-modality EEG for automatic depression screening," *International Journal of Psychophysiology*, vol. 168, no. S, pp. S205–S206, 2021.

[4] C. Wang, C. Wang, W. Li, and H. Wang, "A brief survey on RGB-D semantic segmentation using deep learning," *Displays*, vol. 2020, Article ID 102080, 2021.

[5] J. He, J. Zhou, J. Dong, Z. Su, and H. Lu, "Revealing the effects of microwell sizes on the crystal growth kinetics of active pharmaceutical ingredients by deep learning[J]," *Chemical Engineering Journal*, vol. 428, 2022.

[6] G. Fortino, M. C. Zhou, M. M. Hassan, M. Pathan, and S. Karnouskos, "Pushing artificial intelligence to the edge: emerging trends, issues and challenges," *Engineering Applications of Artificial Intelligence*, vol. 2021, Article ID 104298, 2021.

[7] S. Chatterjee, P. Rana Nripendra, K. Dwivedi Yogesh, and M. Baabdullah Abdullah, "Understanding AI adoption in manufacturing and production firms using an integrated TAM-TOE model," *Technological Forecasting and Social Change*, vol. 170, 2021.

[8] A. F. Blackwell, A. Damena, and T. Tegegne, "Inventing artificial intelligence in Ethiopia," *Interdisciplinary Science Reviews*, vol. 46, no. 3, pp. 363–385, 2021.

[9] F. Cong, Y. Liu, and J. Zhang, "A taxonomical review on recent artificial intelligence applications to PV integration into power grids[J]," *International Journal of Electrical Power & Energy Systems*, vol. 132, 2021.

[10] O. Ziad and J. Topol Eric, "Artificial intelligence, bias, and patients' perspectives[J]," *The Lancet*, vol. 397, Article ID 10289, 2021.

[11] S. Khan and M. R. Rabbani, "Artificial intelligence and NLP - Based Chatbot for islamic banking and finance," *International Journal of Information Retrieval Research*, vol. 11, no. 3, pp. 65–77, 2021.

[12] Y. Song, Y. Luo, and Y. Shen, "3D reconstruction of grid structure based on binocular vision and image recognition," *ACM Transactions on Computer Systems* , vol. 27, no. 4, pp. 16–22, 2021.

[13] S. Edouard, "Learning human insight by cooperative AI: shannon-Neumann measure[J]," *IOP SciNotes*, vol. 2, no. 2, 2021.

[14] Q.-H. Meng Max, "Bridging AI to robotics via biomimetics [J]," *Biomimetic Intelligence and Robotics*, vol. 1, 2021.

[15] G. Gorincour, O. Monneuse, A. Ben Cheikh et al., "La gestion des urgences abdominales de l 'adulte à l'aide de la télémédecine et de l'intelligence artificielle," *Journal de Chirurgie Viscérale*, vol. 158, no. 3, pp. S28–S33, 2021.

[16] S. Stefano, C. Antonio, Y. Bardia, P. Stefano, R. Leonardo, and P. V. Maldague Xavier, "Maximizing the detection of thermal imprints in civil engineering composites via numerical and thermographic results pre-processed by a groundbreaking mathematical approach[J]," *International Journal of Thermal Sciences*, vol. 177, 2022.

[17] M. H. Nguyen, S. Yoon, S. Ju, S. Park, and J. Heo, "B-EagleV: visualization of big point cloud datasets in civil engineering using a distributed computing solution," *Journal of Computing in Civil Engineering*, vol. 36, no. 3, 2022.

[18] H. Bae, M. Polmear, and D. R. Simmons, "Bridging the gap between industry expectations and academic preparation: civil engineering students' employability," *Journal of Civil Engineering Education*, vol. 148, no. 3, 2022.

[19] R. P. K. G. Babu and H. Mudavath, "International conference on innovative and sustainable technologies in civil engineering (ISTCE-2021)[J]," *IOP Conference Series: Earth and Environmental Science*, vol. 982, no. 1, 2022.

[20] F. El Khazanti, R. Ahmed, A. Harrou, H. Nasri, Y. Ettayea, and M. El Ouahabi, "Assessment of a mining-waste dump of galena mine in the east of Morocco for possible use in civil engineering[J]," *Journal of Ecological Engineering*, Prepublish, 2022.

[21] A. Onur and F. Catbas, "Necati. Editorial: human-induced excitations and vibrations serviceability of civil engineering structures," *Frontiers in Built Environment*, vol. 23, 2022.

[22] V. O. U. F. F. O. Marcel, T. I. Franklin, F. H. Kemtchou, K. A. M. G. A. Djoumen Tatiana, and N. G. A. P. G. U. E. François, "Physical and mechanical

characterization of pyroclastic materials in Baleng area (Bafoussam, West-Cameroon): implication for use in civil engineering[J]," *Case Studies in Construction Materials*, vol. 13, 2022.

[23] S. Younger, D. Parry, and D. Meigh, "Preparing for the future: the impact of climate change on the civil engineering profession," *Proceedings of the Institution of Civil Engineers-Civil Engineering*, vol. 175, no. 2, pp. 87–93, 2022.

[24] M. Mishra, B. Lourenço Paulo, and G. V. Ramana, "Structural health monitoring of civil engineering structures by using the internet of things: a review[J]," *Journal of Building Engineering*, vol. 48, 2022.

[25] H. M. Shiferaw, "Evaluating practical teaching approach in civil engineering training among public universities of Ethiopia: students' view and opinion," *African Journal of Science, Technology, Innovation and Development*, vol. 14, no. 1, pp. 216–224, 2022.

[26] S. R. Vadyala, S. N. Betgeri, J. C. Matthews, and E. Matthews, "A review of physics-based machine learning in civil engineering," *Results in Engineering*, vol. 13, Article ID 100316, 2022.

Hindawi
Scientific Programming
Volume 2023, Article ID 9878425, 1 page
https://doi.org/10.1155/2023/9878425

Retraction

Retracted: Application Research and Case Analysis of Landscape Design in Artificial Intelligence Platform

Scientific Programming

Received 18 July 2023; Accepted 18 July 2023; Published 19 July 2023

This article has been retracted by Hindawi following an investigation undertaken by the publisher [1]. This investigation has uncovered evidence of one or more of the following indicators of systematic manipulation of the publication process:

(1) Discrepancies in scope
(2) Discrepancies in the description of the research reported
(3) Discrepancies between the availability of data and the research described
(4) Inappropriate citations
(5) Incoherent, meaningless and/or irrelevant content included in the article
(6) Peer-review manipulation

The presence of these indicators undermines our confidence in the integrity of the article's content and we cannot, therefore, vouch for its reliability. Please note that this notice is intended solely to alert readers that the content of this article is unreliable. We have not investigated whether authors were aware of or involved in the systematic manipulation of the publication process.

Wiley and Hindawi regrets that the usual quality checks did not identify these issues before publication and have since put additional measures in place to safeguard research integrity.

We wish to credit our own Research Integrity and Research Publishing teams and anonymous and named external researchers and research integrity experts for contributing to this investigation.

The corresponding author, as the representative of all authors, has been given the opportunity to register their agreement or disagreement to this retraction. We have kept a record of any response received.

References

[1] Y. Cao, "Application Research and Case Analysis of Landscape Design in Artificial Intelligence Platform," *Scientific Programming*, vol. 2022, Article ID 7122276, 10 pages, 2022.

Hindawi
Scientific Programming
Volume 2022, Article ID 7122276, 10 pages
https://doi.org/10.1155/2022/7122276

Research Article

Application Research and Case Analysis of Landscape Design in Artificial Intelligence Platform

Yunxia Cao

ZheJiang Guangsha Vocational and Technical University of Construction, Dongyang 322100, Zhejiang, China

Correspondence should be addressed to Yunxia Cao; 20192519@zjgsdx.edu.cn

Received 16 August 2022; Revised 13 September 2022; Accepted 19 September 2022; Published 5 October 2022

Academic Editor: Lianhui Li

Modern landscape greening plays an important role in the construction of modern cities and plays a positive role in improving the natural environment of cities and building a good image of cities. With the continuous progress of society and technology, human's understanding of artificial intelligence is deepening, and intelligent technology is gradually integrated into all aspects of life. Because media technology has rich design elements and can carry out rich design structures, it will be more intuitive to use multimedia means for garden landscape design. Therefore, for meeting people's requirements for the diversification of modern urban gardening construction, this study makes a deep analysis of the current status and problems of landscape design and tries to study the effective application methods of artificial intelligence technology in landscape design, to promote the combination of landscape design and artificial intelligence design. At the same time, the combination of AI lighting planning, AI water landscape planning, AI sprinkler planning, and AI paving planning is used to illustrate the application of AI in the specific project design of landscape design. The use of artificial intelligence not only promotes the innovation and optimization of landscape design, but also ensures the quality of modern landscape design and effectively improves the efficiency of modern landscape design.

1. Introduction

In the contemporary society, with the development of society, the design ideas, and methods of landscape architecture are increasingly enriched, coupled with the continuous improvement of social economy and technology level, people also put forward higher requirements for landscape design. People's economic level has been greatly improved, and their comprehensive quality has been improved. Their taste is also very different from that of the past, which can be reflected in all aspects of life. For example, theme parks and fitness squares have more and more requirements for landscape architecture. In addition, with the rapid development of science and technology, it has entered the era of big data, and landscape architecture design has also undergone great changes. With the development of modern civilization, modern landscape gardening design means are increasingly rich. At the same time, the steady development of social economy and technology has also led to the improvement of the requirements for modern urban landscape greening. The current stage of modern landscape architecture design is restricted by backward design concepts and inconsistent design schemes with reality, which is not conducive to improving the quality and efficiency of modern landscape architecture design, nor can it meet people's growing spiritual and entertainment needs [1–5]. Artificial intelligence technology has been rapidly applied to many fields of landscape architecture because of its high-efficiency data knowledge transformation ability, strong analytical ability, strict reasoning, and accurate ability to select the best. Artificial intelligence technology can not only convert the complex qualitative description in landscape architecture into quantitative analysis through efficient and accurate calculation of some relevant data, but also solve some difficult problems in landscape architecture research and reveal the internal mechanism behind the phenomenon through the establishment of intelligent models, so it is widely used in landscape architecture research.

From the point of view of today's society, landscape design has some limitations in the following areas, which

limits the development of landscape design. First, the design concept of landscape architecture is not advanced enough. According to the current situation of landscape design in Chinese gardens, traditional experience and imitation of other works are often the main design methods. In this application scenario of landscape architecture design, it will inevitably lead to innovation and uniqueness in landscape design [6–8]. At the same time, there is no certain concept of environmental protection in the design process, such as blind pursuit of beauty. Therefore, its design is often difficult to effectively play the actual utility of the landscape in the garden. At the present stage, China advocates the development of green economy. The precondition of green economy is to protect the environment and then promote the rapid development of economy on the basis of it again [9]. In addition, due to the involvement different cities, there will be great differences in culture, coupled with the existence of the same human characteristics, and landscape design can only fully reflect these different characteristics to meet the real needs of landscape design. However, in the current landscape design, these different properties are ignored, leading to appear in the landscape design a lot of similar scenes.

Second, the technical level of landscape design needs to be further improved. In the design of landscape architecture, art, and technology are usually integrated, which not only involves many fields, but also requires designers to have a rich variety of professional knowledge and technology, so that more different styles of landscape design can be completed with high quality and efficiency. However, in the current landscape design, designers do not have more professional expertise and technology, and cannot integrate art and technology [10–12]. Therefore, it will have a certain impact on the quality and effect of landscape design. In addition, due to the relatively backward construction technology of gardening landscape in our country at this stage, even if a large number of high-quality designs are developed, it is difficult to implement them in gardens, which will lead to the setback of gardening landscape design.

Finally, there are often differences between design and reality. From the original intention of landscape design, it is a way to reflect the improvement of living environment and landscape design. However, for different areas, their living environment also has different characteristics, and considering different places, the climate and culture are also different. Therefore, when designing landscape architecture, it should be based on local actual needs to ensure that the landscape design conforms to the actual situation [13]. In the real society, some landscape gardens have invested a lot of manpower, material, and financial resources in the design process, but they have not got relatively excellent design scheme. This is because before the gardening landscape design work, no comprehensive collection and collation of data, coupled with the fact that the city is not the main basis, will have a big impact on the effect of the entire design [14].

On this basis, in order to ensure that the design of landscape architecture can be synchronized with the times, improve the efficiency of design planning, and develop high design technology. Therefore, the introduction of advanced

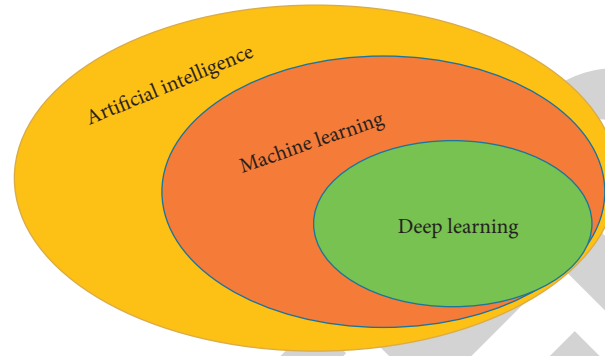

Figure 1: Scope of AI technology.

AI technology ensures that the leading technology in combination with landscape design, so as to maximize the effectiveness of landscape design.

2. Principles of Artificial Intelligence Platform

Artificial intelligence (AI) is a comprehensive technology to simulate various human behaviors with the help of high-performance computing platform on the basis of studying human behavior rules and thinking modes [15–17]. It mainly includes machine learning and in-depth learning technology, as shown in Figure 1. Until now, in the research of AI technology, the practical significance of intelligence has not been well reflected, often closely combined with human. However, through nearly 50 years of research, AI technology has been widely developed in all areas of the world. For example, in machine manufacturing, these technologies fully reflect the advantages of AI. Further development of AI technology can create a more intelligent society for people. From this aspect of landscape design, designers often combine artistic features with science and technology to artificially transform a certain area of the city and create a harmonious and beautiful urban atmosphere between people and nature, which is landscape design. Therefore, virtual tour technology, media, and multimedia technology are mainly used in landscape design [18].

2.1. AI Technology. There are two types of artificial intelligence: simulation, deduction, demonstration, and algorithm. The simulation deduction and demonstration further subdivide artificial intelligence into "reasoning type" capable of logical reasoning and theorem proving; "learning type" capable of deep learning and support vector machine; it is a "knowledge-based" expert system. The algorithm divides artificial intelligence into "symbolism" type that uses logical reasoning method to deduce the whole theoretical system to simulate the process of human like intelligence; the "connectionist" type that uses machines to simulate the neural system and connection mode of the human brain; a new method of controlling intelligence through behavioral activities is "behaviorism" with quantitative research attributes. According to the functions and attributes of artificial intelligence technology and its application in landscape architecture research, there are three types of artificial

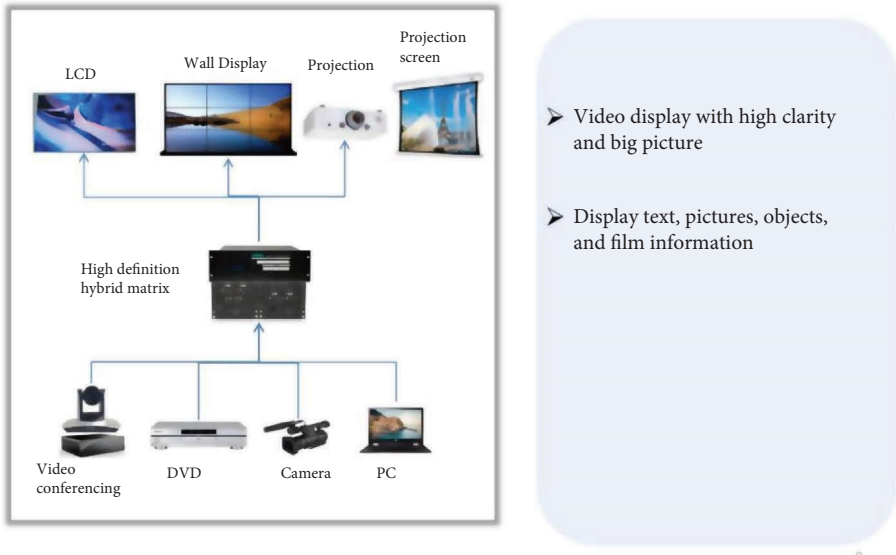

Figure 2: Virtual roaming technology architecture.

intelligence technology currently applied in landscape architecture: intelligent random optimization, artificial life, and machine learning.

Random optimization method is an optimization algorithm that generates and utilizes random elements. Randomness includes two aspects, one is the randomness of the data, and the other is the randomness of the algorithm itself. In the research of landscape architecture, intelligent random optimization method is mainly used to seek the optimal solution of optimization problems. Because the time cost of trying all possible solutions to find the optimal solution is too high, and the random optimization method speeds up the search process, it is easy to find the global optimal solution. Genetic algorithm and simulated annealing are common stochastic optimization methods.

Machine learning includes three types: (1) it directly simulates the tree process of human judgment on concepts, and its representative algorithm is decision tree, which is called semiotic learning. (2) Connectionist learning, represented by artificial neural network, has the best application effect in the field of engineering. (3) It mainly combines the theoretical achievements of inferential statistics, which is represented by support vector machine, so it is called statistical learning. Machine learning can mainly solve the impact of each element on landscape results, scoring problems, and classification problems in landscape architecture. Connectionist learning and symbolism are widely used, such as convolutional neural networks, artificial neural networks, random forests, and decision trees and so on.

2.2. Virtual Roaming Technology. In recent years, with the rapid development of virtual three-dimensional technology, there are many new branches of virtual reality technology, among which virtual tour is an innovative development of virtual reality technology [19–21]. Virtual tours are often used to showcase design results and put people in a virtual three-dimensional environment. Through dynamic interaction, the immersion type of multi-angle and omnidirectional inspection of future buildings is carried out. This is beyond the traditional architectural effect maps. Virtual tour technology showcases the design results while also considering the overall audience. The architecture of the multimedia system is shown in Figure 2.

2.3. Landscape Design with the Media or Multimedia. With the continuous development of science and technology, various countries have increased their research efforts on new media, an emerging industry, and promoted the development of new media in many fields. In urban landscape design, multimedia is designed from a more scientific, advanced, and diversified perspective, matching with the information network of modern society, broadening the scope of design, broadening people's horizon, and changing the traditional design theory. The perfect integration of new media and landscape design marks the initial formation of modern urban landscape design, and also reflects the inextricable connection between them. The emergence of new media has made the Chinese urban landscape design transition and transformation from traditional artificial design to more modern design. New media art can not only give modern landscape design a new life, but also help designers directly absorb nutrients and knowledge through the visual experience and intuitive feeling conveyed by new media. New media use computers and other equipment to process information and images, use information and digital technology means for landscape design, expand the creative space, so that the human design concept and computer together organically, and is an important breakthrough in design [22, 23]. This has significantly broadened the original boundaries and scope. Using only multimedia for landscape design, as shown in Figure 3, is more intuitive with animation effects and certain visualizations.

In modern garden landscape design, we adopt advanced digital media technology, give full play to the advantages of

Figure 3: Visualization of landscape design using multimedia technology.

digital media technology, integrate landscape design resources, combine the application of modern design elements, form diversified design styles, and meet the personalized needs of modern people for landscape with the support of rich landscape design content. During the use of digital media technology, we can integrate the elements of the times, adjust the design style and scheme content, and automatically convert and process different design forms, so as to ensure that design is no longer limited to traditional paper design, but with the help of digital media technology, we can introduce innovative design ideas and modern design elements to form a more diversified and three-dimensional aesthetic orientation. Using digital media technology to carry out garden landscape design can integrate application, transform application, refine application design elements, integrate with modern social elements, and improve the aesthetics of design. On the one hand, digital media technology is used in the specific design. With the support of advanced technology, various artistic elements are readjusted and processed to integrate into modern design and enhance the sense of design art; on the other hand, through the network platform in digital media technology, we can provide a variety of aesthetic options, so that the design content is full of strong sense of art, and increase the artistic expression channel of the design, so that we can collect more creative content and elements of garden landscape design with the help of advanced digital media technology, and fundamentally improve the aesthetics of the design. In the process of innovative use of advanced digital media technology, the quality and level of each design can be improved. The application of digital media technology can broaden the scope of relevant design, integrate art theoretical knowledge and design practice, and broaden the source channel of design art and creativity; ensure the depth of design, create a mature landscape design system, ensure the efficient implementation of design work, and fundamentally improve the design quality and effect; by using the analog system and design research system in digital media technology, this paper analyzes whether there are problems in landscape architecture design and puts forward corresponding rectification suggestions and countermeasures. Through effective measures, complete the tasks of landscape architecture design, improve the current development situation, highlight the positive role and advantages of digital media technology in landscape architecture design, and form a systematic working mode and system.

3. Relationship between Landscape Design and Artificial Intelligence

In the modern landscape design, the design concept is backward and the technical level is not high. Design divorced from practical problems, the emergence of artificial intelligence technology, can solve these problems to a large extent. Changing landscape design with intelligent design not only allows us to play better, but also to engage with our environment more effectively, like smart lighting. In this way, we are not only protected from light pollution, but also can be a free man living in harmony with ourselves [24]. The combination of intelligent public facilities and background music not only brings people a kind of enjoyment, but also helps relieve people's psychological pressure. A large part of the carrier of landscape design is green plants and public facilities. In the past, park landscape was mostly for its own amusement, and artificial intelligence landscape can share the source, protect the environment, and help each other. Intelligent garden design is also conducive to the promotion of local cultural customs and do complement each other. Under the premise of not violating the law of nature, set a variety of interests as one.

The elements of landscape planning and design include natural landscape elements and artificial landscape elements. Among them, natural landscape elements mainly refer to natural landscapes, such as large and small hills, ancient and famous trees, stones, rivers, lakes, oceans, etc., The artificial landscape elements mainly include cultural relics, cultural

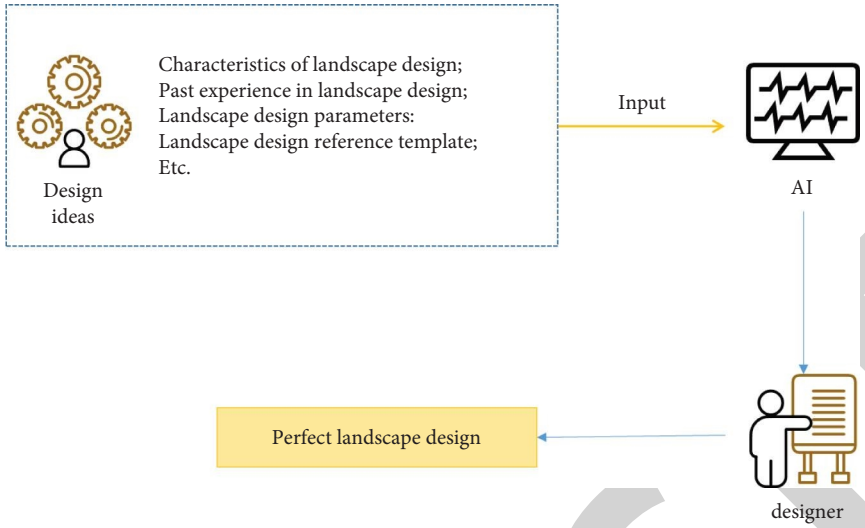

Figure 4: Relationship between designer and AI landscape design.

sites, landscaping, art sketches, trade fairs, buildings, squares, etc., These landscape elements provide a lot of materials for creating a high-quality urban space environment. However, to form a unique urban landscape, it is necessary to systematically organize various landscape elements and combine geomancy to form a complete and harmonious landscape system and an orderly spatial form.

The gradual improvement of scientific and technological level has played a great role in promoting the development of AI technology [25]. In landscape design, the application of AI technology can often effectively solve many adverse factors in the process of landscape design. In the past, some technical problems were often involved in the work of landscape design. It is difficult to ensure efficient and fast solution of problems when some technicians do not have enough knowledge reserve. In the long run, the quality and effect of landscape design will be affected. The application of artificial intelligence technology in landscape design not only helps to avoid light pollution, provides opportunities to get along with nature, but also alleviates psychological pressure. In addition, landscape design focuses on green plants and public facilities. On this basis, the application of artificial intelligence technology can achieve artificial intelligence landscape, promote resource sharing, provide favorable conditions for the complementary of landscape design and local culture, and ensure the maximum improvement of the actual benefits of the landscape.

At present, the concept of landscape design is still not closely related to society, so it is easy to see scenes where the design scheme does not conform to the actual situation. Therefore, the application of AI technology to design can greatly avoid such problems. In the process of landscape design in the current society, a large amount of information needs to be collected and sorted out in advance by designers, and there are also many technical problems that need to be adjusted, which requires designers to have enough knowledge reserve. Through the application of AI technology, computer programs will complete their own retrieval, collation and display of required data, technical data, similar designs, which to some extent reduces the difficulty of design. The relationship between designers and AI design is shown in Figure 4. At the same time, the introduction of AI into landscape design can provide better conditions for the combination of human and environment. For example, according to AI lighting technology, light pollution can be effectively adjusted, and the actual utility of landscape can be further enhanced.

Rebuilding landscape design with intelligent design not only allows us to have a better recreation, but also allows us to participate more effectively in the environment. Intelligent lighting, for example, not only keeps us free from light pollution, but also makes us a free person living in harmony with nature. The combination of intelligent public facilities and background music can not only bring people a kind of enjoyment of life, but also help to alleviate people's psychological pressure.

4. The Role of Artificial Intelligence in Landscape Design

As shown in Figure 5, each step of the landscape design phase can be participated in by AI technology.

4.1. Site Condition Analysis Phase. Investigation and analysis of site conditions is a key task of modern landscape design and a basic element to ensure the high practicability of design schemes. In this stage of practice, many projects can be completed using artificial intelligence technology.

For example, in the process of remotely scanning and taking pictures of a hill using an unmanned aerial vehicle, a 3D image of the hill in the range needs to be generated in the software and the corresponding vertical information obtained. In this section, manual operations are still required during the above operations. Once the routes are set, the UAV can automate the acquisition of required data information based on the settings. Similarly, in the landscape design, human behavior needs to be considered, and the

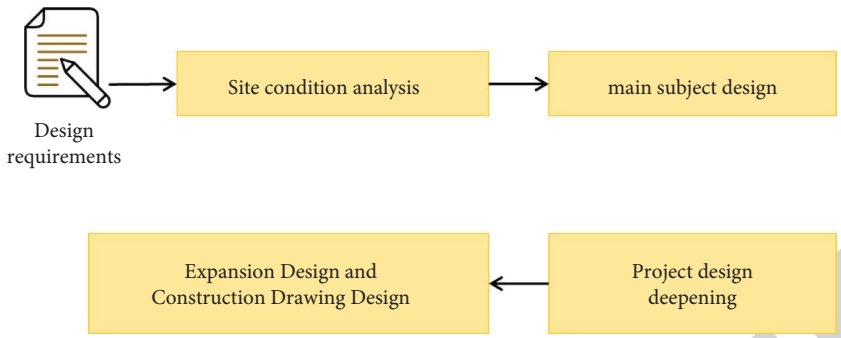

Figure 5: Landscape design stage steps.

Figure 6: Design elements and drawings in AI.

behavior of human in the landscape needs to be analyzed in advance in Guilin. The traditional way of working for this task is to make final design decisions based on-site survey, planning information and work experience around the site. By using AI technology, the software system can automatically analyze and determine the direction and pattern of crowd gathering, avoiding the subjectivity of experience.

4.2. Project Conceptual Design Phase. In the concept stage of landscape greening, designers are required to complete the preliminary design drawings according to the actual needs. However, due to some subjective and relatively abstract needs, the current level of AI technology can hardly be completed by itself, and manual help is still needed. However, it is not impossible to design with AI. Current AI technology has a high advantage in collecting information. In the original process of finding ideas, designers tend to store according to their previous experience, relying on the past design, although it will be efficient, but easy to produce uniform but poor results. But now, with the help of AI technology, AI can automatically retrieve and store related designs, or it can automatically design based on large data. The elements and design drawings in AI are shown in Figure 6. Designers just need to enter keywords into the AI system to get new designs and enhance their uniqueness.

4.3. Design Deepening Stage. AI technology plays a more advantageous role in the design deepening phase, especially because the conceptual framework has been initially defined in the previous conceptual design phase of the project. So, this stage only needs to start the specific work layout, including material selection, color matching, determining the size of each detail part, each streamline relationship, the distribution of each function space, and so on. At this point, AI technology can help designers make decisions.

4.4. Expansion Design Phase and Construction Drawing Design Phase. When this stage is reached, the landscape design scheme has initially emerged, which can quickly achieve the operability of the scheme according to AI and solve its potential minor imperfections. At the same time, if the design needs need to be changed, AI technology can give full play to its advantages and help designers to adjust and change the landscape design through artificial intelligence technology.

Taking artificial neural network (ANN) as an example, ANN can interact with the real world like biological neural system and is composed of simple units and parallel interconnected networks. In the field of cognitive science and machine learning, artificial neural networks have learning ability. The network will automatically recognize

similar images through learning. This function is of a great significance to the prediction problem in the field of landscape architecture; moreover, it has strong expression ability and can fully approach complex nonlinear relations. The ability of associative memory is also a feature of artificial neural networks. When modifying or adding new features, only the parameters corresponding to the new features are trained, which has little effect on the original network parameters. Therefore, artificial neural network can provide scientific and efficient research methods and theoretical basis for landscape architecture design and resource management. In recent years, artificial neural networks have been widely used in simulation prediction, evaluation, and landscape classification.

5. Application of AI in Landscape Design

Through the intervention of AI technology, the landscape construction has begun to transform from traditional to modern, and the design mode of AI has endowed the modern landscape construction with new significance. In the past, traditional design concepts pursued practicality and function, ignoring the satisfaction of aesthetic feelings. AI uses computers to make perfect processing in graphics, sound and animation, and brings wonderful visual experience to people, so as to produce beautiful effects. The new design method innovates the landscape design, satisfies people's pursuit of beauty, and makes the modern landscape design enter a new era. [26–28]. Artificial intelligence will energy technology applied in the landscape construction, can make up for the inadequacy of human technology, break through the technical problems, artificial unable to complete the construction work, for example, in the early stages of the design, artificial intelligence can be used to calculate the accurate virtual images, simulate the real design, improve design scheme is practical and scientific nature in the design stage of implementation. artificial intelligence can calculate the actual topography, climate, temperature, and other corresponding plant and structural material types through a large amount of data, so as to carry out site construction more scientifically and effectively, and achieve the purpose of improving the quality of the project [29, 30].

5.1. Application of AI in Landscape Architecture Construction. The application of artificial intelligence technology in gardening construction can make up for the shortage of artificial technology, break through the technical difficulties, and complete the construction work that cannot be completed by artificial. For example, at the beginning of the design, artificial intelligence is used to calculate accurate virtual images and simulate real design scenarios, so as to improve the feasibility and scientific of the design scheme. In the design and implementation stage, AI can calculate plant species and building materials corresponding to the actual terrain, climate, and temperature through large data, so as to carry out field construction more scientifically and effectively, and to achieve the purpose of improving the project quality.

5.2. Application of AI in Water Landscape Design. Water landscape plays an important role in landscape design, and its design is often closely related to the effect of the whole landscape design. In the past landscape design, fake waterfalls, artificial hills, simulated fountains, and so on will be introduced to expand and enrich the landscape of the whole garden. Such a design can bring visual appreciation to a certain extent, but lacks vitality, cyclicity, and sustainability, and has a relatively high maintenance costs in the later stage, and is easy to cause tourists to fall into aesthetic fatigue. Based on this, AI technology will play a very important role in water landscape design.

In practice, the role of smart sensor technology can be fully used to form light shadows pools, music fountains, and so on, to build a water landscape system with sustainable recycling performance, giving more vitality to the water landscape. For example, you can set up an open space in the center of a fountain and install a gravity sensor on its bottom. When the gravity of the corresponding surface area reaches a certain value, the flow of water and light from the surrounding fountain turns on and stops within 30–60 seconds. At this time, people can take photos and play in the center of the fountain to interact with the water view. In this way, the purpose of improving the effect of water landscape design is achieved, and the upgrade of the whole modern landscape design is also promoted, the flow of which is shown in Figure 7.

5.3. Application of AI in Ground Paving. In landscape design, the paving of the ground should first have a hardening effect and preferably be enjoyable to enhance the visual aesthetics. However, the traditional floor paving only has a hardening effect, it is just an ordinary paving, wasting the value of appreciation [31]. Using large data in AI technology for color analysis and changing the color of the ground paving according to different natural light can make the paving not only have hardening effect, but also display certain visual effect, and achieve the unified design effect of aesthetics and function.

Ground paving is also an important content in modern landscape design. On the basis of guaranteeing its intensity (guaranteeing its function), we need to further optimize its visual effect and aesthetic level. However, in the past landscape paving design, under the condition of ensuring the overall function, it is difficult to obtain more rich and diverse visual effects, and the overall aesthetic feeling is not ideal. With the application of artificial intelligence technology, the above design goals can be achieved and the coexistence of function and aesthetics can be achieved. In practice, large data technology can be used to carry out color analysis, adjust the color of ground paving according to natural light, and improve the aesthetic degree of garden tiles, as shown in Figure 8. At the same time, it can also play the advantage of projection technology, put dynamic images on the ground, and promote the upgrade of landscape ground paving design.

In addition, when carrying out ground paving design relying on artificial intelligence technology, you can also

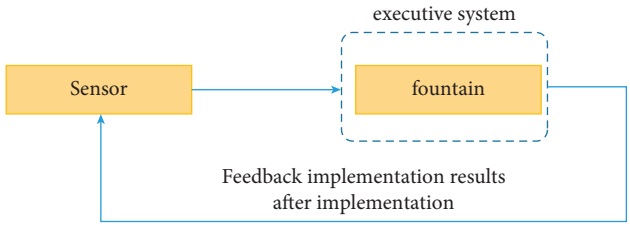

Figure 7: Intelligent water landscape design diagram.

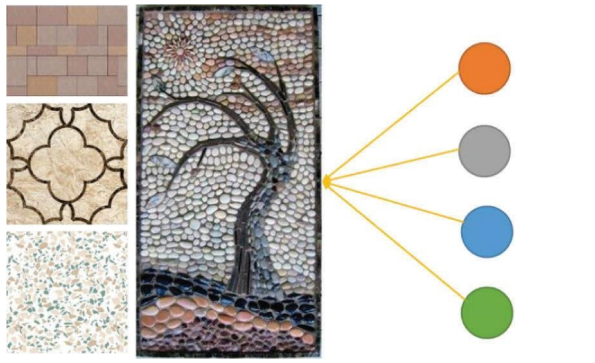

Figure 8: Dynamic adjustment of the paving image under different light sources.

refer to the setting of "stair piano" to create similar landscapes such as "ground piano board," which will attract people to the landscape garden experience, realize the interaction between the landscape and people, and enrich people's experience. This will make the landscape interact with people and enrich their experience.

5.4. The Application of Artificial Intelligence in Visual Lighting. In the past, in landscape design, lighting paid more attention to function (lighting) and atmosphere adjustment, and relatively ignored the aspects of humanization and interaction. The emergence of artificial intelligence technology has brought a new visual experience to lighting design. The application of artificial intelligence technology can bring more rich visual experience to people and make up for the defects of lighting landscape design in the past landscape architecture. For example, smart lighting includes an intelligent sensor system that can effectively perceive the light in the environment, and on this basis, adjusts the light intensity and color of the lighting to reflect the humanization and interaction of the lighting landscape.

In practice, artificial intelligence technology is widely used in three aspects of modern landscape lighting design:

(1) time controller and latitude and longitude controller. Based on the change of latitude and longitude in different areas, the accurate prediction of time change can be achieved, and on this basis, the landscape lighting system can be intelligently controlled.

(2) GPRS wireless landscape lighting remote monitoring device. With this equipment, the gardening administrator can grasp the actual operation of all the lights in the gardens in real time, comprehensively and truthfully. Through the analysis of these data information, the parameters such as the electrical power of lighting fixtures can be determined, which can provide data information support for fault analysis and treatment, and ensure the long-term stable operation of the lighting system in gardens.

(3) Semiconductor landscape lighting. Depending on the reasonable adjustment of lighting time and intensity, and on the basis of meeting the actual lighting needs of modern landscape gardens, the use of electric energy is reduced.

In the future, landscape design and artificial intelligence technology can also be applied in more areas, such as: the intellectualization of background music, combining people with music, can not only heal the mind, enlighten life, but also promote national culture; intelligent lighting not only combines buildings with people organically, but also creates a living place free from light and pollution to better entertain the public without affecting others. Intelligence of public facilities, such as changing some garbage cans to smart robot garbage cans, can be moved to facilitate garbage disposal etc.,

6. Discussion on the Application of AI in Landscape Design

Will designers be replaced by AI? What is the meaning?

It is found that the algorithm can summarize the universal laws of site design through a large number of mature cases, such as "the relationship between layout and site conditions," "the relationship between the layout in the park and the layout outside the park," "the relationship between spatial functions and specific design language," and even summarize some abstract design feature information. However, the design work is far from this. Take a common example of design work. Assuming that a large-scale country park is to be planned at this time, it is likely to experience the following situations: party A proposes that it should adhere to national policies and make "characteristics," but the budget is not high. After a week of discussion, we finally decided to take "carbon neutrality" as the main goal. At this time, I immediately encountered a new problem: how to calculate the carbon reserves? How to balance the revenue and expenditure of carbon source and carbon sink? After another week of discussion, the overall technical route was finally defined. However, once the report was made, there was a new problem: how to make features? At this time, we need to summarize the existing relevant planning and design cases, study the characteristics of the site, and study how to put forward a scientific and objective overall planning and design scheme for the site under the condition of low budget. In the course of design revision, we will also face various problems, ranging from land policy and ecological pattern to special budget, materials, and plant selection. In contrast, a designer is an expert in solving problems, and landscape architecture is a comprehensive discipline that balances society, nature, and economy. These are the meanings of

designers' existence, and also abstract problems that cannot be solved by AI alone. Therefore, automatic design is only a link in the design work.

Therefore, the application of artificial intelligence in landscape architecture design belongs to the exploration of new productivity in landscape architecture industry and the exploration of new production forms in landscape architecture industry. As the landscape architecture industry has become normal to work overtime and stay up late for repetitive drawing, the generation system driven by artificial intelligence can also achieve the production efficiency of thousands of solutions per second. Why is such an amazing productivity meaningless? And mining the universal laws in planning and design with the help of generative confrontation network to build a new human-machine collaboration method, which is only focused on the application research of a small stage in the design industry workflow. The comprehensive intelligent upgrading combining BIM, Lim, UAV, Internet of Things and other cutting-edge technologies will come in the near future, and the new human-machine cooperation forms matching the new productivity will also be accelerated.

7. Conclusion

Explore a more technical parameterized design method for architectural landscape design, combining artificial intelligence with landscape planning and design, and developing a landscape planning and design method that integrates artificial intelligence parameterized analysis. This is a new design branch, which is an extension of landscape design method based on artificial intelligence technology.

Multimedia is becoming more and more important in landscape applications. Due to the public demand and the diversity of social strata, contemporary landscape also shows a diversified trend. Although the future landscape may not necessarily be developed in the direction of multimedia, the future landscape will increasingly use multimedia technology, which represents one of the future directions of landscape development.

Electronic information expressed by multimedia devices has become an important element of landscape design, carrying the fusion of different cultures and technologies in a new form.

8. Limitations and Future Work

Although artificial intelligence technology is more and more applied in landscape architecture research, the ability of artificial intelligence to solve the uncertainty and complexity problems of landscape architecture still fails to meet people's pre-requirements, and it is even more difficult to integrate the uncertainty and complexity problems of landscape architecture into a system framework. First of all, the technology of integrating a variety of artificial intelligence methods is not perfect. At present, there is no more suitable advanced architecture for integrating a variety of artificial intelligence methods. Secondly, to build an artificial intelligence model in landscape architecture research, we need not only landscape architecture knowledge, but also computer science, geography, biology, and other multidisciplinary knowledge. If there is a lack of professional knowledge, we cannot build an ideal artificial intelligence model. This requires that each modeler should have a wide range of knowledge. Although the application of artificial intelligence technology in landscape architecture is not mature at present, with the rapid development of artificial intelligence technology, more artificial intelligence will be applied to landscape architecture research. The intelligent development of landscape architecture in the future needs to actively try to integrate a variety of technologies to establish a landscape model with mixed artificial intelligence methods, and accelerate the automation level of landscape architecture research.

Data Availability

The experimental data used to support the findings of this study are available from the author upon request.

Conflicts of Interest

The author declares no conflicts of interest regarding the present study.

References

[1] T. Teng and C. Qu, "Urban landscape design based on sustainable development innovation," *Open House International*, vol. 43, no. 1, pp. 68–72, 2018.

[2] E. B. Rogers, *Landscape Design: A Cultural and Architectural History*, Harry N. Abrams, China, 2001.

[3] M. L. Cadenasso and S. Pickett, "Urban principles for ecological landscape design and maintenance: scientific fundamentals," *Cities & the Environment*, vol. 1, no. 2, pp. 9–13, 2008.

[4] H. Liu and Y. P. Xia, "Aquatic plants in landscape design," *Journal of Chinese Landscape Architecture*, vol. 1, no. 9, pp. 4120–4132, 2003.

[5] O. Dusan, "Landscape architecture and its articulation into landscape planning and landscape design," *Landscape and Urban Planning*, vol. 4, no. 8, pp. 41–52, 1994.

[6] H. Yang, B. Y. Liu, and U. Patrick, "Traditional Chinese medicine as a framework and guidelines for therapeutic garden design," *Chinese Landscape Architecture*, vol. 11, no. 7, pp. 36–42, 2009.

[7] L. I. Bo-Gang, "The connotation of plant culture in Chinese classical garden and its enlightenment for modern garden design," *Journal of Anhui Agricultural Sciences*, vol. 6, no. 9, pp. 42–48, 2009.

[8] S. S. A. Sun, "Study of the theories of Chinese landscape planting related to the compositon of garden design," *Acta Horticulturae Sinica*, vol. 234, p. 23, 1964.

[9] R. C. Corry and J. I. Nassauer, "Limitations of using landscape pattern indices to evaluate the ecological consequences of alternative plans and designs," *Landscape and Urban Planning*, vol. 72, no. 4, pp. 265–280, 2005.

[10] M. Najafi, K. Zhang, and M. Sadoghi, "Hardware acceleration landscape for distributed real-time analytics: virtues and limitations," in *Proceedings of the 2017 IEEE 37th*

Hindawi
Scientific Programming
Volume 2023, Article ID 9890860, 1 page
https://doi.org/10.1155/2023/9890860

Retraction

Retracted: Construction and Application of College Smart Party-Building Platform Integrating Artificial Intelligence and Internet Technology

Scientific Programming

Received 18 July 2023; Accepted 18 July 2023; Published 19 July 2023

This article has been retracted by Hindawi following an investigation undertaken by the publisher [1]. This investigation has uncovered evidence of one or more of the following indicators of systematic manipulation of the publication process:

(1) Discrepancies in scope
(2) Discrepancies in the description of the research reported
(3) Discrepancies between the availability of data and the research described
(4) Inappropriate citations
(5) Incoherent, meaningless and/or irrelevant content included in the article
(6) Peer-review manipulation

The presence of these indicators undermines our confidence in the integrity of the article's content and we cannot, therefore, vouch for its reliability. Please note that this notice is intended solely to alert readers that the content of this article is unreliable. We have not investigated whether authors were aware of or involved in the systematic manipulation of the publication process.

Wiley and Hindawi regrets that the usual quality checks did not identify these issues before publication and have since put additional measures in place to safeguard research integrity.

We wish to credit our own Research Integrity and Research Publishing teams and anonymous and named external researchers and research integrity experts for contributing to this investigation.

The corresponding author, as the representative of all authors, has been given the opportunity to register their agreement or disagreement to this retraction. We have kept a record of any response received.

References

[1] H. Chen and J. Su, "Construction and Application of College Smart Party-Building Platform Integrating Artificial Intelligence and Internet Technology," *Scientific Programming*, vol. 2022, Article ID 8569301, 9 pages, 2022.

Hindawi
Scientific Programming
Volume 2022, Article ID 8569301, 9 pages
https://doi.org/10.1155/2022/8569301

Research Article

Construction and Application of College Smart Party-Building Platform Integrating Artificial Intelligence and Internet Technology

Huoxin Chen and Jin Su

North China Electric Power University, Hebei, Baoding 071000, China

Correspondence should be addressed to Huoxin Chen; 51551256@ncepu.edu.cn

Received 25 July 2022; Revised 19 September 2022; Accepted 23 September 2022; Published 4 October 2022

Academic Editor: Lianhui Li

In the era of "Internet +," the deep integration of party building in colleges and universities and information technology is the objective need for the modernization of the party's government in colleges and universities and the realization of science. Starting from the concept of the smart party-building platform in colleges and universities, this study analyzes the current situation of the informatization and intelligence of party-building work in colleges and universities. Combined with the current development needs of the party-building work in colleges and universities, starting from the significance of the construction of the smart party-building platform in colleges and universities, the ideas and main research studies on the construction of the smart party-building platform in colleges and universities are expounded. Contents describe the construction path and implementation method of the university wisdom party-building platform in order to construct a reasonable and efficient university wisdom party-building platform construction plan.

1. Introduction

With the rise of "Internet +," the self-construction of grass-roots party organizations in colleges and universities, and the continuous increase in the scale of party members, the pressure on party affairs' management staff has increased, and some colleges and universities have begun to seek more intelligent management models' concept which came into being. The so-called smart party building in colleges and universities [1] is the era title of informatization and digitization of party building in colleges and universities in the new stage of informatization development [2]. The level of party members of teachers and students expands the party's presence and digital influence in colleges and universities, improves the service level of party organizations in colleges and universities, and consolidates the new platform, new model, and new form of party organization management ability in colleges and universities [3]. The formation of smart party building in colleges and universities [4, 5] has gone through a process from scratch, from slogan to initial realization. In the beginning, everyone focused on the research on the necessity and possibility of Internet + party building in colleges and universities, and how to build the Internet + The new system of party building in colleges and universities has become the main theme of the reform of major colleges and universities [6]. The focus of the research is on how to integrate party building in colleges and universities into the mobile Internet platform [7]. Subsequently, a very small number of colleges and universities began to carry out research on the realization and application of smart party building, trying to take "Internet + student growth" as their work idea, such as the "NetEase Class" of Southwest Petroleum University. However, in general, the existing research on high-intelligence party building

platforms [8] is still at a relatively shallow level, and the constructed platforms also generally have the characteristics of a single function, weak data sharing, and poor versatility.

Smart party building is a new application of information technology in the field of party building in the "Internet +" era [9]. Making full use of information technology means building a new smart party building platform to give full play to the smart party building platform to closely connect with the masses, standardize the management of party members, and improve service levels and scientific levels [10]. It is a necessary measure to train qualified builders and reliable successors of the party and the country, and it is an inevitable choice to promote the quality of party-building management in my country's colleges and universities [11–13]. Contemporary college students are all post-90s and digital natives. Almost every college student has more than one mobile phone or mobile terminal. Contemporary college students are very active netizens, who provide sufficient prerequisites for the "Internet + Smart Party Building Platform." It is realistic to build a smart party building platform and strengthen the innovative practice research of college students' party building work, and it is a necessary way to make the party building work in colleges and universities intelligent in the new era [14].

To build a reasonable platform for party building wisdom in colleges and universities, it is necessary to grasp the important advantages of smart party building in colleges and universities from the perspective of theory and practice, strengthen the integration of network, information technology, and party building, and integrate resources so that the management of party building in colleges and universities will become informatized and the forms of publicity will become diversified [15]. Party-building services are becoming smarter, and the following points must be done. (1) Clarify the new tasks and new requirements of the smart party-building platform in colleges and universities, make full-use of the communication power of the mobile Internet, use big data means to integrate resources, and actively explore the use of modern information [16]. (2) Establish a platform for smart party building in colleges and universities. Establish an party member electronic information management system to achieve unified, refined, and standardized management of all party members, and achieve scientific and orderly management of party member information and oral work; establish an online party member examination system to make party member development work smarter; establish an online party school classroom. Develop the APP client of the party building learning platform, transfer the ideological education of colleges and universities to the Internet, and realize the normalization of online education through theoretical learning [17]. (3) Explore the management methods of the smart party building platform in colleges and universities. Strengthen the analysis and judgment of data, improve the accuracy of services, and use relevant policy support and technical means to ensure the safe and effective operation of the party-building platform [18]. Functional modules of the smart party building platform are shown in Figure 1.

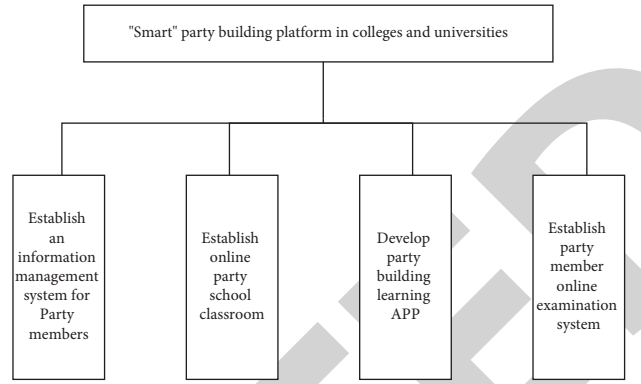

Figure 1: Functional modules of the smart party building platform.

2. The Goal of Building a Party Building Platform That Integrates Internet Technology

In order to implement the requirements of the central party building work, the party and government departments of colleges and universities should make full use of information technologies such as the Internet, cloud computing, big data, and artificial intelligence. Smart management: through the establishment of a smart party building platform, party members are connected to the Internet, the organization is built on the cloud, and the Internet can be integrated into the work, life, and study of party organizations and party members in a timely and effective manner, so as to realize scientific decision-making, learning, and education of party organizations. Use data to achieve precision, use intelligence to achieve prediction, and help provide comprehensive services for teachers, students, and party members in colleges and universities in the digital space [19].

The current smart party building work is carried out in various forms [20]. It is no longer bound by traditional methods. Instead, it uses the Internet to realize party building informatization, establish a smart party building system, and facilitate the implementation of the party's line, principles, and policies, so as to realize the realization of the party central committee. With the proposed goal of strictly governing the party, the smart party building platform provides platform convenience, time convenience, and space convenience for realizing the party building work goals.

The construction of party-building cloud platforms in colleges and universities must be closely integrated with the spirit of the 19th National Congress of the Communist Party of China; it must be integrated with the political and ideological work of schools. The content of the platform should be in line with national conditions, party conditions, and school conditions, and in line with the law of teacher and student growth. Clarify the purpose of building a cloud platform for smart party building in colleges and universities under the new situation and fully reflect the practicality, practicability, and effectiveness of the platform [21] so that teachers and students can learn more efficiently and work well, and party building organizations are more effective, so as to ensure end customers. The number of party members

engaged in online self-learning facilitates, to the greatest extent, the study and lives of the majority of party members, teachers, and students. Second, optimize the top-level design and improve the platform functions. Under the background of "Internet +," the smart party building work in colleges and universities is highly political, professional, and systematic. The construction of the smart party building cloud platform should be regarded as part of the smart campus construction, and college leaders should attach great importance to the smart party building cloud platform. Top-level design and overall planning: give full play to the advantages of the network platform, summarize the main characteristics of the new era and new technology applications, analyze the main problems, and study how to establish and improve the platform design and guarantee mechanism. Establish the concept of "big party building" and improve the platform modules and functions [22], including party building publicity, party member service, party affairs management, party member education, party discipline supervision, party member evaluation, and other modules. Use learning platforms, such as portal terminals, mobile apps, and WeChat public accounts, to give full play to the intercommunication, mutual integration, and interaction functions of "Internet +" and realize the design goal of the smart party building cloud platform. The rapid development of "Internet +" technology has brought great changes to the management of colleges and universities. At present, most domestic colleges and universities have their own complete website construction. With the increase in party affairs' work, it is imperative to open a special portal website for party building on the school homepage. The portal website must have a group of professional management personnel and work according to national laws, top-level reality, and the actual situation of the school. Do a good job in the planning of each module, daily update of content, interconnection and interaction, question answering, background management, etc., and do a good job in the management of WeChat public account platform and mobile APP receiving platform, rather than one or several topics at present module link, and manage lax state. It can really play the role of the portal website and bring convenience to the study and lives of party members. Second is the construction of the WeChat public account platform of the Object Wisdom Party Building. Relying on "Internet +" thinking, the WeChat public account receiving platform for college wisdom party building can transmit text, pictures, videos, and other information anytime and anywhere, allowing college party members and cadres to break the limitations of time and space to browse and read the party's policies and information anytime, anywhere, and learn the latest. The tasks and priorities of the work are well illustrated and immersed. Online party member education is carried out through the WeChat public account, interactive communication, understanding of party members' ideological dynamics, and understanding of the deficiencies in party building work so as to improve the management level and improve the effect of learning and education. Third is the construction of the mobile APP platform of the object wisdom party building. Under the "Internet +" environment, the construction of the party building mobile APP platform is very convenient. For example, the "Learning to Strengthen the Country" mobile APP platform that all our party members are paying attention to every day is good learning receiving platform. Use the mobile phone APP smart party building platform to push news content from time to time, carry out online comments and points learning, and regularly promote the Communist Party members' mobile newspapers with clear themes and vivid content to attract the attention of party members and cadres. Improve the attention of party members and cadres through points ranking, points exchange, etc., so that party members and cadres can improve themselves through learning and fully understand the importance of learning to strengthen the country and the school.

To achieve platform convenience [23], the smart platform built by the smart party building contains a variety of functions, which are intended to transfer the offline activities of the smart party building work to the online, which is more conducive to the development of the smart party building work, and the offline activities are transferred to the online, so that more party members can view and participate at the same time, and there will be no crowding when offline activities are carried out. The party building platform solves this problem very well. Give full play to the supervisory role of the masses. To achieve time convenience, traditional party building work requires smart party building to commute to get off work regularly. When there is a need for study, training, or business trips, you cannot participate in the party-building work of the unit, and you can only go back to the unit to carry out tutoring, resulting in tight working hours; the effect of tutoring is also unsatisfactory. Due to the inconvenience of space, the traditional party building work is difficult to convey information due to the inconvenience of space, and the policies and lines of the Party Central Committee may be "changed" when they are communicated to the grassroots. The establishment of the smart party building platform has solved this problem very well. Party members can use the examination function to strengthen the study of party regulations and party constitutions. The party rules and regulations are imprinted in the heart. The "smart party building" platform system is different from other party building platforms used in colleges and universities in the past [24]. The objects it serves not only are limited to party members and comrades but also include all party identities inside and outside the party, from party applicants to official party members (Figure 2).

The significance of artificial intelligence and Internet technology applications in party building work is mainly reflected in the following three aspects. The use of big data technology to achieve innovation in party building work: after the adoption of cloud computing big data technology, on the one hand, the teaching and labor party branch and student party branch of our college party affairs' workers at the highest level can understand the work dynamics of party organizations in a timely manner based on real-time data and clarify the direction of each party affairs' activity. Data technology provides great convenience. On the other hand, through the analysis of online data on the platform [25], we

Figure 2: Service objects of the "smart team building" platform system.

can more accurately understand the needs of each party member in terms of learning dynamics, work and life, etc., which is conducive to the higher-level party organizations carrying out intraparty care and drawing closer relationships with teachers and students.

3. The Construction of the Platform

For the construction of the cloud platform for smart party building in colleges and universities, it is necessary to grasp the principles and construction methods of platform construction according to the tasks and goals of platform construction. At the same time, plan and design each functional module, build it in one step, and formulate a sound management system to ensure the normal operation of the platform.

3.1. Technical Route. The platform technology architecture is divided into four layers. The bottom layer is the hardware layer, which adopts a safe and reliable elastic cloud platform, which can be elastically expanded according to the size of party members. The data layer is the three core databases of the three party building platforms. The middle layer is the business layer, with the AI intelligence engine as the core, providing a storage engine, search engine, analysis engine, content engine, learning engine, data cache, and other capabilities. The top layer is the user access layer, which is mainly used for external publicity and serving party members and the masses. There are four access methods for the server: portal website, mobile app, WeChat public account, and interactive terminal all-in-one. Party workers, party members, and the masses can easily obtain party building resources and services through different channels. Party organizations can conduct organizational work, content updates and decision-making analysis through a unified management platform [26]. The technology roadmap is shown in Figure 3.

3.2. Functional Framework. A functional framework is shown in Figure 4. The three core databases of the platform include the party member and organization information database, party building information and learning content database, and party member and organizational behavior database, which are used to support the realization of "party building publicity, learning, and education, interactive services, party affairs' management, and party member evaluation." The Party Building Propaganda Center is a column where the party organization publishes important news within the party, and it is a new frontier for party building propaganda; the Learning and Education Center is the "handheld party school" for party members, providing party members with original texts, VR, courses, and other forms of learning content; the party member interactive service center allows party members to post "work, achievements, and highlights" to form a party building work atmosphere that loves interaction and diligent sharing; the party affairs' management center can help party organizations at all levels manage party member information, carry out organizational life, and transfer online. Receive party work such as organizational relations and online collection of party dues; the party member evaluation center generates a medical report by conducting consultations on party members' learning effects and recommends learning content to improve party members' learning effects; the scientific decision-making center for party building provides party organizations at all levels. The AI intelligent engine is the core of the system. Through natural language analysis of party members' speeches and discussions, it depicts party members' portraits and knowledge maps and accurately recommends learning content based on the analysis results.

3.3. Functional Module Design. Platform functions need to be divided and designed from the perspective of user usage habits according to business needs and business processes and follow the standards of identity authentication, information security, sharing, and exchange of the national organization system.

3.3.1. Party Building Information. Party organizations at all levels can publish hot information, advanced models, and clean government models through the party building information module and provide innovative and dynamic propaganda content such as audio and video integration, pictures, and texts. Party members can learn the basic knowledge and theory of the party anytime and anywhere through the three access methods of the platform. Information must be reviewed by the administrator before it can be placed in the corresponding section. The system follows the principle of "which level is the approval level and which level is the release level." For example, the information approved by the branch secretary is open to view by all party members under the branch; if the information has been submitted to the higher-level organization department for approval, all party members under the party organization can view it. In terms of information content recommendation, the platform realizes personalized and accurate push of learning content based on the correlation characteristics and popularity characteristics of party member portraits, learning environment, and party-building content so that the majority of party members can keep abreast of the party and public sentiments they are concerned about. The organizational activity management process is shown in Figure 5.

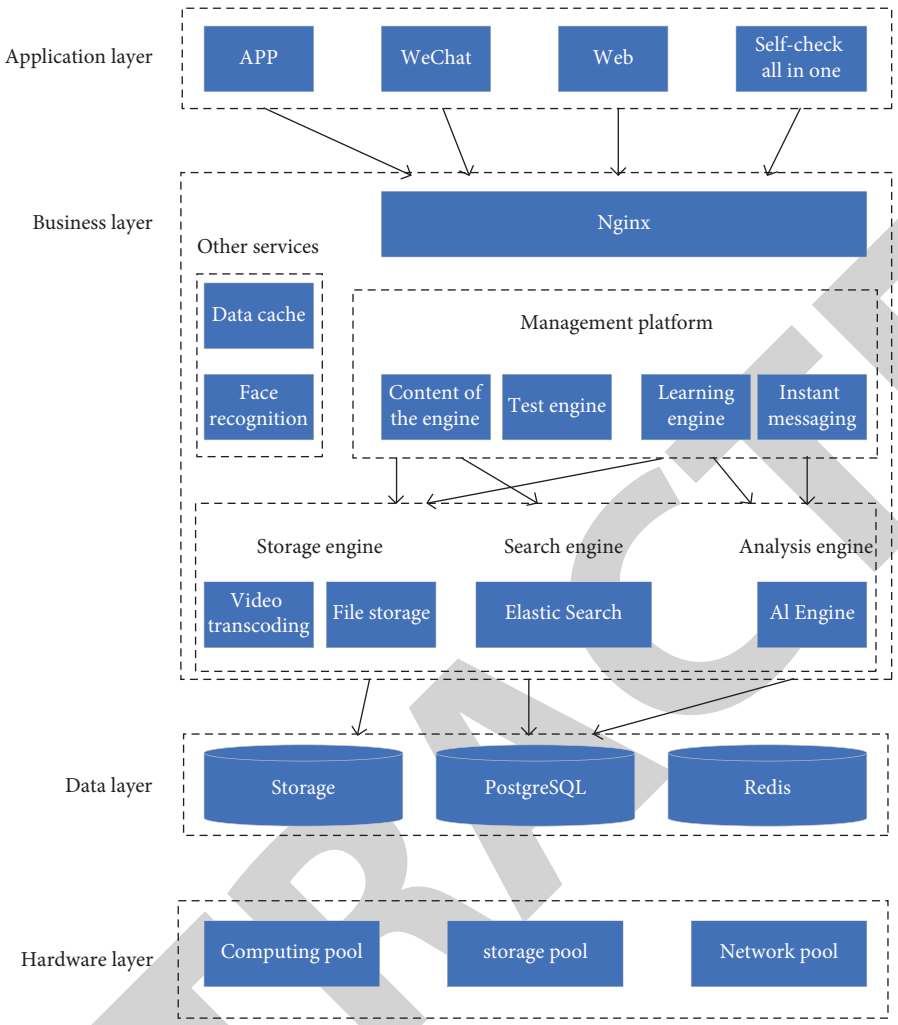

Figure 3: Technology roadmap.

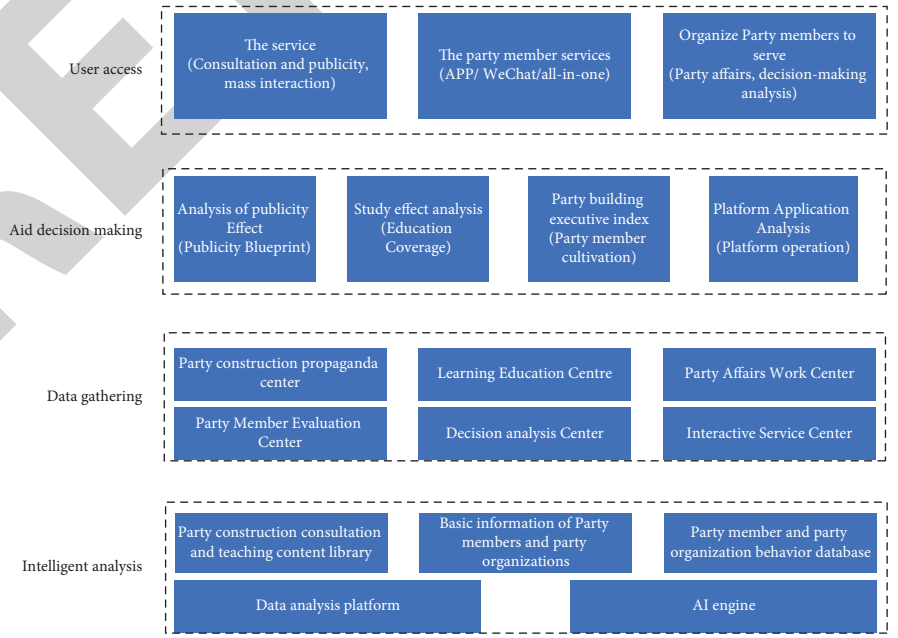

Figure 4: Functional framework.

Party workers initiate organizational activities through the app and set the theme, time, and participants of the event. Before the event starts, the platform automatically pushes information to each party member. After receiving the event notification, individual party members can feed back their opinions to the branch. After the event starts, party members check in after locating them through the app, and the system automatically records and counts the check-in situation. After the event, party workers can upload event pictures and event summaries, and party members can share their experiences.

3.3.2. Party Member Interaction. The party member interaction module realizes the real-time networking of party member management and organizational life. Party members can share their experience and thoughts on party building work, advanced deeds and pioneer stories around them, or the effectiveness of paired assistance work on the platform in the form of a "circle of friends." On the basis of giving full play to the vanguard and exemplary role of the Communist Party members, we launch extensive propaganda. Let the communication and interaction between party members and party organizations and party members and nonparty members no longer be limited by time and space and be able to initiate communication and interaction at any time and any place; changing the previous study relying on on-site lectures, opinions must be presented face-to-face, and evaluations are all thrown around.

3.3.3. Party Affairs' Management

(1) Organizational Management. The organization management module is used to maintain the information database of party organizations and party members and realize the management of adding, deleting, and querying information for party organizations and party members. Party organization information includes party organization code, party organization name, superior party organization code, party organization type, party organization structure, location information, and other information. Support a multilevel tree organization tree, which is consistent with the data format of the Central Organization Department system. Party member information includes name, gender, ethnicity, place of origin, education background, date of birth, contact number, ID number, whether the party has lost contact, job position, code of party organization affiliation, administrative region affiliation, and other information. The format of party members conforms to the "Regulations for Information Collection and Reporting of the National Party Member Information Database of the Organization Department of the Central Committee."

(2) Work Ledger. This module provides two categories of work ledger management of party organization and party affairs work. The party organization ledger includes the party committee work ledger, the party general branch work ledger, and the party branch work ledger. The platform for party building work standardizes the configuration of work items, and this module can provide two categories of work ledger management of party organization and party affairs' work according to the organization. The party organization ledger includes the party committee work ledger, the party general branch work ledger, and the party branch work ledger. The platform party building work standardizes the configuration of work items and can be stratified according to the organization.

(3) Work Assessment. This module provides an online assessment function for party (general) branches and party members. Party (general) branch assessment includes branch self-assessment, branch mutual assessment, leading group scoring, and publicity of assessment results. The assessment of party members includes self-assessment of party members, democratic assessment, scoring by the leading group, and publicity of assessment results. The platform automatically provides the basis for assessment indicators and calculates quantitative scores based on party-building data, which greatly reduces the complexity and workload of assessment work and improves assessment standardization and transparency.

(4) Task Management. The party building work management department can decompose and issue various daily or periodic important work items to the responsible department or person in charge for processing, set the type and completion time of the task, and conduct real-time tracking and penetrating supervision of the task. Party workers can use text messages to remind or urge the responsible person, and the responsible person can also give feedback on the implementation of the work in the task management process. The platform can centrally monitor and summarize key tasks, which is conducive to strengthening the implementation of various party-building work items and forming efficient cooperation in party-building work.

(5) Cadre Management. This module establishes a complete information file of party members and cadres, records the basic information of party members and cadres, resumes, work experience, family situation, important social relations, elected representatives, and committee members, and realizes the daily management of cadres, learning, and examination, assessment, and selection. Full coverage standardizes the whole process of management cadre assessment, provides cadre selection and appointment and management assessment supervision mechanism, and provides information support for colleges and universities to select and employ personnel and conduct cadre assessment.

3.4. Online Teaching. Online teaching is divided as follows.

3.4.1. Online Learning. Relying on "new media" for learning and interaction has become the new normal in the education and training of party members and cadres. The online learning module can provide party members with content such as national policies, party history MOOCs, school regulations, party work priorities, party affairs research,

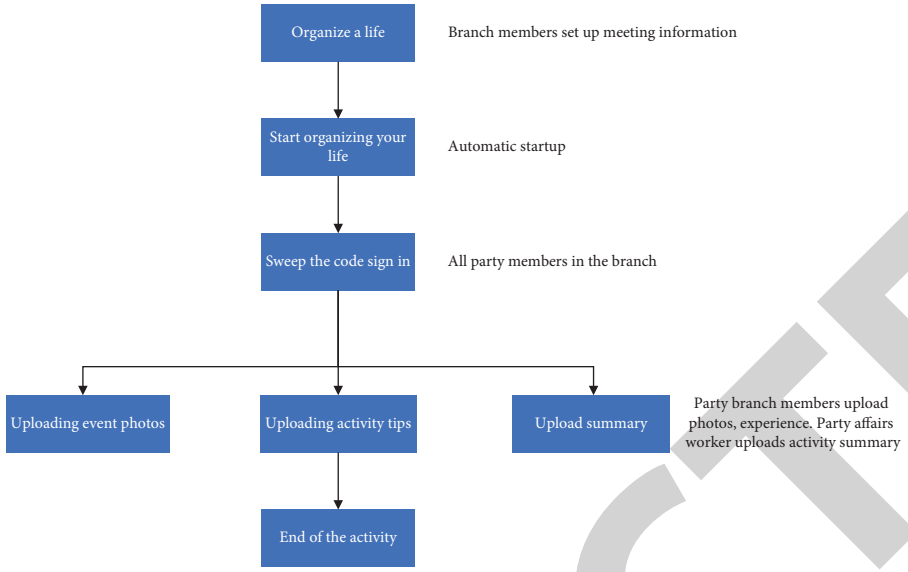

Figure 5: Organizational activity management process.

agricultural history and school history, and VR representation of red scenic spots. The platform records the learning content, time, comments, and other learning behavior data of party members for evaluation and analysis of learning effects.

3.4.2. Exam Management. Exam management is divided into three parts: question management, paper management, and examination management. The range of test questions includes the platform's own question bank and a user-uploaded question bank, and the types of questions are multiple-choice, multiple-choice, and judgment. Administrators can batch import test questions through an Excel spreadsheet. Before the test, the administrator can automatically generate test papers with random questions from the question bank or manually select the test questions to form the test paper and set the test time, question score, test object, and other information on the test paper. After party members submit test papers through computers or mobile phones, the platform will automatically grade the papers and calculate the total score.

3.5. Intelligent Analysis. Intelligent analysis is as follows.

3.5.1. Portraits of Party Members. The image of party members and cadres is related to not only the mass base, influence, and appeal of the party members and cadres but also the image of the party and the prestige of the party organization. This module creates three-dimensional portraits of party members from 26 categories and 145 subcategories. The platform intelligently analyzes the learners' thinking patterns of perceiving and processing information from the semantics and context of comments and categorizes the work behavior styles of party members into four categories: perception, observation, thinking, and hands-on. The machine learning algorithm based on feature extraction compares the text features of the comments with the built-in keyword knowledge base of the system. The level outlines the overall level of party members' learning effects, synthesizing the semantic, context, and keyword features of the review text and mining the relatively stable and lasting characteristics of the learners in most cases, that is, the personality traits through the learners' behavior forms in different times and situations. And from the personality traits of 16 dimensions such as gregariousness, self-discipline, and intelligence, it provides a reference for personnel placement, adjustment, and rational use of party member resources.

3.5.2. Party Building Decisions. The party-building decision-making module realizes the function of supervising and controlling the work of party members and party organizations online. Party workers can supervise the attendance of party members and track and manage the activities of lower-level party organizations and grassroots party organization meetings. This module visually displays the statistical data of the party organization, the statistical data of organizational life, the statistical data of democratic appraisal, the statistical data of the "three meetings and one lesson" learning, the statistical data of the party members' learning effect, etc. Through trend analysis, party affairs' workers can understand the work of grassroots party building and changes in party building indices, and review the effect of special education in real time, so as to adjust and optimize party member education strategies in a targeted manner to achieve precise policy implementation.

4. Conclusion

To sum up, under the background of "Internet +," information technology provides a more complete and convenient way for the cloud platform of smart party building in colleges and universities and promotes the advancement of party member education, management, and service with the

times. In the construction of the smart party building cloud platform, it is necessary to clarify the construction goals to ensure the wisdom of the party building management work. With the innovation and improvement of the smart party building cloud platform, it promotes the development of party building work in colleges and universities, enhances the vitality of party building work, and brings new vitality to party building work. At the same time, it also provides new ideas for the development of college construction work, promotes the progress of grassroots teachers and students in colleges and universities, and ensures the quality of grassroots party members. The online education management method of party members will improve the efficiency of party affairs' work. The four advantages of the "smart party building" platform will also be the necessary methods and means of party building work in the future. From the perspective of "Internet + big data," party building work will surely move forward steadily on the road of high efficiency and technology.

Data Availability

The dataset can be obtained from the corresponding author upon request.

Conflicts of Interest

The authors declare that they have no conflicts of interest.

References

[1] M. Lu, "Practice and exploration of "wisdom party building" applied to party member education in colleges and universities," *International Journal of Educational Technology*, vol. 2, no. 3, 2021.

[2] Z. Zhang and M. Zhu, "Exploring the work paths of smart party building for the private colleges and universities in the new era," in *Proceedings of the 4th International Seminar on Education Research and Social Science (ISERSS 2021)*, January 2022.

[3] J. Sun, T. Liu, Y. Wang, P. Zhang, and D. Yang, "Application of big data analysis and cloud computing in network platform building," *Journal of Physics: Conference Series*, vol. 2033, no. 1, 2021.

[4] C. Zhang, Y. Li, and Z. Wang, "The study of research-oriented learning platform building based on MAS," in *Proceedings of the 2015 International Conference on Computer Science and Information Engineering(CSIE 2015)*, pp. 415–419, September 2015.

[5] P. H. Yen, "The information platform building for marine logistics in taiwan," in *Proceedings of the 2016 International Conference on Sustainable Energy, Environment and Information Engineering (SEEIE 2016)*, pp. 343–348, 2016.

[6] C. E. Zhang, X. F. Hou, and Y. F. Zhang, "The application research of data mining in research-oriented learning platform building," *Applied Mechanics and Materials*, vol. 3147, pp. 548-549, 2014.

[7] Y J. Yang, H. Liu, and Y. Han, "Universities' cloud storage platform building research," *Advanced Materials Research*, pp. 846-847, 2013.

[8] Y. Luo and X. Q. Zhang, "Cloud-based platform building research of teaching resources," *Applied Mechanics and Materials*, vol. 2560, pp. 347–350, 2013.

[9] H. Zhang, J. Yang, and M. Chen, "The reacher of university network teaching platform building based on empathy," in *Proceedings of the 2010 International Conference on Management Science and Engineering (MSE 2010)*, vol. 2, pp. 391–394, ZheJiang, China, 2010.

[10] Z. H. A. O. Jun-feng, "Study of R-TOPSIS method and application of R-TOPSIS method in E-commerce platform building,"vol. 03, pp. 360–363, in *Proceedings of the 2011 3rd IEEE International Conference on Information Management and Engineering(ICIME 2011)*, vol. 03, pp. 360–363, Institute of Electrical and Electronics Engineers, Beijing 100083,China, 2011.

[11] A. J. F. d'Apice and P. J. Cowan, "Building on the GalKO platform," *Transplantation*, vol. 84, no. 1, pp. 10-11, 2007.

[12] D. A. Quistberg and A. V. Diez Roux, "Information technology - information and data platforms; researchers from drexel university discuss findings in information and data platforms (building a data platform for cross-country urban health studies: the salurbal study)," *Information Technology Newsweekly*, vol. 96, no. 2, pp. 311–337, 2019.

[13] S. Jongstra, C. Beishuizen, S. Andrieu et al., "Development and validation of an interactive Internet platform for older people: the healthy ageing through Internet counselling in the elderly study," *Telemedicine and e-Health*, vol. 23, no. 2, pp. 96–104, 2017.

[14] D. Li, S. Meng, B. Qi, C. Liu, and J. Zhu, "Research on development and application of intelligent cluster management platform for shield machine," in *Proceedings of the IOP Conference Series: Earth and Environmental Science*, vol. 861, no. 5, p. 052072p. 052072, 2021.

[15] H. Wu and J. Hu, "Artificial intelligence platform construction and integration based on multi-sensor fusion," in *Proceedings of the MATEC Web of Conferences*, p. 359, Laibin, Guangxi, May 2022.

[16] S. Guo, "Research on the innovation path of organizational personnel and party building work in higher vocational colleges," *Journal of Social Science and Humanities*, vol. 3, no. 10, 2021.

[17] Di Jin and Y. Hu, "Theoretical research and practice on brand building of colleges grass-roots party construction," *International Journal of Education and Teaching Research*, vol. 2, no. 4, 2021.

[18] D. Jing, "The party building leads the innovative exploration of grassroots governance in rural pastoral areas under the concept of Co-governance," *Scientific and Social Research*, vol. 3, no. 5, pp. 125–131, 2021.

[19] F. Yu, "The transmission of the spirit of party building: a functional elaboration of the nurturing ideology of civics——teaching ethics and rule of law Class as an example," *Frontiers in Educational Research*, vol. 0, no. 11, p. 4, 0, 2021.

[20] Wu Jiang, "Research on the party building work of private colleges and universities in the background of "Internet+"," *Advances in Vocational and Technical Education*, vol. 3, no. 4, 2021.

[21] R. Ahmad Mir, "The effective integration of party construction and human resources in state-owned enterprises in the new period," *International Journal of Management Science Research*, vol. 4, no. 3, 2021.

[22] Y. Deng and H. Lu, "Exploration and practice of the working mechanism of the party construction of higher vocational college students under the background of new media,"

Hindawi
Scientific Programming
Volume 2022, Article ID 7116988, 8 pages
https://doi.org/10.1155/2022/7116988

Research Article

Research on Intelligent Power Marketing Inspection Model Based on Knowledge Graph

Jinghua Wang,[1,2] **Bingxu Chen**,[1] **Yue Wang**,[1] **Zihan Xu**,[1] **and Wanru Zhao**[1]

[1]*State Grid Shanghai Municipal Electric Power Company, Shanghai 200030, China*
[2]*Shanghai Jiao Tong University, Shanghai 200030, China*

Correspondence should be addressed to Jinghua Wang; jane950110@sjtu.edu.cn

Received 9 August 2022; Revised 13 September 2022; Accepted 22 September 2022; Published 4 October 2022

Academic Editor: Lianhui Li

The traditional topic-based auditing model lacks the ability of multi-object and multi-abnormal correlation auditing, which makes it impossible to solve the multi-scenario and multi-factor correlation-based auditing problem. This paper designs an intelligent power marketing audit model based on a knowledge graph. First, an entity identification and relationship extraction method for power marketing business based on NLP (natural language processing) and sequence annotation technology is proposed, and the description content is imported into the knowledge graph database; then, semantic disambiguation and knowledge are carried out by using bidirectional encoder representation from transformers (BERT). Link to build a knowledge map of business audit rules: Finally, an experimental analysis is carried out by taking the copying and receiving business with a large business volume in the marketing audit work as an example, and it is verified that the proposed model can effectively improve the information analysis ability and the audit accuracy of the audit work.

1. Introduction

As a basic work of power supply enterprise, power marketing audit plays a very important role in ensuring the economic market order of power enterprises and improving their economic interests [1]. It is not only related to the survival and development of the power supply enterprise itself, but also directly affects the smooth operation of the entire power system and even determines whether the national economy can continue to develop rapidly [2]. The development process over the years can be roughly summarized into the following three stages. The first stage: According to the work experience, conduct random inspection of the marketing business, the main purpose is to find problems. The second stage: Based on the statistical sampling technology, referring to the business audit scoring system, the overall marketing business is audited, and the main purpose is to evaluate the marketing business of each department. The third stage: Build a three-in-one audit system, including online audit, sampling audit, and special audit, to supervise the quality of marketing business from different dimensions, the main purpose is to reduce the problem rate of marketing business to the greatest extent and improve the level of marketing business.

However, with the continuous acceleration of smart grid construction, the business scope of power marketing is more extensive [3]. The current electric power inspection work faces some difficulties, such as the traditional inspection work mode can no longer meet the requirements of current social development, and there are still problems such as backward inspection methods and low efficiency. Therefore, effective measures must be taken to solve these problems. It is necessary to reform and innovate it, use intelligent inspection to improve the continuity and integrity of marketing inspection work, and promote the continuous improvement of marketing management level [4].

As a new type of semantic network analysis technology, knowledge graph connects all knowledge points in series through the correlation between things, displays them in the form of graphs with different structures, and has significant information analysis capabilities [5–7]. In this paper, the construction of an intelligent power marketing audit model

based on knowledge graph is introduced by taking the copy-checking and collection business with a large business volume in the marketing audit work as an example. According to the traditional marketing audit sampling plan, this business will be allocated more audit samples, so it must invest more manpower and material resources. However, because the sample problem rate of this business is relatively low, most of the audit personnel's time is spent checking samples without problems, resulting in a waste of human resources. Through the use of deep learning algorithms to complete knowledge identification and extraction, realize the construction of business audit rules knowledge map, greatly improve the accuracy and control efficiency of this marketing business audit, and effectively ensure the management ability and work efficiency of business audits.

The main contributions of this paper are the following triple:

(1) Propose an entity identification and relationship extraction method for power marketing business based on NLP natural language processing and sequence labeling technology, break through the original audit topic labels, and realize the construction of a three-dimensional label database that combines the basic attributes of customers with hierarchies and classifications.

(2) Carry out semantic disambiguation and knowledge linking based on bidirectional encoder representation from transformers (BERT), generate a knowledge map of business audit rules, check and analyze business content according to its own search rules, and realize intelligent management and control of audit business.

(3) According to the constructed intelligent power marketing audit model based on knowledge graph, take the copying and receiving business with large business volume in marketing audit work as an example to carry out experimental analysis to verify that the proposed model can effectively improve the information analysis ability of audit work.

2. Status Quo of Electric Power Marketing Business Inspection and Research

2.1. Current Status of Research on Extraction of Knowledge Elements in Power Marketing Business Inspection. The research of foreign experts and scholars on power marketing audit management mainly focuses on the mode of marketing audit and the division of supervision power [8]. After research, Li et al. concluded that the functions of power inspection mainly include: inspection, investigation, and execution [9].

The degree of marketization of electricity in the United States is relatively high, and the state-level government enjoys great autonomy. Therefore, the supervision of marketing activities in the United States is not unified by the state, but each state conducts it separately under the guidance of national laws. This model makes the marketization of the power industry very deep, but it is not conducive to the overall regulation and management of the power grid [10].

From the perspective of foreign advanced power companies, some power companies with advanced management have incorporated marketing audit work into their daily marketing work, and rely on the strong support of information systems to effectively monitor data [11]. For example, the marketing information system of Tokyo Electric Power Company of Japan is inclined to the checking of relevant data and logic, and through the automatic review and judgment of the system, the correctness of business execution is ensured [12]. Due to the different business environment of foreign power companies, customers have less breaches of electricity usage and electricity theft, and the internal management of power supply companies is relatively complete. Considering the operating costs, they rarely consider setting up special inspection departments. The inspection of the industry mainly focuses on the supervision of the legal operation and service quality of the electric power enterprises by the electric power supervision department. Of course, in the foreign situation, through systematic analysis and design, streamlining business categories and simplifying business processes is also the key to improving the quality of marketing work [13].

In China, the State Grid Corporation of China was formally established on December 29, 2002. Its main business is power network operation and power market sales. It is mainly engaged in power transmission, and is responsible for voltage conversion, user power distribution, wholesale power sales, and other businesses. It is closely related to the country. The important state-owned backbone enterprises of energy security and national economic construction are the guarantee for the stable development of the national economy and society. The current development of my country's power industry has entered a new stage, and the market-oriented reform will be further accelerated. However, the current level of power marketing in our country cannot meet the needs of the development of the times, the development of demand-side response is not in place, power companies have not deeply studied the potential information of users, lack the necessary system support technology, and lack a perfect service system and user behavior analysis methods. We need to change marketing concepts, adjust marketing strategies, and study new marketing models to meet market demands [14].

The power marketing audit work is in the early stage, but the power enterprises have realized that in the current process of power system reform, the power marketing audit work, as a business control within the enterprise, is particularly important for the improvement of their own management quality [15]. In recent years, electric power companies have also attached more importance to marketing audit work, but it is only a staged and temporary work arrangement. Marketing audit has not been deeply studied and implemented as an independent topic, and a scientific and systematic management system has not been formed. Therefore, there are still many problems. For example, the closed-loop management of marketing audit work is not in place, and there is a lack of tracking and monitoring of the

work. Many of the problems found have not been solved in the end [16]; there is no effective real-time monitoring system for key business windows and front-line service specifications; it lacks a powerful online inspection function and fails to plug loopholes from the source [17]; at the same time, in the face of the ever-expanding mass of customer information and data, it is impossible to pass the traditional method. Effective inspections are carried out manually, and there are problems such as the lack of a professional work team.

In order to solve the work bottleneck of power marketing audit, in 2009, the State Electricity Regulatory Commission issued the "Opinions on Further Doing a Good Job in Electric Power Marketing Audit," requiring that the marketing audit work of power supply enterprises should be increased in all power systems and properly handled in accordance with the laws and regulations. Electricity violations of laws and regulations can comprehensively and effectively maintain the order of the electricity market [18]. On the basis of the theoretical research on marketing audit, State Grid Corporation has issued a series of guiding documents on marketing audit to guide the power supply enterprises in various provinces and cities to strengthen the construction of marketing audit, strive to improve the level of information management, and establish a unified power marketing audit and monitoring platform.

2.2. Research Status of the Construction of Power Marketing Business Inspection Rule Map. Through the vigorous promotion and widespread use of smart meters and power consumption information collection systems, researchers have a large amount of user power consumption data to carry out management and operation decisions based on power data analysis and optimize power supply services [19]. However, in the operation and maintenance business of the domestic power sector, most power sectors use traditional statistical analysis methods or simple threshold determination to detect abnormalities. This method has great limitations. Not only is it difficult to detect the event information contained in abnormal electricity consumption data, but the utilization rate and accuracy of electricity consumption data are also low. The earliest prototype of the knowledge graph was developed from the ontology knowledge base. With the development of time, the World Wide Web appeared, and the concept of data link was introduced, which made the nodes in the semantic web linked and formed a network-like structure. The concept of knowledge graph was formally proposed by Google in 2012 [20]. It is a semantic network knowledge base that stores, uses, and displays existing knowledge in the form of a structured multi-relationship graph. By fusing multiple entity-relationship triples, a multi-relationship graph containing multiple different entity nodes and multiple types of relationship edges is formed, that is, a knowledge graph. The existing larger knowledge graphs include the English Google Knowledge Graph, and the data comes from Freebase, CIA's World Profile and Wikipedia, etc.; the Chinese General Encyclopedia Knowledge Graph (CN-DBpedia) proposed by Fudan University [21], the data comes from many encyclopedia websites. The above knowledge graphs are all general domain knowledge graphs, and in recent years, research on the construction of domain knowledge graphs has also been widely carried out in the fields of power grid, medicine, and finance.

In the field of electric power, Meng et al. [22] used dependency parsing combined with rules to extract entity-relation triples in the electric power field. Based on the domain dictionary combined with the remote knowledge base, this paper aligns the entity-relationship triples of the encyclopedia corpus, uses the LTP tool to perform Chinese word segmentation, part-of-speech tagging and constructs the dependency syntax table, combines the rules to mine entity triples, and constructs the domain knowledge of power dispatching Atlas. Finally, Neo4j is used for storage, and the visualization page that comes with the graph database is used to display the knowledge graph structure. Based on the power user dictionary, Ref. [7] used syntactic information combined with part-of-speech association rules to analyze the main parts and components of the power transformer operation regulations. Knowledge extraction is performed for corresponding operations, a knowledge graph of power transformer operation specifications is constructed, and Neo4j is used to store it; in [23, 24], authors used deep learning and conditional random field model for entity extraction, and uses attention mechanism combined with bidirectional threshold recurrent neural network for relation extraction, build a power dispatching knowledge graph, and use the Redis database for storage.

3. Marketing Business Audit Rules Information Collection

To construct digital audit rules, first of all, we must collect and sort out the business audit information content required by the enterprise, and complete the work of entity extraction and relationship mining. For the marketing business, because the tasks undertaken by each department have a certain degree of dispersion and independence, it is necessary to collect scattered management rules in a unified database. The internal digital audit rules of each department are systematically copied and extracted, sorted by department, and the data is preprocessed according to the content of the business rules of the data processing system.

After integrating all the normal digital audit rules, the relationship mining of business rules is carried out. According to the audit theme and core rules formulated by the enterprise, relevant audit rules matching the theme core rules are formulated. In the business rule database, relevant keywords are extracted according to the content requirements of the rules and sorted according to the degree of association. The associated business rules construct the association relationship according to the business rules to which the keywords belong. The knowledge map information business relationship is shown in Figure 1.

The above analysis tentatively builds the connection between digital audit rules. To make the knowledge map of digital audit rules intelligent, it is necessary to use relevant

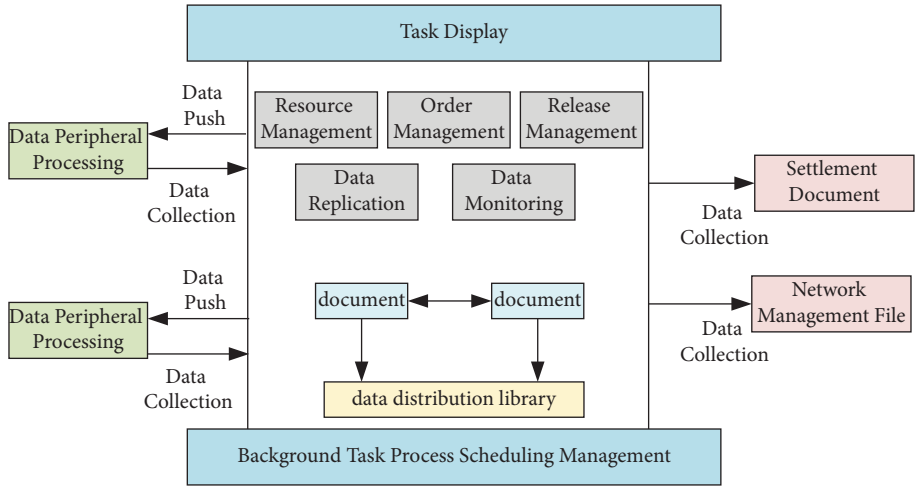

Figure 1: Knowledge graph information business relationship.

languages to describe the content and keywords of business rules. The content of the initially generated digital audit rules with associated relationships is retrieved through the system retrieval program to retrieve the relevant description content and participate in the knowledge map of the digital audit rules, which helps to make the knowledge map more intelligent.

4. The Construction of Intelligent Power Marketing Inspection Model

The construction process of the intelligent power marketing inspection model based on knowledge graph includes three main links: knowledge element identification, relationship analysis, and inspection rule graph construction.

4.1. Knowledge Element Identification and Relation Extraction of Power Marketing Business Audit Rules. Use natural language processing (NLP) and deep learning model algorithms to perform entity recognition on digital audit knowledge. The digital audit rule information source collected and sorted in the early stage is transmitted to the data processing system. The system data processing program first determines the content knowledge entity from the business rule content, extracts the keyword features of the determined knowledge entity, mainly including lexical features, language features, and related features, gives relevant descriptions of knowledge entities according to the characteristics, and then marks the description information as the content of knowledge entities accordingly.

NLP is mainly responsible for the mutual conversion of business rule content with relevant language descriptions in computer language and natural language, so as to realize natural language communication between humans and machines. Identify and analyze knowledge entities in knowledge graphs based on natural language processing technology. Knowledge entity recognition usually builds a knowledge map of digital audit rules based on related dictionaries, and the related dictionaries of business audit rules can be selected as the identification basis. The key words in the dictionary and their related features are introduced into the recognition program, and then the deep learning algorithm is used to realize the association operation of the power marketing business rules knowledge graph sample information data. The relationship between knowledge entities and related terms is determined based on the degree of association obtained by the operation. The keyword feature determination formula of knowledge entity and relationship recognition operation is as follows:

$$s = \left\{ \begin{array}{ll} 1, & e = E \\ 0, & e \neq E \end{array} \right\}. \tag{1}$$

In formula (1), s represents the feature determination result of the word, e represents its corresponding description feature, and E represents a related word. The closer the operation result is to 1, the higher the correlation between the two words, and the stronger the relationship between words. Then calculate the frequency of the word appearing in the document or web page to which it belongs. The formula is as follows:

$$P = c_i n_i \times \log \frac{W}{t_i}. \tag{2}$$

In formula (2), P represents the frequency of the word appearing in the document or web page to which it belongs, $c_i n_i$ represents the number of times the word c_i appears in the document or web page n_i, W represents the total number of documents in the knowledge graph database, and t_i represents the occurrence of the word c_i in the document. Related vocabulary tree: According to this formula, the importance of vocabulary and related documents can be obtained, and then the relationship between multiple documents can be obtained.

Based on the feature method, the relationship recognition and judgment of key words are carried out, and the obtained feature recognition result is shown in Figure 2.

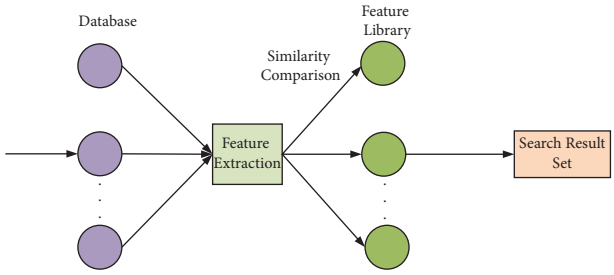

Figure 2: Feature recognition results.

It can be seen from Figure 2 that there is language processing and relationship recognition between the acquired knowledge entity vocabulary and its related vocabulary and documents. Taking knowledge entity language as the analysis object, various recognition methods such as character features, part-of-speech features, and meaning content are selected according to the description features. More specifically, the characteristic relationship can be determined based on the relevant vocabulary classification in the digital auditing rules, such as person name, place name, institution name, and professional work vocabulary. The key words or languages of the knowledge graph of digital audit rules mainly include audit targets, problem descriptions, quick output, audit topics that match the audit targets, and business control rules.

Based on the descriptive features, analyze the feature recognition of related words and sentences, infer the nature of the relationship between the two, give the definition of the relationship, add the description of the related entry, and the subordinate documents of both parties participate in the establishment of the relationship map between the two words or languages. For the determination of the content relationship of the document, it is necessary to take the correlation degree of the two sides of the keyword as the starting point, integrate the determination results of the relationship description in other languages and the relationship judgment results, establish the relationship, and annotate the relationship description entry.

4.2. Construction of Knowledge Map for Power Marketing Business Inspection. After the knowledge feature extraction and relationship identification of the power marketing business audit rules are completed, the relationship processing data resources between them are integrated into the construction of the knowledge map of digital audit rules. The knowledge entity information and related data after analysis and processing are divided according to a certain relationship, and imported into the model building system database in batches. The system uses Cypher language to write the framework program of the vocabulary and document relationship model. Cypher can perform key description queries on associated nodes and all relational features in vocabulary or documents on the system resource database and the Internet platform, and based on the retrieved relational results, further improve the relational network and relational description between words. The layers are progressive, and a network of interconnected relationships is established. At the same time, Cypher can also individually judge the degree of association between them according to the queried relational information, and construct relational networks with different degrees of closeness according to the degree of association. Therefore, after the user uses this knowledge graph, the system will recommend the information content with a greater degree of relevance according to the degree of relevance between the search keywords, while the number of recommendations for other content will decrease in turn according to the degree of relevance, and the user can enjoy the relative individuality, and intelligent retrieval services. In addition, the graph is in a synchronous connection state in the system database, the retrieval content will be associated and recorded, the input information resources will be updated constantly, and the knowledge graph will be maintained in real time, ensuring that the business audit rules and related work content of the enterprise unit are recorded truly and completely.

At the same time, the digital audit based on the knowledge graph has an inspection function, which can check and analyze the business content according to its own search rules. For the problematic parts, it can automatically point out errors, modify and correct, intelligently analyze the original information of the audit work order and the description of the reasons for the audit, and propose the audit. Verification steps, guidelines for rectification measures and other feedback information, judging the type of cause of abnormal situation, labeling the cause of the problem, assisting business personnel to operate, improving the efficiency of inspection rules creation and maintenance management, providing intelligent support for business management and control, using Python language to train knowledge graphs module operation. Figure 3 shows the workflow of digital inspection based on a knowledge graph.

Select the quarterly business work order of the enterprise as the experimental object to conduct problem inspection to examine the problem type. The content of the company's business work order and other information resources are sent to the knowledge graph processing system. Through vocabulary extraction, classification, and feature extraction, the relationship between vocabulary and language based on their respective characteristics and related descriptions is described and marked, and then the business rules are tested through the information dataset. Whether the content of the information is correct can be used to determine whether there is a problem with the work order information. The knowledge graph system internally judges the content of the information about the degree of association between different files or words based on its keywords and relationship descriptions. If there is a problem, mark the cause of the problem, and finally display it through the user. The interface outputs the test results.

5. Experimental Study

In order to test the practical application effect of the intelligent power marketing inspection model research based

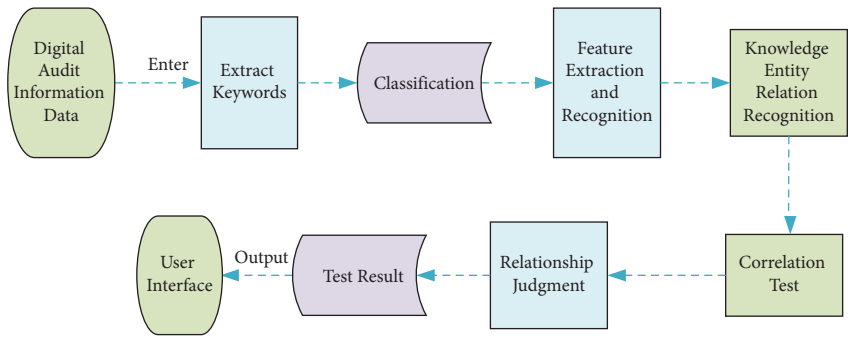

Figure 3: Digital audit workflow based on knowledge graph.

Table 1: Data information.

Abnormal electricity bill	Label
Community supporting charges are not standardized	Inaccurate billing standards Charges are not timely Inconsistency in the amount charged The supporting fee is not implemented for the newly built public-transformation station area Inaccurate billing standards
Abnormal charges for high reliability power supply	Receivable but not received Excess charge Wrong fee type Receivables do not match Escape fees
Abnormal charges	There is a record of overdue payment Payment takes too long Late payment of fees Phased allocation not implemented The same account pays more than 3 times in a single day Advance receipt is not timely
Abnormal refund	Too many cheques returned in the current year Irregular refund Cash refund is not standardized Cancellation prepaid but not refunded

on knowledge graph, this paper conducts experimental research. This paper uses Python as the programming language to simulate the running environment of the method in this paper as the following configuration: The system configuration is Windows 11 Home Chinese version, the processor configuration is 12th Gen Intel (R) Core (TM) i7-12700H 2.30 GHz, 16G RAM.

The data source selects the abnormal electricity bill label as the experimental sample, the collected information is shown in Table 1, and the knowledge map is drawn through the intelligent electricity marketing inspection model of the knowledge map.

According to Table 1, the knowledge graph construction based on tags is shown in the following figure.

From the information in Figure 4, it can be seen that the intelligent electricity marketing inspection based on the knowledge graph can construct a knowledge graph according to the abnormal electricity bill labels, and can intuitively see the connection between various abnormal expenses. Mining and integration. It connects structured and unstructured data and uses it as a whole to mine previous hidden knowledge and simplify complex business problems.

Combined with the characteristics of the audit model, it is fully applied to various channels such as online audit, special audit, and on-site audit. In the first half of 2021, the audit model was applied to mine 84 failure points of front-end risk management and control, and 67,300 cases of various businesses were corrected, mainly including: 12,400 cases of electricity and electricity billing, 13,700 cases of reporting and installation management, and 5,200 cases of electricity bill management. For example, 3,500 cases of meter reading management, 12,800 cases of electric energy meter elimination management; 16.32 million yuan of errors in electricity bills and business expenses were corrected.

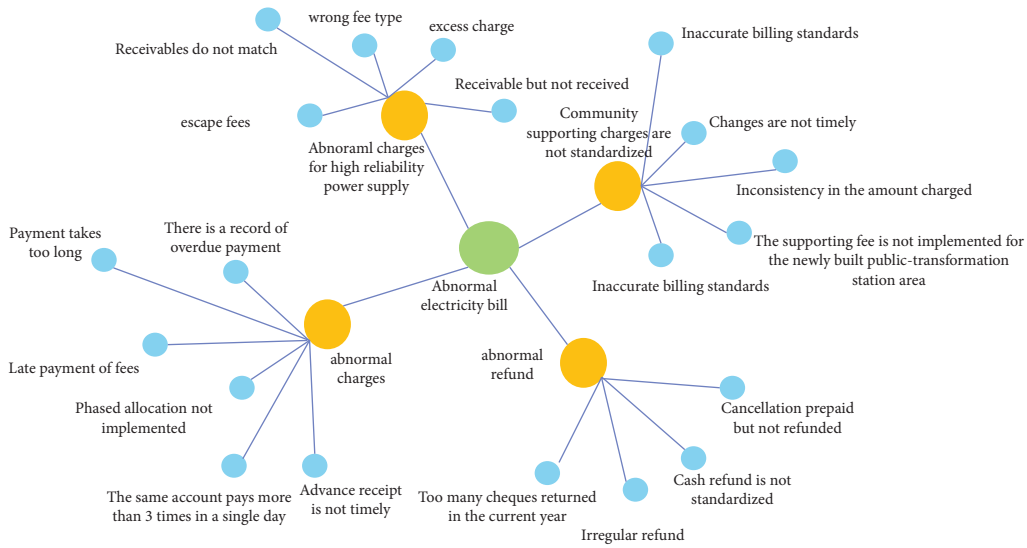

Figure 4: Construction of knowledge map of power marketing inspection rules.

6. Conclusion and Outlook

The application of the audit model in power marketing management gradually builds a closed-loop iterative closed-loop working method for online auditing of marketing business errors, including risk mining, model building, verification evaluation, and classified application. Based on the visualization value of knowledge graph, this paper proposes a new idea of applying knowledge graph to marketing audit work. And by selecting typical application scenarios in actual work, the practicability and effectiveness of the proposed model are verified by cases. The results show that the model can gradually restore complex scenes by using graphs, accurately find abnormal points, and effectively improve marketing lean, digital management level.

In the follow-up research, big data will become the basic driving force for power supply companies to mine risks and improve efficiency. Only by embedding "abstract" data into the audit model can marketing data reflect its value for me. In the future business process of big data, through data mining and knowledge graph to realize the visualization of audit management, look for business loopholes, innovate business methods, and constantly improve the defense system for marketing business errors.

Data Availability

The dataset can be accessed upon request.

Conflicts of Interest

The author declares that there are no conflicts of interest.

References

[1] H. J. Salunkhe, B. S. Kamble, and A. P. Acharya, "Energy management and energy audit in area of western Maharashtra," *Energy*, vol. 10, no. 2, 2022.

[2] Z. Jiang and Z. Liu, "Can wind power policies effectively improve the productive efficiency of Chinese wind power industry?" *International Journal of Green Energy*, vol. 18, no. 13, pp. 1339–1351, 2021.

[3] M. Hamwi, I. Lizarralde, and J. Legardeur, "Demand response business model canvas: a tool for flexibility creation in the electricity markets," *Journal of Cleaner Production*, vol. 282, Article ID 124539, 2021.

[4] W. Wang, X. Liu, and X. Zhao, "Design of intelligent substation communication network security audit system," in *Proceedings of the 2019 IEEE 4th Advanced Information Technology, Electronic and Automation Control Conference (IAEAC)*, pp. 389–397, Springer, Singapore, December 2021.

[5] J. Bai, L. Cao, S. Mosbach, J. Akroyd, A. A. Lapkin, and M. Kraft, "From platform to knowledge graph: evolution of laboratory automation," *JACS Au*, vol. 2, no. 2, pp. 292–309, 2022.

[6] J. Xie, S. Wang, X. Zhou, B. Sun, and X. Sun, "Credit evaluation method of generating companies considering the market behavior in China electricity market," *Energy Science & Engineering*, vol. 9, no. 9, pp. 1554–1567, 2021.

[7] J. Wang, X. Wang, C. Ma, and L. Kou, "A survey on the development status and application prospects of knowledge graph in smart grids," *IET Generation, Transmission & Distribution*, vol. 15, no. 3, pp. 383–407, 2021.

[8] R. Kostyrko, T. Kosova, L. Kostyrko, L. Zaitseva, and O. Melnychenko, "Ukrainian market of electrical energy: reforming, financing, innovative investment, efficiency analysis, and audit," *Energies*, vol. 14, no. 16, p. 5080, 2021.

[9] S. Li, Y. Han, X. Yao, S. Yingchen, J. Wang, and Q. Zhao, "Electricity theft detection in power grids with deep learning and random forests," *Journal of Electrical and Computer Engineering*, pp. 1–12, 2019.

[10] C. Xu, F. Wen, and I. Palu, "Electricity market regulation: g," *Energy Conversion and Economics*, vol. 1, no. 3, pp. 151–170, 2020.

[11] E. Heiskanen, E. L. Apajalahti, K. Matschoss, and R. Lovio, "Incumbent energy companies navigating energy transitions: strategic action or bricolage?" *Environmental Innovation and Societal Transitions*, vol. 28, pp. 57–69, 2018.

[12] Z. Zhang and W. C. Hong, "Electric load forecasting by complete ensemble empirical mode decomposition adaptive noise and support vector regression with quantum-based dragonfly algorithm," *Nonlinear Dynamics*, vol. 98, no. 2, pp. 1107–1136, 2019.

[13] T. Kasim, M. Haracic, and M. Haracic, "The improvement of business efficiency through business process management," *Economic Review: Journal of Economics and Business*, vol. 16, no. 1, pp. 31–43, 2018.

[14] E. Mengelkamp, J. Gärttner, K. Rock, S. Kessler, L. Orsini, and C. Weinhardt, "Designing microgrid energy markets: a case study: the Brooklyn Microgrid," *Applied Energy*, vol. 210, pp. 870–880, 2018.

[15] Z. Y. She, G. Meng, B. C. Xie, and E. O'Neill, "The effectiveness of the unbundling reform in China's power system from a dynamic efficiency perspective," *Applied Energy*, vol. 264, Article ID 114717, 2020.

[16] F. Li, K. Tomsovic, and H. Cui, "A large-scale testbed as a virtual power grid: for closed-loop controls in research and testing," *IEEE Power and Energy Magazine*, vol. 18, no. 2, pp. 60–68, 2020.

[17] A. Bublitz, D. Keles, F. Zimmermann, C. Fraunholz, and W. Fichtner, "A survey on electricity market design: i," *Energy Economics*, vol. 80, pp. 1059–1078, 2019.

[18] P. Komada, I. Trunova, and O. Miroshnyk, "The incentive scheme for maintaining or improving power supply quality," *Przeglad Elektrotechniczny*, vol. 95, no. 5, pp. 79–82, 2019.

[19] P. W. Saługa, K. Szczepańska-Woszczyna, R. Miśkiewicz, and M. Chlad, "Cost of equity of coal-fired power generation projects in Poland: its importance for the management of decision-making process," *Energies*, vol. 13, no. 18, p. 4833, 2020.

[20] X. Chen, S. Jia, and Y. Xiang, "A review: knowledge reasoning over knowledge graph," *Expert Systems with Applications*, vol. 141, Article ID 112948, 2020.

[21] B. Xu, J. Liang, C. Xie, B. Liang, L. Chen, and Y. Xiao, "CN-DBpedia2: an extraction and verification framework for enriching Chinese encyclopedia knowledge base," *Data Intelligence*, vol. 1, no. 3, pp. 271–288, 2019.

[22] F. Meng, S. Yang, and J. Wang, "Creating knowledge graph of electric power equipment faults based on BERT–BiLSTM–CRF model," *Journal of Electrical Engineering & Technology*, pp. 1–10, 2022.

[23] P. Liu, W. Jiang, X. Wang, H. Li, and H. Sun, "Research and application of artificial intelligence service platform for the power field," *Global Energy Interconnection*, vol. 3, no. 2, pp. 175–185, 2020.

[24] J. V. De Sousa, D. V. Coury, and R. A. S. Fernandes, "A survey on cloud computing applications in smart distribution systems," *Electric Power Components and Systems*, vol. 46, no. 14-15, pp. 1554–1569, 2018.

Hindawi
Scientific Programming
Volume 2022, Article ID 3229355, 9 pages
https://doi.org/10.1155/2022/3229355

Research Article

The Restriction Factors and Mechanism Analysis Model Design of the Commercial Serious Disease Insurance in Connection with Serious Disease Insurance

Hongguang Chen, Jiaqi Yuan, and Jinsong Pei

Beijing Jiaotong University, Beijing 100044, China

Correspondence should be addressed to Hongguang Chen; 17113124@bjtu.edu.cn

Received 23 July 2022; Revised 14 August 2022; Accepted 23 August 2022; Published 3 October 2022

Academic Editor: Lianhui Li

Based on the internal and external constraints of serious disease insurance and commercial serious disease insurance, the logistic model of "whether you are willing to connect with commercial serious disease insurance on the basis of serious disease insurance" and "to understand the objective conditions of the connection between serious disease insurance and commerci"a" serious disease insurance" is designed. Based on the empirical research on the micro survey panel data of 6 municipal districts in W City in April 2020, the following research results are obtained: among the many influencing factors, "health status," "per capita family income," "gender," "age," "education level," "number of children," "operating rules," "public value recognition," "settlement linkage" Internal Factors of "Information Mastery" and "Implicit Restrictions." Therefore, the family should be insured in the optimal allocation of family members in the order of "family pillar-children-the elderly" and the scientific layout of insurance products on the basis of family per capita income. The government should promote the institutional integration by strengthening the mechanism construction, building an information platform, and optimizing the management system, so as to promote the health big data sharing, and provide a superior environment for the connection between serious disease insurance and commercial serious disease insurance.

1. Introduction

As the social environment changes, people's health is threatened. In particular, serious diseases have a great impact on patients and their families. According to statistics, about 44 million families worldwide face high medical costs every year due to serious diseases. Of these, about 25 million families and more than 100 million families are trapped in poverty due to spending money for curing serious illness [1, 2]. However, serious illness insurance can reduce family medical expenses, improve family labor participation, and achieve poverty reduction. Due to the rapid rise of "non-compliance" medical expenses, the unreasonable "threshold" of serious illness insurance, the development trend of younger diseases, the out-of-pocket expenses, and out-of-pocket burden cannot be reduced, and the incidence of catastrophic expenditure is still on the rise. Therefore, commercial serious illness insurance receives more and more attention [3–5]. Commercial serious illness insurance is a kind of supplementary medical insurance set according to the market demand to make up for the lack of social medical security [6]. Compared with serious illness insurance, commercial serious illness insurance has more types and a higher level of security. In the face of serious disease risk, it is necessary to choose commercial serious disease insurance [7–9]. On the basis of medical insurance reimbursement method and medical insurance payment method selection, the implementation of one-time payment method can alleviate the economic problems after the occurrence of serious diseases. This is also in line with the requirements outlined in the 2016 Healthy China 2030 Annual Plan Outline, such as "a sound multilevel medical security system

with basic medical security as the main body and various other forms of supplementary insurance and commercial medical insurance systems."

On the basis of commercial serious illness insurance, this paper deeply analyzes the factors that affect the cohesion of commercial medical insurance and social medical insurance from both internal and external aspects, uses questionnaire data to verify the reliability of the constraints, and accordingly proposes a linkage mechanism for the insured and the government to promote the two, so as to further optimize China's medical insurance mechanism..

2. The Choice of Factors

2.1. Intrinsic Constraints

2.1.1. Per Capita Family Income. At present, the purchase cost of commercial serious illness insurance is generally higher, and the insurance amount is not too high. If the amount of insurance increases, the family burden increases. Family per capita income is high, the economy is relatively loose, the insurance premium payment ability is higher, and the willingness to buy commercial serious illness insurance is higher. For families with relatively high family per capita income, their daily living expenses are also relatively high, and the demand for buying commercial serious illness insurance is also relatively high.

2.1.2. Number of Children. For the connection between serious illness insurance and commercial serious illness insurance, the number of family children can affect commercial serious illness insurance. The more children, the greater the financial pressure, and the lower the family's ability to resist risk. To reduce the risk and transfer the risk, the higher the need to buy commercial critical illness insurance. The fewer the children, the less the financial pressure of the family, the higher the family's ability to resist risks, which will not attract purchases, and the lower the desire to buy.

2.1.3. Personal Age. With the growth of age, children's growth, education, and marriage, the demand for economy is growing, and the source of economy is getting weaker. Facing the pressure of work and economy, in order to prevent health risks, people turn to commercial serious illness insurance to strengthen the cohesion of purchasing intentional serious illness insurance and commercial serious illness insurance.

2.1.4. Health Status. Their health status is directly related to the purchase intention. In the face of some possible hidden diseases, once it appears, the family cannot bear it. Therefore, people with poor health will have strong desire to buy commercial serious illness insurance, affecting the connection between serious disease insurance and commercial serious illness insurance.

2.1.5. Gender. In terms of the development law of human function, women and men suffer from serious diseases differently, and the probability of serious diseases in different diseases is also different. Therefore, gender affects the connection between serious disease insurance and commercial serious disease insurance.

2.1.6. Education Level. People with relatively high education level have a strong sense of insurance awareness, coupled with the nature of their work, and their willingness to buy commercial serious illness insurance is stronger than those with relatively high education level. Therefore, the level of education affects the connection between serious disease insurance and commercial serious disease insurance to a certain extent.

2.2. External Constraints

2.2.1. Operation Rules. Due to the professional connection between serious disease insurance and commercial serious disease insurance, the insured do not understand the operation norms and detailed rules of the connection. Therefore, we need to be clear in the relevant systems and policies of serious disease insurance or commercial serious disease insurance, but at present, we need to be clear in the deep connection of the two and coordinated development operation guidance basis. As the insured, only by mastering these foundations, can we better promote the connection between the two.

2.2.2. Integration. In recent years, many local governments have entrusted serious disease insurance to insurance companies to improve their professionalism. Some local governments also purchase insurance companies on serious disease insurance services, which are all operated by insurance companies. As an important product project of insurance companies, commercial serious illness insurance can strengthen the integration and development of the two based on the operation mode of serious illness insurance, and lay a foundation for the connection between serious illness insurance and commercial serious illness insurance.

2.2.3. Invisible Limit Clause. Serious disease insurance is the second reimbursement after basic medical treatment insurance reimbursement. It strictly follows the condition requirement of basic medical treatment insurance implementation, its clause is clear, and limit condition is clear. However, for commercial serious illness insurance, insurance companies have strict restrictions on serious illness compensation in order to improve profits. They usually stipulate in the contract documents that at first glance there are many clauses, but once the disease occurs, they do not meet the conditions of the contract. These "invisible restrictions" are not conducive to coordination with serious illness insurance, and it is difficult to provide a higher level of security, which restricts cohesion.

2.2.4. Information. In the connection between serious illness insurance and commercial serious illness insurance, data sharing is the key point. The emergence of information bottlenecks tends to lead to the lack of data in both serious illness insurance and commercial serious illness insurance, and the inability to share data related to disease treatment and inspection. Insurance companies, in particular, are unable to master basic medical information. Information acquisition is lagging behind, and residents' health is difficult to be accurate. This is not conducive to the price and safety of commercial serious illness insurance, and the cost performance is low. Therefore, promoting the data and information sharing of serious disease insurance and commercial serious disease insurance is conducive to the connection between the two.

2.2.5. Public Value Recognition. Serious disease insurance is essentially a national medical insurance, which needs to cover all the basic medical insurance of the participants. However, the coverage rate of commercial serious disease insurance is about 10%. It limits the selectivity of people, such as limiting age groups and high-risk occupations. Human identity affects the public value attribute of commercial serious illness insurance to a certain extent.

2.2.6. Settlement Linkage. As the serious illness insurance and commercial serious illness insurance belongs to different institutions or unit's, the cohesion will need to optimize the cost settlement platform and realize the linkage development. Under the asymmetric information of the medical system, how to strengthen the optimization of settlement, especially the issue of advance funds for serious illness insurance, and build a cost linkage cooperation platform between insurance companies and hospitals is conducive to serious illness insurance and commercial serious illness insurance.

3. Empirical Analysis

3.1. Data and Models

3.1.1. Data Procurement. This paper gives questionnaires to urban and rural residents who buy basic medical insurance and investigates 600 residents in a city on "whether they are willing to connect commercial serious illness insurance on the basis of serious illness insurance" and "whether to understand the objective conditions for the connection between serious disease insurance and commercial serious illness insurance."

The questionnaire was jointly carried out both on the Internet and on the spot.

The distribution scope of the questionnaire included 6 districts such as WC, HK, HP, DXH, JX, and CD districts. A total of 600 questionnaires were issued and 562 were recovered, including 548 valid questionnaires with an effective rate of 97.5%.

In view of the internal constraints of the connection between serious disease insurance and commercial serious illness insurance, a questionnaire survey was conducted on the family per capita income, number of children, personal age, their own health status, gender, education level of urban and rural residents who have purchased basic medical insurance, and whether they are willing to connect with commercial serious illness insurance on the basis of serious disease insurance. For the external constraints on the connection between serious illness insurance and commercial serious illness insurance, from the aspects of operation rules, integration, implicit constraints, information, public value recognition, settlement linkage, product design, etc., questionnaire survey on whether urban and rural residents who purchase basic medical insurance understand the objective conditions for the connection between serious illness insurance and commercial serious illness insurance. Considering that some variables are ranging variables, all variables are assigned to facilitate processing, and the assignment situation of each variable is shown in Table 1.

In order to test the statistical value of the questionnaire, the reliability and validity were tested. KMO test coefficient is 0.874, its value is greater than 0.5, Bartlett spherical test P value is 0.002, less than 0.001, the questionnaire validity is statistically significant.*p*value is 0.002, less than 0.001, questionnaire validity has statistical value. Cronbach α system value is 0.898, and the questionnaire's reliability is good and has statistical value".

3.1.2. Model Specification. Since the dependent variables of this paper "whether you are willing to connect with commercial serious disease insurance on the basis of serious disease insurance" and "whether you understand the objective conditions of the connection between serious disease insurance and commercial serious disease insurance" are both virtual variables, the linear regression model is estimated to make the research results bias for this discontinuous variable. In addition, considering that the selected internal constraints have different attributes in the demographic category, while the external constraints all belong to distance variables, the correlation between each independent variable is low, and the logistic regression model is sensitive to multiple colinearity of independent variables, the logistic model is used for analysis. Among them, the following calculation formula [10–15] for the internal constraints is studied:

$$\mathrm{Ln}\left(\frac{p_i}{1-p_i}\right) = \beta_0 + \sum_{1}^{n} \beta_{i,n} X_{i,n}. \tag{1}$$

In the above formula, p_i denotes i respondents are willing to connect on the basis of serious illness insurance, $1 - p_i$ denotes i respondents are unwilling to connect on the basis of serious illness insurance, $X_{i,n}$ denotes gender, age, education, family per capita income, health, and children, $\beta_{i,n}$ denotes gender, age, education, family per capita income, health, children, and other independent variable regression coefficient, β_0 denotes constant items. As the external constraints of classification number is greater than 2, here

Table 1: Variable assignment of both intrinsic and external constraints.

Intrinsic constraints	Variable classification	Assignment	External constraints	Variable classification	Assignment
Sex	Man	1	Rules of operation fusion situation invisible restrictions	Has not yet been introduced	1
	Woman	2		Understand a little	2
Age	<30	1	Information mastery public value recognition settlement linkage	Be familiar with	3
	30–45	2		Insufficient fusion	1
	>45	3		Fusion in general	2
Degree of education	High school and below	1	Products design external constraints rules of operation	The fusion is very good	3
	Undergraduate degree and junior college degree	2		Disagree	1
	Bachelor degree or above	3		Self-identity	2
Household incomes per capita	RMB 2,500/month or less	1	Fusion situation invisible restrictions information mastery	Strongly agree with	3
	RMB 2501–5000 yuan/month	2		Information sharing has not yet been implemented	1
	More than 5,000 yuan/month	3		Understand a little	2
Health condition	Preferably	1	Public value recognition Settlement linkage products design	Familiar with information	3
	Same as	2		Does not match with social security	1
	Range	3		There is a certain commonality	2
Number of children	Not have	1	External constraints rules of operation fusion situation	Match with social security	3
	1	2		Linkage and cooperation have not yet been realized	1
	≥2	3		Understand a little	2
			Invisible restrictions	Understand thoroughly	3
				Has not yet been developed	1
				Understand a little	2
				Understand thoroughly	3

the second and third categories are expressed to understand to study into 0-1 variables. But $X_{i,n}$ denotes the operating rules, public value recognition, settlement linkage, information grasp, invisible limit terms, fusion, product design, and other independent variables, $\beta_{i,n}$ denotes the regression coefficient of their respective variables.

3.2. Intrinsic Constraints. The misjudgment matrix was constructed to compare the difference size between the predicted value and the actual value. Secondly, each explanatory variable was introduced into the model one by one, and the rationality of the logistic regression model was judged by the significant level of the variables. After the introduction of a new variable, if the variable-2 log-likelihood value is less than the results in the previous step and the pAfter introducing a new variable, if the logarithmic likelihood value of the variable - 2 is less than the result of the previous step, and the p value is less than 1%, it indicates that the explanatory variable has a significant correlation with the explanatory variable "on the basis that the major disease insurance is willing to join the commercial major disease insurance," and the logistic regression model "on the basis that the major disease insurance is willing to join the commercial major disease insurance" is reasonable [16–20]. Table 2 shows the regression results in the final step, and the odds ratio reflects the explanatory variables screening process and regression system, the final model includes "health status," "sex," "per capita income," "gender," "age," "education," and "number of children." Logistic regression model variables in the p value of each explanatory variable coefficient is less than 0.05 significance level, so on the basis of serious disease insurance, linear relationship is retained in the model equation.

Comparing the misjudgment matrix of the initial situation and the misjudgment matrix after introducing all the explanatory variables, the following can be found (see Table 3): in the process of gradually introducing the explanatory variables, the accuracy rate of the model gradually increases from 54.7% to 89.7%, and the prediction accuracy is relatively high. To sum up, "on the basis of serious illness insurance is willing to join commercial serious illness insurance," logistic regression model analysis shows that "health," "family per capita income," "gender," "age," "education," "children," and so on for residents on the basis of serious illness insurance cohesion commercial serious illness insurance will restrict. Therefore, in the serious illness insurance and commercial serious disease insurance, we should pay attention to combine the above six factors design of policy-holder, in order to enhance the purchase intention of the policy holder.

3.3. External Constraints. Similar to the analysis of intrinsic constraints, a misjudgment matrix was first constructed to compare the magnitude of the difference between the

Table 2: The logistic regression results of the internal factors connected between commercial critical illness insurance and serious illness insurance.

	Coefficient estimate	Free degree	The odds ratio
Health condition	0.650 * * * (0.000)	1	1.915
Household incomes per capita	0.695 * * * (0.000)	1	2.003
Sex	0.643 * * * (0.001)	1	1.902
Age	0.623 * * * (0.001)	1	1.864
Degree of education	0.546 * * * (0.001)	1	1.727
Number of children	0.390 * * * (0.007)	1	1.476
Constant term	−6.629 * * * (0.000)	1	0.001

Note. p value in parentheses; * * * is significant at 1%.

Table 3: Results of logistic progressive regression model.

Observed			Predicted		
			Connect with commercial serious illness insurance		Percent correction
			Yes	No	
Step 0	Connect with commercial serious illness insurance total percentage	Yes	0	248	0.0
		No	0	300	100.0
			—	—	54.7
Step 1	Connect with commercial serious illness insurance total percentage	Yes	130	118	52.4
		No	83	217	72.3
			—	—	63.3
Step 2	Connect with commercial serious illness insurance total percentage	Yes	181	67	73.0
		No	65	235	78.3
			—	—	76.2
Step 3	Connect with commercial serious illness insurance total percentage	Yes	189	59	76.2
		No	55	245	81.7
			—	—	79.5
Step 4	Connect with commercial serious illness insurance total percentage	Yes	195	53	78.6
		No	49	251	83.7
			—	—	81.7
Step 5	Connect with commercial serious illness insurance total percentage	Yes	206	42	83.1
		No	38	262	87.3
			—	—	85.7
Step 6	Connect with commercial serious illness insurance total percentage	Yes	218	26	89.3
		No	28	272	90.7
			—	—	89.7

predicted value and the actual value. Secondly, each explanatory variable was introduced into the model one by one, and the rationality of the logistic regression model was judged by the significant level of the variables [21–26]. If the log-likelihood value of each newly introduced variable is less than the result in the previous step, and the p value is less than 1%, it indicates a significant correlation between the explanatory variable and "understand the objective conditions of the connection between serious disease insurance and commercial serious disease insurance."

Table 4 shows the regression results of the final step. The final model includes explanatory variables such as "operating rules," "recognition of public value," "settlement linkage," "information mastery," and "invisible restriction clause". Since the p value of each explanatory variable coefficient is less than 0.05 significance level, the linear relationship of serious disease insurance and commercial serious disease insurance in the logistic regression model is significant in the model equation.

In the process of gradually screening, the final model failed to enter the fusion situation and product design of two explanatory variables. Due to the introduction of the two explanatory variables after probability p value of 0.099 and 0.140, respectively, more than 0.05 lead to "the serious illness insurance and commercial serious illness insurance cohesion objective conditions understanding." Logistic regression model linear variable linear relationship is not significant and, therefore, is not retained in the model equation.

To sum up, "the understanding of the objective conditions for the connection between serious illness insurance and commercial serious illness insurance"

Table 4: Logistic regression results of external factors linking between commercial critical illness insurance and serious disease insurance.

	Coefficient estimate	df	The odds ratio
Rules of operation	0.578 ∗ ∗ ∗ (0.000)	1	1.783
Settlement linkage	0.476 ∗ ∗ ∗ (0.000)	1	1.609
Information mastery	−0.534 ∗ ∗ ∗ (0.000)	1	0.586
Public value recognition	−0.503 ∗ ∗ ∗ (0.000)	1	0.605
Invisible restrictions	0.549 ∗ ∗ ∗ (0.002)	1	1.731
Constant term	−1.061 (0.071)	1	0.346
Fusion situation	2.723 (0.099)	1	—
Products design	2.181 (0.140)	1	—

Note. p value in parentheses; ∗ ∗ ∗ is significant at 1%.

Table 5: Results of the progressive regression model.

Observed			Predicted		
			Understand the objective conditions of connecting commercial serious disease insurance		Percent correction
			Yes	No	
Step 0	Understand the objective conditions of connecting commercial serious disease insurance	Yes	0	246	0.0
		No	0	302	100.0
	Total percentage		—	—	55.1
Step 1	Understand the objective conditions of connecting commercial serious disease insurance	Yes	90	156	36.6
		No	82	220	72.8
	Total percentage		—	—	56.6
Step 2	Understand the objective conditions of connecting commercial serious disease insurance	Yes	114	132	46.3
		No	87	215	71.2
	Total percentage		—	—	60.3
Step 3	Understand the objective conditions of connecting commercial serious disease insurance	Yes	154	92	62.6
		No	84	218	72.2
	Total percentage		—	—	68.1
Step 4	Understand the objective conditions of connecting commercial serious disease insurance	Yes	187	59	76.0
		No	71	231	76.5
	Total percentage		—	—	76.6
Step 5	Understand the objective conditions of connecting commercial serious disease insurance	Yes	201	45	81.7
		No	54	248	82.1
	Total percentage		—	—	82.2

Logistic regression model analysis shows that "operating rules," "public value recognition," "settlement linkage" information, and "hidden restrictions" have an impact on the objective situation of the connection between serious illness insurance and commercial serious illness insurance. Therefore, in the connection between serious illness insurance and commercial serious illness insurance, attention should be paid to combining the applicant's demand for mastering the above five factors, strengthen design and optimization.

3.4. Internal-External Constraints. The internal and external constraints are introduced into the model, and the model is used to be tested again, in order to screen the constraints more accurately. The model regression results are presented in Table 6.

First, the p value of the parameter likelihood ratio test of the logistic regression model was less than 0.05, indicating a statistical significant OR value for at least one of the 13 variables, so the fitted model was statistically significant. Second, the p value (0.409) of the Hosmer and Lemeshow tests is greater than 0.05, indicating that the information in the current data has been fully extracted, and the model has a better goodness of fit. Finally, the results of the logistic regression for each intrinsic and extrinsic factor indicate that the six intrinsic factors and the five extrinsic factors described above are plausible, and that there is no multicollinearity between the internal and extrinsic factors.

Therefore, in the process of connecting commercial serious illness insurance and serious illness insurance, we pay attention to the design of the "health status," "family per capita income," "gender," "age," "level," "education," "number," and other children, to enhance the purchase intention of the insured. In addition, we should fully obtain the understanding of the "operation rules," "public value recognition," the "settlement linkage," "information

Table 6: Logistic regression results of intrinsic-extrinsic factors between commercial critical illness insurance and serious disease insurance.

	Coefficient estimate	df	The odds ratio
Age	0.643 * * * (0.003)	1	1.902
Degree of education	0.539 * * * (0.002)	1	1.714
Invisible restrictions	0.564 * * * (0.008)	1	1.757
Rules of operation	0.209 * * (0.038)	1	1.233
Household incomes per capita	0.575 * * * (0.002)	1	1.776
Public value recognition	−0.779 * * * (0.000)	1	0.459
Fusion situation	0.391 * * (0.013)	1	1.478
Settlement linkage	0.275 * * (0.046)	1	1.317
Information mastery	−0.600 * * * (0.000)	1	0.549
Products design	−0.548 * * * (0.001)	1	0.578
Number of children	0.409 * * (0.013)	1	1.505
Health condition	0.760 * * * (0.000)	1	2.139
Sex	0.752 * * * (0.001)	1	2.121
Constant	−5.814 * * * (0.000)	1	0.003
Likelihood ratio test	195.739 * * * (0.000)	13	—
The Hosmer and Lemeshow tests were performed	13.071 (0.409)	8	—

Note. p value in parentheses; * * * and * * * are significant at 1% and 5% levels, respectively.

mastery," and "invisible restrictions" and strengthen the design and optimization of insurance products.

4. Linkage Mechanism between Commercial Serious Disease Insurance and Serious Disease Insurance

4.1. Promote the Connection between Serious Disease Insurance and Commercial Serious Disease Insurance Based on Internal Factors

4.1.1. Optimize the Insurance Order and Insurance Items of Family Members Based on Their Age and Health Status. When purchasing health insurance, families first consider children, but from a professional perspective, adhere to the configuration order of family pillars, children, the elderly, and optimize the insurance order of family members. Not only that, as far as insurance projects are concerned, family support is the safety foundation of families. We need to adhere to the insurance principle of "income pillar should be given priority," strengthen the purchase of commercial critical illness insurance to supplement basic medical insurance and serious illness insurance, and ensure that family pillars will not cause family difficulties when they are ill; For children, its premium is relatively low. Adhere to the principle that "child protection should be comprehensive." It can be comprehensive and long-term. Try to buy an insurance with comprehensive protection function. If the insurance amount of commercial serious disease insurance can be increased, promote its protection from the perspective of physical protection. In terms of product selection, you can choose partial payment products. For the elderly, especially family members over 50 years old, the insurance premium is high and the protection is not strong. Therefore, we can purchase products from accident insurance and cancer prevention insurance by adhering to the principle that accidental cancer prevention is necessary for the elderly.

4.1.2. Scientific Layout of Insurance Product Allocation Sequence Based on Family per Capita Income. First, the priority guarantee type to buy financial management type. On the basis of the basic "security" insurance allocation, the per capita family income is surplus, we can consider financial insurance products, and even some wealthy families can use commercial serious disease insurance to do a good job in asset inheritance. Second, choose commercial serious illness insurance according to the per capita family income. The family per capita income is low and can buy consumer commercial serious disease insurance. This kind of insurance is usually paid every year. This kind of premium takes into account the risks of different ages, and also from the gender perspective. Different people, different genders, different ages, different premiums, small amount of insurance benefits, and high leverage ratio.

4.2. Link Serious Disease Insurance with Commercial Serious Disease Insurance Based on External Conditions

4.2.1. System Integration. First, strengthen the construction of market mechanism. Serious disease insurance should not only rely solely on the government but also give full play to the market mechanism. Let alone exclude the market allocation of insurance resources. We should leave enough market space for commercial serious disease insurance, so as to ensure the scientific use of insurance resources. The common development of the two mechanisms of serious disease insurance and commercial serious disease insurance needs to start with the top-level design and constantly optimize the service supply connecting the serious disease insurance and commercial serious disease insurance. Second, strengthen the construction of a multiagent coordination mechanism. Relevant government departments shall take the lead in establishing the coordination structure of medical insurance, to give full play to the leading role of the government, promote strengthened cooperation among relevant subjects, and jointly discuss and formulate

specific methods and detailed rules for the connection between serious disease insurance and commercial serious disease insurance. To increase the government's support for commercial critical illness insurance, the relevant government functional departments and medical institutions can establish a cooperative promotion mechanism with insurance companies to interpret the public value, supporting policies and insurance conditions of commercial critical illness insurance to the public, so as to stimulate the public's demand for medical treatment and health security.

4.2.2. Build a Cohesion Platform. First, establish a health big data information platform. From the perspective of collaborative public management, build health big data information platform, realize the information data sharing between the related subject, help to reduce adverse selection risk and moral hazard, effectively improve the efficiency of medical insurance costs, is also conducive to the insurance institutions using health data information platform accurate positioning, according to different groups design, develop personalized commercial health insurance, such as health insurance products. Second, promote the integration construction of commercial health insurance, hospital, and medical insurance fee settlement platforms. Commercial insurance institutions shall be encouraged and guided to participate in the development, construction, and maintenance of unified settlement platforms for commercial health insurance compensation expenses, such as medical expenses and commercial serious disease insurance, so as to provide convenient direct compensation and claim settlement services for the insured.

4.2.3. Optimize the Management System. First, strengthen operational risk management to provide a superior environment for the connection between serious disease insurance and commercial serious disease insurance. Develop an innovative new model of medical insurance cooperation. Commercial health insurance institutions should establish a service framework combining insurance provision and health management, try to get involved in medical institutions through investment and establishment, merger and acquisition, and strategic cooperation, and increase the complementary advantages and win-win development of insurance industry and medical and health service industry. Second, we will strengthen the reform of the medical system to build a benign space for the connection between serious disease insurance and commercial serious disease insurance. We will strengthen the construction of the government's supervision capacity for the health industry, and at the same time, improve the patient reporting channels, establish a sound and effective supervision network, and strictly investigate and punish any violations found in time. We will resolutely crack down on illegal and unreasonable acts such as arbitrary fees and excessive medical treatment and ensure that medical institutions return to formality and public welfare. We will improve the environment for the orderly development of social security, constantly promote the sustainable development of social security programs, and serve the well-being of the people.

5. Conclusion

This paper is based on the basis and feasibility of connecting commercial serious illness insurance and serious disease insurance, centering on the internal constraints and external constraints of the participants of serious disease insurance and commercial serious disease insurance, respectively. The logistic model of "whether you are willing to connect with commercial serious disease insurance on the basis of serious disease insurance" and "to understand the objective conditions of the connection between serious disease insurance and commercial serious disease insurance" is designed. Based on the microsurvey panel data of the six municipal districts of W city in April 2020, the model was estimated using the maximum likelihood estimation method. The study found that, among many influencing factors, "family members," "health status," "family per capita income," "gender," "age," "education level," "number of children," internal factors as well as external factors such as "operation rules," "public value recognition," "settlement linkage," "information mastery," and "hidden restriction clauses" "have a significant constraint on residents" willingness to connect commercial serious disease insurance on the basis of serious disease insurance. "Fusion situation" and "product design" and other factors have no obvious impact on it. Accordingly, the family should adhere to when being insured "family pillar-child-old man," and the order optimizes the insurance order of configuration family members, with "income pillar wants priority," "children safeguard should be comprehensive," "old man accident prevents cancer prevention is very necessary." The principle chooses appropriate insurance project. At the same time, insurance products should be scientifically distributed based on the per capita family income of families and give priority to the basic "guarantee" insurance allocation of commercial serious disease insurance + serious disease insurance. On the basis of the surplus of the per capita family income of families, financial management insurance products should be considered. In view of the external constraints, the problems existing in the connection process between commercial serious disease insurance and serious disease insurance are imperfect, the connection information sharing and information platform construction need to be promoted, and the connection management system still needs to be strengthened. System integration should be promoted by building market mechanism, improving the coordination mechanism, improving commercial insurance legal system, promoting the interconnection and information sharing of health big data and integrated settlement platform of commercial health insurance, hospital and medical insurance expenses, and competition mechanism.

Data Availability

The dataset can be accessed upon request to the corresponding author.

Conflicts of Interest

The authors declare that they have no conflicts of interest.

Acknowledgments

This study was supported by the China Academy of Labor Security Sciences Project: Research on Labor Security Regulations in Typical Countries along the "the Belt and Road" (RS2017-06).

References

[1] Z. Chen and S. Min, "Study on poverty reduction effect of serious disease insurance - empirical analysis based on CFPS data," *Journal of Jinan Philosophy and Social Sciences edition*, pp. 1–16.

[2] Y. Li and Y. Luo, "Whether serious illness insurance improves the security status of medical disadvantaged groups-takes the elderly and low-income groups as an example," *Journal of Guangdong University of Finance and Economics*, vol. 35, no. 06, pp. 100–110, 2020.

[3] J. Liu, L. Zhang, and C. Yang, "Family critical disease insurance selection strategy study-based on analysis of insurance product rate," *Price Theory and Practice*, no. 11, pp. 99–102, 2018.

[4] Q. Gong, "Research on the connection between personal medical insurance account and commercial insurance system," *New Finance*, no. 05, pp. 60–64, 2018.

[5] Q. Z. Shao and C. Jia, "Competition and cooperation of -from the perspective of social insurance and commercial insurance in China," *Shanghai Economic Research*, no. 03, pp. 11–19, 2009.

[6] L. Jing, "On the quasi-public goods of commercial medical insurance and the social liability of insurance companies-the enlightenment and reference of obamacare reform," *Jiangxi Social Science*, vol. 34, no. 09, pp. 192–196, 2014.

[7] H. Li and J. Du, "Study on the dual construction of social medical insurance and commercial medical insurance in China," *Henan Social Sciences*, vol. 19, no. 04, pp. 143–145, 2011.

[8] J. Zhou, "Does social medical insurance squeeze out commercial medical insurance? Evidence of-from basic medical insurance for town residents," *Journal of Jinan*, vol. 42, no. 02, pp. 99–109, 2020.

[9] H. Peng, Q. Zheng, and Y. Guo, "Will the expansion of social medical insurance in China promote the development of commercial health insurance?" *Financial Research*, no. 05, pp. 97–110, 2017.

[10] X. Guo and G. Zhao, "Establishment and verification of logistic regression model for qualitative diagnosis of ovarian cancer based on MRI and ultrasound signs," *Computational and Mathematical Methods in Medicine*, vol. 2022, no. 21, Article ID 7531371, 1-8 pages, 2022.

[11] L. H. Li, J. C. Hang, Y. Gao, and C. Y. Mu, "Using an integrated group decision method based on SVM, TFN-RS-AHP, and TOPSIS-CD for cloud service supplier selection," *Mathematical Problems in Engineering*, vol. 2017, no. 29, pp. 1–14, 2017.

[12] H. Jiang, "Design and implementation of smart community big data dynamic analysis model based on logistic regression model," *Computational Intelligence and Neuroscience*, vol. 2022, no. 21, Article ID 4038084 1-11 pages, 2022.

[13] L. H. Li, J. C. Hang, H. X. Sun, and L. Wang, "A conjunctive multiple-criteria decision-making approach for cloud service supplier selection of manufacturing enterprise," *Advances in Mechanical Engineering*, vol. 9, no. 3, Article ID 168781401668626, Mar 16 2017.

[14] R. Qin, "Identification of accounting fraud based on support vector machine and logistic regression model," *Complexity*, vol. 2021, no. 20, Article ID 5597060, 1-11 pages, 2021.

[15] Q. Kang, "Correlation analysis of stocks and PMI index based on logistic regression model," *Journal of Sensors*, vol. 2021, no. 20, Article ID 1089266, 1-12 pages, 2021.

[16] Y. Deng and R. Zhu, "Analysis of teaching effect of English classroom mind map based on a logistic regression model," *Journal of Sensors*, vol. 2022, no. 12, Article ID 3356919, 1-11 pages, 2022.

[17] L. Li, C. Mao, H. Sun, Y. Yuan, and B. Lei, "Digital twin driven green performance evaluation methodology of intelligent manufacturing: hybrid model based on fuzzy rough-sets AHP, multistage weight synthesis, and PROMETHEE II," *Complexity*, vol. 2020, no. 6, Article ID 3853925, 1-24 pages, 2020.

[18] S. S. Alshqaq, A. A. Ahmadini, and A. H. Abuzaid, "Some new robust estimators for circular logistic regression model with applications on meteorological and ecological data," *Mathematical Problems in Engineering*, vol. 2021, no. 20, Article ID 9944363, 1-15 pages, 2021.

[19] L. Li and C. Mao, "Big data supported PSS evaluation decision in service-oriented manufacturing," *IEEE Access*, vol. 8, pp. 154663–154670, 2020.

[20] P. Lu, H. Wang, and D. Tolliver, "Prediction of bridge component ratings using ordinal logistic regression model," *Mathematical Problems in Engineering*, vol. 2019, no. 52, Article ID 9797584, 1-11 pages, 2019.

[21] D. Xiao, X. Xu, and L. Duan, "Spatial-temporal analysis of injury severity with geographically weighted panel logistic regression model," *Journal of Advanced Transportation*, vol. 2019, no. 12, Article ID 8521649, 1-1pages5, 2019.

[22] L. Li, T. Qu, Y. Liu et al., "Sustainability assessment of intelligent manufacturing supported by digital twin," *IEEE Access*, vol. 8, pp. 174988–175008, 2020.

[23] H. Jiang, B. Hu, Z. Liu et al., "Huanyu.Detecting depression using an ensemble logistic regression model based on multiple speech features," *Computational and Mathematical Methods in Medicine*, vol. 2018, Article ID 6508319, 2018.

[24] L. Li, B. Lei, and C. Mao, "Digital twin in smart manufacturing," *Journal of Industrial Information Integration*, vol. 26, no. 9, Article ID 100289, 2022.

[25] Z. Nie, X. Bai, L. Nie, and J. Wu, "Optimization of the economic and trade management legal model based on the support vector machine algorithm and logistic regression algorithm," *Mathematical Problems in Engineering*, vol. 2022, no. 25, Article ID 4364295, 201-209 pages, 2022.

[26] J. Lyu, "Construction of enterprise financial early warning model based on logistic regression and BP neural network," *Computational Intelligence and Neuroscience*, vol. 25, no. 21, Article ID 2614226, 57-59 pages, 2022.

Hindawi
Scientific Programming
Volume 2023, Article ID 9857484, 1 page
https://doi.org/10.1155/2023/9857484

Retraction

Retracted: College Students' Ideological and Political In-Depth Teaching Community Based on Core Literacy Model

Scientific Programming

Received 18 July 2023; Accepted 18 July 2023; Published 19 July 2023

This article has been retracted by Hindawi following an investigation undertaken by the publisher [1]. This investigation has uncovered evidence of one or more of the following indicators of systematic manipulation of the publication process:

(1) Discrepancies in scope
(2) Discrepancies in the description of the research reported
(3) Discrepancies between the availability of data and the research described
(4) Inappropriate citations
(5) Incoherent, meaningless and/or irrelevant content included in the article
(6) Peer-review manipulation

The presence of these indicators undermines our confidence in the integrity of the article's content and we cannot, therefore, vouch for its reliability. Please note that this notice is intended solely to alert readers that the content of this article is unreliable. We have not investigated whether authors were aware of or involved in the systematic manipulation of the publication process.

Wiley and Hindawi regrets that the usual quality checks did not identify these issues before publication and have since put additional measures in place to safeguard research integrity.

We wish to credit our own Research Integrity and Research Publishing teams and anonymous and named external researchers and research integrity experts for contributing to this investigation.

The corresponding author, as the representative of all authors, has been given the opportunity to register their agreement or disagreement to this retraction. We have kept a record of any response received.

References

[1] F. Yanju, D. Chao, and L. Man, "College Students' Ideological and Political In-Depth Teaching Community Based on Core Literacy Model," *Scientific Programming*, vol. 2022, Article ID 5481853, 9 pages, 2022.

Hindawi
Scientific Programming
Volume 2022, Article ID 5481853, 9 pages
https://doi.org/10.1155/2022/5481853

Research Article

College Students' Ideological and Political In-Depth Teaching Community Based on Core Literacy Model

Feng Yanju,[1] Dong Chao,[1] and Li Man [2]

[1]*School of Marxism, Hebei Vocational University of Industry and Technology, Shijiazhuang 050091, Hebei, China*
[2]*Changchun College of Humanities, Changchun 130117, Jilin, China*

Correspondence should be addressed to Li Man; liman@ccrw.edu.cn

Received 13 August 2022; Revised 25 August 2022; Accepted 31 August 2022; Published 3 October 2022

Academic Editor: Lianhui Li

With the development of the times, building a learning community in ideological and political teaching has become an urgent need for teaching reform. In ideological and political teaching, the common vision of teachers and students is to carry out cooperative exploration and ultimately realize the progress and growth of common teachers and students, and implement the core of political science. Learning community in ideological and political teaching has the characteristics of group symbiosis, common value, cooperation and sharing, and democratic openness. Therefore, building a learning community in ideological and political teaching is conducive to the formation of a new teaching model of cooperative inquiry and the establishment of equality and democracy. The new teacher-student relationship can cultivate students' higher-order thinking and promote more meaningful learning. It has been proved by practice that it is valuable to construct a learning community in the ideological and political teaching of universities. Teachers and students should change the traditional teaching concept. University political teachers should carefully prepare lessons, set up teaching design, be considerate to students, be close to reality, be close to knowledge itself, enhance the communication and interaction between teachers and students, and students and students, and actively build a learning community in the process of ideological and political teaching. To enable students to get new knowledge, solve challenging problems, and finally achieve progress and growth.

1. Introduction

At present, core literacy has become a topic that the country and even the world focus on. Countries try to use "core literacy" as a guide for curriculum reform; explore curriculum standards, teaching reforms, and teaching practices that match the cultivation of students' core literacy; and make it gradually become a practical concept of international education. Our country also conforms to the development trend of international education reform and pays attention to the core literacy of students, and the ideological and political course, as a subject with the fundamental task of morality and cultivating people, has naturally become an important position for cultivating students' core literacy. The cultivation of subject core literacy is very important. However, in the current ideological and political teaching, there are still various shallow teaching problems such as aiming at "exam-oriented education," overemphasizing the authority of textbook knowledge, formalizing the teaching process, paying attention to the performance of open classes, and flashy teaching results. This is not conducive to the cultivation of students' core literacy and will limit their all-round development. In-depth teaching is a reform of shallow and formalized teaching. The purpose of studying in-depth teaching is to propose effective solutions to the problems existing in current teaching. The teaching of ideological and political courses from the perspective of core literacy is to pay attention to the dialogue between students and knowledge, especially the value and meaning behind knowledge, in an open form so that students can gradually cultivate their knowledge in the process of mining the value and meaning behind knowledge. The core qualities of political identity, scientific spirit, awareness of the rule of law, and public participation are all innovations that promote

teaching activities. It has the functions of being conducive to the independent construction of students' knowledge, the development of scientific thinking, and the implementation of emotional education. However, there are still some problems in the practice of in-depth teaching of ideological and political courses that need to be improved and perfected. In the current teaching of ideological and political courses, due to the limitations of teachers' unclear grasp of the concept of in-depth teaching, the deep-rooted thinking of teachers in exam-oriented education, and the attitude of teachers who have no intention of in-depth teaching, the problem design ability of teachers' core literacy of ideological and political courses and the core literacy of ideological and political courses are not enough. The ability of teaching implementation and the teaching reflection ability of the core literacy of ideological and political courses need to be improved. Students are accustomed to passively accepting knowledge, graffiti-style learning, "picture reading," and other learning methods. Their learning methods are lagging and cannot adapt to in-depth teaching, and the evaluation system is not perfect. Teachers' enthusiasm and other reasons have hindered the practice of in-depth teaching, which is not conducive to the cultivation of students' core literacy. With the research on in-depth teaching, the theoretical and practical system of in-depth teaching is gradually being established and improved, which has reference significance for the teaching practice of ideological and political courses in the future. [1–5].

2. Related Works

The research on deep learning can be traced back to the mid-1950s. Some scholars start from the learning process of students and use shallow learning and deep learning as the reading methods of academic papers for college students so as to adjust the teaching methods according to these two states. American scholars Ference Marton and Roger Saljo were the first to make this point. They believe that shallow learning is passive and mechanical, students' inquiry process lacks self-awareness and the ability to think independently, the content of learning is boring and far from students' life, and students lack emotional experience and thinking skills during learning. On the contrary, deep learning emphasizes the initiative and comprehension of students' learning, emphasizes that students should use critical thinking to understand knowledge; attaches importance to new and old knowledge, knowledge of various disciplines, and the connection between theory and practice; and improves students' transference. Since then, many scholars have conducted comparative studies on the two, put forward the value of deep learning, and explored strategies to promote deep learning for students. For example, "problem-based learning (PBL)" originated from medical education uses "problems" as clues to students' learning and activities, prompting students to change their previous learning methods and change from passive acceptance to active inquiry. Another scholar proposed "self-directed learning." A typical example is an American scholar Tough, A who proposed in 1971 that "students should learn to plan, monitor, and reflect on their own." Students establish learning goals in autonomous learning. Through the learning process, they can have a deep understanding of the content, form a summary, and reflect in the learning process. Another scholar proposed the deep learning route (DELC), the deeper learning cycle. For example, Eric Jensen and LeAnn Nickelsen proposed in "7 Powerful Strategies for Deep Learning" to carry out in-depth learning from seven perspectives: "design standards and courses, pre-assessment, building a learning culture, previewing prophets, acquiring new knowledge, deep processing of knowledge, and learning evaluation," which enriches the practical strategies of deep learning. In recent years, the research of some scholars has gone beyond the previous research vision, not only based on the aspects of educational technology such as instructional design and learning technology but also based on the new concept of learning and knowledge, research, and new interpretations. The most representative of them is the research carried out by the "Learning in Depth" (LID) project team led by Professor Egan of Fraser University in Canada, which implements deep learning based on experiments. The path and the basic principles of its implementation are discussed, and the role of deep learning on student learning, teacher professional growth, and school reform is analyzed. The research focuses on classroom learning and teacher teaching, and even research on deep learning focuses on teachers' guidance on how students learn and how they learn. Aigen's deep learning research has made it clear that teachers also attach importance to the guidance of teachers in the process of deep learning, guide students to focus on the in-depth understanding of knowledge, and promote students to deepen their understanding of knowledge in the process of gradual in-depth learning. Eigen's research on deep learning pays attention to the importance of teachers to students' deep learning, and the connection between deep teaching and deep learning, so the focus of the research gradually shifts from a single learning technology to a two-way activity that combines teacher teaching and student learning. The research on deep learning also shows the characteristics of the combination of deep learning and deep teaching. [6–12].

3. Related Theories and Research Methods

3.1. Community. A community is a tightly connected whole. From the perspective of the etymology, "common" means "everyone does it together; what belongs to everyone is public"; "body" means "group, collective,"; and the community is that everyone does things together, belongs to everyone's collective, mutual help, and no one can do without another, mainly emphasizing that there is a deep emotional foundation between members and a collective or collective organization that depends on each other. The word community comes from the German "Gemeinschaft" and is translated as Community in English; the most common meaning is "society," with derived meanings of "residents" and "regions."

The earliest description of the community was by the German classical sociologist Tennis. He divided the community into several aspects: the community linked by blood,

the community linked by emotional needs, and the community linked by region. They are all interdependent, share weal and woe, recognize and tolerate each other, and have a strong sense of collective belonging. The concept of "community" originated in the field of sociology, has gradually been widely studied in other fields such as education and politics, and has enriched the connotation and extension of the community from different angles, such as the political community in the field of politics, the scientific community in the field of natural and human sciences, etc. With the rise of research on the community, community not only emphasizes the close relationship between members because of blood relationship and geographical location but also emphasizes the organization of collective members relying on common goals. In pedagogy, the commonly mentioned community refers to the learning community, such as Palmer's theory of debate; he believes that "the real community is recognized through debate," and the composition of community members is not limited by blood regions, etc. More emphasis is placed on organisms that identify with each other by arguing with each other. At the same time, the debate process is not closed, but open and shared. The format of the debate is not monotonous for the sake of debate, but to encourage members to fully express and listen to their views, learn together, and achieve common goals. Such communities are more focused on emphasizing the learning process. Although the community in pedagogy and the community in sociology have similarities, they both emphasize mutual recognition and sharing, but there are great differences between the two. Community in pedagogy emphasizes that learners cooperate with each other and grow together in the learning process, while the community in sociology is based on relevant research based on factors such as region, blood relationship, and spirituality. Even so, the concept of community in the field of sociology can also serve as a reference for the concept of community in pedagogy. The concept of community in pedagogy relies on the concept in the field of sociology, but it is not equivalent to its connotation in sociology. The vast groups with different identities in different regions can be summarized as a collective with common goals, mutual cooperation and sharing, mutual recognition, and close connection. [13].

3.2. Learning Community. The learning community idea can be traced back to Dewey's empirical education theory. Dewey believes that the essence of education is: "education is life, school is society, education is growth, education is the reorganization and transformation of experience." In fact, what is emphasized is that schools are not only places to learn knowledge and skills but they also advocate various social activities, emphasize exchanges and cooperation between people, and promote the all-round development and personality development of each student. The concept of the learning community is derived from the learning organization theory. In 1990, the scholar Peter Senge put forward the famous learning organization theory, which refers to the collective that each subject can release their sense of collective identity, cultivate their personality, expand their abilities, and continue to learn together. [14] The learning organization mainly includes five elements: common vision, system thinking, common learning, self-realization, and mental model. Although he did not directly point out the concept of the learning community, he accelerated the process of the concept of the learning community becoming known to the world. In 1995, Boyer put forward the concept of the learning community for the first time. He believed that a learning community is an organization where members share common goals and communicate and cooperate with each other. After 2000, Sato, known as the first person in Japanese educational theory, further developed the learning community theory according to the problems of lonely learning in Japan at that time and regarded the learning community as a new teaching model and a new type of learning community. Learning the organizational form, he believes that the main purpose of the learning community is to accept all differences, that is, to respect and accommodate the differences of each member. And in the description of the global picture of the "classroom revolution" in the 21st century, the school reform philosophy based on the "learning community" is expounded.

3.3. The Elements of the Learning Community in Ideological and Political Teaching in Colleges and Universities. Scholars have different generalizations of what constitutes a learning community. Some scholars believe that it includes five elements: learners, facilitators, learning tools, resources, and learning contexts; some scholars divide it into seven elements: learning subjects, resources, learning methods, curriculum knowledge, shared vision, learning context, and target effects. According to the analysis of the concept and constituent elements of the learning community and the characteristics of the ideological and political teaching of college students, this study believes that the constituent elements of the learning community in the ideological and political teaching of college students mainly include learners, common vision, interactive means, learning situations, and learning resources—5 aspects. All elements influence and depend on each other and jointly promote the sustainable development of the learning community in the ideological and political teaching of college students. [15].

3.3.1. Learners. College students and ideological and political teachers are the main learners of the learning community in the ideological and political teaching of college students. Through certain teaching activities, teachers and students can communicate and interact. Teachers and students are learners with equal status. Teachers and students have their own advantages and personalities. In the ideological and political teaching of college students, ideological and political teachers and students help each other, share knowledge, and jointly solve challenging problems. Special attention should be paid here. Teachers do not blindly instill knowledge but guide and help students in the teaching process. Ideological and political teachers are not managers, but more of a service provider for students' learning. At the

same time, they are also learners. Lifelong learning, or more reflective dialogue with students, can better promote the effective and sustainable development of the learning community in the ideological and political teaching of college students. [16].

3.3.2. Common Vision. The common vision and the common goal are closely related, but in addition to the common goal itself, the common vision also emphasizes that members take the initiative to achieve the learning goal based on the common emotional needs, that is, the common goal of the community. The "Ideological and Political Curriculum Standards" proposes that "the fundamental task of college students' ideological and political teaching is to build morality and cultivate people, further strengthen the education of socialist core values, and emphasize the construction of an active subject curriculum dominated by cultivating the core literacy of ideological and political subjects." Therefore, college students' thinking of the common vision of the learning community in political teaching should not be limited to the achievement of knowledge and skills but should focus more on building morality and cultivating people, implementing the core literacy of disciplines, and promoting the all-round development of each student.

3.3.3. Interaction. Internet + tradition is an interactive means of the learning community in the ideological and political teaching of college students. For students in the traditional ideological and political teaching of college students, generally a class is a group. Although everyone knows each other, the communication and interaction with each other is not enough, and it is only limited to the interaction in the school classroom. Therefore, from the perspective of the composition of the learning community in the ideological and political teaching of college students, it is very important that the interaction means among the members of the learning community. In today's information age, knowledge is updated rapidly, and traditional means of interaction are no longer the main way. More members will use some popular communication tools, such as e-mail, Weibo, QQ group, WeChat group chat, etc. The real-time synchronous and non-real-time asynchronous communication of network media tools promotes the exchange and feedback of information among the participants of the learning community in the ideological and political teaching of college students.

3.3.4. Learning Situation. Carrying out the activity-based curriculum oriented to implement the core literacy of the discipline is the main learning situation of the learning community in the ideological and political teaching of college students. The learning situation is also an important factor in the teaching process of ideological and political courses. It is the so-called "flesh worms, fish withered worms." It emphasizes the importance of internal environmental changes to the development of things, and the reference to teaching also reflects the learning situation. Wang Fuzhi, a Confucian scholar in the late Ming and early Qing dynasties, believed that people's ideology and behavior are closely related to the environment in real life, and the natural learning situation is closely related to people's thinking and behavior. The environment of ideological and political teaching has the characteristics of being extensive, dynamic, specific, and creative. Therefore, it is necessary to pay attention to the creation of the learning environment of the learning community in the ideological and political teaching of college students, not only to consider the environment and characteristics of ideological and political teaching but also to consider the personality and characteristics of the students. Appropriate learning situations can promote ideological and political teaching to achieve a multiplier effect. [17].

3.3.5. Learning Resources. Explicit knowledge + invisible knowledge is the learning resource of the learning community in the ideological and political teaching of college students. Learning resources are an indispensable element and the learning information of the learning community in the ideological and political teaching of college students and generally exist relying on certain carriers, such as books, courseware, exercises, cooperation, and dialogues. Therefore, learning resources include both explicit knowledge and implicit knowledge. Traditional teaching tends to ignore the learning resources in cooperation and exchange, and the learning community attaches great importance to the learning resources obtained in the process of communication, cooperation, and reflective dialogue between teachers and students and between students and students. This is also in line with the activity-based curriculum emphasized by the ideological and political curriculum standards for college students, which promotes the activity of the curriculum content and the curriculum of the activity content and realizes the common progress of teachers and students in the blending of explicit knowledge and invisible knowledge. [18].

4. Construction of College Students' Ideological and Political Teaching Community Based on the Learning Community

4.1. Teaching Design Based on the Concept of the Learning Community. According to the connotation of the learning community, the value of the learning community should be recognized. First of all, it is necessary to form a correct cognition of the learning community, instead of putting wrong labels such as time-consuming and formalism. According to the connotation of the learning community, it can be understood that the learning community is an organic organization for teachers and students, students and students to learn from each other, help each other, achieve common goals, and cultivate socialist core values. Based on this, building a learning community in the ideological and political teaching of colleges is conducive to forming a new teaching model of cooperative inquiry, establishing a new teacher-student relationship of equality and democracy, and, at the same time, cultivating students' higher-order thinking and promoting more

meaningful learning. The content of this lesson is selected from "Truth is Concrete and Conditional" in "Life and Philosophy." The whole teaching design is shown in Table 1.

4.2. Teaching Implementation Based on the Concept of the Learning Community

4.2.1. Correct Concept. Form a correct cognition of the learning community. According to the connotation of the learning community, the value of the learning community should be recognized. First of all, it is necessary to form a correct cognition of the learning community, instead of putting wrong labels such as time-consuming and formalism. According to the connotation of the learning community, it can be understood that the learning community is an organic organization for teachers and students, students and students to learn from each other, help each other, achieve common goals, and cultivate socialist core values. Based on this, building a learning community in the ideological and political teaching of colleges is conducive to forming a new teaching model of cooperative inquiry, establishing a new teacher-student relationship of equality and democracy, and, at the same time, cultivating students' higher-order thinking and promoting more meaningful learning. [19].

4.2.2. Clear Goals. Play the leading role of the common vision in the ideological and political teaching of the university. Because the learning community has the characteristics of political identity and cooperation and openness, it should play the leading role of the common vision in the learning community. A shared vision is a common goal that members of a learning community have and are willing to work towards. In other words, a shared vision includes both common goals and emotional appeals that members are willing to work towards. A shared vision is not simply equivalent to the improvement of academic performance, it is more focused on exploring and solving problems in cooperation and communication and ultimately enables students to actively build new knowledge and promote the achievement of key abilities and necessary characteristics.

4.2.3. Positioning Practice. We should fully respect the dominant position of students, carry out interactive teaching that stimulates students' interest in learning, and promote students to actively build new knowledge in the process of teacher-student and student-student cooperation and interaction. Interactive teaching emphasizes two-way interaction, which is different from teacher-led and invalid interaction or blind interaction of students. It is necessary to change the traditional single self-directed and self-acted teaching but to develop a dialogue and communication method that includes multiple factors such as cognition, behavior, and emotion. Interactive teaching is based on an equal and harmonious modern teacher-student relationship. Students and students, teachers and students understand each other, respect each other, and achieve common progress and common development in the process of cooperative exploration. In the current ideological and political teaching in universities, there is more interaction on the surface, the form is lively, and there is no real knowledge. For example, in the class "Entering the International Society," a teacher guided students to hold a debate on whether China and the United States are rivals or partners. This does not conform to the cognitive characteristics and processes of students. In the information age, many students understand that China and the United States are both rivals, but also partners. Therefore, such debates can easily lead to ineffective interactions. The dialectical thinking that China and the United States are both opponents and partners is not easy to form in this debate. Interaction exists all the time, but effective interaction is rare. How to really achieve effective "interaction?" First, the interaction method must be properly combined with subject knowledge. That is to say, the selection of interactive materials or methods should not be separated from the corresponding subject knowledge. To truly realize the curriculum of the activity content and the activity of the course content, the two should not be separated from each other, but must be closely integrated. Change the traditional curriculum content curriculum, but also avoid the ineffective interaction of the activity content. Second, the interactive way should be promoted to stimulate students' interest in learning. The material selected or the situation created should be based on the psychological characteristics of students, which can stimulate students to learn actively. Failure to unilaterally understand interaction is commonly used in front and back discussions between four people. The selected discussion topics are not close to students, close to life, and close to reality. Effective interaction will definitely not be possible, and students will feel tired of learning. [20].

Third, the layout of traditional learning spaces should be changed. Do a good job in the spatial setting of the learning community and the spatial distance of students' seats is closely related to the psychological distance between teachers and students, and students and students. The narrowing of the space distance can shorten the psychological distance between teachers and students, which makes it easier to listen, communicate and cooperate, and achieve effective interaction. Japanese scholar Sato Xue believes that the physical space environment of learning can be changed to promote the effective interaction between teachers and students, and students and students. The traditional seedling-style desks and chairs cannot carry out more nonverbal communication, which is not conducive to attentive listening between teachers and students, and students and students, and is not conducive to mutual in-depth exchanges and cooperation. The sitting situation in the classroom is to form a classroom that listens attentively to each other and build the physical foundation of a learning community. Generally, there are the following requirements: as shown in the figure below, the group members should sit face-to-face and look at each other; appropriate distance will neither affect the communication between group members nor the connection between groups; the arrangement of the classroom should be as flexible as possible to facilitate students to change the group form; as far as possible, all students should always be with their own group companions together, as shown in Figures 1–3.

Table 1: Learning community concept instructional design sheet.

Textbook analysis	The content of this lesson is selected from "Truth is Concrete and Conditional" in "Life and Philosophy." This article mainly explains the conditionality and specificity of truth and the relationship between true questions and falsehoods and then understands that the process of pursuing truth is never-ending and not smooth, so we begin the process of pursuing truth.	
Study situation analysis	Students have acquired certain philosophical thinking ability in the study of relevant philosophical knowledge points. However, their understanding is relatively scattered, simple, and one-sided, so teachers need to teach systematically to help students comprehensively master knowledge, broaden their understanding, and improve their rational thinking ability. In view of the situation of this course, students have already mastered the relevant knowledge of "truth" and they need to further study the characteristics of truth and the relationship between truth and falsehood.	
Teaching objectives	1. Master the conditionality and specificity of truth and understand the relationship between truth and error. 2. Cultivate students to identify with the philosophical method of dialectical materialism, enhance the ability to actively participate in life and know how to use dialectical thinking to deal with real-life problems, and at the same time improve students' practical ability. 3. Cultivate students' scientific spirit of rational analysis of truth, encourage students to take on the important responsibilities of the times, and strive to pursue the truth.	
Teaching focus	Set by	Truth is conditional 1) First of all, students have learned the relevant knowledge of truth, but they do not have a special understanding of the relationship between truth and falsehood, and the applicable conditions of truth. 2) Second, combined with the requirements of core literacy and the new curriculum concept, it is necessary to cultivate students to establish a scientific spirit and the ability to guide life using the method of dialectical materialism—this is the focus of teaching.
	How to stand out	1) Carry out activity-based courses, teachers and students interact and communicate, analyze and demonstrate knowledge points in turn, and help students fully understand that truth is a conditional philosophical principle. Under the guidance of teachers, students can intuitively experience the changing process of the two experiments of "black wolfberry soaking in water," actively build new knowledge, and understand that truth has its own applicable conditions and scope. 2) Make the content of the course active and the content of the activities into a curriculum, through the interaction between teachers and students, strengthen the guidance of students' values, and cultivate students' scientific spirit.
Teaching difficulties	Set by	Truth is concrete 1) Concrete is a word that is often used in daily life, but for students, the specific understanding of truth is not deep enough, and it is easy to ignore the two dimensions of time and space contained in it, and then they cannot better grasp the truth and falsehood.
	How to break through	1) Use case analysis to analyze from the two dimensions of space and time so that students can understand that the truth must conform to the actual situation of the local and the time.
Teaching method	Pedagogy is based on the concept of the learning community	

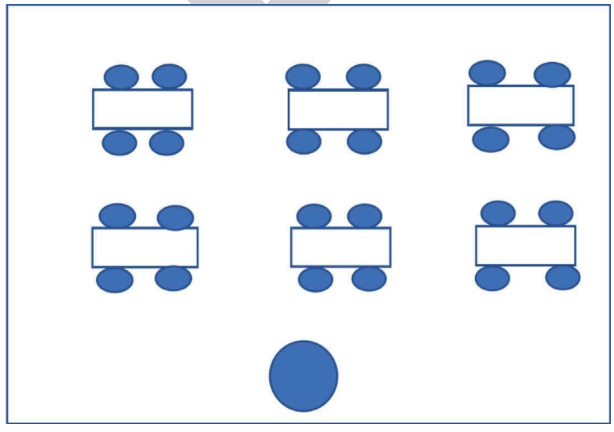

Figure 1: Sitting in a row in the classroom of the learning community: sitting in groups around the front and back.

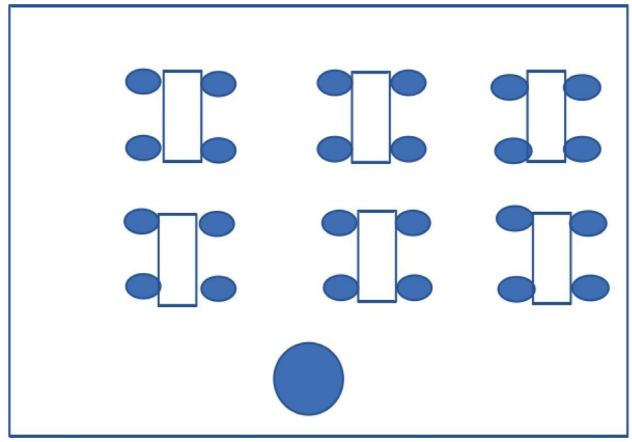

Figure 2: Sitting in a row in the classroom of the learning community: sitting in groups around the left and right sides.

4.2.4. Specific Implementation. First, the spatial arrangement should be completed. In the classroom teaching of "Truth is Concrete and Conditional," it is necessary to build a learning community. First, a classroom atmosphere centered on listening must be created. To cultivate the relationship of mutual trust and mutual respect between

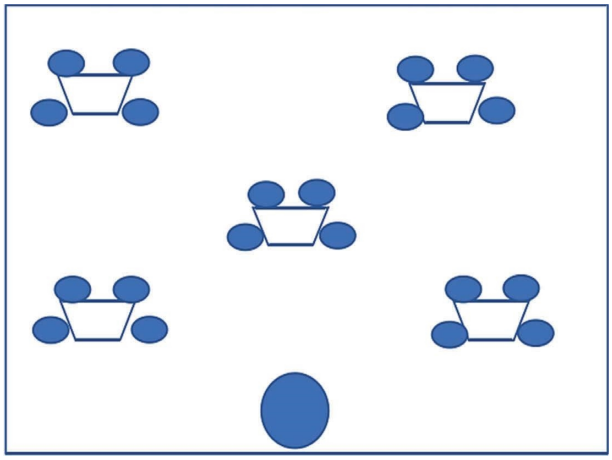

Figure 3: Sitting in a row in the classroom of the learning community: U-shaped sitting in groups.

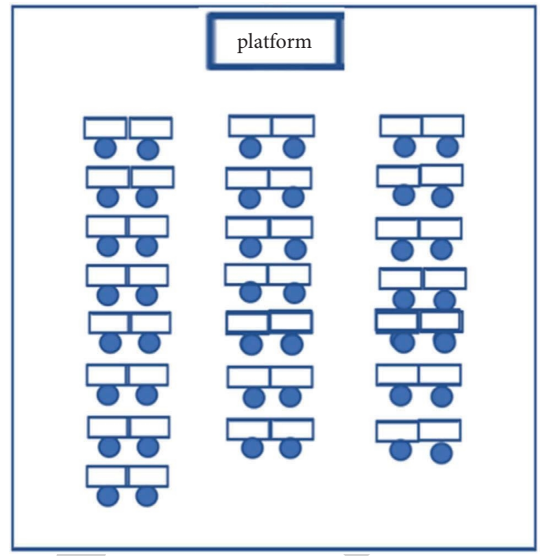

Figure 4: Traditional classroom space layout.

teachers and students, and students and students, it is necessary to change the traditional classroom space layout, create a space layout that facilitates face-to-face communication and cooperation between peers, remove the podium, and reduce the spatial distance between teachers and students. Teachers should take turns walking around different groups, as shown in Figure 4 below.

Figure 5 shows the classroom space layout of the learning community.

Second, assigning team members. The team members should be matched according to the actual situation. Since the selected experimental class has 48 people, it is determined in advance that every four people will form a group. First of all, let the students apply for registration independently, which students are willing to form a group with, and explain the reasons for the application. Then, according to the teacher's daily observation and understanding and the students' evaluation of others and other factors, the group members are preliminarily determined. Finally, the list of group members is announced to the students, and those who are dissatisfied can make corrections according to the actual situation. After the four members of the group are determined, based on self-recommendation, democratic recommendation, and teacher evaluation, a leader, a timekeeper, a main speaker, and a recorder are determined for each group. During the actual operation, their identity can also be adjusted appropriately. It is convenient for everyone to communicate and cooperate in depth in the three cooperative exploration activities in the class "Truth is Concrete and Conditional," and complete the active construction of knowledge. [21–23].

Third, establishing a common vision. Before the class, the teacher guides everyone to understand that the goal we need to accomplish together in this class is to cooperate in depth based on mutual trust with peers and teachers, to master the conditional and specificity of truth, and to understand the relationship between truth and falsehood; and the ability to actively participate in life and know how to use dialectical thinking to deal with real-life problems, to develop the scientific spirit of rational analysis of truth, to be

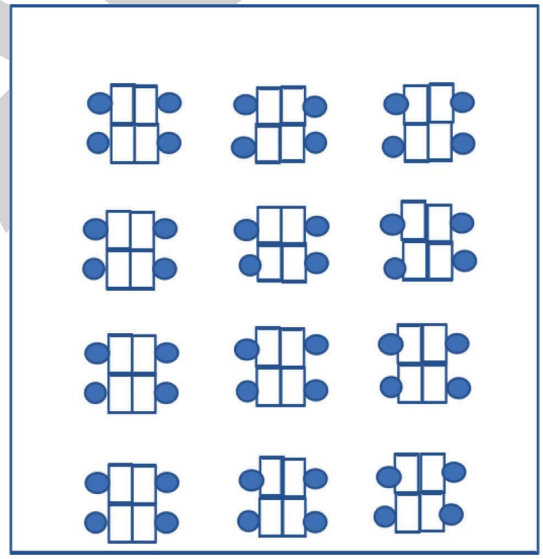

Figure 5: Classroom space layout based on the learning community.

brave to take on the important tasks of the times, and to strive for truth.

Fourth, solving challenging problems. The goal of building a learning community is that students can solve problems and consider the unity of learning and use. Teachers organize students to review textbooks in advance to understand the connotation of truth, so that students can solve problems independently in the teaching process, understand that truth is conditional and specific, and at the same time understand the reasons. This also requires teachers to focus on giving guidance in the teaching process, rather than directly giving answers or results, so that students can explore independently; actively build knowledge; solve challenging problems; and implement the core literacy of disciplines, scientific spirit, and political identity.

Table 2: Comparison of the effect of classroom teaching based on the learning community and the effect of traditional classroom teaching.

Compare items	Traditional classroom teaching	Classroom teaching based on the learning community
Degree of organization	Emphasize pre-class presupposition	Emphasize classroom generative
Learning purpose	Utilitarian (emphasizes the difficulty of the exam)	Nonutilitarian, self-fulfillment
Learning process	Passive participation in the classroom; the classroom atmosphere is dull	Actively participate in the classroom; the classroom atmosphere is active
Learning outcomes	Mechanical memory knowledge, unable to complete challenging problems	Deep learning, capable of solving challenging problems
Evaluation method	Based on external evaluation	Based on self-evaluation
Learning value	Simply acquire knowledge	While mastering knowledge, also acquired the ability of unity and cooperation
Study time	Long time, low efficiency	Short time, high efficiency

Fifth, evaluating group cooperation. After class, the evaluation is made based on the teacher's observation and the record of each group's recorder. The method of evaluation can be either self-evaluation or other evaluation, and the content of evaluation is also diverse. It can be the evaluation of students' completion of teaching tasks, the effect of group cooperation and exploration, and the teaching design of teachers. According to the evaluation results of teachers and students, it is necessary to analyze which aspects can be done better, which aspects have what kind of achievements and experience, etc.

4.3. Evaluation of the Effect of Teaching Implementation Based on the Concept of the Learning Community. On the whole, the effect of classroom teaching based on the learning community is obviously better than that of traditional classroom teaching. According to the evaluations of teachers, students, and teachers listening to the lectures, it is found that in the classroom teaching based on the learning community, students actively participate in the teaching process, actively explore new knowledge, actively communicate and interact with group members, and can solve challenging problems. The degree, learning purpose, learning process, and learning results are superior to traditional classroom teaching in many aspects as shown in Table 2.

From the perspective of solving challenging problems, building a learning community in the ideological and political teaching of colleges is an efficient teaching method. Through experiments, it is found that building a learning community in the ideological and political teaching of colleges seems to be time-consuming, but in fact it is highly efficient. Taking "truth is specific and conditional" as an example, the spatial layout was changed, the division of labor among group members was determined, and interactive teaching was carried out under the guidance of a common vision, in a democratic and equal teaching atmosphere, and students not only master the truth, but also transfer knowledge, solve the problems of low classroom participation, difficult to understand course knowledge, and mostly mechanical memory methods under the traditional teaching mode. Practice has proved that building a learning community in the ideological and political teaching of universities can save time and achieve efficient learning. The traditional misunderstanding that it is a waste of time to build a learning community is not valid in the teaching process of teachers and the learning process of students. Although the time spent by ideological and political teachers in preparing lessons will increase, it is not a waste of time, but a responsibility that should not be shied away.

5. Conclusion

High school ideological and political teaching based on the learning community is a teaching model that emphasizes the coexistence of cognition and emotion and combines respect for individuality and all-round development under the background of the new curriculum reform. In this kind of course teaching, teachers and students, students and students cooperate with each other, have dialogue and reflection, and achieve common growth and progress, which is also the requirement of ideological and political courses in the new era. In the process of frontline ideological teaching, there are still problems in the teacher-student relationship, classroom interaction, evaluation system, etc., which seriously hinder the effective implementation of the learning community. Entering the new era, higher requirements have been placed on high school political teachers in terms of comprehensively advocating and implementing the core values of socialism, promoting the all-round development of students, and cultivating students' key abilities and necessary characters. Building a learning community in ideological and political teaching aims to break through the traditional political indoctrination education, change the discordant and unequal teacher-student relationship, and reshape the curriculum of the activity content and the political classroom of the activity of the curriculum content. Based on the zone of proximal development theory and the principle of teaching and learning, students are promoted to actively build knowledge and complete challenging problems, change their prejudice against political classrooms, enhance their sense of political learning, and make them love and enjoy political classrooms again.

Data Availability

The dataset can be obtained from the corresponding author upon request.

Hindawi
Scientific Programming
Volume 2022, Article ID 5408200, 10 pages
https://doi.org/10.1155/2022/5408200

Research Article

The Design of a Moral Education Evaluation System for College Students Based on a Deep Learning Model

Tianji Liu, Bao Ru, and Yeqing Zhang

North China University of Science and Technology, Tangshan, Hebei 063210, China

Correspondence should be addressed to Tianji Liu; liutianji@ncst.edu.cn

Received 23 July 2022; Revised 6 September 2022; Accepted 12 September 2022; Published 30 September 2022

Academic Editor: Lianhui Li

With the rapid development of deep learning, its application in the field of education has gradually attracted attention. This study introduces a deep learning-based moral education evaluation system for college students. The evaluation of the ideological and political education of college students is an important driving force to strengthen and improve the ideological and political education of college students, and its connotation is very rich. However, at present, there are many difficulties in the evaluation of ideological and political education in colleges and universities, such as narrow evaluation objectives, monotonous evaluation structures, lack of pertinence in the evaluation process, and subjective evaluation standards. The internal mechanism and external mechanism of the evaluation mechanism, the qualitative analysis and quantitative analysis of the evaluation method, the absoluteness and relativity of the evaluation standard, the dynamic and static evaluation process, and the systematic and specialized evaluation are combined to ensure the college students' thinking the objectivity and effectiveness of political education evaluation.

1. Introduction

As the evaluation of the ideological and political education of college students is an important evaluation [1] and feedback on the development of ideological and political education, it is effective for discovering, analyzing, and correcting the dilemma of ideological and political education and constructing [2, 3]. Carrying out ideological and political education is an important task in colleges and universities, and the sustainable development of ideological and political education is an important subject entrusted by the times. Under the new historical conditions, facing the complicated new situation at home and abroad, the ideological and political education of college students can only be strengthened and not weakened. It has become an urgent task of higher education to realize the sustainable development of ideological and political education for college students. A sustainable ideological and political education system for college students plays an important role in improving the overall effect of ideological and political education and promoting its in-depth development. The evaluation system of college students' ideological and political education is a systematic project, and its connotation is also rich [4–6]. Bloom regards evaluation as the most fundamental factor in a hierarchical model of human thinking and cognitive processes. According to his model, evaluation and thinking are the two most complex cognitive activities in the model of human cognitive processing. He believes that evaluation is the process of making value judgments on certain ideas, methods, and materials [7]. It is the process of using criteria to evaluate the accuracy, effectiveness, economy, and satisfaction of things. Taking various factors into consideration, evaluation refers to the process of quantitative and nonquantitative measurement of all aspects of the evaluation object by the evaluator according to the evaluation criteria and finally drawing a reliable and logical conclusion [8]. Among them, the so-called evaluator, who is also called an evaluator, is mainly a subjective agent who evaluates a certain object. The second is the system, which generally refers to the whole of a certain range or the same kind of things combined according to a certain order and internal connection, which is a system composed of

different systems. The content in the system should involve subjects, objects, laws, principles, standards, etc. The last is the ideological and political education of college students, which defines the scope and content; that is, the process of evaluation, analysis, and construction of the system should be carried out around the ideological and political education of college students [9]. When defining the evaluation system of ideological and political education for college students, it is necessary to base it on these keywords, and the key points should be considered from the following aspects.

First, there must be a definite subject in evaluating the ideological and political education of college students. To study the promoting effect of ideological and political education on the economy, we must first recognize the essence of ideological and political education and then explore at what level it can have a functional connection with the economy. It will clarify the nature of ideological and political education and study its effects on the economy from the macro- and microlevels. This subject should include both macro- and microaspects. Judging from the current domestic specific participation in the evaluation, the subjects are mainly the relevant national education administrative departments, education supervisory and scientific research institutions, and ideological and political educators in colleges and universities [10].

Second, the ideological and political education of college students must have a definite object. The object of ideological and political education evaluation of college students is throughout the whole process of ideological and political education [11, 12]. There is content at the top of the ideological and political education system, such as educational policies, educational principles, and educational goals, as well as ideological and political education. The middle end is the content of the process, such as educational content, educational methods, forms, and means of education, and the content of the lower end of ideological and political education, such as the evaluation of ideological and political educators, and the evaluation of college students receiving ideological and political education [13].

The third is the method of ideological and political education for college students [14]. The methods and means of ideological and political education for college students should be diverse, which is a combination of qualitative and quantitative analysis. Especially with the upgrading of modern statistics and analysis methods, the means and methods of evaluation should also keep pace with the times, using advanced measurement methods. Statistical technology uses the latest theoretical and practical achievements in natural science and social science to scientifically analyze the collected data. The current ideological and political education evaluation system lacks a clear line in the operation process, and there is no unified standard. The ideological and political education evaluation system that has been recognized in practice has not yet been established. Educational measurement believes that the essence of educational evaluation lies in value judgment, and the object threshold lies in the development and change of the educated and various factors that constitute the change [15]. The evaluation process of ideological and political education of college students reflects the process and nodes of evaluating the implementation of ideological and political education of college students. Whether the evaluation process is smooth, orderly, and scientific directly determines the final evaluation result. At present, the evaluation process of the ideological and political education of college students in my country involves a wide range of aspects, and the system is too large. Especially, in the connection between evaluation and the definition of responsibilities, there is a disordered state to a certain extent, which leads to rupture and blurred boundaries in the evaluation process. At the same time, the evaluation relies too much on quantitative methods, emphasizes too much on the application of scientific methods and technical methods of evaluation, and integrates some comprehensive educational issues and in-depth activities of ideological and political education that cannot be quantified and activities that reflect changes in college students' ideological and political education. The final purpose of the evaluation is to formulate corresponding policies and systems based on this [16].

2. Related Works

Most of the existing intelligent teaching systems use technologies such as image recognition, AR/VR, and speech recognition and rarely use deep learning.

The design of deep learning evaluation is a process of reasonably selecting evaluation methods and organizing evaluation content according to learning objectives. Bloom's educational goal classification theory, which is the most influential and widely used in the world today, divides educational goals into three areas: cognition, motor skills, and emotion. The specific classification rules commonly used in the corresponding fields are Bloom's cognitive goals. The taxonomies used are Simpson's Motor Skill Target Taxonomy, and Kraswall's Affective Target Taxonomy. These three classification methods are also the theoretical basis for the design of deep learning evaluation, according to which a deep learning evaluation system of cognition, motor skills, and emotion can be constructed, and the goal level to be achieved by deep learners can be comprehensively clarified.

Although Bloom has made a detailed division and elaboration of cognitive goals, there are still some limitations: the change in learner behavior is the evaluation goal, but the description of behavior goals is not clear enough, especially when the target is relatively high. When thinking activities of higher order, take the linear accumulation of thinking complexity as the classification clue, simply use the transfer to explain the transformation from low-level target learning to high-level target learning, and artificially distinguish the knowledge content from the process, ignoring the high-level target learning, a way to evaluate thinking ability. Famous educational psychologists Biggs and Chris put forward the SOLO taxonomy, aiming at the complexity of thinking structure in their reflection on Bloom's taxonomy, in order to make up for the deficiency of Bloom's taxonomy in the evaluation of higher-order thinking ability. The development of higher-order thinking is closely related to the realization of deep learning. Deep learning is to learn

the inherent laws and representation levels of sample data, and the information obtained during these learning processes is of great help to the interpretation of data such as text, images, and sounds. Its ultimate goal is to enable machines to have the ability to analyze and learn like humans and to recognize data such as words, images, and sounds. Deep learning is a complex machine learning algorithm that has achieved results in speech and image recognition far exceeding previous related technologies. Deep learning is higher-order learning with higher-order thinking as its core feature. Therefore, in the evaluation of deep learning, the evaluation of learners' thinking quality, especially the level of higher-order thinking ability, is particularly important.

To sum up, since deep learning has the commonality of general learning forms, the evaluation of deep learning can be based on the three perspectives of traditional cognition, motor skills, and emotion. The theoretical basis of the motor skills target classification and Kraswall's affective target classification, and the achievement of expected goals such as unstructured deep knowledge, higher-order cognitive skills, and high-level motor skills is the realistic standard. However, considering the particularity of deep learning, with higher-order thinking as the core feature, it is obvious that the evaluation of deep learning should pay more attention to the development of learners' higher-order thinking, that is, based on Biggs' SOLO classification method, to evaluate the level of the learner's thinking structure, which then determines the level of cognitive development. Therefore, in the traditional three-dimensional learning evaluation system of cognition, motor skills, and emotion, the SOLO taxonomy, which pays more attention to the development of higher-order thinking, should be incorporated to construct a theoretical system of deep learning evaluation, as shown in Figure 1. The learning objectives of these four dimensions of cognition, thinking structure, motor skills, and emotion are not isolated and mechanically segmented individuals, but an interconnected organic whole, which together provides theoretical guidance for comprehensive evaluation of the effect of deep learning. However, in practice, free combination, organic integration, and flexible application should be carried out according to the nature and objectives of the curriculum.

Bloom's classification of educational goals and educational evaluation theory has had a huge impact on the field of education since they were put forward, and his classification of cognitive goals is still widely used today. According to the level of thinking and the cognitive level attained by the learner, he divides cognitive goals into six levels from low to high: knowing, comprehending, applying, analyzing, synthesizing, and evaluating. This taxonomy defines knowledge and cognitive skills at the operational level, which can better guide the measurement and evaluation of learning outcomes, but does not clarify how to convert knowledge into skills. To address the relationship between knowledge and cognitive skills, Anderson et al. revised the taxonomy, classifying learning outcomes in the cognitive domain into factual knowledge, conceptual knowledge, procedural knowledge, and metacognitive knowledge. There are four types of knowledge, and the cognitive process of acquiring this knowledge is divided into six levels from low to high: memory, understanding, application, analysis, evaluation, and creation.

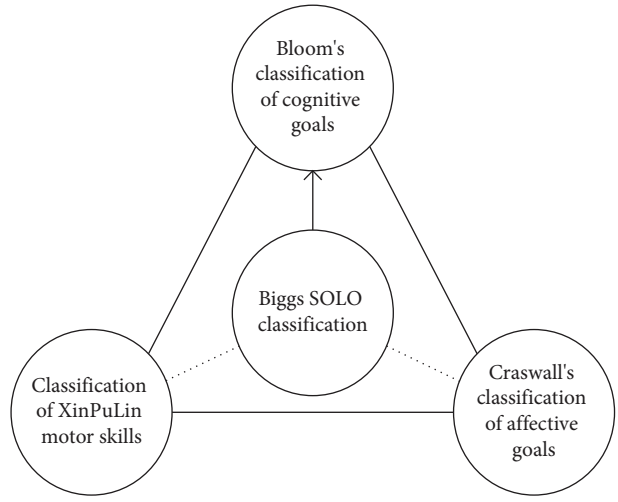

Figure 1: Deep learning evaluation of the multidimensional theoretical system.

According to the understanding of deep learning and shallow learning, shallow learning focuses on scattered, isolated, and currently learned knowledge and is all structured shallow knowledge such as specific facts, information, details, and concepts; deep learning requires learners to establish connections between old and new knowledge in order to master unstructured knowledge such as tacit knowledge, complex concepts, and deep knowledge. Therefore, shallow learning is a simple description, memory, or copy of shallow knowledge, and its cognitive level stays at the lower level of "memory and understanding," which involves low-level mechanical memory, simple retrieval, and shallow understanding. On the contrary, deep learning is a deep understanding and transfer application of knowledge, and its cognitive level is at a higher level of "application, analysis, evaluation, and creation," and most of the activities involved are ill-structured problem-solving metacognition, creative thinking, and other higher-order thinking activities, which require the acquisition of higher-order cognitive skills.

3. The Design of the Student Moral Education Evaluation System

3.1. Research on the Classification of Students' Moral Education Based on the CHAID Decision Tree. CHAID analysis, chi-square automatic interactive detection, is a classification method that uses chi-square statistics to determine the best segmentation and build decision trees. CHAID is a commonly used decision tree, which can automatically search for multiple independent variables, generate the scheme of the maximum difference variable, and finally, output an intuitive tree structure graph. This topic is to find multiple variables (disciplinary items) in the moral education data of students and use chi-square statistics to find the best

segmentation and subcase to build a tree in several moral education periods (normal period, education period, dangerous period, and semester processing period), a framework for reshaping the structure. Through the results of the decision tree, we find out the factors that affect the variables (disciplinary items), finally classify the moral education period (normal period, education period, dangerous period, and semester processing period), and finally get the corresponding rules for each semester through the CHAID decision tree.

3.2. System Architecture Design. Today, the mainstream system architectures are C/S and B/S[17]. These two structural technologies are very mature and have their own characteristics. The B/S system is the abbreviation of Browser/Server. Customers only need to install a browser (Browser) on their personal computer, and the server-side (Server) installs the database. The B/S architecture is a network-based architecture. A C/S distributed mode is a computer term. C refers to Client, S refers to Server, and C/S mode refers to client/server mode. It is a mode in which computer software works together, usually with a two-layer structure. The server is responsible for data management, and the client is responsible for completing the task of interacting with the user. The server side is maintained by professional managers, and the client side is the browser on the client. All operations of the user are sent by the client's browser and then sent to the server through the network. The server processes the client's request accordingly and then returns the request to the client. The structure of the B/S mode is shown in Figure 2.

The advantages of the B/S architecture are that the server side is managed and maintained by professionals, the client side only needs a browser to complete the corresponding request operation, and the technical difficulty is low. Based on the B/S architecture, schools do not need to purchase new equipment, and the moral education system is applied to the local area network, so the ease of use and security are improved.

3.2.1. Theoretical Knowledge of Frame Design.

(1) Performance prediction based on the BP neural network model: the BP neural network algorithm is a supervised classification method. The main idea of the performance prediction model is to input learning samples and use the backpropagation algorithm to determine the weights and biases of the network. Repeated adjustments and training are performed to make the output vector as close to the expected vector as possible. When the sum of squared errors of the output layer of the network is less than the specified error, the training is completed, the weights and deviations of the network are saved, and the classification model is trained. The BP neural network can be used to predict the corresponding offline learning performance by analyzing the characteristics of online learning behavior. A fully connected network is a feedforward network consisting of an input layer, an output layer, and several hidden layers. As shown in the figure below, the input layer is composed of ddd neurons, which are used to input each feature value of the sample; the network can have several hidden layers, and the number of neurons in each hidden layer is also uncertain. Compared with the current fully connected networks of deep learning, the simple BP neural network can maintain a lower computational complexity under the condition of achieving the same effect.

(2) Online learning behavior regularity is analysed by analyzing the user's online learning behavior definition and calculating the corresponding actual entropy value to evaluate the individual's learning behavior regularity and analyze the relationship between the regularity and the user's performance. Theoretically, by calculating the number of days between each time a student logs in, plus the number of logins in an experimental period, the online learning time distribution can be accurately depicted. The user's learning time characteristics are mapped to a two-dimensional coordinate system for visualization, and a user's learning time scatter diagram is made. The maximum, minimum, and average time intervals of each user's login time interval and the truncated average value of the maximum and minimum values are separately counted, and the relationship between them and the performance is analyzed. The most relevant ones are selected and added to the model to enhance the prediction accuracy of the model.

(3) Student sentiment analysis based on microexpression recognition and clustering of the article recognizes the facial microexpressions of users during online learning, including 6 categories of anger, doubt, happiness, fear, dullness, and sadness, to clarify the students' learning emotions and network links between online learning behaviors. Users with different emotions and learning habits are classified by the clustering algorithm. This study proposes an offline classroom quality two-way evaluation system based on classroom information, which has good interactivity and practicability and can provide teaching feedback, classroom discipline supervision, intelligent attendance, and other functions.

3.2.2. System Architecture. The schematic diagram of the structure of the offline classroom quality two-way evaluation system designed in this study is shown in Figure 3, including student terminals, classroom terminals, educational affairs terminals, and cloud servers, in which each terminal and cloud server are connected through mobile network communication.

The industry name for cloud servers is actually called computing units. The so-called computing unit means that

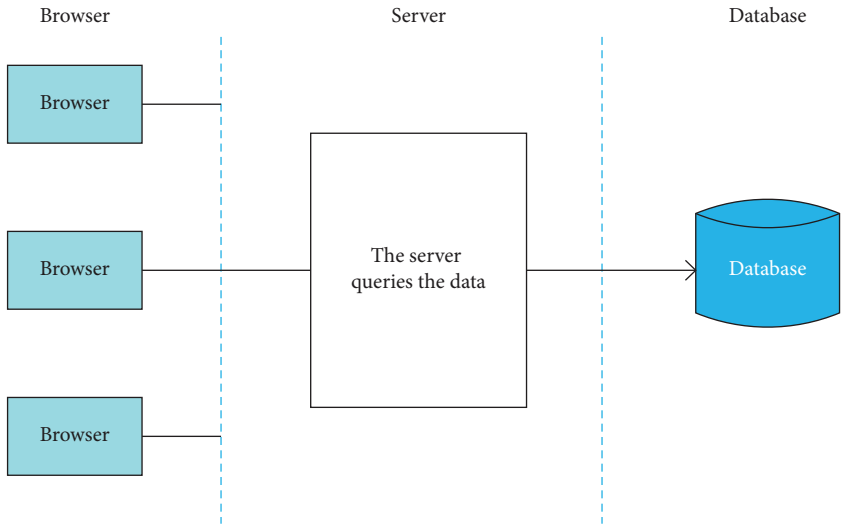

Figure 2: B/S mode.

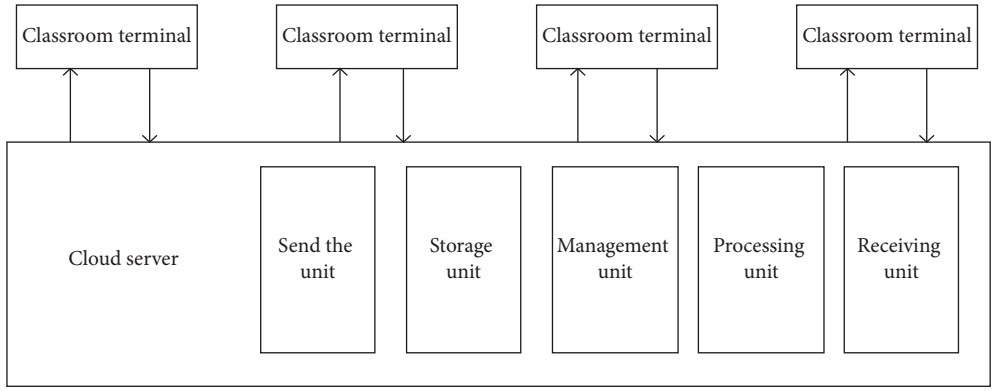

Figure 3: Structure diagram of the two-way assessment system for classroom quality.

this server can only be regarded as a person's brain, which is equivalent to the CPU of an ordinary computer, and the resources inside are limited. If you want to get better performance, one solution is to upgrade the cloud server, and the other is to deploy other software that consumes computing unit resources on the corresponding cloud service. For example, the database has a dedicated cloud database service, and static web pages and pictures have a dedicated file storage service. In this study, through the development of the front-end client of the mobile intelligent terminal and the classroom terminal, combined with the construction of the cloud server and the establishment of the background database, a two-way evaluation system is formed. The use of the client and the data collection of the classroom terminal are based on image processing technology, and classroom data are collected by using a camera and through frame processing. At the same time, a cloud server is built based on deep learning technology, and the collected classroom information is identified and analyzed through the image target detection model, face segmentation, and face detection models, so as to improve and update the stored information and feedback information. In addition, the cloud server is also used for data transmission between clients, classroom terminals, and databases, forming a two-way evaluation system.

The classroom terminal is setup in the classroom; as shown in Figure 4, it consists of a network communication unit, a data acquisition unit, a terminal control unit, and a frame processing unit. The network communication unit communicates with the cloud server and receives the control signal sent by the cloud server. The terminal control unit controls the data acquisition unit to collect classroom data according to the control signal received by the network communication unit, and the classroom data include images and videos. The frame processing unit cuts the collected video into frame images in chronological order and judges the current frame image. If the similarity between the current frame image and the previous frame image is greater than the set similarity threshold, the current frame image is deleted. Implement frame acceleration and processing of video streams. The network communication unit sends the video frames processed by the frame processing unit and the collected images and videos to the cloud server for storage and processing.

As mobile clients, the teacher terminal, educational affairs terminal, and student terminal mainly have the

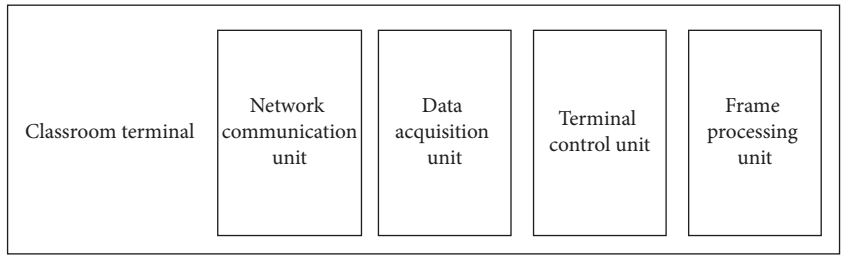

Figure 4: Schematic diagram of the composition of the teacher's terminal.

functions of sending, receiving, and displaying, that is, sending image and text information to the cloud server and receiving and displaying the data returned by the cloud server. The cloud server is mainly used to perform attendance analysis, class attendance analysis, classroom behavior analysis, classroom expression analysis, classroom seat analysis, etc., on the received data, and feedback the analysis results to the mobile client terminal. Among them, the subunit composition of the processing unit is shown in Figure 5, including the attendance analysis and feedback subunit, class attendance analysis and feedback subunit, classroom behavior analysis and feedback subunit, classroom expression analysis and feedback subunit, and classroom seat analysis and feedback subunit. These five subunits all use deep learning models to analyze and provide feedback on classroom data.

3.2.3. System Modules. Fast R-CNN takes the entire image and a series of candidate boxes generated on the image as input and calculates the feature map through the convolutional layer and the pooling layer. For each candidate box, a fixed-length feature vector is extracted from the feature map region corresponding to each candidate box using the ROI pooling layer described below. After the fixed-length feature vector is calculated by several fully connected layers, it is divided into two branches. One branch uses the SoftMax method to classify the images in the candidate frame, and the other branch returns the offset and scaling of the target frame relative to the candidate frame.

(1) Target detection module based on FastR-CNN: the main function of the target detection module in the offline system is to detect and identify students' classroom behavior and students facial expressions in classroom video frame images. The steps of using the FastR-CNN network to identify objects include

(1) Extract features using the CNN model [18, 19].
(2) Selection and mapping of candidate regions.
(3) Target classification and boundary regression. The schematic diagram of the structure of FastR-CNN used in this study is shown in Figure 6.

The image is input into the CNN network, and the feature map is obtained through a series of convolution and pooling operations [17, 20–22]. Then, the selection and mapping of candidate regions are carried out. The selection of candidate regions refers to prefinding the position of possible targets from the original image, that is, the region of interest (RoI). FastR-CNN uses the selective search method to select about 2000 candidate regions. This method combines exhaustive search and segmentation methods, which greatly reduces the search time of candidate regions and improves selection accuracy. The mapping of the candidate region refers to mapping the position of the candidate region in the original image to the feature map. FastR-CNN achieves a reduction in computational complexity by adding an RoI pooling layer after the convolutional layer to map each candidate region into a single fixed-scale feature vector.

Finally, target classification and boundary regression are performed. FastR-CNN uses SVD decomposition to calculate the feature vectors obtained in the previous step through their respective fully connected layers to obtain two output vectors for classification and regression. [23].

(2) Face detection module based on FaceNet.

The main functions of the face detection module in the offline system are the detection and recognition of students' faces in-classroom images. Based on the high cohesion of the same face photos and low coupling of different face photos, FaceNet uses the CNN network model and the TripleLoss function for face detection [24]. Firstly, CNN feature extraction is performed, the face image is input into the CNN network, the feature vector is obtained after convolution and pooling operations, and the mapping of the face to the Euclidean space is realized. The network is trained on the condition that the distance between the face and the object is always smaller than the distance between different individual faces.

The goal of the TripleLoss function is to map the face features of the same individual to the same area of space so that the distance between the faces of the same individual is smaller than the distance between different individuals; that is, the intraclass distance is smaller than the interclass distance. Specifically, the triplet consists of Anchor, Positive, and Negative. Anchor represents a random sample in the dataset, Positive represents a sample belonging to the same class as the Anchor, and Negative represents a sample belonging to a different class from the Anchor. In the training process, the ternary loss

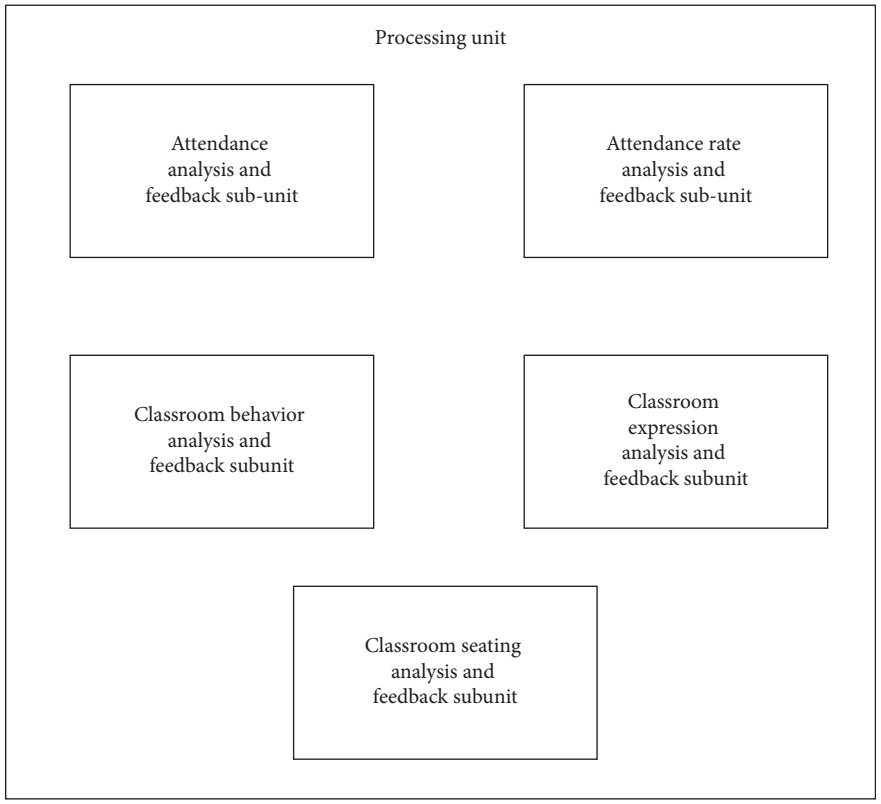

Figure 5: Schematic diagram of the subunit composition of the processing unit.

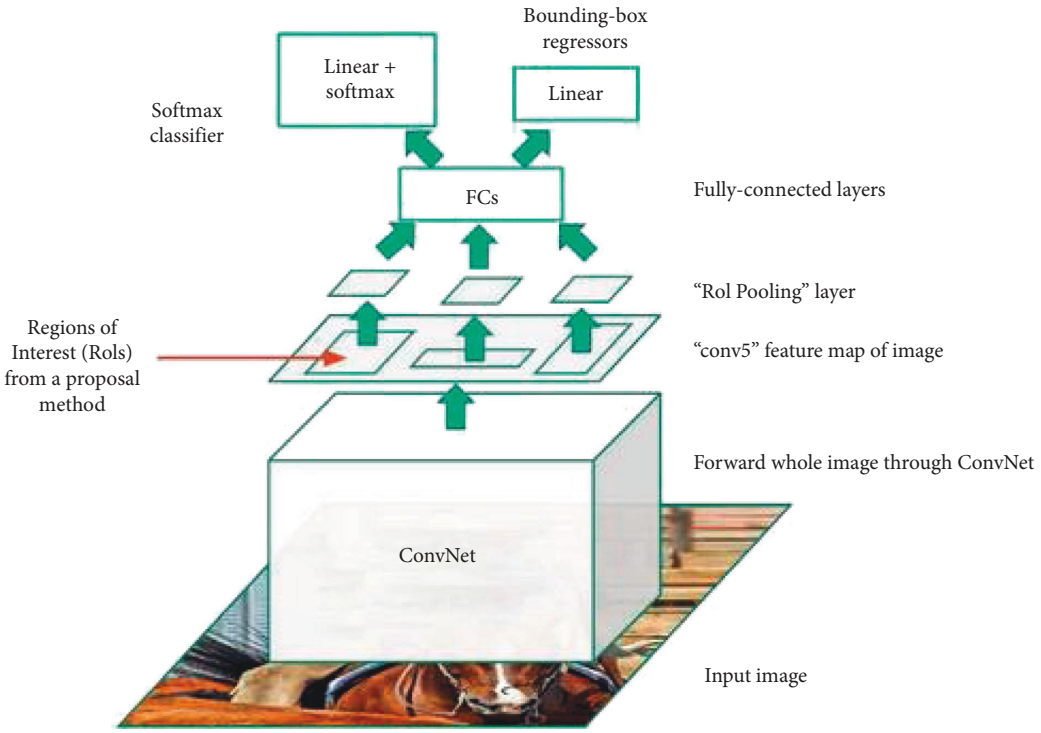

Figure 6: Schematic diagram of the structure of FastR-CNN.

function makes the distance between Anchor and Positive as small as possible and the distance between Anchor and Negative as large as possible and makes a gap between intraclass and interclass distances [25].

(3) Face segmentation module: The main function of the face segmentation module in the offline system is to detect the number of faces in the classroom images and combine them with the face detection module for data analysis. The specific process of the face segmentation model to achieve face segmentation is to input the original image, create an image pyramid based on a certain scaling factor, and obtain scaled images of different scales and resolutions. The Resnet-101 network is used for feature extraction and candidate frame boundary regression for all zoomed images, and the frame that best matches the face position is obtained.

Then, the nonmaximum suppression method (NMS) is used to fuse the bounding boxes corresponding to all the zoomed images to obtain the final detection result, that is, the coordinate value of the face. And according to the returned coordinate values, the cv2 module in OpenCV is used to crop, segment, and temporarily store the face.

For group photos of a class, too many people will lead to smaller faces or too little information. In order to minimize the impact of these situations on the results, the surrounding information (such as shoulders and hair) is positioned for auxiliary positioning and returns the position coordinates of each face.

3.3. Experimental Results and Analysis.

(1) Analysis of online learning regularity: after obtaining the maximum, minimum, and average values of each user's online learning time interval and the truncated average value after removing the extreme values at both ends, each experimental object is divided into 4 values. The rank-ordering. At the same time, the user's real evaluation results are sorted.

Calculate the user's actual entropy function, give the corresponding ranking, and then draw the Spearman correlation scatter diagram between the actual entropy and the score ranking according to the user's actual score, as shown in Figure 7.

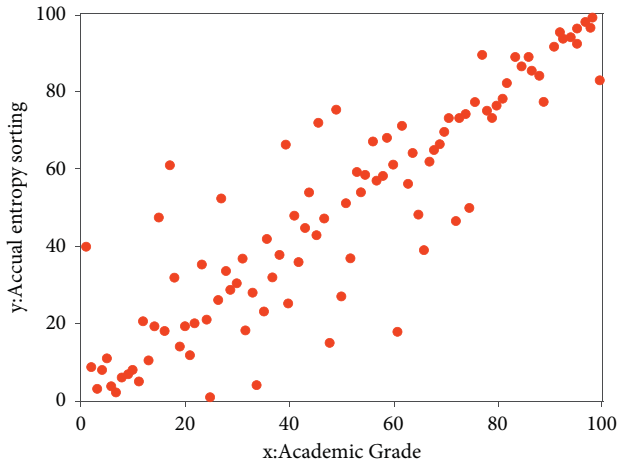

Figure 7: Actual spearman correlation scatter plot.

It can be calculated that the Spearman correlation has obvious positive correlation characteristics. Intuitively, users with more regular learning time periods are more self-disciplined. In learning, users periodically review the knowledge they have learned, and their performance in performance evaluation is better. Combining the abovementioned rank correlation of time difference and the rank correlation of actual entropy function, the study adds the score of actual entropy function as the dimension of time regularity into the model, conducts relevant training on the BP neural network, and finally makes the test set's score. The accuracy rate rose to 74.7900%, achieving the purpose of enhancing the prediction accuracy of the model by fully mining the learning log records of online users.

(2) Sentiment analysis based on microexpression recognition and clustering: according to the microexpression analysis of users during online learning, the number and proportion of various expressions were counted, and the emotional scores of 101 users in four dimensions were obtained in the experiment. The k-means clustering algorithm is an iterative clustering analysis algorithm. The steps are as follows: predivide the data into K groups, randomly select K objects as the initial clustering centers, and then calculate the clustering of each object and each seed. Cluster centers and the objects assigned to them represent a cluster. Each time a sample is assigned, the cluster center of the cluster is recalculated based on the existing objects in the cluster. This process will repeat until a certain termination condition is met. Termination conditions can be that number (or a minimum number) of objects is reassigned to different clusters, number (or a minimum number) of cluster centers changes again, and the sum of squared errors is locally minimized. The emotional dimension data obtained by processing are subjected to K-means clustering analysis to obtain the emotional classification results. The K-means clustering results show that when $K = 3$, the clustering results are the best, that is, the measurement function values of the distances between each point and various centroids. Minimum: according to the emotional data, the emotional attributes of 101 users are divided into three categories. Through the processing of the similarity matrix, the users are exchanged for the rows and columns of the matrix, and the users who are in the same category are exchanged together. In this way, users of the three categories are all concentrated together, and in the visualization of the heat map, you will see that there

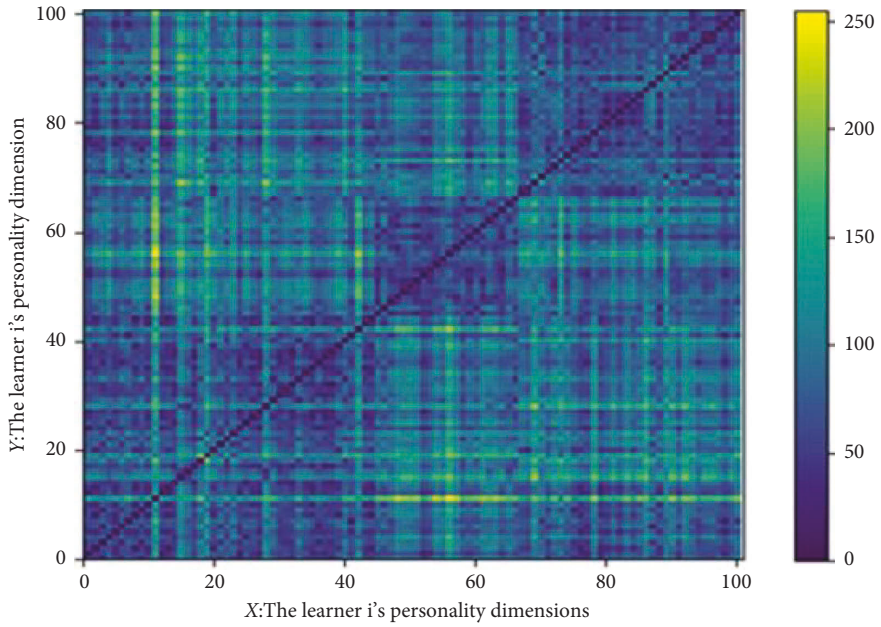

Figure 8: Visualization of the similarity matrix heatmap after clustering.

are three diagonal blocks on the diagonal, which indicates that the clustering effect is obvious. The similarity matrix heat map after clustering is shown in Figure 8.

In these three categories, students with higher academic performance are obtained; that is, students whose performance category is marked as level 1, and the union of their common online learning characteristics is extracted.

The classroom behavior analysis and feedback subunit retrieves and uses the trained image target detection model to detect classroom behaviors (such as students raising their hands, standing, sleeping, and teacher interaction) in the video frame images in the data storage module and uses face segmentation The detection model recognizes the location of students and counts the types and times of classroom behaviors, updates the student identity to the classroom behavior data and student feedback information; and updates the location of students with classroom behaviors and behavior types and times to the classroom behavior data. According to the classroom behavior, the total number of behaviors in the data calculates the interaction rate (the ratio of the number of interactions to the total number of people), evaluates the teaching quality of teachers, and updates the interaction rate and evaluation results to the classroom behavior data and teacher feedback information. Expression Analysis and Feedback Subunit uses the face segmentation and face detection models to identify the student's face in the video frame image in the data storage module and uses the image target detection model to identify and classify the student's expression, including angry, doubtful, happy, afraid, plain, and sad6. Class: Classify and count the recognition results of students' expressions, and calculate the proportion of each expression and further evaluate the teacher's teaching method according to the expression data so that the teacher can make corresponding adjustments to the teaching method according to the results. Students with a large number of times generate corresponding reminder suggestions for course preview, update the expression ratio results to the classroom student data and teacher feedback information, and update the reminder suggestions to the student feedback information.

4. Conclusion

"The assessment and evaluation system of the teaching of ideological and political theory courses in colleges and universities should focus on the unity of the internalization and externalization of the course content and the unity of knowledge and action." It is worth thinking about and exploring to solve the difficult problems in the construction of ideological and political education in colleges and universities. The innovation of the evaluation mechanism of the ideological and political theory course requires not only the research and development of technical personnel but also the cooperation of the ideological and political theory course educators and educated. However, no matter what kind of innovation, the focus is still "people-oriented." The most important thing about technological innovation is to help people's practice. Using deep learning technology to innovate the evaluation mechanism of ideological and political theory courses in colleges and universities will help educators fully understand the dynamic absorption of educated and educational content and will play an important role in improving the effectiveness of ideological and political theory courses in colleges and universities.

Data Availability

The dataset can be accessed upon request.

Conflicts of Interest

The authors declare that they have no conflicts of interest.

References

[1] X. Jiang and P. Wang, "Exploration of moral education system in universities," in *Proceedings of the 2019 Asia-Pacific Conference on Advance in Education,Learning and Teaching(ACAELT 2019)*, pp. 551–555, Francis Academic Press, Guangzhou, China, April 2019.

[2] W. Zhang, "Mechanism and path of creating learning space of "micro ideological and political education" in colleges and universities in the new era," *Journal of Innovation and Social Science Research*, vol. 6, no. 9, 2019.

[3] J. Yin, "An analysis of the idea, system and strategy of moral education in American colleges and universities," *Frontiers in Educational Research*, vol. 2, no. 3, 2019.

[4] L. Zhang, "The construction of female college students developmental moral education system," in *Proceedings of the 2015 3rd International Conference on Education,Management, Arts, Economics and Social Science*, pp. 958–961, Changsha, China, December 2015.

[5] S. Wang, "The basis and value of moral education system," in *Proceedings of the 2014 2nd International Conference on Social Science and Health*, pp. 147–152, Guangzhou, China, December 2014.

[6] F. K. Oser, W. Althof, and A. Higgins-D'Alessandro, "The Just Community approach to moral education: system change or individual change?" *Journal of Moral Education*, vol. 37, no. 3, pp. 395–415, 2008.

[7] M. Huang, "Improving the moral education system in higher vocational colleges with the concept of practical education," in *Proceedings of the 2020 5th International Conference on Humanities Science and Society Development (ICHSSD 2020)*, Xiamen, China, May 2020.

[8] S. Zou, "Significance and Implementation Path to Construct Civil Moral Education System in the New Era," in *Proceedings of the 2019 1st International Education Technology and Research Conference*, Seville, Spain, November 2019.

[9] P. Zhang and Y. Feng, "Enlightenment of locke's moral education thought to the moral education of Chinese secondary vocational school students," *Journal of Research in Vocational Education*, vol. 4, no. 2, 2022.

[10] D. Katy, "Kantian moral education and gendered socialization," *Educational Theory*, vol. 71, no. 6, p. 3, 2022.

[11] Y. Xiong, "Research on the function of the student organization in moral education," *Advances in Educational Technology and Psychology*, vol. 5, no. 9, 2021.

[12] Y. Leighanne, "Moral education, modernization imperatives, and the people's elementary reader (1895): accommodation in the early history of modern education in korea," *Acta Koreana*, vol. 18, no. 2, 2021.

[13] X. Chen and W. Zhou, "Research on moral education and ideological leadership of higher vocational students under the new media environment," in *Proceedings of the 2nd International Conference on Humanities, Arts, and Social Sciences (HASS 2021)*, pp. 430–434, Athens, Greece, December 2021.

[14] Y. Duan, "Research on problems and countermeasures of moral education in middle school," *International Journal of Education and Teaching Research*, vol. 2, no. 3, 2021.

[15] E. M. Kharlanova, S. V. Roslyakova, N. V. Sivrikova, T. G. Ptashko, and N. A. Sokolova, "Studying students' opinions as a stage of designing proactive preparation for provid-ing moral education," *Science for Education Today*, vol. 11, no. 4, pp. 46–63, 2021.

[16] S. Zhang, "Research on school wushu education strategy from the perspective of moral education," *Frontiers in Sport Research*, vol. 20, no. 70, 2020.

[17] X. Cheng and G. Dang, "The research of embedded remote monitoring system based on B/S framework," *IJWA*, vol. 9, no. 1, 2017.

[18] J. E. Valdez-Rodríguez, H. Calvo, E. Felipe-Riverón, and M. A. Moreno-Armendáriz, "Improving depth estimation by embedding semantic segmentation: a hybrid CNN model," *Sensors*, vol. 22, no. 4, p. 1669, 2022.

[19] W. Dang, D. Lv, R. Li et al., "Multilayer network-based CNN model for emotion recognition," *International Journal of Bifurcation and Chaos*, vol. 32, no. 1, 2022.

[20] F. Chen, J. Zheng, and Y. Tang, "Modified LSTM-CNN Model for Arrhythmia Classification with Mixed Handcrafted Features," in *Proceedings of the 2021 33rd Chinese Control and Decision Conference (CCDC)*, pp. 486–490, Kunming, China, May 2021.

[21] X. Liu, G. Li, Xu Luo, and Y. Wu, "Predictive analysis of class Attention based on CNN model," *Journal of Physics: Conference Series*, vol. 9, no. 2, p. 1852, 2021.

[22] I. Emrah, "COVID-19 disease severity assessment using CNN model," *IET Image Processing*, vol. 15, no. 8, 2021.

[23] X. Cheng and G. Dang, "The research of embedded remote monitoring system based on B/S framework," in *Proceedings of the IOP Conference Series: Materials Science and Engineering*, p. 740, Borovets, Bulgaria, November 2020.

[24] Q Guo Dang and Y Cheng, "The research of embedded remote monitoring system based on B/S framework," *Applied Mechanics and Materials*, vol. 3744, pp. 4713–4715, 2015.

[25] D. Li and Z. Wang, "The development of intelligent home remote monitoring system based on B/S framework," in *Proceedings of the 2014 2nd International Conference on Computer,Electrical,and Systems Sciences,and Engineering(CESSE 2014 V1)*, pp. 291–298, Dhaka, Bangladesh, December 2014.

Hindawi
Scientific Programming
Volume 2023, Article ID 9837098, 1 page
https://doi.org/10.1155/2023/9837098

Retraction

Retracted: System Analysis of the Learning Behavior Recognition System for Students in a Law Classroom: Based on the Improved SSD Behavior Recognition Algorithm

Scientific Programming

Received 18 July 2023; Accepted 18 July 2023; Published 19 July 2023

This article has been retracted by Hindawi following an investigation undertaken by the publisher [1]. This investigation has uncovered evidence of one or more of the following indicators of systematic manipulation of the publication process:

(1) Discrepancies in scope
(2) Discrepancies in the description of the research reported
(3) Discrepancies between the availability of data and the research described
(4) Inappropriate citations
(5) Incoherent, meaningless and/or irrelevant content included in the article
(6) Peer-review manipulation

The presence of these indicators undermines our confidence in the integrity of the article's content and we cannot, therefore, vouch for its reliability. Please note that this notice is intended solely to alert readers that the content of this article is unreliable. We have not investigated whether authors were aware of or involved in the systematic manipulation of the publication process.

Wiley and Hindawi regrets that the usual quality checks did not identify these issues before publication and have since put additional measures in place to safeguard research integrity.

We wish to credit our own Research Integrity and Research Publishing teams and anonymous and named external researchers and research integrity experts for contributing to this investigation.

The corresponding author, as the representative of all authors, has been given the opportunity to register their agreement or disagreement to this retraction. We have kept a record of any response received.

References

[1] Q. Guo, "System Analysis of the Learning Behavior Recognition System for Students in a Law Classroom: Based on the Improved SSD Behavior Recognition Algorithm," *Scientific Programming*, vol. 2022, Article ID 3525266, 11 pages, 2022.

Hindawi
Scientific Programming
Volume 2022, Article ID 3525266, 11 pages
https://doi.org/10.1155/2022/3525266

Research Article

System Analysis of the Learning Behavior Recognition System for Students in a Law Classroom: Based on the Improved SSD Behavior Recognition Algorithm

Qingmei Guo

Shengda University of Economics, Business & Management, Zhengzhou 451191, Henan, China

Correspondence should be addressed to Qingmei Guo; 100082@shengda.edu.cn

Received 19 July 2022; Revised 10 August 2022; Accepted 7 September 2022; Published 30 September 2022

Academic Editor: Lianhui Li

Classroom teaching activities have always been the focus of research in the field of pedagogy. The main body of classroom teaching activities is students, and students' classroom behavior status can reflect classroom efficiency to a certain extent, making it an important reference index for classroom quality assessment. With the rapid development of artificial intelligence, school education is gradually becoming more intelligent. At present, most of the classrooms are equipped with video equipment. These videos record the real behavior status of the students in the classroom. For example, by analyzing the data, combining artificial intelligence, deep learning, and other related technologies with education to develop behavioral intelligence, the analysis system has a certain positive effect on helping the reform of classroom education. This study proposes an improved SSD behavior recognition model. The network model is optimized and the model convergence speed is accelerated based on the RMSProp optimization algorithm Through a database of 2,500 images of five behaviors, including raising hands, sitting up, writing, sleeping, and playing with mobile phones, and using them as object detection datasets, we use the OpenCV library to extract frames from classroom screen recording videos as image data sources for student behavior recognition and face recognition. Finally, an improved method is proposed to change the virtual network to MobileNet and complete the fusion function. The results show that compared with the traditional SSD method, the improved model has a significantly improved effect in recognizing small objects and the recognition speed is not significantly reduced.

1. Introduction

Nowadays, legal education is mainly based on teaching in class. In the traditional teaching model, the students are passive and have scattered knowledge. The cultivation of character, emotion, ability, and other aspects has not achieved the best effect. The various disadvantages appear gradually and cannot adapt to the requirements of modern society [1]. The legal teaching in the class includes civil law, criminal law, labor law, and other law departments. The knowledge is scattered and complex, lacking the complete knowledge structure system that cannot be systematically in-depth learning, resulting in the teaching in class being still at the surface level of understanding. The learning effect has not been substantially changed [2]. With the acceleration of the popularization of higher education in China, knowing how to guarantee and improve the quality of teaching and ensure the quality and scale of coordinated development is one of the main problems faced by Chinese colleges and universities.

Under this profound background, it is an effective way to comprehensively deepen the curriculum reform to carry out the construction of a classroom mode of promoting in-depth learning, research methods and strategies based on questions and tasks and summarize the application rules of in-depth knowledge [3]. The shallow monologue and infusing filler in class are gradually replaced by new paradigms such as cooperative inquiry and in-depth dialogue and communication. The new paradigms with exchange and communication as the central theme make classroom teaching achieve a qualitative leap. Deep learning emphasizes the deep digging of knowledge and the inquiry into the nature of things for

students, which requires the students to master the connection between knowledge generation and the knowledge system. It focuses on cultivating critical thinking and problem-solving skills for the students, which are necessary to adapt to society and still have learning abilities after entering the organization [4, 5].

As the main body of classroom teaching, their classroom behavior reflects their acceptance of knowledge and directly affects the teaching quality of teachers. The traditional education in the classroom and the status of the students can only be understood through the teacher's observation in the class, the workload is enormous, and the results are relatively one-sided. The target detection method is used to identify student behavior that can count the number of each behavior quickly in class, which is convenient and has high accuracy compared with the manual method. Therefore, the deep learning that is used to analyze classroom status and the development of artificial intelligence to improve teaching quality is the critical direction of educational research in the future, which has significant research value.

2. Related Work

The theoretical research of deep learning and classroom practice analysis is carried out almost simultaneously in foreign countries. The academic study of deep learning provides a strong foundation for classroom teaching research. Meanwhile, classroom practice research also directly enriches the theoretical investigation of deep understanding.

Rushton [6] investigated the influence of assessment methods on deep learning and highlighted the vital role of formative assessment in promoting deep understanding. The use of formative assessment for teachers to encourage students' deep learning was advocated. Hornby et al. [7] experimented on the first-year students for three cycles, and the design philosophy of Meyers and Nulty was adopted. Through the comparison between the experimental group and the control group many times, improvement and adjustment updates proved that deep learning could improve students' learning effects. Khosa et al. [8] conducted, through experimental research, pre-test and post-test that were arranged in the form of questionnaires, the promotion effect of collaborative learning on deep learning was discussed, and students were advocated to achieve the goal of deep learning through collaborative learning. Aubre and Raath [9] clarified the learning degree through case studies that deep learning and shallow learning under problem learning mode could promote geography standard university students to achieve the goal of deep understanding. Nina [10] guided critical thinking by enhancing the interaction between teachers and students in the network environment. The research focuses on deep learning practice in the classroom. James and Richard [11] designed a comprehensive evaluation method based on constructivism to guide and promote deep learning.

Above all, deep learning mainly focuses on classroom teaching in the practical application and technical support of deep learning research in foreign research. The experimental application research had an extended period. Though the repeated verification experiment to reach appropriate strategy and methods can promote deep learning and provide a reference for the development of classroom teaching, the support of technology for deep understanding was mainly reflected in deep knowledge in the information environment, which responded to the requirements of learning levels in the information age and promoted the effective development of deep learning for higher education learners.

Unlike foreign studies, the research of deep learning in China only stayed at the stage of logical thinking in philosophy. Deep knowledge was combined with practical teaching only in recent years.

Xu [12] combined textbook drama with deep learning. It expounds on the primary connotation of deep learning and puts forward effective strategies to promote deep learning. Wu [13] took political teaching as an example, which pointed out that teachers play an essential role in promoting deep learning and putting forward a teaching model and teaching strategy based on deep learning. Zhang et al. [14] compared deep learning with shallow learning and concluded with the critical understanding that deep learning advocated active learning, lifelong learning, and emphasis on knowledge. Zeng and Dong [15] found that deep learning was mainly "deep" in three aspects:

The achievement of training objectives and results

The level of thinking processing

The level of multidimensional input

Guo [16] carried out a series of research on depth teaching and proposed that depth learning cannot be separated from the guidance and help of teachers and stressed that learners should carry out depth learning under the direction of teachers.

Through the research on the teaching practice in the classroom of deep learning in China, although existing studies have noticed the critical role of the school in promoting deep understanding, most of the research remained at the descriptive level, lacking the support of theories and experiments. Based on MobileNet's deep separable convolution structure and feature fusion theory, this paper proposed an improved SSD algorithm, constructed behavioral data sets, and trained the improved SSD network model. The SSD and enhanced models were used to identify the five behaviors of sitting in class, raising hands, writing, sleeping, and playing with mobile phones, and the recognition results were compared. The research aimed to respond to the requirements of learning levels in the information age and promote the effective development of deep learning for higher education learners.

3. The Theory and Technology of Classroom State Analysis

3.1. The Deep Learning Theory

3.1.1. Activation Function. Neural networks are commonly used in deep learning networks, the smallest of which are

neurons, in which two functions are linear and nonlinear, respectively. The former output has no relationship with the number of layers and is always linear, so the use field is limited[17]. However, in reality, neural networks are required to deal with various nonlinear problems, so a function is used to activate the results, and the web, after processing, can solve nonlinear problems. The calculation process of the activation function is shown in Figure 1, the input is put into the neuron, and the neuron performs the linear calculation on it and outputs it into the activation function; thus, a nonlinear result can be obtained [18]. The neural network with an activation function is more powerful.

(1) Sigmoid Function. The sigmoid function originated in the biological field, and another name for it is the logistic function. The output is controlled between 0 and 1, so it is used to activate the output results of the network layer [19]. The formula is as follows: The sigmoid function is often used in dichotomous problems, and the results are better in some aspects, but the derivation calculation is cumbersome, and the phenomenon of disappearing gradient exists.

$$f(z) = \frac{1}{1 + e^{-z}}, \tag{1}$$

where f(z) is the loss function and z represents the input value.

(2) ReLu Function. The linear rectifying function is widely used in image recognition and computer vision. The output is the maximum value of input X and 0. The formula is as follows. Compared with the Sigmoid function, this method has complex power operation and fast calculation speed. In the calculation process, some neurons will be set to 0 to make the network become sparse and effectively reduce the overfitting phenomenon[20].

$$f(x) = \max(x, 0), \tag{2}$$

where $f(x)$ is the loss function and x represents the input value.

(3) SoftMax Function. This function, also known as the normalized exponential function, computes the output between 0 and 1, and the sum of the probabilities of all the outputs is 1. The formula is as follows: The SoftMax function works well for multicategory tasks but not well for keeping the same categories close together and separating different categories.

$$f(x)_j = \frac{e^{x_j}}{\sum_{k=1}^{k} e^{x_k}} \ (j = 1, 2, \cdots, k), \tag{3}$$

where $f(x)_j$ is the loss function, x_j is the JTH value of the input, and k is the number of input values.

3.1.2. Convolutional Neural Network. Convolutional neural networks, also known as convnets, are the foundation of deep learning, and their design is based on biological ideas. They refer to areas of interest in an image. The primary network structure is divided into three layers: input data, output data, and the middle layer. The input layer can process multidimensional data before data are input to the network, which should be unified in the channel, time, and frequency. The output layer outputs corresponding results for different problems, and the middle layer is divided into the convolution layer, pooling layer, and whole connection layer.

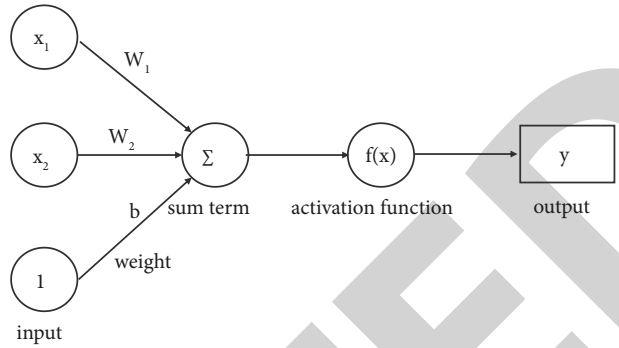

Figure 1: The calculation process for the activating function.

The main mechanism of convolutional neural networks is that when the network is connected to a network, two neurons are related, but convolutional neural networks are only partially protected. I have an $N-1$ layer of neurons connected to N layers of neurons [21–25]. As shown in Figure 2, the special part connects layer $N-1$ and layer N. The left is the fully connected mode and the right is the partially connected mode. The parameter on the right is much smaller than the parameter on the left.

3.2. Face Recognition Method. MTCN face detection algorithm, affine transform face alignment, and NSightface face comparison algorithm. The face data set is first prepared, and the MTCNN algorithm and affine transformation complete face detection and alignment. Finally, the aligned faces were put into InsightFace for face comparison, and the results were obtained.

The face recognition algorithm refers to the recognition of video images in the face recognition model extracted by artificial features and the model selected in this paper. The comparison result of the artificial feature extraction method is 0.9, and the comparison result of MTCNN-InsightFace is 0.95. The accuracy of the MTNC-InsightFace face recognition model is 4% higher than that of the manual feature method, and the speed is much faster, which fully meets the needs of the actual attendance function.

3.3. Image Preprocessing Method. The influence of image noise will affect the information effect, so to ensure the required quality of the image used for operation, it is necessary to deal with it before using it. The commonly used methods include denoising, histogram equalization, normalization, and grayscale image generation.

3.3.1. Grayscale Method. The RGB model color images can get more than 16 million values for one pixel, which will increase the workload of image recognition processing.

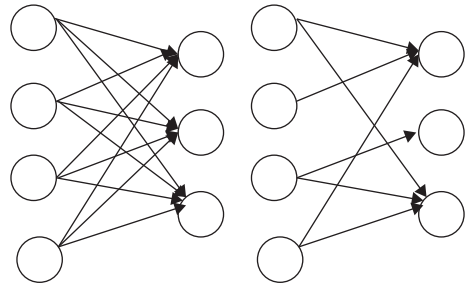

Figure 2: Comparison of full connection (a) and local connection (b).

Graying is $R = G = B$, ranging from 0 to 255 for a single pixel. There are many kinds of grayscale methods, mainly by seeking the average value of each pixel to grayscale, seeking the maximum value of pixels to grayscale, and seeking the weighted mean value of pixels to grayscale, the corresponding function in OpenCV tools is often used.

3.3.2. Denoising Method. The standard denoising methods include mean filter, median filter, Gaussian filter, and bilateral filter. Mean filtering belongs to linear filtering. The average of each pixel value and the surrounding pixel value is taken as the pixel value of the point. Mean filtering will destroy image details in denoising and is suitable for Gaussian noise. Median filtering is to sort the values of a pixel point and the surrounding pixels and find the intermediate value as the final pixel value, which is suitable for denoising impulse noise. The goal of Gaussian filtering is to take the mean of each pixel and the surrounding pixels after weighting and replacing the original pixel. The weight of the center point of Gaussian filtering is more significant than that of the periphery, highlighting the key points more than that of the mean filtering. However, only the spatial distance of pixel value is considered without considering the similarity, which is sufficient to cause image blur. Bilateral filtering takes spatial distance and similarity as indexes and can protect edge characteristics while removing noise.

4. Improvement of the SSD Behavior Recognition Algorithm

The behavior in class helped analyze the quality of listening and teaching effects. Five common postures, including sitting in class, raising hands, writing, sleeping, and playing with mobile phones, were selected for identification and research. The shortcomings of the target detection SSD algorithm were obtained by analyzing the characteristics of students' behavior, and an improved SSD algorithm was proposed. Meanwhile, the implementation process of the classroom behavior recognition model was introduced in detail.

4.1. The Construction Process of the Recognition Model for Behaviors in Class. The model construction mainly includes determining network structure, preparing training data, model training, and testing, etc. The behavior recognition model design process was obtained as shown in Figure 3. [2, 22, 26].

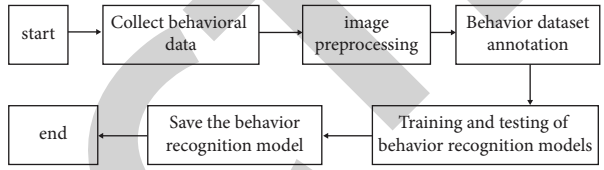

Figure 3: Identification process of behavior in class.

The first step was to prepare student behavior images. Two thousand five hundred images were collected, including raising hands, sitting, writing, sleeping, and playing with mobile phones, with 500 pictures for each behavior. Then, they built a behavior recognition database. The collected 2500 images were preprocessed and labeled, and the photos were divided into three parts: a training set, a test set, and a verification set according to proportion. Finally, the model was trained and tested. The initial model was obtained by putting the training set into the behavior recognition network model for training. The validation set was used to verify the model, and the network model parameters were adjusted according to the verification results. We put the test data into the model to get the results, analyze the results, and determine any differences from expectations. We decide whether to continue the training model according to the comparison results and saved the behavior recognition model with a better effect for subsequent class behavior recognition.

4.2. Improved SSD Algorithm. The improvement strategies were proposed for the primary network and small target detection of the traditional SSD algorithm. Instead of VGG16, a lightweight network was used to reduce the number of parameters to improve the detection speed. The high-level semantics were fused to the low level to enhance the small target detection effect. The improvement principle and process will be introduced in detail as follows:

4.2.1. Improvements to the Underlying Network. The goal of improving the primary network was to replace the original backbone network, VGG16, with a lightweight network. The

Table 1: Comparison of VGG16 and MobileNet in the imagenet dataset.

Model	ImageNet accuracy (%)	Million mult-adds	Million parameters
MobileNet	70.6	569	4.2
VGG16	71.5	15300	138

MobileNet network used deep devolution instead of ordinary convolution to reduce the number of parameters. MobileNet had only 4.2 million parameters compared with 133 million parameters in VGG16. By analyzing the test results of both in the ImageNet data set, as shown in Table 1, the speed of MobileNet was greatly improved. At the same time, the accuracy was only 0.9 percentage points lower than that of VGG16. Therefore, based on the original MobileNet, this paper was used as SSD's primary network after some modifications.

(1) Improvement of MobileNet. MobileNet was faster and less computational than VGG16 because it had two differences. First, depth separable convolution was used for network composition. On the other hand, the width coefficient and resolution coefficient were also used. When the image was input into the network, a set of graphs containing feature information should be obtained through deep convolution operations, respectively, and some other feature graph information should be received by point convolution operations after the BN and ReLu operation of the feature graph, and then, the results should be obtained through BN and ReLu operations again. We change the MobileNet input size from 224×224 to 300×300. In order to increase the information capacity of the feature map and improve detection accuracy, increasing the input size can make essential preparation for the combination of the two networks.

(2) Replacement of SSD Primary Network. The first 14 improved deeply separable convolutional layers were selected from the improved MobileNet(300×300) network to replace VGG16 as the backbone network of the enhanced algorithm. In order to increase the feature extraction capability of the model, eight ordinary convolutional layers of decreasing size were connected behind the replaced primary network in order to further obtain deeper information about the image. The size of the eight convolutional layers is shown in Table 2.

Finally, a classification layer for judging categories and a nonmaximum suppression layer for screening regression boxes were connected to the end of the network to complete the replacement of the primary network. The basic network structure after the replacement is shown in Table 3. Deep convolution and subsequent 1×1 point convolution were regarded as one layer, and there were 14 layers, respectively, denoted as Conv0 to Conv13, where $s1$ represents step size 1, $s2$ represents step size 2, and Conv DW represents deep convolution and then convolved with a 1×1 point to process the channel.

The same as with the original SSD, 6 feature layers were selected to complete feature extraction and target detection. The depth of layers was considered in the selection, as it was too shallow to extract enough image information. The 6 characteristic layers selected in this paper were Conv11, Conv13, Conv14_2, Conv15_2, Conv16_2, and Conv17_2, which decrease in size from front to back to achieve multiscale prediction.

4.2.2. Feature Fusion of the Network Model. The replacement of a primary network improved the detection speed but did not improve the accuracy of small target detection. Improving model performance by integrating features of different scales was the common improvement strategy [9, 27].

Combined with the structure of the network model and the characteristics of each feature fusion method, the ADD feature fusion method was selected by the researchers for the network fusion operation. During the fusion, the fusion layer was selected first. Conv17_2 and Conv16_2 were too small to have much information. Only Conv11, Conv13, Conv14_2, and Conv15_2 were chosen for the fusion operation. The specific fusion steps were as follows.:

In the first step, the size of Conv15-2 changed from 3×3 to 5×5 after up-sampling, and then, it was fused with Conv4-2 by the add method. Finally, the fusion results were normalized to obtain the characteristic layer.

The second step: an upsampling operation was carried out on conv14_2_r with the size of 5×5 to make it the same size as Conv13 with the size of 10×10. The two were fused and normalized by the ADD method to obtain the new feature layer CONV13_r.

The third step: the feature layer conv13-R obtained in the previous step was up-sampled to receive the exact size of 19×19 as Conv11. The add feature fusion method was also used for fusion, and finally, normalized.

4.2.3. Model Optimization Algorithm. Model training requires continuous attention to the change of loss function. The constant decrease in loss function value indicates that the result of model training was closer to the natural consequence. In order to accelerate the decline speed, optimization algorithms were usually used, such as Momentum, RMSprop, and Adam. This paper adopts the RMSProp (Root Mean Square Prop) optimization algorithm proposed by Geoffrey E. Hinton. In this algorithm, the historical gradient of each dimension was squared and superimposed. The decay rate was introduced simultaneously to obtain the sum of the historical rise. The learning rate was divided by the result obtained above when the parameters were updated. After using the algorithm, the gradient direction changes in a small range, which speeds up the convergence of the network. The specific calculation formula was shown as follows:

Table 2: Size of eight convolution layers.

Name of the layer	Conv 14-1	Conv 14-2	Conv 15	Conv 15-2	Conv 16-1	Conv 16-2	Conv 16-1	Conv 17-2
Layer size	10×10	5×5	5×5	3×3	3×3	2×2	2×2	1×1

Table 3: Basic network structure after replacement.

Convolutional layer name	Convolution method/step length	Convolution kernel shape	Input size
Conv0	Conv/$s2$	$3\times3\times3\times32$	$300\times300\times3$
Conv1	Conv dw/$s1$	$3\times3\times32$dw	$150\times150\times32$
	Conv/$s1$	$1\times1\times32\times64$	$150\times150\times32$
Conv2	Conv dw/$s2$	$3\times3\times64$dw	$150\times150\times64$
	Conv/$s1$	$1\times1\times64\times128$	$75\times75\times64$
Conv3	Conv dw/$s1$	$3\times3\times128$dw	$75\times75\times128$
	Conv/$s1$	$1\times1\times128\times128$	$75\times75\times128$
Conv4	Conv dw/$s2$	$3\times3\times128$dw	$75\times75\times128$
	Conv/$s1$	$1\times1\times128\times256$	$38\times38\times128$
Conv5	Conv dw/$s1$	$3\times3\times256$dw	$38\times38\times256$
	Conv/$s1$	$1\times1\times256\times256$	$38\times38\times256$
Conv6	Conv dw/$s2$	$3\times3\times256$dw	$38\times38\times256$
	Conv/$s1$	$1\times1\times256\times512$	$19\times19\times256$
Conv7	Conv dw/$s1$	$3\times3\times512$dw	$19\times19\times512$
	Conv/$s1$	$1\times1\times512\times512$	$19\times19\times512$
Conv8	Conv dw/$s2$	$3\times3\times512$dw	$19\times19\times512$
	Conv/$s1$	$1\times1\times512\times512$	$19\times19\times512$
Conv9	Conv dw/$s1$	$3\times3\times512$dw	$19\times19\times512$
	Conv/$s1$	$1\times1\times512\times512$	$19\times19\times512$
Conv10	Conv dw/$s2$	$3\times3\times512$dw	$19\times19\times512$
	Conv/$s1$	$1\times1\times512\times512$	$19\times19\times512$
Conv11	Conv dw/$s1$	$3\times3\times512$dw	$19\times19\times512$
	Conv/$s1$	$1\times1\times512\times512$	$19\times19\times512$
Conv12	Conv dw/$s2$	$3\times3\times512$dw	$19\times19\times512$
	Conv/$s1$	$1\times1\times512\times1024$	$10\times10\times512$
Conv13	Conv dw/$s1$	$3\times3\times1024$dw	$10\times10\times1024$
	Conv/$s1$	$1\times1\times1024\times1024$	$10\times10\times1024$

$$S_{dR} = \beta S_{dR} + (1-\beta)(dR)^2,$$
$$R = R - \rho\frac{dR}{\sqrt{S_{dR}+a}}, \tag{4}$$

where, β is the rate of decay, S_{dR} is Cumulative gradient variable, ρ is learning rate, a is the constant that is not zero, and R is the parameter.

4.3. Behavioral Database Building Methods. The good classification effect of the deep learning network model should be based on a large number of data, which constitute an image database. At present, there was no database specially used for classroom behavior recognition.

4.3.1. Data Set Acquisition and Enhancement. The data set came from classroom surveillance videos and network pictures. In order to ensure the recognition effect, the video images need to be processed before being used as the data set, from which video segments including raising hands, sitting up, sleeping, and writing were selected. OpenCV was used for frame sampling of the selected video, and the pictures containing the above five actions were selected for saving. 1000 image data were collected in this experiment, and some graphic data are shown in Figure 4.

The precision of model training needed a large amount of data as support, so data enhancement was used to increase the amount of data, which included flipping the image horizontally, left-right, and randomly, translating the image horizontally and vertically, and randomly changing the color of the image. After data enhancement, the dataset for this paper contains 2500 images.

4.3.2. Data Set Preprocessing. The collected color image would increase the model trained workload, and the image was prone to contain noise due to the influence of the external environment, so the data set needs to be processed by grayscale and denoising methods, and sharpened by the object enhancement method.

(1) Grayscale processing. The mean value of each pixel point was calculated to realize grayscale processing. The calculation formula was as follows. The comparison before and after gray processing used the formula as shown in Figure 5.

Figure 4: Comparison of NMS effects on graphic data (hand up, mobile phone, sleep, lecture, writing).

$$R = G = B = \frac{(R + B + G)}{3}, \tag{5}$$

where, R, G, and B are three color channels.

(2) Bilateral filtering denoising technology. The bilateral filtering denoising technology was adopted. In an operation similar to Gaussian filtering, each pixel of the image was scanned once, and the weighted sum of the pixel values and corresponding position weights was added on the basis of the operation of obtaining the weighted sum of each pixel value in the field and corresponding position weights. In the calculation, the closer the center was, the greater the weight was, and the closer the pixel value was, the greater the weight was. The specific formula was as follows.

$$\begin{aligned} G_s &= \exp\left(-\frac{\|p-q\|^2}{2\sigma_s^2}\right), \\ G_r &= \exp\left(-\frac{\|I_p - I_q\|^2}{2\sigma_r^2}\right), \end{aligned} \tag{6}$$

where G_S is the spatial distance weight, G_r is the Pixel weight, q is the central store of Window, p is any point, I_q is the input image, and I_p is the filtered image.

$$\begin{aligned} W_q &= \sum_{p \in S} G_s(p) G_r(p) \\ &= \sum_{p \in s} \exp\left(-\frac{\|p-q\|^2}{2\sigma_s^2}\right) \exp\left(-\frac{\|I_p - I_q\|^2}{2\sigma_r^2}\right), \end{aligned} \tag{7}$$

where W_q is the sum of the weights of each pixel value.

Gaussian filtering mainly played the role of image smoothing. In the critical part of the image, there would be obvious color or light and shade transformation, which was reflected at the pixel level, that was, the pixel values on both sides differed greatly, and the difference gradually increased with the distance. In this case, the G_r value was close to 0, and the whole filter result was also 0. The two images that were, respectively, processed by the method used in this paper (left) and Gaussian filtering (right) are shown in Figure 6.

Figure 5: Image grayscale noise comparison.

Figure 6: Image denoising.

(3) Objective to enhance. Unsharpen Mask (USM) was used to enhance the target. The input image was processed with a low-pass filter to obtain the low-pass component, and the difference between the original image and the component was calculated to obtain the high-pass component, and the sharpened image was obtained by superposition the high-pass component on the basis of the original image. The Gaussian fuzzy method was usually used to obtain low-pass components. The calculation formula was as follows.

$$y = \frac{(x - w \times z)}{(1 - w)}, \tag{8}$$

where y is the output image, x is Gaussian Blur, ranging from 0.1 to 0.9, usually 0.6, z is the weight value.

We input each pixel in the image for USM operation and obtain the pixel value after sharpening each pixel, thus forming the whole sharpened image to complete the target enhancement. The classroom behavior imaged after target enhancement is shown in Figure 7.

4.3.3. Data Set Annotation. Annotation tool uses the LabelImg image annotation tool. The software processes the image according to the format of the Pascal VOC data set. Before labeling, the preprocessed image needed to be saved in Pascal VOC format. After labeling, some basic information about the image, including storage location, size, and category name, was automatically saved in XML files.

Figure 7: Image sharpening.

Table 4: Experimental environment.

Operating system	Windows
Hardware environment	Intel core i5; NVIDIA GeForce GTX1080
Programming environment	Python3.5
Software engineering	Keras deep learning framework, anaconda carrying platform; OpenCV computer vision library

Table 5: Comparison of recognition effects of different models.

Monitoring framework	Based on the network	Whether feature fusion	Average accuracy (mAP) (%)	Detection speed (fps)
SSD	VGG16	No	84.00	22.0
MobileNet-SSD	MobileNet	No	76.14	27.1
Feature fusion of MobileNet-SSD	MobileNet	Yes	83.08	24.6

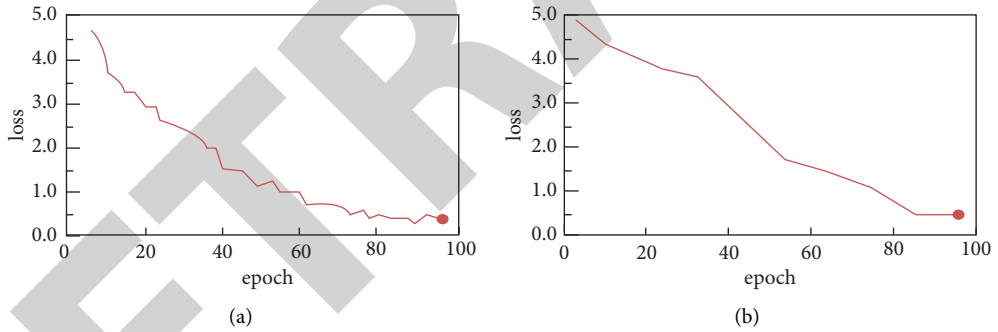

Figure 8: Loss variation.

Table 6: Comparison of the accuracy of five classroom behavior tests.

Model checking	Listen to lecture (%)	Play phone (%)	Raise hand (%)	Writing (%)	Sleep (%)
SSD	89.53	79.74	86.27	77.09	87.66
Improved model	89.31	80.15	87.76	82.12	86.04

5. Experimental Study on the Improved SSD Algorithm

The traditional SSD algorithm, the unimproved MobileNet-SSD algorithm, and the improved MobileNet-SSD algorithm were compared and analyzed from three aspects of training difficulty, detection accuracy, and detection speed.

5.1. Experimental Environment and Parameter Setting. The 500 images were selected for each action in the test training set and 2500 images were selected for each action in the test set. During the training, batch size was set to 4, 625 batches were needed for 2500 training sets, and the epoch was set to 100, that was, 62500 iterations in total. Among them, the learning rate of the first 5000 times was 10^{-4} and the learning rate of the latter was 10^{-5}. The test environment is shown in Table 4.

5.2. Model Evaluation Criteria. In this paper, the model was evaluated by single frame image detection time and Mean Average Precision (mAP) of image detection, which was the mean value of all AP values. AP was the area below the curve

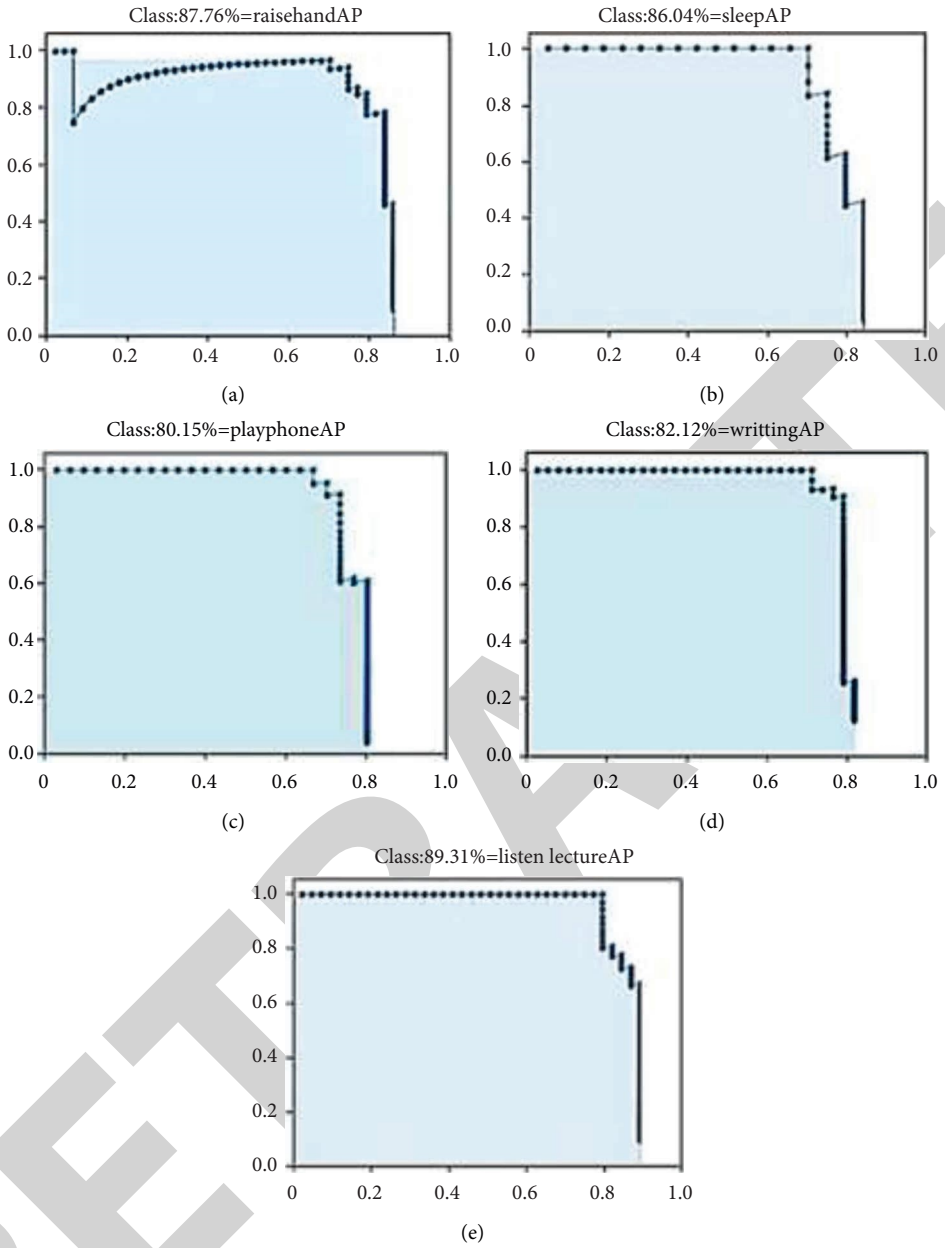

Figure 9: Identify accuracy.

composed of precision and recall. The formula for accuracy was as follows:

$$\text{Precision} = \frac{\text{TP}}{\text{TP} + \text{FP}}, \tag{9}$$

where TP is the classifier that divides the target into positive samples and the number of samples that are actually positive samples and FP is the number of samples that the classifier considers positive but is actually negative.

The whole formula represents the proportion of positive samples considered by the classifier to positive samples recognized by the whole classifier, reflecting the model's precision function.

The recall rate formula was as follows:

$$\text{Recall} = \frac{\text{TP}}{\text{TP} + \text{FN}}, \tag{10}$$

where TN is the number of samples that the classifier treats as negative samples but is actually positive samples.

The whole formula represents the proportion of the samples considered positive and confirmed positive by the classifier to all positive classes, reflecting the model's recall function.

5.3. Model Experiment Process

5.3.1. Preparation of Documents Required for the Test. Before model training, the train. txt file was generated by running the code, which was used to store the training set information.

5.3.2. The Model Training. The training started with an image file load call annotation_path = "train.txt" to reference the resulting train. Then, we identify the category setting. The test needed to identify five behaviors and backgrounds, a total of six categories, namely, NUM_CLASSES = 6. Finally, the network structure was loaded and trained, The model = r_mSSD300() method was used to load the improved model and then accorded to the parameter settings for training. Repetitive training can obtain a better model and save as the behavior recognition model in this paper.

5.4. The Analysis of Model Experiment Results. The traditional SSD algorithm, MobileNet-SSD, and mobile net-SSD with feature fusion were trained in the same experimental environment and parameters, and the three algorithms were compared through the test set. The data used in the test were self-made data sets. The average accuracy and detection speed (detection time per frame) of classroom behavior detection obtained by different models are shown in Table 5.

As seen from Table 4, classroom behavior recognition experiment, compared with the traditional SSD algorithm, the feature fusion MobileNet-SSD improved the detection speed by 2 frames per second, and the average detection accuracy reached 83.08%. Compared with a mobile net-SSD model without feature fusion, the speed was reduced by 2.5% and the accuracy was improved by 6.94% due to the increase in network parameters by fusion. The analysis results showed that the detection speed and recognition accuracy of the proposed algorithm was improved obviously.

The difficulty of model training can be judged by comparing the curve of the loss function during training. With the same parameters, the loss function curve of mobile net-SSD and SSD models with feature fusion was taken when the epoch was 100 iterations for 50000 times, as shown in Figure 8. The loss values of both models continued to decrease, proving that both models were reasonable. During the training, it took 6 days for the loss of the model used in this paper to drop below 0.5, while the original SSD model took 8 days. In addition, the loss value of the model in this paper decreased rapidly, so the training difficulty of the model in this paper was less than that of the traditional SSD model.

The mobile Net-SSD model with SSD and feature fusion was used to test the five actions of students in the test set: listening in class, raising hands, writing, sleeping, and playing mobile phones. The detection accuracy (AP) of each action is shown in Table 6.

It can be seen from Table 6 that compared with the original SSD algorithm, the mobile net-SSD algorithm based on feature fusion in this paper had improved the detection effect of small targets in the five actions, among which the writing improvement reached the highest level of 3.03%, indicating that the model in this paper had improved in small target recognition. Observing the mobile net-SSD recognition result of feature fusion, among the five movements, listening accuracy was the highest, followed by raising hands, and writing and playing on mobile phones were the lowest. Through analysis, the reasons for this result were as follows: compared with other movements, the two activities were more prone to occlusion, especially in the recognition process. It was easy to be confused with other hand movements, so the correction effect was not as good as the other three movements. To more intuitively display the recognition accuracy rate of the model in this paper on the five actions, the line graph is shown in Figure 9, where the shaded area was the accuracy rate.

6. Conclusion

Because of the subjective one-sidedness of traditional legal classes in which students' state was observed artificially, intelligent analysis was introduced into the category, and the deep learning method was proposed to identify students' classroom behavior. The model algorithm was integrated into the system to expand it, and the legal class state analysis system was designed and implemented. The following conclusions were drawn:[28].

(1) The design process of the class behavior recognition model was analyzed, and the images of listening in class, raising hands, writing, sleeping, and playing with mobile phones were selected as the student behavior database after grayscale, noise reduction, and image enhancement practice improved behavior recognition models.

(2) Based on the principle of deeply separable convolution, the improved SSD method was used to analyze student states. Changing the original SSD base network from VGG16 to the improved MobileNet network, using add feature fusion method to replace the network, reducing the basic network parameters, and integrating in-depth information into the shallow layer, the detection effect and speed of small targets were improved.

(3) The improved model was trained and used for student behavior recognition. We identify the population distribution of five behaviors in a class, obtain the population's proportion in the set severe, good, average, poor, and other five states, and complete the analysis test of student status.

(4) The university class state analysis system based on deep learning helps users intuitively analyze the state information of students in a single or multiple classes which is convenient for understanding the class situation of law students and provides a reference for course adjustment.

Data Availability

The dataset can be accessed upon request to the corresponding author.

Conflicts of Interest

The authors declare that they have no conflicts of interest.

Hindawi
Scientific Programming
Volume 2022, Article ID 2202052, 10 pages
https://doi.org/10.1155/2022/2202052

Research Article

Durability Analysis of Small Assembled Buildings in Irrigation Canal System

Zhang Xiao[1] and Wenzheng Wu[2]

[1]*Yellow River Institute of Hydraulic Research, YRCC, Zhengzhou 450000, Henan, China*
[2]*China Pharmaceutical University, Nanjing 210009, China*

Correspondence should be addressed to Wenzheng Wu; wuwenzheng@stu.cpu.edu.cn

Received 9 August 2022; Revised 9 September 2022; Accepted 14 September 2022; Published 30 September 2022

Academic Editor: Lianhui Li

With the rapid development of agricultural economy, people are paying more and more attention to how to apply high-efficiency technologies that save resources to improve agricultural production efficiency, so water-saving irrigation technology has gradually developed. China's agricultural irrigation technology is relatively backward. In addition to the inappropriate irrigation methods and irrigation systems, problems such as siltation, seepage, and frost heave damage in irrigation canals have seriously affected the durability and service life of the canals. The backward irrigation technology seriously restricts the development of agricultural water-saving irrigation. Compared with large irrigation channels, the fabricated reinforced concrete small irrigation channels studied in this paper are less prone to frost heave damage and infiltration problems, and have the advantages of standardized production, simple transportation and installation, and convenient maintenance. In order to study the durability issues such as the basic characteristics, frost heave damage, and service life of fabricated irrigation channels, this paper takes the channel concrete and the formed channel as the research objects, and discusses the research on the properties of the channel concrete through theoretical research, numerical analysis, experiments, and other methods. Strength properties, water penetration resistance, cyanide ion penetration resistance and frost resistance; simulate the seasonal frost heave failure process of the channel; finally, on the basis of the test data, the service life aims to explore the safety and applicability of the fabricated reinforced concrete irrigation channel during the design use period.

1. Introduction

With population growth and social development, water shortage has become a prominent problem faced by our country. Coupled with serious water pollution and uneven distribution of water resources, the contradiction between water supply and demand has become prominent and worsened, which has seriously affected people's quality of life and restricted the social progress and economic development. For a large agricultural irrigation country like China, the country's largest water consumption is agricultural water. According to the 2014 China Water Resources Bulletin, China's total water resources are about 2.73 trillion m^3, a decrease of 1.6% compared to previous years. Water consumption accounts for 22.3% of it, of which agricultural water consumption is about 386.9 billion m^3, accounting for 2/3 of the total water consumption, and the water used for the development of irrigation has reached 90%~95% of agricultural water consumption. Therefore, the channel Low water delivery efficiency directly affects the benefits of agricultural production in irrigated areas. According to calculation and analysis, the national average irrigation water utilization coefficient is 0.502, which is far lower than 70% to 80% of the irrigation water utilization rate in developed countries. The waste of water resources will also cause the groundwater depth to rise in some areas, leading to soil salinization, reducing the area of arable land required for agriculture and increasing investment costs. Channels are

still the main water delivery facilities in China's irrigation areas. The annual water loss of canal system engineering is about $1730 \times 108\ m^3$. Channel engineering using antiseepage technology can reduce water loss by 70% to 90%. Water agriculture and alleviating the contradiction between supply and demand of water resources, it is necessary to establish a set of safe and reliable transmission and distribution canal system to improve the effective utilization of agricultural irrigation water. With the wide application of channel antiseepage technology in water-saving irrigation, the area of water-saving irrigation projects in China reached 407 million mu by the end of 2013, of which the channel antiseepage irrigation area accounted for about 27% of the total area. According to the plan of the Ministry of Water Resources, before 2020, the area of irrigation projects in the country should be increased to more than 60% of the effective irrigation area, the efficient irrigation area should be increased to more than 30% of the effective irrigation area and, the effective utilization coefficient of agricultural irrigation water should be raised to more than 0.55. It can be seen that the construction of channel lining and antiseepage projects directly affects agricultural production and plays a vital role in improving agricultural water use efficiency and the development of water-saving agriculture [1–7].

Through statistical research, there are relatively serious frost heave damage problems in canal buildings in many irrigation areas across the country. According to the frost heave disaster investigation of canal engineering, water transmission channels without antifreeze heave measures generally have frost damage problems, and frost heave produces many cracks. Under the action of water flow, the canal base stop will gradually get swept away, and then slumps will occur, causing channel damage and affecting the normal use of the channel. Therefore, the prevention of frost heave damage in the irrigation channel is also one of the key research issues of channel antiseepage technology. The small prefabricated buildings of the irrigation canal system have many advantages and are also widely used in farmland water conservancy and land improvement projects. However, there is a lack of systematic theoretical and experimental research on the durability performance of small prefabricated buildings in irrigation canal systems. This paper intends to simulate the durability of small prefabricated buildings in irrigation canal systems through laboratory tests, theoretical analysis, and numerical simulation.

2. Related Work

In the study of the most complex structural buildings in hydraulic engineering, the many advantages of prefabricated buildings have been favored by designers. In 1932, the structure of the powerhouse and the lock equipment of the Swell Hydropower Station used prefabricated concrete structures. The Sydney built in 1985. The Mo Hydropower Station became the largest prefabricated hydropower station in the world at that time. The research and application of prefabricated water conservancy projects was carried out. In 1955, in order to improve the engineering quality of power plants, speed up the construction progress, and reduce the labor force, the Soviet Union proposed the industrialization of construction, the development of prefabricated infrastructure, and the maximum mechanization of manufacturing and installation. In the 1970s, the United States became popular with prefabricated products, and successively issued a series of strict standards of industry behavior, which have been used to this day. Ballar and Harper optimized the installation scheme of prefabricated walls, columns, beams, and slabs using genetic algorithms from the perspectives of efficiency and construction technology. And its research results show that in the case of reasonable design and organizational design, the prefabricated technology is superior to the traditional construction method in terms of technology and efficiency. The connection method of prefabricated buildings is the technical difficulty of prefabricated building technology, and it is also the key point in the development process of prefabricated buildings. A reasonable connection method not only improves the quality of prefabricated buildings, but also facilitates construction and reduces prefabrication time. Piltant expounds the prefabrication principle and method of using bolts to connect statically indeterminate prestressed members. It is also pointed out that due to the statically indeterminate characteristics of concrete structures, their manufacture is standardized, the assembly work is reduced to a minimum, and its standardization can greatly reduce the weight of concrete structures. The craftsmanship of prefabricated buildings is different from that of traditional buildings, and the proportion of concrete materials used will also change accordingly. Optimal design requires continuous development to obtain an ideal mix of precast concrete with high early strength, good workability, and economical utility. Jinglin chooses low alkalinity sulfate cement to mix with ordinary Portland cement and adds polycarboxylate superplasticizer and sodium sulfate. The ideal prefabricated concrete mix ratio with higher early strength was selected through orthogonal tests. The research on prefabricated buildings for water conservancy projects in my country began in the 1950s and 1960s. In 1955, at the National Water Conservancy Construction Conference held by the Ministry of Water Resources, Heilongjiang Province introduced the construction experience of prefabricated aqueducts. Since then, this advanced design and construction method has begun to attract attention from all over the world. In 1956, 80% of the hydraulic structures in Zhanjiang were prefabricated, and more than 40,000 structures were built successively, with more than 20 types of structures. In the initial stage of promotion, it was mainly in the form of "building blocks," and light-weight structures were gradually applied, and then steel mesh cement and prestressed concrete components were used. The prefabricated building mold developed by Gaoyou City has gone through the development process from wood mold to steel-wood combination to mechanized assembly line production. At present, three series of irrigation, drainage, and transportation have been formed, with 10 varieties and 38 models, which can be used for clay and sandy areas in hilly, polder,

and plain areas. This achievement has passed the ministerial-level appraisal in November 1992. With the development of information technology, the combination of prefabricated building components and digital technology is the research direction of more and more researchers. The organization and management of information technology can add icing on the cake to the development of prefabricated buildings and promote the development of prefabricated buildings in the direction of modernization. Among them, Mei Yue finds the way of thinking of digital architecture and its corresponding assembly construction and general construction process method and applies it to small design practice activities. With the country's increasing investment in water conservancy project construction year by year, prefabricated slab bridges are also widely used in various water conservancy projects, but as the connection method of prefabricated slab bridges, hinge joints are one of the most prone to disease. [8–14].

3. Durability Parameter Test of Small Prefabricated Buildings in Irrigation Canal System

The object of this test study, the prefabricated concrete U-shaped channel, is mainly used as a water conveyance and diversion channel. In practical engineering applications, the main technical indicators are strength, antiseepage, antifreeze, antichloride ion penetration, and so on. In order to more clearly understand the durability of prefabricated concrete U-channel, it is necessary to test the above indicators of concrete. In this research, by designing different concrete compounding, the concrete test specimens were prepared in the laboratory. The strength characteristics, impermeability, frost resistance, chloride ion permeability resistance of concrete, etc., select the concrete mix ratio suitable for different conditions to meet the working conditions of the corresponding project. The durability can provide the necessary quantitative parameters. In this concrete durability test, the concrete design strength of the fabricated U-shaped channel is C 3 0, and the design slump is 160–180 mm, which is fluid concrete.

3.1. Test Raw Materials. All know, the quality of the raw materials used for mixing concrete may lead to great differences in the performance of concrete. Therefore, the selection of concrete raw materials is crucial to the durability of concrete in the concrete-reduction test. The raw materials required for this experimental study are as follows: cement, coarse and fine aggregates, tap water, mineral powder, fly ash, mineral powder, and water-reducing agent [15].

3.1.1. Cement. In engineering production, cement is an extremely important building material and engineering material, and together with steel and wood, it is called the three major materials of capital construction. This test uses P0.42.5 cement, the chemical composition of cement is shown in Table 1, and its main mechanical properties are shown in Table 2. The properties of various materials are introduced below. Selecting reasonable materials in engineering construction is the key to engineering quality [16].

Table 1: Chemical composition of cement.

Chemical cost of cement (%)					
Sio_2	Al_2O_3	Fe_2O_3	Cao	Mg0	So_3
22.03	8.52	3.76	6 1.37	2.23	2.01

3.1.2. Coarse Aggregates. The aggregate in concrete accounts for about 3/4 of its total volume. Rock particles with a particle size of less than 5.00 mm are called fine aggregates, while those larger than 5.00 mm are called coarse aggregates. Commonly used coarse aggregates include pebbles and gravel. This concrete test uses 5–25 crushed stone on the market. After indoor measurement, the physical index of coarse aggregate is shown in Table 3 and its gradation is shown in Table 4.

3.1.3. Fine Aggregate. Divided into natural sand and artificial sand according to their different production processes and methods. Natural sand can be divided into river sand, sea sand, and mountain sand according to their different sources. Artificial sand can be divided into coarse sand, medium sand, fine sand, and extrafine sand according to the size of the fineness modulus. This test uses medium and fine sand in the building materials market. The fineness modulus of the sand is $Mx = 2.6$, the physical index is shown in Table 5, and the sand particle gradation is shown in Table 6.

3.1.4. Fly Ash. Fly ash is a pozzolanic material with a certain activity. When fly ash is probed into concrete, it can improve the workability of concrete, reduce water consumption, reduce water-cement ratio, and increase the strength of concrete. In this test, the fly ash used is F-class TI grade fly ash with a fineness of 11% and a water demand ratio of 97%.

3.1.5. Mineral Powder. Mineral powder is a concrete admixture obtained by grinding granulated blast furnace slag. It is a powder material that reaches the specified activity index after drying and grinding of granulated blast furnace slag. When grinding slag, a small amount of grinding aid is allowed. The input should be below 144. Mineral powder has potential hydraulic properties, and the main mechanism of action in cement concrete is the cementation effect and the microaggregate effect. The mineral powder that has been separately ground has a surface roughness smaller than that of cement particles, so it also has a certain morphological effect, which can reduce water and increase the fluidity of concrete. In this test, S95 grade granulated blast furnace slag powder was selected, and its surface area was 428 F/kg. The main chemical components are shown in Table 7 [17].

3.1.6. Water Reducer. Adding water reducer to concrete can change the rheological properties of cement paste, thereby changing the internal structure of concrete, thereby

Table 2: The main mechanical properties of cement.

Fineness (80 μm)	Initial setting time (min)	Final setting time (min)	Compressive strength (MPa)			Flexural strength (MPa)		
			3 d	7 d	28 d	3 d	7 d	28 d
4.5%	80	215	28.6	40.3	50.8	5.10	6.45	7.96

Table 3: Physical index of stone.

Specification (mm)	Bulk density (kg/m^3)	Apparent density (kg/m^3)	Mud content (%)	Content of needlelike flakes (%)
5–30	1490	2763	0.8	6.0

Table 4: Grading table of stones.

Specifications (mm)	>25	>20	>16	>10	>5	>2.5
The proportion	8	—	54	—	93	99

Table 5: Physical properties of sand.

Name	Fineness modulus	Apparent density (kg/m^3)	Bulk density (kg/m^3)	Mud content (%)	Mud content (%)
River sand	2.6	2680	1456	2.0	0.6

Table 6: Grain gradation of sand.

Screen size (mm)	>10	>5	>2.5	>1.25	>0.63	>0.315	0.16
Cumulative screening (%)	0	3	10	43	65	91	98

Table 7: Chemical composition of mineral powder (%).

Sio_2	Al_2O_3	Fe_2O_3	Cao	Mg0	So_3	Burn vector
35.23	12.31	3.48	40.38	7.6	—	0.95

improving other properties such as concrete mechanics. In this concrete test, polycarboxylate water-reducing agent was selected as the water-reducing agent.

3.2. Test Mix Ratio. When mixing concrete in engineering construction, the durability of concrete will be completely different when different proportions of materials are adopted. Therefore, in order to obtain concrete that meets the requirements of design quality, it is necessary to calculate the proportion of various materials in the concrete, and through experimental comparison, the concrete mix ratio that meets the durability requirements under the corresponding construction conditions and operating environment is obtained.

In order to study the strength characteristics and durability of the concrete of the prefabricated irrigation canal under different working conditions, three kinds of concrete mix ratios are listed in this experimental study, including the original mix ratio (the mix ratio adopted by the manufacturer) (I), the Add fly ash (II) on the original basis, and then add water-reducing agent (III). The purpose of designing three different concretes is to compare various performance parameters of concrete with different mix ratios, study the applicable environment of concrete with various mix ratios, and meet the safe and applicable durability performance of the channel. See Table 8 for the description of the proportions of three different concretes. [18].

In calculating fly ash in the mixing ratio of (mineral powder) concrete, fly ash (mineral powder) is usually added in two different ways, namely, the method of replacing cement with an equal amount and the method of replacing cement with an excess amount [19].

(1) Equal replacement of cement method, refers to the replacement of cement by the probing fly ash (mineral powder) in equal amount, which can reduce the calorific value of concrete, and can significantly improve the workability and impermeability of concrete, and is often used in mass concrete. The sand replacement method keeps the amount of cement in the concrete unchanged, and hangs fly ash (mineral powder) to reduce the fine aggregate. This kind of concrete has excellent cohesion, water retention

Table 8: Test concrete mix description.

Group	Describe	Water-cement ratio	Sand rate
I	Original mix	0.50	0.41
II	Add fly ash	0.45	0.41
III	Add fly ash, water reducer	0.45	0.41

workability, and impermeability. (2) Oversubstituting cement method, that is, based on the reference concrete mix ratio, according to the principle of equal strength, using the oversubstituting method to adjust the proportion of cement. When calculating the mix ratio in this concrete test study, according to the actual situation of the project, it is planned to use the excess substitution method to design the concrete mix ratio. The use of the excess substitution method to design the mix ratio can determine an economical concrete mix ratio. The design method is completed through testing and trial matching.

3.3. Fabrication and Maintenance of Concrete Specimens. This concrete test plans to complete the concrete strength (tensile, compressive) test, penetration test, freeze-thaw test, and chloride ion resistance penetration test. After statistics, the test pieces to be produced for each group of mix ratios are shown in Table 9. In order to prevent the loss of specimens during the test, there should be excess concrete specimens in each group of mix ratios.

According to the "Standard," the concrete specimens that are formed and demolded should be sent to a standard curing room with a temperature of $20 \pm 2^{\circ}C$ and a relative humidity of more than 95% in time for curing. And the concrete sample should not be washed with water directly. The standard curing age is 28 d, and the test specimens for 7-day compressive strength test shall be taken out for testing at 7 d, and other specimens shall be treated at the corresponding time according to the specifications.

3.4. Experimental Study on the Properties of Concrete Mixtures. The concrete mixture is made by mixing the constituent materials in a certain proportion, and its workability is the most important property of fresh concrete. The workability of the mixture refers to the performance of the mixture that can meet the requirements of the concrete construction process (mixing, transportation, pouring, and vibrating) under the premise of no segregation and bleeding.

The workability of concrete mixture includes fluidity, cohesion, and water retention. Because of its complex connotation, "slump" is used to measure the fluidity, cohesion, and water retention of concrete mixture, so as to evaluate concrete workability of the mixture. During the process of obtaining the mixture in this test, the slump of the mixture was measured, and the statistics are shown in Table 10 [20–22].

4. Durability Analysis and Prediction of Small Prefabricated Buildings in Irrigation Canal System

For any building structure, when designing and constructing, the designer will consider the probability that the building will be used in the expected life time in the future, which is an important basis for judging the "cost-effectiveness" of the building structure. The basic purpose of hydraulic structure design is to make the structure meet various functional requirements predetermined by the design within the predetermined service period, so as to be safe, reliable, economical, and reasonable. The functional requirements of general engineering structures mainly include three aspects.

Safety, serviceability, and durability are commonly referred to as structural reliability. In the design process, in order to obtain the structural reliability that meets the requirements, it is necessary to properly handle the relationship between the two opposites in the structure. On the one hand, the load effect caused by the action (load) applied to the structure, time external force on the structure (such as self-weight, live load, wind load, and water pressure), and other loads (such as humidity deformation, foundation settlement, and earthquake action) cause deformation of the structure. The structural resistance ($R3$) composed of the section size, the number of reinforcements, and the strength of the material is mainly related to the degree of agreement between the structural size of the structural member, the number of reinforcements, the material properties, and the calculation mode of the resistance to the actual situation.

The above load effects and structural resistance R are functions of random variables, so the design of building components is mainly to study the structural resistance 091 used when these two random functions satisfy a certain probability.

4.1. Structural Limit States and Failure Probability. Reinforced concrete structures are widely used in engineering. In the process of design and construction, with the accumulation of experience, the design theory also develops continuously. The process can be divided into three stages: the design method according to the allowable stress, the design method according to the failure stage. The lifetime and prediction in this paper are based on the limit state design concept.

In the engineering field, the limit state of a building structure is generally divided into "bearing capacity limit state" and "normal service limit state" value, mainly considering the applicability and durability of the structural reliability, while the ultimate bearing capacity state refers to the structure or component reaching the maximum bearing capacity or reaching the deformation that is not suitable for continuous bearing. The main consideration is the safety of the structure. The limit state of the structure can be represented by the limit state function Z. In general, many

Table 9: Statistical table of concrete specimens (single group mix ratio).

Type of test	Test specifications	Number of test pieces	Remark
Cube compression	150 mm × 150 mm × 150 mm	6/group	7 days, 28 days old
Split tensile	150 mm × 150 mm × 150 mm	3/group	28 days old
Impermeability test	$D1 = 175$ mm $D2 = 185$ mm $H = 150$ mm	4/group	28 days old
Freeze-thaw test	100 mm × 100 mm × 400 mm	5/group	28 days old
Antichloride test	$R = 100$ mm $H = 50$ mm	3/group	28 days old

Table 10: Measured slump of mixtures.

Group	I		II		III	
	Measurements	Average value	Measurements	Average value	Measurements	Average value
Slump (mm)	175.0 168.0 162.0	1 68.3	165.0 172.0 169.0	168.7	175.0 164.0 168.0	169

factors that affect the limit state are represented by two variables: load effect and structural resistance R, then,

$$\begin{aligned} Z &= g(R, S) \\ &= RS \end{aligned}. \tag{1}$$

Obvious from the above equation that, when $Z > 0$ (i.e., $R > S$), the structure is safe and reliable; when $Z < 0$ (i.e., $R < S$), the structure fails; and when $Z = 0$ (i.e., $R = S$), it means that the structure is positive In the limit state, so when $Z = 0$ is called the limit state equation of the structure. Since, both R and S are random variables, function B is a random function whose value is not a fixed value and should be described by means of probability theory. In probability theory, failure probability P is generally used to represent the reliability of the structure.

Assuming that $F(Z)$ is the probability density distribution function of the functional function Z, then when $Z < 0$, the formula (2) of the failure probability represents the area of the shaded part of the probability distribution curve in Figure 1.

$$\begin{aligned} p_f &= p(Z < 0) \\ &= \int_{-\infty}^{0} f(Z)\mathrm{d}z \end{aligned}. \tag{2}$$

If it is assumed that the two random variables, the structural resistance R and the load effect S, obey the normal distribution, and their mean and standard deviation are μ_R, μ_S, σ_R, and σ_s, respectively, it can be known from probability theory that the functional function B obeys a positive distribution, with the mean and standard deviation of Z being μ_z and σ_z, respectively. Then, the probability density function of the Z normal distribution is as follows:

$$f(z) = \frac{1}{\sqrt{2\pi}\sigma_z} \exp\left[-\frac{(z-\mu_z)}{2\sigma_z^2}\right]. \tag{3}$$

Putting equation (3) into equation (2), we can get the following equation:

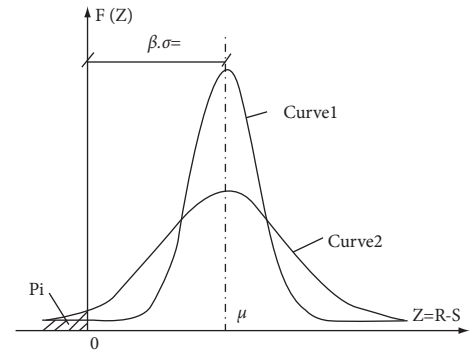

Figure 1: The probability density distribution curve of Z, β, and p_f relationship.

$$p_f = \int_{-\infty}^{0} \frac{1}{\sqrt{2\pi}\sigma_z} \exp\left[-\frac{(z-\mu_z)}{2\sigma_z^2}\right]\mathrm{d}z. \tag{4}$$

In the actual engineering design, it is more complicated to use formula (4) to calculate the failure probability P, so the reliability index is generally used to measure the reliability of the structure.

When the building structure resistance R and load effect S obey the overall distribution, the corresponding relationship between the failure probability p_f and the reliability index β is listed in Table 11. In the design process, when the structural reliability index is determined, the structural failure probability can be obtained, and then the limit state method is adopted to design the structure.

In the design of concrete structures, the probabilistic limit state design concept is mainly used for structural design, so the basic theory adopted in the life prediction of fabricated reinforced concrete irrigation canals is the limit state design theory. The following is the prediction of the service life of the prefabricated irrigation canal under the carbonization condition and the chloride ion environment based on the probability reliability theory, and a certain reference is given for the durability evaluation of the canal concrete.

Table 11: Correspondence between p_f and β.

Beta	p_f
1.0	1.59×10^{-1}
1.5	6.68×10^{-2}
2.0	2.28×10^{-2}
2.5	6.21×10^{-3}
2.7	3.47×10^{-3}
3.0	1.35×10^{-3}
3.2	6.87×10^{-4}
3.5	2.33×10^{-4}
3.7	1.08×10^{-4}
4.0	3.17×10^{-5}
4.2	1.33×10^{-5}
4.5	3.40×10^{-6}

4.2. Life Prediction of Fabricated Irrigation Channels under Carbonation Conditions. The life of the fabricated reinforced concrete irrigation channel under carbonation mainly includes two stages: (1) the time from the concrete surface to penetrate the steel surface; (2) the steel bar begins to corrode until the structural failure occurs. For the corrosion of steel bars, the participation of water and chloride ions is required, so the life prediction part is placed in the later stage of chloride ion steel corrosion. This section only analyzes the time required for the carbonization of the concrete cover.

For the prediction of the concrete carbonation life of the fabricated reinforced concrete irrigation channel, we should first measure the thickness of the steel protective layer, and obtain the average value, mean square error and variation coefficient of the concrete protective layer thickness.

According to the empirical formula, the carbonization rate coefficient of the channel concrete is obtained, the mean square error and variation coefficient of the concrete carbonization coefficient are obtained, and the carbonization life of the concrete is obtained according to formula (4). After measuring the thickness of the protective layer of the irrigation channel in the manufacturing factory, the sample data obtained are shown in Table 12.

According to the knowledge of statistical theory, the average thickness of concrete protective layer can be obtained as μ_c,

$$\mu_c = \frac{1}{N}\sum_{i=1}^{N} x_c = \frac{1}{40}\sum_{i=1}^{40} x_c = 24.9mm\ . \tag{5}$$

Its mean square error σ_c is,

$$\begin{aligned}\sigma_c &= \sqrt{\frac{1}{N}\sum_{i=1}^{N}(x_c-\mu_c)^2}\\ &= \sqrt{\frac{1}{40}\sum_{i=1}^{40}(x_c-\mu_c)^2}.\\ &= 3.12mm\end{aligned} \tag{6}$$

According to the above equation, the carbonization coefficient (in years) is calculated by formula (5), as follows:

$$K = \gamma_1\gamma_2\gamma_3\left(12.1\frac{W}{C} - 3.2\right). \tag{7}$$

In formula 5: the main reference values are γ_1, γ_2, and γ_3.

For the concrete of the prefabricated irrigation channel of the research object, in formula (7), since slag cement is used, the γ_1 value is 1.0; the content of fly ash is 14%, the γ_2 value is 1.1; the channel is mainly used in the northern region, and γ_3 the value is 1.1. Value 1.1: Calculated according to the mix ratio, the water-cement ratio is 0.45, and the above parameter values are taken with AR.

$$K = 1.0\times1.1\times1.1\times(12.1\times0.45-3.2) = 2.72. \tag{8}$$

According to the research, the K value obeys the normal distribution. According to the experience, the mean value μ_k is taken as 2.58 and the standard deviation σ_k is obtained according to the error function. In this study, the value is 0.65.

Substituting $\mu_c = 24.9$ mm, $\sigma c = 3J2$ mm, $\mu_k = 2.58$, and $\sigma_k = 0.65$ into formula (7), and then according to the corresponding values of failure probability P_f and reliability in Table 11, it can obtained carbonation life of fabricated reinforced concrete irrigation channels. According to the calculation, when the failure probability P is 2.28×10^2, its reliability β is 2.0, and the life period $t = 394.4$ years is obtained. The probability of layer carbonization is $P_f = 2.28\times10^2$.

After calculation, it is obtained that the service life of the prefabricated reinforced concrete irrigation canal under the carbonation condition is very long. But only under ideal carbonization conditions, there are not many factors considered in the analysis of the carbonization rate coefficient, so this does not represent the service life of the actual channel. The corrosion time of steel bars is solved in the next section.

4.3. Prediction of Channel Life under Chloride Erosion. To analyze the life of concrete in the chloride ion environment, that is to analyze the time T_1, T_2, and T_3 of the three stages of steel corrosion, and finally unify the three times, that is, the concrete is caused by chloride ions. The time of destruction is analyzed from three aspects.

4.3.1. T_1. The time T_1 is the time for chloride ions to reach the steel bar from the concrete surface. It can be considered here that in the original concrete, the nitrogen ions on the steel bar surface are very small, which is not enough to cause the steel bar to corrode. The time T_1 is when the concrete is exposed to the chloride ion environment until the surface of the steel bar begins to accumulate chloride ions.

This time, the approximate probability design method is mainly used to analyze the time T_1. Considering the partial coefficients in the analysis, the endurance limit state equation of the concrete structure corroded by chloride ions can be expressed as follows:

Table 12: The measured value of the thickness of the protective layer of the irrigation channel (mm).

22.8	27.4	22.6	22.3	31.8	21.5	28.1	22.6	20.6	23.1
22.6	26.0	26.0	27.7	26.3	27.8	21.3	25.7	22.5	24.3
22.6	25.6	23.9	21.6	22.5	22.4	23.3	25.1	27.4	22.7
35.8	23.2	27.3	23.2	30.4	25.2	23.1	26.4	28.6	23.7

Table 13: Parameter value table.

Parameter category	k	h_0	θ	λ
Value	12.5 a/mm	0.15 mm	0.01 mm	6.0

$$\begin{aligned} g &= c_{cr}^{d} - c^{d}(x,t) \\ &= c_{cr}^{d} - c_{s,cl}^{d}\left[1 - \operatorname{erf}\left(\frac{x^{d}}{\sqrt[2]{D_{cl}^{d}(t_{SL}).t_{SL}}}\right)\right] \\ &= 0, \end{aligned} \tag{9}$$

where c_{cr}^{d} is the design value of critical chloride ion concentration for steel corrosion, $c_{s,cl}^{d}$ is the set value of chloride ion concentration on the concrete surface, x^{d} is the statistical value of the thickness of concrete protective layer survey, $D_{cl}^{d}(t_{SL})$ is the test value of nitrogen ion diffusion coefficient of concrete, and t_{SL} is the exposure time of concrete elements.

It can be seen from the above formula that the life estimation model that determines the resistance of concrete to chloride ion damage mainly depends on four parameters: the thickness of the concrete protective layer, the chloride ion concentration on the concrete surface, the critical chloride ion concentration, and the nitrogen ion diffusion coefficient. Given these four parameters, the service life and durability design diagram of the channel concrete can be estimated. This paper only needs to predict the service life, and it can be solved directly by the endurance limit state equation. DuraCrete gives the endurance limit state equation for calculating the durable service life of concrete structures.

$$\begin{aligned} g &= c_{cr}^{d} - c^{d}(x,t) \\ &= c_{cr}^{d} - c_{s,cl}^{d}\left[1 - \operatorname{erf}\left(\frac{x^{d}}{\sqrt[2]{t/R_{cl}^{d}(t)}}\right)\right], \\ &= 0 \end{aligned} \tag{10}$$

When predicting the service life of concrete, considering that the repair cost is lower than the cost required to reduce the risk, the time B when the steel bar begins to corrode can be passed. The following expression can be obtained:

$$t_i^{d} = \left[\left(\frac{2}{x^{c} - \Delta x}.\mathrm{ref}^{-1}\left(1 - \frac{c_{cr}^{c}}{\gamma_{c_{cl}}}.\frac{1}{A_{C,cl}^{c}}\right)\right).^{-2}\frac{R_{0,cl}^{c}}{K_{c,cl}^{c}.K_{c,cl}^{c}.t_0^{n_{cl}^{c}}.\gamma_{R_{cl}}}\right]^{1/1-n_{cl}^{c}}. \tag{11}$$

Small prefabricated building irrigation canal system, which is the research object of this paper, is similar to the external channel environment, the example in DuraCrete is referred to when determining the parameters and partial coefficients.

The model analyzed in this section is a fabricated concrete irrigation channel. The average thickness of the protective layer is $x^{c} = 24.9$ mm, its safety margin is $\Delta x = 5$ mm, and its antichloride ion permeability coefficient is $D_{\mathrm{RCM},0} = 9.41 \times 10^{-12}$ m^2/s (using the value of the third group mix ratio), correspondingly $R_{0,cl}^{0} = 3.3698 \times 10^{-3}\mathrm{year}/mm^2$, the environmental parameter is 0.92, and the curing condition parameter value is 0.79, the test period is 28 days, the attenuation coefficient is 0.37, and the corresponding subitem coefficient is 3.25. Substitute the above values into equation (9) we get the following equation:

$$\begin{aligned} t_i^{d} &= \left[\left(\frac{2}{x^{c} - \Delta x}.\mathrm{ref}^{-1}\left(1 - \frac{c_{cr}^{c}}{\gamma_{c_{cl}}}.\frac{1}{A_{C,cl}^{c}}\right)\right).^{-2}\frac{R_{0,cl}^{c}}{K_{c,cl}^{c}.K_{c,cl}^{c}.t_0^{n_{cl}^{c}}.\gamma_{R_{cl}}}\right]^{1/1-n_{cl}^{c}} \\ &= \left[\left(\frac{2}{25-5}.\mathrm{ref}^{-1}\left(1 - \frac{0.8}{1.2}.\frac{1}{7.76 \times 0.45 \times 1.2}\right)\right).^{-2}\frac{3.3698 \times 10^{-3}}{0.92 \times 0.79 \times 0.0767^{0.37} \times 3.27}\right]^{1/1-0.37}. \end{aligned} \tag{12}$$

Solution: $T_1 = 6.9$ years.

4.3.2. T_2. In actual engineering, the natural environment in which the concrete building structure is located is quite complex. In the process of research and analysis, it is difficult to determine the depassivation time of concrete. Usually, we think this time period is a random variable. Many research results show that when the concrete structure is in an environment with a relatively stable chloride ion source, the depassivation time of the steel bars in the concrete is shorter because the speed of cyanide ions intrusion into the concrete is much faster than the carbonization speed. In the corrosion life, the depassivation time is often considered to be zero, that is, the steel bar is always in an activated state.

4.3.3. T_3. Time B is the development stage of steel bar corrosion, and the steel bar begins to undergo pitting corrosion, which then develops into pit corrosion, and finally produces rust, causing rust expansion and cracking. The corrosion pit at this stage reaches a certain depth, which is usually called the critical depth. In the limit state design method based on probability theory, we regard the depth of the steel corrosion pit reaching a critical depth as the limit state of the durability life of the reinforced concrete. After research, it is considered that the pit corrosion depth on the steel bar obeys the Poisson distribution, and the time length of the steel corrosion development stage based on the failure probability is proposed, and the expression is as follows:

$$T_3 = k\theta \ln\left\{\frac{\ln\left[1 - F_T(t)\right]\left(1 - \exp\ \left(h_0/\theta\right)\right)}{\lambda} + 1\right\}. \quad (13)$$

In the above formula, k is proportionality constant, also known as reinforcement corrosion rate, h_0 is the depth of the pit at the limit state, θ is the average depth of the initial pits, and λ is Poisson flow strength in a Poisson distribution.

For steel bars in fabricated concrete irrigation, by comparing the statistical analysis data of steel bar corrosion in other chloride ion environments, the parameters in formula (13) can be determined as shown in Table 13.

Substitute the parameters in the table into formula (9), and taking the failure probability as 5%, we get the following equation:

$$T_3 = k\theta \ln\left\{\frac{\ln\left[1 - F_T(t)\right]\left(1 - \exp\ \left(h_0/\theta\right)\right)}{\lambda} + 1\right\}$$

$$= 12.5 \times 0.01 \times \ln\left\{\frac{\ln\left[1 - 5\%\right]\left(1 - \exp\ \left(0.15/0.01\right)\right)}{6.0} + 1\right\}. \quad (14)$$

It can be seen by calculation: $T_3 = 12.8$ years, which means that the probability of corrosion damage to the steel bars of the prefabricated irrigation canal concrete after being exposed to the nitrogen ion environment for 12.8 years is 5%.

To sum up, the time required for the corrosion damage of the steel reinforcement of the fabricated concrete irrigation channel in the chloride ion environment is $T_1 + T_2 + T_3 == 6.9 + 0 + 12.8 = 19.7$ years. The service life in the chloride ion environment is 20 years, which meets the life cycle of the general channel.

5. Conclusion

Water-saving irrigation technology refers to the general term for irrigation methods, measures, and systems that significantly save water than traditional irrigation technologies. There is a lack of systematic research on the strength, penetration, freeze-thaw, and other durability of fabricated reinforced concrete irrigation channels. Some durability problems arising from the production and operation of fabricated irrigation channels are analyzed for research.

This study firstly introduced the carbonization mechanism, carbonization rate, and influencing factors of the concrete protective layer, gave the concrete soil carbonization model and life criterion, and predicted the life of concrete under carbonation conditions according to the probability limit state method. Then, the corrosion mechanism of reinforced concrete in nitrogen ion environment and the model and random model of chloride ion intrusion into concrete are introduced, the life criterion of concrete in chloride ion environment is given, and the use of concrete in chloride ion environment according to the probability limit state method is analyzed.

By comparing and analyzing the carbonization life of concrete and the service life in the chloride ion environment, we get that the concrete life in the chloride ion environment is much smaller than the carbonization life. Of course, in the actual engineering structure environment, it is not possible to only carbonize the concrete, but there is often the corrosion of the steel bar by nitrogen ions and the electrochemical reaction. Therefore, in the follow-up research, the service life and durability evaluation of channel concrete should be predicted in the case of concrete carbonation and other coupling conditions.

Data Availability

The dataset can be accessed upon request.

Conflicts of Interest

The authors declare that they have no conflicts of interest.

Acknowledgments

This paper is the research result of the special project of basic scientific research business expenses of the Yellow River Water Conservancy Research Institute, "optimal design and demonstration of small prefabricated buildings in irrigation canal system" (Project No.: hky-jbyw-2021-08).

References

[1] J. A. Lozano-Galant and I. Paya- Zaforteza, "Analysis of Eduardo Torroja's Tempul Aqueduct an important precursor of modern cable-stayed bridges, extradosed bridges and

prestressed concrete," *Engineering Structures*, vol. 150, pp. 955–968, 2017.

[2] D. Keenan-Jones, D. Motta, M. H. Garcia, and B. W. Fouke, "Travertine-based estimates of the amount of water supplied by ancient Rome's Anio Novus aqueduct," *Journal of Archaeological Science Reports*, vol. 3, pp. 1–10, 2015.

[3] Y. Benjelloun, J. D. Sigoyer, J. Carlut et al., "Characterization of building materials from the aqueduct of Antioch-on-the-Orontes (Turkey)-ScienceDirect," *Journal of Field Robotics*, vol. 33, no. 5, pp. 561–590, 2016.

[4] S. Subathra, A. Sekar, S. Fazeela Mahaboob Begum, and M. Balamurugan, "Analysis & design of an aqueduct," *Materials Today Proceedings*, 2021.

[5] D. Qiuhua, Y. Lufeng, and L. Menglin, "Study on the effects of the bent-height on the seismic performance of the aqueduct-water coupling structure," in *Proceedings of the Second International Conference on Mechanic Automation & Control Engineering*, pp. 7758–7761, Inner Mongolia, China, July 2011.

[6] P. Buitelaar, "Ultra-high performance concrete: developments and applications during 25 years," in *Proceedings of the International Symposium on Ultra-High Performance Concrete*, pp. 25–35, Kassel, Germany, September 2004.

[7] P. Richard and M. Cheyrezy, "Composition of reactive powder concretes," *Cement and Concrete Research*, vol. 25, no. 7, pp. 1501–1511, 1995.

[8] W. Kay, A. E. Naanman, and G. J. Parra-Montesinos, "Ultra high performance concrete with compressive strength exceeding 150 MPa," *ACI Materials Journal*, vol. 108, no. 6, pp. 46–54, 2011.

[9] P. Richard and M. Cheyrezy, "Reactive powder concretes with high ductility and 200-800 MPa compressive strength," *Aci Special Publication*, vol. 114, pp. 507–518, 1994.

[10] M. M. Reda, N. G. Shrive, and J. E. Gillott, "Microstructural investigation of innovative UHPC," *Cement and Concrete Research*, vol. 29, no. 3, pp. 323–329, 1999.

[11] C. Porteneuve, H. Zanni, J. P. Korb, and D. Petit, "Water leaching of high and ultra high performance concrete: a nuclear magnetic resonance study," *Comptes Rendus de l'Academie des Sciences - Series IIC: Chemistry*, vol. 4, no. 11, pp. 809–814, 2001.

[12] C. Porteneuve, H. Zanni, C. Vernet, K. O. Kjellsen, J. P. Korb, and D. Petit, "Nuclear magnetic resonance characterization of high-and ultrahigh-performance concrete: application to the study of water leaching," *Cement and Concrete Research*, vol. 31, no. 12, pp. 1887–1893, 2001.

[13] C. Alonso, M. Castellote, I. Llorente, and C. Andrade, "Ground water leaching resistance of high and ultra high performance concretes in relation to the testing convection regime," *Cement and Concrete Research*, vol. 36, no. 9, pp. 1583–1594, 2006.

[14] K. Habel, M. Viviani, E. Denarié, and E. Bruhwiler, "Development of the mechanical properties of an ultra-high performance fiber reinforced concrete (UHPFRC)," *Cement and Concrete Research*, vol. 36, no. 7, pp. 1362–1370, 2006.

[15] I. H. Yang, C. Joh, and B. S. Kim, "Structural behavior of ultra high performance concrete beams subjected to bending," *Engineering Structures*, vol. 32, no. 11, pp. 3478–3487, 2010.

[16] D. Yoo, *Performance Enhancement of Ultra-high-performance Fiber-Rein-Forced Concrete and Model Development for Practical Utilization*, Korea University, Seoul, Republic of Korea, 2014.

[17] D. Y. Yoo, J. J. Park, S. W. Kim, and Y. S. Yoon, "Early age setting, shrinkage and tensile characteristics of ultra high performance fiber reinforced concrete," *Construction and Building Materials*, vol. 41, pp. 427–438, 2013.

[18] D. Y. Yoo and N. Banthia, "Mechanical properties of ultra-high-performance fiber-reinforced concrete: a review," *Cement and Concrete Composites*, vol. 73, pp. 267–280, 2016.

[19] R. J. Thomas and A. D. Sorensen, "Review of strain rate effects for UHPC in tension," *Construction and Building Materials*, vol. 153, pp. 846–856, 2017.

[20] K. Shirai, H. Yin, and W. Teo, "Flexural capacity prediction of composite RC members strengthened with UHPC based on existing design models," *Structures*, vol. 23, pp. 44–55, 2020.

[21] P. Y. Blais and M. Couture, "Precast, prestressed pedestrian bridge world's first reactive powder concrete structure," *PCI Journal*, vol. 44, no. 5, pp. 60–71, 1999.

[22] M. Rebentrost and G. Wight, "Experience and applications of ultra-high performance concrete in Asia," in *Proceedings of the 2nd International Symposium on Ultra- High Performance Concrete*, pp. 19–30, Kassel, Germany, March 2008.

Hindawi
Scientific Programming
Volume 2022, Article ID 1994257, 10 pages
https://doi.org/10.1155/2022/1994257

Research Article

Analysis of the Impact of Change Propagation within Complex Product Modules

Ying Xiang,[1] **Zhenxing Wei**,[2] **and Tianhang Xu**[2]

[1]*College of Mechanical and Electrical Engineering, Shaanxi University of Science and Technology, Xi'an 710021, Shaanxi, China*
[2]*School of Mechatronic Engineering, Xi'an Technological University, Xi'an 710021, Shaanxi, China*

Correspondence should be addressed to Ying Xiang; yingcara@hotmail.com

Received 1 July 2022; Accepted 7 September 2022; Published 30 September 2022

Academic Editor: Lianhui Li

Based on the design structure matrix, the changing dependency analysis method is used to study the law of change propagation between parts in the process of product change, in view of the complexity of the product structure and the strong correlation between parts. First, the product components are divided into different modules according to different requirements, and a design structure matrix with weights is established according to the change dependencies between the components within the modules; then, a part changes propagation network is established to analyze the change dependency degree between parts and the influence of the part propagation mode on change propagation and to analyze the possible change propagation impact of part changes. The feasibility and rationality of the method are verified using the frame module as an example. The experimental results show that the method is effective in predicting the changing risk of a part and analyzing the change propagation impact arising from a part change.

1. Introduction

In the context of economic and trade globalization, manufacturing companies face the challenge of changing market rules, the emergence of relevant new technologies, and the rise of individual customer needs. In order to maintain their competitiveness in the market and to meet the diverse needs of their products, companies inevitably have to make engineering changes to their products. In the engineering change process, module change propagation means that: a change in one component causes a change in other components within the same module, which may also have a change impact on other modules and thus on the whole product [1]. The study of change propagation is a major element in engineering change, and the direction of change propagation affects the outcome of engineering change.

When changes are made to modules, further research is required into the impact of module change propagation, where the prediction of module change outcomes is central to change propagation. In terms of the risk of change communication, Eckert et al. [2] studied the basic causes of product changes and the risks arising from the changes, providing an in-depth analysis of the problems arising from the product change process. Loch et al. [3] used five strategies to reduce the processing time of engineering change orders: capacity flexibility, load balancing, combining tasks, sharing resources, and batch size reduction, with special attention to the impact of engineering changes; Rui et al. [4] predicted the impact of change propagation by clustering and grading parts through a graph-theoretic approach based on a design structure matrix, specifically analyzing the characteristics of three types of change propagation: water-wave propagation, bloom propagation, and avalanche propagation; Xiang et al. [5] constructed a risk analysis model for engineering changes in complex products from two perspectives: direct and indirect impacts between Hub nodes in a complex product design network. Yupeng et al. [6] applied complex network theory to model the structure of complex products by considering three factors, namely, function, structure, and change risk, in the modular division of complex products and established a

network model of complex product parts with parts as nodes and the association relationship of parts as edges. Liang et al. [7] analyzed the propagation of engineering changes in complex products by combining the design structure matrix, defined the risk of engineering changes in two dimensions of direct and indirect influence, and constructed a risk analysis model of propagation of engineering changes in complex products of the perspective of comprehensive risk. Fan et al. [8] studied change propagation from the aspect of feature association, classified the types of feature association units in product design, and analyzed the change propagation characteristics, change propagation mode, and change propagation process of association units; Zhongwei et al. [9] analyzed the causes and characteristics of avalanche propagation with respect to the constraint conflicts and the number of affected parts and predicted the avalanche propagation by using the directed graph method and knowledge related to complex networks.

In the context of changing communication research methods, Cohen et al. [10] proposed a C-FAR method to evaluate and predict the results of engineering changes, modeling the product information about the EXPRESS language, demonstrating the propagation process of engineering changes, and qualitatively evaluating the results of engineering changes. Congdon et al. [11] applied multiple network theory about complex product modeling to analyze the influence mechanism of different association relationships of the propagation of engineering changes, in view of the fact that the joint effect of multiple association relationships between parts and components was not considered comprehensively in the traditional complex product engineering change propagation impact assessment process. Yongze et al. [12] developed software for engineering change analysis based on the directed graph method of engineering change propagation analysis, which can analyze the propagation, coordination, absorption, and control of part changes in engineering changes and can improve the accuracy and efficiency of engineering change analysis and evaluation. Qin et al. [13] tracked and collaboratively sensed change propagation and predicted the impact range of change propagation through engineering change management. Mengze et al. [14] established a complex product part network model by taking the part connection relationship as the edge and defining the change propagation intensity as the edge weight while considering the change propagation intensity. Xianfu et al. [15] represented the association relationship between product parts based on the design structure matrix, analyzed the association propagation path of master parts, calculated the module association dependency, and determined the priority order of modules. According to the change propagation characteristics of components, Jianfen et al. [16] constructed a multi-objective optimization model and used a nondominated ranking genetic algorithm to solve the model and obtain the Pareto optimal solution set, which can provide an important basis for designers to select the optimal design change solution. All of the above are studies of change propagation for components or basic elements of a product, whereas in practice, there are numerous components in a product, and it would be a large and difficult task to conduct a change study for each component.

On the basis of the above research, this paper establishes a change propagation model within a complex product module by dividing the complex product into modules and dividing it into a number of basic module units, taking the module as the basic elements of change propagation research, as shown in Figure 1, to research the change propagation impact of the module Firstly, we analyze the change propagation impact on parts and components within the module where the changed parts are located and find out the change impact produced by the changes of the parts in the module.

1.1. Type of Propagation of Component Changes within a Module. There is a strong correlation between the components in any given module. The parts are related to each other in a network, which is complex and uncertain. In the network, when a change occurs to a component, the change will propagate along different paths according to the relationship between the components and will have a change propagation effect on the associated components. How to determine the scope of change that the change may cause is key. Change propagation between components and parts can be divided into six forms: direct propagation, bi-directional propagation, indirect propagation, circular propagation, diffusion propagation, and clustering propagation.

(1) Direct propagation: the effect of a change in part A is propagated in one direction to part B causing a change in part B. This change propagation relationship can be observed directly.

(2) Two-way propagation: the effect of a change in part A is propagated to part B, and the change in part B in turn affects part A. The two affect each other.

(3) Indirect propagation: The effect of a change to part A is propagated to part B and then indirectly to part C. There is no direct link between part A and part C and this change propagation is not easily observed directly.

(4) Circular propagation: The influence of changes in part A is propagated to part B and then indirectly to part C. Changes in part C in turn acts on part A, causing the part itself to change repeatedly and iteratively, but this does not mean that the cycle is dead, and can be stopped by the coordination of changes in part or the absorption of changes by parts.

(5) Diffusion propagation: The effect of a change to part A is simultaneously propagated to parts B and C at the next A level, and change propagation occurs. During the change propagation process, diffusion increases the number of parts involved in and affected by the change propagation, which may eventually lead to an avalanche of propagation, making the change propagation impact uncontrollable.

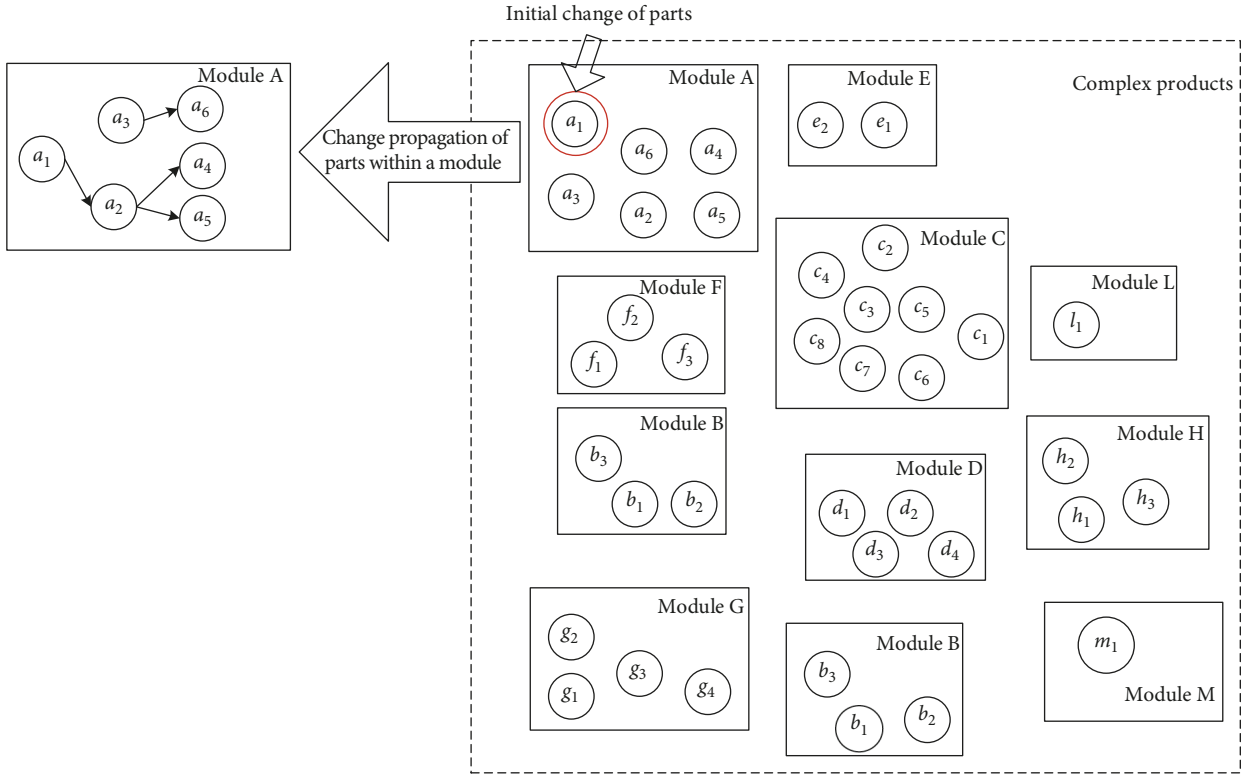

Figure 1: Change propagation model within a complex product module.

Table 1: Types of inter-part change propagation.

Number	Illustration	Type
1	A → B	Direct transmission
2	A ↔ B	Two-way transmission
3	B; A → B; B → C	Indirect transmission
4	B; A → B; B → C; C → A	Ring transmission
5	B; A → B; A → C	Spread transmission
6	B → A; C → A	Gather transmission

(6) Clustered propagation: The change impact on part A and part B is propagated to part C at the same time, and the change propagation is clustered so that part C has to meet the change design requirements of both part A and part B. In the change propagation process, clustering reduces the number of parts involved in the change propagation and the number of parts affected by the change, reducing the area affected by the change propagation.

The six types of change propagation are represented in a table, as shown in Table 1.

2. Establishing a Parts Change Communication Network

The Design Structure Matrix (DSM) is the primary method for studying the propagation of changes in product design. The link between the elements of the matrix rows expresses the change dependencies that exist on parts. In the binary Boolean DSM, a "0″ means that no change dependency exists on two parts and a "1" means that a changing dependency exists on two parts. In actual manufacturing, the degree of change dependency on parts varies, with some parts having a strong change dependency and others having a weak dependency. It is not possible to classify the dependencies on parts into just two types: those with change dependencies and those without. This is defined by the five-

	a_1	a_2	a_3	a_4	a_5	a_6
a_1	–	1	0.7	0	0	0
a_2	1	–	0.7	0	0	0.5
a_3	0.7	0.7	–	0.3	0.5	0.3
a_4	0	0	0.3	–	0	0
a_5	0	0	0.5	0	–	0
a_6	0	0.5	0.3	0	0	–

Figure 2: Digital DSM.

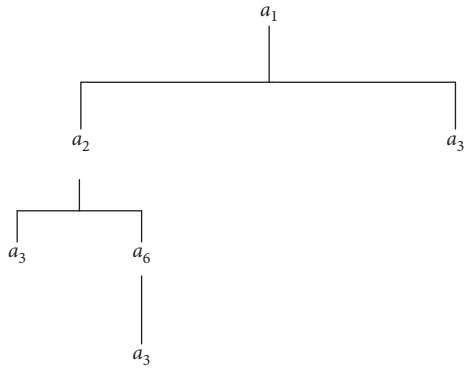

Figure 3: Change propagation impact tree.

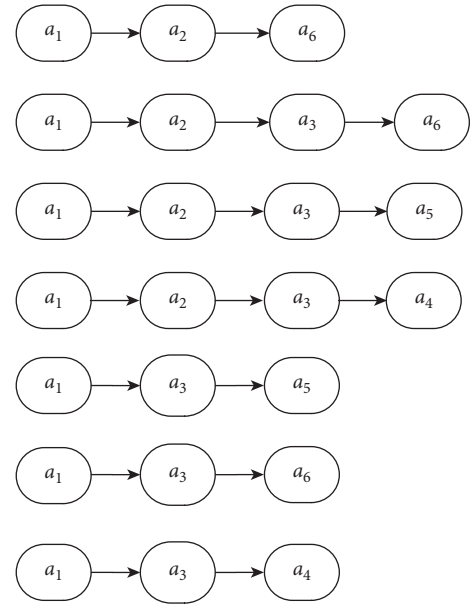

Figure 4: Change propagation chain.

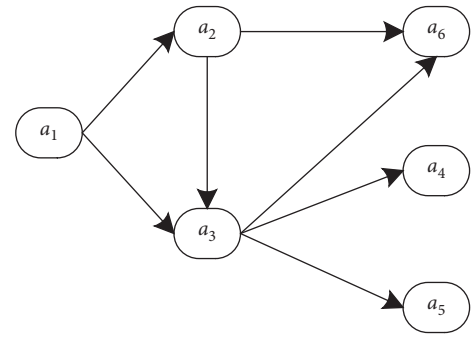

Figure 5: Change dissemination network.

point weighting method [17] using a number between 0 and 1, depending on the strength of the changing dependency on two parts. The number 1 indicates that there is a strong change dependency on two parts, and a change in one part will have a change impact on the other part, while the number 0 indicates that there is no change dependency on two parts, and a change in a part will not have a change impact on the other part. According to the change dependency relationship between parts and the change dependency strength, the numerical design structure matrix is established, as shown in Figure 2.

The change dependency on two elements can be visually represented by a numerical DSM, which reveals the change impact on a change to part a_1 from part a_2. This change propagation influence is a direct change influence and there are also indirect change influences on the change propagation process, for example, a change in part a_1 can cause a change to parts a_3 and a_6 through a change to part a_2. The design structure matrix does not represent the indirect change impact, so a change impact tree is created based on the numerical DSM created. Assuming that part a_1 is the initial changed part and a_3 is the change termination part, create a change impact tree for part a_1 to part a_3 as shown in Figure 3.

During the change propagation process, a part is said to be the initial change part when a change in a part causes the change propagation to occur. Change propagation starts with the initial change part and proceeds according to the change dependencies on the parts until the change is terminated. Firstly, parts in a changing dependency on the initial changed part will have a change impact, with different change dependencies having different change impacts on the part, and secondly, the part affected by the change will also have a change impact on the parts with which it has a changing dependency until the change propagation ends at a particular part. An analysis of the change propagation influenced tree created shows that when the initial parted a_1 starts to make changes, it directly affects parts a_2 and a_3 for changes, while changes to part a_2 affect a_3 and 6 for changes, and changes to part 6 have a change influence on a_3. It can be seen that during the propagation of changes in $a_1 \longrightarrow a_3$, a_1

can affect a_3 directly and a_1 can also have an indirect change impact on a_3 through other parts.

The indirect effects of change propagation cause change to be propagated through a number of different propagation paths, each of which can be represented by a propagation chain, as shown in Figure 4.

Using the digital DSM as a tool, the change propagation network in the network is represented by a directed graph $G(V, \mathrm{E})$, where $V = \{x \mid x = 1, 2, 3, \cdots, n\}$, denotes the set of directed graph vertices and x denotes a part within a module. $E = \{(x, y) \mid x, y \in n, x \neq y\}$ is a directed edge, indicating the existence of a change propagation relationship between part x and part y. In a directed graph $G(V, \mathrm{E})$, the individual change propagation chains described above intersect with each other to form a change propagation network [18]. This is shown in Figure 5.

The change propagation networks to provides a clear view of the initial change parts in a module and the change effects of the initial change parts in other parts, as well as a general view of the paths along which changes are propagated [19]. In the change propagation network, not only direct change effects on parts can be identified, but also indirect change effects. In a network, however, it is not possible to know exactly the magnitude of the propagation dependencies on parts, to determine along which specific paths the change propagation will take, and also to determine the magnitude of the change propagation range. Therefore, there is still a need to study and analyze the change dependencies on parts.

3. Change Propagation Impact Analysis Method Based on Change Dependencies

3.1. Changing Dependencies. When a change activity occurs to a product, due to the high degree of cohesion within the module, there is a high degree of correlation between parts in the module and a high degree of change dependency. When a part starts to change, the change propagates according to the dependencies on the parts, and the complex dependencies between the parts make there are multiple paths for change propagation, the change propagation has a wide range of influence and it is difficult to control the direction of change propagation. If the change propagation path of a part in a module can be determined, the change propagation impact on the part change in the module in which it is located is discovered, the propagation impact between modules is then studied, and the product change results are eventually discovered. If the propagation of change in parts affects the module in which it is located to change in size, structure, or function, then this module will be used as the initial change module, and the propagation impact on the initial change module on other modules will be further investigated between modules to discover the propagation impact on changes in the product. However, when the change propagation of the part will not have a change impact on the module in which it is located, then this module will not change and will not have a change impact on other modules.

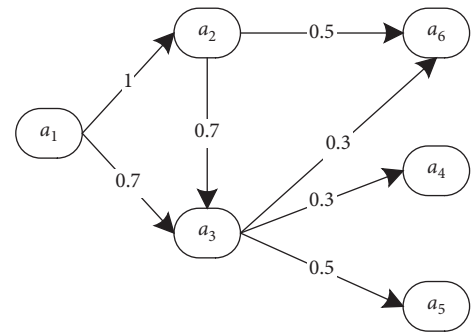

Figure 6: Change dependencies between parts in the change propagation network.

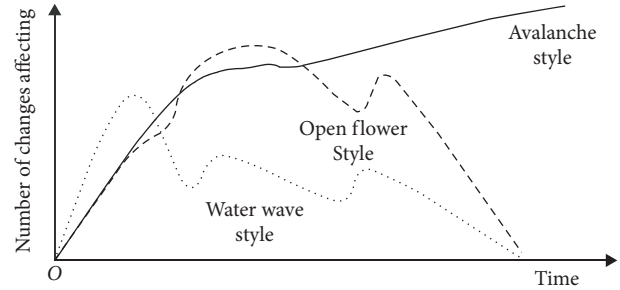

Figure 7: Change propagation impact.

Parts in the same module have strong dependencies on each other, and too much dependency between parts can lead to change propagation going along multiple paths, increasing the scope of change propagation impact. The greater the dependency on parts, the greater the degree to which changes in a part affected changes in another part, and the greater the change transfer of the two parts, making change propagation more difficult to control. Combining the numerical DSM and the change propagation network, the changing dependency on two elements x and y in adjacent cells are represented by $W(x, y)$ and takes a value in the range $[0, 1]$. The value of $W(x, y)$ is obtained according to the numerical DSM established. The value of W is obtained according to the numerical DSM established. $W(x, x)$ represents the degree of change dependency on the component itself and takes the value of 1. Figure 6 shows the addition of change dependencies on the change propagation network [20].

Figure 6 shows that the change propagation of part a_1 spreads and has a simultaneous change impact on parts a_2 and a_3. Due to the close direct change dependency between part a_1 and part a_2, the change impact of part a_1 on part a_2 is greater and change propagation is easily formed.

3.2. Part Change Propagation Impact Analysis. Change propagation impacts are divided into three types: ripple propagation, blossom propagation, and avalanche propagation, as shown in Figure 7.

As can be seen in Figure 7, the water-wave propagation, the initial change causes a part of the parts to be changed, but after a short period of time, the number of parts involved in

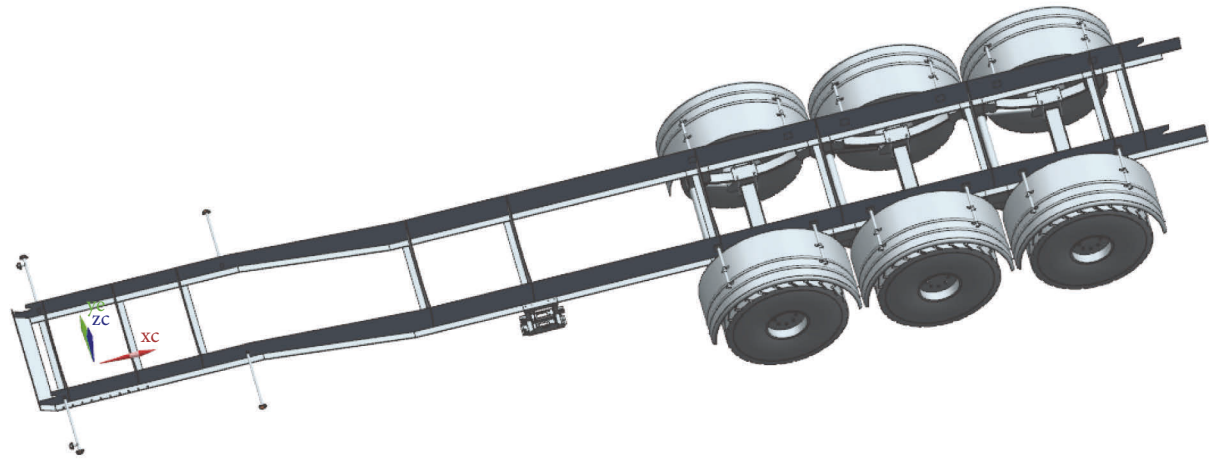

Figure 8: Schematic diagram of the frame module.

the change rapidly decreases and eventually stays at a certain number, because the propagation method of parts is mainly direct propagation, so the change propagation influence is weak. Blossom propagation, where the initial change causes a large number of parts to change, and after a while, the number of parts involved in the change begins to decrease and eventually remains at a reasonable number, due to the existence of indirect and diffusion propagation between parts, which can lead to a rapid increase in the number of changed parts. After a period of time, the number of parts involved in change propagation decreases because, during the change propagation process, some parts have a certain ability to absorb the change. The parts affected by the change propagation absorb the change propagation completely or partially so that the parts with which there is a propagation dependency do not need to be changed or only partially changed, and therefore the change propagation stops or decreases. In avalanche propagation, the initial change causes a large number of parts to change, with the increase of time, the number of changes continues to grow, eventually leading to the number of change impact that is difficult to control, as the avalanche effect, due to the propagation of parts for the diffusion of propagation, the impact of change of a part will be spread to several parts with its change dependency at the same time, making the propagation of change spread, increasing the scope of change propagation impact, and this increases the development cost and reduces the productivity of the product [21]. Therefore, an avalanche of change propagation should be avoided as much as possible.

As can be seen in Figure 6, part a_1 is the initial change part. In the entire change propagation network, the propagation of part a_1 to parts a_2 and a_3 is diffuse, with changes to a_1 affecting changes to both a_2 and a_3, causing changes to propagate along both change paths. The propagation of changes from part a_2 to part a_3 and part a_6 is diffuse, extending the change propagation range. The change propagation of part a_6 is agglomerative and absorbs the change propagation of part a_2 and part a_3, reducing the change propagation impact and creating a blossoming change propagation impact. Part a_3 has both diffuse and convergent propagation. If the change propagation is absorbed in whole or in part at part a_3, the change propagation will be reduced, making the propagation path manageable, but if the change propagation is diffused at part a_3, increasing the range of change propagation, an avalanche of change propagation may occur, making the change propagation difficult to control. Part a_3 is therefore more likely to change and has the greatest impact on changes to the module as a whole. When studying the impact of changes to parts within a module, it is important to prioritize the analysis of the risk of change propagation for part a_3 in order to better control the scope of change propagation.

From the above analysis, it can be concluded that the change propagation impact is mainly determined by the changing dependency between parts and the change propagation mode of the parts. All parts within a module are affected by the initial change. In order to avoid uncontrollable effects of the design change on the product, the changing risk of the part should be analyzed and predicted before the change is made, in order to avoid an avalanche of change propagation effects [22]. In this paper, the change risk value is used to represent the magnitude of the comprehensive change risk of a part, and the change impact that the change propagation of the initial change part will have on the module in which it is located. The changing risk value is expressed in terms of R. Combining the change dependency degree $W(x, y)$ between parts, the changing risk valued calculation formula is obtained as follows:

$$R = \frac{1}{k} \sum_{j=1}^{n} \frac{\sum_{i=1}^{m} W\left(x_i, y_j\right)}{m}. \tag{1}$$

In the formula, k indicates the number of all parts in the module; m indicates the number of parts that have a change propagation effect on the change part; y_j the

	a_1	a_2	a_3	a_4	a_5	a_6	a_7	a_8	a_9	a_{10}	a_{11}	a_{12}
a_1	–	1	0.7	0.5	0	0.7	0	0	0.3	0.5	0.3	0.3
a_2	1	–	1	0.5	0	0.5	0	0.3	0	0	0.3	0.3
a_3	0.7	1	–	0.3	0	0.5	0	0.3	0	0.3	0	0
a_4	0.5	0.5	0.3	–	0	0	0	0	0	0	0.3	0
a_5	0	0	0	0	–	0.7	0.7	0	0	0	0	0
a_6	0.7	0.5	0.5	0	0.7	–	0	0	0	0	0	0
a_7	0	0	0	0	0.7	0	–	0	0.5	0.3	0	0
a_8	0	0.3	0.3	0	0	0	0	–	0.5	0	0	0
a_9	0.3	0	0	0	0	0	0.5	0.5	–	0.3	0	0
a_{10}	0.5	0	0.3	0	0	0	0.3	0	0.3	–	0	0
a_{11}	0.3	0.3	0	0.3	0	0	0	0	0	0	–	0.3
a_{12}	0.3	0.3	0	0	0	0	0	0	0	0	0.3	–

Figure 9: Digital DSM for the change of components in the frame module.

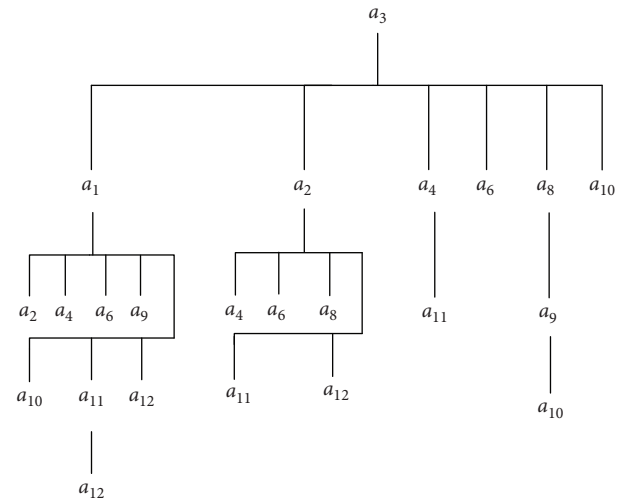

Figure 10: Part change propagation impact scope tree.

number of parts that produce the propagation effects of the change; and n indicates the number of change parts in the module.

By calculating change risk values for key nodes and comparing the magnitude of the change risk values, larger values indicate that an avalanche of change propagation impacts are likely to occur, and therefore, changes to the part need to be controlled so that change propagation is within manageable limits.

4. Example Validation

Using the frame module in Figure 8 as an example, the effect of change propagation on the components within the frame module is investigated when the cross member is the initial change part, and the content of this chapter is verified.

As can be seen in the schematic diagram of the frame module, the components contained in the frame module are the wing, web, cross member, front cover, axle, bearings, tires, fenders, struts, spare wheel carrier, front tail light, and side indicators, 12 components.

Due to the change dependencies on components, changes do not occur in isolation. Changes in the initial component will cause changes in other components that are related, and changes will continue to propagate until an equilibrium is reached. In the actual change propagation process, the change propagation method is divided into the direct propagation method and the indirect propagation method. The direct change relationship between two components can be expressed by establishing a design structure matrix with links between the elements of the matrix. The change dependencies on parts result in several different propagation paths, which are represented by the change propagation chain to parts. Finally, the change propagation chains are intersected in a directed graph to form a change propagation network of the parts.

4.1. Creation of Digital DSM for Component Changes in the Frame Module. By means of the five-point weighting method, the change dependencies on the 12 components in the frame module are specified by numbers between 0 and 1, and the components are arranged in a uniform order above and to the left of the matrix to create a 12×12order numerical DSM, as shown in Figure 9.

From the diagram it can be observed that the initial change to part beam a_3 has a direct change propagation impact on parts a_1, a_2, a_4, a_6, a_8, and a_{10}, while part a_2 also has a change impact relationship on parts a_4, a_6, a_8, a_{11}, and a_{12}, so a change to part a_3 may also have an indirect change propagation impact on parts a_{11} and a_{12}. A change propagation tree based on the numerical DSM for part changes is shown in Figure 10.

4.2. Chain of Propagation of Component Changes. Through the part change propagation influence range tree, it can be seen that there are multiple change propagation paths to part change propagation. A change propagation chain is used to represent a propagation path to represent all part change propagation paths within the frame module, as shown in Figure 11.

4.3. Establishing a Network for the Dissemination of Component Changes within the Frame Module. The change propagation network in the network is represented by a directed graph $G(V, \mathrm{E})$, where $V = \{x \mid x = 1, 2, 3, \cdots, 12\}$, the set of directed graph vertices, x represents the parts in the frame module, and $E = \{(x, y) \mid x, y \in 12, x \neq y\}$ is a directed edge, indicating that there is a change propagation

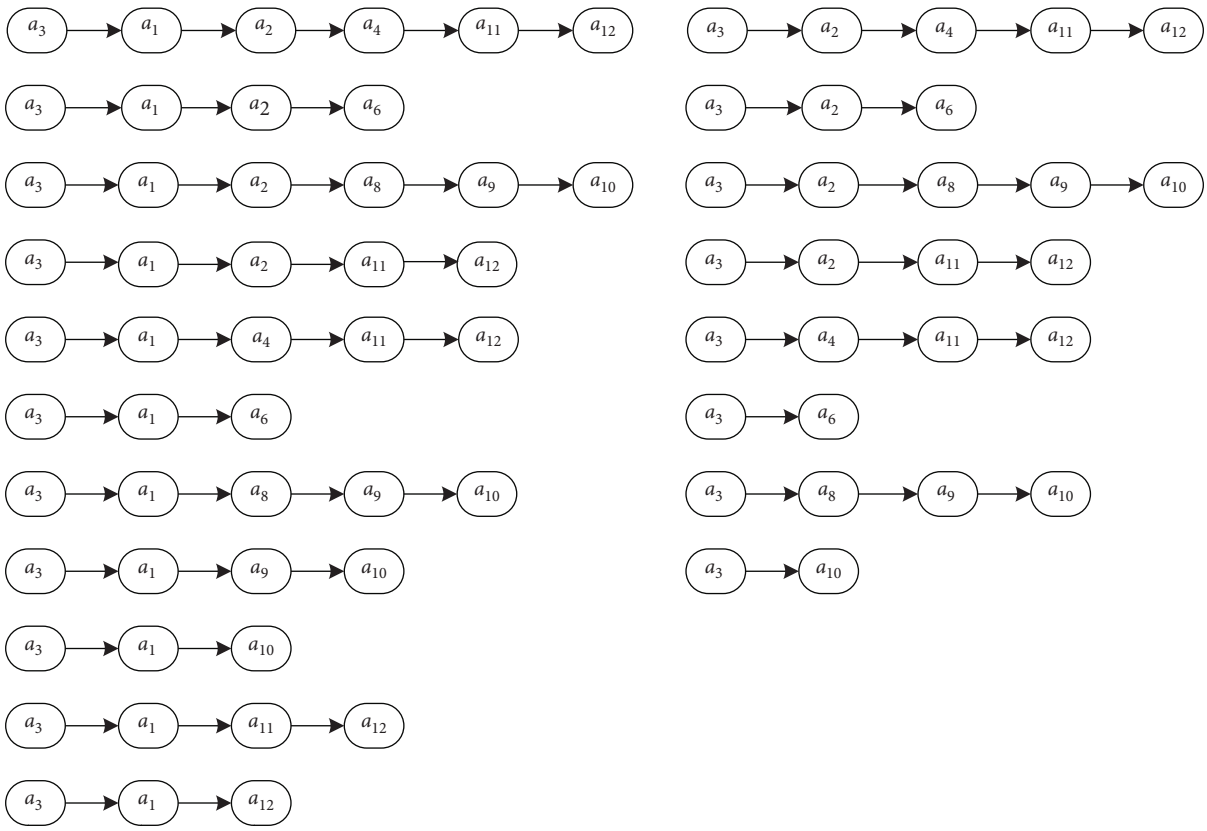

Figure 11: Part change propagation chain.

relationship between parts and parts. In the directed graph $G(V, \mathrm{E})$, the change propagation chains of each part in Figure 11 are intersected to form a part changed propagation network, combined with a numerical DSM, with $W(x, y)$ representing the changing dependency between two elements x and y of adjacent cells, taking a value range of $[0, 1]$, to establish a change propagation network containing change dependencies between parts as shown in Figure 12.

It can be seen from Figure 12 that when the initial change part a_3 produces a change, the change propagation of part a_1 and part a_3 in the whole change propagation network is diffusion propagation, and there are many parts affected by the change of part a_1 and part a_2. Therefore, when studying the change propagation impact on parts in the frame module, the part change risk value [23] is calculated according to (1), and the change propagation risk of part a_1 and part a_2 is analyzed in priority in order to better control the change propagation range.

The change risk value for change propagation through part a_1 after the initial change in part a_3 is:

$$R(a_1) = \frac{1}{12}\left(0.7 + 1 + 1 + \frac{0.5 + 0.5}{2} + \frac{0.7 + 0.5}{2} + 0.3 + 0.3 + \frac{0.5 + 0.3}{2} + \frac{0.3 + 0.3}{2} + \frac{0.3 + 0.3}{2}\right) = 0.45. \tag{2}$$

Then the change risk value for change propagation through part a_2 after the initial change in part a_3 is

$$R(a_2) = \frac{1}{12}\left(\frac{1 + 1 + 0.5 + 0.5 + 0.3 + 0.5 + 0.3 + 0.3 + 0.3/2 + 0.3 + 0.3/2}{2}\right) = 0.196. \tag{3}$$

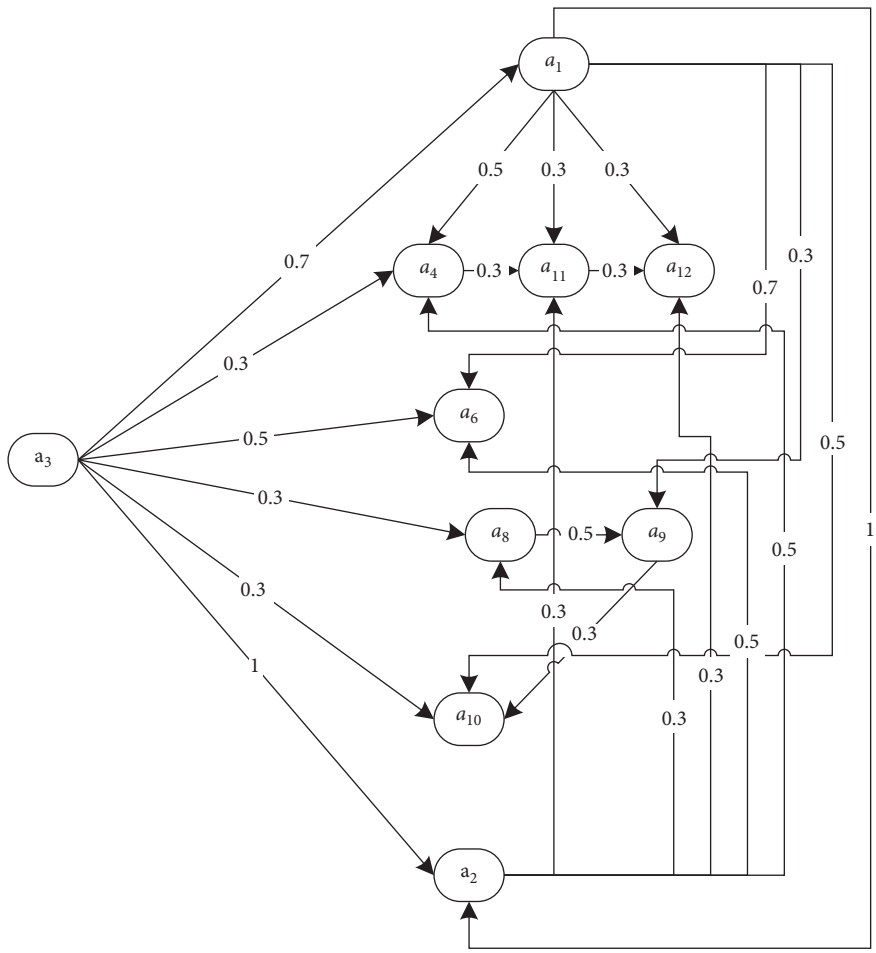

Figure 12: Change propagation network with change dependencies.

It can be seen that $R(a_2) < R(a_1)$, which indicates that the change in the initial part a_3 cross member has a greater impact on the propagation of the change to the part a_2 wings than to the part a_2 web, and therefore the risk of change propagation through part a_1 is greater, indicating that if changes are made to the wing during the frame change process, it may cause the number of change parts to increase, and there is also the possibility of avalanche changed propagation, so attention should be paid to the propagation impact of the change from changes to the wing during the change process.

5. Conclusions

This paper focuses on the change propagation impact on parts within a module. Based on the direct change propagation relationship between parts, a digital DSM of parts is created for parts in the same module, the indirect change propagation relationship between parts is assessed through the DSM, a change propagation chain of parts is constructed, and finally, a change propagation network is formed in the directed graph to describe the propagation path of part changes. By analyzing the degree of change dependency on each part and the impact of the part propagation method on change propagation, the possible paths of change propagation are determined, and based on the calculation of the change risk value, the change risk value of the key node is calculated, the possible change propagation impact of the part change through this node is evaluated, the changing risk of the part is predicted, and the change of the part is controlled in advance to avoid the uncontrollable impact of the change design on the product.

Data Availability

The data used to support the finding of this study are available from the corresponding author upon request.

Conflicts of Interest

The authors declare that there are no conflicts of interest regarding the publication of this paper.

Acknowledgments

This project was supported by the Shaanxi Science and Technology New Star Project (Grant nos. 2020KJXX-071), Key R&D Project in Shaanxi Province (2021NY-171), Shaanxi Science and Technology Resources Open Sharing

Platform (Grant nos. 2021PT-006), and Shaanxi Provincial Department of Education Special Scientific Research Project (Grant no. 20JK0075).

References

[1] Y. Li and P. Lin, "Research on parallel change propagation model for complex products," *Computer Integrated Manufacturing Systems*, vol. 23, no. 4, p. 7, 2017.

[2] C. Eckert, P. J. Clarkson, and W. Zanker, "Change and customisation in complex engineering domains," *Research in Engineering Design*, vol. 15, no. 1, pp. 1–21, 2004.

[3] C. H. Loch and C. Terwiesch, "Accelerating the process of engineering change orders: capacity and congestion effects," *Journal of Product Innovation Management*, vol. 16, no. 2, pp. 145–159, 1999.

[4] R. He, *Research and Development of Engineering Change Management System Based on Design Structure Matrix*, Nanjing University of Aeronautics and Astronautics, Nanjing, 2008.

[5] X. Su, Y. Yu, Z. Yu, Z. Wang, and F. Wu, "Research on risk propagation of engineering changes based on Hub nodes of complex product design network[J]," *Modern Manufacturing Engineering*, no. 06, pp. 23–31, 2018.

[6] Y. Li, W. Xie, and X. Wang, "A modular approach for complex products considering change risk," *Journal of Mechanical Engineering*, vol. 57, no. 9, p. 12, 2021.

[7] C. Liang, Yu Zheng, and S. Li, "A change propagation evaluation method based on product feature network," *Computer Integrated Manufacturing Systems*, vol. 25, no. 11, p. 8, 2019.

[8] Y. Fan and X. Tang, "Product engineering change propagation based on feature association," *Journal of Beijing University of Aeronautics and Astronautics*, vol. 38, no. 08, pp. 1032–1039, 2012.

[9] Z. Gong, H. Yang, and M. o. Rong, *Prediction Methods for Avalanche Propagation of Engineering changes*, Aerospace Manufacturing Technology, no. 05, pp. 71–74, Beijing, 2013.

[10] T. Cohen, S. B. Navathe, and R. Fulton, "C-FAR, change favorable representation," *Computer-Aided Design*, vol. 32, no. 5-6, pp. 321–338, 2000.

[11] C. Li, Z. Zhang, C. Cao, and F. Zhang, "Multi-network-based propagation impact assessment of complex product engineering changes," *Computer Applications*, vol. 40, no. 4, pp. 1215–1222, 2020.

[12] Y. Fang, S. Xie, J. Chen, and Wu Xu, "Research on propagation analysis of engineering changes based on directed graphs," *Beijing:Journal of Graphology*, vol. 33, no. 05, pp. 132–136, 2012.

[13] Q. Zhang, Mo Rong, and Z. Gong, "Research on process control-oriented engineering change system," *Aviation manufacturing technology*, no. 11, pp. 82–85+95, 2012.

[14] M. Li, J. Sheng, Y. Li, and W. Qi, "Multi-objective path optimization for complex product design change propagation," *Mechanical Design and Manufacturing*, no. 6, pp. 294–297, 2020.

[15] X. Cheng, C. Wan, H. Qiu, and L. Wan, "Inter-module association analysis and decoupling strategies in modular product design," *Computer Integrated Manufacturing Systems*, vol. 26, no. 4, pp. 1043–1051, 2020.

[16] J. Luo, M. Li, Li Ting, and H. Ren, "Multi-objective genetic algorithm-based change propagation optimization for complex product design," *Machine Design*, vol. 7, no. 10, 2020.

[17] Z. Du, *Research on the Application of Design Structure Matrix in Complex Product Development*, Lanzhou University, p. 5055.

[18] Y. Dong, *Evolutionary Dynamics of Distributed Modular Product Systems*, Zhejiang University, Hangzhou, 2006.

[19] H. Yang, L. Lu, and Q. Zhang, "A structural model of Internet based on complex networks," *Shenyang:Control Engineering*, vol. 17, no. 03, pp. 380–383, 2010.

[20] A. Barrat, M. Barthélemy, and A. Vespignani, "Modeling the evolution of weighted networks," *Physical Review A*, vol. 70, no. 6, Article ID 066149, 2004.

[21] R. He, D. Tang, and J. Xue, "Research on propagation of engineering changes based on design structure matrix," *Beijing:Computer Integrated Manufacturing Systems*, no. 04, pp. 656–660, 2008.

[22] Y. Yu, *Research on the Propagation Risk of Complex Product Engineering Changes*, Jiangsu University of Science and Technology, Jiangsu, 2017.

[23] M. á. Serrano, M. Boguñá, A. Díaz-Guilera, and Albert, "Competition and adaptation in an internet evolution model," *Physical Review Letters*, vol. 94, no. 3, Article ID 038701, 2005.

Hindawi
Scientific Programming
Volume 2022, Article ID 2190032, 9 pages
https://doi.org/10.1155/2022/2190032

Research Article

The Application of Diversified Blended Models in Teaching British and American Culture Based on Big Data Analysis

Fang Fang

School of Foreign Language, Yancheng Teacher's University, Yancheng 224001, Jiangsu, China

Correspondence should be addressed to Fang Fang; fangf@yctu.edu.cn

Received 4 August 2022; Revised 26 August 2022; Accepted 30 August 2022; Published 29 September 2022

Academic Editor: Lianhui Li

Language is a symbol reflecting ideas and is an important medium for people to realize information transfer and communication. Culture is all the material and spiritual wealth created during the historical development of human society. Language and culture are inseparable. When we learn a language, we must also understand the cultural content it contains. Learning English requires an understanding of the culture of British and American countries, and thus teachers must necessarily teach culture in the English classroom. At present, the software and hardware of Internet technology in our country have been developed in-depth, and the total amount of big data has been in the trend of growth, and China has officially entered the era of big data. This paper takes the reform of teaching mode of British and American culture courses as the main research object and explores how to build a diversified and blended teaching mode based on the existing teaching mode and integrating various online teaching resources under the premise of various technologies in the background of "big data." In order to accelerate the integration and optimization of such course resources, promote the development of theoretical teaching and practical teaching of such courses and improve students' professional ability.

1. Introduction

With the in-depth development of the Internet of Things, computer networks, mobile self-media, and other technologies, the total amount of global data has shown explosive growth according to the set, and human society has entered the era of accelerated development of big data. The concept and value of big data have been gradually accepted by the public; workers are also fully aware of the typical application and extensive prospects of big data in the field of education [1]. At present, many colleges and universities are actively exploring various forms of curriculum practice teaching reform programs according to the actual needs of teaching work, drawing on the existing advanced teaching models, and adjusting teaching and training programs in real-time [2–5].

Once upon a time, students could only ask their teachers for advice if they had knowledge or problems they did not understand, but with the advent of the big data era, many problems students can solve by looking up relevant information through the Internet. The blended teaching mode is a new teaching mode adapted to the era of big data. This teaching mode not only retains the traditional class teaching but also makes full use of the advantages of the network information platform and rich network resources. The application of blended teaching mode makes a major breakthrough in British and American culture education, which not only improves students' learning initiative but also enhances their comprehensive learning ability and lays a solid foundation for their future study and work [6].

A qualified teacher of English culture needs to have a solid knowledge of culture in addition to background knowledge of the culture of English-speaking countries. A good teacher should not only have a broad knowledge of culture but also make it an important task to develop students' cultural sensitivity and self-awareness. Good teachers should be able to familiarize themselves with "the deep and hidden culture of the national psychology, values, and ways of thinking of the target language" [7, 8] and develop their own cultural literacy in English. In addition to professional

competence, qualified and excellent teachers should have high intercultural communication skills, be able to actively explore cultural teaching, and pay attention to the cultivation of students' intercultural awareness and intercultural communication skills [9].

This paper aims at the problems such as the low flexibility and inactive classroom atmosphere in the traditional cramming English culture teaching, face the theoretical, technical, and application challenges, and address the fundamental issues of how to analyze and model big data on teaching and learning, how to build a diversified blended model based on big data analysis, and study its application in teaching British and American culture in order to give full play to the leading role of teachers and yet stimulate students' learning autonomy in many ways.

2. Concept Explanation

2.1. Big Data. Big data era is a new era of mass production, dissemination, and utilization of data with the rapid development of Internet technology. Big data are a huge collection of data, and the scale of data contained in the collection is huge, far beyond the scope of the traditional sense. The processing power of traditional computers cannot meet the needs of the big data era, and traditional tools and software cannot be used to store, analyze and manage big data. In order to solve this problem, computer scientists apply cloud computing to human data computing. Cloud computing technology can effectively solve the problem of storing human data and can calculate, analyze, and predict human data [10]. This can enable us to do effective use of big data and to dig deeper into the hidden data.

The arrival of the big data era provides people with opportunities and capabilities to conduct in-depth research in more fields. People use cloud computing technology to analyze, process, integrate, and mine big data, so as to obtain new knowledge and explore the laws of the real world. This has brought influence and changes to the teaching of British and American culture.

In the field of educational learning, five major applications of big data technologies include [11]: prediction: awareness of the likelihood of anticipated facts. For example, to have the ability to know when a student has intentionally answered incorrectly despite the fact that he or she is in fact capable. Clustering: discovering data points that are naturally clustered together. This is useful for grouping students with the same learning profile and interests together. Modeling: using learning models developed through big data analysis. Associations: discover relationships between variables and decode them for future use. This is useful for exploring the reliability of students' ability to answer questions correctly after asking for help. Decision-making: create a visual reference for decision-making in instructional management. For clarity, Figure 1 counts six areas, where big data and education intersect.

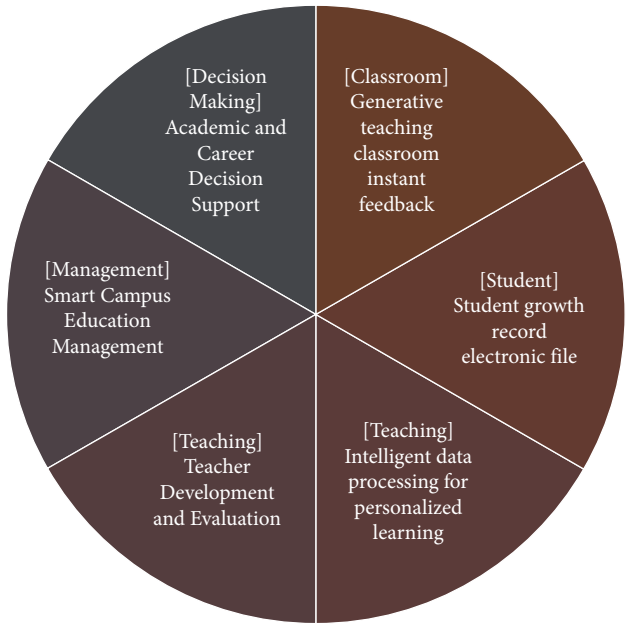

Figure 1: Six areas where big data and education intersect.

2.2. Diversified Blended Teaching Mode. Diversified blended teaching refers to a diversified and multiplatform teaching method that combines the advantages of traditional classroom teaching with information technology [12]. Blended teaching optimizes the selection and combination of all teaching elements to play the leading role of teachers to guide, inspire, and monitor the teaching process, while fully reflecting the initiative, enthusiasm, and creativity of students as the subjects of the learning process [13]. The key to the blended teaching model is the use of appropriate technological means for content presentation and transmission for specific teaching contents and learners.

In terms of form, blended instruction includes a mix of both offline and online learning, a mix of teacher-led activities and active student participation, a mix of student-led learning and collaborative group learning, a mix of multiple teaching resources, a mix of multiple learning environments, and other different dimensions. It should be noted that multiple blended teaching should combine teaching objectives and students' characteristics. For example, a classroom with mastery of knowledge as the main teaching goal can adopt the traditional classroom teaching mode based on teacher activities to highlight systematic lectures and training, while when the teaching goal is to strengthen practical skills development, teachers should adopt more information-based teaching mode to highlight students' independent learning and active exploration [14, 15]. In a word, blended teaching is neither a teaching model that simply emphasizes the application of an online learning environment and ignores the importance of classroom teaching nor a teaching model that unilaterally

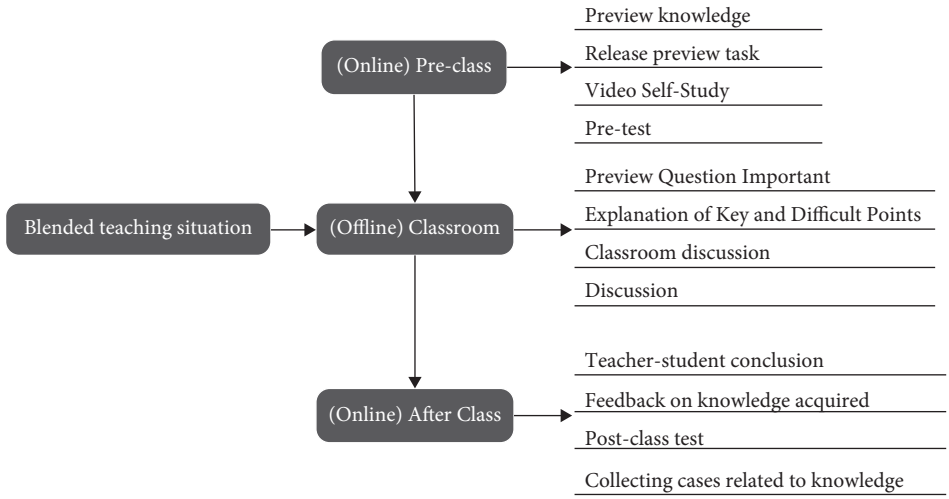

Figure 2: The flow of the diversified blended teaching model.

focuses on students and ignores the leading role of teachers; blended teaching both faces the advantages of traditional classroom and fully reflects the characteristics of the information age. The process of blended teaching model is shown in Figure 2.

2.3. Definition of Culture

2.3.1. Culture. Ancient and modern interpretations of the concept of culture are inseparable from those of nature and human society. Culture is an evolution of the concepts of astronomy and humanities, referring to the composition of natural celestial bodies and their laws, and the composition of human society and its laws, respectively. Culture is an evolution of the concepts of astronomy and humanities, referring, respectively, to the composition of natural celestial bodies and their laws and the composition of human society and its laws. The original meaning of culture is to teach and educate with literature, which is an abbreviation of human culture, and "the cultivation of human temperament and the education of moral character" are all part of cultural education. Culture is explained in the dictionary in a narrow sense as the ideology of society and the institutions and organizations that correspond to it, and in a broad sense as the sum of all the material and spiritual wealth created in the course of human social and historical practice [16]. Whatever is good for human development in material and spiritual terms is called culture. Culture is present throughout life activity; it is an innate, humanistic phenomenon. In general, culture is the sum of what people think, say (verbal and nonverbal), do, and feel [17].

In English, "culture" is an evolution of the Latin "cultus/cultura," which means "to dwell, to cultivate, to practice, to pay attention to, and to fear the spirits" [18]. It also has a derivative meaning for the cultivation of human temperament and moral character. Samuel Pufendorf first introduced culture as an independent concept, arguing that "culture is the sum of what is created by human activity and depends on man and society for its existence." Louis Kroeber and Clyde Kluckhohn, after compiling more than 300 definitions of culture from experts in several fields of study, grouped culture into six categories, including "descriptive, historical, normative, psychological, structural, and genetic." Meanwhile, an integrity definition of culture was made, that is, culture is a kind of "external and internal behavior patterns," and culture enables us to obtain and convey information using symbols.

Throughout the different definitions of culture by scholars, both material and spiritual dimensions are inseparable from the analysis. The concept of culture used in this study refers to the material and spiritual wealth created by human society in the course of its historical development.

2.3.2. Cultural Infiltration. Culture is a valuable asset created during the historical development of human society. "Infiltration" refers to the flow of water between the pores of the soil, within the cracks of hydraulic buildings, and between intersections, and also refers to the operations of the army to secretly infiltrate into the enemy's interior and rear by taking advantage of gaps in the enemy's deployment. It can also be used as a metaphor for the gradual entry of a force into other areas. In present-day terms, cultural infiltration is the use of media, multinational corporations, etc., by more developed countries or regions to promote their own culture to other countries, thus achieving both economic benefits and assimilation into other countries. The interpretation of culture as a medium for the powerful forces to instill values in the weaker countries is a passive and unconscious process of accepting foreign culture. Cultural infiltration is the infiltration of cultural factors into language teaching, which can be done through the operation of lexical mining, grammatical prompting, and translation comparison.

The cultural infiltration explored in this study refers to the active and conscious understanding or introduction of foreign cultures in order to enhance cross-cultural awareness and achieve the ability to communicate appropriately

and effectively across cultures. From the learner's perspective, cultural penetration refers to the language learner's active and conscious action to learn about foreign cultures. From the teacher's perspective, cultural penetration refers to the teacher's activities in teaching culture in the classroom.

3. Review of Research on Teaching British and American Culture

3.1. Research on Teaching British and American Culture Abroad

3.1.1. Teaching Awareness. Between the 1940s and the 1960s, academic research on the culture of the target language and the culture of the native language gradually shifted to the study of the teaching of cultural penetration in foreign language teaching. Fries Charles theoretically discussed the connection between language teaching and culture teaching, and the importance and necessity of culture teaching in foreign language teaching. He argued that cultural learning and language learning are inseparable and that the process of learning a language is also the process of forming students' cultural awareness, and that cultural factors should be infused into language learning. By enhancing students' knowledge of the culture of the target language, they can effectively master and use the target language [19]. Lado stated that by studying the linguistic differences and learning barriers between learners' native language and the target language, concluded that appropriate comparative analysis of native language and target language culture in language teaching can help achieve effective second language teaching. Brooks Atkinson conducted a study on the practical aspects of culture teaching, and he emphasized that culture teaching should always be carried out throughout the whole process of foreign language teaching, and teachers should choose different cultural contents at different teaching stages [20].

From the 1970s to the beginning of the 21st century, research on culture teaching and learning gradually flourished. The discussion of culture teaching in this period focused on the positive effects of culture teaching on language learning. Chastain Kevin discussed the reasons for conducting culture teaching in terms of the need for cultural understanding, the realization of intercultural communication, and personal interest [21]. Louise Damen argued that "culture, although excluded from the curriculum, cannot really be ignored by teachers in language teaching, it is hidden in foreign language learning and should be one of the basic skills for mastering a foreign language." Byram argued that "one acquires culture as one acquires language" [22]. Klippel John stated that cultural knowledge plays a supporting role in teaching culture and that mastering the cultural knowledge behind a language is the beginning of learning a language. Eugene Nida introduced culture into the translation of the English language. Kim discussed the current situation of culture teaching in English classrooms in urban and rural elementary schools in Korea from the perspective of teachers and students. From the study, it was concluded that teachers and students recognize the role of English culture in English education, but in practice, teachers still fail to adequately teach culture and students do not receive adequate cultural education [23]. Leshem conducted a period of observation in an Israeli junior high school English classroom to study the distance between the cultural background of teachers and students and the culture of the target language. The classroom observations concluded that there is a general problem of implicit cultural dynamics in English language teaching, i.e., the extent to which learners' knowledge of the target language culture affects the effectiveness of teachers' language instruction [24].

3.1.2. Teaching Strategies. From the 1980s to the 1990s, the idea of teaching cultural penetration in the classroom was generally recognized, and foreign scholars' research on teaching cultural penetration lies in exploring specific and feasible cultural penetration strategies. Hans argued that in foreign language teaching, the content of cultural introduction should focus on people in the target language country, such as their lifestyles, behavioral habits, and ways of thinking [25]. Thomas James pointed out that pragmatic language failures and communicative language failures are the root causes of cross-cultural pragmatic failures. Seelye introduced culture capsules, culture clusters, and culture assimilators. Seelye introduced classroom culture introduction methods such as culture capsules, culture clusters, and culture assimilators, and discussed how to measure the effect of culture learning [26]. Byram Mike, after studying audiovisual and auditory methods, suggested that grammar and cultural introduction should also be linked together in ELT [27].

At the beginning of the 21st century, cultural infusion strategies began to focus on design from the perspective of teachers and learners. Patrick Moran advocated teaching culture through experiential language instruction that reinforces cultural connotations, student interventions, expected or achieved outcomes, learning content, and the intrinsic connections between teachers and students. Frank has investigated how teachers can integrate cultural knowledge into the English classroom in the English classroom. He suggested that teachers can promote learners' cross-cultural understanding by organizing activities that increase cultural awareness, such as assigning networking tasks, role-playing, and cultural observation [28].

3.2. Research on Teaching British and American Culture in China

3.2.1. Teaching Awareness. From the end of the 20th century to the beginning of the 21st century, improving learners' intercultural communication skills is one of the insurmountable topics of cultural penetration studied by domestic scholars. Cao believed that culture teaching in English language teaching is composed of both cultural knowledge and cultural understanding. Cultivating students' intercultural communication skills requires a

combination of the strengths of both cultural knowledge and cultural understanding, with emphasis on both the learning of cultural knowledge and the cultivation of cultural understanding. Tan Ling proposed that English teaching in colleges and universities should implement a joint approach of language teaching and cultural background knowledge transfer from the perspectives of the connotation of intercultural awareness, the importance, and necessity of strengthening intercultural awareness, and gives suggestions on the ways to enhance intercultural awareness. Gao Dongjun, from the perspective of the relationship between language and culture, explained the role of learning the culture behind language in enhancing students' language application and intercultural communication skills and calls for teachers to introduce English culture in their teaching. Lv believed that "the real purpose of English teaching is to achieve accurate, appropriate and effective communication," and that this goal needs to be achieved by paying attention to the cultivation of students' intercultural communication skills so that they can become intercultural communication talents with a high level of intercultural literacy.

Cultural penetration in the classroom has been recognized by most researchers, and research has begun to focus on the cultural teaching experiences of teachers and learners. Xiao Bin discussed the necessity of cultivating students' intercultural awareness of the dialectical relationship between language, culture, and teaching, and suggested that vocabulary teaching and organizing cultural activities can be used in English teaching to cultivate students' cultural awareness. Shi Rui researched cultural teaching in the higher-level English classroom and concluded that cultural input while teaching English is the key to solving students' linguistic errors. Language and culture run through the English classroom, and classroom teaching should increase cultural input in English to improve students' practical English application skills. Li suggested that cultural differences determine language differences and it is important to include an introduction to the background of cultural knowledge of the language in teaching. Cultural teaching should go hand in hand with language teaching. Cultural teaching is helpful to help students understand the culture behind the language, improve their perception of the cultural differences between Chinese and Western cultures, and enhance their intercultural communication skills. Yu Zhihao and He Huibin studied the issue of developing Anglo-American cultural awareness in a special group of ethnic minority students. They talked about the dilemmas faced by cultivating the British-American cultural literacy of minority students from the issue of supplementing cultural knowledge to constructing students' humanistic spirit and suggested that students should be guided to transform their perspectives and concepts in the teaching process and learn British-American cultural knowledge with a developmental perspective. From the meaning of intercultural awareness, Lu Kaifeng analyzed the significance and necessity of intercultural awareness in English learning. He suggested that teachers should make full use of multimedia technology to infuse intercultural awareness into classroom teaching. Zeng Lili reflected on the status quo of teachers' old teaching concepts and single way of evaluating teaching effects in English teaching and advocates that teachers should study teaching concepts and adopt diversified teaching modes and evaluation methods in culture teaching.

3.2.2. Pedagogical Strategies. Starting from 2010, the research on teaching strategies of cultural penetration has been characterized by the development of theoretical teaching strategies and teaching-aid technology. Wu Xianyun proposed that strengthening the learning of British and American culture and enhancing the awareness of cross-cultural communication meet the needs of English teaching reform. Teachers should make full use of existing multimedia aids, such as using pictures, audio, and video in teaching, to increase students' active participation in class. Based on the theory of multiple intelligences, Lu Tian suggested that teachers need to adopt diversified teaching designs in classroom teaching to provide more development opportunities for cultivating students' intercultural communication skills. Du Haiyan proposed that teachers can stimulate students' interest in cultural learning through the comparison method, test correction, and the creation of cross-cultural situations in response to the negative perceptions of students in the process of cultural teaching. Sun Lei introduced idioms as "concise phrases or short sentences that have been used by language users for a long time," through which English learners can learn the language and Western culture and improve their intercultural communication skills. Li believed that teaching culture can be carried out by comparing cultural differences, using online media, expanding cultural resources in English textbooks, and organizing English-related activities. Mao Mingming believed that cultural penetration is an important part of high school English reading teaching, through which students' reading speed and comprehension can be improved, and is an important way to develop students' cross-cultural awareness and cross-cultural communication skills. Guan Jiangang researched the strategies of teaching English culture in high school and proposed three forms to cultivate students' cross-cultural awareness, such as innovating English teaching theories, creating English teaching contexts, and organizing extracurricular activities.

4. Construction of Blended Teaching Model Based on Big Data Analysis

In order to accelerate the integration and optimization of the resources of these courses, promote the development of theoretical and practical teaching of these courses, and improve the ability of students in related majors to solve practical problems, we explore and practice in the British and American culture courses that have been offered in our university. The blended teaching model constructed in this paper contains the following three parts: the analysis model of teaching behavior based on educational big data, the construction of a blended teaching platform for British and

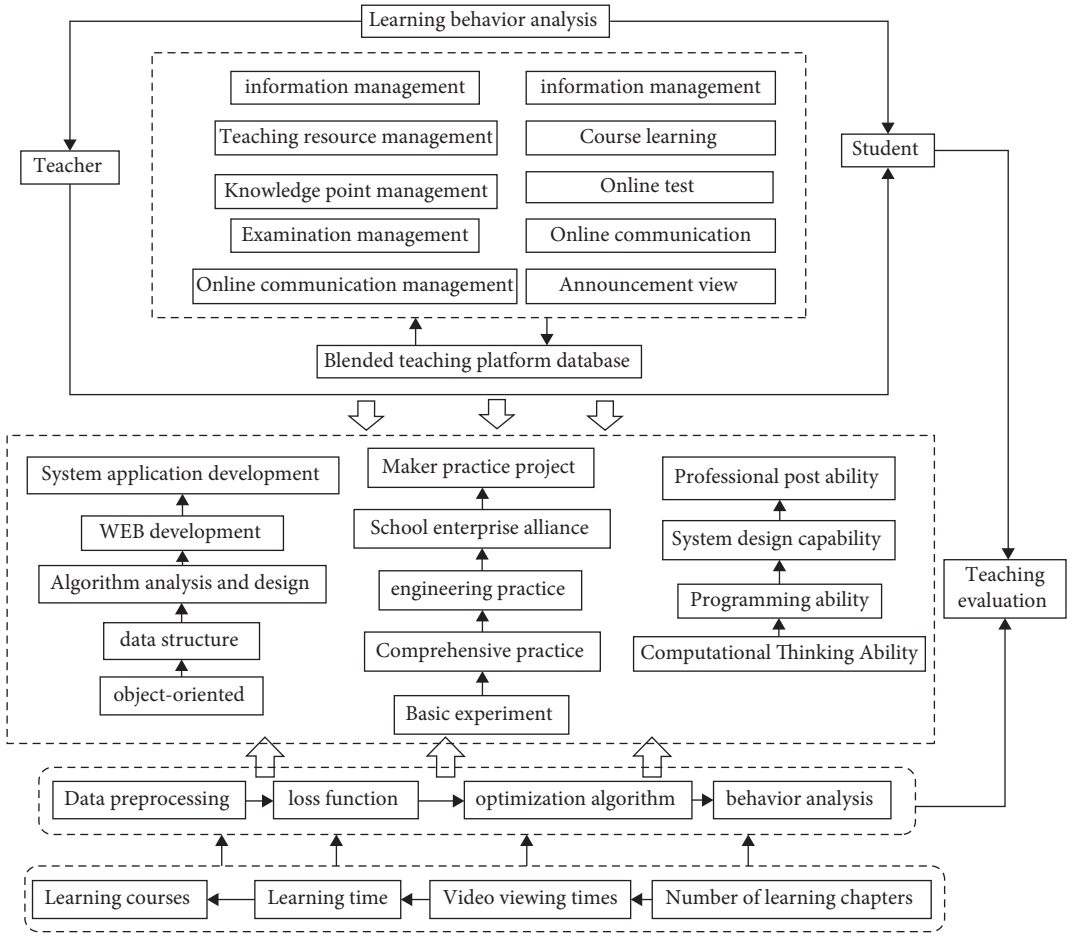

Figure 3: The overall structure of the diversified blended teaching model.

American culture courses, and the construction of a blended teaching model based on big data background. The overall structure diagram is shown in Figure 3.

4.1. Teaching Behavior Analysis Model Based on Education Big Data. Under the teaching environment of "Internet+," the teaching process will generate a large amount of teaching-related data. How to make full use of these teaching big data and analyze students' learning behaviors based on their related information and learning records is the first theoretical problem that needs to be solved in this paper. In view of the lack of abundant teaching data for British and American culture courses, this paper adopts the open data set of MOOC platform to analyze and establish the learning behavior analysis model. The existing learning behavior records include course code, course name, registration time, start time, end time, course days, number of students enrolled, number of students who passed the exam to obtain the certificate, pass rate, and other record information. In this paper, learners' age, gender, educational background, learning time, number of learning events, number of sampling statistics learning, number of watching videos, number of learning chapters, and number of posting on learning forums are selected as the basis of learning effect evaluation, and the support vector machine regression (SVR) algorithm is used to predict the learning behavior. The mathematical model of the support vector machine regression algorithm is shown in Figure 4, in which $f(x)$ denotes the learning effect, x denotes the relevant evaluation basis affecting the learning effect, w denotes the weight

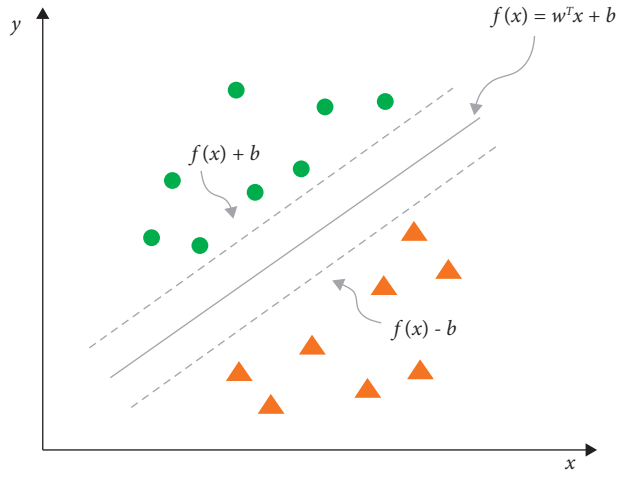

Figure 4: Mathematical model of support vector machine regression algorithm.

obtained by regression, and b denotes the deviation, then its regression model expression is given as follows:

$$f(x) = w_1 x_1 + w_2 x_2 + \cdots . w_n x_n + b. \quad (1)$$

4.2. The Construction of Blended Teaching Platform Based on Learning Analysis. The theory of blended teaching shows that in the teaching process, the teacher's leading role should be played; at the same time, the main role of students should be reflected, and the students' learning initiative should be fully stimulated. In the blended network teaching mode, in order to reflect the teacher's leading role in monitoring the learning process, the teacher needs to upload all relevant teaching materials, teaching videos, and other tutorial materials in advance; while students can complete classroom teaching, after-class homework and discussion, and communication independently through the network teaching platform according to the teaching arrangement given by the teacher. On the other hand, teachers and students will generate a large amount of teaching-related data in the process of completing teaching through the online platform. For example, the number of times of login, login time, students' learning content, learning hours, homework times, homework time, test times, test time, test scores, and many other teaching-related data, how to collect, analyze, count and visualize these data, and establish learning analysis and prediction model according to the relevant course characteristics, so as to implement real-time monitoring of students' learning process and learning effect, and provide a dynamic reference for teachers.' It provides a visual reference for teachers' dynamic management and provides relevant management data for teaching managers.

Based on the abovementioned analysis, the blended teaching platform based on learning analysis built in this project contains the following contents: (1) teacher module: the teacher function module contains personal information management, teaching resource management, teaching announcement management, teaching knowledge point management, test question management, and other parts; (2) student module: the student function module contains personal information management, course learning, online communication, announcement viewing and other functions; (3) learning analysis module: the learning analysis module contains functions such as learning data collection, online communication analysis, online learning analysis, and learning test analysis. The system function diagram of this platform is shown in Figure 5.

4.3. Construction of Blended Teaching Mode Based on Big Data Analysis. The blended teaching mode based on big data analysis is constructed in this paper, taking the British and American culture course of our university as the research object, using the blended teaching platform based on learning analysis as the teaching means, and taking various engineering practice projects of our university as the carrier, collecting the practical teaching links such as course experiment, course design, professional practical training and graduation design, and adopting the basic teaching principle of combining online/offline to realize the integration and optimization of teaching resources, guidance and supervision of teaching process, and overall improvement of teaching quality. It adopts the basic teaching principles of online/offline combination to realize the integration and optimization of teaching resources, supervision of teaching process, and overall improvement of teaching quality.

The project collects teaching data online and adopts a big data analysis model to analyze, visualize and give feedback on teaching data, providing data basis for teachers' teaching process, students' learning planning, and teaching evaluation. The teaching mode constructed in this paper contains the following core contents: (1) project-oriented blended teaching mode: for the characteristics of theoretical courses and practical projects of programming courses, the blended teaching mode oriented to creative practice projects, joint school-enterprise projects, engineering practice projects, comprehensive practice projects, and basic experiment projects is constructed. Based on the blended teaching platform that has been built, various forms of online/offline blended teaching are carried out to effectively improve students' programming levels. (2) Data analysis-oriented multiple blended evaluation mode: based on the blended teaching platform, the platform teaching data are collected in real-time, and the teacher-student two-way evaluation mechanism is implemented. Based on the two-way evaluation results, combined with the platform teaching data, a reasonable teacher-student teaching evaluation model is established to build a foundation for reasonable tracking and evaluation of teaching quality.

4.4. Upgrading and Reengineering of the System under Big Data. The research on big data in education has developed a cone mesh educational system structure, which includes more directions of educational data mining and also a basic system architecture with new resources, and originally, relatively independent resource systems have been opened up to form a system framework with multiple elements. The cone mesh structure requires more management systems, there must be more teaching elements, and many related elements must also have their own independent small modules, and after integration, the overall teaching system framework is formed. Traditional classroom teaching and network distance learning resource system include many teaching resource database building systems, which can form a recursive system structure. The teaching and learning system under education big data can form independent minisystems by studying the correlation relationship, which can add more elements to the teaching and learning system.

The concept of educational big data includes more sources of educational data with multiple types of data. Traditional educational data does not have a large amount of information, but this educational big data contains a large amount of information. The data can bring together more pedagogical elements, which can be relatively independent or can be built into a simpler pedagogical system structure so

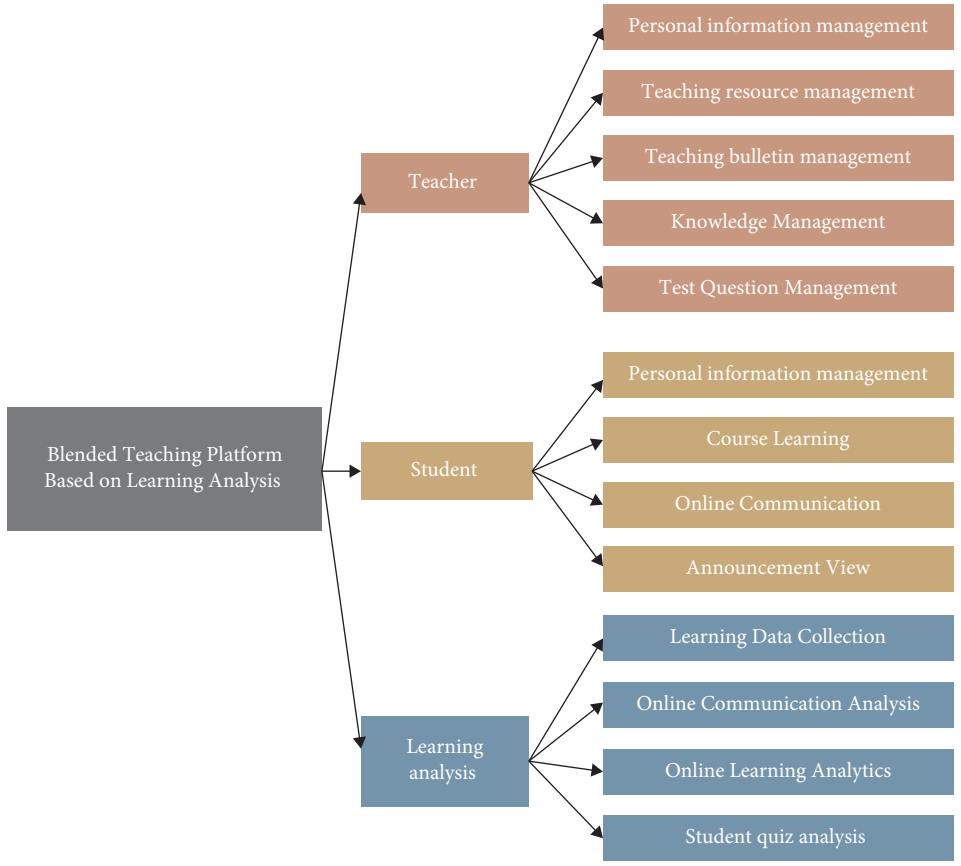

Figure 5: The system function diagram of this platform.

that it can better meet the standards related to the documentation of learning resources and can better meet the needs of scalability. In the beginning, the simplified system does not have much big data or perfect functions. In the subsequent use, the data need to be improved continuously, and the structure and functions of the system must also be improved, but the current data of the new teaching system structure has certain limitations, and the functions of the simplified system are relatively limited and must be upgraded only after manual intervention. The construction of the simplified system structure needs to learn the principles of design configuration before it can have perfect functions. The teaching support system can be better constructed in conjunction with the teaching content and can improve the system's functions to make it faster and more relevant.

With the development of artificial intelligence technology, data construction has become a new research trend. Building a simple teaching system includes rules and teaching cases, the system does not involve other cases, but it cannot be limited to the relationship between the data, but also can focus on upgrading the teaching system, education big data research constructs a cone mesh structure, this model has better internal modules and system as a whole, the platform is more good openness, avoiding some unreasonable construction. The study of educational big data can be more clear educational objectives, and clarify the design of teaching and learning, combined with the relationship between the elements, can have more problem-solving ideas. Education big data integrates the teaching system, realizes the deduction problem, and can send the problem to the teacher actively, the teacher can study according to the learning environment, build advanced teaching logic thinking, promote the formation of advanced teaching architecture, can make the university have more scientific teaching system management.

5. Conclusion

This paper takes the reform of teaching mode of British and American culture courses in our university as the main research object and explores how to analyze teaching data and predict teaching behavior under the technical premise of "big data" background; how to build a blended teaching platform with data analysis function based on existing multiple online teaching resources; and explore and practice in the British and American culture courses that have been offered in our university. In addition, we will explore and practice in the British and American culture courses offered by our university to build a blended teaching model based on data analysis. The teaching method of multivariate mixed mode based on big data analysis is to teach British and American cultures to students. Unlike traditional instillation teaching, through the analysis of data, teachers can better follow the principle of students' subjective initiative in learning and conduct cultural teaching in a heuristic-

induced way. For example, in the knowledge question-and-answer session, teachers give representative keywords by constantly asking questions, and guide students to correct themselves and find answers themselves. At the same time, teachers consider the differences in knowledge acceptance among students, strictly control the process of cultural teaching, and ensure the implementation of effective cultural teaching activities. We will accelerate the integration and optimization of the resources of these courses, promote the development of theoretical and practical teaching of these courses, and improve the ability of students in related majors to solve practical problems.

Data Availability

The dataset can be accessed upon request.

Conflicts of Interest

The author declares that there are no conflicts of interest.

References

[1] Y. Wang, "Big opportunities and big concerns of big data in education," *TechTrends*, vol. 60, no. 4, pp. 381–384, 2016.

[2] X. Jia, "Research on the Role of Big Data Technology in the Reform of English Teaching in universities," *Wireless Communications and Mobile Computing*, vol. 2021, Article ID 9510216, 13 pages, 2021.

[3] X. Li, X. Fan, X. Qu et al., "Curriculum reform in big data education at applied technical colleges and universities in China," *IEEE Access*, vol. 7, pp. 125511–125521, 2019.

[4] S. Diao, "The reform of teaching management mode based on artificial intelligence in the era of big data," *Journal of Physics: conference Series. IOP Publishing*, vol. 1533, no. 4, Article ID 042050, 2020.

[5] B. Williamson, "The hidden architecture of higher education: building a big data infrastructure for the "smarter university"," *International Journal of Educational Technology in Higher Education*, vol. 15, no. 1, pp. 1–26, 2018.

[6] I. Harumi, "A new framework of culture teaching for teaching English as a global language," *RELC Journal*, vol. 33, no. 2, pp. 36–57, 2002.

[7] M. Saville-Troike, "Teaching English as a Second culture," *ON TESOL*, vol. 74, 1975.

[8] S. L. McKay, "Teaching English as an international language: the role of culture in Asian contexts," *Journal of Asia TEFL*, vol. 1, no. 1, 2004.

[9] K. Kitao and S. K. Kitao, *English Teaching: Theory, Research and Practice*, Chiyoda-ku, Tokyo, 1995.

[10] M. I. Malik, S. H. Wani, and A. Rashid, "Cloud computing-technologies," *International Journal of Advanced Research in Computer Science*, vol. 9, no. 2, 2018.

[11] C. Fischer, Z. A. Pardos, R. S. Baker et al., "Mining big data in education: affordances and challenges," *Review of Research in Education*, vol. 44, no. 1, pp. 130–160, 2020.

[12] S. Z. B. Tahir and N. Mufidah, "Multi-blended learning model for remote area schools in pandemic Covid-19 situation," *Journal of Teaching and Education for Scholars*, vol. 1, no. 1, pp. 38–46, 2022.

[13] M. Jiang and X. Wu, "Exploration and practice of college English multi-blended teaching model based on OBE concept [J]," *Open Journal of Modern Linguistics*, vol. 12, no. 4, pp. 367–379, 2022.

[14] M. C. B. Umanailo, "Designing English Teaching Model at the Remote Area Schools of Maluku in Covid-19 Pandemic Situation," in *Proceedings of the 11th Annual International Conference on Industrial Engineering and Operations Management*, Singapore, March 2021.

[15] S. Q. Jiang, L. I. Hui, and H. U. An-Jun, "A study on blended teaching design of comprehensive English course in higher vocational colleges based on production-oriented approach," *Journal of Qingdao Ocean Shipping Mariners College*, vol. 40, no. 3, pp. 71–74, 2019.

[16] "Teachers' education," *Ciência & Educação (Bauru)*, vol. 22, 2016.

[17] T. Dympna and E. Wallace, "Ensuring Effective Intercultural Communication in the Emergency department," *Emergency Nurse*, vol. 30, 2022.

[18] T. Clemmensen, "The Cultural Usability (CULTUSAB) Project: Studies of Cultural Models in Psychological Usability Evaluation Methods," in *Proceedings of the International Conference on Usability and Internationalization*, Springer, Berlin Heidelberg, July 2007.

[19] C. Fries, *Teaching and Learning English as a Foreign Language*, University of Michigan Press, Michigan, 1945.

[20] R. Lado, *Linguistic across Cultures*, University of Michigan Press, Ann Arbor, 1957.

[21] K. Chastain, *Developing Second Language Skills*, Rand Mc Nally College Publishing Company, USA, 1976.

[22] M. Byram, *Culture Studies in Foreign Language Education*, Multilingual Matters, Clevedon, 1989.

[23] E. Y. Kim, *A Study of Culture Teaching in English Classes in Korea and Rural Elementary Schools in the Republic of Korea*, Mc Gill University, Canada, 2005.

[24] S. Leshem, "Unravelling cultural dynamics in TEFL: culture tapestries in three Israeli schools[J]," *Teachers and Teaching: Theory and Practice*, vol. 12, no. 06, pp. 639–656, 2006.

[25] S. Hans, *Fundamental Concepts of Language Teaching*, Oxford University Press, London, 1983.

[26] N. Seelye, *Teaching Culture: Strategies for Intercultural Communication*, National Textbook Company, Lincolnwood Illinois, 1993.

[27] C. Byram, *Teaching and Learning Language and Culture*, Multilingual Matters, Cleve don, Avon, 1994.

[28] J. Frank, "Raising cultural awareness in the English language classroom," *English Teaching Forum*, vol. 51, no. 4, p. 2, 2013.

Hindawi
Scientific Programming
Volume 2023, Article ID 9760437, 1 page
https://doi.org/10.1155/2023/9760437

Retraction

Retracted: The Integrated Development of Furniture Design and Children's Characteristics Based on Artificial Intelligence

Scientific Programming

Received 18 July 2023; Accepted 18 July 2023; Published 19 July 2023

This article has been retracted by Hindawi following an investigation undertaken by the publisher [1]. This investigation has uncovered evidence of one or more of the following indicators of systematic manipulation of the publication process:

(1) Discrepancies in scope
(2) Discrepancies in the description of the research reported
(3) Discrepancies between the availability of data and the research described
(4) Inappropriate citations
(5) Incoherent, meaningless and/or irrelevant content included in the article
(6) Peer-review manipulation

The presence of these indicators undermines our confidence in the integrity of the article's content and we cannot, therefore, vouch for its reliability. Please note that this notice is intended solely to alert readers that the content of this article is unreliable. We have not investigated whether authors were aware of or involved in the systematic manipulation of the publication process.

Wiley and Hindawi regrets that the usual quality checks did not identify these issues before publication and have since put additional measures in place to safeguard research integrity.

We wish to credit our own Research Integrity and Research Publishing teams and anonymous and named external researchers and research integrity experts for contributing to this investigation.

The corresponding author, as the representative of all authors, has been given the opportunity to register their agreement or disagreement to this retraction. We have kept a record of any response received.

References

[1] W. Zhang and S. Li, "The Integrated Development of Furniture Design and Children's Characteristics Based on Artificial Intelligence," *Scientific Programming*, vol. 2022, Article ID 6036160, 9 pages, 2022.

Hindawi
Scientific Programming
Volume 2022, Article ID 6036160, 9 pages
https://doi.org/10.1155/2022/6036160

Research Article

The Integrated Development of Furniture Design and Children's Characteristics Based on Artificial Intelligence

Wenbo Zhang and Si Li

Nanchang University, College of Science and Technology, Jiangxi, Nanchang 330022, China

Correspondence should be addressed to Wenbo Zhang; 2018030600032@jlxy.nju.edu.cn

Received 24 July 2022; Revised 24 August 2022; Accepted 5 September 2022; Published 28 September 2022

Academic Editor: Lianhui Li

Furniture is one of the most enduring items that children grow up with. However, there is a big gap between children's rapidly growing physical and mental needs and existing children's furniture. It is necessary to design children's furniture that is both interesting and multifunctional from the perspective of children's physiology and psychology. In the context of artificial intelligence, this paper applies the artificial intelligence design concept to the design of children's furniture and discusses the necessity and design principles of its application in the design of children's furniture from the aspects of society, children, and development trends.

1. Introduction

For modern residents with ever-increasing living environment requirements, it is also necessary to provide children with a living environment that is more in line with their physical and mental growth. After investigation, it was found that the central consumers of modern families tend to be children. Therefore, the proportion of furniture sales of series furniture specially made for children continues to grow, which has also attracted the interest of many manufacturers. However, the segmentation of China's furniture market is not enough, and the children's furniture market has yet to be developed [1]. According to relevant data, children with separate bedrooms and furniture account for about 10.2% of Chinese families, and about 45.6% of families want to buy furniture for children. China's furniture industry has a profound history, and its manufacturing theory system is also becoming more and more mature. However, as a rising star, children's furniture is still in its infancy in terms of design and R&D, and production and lacks a theoretical system with guiding significance [2]. In the early 1980s, furniture for children was designed and manufactured only by individual adult furniture manufacturers. Due to the lack of designers in the professional field, the finished product is just a miniature version of adult furniture. It was not until 1998 that the production scale of children's furniture gradually expanded. With the continuous development of the times, children became the main group of consumers, and more and more manufacturers turned their attention to the children's furniture market. In 2001, children's furniture began to form an independent category separated from furniture design, formed its own design and manufacturing system, and gradually improved. At the same time, a number of local children's furniture brands have emerged in China [3].

Through the analysis of China's furniture market, the development situation of furniture designed for adults is relatively optimistic. Compared with adult furniture, children's furniture is still in its infancy. There are only a handful of designer teams specializing in the field of children's furniture. Secondly, the size of children's furniture does not take into account the physical and psychological development characteristics of modern children, and can only meet short-term use. Once again, it reflects the necessity of applying the concept of growable design in the design of children's furniture. In the article "A Preliminary Study on the Grow ability Design of Children's Furniture," the author Min Lihong [4] pointed out that because children are in the

stage of continuous growth, the fixed size of furniture cannot meet the needs of children's continuous physical and psychological growth, and should design a set of furniture that accompanies the growth of children. However, this study only discussed the growability of children's furniture from a shallower level and did not specifically and deeply study the growth characteristics of children at various stages and the changes in needs [5].

After the birth of a child in Western countries, parents have already prepared a children's room for the child. This way of parenting is very different from China. At the same time, the research on children's environment design and home furnishing design in developed countries started earlier, and the research on manufacturing and production and theoretical system research is also relatively complete and mature. In the United States, children's furniture pays more attention to personalized design. Modular furniture design and the concept of multifunction are also very mature [6]. Designers in some parts of Europe, on the other hand, pay more attention to safety, and their furniture pays more attention to environmental protection and health. In terms of materials, natural solid wood is often used. The focus of the design is firstly to understand children's physical and mental development needs, secondly to take children's behavior as a design guide, and finally to help children grow in a safe and comfortable environment, which also reflects the care for children's growth. Therefore, versatility, practicality, and flexibility have become synonymous with foreign children's furniture design. Flexibility means that children's furniture can be flexibly adjusted according to children's growth needs and grow with children [7]. It can be seen that foreign designers have also applied the concept of growth to the design of children's furniture. Although children's furniture rose early in Western countries and had relatively complete theoretical and practical foundations, the main research object is the physiological and psychological characteristics of Western children, which is not fully applicable to Chinese children. Moreover, the design thinking of the growth concept applied to children's furniture has not been systematically summarized and summarized. However, their design research methods and design ideas are still worthy of study and reference by Chinese designers and some local enterprises [8].

In the concept of biology, the word "growth" is summarized as the process of growth and maturation of living organisms from small to large. When "growth" is used as the guide of children's furniture design, it is understood that in the process of children's physical and psychological growth, children's furniture can make corresponding adjustments and improvements according to the changes in their growth, so as to meet the different needs of children, age period requirements [9]. In the article "Research on the Growable Design of Children's Furniture," Liu Bowen mentioned that the design of the growable includes two meanings: (1) *Intuitive Growth*. In order to meet the needs of children's growth, the scale of the furniture can be adjusted freely, such as the extension of length and width. Functionally, it can be extended and transformed according to children's different life states, such as life, learning, or time periods such as games. The shape can be changed by adding, subtracting, or replacing parts according to the child's preference. Modular design is a good example. (2) *Indirect Growth*. This is a relatively invisible growth, not easy to detect. But this kind of growth has a subtle effect on children's physical and mental effects [10].

2. Research Ideas for the Subject

2.1. Definition of Research Objects. The term "child" in the United Nations Convention on the Rights of the Child refers to "any person under the age of 1, unless the law applicable to him stipulates that the age of majority is less than 10 years." In the development of psychology, there is a very important research feature, that is, age segmentation. Most psychologists agree that the development of people's lives in different age groups presents different rules, so the age-based research method has become popular and also has scientific rationale. American psychologist Robert Feldman divides it like this: prenatal period (fertilization to birth), infancy and toddler period (birth to 3 years old), preschool (3 years to 6 years old), middle childhood (6 years old to 12 years old), adolescence (12 years old to 20 years old), and early adulthood (20 years old to 40 years old), middle adulthood (40 years old to 60 years old), and late adulthood (60 years old to death) [11]. After reading the relevant psychological works, the author found that the views were recognized by most of the research scholars. The special research carried out from the age group can help the author to carry out the special research. According to the combination of children's growth characteristics and developmental psychology, this subject takes 3- to 12-year-old children as the research object. Because the age group of 0–3 years old is usually called infants and young children, they usually cannot take care of themselves in daily life, and the requirements for furniture are also different, and the age group of 12–18 years old is also called the juvenile chapter, which is a child at this stage. Children aged 3–12 are selected as the research objects, including between preschool and adolescence. There is a big change in the living environment of children at this age, and the center of life gradually shifts from home to school. For children, this stage marks the beginning of formal education, and in this stage, the physical and cognitive development is very obvious [12]. Changes in the status of children, changes in environmental pressure, and changes in the living environment make children's psychology take a qualitative leap. This stage is also an important period of personality development. The research on children at this stage is of great value in guiding the design of children's furniture. Therefore, selecting children at this stage as the research object and analyzing their physiological and psychological characteristics can provide an important basis for the design and research of children's furniture at this stage [13].

2.2. Research Methods

2.2.1. Document Law. We consult domestic and foreign monographs and periodicals on children's furniture design and children's physical and psychological growth such as

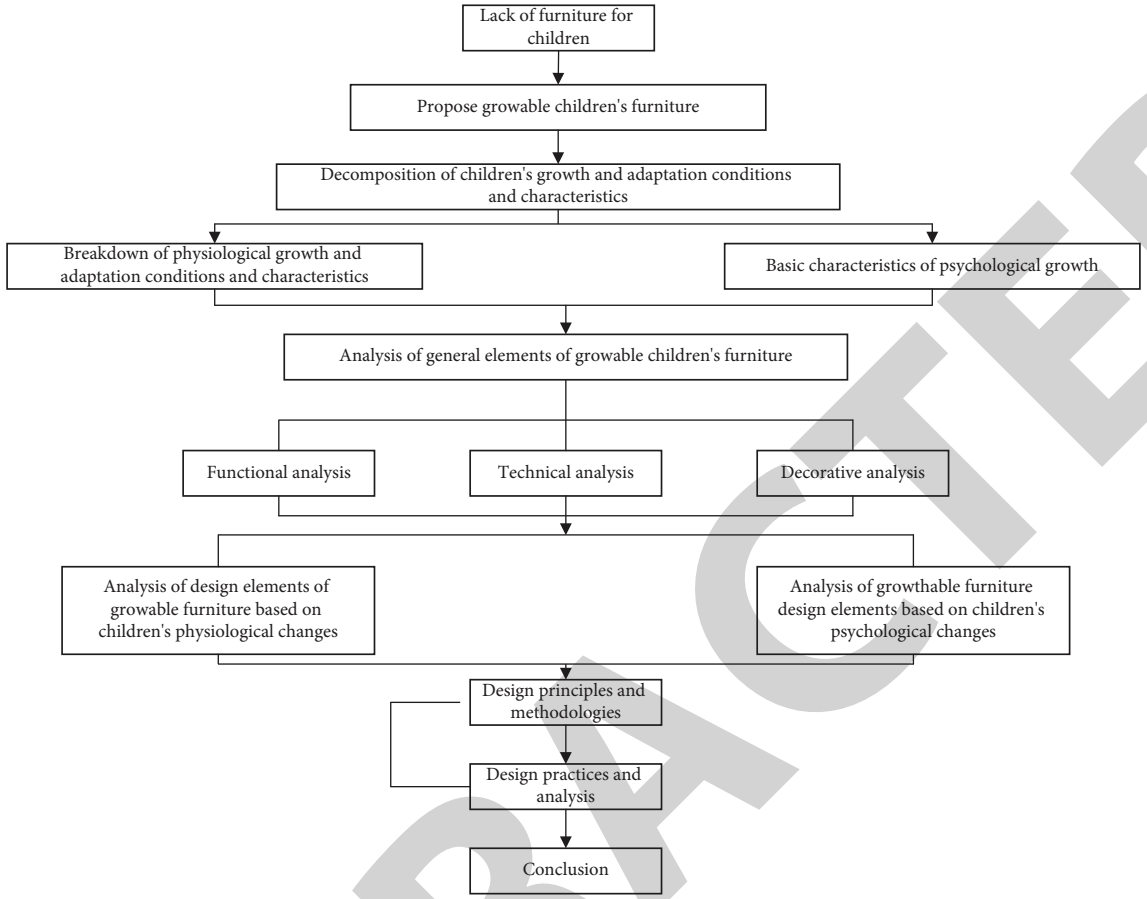

Figure 1: Research technology roadmap.

"Research on Contemporary Furniture Design Theory," "Furniture Modeling Design," "Introduction to Furniture Design," and other monographs, as well as "Forest Products Industry," "Decoration," "Packaging Engineering," "International Wood Industry," "Wood Industry," "Furniture" and "Interior Decoration," "Furniture," and other professional journals and professional websites such as Tiantian Furniture Network and Design Online.

2.2.2. Comparative Research Method. We compare different research objects and different themes to design research procedures and methods, and find out the basic ideas and methods of research. In the course of the research, the physiological and psychological characteristics of children in different periods were compared and analyzed to find out their different physiological and psychological characteristics at different ages.

2.2.3. Deductive Method. The connotation related to the design of the research object is deduced, and the content of the furniture design work is deduced according to the general principles.

2.2.4. Induction. Through the analysis of elements at different levels and different connotations, the basic principles and methods of the design of children's furniture that can grow are summarized.

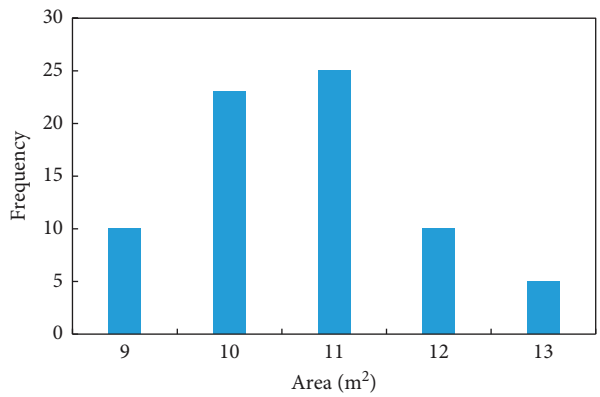

Figure 2: Histogram of indoor area of children's room.

2.3. Technical Circuit. The technology roadmap is shown in Figure 1.

2.4. Research on Children's Room Space

2.4.1. Survey on the Area of Children's Rooms. Here, bedroom refers to the living room. The so-called space is the area

where the specific things that the eyes can see and the hands can touch. The child's room space refers to the room where the child lives. In such an area, it can not only be used to place the furniture used by the child but also provide a certain activity space for the child [14].

Take an ordinary family of three with two bedrooms as an example, such a family will basically arrange a children's room. The area of children's rooms is generally not very large, and most of them are small bedrooms. When consumers buy furniture for their children, they generally configure corresponding furniture items according to the indoor area. Therefore, the small size of children's room should be considered as a constraint factor when designing children's furniture [15]. Through the investigation of the area of some children's rooms in a certain area, the following results are obtained as a histogram, as shown in Figure 2.

In Figure 2, we can see the area of children's room is mainly between 9 and 13 square meters, of which the small area of about 11 square meters occupies most of the room. That is, the space of only ten square meters is often a comprehensive activity place for children to rest, play, and learn.

The design of the children's room affects the child's character and the healthy growth of body and mind to a certain extent. For a small space, how to arrange the children's furniture reasonably and leave a spacious play space for them is a question worth considering.

2.4.2. Division and Layout of Children's Living Room Space. The quality of the environment affects a person's growth, especially for children in early childhood. In their environment, only the children's room can be arranged and arranged by parents. So for the majority of small-area living rooms, how can a reasonable division and layout create a healthy and safe growth environment for children?

2.4.3. Functional Area Division of Children's Room. Every young child will perform some essential activities in daily life, such as sleeping, dressing, learning, playing, and so on. According to the needs of these daily activities, we can divide the children's living space into five functional areas, namely, sleeping area—area for sleeping and resting; storage area—area for placing clothes and toys; learning area—area for reading and drawing; game area—area for building blocks and playing games; and communication area—area for communicating with friends. The following mainly starts from the necessity of each functional area, the environment required for the development of children's characteristics, and the cultivation of good habits, and conducts specific analysis and discussion on the above functional areas [16]:

Sleeping functional area: the sleeping area is the most important functional area in the children's room. Sleep plays a very important role in human life, especially for young children [17]. Good and adequate sleep quality is conducive to promoting the growth and development of young children and enhancing disease resistance. The main piece of furniture in the sleeping area is the bed, the place where the toddler can rest and recover. Secondly, other auxiliary furniture can be added according to actual needs, such as bedside tables, which can be used to store books, dolls, etc. Excessive energy during the day makes it difficult for children to fall asleep at night. At this time, a quiet and comfortable environment is especially needed so that children can fall asleep early [18]. The layout of the bed should avoid affecting the sleep of children, such as doors, windows, and objects that stimulate children's vision, or place the bed in an area with weak light to create a good resting environment for children. In addition, parents should guide their children to form good sleep habits from an early age to ensure that children have adequate sleep [19].

Storage function area: children will inevitably have many clothes, hats and toys, so the children's room is inseparable from the necessary storage space. Since the children's room itself is not large in size and there are many types of toys, it is very necessary to allocate storage space reasonably. It can be classified and partitioned according to the needs of children's activities, which not only improves the activity efficiency but also makes the room beautiful [20].

Children like to throw and litter, which makes the originally small space more messy and disorderly. If you put a few activity storage boxes in the game area, you can not only summarize many scattered toys but also take them easily when playing. In addition, puppet toys can be placed on the clapboard at the head of the bed, which can be displayed on the one hand, and can be hugged to sleep when the child sleeps; and clothing items can be stored in a low closed wardrobe, preferably both at the same time. The multifunctional locker not only uses one thing for multiple purposes but also frees up more space for the freedom and comfort [21].

Learning functional area: when children are three years old, they will enter kindergarten to learn knowledge, and learning will become an indispensable part of their life. Therefore, there should be desks, chairs, and other reading and drawing areas in the children's room.

Early childhood is an important period for the development of speech and thinking, and the development of these mental abilities is closely related to the development of intelligence. Through various learning activities, a large amount of specific and rich knowledge and experience and a higher language level can be accumulated for children, which can promote the development of children's thinking ability and improve their cognition [22]. Attention in early childhood is dominated by highly developed unintentional attention, and it is easy to be attracted by bright and novel things. Therefore, the desk can be placed near the window to avoid objects such as beds and dolls that cause unintentional attention of young children; secondly, the height of the seat should be suitable for

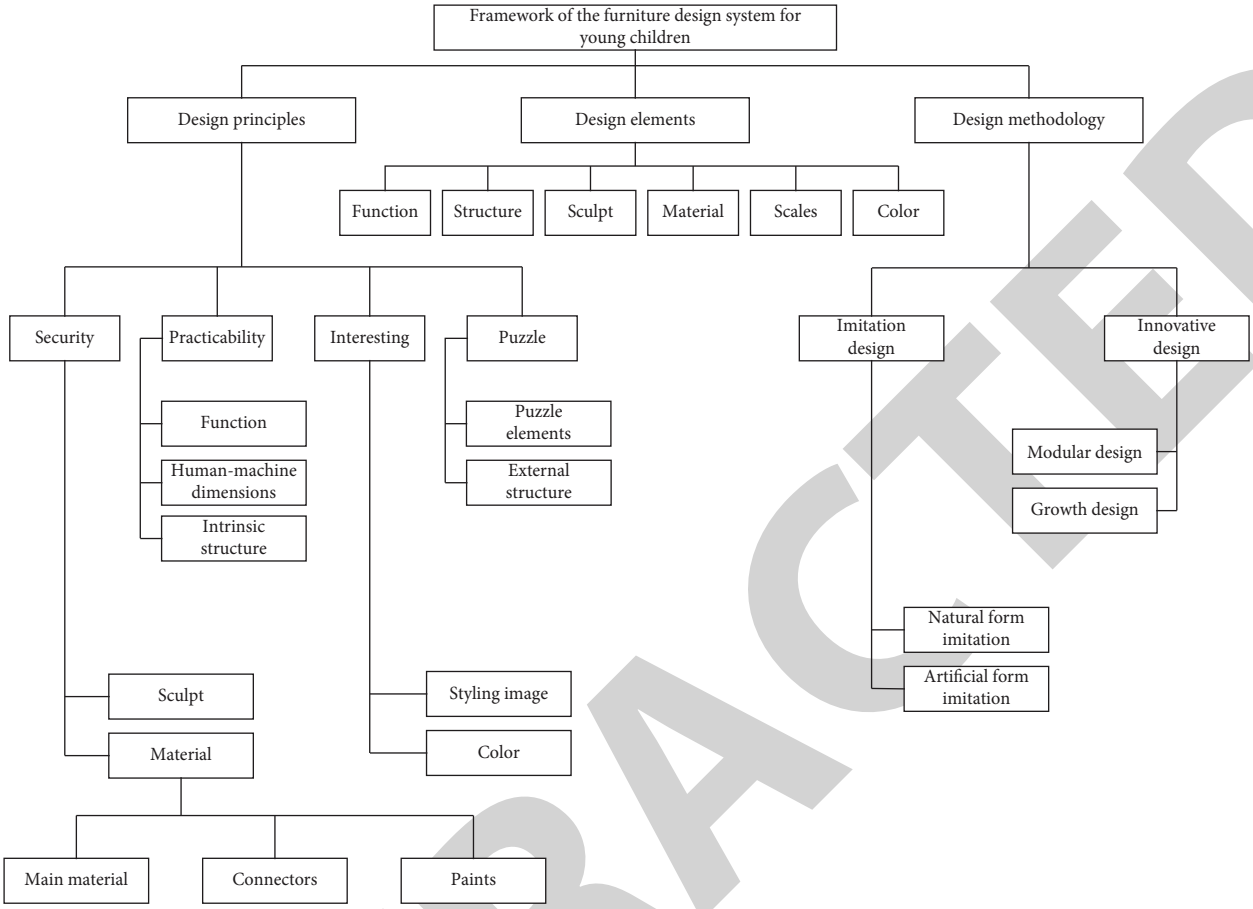

Figure 3: Framework diagram of children's furniture design system.

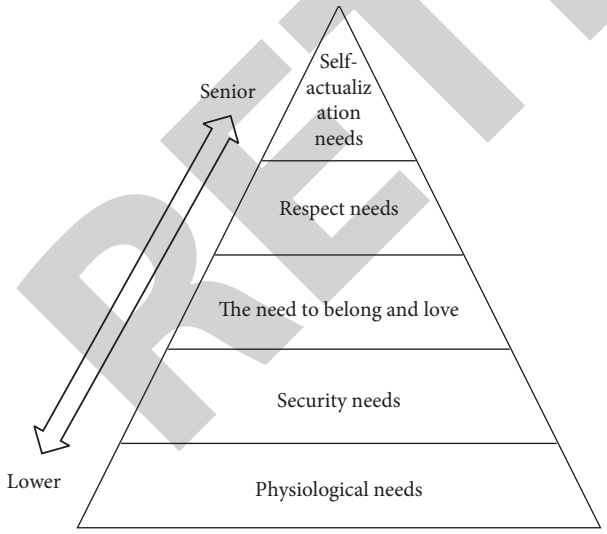

Figure 4: Maslow's hierarchy of needs diagram.

children's physical conditions, which is conducive to the formation of good writing posture and study habits. A table and chair with growth is a good choice. It can not only adjust the height to meet the growing needs of children but also prolong the use of furniture life [22].

Game function area: Mr. Chen Heqin, a famous educator in our country, said: "Children are born active, and play is their life." Indeed, play is their most basic and favorite activity, especially for preschool children, the place to play is an integral part of life, so the extra floor space in the children's room becomes the children's play main venue.

The lively and energetic nature of young children makes the play area as regular and wide as possible to ensure the safety and comfort of the children's play environment and avoid unnecessary bumps and squeezes [23]. The play area must be fun and beneficial so that children can enjoy themselves and promote cognitive development. Therefore, some interesting and educational toys can be prepared for young children, so that they can recognize the world around them while playing. In addition, the play area needs a certain storage space to store children's various toys, such as toy storage boxes can play an excellent role, can be stacked and stored to keep the room in order, and toys can also be classified according to the color of the storage box, which is convenient for children to find. You can also arrange one or two storage boxes with pulleys for children, which can be packed as they play, which can better cultivate children's good habit of timely storage and do-it-yourself [24].

Communication function area: if the indoor space of the children's room is sufficient, a relaxed communication world can be arranged for the children. This space does not need to be deliberately arranged. It can be a few soft cushions placed on the free ground, high and low steps, or a rippling swing. In this happy and comfortable little world, you can communicate happily with your partners, and you can also tell your parents about your heart and bring closer the parent-child relationship.

3. Establishment of Children's Furniture Design System Based on ABAQUS

Because of the guidance of mature theoretical knowledge, furniture designers have designed a large number of furniture products with unique shapes and different styles. The design of children's furniture started late, and the design system of children's furniture still needs to be improved and developed. The practice has proved that only with systematic and perfect theoretical guidance, it is possible to design good furniture products, and the same is true for children's furniture design. Figure 3 shows the frame diagram of the children's furniture design system.

3.1. Design Principles of Children's Furniture

3.1.1. Security. Safety is one of the indispensable design principles in product design, and it is also the first principle of furniture design for children. Products are designed for people, and ultimately serve people, to ensure that people are safe and pleasant in the process of use. If a commodity does not even have the most basic safety guarantee, no matter how good-looking it is, it has no real use value, and there is no market. In recent years, the safety of children's furniture has been frequently exposed on the Internet, TV, newspapers, and other media. The health and safety of children cannot be guaranteed, which makes parents feel confused and worried when purchasing furniture. In view of the safety problems existing in the use of children's furniture, some parents choose to buy it in advance, while others use thick and soft accessories to hide the places with potential safety hazards. The style turned to the safety and environmental factors of furniture to ensure that children grow up in a healthy environment. According to the current market research data, there are certain safety hazards in children's furniture mainly in terms of materials and shapes.

Figure 4 shows the schematic framework of Maslow's hierarchy of needs theory. Maslow puts people's physiological needs at the bottom, indicating that this is the foundation and guarantee of all human activities, and puts safety needs at the penultimate level, that is, on the premise of ensuring that people are fed, clothed, warm, and sheltered well, and people's safety will be the number one need. Scholars such as Xu Deshu have different views on this and especially believe that in today's world, Maslow's hierarchy of needs theory needs to be revised.

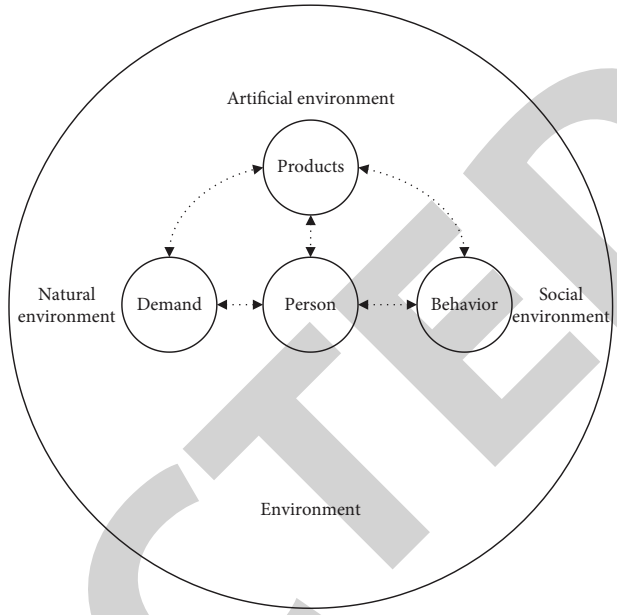

Figure 5: Complete human-machine system.

3.1.2. Practicality. Buying furniture for young children is not only about the aesthetics of the bedroom, but the practicality of the furniture is also very important. Here, practical means that the furniture must have a variety of perfect functions and ensure that the use of the furniture is maximized. For children in early childhood, furniture should first meet its own direct use, meet the physical and psychological needs of children, and be sturdy and durable, children's different use requirements, so as to create a comfortable and convenient environment for learning and life [9]. The practicality of children's furniture is mainly considered from three aspects: function, size, and structure.

3.1.3. Interesting. In addition to meeting people's basic functional needs, furniture should also reflect modern people's needs for visual and psychological aesthetics such as novelty, strangeness, and fun. Children are often curious about interesting things and yearn for beautiful and novel things. We can design interesting furniture according to this characteristic of children. The interesting design of children's furniture, generally through the use of imitation, abstraction, deformation, and other methods, reflects the things in nature and real life into the furniture, so as to satisfy children's curious childlike psychology, thereby bringing more happiness and surprises to children, to create a relaxed and happy living atmosphere. The fun of children's furniture can be reflected in the shape and color.

3.1.4. Intellectual Property. For young children, everything in the world is novel and interesting, and there is a lot of knowledge that they need to learn and master. According to child psychology researchers, 95% of young children can acquire more knowledge and skills in the atmosphere of the play. In early childhood, the main daily activity is games, and the furniture that accompanies them to grow

up will also become part of their entertainment games. It can be seen that furniture also plays a positive role in children's puzzle and inspiration. Early childhood is an important period in the development of various abilities in a person's life. At this time, children have a wide range of interests and hobbies, and their curiosity and thirst for knowledge are strong. It is the best and fastest period to absorb knowledge and learn various skills. Therefore, in the functional design of furniture, while the furniture meets the needs of children and the appearance is beautiful, we can fully consider how to allow children to acquire cognition, develop intelligence, and accelerate various intelligences in the colorful environment stimulation and simple and pleasant furniture operation, and the development of nonintellectual factors, such as attention, observation, spatial imagination, logical thinking, hands-on ability, hand-eye coordination, social skills, and so on. Young children are lively and active, their self-control is still in the developing stage, and they cannot keep a long focus on something or something. Therefore, in the process of furniture design for children, according to this characteristic of children, various knowledge, such as different shapes, colors, and numbers, can be subtly integrated into furniture products, and at the same time, the furniture should be full of interest, so as to stimulate children's interest and arouse their attention, and to cultivate their good habit of love to learn.

3.2. The Application of Ergonomics in Product Design. In product design, the most important point is to make the product match the physiological characteristics of human beings; otherwise, it will cause the product to be unsmooth and even cause harm to people. The significance of ergonomics for product design is as follows: first, it provides human-scale parameters for the consideration of "human factors" in industrial design. The study of ergonomics provides data such as human body structure scale, human physiological scale, and human psychological scale for product design to comprehensively consider "human factors," which can be effectively used in product design. The second is to provide a basis for the functional rationality of "products" in product design: how to optimize the various functions of "products" related to people and create "products" that are in harmony with people's physiological and psychological functions, and it is a new topic in the functional problem of today's product design. The third is to provide design guidelines for considering "environmental factors" in product design: by studying the human body's response and adaptability to various physical factors in the environment and analyzing the impact of environmental factors on the human body's physiology, psychology, and work efficiency. Figure 5 is a schematic diagram of the complete human-machine system.

The definition of safety ergonomics is an emerging discipline that uses the principles and methods of ergonomics to solve the safety problems of the human-machine interface from the perspective of safety. As a branch of the applied discipline of ergonomics, it takes safety as the goal and ergonomics as the condition, an important branch. Human refers to the person who is active, that is, the security subject; machine is a broad sense, which includes labor tools, machines (equipment), labor means and environmental conditions, raw materials, technological processes, and other substances related to people.

Specifically, the task of safety ergonomics is to provide engineering technical designers with reasonable theoretical parameters and requirements for the human body, such as (1) the comfortable range of human work (optimal state); (2) the allowable range of the human body (guarantee work efficiency); (3) the safety range of the human body (minimum and environmental requirements that will not cause harm); and (4) how all safety protection facilities adapt to various human use requirements:

(1) The research scope and content of safety ergonomics mainly include the following aspects:
    (1) Study on the various characteristics of people in the human-machine system. The characteristics of people in the human-machine system refer to the physiological characteristics and psychological characteristics of people. Physiological characteristics include human morphological skills, static and dynamic human scales, human biomechanical parameters, human information input, processing, and output mechanisms and capabilities, and physiological factors for human operational reliability. Psychological characteristics include people's psychological process and personality psychological characteristics, people's psychological state during labor, psychological factors of safe production, and analysis of psychological factors of accidents. These characteristics are the basic theoretical part of safety ergonomics and the main basis for solving safety engineering technical problems.
    (2) Research on the rational distribution of human-machine functions. The main contents of this research are as follows: the respective functional parameters of human and machine, the adaptability and the conditions for exerting their functions, and the methods of human-machine function allocation in various human-machine systems.
    (3) Research on various human-machine interfaces. Human-machine interface is the field in which human-machine contacts or interacts with each other in information exchange or function. The main contents of the control human-machine interface research are as follows: the matching of machine displays device and human information channel characteristics, the matching of machine manipulator and human motion characteristics, and the matching of display and manipulator performance, so as to research different systems. For the tool-like human-machine interface with the largest number in the field of life and production, its applicability and comfort are mainly

studied, that is, how to make it match the shape function, size range, feel, and somatosensory of the human body. For the environment, it mainly studies the impact degree, threshold range and control methods of the physical environment, chemical environment, biological environment, and aesthetic environment of the operation on people. For special environments, it is also necessary to study the human life support system.

(4) Research on operation methods and workload. The research on working methods includes the research on working posture, body position, force, working order, reasonable working tools and work card measuring tools, etc. The purpose is to eliminate unnecessary labor consumption. Workload research mainly focuses on the measurement, modeling (using simulation technology to establish biomechanical models of various operations), and analysis to determine the appropriate workload, work rate, schedule, and study work fatigue and its safety, production relations, etc.

(5) Analysis and research of work space. The main research is on the space range required to ensure safe and efficient operation, including the best viewing area for people, the best working area, the least assembly time, and the minimum safety protection range.

(6) Research on accidents and their prevention. According to a large number of foreign statistics, nearly 80% of accidents are caused by human error. Therefore, the research on accidents and their prevention is not only the foothold of safety ergonomics but also its fundamental purposes such as human factors, human error analysis, and preventive measures.

(2) The application of ergonomics in the design of children's furniture:

In the design of children's room environment, it is necessary to consider its functionality from the perspective of ergonomic "human factors," furniture scale, and visual quality. In terms of furniture scale, children are small and grow quickly, so there are special scale requirements for the choice of children's furniture design. In the design of children's furniture, it should pay attention to the following issues:

(1) The height of the furniture should be suitable for children, so that their hands can reach the things on it. For example, the height of the clothes rail in the wardrobe should be suitable for children to take it.

(2) The doors and drawers of the cabinet should be easy to push and pull, and not too tight; otherwise, the child will lose interest; the size of the drawers in the wardrobe should also be in line with the child's usage habits.

(3) Tables and chairs should conform to ergonomic principles, so that children can develop good sitting and lying habits. The discomfort caused by poor sitting posture and furniture will affect the healthy development of children. Flexibility is also a practical aspect. Children are always growing. When buying children's furniture, we pay attention to whether the furniture can be used continuously. The sustainable use mentioned here does not refer to the service life of a set of furniture, but to meet the needs of children in various growth periods, and will not lose practicality due to age. For example, you can choose desks and chairs that can be adjusted in height to suit the needs of children's growth.

4. Summary

At present, the children's furniture industry is still in an immature stage. The concept of artificial intelligence also needs to be continuously researched and summarized. The application of mature artificial intelligence concepts in children's furniture design is not only conducive to the development of children's physical and mental health but also to the cultivation of their creative ability, hands-on ability, and parent-child interaction, and communication has a certain promotion effect. The application of its concept in the design needs to start from the two aspects of children's body and mind. The design principles proposed in the article must also be based on the standardization of furniture and hardware components. Through the research on children's furniture design, the design theory of artificial intelligence concept provides a theoretical reference for the design of children's furniture. At the same time, in the future design of children's furniture, designers should consider how to improve the quality of children's furniture, reduce the cost of children's furniture that can be grown, and, from the perspective of children, to truly serve children and create for good living environment for them.

Data Availability

The dataset can be accessed upon request to the corresponding author.

Conflicts of Interest

The authors declare that there are no conflicts of interest.

Acknowledgments

The authors thank Science and Technology Research Project of Jiangxi Provincial Department of Education, Research on Green Ecological Furniture Design Practice Based on Ergonomic Data Analysis (no. GJJ217803).

References

[1] M. H. Bornstein, D. L. Putnick, and G. Esposito, "Skill-experience transactions across development: bidirectional relations between child core language and the child's home

Hindawi
Scientific Programming
Volume 2023, Article ID 9761635, 1 page
https://doi.org/10.1155/2023/9761635

Retraction

Retracted: Redistribution of Resources: Sustainable System Mechanisms for Enterprise Migration

Scientific Programming

Received 18 July 2023; Accepted 18 July 2023; Published 19 July 2023

This article has been retracted by Hindawi following an investigation undertaken by the publisher [1]. This investigation has uncovered evidence of one or more of the following indicators of systematic manipulation of the publication process:

(1) Discrepancies in scope
(2) Discrepancies in the description of the research reported
(3) Discrepancies between the availability of data and the research described
(4) Inappropriate citations
(5) Incoherent, meaningless and/or irrelevant content included in the article
(6) Peer-review manipulation

The presence of these indicators undermines our confidence in the integrity of the article's content and we cannot, therefore, vouch for its reliability. Please note that this notice is intended solely to alert readers that the content of this article is unreliable. We have not investigated whether authors were aware of or involved in the systematic manipulation of the publication process.

Wiley and Hindawi regrets that the usual quality checks did not identify these issues before publication and have since put additional measures in place to safeguard research integrity.

We wish to credit our own Research Integrity and Research Publishing teams and anonymous and named external researchers and research integrity experts for contributing to this investigation.

The corresponding author, as the representative of all authors, has been given the opportunity to register their agreement or disagreement to this retraction. We have kept a record of any response received.

References

[1] Y. Wang, Y. Liang, Y. Wang, Z. Li, and C. Guo, "Redistribution of Resources: Sustainable System Mechanisms for Enterprise Migration," *Scientific Programming*, vol. 2022, Article ID 2898460, 17 pages, 2022.

Hindawi
Scientific Programming
Volume 2022, Article ID 2898460, 17 pages
https://doi.org/10.1155/2022/2898460

Research Article

Redistribution of Resources: Sustainable System Mechanisms for Enterprise Migration

Yuan Wang,[1] **Yanxi Liang**,[2] **Yu Wang**,[1] **Zihao Li**,[1] **and Chengjin Guo**[1]

[1]*International Business School, Jinan University, Guangzhou, China*
[2]*School of Finance, Nankai University, Tianjin, China*

Correspondence should be addressed to Yu Wang; twygs@jnu.edu.cn

Received 30 June 2022; Revised 24 July 2022; Accepted 26 August 2022; Published 28 September 2022

Academic Editor: Debo Cheng

The comprehensive reasons for the cross-regional flow of enterprises in their own economy are studied in this paper. Most traditional enterprise migration research focuses on the impact of a single factor. Even the research on the influence of multiple factors often ignores the interaction of various factors. Therefore, this paper proposes and logicalises the "push and pull" mechanism of enterprise migration to address the limitations of previous research. Through bibliometric analysis and investigation, we systematically think about the factors that affect the corporate migration mechanism and improve the Push-Pull Theory. Besides, by deploying a conceptual system dynamics model, this paper explains how various factors affect enterprise migration. In addition, we discussed how to adopt systems thinking to promote the development of emerging economies. We selected and tested 6 companies that migrated in China, and the results are in line with reality. The conclusion supports the theory that systematic thinking and decision-making influence corporate behaviour.

1. Introduction

With the deepening of globalization, cross-border migration and investment of enterprises have become very common [1]. However, due to market orientation or cost orientation, many enterprises choose to migrate within their territory [2]. This situation has been increasing in emerging economies under economic transition in recent years [3–5]. The migration of enterprises in the country affects the flow of capital, personnel, and market structure change [6]. Therefore, it is essential and urgent to study the antecedents of enterprise migration when considering the impact on the overall regional economy.

The existing literature expands our understanding of the antecedents of enterprise migration from a single factor affecting enterprise migration [2, 7–11]. However, as a microeconomic system, the migration of enterprises is not affected by just a single factor but by a series of interactive economic factors [12]. The existing research has not considered the influencing factors of enterprise migration behaviour from the enterprise's overall internal and external environment, which is regrettable. On the one hand, it is common for enterprises to be affected by external factors (such as administrative orders) and internal governance structure, especially in emerging economies [2, 9]. For example, some enterprises in Dongguan City, Guangdong Province, China, have moved to Northwest China due to the combined effect of environmental protection regulation requirements and enterprise human resource costs. On the other hand, relevant studies show that the migration behaviour of enterprises has anthropomorphic characteristics at the same time, which is deeply influenced by corporate symbols such as executives [13]. Especially when the executive power structure is relatively centralized, relocation behaviour is usually affected by the executive team's background. In the existing research, there is a lack of systematic consideration of the above factors [14].

1.1. Overview of Push-Pull Theory. In this study, to narrow the gap between the above theory and practice, we use system dynamics theory and high-level echelon theory for

reference to develop our theoretical model. At the same time, we build a Push-Pull theoretical model of the interaction between internal and external factors and finally explain the motivation system model of enterprise migration behaviour. Specifically, we believe that enterprises' choice of migration behaviour is affected by internal and external factors. The influence of these two parts does not act alone on enterprises' strategic decision-making but interacts with each other. We define this mechanism as the Push-Pull Theory. We explain the Push-Pull Theory model from three aspects: first, the external environment of the enterprise is constantly changing, which promotes or inhibits the migration of the enterprise; second, the internal environment of the enterprise is continually evolving, enabling the enterprise to change or driving the enterprise to maintain the status quo; third, the external environment of the enterprise interacts with the internal information of the enterprise, comprehensively promoting the enterprise to make migration decisions or driving the enterprise to maintain the current business strategy.

1.2. The Logic of Push-Pull Theory. We make a detailed theoretical analysis of the above three aspects. According to the organizational change management theory within the enterprise, there are two forces to promote organizational change and maintain the enterprise's current situation [15, 16]. We believe that the power to encourage organizational change is reflected in the process of enterprise migration, which represents the internal thrust of the enterprise; the strength of maintaining the current situation of the organization is reflected in the process of enterprise migration, which is expressed as the pull force within the enterprise. At the same time, we deduce the deeper mechanism of these two forces and the game process. Based on the high echelon theory, our theory holds that the senior management team, as the direct decision-maker of the enterprise, has a direct impact on the operation of the enterprise according to the signal transmission theory [17]. Therefore, the will of the senior management team plays a vital role in the internal decision-making of the enterprise [18]. Specifically, we believe that the top management team's attachment to the current location of the enterprise is a pull that hinders the migration behaviour of the enterprise [19]. At the same time, the yearning and pursuit of the top management team for the target location of enterprise migration is the thrust to promote the migration behaviour of enterprises. In such a "push-pull" game, enterprises eventually have a preference for whether to migrate internally.

Outside the enterprise, the macroenvironment has a significant impact on the enterprise, and our theory divides this influence into the dual effect of government and market [20]. In terms of the power of market entities on enterprise migration decisions, we use the Push-Pull Theory to supplement the commonly used "cost-profit" orientation theory [21]. Different positions of enterprises in the market affect their decision-making, which is reflected in market share, upstream and downstream bargaining power, and so on [22]. However, the ultimate goal of enterprises is to achieve greater profits. In the market environment, the overall industrial development represents the difficulty for enterprises to obtain profits [22]. With mature development and close to perfect competition, enterprises will face lower entry costs and smaller profits in the market and industry. In unknown or immature markets and industries, enterprises face more significant development costs and higher profits. We believe that cost and profit will become an important reason to drive or hinder enterprise migration [23]. At the same time, we also include exogenous factors not considered in traditional theories, such as the overall market prospect and market public opinion environment, into the Push-Pull Theory [19, 24]. We believe that these exogenous factors will promote or hinder migration with a multiplier effect. The power of "push" and "pull" is more direct in the impact of the government on the decision-making of enterprise migration. The government's influence on enterprises due to compulsory policies such as environmental regulation is the "push" power of enterprise migration [25]. The government's tax preference and financial support are the "pull" power of enterprise migration [26]. The interaction between the push power and pull power constitutes the external constraints of the government on enterprise migration. According to the theory of new structural economics, the influence of government and market on enterprises is not acting alone, their mechanism of action is dynamically related to the social context [27, 28]. We incorporate this relationship into the Push-Pull Theory to explain the game impact of two factors on enterprises. Due to the resource endowment and resource allocation, the market will guide the agglomeration and migration of enterprises. To optimize the allocation of regional economic structure and achieve some noneconomic objectives of the government, the government will use government authority, such as administrative regulation and tax guidance, to enable enterprises to achieve agglomeration and migration [9]. However, when the market fails to realize the authority appeal of the government, the administrative regulations of the government will affect the location choice of enterprises in a way contrary to market forces. For example, high-polluting enterprises in China's coastal areas will migrate to inland areas with high costs and small profits due to environmental protection regulations [29]. Market tax is the cornerstone of government finance.

Furthermore, governments can use market taxation as a powerful tool for environmental regulation [29]. However, when the government's administrative regulation affects industrial development to a certain extent, the government's authority will be weakened. Then the government will reduce the restrictions on companies' migration behaviour. The game between government power and market power will promote or pull the migration of enterprises in the form of environmental impact.

The above two internal and external factors will also produce a "push-pull" effect inside enterprises. Due to the association between the internal senior management team and government personnel, the government has a direct impact on the production factors such as tax preference and

land rental of the enterprise and promotes the internal migration intention of the enterprise to the place where the government is located [30]. Moreover, the market has a more direct impact on the inner mood of the enterprise. First, the market cost and the profits obtained by the enterprise in the current regional market are relatively transparent, and the development prospect of the enterprise's industry in the current regional market is also relatively transparent, which will directly or indirectly promote or stimulate the generation of internal decisions of the enterprise migration. The "narrative economic theory" discusses the influence of market emotion and narration on the people [31, 32]. We extend this influence to enterprise decision-making and improve the Push-Pull Theory. Specifically, we believe that the market public opinion environment will trigger the emotional fluctuation of the enterprise's senior management team. Because the senior management team is not an entirely rational person, this emotional fluctuation will affect the enterprise's decision-making to a certain extent [33]. Therefore, we have made a relatively complete explanation for the Push-Pull Theory.

1.3. Push-Pull Theory and Reality Connection. There are three reasons why this paper chooses China as the actual comparison of the model construction of this paper. These three reasons can prove that our research has practical significance. Cross-border mergers, acquisitions, and corporate migration are becoming more common. This trend is closely related to the development of information technology [34]. The migration trend of multinational enterprises is constantly active and has attracted the attention of academic circles. However, different from the cross-enterprise migration, the cross-regional migration of enterprises in their own country has the same beginning as the migration of multinational enterprises. Still, its internal logical mechanism and migration process is different. As the largest developing country, China has a large geographical area and different degrees of development. The cross-regional migration of enterprises is in line with the goal of global enterprise migration from resource allocation. However, in terms of internal motivation, due to the convergence of Chinese culture, it also meets the characteristics of domestic enterprise migration in a general sense [35]. At the same time, China has a perfect industrial chain, and the domestic migration needs of Chinese enterprises are different from the migration demands of traditional multinational enterprises seeking to embed themselves into the international industrial chain. At the same time, due to the advantages of the whole industrial chain, Chinese enterprises consider more the conditions of government and market economy in migration and make more rational and wise decisions to adapt to the ecosystem. This decision-making consideration is from the enterprise itself, considers the industry and social development, and may contribute. As China's economy is undergoing transformation and enterprises are also experiencing the process from initial development to digital production, this creates much space for enterprises to migrate and seek better development [36, 37]. Some studies show that the migration behaviour of domestic enterprises in China has become active in recent years [2].

Second, China has a vast geographical area, in which the degree of economic development in each region is uneven. At the same time, due to different considerations, local governments provide various policies for different types of enterprises, which creates excellent and low-cost conditions for enterprise migration [38–40]. By observing and analyzing the choice of enterprises under different conditions, it is found that the decision of enterprise migration in different countries has different meanings. For emerging economies such as Southeast Asia, learning from China's experience is helpful to realize the optimal allocation of domestic resources. For developed economies such as the United States, the migration process plays a guiding role in attracting overseas enterprises to return and the migration of domestic enterprises [41–43]. For example, the investment and establishment process of the Chinese enterprise "Fuyao Glass" in the United States is similar to the enterprise migration mechanism studied in this paper. This paper hopes that this research will make academic contributions to the realization of "Reindustrialization" in the United States.

Third, the existing research on the antecedents of enterprise migration mainly focuses on a single factor and few studies on the antecedents of enterprise migration from a comprehensive and dynamic perspective.

1.4. Possible Contribution of Push-Pull Theory. This study has made marginal contributions to the antecedents of enterprise migration and the application of new fields of system dynamics. Firstly, this study constructs a dynamic Push-Pull Theory affecting enterprise migration. In recent years, the literature mainly analyzes the enterprise migration behaviour from the perspective of "benefit-cost" from enterprises. Related to this kind of literature, we focus on enterprises' decision-making under the influence of internal and external environment and find that enterprises' migration behaviour is a dynamic decision-making process rather than a simple element in the market-oriented dynamic decision-making, which is a discovery about enterprises' migration behaviour. Secondly, this research combines the method of bibliometric analysis with systematic thinking. By doing so, we ensure that the internal and external factors affecting enterprise migration are as comprehensive as possible to analyze the migration behaviour of enterprises in line with reality. Finally, this research analyzes the help of systematic thinking and decision-making for the government and enterprises through the systematic discussion of government policies and enterprise policies.

1.5. Introduction to Each Part of the Paper. In order to report our findings, this paper is organized as follows. In the introduction part, our theory is proposed and logicalised. This discussion about our theory is not only based on practical considerations but also based on classical literature and theory. Section 2 conceptualizes our theory in the form of index summary. These selected important indicators come from important literature. Therefore, in this part, this paper reviews the literature related to enterprise migration

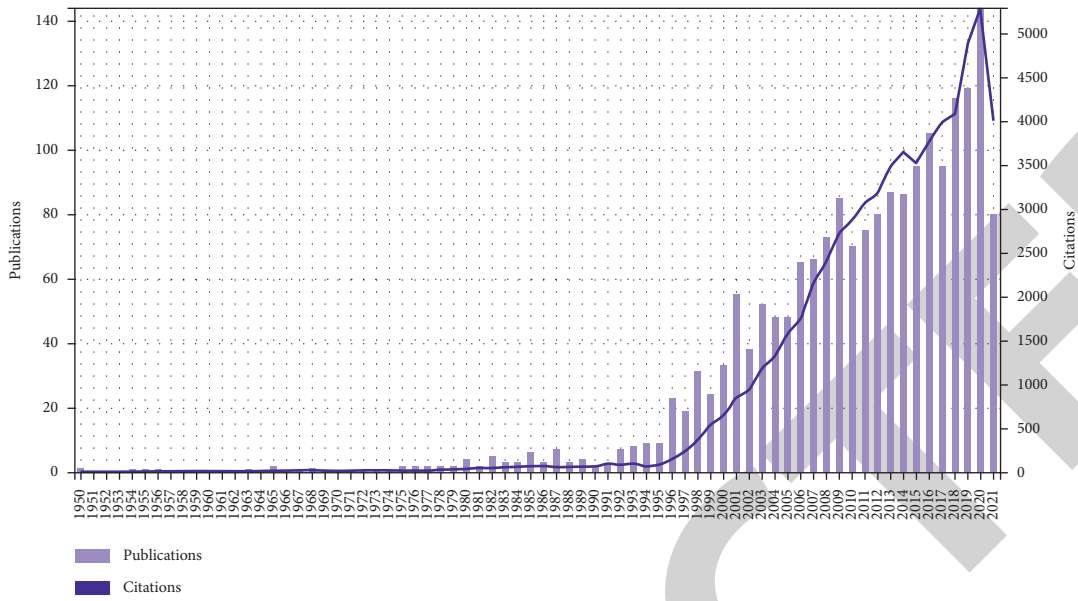

Figure 1: Thematic research trend chart.

behaviour on the basis of literature measurement. Section 3 systematizes our theory through the system dynamics model. The causal relationship between each indicator element is analyzed and displayed in this part. Section 4 discusses our theory in reality. This part discusses the policies that the government may adopt and their impact and how enterprises can make better development by means of relocation. In addition, we discussed how to use systematic thinking to promote the development of emerging economies.

2. Theoretical Background and Literature Review

2.1. Data Collection and Research Trends. This paper takes the core database in the Web of Science as the source for literature retrieval. To ensure the total quantity of literature collection, this paper selects "article" and "conference paper" and searches the literature with the theme of "firm migration." After deleting irrelevant information documents, 1513 core documents with the theme of "firm migration" from 1996 to 2021 were obtained. On this basis, this paper analyzes the research trend of enterprise migration behaviour. Figure 1 shows the research trend of enterprise migration behaviour from 1996 to 2021.

As shown in Figure 1, the trend of enterprise migration behaviour research is on the rise. After 2017, the research enthusiasm continues to rise. In 2020, the number of researches on enterprise migration has increased significantly month on month compared with 2019, indicating that the research on enterprise migration behaviour is currently in the field of hot academic topics.

2.2. Literature Cocitation Analysis. The research network of scientific research citation is the knowledge base of scientific research. The cocitation clustering of Cite-Space literature can reflect the frontier of discipline research. At the same time, the cocitation paper can explain the high academic value of the article. The following literature collection of this paper will start with the factors affecting enterprise migration adopted in the cocitation contribution.

As shown in Figure 2, the cluster is named by the LLR algorithm. Among the cocitation clustering, there are seven categories with more than 25 pieces of literature. We analyzed the seven cluster pieces of literature and collected and sorted the top 100 cited pieces.

2.3. Literature Review and Index Selection. The location of economic activities has been a concern by scholars since its birth. Previous studies mainly provided three methods: neoclassical, behavioural, and institutional [44]. Neoclassical method believes that the location of enterprises for economic activities is based on the strategy of profit maximization and cost minimization. The behavioural approach holds that the motivation of enterprise migration is to better deal with imperfect market information and market uncertainty. Unlike the neoclassical method, the behavioural method believes that the decision-making process of business owners is based on noneconomic factors. The institutional approach holds that, in the process of enterprise location selection, we should not only consider whether the economic environment of the location is suitable for the development of the company but also consider the institutional environment of the location, for example, customers, suppliers, trade unions, regional systems, and government.

At present, the research on the antecedents affecting enterprise migration behaviour generally believes that three groups of main factors affect enterprise migration. They are internal enterprise characteristics, site characteristics, and regional characteristics [12]. Through these three factors and the internal characteristics of enterprises, we consider the site characteristics and regional characteristics of enterprises' moving places and moving places. This research idea is to

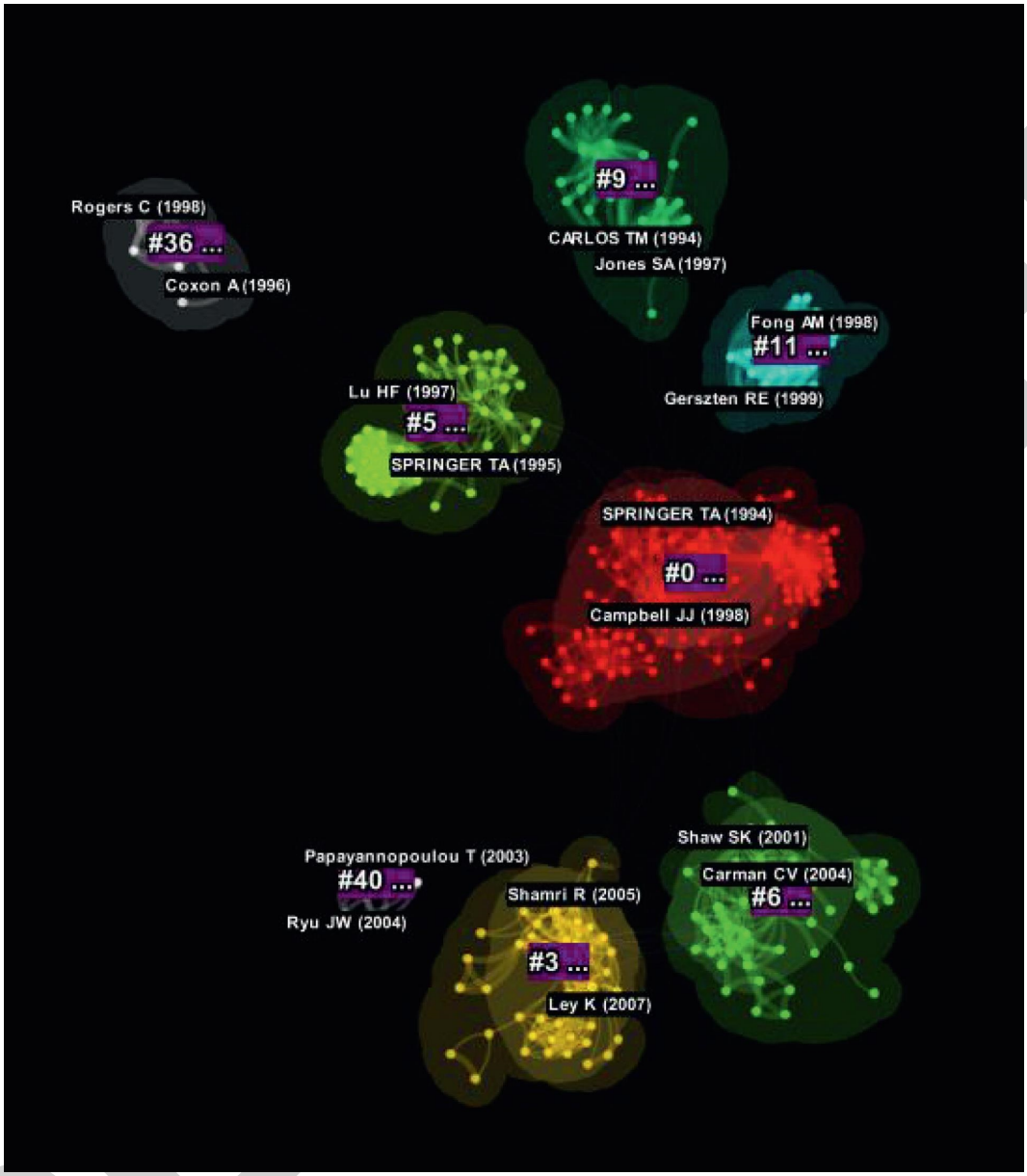

Figure 2: Literature clustering results.

expand institutional methods, which comprehensively consider the influencing factors in enterprise migration.

The neoclassical research viewpoint about how relocated enterprises determine where to move in is generally accepted. Economic factors will affect the migration of enterprises. While integrating the institutional approach into the research, the existing research [11] believes that the policy elements under regional characteristics will affect enterprise migration. For China, an emerging economy with a strong government call, it is more important to consider the impact of policies. Previous studies have shown that the main factor of company relocation is the internal characteristics of the enterprise. Specifically, it is mainly due to the lack of expansion space and the personal factors of business owners [45]. Therefore, when introducing the Push-Pull Theory and considering the internal factors of enterprises, this paper analyzes the internal characteristics of enterprise migration through the interaction and game between considering enterprise development strategy factors and considering enterprise owners' emotional factors.

2.3.1. External: Economic Market Indicators. Firstly, we review the literature and select the indicators related to the economic market in enterprise migration. Some studies show that [46], in the process of overall migration, enterprises will first analyze the current economic level in the region and the economic level in the target region and target to bring their industries into the macroeconomic level to evaluate their industrial development. In the case of enterprise move, the factors that promote the decision to relocate are mainly related to the enterprise's performance

indicators. The consensus that explains the location and relocation of enterprises is that enterprises often look for the most profitable location for relocation and give up their current location. In previous studies [10, 45–49], the relocation behaviour of an enterprise can be conceptualized as a trade-off between the expected cost and expected benefit of the new location compared with the current location. We accept this consideration and fully consider the cost and expected income of the enterprise. In terms of enterprise cost, land cost, raw material cost [50], labor cost, management cost, and transportation and logistics cost [45] in the business process of enterprises are regarded as essential costs in the traditional perspective. We also consider the two costs considered in the new enterprises that attach importance to innovation: the degree of information, technology circulation and the degree of talent activity [12]. When making choices, enterprises should consider the cluster effect caused by the agglomeration of other enterprises. The impact of agglomeration externality on enterprise cost mainly lies in the scale benefits of the cluster allocation of resources and its contribution to the high production process of competitors [10]. We consider the degree of this industrial cluster. Previous studies on industrial agglomeration have been very mature. The positive externalities caused by the spatial concentration of companies in the same industry and the interdependence between companies in different industries are often taken into account in relocation research [51]. Predecessors used various specialization and diversity indicators to capture the externalities caused by agglomeration. See the studies by Groot et al., Mameli et al., and Hong for an overview [52–54]. In previous studies, it is generally believed that the agglomeration has a one-way impact on enterprise decision-making. We believe that the benefits brought by industrial clusters lie in the production cost of enterprises. Due to the accumulation of enterprises, it also reacts to the industry, promotes the full development of the industry and market opening, and improves the degree of complete market competition. In the open market, the market public opinion environment tends to be good [55]. At the same time, due to the increase of industrial enterprise clusters, the cluster externality and strategic interaction between enterprises are increased. For the enterprise, the overall industrial supporting degree is improved, and the market is promising for the industrial market in the region [56].

2.3.2. External: Policy Indicators. We review the literature and select indicators of policy-related influencing factors in the process of enterprise migration. It is found that land rent has an essential impact on enterprise agglomeration and enterprise migration (geographical location spillover). Similarly, land preference is also a form of land rent reduction in China. At the same time, in the development of enterprises, to reduce their costs, they pay great attention to tax and credit (see the studies by de Mooij and Ederveen's literature review in 2003) [57]. In China, due to the different preferential tax policies issued by various regions, the impact on enterprise migration is also different. Most of China's banks and other financial institutions are owned by the state. Their credit payment level is closely related to the local government's policies, which also affects the financial support of enterprises. Worldwide, the openness and transparency of government are essential for enterprises. Recent research on the investment of Chinese enterprises in Cambodia shows that [58] the Cambodian government has an inhibitory effect on the degree of market opening and reduces the desire of enterprises to invest locally due to corruption and other acts. For China, due to the different attitudes of local governments toward investors, they have different administrative efficiency in the face of the relocation demands of relocated enterprises, affecting the operating costs in the process of enterprise relocation and constituting different operating environment characteristics. At the same time, in addition to practical considerations such as space scale [59], the Chinese government has strict restrictions on whether enterprises can enter the local area due to factors such as environmental regulation and total factor productivity. These restrictions together constitute a level playing field in the local market. Generally speaking, the government constructs the hardware environment and cost of local enterprise clusters through investment, credit, land rent, and other dimensions, restricting the migration of enterprises through policy regulation, environmental regulation, access approval, and other methods. These "push" or "pull" play a regulatory role in the development of enterprises. Together, they constitute the policy environment for enterprises to move in and out.

2.3.3. Interior: Strategy. The enterprise's strategy is essential in the choice of location. The role of internal factors is well known in the literature on relocation. In particular, Sleuwaegen and Pennings [50] found that older companies are more integrated into their spatial environment and therefore show less mobility behaviour. Other empirical studies have also confirmed this characteristic [60]. Generally speaking, the essential strategy of enterprises lies in profitability. The profitability of enterprises promotes the growth of enterprises and finally realizes the promotion of enterprise scale. Company size is another crucial factor affecting relocation costs and organizational tasks, which will affect relocation tendency [59, 61, 62]. In particular, because these problems are significant for large companies, the more the employees, the lower the mobility tendency [11]. At the same time, recent studies have found that enterprise size has an important impact on enterprises' overseas investment. After considering the external financial indicators of the enterprise, we found that the enterprise's decision-making has the characteristics of "personification." For example, previous studies found that the tertiary industry companies, especially commercial services, are more "loose" [51, 61, 63, 64]. The degree of enterprise internal control effectively promotes the perfection of the enterprise decision-making process, especially in the significant behaviour of enterprise migration. According to the signal transmission theory, enterprises' perfect information disclosure will release good signals to the market and promote the popularity of enterprises. Due to government policy, environmental protection regulation, market public opinion supervision, environmental

protection, and social responsibility performance are also considered in the enterprise migration behaviour. At the same time, another enterprise feature that affects the relocation choice is the industry [51]. When the enterprise creates and upgrades, it will tend to the area where innovation factors gather, but when the enterprise's industry concentrates on the industrial chain, it will tend to the developed areas of the supply chain [64]. The strategic decisions of the enterprise for different objectives jointly promote the migration decision-making output of the enterprise. We analyze the game of the enterprise's internal strategy through the explicit indicators of the enterprise and deduce the "push-pull" game process.

2.3.4. Interior: Executive Behaviour. In the traditional research on enterprise migration behaviour, it is considered that enterprise migration is entirely rational. However, in the research process of enterprise migration, Chinese scholars bring the branding theory into the research field of vision and find that the migration behaviour of enterprises has a particular location preference. There is evidence that certain aspects of the living environment, such as cultural and natural facilities [65], make specific locations more attractive to companies. We use the Push-Pull Theory to construct this irrational decision-making process within the enterprise. Specifically, the preference of business owners or decision-making teams for particular locations in enterprises is the pull of enterprise migration.

In contrast, the "strangeness" and maladjustment of business owners or decision-making teams to the current environment are the thrust of enterprise migration. Specifically, this location preference is related to the adventurous spirit of business owners and local complexes. According to the high echelon theory, enterprises are affected by the decision-making behaviour of senior managers [66], which is quantified by the characteristics and background of senior managers [67]. In China, an emerging economy, many business owners and managers leave their original areas to seek higher salaries and more promising development prospects. At the same time, the cultural background of different regions has different effects on managers' behaviour and decision-making, which plays an essential role in China's enterprise migration and investment cases. For example, some managers in Fujian Province of China choose to establish manufacturing factories in their birthplace because they can attract the capital of returned or overseas Chinese with their hometown geographical advantages. This influence is primarily reflected in the executive education experience [68]. At the same time, as the current situation, many managers choose to operate in areas away from their original regions, which is related to the managers' adventurous spirit [69]. At present, the overseas background of executives is widely used to quantify the adventurous spirit of executives [70]. In the nonnative place, the enterprise managers pull enterprise migration out of their attachment to the native environment. In the original place, enterprise managers yearn for a better market environment, resulting in the pull of enterprise migration.

The Push-Pull Theory in two different situations constitutes an implicit expression of the internal migration choice of the enterprise. We attribute this expression to the "push-pull" interaction between the "adventure spirit" of the enterprise background and the "local complex" of the enterprise background. On the explicit background expression of enterprise internal decision-making, we mainly build a Push-Pull Theory through the "rationality" and "sensibility" of enterprise managers' decision-making to demonstrate the manager's straight game behind the explicit enterprise decision-making. Precisely, executive power will determine the degree of decision-making in the enterprise, which is determined by the executive team, which is very important for the migration behaviour of the enterprise. The excessive power of the top management team will make managers have overconfidence [71], which will have a short-sighted effect when managers make decisions [72], thus affecting rational judgment [73].

The existing research on relocation decision-making of enterprises generally believes that the academic background of executives encourages executives to take more rational considerations in decision-making output. This allows companies to consider market conditions and corporate social value when making relocation decisions rather than rely on personal preference. The interweaving of rationality and perceptual feelings among the senior management makes the management team face the "push and pull" of internal changes when deciding to relocate. At the same time, we consider that executives' political background, overseas background, and education experience all have an important impact on executives' behaviour. We believe that executives and the government of the region where the enterprise is located have a political background, which will create a pull to hinder enterprise migration due to branding theory and rent-seeking behaviour. However, the political background that senior executives do not have with the target location's local government will push the enterprise migration. This game of "push-pull" forces plays moderating effect in enterprise decision-making. We have also fully considered selecting indicators to ensure that they align with reality and academic reality.

3. Establishment of System Dynamics Simulation Model

3.1. Model Conceptualization. The system boundary is determined in the following ways. The system behaviour of system dynamics research is based on the interaction of internal factors of the system [74]. It is assumed that the system behaviour is not affected by the changes in the system's external environment and is not controlled by internal factors of the system. Therefore, the system boundary is to determine which indicators should be taken into account in the model. Within the boundary, all indicators related to the research conceptual models and variables crucial to emotional problems should be considered; on the contrary, those concepts and variables outside the boundary should be excluded from the model. Our boundary is determined as the composition of the above-screened variables.

Based on determining the boundary, we carry out a causal analysis. The research of system dynamics focuses on

the system dynamics of the self-feedback mechanism. To study the feedback structure of the system, we have to first analyze the relationship between the whole and part of the system, tracing the causality and mutual relationship and reconnecting the variables to form a loop. In system dynamics, we often use a causality diagram to show the loop and analyze the factors and events in the enterprise relocation behaviour with various cause-effect diagrams, flow charts, and tree structure analysis diagrams.

For our system, we use the following causal loop to analyze the relationship between various variables. We believe that the variables we select guide the enterprise to generate behaviour through causality. We divide this guidance process into four subsystems, and their relationship is shown in Figure 3.

In the economic subsystem, there is such a relationship. Land, labor, management, transportation, and logistics costs will hinder the development of the industry to which the enterprise belongs. It should be noted that there are many similar cost factors, and we only select some more important ones for representative demonstration. Similarly, rich raw materials, timely information and technology, promising talents, and an open market can promote the enterprise's industry. As a critical element, innovation ability plays a similar role as a catalyst in a regional economy. Therefore, we will build a separate dimension for the relevant variables to promote enterprise innovation, and it will play a moderating effect. The number of colleges and universities, science and technology investment, and education economy in the region-cost input and the number of employees in high-tech industries can play an essential role in the vitality of industrial innovation. At the same time, the innovation industry will be widely concerned for it is closely related to the market public opinion environment. All these factors are significantly associated with the overall economic level of the region. Regional industrial development level and regional economic level of regional inequality are cause and effect. This relationship is shown in Figure 4.

We express this causal logic according to the following formula:

$$\begin{aligned}
&\text{regional industrial development level}\\
&\quad\longrightarrow \text{degree of market openness}\\
&\quad\longrightarrow \text{positive market public opinion}\\
&\quad\longrightarrow \text{industrial development assistance}\\
&\quad\longrightarrow \text{regional industrial development level},\\
&\text{industrial development assistance}\\
&\quad\longrightarrow \text{degree of industrial cluster}\\
&\quad\longrightarrow \text{degree of industrial supporting}\\
&\quad\longrightarrow \text{regional industrial development level}\\
&\quad\longrightarrow \text{degree of market openness}\\
&\quad\longrightarrow \text{favorable market public opinion}\\
&\quad\longrightarrow \text{industrial development assistance}.
\end{aligned} \tag{1}$$

There is such a relationship with the subsystem of government policies. Due to the outstanding macrocontrol ability of the Chinese government, we pay attention to the policy ability in China. The government will directly impact the production cost of enterprises through land rent preference and tax preference. At the same time, the government will set up an industrial guidance fund. Through credit support, it will affect the technology and finance index of the region, thus affecting the financing cost of enterprises. These measures will be directly reflected indirect or invisible industrial inputs. The result of these industrial inputs is the industrial supporting facilities in the government's location, thus affecting the overall production infrastructure and environment. The government sets negative clearing for enterprises in some industries. It has a poor business environment due to its corruption and rent-seeking, which hinders the improvement of the fair competition environment index. Government administrative efficiency plays a regulatory role in this cause and effect. This relationship is shown in Figure 5.

We describe the causal logic of the policy dimension according to the following formula:

$$\begin{aligned}
&\text{business environment index}\\
&\quad\longrightarrow \text{fair playing field index}\\
&\quad\longrightarrow \text{administrative efficiency}\\
&\quad\longrightarrow \text{the level of improvement of regional policies}\\
&\quad\longrightarrow \text{business environment index},\\
&\text{business environment index}\\
&\quad\longrightarrow \text{tax preference}\\
&\quad\longrightarrow \text{government inverstment in industrial parks}\\
&\quad\longrightarrow \text{government industrial supporting facilities}\\
&\quad(\text{degree of perfection}) \longrightarrow \text{infrastructure index}\\
&\quad\longrightarrow \text{regional policy supporting index}\\
&\quad\longrightarrow \text{the level of improvement of regional policies}\\
&\quad\longrightarrow \text{business environment index}.
\end{aligned} \tag{2}$$

Internally, we also consider the enterprise strategy subsystem. From a financial perspective, enterprise profitability will directly affect enterprise growth. The enterprise growth process is reflected in the enterprise's existing scale, and the enterprise scale supports the enterprise's investment strategy. These investment processes affect the enterprise's spatial distribution strategy, such as the establishment of branches. At the same time, in the capital market, due to the theory of signal transmission, the investment strategy of enterprises also interacts with the popularity of enterprises. The interaction between enterprise internal control and governance and enterprise popularity affects enterprise information disclosure in the explicit social dimension. The existing studies generally believe that enterprises with better information disclosure systems will better fulfil their social responsibilities. In space, on the other hand, corporate behaviour is closely related to social responsibility and social value. This relationship is shown in Figure 6.

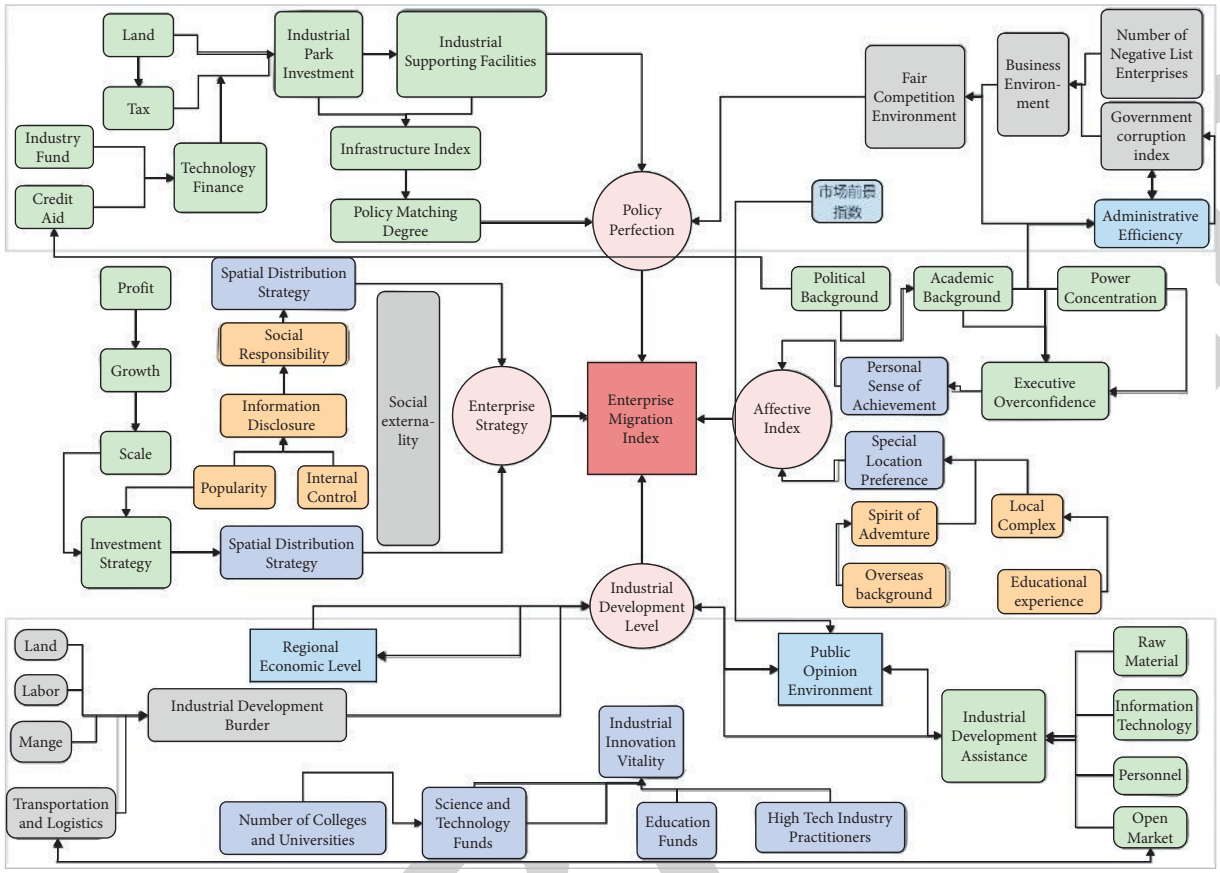

Figure 3: Model causality diagram.

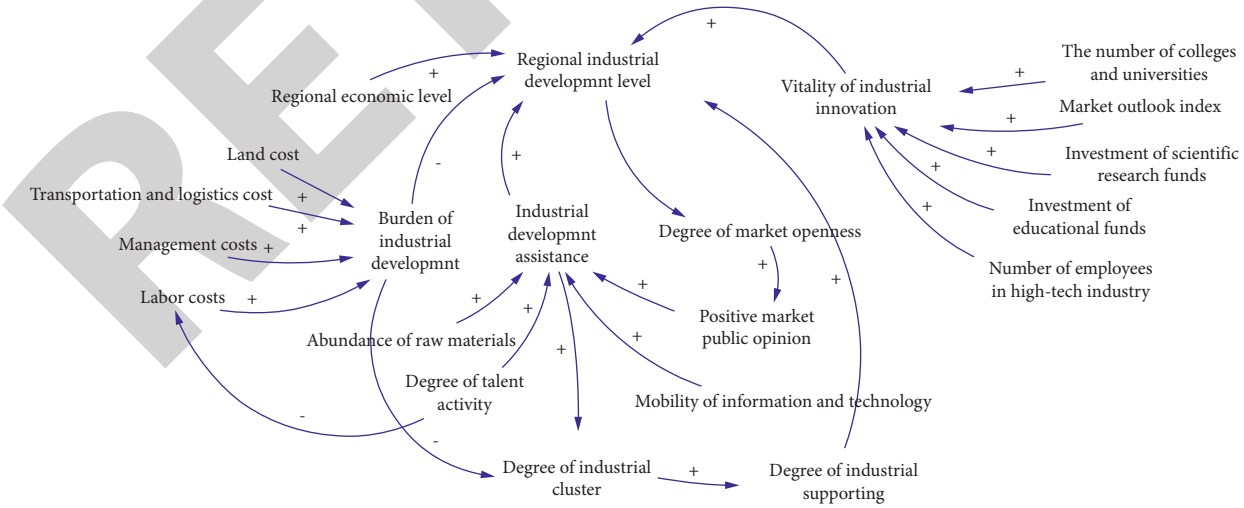

Figure 4: Economic factors.

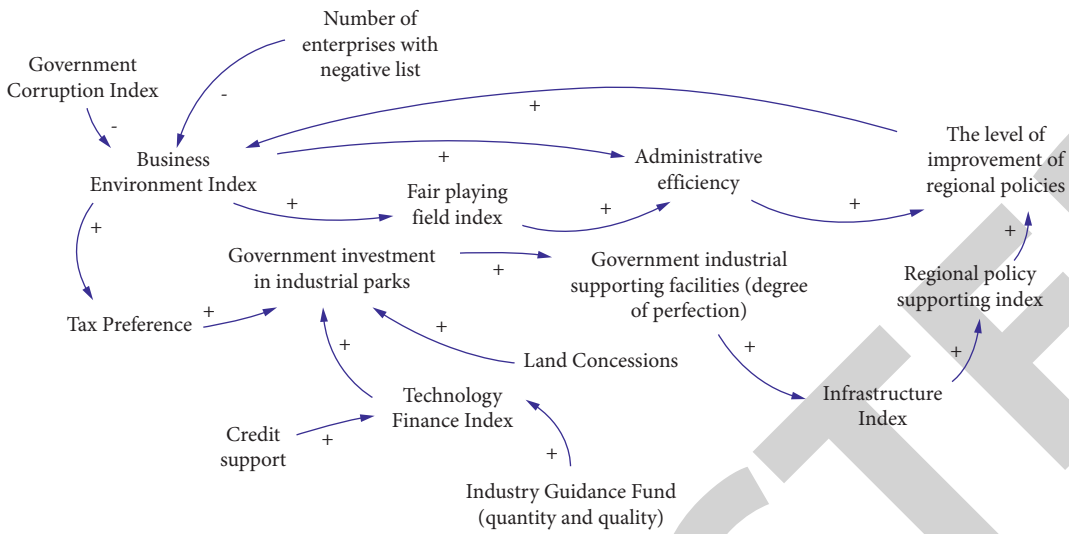

Figure 5: Policy factors.

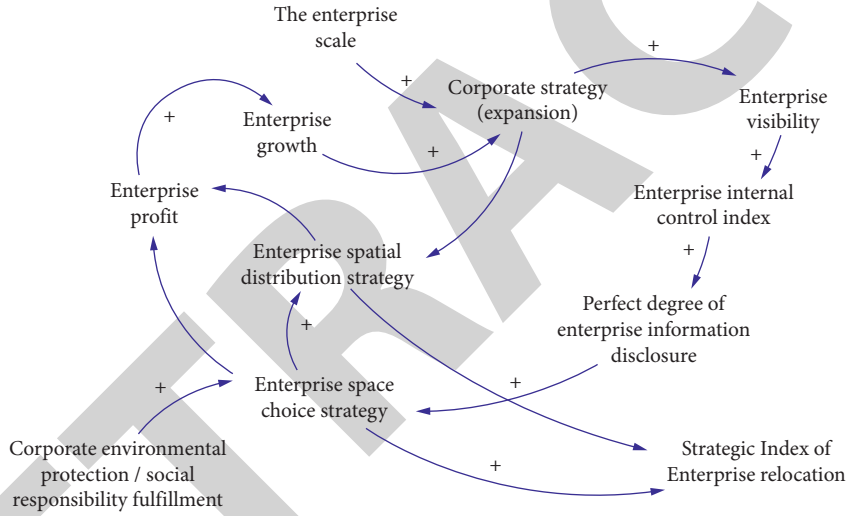

Figure 6: Enterprise strategy.

The internal logic of the enterprise has the following causal relationship:

enterprise growth
⟶ enterprise strategy (expansion)
⟶ enterprise visibility
⟶ enterprise internal control index
⟶ perfect degree of enterprise information disclosure
⟶ enterprise spatial choice strategy
⟶ enterprise spatial distribution strategy
⟶ enterprise profit
⟶ enterprise growth. (3)

After considering the completion of the external subsystem of the enterprise, we analyze the causality of the internal subsystem of the enterprise's migration. The political background of senior executives will affect the land preference and tax preference given to enterprises by the local government. Due to the unique background of Chinese culture, the political background, academic background, and centralized power of senior executives will affect the overconfidence of senior executives. This kind of self-confidence affects executives' sense of personal achievement. At the same time, we also consider the growth background of executives. Executives' overseas background and educational experience will affect their extroversion and willingness to return, thus affecting executives' particular location preferences. This relationship is shown in Figure 7.

The main causal loops are shown in the following formula:

$$\text{local complex} \longrightarrow \text{adventurous spirit}. \quad (4)$$

Based on this, we constructed the causal circuit diagram as shown in Figure 8.

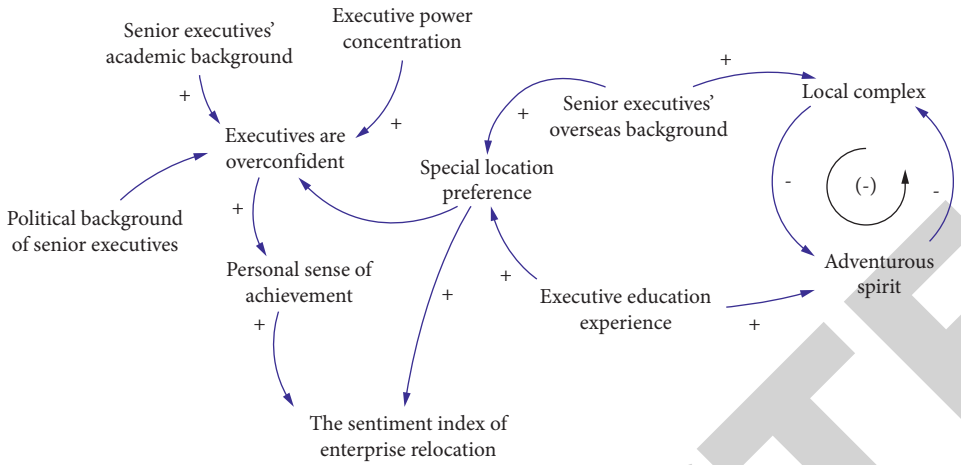

Figure 7: Enterprise emotion.

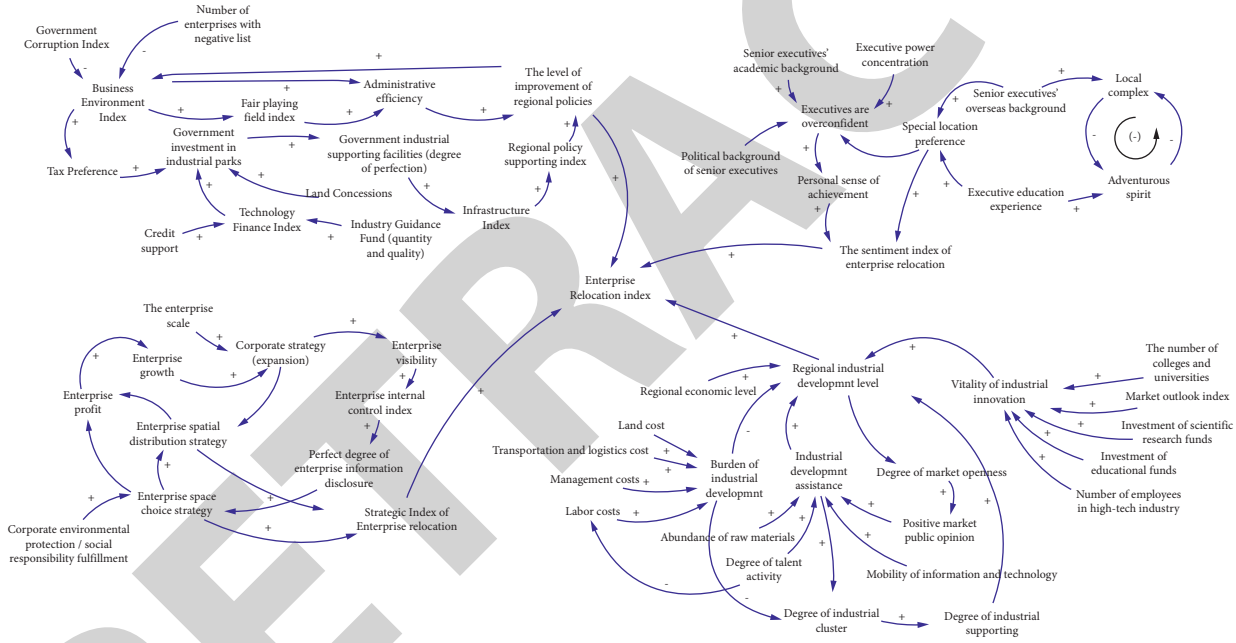

Figure 8: Total cause and effect diagram.

3.2. Model Parameterization. There are five kinds of system dynamics equations, namely, horizontal equation (L), rate equation (R), auxiliary equation (a), constant equation (c), and initial value equation (n). The horizontal equation and rate equation are the core of the model.

Horizontal equation (L) is the basic equation of system dynamics; that is,

$$L_{(t)} = L_{(0)} + \int_0^t \left(\sum R_{in}(t) - \sum R_{out}(t) \right) dt. \quad (5)$$

In the dynamic formula, $L_{(t)}$ represents the value of the quantity L in the state at time t. $L_{(0)}$ represents the initial value, and $\sum R_{in}(t)$ represents the input flow of the state variable. $\sum R_{out}(t)$ represents the output stream of the state variable. $\sum R_{in}(t) - \sum R_{out}(t)$ represents the net inflow of the state variable.

The above integral equation shows that the value of the state variable at time t is equal to the initial value of the state variable plus the accumulation of net flow change over time. What needs to be explained here is that we mainly consider the characteristics of such variables when setting variables belonging to flow and interface data.

In addition, the rate equation is expressed as a function of state variables and constant.

$$R = f(L, \text{constant}). \quad (6)$$

The purpose of designing a system flowchart according to the relationship between various factors in the system of enterprise relocation behaviour is to reflect the characteristics and characteristics of different variables that cannot be reflected in the causal relationship of the system. The flow

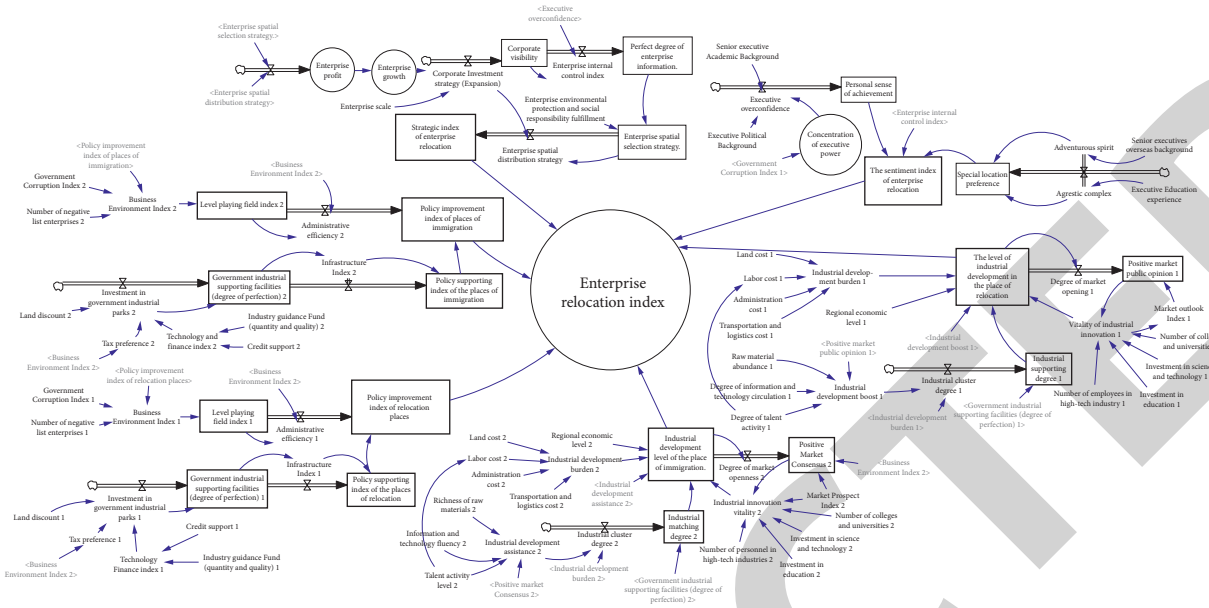

Figure 9: Flowgraph.

diagram makes the internal mechanism of the system clearer, further quantifying the variables in the causality diagram and finally realizing the simulation of enterprise relocation behaviour. The flow diagram of the simulation system is shown in Figure 9.

The model successfully passes the conventional system dynamics confidence-building tests using the practical guide provided by Barlas [74]. We also analyze the six enterprises from China through the above model to ensure that our model is in line with reality. These companies have the same characteristics: they have migrated. At the same time, we compared their simulation index with the actual situation and found that this model can better simulate the process of enterprise relocation.

4. Discussion

This part discusses the policies that the government may adopt and their impact and discusses how enterprises can make better development by means of relocation. In addition, we discussed how to use systematic thinking to promote the development of emerging economies. As a supplement, we analyze the possible contributions and shortcomings of this paper. Future research is also planned.

4.1. Government Policy

4.1.1. Government Policy A: Administrative Convenience. In our theory, we systematically consider the government's impact on administrative facilitation given to enterprises. Local governments are easier to attract enterprises to relocate because administrative facilitation such as preferential land rent and credit support is given to firms. The case of Policy A is verified in Case 1. However, the reality is that enterprises often relocate to the local area due to administrative convenience and then relocate out of the area again due to the low degree of market opening or other policy disadvantages. We contend that other disadvantages in the system offset the attractiveness of administrative convenience for firms in such cases.

The government's effective measures should combine more significant attraction with more vital constraint conditions for enterprises. Specifically, the government can transfer land rights with low added value. For example, the case of Guangdong Province, China, shows that the government transferred the right to develop unexplored islands far from cities to high-tech enterprises. The government has given away land with low value-added. Enterprises have obtained almost zero cost of production land, a win-win situation for both parties. Once the enterprises invest in this place, their desire to relocate is reduced because of sunk costs. Conditional and substantial credit support works equally well, and such policies can reduce the relocation behaviour of enterprises.

4.1.2. Government Policy B: Environmental Regulation. Governments have imposed environmental regulations on high-polluting enterprises within their borders to protect the environment in emerging economies. Such regulations encourage companies to move out and find lower-cost locations for production. For more developed regions, such inlaws and policies can help themselves achieve environmental protection and industrial structure optimization. However, it would be an environmental disaster for the rest of the economy. The whole economy is a dynamically adjusted system. In our theory, such restrictive environmental regulations reduce the openness of regional markets. It will reduce the attractiveness of the business and increase the cost of doing business.

Effective government measures should combine environmental regulation with administrative facilitation. It

promotes its sustainable development while ensuring that the overall utility of the enterprise remains roughly unchanged. To be specific, the government should regulate the pollution emission of enterprises by-laws or policies but, at the same time, provide credit support to enterprises to help them upgrade equipment to achieve sustainable production. This policy can achieve higher efficiency and more sustainable production of enterprises and avoid the relocation of enterprises.

4.1.3. Discussion: Systematically Building Policy Systems for Sustainable Development. Theory suggests that policy alone plays a small role in the circular loop. Changes in other factors often offset it. Due to irrational policies, it sometimes has the opposite effect to that intended by policy settings. Real cases from China validate this view.

Therefore, the systematic construction of the policy system should be emphasized. In the overall system that affects enterprise migration, policies can help enterprises achieve sustainable development in the case of realizing the coordination of multiple policies. This development is not just good for business. It also helps local governments develop sustainable and economic requirements. In reality, such systematic policy system construction requires policymakers to systematically consider the interaction mechanism between various policies and requires that policy implementers engage in systematic policy practices geared toward sustainable development goals.

4.2. Enterprise Strategy

4.2.1. Enterprise Policy A: Market Orientation. When an enterprise is first established, it often does not reasonably estimate its development prospects. This leads to obstacles to market expansion after a certain point of development. This encourages companies to move closer to the market. However, with the increase in informatization, the time lag between enterprise decision-making in emerging economies has decreased. At the same time, with the improvement of infrastructure and the reduction of logistics and transportation costs, the distance from the market is no longer the primary consideration for enterprises to consider when facing the market. However, there is undeniable that enterprises tend to gain more significant market opportunities after relocating to the region close to the market.

Enterprises should also pay attention to the following factors when making market-oriented migration decisions. First, enterprises need to estimate the current location and destination costs reasonably. Such cost estimation should include the direct cost and consider the implicit cost such as corporate reputation and cultural adaptation. All costs will have a comprehensive effect on the enterprise and reduce the development expectation. Second, companies should consider the sustainability of migration destination development. For example, large cities have a high steel demand, but they are more likely to introduce environmental regulations. Then iron and steel enterprises to migrate for this unsustainable production should be estimated.

4.2.2. Enterprise Policy B: The Game between Cost and Innovation. When making migration decisions, enterprises often grapple with low cost or potential innovation. Due to the accumulated advantages of the current location of the enterprise, the production cost of the enterprise is low. However, enterprises have less incentive to innovate products. On the contrary, although the production cost of enterprises in some highly developed cities is higher, the innovation potential of enterprises is higher due to the rich resources and fierce competition. For the current development of enterprises, enterprises may choose the current location to reduce costs. However, enterprises can only achieve sustainable innovation.

Enterprises need to consider many aspects when migrating. In the perfect competitive product market, enterprises focus on innovation to achieve sustainable development. However, the enterprise's product innovation should consider factors such as its current financial status and the vitality of the internal personnel structure of the enterprise. These factors are crucial to the success of an enterprise's innovation. In the oligopoly product market, enterprises can realize market barriers only by cost priority strategy. For example, Coca-Cola's global localization production strategy and cost control strategy have promoted Coca-Cola's monopoly position.

4.2.3. Discussion: Systematic Decision-Making for Sustainable Development. The migration decision of an enterprise has an important systemic connection with the enterprise itself and the external environment of the enterprise. In the process of decision-making, enterprises can adopt systematic thinking to make decisions on behaviour. This kind of systematic decision-making does not only consider factors that affect the enterprise. A reasonable assessment of the company's own conditions should be made to analyze the impact of the interaction of the company's decision-making with external conditions. The impact of this feedback on the company itself should also be considered. In reality, companies often pay too much attention to external factors and neglect their own internal environment. This neglect causes the enterprise to affect the internal structure of the enterprise after its decision-making behaviour, thus causing unsustainable consequences for the enterprise.

Based on the above, companies should systematically think and make decisions when making migration decisions and other major business behaviours. This kind of systematic decision-making requires enterprises to embed themselves in the overall economic system and rationally analyze the impact and secondary impact of decision-making.

4.3. Theoretical Contributions. The possible marginal contributions of this paper in theory and practice mainly include the following two aspects. First, in terms of theoretical innovation, we systematically put forward the Push-Pull Theory for the internal logical motivation of enterprise migration behaviour. We supplement existing research on enterprise migration behaviour from dynamic evolution and factor game theoretical perspectives. In the existing studies,

the promotion and pull of factors are put forward for the migration behaviour of enterprises to a certain extent [75–79]. However, this theory is scattered and analyzed by fewer factors. Therefore, we combine the relatively mature factors affecting enterprises in academia with reality, incorporating the essential decision-making factors into the enterprise migration game and integrating the enterprise migration process into the factor game of the overall macroenvironment. We express it concisely in the form of "push-pull," which is a powerful supplement to the improvement of the theory of enterprise migration. At the same time, in addition to the systematic evolution analysis of the explicit factors of enterprise migration, we also include the internal implicit factors affecting enterprise migration into the research theory for more comprehensive research on enterprise migration.

The above factors have essential research value under the background of the optimal allocation of the global industrial chain and the reindustrialization of developed countries. In practical considerations and concerns, our research provides a theoretical basis for the government and the market to analyze enterprise migration's internal motivation and logical mechanism. This Push-Pull Theory helps the government to optimize the regional industrial layout and enterprises to make reasonable decisions through systematic thinking.

4.4. Practical Implications. The possible practical contributions of this paper are mainly in the following three aspects. First of all, this paper proposes systematic thinking and policy systems for emerging economies that hope to complete economic transformation through enterprise migration. Secondly, this paper puts forward methods and cases of systematic thinking about how companies can achieve sustainable development through migration. Finally, this paper gives realistic cases and systematic countermeasures to the behaviour mechanism of the economic system for microsubjects.

4.5. Future Research Directions. Further research can be carried out from the following two aspects: first, the expansion and improvement of the enterprise migration system, such as adding more dimensions, and second, the relocation behaviour of enterprises in other countries with unique political and economic conditions, which are valuable to study to promote the universality of the system structure.

5. Conclusions

With the development and transformation of emerging economies, many companies are facing an urgent need for migration. Although there are many explanations for corporate migration behaviour in existing studies, they all ignore the systemic reasons and systemic effects of corporate decision-making. This research attempts to explain the behavioural mechanism and impact of corporate migration through systematic thinking.

This paper constructs a Push-Pull theoretical model of the interaction of internal and external factors in the enterprise and finally explains the motivation of the enterprise's migration behaviour. Specifically, the choice of migration behaviour of enterprises is affected by internal and external factors. The influence of these two parts does not act on the strategic decision-making of the enterprise alone but interacts. We define this mechanism as the Push-Pull Theory. We explain the Push-Pull Theory from three aspects: (1) The external environment of the company (economic environment and government regulations) is constantly changing, which promotes the migration or stay of the company. (2) The internal environment of the company (senior management's emotions and management decision-making) is constantly changing, which promotes enterprise reform or drives the enterprise to maintain the status quo. (3) The external environment of the enterprise interacts with the internal information, comprehensively promoting the enterprise to make a migration decision or pulling the enterprise to maintain the current business strategy. This paper conceptualizes the theoretical mechanism and summarizes the influencing factors of these three aspects through bibliometric analysis and the actual situation. Besides, it systematizes these factors and explains the causal feedback of the enterprise migration mechanism by constructing a system dynamics model. Furthermore, it discusses the Push-Pull Theory in the real world. Through a systematic and logical analysis of the policy impact of the government and enterprises, we reiterated the importance of systematic thinking in the process of sustainable economic development.

The migration behaviour of enterprises is closely related to the overall economic system. The upgrading of the industrial structure and sustainable development of emerging economies requires not only attention to current resources but also consideration of the overall impact of changes in the location of enterprises. The challenges ahead are huge if we want companies and economies to develop efficiently. This trend requires systematic thinking and practice.

Disclosure

Any errors of omission and/or commission in this version of the paper are the sole responsibility of the authors.

Data Availability

The dataset can be accessed upon request.

Conflicts of Interest

The authors declare that they have no conflicts of interest.

Acknowledgments

The authors would like to thank Xiaohui Tao and Junbin Fang for their thoughtful comments on earlier drafts of this paper and Jiacong Wu for his careful examination. This research was funded by the National Natural Science Foundation of China under Grant no. 71772075 and

7217020185; Ministry of Science and Technology National Foreign Technical Program, no. G2021199032L; National Social Science Major Preresearch Project of Jinan University, no. 12622204.

References

[1] S. Ali, Z. Yusop, S. R. Kaliappan, and L. Chin, "Dynamic common correlated effects of trade openness, FDI, and institutional performance on environmental quality: evidence from OIC countries," *Environmental Science and Pollution Research*, vol. 27, no. 11, pp. 11671–11682, 2020.

[2] T. Tang, Z. Li, J. Ni, and J. Yuan, "Land costs, government intervention, and migration of firms: the case of China," *China Economic Review*, vol. 64, Article ID 101560, 2020.

[3] G. Beyer and R. P. Shaw, "Migration theory and fact: a review and bibliography of current literature," *International Migration Review*, vol. 10, no. 1, p. 107, 1976.

[4] S. Grimes, "Residential segregation in Australian cities: a literature review," *International Migration Review*, vol. 27, no. 1, p. 103, 1993.

[5] O. Hart, "Thinking about the firm: a review of daniel spulber's the theory of the firm," *Journal of Economic Literature*, vol. 49, no. 1, pp. 101–113, 2011.

[6] A. Chen, T. Dai, and M. D. Partridge, "Agglomeration and firm wage inequality: evidence from China," *Journal of Regional Science*, vol. 61, no. 2, pp. 352–386, 2020.

[7] G. Bettin, P. Bianchi, F. Nicolli, L. Ramaciotti, and U. Rizzo, "Migration, ethnic concentration and firm entry: evidence from Italian regions," *Regional Studies*, vol. 53, no. 1, pp. 55–66, 2018.

[8] J. P. Broschak, E. S. Block, S. Koppman, and I. Adjerid, "Will we ever meet again? The relationship between inter-firm managerial migration and the circulation of client ties," *Journal of Management Studies*, vol. 57, no. 6, pp. 1106–1142, 2019.

[9] R. E. Owens and P.-D. G. Sarte, "Analyzing firm location decisions: is public intervention justified?" *SSRN Electronic Journal*, 1999.

[10] T. Niedomysl, J. Källström, S. Koster, and J. Östh, "Interregional migration of business owners: who moves and how does moving affect firm performance?" *Regional Studies*, vol. 53, no. 4, pp. 503–516, 2019.

[11] J. DijkDijk and P. H. PellenbargPellenbarg, "Firm relocation decisions in The Netherlands: an ordered logit approach," *Papers in Regional Science*, vol. 79, no. 2, pp. 191–219, 2005.

[12] K. Kronenberg, "Firm relocations in The Netherlands: why do firms move, and where do they go?" *Papers in Regional Science*, vol. 92, no. 4, pp. 691–713, 2013.

[13] D. J. A. Phillips, "A genealogical approach to organizational life chances: the parent-progeny transfer among silicon valley law firms, 1946-1996," *Administrative Science Quarterly*, vol. 47, no. 3, pp. 474–506, 2002.

[14] M. Kroll, B. A. Walters, and P. Wright, "Board vigilance, director experience, and corporate outcomes," *Strategic Management Journal*, vol. 29, no. 4, pp. 363–382, 2008.

[15] B. Burnes, "Complexity theories and organizational change," *International Journal of Management Reviews*, vol. 7, no. 2, pp. 73–90, 2005.

[16] N. M. Alsharari, "Management accounting and organizational change: alternative perspectives," *International Journal of Organizational Analysis*, vol. 27, no. 4, pp. 1124–1147, 2019.

[17] J. Kim, "Extending upper echelon theory to top managers' characteristics, management practice, and quality of public service in local government," *Local Government Studies*, vol. 22, pp. 1–22, 2021.

[18] E. Kremp and E. StößStöß, "Estimating the Borrowing Behavior of French and German Firms. An Econometric Analysis/Verschuldungsverhalten französischer und deutscher Unternehmen. Eine ökonometrische Analyse," *Jahrbucher für Nationalokonomie und Statistik*, vol. 221, no. 5-6, pp. 620–647, 2001.

[19] S. Bensassi and L. Jabbour, "Beyond experience and capital. Is there a return to return migration?" *Journal of Development Studies*, vol. 58, no. 4, pp. 730–751, 2021.

[20] D. Nehring and Y. Hu, "From public to commercial service: state-market hybridization in the UK visa and immigration permit infrastructure, 1997-2021," *British Journal of Sociology*, vol. 72, no. 5, pp. 1325–1346, 2021.

[21] R. J. Kauffman, D. Lee, J. Lee, and B. Yoo, "A hybrid firm's pricing strategy in electronic commerce under channel migration," *International Journal of Electronic Commerce*, vol. 14, no. 1, pp. 11–54, 2009.

[22] C. Viet Nguyen and Q. Duy Phung, "Does firm agglomeration induce migration? Evidence from vietnam," *Economics Bulletin*, vol. 40, p. 3325, 2020.

[23] M. Hedfeldt and M. Lundmark, "New firm formation in old industrial regions - a study of entrepreneurial in-migrants in Bergslagen, Sweden," *Norsk Geografisk Tidsskrift - Norwegian Journal of Geography*, vol. 69, no. 2, pp. 90–101, 2015.

[24] R. Martin and D. Radu, "Return migration: the experience of eastern Europe1," *International Migration*, vol. 50, no. 6, pp. 109–128, 2012.

[25] L. Zhao, Z. Yu, and Y Onuma, "A theory of mutual migration of polluting firms," *Canadian Journal of Economics/Revue canadienne d'<html_ent glyph="@eacute;" ascii="e"/>conomique*, vol. 38, pp. 900–918, 2005.

[26] J. Yang and C. Zhou, "Does industrial clustering mitigate the sensitivity of firm relocation to tax differentials? The role of financing," *Finance Research Letters*, vol. 40, Article ID 101681, 2021.

[27] J. Y. Lin, "New structural economics: the third generation of development economics," *Asian Education and Development Studies*, vol. 9, no. 3, pp. 279–286, 2019.

[28] J. Cameron, "Development economics, the new institutional economics and NGOs," *Third World Quarterly*, vol. 21, no. 4, pp. 627–635, 2000.

[29] M. Li, W. Du, and S. Tang, "Assessing the impact of environmental regulation and environmental co-governance on pollution transfer: micro-evidence from China," *Environmental Impact Assessment Review*, vol. 86, Article ID 106467, 2021.

[30] S. Osterloh and F. Heinemann, "The political economy of corporate tax harmonization - why do European politicians (Dis)Like minimum tax rates?" *SSRN Electronic Journal*, 2008.

[31] G. Ferguson-Cradler, "Narrative and computational text analysis in business and economic history," *Scandinavian Economic History Review*, vol. 25, pp. 1–25, 2021.

[32] M. Mordhorst and S. Schwarzkopf, "Theorising narrative in business history," *Business History*, vol. 59, no. 8, pp. 1155–1175, 2017.

[33] R. Mannion, S. Harrison, R. Jacobs, F. Konteh, K. Walshe, and H. T. Davies, "From cultural cohesion to rules and competition: the trajectory of senior management culture in English NHS hospitals, 2001-2008," *Journal of the Royal Society of Medicine*, vol. 102, no. 8, pp. 332–336, 2009.

[34] N. Crespo and M. P. Fontoura, "Determinant factors of FDI spillovers - what do we really know?" *World Development*, vol. 35, no. 3, pp. 410–425, 2007.

[35] K. Li, "Convergence and de-convergence of Chinese journalistic practice in the digital age," *Journalism*, vol. 19, no. 9-10, pp. 1380–1396, 2018.

[36] J. Husár and D. Dupláková, "Material flow planning for bearing production in digital factory," *Key Engineering Materials*, vol. 669, pp. 541–550, 2015.

[37] J. C. Aurich, C. Steimer, H. Meissner, and N. Menck, "Einfluss von Industrie 4.0 auf die Fabrikplanung/Impact of Industry 4.0 on factory planning - effects of the special characteristics of cybertronic production systems on factory planning," *Wt Werkstattstechnik Online*, vol. 105, no. 04, pp. 190–194, 2015.

[38] L. Chen and B. Naughton, "An institutionalized policy-making mechanism: China's return to techno-industrial policy," *Research Policy*, vol. 45, no. 10, pp. 2138–2152, 2016.

[39] T. Kenderdine, "China's industrial policy, strategic emerging industries and space law," *Asia & the Pacific Policy Studies*, vol. 4, no. 2, pp. 325–342, 2017.

[40] C. Scartascini and M. Tommasi, "The making of policy: institutionalized or not?" *American Journal of Political Science*, vol. 56, no. 4, pp. 787–801, 2012.

[41] M. Dietrich and B. Z. Rumer, "Investment and reindustrialization in the soviet economy," *The Russian Review*, vol. 46, no. 1, p. 109, 1987.

[42] "Aleksey BALASHOV reindustrialization of the Russian economy and the development of the military-industrial complex," *Social Sciences*, vol. 47, pp. 11–23, 2016.

[43] V. Kondrat'EVKondrat'ev, "Reshoring as a form of reindustrialization," *World Economy and International Relations*, vol. 61, no. 9, pp. 54–65, 2017.

[44] A. K. Dutt, "Macroeconomic theory after the crisis," *Review of Radical Political Economics*, vol. 43, no. 3, pp. 310–316, 2011.

[45] A. Holl, "Start-ups and relocations: manufacturing plant location in Portugal," *Papers in Regional Science*, vol. 83, no. 4, pp. 649–668, 2004.

[46] R. E. Rawstron and B. R. Hutchinson, "Cardiac monitors," *BMJ*, vol. 2, no. 5318, p. 1545, 1962.

[47] D. M. S. Manj and S. s. Manj, "Shahbaz عورت کی معاشی سرگرمیاں اور عصری سماج: سیرت طیبہ کے تناظر میں," *Rahatulquloob*, vol. 3, no. 2, pp. 38–52, 2019.

[48] J. M. Arauzo-Carod and J. M. Reseña, "Reseña," *Investigaciones de Historia Económica*, vol. 7, no. 2, pp. 341-342, 2011.

[49] Y. Liu, B. Yan, Y. Wang, and Y. Zhou, "Will land transfer always increase technical efficiency in China?-A land cost perspective," *Land Use Policy*, vol. 82, pp. 414–421, 2019.

[50] L. Sleuwaegen and E. Pennings, "International relocation of production: where do firms go?" *Scottish Journal of Political Economy*, vol. 53, no. 4, pp. 430–446, 2006.

[51] F. Targa, K. J. Clifton, and H. S. Mahmassani, "Influence of transportation access on individual firm location decisions," *Transportation Research Record: Journal of the Transportation Research Board*, vol. 1977, no. 1, pp. 179–189, 2006.

[52] S. P. T. Groot, H. L. F. de Groot, and M. J. Smit, "Regional wage differences in The Netherlands: micro evidence on agglomeration externalities," *Journal of Regional Science*, vol. 54, no. 3, pp. 503–523, 2014.

[53] F. Mameli, A. Faggian, and P. Mccann, "Estimation of local employment growth: do sectoral aggregation and industry definition matter?" *Regional Studies*, vol. 48, no. 11, pp. 1813–1828, 2014.

[54] S. H. Hong, "Agglomeration and relocation: manufacturing plant relocation in Korea," *Papers in Regional Science*, vol. 93, no. 4, pp. 803–818, 2014.

[55] C. C. Coughlin, "Globalization Deserves Some Props," *Economic Synopses*, vol. 2008, 2008.

[56] A. Cieślik, "Regional characteristics and the location of foreign firms within Poland," *Applied Economics*, vol. 37, no. 8, pp. 863–874, 2005.

[57] R. A. de Mooijde Mooij and S. Ederveen, "Taxation and foreign direct investment: a synthesis of empirical research," *International Tax and Public Finance*, vol. 10, no. 6, pp. 673–693, 2003.

[58] D. O'Neill, "Playing risk: Chinese foreign direct investment in Cambodia," *CONTEMPORARY SOUTHEAST ASIA*, vol. 36, no. 2, p. 173, 2014.

[59] M. De Bok and F. Sanders, "Firm relocation and accessibility of locations," *Transportation Research Record: Journal of the Transportation Research Board*, vol. 1902, no. 1, pp. 35–43, 2005.

[60] V. Strauss-Kahn and X. Vives, "Why and where do headquarters move?" *Regional Science and Urban Economics*, vol. 39, no. 2, pp. 168–186, 2009.

[61] B. Sleutjes and P. Beckers, "Exploring the role of the neighbourhood in firm relocation: differences between stayers and movers," *Journal of Housing and the Built Environment*, vol. 28, no. 3, pp. 417–433, 2013.

[62] C. Y. Nguyen, K. Sano, T. V. TranTran, and T. T. DoanDoan, "Firm relocation patterns incorporating spatial interactions," *The Annals of Regional Science*, vol. 50, no. 3, pp. 685–703, 2013.

[63] A. E. BrouwerBrouwer, I. Mariotti, and J. N. van Ommerenvan Ommeren, "The firm relocation decision: an empirical investigation," *The Annals of Regional Science*, vol. 38, no. 2, pp. 335–347, 2004.

[64] A. Weterings and J. F. Knoben, "Footloose: an analysis of the drivers of firm relocations over different distances," *Papers in Regional Science*, vol. 92, no. 4, pp. 791–809, 2013.

[65] L. L. Love and J. L. Crompton, "The role of quality of life in business (Re)location decisions," *Journal of Business Research*, vol. 44, no. 3, pp. 211–222, 1999.

[66] P. Trueman, "Standby redundancy," *Data Processing*, vol. 28, no. 7, pp. 374–378, 1986.

[67] L. S. Bamber, J. X Jiang, and I. Y. Wang, "What's my style? The influence of top managers on voluntary corporate financial disclosure," *The Accounting Review*, vol. 85, no. 4, pp. 1131–1162, 2010.

[68] J.-H. Kwak, H.-G. Kwak, and J.-K. Kim, "Behavior of circular CFT columns subject to axial force and bending moment," *Steel and Composite Structures*, vol. 14, no. 2, pp. 173–190, 2013.

[69] Z. Hao, "Research on the positive role of outward-bound in promoting college students' mental health," *Education And Management In Sports*, vol. 2, 2010.

[70] P. Lin, B. Lin, M. Lin, and C. Lin, "Empirical study of factors influencing performance of Chinese enterprises in overseas mergers and acquisitions in context of belt and road initiative-A perspective based on political connections," *Emerging Markets Finance and Trade*, vol. 56, no. 7, pp. 1564–1580, 2020.

[71] X. Lu, Y. Sheng, and J. Wang, "The influence of executive compensation incentives on R&D investment: the moderating effect of executive overconfidence," *Technology Analysis & Strategic Management*, vol. 32, no. 10, pp. 1169–1181, 2020.

Hindawi
Scientific Programming
Volume 2022, Article ID 6173981, 8 pages
https://doi.org/10.1155/2022/6173981

Research Article

Application of Convolutional Networks in Clothing Design from the Perspective of Deep Learning

Cheng Yi

JiangXi Institute of Fashion Technology, Nanchang 330201, Jiangxi, China

Correspondence should be addressed to Cheng Yi; yicheng@jift.edu.cn

Received 3 August 2022; Revised 13 September 2022; Accepted 17 September 2022; Published 27 September 2022

Academic Editor: Lianhui Li

A convolutional neural network (CNN) is a machine learning method under supervised learning. It not only has the advantages of high fault tolerance and self-learning ability of other traditional neural networks but also has the advantages of weight sharing, automatic feature extraction, and the combination of the input image and network. It avoids the process of data reconstruction and feature extraction in traditional recognition algorithms. For example, as an unsupervised generation model, the convolutional confidence network (CCN) generated by the combination of convolutional neural network and confidence network has been successfully applied to face feature extraction.

1. Origin and Development of Convolutional Neural Network

With the development of society, people cannot process data with general statistical knowledge due to the increasing amount of data and the increasing number of dimensions; therefore, processing big data has become a significant problem we face. Machine learning can be divided into supervised learning and unsupervised learning. The core is to classify the characteristics of the data. It can be labeled as data characteristics and by the supervision of learning, these labels can be classified, thus achieving the purpose of feature classification, such as data feature if there is no label, and you can only rely on unsupervised learning to identify these features for clustering [1]. On the other hand, deep learning, commonly referred to by people, relates to machine learning through deep networks, namely multiple networks, such as convolutional neural networks (CNN). The concept of deep learning comes from the research of artificial neural networks, which is a method of data representation learning in machine learning. Deep learning has made breakthrough achievements in image classification, speech recognition, target detection, and other aspects in recent years, showing its excellent learning ability [2]. With the research's deepening, the convolutional neural network structure is constantly optimized, and its application field is gradually extended. For example, Alibaba, Baidu, Google, and other companies are conducting deep learning research on speech recognition. And the use of face recognition, image search, and human behavior recognition is a reasonable prospect of technology. It can be used in medicine, biology, and other fields. Deep learning can also be divided into supervised and unsupervised learning.

CNN first originated in 1962. Biologists Hubel and Wiesel found that Ding is a cell that covers the whole visual well and is very sensitive to the local, visible input space area, called the receptive field. In 1980, Fukushima proposed a neocognitron with a similar structure based on the receptive field. Neocognitron is a self-organizing multilayer neural network model that can stimulate the upper layer's local receptive field to respond to each layer. At the same time, it is also the primary learning method for convolutional neural networks in early learning. Subsequently, Saad et al. proposed and designed the convolutional neural network LeNet-5 model for character recognition based on neocognitron [3]. The basic structure of LeNet-5 comprises an input layer, a revolutionary layer, a pooling layer, a complete connection layer, and an output layer. The system succeeded

in small-scale hand and number recognition but still has significant limitations. In 2012, CNN made a historic breakthrough. The emergence of alexnetu2 made CNN the core algorithm model in image classification. Compared with the traditional CNN model, Alexie improves the algorithm and realizes multi-GPU parallel computing. With the support of a large amount of data, the error rate of the top-5 is getting lower and lower, which has now reduced to about 3.5% [4]. Recently, GoogLeNet, with a deeper VGg structure and network in network structure, has emerged, and the emergence makes it possible to train hundreds or even thousands of neural networks.

2. Characteristics of Convolutional Neural Network

2.1. Local Perception Method. The local sensing method uses a convolutional neural network method to reduce the number of data parameters. From local cognition to global cognition is a method of people's understanding of the outside world, which is also applicable in image processing. The spatial connection of images is also closely related to the relationship of local pixels, but if the interval is far away, the relationship with spatial pixels is weak.

As in conventional neural networks, neurons in the input layer need to be connected to neurons in the hidden layer. But here, instead of connecting every input neuron to every hidden neuron, connections are created only in a local region of an image.

Therefore, each neuron on the convolutional neural network must only perceive it locally. Then the complete connection layer will comprehensively analyze and summarize the locally perceived parameter information to obtain the global information parameters.

The correlation between local pixels is strong and the correlation between distant pixels is weak. Inspired by the human visual reception system, visual neurons receive only local information, i.e., each neuron does not respond to the global. Our observation of the outside world is from local to global, not pixel by pixel but area by area, through which we get local information and then the aggregation of this local information before we get the global information. Assuming that each implicit layer neuron is constructed by perceiving only two input neurons. It can also be 3 or 4, which is mainly related to the size of the image and the size of the feature that we want to obtain.

2.2. Weight Sharing. Compared with the local sensing method, weight sharing has more significant advantages. The Lenet-5 model proposes the weight-sharing network. The Lenet-5 model proposes the weight-sharing network because of too many parameters. The weight-sharing network first simplifies the structure, then reduces the number of training parameters with more application space. This means that all neurons in the first hidden layer detect the same feature at different locations in the image. This mapping from the input layer to the hidden layer is also called feature mapping (or filters, kernels), because the weights are shared so that the features are detected in the same way. The weights of this feature mapping are called shared weights, and its deviation is called shared bias.

For example, a neuron in a nerve needs 100 information parameters, so these 100 information parameters are equivalent to an extraction method and are independent of location [5]. A convolutional neural network can extract the corresponding features from these 100 parameters and then apply them to other parts of the image. Generally speaking, it is to randomly pull a small amount from a large-scale image to an image to extract a small amount from a large-scale painting randomly. Then the extracted small part can be learned to become a feature detector, which can be applied to any image. Then through convolution learning processing with the original image, different characteristic values at different positions in the original image can be obtained.

2.3. Multiconvolution Kernel. In the weight-sharing network, the local features extracted by observing the case cannot meet the requirements of image processing, so the help of a convolution kernel is needed. Each shared weight parameter is a convolution kernel, and multiple convolution kernels can solve this problem [6]. Each convolution kernel will generate an image after local feature extraction and weight sharing, and multiple convolution kernels will form various photos, which can be regarded as multiple channels. As shown in Figure 1, the process of convolution operation with four convolution kernels, that is, four channels, is offered. In this process, the convolution results on the four channels are added first, and then the value of the function is taken. The value obtained is the value of $W1$ and $W2$.

2.4. Model of the Convolutional Neural Network. Because of their high fault tolerance and nonlinear description ability, neural networks have been widely studied and applied, especially in pattern classification. Their primary classification mode of pattern classification is based on feature classification, so some features must be extracted before sorting. The classification model is shown in Figure 2. Samples are extracted from the input and required features F_1, $\underline{F_2}$ ... F_n, then classifies to get the output.

A convolutional neural network is a feedforward neural network that can extract the topology structure from a two-dimensional image and use the backpropagation algorithm to optimize the network structure and solve the unknown parameters in the network. A convolutional neural network is often used to study two-dimensional image recognition problems. It only needs a small preprocessing; the recognition range is vast and can allow the image to change. The traditional classification model is shown in Figure 2. Firstly, the image should be input, and complex preprocessing is carried out to extract features. Then, the classification is done according to the extracted features, and the results are given at the output end. The difference between the classification model of a convolutional neural network and the traditional model is that it can directly input a two-dimensional image into the model and then give the classification result at the output end, as shown in Figure 3. Its advantage is that it does

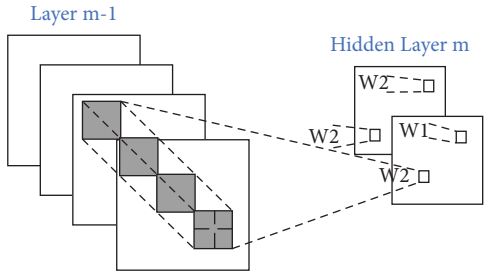

Figure 1: A multiconvolution kernel.

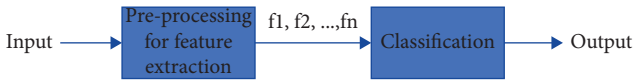

Figure 2: Classification model.

not need complex preprocessing and ultimately puts feature extraction and pattern classification into a black box. It obtains the required parameters of the network through continuous optimization and gives the required type in the output layer. The core of the network is the structural design of the network and the solution of the network. This solution structure has higher performance than many previous algorithms, such as complex texture processing, good feature extraction effect but boundary extraction algorithm, feature processing based on wavelet network, and SVM with special classification effect. These algorithms require much computation when extracting features.

3. Remote Sensing Image Research Based on Convolutional Neural Networks and Its Application in the Design Field

Convolutional neural networks have made significant breakthroughs in machine learning in recent years, mainly thanks to big data and computer performance. Studies have shown that constantly deepening network layers can effectively improve network expression of identities of vast amounts of dataset [7]. The network structure of wider deepen let convolutional neural network become very complex, and depth of retraining a convolution of the new model via the network requires a lot of training samples to adjust the network weights. This is not the reality for small datasets. The proposed migration theory enables small data sets to share the development results of convolutional neural networks and deploy large networks into practical applications.

Remote sensing is a comprehensive Earth observation technology developed in the 1960s that has become one of the leading technologies for studying Earth resources and the environment. After years of development, remote sensing technology has achieved the ability to perform hyperspectral, high spatial resolution, and real-time Earth observation. Currently, the ground resolution of remote sensing images can reach a centimeter level. Remote sensing image classification is one of the essential applications of remote sensing technology, which has critical applications in

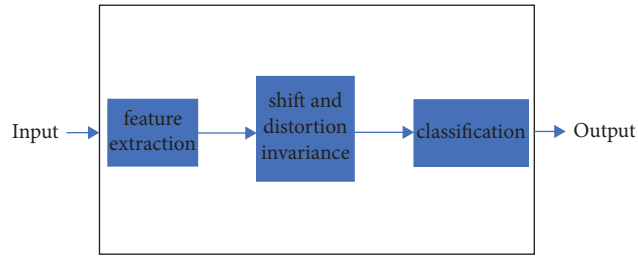

Figure 3: Convolutional neural network classification model.

land use, urban planning, environmental monitoring, etc. It has vital significance for battlefield environment analysis in the military [8]. This paper applies the migration theory to the classification of remote sensing images with the pretrained VGG-16, GoogLeNet, and RESNET-152. Training tests were carried out on the remote sensing image datasets UC Merced and Siri-WHU, and the experimental results were analyzed in detail [9].

3.1. Migration Theory. For a multilayer convolutional neural network, the initial layer extracts more general features of the image. As the network structure becomes deeper, shallow features are combined into advanced features and further transformed into semantic features to achieve classification. For the convolutional neural network trained on ImageNet's extensive image data set, the bottom layer of the convolutional neural network has been prepared with much detailed information, and what needs to be trained prepared is in the combination information of these features at the top layer and the classification information of the final fully connected layer, which also proves that the convolutional neural network has the ability to transfer learning to a certain extent. There are usually two ways to apply transfer theory to convolutional neural networks.

(1) The trained network model is used as a feature extractor. The last complete connection layer of the trained network is removed, and the rest of the network is used as a feature extractor. For the Alex grid work, removing the last convolutional layer will generate a 4096-dimensional feature vector, which will be used to train a linear classifier for practical tasks [10].

(2) They are fine-tuning the trained network with new data sets. For networks pretrained on large databases, the weight parameters of the network are fine-tuned on the new database by a backpropagation algorithm. The features extracted from the first few layers of the pretrained network are usually general. In contrast, those removed from the last layer are related to the task of data set classification. During fine-tuning, you can adjust the parameters of different network layers. You can adapt and change the parameters of all network layers. You can also change the parameters of the first several network layers and fine-tune the parameters of the last network layers.

3.2. Deep Convolutional Neural Network

3.2.1. GoogLeNet Network Model. Lenet-5, AlexNet, and VGGNet are the accumulation of multiple convolutional layers, only deepening in depth. GoogLeNet expands the width of the network while increasing the network depth. The network depth of GoogLeNet is 22 layers [11]. Its primary grouping unit, inception, is shown in Figure 4.

The features of different scales can be obtained by using multiple convolutional kernels of different scales at the same layer, and better features can be obtained by fusion of the accepted elements than by using a single convolutional kernel. The initial Inception architecture does not use a $1 * 1$ convolutional kernel, which has the advantage of reducing a large number of network parameters. For an input with a 256-dimensional feature, the parameter can be reduced by 1/9 by using $1 * 1$. The parameters of GoogLeNet are 1/12 of those of 8-layer AlexNet [12].

3.2.2. ResNet-152 Network Model. ResNet is a residual network model that solves the gradient dispersion problem of the original deep learning network as the number of network layers increases. As a result, shallow network parameters cannot be updated in the backpropagation process, and the network depth cannot be further deepened. ResNet uses a shortcut to connect the inputs and outputs of a module during model design. In the process of backpropagation updating weights, ResNet gradient signals can be directly transmitted to the upper network through shortcuts, which solves the problem of gradient disappearance and makes the network layers of the deep learning network reach 152 layers. The essential components of ResNet are shown in Figure 5.

4. Application of Convolutional Neural Network in Clothing Design

With the rapid development of computer technology, computer-aided design has emerged endlessly and is widely used in business, industrial medicine, art design, entertainment, and other fields. At present, the applications of juice computers in the clothing industry include clothing computer-aided design (clothing CAD), clothing enterprise management information system (MIS), and clothing cutting machine technology system, as well as clothing sales system, clothing fitting system, and contactless clothing measurement system.

Clothing CAD (computer aided design) technology; that is, computer-aided clothing design technology, is a unique technology that uses computer software and hardware technology to input, design, and output new clothing products and clothing processes according to the basic requirements of clothing design [13]. It is a comprehensive high-tech that integrates computer graphics, databases, network communication, and other computer and other fields of knowledge to realize product technology development and engineering design. It is called the interdisciplinary subject of art and computer science. It is a new art school based on cutting-edge science, which is different from any prior art. Clothing CAD technology integrates designer Ding's ideas and technical experience and, through the powerful computing function of the computer, makes clothing design more scientific and efficient and provides a modern tool for clothing designers. It is an essential means of future fashion design [14].

The clothing CAD system mainly includes fashion design system, pattern design system, grading system, marking system, fitting design system, and management system.

4.1. Introduction to Garment Design CAD. The clothing CAD was developed in the United States in the early 1960s. Currently, the popularity of clothing CAD in the United States, Japan, and other developed countries has reached more than 90%. China's clothing CAD technology started late; although the development speed is breakneck, there is still a big gap with foreign technology.

The popularization, application, and popularization of clothing CAD is a vital tent and long-term task of clothing technology transformation in China. Garment CAD software is a common standard in the modern garment industry, and it also improves the production efficiency and product quality of garment enterprises [15]. After entering the WTO, China's clothing industry will further develop rapidly. Therefore, using and promoting clothing CAD software is an inevitable trend for further developing China's clothing industry.

4.2. 3D Digital Design Technology. In the current international manufacturing field, manufacturing technology is developing from traditional manufacturing methods to advanced manufacturing technology. The informatization of the manufacturing industry has become an important trend in the development of the manufacturing industry. The core of the digital construction of manufacturing enterprises is the digital design and manufacturing of products and the integration of related digital technologies. Three-dimensional digital design technology is gradually becoming a hot spot in the application of enterprise design, and it is also a necessary tool for enterprises to deepen their application. As an essential part of information technology, CAD combines the high-speed and massive data storage, processing, and mining capabilities of computers with people's comprehensive analysis and creative thinking capabilities and plays a vital role in accelerating the development of engineering and products; it shortens the design and manufacturing cycle; improves quality; reduces costs; and enhances the market competitiveness and innovation ability of enterprises. Whether it is military or civil industry, construction or manufacturing, processing industry, machinery, electronics, light textile products, literature and sports, film and television advertising production, three-dimensional digital design technology is indispensable [16]. Three-dimensional digital design technology is an essential technical basis for enterprise informatization, and it is also an admission ticket for enterprises to enter the international market.

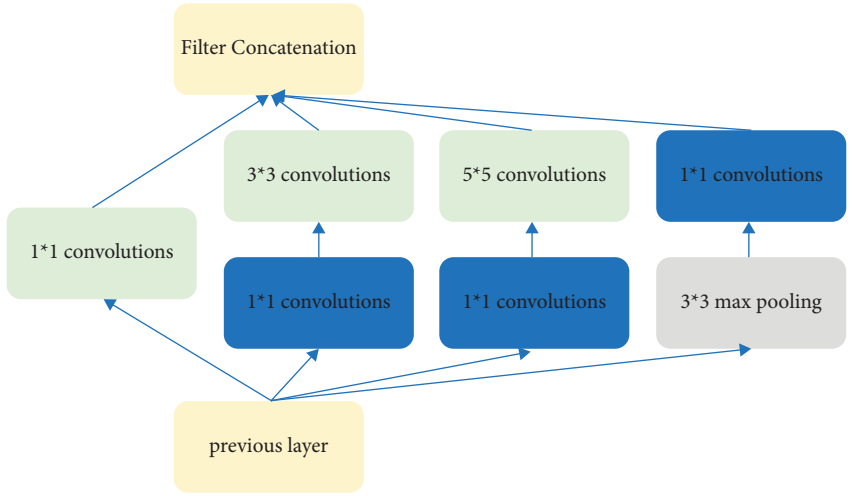

Figure 4: GoogLeNet network.

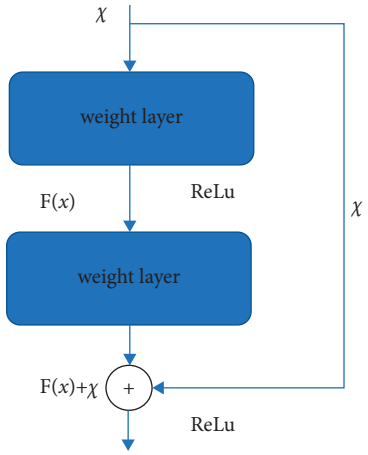

Figure 5: ResNet workflow model.

4.2.1. Working Principle of 3D CAD Technology. The clothing size based on the mass production of clothing cannot accurately reflect the body characteristics of people. The establishment of human body databases of all kinds of people is being carried out at home and abroad. Through three-dimensional anthropometry on many people with different skin colors, regions, ages, and heights, we collect various body size data of the human body and establish a database to provide essential data for formulating clothing specifications and sizes [17].

Three-dimensional anthropometry generates a virtual three-dimensional human body by acquiring the human body's vital geometric parameters, establishing a static and dynamic human model, and forming a complete set of systems with the functions of virtual human body display and dynamic simulation. On this basis, 3D clothing CAD generates the three-dimensional effect of clothing fabric, realistically displays the three-dimensional color image of the dressing impact on the screen, and expands the three-dimensional design into plane clothing pieces [18]. Using advanced computer image capture and recognition technology, laser measurement and positioning technology, numerical control technology, three-dimensional computer software, and data processing technology, the working principle of the system is standing on a unique working platform. Four laser heads are used that can move up and down scan the human body from the top of the head to the heel in four directions and read the position and color information of the human body into the computer and then use special software to process the measured human body information to obtain detailed and accurate size and color information of each characteristic part of the human body and generate standard data formats that can be read by 3D CAD software and animation software.

The basis of 3D garment CAD is 3D anthropometry [19]. The three-dimensional human body measurement system has been commercialized abroad, and its technology has been relatively mature. France, the United States, Japan, and other countries can complete the three-dimensional human body using the natural light grating principle in 40 milliseconds, 10 seconds, and 1.8 seconds, respectively, measurement data. The commonly used three-dimensional anthropometry technology in the world is generally non-contact. The image formed by the light projected onto the human body surface is captured by photosensitive equipment. Then the three-dimensional characteristics of the human body are described by computer image processing. The three-dimensional human body measurement system has many advantages over traditional measurement technology, such as short measurement time and extensive data.

4.2.2. Application Status of 3D Garment CAD. At present, there are two main types of applications of 3D garment CAD in foreign markets:

First, it is used for customization: to measure the human body parameters of specific customers and their specific requirements for clothing styles (such as relaxation, length, width, and other preference information), carry out clothing design, and regenerate into corresponding plane clothing

samples [20]. Such products can be remotely controlled through the Internet, among which the systems of the United States, Britain, France, Germany, Japan, and Switzerland are more advanced.

Second, it is used to simulate the fitting system. Interactive clothing design is carried out through the three-dimensional measurement of a customer's body shape, and the corresponding plane clothing samples are regenerated. Such applications can also be realized by using the Internet for remote control of e-commerce. For example, Lands' End company in the United States can establish a virtual human model of customers on the Internet. Through simple operations, customers can try on the company's clothes and carry out the three-dimensional interactive design until they are satisfied.

Presently, some foreign products can realize three-dimensional clothing wearing, matching design and modification, reflect the animation effect of clothing wearing comfort, simulate the three-dimensional suspension effect of different fabrics, and realize 360-degree rotation and other functions [21]. Among them, the three-dimensional garment CAD software developed by the United States, Japan, Switzerland, and other countries is relatively advanced, such as the concept 3D garment design system launched by CDI company of the United States, the 3D plan of lick company of France, the am-ee-sw3d system of Gerber company of the United States, the 3D system of Pad Company of Canada, the 3D design of Toyo textile company of Japan, etc.

4.2.3. Huge Benefits of 3D CAD Technology. 3D CAD technology can significantly improve the design efficiency and quality of products and projects, working conditions, and competitiveness of products and projects in the market [22]. Statistics from foreign countries show that the application of 3D CAD design technology can reduce engineering design cost by 13%–30%. It can reduce the time from product design to production by 30%–60%, improve product quality by 5–15 times, and increase the breadth and depth of problem analysis by 35 times. Also, it improves product productivity by 40–70% and increases the productivity of input equipment by 2–3 times while reducing the processing process by 30%–60% and labor costs by 5–20%. The research, development, and wide application of 3D digital design technology can promote the development of China's software industry, especially the development of the application software industry [23]. This will accelerate the technological transformation of traditional industries and products and promote the rapid development of conventional disciplines. The resulting direct and indirect economic benefits are enormous, and their social benefits are immeasurable.

5. Development Trend of Garment CAD Technology

5.1. Development Status of Three-Dimensional CAD for Clothing. With the development of computer technology and the social economy in China, people have higher and higher requirements regarding clothing quality, fit, and individuality. The existing two-dimensional clothing CAD technology can no longer meet the CAD application requirements of the textile and clothing industries. It is urgent to develop clothing CAD from the current plane to a three-dimensional design. Therefore, in recent years, three-dimensional clothing CAD, virtual reality clothing design, and other aspects of theoretical research and practical applications both at home and abroad.

According to Autodesk's widespread application of CAD statistics. Currently, about 30% of the users in the world use 3D CAD for product design, and the remaining 70% still use 2D CAD design [24]. Three-dimensional CAD has been widely used in the world. Still, in the clothing field, the development and application of three-dimensional CAD are lagging because clothing is not like solid products in the machinery and electronics industry; its texture is flexible and will change with different external conditions, so it is not easy to simulate. In particular, the transformation of garment CAD from two-dimensional to three-dimensional needs to solve the technical problems of fabric texture and dynamic performance, three-dimensional reconstruction, realistic and flexible surface modeling, and the transformation from a three-dimensional garment design model to a two-dimensional plane garment. These problems lead to a long development cycle and great technical difficulty in 3D garment CAD.

5.2. Development Trend of Garment CAD Technology. In recent years, the CAD technology in achieving rapid development at the same time also exposed the problems in the story; the main problem is the unit's placing too much emphasis on the development of technology, emphasizing the system's generality and ignoring the product's whole life cycle of the design process-oriented design, dismissing the application of network technology, ignoring butyl database, the development of the characteristic library, and so on [25]. Given these problems, combined with the latest evolution of manufacturing information technology, CAD technology developers put forward a three-dimensional digital design system for industry and process (product life cycle). This system has become a hot spot for research and development at home and abroad. It is regarded as the only way to deepen CAD technology's application and leap in evolution.

The original CAD system and its supporting technology have been integrated into CIMS (Computer Integrated Manufacturing System) [26]. Another garment CAD system development trend is establishing the interface and integration with CAM, MIS, PDM, ERP, etc.

With the rapid development of the Internet in recent years, it is expected that online fashion design will gradually become mainstream. Under the increasingly specialized and globalized production and management mode, the CAD system based on the network can realize data sharing and standardization. The parallel product design will also support the efficient and rapid CAD system. To effectively enhance the market size and product profits, the integration of apparel CAD and e-commerce is also an inevitable trend.

An Internet-based remote data transmission and monitoring system for garment enterprises is coming out, which also provides adequate technical support for the networking of garment design and the informatization of garment enterprises.

In recent years, the United States, France, Germany, Japan, and Switzerland have also developed the research and development of Virtual garment CAD and started the application research of ultra-dimensional garment design [27]. Is the so-called super-d clothing design, super-dimensional visual design, for fashion designers in fashion design not only consider a one-dimensional line, two-dimensional plane, three-dimensional body, 4 d, and 5 d design elements such as the meaning of, and feel the person's psychology, the aesthetic view of people's vision, and the interest of the people, and many other factors, paying attention to the use of environmental psychology and ornamental psychology. Through visual, auditory, and tactile means, clothing designers use virtual reality design technology, virtual reality computer display environment for clothing designs, virtual reality design technology and virtual reality computer display environment for clothing design. This virtual clothing CAD technology, the use of network transmission, and the creation of virtual reality technology make the designer able to work in the environment of virtual garment design; the outdoor reading computer hardware equipment still needs data gloves, clothing, and so on for digital human body sensor and helmet stereoscopic display devices such as displays, shutter glasses, and other related equipment [28]. This virtual reality design technology realizes the automation of clothing design.

Currently, all clothing CAD products are more complex, and it takes professional and technical personnel a considerable amount of time to learn and apply them thoroughly, which is also an important reason for the slow popularization of CAD products [29]. Therefore, it is expected that garment CAD products in the future will develop towards high intelligence. More garment model modules and design wizards will be established to provide intelligent support for designers. This academic support includes self-learning, self-organization, self-adaptation, self-correction, parallel search, associative memory, pattern recognition, automatic knowledge acquisition, and other intelligent technologies [30] which step by step become easy to learn like WINODWS operating software. In the future, with the development of hardware technology, embedding software into the human body measurement instrument to become a brilliant clothing design silly machine will become a reality.

Since AlexNet made a breakthrough in the ImageNet competition in 2012, deep learning based on the convolutional neural network has become a common research hotspot for various enterprises and many scholars and has made great breakthroughs in natural images, language processing, and other aspects. With theoretical innovations and improved computational performance, modern convolutional neural networks are evolving in a wider and deeper direction, but eschewing the development in depth. But it is necessary to increase the depth of network computation to improve the learning ability of the model for better region classification and interclass differences. The clothing design work can rely on computer-aided design, fabric organization, pattern, and clothing modeling design out. Based on the CAD system, this paper presents the situation of the fabric directly and improves the efficiency of garment design. To sum up, under the diversified network environment, computer technology develops rapidly and has a wide range of applications, which are applied in all aspects of clothing design, production, and sales. According to the content and requirements of clothing design, the content and form of computer-aided design can be flexibly used to minimize the production costs in the process and improve the quality and efficiency of clothing design and production. Throughthe prediction, the garment fabric, style, color, and other popular elements, trends have an intuitive understanding of comfort, fit, beautiful quality clothing design to meet the needs of consumers and for China's garment industry to open up a broader space for competition and development.

Data Availability

The dataset is available upon request.

Conflicts of Interest

The author declares that there are no conflicts of interest.

Acknowledgments

The authors thank Jiangxi Education Department Science and Technology Project: Antisweating and Antibacterial functional Autumn clothing Design Research (No. GJJ202409).

References

[1] Z. Li, F. Liu, W. Yang, S. Peng, and J. Zhou, "A Survey of Convolutional Neural Networks: Analysis, Applications, and Prospects," *IEEE Transactions on Neural Networks and Learning Systems*, pp. 1–21, 2021.

[2] M. Jogin, M. S. Madhulika, G. D. Divya, R. K. Meghana, and S. Apoorva, "Feature extraction using convolution neural networks (CNN) and deep learning," in *Proceedings of the 2018 3rd IEEE International Conference on Recent Trends in Electronics, Information & Communication Technology (RTEICT)*, pp. 2319–2323, IEEE, Bangalore, India, May 2018.

[3] A. Saad, T. A. Mohammed, and S. Al-Zawi, "Understanding of a convolutional neural network," in *Proceedings of the 2017 International Conference on Engineering and Technology (ICET)*, pp. 1–6, IEEE, Antalya, Turkey, August 2017.

[4] M. Tan and Q. Le, "EfficientNet: rethinking model scaling for convolutional neural networks," in *Proceedings of the 36th International Conference on Machine Learning*, vol. 97, pp. 6105–6114, July 2019.

[5] P. Y. Simard, D. Steinkraus, and J. C. Platt, "Best practices for convolutional neural networks applied to visual document analysis," in *Proceedings of the Seventh International Conference on Document Analysis and Recognition*, vol. 2, p. 958, IEEE, Edinburgh, UK, August 2003.

[6] C. Nebauer, "Evaluation of convolutional neural networks for visual recognition," *IEEE Transactions on Neural Networks*, vol. 9, no. 4, pp. 685–696, 1998.

[7] A Krizhevsky, I Sutskever, and G. E Hinton, "ImageNet classification with deep convolutional neural networks," *Advances in Neural Information Processing Systems*, vol. 25, 2012.

[8] K. Miyake and S. Miyake, "Neocognitron: a new algorithm for pattern recognition tolerant of deformations and shifts in position," *Pattern Recognition*, vol. 15, no. 6, pp. 455–469, 1982.

[9] R. U. Khan, X. Zhang, and R. Kumar, "Analysis of ResNet and GoogleNet models for malware detection," *Journal of Computer Virology and Hacking Techniques*, vol. 15, no. 1, pp. 29–37, 2019.

[10] J.-H. Kim, S.-Y. Seo, C.-G. Song, and K.-S. Kim, "Assessment of electrocardiogram rhythms by GoogLeNet deep neural network architecture," *Journal of Healthcare Engineering*, vol. 2019, pp. 1–10, 2019.

[11] P. Aswathy and D. Mishra, "Deep GoogLeNet Features for Visual Object Tracking," in *Proceedings of the 2018 IEEE 13th International Conference on Industrial and Information Systems (ICIIS)*, pp. 60–66, IEEE, Rupnagar, India, December 2018.

[12] Z.-W. Zhang and J. Zhang, "Feature extraction and image retrieval based on AlexNet," in *Proceedings of the Eighth International Conference on Digital Image Processing (ICDIP 2016), SPIE Proceedings (ICDIP 2016)*, vol. 10033, pp. 65–69, August 2016.

[13] L. Li Zhi and S. Yubao, *Convolutional Neural Networks for Clothes Categories*, pp. 120–129, Computer Vision, 2015.

[14] J. Huang, H. Ruhan, and W. Xinglong, "Real-time clothing detection with convolutional neural network," in *Recent Developments in Intelligent Computing, Communication and Devices*, pp. 233–239, Springer, Singapore, 2019.

[15] R. A Castellino, "Computer aided detection (CAD): an overview," *Cancer Imaging*, vol. 5, no. 1, pp. 17–19, 2005.

[16] N. Zhang, "Research on the application of computer aided Design in clothing Design teaching in higher vocational colleges," *Turkish Journal of Computer and Mathematics Education (TURCOMAT)*, vol. 12, no. 3, pp. 4817–4821, 2021.

[17] L. Jun, "The realization of 3-D garment art design in CAD software," in *Proceedings of the Advanced Technology in Teaching - Proceedings of the 2009 3rd International Conference on Teaching and Computational Science (WTCS 2009)*, pp. 549–554, Springer, Berlin, Heidelberg, June 2012.

[18] N. Magnenat-Thalmann, "Designing and animating patterns and clothes," in *Modeling and Simulating Bodies and Garments*, pp. 139–159, Springer London, London, 2010.

[19] F. Preston and J. D. Preston, "CAD/CAM imaging in dentistry," *Current Opinion in Dentistry*, vol. 1, no. 2, pp. 150–4, Apr. 1991.

[20] J. Gu and T. Chen, "Recent advances in convolutional neural networks," *Pattern Recognition*, vol. 77, pp. 354–377, 2018.

[21] A. Verma and G. K. Verma, "Convolutional neural network: a review of models, methodologies and applications to object detection," *Progress in Artificial Intelligence*, vol. 9, no. 2, pp. 85–112, 2020.

[22] M. Defferrard, X. Bresson, and P. Vandergheynst, "Convolutional neural networks on graphs with fast localized spectral filtering," *Advances in Neural Information Processing Systems*, vol. 29, 2016.

[23] E. R Boulter, "Positioning models in science education and in design and technology education," in *Developing Models in Science Education*, pp. 3–17, Springer, Netherlands, 2000.

[24] S. Lu, P. Y. Mok, and X. Jin, "A new design concept: 3D to 2D textile pattern design for garments," *Computer-Aided Design*, vol. 89, pp. 35–49, 2017.

[25] Y. Gao, "Application of 3D digital technology in the substation design," *IOP Conference Series: Materials Science and Engineering*, vol. 782, no. 3, p. 032066, 2020.

[26] A. S. M. Sayem, R. Kennon, and N. Clarke, "3D CAD systems for the clothing industry," *International Journal of Fashion Design, Technology and Education*, vol. 3, no. 2, pp. 45–53, 2010.

[27] H. Rödel, A. Schenk, C. Herzberg, and S. Krzywinski, "Links between design, pattern development and fabric behaviours for clothes and technical textiles," *International Journal of Clothing Science & Technology*, vol. 13, no. 3/4, pp. 217–227, 2001.

[28] Y.-J. Liu, D.-L. Zhang, and M. M.-F. Yuen, "A survey on CAD methods in 3D garment design," *Computers in Industry*, vol. 61, no. 6, pp. 576–593, 2010.

[29] C. Robson, R. Maharik, A. Sheffer, and N. Carr, "Context-aware garment modeling from sketches," *Computers & Graphics*, vol. 35, no. 3, pp. 604–613, 2011.

[30] M. Jankoska, "Application CAD methods in 3D clothing design," *Tekstilna industrija*, vol. 68, no. 4, pp. 31–37, 2020.

Hindawi
Scientific Programming
Volume 2023, Article ID 9803061, 1 page
https://doi.org/10.1155/2023/9803061

Retraction

Retracted: Tobacco Leaves Disease Identification and Spot Segmentation Based on the Improved ORB Algorithm

Scientific Programming

Received 18 July 2023; Accepted 18 July 2023; Published 19 July 2023

This article has been retracted by Hindawi following an investigation undertaken by the publisher [1]. This investigation has uncovered evidence of one or more of the following indicators of systematic manipulation of the publication process:

(1) Discrepancies in scope
(2) Discrepancies in the description of the research reported
(3) Discrepancies between the availability of data and the research described
(4) Inappropriate citations
(5) Incoherent, meaningless and/or irrelevant content included in the article
(6) Peer-review manipulation

The presence of these indicators undermines our confidence in the integrity of the article's content and we cannot, therefore, vouch for its reliability. Please note that this notice is intended solely to alert readers that the content of this article is unreliable. We have not investigated whether authors were aware of or involved in the systematic manipulation of the publication process.

Wiley and Hindawi regrets that the usual quality checks did not identify these issues before publication and have since put additional measures in place to safeguard research integrity.

We wish to credit our own Research Integrity and Research Publishing teams and anonymous and named external researchers and research integrity experts for contributing to this investigation.

The corresponding author, as the representative of all authors, has been given the opportunity to register their agreement or disagreement to this retraction. We have kept a record of any response received.

References

[1] M. Xu, L. Li, L. Cheng et al., "Tobacco Leaves Disease Identification and Spot Segmentation Based on the Improved ORB Algorithm," *Scientific Programming*, vol. 2022, Article ID 4285045, 12 pages, 2022.

Hindawi
Scientific Programming
Volume 2022, Article ID 4285045, 12 pages
https://doi.org/10.1155/2022/4285045

Research Article

Tobacco Leaves Disease Identification and Spot Segmentation Based on the Improved ORB Algorithm

Min Xu, Lihua Li, Liangkun Cheng, Haobin Zhao, Jiang Wu, Xiaoqiang Wang, Hongchen Li, and Jianjun Liu

China National Tobacco Corporation Henan Company, Zhengzhou 450002, Henan, China

Correspondence should be addressed to Jianjun Liu; kh@bbc.edu.cn

Received 28 June 2022; Revised 24 August 2022; Accepted 29 August 2022; Published 27 September 2022

Academic Editor: Lianhui Li

In order to improve the problems of poor accuracy and low efficiency in tobacco leaves disease recognition and diagnosis and avoid the misjudgment in tobacco disease recognition, a disease recognition and spot segmentation method based on the improved ORB algorithm was proposed. The improved FAST14-24 algorithm was used to preliminarily extract corners. It overcame the deficiency of the sensitivity of the traditional ORB corner detection algorithm to image edges. During the experiment, 28 parameters were obtained through the extraction of color features, morphological features, texture, and other features of tobacco disease spots. Through the experimental comparisons, it was found that the fitness of the improved ORB algorithm was 96.68 and the cross-checking rate was 93.21%. The validation and recognition rate for samples was 96%. The identification rate of tobacco brown spot disease and frog eye disease was 92%, and the identification rate of 6 categories in different periods was over 96%. The experimental results verified the effects of the disease identification fully.

1. Introduction

Tobacco is an important economic crop of China. The tobacco-related industry is also an important industry in China's social economy [1, 2]. The tobacco industry provides an important support for social and economic development every year. At the same time, the existence of tobacco diseases also seriously restricts the output and the overall quality of tobacco, which directly affects the economic development of the tobacco industry and the overall income of tobacco farmers. Therefore, many Chinese scholars have never stopped their research on tobacco diseases. The effective identification and rational control of tobacco diseases not only relate to the physiological health of tobacco leaves but also directly relate to the yield and the final quality of tobacco leaves. And for different regions and different types of tobacco, the corresponding disease types are also different. And the pathology of leaf disease is relatively complex [3, 4]. In order to deal with the problems of poor accuracy and low efficiency in tobacco disease diagnosis, a better and an improved ORB algorithm for disease recognition and disease spot segmentation was proposed and the effects of the disease recognition were verified through experiments.

2. Literature Review

At present, the research on plant disease identification mainly focuses on crop and cash crop diseases. The traditional disease detection was mainly based on manual recognition. The method of manual recognition was low in efficiency and accuracy. Before the rise of deep learning, the traditional disease recognition methods were mainly based on shallow machine learning algorithms, such as SVM and Bayesian classifiers [5, 6]. Some scholars used the statistical learning method of the naive Bayes classifier to realize the classification and recognition of maize leaf diseases, and the diagnostic accuracy of five maize leaf diseases was above 83%. Based on H-threshold segmentation, iterative binarization, image morphology operation, contour extraction, and other algorithms, the texture, color, and shape features of the disease image were extracted. The genetic algorithm was used to optimize the selection of classification features,

and the Fischer discriminant method was used to identify three common maize leaf diseases. According to the features of the maize leaf disease images, a multiclassifier composed of a support vector machine (SVM) was proposed to identify the maize leaf diseases. Experimental results showed that this method was suitable for a small sample and achieved a good classification effect. A support vector machine (SVM) was used to classify cucumber diseases, and the shape, color, texture, and onset time of the disease spots were extracted. The SVM classifier was used to select four common kernel functions for recognition. The results showed that the SVM method had a good classification effect in dealing with small sample problems [7, 8]. A tobacco disease image retrieval method based on the spot feature fusion was proposed to diagnose 7 common tobacco diseases with high recognition accuracy. Five common tobacco diseases were studied and an image processing method based on SVM and ResNet was proposed to diagnose tobacco diseases with an accuracy of 89%. By using image processing and data mining methods, some scholars introduced the disease recognition system based on the double clustering technology. The leaf image was captured by a nonlocal median filter and the noise was removed. Through the double clustering method, anthrax and white leaf diseases of grapes, cucumbers, and tomatoes were segmented. The pattern matching method was used to compare the segmented parts with diseased leaves, which achieved a high recognition accuracy. A method of identification and classification of leaf diseases by digital image processing and machine vision was proposed. Firstly, the leaf images were preprocessed and the features were extracted. And, the leaves were identified by the training and classification based on the artificial neural network. Secondly, the defect region segmentation based on K-means, the feature extraction of the defect part, and the classification of diseases in leaves based on ANN were carried out. A method of tea leaf disease recognition (TLDR) was proposed [9, 10]. The tea image was clipped, resized, and converted into the threshold value in the image processing. Then, the feature extraction method was adopted and the neural network integration was used for the pattern recognition. The recognition accuracy was 91%. Three different convolutional neural network architectures were proposed. Context nonimage metadata were integrated into the image-based convolutional neural network. Combined with the advantages of learning from the entire multicrop dataset, the complexity of the disease classification task was reduced. VGG16 and SingingV3 networks were used to detect and identify the rice pests and diseases, and a two-level small CNN architecture was proposed. Compared with MobileNet, NASNet-Mobile, and SqueezeNet networks, the identification accuracy was 93.3% [11, 12].

3. The Improved ORB Algorithm

3.1. The Improved FAST Corner Detection Algorithm. FAST algorithm is a fast corner detection algorithm at present, but it will produce false detection of some edge points, resulting in the existence of some false corners. Point p is a point on the edge, but it is not a corner point. If the traditional FAST9-16 algorithm is used for detection, it meets the requirement that the gray value of more than 9 continuous pixels in the neighborhood of 16 pixels is sufficiently different. So, the system will identify it as a corner point, and the point p is only an edge point [13, 14].

Therefore, in order to exclude the interference of such edge points on the detection results, the FAST algorithm is improved as follows: 24-pixel points around the pixel point p are taken as the detection template, the gray value of the point p is I_p, and a threshold T is set. If 14 consecutive pixel points among 24-pixel points have a gray value greater than $I_p + T$ or less than $I_p - T$, then the point p is a corner point. And taking the p point as an example, the improved FAST14-24 algorithm does not identify the p point as a corner point, overcoming the deficiency of the traditional FAST9-16 corner point detection algorithm which is sensitive to edges.

3.2. Feature Descriptor Design. The comparison criterion of the gray mean is defined as follows:

$$\tau(p; x, y) = \begin{cases} 1, & p(x) < p(y), \\ 0, & p(x) \geq p(y). \end{cases} \tag{1}$$

In formula (1), $p(x)$ is the mean pixel value of pixel point 5×5 neighborhood. If there are m comparison point pairs, then the m bits binary descriptor is generated.

$$f_n(p) = \sum_{1 \leq i \leq m} 2^{i-1} \tau(p; x, y). \tag{2}$$

Suppose the coordinate of the feature point is O, then OC is the direction of the feature point, and the calculation formula of the direction angle is as follows:

$$\theta = a \tan 2(m_{01}, m_{10}). \tag{3}$$

In formula (3), the centroid of the image gray expression is as follows:

$$C = \left(\frac{m_{10}}{m_{00}}, \frac{m_{01}}{m_{00}} \right). \tag{4}$$

Add the direction of feature points obtained from formula (3) to the descriptor. We define a $2 \times m$ matrix Q as follows:

$$Q = \begin{pmatrix} x_1, x_2, \ldots, x_{m-1}, x_m \\ y_1, y_2, \ldots, y_{m-1}, y_m \end{pmatrix}. \tag{5}$$

In formula (5), (x_i, y_i) is a test point pair. Let the corrected feature point pair matrix be

$$Q_\theta = R_\theta Q. \tag{6}$$

In formula (6), R_θ is the rotation matrix corresponding to the direction of the feature point θ. The descriptor with rotation invariance obtained is as follows:

$$g_m(p, \theta) = f_m(p) | (x_i, y_i) \in Q_\theta. \tag{7}$$

The Shi-Tomasi algorithm is used to optimize feature points. The Shi-Tomasi algorithm takes the smaller of the

two eigenvalues and compares it with the given minimum threshold. If it is larger than the minimum threshold, a strong corner point will be obtained [15, 16]. The Shi-Tomasi algorithm detects corners by calculating the gray level of local small windows $W(x, y)$ moving in all directions. The gray scale change $E[u, v]$ generated by the window translation $[u, v]$ is as follows:

$$E[u, v] = [u, v]W\begin{pmatrix} u \\ v \end{pmatrix}. \tag{8}$$

In formula (8), M is the autocorrelation matrix of 2×2, which can be calculated by the derivative of the image as shown.

$$M = \sum_{x,y} w(x, y)\begin{pmatrix} I_x^2 & I_x I_y \\ I_x I_y & I_y^2 \end{pmatrix}. \tag{9}$$

The two eigenvalues $\lambda_{\max}$ and $\lambda_{\min}$ of the matrix M are analyzed. Since the uncertainty of larger curvature depends on smaller corner points, the corner response function is defined as $\lambda_{\min}$. The Shi-Tomasi algorithm is used to calculate the corner response function $\lambda_{\min}$ of each point for the feature points initially extracted by the improved FAST corner detection algorithm. According to $\lambda_{\min}$, the point with the maximum response value of the first N is determined as the feature point. There are at least two strong boundaries in different directions around the screened feature points, which are easy to identify and are stable [17, 18].

The feature descriptors in the research are designed by a retina-like model. The distribution of sampling points is similar to the structure of the retinal receptive field. The location of feature points is the central point, and the sampling points are evenly distributed on 7 concentric circles, with 6 sampling points on each concentric circle. In terms of the value of sampling points, the research takes the gray mean of the sampling point field as the description of sampling points, just like the ORB algorithm. The difference lies in that ORB uses an equal field to describe sampling points. The research uses square neighborhood descriptions with different side lengths for sampling points on concentric circles [19, 20]. From the intermediate feature point outwards, the sampling side length of each layer is 1, 3, 5, 7, 9, 11, 13, and 15, respectively.

The improved retina-like descriptors are obtained by comparing the results of the neighborhood gray mean of sampling points. Let F be a feature point descriptor, then

$$F = \sum_{0<i<N} 2^i T(P_{ab}), \tag{10}$$

$$T(P_{ab}) = \begin{cases} 1\,(I(P_a) - I(P_b) > 0), \\ 0, \text{others}. \end{cases} \tag{11}$$

N is the dimension of the feature vector ($N = 512$ in the research). P_a is the position of the sampling point to the midpoint $a.P_b$ is the position of the sampling point to the midpoint $b.I(P_a)$ and $I(P_b)$ are the gray mean values of the sampling point in the sampling neighborhood.

For the matching of binary feature description vectors, the Hamming distance is generally used as the similarity measure between descriptors. The Hamming distance is as follows:

$$\mathrm{HM}_{\mathrm{dis\,tan\,ce}} = F_1 \oplus F_2. \tag{12}$$

By determining the threshold of the Hamming distance, the matching of feature vectors can be judged.

3.3. MSRCR. The reflectivity is determined by the object itself and varies without the influence of the emitted light. That is, the object image can be expressed as the product of the reflected image and illumination image, as shown in the formula:

$$S(x, y) = R(x, y) \cdot L(x, y). \tag{13}$$

After the logarithmic processing of both sides of formula (13) is carried out, the following formula can be obtained:

$$\log(R(x, y)) = \log(S(x, y)) - \log(L(x, y)). \tag{14}$$

In formula (14), $S(x, y)$ is the image of the object, $R(x, y)$ is the reflection component of the object itself, and $L(x, y)$ is the illumination component.

By constructing the Gaussian surround function, the Gaussian surround function is used to filter the three channels of RGB image to obtain the estimated light component. The reflection component can be obtained by subtracting the original image and light component in the logarithmic domain; thus, obtaining the output image as shown in the formula.

$$\begin{aligned} r_i(x, y) &= \log\left(R_i(x, y)\right) = \log\left(\frac{s_i(x, y)}{L_i(x, y)}\right) \\ &= \log\left(S_i(x, y)\right) - \log\left(S_i(x, y) * G(x, y)\right). \end{aligned} \tag{15}$$

The formula for the color recovery factor is calculated as follows:

$$C_i(x, y) = \beta\left(\log\left(\partial S_i(x, y)\right) - \log\left(\sum_{i\in(R,G,B)} S_i(x, y)\right)\right). \tag{16}$$

The MSRCR algorithm can not only ensure the gray level of the disease image and remove the influence of the uneven lighting during the shooting but can also improve the saturation of the image color to a certain extent when processing the disease image, which has the best color retention effect on the image.

3.4. Analysis of Experimental Results. All experiments were performed on a P computer environment with a 2.20 GHz CPU and 4 GB memory, and VC++ programming language was used in VS2010.

3.4.1. Analysis of the Distribution of Feature Points. To evaluate the merits and demerits of feature point detection methods, the repetition rate method is often used, so that m_1

and m_2 feature points are detected in two images to be matched. Then, the repetition rate is calculated as follows:

$$R = \frac{C(m_1, m_2)}{\min(m_1, m_2)}. \tag{17}$$

In formula (17), $\min(m_1, m_2)$ is the least number of feature points in the two images. $C(m_1, m_2)$ refers to the corresponding feature points, and the corresponding feature points should meet the following two definitions.

(1) Position error of feature points:

$$\varepsilon_L = |x_a - H \cdot x_b| < 1.5\ pixel. \tag{18}$$

(2) Surface error of feature area:

$$\varepsilon_s = \left|1 - s^2 \frac{\sigma_a^2}{\sigma_b^2}\right| < 0.2. \tag{19}$$

In formula (19), s is the actual scale scaling factor between images and σ_a, σ_b is the feature scale of two feature points.

The ORB feature point detection algorithm and the improved algorithm in the research are used to calculate the repetition rate of feature points for images, respectively, as shown in Table 1.

As can be seen from Table 1, for images with scale transformation, rotation change, illumination transformation, noise interference, and perspective transformation, the improved feature point detection algorithm in the research has improved the repetition rate compared with the ORB feature point detection algorithm. This is because the improved FAST14-24 algorithm is used in the research to eliminate some pseudo-corner points on the edge and eliminate certain interference. In the process of the feature point optimization, the Shi-Tomasi algorithm is used to select feature points with large curvature changes, which are easy to identify and are stable [21, 22]. The feature point matching performance test is conducted on the test images, and the correct matching point pairs of each image are counted as shown in Table 2.

As can be seen from Table 2, the improved ORB feature extraction algorithm in the research improves the matching accuracy by about 18% ~ 65% compared with the traditional ORB algorithm. Specially for the images with light changes, the matching accuracy of the proposed algorithm is significantly better than that of the traditional ORB algorithm, with an increase of 65.8%. Experimental results show that the proposed algorithm is superior to the traditional ORB algorithm in both matching accuracy and robustness for various types of image matching.

4. Identification and Extraction of Tobacco Leaf Disease Data and Segmentation of Disease Spots

4.1. Feature Extraction of Tobacco Spot Image

4.1.1. Color Features. The color feature is widely used in image recognition because of its intuitiveness. In a broad sense, it can be understood that color feature, like texture feature, is used to express the surface attribute information of the scene in the image, but the attribute information expressed by the two is different. It describes the surface properties of the scene corresponding to the image region and is also a global feature. In the research, color moments are used to extract color features based on experimental requirements [23, 24]. The color moment can be understood as saving the information of the image color channel in the form of numerical size. The features of color moments are also different in terms of color information presented by different color channels. In an image, first-order moment (mean), second-order moment (variance), and third-order moment (skewness) are used to express the sufficient color information distribution according to the distribution of all information contained in the color. For example, most of the pictures we often come in contact with are RGB color space models, and there are 9 kinds of information to be extracted from this space model. In the three components R, G, and B, the corresponding first-, second-, and third-moment information is extracted from each component.

In the research, color moment features of RGB and HSV channels need to be extracted, and each extracted color moment has a total of 9 features. The corresponding color moments of the three components of the image constitute a 9-dimensional histogram vector, and the color feature information extracted from each image has a total of 18 dimensions. The model information is shown in Tables 3 and 4.

4.1.2. Morphological Features. The methods of morphological feature extraction [25–27] are as follows: the first is the boundary feature method, which is used to obtain shape parameters of image data information by describing boundary features. The second is the Fourier shape descriptor method, which is based on the mathematical idea of Fourier transform as a shape description, using the closure and periodicity of binary image boundary to reduce its dimension. The third is the shape parameter method for the quantitative measurement of fixed shape, which is based on the representation and matching of shape. The fourth is the shape invariant moment method, which is based on the moment of the region occupied by the target as a shape description parameter. According to the different appearance features of tobacco disease spots in different periods, four feature parameters of tobacco disease spots are extracted, including rectangularity, roundness, complexity, and compactness. The details are shown in Table 5.

4.1.3. Texture Features. Texture features describe the surface properties of the image, such as the patterns on the surface of butterflies, zebra lines, tree rings, and so on [28, 29]. The feature information is based on the statistical features of the whole gray image. Texture features have rotation invariance and strong resistance to noise. In the research, according to the features of spots in the early, middle, and late stages of the two diseases, six texture feature parameters, namely, energy, contrast, correlation, entropy, homogeneity, and

Table 1: Comparison of repetition rates of feature points.

ORB algorithm			Text algorithm		
Repeat points	Total points	Repetition rate	Repeat points	Total points	Repetition rate
255	500	0.510	285	500	0.546
105	389	0.286	139	373	0.385
161	500	0.322	185	500	0.368
220	500	0.442	240	500	0.480

Table 2: Comparison of feature point matching performance.

ORB algorithm correct matching point	Text correct algorithm matching point	Enhancement rate (%)
182	215	18.1
101	124	22.8
165	231	65.8
74	105	40.5

Table 3: Selected color feature information of six images of tobacco brown spot disease and frog eye disease in the early, middle, and late stages (RGB color space model).

	RGB first-order color moment			RGB second-order color moment			RGB third-order color moment		
Early stage of brown spot disease	1.238	1.060	0.875	1.340	1.359	1.329	1.245	1.232	1.242
Middle stage of brown spot disease	8.569	6.879	6.085	3.196	3.199	3.198	2.174	2.176	2.175
Late stage of brown spot disease	8.808	7.935	5.143	11.580	11.285	11.210	5.133	5.070	5.634
Early stage of frog eye disease	0.521	0.513	0.493	0.758	0.765	0.761	0.843	0.853	0.598
Middle stage of frog eye disease	2.767	2.541	2.063	1.822	1.819	1.012	1.511	1.500	1.504
Late stage of frog eye disease	5.961	4.924	3.258	2.820	2.811	2.802	2.008	2.001	2.005

Table 4: Selected color feature information of six images of tobacco brown spot disease and frog eye disease in the early, middle, and late stages (HSV color space model).

	HSV first-order color moment			HSV second-order color moment			HSV third-order color moment		
Early stage of brown spot disease	0.003	0.007	0.875	0.045	0.071	0.059	0.245	0.232	0.142
Middle stage of brown spot disease	0.006	0.018	0.085	0.050	0.099	0.198	0.074	0.176	0.175
Late stage of brown spot disease	0.149	0.120	0.143	0052	0.085	0.021	0.133	0.070	0.111
Early stage of frog eye disease	0.002	0.002	0.002	0.058	0.065	0.760	0.043	0.153	0.120
Middle stage of frog eye disease	0.004	0.009	0.011	0.045	0.019	0.012	0.011	0.500	0.504
Late stage of frog eye disease	0.008	0.025	0.023	0.060	0.011	0.002	0.008	0.001	0.005

Table 5: Selected morphological feature information of six pictures of tobacco brown spot disease and frog eye disease in the early, middle, and late stages.

	Rectangularity	Roundness	Complexity	Compactness
Early stage of brown spot disease	0.9973	0.3175	0.8753	0.3172
Middle stage of brown spot disease	0.9663	0.3.66	2.8785	0.6033
Late stage of brown spot disease	0.9149	0.2184	4.4143	0.2185
Early stage of frog eye disease	1.0002	0.3258	0.0281	0.3184
Middle stage of frog eye disease	0.9899	0.3151	0.2634	0.3158
Late stage of frog eye disease	0.8799	0.3157	3.9754	0.3107

uniformity, are needed as texture feature parameters as shown in Table 6.

4.2. Image Feature Optimization of Tobacco Leaf Spots Based on PSO and ORB

4.2.1. Algorithm Principle. Particle swarm optimization takes the feasible solution space of the optimization problem as its search space and randomly generates the initial population in the search space. An individual is a particle without volume or mass [30]. The spatial position of each particle is a feasible solution to the optimization problem. The fitness of a particle is a measure of its position in space. The particle dynamically adjusts its flight speed and space position in the search space to search for the optimal space position and for finding an optimal solution to the problem [31, 32]. The PSO algorithm is used to reduce the original data dimension, and relatively few features are used to achieve better results. In the research, the PSO algorithm was used for the feature optimization of color features, texture features, and shape features extracted above. The algorithm flow is shown in Figure 1.

The ORB algorithm is a fast feature point extraction and description algorithm [33, 34]. To extract feature points, a scale pyramid is first constructed to make feature points meet scale invariance to a certain extent. Secondly, for each layer of the image pyramid, the FAST algorithm is used for the preliminary extraction of corner points. If the gray value of a pixel and enough pixels in its surrounding area differ sufficiently from the gray value of the point, the pixel is considered a FAST corner point. Furthermore, the Harris corner detection method was used to sort the feature points according to the response function of feature points. And, the first N corner points with good curvature are selected as the feature points according to the sorting results. Finally, the gray center of the mass method is used to determine the direction of feature points, and Rosin defines the moments of image blocks.

For discrete problems, the spatial position of the particle is represented as a vector composed of 0 and 1. For each iteration, it becomes difficult to calculate the velocity and spatial position of the particle in the search space.

4.2.2. Feature Selection Results. A total of 28 normalized features are selected in the early, middle, and late stages of brown spot disease and frog eye disease. After using the particle swarm optimization algorithm for 15 times, the feature selection results are derived which are shown in Table 7.

Table 7 shows that the fitness of the tenth group of data is 95.23, and the cross-validation rate is 93.31%. The recognition rate of the verification set is 96%, which also reaches the maximum value. The feature optimization is a 13-dimensional feature parameter. Therefore, the tenth group of optimization results is selected for the next step of classification recognition, namely, R1, B2, H1, S1, H2, V2, S3, rectangularity, complexity, energy, contrast, entropy, and average grayscale.

4.3. Classification and Recognition of Tobacco Leaf Disease Spots Based on SVM.

Pattern recognition refers to the analysis and processing of all kinds of information representing things through computer technology. It is an integral part of artificial intelligence. Classifiers, also called discriminant models, are used in pattern recognition. The support vector machine (SVM) is one of the commonly used classifiers, which is commonly used in image retrieval, target tracking, face recognition, and other fields. In this research, a support vector machine (SVM) was used to classify the optimized feature parameters, so as to realize the classification and recognition of the early similar diseases of tobacco leaves (brown spot disease and frog eye disease) and the early, middle, and late stages of the two diseases.

In real use, most are discrete, namely, nonlinear. Through the nonlinear mapping, the space samples are mapped to a high-dimensional feature space, constructing the optimal separating hyperplane again. At this time, considering that there is still linear inseparability caused by a small number of samples after nonlinear mapping to a high-dimensional feature space, relaxation variables need to be added. The penalty factor is added to the objective function, which plays a role in controlling the punishment degree of misclassification samples. The discrete classification problem can be regarded as a quadratic programming problem. The SVM is a binary classification algorithm, which can separate two different types of samples. But in the research process, six types of samples will appear at most, so it is necessary to construct appropriate multiclassifiers. Currently, there are two main methods to construct SVM multiclassifiers: direct method and indirect method. In this research, the one-to-one classification method of indirect method is used to design an SVM between any two different samples. Therefore, samples of N different categories need $n(n-1)/2$ SVMs. During the classification, the category with the most votes is the category of samples, as shown in Figure 2. The one-to-one classification method of the SVM function is adopted in MATLAB, and there are at the most six types of data in the research study. Figure 2 is an example diagram of the one-to-one classifier of the support vector machine. In this study, the main research is aimed at the early diseases of tobacco brown spot and frog eye disease, and the middle and late stages of tobacco brown spot and frog eye disease are added as the references in the classification process.

Two kinds of classification problems are solved, that is, the sample of one class at a time is selected as the positive class sample, and the sample of the negative class becomes only one class (called the "one-to-one" method). According to the maximum category adopted in the research, there are six categories. For this pair of one-category devices, the first one only answers "is it the first or the second," the second one only answers "is it the first or the third one," and the third one only answers "is it the first or the fourth one". There should be 15 such classifiers ($n(n-1)/2$ SVM classifiers are constructed if there are n categories). Although the number of classifiers is increased, the total time spent in the training stage is less than that of the "one-to-others" method, which is a directed acyclic graph, so this method is also called the DAG SVM.

Table 6: Selected texture feature information of six images of tobacco brown spot disease and frog eye disease in the early, middle, and late stages.

	Energy	Contrast	Correlation	Entropy	Homogeneity	Uniformity
Early stage of brown spot disease	0.9785	11.0598	0.9669	0.2087	0.9923	1.0851
Middle stage of brown spot disease	0.9065	31.3123	0.9880	0.8315	0.9638	7.3023
Late stage of brown spot disease	0.1854	50.2683	0.9860	8.1253	0.5632	9.8857
Early stage of frog eye disease	0.9932	5.0987	0.9789	0.0652	0.9982	0.5070
Middle stage of frog eye disease	0.9639	12.1158	0.9887	0.3095	0.9868	2.5544
Late stage of frog eye disease	0.9200	19.1023	0.9885	0.6851	0.9756	5.0451

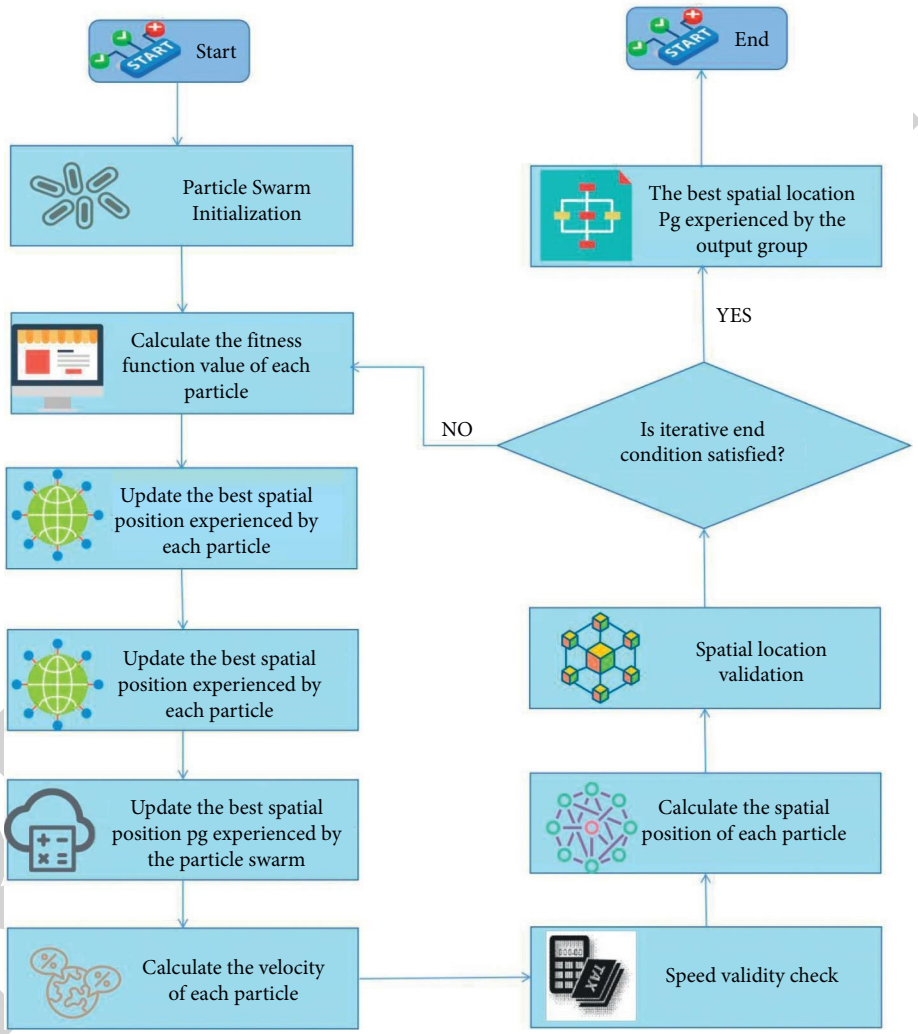

Figure 1: Flow chart of the PSO algorithm.

The classifier used in the research determines whether these categories belong to the first or the sixth category in the "1 to 6" classification process. It continues to judge the category according to the order shown in the above figure and runs the judgment until all six categories of data are identified. At this time, 15 classifiers are actually called, which can accurately distinguish different classes.

4.4. Analysis of Identification Results. The total number of samples in the research is 1200 groups, including 600 groups of tobacco frog eye disease and 600 groups of brown spot disease, including 200 groups in the early, middle, and late stages, respectively. 150 groups are selected as the training data, and 50 groups are selected as the test data. The color features, morphological features, and texture features extracted above are normalized and optimized by the

Table 7: Experimental results of feature selection of particle swarm optimization for 15 times.

Number of experiments	Binary representation of feature-preferred combinations	Adaptability	Cross-validation rate (%)	Verification set recognition rate (%)
1	01011011001011011010010101	94.23	88.57	94.00
2	10010110000101010010100011	94.15	88.69	93.67
3	00010010101101101010011110	98.65	89.23	91.00
4	11010100111000010011001000	95.56	87.87	95.67
5	00011001100101111101010110	92.15	92.66	8933
6	10001001000100001010111011	93.26	86.71	92.67
7	00101001101101101110011011	94.31	87.24	93.00
8	10011001000110011010110011	94.11	89.31	94.00
9	00011001010011110011001111	95.68	88.65	92.65
10	10000100011010101011001010	95.26	93.31	96.00
11	10010100100010110110101110	94.37	92.33	94.33
12	11010100010011011001001010	92.31	89.23	93.00
13	11010100010011011001001010	91.36	87.56	92.00
14	11011101010011001100100011	95.15	86.26	89.23
15	00010101010100100110010101	98.26	91.22	97.65

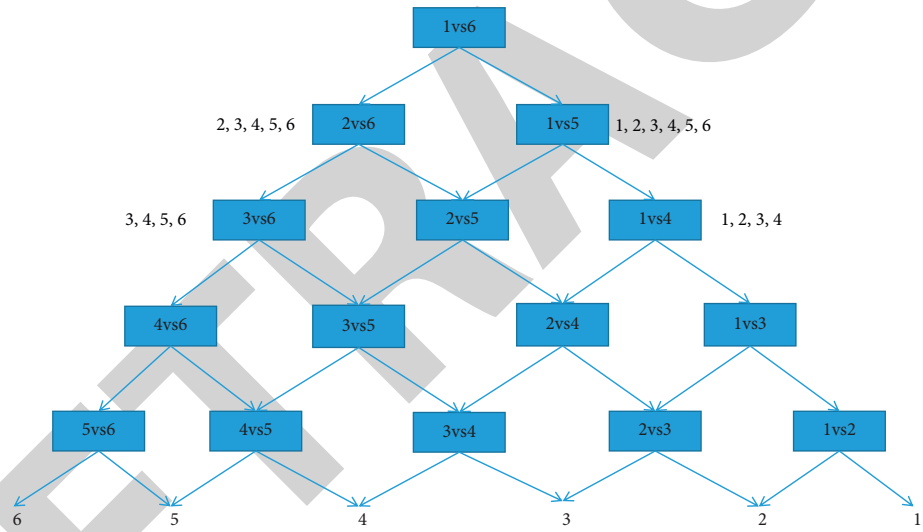

Figure 2: Sample diagram of the one-to-one classifier of SVM.

particle swarm optimization algorithm. Finally, the SVM classification model is established for recognition. The test recognition results are shown in Table 8.

The identification rate of early disease samples of frog eye disease is 90% and that of brown spot disease is 94%. According to Figure 3, the external morphology of frog eye disease and brown spot disease in the early stage is very similar. Brown spot disease has patches of different widths around the spot in the early stage, but frog eye disease does not. The early stage of brown spot disease is characterized by round spots, and the color of the spots is mostly yellowish brown. The early stage of frog eye disease is characterized by round spots which are brown, tawny or dirty white, or mostly brown. The identification rate of frog eye disease is lower than that of brown spot disease based on the color and halo of frog eye disease and brown spot disease and is shown in Table 9.

The number of identification errors in the early, middle, and late stages of frog eye disease samples is 4, 1, and 1, respectively. The number of identification errors in the early, middle, and late stages of brown spot disease samples is 4, 2, and 0, respectively. The early stage of frog eye disease is characterized by round spots which are brown, tawny or dirty white, or mostly brown. There is no significant difference in the area of the middle and late stages of frog eye disease. The actual measurement shows a width range of 0.5 cm-1 cm. The middle stage of frog eye disease is gray parchment in the center, and the gray mold layer and perforation damage are produced in the late stage of frog eye disease. The early stage of brown spot disease is characterized by round spots, and the color of the spots is mostly yellowish brown. In the middle stage, there are obvious rims and the area of the lesion gradually becomes larger. The actual measurement in the field shows a width range of

Table 8: Early identification rates of frog eye disease and brown spot disease.

Disease type	Time of the disease	Training sample	Test sample	Test the correct sample	Test correct sample recognition rate (%)
Brown spot disease	Early	150	50	47	94
Frog eye disease	Early	150	50	48	96
Total		300	100	95	95

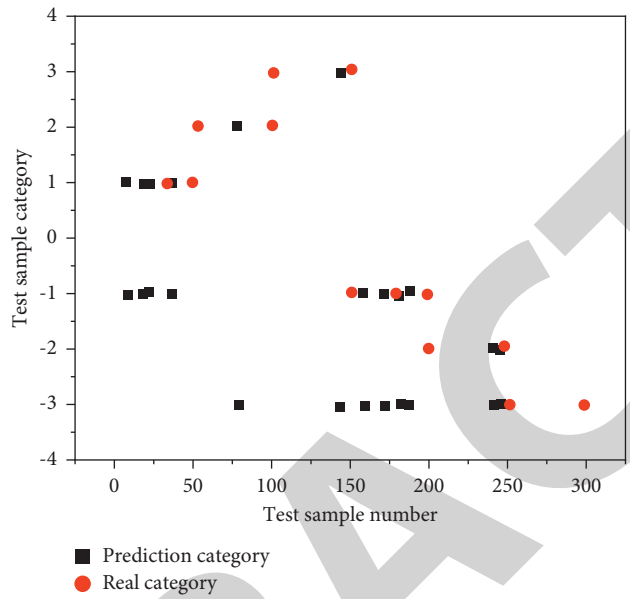

Figure 3: Classification results of tobacco brown spot in the early, middle, and late stages and tobacco frog eye disease in the early, middle, and late stages.

Table 9: Identification rates of brown spot disease and frog eye disease in different periods.

Disease type	Time of the disease	Training sample	Test sample	Test the correct sample	Test correct sample recognition rate (%)
Brown spot disease	Early	150	50	47	94
	Middle	150	50	49	98
	Late	150	50	49	98
Frog eye disease	Early	150	50	48	96
	Middle	150	50	45	90
	Late	150	50	50	100
Total		900	300	288	96

0.6 cm-2 cm. The width of a single spot in the late stage ranges from 4 cm to 10 cm, and the whole leaf surface will be necrotic if multiple disease spots are linked together.

On the other hand, in order to further improve the efficiency of recognition, a deep learning framework is used. After the data enhancement, a total of 2668 original crop leaf disease images are analyzed. 20 labels are assigned to each image in the dataset, each label representing a crop disease. Through the data enhancement, the original data images are extended to the sample set with 32016 images. Through transfer learning, the parameter weights of the last layer are retrained, and then the recognition accuracy of the four groups of experiments on several deep learning frameworks is compared with the verification set. Other parameters are shown in Table 10.

First, it is determined that the dataset contains 32,016 images after data enhancement of the original images, and the influence of different center loss weights λ on the supervision effect is tested. Then, in the best λ case, four groups of experiments are carried out to cross-verify the influence of data enhancement and joint supervision on the model. The verification combination is shown in Table 11.

The specific experimental results are presented in Figures 4 to 6.

After the abovementioned figure is iterated, the recognition accuracy curve gradually becomes stable and rises. Similarly, after 5000 iterations, the loss gradually declines gently. Experimental results show that the two-stage ADGACCNN network structure can effectively improve the generalization ability of the model and reduce the

Table 10: Parameter selection of deep learning framework.

Parameter selection
1. Deep learning framework selection: AlexNet, VGG-16, and GoogleNet
2. Model training method: transfer learning
3. Training-test set distribution: the training set is 80%, and the test set is 20%

Table 11: Cross-validation combinations.

Experiment serial number	Portfolio to be verified
1	CNN
2	AD-GAC CNN
3	CNN + joint supervision
4	AD-GAC CNIN + joint supervision

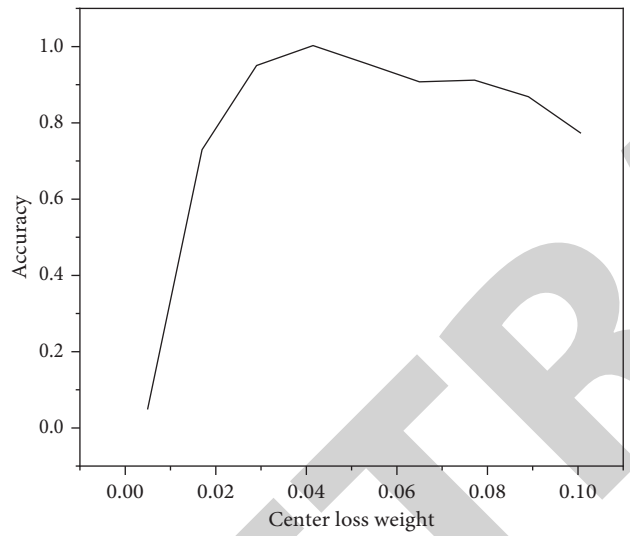

Figure 4: Influence of the weight loss of test center on the recognition accuracy of B + C sets on AlexNet.

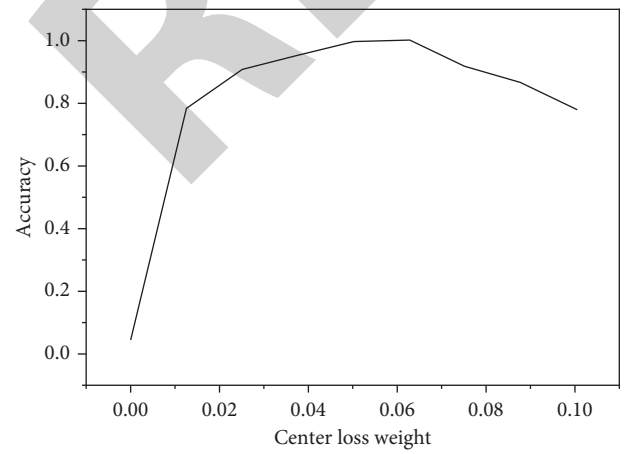

Figure 5: Influence of the weight loss of test center on the recognition accuracy of B + C sets on VGG-16.

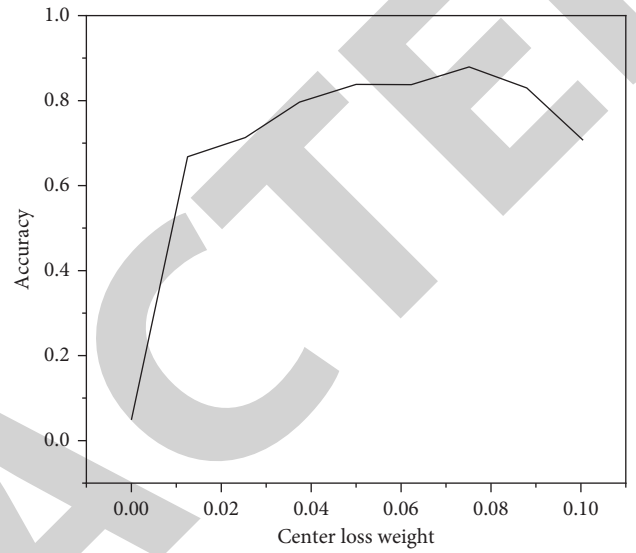

Figure 6: Influence of the weight loss of test center on the recognition accuracy of B + C sets on GoogleNet.

occurrence of the overfitting phenomenon. When using the central loss function and softmax function as the joint supervision mechanism, the model can effectively reduce the intraclass distance and increase the interclass distance. When the two methods are simultaneously applied to the model, the recognition accuracy of the model is increased by nearly 10% compared with that of the model without either method. It can be seen that it has obvious significance for spot recognition tasks for small samples under complex backgrounds and also has reference significance for other types of recognition tasks.

5. Conclusion

The main content of the research was to investigate the early segmentation and recognition of brown spot disease and frog eye disease, which have high similarities to tobacco diseases. The images of two tobacco diseases (brown spot disease and frog eye disease) under complex background were used as segmentation objects.

(1) The commonly used segmentation methods and theories of crop diseases, especially tobacco leaf diseases, were summarized, and the segmentation methods of tobacco leaf diseases under complex backgrounds were emphatically investigated. In view of the difficulty in segmentation of images of two tobacco leaf diseases (brown spot disease and frog eye disease) under complex background in field

practice, a multistep segmentation method based on saliency detection and seed point selection was proposed, which combined the mean shift smoothing preprocessing with simple linear iterative clustering preprocessing. It was suitable for image segmentation in a complex field environment, and the effectiveness of the method was proved.

(2) According to the realization forms of the two diseases in different periods, the color features, morphological features, and texture features were extracted, with a total of 28 dimensions of color feature information. After that, the particle swarm optimization algorithm was used to optimize the features and reduce the dimensions to 13 dimensions, greatly reducing the workload in the recognition classifier.

(3) According to different external forms of brown spot disease and frog eye disease in the early, middle, and late stages (six categories), the different diseases of the image color features, shape features, and texture features were extracted. A total of 28 dimensional data features were extracted from each category. Then, feature optimization was carried out by the particle swarm optimization algorithm, and finally, 13 dimensional feature parameters were obtained. The recognition rate of the verification test set reached 96%. In the recognition process, a support vector machine was used to classify tobacco brown spot disease and tobacco frog eye disease. The recognition rate of tobacco brown spot disease and frog eye disease in the early stage reached 92%, and the recognition rate of six categories of the early, middle, and late stages of the two diseases reached 96%.

Data Availability

Data are available upon request.

Disclosure

Authors Min Xu, Lihua Li, Liangkun Cheng, Haobin Zhao, Jiang Wu, Xiaoqiang Wang, Hongchen Li, and Jianjun Liu are affiliated to and funded by China National Tobacco Corporation Henan Company. The authors attest that China National Tobacco Corporation Henan Company has had no influence on design of this study or its outcomes.

Conflicts of Interest

The authors declare that they have no conflicts of interest.

Acknowledgments

The authors would like to thank China National Tobacco Corporation Henan Company as this research was funded by the Project of China National Tobacco Corporation Henan company (2021410000240021) and the Project of China Tobacco Zhejiang Industry Co, Ltd. (ZJZY2021B009).

References

[1] T. Fang, P. Chen, J. Zhang, and B. Wang, "Crop leaf disease grade identification based on an improved convolutional neural network," *Journal of Electronic Imaging*, vol. 29, no. 01, p. 1, 2020.

[2] N. Yuvaraj, K. Srihari, G. Dhiman et al., "Nature-inspired-based approach for automated cyberbullying classification on multimedia social networking," *Mathematical Problems in Engineering*, vol. 2021, pp. 1–12, 2021.

[3] X. F. Du, J. S. Wang, and W. Z. Sun, "Unet retinal blood vessel segmentation algorithm based on improved pyramid pooling method and attention mechanism," *Physics in Medicine and Biology*, vol. 66, no. 17, Article ID 175013, 2021.

[4] X. Zhou, J. Yu, W. Zhang, A. Zhao, and M. Zhou, "A multi-objective optimization operation strategy for ice-storage air-conditioning system based on improved firefly algorithm," *Building Service Engineering Research and Technology*, vol. 43, no. 2, pp. 161–178, 2022.

[5] J. Bi, S. Yin, H. Li, L. Teng, and C. Zhao, "Research on medical image encryption method based on improved krill herb algorithm and chaotic systems," *International Journal on Network Security*, vol. 22, no. 3, pp. 486–491, 2020.

[6] X. Wang, L. Jiang, L. Li et al., "Joint learning of 3d lesion segmentation and classification for explainable covid-19 diagnosis," *IEEE Transactions on Medical Imaging*, vol. 40, no. 9, pp. 2463–2476, 2021.

[7] M. S. Pradeep Raj, P. Manimegalai, P. Ajay, and J. Amose, "Lipid data acquisition for devices treatment of coronary diseases health stuff on the internet of medical things," *Journal of Physics: Conference Series*, vol. 1937, no. 1, Article ID 012038, 2021.

[8] B. Ye, X. Yuan, Z. Cai, and T. Lan, "Severity assessment of covid-19 based on feature extraction and v-descriptors," *IEEE Transactions on Industrial Informatics*, vol. 17, no. 11, pp. 7456–7467, 2021.

[9] X. Huang, W. Chen, and W. Yang, "Improved algorithm based on the deep integration of googlenet and residual neural network," *Journal of Physics: Conference Series*, vol. 1757, no. 1, Article ID 012069, 2021.

[10] Q. Wang, J. Wang, and M. Zhu, "Research on emotion recognition algorithm based on improved bp neural network," *Journal of Physics: Conference Series*, vol. 1976, no. 1, Article ID 012002, 2021.

[11] H. Cao, "Analysis of English teaching based on convolutional neural network and improved random forest algorithm," *Journal of Intelligent and Fuzzy Systems*, vol. 2, no. 2, pp. 1–11, 2020.

[12] X. Liu, C. Ma, and C. Yang, "Power station flue gas desulfurization system based on automatic online monitoring platform," *Journal of Digital Information Management*, vol. 13, no. 06, pp. 480–488, 2015.

[13] L. F. Zhu, J. S. Wang, H. Y. Wang, S. S. Guo, and W. Xie, "Data clustering method based on improved bat algorithm with six convergence factors and local search operators," *IEEE Access*, vol. 23, no. 99, p. 1, 2020.

[14] C. Huang, H. Ding, and C. Liu, "Segmentation of cell images based on improved deep learning approach," *IEEE Access*, vol. 15, no. 99, p. 1, 2020.

[15] J. Zhang and J. S. Wang, "Improved whale optimization algorithm based on nonlinear adaptive weight and golden sine operator," *IEEE Access*, vol. 9, no. 99, p. 1, 2020.

[16] M. Abdel-Basset, R. Mohamed, M. Elhoseny, R. K. Chakrabortty, and M. Ryan, "A hybrid covid-19

Hindawi
Scientific Programming
Volume 2022, Article ID 7777211, 11 pages
https://doi.org/10.1155/2022/7777211

Research Article

An Intrusion Detection Method Based on Fully Connected Recurrent Neural Network

Yuhong Wu[1] **and Xiangdong Hu**[2]

[1]*College of Computer Science and Technology, Chongqing University of Posts and Telecommunications, Chongqing, China*
[2]*School of Automation, Chongqing University of Posts and Telecommunications, Chongqing, China*

Correspondence should be addressed to Xiangdong Hu; huxd@cqupt.edu.cn

Received 11 July 2022; Revised 23 August 2022; Accepted 1 September 2022; Published 26 September 2022

Academic Editor: Lianhui Li

Now, the use of deep learning technology to solve the problems of the low multiclassification task detection accuracy and complex feature engineering existing in traditional intrusion detection technology has become a research hotspot. In all kinds of deep learning, recurrent neural networks (RNN) are very important. The RNN processes 41 feature attributes and maps them to a 122-dimensional high-dimensional feature space. To detect multiclassification tasks, this study proposes an intrusion detection method based on fully connected recurrent neural networks and compares its performance with previous machine learning methods on benchmark datasets. The research results show that the intrusion detection system (IDS) model based on fully connected recurrent neural network is very suitable for classification of intrusion detection. Classification methods, especially in multiclassification tasks, have high detection accuracy, significantly improve the detection performance of detection attacks and DoS attacks, and it provides a new research direction for the future attempts of intrusion detection methods for industrial control systems.

1. Introduction

With the achievements of deep learning in image recognition, speech recognition, etc, it also provides a new method and idea for researchers in the field of intrusion detection to carry out related work.

Recurrent neural networks (RNN) were important. In 2007, Rachid et al. applied RNN and standard neural network to the field of intrusion detection and conducted experiments on the constructed small sample dataset. The experimental results showed that the detection and classification performance based on the RNN was relatively general on the small sample dataset, which was lower than the neural network under the same conditions. In 2010, Mansour et al., considering the complexity of the fully connected neural network structure, constructed a partially connected RNN, and the features between groups were constructed into a fully connected recurrent neural network, and there was no information between the features between groups [1–3]. Contact feedback to reduce model training time and achieve better detection results on the datasets you build. Although the locally connected recurrent neural network structure shortens the training time, the features were artificially classified, and the connections and roles between different groups of features were not considered.

After in-depth analysis, this study proposes an intrusion detection model based on fully connected recurrent neural network. Forty one feature attributes were processed and mapped into a 122-dimensional high-dimensional feature space, and features were no longer grouped and classified. Considering the relationship between features, this study investigates the detection ability of fully connected recurrent neural networks under multiclassification tasks.

2. Recurrent Neural Network (RNN)

Currently, recurrent neural networks (RNN) are mainly used to solve dynamic system problems involving time series

of events. Structurally, a RNN includes a hidden layer, an input layer, and an output layer [4–6]. The current output is related to the previous output, and the nodes of each hidden layer are no longer disconnected. Therefore, the main work is achieved through the loop of the hidden layer itself. Essentially, an RNN is a unidirectional information flow from the input layer to the hidden layer, combined with a unidirectional information flow from the last sequential hidden layer to the current hidden layer. Figure 1 visually compares the differences between traditional neural networks and RNN.

Figure 2 shows the structure of the RNN after expansion. All states before time series t will be represented as outputs at time series t-1 and affect the time series t. Therefore, a RNN is a learning model with a dynamic deep structure. If the hidden unit is regarded as the storage space of the entire network, when the RNN is expanded according to the time series, it can be considered that the RNN has memorized all the information so far, which is a typical end-to-end learning method. Theoretically, a RNN can learn arbitrarily long sequence information and can remember end-to-end information, reflecting the "depth" of deep learning.

Obviously, in training, the training of RNN includes forward pass and backward pass. Similar to the traditional neural network training algorithm, the forward pass is output according to the time sequence, and the reverse pass is to pass the accumulated residuals of the previous period back through the RNN. During forward propagation, the hidden layer output (h_t) is

$$h_t = \sigma\left(W x_t + U h_{t-1} + b_h\right), \tag{1}$$

where σ is the activation function, x_t is the input vector of the time series t, h_t is the output of the hidden layer, W is the weight matrix, U is the self-circulating weight matrix, and b_h is hidden layer bias.

2.1. Intrusion Detection System (IDS) Based on Fully Connected Recurrent Neural Network. The overall framework of the intrusion detection model is shown in Figure 3, which mainly includes five steps [7–10].

Obviously, the training of the FCRNN-IDS has two aspects: forward propagation and weight fine-tuning. The forward propagation was responsible for the operation of the output data, and the fine-tuning of the weights was to update the weights by passing the accumulated residuals [11], which was no different from ordinary neural network training. The training was divided into two steps: first, the forward propagation algorithm was used to calculate its output value for each training sample of the input model. Then, using the weight fine-tuning algorithm, the entire model parameters were fine-tuned through backpropagation, and finally, a complete fully connected RNN classification model was obtained.

According to Figure 2, Algorithm 1 is a forward propagation algorithm, and Algorithm 2 is a weight update algorithm, respectively. Calculate the output $\hat{y}_i$ of each instance x_i using the forward propagation algorithm.

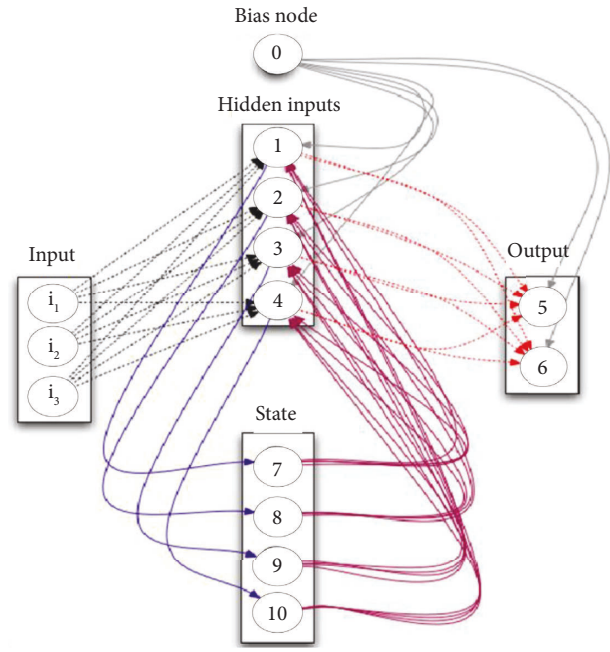

Figure 1: RNN structure.

3. Experiment

3.1. Data Sources. The dataset used in the experiment is a new benchmark dataset NSL-KDD [12–15]. This dataset is widely used.

3.2. Data Feature Extraction and Selection. Each connection record in the NSL-KDD contains 41 feature attributes [16–19]. Among them, 41 features can be divided into 4 categories:

(i) Basic features (9 types in total, numbered 1 to 9)

(ii) Content features (13 types in total, serial numbers 10 to 22)

(iii) Time-based network traffic statistics (9 types in total, serial numbers 23~31)

(iv) Host-based network traffic statistics (10 types in total, serial numbers 32~41)

3.3. Data Preprocessing. Using the NSL-KDD dataset, each connection record consists of 41 feature attributes, including 3 non-numeric feature attributes. Data preprocessing mainly includes two parts: numericalization of nonnumerical feature attributes. After one-hot encoding, the attribute feature 'protocol_type' corresponds to the binary feature vectors (1, 0, 0), (0, 1, 0), and (0, 0, 1). The other two nonnumerical attribute properties "service" and "flag" have 70 and 11 values, respectively. After such digital processing, the original 41-dimensional feature vector was converted into a 122-dimensional high-dimensional feature vector. On the one hand, one-hot encoding solves the problem of nonnumerical data conversion, making the calculation of "distance" between features more reasonable.

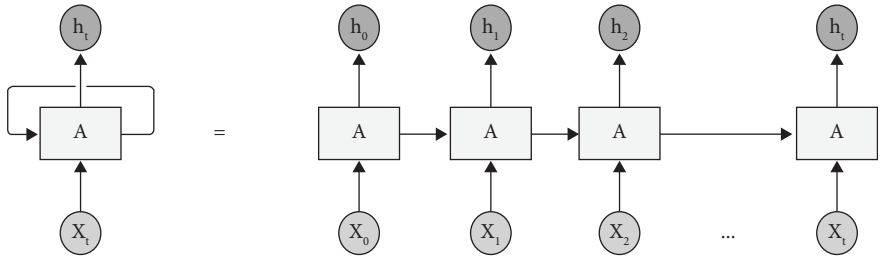

Figure 2: Unrolled RNN.

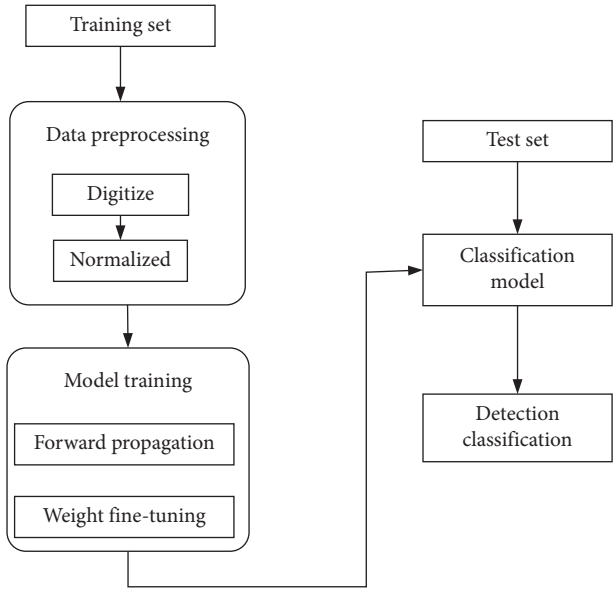

Figure 3: Framework of intrusion detection system based on fully connected recurrent neural network (IDS-FCRNN).

Input: the training sample was x_i ($i = l$, 2, m), the weight matrix was W_{hx}, W_{hh}, and W_{yh}, the bias was b_h and b_y, the activation function e uses the sigmoid function, and the classification function g uses the SoftMax function.
Output: the output value $\widehat{y}_i$ corresponding to the training sample X_i

(1) for xi from 1 to m do
(2) $t_i = W_{hx}x_i + W_{hh}h_{i-1} + b_h$
(3) $h_i = sigmoid(t_i)$
(4) $s_i = W_{yh}h_i + b_y$
(5) $\widehat{y}_i = SoftMax(s_i)$
(6) End for

Algorithm 1: Forward propagation algorithm.

Input: the training sample was (x_1, y_1) ($i = 1$, 2, ..., m).
Initialization: the initialization model parameter was $\theta = \{W_{hx}, W_{hh}, W_{yh}, b_h, b_y\}$
Output: the fine-tuned model parameter was $\theta = \{W_{hx}, W_{hh}, W_{yh}, b_h, b_y\}$

(1) For each sample x_i, input a fully connected RNN, the output $\widehat{y}_i$ of x_i was calculated by Algorithm 2.1
(2) Calculate the cross-entropy $L(y{:}\widehat{y}_i)$ between the output value of each sample and the label value: $L(y{:}\ \widehat{y}_i) \leftarrow -\sum_i \sum_i y_{ij} \log\ (\widehat{y}_{ij}) + (1 - y_{ij}) \log\ (1 - \widehat{y}_{ij})$
(3) For each network model parameter θ_i in θ, calculate the partial derivative δ_i: $\delta_i \leftarrow dL/d\theta_i$
(4) Make the error propagate back along the network and update each network model parameter θ_i in θ: $\theta_i \leftarrow \theta_i + \eta\delta_i$
(5) If $t = k$, save the model parameters and the algorithm ends
(6) If $t < k$, then $t = t + 1$, turn to 1.

Algorithm 2: Weight fine-tuning algorithm.

The first step was that the data value space was too large. Feature attributes such as "duration[0, 58329]," "dst_bytes [0,1.3 × 109]," and "src_bytes[0,1.3 × 109]," which were correspondingly scaled by the logarithmic correction method as "duration[0, 4.77]," "dst_bytes[0, 9.11]," and "src_bytes[0, 9.11];" then, make each instance lie on the same order of magnitude on this feature. The second step was to normalize the data to the [0, 1] value range according to the following formula:

$$x_i = \frac{x_i - \text{Min}}{\text{Max} - \text{Min}}, \tag{2}$$

where x_i was the attribute eigenvalue, Min was the minimum value, and Max was the maximum value.

3.4. Test Plan. This study adopts the comparative test method to detect the accuracy of FCRNN-IDS.

3.4.1. Comparative Experiment 1: Comparison with Traditional Machine Learning Methods. Using the same dataset NSL-KDD, the detection accuracy of seven traditional machine learning algorithms [20–33] such as decision tree, Naive Bayes, Naive Bayes tree, random tree, random forest, support vector machine, multilayer perceptron, and the detection accuracy of the FCRNN-IDS model in the case of 2-class (normal, abnormal) and 5-class (normal, probe, Dod, R2L and U2R) were studied and compared.

In [5], the authors investigated the anomaly detection performance of the above 7 classification algorithm models on the NSL-KDD benchmark dataset using Weka machine learning and data mining tools. Under the 2-class task, Figures 4 and 5 show the detection accuracy of KDDTest+ and KDDTest-21 by seven traditional machine learning methods, respectively. This study takes the research results of [5] as one of the comparative experiments; under the 2-class task, it was compared with the detection model based on fully connected recurrent neural network.

3.4.2. Comparative Experiment 2: Comparison with Recent Similar Literature. Wang and Cai [8] studied the performance of artificial intrusion detection systems under two and five types of tasks based on the same benchmark dataset NSL-KDD. The experimental results show that, under the dataset KDDTest+, the highest detection rate of the model was 81.2% under the 2-class classification; the highest detection rate of the model was 79.9% under the 5-class classification.

Deng et al. [9] proposed three-layer partially connected recurrent neural network architecture with 41 features as input and 4 intrusion categories and normal category as output. Taking the KDD99 dataset as the benchmark, some connection records were selected as the training set and the test set, respectively. The results show that the highest detection accuracy of the model was 94.1%. On the test set, the training time was set at 1383 seconds.

4. Results' Analysis

4.1. Experimental Results of 2-Class Tasks. As mentioned earlier, the 41-dimensional feature vector was mapped to a 122-dimensional feature vector, so in the 2-class experiment. Figure 6 shows the detection accuracy of the FCRNN-IDS model on the training set with different structures and Learningrates.

As shown in Figure 7, it shows the detection accuracy of the FCRNN-IDS model on the test set KDDTest+ with different structures and Learningrates. As can be seen from Figure 7, when the Learningrate was 0.1 and the number of HiddenNodes was 80, the detection accuracy of the model on the test set KDDTest+ was 83.28%.

Figure 8 shows the detection accuracy of the FCRNN-IDS model on KDDTest-21 with different structures and Learningrates. As can be seen from Figure 8, when the Learningrate was 0.1 and the hidden node was 80, the model has the highest detection accuracy on KDDTest-21, which was 68.55%.

The experimental results were as follows.

As shown in Table 1, the number of HiddenNodes was 80 and the Learningrate was 0.1, which obtains high detection accuracy. Figure 9 details the variation in detection accuracy of the FCRNN-IDS model iteratively trained on the KDDTrain+, KDDTest+, and KDDTest-21.

Ashfaq e al. [5] studied the detection accuracy of classification algorithms such as J48, Multilayer Perception, Naive Bayes, Support Vector Machine, and Random Forest. The results are shown in Figures 4 and 5; the artificial neural network algorithm has the highest detection accuracy on the test set KDDTest+ in the 2-class task, reaching 81.2%, which was the latest literature on the application of related algorithms. The above model experimental results were all based on the dataset NSL-KDD, so they had similar comparison conditions.

As shown in Figure 10, the three algorithm models showed good classification and detection performance, especially the Naive Bayesian tree on the test sets, KDDTest+ and KDDTest-21. Better classification and detection performance: the detection accuracy of this method was high, 82.02% and 66.16%, respectively.

Compared with the detection method based on artificial neural network proposed in [8], FCRNN-IDS has the highest detection accuracy under the 2-class task, which was 81.2%, and the detection accuracy under the 2-class task was also higher. Table 2 shows the confusion matrix of the ANN-based detection model on the test set KDDTest + when performing the 2-class task. Table 3 presents the confusion matrix of FCRNN-IDS on KDDTest + under the 2-class task.

Therefore, when performing 2-class tasks, FCRNN-IDS further improved the detection ability of attack behavior, improved the accuracy, and reduced the false positive rate.

4.2. Experimental Results of Multiclassification Tasks. Figure 11 shows the detection accuracy of FCRNN-IDS on the training set with different structures and

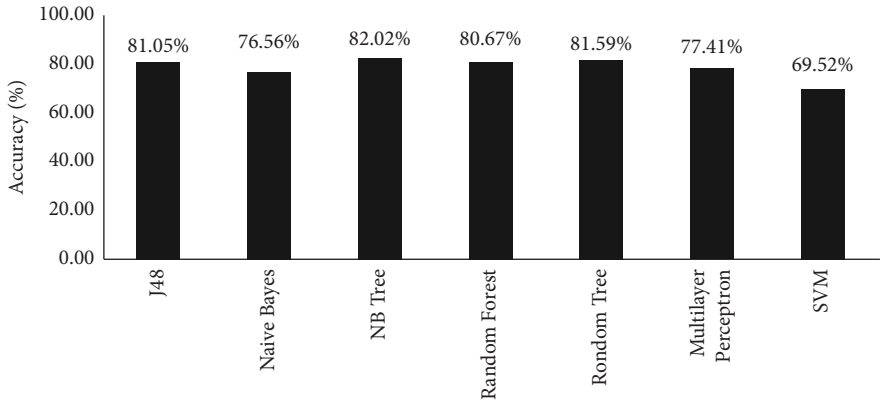

Figure 4: Detection accuracy of traditional machine learning methods in the test set KDDTest+ (2-class).

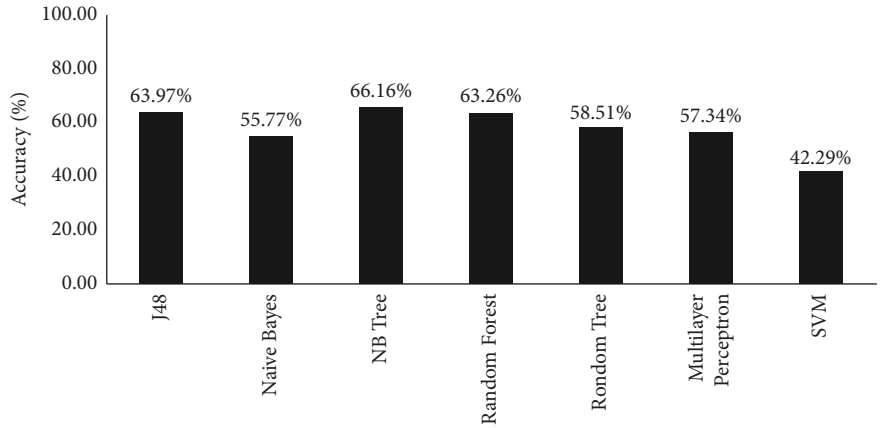

Figure 5: Detection accuracy of traditional machine learning methods on the test set KDDTest-21 (2-class).

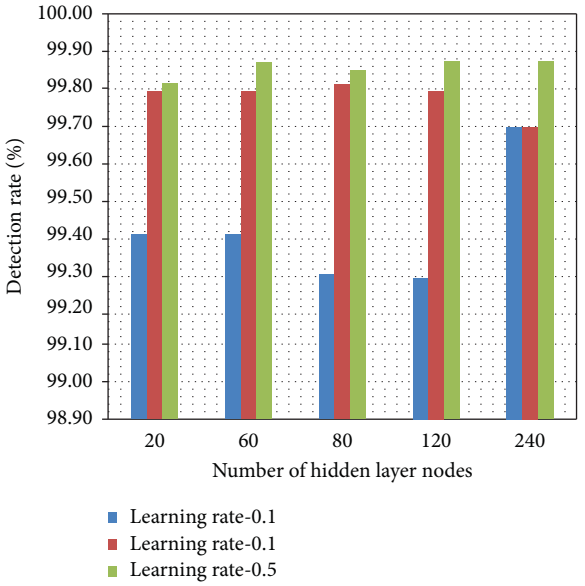

Figure 6: The accuracy of the model on the training set under different structures and Learningrates (2-class).

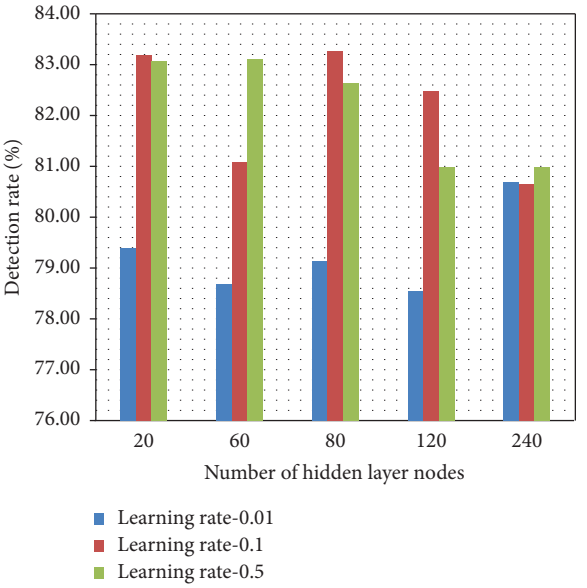

Figure 7: Detection rate of the model on KDDTest+ with different structures and Learningrates (2-class).

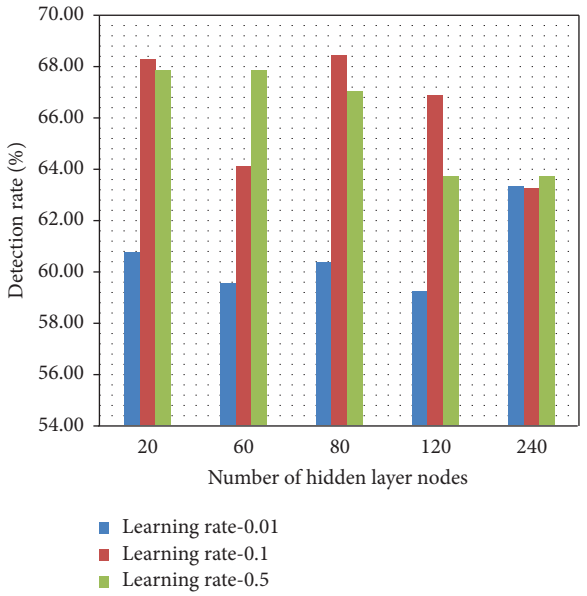

Figure 8: Detection rate of the model on KDDTest-21 under different structures and Learningrates (2-class).

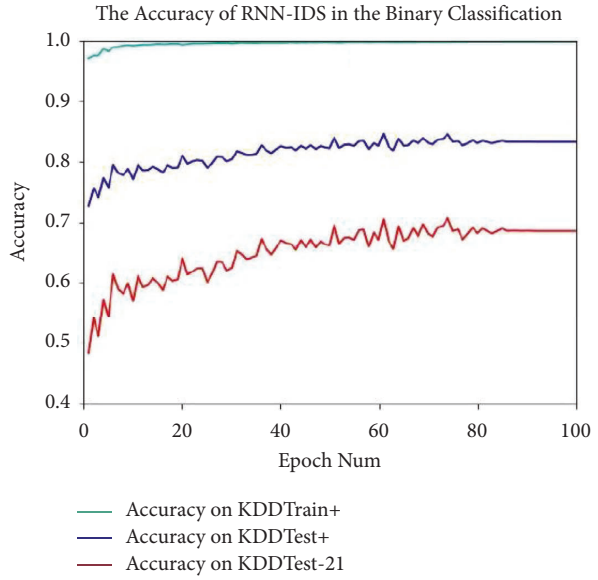

Figure 9: Detection performance of the model on the dataset (2-class).

Table 1: Model detection accuracy (2-class) under different structures and Learningrates.

	KDDTrain^{+}	KDDTest^{+}	KDDTest^{-21} (%)
HiddenNodes = 20, Learningrate = 0.01	99.40%	79.37%	60.76
HiddenNodes = 20, Learningrate = 0.1 rate = 0.1	99.79%	83.18%	68.23
HiddenNodes = 20, Learningrate = 0.5	99.81%	83.09%	67.84
HiddenNodes = 60, Learningrate = 0.01	99.39%	78.72%	59.54
HiddenNodes = 60, Learningrate = 0.1	99.79%	81.06%	64.08
HiddenNodes = 60, Learningrate = 0.5	99.87%	83.11%	67.82
HiddenNodes = 80, Learningrate = 0.01	99.29%	79.16%	60.34
HiddenNodes = 80, Learningrate = 0.1	99.81%	83.28%	68.55
HiddenNodes = 80, Learningrate = 0.5	99.85%	82.66%	66.99
HiddenNodes = 120, Learningrate = 0.01	99.28%	78.55%	59.25
HiddenNodes = 120, Learningrate = 0.1	99.79%	82.48%	66.83
HiddenNodes = 120, Learningrate = 0.5	99.87%	80.97%	63.69
HiddenNodes = 240, Learningrate = 0.01	99.69%	80.69%	63.28
HiddenNodes = 240, Learningrate = 0.1	99.69%	80.67%	63.28
HiddenNodes = 240, Learningrate = 0.5	99.87%	80.97%	63.69

Learningrates. As can be seen from the figure, when the Learningrate was 0.5 and the hidden node was 60, the model has the highest detection accuracy on the training set, which was 99.87%.

As shown in Figure 12, from the detection accuracy of FCRNN-IDS on the test set KDDTest + under different structures and Learningrates, it can be seen that the Learningrate was 0.5 and the hidden node was 80; the model has the highest detection accuracy in the test set KDDTest+, which was 81.29%.

As shown in Figure 13, from the detection accuracy of FCRNN-IDS on the test set KDDTest-21 under different structures and Learningrates, the Learningrate was 0.5 and the number of HiddenNodes was 80; the model has the highest detection accuracy on the test set KDDTest-21, which was 64.67%.

Table 4 shows the detection accuracy of FCRNN-IDS on the training set and 2 test sets when performing multiclass detection tasks with different network structures and different Learningrates. Obviously, the experimental results on multiclassification tasks show that different network structures and Learningrates can affect the detection ability of the FCRNN-IDS. As shown in Table 4, when the hidden layer of the FCRNN-IDS was set to 80 nodes and the Learningrate was set to 0.5, the model has higher detection accuracy on the KDDTest-21 and KDDTest + test sets, which was 81.29% and 64.67%.

In order to compare the detection accuracy of various algorithms, similar to the 2-type task experiment, J48, Naive Bayes, Random Forest, and multilevel models were established through data mining software Weka and open source machine learning. Using 10 layers of cross-validation in the training set KDDTrain+, model training was performed using 7 machine learning algorithm models including layer perceptrons and support vector machines, and then, the model detection accuracy was tested in the

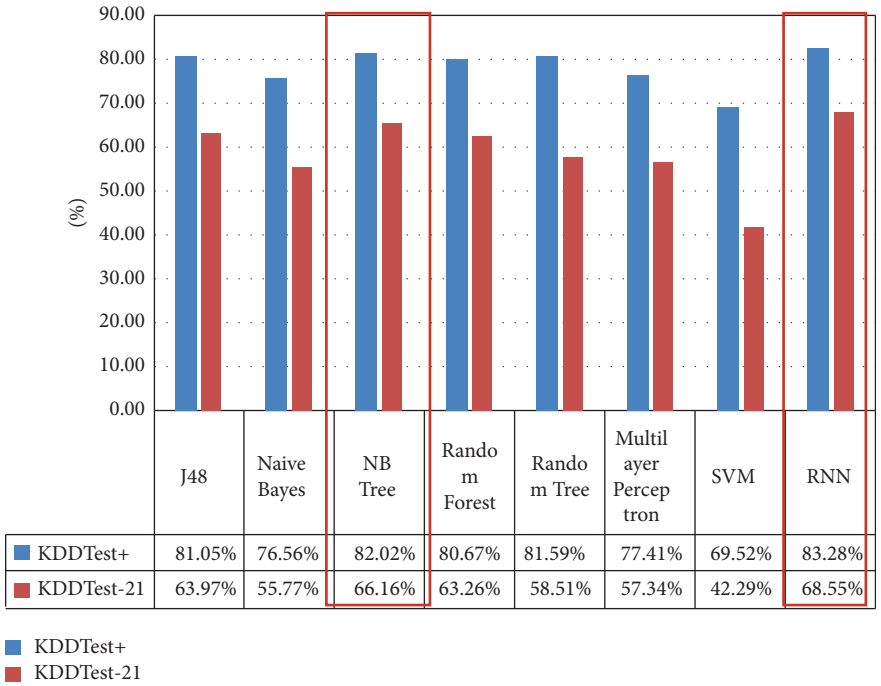

Figure 10: Detection accuracy of different models under 2-class tasks.

Table 2: Confusion matrix of the detection model based on artificial neural network on KDDTest$^+$ (2-class).

Actualclass	Predictedclass	
	Abnormal	Normal
Abnormal	8900	3933
Normal	314	9397

Table 3: Confusion matrix of model on KDDTest$^+$ (2-class).

Actualclass	Predictedclass	
	Abnormal	Normal
Abnormal	9362(↑)	3471
Normal	298	9413(↑)

test set. The experimental results are shown in Figure 14. Compared with the previous 2-class task, the detection accuracy of the traditional classification model generally drops under the multiclass task. Multilayer perception has the highest detection accuracy on the test sets KDDTest+ and KDDTest-21, 78.10% and 58.40%, respectively.

Under the same conditions, the neural network-based classification model achieves a detection accuracy of 79.9% when performing multiclassification tasks. Obviously, FCRNN-IDS performs better than other neural network-based detection models when performing multiclassification tasks.

Tables 5 and 6 show the confusion matrices of the neural network-based detection model and the fully connected recurrent neural network-based detection model on the test set KDDTest+, respectively.

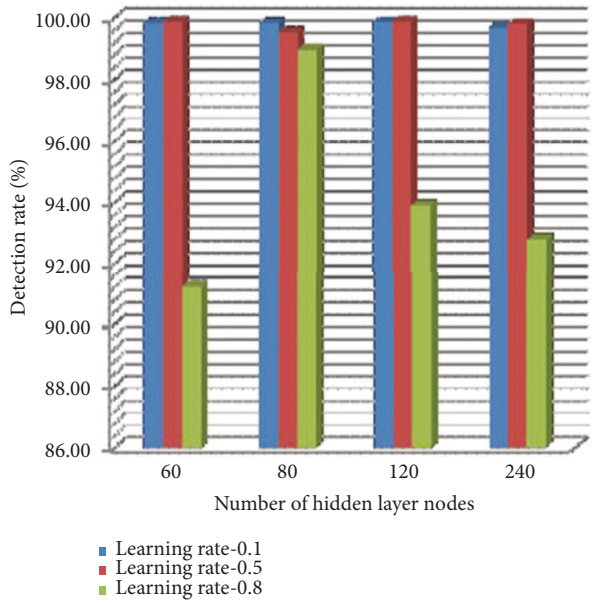

Figure 11: Detection rate of the model on the training set (multiclass).

Comparing the detection results in Tables 5 and 6, it can be seen that, in terms of correctly detecting DoS attacks, detection attacks, and U2R attacks, the detection model based on the RNN was fully connected to correctly detect more than 429 and 165 detection models based on neural networks, respectively, 2 contact records. Of course, in terms of correctly detecting normal connection records and R2L attack categories, the detection model

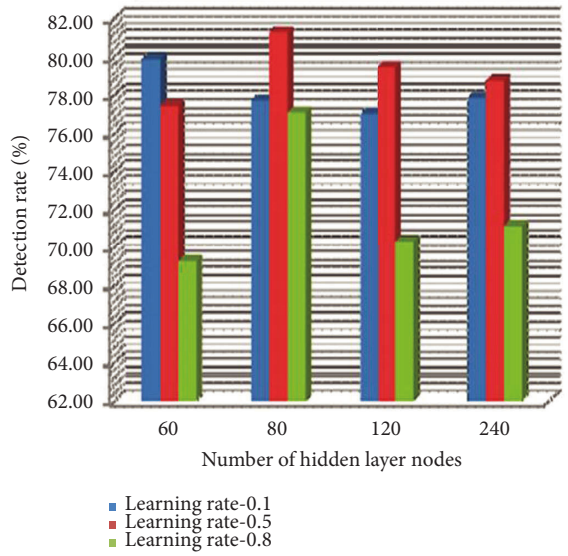

Figure 12: The detection rate of the model on the test set KDDTest^{+} (multiclassification).

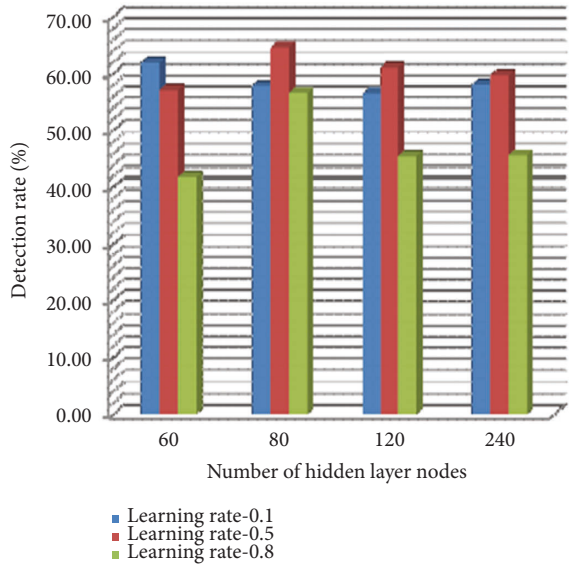

Figure 13: Detection rate of the model on the test set KDDTest^{-21} (multiclassification).

based on the fully connected RNN correctly detected 20 and 272 fewer connection records than the neural network, respectively.

The confusion matrices of the four attack types detected by the model on the test set KDDTest+ are shown in Tables 7–10. Table 10 shows that the model false positives and recalls vary according to the type of attack. Table 11 shows the recall and false positive rates for different attack types.

In order to compare the detection performance of the fully connected neural network model and the partially connected RNN model proposed in [9] for intrusion detection, the training set and test set were constructed according to the method mentioned in [9], as shown in Table 12. In the experiments, the model was set to 20 HiddenNodes, the Learningrate was 0.1, and the training epoch was 50 times. The detection accuracy of the trained model on the test dataset reaches 97.09%, which was higher than 94.1% in the literature.

As shown in the experimental results above, the fully connected model proposed in this study has stronger feature space modeling ability and higher accuracy. Of course, without GPU acceleration, the model training time based on the fully connected RNN was 1765 seconds, which was higher than the training time of the model based on the partially connected RNN at 1383 seconds.

Table 4: Accuracy of models with different structures and Learningrates (multiclassification).

	KDDTrain^{+}	KDDTest^{+}	KDDTest^{-21} (%)
HiddenNodes = 60, Learningrate = 0.1	99.84%	79.87%	61.98
HiddenNodes = 60, Learningrate = 0.5	99.87%	77.46%	57.18
HiddenNodes = 60, Learningrate = 0.8	91.23%	69.29%	41.85
HiddenNodes = 80, Learningrate = 0.1	99.82%	77.73%	57.84
HiddenNodes = 80, Learningrate = 0.5	99.53%	81.29%	64.67
HiddenNodes = 80, Learningrate = 0.8	98.97%	77.09%	56.64
HiddenNodes = 120, Learningrate = 0.1	99.85%	77.02%	56.55
HiddenNodes = 120, Learningrate = 0.5	99.87%	79.44%	61.11
HiddenNodes = 120, Learningrate = 0.8	93.90%	70.32%	45.49
HiddenNodes = 160, Learningrate = 0.1	99.68%	77.85%	58.05
HiddenNodes = 160, Learningrate = 0.5	99.80%	78.73%	59.71
HiddenNodes = 160, Learningrate = 0.8	92.79%	71.15%	45.64

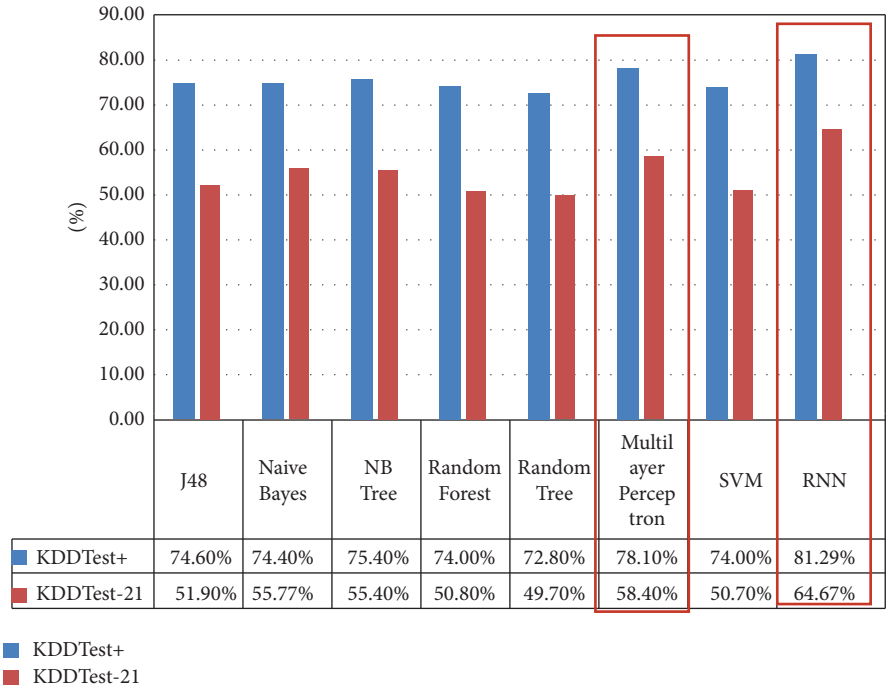

Figure 14: Detection accuracy of different classification models under 5-class tasks.

Table 5: Confusion matrix of the neural network-based detection model on the test set KDDTest^{+} for multiclassification tasks.

Actual class	Predicted class				
	Normal	DoS	R2L	U2R	Probe
Normal	9397	65	23	6	220
DoS	1515	5798	0	0	145
R2L	1789	2	952	6	5
U2R	144	6	10	21	19
Probe	403	164	0	0	1854

Table 6: Confusion matrix of the model on the test set KDDTest$^+$ for multiclassification tasks.

Actual class	Predicted class				
	Normal	DoS	R2L	U2R	Probe
Normal	9377 (1)	88	2	6	238
DoS	1011	6227 (f)	125	0	95
R2L	2058	0	680 (1)	6	10
U2R	149	0	11	23 (f)	17
Probe	231	166	5	0	2019 (f)

Table 7: DoS type confusion matrix.

Actual class	Predicted class	
	DoS	Others
DoS	6227	1231
Others	254	12099

Table 8: R2L type confusion matrix.

Actual class	Predicted class	
	R2L	Others
R2L	680	2074
Others	143	17646

Table 9: U2R type confusion matrix.

Actual class	Predicted class	
	U2L	Others
U2R	23	177
Others	12	18303

Table 10: Probe type confusion matrix.

Actual class	Predicted class	
	Probe	Others
Probe	2019	402
Others	360	16307

Table 11: Recall and false positive rates for different attack types.

Attack type	False positive rate (%)	Recall rate (%)
DoS	2.16	83.49
U2R	0.17	11.50
R2L	0.81	24.69
Probe	2.17	83.40

Table 12: Dataset composition.

Class	Number of training set samples	Number of test set samples
Normal	19454	12118
DoS	78290	45970
Probe	822	834
U2R	12	48
R2L	226	3238

5. Conclusion

Compared with traditional machine learning classification models, fully connected recurrent neural network, as a deep learning method, has stronger feature representation ability, can more comprehensively map high-dimensional feature space into low-dimensional feature representation, and has the ability to express complex functions. Therefore, the detection model based on the fully connected RNN can detect a large number of abnormal attack records in binary and multiclassification tasks, improve the accuracy of intrusion detection, and reduce the false positive rate. For example, in terms of correctly classifying abnormal records, the fully connected recurrent neural network-based detection model correctly detected 462 more records than the neural network-based detection model when performing a 2-class task [34].

The main contributions of this study are as follows:

(1) A new intrusion detection system based on fully connected recurrent neural network (FCRNN-IDS) was proposed, the training method of the model was studied, and the detection rate of models with different structures and different Learningrates was studied.

(2) Using the dataset NSL-KDD, the detection performance of seven traditional machine learning methods in 2-class and multiclass tasks was studied, respectively. It lays a foundation for FCRNN-IDS with traditional learning methods.

(3) The detection accuracy of FCRNN-IDS in 2-class and multiclassification tasks was studied, the performance of FCRNN-IDS in detecting various types of attacks was deeply analyzed, and the performance of FCRNN-IDS in detecting various types of attacks was compared.

Data Availability

The dataset can be obtained from the corresponding author upon request.

Conflicts of Interest

The authors declare that they have no conflicts of interest.

References

[1] P. Torres, W. Lu, C. Catania, S. Garcia, and C. G. Garino, "An analysis of recurrent neural networks for botnet detection behavior," in *Proceedings of the 2016 IEEE Biennial Congress of Argentina (ARGENCON)*, pp. 1–6, IEEE, Buenos, Aires, Argentina, June 2016.

[2] S. Kudugunta and E. Ferrara, "Deep neural networks for bot detection," *Information Science*, vol. 467, pp. 312–322, 2018.

[3] M. Tavallaee and S. Garcia, "A Detailed Analysis of the KDD CUP 99 Data set," in *Proceedings of the 2009 IEEE Symposium on Computational Intelligence for Security and Defense Applications*, pp. 1–6, IEEE, Ottawa, ON, Canada, July 2009.

[4] P. S. Bhattacharjee, A. K. Fujail, and S. A. Begum, "Intrusion detection system for NSL-KDD data set using victories fitness

function in genetic algorithm," *Advances in Computational Sciences and Technology*, vol. 10, no. 2, pp. 235–246, 2017.

[5] R. A. R. Ashfaq, X. Z. Wang, J. Z. Huang, H. Abbas, and Y. L. He, "Fuzziness based semi-supervised learning approach for intrusion detection system," *Information Sciences*, vol. 468, pp. 470–486, 2019.

[6] B. Ingre and A. Yadav, "Performance Analysis of NSL-KDD Dataset Using ANN," in *Proceedings of the 2015 International Conference on Signal Processing and Communication Engineering Systems (SPACES)*, pp. 93–95, IEEE, Guntur, India, January 2015.

[7] M. Sheikhan, Z. Jadidi, and A Farrokhi, "Intrusion detection using reduced-size RNN based on feature grouping," *Neural Computing & Applications*, vol. 21, no. 6, pp. 1185–1190, 2012.

[8] Y. Wang and W.. Cai, "A deep learning approach for detecting malicious JavaScript code," *Security and Communication Networks*, vol. 9, no. 11, pp. 1520–1534, 2016.

[9] L. Deng, D. Li, and X. Yao, "Mobile Network Intrusion Detection for IotSystem Based on Transfer Learning Algorithm," *Cluster Computing*, vol. 22, no. 2, pp. 1–16, 2020.

[10] Z. Li and W. Ou, "Network communication intervention strategy for probabilistic model detection," *Small Micro Computer System*, vol. 38, no. 6, pp. 1175–1180, 2019.

[11] S. Wang, "Research on computer maintenance methods based on virus prevention and control[J]," *Electronic Components and Information Technology*, vol. 3, no. 08, pp. 108–111, 2019.

[12] Z. Sanaei, S. Abolfazli, A. Gani, and R. Buyya, "Heterogeneity in mobile cloud computing: taxonomy and open challenges," *IEEE Communications Surveys & Tutorials*, vol. 16, no. 1, pp. 369–392, 2014.

[13] W. Meng, E. W. Tischhauser, Q. Wang, Y. Wang, and J Han, "When intrusion detection meets blockchain technology: a review," *IEEE Access*, vol. 6, pp. 10179–10188, 2018.

[14] K. Wang, M. Du, S. Maharjan, and Y. Sun, "Strategic honeypot game model for distributed denial of service attacks in the smart grid," *IEEE Transactions on Smart Grid*, vol. 8, no. 5, pp. 2474–2482, 2017.

[15] X. Liu, P. Zhu, Y. Zhang, and K. Chen, "A collaborative intrusion detection mechanism against false data injection attack in advanced metering infrastructure," *IEEE Transactions on Smart Grid*, vol. 6, no. 5, pp. 2435–2443, 2015.

[16] Y. Xiao, *Research and Analysis of Virus Propagation Model and Immune Strategy in Complex Network*, Southwest University, 2016.

[17] C. Network, *Based Application Recognition*, 2017, https://www.cwasco.com/c/en/us/products/ios-nx-os-softwwere/network-based-application-recognition-nbar/index.html?dtid=osscdc000283 (MBAR)[EB/OL].

[18] P. Ponmurugan, C. Venkatesh, M. D. Priyadharshini, and S. Balamurugan, "Intrusion detection strategies in smart grid," in *Design and Analysis of Security Protocol for Communication*, pp. 211–233, Scrivener Publishing, 2020.

[19] K. Song, P. Kim, V. Tyagi, and S. Rajasekaran, "Artificial Immune System (AIS) Based Intrusion Detection System (IDS) for Smart Grid Advanced Metering Infrastructure (AMI) Networks," *CS4624: Multimedia, Hypertext, and Information Access*, Virginia Tech, 2018.

[20] Y. Cui, "Modeling of Ideological and Political Education System in Colleges and Universities Based on Naive Bayes-BP Neural Network in the Era of Big Data," *Mobile Information Systems*, vol. 2022, Article ID 7609697, 9 pages, 2022.

[21] M. Chen, J. Cheng, G. Ma, L. Tian, X. Li, and Q. Shi, "Service Composition Recommendation Method Based on Recurrent Neural Network and Naive Bayes," *Scientific Programming*, vol. 2021, Article ID 1013682, 9 pages, 2021.

[22] L. Li, B. Lei, and C. Mao, "Digital twin in smart manufacturing," *Journal of Industrial Information Integration*, vol. 26, no. 9, Article ID 100289, 2022.

[23] L. Li, T. Qu, Y. Liu et al., "Sustainability assessment of intelligent manufacturing supported by digital twin," *IEEE Access*, vol. 8, pp. 174988–175008, 2020.

[24] Z. Zhang and S. Zhang, "Application of internet of things and naive Bayes in public health environmental management of government institutions in China," *Journal of Healthcare Engineering*, vol. 2021, p. 7, 2021.

[25] J. Yang, Y. Huang, R. Zhang, F. Huang, Q. Meng, and S. Feng, "Study on PPG Biometric Recognition Based on Multifeature Extraction and Naive Bayes Classifier," *Scientific Programming*, vol. 2021, Article ID 5597624, 12 pages, 2021.

[26] Y. Xiong, M. Ye, and C. Wu, "Cancer classification with a cost-sensitive naive Bayes stacking ensemble," *Computational and Mathematical Methods in Medicine*, vol. 2021, p. 12, 2021.

[27] L. Li, C. Mao, H. Sun, Y. Yuan, and B. Lei, "Digital twin driven green performance evaluation methodology of intelligent manufacturing: hybrid model based on fuzzy rough-sets AHP, multistage weight synthesis, and PROMETHEE II," *Complexity*, vol. 2020, no. 6, Article ID 3853925, 24 pages, 2020.

[28] P. Tao, H. Shen, Y. Zhang, P. Ren, J. Zhao, and Y. Jia, "Status forecast and fault classification of smart meters using LightGBM algorithm improved by random forest," *Wireless Communications and Mobile Computing*, vol. 2022, p. 11, 2022.

[29] R. Li, W. Zhang, S. Shen et al., "An intelligent heartbeat classification system based on attributable features with AdaBoost+Random forest algorithm," *Journal of Healthcare Engineering*, vol. 2021, Article ID 9913127, 19 pages, 2021.

[30] L. Li and C. Mao, "Big data supported PSS evaluation decision in service-oriented manufacturing," *IEEE Access*, vol. 8, no. 99, pp. 154663–154670, 2020.

[31] P. Fan, "Random Forest Algorithm Based on Speech for Early Identification of Parkinson's Disease," *Computational Intelligence and Neuroscience*, vol. 2022, Article ID 3287068, 6 pages, 2022.

[32] H. Alla, L. Moumoun, and Y. Balouki, "A Multilayer Perceptron Neural Network with Selective-Data Training for Flight Arrival Delay Prediction," *Scientific Programming*, vol. 2021, Article ID 5558918, 12 pages, 2021.

[33] F. Sayyahi, S. Farzin, and H. Karami, "Forecasting daily and monthly reference evapotranspiration in the aidoghmoush basin using multilayer perceptron coupled with water wave optimization," *Complexity*, vol. 2021, Article ID 6683759, 12 pages, 2021.

[34] J. Woodbridge, H. S. Anderson, A. Ahuja, and D. Grant, "Predicting domain generation algorithms with long short-term memory networks," 2019, https://arxiv.org/abs/1611.00791.

Hindawi
Scientific Programming
Volume 2022, Article ID 8577034, 7 pages
https://doi.org/10.1155/2022/8577034

Research Article

A Method of Personal Music Psychological Recognition Based on Psychological and Physiological Signals

Peijie Pang

Department of Music, Taiyuan University, Taiyuan, Shanxi 030000, China

Correspondence should be addressed to Peijie Pang; pangpeijie@tyu.edu.cn

Received 12 July 2022; Revised 3 August 2022; Accepted 11 August 2022; Published 26 September 2022

Academic Editor: Lianhui Li

We can hear sweet and touching music in our daily life. We like listening to music because music can affect our emotions. Dynamic music makes us very excited. When we are sad, hearing beautiful music can make us happy. In physiology, music affects many physiological processes. It can inhibit fatigue and affect pulse, respiratory rate, and blood pressure level. "Listening music helps improve mood." Although the pursuit of personal happiness is likely to be considered a self-centered adventure, research shows that happiness is positively correlated with socially beneficial behavior, better health, higher income, and better interpersonal relationships. Another reason why we like music and music can be used very effectively for various therapeutic goals is that music is used in many ways in our society. When a group of people come together to sing a chorus or engage in musical activities, concerts establish new ties between people and make them closer. People grow up listening to lullabies from birth. When they die, they end their lives with funeral music (songs). It may be said that one's life begins with music and ends with music. Through music, we sing about social phenomena, express ourselves, and communicate with others. The themes and hidden contents that the music production society is unwilling to express publicly are not limited by any judgment. It should be noted that the functions of the above music are flexibly applied according to personal conditions, rather than being classified and limited by functions.

1. Introduction

Music is a wonderful sound composed of tone, timbre, and rhythm, which gives people unique aesthetic experience [1]. Therefore, if we need to know more about these experiences, we need more empirical research from outside the laboratory. At present, exploratory research has measured the aesthetic experience (emotion and absorption caused by music) of 95 participants, as well as the research on the response of fast-paced and slow-paced music to people's physiology [2]. These participants played romantic, classical, rock, and modern music in four concerts. One of the musical movements of modern works is deduced from the recording. So, the first result emphasizes the influence of two key parts of the framework on aesthetic emotion: (1) unfamiliar contemporary works lead to higher negative emotion, which is caused by the rising and falling trajectory of emotion by the programming sequence. Nevertheless, this experience is printed into a highly praised concert as a whole. (2) Compared with the low participation of live recorded music, the vitality factor becomes obvious. Secondly, the participants' reactions made them observe how more musical works were perceived [3]. The opening and closing movements caused more positive responses, compared the characteristics of the internal parts, and caused lower arousal and complex emotions. However, will the speed of music rhythm affect people's emotional and physiological indicators? Edworthy and Waring found in previous studies and their own that fast-paced music can cause positive performance of participants better than slow-paced music. In the study by Brownley McMurray and Hackney, fast-paced music can improve the physiological response of participants better than slow music [4]. And, some scholars (Nethery, Harmer, Taaffe, etc.) have discussed the impact of inserting music during sports on athletes and how different music affects them, which has also produced many different

arguments and opinions, so 26 athletes were invited to do experiments. The results showed that the heart rate of athletes with music was higher, and the exercise time with music insertion was longer than that without music insertion. Therefore, they believe that music can affect athletes' psychological and physiological reactions during sports because music can stimulate athletes' blood flow [5].

1.1. Aesthetic Experience of Live Concert. Although there are still emotional frameworks and aesthetic experience in music at present, there are still problems of ecological effectiveness in listening and stimulation. Up to now, research is usually carried out in a highly controlled laboratory environment, using relatively short music works or single movements and short films. Classical laboratories usually neither include works of whole or multiple movements nor do they choose the so-called key influence of the framework of auditory generation. Although in theory, the background and scene are considered to be the combination of artistic visual aesthetic experience. The main purpose of this study is to explore the aesthetic experience of listening music in the current real environment, that is, performing music live in the concert hall, including the string quintet of contemporary composers Brett Dean, Ludwig van Beethoven, and Brahms. These writers are very representative in contemporary times. For example, Ludwig van Beethoven's concert has been widely spread until now, and they are very famous pianists. This study takes their works as an experiment, which is very representative. In a fixed course, dedicated listening is the framework of the concert. We chose a term introduced by a sociologist Irving Goffman, namely, framework Goffman [6] in order to understand the relationship between music-related behavior and situational factors. According to Goffman, these frameworks will also affect aesthetic experience and appreciation, and the impact of the contemporary realistic environment, situation, framework, or background is also recognized by the institute. for example, cinemas [7], theatres (Cardizzi et al., 2020) [8], and so on. In fact, research shows that some concerts enhance the experience of music listening, and live music performance provides people stronger (positive) response [9]. Compared with the same performance, the live performance of the video in the Church can arouse the emotional input and feelings of the participants [10] and can be appreciated with more concentration. A series of works performed in the concert are presented in the expected order. Emotions fluctuate during the performance of different musical works [11]. During the performance of classical works, complex and positive emotional fluctuations rise, contemporary works decline, and romantic works rise again. Tension and excitement fluctuate greatly in contemporary works and are significantly higher than classical and romantic works [12]. It can be seen that the emotional range of the less familiar works is different from that of the other two familiar works. Classical concerts put it in famous classical works through different arrangement ideas, including new works, so as to increase people's love for it.

2. Measurement of Aesthetic Experience

In the measurement of aesthetic experience, we use the mixed test experimental model because the conclusions obtained from different model experiments are more comprehensive and illustrative. We select models from different latitudes and test the physiological and psychological data to get a high aesthetic experience. Aesthetic experience has many dimensions, but the most critical is the emotion and absorption induced by music. Other scholars' research data show that people can get more emotional experience beyond music itself from music through physiological response [11], for example, perception of beauty, pleasure, excitement, and so on. Studies have shown that people can witness faster heart rate and respiration when listening music, resulting in an increase in the frequency of skin conductive response—shivering [13]. The key of absorption in the aesthetic discourse of classical music has been discussed by music history literature. This is related to the perception of participants and is different from the "daily" psychological state [14]. The valuable measure of music aesthetic experience at the concert is the performance of absorption state and the difference between the feeling emotion we need and the feeling emotion [17]. In addition, the measurement of experienced emotions through continuous, nonintrusive methods is the use of cardiovascular, electromechanical, and skin conductive responses such as heart and respiratory rate and sweat gland secretion increases (measured by skin conductive response), which is activated by sympathetic nervous division of the autonomic nervous system to stimulate events and, from this reaction, to increase sensory participation. And, facial muscle activity is also known as a measure of behavior, and it can feed back the imitation of several discrete emotions and induce emotions to a certain extent [16]. The emotion of music is generated within the audience. Using the concept of latitude (valence arousal) or classification (such as sadness and happiness) emotion, studies have shown that "happy" music can evoke higher skin conductive induction amplitude than "sad," and thus faster heart rate and breathing. Through the combination of sound and lyrics, many different types of information can be conveyed [17]. For example, music can depict and create a self or group image, and music can also be used to exchange political information. Research shows that music can convey emotional information. And, the speed of the rhythm will affect people's vitality. Speeding up the rhythm will lead to a greater possibility of sympathetic arousal. Using the measurement of skin conductive response, in the following experiments, we compare slow-paced and fast-paced classical music with rock music excerpts and silence [5]. As expected, the frequency of skin conductance response (SCR) during music processing was higher than that during silence. Skin conductive response level (SCL) data show that fast-paced music can "enhance information or emotional content" more than slow-paced music. Using people's psychological response to music to improve sympathetic nerve and finding higher skin conductive response in fast-paced music, people can expect

various emotions induced by music, so as to get a better aesthetic experience.

2.1. Aesthetic Experience of Vision and Hearing. In the aesthetic experience of vision and hearing, we use the principle of the mixed test experimental model. By comparing live concerts with recorded concerts, we draw a conclusion in these experimental model assumptions that there is not much difference. At the same time, the research theory believes that the combination of visual and auditory information may be more easily aroused in music aesthetic experience [16, 17] and enhance the experience by enhancing the uniqueness and creativity in the current performance, We expect that live concerts will cause a stronger positive aesthetic experience than recorded concerts. According to the current research, compared with 256 movements, the participation of live performance will be greater, the degree of liking will be higher, and the attention will be more focused. This is due to the lack of a major factor, namely, vitality [20]. This is true even if you are watching the same performance of the same musician. However, compared with other studies, namely, visual recording [10] and live performance, recorded visual and live performance did not show other differences in self-report and physiological reactions. This leads to the assumption that the situation regulates the aesthetic experience and points out that the framework [6] is a key component of modeling the aesthetic experience. In other words, the emotional difference is related to the framework of the concert site, and it is not necessarily due to the recording. The aesthetic experience of vision and hearing cannot be judged because of whether it is also on the spot. According to experimental research, it is not on the spot that the aesthetic experience is better than that of recording screen. On the contrary, it is more important whether it can attract people's attention and be more energetic. The higher the degree of liking, the stronger the aesthetic experience of vision and hearing.

3. The Adjustment of Music to Emotion

Different music has different effects on emotion. Some studies have shown that, under various emotional conditions, the relaxation degree of self-report of participants who are silent and self-selected is the highest, while the relaxation degree of self-report of rock listeners is the lowest, and there is no obvious physiological difference between groups. Rickard combined self-report of enjoyment, familiarity, and emotional impact with psychophysiological tests to evaluate the effect of music on emotional regulation. Physiological and psychological measurements include shivering, muscle tone, skin temperature, and skin conductance. Although the plot of the film is a song with strong emotional power and strong emotional power of self-selection and although easy and exciting music does not have emotional power, it can regulate emotions. Rickard found that 95 people who attended the concert thought they were in a good mood, and their self-reported measurement scores would be higher, resulting in the largest increase in skin conductance and shivering [21]. However, no correlation was found between these effects and participants' music training or gender. Krumhansl [22] discussed how college students' emotions are stimulated by the peripheral nervous system of the brain. When listening, half of the participants made dynamic emotional judgments from their feelings of music and collected their physiological data from the other half of the participants. All participants' feelings in the work will be filled in a questionnaire for evaluation. From this, we can know that, in all music, no matter what discrete emotions you show, your respiratory rate and blood pressure will increase, and your heart rate will decrease. In addition, all extracts will lead to sympathetic nervous system measurements (i.e., finger temperature and skin conductivity). In Krumhansl's research data, discrete emotions also have a major impact. What can lead to greater sympathetic activation is the excerpt of happiness, followed by fear and sadness. The dynamic characteristic of this effect over time is a statistical analysis of the Pearson r value between the calculation time and the skin conductivity level. As we expected, given the deceleration nature of autonomic nerve activation during the experiment, the results showed that the negative correlation was greater with the development of music over time. Research on mood in testing mode (major or minor) and rhythm shows that increasing rhythm will affect mood more than mode. Kent [23] and Kellaris and Kent [24] asked the participants to listen to original works, marking these works as tonal (atonal, minor, and major), textural (popular and classical), and rhythmic. Participants reported their excitement and pleasure from these original works. The results showed that the greater self-report pleasure was the increase of rhythm from classical music, but in pop music, it was more able to mobilize participants' emotions, and the tone had nothing to do with the awakening of self-report. But there is no doubt that music can "transmit" emotions and regulate emotions [25]. However, there are still differences in the literature of music psychologists on how to better empirically and theoretically solve this problem 26–30. The first is that the cognitive calculus that prompts the need for recognition in the score is excluded by emotionalists, and this kind of musical emotional response is described as another emotion, which is different. The other is the cognitive approach, which describes the emotional response of music as the cognitive recognition of the clues of the music audience to the music itself. There are two ways to interpret music: social influence and cultural influence. However, there are still many differences in music's emotional expression and quotation [31].

4. The Influence of Music on Sports

Scholars have long pointed out that the insertion of music can improve the performance of athletes. If inserting music can improve the performance of athletes, the use of music in competition or training is very important. But there is still no way to clearly say the impact of music on people's psychology and physiology. However, there are traces of music use in many sports fields. Many studies have shown that music has an impact on sports performance and can

improve sports performance 32, 33. In terms of discussing whether music has an impact on people's exercise, Eliakim et al. conducted experiments on 26 athletes, inserted music in their warm-up stage, and tested the temperature and heart rate after the warm-up. The results showed that the group with music insertion has higher temperature and heart rate, and the peak value of anaerobic exercise is also higher than other groups with music insertion [34]. It was also found that those with music insertion lasted longer than those without music insertion. In sports, people often affect sports performance because of physiological and psychological factors inside the human body, such as pain and anxiety. Nethery [35] showed that the level of wakefulness measured during exercise in the inserted music group was lower than that in the distracted and undisturbed group. In Nethery's study, it was verified that the degree of arousal in the music group was lower than that in the nonmusic group and the video group. The fact proved that if the athletes had a small amount of attention, they could be stimulated by some attention diversion, such as music insertion, and the stimulation was received by the sensory receiver to form some short-term memories caused by music stimulation [36]. If the impact of this short-term memory was large enough, it can cover the working memory formed by pain or anxiety caused by exercise, so that the brain can preferentially check the stimulation given by music so as to forget the pain and anxiety caused by exercise. Therefore, music can effectively reduce the level of wakefulness and distract athletes to a large extent [32]. Figure 1 is a general model of the theory that music stimulates the brain. But in the future, we need to further understand the impact of music on sports, such as whether the same music has the same impact on male athletes and female athletes and whether male and female athletes are more sensitive to aesthetic music, which is worthy of our experimental research.

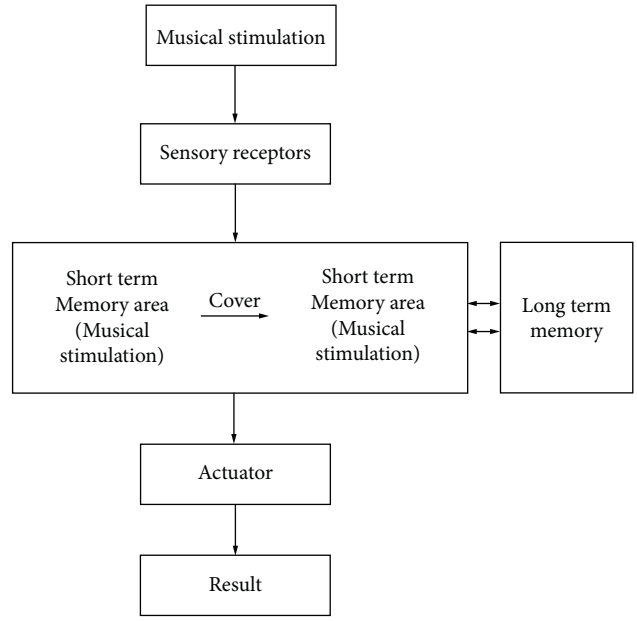

Figure 1: Theoretical model of how music stimulates the brain.

5. Experiment

Different music choices are selected among rock music, swing music, and classical music types, and the following assumptions are tested according to similar experimental designs [37]:

H1: in the selection process of different music, participants showed less deceleration in SCL when listening to fast-paced music than slow-paced music.

H2: there will be genre × rhythm interaction, which is activated on the sympathetic nervous system. Increasing rhythm will lead to greater SCR activity in classical music than rock and swing music types we are more familiar with.

5.1. Method. To better solve these assumptions, we designed and implemented a 2 (type) × 3 (rhythm) × 6 (presentation order) hybrid test experiment. The two main internal factors are music rhythm (fast rhythm and slow rhythm) and genre (rock, swing, and classical).

5.2. Experimental Process. In the experiment, six participants were randomly assigned, and the theme factor was the order of presentation. Twenty-seven graduate students agreed to participate in the experiment in exchange for graduate course credits. However, due to equipment failure, the skin conductance data of 7 students could not be used, and these 7 students also received the same credit reward. During the experiment, these participants heard the following six music clips, including slow classical, slow rock, fast classical, fast rock, and two silent clips. The slow-paced (75 BPM) classic clip features Pachelbel"s "Canon in D major." The slow tempo (74 BPM) swing clip features the Squirrel Nut Zippers' Mean to Be. The fast-paced (140 BPM) classical editing features the ending of Rossini's "William Tell Overture." The fast-paced (138 BPM) rock clips are taken from the cut's "She Sellers Sanity." In the video, these sounds divide the system into six unique sequences. After each auditory choice, the movie clips of pop music will follow closely, and the time will be maintained between 90 seconds and 115 seconds. These six movie clips are sorted by the system according to different types, so that there is not only any music choice next to each movie clip. As far as the current test is concerned, what is more relevant is that the research results are applied to the speed of music rhythm, which is consistent with the more subjective arousal level of interest during programming, rest, and programming sequence [38]. The SCR frequency data presented in these six movie clips is 2 (rhythm) × 3 (genre) repeated test MANOVA. Although the figures of these SCR frequencies are similar to those we predicted, the only surprising result is the main influence of genre (f (2, 40) = 6.947, P = 003, $\varepsilon 2$ = .2207). Regardless of the rhythm, classic genres can more arouse the activation of participants. In order to solve hypothesis 1, participants' SCL in fast-paced music was compared with slow-paced music, the change value was

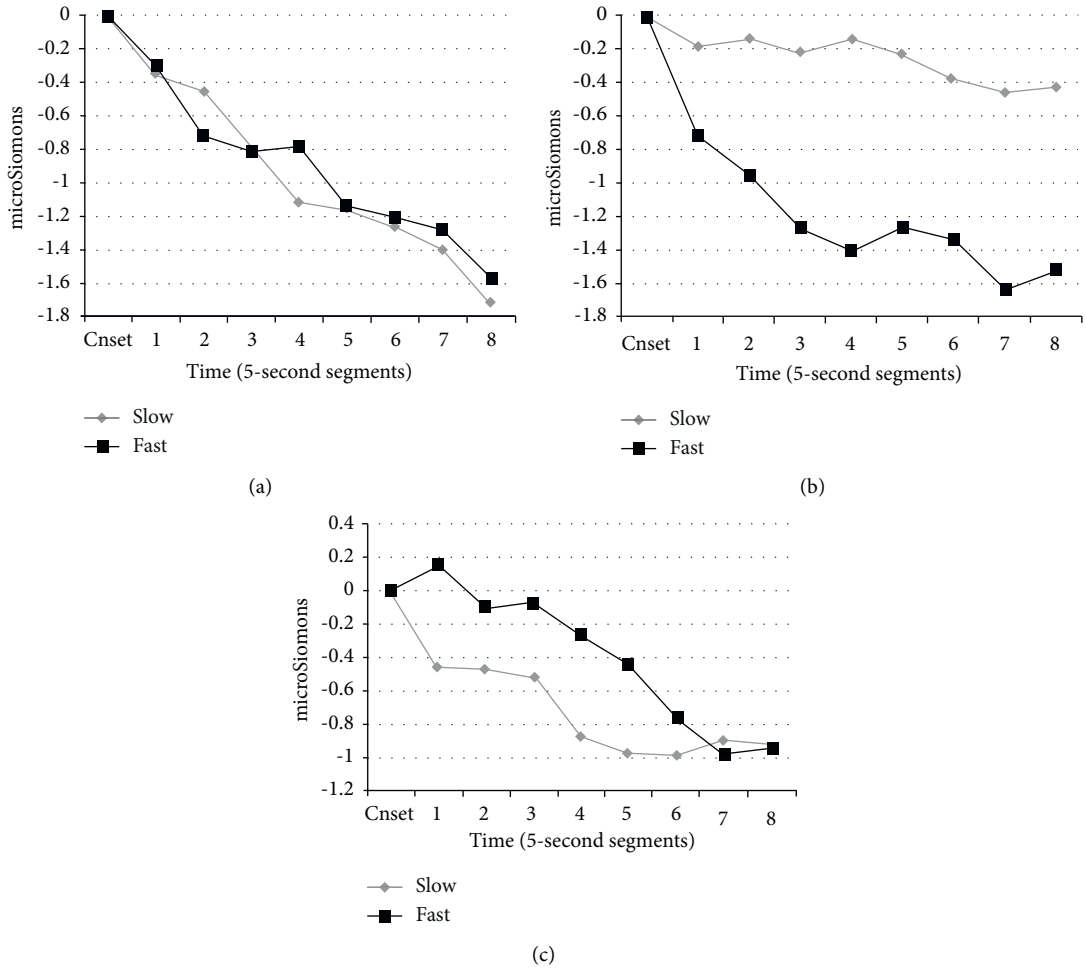

Figure 2: Tempo × genre × time on SCL. (a) Rock genre. (b) Classical genre. (c) Swing genre.

submitted to 2 (rhythm) × 3 (genre) × 8 (time) repeated test MANOVA, and the result was close to significance (f (16256) = 1.502, P = 099, ε 2 = . 0287).

5.3. Results and Experimental Analysis. This group of experiments attempts to test two broad hypotheses. First, when participants hear fast-paced music, they show less deceleration in SCL than slow-paced music. Second, the increase of rhythm will lead to greater SCR activity of classical music than rock and swing music types we are more familiar with [38]. According to the collected participant data, these two hypotheses have been confirmed. The data show that, as time goes on, rock music is not affected by rhythm. However, rhythm has obvious influence on the other two types. However, faster rhythms increase sympathetic activation in the swing type and decrease activation in the less familiar classical type, as shown in Figure 2, which is contrary to our expectations. In the selection of classical music that may be less familiar, the activation response of slow rhythm (even if the change score is initially higher than the baseline level) is greater in fast rhythm than in relatively familiar swing music. Therefore, by analyzing the experimental data, it is proved that the familiarity assumption around classical and rock proposed by hypothesis 2 is not tenable in accurately predicting the direction of this interaction. The experiment uses psychological and physiological factors to verify the existence of any music, whether slow or fast-paced, classical music or rock music, which will increase the excitement of people's sympathetic nervous system. Over time, the genre of music may alleviate the impact of any rhythm on skin conductance. Through data analysis, when using SCL as attribute measurement to confirm the dynamic characteristics of music processing, it is predicted that music with a slower beat will cause less sympathetic activation than music with a faster beat. People are using all the spontaneous SCR frequency counts, so the whole listening period is summarized across time, and no major impact is found. On the contrary, in the interaction with genres, the increase of rhythm in the processing of rock music leads to a significant increase in SCR, while the increase of rhythm in the processing of classical music leads to a significant increase in SCR. In slow-paced classical music, participants can adapt to the expected genre and the rapid start of a single note in the rhythm pairing [39]. Through the analysis of the two hypotheses, we can better confirm that the speed of rhythm and

genre are related to the presentation of SCL, but it is untenable to propose that it is related to familiarity, and in the interaction of genres, classical music is higher than rock music SCL.

6. Conclusion

The extraction of key words in this paper is a relatively extensive field. The psychological construction of music combines psychological and physiological signals. That is, the collection of aesthetic experience and physiological experience created by emotion and absorption caused by music. The type of music and the speed of rhythm can convey many different types of signals through different combinations [40]. Based on the scenes of classic classical concerts, this paper discusses the aesthetic experience of music works with different musical styles and fast and slow rhythms, as well as the adjustment of music to our emotions and sports performance. According to the research data, the speed of rhythm can increase the excitability of the sympathetic nervous system, and if in the same type of music, fast-paced music is easier to activate the sympathetic nerve than slow-paced music. Emotional reactions and some physiological reactions reflect the changes in the form of sonata represented by motor function in familiar classical music works. Of course, it does not follow such a trajectory in unfamiliar contemporary works [40]. Use music to reduce athletes' arousal and divert attention, reduce sports pain, and improve sports performance. Moreover, music can improve our psychological feelings, promote the motivation of activities, and increase their attachment. In addition, some scholars Zhou [41] believe that not the same kind of music has the same impact on everyone. Some scholars have also proposed that a type of music has an impact on one person, but not necessarily on others. So far, many scholars' research on the impact of music intervention on the human body is still growing. André Previn said, "there are a million things in music that I do not know. I just want to narrow this number [42]." In addition to the speed of the music rhythm, we should also evaluate the type. Perhaps, as our understanding of the awakening caused by music increases, our ability to predict the effect of music will be improved. Then, we can start to study the impact of music on human psychology and physiology, so as to make our research more in depth and breadth [41].

Data Availability

The dataset can be accessed upon request.

Conflicts of Interest

The authors declare that they have no conflicts of interest.

References

[1] C. L. Pelletier, "The effect of music on decreasing arousal due to stress: a meta-analysis," *Journal of Music Therapy*, vol. 41, no. 3, pp. 192–214, 2004.

[2] N. S. Rickard, "Intense emotional responses to music: a test of the physiological arousal hypothesis," *Psychology of Music*, vol. 32, no. 4, pp. 371–388, 2004.

[3] K. Bartoń, "MuMIn: multi-model inference," 2015, http://r-forge r-project.org/projects/mumin.

[4] T. Baumgartner, M. Esslen, and L. Jäncke, "From emotion perception to emotion experience: emotions evoked by pictures and classical music," *International Journal of Psychophysiology*, vol. 60, no. 1, pp. 34https–43, 2006.

[5] E. Brattico and M. Pearce, "The neuroaesthetics of music," *Psychology of Aesthetics, Creativity, and the Arts*, vol. 7, no. 1, pp. 48–61, 2013.

[6] Goffman, *Comparison of Framing Models of Concerts, Ie Differences that Affect Aesthetic Experience and Appreciation*, 1974.

[7] S kostoulas, "MuMIn: multi-model inference," *R package version 1*, vol. 43, In Juslin, P. & Sloboda, J.A. (Eds.), Music and emotion: Theory and research. Oxford: Oxford University Press, 223 248, 2015.

[8] D. L. Cardizzi and Filion, "The electrodermal system," *Psychophysiology: Human Behavior and Physiological Response*, Hillsdale, Lawrence Earlbaum Associates, Publishers, 2020.

[9] Gabrielsen, lindstromwick, and Lamont, "Affective reactions to acoustic stimuli," *Psychophysiology*, vol. 37, 2011.

[10] K. R. Scherer and coutinho, "Emotional effects of music: production rules," in *Music and Emotion: Theory and Research*, P. N. Juslin and J. A. Sloboda, Eds., pp. 361–392, Oxford University Press, New York, 2007.

[11] D. Bates, M. Mächler, B. Bolker, and S. Walker, "Fitting linear mixed-effects models using lme4," *Journal of Statistical Software*, vol. 67, no. 1, pp. 1–48, 2015.

[12] S. Bannister, "A survey into the experience of musically induced chills:Emotions, situations and music," *Psychology of Music*, vol. 48, no. 2, pp. 297–314, 2020.

[13] Blood and Zatorre, "Oxford University Student Experiment Group, Response of skin conductance to tremor frequency in experimental controls, 2004," *Psychology of Music, Oxford: Oxford University Press*, vol. 18, no. 3, pp. 152–163, 2004.

[14] D. E. Berlyne, *Conflict, Arousal, and Curiosity*, McGraw-Hill Book Company, New York, NY, US, 1960.

[15] Gabrielson and schubert, "Study the effects of music on various tissues of the human body during exercise, Effect of music on perceived exertion, plasma lactate, norepinephrine and cardiovascular hemodynamics during treadmill running," *International journal of sports medicine*, vol. 19, no. 1, pp. 32–37.

[16] C. Cannam, C. Landone, and M. Sandler, "Sonic Visualiser: An Open Source Application for Viewing, Analysing, and Annotating Music Audio Files," in *Proceedings of the 18th ACM international conference on Multimedia*, p. 1467, New York, NY, USA, October 2010.

[17] Sellnow & sellnow, "The biological impact of listening to music in clinical and nonclinical settings: a systematic review," *Progress in Brain Research*, vol. 237, pp. 173–200, 2018.

[18] J. Cohen, *Statistical Power Analysis for the Behavioural Sciences*, 1988.

[19] D. Huron, "Aesthetics," *The Oxford Handbook of Music Psychology*, pp. 1–14, 2008.

[20] B. Calvo-Merino, C. Jola, D. E. Glaser, and P. Haggard, "Towards a sensorimotor aesthetics of performing art," *Consciousness and Cognition*, vol. 17, no. 3, pp. 911–922, 2008.

[21] A. J. Cohen, *Music in Performance Arts: Film, Theatre and Dance*, pp. 1–16, The Oxford Handbook of Music Psychology, 2008.

[22] C. L. Krumhansl, "An exploratory study of musical emotions and psychophysiology," *Canadian Journal of Experimental Psychology/Revue canadienne de psychologie expérimentale*, vol. 51, no. 4, pp. 336–353, 1997.
[23] Kent, *Effects of Relaxing Music on Salivary Cortisol Level after Psychological Stress*, 1993.
[24] J. J. Kellaris and R. J. Kent, "An exploratory investigation of responses elicited by music varying in tempo, tonality, and texture," *Journal of Consumer Psychology*, vol. 2, no. 4, pp. 381–401, 1993.
[25] N. Cook, "The perception of large-scale tonal closure," *Music Perception*, vol. 5, no. 2, pp. 197–205, 1987.
[26] T. G. Bever, "A cognitive theory of emotion and aesthetics in music," *Psychomusicology: A Journal of Research in Music Cognition*, vol. 7, no. 2, pp. 165–175, 1988.
[27] W. W. Gaver and G. Mandler, "Play it again, Sam: on liking music," *Cognition & Emotion*, vol. 1, no. 3, pp. 259–282, 1987.
[28] P. Juslin and J. A. Sloboda, *Music and Emotion: Theory and Research*, Oxford University Press, Oxford, 2001.
[29] R. W. Lundin, *An Objective Psychology of Music*, Robert E. Krieger Company, Malabar, FL, 1985.
[30] J. A. Sloboda, "Music structure and emotional response: some empirical findings," *Psychology of Music*, vol. 19, no. 2, pp. 110–120, 1991.
[31] E. Coutinho and K. R. Scherer, "Introducing the GEneva Music-induced Affect Checklist (GEMIAC): a brief instrument for the rapid assessment of musically induced emotions," *Music Perception*, vol. 34, no. 4, pp. 1225–1228, 2017a.
[32] J. Edworthy and H. Waring, "The effects of music tempo and loudness level on treadmill exercise," *Ergonomics*, vol. 49, no. 15, pp. 1597–1610, 2006.
[33] M. Eliakim, Y. Meckel, D. Nemet, and A. Eliakim, "The effect of music during warm-up on consecutive anaerobic performance in elite adolescent volleyball players," *International Journal of Sports Medicine*, vol. 28, no. 4, pp. 321–325, 2007.
[34] F. D. Carpentier, S. Knobloch, and D. Zillmann, "Rock, rap, and rebellion: comparisons of traits predicting selective exposure to defiant music," *Personality and Individual Differences*, vol. 35, no. 7, pp. 1643–1655, 2003.
[35] Nethery, "The framing effects of emotion: can discrete emotions influence information recall and policy preference?" *Communication Research*, vol. 30, pp. 224–247, 2002.
[36] C. H. Hansen and R. D. Hansen, "Music and music videos," in *Media Entertainment: The Psychology of its Appeal*, D. Zillmann and P. Vorderer, Eds., pp. 175–196, Lawrence Erlbaum Associates, Mahwah, NJ, 2000.
[37] M. B. Holbrook and P. Anand, "Effects of tempo and situational arousal on the listener's perceptual and affective responses to music," *Psychology of Music*, vol. 18, no. 2, pp. 150–162, 1990.
[38] G. Husain, W. F. Thompson, and E. G. Schellenberg, "Effects of musical tempo and mode on arousal, mood, and spatial abilities," *Music Perception*, vol. 20, no. 2, pp. 151–171, 2002.
[39] M. G. Judge, "Back to the future," *First Things*, vol. 95, pp. 14–16, 1999, Aug/Sept.
[40] P. N. Juslin and P. Laukka, "Communication of emotions in vocal expression and music: different channels, same code?" *Psychological Bulletin*, vol. 129, no. 5, pp. 770–814, 2003.
[41] L. Zhou, "Alternative health music therapy," *Health World*, vol. 249, pp. 15–17, 2006.
[42] D. T. Lykken and P. H. Venables, "Direct measurement of skin conductance: a proposal for standardization," *Psychophysiology*, vol. 8, no. 5, pp. 656–672, 1971.

Hindawi
Scientific Programming
Volume 2022, Article ID 9451500, 8 pages
https://doi.org/10.1155/2022/9451500

Research Article

Influence Model Design of National Culture in Shaping the Organisational Management Cultures: The Case between China and the USA

Yiwen Shi and Pingqing Liu

Beijing Institute of Technology, Beijing 100081, China

Correspondence should be addressed to Pingqing Liu; 2021214937@ecut.edu.cn

Received 4 July 2022; Revised 12 August 2022; Accepted 16 August 2022; Published 24 September 2022

Academic Editor: Lianhui Li

This research topic investigates the inquiry on how national cultures shape the organisational management cultures. Similarities and differences between the national cultures of China and the USA are being scrutinised for the purpose to examine the impacts of such features on the management cultures and strategies of organizations located in these two main world financial centres so as to achieve a majority of data to confirm how national culture relates and assists to shape the organisational management. This research uses the data collection methods of non-governmental organizations, including the invitation of participants or volunteers via social media, working emails, and invitation letters, involving the issues such as designing human rights and privacy. The result has established that high mobilization of culture differences in the USA had a notable positive consequence on companies' organisational management culture. Alternatively, the Chinese cultures may bring some positive effect to the companies' culture, but it was only significant to shape management culture influence in their domestic companies, excluding most of the multinational companies. Moreover, the differences in national cultural characteristics will greatly affect each organisation to choose their own management strategies. Raising up for cross-cultural and transnational management will be a huge challenge for organizations to take, especially if countries wish to establish bilateral or trilateral business relations and partnerships.

1. Introduction

1.1. Research Background. One of the key formation factors in an organisation's culture includes its national culture's history and environment, and it has been proven by studies that national culture affects the organisational management system greatly in many aspects [1]. Although national and organisational cultures are used to be classified as different phenomena, it is interesting to investigate the linkage between them and discover how national culture can influence an organisation's practices. In this case, the similarities and differences between the national cultures of China and the USA will be analyzed, and the outcome of the analysis will be used for further investigation on the impacts of management cultures of organizations located in these two countries. By this approach, this research can recall the attention of building up a well-established organisational management culture, which is essential to take national cultures into account since national culture conducts the employees' decisions, devotions, and standards of behaviour [2]. The aim and objectives of this essay is to guide readers for understanding that the national culture formed the common characteristics of human. This will further influence the responses to its organizations, resulting in a company's identical organisational management cultures, especially in a country's domestic companies. Therefore, it is essential and important to recognize the relationship between the national and organisational culture, proving that the differences in national cultures will have a great influence on how managers chose their strategies and supervised their organizations. Additionally, the challenges of high mobilization of culture differences faced by cross-cultural and multinational companies will be discussed for the purpose of examining some practicable solutions.

Table 1: Definition of national cultures.

Authors	Years	Classification of national culture systems
Kluckhohn and Strodtbeck	1961	Human nature orientation and time orientation based on relationship
Tony Morden	1985	It is defined as the collective mental programming in a society. Organisation's management and human resources supplies were mostly included environmental and local aspects
Trompenaars and Hampden-Turner	1997	Idea of individualism vs. communitarianism; universalism vs. particularism; internal direction vs. outer direction
Hofstede	2001	Power distance such as equality; individualism vs collectivism; focus on the level how employees are essential for a future-oriented running system rather than a short-term oriented running system
House et al.	2004	Focus on the points related to future orientation, gender equality, and power distance
Tony Smale	2016	National culture establishes human behaviour and cognition as a salient way since it is a psychological process of initiative, creativity, and innovation
Mike Berrell	2021	National culture generally describes the beliefs, value, and behaviours shared by the population of a sovereign nation and particularly refers to specific national characteristics such as religion, history, language, and ethnic

1.2. Theoretical Background

1.2.1. Theory of National Culture. Culture is not fabricated, but it is something that evolves with human, and it is the fundamental sources to create nationalism of a country. Since the nineteenth century, national culture is given by the definition of a comprehensive and multiplex system mixed with the elements of action, values, history, knowledge, and beliefs, which are identical by the particular social community and form their own practices. Hofstede realized that according to the past of historical process, nations were created as a part of social organisation, leading to a concept of culture to be closely related to the nation rather than the states [3]. If the countries obtain some particular historical practices nor heritages, it is likely to favour the further integration, original language, education system, and political system that are the examples of the most significant symbolic signature of a country since they obtain an excessive emotional load.

1.2.2. Organization and Management Culture. The reason why organisational culture has more than one interpretation is because this culture is made by the combination of values fabricated by humanity. To be more attributed to this notion, social sciences described organisational culture as everything generated by human themselves without arising from nature, and this culture reflects the deliberated situation and human activity gaining from the past [4]. The organisation and management theory is used to evaluate organisational cultures as a rational action, which is acceptable to identify the organisation with their effectiveness. To conclude the refinement of the organisational culture, we can apply the definition in the following statements:

(i) Organisational management culture is the creation of social network that assists in maintaining the organisation.

(ii) Organisational management culture is holistic and used to unite the company, remains stable, and minimises uncertainty to achieve internal integration and provide a working environment for the employees.

(iii) The process of organisational culture is shaped and developed with a long history, and it will be inertial (ongoing). When the process has finished, the result will be shown during the deal in environmental problems and other internal coordination.

(iv) Organisational management culture shows the process of cultural evolution and the process of socialisation.

1.3. Research Review

1.3.1. Section 1: National Culture Concept and the Corresponding Scopes. In general, cultures are separated according to the levels starting from individual, group, organisational, industrial, national, and geographic regions [5]. It is arranged according to the internal elements such as work outlook, history, goals and values, work role, communication mode, technical practice, customary rules, and other cultural activities, as well as cultural systems such as law, education, religion, economy, politics, and family status. Meanwhile, the term national is defined as the combination of economic, social, political institutions and culture group as to influence organizations on managing their people in divergent environments. Hofstede defined national culture as the general formation of the mind behaviour that helps to distinguish different human groups from one another. To be more precise, national culture can be used as the assumptions of practise by a given group because they are commonly influenced by the same attitudes, values, and beliefs of the same group members since they were young [6]. Hence, national cultural concepts are the collective programming activities made of and values from the past experiences [7]. Table 1 shows the definition of the national culture concept since 1961 to 2020 to explain how the dimensions changed over the past several decades.

1.3.2. Section 2: Hofstede's Six Dimensions of Culture

(1) Power Distance. Solutions to money and power problems because in some countries, hierarchical status and inequality may often occur in specific cultures [8]. This degree of inequality is measured by Power Distance Index (PDI). A low PDI marks also represent that power in the society is equally shared and dispersed, and citizens will be expected to reject if

Table 2: Hofstede's power distance index.

Power distance index					
Country	PDI	IDV	MAS	UAI	LTO
Malaysia	104	26	50	36	
Guatemala	95	6	37	101	
Panama	95	11	44	86	
Philippines	94	32	64	44	19
Mexico	81	30	69	82	
Venezuela	81	12	73	76	
China	80	20	66	40	118
South Africa	49	65	63	49	
Hungary	46	55	88	82	
Jamaica	45	39	68	13	
United States	40	91	62	46	29
Netherlands	38	80	14	53	44
Australia	36	90	61	51	31
Costa Rica	35	15	21	86	
Germany	35	67	66	65	31

power was distributed unfairly [9]. With the references of the map, a high PDI country like Malaysia that scored 100 marks is not going to initiate any action of unfairness but willing to be guided and follow the instructions by the governments.

(2) Individualism vs. Collectivism. The dimension of this emphasis is the unity of culture. Starting with the individualistic cultures, most people will have the mentality of independent and put themselves in the first place. People is likely to focus on the advantages of themselves and immediate family first, leading to a less tightly knit society. On the other hand, the collectivist cultures present the concept of "we" as a replacement of "I." Citizens are connected with each other's closely and willing to cooperate together. Psychologists believed that a country will be more benefited as a group than the self-esteem from the group mentality because citizens will have a higher sense of belongings [10]. This dimension is normally the easiest to perceive from the culture. According to the individualism versus collectivism score (IDV), countries such as America and Australia have a high score in individualism (IDV), indicating that they have weak interpersonal connection and the marketing campaign started in this country can be accepted and well understood. In contrast, cultures in countries such as China and Japan score low in individualism. Citizens are likely to work for their own intrinsic rewards and care less for others.

(3) Masculinity Versus Femininity (MAS). This dimension focuses on the distribution of works and responsibilities between men and women. Masculine societies present that the gap between men and women is less, while men are expected to acquit themselves assertively. The action of showing the success to others and voice out your feeling are seen to be positive characteristics in the society. However, feminine societies appear to be a great overlap between the female and male roles. A good relationship between the supervisors will be placed at first to prevent arguments [11]. The largest gap between the value of men and women is in Austria and Japan, and their MAS score is 79 and 95, respectively. The reason why they have such high scores is basically the men showed their "tough" during work and behaviours. By the studies of Samsung companies in Japan, the working style is closely related to the hierarchical and deferential style. The long working hours and low percentage for female employees to achieve advancement are developed to their organisational culture [12]. The USA and China have scored a close mark of 62 and 66, respectively, according to Table 2. This similarity can prove that although earning money and gaining achievement in both countries are important, citizens in the USA and China are also eager to maintain their relationship more orientally and achieve the quality of life. Workers may focus more on work-life balance and the flexibility in workspace. Therefore, the organisational management team of these countries can adjust their environment and workload according to this culture.

(4) Uncertainty Avoidance. This dimension can demonstrate how well the citizens can cope with anxiety and try to control their life in predictable and manageable methods. Alternatively, countries with a low uncertainty avoidance index are described with an open, relax, and inclusive living style. However, Hofstede pointed out that countries with high score may also acquire the personality of risk adverse, and they are likely to reduce ambiguities as low as they can in order to escape from failure [13]. With the glance of Hofstede's model, countries with a low UAI scale can also represent the cultural tendency with a safe and conservative decision style, and this can be represented by Singapore that has scored a low mark of eight. The USA and China have scored a close mark in the Uncertainty Avoidance Index too. The citizens in both countries are likely to have the national culture of innovation and desperate to take opportunities on their own life instead of following behind others.

(5) Long-Versus Short-Term Orientation. Long- and short-term orientation can display how a culture choose its decisions when dealing about the questions of the present and future. The characteristics of a country with long-term

orientation are described as more modest and pragmatic, and the citizens will prevent from any changes but emphasize more on customs and traditions [14]. As for short-term oriented countries, citizens are likely to focus on short-term gains and stick with consistency and truth. The USA is defined as a short-term orientation since the country reflects a great sense of social standards and nationalism. In term of business, this measure can measure how successful can a business be. If the business has a short-term orientation style, their goal is to get quick results as soon as possible on a quarterly basis. Meanwhile, a business with long-term orientation tends to be more patience and accepts short-term losses to achieve long-term gains [15].

(6) Indulgence vs. Restraint. As for the final dimension, it focuses on the natural human response, which is the level of urgent to satisfy desire. Different cultures will answer this dimension by choosing either appreciate (indulgence) or reject (restraint) this desire. Restrained culture countries tend to obtain characteristics such as pessimism and cynicism, and they stick closer with moral rules that contrast with those indulgence countries. Indulgence countries are prone to grab the chances of opportunities, be more carefree, and enjoy their spare time, and they have a low IVR score too. Eastern European countries and China are the good examples with a low IVR score. Employees only allow themselves a little time on leisure activities. At the same time, they are controlled with a restrained culture and present themselves in a more pessimistic way. The USA culture is different as they are more optimistic and allow the freedom of speech of citizens, feedback, and mentoring, which will prioritize at the first place to improve the countries [16, 17].

The six cultural dimensions will be scored on the scale within 0 to 100 for each dimension, and they will intertwine with each other and influence the countries when time passes. For instance, countries with long-term orientation will likely correlate the countries with the characteristics of uncertainty avoidance since both characteristics are related to the adherence of traditions. By applying Hofstede's six dimensions of culture models, it can provide a correct framework for organizations to compare and contrast every culture and achieve success by choosing suitable strategies. In the case of the USA, high individualism is their historical significance. Therefore, organizations can apply employees' rights and individual freedom to maintain their loyalty to the companies.

1.4. Comparative Analysis of the National and Organisational Management Cultures in China and the USA

1.4.1. China National Culture. The long history of the Chinese traditional culture has formed their unique characteristics. The national culture values have influenced the Chinese people to become harmonious, wise, honest, loyal, and hard-working [18–22]. Since the core value of harmony is described as "balancing the coordination between working," it has been proven that the working performance of the Chinese is based on the personal relationship and used to be peaceful. The organizations will put more focus on the social relationship among the employees since the management teams are used to organise team-building regularly. The outstanding team spirit and loyalty lead to the practice of organisation to be prudence and obedient. The Chinese organizations are used to follow all the rules and laws without any reformation in the practices. Moreover, the situation of working overtime in China is common too since the Chinese are taught by the idea on sacrificing themselves in order to accomplish others when they were young. Therefore, the work-life balance is comparatively poor in China.

1.4.2. The USA National Culture. Studies have listed out that the American national culture is basically recognized as being freedom oriented and individualistic. Americans advocate privacy and equality, and their personalities are accustomed to independence, individualism, hospitality, and future achievement orientation. Comparing with Hofstede's formation of national cultures, Americans are described as a high individualistic group of people who may not cooperate well during the group missions. The independent and aggressive personality may lead them to decision-making based on their self-interest instead of the positive benefits for the economy at large scale, affecting the loyalty as well. However, Americans are described as creativitive and future achievement oriented due to the education system when they were young; therefore, they may be likely to break the rules and innovate new ideas for the organizations. The working overtime practice is rare in the USA since they are more aware on the work-life balance and health practices.

In contrast, the managers in the USA are likely to be more individualistic, the management cultures may be more sensitive to the relative power of division managers and the power struggles, and the employees may have a greater competition among themselves. Interesting, China and the USA have a similar score in masculinity and has a biggest gap between individualism, displaying a phenomena that both countries are driven by the desire of achievement and success. However, the citizens in China may have a greater sense to achieve success for a society as a whole, while the USA has a stronger desire to attaining personal goals instead of assisting the countries.

2. Research Methods and Processes

2.1. Research Methods. For the purpose to disclose the research questions mentioned in Section 1.2.2, a combination of quantitative and qualitative methods that were applied to reveal the affection of national culture shapes the organisational management cultures. The research method comprises two major approaches of data collection: (1) a free anonymous questionnaire with employees and directors working in China, the USA, or multinational companies and (2) semi-Zoom interviews with employees or directors who volunteer to participate when filling the questionnaire e--mail. The Zoom interviews are held in different subareas within the same organizations so as to achieve the maintenance of common institutional context.

Table 3: Questionnaire.

Questions	The content of the problem
Question 1	Home countries you grew up before 18 years old?
Question 2	Which characteristics will you use to describe the citizens and society in your home countries?
Question 3	Type of companies you are working for?
Question 4	Which national culture variables have influence the most in the company you are working?
Question 5	Which organisational management variables are essential in your workplace?
Question 6	Challenges faced by your companies?
Question 7	To what extent you agreed that national culture variables shaped the organisational management cultures?
Question 8	To what extent you concern about work-life balance?
Question 9	Do you agree that China and the USA companies have different organisational management cultures?
Question 10	Possible solutions to shape an appropriate organisational management culture for multinational employees?

2.2. Research Processes

2.2.1. Data Collection and Recruitment. The empirical data in this research is observed from some major market within China and the US, and data is collected from open databases, questionnaire survey, and on-site observation to identify how national culture helps to shape the organisational management culture. The questionnaire is set up in Table 3.

Four research questions were superscribed within the options in the questionnaire. The reason for applying questionnaires to collect both qualitative and quantitative data is to ensure the consistency, while the questionnaire can provide the opportunity to analyze significant trends and differences between China and the USA cultures statistically. The survey is composed by the online questionnaires to prove the relationship between the national culture and organisational management cultures, and responses are collected in a costless and efficiency way. The survey has collected 166 suggestions from both genders of employees and directors located in the United States and Shanghai, China, with the age over 18 years old. Sheets of questionnaires are presented to participants though working e-mail and letter, and participants are accepted to fill in the answer anonymously to protect their privacy. Participant information sheets were sent and provided in the attachment of mail and website with the description about the aim of this research. Data is legally saved in the data protection system and will be deleted after the data analysis has been finished. Although the questionnaire may produce less in-depth responses, it can reveal the ideas of society directly. The responses are open ended and being taken for a grounded approach, and key categories can be identified through the data results. Responses may be answered with more than one option, and the multiple options will be classified as sophisticated responses. Following question 2, we get the following example (Table 4).

Throughout the quantitative analysis via correlational research, research object can be further refined so as to facilitate the understanding of the nature of things and predict the future of research. Data will be collected and analyzed using Microsoft Excel and "Survey Monkey" to conduct quantitative analysis.

Table 4: Meta-ethical questionnaire response options (question 2).

Answer choices	Responses (%)
(i) The most important priority	19.05
(ii) A top priority, but not the most important	14.29
(iii) Not very important	57.14
(iv) Not important at all	9.52

Table 5: Group of participants collected in the questionnaire.

Home countries	Male	%	Female	%	Total
China	56	67.47	27	32.53	83
The USA	47	66.20	24	33.80	71
Europeans	4	80.00	1	20.00	5
Others	2	28.57	5	71.43	7
Total	109	65.66	57	34.34	166

2.2.2. Data Analysis

(1) Section 1: Participants. Gender, age, and the employment times are collected before the questionnaires started. The collective data has achieved upon 166 responses, and the breakdown of the group of participants is shown in Tables 5 and 6, representing the similar pattern of response in terms of the whole questionnaires.

(2) Section 2: Questionnaire and Zoom Interview Analysis. From the questionnaire, more than half of the participants are having their home countries in China, and they agreed that national culture has changed their personality during the teenage stage, influencing their working attitude when they joined into the organizations. During the zoom interview, two participants who are working in Apple, which is a multinational company, revealed that they avoid changing any management style but prefer to stay with the management scheme. Alternatively, the employers in the USA Apple department prefer an effective management style with appropriate communication and feedback collections from the workers and costumers. The differences of organisational management culture are most significant in questions 6 and 8 of the questionnaire. Organisations in China are used to

Table 6: Type of companies collected in the questionnaire (question 3).

Answer choices	Responses (%)
(i) Registered or incorporated companies	4.76
(ii) Multinational companies	33.33
(iii) Companies limited by guarantee	14.29
(iv) Unlimited companies	14.29
(v) Public company	9.52
(vi) Private company	14.29
(vii) One person company	4.76
(viii) Country-based company	4.76

have less concern about the components of leadership since they have an uncertainty avoidance and restraint personality. As a result, companies in China are likely to provide a regulations guide based on bureaucracy and leaders did not accept the opinions from the perspective of his/her teams. Long-term improvement is not increased as fast as the USA since the US organizations prefer an impersonal strategy of rules to satisfy every employees. In China, important decisions can be only determined by directors since they believed that they have more authority and knowledge. For example, the outcome statistics of question 2 in the questionnaire (Table 7):

According to the result of question 4 in the questionnaire, there is a close relationship between language and management cultures since the two variables affect each other interactively. Culture is empowered and developed though its original home language, and the way of presenting the language can become the method of employees to express and receive information directly. More than 70% of the participants agreed that language is an essential component to shape an organisational management culture, proving the importance of adopting appropriate language skills that can motivate employees and enhance efficiency during workplace. Question 4 in the questionnaire of empowerment within organizations leading to high productivity and high performance has revealed that the empowerment in language within the organizations can assist the leadership skills and achieve high productivity and performance to satisfy the needs of goals of companies (Table 8).

During the interview of managers in the USA Apple, the results have shown that they are desperate to learn about different cultures in order to adapt the modern way of business management from the parent company in the United States of America. Set up Table 9 as follows:

In the questionnaire, both managers chose to set up a department to sense the culture in an organization and enhance their own communication system to solve the problems faced by the multinational companies. This management culture has positive correlated with the indulgence and low uncertainty avoidance in their national culture characteristics. Comparing with the management style in the USA, China organizations are not able to bring the essence of the USA management into their organizations because of the reason on their high power distance,

Table 7: Characteristics to describe the citizens and society in your home countries.

Answer choices	Responses (%)
(i) Oligarchy	4.00
(ii) Absolute monarchy (absolutism)	16.00
(iii) Concern in power distance	4.00
(iv) Individualism	76.00
(v) Collectivism	20.00
(vi) Masculinity	8.00
(vii) Uncertainty avoidance	4.00
(viii) Long-term orientation	72.00
(ix) Short-term orientation	12.00
(x) Indulgence	12.00
(xi) Restraint	56.00

Table 8: National culture variables that influence the most.

Answer choices	Responses (%)
(i) Language religion	72.00
(ii) History and traditions	32.00
(iii) Social organization	20.00
(iv) Value and attitudes	24.00
(v) Education practice	64.00
(vi) Political system (including rules and regulations)	28.00

individualism, and relative high collectivist culture. Since China is classified as a short-term orientation culture, the USA companies may have achieve a more effective and efficient working style compared with the Chinese subsidiary. Communicating with foreign employees had revealed the most concerned questions by the questionnaires. When facing the misunderstandings of communication, the managers with the USA national cultures are likely to be keen on finding the reasons and solutions even they felt frustrated, proving that a high significant influence of national culture helps to shape the managing and communicating practices in the USA organizations. Table 10 shows the national culture variables that influence the most (questionnaire question 4).

Finally, a social organisation presenting the importance level of family as well as the level of spirituality is revealed as comparatively different in China and the USA. Participants from the USA appear to have indulgence characteristics, and the national variables are revealed in question 8 of the questionnaires. According to the OECD Better Life Index, the United States ranked 28th in work-life balance and it is higher than China, which is not disclosed in the top 40 of the list in this category. Governments in the USA are likely to provide welfare state and listen to the opinions of the society, resulting in a better work-life balance compared with China. This will further affect the organisational management culture since the directors in the companies may care on the pressure of employees and prevent them from over working hours. This is a healthy working condition, and China should adopt this culture from the USA. Table 11 shows to what extent you concern about work-life balance (question 8).

Table 9: Interview questionnaire.

	Definitely my opinion	More or less what I believe	Neither statement represents my view	More or less what I believe	Definitely my opinion
Set up a department to sense the culture in an organization					
Enhancing the communication system					
Embrace transparency and inspire employee autonomy					
Recognize and reward valuable contributions					
Promote a team atmosphere by organizing regular workshops					
Encourage regular feedback					

Table 10: National culture variables that influence the most (questionnaire question 4).

Answer choices	Responses (%)
(i) None of the above	0.00
(ii) Identifying new opportunities	28.00
(iii) Innovating new products and ideas	32.00
(iv) Adapt global business models to the local market	16.00
(v) Communicating with foreign employees	60.00
(vi) Identifying regional and subculture differences	28.00
(vii) Understanding multinational business model	12.00
(viii) Adapting management practices across cultures	12.00

Table 11: To what extent you concern about work-life balance (question 8).

Answer choices	Responses (%)
(i) The most important priority	16.00
(ii) A top priority, but not the most important	20.00
(iii) Not very important	52.00
(iv) Not important at all	12.00

3. Conclusion

This research uses the data collection methods of non-governmental organizations, including the invitation of participants or volunteers via social media, working emails, and invitation letters, involving the issues such as designing human rights and privacy. The survey conducted by this research project has been conducted ethically, keeping in mind privacy, consent, and appropriate reporting of those involved in this study. All data are saved anonymously and will be erased from the database after the analysation completed. After completing the entire study, it was found that the result has established that high mobilization of culture differences in the USA had a notable positive consequence on companies' organisational management culture. In addition, after the study, it was also found that raising up for cross-cultural and transnational management will be a huge challenge for organizations to take, especially if countries wish to establish bilateral or trilateral business relations and partnerships. For a large part, China is geographically far away from the United States. However, the data size may be too small to represent each of the characteristics of the national cultures. The survey focuses on the company's case in the United States of America and China, representing that the results drawn from the questionnaires and analysis are only applicable to China and its similar cities. Not all participants taken part in the survey are working in a multinational companies, resulting in the challenges and solutions to multinational companies that may face the differences in data. The questionnaire results and recommendations may be suitable for the future development and management strategies in China and the USA due to the cultural and geographical differences.

Data Availability

The dataset can be accessed upon request.

Conflicts of Interest

The authors declare that they have no conflicts of interest.

References

[1] A. V. G. De Hilal, "Brazilian national culture, organizational culture and cultural agreement: findings from a multinational company," *International Journal of Cross Cultural Management*, vol. 6, no. 2, pp. 139–167, 2006.

[2] M. De Silva Kanakaratne, J. Bray, and J. Robson, "The influence of national culture and industry structure on grocery retail customer loyalty," *Journal of Retailing and Consumer Services*, vol. 54, Article ID 102013, 2020.

[3] W. P. Dorfman and J. P. Howel, "Dimensions of national culture and effective patterns and revisited, leadership patterns: Hofstede revisited," *Advances in International Comparative Management*, vol. 3, pp. 127–150, 1988.

[4] M. Erez, "Culture and job design," *Journal of Organizational Behavior*, vol. 31, no. 2-3, pp. 389–400, 2010.

[5] I. Franceschini, "Labour NGOs in China: a real force for political change?" *The China Quarterly*, vol. 218, no. 218, pp. 474–492, 2014.

[6] G. Hofstede, "National culture in four dimensions," *International Studies of Management & Organization*, vol. 13, no. 2, pp. 46–74, 1983.

[7] G. Hofstede, "Identifying organizational subcultures: an empirical approach," *Journal of Management Studies*, vol. 35, no. 1, pp. 1–12, 1998.

[8] E. Karahanna, J. Evaristo, and M. Srite, "Levels of culture and individual behaviour:AnPerspective, integrative perspective,"

Journal of Global Information Management, vol. 13, no. 2, pp. 1–20, 2005.

[9] W.-H. Lai and C.-W. Yang, "Barriers expatriates encounter during cross-cultural interactions," *Journal of Enterprising Culture*, vol. 25, no. 03, pp. 239–261, 2017.

[10] J. Leerssen, "Nationalism and the cultivation of culture," *Nations and Nationalism*, vol. 12, no. 4, pp. 559–578, 2006.

[11] D. Leidner and T. Kayworth, "Review: a review of culture in information systems research: toward A theory of information technology culture conflict," *MIS Quarterly*, vol. 30, no. 2, pp. 357–399, 2006.

[12] R. Magnier-Watanabe and D. Senoo, "Shaping knowledge management: organization and national culture," *Journal of Knowledge Management*, vol. 14, no. 2, pp. 214–227, 2010.

[13] C. Mora, "Cultures and organizations: software of the mind intercultural cooperation and its importance for survival," *Journal of Media Research*, vol. 6, no. 1, p. 65, 2013.

[14] C. E. Nicholls, H. W. Lane, and M. B. Brechu, "Taking self-managed teams to Mexico [and executive commentary]," *The Academy of Management Executive*, vol. 13, no. 3, pp. 15–27, 1999.

[15] M. H. Onken, "Temporal elements of organizational culture and impact on firm performance," *Journal of Managerial Psychology*, vol. 14, no. 3/4, pp. 231–244, 1999.

[16] J. Li, K. Lam, and G. Qian, "Does culture affect behavior and performance of firms? The case of joint ventures in China," *Journal of International Business Studies*, vol. 32, no. 1, pp. 115–131, 2001.

[17] R. Jia, M. Kudamatsu, and D. Seim, "Political selection in China: the complementary roles of connections and performance," *Journal of the European Economic Association*, vol. 13, no. 4, pp. 631–668, 2015.

[18] L. Li, B. Lei, and C. Mao, "Digital twin in smart manufacturing," *Journal of Industrial Information Integration*, vol. 26, no. 9, Article ID 100289, 2022.

[19] L. Li, T. Qu, Y. Liu et al., "Sustainability assessment of intelligent manufacturing supported by digital twin," *IEEE Access*, vol. 8, pp. 174988–175008, 2020.

[20] L. Li and C. Mao, "Big data supported PSS evaluation decision in service-oriented manufacturing," *IEEE Access*, vol. 8, pp. 154663–154670, 2020.

[21] L. Li, C. Mao, H. Sun, Y. Yuan, and B. Lei, "Digital twin driven green performance evaluation methodology of intelligent manufacturing: hybrid model based on fuzzy rough-sets AHP, multistage weight synthesis, and PROMETHEE II," *Complexity*, vol. 2020, no. 6, Article ID 3853925, 24 pages, 2020.

[22] G. K. Stahl and R. L. Tung, "Towards a more balanced treatment of culture in international business studies: the need for positive cross-cultural scholarship," *Journal of International Business Studies*, vol. 46, no. 4, pp. 391–414, 2015.

Hindawi
Scientific Programming
Volume 2023, Article ID 9873894, 1 page
https://doi.org/10.1155/2023/9873894

Retraction

Retracted: Rapid Identification of Tobacco Mildew Based on Random Forest Algorithm

Scientific Programming

Received 18 July 2023; Accepted 18 July 2023; Published 19 July 2023

This article has been retracted by Hindawi following an investigation undertaken by the publisher [1]. This investigation has uncovered evidence of one or more of the following indicators of systematic manipulation of the publication process:

(1) Discrepancies in scope
(2) Discrepancies in the description of the research reported
(3) Discrepancies between the availability of data and the research described
(4) Inappropriate citations
(5) Incoherent, meaningless and/or irrelevant content included in the article
(6) Peer-review manipulation

The presence of these indicators undermines our confidence in the integrity of the article's content and we cannot, therefore, vouch for its reliability. Please note that this notice is intended solely to alert readers that the content of this article is unreliable. We have not investigated whether authors were aware of or involved in the systematic manipulation of the publication process.

Wiley and Hindawi regrets that the usual quality checks did not identify these issues before publication and have since put additional measures in place to safeguard research integrity.

We wish to credit our own Research Integrity and Research Publishing teams and anonymous and named external researchers and research integrity experts for contributing to this investigation.

The corresponding author, as the representative of all authors, has been given the opportunity to register their agreement or disagreement to this retraction. We have kept a record of any response received.

References

[1] Z. Jiang, W. Zhang, H. Huang et al., "Rapid Identification of Tobacco Mildew Based on Random Forest Algorithm," *Scientific Programming*, vol. 2022, Article ID 1818398, 10 pages, 2022.

Hindawi
Scientific Programming
Volume 2022, Article ID 1818398, 10 pages
https://doi.org/10.1155/2022/1818398

Research Article

Rapid Identification of Tobacco Mildew Based on Random Forest Algorithm

Zhimin Jiang,[1] Wenjun Zhang,[2] Haixia Huang,[3] Zhengguang Zhai,[2] Dairong chen,[4] Yongfeng Ai,[4] Bo Li,[1] and Xiaoxiang Chen [1]

[1]*China Tobacco Zhejiang Industry Co Ltd., Hangzhou 310008, Zhejiang, China*
[2]*Hunan Tobacco Corporation Changsha Company, Changsha 410007, Hunan, China*
[3]*Guangxi Zhuang Autonomous Region Tobacco Corporation Baise Company, Baise 533000, Guangxi, China*
[4]*Guizhou Tobacco Corporation Tongren Company, Tongren 0856, Guizhou, China*

Correspondence should be addressed to Xiaoxiang Chen; ql@bbc.edu.cn

Received 19 August 2022; Revised 27 August 2022; Accepted 1 September 2022; Published 24 September 2022

Academic Editor: Lianhui Li

In order to further improve the identification efficiency of tobacco mildew, a rapid identification model of tobacco mildew based on random forest algorithm was proposed in this study. In order to ensure the feasibility and pertinence of the model study, this study takes redried leaf tobacco as the research object, selects high-temperature and high-humidity environment as the experimental conditions, and obtains the sample data of the degree of tobacco mildew under different experimental conditions. At the same time, this paper constructs a rapid identification model of tobacco mildew with the help of random forest algorithm. Through the model experimental results, it is found that the accuracy of the model for the rapid identification of training samples can reach 93.82%, while the accuracy of independent testing is 94.84%. The experimental results fully reflect the availability and efficiency of the random forest algorithm model in the rapid identification of tobacco mildew.

1. Introduction

Tobacco leaf is a special leaf plant. In most cases, tobacco leaves need to be stored for a period of time after harvest, and tobacco leaf storage is directly related to the quality of tobacco leaves, because the tobacco leaves in the mature stage can only enter the cigarette production after being harvested through special processes such as baking, purchasing, transportation, redrying, and aging. However, it takes a long time for the tobacco leaves to be harvested and made into finished cigarettes. If the tobacco leaves are not properly managed in the storage process, it is easy to mildew and then form mold. Mold is a relatively wide range of fungal microorganisms. Its growth environment is relatively simple. As long as it meets the requirements of appropriate temperature and humidity, it will quickly reproduce, and then the tobacco leaves will become moldy, which will seriously affect the quality of tobacco leaves and even cause the deterioration of tobacco leaves. Based on this background, this paper starts with the process and key points of tobacco mildew and combines random forest algorithm to identify tobacco mildew more accurately and efficiently.

2. Literature Review

There are many related research works on the detection technology of the internal components of tobacco leaves after mildew, which can be roughly divided into the following types: using the near-infrared technology to detect specific components, such as using the near-infrared spectroscopy technology to establish and verify the quantitative prediction model of ergosterol, establish the GBA algorithm, screen the characteristic wavelengths of the basic spectral data, and establish the PLS-DA discrimination model [1]. The model is applied to the identification of tobacco leaf samples, and the accuracy is as high as 95.79%. The characteristics of grain respiration and microbial activity were explored by using carbon dioxide technology detection,

reserve pest detector, and colony counting method, so as to obtain the characteristics of carbon dioxide gas produced by grain respiration and microbial activity, respectively. Amino acid analyzer was used to determine the specific content of free amino acids in moldy tobacco leaves. At the same time, the changes of amino acid content were divided into two categories: the absolute content increased and the absolute content decreased. GC-MS technology was used to determine the changes of volatile components in tobacco before and after mildew. Some studies have shown that substances with large changes are obtained by comparing before and after mildew, and then the content changes of these substances are used to establish a model, so as to infer whether it is mildew [2].

At present, the most widely used control technology is chemical control, which uses a variety of reagents. The most common antifungal agents in food include benzoic acid, sodium benzoate, sorbic acid, and propionic acid, but the mechanism of action is too small, and harmful gases may be generated after high temperature. Therefore, only staying in the previous research on antimildew agents cannot meet the needs of modern social development and people's attention to health. For this reason, many researchers began to turn to other chemical control agents with less toxic and side effects and better effects [3]. Some scholars pointed out that dimethyl fumarate has the strongest inhibitory effect on mold in tobacco leaves. Some researchers selected four kinds of fungicides, 75% dakonine, 40% hexin, 98% kangzhuolin, and 100% dimethyl fumarate, for toxicological and antimildew tests. The results showed that, through bioassay, 40% nucleostar had the best antibacterial spectrum and antibacterial effect, and dimethyl fumarate was the second. Kangzhuoling is also a safe and efficient biological fungicide. Some scholars have used organic acid mold inhibitor KMC-LF2 to conduct mold proof test on corn and found that it has good mold proof effect [4]. In recent years, some researchers have also studied the control of microwave technology. Some scholars have studied the effects of pulse microwave on the mortality of rice weevil and parasitic *Aspergillus*, rice temperature, broken rice rate, and burst waist rate of rice and their sensory quality. The results showed that, with the increase of pulse microwave intensity, the mortality of rice weevil and parasitic *Aspergillus* increased, the hatching rate of insect eggs decreased significantly, the sensory quality remained basically unchanged, the rice temperature increased gradually, and the broken rice rate and waist burst rate also increased [5].

3. Introduction to Random Forest Algorithm

Random forest (RF) is an aggregation distribution algorithm that contains multiple decision trees and poll strategies. The main idea of RF is to select randomly (not all) vectors to grow a tree in a class, and the only difference between them when designing a tree is a small number of differences [6]. In other words, implementation variables and patterns are randomly divided. This random number is called random existence because it is used in division or regression analysis. The final decision tree is generated by voting through the potential random vector tree; that is, select the "class" with the most votes as the category of the corresponding sample [7].

3.1. Decision Tree. Deciduous trees are formed by root nodes, leaves, and petals. The algorithm can be seen from the 1970s and 1980s. The most commonly used algorithms are the ID3 logging algorithm, the C4.5 logging algorithm, and the push logging algorithm [8].

3.1.1. ID3 Decision Tree Algorithm. ID3 algorithm is based on entropy in information theory. Suppose that an event has k optional results, and the probability of each result is shown in the following formula:

$$P_i(i = I, ..., k). \tag{1}$$

After observing the result of this event, its information is described by entropy, and the definition is shown in the following formula:

$$I = -\left(P_1 \log_2 P_1 + P_2 \log_2 P_2 + ... + P_k \log_2 P_k\right) = -\sum_{i=1}^{k} P_i \log_2 P_i. \tag{2}$$

If the characteristic divides N samples into m parts and there are N_m samples in each part, the impurity reduction is expressed by the two following formulas:

$$\Delta I(N) = I(N) - \left(P_1 I(N_1)\right) + \left(P_2 I(N_2)\right) + ... + \left(P_m I(N_m)\right), \tag{3}$$

$$P_m = \frac{N_m}{N}. \tag{4}$$

First, calculate the entropy purity of the samples in the current leaf node, split the current node with different features, compare the information gain in the split node, that is, the uncertainty reduction (3), and take the feature with the maximum information gain as the best node feature. If the subsequent nodes only include one type of samples, the branches and leaves stop growing, and the final node is called a leaf node. If the subsequent nodes include different kinds of sample sets, continue to iterate the above steps until each branch reaches the leaf node [9].

3.1.2. C4.5 Decision Tree Algorithm. C4.5 algorithm uses information gain rate replacement formula to obtain information gain, as shown in the following formula:

$$\Delta I_R(N) = \frac{\Delta I(N)}{I(N)}. \tag{5}$$

Moreover, C4.5 algorithm can also solve the characteristic problems with continuous values. The basic principle is as follows: assuming that the numerical characteristic x has n values in the training sample, arrange these values in order from small to large, and obtain the following formula:

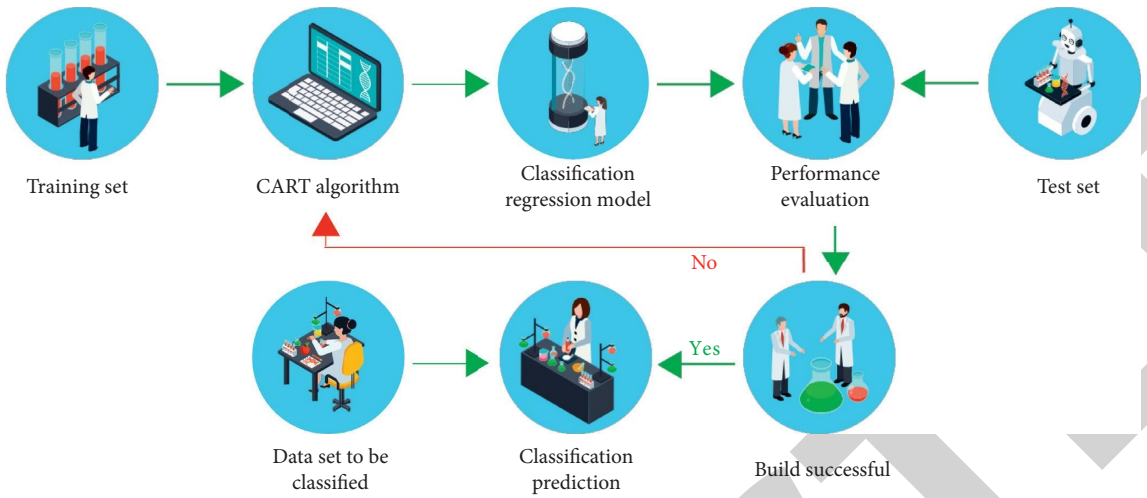

Figure 1: Flow chart of constructing classification regression tree.

Table 1: Advantages and disadvantages of decision tree.

Advantages
1. There is no need to introduce a priori assumption.
2. The decision tree is relatively simple to understand, its logical thinking is easier for people to understand, and it is easy to realize in practical application.
3. It has good stability for outliers and noise. The decision tree does not classify the data according to the specific value, and the outliers in the data have little impact on the whole result.
Disadvantages
1. In the process of top-down recursive construction, nodes store less and less information, and too little information will cause data fragmentation.
2. In the process of modeling, the unstable splitting of leaf nodes will cause overfitting.

$$v_i (i = I, \ldots, n). \tag{6}$$

Using dichotomy to divide the array, there are $n-1$ kinds of division methods. The information gain rate of each partition method is calculated. The continuous feature vector is changed into binary feature by selecting the method with the maximum gain rate, and then the decision tree is constructed together with other nonnumerical features. For the problem of feature discretization into multiple numerical values, the principle of the algorithm is the same; just increase the number of division methods.

3.1.3. Cart Decision Tree Algorithm. When constructing the classification regression tree model, we first randomly divide the sample set into training set and test set and then use cart algorithm to build the model in the training set, so as to obtain the classification regression model. Then we evaluate its performance through the test set. After successful construction, we apply this model to classify and predict the data of unknown categories. If the model construction fails, we return to the modeling process again and then conduct effective modeling and analysis through appropriate eigenvalues until the model is successfully constructed. Figure 1 shows the flow diagram of constructing classification regression tree [9].

Compared with neural network, support vector machine, and Bayesian algorithms, decision tree has its own advantages and disadvantages, as shown in Table 1.

3.2. Random Forest Model. Random forest is a model established by using a large number of decision trees (7).

$$\{h(x, \theta_k), k = 1, \ldots, K\}, \tag{7}$$

where $\{\theta_k\}$ represents a random vector subject to independent identically distributed, K is the number of decision trees, and each tree is the known variable x for optimal voting.

For the training sample set (8), N is the total number of samples, the object in X has an M-dimensional feature vector, and Y includes F different categories of information.

The classifier overemphasizes the classification of training samples, which makes the prediction of test samples worse. This phenomenon is called overfitting [10]. In the process of model construction, a variety of error analysis will be introduced. For random forest, generalization error is the key point to describe the overfitting problem. The generalization error is described by the edge function as follows:

$$mg(X, Y) = av_k I(h_k(X) = Y) - \max_{j \neq Y} av_k I(h_k(X) = j). \tag{8}$$

This function expresses the difference between the average value of correct votes obtained by correctly classifying random vector X into Y and the average value of votes obtained by other categories. The larger the function value is, the higher the classification accuracy is. Then the generalization error is defined as follows:

$$PE^* = P_{X,Y}(mg(X,Y) < 0). \tag{9}$$

According to the inference of the theorem of large numbers, the generalization error will eventually converge to the extreme value as the number of decision trees k increases, as shown in the following expression:

$$\lim_{k \longrightarrow \infty} PE^* = P_{X,Y}\left(P_\theta(h(X,\theta) = y) - \max_{j \neq Y} P_\theta(h(X,\theta) = j) < 0\right). \tag{10}$$

By solving the expected value of the edge function and the inference of Chebyshev inequality, an upper bound of the generalization error can be obtained as follows:

$$PE^* = \frac{\overline{\rho}(1-s)^2}{s^2}, \tag{11}$$

where $\overline{\rho}$ represents the mean value of the correlation factor ρ between trees and s represents the performance strength of the classifier. In order to better analyze the final performance of the classifier, the correlation factor and performance intensity are described by $c/s2$ ratio, and the smaller the ratio, the better the effect of the classifier, which is defined as follows:

$$\frac{c}{s2} = \frac{\overline{\rho}}{s^2}. \tag{12}$$

3.3. Random Forest Algorithm Regression Model. Suppose that the training set is taken from the distribution of random variables X and Y, which is similar to many predictors (see the following equation):

$$E_{XY}(Y - h(X))^2. \tag{13}$$

The above formula is the mean square random error, where $h(X)$ is the predicted value of the classifier. Since the predicted value is the average value of all trees, the form of mean square random error is as follows:

$$E_{XY}(Y - av_k h(X,\theta_k))^2. \tag{14}$$

When the total number of trees K is increasing, it is finally expressed as follows:

$$E_{XY}(Y - av_k h(X,\theta_k))^2 \longrightarrow E_{XY}(Y - E_\theta h(X,\theta_k))^2. \tag{15}$$

The regression function is expressed as follows:

$$Y = E_\theta h(X,\theta_k). \tag{16}$$

In practical application, it is often considered that the value of K is large enough and is replaced by the following:

$$Y = av_k h(X,\theta_k). \tag{17}$$

The average generalization error PE can be expressed in the form of a single tree as follows:

$$PE(\text{tree}) = E_\theta E_{XY}(Y - h(X))^2. \tag{18}$$

Table 2: Update of incremental random forest model.

Algorithm 3.3 incremental random forest←Update (x, y)
Steps:
1: For $t < 1$ to T do
2: For k←1 to P = Poisson (1) do
3: l = navigateToLeaf (x);
4: updateLeaf (l, (x, y));
5: If shouldSplit (l) then
6: Arg $\max_{\text{deD}} \Delta L$ (l,d);
7: createChild (l, d);
8: Endif
9: if P←0 then
10: $OOBE_t$←updateOOBE (t, (x, y));
11: End if
12: If s drawn from bern ($OOBE_t$)
13: rebuildTree (T);
14: Endif
15: End for
16: End for

Table 3: Node splitting conditions.

Algorithm 3.4 split function shouldSplit (l)
Steps:
1: If diffCluster (l) < 2 then
2: Return *false*;
3: If ΔL (l, d) > $\alpha \forall d \in D$ then
4: Return *false*;
5: Return *true*;

Through mathematical derivation and calculation, the average generalization error RE(forest) of random forest has an upper bound, and the form is as follows:

$$RE(\text{forest}) \leq \overline{\rho} PE(\text{tree}), \tag{19}$$

where $\overline{\rho}(0 < \overline{\rho} < 1)$ is the correlation factor. This formula shows that the generalization error of the whole random forest is $\overline{\rho}$ times that of a single decision tree, and rational design of the random forest model can better reduce the generalization error.

3.4. Incremental Random Forest. In the process of incremental random forest growth, we need to pay attention to two necessary factors: one is to sample the data set online, and the other is to reconstruct the splitting rules of nodes. Random forest generates a large number of test sets according to the characteristic randomness and then continuously calculates the quality measure of the test set to select the best splitting criterion. There are a large number of test sets at the nodes of each random tree when splitting. If the random forest randomly selects the set threshold instead of the threshold for a certain feature, it is called extreme random forest. The modeling time is long and the data cannot be updated in real time, but the accuracy of classification has been greatly improved. Tables 2 and 3 show the updating and node splitting conditions of the incremental random forest model.

This section selects 6 groups from UCI database 1 [9–11] as experimental data: Colon, Leukemia, Prostate, Lung,

Table 4: Comparison results of data classification.

UCI data	Training/testing	Category	Features	Random forest	Incremental random forest	OAB
Colon	6000/2150	2	62	0.107 ± 0.007	0.109 + 0.008	0.157 ± 0.010
Leukemia	7129/2500	2	72	0.128 ± 0.009	0.124 ± 0.008	0.188 ± 0.013
Prostate	6034/2300	2	102	0.109 ± 0.006	0.114 ± 0.006	0.215 ± 0.009
Lung	12533/4000	2	181	0.103 ± 0.008	0.108 ± 0.007	0.152 ± 0.011
Lymphoma	4026/1500	3	62	0.115 ± 0.010	0.118 ± 0.009	0.176 ± 0.013
SRBCT	2308/1000	4	63	0.113 ± 0.009	0.109 ± 0.006	0.189 ± 0.011

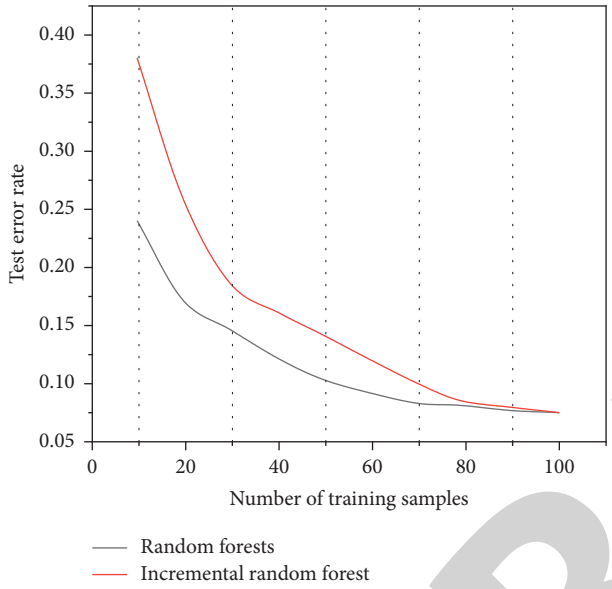

Figure 2: Effect of training sample number.

Lymphoma, and SRBCT. In the experiment, the total number of random trees is set to 100, and the number of randomly selected features is set to 10. In the experiment, the data are repeated 5 times and the average value is calculated. The standard deviation of classification error is shown in Table 4. The classification result of incremental random forest is very similar to that of original random forest. The prediction performance of the two methods is more accurate than that of OAB algorithm [11]. The main reason for the poor performance of OAB algorithm is that OAB algorithm can only solve the binary classification problem and cannot obtain the overall distribution of multifeature space in the data training process. Change the number of samples in the SRBCT data and compare the test error rates of the two methods. It can be concluded from Figure 2 that, with the gradual increase of the number of samples, the performance of the incremental random forest converges to the original algorithm.

4. Tobacco Mildew Image Recognition Based on Random Forest Algorithm and Neural Network

4.1. Simulation Experiment. In order to verify the effectiveness of the convolution neural network model for tobacco image classification, the tobacco image data set

Table 5: Experimental environment configuration.

Configuration	Content
CPU	Intel i7-8700
Computer memory	32 G
Computer operating system	Linux Ubuntu 19.10
GPU	NVIDIA GTX 1080 Ti
Deep learning framework	PyTorch

produced in this paper will be used to carry out experiments on the convolution neural network model and four classical convolution neural network models. During the whole experiment, each model was trained by multiple epochs to obtain the best parameters of the model, and the accuracy change curve of the training set and the test set was obtained, so as to visually see the effect and comprehensive performance of each model [12].

4.1.1. Experimental Environment and Data Set. The experiment in this chapter is carried out under the PyTorch framework. The specific software and hardware environment configuration of the computer used in the experiment is shown in Table 5. The main experiment environment is to use Ubuntu19.10 system + PyTorch deep learning framework + Python 3.6 and use the GPU with NVIDIA GeForce GTX 1080 Ti and 64g display memory to accelerate the experiment. The data set used in the experiment is a self-made tobacco leaf image data set. The tobacco leaf image data set mainly includes four categories of tobacco leaf image data: normal tobacco leaf, moldy tobacco leaf, green miscellaneous tobacco leaf, and variegated tobacco leaf. Each category has 3500 tobacco leaf images in the three categories of moldy tobacco leaf, green miscellaneous tobacco leaf, and variegated tobacco leaf. There are 4500 pieces of tobacco leaf data in the normal tobacco leaf category, and there are 15000 pieces of tobacco leaf image data in total. The tobacco leaf image data set is divided into 2 subsets in the ratio of 4 : 1, including 12000 training sets and 3000 test sets, so as to facilitate the use of experiments [13].

4.1.2. Experimental Design. In this paper, the tobacco leaf image data set is used as the experimental data, and the simulation experiments are carried out on four classical convolutional neural network models and the convolutional neural network model built in this paper. In the process of experiment, after many experiments, the model parameters and learning rate that can optimize the performance of the model are finally obtained. Then, they are applied to the

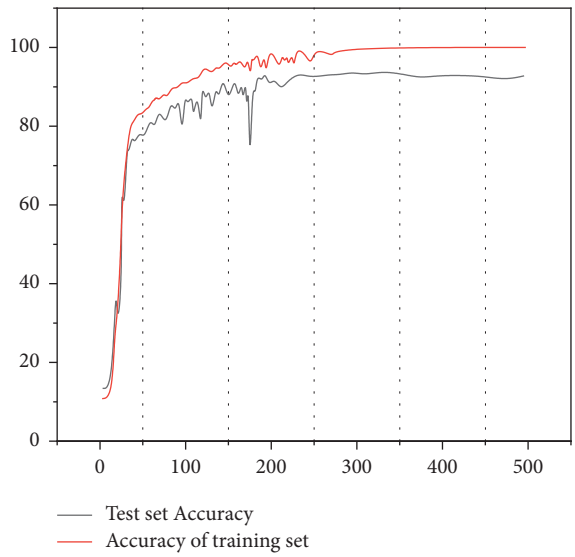

Figure 3: AlexNet model experiment results.

tobacco leaf image test set made in this paper for recognition [14]. During the experiment, the convolution neural network model has passed through 500 epochs, and the accuracy of the model test set is relatively stable. In addition, the visualization tool TensorboardX of PyTorch is used in the experiment. Its main function is to save and upload the data after model training to TensorboardX. TensorboardX is used to upload the coordinate data of the corresponding points of accuracy and generate csv files during model training. As the number of epochs increases, the accuracy change curve in the experiment is drawn. According to the change of the curve, we can more intuitively see the accuracy change and model effect of this test [15].

4.2. Analysis of Experimental Results

4.2.1. Results. Input the tobacco leaf image data set to AlexNet model for experiment. The network parameters are set as follows: the learning rate is set to 0.001, the dropout is set to 0.5, and the batch size is set to 64. This simulation experiment is based on 500 epochs and has been tested for many times. The accuracy change curve of AlexNet model simulation experiment is shown in Figure 3.

According to the experiment, the classification accuracy of AlexNet model test set is 95.5%. As can be seen from Figure 3, the convergence speed of the model is slow, and the accuracy of the model test set is relatively stable.

4.2.2. Result Analysis. We have made statistics on the test set loss value, training time of each epoch, and test set accuracy of the convolutional neural network model and four classical convolutional neural network models built in this paper [16]. The statistical results are shown in Table 6.

For the traditional image classification technology, this paper uses the HOG + SVM and HOG + KNN image classification methods. The main process is to first extract the HOG (histogram of oriented gradient) feature of the tobacco

Table 6: Comparison of experimental results of different convolutional neural network models.

Model	Loss	Time of each iteration (s)	Accuracy (%)
AlexNet	±0.002543	98	95.53
VGGNet16	±0.001822	120	96.23
GoogLeNet	±0.002015	132	96.56
ResNet18	±0.001555	115	97.36
This paper's model	±0.001424	85	98.08

Table 7: Comparison of experimental results of different algorithms.

Classification algorithm	Running time	Accuracy (%)
HOG + SVM	25 mins	71.36
HOG + KNN	13 mins	74.62
This paper's model	13 h	98.08

ptdata image and then use the support vector machine (SVM) algorithm and KNN algorithm for image classification [17]. The specific experimental process of traditional image classification method in this paper is as follows:

(1) HOG + SVM image classification method. Firstly, the moldy tobacco leaves, green miscellaneous tobacco leaves, and variegated tobacco leaves in the data set are taken as positive samples, and the normal tobacco leaves are taken as negative samples. Then the HOG features of positive and negative samples are collected to establish Feature Engineering, and then the support vector machine is used for image classification. As for support vector machine, LibSVM is used in this paper. It is a software library of support vector machine. It has the advantages of less input parameters and fast operation speed. It can easily classify or regress data.

(2) HOG + KNN image classification method. Firstly, take the moldy tobacco leaves, green miscellaneous tobacco leaves, and variegated tobacco leaves in the data set as positive samples and normal tobacco leaves as negative samples, and then collect the HOG characteristics of positive and negative samples to establish Feature Engineering [18]. For the KNN algorithm, this paper uses the KNeighborsClassifier function encapsulated by sklearn, where the K value is set to 3. The experimental results of the convolution neural network model built in this paper are compared with the experimental results of the traditional image classification methods. The comparison results are shown in Table 7.

The structure of the actual circulatory neural network formed when the image data generated in this form is used for image distribution. This text is much larger than the traditional image distribution method. In terms of runtime, the training time for curved neural network structures is much longer than that for traditional image distribution

methods, but traditional image distribution methods require more time to remove image features and establish functional engineering before splitting [19].

5. Fast Identification Experiment of Tobacco Mildew

5.1. Materials and Instruments. 116 kinds of redried leaf tobacco collected from 2015 to 2017 were selected from different places of origin, different parts, and different grades, so as to fully consider the different effects of different places of origin, different parts and grades, and different types and quantities of mold in tobacco leaves on the mildew of tobacco leaves. The samples were provided by a tobacco company. The instruments are as follows: TRH-1250 constant temperature and humidity box (for sample mildew test); MPA Fourier transform near infrared spectrometer; KBF constant temperature and humidity chamber (for microbial counting experiment); Double Biocao RNA/DNAultra clean workbench; Ba-2s flapping sterile homogenizer; MS204 balance; Milli-Q Integral 10 ultra pure water machine [20].

5.2. Preparation of Moldy Samples. Put the redried tobacco leaf sample under the environment of temperature $(22 \pm 2)^{\circ}$ C and humidity $(60 \pm 5)\%$ for 48 h. Put the balanced samples into the constant temperature and humidity box, adjust the temperature and humidity to 25°C and 85%, respectively, and carry out the tobacco mildew test. Take 21 days as the cycle, and take samples according to the following methods:

(1) The first sampling shall be carried out on day 0, that is, before putting the sample into a box with a constant temperature of 25°C and humidity of 85%.

(2) On the 3rd to 9th day, take the 2nd to 4th sampling, respectively, at the interval of 3 days.

(3) On the 11th to 21st day, take the 5th to 10th sampling, respectively, at 2-day intervals.

This process can completely collect the sample state that the redried tobacco leaves have never been mildewed to near mildewed and then to mildewed.

5.3. Mould Counting Test. According to YC/T 472-2013 microbiological examination of tobacco and tobacco products mold count, the mold count of redried tobacco samples with different degrees of mildew was detected. According to the mold count test results, the mold degree is divided into the following: nonmoldy samples (mold count $<2\times10^3$ CFU/g), adjacent moldy samples (2×10^3 CFU/g ≤ mold count $<10^4$ CFU/g), and moldy samples (mold count $\geq 10^4$ CFU/g).

5.4. Near-Infrared Spectrum Data Acquisition. MPA Fourier transform near-infrared spectrometer was used in the experiment. The spectrum acquisition range was 4000 ~12000 cm^{-1}, the resolution was 8 cm^{-1}, and the scanning times were 64. The tobacco samples with different degrees of mildew were loaded into the sample cup, and the near-infrared spectra of each sample were collected as the basic spectral information of each tobacco sample. Repeat the loading and determination for each sample twice, and then calculate the average result as the final spectrum [21].

Near-infrared spectroscopy is affected by a series of chemical and physical factors of samples. It is necessary to take mathematical pretreatment methods to reduce system noise, such as baseline change and light scattering. In this study, after comparing the first derivative (1-Der), second derivative (2-Der), multivariate scattering correction (MSC), standard normal variable (SNV) correction, and other preprocessing methods, discrete wavelet transform (DWT) is used to preprocess near-infrared spectral data [22].

The essence of wavelet transform is to decompose the signal into wavelet subspaces with different scales and frequencies. Choosing various mother wavelets according to the waveform or length makes wavelet transform more effective and flexible than other signal preprocessing methods in extracting the features of signals. Through wavelet transform, the signal is decomposed into low-frequency signal and high-frequency signal, approximation coefficient, and detail coefficient [23–29]. When wavelet transform is used to preprocess the near-infrared spectrum, there are two ways to establish the correlation model between independent variables and near-infrared signals: first is to reconstruct the spectrum with approximate coefficients and detail coefficients after denoising or data compression and to establish a model between the reconstructed spectrum and independent variables; second, the wavelet coefficients obtained by wavelet decomposition are directly used as variables to establish the model. Obviously, the latter method is much more convenient, time-saving, and widely used. In this study, wavelet coefficient was used as a variable to establish a prediction model for the mildew degree of redried tobacco leaves.

6. Results and Discussion

6.1. Classification of Moldy Tobacco Leaves. After the mildew experiment, 1160 tobacco samples with different degrees of mildew were obtained from 116 kinds of single flue-cured tobacco, which were sampled 10 times at different stages. Microbiological tests were carried out on 1160 samples according to YC/T 472-2013 microbiological examination of tobacco and tobacco products mold count. The research results of some scholars show that when the mold number reaches a certain amount (about 104 CFU/g), it will start to grow rapidly. In order to give early warning of tobacco mildew, it is necessary to prejudge the samples near mildew. Therefore, 104 CFU/g is taken as the critical point to judge the "near mildew" samples. According to the method of determining the degree of tobacco mildew, the tobacco mildew was finally divided into three categories: nonmildew, near mildew, and mildew. The three types of samples obtained from mildew test are shown in Table 8.

6.2. Near-Infrared Spectral Pretreatment. The original near-infrared spectra of 1160 redried tobacco samples with

Table 8: Classification of mildew degrees of tobacco leaf samples.

Mildewing degree	Sample quantity	Mold count (CFU/g)
Nonmildew	548	$<2\times10^3$
Near mildew	102	$[2\times103, 10^4)$
Mildew	510	$\geq10^4$

Table 9: Training results of random forest model based on different wavelet coefficients.

Wavelet coefficient	Variable length	Recognition rate/%	Recognition rate 1/%	Recognition rate 2/%	Recognition rate 3/%
cd1	1051	78.53	77.81	45.59	85.88
cd2	540	80.85	81.10	58.82	85.00
cd3	284	82.79	80.82	58.82	89.71
cd4	156	90.94	90.68	80.83	93.24
cd5	92	84.22	90.14	73.53	80.00
cd6	60	82.28	87.95	72.06	78.24
cd7	44	81.76	83.29	70.59	82.35
cd8	36	79.69	83.56	70.59	77.35
cd9	32	79.04	79.45	58.82	82.65
cd10	30	74.77	81.37	36.76	75.29
cd11	29	73.48	79.73	35.29	74.41
ca11	29	59.51	67.67	27.94	57.06
[cd4, cd5]	248	93.40	93.42	91.17	93.82
Primitive harmonic	2074	69.73	73.15	30.88	73.82

different degrees of mildew can be obtained from the original near-infrared spectra during the mildew process of redried tobacco. According to the principle of near-infrared spectroscopy, the near-infrared spectral absorption band of the sample is the frequency doubling and merging of hydrogen containing groups (O-H, N-H, C-H) in the mid infrared spectral region, as well as the superposition of differential absorption bands. When tobacco is mildewed, the organic substances such as C source and N source in the sample will change due to the catabolism of mold, and some chemical components related to the composition of mold cell wall such as ergosterol and chitin will be produced. Therefore, in theory, the near-infrared absorption bands of tobacco leaves with different degrees of mildew will change with the change of chemical composition in the sample. However, on the one hand, it is due to the serious overlap of near-infrared spectra; on the other hand, tobacco mildew is a complex process, and the changes of chemical components are also extremely complex. It is difficult to directly extract the information related to the degree of mildew from the near-infrared spectra of tobacco leaves and give a reasonable spectral analysis. It can be seen from the final results that the absorption bands related to mildew in the near-infrared spectra of tobacco leaf samples are difficult to be directly judged from the spectra.

In this study, discrete wavelet transform (DWT) was used to decompose the original near-infrared spectra of redried tobacco leaves in the process of mildew. When using DWT to process NIR spectra, there are two factors to be considered: the selection of mother wavelet and the determination of decomposition level. At present, there is no theory to follow for the selection of mother wavelets. The study investigated the influence of 15 mother wavelets, five Daubechies series wavelets (db2, db4, db6, db8, and db10), five Symlets series wavelets (sym2, sym4, sym6, sym8, and sym10) and five Coiflets series wavelets (coif1, coif2, coif3, coif4, and coif5), on the recognition accuracy of moldy tobacco leaves. The results of Daubechies series wavelets are basically the same, but, in general, the prediction results are better than those of the other two types of wavelets. Finally, db6 is determined as the mother wavelet. When determining the decomposition level, the dimension n of the input data should generally be considered, which generally does not exceed log2 (N). For the extraction of useful information, the decomposition level should be as large as possible. In this study, there are 2074 data points in the near-infrared spectrum, so this paper selects 11 as the decomposition level of wavelet transform. After each level of decomposition, a detail coefficient vector and an approximate coefficient vector are obtained. The approximation coefficient is further decomposed to obtain the detail coefficient and approximation coefficient until the 11th decomposition level. Finally, the vectors obtained by wavelet transform include the approximate coefficients (ca) of the spectral signal of each sample at the last decomposition level and the detail coefficients (cd) at all decomposition levels. A total of 12 groups of wavelet coefficients, ca11, cd11, cd10, ..., cd1, are obtained.

6.3. Establishment of Identification Model of Tobacco Mildew Degree. To compare the reception results of the different models, 1160 models were divided into training and test modes. Approximately 2/3 of the models are used as training, and 1/3 of the models are based on experiments. Finally, 773 models were selected for the training, of which 365 were standard, 68 were standard, and 340 were standard. The remaining 387 models were used as standardized

Table 10: Comparison of training results of cigarette model, cut tobacco model, cigarette end model, and comprehensive model.

Model	Total recognition rate/%	Recognition rate_1/%	Recognition rate_2/%	Recognition rate_3/%
Smoke model	93.40	93.42	91.17	93.82
Cut tobacco model	94.05	94.25	91.17	94.41
Smoke model	94.95	95.62	92.65	94.71
Integrated model	80.60	80.55	73.53	82.06

Table 11: Prediction results of test set based on [cd4, cd5] random forest model.

Parameter	Unmodified samples	Adjacent moldy samples	Moldy samples	Total
Number of test set samples	183	34	170	387
Accurately predict the number of samples	175	31	161	367
Correct prediction rate/%	95.63	91.18	94.71	94.84

experiments. This document categorizes mold-free designs, mold designs, and multimold designs as "1," "2," and "3," respectively. The accuracy of the training procedures and examination procedures is determined by the fees and assumptions.

It can be seen from Table 9 that the number of variables from cd1 to cd11 and ca11 and from 1051 to 29 decreases in turn. Among them, the random forest model constructed by the wavelet coefficient cd4 with a small number of variables (92) has the highest recognition rate: the total recognition rate is 90.04%, the recognition accuracy rate of nonmildewed samples is 90.68%, the recognition accuracy rate of near mildewed samples is 80.88%, and the recognition accuracy rate of mildewed samples is 93.24%, which are higher than the recognition ability of other wavelet coefficients.

As can be seen from Table 10, from the perspective of model accuracy, the prediction accuracy of the end of tobacco model > cut tobacco model > piece tobacco model > comprehensive model is similar to those of the end of tobacco model, cut tobacco model, and piece tobacco model.

In the measurement model, the flue gas model was used to calculate the sample size, and the calculated results are shown in Table 11. As shown in Table 11, 175 of the 183 models were correctly calculated, not moldy. The accuracy is 95.63%. Out of 34 samples close to the fungus, 31 samples were calculated correctly, with an accuracy of 91.18%; 161 out of 170 yeast samples were calculated correctly, with an accuracy of 94.71%. The accuracy of the test lumped forecast is 94.84%. The results showed that the model established by this method could effectively identify tobacco samples with different degrees of mildew.

7. Conclusion

In this study, the redried tobacco leaf was taken as the research object, the experimental conditions were high-temperature and high-humidity environment, and the sample data of tobacco mildew degree were obtained under different experimental conditions. In this paper, a rapid identification method of tobacco samples with different degrees of mildew was established by near-infrared spectroscopy, which provided a basis for early warning of tobacco mildew. The wavelet transform was used to process the spectral data, and [cd4, cd5] was selected as the spectral variable to establish the random forest recognition model of tobacco leaves with different degrees of mildew. The recognition rate and prediction rate of the model were 93.82% and 94.84%, respectively. The satisfactory recognition rates were achieved for the normal tobacco leaves, the adjacent moldy tobacco leaves, and the moldy tobacco leaves. It can be seen that near-infrared spectroscopy combined with wavelet transform and random forest algorithm can effectively identify tobacco samples with different degrees of mildew. This method can be considered feasible to quickly predict the degree of tobacco mildew.

Data Availability

The data set can be obtained from the corresponding author upon request.

Conflicts of Interest

The authors Zhimin Jiang, Bo Li, and Xiaoxiang Chen are affiliated to and funded by China Tobacco Zhejiang Industry Co., Ltd. The authors attest China Tobacco Zhejiang Industry Co., Ltd. has had no influence on design of this study or its outcomes.

The authors Wenjun Zhang and Zhengguang Zhai are affiliated to and funded by Hunan Tobacco Corporation Changsha Company. The authors attest Hunan Tobacco Corporation Changsha Company has had no influence on design of this study or its outcomes.

The authors Dairong Chen and Yongfeng Ai are affiliated to and funded by Guizhou Tobacco Corporation Tongren company. The authors attest Guizhou Tobacco Corporation Tongren company has had no influence on design of this study or its outcomes.

Acknowledgments

This research was funded by Project of China Tobacco Zhejiang Industry Co, Ltd. (ZJZY2021B009), Project of Hunan Tobacco Corporation Changsha Company (21-

Hindawi
Scientific Programming
Volume 2022, Article ID 7202627, 11 pages
https://doi.org/10.1155/2022/7202627

Research Article

A Rapid Temporal Bone Localization Method Based on Machine Visual Detection Markers

Li Jian-jun,[1] **Zhuo Jian-ye**,[1] **Wu Yue**,[1] **Wang Zuo**,[2] **Yao Zhen**,[1] **Jia Huan**,[3] **Wang Zhao-yan**,[3] **Chen Ying**,[3] **Zhou Dao-min**,[4] **and Yu Ming-zhou**[1]

[1]*China Jiliang University, Hangzhou 310018, China*
[2]*Maanshan University, Maanshan 243100, China*
[3]*Shanghai Ninth People's Hospital, Shanghai 200125, China*
[4]*Zhejiang Key Laboratory of Neuroelectronic and Brain Computer Interface Technology, Hangzhou, China*

Correspondence should be addressed to Li Jian-jun; 13a0104121@cjlu.edu.cn

Received 25 July 2022; Revised 9 September 2022; Accepted 12 September 2022; Published 23 September 2022

Academic Editor: Lianhui Li

The number of hearing-impaired people is increasing year by year; robotic cochlear drilling surgery is one of the safest methods to treat deafness. Looking at the issue of low efficiency of temporal bone posture positioning in cochlear implantation robotic drilling, a novel auxiliary ring marker temporal bone positioning method was proposed to improve temporal bone posture positioning efficiency, optimize the operation time, and reduce auxiliary injuries caused by the surgery. First, the temporal bone visual positioning assistant ring was designed based on the requirements for cochlear robotic drilling surgery. The target detection was conducted on the auxiliary ring and image processing and feature point extraction methods were designed. Then, the three-dimensional coordinates of the measured feature points were obtained by binocular vision, and the auxiliary ring and temporal bone postures were estimated. Finally, the auxiliary ring and temporal bone localization methods were validated. The experiment results indicated that the temporal bone was located quickly and effectively in a total time of about 33 ms, which was faster and more accurate than traditional visual localization methods and could satisfy real-time temporal bone localization during surgery. This study can reduce the time of temporal bone visual positioning in cochlear implant drilling operations, greatly improving the robot's capabilities to extract visual information during the operation, which has a better auxiliary role for future research and applications of the cochlear implant drilling operation.

1. Introduction

Cochlear implant drilling is a new surgical procedure that optimizes the surgical method and reduces surgical trauma [1, 2]. As robot technology has developed, robot drilling surgery has gradually become more acceptable [3, 4]. Compared with human-performed operations, robotic operations for cochlear drilling have shown far more advantages than the former, which is conducive to an effective, quick, and safe methodology for cochlear drilling [5]. Human beings have innate advantages in visual information perception and can quickly extract and identify information and content during surgery; however, there is no perfect computer model in this field, and the weak visual information processing ability is the key to the challenges facing robotic surgery for cochlear implant drilling [6]. In recent years, temporal bone visual localization as the core technology for robotic drilling surgery has garnered an increasing amount of attention. The goal is to map the positions of key tissue structures in the ear and plan the drilling path of surgery by using the postures of human temporal bones [7].

Currently, many scholars are studying the rapid temporal bone localization method, but most of them still abide by the traditional image detection marker method. Cho et al. proposed registering the locations of surgical wounds using a tripod visual calibration rod as a marker [8]. The calibration rod could provide reliable geometric feature

information and facilitate calculating wound location, but the registration method for implanting the calibration rod was cumbersome and would easily affect the operating space. Dillon et al. used titanium screw implantation on temporal bones to simplify the challenges inherent to marker implantation [9], but the locations where the titanium screws were implanted were random and riddled with uncertainties, and it is difficult for computers to obtain such random information. Jia et al. proposed a short-flow visual registration method of the malleus, which can effectively improve registration accuracy for intra-aural structures and reduce any damage caused by the registration process [10], but this method requires a surgeon to have a lot of clinical experience.

In conclusion, the temporal bone localization markers used now cannot satisfy the requirements for rapid detection in computer vision. To solve the aforementioned problems, this paper proposed a temporal bone localization method based on an auxiliary ring, named the Deep (DL-M), and functions based on a combination of deep learning target detection, computer vision, and medical requirements of cochlear implant drilling surgery. The DL-M reduces extraction time for feature points and matching calculation of irrelevant features through image processing. Compared with BM, SGBM, and other methods, DL-M is faster, and its overall duration is about 40 ms, which meets the requirement for real-time detection of more than 20FPS. The average detection accuracy of the auxiliary ring is less than $\pm 0.63^{\circ}$.

2. Principles of Auxiliary Temporal Ring Bone Localization

In the robotic drilling operation for a cochlear implant, a surgical approach from the mastoid surface of the temporal bone to the tympanic step needs to be drilled, so it is necessary to locate the temporal bone in the body to determine the drilling point and the direction of approach [11]. Since there is no fixed and easily identifiable feature information for the temporal bone, it is difficult to calculate its pose through vision. Therefore, it is necessary to plant external markers to establish the spatial relationship between the markers and the temporal bone and to detect and calculate the pose information for external markers to obtain the current pose information for the temporal bone. Therefore, during robotic cochlear implant drilling surgery, temporal bone position and pose information detection are obtained by detecting temporal bone visual markers.

2.1. Temporal Bone Positioning Auxiliary Ring. During cochlear implant drilling, the temporal bone with implant markers was initially scanned with high-precision CT, and its three-dimensional image was reconstructed. Then, the relative position of the tissue structure in the ear was calculated to plan the drilling path based on the surgical conditions, and the relative postural relationship between the path and markers was calculated. Finally, the robot drills the planned surgical approach through the relative postural relationship between the postural information from the markers and the path [12, 13]. Therefore, temporal bone markers should not only have a clear shadow in a CT scan but also visual features that can be detected by machine vision. The traditional locating method with external markers is random and subjective, and the irregular pattern is not conducive to machine vision detection and analysis. There are three main effects of robotic drilling. First, the spatial location of marker planting is too single, which will affect the calculation of depth information, which will lead to a large relative position error between marker and tissue structure. Second, too many marker points will cause secondary damage to the temporal bone. Third, it is difficult for robots to detect and analyze the traditional irregular planting location distribution. To resolve these issues, a robotic drilling auxiliary ring for cochlear implantation was proposed and designed, as shown in Figure 1.

The auxiliary ring is structurally divided into three parts: the inner ring, the outer ring, and the attached titanium sphere. The inner ring is nested in the outer ring, and the titanium sphere is attached to the torus of the outer ring and is sequentially mapped. The effects of traditional markers and auxiliary ring implantation are shown in Table 1. By using the auxiliary ring as the temporal bone visual registration marker, up to three wounds on the temporal bone can be fixed, thus reducing temporal bone injuries in the implanting process. The use of a circular structure is more in line with human engineering properties. The titanium spheres attached to the outer ring can be used as markers in CT scan reconstruction instead of titanium nails. The inner and outer ring structure adds visual features that are easy to detect on the auxiliary ring surface. The feature points of colors, fixed shapes, and distribution laws are beneficial to computer vision processing and analysis.

2.2. Binocular Vision Measurements. In the cochlear implant drilling operation, the auxiliary ring spatial position should be calculated, and real-time feedback of image information during the operation is needed. Binocular vision was used to locate the auxiliary ring. Based on the parallax principle, binocular vision reconstructs the three-dimensional coordinates of the target in space according to the two-dimensional coordinates of the measured target in the left and right images combined with the transformation relationship between each coordinate [14]. Binocular ranging needs to calibrate the binocular camera, determine the transformation relationship between the world coordinate system, pixel coordinate system, and camera coordinate system, and finally calculate the rotation matrix and translation vector between the internal and external camera parameters and the left and right cameras. The calibration tool for the STEREO Camera Calibrator in MATLAB was adopted, and Chang's calibration method was employed to calibrate the internal and external parameters of the left and right cameras. The calibration results are shown in Figure 2.

According to the mapping relationship between the projections, external parameters, and internal parameters, the distortion coefficients were obtained after the left and

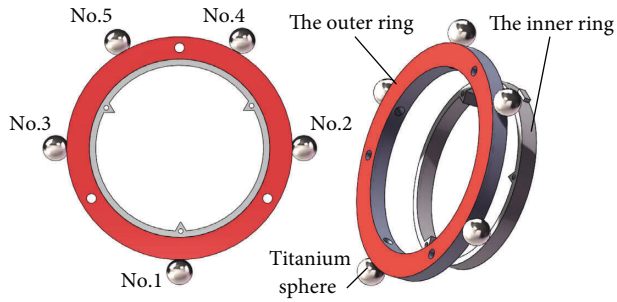

Figure 1: Auxiliary ring 3D model.

Table 1: Statistics of auxiliary ring model test results.

Target object identification	Real quantities	Quantity checks	Missed checks	Error checks
Outer ring	130	131	1	2
Titanium spheres	650	664	5	19

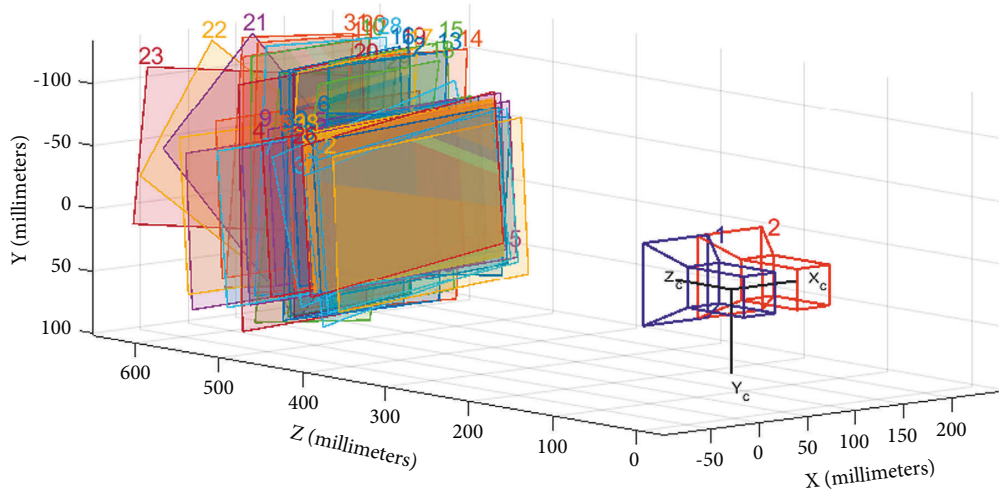

Figure 2: Binocular vision stereo calibration.

right cameras were calibrated, and the projection matrices of the cameras were $M_l\, M_r$, respectively, allowing the world coordinates of any point in space to be (X, Y, Z), then the following formula can be obtained:

$$\begin{cases} Z_{cr}\begin{bmatrix} u_r \\ v_r \\ 1 \end{bmatrix} = M_r \begin{bmatrix} X_c \\ Y_c \\ Z_c \\ 1 \end{bmatrix} = \begin{bmatrix} m_{11}^r & m_{12}^r & m_{13}^r & m_{14}^r \\ m_{21}^r & m_{22}^r & m_{23}^r & m_{24}^r \\ m_{31}^r & m_{32}^r & m_{33}^r & m_{34}^r \end{bmatrix} \begin{bmatrix} X_c \\ Y_c \\ Z_c \\ 1 \end{bmatrix} \\ Z_{cl}\begin{bmatrix} u_l \\ v_l \\ 1 \end{bmatrix} = M_r \begin{bmatrix} X_c \\ Y_c \\ Z_c \\ 1 \end{bmatrix} = \begin{bmatrix} m_{11}^l & m_{12}^l & m_{13}^l & m_{14}^l \\ m_{21}^l & m_{22}^l & m_{23}^l & m_{24}^l \\ m_{31}^l & m_{32}^l & m_{33}^l & m_{34}^l \end{bmatrix} \begin{bmatrix} X_c \\ Y_c \\ Z_c \\ 1 \end{bmatrix}. \end{cases} \tag{1}$$

In the above formula, $Z_{cr}\, Z_{cl}$is the distance from the projection of a point in space on the optical axis to the optical center; $M_r\, M_l$ is the projection matrix of the camera; and (X, Y, Z) is the world coordinate of a point in space.

3. Auxiliary Ring Positioning Method

The temporal bone auxiliary ring positioning method DL-M proposed in this paper for cochlear implant drilling surgery can generally be divided into three parts: target region detection, feature point extraction, and position and pose a solution. The specific realization process is shown in Figure 3. First, the outer ring of the input image and the target region of the characteristic titanium spheres are detected by the trained deep learning model. Next, the feature points in the boundary box are extracted quickly, and the image coordinates are calculated. Then, binocular vision measures the three-dimensional coordinates of the feature points. Finally, the pose information for the auxiliary ring is solved according to the three-dimensional coordinates of the feature points.

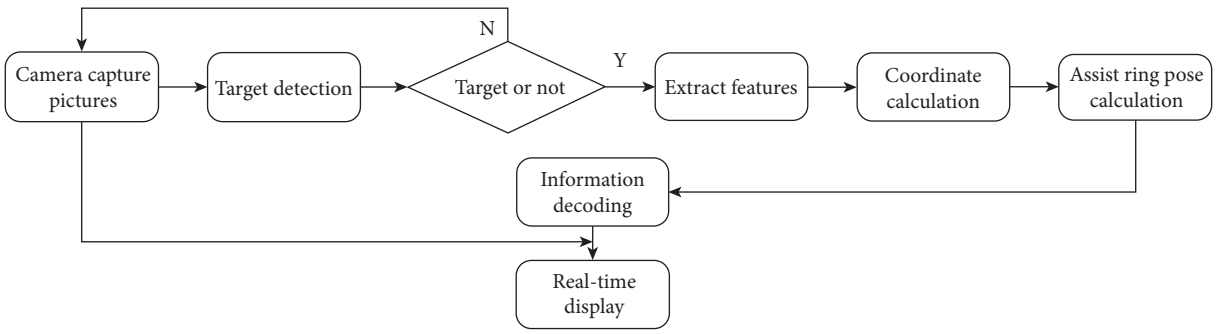

Figure 3: Auxiliary ring positioning method flow.

3.1. Auxiliary Ring Target Detection. How to efficiently identify an object to be measured is always one of the most important challenges for machine vision. Due to the influence of light, blood stains, instruments, and other factors, it is difficult to obtain the characteristic information of the auxiliary ring quickly and accurately through traditional detection methods in cochlear implant drilling surgery. Due to the development of the Convolutional Neural Network, deep learning algorithms based on the Convolutional Neural Network, it has gradually become the main method of target detection. Compared with traditional detection methods, deep learning algorithms are more advantageous in terms of speed, precision, and structure [15, 16]. In drilling surgery, the deep learning target detection algorithm can quickly and accurately identify the characteristic information of the auxiliary ring in complex surgical environments and accelerate auxiliary ring positioning.

To accurately and quickly detect the target auxiliary ring in a complex surgical environment, the YOLOV3 method was employed in this paper to detect the target related to the auxiliary ring [17]. The outer ring and titanium spheres were used as detection models for training auxiliary rings to obtain the boundary information of the outer ring and titanium spheres. The K-means clustering algorithm was used to calculate the prior parameters of anchor points in the data set, and the method for initiating random numbers in the clustering algorithm was changed. By analyzing the data set, 9 anchor points are given for the initial calculation, which can help the network better adjust the size of the bounding box while learning. In this experiment, the outer ring region and titanium sphere regions from about 650 images of the auxiliary rings with a different attitude in different environments were labeled, and the PASCAL VOC2007 dataset was established.

3.2. Feature Extraction. After the target features of the outer ring and titanium spheres were obtained by target detection, the target feature information in the boundary box should be further extracted, as shown in Figure 4. Firstly, the image of the attitude auxiliary ring was preprocessed by filtration and equalization. Secondly, the contour information in the boundary box of the outer ring was detected, screened, and fitted, and the fitted contour dataset was reconstructed by using relevant mathematical functions. Then, the reconstructed ellipse dataset was matched with the original contour dataset to determine whether the contour was the target contour that met the conditions. Finally, the center of the fitted ellipse was calculated, which was the two-dimensional coordinate of the center of the auxiliary ring.

To reduce the image processing duration, RoI segmentation was conducted on the original image in the range of the bounding box information output after target detection, and image pre-processing was conducted within RoI to reduce the amount of image pre-processing calculations. Bilateral filtering removed the noise in images in the region of interest and the image edge information was retained. Then the target feature points were extracted by ellipse detection and a region growing algorithm. Finally, the feature points of the left and right cameras are matched to provide reliable matching points for binocular vision calculation.

3.3. Posture Calculating. After the matching target feature points were obtained, the characteristic coordinates of the auxiliary ring were obtained through the principles of binocular vision, and the auxiliary ring position and pose information were further calculated. The specific process is shown in Figure 5.

The feature points matched by the left and right images were substituted into (1), and irrelevant variables were eliminated. The least square fitting method solved the three-dimensional coordinates for the feature points. $(x_i, y_i, z_i)i \in (1, 5)$, (q_x, q_y, q_z) represented the coordinates of the centers of the corresponding 1–5 titanium spheres and the corresponding inner ring. The obtained coordinates were the three-dimensional space coordinates for the auxiliary ring from the image plane coordinates. Given the world coordinates of the camera, the coordinate values of the auxiliary ring in the world coordinates can be obtained through coordinate transformation. To coordinate with each serial number corresponding to an individual sphere, this paper combined with the distribution rules of auxiliary ring attached titanium ball, and designed the coordinate collation of feature points by considering the intensive degree of space points. The intensive degree ρ_i of the coordinate distribution concerning the titanium cue ball was calculated by using the formula (5), the feature points were ordered by relative intension of ρ_i, and, thus, the titanium

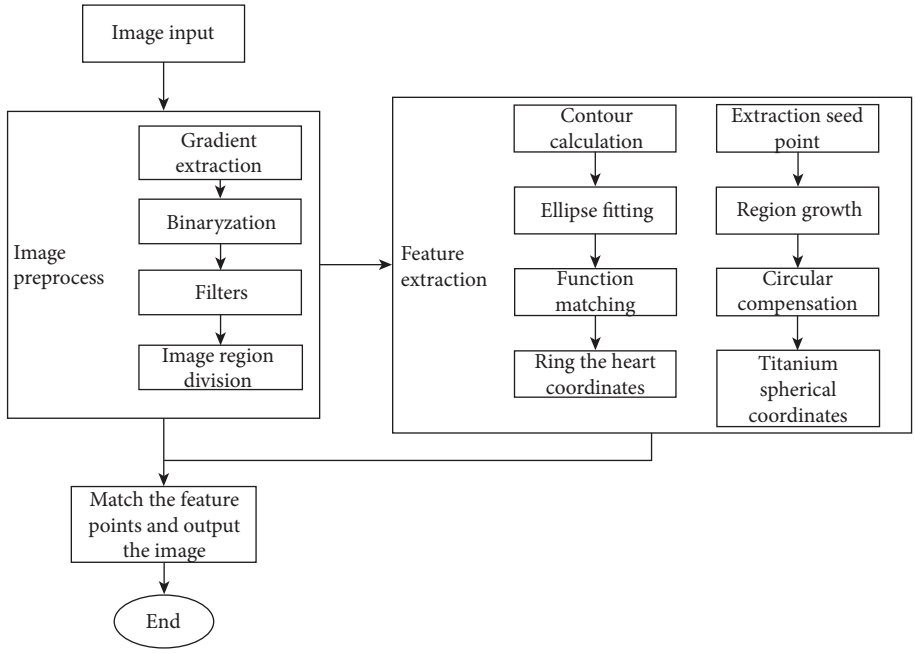

Figure 4: Feature point extraction process.

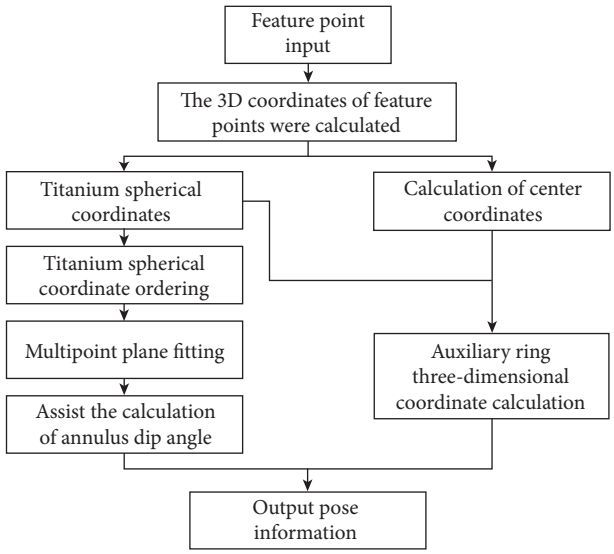

Figure 5: Pose and pose calculation process.

spherical coordinate in the image corresponded with the actual serial number of the ball. It can provide accurate characteristic correspondence information for the ring attitude solution.

According to the regular distribution of titanium spheres, a virtual average point of titanium spheres is:

$$\mathrm{p}^{\mathrm{avg}} = \frac{\mathrm{sum}\left(\mathrm{p}^{\mathrm{j}}\right)}{\mathrm{j}}. \tag{2}$$

Find the square of the absolute distance between each point and the average point.

$$\rho = \frac{1}{d^2} = \left(p^j - p^{\mathrm{avg}}\right)^2, \tag{3}$$

(2) and (3) are simultaneously established, and the irrelevant variables are eliminated to obtain:

$$\rho_{\mathrm{i}} = \frac{1}{\sum_k \left(\mathrm{p}_{\mathrm{k}}^{\mathrm{i}} - \overline{\sum_{\mathrm{j}=1}^{5} \mathrm{p}_{\mathrm{k}}^{\mathrm{j}}}\right)^2} \{\mathrm{k} = (\mathrm{x}, \mathrm{y}, \mathrm{z})\}, \tag{4}$$

Setting the auxiliary ring attitude as the initial attitude when the width coordinate of the line between the No. 1 titanium sphere and the ring center is perpendicular to the image. The rotation angles around the X, Y, and Z coordinate axes are defined as $\theta_x, \theta_y, \theta_z$, respectively. The initial angle is defined as when the No. 2 titanium ball and the No. 3 titanium ball are parallel to the X-axis of the spatial coordinates. The connection between the center of the No. 2 titanium ball and No. 3 titanium ball is parallel to X, so the rotation angle around the z-axis can be obtained only by calculating the tangent value of the connection and X, so θ_z can be expressed as:

$$\theta_{\mathrm{z}} = \tan^{-1}\left(\frac{\mathrm{y}_3 - \mathrm{y}_2}{\mathrm{x}_3 - \mathrm{x}_2}\right). \tag{5}$$

To reduce errors in angle calculation caused by visual detection and feature extraction, the three-dimensional coordinates of the spherical center were substituted into the spatial plane equation to fit the auxiliary ring plane by the spatial multipoint SVD plane fitting method to reduce the errors caused by binocular vision measurements and optimize the attitude calculation results.

$$AX = \begin{bmatrix} x_1 - \overline{x} & y_1 - \overline{y} & z_1 - \overline{z} \\ x_2 - \overline{x} & y_2 - \overline{y} & z_2 - \overline{z} \\ x_3 - \overline{x} & y_3 - \overline{y} & z_3 - \overline{z} \\ & \cdots & \\ x_n - \overline{x} & & z_n - \overline{z} \\ & y_n - \overline{y} & \end{bmatrix} \begin{bmatrix} a \\ b \\ c \end{bmatrix} = 0. \quad (6)$$

Taking the residual difference between the selected feature points and the fitting plane as the goal of minimization optimization, the fitting objective function is $\min\|AX\|$, with constraint $\|X\| = 1$through a singular value decomposition $A = \mathrm{UDV}^{\mathrm{T}}$. The feature vector corresponding to the minimum singular value was the coefficient vector of the fitting plane. The geometric meaning of a, b, c was the coordinate component values of the normal plan vector, so θ_x, θ_y can be expressed as:

$$\begin{cases} \theta_x = \tan^{-1}\left(\dfrac{a}{c}\right) \\ \\ \theta_y = \tan^{-1}\left(\dfrac{b}{c}\right) \end{cases}. \quad (7)$$

Through the aforementioned coordinate calculation of feature points and plane fitting operation, the spatial coordinate position of the auxiliary ring under the camera plane was obtained. Since the spatial relationship between the temporal bone and the auxiliary ring was obtained by preoperative CT scanning, the spatial position of the temporal bone and structural tissue in the ear could be obtained by coordinate transformation.

4. Rapid Extraction of Auxiliary Ring Features

In the temporal bone auxiliary ring visual positioning method, the key to pose detection is to extract the set features quickly and accurately. The more traditional BM or SGBM needs to calculate the pixel points of an entire image, and the algorithm takes a long time and is prone to producing parallax holes, which is not conducive to extracting specific feature points. In this paper, the DL-M feature point extraction scheme can quickly and accurately extract target features and, through improved ellipse matching, regional growth point selection and matching methods, accelerate target feature extraction.

4.1. Ellipse Matching Based on Image Moments. While detecting contour ellipse in the auxiliary ring, because the input contour was not screened in the Hough ellipse fitting, it is impossible to judge whether the original contours before fitting are an elliptic contour. To solve this problem, based on the concept behind the Hu moments image moment, this paper calculated the Hu-moment for the fitting contour and the original contour and judged it, which greatly eliminated any interference from nonelliptical contours. On this basis, a contour screening mechanism was added to reduce the computational burdens for ellipse recognition. After fitting the selected contour, the mathematical expression for the fitting ellipse was established by using the rotation matrix information returned by the fitting, and the fitting ellipse pixel group was reconstructed. The calculation formula is:

$$\mathrm{Vponit}(x, y) = \begin{cases} P_i^x = x\cos\varphi - \sqrt{\left(1 - \dfrac{x^2}{a^2}\right)b^2}\ \sin\varphi \\ \\ P_i^y = \sqrt{\left(1 - \dfrac{x^2}{a^2}\right)b^2}\ \cos\varphi + x\sin\varphi \\ \\ \varphi = \dfrac{\mathrm{angle} * \pi}{180} \end{cases}. \quad (8)$$

The geometric moments for the reconstructed elliptic contour and the original image contour were calculated, and the reciprocal deviations of the geometric moments were calculated to accumulate the moment errors in the original contour and reconstructed contours. The specific calculation formula is:

$$M_x = \sum_{i=1}^{M}\sum_{j=1}^{N} i^p j^q f(i, j),$$
$$I(A, B) = \sum_{i=1}^{7}\left|\frac{1}{m_i^A} - \frac{1}{m_i^B}\right|. \quad (9)$$

The accumulated error function was then normalized. When the fitted ellipse contour was similar to the original contour, $I(A, B)$ approached 0; otherwise, it approached 1. The maximum threshold was set to limit the errors between its geometric moments, and then the similarities between the two were judged.

4.2. Obtaining the Planar Center of the Titanium Spheres. While calculating the titanium sphere centers by the angle of view, part of the titanium sphere boundaries will be blocked by the outer ring plane, so they cannot be completely detected in the image. In this paper, the region-growing algorithm [18] and circle compensation were used to calculate the image coordinates of the titanium sphere centers. The challenge for the regional growth algorithm was selecting the seed starting point. Usually, the seed point is judged artificially, or the starting point of the seed is obtained by using a clustering algorithm adhering to a certain set of rules. This method was difficult to apply to the seed point selection for the titanium spheres because of their small size and indistinct features.

To solve the aforementioned problem, the region growth algorithm was designed in combination with the titanium sphere boundary box information obtained from YOLOV3 target detection. The specific process is shown in Figure 6. The midpoints of the titanium sphere beam boxes were utilized as the growth starting points, and the shape of the visible portions of the titanium spheres were described, and the field pixel values and growth sizes at the midpoints of the titanium sphere beam boxes was limited to exclude any incorrectly detected targets during target detection. The

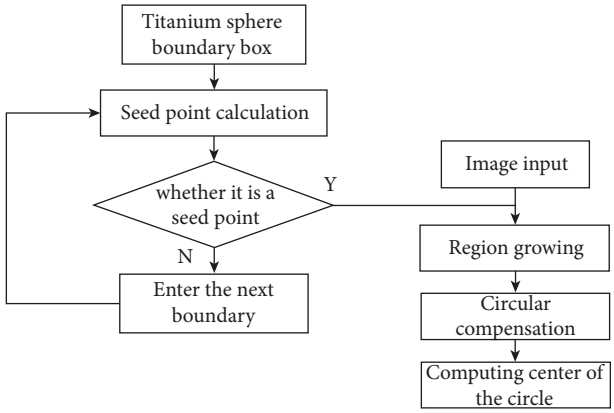

Figure 6: Calculation process for center coordinates.

minimum circumferential circle was used to complete the spherical surfaces of the titanium spheres, and their centers were calculated.

4.3. Feature Point Matching Based on Polar Constraints. After the feature points on the auxiliary rings from the left and right images were obtained through the aforementioned calculation, the order of the titanium spheres in the left and right images was different. Based on the concept of polar constraints, this paper matches the feature points of the titanium spheres, and the main process is:

(1) Calculated the polar equation on the right image plane through the coordinates of the characteristic points of the centers of the titanium spheres on the left image plane.

(2) Calculated the distances between the feature points in the right image and the polar line, and found the right feature points with the smallest distances after feature traversal. The smallest point was the matching point of the left image in the right image.

(3) The matching feature information was stored, and the distance error was analyzed. If the error was greater than the set value, the point was brought into the region again for growth calculation.

With this method, the target feature points for the centers of the titanium spheres could be accurately matched. When compared with the traditional matching methods BM or SGBM based on polar line constraints, the calculation of useless coordinates during feature matching can be reduced. In addition to accelerating the matching speed, the precision of regional growth feature points was also calculated and analyzed.

5. Results and Discussion

In this paper, the method that calls for drilling an auxiliary ring for cochlear implants was used as the test object to detect features and calculate position and pose information. Firstly, the trained auxiliary ring model was tested on the test set, and the average detection rate, the missed detection rate, and the false detection rate were calculated, and the effect of the model was evaluated by comparing it with the detection method. Then, the method of extracting feature points is verified to evaluate its reliability. Finally, the pose information of the auxiliary ring under different positions and postures is measured and the error is analyzed.

In the target detection experiment, 130 test pictures were tested, and some of the test results are shown in Figure 7. Among them, the number of auxiliary rings was 130, and the number of titanium spheres was 650. The number of detections, missed detections, and false detections for the model was statistically analyzed, and the results are shown in Table 1. It can be observed that the model presented in this paper has a high recognition rate for both the outer ring and the titanium spheres on the auxiliary ring, and the detection effect for the outer ring was better than that of the titanium sphere.

Using auxiliary ring structure characteristics of the feature point extraction scheme design, by combining deep learning target detection and image processing with a feature point detection method that incorporated a feature point matching method based on polar constraints, a large number of target detections were decreased, and the time needed for binocular image feature matching quickly extracted accurate target feature points. The specific process and effects are shown in Figure 8.

To better evaluate the current morphology and measurement data for the auxiliary ring during the operation, this paper used QT to design the image interactive interface. Multithreading displayed current image information in real time and controlled target detection, image processing, and information transmission programs, as shown in Figure 9. In the figure on the left, the image content obtained in real time by the left and right cameras was provided for real-time observation during the experiment. The image on the right is the target detection effect. The image in the lower right corner displays the current coordinate information of the auxiliary ring in real time. The interface of information transmission is also reserved in the program, which makes preparation for the interaction between the surgical robot and visual information.

The auxiliary ring was fixed on the experimental platform with a variable dip angle, and the auxiliary ring position and attitude were measured by changing the platform angle and setting the auxiliary ring dip angle. The binocular camera was placed about 25 cm above the experimental platform. To eliminate any error interference caused by the camera's own attitude, the camera was fixed, and the error between the actual and measured angle changes was calculated through the differences in experimental angle measurement. The position and attitude information of the auxiliary ring under random different attitudes were measured several times (greater than 50), and the standard deviations and maximum deviations obtained from all measurements were counted. The test results are shown in Table 2. Experimental data shows that the method has relatively high accuracy and small measurement fluctuations in the test environment, and the measurement results have good stability.

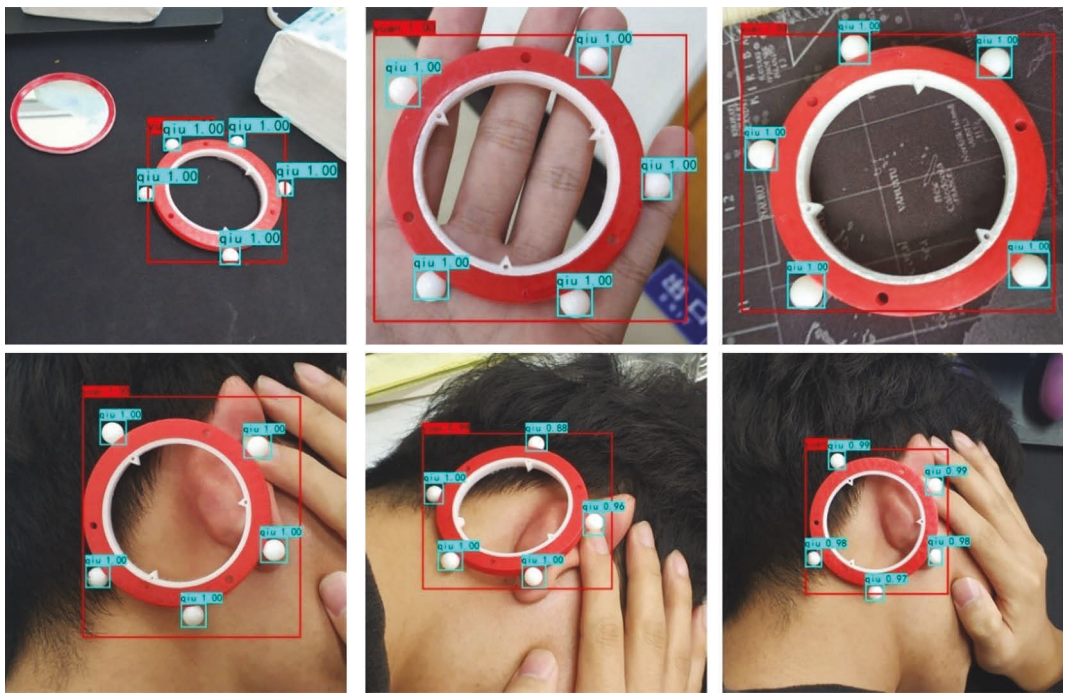

Figure 7: This is a figure. Schemes follow the same formatting.

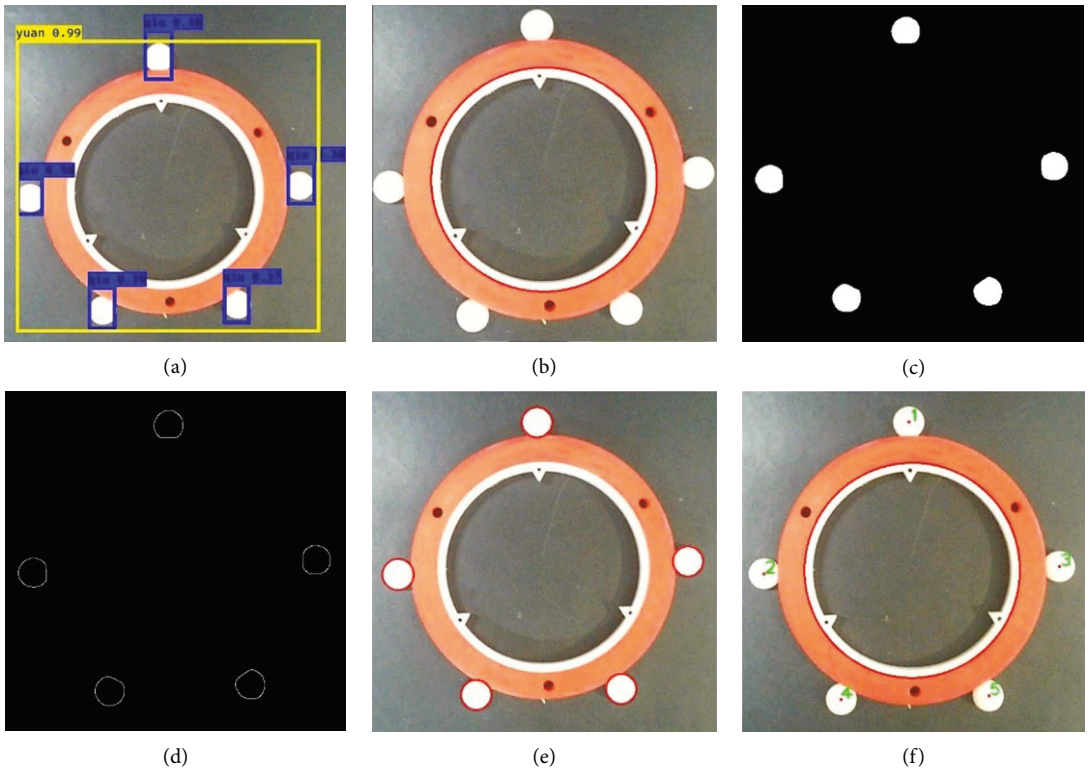

Figure 8: Feature Point Extraction Effect. (a) Target detection; (b) ellipse fitting; (c) region growing; (d) contour detection; (e) compensation outline; and (f) final exaction effect.

In robotic surgery, the use of titanium nails as markers does not give a fixed structure. The use of a triangulation bar usually requires the secondary calibration in the operation, which takes time and has a certain impact on the operating space. The auxiliary ring of cochlear implant drilling used in this paper adopts the combination of simple shapes, colors, and materials, which not only meets the positioning requirements of the auxiliary robot cochlear implant drilling

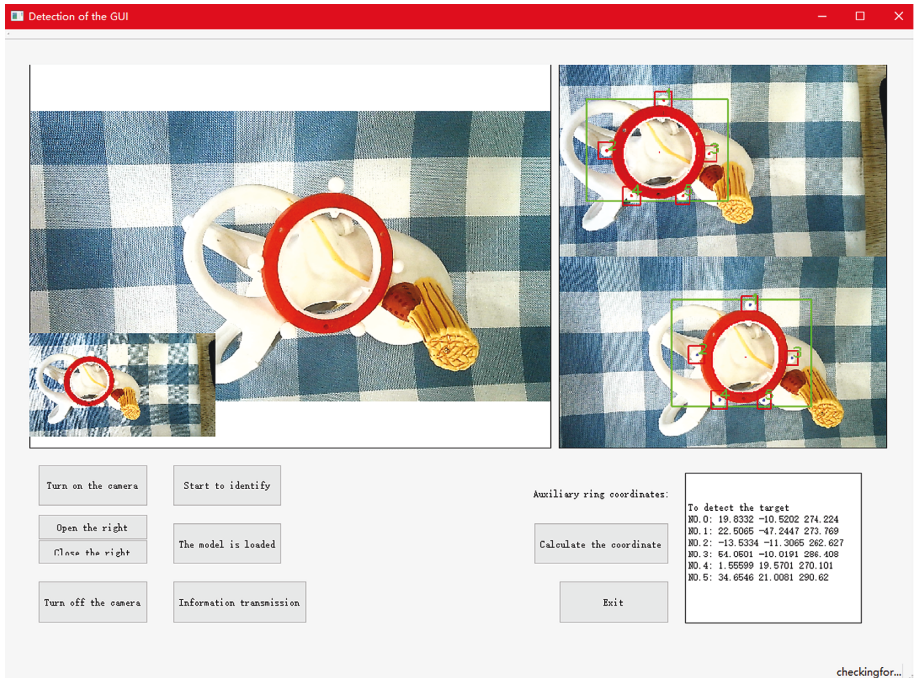

Figure 9: GUI interactive interface.

Table 2: Position and angle measurement results statistical table.

Measuring object	Max deviation	Standard deviation
X/Y	0.562 mm	0.287 mm
Z	1.331 mm	0.718 mm
$\theta x/\theta y$	0.632°	0.265°
θz	0.312°	0.205°

Table 3: Comparisons of marker implanting effects.

Marker object	Volume	Number of wounds	Visual features	Feature fixed	Workspace impact
Titanium nail	Smallest	3~5	Shape	N	Minimal
Tripod visual calibration rod	Biggest	3~5	Shape	Y	Greatest
Auxiliary ring	Smaller	2~3	Shape, color	Y	Less

surgery but also provides enough operating space. It has certain advantages compared with titanium nail implantation or the use of a visual calibration rod. The effects of traditional markers and auxiliary ring implantation are shown in Table 3.

In this paper, the deep learning algorithm was combined with the binocular vision image processing auxiliary ring detection method DL-M. The neural network method is used to train the model of specific auxiliary rings in advance, and the deep learning target detection method is applied to medical-assisted detection, which is faster and more accurate than the traditional target detection method, and the detected perceptual region helps to reduce the computational effort and difficulty in the subsequent feature extraction. Compared with the traditional binocular vision matching algorithms, such as BM and SGBM, the detection speed and matching effect were improved. The DL-M method used in this paper is similar to the BM matching algorithm in speed, but the effect is more accurate. In this paper, the DL-M method eliminated the duration of useless feature point matching and 3D coordinate calculation and utilized a fast image processing method to increase the accuracy of effective feature extraction for the auxiliary ring. In this paper, an image with a resolution of $1280 * 720$ was used to compare three visual matching algorithms, and the results are shown in Table 4.

Based on the aforementioned experiments, it can be seen that the DL-M method designed to detect the temporal bone in cochlear implant surgery using the auxiliary ring as the temporal bone marker in this paper can quickly and accurately detect the auxiliary ring, extract the features, solve the relative pose information, and then calculate the temporal bone pose. It reduces the duration spent on temporal bone localization while the cochlear implant robot drills, and the average detection and calculation efficiency is about 25FPS, which is a great improvement over traditional medical image navigation systems and binocular matching algorithms. The average attitude measurement accuracy is

Table 4: Comparison of method effects.

Method	Duration (ms)	Matching effect
BM	41	Poor
SGBM	305	Better
DL-M	40	Best

about ±0.6°. The high frequency detection ability can further compensate for measurement errors and meet the requirements for the real-time acquisition of temporal bone postures in cochlear implant drilling surgery.

6. Conclusions

Combined with target detection, image processing, and binocular vision, this paper proposes a fast and real-time detection and calculation method for temporal bone marker localization in cochlear implant robot drilling surgery. The detection rate for auxiliary ring features is about 97%, and the overall detection and calculation time is about 40 ms. The average attitude measurement accuracy is ±0.63°. The position and attitude information of the auxiliary ring can be obtained quickly, and the rapid calculation for the auxiliary ring position and pose can reduce the time of temporal bone visual positioning in cochlear implant drilling operations, greatly improving the robot's capabilities to extract visual information during the operation, which has a better auxiliary role for future research and applications of cochlear implant drilling operation. Since the accuracy of visual positioning is closely related to the binocular camera itself, the positioning accuracy of this method is still very limited. The accuracy of measurement may not yet fully meet the requirements of surgical positioning. The accuracy of the detection calculation is limited by camera performance, and the future research direction is to improve the accuracy of target detection and visual measurement, and our team will continue to conduct in-depth research in this direction. With the improvements in binocular vision technology and camera performance, this method will also make the research results more robust, and the use of this method will also obtain higher measurement accuracy, which our team will investigate here next.

Data Availability

The datasets used and/or analyzed during the current study are available from the corresponding author on reasonable request.

Conflicts of Interest

The authors declare that there are no conflicts of interest regarding the publication of this paper.

Acknowledgments

This research was funded by the National Natural Science Foundation of China (51705493) and the Natural Science Foundation of Zhejiang Province (LY17E050016).

References

[1] L. Bruschini, F. Forli, A. D. Vito, and S. Berrettini, "A new surgical approach for direct acoustic cochlear implant: a temporal bone study," *Clinical and experimental otorhinolaryngology*, vol. 9, no. 4, pp. 314–318, 2016.

[2] P. Dai and Y. Jiang, "Precise and minimally invasive cochlear implant surgery," *Journal of Otology*, vol. 16, no. 6, pp. 9–13, 2018.

[3] T. Williamson, X. Du, B. Bell et al., "Mechatronic feasibility of minimally invasive, atraumatic cochleostomy," *BioMed Research International*, vol. 2014, pp. 1–7, Article ID 181624, 2014.

[4] Y. Y. Yuan and P. Dai, "Surgical strategy of minimally invasive cochlear implantation," *Zhonghua Yixue Zazhi*, vol. 101, no. 2, pp. 87–91, 2021.

[5] H. Jia, J. X. Pan, Y. Li et al., "Preliminary application of robot-assisted electrode insertion in cochlear implantation," *Zhonghua er bi yan hou tou Jing wai ke za zhi= Chinese Journal of Otorhinolaryngology Head and Neck Surgery*, vol. 55, no. 10, pp. 952–956, 2020.

[6] Y. Zhao, B. M. Dawant, and J. H. Noble, "Automatic electrode configuration selection for image-guided cochlear implant programming," *Medical Imaging 2015: Image-Guided Procedures, Robotic Interventions, and Modeling*, vol. 9415International Society for Optics and Photonics, Bellingham Washington USA.

[7] J. Wang, H. Liu, J. Ke et al., "Image-guided cochlear access by non-invasive registration: a cadaveric feasibility study," *Scientific Reports*, vol. 10, no. 1, pp. 18318–18413, 2020.

[8] B. Cho, N. Matsumoto, S. Komune, and M. Hashizume, "A surgical navigation system for guiding exact cochleostomy using auditory feedback: a clinical feasibility study," *BioMed Research International*, vol. 2014, Article ID 769659, 7 pages, 2014.

[9] N. P. Dillon, R. Balachandran, and R. F. Labadie, "Accuracy of linear drilling in temporal bone using drill press system for minimally invasive cochlear implantation," *International Journal of Computer Assisted Radiology and Surgery*, vol. 11, no. 3, pp. 483–493, 2016.

[10] J. Ke, S. Zhang, C. Li, Y. Zhu, L. Hu, and F. Ma, "Application of bonebed-malleus short process registration in minimally invasive cochlear implantation," *Computer Assisted Surgery*, vol. 21pp. 30–36, sup1, 2016.

[11] S. Duret, C. Guigou, M. Grelat, and A. Bozorg-Grayeli, "Minimally invasive cochlear implantation assisted by intraoperative CT scan combined to neuronavigation," *Otology & Neurotology*, vol. 41, no. 4, pp. e441–e448, 2020.

[12] B. Copson, S. Wijewickrema, X. Ma, Y. Zhou, J. M. Gerard, and S. O'Leary, "Surgical approach to the facial recess influences the acceptable trajectory of cochlear implantation electrodes," *European Archives of Oto-Rhino-Laryngology*, vol. 279, no. 1, pp. 137–147, 2021.

[13] A. Karkas, N. M. d. Champfleur, A. Uziel, M. Mondain, J. L. Puel, and F. Venail, "Benefit of preoperative temporal bone CT for atraumatic cochlear implantation," *Otology & Neurotology*, vol. 39, no. 3, pp. 186–194, 2018.

[14] X. Sun, Y. Jiang, Y. Ji et al., "Distance measurement system based on binocular stereo vision," *IOP Conference Series: Earth and Environmental Science*, vol. 252, no. 5, p. 052051, Article ID 052051, 2019.

[15] B. R. Kiran, D. M. Thomas, and R. Parakkal, "An overview of deep learning based methods for unsupervised and semi-

supervised anomaly detection in videos," *Journal of Imaging*, vol. 4, no. 2, 2018.

[16] T. Fan, "Research and realization of video target detection system based on deep learning," *International Journal of Wavelets, Multiresolution and Information Processing*, vol. 18, Article ID 1941010, 01 pages, 2020.

[17] J. Redmon and A. Farhadi, *YOLOv3: An Incremental Improvement*, arXiv e-prints, 2018, https://doi.org/10.48550/arXiv.1804.02767.

[18] S. Kamdi and R. K. Krishna, "Image segmentation and region growing algorithm," *International Journal of Computer Technology and Electronics Engineering (IJCTEE)*, vol. 2, no. 1, pp. 103–107, 2012.

Hindawi
Scientific Programming
Volume 2023, Article ID 9815350, 1 page
https://doi.org/10.1155/2023/9815350

Retraction

Retracted: Deep Learning Analysis of English Education Blended Teaching in Virtual Reality Environment

Scientific Programming

Received 26 September 2023; Accepted 26 September 2023; Published 27 September 2023

This article has been retracted by Hindawi following an investigation undertaken by the publisher [1]. This investigation has uncovered evidence of one or more of the following indicators of systematic manipulation of the publication process:

(1) Discrepancies in scope
(2) Discrepancies in the description of the research reported
(3) Discrepancies between the availability of data and the research described
(4) Inappropriate citations
(5) Incoherent, meaningless and/or irrelevant content included in the article
(6) Peer-review manipulation

The presence of these indicators undermines our confidence in the integrity of the article's content and we cannot, therefore, vouch for its reliability. Please note that this notice is intended solely to alert readers that the content of this article is unreliable. We have not investigated whether authors were aware of or involved in the systematic manipulation of the publication process.

In addition, our investigation has also shown that one or more of the following human-subject reporting requirements has not been met in this article: ethical approval by an Institutional Review Board (IRB) committee or equivalent, patient/participant consent to participate, and/or agreement to publish patient/participant details (where relevant).

Wiley and Hindawi regrets that the usual quality checks did not identify these issues before publication and have since put additional measures in place to safeguard research integrity.

We wish to credit our own Research Integrity and Research Publishing teams and anonymous and named external researchers and research integrity experts for contributing to this investigation.

The corresponding author, as the representative of all authors, has been given the opportunity to register their agreement or disagreement to this retraction. We have kept a record of any response received.

References

[1] W. Wu and C. Qiu, "Deep Learning Analysis of English Education Blended Teaching in Virtual Reality Environment," *Scientific Programming*, vol. 2022, Article ID 8218672, 11 pages, 2022.

Hindawi
Scientific Programming
Volume 2022, Article ID 8218672, 11 pages
https://doi.org/10.1155/2022/8218672

Research Article

Deep Learning Analysis of English Education Blended Teaching in Virtual Reality Environment

Wen Wu [1] **and Chen Qiu** [2]

[1]*International School, Xi'an Siyuan University, Xi'an, Shaanxi, 710038, China*
[2]*Student's Affairs Division, Xi'an Jiaotong University, Xi'an, Shaanxi, 710048, China*

Correspondence should be addressed to Chen Qiu; qiuchenxjtu@xjtu.edu.cn

Received 30 May 2022; Revised 13 June 2022; Accepted 20 June 2022; Published 23 September 2022

Academic Editor: Lianhui Li

The rapid development of computer software and hardware, network technology, and various Internet platforms has brought mankind into a new era. In recent years, "virtual reality" can be regarded as a huge hot spot, whether in the field of industry, education, or research. At present, although the heat has subsided a little, the technical teams involved in various fields are also working collectively to continuously innovate. Based on the mixed teaching mode of English education, this article conducts in-depth research on deep learning and virtual reality technology, integrates deep learning and virtual reality learning environment, and builds a learning model of English education learning environment based on virtual reality. The teaching design of the course aims to fully combine the main content of deep learning with the virtual reality environment. Through experimental research, it is explored whether the learning environment based on virtual reality can promote deep learning. The relevant data of the experimental class and the control class are collected through questionnaires, starting from the four dimensions of motivation dimension, investment dimension, strategy dimension, and result dimension, and conduct a comparative analysis, and use the auxiliary interview method to understand the experience of students and teachers on virtual reality equipment and put forward relevant suggestions.

1. Introduction

With the continuous development of society and the continuous integration of education and information technology, the country's education informatization has also ushered in rapid development. The continuous popularization of the Internet, virtual technology, cloud computing, etc. provides education with an interactive and cooperative teaching environment of "Internet +." The rapid development of these technologies will promote the development of education and teaching, and change the demand for talents and the form of education. Among them, the rise and development of virtual reality (VR) technology will have an increasingly important impact on future education forms. As a new technology applied to the field of education, virtual reality has gradually become a brand-new educational method to help teachers teach and promote the development of education, enriching the dimension of education from the aspects of the learning process and results. Different from the traditional teaching mode and teaching environment where the teachers of traditional education stand on the podium, Internet technology and virtual reality technology are fully utilized, so that the teaching mode and students' learning environment have undergone great changes, and they can intuitively feel the real and specific This kind of learning environment relieves the pressure on schools and learner resources, can help students become participants in the learning environment, knowledge is more easily accepted and recognized by students, and promotes students' enthusiasm for learning. The continuous improvement of learning enthusiasm can make students' thinking continue to expand, and also can make students' interest in learning continue to improve, which has a very important positive effect on students' learning efficiency. It can be seen that the

in-depth application of virtual reality technology in education and teaching and the exploration of innovative education and teaching models are highly valued by the country, and the application of virtual reality in education has also become one of the main directions of virtual reality research and development. Its application will inject new vitality into traditional teaching. In the era of an increasingly informatized and globalized knowledge economy, learners are faced with complex and diverse social and learning environments. Based on this, American scholars and all walks of life have launched "deep learning" activities to help students be able to have a comprehensive understanding of people's daily life, daily work, and university life in the future. In order to achieve the goal of deep learning, teachers should adopt new and effective teaching modes and teaching strategies, so that students are not limited to shallow understanding, but stay at the shallow learning level. Students build new knowledge on the basis of existing knowledge and experience and transfer it to new situations, so as to achieve deep learning. The immersion, interactivity, and conception of virtual reality technology provide technical support for deep learning. It can not only create and reproduce the existing scenarios in reality but also create and conceive scenarios that cannot be experimented with or not in reality, which helps to effectively enhance the state of students' deep learning. Therefore, the deep learning and virtual reality learning environment integrate, build a learning model of English education blended teaching based on the virtual reality learning environment, and carry out teaching design according to the learning model and related courses, aiming to fully combine the main content of deep learning and virtual reality environment, so that students can learn more. The state of learning has been effectively improved, and the students' learning efficiency has been continuously improved [1–10].

2. Related Works

With the continuous change of VR technology, virtual reality has been widely used in medicine, education, film and television, and other fields and in the educational application of virtual reality technology. The earliest country to apply virtual reality technology in education is the United States, where it is widely used in military teaching. The research and application of VR technology in the United Kingdom is the most advanced country among all European countries; at the same time, the University of Nottingham has achieved excellent results in the application of virtual reality technology in the field of education. VR technology is used in the field of education to help students with physical disabilities and learning difficulties to further improve their learning efficiency. In virtual reality, learners interact with the learning environment according to the specific object content. This interaction is immediate, and the virtual environment can react in real-time based on the learner's behavior, for example, providing language input to learners in a targeted manner. The combination of virtual technology and education can also improve student outcomes. Research has found that students in VR English teaching classes get higher grades than other students, and VR also helps with memory retention. EdTech reports on a recent study that showed a nearly 9% increase in memory retention for students who learned in a VR immersive environment. Virtual reality technology has a wealth of practical experience in the field of education. However, there are obvious limitations in the application of virtual reality technology in today's education field. Deep learning makes virtual reality education more rigorous. Using new software and hardware equipment and combining intelligent learning environments for deep learning can better promote students' self-learning and lifelong learning. Learning, thus cultivating new talents to adapt to the development of the times. The application of virtual reality education not only provides unique advantages for learners in the learning environment, interactive environment, and experimental environment but also requires strengthening and improving the self-awareness and initiative of learners in autonomous learning, which is in line with the established goals of deep learning at all stages. Immersion, interactive functions, and conception in the virtual reality environment provide support for deep learning. Deep learning is a situation-based learning method. If knowledge cannot be applied to new and real situations to solve problems, only superficial understanding, mechanical memory, and simple copying, then this kind of learning will still remain on a shallow learning level. This research will be based on virtual reality technology combined with English education mixed teaching courseware, allowing students to experience English learning in virtual scenes, so as to carry out in-depth learning. In the process of English mixed teaching practice, virtual reality technology can provide the interaction of real role models and dialogue scenes [11–15].

3. Related Theories and Technical Methods

3.1. Virtual Reality Technology

3.1.1. Virtual Reality System. Virtual reality is a simulation technology that uses a computer to create a near-real virtual environment that is dynamic, three-dimensional, and fully immersive when the user interacts with it. According to different functions and implementation methods, virtual reality systems can be divided into four categories such as wearable virtual reality systems, desktop virtual reality systems, augmented virtual reality systems, and distributed virtual reality systems. According to the scenario materials and suggestions in the learning activities in the English teaching curriculum standards, combined with the results of the school's pre-investigation, the virtual reality system in this study is planned to use a wearable virtual reality system. Due to the uneven situation of VR hardware in schools at this stage, the selection of the type of virtual reality system will be based on the VR teaching resources and hardware status of the selected high schools' virtual reality system. Wearable virtual reality systems are also known as "immersive virtual reality systems." Users enter a virtual environment with hardware devices such as virtual reality glasses and digital helmets and then interact with the virtual environment through sensing devices such as data gloves (Figure 1) [16].

Figure 1: Selected school virtual reality device.

3.1.2. VR Teaching Resources. English teaching resources refer to many materials and conditions that can be used by teachers in all aspects of English teaching, including English course textbooks, English teaching cases, relevant English video pictures, PPT English teaching courseware, as well as teachers' resources, teaching aids, and teaching infrastructure such as desks. In a broad sense, English teaching resources can refer to all elements used by teachers in the process of English teaching, including people, money, materials, and information that support and serve teaching; in a narrow sense, English teaching resources (learning resources) mainly include teaching materials, teaching environment, and teaching support system. The VR English teaching resources in this study belong to the narrow English teaching resources in the broad and narrow sense, including (1) VR hardware equipment: wearable complete sets of virtual reality glasses for English teaching, virtual reality all-in-one machine. (2) VR software resources: virtual reality software resources that are matched with equipment, related to courses, and developed maturely. (3) VR supporting classrooms: VR supporting classrooms that can properly store and easily access VR-related hardware equipment, have enough space for students to interact and explore independently with the virtual environment, and have an interactive learning space design.

3.2. Deep Learning Theory. According to the subject core literacy and course objectives of the English blended teaching course, carefully analyze the English textbooks used, collect data on virtual reality and deep learning, and draw lessons from the famous teaching reform experts LeAnn Nickelsen and Eric Jensen in their works. Based on the study of learning, a detailed process system is constructed, and based on each link of the model, a complete deep learning process is formed (Figure 2) [17].

Based on the theoretical framework of deep learning, this research constructs a deep learning model based on a virtual reality environment (Figure 3).

Analyze the current students' understanding of virtual reality, based on the deep learning model, combine virtual reality and English courses, follow the basic principles of teaching design, and construct a virtual reality environment-based English mixed teaching curriculum design framework (Figure 4) [18–20].

4. Research Design and Result Analysis of Mixed Deep Learning in English Education Based on Virtual Reality Environment

4.1. Experimental Design

4.1.1. Experimental Theme. Through the case of a VR educational game called "In Order To Dr.," an experimental class and a control class were set up, and the traditional teaching methods and the teaching methods with the help of VR educational games were used to conduct comparative experimental teaching in the English mixed teaching classroom. Taking Unit 1: Where did you go on vacation? For the experimental class in the first week as an example, the teaching objectives are drawn up, as shown in Table 1 [21].

4.1.2. Experimental Variable. Independent variable: whether to adopt the English blended teaching-learning mode based on a virtual reality environment.

Dependent variable: whether it helps to promote deep learning, that is, whether it has achieved the promotion of problem-solving ability, communication, active cooperation, knowledge processing level, and reflective evaluation level.

Irrelevant variables: students' initial cognition, operational level, mastery of basic knowledge, and grades in English class.

Number of students, teachers, English teaching content, study hours, etc.

4.1.3. Experimental Hypothesis. In view of the existing problems in the current English mixed teaching and the current teaching practice research of virtual reality, the design and construction.

The deep learning teaching mode of the English blended teaching course is based on the virtual reality environment,

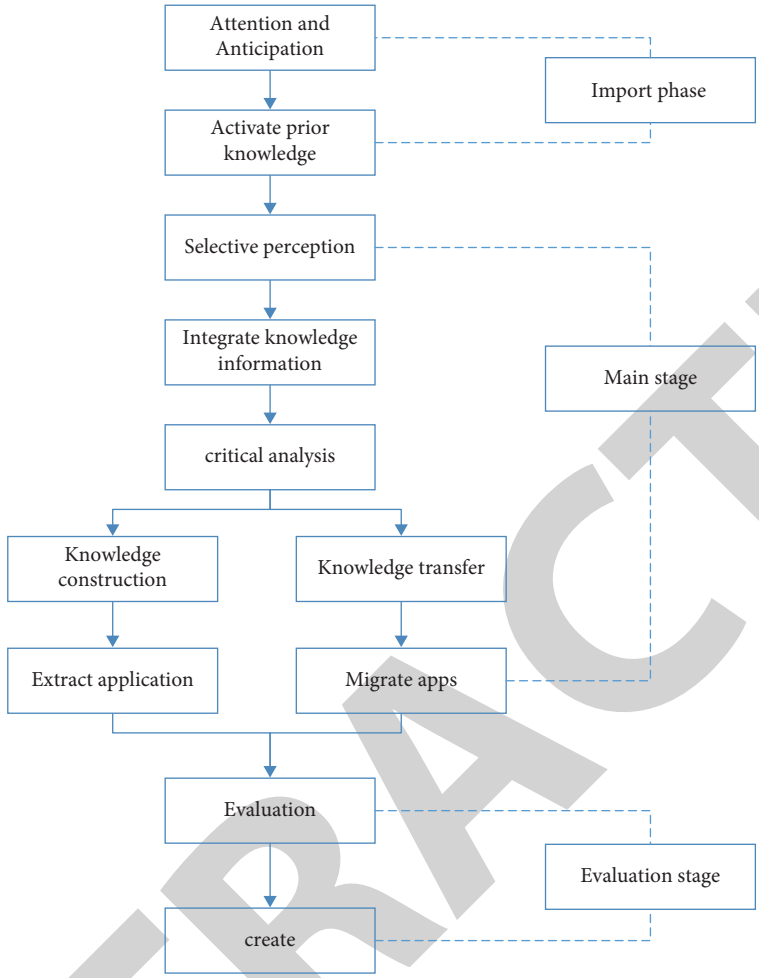

Figure 2: The deep learning process.

and the experimental research on the effectiveness of this teaching mode. The experimental hypotheses proposed in this experimental study are as follows:

Hypothesis 1. the level of deep learning in the English learning environment based on virtual reality is significantly improved compared with the control class in the traditional teaching environment.

Hypothesis 2. the motivation level in the English learning environment based on virtual reality is significantly improved compared with the control class in the traditional teaching environment.

Hypothesis 3. the problem-solving ability in the English learning environment based on virtual reality is significantly improved compared with the control class in the traditional teaching environment.

Hypothesis 4. the ability of communication, communication, and cooperation in the English learning environment based on virtual reality is significantly improved compared with the control class in the traditional teaching environment.

Hypothesis 5. the knowledge processing level in the English learning environment based on virtual reality is significantly improved compared with the control class in the traditional teaching environment.

Hypothesis 6. the level of reflective evaluation in the English learning environment based on virtual reality is significantly improved compared with the control class in the traditional teaching environment.

4.1.4. Experiment Process. According to the specific content of the research topic and the actual situation, the specific process designed in this article is shown in Figure 5.

4.2. Matching of VR Teaching Resources. Learn about school VR equipment availability. The classroom is a smart classroom that integrates modern educational technologies such as smart blackboards, smart tablets, smart recording and broadcasting, and VR teaching equipment. In order to promote students' communication and discussion, the desks are set up with closed polygons, and the classroom setting conforms to the characteristics of the teaching mode designed in this study, which is mainly based on

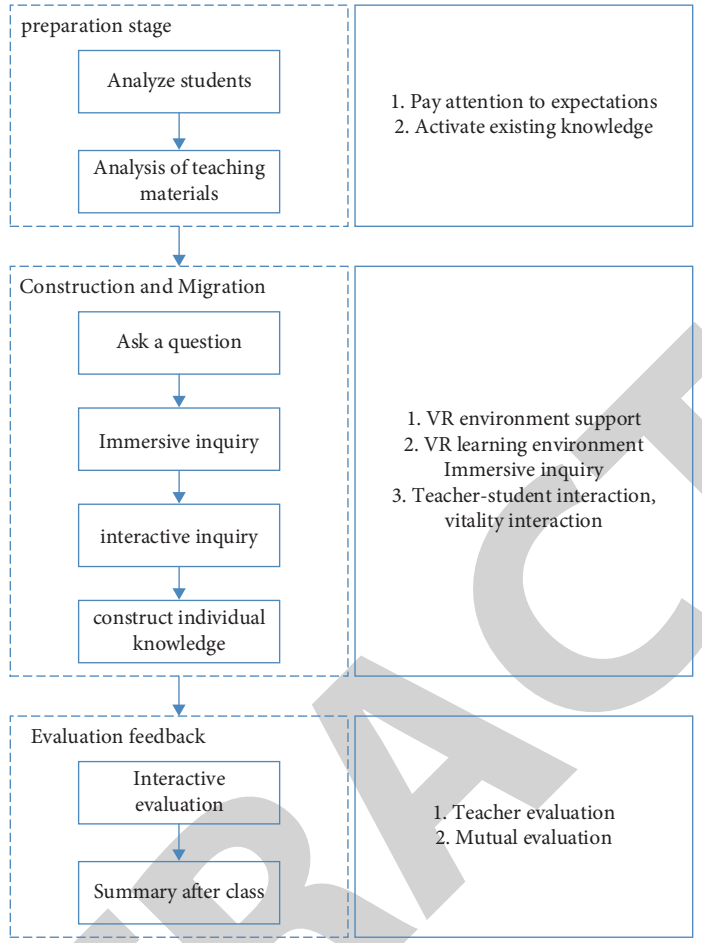

Figure 3: Deep learning model based on virtual reality environment.

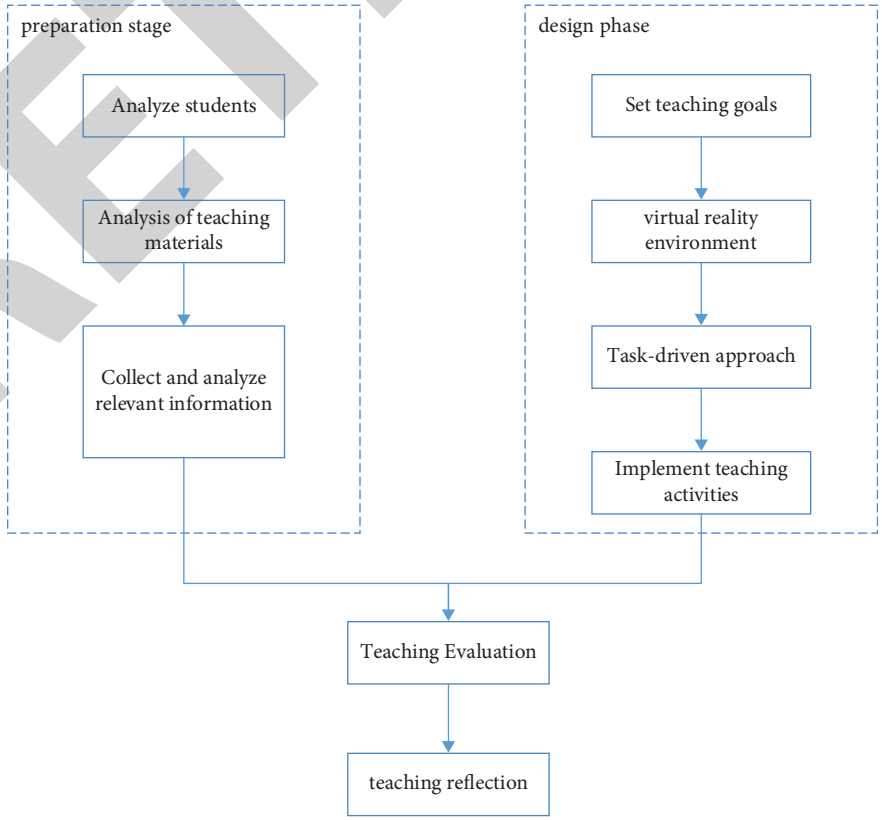

Figure 4: Instructional design framework.

Table 1: English teaching objectives.

Teaching objectives	1. Knowledge and skills: understand the meaning and usage rules of indefinite pronouns, learn to use Where and How to ask questions in English activity conversations, and learn to use Did to ask questions about what happened in the past. Master the following words: wonderful, most, something, nothing, of course, everyone, myself, yourself, anyone, anywhere. Master the following sentence patterns: a. Where did you go on vacation?—I went to the mountains. *b*. Where did Tina go on vacation?—he went to the beach. *c*. Did you go with anyone?—Yes, I did./No, I didn't. 2. Process and method: the teacher's demonstration and the VR educational game explain the use of the context in the simple past tense. Conduct group inquiry learning to complete the contextual use of the simple past tense in VR educational games. Use special interrogative sentences in the simple past tense, general interrogative sentences, and their affirmative and negative answers. 3. Emotional attitudes and values: feel the convenience of past tense in English expression, and improve the ability to use information technology to solve problems in real contexts. In the process of learning with VR educational games, cultivate a rigorous and realistic learning attitude.
Difficulties in teaching	Past tense in the correct context, the use of reflexive pronouns such as yourself, myself, and the use of the indefinite pronoun something, anything, someone, anyone, and other words.

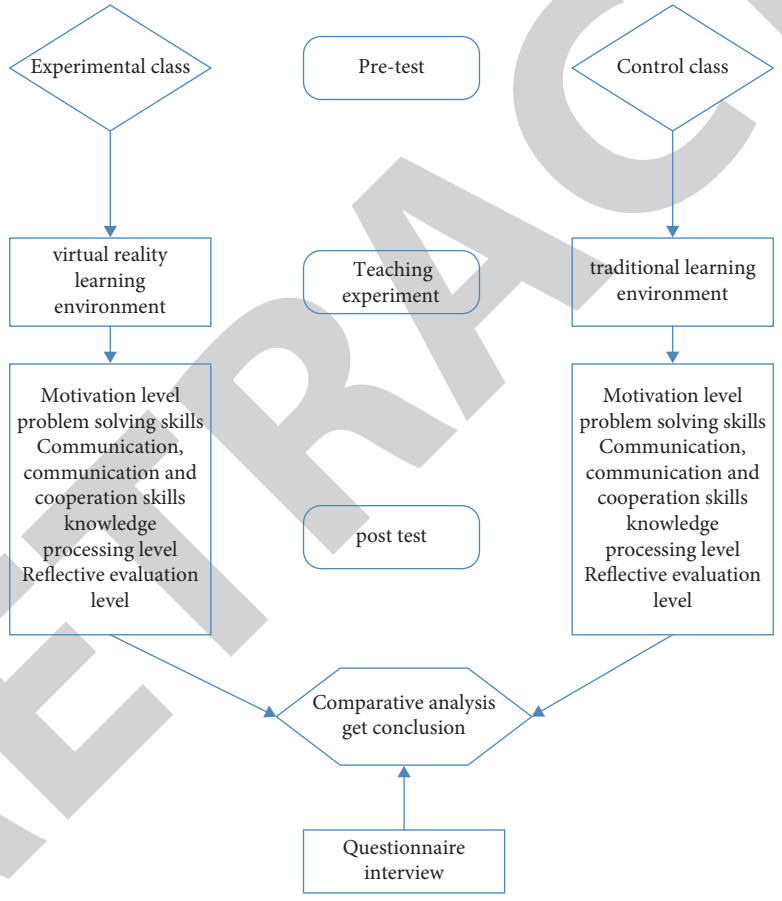

Figure 5: Experimental process design.

independent inquiry and cooperative inquiry. High school B sets up the VR teaching equipment in an independent VR classroom. As shown in Figure 6, the desks of the students in this classroom are set in rectangles, and the teachers have no other educational information equipment except VR equipment.

VR Science Corner is the first VR Science Corner in China that truly combines VR technology with science education. It aims at popular science knowledge points; uses virtual reality technology and virtual reality equipment; is based on high-quality VR science resources; breaks the traditional form of science education courses. Time provides immersive science knowledge learning and experience in order to realize various personalized teaching methods such as independent learning and inquiry-based learning, and enhance students' interest in learning. As shown in Figure 7.

However, each VR classroom is equipped with only one VR all-in-one machine, which is difficult for classroom teaching. Therefore, in the English classroom, another VR equipment for English classroom teaching is set up. VR/AR education brand Class VR product, its initial interface is shown in Figure 8.

Figure 6: VR classroom.

Figure 7: Placement of VR all-in-one.

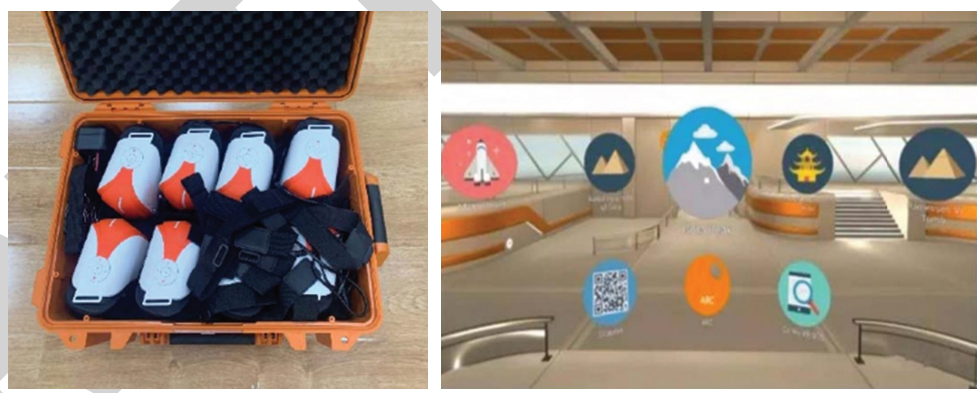

Figure 8: Class VR and initial interface.

4.3. Teaching Objective Design. To promote deep learning of English education blended teaching. Through the implementation of a virtual reality-based teaching model designed to promote deep learning in English education blended teaching courses, through quasi-experimental research, to explore whether the virtual reality learning environment can help promote students' deep learning.

4.3.1. Design of Teaching Activities. Teaching activities to promote students' in-depth learning means that students, under the guidance of teachers, carry out constructive activities based on existing knowledge, solve problems in different situations through experiments, analysis, summarization, etc., and finally form higher order thinking and complete shallow learning. The design of activities to promote deep learning mainly includes the form of activities, the selection of teaching resources, and the methods of implementing activities. These designs need to be closely combined with the in-depth learning objectives determined in the design of teaching objectives, especially the activities necessary for driving questions and content questions determined according to the objectives, to ensure the development of students' core literacy of English subjects and the

construction of self-knowledge systems, so as to promote high-level learning. The formation of order thinking.

At present, students' lack of initiative in learning English and lack of enthusiasm for learning are actually related to the current "dead" classroom. How to make the classroom really live, it is definitely necessary to design a variety of activities. The rational use of VR teaching resources is the key to changing this situation. Therefore, important activities that require teacher guidance should be given sufficient time for students to prepare in the classroom, and secondary students or activities that students are expected to be capable of should be completed after class. The purpose of deep learning includes the acquisition of disciplinary thinking methods, the cultivation of higher order thinking, etc., all of which require students to truly carry out activities independently, which cannot be achieved by teachers' elaboration alone. Of course, to ensure the quality of the activity, it is necessary to integrate various factors, such as whether the activity design is in line with the goals of deep learning; whether the students are given enough time; whether the students have enough opportunities to experience; the activity design of each link; and whether it is organically combined and matched with the purpose. Therefore, the teaching mode in this study requires teachers to design a study guide program for students to use in the course content in the teaching process. The purpose is to gradually guide students to achieve in-depth learning in the stages of autonomous exploration of VR experience and group discussion and cooperative exploration. Make students enter the virtual environment with questions to explore, and take part in group discussion and exploration with tasks.

4.3.2. Teaching Evaluation Design. In fact, most learners cannot complete deep learning the first time, and most people can only complete simple learning, that is, the "knowledge" level. The completion of deep learning requires continuous evaluation and feedback. It can be said that without evaluation and feedback mechanisms, it is almost impossible for learners to learn abstract and complex cognitive skills. Many studies have shown that evaluation can promote the improvement of course performance, promote learners to consolidate and internalize information, and is conducive to the path to understanding, comprehension, synthesis, evaluation, higher order thinking, and deep learning. Provide continuous evaluation to students so that as students engage in learning activities, they can continue to see, hear, and experience the results of their efforts.

4.4. Experimental Results and Analysis. By randomly distributing questionnaires to other students, the purpose is to ensure the rigor and rationality of the questionnaires, and the reliability and validity of the recovered effective questionnaires are tested using SPSS 23.0. This questionnaire sets the current situation of students' deep learning into four dimensions: motivation dimension, investment dimension, strategy dimension, and outcome dimension, which are mainly reflected in the level of reflection and evaluation, knowledge processing level, active cooperation ability, communication ability, problem-solving ability, and motivation. Basic information such as level mainly includes the following types of questions and the details are given in Tables 2 and 3.

4.4.1. Questionnaire Reliability and Validity Analysis. The Cronbach's alpha coefficient of the posttest questionnaire dimension is 0.929, which is greater than 0.8, indicating that this questionnaire has very high consistency and the design content of this questionnaire is reasonable.

The KMO value of the posttest questionnaire is 0.717, which is greater than 0.6, indicating that the questionnaire has good validity and is suitable for exploratory primer analysis; the significance of Bartlett's spherical test value is less than 0.05, reaching a significant level, indicating that the questionnaire contains items suitable for performing factor analysis.

4.4.2. Group Statistics

(1) Dimensional analysis. From the analysis in Table 4, we can see that from the perspective of motivation, the averages of the experimental class and the control class are 4.8308 and 4.2923, respectively, with a difference of 0.5385; from the perspective of investment, the averages of the experimental class and the control class are 4.7322 and 4.1994, respectively, with a difference of 0.5385. 0.5328; from the perspective of the strategy dimension, the averages of the experimental class and the control class are 4.7590 and 4.3949, respectively, with a difference of 0.3641; from the perspective of the result dimension, the averages of the experimental class and the control class are 4.7885 and 4.3590, respectively, with a difference of 0.4295; thus it can be seen that the mean value of each dimension of the experimental class is greater than the mean value of each dimension of the control class.

(2) Ability level analysis. From the analysis in Table 5, it can be seen that from the perspective of motivation level, the mean of the experimental class is 4.8376, and the mean of the control class is 4.8376.

The average value of the experimental class is 4.2735, a difference of 0.5641; from the perspective of problem-solving ability, the average value of the experimental class is 4.7650, and the average value of the control class is 4.4017, a difference of 0.3633; from the perspective of communication, communication, and cooperation ability, the average value of the experimental class is 4.7564, and the average value of the control class is 4.7564. The average value of the experimental class is 4.3419, a difference of 0.4145; from the perspective of knowledge processing level, the average value of the experimental class is 4.7607, and the average value of the control class is 4.2393, a difference of 0.5214; from the perspective of reflection evaluation level, the average value of the experimental class is 4.7404, and the average value of the control class is 4.7404. It is 4.3173, with a difference of 0.4231; it can be seen that the mean value of each dimension

Table 2: The distribution of deep learning according to dimension question type.

Dimension	Number of questions	Question number
Motivation dimension	5	Q3, Q4, Q5, Q6, Q7
Input dimension	9	Q8, Q9, Q10, Q11, Q12, Q13, Q14, Q15, Q16
Policy dimension	10	Q17, Q18, Q19, Q20, Q21, Q22, Q23, Q24, Q25, Q26
Outcome dimension	8	Q27, Q28, Q29, Q30, Q31, Q32, Q33, Q34

Table 3: Deep learning questionnaire distribution of question types according to ability levels.

Ability level	Number of questions	Question number
Motivation level	6	Q3, Q5, Q6, Q7, Q15, Q18
Problem-solving skills	6	Q4, Q12, Q17, Q20, Q23, Q30,
Communication, communication, and cooperation skills	6	Q11, Q13, Q14, Q19, Q31, Q32
Knowledge processing level	6	Q8, Q9, Q10, Q16, Q21, Q33
Reflective evaluation level	8	Q22, Q24, Q25, Q26, Q27, Q28, Q29, Q34

Table 4: Posttest four-dimension group statistics.

	Class	N	Average value	Standard deviation	Standard error mean
Motivation dimension	Experimental class	39	4.8308	0.24078	0.03856
	Control class	39	4.2923	0.38620	0.06184
Input dimension	Experimental class	39	4.7322	0.31086	0.04978
	Control class	39	4.1994	0.40879	0.06546
Policy dimension	Experimental class	39	4.7590	0.36398	0.05828
	Control class	39	4.3949	0.40194	0.06436
Outcome dimension	Experimental class	39	4.7885	0.33339	0.05338
	Control class	39	4.3590	0.41575	0.06657

Table 5: Posttest five ability level group statistics.

	Class	N	Average value	Standard deviation	Standard error mean
Motivation level	Experimental class	39	4.8376	0.26070	0.04175
	Control class	39	4.2735	0.34937	0.05594
Problem-solving skills	Experimental class	39	4.7650	0.30038	0.04810
	Control class	39	4.4017	0.41836	0.06699
Communication, communication, and cooperation skills	Experimental class	39	4.7564	0.32183	0.05153
	Control class	39	4.3419	0.35858	0.05742
Knowledge processing level	Experimental class	39	4.7607	0.31250	0.05004
	Control class	39	4.2393	0.46641	0.07469
Reflective evaluation level	Experimental class	39	4.7404	0.39982	0.06402
	Control class	39	4.3173	0.44040	0.07052

of the experimental class is greater than the mean value of each dimension of the control class.

(3) Independent sample t-test. An independent sample t-test was performed on the data of the survey results using SPSS data statistical analysis software. The analysis of the results is carried out from four dimensions (motivation dimension, investment dimension, strategy dimension, and outcome dimension). From Table 6, we can see that the independent sample t-test results of the motivation dimension of the experimental class and the control class show that there are significant differences between the two teaching environments ($t = 7.389$, $p < 0.001$), the motivation dimension of students based on virtual reality learning environment is significantly higher than that of students based on traditional teaching form; the independent sample t-test results of the input dimension of experimental class and control class show that the two teaching environments exist significant difference ($t = 6.479$, $p < 0.001$), students based on virtual reality learning environment have significantly higher input dimension than students based on traditional teaching form; independent sample t-test results of strategy dimension of experimental class and control class show that the two. There is a significant difference in the teaching environment ($t = 4.193$, $p < 0.001$), and the students' strategy dimension based on the virtual reality learning environment are significantly higher than that of the students based on the traditional teaching form; the independent sample t-test results of the experimental class and the control class's outcome dimension. It shows that there is a significant difference between the two teaching environments ($t = 5.033$,

Table 6: Sample t-test in four dimensions of posttest.

	t	Degrees of freedom	Significance (two-tailed)	Mean difference	Standard error
Motivation dimension	7.389	63.664	p	0.53846	0.07288
Input dimension	6.479	76	p	0.53276	0.08223
Policy dimension	4.193	76	p	0.36410	0.08683
Outcome dimension	5.033	76	p	0.42949	0.08683

Table 7: Independent sample t-test for posttesting five ability levels.

	t	Degrees of freedom	Significance (two-tailed)	Mean difference	Standard error
Motivation level	8.081	70.303	p	0.56410	0.06980
Problem-solving skills	4.405	68.954	p	0.36325	0.08247
Communication, communication, and cooperation skills	5.373	76	p	0.41453	0.07715
Knowledge processing level	5.799	66.395	p	0.52137	0.08990
Reflective evaluation level	4.442	76	p	0.42308	0.09525

$p < 0.001$), and the outcome dimension of students based on the virtual reality learning environment is significantly higher than that of students based on the traditional teaching form. The experimental results show that there are significant differences in the four dimensions of the experimental class and the control class, and the experimental class is significantly higher than the control class in the four dimensions of motivation, investment, strategy, and results.

Use SPSS data statistical analysis software to conduct an independent sample t-test on the data of the survey results. From the analysis in Table 7, it can be seen that the independent sample t-test results of the motivation level of the experimental class and the control class show that there are significant differences between the two teaching environments ($t = 8.081$, $p < 0.001$), the motivation level of students based on virtual reality learning environment is significantly higher than that of students based on traditional teaching form; the independent sample t-test results of the problem-solving ability of experimental class and control class show that there are significant differences between the two teaching environments ($t = 4.405$, $p < 0.001$), the problem-solving ability of the students based on the virtual reality learning environment was significantly higher than that of the students based on the traditional teaching form; There is a significant difference between the two teaching environments ($t = 5.373$, $p < 0.001$). The students' communication, communication, and cooperation abilities based on the virtual reality learning environment are significantly higher than those based on the traditional teaching form. The independent sample t-test results show that there is a significant difference between the two teaching environments ($t = 5.799$, $p < 0.001$), and the knowledge processing level of students based on the virtual reality learning environment is significantly higher than that of students based on traditional teaching form. The independent sample t-test results of the reflective evaluation level showed that there was a significant difference between the two teaching environments ($t = 4.442$, $p < 0.001$), and the reflective evaluation level of students based on the virtual reality learning environment was significantly higher than that of students based on traditional teaching form.

5. Conclusion

In the information society, the progress of science and technology is reflected in all aspects, and high technology and new technology are constantly integrated into us.

The integration of modern technology into education and teaching can better improve the quality of teaching. As a modern technology, virtual reality technology, its interactive and immersive characteristics can make users feel immersive and inject into education. New vitality, the combination of virtual reality technology and education will create a different spark, which will also help deep learning.

In this study, the teaching application of virtual reality, the research level of deep learning and the two learning theory, embodied cognitive learning theory, and situational cognitive learning theory, an instructional design based on virtual reality to promote students' deep learning is constructed and applied in the actual English class, observe students' performance through teaching experiments, collect questionnaires and analyze data by distributing questionnaires after teaching is completed, and find that the learning environment based on virtual lines is conducive to the improvement of students' in-depth learning, whether it is classroom discipline or group discussion, The overall engagement of the students in the experimental class is significantly higher than that of the students in the control class. Based on the analysis results of the four dimensions of motivation, engagement, strategy, and outcome of the deep learning questionnaire, the experimental class has a higher level of engagement in each dimension. The performance level is higher than that of the control class, which provides a new idea for promoting the deep learning of English courses.

Virtual reality provides a new teaching environment for teaching. Virtual reality technology needs to be skillfully combined with the teaching mode, which subverts the traditional teaching environment and provides a more effective way for the realization of deep learning. Due to the limitations of the research, this research is only at the initial stage of related research, and future research can add experimental measurement methods, collect, and use a variety of data, such as comprehensive analysis through eye trackers,

Hindawi
Scientific Programming
Volume 2022, Article ID 4131316, 7 pages
https://doi.org/10.1155/2022/4131316

Research Article

The Analysis and Implementation of Film Decision-Making Based on Python

Han Zhang[1] **and Yao Wu**[2]

[1]*Capital Normal University, Beijing 100089, China*
[2]*Communication University of China, Beijing 100024, China*

Correspondence should be addressed to Han Zhang; 6592@cnu.edu.cn

Received 9 July 2022; Revised 14 August 2022; Accepted 22 August 2022; Published 23 September 2022

Academic Editor: Lianhui Li

With the growing development of the era of big data, data acquisition and analysis have become hot spots, and Python-based crawler technology is one of the most widely used tools in data analysis work at present. In this paper, we apply Python crawler key technology to acquire data of movie list and hot movies on Cat's Eye movie network, analyze data based on Python development environment Spyder, use the Numpy system to store and process large data, Chinese Jieba word separation tool to crawl data for word separation text processing, Snownlp library to process text sentiment, and finally by the word cloud map and web dynamic map display information such as viewers' emotional tendency and movie rating statistics, and provide decision support for users' movie viewing.

1. Introduction

With the rapid development of web technology, the amount of web information is also growing rapidly [1, 2]. In order to better meet the personalized needs of users, various recommendation systems have emerged, which automatically establish the connection between users and information by studying their interest and preferences, thus helping users to discover their potential needs from the huge amount of information. Python is an open source, free, cross-platform interpreted high-level dynamic programming language, and its powerful functions and simplicity make it the preferred language for Internet application development.

Scholars at home and abroad have also made many contributions to the research of film rating prediction. Karl Persson collected the attribute and feature information of 3,376 Hollywood movies from the IMDB website and constructed a random forest model and a support vector machine model to predict the movie ratings. Liu Changming proposed a hybrid prediction model of movie scoring based on the machine learning algorithm and movie features and predicted movies on Douban [3, 4]. Lu Junzhi (Spark Mllib machine learning framework, 2018) built a movie score prediction model through the random forest regression algorithm, with good results. In general, domestic and foreign scholars have studied the prediction of films, but the prediction of foreign film is more mature, and there is still room for improvement in domestic research on film prediction models.

In this paper, the movie data are obtained from Douban website, and a total of 91,368 movie records are crawled for movie ratings, number of ratings, number of stars, genres and tags, etc [5, 6]. The data are analyzed based on Python's integrated development environment, using Numpy for storing and processing data, pandas for data analysis, and matplotlib, and this data analysis project is mainly composed of three parts: production and quality analysis of the movie industry, analysis of Douban rating factors, and prediction of rating models, which can be used to intuitively grasp movie-viewing orientation and quickly find preferred high-quality movies through data visualization.

2. Python-Based Movie Data Acquisition

2.1. Introduction to Python. Python is a high-level combination of interpreted, compiled, interactive, and object-oriented scripting language that is powerful, syntactically simple, and easy to maintain. It is a great language for beginners because of its highly readable design, its more distinctive syntax than other languages, and its support for a wide range of applications [7, 8].

2.2. Movie Ranking Acquisition Techniques. For the movie ranking acquisition, we mainly use the re module and the request the HTTP client library to get the data of the Hot 100, Most Anticipated, Domestic Box Office, North American Box Office, and Top 100 lists. We use the browser to login to the CatEye movie page, view the html body data of the page, analyze the html structure of the page, extract the URL information using regular expressions, and then collect the data in the next step. The key code is as follows:

```
def getOnePage(url)
response = requests.get(url, headers = header)
if response.status_code = = 200:
allTop = re.findall("<dd>. *?board-index-(\d+). *?
title = "(. *?)". *?/p>. *? </dd>", response.text, re.S)
return allTop, response.text
```

2.3. Movie Data Fetching Techniques. The movie data acquisition mainly uses requests HTTP client library, json package, random library, csv function package, datatime module, and re module. re module and requests library and random library are mainly used to crawl data, json package is used to convert the acquired data format to json format, datatime module the csv function package is used to store the data [9, 10]. The User-agent proxy mechanism is used to represent the requester's information, the User-agent can be collected and saved, and the User-agent can be dynamically changed during the crawling process to prevent the data from being terminated due to frequent acquisition. In this paper, the movie "Spirited Away" is selected for analysis according to the hot word-of-mouth list, and finally, 13318 records are obtained for visualization using Python crawler technology.

3. Acquisition of Douban Top 250 Movie Data

3.1. Introduction of Concepts Related to Douban Top 250 Movie List. Douban is a sharing and review community website that provides users with information about books, movies, music, and others. Douban.com is a community website that provides users with information about books, movies, music, and other works, with descriptions and comments provided by users, and is one of the most unique Web 2.0 websites [11, 12]. As an important part of Douban.com, Douban Movies provides users with movie-related information, such as descriptions, schedules, ticket prices, and reviews of currently released movies. The Top 250 movie list is based on the number of people who have seen each movie and the reviews it has received and represents the movie preferences of the majority of users.

3.2. Data Acquisition and Cleaning. In this paper, we choose Octopus collector to crawl the information of Douban Top 250 movie list and enter the URL of Douban Top 250 movie "https://movie.douban.com/top250" on the home page to enter the interface of the collection process [13, 14]. The total number of information crawled was 250, and 20 fields were obtained after data cleaning with the Pandas library in Python, namely, movie name, score, number of ratings (num), number of five-star ratings (star5), number of four-star ratings (star4), number of three-star ratings (star3), number of two-star ratings (star2), and number of one-star ratings (star3). (star1), short reviews (short), director (director), writer (writer), actor1, actor2, actor3, type1, type2, region of production (region), year of release (year), month of release (month). year, month, and time.

4. Exploratory Analysis of Douban Top 250 Movies

4.1. Number of Movies in Each Region. The origins of Douban Top 250 movies are divided into UK, USA, Italy, France, Korea, Japan, and China, as shown in Figure 1. Since the number of movies from the remaining regions is small, it is not shown in this paper. In the Douban Top 250 movie list, there are 114 American movies, accounting for 45.6% of the overall total. This is followed by a total of 41 Chinese movies, including 16 movies from Mainland China, 19 movies from Hong Kong, and 6 movies from Taiwan. In addition, there were 32 Japanese films, 17 British films, and 10 Korean films [15, 16]. It can be seen that Western countries have some influence on Chinese film culture. Since most of the users of Douban are young people, the reason why American movies are highly rated by young people is inseparable from their movie culture and dissemination. In addition, further analysis of Japanese movies shows that most of the movies are anime, which is an important part of Japanese soft culture and reflects the preference of young people for anime culture.

4.2. The Overall Distribution of Movie Ratings. Because the list of Top 250 movies is selected, the ratings of movies are relatively high, concentrated in the range of 8~10, and the number of movies with each score is shown in Figure 2.

As we can see from Figure 2, the lowest rating among the movies crawled is 8.3 and the highest is 9.7.93.2% of the movies which are rated 8.5~9.3, and most of them are rated 8.5 and above, indicating that the quality of these movies is relatively high. In addition, there are very few movies with high ratings, which shows that audiences have different preferences for movies, and movies that seem to be highly rated by some people are not liked by all [17, 18].

4.3. Analysis of Movie Genres. In order to better understand the movie genres that viewers pay attention to, we first use the wordcloud word generation library in Python to create a word cloud map of Douban Top 250 movie genres.

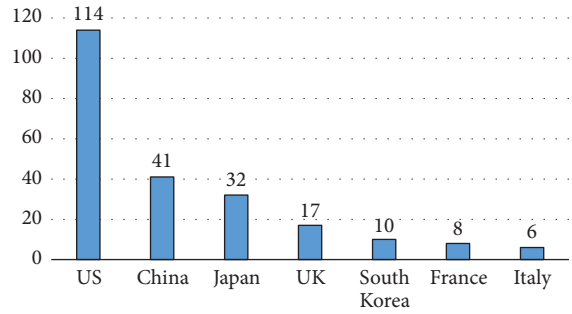

Figure 1: Number of movies in each region.

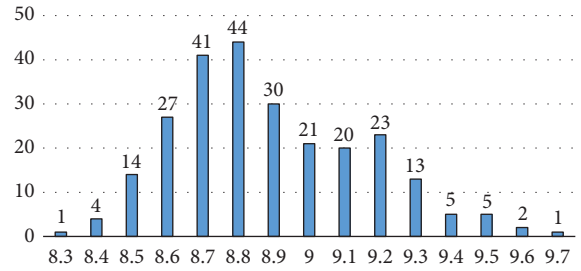

Figure 2: Number of movies for each score.

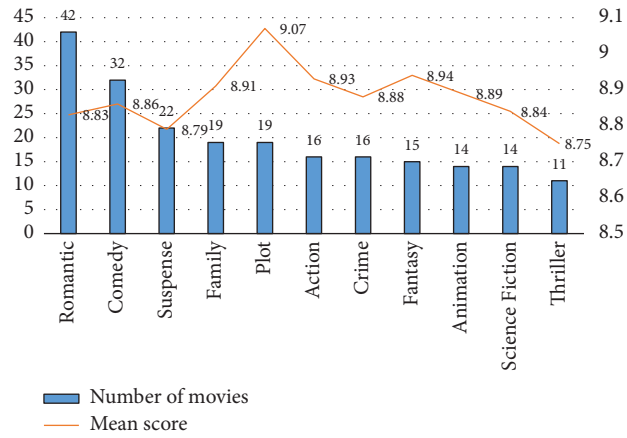

Figure 3: Number of movies for each score.

The movies with the highest frequency in the list are romance movies. This is followed by comedy, suspense, family, and drama movies, and song and dance movies appear very infrequently [19, 20]. After further statistical analysis, the movie genres in the Douban Top 250 movie list are mainly divided into 20 types, such as romance, comedy, suspense, family, drama, action, and crime. According to the classification and number of movies, the movie genres with more than 10 movies were selected for the analysis of the number of movies and rating averages, as shown in Figure 3.

As can be seen from Figure 3, there are ten categories of movies with a number of movies greater than 10. The most movies are in the romance category, with 42 movies in total. The next category is comedy, with 32 movies. There are 22 suspense movies, 19 family movies, 19 drama movies, and 16 action and crime movies. The number of movies in the fantasy, animation, science fiction, and thriller categories is relatively small, but all of them have more than 10. In addition, the average rating of most types of movies is around 8.9 points. The highest is drama movies with an average rating of 9.07, and the lowest is thriller movies with an average rating of 8.75.

5. Python-Based Visual Analysis of Movie Data

5.1. Sentiment Analysis and Word Cloud Generation. Snow NLP is a class library of Python, which can easily process Chinese text content, call the classification method under sentiment, and score the emotional tendency of the review, between 0 and 1; the more positive emotional tendency corresponds to a higher score, as shown in Figure 4. We can find that the user reviews of the movie "Spirited Away" are mostly positive tendency words, which means the movie has more positive comments.

Using the lexicon-based sentiment analysis method, the text is borrowed and analyzed through the sentiment dictionary and rules, and the sentiment value is calculated by traversing the sentiment words, degree words, negation words, matching words, and exclamation words, and finally, the sentiment value is used as the basis for the sentiment tendency of the text [21–23]. The specific operation process is "text preprocessing, text word splitting—exact pattern word splitting, customizing common word removal database, removing individual words, doing word frequency statistics on word splitting, getting the top 100 most frequent words, reading positive and negative word database, counting positive words and negative words, and drawing word cloud." Through the word cloud chart, we found that the overall feeling of the audience for the film is good and classic, and we also found that the most watched cities in China are Beijing, Guangzhou, Shenzhen, and Shanghai.

5.2. Movie Star Rating Analysis. The Pie component in the Pyecharts library is imported and used to generate pie charts [24, 25]. Pandas incorporates a large number of libraries and some standard data models, providing the tools needed to manipulate large data sets efficiently, and the movie ratings are grouped and summed using Pandas to derive the percentages, which are finally displayed in the form of dynamic graphs on web pages, as shown in Figure 5.

Three pieces of information are captured according to the html structure: the rating level for each account; the review message for each account; and the http link to jump to the next review page. After acquiring all the information and processing the information, the total number of each star rating and how many accounts in total were rated were calculated [26–28]. Through the results, it can be found that 78.97% of the viewers were five-star positive, and the overall rating of the movie was high and worthy of recommendation. The key code for star rating analysis is as follows.

```
import pandas as pd from pyecharts import Pie # Import Pie component for generating pie charts.
```

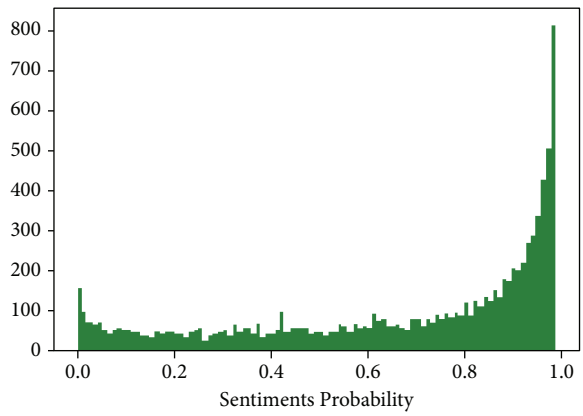

Figure 4: Effect diagram of emotion analysis.

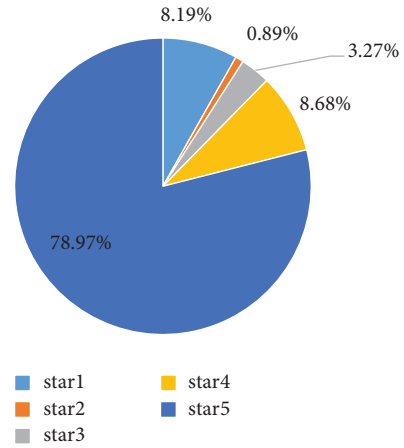

Figure 5: Scale diagram of star evaluation.

```
# pandas.
df = pd.read_csv("D:comments.txt," encoding = "gb18030," names = ["id ," "NickName," "userLevel," "cityName," "content," "score," "startTime"])
attr = ["one-star," "two-star," "three-star," "four-star," "five stars"] score = df.groupby("score").size() # sum by group.
value = [
score.iloc[0] + score.iloc[1] + score.iloc[1],
score.iloc[3] + score.iloc[4],
score.iloc[5] + score.iloc[6],
score.iloc[7] + score.iloc[8],
score.iloc[9] + score.iloc[10],
]
pie = Pie("Spirited Away Star Ratings Ratio," title_pos = "left," width = 600)
pie.use_theme("dark")
pie.add("rating," attr, value, center = [40, 50], radius = [25, 75], rosetype = "raea," is_legend_ show = True, is_label_show = True)
pie.render("rating-star.html")
```

6. Douban Top 250 Movie Rating Prediction

In this paper, the random forest regression algorithm, regression tree algorithm, and gradient boosting regression algorithm were selected to train and predict the ratings of Douban Top 250 movies. By evaluating the prediction results of the three algorithms, the gradient boosting regression algorithm was selected to predict the ratings of the experimental data [29, 30].

6.1. Introduction of the Algorithms

6.1.1. Random Forest Regression Algorithm. The random forest regression algorithm is a fusion algorithm constructed based on a decision tree classifier, which is composed of multiple decision trees. The algorithm performs multiple sampling from the sample data by sampling with put-back, constructs a corresponding decision tree for each sample subset, then averages or votes on the prediction results of all decision trees, and then selects the optimal prediction result. The advantage of this algorithm is that it is insensitive to the correlation between variables and avoids the effect of multicollinearity [31–33].

6.1.2. Regression Tree Algorithm. The decision tree regression algorithm is a relatively common algorithm for regression and classification, where data are regressed by rules in order to construct a regression tree model. Creating a decision regression tree requires using the values obtained from the observed data to establish a rule for constructing a model in which each characteristic attribute is a variable, and after classifying, a variable according to the rule so that the sum of squared residuals of the two parts is minimized to form a regression tree with good results.

6.1.3. Gradient Boosting Regression Algorithm. The gradient boosting regression algorithm is a representative algorithm in machine learning algorithms, which can be used for regression or classification problems, and the common gradient boosting algorithms include AdaBoost and gradient boosting algorithms. In this paper, the gradient boosting algorithm is used to predict movie ratings, and the principle of the gradient boosting algorithm is to evaluate the reliability of the model using a loss function [34, 35]. According to the established loss function, each iteration of the model will refine the model according to the direction of gradient descent, gradually reducing the value of the model's loss function. The gradient boosting algorithm is based on regression trees for model construction, and the residuals of the previous tree are used as the next learning target, so as to construct new regression trees until the residuals of the model reach the allowed range.

6.2. Model Construction and Result Analysis

6.2.1. Feature Selection and Data Processing. By processing the feature information, this paper selects 9 feature variables

for modeling according to the characteristics of each feature information and referring to related literature, which are score, num, star5, star4, star3, star2, short, time, and year, where score is used as the target variable and the other 8 variables are used as predictor variables [36, 37]. In this paper, we divide 250 data into training set and test set by train_test_split ( ) in sklearn.model_selection, then standardize both training set and test set data of predictor variables by using StandardScaler ( ), and use the standardized data to build the prediction model.

6.2.2. Model Construction. In this paper, the random-forest classifier and gradient boosting regressor in sklearn.ensemble are used to implement the random forest algorithm and the gradient boosting regression algorithm, and the tree package in sklearn is used to implement the regression tree algorithm. The processed training set data are used to construct the random-forest regression model, gradient boosting regression model, and regression tree model, respectively, using these three algorithms, and the corresponding values, i.e., movie ratings, are predicted for the test set using the predict( ) method.

The error results obtained from the three models are shown in Table 1.

From Table 1, we can see that the gradient boosting regression model has the best evaluation result, with the model prediction accuracy reaching 91.16%, the mean square error only 0.5974, and the average absolute error 0.6268, which is obviously better than the other two models. Therefore, the gradient boosting regression model is selected in this paper for movie rating prediction of experimental movie data. The prediction results are shown in Table 2. It can be seen that the errors between the predicted and actual ratings of the five movies are small, and the prediction results are highly accurate [38].

Table 1: Error comparison of the three models.

Model	Accuracy rate	R^2	MSE	MAE
Random-forest	0.2540	0.7040	2.0000	1.0793
Regression tree	0.74860	0.7486	1.6984	0.9683
Gradient boosting	0.9116	0.9116	0.5974	0.6268

Table 2: A part of the movie score prediction results.

Movie	Prediction score	Actual ratings
Gone with the Wind	9.1775	9.3
Contratiempo	8.8002	8.8
Little Woods	8.9806	9.0
How to Train Your Dragon	8.7177	8.7
Days of Being Wild	8.5237	8.5

7. Thinking and Countermeasures

In recent years, the habit of movie-going in China has not only created the prosperity and development of the movie market but also put forward higher requirements for movie workers. China is undoubtedly a big movie country, but there is still a small gap from being a strong movie country, and how to get out of the country and further enhance the cultural influence of domestic movies is perhaps the next step that should be considered.

7.1. Improve the Quality of Movies. People often hope that a "good movie" with high rating can get a high box office to match it, instead of relying on publicity and marketing and the participation of big popular stars, so as to promote the benign development of the film industry and promote more high-quality films [29]. The era of relying on large-scale marketing and publicity to obtain the market has long passed, and the final factor that attracts the audience to enter the theater is still the film's choreography and production. As a big movie country, the rate of bad movies is much higher than that of other countries, so it is important for all filmmakers to set the right attitude and do a good job in film arrangement and production, not to meet the market demand, but to make films that really resonate with the public and cause society to think [39].

7.2. Create Diversified Cinema Lines. The full explosion of the movie market is destined to be accompanied by the diversification of people's movie-going preferences [30–39]. In the future development of domestic movies, under the influence of the new film industry pattern, movie genres will become more and more abundant, and traditional comedies and romances will join hands with new genres such as suspense and crime to the screen. It will be difficult to summarize the genre of a movie with one or two genres, and there will be more and more movies with multiple genres at the same time, and their structure and methods will be more mature.

8. Conclusion

In this paper, we use Python crawler technology combined with Python library to analyze the data of movie information on Douban website, clean and analyze the scattered movie data, and use word cloud and charts to visualize and display the data to achieve self-interpretation. The user evaluation data are focused in multiple dimensions and levels, and the patterns and features of the data are discovered to make it have reference value for the audience's movie viewing behavior. For the construction of the movie score prediction model, three algorithms of random forest, regression tree, and gradient lifting are adopted. The model evaluation results show that the best prediction effect is the gradient boosting regression model, with an accuracy of 91.16%. This model was used to score the five films, and the prediction score and the actual score were very close. In the next step, the program will be further extended so that it can be developed into a complete film evaluation visualization system equipped with a user interface for smooth operation. At the same time, it will focus on dynamic data crawling for mobility so that it can achieve multiple data acquisition and evaluation and can play a greater role in public opinion analysis in the future.

Data Availability

The dataset can be accessed upon request.

Conflicts of Interest

The authors declare that they have no conflicts of interest.

Acknowledgments

This work was supported in part by the Beijing Municipal Social Science Program (Grant 20YTC032) and Beijing Municipal Education Commission and Scientific Research Program (Grant SM202110028014).

References

[1] X. Yang, X. Chang, X. Yu, and N. Li, "A study of Chinese film industry based on social networks and decision trees," *Film Literature*, vol. 5, pp. 3–12, 2019.

[2] Y. Y. Zhang, "Design and implementation of a movie recommendation system based on collaborative filtering," *Computer Knowledge and Technology*, vol. 15, no. 6, pp. 70–73, 2019.

[3] Y. J. Wu and N. Huang, "Research on movie word-of-mouth based on Python technology," *Computer Networks*, vol. 45, no. 9, pp. 42-43, 2019.

[4] Y. Zhang, "Design and implementation of a Python-based recommendation system," *Computer Age*, vol. 6, pp. 59–62, 2019.

[5] L. Pei, "Design and implementation of a Python-based data crawler for Douban movies," *Electronic Technology and Software Engineering*, vol. 13, pp. 176-177, 2019.

[6] F. Wu, J. Qian, and J. Liu, "A research on box office prediction based on C5.0 decision tree algorithm," *Science and Technology Square*, vol. 4, pp. 186–192, 2016.

[7] W. Cheng and X. Li, "Research on movie data crawling and data visualization analysis based on Python," *Computer Knowledge and Technology*, vol. 15, no. 31, pp. 8–10+12, 2019.

[8] W. Li and L. Zheng, "Box office prediction of domestic movies based on random forest regression model," *Journal of Hubei University of Technology*, vol. 35, no. 1, pp. 114–117, 2020.

[9] W. Gao, P. Sun, and D. Li, "Visual analysis of movie data based on Python crawler," *Journal of Shenyang University of Chemical Technology*, vol. 34, no. 01, pp. 73–78, 2020.

[10] J. Zhou, J. Liang, and J. He, "Analysis of residents' consumption opinion on domestic science fiction movies and box office prediction--Wandering Earth as an example," *China Collective Economy*, vol. 34, pp. 142–144, 2020.

[11] X. Tu, "Emotional tendency analysis of movie reviews based on Python crawler," *Modern Computer(Professional Edition)*, vol. 35, pp. 52–55, 2017.

[12] Z. M. Han, B. H. Yuan, Y. Chen, N. Zhao, and D. A. G. O. Duan, "An effective GBRT-based early movie box office prediction model," *Computer Application Research*, vol. 35, no. 2, pp. 410–416, 2018.

[13] S. Tian, "Crawling data of Douban movie TOP250 based on python and conducting analysis," *Communication World*, vol. 10, pp. 261-262, 2018.

[14] W. Tang, "Design and implementation of personalized video recommendation system based on Web mining," *Electronic design engineering*, vol. 26, no. 18, pp. 102–106+112, 2018.

[15] L. Tang, "Research on the classification of emotional tendency of online movie reviews," *Journal of Zunyi Normal College*, vol. 20, no. 6, pp. 160–164, 2018.

[16] J. Yue, X. Wang, and M. Yang, "Python based data crawling and analysis of Douban website," *Computer Knowledge and Technology*, vol. 16, no. 32, pp. 51–53, 2020.

[17] Y. Qin, "Research and implementation of a Python-based collaborative user filtering recommendation system," *Computer Knowledge and Technology*, vol. 16, no. 31, pp. 234–236, 2020.

[18] J.-Yi Feng, Chen, Qi-Qi, and Bo-H. Chen, "Research on movie data analysis based on decision tree algorithm," *Information Recording Materials*, vol. 21, no. 12, pp. 153-154, 2020.

[19] J. Geng and M. Guo, "Data mining and rating prediction of Douban Top 250 movies," *Hebei Enterprise*, vol. 2, pp. 11–13, 2021.

[20] L. Liu and Y. Liu, "Design and implementation of movie recommendation system," *Internet of things technology*, vol. 11, no. 3, pp. 86–88+92, 2021.

[21] W. Wang, H. Yu, and G. Fan, "A matrix decomposition movie recommendation algorithm incorporating classification and contextual preference," *Journal of East China University of Science and Technology*, vol. 47, no. 3, pp. 348–353, 2021.

[22] J. Zhang and H. Mao, "Visualization of douban movie data collection and analysis based on python," *Electronic Production*, vol. 2021, no. 16, pp. 47–49.

[23] Y. Yang, "Python based movie information crawling and data visualization analysis," *New Industrialization*, vol. 11, no. 7, pp. 71–73, 2021.

[24] Y. Wang, "A light analysis of factors affecting movie box office based on data mining," *Communication World*, vol. 2, pp. 236-237, 2017.

[25] W. L. Cai, Q. C. Zhou, Y. T. Liu, and L. J. Qin, "Visual analysis of Douban movie review data based on Python crawler," *Modern Information Technology*, vol. 5, no. 18, pp. 86–89+93, 2021.

[26] R. Wang and J. Lv, "The thematic mining of the multi-clue narrative of the film "Contagion": a corpus+ approach to film and television evaluation," *Popular Literature and Art*, vol. 20, pp. 127–129, 2021.

[27] H. Liu, F. Li, J. Yu, C. Cui, and R. Ge, "Design and implementation of movie recommendation system based on movie review mining," *Electronic Technology*, vol. 47, no. 12, pp. 83–86, 2018.

[28] Y. Jiang, L. Gan, W. Chen, and Wuzhou, "The application of data mining technology in movie recommendation," *Computer Knowledge and Technology*, vol. 15, no. 18, pp. 254–256, 2019.

[29] G. Su and Yu Su, "Python-based configurable network crawler," *Journal of Ningde Normal University (Natural Science edition)*, vol. 30, no. 4, pp. 364–368, 2018.

[30] Y. Wang, "Research on microblog data based on Python," *Information and Computer (theoretical edition)*, vol. 23, pp. 93-94, 2018.

[31] Q. He and B. Hu, "Research on the influencing factors of film consumption and box office forecast in the digital era: based on the perspective of machine learning and model integration," *Wireless Communications and Mobile Computing*, vol. 2021, Article ID 6094924, 10 pages, 2021.

[32] L. Li and C. Mao, "Big data supported PSS evaluation decision in service-oriented manufacturing," *IEEE Access*, vol. 8, Article ID 154663, 2020.

[33] L. Li, C. Mao, H. Sun, Y. Yuan, and B. Lei, "Digital twin driven green performance evaluation methodology of intelligent

manufacturing: hybrid model based on fuzzy rough-sets AHP, multistage weight synthesis, and PROMETHEE II," *Complexity*, vol. 2020, no. 6, Article ID 3853925, 24 pages, 2020.

[34] J. Xiao, X. Li, S. Chen, X. Zhao, and M. Xu, "An inside look into the complexity of box-office revenue prediction in China," *International Journal of Distributed Sensor Networks*, vol. 13, no. 1, Article ID 155014771668484, 2017.

[35] S.-M. Choi, H. Lee, Yo-S. Han, Ka L. Man, and W. K. Chong, "A recommendation model using the bandwagon effect for E-marketing purposes in IoT," *International Journal of Distributed Sensor Networks*, vol. 11, no. 7, Article ID 475163, 2015.

[36] L. Li, B. Lei, and C. Mao, "Digital twin in smart manufacturing," *Journal of Industrial Information Integration*, vol. 26, no. 9, Article ID 100289, 2022.

[37] L. Li, T. Qu, Y. Liu et al., "Sustainability assessment of intelligent manufacturing supported by digital twin," *IEEE Access*, vol. 8, Article ID 174988, 2020.

[38] W. Xiao-Ling, L. Zhi-Long, and Z. Madina, "Machine Learning-Enabled Development of Model for Japanese Film Industry," *Security and Communication Networks*, vol. 2022, Article ID 7637704, 9 pages, 2022.

[39] J. Lv and Y. Tao, "Development and performance evaluation of digital technology and radio and television integration based on big data model," *Journal of Sensors*, vol. 2022, Article ID 1843753, 11 pages, 2022.

Hindawi
Scientific Programming
Volume 2022, Article ID 3922377, 11 pages
https://doi.org/10.1155/2022/3922377

Research Article

Face Recognition Model Design Based on Convolutional Neural Networks

Shangtao Zhang

The Internet of Things and Artificial Intelligence College, Fujian Polytechnic of Information Technology, Fuzhou 350003, Fujian, China

Correspondence should be addressed to Shangtao Zhang; zhangshangtao@fjpit.edu.cn

Received 7 July 2022; Revised 15 August 2022; Accepted 23 August 2022; Published 22 September 2022

Academic Editor: Lianhui Li

With the rapid development of computer science and Internet technology, face recognition technology is widely used in such as public security, judicial and criminal investigation, public security, information security and access control system, such as public security system need to find out the criminals in the system library, or from the entrance control system quickly identify and match the identity of relevant personnel information. As a stable, intuitive and highly recognizable biometric feature, human face is being paid more and more attention by researchers. Compared with other bioinformation recognition methods, face recognition is characterized by direct, friendliness and convenience. Users are not easy to resist, and compared with other recognition technologies, they are easy to be accepted by users, so it has received attention and research. This paper designs a face recognition system based on a convolutional neural network. Compared with the traditional face recognition method, the convolutional neural network model does not need manual complex and time-consuming feature extraction algorithm design, only need to design an effective neural network model, and then end-to-end training on a large number of training samples for simple and efficient training, can get a good identification effect. The design uses the target detection algorithm to conduct accurate, real-time, efficient face recognition, and can accurately identify the people in the camera.

1. Introduction

1.1. Research Background. The narrow sense of facial recognition technology refers to a computer vision technology that performs authentication or search by analyzing and comparing facial visual feature information. Some of the more common recognition technologies in daily life, such as fingerprint recognition, belong to the same field and the field of biological information recognition, and facial recognition technology is also widely used in daily life. This authentication method has many advantages compared with the traditional identity authentication. Password, card, certificate as the featured authentication technology, biometric technology is difficult to forge, and there will not be lost, biometric technology has become the most secure and the most reliable authentication technology in the world.

In the information age, information protection is particularly important, and China attaches great importance to public security, and the demand for security protection application of new technologies and new products is strong. Face recognition technology uses the difference of individual facial characteristics to realize human identity characteristics recognition. Face is the most direct performance and the most unique biological feature in biology, which makes face recognition technology have unique recognition advantages. Based on this advantage, face recognition has shown great potential in the application of many fields, especially to the public security investigation system [1].

In today's Internet + environment, O2O, P2P, B2C, B2B and other forms of network business model gradually emerging, and in various network business model the most important key technology is network payment, network payment security problem determines the development of business model, so safe, fast network payment is the urgent need of modern society, face recognition is easy to forget, theft, and convenient and fast, security has become a new way of network payment [2].

Face recognition technology as the security of the city, realize the convenient life core technology, with the

construction of intelligent information city in China, some high-tech company investment and strategic transfer, make the application of face recognition technology more and more wide, brush face payment, brush face clock function application, can say the new era of face recognition application has come.

1.2. Research Meaning. Face recognition has some characteristics that other recognition methods do not have, making it has unique advantages in specific applications [3, 4]:

1.2.1. Non-Contact, Imperceptible. Face recognition is generally carried out under conditions with visible light or infrared interaction with visible light and if the face is exposed to light, it is difficult to camouflage and change. Therefore, face recognition can easily access to identity information but cannot be detected and disgusted. This can play a great role in the arrest process of criminal suspects, because criminal suspects generally have a high vigilance, it is difficult to gain their trust, get their identity information. Face recognition does not require direct contact between people and the device, and other methods such as fingerprint recognition require contact with the device. On the one hand, it is not easy to be noticed that the collection can be completed inadvertently, without too much intervention from the staff. The collection person will not resist, because the face compared with fingerprint, iris and other characteristics are exposed characteristics, and we can accept it. On the other hand, it is clean and hygienic, and will not spread infectious diseases. During the epidemic prevention and control period, non-contact even reflects the unique advantages that other identification methods do not have [5, 6].

1.2.2. Concurrency, Equipment Requirements are Single. Face recognition for equipment requirements are mainly high pixel camera, the equipment requirements of a single. With the improvement of smartphone front camera pixels, more and more smartphone brands regard human recognition as an important way to unlock it. With people's increasing requirements for urban security, the urban video surveillance system is increasingly perfect, and the number of high-performance cameras is increasing greatly. Compared with fingerprint recognition, iris recognition and other recognition devices, face recognition has obvious hardware basic advantages. And the price of face recognition equipment has significant advantages compared with the price of other recognition devices, and the price of face recognition equipment belongs to the acceptable range of users [7]. At the same time, with the improvement of the monitoring system, it can also be used to find the lost property and accurately crack down on the crime of population trafficking and other functions, because the surveillance can save the video and restore the scene at that time, which is impossible for other recognition methods. With the increasing accuracy of face recognition, face recognition will become a large-scale social recognition technology [8].

1.2.3. Natural Advantage. The advantage of nature is simply being able to distinguish with human eyes, rather than having to be processed by the device to distinguish [9]. Face recognition is very simple, just a few seconds after standing in front of the camera, users do not need to be trained, and do not need to carry documents. It also improves security. Fingerprint and iris recognition humans cannot be distinguished by the naked eye and must be scanned through devices, so they are not natural. Criminals have the opportunity to cheat devices by collecting fingerprints and iris to commit crimes [10, 11].

1.3. Development Trends

Stage 1: The initial stage of face recognition technology. In the initial stage of face recognition technology to Parke, mainly on the face gray scale graph model research, at this stage has no key progress, basic in practical application is with artificial to identify, identification efficiency is very low, recognition effect is poor, it is easy to identify error, and manual operation is too large, the system has no automatic recognition ability [12, 13].

Stage 2: The transition stage of face recognition technology. The excessive stage of face recognition technology has achieved many very important results, pointing out the direction for face recognition technology. After going through the initial stage, the researchers study face recognition as one of the pattern recognition problems. The geometric structure features of the human face, such as the relative position and distance of the nose, eyes and mouth, constitute the feature vectors, which are matched for face recognition. The main characters are AJ Goldstein [5], LD Harmon and AB Lesk use geometric feature parameters to represent the front image of the face; Kaya uses statistical methods to study the Euclidean distance as the face features; Kanade [6] has designed a semi-automatic backtracking recognition system. The Turk of MIT and the characteristic face method proposed by Pentland are of great significance, and they are the most representative method during this period. Face Recognition technology Test has created its own FERET face image library, using it to evaluate various algorithms and look for algorithm flaws and improvements [14].

Stage 3: Face recognition technology gradually mature stage. With the improvement of computer computing power, the concept of artificial intelligence and machine learning, face recognition technology has had a new development. At this stage, automatic face recognition has been available. At this stage, the research focus has gradually shifted to face recognition under non-ideal conditions. The current face system will still be affected by expression changes, posture changes, light conditions. The main characters include face recognition based on light cone model under multi-pose and multi-illumination conditions proposed by Georghiades, face image recognition based on

multi-pose and 3D deformation model under multi-illumination conditions proposed by Blanz, and face recognition method for statistical learning of support vector machine SVM.

2. The Theoretical Basis of the Convolutional Neural Networks

2.1. Artificial Neural Nets. Artificial neural network is a mathematical model that mimics the coping mechanism of the human neural system and the process of external excitation, according to the principle of various information, as shown in Figure 1. This mathematical model has some features similar to biological systems, such as nonlinearity, robustness, non-limitation, very qualitative, fault tolerance, and fuzzy information that can be processed. Therefore, this model has achieved good results in pattern recognition, image processing and other aspects. Simply put, the artificial neural network first provides some data with the input-output mutual response relationship, and then analyzes the relationship between the two, to get the law, and to predict the corresponding results of the new input data according to this law. Convolutional neural network belongs to a kind of artificial neural network, so mastering artificial neural network is beneficial to understand convolutional neural network. Figure 1 shows a cerebellar model arithmetic computer.

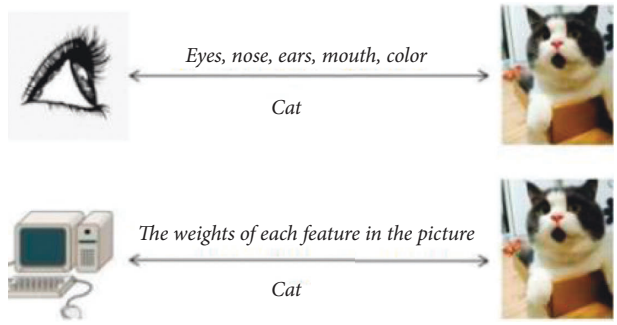

Figure 1: Cerebellar model arithmetic computer.

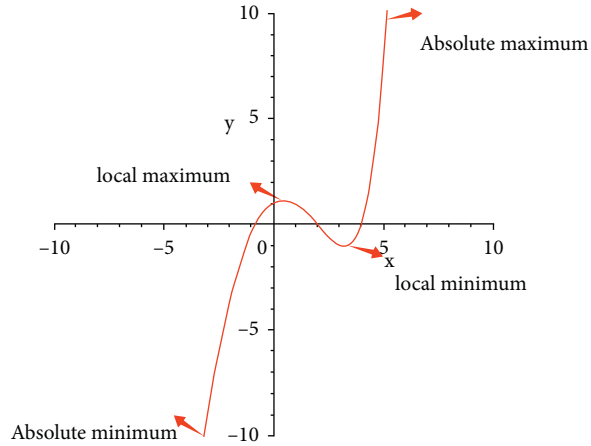

Figure 2: A function image of a certain loss function.

2.1.1. Loss Function. The loss function [9] is used to measure how well the model predicts results at a time. Using the input and output of a set of data to adjust the parameters in the model to achieve the required performance, the process is supervised learning. Take it as an example, and arbitrarily choose a model that corresponds to a function, and for any input, the model will output a corresponding output result. The output may be the same as the true value, but there may be some error. At this point, a function is needed to describe the error of the model output, which is known as a loss function.

2.1.2. Gradient Descent. In order to reduce the error between the output of the model and the real value, the minimum value of the loss function is actually found. In practice, we generally iterate through gradient descent to find the minimum value of the loss function, a function image shown in Figure 2.

Assuming that the vertical axis of the function curve is the loss function value of the model, and the horizontal axis is a certain parameter value of the model, the loss function of the best predicted model that we want to obtain must be minimal. As can be seen from Figure 2, the image has two stagnation points, respectively, the maxima and minima of the function, but the minimum value of the function is only one. For machine learning models, the vast majority of them cannot directly obtain the minimum value through calculus, so we can only try to obtain the global minimum value through the step-by-step iteration method.

For a unary function, you can find the minimum value of the function method can be divided into several steps, each time along the derivative is negative way. For multivariate functions with multiple independent variables, it can be gradually found gradually along the direction of its gradient descent, which is the gradient descent algorithm. To get the minimum value of the loss function, you need to get the gradient of the loss function, and then update it in the direction where the gradient is negative, where parameter η is known as the learning rate, the gradient descent convergence case at different learning rates is shown in Figure 3.

It can be seen that either too large or too small of the learning rate setting will affect the convergence effect, so a suitable learning rate is very important for the convergence of the model.

2.1.3. Optimizer. The learning rate parameter has a great impact on the quality of the trained model, but this parameter is not easy to set, either too large or too small. Therefore, one hopes that the model can both converge quickly and get a good result during the training process. Some scholars have proposed an optimizer that can automatically adjust the learning rate. By introducing the concept of momentum to adjust the speed of gradient descent, so that it can accelerate the decline when it should fall faster, and then converge quickly. There are many such optimizers,

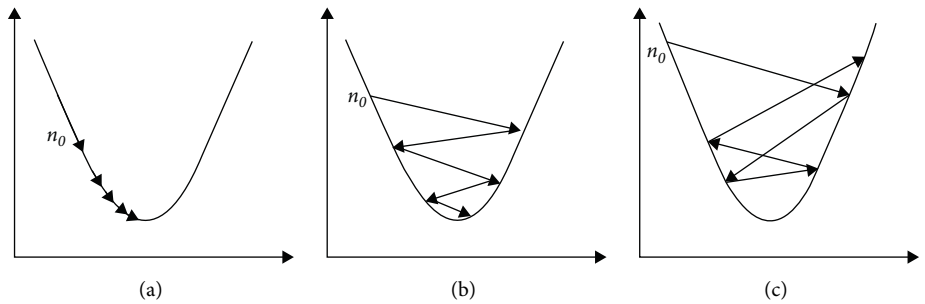

Figure 3: Convergence case of the gradient descent at different learning rates. In Figure 3 (a) the learning rate is too hours. The small learning rate setting can find the minimum, but the convergence rate is slow and easier to enter the local minimum. (b) When the learning rate is set to moderate. The convergence process of the model is oscillating and converges faster. (c) This is shown when the learning rate is set to be too large. The convergence process of the model is violently volatile and difficult to converge.

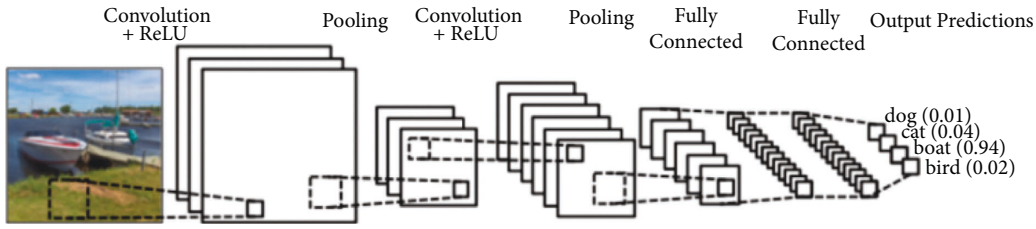

Figure 4: Traditional convolutional neural network architecture.

such as RMSprop, Adagrad, Adadelta, Adam, etc. This design uses the Adam optimizer, which mainly has significant advantages:

(i) Easy to use, fast operation speed

(ii) Memory footprint is not high, and the computer configuration requirements are low

(iii) Suitable for the unstable objective functions.

In general, the Adam optimizer is highly efficient, simple to call to, and it is perfect for this design.

2.1.4. Error Backpropagation Algorithm. The error backpropagation algorithm in the 1980s is one of the most widely influential, Rumhart et al. the core content of the error backpropagation algorithm [11] is to divide the learning process into forward propagation process and backpropagation process. The forward propagation process is the input sample from the input layer, and the output layer from the hidden layer. If the actual output of the output layer does not match the desired output, the backpropagation process enters the error. Error backpropagation is to input the output error to the input layer through the hidden layer in some form, and the main purpose error is apportioned to all the units in each layer to obtain the error signal of each layer and correct the weights of each unit.

2.2. Convolutional Neural Network. Convolutional neural network is a feedforward neural network with deep structure composed of many layers. As shown in Figure 4, a typical convolutional neural network architecture is seen. The structure of convolutional neural network (CNN) includes convolutional layer, pooling layer, rectifier linear unit (ReLU), and fully connected layer.

2.2.1. Convolutional Layer. Convolutional layer [12] is the main building module used by convolutional networks, which performs most computationally heavy work. The main work of the convolutional layer is to extract the feature [13] from the input data of the image. Convolution preserves the spatial relationships between pixels by learning image features using small squares of the input image. Input images were convolved by using a set of learnable neurons. A feature graph or an activation graph is generated in the output image, which is then input to the next convolutional layer as input data. Layers of deep convolution is designed to extract the information of the various dimensions of the image, as shown in Figure 5, and the different features in the images are obtained through multiple extraction.

2.2.2. The ReLU Activation Function Layer. ReLU [14] is a nonlinear function, also known as a modified linear unit, and is a common activation function commonly used in artificial neural networks, as shown in Figures 6. This means that the operation will be applied to each pixel, reconstructing all negative values in the feature graph to zero. To understand how ReLU works, we assume that there exists a neuronal input with an input of x, whose function is defined as:

$$f(x) = max(0, x). \tag{1}$$

As shown in the schematic diagram of the neuron model in Figure 7, from formula $y = \sum (w * x) + b$, the function of

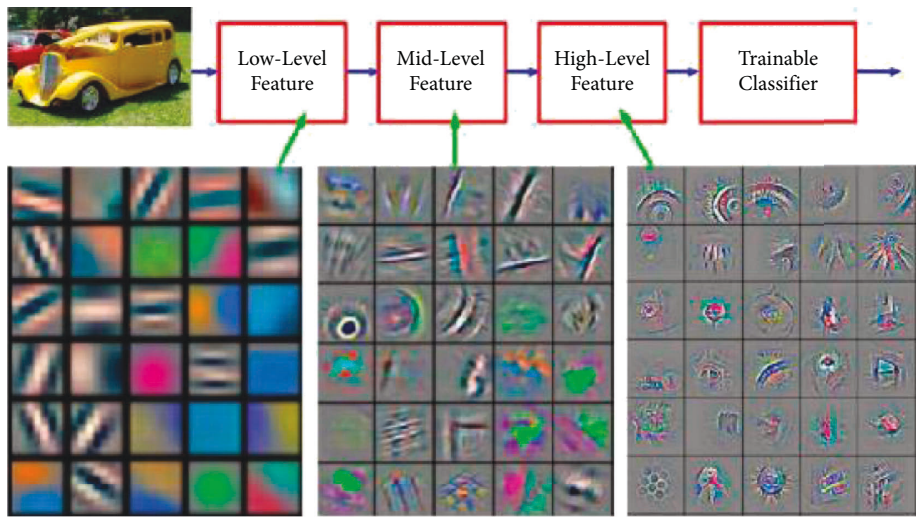

Figure 5: The effect of multiple convolutions.

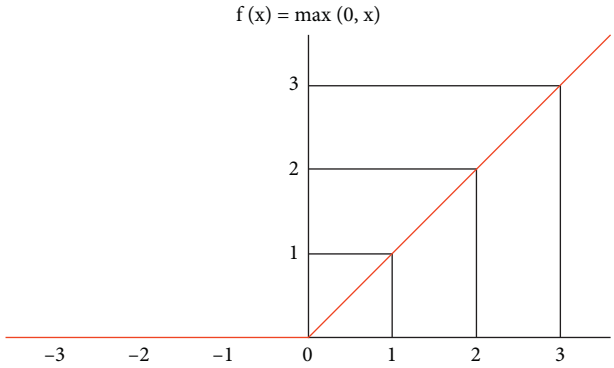

Figure 6: ReLU function.

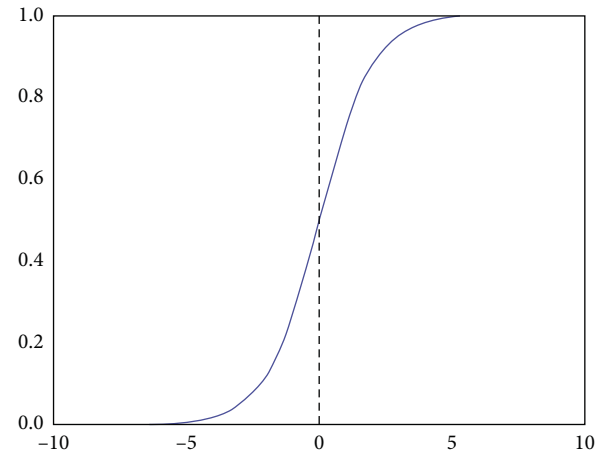

Figure 8: The Sigmoid function image.

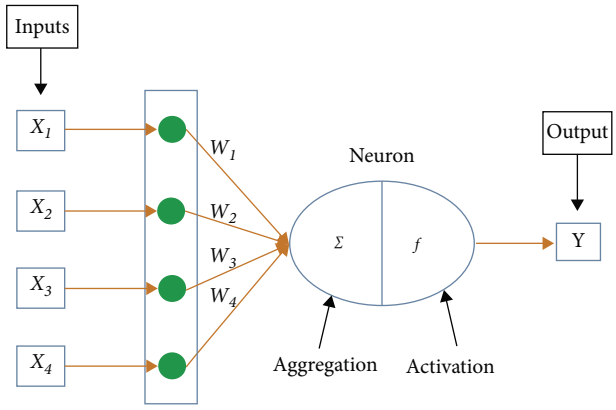

Figure 7: Schematic representation of the neuronal model.

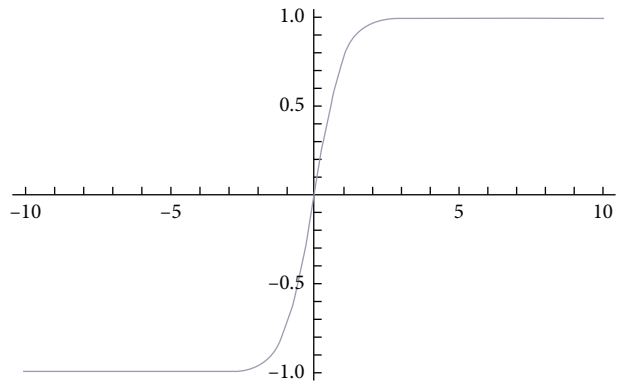

Figure 9: Tanh functional image.

using the ReLU activation function is to change the original linear output to the nonlinear output, and in practical industrial applications, more often, there are various nonlinear distributions.

The activation function also has the Sigmoid function and the Tanh function, as shown in Figures 8 and 9. The output of these two functions when x tends to infinity is 0 and 1, −1 and 1, respectively, but finding the gradient requires the first partial derivative of the function. When the value of the function is constant, the partial derivative of the function is 0, and the gradient does not exist, which is called gradient vanishing. Eventually the weight w, and the bias b cannot be updated. However, when the ReLU function approaches 0 at x, the derivative of the ReLU function exists

with a value of 1, which can reduce the computational amount of backpropagation. The gradient explosion problem occurs in the Sigmoid function, because the Sigmoid function is an exponential function, causing the problem of too large data in the result.

2.2.3. Pooling Layer. The function of the pooling layer is to reduce the size of the matrix, and can reduce the amount of operation in subsequent operations. The pooling layer reduces the broadband and height of the matrix and does not change the depth of the matrix to extract the main features of the matrix. However, there is no denying that after the pooling layer, the characteristics of the matrix will be lost. Pooling layers generally subsample each region through nonlinear operations such as average pooling or maximum pooling. Thus achieving better generalization, faster convergence, and better robustness to translation and distortion. The pooling layer is usually located behind the convolution layer. The process of maximum pooling is shown in Figure 10.

2.2.4. Fully Connected Layer. The convolution layer is the extraction of local features, the full connection is the extracted local features reintegrated through the weight matrix into a new graph, because all the extracted local features are called the full connection layer (Figure 11).

After layers of convolution and pooling, to extract the local features in the picture, and the first connected layer has activated a part of the neurons, the role of the fully connected layer is to integrate the relevant output to the second fully connected layer of some neurons, through the combination we can know that these features integrated is a cat.

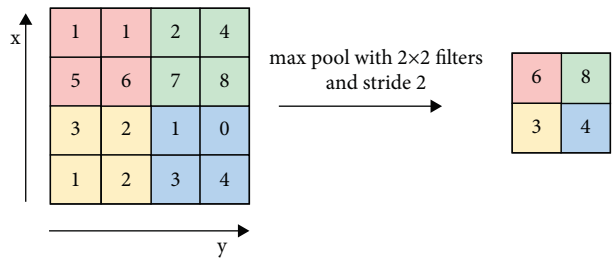

Figure 10: Maximum pooling process.

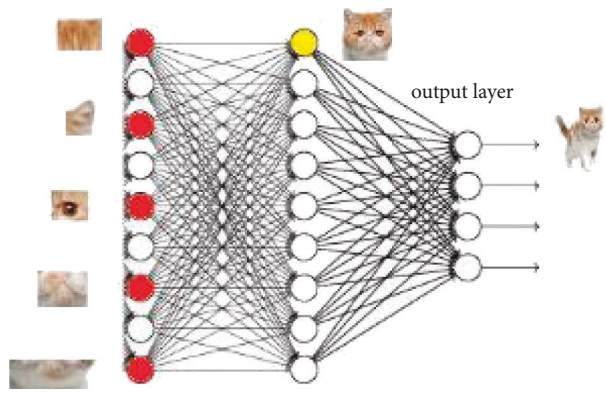

Figure 11: The role of the fully connected layer.

3. Design of the Face Recognition System

3.1. Overall Flow of the System. The convolutional network-based face recognition system is designed to detect the faces from the camera display images and compare them with the previously trained faces in the database to determine whether they belong to be the same person.

(i) Photo collection: complete video image acquisition from the camera.

(ii) Face detection: detect whether there is a face in the image, and send the picture input to the image for pre-processing. If there is no face, return to the collection stage.

(iii) Image pre-processing: face correction and cutting of face pictures.

(iv) Image feature extraction: face feature extraction through convolutional neural network.

(v) Feature matching: the extracted feature vector is compared with the feature vector of the face pictures in the library to get the judgment results.

3.2. Introduction of the Development Language and Library. Python is a fully object-oriented language. The most obvious feature that distinguishes the Python language from other languages is its simplicity. Python is the most concise of all programming languages, although it is also easy for beginners to learn from python languages, and python has many excellent libraries to help you develop. In addition, compared to other programming languages, Python can often achieve the same function with the shortest code.

3.2.1. OpenCV Storeroom. Mention computer perspective has to mention OpenCV, it is a very widely used computer vision library, OpenCV contains hundreds of computer vision, machine learning, image processing and other related algorithms, it not only contains the classic algorithm also contains now the most advanced computer vision and machine learning algorithm, it can be used to detect and identify the face, extract 3 d model of objects. Its powerful capabilities make OpenCV widely used in many fields, such as robot navigation and searching for objects, stitching together street scenes in cities, autonomous driving by unmanned cars, and so on. In this design, the OpenCV library needs to be used for processing the images.

3.2.2. Tensor Flow. Tensor Flow is a very important software library that often appears in the field of machine learning and deep learning, and its function mainly is to perform some high-performance numerical calculation and analysis. Tensor is a tensor, which represents the transmission of data between nodes, and Flow is a data stream, which refers to the various nodes of the data operation diagram in the form of a stream.

3.2.3. Numpy Storeroom. The Numpy library is the basic library of Python in the field of scientific computing, and many machine learning and deep learning studies rely on the Numpy library. The Numpy library mainly implements the computation of matrices, which can calculate the higher order, a large number of matrices, vectors, and also have relatively rich functions. The Numpy library is an important scientific computational library.

3.3. Overall Design of Face Recognition System

3.3.1. The Design of the Convolutional Neural Network. Convolutional neural network design is the core content of this design. The main principal of convolutional neural network is the face feature extraction and the training of neural network model, so the structure of convolutional neural network will determine the effect of face recognition behind [15–28]. The convolutional neural network system has designed eight layers of neural network, including three convolutional layers, three pooling layers, one fully connected layer and one output layer.

The first convolution layer: The layer of depth convolution is to extract the information of various dimensions in the image, increase the number of channels of the image, and the size of the image remains unchanged. The input image size is $64 \times 64 \times 3$, and the image size output after convolution is $64 \times 64 \times 32$. The convolution kernel size is (3, 3), the convolution step length is 1 step, and the padding fills the SAME and the image boundary pixels during the convolution process. The number of input channels is 3, and the number of output channels is 32.

The second maximum pooling layer: The main purpose is to reduce the size of the matrix, and it can reduce the amount of operation in subsequent operations. At this time, the input image size is $64 \times 64 \times 32$, the sampling size of the pooling layer is 2×2, and the output image length and width are generally the input image, so the output of the pooling image is $32 \times 32 \times 32$, which reduces the calculation amount of the image. The drop layer randomly drops some neurons with a certain probability to obtain a faster training speed.

The third convolution layer: with the input image size $32 \times 32 \times 32$, output image size $32 \times 32 \times 64$, convolution core size (3, 3), input channel 32, output channel 64, and convolution step size 1.

The fourth pooling layer: the input image size is $32 \times 32 \times 64$, the sampling size of the pooling layer is 2×2, and the output of the pooling image is $16 \times 16 \times 64$, which further reduces the information of the image, and is conducive to the calculation.

The fifth convolutional layer: with input image size $16 \times 16 \times 64$, output image size $16 \times 16 \times 64$, convolution kernel size (3, 3), input channel 64, output channel 64, and convolution step size 1.

The sixth pooling layer: The input image size is $16 \times 16 \times 64$, the sampling size of the pooling layer is 2×2, and the output of the image after pooling is $8 \times 8 \times 64$.

The seventh fully connected layer: In order to enhance the nonlinearity of the neural network and limit the size of the network, a fully connected layer is fully connected. Each neuron of the fully connected layer is connected to the neurons of the previous layer, and the picture of the input of $8 \times 8 \times 64$ is compressed into a one-dimensional vector of 1×512.

The eighth layer output layer: The output of the system is divided into two categories, one is the face saved in the database, the other one is not saved in the database face, so as to realize the recognition function. The input picture of the output layer is 1×512, and the output picture is 1×2.

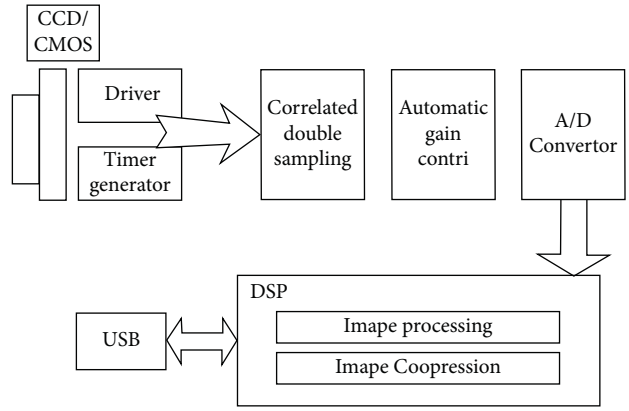

Figure 12: How the USB camera works.

3.3.2. Monitoring Picture Acquisition Subsystem. This design uses a USB digital camera using a new data transmission interface. It can be inserted directly into the computer USB interface, which is easy to operate, and the cost is lower compared with the traditional surveillance camera. The working principle is shown in Figure 12. First, the image screen is collected by the lens, and then the light sensor components and control components inside the camera process the image into a digital signal, and finally input to the computer through the port or USB connection.

3.3.3. Face Detection. Dlib comes with a Hog-SVM-based face detector, a widely used face detection model consisting of five HOG filters forming forward, left, right, forward but left, forward but right.

This recognition pattern is the fastest method to detect on the CPU, which is suitable for both frontal and slightly negative faces, and also works properly under small occlusion, and basically this method satisfies most cases. The main drawback is the inability to detect small faces, as the minimum face size trained by the authors is $80 * 80$. Therefore, you need to ensure that the face size should be greater than the face size in the program. Not suitable for side and extreme facade, such as overlooking and

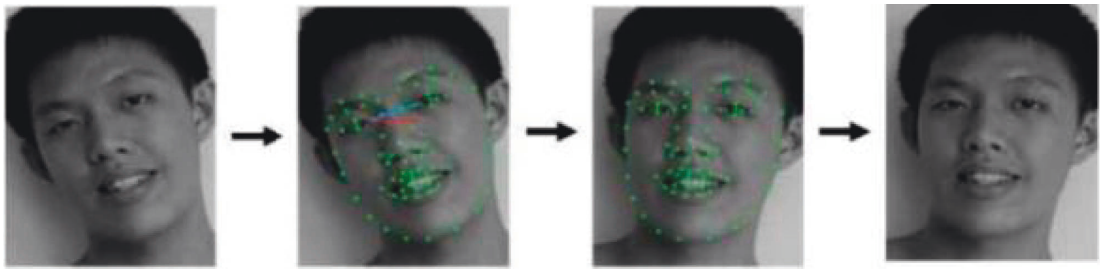

Figure 13: Face alignment process.

overlooking, face detect face detected. It also does not work under severe shielding.

3.3.4. Image Processing. Preprocessing of an image usually includes image grayscale processing, image data normalization processing, and transforming the dimensions of an image, and the like. Face correction is because to the photos of the machine whether crooked head, bow or head, position is not right, so need to cut the face first, for each feature little positioning, then according to the point positioning a coordinate, compared with the coordinates of the real face, the Angle of the difference, is the Angle of the head crooked, the reverse rotation image, the image is positive, as shown in Figure 13 below.

The gray scale of the image is to reduce the information of the image and reduce the amount of calculation of the computer, and the size transformation of the image is to minimize the impact of the image background on the picture.

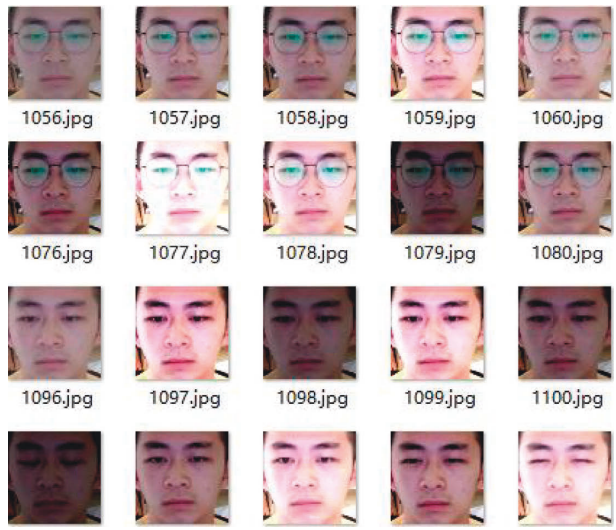

Figure 14: Face picture collection.

3.3.5. Eigenvector Contrast. The known face feature vectors are stored in the database, so for face recognition, the feature vectors must be compared. First, we need to send the face images in the video to the convolutional neural network, which generates the image feature vector through the convolution and pooling operations. The extracted face features will be used as the main basis for judgment, calculating the similarity of the feature vector of the picture in the video and the extracted feature vector of the face. The vectors have both size and direction, and if the angle between the two vectors is very small, then the two vectors are very close. By comparing the angles between vectors, the two targets are similar. The same face has smaller vector angles; different faces have larger vector angles.

4. Implementation of the Face Recognition System

4.1. Implementation of the Face Recognition System. Face detection is conducted through Dlib's frontal_face_detector feature extractor, and the face interception is detected, while adjusting the contrast and brightness of the picture. The contrast and brightness values are random, which can increase the diversity of the sample. Finally, the size of the picture is re-set to 6464 and saved in the database. In this way, I collected 10,000 pictures of my own camera monitoring faces, in which the brightness of the background, human expression and posture, facial shielding, glasses removal and other aspects were changed. The process of face image collection is shown in Figure 14.

After building one's own face library, you also need other people's faces to train the convolutional neural network. Other people's face photos can be extracted on the Internet through python, or some face databases in the face recognition field have been made, such as Yale Yale Faces, Cambridge ORL Faces, and FERET Faces of the US Department of Defense. In this design, choose to use the LFW face database, which was produced by the University of Massachusetts, and is an unconstrained face picture in a natural scene dataset collected from the Internet. The database stores images of more than 5,000 prominent faces and nearly 14,000 photos. It is well known in academia and often appears in a variety of deep learning papers related to face recognition. After downloading the LFW face library on the official website of the University of Massachusetts, do the same operation, intercept the face picture, change the size of the picture to 6464, and save it in the face database, as shown in Figure 15. So far, the face library needed for this design is established.

4.2. Training of Convolutional Neural Networks. The main training step of the convolutional neural network is to first read into the made face database, and transform the data and

Figure 15: LFW face database face extraction.

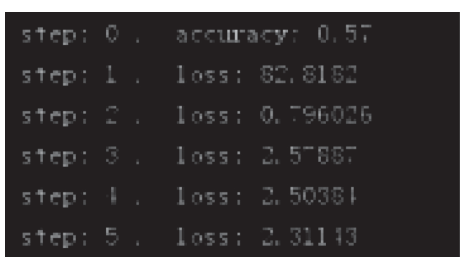

Figure 16: Training process 1 of neural networks.

labels of the face images into arrays. These images are then divided into test set and training set. In this design, the ratio between test set to training set is 20 : 1, and it is normalized. Finally, the face pictures were introduced into the convolutional neural network for training.

The training process is shown in Figures 16–18. It can be seen that as the value of the continuous training loss function becomes smaller and smaller, the accuracy of the model identification is also more and more high, which is the advantage of the convolutional neural network.

4.3. Implementation of Face Recognition. The main realization step of face recognition is to open the camera to obtain pictures and grayscale. Face detection is conducted through the frontal_face_detector feature extractor brought by Dlib, import the convolutional neural network that has been trained, and finally the face recognition function is realized through feature vector comparison.

After realizing the function of face recognition, in order to simply understand the recognition effect of the system, the system was conducted a simple test, the content of 100 face tests, the test results of 97 times successfully identified author's face and other people's faces, as shown in Figure 19.

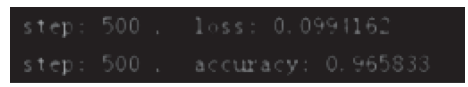

Figure 17: Training process 2 of neural networks.

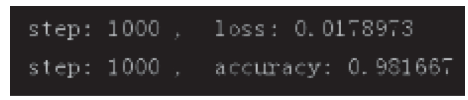

Figure 18: Training process 3 of the neural networks.

Figure 19: Successfully identifying.

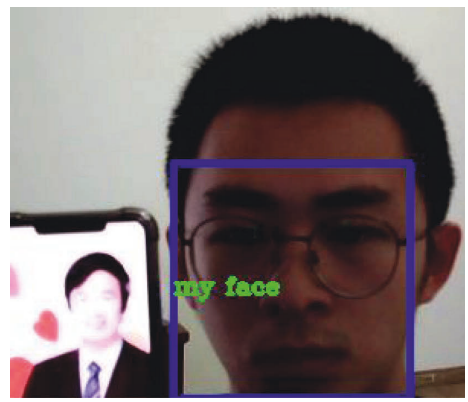

Figure 20: Failure to identify the human face in the mobile phone.

Sometimes, it failed to identify someone else's face on the phone, which could be affected by the camera resolution and the brightness of the phone's display, as shown in Figure 20.

There were 2 more times of identifying other people's face as author's, as shown in Figure 21.

4.4. Advantages and Disadvantages of the System. After many experiments, the system has the following advantages:

(i) The system can identify the face relatively accurately and stably, and can quickly conduct image preprocessing, and the face contour is surrounded by a frame.

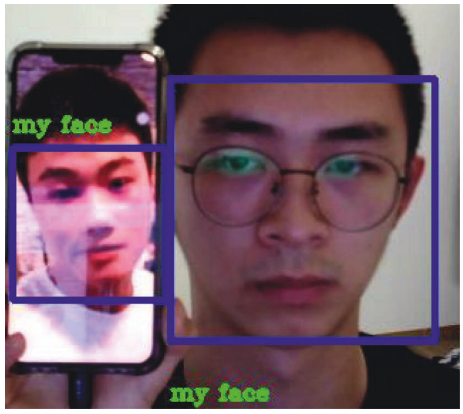

Figure 21: Identify someone else's face as mine.

(ii) The system's recognition and response speed is fast. The system uses the GPU for computational acceleration, which greatly accelerates the response speed of the system. Basically can meet the requirements of real-time identification.

(iii) The system is not sensitive to the light transformation, and the light conditions are constantly changing during the experiment, but the system can still be accurately identified, which is conducive to the application in real life.

(iv) The recognition rate of the system is high. In addition to a few identification errors, the system recognizes most of the time to meet the design requirements. The system has good posture, expression and without cover.

The system mainly has the following shortcomings:

(i) To achieve a good recognition effect requires a lot of face picture training. If fewer pictures participate in the training, the recognition effect will be relatively poor.

(ii) High requirements for computer hardware. The training of convolutional network requires graphics cards with computing power above 3.0, and high CPU, memory and graphics card video memory occupancy.

(iii) The functions of the system can be further improved, such as the number of faces in the database can be increased, and the logging function can be increased to save the data of people in and out to view.

(iv) The functions of the system can be further improved, such as the number of faces in the database can be increased, and the logging function can be increased to save the data of people in and out to view.

5. Conclusion

Face recognition is an identification technology through human facial information. Convolutional neural network has been active in the field of AI deep learning in recent years. This design realizes a face recognition system based on convolutional neural network. And the development process of biometric recognition, face recognition technology was investigated and made a brief introduction, and the advantages of face recognition technology were summarized and summarized. The basic theoretical knowledge loss function of convolution neural network, gradient descent algorithm and error backpropagation algorithm are also summarized. A convolutional neural network model is designed, and using its excellent feature extraction ability, combined with monitoring screen collection and face detection modules to design a convolutional neural network-based face recognition system, with good recognition effect.

Although the face recognition system completed in this paper has a good recognition effect, there is still a big gap with the best recognition ability at present, and we still need to continuously improve the recognition ability of the system in the future work. In addition, the system functions are too few, but also can add many functions such as diary recording, face tracking function.

Data Availability

The dataset can be accessed upon request.

Conflicts of Interest

The authors declare that they have no conflicts of interest.

Acknowledgments

This study was supported by the Young and Middle-Aged Teachers Education Research Project of Fujian Province (No. JAT210737).

References

[1] X. Zhao, "Summary of the development of biometric identification technology," *Criminal Technology*, vol. 06, pp. 46–50, 2011.

[2] M. Selight, *Research on Several Key Issues in Face recognition*, Institute of Computer Technology,Chinese Academy of Sciences, Beijing, China, 2004.

[3] Y. Lang, "Face Recognition Based on Convolutional Neural network," Master's Thesis, Southeast University, Nanjing, China, 2015.

[4] L. Gen, *Face Recognition Based on Local Features and Evolutionary algorithms*, PhD Dissertation, Jilin University, Jilin, China, 2014.

[5] A. J. Goldstein, L. D. Harmon, and A. B. Lesk, "Identification of human faces," *Proceedings of the IEEE*, vol. 59, no. 5, pp. 748–760, 1971.

[6] T. Kanade, "Picture Processing System by Computer Complex and Recognition of Human faces," *Computer Graphics and Image Processing*, vol. 2, 1974.

[7] X. Wang, "Automatic Face Recognition Algorithm Research Based on Statistical learning," doctoral Dissertation, Hefei: University of Science and Technology of China, Hefei, China, 2007.

[8] Vanin, "Research and Implementation of Face Recognition Based on Convolutional Neural Network," Master's Thesis, University of ESTC, Chengdu, China, 2013.

[9] T. Wang, *Python Face Recognition from Introductory to Engineering practice*, China National Machinery Industry Press, Beijing, China, 2019.
[10] Y. Zhang and G. Huang, *AI Tutorial*, Higher Education Press, Beijing, China, 2008.
[11] X. Qiu, *Neural Networks and Deep learning*, China National Machinery Industry Press, Beijing, China, 2020.
[12] T. Rashid, *Python Neural Network Programming*, People's Post and Telecommunications Publishing House, Beijing, China, 2018.
[13] D. Tang, *Research on Image Characteristic Extraction and Matching Technology in Face Recognition*, PhD Dissertation, University of Science and Technology of China, Hefei, China, 2007.
[14] S. Xu, "The Application of the Convolutional Neural Network," Master's Dissertation, Nanjing Forestry University, Nanjing, China, 2013.
[15] Y. Wang, X. Peng, W. Huang, and M. Wang, "A convolutional neural network for nonrigid structure from motion," *International Journal of Data Mining and Bioinformatics*, vol. 2022, Article ID 3582037, 8 pages, 2022.
[16] S. Huang, J. Luo, K. Pu, and M. Wu, "Diagnosis System of Microscopic Hyperspectral Image of Hepatobiliary Tumors Based on Convolutional Neural Network," *Computational Intelligence and Neuroscience*, vol. 2022, Article ID 3794844, 13 pages, 2022.
[17] L. Li, B. Lei, and C. Mao, "Digital twin in smart manufacturing," *Journal of Industrial Information Integration*, vol. 26, no. 9, Article ID 100289, 2022.
[18] L. Li, T. Qu, Y. Liu et al., "Sustainability assessment of intelligent manufacturing supported by digital twin," *IEEE Access*, vol. 8, Article ID 174988, 2020.
[19] T. Tian and F. Nan, "A Multitask Convolutional Neural Network for Artwork Appreciation," *Mobile Information Systems*, vol. 2022, Article ID 8804711, 8 pages, 2022.
[20] Y. Liu, "Innovation of teaching method of digital media art based on convolutional neural network," *Advances in Multimedia*, vol. 2022, Article ID 6288890, 11 pages, 2022.
[21] B. Cao, C. Li, Y. Song, and X. Fan, "Network Intrusion Detection Technology Based on Convolutional Neural Network and BiGRU," *Computational Intelligence and Neuroscience*, vol. 2022, Article ID 1942847, 20 pages, 2022.
[22] L. Li and C. Mao, "Big data supported PSS evaluation decision in service-oriented manufacturing," *IEEE Access*, vol. 8, pp. 154663–154670, 2020.
[23] L. Li, C. Mao, H. Sun, Y. Yuan, and B. Lei, "Digital twin driven green performance evaluation methodology of intelligent manufacturing: hybrid model based on fuzzy rough-sets AHP, multistage weight synthesis, and PROMETHEE II," *Complexity*, vol. 2020, no. 6, 24 pages, Article ID 3853925, 2020.
[24] J. Yao and Y. Chen, "A motion capture data-driven automatic labanotation generation model using the convolutional neural network algorithm," *Wireless Communications and Mobile Computing*, vol. 2022, Article ID 2618940, 9 pages, 2022.
[25] T. Wang, H. Xu, Y. Hai, Y. Cui, and Z. Chen, "An improved crop disease identification method based on lightweight convolutional neural network," *Journal of Electrical and Computer Engineering*, vol. 2022, pp. 1–16, Article ID 6342357, 2022.
[26] C. Liu, S. Sanober, A. S. Zamani, L. R. Parvathy, R. Neware, and A. W. Rahmani, "Defect Prediction Technology in Software Engineering Based on Convolutional Neural Network," *Security and Communication Networks*, vol. 2022, Article ID 5058461, 8 pages, 2022.
[27] S. He, "Research on Tourism Route Recommendation Strategy Based on Convolutional Neural Network and Collaborative Filtering Algorithm," *Security and Communication Networks*, vol. 2022, Article ID 4659567, 9 pages, 2022.
[28] B. Gao, "Application of Convolutional Neural Network in Emotion Recognition of Ideological and Political Teachers in Colleges and Universities," *Scientific Programming*, vol. 2022, Article ID 4667677, 8 pages, 2022.

Hindawi
Scientific Programming
Volume 2023, Article ID 9857605, 1 page
https://doi.org/10.1155/2023/9857605

Retraction

Retracted: Design and Implementation of Music Teaching System Based on J2EE

Scientific Programming

Received 18 July 2023; Accepted 18 July 2023; Published 19 July 2023

This article has been retracted by Hindawi following an investigation undertaken by the publisher [1]. This investigation has uncovered evidence of one or more of the following indicators of systematic manipulation of the publication process:

(1) Discrepancies in scope
(2) Discrepancies in the description of the research reported
(3) Discrepancies between the availability of data and the research described
(4) Inappropriate citations
(5) Incoherent, meaningless and/or irrelevant content included in the article
(6) Peer-review manipulation

The presence of these indicators undermines our confidence in the integrity of the article's content and we cannot, therefore, vouch for its reliability. Please note that this notice is intended solely to alert readers that the content of this article is unreliable. We have not investigated whether authors were aware of or involved in the systematic manipulation of the publication process.

Wiley and Hindawi regrets that the usual quality checks did not identify these issues before publication and have since put additional measures in place to safeguard research integrity.

We wish to credit our own Research Integrity and Research Publishing teams and anonymous and named external researchers and research integrity experts for contributing to this investigation.

The corresponding author, as the representative of all authors, has been given the opportunity to register their agreement or disagreement to this retraction. We have kept a record of any response received.

References

[1] Y. Zhu and S. Liang, "Design and Implementation of Music Teaching System Based on J2EE," *Scientific Programming*, vol. 2022, Article ID 2179882, 10 pages, 2022.

Hindawi
Scientific Programming
Volume 2022, Article ID 2179882, 10 pages
https://doi.org/10.1155/2022/2179882

Research Article

Design and Implementation of Music Teaching System Based on J2EE

Yuanyuan Zhu[1] **and Shuo Liang**[2]

[1]*Academy of Music, Jiangsu Normal University, Xuzhou, Jiangsu 221116, China*
[2]*Beijing Kuanteng Heyi Technology Co, Ltd, Beijing 100020, China*

Correspondence should be addressed to Yuanyuan Zhu; 6020130032@jsnu.edu.cn

Received 10 July 2022; Revised 15 August 2022; Accepted 20 August 2022; Published 22 September 2022

Academic Editor: Lianhui Li

In order to improve the quality and management efficiency of music education, research on the music education system based on J2EE is carried out. The music education system adopts J2EE technology, UML modeling technology, SQL Server 2012 database, Web programming technology, MVC mode, etc., which can effectively guarantee the operation performance and security performance of the system in the later application. By analyzing the background, current situation, and demand for the music education system, the design and implementation of the music education system based on J2EE are proposed, the overall realization of system management functions, music teaching management functions, music course management functions, and other functions.

1. Introduction

With the popularization of concept-based teaching methods such as quality education and comprehensive education in schools, my country has invested more energy in art education. In particular, cultivating evangelists in art education, the Art Department of Yun Normal University has entered a new stage in its music teaching management under this background. Through a series of means to make teaching more scientific and standardized. The rapid economic and social development has changed people's long-standing production and living patterns to a considerable extent. In terms of education, the increasingly accelerated social rhythm makes the traditional face-to-face centralized teaching mode gradually unable to meet people's increasing learning needs [1]. In recent years, with the rapid development of computer and multimedia technology, and information-based online teaching method based on the Internet has been gradually accepted and recognized by people. At present, the popularity of the Internet in my country is increasing day by day, and the online teaching mode has gradually become a normalization that relies on and complements the traditional offline teaching mode due to its advantages of fast dissemination, wide-coverage, and less impact on time and space. Educational model [2]: at the end of 2019, the novel coronavirus pneumonia (COVID-19) outbreak broke out all over the world, and people's social environment was greatly affected. Due to the epidemic, the teaching of domestic primary and secondary schools and colleges and universities was also unable to provide normal classroom teaching activities as scheduled, making the online teaching-based remote teaching mode the main teaching method of various educational institutions during the epidemic. Although the epidemic situation in my country has basically been effectively controlled, the development of the epidemic situation is still relatively severe on a global scale. Therefore, effectively reducing social activities through online teaching is still one of the main methods to effectively prevent and control the epidemic. In this context, people's attention to music teaching system research has gradually increased [3].

The realization process of the music education system is very complicated, and it is necessary to study the practical activities of music education based on theoretical

knowledge. However, many current ITS systems do not have this basic knowledge, so the educational process achieved is too simple [4]. This paper starts from the development status of music education at home and abroad and develops a music education system based on J2EE according to the basic requirements and characteristics of music education. This paper adopts J2EE development technology, overall use of UML modeling, SQL Server 2012, JAVA language, MVC mode, and Web programming technology from the actual needs, to provide a basic guarantee for music education. The specific content of the music education system based on J2EE is mainly reflected in the following aspects: design and implementation of system management functions, design, and implementation of music resource management functions, design and implementation of music course management functions, etc. [5].

With the increase of music teaching needs and users, the demand for music teaching curriculum resource data and network bandwidth resources has also shown explosive growth. The service provision capability of traditional music teaching systems has been unable to meet the increasing demand for music curriculum data dissemination. Therefore, it is very necessary to use the more advanced cloud computing distributed network technology and network load balancing algorithm to optimize and upgrade the service provision capability of the music teaching system [6].

This paper analyzes the existing problems and status quo of the music teaching model of the Department of Art of Yunshi University and uses the object-oriented analysis and design ideas in combination with the actual situation, combined with J2EE computer technology, to realize the informatization, scientific, and standardization of music teaching. This system uses the open-source SSH (Spring Structs Hibernate) as the basic framework of the system and uses SQL Server with excellent security and operability as the database [7]. Using the MVC model to design the Struts architecture ensures that the system has good maintainability and at the same time enhanced data. The importance of music teachers in the traditional teaching mode is relatively high, and most of them teach in the form of face-to-face teaching. The traditional teaching mode has a single method and lacks of change in content, which leads to poor information transmission in a short period of time [8]. At present, the desire of students who study music in schools is relatively high, and the "narrow" information input forms a great contrast with reality, which cannot meet the needs of students who study music. Through this complete system, it can be a good teaching environment. It is an improvement of the teaching system, which makes music teaching appear in multiple dimensions while reducing the teaching pressure on teachers. On the other hand, it can meet the needs of students for music learning. Processing power: realizes the separation of data and view, and technology makes the system into a system with strong scalability and maintainability. This paper mainly assists students in the initial construction of a new model of music teaching from the aspects of cultivating students' interest in learning, adjusting teaching goals, expanding teaching content, innovation, teaching evaluation, and improving teaching methods [9]. The teaching mode emphasizes the coordination of covering music, performance, and enjoying unified comprehensive teaching so that students can get a comprehensive and rich music aesthetic experience, and learning can create a new realm of their own personality, and gradually improve the quality and personalization of modern music. Comprehensive healthy development. This subject takes the informatization of the music teaching system as the research content and realizes the teaching system based on WEB, which can not only optimize knowledge but also apply the project-based collaborative teaching mode technology to the informatization of the music education system. This teaching system builds applications on the B/S structural framework development environment and multilayer system architecture to assist music teaching activities [10].

2. Introduction to Related Technologies

2.1. J2EE. J2EE includes the following three component types: one is the in-app program, which is mostly used for internal training computers; the second is Servlet and JSP components, which are often used in some Internet; the third is the EJB component, which completes its functions on the server-side. J2EE belongs to JAVA, and its programming method is similar to JAVA, but there are some substantial differences. J2EE components can be used in application programs, and at the same time, they can be consistent with the J2EE specification [11].

Since J2EE has a complete set of specifications, in general, J2EE can be regarded as a constraint of the JAVA2 platform on music education. In addition, J2EE has many advantages; for example, it can meet various requirements of the bottom layer of the system through containers, and the development speed of system personnel has been greatly improved. J2EE uses the middle-tier integration framework for program development, which reduces the cost of system development, and not only improves its performance but also ensures the security of system operation [12].

2.2. JAVA Language. At the end of the 20th century, in order to design a cross-platform and distributed software system, Sun Computer Systems researched and launched the JAVA language in the United States, which is an object-oriented design language. For software developers, learning JAVA is simpler to use, and can also perform exception handling and automatic collection of discards. The programming language has functions such as porting and interpretation, so it has been widely used after its launch [13].

After continuous development, JAVA has been continuously expanded on the basis of the original programming language and has become a mainstream technology in the computer software industry. Chip technology, Internet connection technology, and other fields [14]: based on the many advantages of JAVA, its application is also very wide, and its main application directions include game systems developed in large numbers today and mobile Internet-related systems. At the same time, it is also widely used in many colleges and universities, such as educational

administration, college teaching, and other management systems. At the same time, due to its various advantages, it is often used in the relevant information systems of government departments [15].

2.3. UML Modeling Technology

2.3.1. Introduction to UML. UML (Unified Modeling Language) is the best way to represent program visualization. It is commonly used in current program design. In short, using this UML pattern to design programs makes the program layering more obvious, and the later testing of software design. And the maintenance is simpler, for developers, it will greatly reduce their development and testing time [16].

In this mode, graphical structural use case diagrams, sequence diagrams, activity diagrams, class diagrams, and state diagrams are used. These diagrams can realize many functions, including the whole process of a subject from production to demise. The standard is separated, and the original complete program is divided on the basis of these three blocks, so as to facilitate the operation of the program [17].

The UML view is mainly used to display the results of program processing. The relevant programmers can analyze the program according to the display. When using the WEB for related operations, the MODEL needs to be converted into the HTML running mode first. In the operating environment of the system, its own visual graphics can display the program, UML is a program that helps to generate view-related content and interact efficiently with clients [18].

M in UML design mainly refers to the data model object. In the whole process, the control layer of the use case diagram transfers the relevant model objects that need to be processed to the view layer, and the related operations are displayed in the view layer. In the whole process, the data model is a designed complex of calculation rules, processing flow and analysis rules, through which data is processed and displayed. The control layer is the bridge linking the view and the model layer, matching the two to facilitate processing and operation, which also makes the data and logic interfaces between the various layers of the program more coupled under the UML design. The use of this technology makes the systematic testing of music education systems simple and convenient [19].

2.3.2. Advantages of UML and Its Application in This System. The most important function in UML, the realization of visualization technology, has always been one of the basic application frameworks on the Web, and its practical cases can be seen everywhere. Its basic core includes use case diagrams, sequence diagrams, and class diagrams. Key content: the first function is to realize the application demonstration function of system-related functions, the second function is to realize the business logic layer demonstration function, the third function is to realize the data access demonstration function, and the last main function of the domain model layer is to solve modeling problems. Each layer performs its own duties in its own field and has its own tasks. UML separates and isolates the entire interface operation function of the system as a whole, and reduces the degree of interaction and coupling, which is important for the subsequent maintenance and expansion work. It is of great help to the design scheme and technical development of the entire research and development process of Web applications [20].

2.4. MVC Pattern. The abbreviation of the three concepts of model, view, and controller is represented by MVC. Through these three parts, the software design part in the WEB development process is realized, the rapid development, upgrade and maintenance of the system is realized, and modularization is provided for designers selection, which greatly optimizes the efficiency of program development. The schematic diagram of the MVC mode function implementation is shown in Figure 1 [21].

2.5. SQL Server2012 Database Technology. SQL Server 2012 is based on the research and design of the previous version of SQL Server. It has been greatly improved on the previous version, and its cohesion, practicality, integration, and other properties have been further strengthened. Therefore, the software is more widely used in practical applications and can adapt to the daily data management needs of various software with increasing update frequency. Its practical application market is very large, but it is mainly used in the data information management system of large and medium-sized enterprises [22].

This version inherits the layered structure of its previous version. The first is the protocol layer. This layer is mainly used to operate and process-related data information, such as format changes, data-related operations, and structural responses of operations. Developers can directly operate this layer, and perform a series of required operations on the data through this layer. At the same time, developers can use this layer to change the format of data information and change its format to the desired pattern that can be recognized. The result of its modification is sent to the next layer, where the data is converted again as required. This time the data can be converted to the data information format that can be recognized and used by the user, so as to facilitate the user to match the required data and access to the data information, so it is called the access layer [23].

The characteristics and advantages of this system are summarized in the following four points: (1) broad applicability, (2) strong security, (3) high availability, and (4) scalability.

2.6. Web Programming Technology. The WEB programming technology adopted by the music education system is the current mainstream development technology system, including the development of the WEB terminal, the development of the mobile terminal, the development of the web interface and the development of database, and the development of the system realized from multiple perspectives. The development technology used for the system studied in

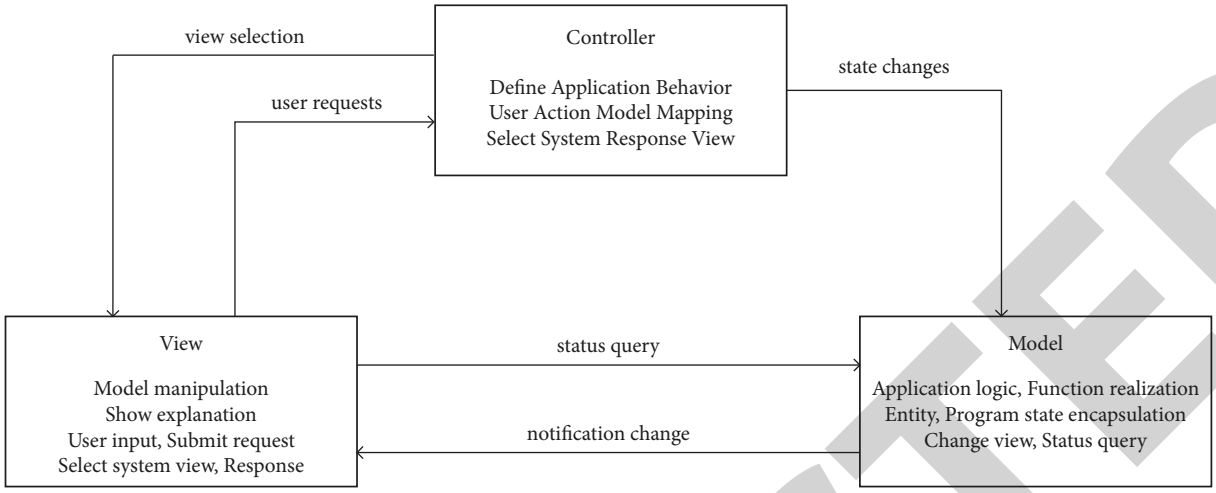

Figure 1: Schematic diagram of MVC mode function implementation.

this paper is implemented based on a three-tier architecture, including the design of the presentation layer, the business logic layer, and the data persistence layer, and is developed around the object instance of the music education system [24].

3. Demand Analysis of the Music Teaching System

3.1. Analysis of Functional Requirements

3.1.1. Information Release Module. The information release management part mainly includes two functions, one is to release news information, and the other is to release announcement information. The news information is for all users of the music teaching auxiliary system, and the management content includes news editing, news release, and news maintenance; the announcement is mainly for registered users, that is, teachers, students, or administrators, similar to news management.

3.1.2. Document Management Module. The music teaching auxiliary management system includes part of the official document management function, which manages the official document processing in the school teaching and office process. Official document management mainly completes the entire process from drafting, and approval to document issuance in learning. With the help of network technology and computer technology, the school's office work can be paperless, improve work efficiency, and supervise the circulation process of official documents.

3.1.3. Teaching Resource Management Module. The teaching resource management module mainly realizes the management of self-study resources, including music audio and video, homework exercises, music knowledge popularization, and other parts.

3.1.4. Auxiliary Teaching Management Module. The auxiliary teaching management module is mainly responsible for the system administrator, which realizes the management of courses, management of students' online examinations and exercises, interactive management of Q&A, discussion, and performance analysis.

3.1.5. System Management Module. The system management in the music teaching assistant is mainly used to serve the related activities of students and teachers, provide support for the normal operation of the system, and coordinate the collaboration and communication of different modules. This part of the management can be divided into music-assisted teaching, log management, and user management. The specific contents are as follows:

(1) Music-assisted teaching: auxiliary teaching management is mainly through the statistics and analysis of existing data; school leaders or teachers conduct auxiliary decision-making management in order to improve teaching quality and management level.

(2) Log management: the log management part is divided into two parts: operation log and system log. The operation log completes the management of all functional operation records; the system log completes the record management of the system running process.

(3) User management: manages user identities such as teachers, students, leaders, and managers, as well as user basic information.

3.2. Model Analysis

3.2.1. Object Model Analysis. The needs of music teaching auxiliary management are mainly reflected through the use case model, which can build a bridge between ordinary customers and system implementers, allowing users to describe their own needs and the functions to be achieved by the required system in the most detailed way. There is a

particularly important relationship between the refinement of the use case diagram and the modularity of the use case diagram. The modeling of this system is to use UML to visualize the system functions and specific feasible methods. To achieve the goals of all parties, the first is customer needs, which must be easy for users to understand, and the second is to allow developers to fully understand so that development work can begin [25].

The establishment of use cases must focus on system participants. From this point of view, the premise of use case determination should be to conduct a series of analyses on the actual participants in the system and their related information and then combine the actions and behaviors of all participants. Only in this way can the functions required by customers be realized, and then specific and available use case analysis can be obtained. The language used for unified modeling can describe the use case from several aspects, and its participants and various subtle interrelationships between them. Solving these problems can specifically determine the construction of the use case.

We do the design work required for the use case from the top down, and the principle is progressively deeper. We will first establish the most basic use cases according to the specific needs of the project at the beginning, and then refine the use cases step by step on this basis to achieve deeper customer needs and target analysis. Figure 2 shows the school leadership using a case diagram.

School leaders mainly carry out operations such as official document handling, news and announcement browsing, and auxiliary decision-making management (music teaching).

Music teachers mainly carry out operations such as music examination question bank management, music courseware management, student field communication, and homework and examination management. The example of music teachers is shown in Figure 3.

Students mainly conduct music-related question consultation, online learning, and online testing, among which question consultation includes music knowledge, exam-related, and amateur discussions. The example of student use is shown in Figure 4.

System administrators mainly perform user management (including teacher management, student management, and authority management, leaders belong to teacher management and assign higher-level authority), log management, system settings and information release (including news management and announcement management), and other operations.

3.2.2. Data Model Analysis. The analysis of the data model is mainly carried out by means of the data flow chart, which can systematically and comprehensively describe the data logic of the music teaching auxiliary management system. In the process of information storage, processing, and flow reflection, the data flow diagram is mainly realized by means of centralized and general symbols. The characteristics of the data flow graph are mainly composed of the following two aspects:

(1) Abstraction: abstract data information into specific information storage, processing and flow, and reduce unnecessary object processes

(2) Generality: express all requirements as a whole, and associate all related information or business processing

A data flow diagram consists of the following four basic elements, namely, external entities, data flow, processing (function), and data storage. Each module uses a data flow diagram to represent the source of data and the relationship between data. The top-level data flow of the system is shown in Figure 5.

3.3. Analysis of Nonfunctional Requirements

3.3.1. Performance Requirements

(1) Performance. The safe and reliable operation time of the music teaching auxiliary platform is not less than ten years; the number of simultaneous online teachers and students is not less than 400; the response time of business processing shall not exceed five seconds; in order to adapt to the continuous increase of functions, automatic expansion support is required; all data transmissions must be stable and secure;

(2) Security. Security requirements mainly include data transmission encryption, data backup, and virus prevention.

Data transmission encryption: different levels of users set different access rights, and MD5 encryption is performed for user authentication; Data backup: data backup is performed regularly to ensure safe operation; Virus prevention: because it is in the form of a network, virus prevention and awareness enhancement are required.

(3) Scalability. In the process of music teaching, various teaching methods, teaching modes, and functions are changing with each passing day, and need to be maintained and upgraded from time to time. Therefore, the auxiliary teaching system must be scalable and configurable.

The auxiliary management of music teaching is realized by modularization, which improves the reusability and maintainability of the code by reducing the association between different modules.

The upgrade of the system must not affect the normal operation and only needs to be upgraded online on the server-side.

3.3.2. Design Goals. The design goals of the music teaching assistant management system based on J2EE mainly include the following aspects:

Practicality: simultaneously design information functions based on traditional operation methods to provide a concise and clear operation interface for teachers and students when teaching or learning music; Fault tolerance: when data errors are caused by a program running or

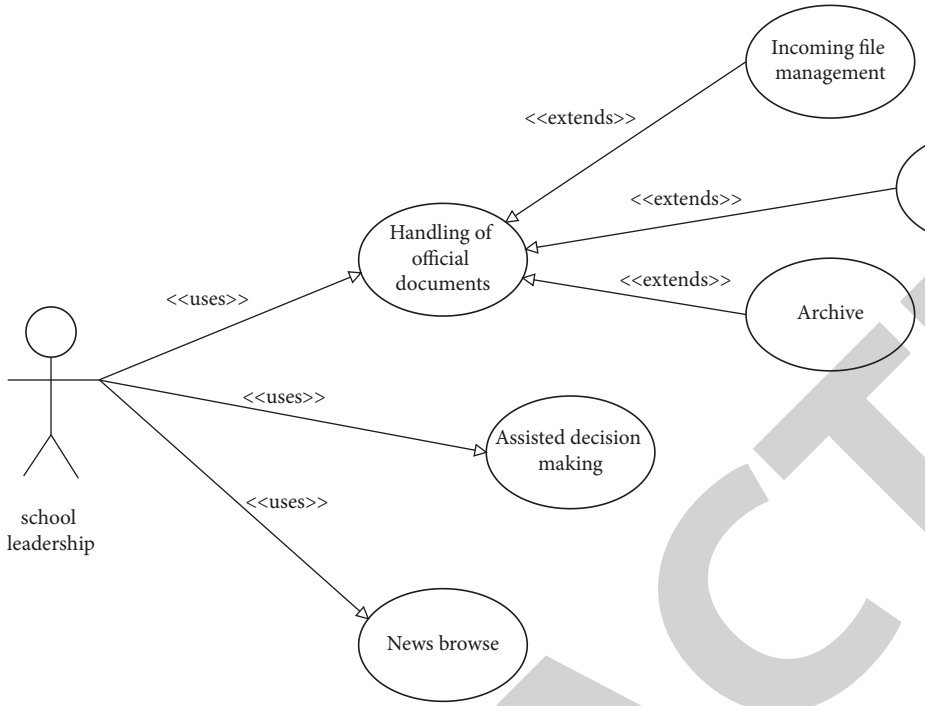

Figure 2: School leadership use case diagram.

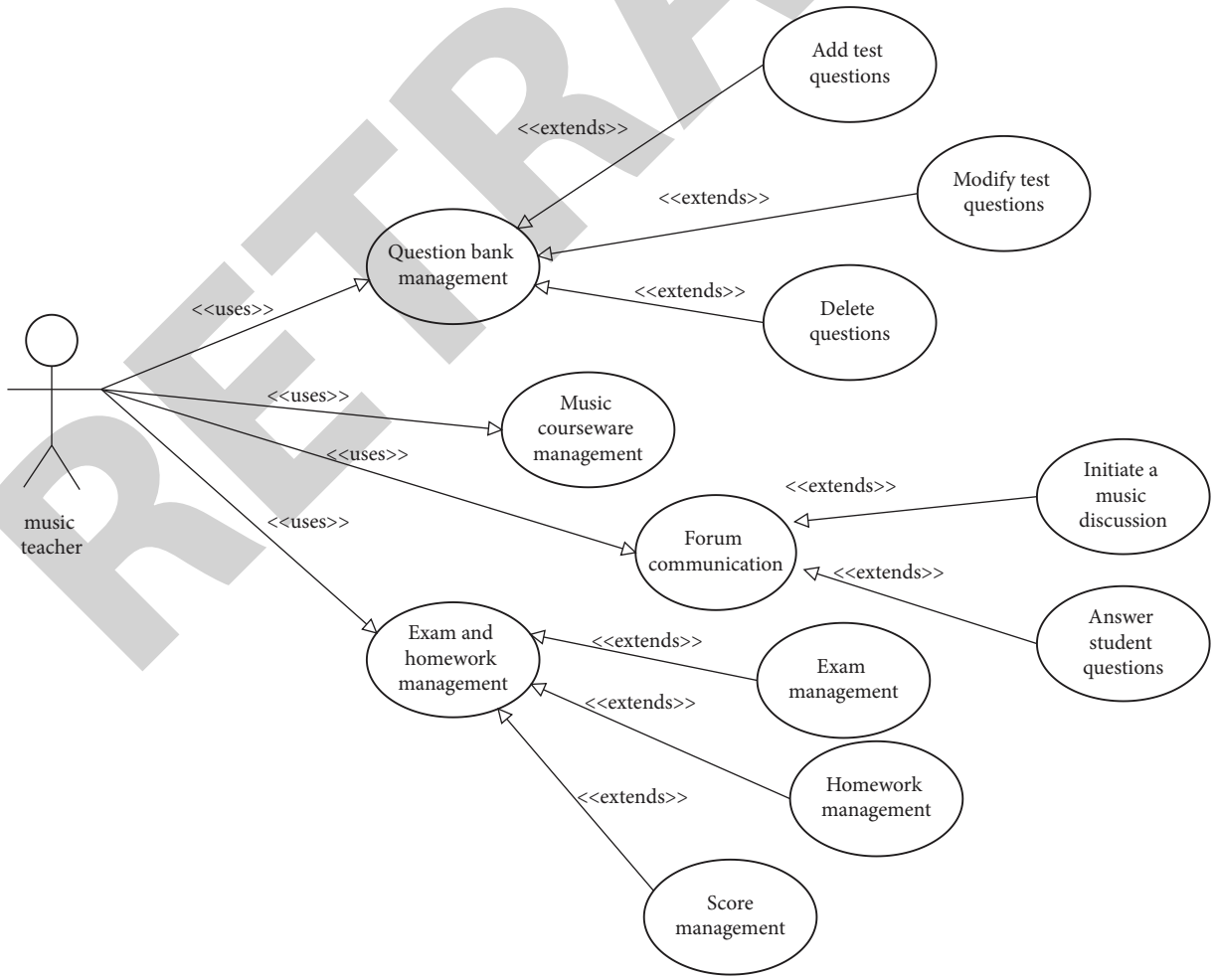

Figure 3: Music teacher use case diagram.

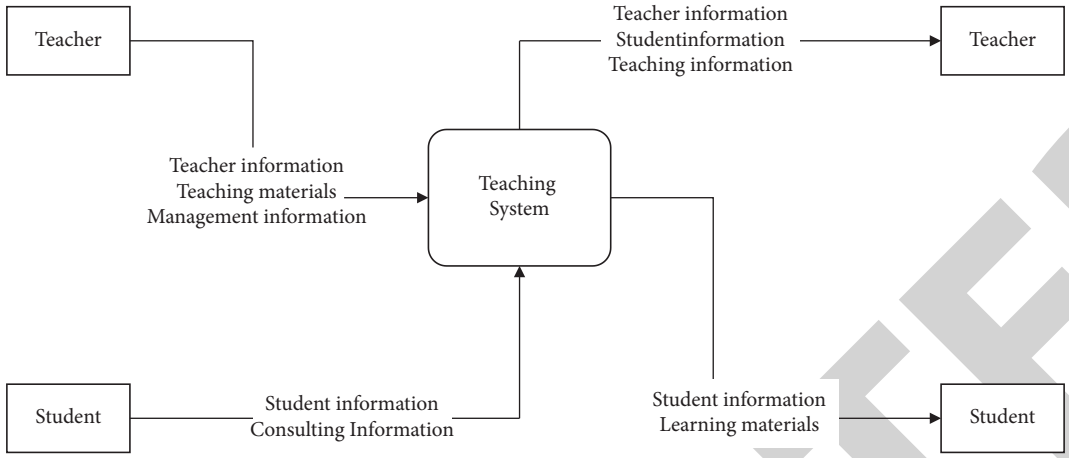

Figure 4: System top-level data flow diagram.

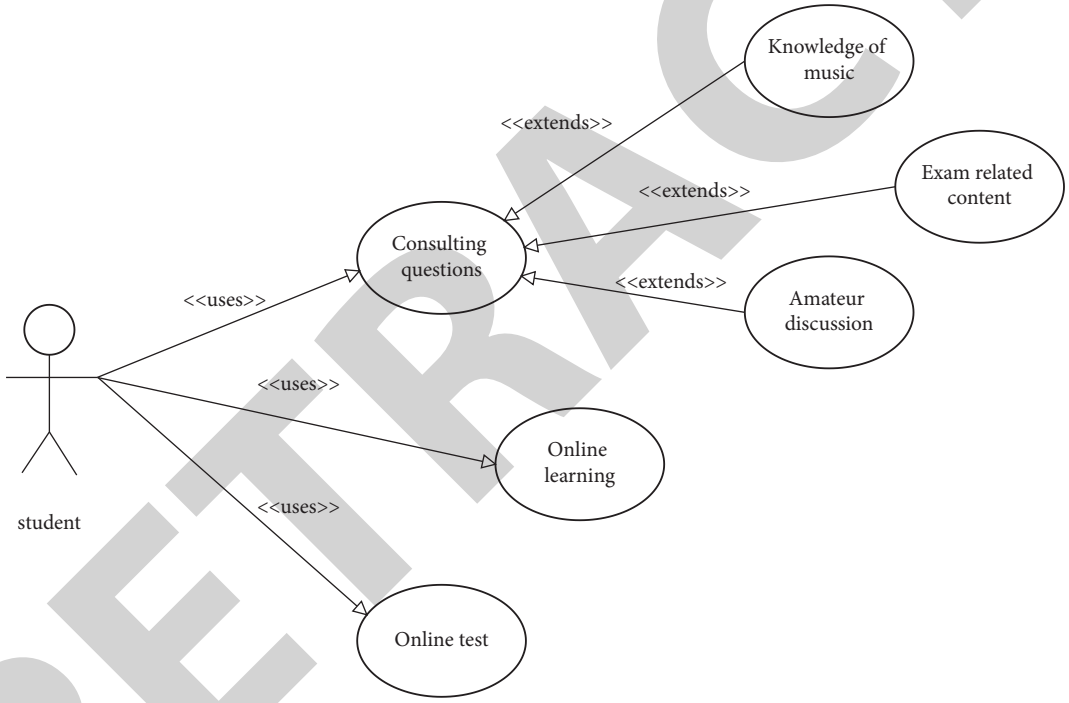

Figure 5: Student use case diagram.

misoperation, the system must have good fault tolerance capabilities, such as error prompts and automatic rollbacks, and both security and reliability must be guaranteed during the fault tolerance process.

Versatility: the system cannot be limited to a specific browser access form to meet the needs of learners and operators' operating habits;

Openness: the system adopts a standardized processing form and provides a good extension interface in the research of music teaching curriculum setting to ensure that the system can be used in multiple platforms and environments.

Timeliness: as long as there is a network, the learning and management of music-related courses and knowledge can be carried out at any time.

Stability: we use a data management system to achieve data management, use J2EE technology and MVC design pattern to achieve system development, and ensure the stability of system operation.

The music teaching assistant management platform has the characteristics of real-time communication, functional versatility, and object openness.

4. Design of the Music Teaching System

4.1. Overall Design. The overall design of the system includes functional structure design and architecture design, which can generally be simplified as a modular design. When carrying out modular design, not only should the entire system be divided into components, but also the

communication between modules, module continuity, module protection, module solvability, and module combination should be designed. If you want to improve the continuity principle, you need to maintain the black box characteristics between modules, which are transparent to other modules. If the protection of the module needs to be improved, it is necessary to protect the variables inside the module to prevent the misuse of other modules, and special consideration should be given to the exception handling of the module.

When carrying out the modular design of the system, it is necessary to meet the loose coupling between modules and the high cohesion characteristics within the modules. Modules must be able to function independently to complete the design, but the size of the modules needs to be controlled. The nature of modules can be summarized as interchangeability, pluggability, and boundedness, which mainly include three aspects: (1) When the internal requirements of a module change, the changes do not affect the normal operation of other modules; (2) When a module needs to be deleted, only the functions handled by this module are affected; (3) If a new module implements the same function and has the same operation interface, it will not affect the operation of the entire system after replacement.

4.1.1. Functional Structure Design. The music-assisted teaching management system is mainly composed of modules such as information release, official document management, teaching resource management, auxiliary teaching management, and system management. The information release module is further divided into school news, notice announcements, and BBS. Document management, document receipt management, and filing management; teaching resource management includes courseware management such as music videos, homework management, and music knowledge management; auxiliary teaching management is divided into course management, online examinations, Q&A discussions, and performance analysis; system management is divided into teachers student management, system settings management, log management, and auxiliary decision-making management. The functional structure of the music-assisted teaching management system is shown in Figure 6.

4.1.2. Architecture Design. The design of the music teaching assistant management system adopts a three-tier system structure. The architecture of the system is mainly divided into three layers: Web Server layer (display layer), Application Server layer (control layer), and Database Server (data access layer). The display layer is mainly composed of the Web UI Layer and Web Service Layer, using JSP and other technologies to achieve interaction with the client; the control layer mainly uses the core frameworks such as Spring to complete the business logic processing of the auxiliary teaching system, calls the data access layer to process the business request sent by the client, and displays the processing result to the user. The specific form of interaction is displayed to the client for users to view and browse; the data access layer mainly realizes the interaction between the business logic layer and the database, preventing business requests from directly accessing the database, causing data inconsistency, and ensuring data security and integrity.

4.2. Database Design. In the process of information service, information management, and resource development, system users and design developers have concluded an important experience that database technology is the most effective way to manage data. With the advancement of network technology and computer technology, data management through databases has become an important consensus. In order to complete the sharing, integrity, and consistency of system data, both large-scale management systems and small-scale transaction processing are using database technology to complete data management. At present, the important criteria for measuring the degree of a country's informatization construction are the frequency of database use, the amount of database information, and the scale of the database.

4.2.1. Database Design Principles. The database design of the music-assisted teaching management platform mainly serves the business knowledge base of music-assisted teaching management. Through the management of the database, the processing of knowledge data and business data is optimized. When designing a database, the following aspects are considered important criteria:

(1) Verification is based on database design specifications, and data structure design is carried out in a standardized form to ensure the consistency and normal operation of data operations.

(2) Normative naming: the naming specification is helpful for unified management and upgrades maintenance in the later stage. Therefore, when designing databases and tables, the naming must strictly follow the normative standards and annotate all column information.

(3) Data redundancy and the standardization of data paradigms will affect the retrieval speed of later data. Therefore, when designing data tables, it is necessary to master various degrees in order to achieve the highest value of retrieval and reduce system response time.

(4) Security: strict identity authentication management is implemented, and users with different permissions have different degrees of access to data and operations to improve data security.

(5) Concurrency control: through the use of triggers and stored procedures, the simultaneous operation of the table is strictly controlled to ensure the control of simultaneous modification access, and reduce data inconsistency, and the query can be exempted from this control. Through the above analysis, it can be seen that when designing the database of the music teaching assistant management platform, in order to

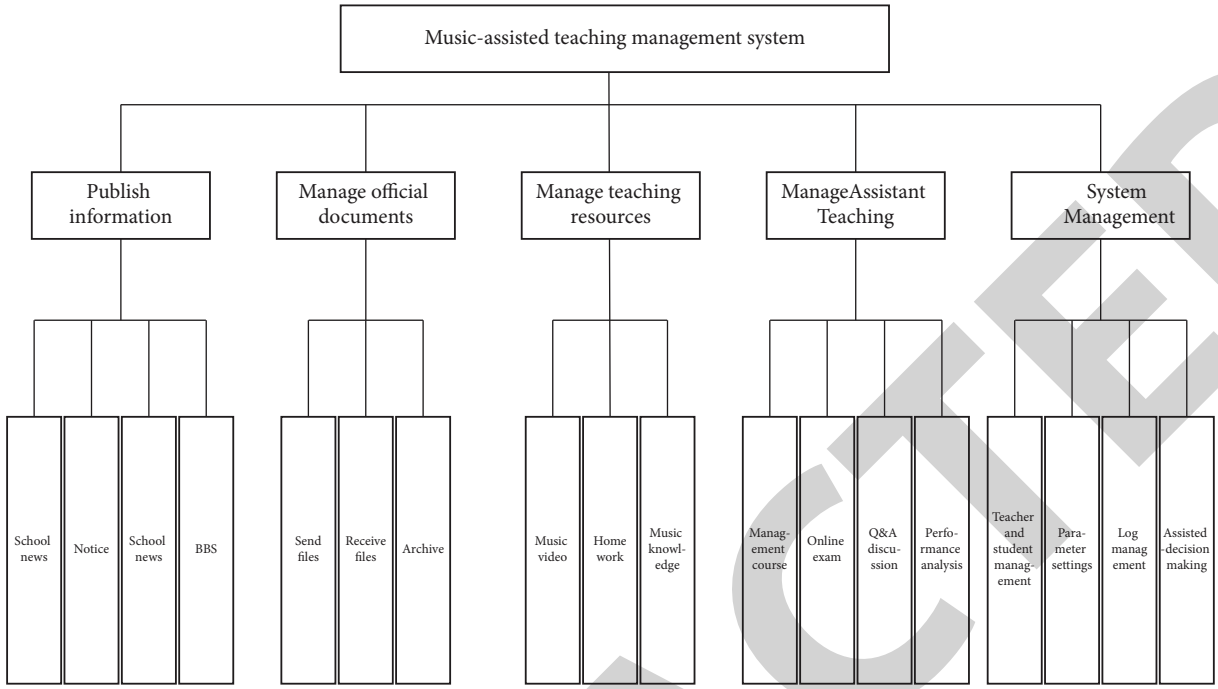

Figure 6: System function structure diagram.

realize the BC paradigm mode, the third paradigm should be used as the main basis.

4.2.2. Conceptual Structure Design. The conceptual schema design of the database is to abstract the existing data. Abstraction refers to the man-made processing of concepts, affairs, and relationships between people, extracting common features that are needed, and ignoring unnecessary parts. The extracted features are described in detail and finally form a certain model structure. This system adopts SQL Server2005 as the database development tool to realize the design and realization of a relational database.

5. Summary

This dissertation mainly studies and expounds on the design and development of the music teaching assistant system. First of all, this thesis analyzes the development significance, application, and development feasibility of the interactive multimedia network teaching system from the background and feasibility analysis. In the requirement analysis stage, the analysis of the system needs and the compilation of related manuals is to list all the requirements of the user for the system to be designed, to establish the model of the music teaching assistant system to be developed, and the design and implementation of its functions to facilitate the development of this system. Let our software design team have a very thorough knowledge of the functions to be completed by the entire software so that we can know what to do when developing and designing, which is beneficial to software development and development progress control and quality control. In addition, it also provides a basis for further upgrades in the future, so that the corresponding deficiencies can be quickly located during the upgrade, and the development cycle of software upgrades can be improved. The development of this system has reached a good level in function and technology, but it still has its own defects. First of all, it is not perfect in terms of module functions, and secondly, some functions are not considered enough, but I believe that through the continuous improvement of our team, this system will eventually be put into practical use.

Data Availability

The dataset can be accessed upon request.

Conflicts of Interest

The authors declare that there are no conflicts of interest.

Acknowledgments

The authors thank Xuzhou Science and Technology Key Project, "The Remote Intelligent Interactive Music Teaching System" (no. KC19246).

References

[1] H. Yan, "Design of online music education system based on artificial intelligence and multiuser detection," *Algorithm[J]. Computational Intelligence and Neuroscience*, vol. 2022, Article ID 9083436, 11 pages, 2022.

[2] M. Liu, "Research on the application value of orff music education system in college music education based on computer new media technology[J]," *Journal of Physics: Conference Series*, vol. 2021, no. 3, 1992.

Hindawi
Scientific Programming
Volume 2022, Article ID 9943965, 8 pages
https://doi.org/10.1155/2022/9943965

Research Article

Personalized Course Recommendation Method Based on Learner Interest Mining in Educational Big Data Environment

Ruiping Zhang

Department of Preschool Education, Anyang Preschool Education College, Anyang, Henan 456150, China

Correspondence should be addressed to Ruiping Zhang; zhangruiping@ayyz.edu.cn

Received 23 August 2022; Revised 1 September 2022; Accepted 12 September 2022; Published 21 September 2022

Academic Editor: Lianhui Li

Aiming at the problems of low accuracy and large limitations of the current personalized course recommendation method in the educational big data environment, a personalized course recommendation method based on learner interest mining in the educational big data environment is proposed. First, a corresponding online course recommendation model framework is proposed by adopting GRU, which can effectively solve the problems of gradient disappearance and gradient explosion in the process of training the RNN neural network. Then, by introducing an auto-regressive language model, XLNet (Generalized Autoregressive Pretraining for Language Understanding), the information missing problem under the Mask mechanism in the BERT model is effectively optimized, and bidirectional prediction is achieved. Finally, by introducing a temporal attention mechanism into the model, enough attention is assigned to highlight local important information on key information, which improves the quality of hidden layer feature extraction, and a high-accuracy personalized course recommendation based on learner interest mining is realized. The proposed algorithm is compared with the other three collaborative filtering algorithms and the RNN algorithm through simulation experiments. The results show that the precision, recall, and $F1$-measure of the proposed algorithm in the personalized course recommendation results for different types of courses under the condition of the same database are all optimal. The largest values were 92.1%, 89.3%, and 90.7%, respectively. The overall performance is better than other comparison algorithms. This method can improve the accuracy and optimization limitations of personalized courses and can fully tap the interests of learners. It is of great significance for learners to choose personalized courses in the current educational big data environment.

1. Introduction

Since entering the twenty-first century, people's production and lives are changing with each passing day under the influence of the Internet. In terms of education, learners' learning methods have also undergone great changes. The "education informatization" and "Internet + education" are just bred under the new trend of the Internet, and are also the only way for future educational development [1–3]. Education under the Internet environment helps to promote the development of personalized education and promotes the reform of the education system and education mode. The personalized education concept that varies from person-to-person breaks the traditional education and teaching methods. At the same time, various educational institutions also take this opportunity to build online learning platforms, constantly enrich high-quality educational resources, and provide students with more convenient learning experiences and high-quality online learning courses. Supporting education modernization through education informatization, unremittingly helping the innovation and development of education, forming a new education service system, and creating a new mode of integrated development of online and offline education [4–6].

The widespread sharing of a large number of high-quality curriculum resources under the internet environment provides convenience for learners. Learners can arrange learning according to their own time to meet their personalized learning needs [7, 8]. However, online learning has changed people's learning styles, which also shows some disadvantages. There are three specific problems. First, at present, there are many kinds of courses on the online

learning platform. Different courses are often classified by simple labels and course names, and the unstructured text information in the course description is not fully utilized, resulting in an unclear classification of courses [9, 10]. Second, in view of the rapid development and expansion of the online learning platform, the learning resources on the platform are gradually accumulated. In order to increase the activity of the platform, some online platforms simply pursue the number of courses on the platform and do not do good supervision on the quality of resources on the platform, resulting in the poor quality of some course resources on the platform. Because these inferior resources are not filtered, it has a great impact on the learning effect of the learners [11, 12]. Third, for the learners of the course, the online learning platform cannot provide targeted learning guidance and personalized recommendation to the learners based on the user's learning style preference and the similarity between the course content and the prerequisites of the course. As a result, users often lose their direction when faced with many online courses and cannot quickly find which courses they need. It ultimately reduces the user's learning experience and learning efficiency [13–15]. Therefore, in view of the above problems, this paper proposes a personalized course recommendation method based on learner interest mining in the educational big data environment to solve the problem of low accuracy and limitations of the personalized course recommendation method in the current educational big data environment.

2. Related Works

Aiming at the problems existing in the current network education field, it is an important work in the field of intelligent education to study how to fully mine and explore the valuable data of the online education platform and find the relationship between learners and learning resources. On this basis, we accurately recommend the required courses for learners by using multi-source heterogeneous learning behavior data [16, 17]. Reference [18] calculated the importance of external attribute tolerance and internal attribute quality value on the course and built the LDA user interest model on this basis to calculate the user's preference for the topic and realize the recommendation of personalized learning resources. However, this method does not actually divide the user's access sequence into different interest segment sequences according to time, so the recommendation accuracy is low. Reference [19] developed an ontology-based hybrid filtering system framework for the recommendation and selection of higher education courses in universities, that is, ontology-based personalized course recommendation. This method is used for personalized course recommendations according to users' personal needs. However, this method is slow in computation and weak in generalization. Reference [20] designed a personalized online education platform based on a collaborative filtering algorithm by applying the recommendation algorithm in the recommendation system to the online education platform. This method is based on the hybrid programming mode of cross-platform compatible HTML5 and a high-performance framework. But this method does not give a new personalized recommendation algorithm. It is inefficient for a large-scale online learning system. Reference [21] proposed a deep learning method of recommending MOOC (massive open online courses) to students based on the multiattention mechanism of learning record attention, word-level review attention, sentence-level review attention, and course description attention. This method integrates multiple data sources, takes students' learning behavior as the basic basis, and realizes personalized course recommendations. However, the computational efficiency of this algorithm will decrease significantly with the increase in data volume, and it cannot be well applied to the case of sparse data. Reference [22] studied and analyzed the English course recommendation technology by combining the bee colony algorithm and the neural network algorithm. Through the deep learning model, the document vector was used to train the acquired text, and the collaborative filtering method was used to realize the recommendation of user courses. However, this method has limitations when it is used in large-scale E-learning systems due to the complexity of computing requirements. Based on the recommendation standard of traditional MOOCs, reference [23] constructed the ontology model of learning participants for the matching process of the personalized recommendation system introduced by MOOC. This method comprehensively considers the knowledge level, ability, and learning speed of learners. However, this method is difficult to obtain the prior distribution, and it is difficult to characterize the high-dimensional semantics of users. Reference [24] analyzed the research status of robust recommendation technology based on the text vector model and support vector machine and constructed the corresponding sustainable economic learning curriculum recommendation model. However, the recommendation accuracy of this method is low and needs further improvement.

Based on the above analysis, a personalized course recommendation method based on learner interest mining in the education big data environment is proposed to solve the problems of low accuracy and large limitations of the personalized course recommendation method in the current education big data environment. The basic ideas are as follows: ① using GRU to solve the problems of gradient disappearance and gradient explosion in the process of RNN training. ② Based on the autoregressive language model XLNet, the bidirectional prediction is realized by learning the sequence feature information of different sorting. ③ Time attention mechanism is used to calculate the probability weight of the word vector at different times through the probability weight distribution so that the important words get more attention. Compared with the traditional personalized course recommendation method, the innovation points of the proposed method are

(1) The GRU-coded module can reduce parameters while obtaining the equivalent result value and eliminate the gradient disappearance and explosion problems in the training process.

(2) Using the autoregressive language model XLNet, the problem of missing information under the Mask mechanism in the BERT model is effectively optimized.

(3) The temporal attention mechanism is used to allocate sufficient weight to improve the quality of feature extraction of the hidden layer.

3. Personalized Course Recommendation Method Based on Learner Interest Mining in the Education Big Data Environment

3.1. Model Framework (XATGRU). A recurrent neural network (RNN) is a kind of a time recurrent network, which can be regarded as the result of the same neural network structure circulating on the time axis many times. Compared with other deep neural networks, RNN is better at processing sequence data because of its structural characteristics. Theoretically, RNN can process any length of time series data, but in practical application, it is found that gradient disappearance and gradient explosion will occur in the process of RNN training. This is because the traditional RNN model tends to update in the right direction according to the weights at the end of the sequence. Small GRU parameters reduce the risk of overfitting, and the GRU solves the problems of gradient disappearance and gradient explosion in the process of RNN training neural network and can retain the information from a long time ago. The network structure of GRU is generally similar to that of RNN, but the structure of the hidden layer is more complex. The online course recommendation model framework based on GRU is divided into input, processing, and output sections according to functions, as shown in Figure 1 below.

The input part is mainly to convert the records that the user initially learned into the data format needed for GRU network computing, that is, the vector representation of each user's learning course. The processing part mainly processes the input data through the GRU network and then obtains the output result. It is necessary to determine the structure of the GRU network, including the total number of layers, the step length of time, and the connection settings between layers. This paper takes the number of courses as the number of eigenvalues, which defines the dimensions of input data and output data, namely the number of neurons in the input layer and output layer. The length of the user's learning sequence determines the time step required for each calculation. The maximum time step is defined as the maximum value of the user's learning sequence. At the same time, the length of the sequence should be specified when reading each user's learning sequence. Thus, the structure of the entire GRU network model is clear. The Softmax layer maps the value of the output vector of the GRU processing layer to the (0, 1) interval, and the output part can take the last dimension of the Softmax layer processing result to determine the final recommended course vector. Because the role of the softmax layer is to convert the output results of the neural network, the output results are expressed in the form of probability.

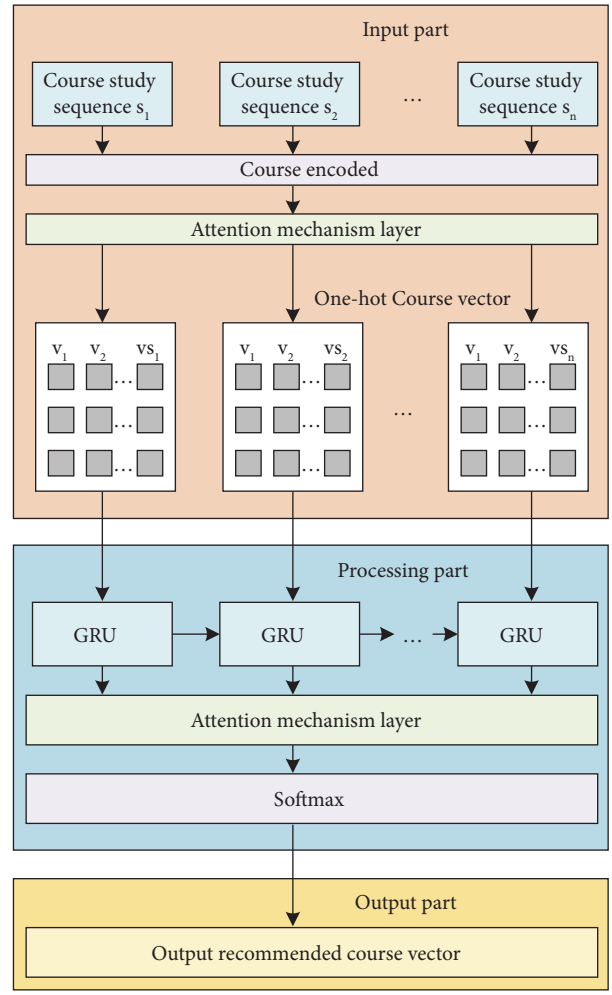

Figure 1: Personalized course recommendation model framework.

3.2. XLNet Pre-Training Model. Unsupervised learning models are divided into Auto-Regressive (AR) language model and Auto-Encoding (AE) language model. Different from the traditional AR language model, the AE language model represented by BERT realizes bidirectional prediction. XLNet realizes bidirectional prediction based on the AR language model. Its core idea is to rearrange the input sequence through the Attention Mask matrix in Transformer. At the same time, it does not change the original word order, and effectively optimizes the information missing problem under the Mask mechanism in the BERT model. Because the mask mechanism in the pretraining stage mainly predicts the words out of the mask by masking some words. The Mask mechanism of XLNet is shown in Figure 2.

In Figure 2, the light-colored circle indicates that the model can take its position information into account, and the dark-colored circle indicates that the model cannot take the position information into account. Taking the input vector $x = (x_1, x_2, x_3, x_4, x_5)$ as an example, a rearrangement combination of x is represented by $\tilde{x} = (x_3, x_2, x_5, x_4, x_1)$. As for the vector $\tilde{x}$, since x_3 is located at the first position of the sequence, other word information cannot be used, and only the previous implicit state

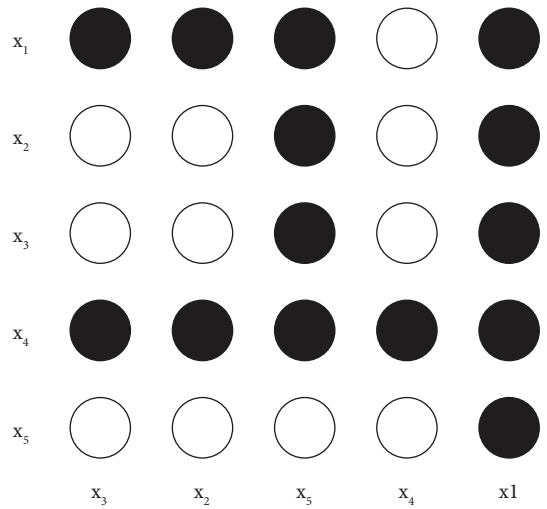

Figure 2: The realization principle of the Mask mechanism of XLNet.

information can be used. x_5 is located at the third position in the sequence, and the first three position information can be used.

Given that the sequence length is A, the total number of sorting methods $n = A!$. The model can learn various contexts through n various sorting methods. In practical application, XLNet randomly takes samples of partial permutation in n. The formula of the full permutation model is shown in the following formula:

$$\max(\alpha) S_{w \sim W_A} \left[\sum_{a=1}^{A} \lg P_\alpha \left(x_{w,a} \mid X_{w<a} \right) \right], \tag{1}$$

where S represents the sequence set. $w \sim W_A$ represents all possible text arrangements. $x_{w,a}$ represents the current word. $X_{w<a}$ represents the previous words of $a-1$. P represents the probability that the prediction result is the current word. α represents a parameter.

The core of XLNet is Transformer-XL, which introduces the idea of relative position encoding and recurrent mechanism on the basis of transformer structure. The transformer specifies that the input sequence is a fixed length sequence in the training. After the long sequence is segmented in the training, the model cannot make use of the links between the segments, which will cause the problem of missing information. Transformer-XL inserts implicit state information between segments. The prediction of the current segment can use the information of the previous segment through implicit state information, so the model can learn more long-term semantic information. The information transmission mode of the recurrent mechanism between the two segments is shown in Figure 3.

In Figure 3, the red dotted line represents the memory information. The cache information from Segment 1 can be used in Segment 2 training. XLNet realizes the transfer of historical information through this mechanism.

The Transformer encodes the absolute position into a vector in the form of a sine function. The upper layer can learn the relationship between the relative positions of two

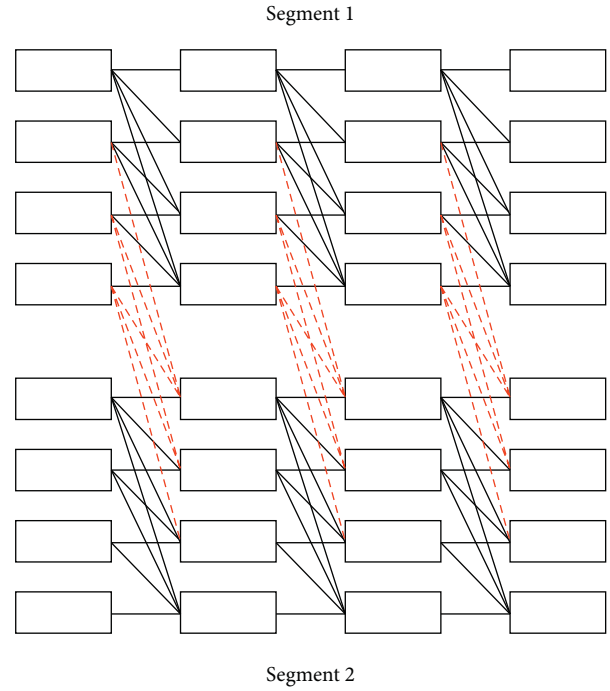

Figure 3: Information transmission mode of recurrent mechanism between two segments.

words through this vector. The calculation formula is shown in the following formula:

$$\begin{cases} e_{t+1} = f\left(e_t, L_{t+1} + U_L\right), \\ e_t = f\left(e_{t-1}, L_t + U_L\right), \end{cases} \tag{2}$$

where e_t represents vector encoding at time t. L represents the position encoding of the current segment text vector. U_L represents the position code, which is the same in different segments. The model cannot accurately determine the specific position of each segment through vectors. The absolute position code is the same for the same position encoding of each segment, while Transformer-XL can use the historical information of different segments. Considering that different segments and words with the same position code have different information contributions to the current segment, Transformer-XL uses the idea of relative position encoding, which calculates the relative distance according to the current position and the position to be used when calculating attention.

Taking the Transformer-XL framework as the core, XLNet can obtain more accurate word vector representation by introducing the recurrent mechanism and relative position encoding. XLNet considers bidirectional semantic information and mining long-term historical information.

3.3. Data Normalization. The neural network usually needs to normalize the input data before calculation to limit the data to a certain range, which ensures that the model can converge quickly and have the same metric for data characteristics. Here, One-Hot encoding is used to normalize the input data. The one-hot encoding adopts binary vector form,

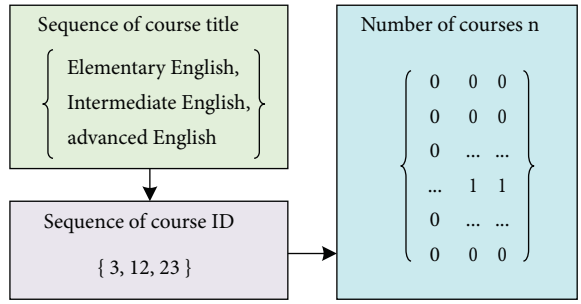

Figure 4: Data normalization.

so courses need to be mapped into integer values. That is, each course corresponds to a course number. Then, the course number is represented as a binary vector. The value of the element whose subscript is the number in the vector is marked as 1, and the other elements are all 0. For example, $\{0, 0, 1, 0, \ldots, 0\}$ represents the course whose course number is 3. First, the original learning records of users in the database are read and converted into the format of the user's course sequence. Then, each course in the course sequence is represented by a vector. The method of representing the user course sequence by vectors is shown in Figure 4.

3.4. GRU. GRU is a variant of RNN and has fewer parameters than LSTM. The basic structure of GRU is shown in Figure 5.

The data update formula of the basic unit in GRU is shown in the following formula:

$$\begin{cases} g(t) = \sigma\left[\omega(g)x_t + U(g)h_{t-1}\right], \\ c(t) = \sigma\left[\omega(c)x_t + U(c)h_{t-1}\right], \\ h_{0t} = \tanh\left[c(t) \circ Uh_{t-1} + \omega x_t\right], \\ h_t = [1 - g(t)] \circ h_{0t} + g(t) \circ h_{t-1}, \end{cases} \tag{3}$$

where $g(t)$ is the update unit module, which is responsible for determining how much h_{t-1} pass to h_t. If $g(t) \approx 1$, h_{t-1} will almost be directly copied to h_t. On the contrary, if $g(t) \approx 0$, it will not be directly passed to h_t. The reset gate $c(t)$ determines how much of the previous memory module information will flow to the current h_t. The symbol $\circ$ represents the operation of dot product. Compared with LSTM encoding, GRU encoding modules not only have fewer parameters but can also obtain equivalent result values. The bidirectional GRU module can not only use the past information but also combine the future word information.

3.5. Attention Mechanism. The attention mechanism is outstanding in speech recognition, machine translation, part of speech tagging, and other serialized data. The attention mechanism can be used alone or as a layer of other hybrid models. It can be placed after the text vector input layer or after the training data of other network models. Through automatic weighting transformation of the data, connecting two different parts to make the whole system perform better and highlight keywords . The attention mechanism is like the principle that the human brain observes something, such as people observing a painting in order to describe the content of some paintings. They will first observe the words in the title of the picture, and then they will observe the part of the picture that expresses the theme purposefully according to their judgment. When describing this painting, people often describe the most relevant content of this painting first, and then describe other aspects. The attention mechanism is a mechanism that highlights local important information by allocating sufficient attention to key information. It can generally be divided into two types: temporal attention mechanism and spatial Attention mechanism. The temporal attention mechanism is mainly used here. The attention mechanism is a kind of attention resource allocation mechanism similar to the human brain. It calculates the probability weights of word vectors at different times through probability weights, so that some words can get more attention and finally improve the quality of feature extraction of the hidden layer. The basic structure of the attention mechanism is shown in Figure 6.

4. Experiments and Analysis

4.1. Experimental Environment and Dataset. The relevant parameters of the simulation experiment environment are shown in Table 1.

The experimental dataset comes from the actual operation data of an online teaching website, with 14370 users and 816 courses, it is mainly related to some courses related to computer subjects. The data mainly includes the user's learning records and scoring records. From May 2018 to July 2021, a total of 157825 records were recorded. Among them, the training set accounts for 80%, a total of 126260 records, and the test set account for 20%, a total of 31565 records.

4.2. Evaluation Index. The performance of the model is measured by the results of the model extraction and the actual results. The evaluation indexes include precision (P), recall (R), and $F1$-measure ($F1$). The calculation methods of different evaluation indexes are shown in the following formulas (4)–(6).

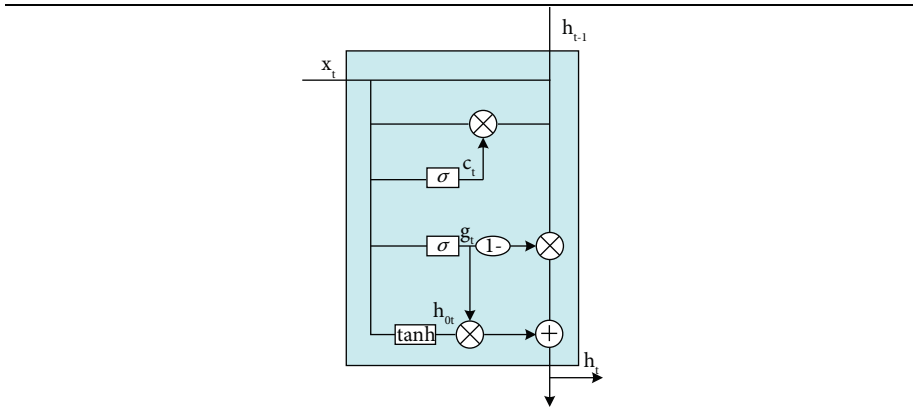

Figure 5: Basic structure of GRU.

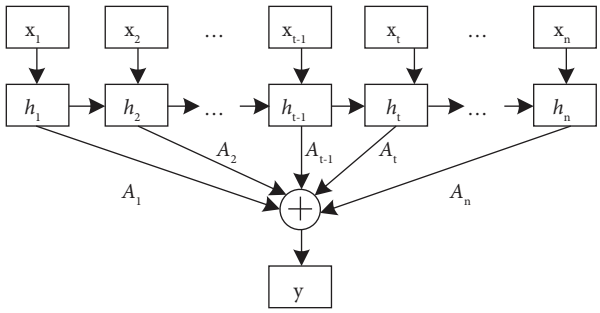

Figure 6: The basic structure of the attention mechanism.

$$P = \frac{S_T}{S}, \tag{4}$$

$$R = \frac{S_T}{S_G}, \tag{5}$$

$$F1 = 2 \cdot \frac{P \cdot R}{P + R}, \tag{6}$$

where S_T is the number of knowledge entities and relationships correctly identified by the model. S is the number of knowledge entities and relationships identified by the model. S_G is the number of all labeled knowledge entities and relationships.

4.3. Model Training. In order to verify the effect of our model, the comparison model is the classical Pipeline model. The experimental results on the dataset are shown in Table 2.

The overall $F1$ of the two models is shown in Figure 7.

From the above experimental results, it can be seen that for the task of entity recognition and relationship extraction, the proposed personalized course recommendation model XATGRU based on learner interest mining in the education big data environment has improved in precision, recall, and $F1$-Measure compared with the Pipeline model.

4.4. Experimental Comparison and Analysis. In the following, the personalized course recommendation method proposed in this paper is compared with the collaborative filtering algorithm in reference [20, 21, 23]. The indexes of recommendation results of different methods under the same dataset are shown in Table 3.

The following is a comparative analysis of the personalized course recommendation method proposed in this paper and the RNN algorithm. The indexes of recommendation results of different methods under the same dataset are shown in Figure 8.

It can be seen from Table 3 and Figure 8 that when the same database is used, compared with the collaborative filtering algorithm in reference [20, 21, 23] and the traditional RNN algorithm, the precision, recall, and $F1$-Measure of the proposed algorithm for personalized recommendation results of different types of courses are optimal, and the maximum values are 92.1%, 89.3%, and 90.7%, respectively. This is because the introduction of GRU solves the problems of gradient disappearance and gradient explosion in the training process. The XLNet model based on autoregressive language is used for bidirection prediction. The missing information caused by the Mask mechanism in the BERT model is effectively optimized and greatly improves the accuracy of personalized course recommendations.

Table 1: Simulation experiment environment parameters.

Name	Parameter
System environment	Windows 10 professional
Memory size	16 GB
Deep learning framework	TensorFlow-DPU 1.11.0

Table 2: Model training results.

Model		Pipeline	XATGRU
Entity	P	0.812	0.913
	R	0.754	0.905
	$F1$	0.792	0.912
Relation	P	0.542	0.668
	R	0.379	0.573
	$F1$	0.465	0.602

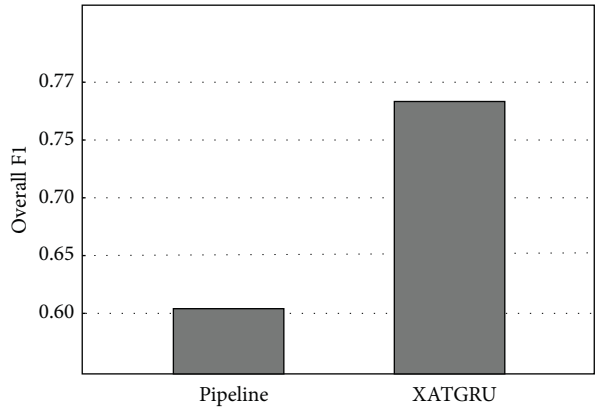

Figure 7: The overall $F1$ of two models.

Table 3: The indexes of recommendation of different methods under same dataset.

Category		Proposed method	Ref. [20]	Ref. [21]	Ref. [23]
Course 1	P	0.910	0.852	0.821	0.847
	R	0.881	0.833	0.801	0.812
	$F1$	0.895	0.842	0.811	0.829
Course 2	P	0.921	0.849	0.818	0.838
	R	0.893	0.835	0.821	0.827
	$F1$	0.907	0.842	0.819	0.832
Course 3	P	0.908	0.861	0.842	0.850
	R	0.879	0.842	0.813	0.824
	$F1$	0.893	0.851	0.827	0.837

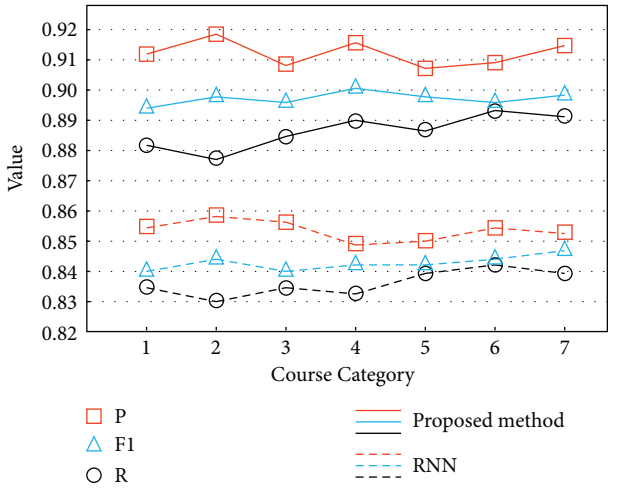

Figure 8: The comparison results between the proposed method and RNN.

5. Conclusion

In view of the low accuracy and large limitations of personalized course recommendation methods in the current education big data environment, a personalized course recommendation method based on learner interest mining in the education big data environment is proposed. The proposed method is verified by simulation experiments. The results show that the network structure of GRU is more complex, but it can effectively solve the gradient disappearance and gradient explosion problems in the training process of RNN, and the number of parameters is small, which can reduce the risk of overfitting. This neural network can improve the accuracy of personalized course recommendation methods and solve the problem of large limitations. XLNet based on the autoregressive language model can effectively optimize the information missing problem under the Mask mechanism in the BERT model and realize bidirectional prediction. The temporal attention mechanism can change the importance of different words by means of probability weight distribution, thus improving the quality of feature extraction in the hidden layer and the accuracy of personalized course recommendations. This method is of great significance to solve the problem of low accuracy and limitations of personalized course recommendation methods in the current educational big data environment. Future work will further study the relationship between course reviews and courses. On this basis, consider mining the information from course reviews to discover the relationship between courses from a diversified perspective and to achieve more accurate personalized course recommendations.

Data Availability

The data used to support the findings of this study are included within the article.

Conflicts of Interest

The author declares that there are no conflicts of interest regarding the publication of this paper.

References

[1] T. Morrow, A. R. Hurson, and S. S. Sarvestani, "Algorithmic support for personalized course selection and scheduling," in *Proceedings of the 44th Annual IEEE-Computer-Society International Conference on Computers, Software, and Applications (COMPSAC), ELECTR NETWORK*, pp. 143–152, Madrid, Spain, July, 2021.

[2] H. T. Chang, C. Y. Lin, and L. C. Wang, "How students can effectively choose the right courses: building a recommendation system to assist students in choosing courses adaptively," *Educational Technology & Society*, vol. 25, no. 1, pp. 61–74, 2022.

[3] L. Chen, L. Zhang, S. S. Cao, Z. Wu, and J. Cao, "Personalized itinerary recommendation: deep and collaborative learning with textual information," *Expert Systems with Applications*, vol. 144, no. 3, Article ID 113070, 2020.

[4] Y. Yang, Y. Zhu, and Y. Li, "Personalized recommendation with knowledge graph via dual-autoencoder," *Applied Intelligence*, vol. 52, no. 6, pp. 6196–6207, 2021.

[5] K. Wang, T. T. Zhang, T. Q. Xue, Y. Lu, and S. G. Na, "E-commerce personalized recommendation analysis by deeply-learned clustering," *Journal of Visual Communication and Image Representation*, vol. 71, no. 12, Article ID 102735, 2020.

[6] H. Jung, Y. Jang, and S. Kim, "KPCR: knowledge graph enhanced personalized course recommendation," in *Proceedings of the 34th australasian joint conference on artificial intelligence (AI)*, pp. 739–750, Univ Technol Sydney, ELECTR NETWORK, Sydney, NSW, Australia, February, 2022.

[7] Z. Ali, P. Kefalas, K. Muhammad, B. Ali, and M. Imran, "Deep learning in citation recommendation models survey," *Expert Systems with Applications*, vol. 162, no. 2, Article ID 113790, 2020.

[8] L. B. Cao and C. Z. Zhu, "Personalized next-best action recommendation with multi-party interaction learning for automated decision-making," *PLoS One*, vol. 17, no. 1, Article ID e0263010, 2022.

[9] X. F. Zhang, M. F. Li, D. W. Seng, X. Chen, and X. Chen, "A novel precise personalized learning recommendation model regularized with trust and influence," *Scientific Programming*, vol. 2022, no. 6, Article ID 8479423, 15 pages, 2022.

[10] S. Kim, W. Kim, and H. Kim, "Learning path construction using reinforcement learning and bloom's taxonomy," in *Proceedings of the 17th International Conference on Intelligent Tutoring Systems (ITS)*, pp. 267–278, Univ W Attica, ELECTR NETWORK, Athens, Greece, June, 2021.

[11] Z. Shi and W. Wang, "Design of personalized recommendation system for swimming teaching based on deep learning," *Security and Communication Networks*, vol. 2021, no. 9, Article ID 1211059, 7 pages, 2021.

[12] L. Zeng, M. Peng, and Y. Liu, "Personalized hashtag recommendation using few-shot learning," *Journal of Chinese Information Processing*, vol. 35, no. 9, pp. 102–112, 2022.

[13] F. Liu and W. W. Guo, "Personalized recommendation algorithm for interactive medical image using deep learning," *Mathematical Problems in Engineering*, vol. 2022, no. 23, 10 pages, Article ID 2876481, 2022.

[14] W. J. Jiang, Z. A. Pardos, and Q. Wei, "Goal-based course recommendation," in *Proceedings of the 9th International Conference on Learning Analytics and Knowledge (LAK)*, pp. 36–45, Arizona State Univ, Tempe, AZ, USA, March, 2019.

[15] E. G. Mantouka and E. I. Vlahogianni, "Deep reinforcement learning for personalized driving recommendations to mitigate aggressiveness and riskiness: modeling and impact assessment," *Transportation Research Part C: Emerging Technologies*, vol. 142, no. 5, Article ID 103770, 2022.

[16] Y. C. Chou, C. T. Chen, and S. H. Huang, "Modeling behavior sequence for personalized fund recommendation with graphical deep collaborative filtering," *Expert Systems with Applications*, vol. 192, no. 13, Article ID 116311, 2022.

[17] C. F. Tang and J. Zhang, "An intelligent deep learning-enabled recommendation algorithm for teaching music students," *Soft Computing*, vol. 15, no. 7, pp. 18–26, 2022.

[18] Q. Lin, S. He, and Y. Deng, "Method of personalized educational resource recommendation based on LDA and learner's behavior," *International Journal of Electrical Engineering Education*, vol. 12, no. 5, pp. 128–136, 2021.

[19] M. E. Ibrahim, Y. Y. Yang, D. L. Ndzi, G. Yang, and M. Al-Maliki, "Ontology-based personalized course recommendation framework," *IEEE Access*, vol. 7, no. 13, pp. 5180–5199, 2019.

[20] J. Li and Z. Ye, "Course recommendations in online education based on collaborative filtering recommendation algorithm," *Complexity*, vol. 2020, no. 23, Article ID 6619249, 332 pages, 2020.

[21] J. Fan, Y. C. Jiang, Y. Z. Liu, and Y. Zhou, "Interpretable MOOC recommendation: a multi-attention network for personalized learning behavior analysis," *Internet Research*, vol. 32, no. 2, pp. 588–605, 2022.

[22] Y. Fang and J. N. Li, "Application of the deep learning algorithm and similarity calculation model in optimization of personalized online teaching system of English course," *Computational Intelligence and Neuroscience*, vol. 2021, no. 6, Article ID 8249625, 66 pages, 2021.

[23] S. Assami, N. Daoudi, and R. Ajhoun, "Learning actor ontology for a personalised recommendation in massive open online courses," *International Journal of Technology Enhanced Learning*, vol. 12, no. 4, pp. 390–410, 2020.

[24] XF. Ma, "Recommendation of sustainable economic learning course based on text vector model and support vector machine," *Journal of Intelligent and Fuzzy Systems*, vol. 40, no. 4, pp. 7135–7145, 2021.

Hindawi
Scientific Programming
Volume 2022, Article ID 7699998, 13 pages
https://doi.org/10.1155/2022/7699998

Research Article

Prediction of New Media Information Dissemination Speed and Scale Effect Based on Large-Scale Graph Neural Network

Chen Qiumeng[1] **and Shen Yu**[2]

[1]*Minzu Normal University of Xingyi, Guizhou, Xingyi 562400, China*
[2]*Huanghe Science and Technology University, Foreign Languages School, Zhengzhou, China*

Correspondence should be addressed to Shen Yu; shenyu@hhstu.edu.cn

Received 9 July 2022; Revised 22 July 2022; Accepted 30 August 2022; Published 21 September 2022

Academic Editor: Lianhui Li

In recent years, because of the popularity of the internet and mobile devices, the dissemination of new media in social networks has attracted extensive attention from scholars and the industry. Scale prediction or propagation speed prediction is to use the initial data to predict the propagation scale of the network. In the complex and changeable social network, how to accurately predict the cascading scale of new media information is the biggest problem at present. In the process of new media information transmission, because of the role of new media information transmission in guiding public opinion, the current hierarchical model of new media information transmission lacks the overall and local models. To solve this problem, a global structure modeling method is proposed. In addition, because of the uncertainty of new media information dissemination, a method of bidirectional recurrent neural network prediction and algorithm complexity is used, and a new method based on large-scale graph neural network is constructed. A prediction method of new media information dissemination speed and scale based on large-scale graph neural network. Through comparative experiments with previous research models, it is found that the NWIDF model constructed in this paper has a good prediction effect.

1. Introduction

In recent years, the modeling and prediction of new media information cascade has attracted extensive attention in the academic field and industry [1]. In recent years, with the improvement of computing power, prediction models based on deep learning have been successful in many tasks.

Existing models based on deep learning can be roughly divided into three categories: (1) models based on information content, such as text, image, video, and other multimedia content, which usually use technology from the field of computer vision and natural language processing to learn the effective representation of information content. (2) Based on time series model, it relies on recurrent neural network, pooling mechanism, and attenuation mechanism to linearly model the information cascade in social networks and [2] (3) model based on the graph structure, such as information cascade graph or global graph. As per reference [3], these models typically use graph neural networks and graph representation learning techniques to learn efficient structures of nodes, edges, and graphs to represent information. Other deep learning technologies, such as variational reasoning and reinforcement learning, are also used for information cascade scale prediction. In many cases, multimode, multiscale, and multitask learning techniques can be used to improve prediction performance. Deepcas [4] is the first model to model and predict the scale of information cascade using graph representation learning technology. It borrows the idea of deepwalk model [5] and uses the random walk method to sample the information cascade graph. The sampled node sequence is input into the bidirectional gated loop unit [6], and then the node embedding is obtained in cooperation with the attention mechanism [7]. The prediction of the deepcas model is end-to-end, and therefore, it does not depend on the manual functional design. Subsequently, in document [8], the author proposed

the dcgt model, which adds the modeling of node content to deepcas. The purpose of the deephawkes model [9] is to combine the advantages of the generated model with the advantages of deep learning technology, so as to simultaneously consider the predictability and good prediction performance. The ANPP model [10] uses g1ove [11] for the text embedding of information content and node2vec [12] for user graph embedding. ANPP uses the attention mechanism to aggregate the obtained representations and time-series feature vectors. The Dtcn model [13] predicts the popularity of Flickr images by learning user and image embedding, pore context of shared sequences, and multistep temporal attention mechanism. The dtcn model uses RESNET [14] and long-term and short-term memory artificial neural networks [15] to simulate the visual and temporal dependence of pictures, respectively. The recursive cascade convolution network [16] regards the information cascade graph as a series of subinformation cascade graphs, and then, it uses the dynamic multidirectional graph convolution network to learn the structural information of the information cascade.

Although the model based on deep learning has achieved good results in the information cascade prediction task, it also faces many limitations and challenges. The computational consumption of the deep learning model is generally greater than that of the other two types of models. To obtain satisfactory prediction results, engineers usually need to perform complex parameter optimization and model training and face the risk of data overfitting. At the same time, in the prediction of the cascade scale of new media information, there is a lack of modeling of global and local communication structures, ignoring hierarchical modeling, and it is unable to cope with changes and uncertainties in the process of information dissemination. Therefore, the article starts from this angle, and relevant research is carried out.

2. Related Work

The modeling and prediction of new media information cascades have attracted extensive attention in academia and industry in recent years [1]. In recent years, with the improvement of computing power, prediction models based on deep learning have been successful in many tasks.

Existing deep learning-based models can be roughly divided into three categories: (1) models based on information content, such as text, images, videos, and other multimedia content, these models usually use technologies from the fields of computer vision and natural language processing to effectively represent the content learning of information; (2) time-based models of sequences, which linearly model information cascades in social networks and rely on techniques such as recurrent neural networks, pooling mechanisms, and attention mechanisms [2]. (3) Models based on graph structures, such as information cascade graphs or global graphs, etc. [3], usually use graph neural networks and graph representation learning techniques to learn effective structural representations of nodes, edges, and graphs. Other deep learning techniques, such as variational inference, reinforcement learning, etc., are also used in information cascade scale prediction. In many cases, techniques, such as multimodal, multiscale, and multitask learning, are used to improve the prediction performance. DeepCas [4] is the first model to use graph representation learning techniques to model and predict the scale of information cascades. It borrows the idea of the DeepWalk model [5] and uses a random walk method to sample the information cascade graph. The sampled node sequence is input into the bidirectional gated recurrent unit [6], and it cooperates with the attention mechanism [7] to obtain the node embedding. The predictions of the DeepCas model are end-to-end and thus do not rely on manual feature design. Subsequently, in literature [8], the authors propose the DCGT model, which adds the modeling of node content to DeepCas. The purpose of the DeepHawkes model [9] is to combine the advantages of generative models with the advantages of deep learning techniques, thereby taking into account both predictive interpretability and good predictive performance. The ANPP model [10] uses G1oVe [11] for the textual embedding of information content and node2vec [12] for user graph embedding. ANPP uses an attention mechanism to aggregate the acquired representations and time series feature vectors. The DTCN model [13] predicts the popularity of Flickr images by learning user and image embeddings, sharing temporal context of sequences, and a multistep temporal attention mechanism. The DTCN model uses ResNet [14] and Long Short-Term Memory Artificial Neural Network [15] to model the visual and temporal dependencies of pictures, respectively. Recurrent Cascade Convolutional Networks [16] treat the information cascade graph as a series of subinformation cascade graphs, and then, it use a dynamic multidirectional graph convolutional network to learn the structural information of the information cascade.

Although deep learning-based models have achieved good results on information cascade prediction tasks, they also face many limitations and challenges. The computational consumption of deep learning models is generally larger than that of the other two types of models. The main reason is that deep learning learns the deep nonlinear network structure, and its essence is to approximate complex functions and represent the distributed representation of the input data. Deep learning can learn the essential characteristics of the dataset. But the problem may often involve causal reasoning, logical reasoning, and dealing with uncertainty, which is obviously beyond the ability of traditional deep learning methods. Hence, the predictions of deep learning models lack interpretability, because neural networks are essentially a "black box model." Secondly, the computational consumption of deep learning models is generally higher than that of feature engineering-based prediction models and probability-based generation. The model should be bigger. To achieve satisfactory prediction results, engineers often need to perform complex parameter tuning, model training, and face the risk of overfitting the data. At the same time, in the prediction of the cascade scale of new media information dissemination, there is a lack of modeling of the global and local dissemination structure, ignoring hierarchical modeling and inability to deal with

changes and uncertainties in the process of information dissemination. Therefore, the paper starts from this perspective, and related research is conducted.

3. Related Theories

3.1. Bayesian Graph Neural Network. A Bayesian network is a probabilistic graphical model. By adjusting the preset parameters or the prior knowledge of the model through sample data, the parameters of the Bayesian network or the posterior probability of the model are inferred to express uncertainty. The uncertainty of the node characteristics of new media information dissemination is mainly manifested in the uncertainty caused by noise data, missing or repeated data, etc., in the process of feature extraction and the uncertainty of the relationship between different characteristics of nodes and node labels. A probabilistic graph model that can solve uncertainty through the Bayesian graph neural network identifies hot topics in new media information, compares the prediction of node labels under different features, integrates the prediction of node labels by all features, and then judges the uncertainty of node features.

In the dissemination of new media information, as the network structure is not fully known and constructed by domain experts, it usually leads to missing important edges, adding false edges and other problems, resulting in poor model prediction effect and poor robustness.

This paper needs to propose a way to add missing important edges and prune irrelevant and spurious edges. In other words, the network structure needs to be reconstructed. The Bayesian graph neural network is used to solve the uncertainty problem of the node relationship in the reconstructed network.

Generally speaking, a neural network can be regarded as a conditional distribution model $p(Y \mid X, W)$, i.e., the distribution of labels Y under the condition of input feature X and neural network weight W. Then, the learning process of the neural network can be regarded as maximum likelihood estimation. Based on this, the researchers proposed a Bayesian neural network [17], which, firstly, obtained the weight probability $p(W \mid D)$ of the neural network based on the dataset not only to find its maximum posterior value but also to be used for the neural network. Networks introduce uncertainty. The prediction Y for a new input x can be obtained by integrating the posterior distribution of W, and the process can be expressed as follows:

$$p(y|x, X, Y) = \int p(y \mid x, W)p(W \mid X, Y)dW. \quad (1)$$

However, since the posterior distribution (formula (1)) of the Bayesian neural network is often difficult to calculate directly, researchers have adopted different methods to approximate it [18–21].

This paper considers reconstructing the network structure with a random graph generation model to solve the uncertainty of the network structure.

3.2. Random Block Model. The random block model is a generative model for random graphs. The model tends to generate graphs that contain populations, i.e., subsets characterized by a certain edge density interconnected. For example, edges may be more common within a community than between communities. The stochastic block model is important in statistics, machine learning, and network science, and in graph data, it serves as a useful benchmark for the task of recovering community structure. Reconstructing the network structure in this way can aggregate nodes with strong correlations in the network, while nodes with weak correlations will have certain edges if they are directly pressed.

The random block model has the following parameters:

(1) The number of vertices n

(2) Divide the vertex set $\{V_1, V_2, \cdots, V_n\}$ into disjoint subsets $C_1, C_2, \cdots, C_r$ called groups

(3) A symmetric matrix P of edge probabilities

Randomly sample the edge set: any two nodes $V_p \epsilon C_i$ and $V_q \epsilon C_j$ are connected by an edge with probability P_{ij}.

Its generation process is shown in Algorithm 1.

The group membership of each node depends on the context, i.e., each node may have different memberships when interacting with or being interacted with by different nodes. Statistically, each node is a mixture of group-specific interactions. After the random block model is represented by a generative graph, the network can be reconstructed and applied to the graph neural network to solve the uncertainty of the network structure.

3.3. New Media Information Dissemination Mechanism. In this paper, we mainly explain the mechanism of new media information dissemination from two perspectives, namely information cascade graph and user social network (global graph).

Cascade graph: given the new media information microblog I and its corresponding forwarding information cascade C, the information cascade graph can be defined as $\zeta_c = (v_c, \varepsilon_c)$, where $v_c = \{u_i | 1 < i \leq M\}$ is a part of the user nodes participating in the information cascade, $\varepsilon_c \in v_c \times v_c$ is a set of edges with a number of $M = |C|$, representing all user interactions in the information cascade graph. A schematic diagram of a cascade graph growing over time is shown in Figure 1.

$$C(t_0) \longrightarrow \cdots \longrightarrow C(t_n). \quad (2)$$

Global Graph: the global graph contains all the nodes and edges in the social network, which can be defined as $\zeta_g = (v_g, \varepsilon_g)$. The edges represent different node relationships in the information cascade. An example of a typical global graph is the user's follow du and followed network in TikTok.

In this paper, the information cascade graph represents the local propagation characteristics of information in the network, while the global graph represents the associations between nodes in the whole network. Taking TikTok as an

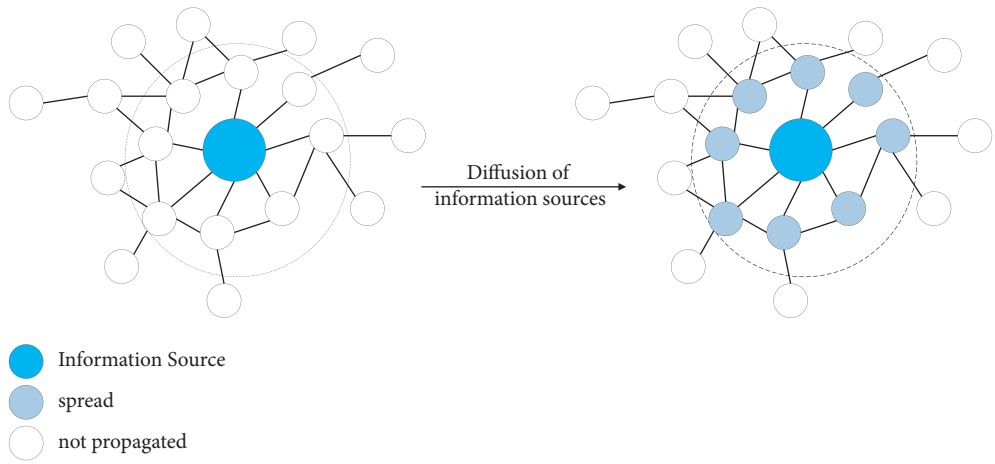

Figure 1: Cascading diagram of media information.

example, the following relationships, forwarding relationships, and historical behaviors among users can all be reflected in the structure of the global graph. The previous work [8–10] simply used features, such as the number of followers of the user (which can be regarded as the degree of nodes) as the structural features of the user, which cannot fully capture the user's influence, preference, and other attributes. There are a few other works [14, 17] that use other types of structural features. But, they also all make strong assumptions about the intrinsic mechanism of information dissemination, or face the risk of overfitting on specific data, resulting in their poor generalization performance, and when migrating to other applications or data platforms (with different propagation mechanism or propagation mechanism unknown) is less effective.

4. New Media Information Dissemination and Scale Prediction Path Based on Large-Scale Graph Neural Network

4.1. The Overall Architecture of the Prediction Model. This section builds the general framework of the NWIDF prediction model. It consists of four parts: structure learning, time series propagation, new media information uncertainty propagation, and predictor. Structural learning mainly captures and models the contextualized structural patterns in information cascade graphs and the implicit relationships of users in social networks. It leverages techniques from graph signal processing to learn structural representations of information cascades: local structure modeling based on wavelet maps and user global structure modeling based on sparse matrix factorization. Temporal propagation uses a bidirectional recurrent neural network to model temporal dependencies in information propagation. The uncertain propagation of information in new media uses a variational autoencoder to model changes and uncertainties in information propagation and information growth, and it uses a regularized flow to estimate the posterior distribution of hidden variables for a series of complex and flexible transformations. The predictor combines recurrent neural networks and variational inference to learn high-order representations of the information cascade, and finally, it uses a multilayer perceptron to make predictions about the final size of the information cascade, as shown in Figure 2.

As the core of the NWIDF model system, the new media information person is the main body of information production, transmission, processing, and management. Information people usually include are users and platforms. Users can enhance the quality impact of new media platforms by accepting feedback and continuously optimizing. New media information technology is the support of information activities. Through the collection, processing, dissemination, and feedback of information, the continuous operation of the NWIDF model system is realized.

4.2. Modeling of New Media Information Cascade Structure under Large-Scale Graph Neural Network

4.2.1. New Media Information Cascade Learning Structure. In the new media information dissemination mode, the cascade graph is introduced $C_i(t)$, which is represented as an adjacency matrix, and a self-loop is added to each node, as shown in Figure 3. Then, according to the arrival time of each node in the cascade graph $C_i(t)$, one-hot encoding (One-Hot Code) is performed to represent the node characteristics. Divide the observation window $[0, T$ into disjoint fine l-grained time intervals, then encode each time interval.

At the $t_m (0 < m < l)$ moment, the node V_i forwards to the node. Then, V_j the adjacency matrix of the $a_i^{t_m}$ cascaded graph at this moment $C_i(t)$ is 1, and the rest are 0. The adjacency matrix embedding for the cascaded graph $C_i(t)$ is encoded as follows:

$$A_i^T = \left\{a_1^{t_l}, a_2^{t_l}, \cdots, a_i^{t_{i-l}}\right\}. t_j \epsilon [0, T,\ j \epsilon [1, l. \tag{3}$$

To capture the global graph structure information in the process of cascading information diffusion in new media, we use a graph convolutional network to learn the Markov process embedded in [22] information diffusion, i.e., it will converge to a stable value after a period of diffusion. Normal distribution will converge to a stable distribution after a

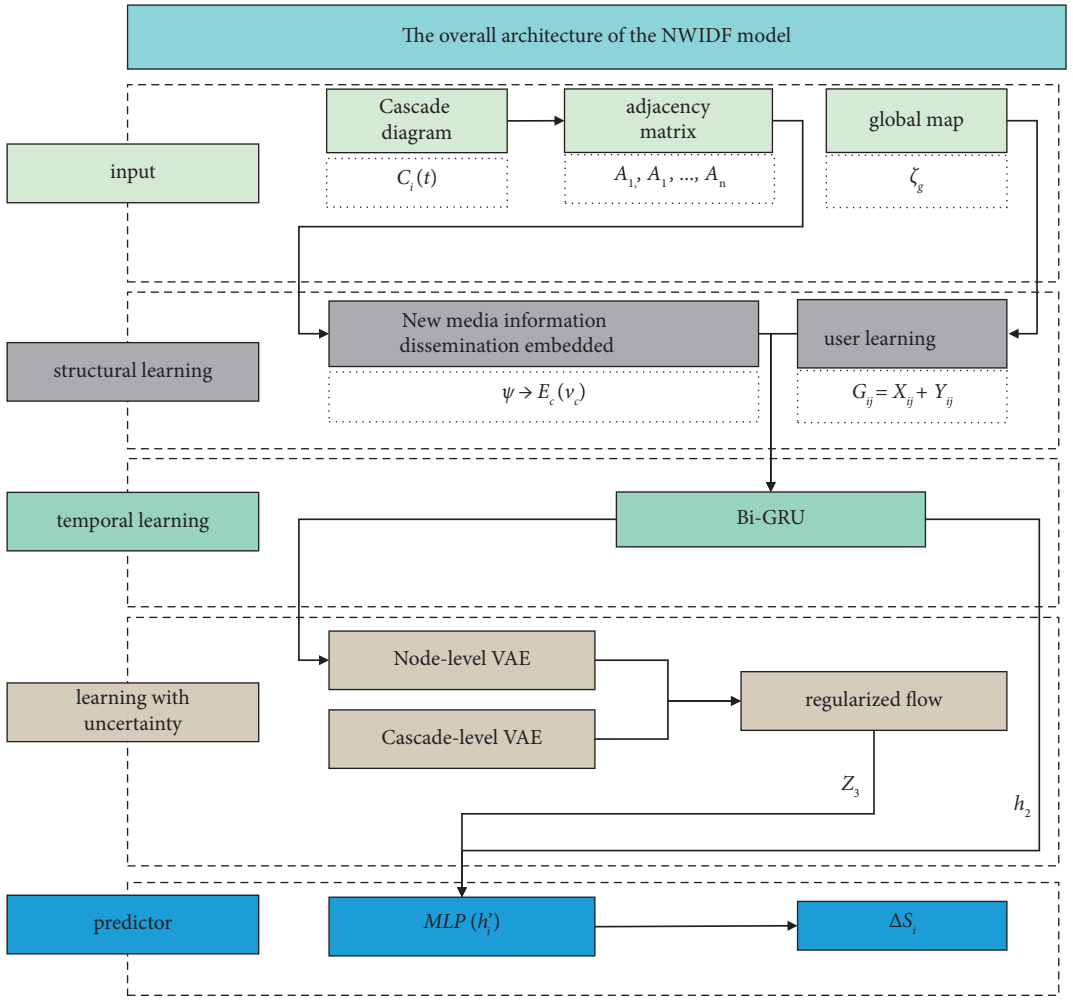

Figure 2: The overall architecture of the NWIDF model.

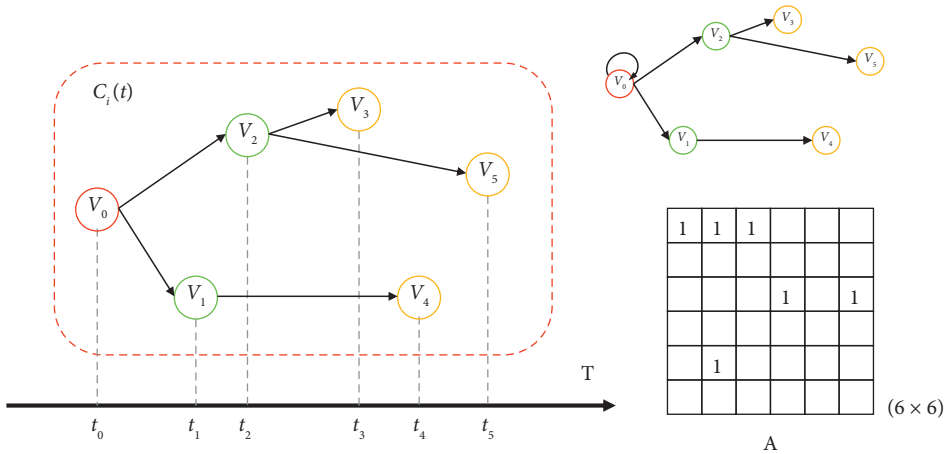

Figure 3: Cascaded subgraph sequence sampling representation.

period of time, similar to the normal distribution [23]. Therefore, let the cascaded Laplacian matrix Δc conform to the random walk characteristics of the cascaded graph, and let the Markov state transition probability matrix $P = D^{-1}A$. According to the graph convolution network formula, the Lapuas matrix can be obtained Δc as follows:

$$\Delta c = D^{-1/2}(D-A)D^{-1/2} = D^{-1/2}(I-P)D^{-1/2} \approx \Phi^{1/2}(I-P)\Phi^{-1/2}. \tag{4}$$

D represents the degree matrix of the cascade graph, and K represents the number of captured neighborhood layers.

$\Lambda = \mathrm{Diag}(\lambda_0, \lambda_1, \cdots, \lambda_{M-1})$ is the eigenvalue of the adjacency matrix satisfying the condition of $\lambda_0 < \lambda_1 \leq \cdots \leq \lambda_{M-1}$, where U is the eigenvalue decomposition. We can then compute $u_i \epsilon v_i(t_0)$ the graph wavelet for each node $\Psi_{u,s}$ as follows:

$$\Psi_{u,s} = U\mathrm{Diag}(g_s(\lambda_0), \cdots, g_s(\lambda_{M-1}))U^T \delta_u, \tag{5}$$

where δ_u is the one-hot encoded vector of node u, and the filter kernel g_s is a continuous function defined on R^+. Here, we use the Heat kernel function $g_s(\lambda) = e^{-\lambda s}$, where s is a scale parameter defined on the spectrum $(\lambda_l)_{l=0,\cdots,M-1}$.

In particular, for a given node u_i and a scale parameter s, the empirical feature function is formally defined by the following formula:

$$\varphi_{u,s}(p) = \frac{1}{M}\sum e^{ip\Psi_{m,u,s}}, \Psi_{m,u,s} = \sum_{l=0}^{M-1} g_s(\lambda_l)U_{ml}U_{ul}, \tag{6}$$

where $\Psi_{m,u,s}$ is the m^{th} wavelet coefficient of $\Psi_{u,s}$. Then, the embedding of node u_i in the information cascade graph can be obtained by concatenating the real and imaginary parts.

$$E_c(u_i) = \left[Re\varphi_{u,s}(p), Im\varphi_{u,s}(p)\right]_{p1,p2,\cdots,p\,d}. \tag{7}$$

The dimension of the node embedding $E_c(u_i)$ is $d_c = 2d$, and the first element of the embedding is set as the weight of the node edge, which is defined and regularized by the following formula:

$$W_u = \frac{\left(t_j - t_0\right)}{t_0} \in [0,1], 0 < t_0 \leq t_j. \tag{8}$$

From the perspective of sentences, the emotion of a long sentence is mainly determined by several keywords connected to the root node, and the function of other words is ignored, resulting in the lack of key information. In recent years, the rapid development of Internet+ has made the sentiment analysis of comment texts occupy a certain proportion in user-based big data analysis. Compared with the inflexibility of traditional machine learning methods, deep learning methods can be more efficient and accurate. The emotional information is contained in the text, so obtaining text emotional information through deep learning is a relatively popular research field at present, and it has achieved good research success. Since the machine cannot directly recognize the plain text input, it is necessary to vectorize the text to convert the text into a numerical form that the machine can recognize.

To solve the problem of the adjacency matrix generated by the dependency tree containing a large number of zero elements, there may be information loss and data sparseness. In this paper, a global graph matrix is constructed, and a layer of identity matrix is added to the original adjacency matrix, which is the global graph matrix. The construction of the global matrix in this paper is shown in equations –(11).

$$X_{ii} = 1, \tag{9}$$

$$X_{ij} = 1, \mathrm{OR} X_{ij} = 0, \tag{10}$$

$$Y_{ij} = 1, \tag{11}$$

$$G_{ij} = X_{ij} + Y_{ij}. \tag{12}$$

$X_{ii} = 1$ means that all elements on the diagonal of the adjacency matrix are set to 1, which means that each node in the graph performs a self-loop operation. The formula $X_{ij} = 1$ indicates that the i^{th} node has a directed connection to the j^{th} node. $X_{ii} = 0$ indicates that there is no connection between the $Y_{ij}i^{\text{th}}$ node and the j^{th} node, and when generating the adjacency matrix, a unit matrix is added, which means that an edge is added between each node in the graph structure to connect. This allows the graph structure to contain global dependency information. G_{ij} represents the connection of all nodes in the graph, which is the global graph matrix. This operation allows each word to play a corresponding role, avoiding data sparse and incomplete information.

Compared with the node embedding in the information cascade graph, the node embedding in the global graph expresses a very different concept of information propagation in the global graph. For the information cascade graph, whether for those influential nodes, hub nodes connecting different communities, or inconspicuous leaf nodes, nodes with similar structural positions will have similar node embeddings even if they are very far apart in the graph. This positional property is captured by the propagation mode of the graph wavelet. For the global graph, the low-dimensional continuous embeddings learned by the model preserve the neighbors of nodes in the global graph. Hence, nodes with similar preferences and behaviors will have similar spatial embeddings.

Unlike information cascade graphs, global graphs often contain up to millions of nodes and edges, making representation learning on them very difficult. Existing graph learning models [15, 18] are difficult to directly apply to practical information cascade prediction problems. The text uses sparse matrix factorization to process and model large-scale global graphs efficiently and in a scalable manner ζ_c ζ_g.

4.2.2. Temporal Propagation Build. In the above, we used graph wavelets and sparse matrix factorization to generate embeddings that encode the structural information of users in information cascade and global graphs. In particular, they are characterized by the following: (1) structurally equivalent nodes in an information cascade graph will have similar embeddings (refer to [20]). For

example, hub nodes have stronger propagation capabilities than leaf nodes. (2) Adjacent nodes in the global graph will have similar embeddings, i.e., adjacent nodes will have similar preferences for disseminating specific information.

In addition to the structural information contained in the information cascade, time series information is considered to be one of the most important features in the scale prediction problem of the information cascade, and it has a key impact on the final scale of the information cascade. To capture the temporal nature of information cascades, we use bidirectional gated recurrent units (BiGRUs) to model the cascade effects in information. Recurrent neural networks are widely used in the modeling of time series data, and they are used to model time series features in information dissemination. The calculation formula of BiGRU is shown in formulas (12)–(14), which can be expressed in the formula. The hidden state of the forward output at the moment is expressed in watts. The hidden state of the reverse output at time, Q_c, represents the hidden state of the output, ω_c represents the input, and ω_c and v_c represent the weight matrix, where b_c is the bias vector.

$$\overrightarrow{Q}_c = GRU\left(\overrightarrow{Q}_{c-1}, \omega_c\right), \tag{13}$$

$$\overleftarrow{Q}_c = GRU\left(\overleftarrow{Q}_{c-1}, \omega_c\right), \tag{14}$$

$$Q_c = \omega_c \overrightarrow{Q}_c + v_c \overleftarrow{Q}_{c-1} + b_c. \tag{15}$$

BiGRU includes the process of forward GRU and reverse GRU transfer. Bidirectional GRU can enrich the representation of contextual information based on aspect words and enhance the interaction of information in a complementary form, so that more useful information can be captured compared to unidirectional GRU. Usually, two-way GRU will also perform better than one-way GRU. Deep BiGRU is to continuously expand the depth of the neural network. On the basis of one layer of BiGRU, the method of superimposing multiple layers of BiGRU is to use the output of each BiGRU layer as the input of the corresponding node of the next layer of BiGRU.

However, only using the hidden state of the last layer of the RNN has certain drawbacks for information cascade prediction. It is because of the flat sequence generation process in recurrent neural networks, where the embedding of each node is dependent on the node embedding at the previous time. The problem is that the model is forced to generate all higher-order information in a deterministic and step-by-step manner. This setting has significant limitations for exploring uncertain dependencies in information cascades. In addition, because of the limitations of RNNs themselves, these models cannot handle long-term dependencies, and their predictive performance may drop significantly when the length of the information cascade is very long.

4.2.3. Uncertainty Modeling of New Media Information. An information cascade C consists of a growing sequence of participants, each of which is associated with a learned representation that represents a specific stage of information dissemination. In the above, for each node in the information cascade graph and global graph, we use graph wavelet and sparse matrix factorization to learn its embedding representation $E_c(u_i)$ and $E_g(u_i)$ for the node, respectively. In a more general sense, any other type of graph representation learning method can be used to enhance the learning ability of the model, for example, text and image embeddings. Without causing ambiguity, we use R_i, $(i\epsilon|v_c|)$ to represent each participant in the information cascade C, i.e., $R_i = \text{Concat}(E_c(u_i), E_g(u_i))$.

Let Enc(•) be the input encoder and Dec(•) be the reconstructed input decoder. The deep variational autoencoder based on neural network can be defined as follows:

$$\begin{aligned} &z_i = Enc(R_i), \overline{R_i} = Dec(z_i), for\, i = 1, 2, \cdots, M, \\ &u_i = NN(R_i), \log\sigma_i^2 = NN(R_i), z_i \sim \mathrm{N}\left(u_i, \sigma_i^2\right), \end{aligned} \tag{16}$$

where $\overline{R_i}$ is the reconstructed input and $z_i \epsilon R^d$ is the hidden vector. The variational autoencoder accepts high-dimensional data as input and generates a compressed hidden representation that is sampled from a conditional prior distribution with standard deviation μ and variance $\log\sigma^2$. The original input is then reconstructed from this hidden representation.

In order to learn an efficient probability-based representation from the information cascade data, which captures the variation and uncertainty of the information cascade propagating in the network, the variational autoencoder samples $\log\sigma^2$ and μ andfrom the output vector of the encoder. Then, use the reparameterization trick to sample the hidden vectors from the Gaussian distribution [22].

$$z_i = u_i + \sigma_i \varepsilon, \varepsilon \sim \mathrm{N}(0, 1). \tag{17}$$

Given a hidden random variable $Z \epsilon R^{d_z}$ (in this paper, it is referred to Z_2 learned in higher-order variational autoencoders, the regularization flow is a class of generative models that transforms the observed vector Z into the required target hidden vector Z^k. The transformation consists of a series of K invertible mappings (invertible mappings). The Jacobian matrix of the transformation is computable, and the function is differentiable. In more detail, the regularization flow uses the mapping function $f : Z \longrightarrow Z'$, which is defined as follows:

$$q(Z') = q(Z)\left|det\frac{\partial f^{-1}}{\partial Z'}\right| = q(Z)\left|det\frac{\partial f}{\partial Z'}\right|^{-1}, \tag{18}$$

where $q(Z)$ is the distribution of the random vector Z and the transfer function f is invertible. To obtain an effective probability density $q_k(Z^{(k)})$from the initial density $q_0(Z)$, a series of hierarchical transformations of K regularization flows successively use equation (15) to calculate the target density.

Step 1: for each node$V_n$do
Step 2: constructing K-dimensional mixed membership vectors $\pi_n \sim \text{Dirichlet}(\alpha)$
Step 3: for each node pair(V_p, V_q)do
Step 4: constructor class initialization indicator variable $Z_{p\longrightarrow q} \sim \text{Multinomial}(\pi^p)$
Step 5: construct category indicator variable receiver $Z_{q\longrightarrow p} \sim \text{Multinomial}(\pi^q)$
Step 6: sample their interaction values $Y(p,q) \sim \text{Bernoulli}(Z_{p\longrightarrow q} \text{B} Z_{q\longrightarrow p})$

Algorithm 1: Generation process.

$$Z^k = f_k\left(Z^{(k-1)}\right) = f_k\left(f_{k-1}\left(\cdots f_2\left(f_1(Z)\right)\right)\right)$$

$$\ln q_k\left(Z^{(k)}\right) = \ln q_0(Z) - \sum_{k=1}^{k} \ln det\left|\frac{\partial f_k}{\partial Z'}\right| = q(Z)\left|det\,\frac{\partial f}{\partial Z^{(k)}}\right|. \tag{19}$$

If the mapping function is appropriate, then the learned mixture distribution of hidden random vectors more closely matches the distribution of the real data than the simple independent Gaussian distribution.

4.2.4. New Media Information Dissemination Speed and Scale Effect Predictor. Previous studies have found that information cascades have a time decay effect, i.e., the influence of one node on other nodes decreases over time [57]. In this paper, a nonparametric time decay function is used $\lambda_{f(T-t_j)}$, and according to the literature [25], we get the following:

$$h_i' = \sum_{j=1}^{R_i(T)} \lambda_{f\left(T-t_j\right)} h_{j.}' \tag{20}$$

Among them, $f(T-t_j) = \left\lfloor t_j - t_0/T/l \right\rfloor$, and R_T indicates the forwarding amount of h_i' new media information, indicating that the time decay function is considered.

The hidden state of the number.

The last part of the NWIDF model is composed of fully connected layers (MLP). According to the previous calculation h_i', it can be calculated ΔS_i as follows:

$$\Delta S_i = MLP\left(h_i'\right). \tag{21}$$

The final task is to predict the increment of information dissemination within the specified time interval, introducing MeanSquare Log-Transformed Error (MSLE), namely, the following:

$$MSLE = \frac{1}{N}\sum_{i=1}^{N}\left(\log \Delta S_i; -\log \Delta \widetilde{S}_i;\right)^2. \tag{22}$$

As the loss function loss, use the Adam optimizer to optimize the loss value to make it optimal (minimum).

Through the above synthesis, the following training process can be performed as shown in Algorithm 2.

5. Experiment Setup and Results Analysis

5.1. Test Setup

5.1.1. Dataset. To evaluate the effectiveness and scalability of NWIDF models in information cascade prediction, experiments are conducted using publicly available datasets and compared with previous studies. The data information statistics of the dataset are shown in Table 1.

Weibo [25]: this dataset selects all the original posts generated by Sina Weibo on June 1, 2016, and tracks all retweets of each post over the next 24 hours, including a total of 119,313 posts. Figure 4(a) shows the distribution of the cascade size; Figure 5(a) shows the prevalence of the cascade, showing that after 24 hours, the prevalence reaches saturation. This paper follows a similar setup to CasCN [26], i.e., observation time window $T = 1$, 2, 3 hours. Finally, the stacks are sorted according to the stacking time after preprocessing, and the top 70% of the stacks are selected as the training set for the stacks, and the rest are equally divided into the validation set and the test set.

HEP-PH [27]: the HEP-PH dataset (High Energy Physics Phenomenology Dataset) comes from the electronic version of the arXiv paper citation network. The data covers papers from January 1993 to April 2003 (124 months), in which there are citations for all 34,546 papers. If paper i cites paper J, the paper citation graph contains directed edges from i to j. If a paper cites or is cited by a paper outside the dataset, the graph will not contain information about this. Figure 4(b) shows the distribution of cascade sizes, and Figure 5(b) shows the prevalence of cascades. For the observation window, $T = 3$, 5, and 7 years were chosen, corresponding to the prevalence reaching 50%, 60%, and 70% of the final scale, respectively, as shown in Figure 5(b). Then, 70% of the cascades are collected for training, and the rest are split equally into validation and test sets.

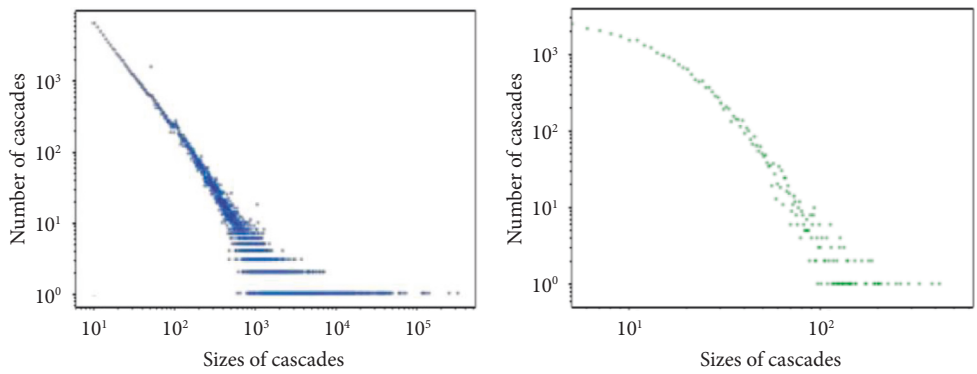

Figure 4: Cascade size distribution graph, the X-axis is the cascade size, and the Y-axis is the number corresponding to different cascade sizes. (a) Weibo dataset. (b) HEP-PH dataset.

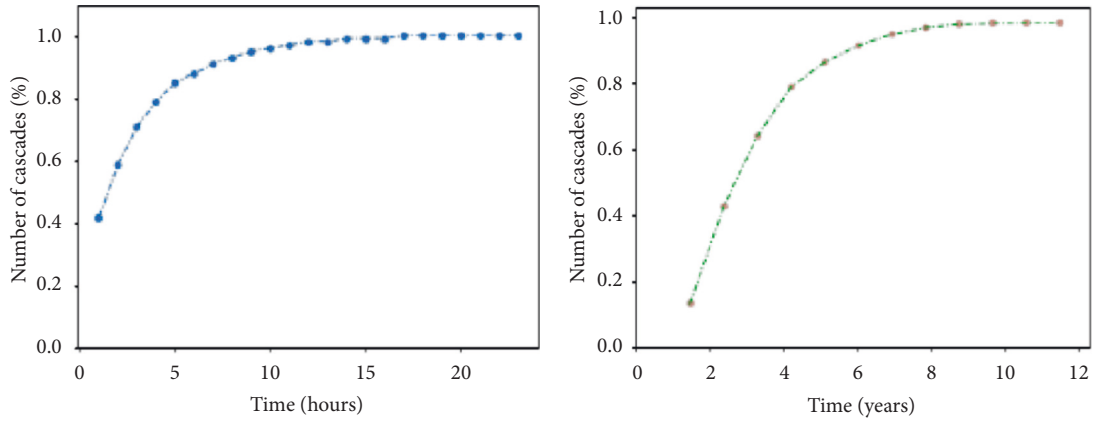

Figure 5: Percent distribution between time and number of cascades. (a) Weibo dataset. (b) HEP-PH dataset.

5.1.2. Benchmark Model Selection. From traditional cause analysis methods, hydrological statistics methods, time series analysis methods, etc., to modern artificial neural networks, wavelet theory, gray system and turbidity theory, each method has its own advantages because of its different mechanisms and applicable environments. To verify the effectiveness of our proposed NWIDF model in predicting the scale of information cascades, we choose three basic models: a feature engineering-based model (Topo-LSTM model [29]), a statistical generative model-based DeepHawkes model [25], and a deep learning based model CasCN model [26]. The comparative model is the latest model with high reliability in the research field, which can supplement and improve the comparative analysis research.

5.1.3. Parameter Setting. All experiments in this paper are performed on Ubuntu 16 operating system, Intel Core i9-9980XE CPU, 1286 memory, and NVIDIA TiTan RTX (24G) graphics card.

For DeepCas [28], DeepHawkes [25], Topo-LSTM [29], and CasCN [26], refer to DeepCas to set the user's embedding dimension to 50. The number of hidden units in the fully connected layer of the recurrent neural network is 32 and 16, respectively. The user learning rate 5×10^{-4}, and the other learning rate is 5×10^{-3}. The batch size of each iteration is 32, and when there are 50 consecutive iterations, the loss of the validation set does not drop, and the model training process will stop. The time interval for Weibo dataset was set to 10 minutes, and the time interval for HEP-PH was set to 2 months.

This paper uses Tensorflow to implement the NWIDF model and uses the Adam optimizer to optimize the parameters through gradient descent. Except that, the embedding neighborhood layer of graph representation learning adopts $K = 2$, and the rest of the model parameter settings are consistent with the above models.

5.1.4. Evaluation Indicators. According to the existing work, a standard evaluation metric, MSLE (see equation (22)), is selected in the experiment to evaluate the linking accuracy. Note that the smaller the MSLE, the better its prediction performance.

input: cascade graph C, sequence of cascade graph adjacency matrices $A = \{A_1^T, A_2^T, \cdots\}$, time window of observation $\Delta c = \{\Delta c_1, \Delta c_2, \cdots\}$
output: predicted information cascade incremental scale $\Delta S = \{S_1, S_2, \cdots\}$
(1) the Laplacian matrix of the Δc concatenated graph C;
(2) the graph wavelet $\varphi_{u,s}$ for each node u_i;
(3) compute the node embeddings of the information cascade graph $E_c(v_c)$;
(4) Calculate the node embedding of the global graph $E_g(v_g)$;
Calculate the global matrix $G_{ij} = X_{ij} + Y_{ij}$
(5) while not converge do
(6) Train a bidirectional gated recurrent unit to acquire h_2;
(7) for $|v_c|$ each user in the pair i do
(8) calculate z_i
(9) end for
(10) get $\overrightarrow{Z_1} = \{z_1, z_1, \cdots, z_{|v_c|}\}$;
(11) Train a cascaded variational autoencoder to obtain Z_2;
(12) Obtained by K transformations Z_3;
(13) Combining sums $h_2$and Z_3 sums $\Delta S_i = MLP(h_i')$ to make final scale incremental forecasts;
(14) end while

Algorithm 2: Learning process of the NWIFD model.

5.2. Result Analysis

5.2.1. Experimental Comparative Analysis

(1) Performance Comparison of the Benchmark Version. The benchmark version of the NWIDF model proposed in this paper will be experimentally compared with previous cascade prediction models on real datasets.

The DeepCas model [28] is the first deep learning architecture for information cascade prediction, which represents a cascade graph as a set of random walk paths, piped through a bidirectional GRU neural network with an attention mechanism to predict the size of the cascade. It mainly uses the information of structure and node identity for prediction.

The DeepHawkes model [25] integrates the predictive power of end-to-end deep learning into the interpretable factors of the Hawkes process for popularity prediction. The combination between deep learning methods and cascade dynamics modeling processes bridges the gap between the prediction and understanding of information cascades. This method belongs to both generative and deep learning-based methods.

The Topo-LSTM model [29] is a directed acyclic graph structure (DAG structure) RNN that takes a dynamic DAG as input and generates topology-aware embeddings as output for each node in the DAG, thereby predicting the next node.

Pak et al. proposed a particulate matter (PM) prediction model (CNN-LSTM) based on spatiotemporal convolutional network and long short-term memory network and applied it to the concentration prediction of PM2.5 in Beijing. Using mutual information to analyze the spatial-temporal correlation, considering the linear and nonlinear correlation between the target and the observed parameters and combining the historical air quality and meteorological data, the spatial-temporal eigenvectors reflecting the linear and nonlinear correlation between the parameters are constructed. (STFV), CNN-LSTM prediction model extracts the inherent relationship between PM2.5-related latency air quality and meteorological input data through CNN and reflects the long-term historical process of input time series data through LSTM, using 384 monitoring stations across the country for 3 years The validity of the model is verified by the air quality data and meteorological data. [26].

Singh et al. used deep learning for stock prediction and proposed a stock prediction model based on 2-dimensional principal component analysis (PCA) and deep neural network (DNN), which combined the closing price, highest price, and lowest price. 36 indicators, such as opening price, are used as the input of the stock prediction model, and the original data matrix is projected into the projection matrix by (2D)2PCA. The dimension of the input sample is reduced, and then the dimension-reduced data is used as the input of DNN in the prediction model. Finally, get the predicted closing price. Compared with the radial basis function neural network (RBFNN), in the stock forecast of Google in Nasdaq, the network (RBFNN) rate is improved by 4.8%, and the actual return (i.e., the correlation coefficient with the predicted return of information dissemination) is 17.1% higher than that of RBFNN [27].

The CasCN model [26] combines the deep learning framework of structure and time, uses graph convolutional network to capture network spatial structure information, and incorporates temporal decay function using a recurrent neural network to achieve the more efficient use of temporal information. This model is a deep learning method.

Table 2 summarizes the performance comparison between the NWIDF model and other model benchmarks on the Weibo and HEP-PH datasets. The comparison of the NWIDF model with the DeepCas model proves that it is not enough to simply embed nodes as a graph representation, and it cannot represent the graph as a set of random paths. Because DeepCas fails to consider timing information and

Table 1: Dataset information statistics table.

Dataset		Weibo_			HEP-PH		
Post–papers edges T	All	119313			34546		
	All	8466858			421578		
		1 hour	2 hours	3 hours	3 years	5 years	7 years
Cascades	Train	25145	29515	31780	3458	3467	3478
	Val	5386	6324	6810	837	839	848
	Test	5386	6324	6810	837	839	848
Avg.nodes	Train	28.58	29.3	29.48	5.27_	5.27_	5.27_
	Val	28.71	29.47	29.69	4.32_	4.93_	4.27_
	Test	29.11	29.77	30.21	4.91_	4.27_	4.28_
Avg.nodes	Train	27.78	28.54	28.74	4.27_	4.27_	4.27_
	Val	27.91	28.7	28.94	3.31_	3.93_	3.95_
	Test	28.32	29.01	29.48	3.91_	3.27_	3.28_

Table 2: Performance comparison table (MSLE).

Data set	Weibo (hours)			HEP-PH (year)		
	1	2	3	3	5	7
DeepCas	2.958	2.689	2.647	1.765	1.538	1.462
Topo–LSTM	2.772	2.643	2.423	1.684	1.653	1.573
Deep–Hawkes_	2.441	2.287	2.252	1.581	1.47	1.233
CasCN	2.242	2.036	1.916	1.004	0.917	0.887
NWIDF	**2.123**	**2.012**	**1.776**	**0.939**	**0.843**	**0.812**

Table 3: Global graph for information cascade prediction performance comparison table (MSLE).

Data set	Weibo (hours)			HEP-PH (year)		
	1	2	3	3	5	7
CasCN $K=2$	2.242_	2.036_	1.916_	1.004_	0.917_	0.887_
NWIDF–All $K=1$_	2.136_	2.074	1.858_	1.02_	0.892_	0.842_
NWIDF–All $K=2$	2.099_	2.028_	1.835_	0.92_	0.907_	0.867_

topology of cascaded graphs, its performance is worse than other deep learning-based methods. Topo-LSTM also lacks the processing of timing information, resulting in its poor performance. Although the DeepHawkes models cascades in a generative manner, it does not perform optimally because of its weak ability to learn structural information. CasCN considers temporal information and spatial topology but ignores the fusion between the two features. Finally, the NWIDF model proposed in this paper performs information cascade prediction (tweet retweets and paper citations) on both datasets, which is significantly better than other models. For example, in the Weibo dataset for 1, 2, and 3 hours, the MSLE values were 2.123, 2.012, and 1.776, respectively. Observing in the HEP-PH dataset for 3, 5, and 7 years, the MSLE values are 0.939, 0.843, and 0.812, respectively. The data shows that a good prediction effect has been achieved. Compared with CasCN, the prediction errors of the NWIDF model proposed in this paper are reduced by 5.31%, 1.18%, 7.31%, and 6.47%, 8.07%, 8.46%, respectively, thus confirming the effectiveness of the model.

5.2.2. The Influence of Global Graph on Information Cascade. NWIDF-All: we removed the structure learning module in the NWIDF model. For NWIDF-All, all nonroot nodes in the information cascade graph are directly connected to the root node, and we do not use global graph information.

Firstly, the validity of the bidirectional recurrent neural network is verified, and experiments are designed. Construct a shortened version of NWIDF-GRU, namely, BiGRU in the benchmark version, and then compare it with CasCN, which is equivalent to NWIDF-GRU, adding attention mechanism on the basis of the CasCN model. During the experiment, the parameters of the two are the same, and the experimental results when the sampling neighborhood layers $K=1$, 2 are shown in Table 3.

The performance comparison of the embedding layer $K=1$, 2 and the CasCN model $K=2$ is given in Table 3. According to Table 3, it can be seen that when $K=2$, the NWIDF model proposed in this paper is better than the CasCN model because the node embedding of the global graph is considered, which can couple the timing information and the spatial structure information. When $K=1$, after observing in Weibo for 2 hours, the MSLE of NWIDF-All is larger than that of CasCN. As $K=1$, the spatial structure information taken is insufficient, resulting in slightly lower results.

Then, the effect of timing information on cascade prediction is verified. Analyze the variant NWIDF-BiGRU of NWIDF, i.e., remove the bidirectional recurrent neural network from the NWIDF model proposed in this paper, and use BiGRU to compare with CasCN, which is equivalent to NWIDF-BiGRU, which is generated by replacing LSTM in the CasCN model with the BiGRU model. From the data in Table 4, it can be seen that when $K=2$, the MSLE = 1.783 observed by Weibo for 3 hours and the MSLE = 0.84 observed by HEP-PH for 7 years are better than the MSLE of CasCN. Thus, the importance of timing information in information cascade is confirmed.

Finally, to verify the impact of time series information and spatial information on cascade prediction, we use BiGRU on the basis of CasCN, add a structure learning mechanism, and then adjust the number of embedded neighborhood layers K to compare with CasCN, respectively. It can be seen from the data in Table 5 that when $K=1$,

Table 4: Time series network impact cascade prediction performance comparison table (MSLE).

Data set	Weibo (hours)			HEP-PH (year)		
	1	2	3	3	5	7
CasCN $K=2$	2.242_	2.036_	1.916_	1.004_	0.917_	0.887_
NWIDF–BiGRU $K=1$	2.198_	2.075	1.872_	0.995	0.845_	0.884_
NWIDF–BiGRU $K=2$	2.17_	2.065_	1.783_	0.946	0.826_	0.84_

Table 5: Time series space impact cascade prediction performance comparison table (MSLE).

Data set	Weibo (hours)			HEP-PH (year)		
	1	2	3	3	5	7
CasCN $K=2$	2.242_	2.036_	1.916_	1.004_	0.917_	0.887_
NWIDF $K=1$	2.18_	2.032_	1.801_	0.973_	0.819_	0.807_
NWIDF $K=2$	2.123_	2.012_	1.776_	0.939_	0.843_	0.812_

2 on Weibo and HEP-PH datasets, MSLE values are smaller than those of CasCN, indicating that the model proposed in this paper is better than CasCN in terms of time series information and spatial topology information. The capture is more comprehensive, which improves the efficiency of the model and reduces the loss rate.

The above experiments show that time series information and spatial structure information have an important impact on the information cascade prediction effect. The combination of the two can better ensure the accuracy of prediction. The capture of information is also more comprehensive, which also makes the model more generalizable.

6. Conclusion

Under the background of the wrong public opinion orientation caused by the rapid spread of new media information and its wide spread, it is of great practical significance to carry out the prediction of the spread of new media information and the scale effect. Based on the fact that the current hierarchical model of new media information dissemination lacks global and local models, this paper starts from the characteristics that new media information conforms to node dissemination and conducts prediction research on the speed and scale effect of new media information dissemination. The main research contents are as follows [24]:

(1) The modeling method of local and global propagation of the characteristics of new media information propagation is proposed, and considering the uncertainty and scale effect of information propagation, a graph neural network-based NWIDF model is proposed, which starts from the information cascade structure. Graph the structure learning for information propagation based on locality and globality.

(2) On the two large-scale information cascade datasets of Facebook and TikTok, the current mainstream and advanced prediction models are applied to carry out experimental research, and it is found that the NWIDF model has better prediction effect and performance. To a certain extent, it can predict the spread and scale of new media information and public opinion, control the rapid spread of wrong public opinion, and quickly cut off the communication channel to provide more advanced ideas.

In this paper, the NWIDF model is the hotspot of current network and graph neural network research. The main difference in speed is the large-scale graph and scale effect of new media information dissemination, and other types of features are caused by the complexity of the research content. In this paper, the NWIDF model is not extended to other types of features, such as learning various content features (number of user attention, h-index of authors, historically published articles, etc.). However, it provides a richer theoretical and practical basis for the future use of more powerful and complex graph neural networks, such as heterogeneous information networks with multiple node types and edge types. The model can be generalized to other types of graph-based business applications, such as virus information diffusion, interpretable information prediction, rumor detection, epidemic control, etc.

Data Availability

The dataset can be accessed upon request.

Conflicts of Interest

The authors declare that there are no conflicts of interest.

References

[1] A. Tatar, M. D. De Amorim, S. Fdida, and P. Antoniadis, "A survey on predicting the popularity of web content," *Journal of Internet Services and Applications*, vol. 5, no. 1, p. 8, 2014.

[2] Z. Zhang, F. Zhang, and X. Chen, "Etc. Information cascade prediction model based on hierarchical attention," *Computer Science*, vol. 46, no. 6, pp. 210–209, 2020.

[3] X. Xu, F. Zhou, K. Zhang, S. Liu, and G. Trajcevski, "CasFlow: exploring hierarchical structures and propagation uncertainty for cascade prediction," *IEEE Transactions on Knowledge and Data Engineering*, vol. 8, p. 1, 2022.

[4] C. Li, J. Ma, X. Guo, and Q Mei, "Deepcas: an end-to-end predictor of information cascades," in *Proceedings of the The Web Conference (WWW)*, pp. 577–586, Perth, Australia, April 2017.

[5] B. Perozzi, R. Al-Rfou, and S. S.. Deepwalk, "Online learning of social representations," in *Proceedings of the ACM SIGKDD Conference on Knowledge Discovery and Data Mining (KDD)*, New York, USA, August 2014.

[6] J. Chung, C. Gulcehre, K. H. Cho, and Y Bengio, "Empirical evaluation of gated recurrent neural networks on sequence modeling," 2014, https://arxiv.org/abs/1412.3555.

[7] D. Bahdanau, K. Cho, and Y. Bengio, "Neural machine translation jointly learning to align and translate," in

Proceedings of the International Conference on Learning Representations (ICLR), pp. 1–15, San Diego, CA, USA, May 2015.

[8] C. Li, X. Guo, and Q. Mei, "Joint Modeling of Text and Networks for cascade prediction," *International Conference on Web and Social Media (ICWSM)*, vol. 12, pp. 640–643, 2018.

[9] G. Chen, Q. Kong, and W. Mao, "An attention-based neural popularity prediction model for social media events," in *Proceedings of the IEEE International Conference on Intelligence and Security Informatics*, pp. 161–163, Beijing, China, July 2017.

[10] J. Pennington, R. Socher, and C. D. M.. Glove, "Global vectors for word representation," *Conference on Empirical Methods in Natural Language Processing*, vol. 15, pp. 1532–1543, 2014.

[11] A. Grower and J. L.. node2vec, "Scalable Feature Learning for networks," in *Proceedings of the ACM SIGKDD Conference on Knowledge Discovery and Data Mining (KDD)*, pp. 855–864, San Francisco, California, USA, August 2016.

[12] B. Wu, W.-H. Cheng, Y. Zhang, and Q Huang, "Sequential prediction of social media popularity with deep temporal context networks," in *Proceedings of the International Joint Conference on Artificial Intelligence (IJCAI)*, pp. 3062–3068, Melbourne, Australia, August 2017.

[13] K. He, X. Zhang, S. Ren, and J Sun, "Deep residual learning for image recognition," in *Proceedings of the IEEE/CVF Conference on Computer Vision and Pattern Recognition (CVPR)*, pp. 770–778, Las Vegas, Nevada, USA, June 2016.

[14] S. Hochreiter and J. Schmidhuber, "Long short-term memory," *Neural Computation*, vol. 9, no. 8, pp. 1735–1780, 1997.

[15] X. Chen, F. Zhou, K. Zhang, and G Trajcevski, "Information diffusion prediction via recurrent cascades convolution," in *Proceedings of the International Conference on Data Engineering (ICDE)*, pp. 770–781, Macao, China, April 2019.

[16] Q. Cao, H. Shen, J. Gao, and B Wei, "Popularity prediction on social platforms with coupled graph neural networks," in *Proceedings of the ACM International Conference on Web Search and Data Mining (WSDM)*, pp. 70–78, Bingzheng Wei, January 2020.

[17] D. K. Hammond, P. Vandergheynst, and R. Gribonval, "Wavelets on graphs via spectral graph theory," *Applied and Computational Harmonic Analysis*, vol. 30, no. 2, pp. 129–150, 2011.

[18] C. Donnat, M. Zimik, D. Hallac, and J Leskovec, "Learning structural node embeddings via diffusion wavelets," in *Proceedings of the ACM SIGKDD Conference on Knowledge Discovery and Data Mining (KDD)*, pp. 1320–1329, UK, London, July 2018.

[19] E. Lukacs, *Characteristic functions[M]*, Griff'm, London, UK, 1970.

[20] J. Zhang, Y. Dong, Y. Wang, and J Tang, "ProNE: fast and scalable network representation learning," in *Proceedings of the International Joint Conference on Artificial Intelligence (IJCAI)*, pp. 4278–4284, Macao, China, August 2019.

[21] T. Tao, *Topics in Random Matrix theory*, American Mathematical Society, Washington, DC, USA, 2012.

[22] W. Fan, Y. Ma, Q. Li, and Y He, *Graph Neural Networks for Social Recommendation*, in *Proceedings of the The World Wide Web Conference*, pp. 417–426, San Francisco, CA, USA, May 2019.

[23] J. Atwood and D. Towsley, "Diffusion-convolutional neural networks," *Advances in neural information processing systems*, vol. 29, 2016.

[24] J. Cheng, L. Adamic, P. A. Dow, and J. M Kleinberg, "Can cascades be predicted?" in *Proceedings of the The Web Conference (WWW)*, pp. 925–936, Seoul, Korea, April 2014.

[25] Q. Cao, H. Shen, K. Cen, and O Wentao, "Deephawkes: bridging the gap between prediction and understanding of information cascades," in *Proceedings of the 2017 ACM on Conference on Information and Knowledge Management*, pp. 1149–1158, Singapore, November 2017.

[26] X. Chen, F. Zhou, K. Zhang, and T Goce, "Information diffusion prediction via recurrent cascades convolution," in *Proceedings of the 2019 IEEE 35th International Conference on Data Engineering (ICDE)*, pp. 770–781, Macao, China, April 2019.

[27] J. Leskovec, J. Kleinberg, and C. Faloutsos, "Graphs over time: densification laws, shrinking diameters and possible explanations," in *Proceedings of the eleventh ACM SIGKDD international conference on Knowledge discovery in data mining*, pp. 177–187, Chicago, Illinois, USA, August 2005.

[28] C. Li, J. Ma, X. Guo, and M Qiaozhu, "Deepcas: an end-to-end predictor of information cascades," in *Proceedings of the 26th international conference on World Wide Web*, pp. 577–586, Perth, Australia, April 2017.

[29] J. Wang, V. W. Zheng, Z. Liu, and C.C. C Kevin, "Topological Recurrent Neural Network for Diffusion Prediction," in *Proceedings of the IEEE International Conference on Data Mining (ICDM)*, pp. 475–484, New Orleans, LA, USA, December 2017.

Hindawi
Scientific Programming
Volume 2022, Article ID 3601265, 12 pages
https://doi.org/10.1155/2022/3601265

Research Article

Generic Structure Construction of 3D Assembly Model Based on Conjugate Subgraph

Hu Qiao,[1] Liang You,[1] Sibo Hu,[1] Shanshan Liu,[1] and Ying Xiang[2]

[1]*School of Mechatronic Engineering, Xi'an Technological University, Xi'an 710021, Shaanxi, China*
[2]*College of Mechanical and Electrical Engineering, Shaanxi University of Science and Technology, Xi'an 710021, Shaanxi, China*

Correspondence should be addressed to Ying Xiang; yingcara@hotmail.com

Received 24 June 2022; Accepted 3 August 2022; Published 19 September 2022

Academic Editor: Lianhui Li

As an important resource under the background of digital design technology, 3D assembly model plays a great role in many complex product design occasions. Based on the existing 3D model database, how to find and reuse the effective information that meets their own needs in many models is one of the important ways to provide design efficiency. The research content of this paper is to build a general assembly model according to the requirements of 3D assembly model. Based on the common structure, the general structure aims to integrate as much model information as possible to meet the design needs of designers in different periods and conditions. Due to the large number of components in the 3D assembly model, blindly improving hardware cost is the root of the problem. To improve quality and efficiency from the source, we need to start with the source of input. This paper simplifies the analysis of 3D assembly model information, which can not only improve the construction efficiency of the general structure of 3D assembly model but also highlight the assembly characteristics of 3D assembly model and facilitate the matching of assembly features during the construction process. Firstly, based on the attributes of assembly features and matching relationship, combined with the idea of conjugate, the matching problem between two features in the model is solved by using the idea of conjugate subgraph matching. Secondly, based on the Ullmann algorithm, combined with the definition of conjugate subgraph and related optimization operations, a conjugate subgraph matching algorithm based on vertex screening is proposed. Finally, the construction process of the general structure is proposed, and the general structure of 3D assembly model is established.

1. Introduction

With the progress of the times and the innovation of science and technology, CAD model has made a qualitative leap in the traditional function. 3D assembly model contains much reusable information reflecting the design intention, such as structure, function, and attributes. In the design and manufacturing of products, scholars at home and abroad have done a lot of research on the mining and reuse of relevant information for CAD models [1–8]. In the process of information reuse, designers often pay more attention to local similarity comparison. Because the overall similarity almost does not exist, and the local similarity is easy to analyze and obtain, it can also better realize the reuse of model information. The construction of the general structure of 3D assembly model and the related research on design reuse are essentially the matching process of subgraph isomorphism. The process of building a general structure is mainly isomorphic matching and updating, until a comprehensive and general 3D assembly model general structure is generated. The design reuse of 3D assembly model mainly carries out subgraph isomorphic matching and semantic information matching with the general structure according to the information corresponding to the design intention provided by the designer, to provide a series of model structure information with reference value. For the NP complete problem of subgraph isomorphism, scholars at home and abroad have conducted in-depth research and achieved many results, which have been widely used in many fields.

Ullmann [9], based on the backtracking method, simplified the mapping matrix in the matching process and carried out corresponding isomorphic matching according to the adjacency relationship between vertices. Wang [10]

combined the advantages of Ullmann algorithm and VF2 algorithm, first pruned through the adjacency relationship between vertices based on Ullmann algorithm. Then, based on VF2 algorithm, the vertex matching order is changed to realize fast pruning. Ma et al. [11] proposed filtering and simplification based on Ullmann algorithm. The corresponding isomorphic matching process is carried out through neighbor filtering, partial simplification, and the selection order of adding matching graph vertices. Choi et al. [12] considered various design problems and analyzed the incremental hybrid genetic algorithm for subgraph isomorphism problem to improve the performance of the algorithm. Fehér et al. [13] proposed a subgraph isomorphism algorithm based on MapReduce framework to match font patterns in any large map. Chen et al. [14] provided a method to solve the isomorphism problem of the maximum common subgraph by generating a weighted graph, in which the weight represents the probability that the associated link is in the maximum common subgraph of two input graphs. Xu et al. [15] proposed extended subgraph matching and, combined with the different characteristics of Ullmann algorithm and QuickSI, gave the corresponding edging algorithm to optimize the processing of distance information. Rong et al. [16] constructed the information representation of process model based on attribute adjacency graph and improved the subgraph isomorphism algorithm to obtain processing features. Tang [17] proposed a similarity evaluation method based on improved random walk graph matching for 3D part models and a similarity evaluation method based on tree graph matching for 3D assembly models, to improve the matching efficiency. Dong et al. [18], based on algebraic theory, taking unlabeled graph as the research object, established subgraph isomorphism algorithms from two aspects of eigenvalue construction and degree sequence, to realize the graph isomorphism matching of directed graph and undirected graph.

This paper studies the model representation method based on attribute assembly feature adjacency graph and puts forward a general structure construction method of 3D assembly model. Firstly, this method analyzes the related concepts such as assembly features and assembly relationship, introduces the idea of conjugate, and gives the definition of practical guiding significance between the matched part features. Based on the matching algorithm of conjugate subgraphs, the matching problem is solved by combining the matching algorithms of conjugate subgraphs. Finally, the construction process of general structure is formed, and the general structure of 3D assembly model is established.

2. Materials and Methods

2.1. Method for Representation of 3D Assembly Model Information. The representation of 3D assembly model information should include topological structure information that can express the structural resources related to the model, semantic information such as part name, type, and function, and some characteristic information that can express the matching relationship between parts.

Graph model representation takes graph theory as a tool and is mainly composed of nodes and edges. Graph model can be used to describe the connection relationship between structures of 3D assembly model. In the process of design and manufacturing, there are also mature methods and properties to solve relevant problems based on graph theory. Therefore, the representation method of graph model is favored by scholars and applied to many research fields.

2.1.1. Definition of Feature Adjacency Graph of Attributed Assembly

Definition (1): Attributed Adjacency Graph (AAG). It mainly takes the part face as the node and the adjacency relationship between faces as the edge of the graph representation model to represent the topological relationship of the part, which is often expressed by $G = \{V, E, \alpha, \beta\}$, wherein V represents the set of nodes, and any element v_i in the set meets the corresponding relationship with one side in the part; E represents the set of edges, which is the adjacency relationship of faces, and any element in the set has an element in V corresponding to it, mainly including the geometric type of faces, the number of edges of faces, and so on; and β represents the attribute set of edges, and any element in the set has an element in E corresponding to it, mainly including the type of edges and the position relationship of adjacent faces.

In this paper, the shape features of the model are divided into assembly features and nonassembly features. The assembly features include the assembly information in the parts, which is used to construct the main shape of the parts, which plays a decisive role in the assembly process of the 3D assembly model. Nonassembly features are auxiliary features in parts, which are local modifications of part information, and play little role in the assembly process of 3D assembly model. Based on the AAG of 3D model, this paper first maintains the assembly feature information in the part model and then uses semantic nodes to replace other information in the model, so as to construct the attributed assembly feature adjacency graph of parts. Its definition is as follows.

Definition (2): Attribute Assembly Feature Adjacency Graph. It is a graphic representation that focuses on the assembly features in the part model, which is represented by $G = \{V, E, \alpha, \beta, V_0\}$, where V represents the set of nodes, and any element v_i in the set corresponds to one side f_i in the part assembly feature; E represents the set of edges, and any element e_j in the set corresponds to the side composed of adjacent faces f_n and f_m in the part assembly feature; α represents the attribute set of the node, mainly including the geometric type of the face, the number of sides of the face, and so on; and β represents the attribute set of edges, mainly including the type of edges and the positional relationship of adjacent faces and so on. $V_0 = \{I_N, I_F, I_C\}$ represents the semantic node of the part. It is the semantic expression of other information in the part except assembly features, including semantic information such as part name (I_N), function (I_F), and category (I_C).

2.1.2. Construction of AAG of the 3D Assembly Model. From the 3D model assembly, designers can obtain comprehensive assembly information. For example, two parts in contact with each other in an assembly can be divided into contact connection and assembly connection by judging whether they have assembly properties, while assembly link represents the fact that the two parts have assembly properties and then analyzes the connection relationship. The assembly properties can be divided into riveting, key connection, pin connection, thread connection, and so on. In the process of model reuse, designers should focus on the mating connection between parts. This paper classifies and codes the connection relationship of assembly link and the contact type of mating surface, as shown in Tables 1 and 2. For example, the code "a3" represents the fact that the part assembly link relationship is riveting, and the contact type of mating surface is cylindrical-cylindrical contact.

Taking the assembly process of the 3D assembly model shown in Figure 1 as an example, the 3D assembly model shown in Figure 1(c) is assembled and combined by part A shown in Figure 1(a) and part B shown in Figure 1(b). By searching the assembly features corresponding to the model and relevant process documents, it can be obtained that the connection relationship between parts is "threaded connection," and the contact type of mating surface is "cylindrical-cylindrical contact."

Based on the construction steps of AAG of 3D assembly model, parts A and B are represented by graph models as shown in Figures 2(a) and 2(b), and the shaded part represents the mating surface. Then, code according to the contact coding rules of the mating surface above, so that the mating surfaces are assembled into a node, which is named as the mating node, that is, the node marked "d3" in the figure ("d" refers to "threaded connection" and "3" refers to "cylindrical-cylindrical contact"). Thus, the model AAG is constructed, and the results are shown in Figure 2(c).

2.2. General Structure Construction of the 3D Assembly Model Based on Conjugate Subgraph. Based on the model representation method in Section 2.1, this section realizes the construction of general structure of 3D assembly model through three steps. Firstly, the related concepts such as assembly features and fit relationship are analyzed, and the idea of conjugate is introduced to give the definition of matching part features with practical guiding significance. Then, based on the graph isomorphism algorithm and the related properties of conjugate subgraphs, the matching problem of assembly features in 3D assembly model is solved by conjugate subgraph matching algorithm based on vertex screening. Finally, the construction process of general structure is formed, and the general structure of 3D assembly model is established.

2.2.1. Relevant Definitions and Concepts

(1) Assembly Features. In the current industrial design and manufacturing, most of the features are defined as the combination of shape and function. The feature is the specific mapping of relevant shapes and is endowed with specific multisource information. In the 3D assembly model, the assembly feature is the information that represents the assembly attributes of parts; that is, it represents the assembly information such as methods and attributes contained in the cooperation between parts [19].

Table 1: Classification code of connection relationship type.

Serial number	Code	Connection relationship type
1	*a*	Riveting
2	*b*	Key connection
3	*c*	Pin connection
4	*d*	Threaded connection
5	*e*	Other

Table 2: Classification code of contact type of mating surface.

Serial number	Code	Contact type of mating surface
1	0	Plane-plane contact
2	1	Tooth-tooth contact
3	2	Plane-tooth contact
4	3	Cylindrical-cylindrical contact
5	4	Other

(2) Assembly Relationship. In the 3D assembly model, the assembly relationship plays an important role in the model expression, which can be regarded as the constraint relationship among the corresponding points, lines, and faces in the model. Analyzing the assembly relationship from the perspective of engineering design, there are many forms of assembly relationships in the actual design and manufacturing such as surface fitting, alignment, isometric surface reversing, isometric surface of the same direction, coaxial, etc., same direction isometric, coaxial and so on [20]. However, the most commonly used assembly relationships mainly include surface fitting and coaxial assembly for the consideration of assembly stability and economy.

(1) Face fitting: the two surfaces of parts in the assembly contact with opposite normal vectors. In the bolt connection shown in Figure 3, the end faces of part A and part B fit together, and the red part indicates the assembly part of surface fit.

(2) Coaxial assembly: the axes of two feature surfaces are collinear. In the bolt connection shown in Figure 3, part A and part B are coaxial with the bolt respectively, and the blue part indicates the coaxial assembly position.

(3) Conjugate Subgraph. In the actual design and manufacturing, there are many matching relationships such as those shown in Figure 3. Through the analysis of many assembly relationships, it can be observed that the topological structures of the two parts to be assembled in the 3D assembly model are usually the same, and the surface normal vector and edge attributes are often opposite. Based on the attribute assembly feature adjacency graph of parts, the idea of conjugate is introduced to express the assembly relationship between 3D assembly models. Yoke in life refers to the shelf on the back of two cows. It can play the role of allowing two cows to walk synchronously. Conjugation means that two parts are assembled with each other

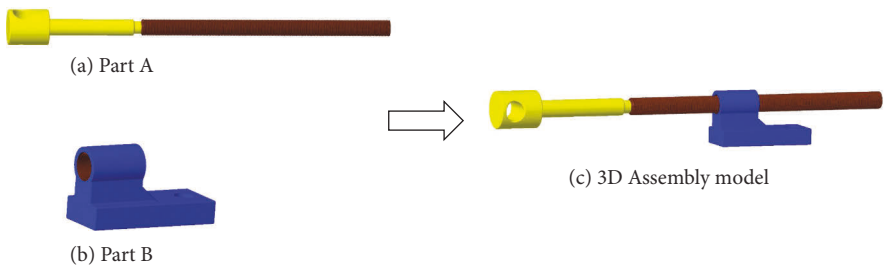

Figure 1: Assembly diagram of 3D assembly model. (a) Part A, (b) part B, and (c) 3D assembly model.

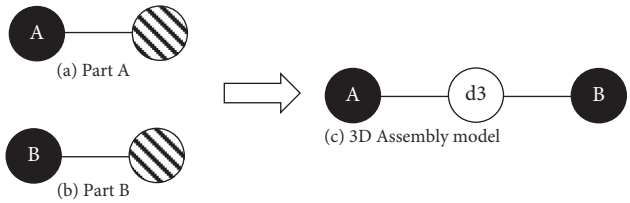

Figure 2: Construction diagram of AAG of the 3D assembly model. (a) Part A, (b) part B, and (c) 3D assembly model.

according to specific laws, commonly known as twinning. Twins are similar in general and slightly different in detail. Therefore, the definition of conjugate subgraph is as follows.

Definition (3): Conjugate Subgraph. In the 3D assembly model, there are two parts assembled with each other, and their attribute assembly features are adjacent to some assembly feature parts (subgraphs) represented by the graph. The two subgraphs have the same topological connection form, but the edge attributes in the graph are just opposite, so the two subgraphs are called common yoke subgraphs.

A 3D assembly model of a slider coupling is composed of Part 1, Part 2, and Part 3, shown in Figure 4. Traverse each face of the three parts of the slider coupling, and extract the geometric attributes and relevant semantic information of the fitting surface of the part assembly features as the node attributes based on the relevant definitions of the attribute assembly feature adjacency graph and conjugate subgraph. Identify the relationship between adjacent faces as the attributes of corresponding edges, so as to construct the corresponding attribute assembly feature adjacency diagram of each part, as shown in Figure 5. Among them, the two corresponding subgraphs in the green coil are conjugate subgraphs with assembly relationship between parts.

By observing the conjugate subgraph shown in Figure 5, the following properties can be obtained:

(1) Conjugate subgraphs have the same topology

(2) The face type, assembly requirements, and other attributes of each corresponding vertex in the figure are the same, but the face normal vector is opposite

(3) The attributes of the corresponding edges in the figure are opposite; for example, the concavity and convexity are opposite

(4) General Structure of the 3D Assembly Model. The common structure of the 3D assembly model is known. Each part in the common structure has several assembly features. Each part in the common structure is matched through the conjugate subgraph to match the parts and components with conjugate relationship, because, in the current assembly scene, there are often more than one component matching with the assembly features of the part. After conjugate subgraph matching, a set of AAG that meet the assembly requirements may be obtained. Therefore, a general set corresponding to the part is constructed, and its definition is shown in Definition 4.

Definition (4): General Set. The function of this set is to store the AAG of parts and components that meet the conjugate relationship with a part, which is expressed by a formula. Any graph in the set and all the adjacency graphs meet the conjugate subgraph matching with the attribute assembly feature adjacency graph of the part.

Until all the parts and components in the current scene are matched, the general set corresponding to each part meeting the conjugate relationship in the common structure is constructed, and finally a complex AAG is obtained, which is the general structure of 3D assembly model.

2.2.2. Method for Assembly Feature Matching Based on the Conjugate Subgraph. The matching problem of assembly features is basically the matching problem of conjugate subgraphs. The matching problem of conjugate subgraphs is essentially the matching problem of subgraph isomorphism. The main process includes the following steps: in the current matching environment, convert the components to be matched into the corresponding AAG representation. The conjugate subgraphs are matched with the parts and components in the common structure of the 3D assembly model, that is, the conjugate subgraphs that meet the same structure, the same node surface type, assembly requirements, and other attributes, and the opposite surface normal vector and the opposite edge attributes are searched for matching.

(1) Ullmann Algorithm. Ullmann algorithm mainly stores the matrix of the mapping relationship between the vertices of any two graphs, to judge the isomorphism of the two graphs. After one operation, this algorithm can enumerate all *isomorphic* subgraphs, so it is also called enumeration algorithm.

It is known that there are two AAG G_A and G_B, n_A and n_B represent the number of vertices of the two graphs, respectively, s_A and s_B represent the number of edges of the two

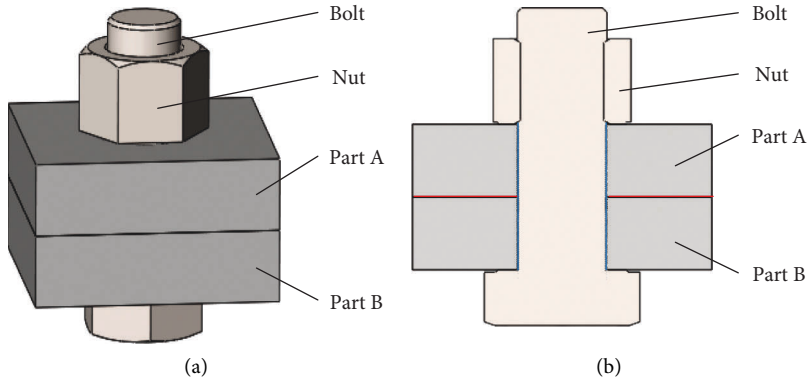

Figure 3: Bolt connection and bolt connection section. (a) Bolted connection. (b) Bolted connection section.

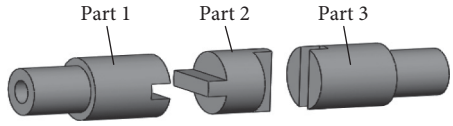

Figure 4: Slider coupling.

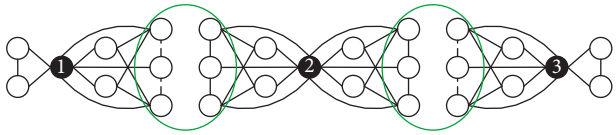

Figure 5: Attribute assembly feature adjacency diagram of slider coupling.

graphs, respectively, $n_A < n_B$, and $s_A < s_B$. $M_A = [a_{ij}]$ and $M_B = [b_{ij}]$ represent the adjacency matrix of the two graphs, respectively. The vertex correspondence between G_A and G_B is represented by vertex mapping matrix $\boldsymbol{M}$, where $\boldsymbol{M}$ is $n_A \times n_B$ matrix and m_{ij} is an element in $\boldsymbol{M}$, which mainly refers to the elements in row i and column j of the matrix, representing the matching relationship between node i of G_A and node j of G_B. If there is no mapping relationship between node i of G_A and node j of G_B, then $m_{ij} = 0$. If there is a mapping relationship between node i of G_A and node j of G_B, then $m_{ij} = 1$. If and only if each row in $\boldsymbol{M}$ has only one element $m_{ij} = 1$ and each column has at most one element $m_{ij} = 1$, it is said that the subgraphs of G_A and G_B are isomorphic.

When G_A and G_B satisfy the isomorphism condition of subgraphs, the elements in vertex mapping matrix $\boldsymbol{M}$ will remain unchanged. This is because when the element in $\boldsymbol{M}$ conforms to the formula

$$(\forall x)\left((a_{ix} = 1) \Rightarrow (\exists y)\left(m_{xy} \bullet b_{yj} = 1\right)\right) \quad (1 \le x \le n_A, 1 \le y \le n_B). \tag{1}$$

Then, in $\boldsymbol{M}$, the elements $m_{ij} = 1$ will not change. Therefore, $\boldsymbol{M}$ constructs the vertex mapping relationship between G_A and G_B. If any two vertices in G_A have adjacency relationship, two adjacent vertices with vertex mapping relationship with G_A can also be found in G_B, so that the edge also has corresponding mapping relationship.

The basic idea of Ullmann algorithm is as follows: in the whole process of isomorphic matching, always check whether each row in $\boldsymbol{M}$ has an element $m_{ij} = 1$. If the element is not found, it means that there is no corresponding vertex in G_B that matches the vertex of G_A, and then the isomorphism condition is not tenable, so exit the program. If this element exists, then the matrix $\boldsymbol{M}$ is traversed in turn, and finally an isomorphic subgraph that meets the needs of the designer can be matched.

To sum up, the basic steps of Ullmann algorithm are as follows:

Input: G_A and G_B

Input: isomorphic subgraph.

Step 1. Initialize the vertex mapping matrix $\boldsymbol{M}$ and the incidence matrix M_0, whose size is $n_A \times n_B$.

Step 2. Define Atlas G_0 to store matching pairs of vertices.

Step 3 Starting from $r = 1$, traverse each row $r = r + 1$ in $\boldsymbol{M}$. If there is an element $m_{ij} = 1$, store the vertex matching pairs of graphs G_A and G_B corresponding to m_{ij} in G_0. The matching value of the vertex of the corresponding graph G_B in M_0 and other vertices is 0. Until $r = n_A + 1$, jump to step 6.

Step 4. Traverse all vertices in Atlas G_0; if there is a corresponding mapping relationship between the two vertices, $m_{pq} = 1$. If not, $m_{pq} = 0$.

Step 5. In the mapping matrix obtained by traversing step 4, if each row of the matrix has only one 1, and each column has at most one 1, then the subgraph of G_0 is isomorphic, and step 3 is repeated according to the matrix elements in M_0. Otherwise, the subgraph is not isomorphic, and step 3 is returned.

Step 6. At the end of the algorithm, the vertex pairs in G_0, that is, the isomorphic subgraphs of G_A and G_B, are output.

Ullmann algorithm adopts the method of depth first in matching. The whole process uses Boolean matrix to record relevant data. When there is no mapping relationship between them, it returns the nearest matching node and reexplores other matching objects. At the same

Table 3: Symbolic meaning.

Symbol	Meaning
$\boldsymbol{M}$	Mapping matrix
V_1, V_2	Vertex set: the function of the two sets is to store the matched vertices during the operation of the algorithm
m_{rc}	Elements in row r and column c in $\boldsymbol{M}$
o_c	Column C occupancy mark
B	Initialize fallback flag
L	Row count

time, while matching, check the adjacency of matching point pairs, eliminate mismatched nodes, and improve the efficiency of the algorithm. Ullmann algorithm is a mature graph isomorphism algorithm with high retrieval efficiency.

Although Ullmann algorithm is relatively mature, its retrieval efficiency is better. However, in practical engineering applications, the working time of Ullmann algorithm is exponentially related to the size of AAG. Therefore, in contrast, the whole matching process is also time-consuming. The local structure of the assembly model obtained by matching isomorphic subgraphs is also mixed. Therefore, it does not achieve better economic value and social value, and its retrieval accuracy needs to be improved accordingly. The main reasons for the poor retrieval accuracy include the following: first, in the matching process, the attributes contained in the vertices are limited and cannot be matched accurately. The consequence of fuzzy matching is the low accuracy. Secondly, isomorphic matching focuses mostly on vertices and has less constraints on edge attributes, resulting in low accuracy and efficiency.

(2) Conjugate Subgraph Matching Based on Vertex Filtering. In order to improve the retrieval accuracy of subgraph isomorphism and the efficiency of the algorithm, and to meet the needs of constructing the general structure of 3D assembly model, a conjugate subgraph matching algorithm based on vertex screening is proposed. The algorithm is mainly based on Ullmann algorithm and improves the algorithm through the following aspects:

(1) Before the algorithm starts running, the vertices of the two input graphs are filtered by using the same properties of the node attributes of the conjugate subgraph. The face type is one of the main constituent elements of the node attribute. In the 3D assembly model, if the face type is a plane, the corresponding graph should also have a plane, and if the face type is a surface, the corresponding graph should also have a surface. If there is no corresponding face type in the graph, there is no need to enter the algorithm for conjugate matching and return directly. Secondly, if the number of vertices of the subgraph is more than that of the large graph, it is impossible for the subgraph to be isomorphic and return directly. Finally, if there are a certain number of specific graphs in the subgraph, but the graph does not exist in the large graph or the number is less than the subgraph, the isomorphism cannot succeed and is returned directly. Through the above judgment, many invalid matches can be eliminated to a great extent, so as to reduce the complexity of conjugate subgraph matching algorithm and improve work efficiency.

(2) The conjugate subgraph matching model is represented based on the attribute assembly feature adjacency graph. Therefore, the attribute assembly feature adjacency graph of the model contains semantic nodes representing semantic information such as part name, category, and function, as well as matching nodes of connection relationship. In the matching, relevant information is extracted, vertex- and edge-related attributes are added, and the similarity calculation method in [21] is used to judge in the conjugate matching process, so as to make the conjugate matching achieve accurate matching, remove invalid matching as much as possible, and improve the matching accuracy.

(3) When the algorithm is in normal operation, according to the principle that the subgraphs formed by the vertex set V_A on the current small graph and V_B on the large graph must also be isomorphic, it can judge whether the subgraphs composed of V_A and V_B are isomorphic, and whether the attributes of the edges corresponding to the corresponding vertices meet the opposite properties of the corresponding edge attributes of the conjugate subgraph, so as to judge the effectiveness of the newly found columns, effectively eliminate invalid matches, and improve matching accuracy and efficiency.

In order to facilitate the description of conjugate subgraph matching algorithm, the definitions of relevant symbols in the algorithm are shown in Table 3.

To sum up, the basic steps of the algorithm are as follows.

Step 1. Pretreatment.

The specific content of preprocessing is to initialize $\boldsymbol{M}$ according to the relevant properties of conjugate subgraphs, mainly to judge the elements with the value of 1 in $\boldsymbol{M}$ to see whether 1 can be set to 0. Since the number of elements with 1 in $\boldsymbol{M}$ is also limited, the steps of preprocessing process are also limited until no element in $\boldsymbol{M}$ can be set to 0. The specific principles are as follows.

If the vertex attributes of the two graphs do not conform to the conjugate subgraph, and the corresponding node attributes of each conjugate subgraph are the same, the elements corresponding to the vertices in matrix $\boldsymbol{M}$ are set to 0.

After initialization, perform vertex filtering. If the following conditions are met, exit conjugate subgraph matching; if not, enter step 2:

(1) In $\boldsymbol{M}$, if none of the elements in a row is 1, this indicates that a node in the matched subgraph does not exist in the large graph to be retrieved.

(2) In $\boldsymbol{M}$, if $r > c$, it means that the matched subgraph is larger than the large graph to be retrieved.

(3) The number of nodes in the matched subgraph is greater than the number of similar nodes in the large graph to be retrieved.

Step 2. Initialize V_1 and V_2 so that $V_1 = 0$ and $V_2 = 0$.

Step 3. Start traversing from the first row of matrix $\boldsymbol{M}$. If element $m_{rc} = 1$, add the vertices corresponding to this element to V_1 and V_2, respectively, and set O_C as true, B as false, and L as r.

Step 4. $r + 1$, traverse matrix $\boldsymbol{M}$. If B is false, enter this line and run step 5. Otherwise, go back to line r and run step 6.

Step 5. Traverse row I in $\boldsymbol{M}$, starting from column 0:

(1) If $m_{ij} = 1$, and the column is not occupied, add the matching vertices to V_1 and V_2, respectively, and judge the conjugate subgraph matching. If the conditions such as the same conjugate subgraph structure, the same vertex face type and other attributes, the opposite face normal vector, and the opposite edge attributes are met, set O_j to true and execute step 10. Otherwise, delete the matching vertices, $L + 1$.

(2) Otherwise, $L + 1$.

Step 12. O_c in row r is false. Delete the matching vertex and traverse row I of the matrix from column $c + 1$:

(1) If $m_{ij} = 1$, and the column is not occupied, add the matching vertices to V_1 and V_2, respectively, and judge the conjugate subgraph matching. If the conditions such as the same conjugate subgraph structure, the same vertex face type and other attributes, the opposite face normal vector, and the opposite edge attributes are met, set O_j to true and B to false, and execute step 10. Otherwise, delete the matching vertex, $L + 1$.

(2) Otherwise, $L + 1$.

Step 13. If the number of columns of L and $\boldsymbol{M}$ is equal, or $c + 1$ in step 12 is equal to the number of columns of $\boldsymbol{M}$, set B to true and step back one row. Otherwise, go to the next line.

Step 14. After traversing $\boldsymbol{M}$, if V_1 and V_2 sets are not empty sets, the vertices in the set are the matched conjugate subgraphs and output. Otherwise, the algorithm ends and the subgraph is not conjugate.

To sum up, compared with Ullmann algorithm, the conjugate subgraph matching algorithm based on vertex filtering first initializes the mapping matrix based on the characteristic attributes of the conjugate subgraph in the preprocessing stage and, at the same time, carries out vertex filtering before the conjugate subgraph matching to screen and eliminate the subgraphs that do not meet the requirements, reduce the number of invalid matching processes, and improve the matching efficiency of the conjugate subgraph. Then, in the process of conjugate subgraph matching, according to the principle that the subgraphs composed of two matched sets of V_1 and V_2 must be isomorphic, combined with the relevant properties of conjugate subgraphs, judge the newly added vertices and edges and screen and eliminate the vertices that do not meet the requirements, so as to improve the matching efficiency of conjugate subgraphs.

2.2.3. Construction of General Structure. The general structure of 3D assembly model takes the common structure as the main body and combines the multisource and discrete noncommon structure information with it through the assembly feature matching algorithm based on conjugate subgraph to construct a complex and comprehensive expression form of 3D assembly model. Not only can the general structure reflect the reusable common structure information such as functions, structures, and attributes in a group of 3D assembly models, meet the needs of the public, and provide designers with the general structure of the group of models and relevant functions, attributes, design experience, and other information, but it also can reflect the relevant information of many personalized structures and include as many qualified structures as possible, so as to meet the various personalized needs of designers at different stages and under different conditions and provide comprehensive and detailed reusable information for designers in design and manufacturing.

To sum up, the construction steps of general structure of 3D assembly model are as follows:

Step 1: define n general sets (n is the number of parts in the common structure of the 3D assembly model) and initialize them to store the AAG that satisfies the conjugate matching with the part in the matching process.

Step 2: input the common structure of the 3D assembly model and the AAG Atlas corresponding to the parts and components to be matched. The Atlas mainly stores the AAG corresponding to each part and component in the model.

Step 3: based on the matching algorithm of conjugate subgraph in Section 2.2.2, traverse each part in the common structure of 3D assembly model, and match each component in the current component graph set with the AAG of the current part in turn. For the k-th part in the common structure,

(1) If the conjugate matching is satisfied, the AAG corresponding to the component is added to the

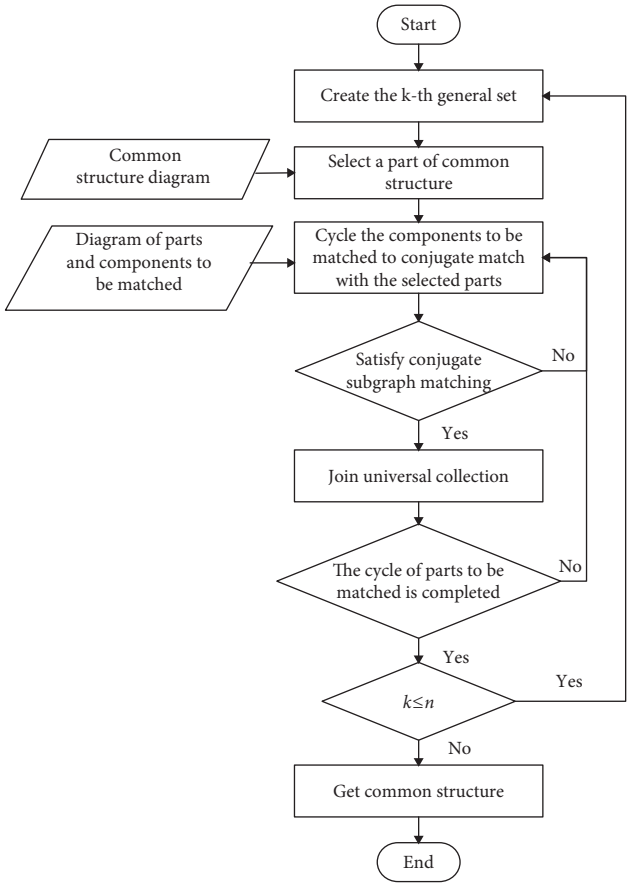

Figure 6: General structure construction flowchart of the 3D assembly model.

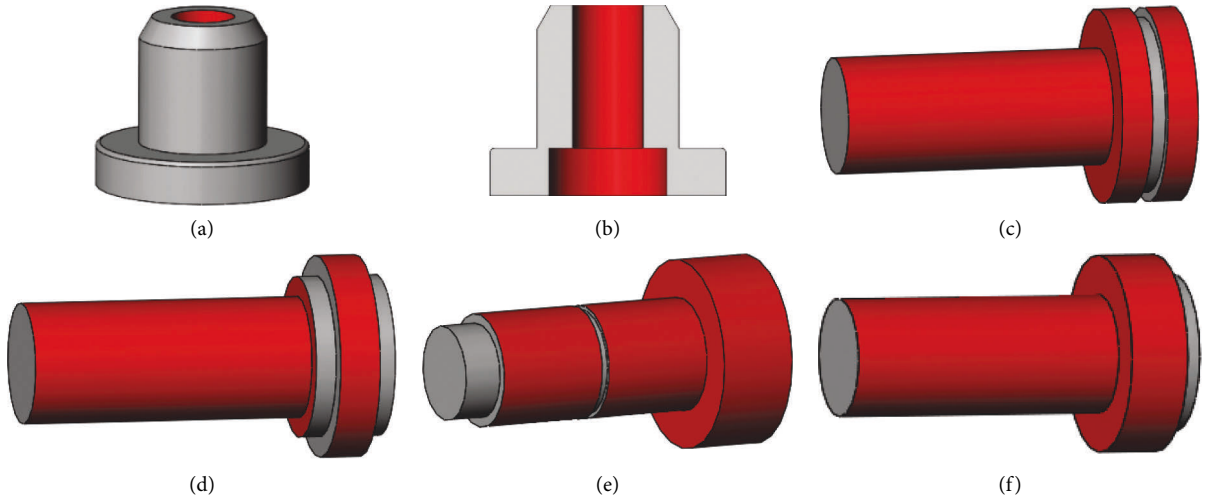

Figure 7: Hydraulic piston cylinder and piston rod. (a) Piston cylinder. (b) Piston cylinder section. (c) Piston rod 1. (d) Piston rod 2. (e) Piston rod 3. (f) Piston rod 4.

general set corresponding to the k-th part, the general structure state of the added 3D assembly model is updated, and the next component to be matched is selected to continue to judge the conjugate subgraph;

(2) If the conjugate matching is not satisfied, skip directly, and select the next component to be matched to continue to judge the conjugate subgraph.

Step 4: until all components in the current component diagram set to be matched are traversed, the general set

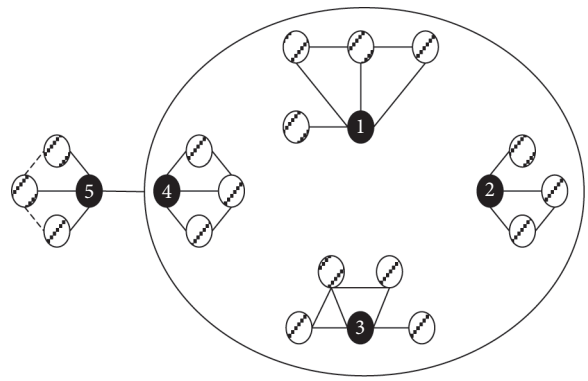

Figure 8: Example of general set of 3D assembly model. 1: piston rod 1; 2: piston rod 2; 3: piston rod 3; 4: piston rod 4; 5: piston cylinder.

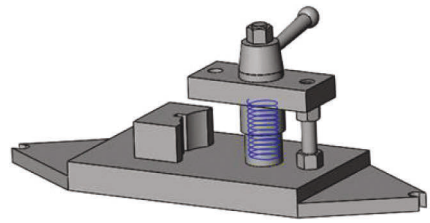

Figure 9: Fixture 3D assembly model.

corresponding to the part is constructed, and the part in the next common structure is selected to enter step 3.

Step 5: repeat the above steps until all parts in the common structure of the 3D assembly model are traversed, and the corresponding general set of parts is obtained, so that the general structure of the 3D assembly model can be constructed. The general assembly flowchart is shown in Figure 6.

As shown in Figure 7, there are one piston cylinder part and four piston rod parts of hydraulic transmission in machine tool accessories. Figures 7(a) and 7(b), respectively, represent the 3D model and sectional view of piston cylinder parts, parts 7(c)–7(f), respectively, represent piston rod parts of different specifications and models, and piston rod parts 1–4 meet the conjugate subgraph matching with piston cylinder parts, which can be assembled with piston cylinder parts. In the figure, the red part is the assembly feature part, and the gray part is the nonassembly feature part.

For the piston cylinder parts and piston rod parts in Figure 7, the assembly feature information is retained, and the nonassembly feature information is simplified, so as to construct the attribute assembly feature adjacency diagram corresponding to each part respectively. According to this information, the general structure is constructed, and the corresponding general set is established. The results are shown in Figure 8. The part circled by the coil is the relevant content represented by the general set. The shaded part is the assembly feature part matched between parts, and the virtual and real lines used for the connection between conjugate nodes represent the edges with opposite attributes in the assembly feature of parts.

To sum up, this method constructs the general structure of 3D assembly model based on comprehensively considering the relevant information of common structure and noncommon structure of 3D assembly model, which has a certain reference value for obtaining design commonness and mining and reuse of 3D assembly model meeting design individuality.

3. Discussion

In order to verify the feasibility of the general structure construction of the 3D assembly model based on conjugate subgraph, the 3D assembly model of a machine tool fixture is selected as the research object, and the method in this paper is used to describe it in detail and step by step to verify the rationality and feasibility of the relevant methods.

Taking the 3D assembly model of a machine tool fixture shown in Figure 9 as the verification object, a detailed example verification process is carried out based on the general structure construction of conjugate subgraph.

Firstly, based on the AAG, the relevant information of assembly features in the 3D assembly model is retained, and semantic nodes are used to replace other information of parts. The corresponding attribute assembly feature adjacency graph is constructed for all parts in the model. The representation results are shown in Table 4. In the table, the red part in the part model corresponds to the assembly feature part of the part. The black node of the attribute assembly feature adjacency graph corresponds to the semantic node containing much semantic information of the part.

Then, based on the construction method of AAG of 3D assembly model, the corresponding AAG of 3D assembly model is constructed, and the representation results are shown in Figure 10.

Table 4: Attribute assembly feature adjacency diagram of each part in the fixture.

Serial number	Part name	Part model	Attribute assembly feature adjacency graph
1	Floor	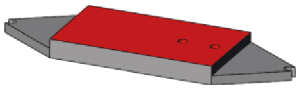	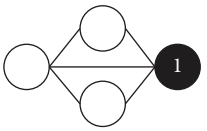
2	Positioning block	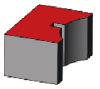	
3	Pressing plate	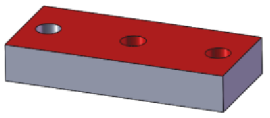	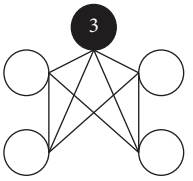
4	Handle		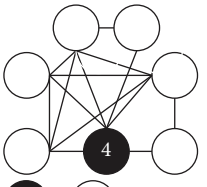
5	Support 1		
6	Nut	 ×3	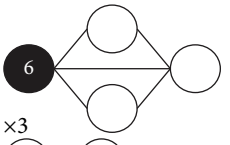 ×3
7	Spring	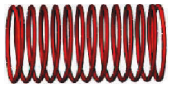	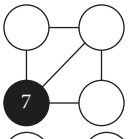
8	Spring protective sleeve	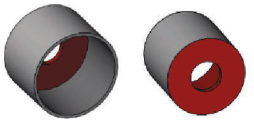	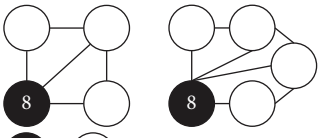
9	Support 2		
10	Cylindrical pin		
11	Rotating parts		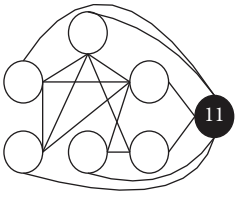

The conjugate subgraph matching algorithm based on vertex screening goes through the general structure construction process in turn and then establishes a comprehensive and rich general structure expression. The experimental results are shown in Figure 11.

By analyzing the general structure of the 3D assembly model constructed in Figure 11, it can be seen that the structure displayed outside the coil is the common structure of the 3D assembly model, which represents the general composition of the model components, mainly including bottom plate, pressing plate, positioning block, support, nut, and other parts. The part circled by the coil is the general set corresponding to Part 9 (support 2) in the general structure of the 3D assembly model, that is, the noncommon structure of the 3D assembly model, which represents the product structure of different designers according to different application scenarios, functional requirements, structural optimization, and other different design concepts.

Through the above analysis, designers have a specific understanding of the general composition of this group of 3D assembly structures, and the corresponding general set contains many personalized structures to meet the design needs of different designers.

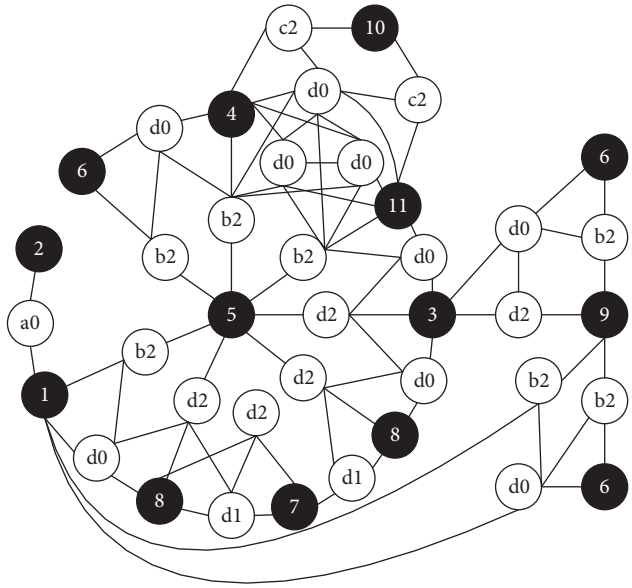

Figure 10: Fixture AAG. 1: floor; 2: positioning block; 3: pressing plate; 4: handle; 5: support 1; 6: nut; 7: spring; 8: spring protective sleeve; 9: support 2; 10: cylindrical pin; 11: rotating parts.

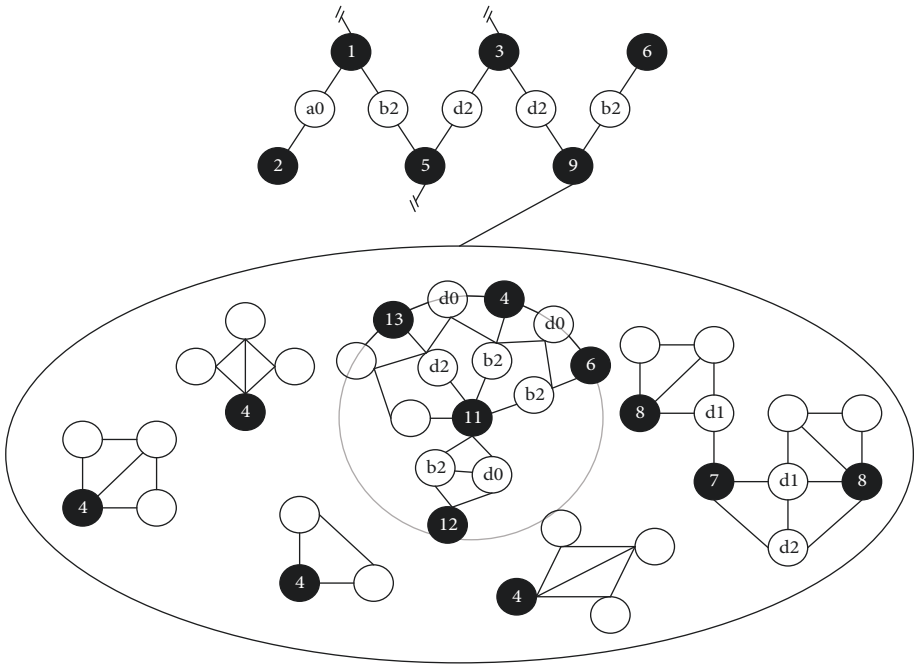

Figure 11: General structure of 3D assembly model. 1: floor; 2: positioning block; 3: pressing plate; 4: handle; 5: support 1; 6: nut; 7: spring; 8: spring protective sleeve; 9: support 2; 10: cylindrical pin; 11: rotating parts; 12: connecting rod; 13: swing rod; 14: sleeve; 15: screw.

4. Conclusion

By analyzing the concepts of assembly feature, assembly relationship, and conjugate in 3D assembly model, a general structure construction method based on conjugate subgraph is proposed in this paper. On the basis of relevant definitions and concepts, based on the relevant characteristics of conjugate subgraphs and preprocessing, the efficiency is improved, and the conjugate subgraph matching algorithm based on vertex screening is used to solve the matching problem of assembly features in 3D assembly model. On this basis, taking the common structure as the core, the construction steps of the general structure of 3D assembly model are designed, so as to build a general structure expression

form with comprehensive information, reduce the matching times in the process of information retrieval, and improve the reuse efficiency of model design.

In the process of product design and manufacturing, designers have many objective and subjective requirements for the information of 3D assembly model, which have many uncertainties. Therefore, the design intention can be analyzed concretely in the follow-up, and its constituent characteristics can be summarized to build a more comprehensive semantic information expression standard that highlights the design personality.

Data Availability

The data used to support the findings of this study are available from the corresponding author upon request.

Conflicts of Interest

The authors declare that there are no conflicts of interest regarding the publication of this paper.

Acknowledgments

This work was supported by Shaanxi Science and Technology Resources Open Sharing Platform (Grant no. 2021PT-006) and Shaanxi Science and Technology New Star Project (Grant no. 2020KJXX-071).

References

[1] K. Lupinetti, L. Chiang, F. Giannini, M. Monti, and J. P. Pernot, "Regular patterns of repeated elements in CAD assembly model retrieval," *Computer-Aided Design and Applications*, vol. 14, no. 4, pp. 516–525, 2017.

[2] G. song, *"Semantic Based Assembly Model Retrieval [D]" Hangzhou*, Springer, Berlin/Heidelberg, Germany, 2011.

[3] D. McWherter, M. Peabody, W. C. Regli, and A. Shokoufandeh, "Transformation invariant shape similarity comparison of solid models," in *Proceedings of the ASME Design Engineering Technical Conference*, pp. 46–57, Philadelphia, January 2001.

[4] Hu Qiao, Y. Zhou, and Yu Bai, "Automatic semantic annotation method of MBD model using feature recognition technology [J]," *Journal of Huaqiao University*, vol. 39, no. 05, pp. 750–755, 2018.

[5] C. L. Sun, D. Y. Ning, W. Xiong, and H. T. Wang, "Feature based CAD model retrieval technology in engineering field," *Computer integrated manufacturing system*, vol. 20, no. 04, pp. 747–754, 2014.

[6] H. Qiao, Q. Wu, S. Yu, J. Du, and Y. Xiang, "A 3D assembly model retrieval method based on assembly information," *Assembly Automation*, vol. 39, no. 4, pp. 556–565, 2019.

[7] R. Wu, *Research on Key Assembly Technologies for Process Reuse [D]" Changsha*, National University of Defense Technology, Changsha, China, 2008.

[8] T. Zheng, *"Research on 3D CAD Model Retrieval Technology [D]" Wuhan*, Huazhong University of Science and Technology, Wuhan, China, 2009.

[9] J. R. Ullmann, "An algorithm for subgraph isomorphism," *Journal of the ACM*, vol. 23, no. 1, pp. 31–42, 1976.

[10] H. Wang, *"Research on Query Technology of Accurate Subgraph Database [D]" Harbin*, Harbin Institute of technology, Harbin, China, 2014.

[11] F. Yuan, *"Research and Implementation of Subgraph Isomorphism Algorithm Based on Spark [D]" Changchun: Northeast*, Normal University, Cebu, Philippines, 2018.

[12] H. G. Choi, J. Kim, Y. Yoon, and B. R. Moon, "Investigation of incremental hybrid genetic algorithm with subgraph isomorphism problem," *Swarm and Evolutionary Computation*, vol. 49, pp. 75–86, 2019.

[13] P. Fehér, M. Asztalos, T. Vajk, T. Mészáros, and L. Lengyel, "Detecting subgraph isomorphism with MapReduce," *The Journal of Supercomputing*, vol. 73, no. 5, pp. 1810–1851, 2017.

[14] A. C. L. Chen, A. Elhajj, S. Gao, A. Sarhan, A. Afra Kassem, and R. Alhajj, "Approximating the maximum common subgraph isomorphism problem with a weighted graph," *Knowledge-Based Systems*, vol. 85, pp. 265–276, 2015.

[15] Xu Kaixuan, *"Optimization Algorithm and Experimental Research of Extended Subgraph Matching Problem [D]" Shanghai*, Fudan University, Shanghai, China, 2011.

[16] Mo Rong, L. Liu, N. Wan, and J. Li, "3D process model machining feature environment matching," *Mechanical Science and Technology*, vol. 34, no. 4, pp. 549–554, 2015.

[17] W. Tang, *"Similarity Evaluation of 3D CAD Model Based on Efficient Map Matching [D]" Hangzhou*, Zhejiang University, Hangzhou, China, 2010.

[18] A. Dong, L. Gao, and J. Zhao, "Subgraph isomorphism algorithm in graph pattern mining," *Practice and understanding of mathematics*, vol. 41, no. 13, pp. 105–112, 2011.

[19] G. Wang, Y. Wang, and Z. Li, "Assembly modeling method supporting top-down die design," *China Mechanical Engineering*, no. 01, pp. 56–58, 1998.

[20] Z. Liu, *"Research on Theory, Method and Application of Product Assembly Modeling in Process and History Oriented Virtual Environment [D]" Hangzhou*, Zhejiang University, Hangzhou, China, 2002.

[21] Mi Zuo, *General Structure Mining and Information Reuse Method of 3D Assembly [D]" Xi'an*, Northwest University of technology, Seattle, Washington, 2016.

Hindawi
Scientific Programming
Volume 2023, Article ID 9878574, 1 page
https://doi.org/10.1155/2023/9878574

Retraction

Retracted: Optimization Method of Urban Square Public Space from the Perspective of Contextualism

Scientific Programming

Received 18 July 2023; Accepted 18 July 2023; Published 19 July 2023

This article has been retracted by Hindawi following an investigation undertaken by the publisher [1]. This investigation has uncovered evidence of one or more of the following indicators of systematic manipulation of the publication process:

(1) Discrepancies in scope
(2) Discrepancies in the description of the research reported
(3) Discrepancies between the availability of data and the research described
(4) Inappropriate citations
(5) Incoherent, meaningless and/or irrelevant content included in the article
(6) Peer-review manipulation

The presence of these indicators undermines our confidence in the integrity of the article's content and we cannot, therefore, vouch for its reliability. Please note that this notice is intended solely to alert readers that the content of this article is unreliable. We have not investigated whether authors were aware of or involved in the systematic manipulation of the publication process.

Wiley and Hindawi regrets that the usual quality checks did not identify these issues before publication and have since put additional measures in place to safeguard research integrity.

We wish to credit our own Research Integrity and Research Publishing teams and anonymous and named external researchers and research integrity experts for contributing to this investigation.

The corresponding author, as the representative of all authors, has been given the opportunity to register their agreement or disagreement to this retraction. We have kept a record of any response received.

References

[1] M. Zhang and M. Lee, "Optimization Method of Urban Square Public Space from the Perspective of Contextualism," *Scientific Programming*, vol. 2022, Article ID 3811260, 8 pages, 2022.

Hindawi
Scientific Programming
Volume 2022, Article ID 3811260, 8 pages
https://doi.org/10.1155/2022/3811260

Research Article

Optimization Method of Urban Square Public Space from the Perspective of Contextualism

Min Zhang and Min Lee

Department of Spatial Culture Design, Graduate School of Techno Design, Kookmin University, Seol 02702, Republic of Korea

Correspondence should be addressed to Min Lee; liwen@kookmin.ac.kr

Received 5 July 2022; Revised 28 August 2022; Accepted 31 August 2022; Published 17 September 2022

Academic Editor: Lianhui Li

In the era of rapid development of science and technology, in order to attract the public's attention, many architectural designs unilaterally pursue nonmainstream design, completely ignoring the surrounding environment and historical context. The original spatial features and scales have disappeared, and the root cause is that the spatial shaping is separated from the urban context. Urban design that continues the urban context is not only a method to solve specific urban space problems and contradictions but also an important means to build a beautiful urban space and achieve sustainable development. The urban design of the two banks of the Pinghe River in the east of Foshan is based on the sorting and analysis of the material and spiritual elements of the context of the base. This article will go back to the trend of Western architectural contexts and discuss how to design new buildings while respecting the historical context of the city through rational speculation on the two dimensions of contextualism architectural theory, space and time, combined with architectural cases.

1. Introduction

In the 1930s, many Chinese architects returned from overseas and brought back Western modernist architecture. In the 1980s, the trend of Western architectural theory arose again in my country. People gradually realize that Western architectural theory is an effective design method, and more architects try to apply these theories to modern architectural urban design. While studying western architectural theory, it is also necessary to emphasize the confidence of national culture, and the attention to architectural urban context has become a focus topic. Looking at the development of Chinese architectural culture in recent years, the buildings that are deliberately symbolic, strange and vulgar, and extremely discordant with the surrounding environmental conditions are increasing. Many buildings with strange images have become a topic of discussion among netizens after dinner, and there is even a list of the top ten ugly buildings in China that is reviewed every year. Either the company's products are unmodified as the appearance model, or the model expresses the blind worship of sexual culture, or imitates and plagiarizes Western architecture. Many buildings try to use the "ugly" name. A lot of buildings try to make a name for themselves as "ugly." Architecture is a part of a specific history and a specific urban background, and it is a macro-spatial combination, which should fully consider its environment and historical background. There have been many great cities in Chinese history, such as Yecheng and Chang'an, which were planned in an orderly manner. The symbols of history should not be forgotten, and the design of the building should be completed in the macro urban context. It should be done in a macro urban context. Recalling the trend of Western architectural theory, contextualism has always been controversial. Many buildings produced under contextualism are not coordinated with the existing environment, and the design is conservative. In modern architectural design, we should hold a rational and speculative attitude, understand contextualism, use it as a technique of urban design, and consider and learn from the architectural environment and history [1].

The word context originated from the field of linguistics. It is a historical category developed in a specific space, and its

extension contains extremely broad content, which is interpreted as the context of the culture in a narrow sense [2]. The thought of context has a long history. In China, it was first introduced into the field of architecture and then gradually extended to cities. Due to the lack of in-depth research on the ambiguity and uncertainty of the context theory and its slow development, it has not formed an independent theoretical system and has been widely used in architecture, cities, and landscapes in the form of theoretical concepts. Today, the meaning of context in the city has been comprehensively updated and inherited [3]. "The current context is based on the specific situation of our country, drawing on Western contexts to develop and innovate, giving Chinese culture a way of interpreting it, and imbuing it with new cultural connotations. It not only represents the cultural essence of the past but also points to the most current cultural essence. Vibrant cultural genes pay more attention to the potential for future cultural innovation. The systematic project of promoting and inheriting culture is called "New Context Doctrine." In the concept of the new context doctrine, the understanding of context is no longer limited to the old and the new. To solve the problem of cohesion, we should conduct an in-depth and three-dimensional excavation of its connotation, adapt to the needs of sustainable development of urban culture, and reveal the evolution law of context [4].

In terms of ideology, the development of the "city color pulse" is rooted in the concept of the collective unconscious created by Jung, which is an inherent deep unconscious. "The level of the collective unconscious is unconscious, and it contains the influence of the experiences accumulated by all generations in the past, including distant ancestors [5]." The fundamental reason for its formation is the common environment, that is, the environment with the social and cultural place, and it includes all indoor and outdoor man-made environments and natural environments. The fundamental feature of this environment is what Schultz calls the "spirit of place," which creates and perpetuates the collective unconscious and its archetypes that exist in the deepest part of the human spirit. The traditional color ideology was formed earlier; from ancient times, the color cognition was developed from the fear of life to the ideology of color symbols as totem worship. In the Yangshao culture, Xia, and Shang dynasties, the color aesthetic psychology gradually formed. In the Zhou dynasty, the simple materialist worldview "Five Elements Theory" was combined with the worship of five colors, five numbers, heaven, Earth, human beings, and gods, forming a combination of time, space, human relations, and ritual system, the "Five Elements of Color Science" [6]. During the Tang and Song dynasties, the traditional "five-color aesthetics" was finally formed. Nowadays, with the introduction of the rational western color theory system, the traditional "five elements of color theory" has been gradually ignored. Although the simple color concept has not formed a color science system, the aesthetic awareness of the five colors has been deeply rooted in the hearts of the people and has become a national color feature [7] (as shown in Figures 1–3).

Figure 1: A corner of the square.

Figure 2: Landscape greening screenshot.

The connotation of architectural "context" includes two main lines of cognition: One is the spatial dimension, which refers to the physical space environment in which the building is located, including the natural environment and artificial environment; the other is the time dimension, which refers to the generation and development of buildings and the social and cultural background on which it depends. The so-called continuity of spatial context emphasizes the expression of the building in the spatial relationship of the neighborhood and respects the regionality of the building [8]. Robert Stern believed that "Architecture is a part of the whole" and "The new building should be adapted to the environment" [9]. In 1950, Venturi believed that architecture does not exist in isolation by itself but should be related to the whole between architecture and urban space, and form part of the whole of urban space. This is consistent with the "whole prior to the part" view emphasized in Gestalt psychology and the "text prior to sentence" idea advocated by Frege in the field of linguistics [10]. Whether there is a unified context between the building and other buildings reflects whether the relationship between the part and the

Figure 3: Square stone bench.

whole is harmonious. When a building is harmonious in its site, it will likely disappear into the site and the urban environment. People often think that this is a lack of design and is just a replica. However, the overall connotation of the city is magnified, and a new building that is in harmony with the urban context should be a work that skillfully uses the connotation of contextualism and design skills, rather than a simple and crude plagiarism [11].

2. The Concept, Spatial Value, and Constituent Elements of the Urban Context

2.1. The Concept of the Urban Context. The word context is derived from "Context." As a term used to express the logical relationship between upper and lower contexts, it can also indicate the background and conditions in which things occur. Things can only develop if they are connected with a specific background environment. If the context is the soil of urban development, then the space shaped by urban design is the creation based on the context and soil. Context is the background of urban development and is related to many essential elements that affect urban development. All explicit and implicit elements related to the formation and development of a city can be included in the category of urban context [12].

Context is the connection in time and space between things created by human beings and things. It has both the "synchronicity" of horizontal time and space and the "diachronic" of vertical time and space [13]. By extension to the field of urban research, the basic connotation of urban context can be obtained, that is, in the process of historical development and under specific conditions, there is a dynamic and internal relationship between people and the natural environment, the built environment, and the corresponding social and cultural background, and the sum of essential connections [14].

After fully considering the style and morphological characteristics of the existing buildings on the plot, first choose to carry out roof renovation for the buildings with a north-south strip in the block volume, and make certain innovations in the sloping roof, connecting with glass in the middle to adapt to the building volume The problem of lighting difficulties caused by it; second, repair the facades of the buildings along the street, strengthen the interface characteristics of the buildings along the street, try to control the height of the buildings on both sides of the alley and the parking lane, and ensure the integrity and unity of the style along the street. Through historical research, sorting out the width of the street and the height of the buildings on both sides, and on the premise of respecting the history, the comfort of the street is improved and adjusted to a certain extent, and the width of the two streets and alleys is controlled to be about 3.0 ~ 3.5 m. The building height is controlled below 5 m. Finally, when repairing the original courtyard with missing texture, the newly added building should echo the style and volume of the original building and make appropriate adjustments on the premise of respecting the history to adapt to modern life and create a comfortable living environment [15].

2.2. The Spatial Value of Urban Context. Public space is the main place where residents work and live and is an important part of urban space (as shown in Figure 4). The public space that concentrates on the urban context and public activities can fully demonstrate the city's heritage, charm, and vitality [16]. With the continuous acceleration of the urbanization process, driven by the short-sighted construction goals, the problems of monotony and low-quality urban space have become increasingly prominent, and the original spatial characteristics and scales have disappeared. The root cause of this problem is that today's spatial shaping is divorced from the context of the city. First of all, the internal streets and alleys should be fully sorted out, and the additional buildings should be demolished to make the originally narrow and blocked internal streets and alleys open and transparent so as to enhance the comfort of the living space and further solve the hidden dangers of safety. The facades of the buildings on both sides of the streets should be unified in style, embellished with appropriate historical and cultural elements, and appropriate building concessions should be made to create micro-ecological nodes to create street landscape ecological corridors. Second, on the basis of dismantling buildings with incompatible styles, guided by the spatial layout of traditional courtyards in the old city, dismantling structures that destroy the courtyard pattern, rebuilding new buildings in areas where the pattern is vacant, and ensuring that it is compatible with the existing historic buildings and the traditional courtyards are in harmony, fully continuing the courtyard space pattern of the historical and cultural blocks, and creating a comfortable living and leisure space for the residents. Finally, retain the existing ancient trees in the plot, use them to create landscape space nodes, recreate the historical living space scene of the block, and create a comfortable and livable external living space [17].

Therefore, it is necessary to clarify the relevant elements of urban context and urban space design, comprehensively use urban design methods and context analysis and refinement methods, continue the context, and focus on the

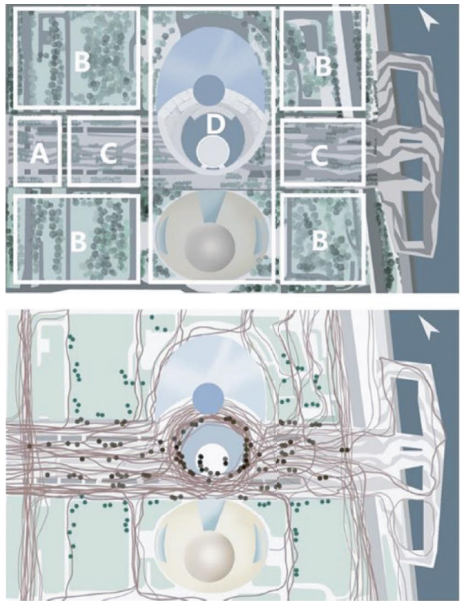

Figure 4: Functional zoning, crowd movement trajectory, and parking location of the civic square.

inheritance and innovation of the context in the design of urban public spaces so as to create a "cultural context." The key to establishing a city's image, increasing its charm, and enhancing its competitiveness is to realize the harmony between man and the environment, and the harmony between history and modernity [18].

2.3. Elements of the Urban Context

2.3.1. Material Elements. It is divided into two categories: one is the structural elements formed by the long-term accumulation of urban space; the other is the spatial form elements formed from the local climate, materials, and culture [19].

Structural elements include urban pattern, urban context, and urban texture. Structural elements are closely linked to the daily activities of residents through the perception of macro-spatial relationships such as axes, geographic markers, and skylines, and local structural elements should be respected in urban design. Spatial form elements refer to a variety of elements including urban skylines, urban landmarks, historical relics, dynamic place areas, and distinctive local spaces (such as spatial scale, shape, texture, color, interface, etc.) [20].

2.3.2. Spiritual Elements. Spiritual elements mainly refer to the regional culture of a city. It is the sum of various spiritual resources, including the morals, beliefs, customs, and arts of the city, as well as the habits and all other abilities learned by each city member [21]. Spiritual elements, as an abstract concept, are the essential attributes of "people" that govern activities in a specific urban space. Only by thoroughly analyzing and classifying urban regional culture, creating suitable local culture and habits in specific urban places, and providing unique cultural activity space can we create an urban space full of vitality and a sense of place belonging [22].

3. Urban Space Construction Methods from the Perspective of Context

For urban design, context continuation is to advocate in the design of specific sections, through the analysis and research of the urban context, to maintain the continuity of the original space, culture, and life and highlight the characteristics of the city. This concept limits the problem of urban characteristics to the category with space as the basic research object, which makes the work goal of urban design clear. By summarizing excellent cases at home and abroad and the continuous improvement of urban design experience, the urban design method based on the purpose of context continuation can be summarized in the following three points [23]. Through the urban design, the spatial elements of the base are sorted out, the original "Wang Jigang-Green Island Lake" space corridor is retained, and the axis of "Green Island Lake-Jihua Road" is listed as the two major axes; at the same time, through sorting out, the topography and local settlement texture have extracted four characteristic elements of "lakes, hills, islands, and swells." As an open public activity space, "lake" is one of the important ecological landscape elements, and various public activities can be carried out; it is the core area of public activities and the core of gathering popularity; "Chong" is an important link for the functional connection of various groups. On the axis, this urban design clarifies the original landscape axis of "Green Island Hu-Wang Jigang," which serves as the principal basis for urban design to organize space and connect the two banks of the river. In terms of group relationships, the base is divided into three groups with different themes. Each group grows from existing elements and connects with the road network, rail transit stations, and water buses. The "*S*"-shaped lake gushing texture belt connects the "three groups on both sides of the strait" to form a spatial pattern of "one belt, three centers, two axes, and three groups", and based on this, the spatial layout of urban design is guided. The Green Island Lake Smart Group not only concentrates on the main production and service functions of the Shanxi area but also owns the important water system resource of Green Island Lake. Therefore, the urban design positions this group as a comprehensive display of the cultural characteristics of Lingnan water towns and a provision for the Guangfo area. The intelligent highland of comprehensive services, through this intelligent group, strives to integrate the vitality of multiple waterfronts, realize the organic complementarity of main functions, and make it a springboard for connecting the two banks of the Dongping River and realizing the integrated development of the Ronghe River, creating the iconic core of Shanxi. space. The central wisdom island is the core area of the entire design, and it is also the area that the axis of Wang Jigang and Lvdao Lake traverses. In the urban design, the spatial development model of the landscape city should be introduced, that is, to follow the natural

landscape space and create architectural space. Make it complement each other with the landscape axis accumulated in the context. The building space is created with green buildings and earth-covered buildings as the core elements, and the second-floor platform is organically combined with the platform across the embankment to build a core space with good accessibility and fun and at the same time reflect the image of a waterfront city [24].

3.1. Capture of Context. The development of a city must be accompanied by the renewal of space. The context allows people to find the basis for the creation of spatial characteristics from the traditional and localized content and forms from time to time. By extracting the elements of local context and summarizing their unique arrangement, urban design can subtly inject a localized atmosphere that strengthens environmental history and continuity into new spaces and enhances the place appeal of the space [25].

3.2. Transplantation of Context. In the process of urban design, the issues of "new" and "dilapidated" must be considered. For many issues such as whether to keep the urban context elements as they are after refining the urban context elements, and whether the original urban space cannot coexist with the new development, the author believes that the key lies in whether the context elements can be transformed into design principles in the design. We transform the complex "semantics" of the original context elements into a simple space "language" so that the urban design integrates and presents the structural relationship and characteristic symbols of traditional space.

3.3. The Shaping of the Contextual Characteristic Space. After extracting the local contextual elements and completing the transplantation work, the basic materials of urban design are obtained. By clarifying key areas, shaping a new spatial structure system, sorting out and arranging elements at all levels, and optimizing the arrangement of original elements, the new space has both historical continuities and adapts to the requirements of the new era. In terms of details, through the introduction of new functions, new materials, and new technologies, symbolic traditional cultural elements are added so that the precipitation of history and time can be displayed in the new urban space [26].

4. Optimization and Promotion Strategies of Urban Square Public Space from the Perspective of Contextualism

Public space is an important part of the urban innovation ecosystem. It is not only an important part of the material elements of the urban innovation zone but also the specific bearing and expression of economic and network elements, and is the spatial basis for "stimulating agglomeration." Through the understanding of the theoretical basis of the urban innovation zone, this paper believes that the public space of the urban innovation zone should reflect the characteristics of its three components, so the construction of the public space of the urban innovation zone should comply with the three principles of accessibility, openness, and network.

The physical elements of the urban innovation district enhance the innovation ecosystem by providing a compact and efficient mix of functions and street connections, so the public spaces of the urban innovation district need to be accessible to enable the connection between the physical elements. Public space is an important part of physical elements, including neighborhood scale public space. In order to make full use of the high quality public space, it is necessary to integrate the public space with exhibitions, concerts, restaurants, residences, and so on into a compact, functional mixed area. Connectivity that connects Category 1 (public realm) and Category 2 (private realm) physical assets is critical to public spaces in urban innovation districts, including walkable and cyclable street networks, among others. Based on the same concept, high-quality and convenient public transportation serves the interconnection of cities and regions. The transportation infrastructure such as Barcelona's ring road and high-speed rail to Paris, Boston's Silver Line, and Sydney's northern M2 railway line are all urban infrastructure. The public space of the innovation district brings a large flow of people.

The management of the public space of the urban innovation district needs to follow the principle of openness to promote the diffusion of innovative activities and creative ideas in the public space. The urban innovation zone emphasizes the importance of spatial proximity and aggregation of economic activities. However, due to the blurred boundary of the urban innovation zone and the blurred boundary between work and life, the public space and the private space have proximity to economic activities. Circulating information has the characteristics of "liquid" and lack of openness, and information spillover cannot be realized, so the appearance of good ideas will disappear without circulation and diffusion. According to the Twelve Principles of Urban Innovation Districts published by the Brookings Institution, public spaces make innovation visible and open. Open innovation events help spark the curiosity of potential innovators, spark dialogue among neighbors, and spread innovations. Thus, in the urban innovation district, the public space becomes an outdoor testing ground for testing the initial results of innovation. The Boston District District Hall is itself a product of innovation, creating a new public space for the purpose of promoting a culture of innovation, the Innovation Hall. Opening District Hall in the BSID as a pilot project also accommodates a variety of innovative activities.

The social element of the city innovation district emphasizes the importance of social interaction, which not only lies in the strong ties between similar fields and departments but also focuses on the establishment of new ties between fields and departments, that is, weak ties. The public space serves as a key container for establishing weak ties, providing opportunities for chance encounters, networking, and knowledge spillovers. Creating an innovative atmosphere is

a new public interest represented by public space in urban innovation zones under the background of sharing economy and technological innovation. Networking is essential for public spaces, such as a series of activities to learn and develop new skills and build social interaction. High-frequency social interactions among innovative populations tend to be concentrated in a few specific "hot spots," which may occur naturally. In addition, the innovation district requires a series of catalyst activities to reactivate neglected public spaces. Therefore, public space is the link between these "innovation hotspots." In addition to forming a visible public network, it is more important to establish an internal interactive network relationship of competition, collaboration, and learning.

Spatial location is an important factor affecting the layout and form of public space in urban innovation districts. The Huanghuagang Science and Technology Park area is located in the old city of Guangzhou. Due to the tighter land use, the development intensity is often greater and the construction density is higher, showing the characteristics of compact urban space. During the process of urbanization, the surrounding living facilities are gradually supplemented. The surrounding communities are more closely connected, forming a mixed-function area. The overall layout of the land is larger, and the layout mode of multiple independent parks is adopted, which has more flexibility; at the same time, it has more abundant natural resources, and the planning considers the natural ecology, the interaction of the environment. In general, the core area of the main city is limited due to the limited urban space and limited space development of the science and technology park. The main open space is arranged along the road, and the street has become an important vitality center. On the other hand, due to the lack of interaction between public innovation space and public open space, the low degree of innovation openness is also the reason for the lack of vitality of public space.

A reasonable layout can improve the utilization rate of local accessibility of public space in the innovation zone. Traditional parks are generally relatively closed, and physical measures such as the establishment of walls are used to isolate the park from the residential community, which is not conducive to the integration of the park into the surrounding communities. Improving the local accessibility of public spaces in the urban innovation zone is conducive to keeping the park open and flowing. MPID has designed a variety of options for walking or cycling into the Lane Cove National Park from the track site while enhancing the density of the road network combined with the road network layout of public spaces to improve the accessibility of public spaces. Shenzhen Huaqiangbei District was born out of Shangbu Industrial Zone and continued the characteristics of openness of industrial blocks. The pattern of "small plots, dense road network" broke down the walls that were drawn as the ground to enhance the communication between plots, making the streets easier to communicate with each other. It has become a highly accessible public space in itself, which is friendly and approachable to pedestrians. In the practice of Guangzhou in recent years, the urban design and control planning optimization of Pazhou West District emphasizes the urban development concept of "compact, intensive, efficient, and complex." The arcade street of more than 2 kilometers is implemented on the ground, the three-dimensional park platform is built in the air, and the underground is connected through the vertical traffic module, ground, and air public spaces to realize the interconnection of public spaces. Figure 5 shows the optimization strategy proposed in this paper.

Providing a walkable environment in public space is an important condition for crowds to gather. High-density technology parks need to avoid rapid and massive traffic and people; planning new technology parks should avoid lack of consideration of spatial scale and one-sided pursuit of landscape ecology The effect is to blindly build wide green isolation belts and huge square nodes. Shared communication space is an important feature that distinguishes the urban innovation district from other urban spaces. Similar to the community service center in each community, the shared communication space is a special public space built by the urban innovation district to stimulate innovation vitality, providing an open place for the exchange of ideas for the innovation district, allowing more people to get in touch with the ongoing innovation activities and promote the improvement of the innovation ecosystem. The purpose of building a shared communication space is to encourage knowledge sharing and information exchange. From the perspective of economic factors, building a rich and available shared communication space is conducive to promoting the exchange and collision of ideas. Around the world, regions building urban innovation districts actively build shared exchange spaces to provide venues for knowledge flow. Innovation districts in Barcelona and Stockholm, for example, have developed workshops and informal meeting spaces to encourage such exchanges; Research Triangle Park in North Carolina is a successful cluster, but they have found that the lack of venues for the exchange of ideas limits the They go further; they try to redevelop their physical spaces to allow for active interaction.

Network innovation is created from the bottom up. Urban innovation districts cannot be achieved with a single order. Various event planning and construction are needed to promote collaboration between industries and departments and to foster innovative networks and a culture of exchange and sharing. Providing a public space that promotes communication and interaction is a prerequisite for nurturing weak interpersonal ties, and an innovative atmosphere is a catalyst for building a weak interpersonal network. The atmosphere is closely related to various scenarios, such as rich innovative activities, street art, nightlife, etc., to enhance social vitality and business interaction, attract, retain, and nurture innovative people and innovative enterprises. The existing newer science and technology parks in the urban area are located in the core area of the main city and often have a certain compact and mixed physical space foundation, such as Huanghuagang Science and Technology Park, Keyun Road, Longkou East Community, etc. At the same time, the limited space and the early construction period bring problems such as a single type of public space

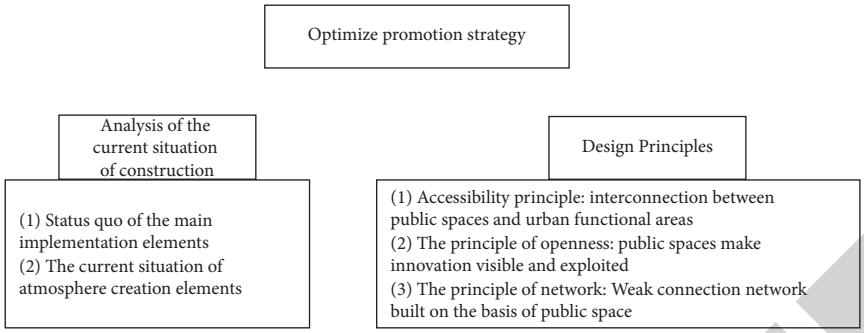

Figure 5: Optimization promotion strategy.

and outdated facilities. Aiming at the main contradiction of limited development space, the optimization strategy can control and guide the interaction and continuity between the existing building space and the public space so as to expand the shared communication space with suitable functions and the public retail space with various choices. Therefore, the strategies for improving the openness of the existing urban renewal technology parks can be summarized as follows: focus on the combination of dots and lines in the surrounding area to create a public space with a continuous interface, encourage the opening of the ground floor of the building to improve the interface quality of the public space, and pay attention to street management to avoid sidewalks and subways. The entrance and exit become the storage yard for shared bicycles.

5. Conclusion

In the process of rapid urbanization, the urban design with the theme of continuation of the urban context adheres to the spirit of the "Beijing Charter", advocates cultural diversity, maintains cultural diversity, and adheres to the path of regionalization and modernization of modern buildings to demonstrate the Chinese characteristics of modern regional cities. The urban design of the two banks of the Pinghe River in the east of Foshan adopts the methods of extraction, abstraction, and construction and adopts the design idea of respecting the city's history and culture so as to achieve the sustainable development of the city's vitality and cultural continuity. Urban design that continues the urban context is not only a method to solve specific urban space problems and contradictions but also an important means to build a beautiful urban space and achieve sustainable development.

Data Availability

The dataset can be accessed upon request to the corresponding author.

Conflicts of Interest

The authors declare that they have no conflicts of interest.

References

[1] R. Malte, "Mercenaries in/and history: the problem of ahistoricism and contextualism in mercenary scholarship," *Small Wars and Insurgencies*, vol. 33, no. 1-2, 2022.

[2] H. C. Stoeklé and C. Hervé, "Ownership of genetic data: between universalism and contextualism?" *The American Journal of Bioethics*, vol. 21, no. 12, pp. 75–77, 2021.

[3] K. J. Ravi, "Contextualism preserved," *Philosophical Perspectives*, vol. 35, no. 1, 2021.

[4] F. Testini, "Genealogical solutions to the problem of critical distance: political theory, contextualism and the case of punishment in transitional scenarios," *Res Publica*, vol. 28, 2021 (prepublish).

[5] J. Bebb, "Demarcating contextualism and contrastivism," *Philosophy*, vol. 97, no. 1, pp. 23–49, 2021.

[6] S. Bonzio, G. Cevolani, and T. Flaminio, "How to believe long conjunctions of beliefs: probability, quasi-dogmatism and contextualism," *Erkenntnis*, vol. 5, pp. 1–26, 2021, (prepublish).

[7] E. Pérez-Navarro, "No matter who," *Theoria: An International Journal for Theory, History and Foundations of Science*, vol. 36, no. 2, 2021.

[8] J. Vedran, "Strategic use of context in the interpretation of political discourses: an encounter between theory of hegemony and linguistic contextualism," *Politicka Misao: Časopis Za Politologiju*, vol. 58, no. 1, 2021.

[9] S. Lebens, "Will I get a job? Contextualism, belief, and faith," *Synthese*, vol. 199, no. 3-4, 2021.

[10] F. Martin and B.-H. Dermot, "In support of reacquainting functional contextualism and interbehaviorism," *Journal of Contextual Behavioral Science*, vol. 19, 2021.

[11] W. Ron, "Linguistic evidence and substantive epistemic contextualism," *Logos & Episteme*, vol. 12, no. 1, 2021.

[12] R. Wilburn, "What IS the relation between semantic and substantive epIStemic contextualISM?" *Logos & Episteme*, vol. 12, no. 3, pp. 344–366, 2021.

[13] D. P. Miller, "Depicting watt: contextualism, myopia and the long view," *Metascience*, vol. 29, 2020 (prepublish).

[14] J. Berškytė, "Rollercoasters are not fun for mary: against indexical contextualism," *Axiomathes*, vol. 31, 2020.

[15] C. Zeng and B. Guo, "A study on the measurement and optimization of urban innovation capability from the perspective of two-stage efficiency," *Science & Technology Progress and Policy*, vol. 31, no. 17, pp. 32-33, 2014.

[16] X. Ma, X. Chen, Y. Du et al., "Evaluation of urban spatial resilience and its influencing factors: case study of the

Hindawi
Scientific Programming
Volume 2022, Article ID 4786623, 10 pages
https://doi.org/10.1155/2022/4786623

Research Article

Big Data Model of Digital Employees of High-Tech Enterprises under the Background of Digital Transformation

Manhang Li

School of Public Affairs and Administration, University of Electronic Science and Technology of China, Chengdu 611731, China

Correspondence should be addressed to Manhang Li; 2019160901024@std.uestc.edu.cn

Received 15 July 2022; Revised 14 August 2022; Accepted 24 August 2022; Published 16 September 2022

Academic Editor: Lianhui Li

This paper firstly conducts a theoretical analysis on the digital transformation of enterprises. Theories such as Marxism and new institutional economics related to the digital transformation of enterprises are sorted out. Secondly, it conducts an empirical analysis on the digital transformation of high-tech enterprises. This paper summarizes the three major transformation paths of the existing production service digitization, marketing model digitization, and industrial digitization. Based on the data analysis of the questionnaire, this paper summarizes the difficulties of digital transformation of high-tech enterprises, mainly due to the lack of transformation ability, resulting in "cannot transfer"; the lack of self-development conditions and digital transformation, resulting in "will not transfer"; digital transformation lacks full guarantee, resulting in "do not dare to turn." And based on the analytic hierarchy process, the influencing factors of the digital transformation of high-tech enterprises are analyzed, and the relative importance of each factor is obtained.

1. Introduction

With the introduction of new development and new development strategies, China's economic development has undergone tremendous changes. The term "digital economy" was first coined in government work in 2017, and it has had a profound effect on the optimization of the economy by the prosperity of emerging industries such as the digital economy. And accelerating the development of the digital economy and promoting the combination of digital economy have become a hot topic. With the rise of digital technologies such as big data, cloud computing, and artificial intelligence, digital technology has become an important means for modern enterprises to adapt to the changes of the times, implement national strategies, and improve their competitiveness. According to a survey report by IDC on CEOs of 2,000 companies, up to now, 67% of companies regard digital transformation as the core of their corporate strategy, and 70% of China's 1,000. The "2019 Chinese Enterprise Digital Transformation Index Research" published by Accenture on September 10, 2019, shows that China's "ideal digital company" was a measure in 2018, with a comprehensive score of 45, up from 37 in the same period last year, 20%. This shows that China's e-commerce has entered a new stage, and it is also a new digital age [1].

In order to maintain the stable development of enterprises, it is necessary to conform to the development trend of the times and the digital age although many companies regard digital transformation as a strategic focus and have invested in many companies' systems and equipment on the basis of digitalization [2, 3]. However, the "2019 Chinese Enterprise Digital Transformation Index Research" pointed out that although China has achieved a substantial increase in revenue and sales, in terms of digital transformation, only 9 aspects have achieved obvious results, and many companies are still unable to achieve expected goals and effect, facing the difficulty of transformation. How to promote the digital economy of enterprises to achieve higher performance has become an important topic of concern to the industry and theoretical circles. This dissertation takes high-tech companies as the center and discusses their digital transformation. Most of the previous literature on the transformation of high-tech companies has discussed the transformation strategies of high-tech companies from a

macro perspective, but the results are inconsistent with the digital transformation trend of high-tech companies; only a few scholars have focused on the digital transformation of high-tech industries. However, due to the lack of accurate understanding, their digital research mainly focuses on the network. In the digital age, the digital transformation of high-tech industries involves a relatively narrow scope and a relatively shallow level.

2. Overview

2.1. Digital Economics. The "digital economy" was first proposed in 1994, and its meaning is constantly changing. The connotations of various concepts and researches on the digital economy are getting richer and richer. So far, there is no consensus on this issue, whether domestically or in academia. The definition of digital economy in European and American countries is mostly defined from the perspective of industry and products, which focuses on the interaction between technology and people, but the definition of industry is relatively simple in general, involving telecommunications, audio-visual, software, Internet, and other industries [4]. And on this basis, the communication, audio-visual, and other technologies have been deeply analyzed. When China defines the digital economy, what it considers is the entire relevant behavior, that is, the changes that occur on the basis of the occurrence and development of an economic system, that is, the combination of economy and technology. The "G20 Digital Economy Development and Cooperation Initiative" was officially released by China at the 2016 G20 Summit. The initiative focuses on China's ideas in promoting economic growth and strengthening cooperation with other countries. The digital economy is a kind of production factor that uses digital technology as the medium to effectively utilize digital technology to achieve economic optimization and improve efficiency. It is pointed out that the digital economy is the combination of industry and industry with communication as the main content. In the context of the digital economy, digital information is regarded as the main means of production. The new socioeconomic form came into being after the two major development forms of agriculture and industry [5]. Compared with the conventional model, the new economic model has brought a large amount of digitalization of production and operation, and these new means of production are new means of production based on data. In short, the digital economy is a huge economic change. Its combination with modern technology allows enterprises and users to communicate efficiently, so that the circulation of products and services will develop in a more convenient and scientific direction. Through the digital economy, all aspects of each link can be effectively integrated, so as to achieve better development.

2.2. Data Processing. "Digitalization" is an important part of the digital economy. With the passage of time and the continuous innovation of technology, the meaning and external expansion of numbers have become more and more diverse. Digital technology is the integration and optimization of traditional information systems. Through integration and optimization, the operation of enterprises can be improved, and new technologies can be improved through new technologies, so that they can meet the needs of digitalization.

2.3. Digital Conversion. How to carry out digital transformation has become a common concern of both the theoretical and practical circles. Huawei believes that digital transformation is the use of a new generation of digital technologies to build a digital society with full perception, full link, full scene, and full intelligence, thereby reconstructing traditional management and business models. By innovating and reconstructing the way of operation of the enterprise, we can obtain the victory of the enterprise. Kingdee regards digital transformation as the digital transformation of enterprises; that is, enterprises use digital technologies to apply technologies such as the Internet of Things, cloud computing, big data, mobile, and intelligence to enterprises and plan and implement business model transformation, management, and operation transformation. Enterprises and employees bring new digital value enhancement and continuously improve the new core competitiveness of enterprises in the digital economy environment [6].

There are differences in the understanding of "digital transformation" in academic circles. Gemini believes that digital technology is the fundamental improvement of company performance through digital technology and through the use of digital technology to break down the information barriers between various departments, thereby improving the efficiency of company operations. Experts such as Berman believe that the essence of digital transformation is to reconstruct the value of customers and use digital technology to change the way of production and operation, thereby changing the value and operation of traditional manufacturers, thereby promoting their development in the digital age. The main proposition of Wang Hua in China is as follows: digital transformation means that the company's production and services can be realized through digital technology, the company's operations and operations can be combined with digital technology, and the company, customers, and the market can achieve, through comprehensive technological transformation, interaction and communication and constantly promote the comprehensive innovation of the market, business system, and customers, thereby improving operating efficiency.

Based on the above theories and the actual experience of enterprises, the concept of enterprise digital and the innovation of product models and business models accelerate the transformation and upgrading of enterprises through digital means and seek new paths for innovation and development. Big data application, intelligence, and networking are important features of the transformation of the digital economy.

3. Mechanism Analysis of the Driving Force of Digital Transformation of Enterprises

With the development of economy and society, and the continuous progress of the times, emerging industries such as the Internet and e-commerce have emerged as the times require. In the research of emerging fields, the basic principles of Marxism can still be used as the basic theory to build the theoretical logic of related research. Based on the actual national conditions of China, it still has extremely important practical guiding significance to apply the basic principles of Marxism directly or indirectly to the research of economic or social topics in the new era. The pursuit of excess profit is the subjective motivation and fundamental driving force of the digital transformation of enterprises [7]. Marx believed that the productivity of social labor is affected by many factors. With the integration and development of large industry and the digital economy, the creation and accumulation of real wealth depend more on the average level, iteration speed, and application of science and technology in the current society, rather than the simple accumulation of labor time. Therefore, the advancement of digital technology is a key factor in promoting the transformation of social productivity, resulting in changes in the economic form and gradually forming a digital economy.

3.1. Digital Technology Lays a Technical Foundation for the Digital Transformation of Enterprises. The development and progress of digital information technology have laid the necessary technical foundation for enterprises to carry out digital transformation. On the one hand, the advancement of digital information technology can improve the labor productivity of enterprises in digital production. Using Marx's relevant viewpoints for analysis, we can see that the development and application of digital information technology determine the proportion of capital divided into constant and variable parts. However, in the current situation where the nature of society is certain and the speed of development is relatively stable, the accumulation of wealth is closely related to the development of human beings. Therefore, when the production department of the enterprise is reasonably and effectively equipped with digital software and hardware facilities and high-tech talents, the labor productivity of the production department of the enterprise will be greatly improved [8]. In the era of digital economy, as long as a certain department takes the lead in completing digital transformation and realizes the transformation of production methods, "it will inevitably lead to changes in the production methods of other departments." It is worth noting here that, in the process of digital production, digital information technology and the corresponding digital hardware and software facilities "always enter the labor process in their entirety but always only partially enter the value appreciation process." Digital technology and digital production equipment itself do not create value, but they gradually transfer their own value to the digital products they produce or the digital services they provide. In this sense, digital technology and digital production equipment are a digital component of the value of a product or service.

On the other hand, the advancement of digital information technology promotes the digitization of collaboration and the specialization of division of labor among various departments of the enterprise, which is conducive to promoting the digital transformation of enterprise organizations. The development of digital information technologies such as the Internet and SG makes collaboration not limited by time and space, which is conducive to expanding the scope of collaboration and greatly improving the efficiency of collaboration [9]. The digital production operation of an enterprise under the technological progress itself is a huge and complex system, which requires a large number of local workers to divide and cooperate. As Marx put it: "Not to mention the new forces arising from the fusion of many forces into one total force, in most productive labor, social contact alone evokes a sense of competition and a peculiar invigoration of energy that elevates everyone. The application of digital information technology provides technical support for expanding the influence of this social contact, promotes the digital and efficient transformation of enterprise organizations, and greatly improves the work efficiency of enterprise workers."

3.2. Participation and Distribution of Data Is a Necessary Condition for Digital Transformation of Enterprises. The reason why nonphysical data can participate in the distribution is that it is gradually capitalized with the development of the digital economy. It has the nature of capital and is also a special kind of capital. Combined with the analysis of the basic principles of Marxism, it can be seen that, in the digital network formed by the application of related, the data generated in the daily use of social media will be transformed into capital through two stages:

First, the commercialization stage: users need to consume a certain amount of physical and mental energy in the process of using social media, and the relevant data generated based on this exists in the form of labor products; when these digital labor products are "exchanged, transferred to use as use value, and use it in the hands of people," it becomes a data commodity; that is, in the market economy, the data generated through digital labor is exchanged for the purpose of profit, and it exists in the form of a commodity.

The second is the capitalization stage: the digital labor that users use various software to generate data in their daily life is unpaid labor and still has the nature of "exploitation." Large-scale Internet companies such as Amazon, based on the volume of their digital business and the advantages of related digital technologies, freely occupy the digital labor of users and the data value they generate [10, 11]. According to the needs of business development, the relevant data generated by the digital labor that they possess for free are extracted, processed through digital technology to form a data group, exchanged, and sold, and their data products are sold, "and most of the money obtained from this are reconverted into capital" and used for the additional

production materials and labor required for the continuous digital development of enterprises, and data commodities are transformed into digital capital. In this process, data exists in the form of capital.

Participation in the distribution of data mainly involves two aspects: on the one hand, data as a factor of production participates in the distribution. According to the relevant theoretical analysis of factor distribution theory, data has become a special production factor, and its distribution principle is determined by social production relations. In a capitalist society, how data is distributed as a factor of production is determined by the owners of the data, the capitalists. In a socialist society, public data resources are shared by the whole people, while nonpublic data resources are distributed by the market under established legal conditions. Another aspect is that data participates in distribution as the final product. In China, the distribution of data products needs to meet the relevant requirements of the basic distribution system, which is mainly determined by the amount of labor paid by the laborers in the process of data collection, analysis, and application.

3.3. Pursuit of Excess Profit Is the Fundamental Driving Force for Digital Transformation of Enterprises. In the digital age, the "labor" expounded by Marx in the labor value theory combines digital information and other modern technologies to form a new form of labor, that is, digital labor. According to the relevant elaboration of labor value theory, digital labor includes concrete labor and abstract labor. A user posts videos, images, comments, etc. in social media. This kind of labor consumption based on a certain purpose constitutes the specific labor of digital labor. The specific content published can meet certain needs of people. Therefore, there is the specific labor of digital labor. The generated data information can create use value for the economy and society; the digital behavior of all users, such as web page search and browsing behavior, has no specific form. Human labor in the general sense forms the abstract labor of digital labor, which is given to commodity producers. The demand information about the size, shape, and function of the designed product can be produced based on the application of related technologies to create value, which reflects the relationship between data producers, information users, and commodity sellers in the social production process in the digital age social relationship. The amount of value of goods produced based on the use of digital technology is determined by the socially necessary labor time [12]. The higher the "development level of science and the degree of its application in craftsmanship" in the field of digital information are, the higher the productivity of digital labor is, and the smaller the value of the digital goods it produces. From the relevant analysis of the theory of surplus value production, it can be seen that, in the early stage of the development of the digital economy, individual entrepreneurs used digital information technology to improve the labor productivity of enterprises and carried out digital production and operation. The labor time consumed by the same commodity shows that the commodity value produced by individual entrepreneurs based on digital information technology is lower than the social value, thus obtaining excess surplus value. Based on this, the individual production price of the commodity will be lower than the social production price, and enterprises that use digital information technology for digital operations will obtain additional profits that are more than average profits, that is, excess profits. Due to the existence of the law of market competition, the practice of individual entrepreneurs using digital information technology for production and operation to obtain excess profits will be replicated and promoted by other entrepreneurs in their industry, which will eventually attract more enterprises to improve their digital production and operation capabilities and conduct digitalization [13].

To sum up, the pursuit of excess profit is the fundamental driving force and subjective motivation for enterprises to improve production technology and carry out digital transformation. In the era of digital information, the pursuit of excess profits by various entrepreneurs is conducive to improving the level of labor productivity in society and promoting the pursue more Excessive profits, thus forming a virtuous circle.

4. Big Data Model for Digital Evaluation of High-Tech Enterprises

There are currently three ways to distribute the income of estimating the coefficients of the digital combination: one-way ANOVA, historical simulation, and Monte Carlo simulation.

4.1. The Variance-Covariance Method. This method is one of the most common VaR values and belongs to the parametric method. On this basis, the statistical method is used to predict the income distribution of the digital coefficient, and the historical data are used to estimate it, such as variance and correlation coefficient, thus obtaining an overall under certain credibility. The VaR value of the asset is

$$\mathrm{VaR} = z_\alpha \sigma_p \sqrt{\Delta t}, \tag{1}$$

where σ_p is the standard deviation of the entire portfolio return, z_α is the quantile of level α, and Δt is the holding period. According to the above formula, the VaR value can be obtained only by calculating the variance. The commonly used variance prediction methods include the RiskMetrics method and the GARCH method.

4.1.1. Risk Metrics Method. The RiskMetrics digital control model was launched by the digital management department of JPMorgan in October 1994. It is the world's first quantitative VaR model. Its main idea comes from the exponential moving average method (EWMA), which takes unequal weights on the data in the time series. To simplify the assigned weights, it introduces a parameter λ, called

attenuation factor, whose value is between 0 and 1. For the estimation of λ, the principle of root mean square error (RMSE) is usually used; that is, the value of λ that minimizes the root mean square error of the prediction is selected:

$$\sigma_t^2 = (1-\lambda)\sum_{i=1}^{\infty}\lambda^i r_{t-i}^2. \tag{2}$$

The exponential moving average method estimates the standard deviation of returns. The variance estimation formula can be written in an iterative form, which will help the use of computers process huge data. RiskMetrics based on the normal method has some drawbacks: it relies on the normality of position returns and is a partial method and a thoroughly linear method, while being computationally cumbersome.

4.1.2. GARCH Class Methods. The 2003 Nobel Laureate in Economics Robert Engle first introduced the ARCH model in 1982 to model variance. In 1987, Bollerslev extended the autoregressive conditional heteroscedasticity (ARCH) model and developed it into a generalized ARCH model, namely, the general autoregressive conditional heteroscedasticity (GARCH) model. Over the years, GARCH models have become a large family of many different types. A large number of empirical studies have shown that GARCH-type models have the characteristics of good description of financial time series, that is, the ability to deal with the time-varying and thick-tailed distribution of variance.

$$r_t = \mu + \varepsilon_t, \tag{3}$$

where μ is the unconditional mean and ε_t is the disturbance term. The conditional variance equation of GARCH-like models provides a simple analytical form for the stochastic volatility process in financial return data. The GARCH (p, q) model predicts volatility as follows:

$$\begin{aligned}\sigma_t^2 &= \omega + \alpha_1\varepsilon_{t-1}^2 + L + \alpha_p\varepsilon_{t-p}^2 + \beta_1\sigma_{t-1}^2 + L + \beta_p\sigma_{t-p}^2 \\ &\cdot\left(\omega > 0, \alpha_1, L, \alpha_p \geq 0, \beta_1, L, \beta_p \geq 0\right).\end{aligned} \tag{4}$$

The choice of the conditional variance equation and the assumption of the independent and identical distribution of the residuals are two key factors. With the application of GARCH-type models in the financial field, two obvious problems have gradually emerged in general GARCH-type models: first, the nonnegativity constraints on coefficient parameters are too strong, which excessively restricts the dynamics of conditional variance. Second, the conditional variance σ_t in GARCH-like models is a symmetric function of ε_t, which depends only on the magnitude of ε_t and not on its sign. Obviously, this is not true because interest rate movements in financial markets have a leverage effect, and the rise and fall of stocks will have an uneven impact, and the fall of stocks will have a greater impact on subsequent volatility. This means that the preferred mode handles both positive and negative types of residuals in an asymmetric manner.

4.2. Historical Simulation Method. By analyzing the frequency of portfolio income in a certain period, the method finds the historical rate of return and the current minimum rate of return of the index within a certain confidence interval [14]. The model does not need to assume the statistical distribution of various market factors and can fully reflect the real changes of various market factors, so that it can solve the problem of abnormal distribution. The simulation algorithm is easy to implement and suitable for various types of positions and digital calculations in various markets. However, because this model assumes that future market factors and past historical changes are exactly the same, which is inconsistent with the real financial market, especially in the recent large-scale range, past data cannot be used to predict future stock markets and make accurate expectations, so historical simulation techniques are employed without any warning of unforeseen numbers. In addition, it is difficult to meet the above requirements because of the many specific data required for historical allocation of portfolio returns.

4.3. Monte Carlo Simulation. Return on assets or market factor returns are not derived from historical observations, but we use tools to generate a huge amount of possible random data that conform to historical distributions, thereby constructing a portfolio, possible gain or loss, and then get an estimate of the digitized value at a given confidence level [15]. This method is extremely efficient and flexible because it does not require normality assumptions about the distribution of asset values, can be used for arbitrarily distributed return assumptions, does not require linear relationships between digitized factors, and also applies to variance changes with time, when the distribution is tail, in extreme value scenarios, and other special situations. However, the process used to generate data in the simulation process is random, which makes it subject to a certain degree, and this method has a large amount of calculation, a long calculation time, and is more complicated than other methods.

5. VaR Measurement Analysis of Market Digitization of Small- and Medium-Sized Private Enterprises

By processing the closing prices of 423 small- and medium-sized private listed companies from January 4, 2016, to December 31, 2020, a logarithmic daily rate of return sequence containing 1215 data was obtained.

5.1. Basic Statistical Data Analysis. The normality test of financial time series can generally be tested by calculating the mean, skewness, kurtosis, and Jarque–Bera statistics. The daily rate of return was analyzed using EViews software to obtain the histogram and descriptive statistics of the logarithmic daily rate of return series (Figure 1).

From the chart, we can see that the deviation value of the portfolio is above 0, and the distribution is positive, indicating that there is a right tail in the return distribution.

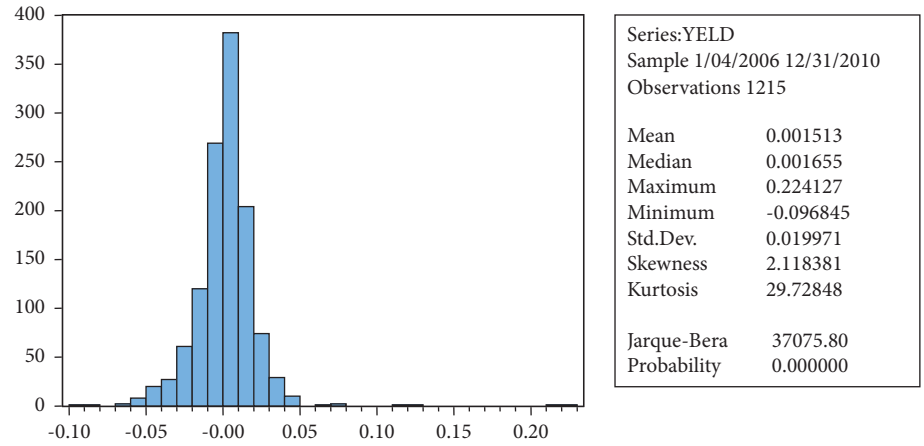

Figure 1: Descriptive statistics of log daily returns and their histograms.

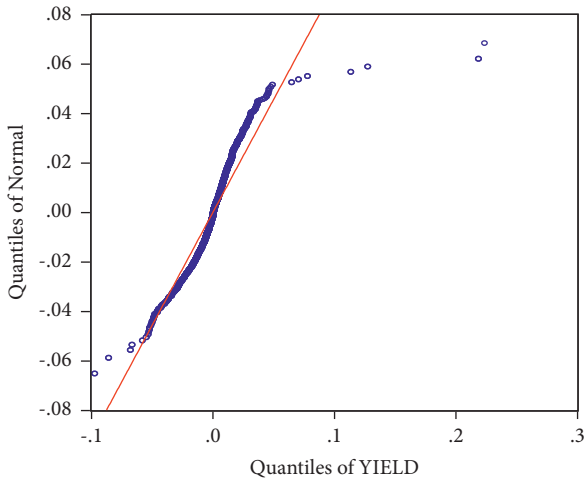

Figure 2: QQ plot of log daily returns.

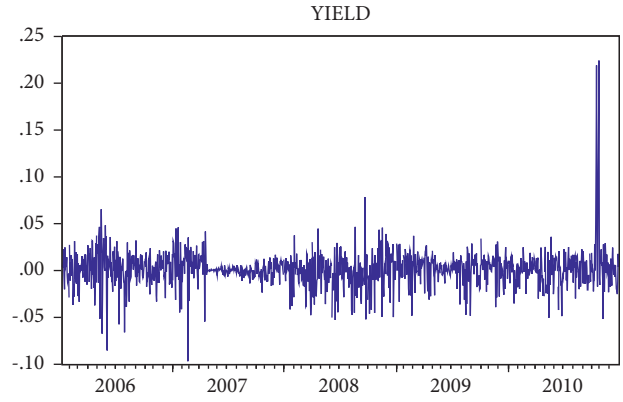

Figure 3: Logarithmic daily return time series chart.

Kurtosis is used to describe this type of steep slope, which is much higher than the normal 3 peaks, which means that the frequency distribution is much more dense than normal. The Jarque–Bera statistic is used to detect the normal distribution of a series, and the threshold for 5% significance of this statistic is 5.99 under the assumption that the condition is 2. The value of the Jarque–Bera standard test statistic here is above the threshold of 5.99, which, in terms of the probability of the JB statistic, shows that a 0 assumption negates a normal distribution. The average return is not too far from zero, and it is also insignificant compared to the standard deviation. It is clear from the curve that there is a sharp rear tail in the distribution of returns. The average daily returns of small- and medium-sized board stocks show abnormal characteristics.

In addition, the QQ chart can more directly detect the normal distribution of returns (Figure 2).

The QQ plot compares the quantiles of a sample with the quantiles of a normal distribution. If the return distribution of the index is a normal distribution, then it should be a straight line on the QQ chart, and it can be seen from the figure that the line is a curve rather than a straight line, so the distribution of the logarithmic daily return series is not a normal distribution. In addition, looking at the time series of the logarithmic-day yield series in Figure 3, we can see that there is a clustering effect in yield fluctuations. The QQ plot also shows that this thick-tailedness is asymmetric.

5.2. Stationarity Test. The ADF method controls for higher-order serial correlations by adding a lagged difference of the dependent variable y_t to the right-hand side of the regression equation, as shown in Figure 4.

$$\Delta y_t = \gamma y_{t-1} + \sum_{i=1}^{p} \beta_i \Delta y_{t-1} + u_t, t = 1, 2, \ldots, T, \tag{5}$$

$$\Delta y_t = \gamma y_{t-1} + \alpha + \sum_{i=1}^{p} \beta_i \Delta y_{t-1} + u_t, t = 1, 2, \ldots, T, \tag{6}$$

$$\Delta y_t = \gamma y_{t-1} + \alpha + \delta t + \sum_{i=1}^{p} \beta_i \Delta y_{t-1} + u_t, t = 1, 2, \ldots, T. \tag{7}$$

5.3. ADF Inspection. Model (7) is a time variable, which represents a certain trend of the time series over time. The null hypotheses are all H0: $\gamma = 0$; that is, there is a root of unity

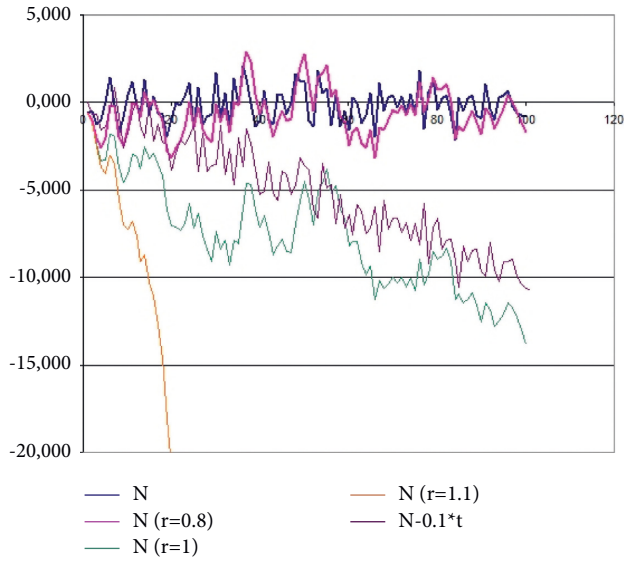

Figure 4: Stationarity test.

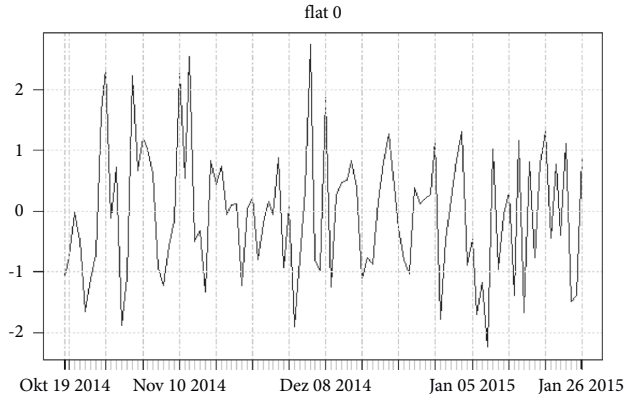

Figure 5: ADF test.

Table 1: ADF test.

Null hypothesis: Yield has a unit root			
Lag Length: 0 (fixed)		*t*-statistic	Prob.*
ADF test statistic		−29.73025	0.0000
	1% level	−3.435523	
	5% level	−2.863712	
	10% level	−2.567977	
Akaike Info criterion	−5.0105	Schwarz criterion	−5.00209

(Figure 5). The difference between model (7) and the other two models is whether it contains constant term and trend term. The actual test starts with model (7), then (5), (6): when to reject the null hypothesis, that is, the original sequence does not have a unit root and is a stationary sequence, and when to stop testing. Otherwise, continue to check until (5) is completed. The results shown in the table were obtained under the principle of minimum AIC and SC (Table 1).

From the test results, at the three significance levels of 1%, 5%, and 10%, the critical values of the unit root test are −3.435523, −2.863712, and −2.567977, the hypothesis $H0$

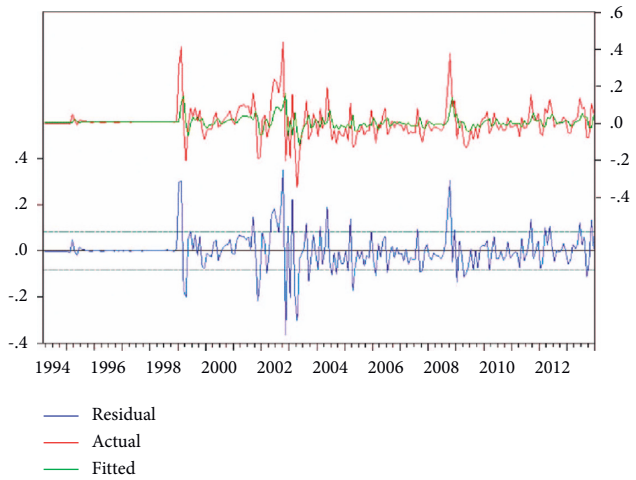

Figure 6: ARCH effect test.

Table 2: ARCH-LM test.

F-statistic	46.35092	Probability	0.00000
Obs ∗ R-squared	133.56369	Probability	0.00000

indicates that the difference series of daily returns does not have a unit root, and the logarithmic daily returns are stationary series.

5.4. ARCH Effect Test. In 1982, Engle proposed the Lagrangian multiplier test, namely, the LM test, to test whether there is an ARCH effect in the residual sequence. This particular specification of autoregressive conditional heteroskedasticity is due to the discovery that, in many financial time series, the magnitude of the residuals is related to the most recent residual value. The LM test statistic was calculated by an auxiliary test regression (Figure 6). There is no ARCH effect in the residual sequence up to the p-order, and the following regression is required:

$$u_t^2 = \beta_0 + \left(\sum_{s=1}^{P} \beta_s u_{t-s}^2 \right) + \varepsilon_t, \tag{8}$$

where u_t is the residual. This formula represents a regression of the residual squared u_t^2 on a constant and lag u_{t-s}^2 up to the p-order residual squared. This test regression has two statistics:

(1) The F statistic is an omitted variable test for the joint significance of the lags of all squared residuals;

(2) The $T * R2$ statistic is Engle's LM test statistic, T is the number of observations, and $R2$ is the regression test. The exact finite-sample distribution of the F statistic under the null hypothesis is unknown, but the LM statistic is in general asymptotically subject to the $\chi^2_{(p)}$ distribution.

Table 2 is the test result of ARCH-LM, and the result shows that the P value is zero, rejecting the null hypothesis. This indicates that the residual series has an

ARCH effect; the residual squared correlation plot shows that the Q statistic of the residual squared series is significant, which also indicates that the residual series has an ARCH effect.

6. Discussion of Results

As an important part of developing the digital economy and an important part of China's digital strategy, the digital transformation of enterprises is of great significance to boosting the Chinese economy. Based on the data of high-tech listed companies from 2016 to 2020, this paper studies the impact of digital transformation on enterprise performance from multiple perspectives such as dynamic effects and heterogeneity and studies the mediation of its impact. Finally, robustness and endogeneity tests were carried out. This paper mainly draws the following conclusions: first, digital transformation can effectively improve enterprise performance and can continue to improve enterprise performance for a long time, and the effect is more obvious in enterprises with a high degree of digital transformation. Second, considering that differences in the company's own attributes and macro-environmental conditions may have different effects on corporate performance, we empirically test the impact of digital transformation on the effects of digital transformation from a micro perspective (property nature, corporate age) and a macro perspective impact on business performance [16]. It is found that, compared with non-state-owned enterprises, digital transformation can significantly improve enterprise performance in state-owned enterprises, but for non-state-owned enterprises, it does not play a boosting role; from the perspective of enterprise age, digital transformation can effectively improve enterprise performance, but compared with young enterprises, mature enterprises have better performance improvement effect; from the perspective of macroeconomic environment, no matter the macroeconomic environment is good or bad, digital transformation can improve enterprise performance, but the performance improvement effect is more effective when the environment is good for obvious reasons; digital transformation can improve business performance as far as the financial cycle is concerned, but it works better in a bull market [17]. Third, from the perspective of the transmission mediation path, operating costs and labor productivity have a partial mediating effect in the relationship between digital transformation and corporate performance; that is, digital transformation improves corporate performance by reducing operating costs and improving labor productivity. Fourth, considering that the impact of digital transformation on enterprise performance is inseparable from government support, we further embedded government governance elements to study the paradigm of "digital transformation and enterprise performance." The policy effect exerted is inefficient, while the government focuses on refined governance in the micro-field; that is, the policy effect exerted in the form of targeted subsidies is extremely efficient.

This research provides important practical implications for exploring new driving forces for improving corporate performance and thus promoting the high-speed and high-quality development of the digital economy: first, to promote enterprises to actively promote digital transformation, drive flexible production, intelligent manufacturing, and digital management and sales. Promote the value of data, accelerate the deep integration and integration of new-generation technologies such as big data, cloud computing, Internet of Things, and 5G with enterprises, promote cloudification and integration of core systems, and continuously promote enterprises to digitalize transformation of modern business models. Strengthen the interconnection of data, knowledge, and services between enterprises, tap synergies between enterprises, promote the online, intelligent, and digitalization of commercial trade, realize the rapid matching of data and services, and improve the agility to respond to changes in business needs. Customers provide personalized customized services to form a digital ecological cluster that "gets what they need, mutual benefit and win-win," so as to improve corporate performance. For example, home appliance companies can use the smart TV terminals sold by the company as the basis to develop third-party businesses, such as cooperating with Internet companies to collect statistics and data on users' use of watching videos, music, education, games, and other content services, conducting in-depth analysis of these data, and using public services and other means to spread brands to users and gradually form a ten million-level user platform and realize the development model of "user + terminal." In addition, we should also pay attention to the digital transformation of non-state-owned enterprises and young enterprises, promote small-scale enterprises to go to the cloud platform, improve the external economic environment of enterprises, and promote the sustainable development of all-round overall digital economic benefits. Second, help enterprises to improve labor production efficiency through digital transformation and promote the quality and efficiency of digital transformation. In-depth mining, collection, and analysis of enterprise internal data information such as enterprise equipment, personnel, and logistics focus on analyzing this data information and classify and refine it. Identify possible integrated processes and steps that can be omitted and rationally use data core resources to promote intelligent, digital, and networked reforms in the manufacturing industry and promote enterprise innovation [18]. Promote the coordinated development of upstream and downstream enterprises in the industry chain and increase the added value of products based on the transformation needs of key business scenarios [19–21]. For example, companies can rely on the company's procurement channels, distribution systems, and terminal network advantages and use digital technology to eliminate information between upstream and downstream enterprises in the supply chain. Asymmetric tangerine is innovating the supply chain service model and improving the circulation efficiency of the supply chain; on the other hand, it extensively collects and stores consumer group information and conducts in-depth analysis to form

customer portraits and implement precise marketing, thereby improving labor production efficiency, reducing operating costs, management costs, and investment costs, and improving enterprise performance and sustainable competitiveness, based on long-term development [22–28]. Finally, strengthen government governance, and distribute government subsidies in a reasonable and targeted manner. As an important driving force for enterprises' digital transformation, the government must give full play to the "promising government" effect. Relying on ABCD technology to promote government digital management, establish a professional information consulting platform, technical guidance platform, etc., to achieve efficient, active, precise, and flexible government governance, formulate a digital governance system that matches the digital economy, and give full play to the market role of resource optimization and allocation in digital transformation, creating a good external ecological environment for digital transformation and improving the efficiency of government digital services [29–33]. Strengthen the construction of infrastructure, optimize the industrial structure, form a digital development strategy, actively introduce relevant policies to provide technical support for the digital transformation of enterprises, and provide targeted financial support for the transformation of enterprises, so as to alleviate the financial difficulties faced by enterprises. In addition, attach importance to the protection and open sharing of data, break down digital barriers, and appropriately and reasonably open part of the data resources for commercial purposes within the scope of government monitoring to reputable companies, reducing the difficulty and cost of data collection. Improve the level of communication and interaction between government and enterprises, understand the actual difficulties of enterprises, and help them get out of the predicament.

7. Conclusion

Digital transformation is the all-round reshaping of internal and external processes, production methods, and management methods of enterprises in the digital economy era in the face of big data, Internet of Things, cloud computing, 5G, and other information technologies. There are many intermediary paths for corporate performance, and the current research on the impact of the digital transformation of physical enterprises on performance from the perspective of the digital economy mainly studies such as communication and collaboration costs and investment costs, agency costs, logistics costs, research, and development costs. Regarding the intermediary path in terms of cost, relatively, this paper mainly reveals the intermediary path that digital transformation affects enterprise performance, such as reducing costs and improving labor productivity, and then enriches and improves the mediation path in the paradigm of digital transformation and enterprise performance in this field.

Data Availability

The dataset can be accessed upon request.

Conflicts of Interest

The author declares no conflicts of interest.

References

[1] F. Wu, H. Hu, H. Lin, and X. Ren, "Enterprise digital transformation and capital market performance: empirical evidence from stock liquidity," *Management World*, vol. 37, no. 7, pp. 159–162, 2021.

[2] X. Li, Z. Li, and L. Gao, "Research on digital transformation and intelligent upgrade path of discrete manufacturing industry," *China Engineering Science*, vol. 24, no. 2, pp. 119–121, 2022.

[3] W. Chen and J. Wang, "Dependency upgrade: digital transformation strategies of participants in platform ecosystem," *Management World*, vol. 37, no. 10, pp. 20–25, 2021.

[4] L. Huang, H. Zhu, W. Liu, and M. Li, "Digital transformation and management of enterprises: research framework and prospects," *Journal of Management Science*, vol. 24, no. 8, pp. 10–14, 2021.

[5] B. Li and S. Yin, "Research on ICT enterprise ecological partner selection in the background of digital transformation—based on prospect theory and field theory," *Management Review*, vol. 32, no. 5, pp. 157–164, 2020.

[6] Y. Lu, B. Zhao, and S. Chang, "Decision logic, learning from failure and the performance of enterprise digital transformation," *Foreign Economics and Management*, vol. 43, no. 9, pp. 159–166, 2021.

[7] C. Maomao, J. Wang, and W. Wang, "Research on the influence mechanism of enterprise innovation performance in the background of digital transformation—based on the hybrid method of NCA and SEM," *Science Research*, vol. 40, no. 2, pp. 13–22, 2022.

[8] R. Guo, M. Han, T. Shao, and T. Zhang, "The opportunity development mechanism of digital transformation enterprises from an ecological perspective: based on a double case study of haier and suning," *Foreign Economics and Management*, vol. 43, no. 9, pp. 25–32, 2021.

[9] B. Lu, Z. Yin, and Y. Zhang, "An exploratory study on the process and mechanism of digital transformation of traditional enterprises," *Research Management*, vol. 43, no. 4, pp. 110–114, 2022.

[10] X. Wang, T. Nie, and J. Meng, "The influence of political connections on the digital transformation of small and medium-sized enterprises: the mediating role of policy perception ability and market perception ability," *Research Management*, vol. 43, no. 1, pp. 91–94, 2022.

[11] C. Zhao, W. Wang, and X. Li, "How digital transformation affects the total factor productivity of enterprises," *Finance and Trade Economics*, vol. 42, no. 7, pp. 106–114, 2021.

[12] B. Wang and J. Mao, "How can traditional enterprises achieve digital transformation through intrapreneurship?—a strategic evolution perspective based on resource matching," *Management Review*, vol. 33, no. 11, pp. 114–119, 2021.

[13] L. Liang, R. Jin, and J. Song, "Research on the digital transformation path selection mechanism of third-tier military enterprises under the digital economy," *Science and Technology Progress and Countermeasures*, vol. 39, no. 7, pp. 95–109, 2022.

[14] Z. Yang and L. Qi, "Review of foreign digital innovation research and its enlightenment to the digital transformation of Chinese manufacturing enterprises," *Scientific Management Research*, vol. 39, no. 4, pp. 58–62, 2021.

[15] H. Tian, Z. Niu, and C. He, "Experiences, practices and development prospects of digital transformation of construction enterprises," *Construction Economy*, vol. 42, no. 10, pp. 61-62, 2021.

[16] G. Hou and C. Gao, "Research on the influence of enterprise network structure on enterprise innovation performance from the perspective of digital transformation capability," *Science and Technology Management Research*, vol. 42, no. 1, pp. 56–61, 2022.

[17] L. Yang, G. Pan, and G. Hou, "Behavioral evolution of key participants in digital transformation of SMEs," *Science and Technology Management Research*, vol. 42, no. 6, pp. 12–17, 2022.

[18] C. Wang and H. Chen, "Research on digital transformation of enterprises in the context of digital economy," *Management Modernization*, vol. 41, no. 2, pp. 30–34, 2021.

[19] X. Tan, Y. Dong, and T. B. Fang, "Competition, Combination of Industry and Finance, and Enterprise Innovation: Evidence from China," *Complexity*, vol. 2022, Article ID 6594964, 2022.

[20] M. Bai, "An Empirical Study on the Relationship between Stock Price Information and Enterprise Innovation Management Based on Information Learning Mechanism," *Computational Intelligence and Neuroscience*, vol. 2022, Article ID 9425405, 2022.

[21] L. H. Li, J. C. Hang, Y. Gao, and C. Y. Mu, "Using an integrated group decision method based on SVM, TFN-RS-AHP, and TOPSIS-CD for cloud service supplier selection," *Mathematical Problems in Engineering*, pp. 1–14, 2017.

[22] J. Wang, X. Wang, and H. Wen, "The use of BP neural network algorithm and natural language processing in the impact of social audit on enterprise innovation ability," *Computational Intelligence and Neuroscience*, vol. 2022, Article ID 7297769, 2022.

[23] L. Li, C. Mao, H. Sun, Y. Yuan, and B. Lei, "Digital twin driven green performance evaluation methodology of intelligent manufacturing: hybrid model based on fuzzy rough-sets AHP, multistage weight synthesis, and PROMETHEE II," *Complexity*, vol. 2020, no. 6, pp. 1–24, 2020.

[24] P. Zhang, E. Zhou, Y. Lei, and J. Bian, "Technological innovation and value creation of enterprise innovation ecosystem based on system dynamics modeling," *Mathematical Problems in Engineering*, pp. 2021–13, 2021.

[25] R. Wu, Z. Wang, and Q. Shi, "Increment of heterogeneous knowledge in enterprise innovation ecosystem: an agent-based simulation framework," *Complexity*, pp. 2021–16, 2021.

[26] L. Li, B. Lei, and C. Mao, "Digital twin in smart manufacturing," *Journal of Industrial Information Integration*, vol. 26, no. 9, Article ID 100289, 2022.

[27] L. Li, T. Qu, Y. Liu et al., "Sustainability assessment of intelligent manufacturing supported by digital twin," *IEEE Access*, vol. 8, pp. 174988–175008, 2020.

[28] K. Gao and L. Ma, "Security Regulation and Enterprise Innovation in Communication Industry," *Security and Communication Networks*, vol. 2021, Article ID 3307493, 2021.

[29] L. Li and C. Mao, "Big data supported PSS evaluation decision in service-oriented manufacturing," *IEEE Access*, vol. 8, pp. 154663–154670, 2020.

[30] X. Wang and C. Jiang, "The signal effect of new energy vehicles promotion on enterprise innovation," *Complexity*, pp. 2021–10, 2021.

[31] L. H. Li, J. C. Hang, H. X. Sun, and L. Wang, "A conjunctive multiple-criteria decision-making approach for cloud service supplier selection of manufacturing enterprise," *Advances in Mechanical Engineering*, vol. 9, no. 3, pp. 168781401668626–1687814016686264, 2017.

[32] T. Liu, X. He, X. Guo, and Y. Zhao, "The influence of the network evolutionary game model of user information behavior on enterprise innovation product promotion based on mobile social network marketing perspective," *Mathematical Problems in Engineering*, vol. 2022, Article ID 1416488, 12 pages, 2022.

[33] B. A. Luo, "Method for enterprise network innovation performance management based on deep learning and Internet of Things," *Mathematical Problems in Engineering*, vol. 2022, Article ID 8277426, 11 pages, 2022.

Hindawi
Scientific Programming
Volume 2022, Article ID 8329745, 10 pages
https://doi.org/10.1155/2022/8329745

Research Article

Research on Modern Book Packaging Design Based on Aesthetic Evaluation Based on a Deep Learning Model

Wen Wen

Journalism & Communication Department, Anhui News and Publishing Vocational College, Hefei, Anhui 230601, China

Correspondence should be addressed to Wen Wen; 2007020061@ahcbxy.edu.cn

Received 6 August 2022; Revised 30 August 2022; Accepted 2 September 2022; Published 15 September 2022

Academic Editor: Lianhui Li

Through the analysis of the application and development of deep learning in the field of book design and publishing, the article expounds on the positive impact of deep learning on book design and publishing, discusses the shortcomings of deep learning in creative ability, aesthetic ability, emotion, etc., and then discusses the design and publishing of books. The future development direction of intelligent aided design and intelligent personalized design is proposed to provide a reference for researchers in deep learning and book design and publication.

1. Introduction

Deep learning was first proposed at the Summer Symposium on Deep Learning at Dartmouth College in Hanover, the USA, in 1956 [1]. Due to the wide range of research fields, the concept of deep learning is also divided. At present, the more recognized definition in the academic circle comes from the book "Deep Learning: A Modern Approach" by Stuart Russell and Peter Norvig: "deep learning" is the research and design of "intelligent agents" [2], and "an intelligent agent refers to a system that can observe the surrounding environment and take actions to achieve the goal." Today, deep learning has been widely used in speech recognition, machine vision, data mining, etc., and the cross-border between deep learning and publishing and design has gradually emerged [3]. Content is the starting point of book publishing, and content is often summarized and compiled by writers and scholars through learning, reading, investigation, and research, and this process requires a lot of time and energy to complete. In ancient times, people recorded text and image content by handwriting, and it was not until the advent of printing that books published close to modern times were widely disseminated. In recent years, we can even use speech recognition technology to allow computers to quickly convert language into text through "dictation," which is just the tip of the iceberg for deep learning [4]. In September 2015, Tencent developed a manuscript writing robot, Dreamwriter, which can generate manuscripts in a very short time. After more than two years of development, Dreamwriter has been able to generate templates through automatic learning, which has expanded from the initial financial field to movies, cars, games, and many other fields. In addition, Xinhuanet, Yicai, and other media also put the writing robot into use, and the content is mainly based on event description and analysis data. Poems and novels that require more complex rhetoric and grammar can also be completed by robots. For example, the poems created by Xiaobing, a poetry-writing robot developed by Microsoft (Asia) Internet Engineering Institute, have been submitted to newspapers and periodicals under multiple pseudonyms, and all of them have been received to publish invitation [5].

Since the end of 2013, a senior researcher from Microsoft Research Asia and an information design expert from the Academy of Arts and Design of Tsinghua University have been working on research in the field of the automatic layout. This research combines aesthetic principles in design with computable image features to creatively propose a computable prototype of an automatic typesetting framework. The prototype optimizes a series of key issues, such as the visual weight of text and pictures, the weight of visual space, the color harmony factor in psychology, and the importance of information in visual cognition and semantic

understanding. The prior knowledge of experts in the fields of text semantics, design principles, and cognitive understanding is integrated into the same multimedia computing framework, creating the research direction of automatic visual text layout design [6]. At the 2017 Yunqi Conference Shanghai Summit, Alibaba iDST algorithm experts shared research titled "Visual Design in the Era of Deep Learning," proposing that automated and controllable visual content can be generated through deep learning. The process of intelligent design includes the spatial layout of design elements, color matching, background adaptation, font synthesis, style recommendation, intelligent interaction, etc. Among them, "automation" can automatically adapt to various sizes, automatically learn various styles, and automatically adapt to the number of elements; "controllable" means predictable and modifiable results. The introduction of deep learning into other fields seems unstoppable. In fact, most of the time, deep learning cannot be presented as an independent subject, and deep learning is more about transforming the process and mode of work in other fields [7].

Jane Hazus, the chief economist at Goldman Sachs Group, said: "In general, AI seems more likely to capture more valuable things in statistics than the last wave of innovation, and deep learning can reduce costs, reduce labor input for high value-added production types." China's modern book publishing industry is still dominated by paper media, and a series of work in publishing activities from topic selection, drafting, editing, and reviewing, to design publishing, and distribution is required. High value-added artificial brain power is to participate in the completion. Deep learning can improve the efficiency of book design and publication in the following three aspects [8].

The first is intelligent topic selection. The terminal of book publishing and distribution must be readers. The pain point of the traditional publishing topic selection process is that the distance between publishers and readers is too far. Book publishing forms a one-way process, and readers can only passively accept it. Or the publishing house obtains the data required by readers through traditional research and consultation methods and then selects a topic for publication and distribution, which must go through a long period of time. For some books whose market demand changes rapidly traditional data acquisition, the way will bring hysteresis [9]. It can be seen that data will be the source of future productivity. Based on deep learning and big data, readers' purchase and reading behaviors can be effectively recorded, the needs of the audience can be outlined through data, and the direction of topic selection will be more accurate.

The second is smart editing. The traditional editing work mainly includes drafting, revision, and proofreading. It should be said that each part requires a lot of time, and the error rate that occurs manually cannot be ruled out. Deep learning can be said to be the core technology of the current deep learning development. After the speech recognition and natural language processing technology has developed to a certain level, the language and grammar in the work can be corrected, and then, it can undertake a lot of tedious and time-consuming work. These problems can be solved by deep learning technology based on massive data support and with deep learning capabilities. However, modern editors can shift the focus of their work to the core values of judgment and decision making that cannot be completed by deep learning for the time being [10].

The third is intelligent design [11]. As a very important work in book publishing, book design affects the sales of books to a certain extent, and people are not satisfied with absorbing text content when reading. The graphic arrangement part of book design is the part of the largest workload after the overall creative design positioning of the book is completed in the early stage, and now, it is mainly completed by designers using arrangement software. According to the application research content mentioned above, the designer can analyze the reading audience according to the deep learning, propose a highly targeted book planning and design plan, and use the automatic layout software to arrange and adjust the content, effectively improving the work efficiency, and reduce the work intensity of design practitioners.

2. Knowledge about Deep Learning

2.1. Basics of Convolutional Neural Networks. Convolutional neural network (CNN) is a type of artificial neural network. It draws on the sparse response characteristics of biological neural networks and replaces the original fully connected layer with local connections to avoid overfitting in the training process due to too many model parameter problems [12]. The weight-sharing network structure of a convolutional neural network significantly reduces the complexity of the network, reduces the number of weights, and reduces the demand for training data. It is a research hotspot in the fields of speech analysis, image recognition, and target detection [13].

The general working principle of the convolutional neural network is as follows: first, the entire image is input into the convolutional neural network, and the network starts from the bottom pixel to learn the filters. These filters are used to extract the local edge and texture features of the image and then the middle layer filters. We learn the feature map processed by the upper-level edge filter and then extract the features that can describe different types of targets, and then learn those global features that describe the entire target by the high-level filter, and finally realize the target in the image through the nonlinear fitting of the activation function [14]. In the whole image recognition process, the network automatically learns the parameters of various types of filters from the image data. Its rich feature expression ability realizes the target recognition in the image and solves the problem of the traditional image recognition algorithm. Perform manual feature extraction and data reconstruction on image data. Figure 1 shows the development of convolutional neural networks.

The starting point of the development of convolutional neural networks is the neurocognitive machine model. LeCun, the originator of deep learning, proposed the first convolutional neural network model LeCun in 1989. Since

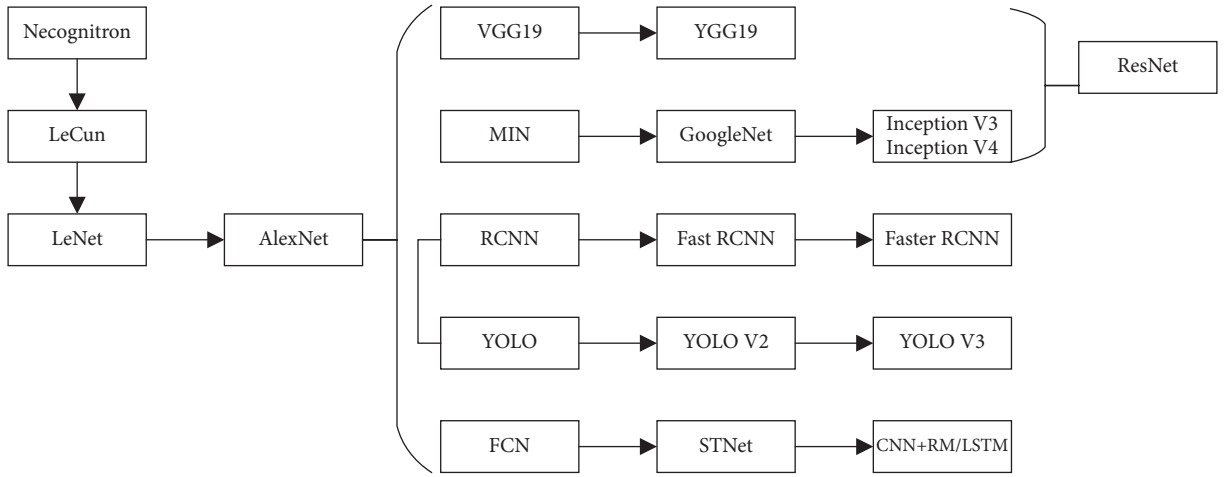

Figure 1: Development of convolutional neural networks.

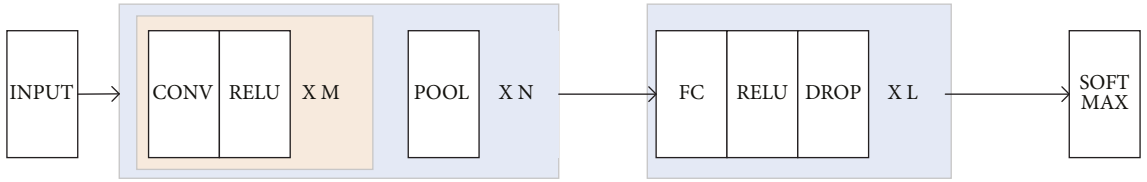

Figure 2: Classic convolutional neural network framework.

then, LeCun proposed the LeNet neural network model in 1998, but at that time, due to the superiority of hand-designed SVM and other classifiers, the convolutional neural network did not attract public attention along with the proposal of methods such as ReLU and Dropout, as well as the historical opportunities brought by GPU and big data, and the proposal of AlexNet in 2012 ushered in a historic breakthrough in convolutional neural networks. The evolution process of the convolutional neural network after AlexNet mainly consists of four directions: increasing the number of network layers and deepening the depth; enhancing the function of the convolutional layer from classification tasks to detection tasks; and adding new functional modules [15].

2.2. Convolutional Neural Network Architecture. A classic convolutional neural network for image classification mainly consists of five parts: input layer, convolutional layer, pooling layer, fully connected layer, and softmax layer. Usually, the network has only one input layer and one softmax output layer, and the convolution layer in the network can appear multiple times. The pooling layer is often located between the convolutional layers for data dimensionality reduction. The convolutional layer and the pooling layer are often connected in several adjacent convolution and pooling layers like this, which constitute a feature extraction layer of the network [16]. After multiple feature extraction and compression, the image data are input to the fully connected layer, and finally, the probabilistic classification result is output through the softmax layer. Figure 2 shows a classic convolutional neural network structure, in which M, N, and L are integers greater than zero to indicate the number of repetitions of the unit where it is located.

2.2.1. Convolutional Layer. The convolutional layer is the core part of the convolutional neural network. Its function is to extract the features of the input image. The convolutional layer completes the feature extraction through the convolution kernel. Each convolution kernel contains parameters such as size, stride, and edge padding. In shallow networks, convolution kernels extract low-level features, such as edges and corners, and in high-level networks, convolution kernels extract high-level features, such as faces, dogs, and cars [17]. Figure 3 shows the convolution operation process in the convolution layer.

In Figure 3, the input picture is a two-dimensional activation map K obtained after the convolution layer operation of the convolution kernel K, and its size is obtained by the following formulas:

$$h_{out} = \left(\frac{h_{in} - h_f + 2p}{s_h}\right) + 1, \tag{1}$$

$$w_{out} = \left(\frac{w_{in} - w_f + 2p}{s_w}\right) + 1, \tag{2}$$

$$d_{out} = k. \tag{3}$$

In formulas (1)–(3), h_{out} and w_{out} are the height and width of the output image,h_{in} and w_{in} are the height and width of the input image, as well as the height and width of the h_f convolution kernel, w_f is the width of the s_h

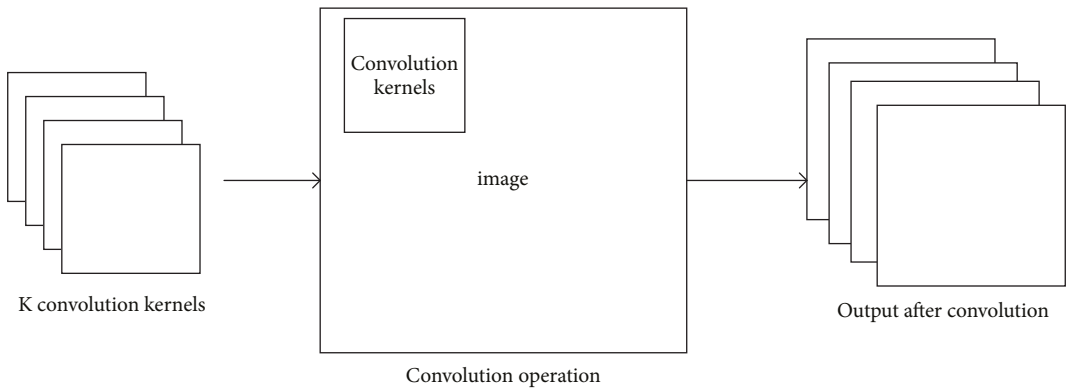

Figure 3: Convolution operation process in the convolution layer.

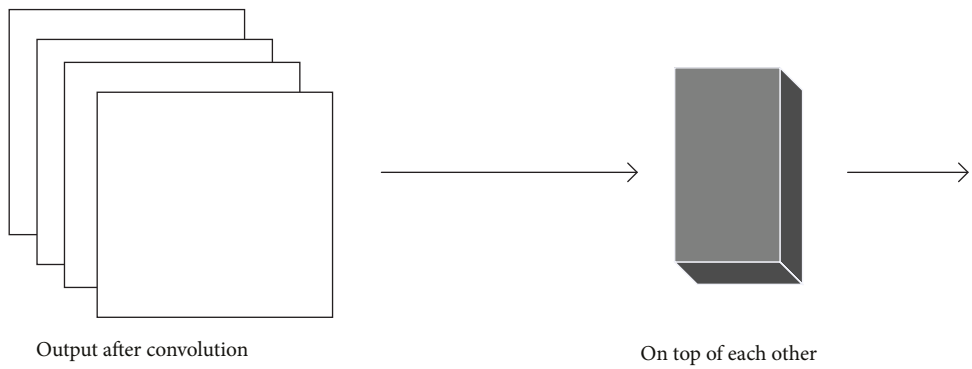

Figure 4: Activation maps are stacked and fed into the next convolutional layer.

convolution kernel, the sliding step size of the convolution kernel in the vertical direction and the s_w convolution kernel. The sliding step size in the horizontal direction p is the number of pixels to be supplemented by the edge, in which d_{out} is the dimension of the output.

Figure 4 shows that the K activation maps obtained after the convolution operation are stacked as the input to the next convolutional layer.

2.2.2. Pooling Layer. The function of the pooling layer is mainly to reduce the size of the feature map, and it is often used in the middle of two convolutional layers to reduce network parameters and reduce the overfitting of the model. Common types of pooling operations are max pooling and average pooling [18]. The maximum pooling operation is usually used in the middle of the convolutional network to reduce the size of the feature map, and the average pooling operation is generally used at the end of the network to replace the fully connected layer and reduce network parameters. Common pooling sizes are 2×2 and 3×3, and strides are usually 1×1 and 2×2.

If the size of the input feature map is $w_{in} \times h_{in} \times d_{in}$, the size after the pooling operation is

$$w_{out} = \left(\frac{w_{in} - w_f}{s_w}\right) + 1, \tag{4}$$

$$h_{out} = \left(\frac{h_{in} - h_f}{s_h}\right) + 1, \tag{5}$$

$$d_{out} = d_m. \tag{6}$$

In equations (4)–(6), w_{out} and h_{out} are the width and height of the output feature map, w_f and h_f are the width and height of the pooling window size, s_w and s_h are the horizontal and vertical strides, and d_{out} are the output dimensions. After the pooling operation, the size of the feature map is reduced to varying degrees according to the pooling window size and stride size [19].

2.2.3. Activation Layer. The main function of the activation layer is to introduce a nonlinear activation function, thereby increasing the nonlinearity of the network. The commonly used nonlinear activation functions are Sigmoid, Tanh, ReLU, ELU, Leaky ReLU, etc. Usually, an activation layer immediately follows each convolutional layer. For the input $w_{in} \times h_{in} \times d_{in}$ feature map, the output size after the activation layer is

$$w_{out} = w_{in}, \tag{7}$$

$$h_{out} = h_{in}, \tag{8}$$

$$d_{out} = d_{in}. \tag{9}$$

From equations (7)–(9), the activation layer usually does not change the size of the input feature map.

2.2.4. Fully Connected Layer. The convolution layer and pooling layer are mainly to complete the extraction of image features, while the fully connected layer is mainly to complete the classification task [20]. The fully connected layer is located at the end of the convolutional neural network, and the fully connected layer is usually followed by a softmax layer to calculate the final output of the network for each classification probability.

2.3. Data Augmentation. In deep learning, the training of the model often relies on a large amount of data to learn the parameters of the network, especially the deep network. However, in reality, it is often difficult to obtain enough data due to the limitation of practical conditions, and sometimes, a lot of manpower and material resources are wasted [21]. Data enhancement is to make some changes to the original data, but for the network model, it is "new" datum, thus easing the data requirements for deep learning model training. Data augmentation can improve the generalization ability of the model and improve the robustness of the model. Common data augmentation methods are flipping, rotating, scaling, cropping, translation, adding noise, etc. Compare model performance on the test set with and without data augmentation. It can be seen from the experiments that for the same model and the same dataset, when data augmentation is used, the accuracy and recall rate of the model on the test set are much better than when data augmentation is not used. It can be seen that, without adding any additional investment, the performance of the model can be significantly improved only through data augmentation operations.

2.4. Transfer Learning. Transfer learning refers to the simple adjustment of a model trained on one problem to make it suitable for a new problem. There are two common types of transfer learning. One is to use models trained on other datasets such as ImageNet datasets such as VGG, ResNet, and Inception as feature extractors, remove the final classification layer of the model, and replace it with new ones. This kind of transfer learning is suitable for the classification problem with a small dataset and is similar to the classification problem of the original model [22]; the other is fine-tuning that refers to replacing the last classification layer of the trained model with the classification layer of the new problem, initializing the classification layer, keeping the parameters of other layers unchanged, and then training the new classification layer separately, after a few rounds of iteration (warm-up) "Unfreeze" other layers to continue training, fine-tuning the parameters of the entire model. This method is suitable for a relatively large dataset of new problems and is similar to the problem of the original model. Since the first layer of the convolutional neural network generally extracts low-level features such as texture, corners, and colors, the features extracted by the closer convolutional layers are more advanced, abstract, and task-oriented, so during training, you can "Unfreeze" the later convolutional layers of the original model, keeping the initial convolutional layer parameters unchanged [23].

3. Modern Book Packaging Design Based on BBE Network Aesthetic Evaluation

3.1. Object Detection Task Overview. Image classification, object detection, and image segmentation are the three major tasks of deep learning applied to the field of image processing. Image classification means that when an input image is given, the deep learning algorithm needs to analyze and identify what all the objects in the image are, that is, the category they belong to; target detection means that when an input image is given, the deep learning algorithm needs to detect the specific positions of all objects in the image, and also be able to identify the category to which they belong; the image segmentation task is aimed at pixels in the image, which means that the deep learning algorithm needs to distinguish all pixels in the input image, that is, determine which pixels in the image belong to which targets [24].

3.2. Book Packaging Design Based on Object Detection. Object detection tasks in deep learning are classified into two-stage algorithms and one-stage algorithms.

3.2.1. Two-Stage Algorithm. The two-stage algorithm is characterized by high detection accuracy and slow detection speed. With the development of the two-stage algorithm, the tasks of each stage of target detection are integrated into a deep neural network [25]. Two-stage algorithms include RCNN, SPPNet, Fast-RCNN, Faster-RNN, and Mask-RCNN. The first two-stage algorithm was the R-CNN algorithm, followed by Fast R-CNN and Faster R-CNN gradually enabling object detection to be trained end-to-end. The principle of the two-stage algorithm is multistep. First, a large number of candidate frames are generated in the image, and then, the features of the selected regions of the candidate frames are extracted. Finally, according to the results of the feature extraction, more refined classification and localization operations are performed in the high-level network. It is precise because of the step-by-step detection process of the two-stage algorithm that the detection accuracy of the algorithm is high, and the detection speed is relatively slow.

The Faster R-CNN model is shown in Figure 5, and the algorithm completes the target detection step by step. First, we complete the work of extracting features from the input image. Then, the extracted feature maps are filtered through the region generation network. Finally, using the filtered feature map, the

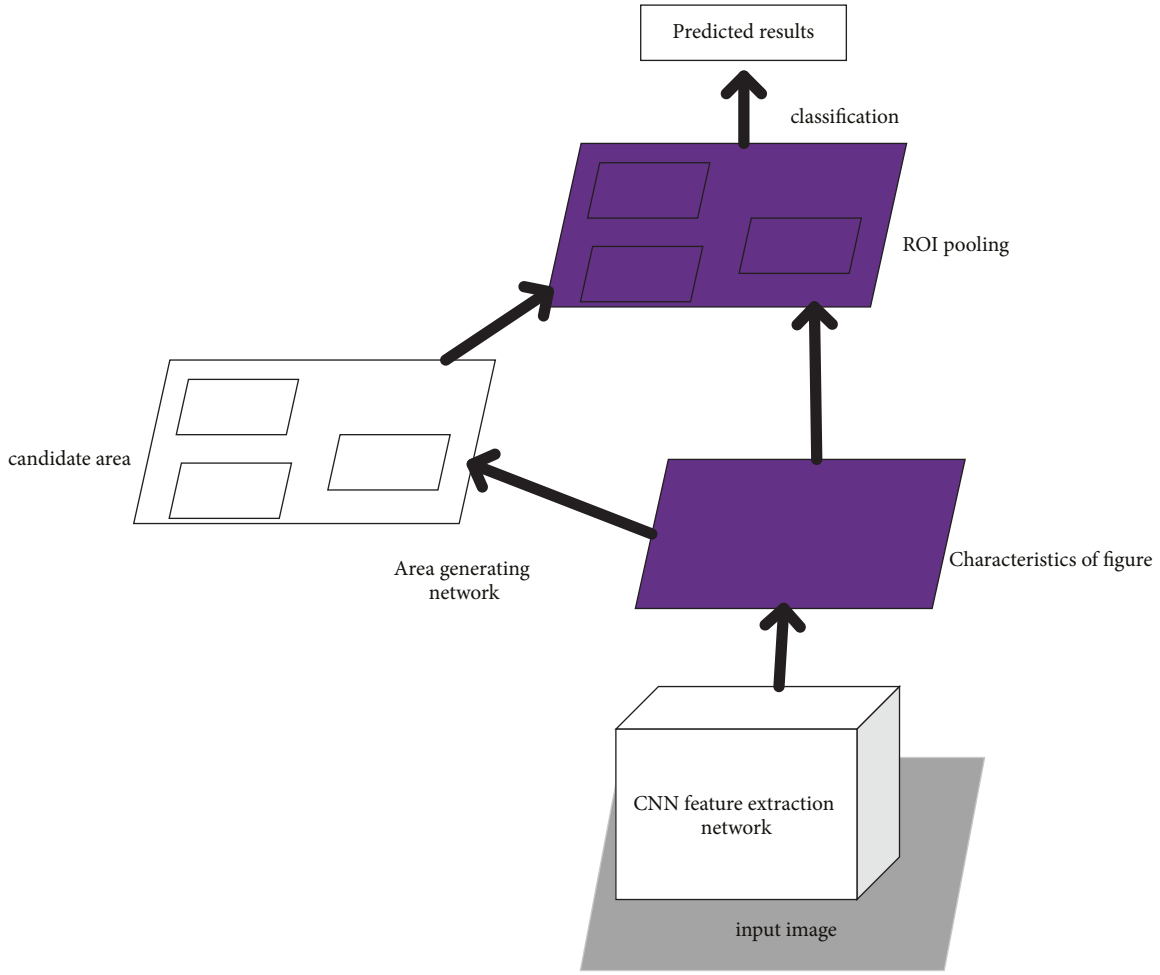

Figure 5: Faster R-CNN network model.

classification and localization of the target object are completed. Faster R-CNN has a unique area generation network, which enables the algorithm to perform more refined detection and identification. At the same time, because of the more complex network structure, the detection speed and training speed of the algorithm are relatively slow, and the computing performance of the hardware device is required high, and it is generally difficult to achieve real-time detection [26].

3.2.2. One-Stage Algorithm. The classic one-stage algorithm can be mainly divided into two series, namely, YOLO and SSD. The one-stage algorithm integrates feature extraction, classification, and regression into a deep learning network framework, and the detection speed is very fast.

YOLO is a representative of a one-stage target detection algorithm. The principle of the algorithm is to generate a large number of a priori frames on the input image, and then directly classify and locate the area selected by the a priori frame, that is, directly output the target object in the input image. Specifically, the image is first divided into grids, and then, a large number of prediction boxes are generated for each grid, and finally, the final prediction box is obtained through operations such as nonmaximum suppression and threshold analysis. Figure 6 shows the model architecture of the YOLO network, in which the input image is divided into 7×7 grids, and each grid has 30 data, including the coordinate offset of 2 bounding boxes, the target confidence, and the probability over a class. The YOLO algorithm does not perform well in detecting objects that are close to each other and small objects, because each grid of the algorithm only predicts two bounding boxes that belong to only one class, and when target objects with different aspect ratios appear in the image, the generalization ability of the algorithm is weak.

The difference between the SSD algorithm and YOLO is that the SSD algorithm directly uses CNN for detection. The SSD network has the following characteristics. First, SSD uses a multiscale strategy to detect target objects of different sizes in the image by extracting feature maps of different scales in the image, which helps to improve the detection accuracy of the network. Second, in order to simulate the size of different target objects in the image, the SSD network uses a priori frames with different aspect ratios and different sizes, which helps to improve the detection effect of the network on small target objects. Positioning will be more accurate. In general, the SSD algorithm not only takes the advantages of the YOLO algorithm but also draws on the candidate region generation network of the two-stage

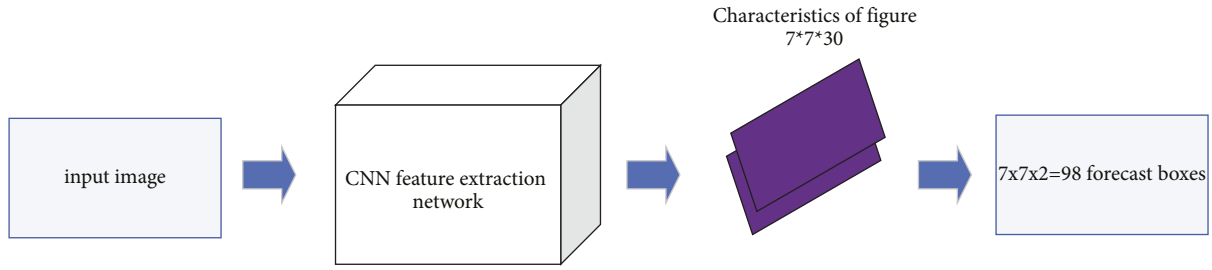

Figure 6: YOLO network model.

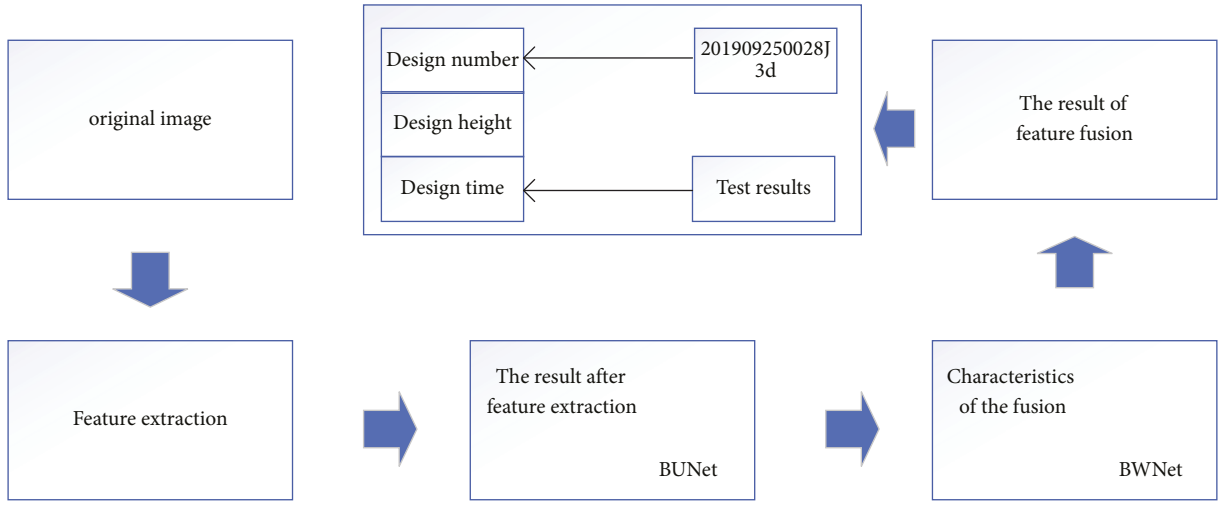

Figure 7: Overall design.

algorithm to achieve the speed of the one-stage algorithm and the accuracy of the two-stage algorithm, which is a relatively balanced accuracy and speed algorithm [27].

3.3. Overall Scheme and Algorithm Framework Design. The detection method of target detection can realize the end-to-end detection of inkjet character defects. However, due to the diversification of book design types, a large number of training sample datasets are required, and the detection accuracy is also easily interfered with by various factors. It is difficult to meet the requirements of industrial applications. The idea of the detection algorithm in this paper is to first obtain the category and position of each book through target detection. The overall design scheme is shown in Figure 7.

The BBE target detection network based on convolutional neural network has powerful feature extraction ability and has high detection accuracy and speed, which is very suitable for practical industrial detection. First, the collected images are input into the feature extraction network BUNet designed based on the EfficientNet core module for processing, and then, the extracted effective features are input into the designed feature fusion network BWNet for feature refinement and abstraction, and then, the fused features are classified and positioned through the classification network and the regression network, respectively. Finally, the quality inspection standards (number of code, height, and time) are set. We compare them to obtain the final overall detection result.

The structural framework of the BBE network, the feature extraction network, the feature fusion network, and the classification and regression network constitute the main frame structure of the algorithm network. The feature extraction network BUNet achieves good recognition with a small amount of parameters. The backbone of the feature extraction network is a general convolutional layer, which is used to perform convolution processing on the input image, and then continuously extract the depth features of the inkjet characters by connecting 7 basic modules with a total of 23 basic units (basic unit). It is based on the improvement of the core structure of EfficientNet. Based on the feature map pyramid network (FPN), the feature fusion network BWNet adds many connections to the network, fuses the feature maps of multiple intermediate layers, and continuously performs up and down weighted sampling and fusion features. It is a fast normalized multiscale weighting feature map pyramid network. The classification and regression networks are separate, the classification network classifies the target in the prior box, and the regression network adjusts the size and position of the prior box until the final prediction box is obtained. Finally, the redundant prediction frame is removed by the operation of nonmaximum suppression, and the category and position information of the inkjet characters are obtained.t

3.4. Feature Extraction Network Design

3.4.1. EfficientNet Algorithm. EfficientNet network was proposed by Google in 2019. On the basis of other networks, it improves the detection accuracy while greatly reducing the network parameter calculation, and has high detection accuracy and speed. To improve network performance, the following points should be paid attention to: (1) first, the network must be able to converge and be able to be trained; (2) the amount of parameters of the network should be minimized to ensure the high precision and speed of the network, and the model should be easy to train; and (3) improve the network structure, enabling it to learn useful deep features. The EfficientNet network does the above points well, and the network model uses a small amount of parameters to obtain good accuracy.

The construction of CNN often has the following characteristics: (1) increase the depth through the residual structure to improve the expressive ability of the network; (2) increase the number of feature layers extracted by each layer of the network, realize the extraction of multiscale features, and improve the width of the network and learn more features; and (3) increase the resolution of the input image, enrich the feature information that the network can learn, and improve the accuracy of the network. The EfficientNet network combines the above characteristics and adjusts the depth, height, and resolution of the input image to obtain a series of lightweight networks with balanced speed and accuracy.

3.4.2. Feature Extraction Network: BUNet. The feature extraction network in this paper is based on the core module of EfficientNet, which is designed, and the algorithm is based on a modular design, and the feature extraction capability of the network can be changed according to the needs of the task. The backbone of the network is a stack of 7 basic modules (23 basic units) with powerful feature extraction capabilities. At the end of the network are two max pooling layers of size 3×3, which are mainly used to downsample the extracted feature maps to make the obtained features more refined. Finally, 5 effective feature layers are selected from the network as output features. Among them, (BUConvk, $3 \times 3) \times n$ is the basic unit based on the inverted bottleneck structure, BU is the basic unit, k is the number of convolution kernels, n is the number of basic units, and the size of the convolution kernel is 3×3. Since the feature extraction network in this paper is continuously stacked by the same basic unit (basic unit), it is named BUNet.

3.5. Basic Unit. The basic unit of this paper is an inverted bottleneck structure as a whole, and many optimization strategies are added. After each calculation by a downsampling module, the resolution of the feature map is reduced to 1/2 of the original. First, the input channel is subjected to 1×1 convolution, BatchNorm normalization, and Swish activation operations, and then calculated by an improved depthwise separable convolution (xDepthwise Conv2d), which also performs normalization and activation operations, and then increases. An attention mechanism on channels is finally reduced by 1×1 convolution and normalized, and then connected to the large residual edge. The two most important operations in the base unit are the depthwise separable convolution and the inversion bottleneck structure.

3.5.1. Depthwise Separable Convolution. Depthwise separable convolution is composed of depthwise convolution and point-by-point convolution. Different from ordinary convolution operations, depthwise separable convolution reduces a lot of convolution calculations, which is widely used in most lightweight detection networks. For a three-channel input image, a depthwise convolution kernel is used to process one of the channels, and then, the number of channels of the output feature map is adjusted by point-by-point convolution. Point-by-point convolution is actually a 1×1 convolution, which can be used to adjust the number of output channels of the network, which plays a role in feature fusion to a certain extent and ensures the information exchange between each channel in the input feature map.

3.5.2. Inverted Bottleneck Structure. Residual structure and bottleneck structure are proposed in the ResNet network, which can solve the problem of gradient disappearance and gradient explosion caused by the deepening of the network, thus solving the problem that deeper networks are difficult to train. The residual structure has a bypass branch to connect the input directly to the output, so that the subsequent network layers can directly learn the residual between the input and the nonlinear convolution output, which not only protects the integrity of the input information but also simplifies the network. *Learning Goals and Difficulty*. The bottleneck structure first uses a 1×1 convolution to reduce the number of input channels. After the convolution calculation is completed, a 1×1 convolution is used to restore the number of output channels. This structure can not only improve the expressiveness of the network but also the computational complexity of the entire network can be reduced.

The inverted bottleneck structure first uses a 1×1 convolution to increase the dimension of the input channel. After the convolution calculation is completed, a 1×1 convolution is used to restore the number of output channels; that is, channel expansion is performed first, and then, channel compression is performed. The inverted bottleneck structure can learn more deep features in the middle convolutional layer of the network by first expanding the input feature map, and finally summarize and filter out useful features; that is, the inverted bottleneck structure can learn more about the input channel. Useful features have stronger feature extraction capabilities. The depthwise separable convolution (DWConv) is also applied in the inverted bottleneck structure. The operation of dilating and then compressing the feature channel does not increase the amount of computation, and the memory efficiency of the inverted design is much higher. The experimental effect is also better.

3.6. Network Optimization. The optimization strategy in the basic unit is elaborated below.

3.6.1. Improved Depthwise Separable Convolution. This section improves the depthwise separable convolution. Specifically, the number of input feature channels is adjusted by point-by-point convolution, and then, the feature extraction operation is completed by depthwise convolution. Among them, the depth convolution of 3×3 is split into two asymmetric convolutions of 1×3 and 3×1, which will not affect the function of the convolution, but can greatly reduce the calculation amount of the convolution. This can not only speed up the calculation speed of the network but also deepen the depth of the network and improve the nonlinear expression ability of the network.

3.6.2. Channel Attention Mechanism. After completing the convolution calculation for feature extraction, an attention mechanism is applied to the feature channels, which allows the network to learn and pay more attention to the channel where the effective features are located. First, perform global average pooling on the features extracted by the convolution operation, and reshape the feature channel into a dimension that can be convolved, then compress and expand the feature channel through 1×1 convolution, and use the Sigmoid function to obtain a ratio between 0 and 1. The probability value between them is the attention level of the channel. Finally, different feature channels are multiplied by their attention levels to obtain different levels of depth features.

3.6.3. Linear Activation Dimensionality Reduction and Element-Level Reduction Operations. The nonlinear activation function in the network can enhance the nonlinear expression ability of the network, and at the same time, it will also cause the model to lose part of the feature information, and the downsampling operation itself will also discard part of the feature information. If the feature channels are downsampled and processed with nonlinear activation functions at the same time, the expressive ability of the network will be reduced and the performance of the model will be reduced. In this paper, when 1×1 convolution is used to reduce the number of feature channels, the Swish function is not used as the activation function, and it is directly activated linearly to retain more feature information, ensure the expressive ability of the network, and thus ensure the performance of the model. The operation of using linear activation to retain more feature information is also mentioned in the MobileNet-v2 network model.

Element-level operations will not bring too much extra computation, but too many element-level operations will increase the memory consumption of the computer, reduce the calculation speed, and affect the performance of the model. Finally, the output channel after dimensionality reduction and the large residual edge (input) are stitched and fused by point convolution.

4. Conclusion

With the advancement of science and technology, digital technology has developed rapidly, and technological innovation has made people's cognition of the world more intuitive and vivid. The original perceptual cognition method is reorganized with a rigorous mathematical model, and various design elements are presented rationally and digitally. This new expression method will definitely bring a new design thinking and artistic presentation. The evolution of art design is rooted in society, and so it is the rise of digital media art. With the continuous development of digital art, the form and function of art design are constantly enriched and improved. As a discipline, we should also cater to the diversified development trend of design, and build a new theoretical system and thinking mode for the cultivation of artistic talents in line with social development. We should not only pay attention to the inheritance of traditional culture and the learning of advanced design theory but also keep up with the pace of the times, quickly master digital technology, continuously expand creative thinking, and comprehensively improve our operational capabilities. Only in this way can a scientific and sustainable design teaching system be built.

Data Availability

The dataset that supports the findings of the study can be accessed upon request.

Conflicts of Interest

The author declares that there are no conflicts of interest.

References

[1] P. Aditya, M. Doron, and C. Caicedo Juan, "Image-based cell phenotyping with deep learning," *Current Opinion in Chemical Biology*, vol. 65, 2021.

[2] Y. Ding, J. Chen, and J. Shen, "Prediction of spectral accelerations of aftershock ground motion with deep learning method," *Soil Dynamics and Earthquake Engineering*, vol. 150, 2021.

[3] M. W. Wang, Y. Y. Zhang, and J. Xu, "A deep learning method based on multi-modality EEG for automatic depression screening," *International Journal of Psychophysiology*, vol. 168, no. S, pp. S205–S206, 2021.

[4] C. Wang, C. Wang, W. Li, and H. Wang, "A brief survey on RGB-D semantic segmentation using deep learning," *Displays*, vol. 70, Article ID 102080, 2021.

[5] M. Li and L. Jiang, "Deep learning nonlinear multiscale dynamic problems using Koopman operator," *Journal of Computational Physics*, vol. 446, Article ID 110660, 2021.

[6] O. F. Ertuğrul and M. F. Akıl, "Detecting hemorrhage types and bounding box of hemorrhage by deep learning," *Biomedical Signal Processing and Control*, vol. 71, 2022.

[7] J. He, J. Zhou, J. Dong, Z. Su, and H. Lu, "Revealing the effects of microwell sizes on the crystal growth kinetics of active pharmaceutical ingredients by deep learning," *Chemical Engineering Journal*, vol. 428, Article ID 131986, 2022.

[8] D. J Manuel and O. Lukumon, "Deep learning with small datasets: using autoencoders to address limited datasets in

construction management," *Applied Soft Computing Journal*, vol. 112, Article ID 107836, 2021.

[9] G. Lu, Lu Pan, and Y. Ren, "A Deep Learning Approach for Imbalanced Crash Data in Predicting Highway-Rail Grade Crossings accidents," *Reliability Engineering and System Safety*, vol. 216, Article ID 108019, 2021.

[10] H. Choi, C. Y. Um, K. Kang, H. Kim, and T. Kim, "Application of Vision-Based Occupancy Counting Method Using Deep Learning and Performance analysis," *Energy & Buildings*, vol. 252, Article ID 111389, 2021.

[11] N. M. Esrafilian and H. Fariborz, "Occupancy-based HVAC Control Using Deep Learning Algorithms for Estimating Online Preconditioning Time in Residential buildings," *Energy & Buildings*, vol. 252, Article ID 111377, 2021.

[12] K. Dutta Subrat, S. Sudarshan, B. Abhilasa et al., "Study on enhanced deep learning approaches for value-added identification and segmentation of striation marks in bullets for precise firearm classification," *Applied Soft Computing Journal*, vol. 112, Article ID 107789, 2021.

[13] N. Wang, H. Xu, F. Xu, and L. Cheng, "The algorithmic composition for music copyright protection under deep learning and blockchain," *Applied Soft Computing Journal*, vol. 112, Article ID 107763, 2021.

[14] D. Tian, Q. Ying, X. Jia, R. Ma, C. Hu, and W. Liu, "MDCHD: A Novel Malware Detection Method in Cloud Using Hardware Trace and Deep learning," *Computer Networks*, vol. 198, Article ID 108394, 2021.

[15] R. Xie and A. G. Dempster, "An on-line deep learning framework for low-thrust trajectory optimisation," *Aerospace Science and Technology*, vol. 118, Article ID 107002, 2021.

[16] W. Chao, J. Zhang, and X. Yuan, "DeepTIS: improved translation initiation site prediction in genomic sequence via a two-stage deep learning model," *Digital Signal Processing*, vol. 117, Article ID 103202, 2021.

[17] I. Hussain, S. Tan, B. Li, X. Qin, D. Hussain, and J. Huang, "A novel deep learning framework for double JPEG compression detection of small size blocks," *Journal of Visual Communication and Image Representation*, vol. 80, Article ID 103269, 2021.

[18] R. Liu, R. Yassine, and El Bagdouri Mohammed, "Multispectral background subtraction with deep learning," *Journal of Visual Communication and Image Representation*, vol. 80, Article ID 103267, 2021.

[19] N. Gentner, C. Mattia, K. Andreas, S. Gian Antonio, and Y. Yao, "DBAM: making Virtual Metrology/Soft sensing with time series data scalable through Deep Learning," *Control Engineering Practice*, vol. 116, Article ID 104914, 2021.

[20] J. Guo, Q. Wang, and Y. Li, "Evaluation-oriented façade defects detection using rule-based deep learning method," *Automation in Construction*, vol. 131, Article ID 103910, 2021.

[21] A. Akshay and F. You, "Quantum computing based hybrid deep learning for fault diagnosis in electrical power systems," *Applied Energy*, vol. 303, Article ID 117628, 2021.

[22] L. Gao, T. Liu, T. Cao, Y. Hwang, and R. Reinhard, "Comparing deep learning models for multi energy vectors prediction on multiple types of building," *Applied Energy*, vol. 301, 2021.

[23] X. Li, Y. Yang, Y. Ye, S. Ma, and T. Hu, "An online visual measurement method for workpiece dimension based on deep learning," *Measurement*, vol. 185, Article ID 110032, 2021.

[24] W. Chen, A. N. Wu, and F. Biljecki, "Classification of urban morphology with deep learning: application on urban vitality," *Computers, Environment and Urban Systems*, vol. 90, Article ID 101706, 2021.

[25] S. A. Azimi, A. Hossein, J. S. Chai, K. Martin, G. Abdelhakim, and R. Hofman, "Classification of radioxenon spectra with deep learning algorithm," *Journal of Environmental Radioactivity*, vol. 237, Article ID 106718, 2021.

[26] C. Neha, G. Gupta, V. Vallurupalli, and B. Indranil, "On the platform but will they buy? Predicting customers' purchase behavior using deep learning[J]," *Decision Support Systems*, p. 149, 2021.

[27] M. Huang, B. Zhang, W. Lou, and K. Ahsan, "A deep learning augmented vision-based method for measuring dynamic displacements of structures in harsh environments," *Journal of Wind Engineering and Industrial Aerodynamics*, vol. 217, Article ID 104758, 2021.

Hindawi
Scientific Programming
Volume 2022, Article ID 6397478, 10 pages
https://doi.org/10.1155/2022/6397478

Research Article

Based on Improved Artificial Neural Network Sewage Monitoring Alarm System Method

Liping Chen,[1] Ruichuan Zhao,[2] and Wenzheng Wu[3]

[1]*School of Architecture and Transportation, Ningbo University of Technology, Ningbo 315016, China*
[2]*CCCC Highway Planning and Design Institute Co., Ltd., Beijing 100088, China*
[3]*China Pharmaceutical University, Nanjing 210009, China*

Correspondence should be addressed to Wenzheng Wu; wuwenzheng@stu.cpu.edu.cn

Received 25 July 2022; Revised 9 August 2022; Accepted 16 August 2022; Published 14 September 2022

Academic Editor: Lianhui Li

Sewage discharge has become a key issue affecting the quality of the water environment, and how to effectively monitor and manage sewage discharge behavior has become a key factor to avoid water pollution and improve water quality. However, the current domestic sewage discharge monitoring system is not perfect, resulting in the lack of effective monitoring of enterprise sewage discharge by regulatory authorities, which provides an opportunity for enterprises to steal discharge. In the background of sewage treatment plant, the comprehensive design of sewage monitoring and alarm system is carried out based on the idea of physical information fusion. The design adopts a four-layer information physical architecture, which is divided into four parts: perception communication, fusion processing, push, and execution. In the fusion treatment part, the neural network intelligent algorithm is used to predict the dissolved oxygen, and the oxygen delivery is adjusted according to the predicted value to achieve accurate aeration and optimize the effluent quality. The push and execution parts adopt multiparameter monitoring to realize the smooth operation of equipment and ensure the system security. A new optimal control strategy of dissolved oxygen based on neural network is proposed. Through a large number of experiments and historical data, the intake index and dissolved oxygen value of the aeration tank under the condition of optimal outlet water are obtained as samples. According to the sample training, the BP neural network optimized by particle swarm optimization algorithm is adopted to achieve accurate prediction of dissolved oxygen under different inlet water conditions. The smooth operation of sewage treatment equipment is accomplished by the lower machine and the upper machine. In sewage treatment, each process section collects the equipment status in strict accordance with the order of sewage monitoring facilities. Then the communication network between the upper computer and the lower computer and the sensor is designed. The lower machine adopts PLC as the core, programming PLC through STEP7, and uses PID algorithm to control dissolved oxygen. The PC is developed in C language, so as to realize user login, real-time data display, over-limit fault alarm, report query, user management, etc. The PC integrates MATLAB neural network on the platform to predict dissolved oxygen through mixed programming quantity. The sewage alarm system based on improved artificial neural network is sensitive and has excellent performance. It provides a new idea for intelligent sewage detection and real-time monitoring.

1. Introduction

"Gold mountains and silver mountains are not as good as lucid waters and lush mountains." Water resources protection has always been a major national policy of our country. The Party Central Committee has thoroughly implemented the sustainable development strategy for many years, promoted the construction of a resource-saving and environment-friendly society, improved water treatment and discharge standards, and continuously increased large investment in the construction of livelihood projects related to sewage treatment. From 2011 to 2018, the daily treatment capacity of urban sewage in our country increased from 113.03 million cubic meters to 168.8 million cubic meters, and the number of sewage treatment plants increased from 1,588 to 2,321, an increase of 46% in 8 years. According to relevant policies and regulations, our country will achieve full coverage of sewage treatment in 2020, requiring the urban sewage treatment rate to reach 90% [1–3].

In recent years, more and more attention has been paid to sewage treatment in China. The increase in the number of sewage plants requires more skilled operators and consumes a lot of money. By contrast, automated monitoring systems that manage equipment according to established procedures can reduce the stress of staffing [4]. At the same time, through the accurate measurement of data by measuring instrument, the timely transmission of data by stable high-speed communication network, and the personification of data by intelligent control method, the sewage treatment process can be effectively managed on the basis of energy saving. Therefore, according to the actual needs, the introduction of intelligent control methods and advanced automation equipment, based on the design of sewage treatment monitoring system, has important significance for the development of economic society, in line with the requirements of industry development [5].

In the past decades, technological innovation has brought great changes to our lives, and intelligent algorithms have been widely applied in various fields [6]. The concept of intelligent algorithm has been widely recognized around the world since its introduction. Scholars from all countries agree that it is necessary to give full play to the excellent achievements made by human beings in the field of electronic information, closely combine information and physics, turn industrial system to intelligence, and form cyberphysical system [7]. A mature and intelligent sewage treatment monitoring system can realize real-time monitoring of various parameters of the equipment and, through intelligent methods, according to different sewage water quality, adjust the treatment strategy and adjust the parameter settings in key steps. This can not only reduce energy consumption but also optimize the quality of the effluent after treatment; the intelligent monitoring system can also improve the stability of the equipment and the level of intelligent informatization and reduce production costs; in the end, it can liberate labor and allow technicians. A lot of energy is put on the improvement of sewage treatment process and the development of sewage treatment equipment, so as to realize the requirements of constructing economical production and develop productivity.

2. Related Work

After the industrial revolution in the 19th century, economic and social changes took place in foreign countries, which also led to a series of environmental pollution problems, including water pollution. So far, the sewage treatment system has gone through the stages shown in Table 1.

In foreign countries, the problem of water pollution caused by the development of industrialization appeared earlier. During the 1950s and 1960s, developed countries gradually realized the need for early detection and treatment of sewage.

The United States, with the strongest comprehensive national strength, had built more than 20,000 sewage treatment plants, of which four-fifths were secondary treatment plants. Sweden had a small population and a well-developed sewer system that can collect almost all sewage. Britain and Germany had a sewage treatment plant for every 7,000 people on average, and the treatment effect could basically achieve the effect of secondary treatment, and Germany was the country that developed sewage treatment industry earlier. The largest sewage treatment plant in the United States in the 20th century had a maximum capacity of 5 million cubic meters per day, while Japan's largest sewage treatment plant had a capacity of nearly 2.5 million cubic meters per day.

Now automatic control systems are widely used in sewage treatment plants abroad. A variable number of on-site detection instruments are used, such as physical treatment (precipitation, filtration), drug delivery and pump room and other sewage treatment of each link to monitor, and then measured data through the network to the central control room computer, convenient data recording, storage, and fault alarm. The role of automatic control was not only reflected in the control of equipment but also reflected in the actual processing process. Pierson John used the relationship between ORP (REDOX potential) and the removal rate of COD and ammonia nitrogen to control the ORP in the pretreatment process of poultry wastewater and successfully controlled the content of COD and ammonia nitrogen in effluent below 7% and 65% [8]. Zipper et al. used ORP as a control parameter to shorten the nitrification cycle, reduce the sludge load, and save energy while improving the sewage treatment rate [9]. Puznava et al. kept dissolved oxygen between 0.5 and 3 mg/L in the aeration process through active intervention, extended the denitrification reaction time in nitrification and denitrification, and reduced the aeration capacity in the aeration tank by half on the basis of meeting the water quality discharge standard, which played an energy-saving role [10].

Some detection instruments are placed in the equipment, respectively, and the data in the sewage is collected through the PLC CPU. The lower computer PLC controls and handles the fault, and alarms are sent in time to remind the staff to eliminate the fault. Compared with the Ohio sewage discharge monitoring system in the United States, the chromatographic monitoring method at the river inlet and sending the information back to the computer in the central control room for analysis and processing has achieved good results in organic pollution treatment. At the same time, the control of sewage treatment in developed countries has also achieved a high degree of modernization: according to the process and treatment needs, a multilevel control system is adopted, which is divided into control stations according to its own different conditions. Different intelligent control methods are adopted to realize the automatic control of different control objects. High tech water quality analysis instruments are used to monitor the sewage treatment process online in real time, and the data are transmitted to the computer in the form of reports [11]. For example, the sewage treatment plant built in Geneva in 1989 is unattended, and operators can monitor the system at any time through mobile phones, the Internet, and other media. In Paris, France, the central server effectively monitors and warns organic pollutants by monitoring water quality and

Table 1: Sewage treatment control stages.

Development phase	Characteristic
Manual control stage	Manual detection, recording data, by human control
Semiautomatic control stage	Instrument detection data, manual recording data, mechanical operation
Automatic control stage	Instrument detection record data, storage data, central control operation
Information control stage	Automatic control, engineering optimization, information management, group management

processing data, but the cost is high and information sharing is difficult [12]. Now, almost all factories in the United States have automatically controlled the main process parameters. As regards Macon's sewage treatment plant in the Middle East, although the daily treatment capacity of a single equipment is not strong, its process is relatively perfect. The plant has achieved 24-hour telephone alarm duty, and there are no other staff on duty except normal office workers.

To sum up, the foreign sewage automatic control system has such characteristics: advanced water quality intelligent analysis instrument was used to monitor the water quality of each link of sewage treatment, and the measured accurate data was transmitted to the subcontrol station, which would adjust the control parameters according to the preset intelligent control program. At the same time, it was transmitted to the computer in the central control room by the subcontrol station to record data, generate reports, and generate trend curves. These control stations had different control objects and different control strategies. Both the central control computer and the subcontrol station had redundancy design to ensure the reliability and security of the system. Operators could use telemetry and remote control devices (such as mobile phone networks, telephone lines, Internet, etc.) to respond to alarm information from afar.

3. Improved BP Neural Network Intelligent Prediction Model by Particle Swarm Optimization

3.1. Particle Swarm Optimization. The specific process of particle swarm optimization algorithm is not complicated. At the beginning, a group of particles are randomly generated in the solution space, and each of them represents a possible solution in the space and has a fitness value, which depends on the optimization function. Each particle has another speed to control the direction and distance of its movement. The particles then adjust their search strategy according to the current best particle. The particle adjusts its speed by referring to two extreme values. The first extreme value is the optimal solution found by the particle itself, which is called individual extreme value (p_{best}). The second is the optimal solution currently found for all particles, which is called the global extreme value (g_{best}).

The dimension of solution space that defines particle motion is D, and the number of particles in the initial generated particle group is N, so any particle represents a D-dimensional vector. Here, I particles are taken as an example.

$$X_i = (x_{i1}, x_{i2}, \cdots x_{iD}), \ (i = 1, 2 \ldots N) \tag{1}$$

The velocity of particle i is also a D-dimensional vector.

$$V_i = (v_{i1}, v_{i2}, \cdots v_{iD}), \ (i = 1, 2 \ldots D). \tag{2}$$

The best position that particle i can find at the moment is the individual extremum:

$$p_{\text{best}} = (P_{i1}, P_{i2}, \cdots P_{iD}), \ (i = 1, 2 \ldots N). \tag{3}$$

The best position that can be found for all particle swarms is the global extremum:

$$g_{\text{best}} = (P_{g1}, P_{g2}, \cdots P_{gD}). \tag{4}$$

After the individual and global extreme values are determined, the individual particle changes its velocity and orientation according to the following equation:

$$\begin{aligned} v_i^{k+1} &= w * v_i^k + c_1 r_1 \left(\text{pbest}_i - x_i^k\right) + c_2 r_2 \left(\text{gbest}_i - x_i^k\right), \\ x_i^{k+1} &= x_i^k + v_i^{k+1}. \end{aligned} \tag{5}$$

w in the above equation is called the inertial weight, and c_1 and c_2 are called the learning factors. r_1 and r_2 are random numbers between 0 and 1. In equation (1), the first term on the right side of the equal sign can be understood as a kind of "inertia" that particles are subjected to in the D-dimensional space. This inertia can give particles the ability to keep themselves moving towards the original direction. It provides the particles with an incentive to stay in their original motion. The middle term on the right side of the equation is usually understood as "own experience." Just as people can choose the best way to solve problems according to their previous experience, particles modify their movement strategy according to the best solution they have found before. The right-hand end of the equation is usually understood as "social experience," in which particles communicate through knowledge transfer to obtain the orientation of the best solution in the whole group and then modify their movement strategy according to this orientation, similar to interpersonal communication in human society. Parameter IV represents the speed of the particle itself. $v_i \in [-v_{\max}, v_{\max}]$, $v_{\max}$ represents the maximum speed that the particle can obtain. The setting of the maximum speed ensures that the particle will not lose control of speed [13–15].

3.2. Further Optimization by Particle Swarm Optimization

3.2.1. Improvement of Inertia Weight. In the traditional equation (1), the inertial weight w is set to a constant real number. This method will confine the convergence speed and convergence precision of particles to a specific value, and what is needed in this paper is that particles can choose and adjust their own search strategy according to their own

search period. According to the analysis, it is better to have large w in the equation of PSO at the beginning of searching, which can make the whole group move at a high rate. At the end of the search, it is better for the equation to have smaller w, which enables the whole group to move more precisely to the optimal position. In this paper, a method is designed to decrease as the number of iterations increases, and its slope keeps changing all the time:

$$w(k) = w\left(w\min_{\max} * \exp\left[-15\left(\frac{k}{\text{MAXEPOCH}} \right)^3 \right] \right)_{\min}, \quad (6)$$

where k is the current iteration number of particle swarm; MAXEPOCH is the maximum number of iterations of particle swarm. In this design, $w_{\max} = 0.9$, $w_{\min} = 0.4$, and MAXEPOCH = 1000 are set.

3.2.2. Learning Factor Improvement. In equation (1), c_1 represents "self-experience" and c_2 represents "social experience." Similar to the change of the weight factor, the particle swarm can acquire more "own experience" and less "social experience" at the beginning of the search period, which can make the overall movement rate of the swarm higher. At the end of the search, there is less "self-experience" and more "social experience," which enables the group as a whole to move more accurately to the optimal position. This requires c_1 to start large and then small and c_2 to start small and then large, and, after experimental analysis, linear change is difficult to meet the requirements of the system, the design also adopts nonlinear change, and the specific implementation method is [16–19]

$$c_1 = \frac{4}{\{1 + \exp[\rho * (k/\text{MAXEPOCH}) - 0.5]\}}, \quad (7)$$

$$c_2 = 4 - c_1. \quad (8)$$

To control the descent speed ρ, this design takes 4.

3.3. Specific Flow of Particle Swarm Optimization.

Step 1: initialize the particle swarm, and give the particle number, dimension, initial position, speed, and other parameters.

Step 2: calculate the value according to the fitness equation, and give the overall best position g_{best} and individual best position p_{best}.

Step 3: reset the particle's velocity and orientation according to equations (1)–(5).

Step 4: after particle movement, if the current position is better than p_{best}, then reset p_{best} to the current particle position. If it appears that the current position is better than g_{best}, the best position of the entire particle swarm, then g_{best} is reset to the current particle position.

Step 5: if the value of the fitness equation is lower than the set stop value or the frequency of particle updating position exceeds the set maximum number of iterations, the optimal particle position is output. If the two conditions are not met, go back to Step 3.

3.4. Improved BP Neural Network by Particle Swarm Optimization. BP algorithm adopts the strategy of gradient descent and shows excellent local searching ability under nonlinear condition. If the parameter adjustment is already around the best parameter during the algorithm execution, the global optimization can be achieved in a short time. However, if the parameter adjustment is far from the optimal solution, it may fall into the trap of local optimization. Since BP algorithm adopts the strategy of gradient descent to correct system parameters, here is a vivid analogy: To find the optimal solution, the BP algorithm needs to search in a valley with multiple bumps. The algorithm error is very large. Particle swarm optimization (PSO) belongs to the category of algorithms based on global search. When the search starts, the convergence rate is relatively high. When it approaches the best solution of the whole, the convergence rate of its algorithm is relatively low, and sometimes it cannot meet the requirements. Therefore, such complementary advantages and disadvantages provide us with a way of thinking. If the two can be combined, local optimization can be avoided, while fast convergence can be achieved at the overall optimal point [20–22]. Particle swarm optimization belongs to the category of algorithms based on overall search. When the search starts, the convergence rate is relatively large. When it is close to the overall best solution, the convergence rate of the algorithm is relatively small, and sometimes it cannot meet the requirements. Therefore, the complementary advantages and disadvantages provide us with a way of thinking. If we can combine the two, we can avoid local optima and quickly converge at the overall optima.

In the design, using the design idea of particle swarm, the BP algorithm is optimized through the initial weight and threshold so that the particles can search for the best solution vector in the weight and threshold, and then set the weight of the BP algorithm and the corresponding solution vector of the threshold, and train again. The detailed execution process is as follows: Set the search space dimension of particle swarm optimization algorithm to be equal to the total number of weights and thresholds in BP algorithm, and then the position to which the particle moves is a solution of the weight threshold. The fitness function of particle swarm is shown in the following equation:

$$f = \frac{1}{n} \sum_{j=1}^{n} \sum_{k=1}^{m} (y_k - t_k)^2. \quad (9)$$

In the above equation, n is the number of sample groups collected by training BP network, m is the number of neurons in the last layer of BP network, y_k is the actual efferent value after input sample, and k_t is the ideal efferent value. Given (9), the optimization process can be thought of as keeping f in the equation as small as possible. If the size of f during the operation of the algorithm is lower than the set stop quantity or the frequency of particle updating position

exceeds the set stop number, the algorithm ends. At this point, the weight threshold represented by the optimal particle position is set as the initial weight threshold of the BP network, and then the BP neural network is trained.

3.5. Improved BP Neural Network Algorithm Flow

Step 1: set BP network parameters, such as the number of nodes at each layer. Set the number of individuals in the particle swarm, dimension (threshold number, weighted value number), and other parameters.

Step 2: give the initial position of the particle, assign the corresponding value of the initial particle position to the neural network, calculate the value according to equation (6), and give the overall optimal position g_{best} and individual optimal position p_{best}.

Step 3: reset the particle's velocity and orientation according to equations (1)–(5).

Step 4: after particle movement, if the current position is better than p_{best}, then reset p_{best} to the current particle position. If it appears that the current position is better than g_{best}, the best position of the entire particle swarm, then g_{best} is reset to the current particle position.

Step 5: check whether f in equation (6) is lower than the set stop quantity or the frequency of particle updating position exceeds the set stop number, and go to the next step. If not, go back to Step 3.

Step 6: set the weight threshold represented by the optimal particle position as the initial weight threshold of the BP network, and then train the BP neural network.

3.6. Dissolved Oxygen Improved BP Neural Network Prediction Model Simulation. The initial range of each particle is between [−1, 1]. According to the guidance of literature, the initial individual number of particle swarm $m = 100$, the minimum training stop error is set to 10^{-4}, the maximum iteration number is set to 1000, and the learning factor starts to calculate $c_1 = 2.4861$ according to formulas (7) and (8). $c_2 = 1.5139$, $w_{\max} = 0.9$, $w_{\min} = 0.4$, $v_{\max}$ is set to 2, and ρ is set to 4. The training target precision is 10^{-5}, and the training cycle times are set as 1000 times. Simulation results are shown in Figure 1.

As can be seen from the figure, the fitting effect of the improved neural network is very good, and the error is relatively small, which meets the standard of industrial application.

4. Design of the Lower Computer of the Sewage Monitoring System

4.1. Collecting System Hardware. According to the needs of the overall design scheme of intelligent monitoring in this study, and taking into account the characteristics of each technological process and equipment and facilities in this study, we considered the following points when selecting the collection equipment: First, the collection equipment selected in this study came from regular manufacturers, the industry has a good reputation in the after-sales service, its product quality is superior, and the product maintenance is guaranteed. Second, it is strictly economical, is not blindly demanding the high-end equipment, and, on the premise of ensuring the quality of monitoring, chooses more domestic brands. Then it is necessary to take into account the waterproof performance and corrosion resistance of hardware equipment; the composition of sewage is complex, and the equipment with good water and corrosion resistance effect can work stably. Hardware acquisition system was similar to human perception cells, mainly composed of instruments and sensors. With the booming of intelligent automation industry, its figure widely existed in various plant equipment so as to provide sensory information for monitoring personnel. Because this perceptual information was the basis of subsequent processing, the selection of instruments and other hardware equipment should be fully considered to ensure the effect.

In this paper, the data collection instruments were mainly COD meter, total nitrogen, total phosphorus determination apparatus, suspended solid concentration meter, electromagnetic liquid flowmeter, PH dollars, thermometer, DO dissolved oxygen meter, and liquid level meter, and equipment was started by reading relay internal register [23].

4.2. Programmable Logic Controller (PLC). The core of the lower system of this project was the programmable logic controller, and PLC was used to coordinate the actions of the whole lower system. PLC used its own receiving unit to receive digital or analog signals collected by hardware equipment such as field instruments and transmitted the signal from the upper computer to the lower actuator to control the action of the actuator. All signals must pass through its processing. All signals must pass through its processing and relay, so it is particularly important.

After absorbing the advantages of previous products, the S7 PLC produced by Siemens in Germany integrates the world's most advanced information technology and scientific achievements, especially in processing speed, code running, error self-checking, and information communication. S7 series could be divided into S7-200 type, S7-300 type, and S7-400 type according to the number of input and output ports.

Figure 2 shows the Siemens PLC structure diagram, the hardware modules are relatively independent in layout, but cooperate closely with each other, which is conducive to distributed control, and is also convenient for expansion and maintenance. Programming Languages Multiple programming languages are supported. And supports a variety of communication protocols, fully adapting to the instruments and sensors for parameter collection of various lower computers in sewage plants.

4.3. Communication System Design. The lower computer and the upper computer were connected by industrial Ethernet, which is the most extensive local area network

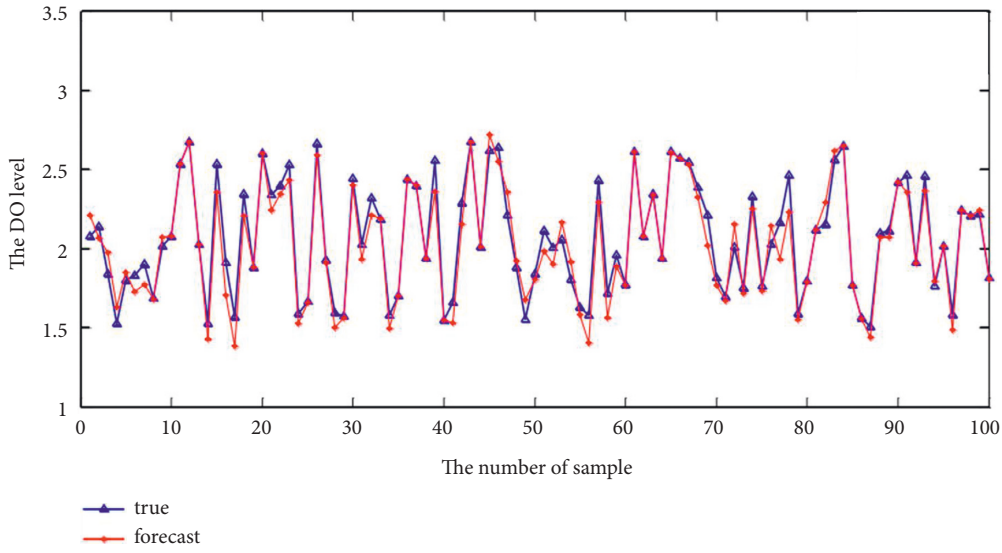

Figure 1: Improved neural network prediction results.

based on the IEEE 802.3 standard and is widely recognized in the world. Comprehensive consideration of industrial Ethernet in quality, compatibility, transmission timeliness, data stability, robustness, attack prevention, and other aspects had been greatly improved. Considering the cost performance, transmission rate, and safety and reliability factors, 100 Mb/s ring network optical fiber industrial Ethernet was selected.

Signals involving digital and analog quantities were directly connected to the input and output ports of the equipment on the corresponding module of PLC. Digital input and output signals were high- and low-level signals, PLC according to the transmission of high level or low level to monitor the state of the field equipment, switch, start and stop, and so forth, in this design was mainly through the relay to operate. Analog signal had two kinds: voltage and current signal; PLC accorded to the numerical conversion formula to convert input and output values [18].

4.4. Programming the Lower Computer. STEP7 development platform was developed by Siemens, which was specially applied to the configuration and programming debugging of PLC of its owned brand. The software function of STEP7 contained many development modules: process equipment management module, symbol table module, program module, and others. When writing the program, the user can choose to connect PLC or not to connect, which will not have a bad influence on the program effect. STEP7 platform could easily set up a complete set of industrial control system solutions. Figure 3 shows the process of establishing the whole industrial control system solution. The programming languages used for S7-300 are Ladder Logic (LAD) programming language, Instruction List Language (STL), and Function Block Diagram (FBD). The Ladder Logic programming language is a unique graphical representation method of the STEP7 programming language. Its grammar rules have many similarities with the relay ladder logic diagram: for example, if information is transmitted to each connection and finally reaches the output, we can find the entire transmission process of the signal according to the diagram.

The PID control program of the system used the PID controller function module FB41 integrated in STEP7 software, and the PID control program was stored in the timing cycle interrupt OB35. When the system starts, FB41 is called through OB35, and the background data block DB20 is created for the function module.

The core control of the lower machine of the system is here. Firstly, the influent COD, suspended solid SS, total nitrogen content, total phosphorus content, flow rate, PH value, and aeration tank temperature were collected by the sensor and stored in the DB block of PLC. The communication network was transmitted to the upper computer, and the upper computer predicted the precise dissolved oxygen (DO) value through intelligent algorithm. It was transmitted down through the communication network and stored in DB block at the address of DB3.DBD208. The actual measured DO value in the aeration tank was also stored in DB block at the address of DB3.DBD32. DB3.DBD208 was connected with SP_INT of FB41 module in PLC (set value), and DB3.DBD32 was connected with PV_IN of FB41 module in PLC (current time value). The algorithm's flow chart is shown in Figure 4.

5. Monitoring System Upper Computer Design

The application development of the upper computer was a very critical task in the intelligent sewage project. The upper computer collected all the information in sewage treatment, and the staff could monitor the sewage treatment site comprehensively through the upper computer in the control room, which not only reduced the amount of operator activity but also saved time. In this study, the key parameters

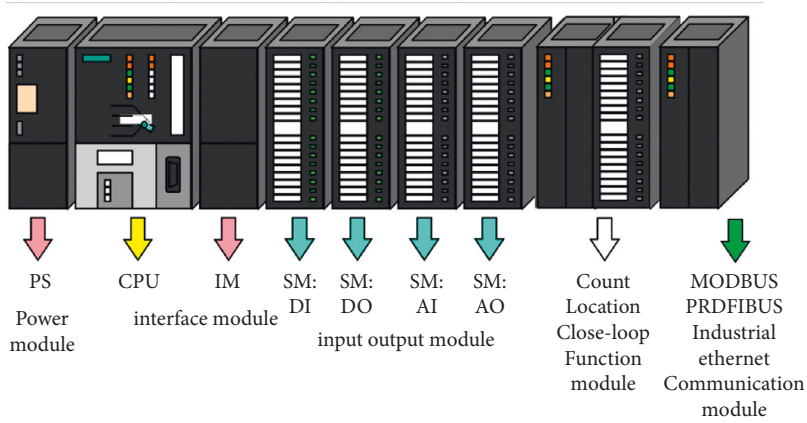

Figure 2: Siemens PLC structure drawing.

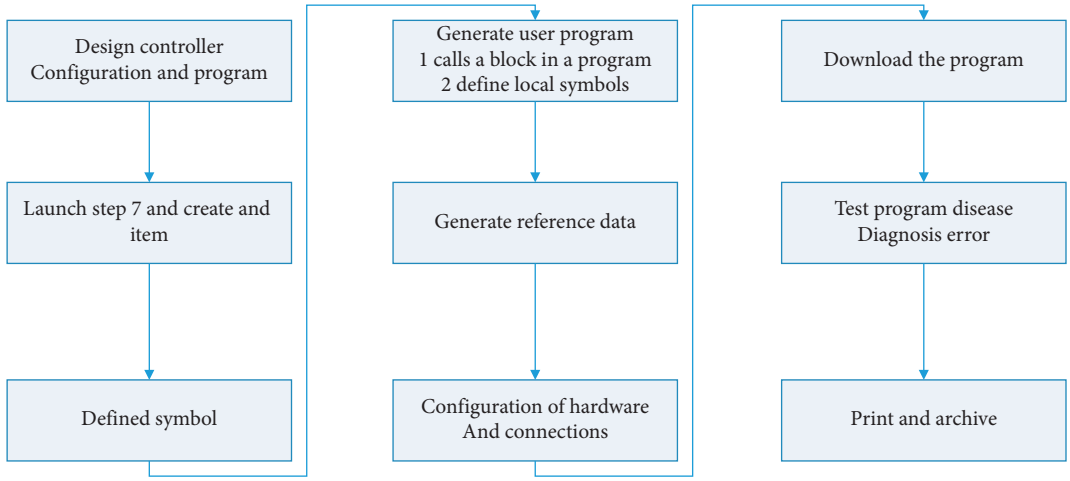

Figure 3: Steps to create an automated project.

of each process section of the factory should be displayed on the main interface first, and then the intelligent dissolved oxygen control algorithm should be integrated into the software and the parameters should be transmitted to the lower computer. The upper computer client software was developed on Visual Studio 2010 platform, and the data was stored and managed in SQL Server 2012 database. The development language was C#.

5.1. C# Communication Implementation. The design of the upper computer hardware used Yanhua brand industrial computer, with excellent performance, through the Ethernet link and Siemens S7-300 PLC to establish a connection. In this design, the IP address of PLC was set as 192.168.0.1. Communication mode was MODBUS/TCP mode of Ethernet network architecture, port number was set as MODBUS, corresponding to 502, and the specific configuration of C# program is as follows:

```
?xml version = "1.0" encoding = "utf-8" ?
<configuration>
  <appSettings>
    <!--Modbus TCP configuration-->
      <add key = "IP" value = "192.168.0.1"/>
      <add key = "Port" value = "502"/>
  </appSettings>
</configuration>
```

5.2. Database Design. The database uses SQL Server 2012, which was mainly divided into three parts. The first part was the report data part, which mainly stored the periodically inserted real-time display data. The second part was the alarm data part, which contained various alarm related information. The third part was the user part, which contained the user related information. Redundant fields were added between each table to realize join query of each table. There were other secondary tables, of course, but only five tables that were closely related to business logic are detailed here. The process section table and data table, respectively, are shown in Tables 2 and 3 [23].

The alarm data part consists of two tables. The first is table of alarms, which displays alarm information, and the second is alarm settings table, and they are shown in Tables 4 and 5, respectively.

The table of users is shown in Table 6.

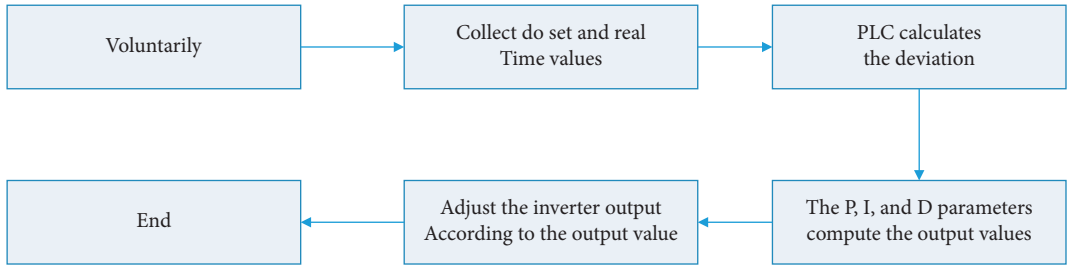

Figure 4: Flow chart of DO control.

5.3. Host Client. The user login module mainly checked the security of the users who entered the remote intelligent management system, so as to prevent the illegal users from misoperating the system or controlling the system illegally after logging in. After the login window was opened, only the legitimate user account could log in to the system. The legitimate user account was manually assigned by the administrator.

The main interface after logging in is the real-time parameter display interface. By directly reading the PLCDB block, it can directly send data and detect key indicators of each process section, including liquid level, PH value, COD, SS, nitrogen and phosphorus content, influent water flow, temperature, whether the device is running, running status, etc.

When the parameter exceeds the threshold or the device displays a fault, the C# program will execute to insert a data into the alarm table in the database, including the alarm date and time (accurate to second) and alarm information, and this data will be extracted by the program in the alarm management interface. The remarks field at the back of each data was manually operated by technicians. When the technicians debug and eliminate the fault, the processing button on the right of the list is manually clicked, and the fault status changes to processed. In this case, a piece of data is inserted into the UserId field of the alarm table in the database, namely, the login user name of the software platform. The value of UserId represents the fault handler, namely, the login user. The data was extracted and displayed in the handler column.

The design and verification of the measurement model of dissolved oxygen in aeration tank were completed by testing and simulation on Matlab platform. For neural networks, which needed a lot of matrix calculation, Matlab modeling and simulation had twice the result with half the effort. At present, scholars at home and abroad in the field of neural network research also relied on Matlab simulation results for comparison. Therefore, the design and performance verification of the dissolved oxygen measurement model mentioned were all carried out in the Matlab environment. In practical application, the running results of Matlab could be called in Windows form written under VS platform through mixed programming and the predicted results could be displayed.

Table 2: Table of process sections.

Field name	Type	Explanation
ProcessId	Int	Process segment ID
ProcessName	String	Name of process section

Table 3: Table of data.

Field name	Type	Explanation
DataId	Int	dataID
DataName	String	Data name
DataValue	Float	Data value
IsAlarm	Bool	To alarm or not to alarm
ProcessId	Int	Process segment ID
SampleTime	Datetime	Data insertion time

Table 4: Table of alarms.

Field name	Type	Explanation
AlarmId	Int	The police ID
AlarmDesc	String	The police described
AlarmTime	Datetime	Time of fire alarming
IsDeal	Bool	Processed or not
DealTime	Datetime	Processing time
UserId	Int	ID of the login user

Table 5: Table of alarm settings.

Field name	Type	Explanation
DataName	String	Data name
ProcessId	Int	Process segment ID
AlarmHigh	Float	Alarm upper limit
AlarmLow	Float	Alarm lower limit
AlarmPRI	Int	Priority

Table 6: Table of users.

Field name	Type	Explanation
UserId	Int	UserID
UserName	String	User name
Password	Varchar (50)	User password
RoleType	Int	Character types
RoleName	String	Role name

6. Conclusion

With population growth and water pollution becoming more and more serious, secondary treatment of sewage is an effective way to reduce water pressure and an important measure to control environmental pollution. Sewage problem is a major problem in China's development; sewage treatment has risen to the national strategy. Design was based on improved artificial neural network; a new system of a set of automatic alarm intelligent monitoring and optimization for wastewater treatment equipment provides a new technical point of view, based on the advanced sewage treatment technology and sewage disposal characteristics, as well as the monitoring and optimization of demand, with the main ideology of physical information fusion and intelligent algorithm as the core. Combining information technology and communication technology to comprehensively monitor various parameters of the sewage plant, once the limit is exceeded, an alarm will be issued, so that the dissolved oxygen in the sewage treatment can be better controlled, so that the equipment of the plant runs smoothly and the effluent quality is better. The design work is summarized as follows:

(1) Using A2/O process, a new optimal control strategy for dissolved oxygen is designed for the key control of dissolved oxygen. Through a large number of experiments and combined with historical data, the intake index and dissolved oxygen value of aeration tank were obtained as samples under the condition of optimal outlet water. According to the samples, the neural network was trained to predict the optimal value of dissolved oxygen under different inlet water conditions. The improved BP neural network is improved by particle swarm optimization. Compared with the traditional BP neural network, the improved neural network has better characteristics.

(2) The sewage treatment in each process is based on the configuration sequence of the monitoring equipment, the design of the upper computer and the lower computer, the communication network between the lower computer and the sensor, and the design of the lower computer system is successfully realized through STEP7 PLC programming.

(3) C# in Visual Studio 2010 was used to develop the upper client platform, and the database used was SQL Server database. The platform realizes user login, real-time data display, overload and fault alarm, report query, and user management, and, through mixed programming, the dissolved oxygen prediction neural network written by Matlab is integrated in the upper computer platform. The parameter value of dissolved oxygen is set through the communication of upper and lower machine [24].

Data Availability

The dataset can be accessed upon request.

Conflicts of Interest

The authors declare that there are no conflicts of interest.

References

[1] H. Y. Kim and C. H. Won, "Forecasting the volatility of stock price index: a hybrid model integrating LSTM with multiple GARCH-type models," *Expert Systems with Applications*, vol. 103, pp. 25–37, 2018.

[2] Y. Kuang, R. Singh, S. Singh, and S. P Singh, "A novel macroeconomic forecasting model based on revised multimedia assisted BP neural network model and ant Colony algorithm," *Multimedia Tools and Applications*, vol. 76, no. 18, pp. 18749–18770, 2017.

[3] Y. Chen, L. Shen, R. Li et al., "Quantification of interfacial energies associated with membrane fouling in a membrane bioreactor by using BP and GRNN artificial neural networks," *Journal of Colloid and Interface Science*, vol. 565, pp. 1–10, 2020.

[4] H. Hong, Z. Zhang, A. Guo et al., "Radial basis function artificial neural network (RBF ANN) as well as the hybrid method of RBF ANN and grey relational analysis able to well predict trihalomethanes levels in tap water," *Journal of Hydrology*, vol. 591, Article ID 125574, 2020.

[5] K. Chapman, G. S. Miller, and H. D. White, "Investor relations and information assimilation," *The Accounting Review*, vol. 94, no. 2, pp. 105–131, 2019.

[6] J. Jawad, A. H. Hawari, and S. Zaidi, "Modeling of forward osmosis process using artificial neural networks (ANN) to predict the permeate flux," *Desalination*, vol. 484, Article ID 114427, 2020.

[7] F. Dong, Q. Lin, C. Li, G. He, and Y. Deng, "Impacts of preoxidation on the formation of disinfection byproducts from algal organic matter in subsequent chlor(am)ination: a review," *Science of the Total Environment*, vol. 754, Article ID 141955, 2021.

[8] P. John, "Real-time monitoring and control of sequencing batch reactors for secondary treatment of a poultry processing wastewater[J]," *Journal of Environmental Engineering*, vol. 126, no. 10, pp. 943–948, 2000.

[9] T. Zipper, N. Fleischmann, and R. Haberl, "Development of a new system for control and optimization of small wastewater treatment plants using oxidation-reduction potential (ORP)," *Water Science and Technology*, vol. 38, no. 3, pp. 307–314, 1998.

[10] N. Puznava, M. Payraudeau, and D. Thornberg, "Simultaneous nitrification and denitrification in biofilters with real time aeration control," *Water Science and Technology*, vol. 43, no. 1, pp. 269–276, 2001.

[11] M. Y. Ren, *Measurement, Automatic Control and Fault Diagnosis of Sewage Treatment plant*, Chemical Industry Press, Beijing, China, 2009.

[12] V. Santiago, "Recent developments on biological nutrient removal processes for wastewater treatment," *Reviews in Environmental Science and Biotechnology*, vol. 3, no. 2, p. 171~183, 2004.

[13] Y. Y. Li, "Brief analysis of B/S and C/S architecture," *Friends of the science*, vol. 15, no. 1, pp. 6–8, 2009.

[14] H. Q. Hu, T. Ma, and Y. Z. Tan, "Remote monitoring system of sewage treatment plant based on VPN and OPC," *Mechatronics technology at home and abroad*, vol. 15, no. 5, pp. 20–22, 2012.

[15] M. Z. Yuan, "Remote Monitoring System for Sewage Treatment Circuit and its implementation," http://www.google.com/patents/CN102681497B.
[16] Q. Li, *Design and Development of Remote Unattended Monitoring System for Jihua Sewage Treatment Plant*, Kunming University of Science and Technology, Kunming, China, 2014.
[17] H. Hong, L. Qian, Y. Xiong, Z. Xiao, H. Lin, and H Yu, "Use of multiple regression models to evaluate the formation of halonitromethane via chlorination/chloramination of water from Tai Lake and the Qiantang River, China," *Chemosphere*, vol. 119, pp. 540–546, 2015.
[18] Y. W. Him and L. Camillo, "Stock price crash risk and unexpected earnings thresholds[J]," *Managerial Finance*, vol. 44, no. 8, pp. 1012–1030, 2018.
[19] F. Liu, H. Gong, L. Cai, and K. Xu, "Prediction of ammunition storage reliability based on improved ant colony algorithm and BP neural network," *Complexity*, vol. 2019, no. 4, pp. 1–13, 2019.
[20] S. Y. Kimura, A. A. Cuthbertson, J. D. Byer, and S. D. Richardson, "The DBP exposome: development of a new method to simultaneously quantify priority disinfection byproducts and comprehensively identify unknowns," *Water Research*, vol. 148, pp. 324–333, 2019.
[21] Y. Liu, C. Hu, and Y. Hong, "Electric energy substitution potential prediction based on logistic curve fitting and improved BP neural network algorithm," *Elektronika ir Elektrotechnika*, vol. 25, no. 3, pp. 18–24, 2019.
[22] H. K. Ghritlahre and R. K. Prasad, "Application of ANN technique to predict the performance of solar collector systems - a review," *Renewable and Sustainable Energy Reviews*, vol. 84, pp. 75–88, 2018.
[23] A. Sethi, "Predictive modeling of CNX Nifty 200 from a valuation perspective," *Asian Journal of Management*, vol. 10, no. 1, pp. 14–18, 2019.
[24] G. D. Martino, "How do investors perceive long-term growth targets and forecast horizons in strategic plans[J]. Evidence from Italian firms," *Issues & Studies*, vol. 7, no. 2, pp. 33–43, 2019.

Hindawi
Scientific Programming
Volume 2022, Article ID 7532076, 12 pages
https://doi.org/10.1155/2022/7532076

Research Article

Improvement of Wolf Pack Algorithm and Its Application to Logistics Distribution Problems

Wei Zheng

Henan Polytechnic Institute, Henan, Nanyang 473000, China

Correspondence should be addressed to Wei Zheng; zhengwei@hnpi.edu.cn

Received 1 August 2022; Revised 16 August 2022; Accepted 26 August 2022; Published 13 September 2022

Academic Editor: Lianhui Li

In logistics distribution systems, the constrained optimisation of the cargo dispensing problem has been the focus of research in related fields. At present, many scholars try to solve the problem by introducing swarm intelligence algorithms, including genetic algorithm, particle swarm algorithm, bee swarm algorithm, fish swarm algorithm, etc. Each swarm intelligence algorithm has different characteristics, but they all have certain advantages for the optimisation of complex problems. In recent years, the Wolf Pack algorithm, an emerging swarm intelligence algorithm, has shown good global convergence and computational robustness in solving complex high-dimensional functions. Therefore, this article chooses to use the Wolf Pack algorithm to solve a multi-vehicle and multi-goods dispensing problem model. First, the principle and process of the Wolf Pack algorithm are introduced, and two improvements are proposed for the way of location update and the way of step update. Then, a mathematical model of the multi-vehicle and multi-goods dispensing problem is developed. Next, the mathematical model is solved using the proposed improved Wolf Pack algorithm. The experimental results show that the proposed improved Wolf Pack algorithm effectively solves the cargo dispatching problem. In addition, the proposed improved Wolf Pack algorithm can effectively reduce the number of vehicles to be dispatched compared with other swarm intelligence algorithms.

1. Introduction

With the progress of science and technology, after reducing the cost of raw materials and improving labour productivity, modern logistics has become a "new source of profit" for enterprises and has received widespread attention from the logistics industry and even from the business community [1, 2]. Especially in the field of commodity circulation, different types of large-scale modern logistics enterprises have emerged. With the rapid development of the logistics industry, the study of logistics distribution has also attracted more widespread attention [3, 4]. How to reduce costs and at the same time improve efficiency, as well as obtain more economic and social benefits, has become a topic of research for experts and scholars.

In modern logistics, the biggest cost of logistics and distribution is the transport cost, which in turn has a lot to do with the vehicle. Therefore, when carrying out distribution operations, the load capacity and volume of the vehicle should be fully considered [5, 6]. By selecting the right transport vehicle, the optimum utilisation of the transport vehicle (100% utilisation) is achieved as far as possible, which is an effective way to reduce distribution costs. However, in practical situations, the space utilisation and load capacity of the vehicle often cannot be maximised at the same time due to the type of goods, packaging methods, etc. These situations can waste transport power and cause an increase in transport costs. In logistics and distribution systems, the issue of cargo dispensing is the most fundamental item [7, 8]. Reasonable dispensing can improve distribution efficiency on the one hand and reduce distribution costs on the other. At present, in the actual cargo dispensing business, it is usually done based on manual estimation methods. There is no uniform planning based on experience alone, which wastes both manpower and material resources [9, 10]. Therefore, the rational allocation of goods is conducive to improving distribution efficiency, reducing distribution costs, and achieving higher

vehicle utilisation. Therefore, due to its extensive application background and important theoretical value, the study of cargo dispensing has become an important research content in the logistics and distribution industry [11, 12].

The key to the cargo dispensing problem is how to maximise the vehicle's capacity and volume, thereby reducing distribution costs and improving distribution efficiency. It is a complex discrete multi-constrained combinatorial optimisation problem, which belongs to the NP problem like the traveler problem and workshop scheduling problem [13, 14]. And for solving NP problems, heuristic algorithms or intelligent optimisation algorithms are the most commonly used techniques. Solving cargo dispensing problems often requires the use of heuristic algorithms or intelligent optimisation algorithms to approximate the optimisation solution.

There have been a number of studies on heuristic algorithms for cargo dispensing and loading problems. For example, Tran et al. [15] constructed a three-dimensional multilayer loading layout optimisation model with the maximisation of combined vehicle load and volume utilisation as the optimisation objective and designed a heuristic algorithm that can quickly develop a reasonable loading solution. Chua et al. [16] combined the two problems of vehicle dispensing optimization and transport path optimization into one and used the classical Dijkstra's algorithm and the improved C–W saving algorithm to solve the optimisation problem for the full-load transportation case and the optimisation problem for the non-full-load transportation case, respectively. Experimental results show that the solution is effective. Du et al. [17] developed an intelligent cargo dispensing model with multidimensional constraints and proposed a hybrid algorithm based on heuristic ideas and fuzzy principles. The test results showed the effectiveness of this intelligent dispensing model. Chao et al. [18] established a cargo dispensing model with the optimisation objective of maximising revenue and minimising expenditure and used a heuristic algorithm to solve it. Finally, the effectiveness of this algorithm was verified by example. However, heuristic algorithms tend to rely too much on personal experience. When the problem is large, heuristics can become "combinatorially explosive." As a result, heuristics are not very efficient when solving large-scale problems and lack global optimisation capabilities, giving only approximate or locally optimal solutions to the problem.

Swarm intelligence algorithms are all inspired by the evolution of organisms in nature, foraging, clustering, and information exchange. At present, the main swarm intelligence optimisation algorithms are simulated annealing algorithms, genetic algorithms, particle swarm algorithms, ant colony algorithms, immune algorithms, etc. These intelligent optimisation algorithms are all easy to implement and have good robustness. When solving complex optimisation problems, the advantages of swarm intelligence algorithms are more obvious. For solving large-scale, multi-constrained complex problems, swarm intelligent optimisation algorithms are more widely used. For example, Jamrus et al. [19] used a genetic algorithm to investigate the optimal placement of containers and developed a corresponding single-vehicle transport dispensing model, while Miao et al. [20] designed a hybrid genetic algorithm and applied it to a multi-species cargo dispensing model. The experimental results showed that the above model could fully utilise the load and volume of the loading tools in a balanced manner. Sicilia et al. [21] used an ant colony algorithm to solve a bi-objective bulk cargo loading model and verified that the proposed model and algorithm were feasible through experiments.

As an emerging swarm intelligence algorithm, the Wolf Pack algorithm exhibits good global convergence and computational robustness in the process of solving complex high-dimensional functions [22, 23]. During the hunting process, each wolf is classified into Alpha, Beta, or Omega wolves according to its different roles. Alpha wolves are always the strongest wolves in the pack and are responsible for directing the pack to capture prey without participating in the roaming, running, or siege process; Beta wolf is an elite unit of wolves, responsible for searching for prey; and Omega wolf is the attack force of wolves and is responsible for quickly closing in on the Alpha Wolf's direction when the Alpha Wolf initiates an attack command, in order to capture prey. Zhu et al. [24] proposed a Wolf Pack algorithm based on ant colony optimisation for solving the TSP problem. An ant colony algorithm was used to initialise the population in order to implement a heuristic crossover operator, while adaptive adjustment of the crossover probability and variation probability was employed. This algorithm achieves good optimisation results for smaller TSP problems. However, when the scale is larger, this algorithm needs further improvement. As an efficient intelligent optimisation algorithm, the Wolf Pack algorithm can provide a practical and effective solution to the cargo dispensing problem, thereby effectively reducing logistics costs (improving dispensing efficiency).

Therefore, this study aims to use the Wolf Pack algorithm to solve the cargo dispensing problem in logistics distribution, so that it can effectively improve the solution quality. Although the Wolf Pack algorithm has good global search performance and superiority-seeking ability, the number of iterations and convergence speed need to be further improved. Therefore, this article improves the traditional Wolf Pack algorithm. In addition, this article provides a brief introduction to the components and classification of the cargo dispensing problem in logistics distribution and establishes a multi-vehicle, multi-goods mathematical model. The improved Wolf Pack algorithm in this article is used to solve this model in order to reduce the number of vehicles used, which can effectively improve the solution quality. The final experimental results validate the performance and application value of the improved algorithm.

The main innovations and contributions of this article include:

(1) Through an in-depth study of the Wolf Pack algorithm, it was found that the location update method of Beta and Omega wolves has certain shortcomings, so the location update and step update of the Wolf Pack algorithm were improved respectively to achieve better optimisation search results.

(2) A mathematical model is described and developed for the multi-vehicle, multi-goods dispensing problem. The constraints of the model are deformed and transformed into a penalty function added to the fitness function. The model is solved using the proposed improved Wolf Pack algorithm to reduce the number of vehicles used, thus effectively improving the quality of the solution.

The rest of the article is organised as follows: In Section 2, the Wolf Pack algorithm is studied in detail, while Section 3 provides the improvements to the Wolf Pack algorithm. In Section 4, the multi-vehicle, multi-goods dispensing problem based on the improved Wolf Pack algorithm is studied in detail, while Section 5 provides experimental results and analysis. Finally, the article is concluded in Section 6.

2. Wolf Pack Algorithm

2.1. Principle of the Wolf Pack Algorithm. Each wolf is classified as an Alpha, Beta, or Omega wolf, depending on the role it plays in the hunting process [25, 26]. Alpha wolves are always the strongest wolves in the pack and are responsible for directing the pack to capture prey without participating in the roaming, running, or siege process; Beta wolf is an elite unit of wolves, responsible for searching for prey; and Omega wolf is the attack force of wolves and is responsible for the [27, 28]. The principle of the Wolf Pack algorithm is shown in Figure 1.

When a wolf perceives a greater concentration of prey than the current Alpha wolf, we consider that wolf to be more likely to capture the prey. That wolf will then replace the Alpha wolf and call the surrounding Omega wolves to approach the current location [29]. When the prey is caught, the earlier the wolf catches the prey, the more food it gets, which approach allows wolves capable of capturing prey to maintain sufficient stamina [30, 31]. Wolves with sufficient physical strength are more likely to catch prey in the later hunting process, thus ensuring the development of wolfs.

The total number of wolves is assumed to be N and the total number of variables is D. The state of an artificial wolf is represented as $X_i = (x_{i1}, x_{i2}, \ldots, x_{iD})$, where$x_{\mathrm{id}}$ denotes the position of the ith artificial wolf in the dth dimension. The objective function is $Y = f(x)$, where Y denotes the concentration value of prey perceived by a wolf, that is the degree of adaptation.

2.1.1. Generation of Alpha Wolves. An Alpha wolf is an optimal value in the initial solution. An Alpha wolf is not fixed. During the iteration, the position of each wolf is updated continuously. If a better solution appears, the Alpha wolf is replaced by another wolf [32, 33].

2.1.2. The Wandering Process of Beta Wolves. Among N artificial wolves, the number of Beta wolves is $S_$num. The scale factor is denoted as a, the number of directions is h, and the wandering step is step_a. The fitness value of the Beta wolves in the initial solution is Y_i. The Beta wolves then take a step forward in a direction ($p = 1,2, \ldots, h$) based on their current position. The position of the advancing Beta wolves in the dth dimension is updated.

$$x_{\mathrm{id}}^{p} = x_{\mathrm{id}} + \sin\left(2\pi \times \frac{p}{h}\right) \times \mathrm{step}_a^d. \tag{1}$$

After updating the Beta wolf's position, the adaptation value Y_i of the Beta wolf's current position is compared with the adaptation value Y_{lead} of the Alpha wolf. If $Y_i > Y_{\mathrm{lead}}$, this Beta wolf replaces the Alpha wolf, and the Omega wolf is called to run towards the current position; otherwise the wandering continues until the maximum number of times $T_{\max}$ is reached.

2.1.3. The Long-Range Raiding Process of Omega Wolves. Except Alpha wolf and Beta wolf, the remaining artificial wolves are Omega wolves. The number of Omega wolves is $_$num. When an Omega wolf receives a call from an Alpha wolf, it will run in the direction of the Alpha wolf. The step length of the long-range raid is step_b. The position of the Omega wolf in the dth dimension is updated at the (k+1)th iteration.

$$x_{\mathrm{id}}^{k+1} = x_{\mathrm{id}}^{k} + \mathrm{step}_b^d \times \frac{\left(g_d^k - x_{id}^k\right)}{\left|g_d^k - x_{\mathrm{id}}^k\right|}, \tag{2}$$

where g_d^k is the position in the d-th dimension of the Alpha wolf at the (k+1)th iteration.

When the distance between the Omega wolf and the Alpha wolf is less than d_{near}, it enters into a siege process of its prey.

$$d_{\mathrm{near}} = \frac{1}{D \times \omega} \times \sum_{d=1}^{D} \left|\max_d - \min_d\right|, \tag{3}$$

where ω is the decision factor and $[\max_d - \min_d]$ is the range of values for the dth dimensional variable.

2.1.4. The Siege Process of Prey. Because Alpha wolves are closest to the prey, the position of Alpha wolves is considered to be the position of the prey G_d^k. The siege step of the wolves in the prey siege process is step_c. Location updates are calculated as follows:

$$x_{\mathrm{id}}^{k+1} = x_{\mathrm{id}}^{k} + \lambda \times \mathrm{step}_c^d \times \left|G_d^k - x_{id}^k\right|, \tag{4}$$

where λ is a random number between [1].

There is a relationship between the step sizes of the three different stages.

$$\mathrm{step}_a^d = \frac{\mathrm{step}_b^d}{2} = step_c^d \times 2 = \frac{\left|\max_d - \min_d\right|}{S}. \tag{5}$$

During the siege process of a wolf pack, the position is updated if the adaptation of the current position is greater than the adaptation of the original position; otherwise, the position remains unchanged.

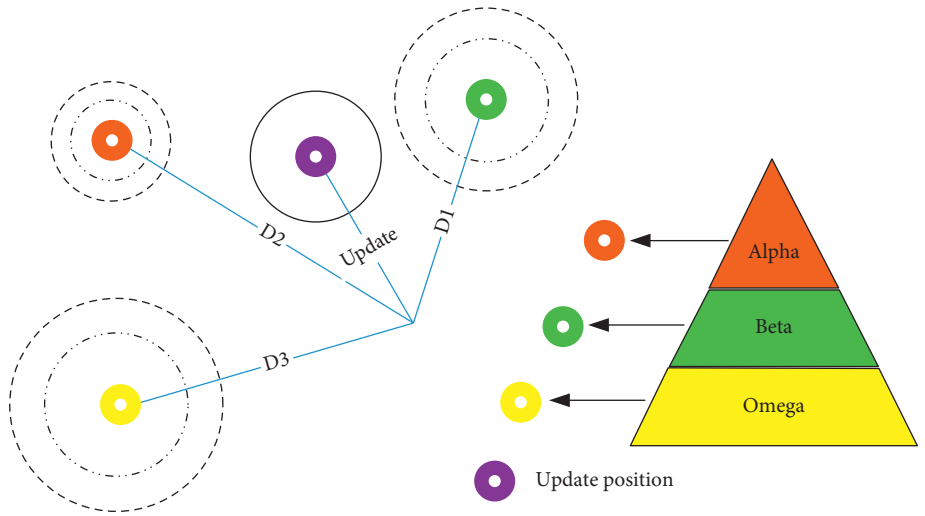

Figure 1: Principle of the Wolf Pack algorithm.

2.1.5. Renewal of Wolf Pack. In order to maintain the quality of the wolf population while preserving the diversity of the pack, the least adapted wolves are selected for culling and new artificial wolves are randomly generated [34–37]. The number of eliminated artificial wolves is the same as the number of newborn artificial wolves. The number of retirements needs to be determined by human experience.

2.2. Flow Chart of the Wolf Pack Algorithm. Figure 2 shows the flow chart of the Wolf Pack algorithm.

The detailed steps of the Wolf Pack algorithm are as follows:

Step 1: Initialise the number of artificial wolves N, the position X_i, the maximum number of generations to be selected $k_{\max}$, the scale factor a, the maximum number of wanderings $T_{\max}$, the distance determination factor ω, and the step size factor S.

Step 2: Follow equation (1) for position update. If the Beta wolf's fitness value Y_i is greater than the Alpha wolf's fitness value Y_{lead}, replace Alpha wolf and jump to Step 3; otherwise, the Beta wolf continues to wander until the maximum number of wanderings $T_{\max}$ is reached.

Step 3: Follow equation (2) for position update. If the fitness value of an Omega wolf Y_i is greater than the fitness value of an Alpha wolf Y_{lead}, replace the Alpha wolf; otherwise, the Omega wolf continues to long-range raid until the distance to the prey is less than the judged distance d_{near}.

Step 4: Begin the wolf pack siege process and carry out the position update according to equation (5), together with the Alpha wolf update.

Step 5: Update Wolf Pack.

Step 6: Determine whether the maximum number of iterations is reached or the optimisation accuracy is achieved. If yes, the output of the optimal solution is carried out; otherwise jump to Step 2.

3. Improvements to the Wolf Pack Algorithm

After an in-depth study of the Wolf Pack algorithm, it was found that position update methods have certain shortcomings for Beta wolf and Omega wolf. Therefore, in this article, the Wolf Pack algorithm is improved in order to achieve better merit-seeking results.

3.1. Location Update. The Beta wolf's position during the wandering phase [38] was updated as follows:

$$x_{\text{id}}^{p} = x_{\text{id}} + \sin\left(2\pi \times \frac{p}{h}\right) \times \text{step}_a^d, \tag{6}$$

where h is the number of directions in Beta wolf's wandering process.

In most cases, the value of h is 4. The calculation shows that there are only two values for updating the position of the Beta wolf.

$$\begin{aligned} x_{\text{id}}^{1} &= x_{\text{id}} + \text{step}_a^d, \\ x_{\text{id}}^{3} &= x_{\text{id}} - \text{step}_a^d, \\ x_{\text{id}}^{2} &= x_{\text{id}}^{4} = x_{\text{id}}. \end{aligned} \tag{7}$$

That is, when Beta wolves wander in each of the four directions, they are only able to obtain two values that are different from their original position. This increases the computational effort and weakens the ability of Beta wolves to wander [39].

Therefore, the updated formula for the wandering phase has been improved in this article.

$$x_{\text{id}}^{p} = x_{\text{id}} + \cos\left(\pi \times \frac{p}{h}\right) \times \text{step}_a^d. \tag{8}$$

When h takes the value of 4, the Beta wolf's position is updated with a value of 3.

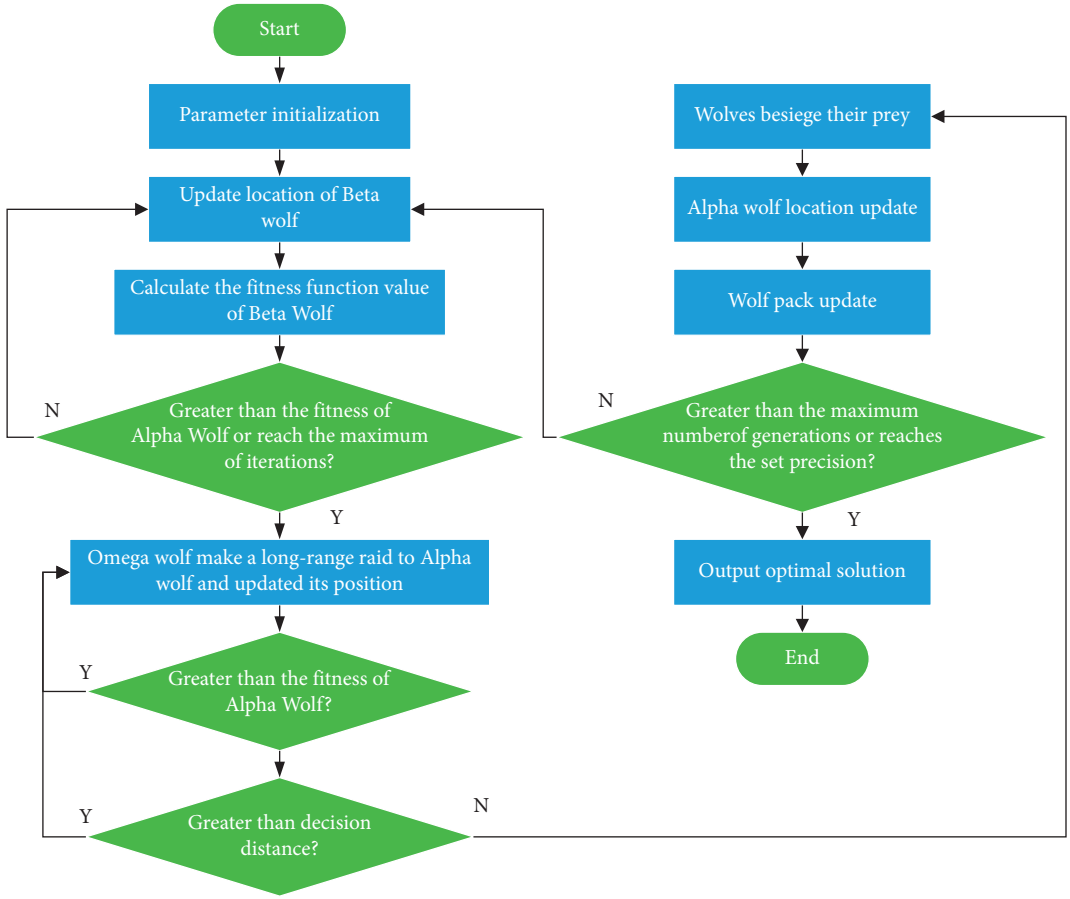

Figure 2: Flow of the Wolf Pack algorithm.

$$x_{\mathrm{id}}^{1} = x_{\mathrm{id}} + \frac{\sqrt{2}}{2}\mathrm{step}_{a}^{d},$$

$$x_{\mathrm{id}}^{3} = x_{\mathrm{id}} - \frac{\sqrt{2}}{2}\mathrm{step}_{a}^{d}, \tag{9}$$

$$x_{\mathrm{id}}^{4} = x_{\mathrm{id}} - \mathrm{step}_{a}^{d}.$$

The improvement ensures that when Beta wolves wander in more than one direction, at most one value can be the same as the original position value.

3.2. Step Size Update. The step size of the long-range raiding and the step size of the siege are always fixed. However, as the distance between the wolves and their prey decreases (increasing number of iterations), both step values should decrease adaptively.

Therefore, this article uses an adaptive approach to improve the update process of the step size.

$$x_{\mathrm{id}}^{k+1} = x_{\mathrm{id}}^{k} + \frac{(1-k)}{k_{\max}} \times \mathrm{step}_{b}^{d} \times \frac{\left(g_{d}^{k} - x_{\mathrm{id}}^{k}\right)}{\left|g_{d}^{k} - x_{\mathrm{id}}^{k}\right|},$$

$$x_{\mathrm{id}}^{k+1} = x_{\mathrm{id}}^{k} + \lambda \times \frac{(1-k)}{k_{\max}} \times \mathrm{step}_{c}^{d} \times \left|G_{d}^{k} - x_{\mathrm{id}}^{k}\right|, \tag{10}$$

where k is the current number of iterations and $k_{\max}$ is the maximum number of iterations.

4. Multi-Vehicle, Multi-Goods Dispensing Problem Based on the Improved Wolf Pack Algorithm

4.1. Description of Cargo Dispensing Problems. As a fundamental part of logistics and distribution, the quality of the cargo dispensing has an impact not only on the efficiency of distribution, but also on the operational efficiency of the entire logistics centre. Therefore, a reasonable cargo dispensing can reduce logistics costs, on the one hand, and improve the efficiency of distribution on the other. The dispensing problem is a complex discrete multi-constrained combinatorial optimisation problem, which belongs to the same NP problem as the travel merchant problem (TSP) and the workshop scheduling problem. The main components of the cargo dispensing problem are goods, vehicles, constraints, objective functions, etc. [40]. The volume and weight of the cargo are the basis for the decision of vehicle allocation. When the volume or weight of the cargo exceeds the volume or capacity of the vehicle, multiple transport vehicles are required to distribute it. A general description of the cargo dispensing problem is shown in Figure 3.

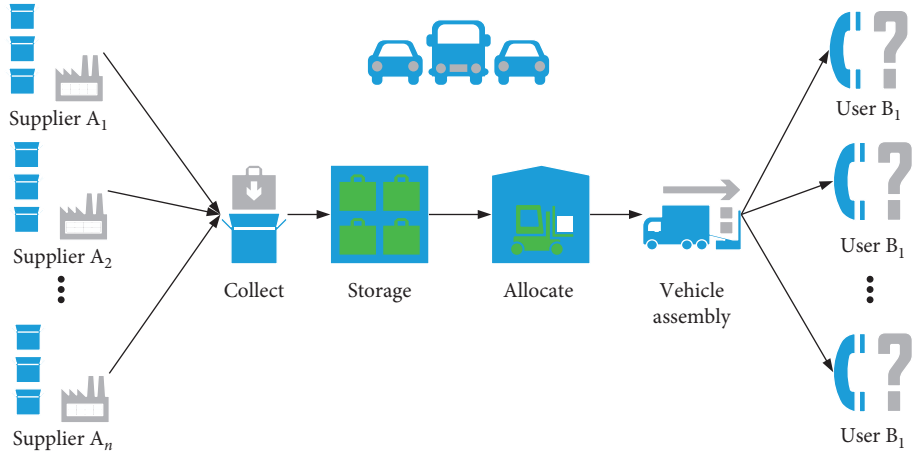

Figure 3: General description of the cargo dispensing problem.

4.2. Problem Description and Mathematical Model. Real-life cargo dispensing problems are very complex, and to facilitate modelling and solution, some cases are simplified: (1) the goods are all shipped to the same distribution centre; (2) the goods are intermixable and not incompatible; (3) there is no priority of goods.

Problem description: In a distribution centre, there are m vehicles of different types. Each vehicle has a maximum weight and a maximum volume of w_k and v_k ($k = 1,2, \ldots, m$), respectively. There are n different goods to be dispensed, with weights and volumes of w_i and v_i ($i = 1,2, \ldots, n$), respectively. Under the condition that the goods are relatively limited, the number of vehicles to be used is required to reach a minimum value.

The mathematical model for the multi-vehicle, multi-goods dispensing problem presented in this article is shown as follows:

$$\min f = \sum_{k=1}^{m} y_k, \sum_{i=1}^{n} x_{ki} w_i \le y_k W_k, \sum_{i=1}^{n} x_{ki} v_i \le y_k V_k, \sum_{k=1}^{m} x_{ki} = 1, \tag{11}$$

$$y_k = \begin{cases} 1, & \text{The } k\text{th vehicle is selected,} \\ 0, & \text{The } k\text{th vehicle is not selected,} \end{cases} \tag{12}$$

$$x_{ki} = \begin{cases} 1, & \text{The } i\text{th shipment is loaded into the } k\text{th vehicle,} \\ 0, & \text{The } i\text{th shipment is not loaded into the } k\text{th vehicle.} \end{cases} \tag{13}$$

The objective function is (11). It can be seen that the objective function is a minimum optimisation problem, that is, the number of vehicles used is the least. The constraint indicates that the total weight of the cargo on the kth *vehicle does* not exceed the capacity of the vehicle. (12) and (13) represent the constraints on the values taken by the variables y_k and x_{ki}.

4.3. Fitness Function. Fitness function is the optimisation index of wolf pack algorithm and the important basis of survival of the fittest in the siege process. In the mathematical model of multi-vehicle and multi-goods allocation, the objective function cannot be directly used as the fitness function due to more constraints. Therefore, this article uses the penalty function to construct the fitness function.

$$\begin{aligned} \min F &= f + c \sum_{k}^{m} \left(\left[\max(0, g_k) \right]^2 + \left[\max(0, h_k) \right]^2 \right), \\ g_k &= \sum_{i=1}^{n} x_{ki} w_i - y_k W_k, \\ h_k &= \sum_{i=1}^{n} x_{ki} v_i - y_k V_k, \end{aligned} \tag{14}$$

where c is the penalty factor.

The optimisation process of the Wolf Pack algorithm is a maximum value problem, so a further transformation has to be performed to obtain the optimisation fitness function of the Wolf Pack algorithm.

$$\text{maxFit}(F) = -F. \tag{15}$$

5. Experimental Results and Analysis

5.1. Experimental Environment and Setup. In order to verify the effectiveness of a multi-vehicle, multi-cargo dispensing model based on the improved Wolf Pack algorithm, simulation tests were carried out using MATLAB. The hardware and software environments associated with the experiments are shown in Table 1. In addition, all experiments involved in this study were carried out in the same hardware and software environment. The parameter settings for the improved Wolf Pack algorithm during the experiments are shown in Table 2.

5.2. Typical Test Function Verification. Five typical continuous complexity functions are selected to verify the effectiveness and feasibility of the proposed improved wolf pack algorithm and to compare it with the traditional wolf pack algorithm.

Table 1: Experiment-related software and hardware environment and parameter settings.

Specification	Parameters
Processor	Intel Core i7
Memory	8 GB
Hard disk	500 GB
Operating systems	Windows 10 Professional
Programming software	MATLAB R2012a

Table 2: Parameter settings for the improved Wolf Pack algorithm.

Parameters	Numerical values
Wolf population	50
Maximum number of iterations	20
Scale factor for Beta wolves	4
Maximum number of wanderings for Beta wolves	20
Number of directions for Beta wolves	4
Distance determination factor	500
Step size factor	1000
Updating the scale factor	6

$$
\begin{aligned}
&F_1 = x_1^2 + x_2^2, -5 \le x_i \le 5, i = 1, 2,\\
&F_2 = 100\left(x_1^2 - x_2\right)^2 + \left(1 - x_1\right)^2, -2.048 \le x_i \le 2.048, i = 1, 2,\\
&F_3 = \left[1 + \left(x_1 + x_2 + 1\right)^2\left(19 - 14x_1 + 3x_1^2 - 14x_2 + 6x_1x_2 + 3x_2^2\right)\right]\times\\
&\quad \left[30 + \left(2x_1 - 3x_2\right)^2\left(18 - 32x_1 + 12x_1^2 + 48x_2 - 36x_1x_2 + 27x_2^2\right)\right], -2 \le x_i \le 2, i = 1, 2,\\
&F_4 = \left(4 - 2.1x_1^2 + \frac{1}{3}x_1^4\right)x_1^2 + x_1x_2 + \left(-4 + 4x_2^2\right)x_2^2, -3 \le x_i \le 3, i = 1, 2\\
&F_5 = 10\cos\left(2\pi x_1\right) + 10\cos\left(2\pi x_2\right) - x_1^2 - x_2^2 - 20, -5.12 \le x_i \le 5.12, i = 1, 2.
\end{aligned}
\tag{16}
$$

In order to illustrate the convergence and optimisation seeking ability of the improved Wolf Pack algorithm in this article, a comparison was made with the genetic algorithm and the traditional Wolf Pack algorithm on the above five test functions. Figure 4 shows the optimisation process curves of the three algorithms on the test function F_1. Figure 5 shows the optimisation curves of the three algorithms on the test function F_2

It can be seen that the genetic algorithm can only converge to a local optimum. Both the traditional Wolf Pack algorithm and the improved Wolf Pack algorithm can converge to the global optimum, while the improved Wolf Pack algorithm converges faster, indicating that the improved Wolf Pack algorithm in this article can greatly improve the efficiency of the search for the optimum. In order to further illustrate the optimisation finding ability of the improved Wolf Pack algorithm in this article, 100 calculations were carried out for each of the five test functions. Then, four metrics, the best value, the worst value, the average value, and the average deviation value (the deviation of the average value from the theoretical optimum value), were used to evaluate the results. A comparison of the test function optimisation results is shown in Table 3.

The best, worst, and average values show that the solution quality of the improved Wolf Pack algorithm is significantly better than that of the genetic algorithm and the traditional Wolf Pack algorithm. The highest accuracy was obtained by the improved Wolf Pack algorithm. In terms of the average deviation value, the improved wolf pack algorithm has the smallest value, that is the smallest difference from the theoretical optimum.

The global search capability of the three algorithms was then judged by the number of convergences. A comparison of the convergence results on the five test functions is shown in Table 4. The maximum number of evolutionary generations was set to 1000. 100 tests were performed for each algorithm. The convergence accuracy was 10^{-3}. These algorithms were considered to have reached the convergence condition when the difference between the optimised value and the theoretical optimum was less than 10^{-3}.

It can be seen that the improved Wolf Pack algorithm converges 100 times on all five test functions, indicating that it is able to achieve global convergence with 100% probability, that is it is more stable. The genetic algorithm has the worst convergence, with only 4 out of 100 experimental tests, indicating that it is prone to fall into the local extreme value trap. Compared to the traditional wolf pack algorithm, the improved wolf pack algorithm takes 40% less time to reach convergence, indicating that it can converge to the global optimum more quickly. Overall, the number of convergence iterations and convergence time of the improved wolf pack algorithm are the lowest.

5.3. Experimental Cases. Suppose a distribution centre has 20 delivery vehicles with a load and volume of 6 t and 10 m^3, respectively. There are 42 different types of goods to be dispensed. The goods now need to be rationally dispensed

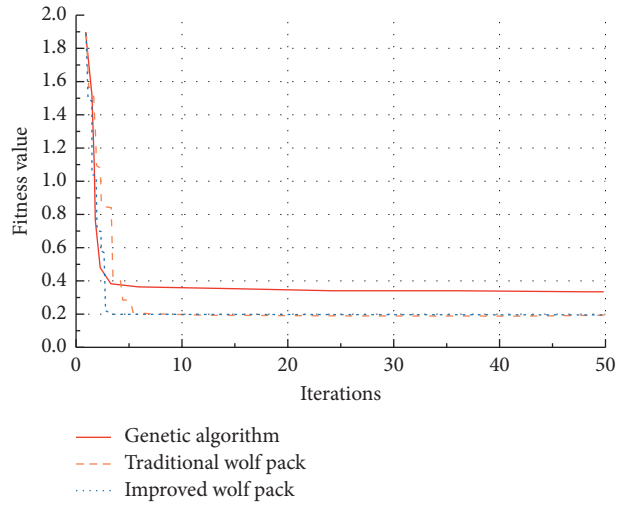

Figure 4: Optimisation curve for the F_1 function.

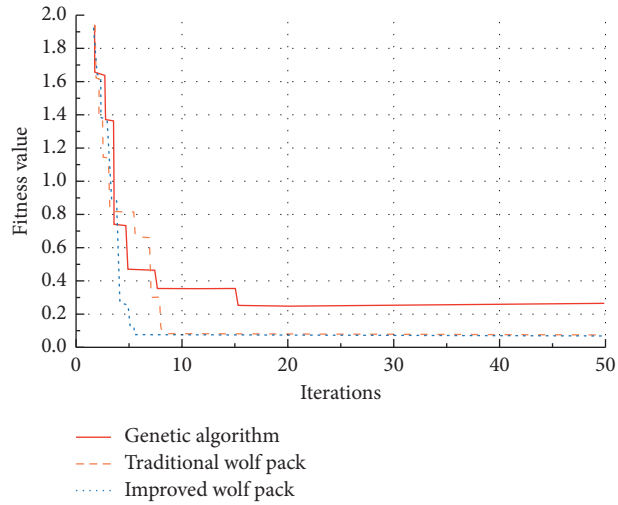

Figure 5: Optimisation curve for the F_2 function.

Table 3: Comparison of test function optimisation results.

Functions	Algorithms	Best value	Worst value	Average	Average deviation value
	Genetic algorithm	2.15E-05	1.0173	0.1302	0.1302
F_1	Traditional Wolf Pack	4.55E-11	1.17E-05	1.65E-07	1.65E-07
	Improved Wolf Pack	4.55E-11	4.55E-11	4.55E-11	4.55E-11
	Genetic algorithm	8.63E-04	2.8217	0.64209	0.64209
F_2	Traditional Wolf Pack	1.08E-10	5.76E-02	2.63E-03	2.63E-03
	Improved Wolf Pack	1.01E-10	1.94E-03	2.30E-04	2.30E-04
	Genetic algorithm	3.0094	96.9906	19.8777	16.8777
F_3	Traditional Wolf Pack	3	3.0002	3 + 7.79E-06	7.79E-06
	Improved Wolf Pack	3	3 + 5.63E-09	3 + 1.47E-09	1.47E-09
	Genetic algorithm	−1.03068005	−0.122028	−0.754928	0.2767
F_4	Traditional Wolf Pack	−1.03162779	−0.999872	−1.0276737	3.95E-03
	Improved Wolf Pack	−1.03162779	−1.03153801	−1.03161098	1.70E-05
	Genetic algorithm	−1.0174	−12.6704	−4.9979	4.9979
F_5	Traditional Wolf Pack	−9.46E-09	−1.2372	−0.1319	0.1319
	Improved Wolf Pack	−9.46E-09	−9.46E-09	−9.46E-09	9.46E-09

Table 4: Comparison of convergence results of test functions.

Functions	Algorithms	Maximum number of iterations	Minimum number of iterations	Average number of iterations	Average convergence time/s	Number of convergences
F_1	Genetic algorithm	1000	84	977	9.157	4
	Traditional Wolf Pack	539	11	46	0.539	100
	Improved Wolf Pack	60	7	26	0.304	100
F_2	Genetic algorithm	1000	2	990	9.433	11
	Traditional Wolf Pack	1000	2	442	5.387	61
	Improved Wolf Pack	947	12	219	2.681	100
F_3	Genetic algorithm	1000	1000	1000	9.582	0
	Traditional Wolf Pack	600	23	115	1.419	100
	Improved Wolf Pack	162	21	66	0.823	100
F_4	Genetic algorithm	1000	1	970	9.905	3
	Traditional Wolf Pack	1000	16	256	3.224	78
	Improved Wolf Pack	326	1	52	0.654	100
F_5	Genetic algorithm	1000	1000	1000	9.462	0
	Traditional Wolf Pack	1000	43	293	3.560	89
	Improved Wolf Pack	355	17	104	1.282	100

Table 5: Number, weight, and volume of goods.

No.	Weight/t	Volume/m^3	No.	Weight/t	Volume/m^3	No.	Weight/t	Volume/m^3
1	1.221	1.05	15	1.040	2.60	29	1.102	2.46
2	1.156	1.98	16	0.805	1.23	30	2.041	2.20
3	0.700	2.00	17	1.220	0.65	31	1.900	2.80
4	1.243	3.14	18	1.000	2.40	32	2.400	3.20
3	1.600	2.86	19	1.782	0.87	33	1.029	3.00
6	1.612	2.17	20	1.100	1.54	34	3.000	1.20
7	2.300	4.80	21	1.030	5.60	35	1.840	1.20
8	1.930	5.20	22	0.730	4.40	36	1.796	3.89
9	1.850	2.30	23	1.030	1.80	37	2.650	1.01
10	1.900	3.80	24	2.430	3.80	38	1.975	123
11	1.120	2.00	25	1.520	4.00	39	0.800	1.00
12	1.431	4.02	26	1.890	5.46	40	1.100	3.20
13	0.600	2.78	27	1.320	3.54	41	1.200	0.80
14	0.306	3.22	28	1.150	1.60	42	2.000	1.10

and the minimum number of vehicles to be used are required. The numbers, weights, and volumes of all goods are shown in Table 5.

The experiment was carried out for 40 calculations. Both the conventional Wolf Pack algorithm and the modified Wolf Pack algorithm yielded an optimal solution of 12 after 40 calculations, which indicates that a minimum of 12 vehicles are required. An optimal dispensing solution is shown in Table 6.

When using the improved particle swarm algorithm (IPSO) to solve the same multi-vehicle, multi-goods dispensing problem, the best value is 13 in 35 out of 40 operations and the worst value is 16. When using the improved genetic algorithm (IGA) to solve the same vehicle dispensing problem, the best value is 13 in 36 out of 40 operations and the worst value is 17. The results of the different algorithms are compared in Table 7 and Figure 6. It can be seen that the improved Wolf Pack algorithm has better optimisation

Table 6: The solution of dispensing.

Vehicle no.	Goods no.	Total weight/t	Total volume/m^3	Load utilisation (%)	Volume utilisation (%)
1	22, 23, 30, 35	5.641	9.6	94.02	96
2	1, 4, 7, 41	5.964	9.79	99.4	97.9
5	9, 16, 18, 27	4.975	9.47	82.92	94.7
7	20, 36, 40, 42	5.996	9.73	99.93	97.3
8	6, 14, 28, 33	4.097	9.99	68.28	99.9
9	2, 10, 19, 29	5.94	9.11	99	91.1
12	5, 17, 26	4.71	8.97	78.5	89.7
13	11, 24, 25	5.07	9.8	84.5	98
14	3, 12, 34	5.131	7.22	85.52	72.2
16	8, 32	4.33	8.4	72.17	84
19	21, 37, 38	5.655	7.84	94.25	78.4
20	13, 15, 31, 39	4.34	9.18	72.33	91.8

Table 7: Optimisation results.

Algorithms	Best value	Worst value	Probability of best value (%)
IPSO [41]	13	16	87.5
IGA [42]	13	17	90
Wolf Pack algorithm	13	15	100
Improved Wolf Pack algorithm	12	12	100

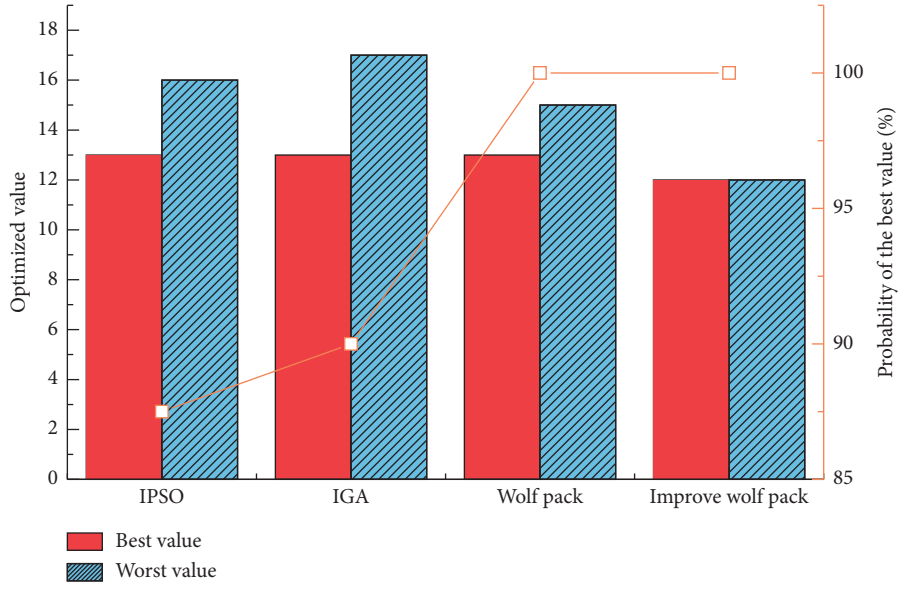

Figure 6: Comparison results of the optimising performance.

capability and better stability in solving multi-vehicle and multi-goods dispensing problems.

6. Conclusion

In this article, a mathematical model of a multi-vehicle and multi-goods dispensing problem is established and constraints are transformed into penalty functions. Simulation results of five typical test functions show that the proposed improved wolf pack algorithm achieves better performance in terms of accuracy and convergence time. Compared with the traditional Wolf Pack algorithm, the time required for convergence of the improved Wolf Pack algorithm is reduced by 40%. The simulation results of the logistics case show that the improved Wolf Pack algorithm has stronger optimising performance and better stability in solving the multi-vehicle and multi-goods dispensing problem, thus effectively reducing the number of vehicles. As the number of vehicles is often limited in actual logistics distribution, subsequent research will consider more realistic constraints to further improve the dispensing model.

Data Availability

The data that support the findings of this study are available from the author upon request.

Conflicts of Interest

The author declares that there are no conflicts of interest.

References

[1] S. Winkelhaus and E. H. Grosse, "Logistics 4.0: a systematic review towards a new logistics system," *International Journal of Production Research*, vol. 58, no. 1, pp. 18–43, 2020.

[2] S. H. Chung, "Applications of smart technologies in logistics and transport: a review," *Transportation Research Part E: Logistics and Transportation Review*, vol. 153, Article ID 102455, 2021.

[3] F. Sgarbossa, E. H. Grosse, W. P. Neumann, D. Battini, and C. H. Glock, "Human factors in production and logistics systems of the future," *Annual Reviews in Control*, vol. 49, pp. 295–305, 2020.

[4] V. Yavas and Y. D. O. Ozen, "Logistics centers in the new industrial era: a proposed framework for logistics center 4.0," *Transportation Research Part E: Logistics and Transportation Review*, vol. 135, Article ID 101864, 2020.

[5] T. M. Choi, "Risk analysis in logistics systems: a research agenda during and after the COVID-19 pandemic," *Transportation Research Part E: Logistics and Transportation Review*, vol. 145, Article ID 102190, 2021.

[6] C. S. Tang and L. P. Veelenturf, "The strategic role of logistics in the industry 4.0 era," *Transportation Research Part E: Logistics and Transportation Review*, vol. 129, pp. 1–11, 2019.

[7] L. Koh, A. Dolgui, and J. Sarkis, "Blockchain in transport and logistics – paradigms and transitions," *International Journal of Production Research*, vol. 58, no. 7, pp. 2054–2062, 2020.

[8] T. S. Clair and J. Guzman, "Contribution volatility and public pension reform," *Journal of Pension Economics and Finance*, vol. 17, no. 4, pp. 513–533, 2018.

[9] X. Qin, Z. Liu, and L. Tian, "The strategic analysis of logistics service sharing in an e-commerce platform," *Omega*, vol. 92, Article ID 102153, 2020.

[10] J. M. Moshref and M. Winkenbach, "Applications and Research avenues for drone-based models in logistics: a classification and review," *Expert Systems with Applications*, vol. 177, Article ID 114854, 2021.

[11] R. Beysenbaev and Y. Dus, "Proposals for improving the logistics performance index," *The Asian Journal of Shipping and Logistics*, vol. 36, no. 1, pp. 34–42, 2020.

[12] M. Pournader, Y. Shi, S. Seuring, and S. L. Koh, "Blockchain applications in supply chains, transport and logistics: a systematic review of the literature," *International Journal of Production Research*, vol. 58, no. 7, pp. 2063–2081, 2020.

[13] I. J. Orji, S. Kusi-Sarpong, S. Huang, and D. Vazquez-Brust, "Evaluating the factors that influence blockchain adoption in the freight logistics industry," *Transportation Research Part E: Logistics and Transportation Review*, vol. 141, Article ID 102025, 2020.

[14] I. M. Ar, I. Erol, I. Peker, A. I. Ozdemir, T. D. Medeni, and I. T. Medeni, "Evaluating the feasibility of blockchain in logistics operations: a decision framework," *Expert Systems with Applications*, vol. 158, Article ID 113543, 2020.

[15] H. Tran, N. Krommenacker, and P. Charpentier, "The Internet of Things for logistics: perspectives, application review, and challenges," *IETE Technical Review*, vol. 39, no. 1, pp. 93–121, 2022.

[16] C. Chua, M. Danyluk, D. Cowen, and L. Khalili, "Introduction: turbulent circulation: building a critical engagement with logistics," *Environment and Planning D: Society and Space*, vol. 36, no. 4, pp. 617–629, 2018.

[17] Y. Du, F. Chen, X. Fan, L. Zhang, and H. Liang, "Research on cargo-loading optimization based on genetic and fuzzy integration," *Journal of Intelligent and Fuzzy Systems*, vol. 40, no. 4, pp. 8493–8500, 2021.

[18] C. Chao, H. Mei, and H. Yanhui, "Study of railway freight vehicle body's dynamic model based on goods loading technical standards," *Procedia Engineering*, vol. 29, pp. 3572–3577, 2012.

[19] T. Jamrus and C. F. Chien, "Extended priority-based hybrid genetic algorithm for the less-than-container loading problem," *Computers & Industrial Engineering*, vol. 96, pp. 227–236, 2016.

[20] L. Miao, Q. Ruan, K. Woghiren, and Q. Ruo, "A hybrid genetic algorithm for the vehicle routing problem with three-dimensional loading constraints," *RAIRO - Operations Research*, vol. 46, no. 1, pp. 63–82, 2012.

[21] J. A. Sicilia, B. Royo, E. Larrode, and A. Fraile, "A decision support system for a long-distance routing problem based on the ant colony optimization metaheuristic," *Procedia-Social and Behavioral Sciences*, vol. 111, pp. 1035–1044, 2014.

[22] L. Xu, B. Wang, X. Du, and Y. Hong, "Prediction method of mine gas emission based on complex neural work optimized by Wolf pack algorithm," *Systems Science & Control Engineering*, vol. 6, no. 3, pp. 85–91, 2018.

[23] Y. Chen, Z. Jia, X. Ai, D. Yang, and J. Yu, "A modified two-part wolf pack search algorithm for the multiple traveling salesmen problem," *Applied Soft Computing*, vol. 61, pp. 714–725, 2017.

[24] Y. Zhu, L. Zhu, Y. Long, and J. Luo, "The Wolf pack assignment rule based on ant colony algorithm and the path planning of scout ants in complex raster diagra," *Journal of Physics: Conference Series*, vol. 1732, no. 1, Article ID 012084, 2021.

[25] F. Yang, "A hybrid recommendation algorithm-based intelligent business recommendation system," *Journal of Discrete Mathematical Sciences and Cryptography*, vol. 21, no. 6, pp. 1317–1322, 2018.

[26] Y. Chen, D. Yang, and J. Yu, "Multi-UAV task assignment with parameter and time-sensitive uncertainties using modified two-Part Wolf pack search algorithm," *IEEE Transactions on Aerospace and Electronic Systems*, vol. 54, no. 6, pp. 2853–2872, 2018.

[27] X. Chen, F. Cheng, C. Liu, L. Cheng, and Y. Mao, "An improved Wolf pack algorithm for optimization problems: design and evaluation," *PLoS One*, vol. 16, no. 8, Article ID e0254239, 2021.

[28] Y. Lu, Y. Ma, J. Wang, and L. Han, "Task assignment of UAV swarm based on wolf pack algorithm," *Applied Sciences*, vol. 10, no. 23, p. 8335, 2020.

[29] L. Zhen, Y. Liu, W. Dongsheng, and Z. Wei, "Parameter estimation of software reliability model and prediction based on hybrid wolf pack algorithm and particle swarm optimization," *IEEE Access*, vol. 8, pp. 29354–29369, 2020.

[30] S. Xu, L. Li, Z. Zhou, Y. Mao, and J. Huang, "A task allocation strategy of the UAV swarm based on multi-discrete wolf pack algorithm," *Applied Sciences*, vol. 12, no. 3, p. 1331, 2022.

[31] S. Xian, T. Li, and Y. Cheng, "A novel fuzzy time series forecasting model based on the hybrid wolf pack algorithm and ordered weighted averaging aggregation operator," *International Journal of Fuzzy Systems*, vol. 22, no. 6, pp. 1832–1850, 2020.

[32] L. Y. Cang and X. P. Dong, "Improved Wolf Pack algorithm for optimum design of truss structures," *Executive Manager*, vol. 6, no. 8, p. 1411, 2020.
[33] Z. Wang, S. Yu, L. Y. Chen, and Y. Li, "Robust design for the lower extremity exoskeleton under a stochastic terrain by mimicking wolf pack behaviors," *IEEE Access*, vol. 6, pp. 30714–30725, 2018.
[34] H. S. Wu, J. J. Xue, R. B. Xiao, and J. Q. Hu, "Uncertain bilevel knapsack problem based on an improved binary wolf pack algorithm," *Frontiers of Information Technology & Electronic Engineering*, vol. 21, no. 9, pp. 1356–1368, 2020.
[35] Y. J. Gao, F. M. Zhang, Y. Zhao, and C. Li, "A novel quantum-inspired binary wolf pack algorithm for difficult knapsack problem," *International Journal of Wireless and Mobile Computing*, vol. 16, no. 3, pp. 222–232, 2019.
[36] J. Hu, H. Wu, R. Zhan, and N. Li, "Hybrid integer-coded Wolf Pack Algorithm for multiple-type flatcars loading problem," *Journal of Rail Transport Planning & Management*, vol. 16, Article ID 100201, 2020.
[37] M. Papin, M. Aznar, E. Germain, F. Guerold, and J. Pichenot, "Using acoustic indices to estimate wolf pack size," *Ecological Indicators*, vol. 103, pp. 202–211, 2019.
[38] X. Feng, K. Hu, and X. Lou, "Infrared and visible image fusion based on the total variational model and adaptive wolf pack algorithm," *IEEE Access*, vol. 8, pp. 2348–2361, 2020.
[39] R. Menassel, B. Nini, and T. Mekhaznia, "An improved fractal image compression using wolf pack algorithm," *Journal of Experimental & Theoretical Artificial Intelligence*, vol. 30, no. 3, pp. 429–439, 2018.
[40] R. Pinto, A. Lagorio, and R. Golini, "The location and sizing of urban freight loading/unloading lay-by areas," *International Journal of Production Research*, vol. 57, no. 1, pp. 83–99, 2019.
[41] H. Saleh, H. Nashaat, W. Saber, and H. M. Harb, "IPSO task scheduling algorithm for large scale data in cloud computing environment," *IEEE Access*, vol. 7, pp. 5412–5420, 2019.
[42] P. Shahrokh and F. Safi-Esfahani, "QoS-based web service composition applying an improved genetic algorithm (IGA) method," *International Journal of Enterprise Information Systems*, vol. 12, no. 3, pp. 60–77, 2016.

Hindawi
Scientific Programming
Volume 2022, Article ID 2711236, 9 pages
https://doi.org/10.1155/2022/2711236

Review Article

A Study of Trends on Human-Machine Interface Design in Modern Vehicles

Jianan Lyu,[1,2] **Zalay Abdul Aziz**,[1] **and Nor Syazwani Binti Mat Salleh**[1]

[1]*Faculty of Art, Computing and Creative Industry, Sultan Idris Education University, Tanjung Malim, Malaysia*
[2]*School of Art and Design, Huizhou University, Huizhou, China*

Correspondence should be addressed to Jianan Lyu; lyujianan@hzu.edu.cn

Received 8 June 2022; Revised 1 August 2022; Accepted 22 August 2022; Published 13 September 2022

Academic Editor: Lianhui Li

This study aims to analyze the development trends of intelligent device interface improvements, specifically the car dashboards, by applying liquid crystal display technology. The methodology used in this study is mainly a comparison and analysis of the improvements that have been made. The objects in the study were several old version dashboards display instruments that were compared against the improved version of the LCDs. This paper analyses the requirements of car operators, with various proficiency for drivers' information, in enhancing the modern car dashboards displays. Besides, this study further delves into ways through which instrument interface intelligently can be improved to adapt effectively to all kinds of drivers. This study also touches on an analytical view of information targeting drivers. This is a scientific technique to determine the extent of information needed from drivers in different circumstances by having precise or averaged information about the drivers; it is easier to integrate this information into the human interface that helps in these modern car operations. The results of the study show that the current LCD Dashboards are valuable, accurate, precise user friendly, and improved with integrated ICT pieces of equipment. This makes them much better than the older traditional systems of the car dashboards.

1. Introduction

The methodology used in this study is mainly a comparison and analysis of the improvements that have been made, to analyze the development trends of intelligent device interface improvements, specifically the car dashboards, by applying liquid crystal display technology. This study shows that current LCD dashboards have been improved by integrating ICT equipment, which makes them much better than the old traditional car dashboard systems. The study reveals the evolution and improvement of modern vehicle dashboard display systems.

The old dashboard display version mainly consisted of mechanics and several movable parts. This made it difficult for the drivers to handle the cars at times. The rate at which the drivers were to multitask to gain full control of these machines was a daunting task. The rates of traffic jams, low speed, and road crashes were significantly high. Besides, it took a long time for one to learn how to manipulate all the instruments on the car's dashboard fully. With a relatively high number of instruments to read, the information provided by these instruments sometimes failed to reflect the real conditions of the car. There are significant steps that have been taken to improve the ancient dashboards. Nonetheless, for high efficiency to be achieved in this human-machine interface, significant developments were also incorporated, both in design and also efficiency. A milestone change from mechanical to digital intelligence dashboard whose contents keep changing was achieved. As demonstrated by the incorporation of the new displays of LCDs and the future transparent dashboards, this Human Machine Interface has more advantages than disadvantages to automobile Human-computer Interaction and Automobile Human-machine Interface [1]. The flexibility of applying the full liquid crystal technology in the dashboard interface in an automobile is a modern method that is software-dependent [2] with more knowledge of science and technology across the globe. Tremendous improvements have been suggested,

and some implemented on ancient automobile products in the right direction in the intelligentization of human-computer interaction. The principle of this change depends on the rapid development and application of corresponding technological advancement, especially in automobile electronics, automobile human-computer interaction, automobile, and human-machine interface. It is projected that several vehicles will fully adopt the liquid crystal display dashboard in the future [3]. This will be integrated by the emergence of varying new dashboard interfaces in the automobile Human-computer Interaction and Automobile Human-machine Interface.

Externally, the design of these brand-new interfaces has a lot of modern development compared to traditional dashboards, suggesting a new requirement for design content and techniques. Besides, there are dynamics in the contents displayed by the new automobile dashboard interface. The displays are variable and diversified-unlike in the traditional mechanical dashboard in which pointers and scale were applied as the generation of hardware. The colors and style of operation are permanent. Furthermore, the liquid crystal display dashboard is a combination of a whole screen [3]. This implies that the kind of pointers, scales, numerals, and texts are simple images displayed and colors whose styles can be changed at will. This helps to meet the demand of different users in different scenarios [2]. It is both entertaining and interactive. Because of the different functions in the display, the dashboard can achieve various functions. For instance, it can display targeted prompts according to various driving procedures and environmental conditions that alert the drivers of the required information. This helps the drivers in quick decision-making. The alert system onboard has been instrumental in helping drivers with poor vision and hearing problems. These warning devices are pivotal in avoiding accidents [4].

The dashboard systems are intergraded with images and audio systems that can be read and heard. This interactive design provides advanced options lacking in old vehicle models. The other important tool in this category is the information demand level interface display. It enables the driver to be flexible, Drivers can make choices promptly, and it also allows for various styles and content according to their taste, driving norms, and varied information required [5]. Sometimes challenges are met in due course of implementing this technology. That is instrument interface cannot fully work out for all drivers.

For most developers to salvage this situation, analytic hierarchy processes have been proposed. Besides simple, effective index weight analysis technique that dwells much on the new liquid crystal display technology in the intelligent development procedure of automobiles, this could help satisfy the drivers' demand that depends on foregoing technology [5]. Furthermore, there is a method that helps in evaluating the demand level of different drivers for varied types of information during driving. From these reviews, it is evident that several changes have been in place to improve the old dashboards to a much better dashboard that is based on the liquid crystal display. There is a possibility of eradication of the traditional dashboard soon if the LCDs are made cheap for all vehicle manufacturers.

2. Related Improvements in Human-Machine Interface Design in Modern Vehicles

Several factors like market demands show advantages of the improved LCD car dashboards. The number of cars sold due to the enhanced dashboards on LCD versions has improved greatly, as shown in Figure 1, along with the market demand for LCDs in different parts of the world for different models. The stiff competition in the market must, therefore, be handled technologically. This is achievable by the introduction of Human Interface Machines, which will be ideal and unique to attract more customers. Besides, Asian countries have the best-growing economy among their rivals worldwide. The growth in the Asian country's economy provides the best business arena and research platform for improved modern vehicles. Through market analysis, the taste for automatic vehicles has taken the day [3], substituting the old manual fashioned vehicles with improved dashboards such as automobile human-computer interaction and automobile human-machine interface. The need to improve their dashboards and other software-related interfaces in the current automated vehicles is greatly a good idea whose time has come [7]. Automated vehicles require a well-integrated human interface that will reduce risks such as accidents through a quick grasp of the information played by the LCD dashboards [8, 9].

Through the improvements of the displays, errors have been greatly reduced since most of the information on the performance of the vehicle is read by machines through a computerized interface system [10]. For this reason, Asian countries like China, Japan, and India have greatly contributed to the improvement that is deemed necessary for the best quality of automobiles they launched in the market. The USA and European car manufacturers have not been underscored in this analysis. The duos have also tried to pump financial and human capital to facelift their modern car production to unmatched standards [5]. I must relate that Russia, Europe, and America produce some of the most sophisticated motor vehicles in the modern world. They boast of their skilled manpower, availability of research funds, and also the staunched willingness to stay aloft among their competitors.

These multifaceted nations have enjoyed producing and selling cars in almost every niche of automobile transport. Their car production cuts across sports, heavy-duty, general transport, military, media, health education, and research. By being capable of extensively researching the current needs, China, America, Russia, Europe, and other stakeholders have played a pivotal role in modernizing their cars [11]. Their industries began by building manual vehicles with too many mechanical systems of display like the pointer speedometer and the oil gauge. These mechanical parts dashboards, with instruments having movable parts, were prone to mechanical breakdown [3]. They also had a short life with low work efficiency. The modern (improved car

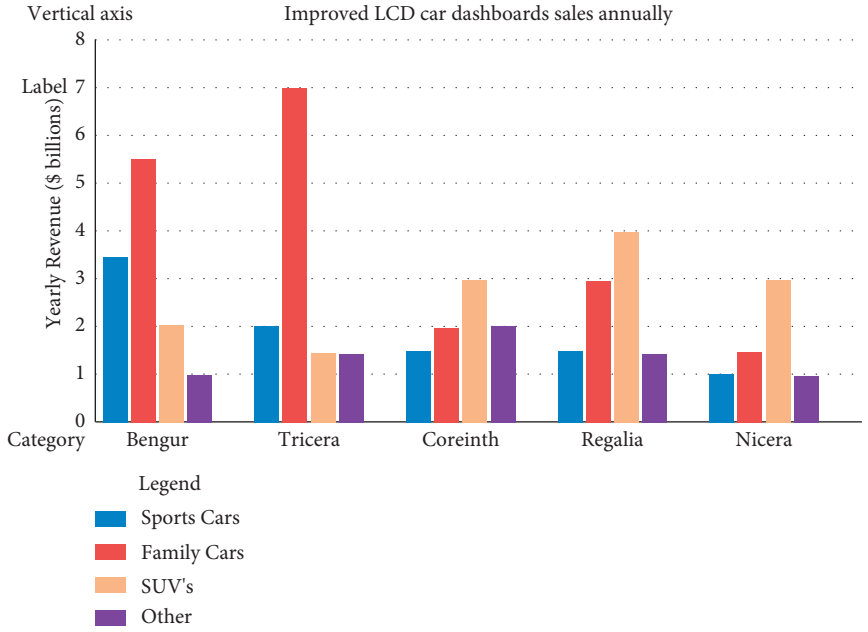

Figure 1: Market demand for LCDs in different parts of the world for different models [6].

dashboards) depend on minimal movable parts. Most of the display mechanisms are electronic-based, and their efficiency is highly improved. Quick readings can be taken at a glance. This reduces the energy spent by the drivers to obtain vital information like engine speed on their car dashboards.

Asian countries have contributed to the development and production of motor cars since the early 1980s. Countries such as Japan, India, China, and Russia are well-known champions of the automobile industry. Due to the growing automobile market, Asian countries have continued to remain relevant in the market to level their production against the USA (Ford), European (British Motor Works) countries, and other parts of the world. The backbone of the economy of these Asian countries is greatly dependent on motor vehicle assembly. Nonetheless, other Asian countries like India and China also offer favorable competition in the manufacture of vehicles in their regions. India produces a good number of its TATA brand vehicles in various models [12]. The market for cars and other heavy-duty automobiles has speedily increased. This is because cars are considered lucrative goods worldwide [3]. With the adoption of this new LCD technology, the dashboard interface design has a lot of importance, aimed to improve, convince, create comfortability, and even lessen driving rules [2]. By doing this, the safety of the drivers and general users is tremendously improved before creating any Human Machine Interface.

Since the advent of the first modern (i.e., digital) automotive display, designers and manufacturers have made significant progress in improving image quality and enhancing device durability [13], facilitating the development of modern automotive HMI designs. Takatoh et al. proposed a new type of optical device with variable transmittance based on the incident angle direction. These devices consist of two liquid crystal devices (LCDs) with a half-wave plate between them, a wide range of transmittances was obtained because no polarizer was used [14]. Yoon et al. [15] proposed a homogeneously aligned liquid crystal device in which the liquid crystal director does tilt as well as twist deformation in a confined area by both vertical- and fringe-electric fields, exhibiting about two times faster decay response time than that of conventional FFS mode with suppressed luminance in the upward direction. In the vehicle display field, the brightness of the backlight is almost more than 10000 cd/m^2, which may enlarge small defects in the display screen to impact display quality. As black uniformity is a crucial characteristic of image quality, Hua et al. [16] reduced the interference stress by controlling the flatness of the backlight and the metal frame, optimizing the design of the buffer strip, and reducing the bending stress by optimizing the structure and shape. The black uniformity of the module was improved by more than 80%. Wang et al. [17] designed a programmable digital power supply TFT liquid crystal display (LCD) screen touch display system based on STM32F7, the system has a clear display effect and fast control response.

3. Research Methodology and Design

3.1. Comparison and Analysis of the Improvements. The research methods were mainly a comparison between old traditional dashboards and modern LCD-based ones. The comparison offered a reflection of the tremendous work done to achieve the current dashboard displays. The popularity of LCDs is due to the high-tech Displays, Customized information, and the true reflection of Information Technology in the application of these great Human Machine interface tools. Up to now, it is premature to conclude that the development is fully done. Nonetheless, the LCD dashboards have a shred of clear evidence to capture the attention of all automobile manufacturers. This technology has proven important due to its unlimited advantages. Factors such as the orientation of the car and the global

Table 1: Comparison between the traditional and the current LCD-based dashboards.

Old car dashboards	LCD car dashboards
Had several mechanical parts	Few mechanical parts
Consumed more electrical power	Consumed less electrical power
Had limited functions	More functions and quite flexible
Manual operations	Dependable on programming
Difficult to operate required more attention	Easy to operate requires less attention
Time-consuming to repair and overhaul	Little time for repair and maintenance
Could not be linked to wireless devices, and the Internet	It can be linked to wireless devices like the Internet

positioning of the vehicles can easily be obtained on an LCD dashboard [18]. The major types of designs available in the market include mechanical meters with LCD Displays, pure mechanical meters, and all LCD.

Furthermore, The LCDs are available in different sizes and measurements, ranging from 4.3 inches to 12.3 inches, depending on their purpose. Wide choices and preferences are well taken care of. The improved versions of car dashboards are integrated with LCDs. The drivers can read the engine temperature, fuel gauge, and speedometer quite easily [19]. The application of computers to program the LCDs is also catered to in the new design. This has also enabled the connection of the current dashboards with wireless devices and even the Internet. The introduction of the touch smart LCDs is also an integral improvement on the car dashboards. The touch screens are easily operated since they don't require many complex mechanical systems. The comparison between the traditional and current LCD-based dashboards is demonstrated in Table 1.

The improved versions of car dashboards are integrated with LCDs. The application of computers to program the LCDs is also catered to in the new design. This has also enabled the connection of the current dashboards with wireless devices and even the Internet.

Among the cars that have adopted the incorporation of the LCDs fully on their dashboard is the EcoJet car. This car runs on a 650-horsepower run by biodiesel fuel. The display is a two-screen mounted on the front part (dashboard). This car entirely depends on the improved dashboard display, which provides basic information about the general state of the vehicle. Microsoft Windows Vista runs the LCDs for the multimedia and navigation control systems. This gives the car an enhanced ability of word processors and the web on the same dashboard. The rare views are also taken care of. The screen can successfully display the rear part of the car, and this display is connected to the camera. The dashboard is quite fascinating and entertaining. The LCDs are fully touch mart enabled. The audio system of this car is embedded with high graphics that can also recognize speech through a series of microphones onboard. This car is a postulation of future vehicles that will fully rely on the improved LCDs. The car borrows a lot of design from the jet airplane. The use of LCDs is not only limited to car displays but general automotive-like high-speed railways [20].

3.2. Evaluation of the Requirements of Car Operators. The operators require displays that can multitask, as shown in Figure 2. The need to display numerous information at once is among the choices and preferences of the current drivers. User-friendliness, entertainment, and beauty are the evaluated factors that the driver requires in their modern LCD dashboards.

3.3. Evaluation of Dashboard Interface in Automobiles. In the early ages (from 1940s to 1960s) of car manufacturing by American companies, the dashboard was less readable. The instruments were chrome-laden and with transparent plastic covers, which at that time were seen as the best methods and styles. The reflection on the chrome surfaces, especially from the sunlight, could even make it difficult for the drivers to take correct readings. This trend continued until the 1980s when wood and chrome were still ramp-ant on building the dashboard displays. Most of the improvements were made in Europe and the Asian-based car manufacturing companies. The dashboards started looking attractive with increased research to make them look much better by these companies. In the wake of the inception of LEDs, LCDs integration in the electronic arena and the possible displays were then made. The current automakers have gone far beyond this age within 20 years. The LEDs and, ultimately, the LCDs have taken the subject of discussion in-car dashboard displays. With the ability to convert the mechanical motion into electrical signals and then into the screens through computer programming, the car displays are much better. The car dashboard displays as major Human Machine Interface increases by adding stylish modern technology in the displays of these machines, as shown in Figure 2 Full interchangeable LCD Dashboard touch smart enabled. The other models of car that included the LCDs on their dashboards were the Audi Quattro. This was a sports car in the early 1990s. The LDC displays in these cars were simpler than the current full liquid crystal displays. The analog systems were reduced in this model in 1991.

Several companies have even gone a notch higher to incorporate the fuel economy gauges in a cluster of some vehicles, e.g., Honda, Mercedes, and British Motor work for companies. This fuel gauge helps in real-time monitoring of these vehicles' fuel consumption, as shown in Figure 3. Further, engine real-time and even mileage readings have been developed in the 2010s to improve the awareness of the drivers on the car performance. These transitions from the ammeters to voltmeters and finally, proper gauges have been developed and improved through the integration of the LCDs and the computer software, as demonstrated in Figure 4. These developments and further improvements have taken time to complete the evolution. With speculations and

Figure 2: Full interchangeable LCD dashboard touch smart enabled [12].

Figure 3: A color-coded fuel economy is not only beautiful but also easy to read: left photo, right column photo [21].

research which is still on to better the dashboard systems, more is yet to be achieved. Car tracking systems have been made possible by this new technology.

Along with influencing factors like the competition for the market, this study also offers a succinct and comprehensive knowledge of the facets like the future of these current developments in the automobile industry [11]. Capturing areas like the market growth for the improved human-machine interface profoundly delves into the crystal liquid display dashboards. Full liquid crystal technology in the dashboard interface in an automobile has a benefit for both the car developers and the car users [5]. The developers are earning cash from their skills and ideas by developing better equipment like the liquid crystal technology in the automobile dashboard interface. Furthermore, car drivers get quality services offered by the designed interfaces while driving, as demonstrated in Figure 3. This is a win-win situation for both the equipment vendors and consumers.

The LCDs in the car display come with various values and functions. Some of the improved display systems help tell the distance between the driver's car and the next car in front. The distances to be estimated by the driver's car can also be adjusted to varied abilities, which helps drivers with high-speed cars to keep safe distances from cars [23]. It avoids accidents since the car drivers can slow down at convenient distances and times, even at sharp bends. Drivers with poor vision have also benefitted from this improved dashboard display [11]. To safely drive, the drivers get the exact distance between the two cars even under poor visibility brought about by the weather. Some of the improved version of these displays is shown below in Figure 5.

LCDs are designed such that their function shifts, the improvement here is that the screen can display some information discretely or as set by the driver, and some situations prompt reverse driving. The strain to turn while the drivers sit to view the back of the car during reverse has also been catered for [24]. The above model LCD is designed in such a manner that during reverse, the display picks the back view movement of the vehicle through some camera at the back. This aids the drivers in making smooth turns by avoiding hitting objects. In modern urban areas, parking a car in front of schools, offices, Walmarts, and even supermarkets has faced a high number of cars with little or no space for parking. It becomes difficult for the lucky ones who get parking spaces again to unpark the car and get to the road [25]. The emergence of this improved version of the Human Machine Interface provided back the vision of the car during

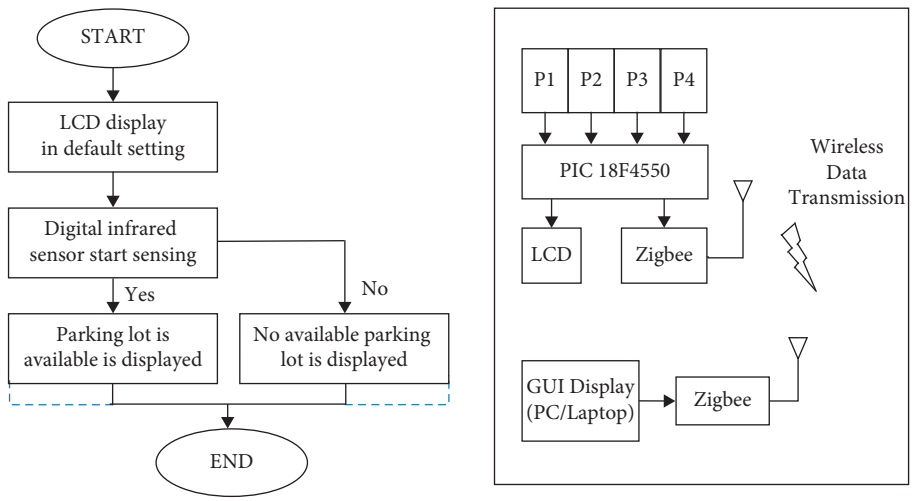

Figure 4: A computerized LCD with android operating systems [22].

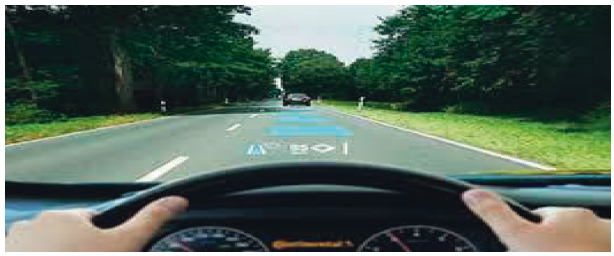

Figure 5: Distance gauge Integrated into the car windscreen for easy reading [4].

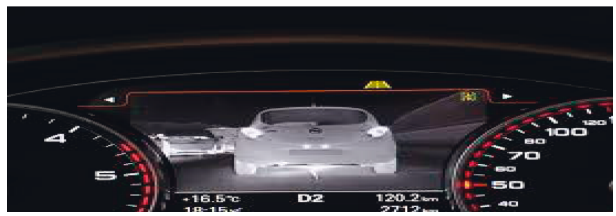

Figure 6: Night vision aid LCD [4].

Figure 7: Reverse assistance LCD [26].

reverse. The drivers find it easier to get the car safely in reverse mode. The improved display is shown below in Figure 6 and Figure 7 during usage.

The application of the above LCDs has dramatically improved the efficiency of the current drivers. The need to be increasingly dependable. The interfaces act as an aid to humans both for safety and accuracy. It is not a matter of production, but the main issue is producing quality at speed. It is equally imperative to highlight the improvements in the design of the LCDs. Through active projects, there are several designs of programmable LCDs [27]. Through these designs, they significantly employ the instrument cluster as an important element of the safety automobiles' passive safety channel and systems [28]. This state of art invention shows the driver the situation of the car through some signals. The energy distribution in the car LCDs is also shown below in Figure 8.

The warnings are informed of collision warnings, terrain warnings and portholes, vision and audio support, parking aids, and even adoptive speed controls. There are several eventualities that prompt signal warnings on the dashboard of a car [29]. Moreover, the car dashboard display systems are smaller to cater to all warnings. Therefore, multitasking designs are integrated into the crystal display system that allows the car to send more than one warning per instrument [30]. This design chiefly helps to create more useful gadgets for a small area in the car dashboard. Another important improvement is the incorporation of an integrated instruments cluster, which has more areas to exploit in terms of visual space [31].

The runtime configurations and flexibility are the key priorities that make these designs important too. This ensures that the driver can make changes due to the prevailing conditions of the road (Bellotti et al.). It is quite clear that the designs play a key role in the adoption of this Human Machine Interface in the motor car industry. These adorable communications tools have made driving more desirable and enjoyable, as they limit the energy and tasks of the driver. These communication tools are equally imperative in line with safety and containment. The best part is the existence of research to improve the improved designs through lab road tests [32].

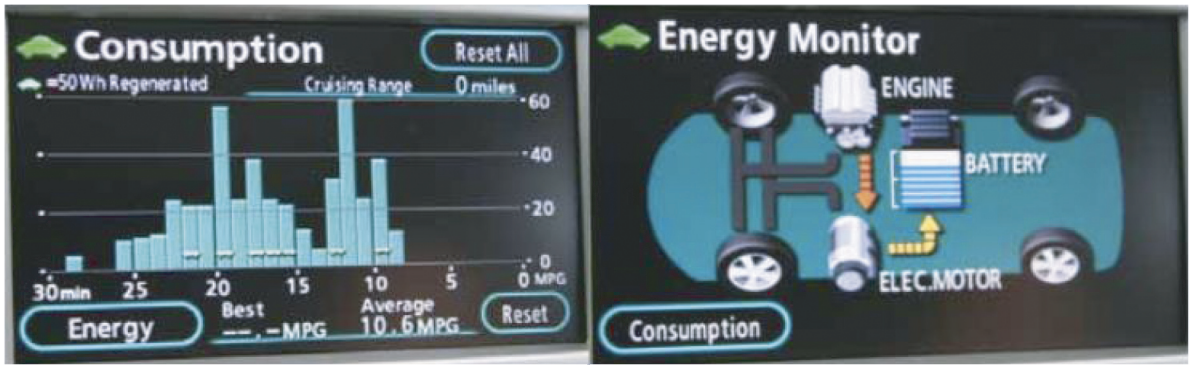

Figure 8: Consumption and energy monitor of a modern improved car (generation Toyota Prius, 2010).

The car developers may choose a number of these OS, depending on the requirements of the display systems. Besides, these operating systems also make it possible to bring plug-and-play and wireless devices into the car. Bluetooth, Wi-Fi, and Ethernet can be connected with the LCDs courtesy of the computer science contributions [33]. The computerized display system also helps link the car to the outside world through the Internet. Connecting the dashboards to the 3G and 4G is possible if the dashboard is compliant [34]. This means that the integration of the Operating System dependent LCDs is not only for the beautiful graphical but also a research and interlinking tool altogether. Every opportunity has got a challenge. Despite the praises hipped on the Human Machine Interface, several challenges such as space and overheating in the dashboards due to the circuit boards of these LCDs are the challenges that continue to face their use [29]. The cars and the software developers have endeavored to develop and harmonize both software and hardware that are complacent, small size, and efficient car dashboard LCDs. This technical problem has derailed the full adoption of all LCDs in the current vehicles.

4. Discussion

All this improvement can be achieved through the following techniques: first and foremost, for this behavioral dashboard interface intelligent to be implemented in automobiles, checking the driving conditions is Key [5]. This can be done by analyzing the driver's behavior, and installing all kinds of sensors should be fully implemented; secondly, choosing and deciding which information should be fed onboard computers based on a designer framework adhering to rules and standards. And finally, the information displayed on the dashboard interface should be a man based on the decision-making results.

From the above analysis, the improved car displays by application of the LCDs have indeed brought a turnaround in the automobile industry. These improvements aim to make the use of modern cars as easy as possible. Besides, the development in information technology has equally boosted the Human-machine Interface Systems like an entire LCD car dashboard [12]. In as much as the technology may face challenges in the application. There are many advantages attached to it in the end. This ranges from accuracy to the safety of the road users and the drivers [11]. The fully LCD dashboard was only typical in the luxurious cars that dominated the global market. It is good news to realize that through research, cheap cars are also embarking on adopting all LCD dashboard systems, which shows a milestone improvement that has taken place since the inception of the LCDs [6]. Some challenges come with every bit of technology. For instance, cars that are computer-dependent are also liable for hacking. Cyber-attacks are currently a menace in every sector like health, finance, transport, and communication. With the advent of this crime, it is pretty challenging to develop dashboards that are computer dependable but free from cyber-attack risks. Taxi companies like UBER face technical and crime problems. Another upcoming challenge that drags behind the implementation of the LCD Car dashboards is the maintenance cost that they come. For a long time in history, the development of LCDs has depended on a better research foundation, which calls for funds for starting and maintaining the automakers that integrate the computer and LCD display in their automobiles.

This Human Machine Interface has also improved and speeded up future designs of the expected cars that will be electric and solar energy-dependent. It is also pivotal to acknowledge the roles played by the computer technicians in integrating all LCDs in the car display system through their scientific knowledge and unwavering spirit of the invention. They have made it possible to coalesce computer science and mechanical science to come up with a human-machine interface [29]. Besides, it is pivotal to note that the core of the LCD dashboard displays has been immensely improved through software development in computer science. The backbone of clear communication between LCDs, the car, and humans lie in the operating system, which is computer software. QNX, WinCE, Android, Linux, and Windows operating systems have made it possible to develop the LCD car dashboards display [34]. These operating systems greatly assist in programmable LCDs.

As the terminal information gate of the IoT era, the LCD devices will also extend to the smart area, which is the intelligent display. On the one hand, the display effect will reach the real world and achieve "zero error output." On the other hand, the display equipment can detective the emotional state of human beings and automatically switch the

information they present in real-time according to their wishes, and then realize "human-machine interaction" [35].

LCD has many advantages and is the main development direction. However, physical interaction is considered the most reliable and efficient [36, 37]. LCD is susceptible to environmental factors, resulting in unstable performance [37]. With the improvement of technology, these problems will eventually be overcome, and the LCD industry will further develop and play an essential role in human-computer interaction.

5. Conclusion

This study shows that the current LCD dashboards are valuable, accurate, precise user friendly, and improved with integrated ICT equipment. This makes them much better than the older traditional systems of the car dashboards. The result indicates the availability of several improved versions of the car dashboards integrated with LCDs. The application of computers to program the LCDs is also catered to in the new design. This has also enabled the connection of the current dashboards with wireless devices and even the Internet. Therefore, the study reveals the evolution and improvements in the modern car dashboard display systems.

This work focuses on the published liquid crystal display technology, studies the development trend of smart device interface improvement, how to apply the still researched and unpublished liquid crystal display technology into smart devices, achieving high human-computer interaction efficiency and accuracy requires other researchers to investigate further. In recent years, the popularity of keywords such as human-vehicle interaction and autonomous driving has continued to increase, and liquid crystal technology, human-computer interaction technology, sensors, and information technology have continued to develop. These all provide research opportunities for researchers. This work is expected to offer broad prospects for future research and help researchers discover potential opportunities for human-vehicle interactions.

Data Availability

The data used to support the findings of this study are available from the corresponding author upon request.

Conflicts of Interest

The authors declare that there are no conflicts of interest.

Acknowledgments

This study was funded by the Natural Science Research Development Fund of Huizhou University (PX-21750).

References

[1] J. Cannon and H. Hu, *Human-machine Interaction (HMI): A Survey*, The University of Essex, Colchester, 2011.

[2] X. Chen and Q. W. Pu, "Electric vehicles LCD instrumentation design based on emWin," *Instrument Technique and Sensor*, vol. 7, pp. 105–108, 2013.

[3] S. Mingyang and Y. Haiyang, "Automobile intelligent dashboard design based on human-computer interaction," *International Journal of Performability Engineering*, vol. 15, no. 2, pp. 571–578, 2019.

[4] C. Edwards, "Car safety with a digital dashboard," *Engineering & Technology*, vol. 9, no. 10, pp. 60–64, 2014.

[5] L. M. Fu, H. Y. Yu, M. Y. Sun, and J. X. Fan, "The automobile intelligent dashboard design to enhance driving safety," *Advanced Materials Research*, vol. 1079, pp. 1010–1013, 2015.

[6] T. R. Fitch and M. L. Oberpriller, *US Patent No. 9*, p. 235, US Patent and Trademark Office, Washington, DC, 2016.

[7] S. K. Prasad, J. Rachna, O. I. Khalaf, and D. N. Le, "Map matching algorithm: real time location tracking for smart security application," *Telecommunications and Radio Engineering*, vol. 79, no. 13, pp. 1189–1203, 2020.

[8] S. Singh, "Audi was pushing more virtual cockpit clusters with Rightware for next-generation A3, A4, Q7, others," *IHS Technology. Retrieved*, 2015.

[9] S. Gibbs, *Audi Builds Hi-Tech 'virtual Cockpit' into the New TT*, The guardian, Kings Place, London, 2014.

[10] G. M. Abdulsahib and O. I. Khalaf, "Comparison and evaluation of cloud processing models in cloud-based networks," *International Journal of Simulation. Systems, Science and Technology*, vol. 19, no. 5, 2019.

[11] K. Wakunami, P. Y. Hsieh, R. Oi et al., "Projection-type see-through holographic three-dimensional display," *Nature Communications*, vol. 7, no. 1, pp. 12954–12957, 2016.

[12] D. Yee and K. S. Perez, *US Patent No. 9*, p. 898, US Patent and Trademark Office, Washington, DC, 2018.

[13] J. Van Derlofske, S. Pankratz, and E. Franey, "New film technologies to address limitations in vehicle display ecosystems," *Journal of the Society for Information Display*, vol. 28, no. 12, pp. 917–925, 2020.

[14] K. Takatoh, M. Ito, S. Saito, and Y. Takagi, "Optical filter with large angular dependence of transmittance using liquid crystal devices," *Crystals*, vol. 11, no. 10, p. 1199, 2021.

[15] J. H. Yoon, E. J. Seo, S. J. Lee et al., "Fast switching and luminance-controlled fringe-field switching liquid crystal device for vehicle display," *Liquid Crystals*, vol. 46, no. 11, pp. 1747–1752, 2019.

[16] L. X.. Hua, B. J. Ping, X.. Bing, and F. H. Yuan, "Improvement research of TFT-LCD module black uniformity," *Chinese Journal of Liquid Crystals and Displays*, vol. 33, no. 4, pp. 271–276, 2018.

[17] P. J. Wang, F. He, G. P. He, C. Chen, X. Guan, and X. Zhang, "Design and implementation of programmable power display system based on STM32F7," *Chinese Journal of Liquid Crystals and Displays*, vol. 36, no. 7, pp. 973–982, 2021.

[18] B. M. Lim, Y. H. Ko, Y. S. Jang, O. H. Kwon, S. K. Han, and S. G. Lee, "A 200-V 98.16%-efficiency buck LED driver using integrated current control to improve current accuracy for large-scale single-string LED backlighting applications," *IEEE Transactions on Power Electronics*, vol. 31, no. 9, pp. 6416–6427, 2016.

[19] A. D. Salman, O. I. Khalaf, and G. M. Abdulsaheb, "An adaptive intelligent alarm system for wireless sensor network," *Indonesian Journal of Electrical Engineering and Computer Science*, vol. 15, no. 1, p. 142, 2019.

[20] F. Railroad Administration, *Information in Cab Displays for High-Speed Locomotives" (PDF)*, US Department of Transportation, Washington, 2005.

[21] Hellwig, *Honda Civic: Unique Gauge Cluster Works Well*, Edmunds, Santa Monica, California, 2017.
[22] L. Shankun, D. Liqian, Z. Qun, and G. Pengcheng, "Design and implementation of vehicle virtual instrument panel and fault diagnosis system," *Computer Applications and Software*, no. 8, p. 52, 2016.
[23] L. Keqiang, "Review of status and prospects of automotive intelligent safety electronics," *Chinese Journal of Automotive Engineering*, vol. 1, no. 1, pp. 5–17, 2011.
[24] G. Q. Zhu, L. Y. Sun, L. H. Sun, and K. Cui, "The analysis of speed instrument danger prompt effect's influence factors," *Industrial Engineering & Management*, vol. 16, no. 4, pp. 129–132, 2011.
[25] T. R. Pryor, *US Patent No. 7,084*, p. 859, US Patent and Trademark Office, Washington, DC, 2006.
[26] *Generation Toyota Prius - 2010 Pictures and Photo Gallery*, , pp. 12–08, Toyota.com, 2009.
[27] F. Bellotti, A. De Gloria, A. Poggi, S. Andreone, P. Damiani, and P. Knoll, "Designing configurable automotive dashboards on liquid crystal displays," *Cognition, Technology & Work*, vol. 6, no. 4, pp. 247–265, 2004.
[28] D. U. A. N. Hong Jie, "The development of a vehicle LCD dashboard based on serial bus," *Microcomputer Information*, vol. 25, pp. 5–1, 2009.
[29] A. Amditis, L. Andreone, K. Pagle et al., "Towards the automotive HMI of the future: overview of the AIDE-integrated project results," *IEEE Transactions on Intelligent Transportation Systems*, vol. 11, no. 3, pp. 567–578, 2010.
[30] G. Takeda and H. Cheng, *US Patent No. 8,913,009*, US Patent and Trademark Office, Washington, DC, 2014.
[31] T. Matsumoto, Y. Nakagawa, K. Matsuhiro, Y. Souda, H. Araki, and K. Ohara, *Improved VHC (Very High Contrast) LCD for Automotive Dashboard Displays*, SAE Technical Paper Series, 1990.
[32] F. Bellotti, A. De Gloria, M. Risso, and A. Villamaina, "AutoGraL: a Java 2D graphics library for configurable automotive dashboards," *Computers & Graphics*, vol. 25, no. 2, pp. 259–268, 2001.
[33] S. M. Choi and J. Van Ee, *US Patent No. 6*, p. 211, US Patent and Trademark Office, Washington, DC, 2001.
[34] S. Y. N. Zhen-zhong, *The Development of Graphical Automotive Instrument Based on the QNX Operating System*, Harbin Institute of Technology, Nangang, Harbin, 2012.
[35] L. Sha, W.. Dan, Y. Z Kun et al., "Key technology trends analysis of TFT-LCD," *Chinese Journal of Liquid Crystals and Displays*, vol. 33, no. 6, pp. 457–463, 2018.
[36] T. Hao, Z. Jianghong, and W. Wei, "Research on human-computer interaction interface design for automobiles," *Journal of automotive engineering*, vol. 2, no. 5, pp. 315–321, 2012.
[37] L. Jianan and A. Abas, "Development of human-computer interactive interface for intelligent automotive," *International Journal of Artificial Intelligence*, vol. 7, no. 2, pp. 13–21, 2020.

Hindawi
Scientific Programming
Volume 2022, Article ID 8995448, 15 pages
https://doi.org/10.1155/2022/8995448

Research Article

Analysis of the Low-Carbon, Environmental-Friendly, Energy-Saving, and Emission-Reduction Evaluation Model of Urban Rail Transit Based on the Spatiotemporal Distribution of Passenger Flow

Hong Zhang [1,2]

[1]*School of Transportation and Logistics, Southwest Jiaotong University, Chengdu 611756, China*
[2]*The Second Research Institute of Civil Aviation Administration of China, Chengdu 610041, China*

Correspondence should be addressed to Hong Zhang; caaczh@my.swjtu.edu.cn

Received 19 July 2022; Revised 13 August 2022; Accepted 20 August 2022; Published 13 September 2022

Academic Editor: Lianhui Li

The development of the urban economy and the effect of linkage radiation are inseparable from the urban transportation system's efficient operation. In the context of the new era, environmental pollution caused by economic development has gradually become an invisible killer that endangers human health and the atmospheric environment. It is a pillar industry of economic development, a key part of urban infrastructure construction, and a necessary guarantee for urban residents to travel and live, and it is important to develop a low-carbon, environmental-friendly, energy-saving, and emission-reduction potential for urban transportation systems. On the basis of a large number of literature research, this paper attempts to establish the role of an urban rail transit system in energy conservation and emission reduction in three aspects: residents' travel behavior, ground transportation operation, and low carbon, energy conservation, and reduced emission under the influence of the urban rail transit system. Based on the temporal and spatial distribution characteristics of urban rail transit passenger flow, a relatively complete energy-saving and emission-reduction evaluation model is established. Through case analysis, it is verified that the model can effectively evaluate the effect of energy saving and emission reduction under different rail transit settings and its spatial and temporal distribution characteristics, and provides ideas and technical guidance for multidimensional quantitative analysis of urban rail transit carbon environmental protection, energy conservation, and emission reduction.

1. Introduction

The rapid development of urban economy and scale has brought earth-shaking changes to people's lives. However, at the same time, this leap-forward development process that exceeds the speed of perfecting urban supporting facilities also makes people pay a corresponding price. Environmental pollution and energy consumption are increasingly threatening the living environment of human beings and the realization of sustainable urban development goals. "Energy saving and emission reduction" has become a huge challenge faced by all fields worldwide. As the pillar industry of urban economic development, the urban transportation system is a key part of urban infrastructure construction, and a necessary guarantee for urban residents to travel and live, energy conservation and emission reduction for the urban transportation system is imperative.

As one of the most important public travel tools in the modern urban transportation system, urban rail transit is a breakthrough to achieve energy conservation, reduced emission, and sustainable development. Compared with the traditional ground transportation mode, urban rail transit, as a large-capacity passenger vehicle driven by electric energy, has developed rapidly in major cities around the world in recent years due to its advantages of low pollution and low energy consumption. Considering the problems faced by the sustainable development of the urban transportation system, it is the key to carry out the energy-saving and emission-

reduction strategy of the urban transportation system. Since the passenger flow of urban rail transit is complex and has significant spatial and temporal distribution characteristics, its energy-saving and emission-reduction effects will have corresponding spatial and temporal differences due to the size of the passenger flow. The mechanism of action has not been fully considered and explored, and there are certain limitations in the application of the model.

Therefore, this paper will make up for the insufficiency of the traditional evaluation model in the analysis of the action mechanism, analyze its energy-saving and emission-reduction action mechanism through the multidimensional influence of the urban rail transit system, build a more reasonable quantitative evaluation method for the energy-saving and emission-reduction effect, and provide technical support and theoretical basis for the implementation of emission-reduction strategies.

2. Related Work

With the continuous deterioration of urban rail transit pollution around the world, researchers in the field of environmental engineering aim to establish regional emission inventories, which are represented by MOBILE [1], COPERT [2], and HBEFA [3]. The research shows [4] that this will lead to the emission measurement results being about 30% higher than the actual emission level, but the construction idea of the MOBILE model has reference significance for the development of the emission model. At this stage, similar modeling ideas are adopted in the widely used urban rail transit energy conservation and emission-reduction evaluation models, that is, by establishing urban transit system scenarios with or without rail, comparing rail transit and rail transit alternative modes of transportation and the emission difference between the two, and then drawing the conclusion of rail transit energy saving and emission reduction. Sostenibile et al. [5] believe that the essential reason for urban rail energy saving and emission reduction is to effectively reduce the per capita emission intensity to achieve the purpose of energy saving and emission reduction. Hodges et al. [6] compared the per capita CO_2 emission factors of different transportation vehicles and found that there is a certain multiple relationship between different transportation vehicles and unit emission factors. Obviously, only the per capita emission intensity of different transportation modes cannot reflect the impact of the complexity of transportation on its emission results. Therefore, Wang et al. [7] established a city-level comprehensive transportation emission model, combined with urban rail transit passenger flow data and average haul distance data to compare the differences in emissions of different modes of transport with macro emissions. The problem with the above model is that its focus is on the emission of urban rail transit, and it cannot truly quantitatively evaluate the emission reduction of urban rail transit.

Therefore, analyzing the quantitative substitution relationship between urban rail transit and other modes of transportation is a solution to break through this bottleneck. The model estimation method of the emission impact after returning the passenger flow to the original travel mode is simple and easy to implement [8, 9], but it is unreasonable to summarize the emission factors under all conditions only with a single comprehensive emission factor value. Based on Chen et al. [10], the above model is optimized, and the model solves the shortcomings of the original model to a certain extent. In recent years, with the increase in the proportion of environmental indicators in urban transportation planning schemes, the research on the evaluation model of urban rail transit energy conservation and emission reduction has also introduced a traffic demand forecast model, which provides a basis for the construction of urban rail transit energy conservation and emission-reduction models and new ideas [11, 12].

The study found that most scholars have discussed and analyzed the evaluation model of urban rail transit energy conservation and emission reduction, and established effective research models from different perspectives; however, there is a lack of full consideration and exploration of the mechanism of urban rail transit energy conservation and emission reduction; there are certain limitations in considering the model application scenarios. The passenger flow of urban rail transit is complex and has significant spatial and temporal distribution characteristics. Therefore, it should be noted that there are corresponding spatial and temporal differences in its energy-saving and emission-reduction effects. Regarding this point, no scholars have yet found a multidimensional analysis of the energy-saving and emission-reduction mechanism of urban rail transit systems to form a more comprehensive and reasonable quantitative evaluation method for energy-saving and emission-reduction effects.

3. Related Theories

3.1. Multidimensional Influence Relationship between Urban Rail Transit and Urban Transportation System. The research goal of this paper was to quantitatively evaluate and explore the energy-saving and emission-reduction effects of urban rail transit on the urban transportation system to which it belongs. Therefore, the impact of the construction and operation of urban rail transit on the urban transportation system is the entry point for the analysis of its energy-saving and emission-reduction mechanism. Based on the research of the previous part, the urban transportation system is a complex system composed of people, vehicles, and roads, and the impact of urban rail transit on the system is shown in Figure 1, including the travel behavior of travelers, the transfer of transportation modes, and ground transportation running changes.

3.2. Characteristics of Urban Rail Transit Passenger Flow Transfer. In the process of the subway network gradually, the attraction degree of urban rail transit to passenger flow is mainly related to the nature of land use along the line and the service level of replacing buses. With the increase in development intensity, residential area density, and population density along the line, the passenger flow will increase, which

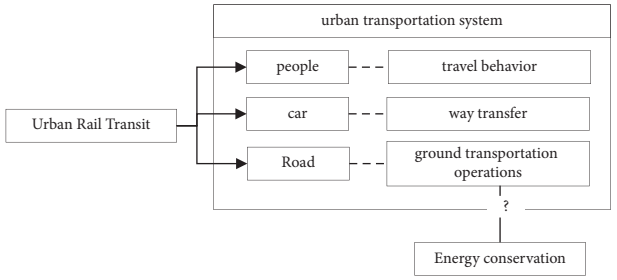

Figure 1: Multidimensional influence of urban rail transit on the urban transportation system.

will also promote the growth of the passenger flow in the original section.

The passenger flow of urban rail transit generally includes three parts: trend passenger flow, transfer passenger flow, and induced passenger flow [13].

3.2.1. Trend Passenger Flow. Trend passenger flow refers to the normal growth of the passenger flow at rail stations and along the line.

3.2.2. Transfer Passenger Flow. Diverted passenger flow refers to the passenger flow that is attracted and transferred to urban rail transit by other modes of transportation, and this part of the passenger flow is usually caused by competition between modes of transportation. A small part of the diverted passenger flow comes from private cars and taxis, while most of them come from regular bus and bicycle trips.

3.2.3. Induced Passenger Flow. Induced passenger flow means that with the rapid construction and operation of urban rail transit lines, land development and population agglomeration along the lines are promoted, the accessibility between different areas of the city is improved, the city's subway service level is improved, and residents' travel intensity is increased, thereby increasing traffic.

3.3. Influencing Factors of Emission Measurement in the Urban Rail Transit Emission Model. This paper will refer to Xie et al. [14] to establish the link between ground transportation operation data and emission measurement results to analyze the mechanism of energy conservation and emission reduction. The established urban road traffic emission model shows that the calculation of ground traffic emissions is shown in formulas (1) and (2):

$$E_{\text{mission}_{i,j}} = EF_{i,v} \times VKT_{i,j}, \tag{1}$$

$$E_{\text{mission}_{\text{net}}} = \sum_{i} \sum_{j} E_{\text{mission}_{i,j}}, \tag{2}$$

$E_{\text{mission}_{i,j}}$ represents emissions of vehicle i on road segment j (g); $E_{\text{mission}_{\text{net}}}$ represents total emissions from the road network (g); $EF_{i,v}$ represents the emission factor for model i at speed v (g/km); $VKT_{i,j}$ represents the vehicle mileage of vehicle type i on road j (pcu·km); i, j, v represent the model, road segment, and speed, respectively.

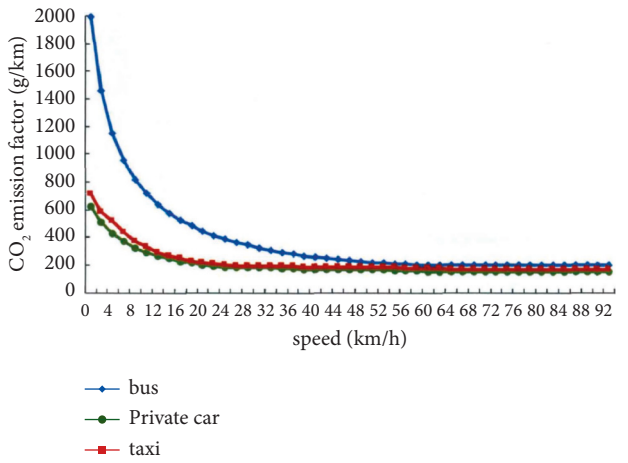

Figure 2: CO_2 emission factor variation curve of different vehicle models with speed.

According to the calculation formula of the transportation emission model shown above, it can be found that the emission factor and VKT are two important components of the road network emission measurement, and they are also the factors that directly affect the emission measurement results.

3.3.1. Relationship between Emission Factor and Speed Change. The emission factor is defined as the amount of emissions produced by a motor vehicle per unit mileage, which is composed of the distribution of vehicle driving conditions and the emission rate as shown in the following formula:

$$EF_{i,v} = \frac{\sum VSP\ Dsitribution \times ER_i}{\overline{v}}, \tag{3}$$

where VSPDsitribution represents the vehicle driving condition distribution based on VSP characterization; ER_i represents the emission rate of model i (g/s); $\overline{v}$ is the average speed (km/m).

From the calculation formula of the emission factor, it can be found that different vehicle types have different emission factor values at different average driving speeds. Therefore, the emission factor is characterized by a distribution curve that changes with speed as shown in Figure 2. The emission factor gradually decreases with the increase in speed, and the emission factor value in the low-speed range is much larger than that in the high-speed range; from the perspective of the relationship between the emission factor and the vehicle model, the emission factor curves of different models have obvious differences with the speed. The low-speed interval is more significant. At the same speed, the emission factor of buses is the largest, followed by social vehicles, and the emission factor of taxis is the smallest.

3.3.2. The Relationship between VKT and Road Flow Calculation. VKT (vehicle kilometer traveled) is the number of kilometers traveled by motor vehicles, which reflects the

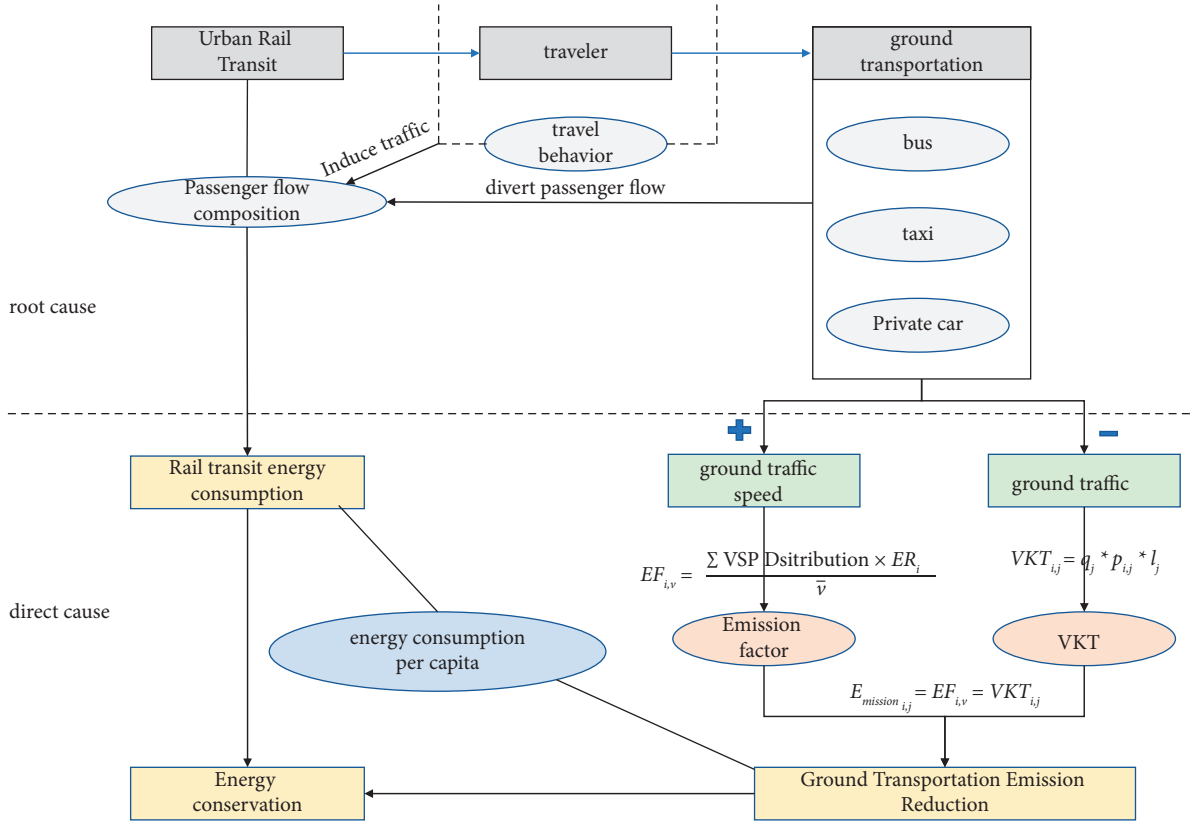

Figure 3: Analysis of the mechanism of low-carbon, environmental-friendly, energy-saving, and emission-reduction action of urban rail transit.

traffic activity level of motor vehicles. It is multiplied by the emission factor to obtain the total emission and emission inventory. It is a key parameter for the coupling of the traffic model and the emission model. The calculation method is shown in the following formula:

$$VKT_{i,j} = q_j * p_{i,j} * l_j, \tag{4}$$

where $VKT_{i,j}$ represents the vehicle mileage of vehicle type i on road j (pcu·km) q_j represents the traffic flow on road segment j (pcu); $p_{i,j}$ represents the proportion of traffic of vehicle i on road j to the total traffic; l_j is the length of road segment j (km).

It can be found that VKT is composed of three parts: road traffic volume, road length, and vehicle model ratio. Therefore, there is a linear positive correlation calculation relationship between VKT and road flow; that is, when the ratio of road and vehicle models is determined, the greater the flow of the road is, the greater the calculation result of VKT is, and the greater the final discharge result of the road is.

3.4. Mechanism and Distribution Characteristics of Low Carbon, Environmental Protection, Energy Saving, and Emission Reduction in Urban Rail Transit

3.4.1. Mechanism of Action. This study summarizes the mechanism of energy saving and emission reduction of urban rail transit based on the corresponding literature [14–22], as shown in Figure 3. It can be found that the mechanism of energy saving and emission reduction of urban rail transit is relatively complex, which is the result of comprehensively considering the multidimensional impact of urban rail transit on the urban transportation system.

The direct reason for energy saving and emission reduction of urban rail transit lies in its impact on the "road" dimension of the urban transportation system. The opening and operation of urban rail transit lines share the traffic pressure in the area where the line radiates, and part of the ground transportation travel demand is transferred to urban rail transit. The traffic flow on the ground is reduced, and the traffic operation in the surrounding area of the line is improved.

The fundamental reason for urban rail transit energy conservation and emission reduction lies in its impact on the two dimensions of "people" and "vehicles" in the urban transportation system. Urban rail transit lines affect the travel behavior of travelers on the line, and on the one hand, some people originally travel on different grounds. Passengers who have completed their trips by means of transportation are transferred to the subway, and on the other hand, it has induced some travelers to generate new travel needs. It can be found that the impact of urban rail transit on the two dimensions of "people" and "vehicles" is also the reason for the formation of urban rail transit passenger flow.

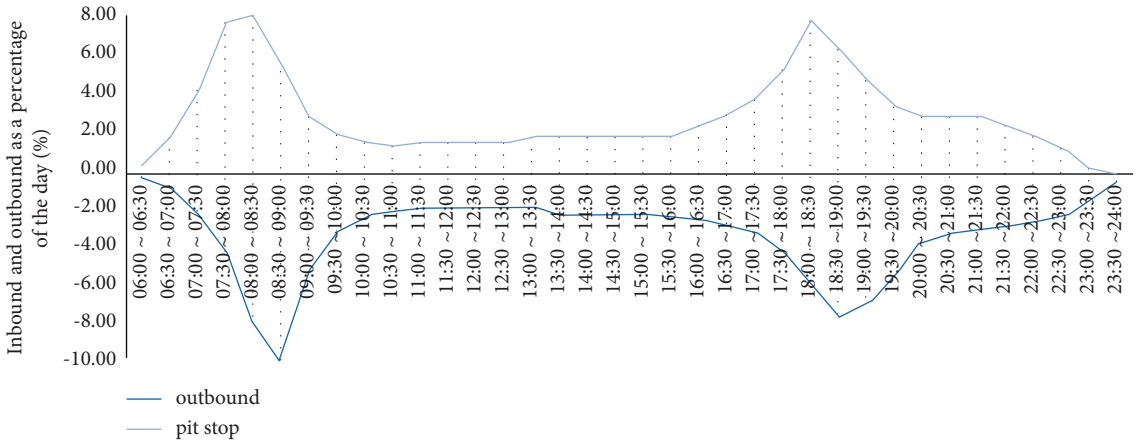

Figure 4: Time distribution of passenger flow in and out of rail transit stations.

3.4.2. Spatial and Temporal Distribution Characteristics of Passenger Flow. Using the urban rail transit AFC (automatic fare collection system), that is, the automatic fare collection system swiping data to analyze the spatiotemporal distribution characteristics of urban rail transit passenger flow, it has the following characteristics.

(1) Imbalance. In the lines or stations of the urban rail transit system, there is a specific phenomenon of the mismatch between the supply of transport capacity and the demand for passenger flow in time, space, and direction. With the formation of the rail transit network, the share of rail transit in urban public transport has gradually increased. The main purpose of travel for passengers is commuting. People who work and go to school take the subway at a fixed time every day. Therefore, in terms of the rail transit network, within one day, the fluctuating state of the passenger flow of the railway shows the unbalanced characteristics of two peaks in the morning and evening, and the time distribution of rail transit passenger flow in and out of the station is shown in Figure 4.

(2) Travel periodicity. In the urban rail transit system, the passenger flow presents a periodic change in a fixed period of time. Since the commuter passenger flow accounts for a large proportion of the daily passenger flow, and its work cycle is carried out in a weekly cycle, the rail transit passenger flow generally presents a cyclical change in the weekly time unit throughout the year. The daily passenger flow curve of rail transit is shown in Figure 5.

(3) Travel tidal nature. In the lines or stations of the urban rail transit system, there are a large passenger flow in one direction and a less passenger flow in the opposite direction at a certain period of time, but the phenomenon of the opposite passenger flow characteristics occurs in another period of time. With the continuous expansion of the city scale, the rail transit system has become an important mode of transportation connecting the central city and surrounding suburbs. Passengers will have different travel modes due to different travel purposes such as work, school, shopping, and business, and rail transit travel presents significant tidal characteristics. During the morning peak period on weekdays, the passenger flow is reflected in the commuting passenger flow generated by passengers going to work and school, and passengers flow from the place of residence to the place of work. In the evening rush hour on weekdays, the passenger flow is reflected in the commuter passenger flow generated by the passengers getting off work and school. The basic flow direction of the passenger flow is opposite to that of the morning rush hour. Passengers flow from the office to the residence. During weekends, there is no obvious morning and evening peak period, and a large number of passengers travel between residential areas, shopping areas, and tourist areas due to travel purposes such as shopping and tourism. In lines with obvious tidal phenomena, the passenger flow of rail transit is unevenly distributed in time and space, which is very likely to cause tension in the capacity of some lines.

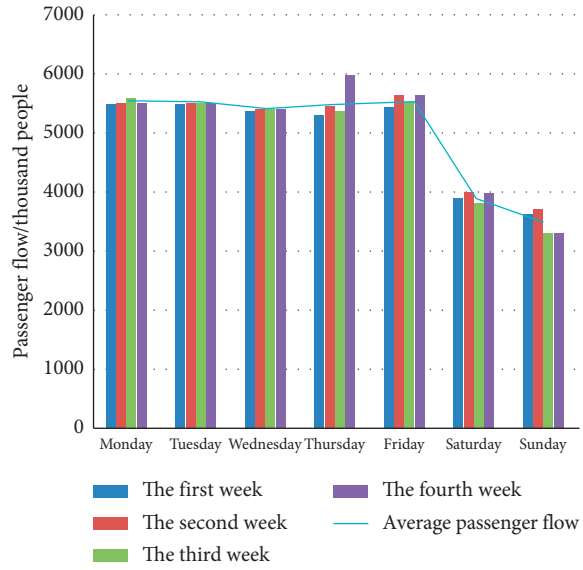

Figure 5: Curve of daily passenger flow of rail transit.

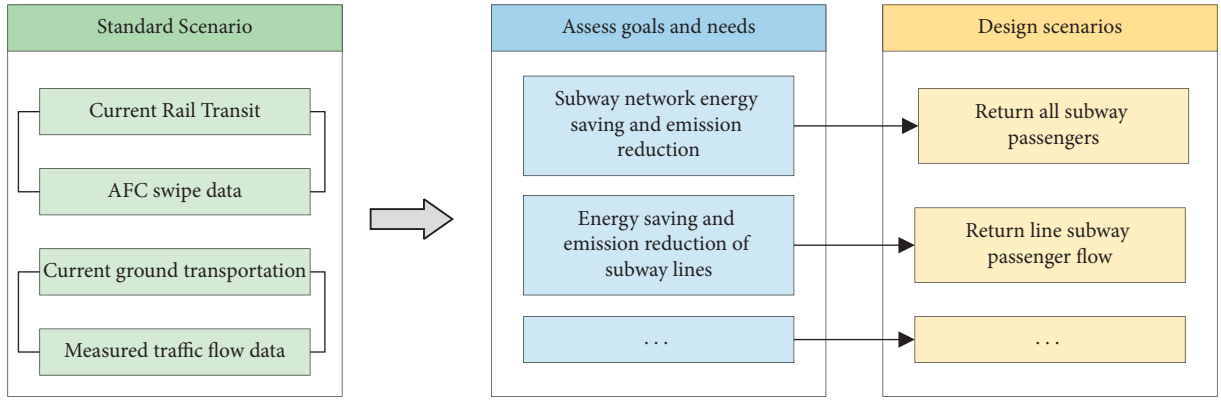

Figure 6: Scenario design flow idea based on low-carbon, environmental protection, energy conservation, and emission-reduction assessment targets.

4. Construction of the Low-Carbon, Environmental-Friendly, Energy-Saving, and Emission-Reduction Evaluation Model for Urban Rail Transit

4.1. Model Building Ideas

4.1.1. Model Assumptions and Scenario Design. From the previous research and analysis, it can be seen that the direct reason for energy conservation and emission reduction of urban rail transit is that the construction and operation of the urban rail transit network shares the passenger flow of ground transportation, improves the operation of ground transportation, and then achieves the effect of energy conservation and emission reduction of urban transportation system. Based on this, this paper makes a reasonable inversion and assumes that when there is no rail transit in the urban transportation system, passengers who originally traveled by subway will return to ground transportation to complete their travel needs. At the same time, considering the complexity and diversity of urban rail energy conservation and emission-reduction assessment targets and needs, this paper takes the current urban rail transit setup as the standard scenario, and forms corresponding design scenarios according to different assessment targets and needs, as shown in Figure 6. Then, this paper analyzes the ground transportation operation under the influence of the standard scenario and the design scenario, respectively, and measures the ground transportation emission difference under the different scenarios, that is, the ground transportation emission reduction under the design scenario and the urban rail transit energy saving and emission reduction of the design scenario. The evaluation of the scenario design helps in comparative analysis and improves the applicability of the model.

Figure 6 shows the scenario design idea of urban rail transit. It can be found that the energy-saving and emission-reduction evaluation model constructed in this paper is suitable for various evaluation objectives, including the evaluation of the energy-saving and emission-reduction effect of the existing subway operation network in the city and energy conservation and emission-reduction assessment. It should be noted that in order to ensure the use of the traffic demand forecast model to analyze the ground traffic operation under its influence in the design scenario, the current urban traffic situation is considered, so the standard scenario in this paper is based on the current urban rail transit and ground traffic as a reference. Therefore, the ground traffic operation situation under the standard scenario is calculated through the measured traffic flow data, and only the design scenario is predicted using the traffic demand forecasting model established in the literature [23] that considers the impact of urban rail transit.

4.1.2. Low-Carbon, Environmental-Friendly, Energy-Saving, and Emission-Reduction Model Framework for Urban Rail Transit. As shown in Figure 7, the urban rail transit energy conservation and emission-reduction evaluation model consists of two parts, namely, ground transportation emission reduction and urban rail transit operation energy consumption. The calculation method is shown in the following formula:

$$E_{\text{save}} = \triangle E_{\text{road}} - \triangle E_{\text{rail}} = \left(E_{B,\text{road}} - E_{A,\text{road}}\right) - \left(E_{A,\text{rail}} - E_{B,\text{rail}}\right), \tag{5}$$

where E_{save} represents the energy saving and emission reduction of urban rail transit in urban transportation system (g); $\triangle E_{\text{road}}$ represents the urban rail transit affecting the energy saving and emission reduction of the ground transportation system (g); $\triangle E_{\text{rail}}$ represents the emission reductions added by urban rail transit to urban transportation systems (g); $E_{A,\text{road}}$ and $E_{B,\text{road}}$ represent surface transportation emissions for standard and design scenarios (g), respectively; $E_{A,\text{rail}}$ and $E_{B,\text{rail}}$ represent rail transit emissions for standard and design scenarios (g), respectively.

Since the emissions generated by the operation of urban rail transit are mainly due to the carbon emissions generated by the consumption of electric energy, the existing research on energy conservation and emission reduction of urban rail transit often only uses carbon emission reduction as the only energy conservation and emission-reduction evaluation index. However, this study believes that the traffic pollution situation including NOx, PM, and other pollutants has become more and more serious in recent years [24]. Based on this, the pollutants and emission indicators evaluated in

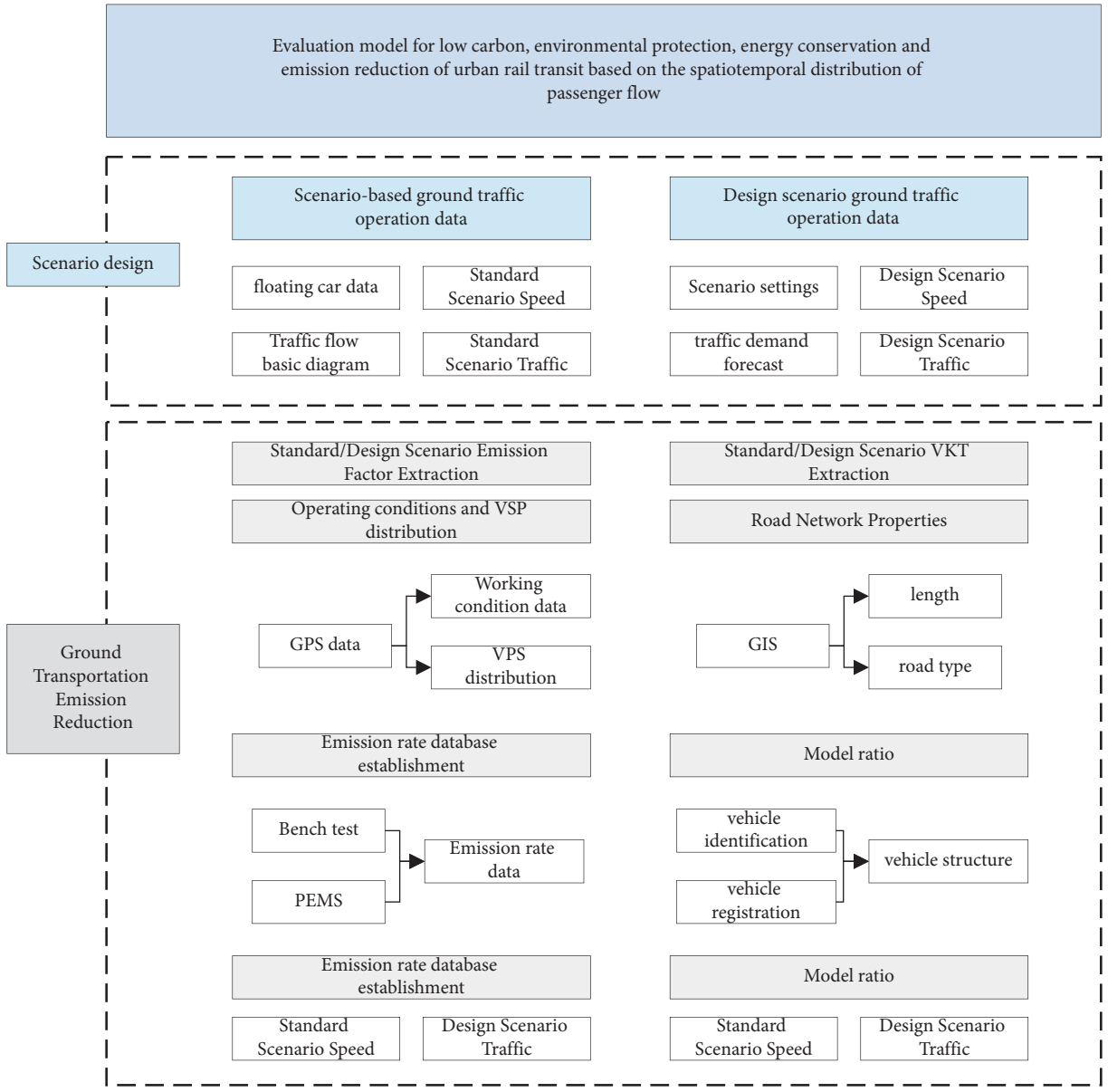

Figure 7: Architecture of the low-carbon, environmental-friendly, energy-saving, and emission-reduction model of urban rail transit.

Table 1: Evaluation indicators for energy conservation and emission reduction.

	Transportation	Emissions	Energy-saving emission indicators
Urban transport system	Rail	CO_2	Indicator 1
		CO_2	
	The traffic	NOx	Indicator 2
		CO	Indicator 3
		HC	Indicator 4
		PM	Indicator 5

this paper for energy conservation and emission reduction are shown in Table 1.

4.2. Calculation of Ground Transportation Emission Reduction under the Influence of Urban Rail Transit. The measurement of ground transportation emission reduction under the influence of urban rail transit is one of the important components of the urban rail transit energy conservation and emission-reduction evaluation model constructed in this paper, and it is also an indicator that reflects the mechanism of urban rail transit energy conservation and emission reduction. Combining the model technical route in Subsection 4.1 and the calculation formula of the

transportation emission model in 3.3, the calculation method of ground transportation emission reduction is shown in formulas (6) and (7):

$$\triangle E_{road} = \sum_{i,v}^{j} EF_{i,v} * VKT_{i,j} = \sum_{i,v}^{j} EF_{i,v} * \left(l_j * q_j * p_{i,j}\right), \quad (6)$$

$$\triangle E_{road} = \sum_{i,v}^{j} EF_{i,v^A} * \left(l_j * q_j^A * p_{i,j}^A\right) = \sum_{i,v}^{j} EF_{i,v^B} * \left(l_j * q_j^B * p_{i,j}^B\right), \quad (7)$$

where $EF_{i,v}$ represents the emission factor for model i at speed v (g/km); $VKT_{i,j}$ is the number of kilometers traveled by vehicle i on road j (km); v^A and v^B represent the ground traffic operating speeds for standard and design scenarios, respectively (km/h); q_j^A and q_j^B are the traffic routes of section j in the standard scenario and the design scenario, respectively (pcu); $p_{i,j}^A$ and $p_{i,j}^B$—are the proportion of vehicle i on road j in the standard scenario and the design scenario, respectively.

According to the above formula, it can be found that the measurement of ground transportation emission reduction under the influence of urban rail transit is mainly composed of emission factor and VKT. The emission factor is mainly affected by the change in ground transportation operating speed under different scenarios, while VKT is mainly affected by the impact of changes in ground traffic flow and vehicle model proportions under different scenarios.

4.2.1. Calculation of Emission Factors under Different Scenarios. According to the introduction of the establishment process of emission factor database and the acquisition method of ground transportation speed data under different scenarios, establishing the relationship between emission factors and speed requires the coupling of traffic operation data and traffic emission data. Therefore, the emission factor database established in this paper is composed of vehicle driving condition distribution data based on specific power and measured vehicle emission rate data.

This section uses the MOVES model developed by the US Environmental Protection Agency (EPA) to establish the vehicle specific power (VSP) parameter to describe and analyze the distribution of vehicle driving conditions. VSP is defined as the output power per ton of mass (including self-weight) moved by the motor vehicle engine [25], and the calculation method is shown in the following formula:

$$VSP = \frac{Av + Bv^2 + Cv^3 + mva}{f}, \quad (8)$$

where v and a are the instantaneous speed and instantaneous acceleration of the motor vehicle, respectively, in m/s and m/s^2; M is the vehicle quality (t); A, B, C, and f are model constant coefficients, only relevant to the vehicle type.

The emission rate is the amount of vehicle emissions per unit time, in g/s. The collection of emission rate data is completed by the bench test based on NEDC (New European Driving Cycle), and the test data cover CO_2, CO, HC, NOx, and PM of various models. Through VSP clustering and interval division, the average emission rate (g/s) of each pollutant and pollutant in each VSP interval can be obtained, that is, the mass of pollutants emitted by the motor vehicle per unit time of driving under specific operating conditions, as shown in Figure 8.

The actual driving speed on the road is an important factor affecting the emission of motor vehicles, which is often ignored in traditional emission models. Therefore, in order to accurately quantify the impact of speed on the emission factor, it is necessary to calculate the emission factor of motor vehicles based on the average speed and to establish speed correction models for emission factors of different vehicle types and fuel types. The calculation method of the emission factor in the usual emission model is shown in the following formula:

$$EF_V = \frac{3600 * \sum VSP\text{Distribution}_i * ER_i}{v}, \quad (9)$$

where EF_V represents the emission factor at average velocity $v(g/\text{km})$; ER_i represents the average emission rate for VSP interval i (g/s); $VSP\text{Distribution}_i$ represents the distribution ratio of VSP interval i.

To sum up, this paper established an emission factor database covering 36 vehicle types and 3 road classes, including CO, CO_2, HC, and NOx emissions. Emission factors for some speed ranges are shown as examples in Table 2.

4.2.2. VKT Calculation in Different Scenarios. The ground traffic flow under the influence of different scenarios is a key step to measure the emission reduction of ground transportation, and it is also the main factor affecting VKT. The ground traffic operation under the influence of the design scenario is based on the analysis of the traffic demand forecasting model established by the literature considering the impact of urban rail transit after the inversion of the subway passenger flow, while the standard scenario is based on the analysis of the current ground traffic operation. In this paper, with the help of the existing research results of the basic traffic flow diagram [26], the relationship between the three elements of the traffic flow of the road segment can be established based on the Van Aerde model, as shown in equations (10)–(12).

$$v = v_f e^{-\rho/\rho_m}, \quad (10)$$

$$q = \rho v_f e^{-\rho/\rho_m}, \quad (11)$$

$$q = -\rho_m v ln \frac{v}{v_f}, \quad (12)$$

where q represents the hourly traffic on a single lane (veh/h); v is the average speed of the road (km/h); ρ is the average density of road sections (veh/km); v_f is the free-flow velocity of the road type to which the segment belongs (km/h); ρ_m is the road segment critical density (veh/km).

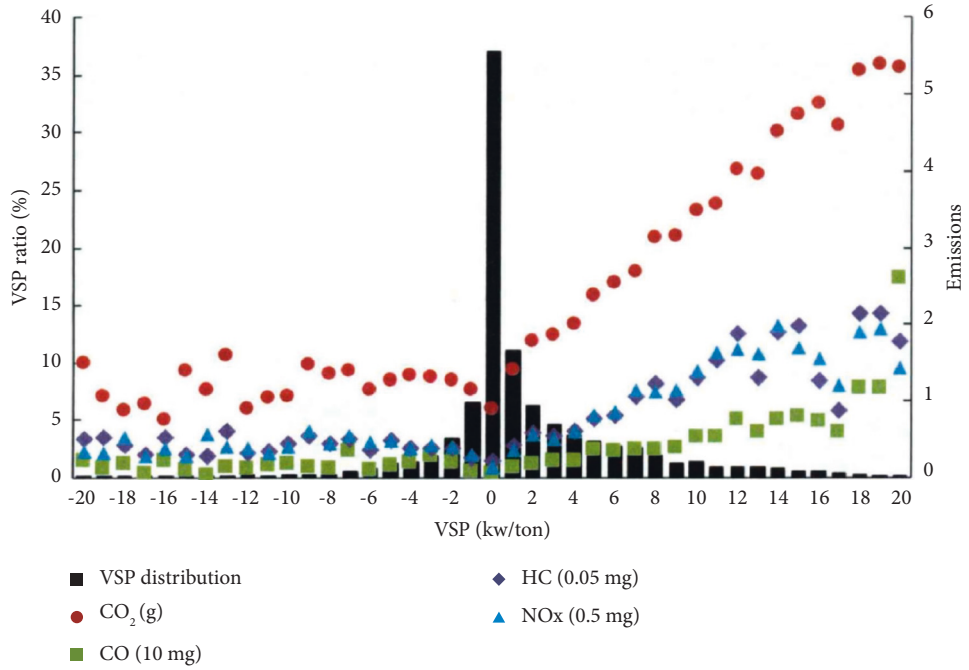

Figure 8: Distribution of emission rates in different VSP intervals.

Table 2: Sample of emission factor database.

Road type	Speed range	CO	CO_2	THC	NO_x
11	0	42.39	5631.03	9.86	46.98
11	1	24.37	3399.37	5.53	26.83
11	2	17.59	2526.35	3.94	19.39
11	3	13.61	1966.97	3.03	14.95
11	4	11.53	1698.62	2.55	12.66
11	5	9.87	1459.58	2.17	10.81
11	6	8.8	1324.12	1.93	9.67
11	7	7.87	1188.26	1.72	8.63
11	8	7.16	1089.2	1.56	7.86
11	9	6.49	992.84	1.41	7.13
11	10	6.01	930.91	1.3	6.64

Note. Road type 11 represents the roads on the left and right sides for vehicles, with six roads on each side including motor vehicle lanes and nonmotor vehicle lanes.

According to the relationship between flow and speed established by the traffic flow basic map, this paper combines the measured floating car data in City A with the traffic flow basic map formula to carry out data regression analysis, and at the same time can calculate the speed-flow inversion method that conforms to City A, as shown in the following formula:

$$q = -\frac{v}{\delta_i} \ln \frac{v}{v_{f_i}}, i = 1, 2, 3, \tag{13}$$

where δ_i and v_{f_i} are model constant parameters; $i = 1, 2, 3$ represent expressway, main road, and sub-branch, respectively.

Due to the large differences in the emissions of the same model, after obtaining the traffic volume and length of a road section, it is necessary to analyze the model structure of the traffic volume of the road section, and then combine it with the corresponding emission factor to calculate the emission. In the actual operation process of road traffic, the proportion of models changes in real time, but it is difficult to obtain the proportion of dynamic models. In this paper, the proportion of models in the standard scenario of fixed model ratio is used for calibration, and the proportion of models in the standard scenario is corrected to obtain the models in the design scenario.

Proportion. The proportion of vehicle models in the standard scenario in this paper is obtained by combining the video recognition data of the license plate and the vehicle management registration data. When a motor vehicle passes through a road section with a camera installed, the license plate number will be recorded. At the same time, by querying the vehicle management registration information, the vehicle model corresponding to the license plate number can be determined to obtain the model proportion data. The proportion data of some models is shown in Table 3.

5. Evaluation and Analysis of Low Carbon, Environmental Protection, Energy Saving, and Emission Reduction in Rail Transit

5.1. Rail Transit Carbon Emission Calculation. The urban rail transit energy conservation and emission-reduction evaluation model constructed in this study considers the energy consumed by rail transit in the operation process. This section takes the track lines covered by City A as the research scope. As shown in Figure 9, based on the AFC credit card data, the average transportation distance and passenger flow of different track lines are counted, and the carbon emission coefficient per person-kilometer of different track lines is combined to calculate the area of rail transit carbon

Table 3: Sample table of model proportion data.

Expressway, main road, and sub-branch		Highway (%)	Main road (%)	Secondary branch (%)
Bus	Class A	2.0	2.0	2.0
	Class B	1.0	1.0	1.0
	Class C	0.0	0.0	0.0
Social vehicle	Class A	0.3	0.3	0.4
	Class B	1.8	1.7	1.9
	Class C	7.5	7.4	8.3
	Class D	10.0	9.8	10.9
	Class E	41.2	40.6	45.1
	Class F	3.3	3.3	3.7

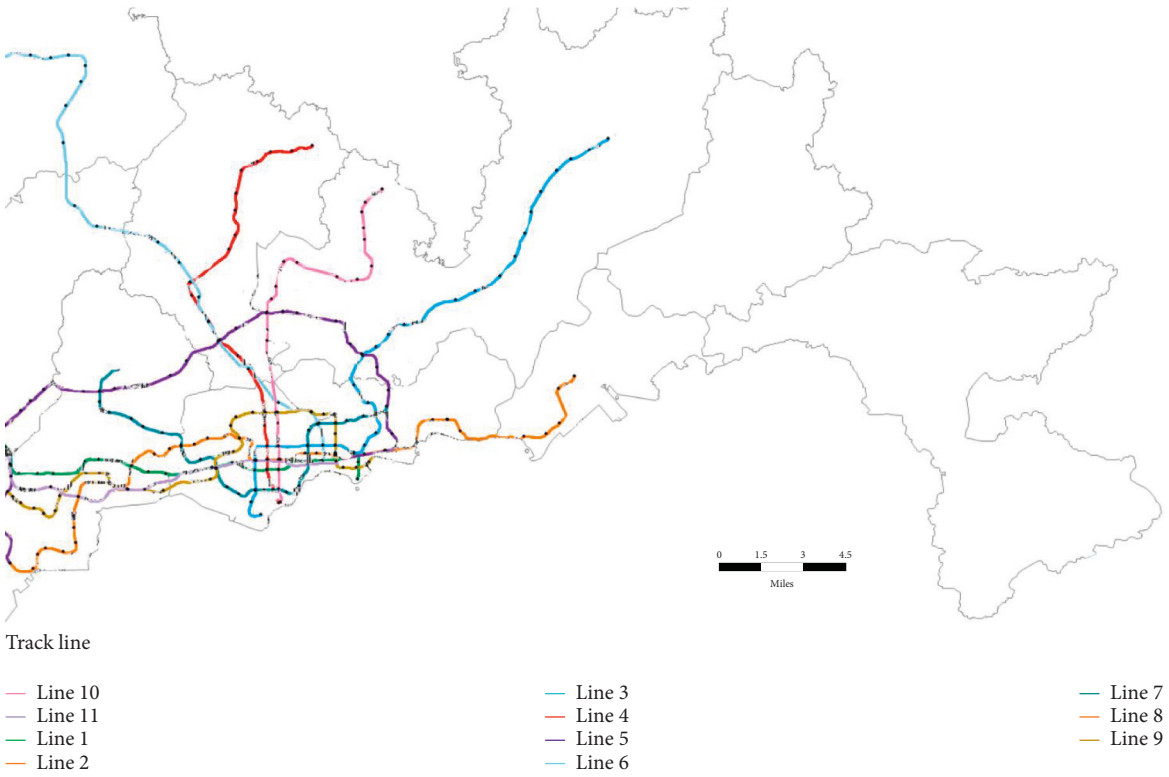

Figure 9: City-covered track route map.

emissions. Figure 10 shows the average transportation distance (km/person) and line occupancy ratio (ratio of average transportation distance to line length) of 11 subway lines within City A. It can be found that the average transportation distance of different lines is quite different. The average haulage occupancy ratio shows that the track occupancy ratio in the surrounding areas of City A is large, while the urban occupancy ratio is small, which is closely related to the spatial separation of passengers' work and residence, which is in line with the characteristics of passenger travel.

In this study, the energy consumption of rail transit is calculated based on the carbon emission coefficient of person-kilometers of different rail transit lines. Therefore, in addition to the average transportation distance of different lines, it is also necessary to calculate the passenger volume of each line. Generally speaking, with the change in subway passenger flow, the subway operating company will adjust the departure interval and station service equipment, so there is a linear correlation between passenger volume and rail transit energy consumption, and considering the urban rail transit constructed in this study. The low-carbon, environmental protection, energy-saving, and emission-reduction evaluation model is based on the temporal and spatial distribution of rail transit passenger flow. Therefore, based on the AFC credit card data, I calculate the morning peak (7 : 00–9:00) and evening peak (17 : 00–19 : 00), respectively. The passenger flow of the line in the three periods of Pingfeng (12 : 00–14 : 00) is shown in Figures 11–13. It can be found that the passenger flow of different lines is the largest during the morning peak, the evening peak is slightly lower than the morning peak, and the passenger flow during the flat peak period drops significantly, accounting for only about 20% of the morning peak passenger flow. At

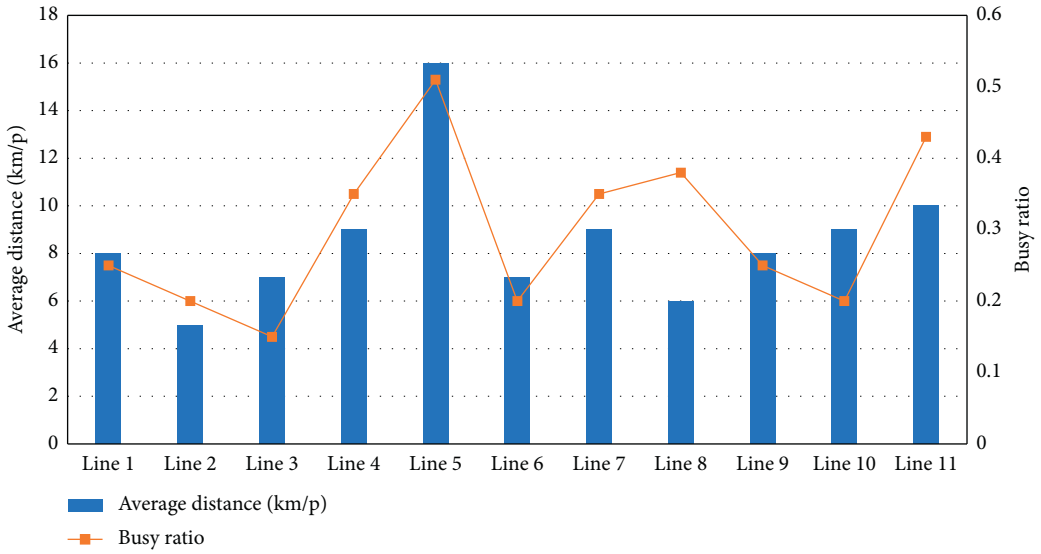

Figure 10: Average distance of rail transit lines in City A.

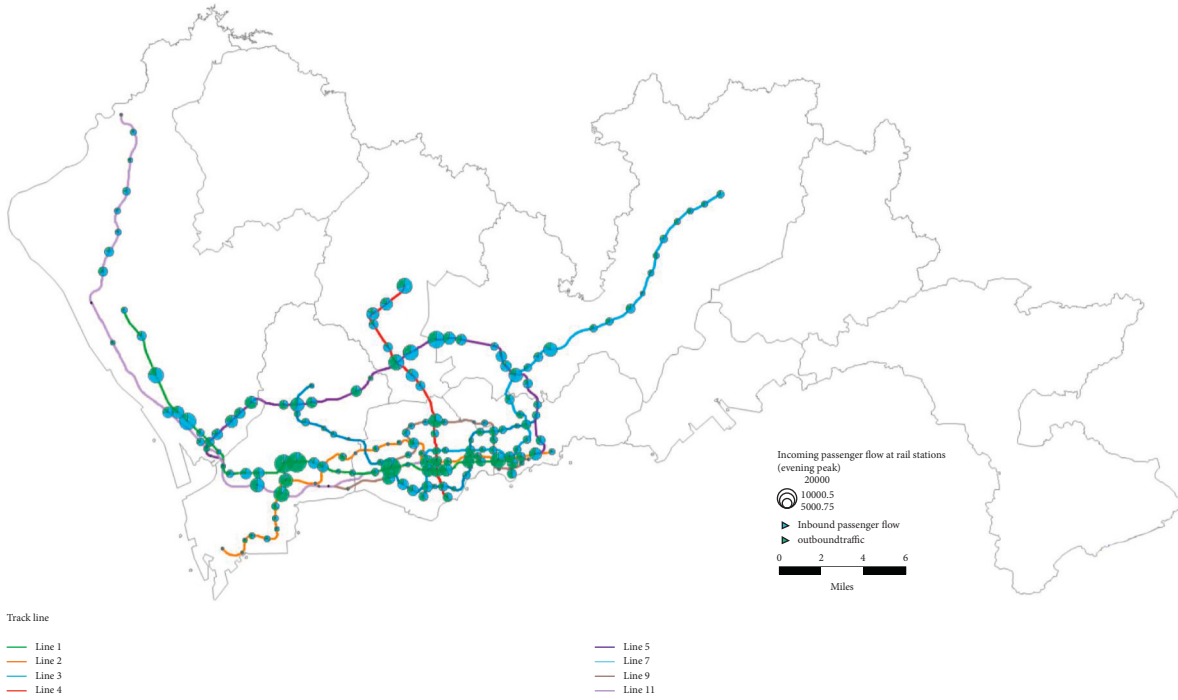

Figure 11: Passenger flow diagram of the rail transit lines in City A in the morning rush hour.

the same time, the difference in passenger flow between lines is also more obvious. The passenger flow of Metro Line 1 and Line 5 is the highest, the passenger flow of Line 2, Line 3, and Line 11 is relatively close, while the passenger flow of Line 4 and Line 9 is the lowest.

To sum up, this study obtained the carbon emission coefficients of 7 subway lines in City A, calculated the average transportation distance of the lines, and counted the passenger volume of each subway line in different periods according to formulas (5)–(14). The carbon emission measurement of rail transit lines can be carried out, and the calculation results are shown in Table 4.

5.2. Energy Conservation and Emission-Reduction Assessment Results. The evaluation indicators of energy conservation and emission reduction in this study include five pollutants and emissions, including CO_2, NOx, CO, HC, and PM. Among them, only CO_2 emissions are generated during the operation of urban rail transit itself. Therefore, the ground

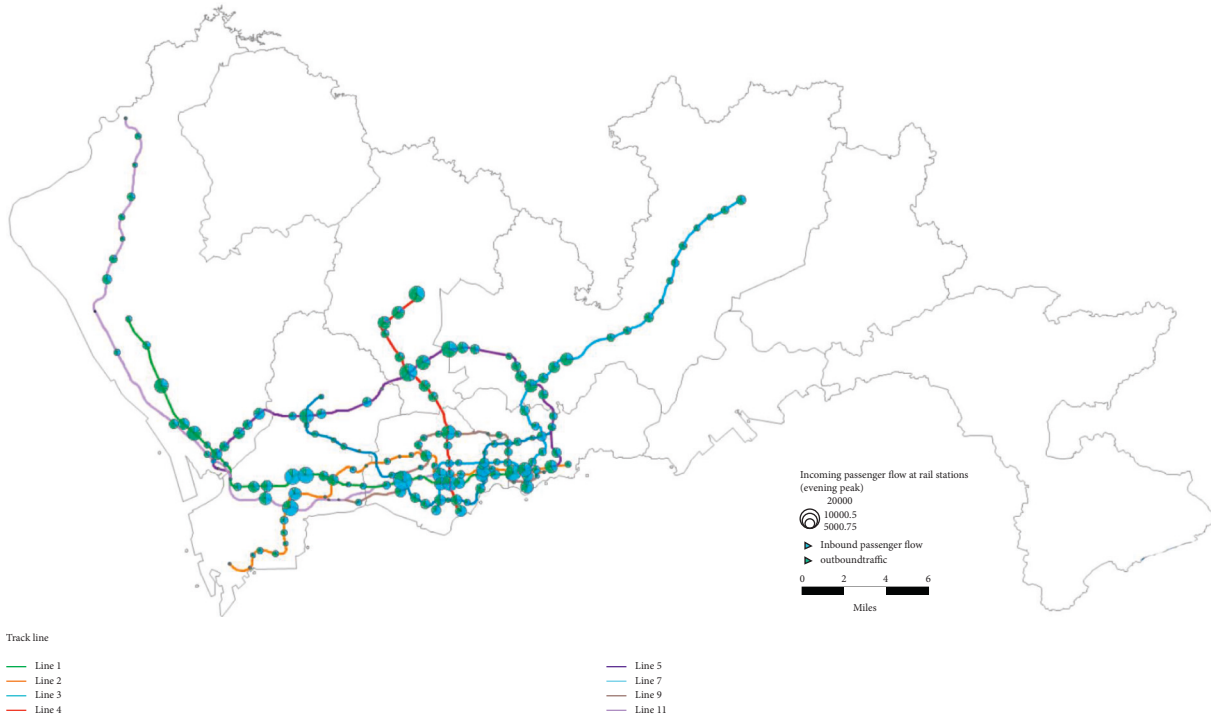

Figure 12: Passenger flow in and out of stations in the evening peak of the rail transit lines in City A.

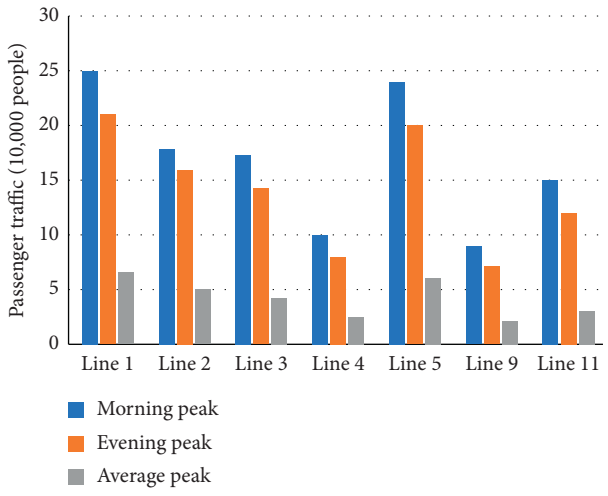

Figure 13: Passenger flow in different periods of rail transit lines in City A.

transportation under the influence of urban rail transit and the CO_2 emission reduction of urban rail transit to the urban transportation system need to be calculated separately, while the ground transportation emission reduction of the remaining four pollutants is the evaluation result of urban rail transit emission reduction, and the calculation methods are shown in the following formula:

$$E_{CO_2-save} = \left(E_{B,CO_2-road} - E_{A,CO_2-road}\right) - \left(E_{A,CO_2-rail} - E_{B,CO_2-rail}\right),$$
$$E_{Other-save} = E_{B,Other-road} - E_{A,Other-road}, \quad (14)$$

Table 4: CO_2 emissions of rail transit lines in City A during each period.

Line	Morning peak (t)	Evening peak (t)	Average peak (t)
Line 1	59.8	50.7	15.1
Line 2	25.1	21.4	6.5
Line 3	58.2	47.2	13.8
Line 4	37.2	31.3	8.8
Line 5	62.4	52.0 1	3.9
Line 9	12.9	10.0	2.8
Line 10	149.7	126.1	34.2
Total	405.3	286.7	85.1

where E_{CO_2-save} represents the CO_2 emission reduction (t); $E_{Other-save}$ represent emissions of pollutants other than CO_2(t); E_A represents standard scenario emissions (t); E_B represents design scenario emissions (t).

It should be noted that the result calculated according to the above formula is the emission increase in the design scenario compared with the standard scenario, and it can be considered as the emission reduction of the standard scenario compared with the design scenario, that is, the emission reduction of urban rail transit on the urban transportation system quantity.

5.2.1. CO_2 Emission Reduction. According to formula (14), it can be found that the evaluation of energy conservation and emission reduction based on the CO_2 indicator is more complicated than that based on other emission indicators. Table 5 summarizes the CO_2 emission values and emission reductions of ground transportation in the standard and design scenarios at different time periods. It can be found

Table 5: CO_2 emission reduction of ground transportation under the influence of urban rail transit.

Period	Standard–ground (t)	Design–ground (t)	Ground emission reduction (t)	Ground emission-reduction ratio (%)
Morning peak	3297	4451	1154	35.0
Evening peak	3782	4778	996	26.3
Average peak	2876	3207	331	11.5

Table 6: CO energy saving and emission reduction under the influence of urban rail transit.

Period	Ground transportation emission reduction (t)	Rail transit emissions (t)	Rail transit emissions (t)	Total emission-reduction ratio (%)
Morning peak	1154	646	508	12.9
Evening peak	996	542	354	8.2
Average peak	331	152	179	6.1

Table 7: Emission reduction of other indicators under the influence of urban rail transit.

Index	Period	Standard scenario (t)	Design scenario (t)	Emission reduction (t)	Emission-reduction ratio (%)
CO	Morning peak	15.3	21.9	6.6	43
	Evening peak	18.2	24.1	5.9	32
	Average peak	10.7	12.9	2.2	21
NOx	Morning peak	2.6	3.6	1 3	38
	Evening peak	3.1	3.9	0.8	26
	Average peak	1.7	0.3	18%	18
HC	Morning peak	1.7	2.5	0.8	47
	Evening peak	2.1	2.7	0.6	29
	Average peak	1.2	1.4	0.2	17
PM	Morning peak	0.077	0.104	0.027	35
	Evening peak	0.089	0.112	0.023	26
	Average peak	0.046	0.054	0.008	17

that in the standard scenario, the ground transportation emissions in the evening peak are 3782 t, slightly higher than the 3297 t in the morning peak. After calculating the emission reduction of ground transportation emissions in the design scenario, the emission reduction of ground transportation CO_2 reached 1154 t in the morning peak period, and the emission-reduction ratio was as high as 35%, followed by about 23% in the evening peak period. Therefore, the CO_2 emission reduction is relatively low, and the emission-reduction ratio is less than 15%. To sum up, it can be considered that urban rail transit effectively reduces the CO_2 emissions of ground transportation. This is consistent with the passenger flow distribution law of urban rail transit and the spatiotemporal distribution law of ground traffic operation under the influence of urban rail transit.

The CO_2 emission reduction of ground transportation is only a part of evaluating the effect of urban rail transit on energy conservation and emission reduction of the urban transportation system. Combined with the measurement results of rail transit carbon emissions in different time periods in Subsection 5.1, the calculation and statistics of the CO_2 emission-reduction results of urban rail transit within City A are shown in Table 6. It can be found that although rail transit generates CO_2 emissions through energy consumption, in the case of this study, urban rail transit still plays a role in reducing CO_2 emissions in the entire urban transportation system, and the emission-reduction effect in the morning peak is still due to the other two. During this period, the total emission-reduction ratio was 12.9%, and the evening peak period was 8.2%. During the off-peak period, due to the less CO_2 emissions generated by rail transit, the total emission-reduction ratio for this period also reached 6.1%.

5.2.2. Reduction of Other Indicators. In addition to CO_2, the energy-saving and emission-reduction evaluation indicators include NO_x, CO, HC, and PM.

The emission of the above four pollutants will not be generated during the transportation operation, so the emission reduction of pollutants in the standard scenario compared with the design scenario is the emission-reduction effect of urban rail transit on the urban transportation system. Therefore, the emission-reduction effects of the above four indicators in different time periods are calculated as shown in Table 7. It can be found that in the evaluation results of the four evaluation indicators, the emissions under the urban rail transit scenario are lower than those under the no rail transit scenario. The emission-reduction effect of the four pollutants is the most obvious during the morning peak. The emission reduction of HC in the morning peak is as high as 47%, followed by the emission-reduction effect of CO, which also exceeds 40%. The emission-reduction effect of the two pollutants of PM is slightly lower, but the emission-

reduction ratio during the morning peak still reaches 38% and 35%, respectively. During the evening peak period, the emission-reduction effect of the four pollutants decreased compared with that during the early peak period, and the emission-reduction ratios of the four pollutants were all within the range of 26%–32%. Compared with the morning and evening peaks, the emission-reduction effect during the flat peak period is significantly lower, and the emission-reduction ratio is about 20% or less. From the comparison results of the emission-reduction effects of the four pollutants in different time periods, it can be found that the emission-reduction effects of different pollutants maintain a good time consistency, and this consistency is directly related to the passenger flow distribution of rail transit.

Through the above analysis of the energy-saving and emission-reduction effects of the urban rail transit network on the urban transportation system during the morning peak hours, evening peak hours, and flat peak hours, it can be found that for the ground traffic speed and flow data in the urban rail transit scenario, it is found that the urban area of City A in the rail transit network within the area effectively relieves the operating pressure of ground traffic in the area, and improves the operating conditions of ground traffic, and the improvement effect has a time-space variation law consistent with the distribution of rail transit passenger flow. For the CO_2 emissions generated by different rail transit lines in different periods of operation, it is found that the CO_2 emissions of rail transit have obvious line differences and time differences. By calculating the emissions of CO_2, NOx, CO, HC, and PM in the presence or absence of urban rail transit, it is found that the construction and operation of urban rail transit reduces the emissions of different emissions, achieving the effect of energy saving and emission reduction. And there are temporal and spatial variation laws consistent with the distribution of rail transit passenger flow.

6. Conclusion

With the rapid development of the economy, the systematic construction and operation of urban rail transit plays a vital role in further improving business efficiency. However, with the intensification of environmental pollution and energy consumption problems, it continues to threaten the living environment of human beings and the sustainability of cities. To achieve the development goals, the research on the emission of urban rail transit has certain practical significance. This paper attempts to take the urban rail transit route as the entry point, deeply and multidimensionally analyzes many factors affecting carbon emissions, and does the following research:

(1) Comprehensively considering the multidimensional impact of urban rail transit on the urban transportation system, a set of relatively complete mechanisms of urban rail transit energy conservation and emission reduction is established, which is the basis for the quantitative evaluation model analysis of urban rail transit low carbon, environmental protection, energy conservation, and emission reduction.

(2) Considering the ground traffic operating speed data in different scenarios, the establishment of the relationship between the emission factor and the speed requires the coupling of the traffic operating data and the traffic emission data, getting rid of the rate for a single emission factor, the establishment of emission factor database, getting rid of the limitations of model scene application, and the improvement of the applicability of model evaluation.

(3) The characteristics of the temporal and spatial distribution of passenger flow were analyzed, and the carbon emissions in different scenarios of morning and evening peaks were quantitatively analyzed. The temporal and spatial variation law of rail transit passenger flow distribution is consistent.

Since this paper uses a certain proportion of vehicles in the calculation of emissions, and the proportion of vehicles changes in real time during road driving, in future research, a dynamic vehicle proportion database can be established to make the calculation of emissions closer to reality.

Data Availability

The dataset can be obtained from the author upon request.

Conflicts of Interest

The author declares no conflicts of interest.

References

[1] US Environmental Protection Agency, *User's Guide to MOBILE6.1 and MOBILE6.2*, U.S.Environmental Protection Agency, Washington, DC, USA, 2003.

[2] L. Ntziachristos and Z. Samaras, *COPERT 4 Computer Programme to Calculate Emissions from Road Transport*, Methodology and Emission Factors, New York, NY, USA, 2007.

[3] M. Keller and P. Wuthrich, *Handbook Emission Factors for Road Transport 3.1/3.2*, Quick Reference, Bern, Germany, 2014.

[4] S. H. Ho, Y. D. Wong, and V. W. C. Chang, "Developing Singapore Driving Cycle for Passenger Cars to Estimate Fuel Consumption and Vehicular Emissions," *Atmospheric Environment*, vol. 97, 2014.

[5] Sosentibile, *CO_2 Emission Reduction from Modal Shift to Railways Pre-study*, University of Bologna-Department of Transport engineering research, 2010.

[6] T. Hodges, *Public Transportation's Role in Responding to Climate Change*, U.S. Department of Transportation Federal Transit Administration, Pennsylvania, PA, USA, 2010.

[7] "Carbon emission from urban passenger transportation in Beijing," *Transportation Research Part D: Transport and Environment*, vol. 41, pp. 217–227, 2015.

[8] L. Li, J. Hu, and D. Shao, "Carbon emission reduction benefit of rapid development of shanghai expo rail transit," *China Environmental Science*, vol. 32, no. 6, pp. 1141–1147, 2012.

[9] H. Jiang and B. Fan, "Research on low carbon economy evaluation of urban rail transit," *Railway Transportation and Economy*, vol. 32, no. 9, pp. 11–15, 2010.

[10] F. Chen, X. Shen, Z. Wang, and Y. Yang, "An evaluation of the low-carbon effects of urban rail based on mode shifts," *Sustainability*, vol. 9, no. 3, pp. 401–412, 2017.

[11] L. Hidenori, F. Atsushi, and L. Paramet, "Measuring Emission Reduction Impacts of Mass Rapid Transit in Bangkok: The Effect of a Full Network," *13th WCTR*, vol. 11, no. 4, pp. 40–42, 2013.

[12] Z. Wang, Y. Huo, and Z. Liu, "Prediction model on energy consumption of highway transportation in inner Mongolia based on ARMA green intelligent transportation system," in *Proceedings of the 7th International Conference on Green Intelligent Transportation System and Safety*, pp. 105–114, Springer, New York, NY, USA, June 2018.

[13] G. Song and L. Yu, "Characteristics of low-speed vehicle-specific power distributions on urban restricted-access roadways in beijing," *Transportation Research Record: Journal of the Transportation Research Board*, vol. 2233, no. 1, pp. 90–98, 2011.

[14] D. Xie, G. Song, Ji. Guo, J. Sun, and L. Yu, *Development and Application of an Online Dynamic Emission Model for Traffc Networks-A Case Study of Beijing*, Present at 98th Annual Meeting of the Transportation Research Board, Washington, DC, USA, 2018.

[15] M. F. Dziauddin, "Estimating land value uplift around light rail transit stations in Greater Kuala Lumpur: an empirical study based on geographically weighted regression (GWR)," *Research in Transportation Economics*, vol. 74, no. 5, pp. 10–20, 2019.

[16] G. Song, F. Zhang, J. Liu, L. Yu, Y. Gao, and L. Yu, "Floating car data based method for detecting flooding incident under grade separation bridges in Beijing," *IET Intelligent Transport Systems*, vol. 9, no. 8, pp. 817–823, 201S.

[17] S. K. Chaturvedi, P. K. Srivastava, and U. Guven, "A brief review on tsunami early warning detection using BPR approach and post analysis by SAR satellite dataset," *Journal of Ocean Engineering and Science*, vol. 2, no. 2, pp. 83–89, 2017.

[18] T. H. DeFries, M. Sabisch, S. Kishan, F. Posada, J. German, and A Bandivadekar, "In-use fuel economy and CO_2 emissions measurement using OBD data on US light-duty vehicles," *SAE International Journal of Engines*, vol. 7, no. 3, pp. 1382–1396, 2014.

[19] H. C. Frey, K. Zhang, and N. M. Rouphail, "Fuel use and emissions comparisons for alternative routes, time of day, road grade, and vehicles based on in-use measurements," *Environmental Science & Technology*, no. 7, pp. 2483–2489, 2008.

[20] L. Zhang, Y. Yin, and S. Chen, "Robust signal timing optimization with environmental concerns," *Transportation Research Part C: Emerging Technologies*, vol. 29, no. 1, pp. 55–71, 2013.

[21] C. Roncoli, N. Bekiarisliberis, and R. C. Carlson, "Special Issue on "Management of Future Motorway and Urban Traffic Systems"," *Transportation Research Part C-emerging Technologies*, vol. 96, pp. 1-2, 2018.

[22] J. Lederer, C. Ott, P. H. Brunner, and M. Ossberger, "The life cycle energy demand and greenhouse gas emissions of high-capacity urban transport systems: a case study from Vienna's subway line U2," *International Journal of Sustainable Transportation*, vol. 10, no. 2, pp. 120–130, 2016.

[23] Z. Yangyang, Z. Ma, Yi Yang, J. Wenhua, and J. Xinguo, "Short-Term Passenger Flow Prediction with Decomposition in Urban Railway Systems," *IEEE Access*, vol. 8, 2020.

[24] H. Wang, X. Yang, and X. Ou, "A study on future energy consumption and carbon emissions of China's transportation sector," *Low Carbon Economy*, vol. 05, no. 04, pp. 133–138, 2014.

[25] Z. Zhai, G. Song, H. Lu, W. He, and L. Yu, *A validation of temporal and spatial consistency of facility- and speed-specific VSP distribution for emissions estimation: a case study in Beijing*, Present at 95th Annual Meeting of the Transportation Research Board, Washington, DC, USA, 2016.

[26] Y. Yue, *Research on the Basic Map of Multi-Level Traffic Flow in Beijing Based on Multi-Source Data*, Beijing Jiaotong University, Beijing, China, 2015.

Hindawi
Scientific Programming
Volume 2023, Article ID 9783528, 1 page
https://doi.org/10.1155/2023/9783528

Retraction

Retracted: Emotion Analysis of Literary Works Based on Attentional Mechanisms and the Fusion of Two-Channel Features

Scientific Programming

Received 18 July 2023; Accepted 18 July 2023; Published 19 July 2023

This article has been retracted by Hindawi following an investigation undertaken by the publisher [1]. This investigation has uncovered evidence of one or more of the following indicators of systematic manipulation of the publication process:

(1) Discrepancies in scope
(2) Discrepancies in the description of the research reported
(3) Discrepancies between the availability of data and the research described
(4) Inappropriate citations
(5) Incoherent, meaningless and/or irrelevant content included in the article
(6) Peer-review manipulation

The presence of these indicators undermines our confidence in the integrity of the article's content and we cannot, therefore, vouch for its reliability. Please note that this notice is intended solely to alert readers that the content of this article is unreliable. We have not investigated whether authors were aware of or involved in the systematic manipulation of the publication process.

Wiley and Hindawi regrets that the usual quality checks did not identify these issues before publication and have since put additional measures in place to safeguard research integrity.

We wish to credit our own Research Integrity and Research Publishing teams and anonymous and named external researchers and research integrity experts for contributing to this investigation.

The corresponding author, as the representative of all authors, has been given the opportunity to register their agreement or disagreement to this retraction. We have kept a record of any response received.

References

[1] Y. Han, "Emotion Analysis of Literary Works Based on Attentional Mechanisms and the Fusion of Two-Channel Features," *Scientific Programming*, vol. 2022, Article ID 8237466, 9 pages, 2022.

Hindawi
Scientific Programming
Volume 2022, Article ID 8237466, 9 pages
https://doi.org/10.1155/2022/8237466

Research Article

Emotion Analysis of Literary Works Based on Attentional Mechanisms and the Fusion of Two-Channel Features

Yanli Han [1,2]

[1]*Henan University of Urban Construction, Pingdingshan, Henan 467000, China*
[2]*University Sains Malaysia, Penang 11800, Malaysia*

Correspondence should be addressed to Yanli Han; 30140617@hncj.edu.cn

Received 25 July 2022; Revised 22 August 2022; Accepted 29 August 2022; Published 13 September 2022

Academic Editor: Lianhui Li

In order to analyze sentiment data of foreign literary works, this paper proposes an algorithm for sentiment classification of literary works. We do this by fusing different features of literary works, which in turn captures more feature information for the classifier. As traditional word embedding models are difficult to achieve fusion with the sentiment features of literary works, we consider a multifeature fusion approach of word embedding features and lexical features of literary works. A two-channel and single-channel comparison is also used to analyze the classification accuracy based on the two feature fusion methods, and a parallel CNN and BiLSTM-attention two-channel neural network model proposed. Finally, the proposed model was evaluated using a real dataset of sentiment reviews of literary works and compared with different classification algorithms in the experiments. The experimental results show that the new hybrid approach has better classification accuracy, recall, and F1 metrics. The proposed methodology is an important guide for the creation of literary works and their screenplays, as it can be used to judge whether a work appeals to readers and, importantly, can also be considered as one of the criteria for the success of a film adaptation of a literary work.

1. Introduction

Since the beginning of the new era, people's attention to contemporary literature has gradually increased, both in terms of genre and content, which is very different from traditional literature, especially in the three areas of values, ideology, and emotional values. Modern and contemporary foreign literature has a more humanistic approach to emotional values than traditional literature, as well as reflects the individual emotions of the author. In the development of foreign literature, the embodiment of emotional value in modern and contemporary foreign literature is more focused on the experience, and through reading it, one can understand the humanistic and personal feelings embedded in the work and thus grasp the author's personality and spiritual experience. In contrast to traditional foreign works, contemporary foreign literature is more open in its expression and more emotive.

A popular foreign work of literature contains a wealth of emotion. The extraction of emotion from a literary work has become a reality, and it is vital to systematically analyze the time series of emotion extracted [1]. Emotion is the soul of a literary work, and existing studies have largely addressed the importance of emotion to a literary work from a qualitative perspective and how the emotion of a literary work changes. This paper will use complexity science methods to quantitatively analyze emotion in foreign literature and its applications.

Online reviews of e-commerce, such as consumer-initiated comments on the quality of goods and services, etc., play a role in the purchasing decisions of potential consumers and directly influence the user stickiness of e-commerce platforms. The process of mining these reviews for positive and negative attitudes in order to identify people's propensity to buy a product is known as sentiment analysis [2] (SA). The goal of sentiment analysis is to extract all the points of view from a document that contains information about the points of view, an analysis method that uses natural language processing and text mining techniques, a method that takes a large amount of data and analyses it to get an understanding

of something. In the early days, sentiment analysis was solved by constructing classifiers methods. Leeuw et al. [3] first proposed to solve the problem of sentiment classification using machine learning algorithms including parsimonious Bayes (NB), they used n-grams models and lexical properties to extract features of film reviews [4]. The main contribution of the fine-grained sentiment analysis method is to extract the corresponding features by syntactic analysis and to compare the experiments with the TF-IDF benchmark model, and their proposed model improves the accuracy (precision), recall (recall), and F1-score in positive or negative evaluations. Wei et al. [4, 5] extracted the features of Chinese hotel reviews by word embedding and put them into classifiers plain Bayesian (NB), support vector machine (SVM), and CNN for comparison, where SVM performed the best in classification. The word embedding approach can extract key information and hierarchical information of words from the comment text, but it cannot extract the information of emotions expressed in the words, so fusing the two features can express the information in the comment more comprehensively.

Now many scholars are very enthusiastic about applying deep learning models to sentiment analysis, applying ever-improving classical deep learning models to this domain, and even proposing new deep learning models in order to solve problems in this domain. TextCNN models were proposed earlier by Mosleh [6], using CNN algorithm to deal with the problem of sentence classification, and obtained better results than previous studies in four out of seven tasks. Liu et al. [7] used Glove to extract features and put them into a very deep CNN model for Twitter sentiment classification experiments, and the results showed that their model had higher accuracy and F1 values than the baseline model. In addition to CNNs, the long short term memory (LSTM) algorithm in deep learning, which is believed to be better at learning contextual information from text, has also been applied to the problem of sentiment classification, and Mansaray et al. [8] used LSTMs to replace the pooling layer in CNNs to perform binary and quintuple classification experiments with higher accuracy than the previously proposed models. In addition, many scholars have combined multiple features in text [9] to achieve better classification results. Nguyen et al. [10] fused word embedding features, sentiment information features, and linguistic knowledge features and overcame the disadvantages of word embedding based on relevant strategies, and their model has advantages over other classical methods. The feature fusion method used in this paper is implemented using the Syuzhet R language package. This is done by extracting the sentiment time series of a literary work to obtain the sentiment score of each sentence in the literary work and then using channel fusion and attention mechanisms to quantitatively analyze the sentiment of a variety of foreign literary works.

2. Model Principles

Since the word embedding model cannot contain the sentiment information of words well, this paper proposes the PWCNN model and PW2CNN model to apply the combination of lexical features to make the information contained in the features richer. While a single CNN model cannot capture the temporal information of a sentence well, adds an attention mechanism, and proposes a parallel classification algorithm PW2CNN and BiLSTMatt model.

2.1. Word2vec + CNN Model. The classical model of TextCNN was [11] proposed by Phan, where each word is a one dimensional vector and a sentence forms a matrix. Convolutional operations are performed by different convolutional kernels, then dimensionality reduction is performed by pooling operations, and finally, binary classification is performed using a sigmoid function.

Earlier, the bag of words (BOW) model represented a vector of word frequencies for each sentence by making a bag of all the words in the document and constructing a corresponding dictionary so that the resulting vector corresponds to the dictionary and represents the frequency of the words. In longer sentence sets, this approach results in a very sparse matrix and the loss of information about the order of words. The word embedding model word2vec takes better account of word position relations [12–14] and solves the problem of oversparsity when vectorizing words with one-hot encoding.

The word embedding model is proposed to better learn word representations quickly and accurately on a large dataset, using the idea of embedding high-dimensional word vectors into a low-dimensional space so that words with adjacent meanings have closer spatial distances. By improving on the BOW model, the continuous bag-of-words model (CBOW) produces a matrix with a dimension of 256×128, which is initially set in the article, with each matrix text represented by 128 dimensions so that the concatenation of words can form a feature vector matrix, which is filled with zeros in the case of a sentence with no more than 256 words.

The word2vec + CNN model is a modification of the classical TextCNN model, where the CNN structure is convolved on the feature matrix of each sentence by a number of different 4×4 convolution kernels. The input text matrix $X \in R^{N \times N}$and filter $W \in R^{N \times V}$, and the two-dimensional convolution is given as follows:

$$c_{ij} = \sum_{U}^{u=0} \sum_{V}^{v=0} w_{uv} x_{i-u+1, j-v+1}. \quad (1)$$

Equation (1) represents the process of multiplying the elements of the text matrix $Xx_{ij}$and the elements w_{uv} of the convolution kernel matrix W to obtain the features c_{ij} using a filter W with a window size of $U \times Vx_{i,j}$ to, $x_{i-u+1, j-v+1}$, which results in multiple feature matrices.

The first layer in Figure 1 is the input layer, the last layer is the output layer, and the layers in between represent the structure [15] of the CNN. This model has two convolutional layers and one pooling layer. The first has 32 convolutional kernels, all of which are 4×4 matrices, and the activation function is a ReLu function. The second convolutional layer has 16 convolutional kernels, all of which are 4×4 in size,

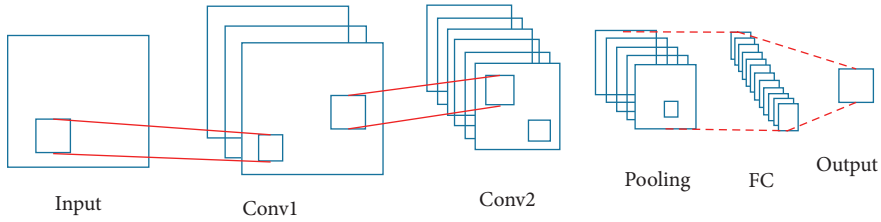

Figure 1: CNN model in 1word2vec + CNN model.

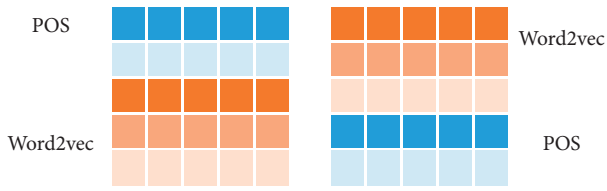

Figure 2: Word vector and lexical vector splicing diagram for word embedding model training.

and also uses the ReLu function. The reason for using the ReLu function is that it is less computationally intensive than the other activation functions and provides better protection against overfitting. The third layer is the maximum pooling layer, with a pooling kernel size of 2×2.

2.2. PWCNN Model. In this experiment, the word2vec + CNN benchmark model is a single-channel CNN model with word2vec as input, and has the same structure as the CNN model in the two-channel PWCNN model, except for the input of the features [16, 17]. The two features are the word embedding word2vec model matrix ($256 \times 128 \times 1$ dimension) and the part-of-speech (POS) feature input matrix ($220 \times 56 \times 1$ dimension).

The lexical annotation determines the lexical annotation of each word in the sentence and uses lexical features to disambiguate on the basis of participles. These lexical words are better able to express the subjective feelings of the reviewer, so the model focuses more on adverbs, verbs, and adjectives. The more important lexical features that the model focuses on are adjectives, adverbs, and verbs, as these lexical features are better at conveying the subjective feelings of the commenter. In addition, punctuation is also important in a sentence and thus is not considered for removal of punctuation when performing subordination and giving the lexicality of the corresponding subword. The PWCNN model splices the word vectors trained by the word embedding word2vec model with the lexical vectors, including two splicing methods, as shown in Figure 2 and Equation (2) [18].

$$X = [X_W, X_P], \tag{2}$$

where X_W denotes the word embedding word2vec model matrix; X_P denotes the lexical annotation feature input matrix.

In addition, the POS features and word2vec features of each sentence are stitched together one by one so that the whole feature matrix is meaningful. The spliced feature vectors are then trained in the same single-channel CNN model as the word2vec + CNN model, mainly to directly compare [19] the experimental results of the feature fusion single-channel model with the benchmark model. Given the difference in structure between the CNN model and the classical TextCNN model, this "top-down" rather than "left-right" splicing was chosen, but the "left-right" splicing is also worth trying. The stitching is also worth trying. At the same time, it was found that the two splicing methods have little effect on the experimental results and made no difference to the CNN. The word vector of fused features was put into the same structure of convolution as mentioned above for the experiments, and the activation function and parameters were set in the same way. The information in the feature vector is extracted through a two-layer convolutional layer, then further reduced and aggregated through a pooling layer, where full connectivity is performed through a random dropout, and to further prevent overfitting (reducing parameters), a dropout is added after this flatten layer, and finally, classification is performed. The experimental model is shown in Figure 3.

This experiment is compared with the word2vec + CNN model to clearly determine whether POS features can play a role in this classification experiment. The experiments prove that the input matrix with POS features does have better classification results. The next step is to further consider a two-channel CNN model based on this single-channel model and explore whether the same features are affected when they enter the same structural CNN model separately.

2.3. PW2CNN Model. It is well known that the two-channel model differs from the single-channel model in terms of the input method. In the single-channel model, the input is spliced with multiple features to obtain the fused features, while in the two-channel model, it is obtained by inputting different features separately [20, 21], and feature fusion can be achieved by matrix splicing. The two-channel CNN model has a matrix of POS features on one side and a matrix of word2vec features on the other side. The two feature matrices are processed separately by the CNN (two convolutional layers, a pooling layer), and the two processed features are "flattened" in the transition layer (the process of turning multidimensional data into one dimensional) and "left-right." The purpose of this is also to preserve the information on both sides.

$$C = [C_1, C_2], \tag{3}$$

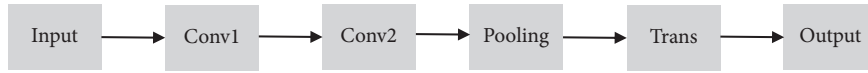

Figure 3: PWCNN model.

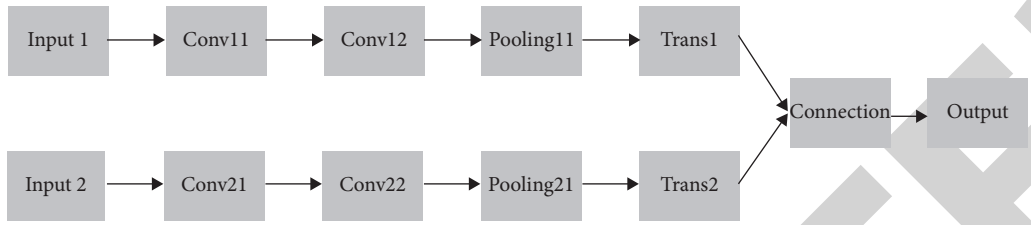

Figure 4: PW2CNN model.

where C_1 denotes the convolutional feature matrix with POS features as input; C_2 denotes the matrix convolutional feature matrix with word2vec model as input.

The overall structure of the model is shown in Figure 4.

In order to ensure comparability between the models, the structure of the CNNs for the dual and single channels was basically kept the same [22], and the comparison of the experimental results revealed that the improvement in the correctness and F1 values on their validation sets was not significant. However, when the CNN on the dual channel side of the model was replaced with a BiLSTM, the results changed significantly, indicating that it is not only the selection of features (the selection of information) but also the selection of the classifier that affects the overall results. When one side of the input is a POS feature, the CNN is able to extract the local features very well. When the other side of the input is a word2vec model, a BiLSTM model that takes into account the context is used, as the word embedding features themselves have information about the word itself. In summary, such a classifier has better experimental results and is the reason why this model is proposed in this paper.

2.4. PW2CNN and BiLSTMatt Models. The proposed PW2CNN and BiLSTMatt model uses the word2vec model [23] for word embedding, CNN, and BiLSTM models for classifier, and incorporates an attention mechanism. As the RNN (recurrent neural network) will lose its ability to learn long-term information, i.e., there is a long-term dependency problem, as the gradient will disappear or explode after multiple propagations with increasing input time series. For this reason, LSTM [24], is introduced into the model design. LSTM removes or adds information to the cell states through a gate structure.

A bidirectional long and short-term memory network (BiLSTM) usually consists of two LSTMs connected, including a positive and a negative one. The positive LSTM captures the past information in the sentence and the negative LSTM acquires the future information in the sentence. In this way, the model is able to extract contextual information, and therefore, the prediction results of the bidirectional LSTM will be more accurate. For the problem of sentiment classification of text, the model is very suitable, as it contains all the forward and backward information in the sentence.

$$\begin{aligned} i_t &= \sigma\left(W_i\left[h_{t-1}, x_t\right] + b_i\right) & c_t &= f_t \odot c_{t-1} + i_t \odot \tilde{c}_t \\ f_t &= \sigma\left(W_f\left[h_{t-1}, x_t\right] + b_f\right) & o_t &= \sigma\left(W_o\left[h_{t-1}, x_t\right] + b_o\right). \\ \tilde{c}_t &= \tanh\left(W_c\left[h_{t-1}, x_t\right] + b_c\right) & h_t &= o_t \odot \tanh C_t \end{aligned} \tag{4}$$

The LSTM network introduces a new internal state $(internalstate)c_t \in R^D$ for information transfer and outputs information to the state $h_t \in R^D$ of the hidden layer b_i, where $f_t \in [0,1]^D$, $i_t \in [0,1]^D$, and $O_t \in [0,1]^D$ are three gates to control the path of information transfer and $\odot$ is the product of vector elements. c_{t-1} is the product of vector elements. $\tilde{c}_t \in R^D$ is the memory unit of the previous moment.

The attention mechanism (AM) [25, 26] is inspired by the human cognitive function of extracting and receiving small portions of important information from a large amount of information and ignoring the rest. Similarly, the essence of the AM is to focus on certain key parts of the input and give them a higher weight. The hidden state of an LSTM model based on the AM at any given moment depends not only on the state of the hidden layer at the current moment and the output at the previous moment but also on the contextual features, which are obtained by a weighted average. This is calculated as follows:

(a) Calculate the attention distribution.

$$a_i = p(z = i \mid \mathbf{X}, \mathbf{q}) = softmax\left(s\left(x_i, q\right)\right) = \frac{\exp\left(s\left(x_i, q\right)\right)}{\sum_{j=1}^{N} \exp\left(s\left(x_i, q\right)\right)}. \tag{5}$$

(b) A weighted average of the input information is calculated based on the attention distribution.

$$att\left(\mathbf{X}, \mathbf{q}\right) = \sum_{N}^{i=1} \alpha_i x_i = E_{z \sim p(z|X,q)}[x]. \tag{6}$$

To calculate the attention distribution is to calculate the probability of selecting the first input vector given the query

Table 1: Information on crawled literature data.

Category	Literary works	Film and television works	Proportion (literature/Film)
Don quixote	4282	1218	3.52
Childhood	4002	2592	1.54
On Earth	4624	1124	4.11
War and peace	5007	1949	2.60
Red and black	4000	2332	1.72

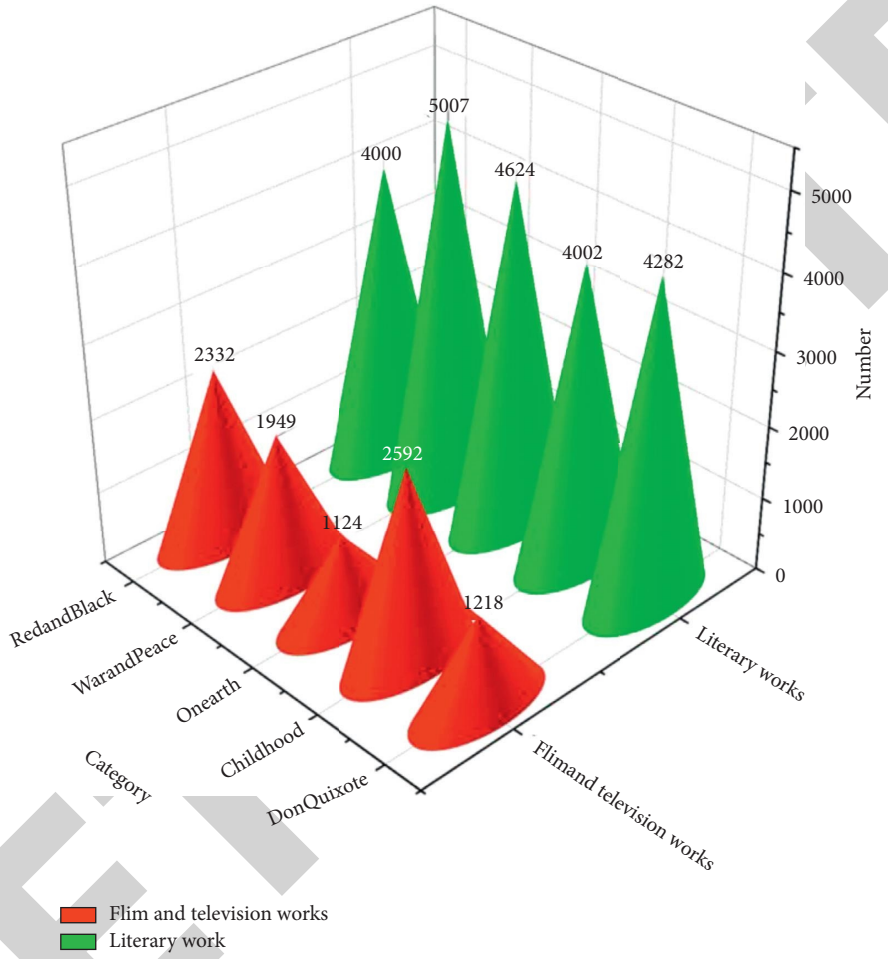

Figure 5: Comparison of the emotional evaluation of literary works and film works.

vector $a_i\mathbf{q}$ and the input $\mathbf{X}$. Where: $z \in [1, N]$ is the attention variable. The first $z = ii$ input vector is selected; a_i is the AM; $s(x_i, q)$is the attention scoring function.

The CNN and BiLSTM were chosen as parallel structures for the model classifier. The CNN model was able to extract a certain class of lexical features (e.g. adjectives, adverbs, nouns) that are more significant for the expression of emotions. The BiLSTM is more suitable for capturing temporal information features [27].

The current state in the bidirectional LSTM should also be related to the contextual features, and the output is influenced by the weighted average of the hidden states of all moments fed into the current state through the attention mechanism. The weights in the attention mechanism are adjusted according to the difference between the output and the real situation. In fact, it can be demonstrated through this experiment that this parallel model gives the best classification results compared to the benchmark model, which not only makes full use of the different feature information but also takes advantage of the different neural network models [28, 29]. This model gives better classification results than the two-channel CNN model, suggesting that the BiLSTM model with the attention mechanism plays an important role.

3. Experimental Preparation

3.1. Data Sets. The datasets used for the experiment were sentiment data from five literary works: Don Giovanni, Boyhood, On Earth, War and Peace, and Red and Black. Table 1 gives information on the number of people, who received positive reviews before and after the five works, were adapted for film and television. The sentiment of each

Table 2: Parameter setting of CNN.

Convolutional layer	Number of convolution kernels	Convolution kernel size	Activation functions
Conv1	32	4 * 4	ReLu function
Conv2	16	4 * 4	ReLu function
Pooling layer	Pooling methods	Pooling kernel size	Dropout function
Pool1	Maximum pooling	2 * 2	0.25

Table 3: F1 values for different experimental models.

Type of experiment	F1 value (%)			
	BASELINE model	PWCNN model	PW2CNN model	PW2CNN & BiLSTMatt model
1	0.942	0.946	0.957	0.960
2	0.944	0.944	0.959	0.963
3	0.948	0.945	0.952	0.954
4	0.945	0.952	0.949	0.961
5	0.947	0.946	0.960	0.963
6	0.940	0.947	0.940	0.963
7	0.946	0.951	0.943	0.950
8	0.942	0.953	0.945	0.955
9	0.944	0.952	0.943	0.957
10	0.945	0.950	0.944	0.959

Table 4: Accuracy of different experimental models.

Type of experiment	Accuracy rate (%)			
	BASELINE model	PWCNN model	PW2CNN model	PW2CNN & BiLSTMatt model
1	0.942	0.944	0.950	0.964
2	0.944	0.944	0.951	0.963
3	0.946	0.941	0.952	0.962
4	0.943	0.952	0.945	0.961
5	0.943	0.942	0.956	0.963
6	0.940	0.947	0.951	0.962
7	0.946	0.951	0.949	0.960
8	0.942	0.953	0.945	0.957
9	0.944	0.948	0.952	0.965
10	0.945	0.950	0.946	0.960

film line was extracted using Syuzhet [30], and the sentiment indices of the novel and film lines were compared to correlate the Hurst indices of the film lines with the Rotten Tomatoes and IMDB ratings.

The results of the comparison of the number of literary works and film and television works that received positive reviews are shown in Figure 5.

3.2. Experimental Environment. In order to validate the performance metrics of the model, the comparison environment was set up as follows: Windows 64 operating system, 64 GB of memory, Intel(R) Xeon(R) CPU E5-2 650v4 @ 2.20 GHz (2 processors), and the model used the Keras deep learning framework.

3.3. Loss Function. The loss function used in the experiments in this paper is a cross-entropy loss function (binary cross-entropy), with the following equation.

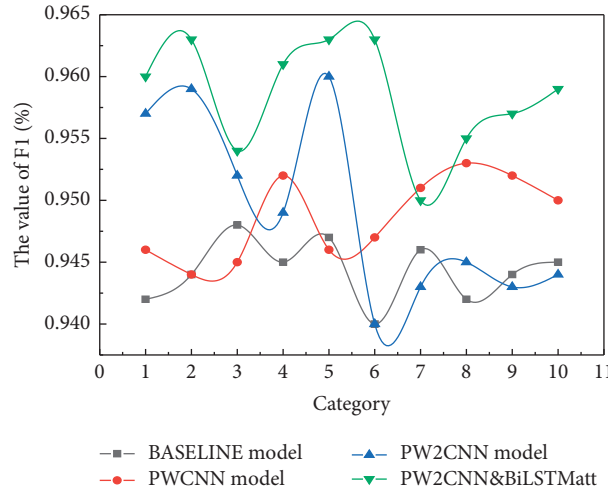

Figure 6: Comparison of the different F1 values for the four models.

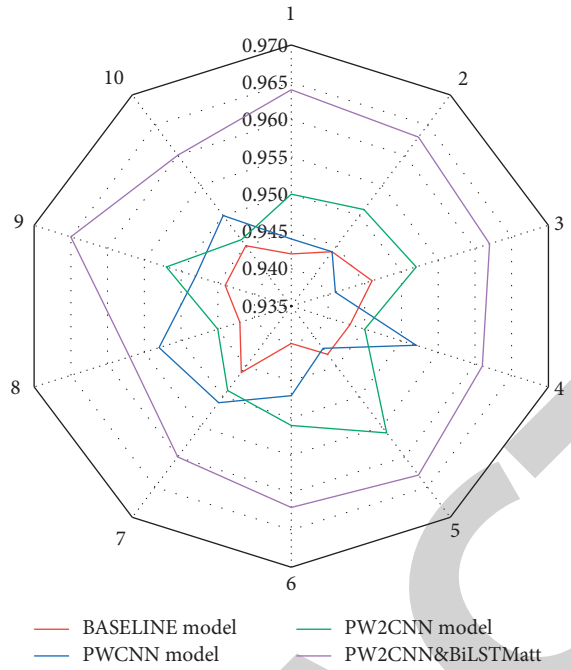

Figure 7: Comparison of the different accuracy rates of the four models.

Table 5: t-test among four models.

Models	BASELINE	PWCNN	PW2CNN	PW2CNN and BiLSTMatt
PWCNN	0.1339	0.3458	0.3141	0.4123
PW2CNN	0.2128	0.36937	0.2821	0.3896
PW2CNN and BiLSTMatt	0.28009	0.3596	0.2431	0.4012

$$loss = -\sum_{n}^{i=1} y_i \lg \widehat{y}_i + (1 - y_i)\lg(1 - \widehat{y}_i). \quad (7)$$

where: y_i is the true discrete category; $\widehat{y}_i$ is the conditional probability distribution of the predicted category labels.

3.4. Experimental Parameters. The hyperparameters on the CNN model in this paper are set as shown in Table 2.

The PW2CNN and BiLSTMatt model puts the long memory model into a parallel structure and adds the attention mechanism, the activation function (AF) of the attention layer in the parallel structure is the softmax function, and the AF of the middle output layer is the ReLu function, and the dropout value of the attention layer is 0.3. For the model with a nonparallel structure, the FC layer and the output layer are also followed by the FC layer and the sigmoid function, respectively, with the dropout value set to 0.5 for the FC layer. The output layer is also followed by the FC layer and the output layer with the same parameters as above, mainly to maintain consistency across multiple models. Four different comparison experiments showed that the best results were obtained with the cross-entropy function as the loss function. In this case, the batch size is set to 64, and the model converges when the epoch is 10, so the epoch is set to 10.

4. Experimental Results and Analysis

4.1. Multimodel Testing. The results of 10 experiments with the four models were compared by the method mentioned previously, and the F1 values and accurate information of the four models are given in Tables 3 and 4. The BASELINE benchmark model is a word2vec + CNN model, the PWCNN is a CNN model with feature fusion, the PW2CNN model is a two-channel CNN model, and the PW2CNN and BiLSTMatt model is a parallel CNN and BiLSTM model (with attention added).

A visual comparison of the F1 values of the four models is shown in Figure 6, and information on the accuracy data of the different experimental models is given in Table 4.

A visual comparison of the accuracy of four of these models is shown in Figure 7.

4.2. Significance Tests between Different Models. The t-test is a method of significance testing that uses a small probability counterfactual method of logical reasoning to determine whether the hypothesis is valid. This test can be used to test the degree of difference between two sample means. The reason for using *the t*-test here is to test whether there is a difference between the experimental results of the different models. Table 5 shows the *t*-test values between the four models.

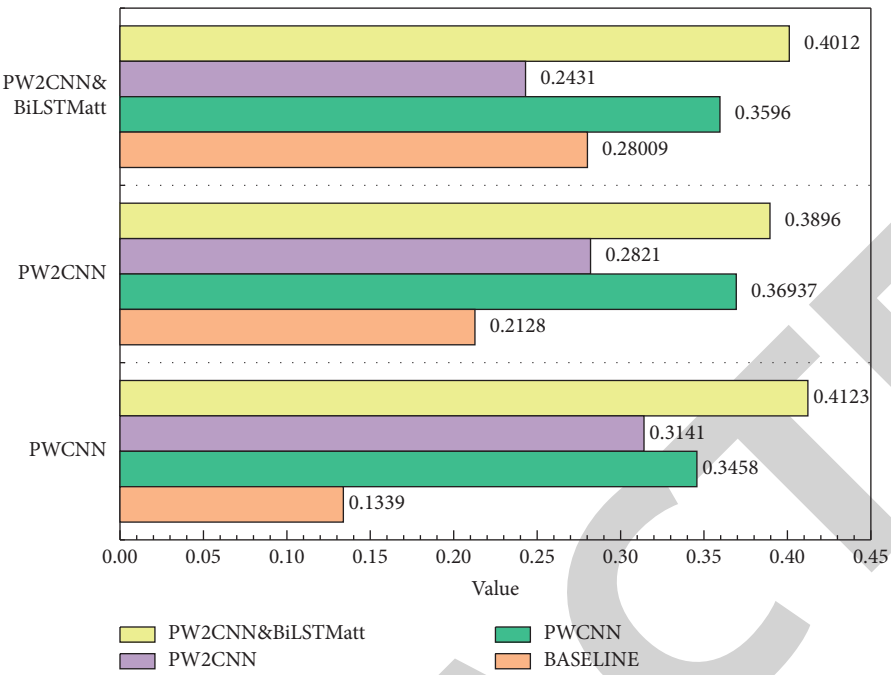

Figure 8: Comparison effect of *t*-test for the four models.

The comparative effect of the *t*-test for the four models is shown in Figure 8.

At a significance level of 0.001, the *p*value of the *t*-test of the PW2CNN&BiLSTMatt model against the BASELINE, PWCNN, and PW2CNN models was less than 0.001. Therefore, there was a difference between the PW2CNN&BiLSTMatt and the BASELINE, PWCNN, and PW2CNN models. Models were all significantly different from each other. In other words, at a significance level of 0.001, the PW2CNN& BiLSTMatt model significantly outperformed the BASELINE, PWCNN, and PW2CNN models. In addition, the *p* value of the *t*-test of the PWCNN model against the BASELINE model (0.003 39) was less than 0.05 at a level of 0.05. Therefore, there was a difference between the PWCNN model and the BASELINE. In other words, the PWCNN is significantly better than the BASELINE model at a significance level of 0.05.

5. Conclusion

A PW2CNN and BiLSTMatt model for sentiment evaluation is proposed for mining and analyzing the sentiment of foreign literary works, using both word vectors and POS feature vectors. These two features are two ways of extracting information from textual data, mainly taking into account the characteristics of words themselves and the characteristics of features containing sentiment information. The role of lexical features in the model is verified by comparing the BASELINE model with the PWCNN model. At the same time, two options are proposed for the fusion of these two features, one is the direct splicing of two vectors and the other is the "fusion" by means of a parallel structural neural network model. A comparison is made between a CNN and a bidirectional long and short-term memory network incorporating an attention mechanism, and experimental results are presented to demonstrate which model is more suitable. The convolutional network is good at capturing local features, while the long and short-term model is more suitable for features containing "temporal" information. Since in the summary of the study of BASELINE and PWCNN models, no comparative experiments with multiple parameters were conducted, but only between models, the study of the effect of multiple parameters on experimental results will be a key direction, in future work.

Data Availability

The dataset can be accessed upon request.

Conflicts of Interest

The authors declare that they have no conflicts of interest.

References

[1] X. Jin, L. Kumar, Z. Li et al., "A review of data assimilation of remote sensing and crop models," *European Journal of Agronomy*, vol. 92, no. 1, pp. 141–152, 2018.

[2] A. G. Laborte, M. A. Gutierrez, J. G. Balanza et al., "RiceAtlas, a spatial database of global rice calendars and production," *Scientific Data*, vol. 4, no. 1, Article ID 170074, 2017.

[3] J. de Leeuw, A. Vrieling, A. Shee et al., "The potential and uptake of remote sensing in insurance: a review," *Remote Sensing*, vol. 6, no. 11, pp. 10888–10912, 2014.

[4] A. Orynbaikyzy, U. Gessner, and C Conrad, "Crop type classification using a combination of optical and radar remote sensing data: a review," *International Journal of Remote Sensing*, vol. 40, no. 17, pp. 6553–6595, 2019.

[5] Y. Wei, X. Tong, G. Chen, D. Liu, and Z Han, "Remote detection of large-area crop types: the role of plant phenology and topography," *Agriculture*, vol. 9, no. 7, pp. 150–153, 2019.

Hindawi
Scientific Programming
Volume 2023, Article ID 9767390, 1 page
https://doi.org/10.1155/2023/9767390

Retraction

Retracted: A Method of Extracting and Identifying College Students' Music Psychological Features Based on EEG Signals

Scientific Programming

Received 18 July 2023; Accepted 18 July 2023; Published 19 July 2023

This article has been retracted by Hindawi following an investigation undertaken by the publisher [1]. This investigation has uncovered evidence of one or more of the following indicators of systematic manipulation of the publication process:

(1) Discrepancies in scope
(2) Discrepancies in the description of the research reported
(3) Discrepancies between the availability of data and the research described
(4) Inappropriate citations
(5) Incoherent, meaningless and/or irrelevant content included in the article
(6) Peer-review manipulation

The presence of these indicators undermines our confidence in the integrity of the article's content and we cannot, therefore, vouch for its reliability. Please note that this notice is intended solely to alert readers that the content of this article is unreliable. We have not investigated whether authors were aware of or involved in the systematic manipulation of the publication process.

In addition, our investigation has also shown that one or more of the following human-subject reporting requirements has not been met in this article: ethical approval by an Institutional Review Board (IRB) committee or equivalent, patient/participant consent to participate, and/or agreement to publish patient/participant details (where relevant).

Wiley and Hindawi regrets that the usual quality checks did not identify these issues before publication and have since put additional measures in place to safeguard research integrity.

We wish to credit our own Research Integrity and Research Publishing teams and anonymous and named external researchers and research integrity experts for contributing to this investigation.

The corresponding author, as the representative of all authors, has been given the opportunity to register their agreement or disagreement to this retraction. We have kept a record of any response received.

References

[1] L. Liang, "A Method of Extracting and Identifying College Students' Music Psychological Features Based on EEG Signals," *Scientific Programming*, vol. 2022, Article ID 1503757, 10 pages, 2022.

Hindawi
Scientific Programming
Volume 2022, Article ID 1503757, 10 pages
https://doi.org/10.1155/2022/1503757

Research Article

A Method of Extracting and Identifying College Students' Music Psychological Features Based on EEG Signals

Li Liang

Music Department of Taiyuan University, Taiyuan, Shanxi 030012, China

Correspondence should be addressed to Li Liang; liangli@tyu.edu.cn

Received 2 July 2022; Revised 13 August 2022; Accepted 16 August 2022; Published 12 September 2022

Academic Editor: Lianhui Li

With the development of information technology, music education in universities is also changing. Traditional music education can not effectively explore the feature of students, resulting in the quality of music education being restricted. The rapid development of Electroencephalogram (EEG) signals has brought a new educational model to music education. Through the extraction of students' psychological features of music by EEG, psychological features can be identified and different educational programs can be formulated according to the results. Multifeature extraction and combination method can improve the accuracy of EEG feature extraction. Using empirical mode decomposition and wavelet packet decomposition of the two kinds of methods to analyze EEG data, respectively, then the average energy, volatility index, sample entropy, and approximate entropy and multiscale features such as permutation entropy and Hurst index, select features in combination, to classify the feature set after the combination, so as to find out the feature of the performance of the optimal combination. The experimental results show that the feature combination of sample entropy and approximate entropy can better represent the main features of EEG psychological characteristic signals after wavelet packet decomposition, and the recognition accuracy is more than 90%.

1. Introduction

In the teaching of traditional music, most of the teachers have followed the same approach as in general subjects, from concept to illustration and back to the concept. This teaching method is dull and inflexible, and students can only passively accept knowledge. If the teacher can not design the teaching plan according to the characteristics of students, music teaching will become the 'stumbling block' of aesthetic education. The quality of music education can be effectively improved if the psychological characteristics of students learning music can be fed back at any time. [1, 2] Musical psychological feature refers to the psychological process including various human psychological factors generated during the interaction between people and music. [3] It includes the mood, preference, interest, and attitude related to music practice. It is a kind of special psychological fuzzy quantity, which includes both the psychological feature component caused by sound directly and the psychological component produced by the subject's thinking about the content of social life. [4–7] It is a current synthesized from two sources. Musical psychological feature is a kind of realistic psychological features with special concretization and music images. Music psychological feature is a kind of artistic psychological feature, which is contained in music and reflected by music, and is also the artistic expression of realistic psychological features in music. [8] Its form and existence have their own feature. Compared with the real psychological feature, musical psychological feature is not only a means of communication between people, but also the connotation of art for people to appreciate. It is expected to arouse the sympathy of others. Therefore, it is more concentrated and generalized than the natural outpouring of psychological feature, and thus has a stronger susceptibility. [9, 10]

psychological feature recognition aims to establish a harmonious man-machine environment and make the computer have higher and more comprehensive intelligence by giving the computer the ability to recognize, understand and adapt to the psychological feature of college students.

psychological feature recognition is an interdisciplinary research field integrating cognitive science, psychology, computer science, and neuroscience. [11–15] It is a difficult and hot topic in the field of cognitive science. With the enhancement of the computing power of computer, the cost of machine learning algorithms is greatly reduced, which lays a solid foundation for the rapid development of machine learning algorithms. Building an appropriate machine learning algorithm model can effectively improve the accuracy of the psychological feature recognition system. [16, 17] At the same time, the development of noninvasive sensing technology and human-computer interaction technology, it also provides a new idea for the development of psychological feature recognition. psychological feature recognition has a broad application prospect, and it can be potentially applied to the field of education. [18].

The modes of musical psychological feature recognition can be divided into physiological signals and non-physiological signals according to the source of signals. In recent years, with the development of wearable and non-invasive physiological signal acquisition devices, the real-time performance and accuracy of physiological signal acquisition are greatly improved, which promotes the development of physiological signals in the field of music psychological feature recognition. Physiological signals such as EEG signals, eye-tracking, and Electrodermal activities (EDAs) are widely used in psychological feature recognition. [19, 20] The reason why EEG signals play an important role in psychological feature recognition based on physiological signals is that the amygdala located deep in the brain is closely related to feelings and psychological features. Multichannel EEG signals can record the measurement results of different parts of the brain including the amygdala, and this information can closely reflect the psychological featured state. With the rapid development of EEG signal acquisition technology, brain-computer interface technology, and artificial intelligence technology, the study of EEG signals has gotten great attention in many countries. [22–26] The US government launched the Human Brain Initiative in 2013 to explore brain mechanisms, advance neuroscience research and develop new treatments for brain diseases that currently have no cure. In the same year, the European Union and Japan also announced their respective "Brain Project". The European Union's Brain Project research focuses on brain-like computing, which uses supercomputers to simulate brain functions; Japan's Brain program focuses on the medical field, studying brain diseases and developing new treatments. In 2016, China listed "brain science and brain-like research" as a major national scientific and technological innovation and engineering project in its planning outline. For the "China Brain Project", experts jointly proposed the layout of "one body and two wings": the "main body" of the research on the neural principles of brain cognition, and the "two wings" of the research on the treatment and diagnosis of major brain diseases and the new technology of brain intelligence. Brain planning has provided impetus for the development of cognitive science and neuroscience. Therefore, psychological feature recognition based on EEG signals has attracted the attention of many scholars. [27–30].

In this paper, we study a kind of effective EEG music psychological characteristic feature extraction algorithm, study how to extract a variety of electrical features and combinations, to seek the feature of the optimal combination, and to improve the accuracy of electrical psychological feature classification, based on EEG signals of music college students psychological feature extraction and recognition technology development to provide technical basis.

2. Brain Electricity

2.1. Acquisition Method of EEG Signal. Dry electrodes are used to collect EEG signals. The electrodes on the device that touches the scalp do not need to be coated or added with conductive materials and can be worn directly on the head to collect EEG signals. The method is easy to operate in the experiment and the equipment is easy to carry, which provides theoretical basis and technical support for the development of portable EEG psychological feature detection therapeutic instruments in the future. However, the cuticle of the scalp has a large impedance, so the extracted EEG signal is not strong.

The other is to obtain EEG signals from a wet electrode, which is attached to the scalp via a conductive paste to reduce the impedance of the cuticle. This collection method can collect more stable and effective EEG signals, but this collection method is not conducive to the application of real life in terms of convenience and comfort.

2.2. EEG Preprocessing. Early EEG research usually involved manual detection and discarding of parts of the signal that contained artifacts, or EEG acquisition experiments designed to avoid artifacts. However, in the actual EEG collection, artifact generation is inevitable. Three methods are commonly used for artifact removal:

(1) Artifact subtraction. Assuming that the collected EEG signal is a linear combination of EEG signal and artifact signal and that the EEG signal is not correlated with the artifact signal, the artifact can be obtained by measurement. This method was used to remove electro-ophthalmic artifacts in the early stage. It is intuitive and has a clear physical meaning, but may lead to the loss of some useful EEG data.

(2) Principal component analysis. The EEG signal is decomposed by the orthogonal principle and the artifacts are removed according to the energy proportion of each EEG component. This method is only related to the covariance matrix of the signal, and although it is better than the pseudo-trace subtraction method, there is still high-order residual information between the signal components because it does not involve the high-order statistical feature of the signal.

(3) Independent Component Analysis (ICA). This blind source separation method has been widely used in EEG for artifact removal and feature extraction. Since this method does not have various noises of

physiological signals, and the sequence of separation signals cannot be determined, this method needs several iterations to obtain a separation matrix, and whether the independent components are artifacts needs manual judgment.

2.3. Feature Extraction Method. EEG feature extraction mainly involves noise reduction, reduction, and correlation removal. In the present research, the commonly used feature extraction methods are divided into time domain frequency domain analysis, space domain analysis, and nonlinear dynamics analysis.

2.3.1. Time Domain Frequency Domain Analysis. Frequency domain analysis of EEG signals mainly focuses on the statistical and geometric feature of EEG signal waveforms. Common analysis methods include probability density, time domain waveforms, autocorrelation, and cross-correlation. The analysis of EEG signals usually focuses on the amplitude, peak, waveform, histogram, mean, and variance of EEG signals. Although the time domain analysis of EEG has the advantage of intuition, it lacks objectivity. At present, the most common time-domain features in research are amplitude feature and amplitude energy feature (Band power, BP), while the most common filtering methods in time domain analysis are: band-pass filter, Laplace filter, full-lead average reference method, Kalman filter and moving average filter. Frequency domain analysis of EEG signals is usually to analyze the correlation and power spectrum of EEG signals. Frequency domain features usually use fast Fourier transform, Adaptive Antoregessive (AAR) model and wavelet transform to extract Power spectral density (PSD), AAR parameters or wavelet frequency band energy. Frequency domain analysis, known as power spectrum estimation, converts EEG signals based on the corresponding relationship between EEG power and frequency, making it easier to observe the distribution and variation of rhythm, as well as the energy distribution of each frequency. However, variance estimation is prone to fluctuation, so it will lead to the loss of higher-order information. Although autoregressive model is easy to estimate parameters, its parameters do not have specific physical meaning, so it cannot be extended in practice. The common time-frequency analysis of EG signal includes short-time Fourier transform, wavelet transform, wavelet packet decomposition, empirical mode decomposition, global empirical mode decomposition and local mean decomposition. What time-frequency analysis has in common is its powerful energy gathering ability. Even if it is impossible to know the relationship between signal changes over time, the corresponding time-frequency relationship can be obtained within a certain range of SNR. This method can easily describe the transient feature of EEG signals, but cannot describe the trend changes of EEG signals.

2.3.2. Airspace Analysis. Spatial domain analysis is to optimize the weighted combination of multilead EEG signals to obtain signal feature with higher signal-to-noise ratio. Common spatial analysis algorithms include principal component analysis (PCA), independent component analysis (ICA), common space model (COSPATIAL mode), Fisher's Criterion (FC), spatial adaptation of data and Canonical correlation analysis (CCA), etc.

2.3.3. Nonlinear Dynamics. In recent years, nonlinear dynamic analysis method has been widely used in EEG signal analysis because EEG signal is a collection of nonlinear coupling by a large number of nerve cells. In nonlinear analysis of EEG signals, one method is to analyze EEG signals through mixed pure theory. The common methods include Lorenz scatter diagram, maximum Lyapunov exponent, correlation dimension, and Hurst exponent. The other method is to analyze EEG signals by information theory. Common methods include permutation entropy, singular value decomposition entropy, LZC complexity, approximate entropy, and sample entropy.

3. Music Psychological Feature of EEG

3.1. Empirical Pattern Decomposition Algorithm of EEG. Empirical Mode Decomposition (EMD) algorithm does not need to set a basis function in advance, and it can decompose EEG signals according to the time-scale feature of EEG signals. Compared with Fourier decomposition which requires pre-setting of harmonic basis function and wavelet decomposition which requires pre-setting of wavelet basis function, the empirical mode decomposition algorithm does not need to set the feature of basis function, so its algorithm can be applied to any type of signal decomposition. EMD algorithm is suitable for the analysis of nonlinear and nonstationary signal sequences and has a high signal-to-noise ratio, so it has obvious advantages in processing nonstationary and nonlinear data. Since the EMD decomposition algorithm is based on local feature of EEG signal time scale, the EMD algorithm is adaptive. EMD algorithm can decompose THE EEG signal into several Intrinsic mode functions (IMF), and each IMF component covers local characteristic signals at different time scales of the original EEG signal. EMD can transform all the time domain signals of EEG signals into a linear steady state, and stabilize the nonstationary EEG data, so that more processing methods can be applied to EEG signals.

3.2. Eigenmode Functions. If the original EEG signal is decomposed by EMD, the original EEG signal can be reconstructed. The instantaneous frequency of a function is meaningful only when it is symmetric and its amplitude is 0 on average over local time periods, and when the point at which its amplitude is 0 is the same as the number of points at the minimax. The instantaneous frequency of each point in the eIGen mode function is meaningful, so the eigen mode function after EMD decomposition of EEG signal needs to satisfy 2 points. First of all, in the time period when the signal exists, the number of maximum and minimum points of the eigenmode function can differ at most by one in the local time period. Secondly, at any time point, the average value of

the envelope of the maximum and minimum values of the eigenmode function in the local time is 0.

The first point to be satisfied is similar to the narrowband requirement for stationary Gaussian signals. The second point that needs to be met is that the instantaneous frequency does not vary with the fluctuation of the asymmetric signal over a local time period. The second point can also be explained by the fact that the local mean of the data is zero, but for nonstationary EEG data, calculating the local mean involves local time scales, which are difficult to define. Therefore, the average value of the envelope formed by the local maximum and the envelope formed by the local minimum is zero, so that the waveform of the EEG signal is locally symmetric. IMF represents the intrinsic vibration mode of the EEG data, where each vibration period of IMF defined by zero crossing has only one vibration mode and does not contain other complex odd waves. IMF may be frequency and amplitude modulated or unsteady and not constrained to be a narrowband signal, while a signal modulated only by frequency or amplitude may also be called IMF.

3.3. Empirical Mode Decomposition Implementation Method. EMD algorithm considers the oscillation in EEG signal as local oscillation. If the evaluation signal $x(t)$ is a variation between two adjacent minimum points at t^- and t^+, a locally high-frequency component $d(t)$ corresponding to the oscillation is defined, where $t^- \le t \le t^+$ where the oscillation is between two minimum values and passes through the maximum. At the same time, it is still necessary to define a local low-frequency component $m(t)$, where $t^- \le t \le t^+$, then $x(t) = m(t) + d(t)$. This method can be used to decompose all the oscillating components of the EEG signal. It can also be applied to all the residual components of the local signal. Therefore, the components of the EEG signal can be decomposed by an iterative method, a process called EMD decomposition. EMD decomposition is performed for a given EEG signal, and the decomposition process is shown in Figure 1.

The EMD decomposition process of EEG signals is as follows:

(1) Find all extreme values of $x(t)$.

(2) The envelope of extreme points is formed by interpolation method. The minimum point forms the lower envelope, which is expressed as $E_{\min}(t)$. The maximum point forms an upper envelope and is expressed as $E_{\max}(t)$.

(3) Calculate the mean value of upper and lower envelope $m(t) = (E_{\min}(t) + E_{\max}(t))/2$.

(4) Extract details $d(t) = x(t) - m(t)$.

(5) Repeat the above steps for residual $d(t)$ until the mean value of $d(t)$ is 0, and the iteration ends.

A screening process is needed during EMD decomposition, and the above EMD decomposition steps are redefined. In this screening process, steps 1–4 of EMD decomposition above are repeated for detail signal $d(t)$ at first, and iteration is not stopped until the mean value of detail signal $d(t)$ is 0 or meets the stop criteria. The detail signal $d(t)$ after iteration stop is called IMF, and the residual signal of detail signal $d(t)$ can be calculated through the fifth step of EMD decomposition above. After the above calculation process, with the generation of residual signals, the number of extreme points gradually decreases. After completing the EMD decomposition of the whole EEG signal, several IMF will be generated.

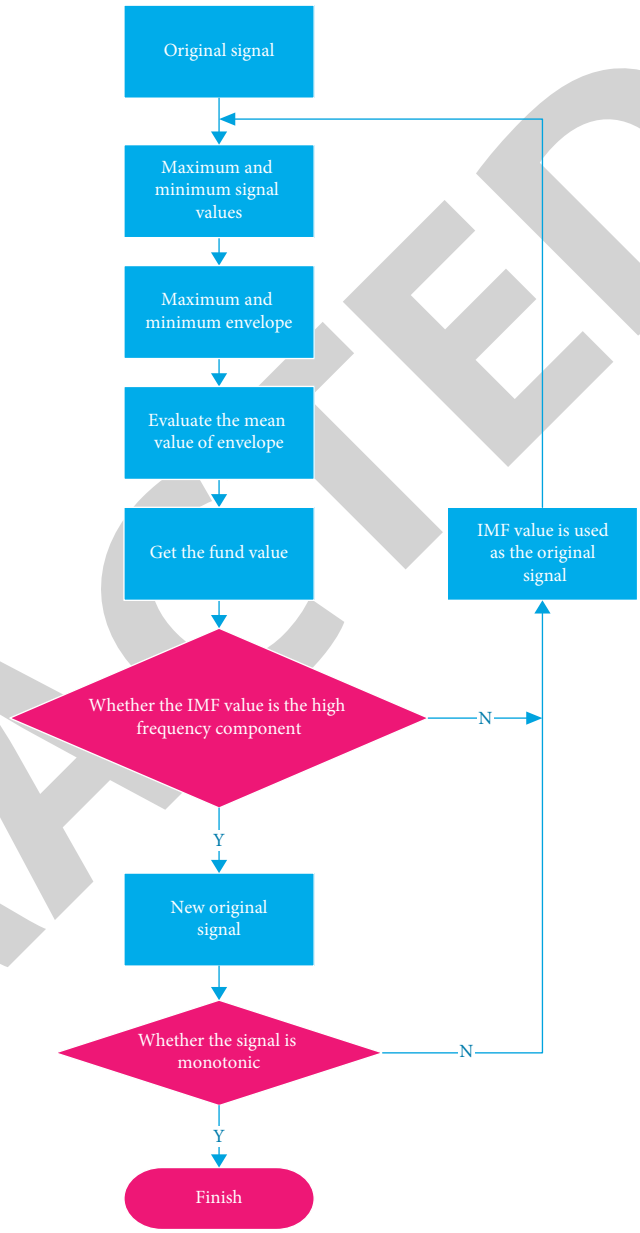

Figure 1: Empirical pattern decomposition process.

3.4. Feature Extraction Algorithm. The EEG signal will produce signal components after decomposition, and the EMD decomposition algorithm is used as an example to solve the average energy and fluctuation index of each component. Through the decomposition of the original EEG

signal by the EMD algorithm, the l-order IMF components can be obtained, but the difference between the frequencies of the IMF components of each order is relatively large, so there is an energy difference between the IMF components of each order, and the average energy of the IMF components of each order can be used as a characteristic value of the EEG signal. The average energy per order IMF component is calculated as follows:

$$E_l = \frac{1}{n}\sum_{t=1}^{n}\left|S_l(t)\right|^2, \tag{1}$$

where S_l is the lth IMF component, n is the number of IMF component data points; E_l is the average energy characteristic of the lth IMF component.

According to the feature of each order IMF component after EMD decomposition, the representative first m-order IMF components are selected for feature extraction so that m average energy feature values can be extracted for each EEG data. Since the amplitude of brain waves varies with changes in musical psychological feature, the average of the sum of amplitude differences of adjacent IMF components is extracted as an eigenvalue, which characterizes the fluctuation intensity of the signal and is called the fluctuation index. Since the intensity of EEG signal changes varies across psychological feature states, the fluctuation index can be used as a measure of the intensity of EEG signal changes, which is defined as:

$$H_{i,j} = \frac{1}{n}\left(\sum_{t=1}^{n}\left|S_i(t) - S_j(t)\right|\right), \tag{2}$$

where $S_i(t)$ is the i-th IMF component after EMD decomposition; $S_j(t)$ is the j-th IMF component; n is the number of data points of the IMF component; H_{ij} is the average of the sum of the absolute values of the differences between the i-th and j-th IMF components, which is the fluctuation index.

The most representative top m-order IMF components are selected for feature extraction after EMD decomposition, so that $m-1$ IMF fluctuation index feature values can be obtained for each EEG data.

Approximate entropy (ApEn) is a nonlinear kinetic parameter that can be used to measure the pattern of EEG signal waveform changes and the unpredictability of EEG signal changes. ApEn characterizes the complexity of an EEG signal by a nonnegative number that is also used to indicate the probability of a change in the EEG signal, whose magnitude increases with the complexity of that EEG time series. Approximate entropy does not require a large number of data points for calculation in practical applications, and approximate entropy can suppress the mixed noise signals in EEG signals and has a strong resistance to interference signals. Since ApEn can analyze single or superimposed random signals, it is very suitable to be used for analyzing EEG signals. Denote a set of original EEG signals by $x(i)$, where $i = 1, 2, ..., n$, and n is the number of data points. The detailed steps to extract ApEn from EEG signals are as follows.

(1) This set of EEG signals $x(n)$ is converted into a set of vectors with dimension d according to the sequence of serial numbers.

$$Y(i) = X(i), X(i+1), \cdots, X(i+d-1), \tag{3}$$

where d is the window length, i is satisfying $i = 1,2, ..., n-d+1$.

(2) Calculate the distance between the i-th vector $Y(i)$ and the j-th vector $Y(j)$.

$$D\{Y(i), Y(j)\} = \max\{|Y(i+k) - Y(j+k)|\}, \tag{4}$$

where i is satisfied by $i = 1, 2, ..., n-d+1$, j is satisfied by $j = 1, 2, ..., n-d+1$, and k is satisfied by $k = 0, 1, ..., d-1$.

(3) When the threshold r is known and r is a nonnegative number, if the number of $D\{Y(i), Y(j)\} < r$ in a set of data points is denoted by $N^d(i)$, and the number of total vectors is denoted by $N-d+1$, and the ratio of these two is denoted by $C_i^d(r)$, the formula for calculating $C_i^d(r)$ for each EEG data series is shown below.

$$C_i^d(r) = \frac{N^d(i)}{(N-d+1)}, \tag{5}$$

where i is satisfied with $i = 1, 2, ..., N-d+1$.

(4) The natural logarithm is taken, and then the average of all the i's is found for the requested logarithm.

$$\phi^d(r) = \frac{1}{N-d+1}\sum_{i=1}^{N-d+1}\ln C_i^d(r). \tag{6}$$

(5) Then the data sequence $X(N)$ is further composed into a set of vectors of dimension $d+1$ according to the serial number, and $C_i^{d+1}(r)$ and $\phi^{d+1}(r)$ can be obtained after repeating the above steps.

$$\mathrm{ApEn} = \phi^d(r) - \phi^{d+1}(r). \tag{7}$$

Since the length of the processed EEG data points is set, the value of the original data point length N is not discussed for the time being. The window length d is also called the embedding dimension, and if the value of d is set larger than 2, the calculated approximate entropy is not used to accurately characterize the EEG signal. If the EEG signal is reconstructed when the value of d is set to 2, the EEG information obtained after reconstruction is more detailed than that portrayed when the value of d is 1, so the value of d is set to 2. The value of the threshold r, also known as the similarity tolerance, is related to the ability of the requested approximate entropy to discriminate between EEG categories. the size of r is more relevant to the scenario of practical application, and $r = 0.2 * std$ is usually chosen, where std denotes the standard deviation of the original time series.

3.5. Holdings of Sample Entropy. Sample entropy (SampEn), which transforms some of the steps in approximate entropy calculation, is also used to measure the complexity of time series and is commonly used in the assessment of physiological time series complexity and in the diagnosis of case states.

Sample entropy algorithm is expressed as follows:

(1) If the time series of an N-dimensional EEG signal is $u(1)$, $u(2)$, ..., $u(N)$, the sequence is obtained by sampling at equal time intervals.

(2) The parameters that determine the calculation results of the sample entropy algorithm are integer d and real number r, where d is the length of the comparison vector and r is the measure of similarity.

(3) Reconstruct d vector $X(1)$, $X(2)$, ..., $X(N-d+1)$, where $X(I) = [u(i), u(i+1), \ldots, u(i+d-1)]$.

(4) For $1i \le N-d+1$, count the number of vectors that meet the following conditions:

$$B_i^d(r) = \frac{(X(j), D[X(i), X(j)] \le r)}{(N-d)}, i \ne j. \tag{8}$$

Among them, the $D[X, X*]$ is defined as $D[X, X*] = \mathrm{Max}|u(a) - u*(a)|$, indicates $X \ne X*$. $u(a)$ represents the element of vector X, and D represents the distance between vector $X(i)$ and vector $X(j)$, which is determined by the maximum difference of the corresponding element. The value range of j is $[1, N-d+1]$, but $j \ne i$.

(5) Find the average value of $B_i^d(r)$ over all I values, denoted as $B^d{}_i(r)$.

$$B^d(r) = (N-d+1)^{-1} \sum_{i=1}^{N-d+1} B_i^d(r). \tag{9}$$

(6) let $k = d+1$, repeat steps 3–4, get $A^k(r) = (N-k+1)^{-1} \sum_{i=1}^{N-k+1} A_i^k(r)$. Among them: $A_i^k(r) = (\text{number of } X(j) \text{ such that } d[X(i), X(j)] \le r)/(N-k), i \ne j$.

(7) Sample entropy (SampEn) is defined as:

$$\mathrm{SampEn} = \lim_{N \longrightarrow \infty} \left\{ -\ln \left[\frac{A^k(r)}{B^d(r)} \right] \right\}. \tag{10}$$

3.6. Multiscale Permutation Entropy. Permutation entropy (PE) is also a nonlinear parameter that can be used to characterize the complexity of an EEG signal. It has the advantages of simple calculation procedures and a strong ability to suppress the mixed noise in EEG signals. Multiscale permutation entropy is calculated on the basis of PE, and its calculation steps are as follows, as shown in Figure 2.

First, the EEG psychological feature time series were coarse-grained. If a group of EEG psychological feature time series is $\{x(i), i = 1, 2, ..., n\}$, then the coarse-granulating method is as follows:

$$y_i = \frac{1}{s} \sum_{i=(j-1)s+1}^{js} x_i, \ 1 \le j \le \frac{N}{s}, \tag{11}$$

where s is a multiscale factor, and y_i is a multiscale time series.

When the scale factor s is 1, it means that the EEG psychological feature time series is the original EEG psychological feature time series, and the entropy calculated by the multiscale permutation entropy algorithm is the permutation entropy value.

Spatial reconstruction time series $\{y(i), i = 1, 2, ..., N\}$, and you get the matrix Y. The length of the time series is N.

$$Y = \begin{bmatrix} y(1) & y(1+\tau) & \cdots & y(1+(d-1)\tau) \\ y(2) & y(2+\tau) & \cdots & y(2+(d-1)\tau) \\ y(j) & y(j+\tau) & \cdots & y(j+(d-1)\tau) \\ \vdots & \vdots & \cdots & \vdots \\ y(k) & y(k+\tau) & \cdots & y(k+(d-1)\tau) \end{bmatrix}, \tag{12}$$

where d is the embedding dimension; τ is the delay factor; k is $k = N-(d-1)$; $y(j)$ is the j-th row component of the reconstruction matrix.

Consider $N-(d-1)\tau$ rows in the above formula as $N-(d-1)$ reconstruction components. The first j a, matrix component $\{y(j), y(j+\tau), ..., y(j+1)\ (d-1)\tau\}$, arranged in ascending order, is available:

Consider the $N-(d-1)\tau$ rows in the above equation as $N-(d-1)\tau$ reconstructed components. Then, the j-th component of the matrix $\{y(j), y(j+\tau), ..., y(j+1)\ (d-1)\tau\}$, rearranged in ascending order, gives the following equation.

$$\%\ y(i+(j_1-1)\tau) \le y(i+(j_2-1)\tau) \le \cdots \le y(i+(j_d-1)\tau), \tag{13}$$

where $j_1, j_2, \cdots, j_d$ is the index value of the column where each element is located in the reconstructed component. If $y(i+(j_p-1)\tau) = y(i+(j_q-1)\tau)$ exists in the reconstructed component and p≠q, then it is necessary to sort the values of j_p and j_q by their magnitude. If $j_p < j_q$, then there is $y(i+(j_p-1)\tau) < y(i+(j_q-1)\tau)$.

Each row of an arbitrary reconstruction matrix has a sequence of reconstruction symbols corresponding to it.

$$S(i) = (j_1, j_2 \cdots, j_d), \tag{14}$$

where i is satisfied by $i = 1, 2, ..., k$, where the value of k is less than d.

Since the dimension of the reconstructed EEG component is d, the arrangement can be obtained as d kind.

If $p_1, p_2, ..., p_k$ is used to denote the probability of occurrence of sequence S(i), the permutation entropy of EEG sentiment time series $x(i)$ can be expressed as the following equation.

$$\mathrm{MPE} = -\sum_{j=1}^{k} P_j \ln P_j. \tag{15}$$

The formula for calculating PE and the range of values of probability P_j shows that MPE is maximum when $P_j = 1/d$ and its value is $\ln(d)$.

$$0 \le \mathrm{MPE} \le 1. \tag{16}$$

Figure 2: Multiscale permutation entropy calculation process.

The numerical size of the ranking entropy measures the complexity of the EEG signal $\{x(i), i = 1, 2, ..., N\}$. a larger value of PE indicates a more complex and random EEG signal, and vice versa.

The three parameters, embedding dimension d and delay factor as well as scale factor, will have an impact on the accuracy of the multiscale alignment entropy calculation results. An EEG psychological feature signal containing high and low arousal is selected from the DEAP database, and the appropriate parameters d, τ, and s are found experimentally. When $d = 3$ and $\tau = 1$, the absolute value difference of the amplitude of the two types of signal alignment entropy with different scale factors s is shown in Figure 3 below. From the figure, it can be seen that the magnitude difference is the largest when s is 1, so $s = 1$ is chosen. According to the previous research, it is known that when $2d \leq 5$ can make a good approximation to the asymptotic distribution by finite series.

Therefore, when $s = 1$ and $\tau = 1$, the absolute value difference of the amplitude of the two types of signal alignment entropy under different d is shown in Figure 4 below. From the figure, it can be seen that the amplitude difference is the largest when d is 5, so $d = 5$ is chosen.

Therefore, when $s = 1$, $d = 5$, the absolute value difference of the amplitude of the two types of signal alignment entropy under different d is shown in Figure 5 below. From the figure, it can be seen that the amplitude difference is the largest when $s = 1$, so it is chosen $\tau = 1$.

3.7. Hurst Index. There are seven main methods for calculating the Hurst index: Aggregate variance method, R/S analysis method, Periodogram method, Absolute value method, Variance of residuals method, Abry-Veitch method, and Whittle method (Whittle estimator). R/S analysis is also called rescaled polar variance analysis, which is usually performed for only a few representative indices due to the complexity of the calculation method.

The Hurst index, calculated by R/S analysis, enables a quantitative description of the long-term dependence of time series information. The Hurst index is able to predict the trend of the EEG signal, but not the duration of new changes. In practical applications usually the system beyond a certain time scale shows a random behavior that is not correlated with the past. The quantity R for determining whether the EEG signal has acyclic cycles can be calculated by the following equation.

$$R_n = \frac{(R/S)_n}{\sqrt{n}}. \tag{17}$$

On the curve plotted by the relationship with lnn, if the curve is a horizontal line, it means that the signal is random and the Hurst exponent is equal to 0.5; if the curve slopes downward, it means that the signal has inverse persistence and the Hurst exponent is less than 0.5; if the curve slopes upward, it means that the signal has persistence and the Hurst exponent is greater than 0.5.

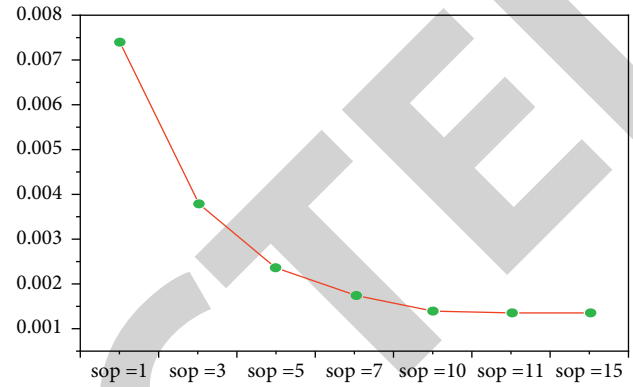

Figure 3: The difference of the average amplitude difference between the two categories at different s values.

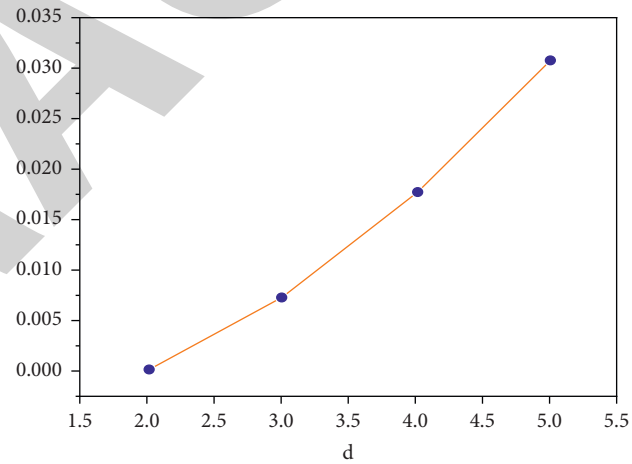

Figure 4: The difference of the average amplitude difference between the two categories at different d values.

4. Experimental Results Analysis of EEG Psychological Feature Extraction

The EMD decomposition algorithm was used to process the EEG signals to obtain the IMF components of each order, and the 11-order IMF components were obtained after the 1-second EEG psychological feature signals on channel Fp1 were decomposed. Fourier transform algorithm was used to transform the IMF components of each order into the frequency domain, and the spectrum graph of each order IMF was obtained. After EMD treatment, the frequency range of each order IMF component is different. The

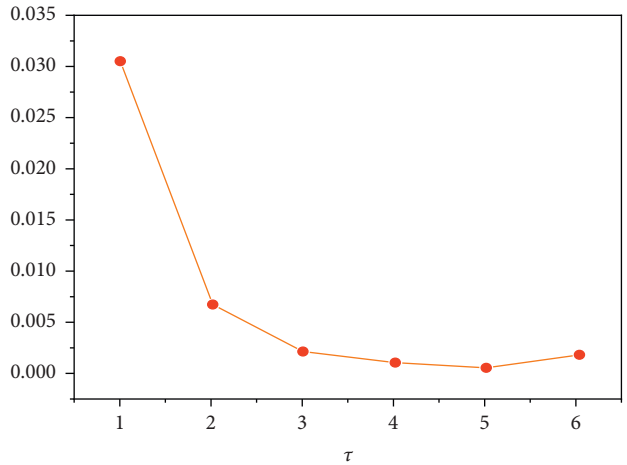

Figure 5: The difference of the average amplitude difference between the two categories at different τ values.

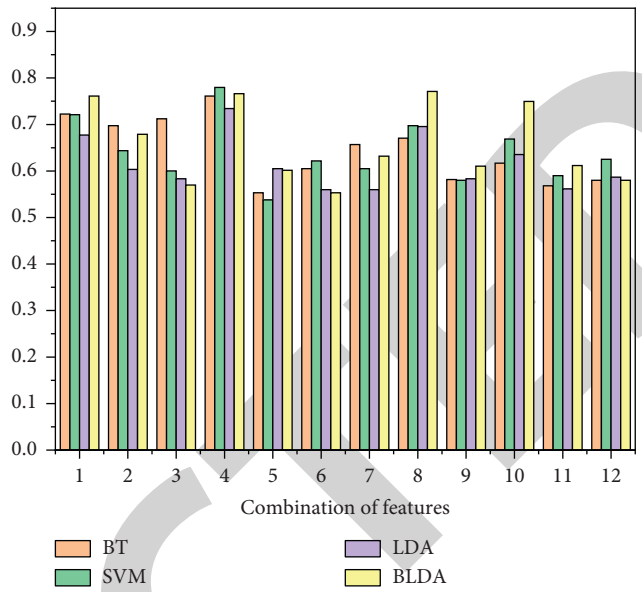

Figure 6: Average classification accuracy of feature combinations.

frequency of each IMF component decreases gradually with the increase of the order, and the higher the order IMF component, the lower the corresponding frequency. If the relevant features of each order IMF component are extracted, the obtained feature vector dimension will be very high, and these feature quantities will also contain many EEG features with little correlation with psychological features, thus reducing the accuracy of EEG psychological feature recognition. Since the frequency range of the EEG, rhythm wave is between 0.5 Hz and 45 Hz, and the IMF components obtained after EMD decomposition, in which the first 6th order IMF components occupy almost 90% of the energy of the EEG signal, the first 6th order IMF components are reconstructed with the original EEG signal on channel Fp1 for 1 second and the EEG signal on channel Fp1 for 1 second after reconstruction. The first 6 orders of IMF components can show the features of the original EEG signal on channel Fp1 for 1 second, so the first 6 orders of IMF components are selected for feature extraction respectively.

The data from the pre-processed DEAP dataset were analyzed in the time-frequency domain, and the EEG data of 32 subjects on 32 channels were decomposed into several eigen-simulation functions using the EMD algorithm. Based on the analysis of appropriate order IMF components, the first 6 order IMF components were selected for time-frequency analysis after EMD decomposition of EEG data from 32 subjects on 32 channels. The average energy features and fluctuation index features are first extracted for each order of IMF components selected as feature set 1 and feature set 2, respectively, and then the FFT transform is applied to the first 6 orders of IMF components after EMD decomposition, and the average energy features and fluctuation index features are extracted as feature set 3 and feature set 4, respectively. Finally, the sample entropy, approximate entropy, multiscale alignment entropy, and Hurst index of the first 6 order IMF components after EMD decomposition are extracted as feature set 5, feature set 6, feature set 7, and feature set 8, respectively. 80% of the extracted EEG sentiment feature set is selected as the training set and 20% as the validation set, respectively. High/low arousal binary classification is performed by four classical classification methods, BT, SVM, LDA, and BLDA, one by one.

As can be seen from Figure 6, the classification accuracy of these features combined is not high, and the accuracy of EEG emotion classification after feature combination is lower than that before feature combination. The highest classification accuracy for the combination of all features is only 77.68%. It is 12.32% lower than the best result of 90% for classification by single features. The possible reasons for this phenomenon are: (1) the combined features produce redundant data, which affects the classification results; (2) when individual features are classified, the amount of feature data is relatively small compared to the combined features, and the classification results of the combined features may be oversaturated; (3) when each feature is classified individually, the feature values of the two categories have certain differences, but after combining them together, the differences between the two The difference between the feature values is reduced.

5. Conclusion

The psychological features of the music of college students are related to their preferences in learning music. It can effectively extract the psychological feature of music, identify and analyze the preferences of students, and develop different learning programs according to different students by combining their own features, so as to maximize the advantages of students. In this paper, multifeature extraction and combination methods are studied to improve the accuracy of mental feature extraction from EEG signals. The EEG emotion data after DEAP centralized preprocessing is processed by the Empirical Mode Decomposition algorithm. Through verification, it is found that the multifeature extraction method can effectively extract psychological feature

data, better reflect the psychological feature of students, and provide good data support for the development of music education programs [21].

Data Availability

The dataset can be obtained from the author upon request.

Conflicts of Interest

The author declares that there are no conflicts of interest.

References

[1] Y. Wang, "RETRACTED: music education: which is more effective – traditional learning or the introduction of modern technologies to increase student motivation?" *Learning and Motivation*, vol. 77, Article ID 101783, 2022.

[2] N. K. A Suarningsih, W Kongsuwan, and C. Kritpracha, "Effect of an education program and traditional music on anxiety in patients with myocardial infarction," *Enfermería Clínica*, vol. 30, no. 7, pp. 52–56, 2020.

[3] G. Sinclair, H. Sinclair, and J. Tinson, "Psychological ownership and music streaming consumption," *Journal of Business Research*, vol. 71, pp. 1–9, 2017.

[4] M. Bigliassi, C. I. Karageorghis, and G. K. Hoy, "Georgia S. Layne, the Way You Make Me Feel: psychological and cerebral responses to music during real-life physical activity," *Psychology of Sport and Exercise*, vol. 41, pp. 211–217, 2019.

[5] S. Nieminen, E. Istók, E. Brattico, M. Tervaniemi, and M. Huotilainen, "The development of aesthetic responses to music and their underlying neural and psychological mechanisms," *Cortex*, vol. 47, no. 9, pp. 1138–1146, 2011.

[6] X. Hu, J. Chen, and Y. Wang, "University students' use of music for learning and well-being: a qualitative study and design implications," *Information Processing & Management*, vol. 58, no. 1, Article ID 102409, 2021.

[7] I. Ruokonen, S. Pollari, M. Kaikkonen, and H. Ruismäki, "The resonaari special music centre as the developer of special music education between 1995-2010," *Procedia-Social and Behavioral Sciences*, vol. 45, pp. 401–406, 2012.

[8] A. Issaka and L. Hopkins, "Engagement with education: music education in a paediatric hospital," *International Journal of Educational Research*, vol. 83, pp. 142–153, 2017.

[9] A. Rauduvaite, J. Lasauskiene, and Music Education, "Some aspects of pedagogical efficiency of popular music integration," *Procedia-Social and Behavioral Sciences*, vol. 197, pp. 910–915, 2015.

[10] R. E. Demirbatir and D. A. Engur, "A A Comparative Examination of the 2013 Musical Aptitude Test Scores of Music Education Students and their 1st Academic year GPA-somparative examination of the 2013 musical aptitude test scores of music education students and their 1st academic year GPAs," *Procedia - Social and Behavioral Sciences*, vol. 197, pp. 815–820, 2015.

[11] A. Juvonen, H. Ruismäki, and K. Lehtonen, "Music education facing new challenges," *Procedia - Social and Behavioral Sciences*, vol. 45, pp. 197–205, 2012.

[12] M. del Mar Bernabé Villodre, "Music education as a tool to improve socio-emotional and intercultural health within adverse contexts in El Salvador," *Procedia - Social and Behavioral Sciences*, vol. 237, pp. 499–504, 2017.

[13] F. Sheng-wei and C. You-bing, "A novel classification strategy of motor imagery EEG signals utilizing WT-PSR-SVD-based MTSVM," *Expert Systems with Applications*, vol. 199, Article ID 116901, 2022.

[14] B. Ari, N. Sobahi, Ö. F. Alçin, A. Sengur, and U. R. Acharya, "Accurate detection of autism using Douglas-Peucker algorithm, sparse coding based feature mapping and convolutional neural network techniques with EEG signals," *Computers in Biology and Medicine*, vol. 143, Article ID 105311, 2022.

[15] Pentari, G. Tzagkarakis, K Marias, P. Tsakalides, K. Marias, and P. Tsakalides, "Graph denoising of impulsive EEG signals and the effect of their graph representation," *Biomedical Signal Processing and Control*, vol. 78, Article ID 103886, 2022.

[16] M. Córdova, H. F. Cifuentes, H. A. Díaz et al., "Design of an EEG analytical methodology for the analysis and interpretation of cerebral connectivity signals," *Procedia Computer Science*, vol. 199, pp. 1401–1408, 2022.

[17] S. Morteza Ghazali, M. Alizadeh, J Mazloum, Y. Baleghi, J. Mazloum, and Y. Baleghi, "Modified binary salp swarm algorithm in EEG signal classification for epilepsy seizure detection," *Biomedical Signal Processing and Control*, vol. 78, Article ID 103858, 2022.

[18] P. M. Ramos, C. B. Maior, M. C. Moura et al., "Automatic drowsiness detection for safety-critical operations using ensemble models and EEG signals," *Process Safety and Environmental Protection*, vol. 164, pp. 566–581, 2022.

[19] G. Kaushik, P. Gaur, and R. R. Sharma, "Ram Bilas Pachori, EEG signal based seizure detection focused on Hjorth parameters from tunable-Q wavelet sub-bands," *Biomedical Signal Processing and Control*, vol. 76, Article ID 103645, 2022.

[20] A. Harishvijey, J. Benadict Raja, and J. B. Raja, "Automated technique for EEG signal processing to detect seizure with optimized Variable Gaussian Filter and Fuzzy RBFELM classifier," *Biomedical Signal Processing and Control*, vol. 74, Article ID 103450, 2022.

[21] R. Nath Bairagi, M. Maniruzzaman, S. Pervin, A. Sarker, S. Pervin, and A. Sarker, "Epileptic seizure identification in EEG signals using DWT, ANN and sequential window algorithm," *Soft Computing Letters*, vol. 3, Article ID 100026, 2021.

[22] Y. Yi, N. Billor, M. Liang, X. Cao, A. Ekstrom, and J. Zheng, "Classification of EEG signals: an interpretable approach using functional data analysis," *Journal of Neuroscience Methods*, vol. 376, Article ID 109609, 2022.

[23] N. Kumari, S. Anwar, V. Bhattacharjee, S. Anwar, and V. Bhattacharjee, "Automated visual stimuli evoked multichannel EEG signal classification using EEGCapsNet," *Pattern Recognition Letters*, vol. 153, pp. 29–35, 2022.

[24] H. R. Hou, Q. H. Meng, B. Sun, Q.-H. Meng, and B. Sun, "A triangular hashing learning approach for olfactory EEG signal recognition," *Applied Soft Computing*, vol. 118, Article ID 108471, 2022.

[25] L D. Sharma, V. K. Bohat, M Habib et al., "Evolutionary inspired approach for mental stress detection using EEG signal," *Expert Systems with Applications*, vol. 197, Article ID 116634, 2022.

[26] W. Dong, R. Li, M. Jiang et al., "Wei Han, Yanhong Zhou, Multi-dimensional conditional mutual information with application on the EEG signal analysis for spatial cognitive ability evaluation," *Neural Networks*, vol. 148, pp. 23–36, 2022.

[27] Bo Jiang, J. Zhu, X. Wang et al., "A comparative study of different features extracted from electrochemical impedance spectroscopy in state of health estimation for lithium-ion batteries," *Applied Energy*, vol. 322, Article ID 119502, 2022.

Hindawi
Scientific Programming
Volume 2022, Article ID 4516499, 14 pages
https://doi.org/10.1155/2022/4516499

Research Article

Application of Collaborative Optimization in Urban Fresh Product Logistics Inventory and Distribution System

Xiaoli Li

Zhengzhou Sias University, Xinzheng 451100, Henan, China

Correspondence should be addressed to Xiaoli Li; 10969@sias.edu.cn

Received 23 July 2022; Revised 25 August 2022; Accepted 29 August 2022; Published 9 September 2022

Academic Editor: Lianhui Li

People's requirements for material needs and living standards are gradually increasing, and consumers' demand for fresh, fruit, and vegetable cold chain foods is also increasing. This paper takes urban fresh agricultural products cold chain logistics as the research object, establishes a collaborative optimization model of urban fresh agricultural products cold chain logistics inventory and distribution based on distribution centers, proposes a partitioning solution strategy for the multidistribution center problem, and proposes a collaborative optimization in urban fresh agricultural products logistics inventory and distribution system. The application of collaborative optimization in urban fresh product logistics inventory and distribution system is proposed.

1. Introduction

In recent years, with the healthy and rapid development of China's national economy, people's requirements for material needs and living standards have gradually increased, and consumers' demand for fresh, fruit, and vegetable and other cold-chain foods has also increased day by day. With this, people's requirements for the safety and freshness of food are also getting higher and higher [1]. According to the analysis of relevant experts, it is because people pay more and more attention to food safety [2], so in recent years the public is more concerned about the safety and freshness of cold chain logistics products, and there are some products in the logistics system in the process of transportation and circulation need to be stored at low temperature and other technical means to maintain the maximum degree of freshness, nutrients, and so on; the cold chain logistics industry was born [3].

Since the establishment of the cold chain logistics system, some cold chain logistics products can be transported and sold over long distances; the seasonality of fresh fruits and vegetables in daily life has gradually become blurred; and the categories of food that people can buy in general are increasingly rich. The development of cold chain logistics benefits from the current high-speed economic situation and people's increasing demand for daily consumption, and it is foreseeable that the development prospect of cold chain logistics will be very broad in the future. In recent years, the rapid development of logistics management, facility planning, safety monitoring, and other logistics-related disciplines has led to the gradual development of the cold chain logistics industry in China [4].

There are many shortcomings in China's cold chain logistics, such as higher costs, the extremely low delivery rate of cold chain logistics and product circulation rate, very backward infrastructure, serious losses of cold chain logistics products during inventory distribution, and so on. This is mainly due to the late start of China's cold chain logistics industry compared with developed countries, the lack of reasonable cold chain logistics system planning, and backward basic logistics facilities [5]. According to professional statistics, the current loss in the process of inventory distribution due to the spoilage of cold chain logistics products has caused a large amount of irretrievable losses in the cold chain logistics industry [6]. Under the guidance of the rapid development of the global economy, China's logistics industry is rising rapidly, and cold chain logistics is also gradually attached to the relevant national departments and the entire logistics industry. The depletion of cold chain logistics products is inevitable, so the research on it to

improve the cold chain logistics network can minimize the loss of cold chain products in the process of inventory distribution and then reduce the cost of cold chain logistics products, and it will also promote the economic and social development of China. Therefore, the cost of loss of goods in circulation considered in the study of the total cost of cold chain logistics network to improve the cold chain logistics network in China has now become an urgent problem [7].

Relying on the rapid development of the Internet [8], fresh product e-commerce has started to enter a golden age of development. Combined with the characteristics of perishability, easy deterioration, and high timeliness requirements of fresh products, high demands are placed on their timeliness of delivery and freshness at the time of delivery [9]. If the quality of the product is significantly degraded at the time of delivery, it will usually be rejected directly. This requires a perfect logistics system to support, through a reasonable logistics system planning to shorten the delivery time of the product, to protect the quality of the product, and at the same time can reduce the cost. With the continuous development of logistics systems and even pharmaceutical logistics systems, managers have gradually realized that there are two important decisions in logistics systems, which are inventory decisions at the tactical level and transportation path decisions at the technical operational level [10]. The two elements are interlinked and highly correlated, and inventory and distribution costs account for a large proportion of the total cost, so the backward phenomenon of benefits between the two is particularly prominent: if we hope that inventory costs are low, we need to reduce the amount of inventory, then the number of deliveries will increase, and distribution costs rise; if we hope that distribution costs are low, we need to make the number of deliveries decrease, and the amount of goods per delivery becomes larger, and then the pressure on warehouse storage becomes larger and Inventory cost increases. Therefore, in order to balance the contradiction between inventory and distribution and achieve the optimization of the logistics system, the inventory and distribution activities of this logistics network should be collaboratively optimized [11].

As the core link of cold chain logistics, inventory and distribution are mutually constrained, and changes in the decision of one link will directly affect the other link, so it is important for the long-term development of enterprises to consider the synergy of the two types of decisions [12]. Based on the existing research, this paper summarizes and refines the relevant concepts of cold chain logistics, constructs a collaborative platform for cold chain logistics supported by blockchain, ensures real-time sharing of inventory and distribution information upstream and downstream of the supply chain through the collaborative platform, focuses on the rational modeling and solution of inventory decision and collaborative arrangement of paths in the secondary network of cold chain logistics on this basis, and discusses the cold chain. It is of strong theoretical and practical significance to discuss the cooperative problem of inventory and distribution of cold chain logistics from the information technology level and business process operation level [13].

Fresh agricultural products are rich in elements and water required for life, and there are more microorganisms with life activities inside them than other products, so deterioration and corruption are the most important characteristics of fresh agricultural products [14]. The supply chain circulation is complicated and complex, mainly including raw materials, production, circulation and processing, sorting, storage, loading and unloading, distribution and sales, and so on. In the process of circulation, slight damage often causes irreversible effects on fresh agricultural products, which can lead to rapid deterioration and even corruption. Therefore, in the process of supply chain circulation, different temperatures need to be set according to the characteristics of different products such as the speed of freshness weakening to ensure product quality. Cold chain logistics of fresh products has the following characteristics compared with room temperature logistics. (1) Precise temperature control and high timeliness: cold chain logistics is more complicated compared with normal temperature logistics, mainly because the object of cold chain logistics is mainly fresh products, and the characteristics of different fresh products have big differences, and they are sensitive to the storage environment temperature, humidity, and light, so in each link of the supply chain, in order to ensure the quality of fresh products and slow down the decline of freshness, the optimal storage environment for fresh products varies greatly. In addition, fresh products have strict requirements on delivery time; cold chain logistics enterprises should deliver the products to the customer's designated location in a timely and accurate manner. Therefore, cold chain logistics enterprises need to plan the distribution path in advance to ensure timely and accurate delivery [15]. (2) More capital investment and frequent daily maintenance: fresh products have the characteristics of perishability and short life cycle and generally have extremely high requirements for temperature and humidity, so they must be equipped with professional refrigerated holding tanks and distribution vehicles in the circulation process. In the process of circulation from the upstream to the downstream of the supply chain, temperature changes are often caused by irregularities in handling and transportation operations.This can lead to the decline of product freshness, affect product quality, and cause damage to goods, which can bring huge capital losses. Therefore, it is necessary to regularly spend a lot of costs to maintain the facilities and equipment of cold chain logistics of fresh products to ensure normal temperature control of refrigeration equipment [16]. (3) Strong equipment expertise and high safety protection: in order to guarantee a constant temperature in the supply chain circulation, packaging materials with good anticollision ability and insulation capacity should be selected, and the selected facilities and equipment must also meet national standards and specifications. At the same time, to ensure product safety, safety protection is required for product information (including production date, expiration date, storage temperature, etc.), health status of distribution personnel, and cleanliness of shipping equipment [17].

Compared with ambient logistics, the main feature of the cold chain logistics operation process is the need for full temperature control of multiple products in the circulation process to delay the decay and deterioration of product freshness and ensure product quality [18]. The operation process of cold chain logistics mainly includes five links: production, storage, circulation and processing, transportation, distribution, and sales. After the raw materials of fresh products are simply processed into semifinished products at suppliers, they are packaged and sorted for transportation to distribution centers for secondary processing to become finished products, and then the products are distributed to retailers for sales, and finally, customers choose delivery or self-pickup according to their needs [19]. The basic operation process of cold chain logistics is shown in Figure 1.

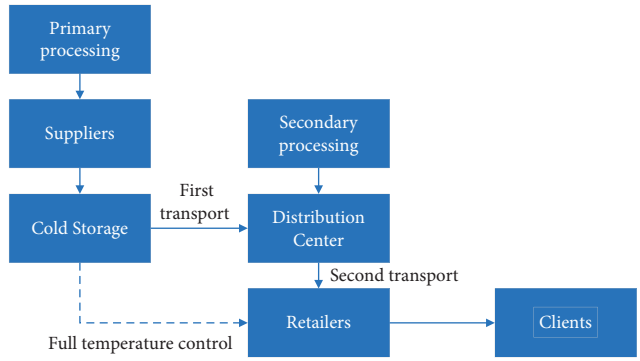

Figure 1: Basic operation process of cold chain logistics.

Collaborative cooperation of logistics enterprises refers to logistics enterprises with autonomy, which adopt unified standards and standardized processes according to certain agreements to complete partial or comprehensive third-party logistics services and play the effect that the whole is greater than the sum of its parts, with the aim of integrating scattered logistics resources and realizing intensive operation [20]. There are three types of collaborative cooperation among logistics enterprises as follows.

The first one is horizontal synergistic logistics [21], that is, the complementary synergistic cooperation among logistics enterprises with different core competencies. On the basis of constructing their own core competitiveness, enterprises choose appropriate other logistics enterprises to reduce costs through collaborative planning and operation. For example, professional transportation enterprises can cooperate with distribution centers, and the transportation enterprises can complete long-distance and high-volume mainline cargo transportation, while the distribution centers can complete activities such as storage, sorting, packaging, and distribution of goods. For enterprises that can only provide logistics services within certain regions due to capacity constraints, they can also complete the whole process of logistics activities through different distribution centers in cooperation. This collaborative approach is flexible and can realize the complementary advantages among logistics enterprises, optimize resource allocation, and enable each enterprise to develop markets and expand business while developing, as shown in Figure 2.

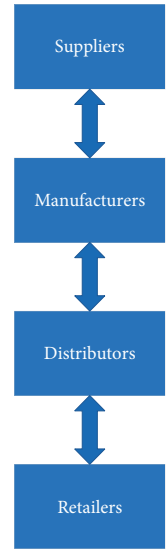

Figure 2: Horizontal collaborative logistics.

The second type is vertical collaborative logistics. Its main form is the collaboration between suppliers, producers, wholesalers, and retailers. This type of synergy can reduce the cost of each logistics enterprise and is conducive to the operational effect of economies of scale. Each logistics enterprise invests and builds together, shares the benefits, and shares the risks and costs, forming a close community of interests, which helps form a stable synergistic relationship among the enterprises. However, there are many specific details involved in the implementation process. For example, the products of different industries have different characteristics and different requirements for logistics, and how to share the expenses and costs among the participating enterprises, which makes collaborative logistics difficult [22], as shown in Figure 3.

The third type is the collaborative logistics realized by the third-party logistics. Provision of necessary logistics services by relatively independent companies. This makes the logistics service system of each enterprise faster and safer. This type of logistics operation is particularly suitable for the replenishment mode of small-lot inventory. However, in the process of third-party logistics cooperation, there are barriers to information communication and exchange of sales data, business plans, development plans, market demand, and so on. Only on the basis of the collaborative exchange of these key information can immediate, accurate, and efficient logistics services be realized and a win-win strategic state be formed [23], as shown in Figure 4.

In the area of fresh product quality losses: Donis-González et al. developed a technique to detect the internal quality parameters of the fresh product without loss of the product. The aim of the study was to detect the internal quality of the fresh product earlier in the production and processing stages of the fresh product supply chain [24]. Prakash studied the effect of ionizing radiation on fresh products and concluded that ionizing radiation has the effect of slowing down the rate of decay of freshness, prolonging the period of spoilage, and destroying bacteria [25].

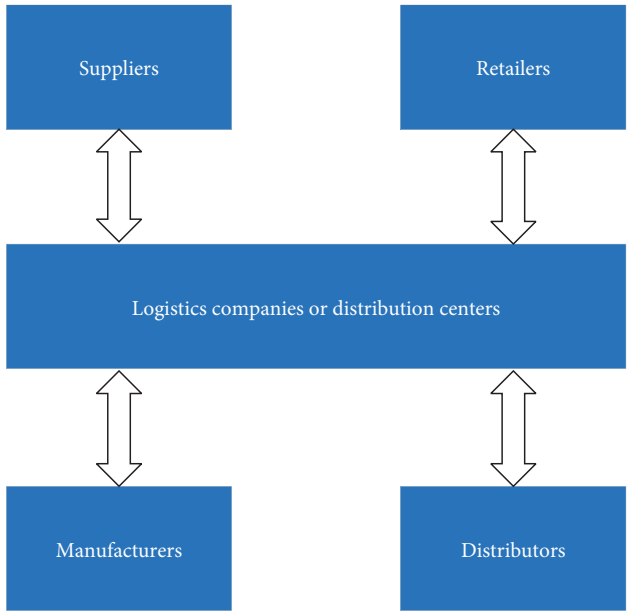

Figure 3: Vertical collaborative logistics.

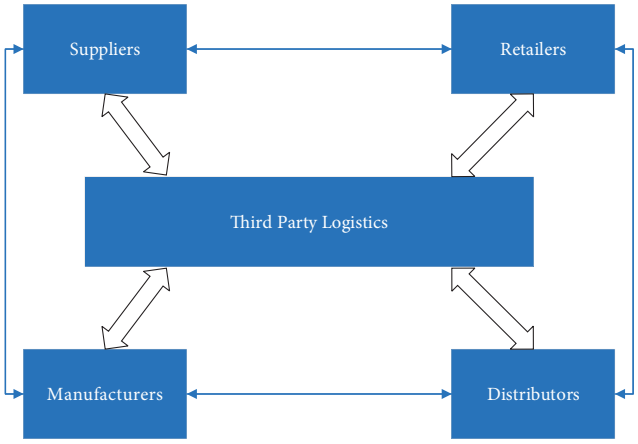

Figure 4: Collaborative logistics realized by the third-party logistics.

Ahumada et al. constructed a planning model on the stochastic allocation of fresh products based on uncertain climate and customer demand, which enables maneuvering selection risk [26]. Piramuthu and Zhao used an exponential function to represent the decaying changes in the quality of fresh product from the perspective of supermarkets and developed a model for fresh product inventory allocation by type and shelf space where demand is influenced by both product shelf display and freshness [27].

For fresh product inventory optimization research: Banerjee and Agrawal analyzed the influence of product selling price and freshness on customer demand and constructed an inventory segmentation control optimization model based on uncertain customer demand, which is only influenced by selling price before selling and determined by product freshness after starting selling [28]. Chan et al. analyzed the effect of supplier productivity on the total cost of the supply chain system and, based on this, proposed an integrated model for constructing an exponential deterioration function of a single supplier corresponding to a single retailer under uninterrupted production conditions, considering the deterioration of the product at the time of delivery and using the production quantity as one of the independent variables affecting the objective function [29]. Hsieh and Dye proposed a customer demand function based on shipment loss neutrality, shipment loss avoidance, and shipment loss finding by analyzing the theory related to reference price effectiveness and integrating reference price effectiveness with inventory control problem and constructed a dynamic pricing model based on this to pursue long-term profit maximization [30]. Nemtajela and Mbohwa reviewed the relationship between FMCG inventory control problems and uncertain customer demand by analyzing the impact of uncertain customer demand on inventory control [31]. Mirzaei and Seifi developed an inventory path optimization model based on freight cost, inventory cost, and cost of goods lost on sale and designed a meta-heuristic algorithm by combining simulated annealing and taboo search [32]. Li et al. studied a demand-dependent and dynamic pricing inventory level model [33].

In the study of inventory and distribution synergy optimization, Anily Federgruen studied a secondary logistics system consisting of distribution centers and multiple retailers and constructed an optimization model to minimize the total cost of the inventory/distribution secondary system by analyzing the inventory and distribution cost of distribution centers and the inventory of each retailer. The solution process is mainly: firstly, the actual demand of each retailer is determined and summed, then the group distribution is carried out according to the design demand of each retailer, and finally the optimal inventory control strategy of the distribution center and the optimal replenishment strategy of retailers are determined [34]. In another paper, she studied a secondary system consisting of a single distribution center and multiple retailers; considered a retailer cost minimization model including inventory holding, fixed order, and transportation costs with a determined sales rate of goods, a limited load of distribution center vehicles, and no time window; and finally verified the feasibility of the model by a heuristic algorithm [35]. Monthatipkul and Yenradee developed an optimization model based on integer programming for a single distribution center and many retailers to determine the optimal inventory control strategy and distribution strategy for the distribution center. Through comparison and analysis, this algorithm was proved to be superior [36].

In terms of multidistribution center vehicle path optimization research, Laporte established a multidistribution center path shortest model based on the shortest distribution center single vehicle type and finally verified the feasibility of the model by genetic algorithm calculation example [37]. Nagy and Salhi established a multidistribution center multivehicle model based on multiple vehicle models and solved it with a genetic algorithm based on the shortest transport distance model [38].

Lack of fresh product spoilage preservation inputs and quality change related studies: in the theoretical studies related to fresh product spoilage, there is more literature on the study of the relationship between time and freshness, but it ignores the effect of the input of preservation cost on the freshness function, which is a binary continuous function about time and preservation cost. At the same time, most of the existing literature have fragmented the relationship between freshness function and quality change function. Most of the literature treat quality change rate as a fixed parameter value; quality change does not happen overnight; it increases with the decay of freshness; quality change is a continuous process; and when the quality change rate reaches a specific value, it causes product spoilage and deterioration. Low degree of synergistic optimization of inventory and distribution: in the study of synergistic optimization of inventory and distribution, the research on each link of the supply chain is more extensive and comprehensive, among which there are relatively more studies on inventory management control and vehicle path planning, but most of the theories only focus on one of the links of the research, so independent research on each link can only achieve local optimization, which is not conducive to maximizing the overall benefits of the system. Although some scholars have proposed the relationship between the quality change function and the product freshness function based on the deterioration rate obeying the three-parameter Weibull distribution, the research is on the integrated inventory model of the three-level system of the supply chain, and the research on the path planning of the distribution vehicles and the multidistribution center problem is missing [39]. Multidistribution center problem: the current research about the supply chain secondary system is limited to the inventory and distribution from a single distribution center and a single commodity, and there is less research about the scheduling problem of multiple distribution centers, multiple yards, and multiple models.

In the operation of the cold chain logistics system, the secondary cold chain logistics network consisting of distribution centers and retailers is the object of study. In a certain period of time, considering the freshness of fresh agricultural products, the distribution center will deliver the products to the retailers according to the optimal distribution path with the optimal quantity and number of times and pursue the process of minimizing the total cost of inventory and distribution. The process of minimizing inventory and total cost of distribution: specifically, within the ordering cycle of the distribution center, the best replenishment quantity and number of replenishment times of each retailer are determined, and the best distribution path from the distribution center to each retailer is determined on this basis so that the total cost of inventory and distribution cost of the distribution center and the total cost of inventory of the retailer are finally realized. In the secondary system center of urban fresh year agricultural products cold chain logistics, if the minimization of distribution center inventory cost is pursued, it will lead to the reduction of the volume of distribution and the increase of the number of deliveries, which indirectly increases the distribution cost of the distribution center. Similarly, the minimization of the most sought-after distribution costs will lead to an increase in the volume of distribution and a decrease in the number of deliveries. The increase in the volume of distribution leads to an increase in the inventory of retailers within a certain period of time, and the inventory holding costs and freshness costs also increase, while the order quantity of the distribution center increases to meet the scale effect pursued by the volume of distribution, leading to an increase in the inventory costs of the distribution center. In short, the relationship between inventory cost and distribution cost is mutually influential and restrictive. By analyzing the relationship between inventory cost and distribution cost in the secondary system of urban fresh agricultural products cold chain logistics under the consideration of freshness cost input, it is determined that the main objects of the synergistic optimization of fresh agricultural products cold chain logistics inventory and distribution are the order quantity of distribution center, the number of delivery times and delivery quantity of each retailer, and the distribution path.

2. Collaborative Optimization Model

Urban cold chain logistics II system is a logistics network based on business flow, logistics, and capital flow with full temperature control. In addition to the functions of sorting and distribution of conventional logistics distribution centers, fresh agricultural products distribution centers also have the functions of fresh products circulation and processing, refrigeration and freshness preservation, fresh packaging, and so on. Therefore, cold chain logistics distribution centers on how to improve refrigeration technology and freshness preservation level, expand radiation radius, and realize cross-regional distribution and other issues have become the focus of research. Therefore, this paper takes the secondary system of urban fresh agricultural products cold chain logistics composed of N distribution centers and M retailers as the research object and firstly determines that the paper constructs a collaborative optimization model of inventory and distribution based on a single distribution center. Secondly, based on the single distribution center inventory and distribution co-optimization model, the thesis proposes a solution strategy for the multidistribution center problem, which is mainly based on partition processing to realize the conversion of multidistribution centers into single distribution centers for a solution.

Freshness, as an important characteristic of fresh agricultural products, is an irreplaceable factor that influences consumers to purchase fresh products, so the demand for fresh agricultural products of retailers must consider the influence of product freshness. As the freshness of fresh products decreases over time, the market demand decreases in line with the actual situation, that is, the fresher the fresh product is, the higher the demand is, so the market demand is positively related to the freshness of the product. In addition to the influence of product freshness on demand, the selling price also has an influence on demand, and the selling price has an inverse relationship with demand. Referring to

the defined equation of the function in the literature on the relationship between product freshness, product selling price, price elasticity, and market demand, the demand function in this paper is derived as follows:

$$D_{ij}(t) = \left(A_{ij} - c_j P_j\right) \bullet \varphi_{ij}(t), \tag{1}$$

where $D_{ij}(t)$ is the demand for product j by retailer i at time t; A_{ij} is the potential market share, which is the maximum rate of demand for product j by retailer i; P_j denotes the product the selling price of product j; c_j is the price elasticity of demand ($c_j > 1$); and$\varphi_{ij}(t)$ is the product freshness function. When product freshness φ_{ij} tends to 0, regardless of how the product sales price is adjusted, the market demand D_{ij} also tends to 0. When the product freshness and price elasticity is certain, the market demand D_{ij} decrease with the increase in sales price P_j.

Based on the freshness model and the inventory level equation, the retailer's inventory level as a function of time is calculated by integration, as follows:

$$I_{ij}(t) = \frac{c_j P_j - A_{ij}}{\left(\alpha_j - \lambda_{bj}\right) \bullet \ln\ \theta_{bj}} \bullet \left[e^{\theta_{bj}^{\left(\alpha_j - \lambda_{bj}\right)t} - \theta_{bj}^{\left(\alpha_j - \lambda_{bj}\right)\frac{\omega_{ij} \bullet T}{n_{ij}}}} - 1 \right], \tag{2}$$

where $I_{ij}(t)$ is the inventory level of retailer i of product j, α_j is the freshness decay coefficient under normal condition of product j, λ_{bj} is the seller's investment factor for product j preservation, θ_{bj} is the initial freshness of the j product at the vendor, ω_{ij} is the replenishment cycle, and n_{ij} is the number of times the distribution center delivers product j to retailer i in an ordering interval.

During the replenishment interval, for the freshness cost of product j at retailer i, which is mainly expressed as the freshness cost, FC_1, invested in the product by the retailer to ensure the freshness of fresh agricultural products, the freshness cost is can be calculated as follows:

$$FC_1 = b_{bj} \bullet Q_{bij}, \tag{3}$$

where b_{bj} is retailer's cost of freshness per unit of product j and Q_{bij} is the number of j products per retailer i purchase. For the cost of goods loss, DC_1, it is mainly due to the cost of spoilage caused by the deterioration of fresh products as the freshness of the product decreases and the rate of spoilage increases over time after arrival at the retailer, as shown in the following equation:

$$DC_1 = \left(Q_{bij} - D_{ij}^{\omega_{ij}}\right) q_j, \tag{4}$$

where $D_{ij}^{\omega_{ij}}$ is the effective demand for product j by retailer in the ww-th replenishment cycle and q_j is the cost of goods loss per unit of fresh product j. Retailers' inventory holding costs, HC_1, are mainly the costs incurred by retailers in storing and maintaining fresh agricultural products for a certain period of time, according to the following equation:

$$HC_1 = C_{bj} \bullet I_{bij}, \tag{5}$$

where C_{bj} is the retailer's inventory holding cost for unit j product and I_{bij} is the weighted inventory for retailer i and product j. In a replenishment interval, the total cost, TC_{ij}, incurred for the product at retailer i, including the cost of freshness, the cost of damage to goods, and the cost of holding inventory, can be calculated as follows:

$$TC_{ij} = FC_1 + DC_1 + HC_1. \tag{6}$$

Assuming that retailer i replenishes fresh product j to the distribution center, the change of inventory level in the distribution center is only affected by the loss of product spoilage in the interval between replenishment periods, so the expression of the change of inventory level in the distribution center at time t is shown in the following equation:

$$I_{dij\,dij}^{\omega_{ij}}(t) = \left(Q_{bij} + Q_{dij}^{\omega_{ij}+1}\right) \bullet e^{\theta_{dj}^{\left(\alpha_j - \lambda_{dij}\right)t} - \theta_{dj}^{\left(\alpha_j - \lambda_{dij}\right)\frac{\omega_{ij} \bullet T}{n_{ij}}}}, \tag{7}$$

where $I_{dij\,dij}^{\omega_{ij}}(t)$ is the inventory level of the distribution center for retailer i of product j at replenishment interval; ω_{ij}, Q_{dij} and Q_{bij} are distribution center, retailer i for each purchase of product j in volume; λ_{dij} is the distribution center's investment factor for product j preservation; and θ_{dj} is the initial freshness of the j product at the distribution center.

In the ordering cycle T of the distribution center, for the procurement cost of product j distributed by the distribution center for retailer i, it is mainly expressed as the sum of the fixed order cost and purchase cost paid by the distribution center to the fresh product supplier, and the procurement cost, BC, is shown in the following equation:

$$BC = h_0 + h_j \bullet Q_{dij}^1, \tag{8}$$

where h_0 is fixed order cost per order for all products and h_j is unit cost per order for product j.

In the distribution center ordering cycle T, for the distribution center to deliver product j at retailer i, the inventory holding cost is mainly expressed as the cost of storage and storage of fresh agricultural products at the retailer in the distribution center, that is, the storage and storage cost, HC_2, of product-weighted inventory in the ordering cycle can be calculated as follows:

$$HC_2 = C_{dj} \bullet \sum_{\omega_{ij}=1}^{n_{ij}} I_{dij}^{\omega_{ij}}. \tag{9}$$

The freshness cost, FC_2, incurred by the distribution center when the distribution center delivers product j to retailer i during the distribution center's ordering cycle T can be calculated as follows:

$$FC_2 = b_{dj} \bullet Q_{dij}^1. \tag{10}$$

In the ordering cycle T, other than $n_{ij} \bullet Q_{bij}$ which is the fresh product that supplied by distribution center j to retailer i, the remaining fresh product will be spoilage depletion, so the cost of spoilage goods loss, DC_2, for the distribution center can be calculated as follows:

$$DC_2 = \left(Q_{dij}^1 - n_{ij} \bullet Q_{bij}\right) \bullet q_j. \tag{11}$$

In addition to the completion of storage, the products in the distribution center also involve a number of other businesses. The relatively fixed costs arising from these business links are additional costs, which mainly include the costs arising from loading and unloading, distribution processing, packaging, sorting, and other business links. The amount of additional costs is mainly affected by the amount of products purchased by the distribution center. In the ordering cycle, the additional costs are mainly caused by the first replenishment period and the initial inventory of the distribution center, that is, the order quantity of the distribution center, so the total additional costs, AC_2, can be calculated as follows:

$$AC_2 = \sum_{i=1}^{N} \sum_{j=1}^{N} C_0 Q_{dij}^1 \bullet x_{ij}, \tag{12}$$

$$x_{ij} = \begin{cases} 1 & \text{Distribution center replenishes product } j \quad j = 1, 2, \ldots \\ 0 & \text{Do not need replenishment product } j \quad j = 1, 2, \ldots \end{cases}, \tag{13}$$

where C_0 is the additional cost per unit of product, that is, the total cost of packaging, sorting, distribution processing, handling, and transportation per unit of product.

In this paper, one distribution path planning is modeled as an example within one ordering interval T of a distribution center. In the retailer's one replenishment interval, the distribution cost is mainly generated by the transportation link, and the transportation cost will vary depending on the transportation distance and the number of transports. For the convenience of modeling, the transportation cost in this paper includes transportation variable cost and fixed cost, and vehicle driver cost. The fixed cost, FC_3, generated by the distribution center vehicle for one delivery to the retailer can be calculated as follows:

$$FC_3 = S \sum_{y=1}^{Z} \sum_{i=1}^{N} X_{di}^y, \tag{14}$$

$$X_{di}^y = \begin{cases} 1 & \text{vehicle y provides delivery service } i = 1, 2, \ldots \\ 0 & \text{Do not provide delivery service} \quad i = 1, 2, \ldots \end{cases}. \tag{15}$$

For the variable cost of transportation, which is mainly affected by the distance from the fresh product distribution center to individual retailers, the variable cost, VC_3, of transportation during the planning period can be calculated as follows:

$$VC_3 = S_1 \sum_{y=1}^{Z} \sum_{i=1}^{N} \sum_{k=1}^{N} d_{ik} Y_i^y X_{ik}^y, \tag{16}$$

$$Y_i^y = \begin{cases} 1 \text{ Provides delivery service for retailer} \quad i = 1, 2, \ldots \\ 0 \text{ Do not provide delivery service for retailer } i = 1, 2, \ldots \end{cases}, \tag{17}$$

$$X_{ik}^y = \begin{cases} 1 & y \text{ vehicle move } from\ i \text{ to } k \quad i, k = 1, 2, \ldots \\ 0 & \text{vehicle do es not move} \quad i, k = 1, 2, \ldots \end{cases}. \tag{18}$$

The vehicle driver cost, DC_3, represents the sum of the costs incurred by the driver driving the vehicle to complete the delivery of all retailers on a route and return it to the distribution center during the order cycle, as shown in

$$DC_3 = S_2 \sum_{y=1}^{Z} \sum_{i=1}^{N} X_{di}^y, \tag{19}$$

where d_{ik} is the distance from node i to point k in the distribution network, S is the fixed start-up costs per vehicle per delivery, S_1 is the unit transportation cost, and S_2 is the driver's labor cost per drive to deliver. In summary, the total cost incurred in the distribution chain during an ordering period in the distribution center, that is, the distribution cost objective function, can be calculated as follows:

$$\min TC_3 = \sum_{y=1}^{Z} \sum_{i=1}^{N} X_{di}^y + S_1 \sum_{y=1}^{Z} \sum_{i=1}^{N} \sum_{k=1}^{N} d_{ik} Y_i^y X_{ik}^y + S_2 \sum_{y=1}^{Z} \sum_{i=1}^{N} X_{di}^y. \tag{20}$$

In the urban fresh agricultural products cold chain logistics system, it is often difficult for a single distribution center to supply the demand for fresh products from supermarkets in the region, and the multidistribution center supply mode appears to meet the demand for fresh products from supermarkets radiating throughout the region. To this

end, this section will propose a multidistribution center solution based on the single-distribution center inventory and distribution cooperative optimization model constructed above. At present, the solution methods for the multidistribution center problem include the partition processing method and the combinatorial optimization method, in which the partition processing method is to partition the retailers according to the distance between the distribution center and the retailers, and different regions are served by different distribution centers to realize the transformation of the multidistribution center distribution problem into a single-distribution center distribution problem for solving. The combinatorial optimization method converts the multidistribution center problem into a complex combinatorial optimization problem and realizes the multidistribution centers to provide services for retailers.

The multidistribution center combination optimization problem is computationally tedious and has harsh adaptation conditions, which are not suitable for the solution strategy of this paper. Therefore, this paper chooses the solution strategy of partitioning the retailers so as to transform the multidistribution center problem into a single-distribution center problem. At this stage, there are many kinds of partitioned distribution methods, mainly the mid-pipeline partitioning method, the scanning partitioning method, center of gravity partitioning method, and so on. The mid-pipeline partitioning method is to partition the retailers through the heavy vertical line of each distribution center connection, which is only applicable to two distribution centers distributed on the same line; scanning partitioning method is to use a kind of successive approximation method for partitioning, which is exponentially increasing and not easy to choose. The center of gravity partitioning method uses the center of gravity of all distribution centers and the line connecting the midpoints of two neighboring distribution centers to partition.

According to the constructed cooperative optimization model of urban fresh agricultural products cold chain logistics inventory and distribution, it is known that the cooperative optimization model consists of the inventory minimization model of the cold chain logistics secondary system and the distribution minimization model, which are interrelated and mutually synergistic, so the model solution algorithm is determined as a two-step cooperative process. Firstly, under the objective function of minimizing the total inventory cost of the cold chain logistics secondary system, the optimal order quantity, distribution quantity, and distribution times are determined in the distribution center. Then, based on the optimal replenishment strategy, the optimal distribution route is solved under the condition that the system distribution cost is minimized, so this paper involves the problem of inventory management control (IMC) and path optimization (PO).

In this paper, a genetic algorithm is used to solve the system inventory cost model. The genetic algorithm is mainly used for optimization problems or discrete problems where the objective function cannot be derived and has strong robustness. The objective function of the secondary system inventory in this paper is designed with numerous constraints, which is difficult to derive, and the approximate optimal solution of the objective function may have certain dispersion, so the genetic algorithm is used to solve this paper.

For PO problems with small computational effort, they can be solved by using Dijkstra's algorithm, branch delimitation, and dynamic programming. The fresh product cold chain logistics distribution optimization model in this paper involves multiple retailers and multiple vehicles, and the model computation will explode exponentially with the increase of relevant parameters. Therefore, the solution methods for such problems mainly include ant colony algorithm, particle swarm algorithm, and simulated annealing method. In this paper, we mainly solve the path optimization problem based on the strong search ability of the ant colony algorithm. Therefore, the collaborative optimization solution flow is shown in Figure 5.

Based on the collaborative optimization model of fresh product cold chain logistics inventory and distribution, this paper adopts a genetic algorithm and an ant colony algorithm to solve the collaborative optimization model. Firstly, we use a genetic algorithm to solve the objective function of minimizing the total cost of secondary system inventory and calculate the optimal number of replenishment, replenishment quantity, and the total cost of minimum inventory for retailers.

The genetic algorithm first generates a random set of the initial population, then calculates the fitness value of individuals in the population using the fitness function transformed by the objective function, and then evaluates the merits of all individuals in the population according to the calculated fitness value, in which the unqualified individuals are selected, crossed, and mutated to produce new individuals, and the new individuals form a new population and continue to iterate repeatedly.

Combining the genetic algorithm solution process and the collaborative optimization model of urban fresh product cold chain logistics inventory and distribution constructed in this paper, the genetic algorithm is designed to meet the cold chain logistics secondary system inventory optimization model, which mainly includes the design of the following links: coding, population initialization, fitness function determination, selection operator, crossover operator, variation operator, and algorithm end rule.

The ant colony algorithm is a bionic algorithm based on the ability of ants to secrete pheromones on the paths they pass through during foraging to achieve mutual communication with other individuals. From the starting point to the end point, other ants are attracted to move to that path by secreting pheromones. As the ants increase, the amount of hormones on the short path becomes more and more, leaving less hormones on the long path. Therefore, the more ants after that choose the path with a greater concentration of pheromones the greater the probability, and vice versa, the smaller the probability.

In the ant colony algorithm of this paper, let there be m ants and n cities, and the state transfer probability of the k-th ant moving from city i to city j at moment t is P_{ij}; the specific algorithm is

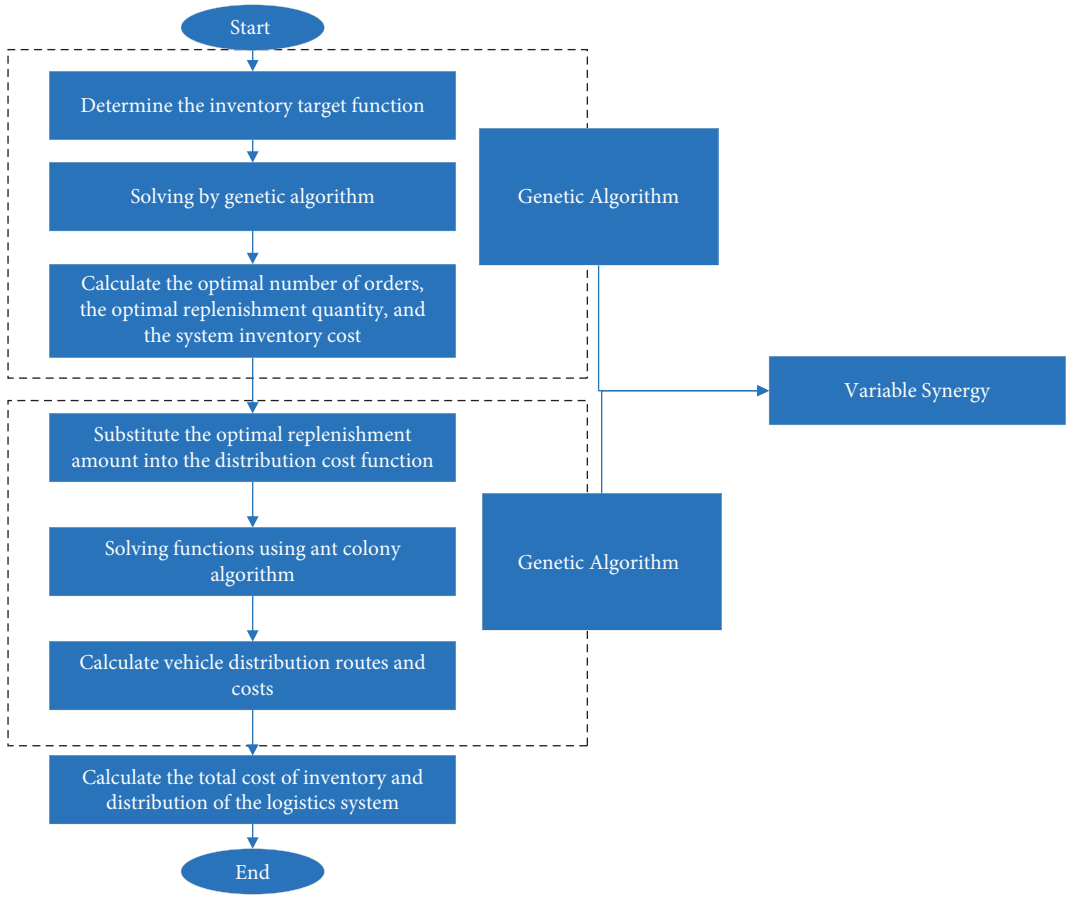

Figure 5: Collaborative optimization solution process.

$$P_{ij}^{k}(t) = \begin{cases} \dfrac{\tau_{ij}^{\alpha}(t)\eta_{ij}^{\beta}(t)}{\sum_{s \in j_k(i)} \tau_{is}^{\alpha}(t)\eta_{is}^{\beta}(t)}, & j \in j_k(i) \\ 0, else, \end{cases} \tag{21}$$

where $\tau_{ij}(t)$ is the amount of pheromone secreted on path (i, j) when the ant moves from city i to city j at time t; η_{ij} is the heuristic function (visibility), which refers to the expected value of ants moving from city i to city j; α is the pheromone inspiration factor; β is the visibility importance expectation heuristic factor; and $j_k(i)$ is the set of cities that ant k untraversed, where $j_k(i) = \{1, 2, \ldots, n\}$.

This paper mainly designs the algorithm of the collaborative optimization model of inventory and distribution of urban fresh agricultural products cold chain logistics. Firstly, according to the characteristics of the constructed inventory optimization model and distribution optimization model, the design idea of the algorithm of this collaborative optimization model is determined, and the solution is finally determined by using a genetic algorithm and ant colony algorithm together, and the relevant theoretical analysis of genetic algorithm and ant colony algorithm is conducted.

3. Results

The object of this case study is a large fresh product retail supermarket in Beijing, which is the first batch of fresh product supermarkets in China, and after years of development, the company operates a chain of fresh product supermarkets covering 24 provinces and cities in China. Up to now, the company has developed more than 900 supermarket chains in the country, with an operating area of more than 6 million square meters, and has been ranked among the top 100 Chinese chains and the top 100 FMCG chains many times. The company has built its own distribution center in the sales region, which is responsible for the storage, processing, and distribution of regional supermarket products.

In recent years, due to the popularity of green concepts, the development of fresh product supermarkets has reached a climax, and many retail supermarkets have begun to transform into fresh product supermarkets, which has led to the expansion of the fresh product market and increased competitiveness. In such a context, the company began to focus on the costs incurred by logistics, seeking ways to "reduce costs and increase efficiency" in the fresh product inventory and distribution chain, seeking to reduce fresh

food cold chain logistics costs and improve cold chain logistics operational efficiency through advanced operational management methods and inventory management control strategies. Therefore, the thesis selects a secondary cold chain logistics network consisting of 18 fresh food supermarket chains and 3 fresh food distribution centers in Beijing to test the synergistic optimization of inventory and distribution according to the needs of the enterprise.

The case designed in this paper is 18 fresh food supermarkets with 3 distribution centers, which belong to the multidistribution center's inventory and distribution cooperative optimization problem. In the process of solving the example, this paper firstly applies the center of gravity method according to the above section to transform the multidistribution center problem into the inventory and distribution of three independent distribution centers and then selects one of the distribution center problems as an example and applies the central solution strategy, distribution optimization problem, single distribution center inventory, and distribution cooperative optimization model and genetic algorithm in the above section to solve the problem.

In order to verify the validity of the synergistic optimization model of cold chain logistics inventory and distribution of fresh agricultural products, this paper analyzes the synergistic optimization of cold chain logistics inventory and distribution of three products in an order cycle $T = 3$ days in the distribution center of this large chain fresh supermarket. The freshness decay coefficients of the three products were $\alpha_1 = 2.2$, $\alpha_2 = 2$, and $\alpha_3 = 2.1$ under the case of freshness preservation measures.

In the secondary cold chain logistics system, the distribution center is responsible for the inventory and distribution of all supermarkets' fresh products, and the instantaneous replenishment and real-time information sharing between the distribution center and supermarkets can be realized. Based on the above coordinates of each fresh food supermarket and distribution center, a plane coordinate system is established on the map.

In order to facilitate the subsequent calculation, each supermarket in the distribution center is numbered; the distribution center is numbered as 0; and supermarket 1, supermarket 2, supermarket 3, supermarket 6, supermarket 8, supermarket 13, supermarket 15, supermarket 16, supermarket 17, and supermarket 18 are numbered as 1 to 10, respectively. Meanwhile, according to the inventory and distribution cooperative optimization model for distribution path planning, the distance between fresh produce supermarkets and the distance to the distribution center are measured.

In this example, the relevant parameters of the distribution center for each product are shown in Table 1.

The relevant parameters of the supermarkets for each product are shown in Table 2.

The maximum market share of 10 supermarkets for the three products, which is the maximum market demand, A_{ij}, is shown in Table 3.

The distribution-related parameters are shown in Table 4.

Among them, this paper is a collaborative optimization model established in the case that the replenishment intervals of various products in supermarkets are different, and the replenishment intervals of the same product in each supermarket are also different. The replenishment intervals of each product are different, Resulting in a distribution path based on the solution of one product that is not suitable for the distribution path of another product, and path planning is a dynamic process. Therefore, in order to facilitate the subsequent solution of path planning, this section specifies that each supermarket replenishes only one product as an example for system inventory optimization and distribution path optimization.

In this paper, the original genetic algorithm is used to obtain the local optimal solution after 50 iterations, that is, the optimal number of replenishment and replenishment quantity for each retailer when the total inventory cost of the distribution center and retailer of the fresh supermarket cold chain logistics secondary system is minimal. The optimal solution is the lowest point of the iterations.

According to the design of the genetic algorithm and the ant colony algorithm, the distribution strategy and distribution path of the distribution center are calculated. (1) The calculation results of the genetic algorithm are based on the inventory and distribution optimization model of fresh agricultural products cold chain logistics, and the inventory optimization solution of the calculation case is carried out using the genetic algorithm to derive the minimum inventory cost of the secondary logistics system of this fresh supermarket chain within one order cycle of the distribution center, including the optimal number of deliveries and the optimal distribution quantity. In the process of designing the genetic algorithm, the relevant parameters are set. The specific values are as follows: pop size of 100, cross possibility of 0.85, mutation possibility of 0.015, and max generation of 50 times.

The objective function of minimizing the inventory cost of distribution centers and retailers is solved by MATLAB genetic algorithm, and the local optimal solution is generated after 100 iterations of operation, and the total inventory cost of distribution centers and retailers in the example tends to be an optimal solution. The optimal replenishment strategy for each retailer within 3 days of an order cycle of the distribution center is shown in Table 5.

The costs associated with the distribution centers of the fresh product supermarket chain and the 10 supermarkets during the ordering interval of the distribution centers include inventory holding costs, freshness costs, damage costs, purchasing costs, and additional costs. Based on the actual research data, the total costs associated with the distribution centers were 127,343.2 RMB, and the total costs associated with the supermarkets were 8945.39 RMB.

Based on the above genetic algorithm solution, the distribution center delivers to 10 fresh food supermarkets within 3 days of the ordering cycle, and the replenishment cycle is calculated based on the number of deliveries to each supermarket. It can be concluded that the replenishment cycle of each supermarket has decimal places, which is not conducive to calculation, so the time is converted into hours

Table 1: The relevant parameters of the distribution center for each product.

Product	Initial freshness	Preservation cost	Cost factor	Fixed cost	Sourcing cost	Inventory cost	Freight costs
1	0.93	0.4	9.5		6	0.3	5
2	0.96	0.38	10	500	9	0.35	7
3	0.95	0.42	9		8	0.4	6

Table 2: The relevant parameters of the supermarkets for each product.

Product	Initial freshness	Preservation cost	Cost factor	Price flexibility	Selling price	Inventory cost	Freight costs
1	0.92	0.6	4.0	1.1	18	0.6	5
2	0.93	0.5	4.5	1.15	22	0.8	7
3	0.93	0.45	3.8	1.2	20	0.75	6

Table 3: The maximum market demand.

Maximum demand	A_{1j}	A_{2j}	A_{3j}	A_{4j}	A_{5j}	A_{6j}	A_{7j}	A_{8j}	A_{9j}	A_{10j}
1	479	486	488	479	481	490	476	492	482	479
2	491	482	472	482	488	473	489	490	489	485
3	487	492	486	483	477	487	493	476	495	492

Table 4: The distribution-related parameters.

Parameter	Packaging and handling costs	Vehicle start-up costs	Unit shipping costs	Driver's labor cost	Vehicle average speed	Max. loading
Symbol	C_0	S	S_1	S_2	v	G
Unit	RMB/kg	RMB/time	RMB/km	RMB/time	km/h	kg
Value	0.4	40	3	100	50	1,000

Table 5: The optimal replenishment strategy for each retailer.

Market	Replenishment product	Replenishment times	Replenishment volume	Actual demand	Spoiled goods
1	1	7	158.98	155.58	3.4
2	2	7	144.82	142.47	2.35
3	1	6	188.22	183.59	4.63
6	3	7	157.57	154.63	2.94
8	2	6	170.82	167.62	3.2
13	3	7	159.22	156.25	2.97
15	3	6	187.31	183.28	4.03
16	1	4	276.98	267.19	9.79
17	2	6	171.30	168.09	3.21
18	2	4	248.71	241.94	6.77

for calculation, the time unit of the distribution service is hours, and the total time of replenishment is 72 hours.

Based on the optimal number of replenishments and the optimal replenishment quantity of each fresh food supermarket calculated by the genetic algorithm and the operating time of each replenishment of the supermarket, the optimal distribution path of the distribution center was solved by using the ant colony algorithm. According to the results of the algorithm, the distribution center makes 17 deliveries for each supermarket within 3 days of an order cycle; and the total vehicle travels 767.2 km; and the total cost of delivery is 4,695.1 RMB. In this paper, we firstly use a genetic algorithm to solve the minimum total inventory cost of distribution centers and fresh food supermarkets and calculate the optimal replenishment quantity and replenishment times for each fresh food supermarket, based on which we use an ant colony algorithm to solve the distribution path with the minimum distribution cost. Therefore, the total cost of the cold chain secondary logistics system of the fresh supermarket chain within one order cycle 3 of the distribution center is 140,983.69 RMB.

In order to further elaborate on the rationality and feasibility of the urban fresh product cold chain logistics inventory and distribution synergy optimization model, this section introduces the data related to inventory and distribution in the actual operation of the fresh product supermarket chain for comparison, which mainly includes the order quantity of the distribution center, the replenishment quantity and the replenishment times of each supermarket.

The distribution center inventory costs, supermarket inventory costs, distribution costs, and total system costs for the actual operation of this fresh product supermarket with separate decisions are compared to the costs associated with the inventory and distribution synergy strategy derived in this paper, as shown in Figure 6.

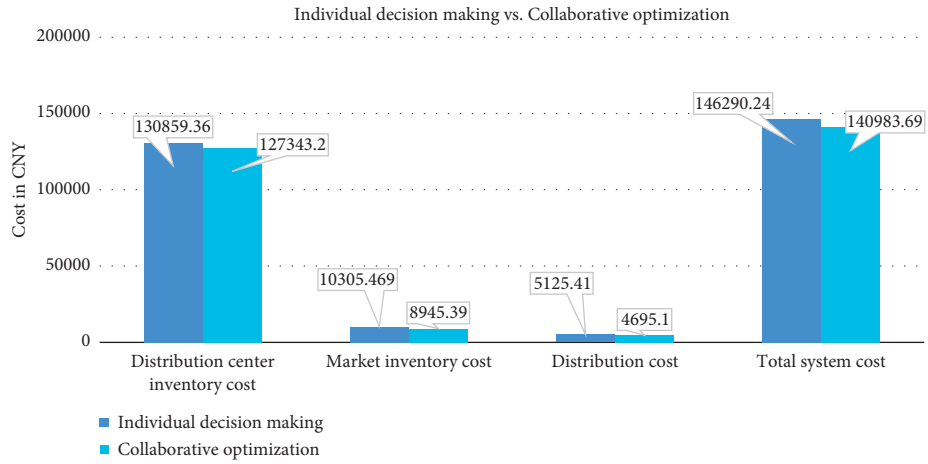

Figure 6: Cost comparison of stand-alone decision-making and collaborative optimization.

Compared with the separate decision, the total cost of the system solution of inventory and distribution co-optimization in this paper is reduced by 5,306.55 RMB. This is because the synergistic optimization model is based on the freshness function and the deterioration rate function of fresh agricultural products, which largely ensures the freshness of fresh products and reduces the deterioration loss of products, thus reducing the cost of goods loss in the distribution center. In addition, the distribution cost is reduced by 430.31 RMB, which is mainly due to the fact that the distribution model is solved in the delivery path with the lowest delivery cost, which reduces the cost of distribution to a certain extent. After solving the collaborative optimization model, the supermarket inventory cost is reduced by 1,360.079. This is due to the fact that the collaborative optimization model in this paper is based on the fact that customer demand is determined by the freshness of fresh products and the sales price. The model ensures that the sales volume of the supermarket increases per unit replenishment cycle and the time that the products occupy the inventory is reduced by minimizing the decay rate of freshness, thus reducing fresh product supermarkets' inventory costs.

4. Conclusion and Discussion

This paper takes urban fresh agricultural products cold chain logistics as the research object; analyzes the relationship among freshness cost input, freshness, and deterioration rate; establishes a collaborative optimization model of urban fresh agricultural products cold chain logistics inventory and distribution based on a single distribution center under the condition that the customer market demand is influenced by both freshness and sales price of fresh agricultural products; and proposes a partitioned solution strategy for the multidistribution center problem. Among them, the main work of the thesis is as follows. (1) The thesis takes the secondary system composed of urban fresh agricultural products cold chain logistics distribution center and retailer as the research object; analyzes the relationship between fresh agricultural products freshness function, deterioration rate function, freshness cost input, and so on; also analyzes the relationship between customer demand and product freshness and sales price; and establishes the urban fresh agricultural products cold chain logistics inventory and distribution collaborative optimization based on single distribution center. The model of optimization is established. (2) The thesis analyzes the structure of the cold chain logistics secondary network with multiple distribution centers for fresh agricultural products, proposes a strategy of partitioning solution, uses the center of gravity partitioning method to partition each retailer, converts the multiple distribution center problem into a single distribution center problem, and finally solves it through the single distribution center inventory and distribution cooperative optimization model. (3) The thesis realizes the combination of a genetic algorithm and ant colony algorithm to solve the problem. Firstly, the genetic algorithm is used to solve the optimal distribution volume and number of deliveries for each retailer by distribution center under the condition that the total sum of inventory cost of fresh product distribution center and retailer inventory cost is minimized. (4) The thesis verifies the feasibility of the collaborative optimization model of inventory and distribution of urban fresh agricultural products cold chain logistics by designing practical arithmetic cases, using MATLAB genetic algorithm and ant colony algorithm, and at the end, the minimum cost, optimal order quantity, optimal distribution quantity, and distribution route are derived. (5) In the modeling process, the relationship between freshness input cost and freshness and deterioration rate is considered more comprehensively, and the effective customer demand is combined with freshness and sales price to design the actual customer demand function. At the same time, the paper comprehensively considers the actual influencing factors, such as the limitation of each retailer on the delivery time and the maximum load capacity of the vehicle.

Based on the above analysis, the following conclusions can be drawn: (1) The cooperative optimization model of inventory and distribution of urban fresh agricultural products cold chain logistics based on the freshness and customer demand influenced by both freshness and sales price is practical and feasible, and the model solution can realize the cooperative

optimization of inventory and distribution of urban fresh agricultural products cold chain logistics secondary system. (2) The algorithm designed in this paper is feasible, and the genetic algorithm and ant colony algorithm of the collaborative optimization model designed in this paper can solve the optimal solution of the secondary system of urban fresh product cold chain logistics through the calculation example. (3) The strategy of the center of gravity partitioning designed in this paper can realize the solution of the problem of multiple distribution centers corresponding to multiple retailers and convert the complex multidistribution center problem into a single distribution center problem to be carried out; therefore, the solution strategy has certain practicality.

The problem of collaborative optimization of inventory and distribution of urban fresh agricultural products cold chain logistics involves complex and uncertain constraints and influencing factors in practice, which needs continuous improvement in practice. Based on the previous theories, this paper further investigates such problems and establishes an inventory-distribution collaborative optimization model for urban fresh product cold chain logistics, considering freshness cost input, freshness, deterioration rate, and customer demand, and designs an algorithm that conforms to the model, but many practical influencing factors are ignored in the modeling and solving process, so there are more problems that need further research, such as: (1) this paper does not study the freshness of fresh agricultural products in the inventory and distribution of loading and unloading, handling, and other aspects of the irreversible damage to product quality caused by irregularities in the operation, but in the actual distribution process, the damage caused by a handling of the product exists, so this factor needs to be taken into account in the subsequent research. (2) The paper only considers the case that the distribution center delivers only one product for each retailer in the solution of the calculation, but in practice, there are multiple products replenished by each retailer, and the replenishment cycle of each product is different for each retailer, so this situation needs to be improved in the subsequent research. (3) The model in this paper is a system optimization model constructed based on the fact that customer demand is influenced by both product sales price and freshness, but in the actual operation of fresh product supermarkets, customer demand is stochastic, so the theory related to stochastic demand should be improved in future research on inventory and distribution optimization.

Data Availability

The data set can be obtained from the author upon request.

Conflicts of Interest

The author declares that there are no conflicts of interest.

Acknowledgments

The authors thank Achievements in The Brand Majors Development Program of Private University of Henan Province (no. [2017]344) and Soft Science Research Programs of Henan Province in 2021: Study On Long Effective Mechanism of Employee-Shared Flexible Employment System of Post Epidemic (no. 212400410343).

References

[1] H. Treiblmaier, "The impact of the blockchain on the supply chain: a theory-based research framework and a call for action," *ERN Networks*, vol. 23, no. 6, 2018.

[2] Z. Han, L. Hua, Y. Fang, Q. Ma, Y. Li, and J. Wang, "Innovative research on refrigeration technology of cold chain logistics," *IOP Conference Series: Earth and Environmental Science*, vol. 474, Article ID 052105, 2020.

[3] P. Dirapan, D. Boonyakiat, and P. B. Poonlarp, "Improving shelf life, maintaining quality, and delaying microbial growth of broccoli in supply chain using commercial vacuum cooling and package icing," *Horticulturae*, vol. 7, no. 11, 2021.

[4] T. Davis, "Effective supply chain management," *Strategic Direction*, vol. 34, no. 4, 2020.

[5] L. L. Yan and S. B. Liu, "Effect of different pre-cooling, packaging and cold storage treatments on quality of broccoli," in *Proceedings of the International Horticultural Congress on Science and Horticulture for People (IHC2010): International Symposium on Postharvest Technology in the Global Market*, 2012.

[6] Y. Jin and X. Jin, "Using k-means clustering to classify protest songs based on conceptual and descriptive audio features," *Culture and Computing*, pp. 291–304, 2022.

[7] M. Saad, "Effect of cooling delays on quality attribute of globe artichoke during cold storage," *Annals of Agricultural Science, Moshtohor*, vol. 57, no. 1, pp. 105–112, 2019.

[8] Y. Jiang, X. Jin, and Q. Deng, "Short video uprising : how # BlackLivesMatter content on TikTok challenges the protest paradigm," *Computers and Society*, 2022.

[9] N. Terry and L. A. Terry, "Recent advances in controlled and modified atmosphere of fresh produce," *Johnson Matthey Technology Review*, vol. 62, no. 1, pp. 107–117, 2018.

[10] L. Yan, X. Jin, and Y. Zhang, "Effects of virtual reality technology in disaster news coverage based on MAIN model," *Communications in Computer and Information Science*, vol. 2022, pp. 122–129, 2022.

[11] L. Li, A. Lichter, D. Kenigsbuch, and R. Porat, "Effects of cooling delays at the wholesale market on the quality of fruit and vegetables after retail marketing," *Journal of Food Processing and Preservation*, vol. 39, no. 6, pp. 2533–2547, 2015.

[12] P. Brat, C. Bugaud, C. Guillermet, and F. Salmon, "Review of banana green life throughout the food chain: from autocatalytic induction to the optimisation of shipping and storage conditions," *Scientia Horticulturae*, vol. 262, Article ID 109054, 1 page, 2020.

[13] W. Pelletier, J. K. Brecht, M. Cecilia do Nascimento Nunes, and J.-P. Émond, "Quality of strawberries shipped by truck from California to Florida as influenced by postharvest temperature management practices," *HortTechnology*, vol. 21, no. 4, pp. 482–493, 2011.

[14] Z. Zhu, Y. Geng, and D. Sun, "Effects of operation processes and conditions on enhancing performances of vacuum cooling of foods: a review," *Trends Food Sci. \& Technol*, 2019.

[15] Z. Hussein, O. J. Caleb, and U. L. Opara, "Perforation-mediated modified atmosphere packaging of fresh and minimally processed produce-A review," *Food Packaging and Shelf Life*, vol. 6, pp. 7–20, 2015.

[16] F. A. R. Oliveira, S. C. Fonseca, J. C. Oliveira, J. K. Brecht, and K. Chau, "Development of perforation-mediated modified

atmosphere packaging to preserve fresh fruit and vegetable quality after harvest/Envasado em atmósfera modificada y películas perforadas para preservar la calidad de frutas y verduras frescas después de su cosecha," *Food Science and Technology International*, vol. 4, no. 5, pp. 339–352, 1998.

[17] A. Akshaya, "Microporous modified atmosphere packaging of food stuffs," *International Journal of Advance Research, Ideas and Innovations in Technology*, vol. 7, no. 3, pp. 713–1496, 2021.

[18] U. L. Opara, O. J. Caleb, and Z. A. Belay, "Modified atmosphere packaging for food preservation," *Food Qual. Shelf Life*, 2019.

[19] P. Qu, M. Zhang, K. Fan, and Z. Guo, "Microporous modified atmosphere packaging to extend shelf life of fresh foods: a review," *Critical Reviews in Food Science and Nutrition*, vol. 62, no. 1, pp. 51–65, 2020.

[20] E. S. Spang, "Food loss and waste: measurement, drivers, and solutions," *Annu. Rev. Environ. Resour*, 2019.

[21] L. M. A. Chan, A. Federgruen, and D. Simchi-Levi, "Probabilistic analyses and practical algorithms for inventory-routing models," *Operations Research*, vol. 46, no. 1, pp. 96–106, 1998.

[22] J. Li, F. Chu, and H. Chen, "A solution approach to the inventory routing problem in a three-level distribution system," *European Journal of Operational Research*, vol. 210, no. 3, pp. 736–744, 2011.

[23] J. Mathur and K. Mathur, "An efficient heuristic algorithm for a two-echelon joint inventory and routing problem," *Transportation Science*, vol. 41, no. 1, pp. 55–73, 2007.

[24] I. R. Donis-González, D. E. Guyer, A. P. Pease, and F. Barthel, "Internal characterisation of fresh agricultural products using traditional and ultrafast electron beam X-ray computed tomography imaging," *Biosystems Engineering*, vol. 117, pp. 104–113, 2014.

[25] A. Prakash, "Particular applications of food irradiation fresh produce," *Radiation Physics and Chemistry*, vol. 129, pp. 50–52, 2016.

[26] O. Ahumada, J. Rene Villalobos, and A. Nicholas Mason, "Tactical planning of the production and distribution of fresh agricultural products under uncertainty," *Agricultural Systems*, vol. 112, pp. 17–26, 2012.

[27] S. Piramuthu and W. Zhou, "RFID and perishable inventory management with shelf-space and freshness dependent demand," *International Journal of Production Economics*, vol. 144, no. 2, pp. 635–640, 2013.

[28] S. Banerjee and S. Agrawal, "Inventory model for deteriorating items with freshness and price dependent demand: optimal discounting and ordering policies," *Applied Mathematical Modelling*, vol. 52, pp. 53–64, 2017.

[29] C. K. Chan, W. H. Wong, A. Langevin, and Y. C. E. Lee, "An integrated production-inventory model for deteriorating items with consideration of optimal production rate and deterioration during delivery," *International Journal of Production Economics*, vol. 189, pp. 1–13, 2017.

[30] T.-P. Hsieh and C.-Y. Dye, "A production-inventory model incorporating the effect of preservation technology investment when demand is fluctuating with time," *Journal of Computational and Applied Mathematics*, vol. 239, pp. 25–36, 2013.

[31] N. Nemtajela and C. Mbohwa, "Relationship between inventory management and uncertain demand for fast moving consumer goods organisations," *Procedia Manufacturing*, vol. 8, pp. 699–706, 2017.

[32] S. Mirzaei and A. Seifi, "Considering lost sale in inventory routing problems for perishable goods," *Computers & Industrial Engineering*, vol. 87, pp. 213–227, 2015.

[33] Y. Li, S. Zhang, and J. Han, "Dynamic pricing and periodic ordering for a stochastic inventory system with deteriorating items," *Automatica*, vol. 76, pp. 200–213, 2017.

[34] S. Anily and A. Federgruen, "One warehouse multiple retailer systems with vehicle routing costs," *Management Science*, vol. 36, no. 1, pp. 92–114, 1990.

[35] S. Anily and J. Bramel, "An asymptotic 98.5%-effective lower bound on fixed partition policies for the inventory-routing problem," *Discrete Applied Mathematics*, vol. 145, no. 1, pp. 22–39, 2004.

[36] C. Monthatipkul and P. Yenradee, "Inventory/distribution control system in a one-warehouse/multi-retailer supply chain," *International Journal of Production Economics*, vol. 114, no. 1, pp. 119–133, 2008.

[37] G. Laporte, "The vehicle routing problem: an overview of exact and approximate algorithms," *European Journal of Operational Research*, vol. 59, no. 3, pp. 345–358, 1992.

[38] G. Nagy and S. Salhi, "Heuristic algorithms for single and multiple depot vehicle routing problems with pickups and deliveries," *European Journal of Operational Research*, vol. 162, no. 1, pp. 126–141, 2005.

[39] A. M. Savelsbergh and M. W. P. Savelsbergh, "A decomposition approach for the inventory-routing problem," *Transportation Science*, vol. 38, no. 4, pp. 488–502, 2004.

Hindawi
Scientific Programming
Volume 2022, Article ID 7648810, 9 pages
https://doi.org/10.1155/2022/7648810

Research Article

Ensemble Investment Strategies Based on Reinforcement Learning

Fangyi Li, Zhixing Wang, and Peng Zhou

Chengdu University of Technology, Chengdu, Sichuan, China

Correspondence should be addressed to Zhixing Wang; wang.zhixing@student.zy.cdut.edu.cn

Received 16 June 2022; Revised 5 July 2022; Accepted 8 July 2022; Published 8 September 2022

Academic Editor: Lianhui Li

Due to the rapid development of hardware devices, the analytical processing and algorithmic capabilities of computers are also being enhanced, which makes machine learning play an increasingly important role in the field of quantitative investment. For this reason, the possibility of replacing traditional human traders with automated investment algorithms that have been trained several times has become a hot topic in recent years. The majority of machine algorithms used in today's stock trading market are supervised learning algorithms, which are still unable to objectively analyse the market and find the optimal solution for market trading on their own. To solve the two major challenges of environment awareness and automated decision-making, this study uses three core algorithms, PPO, A2C, and SAC, to build a set of ensemble automated trading strategies in a deep reinforcement learning-based framework. The *ensemble* trading strategy combines the advantages of each of the three algorithms to make the original reinforcement learning algorithm more adaptive, and to avoid consuming a large amount of memory when training the network, the study uses the PCA method to compress the dimension of the stock feature vector. We test our algorithm on 40 A-share stocks with sufficient liquidity and compare it with different trading strategies. The results show that the ensemble strategy proposed in this study outperforms three independent algorithms and two selected baselines, achieving an accumulated return of around 70%.

1. Introduction

Increasing computer processing power has led to the gradual digitization of financial market transactions, and it has become a reality to use computers to access large amounts of financial market data and complete high-frequency transactions within milliseconds [1]. The massive amount of data in the financial markets is often highly dimensional and noisy, and traditional econometrics cannot accurately quantify this multidimensional market data, so forecasting financial market data has always been a challenging problem in finance [2]. Most of the quantitative trading algorithms in the market today use supervised learning methods, which rely on manual design to select features and construct labels [3]. Quantitative trading systems under this approach require external managers with a certain level of financial knowledge to be able to change labels and parameters in a timely manner in response to market conditions, and therefore, the objectivity and independence of the algorithm cannot be guaranteed [4]. In contrast to supervised learning methods, reinforcement learning methods have the ability to learn control strategies from high-dimensional data [5]. Reinforcement learning methods do not require supervision by external managers and can continuously optimize paths to achieve the best cumulative returns through rewards and penalties during the interaction of market transactions [6].

Although reinforcement learning offers a new way of thinking about the analysis and prediction of financial data, there is still room for improvement. The first is that derivative algorithms on reinforcement learning often ignore the dominance of irrational investor sentiment in financial markets in the pursuit of decision objectivity, and researchers often combine sentiment mining with supervised algorithms, but few apply this to reinforcement learning methods [7]. This study addresses this issue by expressing market sentiment as a sentiment indicator and effectively improving the adaptability of algorithms to irrational markets. Secondly, it has been shown that reinforcement learning relies on a large amount of external environment as input data, but existing trading algorithms tend to select

fewer technical indicators as the spatial state of the underlying investment to alleviate memory pressure [8], making the benefits of reinforcement learning methods less impressive than supervised learning methods. This study uses the PCA algorithm to compress the spatial vector dimension, incorporating more technical indicators to extend the spatial state of the underlying under the same memory pressure. In addition, the researcher found that different agents are suitable for different conditions of the stock market, which means that the model constructed by a single agent does not have the effectiveness and generalization ability in the face of different stock assets and different market environments [9]. So, this study constructs an ensemble strategy of three algorithms: PPO, A2C, and SAC. The ensemble strategy can choose the appropriate agent to maximize the accumulated return for different market environments and situations, so the ensemble strategy is more stable and reliable than a single strategy.

In the design of the ensemble model, we firstly constructed a deep reinforcement learning framework, setting up the environment, state space, and action space. Secondly, we designed a reward and punishment function for the agent to ensure that it can effectively optimize its own decisions. Thirdly, we connect the three different agents effectively through the Sharpe ratio. Finally, we demonstrate the effectiveness of the ensemble algorithm through ablation experiments and two baselines.

The study is structured as follows: Section 2 presents the relevant literature in the same research area, Section 3 describes the theoretical approach used in this study, Section 4 describes the detailed construction process of the ensemble model, Section 5 presents the data processing and empirical results, and finally we place the summary in Section 6.

2. Literature Review

Reinforcement learning has now evolved from its initial stand-alone application to a multiplicity of applications in combination with deep learning. It has been extensively investigated by many researchers in the field of finance due to its ability to effectively deal with continuous decision-making.

In terms of practical applications of reinforcement learning, Moody and Saffell proposed to construct portfolios and trade stocks with recurrent reinforcement learning and eventually proved that the returns of the reinforcement learning strategy were higher than those of the buy-and-hold strategy [10]. Tan et al. added an adaptive network fuzzy inference system as a supplement to the reinforcement learning framework to design a high-frequency trading strategy [11]. Sun and Bi selected convolutional neural networks and LSTM neural networks to build up and down classification models, respectively, based on which a high-frequency trading strategy was proposed and backtested with the main asphalt futures contract and demonstrated that the high-frequency trading strategy based on convolutional neural networks and long- and short-term memory neural networks had better profitability [12]. Dai and Zhang demonstrated that the reinforcement learning model outperformed the buy-and-hold strategy and MACD strategy in stock selection [13]. Lu and Salem applied the long- and short-term memory model (LSTM) to reinforcement learning and backtested it through forex trading, and the results demonstrated that the improved reinforcement learning model could effectively control the number of trades and maintain stable profitability [14]. Hu et al. constructed a cointegrated pair trading model based on the reinforcement learning SARSA algorithm and conducted simulation trading experiments on the Chinese bond market and demonstrated that the model outperformed the traditional model in all aspects and could significantly improve the profitability of the trading system [15].

In terms of algorithm design for reinforcement learning, Zhang and Wang and other scholars (2015) constructed a stock prediction model based on neural networks, which can solve the problem of high dimensionality of input data through genetic algorithms, and the results showed that genetic algorithms can improve model training efficiency [16]. Yung added news headlines for market opinion mining on the basis of stock time-series price data and in this way effectively improved the correct rate of model decisions [17]. Zhou et al. improved the traditional quantitative trading algorithm using the sentiment indicator ARBR, enabling the improved reinforcement learning algorithm to have richer returns in irrational markets [18]. Li et al. proposed a new trading model for deep reinforcement learning, which used two different reinforcement learning methods, stacked denoising self-coding (SDAEs) and long- and short-term memory (LSTM), and can effectively extract features from the raw data to build a robust trading agent, and experimental results show that the model achieves stable risk-adjusted returns in both the stock and future markets [19]. Gabrielsson and Johansson introduced seven new features based on Japanese candlesticks into the reinforcement learning input, and their HFT system outperformed the S&P 500 index and significantly outperformed the basic RRL algorithm in the test [20].

It is therefore easy to see that trading models built on reinforcement learning are well established and widely used in the financial field, achieving good returns in both the equity and foreign exchange markets. In terms of improvements to reinforcement learning algorithms, researchers have focused on improving different neural network structures and expanding the spatial state of the model.

3. Methodology

3.1. Reinforcement Learning Theory. Reinforcement learning is an important machine learning approach in current quantitative trading research [21]. Unlike common machine learning algorithms, the core of reinforcement learning is to allow an agent in an interactive environment to calculate the reward value for different actions using the current action state at the moment and to continuously optimize the agent's internal policy along the direction of the best reward value until the best policy is found [22]. In summary, the reinforcement learning framework consists

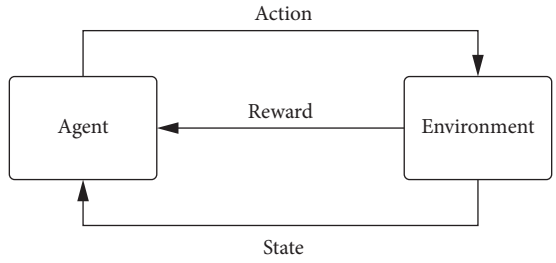

Figure 1: Structure of the reinforcement learning algorithm.

of the interactable state of the agent in the current environment, the different actions resulting from the decision, the policy for the decision made in the current state, the reward function used to calculate the reward value at the end of the action, the value function for the different actions and states, and the environment used to implement the agent interaction process.

The flow of the whole reinforcement learning algorithm is shown in Figure 1. At time t , the agent obtains the current state of the environment S_t and uses the policy function to process S_t to output the action a_t in the current state. After the action is completed, the action a_t will be applied to the environment, causing the environment state to change from S_t to S_{t+1}, and then, the function uses the action transfer state to calculate the reward value τ_t for the action a_t. The agent can use τ_t to continuously optimize future action strategies and ultimately maximize the cumulative reward value. The optimal strategy can be shown in (1), where π is the chosen strategy, γ is the discount rate, T is the total moment of interaction, and a is the state space.

$$\pi^* = \text{argmax}_\pi E_\pi \left\{ \sum_{T=0}^{\infty} \gamma^T r_{t+T} | S_t = S \right\}, \forall S \in S, \forall t \geq 0. \quad (1)$$

3.2. Markov Decision Process. The Markov decision process is the classical algorithm for reinforcement learning modelling, and its main idea is to perform dynamic planning with finding the maximum cumulative payoff on the MDP [23]. If the current state, which contains all relevant historical information, can be used to determine the future cumulative payoff, then we can consider the state to have Markovianity, and this property can be described as follows:

$$P(s_{t+1}|s_t) = P(s_{t+1}|s_t, \ldots, s_2, s_1). \quad (2)$$

We can describe the MDP using a set, as in (3), where S is the state space, which stores all states in the environment, A is the action space, which represents all actions that the agent can interact with, and P is the transfer probability, which represents the probability that an action taken by the agent in a state will result in a state transfer, which we usually identify as needing to satisfy $0 \leq p(s|s_t, a_t) \leq 1$. R is the reward generated by the action.

$$M = \{S, A, P, R, \gamma\}. \quad (3)$$

3.3. A2C. The actor-critic approach is one of the mainstream approaches in reinforcement learning, combining the advantages of both value-based and policy-based classical algorithms [24]. The core idea is to use the value of the state actions predicted by the critic model to optimize the decision-making behaviour of the actor model, and by alternating training, the generated actions can be made to better match the current environment and state. The structure of the model is shown in Figure 2.

Since the original AC model was slow to converge, the A2C algorithm was proposed to reduce the variance of the strategy gradient by adding a baseline to the strategy gradient while keeping the expectation of the strategy gradient random variable constant, allowing for faster convergence.

The gradient formula of the AC algorithm in its original state can be expressed as follows:

$$\nabla_\theta J(\theta) = E_{\pi_\theta}[\nabla_\theta \log \pi_\theta(s, a)(Q_\pi(s, a) - B)]. \quad (4)$$

Since the baseline function B is only related to the state S and not to the action A, the above equation can be derived as follows:

$$\nabla_\theta J(\theta) = E_{\pi_\theta}[\nabla_\theta \log \pi_\theta Q_\pi(s, a)]. \quad (5)$$

Since the baseline function B is a function independent of the action A, we can further optimize the formula using the state value function $V(s)$ as the baseline $B(s)$ and let the dominance function be $A(s, a) = Q(s, a) - V(s)$. Eventually, we can obtain the optimized gradient as follows:

$$\nabla_\theta J(\theta) = E_{\pi_\theta}[\nabla_\theta \log \pi_\theta(s, a) A(s, a)]. \quad (6)$$

In this study, the MLP neural network is chosen to build the A2C algorithm. The algorithm is updated step by step during training, and its training process is seen in Table 1.

3.4. PPO. The principle of the PPO algorithm is to represent the policy parametrically as $\pi_\theta(a|s)$, using a parametrized linear function or neural network to represent the policy [25].

The PPO algorithm strategy gradient is implemented by calculating an estimator combined with a stochastic gradient ascent algorithm, and the updated formula can be seen as follows:

$$\theta_r = \theta_b + \alpha \nabla_\theta J, \quad (7)$$

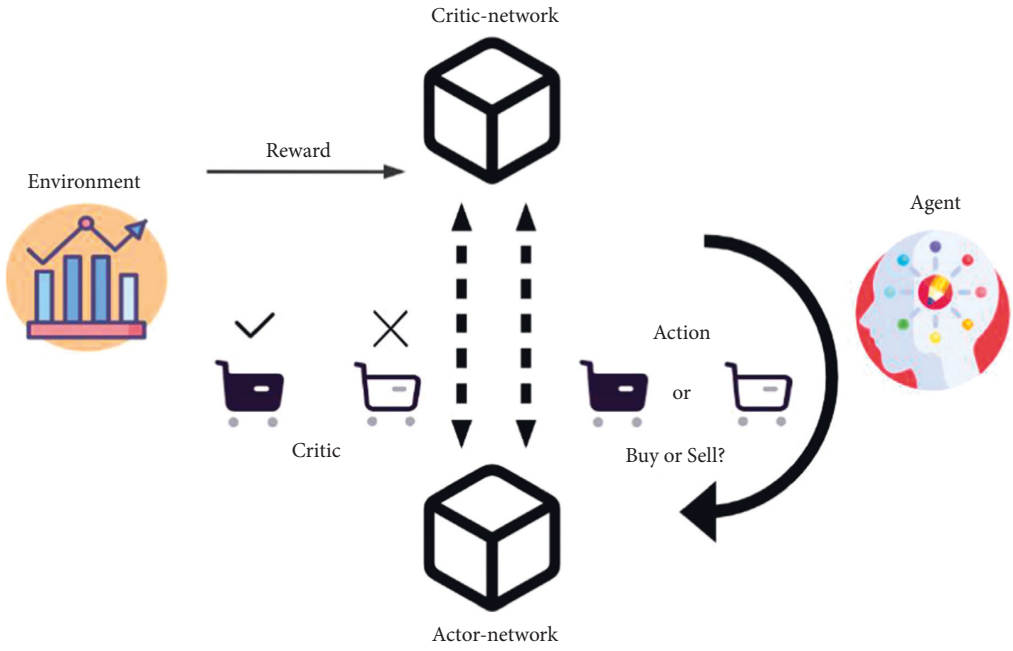

Figure 2: Structure of the actor-critic model.

Table 1: Pseudo-code for the A2C model.

```
Input: environment of the stock market
Output: estimated optimal strategy π(θ)
Initial setup of actor and critic networks
Repeat
  For episodes = 0, 1, 2, . . ., N do:
    Get state S and calculate π(AS; θ|) to get action A
    IF the episode does not end there:
      Get S′ with reward τ
      Using critic networks to obtain return values to estimate Q
      Calculating the gradient using Q values and updating the actor network
      Updating the critic network to reduce the difference
      Update status S
    End
  End
To convergence
```

where θ_b is the policy parameter before the update, θ_τ is the updated policy parameter, α is the learning rate, and ∇_θ is the importance weight. J is the optimization objective, which is the expected value of the future reward in state S.

3.5. SAC. SAC is a heteroskedastic AC algorithm developed for maximum entropy reinforcement learning [26]. Unlike other methodological theories, the SAC algorithm changes the goal of reinforcement learning by the introduction of the concept of entropy, which actually improves the exploratory and robustness of the algorithm [27].

The entropy [28–35] of the distribution x can be expressed as follows:

$$H(p) = E_{X\sim p}[-\ln\ p(x)]. \tag{8}$$

In order not to miss any valid actions and trajectories and to promote strategy randomization for greater robustness and exploration, the maximum entropy reinforcement learning algorithm requires the strategy function to output the action expressed as follows:

$$\pi^* = \operatorname{argmax}_\pi E_{s_t,a_t\sim\rho_\pi}\left[\sum_t r_t + \alpha H(\pi(\cdot|s_t))\right]. \tag{9}$$

4. Ensemble Model Development

The ensemble model can be divided into two parts: the first part is to select a suitable algorithm from A2C, PPO, and SAC as agent, and the second part is to build the state space of the stock through stock price, technical indicators, and sentiment indicators to describe the stock trading market environment [36–39]. When these two parts are completed, the action space and reward function will link the agent with the environment so that the agent

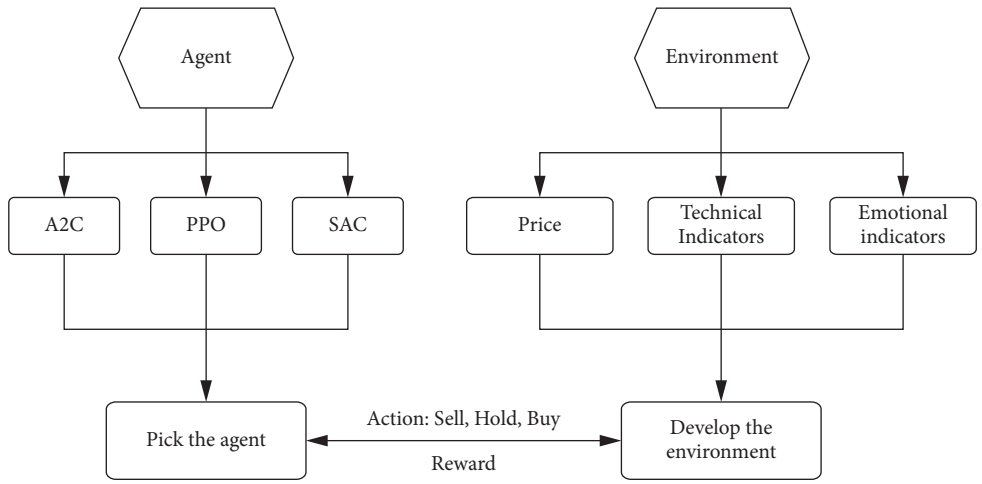

Figure 3: Structure of the ensemble strategy.

can make continuous decisions to maximize the cumulative return. The structure of the ensemble model is shown in Figure 3.

4.1. Select the Agent. In this study, we use a several months' long window to train all three agents simultaneously, and every three months, we retrain our three agents. At the same time, we use the latter three months of the training window to validate the performance of the three different agents and select the agent with the highest Sharpe ratio as the agent of the ensemble strategy for the underlying investment. The following equation shows how the Sharpe ratio is calculated:

$$\text{Sharpe ratio} = \frac{\overline{r}_p - r_f}{\sigma_p}. \tag{10}$$

4.2. Setting Up the Environment. We incorporate the daily opening and closing prices of the stock: the technical indicators of the stock and the sentiment indicator ARBR, which describes market sentiment, as the spatial state of the stock.

It is worth mentioning that to incorporate more indicators as the spatial state of the stock while relieving the memory pressure on the algorithm, we used the PCA algorithm to compress the original 24-dimensional feature vector to 20 dimensions. Figure 4 shows the correlation hotspots of the technical indicators selected by the ensemble model. It is easy to see that there is a large positive correlation between vol10 and vol20 and a large negative correlation between the deviation rate BIAS and MA, so the PCA algorithm can be used to reduce the dimensionality.

4.3. Transaction Cost. Since every transaction in the stock market incurs transaction costs and the rules for transaction costs in the stock exchange vary from country to country, we have set a uniform transaction cost of 0.1% of the value of each transaction.

4.4. Reward Function. We define the reward value as the maximum profit that each group of stocks can take in a given period of time, expressed as follows:

$$r_t = p_t - p_{t-1}, \tag{11}$$

where r_t is the value of the reward currently received, p_t is the price of the stock at time t, and p_{t-1} is the price of the stock at the previous time. The reward value is therefore the difference between the two momentary prices. When the current price is greater than the past price, a positive reward value is obtained; when the current price is lower than the past price, a negative reward value is obtained. The final cumulative return is as follows:

$$R_t = \sum_{t=1}^{T} r_t. \tag{12}$$

4.5. Action Space. To make it easier to calculate the profitability of the ensemble model in the stock market, we do not consider shorting trades in the stock and simply use buy, sell, hold, and wait and see as the action states of the stock. This can be expressed as follows:

$$a = \begin{cases} 1, & \text{Buy}, \\ 0, & \text{Wait and see}, \\ -1, & \text{Sell}. \end{cases} \tag{13}$$

5. Empirical Results

5.1. Data Preprocessing. We select the constituent stocks of the CSI 100 index as the pool of stocks to be traded in the pooled strategy. We use historical daily data from 1 January 2010 to 12 February 2021 for the evaluation of model returns. The stock data used in this study are downloaded via the wind terminal. As mentioned above, we split the historical stock data into two parts: one for the training of the three agents, PPO, A2C, and SAC, and the other for the validation of the three agents, including the adjustment of the learning

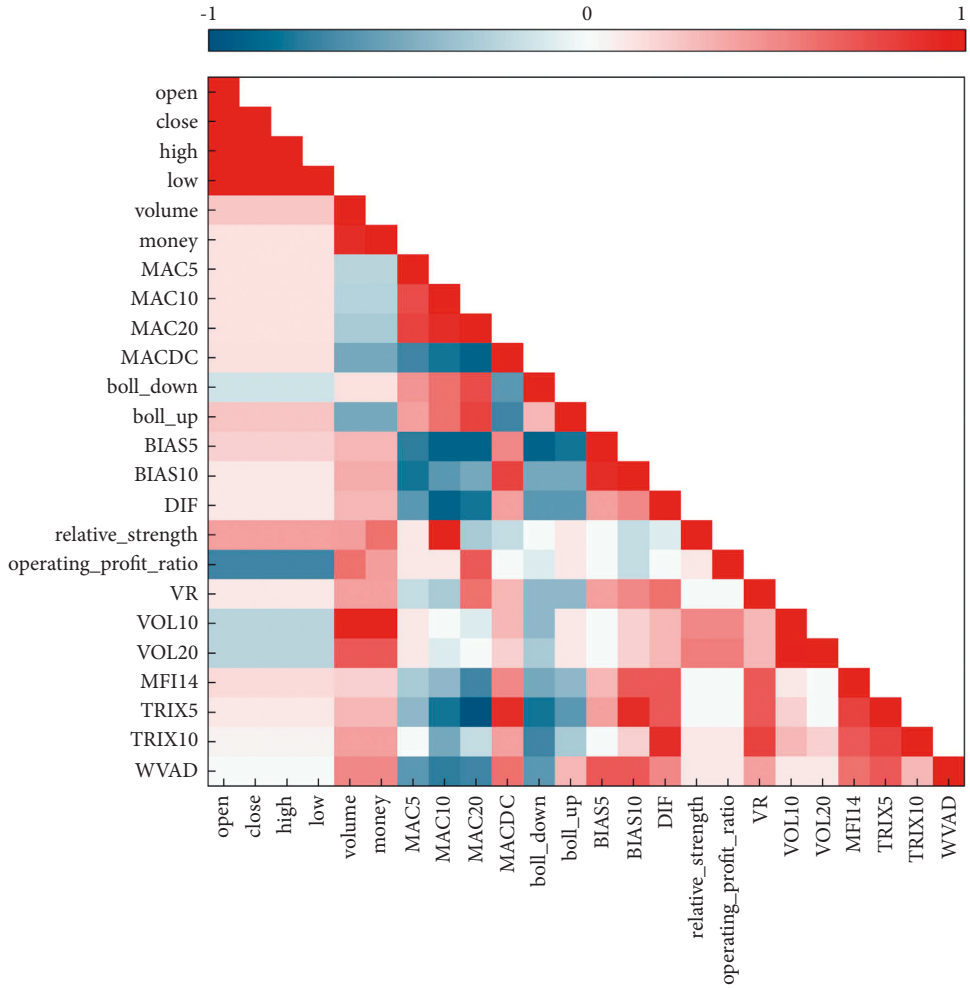

Figure 4: Relevance of selected technical indicators.

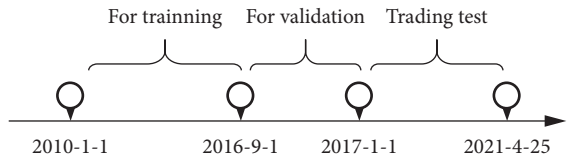

Figure 5: Classification of empirical data.

rate and key parameters. After selecting a suitable agent by comparing the Sharpe ratio, we start the real trading test and compare the results. The three agent's algorithms are MACD, and Min-Variance two baselines. A breakdown of the training data used is seen in Figure 5.

5.2. Test Result. The backtest results of the ensemble model and the comparison model are shown in Figure 6. It is easy to see that the ensemble model achieved a cumulative return of 71.92% and an annual return of 17.98%, which is higher than the remaining two individual agent models with the baseline in terms of return results. More detailed backtesting data are shown in Table 2. The ensemble model has the lowest annual volatility, which proves that the model is more stable and reliable than the other models, while the min-variance model has the highest annual volatility. In terms of the Sharpe ratio, the ensemble model achieved the highest Sharpe ratio, while it had the lowest maximum capital withdrawal rate. Overall, the A2C, PPO, and SAC models all achieved above-baseline returns, demonstrating that all three models have some portfolio management capability. In contrast, the ensemble model achieved a cumulative return of 70%, while its stability, Sharpe ratio, and maximum return were better than the other models, demonstrating the effectiveness of the model in the equity market.

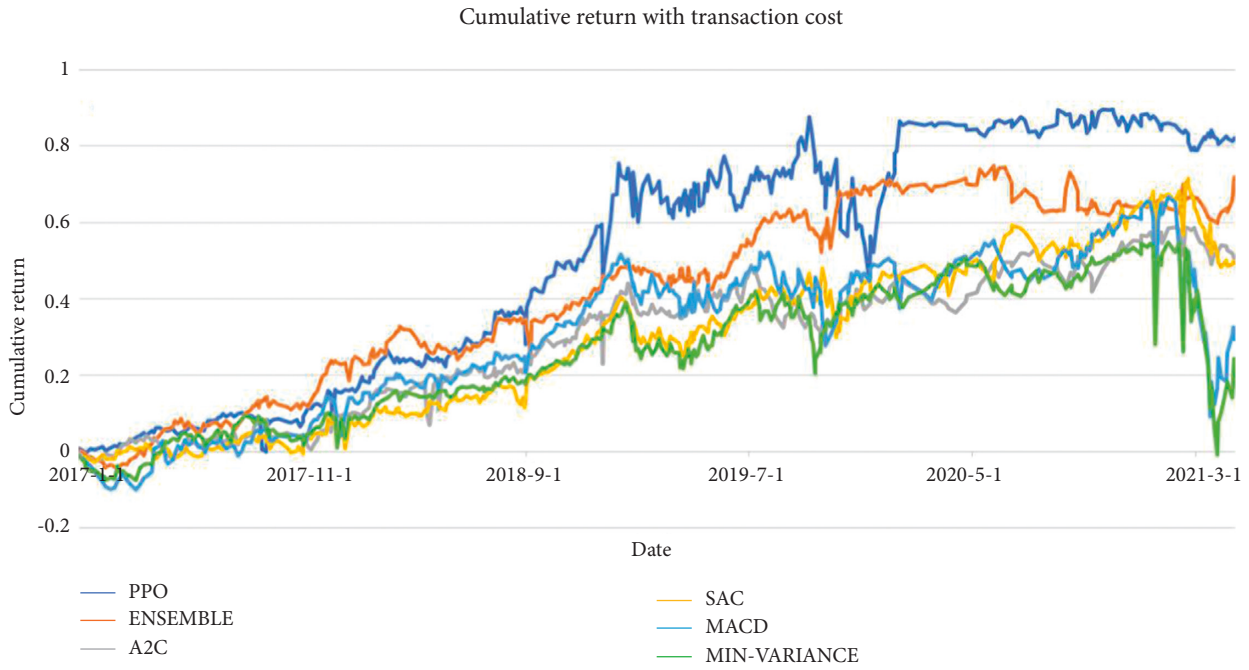

Figure 6: Cumulative return with transaction cost.

Table 2: Backtest results under different strategies.

2017/01/01–2021/04/25	Ensemble	PPO	A2C	SAC	MACD	Min-variance
Cumulative return	71.92%	81.99%	50.73%	49.23%	29.32%	24.27%
Annual return	17.98%	20.5%	12.68%	12.31%	7.33%	6.07%
Annual volatility	9.7%	14.8%	11.3%	14.9%	18.3%	20.1%
Sharpe ratio	1.41	1.12	1.15	0.78	0.42	0.45
Max drawdown	−9.5%	−25.3%	−18.4%	−14.8%	−38.8%	−34.6%

6. Conclusion

In this study, we propose an ensemble trading strategy in a reinforcement learning framework, which selects the appropriate strategy as agent from three strategies, PPO, A2C, and SAC, through the Sharpe ratio, and incorporates more stock indicators and data as the state space of the stock using the PCA method. Through backtesting on the CSI 100, the results show that the proposed model outperforms the two agent models A2C and SAC in terms of return and outperforms all three independent agent models and the two baselines in terms of Sharpe ratio, annual volatility, and maximum retracement, so the ensemble model is innovative and superior and has research and application value.

Data Availability

The dataset can be accessed upon request.

Conflicts of Interest

The authors declare that they have no conflicts of interest.

References

[1] Y. Liu, Q. Liu, H. Zhao, Z. Pan, and C. Liu, "Adaptive quantitative trading: an imitative deep reinforcement learning approach," *Proceedings of the AAAI Conference on Artificial Intelligence*, vol. 34, no. 2, pp. 2128–2135, 2020, April.

[2] X. Guo, T. L. Lai, H. Shek, and S. P. S. Wong, *Quantitative Trading: Algorithms, Analytics, Data, Models, Optimization*, Chapman and Hall/CRC, Boca Raton, FL, USA, 2017.

[3] R. Caruana and A. Niculescu-Mizil, "An empirical comparison of supervised learning algorithms," in *Proceedings of the 23rd international conference on Machine learning*, pp. 161–168, Pittsburgh, PA, USA, June, 2006.

[4] D. H. Lee, "Pseudo-label: the simple and efficient semi-supervised learning method for deep neural networks," *Workshop on challenges in representation learning ICML*, vol. 3, no. 2, p. 896, 2013.

[5] M. Eppe, C. Gumbsch, M. Kerzel, P. D. H. Nguyen, M. V. Butz, and S. Wermter, "Intelligent problem-solving as integrated hierarchical reinforcement learning," *Nature Machine Intelligence*, vol. 4, no. 1, pp. 11–20, 2022.

[6] L. Chen, K. Lu, A. Rajeswaran et al., "Decision transformer: reinforcement learning via sequence modeling," *Advances in Neural Information Processing Systems*, vol. 34, 2021.

[7] F. M. J. Mehedi Shamrat, S. Chakraborty, M. M. Imran et al., "Sentiment analysis on twitter tweets about COVID-19 vaccines using NLP and supervised KNN classification algorithm," *Indonesian Journal of Electrical Engineering and Computer Science*, vol. 23, no. 1, p. 463, 2021.

[8] E. L. Roscow, R. Chua, R. P. Costa, M. W. Jones, and N. Lepora, "Learning offline: memory replay in biological and artificial reinforcement learning," *Trends in Neurosciences*, vol. 44, no. 10, pp. 808–821, 2021.

[9] K. Xia, C. Sacco, M. Kirkpatrick et al., "A digital twin to train deep reinforcement learning agent for smart manufacturing plants: environment, interfaces and intelligence," *Journal of Manufacturing Systems*, vol. 58, pp. 210–230, 2021.

[10] J. Moody and M. Saffell, "Learning to trade via direct reinforcement," *IEEE Transactions on Neural Networks*, vol. 12, no. 4, pp. 875–889, 2001.

[11] Z. Tan, C. Quek, and P. Y. Cheng, "Stock trading with cycles: a financial application of ANFIS and reinforcement learning," *Expert Systems with Applications*, vol. 38, no. 5, pp. 4741–4755, 2011.

[12] D. C. Sun and X. C. Bi, "High-frequency trading strategies based on deep learning algorithms and their profitability," *Journal of University of Science and Technology of China*, vol. 11, pp. 923–932, 2018.

[13] S. X. Dai and S. L. Zhang, "An application of reinforcement learning based approach to stock trading," *Business Management*, vol. 3, pp. 23–27, 2021.

[14] Y. Lu and F. M. Salem, "Simplified gating in long short-term memory (lstm) recurrent neural networks," in *Proceedings of the 2017 IEEE 60th International Midwest Symposium on Circuits and Systems (MWSCAS)*, pp. 1601–1604, IEEE, Boston, MA, USA, August 2017.

[15] B. Hu, J. Li, J. Yang et al., "Reinforcement learning approach to design practical adaptive control for a small-scale intelligent vehicle," *Symmetry*, vol. 11, no. 9, p. 1139, 2019.

[16] W. Zhang and W. Wang, "Deep learning-based stock market forecasting," *Journal of Wuhan University (Natural Science Edition)*, vol. 201439, no. 1, pp. 1–7.

[17] Z. H. Yung, "Deep reinforcement learning stock algorithmic trading system application," *Computer Knowledge and Technology*, vol. 23, pp. 75-76, 2020.

[18] P. Zhou, J. Tang, and Y. Li, "Research on investment strategies of stock market based on sentiment indicators and deep reinforcement learning," in *Proceedings of the International Conference on Statistics, Applied Mathematics, and Computing Science (CSAMCS 2021)*, vol. 12163, pp. 1151–1156, SPIE, April 2022.

[19] Y. Li, W. Zheng, and Z. Zheng, "Deep robust reinforcement learning for practical algorithmic trading," *IEEE Access*, vol. 7, Article ID 108014, 2019.

[20] P. Gabrielsson and U. Johansson, "High-frequency equity index futures trading using recurrent reinforcement learning with candlesticks," in *Proceedings of the 2015 IEEE Symposium Series on Computational Intelligence*, pp. 734–741, IEEE, Cape Town, South Africa, December 2015.

[21] V. Mnih, K. Kavukcuoglu, D. Silver et al., "Playing Atari with Deep Reinforcement Learning," 2013, https://arxiv.org/abs/1312.5602.

[22] G. Dulac-Arnold, D. Mankowitz, and T. Hester, "Challenges of Real-World Reinforcement Learning," 2019, https://arxiv.org/abs/1904.12901.

[23] F. Garcia and E. Rachelson, "Markov decision processes," *Markov Decision Processes in Artificial Intelligence*, pp. 1–38, Wiley, Hoboken, NJ, USA, 2013.

[24] H. Chen, Y. Liu, Z. Zhou, and M. Zhang, "A2C: attention-augmented contrastive learning for state representation extraction," *Applied Sciences*, vol. 10, no. 17, p. 5902, 2020.

[25] L. Engstrom, A. Ilyas, S. Santurkar et al., "Implementation matters in deep rl: a case study on ppo and trpo," in *Proceedings of the International conference on learning representations*, New Orleans, LA, USA, September 2019.

[26] C. Yang and J. Collins, "Deep learning for pollen sac detection and measurement on honeybee monitoring video," in *Proceedings of the 2019 International Conference on Image and Vision Computing New Zealand (IVCNZ)*, pp. 1–6, IEEE, Dunedin, New Zealand, December 2019.

[27] J. Zhang, Q. Wang, and W. Shen, "Message-passing neural network based multi-task deep-learning framework for COSMO-SAC based σ-profile and VCOSMO prediction," *Chemical Engineering Science*, vol. 254, Article ID 117624, 2022.

[28] L. Li and C. Mao, "Big data supported PSS evaluation decision in service-oriented manufacturing," *IEEE Access*, vol. 8, Article ID 154663, 2020.

[29] X. Lu, "Research on biological population evolutionary algorithm and individual adaptive method based on quantum computing," *Wireless Communications and Mobile Computing*, vol. 2022, Article ID 5188335, 9 pages, 2022.

[30] L. Li, C. Mao, H. Sun, Y. Yuan, and B. Lei, "Digital twin driven green performance evaluation methodology of intelligent manufacturing: hybrid model based on fuzzy rough-sets AHP, multistage weight synthesis, and PROMETHEE II," *Complexity*, vol. 2020, no. 6, 24 pages, Article ID 3853925, 2020.

[31] L. Zhang and L. Qiu, "Aerobic exercise fatigue detection based on spatiotemporal entropy and label technology," , p. 2022, Scientific Programming, 2022.

[32] L. Li, T. Qu, Y. Liu et al., "Sustainability assessment of intelligent manufacturing supported by digital twin," *IEEE Access*, vol. 8, Article ID 174988, 2020.

[33] J. Zhang, "A study on mental health assessments of college students based on triangular fuzzy function and entropy weight method," *Mathematical Problems in Engineering*, vol. 2021, Article ID 6659990, 8 pages, 2021.

[34] L. Li, B. Lei, and C. Mao, "Digital twin in smart manufacturing," *Journal of Industrial Information Integration*, vol. 26, no. 9, Article ID 100289, 2022.

[35] Y. Li, F. Ning, X. Jiang, and Y. Yingmin, "Feature extraction of ship radiation signals based on wavelet packet decomposition and energy entropy," *Mathematical Problems in Engineering*, vol. 2022, Article ID 8092706, 12 pages, 2022.

[36] J. C. . Alves, D. M. da Silva, and G. R. Mateus, "Applying and comparing policy gradient methods to multi-echelon supply chains with uncertain demands and lead times. Lecture notes in computer science (including subseries lecture notes in artificial intelligence and lecture notes in bioinformatics), v 12855 LNAI," in *Proceedings of the Artificial Intelligence and Soft Computing - 20th International Conference, ICAISC 2021*, pp. 229–239, June 2021.

[37] L. Sun, M. K Siddique, L. Wang, and S. J. Li, "Mixing characteristics of a bubble mixing microfluidic chip for genomic DNA extraction based on magnetophoresis: CFD simulation and experiment," *Electrophoresis*, vol. 42, no. 21-22, pp. 2365–2374, 2021.

[38] J. Zheng, M. N. Kurt, and W. Xiaodong, "Integrated actor-critic for deep reinforcement learning. Lecture notes in computer science (including subseries lecture notes in artificial intelligence and lecture notes in bioinformatics), v 12894 LNCS," in *Proceedings of the artificial neural networks and machine learning – ICANN 2021 - 30th international conference on artificial neural networks*, pp. 505–518, Bratislava, Slovakia, September 2021.

[39] X. Wenwen, "Application Research of end to end behavior decision based on deep reinforcement learning," in *Proceedings of the 2021 5th International Conference on Electronic Information Technology and Computer Engineering, EITCE 2021*, pp. 889–894, Xiamen, China, October 2021.

Hindawi
Scientific Programming
Volume 2022, Article ID 7496054, 9 pages
https://doi.org/10.1155/2022/7496054

Research Article

Text Feature Extraction and Representation of Chinese Mental Verbs Based on Deep Learning

Yongxue Wang[1] **and Tee Boon Chuan**[2]

[1]*Chinese Studies, Institute of Studies, Universiti Tunku Abdul Rahman, Kajang 4300, Malaysia*
[2]*Institute of Chinese Studies, Universiti Tunku Abdul Rahman, Kajang 4300, Malaysia*

Correspondence should be addressed to Tee Boon Chuan; b20160803111@stu.ccsu.edu.cn

Received 28 July 2022; Revised 19 August 2022; Accepted 25 August 2022; Published 8 September 2022

Academic Editor: Lianhui Li

There are some problems in feature extraction and representation of Chinese mental verbs, such as low accuracy and low efficiency. In order to further improve the computational efficiency and accuracy of Chinese mental verb text, based on deep learning theory, activation function and damage function were used to optimize the original model. Considering the calculation method of model gradient, the optimization model describing the characteristics of Chinese mental verbs is finally obtained. The model can be used to analyze the variation of the characteristic parameters of Chinese verbs and the method of representation. Finally, the model error is analyzed by the method of comparative verification. Relevant studies show that the number of outputs and output results corresponding to softmax function will influence the test results of the model. By comparing the curves, it can be seen that the curve corresponding to the output number has an obvious increasing trend, while the corresponding output result curve has an opposite changing trend. The linear and nonlinear characteristics of the two curves are obvious. The real value of the mean square error function shows a change of linear increase, while the corresponding output value shows a change trend of gradual decline, which indicates that the two kinds of data have different influences on the model under related algorithms. It can be seen from the error data that the gradual increase of independent variables will improve the accuracy of the test results. Five different Chinese mental verb parameters have different manifestations in the deep learning model: among them, declarative verbs fluctuate in a small range and have little corresponding influence. However, the fluctuation of nondeclarative verbs and positive and negative declarative verbs is relatively small, and the curve is relatively stable. Negative verbs have a positive influence on the test output. Double negative verbs have negative effects. Finally, the accuracy of the model is verified by calculating the difference between experimental data and model data. This research can provide theoretical support and model verification method for the application of deep learning model in other fields of Chinese language.

1. Introduction

Deep learning models have been widely applied in artificial intelligence and other fields and also have obvious application prospects in face recognition [1], information security [2], molecular microscopy [3], retinopathy monitoring [4], and other fields. In view of the low calculation accuracy and slow calculation efficiency of partial differential equation in the calculation process, based on deep learning theory, fuzzy analysis method was adopted to extract the features of calculus calculation process, so as to obtain the periodic characteristic parameters. Through damage estimation of characteristic parameters, an optimized deep learning model was obtained [5]. This model can provide new research thinking for the solution of calculus equation and can further improve the solution accuracy of the model and further compress the solution time of the model. Finally, the accuracy of the model was verified by comparing experimental data with model data. Through verification and analysis, it can be seen that relevant theories based on deep learning model can provide reference for solving calculus equation. The analysis and prediction of cancer have always been a difficult medical problem. There were some problems in the process of cancer analysis, such as backward analysis

methods and complicated cancer lesions. In order to further improve and optimize the tissue framework in the process of cancer treatment, artificial intelligence technology was used to analyze the original model based on deep learning model, so as to obtain a new optimization model [6]. This model mainly uses different types of activation functions to analyze the framework of treatment, so as to extract the required data and characteristic indicators. The model algorithm was used to analyze these indexes and find out the changing rules of different indexes. Finally, the deficiencies of existing data can be further optimized according to these calculation and research rules, so as to obtain the final optimization model. Through experimental calculation, different frames and types of the model can be analyzed, and finally, the accuracy of the model can be verified by experimental data.

The above studies mainly started from the fields of industry and medical treatment and failed to provide better solutions to the problems existing in the analysis of characteristic parameters of Chinese mental verbs. Based on deep learning theory, this paper uses activation function and damage equation to analyze and study the text features of Chinese mental verbs. Model gradient analysis was used to further characterize the text features of Chinese verbs so as to find the corresponding representation methods. Finally, the analysis model of Chinese mental verbs based on deep learning theory was obtained. This model can provide research ideas for the analysis of the text characteristics of Chinese mental verbs and use the method of index calculation to analyze the different indicators of Chinese. Finally, the error analysis method was used to verify the model, and the results show that the model has good advantages and application prospects. This study can provide research ideas for the textual analysis of Chinese mental verbs.

2. Theoretical Basis of Deep Learning

Based on the relevant theories of deep learning model, this paper mainly uses activation function and damage function to extract the text features of Chinese mental verbs, so as to get the change rules of Chinese mental verbs under different indicators [7, 8]. In order to introduce the change rules of different indicators into the original deep learning model, model gradient algorithm is adopted to classify and analyze the change rules of different indicators [9, 10]. The common points of indicators were found and introduced into the original model combined with algorithm rules. The optimized deep learning model was obtained by revising the original model. The calculation of model can calculate the text features of Chinese mental verbs, and the calculation results can well reflect the actual change rules of verbs. The ultimate goal is for machines to be able to learn analytically, like humans, and to recognize data such as text, images, and sound. Deep learning is a complex machine learning algorithm that has achieved far more results in speech and image recognition than previous related technologies.

Deep learning model has been widely used in feature extraction of Chinese mental verbs [11, 12]. In order to further illustrate the application process of this model in the field of Chinese mental verbs, the training process of the corresponding deep learning model is obtained through summary analysis, as shown in Figure 1. The coordinates of the corresponding text features of Chinese mental verbs should be extracted first, and then the multipath errors are analyzed as training samples. By importing the model samples into the sample database, and then setting the relevant parameters, the corresponding analysis model of Chinese mental verb text features based on deep learning theory is obtained, and the model is further built. In order to further illustrate the accuracy of the model, the training accuracy of the model should be identified first. If the model does not meet the requirements, the corresponding sample should be imported into the sample input for circulation. If it meets the requirements, the grid of the model should be saved and then analyzed in the output grid under the action of coordinate sequence, so as to finally get the corresponding error mining.

2.1. Activation Function. Each layer of neural network contains several neurons. Through repeated training and learning, the weight value of neuron connection is adjusted, so as to obtain data processing ability [13, 14]. Neuron is the basic element of neural network. Neuron structure consists of input signal, sum, threshold judgment, activation function, and output. Input values of neurons are transmitted by input signals of other neurons through their respective connection weights, and finally, output is generated through activation function processing. xi is the input signal transmitted by other neurons, wi is the corresponding connection weight of other neurons, θ is the threshold, and y is the output, which is output by the following formula:

$$y = f\left(\sum_{i=1}^{m} wixi - \theta\right), \tag{1}$$

where $f(x)$ is the activation function of the neuron.

In the activation function, different parameters have different effects on the output value [15, 16]. The variation rules of output value and activation function under the action of different neurons were further explained, and the calculation indexes of different neurons were obtained as shown in Figure 2. When the number of neurons exceeds 17, the curve increases rapidly, showing the characteristics of nonlinear change, and the increase range of the curve is relatively large. It can be seen from the corresponding activation function that it shows a downward change with the increase of neurons, and then shows a change trend of approximately linear increase with the increase of neurons. The curve then rapidly increased to the maximum value and remained stable, and then decreased rapidly under the action of higher neurons, with a relatively large fluctuation range. Through the curve changes of the two, it can be seen that the overall change is relatively obvious, with opposite change characteristics, which can reflect the actual rule of parameter change.

The activation function in neurons is usually nonlinear. Since the input and output of neurons are linearly correlated, the neuron has more powerful performance and can process

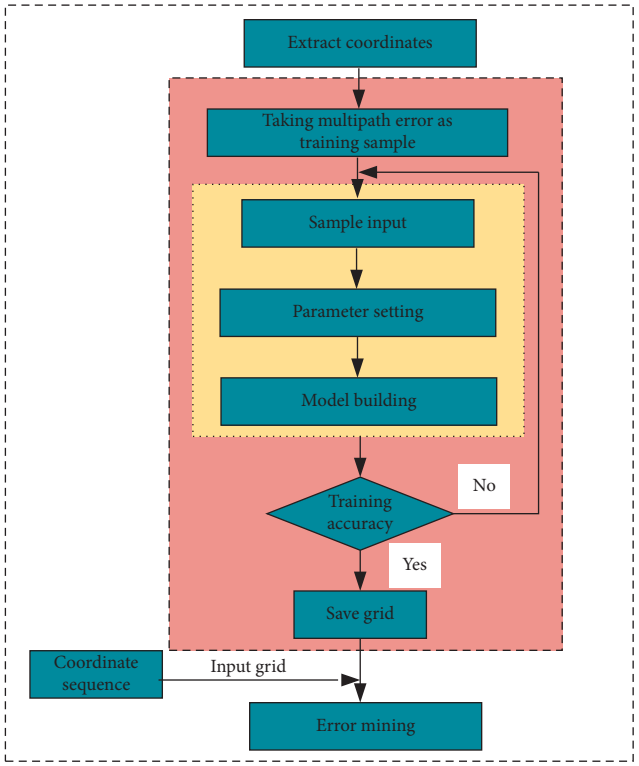

Figure 1: Flow chart of deep learning training.

complex feature information through the nonlinear operation of activation function. The choice of activation function changes with the further research. Common activation functions include the following:

(1) Sigmoid function, its formula is as follows:

$$\sigma(x) = \frac{1}{1 + \exp(-x)}. \quad (2)$$

The characteristic of this function is that its output value varies between (0, 1) and can be used for dichotomies. In information science, Sigmoid function is often used as threshold function of neural network due to its properties of singleton and inverse singleton. The main disadvantages of the Sigmoid function include the following: when the input value is large, the function is not sensitive to its change perception, which easily leads to the situation that the gradient is 0 in the back propagation, resulting in slow update of weight in network training.

(2) Tan h function, its formula is as follows:

$$\tan hx = \frac{\exp(x) - \exp(-x)}{\exp(x) + \exp(-x)}. \quad (3)$$

This function can be regarded as magnifying and translating the Sigmoid function, and its output value varies between [−1, 1], and the output mean value is around 0. Compared with Sigmoid function, Tan h function performs better, has the effect of data center, and can accelerate network training, but it also has the same gradient disappearance. Moreover, the calculated data corresponding to Tan h function have more extensive output results, which makes the research scope of Tan h function more extensive.

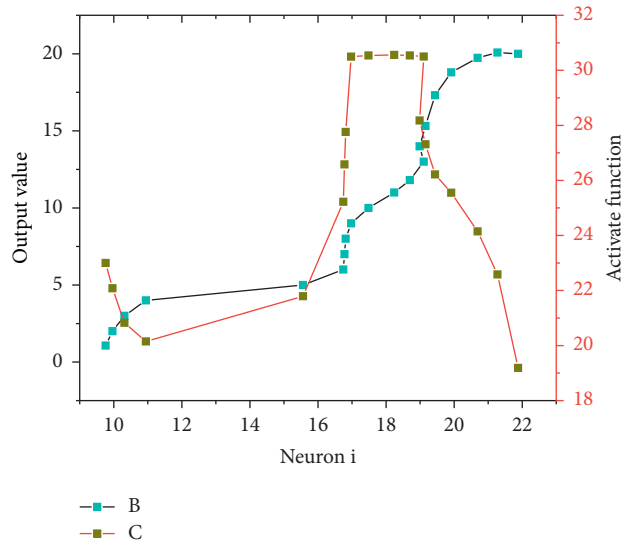

Figure 2: Different neuron computation index.

(3) ReLU function, whose formula is expressed as follows:

$$f(x) = \max(0, x). \quad (4)$$

This function is the most commonly used activation function in neural networks and can accelerate the convergence of network models. Compared with Sigmoid function and Tan h function, ReLU function has the advantage that when the input value is greater than 0, it will not tend to saturation with its change. However, there are also obvious disadvantages: the constant gradient of some neurons is 0, so that the corresponding parameters can never be adjusted, namely, the phenomenon of neuron necrosis.

(4) Leaky ReLU function, whose formula can be expressed as follows:

$$f(x) = \max(ax, x). \quad (5)$$

By introducing constant a, this function solves the neuron failure phenomenon of ReLU function in the region whose input value is less than 0 and effectively reduces the disappearance of gradient.

Leaky ReLU function is an optimization of ReLU function in a linear interval. To further illustrate the accuracy of the optimization, the Leaky ReLU function and ReLU function as well as the calculation results between the parameters have been obtained through calculation and analysis, as shown in Figure 3. The test data show a two-stage variation trend with the increase of independent variables: in the first stage, the curve gradually drops to the lowest

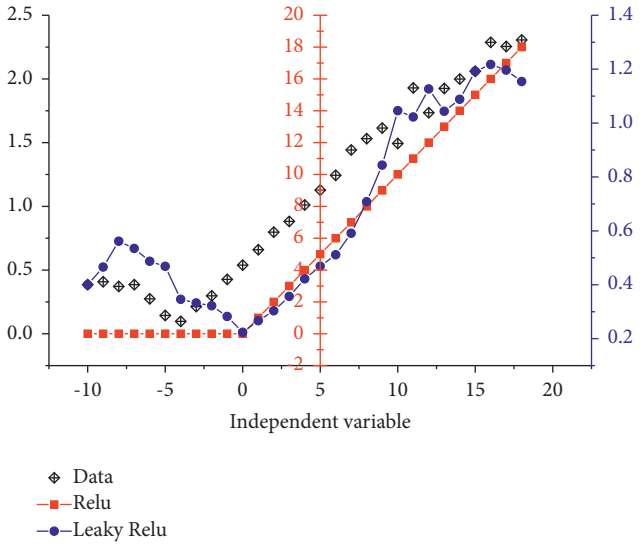

Figure 3: ReLU function optimization results.

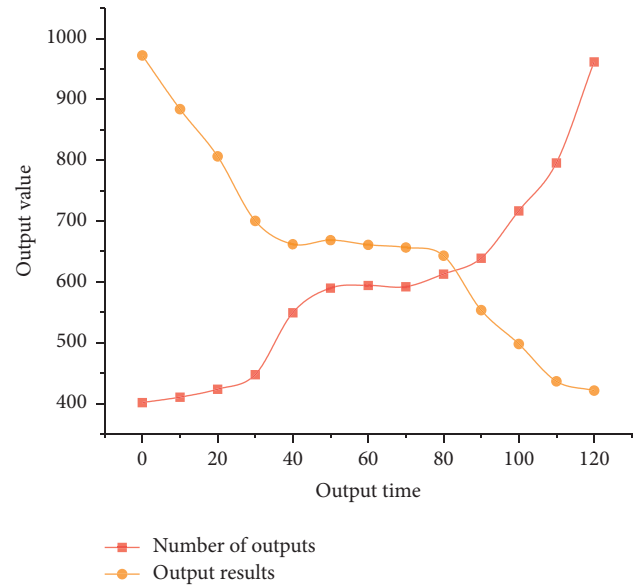

Figure 4: Change value of softmax function at different output time.

point. Then in the second stage, the curve gradually increases to the maximum value, and the increment is basically the same, indicating that the linear characteristics are relatively obvious. The corresponding traditional ReLU function tends to zero in the first stage, which cannot better describe the decline and change of the test data in the first stage. In the second stage, ReLU function showed a trend of linear increase, but it could not reflect the test data well in terms of specific values and could only be consistent with the test data in the trend. Leaky ReLU function can not only explain the change of its linear decline in the first stage but also describe the change trend and specific data in the second stage relatively well. Therefore, the optimized Leaky ReLU function can better reflect the change rule of experimental data.

(5) Softmax function, its formula is as follows:

$$\text{Softmax}(x) = \frac{\exp(x)}{\sum_{i=1}^{I} \exp(x)}, \tag{6}$$

where x is the output of the ith neuron and I is the total number of output neurons of this layer. This function can realize feature mapping and is often used in multiclassification problems.

In softmax function, the number of neuron input and output result will affect the output value. In order to further explain the variation rule of output number and output result under different output time, the time variation curve of softmax function under different output time was calculated as shown in Figure 4. It can be seen from the changes in the figure that the number of output and the change of output result have an opposite trend. Firstly, it can be seen from the number of output that it shows a trend of slow increase with the increase of output time, and then in a higher output time, the curve shows a gradual increase. When the curve increases to the local maximum value, the curve gradually tends to be stable. At a higher output time, the corresponding output value of the output number curve increases rapidly to the maximum value, and the range of the curve is relatively large. The output results show a linear decreasing trend under the action of lower output time, and then the curve gradually tends to be stable. Under the action of higher output time, the corresponding output results tend to be stable. This shows that the number of outputs increases linearly while the output results decrease linearly.

2.2. Loss Function. Loss function is used to calculate the error between the output value and the real value during model training, which can reflect the training effect of the model in real time and provide direction for model training optimization [17, 18]. The smaller the loss function, the better the robustness of the model. Common regression loss functions include mean square error loss and mean absolute error loss. Common classification loss functions include piecewise loss, binary loss, and exponential loss [19, 20].

(1) Mean square error loss function: this function is the most commonly used loss function in regression tasks, and its formula is expressed as follows:

$$\text{MSE} = \frac{1}{N} \sum_{i=1}^{N} (yi - \overline{y}i), \tag{7}$$

where N is the number of true values, yi is the output value of the model, and $\overline{y}i$ is the true value. The loss function does not consider the direction of the error, but only the average value of the error, which can better reflect the error degree between the output value and the real value. Because the variation relationship between the real value and the output value is considered, the loss function is easy to

calculate the gradient. However, since the loss function assumes that the error between the output value and the real value of the model meets the Gaussian distribution, the error of outliers will be too large, resulting in poor robustness.

It can be seen that the real value and the output value have different influences on the specific data of the model by calculating the mean-square error loss function in the loss function. In order to further explain the change rule between the real value and the output value and the corresponding change of the error, the curve of the error value of the mean-square error loss function was obtained through calculation as shown in Figure 5. The true value shows a gradually increasing trend with the increase of the independent variable, and the change amount of the true value decreases is relatively consistent, indicating that its linear characteristics are obvious. With the increase of independent variables, the corresponding output results show a trend of gradual decline, and the slope of decline is constant, which indicates that the real value and the corresponding output value have obvious linear characteristics. The corresponding error is obtained through calculation, and the corresponding error curve is basically maintained at a higher level under a lower independent variable. When the independent variable increases gradually, the curve drops rapidly to the lowest point and tends to be stable gradually under the action of higher independent variable. This indicates that the independent variable will have a certain influence on the test results and also indicates that there is a certain error between the real value and the output value.

(2) Average absolute error loss function, which is given by the absolute error value between the output value and the true value, and its formula is expressed as follows:

$$\mathrm{MAE} = \frac{1}{N}\sum_{i=1}^{N} |yi - \overline{y}i|, \tag{8}$$

where $(yj - \overline{y}j)$ is the learning error. In the process of gradient descent, the loss value of the loss function will be positive or negative 1, which is not conducive to the training of the model. Although the loss function assumes that the error between the output value of the model and the real value satisfies the Laplace distribution, the Laplace distribution is more robust to the processing of outliers.

(3) The piecewise loss function means that the loss is 0 when the output value is equal to the true value and 1 when the output value is unequal. The formula is expressed as follows:

$$F(y, f(x)) = \begin{cases} 0, & y = f(x), \\ 1, & y \neq f(x). \end{cases} \tag{9}$$

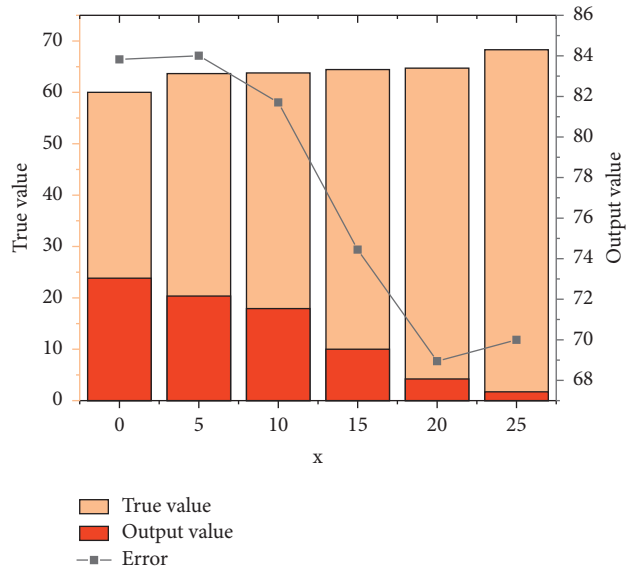

Figure 5: Curve of error of mean square error loss function.

The loss function directly reflects the number of classification errors.

(4) Binary loss function is the most commonly used loss function in model classification loss calculation. It is often used in binary classification problems and can effectively reflect the degree of deviation from the true value of the output value. Its formula is expressed as follows:

$$E(yi, \overline{y}i) = -\sum_{i=1}^{N} p(yi)\log p(yi) - (1 - p(\overline{y}i))\log(1 - p(yi)), \tag{10}$$

where N is the number of true values, $P(yi)$ is the output probability distribution value of the model, and $P(\overline{y}i)$ is the true probability distribution value. In the process of gradient descent, the binary loss function has a good learning characteristic of fast update with large error weight and slow update with small error weight. Considering the probability distribution of model parameters, the calculation results of binary loss function are more consistent with the characteristics of data distribution.

(5) Exponential loss function is often used in model algorithms and is very sensitive to noise and outliers. Its formula is expressed as follows:

$$Z = \exp[-yf(x)]. \tag{11}$$

It can be seen from the above analysis that the classified loss function includes three different loss functions: piecewise function, binary function, and exponential function. There are differences in the calculation formulas of the three different functions, indicating that there are some differences in the corresponding calculation results. In order to further

explain the change rules of different specific functions in the classification loss function, the change curves of the classification loss function are obtained through calculation, as shown in Figure 6. First of all, it can be seen from the test data that the curve first decreases to the lowest point and then gradually tends to be stable. However, when the independent variable gradually increases, the test data show a linear increase in the change law, and its change range is relatively large. As can be seen from the piecewise loss function, when the independent variable is less than 20, the corresponding output value is zero, while when the independent variable is more than 20, the corresponding curve increases. Then, the corresponding output value shows a fluctuation trend and finally gradually tends to decline. The overall variation range of the curve is relatively small. Through the binary loss function, it can be seen that the curve drops first, then fluctuates, and finally gradually rises in three stages. The corresponding range of variation is relatively small, overall between 0.2 and 0.5. It can be seen from the exponential damage function that it has typical exponential function change characteristics. Under the action of small independent variables, the curve shows a rapid downward trend, and then the curve gradually tends to be stable. Under the action of higher independent variable, the curve decreases gradually. This shows that three different loss functions have different typical characteristics, and it is necessary to comprehensively consider two or three functions to accurately describe and analyze the test data.

2.3. Model Gradient Descent. The training process of neural network includes forward propagation and back propagation [21, 22]. Backpropagation is the core part of network training to realize the dynamic adjustment of network training parameters. Forward propagation propagates data from the shallow layer to the deep layer of the neural network until the output layer is cut off [23, 24]. During the calculation of gradient descent, the neural network can obtain the error between the output value and the real value through the loss function. Back propagation is to obtain the updated weight value of neurons calculated by gradient descent method through the errors generated by forward propagation, and then use the chain derivative formula to carry out the back propagation calculation. In gradient descent, the method of partial derivative is usually used to calculate the gradient value of the current parameter. Then a learning rate η is introduced to control the change speed of updating weight value, and the weight updating formula is as follows:

$$W = w - \eta \frac{\partial J(w)}{\partial w}. \tag{12}$$

However, in order to update the parameter values of other layers in the neural network, it is necessary to make further use of back propagation. In this process, the back propagation uses the chain rule to calculate the gradient:

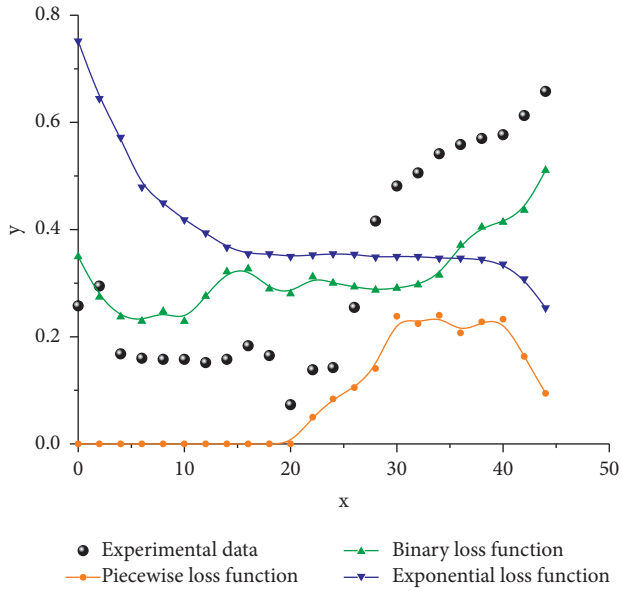

Figure 6: Classification loss function curve.

$$\frac{\partial J(w)}{\partial w} = \frac{\partial J^*(x)}{\partial y} \times \frac{\partial y}{\partial w}, \tag{13}$$

where w is the parameter value of the network and y is the output value of the network activation function.

Therefore, back propagation can pass the updated parameter value to the corresponding position layer by layer through the chain rule using the error function. Thus, the parameter value update formula of layer L network is as follows:

$$W = w - \eta \frac{\partial J(w)}{\partial w} = w - \eta \left[\delta \times \left(x^{l-1} \right)^T \right], \tag{14}$$

where x is the input value.

The accuracy of the model can be further illustrated by analyzing the formula of the model gradient descent and the corresponding calculation results. It can be seen that different learning rates and corresponding parameter values will have different influences on the output results of the model. In order to further illustrate the influence of learning efficiency and parameter values on test data, the model gradient curve was obtained through calculation, as shown in Figure 7. It can be seen from the curve that the learning rate curve and the parameter value curve have different change rules. Firstly, it can be seen from the test data that, with the increase of input value, the corresponding test data first increases and then decreases, and the overall fluctuation range is relatively small. When the input value of the curve gradually increases, the corresponding output results show a trend of gradual increase; when it reaches the maximum value, the corresponding test data gradually decreases with great volatility. This shows that the nonlinear characteristics of the test data are obvious. As can be seen from the learning rate curve, with the increase of input value, the corresponding curve fluctuates in a larger range first, and then gradually increases to the maximum value. As the value

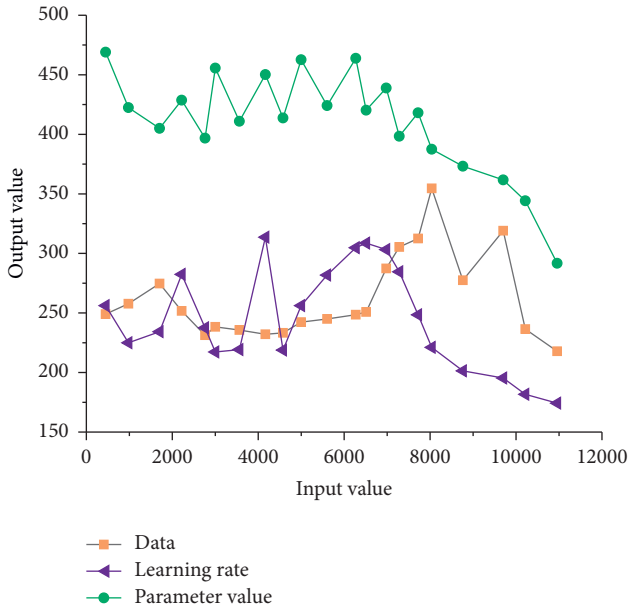

Figure 7: Model gradient curve.

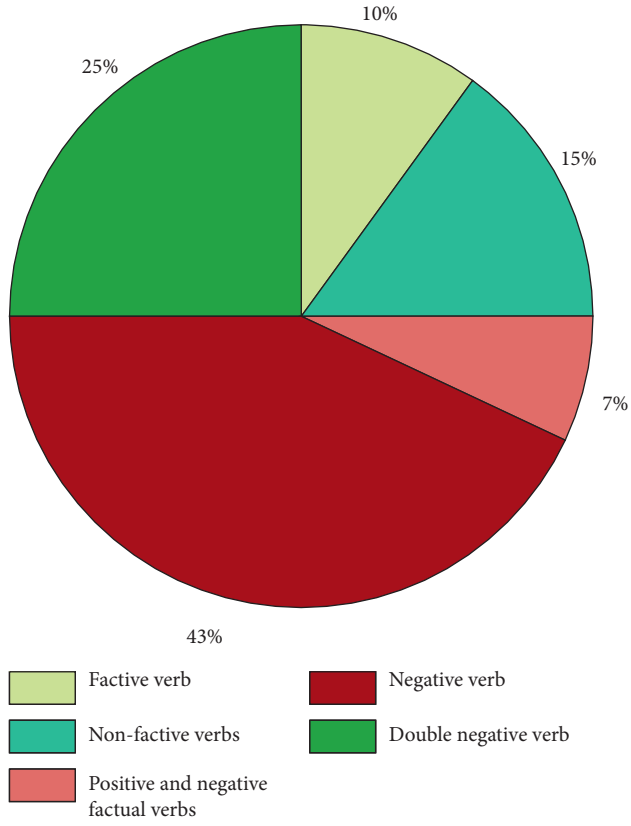

Figure 8: Pie chart of Chinese mental verbs.

increases, the curve drops rapidly and then flattens out. It can be seen from the variation curve of parameter values that the parameter curve fluctuates rapidly under the action of small input values, and the fluctuation range is relatively small. Then, as the input value gradually increases, the corresponding output result gradually decreases to the lowest value.

3. Analysis of the Characteristics of Chinese Mental Verbs Based on Deep Learning

3.1. Text Feature Extraction of Chinese Mental Verbs. There are many problems in the analysis of the textual features of Chinese mental verbs, mainly including the unclear description and analysis of Chinese features. In order to further analyze the characteristics of Chinese mental verb text, five different feature parameters are obtained through analysis: declarative verbs, nondeclarative verbs, positive and negative verbs, negative verbs, and double negative verbs. In order to further explain the proportion of these five verbs in actual Chinese mental verbs, the pie chart of Chinese mental verbs is obtained through statistics as shown in Figure 8. The proportion of declarative verbs is about 10%, while that of nondeclarative verbs is about 15%. The proportion of positive and negative declarative verbs is the smallest, only 7%. Negative verbs make up the most, about 43 percent, while double negatives make up about 25 percent. It can be seen from the above analysis that the proportion of negative verbs is the highest, while the proportion of positive and negative verbs is the lowest.

3.2. Analysis of Text Features of Chinese Mental Verbs Based on Deep Learning. Based on the deep learning model, the activation function and loss function are used to analyze the original model, so as to obtain the optimization value of the deep learning model. The model gradient descent is introduced into the model to obtain the optimized deep learning model, which can be used for the analysis of Chinese mental verbs [25]. In order to further illustrate the application of the deep learning model in Chinese mental verbs, the flow chart of the application of the deep learning model in Chinese mental verbs is obtained through the above analysis, as shown in Figure 9. As can be seen from the computational flow chart of text feature extraction of Chinese mental verbs, the data of Chinese mental verbs are first imported into the model and then divided into different sections according to different feature parameters. Then, the critical value of the model can be obtained according to the verb feature of the calculated value. Based on the critical value, the verb feature can be further clipped and analyzed. The results of clipping and analysis are introduced into the activation function to analyze the change between the activation function and the damage function. Furthermore, the linear difference and gradient descent results are obtained to obtain the reconstruction scheme and model of Chinese mental verbs. Finally, the model calculation results and optimization results are output.

Based on the deep learning model, the activation function and damage function are used to optimize the original model, so as to obtain the optimization model for describing Chinese mental verbs. This optimization model can calculate the characteristic parameters of Chinese mental verbs, and thus obtain the histogram of the calculation results of characteristic parameters of Chinese mental

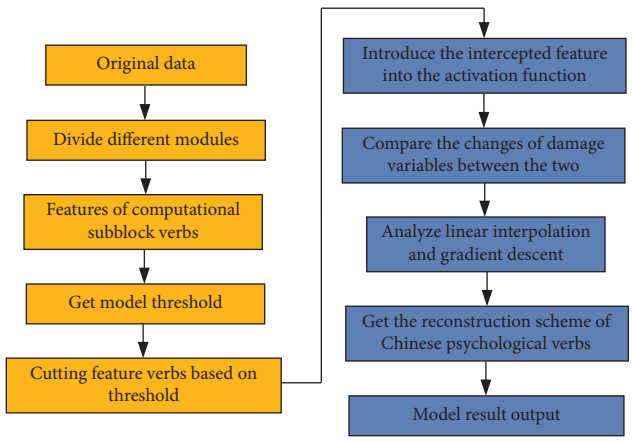

Figure 9: Flow chart of deep learning algorithm.

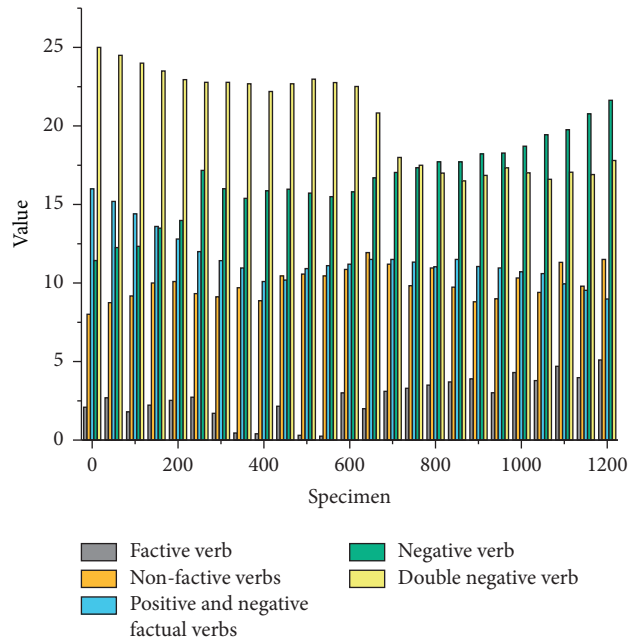

Figure 10: Histogram of calculation of characteristic parameters of Chinese mental verbs.

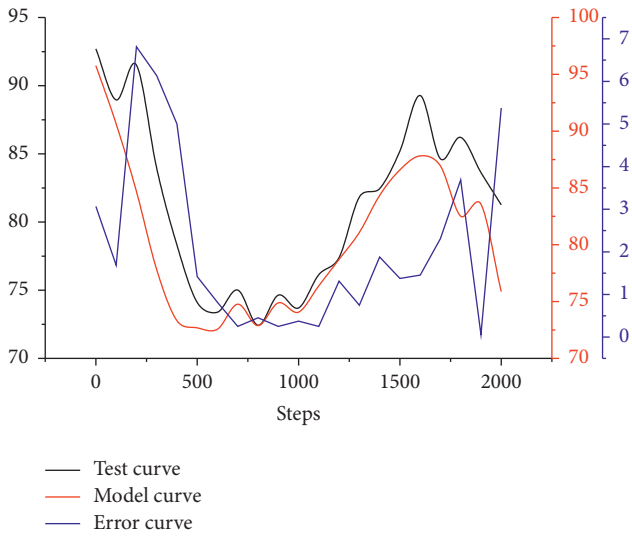

Figure 11: Model validation curve.

verbs, as shown in Figure 10. It can be seen from the figure that different characteristic parameters show different variation trends with different sample parameters. First of all, it can be seen from the calculation results of declarative verbs that the calculation results are relatively small and the overall range of change is relatively small. A trend in volatility in which a curve increases gradually, then drops to a low point, and then increases gradually. While the corresponding nonpredicate verbs show a linear increase trend with the gradual increase of samples. When the curve reaches the local maximum value, the curve gradually decreases to the local minimum value with the increase of samples. As can be seen from the positive and negative narrative verbs, the change of positive and negative narrative verbs gradually decreases with the increase of samples, and the change of positive and negative narrative verbs gradually tends to be stable with the further increase of samples. It shows that with a higher sample size, positive and negative verbs tend to be constant. However, it can be seen from the negative verb that its change increases linearly with the increase of samples, and the overall change range of the curve is relatively large. As can be seen from the change of double negative verbs, the curve has a high output result under the action of small specimens, while the corresponding output result drops to the lowest value rapidly with the increase of samples, and the overall change range is relatively large.

4. Discussion

The optimization model based on deep learning theory can carry out targeted data analysis by considering activation function and loss function. In order to further illustrate the superiority of the calculated results, the test curve, model curve, and corresponding error curve were obtained by summarizing, as shown in Figure 11. As can be seen from the model verification curve, the test curve first presents a V-shaped change with the increase of iteration steps, and then rapidly drops to the lowest point and then carries on a small fluctuation. With the further improvement of iteration steps, the test data gradually increased to the maximum value, and the overall change range was approximately *U*-shaped. The corresponding model curve can better reflect the overall change trend of the test data, and then get the error curve through the comparison between the two. It can be seen from the error curve that the overall error range is within 7%, while with the increase of the number of test steps, the corresponding error range gradually decreases. As the sample increases, the curve is driven by increasing variation. This shows that the error is also *U*-shaped in a certain range. The curve has different error ranges under different iteration steps. Therefore, in practical application, it is necessary to determine the number of iterations according to the specific test data, so as to obtain the optimal calculation results.

5. Conclusion

(1) It can be seen that the output value and the activation function have the same variation range through the change curves of the calculated indexes of different neurons. When the neuron is low, the output value and the corresponding activation function have the same change trend. When the neuron is high, the output value shows a rapid decline, while the corresponding activation function shows a rapid increase.

(2) The comparison curve between Leaky ReLU function and ReLU function shows that the original model can only provide a good description of the second stage of the test data. The optimized activation function can not only explain the change rule of the first stage but also better analyze the experimental data in the key points of the second stage.

(3) Model gradient changes mainly include learning rate and parameter values of the model. By comparing the experimental data, it can be seen that the curve shows obvious fluctuation in the first stage, among which the fluctuation of learning rate is relatively large. The corresponding parameter values change in a small range, and the curves all decline significantly in the second stage.

Data Availability

The dataset can be obtained from the corresponding upon request.

Conflicts of Interest

The authors declare that they have no conflicts of interest.

References

[1] X. Sun, P. Wu, and S. Hoi, "Face detection using deep learning: an improved faster RCNN approach," *Neurocomputing*, vol. 299, no. 19, pp. 42–50, 2018.

[2] A. Rajkomar, E. Oren, K. Chen et al., "Scalable and accurate deep learning with electronic health records," *Npj Digital Medicine*, vol. 1, no. 1, pp. 18–36, 2018.

[3] E. Nehme, L. E. Weiss, and T. Michaeli, "Deep-STORM: super-resolution single-molecule microscopy by deep learning[J]," *Optica*, vol. 5, no. 4, pp. 436–452, 2018.

[4] M. Voets, M. Kajsa, and L. A. Bongo, "Replication study: development and validation of deep learning algorithm for detection of diabetic retinopathy in retinal fundus photographs[J]," *PLoS One*, vol. 10, no. 12, pp. 77–96, 2018.

[5] J. Han, J. Arnulf, and E. Weinan, "Solving high-dimensional partial differential equations using deep learning[J]," *Proceedings of the National Academy of Sciences*, vol. 63, no. 12, pp. 406–423, 2018.

[6] D. Bychkov, N. Linder, R. Turkki et al., "Deep learning based tissue analysis predicts outcome in colorectal cancer," *Scientific Reports*, vol. 8, no. 1, pp. 3395–3412, 2018.

[7] T. Ben-Nun and T. Hoefler, "Demystifying parallel and distributed deep learning: an in-depth concurrency analysis," *ACM Computing Surveys*, vol. 52, no. 4, pp. 4023–4045, 2018.

[8] W. Ma, F. Cheng, and Y. Liu, "Deep-learning-enabled on-demand design of chiral metamaterials[J]," *ACS Nano*, vol. 78, no. 42, pp. 4203–4215, 2018.

[9] Y. Li, W. Shi, and W. W. Wasserman, "Genome-wide prediction of cis-regulatory regions using supervised deep learning methods," *BMC Bioinformatics*, vol. 19, no. 1, pp. 202–225, 2018.

[10] D. S. Kermany, M. Goldbaum, W. Cai et al., "Identifying medical diagnoses and treatable diseases by image-based deep learning," *Cell*, vol. 172, no. 5, pp. 1122–1131.e9, 2018.

[11] A. Voulodimos, N. Doulamis, A. Doulamis, and E. Protopapadakis, "Deep learning for computer vision: a brief review," *Computational Intelligence and Neuroscience*, vol. 2018, no. 12, pp. 1–13, 2018.

[12] A. Kamilaris and F. X. Prenafeta-Boldu, "Deep learning in agriculture: a survey," *Computers and Electronics in Agriculture*, vol. 147, no. 12, pp. 70–90, 2018.

[13] H. Chen, O. Engkvist, and Y. Wang, "The rise of deep learning in drug discovery," *Drug Discovery Today*, vol. 23, no. 6, pp. 63–86, 2018.

[14] Q. S. Zhang, S. C. Zhu, and U. O. California, "Visual interpretability for deep learning:a survey," *Frontiers of Information Technology & Electronic Engineering*, vol. 415, no. 42, pp. 639–657, 2018.

[15] N. Akhtar and A. Mian, "Threat of adversarial attacks on deep learning in computer vision: a survey," *IEEE Access*, vol. 6, no. 5, pp. 14410–14430, 2018.

[16] Y. Tom, H. Devamanyu, and P. Soujanya, "Recent trends in deep learning based natural language processing [review article]," *IEEE Computational Intelligence Magazine*, vol. 13, no. 3, pp. 55–75, 2018.

[17] X. X. Zhu, D. Tuia, and L. Mou, "Deep learning in remote sensing: a comprehensive review and list of resources," *IEEE Geoscience & Remote Sensing Magazine*, vol. 5, no. 4, pp. 8–36, 2018.

[18] E. Nachmani, E. Marciano, and L. Lugosch, "Deep learning methods for improved decoding of linear codes," *IEEE Journal of Selected Topics in Signal Processing*, vol. 85, no. 40, pp. 1–10, 2018.

[19] L. He, K. Ota, and M. Dong, "Learning IoT in edge: deep learning for the internet of things with edge computing," *IEEE Network*, vol. 32, no. 1, pp. 96–101, 2018.

[20] H. He, C. K. Wen, S. Jin, and G. Y Li, "Deep learning-based channel estimation for beamspace mmWave massive MIMO systems," *IEEE Wireless Communications Letters*, vol. 7, no. 5, pp. 852–855, 2018.

[21] Q. Zhang, L. T. Yang, Z. Chen, and P Li, "A survey on deep learning for big data," *Information Fusion*, vol. 42, no. 26, pp. 146–157, 2018.

[22] S. Macaluso and D. Shih, "Pulling out all the tops with computer vision and deep learning," *Journal of High Energy Physics*, vol. 18, no. 10, pp. 736–752, 2018.

[23] A. Cocos, F. Alexander, and A. Masino, "Reply to comment on: "deep learning for pharmacovigilance: recurrent neural network architectures for labeling adverse drug reactions in Twitter posts"," *Journal of the American Medical Informatics Association Jamia*, vol. 780, no. 120, pp. 726–758, 2019.

[24] Z. Rui, R. Yan, and Z. Chen, "Deep learning and its applications to machine health monitoring," *Mechanical Systems and Signal Processing*, vol. 115, no. 15, pp. 213–237, 2019.

[25] R. Brent and L. Boucheron, "Deep learning to predict microscope images," *Nature Methods*, vol. 16, no. 5, pp. 882–896, 2018.

Hindawi
Scientific Programming
Volume 2022, Article ID 2462562, 7 pages
https://doi.org/10.1155/2022/2462562

Research Article

Cloning and Expression Analysis of After-Ripening Related Genes in *Panax ginseng* Seed

Qingling Qu,[1] **Shoujing Zhao**,[2] **and Xuesong Wang**[2]

[1]*Physical Education College, Baicheng Normal University, Jilin 137000, Baicheng, China*
[2]*School of Life Sciences, Jilin University, Jilin 130012, Changchun, China*

Correspondence should be addressed to Qingling Qu; quqingling@bcnu.edu.cn

Received 3 July 2022; Revised 11 August 2022; Accepted 20 August 2022; Published 6 September 2022

Academic Editor: Lianhui Li

Panax ginseng enjoys a wide range of medicinal applications and good economic value, the market demand is large, but *Panax ginseng* seed's after-ripening characteristic seriously restricts development of *Panax ginseng* industry. In this experiment, starting from the main action hormone ABA and GA of *Panax ginseng*, primers of GA and ABA related to *Panax ginseng* seed after-ripening were screened and designed, and the possible relationship between transcription factor WRKY gene and *Panax ginseng* seed after-ripening was probed. Semiquantitative and quantitative real-time PCR of these genes were performed. ABA and GA-related metabolizing enzymes play an important role in the process of *Panax ginseng* seed after-ripening, and WRKY transcription factor regulates gene expression. In this study, we cloned the PgGA2ox gene, which is the key metabolic enzyme of GA, and analyzed the genes by the bioinformatics software, which laid a foundation for studying the molecular mechanism of *Panax ginseng* seed after-ripening.

1. Introduction

Panax ginseng, a valuable medicinal plant, is widely used in human medical treatment and healthcare, and the market demand is on the rise [1]. *Panax ginseng* is a plant of seed propagation, and *Panax ginseng* seeds have not fully developed embryo after natural maturity [2–4]. With the characteristic of postripening, it must be treated by a long period of stratification to break dormancy and germinate. In the main producing areas of *Panax ginseng*, seeds are planted in early August every year and seeded immediately after harvest. Most of the seeds will germinate in the spring of the third year (after 21-22 months) under natural conditions. Many growers cannot promote seed after-ripening, leading to plant failure and seriously affecting economic benefits. The long production cycle restricts large-scale popularization of *Panax ginseng* cultivation to a certain extent, and cultivation process is vulnerable to climate, cultivation conditions, pests, and diseases, resulting in low production of *Panax ginseng* and low economic efficiency. Therefore, it is necessary to find an effective way to improve *Panax ginseng* yield and quality, thereby improving production efficiency [5].

Phytohormone is a minor molecule signal substance, with very small concentration or even close to 0, but plays a very important role in the plant's life cycle. During seed dormancy and germination, hormones regulate the metabolism of proteins and enzymes through signal transduction, regulating seed dormancy and germination [6].

ABA is a positive regulatory factor of dormancy and is involved in induction and maintenance of dormancy, which negatively regulates germination [7–9]. ABA will resynthesize during imbibition of dormant seeds, which is a requirement for seed to remain dormant. ABA produced by the embryo is necessary for dormancy [10]. The decrease of ABA content before germination is due to inhibition of newly synthesized ABA and activation of ABA catabolism.

NCED is the key rate-limiting enzyme in ABA synthesis. There are five types present in *Arabidopsis thaliana*, including AtNCED1, AtNCED3, AtNCED5, AtNCED6, and AtNCED9. AtNCED6 and AtNCED9 are essential ABA biosynthetic enzymes [11, 12]. The expression level of

NCEDs is directly related to ABA content [13]. AtNCED5 and AtNCED6 are highly expressed in the mid to late stages of *Arabidopsis thaliana* embryogenesis [11]. The CYP707A family encodes the ABA 8′-hydroxylase, which is involved in ABA catabolism. CYP707A1 enhances expression at the early stage of seed maturation, while CYP707A2 enhances expression at the late stage of maturation [14]. After seed imbibition, ABA content decreased, CYP707A2 activity increased, and lack of this enzyme will increase ABA content and strengthen dormancy [14, 15].

GA, a positive regulatory factor of germination, can antagonize inhibition of ABA [16]. In the early stage of seed germination, GA can promote embryonic development and material decomposition. According to Kucera, GA exerts two positive effects on seed: enhancing seed vigor and promoting germination; breaking the seed coat bound and weakening the radicle surrounding tissue [17]. Low-temperature stratification can promote GA synthesis, enable ABA/GA changes, and promote dormancy release and seed germination [18].

GA can regulate GA metabolism by controlling the expression of many key enzymes in the GA synthesis pathway through feedforward or feedback regulation. GA synthesis regulation occurs mainly in late course of transduction. GA2-oxidase (GA20ox) can be catalyzed into active GA1, which is a key regulatory enzyme of GA biosynthesis. GA2-oxidase (GA2ox) can catalyze active GA1 to inactive GA34, catalyzing degradation of GA (Henderson et al. [19–21]).

WRKY transcription factor regulates seed germination and growth after seed germination. In 2004, ScWRKY1 transcription factor was isolated from wild potato ovule. ScWRKY1 transcription factor was transiently highly expressed in the embryo of torpedo stage. Its expression level was low in the fruit, root, and stem, suggesting that ScWRKY1 might participate in the embryogenesis process. *Arabidopsis thaliana* AtWRKY10 was expressed in pollen and globular embryos and also expressed in binucleate stage of endosperm development to cell stage. New plant with the gene deleted cannot form seed of normal size. The result showed that WRKY transcription factor played an important role in the embryo growth and in reducing early cellularization of endosperm [22].

In this study, beginning from the key hormones ABA and GA directly related to after-ripening characteristic of *Panax ginseng* seed by removing seed dormancy, the related primers were designed. Semiquantitative PCR and real-time quantitative PCR of these genes were performed. As WRKY transcription factor could regulate seed embryo growth to determine its expression level and understand its relationship with other genes can lay a foundation for the study of molecular mechanism of *Panax ginseng* seed postripening. Table 1.

Table 1: Real-time quantitative real-time PCR primers.

Gene	Primers
GA2ox	F-TTCACAGCACAACTGAGGTT
	R-AGAGTATTGGTCGTAACGGC
GA20ox	F-TCGCCCTAATACCCTTGTC
	R-CGATAGTGTTTCTGTGTGAACC
NCED	F-GTGAGCCTTTCTTTCTTCCTTCG
	R-GAAATCCATACGGAACTCTTGACG
CYP707A	F-GGGGAAACTCTTCAGCTCTACTCCA
	R-TCCGGGCTCGACACCATCACA
WRKY6	F-ATAGTCCGACGAGTGAGAT
	R-CTGCCCATATTTTCTCCAAC
WRKY3	F-AGCGAACGCACTGTGGTAT
	R-CTTGGTTTGAAGGCGAGAA
WRKY27	F-TGGAGGAAGTATGGACAAAA
	R-AGGGTGTGTATGATTGTGCTC
5S	F-TATTCTGGTGTCCTAGGCGT
	R-ATCCTGGCGTCGAGCTATTT

2. Materials and Methods

(1) *Panax ginseng* seeds were purchased from the Tonghua Changlong Forest Farm in Jilin Province. The seed was harvested for lamination treatment, washed with 75% ethanol 3 times, rinsed with distilled water 3 times, and wiped with filter paper, to be placed in sterilized sand with carbendazim treatment, with seed: sand = 1 : 3 at lamination. The stratified seeds were sampled at 45-day intervals, 30 seeds at a time, for a total of 5 samples. The samples were washed and frozen with liquid nitrogen and then stored in a refrigerator at −80°C until use.

(2) Total RNA extraction and cDNA synthesis: Total RNA was extracted in accordance with instructions of RNA extraction kit; and then, reverse transcription synthesis of cDNA was performed in accordance with instructions of reverse transcription kit. The kit was purchased from the Dalian Takara Bio Company.

(3) Quantitative real-time PCR primer design: Primers were designed using the Primer Premier 5.0 software. Semiquantitative and quantitative real-time PCR were performed according to the primer sequence in Table 1, and all primers were synthesized by the Beijing Genewiz Company.

(4) Semiquantitative PCR system and procedures: Reaction system: cDNA 1 μl, upstream and downstream primers 1 μl, Ex Taq enzyme 0.2 μl, dNTP 1 μl, 20 × Ex Taq enzyme buffer 2.5 μl, ddH2O 18.3 μl, final volume of 25 μl; Reaction procedure: predenaturation at 94°C for 5 min; denaturation at 94°C for 30 s, 50°C–60°C (according to different primer changes in Tm value) annealing 30 s, 72°C extension for 30 s, 35 cycles; 72°C extension for 5 min; and storage at 4°C.

(5) Quantitative real-time PCR system and procedures: Reaction system: 2 × SYBR Green Mix 10 μl, upstream and downstream primers 1 μl, cDNA 1 μl, ddH2O 7 μl, final volume of 20 μl; Reaction procedure: 95°,C 5 min; 95°C 15 s, 56°C 15 s, and 72°C 30 s single lighting, 40 cycles; 95°C, 1 min; 65°C, 1 min; solubility curve: target temperature 95°C, initial temperature 65°C, constant temperature time 20 s, and step 0.5°C/s; 30°C, 1 min; and end 4°C.

(6) Cloning the full-length cDNA of PgGA2ox gene: The cDNA of *Panax ginseng* seed was used as template, and PgGA2ox gene was amplified by the following system: 1 μl of cDNA, 1 μl of upstream and downstream primers, 0.2 μl of Ex Taq enzyme, 1 μl of dNTP, 20 × Ex Taq enzyme buffer 2.5 μl, 18.3 μl of ddH_2O, and final volume of 25 μl. PCR reaction annealing temperature was 55°C; the reaction primers were F-ATGGTAGTCTTGCCCAAGCCAACAA and R-TCATGAGGCTGCAATTTTCTCAAAG. PCR products were detected by 1% agarose gel electrophoresis, and extraction of DNA from agarose gel of target amplified fragments was performed according to operation instructions of the DNA purification recovery kit. The recycling products were ligated into pMD18-T vector and transferred into E.*coli* to be cultured on LB medium containing ampicillin. After 12 hours, the colonies were observed. The positive clones were placed in LB medium containing ampicillin for 12 hours' culture before colony PCR amplification. After electrophoresis detection, it was sent to Genewiz for sequencing.

3. Results

3.1. Panax ginseng Embryos in Different Stages of After-Ripening. Dormancy of *Panax ginseng* seed needs to pass through the two stages of morphological after-ripening and physiological after-ripening. Samples were taken 5 times at 45-day intervals and defined as SE1–SE5 stages: SE1, initial phase of morphological after-ripening; SE2, mid-term of morphological after-ripening; SE3, late morphological after-ripening, seed fissure; SE4, initial phase of physiological after-ripening; and SE5, mi-term of physiological after–ripening.

3.2. Semiquantitative PCR Results. The cDNA of seeds of the five stages of *Panax ginseng* embryo after-ripening was used as template, and 5S rRNA was used as internal reference. The seven primers were amplified after the annealing temperature was set based on primer Tm value. Detection was performed with 1% agarose gel electrophoresis, and loading quantity of sample was 5 μl. Picture was taken in the ultraviolet light irradiation after electrophoresis, and gene expression is shown in Figure 1.

From the figure, we can see that most of the genes were in low expression or no expression in the morphological after-ripening stage, GA2ox gene expression in morphological after-ripening stage is higher than that in physiological after-ripening, and CYP707A gene and GA2ox gene expression level tends to be consistent. WRKY transcription factor family showed a completely different expression. WRKY6 expression level in the physiological after-ripening period was higher than that in the morphological after-ripening stage, suggesting that it was associated with seed dormancy. WRKY3 and WRKY27 in morphological and physiological after-ripening stage were in low expression.

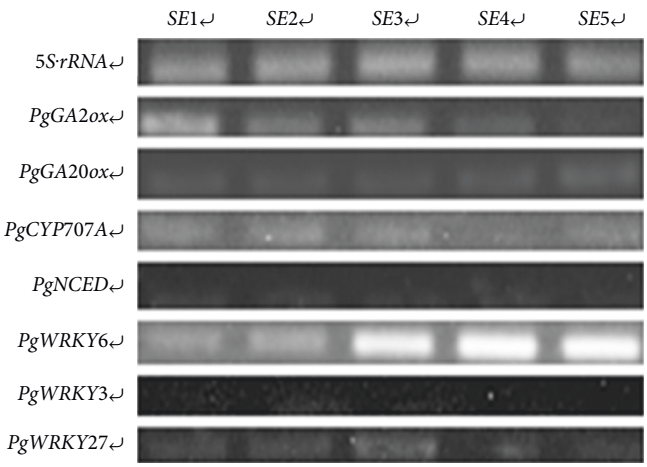

Figure 1: Gel electrophoresis photograph of semiquantitative PCR.

3.3. qRT-PCR Results. With 5S rRNA as internal reference, expression of GA, ABA, and WRKY transcription factor and embryo after-ripening related genes was detected in different period of *Panax ginseng* seed. The experimental data were analyzed by a software that came with quantitative real-time PCR instrument, as shown in Figures 2–4.

GA is a key factor in embryo dormancy and germination, GA2ox is a key gene in GA anabolism and catabolism. The study on action law of these two genes is helpful for the analysis of GA action mechanism in *Panax ginseng* seed after-ripening. The expression of GA20ox gene in physiological after-ripening stage was higher than that in morphological after-ripening stage, and GA20ox gene expression increased gradually in the two periods, which indicated that GA20ox gene played a more important role in physiological after-ripening. The expression level of GA20ox gene decreased in physiological after-ripening stage, quite low in physiological after-ripening stage, but increased slightly at the end of physiological after-ripening stage. It was inferred that the increase of expression level was related to release of seed dormancy.

ABA can induce and maintain dormancy, a positive regulatory factor of dormancy, a negative regulatory factor of germination, which acts antagonistically with GA. NCED is the key rate-limiting enzyme in ABA synthesis. The expression of NCED gene is directly related to ABA content. CYP707A gene is involved in ABA catabolism. The expression level of NCED gene decreased gradually at morphological and physiological after-ripening stages, with the former higher than the latter, indicating that the content of ABA was decreased and the dormancy was gradually broken. The expression level of CYP707A gene declined continuously in morphological after-ripening stage and increased at SE5 stage.

WRKY transcription factor has a special zinc finger structure, which plays an important regulatory role in the process of plant response to biological and abiotic stress, plant development (such as seed germination, dormancy, and leaf senescence). The three WRKY genes showed different expression trends in after-ripening stage of *Panax ginseng* seed. Expression levels of WRKY3 and WRKY27

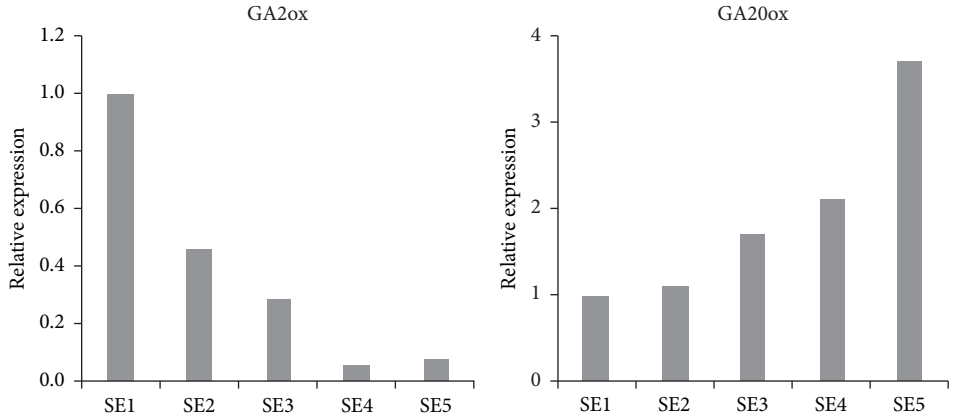

Figure 2: Expression of genes related to GA metabolism in after-ripening stage of *Panax ginseng* seeds.

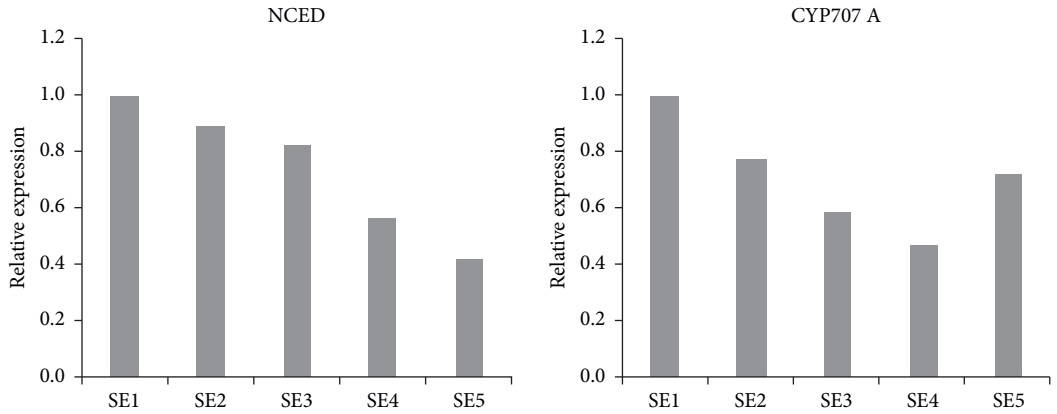

Figure 3: Expression of ABA-related genes in after-ripening stage of *Panax ginseng* seeds.

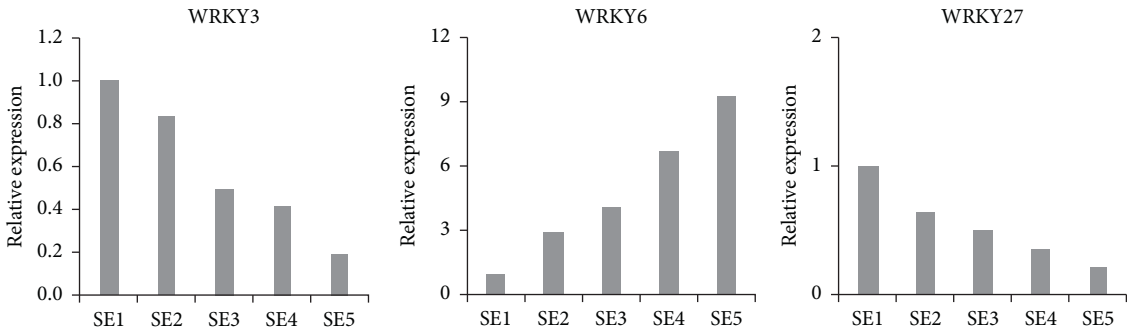

Figure 4: Expression of WRKY transcription factor in after-ripening stage of *Panax ginseng* seeds.

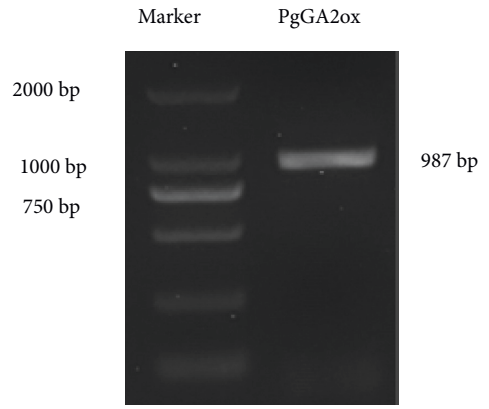

Figure 5: Gel electrophoresis photograph of cloned PgGA2ox gene.

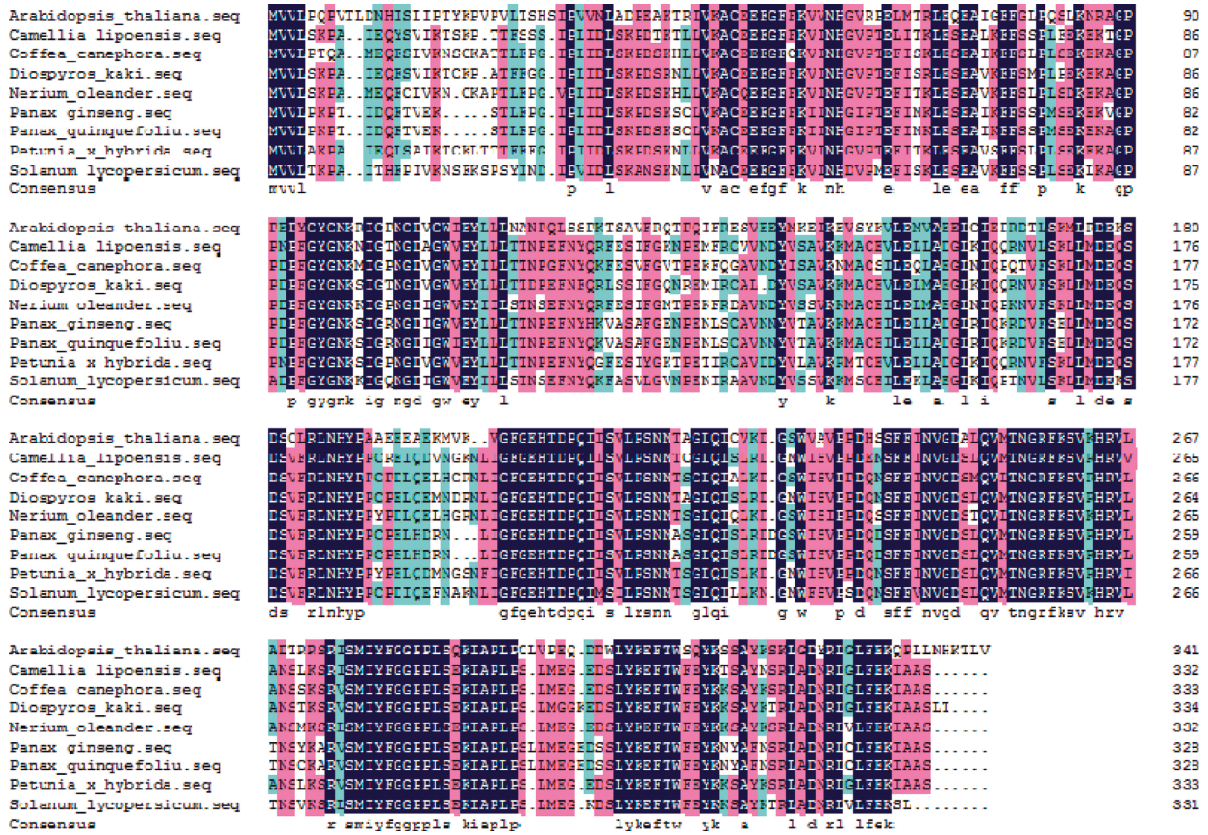

Figure 6: Comparison of amino acid sequence similarity between PgGA2ox and other species.

were low, which decreased in morphological and physiological after-ripening stages. But expression level of WRKY6 was opposite, which gradually increased in physiological after-ripening stage. It is inferred that it is related to release of embryo dormancy and accelerated seed germination.

3.4. Cloning of PgGA2ox Gene of Panax ginseng Seed. The PCR cloning of designed primers was performed using *Panax ginseng* seed cDNA as the template, obtaining a sequence with length of 987 bp. The amplified gene was named PgGA2ox and the nucleotide sequence was submitted to NCBI. GenBank accession number obtained was KT692958.1. The electrophoregram is shown in Figure 5.

3.5. GA2ox Coded Amino Acid Sequence Similarity Analysis and Construction of Phylogenetic Tree. BLASTN analysis was performed on NCBI. It was found that nucleotide sequence of PgGA2ox was similar to gene sequence of *Panax quinquefolius* (KJ802836.1), *Petunia x hybrida* (GU059939.2), and *Camellia lipoensis* (KJ502290.1), with similarity at 99%, 81%, and 80%, respectively. Amino acid sequences coded by PgGA2ox were compared using BLASTP, finding that in terms of amino acid sequence similarity, it was 99% similar to *Panax quinquefolius* (AIL25679.1) GA2ox, 79%, 79%, 79%, 77%, 76%, 73%, 72%, 71%, and 55%, respectively, similar to *Coffea canephora* (CDP06089.1), *Diospyros kaki* (AID65071.1), *Camellia lipoensis* (AHZ13201.1), *Nerium oleander* (AAT92094.1), *Petunia x hybrida* (AFH56955.1)

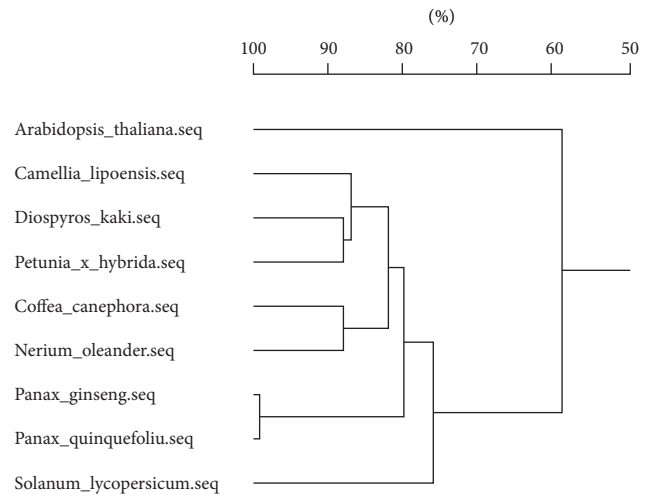

Figure 7: Evolutionary analysis of PgGA2ox.

GA2ox, *Cucurbita maxima* (CAC83090.1), *Solanum lycopersicum* (NP_001234752), *Helianthus annuus* (CAS03784.1), and *Arabidopsis thaliana* (NP_174296.1) gene encoding.

GA2ox is a dioxygenase and 2-ketoglutarate substrate in the GA metabolic pathway. The PgGA2ox protein in the *Panax ginseng* contains a conserved binding amino acid site shared by other plants, i.e., a R residue and a S residue bounded to 2-ketoglutarate, located at positions 226 and 228, respectively, and two H residues and one D residue bound to Fe (Figure 6).

In order to analyze the evolution of PgGA2ox encoded proteins, a phylogenetic tree was constructed using the DNAMAN software (Figure 7). According to the phylogenetic tree, PgGA2ox is most closely related to *Panax quinquefolius*, close to persimmon and *Nerium indicum*, which is consistent with BLASTP result of amino acid sequence.

4. Conclusion

The seed after-ripening is an adaptation of the *Panax ginseng* to the external environment in the long-term evolutionary process. In natural conditions, it helps *Panax ginseng* pass through adverse environment, so that its race multiply, but it brings difficulties to cultivation of mankind. In order to expand cultivation area of *Panax ginseng* and further improve economic benefits of *Panax ginseng*, research on after-ripening mechanism of *Panax ginseng* seed is an urgent problem to be solved. *Panax ginseng* seed after-ripening process is very complex, so current domestic and foreign scholars' study on *Panax ginseng* seed after-ripening process focuses on physiological and biochemical dynamic changes within the seed, seed embryo development changes, and changes in hormones and isoenzyme content in the after-ripening period, but little is reported on the after-ripening mechanism of *Panax ginseng* seed.

In this study, we analyzed the expression rules of GA and ABA hormone-related genes and WRKY transcription factor in *Panax ginseng* seed after-ripening, which is the first of its kind in study of *Panax ginseng* seed dormancy.

GA-related genes: Gibberellin acid synthesis regulation occurs mainly in the late transduction pathway. GA20ox can catalyze GA12 and GA53 into active GA1 and GA4. GA2ox, by β-hydroxylation, can convert active GA1 and GA4 into inactive GA13 and GA14 [23]. The expression level of GA20ox (GA synthetic gene) in the physiological after-ripening stage was higher than that in the morphological after-ripening stage, which proved that low temperature could promote GA synthesis and increase expression of GA synthetic gene, which is consistent with the results of Derkx [24]: low temperature can enhance expression of AtGA20ox1 and AtGA20ox1.

ABA-related genes: C40 carotenoid zeaxanthin was oxidized to violaxanthin, which, after forming 9-cis-epoxy carotenoids, turned to C15 xanthohumol after NCED pyrolysis, a key step in ABA synthesis. CYP707A belongs to P450 monooxygenase family and encodes ABA 8′-hydroxylase, which is involved in catabolism of ABA. The expression level of NCED gene and CYP707A gene was not high in the after-ripening stage of *Panax ginseng* seed, both of which decreased gradually during the whole after-ripening stage, which indicated that endogenous ABA synthesis pathway was closely related to seed after-ripening.

WRKY transcription factor: WRKY gene family is a multifunctional gene family. Molecular biological function of its family members is very rich, including regulation of plant resistance to biological stress and abiotic stress, regulation of plant growth and development, morphogenesis, metabolic regulation, and so on. In addition, WRKY transcription factor is also involved in plant low-temperature response. *Panax ginseng* seeds need to go through low-temperature environment in the after-ripening process. The expression level of WRKY3 and WRKY27 decreased during seed ripening, and WRKY6 was highly expressed in the process of *Panax ginseng* seed after-ripening. Therefore, we speculated that WRKY transcription factor could respond to low temperature regulation, then participate in regulation of metabolism, regulation of gene expression, and finally complete *Panax ginseng* seed after-ripening, which can be further verified in subsequent relevant experiments.

In this study, we cloned for the first time the key gene PgGA2ox for gibberellin acid metabolism during the process of *Panax ginseng* seed after-ripening and obtained GenBank accession number KT692958.1.

The results of this study not only provide a basis for molecular function analysis of PgGA2ox gene but also provide a basis for study on mechanism of after-ripening of *Panax ginseng* seeds.

Data Availability

The data used to support the findings of this study are available from the corresponding author upon request.

Conflicts of Interest

The authors declare that there are no conflicts of interest.

Acknowledgments

The authors thank the National High Technology Research and Development Program of China (863) (2013AA102604), Projects of the National Science Foundation of China (30970259 and 31270337), Research Fund for the Doctoral Program of Higher Education of China (20120061110038), and Jilin Province Science and Technology Development Plan Item of China (20130102041JC).

References

[1] D. Q. Dou, L. Jin, and Y. J. Chen, "Research progress and prospect of chemical composition and pharmacological activity of Panax ginseng," *Journal of Shenyang Pharmaceutical University*, vol. 16, no. 2, pp. 151–156, 1999.

[2] T. Sadler, *The Influence of Climate, Dormancy and Seed Germination in Understanding the Commercial Limitations of Growth of Panax Ginseng C.A. Meyer and Panax Quinquefolius L. And the Mass Micropropagation of These Species*, Panax ginseng, Australia, 2004.

[3] C. P. Zhang, *Mechanism of Different Exogenous Substances Improving Stress Resistance of Coptis Chinensis Seeds and Seedlings under Salt Stress*, Southwest University, Texas, 2012.

[4] Y. Y. Hu, *Study on Seed Germination Characteristics and Seedling Technology of Fritillaria Sichuanensis*, Sichuan Agricultural University, China, 2008.

[5] L. S. Wang and H. L. Sun, "Seed germination and preservation of medicinal plants," *Plant Magazine*, vol. 17, no. 2, pp. 12–21, 1990.

[6] S. Y. Chen, C. T. Chien, J. M. Baskin, and C. C Baskin, "Storage behavior and changes in concentrations of abscisic

acid and gibberellins during dormancy break and germination in seeds of Phellodendron amurense var. wilsonii (Rutaceae)," *Tree Physiology*, vol. 30, no. 2, pp. 275–284, 2010.

[7] J. Lozanojuste, M. Masi, and A. Cimmino, "The fungal sesquiterpenoid pyrenophoric acid B uses the plant ABA biosynthetic pathway to inhibit seed germination," *bioRxiv*, vol. 36, pp. 241–243, 2019.

[8] E. Zdunek-Zastocka and A. Grabowska, "The interplay of PsABAUGT1 with other abscisic acid metabolic genes in the regulation of ABA homeostasis during the development of pea seeds and germination in the presence of H2O2," *Plant Science*, vol. 285, pp. 79–90, 2019.

[9] H. Nonogaki, "Seed germination and dormancy: the classic story, new puzzles, and evolution," *Journal of Integrative Plant Biology*, vol. 61, no. 5, pp. 541–563, 2019.

[10] J. Pan, H. Wang, Y. Hu, and D Yu, "Arabidopsis VQ18 and VQ26 proteins interact with ABI5 transcription factor to negatively modulate ABA response during seed germination," *The Plant Journal*, vol. 95, no. 3, pp. 529–544, 2018.

[11] G. Q. Song, W. Li, S. J. Zhang et al., "Analysis of the relationship between TaNCED1 gene expression and ABA accumulation in wheat under drought and rehydration," *Journal of Triticeae Crops*, vol. 39, no. 4, pp. 400–406, 2019.

[12] S. Z. Ma, Z. W. Sha, Y. N. Lu, X. L. Zhang, L. X. Zhou, and M. D. Bian, "Functional analysis of *Arabidopsis thaliana* cryptochrome in ABA regulated seed germination," *Journal of Jilin Agricultural University*, vol. 40, no. 3, pp. 264–269, 2018.

[13] Z. Wang, D. Chen, C. Yue, H. L. Cao, and Y. L. Guo, "Cloning and expression analysis of CsNCED2 gene in tea plant," *Acta Botanica Boreali-Occidentalia Sinica*, vol. 38, no. 6, pp. 994–1002, 2018.

[14] A. J. Matilla, N. Carrillobarral, and M. D. C. Rodríguez-Gacio, "An update on the role of NCED and CYP707A ABA metabolism genes in seed dormancy induction and the response to after-ripening and nitrate," *Journal of Plant Growth Regulation*, vol. 34, no. 2, pp. 274–293, 2015.

[15] Y. Zheng, Y. Huang, W. Xian, J. Wang, and H. Liao, "Identification and expression analysis of the Glycine max CYP707A gene family in response to drought and salt stresses," *Annals of Botany*, vol. 110, no. 3, pp. 743–756, 2012.

[16] H. Y. Ma, D. D. Zhao, Q. R. Ning et al., "A multi-year beneficial effect of seed priming with gibberellic acid-3 (GA3) on plant growth and production in a perennial grass, leymus chinensis," *Scientific Reports*, vol. 8, no. 1, 14 pages, Article ID 13214, 2018.

[17] D. Koryznienė, S. Jurkonienė, T. Žalnierius et al., "Heracleum sosnowskyi seed development under the effect of exogenous application of GA," *PeerJ*, vol. 7, no. 5, pp. 88–95, 2019.

[18] G. Gogoi, P. K. Borua, and D. Chetia, "GA3 assisted seed dormancy breaking in abelmoschus moschatus medik. subsp. moschatus," *Cercetari Agronomice in Moldova*, vol. 49, no. 4, pp. 27–34, 2016.

[19] J. T. Henderson, H. C. Li, S. D. Rider et al., "*PICKLE* acts throughout the plant to repress expression of embryonic traits and may play a role in gibberellin-dependent responses," *Plant Physiology*, vol. 134, no. 3, pp. 995–1005, 2004.

[20] X. Z. Huang, C. F. Jiang, and L. L. Liao, "Research progress on molecular basis and regulation mode of gibberellin acid mechanism," *Chinese Bulletin of Botany*, vol. 23, no. 5, pp. 499–510, 2006.

[21] A. L. Hauvermale, T. Ariizumi, and C. M. Steber, "Gibberellin signaling: a theme and variations on della repression," *Plant Physiology*, vol. 160, no. 1, pp. 83–92, 2012.

[22] D. Q. Yu, L. G. Chen, and Y. R. Hu, "AtWRKY8 regulates multiple stress signaling pathways in plants," *Chinese Society of Genetics National General Assembly and academic seminar*, vol. 167, 2013.

[23] Y. B. Li, M. Y. Zhu, X. R. Yang et al., "Advances on gibberellin 2-oxidases gene in higher," *Plants Acta Horticulturae Sinica*, vol. 45, no. 9, pp. 1844–1856, 2018.

[24] T. Boonkaew, C. Mongkolsiriwatana, A. Vongvanrungruang, K. Srikulnath, and S. Peyachoknagul, "Characterization of GA20ox genes in tall and dwarf types coconut (Cocos nucifera L.)," *Genes & Genomics*, vol. 40, no. 7, pp. 735–745, 2018.

Hindawi
Scientific Programming
Volume 2022, Article ID 7395678, 7 pages
https://doi.org/10.1155/2022/7395678

Research Article

Food Interactive Packaging Design Method Based on User Emotional Experience

MingDong Song,[1] Juan Xu ,[2] and YingBo Chen[1]

[1]*College of Arts and Design, ZheJiang A&F University, Hangzhou, Zhejiang 311300, China*
[2]*Dean's Office, ZheJiang A&F University, Hangzhou, Zhejiang 311300, China*

Correspondence should be addressed to Juan Xu; cigaba@zafu.edu.cn

Received 6 June 2022; Accepted 2 July 2022; Published 5 September 2022

Academic Editor: Lianhui Li

Based on the interactive food packaging design method based on the user's emotional experience, the specific food packaging design scheme is completed. On the basis of analyzing the current situation of the food industry, this paper discusses the competitive driving factors between the demand side and the enterprise side for food packaging, integrates the user's emotional experience into the reality of food packaging, and focuses on the specific practical solutions based on the user's emotional experience. Incorporating user emotional experience into food packaging design Yuan, 2022 and Liu, 2020 is beneficial to both the impact of food brands and the promotion of product sales. Incorporating user emotional experience has played a very important role in food market competition. At the same time, through practical cases, closely focusing on the user's emotional experience, it innovatively tried to convert users into core designers of product packaging and adopted a small-batch customized production and packaging mode. This plays a certain guiding and reference role for food packaging design. This paper takes the user's emotional experience as the research perspective and interactive packaging as the research object, uses the three-level theory of emotionality as the guide, explores the user's emotional experience path for packaging by means of literature analysis, fieldwork, case analysis, and experiments, and summarizes the design, principles, and methods.

1. Introduction

With the continuous development of the social economy and the advancement of network information technology, people's lives have undergone rapid changes. Social psychologist Maslow once proposed the following. "The development law of human needs is to gradually increase from the lowest level of physiological needs to the highest level of self-realization." When people begin to pursue a high-quality life, consumers' values have also changed, with a desire for more emotional attention. The expectation for commodity packaging [1] has also shifted from simple functional requirements to the emotional experience of commodity packaging [2]. Therefore, it is particularly important to pay attention to the psychology and behavior of consumers to understand their real needs of users [3]. At the same time, the maturation of new media technology, packaging materials [4, 5], and production technology provides the possibility of innovation in future commodity packaging.

Donald Norman proposed that the affective system consists of three distinct, interconnected layers, each of which affects our experience of the world in a specific way. These three levels are the instinct level, the behavior level, and the reflective level in turn. The instinct layer is responsible for the most primitive instincts of human beings. The behavioral layer refers to the process of achieving an effective goal in the shortest time or with the least amount of behavior. The reflective layer is conscious thinking and learning. These three levels create our emotional experience of things. When these three levels are applied in packaging design, they can, respectively, correspond to the user's instinctive experience of the packaging before purchasing the product, the behavioral experience during use, and the information feedback process after use.

Humans have a relatively rich perception system, and feeling is the simplest and most basic form of reflection when people understand the objective world. "People rely on sensory experience to understand the world. The senses are our connection to memory and the connection of emotion." In instinctive experience, vision, hearing, touch, smell, and taste are in the dominant position. When choosing a product in front of the shelf, the shape of the packaging [6], the texture of the material, and the warmth of the color will bring different emotional feelings to users, which will instinctively trigger emotional reactions, thereby promoting consumption behavior.

In the behavior layer, what is concerned is the user's behavior. The highest requirement of behavioral experience is people-oriented. Understand user behaviors and discover unmet or clearly articulated needs of users. But if the experience is puzzling, it will bring a negative emotional impact on the user, and conversely, good design will produce a positive emotional experience [7].

Good design creates a positive emotional experience. The reflective layer is based on the instinctive layer and the behavioral layer. The focus is on information, culture, and identification with the product or the meaning behind the product. A user's lasting memory of an experience comes from the reflective layer and even affects our future use of a product or service. In packaging design, "the instinct layer, the behavior layer, and the reflection layer are intertwined, influenced, and penetrated." By exploring the emotional experience path of packaging users, we can make packaging design that meets the real needs of consumers [3, 8, 9].

2. Current Situation at Home and Abroad

Since the concept of user experience was first proposed in the 1990s, after decades of development, it has been widely used in different fields and has expanded many related concepts. According to "the authoritative ISO 9241-210 standard, "user experience" is regarded as the response process of people's needs to real-world conditions and the realization of desired products, systems, or services."

Analysis of the research status of foreign user experience shows that most scholars study user experience according to different practical problems, select its constituent elements according to the needs of practical problems, and then conduct classification research one by one [10]. For example, [10] covers the content of user experience as actionable, cognitive, motivating, and enlightening. Morvilleclassifies user experience into usability, usefulness, ease of use, reliability, ease of discovery, satisfaction, and value and then evaluates user experience according to the above categories. [13] encapsulates the components of user experience as pleasure, functionality, usability, and pride. From the above research, it can be seen that user experience can be divided into usability, user emotional experience, and user needs. The research scope of this paper mainly focuses on the user's emotional experience. Emotional design refers to integrating the user's emotional needs in the process of the design construction and applying it to the design process. In order to explore the satisfaction of user experience, Partala [14] started from the aspects of emotional experience, psychological needs, and interactive environment, respectively, compared the experience data in the experiment, and concluded that autonomy, competitiveness, and self-esteem are more prominent in psychological needs. In marketing and consumer behavior research, there are also many discussions on emotional experience. [15] proposed that when "emotion" acts on the consumption scene, face-to-face interaction is the main reason for affecting the emotional experience. [16] proposed that "in the process of consumption, the complete experience affects consumers' purchasing preferences, and the influence of emotional factors and shopping experience exceeds the product and service itself." According to empirical research by scholars, 85% of consumers decide whether to buy or continue to use a certain brand through an emotional experience, and only 15% of consumers pay relatively little attention to emotional experience.

In the research scope of the user's emotional experience, the measurement method is also very important. Due to the strong subjectivity of user experience, the measurement of subjective emotion has become a relatively common method. In psychological measurement, PAD emotional model, PrEmo scale, semantic difference method, utility scale, hedonic scale, etc. are all commonly used, and most of them are conducted in the form of questionnaires. In addition, a series of qualitative methods such as interviews and observations can be combined for research. However, subjective emotion measurement methods are still not scientific and accurate to a certain extent. Therefore, using experimental methods to quantify physiological indicators can provide scientific data support for emotional research more objectively. For example, facial recognition technology that compares AI and expression databases, brain wave experiments using EEG amplifiers, and eye movement experiments using gaze tracking are gradually being applied by scholars in user experience research in various fields. In the article "Product packaging and consumers' emotional response. Does spatial representation influence product evaluation and choice?", the author uses facial recognition technology to capture the face image of the measurer when viewing the product packaging image and compares the face modeling method with the expression database. Yes, it is found that visual images on product packaging can affect consumers' emotional perception and purchasing decisions, and it is verified that the foreground position of images on the packaging [10, 17] will reduce consumers' psychological distance and increase positive emotional experience.

In our country, the theoretical research of user experience is still in the process of continuous development. Previous scholars have systematically sorted out the concept, composition, measurement, and evaluation of user experience, focusing on in-depth research on measurement and evaluation methods. These discuss the era background and main application fields related to emotionalization, as well as the current research status and future development trends. If prepurchase feelings and product efficacy meet expectations, emotions will suddenly revive and satisfaction will increase significantly, and vice versa. In the process of consumption,

consumers' personal feelings, temperament, knowledge structure, perceptual experience, attitudes, and values will directly or indirectly affect consumers' emotions and emotional responses.

In the process of user research, researchers have different understandings of user experience due to different research perspectives and backgrounds. The research on user experience in our country has just started, and there is still a lack of in-depth and detailed theoretical research, most of which are analyses and enlightenment of foreign research content. User experience has a high degree of attention in the design discipline, and the number of researchers is increasing year by year. However, most of them are widely used in industrial design disciplines, and less in the field of packaging design [18, 19], and most scholars still focus on qualitative research on the measurement method of user experience, which is not scientific and rational in the method. Objectively provide data support for packaging design [20, 21].

By analyzing the user's emotional experience characteristics and the experience path in the packaging, the corresponding three-level design methods are summarized (Figure 1), which are the perception of the instinct layer, the participation process of the behavior layer, and the feedback of the reflection layer.

3. Research on Packaging Design Based on User Emotional Experience

In order to extensively collect the user's emotional experience information about packaging [22], the authors conduct research in the form of questionnaires. By visiting tourist attractions, specialty stores, exhibitions, and issuing online questionnaires, we conduct research on user needs. Through the survey data results, it is known that the user's demand for food packaging is generally divided into the following points, which can reasonably protect the product and meet the functional requirements of the packaging. It can convey national characteristics and show national customs. Interestingly, research has shown that 63% of users say that the interestingness of packaging will affect users' purchase intention.

Graphics are an important part of the packaging. Compared with text, graphics have stronger visual expressive power and are easier to attract users' visual attention [23, 24] and effectively convey the connotation of products. The immersive graphic isomorphism method puts the product itself or partial content into the context, combines the two-dimensional graphic with the product, conveys the form of images and objects that are both real and illusory, breaks the relationship between the picture and the bottom, and integrates the product into the product. At the same time, the dual expression of semantics can also be integrated, and consumers can receive additional brand information or commodity attributes through the presentation of visual graphics. For example, designer Constantin Bolimond (Figure 2) combines the packaging design of nuts with squirrels and forms a complete design by combining the product itself with the packaging pattern. The image of the squirrel is naive and attractive and metaphorically expresses the invisible meaning of the product.

The realization of any product function is completed by the interaction between people and products, so packaging design should be people-oriented and understand the expectations and usage of packaging by people in all aspects. "Focus on the instinct layer, the user's initial feeling of the packaging, the intuitive feeling of appearance, color matching, material texture, and so on; pay attention to the behavior layer, whether the process of the user using the packaging is simple and easy, and whether the packaging after use can arouse the user's deeper understanding."

Usability is the basic premise of packaging design [25], and it is also the first principle, which can protect the attributes of commodities in the process of commodity circulation. For example, the shape of the food itself will directly affect the structure of the packaging. For example, milk skins, during the production process, in the production process, due to the use of pots and the way the finished product is taken out, most of the unprocessed milk skins are semicircular . The pure milk chews have a thick texture, and a large-caliber short bottle is required when choosing packaging. Milk residue, Bischlager, etc. are all fragile products. In the design of the packaging, it is necessary to take into account the pouch packaging or pressure-resistant packaging. The packaging can only proceed to the next design on the premise of guaranteeing usability. "Sanchun," a dairy food brand in Inner Mongolia, promotes this delicious food as an easy-to-carry food through people-oriented design and packaging (Figures 3 and 4).

On the premise of satisfying usability, ease of use is a further requirement. To measure whether the function and structure of a package are reasonable, through the analysis of the user's psychological needs, physiological habits, and ergonomics, the difficulty of use is determined. Questions such as degree, convenience, and availability for most people come before design [26]. Whether the user's use can be improved in a more convenient way will affect the user's repurchase. Therefore, reducing the time cost for the user's use as much as possible is a high manifestation of ease of use.

After satisfying the principles of usability and ease of use, how to make consumers feel satisfied and happy in the process of selection and use is an important part of pleasantness. Integrate emotional care into packaging, integrate national culture and additional functions, and connect consumers with products through the medium of packaging, thereby generating emotional resonance.

It is very important to add creative graphic elements. In the selection and application of ethnic elements found in the market, most of the graphics are outdated, conservative, and have serious convergence problems. On the basis of retaining the inherent form of ethnic elements, the elements should be simply deconstructed and reconstructed by means of graphic isomorphism, graphic creative expression, etc. to get rid of the convergent packaging of blue sky, white clouds, and green grass and give them a new visual experience [27]. For example, in the kitchen utensil packaging designed by Danish designer Des Jacob Poulsen for Scanwood, the kitchen utensils are isomorphic with the background picture

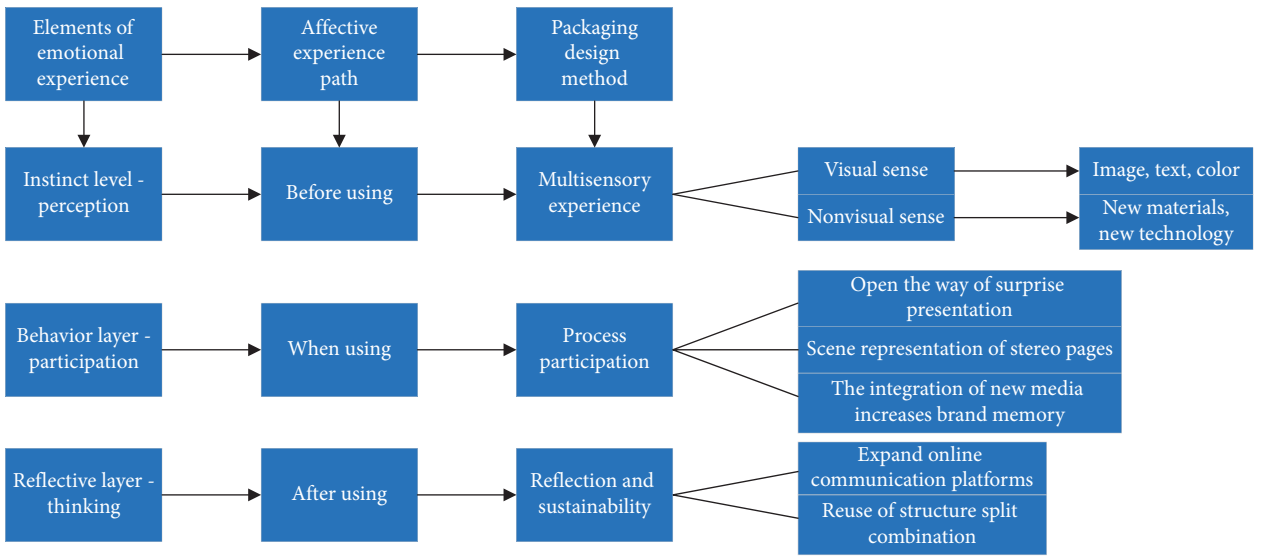

Figure 1: Summary of interactive packaging design methods.

Figure 2: Nut packaging design.

Figure 3: Coffee milk packaging design.

Figure 4: Packing design.

in the packaging, which interestingly expresses the natural and pollution-free characteristics of the product.

Emotional color expression is also very important, and the color is more likely to make users form visual memories. Different colors will bring different psychological hints to users. "The rational use of color can not only highlight the functions and attributes of products but also shape the brand image, expand the effect, gain memory cognition in consumers' minds, and strengthen the perception [28]." For example, McDonald's standard red and yellow color matching, Pepsi's standard blue color, and Sprite's standard

green have formed the inherent brand attributes in the minds of users. Choosing the main tone and auxiliary color corresponding to the product attributes can maximize the overall artistic effect of the sublimation packaging. The integration and sorting of text information is the key point. Text is one of the elements of commodity packaging. It plays the role of information transmission in packaging and annotates the nature of packaging. It is generally divided into the main text, data text, description text, and advertising text. Text content requires information integration and hierarchical induction. The size and direction of the text, the looseness and tightness of the font area, and the hierarchical relationship of the text will affect people's visual experience. By controlling the spacing, line spacing, and combining text, the hierarchical relationship between different elements is clearly listed, allowing users to quickly obtain the required information in the shortest time. The text information on the packaging of dairy food should take into account the reasonable arrangement of ethnic characters and Chinese characters and the style of expression. For example, by extracting the form of Mongolian characters and combining them with Chinese characters, on the premise of maintaining readability, it can add a touch of ethnic charm to the font style.

4. Optimal Design of Food Packaging

In consumer psychology, if users participate in a certain action, they will strengthen their awareness of the product and will develop a sense of trust with the gradual deepening of their awareness. The design that guides user behavior levels in packaging design is related to the way the packaging is used. The design that pays attention to the way of using the packaging of local specialty food can allow users to relieve stress in the process of using the packaging and have a pleasant, satisfying, and self-identified experience [29].

For example, the design of the way in which local food is used should make the packaging easier to use and more valuable. Good ideas usually emerge from certain behaviors. The packaging of local specialty food is usually discarded by users after use [30]. However, if the packaging design of local specialty food can reflect the value of user experience, feelings, and secondary use, it can effectively enhance users' favorable impression of the product and facilitate the promotion of the product, while also playing a positive role in the protection of the natural environment. Souvenir packaging usually has game functions and secondary utilization functions. Figure 5 shows the sweet corn food packaging designed by VRS WPI Vilnius in Lithuania. The designer has skillfully combined the cutting process in the packaging design so that the images of sloths, flamingos, and owls can be used not only as the visual image symbols of the packaging but also as the main body of the toy. They can create beautiful and unique handmade works. The handmade parts of the three types of packaging can be exchanged and shared, which enhances the fun of the packaging design experience process. While promoting the sales of goods, it also virtually reduces the post-promotion cost of the product.

Figure 5: Oho children's sweet corn food packaging.

With the popularization of digital information technology and network, virtual digital packaging has become an inevitable product of the development of modern information technology. Traditional offline consumer groups are diverted by online shopping, and virtual packaging just makes up for the shortcomings of traditional packaging. In recent years, virtual packaging that has emerged one after another not only undertakes the functions of protecting products and displaying goods but also in product promotion and demonstration.

Superimposing virtual images on the original packaging materials through AR technology can expand a large amount of information presentation space and even dynamic display links, allowing consumers to immersively experience the use of products and brand stories through colorful digital content. For example, Baidu joined hands with Yili in December 2015. Through the combination of Baidu's technological innovation and manufacturing and Yili's creation of the global milk industry chain, a brand-new interactive packaging experience can be created[25]. By shooting packaging through mobile phones, global consumers can be led to understanding of all aspects of the global milk industry chain through the form of AR. The living environment, milk processing, and packaging process allows every user to have access to the most authentic Yili. The development of technology has made the application of virtual reality technology in packaging gradually popular, providing technical support for packaging innovation.

Reflecting on the experience of the layer conveys the deep semantics of the product, "focusing on the user's culture, memories, and emotions, increasing the spiritual value and cultural connotation of the product, is a progressive process of user experience from shallow to deep." Also, formulate the next two goals, which are to build an industrial basic innovation system around green packaging, safe packaging, and intelligent packaging. The second is a green production system covering the life cycle of packaging

around cleaner production and green development. This layer focuses on information, culture, and the story behind the product, which is usually an extension of the experience of the product's instinctive layer and behavioral layer.

5. Establishing Packaging Design Patterns

5.1. Brand Positioning and Audience Analysis. Professor Bruce Hanna of the Pratt Institute in the United States once mentioned that designers are all storytellers. The stories told by designers are the behaviors brought out by the design, and the design is the output of the story from a certain perspective. The living background of the light-middle-class people belongs to the era of rational consumption, and they are willing to improve their quality of life and have a greater interest in new things. By 2020, China's light and middle-class population will reach 350 million, becoming the backbone of China's consumer market, while the new middle-class population is still the backbone of urban consumption. In the future, "quality consumption will become the new normal, and the pursuit of high-cost performance will be the main theme of Chinese consumption in the next five years."

5.2. Food Packaging Design. Based on the previous research and experimental data, the author learned that most of the food packaging design uses fashion, gorgeous and creative as semantic phrases to design food packaging and gift boxes.

5.2.1. Instinct Layer. A cultural symbol is a symbolic form of regional cultural connotation and meaning. According to the previous user research and food packaging collection, it is found that most food packaging designs can make users feel the national atmosphere in the shortest time. In the selection and application of ethnic elements, most of the packaging seen in the market has problems such as outdated graphics and conservative and serious convergence. On the basis of retaining the inherent form of ethnic elements, this paper simply deconstructs and reconstructs the graphics to give them a new visual experience. According to the survey, 65% of users believe that when choosing food, whether the original appearance of the food can be presented on the packaging is more important. Therefore, the schematic diagram of the extracted food is used directly in front of the packaging, which is beneficial for the user to obtain the product form through the screen content and reduce the time and cost of purchasing.

5.2.2. Behavior. According to statistics, people will come into contact with at least 30,000 daily necessities in their daily lives and will not leave memories or emotions about each of them in the process. But because of countless repetitions of limbs, it will leave "behavioral memory" during the use of the product. It is necessary to make reasonable use of the user's behavior memory and innovate the packaging under the premise of being easy to use. Look for the features of simplicity, mechanics, and daily from the common packaging box types and guide users to seamlessly connect when picking up the packaging and using the packaging.

In life, most people have countless experiences using the box-type structure. This experience is not paid attention to, and users can open it smoothly without expending extra effort. The difference is that when the lid is picked up, the surrounding structures automatically descend, presenting a series of contents such as product display screen, eating method, production process, and so on, creating an interaction process different from daily experiences, such as making users feel extremely friendly at the same time and feel a little surprised.

5.2.3. Reflection Layer: Deep Communication of National Culture. The experience of the reflection layer conveys the deep semantics of the product, pays attention to the user's culture, memories, and emotions, and increases the spiritual value and cultural connotation of the product. It is a progressive process of user experience from shallow to deep. This layer focuses on information, culture, and the story behind the product, which is usually the progression of the instinctive layer of the product and the extension of the behavioral layer experience. Based on the user's emotional experience, guided by the three-level theory of emotionality, the practical design of food packaging is completed, providing a new development direction for the packaging of national characteristic products.

6. Conclusion

This paper summarizes the principles and methods of interactive packaging design by exploring consumer perception characteristics and emotional experience paths. According to the three aspects of the user's emotional experience in packaging, three methods of interactive packaging design are summarized, cleverly through the color of the image and the arrangement of the text, the emotional expression of cool and warm colors, the fusion of new technology materials, etc. The interactive experience method when using, including the surprise presentation of the opening method, the scene reproduction of the three-dimensional page, and the introduction of AR technology to enhance the brand memory. For information feedback and reuse after use, including adding QR code recognition and broadening the information dissemination platform, designers should focus on a wider audience. Based on the research of this paper, there are the following possibilities for follow-up research: in-depth analysis of consumers' usage needs, behaviors, and psychological characteristics, and perfect packaging design methods. Continue to expand the research scope of packaging design and deeply explore the possibility of packaging innovation in packaging materials, production processes, packaging, transportation, etc. Continue to explore the application of innovative methods in the packaging of ethnic products and broaden the channels for the dissemination of ethnic culture. In the process of protecting the product, the packaging will cause an emotional experience for the user. Paying attention to the psychology

and behavior of users can better guide the packaging design, promote the mutual communication between users and products, trigger a positive emotional experience while increasing the added value of products, and convey national culture in a subtle way.

Data Availability

The dataset can be accessed upon request.

Conflicts of Interest

The authors declare that they have no conflicts of interest.

Acknowledgments

This study was sponsored in part by the National Natural Science Foundation of China (no. 2345678).

References

[1] H. Li, "Effects of Pet Food Packaging Design on Consumers' Mental health," *BASIC & CLINICAL PHARMACOLOGY & TOXICOLOGY*, p. 127, 2020.

[2] L. Motelica, D. Ficai, O. C. Oprea, A. Ficai, and E. Andronescu, "Smart food packaging designed by nanotechnological and drug delivery approaches," *Coatings*, vol. 10, no. 9, p. 806, 2020.

[3] B. Nemat, M. Razzaghi, K. Bolton, and K. Rousta, "The role of food packaging design in consumer recycling behavior-A literature review," *Sustainability*, vol. 11, no. 16, p. 4350, 2019.

[4] Maffei, "Perspectives on food packaging design," *International Journal of Food Design*, vol. 2, no. 2, pp. 139–152, 2017.

[5] "The application and psychology of color in food packaging design," *Advance Journal of Food Science and Technology*, vol. 10, no. 9, 2016.

[6] C. Bou Mitri, M. Abdessater, H. Zgheib, and Z. Akiki, "Food Packaging Design and Consumer Perception of the Product Quality, Safety, Healthiness and preference," *Nutrition & Food Science*, 2020.

[7] N. Babak, R. Mohammad, B. Kim, and R. Kamran, "Sustainability Research," *Recent Findings from University of Boras Has provided New Information about Sustainability Research (The Role of Food Packaging Design in Consumer Recycling Behavior-A Literature Review)*, vol. 11, no. 16, 2019.

[8] S. Raja Intan, B. Azman, and Y. Lim, "The Evaluation of Aesthetic Values on the Two-Dimensional Visual Design Structure: Food Packaging Design," *Wacana Seni Journal of Arts Discourse*, vol. 17, 2018.

[9] K. Chen, "Analysis on the application of color in children's food packaging design," in *Proceedings of 2015 3rd International Conference on Economics and Social Science (ICESS 2015 V86)*, p. 4.

[10] D. Jia, "Research on application of color on food packaging design," in *Proceedings of the 2021 International Conference on Electronic Commerce*.

[11] M. S. Burmester, "Diefenbach/M. Hassenzahl: Psychologie in der nutzerzentrierten produktgestaltung," in *i-com*, J. Ziegler, Ed., vol. 16, no. 2, 2017.

[12] P. Morville, *Communication Design Quarterly Review*, Semantic Studios,, vol. 4, no. 2, Ann Arbor, MI, USA, 2014.

[13] N. V. Gowtham Deekshithulu, Samreen, B. Raj Kiran, and L. R. V. Prasad, ". Comparitive field evaluation of roto drill cum herbicide applicator," *Current Journal of Applied Science and Technology*, 2021.

[14] James Critchlow, "Cold war broadcasting: impact on the soviet union and eastern europe—a collection of studies and documents," in *Journal of Cold War Studies*, A. Ross Johnson and R. Eugene Parta, Eds., no. 2, p. 22, 2020.

[15] C. H. Jeong and N. Ken, "A study on package design methodology through the experience factor analysis," *Journal of the Korean Society Design Culture*, no. 4, p. 22, 2016.

[16] G. Hans Werner and G. Schwedler, "Vergessen, Verändern, Verschweigen. damnatio memoriae im frühen Mittelalter. Köln, Böhlau 2020," *Historische Zeitschrift*, no. 1, p. 314, 2022.

[17] X. Xie, "Ease of use design for food packaging for the elderly," *Frontiers in Art Research*, vol. 1, no. 2, 2019.

[18] "Partnering on Package Design for Food to Go," *Nation's Restaurant News*, 2014.

[19] F. Tobi, C. Coetzee, M. Tarl, and A. Alemayehu, "Engineering - Biosystems Engineering; Studies from University of Stellenbosch in the Area of Biosystems Engineering Described [The Efficacy of Finite Element Analysis (FEA) as a Design Tool for Food Packaging: A review]," *Food Weekly News*, 2018.

[20] T. Fadiji, C. Coetzee, T. Berry, A. Ambaw, and L. Umezuruike, "The efficacy of finite element analysis (FEA) as a design tool for food packaging: a review," *Biosystems Engineering*, p. 174, 2018.

[21] F. Fernqvist, A. Olsson, and S. Spendrup, "What's in it for me? Food packaging and consumer responses, a focus group study," *British Food Journal*, vol. 117, no. 3, pp. 1122–1135, 2015.

[22] N. Babak, R. Mohammad, B. Kim, and R. Kamran, "Design affordance of plastic food packaging for consumer sorting behavior [J]. Resources," *Conservation & Recycling*, p. 177, 2022.

[23] M. Salhieh Sa'Ed, "Designing food packages to attract customers: a systematic approach," *JORDAN JOURNAL OF MECHANICAL AND INDUSTRIAL ENGINEERING*, vol. 14, no. 2, 2020.

[24] A. Fenko, R. de Vries, and T. van Rompay, "How strong is your coffee? The influence of visual metaphors and textual claims on consumers' flavor perception and product evaluation," *Frontiers in Psychology*, vol. 9, p. 53, 2018.

[25] Y. Liu, "Food packaging printing technology trend analysis: a patent analysis approach," *Applied Mechanics and Materials*, vol. 469, p. 469, 2013.

[26] L. Brennan, S. Langley, V. Karli et al., "The role of packaging in fighting food waste: a systematised review of consumer perceptions of packaging," *Journal of Cleaner Production*, p. 281, 2021.

[27] Li Sun, "A Preliminary Exploration on the Artistic Design of Take-Away Food Packaging," in *Proceedings of the 2020 2nd International Conference on Art, Design and Cultural Studies*, East Java, Indonesia, October 2020.

[28] G. Yang, "Research on packaging design of take-out food oriented towards the usability enhancement," in *Proceedings of the 2015 International Conference on Social Science*, Education Management and Sports Education, November 2015.

[29] F. Yuan, "Application and value of hand-painted illustration in food packaging design," in *Proceedings of the 4th International Conference on Art, Design and Cultural Studies (ADCS 2022)*, Wuhan Zhicheng Times Cultural Development Co., Ltd, 2022.

[30] W. Lin, "Application of traditional culture in food packaging design," *International Journal of Educational Technology*, vol. 2, no. 1, 2021.

Hindawi
Scientific Programming
Volume 2022, Article ID 2322562, 14 pages
https://doi.org/10.1155/2022/2322562

Research Article

Signal Control Adaptive Model Based on Microtransformation of Urban Street Space

Cheng Zhao,[1] Yi Xun ,[1] and Lixin Qi[2]

[1]*School of Art & Design, Guangdong University of Technology, Guangzhou 510000, China*
[2]*Guangdong Jingwei Land Surveying and Planning Technology Co., Ltd., Huizhou 516001, China*

Correspondence should be addressed to Yi Xun; xun.yi@gdut.edu.cn

Received 28 June 2022; Revised 11 August 2022; Accepted 16 August 2022; Published 1 September 2022

Academic Editor: Lianhui Li

Cities need to develop, people's lives need to be improved, and the living environment needs to be enhanced. With the strengthening of the national policy of paying attention to people's livelihood, the speed of development, the increase of the number of cars, and the major demolition and construction of streets are in full swing everywhere. However, traffic congestion has become a serious social problem, which greatly affects economic development and people's daily life. Therefore, the study of signal coordination control of urban traffic arteries has become an urgent problem for all countries. In this paper, after a brief introduction of the basic concepts and related technologies of traffic control systems, we focus on the arterial coordinated control system. The adaptive control model studied in this paper reveals the vehicle arrival dynamics from a microscopic perspective, which helps to improve the adaptive control effect and alleviate urban intersection congestion. The use of traffic information acquisition and control systems can promote the application of vehicle networking technology, while moreover helping to provide important model simulations for future street simulation renovation.

1. Introduction

It is urgent to analyze and propose solutions to the current shortcomings and problems of urban street space design and the current situation of urban streets in China. We should use system theory as an analytical tool and philosophical theory support, from the cultural, human, ecological, ethical perspective to analyze the design of urban street space in China and the current situation of the street problems. Street space is not a long and narrow independent space, closed space, but widely permeated to other types of space, and benign interaction. Street space condenses and carries a large amount of information, involving economic, political, and cultural and social factors and reflects not only value orientation but also social ethics. The transformation process of historical districts often involves different social groups, and one social group often influences another group in order to realize its own spatial practice [1]. Street space renovation design must not unilaterally pursue the expansion of traffic flow while ignoring the reduction of pedestrian space; unilaterally pursue individual or local economic or commercial interests while ignoring long-term social and overall interests; unilaterally pursue so-called biased visual aesthetics, personal preferences, and a certain style while ignoring the real life and inner feelings of citizens; unilaterally pursue formal novelty and objective prosperity while ignoring the regulation of microclimate. The unilateral pursuit of formal novelty, objective prosperity, while ignoring microclimate regulation and humane care; the unilateral pursuit of verbal ecological green environmental protection and ignore the true meaning of ecological cycle, the true meaning of the green environment, simply because of the so-called international style, while ignoring the unique flavor of the regional personality with a deaf ear. A good street is not only durable but also useable, pleasant, livable, ecological, harmonious, and humane. It is a dynamic open system with all the characteristics of a system that needs to be constantly improved and evolved to meet the needs of the times and to adapt to the development of people. Street space is the window of the city, recording the history of the citizens, and

every detail gives the space a personalized charm, reflecting the comprehensive quality and public spirit of the citizens. The transformation design of street space needs to be preceded by systematic analysis methods and forward-looking theories, and the transformation plan should be made according to local conditions after careful investigation and research of basic information, meticulous and thorough analysis, feedback and evaluation, and many other procedures of combing and borrowing relevant theoretical research results and comprehensive research.

One of the most important points is that urban traffic congestion has become a serious social problem, and how to regulate and manage urban traffic flow in a rational and scientific way is the focus of attention of the global traffic engineering and theoretical communities. Urban residents are increasingly vulnerable to the problems brought by high urbanization, such as traffic congestion, air pollution, and housing tension. Among them, urban congestion is a common problem in major cities around the world, and it seriously affects the quality of life of residents and the operational efficiency of various services. To solve urban traffic congestion, on the one hand, the layout and proportion of residential land and commercial land should be reasonably arranged from the interactive relationship between land use and traffic, so as to solve traffic congestion from planning; on the other hand, the traffic efficiency of roads and road networks should be improved to reduce the probability of congestion. Urban traffic control signal control intersection, as a key node of the road network, is the most likely location to generate traffic congestion, and if its queue of vehicles spreads without limit, it will seriously affect the traffic efficiency of adjacent intersections. Therefore, the signal control strategy of intersections, as an effective method to alleviate their congestion level, is an important research direction for urban road reconstruction in recent years. According to the traffic flow characteristics of urban arterial roads, it has become one of the important research topics of current intelligent traffic control to design advanced adaptive coordinated control systems for urban traffic arterials by using advanced information technology, communication technology, and control technology to improve the operational efficiency of arterial traffic networks. In addition, with the implementation of the concept of bus priority in major cities, the proportion of buses in the road network has increased significantly. In order to improve the efficiency of bus travel, more and more urban intersections are equipped with bus priority signals. However, existing studies and practices show that vehicle-specific signal priority strategies will inevitably lead to increased delays in normal traffic flows. Especially in the case of a general mix of buses and cars, attention needs to be paid to the signal right-of-way allocation for traffic in different directions. Therefore, a reasonable signal control strategy is particularly important to reduce passenger delays. Conversely, if the signal timing scheme does not correctly reflect the characteristics of real-time traffic flow, it may lead to wasted green time, too short cycles, or underestimated turn times, generating unnecessary waiting time. Studies have shown that up to 40% of excess fuel consumption can be generated due to improper traffic signal timing [2]. It is of practical importance to study and design coordinated signal control systems for urban traffic arteries to solve urban congestion and ensure smooth road flow to promote economic development.

In this paper, after a brief introduction of the basic concepts and related technologies of traffic control systems, we focus on the arterial coordinated control system. With the help of numerical models of arterial traffic delays, we established a set of our own real-time optimization algorithms for arterial coordinated control systems with reference to the current previous control systems. We have collected various literature and technical reports to grasp the current status and development direction of theoretical research in the field of adaptive signal control. In the process of studying the literature, we focused on microscopic simulation-based optimization and control models and organized and summarized the research methods from the perspectives of data collection and traffic flow arrival characteristics. In addition, since developed countries in Europe and the United States started earlier in this field and accumulated rich theoretical foundation and practical experience, this paper pays special attention to the effectiveness of new signal control and optimization methods in comparison with traditional methods based on collecting and organizing relevant data. The phase structure adopted by the signal controller specifies the combination of traffic flow directions for simultaneous release, which will have a certain impact on the final optimization effect. Previous adaptive signal control methods tend to use a four-phase signal structure with simultaneous release of opposing traffic flows, which can only accommodate control requirements where opposing traffic flows are approximately the same. However, in reality, due to the possible deviation of the opposite traffic flow during the peak of the tidal phenomenon, a signal phase structure with higher flexibility in the North American NEMA (National Electrical Manufacturers Association) standard is needed. We then perform adaptive signal optimization and control using a modified dynamic programming (DP) algorithm that is divided into forward recursion and backward recursion. The forward recursive process is combined with the North American NEMA phase structure to invoke a vehicle arrival time prediction model for short-term traffic flow prediction, on the one hand, to estimate the intersection vehicle delay, queue length, and throughput based on the different phase characteristics of vehicles passing through the intersection on the other hand, and finally to determine the optimal green time length and its phase combination for each phase. The optimal phase sequence and duration can be determined through the reverse recursive process, thus completing the optimization of the timing scheme in one go.

The technical route of the research in this paper is shown in Figure 1. The core of the research is an adaptive signal control optimization method for urban intersections based on microscopic simulation. Based on the summary of the current research status, the key issues such as vehicle arrival prediction under microscopic perspective, improvement of traditional dynamic planning algorithm, signal optimization model under the conditions of vehicular network, and

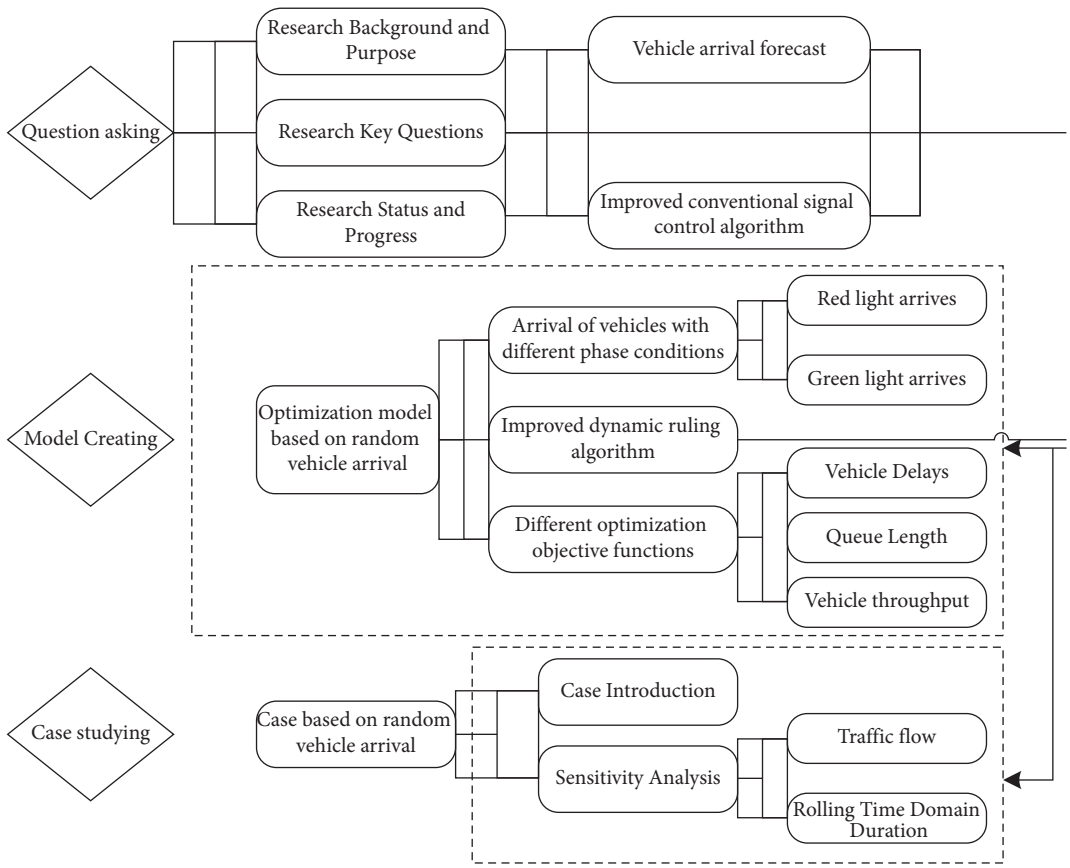

Figure 1: Research technology routes.

distributed signal cooperative optimization are focused on. An improved adaptive signal control model based on random vehicle arrival under different vehicle arrival mode conditions is proposed. Finally, based on the secondary developed VISSIM simulation, the proposed model is verified and analyzed using two real intersection cases, respectively, and finally, the research conclusions are drawn.

In order to verify the feasibility of the method proposed in this paper, a secondary development platform is constructed for signal optimization and collaboration using the simulation software VISSIM, a microscopic traffic simulation software developed by PTV, Germany, which can effectively simulate and analyze the operation of vehicles, pedestrians, and rail traffic under various traffic conditions. In the simulation of road network intersections, the general practice is to input the timing scheme in advance and keep the timing scheme fixed during the simulation process. This practice not only cannot realize the information interaction between VISSIM and the optimization model but also is not conducive to the development and validation of new traffic control models. Therefore, it is necessary to link the VISSIM simulation platform with external programs using the COM interface to achieve signal collaboration and optimization. Real-time interaction between external programs and simulation software can be realized through the VISSIM COM server interface technology. The principle of interaction between VISSIM simulation software and programming is briefly described in Figure 2.

2. Adaptive Control Method Based on Traffic Flow Model

Model adaptation (MA for short) has now become a research hotspot in several fields. Its goal is to maximize the performance of the target task using both source training data and target data. As shown in Figure 3, we train a good original model on rich source/training data and adapt the model with additional task-related data in the application phase to get an adapted model (adapted model) to better fit the target task/target data. Model adaptation can be seen as a way of migration learning.

In addition to the signal control methods that have been applied in existing systems, scholars around the world have developed various adaptive signal control and optimization theories based on different characteristics and applicability conditions for adaptive models in road modification signal control. The existing studies generally need to rely on specific traffic flow models and mathematical optimization methods, which can be classified into the single intersection, arterial, and regional cooperative adaptive signal control methods according to their applicability.

In this paper, we introduce many methods and generalize and unify them. Since the introduced and organized articles span a wide range of concepts in terms of time and geography, we have unified the concepts in this article and tried to show our unified concepts in the form of diagrams or formulas.

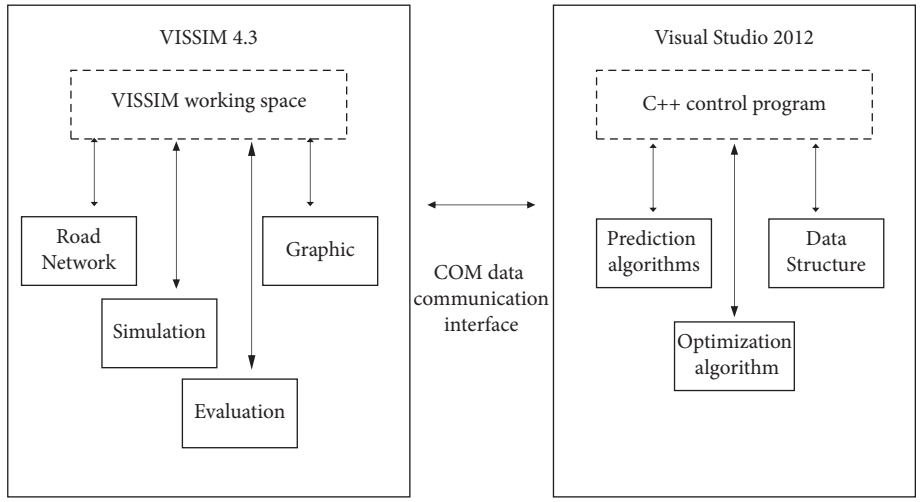

Figure 2: Principle of interaction between VISSIM simulation software and visual studio programming environment.

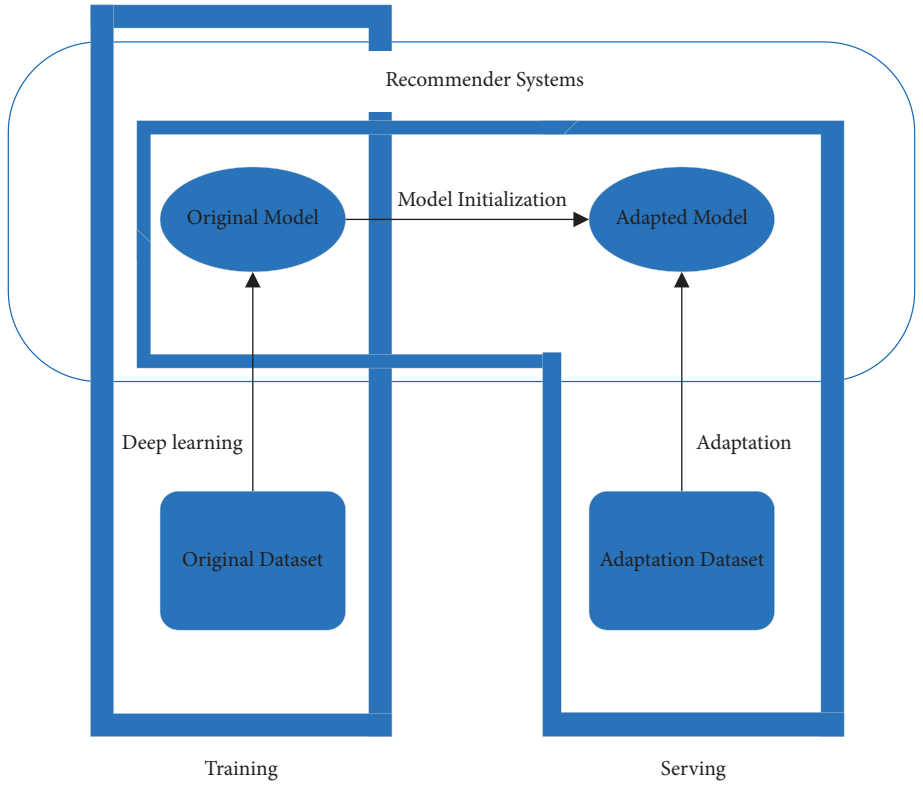

Figure 3: General principles of adaptive models.

There are a large number of level intersections in urban roads, which become the convergence and diversion points of traffic flow. In order to make the traffic flow safely into and out of the intersection, some control method must be used to reasonably allocate the right-of-way so that conflicting traffic flows are separated in time and space, thus ensuring the safe passage of vehicles and pedestrians. Planar intersections can generally be divided into cross-shaped, X-shaped, T-shaped, Y-shaped, and multiway intersection shapes. Due to the complicated traffic organization of multiway intersection, it should be avoided as much as possible.

The signal used to direct traffic always changes step by step in a cycle, and a cycle consists of a finite number of steps. The sum of the step lengths of each step in a cycle is called the signal period, or cycle for short, and is denoted by C. If a cycle has n steps, the step lengths are $t_1, t_2, \ldots, t_n$, then the period formula can be shown by the following formula:

$$C = t_1 + t_2 + \cdots + t_n. \quad (1)$$

In traffic control, in order to avoid conflicts between traffic flow in all directions on the plane intersection,

usually use the method of time-sharing, that is, in a cycle of a certain period of time, the intersection on a certain traffic flow or several traffic flow has the right of way (i.e., the direction of the signal is green or green arrow), and the conflict with the other traffic flow cannot pass (i.e., the signal in the direction of red). In a cycle, the right-of-way obtained by one or more traffic streams on the level intersection is called the signal phase. A cycle of several signal phases, the signal system is said to be a several phase system. The phase can be represented by a directional line segment, the direction of the arrow direction, and the direction of vehicle movement. If a light-controlled intersection is a four-phase system, the first phase of east-west traffic flows straight ahead, the second phase of east-west traffic flows left, the third phase of north-south traffic flows straight ahead, and the fourth phase of north-south traffic flows left, while all right-turning traffic flows are not controlled. The above phase system is generally known as a four-phase signal and can be represented by Figure 4.

Sometimes, in order to improve intersection utilization, the right-of-way of one traffic flow in one phase can be maintained until the next phase, most often for left-turn traffic flows, as shown in Figure 5. Since the left-turn traffic flow of the second and fourth phases is a continuation of the first and third phases, respectively, the step length can be shorter, for example, a few seconds. Therefore, some people call them "half-phases." However, the concept of steps and step lengths is quite simple to describe that the above example is actually four steps in a cycle.

The phase difference is an important concept in the coordinated control system of traffic arteries. The phase difference is divided into absolute phase difference and relative phase difference. In the traffic arterial coordinated control system, all intersections on the arterial have the same signal period, and each intersection designates a certain phase to participate in the coordination, called the coordinated phase. With an intersection on the traffic arterial as the reference intersection, the minimum time difference between the start time of the coordinated phase of other intersections lagging behind the start time of the coordinated phase of the reference intersection is called the absolute phase difference; the minimum time difference between the start time of the coordinated phase of any adjacent intersection along the direction of vehicle travel is called the relative phase difference.

Single intersection signal control is the basis for implementing traffic arterials, regional signal control, and distributed control strategies. Regardless of the adaptive signal control strategy, vehicle arrival prediction based on a single intersection is required. Fang and Elefteriadou [3] proposed a vehicle arrival-dissipation prediction model considering intersection queues, which can solve the problem that the conventional PREDICT algorithm [4] cannot accurately predict the intersection approach lane queue length. However, since the model only microscopically simulates the queue arrival under red light conditions, its vehicle arrival dynamics under green light conditions remain to be investigated. Sun and

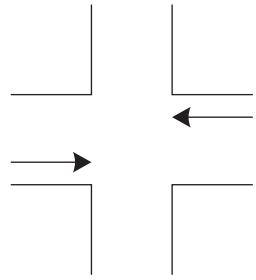

Figure 4: 4-phase signal diagram. (a) Phase 1. (b) Phase 2. (c) Phase 3. (d) Phase 4.

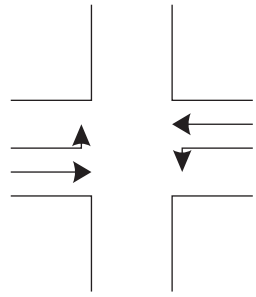

Figure 5: Half-phase signal diagram. (a) Phase 1. (b) Phase 2. (c) Phase 3. (d) Phase 4.

Zhang [5] developed a single-intersection vehicle arrival prediction model under triggered signal control conditions, which is not only applicable to NEMA phase structures but can also be extended to multiintersection cooperative control.

The first single-junction-based adaptive signal control strategy was proposed by Miller [6] in 1963, and since then various adaptive signal control strategies have emerged, such as optimization policies for adaptive control (OPAC) [7], PRODYN [8], UTOPIA [9], and controlled optimization of phases (COP) [10]. The aforementioned signal control strategies use dynamic planning algorithms to adjust the green time in real time based on vehicle arrival predictions, among which the COP algorithm is considered to be the best single intersection adaptive signal control algorithm to date because it is not limited by cycle length and phase sequence. The optimization process of the COP algorithm is divided into two main parts: first, a forward recursive step to calculate the vehicle delay time under each alternative scheme and a backward recursive [11] provide a detailed comparison of the performance of various dynamic planning algorithms. Porche and Lafortune [12] proposed the ALLONS-D adaptive signal control theory in 1999, which uses branch constraint method to calculate the optimal timing scheme, while proposing an "implicit coordination" mechanism, that is, optimizes the signal timing schemes of individual intersections sequentially with the predicted upstream traffic arrivals to achieve cooperative control. This approach requires a shorter prediction time (5–15 s), the detector can be placed in the middle of the road, and takes into account the influence of upstream intersection signal control on the prediction results, but the shorter time step places higher

demands on computer performance. Fang and Elefteriadou [13] proposed a single intersection adaptive signal based on the OPAC algorithm and supporting the NEMA phase control strategy. Feng et al. [14] proposed an optimization algorithm based on the COP algorithm and compatible with NEMA phases in 2015, but its performance suffers due to the introduction of the enumeration algorithm in the two-layer model.

From this, it can be found that adaptive signal timing at individual intersections under the framework of a distributed "implicit coordination" control strategy is still necessary for research, first to further improve the short-term vehicle arrival prediction model at the microlevel, while how to improve the algorithmic optimization effect under NEMA phase conditions is still a frontier issue in the field of traffic control. After all, improving the capacity of individual intersections is still the key to achieving smooth traffic flow.

The earliest traffic arterial signal control systems in the world can be traced back to the six-intersection manual signal control system in Salt Lake City, USA in 1917, followed by the development of a 12-intersection cooperative signal control system based on automatic machine timers by the City of Houston in 1922. In contrast, researchers at this stage generally start by maximizing the green wave bandwidth to achieve cooperative control of arterials. The first computational model for bandwidth optimization was proposed by Morgan and Little [15] in 1964, which was able to optimize a fixed signal timing scheme for two-way arterials to maximize the green wave bandwidth. Subsequently, Little [16] proposed a more advanced mathematical planning model to determine the optimal signal cycle length and the recommended travel speed for a given range. Based on this, Little et al. [17] developed the classical MAXBAND model by combining left-turn traffic and queue lengths. The MULTIBAND model was proposed by Gartner et al. [18] in 1995, which can set different bandwidths for traffic arterials to meet specific traffic flow characteristics.

However, the above studies are based on offline methods, and in order to dynamically adjust the signal timing scheme at arterial intersections, Dell'Olmo and Mirchandani [19] proposed the REALBAND optimization model, which uses a decision tree approach to minimize the number of stops and total delays of arriving convoys as the study object, which has been applied through the RHODES [20] system. The real-time, hierarchical, optimized, distributed, and effective system (RHODES) is a distributed adaptive traffic signal optimization system developed by the University of Arizona, USA, using a hierarchical control structure, that is, a network load distribution layer, a network flow control layer, and an intersection control layer. Its traffic flow prediction algorithm obtains vehicle arrival information through detection coils buried in front of the stop line at upstream intersections, and the model system allows for longer prediction times due to possible phase delays.

However, the common drawback of the above models is that they cannot effectively handle the arterial signal coordination problem under saturated traffic conditions. To address the capacity loss caused by vehicle overflow, Lieberman et al. [21] proposed a real-time cooperative optimal control strategy for oversaturated traffic flow on traffic arterials, which mainly uses Lighthill and Whitham [22], and the traffic flow fluctuation theory proposed by Richards [23] to calculate the fleet depletion time and rate. Hu et al. [24] used the hybrid genetic-simulated annealing algorithm of Li and Schonfeld [25] to optimize the signal timing scheme of traffic arteries under oversaturated traffic flow, including phase sequence, cycle length, and green time, and the results showed that a reasonable phase sequence is crucial to improve the optimization effect.

Given the complexity of the actual system, semiautomatic control has been widely used in the field of cooperative signal control at arterial intersections due to its low installation and usage costs. This signal control strategy is mainly based on triggered control logic that dynamically adjusts the phase difference parameters of key phases at upstream and downstream intersections to achieve cooperative control, and part of the adjustment mechanism is implemented based on offline computation. For example, Jovanis and Gregor [26] improved the traditional optimization method of maximizing the green band by moving the reference point of the phase difference to the end of the straight ahead phase to achieve semitriggered cooperative control. Shoup and Bullock [27] used the travel time of the first vehicle in the passing convoy to dynamically adjust the phase difference parameters. Yin et al. [28], on the basis of a large number of basis, Zhang and Yin [29] proposed a robust optimization model to adjust the cycle time and phase difference, which can effectively deal with the effect of uncertainty in the coordinated phase start time in semitriggered signal control. For the uncertainty of traffic flow, Zhang and Lou [30] proposed an optimization model for semitriggered signal control based on integer programming, which can obtain significant optimization results under lower traffic conditions.

In summary, the research of traffic arterial signal synergy and optimization models generally focuses on the modeling of the phase difference adjustment mechanism based on the traffic flow model, because the signal control parameters set can effectively improve the intersection capacity only when the traffic flow changes are reasonably predicted. However, some of these control models are mainly based on off-line calculations, which cannot well match the real-time fluctuation characteristics of traffic flow. If the traffic flow in different directions can be coordinated, this type of signal control model will be extended to the road network level to achieve larger scale traffic coordination and control.

3. Adaptive Control Model for Random Vehicle Arrival in Urban Roads

The signal period of each intersection in the line control system should be the same so as to ensure the stability of the arterial phase difference. Therefore, the period as the timing parameter of the line control system should refer to the common period of the signals at each intersection in the control model. There are usually two methods to determine the common period: one is to directly take the best period of

the most important intersection in the traffic status of the arterial as the common period; the other method is to calculate the best period of each intersection according to the traffic condition of each intersection and then take the largest value as the common period to avoid the bottleneck effect. This chapter introduces the vehicle arrival model and adaptive signal control optimization method based on a microscopic perspective. The method is mainly applied to traffic signal control in the case of random vehicle arrivals. In order to improve the adaptive signal control algorithm, the NEMA traffic signal phase structure, which is common in North America, is introduced into the original dynamic planning algorithm. In addition, the objective functions of vehicle delay, queue length, and vehicle throughput are established in this chapter. Finally, the implementation framework based on the secondary development of the COM component of the VISSIM simulation software is introduced.

In adaptive signal control, vehicle arrival and dissipation information is an important input variable for the signal optimization algorithm, while the signal timing scheme will conversely affect the changes in traffic dynamics near the intersection. In general, traditional adaptive signal control methods collect vehicle arrival information mainly through upstream detection coils or cameras. If a queued vehicle has not completely left the stop line, whether it starts moving or not, the subsequently detected vehicle travel distance is primarily the distance from the upstream detection coil location to the end of the queue. Therefore, the intersection maximum queue length (distance from the stop line to the end of the queueing convoy) [31] is crucial for estimating the vehicle stopping time. In this section, the trajectory and maximum queue length variation of vehicles arriving at the end of the queue until they leave the stop line are studied from a microscopic perspective to model the vehicle arrival-dispersion process. The proposed model is able to predict the vehicle arrival time at the end of the queue fleet under red light and green light conditions.

3.1. Red Light Arrival. Assume that the distance from the upstream detection coil to the intersection stop line is D. The vehicle passes the detection coil and proceeds at the free-flow speed, vf, and reaches the end of the queue in different lanes according to a certain steering ratio. For simplicity, the deceleration process when the vehicle enters the queue is ignored. The travel time, tt_k, and arrival time, t_k^a, of vehicle k at this distance can be expressed by the following formulas:

$$tt_k = \frac{\left(D - q_{k-1}^{\max}\right)}{vf}, \tag{2}$$

$$t_k^a = t_k^d + tt_k, \tag{3}$$

where $q_{k-1}^{\max}$ is the maximum queue length after the vehicle $k-1$ enters the queueing convoy; t_k^d is the time for the vehicle to pass the upstream detection coil. The initial maximum queue length can be expressed as $q_0^{\max} = n_0 \cdot S$, where n_0 is the number of queued vehicles in the lane and S is the length of the space occupied by the queue.

In Algorithm 1, T_{st} and T_{end} are the start and end times of the red or green light in the phase, which can be used as the range of vehicle arrival times. The set of the vehicle arrival times at the detection coil is also used as one of the inputs to the algorithm, and K represents the number of detected vehicles. If the calculated vehicle arrival time is within the red light time range $[T_{\text{st}}, T_{\text{end}}]$, it is recorded and used in the subsequent optimization algorithm. Also, the maximum queue length value is updated after the vehicle arrives. If the vehicle arrival time is greater than the predefined time range or if no vehicle arrives, Algorithm 1 ends. The algorithm will end.

3.2. Green Light Arrival. After the start of the green time, as the traffic dissipation wave [22] passes, the queued vehicles start one by one and at the following speed vq ($vq < vf$) through the stop line. Depending on whether the end-of-fleet vehicle starts or not, the vehicle arrivals can be divided into two categories: Scenario 1, the arriving vehicle arrives and stops before the dissipation wave passes to the end of the queue and then restarts to cross the intersection. Scenario 2, the arriving vehicle catches up with the started vehicle at the end of the queue at free-flow speed vf and passes the intersection stop line at the following speed vq. The details of the two scenarios are shown as follows.

In Scenario 1, similar to the arrival case during the red light period, vehicles join the stationary queueing convoy, and the maximum queue length continues to increase. According to the traffic flow theory, the start time of the vehicles at the end of the queue corresponds to the time when the dissipation wave ends its propagation [32]. Assuming that the speed of propagation of the dissipation wave of the traffic flow after the start of the green light is v_s, therefore, the start time of the vehicle at the end of the queue after the start of the green light can be determined by the following formula:

$$t_s = T_{st} + \frac{q_0^{\max}}{v_s}. \tag{4}$$

If the vehicle arrives before the start time, t_s, at the end of the queue, the start time of the vehicle at the end of the queue increases accordingly due to the increase in queue length Δt_s, which is calculated as follows:

$$\Delta t_s = \frac{S}{v_s}. \tag{5}$$

In Scenario 2, the end of the line starts moving before the arriving vehicle joins the convoy, so the arriving vehicle first moves forward at free-flow speed vf and then joins the convoy at the following speed vq to pass the stop line. For arriving vehicle $k+1$, its arrival process is similar to that of the previous vehicle, the only difference being that the preceding vehicle k has already started at the t_k^a time. In this case, the final value of the arrival moment is calculated as follows:

$$\Delta t_k^a = \frac{vq \cdot \left[t_k^{a,0} - \max\left(t_{k-1}^a, t_s\right)\right]}{(vf - vq)}, \tag{6}$$

$$t_k^a = t_k^{a,0} + \Delta t_k^a, \tag{7}$$

where Δt_k^a represents the additional travel time required for arriving vehicle k to catch up with the end of the moving queue. The numerator in (6) represents the length of the vehicle $k-1$ traveling forward from the time t_{k-1}^a, and the denominator represents the speed difference. Due to the speed difference between the free-flowing vehicle speed and the following vehicle speed, it is assumed that the arriving vehicle k will catch up and join the convoy at moment t_k^a. The flow of the arrival time and maximum queue length estimation is shown in Algorithm 2.

In Algorithm 2, first initialize the vehicle start time t_s at the end of the queue, the initial value of vehicle travel time tt_1, and the initial value of vehicle arrival time $t_k^{1,0}$. Vehicle arrivals can be divided into two categories according to the relationship between the magnitude of t_k^a and t_s (Step 3): in scenario 1, the maximum queue length continues to increase; in scenario 2, it is necessary to detect whether the arriving vehicle k can catch up with the convoy before the stop line and pass with the following speed vq. If not, subsequent arrivals will continue and the above process will continue until all arrivals have passed the checkpoint. It can be seen that the maximum queue length and the state of the vehicles at the end of the queue are the keys to estimate the vehicle arrival time in this model.

3.3. Real-Time Signal Control Algorithm. The DP algorithm mainly consists of forward and backward recursion algorithms. The forward recursion is mainly used to calculate the optimal green light time and its corresponding objective function value under different control variables. Backward recursion is mainly used to calculate the optimal signal. Backward recursion is mainly used to calculate the optimal signal timing scheme. The details of the forward and backward recursive algorithms are described as follows.

The forward recursive algorithm in the DP algorithm mainly assigns the phase time length and the alternative traffic direction combinations to each phase group. If a phase in the DP corresponds to two alternative traffic direction combinations, the phase group can be omitted assuming that the minimum control variable, $x_j^{\min} = 0$, which means that the minimum green time is zero; otherwise, the minimum green time is a certain determined value (e.g., 10 s). Under the minimum green light time constraint, the state variable corresponding to phase j can be calculated by the following equations:

$$s_j^{\min} = \begin{cases} s_j^{\min} + h\left(x_j^{\min}\right), & j > 1, \\ \max\left\{x_j^{min} - x_e, 0\right\}, & j = 0, \end{cases} \tag{8}$$

$$h(x) = \begin{cases} x + R, & x > 0, \\ 0, & x = 0, \end{cases} \tag{9}$$

where $s_j^{\min}$ is the smallest state variable value in stage j in the DP algorithm, x_e indicates the length of the green time in the end phase of the previous rolling time domain, and R is phase interval, which is the time when there are all yellow or full red light.

In order to simplify the DP algorithm, the maximum green time limit is omitted as it is not often reached in practice. The upper limit of the state variable is T, and the rolling time domain is not bounded by the cycle time. The set of feasible control variables, $X_j(s_j)$, for a given state variable, s_j, can be expressed by the following formula:

$$X_j\left(s_j\right) = \begin{cases} x_j^{\min}, \ \ldots, s_j - s_j^{\min}, & if\ s_j^{\min} < s_j < T, \\ 0, \ \ldots, T - s_j^{\min}, & if\ s_j = T. \end{cases} \tag{10}$$

Using (10), it can be found that each phase in the DP algorithm may correspond to the end phase group of the rolling time domain. If the state variable is equal to the rolling time domain duration, the current phase group may be omitted, and the previous phase group may become the end phase of the current rolling time domain. With supporting variables, c_j is the phase group assigned to DP phase j, which contains two nonconflicting traffic directions; $C_j(i)$ is alternative sets that can be assigned to the two traffic directions in the i phase group. $f_{j(c_j,s_j,x_j)}$ is the objective function value when the state variable is s_j, the control variable is x_j, and the phase group is c_j; $v_j(s_j)$ is the cumulative value of the objective function from DP stage 1 to stage j. We can then summarize Algorithm 3 as the forward recursive algorithm in the DP algorithm:

The forward recursion algorithm first initializes the cumulative state values. In each stage, the DP algorithm calculates the optimal control variables and the green light phases for each condition. The objective function value can be obtained by the model calculation in the next section. The stopping condition of the proposed algorithm differs from the conventional COP algorithm, that is, the algorithm ends when the minimum value of the state variable is greater than the rolling time domain duration T (step 3) and when the objective function value is no longer varies as the phase group increases.

In the backward recursive algorithm, when the optimal function values of all control variables under each phase of the DP algorithm are known, the optimal phase combinations and green light duration in each DP phase can be obtained by the backward recursive algorithm. When the state variable is T, the DP algorithm can be started from the end phase, to phase J where $x_j^*(T) \neq 0$, in order to obtain the optimal control variables, $x_j^*(T)$.

The reasons why the optimal green light duration can be recursively extended through phase J are as follows: first, the stopping condition in Algorithm 3 ensures that no other phase groups can be added at the end of the rolling time domain. Second, for any phase that $j > J$, its corresponding green time length is 0, which can no longer improve the optimization result of the signal timing scheme. At this point, the backward algorithm can be expressed by Algorithm 4 as follows.

With the four algorithms illustrated before, we can then calculate the objective functions or target variables.

For adaptive signal control algorithms, different objective functions often lead to different control effects. Under specific traffic flow or rolling time domain duration

conditions, some objective functions tend to obtain better signal control optimization results. In this text, $f_{j(c_j,s_j,x_j)}$ represents the objective function corresponding to different measurement indicators, including delay, vehicle queue length, and throughput. The objective function and related variables are calculated as follows:

Objective function 1.

$$\min \sum_{t=s_{j-1}+1}^{s_j} \sum_{p=1}^{8} \sum_{l \in L_p} n_l^q(t). \tag{11}$$

Objective function 2.

$$\min \sum_{p=1}^{8} \sum_{l \in L_p} n_l^q\left(s_j\right). \tag{12}$$

Objective function 3.

$$\min \sum_{t=s_{j-1}+1}^{s_j} \sum_{p=1}^{8} \sum_{l \in L_p} n_l^d(t). \tag{13}$$

Objective function 1 denotes minimizing the sum of queue lengths for all lanes from state moment s_{j-1} to s_j for each time step, which is the length of time experienced by all vehicles from the start of the queueing state until they leave the stop line.

Objective function 2 is calculating the minimized queue length, which is the sum of the queue lengths for each lane at the end of each phase group.

Objective function 3 represents the number of vehicles maximized through the intersection, which is the total number of vehicles leaving in each phase. The unit time interval in the above objective function is 1s.

Where l represents certain lane, and L_p is the lane set in phase p, and the relative variables are calculated as follows:

$$n_l^q(t) = n_l^q(t-1) - n_l^d(t) + n_l^a(t), \tag{14}$$

$$n_l^d(t) = \min\left\{v, n_l^q(t-1) + n_l^a(t)\right\} \forall l \in L_p, p \in c_j \cap c_{j-1}, \tag{15}$$

$$n_l^d(t) = \begin{cases} \min\left\{v, n_l^q(t-1) + n_l^a(t)\right\}, & s_{j-1} + R < t \le s_j, \\ 0, & s_{j-1} < t \le s_{j-1} + R, \end{cases} \forall l \in L_p, p \in \frac{c_j}{c_{j-1}}, \tag{16}$$

$$n_l^d(t) = 0, \quad \forall l \in L_p, \quad p \notin c_j, \tag{17}$$

$$n_l^a(t) = A(l,t). \tag{18}$$

In equation (14), the number of vehicles in queue at time t is determined by the number of vehicles in queue, arriving, and departing vehicles at time $t-1$ while departing vehicles could be illustrated by equations (15)–(17). Where v represents vehicle dissipation rate at saturation headway. And $A(l,t)$ in equation (18) denotes the number of vehicles entering the queueing fleet at moment t, obtained mainly based on the vehicle arrival prediction information described in the previous section.

3.4. Implementation Framework and Methodology. This study uses the C++ programming language and Visual Studio 2012 for secondary development of VISSIM simulation software, VISSIM supports C++, JAVA, and VB for secondary development, and compared with other programming languages, using C++ is more convenient to implement various data structures and improve programming efficiency. The following briefly describes the principle of the COM interface of VISSIM simulation software and its application in this study. Figure 6 shows the development framework for implementing the algorithmic model in this section.

In Figure 6, the left side shows the simulation function and interface of the VISSIM simulation platform, and the right side shows the C++ console program of the urban intersection adaptive model built in this paper, which is called by the VISSIM simulation kernel through the COM interface, including the prediction model and dynamic planning algorithm. In VISSIM version 4.3, the simulation engine contains several simulation categories, among which the Net category contains signal-controlled intersections and traffic elements in the road network, including the SignalControllers category, Links category, and Vehicles category. The SignalControllers category is used to control the signal controllers at all intersections in the network, and for each signal intersection, there is a corresponding SignalController category. The adaptive signal control program built in this paper mainly obtains the vehicle arrival trigger information through the detector category, then collects the implemented timing schemes through the SignalGroup category, and finally returns the optimized signal phases and durations to the SignalGroup category to achieve real-time signal timing control.

4. Signal Control Model Based on Random Vehicle Arrival

First, in order to validate the adaptive signal control optimization method based on vehicle microarrivals, the intersection of Jianchuan Road and Humin Road is used as an

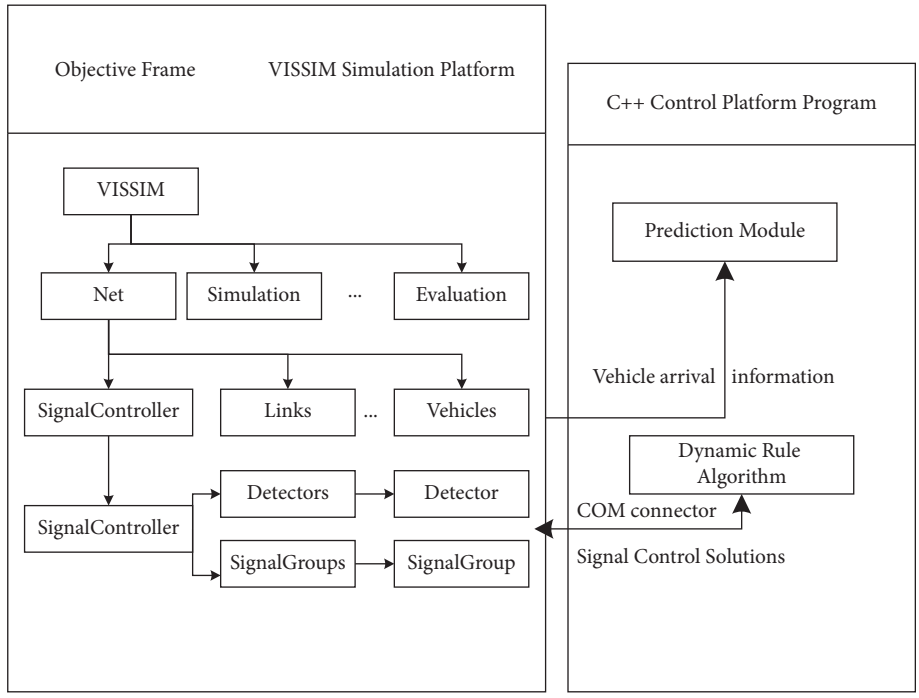

Figure 6: Simulation implementation framework.

empirical case and analysis. This intersection is located in Minhang District, Shanghai, and is an intersection with high traffic flow in the region, and the traffic congestion phenomenon is more obvious in the morning and evening peaks, and there is still room for optimization and improvement of its traffic signal timing. Due to the distance from the upstream signal-controlled intersection, the arrival traffic is less affected by the upstream signal timing; at the same time, there are several nonsignal-controlled intersections in the road section, and the vehicle arrival is more random, so this paper uses the random arrival-based adaptive signal control strategy for signal timing optimization. Figure 7 shows the intersection canalization and its corresponding NEMA phase number, where the intersection left-turn lane length is about 150 m, which may generate an overflow phenomenon under oversaturated flow conditions. In order to implement adaptive signal control, it is assumed that a detection coil is buried 500 m upstream to obtain the vehicle passing time and speed for vehicle arrival time prediction.

In this paper, the average stopping distance, the minimum headway, and the desired speed are selected as calibration parameters when establishing the simulation network in VISSIM. Based on the reasonable prediction, the above parameters are set to 3 m, 2 s, and 35 km/h. The C++ console program is written using VISSIM as the COM interface of the simulation platform. The console program contains a prediction module and an optimization module. The prediction module estimates the vehicle arrival time based on the vehicle information collected from the upstream coil at fixed intervals and passes it to the optimization module for calculation, thus realizing real-time control and optimization of the adaptive signal.

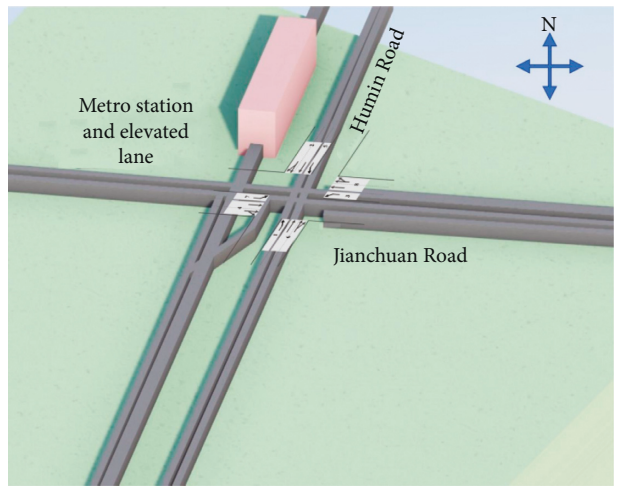

Figure 7: Intersection drainage rendering.

Table 1 shows the traffic flow magnitudes for three different congestion levels with intersection saturation levels measured by intersection capacity utilization (ICU) in the traffic signal timing optimization function where the unit is vehicle per hour (vph). The three categories of traffic flow based on different time periods used in this paper cover the low-moderate-high intersection congestion levels, and their traffic saturation rates gradually increase from 58% to 95%. In VISSIM, the vehicle arrival rate obeys a random distribution by ignoring the effect of upstream intersections on the arrival traffic.

The average vehicle delay (s/veh) output from VISSIM is used to evaluate the control effect of the proposed NEMA phase-based DP algorithm, and the optimal fixed signal timing scheme is calculated and compared with the

Step 1 Let $k = 1$, Initialize tt_1 and t_1^a according to the original queue length.
Step 2 If $T_{st} \le t_k^a \le T_{end}$, while $k \le K$, then record vehicle arrival time, and update $q_k^{max} = q_{k-1}^{max} + S, k = k + 1$; Otherwise end the algorithm.
Step 3 Use equations. (2) and (3) to calculate the arriving time of vehicle k, and move back to step. 2.

Algorithm 1: Define maximum queue length.

conventional four-phase DP algorithm. The conventional four-phase method consists of 1 + 5, 2 + 6, 3 + 7, and 4 + 8 phases of NEMA phases, and the corresponding DP algorithm is similar to the conventional COP algorithm. Assuming that the detection coil is buried in the upstream section 500 m away from the intersection stop line, the vehicle needs about 45 seconds to reach the intersection stop line from the upstream detection coil location under the speed limit of 40 km/h. Therefore, the rolling time domain duration is set to 40 s, so that all vehicles that may reach the end of the queue in the rolling time domain are detected by the upstream coil as much as possible. A sensitivity analysis of the impact of the rolling time domain duration on the performance of the algorithm will be described later.

Table 2 shows the delay data of vehicles passing through the intersection under different signal control strategies, including DP optimization algorithms with vehicle delay, queue length, and vehicle throughput as objective functions, denoted by DP-D (delay), DP-Q (queue), and DP-T (through), respectively. Table 3 shows the comparison results of different adaptive control algorithms with different objective functions and the significance test results at a 95% confidence interval. It is found that the NEMA phase-based DP algorithm proposed in this paper can significantly reduce vehicle delays compared with the four-phase DP algorithm under medium and high traffic conditions, but its optimization effect is not obvious under low traffic conditions.

The simulation results show that the DP algorithm proposed in this paper has different optimization results under different objective functions and traffic flow conditions. Specifically, the DP algorithms (DP-D and DP-T) with vehicle delay and throughput as the objective functions can achieve better optimization results under low traffic flow conditions. However, the optimization results of DP-D and DP-T algorithms gradually decrease as the traffic volume increases. In contrast, the adaptive signal control algorithm DP-Q with queue length minimization as the objective function achieves better optimization results under near-saturation conditions and outperforms the other two control algorithms with the objective function. The reason for this is that under low flow conditions, the queue changes less compared to high flow conditions, so the optimization algorithm as an objective function is not sensitive enough to changes in actual flow, and queue length minimization and queue length minimization are not exactly equivalent to alleviating vehicle delays in all time periods. Combined with the significance test results in Table 3, it can be found that the adaptive signal control algorithm proposed in this paper performs better than the optimal fixed timing scheme except DP-Q under low and medium traffic volumes.

To investigate the variation of the optimal performance of the DP algorithm at different rolling time domain durations, a sensitivity analysis was performed for this case, that is, three DP algorithms with different objective functions were compared under high traffic conditions with rolling times ranging from 20 s to 60 s. As shown in Table 4, the optimization effect of DP-D gradually improves when the vehicle arrival prediction cycle length increases. This is due to the fact that in the longer rolling time domain, the optimization algorithm can effectively evaluate the impact of the signal timing scheme on traffic flow, especially the magnitude of cumulative delay. However, for calculating queue length and throughput, a longer rolling time domain does not lead to improved optimization results. For example, DP-Q mainly uses the queue length at a particular moment as an optimization metric, which requires frequent traffic state updates to obtain better optimization results. dp-t is also insensitive to changes in the rolling time domain, and the data show that it obtains the best signal control results when the rolling time domain duration is close to the travel time of vehicles from the upstream coil to the stop line.

Based on the simulation experiments and data analysis results, the following conclusions can be drawn: first, the DP algorithm proposed in this paper outperforms the optimal signal timing scheme derived from the traditional 4-phase calculation under different traffic conditions; second, the DP algorithm under NEMA phase outperforms the traditional algorithm when the traffic flow is relatively high, and there is an imbalance in the opposite direction. For the three objective functions, the DP algorithms under the principles of minimizing delay and maximizing throughput have similar control effects, while the DP-Q has relatively obvious advantages mainly under saturation traffic. In addition, DP-Q needs to update vehicle arrival data frequently to ensure the optimization results, so it can obtain a better delay control effect under rolling time domain conditions of short time length, so it should be applied in the road sections with adjacent closer upstream and downstream intersections.

5. Conclusion

Leading urban street transformation is conducive to protecting and improving people's livelihood, and providing practical experience for the modeling of street transformation. However, we also find that if road traffic conditions are to be improved. It is necessary to rely on more advanced means of traffic information collection and signal control

Step 1 Let $k = 1$, Initialize t_s,tt_1 and $t_1^{a,0}$.
Step 2 If $T_{st} \le t_k^{a,0} \le T_{end}$, while $k \le K$, then move into step 3. Otherwise, Stop algorithm 2.
Step 3 If $t_k^{1,0} \le t_s$, then update $t_k^a = t_k^{a,0}$, and record the time that the vehicle arriving time t_k^a, update the longest queue distance $q_k^{max} = q_{k-1}^{max} + S$, $t_s = t_s + \Delta t_s$. (Scenario 1) Enter Step 5. Otherwise, use equations (6) and (7) to calculate the time that the vehicle arriving time t_k^a, update the longest queue distance $q_k^{max} = q_{k-1}^{max} - \Delta t_k^a \Delta vq + S$. (Scenario 2) Enter Step 4.
Step 4 If $q_k^{max} \le 0$ or $t_k^a > T_{end}$. Stop Algorithm 2. Otherwise. Record the time that the vehicle arriving time t_k^a, and enter step 5.
Step 5 Update that $k = k + 1$, use equations (2) and (3) to calculate the arriving time of vehicle, $t_k^{a,0}$, and move back to step. 2.

Algorithm 2: Define travel time while green light.

Step 1 Let $j = 1$, Initialize $v_1(0) = 0$, $s_1^{min} = \min\{x_1^{min} - x_e, 0\}$.
Step 2 For $s_j = s_j^{min}, \ldots, T$. When the objective function is minimizing the delay as well as the queue length: $v_j(s_j) = \min_{c_j, x_j}\{f_j(s_j, x_j, c_j) + v_{j-1}(s_{j-1}) | x_j \in X_j(s_j), c_j \in C_j(i)\}$. When the objective function is to maximize vehicle throughput: $v_j(s_j) = \max_{c_j, x_j}\{f_j(s_j, x_j, c_j) + v_{j-1}(s_{j-1}) | x_j \in X_j(s_j), c_j \in C_j(i)\}$. Record $x_j^*(s_j)$ and $c_j^*(s_j)$ as the best signal timing solution.
Step 3 If $s_j^{min} < T$, then $j = j + 1$, $i = i + 1$. And return to Step 2. Otherwise stop Algorithm 3.

Algorithm 3: Define state variables.

Step 1 Let $s_j^* = T$.
Step 2 For any $j = J, J-1, \ldots, 2$, $s_{j-1}^* = s_j^* - h(x_j^*(s_j^*))$.

Algorithm 4: Backward algorithm.

Table 1: Traffic demand and intersection capacity utility (ICU).

Traffic level	West/eastward (vph)	North/southward (vph)	Saturation rate (%)
Low	600/500	600/500	58
Medium	900/800	800/700	78
High	1200/1100	1100/1000	95

Table 2: Control performance under different optimization methods (seconds).

Control strategy	Phase structure	Traffic level		
		Low	Medium	High
DP-D	NEMA	19.2	25.7	52
	4-phase	18.6	28.1	55.1
DP-Q	NEMA	27.4	30.6	50.8
	4-phase	28.4	32.5	53.5
DP-T	NEMA	18.1	25.8	51.8 54
	4-phase	18.2	27.2	

Table 3: Vehicular delay under different optimization methods (seconds).

No.	Low flow rate		Medium flow rate		High flow rate	
	Mean difference	Significant?	Mean difference	Significant?	Mean difference	Significant?
1	−0.4	No	−2.4	Yes	−3.1	Yes
2	−1.0	No	−1.9	Yes	−2.7	Yes
3	−0.1	No	−1.3	Yes	−2.2	Yes

Table 4: Vehicular delay under different lengths of rolling horizon (seconds).

	Rolling time domain duration (s)				
	20	30	40	50	60
DP-D	55.1	52.6	52.0	51.9	50.5
DP-Q	47.9	49.9	50.8	51.4	54.7
DP-T	53.9	53.5	51.8	50.5	52.9

strategies. Therefore, adaptive traffic signal control methods based on different vehicle arrival characteristics information and collection means remain an important research problem in the field of traffic management and control. Although formed traffic signal control systems are commonly installed in large and medium-sized cities in China, the effect of relieving traffic congestion is still limited, and the control effect of predicting vehicle arrival time from the microlevel to improve the signal timing scheme is not good enough. This paper focuses on how to improve the optimization effect of the control model based on the existing adaptive signal control scheme by using new technologies and concepts. On this basis, this paper draws on the latest foreign research results and establishes a vehicle arrival prediction model and an adaptive signal control method according to different information collection hands and vehicle arrival characteristics, and its main research results are as follows.

Starting from the generation and development of adaptive signal control theory, this paper introduces the latest research progress and challenges of its control models and algorithms. This paper argues that it is an important research direction in the future to make reasonable use of the emerging traffic information collection technology, improve the existing signal control methods, realize the linkage and cooperation of different signal controllers under the condition of reasonable computational complexity, and gradually expand the scope of traffic control and cooperation. For individual intersections with strong randomness of traffic arrival distribution, this paper proposes to collect upstream vehicle arrival data by using a loop coil to establish a microlevel vehicle arrival model to predict the vehicle arrival time under different queuing states. The vehicle arrival time estimation models under red and green conditions are developed separately according to the signal states, and their output vehicle arrival times and numbers are the main input variables of the signal optimization algorithm. Subsequently, the classical algorithm is improved by introducing the North American signal control structure NEMA on the framework of the existing COP algorithm. In addition to the traditional delay metrics, a control model with queue length and vehicle throughput as objective functions is developed in this paper. In order to verify the effectiveness of the model, an adaptive signal real-time control program is constructed in this paper based on the principle of the VISSIM simulation COM component, and simulation tests are conducted using the intersection of Jianchuan Road and Humin Road in Shanghai.

Compared with the existing adaptive signal optimization models, the main innovations of this paper are as follows:

(1) The vehicle arrival model describes the dynamic process of vehicles arriving at the end of the queue under red light and green light conditions. Combined with the traffic flow fluctuation theory, the arrival time of vehicles entering the queue is quantitatively calculated, which helps to predict the queue length and estimate the delay time.

(2) The dynamic planning algorithm is improved by combining the characteristics of the NEMA phase structure. The improved optimization algorithm can determine the optimal phase while assigning the green light duration and improve the flexibility of signal control. Meanwhile, based on the objective functions of vehicle delay and queue length, the optimization objective of maximizing the vehicle throughput is proposed, and a better control effect is obtained.

(3) Based on the arrival-dissipation dynamic characteristics of the convoy at the stop line, the corresponding delay estimation constraints are established, which simplify the model construction methods in previous literature. An implicit cooperative-based regulation mechanism is proposed to achieve distributed control at multiple intersections.

The properties of street space are very complex and show different functional properties in different spatial and temporal environments, which is also a key to study and interpret the city. However, with the intensification of the "car-oriented" street space design, the original outdoor platform for interaction, entertainment, rest, and chatting is gradually deprived, which is a mockery of modern civilization. T The study of street space design can be more effective in mastering other spatial design skills. Street space involves social, economic, cultural, ecological, psychological, human, political and other factors, which must be systematically thought, using forward-looking theories, and formulating corresponding countermeasures according to the time and place. There is no one panacea for all streets, and all streets must be considered in a comprehensive manner by investigating regional culture, citizen's lifestyle, street texture, and streetscape characteristics. Second, street space is also the window of the city, most easily remembered and most reflective of the humanistic qualities of the citizens. The transformation of street space is also of practical significance for changing the value orientation, promoting the moral spirit of health and frugality, and maintaining sustainable social development. The starting point of this paper is to establish a new street traffic adaptive model to provide model simulation support for future urban street renovation. However, since the model proposed in this paper is only implemented in the VISSIM simulation platform, whether it can effectively alleviate traffic congestion in the actual road network needs further verification, including calibration and verification of the simulation model. If it can be implemented in the control system, it can also be evaluated by means of hardware-in-the-loop to improve the reliability of the model method.

Data Availability

The dataset can be accessed upon request.

Conflicts of Interest

The author declares that there are no conflicts of interest.

Acknowledgments

The authors thank the Ministry of Education of Humanities and Social Science Project, Research on Dynamic Evaluation of Purchase Intention and Satisfaction of Internet Shopping (no. 18YJC760141) and Guangdong Provincial Social Science Planning Office Project, A Comparative Study of Modern Shophouse Architecture and Culture in the Pearl River Delta and Malaysia Based on Genetic Digitisation Technology (no. GD20CYS15).

References

[1] H. Robert and K. Gunther, *Social Semiotics*, Polity, Cambridge, UK, 1988.

[2] B. R. T. Fambro, S. M. Sangineni, C. A. Lopez, and S. R. Sunkari, "Benefits of the Texas traffic light synchronization (TLS) grant program II," *Texas Transp. Inst.*vol. 7, no. 2, 1995.

[3] F. C. Fang and L. Elefteriadou, "Modeling and simulation of vehicle projection arrival–discharge process in adaptive traffic signal controls," *Journal of Advanced Transportation*, vol. 44, pp. 176–192, 2010.

[4] K. L. Head, "Event-Based short-term traffic flow prediction model," *Transportation Research Record*, vol. 1, pp. 45–52, 1995.

[5] J. Sun and L. Zhang, "Vehicle actuation based short-term traffic flow prediction model for signalized intersections," *J. Cent. South Univ.*vol. 19, no. 1, pp. 287–298, 2012.

[6] A. J. Miller, "Settings for fixed-cycle traffic signals," *Journal of the Operational Research Society*, vol. 14, no. 4, pp. 373–386, 1963.

[7] N. H. Gartner, "OPAC: a demand-responsive strategy for traffic signal control," *Transportation Research Record*, vol. 1, 1983.

[8] J. J. Henry, J. L. Farges, and J. Tuffal, "The prodyn real time traffic algorithm," *IFAC Proc*, vol. 16, no. 4, pp. 305–310, 1983.

[9] V. Mauro and C. Di Taranto, "Utopia," *IFAC Proc*, vol. 23, pp. 245–252, 1990, https://doi.org.

[10] S. Sen and K. L. Head, "Controlled optimization of phases at an intersection," *Transportation Science*, vol. 31, no. 1, pp. 5–17, 1997.

[11] S. G. Shelby, "Single-intersection evaluation of real-time adaptive traffic signal control algorithms," *Transportation Research Record*, vol. 1867, no. 1, pp. 183–192, 2004.

[12] I. R. Porche and S. Lafortune, "Adaptive look-ahead optimization of traffic signals," *J. Intell. Transp. Syst.*vol. 4, pp. 209–254, 1999.

[13] F. C. Fang and L. Elefteriadou, "Development of an optimization methodology for adaptive traffic signal control at diamond interchanges," *Journal of Transportation Engineering*, vol. 132, pp. 629–637, 2006.

[14] Y. Feng, K. L. Head, S. Khoshmagham, and M. Zamanipour, "A real-time adaptive signal control in a connected vehicle environment," *Transportation Research Part C-Emerging Technol.*vol. 55, pp. 460–473, 2015.

[15] J. T. Morgan and J. D. C. Little, "Synchronizing traffic signals for maximal bandwidth," *RAIRO - Operations Research*, vol. 12, no. 6, pp. 896–912, 1964.

[16] J. D. C. Little, "The synchronization of traffic signals by mixed-integer linear programming," *RAIRO - Operations Research*, vol. 14, no. 4, pp. 568–594, 1966.

[17] J. D. C. Little, M. D. Kelson, and N. H. Gartner, "Maxband: a program for setting signals on arteries and triangular networks," *Transportation Research Record*, vol. 795, pp. 40–46, 1981.

[18] N. H. Gartner, S. F. Assman, F. Lasaga, and D. L. Hou, "A multi-band approach to arterial traffic signal optimization," *Transportation Research Part B: Methodological*, vol. 25, no. 1, pp. 55–74, 1991.

[19] P. Dell'Olmo and P. B. Mirchandani, "Realband: an approach for real-time coordination of traffic flows on networks," *Transportation Research Record*, vol. 1, pp. 106–116, 1995.

[20] P. B. Mirchandani and L. Head, "A real-time traffic signal control system: architecture, algorithms, and analysis," *Transportation Research Part C-Emerging Technol.*vol. 9, pp. 415–432, 2001.

[21] E. B. Lieberman, J. Chang, and E. S. Prassas, "Formulation of real-time control policy for oversaturated arterials," *Transportation Research Record*, vol. 1727, pp. 77–88, 2000.

[22] M. J. Lighthill and G. B. Whitham, "On kinematic waves II. A theory of traffic flow on long crowded roads," *Proc. R. Soc. London. Ser. A. Math. Phys. Sci.*vol. 229, pp. 317–345, 1955.

[23] P. I. Richards, "Shock waves on the highway," *RAIRO - Operations Research*, vol. 4, pp. 42–51, 1956.

[24] H. Hu, X. Wu, and H. X. Liu, "Managing oversaturated signalized arterials: a maximum flow based approach," *Transportation Research Part C: Emerging Technologies*, vol. 36, pp. 196–211, 2013.

[25] Z. Li and P. Schonfeld, "Hybrid simulated annealing and genetic algorithm for optimizing arterial signal timings under oversaturated traffic conditions," *Journal of Advanced Transportation*, vol. 49, no. 1, pp. 153–170, 2015.

[26] P. P. Jovanis and J. Gregor, "Coordination of actuated arterial traffic signal systems," *Journal of Transportation Engineering*, vol. 112, pp. 416–432, 1986.

[27] G. E. Shoup and D. M. Bullock, "Dynamic offset tuning procedure using travel time data," *Transportation Research Record*, vol. 1683, pp. 84–94, 1999.

[28] Y. Yin, M. Li, and A. Skabardonis, "Offline Offset Refiner for Coordinated Actuated Signal Control Systems," in *Proceedings of the Transportation Research Board 85th Annual Meeting*, Washington, DC USA, 2006 January.

[29] L. Zhang and Y. Yin, "Robust synchronization of actuated signals on arterials," *Transportation Research Record*, vol. 2080, pp. 111–119, 2008.

[30] L. Zhang and Y. Lou, "Coordination of semi-actuated signals on arterials," *Journal of Advanced Transportation*, vol. 49, pp. 228–246, 2015.

[31] H. X. Liu, X. Wu, W. Ma, and H. Hu, "Real-time queue length estimation for congested signalized intersections," *Transportation Research Part C-Emerging Technol.*vol. 17, pp. 412–427, 2009.

[32] Y. Cheng, X. Qin, J. Jin, and B. Ran, "An exploratory shockwave approach to estimating queue length using probe trajectories," *J. Intell. Transp. Syst.*vol. 16, pp. 12–23, 2012.

Hindawi
Scientific Programming
Volume 2022, Article ID 3724960, 15 pages
https://doi.org/10.1155/2022/3724960

Research Article

The Climate Changes and the Simulation of the Runoff in the Last 50 years (1961–2010) in the Upper Tarim River Basin of Southern Xinjiang, China

Tianjian Lu,[1] Qingquan Xiao,[1] Leiding Ding,[1] Hanyu Lu ,[1,2] Ziyue Huang,[1] and Yongyi Yuan[3]

[1]*College of Big Data and Information Engineering, Guizhou University, Guiyang 550025, China*
[2]*School of Information Engineering, Guizhou University of Engineering Science, Bijie 551700, China*
[3]*Guizhou Liupanshui Sanlida Technology Co Ltd, Liupanshui 532001, China*

Correspondence should be addressed to Hanyu Lu; hylu1@gzu.edu.cn

Received 5 July 2022; Revised 25 July 2022; Accepted 29 July 2022; Published 1 September 2022

Academic Editor: Lianhui Li

The upper Tarim River basin is supporting approximately 50 million people by melting the glaciers and snow, which are highly vulnerable and sensitive to climate change. Therefore, assessing the relative effects of climate change on the runoff of this region is essential not only for understanding the mechanism of hydrological response over the mountainous areas in Southern Xinjiang but also for local water resource management. This study quantitatively investigated the climate change in the mountainous area of the upper Tarim River basin, using the up-to-date "ground-truth" precipitation and temperature data, the Asian Precipitation Highly Resolved Observational Data Integration Towards Evaluation of Water Resources (APHRODITE, 1961–2010, 0.25°) data; analyzed the potential connections between runoff data, observed at Alar station, and the key climatological variables; and discussed the regression models on simulating the runoff based on precipitation and temperature data. The main findings of this study were as follows—(1) both annual precipitation and temperature generally increase at rates of 0.85 mm/year and 0.25 °C/10a, respectively, while the runoff data measured at the Alar station shows fluctuating decreasing trends. (2) There are significant spatial differences in the temporal trends of precipitation; for example, the larger increasing rates of precipitation occur in the Karakoram mountains, while the larger decreasing rates happen in the northwestern Kashgar county. (3) The decreasing trends of temperature mainly occur in Kashgar county and its surrounding areas in summer. (4) Seasonal correlations in precipitation and temperature trends are more significant than those on a monthly and annual scale. (5) The regression model in simulating the runoff in the upper Tarim River basin based on radial basis function (RBF) is better than that based on the least-squares method, with the predictive values based on RBF models significantly better (correlation coefficient, CC ~ 0.85) than those by least-squares models (CC ~ 0.75). These findings will provide valuable information to inform environmental scientists and planners on the climate change issues in the upper Tarim River basin of Southern Xinjiang, China, under a semiarid-arid climate.

1. Introduction

Global climate is changing considerably, characterized by warming over nearly 100 years, and there is a general consensus that increasing average surface air temperature had intensified global hydrological cycles during the 20th century [1–3]. According to the Intergovernmental Panel on Climate Change (IPCC) fifth assessment report [4], by the end of the twenty-first century, the global average surface temperature will increase by 3.7–4.8°C over the 1750 level, and the global average sea level will rise by 0.52–0.98 m because of CO_2 doubling. Global climate change has accelerated regional water circulation and has caused asymmetry in precipitation distribution and high flood frequencies [5–8].

Spatiotemporal changes in global precipitation and temperature have received increasing attention, and the information on trends of precipitation and temperature is the starting point for the accurate assessment of water

resources, flood control, and drought relief, and the understanding of climate change and effective management of water resources. Meanwhile, natural surface runoff is also vital to maintaining surface water balance. For temporal and long-term runoff, the physical process of runoff yield always has a close relationship with climate variables, such as precipitation and temperature [9–11]. In arid and semiarid regions of vulnerable ecology, a small climate fluctuation may cause large environmental variation when human activity overwhelms the natural carrying capacity [12]. For this reason, addressing the impact of regional climate change on runoff volume will support scientific and technological sustainable development of local water resources.

Xinjiang Province, located in Northwest China, is under an inland, arid, or semiarid desert climate, which is not directly affected by the monsoon system [13, 14]. The Tarim basin in Southern Xinjiang Province is a typical inland watershed in an arid area, and the hydrologic processes of the upper Tarim River basin are typical among those in other regions at mid- and high latitudes of the Northern Hemisphere [11]. Various studies have focused on the impacts of climate change on water resources in the Tarim River basin [15, 16]. They concluded that the temperature and precipitation show an upward tendency during the past several decades and a significant jump has been detected for both the two variables around 1986 [10, 17]. Although the streamflow from the headwaters of the Tarim River shows a significant increase and is sensitive to precipitation [18], the streamflow along the mainstream of the river has decreased. This implies that anthropogenic activities such as irrigation and increased population instead of climate change dominated the streamflow change of the river [19]. Recently, various reports have shown a widespread climatic and hydrologic change in the Tian Shan Mountains during the past few decades [20]. For example, temperature demonstrated a significant rising trend (significant level is smaller than 0.001) at a rate of 0.33~0.34°/10a during 1960~2010, which is higher than those of China (0.25°/decade) and the entire globe (0.13°/10a) [21]; precipitation increased substantially in most regions especially for the middle and high latitudes, at a rate of 0.61 mm/*a* [22]; glacier area decreased by 11.5%, and the thickness of snowpack has also decreased [23]. The climate in Northwest China changed dramatically from a warm-dry mode to a warm-wet mode around 1987, and the Chinese Tian Shan Mountains experienced the most dramatic changes during this transition [20].

However, the upper Tarim River basin is relatively unknown in terms of recent climate changes simply due to a lack of meteorological observations in high-altitude areas (Wang et al., [24]. Fortunately, the state-of-the-art dataset (updated in September 2018), Asian Precipitation Highly Resolved Observational Data Integration Towards Evaluation of Water Resources (APHRODITE, 0.25°/daily [25]), provided great valuable precipitation and air temperature data in the Asian over the last half century, from 1951 to 2015. And APHRODITE has been demonstrated to replicate "ground-truth" observations very well [26] and represents the best tool for analyzing historical precipitation variability and change. Therefore, this study aims at revealing the in-depth climate change principles in the upper Tarim River basin and determining the response of runoff to climate change in the region through the analyses of precipitation and temperature.

2. Study Area and Materials

2.1. Study Area. Xinjiang Province of Northwest China accounts for one-sixth of China's land area and has an inland, arid, or semiarid desert climate that is not directly affected by the monsoon system. Local precipitation of a large spatiotemporal variation is concentrated in mountainous areas [15]. The Tarim River basin in Southern Xinjiang is one of the world's largest closed drainage hydrographical systems without outflow. The basin is composed of 114 streams belonging to nine river systems: the Aksu River, Kashgar River, Yarkand River, Hotan River, Kaidu River, Dina River, Weigan River, Kuqa River, and Keriya River. The landforms of the Tarim River basin include mountains (47%), plains (22%), and deserts (31%) [27]. The Tarim River lies entirely within a landlocked area and has a mainstream length of 1,321 km. Water has been imported to the mainstream from nine systems throughout history, and the main causes of this import were climate change and human economic activities. The Qarqan, Keriya, and Dina rivers successively lost surface connections to the mainstream prior to the 1940s, as did the Kashgar, Kongqi, and Weigan thereafter. As a result, only the Yarkant River, Akesu River, Hotan River, and Kaidu River have links with the mainstream of the Tarim River. Three tributary river systems (Aksu, Hotan, and Yarkant River) contributing to the Tarim River converge just above the Alar gauging station, while the Kaidu River flows into the Tarim River at the lower reaches.

The study area (73° E–82° E, 35° N–43° N) is the upper mountain areas of the Tarim River basin (Figure 1(a)). The region is surrounded by high mountains like Tianshan, Eastern Pamir, and Karakoram mountains, which leads to orographic precipitation. Based on the Asian Precipitation Highly Resolved Observational Data Integration Towards Evaluation of Water Resources, the precipitation in the mountainous regions can exceed 300 mm/year in some areas and is mostly in the form of snowfall (Figure 1(b)). However, the average annual precipitation in the region is below 100 mm. The average annual temperatures can range from −12°C to 16°C (Figure 1(c)). The mainstream of the Tarim River is a typical pure dissipation inland river that does not yield water resources by itself and is supplied only by runoff from its upper basin [11, 14, 28]. This runoff is primarily from glacial meltwater and precipitation in mountainous areas. Therefore, hydrologic processes of the mountainous areas are typical of those in other regions at mid- and high latitudes of the Northern Hemisphere [11]. With the backdrop of global climate change, a detailed investigation on changing spatial and temporal features of precipitation will not only help to understand the relationship between climate change and the hydrological cycle, but also be helpful in formulating a regional strategy for water resource management in Southern Xinjiang.

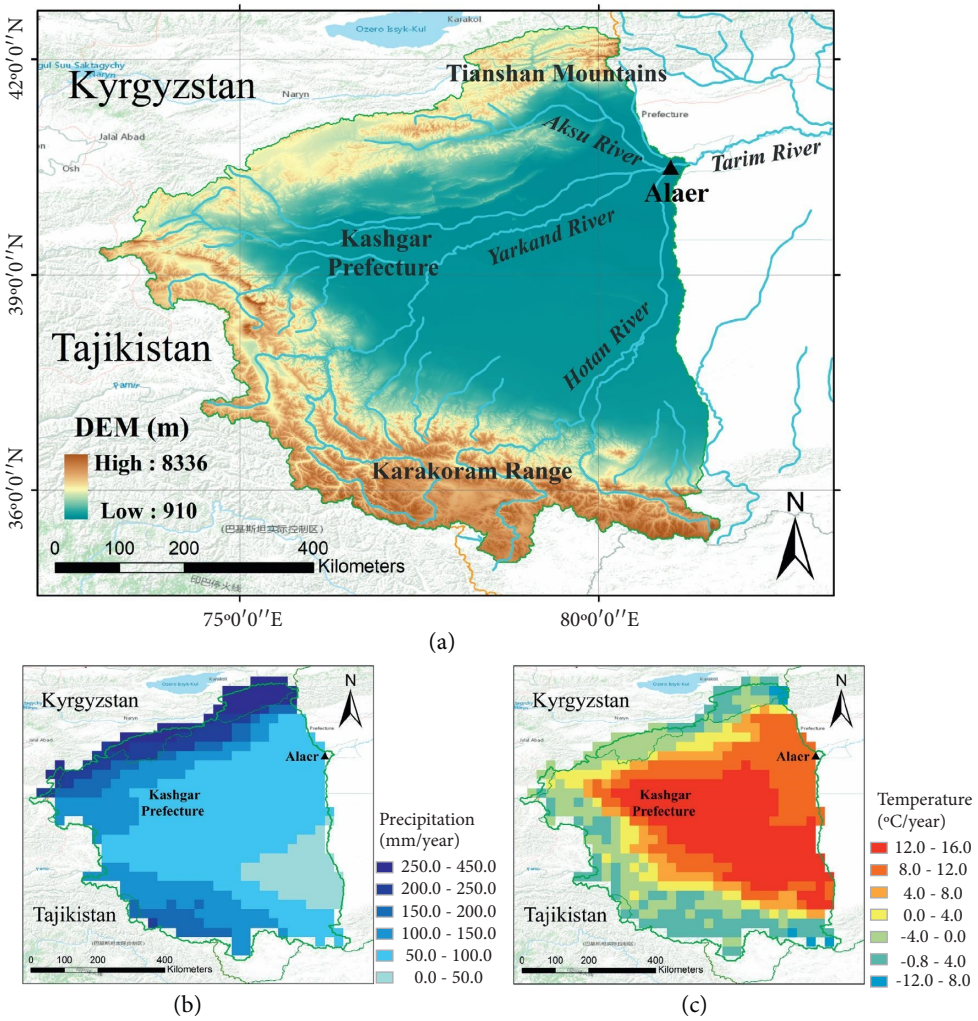

FIGURE 1: (a) The border of the upper Tarim River basin and the spatial patterns of (b) average annual precipitation and (c) average annual temperature over the study area.

2.2. Data. This study employed the new state-of-the-art daily dataset with a resolution of 0.25° (updated in September 2018), Asian Precipitation Highly Resolved Observational Data Integration Towards Evaluation of Water Resources [25, 29, 30], which provided great valuable precipitation and temperature data in the Asian over the last half century, from 1961 to 2010, to reveal the in-depth climate change principles in Southern Xinjiang. The APHRODITE project develops state-of-the-art daily precipitation datasets and daily mean temperature datasets with local meteorological/hydrological agencies for Asia. In terms of precipitation, the APHRODITE's Water Resources project has been executed by the Research Institute for Humanity and Nature (RIHN) and the Meteorological Research Institute of Japan Meteorological Agency (MRI/JMA) since 2006. The datasets are created primarily with data obtained from in situ rain-gauge-observation networks [31].

APHRODITE's daily gridded precipitation was presently the only long-term continental-scale high-resolution daily product and has been demonstrated to replicate "ground-truth" observations very well [26], which was the best tool for studies such as the diagnosis of climate changes, evaluation of Asian water resources, and satellite precipitation estimates. And the APHRODITE data are available online at http://aphrodite.st.hirosaki-u.ac.jp/download/with high-resolution (0.5° and 0.25°) grids for Asia. Furthermore, measured annual runoff data were furnished by the administration of the Tarim River basin and were collected from Alar stations during 1961–2010. And Alar can be seen as the entrance to the Tarim River. Therefore, the runoff measured at the Alar station was considered to be the runoff of the Tarim River in this article.

3. Methods

3.1. Regression Analysis. Rational allocation of water resources is the foundation for the rational allocation of water rights, while the control of runoff prediction in the hydrological site is a prerequisite for the rational allocation of water resources. Therefore, the mathematical model developed to predict runoff timely and accurately for the right to

water management is an extremely important basic job. Runoff prediction is one of the problems in the natural sciences and technology field, and its difficulty is that hydrological changes are subject to various uncertainties and not entirely clear to operation rules. And in mountainous catchments, the quality of runoff modeling depends strongly on the amount and intensity of precipitation and the snow melting.

At present, there are many methods for predicting river runoff such as neural networks, wavelet analysis, and support vector machines. One of the commonly used methods is to calculate the runoff data using statistical methods, and the other is to set up a prediction model according to the evolution of the predicted subject. We used statistical methods including linear regression and nonlinear regression, based on the observed data, to predict and analyze the runoff situations [32–38]. Speaking specifically, based on the monthly runoff data of the upper mountain areas of the Tarim River basin, from the Alar station, during the period of 1961–2010, and precipitation and temperature data in mountainous areas, the influence of the temporal-spatial component of regional precipitation and temperature on monthly runoff was analyzed by using least-squares methods and radial basis function (RBF) neural network.

3.2. Quantitative Error Indicator. In this study, the regression models were established based on the precipitation and temperature data, according to least-squares methods and RBF neural network, and the runoff data were predicted and analyzed by those models. To assess the accuracy of the predictive value of the regression models, four indicators were used in this study: correlation coefficient (*CC*), bias, root mean square error (RMSE), and mean absolute error (MAE) [39]. Among them, *CC* is used to measure the correlation between satellite precipitation data and rain gauge data with the value ranging from 0 to 1. Bias evaluates the degree of bias of satellite precipitation data against the rain gauge data. RMSE and MAE are used to evaluate the overall level of satellite precipitation data error within the range of [0, $+\infty$]. The best possible values are CC = 1, bias = 0, RMSE = 0, and MAE = 0. The equations for the above-mentioned statistics are shown as follows:

$$
\begin{aligned}
CC &= \frac{\sum_{i=1}^{n}(O_i - \overline{O})(P_i - \overline{P})}{\sqrt{\sum_{i=1}^{n}(O_i - \overline{O})^2 \times \sum_{i=1}^{n}(P_i - \overline{P})^2}},\\
\text{bias} &= \frac{\sum_{i=1}^{n}(P_i - O_i)}{\sum_{i=1}^{n} O_i} \times 100\%,\\
\text{RMSE} &= \sqrt{\frac{1}{n}\sum_{i=1}^{n}(P_i - O_i)^2},\\
\text{MAE} &= \frac{1}{n}\sum_{i=1}^{n}\left|P_i - O_i\right|,
\end{aligned}
\tag{1}
$$

where O_i represents the amount of runoff observed at the Alar station, $\overline{O}$ represents the average observed runoff, P_i and $\overline{P}$ are the estimated values of the regression models and their average values, respectively, and n represents the number of pairs of the two runoff factors in the analysis.

4. Results

4.1. Analysis of Climate Change from 1961 to 2010 in the Upper Tarim River Basin. Generally, a linear regression analysis of precipitation and temperature data from 1961 to 2010 found that precipitation and temperature demonstrated significant increasing trends in the upper Tarim River basin at a rate of 0.85 mm/year and 0.25°C/10a, respectively (significant level is smaller than 0.001; Figure 2(a) and Figure 2(b)). Figure 2(c) shows the temporal patterns of the runoff observed at the Alar station, demonstrating the streamflow along the mainstream of the upper Tarim River basin fluctuating in decreasing trends. In terms of precipitation, it showed a continuously increasing trend, while there were still several years (e.g., 1975, 1985, and 1997) with the smallest precipitation volume around 70.00 mm/year, and the largest precipitation occurred in 2010 with the volume around 210.00 mm/year. In terms of temperature, there was a clear horizontal trend at the beginning from 1961 to 1995, while in the afterward period from 1996 to 2010, the temperature demonstrated a more significant increasing trend at a rate of 0.51°C/10a, with the lowest and highest annual temperature happened in 1974 around 4.00°C and in 2006 around 6.46°C, respectively. In the period from 1961 to 1995, the annual variation in precipitation and temperature demonstrated negative correlations (CC ~ -0.24 and $P = 0.168$). And the negative correlations (CC ~ -0.40 and $P = 0.142$) were more significant in the period from 1996 to 2010. In addition, the Tarim River runoff showed a continuous decreasing trend, while there were still several years (e.g., 1978, 1995, and 2010) with the largest runoff volume around 220.00 m^3/s. In the period from 1996 to 2010, the annual variation in runoff and temperature demonstrated significant correlations (CC ~ 0.59 and $P = 0.021$) and the CC value of runoff and precipitation is around −0.27.

The Aksu River, Hotan River, and Yarkand River are all dominated by snowmelt and precipitation replenishment in the mountain areas. Therefore, changes in precipitation and temperature in the river basin have a direct impact on changes in river runoff. However, the increasing trends of precipitation and temperature in the upper Tarim River basin over the last 50 years conflict with the decreasing trend of runoff, indicating that the Tarim River runoff is affected not only by climate change, but also by human activities. Since the 1960s, land reclamation in the upper Tarim River basin has never stopped. The area of an artificial oasis has been continuously expanded, and the area of irrigation has more than doubled. It can be said that human activities are the dominant factor that causes the Tarim River runoff to decrease.

On a seasonal scale, both precipitation and temperature showed increasing trends in all seasons (Figure 3(a) and Figure 3(b)). As for precipitation, the largest and smallest

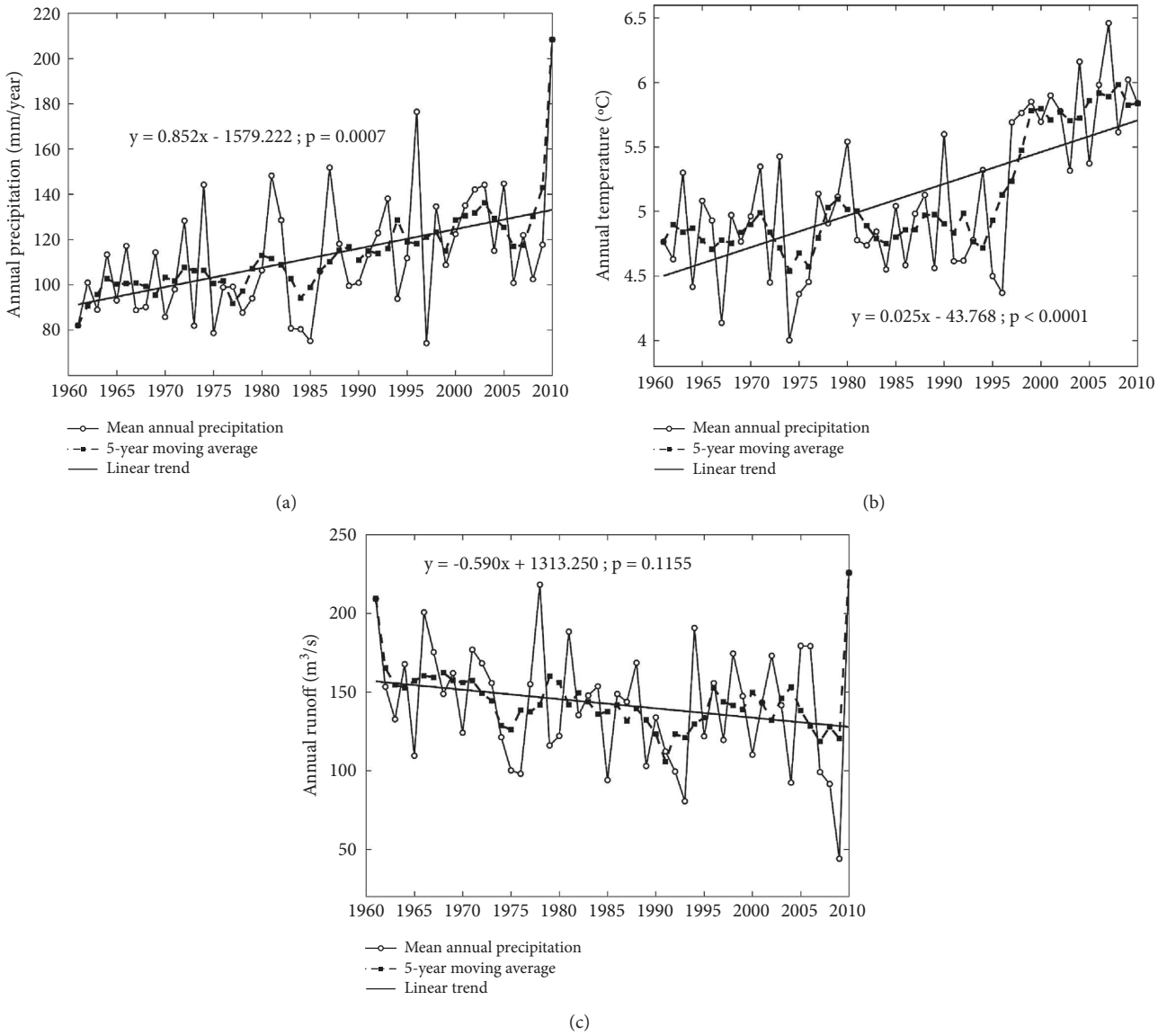

Figure 2: Variations in annual mean. (a) Precipitation, (b) temperature, and (c) runoff in the upper Tarim River basin during the period 1961–2010.

increasing rates happened in summer (JJA; June, July, and August, 0.32 mm/year) and spring (MAM; March, April, and May, 0.16 mm/year), respectively. As for temperature, adversely, the largest and smallest increasing rates happened in winter (DJF; December, January, and February) and spring, respectively. The climate changed with the temperature in winter at a rate of 0.36°C/10a in the upper Tarim River basin, which may bring a great threat to the glacier's accumulations. Meanwhile, the runoff showed decreasing trends in all seasons except spring (Figure 2(c)). The possible reasons are the increase in the arable land area and the continuous expansion of agricultural irrigation areas in the upper Tarim River basin. Although the Tarim River flood season mainly occurs in summer, which is consistent with the period of concentrated water use for agriculture in the basin, a large amount of agricultural water not only occupies the river runoff in summer, but also leads to excessive groundwater extraction. Even in the autumn and winter seasons, even if agricultural water is reduced, the infiltration of precipitation in autumn and winter directly replenishes the groundwater that is lacking due to severe summer mining. As a result, the surface runoff in the Tarim River basin is still reduced in the autumn and winter seasons when it is not the peak period of agricultural water use.

Table 1 lists the change rates of monthly mean precipitation, temperature, and runoff. Precipitation increased with the largest trend occurring in June at a rate of approximately 0.16 mm/year and demonstrated large increasing trends in July and September with rates larger than 0.10 mm/year, while the smallest increasing trend happened in April with the rate of 0.02 mm/year. In terms of temperature, the largest increasing trend happened not in the winter months but in November at a rate of 0.47°C/10a, which was larger than those of the rest months, and the

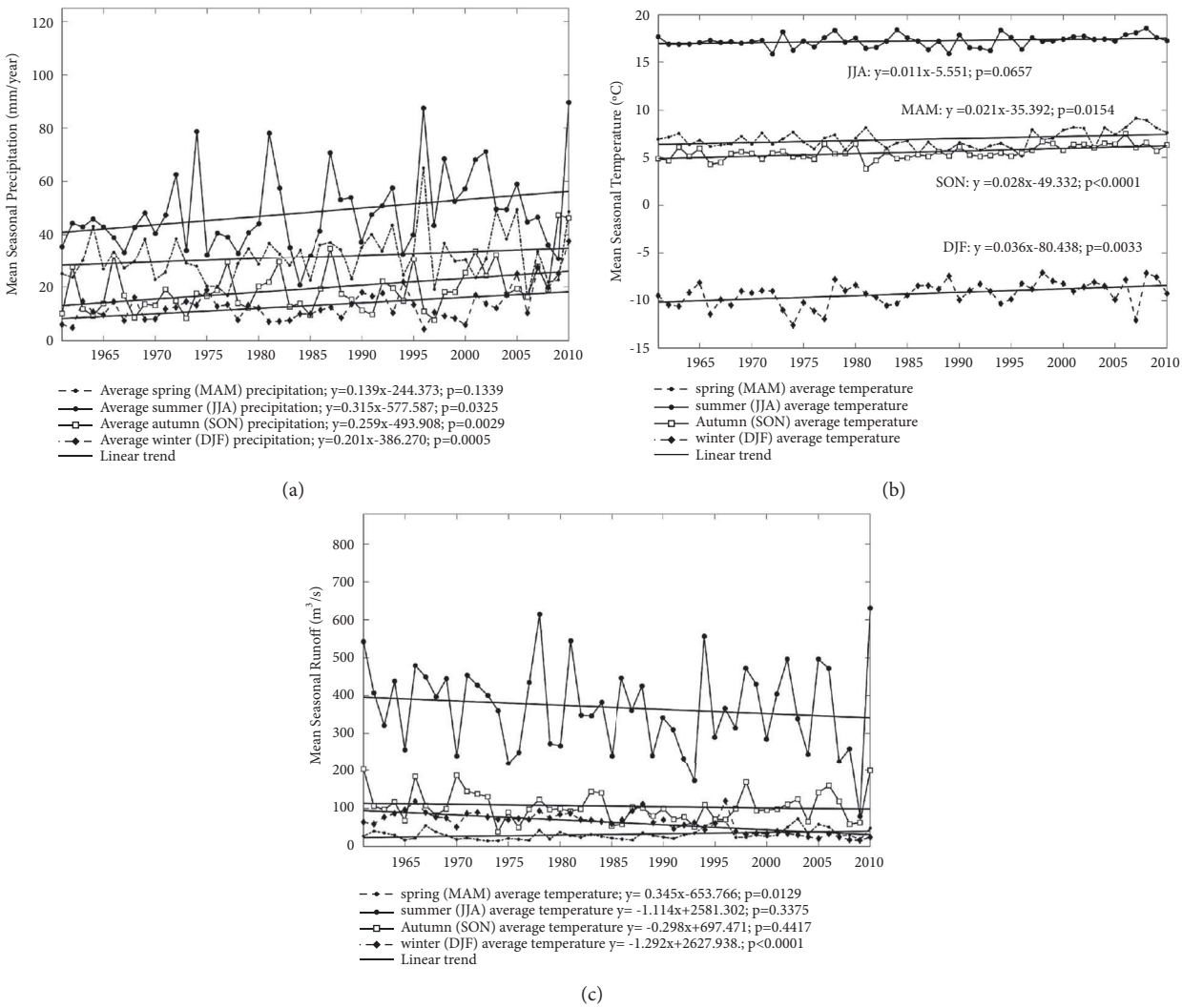

Figure 3: Variations in seasonal mean. (a) Precipitation, (b) temperature, and (c) runoff in the upper Tarim River basin during the period 1961–2010.

Table 1: Change rates of monthly mean precipitation, temperature, and runoff in the upper Tarim River basin during the period 1961–2010.

Trend	Jan	Feb	Mar	Apr	May	Jun
Precipitation trend (mm/month)	0.052	0.042	0.063	0.019	0.054	0.158
Temperature trend (°C/month)	0.026	0.044	0.029	0.018	0.017	0.012
Runoff trend (m^3/month)	-1.125	-0.950	-0.324	0.352	1.008	-0.023
Trend	Jul	Aug	Sept	Oct	Nov	Dec
Precipitation trend (mm/month)	0.124	0.033	0.137	0.087	0.036	0.046
Temperature trend (°C/month)	0.006	0.016	0.017	0.019	0.047	0.045
Runoff trend (m^3/month)	-1.806	-1.515	0.212	0.115	-1.222	-1.801

smallest increasing trend occurred in July at a rate of 0.06°C/10a. Generally speaking, the increasing rates of temperature in cold seasons were larger than those in warm seasons. In addition, the runoff of the upper Tarim River at a monthly scale decreased with the most significant trend occurring in July at a rate of approximately −1.81 m^3/s, and it also showed large decreasing trends in January, August, November, and December with rates smaller than 1.00 m^3/s, while the largest increasing trend happened in May with the rate of 1.01 m^3/s. Besides, positive trends were observed in April, September, and October.

4.2. Spatial Distributions of the Climate Change and Runoff Trends from 1960 to 2010 in the Upper Tarim River Basin. Figure 4 shows the spatial distributions of precipitation trends, at annual and seasonal scales over the upper Tarim River basin from 1961 to 2010. Overall, the annual

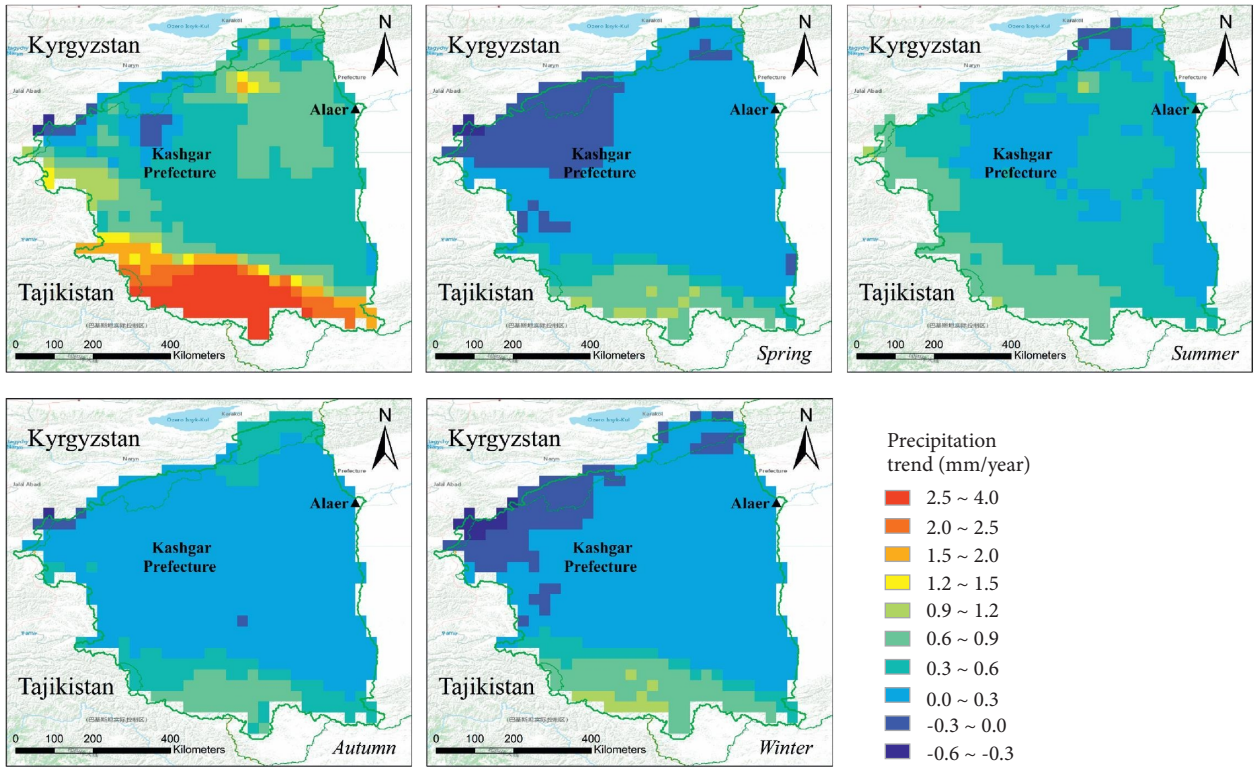

Figure 4: Spatial patterns of variations in (a) annual mean precipitation and spatial patterns of variations of precipitation in (b) spring, (c) summer, (d) autumn, a©(e) winter, during the period 1961–2010.

precipitation trends generally presented an increasing trend from northwest to south, and the differences in precipitation trends in spatial distributions among the four seasons were significant. The regions with the largest precipitation increasing rates were in the southern region, the Karakoram mountains, in intervals larger than 2.50 mm/year. Although most regions showed increasing trends, the decreasing trends occurred in the northwest edges of the upper basin, with the rates varying from −0.60 mm/year to −0.30 mm/year (Figure 4(a)). On the seasonal scale, the decreasing trends were detected in most regions in spring and winter (Figures 4(b) and 4(d)), and the increasing trends were detected in almost all study areas in summer and autumn (Figures 4(c) and 4(e)). Moreover, the increase in precipitation trends in the Karakoram mountains at all seasons was more significant than that in the other regions.

From 1961 to 2010, the annual average temperature in the upper Tarim River basin showed an overall increasing trend, with the increasing rates varying from 0.00°C/10a to 0.30°C/10a in most areas. And the most significant increasing trends were detected in the southeastern region, with the maximum rate around 0.60°C/10a (Figure 5(a)). On the seasonal scale, the spatial pattern of temperature trends in spring was similar to that at an annual scale (Figure 5(b)). And the temperature in the south, in autumn and winter, showed a clear upward trend (Figures 5(d) and 5(e)). In addition, the temperature in summer dropped slightly in some northern areas (Figure 5(c)).

The correlation coefficients between precipitation and temperature varied both spatially and temporally. The precipitation and temperature demonstrated higher correlations at the seasonal scale in most regions with the values of CC varying from 0.5 to 0.9, while the correlations on the monthly scale were generally between 0.3 and 0.7. Meanwhile, the spatial distribution of correlations generally presented an increasing trend from south to north (Figure 6(b) and Figure 6(c)). However, on an annual scale, the relationship between the precipitation and temperature was negative in most areas especially in northwestern regions varying from −0.5 to −0.3, while in the east Karakoram mountains, the correlations were generally fluctuating between 0.3 and 0.5 (Figure 6(a)).

4.3. Analysis of Simulating Runoff Based on Regression Models and Deep Learning Models from 1961 to 2010 over the Upper Tarim River Basin. The spatial distributions of the 50-year average monthly precipitation and temperature over the upper Tarim River basin and the runoff volume observed at Alar are shown in Figure 7. The results show that the runoff of the Tarim River was mainly concentrated in July and August. Considering the precipitation and temperature, the runoff was dominated by snow accumulation in winter, subsequent snow melting in spring, and high precipitation in summer.

Meanwhile, Figure 8 shows the spatial patterns of correlations between monthly precipitation and runoff and those between monthly temperature and runoff for the period 1961–2010. In terms of precipitation, Figure 8(a) shows the correlation coefficients of precipitation and runoff

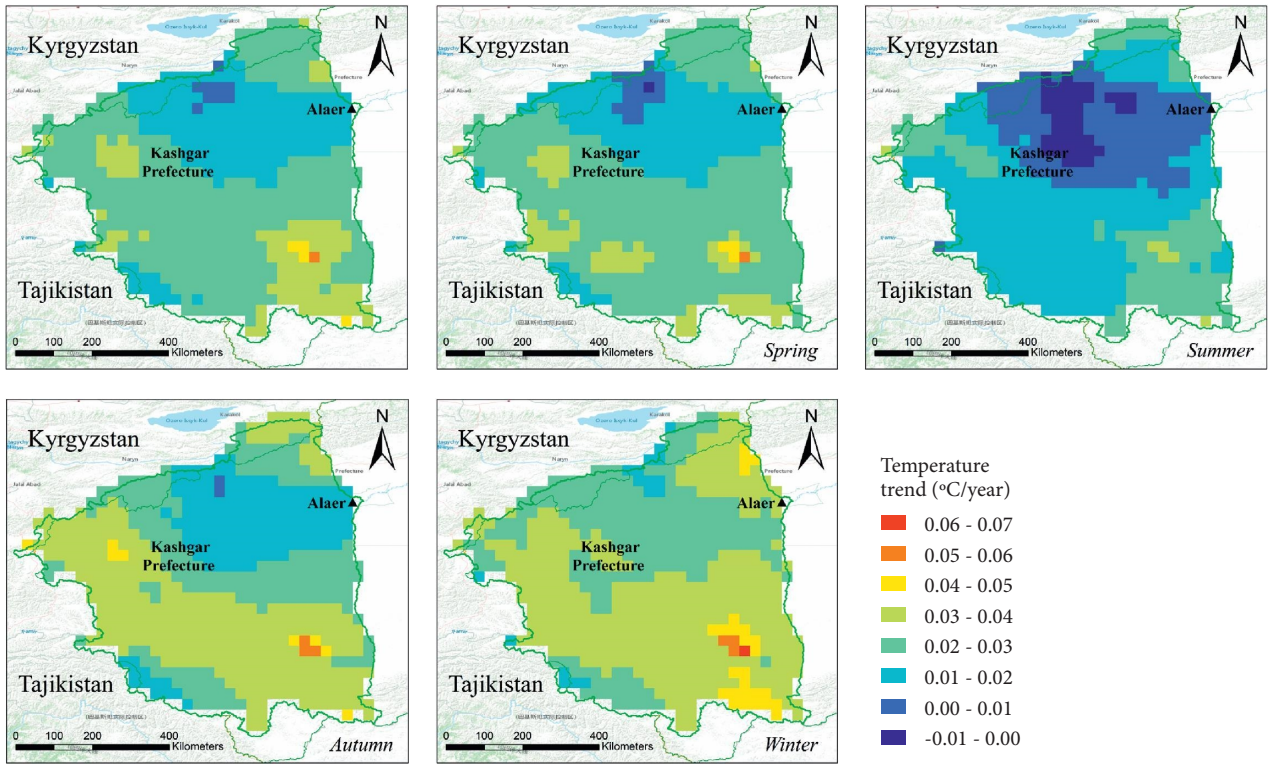

Figure 5: Spatial patterns of variations in (a) annual mean temperature and spatial patterns of variations of temperature in (b) spring, (c) summer, (d) autumn©nd (e) winter, during the period 1961–2010.

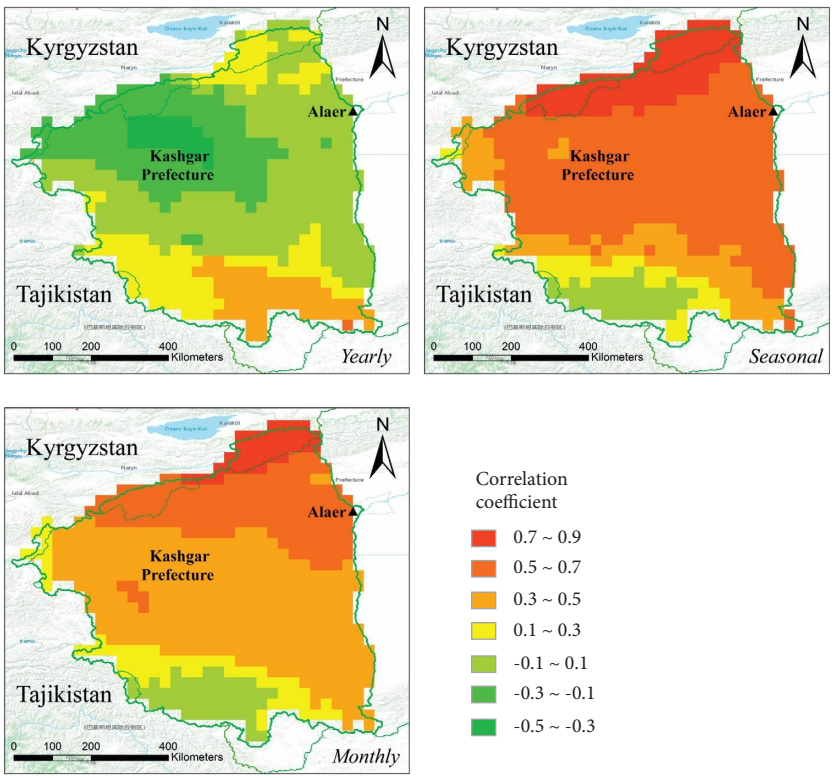

Figure 6: The spatial patterns of correlations between precipitation and temperature at (a) annual, (b) seasonal, and (c) monthly scales in the upper Tarim River basin during the period 1961–2010.

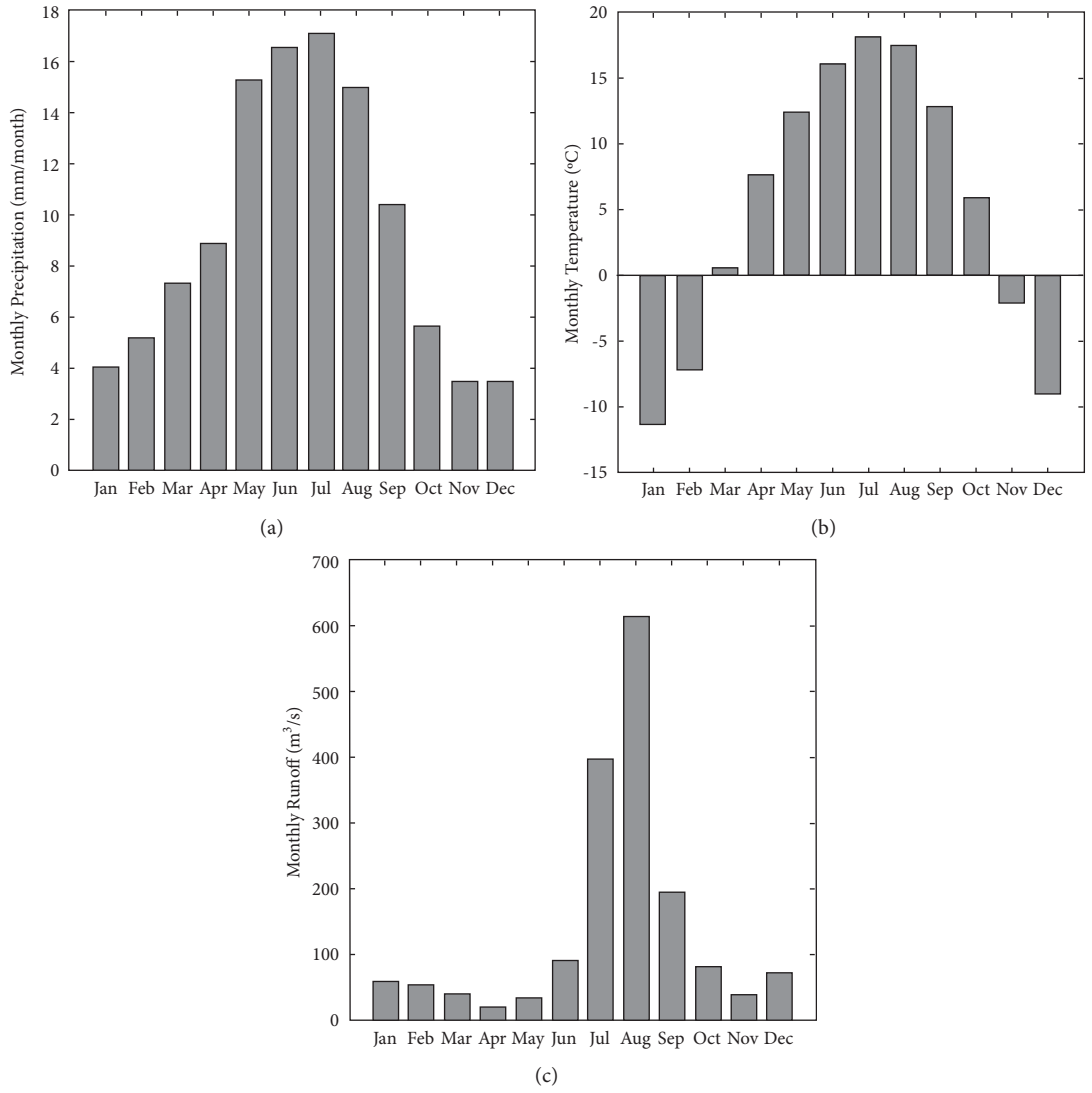

Figure 7: Monthly area averages of (a) precipitation, (b) temperature, and (c) runoff in the upper Tarim River basin during the period 1961–2010.

at the corresponding time and the Figure 8(b) shows the correlation coefficients between precipitation and runoff, with one-month delay to the precipitation. The differences in coefficients in spatial distributions were significant, and the coefficients generally presented an increasing trend from south to north. It can be seen that the impact of precipitation, which occurred in the Tian Shan Mountains, had a more significant impact on the runoff than that occurred in the Karakoram mountains. However, the values of correlations shown in Figure 8(b) were larger than those shown in Figure 8(a) demonstrating that the precipitation might have a great potential impact on the runoff with one-month delay at Alar. In terms of temperature, the runoff-temperature relationship exhibited an overall positive correlation. Similar to the relationship between precipitation and runoff, the temperature had larger correlations with runoff with a one-month delay than those of temperature in the corresponding months.

In the present study, another focus was on comparing the least-squares method models with the deep learning models, radial basis function (RBF) neural network models. A training period of 1961–2000 and an evaluation period of 1961–2000 were identified. We regarded the runoff data as the dependent variable, and the precipitation, temperature, and runoff in the current or previous month as the independent variables. And Table 2 lists a total of 12 regression models based on different independent variables and methods. The weighted data were the correlation coefficient of precipitation or temperature and runoff at each grid point as shown in Figure 8.

While comparing the results, it is to be kept in mind that the data used for calibration and verification are the same among different models. The data from 1961 to 2000 were used to build models and validated using data from 2001 to 2010. Figure 9 demonstrated the temporal patterns of monthly runoff at Alar, in the period from 2001 to 2010,

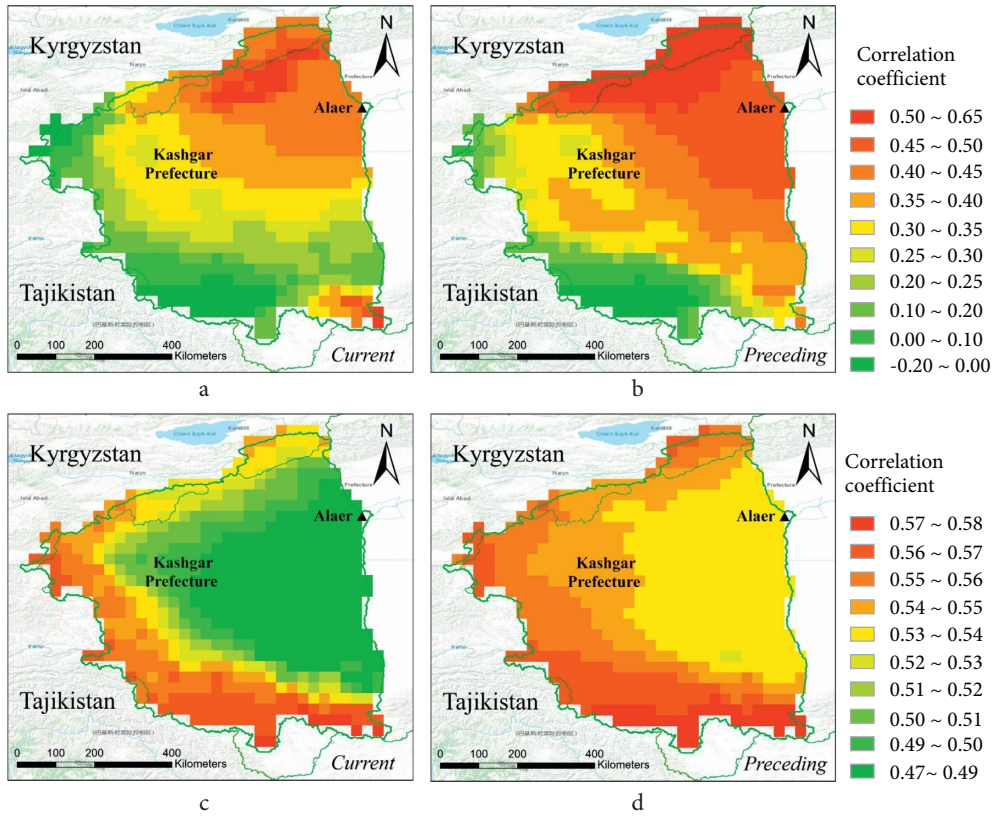

Figure 8: The Spatial patterns of correlations between (a) precipitation and runoff in the corresponding months, (b) precipitation and runoff with one-month delay, (c) temperature and runoff in the corresponding months, and (d) temperature and runoff with one-month delay in the upper Tarim River basin.

Table 2: Summary of models based on different independent variables.

Current			Preceding		Linear fitting	Nonlinear fitting	
Model	P^{cur}	T^{cur}	P^{pre}	T^{pre}	R^{pre}	Least-squares	Radial basis function
Cur	√	√	—	—	—	Cur-LS	Cur-RBF
CurW	√*	√*	—	—	—	CurW-LS	CurW-RBF
Pre	√	√	√	√	—	Pre-LS	Pre-RBF
PreW	√*	√*	√*	√*	—	PreW-LS	PreW-RBF
PreRun	√	√	√	√	√	PreRun-LS	PreRun-RBF
PreRunW	√*	√*	√*	√*	√	PreRunW-LS	PreRunW-RBF

*represents weighted data.

based on observations and different prediction models. The least-squares method models significantly overestimated the runoff in winter and spring, and underestimated the runoff in summer especially in August. In terms of accuracy and consistency, the overall performances of the models based on RBF were better than those of the least-squares method models.

Based on different models, the four quantitative error indicators (CC, bias, RMSE, and MAE) of predictions against the runoff observations were also analyzed (Table 3). In terms of least-squares method models, the models using weighted independent variables outperformed the models using unweighted independent variables. In addition, an increase in the number of independent variables improved the accuracy of the models. The CC (~0.75), bias (~-17.15%), RMSE (~136.40 m^3/s), and MAE (~89.33 m^3/s) of the PreRunW-LS model generally performed better than the other models. In terms of RBF models, although the CC value of PreW-RBF (0.84) is less than the CC of Pre-RBF (0.85), the weighted independent variables still improved the models. Unlike the least-squares method, preceding runoff data as one of the independent variables did not significantly improve the quality of the models in terms of quantitative error indicators. Generally speaking, the PreW-RBF model (CC ~0.84) outperformed the PreRunW-LS model (CC ~ 0.75). Although the bias value of the PreW-RBF model (~30%) was around two times larger than that of the PreRunW-LS model (~17%), and both the RMSE and MAE values of PreW-RBF were significantly smaller than those of the PreRunW-LS, respectively.

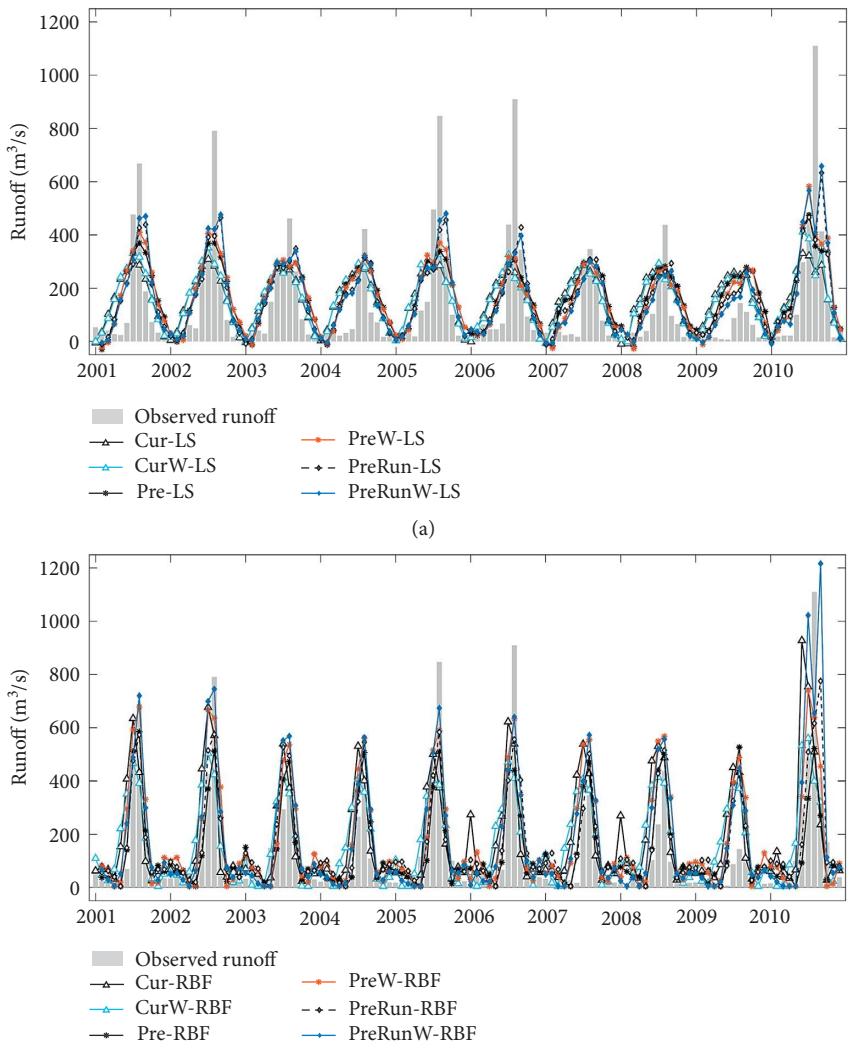

Figure 9: Temporal runoff patterns were predicted by (a) least-squares method models and (b) RBF models, against the observed values, in the upper Tarim River basin during the period 2001–2010.

Table 3: Summaries of the statistical results based on different models, against the runoff observations, in the upper Tarim River basin during the period 2001–2010.

Model	CC	Bias (%)	RMSE (m^3/s)	MAE (m^3/s)
Cur-LS	0.59	14.91	163.85	107.76
CurW-LS	0.62	15.43	160.05	103.01
Pre-LS	0.69	22.90	151.34	104.63
PreW-LS	0.72	20.50	143.61	98.05
PreRun-LS	0.73	19.22	141.45	95.32
PreRunW-LS	0.75	17.15	136.40	89.33
Cur-RBF	0.69	28.17	161.17	104.60
CurW-RBF	0.71	15.95	143.31	90.41
Pre-RBF	0.85	33.68	126.08	84.38
PreW-RBF	0.84	29.61	120.86	82.90
PreRun-RBF	0.82	41.06	146.75	87.95
PreRunW-RBF	0.83	30.19	136.20	75.42

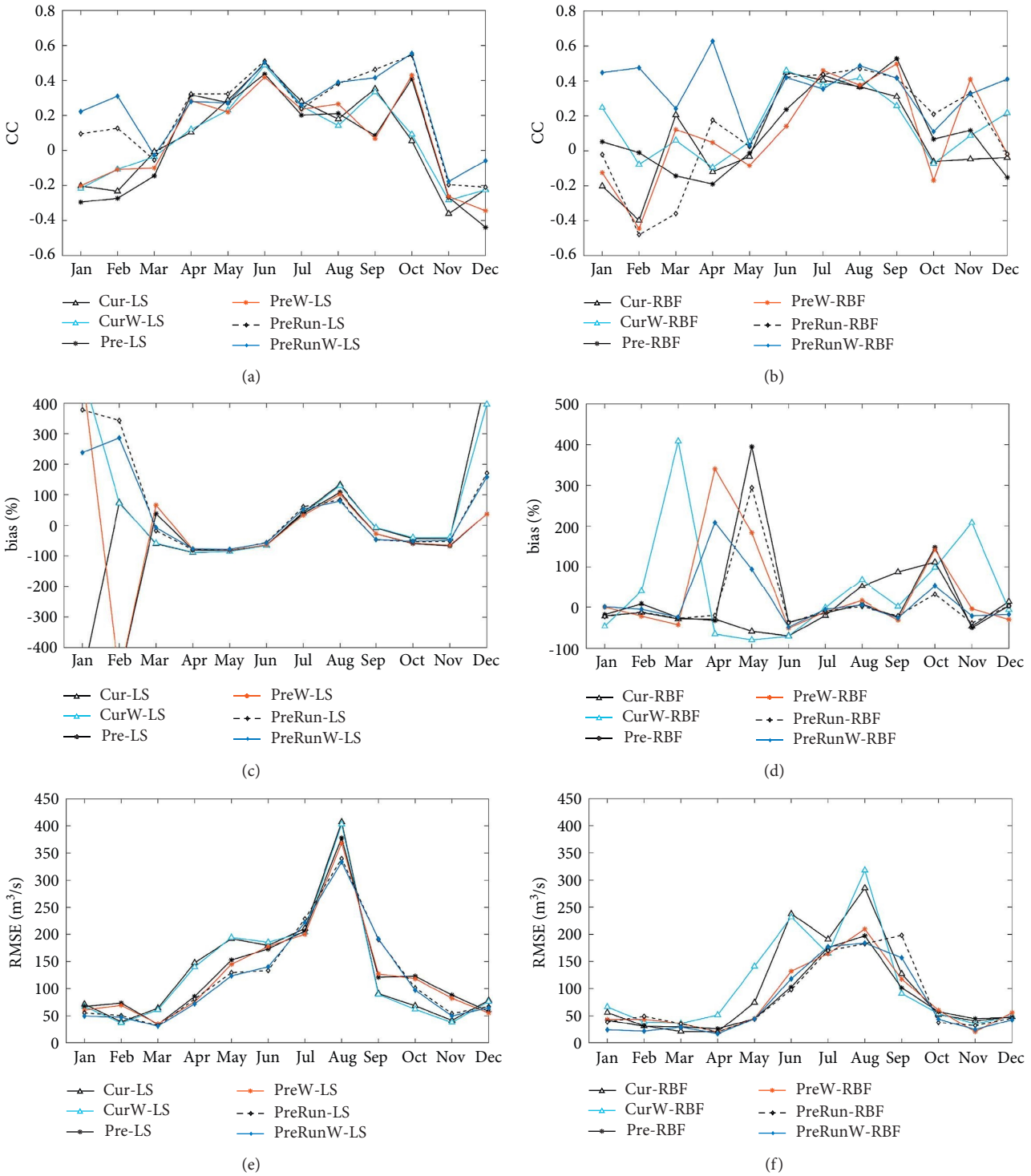

Figure 10: Continued.

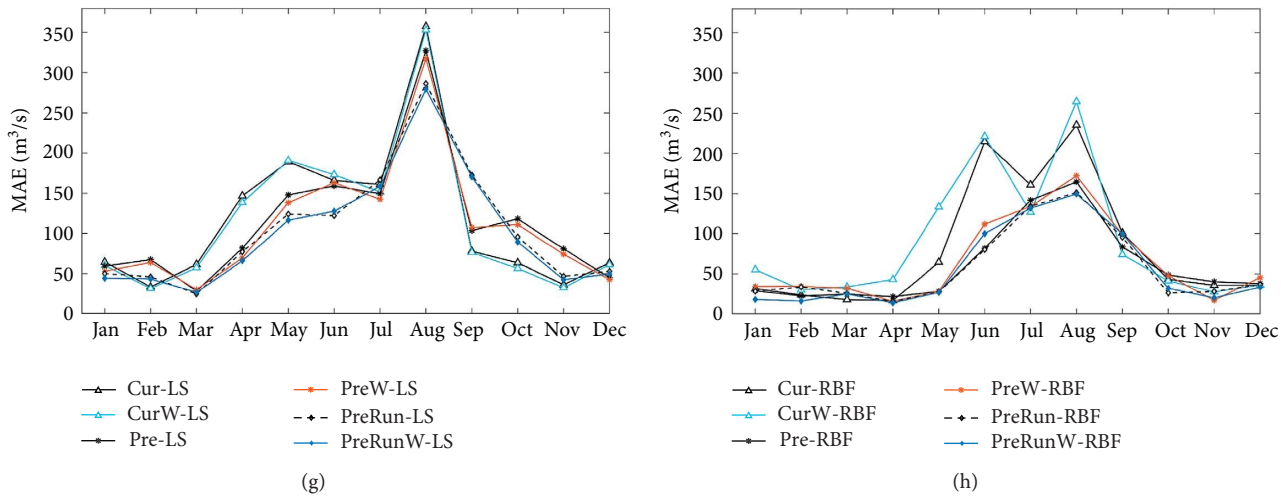

FIGURE 10: Temporal patterns of performances based on least-squares method models in terms of (a) CC, (c) bias, (e) RMSE, (g) MAE, and performances based on RBF models in terms of (b) CC, (d) bias, (f) RMSE, (h) MAE against observations at monthly scale during 2001–2010.

5. Discussions

The Tarim River played a crucial role in the economic and social development of Xinjiang, and the accurate prediction of long-term runoff variation in this basin was important for watershed and flood management. However, frequent floods and droughts in the Tarim River basin were caused by complex forcing factors, so it was challenging to predict when runoff disasters would happen. Many current studies focused on setting up prediction models according to the evolution of the predicted subject. Statistical methods including simple linear or nonlinear methods, in this article, were also considered; it is of great significance for the prediction of runoff in the Tarim River. And the purpose of this study was to be able to quickly predict monthly runoff based on precipitation and temperature data.

Figure 10 demonstrates the temporal patterns of the statistical accuracy indicators evaluating the least-squares method models and RBF models against observed runoff data at the monthly scale. And PreRunW-LS and PreW-RBF models represented the best of the linear and nonlinear models, respectively. The temporal patterns of the CC of least-squares method models and RBF models were different significantly (Figures 10(b) and 10(b)), while the CC values of PreRunW-LS (~-0.20 – ~0.0.5) were significantly larger than those of PreW-RBF (~-0.50 – ~0.50) in winter and spring, especially in February. In terms of bias, PreRunW-LS overestimated the runoff in January and February (as high as ~300%), and PreW-RBF overestimated the runoff in April, May, and October (up to ~350%) against the observed data. However, the bias values of PreW-RBF models were closer to 0.0, in January, February, July, August, and November (Figure 10(d)). As for indicators of RMSE and MAE, the temporal patterns of PreRunW-LS and PreW-RBF were very similar. The RMSE values of PreRunW-LS (~20 m^3/s – ~350 m^3/s) were much larger than those of PreW-RBF (~10 m^3/s – ~200 m^3/s), especially in August (Figure 10(f)); similarly, the MAE values of PreW-RBF (~10 m^3/s – ~150 m^3/s) were also much smaller than those of PreRunW-LS (~20 m^3/s – ~260 m^3/s). In general, neither PreRunW-LS nor PreW-RBF performed better in summer and autumn than in spring and winter. The possible reason might be that in the upper mountainous basin, when the temperature was much lower than the snow melting temperature, the simple linear or nonlinear models were difficult to fit the relationship between temperature and runoff.

Least-squares models and RBF models used a 40-year training period (1961–2000), and forecasts were conducted for the 10-year validation period from 2001 to 2010. The RBF models exhibited promising predictive skills with the correlation coefficient between the observation and the predicted values close to 0.85, which was better than those of the least-squares models. The results have shown that the PreW-RBF model built with the RBF neural networks had some significant advantages for the long-term prediction of runoff and might provide a new and effective tool for the prediction of drought and flood events in the Tarim River basin.

It should be mentioned that the variability of the Tarim catchment hydrology is not only closely linked with the large-scale atmospheric circulation over Asia but also with headstream snow cover because the Tarim River was fed by the glaciers of the mountainous areas. Thus, in addition to the precipitation and temperature data, snow cover or other anomalies may also be an important independent variable for predicting runoff. And we may conduct a further study in the future to analyze the importance of snow cover to the simulation of the runoff.

6. Conclusions

This study quantitatively investigates the climate change in the upper Tarim River basin, using the up-to-date "ground-truth" precipitation and temperature data, the Asian Precipitation Highly Resolved Observational Data Integration

Towards Evaluation of Water Resources (APHRODITE, 1961–2010, 0.25°) data; analyses the potential connections between runoff data, observed at Alar station and the key climatological variables; and discusses the models in simulating the runoff based on precipitation and temperature data. The main findings of this study are as follows:

(1) Both annual precipitation and temperature generally increased at rates of 0.85 mm/year and 0.25 °C/10a, respectively, while the runoff data measured at Alar station showed fluctuating decreasing trends.

(2) There were significant spatial differences in the temporal trends of precipitation, for example, the larger increasing rates of precipitation occurred in the Karakoram mountains, while the larger decreasing rates happened in northwestern Kashgar county.

(3) The decreasing trends of temperature mainly occurred in the Kashgar county and its surrounding areas in summer.

(4) The seasonal correlations in trends of precipitation and temperature were more significant than those on a monthly and annual scale.

(5) The regression model in simulating the runoff in the upper Tarim River basin based on RBF was better than that based on the least-squares method, with the predictive values based on the RBF models significantly better (correlation coefficient, CC, ~ 0.85) than those by least-squares models (CC ~ 0.75).

These findings would provide valuable information to environmental scientists and planners on the climate change issues over the Tarim River basin. [40] [41].

Data Availability

All the data used in this study can be obtained from the corresponding author upon request.

Conflicts of Interest

The authors declare that they have no conflicts of interest.

Acknowledgments

This study was financially supported by the National Natural Science Foundation of China (Grant no. 41901343) and Natural Science Foundation of Guizhou Province (Grant no. [2020]4001) The authors appreciate the contribution of the data providers, including the Chinese Meteorological Data Sharing Service System (http://cdc.nmic.cn/home.do) and the APHRODITE data provider (HYPERLINK "http://aphrodite.st.hirosaki-u.ac.jp/download/" \o "http://aphrodite.st.hirosaki-u.ac.jp/download/"http://aphrodite.st.hirosaki-u.ac.jp/download/).

References

[1] J. D. Milliman, K. L. Farnsworth, P. D. Jones, K. Xu, and L. Smith, "Climatic and anthropogenic factors affecting river discharge to the global ocean, 1951–2000," *Global and Planetary Change*, vol. 62, no. 3-4, pp. 187–194, 2008.

[2] S. J. Déry, M. A. H. Hernández, J. E. Burford, and E. F. Wood, "Observational evidence of an intensifying hydrological cycle in northern Canada," *Geophysical Research Letters*, vol. 36, no. 13, p. L13402, 2009.

[3] T. G. Huntington, "Evidence for intensification of the global water cycle: r," *Journal of Hydrology*, vol. 319, no. 1-4, pp. 83–95, 2006.

[4] Edenhofer and Ottmar, "IPCC, 2014: climate change 2014: mitigation of climate change," *Contribution of Working Group III to the Fifth Assessment Report of the Intergovernmental Panel on Climate Change*, p. 72, Cambridge University Press, Cambridge, New York, NY, USA, 2014.

[5] D. Labat, Y. Godderis, J. L. Probst, and J. L. Guyot, "Evidence for global runoff increase related to climate warming," *Advances in Water Resources*, vol. 27, no. 6, pp. 631–642, 2004.

[6] L. Menzel and G. Bürger, "Climate change scenarios and runoff response in the Mulde catchment (Southern Elbe, Germany)," *Journal of Hydrology*, vol. 267, no. 1-2, pp. 53–64, 2002.

[7] V. Semenov and L. Bengtsson, "Secular trends in daily precipitation characteristics: greenhouse gas simulation with a coupled AOGCM," *Climate Dynamics*, vol. 19, no. 2, pp. 123–140, 2002.

[8] Q. Zhang, Y. David Chen, and J. Chen, "Flood/drought variability in the Yangtze Delta and association with the climatic changes from the Guliya ice core: a wavelet approach," *Quaternary International*, vol. 189, no. 1, pp. 163–172, 2008.

[9] H. Karambiri, S. G. G. Galiano, and J. D. Giraldo, "Assessing the impact of climate variability and climate change on runoff in West Africa: the case of Senegal and Nakambe River basins," *Atmospheric ence Letters*, vol. 12, no. 1, pp. 109–115, 2015.

[10] C. Xu, Y. Chen, W. Li, and Y. Chen, "Climate change and hydrologic process response in the Tarim River Basin over the past 50 years," *Chinese Science Bulletin*, vol. 51, no. S1, pp. 25–36, 2006.

[11] H. Xu, B. Zhou, and Y. Song, "Impacts of climate change on headstream runoff in the Tarim River Basin," *Hydrology Research*, vol. 42, no. 1, pp. 20–29, 2011.

[12] T. Y. Gan, M. Ito, S. Huelsmann et al., "Possible climate change/variability and human impacts, vulnerability of drought-prone regions, water resources and capacity building for Africa," *International Association of entific Hydrology Bulletin*, vol. 61, no. 5-8, pp. 1209–1226, 2016.

[13] S. Reinhard, L. Daniel, V. Pier Luigi, and S. Christoph, "The precipitation climate of Central Asia—intercomparison of observational and numerical data sources in a remote semiarid region," *International Journal of Climatology*, vol. 28, no. 3, 2010.

[14] R. Wang and X. Lu, "Quantitative estimation models and their application of ecological water use at a basin scale," *Water Resources Management*, vol. 23, no. 7, pp. 1351–1365, 2009.

[15] X. Jianhua, L. Weihong, M. Ji, F. Lu, and S. Dong, "A comprehensive approach to characterization of the nonlinearity of runoff in the headwaters of the Tarim River, western China," *Hydrological Processes*, vol. 24, 2010.

[16] Z. X. Xu, Y. N. Chen, and J. Y. Li, "Impact of climate change on water resources in the Tarim river basin," *Water Resources Management*, vol. 18, no. 5, pp. 439–458, 2004.

[17] Y. N. Chen, L. I. Hong, X. U. Chun, and X. M. Hao, "Effects of climate change on water resources in Tarim river basin,

northwest China," *Journal of Environmental Sciences*, vol. 19, no. 04, pp. 106–111, 2007.

[18] L. Chen, C. Liu, and H. Fanghua, "Change of the baseflow and it's impacting factors in the source regions of Yellow River," *Journal of Glaciology and Geocryology*, vol. 28, no. 2, pp. 141–148, 2006.

[19] X. Hao, Y. Chen, C. Xu, and W. Li, "Impacts of climate change and human activities on the surface runoff in the Tarim river basin over the last fifty years," *Water Resources Management*, vol. 22, no. 9, pp. 1159–1171, 2008.

[20] Y. Shi, Y. Shen, E. Kang et al., "Recent and future climate change in northwest China," *Climatic Change*, vol. 80, no. 3-4, pp. 379–393, 2007.

[21] B. Li, Y. Chen, and X. Shi, "Why does the temperature rise faster in the arid region of northwest China," *Journal of Geophysical Research: Atmospheres*, vol. 117, 2012.

[22] B. Li, Y. Chen, Z. Chen, H. Xiong, and L. Lian, "Why does precipitation in northwest China show a significant increasing trend from 1960 to 2010," *Atmospheric Research*, vol. 167, pp. 275–284, 2016.

[23] S. Wang, M. Zhang, Z. Li et al., "Glacier area variation and climate change in the Chinese Tianshan Mountains since 1960," *Journal of Geographical Sciences*, vol. 21, no. 2, pp. 263–273, 2011.

[24] Y. Zhong, B. Wang, C. B. Zou, B. X. Hu, Y. Liu, and Y. Hao, "On the teleconnection patterns to precipitation in the eastern Tianshan Mountains, China," *Climate Dynamics*, vol. 49, no. 9-10, pp. 3123–3139, 2017.

[25] A. Yatagai, K. Kamiguchi, O. Arakawa, A. Hamada, N. Yasutomi, and A. Kitoh, "APHRODITE: constructing a long-term daily gridded precipitation dataset for Asia based on a dense network of rain gauges," *Bulletin of the American Meteorological Society*, vol. 93, no. 9, pp. 1401–1415, 2012.

[26] J. M. A. Duncan and E. M. Biggs, "Assessing the accuracy and applied use of satellite-derived precipitation estimates over Nepal," *Applied Geography*, vol. 34, pp. 626–638, 2012.

[27] F. Xie, W. Mao, J. Zhang et al., "Analysis of streamflow from four source rivers to mainstream of the Tarim River," *Glaciol. Geocryol*, vol. 29, pp. 559–569, 2007.

[28] Y. Chen, K. Takeuchi, C. Xu, Y. Chen, and Z. Xu, "Regional climate change and its effects on river runoff in the Tarim Basin, China," *Hydrological Processes*, vol. 20, no. 10, pp. 2207–2216, 2006.

[29] Y. Ma, G. Tang, D. Long et al., "Similarity and error intercomparison of the GPM and its predecessor-TRMM multisatellite precipitation analysis using the best available hourly gauge network over the Tibetan plateau," *Remote Sensing*, vol. 8, no. 7, p. 569, 2016.

[30] Z. Ma, Y. Xu, J. Peng et al., "Spatial and temporal precipitation patterns characterized by TRMM TMPA over the Qinghai-Tibetan plateau and surroundings," *International Journal of Remote Sensing*, vol. 39, no. 12, pp. 3891–3907, 2018.

[31] Z. Ma, L. Zhou, W. Yu, Y. Yang, H. Teng, and Z. Shi, "Improving TMPA 3B43 V7 data sets using land-surface characteristics and ground observations on the qinghai-tibet plateau," *IEEE Geoence & Remote Sensing Letters*, vol. 15, no. 99, pp. 1–5, 2018.

[32] L. Li, C. Mao, H. Sun, Y. Yuan, and B. Lei, "Digital twin driven green performance evaluation methodology of intelligent manufacturing: hybrid model based on fuzzy rough-sets AHP, multistage weight synthesis, and PROMETHEE II," *Complexity*, vol. 2020, no. 6, pp. 1–24, Article ID 3853925, 2020.

[33] H. J. Lin, L. W. Chou, K. M. Chang, J. F. Wang, S. H. Chen, and R. Hendradi, "Visual fatigue estimation by eye tracker with regression analysis," *Journal of Sensors*, vol. 2022, Article ID 7642777, 1–7pages, 2022.

[34] L. Li, B. Lei, and C. Mao, "Digital twin in smart manufacturing," *Journal of Industrial Information Integration*, vol. 26, no. 9, Article ID 100289, 2022.

[35] L. Li, T. Qu, Y. Liu et al., "Sustainability assessment of intelligent manufacturing supported by digital twin," *IEEE Access*, vol. 8, pp. 174988–175008, 2020.

[36] M. K. Devi, V. P. Vemuri, M. Arumugam et al., "Design and implementation of advanced machine learning management and its impact on better healthcare services: a multiple regression analysis approach (mraa)," *Computational and Mathematical Methods in Medicine*, vol. 2022, Article ID 2489116, 1–7pages, 2022.

[37] L. Li and C. Mao, "Big data supported PSS evaluation decision in service-oriented manufacturing," *IEEE Access*, vol. 8, pp. 154663–154670, 2020.

[38] S. Zhou and C. Kang, "Research on the influencing factors of Russian foreign trade based on R language regression analysis," *Mathematical Problems in Engineering*, vol. 2021, Article ID 5638831, 11 pages, 2021.

[39] Z. Ma, Z. Shi, Y. Zhou, J. Xu, W. Yu, and Y. Yang, "A spatial data mining algorithm for downscaling tmpa 3b43 v7 data over the qinghai-tibet plateau with the effects of systematic anomalies removed," *Remote Sensing of Environment*, vol. 200, 2017.

[40] A. Rutkowska, P. Willems, C. Onyutha, and W. Mlocek, "Temporal and spatial variability of extreme river flow quantiles in the Upper Vistula River basin, Poland," *Hydrological Processes*, vol. 31, no. 7, pp. 1510–1526, 2017.

[41] E. Łupikasza, T. Niedźwiedź, and I. Pinskwar, "Observed changes in AirTemperature and precipitation and relationship between them," in *The Upper Vistula Basin,* Springer International Publishing, Berlin, Germany, 2016.

Hindawi
Scientific Programming
Volume 2022, Article ID 8943314, 10 pages
https://doi.org/10.1155/2022/8943314

Research Article

The Potential of Sino–Russian Energy Cooperation in the Arctic Region and Its Impact on China's Energy Security

Ke Zhang,[1] Maixiu Hu ,[1] and C. N. Dang[2]

[1]*School of Economics and Management, Shanghai Ocean University, Shanghai, China*
[2]*Ho Chi Minh City University of Transport, Ho Chi Minh City, Vietnam*

Correspondence should be addressed to Maixiu Hu; mxhu@shou.edu.cn

Received 28 June 2022; Revised 21 July 2022; Accepted 26 July 2022; Published 31 August 2022

Academic Editor: Lianhui Li

The Sino–Russian Arctic energy cooperation is a successful example based on the comprehensive strategic partnership between the two countries. In order to analyze the impact of Sino–Russian oil and gas resources cooperation in the Arctic on China's energy security, this paper selects 11 influencing factors such as energy self-sufficiency rate and uses the energy security index method to evaluate the three dimensions of energy supply, demand, and environmental security. The assessment results show that China's energy security is mainly affected by the over concentration of energy import sources. At the same time, energy demand and environmental security will also have an important impact on China's energy security. However, relative to energy demand, environmental security factors such as the proportion of clean energy consumption and channel safety factor have a greater impact on China's energy security. After China and Russia strengthen cooperation in oil and gas resources in the Arctic, China's energy security index is expected to increase from 0.4419 in 2020 to 0.5412 in 2025. Therefore, China can use technology, funds, scientific research, and other support to carry out all-round cooperation with Russia in the Arctic waterway, oil and gas exploration and development, and Arctic scientific research.

1. Introduction

With the climate warming and the "Arctic amplification" phenomenon [1], the development and utilization of Arctic energy have attracted more and more attention. As a "major stakeholder in the Arctic," the Chinese government released the first white paper on China's Arctic policy in 2018, which clearly supports Chinese enterprises to actively participate in the development of Arctic oil and gas resources. The Arctic region is rich in oil and gas resources. According to the estimation of the United States Geological Survey (USGS), the total technically exploitable oil and natural gas resources in the Arctic region are 412 billion barrels of oil equivalent, of which 78% are expected to be natural gas and liquid natural gas. However, China has no geographical advantage in participating in the cooperative development of Arctic energy, and the United States and other countries have restricted China's influence in Arctic affairs for a long time, which has hindered China's in-depth participation in Arctic affairs. In recent years, the scale of Russia's development of oil and gas resources in the Arctic has been expanding, and its financial and technical support has also increased, which provides an opportunity for China to participate in the cooperative development of Arctic energy. At present, the Yamal natural gas project, in which China and Russia have cooperated in the Arctic region, has been put into operation since 2017, with a total output of 45.8 million tons by 2020. The project plays a leading role in China's further participation in the development of Arctic energy. Meanwhile, the Sino–Russian Arctic 2 liquid natural gas project under construction will further deepen the cooperation between the two countries in oil and gas resources. The Sino–Russian Arctic oil and gas cooperation not only provides China with the opportunity to jointly develop the Arctic waterway but also on the energy level, the Arctic oil and gas projects have greatly alleviated the need for China's energy structure adjustment. Therefore, the main research content of this paper is to analyze the potential of energy cooperation

between China and Russia in the Arctic region and evaluate the impact of Sino–Russian Arctic energy development on China's energy security.

At present, the research on Arctic energy security is not rare at home and abroad. The existing research is mainly carried out from the perspective of energy policy and the environment. In terms of Arctic energy security policy, Zhang and Xing [2] assessed the political and economic role of the Arctic in international relations from the perspective of China's energy policy strategy. Luo and Li [3] combed the Arctic energy policies of Arctic countries, the European Union, Britain, Germany, Japan, and South Korea and analyzed the game of major powers in the Arctic region and its impact on China's energy security. Korkmaz (2021) [4] studied the characteristics of China's Arctic policy and its links with the "Belt and Road" initiative through the white paper on China's Arctic policy. In terms of the impact of Arctic climate change on China's energy security, Yang et al. [5] analyzed the possibility of Arctic energy development from the perspective of climate change. Pan [6] analyzed the uncertainties and risks faced by the development of oil and gas resources in the Arctic region and put forward countermeasures for China's energy security according to the changes in the Arctic climate and environment. However, there is a lack of research on the specific measurement system and evaluation methods of Arctic energy security in the existing literature.

Based on this, this paper studies the current situation of energy cooperation between China and Russia predicts the potential of energy cooperation between China and Russia in the Arctic region and uses the energy security index method to evaluate the impact of Arctic energy development on China's energy security.

2. Current Situation of Energy Development Cooperation between China and Russia

Among the eight Arctic countries, Russia has the most abundant oil and gas reserves in the Arctic region. According to the USGS assessment, there are 61 large oil and gas fields in the Arctic region, of which 43 are located in the Russian Arctic region, with an oil and gas volume of about 247.4 billion barrels of oil equivalent. In 2017, China and Russia reached an agreement on the construction of the northern waterway and the "ice silk road". In 2016 and 2018, China and Russia formed two joint investigation teams to complete the scientific investigation of the key waters of the "northeast channel". In 2019, China–Russia relations will become "strategic cooperative partners," and China has increased its investment in Russia's Arctic region.

At present, the oil and gas cooperation projects between China and Russia in the Arctic region mainly include Yamal liquid natural gas project and the Arctic 2 natural gas project. Yamal project, integrating natural gas development, processing, liquefaction, and maritime transportation, is a major oil and gas project in the world. The project is jointly operated by CNPC, China Silk Road Fund, Novatec of Russia, and a total of France, holding 20%, 9.9%, 50.1%, and 20% of the shares of the project, respectively. By 2021, all four production lines of the project will be put into production, and the annual production capacity of natural gas will reach 19.75 million tons.

The Arctic 2 liquid natural gas project is the second liquid natural gas project developed by Novatec in the Arctic region after the Yamal project. Novatec of Russia holds 60% of the shares in the project, and CNOOC, PetroChina exploration and Development Corporation, a total of France, and Mitsui property-jogmec consortium of Japan holds 10% of the shares respectively. The project is expected to build three natural gas production lines, with a single production line capacity of 6.6 million tons/year and a total annual output of 19.8 million tons. Novatec plans to put the first natural gas production line into production in 2023 and put all three production lines into production in 2025.

According to the data of the world energy network, the actual output of energy cooperation projects between China and Russia in the Arctic region from 2017 to 2020 is shown in Table 1.

3. Analysis of the Potential of Energy Cooperation between China and Russia in the Arctic Region

According to the USGS assessment results, about 30% of the crude oil, 69.3% of the liquid natural gas, and natural gas in the Arctic region are located in Russia. Table 2 shows the technically recoverable oil and gas resources not found in the Arctic region of Russia. From the perspective of resources, the East Barents basin and Timan bochaola basin, which are rich in oil and gas resources, have a low degree of exploration and have broad exploration and production prospects. China and Russia still have much room for cooperation in the Arctic region. From the perspective of Russia's natural gas exports, Russia's natural gas exports to Japan, South Korea, and other countries in Asia are decreasing in 2020, but its natural gas exports to China have increased by about 35%. As an important oil and gas exporter of Russia in Asia, Russia is bound to strengthen its energy cooperation with China. At the same time, with the smooth progress of the Yamal project, Russia will strengthen the development of Arctic oil and gas resources. In October 2020, the Russian government approved the national security strategy for developing the Arctic region by 2035. The strategy points out that Russia is expected to significantly increase the Arctic natural gas production from 8.6 million tons in 2018 to 43 million tons, 64 million tons, and finally, to 91 million tons in 2024, 2030, and 2035. At the same time, the strategy also plans to increase the proportion of Russian Arctic oil production in the total oil production, from 17.3% in 2018 to 23% in 2030.

The factors that affect the potential of energy cooperation among countries mainly include the scale of energy cooperation, i.e., energy output, import and export volume, investment in energy technology, equipment, and funds, and the closeness of political and diplomatic relations among countries. However, considering the measurability and availability of data, this paper takes the scale of energy

Table 1: Actual total annual production of Yamal 2017–2020.

Particular year	Yamal project	Estimated capacity of a single production line	Actual annual output
2017	In December, the first line was put into operation	5.5 million tons/year	—
2018	In July, the second line was put into operation	5.5 million tons/year	8.6 million tons
2019	—	—	18.4 million tons
2020	—	—	18.8 million tons

Source: World Energy Network.

Table 2: Undiscovered, technically recoverable oil and gas resources in the Russian Arctic (including shared resources with Norway).

	Crude oil (billion barrels)	Natural gas (ten thousand	Crude oil (billion barrels)	Natural gas (ten thousand
Siberian basin	3.66	651.5	20.33	132.57
Yenisei–Khatanga basin	5.58	99.96	2.68	24.92
Laptev Sea continental shelf	3.12	32.56	0.87	9.41
North Kara basin	1.81	14.97	0.39	4.69
Timan bochaola basin	1.67	9.06	0.2	3.38
Lena–Anabar basin	1.91	2.11	0.06	2.32
Scintillation basin	0.10	5.74	0.10	1.16
Northwest raodev shelf	0.17	4.49	0.12	1.04
Lena–Vilyui basin	0.38	1.34	0.04	0.64
Riliangka basin	0.05	1.51	0.04	0.34
Eastern Siberian basin	0.02	0.62	0.01	0.13
East Barents basin	7.41	317.56	1.42	61.7
Eurasian basin	1.34	19.48	0.52	5.11
Total	27.22	1160.9	26.78	247.47

Source: USGS https://earthquake.usgs.gov/. Note: 6 trillion cubic feet of natural gas is equivalent to 1 billion barrels of crude oil.

Table 3: Total annual production from Yamal and arctic 2 2021–2025.

Particular year	Yamal project	Arctic 2 project	Estimated capacity of a single production line	Estimated annual output
2021	Article 4 production line put into operation	—	950000 T/a	2018 million tons
2022	—	—		20.62 million tons
2023	—	The first production line is put into operation	6.6 million tons/year	28.46 million tons
2024	—	The second production line is put into operation	6.6 million tons/year	36.47 million tons
2025	—	All three production lines are put into operation	6.6 million tons/year	44.65 million tons

cooperation as the analysis index of the potential of China and Russia oil and gas resources cooperation in the Arctic region.

As the actual annual output of the Yamal project is higher than the estimated annual output, and the annual output has increased, relevant assumptions need to be made when predicting the annual natural gas production capacity of China and Russia in the Arctic region. Assumption: the annual growth rate of natural gas production in China and Russia in the Arctic region is 1.02, and the actual production capacity of the Arctic No. 2 single production line is 7.39 million tons. The reason is that by 2021, all four production lines of the Yamal project have been completed and put into production, and the estimated annual capacity of the first three production lines is 16.5 million tons. However, according to the report of energy world network Moscow, its actual output will be 18.4 million tons/year in 2019 and 18.8 million tons/year in 2020. Considering the actual production capacity of the mining technology, this paper assumes that the actual annual production capacity of a single production line of the Arctic 2 project is 1.12 times of the estimated annual production capacity. Meanwhile, the first three production lines of the Yamal project will be fully put into production in 2019 and 2020, but the capacity in 2020 is 1.02 times that in 2019, so it is assumed that the annual capacity growth rate of the two projects is 1.02.

Based on the above assumptions, this paper forecasts the output from 2021 to 2025, and the results are shown in Table 3.

4. Selection Basis of Energy Security Assessment Methods and Influencing Factors

4.1. Basis for Selection of Energy Security Assessment Method. Energy security is the core content of a country's national security system. China is relatively short of oil and gas natural resources and has long relied on imports. The long-term stable supply of energy and transportation security has

always been the focus of China's attention. For China, energy security is not just an economic issue of energy supply and demand, but a strategic issue involving energy cooperation and national security among countries. The large-scale natural gas cooperation project between China and Russia in the Arctic region not only stabilizes the overseas supply of China's oil and gas resources but also invests in the construction of the Arctic northeast channel to further expand China's maritime transport channels. But how to quantify its impact on China's energy security is a big challenge. In the existing research, scholars use different measurement methods to quantify energy security. Filipović et al. (2018) [7] used the energy security index (ESI) to analyze and rank the energy security index of EU Member States on the basis of principal component analysis (PCA). Wang et al. [8] proposed a dynamic analysis method of ESI within the framework of FDA (function data analysis), namely desi. The improved desi can dynamically analyze the change in energy security index over time. Ioannidis and Chalvatzis (2017) [9] for the first time, based on the Shannon Wiener diversity index and the Herfindal Hirschman index, combined the diversity of fuel composition with the dependence on energy imports to assess the security of energy supply. Augustis et al. [10] used the ESL energy assessment method to analyze the energy security of the Baltic Sea. Among many energy security assessment methods, the energy security index (ESI) is a common method for quantitative analysis of energy security. It classifies the data related to energy security, calculates the information entropy, and then combines them into a total value. This method can integrate the information of the Russian Arctic region on China's oil and gas resource supply, energy transport safety coefficient, and so on, summarize China's entire energy system, and reflect the characteristics of energy security. And it has been widely studied in the application of assessing and measuring national energy security, and the research results are relatively reliable.

4.2. Basis for Selection of Factors Affecting Energy Security. On the one hand, the selection of factors affecting energy security in this paper can integrate the information of China Russia Arctic energy cooperation, on the other hand, the data should be easy to sort out and a weighted summary. In the existing literature, scholars use different influencing factors to evaluate energy security. Matsumoto et al. (2018) [11] assessed the energy security of EU countries, focusing on energy diversity, import dependence, and supply risks. Radovanovi et al. [12] proposed an energy security index covering environmental and social factors, which was applicable to EU countries from 1990 to 2012. Kruyt et al. [13] combed four dimensions such as the availability of energy security and selected influencing factors from the four dimensions. Song et al. [14] proposed China's energy security index, which includes three dimensions: energy supply, energy consumption, and environment. This dimension can be divided from the supply of oil and gas resources, the proportion of China's oil and gas resources consumption, the energy transportation environment, and other factors to specifically analyze the impact of China Russia Arctic energy cooperation and development on China's energy security. In this paper, the selection of factors affecting energy security is mainly considered from three aspects: first, it can measure the impact of changes in the supply of oil and gas resources on energy security after China's participation in the cooperative development of Arctic energy; Second, it can measure the impact of the utilization of the Northeast waterway on China's energy security; The third is the availability, reliability, and integrity of data. According to the existing literature, this paper selects 11 influencing factors, including 5 energy supply dimensions, 3 energy demand dimensions, and 3 environmental dimensions.

5. Impact Assessment of China Russia Energy Cooperation on China's Energy Security

5.1. Basic Assumptions. In 2018, the first batch of liquid natural gas of the Sino–Russian Yamal project was transported to Rudong terminal in Jiangsu, China, opening a new chapter in Sino–Russian Arctic oil and gas resources cooperation. At the same time, the construction and production of Sino–Russian Arctic No. 2 project will further increase the natural gas delivered to China. However, the specific data that China will import oil and gas resources from the Russian Arctic region after the Arctic 2 project is put into operation is not clear. Therefore, before assessing the impact of Arctic energy development on China's energy security, this paper makes the following assumptions:

Assumption 1. Assumption that China imports oil and gas resources from the Russian Arctic region

China's import of oil and gas resources from Russia's Arctic region accounts for 21% of the total output of bilateral cooperation projects. The reason is that the actual output of liquid natural gas of the Yamal project in 2019 is 18.4 million tons, of which at least 4 million tons will be transported to China, accounting for about 21%. At present, the Sino–Russian Yamal project is progressing very smoothly, and it is also the foundation and important fulcrum for China to participate in the Arctic energy cooperation. The project can also be used as a reference for subsequent cooperation.

Assumption 2. Assumption of influencing factors of energy security

When assessing the impact of the Arctic oil and gas resources cooperation between China and Russia on China's energy security, it is assumed that other factors affecting energy security, except the per capita supply of natural gas, per capita supply of oil and channel safety factors, and maintain the current upward or downward trend. The per capita supply of natural gas, per capita supply of oil and channel safety factors, is evaluated using the data predicted in this paper.

5.2. Accounting and Data Source of Influencing Factors of Energy Security. This paper sorts out the influencing factors of China's energy security from the three dimensions of

energy supply, energy demand, and environment, mainly involving 11 influencing factors such as oil import concentration, energy consumption elasticity coefficient, and channel safety coefficient. It is used to reflect and predict China's energy security from 2010 to 2025. The specific accounting methods and data sources are as follows:

5.2.1. Factors Affecting Energy Supply. The impact of Sino–Russian cooperation in oil and gas resources in the Arctic on China's energy is mainly reflected in the energy supply. The stronger the country's energy supply capacity and the higher the per capita supply, the more its energy security can be guaranteed. In view of this, five factors affecting energy supply security, such as the per capita supply of natural gas, are selected in terms of energy supply security.

(1) Dependence on foreign oil. The proportion of a country's net oil imports in its domestic oil consumption. External dependence on oil = (total annual oil imports − total annual oil exports) total annual oil consumption. The higher the dependence on foreign oil, the higher the risks of energy supply.

(2) Oil import concentration. The proportion of the total export volume of all China's oil import source countries to China's top five oil countries each year in China's net oil import volume. The higher the value, the higher the concentration of China's oil imports and the greater the risk of energy supply.

(3) Energy self-sufficiency rate. Percentage of domestic energy output to total energy consumption. Indicates the extent to which a country's energy production meets its consumption. The higher the energy self-sufficiency rate, the stronger the domestic energy supply capacity and the higher the energy security.

(4) Per capita supply of natural gas. The average amount of natural gas per person in the country can be provided for use. Per capita natural gas supply = total annual natural gas supply of a country/total population of the country in this year. The total natural gas supply includes domestic production and foreign net import. Among them, the natural gas import volume of Russia's Arctic region from 2020 to 2025 is predicted in this paper.

(5) Per capita oil supply. The amount of oil that can be provided for use per capita in the country. Per capita oil supply = annual oil supply of the country/population of the country in the current year. The total oil supply includes domestic production and foreign net import.

5.2.2. Factors Affecting Energy Demand. The energy security of a country is also affected by energy consumption and energy efficiency. High energy consumption means high energy demand, which means that more energy supply is needed to ensure social production and life. The Sino–Russian cooperation on oil and gas resources in the Arctic region has an impact on China's energy efficiency to a certain extent. The increase in the use of natural gas will improve energy efficiency. Efficient energy consumption and a good energy demand structure can reduce energy waste and ensure the full utilization of energy. Therefore, three factors, such as the proportion of oil consumption, are used to measure the security of energy demand.

(1) Elasticity coefficient of energy consumption. In China, this indicator is the ratio of the average growth rate of energy consumption in a certain period to the average growth rate of agricultural GDP in the same period. The elasticity coefficient of energy consumption is affected by energy efficiency, economic structure, and other factors. With the improvement of energy efficiency and the optimization of economic structure, the elasticity of energy consumption will decline.

(2) Energy consumption per unit of GDP. The ratio of total primary energy consumption to domestic GDP. This indicator can reflect the national energy demand level and energy efficiency. Energy consumption per unit GDP = domestic primary energy consumption (ten thousand megajoules)/domestic GDP (ten thousand yuan).

(3) Proportion of oil consumption. The proportion of domestic oil consumption in primary energy consumption. Oil security is particularly important in energy security. The stability of the oil market has an impact on China's energy security, economic security, and even national security.

5.2.3. Environmental Factors. The stable natural gas supply from the Arctic region to China every year can alleviate environmental pressure and contribute to China's realization of "carbon peak" and "carbon neutrality." At the same time, with the further deepening of energy cooperation between China and Russia in the Arctic region, the commercial and economic value of the Northeast passage of the Arctic is becoming greater and greater. The Strait of Malacca has always been responsible for China's energy transport. The full opening of the Northeast passage of the Arctic can reduce the dependence of energy transport on the traditional passage. Assessing the safety of China's energy maritime transport channels, especially the safety factors of the Malacca Strait and the Northeast channel, can further clarify China's energy security situation. In view of this, China's energy and environmental security is measured by the proportion of coal consumption, the proportion of clean energy, and the channel safety factor.

(1) Proportion of coal consumption. The proportion of domestic coal consumption in primary energy consumption. This indicator can reflect the energy consumption structure of a country. Reducing the proportion of coal consumption is conducive to the country's optimization of energy structure and improvement of energy efficiency. It is also a practical need to promote China's clean and low-carbon energy transformation.

Table 4: Waterway safety impact factors and weights.

Classification	Influencing factors and weight	Arctic passage	Strait of Malacca
Hydrology (0.13)	Current and tide (0.21)	0	1
	Sea ice (0.79)	0	1
Meteorology (0.34)	Wind (0.32)	0	1
	Air temperature (0.25)	0	1
	Visibility (0.43)	0	1
Channel (0.09)	Channel width (0.28)	0	1
	Water depth (0.72)	0	1
Traffic (0.15)	Perfection of national laws and regulations (0.45)	0	1
	Number of accidents (0.55)	1	0
Others (0.29)	Port construction (0.17)	1	0
	Navigation equipment (0.27)	0	1
	Pirates (0.25)	1	0
	Icebreaker (0.31)	1	0

(2) Proportion of clean energy. The proportion of domestic clean energy consumption in primary energy consumption. The higher the proportion of clean energy consumption in a country, the more friendly its energy consumption is to the environment and the more conducive it is to the long-term stable development of the social economy.

(3) Channel safety coefficient. Channel safety is an important guarantee for energy maritime transportation. The higher the channel safety coefficient, the higher the overseas supply security of energy. The channel safety factors of ships in the Strait of Malacca and the Northeast channel of the Arctic mainly include hydrological conditions (current and tide, sea ice conditions), meteorological conditions (wind speed, temperature, visibility), channel conditions (navigation width, water depth), traffic conditions (annual traffic accidents, international navigation law), and other conditions (port construction, piracy, navigation facilities). Because the navigation conditions of the channel are fuzzy and complex, the fuzzy analytic hierarchy process is used to measure the channel safety factor. In this paper, five classification conditions are used to form a judgment matrix, and 13 influencing factors are used to form five judgment matrices. The factors in each matrix are compared in pairs, the scaling method is used to assign values, and the weights of each influencing factor are calculated. At the same time, comparing the advantages and disadvantages of various factors in the Arctic channel and the Malacca Strait, the more advantageous one gets a score of 1 and the other 0. The specific weights and scoring results are shown in Table 4.

From the above assessment, the safety factor score of the Arctic channel is 0.2942 and that of the Malacca Strait is 0.7058. The Malacca Strait is superior to the Northeast Arctic channel in sea ice, meteorological conditions, and water conditions, so its final safety factor is also higher than the Northeast Arctic channel. In this paper, the overall safety factor of the channel = the safety factor of the channel of the Malacca Strait, the proportion of the energy freight volume of the Malacca Strait + the safety factor of the Arctic channel, the proportion of the energy freight volume of the Arctic channel. The energy freight volume data of Malacca Strait is from EIA, and the energy freight volume data of the Arctic channel is from the Norwegian ship owners' Association.

The influencing factors and relevant information used in the energy security assessment are as follows:

5.3. Energy Security Assessment and Result Analysis

5.3.1. Introduction of Energy Security Assessment Method. Among many energy security assessment methods, the energy security index method is more objective and interpretable, and its application is the most. This paper will use this method to evaluate energy security. As shown in Table 5 in 4.2, the measurement of China's energy security is divided into three dimensions. Each dimension contains the influencing factors related to this dimension, but the influencing factors of each dimension are quite different. Therefore, assuming that the importance of each influencing factor is not distinguished in the same dimension, the subindicators of each dimension are objectively evaluated through information entropy, and then a comprehensive index is aggregated by assigning weights to each dimension. As each influencing factor has different directions for China's energy security, it is necessary to standardize the data of each influencing factor. The specific steps are as follows:

The first step is to standardize the influencing factors of different attributes or scales into a common scale. Generally, the standardized data is between 0 and 1.

Factors that have a positive impact on China's energy security, such as channel safety factors,

$$x_i(t) = \frac{y(t) - \min[y(t)]}{\max[y(t)] - \min[y(t)]} \left(t_1 \le t \le t_{10}\right); \quad i = 1, \ldots, m, \tag{1}$$

where t is the statistical year, m is the number of influencing factors in each dimension, and $y(t)$ is the original value of each influencing factor; $\min[y(t)]$ and $\max[y(t)]$ respectively

Table 5: Energy security impact factors and data sources.

Classification	Influence factor	Direction of influence	Data sources
Energy supply	Dependence on oil imports (y_1)	−	BP world energy statistical yearbook 2020 National Statistical Yearbook
	Oil import concentration (y_2)	−	General Administration of Customs of China
	China's energy self-sufficiency rate (y_3)	+	BP world energy statistical yearbook 2020
	Per capita supply of natural gas (y_4)	+	National Statistical Yearbook, predicted value of this article
	Per capita oil supply (y_5)	+	National Statistical Yearbook
Energy needs	Energy consumption elasticity (y_6)	−	National Statistical Yearbook
	GDP energy intensity (y_7)	−	BP world energy statistical yearbook 2020 National Bureau of Statistics
	Proportion of oil consumption (y_8)	−	National Statistical Yearbook
	Proportion of coal consumption (y_9)	−	National Statistical Yearbook
Environment	Proportion of clean energy consumption (y_{10})	+	National Statistical Yearbook
	Channel safety factor (y_{11})	+	EIA Norwegian Shipowners Association

represent the minimum and maximum values of influencing factor I in each dimension.

Factors that have a negative impact on China's energy security, such as energy consumption elasticity,

$$x_i(t) = \frac{y(t) - \max[y(t)]}{\min[y(t)] - \max[y(t)]} \left(t_1 \le t \le t_{10}\right); \quad i = 1, \ldots, m. \tag{2}$$

The second step is to use the function information entropy to measure the proportion of each influencing factor of the operator dimension

$$P_i = \frac{x_i(t)}{\sum_{k=1}^{m} x_i(t)} \left(t_1 \le t \le t_{10}\right). \tag{3}$$

The third step is to calculate the information entropy of the influencing factors included in each dimension

$$E_i = \left[\ln\left(t_{10} - t_1 + 1\right)\right]^{-1} \cdot \sum_{k=1}^{m} P_i \cdot \ln\left(P_i\right). \tag{4}$$

The fourth step is to calculate the weight of influencing factors included in each dimension

$$\omega_i = \frac{1 - E_i}{m - \sum_{k=1}^{m} E_i} \left(0 \le \omega_i \le 1\right). \tag{5}$$

The fifth step is the energy security index of each dimension

$$\mathrm{ESI}(t) = \sum_{k=1}^{m} \omega_i(t) \cdot x_i(t), \left(t_1 \le t \le t_{10}\right)\left(0 \le \omega_i \le 1\right). \tag{6}$$

Finally, reasonably allocate weights to each dimension, summarize the security indexes of each dimension, and form a comprehensive China energy security index

$$\mathrm{TESI}(t) = \sum_{d}^{D} \alpha_d \cdot \left[\sum_{k=1}^{m} \omega_i(t) \cdot x_i(t)\right], \tag{7}$$

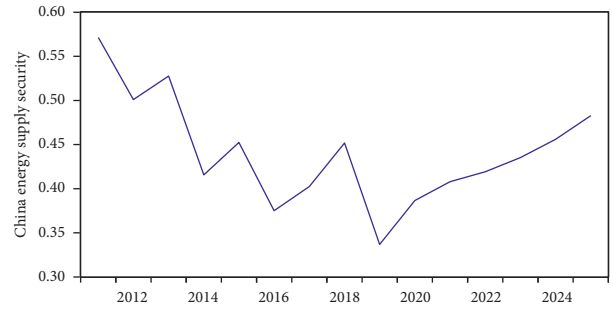

Figure 1: China's energy supply security index 2011–2025.

where d represents different dimensions, D represents the total number of dimensions, and α_d represents the weight of different dimensions. According to the research of Ang et al. [15], the weights of energy supply, energy demand, and environment are 50%, 25%, and 25%, respectively. Giving a higher weight to the dimension of energy supply is to emphasize the importance of uninterrupted energy supply. Since all influencing factors have been subject to positive standardization, a larger Tesi (T) means a safer level of energy security.

5.3.2. Energy Security Assessment Results

(1) Evaluation Results of Three Dimensions of Energy Security. According to the above calculation method, the energy security assessment [16–22] results of three dimensions are calculated respectively, as shown in Figures 1–3 below. Obviously, the fluctuation of the evaluation results of each dimension is different. The assessment results of China's energy supply security are shown in Figure 1, which shows a downward trend before 2020. This downward trend also reflects that China has always been highly dependent on energy imports, with concentrated sources of energy imports, and a low per capita supply of oil and natural gas. In fact, limited by domestic energy resources, China's dependence on oil imports has reached 73% in 2020, and the

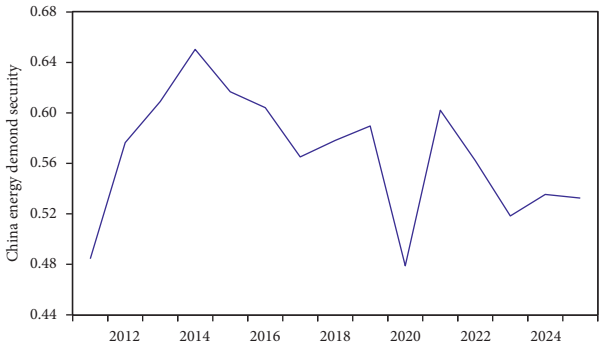

Figure 2: China energy demand security index 20011–2025.

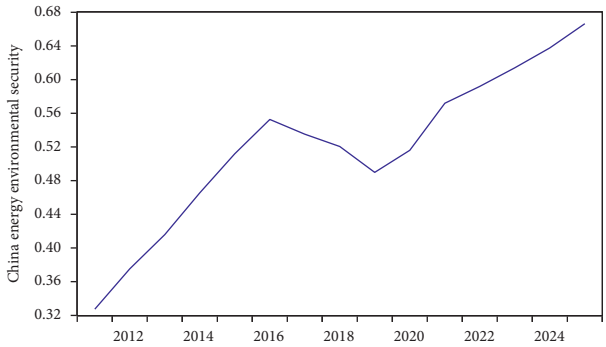

Figure 3: China environmental security index 2011–2025.

concentration of oil imports is 57%. China's energy supply faces great risks. After considering the long-term oil and gas resources cooperation projects between China and Russia in the Arctic region, it can be seen from Figure 1 that the energy supply security index has rebounded significantly after 2020 because China's oil and gas resources, especially the import of natural gas, have been protected to a great extent.

The energy demand security assessment index is shown in Figure 2, which fluctuates from 2011 to 2025 and reaches a trough in 2020. After 2014, the energy demand security index has decreased significantly. The possible reason is that in the past, the proportion of oil consumption increased by an average of about 0.2% every year. From 2014 to 2015, the proportion of oil consumption in primary energy consumption increased from 17.3% to 18.4%. Since 2015, the proportion of oil consumption has been relatively stable, and the fluctuation of the energy demand security index is mainly due to the increase of the energy consumption elasticity coefficient (the value in 2020 is 0.96). After 2020, with the further deepening of natural gas cooperation between China and Russia, the proportion of clean energy consumption such as natural gas has increased, and the energy structure has been optimized, which has played a significant role in improving the security of energy demand. But at the same time, the increase in the proportion of oil consumption makes the energy consumption elasticity index unable to rise all the time, so the security of energy demand fluctuates.

The energy and environmental security assessment index is shown in Figure 3, which shows an overall upward trend from 2011 to 2025. Among the three environmental factors,

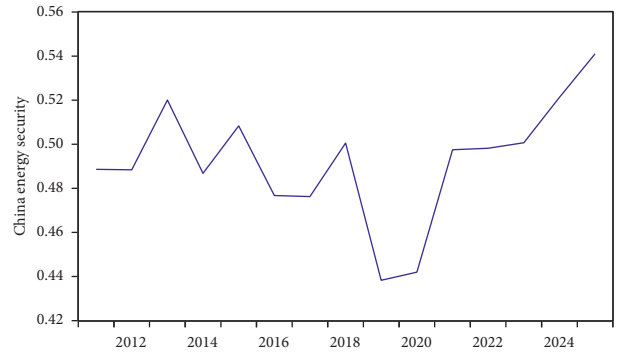

Figure 4: China's energy security index 2011–2025.

the proportion of coal consumption has a negative impact on the environmental index, and the proportion of clean energy and channel safety factor have a positive impact on it. With the further deepening of oil and gas resources cooperation between China and Russia in the Arctic region, the Northeast passage of the Arctic has been more utilized, and China's energy transportation has become less dependent on the Malacca Strait. At the same time, the increased use of natural gas has reduced the pressure of energy consumption on the ecological environment. Under the joint action of the two aspects, the growth rate of the energy and environmental security index will increase after 2020.

(2) Overall Assessment Results of China's Energy Security. With reference to the predetermined weights, the evaluation results of China's energy security index are obtained by using the final summary formula in 3.3.1, as shown in Figure 4 below. In fact, in 2011, China put forward many favorable energy policies, such as promoting diversified and clean energy development and closing small coal mines, which improved the level of energy security. However, China's domestic energy resources have long been more coal and less oil and gas. In 2019, China's oil import concentration reached 62%, posing challenges to the security of the energy supply, which led to a sharp decline in the energy security factor. With China actively expanding energy channels, strengthening cooperation with Russia on oil and gas resources projects in the Arctic region, and improving energy efficiency, China's overall energy security level has maintained a steady rise. After considering the Arctic energy cooperation with Russia, China's energy security level is expected to rise from 0.4381 in 2019 to 0.5412 in 2025. The continuous promotion of China–Russia Arctic energy cooperation and the construction of the Arctic waterway has reduced China's dependence on energy imports from the Middle East, reduced the constraints of the Malacca Strait, increased the proportion of clean energy consumption, optimized the energy structure, improved energy efficiency, and improved the level of energy security.

6. Conclusion

This study uses the energy security index method to evaluate the impact of oil and gas development cooperation between

China and Arctic countries, especially Russia, on China's energy security. From the final results of the evaluation, it has an impact on China's energy supply security, energy demand security, and environmental security. The specific conclusions are as follows:

(1) China's energy security risks are mainly affected by the over concentration of energy import sources. Therefore, diversifying energy imports and reducing energy imports from volatile regions such as the Middle East can effectively disperse China's energy supply risks.

(2) Energy demand and environmental security will also have an important impact on China's energy security. However, compared with energy demand, environmental security factors such as the proportion of clean energy consumption and channel safety factor have a greater impact on China's energy security. Therefore, increasing the proportion of clean energy consumption, reducing the dependence on energy import channels in the Malacca Strait, and diversifying energy import transport channels can effectively ensure China's energy security.

(3) Strengthening energy cooperation with Russia in the Arctic region can greatly enhance China's energy security. Therefore, with the support of technology, funds, and scientific research, China can carry out all-round and multifield cooperation with Russia in the construction of Arctic waterway, port infrastructure, icebreaker technology, oil and gas exploration and exploitation technology, and Arctic scientific research.

Data Availability

The dataset can be accessed upon request.

Conflicts of Interest

The authors declare that they have no conflicts of interest.

Acknowledgments

This study was supported by the National Social Science Foundation of China: Study on the Evolution of "Arctic Passage" and World Trade Pattern and Geopolitical Pattern (17BGJ059), and major projects supported by the Ministry of Education for Philosophy and Social Sciences Research in the later stage: "Study on the Development and Utilization of Arctic waterway" (20JHQ016).

References

[1] M. Yang, S. Ge, and R. Zhang, "Climate change and Arctic response: opportunities, challenges and risks," *Chinese Soft Science*, vol. 13, no. 06, pp. 17–25, 2016.

[2] S. Zhang and Li Xing, "China's energy security and China's Arctic strategic positioning," *International observation*, vol. 21, no. 04, pp. 64–71, 2010.

[3] Y. Luo and F. Li, "Great powers' Arctic game and China's Arctic energy security -- Also on the promotion path of the "ice silk road," *International Security Studies*, vol. 38, no. 02, p. 91, 2020.

[4] H. Korkmaz, "Understanding China's arctic policy in the context of Belt and road initiative," *IJPS*, vol. 3, no. 1, 2021.

[5] Z. Yang, J. Cui, S. Han, P. Guo, and H. Fan, "Impact of Arctic ecological security on China's national security and Countermeasures," *Marine Environmental Science*, vol. 32, no. 04, pp. 629–635, 2013.

[6] M. Pan, "Opportunities and risks: impact of arctic environmental change on China's energy security and Countermeasures," *Chinese Soft Science*, vol. 18, no. 09, pp. 12–21, 2014.

[7] S. Filipović, M. Radovanović, and V. Golušin, "Macroeconomic and political aspects of energy security – exploratory data analysis," *Renewable and Sustainable Energy Reviews*, vol. 97, pp. 428–435, 2018.

[8] D. Wang, S. Tian, L. Fang, and Y. Xu, "A functional index model for dynamically evaluating China's energy security," *Energy Policy*, vol. 147, Article ID 111706, 2020.

[9] A. Ioannidis and K. J. Chalvatzis, "Energy supply sustainability for island nations: a study on 8 global islands," *Energy Procedia*, vol. 142, pp. 3028–3034, 2017.

[10] J. Augutis, R. Krikštolaitis, L. Martišauskas, S. Urbonienė, R. Urbonas, and A. B. Ušpurienė, "Analysis of energy security level in the Baltic States based on indicator approach," *Energy*, vol. 199, Article ID 117427, 2020.

[11] K. Matsumoto, M. Doumpos, and K. Andriosopoulos, "Historical energy security performance in EU countries," *Renewable and Sustainable Energy Reviews*, vol. 82, pp. 1737–1748, 2018.

[12] M. Radovanović, S. Filipović, and D. Pavlović, "Energy security measurement – a sustainable approach," *Renewable and Sustainable Energy Reviews*, vol. 68, pp. 1020–1032, 2017.

[13] B. Kruyt, D. P. van Vuuren, H. J. M. de Vries, and H. Groenenberg, "Indicators for energy security," *Energy Policy*, vol. 37, no. 6, pp. 2166–2181, 2009.

[14] Y. Song, M. Zhang, and R. Sun, "Using a new aggregated indicator to evaluate China's energy security," *Energy Policy*, vol. 132, pp. 167–174, 2019.

[15] B. W. Ang, W. L. Choong, and T. S. Ng, "A framework for evaluating Singapore's energy security," *Applied Energy*, vol. 148, pp. 314–325, 2015.

[16] L. Li, B. Lei, and C. Mao, "Digital twin in smart manufacturing," *Journal of Industrial Information Integration*, vol. 26, no. 9, Article ID 100289, 2022.

[17] L. Li, T. Qu, Y. Liu et al., "Sustainability assessment of intelligent manufacturing supported by digital twin," *IEEE Access*, vol. 8, pp. 174988–175008, 2020.

[18] T. T. Li and J. Xu, "Energy security and economic development based on complex computer system dynamic model," *Wireless communications & mobile computing*, vol. 2022, Article ID 2800308, 10 pages, 2022.

[19] L. Li and C. Mao, "Big data supported PSS evaluation decision in service-oriented manufacturing," *IEEE Access*, vol. 8, pp. 154663–154670, 2020.

[20] L. Li, C. Mao, H. Sun, Y. Yuan, and B. Lei, "Digital twin driven green performance evaluation methodology of intelligent

manufacturing: hybrid model based on fuzzy rough-sets AHP, multistage weight synthesis, and PROMETHEE II," *Complexity*, vol. 2020, no. 6, pp. 1–24, 2020.

[21] M. K. Hasan, A. Alkhalifah, and M. A. Hossain, "Blockchain technology on smart grid, energy trading, and big data: security issues, Challenges, and Recommendations," *Wireless communications & mobile computing*, vol. 2022, Article ID 9065768, 26 pages, 2022.

[22] P. Li, J. S. Zhang, J. Xu, and P. Wang, "A dynamic approach to measuring China's provincial energy supply security along "the Belt and road," *Mathematical Problems in Engineering*, vol. 2018, Article ID 3605024, 16 pages, 2018.

Hindawi
Scientific Programming
Volume 2022, Article ID 9087653, 12 pages
https://doi.org/10.1155/2022/9087653

Research Article

Evaluating the Effectiveness of Teaching Experimental Design in Universities in the Context of Information Technology

Fang Zhang[1] **and Shenggong Guan**[1,2,3]

[1]*College of Civil Engineering, Shaoxing University, Zhejiang, Shaoxing 312000, China*
[2]*Key Laboratory of Rock Mechanics and Geohazards of Zhejiang Province, Zhejiang, Shaoxing 312000, China*
[3]*Zhejiang Collaborative Innovation Center for Prevention and Control of Mountain Geologic Hazards, Zhejiang, Shaoxing 312000, China*

Correspondence should be addressed to Shenggong Guan; guanshenggong@usx.edu.cn

Received 3 July 2022; Revised 14 August 2022; Accepted 18 August 2022; Published 29 August 2022

Academic Editor: Lianhui Li

Experimental instructional design is an important pedagogical component of university teaching and learning, an important means of cultivating students' innovative spirit and practical skills, and has an important status and role that cannot be replaced by any other means of teaching and learning. Assessment for learning as learning, assessment for learning, and assessment as learning are three paradigms of educational assessment that complement each other in achieving curricular and pedagogical goals and together form learning-based assessment. As an important component of national science and technology development, measuring the effectiveness of laboratory instructional design in universities and research institutions is of special significance. This paper presents the authors' research on the background, evaluation characteristics, evaluation content, and methods of experimental teaching evaluation in the information technology environment, with examples of their application.

1. Introduction

Experimental teaching is an important teaching content of science and technology teaching is an important means to cultivate students' innovative spirit, and practical ability has an important status and role that cannot be replaced by any other teaching methods and means [1].

Informatization is a symbol of the 21st century, with the process of informatization, the core of modern computer education technology is developing rapidly, laboratory teaching equipment is gradually digitalized, computerized, and networked, and the era of informatization of laboratory teaching has arrived. Make full use of modern information technology educational tools to significantly improve teaching methods, teaching efficiency, and teaching quality [2]. Laboratory teaching informatization, so that experimental teaching from teaching methods [3], teaching effectiveness, and teaching quality has been improved, so that the experimental management to a new level [4]. Obviously, education, classroom teaching, and experimental teaching in the 21st century are inevitable and necessary for gradual informatization.

Effective teaching in information-based teaching differs from traditional effective teaching in that it refers to effective teaching in the teaching environment supported by information technology. IT-supported teaching breaks the limitations of time, space, and resources in traditional teaching, and can make full use of the advantages of information technology to carry out various teaching modes based on information technology, such as project-based teaching mode, problem-based teaching mode, network collaborative learning teaching mode, and case-based learning mode, which are conducive to the improvement of teaching quality and the full development of students. The application of information technology in teaching does not mean that effective teaching happens. Some studies have shown that the reasons for successful IT teaching should be attributed more to good instructional design and adequate preparation

for teaching. Therefore, to examine whether informationalized teaching is effective, it is still necessary to start from whether teaching accomplishes teaching objectives and promotes students' learning, and to synthesize various factors such as teaching purposes, application of informationalized teaching mode, application of information technology, and teaching process, so as to explore the objective rules of the effectiveness of informationalized teaching.

Educational assessment is the wind vane and baton of educational reform and development [5]. Due to the long-term, generative and delayed nature of education and the indirect, implicit and subjective nature of assessment, the scientific and effective organization and implementation of educational assessment have been a difficult problem in educational teaching practice [6]. Educational evaluation is related to the direction of educational development, and it is gradually shifted to the following direction: improving result evaluation, strengthening process evaluation, exploring value-added evaluation, improving comprehensive evaluation, and establishing a scientific educational evaluation system and mechanism for different subjects and characteristics of different levels and types of education.

Evaluation of laboratory teaching is a necessary method and tool to analyze and recognize the pedagogical quality and efficiency of laboratory teaching. It is also often assumed that the act of measuring memory does not change memory [7], and most educational practices are focused on strengthening the process of students' processing of knowledge, that is, getting it into their heads. Nowadays, the purpose of evaluation of experimental teaching in the informationized environment is to recognize the laws, problems, and shortcomings of experimental teaching in the informationized environment, to provide a basis for the improvement of experimental teaching quality, experimental teaching improvement, experimental teaching research, and experimental teaching development, in order to meet the needs of talent training in universities in the information era. In the study of how students learn [8], there is no mention of a method about retrieval [9]. This method of retrieval memory is still controversial in specific teaching [10]: whether it is effective [11], ineffective [12], or vague [13]. For a long time, universities across the country have invested a lot of human and financial resources in the field of experimental teaching, accumulated rich experience in experimental teaching, and cultivated a large number of talents, and the evaluation system of classroom theory class teaching is relatively mature, but the evaluation system used to evaluate the quality of experimental teaching has been little studied [14]. With the involvement of information technology in experimental teaching and the increasing requirements for the evaluation of scientific teaching concepts [15] year by year, it is urgent to study and develop the evaluation system of experimental teaching in the new situation to evaluate and monitor experimental teaching.

Whenever new media technologies emerge, some researchers are always eager to introduce these new media technologies into teaching, expecting to use the advantages of new media technologies to improve teaching or solve problems in teaching [16]. However, as the cult of modern media cools down [17], people gradually shift from the blind pursuit of media technology to the research on the effectiveness of information technology teaching applications, but always fall into the awkward mode of "introducing new technology, a successful experiment and a failed promotion." In this era of information technology, what is wrong with the research on the effectiveness of experimental technology teaching application, and why the research results cannot be promoted to the general practice? And now, the integration of a variety of high-end information technology wisdom classrooms into the vision of educational technology researchers, and how we should be sensible to the configuration of various technologies in the wisdom classroom, the wisdom classroom pragmatic introduction to teaching life? There is an urgent need to find a scientific rationale for the pedagogical application of experimental technologies.

Research on the effectiveness of experimental instructional designs often uses a simple two-class comparison experiment, but such comparison experiments are difficult to prove the instructional effectiveness of experimental designs because of the many gaps in empirical research in this way.

1.1. Misplacement of the Research Question. Comparative experiments on technology application generally explore the question of which is superior between teaching with or without the involvement of a particular technology or between teaching with the involvement of different experimental technologies and attribute the advantage to the application of a particular technology. In pedagogical practice, however, the primary task is to apply technology to improve instruction (practical goal) rather than to demonstrate the superiority of a particular technology (theoretical goal). It is the technology that has specific functions, and these objective functions do not need to be tested repeatedly in pedagogical research. In reality, when different people use the same technology, there will certainly be differences in the extent to which the technology functions are used, but this difference is not caused by the technology itself, but by multiple factors outside the technology. For an emerging technology, the acceptance or rejection of it should not be decided by the merits of its performance. Therefore, the basic question of technology application research is not to prove the superiority of a particular technology, but to explore what particular experimental techniques are most applicable and how they can be combined with other pedagogical elements to achieve optimal results. It is the study of the instructional system associated with the technology that is more important than the study of its advantageous functions.

1.2. Poor Definition of the Comparison Item. Contrast experimental research often judges the merits of technology by the good or bad teaching effect, and inadvertently mistakenly takes the technology as a whole (with or without, this or that) as a contrast item to study. However, technology and its products often contain multiple attributes and functions,

and they have completely different effects on teaching and learning, so it is difficult to say what is being compared by using the technology as a whole as a comparison item. Imagine the need to compare visual media and auditory media in terms of the intuitiveness of content presentation. For example, is there a direct comparison between a computer + projector and a blackboard? Comparing technologies in general terms, the conclusions obtained are hardly indicative of the problem. That is, technology products are only meaningful when compared in terms of the same type of information and pedagogical function. Moreover, comparisons of the role of the same technology product in different instructional contexts are interesting, but unfortunately less often done.

1.3. Evidence of Ineffectiveness. The general idea of validity testing of technology instructional applications is to compare the effectiveness of the experimental and control classes and to attribute the improvement in instructional effectiveness to the application of technology. There are two loopholes in this. First, effectiveness here usually refers to the effect of an educational intervention in a specific context, which is actually based on "client satisfaction," such as improved academic performance, increased motivation, positive learning attitude, and good experience with a technology product [18]. However, "client satisfaction" is not an "objective" effect. Second, the effect of teaching is the result of complex interactions between the elements of teaching activities, which reflects the overall operation of teaching activities and cannot be attributed to any local elements of teaching. Therefore, we cannot conclude the effectiveness of technology application in terms of teaching effectiveness [19]. To take a step back, even if technology is effective, it is only effective in a specific teaching context and does not have a universal applicability out of context. Due to the non-reproducibility of teaching activities, we simply cannot prove the pedagogical validity of technology in the doctrine. In fact, all tests are only tests of the feasibility in a particular context.

1.4. Defective Experimental Design. This phenomenon can be considered to be widespread at home and abroad. Single-factor isogroup experiments are the simplest experimental teaching comparison study experiments, and these experimental designs are still so, and other multifactor experimental teaching comparison experiments are even more seriously flawed in their design. This phenomenon, although directly related to designer literacy, is not essentially caused by the experimental designer, but by the faulty rationale of experimental teaching comparison experiments. Unlike other scientific experiments, teaching experiments with evidence of teaching effectiveness have to consider the individual person as a variable because the individual person as a whole is involved in the experimental process [20]. However, the individual person is in an open self-creation process and cannot be objectified or conceptualized, so we cannot treat the individual person in a teaching experiment as a variable (operationally speaking, i.e., not controllable), and the teaching effect is indeed inseparable from the unique contribution of the individual student, so with the teaching effect as the grip, the comparison experiment, no matter how strictly the experimental environment is controlled, can hardly show that the achievement of the teaching effect and The use of technology is directly related. Therefore, no matter how the comparison experiment is designed, it will have doctrinal flaws, and no researcher will be able to recover from this research rationale. It is for this reason that the field of education refers to these types of teaching experiments as "quasi-experiments. Such quasi-experiments have some exploratory research value, but they can only test the feasibility of local methodological elements. Such feasibility, of course, does not require such empirical studies, which are often obvious.

1.5. Treating Quasi-Conclusions as Conclusive. The conclusions drawn from quasi-experiments in teaching should be "quasi-conclusions." However, both researchers and practitioners have "inadvertently" promoted quasi-conclusions as generalized definitions, which has led to nothing but confusion and dogma in teaching practice. When people experiment with technology applications, they generally delve into the functional characteristics of a particular technology, customize the content for that technology, and provide as much support as possible in terms of resources, funding, and policies, so that the functionality of the technology is brought to a higher or even higher level, with satisfactory results. You can imagine how costly this kind of teaching experiment is. In fact, although this kind of teaching experiment is a teaching experiment in a "real situation," it is not a teaching experiment in a "natural situation," because this kind of teaching experiment is a nonstandard teaching practice. The teaching application of media eventually goes back to the routine work of regular cost, and most of the support equipped for the experiment will be withdrawn. So, is the specific functionality of the technology really needed in regular teaching? If so, will its actual utility be as good as it was during the experiment? These are all uncertainties. If we cannot use the quasi-conclusions of the experiment to address these issues in regular teaching, the quasi-conclusion is naturally useless. At best, it tells us that someone has "worked" before.

We can think about this issue from a different perspective: the pedagogical use of technology may indirectly affect the effectiveness of teaching and learning by increasing the "goal-means" coherence of the teaching system, student engagement, or the adaptability of the teaching system under certain conditions. Therefore, research on the use of technology should examine more the actual role and contribution of technology products in conventional teaching and learning rather than proving its pedagogical effectiveness in isolation [21]. Such empirical studies, while not getting bogged down in quasi-experiments, require an information flow-based approach to instructional systems analysis in order to explore the details of the role of technology products in teaching and learning.

Experimental teaching design validity analysis is a very important experimental design issue [22]. The study of the

relative validity of each basic unit facilitates the improvement of the experimental management model and the development of rational planning, thus maximizing the effectiveness of experimental design [23]. Scientific measurement of experimental design validity can reflect the degree of effective subjective efforts to improve experimental design, which can have a motivating effect on each unit [24]. For measuring the effectiveness of teaching experimental design, hierarchical analysis has been used in the past to analyze the good and bad experimental design of each unit. That is, the weight parameters of each research outcome index are determined by hierarchical analysis, and then each index is multiplied by its respective weight and summed, and the result is used as the final comparative score of each unit. Such a measurement method is hardly motivating for the assessment unit. Because the number of indicators of units with good foundation conditions is often higher, the weighted sum is naturally in the upper level, while the units with poor foundation conditions, no matter how hard they work, the results are limited, and the weighted sum is not likely to be in the upper level, which greatly affects the motivation of the subjective efforts of units with poor foundation conditions, or worse, some units with good foundation conditions rest on their laurels and do not think about making progress, resulting in assessment scores are still at the top, while they have actually regressed.

In this paper, the idea of the binary relative effectiveness of measuring the economic efficiency of enterprises is transferred to measuring the effectiveness of teaching experiment design in colleges and universities, that is, the results of the effectiveness of teaching experiment design of each college and university measured by the hierarchical analysis method are taken as a measure of the basic conditions of each college and universities, and it is regarded as an input, while the corresponding current results measured by the hierarchical analysis method are regarded as an output, as the C^2GS^2 model in the Data Envelope Analysis (DEA) method [25] is used to calculate the relative evaluation results among the evaluation units. This relative evaluation result can eliminate the influence caused by the objective base conditions of each university, and it can make the decision units with different base conditions have the same "benchmark" to achieve the purpose of fair and objective evaluation. It truly reflects the validity of the experimental design. We call this evaluation method the second relative assessment method. By using the binary relative assessment method to evaluate the effectiveness of teaching experiment design in each university, universities with different basic conditions can be stimulated. Against the above background, this study focuses on the problems related to the experimental teaching evaluation system in the information technology environment.

2. Establish the General Index System and Participation Parameters

The research on teaching application of technology must go beyond the old idea of comparative experimental research with no benefit as mentioned above, and start from teaching system analysis to study the teaching function of technology products in normal teaching. At present, there are two main perspectives of teaching system analysis: one is to view the teaching system as a human behavioral system and analyze the behavior of students and the relationship between them; the other is to view the teaching system as an information system with specific functions, inferring the overall properties of teaching from the local characteristics of information flow and revealing the relationship between information flow and teaching functions [26]. The method of analyzing the teaching system from the perspective of behavioral system suffers from the defects of a complicated and confusing coding system, mechanical and arbitrary cut scores, weak interpretation of results, etc. Moreover, it mostly analyzes the external behavior of students and rarely involves technical elements, and even if the technical dimension is involved in the improved scale, it only judges whether a media is used at the operational level, but there is still no way to know what specific role the media information plays for teaching. In addition, understanding or describing the teaching system from the external verbal behaviors of teachers and students ignores the flow of knowledge and information behind the behaviors and fails to establish a link between teaching behaviors and teaching effects, and the research findings are neither supported nor real teaching guidance.

The IIS (Instructional Information Set) diagram analysis method focuses on the relationship between the marked information of IIS output by three types of information processing subjects, namely, teachers, students, and information media, in the teaching system and the teaching function, and infers the overall properties of teaching from the local characteristics of the information flow in these teaching processes. Here, the teaching system refers to a system of information flow among three types of information processing subjects, namely, teachers, students, and information media, which is essentially an information system composed of students, information media, and teachers and their input information and output information plus the IIS expressing socially shared knowledge set. The conceptual model of the teaching system is shown in Figure 1.

Information processing of teacher (IPT), Information processing of learner (IPL), and Information processing of media (IPM) represent the processing of information by teachers, learners, and information media, respectively. *{X}* and *{Y}* represent the input and output of their information processing processes. In the conceptual model, the information output Y from the three information processing subjects is extracted and structured as "input information items" with the representation format "<contributor> <operation> <information type> <representation form> <IIS subgraph> [<information quality>] [<content annotation>]" (as shown in Figure 2), and the set of information outputs Y is abstractly summarized as the Instructional Information Set IIS, which is used to characterize the shared nature of knowledge. Other elements that are not directly related to information processing are categorized as environmental elements of the instructional system, such as

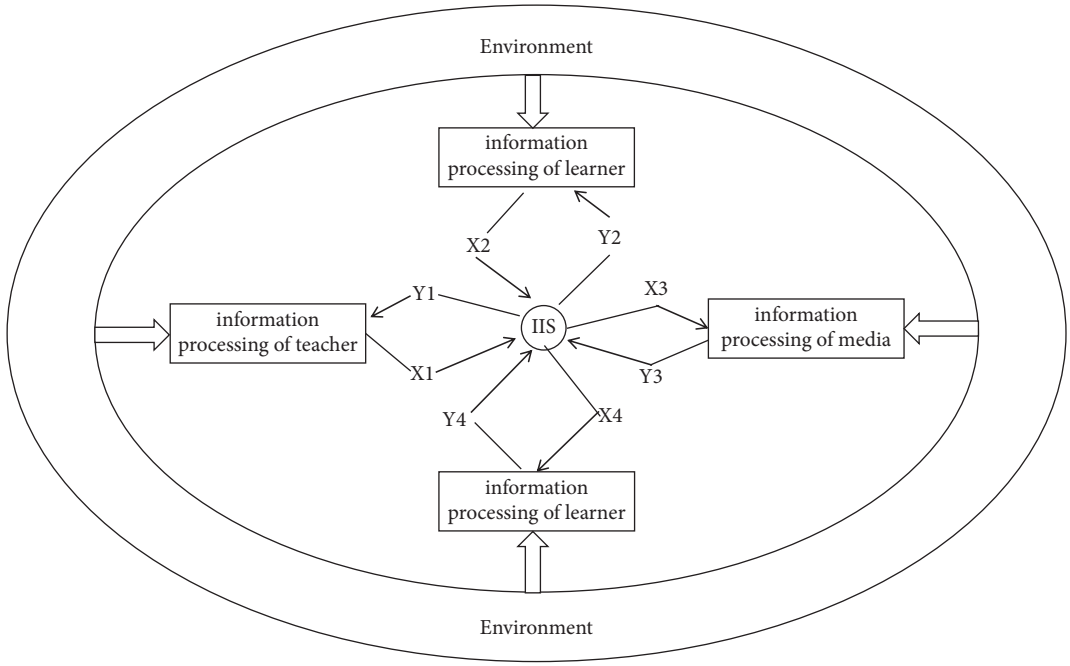

Figure 1: Conceptual model of general experimental teaching system.

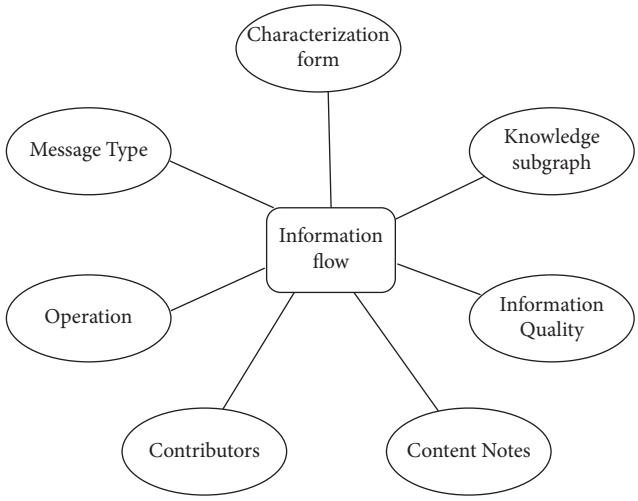

Figure 2: General representational structure of information flow for experimental teaching.

students' prerequisite knowledge skills, teacher-student relationships, and students' motivation levels. Environmental factors have an impact on the instructional system, but these impacts are ultimately expressed through externalized information output. The conceptual model of the instructional system reflects not only the relationship of information flow among three types of subjects: teachers, students, and information media, but also the contribution of this multi-subject information flow to social knowledge construction, which is reflected in the amount of activation of knowledge points by the information flow. The IIS diagram analysis method specifies that only the information flows of "answer," "knowledge semantics" and "factual examples" correspond to the IIS knowledge subgraphs, and only the information flows of Only the subgraphs containing IIS knowledge can contribute to the activation of knowledge points. Although the specific externalized behaviors or verbal information of teachers and students in the teaching process cannot be reproduced, the IIS knowledge subgraph behind the specific behaviors or information flow is an objective graph, and only the information flow that contains the IIS knowledge subgraph has value, and the specific expressions of the information flow have no essential influence on the operation results of the teaching system, so the teaching system in the sense of this information flow is reproducible. This reproducibility of the research object ensures the reproducibility and scientificity of the whole empirical study.

Research on the application of media technologies based on information flow analysis opposes the verification of the pedagogical effectiveness of technologies through comparative experiments and advocates the analysis of the actual pedagogical functions of specific technological products in the context of regular teaching [27]. Therefore, instead of interfering with teachers and students to deliberately use a certain technology in the teaching process, the researcher provides a variety of media technology choices and allows them to make their own trade-offs according to their needs, and then conducts an information flow analysis of the teaching activity process to determine in detail the real role of the selected technology product in the teaching process and the actual dependence of teaching on it [28].

Traditional experimental teaching methods are mostly validation experiments students rely on detailed laboratory handouts to guide each step of the experiment students carefully and cautiously operate inevitably to obtain the expected experimental data thus achieving verification of theoretical learning [29]. However, due to the limitations of

experimental conditions, time, consumption of equipment, equipment integrity, laboratory management, etc. students rely on the teacher's guidance and lack of active thinking, creative thinking, and research on experimental refutation thus the students are trained in experimental ability are less competent. The introduction of computer-assisted teaching with its multimedia, interactivity, and simulation makes the whole teaching process more active and efficient [30]. The use of computer simulation can facilitate the examination of students' design ideas repeatedly modified and optimized and also make many experiments that could not be realized in the laboratory in the past to obtain simulation effects. At the same time, the local area network of experiments, the intelligence, interactivity, and reliability of experimental instruments and virtual instruments to achieve student-oriented personalized teaching reduces the duplication of teachers' work and laboratory management workload makes open laboratories possible and also creates conditions for remote experimental teaching in distance education [31].

The key to the reform of experimental teaching is the reform of experimental teaching mode with students as the main body of the experimental teaching mode of the experimental process to design comprehensive. The design of comprehensive experiments requires students to have strong basic knowledge and wide knowledge with certain innovative abilities. Informatization experimental environment due to the large amount of experimental data storage, experimental program optional, high comparability, experimental data easy to analyze and calculate digital equipment to make the experimental data sampling easy to experiment in the system with a computer to facilitate rapid processing [32]. Based on the above information environment fully mobilizes the enthusiasm, initiative, and creativity of students in the experiments while also providing technical support for the student-led teacher-led experimental teaching design. Of course, to achieve the change of teaching mode must also have the practice and scientific evaluation of the experimental teaching process guided by the theory of learning-based instructional design and other educational technology.

3. Comprehensive Algorithm for Measuring the Validity of Experimental Instructional Design

Before teaching, interviews and questionnaires were conducted with database-related experts, teachers, and former students to understand the learning needs of the database course and to analyze the needs in order to prepare for conducting the effectiveness study. Based on this, we designed the teaching program and prepared the teaching materials according to the available technology and equipment. Then, the first phase of teaching "case study and collaborative web-based learning," i.e., "instructional design," was conducted. During the teaching process, changes and problems were recorded, and after the "instructional design" was completed, research was conducted to understand the effectiveness of the teaching at this stage by means of interviews and questionnaires. After analyzing the effectiveness of the teaching, the teaching plan is revised and adjusted, and the next stage, i.e., the "multimedia courseware production" stage, is carried out until the end of this stage of teaching. After all the teaching is finished, we summarize the whole teaching and research process and propose a model for analyzing the effectiveness of information technology teaching for undergraduates. The model is shown in Figure 3.

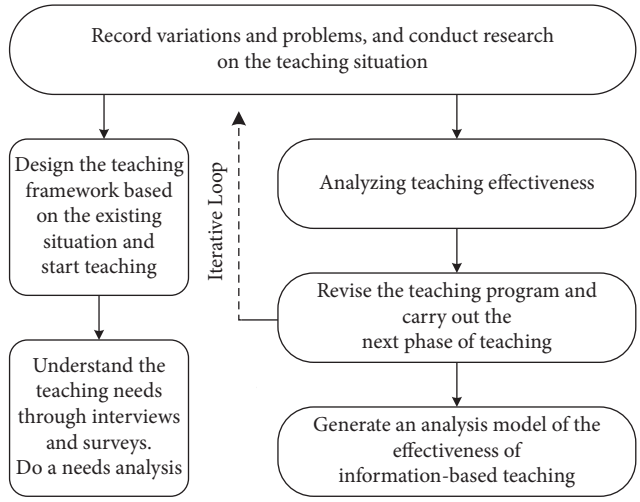

Figure 3: Framework for the implementation of data-based informational teaching experiment design.

In the study, the effectiveness of stage-specific teaching is mainly understood by means of questionnaires to find out the existing problems and analyze the effectiveness. The analysis of the effectiveness of informatization teaching should comprehensively examine the implementation effect of informatization teaching mode, the application of information technology, and the teaching process to see whether the teaching effect meets the purpose of teaching and whether it effectively promotes students' learning. Based on such considerations, this paper proposes the analysis model of information-based teaching effectiveness as shown in Figure 4 and uses it to analyze the effectiveness of information-based teaching on the basis of questionnaire survey. First, the purpose of teaching is determined according to the learning needs, and the teaching process is analyzed, mainly from examining two aspects: the information technology teaching model and the application of information technology. Then, we analyze what kind of teaching effect is produced after the teaching process and whether it conforms to the teaching purpose. There are many cases between the two extremes of fully conforming and not conforming at all, as shown by the double arrows in the figure. The author divides the teaching effect into five levels, and there are several cases between very effective and completely ineffective such as relatively effective, generally effective, and less effective.

Through the analysis of the effectiveness of experimental teaching, several main factors affecting the teaching effect were summarized: the knowledge and skill reserve before the experiment, the expected results and innovation of the

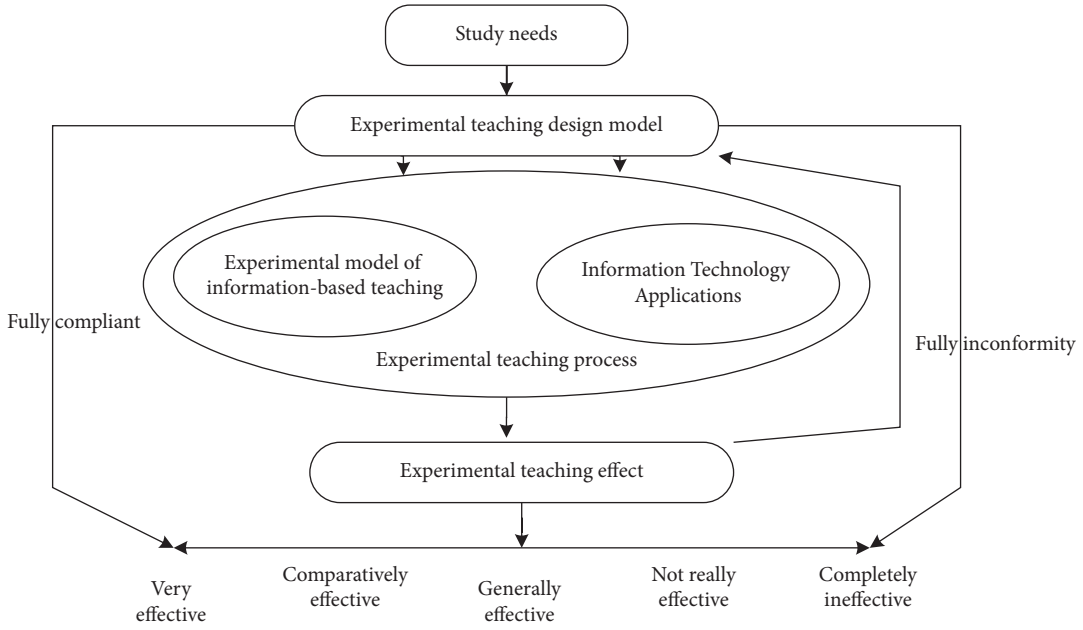

Figure 4: Analysis model of the effectiveness of information-based experimental teaching design.

Table 1: Findings on the factors influencing the effectiveness of information-based experimental teaching design.

	High impact (%)	Some impact (%)	No impact (%)	N/A (%)
Experiment content	62	26	12	0
Experiment management	4	45	39	12
Experiment results	60	29	10	1
Informational environment	18	25	57	0
Experiment knowledge and skill base	32	43	24	1

experiment, the content of the experiment, the experiment management, the information environment, etc. The specific contents and the results summarized by the questionnaire research are shown in Table 1:

At this point, traditional information technology effectiveness research has come to an end. However, innovative effectiveness measurement must be supported by data or models. Therefore, we reanalyze the data summarized above to come up with a more effective evaluation method. As mentioned in the introduction part of DEA, in this paper we will analyze and summarize the data from the survey results again by using the binary relative evaluations.

The binary relative evaluation method for the analysis of the effectiveness of experimental design teaching in colleges and universities was carried out in two stages. First, the previous and current composite indices of the effectiveness of experimental design teaching in each university are measured by using the hierarchical analysis method, and then they are regarded as input and output, respectively, and their binary relative evaluations are measured by using the data envelopment analysis method. When using the hierarchical analysis method to measure the composite index of the management effectiveness of each university, a system of indicators of the effectiveness of experimental design teaching in universities and selected weight parameters are established. The intent of this method is to establish the system of measuring the effectiveness of experimental teaching design in universities using the principles of system engineering and hierarchical analysis.

After the analysis of the above-mentioned survey results, some relatively important evaluation factors were determined, but due to the instability and limitation of the survey sample, we made a deeper weighting of the summarized influencing factors through the hierarchical analysis method. The specific method is derived from the following hierarchical analysis. The algorithm of the maximum characteristic root $\lambda_{\max}$ is shown in equation (1); the consistency index CI is shown in equation (2); the consistency ratio CR is shown in equation (3). The judgment matrix of A-B and the judgment matrix of B-C are shown in equations (4) and (5):

$$\lambda_{\max} = \sum_{i=1}^{n} \left[(AW)_i / nW_i \right], \tag{1}$$

where i is the i-th factor, A is the Judgment Matrix, W_i is the i-th weighting factor.

$$CR = (\lambda_{\max} - n)/(n-1). \tag{2}$$

The average random consistency index, RI, is obtained by taking the arithmetic mean of the eigenvalues of the random judgment matrix after several iterations of the calculation.

$$CR = CR/RI. \tag{3}$$

When CR < 0.1, the consistency of the A-matrix is generally considered to be acceptable.

$$A = \begin{bmatrix} 1 & 1 & 1 & \frac{1}{3} & \frac{1}{5} & \frac{1}{2} \\ 1 & 1 & 1 & \frac{1}{3} & \frac{1}{5} & \frac{1}{2} \\ 1 & 1 & 1 & \frac{1}{3} & \frac{1}{5} & \frac{1}{2} \\ 3 & 3 & 3 & 1 & \frac{1}{3} & 2 \\ 5 & 5 & 5 & 3 & 1 & 4 \\ 2 & 2 & 2 & \frac{1}{2} & \frac{1}{4} & 1 \end{bmatrix}, \tag{4}$$

where $\lambda_{\max} = 6.061, CI(6) = 0.012, RI(6) = 1.24, CR \approx 0.01$.

And the weighting factor is: $W = 0.074, 0.074, 0.074, 0.210, 0.438, 0.130$

$$B = \begin{Bmatrix} 1 & 7 & 3 \\ \frac{1}{7} & 1 & \frac{1}{5} \\ \frac{1}{3} & 5 & 1 \end{Bmatrix}, \tag{5}$$

where $\lambda_{\max} = 3.050, CI(3) = 0.025, RI(3) = 0.58, CR = 0.043$.

And the weighting factor is: $W = 0.649, 0.072, 0.279$

The final structural model and weight parameters of the index system for the effectiveness of experimental teaching design in universities using hierarchical analysis are shown in Figure 5.

In order to give a true reflection of the improvement of the management level of each university due to subjective efforts, each university with different basic conditions should have different reference standards, and the index of the effectiveness of experimental design teaching in each university measured by hierarchical analysis reflects to some extent their different basic conditions, so it can be used as a reference standard to measure the basic conditions of different universities, and we call it the reference index. The current index of the effectiveness of experimental design teaching in each university can also be measured by the hierarchical analysis method, and we call it the current index. We know that the level of experimental design teaching in each university can be fairly measured only in the dynamic change, so we introduce the concept of index state and possible set of index state.

Let x_i, y_j be the reference index and current index of the j-th college, respectively, and call the array (x_i, y_j) the index state of the jth college, called the convex set, T, as in (3)

$$T = \left\{ (x, y) \middle| \sum_{j=0}^{n} \lambda_j x_j \le x, \sum_{j=0}^{n} \lambda_j y_j \le y, \sum_{j=0}^{n} \lambda_j = 1, \lambda_j \ge 0, j = 0, 1, 2, \ldots, n \right\}, \tag{6}$$

where $(x_0, y_0 =) = 0$.

From DEA model [25], we obtain (4):

$$\begin{aligned} &Max\, Z, \\ &\sum_{j=0}^{n} \lambda_j x_j \le x_{j0}, \\ &\sum_{j=0}^{n} \lambda_j y_j \le y_{j0}, \\ &\sum_{j=0}^{n} \lambda_j = 1, \lambda_j \le 0, j = 0, 1, 2, \ldots, n. \end{aligned} \tag{7}$$

If the optimal value $Z^* = 1$, the university is said to be on the frontier of the set of possible exponential states T. So the binary relative evaluation N of the college can be derived from (5):

$$\eta = 1/Z^* \times 100\%. \tag{8}$$

As $1/Z^* = y/\overline{y}$, the binary relative evaluation represents the percentage of the current index of each university in the maximum current index that can be achieved under the same reference conditions.

4. Results

In this paper, the effectiveness of experimental design teaching in 15 universities from 2014 to 2017 was measured using the above-mentioned binary relative evaluation method. The selected data sources were "2014 National Compendium of Science and Technology Statistics of Higher Education Institutions" and "2018 National Compendium of Science and Technology Statistics of Higher Education Institutions" prepared by the Department of Science and Technology, Ministry of Education and published by Higher Education Press [33]. In order to protect the privacy of local schools and to comply with the relevant protocols, the abbreviated names of these universities are protected in this paper.

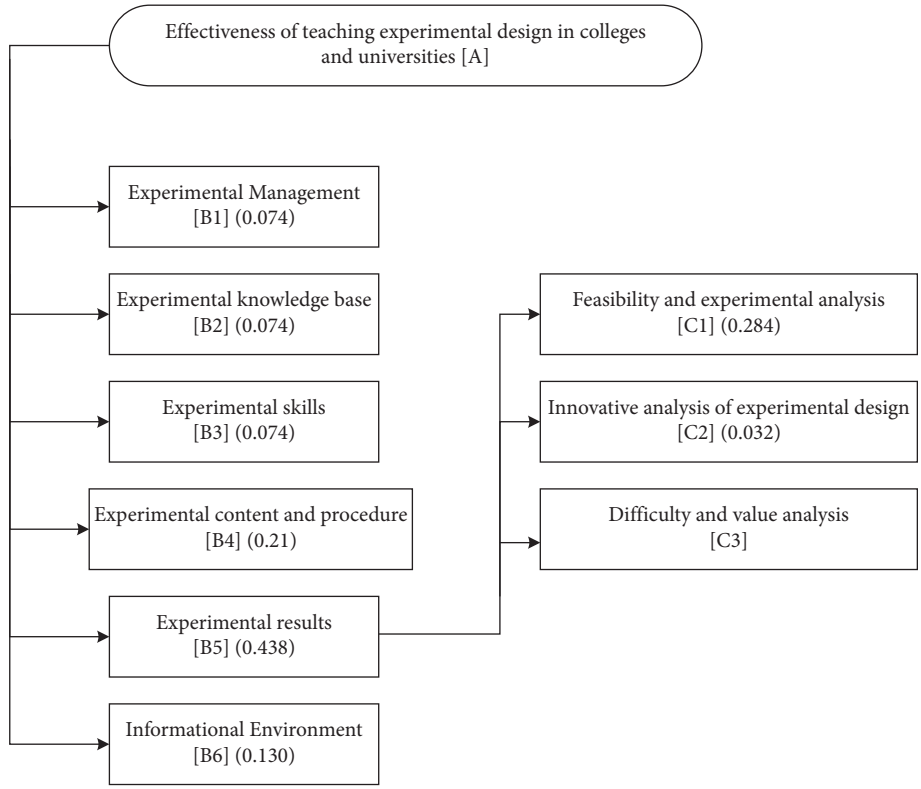

Figure 5: Hierarchical structure model and weight parameters of experimental design teaching effectiveness index system in colleges.

Table 2: Reference and current indices of binary relative evaluation of the effectiveness of experimental design teaching in 15 universities.

No.	College	2014 R.I.	2014 C.I. 2015 R.I.	2015 C.I. 2016 R.I.	2016 C.I. 2017 R.I.	2017 C.I.
1	H Technical University	1.0000	1.0000	1.0000	1.0000	1.0000
2	H University of Engineering	0.4277	0.1981	0.1935	0.3122	0.4301
3	D University of Petroleum	0.3840	0.3363	0.3365	0.3677	0.4163
4	A University	0.0573	0.0483	0.0564	0.0852	0.0751
5	H Polytechnic University	0.3722	0.3350	0.2786	0.3645	0.3655
6	H University of Architecture	0.1449	0.1725	0.2091	0.1720	0.2346
7	A School of Mining	0.0378	0.0830	0.0502	0.0435	0.0655
8	J University	0.1185	0.0544	0.0557	0.0908	0.0656
9	A University of Agriculture	0.0723	0.1235	0.0889	0.0800	0.0555
10	D University of Agriculture	0.1181	0.1080	0.1993	0.1688	0.1394
11	D University of Forestry	0.2110	0.1779	0.1873	0.1985	0.1609
12	H University of Medical Science	0.1450	0.2765	0.1945	0.2584	0.3193
13	A University of Chinese Medicine	0.0936	0.0130	0.1036	0.1809	0.2334
14	M School of Medicine	0.0267	0.0156	0.0147	0.0036	0.0037
15	Q School of Medicine	0.0189	0.0158	0.0153	0.0147	0.0097

However, due to the specificity of the related professions involved, the nature of the terms in the names of the schools is retained. For example, in this paper, the abbreviation of Harbin Institute of Technology, one of the leading industrial institutions in China, is coded as H Technical University. The results of the binary relative evaluation of the effectiveness of experimental design instruction in the 15 target universities in this paper are shown in Tables 2–4.

From the results, we can see that the schools with high binary relative values can be divided into two cases: one case is the schools with high reference index and current index, such as H Technical University. Medicine in 2015, and A University in 2016. The schools with a lower binary relative evaluation can also be divided into two cases: one is a school with a larger decrease in the current index, such as A University of Agriculture in

Table 3: Binary relative evaluation of the effectiveness of experimental design teaching in 15 universities.

College	Binary relative evaluation value			
	2014	2015	2016	2017
H technical University	1.0000	1.0000	1.0000	1.0000
H university of Engineering	0.3841	0.6906	1.0000	1.0000
D University of Petroleum	0.7025	0.8324	0.8469	0.8744
A University	0.4086	0.4053	0.8651	0.6152
H Polytechnic University	0.7147	0.6912	0.9473	0.7720
H University of Architecture	0.6243	0.8130	0.5284	0.9781
A School of Mining	1.0000	0.2883	0.4963	1.0000
J University	0.2379	0.3883	0.9336	0.5059
A University of Agriculture	0.8501	0.7170	0.5154	0.4825
D University of Agriculture	0.4738	1.0000	0.5322	0.5919
D University of Forestry	0.5353	0.4148	0.6548	0.5834
H University of Medical Science	1.0000	0.5548	0.8254	0.8939
A University of Chinese Medicine	0.0708	1.0000	1.0000	0.9264
M School of Medicine	0.2661	0.1384	0.1403	0.6826
Q School of Medicine	0.3807	0.1438	0.5502	0.4382

Table 4: Ranking of the binary relative evaluation of the effectiveness of experimental design teaching among the 15 universities.

College	Ranking			
	2014	2015	2016	2017
H Technical University	1	1	1	1
H University of Engineering	9	6	1	1
D University of Petroleum	4	2	5	5
A University	8	9	4	8
H Polytechnic University	3	5	2	6
H University of Architecture	5	3	10	2
A School of Mining	1	11	12	1
J University	12	10	3	11
A University of Agriculture	2	8	11	12
D University of Agriculture	7	1	9	9
D University of Forestry	6	4	7	10
H University of Medical Science	1	7	6	4
A University of Chinese Medicine	13	1	1	3
M School of Medicine	11	13	13	7
Q School of Medicine	10	12	8	13

2017, and the other is a school with a lower reference index and a lower current index, such as M School of Medicine and Q School of Medicine.

5. Conclusion

A teaching process without an evaluation system is unscientific and unlikely to succeed in experimental teaching as well. The study of a more complete, comprehensive, and operational evaluation system is the urgent need for the development of experimental teaching in the information technology environment to improve the quality of experimental teaching testing standards. The scientific evaluation system should be both a certain standard requirements and to meet the actual situation of an evaluation system needs time to establish and improve the need for continuous improvement and development in practice. With the implementation of the evaluation system application evaluation system will continue to be modified and improved. Higher education laboratory courses due to different professional disciplines experimental content is also different according to the characteristics of the discipline can be applied as above evaluation system.

By using design-based research paradigm to study the effectiveness of informatization teaching, researchers and teachers have a deeper understanding of the factors affecting the effectiveness of informatization teaching. It has some significance to grasp the law of informatization teaching and better use information technology in teaching practice to promote the development of informatization teaching and education informatization. The science of information flow analysis itself is the foundation of teaching analysis research. If information flow analysis is combined with teaching behavior analysis and social network analysis, it must be able to analyze teaching activities in an all-round way.

The strengths of the assessment method described in this paper are: first, it enables students with various characteristics to have the opportunity to be recognized and encouraged because human intelligence is diverse and each student has his or her own superior intelligence; second, it conveys the important idea that learning is complex and that key learning outcomes usually have multiple manifestations and require different skills to be fully demonstrated; and finally, when using performance-based assessment and authentic assessment, it helps to stimulate students' interest and engagement in learning. Improving outcome assessment, strengthening process assessment, exploring value-added assessment, and sound comprehensive assessment necessarily rely on multidimensional assessment methods. It should be clear that the most important concern is the quality, not the quantity, of assessment, and that it is not better to use more assessment methods for a particular concept to be assessed, but rather to choose the assessment methods that match the purpose of the assessment as much as possible. This principle needs to be strictly observed when selecting assessment methods, taking into account the type of learning objectives and their characteristics.

To make the evaluation results highly reliable and comparable, the key issue is to develop a scientific and feasible quantitative index system. When constructing the evaluation index system of information-based teaching, we can draw on the more mature evaluation index systems of other disciplines, then combine the characteristics of computer-assisted teaching to select evaluation indexes, and determine the weight of each index according to its role in teaching, so that the indexes play an objective and comparable role in the process of quantification. At the same time, when selecting the indicators, we should pay attention to the fact that there should not be too many or too few indicators. Too many evaluation indicators are not easy to operate, and too few indicators are not differentiated enough. Therefore, the index system should be improved continuously in teaching practice to avoid the overlapping of index factors and repeated weighting, so that it can be more suitable for the needs of teaching evaluation.

In summary, it can be seen that the reference index is used as the reference standard for the experimental design and teaching effectiveness of colleges and universities. It is more appropriate to use the binary relative evaluation value as an indicator of the effectiveness of the experimental design teaching in various colleges and universities. This can eliminate the injustice to evaluate the effectiveness of experimental design teaching in colleges and universities due to the quality of objective basic conditions. Thus it truly reflects the management effect produced by people's subjective efforts. In addition, the method of binary relative evaluation is used to calculate the effectiveness of experimental design teaching in all colleges and universities.

Data Availability

The dataset can be accessed upon request.

Conflicts of Interest

The authors declare that there are no conflicts of interest.

References

[1] H. Posadas and E. Villar, "Using professional resources for teaching embedded SW development," *IEEE Revista Iberoamericana de Tecnologias del Aprendizaje*, vol. 11, no. 4, pp. 248–255, 2016.

[2] H. Xie, K. Liang, X. Jiang, K. Chen, G. Wang, and K. Xie, "Study on reform of electronic technology experimental teaching under background of 'new engineering," *International Journal of Education*, 2021.

[3] G. Brandhofer and M. Miglbauer, "Digital competences for teachers - the Digi.Kompp model in an international comparison and in the practice of Austrian teacher training," *International Journal of Education*, 2020.

[4] X. Geng, L. Shen, Y. Deng, and L. Lin, "Discussion on the Talent Training of Universities with Industry Characteristics from the Perspective of Courses," *International Journal of Education*, vol. 8, 2020.

[5] C. J. Roettger, L. O. Roettger, and F. Walugembe, "Teaching: More than Just Lecturing," *Journal of University Teaching & Learning Practice*, vol. 4, 2007.

[6] A. A. Tzacheva and A. Easwaran, "Emotion Detection and Opinion Mining from Student Comments for Teaching Innovation Assessment," *International Journal of Education*, vol. 9, 2021.

[7] J. D. Karpicke and H. Roediger iii, "Repeated retrieval during learning is the key to long-term retention," *Journal of Memory and Language*, vol. 57, no. 2, pp. 151–162, 2007.

[8] K. Kampourakis, R. Duschl, H. Schweingruber, and A. Shouse, "R. Duschl, H. Schweingruber, and A. Shouse: taking science to school: learning and teaching in grades K-8," *Science & Education*, vol. 22, no. 5, pp. 1265-1266, 2013.

[9] F. I. M. Craik and E. Tulving, "Depth of Processing and the Retention of Words," *Journal of Experimental Psychology: General*, vol. 104, 1975.

[10] J. D. Karpicke and H. L. Roediger, "The critical importance of retrieval for learning," *Science*, vol. 319, no. 5865, pp. 966–968, 2008.

[11] H. Pashler, D. Rohrer, N. J. Cepeda, and S. K. Carpenter, "Enhancing learning and retarding forgetting: choices and consequences," *Psychonomic Bulletin & Review*, vol. 14, no. 2, pp. 187–193, 2007.

[12] H. L. Roediger and J. D. Karpicke, "Test-enhanced learning," *Psychological Science*, vol. 17, no. 3, pp. 249–255, 2006.

[13] M. A. Pyc and K. A. Rawson, "Testing the retrieval effort hypothesis: does greater difficulty correctly recalling information lead to higher levels of memory?" *Journal of Memory and Language*, vol. 60, no. 4, pp. 437–447, 2009.

[14] J. D. Novak, "Results and implications of a 12-year longitudinal study of science concept learning," *Research in Science Education*, vol. 35, no. 1, pp. 23–40, 2005.

[15] M. Fleer, "Understanding the dialectical relations between everyday concepts and scientific concepts within play-based programs," *Research in Science Education*, vol. 39, no. 2, pp. 281–306, 2009.

[16] Y. Jiang and X. Jin, "Using k-means clustering to classify protest songs based on conceptual and descriptive audio features," in *Culture and Computing*, pp. 291–304, 2022.

[17] Y. Jiang, X. Jin, and Q. Deng, *Short Video Uprising: How # BlackLivesMatter Content on TikTok Challenges the Protest Paradigm*, 2022.

[18] J. Kittur, "Measuring the programming self-efficacy of electrical and electronics engineering students," *IEEE Transactions on Education*, vol. 63, no. 3, pp. 216–223, 2020.

[19] J. K. L. Leung, S. K.-W. Chu, T.-C. Pong, D. T. K. Ng, and S. Qiao, "Developing a Framework for blended design-based learning in a first-year multidisciplinary design course," *IEEE Transactions on Education*, vol. 65, no. 2, pp. 210–219, 2022.

[20] D. M. Lee, "Enhancing research quality through analytical memo writing in a mixed methods grounded theory study implemented by a multi-institution research team," in *Proceedings of the 2019 IEEE Frontiers in Education Conference*, pp. 1–7, IEEE, Covington, KY, USA, October 2019.

[21] L. Yan, X. Jin, and Y. Zhang, "Effects of virtual reality technology in disaster news coverage based on MAIN model," in *HCI International 2022 Posters*, pp. 122–129, 2022.

[22] J. Rohde, L. Musselman, B. Benedict et al., "Design experiences, engineering identity, and belongingness in early career electrical and computer engineering students," *IEEE Transactions on Education*, vol. 62, no. 3, pp. 165–172, 2019.

[23] H. Fan, X. Wu, R. Ghannam, Q. Feng, H. Heidari, and M. A. Imran, "Teaching embedded systems for energy harvesting applications: a comparison of teaching methods adopted in uestc and kth," *IEEE Access*, vol. 8, pp. 50780–50791, 2020.

[24] A. L. Campbell, I. Direito, and M. Mokhithi, "Developing growth mindsets in engineering students: a systematic literature review of interventions," *European Journal of Engineering Education*, vol. 46, no. 4, pp. 503–527, 2021.

[25] A. Charnes, W. W. Cooper, B. Golany, L. Seiford, and J. Stutz, "Foundations of data envelopment analysis for Pareto-Koopmans efficient empirical production functions," *Journal of Econometrics*, vol. 30, no. 1-2, pp. 91–107, 1985, https://doi.org/10.1016/0304-4076(85)90133-2.

[26] J. W. Pellegrino, N. Chudowsky, and R. E. Glaser, *Knowing what Students Know: The Science and Design of Educational Assessment*, National Academies Press, 2001.

[27] D. D. Dsouza, D. Nayak, and E. J. Machado, "Sentimental Analysis of Student Feedback Using Machine Learning Techniques," *International Journal of Recent Technology and Engineering*, vol. 8, 2019.

[28] C. D. Barnes, P. Kohler-Evans, and R. A. Wingfield, "Are we effectively teaching today's college student?" *International Journal of Education*, vol. 8, 2020.

[29] X. Geng, "Discussion on large-scale online education practices amid the novel coronavirus outbreak," *International Journal of Education*, vol. 8, 2020.

[30] W. L. McCarty, S. R. Crow, G. A. Mims, D. E. Potthoff, and J. Harvey, "Renewing Teaching Practices: Differentiated Instruction in the College Classroom," vol. 6, 2016.

[31] M. Miron, "Students' evaluation and instructors' self-evaluation of university instruction," *Higher Education*, vol. 17, no. 2, pp. 175–181, 1988.

[32] J. D. Novak, "The promise of new ideas and new technology for improving teaching and learning," *Cell Biology Education*, vol. 2, pp. 122–132, 2003.

[33] M of E of the P R C, *Compendium of Science and Technology Statistics for Higher Education Institutions*, Higher Education Press, Beijing, 2020, 2018.

Hindawi
Scientific Programming
Volume 2022, Article ID 2120264, 9 pages
https://doi.org/10.1155/2022/2120264

Research Article

Research on the Optimization of International News Communication Teaching Mode Based on Cluster Analysis under the Background of Big Data

Yu Cheng and Zongyi Zhou

Rajamangala University of Technology Rattanakosin, 96 Phutthamonthon Sai 5 Road, Salaya, Phutthamonthon District, Nakhon Pathom 73170, Thailand

Correspondence should be addressed to Yu Cheng; cheng.yu@rmutr.ac.th

Received 21 June 2022; Revised 12 July 2022; Accepted 18 July 2022; Published 29 August 2022

Academic Editor: Lianhui Li

With the rapid development of the Internet, the new and advanced teaching mode is becoming increasingly popular, which has become a focus in the field of education in recent years. Therefore, the research and development of online teaching platforms have become a hot topic. This article takes international news communication as the research background, aiming at the unclear existing level and weak target. The teaching mode of the single teaching form puts forward the "embedded online intelligent teaching platform." A set of online innovative teaching platforms for large embedded systems is studied and established. The improved clustering analysis uses the GBKM clustering analysis algorithm to integrate grid clustering and K-means clustering and introduces the new meshing algorithm and the new function to calculate the density threshold. Through theoretical analysis and experimental verification, the superiority of the GBKM algorithm is demonstrated. As the GBKM clustering analysis algorithm is the core algorithm of a personalized smart learning system, it is applied to an online intelligent teaching platform. The experimental results show that the teaching effect of the optimized teaching mode is significantly improved.

1. Introduction

In October 2018, the Ministry of Education of China and the Propaganda Department of the Central Committee of the Communist Party of China issued "Opinions on Improving the Training Ability of Journalism and Communication Talents in Colleges and Universities and Implementing the Education and Training Plan 2.0 for Excellent Journalism and Communication Talents," strengthening and improving the construction of international journalism and communication in colleges and universities; building first-class global journalism and communication specialty with Chinese characteristics and world level; fully implementing the fundamental task of moral education; educating people with the theory of socialist journalism with Chinese characteristics; and cultivating a large number of high-quality all-media compound expert news communication reserve talents with national feelings and global vision [1].

Foreign scholars believe that teachers with news work experience must undertake international news communication teaching activities, and experienced teachers must guide students. Educators continue to work hard to cope with the transformation of the media industry, and journalism students in grades 2 and 3 of the University of Missouri have their newspapers in a real community work club [2]. In recent years, foreign news colleges and universities have paid particular attention to data journalism education. From "number one" to "visual first," news technology has changed continuously, rapidly changing the media pattern, and even the flagship store of the New York Times is trying to keep up with the trend of the times [3].

The traditional theoretical classroom still dominates the shaping of college students' journalism concept in China.

Domestic scholars have new thoughts on the whole journalism discipline [4]. Some theories of journalism have not adapted to the reality of media diversification, function diversification, and structure diversification. Re-understanding the media and communication will become the key to the teaching and research of news communication [5]. Journalism must make changes in two aspects. Firstly, journalism should not only open up new research fields but also break through the original professional and disciplinary restrictions; learn from and accommodate the research results, research methods, and theoretical systems of other disciplines; and achieve interdisciplinary integration [6]. Secondly, news colleges need to break through the teaching framework of mass communication; adjust the training scheme of news students; and change the curriculum system, teaching mode, and target orientation [7].

Throughout the international journalism and communication professional teaching mode, too old teaching model is not in line with China's national conditions, so they continue to propose new models. This article presents the "personalized intelligence" teaching model—implementing an embedded online intelligent teaching platform. By offering an improved GBKM clustering analysis algorithm, a new meshing algorithm, and a new function to calculate the density threshold, the GBKM clustering analysis algorithm is applied to the online intelligent teaching platform. In this article, a personalized, innovative learning system is designed. The GBKM clustering analysis algorithm is the core performance analysis algorithm. The students' personality characteristics are obtained by clustering analysis of students' performance records. According to the analysis results, the personalized intelligent learning system provides a personalized learning guide for students and achieves a satisfactory' personalized intelligence' teaching effect. Through theoretical analysis and experimental proof, the superiority of the GBKM algorithm is demonstrated, and the clustering process has achieved good results.

2. GBKM Clustering Analysis Algorithm

K-means is one of the most widely used clustering analysis algorithms and is a classical algorithm to solve the clustering problem [8, 9]. Because of the shortcomings of excessive dependence on the initial clustering center point of k and because of the large amount of computation, it is not efficient in time. At present, there are many improvements to the K-means algorithm. For example, the efficiency of grid clustering algorithms such as the K-means based on genetic algorithm, the K-means with penalty factor, and the PBKP algorithm is very high, and clusters with arbitrary shapes can be found. However, there are also various defects in grid clustering. For example, it depends on the selection of the density threshold. At present, there are many improved grid clustering algorithms, such as bipartite grid clustering, adaptive grid clustering, GCHL, etc [10, 11].

In view of the shortcomings of the above algorithms, this article proposes an improved clustering analysis algorithm based on their advantages. GBKM clustering analysis algorithm has achieved satisfactory results through data testing and its application to practical systems.

2.1. Basic Concepts of Algorithm. If $A = (D_1, D_2, \ldots, D_n)$ is n bounded domains, then $S = D_1 \times D_2 \times \cdots \times D_n$ is an n-dimensional space, and $D_1, D_2, \ldots, D_n$ is regarded as the dimension of S. The algorithm's input is a set of points in n-dimensional space, defined as $V = \{v_1, v_2, \ldots, v_n\}$, where $v_1 = \{v_{i1}, v_{i2}, \ldots, v_{\text{in}}\}$ represents the i-point. $v_{ij} \in D_j$ represents the j-dimensional component of the i-point [12].

Definition 1. Network unit

Assuming that the value on the i dimension is in the interval $[l_i, h_i]$, $i = 1, 2, \ldots, n$ each size is divided into p disjoint left-closed and right-open equal-length intervals, so the data space is divided into p'' grid cells. The length of the grid element on the i dimension is $\delta_i = ((h_i - l_i)/p)$, and the j interval on the i dimension can be obtained by the following formula:

$$I_{ij} = [l_i + (j-1)\delta_i, l_i + j\delta_i], \quad j = 1, 2, \ldots p. \tag{1}$$

Definition 2. Grid unit density

The density $Den\ (\ C_i\ )$ of the cell C_i is defined as the number of data points in the cell.

Definition 3. Density threshold

Set the density threshold *Minpts*, the grid whose density is greater than the density threshold *Minpts* is "dense unit," and the data in the unit whose density is less than the density threshold is "free data."

Definition 4. Cluster focus

Given the cluster $K_i = (t_{i1}, t_{i2}, \ldots, t_{\text{in}})$, the mean cluster center is defined as

$$Z_i = \left(\frac{1}{n_i}\right) \sum_{x,y \in K_i} (x, y)^2, \tag{2}$$

where n_i is the number of objects in cluster K_i, and x and y are pairwise different objects in cluster K_i.

Definition 5. Intermediate clustering

The sample space is divided, the unit grid set is defined, the density of the grid unit is calculated, and a grid clusters the dense team. This process, called intermediate clustering, only contains densely distributed points and does not contain all the books. The cluster generated by intermediate clustering is called a medium clustering cluster.

Definition 6. Postclustering

After the intermediate clustering, the center of each medium cluster is calculated as the initial center point, and then the remaining accessible data are K-means clustering. This process is called postclustering, and the clusters are called postclustering clusters.

2.2. The Basic Idea of the Algorithm. Firstly, based on grid clustering analysis, the sample space is divided, and the grid cell set is defined. The object is mapped to the corresponding grid cell, and the density of the grid cell is calculated. The unit with thickness is more incredible than the density threshold r, and the data with a density less than the density threshold r are marked. The adjacent dense units are merged to form an "intermediate cluster," which does not contain discrete free data. It calculates the center of gravity of the middle group as the initial cluster center [13], calculates the distance between free data and each cluster center, and the accessible data are assigned to the nearest intermediate cluster to form the "postcluster." The initial clustering center of each postclustering is recalculated. The algorithm terminates if there is no change; if there is a change, the clustering is repeated until the clustering conditions are met [14].

Grid definition itself is a complex problem. Grid size and placement have a significant impact on the clustering results. How to divide the grid is of great significance to the advantages and disadvantages of the algorithm. In the GBKM algorithm, a new function is introduced for meshing: $\delta = ((\sum_{i=1}^{n} \sqrt{l_i})/n)$ and li are the lengths of the i component, $i = 1, 2, \ldots, n$.

At the same time, grid-based clustering is very dependent on the selection of density threshold τ. Too large or too small τ will affect the algorithm's performance. A new algorithm is proposed for determining the density threshold in the GBKM algorithm: Minpts = $([\sum_{i=1}^{N} \mathrm{Den}(C_i)^2]^{(1/2)}/N)$, where $\mathrm{Den}(C_i)$, $i = 1, 2, \ldots, N$ is the density value of N dense units with the highest density [15]. The value of N depends on the specific data. In general, $\mathrm{Den}(C_i)$ is arranged in descending order. If $\mathrm{Den}(C_i)$ display density has a significant jump, then $N = I$.

2.3. Steps of the Algorithm. According to a description of the basic idea, the basic steps are as follows:

Step 1: Divide the data space into m disjoint, equal-length grid cells and define the grid cell set;

Step 2: Assign the object to the appropriate unit;

Step 3: Calculate the density of each unit;

Step 4: Mark the grid with a density more remarkable than the density threshold *Minpts* as "dense unit," and mark the data in the division with thickness less than the density threshold as "free data."

Step 5: Repeat any dense unit that is not clustered, merge its adjacent thick units into a cluster until all wide units are clustered to form K "intermediate clusters";

Step 6: Calculate the center of gravity $Z_i^{(1)}$ of the K intermediate clustering as the initial clustering center;

Step 7: Repeat any accessible data object, calculate the distance between $\mathrm{dis}(x_i, C_i)$ and k initial clustering centers, where x is the accessible data object, C_i is the first class, if $\mathrm{dis}(x, C_i)$ is the smallest, then $x \in C_i$; until no longer exists free data, forming "postclustering";

Step 8: Recalculate the center of gravity of the clustering $Z_i^{(1)}$, if $|Z_i^{(1)} - Z_i^{(0)}| \le \varepsilon$, the clustering ends. Otherwise, continue K-means clustering until $|Z_i^{(i+1)} - Z_i^{(i)}| \le \varepsilon$ completes clustering.

2.4. Implementation of the Algorithm. The GBKM algorithm is written in Java language, and the editing environment is Eclipse. Eclipse is an open-source extensible application platform which provides a first-class Java integrated development environment for programmers [16]. The implementation of the algorithm is mainly divided into six parts. The first part defines various variables, methods, and classes, among which the most important is to define a public class cluster class, which describes the cluster generated by the clustering process, including the variable of cluster members, the variable of cluster centroid, and the method of updating the cluster centroid. The second part is the definition of the GetData (int cid, int analysis) method, the function of this method is to read data from the database and store it in the array folder after initialization; the third part is the definition of Grid () method. The function of this method is to divide the data space into grids and map the data objects to the Grid one by one. The fourth part is the method of clustering process preCluster (). The fifth part is the method of storing and displaying the clustering results. The sixth part is the main program entry (), which mainly generates the object of the above class and then calls the method of the thing to realize the whole clustering process.

3. International News Communication Intelligent Teaching Optimization

The development of an embedded network intelligent teaching system platform plays a good role in solving embedded professional theory teaching and market demand-oriented application teaching mode optimization. It can quickly improve embedded talents' training effect and efficiency and solve the bottleneck of market demand for skills. At the same time, it is of great significance to the research and development of international news communication teaching platforms.

3.1. Development Tools and Models

3.1.1. Development Tools. The system used JSP (Java Server Pages) technology framework to generate dynamic, interactive web server applications. JSP technology is the traditional web HTML file (*.htm, *.html) into the Java program segment (scriptlet) and JSP tags, resulting in a JSP file (*.jsp). JSP uses tags and scriptlets to encapsulate the processing logic that generates dynamic web pages, accesses the application logic of resources existing in the server, and separates the web logic from the web design and display. It supports the reusable component-based design and makes developing web-based applications rapid and easy [17].

The web server of this system uses Tomcat 5.0 as a Servlet container, which passes page requests to Serverlets and returns the results to users. When a user requests access to a

Servlet, it encapsulates the user's request information in the ServletRequest object, then passes the Request object and Response object to the Servlet requested by the user, and the Servlet writes the results of the response to the ServletResponse object. Then Tomcat transmits the response results to the user.

SQL Use server 2000 is d in the background database, and JavaBean is used to connect the database and query and update the data. Using advanced B/S (Browser/Server) architecture, page design uses the current international popular web production tool Dreamweaver 2004 and EditPlus for editing; the script language is JavaScript; page image processing uses PhotoshopCS and Flash 5.0.

3.1.2. Development Model. This system is composed of people and computers for information collection, storage, knowledge transfer, and use. With the development of science and technology, the expansion of information, and the explosion of knowledge, how to effectively collect information and transfer knowledge has become the development purpose of this system. Therefore, it is imperative to develop a plan that considers the development and operation efficiency and meets the asynchronous real-time processing function. The development of this system uses the MVC model. MVC pattern is the abbreviation of "Model-View-Controller," translated into Chinese as "Pattern-View-Controller." That is, an application's input, processing, and output processes are divided into three layers according to model, view, and controller, namely a model layer, a view layer, and a control layer.

View represents the user interaction interface. For web applications, it can be summarized as an HTML interface. An application may have many different views. The processing of the MVC design pattern for a view is limited to collecting and processing data on the view and the user's request, but not the processing of business processes on the view. Handling of business processes is handed over to model processing. Model is the processing of business processes/states and formulating of business rules. The model accepts the data requested by the view and returns the final processing results. Model design is the core of MVC. When receiving requests from the user, the model is matched with the view and the user's request together without any data processing is completed. The separation of model, view, and controller enables a model to have multiple display views. If the user changes the model's data through a view controller, all views that depend on these data will change. When data changes, the controller notifies all views of the change. Models, ideas, and controllers are updated synchronously according to their relationships and primary functions [9].

The view is in the web tier or client tier in this system. That is, JSP is the page display part. A controller is also in the web tier, implemented by Servlet, the logic part of page display. The model is in the middle tier, implemented with JavaBean on the server side, and implementing logical relationships, as shown in Figure 1.

3.2. Design and Implementation of a Resource Center. As a learning website, providing students with as many learning materials and software download as possible is the proper service function of the website. The resource center module of this website includes nine submodules, as shown in Figure 2: search module, e-book module, curriculum resource module, software download module, learning material module, free resource area module, the latest resource area module, the hottest resource area module, and other resource areas.

Based on the above module system diagram:

Search module: the user inputs keywords, and the system will display the matching records in the database according to fuzzy matching.

Electronic book module: provides users free downloads of electronic books, such as PDF, superstar, and other formats, covering all aspects of embedded learning.

Curriculum resource module: it lets users download free courses or other courses produced by this website. With the curriculum resource center, students can easily find free learning courseware.

Software download module: Module more professional in the embedded aspect can obtain the professional information common download site that does not provide..

Updated resource area: the resources provided by this area are the latest with the help of this website.

Learning material module: the module mainly provides students with more whole, suitable learning materials, such as related technology frontier articles, excellent students' learning notes, etc.

Free resource area: this area provides free downloads to students.

The hottest resource zone: the zone aims to make the most popular resources present in a unique position on the website so that students can understand the current trend of resources.

Other resource areas: it lets users download a window of resources other than free, up-to-date, and hottest resources to display the site's resources more fully on the page.

According to the above description, the logical function of the resource center is clear. First, users select the module after entering the resource center, view the resource information, and then download it online, which can also view the resource's relevant resources and the website's outstanding recommendations.

4. Case Study

One of the main applications of improved clustering analysis algorithms is the personalized intelligent learning system of embedded online innovative teaching platforms. GBKM clustering algorithm is used to cluster the students' scores. According to the clustering analysis results, different learning plans and suggestions are given for international students. At the same time, the results of the analysis are transmitted to the intelligent test paper generation system. The system changes the structure of the following examination paper of the students, truly achieves "individualized teaching", improves the intelligence of the website, and truly

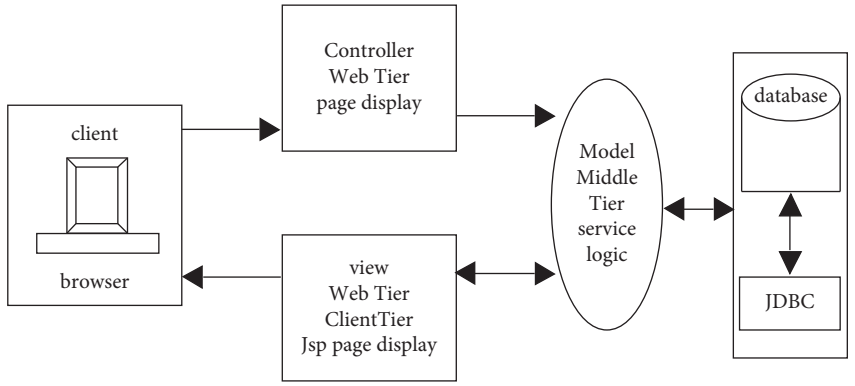

Figure 1: The design of the model.

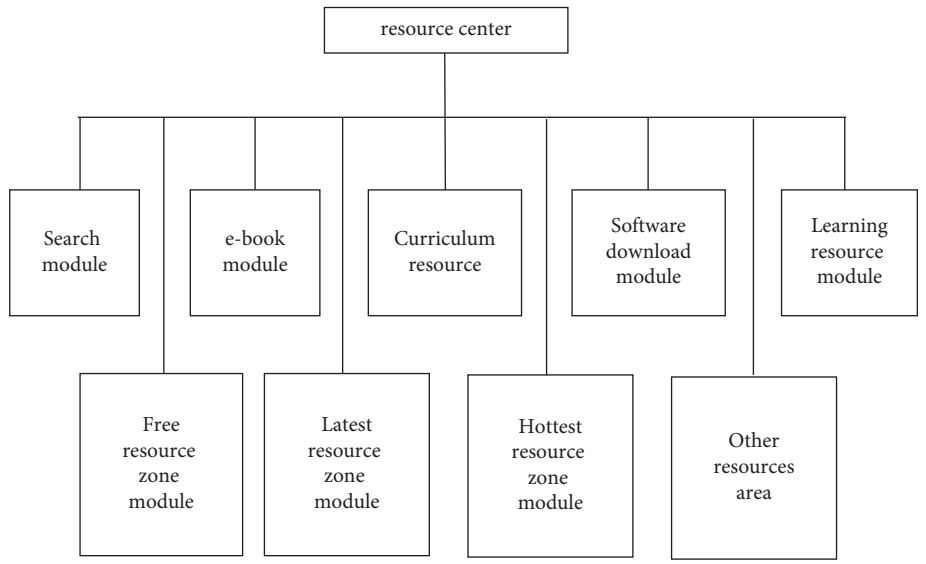

Figure 2: The module system of resource center plans.

realizes the "personalized" and "intelligence" of online teaching.

The page display of performance analysis is designed in JSP and CSS style. GBKM algorithm uses Java to compile JavaBean file from Eclipse environment and calls this bean file by JSP page.

In the specific application of the performance analysis system, the GBKM clustering algorithm not only completes the primary function of clustering the relevant data but also completes the analysis of the characteristics of the cluster formed after clustering and how to display it on the page. At the same time, it stores the analysis results in the corresponding database table. The related database table records are updated, such as updating the proportion of each chapter in the testStru table CHAPTERSCORE. For subsequent use, after completing the clustering and analyzing the characteristics of the cluster, the analysis of students' personality characteristics and the display of various learning suggestions are realized on the JSP page.

Calling a bean file in Jsp is done by introducing the package util where the bean file resides. The specific presented method:

When calling, a GetData object is created in the analysis package and the object is instantiated. Then call various methods in GetData class are called to implement multiple mechanisms. The code segment is as follows:

```
analyse.GetData gbkm = new analyse.GetData (cido,ido);
gbkm.GetDatal ();
gbkm.Grid(); System.out.println ("main");
gbkm.preCluster(); gbkm.getPreCluster();
out.print (gbkm.ShowOut());
```

The realization of viewing the previous performance analysis results mainly depends on the analysis of the performance analysis result record table. The USERID, COURSE ID, and TEST TIME fields in the table store the student's latest test time for a specific course. These three fields are consistent with the three fields of USERID, COURSE ID, and TEST TIME in the test history information table. The three fields uniquely identify the analysis results of the previous test and obtain the values of these three fields in the JSP page of analysis. The last examination

Table 1: Structure of examination paper table.

Field name	Field ID section	Property	Length	Pkey	Null
Serial number	ID	Int	4	O	O
Course number	SUBJECTID	Int	4		
Category name	STRUTEXT	Varchar	100		
Total number of sections	CHAPTERNUMBER	Char	3		
Chapter scores	CHAPTERSCORE	Varchar	50		

results can be viewed for study and reference by calling the corresponding records in test history.

4.1. Database Table Design. This section mainly introduces the database table design involved in the personalized intelligent learning system, including the test paper structure table, the score analysis result record table, and the test history information table.

Table 1 is the test paper structure table, identified as testStru, and the data source is the change and addition of the background paper structure. This table mainly controls the composition structure of the test paper. CHAPTERSCORE is the proportion of each chapter in the intelligent test paper generation. According to the value of this field, the savvy test paper generation can adjust the structure of the test paper obtained by each savvy test paper generation, namely the proportion of each chapter.

Table 2 is a record of the performance analysis results, which is identified as analysis. The data source is updated after the performance analysis. It records the course number and examination time of the students' last performance analysis, mainly for calling the corresponding information when the students want to view the results of the previous research.

Table 3 is the test history information table identified as test history. The data source is generated automatically by the system after online testing. CHAPTERPER is the proportion of the following test section: CLUSTERED is the student's class number, CLUSTERMEMBER is the class member the student belongs to, and CLUSTERCENTER is the clustering center of the type that the student belongs. SCORE records the examination results, and PNSCORE records each chapter's scores. The table records the information after each examination, including the information obtained from the scoring and the analysis of the result.

4.2. Evaluation of Personalized Intelligent Learning System. In the specific application of the GBKM clustering algorithm in the personalized intelligent school system, as the core algorithm of performance analysis, the corresponding records in the database are successfully read, and the GBKM clustering completes analysis effectively. The characteristics of clusters formed after clustering are analyzed, and the results are displayed on the browser page. At the same time, stored the analysis results in the corresponding database table test history and updated the records of the corresponding database table, such as updating the CHAPTERSCORE of each chapter in the testStru table for subsequent use.

Table 2: The pre-analyze table.

Fieldname	Field ID section	Property	Length	Pkey	Null
Serial number	ID	Int	4	O	O
Student no.	USERID	Varchar	4		O
Course number	COURSEID	Varchar	100		O
Test time	TESTTIM	Datetime	3		O

Multiple GBKM clustering analyses were conducted on 78 test records in the database, and the clustering results were roughly the same, as shown in Table 4.

By comparing the characteristics of each class, the course members are very similar to those of the class. In contrast, the differences between the course and the style are significant, and each type's clustering center can represent each class's characteristics. Due to the fast and effective clustering and analysis of the GBKM clustering algorithm, the system can understand the factors of each student's grace and give personalized learning suggestions and guidance according to this feature, increase the system's intelligence, and improve students' learning efficiency and effect. Taking "Introduction to Journalism" as an example, this article compares a series of data. The change of data can better and more intuitively see the transformation of test paper parameters, concluding that the evolution of test paper parameters impacts students' learning.

Firstly, the proportion of original questions in this course is given and then this information is stored in the database table testStru (Table 5).

When students do not perform performance analysis, the structure of the test paper, i.e., the number of points in each chapter, is carried out in following Table 6. The system will set the number of questions according to the specified percentage and will not increase or decrease the number of questions considering students' factors.

Observe the scores of each chapter derived from the database test history table, as shown in Table 6. In this table, the scores of each chapter are expressed in the form of "1 @ 9.5 # 2 @ 9.0 # 3 @ 16.5 # 4 @ 11.0 # 5 @ 11.5 # 6 @ 9.0 # 7 @ 7.0 # 8 @ 9.0 #," where @ is the number of chapters and the equal score of this chapter, for example, 1 @ 9.5 is the score of the first chapter 9.5; # is separated from chapters, such as 1 @ 9.5 # 2 @ 9.0, # is the first chapter, # is the second chapter. In Table 6, the test scores of different students and each student at different times are not the same. That is, different and the same students have different degrees of mastery of knowledge at different times. Suppose all the questions are with the proportion of questions in Table 5. In that case, the examination will lead to different levels of students with different

Table 3: Test history table.

Field name	Field ID	Property	Length	Pkey	Null
Serial number	ID	Int	4	O	O
Test no.	TID	Varchar	50		
Examinee number	USERID	Varchar	20		
Course number	CID	Int	4		
Test time	TEST TIME	Datetime	8		
Array of test numbers	ANSWER	Text	16		
Test score	SCORE	Decimal	9		
Chapter score	PNSCORE	Varchar	200		
Class member	CLUSTERMEMBER	Varchan	200		
Class-center	CLUSTERCENTER	Varchan	200		
Class-mark	CLUSTERID	Varchar	200		
Section question ratio	CHAPTERPER	Varchar	200		
Degree of difficulty	HARD	Chan	1		

Table 4: The clustering of GBKM.

Class-mark	Members of the class
0	35, 36, 42, 43, 45, 58, 61, 65, 67, 74
1	8, 26, 30, 31, 32, 33, 34, 37, 38, 44, 46, 47, 49, 50, 51, 52, 54, 55, 56, 59, 60, 62, 64, 66, 69, 70, 71, 72, 81
2	48, 75, 76, 77, 78, 79, 80, 82
3	16, 17, 18, 19, 53, 63, 73, 83, 93
4	7, 9, 10, 11, 12, 13, 14, 15, 20, 21, 22, 23, 24, 25, 27, 28, 29, 39, 40, 41, 57, 68

Table 5: Original question's proportion of every chapter.

The section	1	2	3	4	5	6	7	8
Proportion of questions per chapter (%)	10	10	20	15	15	10	10	10

Table 6: Student's score of every chapter.

Students ID	Examination of time	Scores per chapter
0001	2021-5-30	1@9.5#2@9.0#3@16.5#4@11.0#5@11.5#6@9.0#7@7.0#8@9.0#
0001	2021-6-11	1@6.0#2@7.5#3@15.0#4@12.5#5@11.5#6@8.5#7@7.5#8@9.5#
0001	2021-10-8	1@6.5#2@10.0#3@19.5#4@14.0#5@13.5#6@9.5#7@8.0#8@10.0#
0002	2021-6-12	1@6.3#2@7.6#3@15.4#4@12.0#5@12.0#6@10.0#7@9.0#8@6.0#
0003	2021-6-12	1@8.3#2@9.2#3@19.5#4@15.0#5@14.5#6@8.5#7@9.5#8@8.0#
0004	2021-6-12	1@8.5#2@9.0#3@17.0#4@13.0#5@12.5#6@6.5#7@6.5#8@8.0#

foundations to test the same topic. The same student always repeats the examination of familiar knowledge points, and unfamiliar knowledge points may not be tested. Therefore, how to change the proportion of questions for different students at different test times to achieve targeted testing has become the focus of the personalized intelligence of this system. Therefore, after the performance analysis, the intelligent learning system will change the proportion of each chapter of the students according to the analysis results. For example, Table 7 shows the proportion of each class chapter after cluster analysis. As Table 6, 1 @ 11% # 2 @ 8% means that the proportion of the first chapter is 11% and the second chapter is 8%.

Table 8 shows the classes of different students and the proportion of each chapter. From this table, we can see the differences among students and their different balance of questions. The system can carry out individualized intelligent education for international students.

Table 9 shows that students have achieved different results at different test times, belonging to different categories and proportions of questions. Over time, the students' knowledge of each chapter also changes. The ratio of students' questions in each chapter also changes, which realizes the function of individual questions.

From the above analysis, the GBKM algorithm is applied to the personalized intelligent learning system and the implementation of personalized philosophical teaching for different students in different periods. It dramatically enhances the intelligence of embedded online innovative teaching platforms.

Table 7: Question's proportion of every chapter after clustering.

Kind ID	Proportion of each chapter	Class size
0	1@11%#2@8%#3@18%#4@13%#5@18%6@12%7@12%8@10%#	10
1	1@10%#2@9%#3@20%#4@16%#5@18%#6@12%#7@8%#8@7%#	29
2	1@11%#2@11%#3@19%#4@14%#5@16%#6@7%#7@11%8#@11%#	8
3	1@12%#2@9%#3@18.5%#4@13.5%#5@15%#6@9%#7@15%#8@9%#	9
4	1@7.9%#2@7%#3@21.7%#4@16.3%#5@15%#6@11%#7@10.6%#8@10.5%#	22

Table 8: Different student's cluster.

Student ID	Kind ID	Proportion of each chapter
Admin	4	1@7.9%#2@7%#3@21.7%#4@16.3%#5@15%#6@11%#7@10.6%#8@10.5%#
0009	0	1@11%#2@8%#3@18%#4@13%#5@18%6@12%7@12%8@10%#
0020	3	1@12%#2@9%#3@18.5%#4@13.5%#5@15%#6@9%#7@15%#8@9%#
0019	0	1@11%#2@8%#3@18%#4@13%#5@18%6@12%7@12%8@10%#
0021	2	1@11%#2@11%#3@19%#4@14%#5@16%#6@7%#7@11%8#@11%#
0007	1	1@10%#2@9%#3@20%#4@16%#5@18%#6@12%#7@8%#8@7%#
0008	1	1@10%#2@9%#3@20%#4@16%#5@18%#6@12%#7@8%#8@7%#

Table 9: Question's proportion of every chapter of 0009.

Examination of time	Kind ID	Question proportion
2021-6-12	4	1@10%#2@9%#3@20%#4@16%#5@18%#6@12%#7@8%#8@7%#
2021-6-12	0	1@7.9%#2@7%#3@21.7%#4@16.3%#5@15%#6@11%#7@10.6%#8@10.5%#
2021-6-12	1	1@11%#2@8%#3@18%#4@13%#5@18%6@12%7@12%8@10%#

5. Conclusion

Because the teaching mode of international news communication is too single, the teaching mode and implementation method are improved. The application of cluster analysis algorithms in teaching is studied in depth. GBKM clustering analysis algorithm is proposed to improve the traditional clustering analysis algorithm. Standard tests verify the convergence and effectiveness of the GBKM clustering analysis algorithm, which is successfully applied to the personalized intelligent learning system of an embedded online smart teaching platform. The main innovative work of this article is as follows:

(1) By studying the implementation of the online teaching platform and related technologies, the concept of "personalized intelligent teaching is proposed," the embedded online intelligent teaching platform is realized using various popular technologies, and the overall style and architecture of the online teaching platform are designed as *d*.

(2) The clustering analysis algorithm is studied, and an improved clustering analysis algorithm—GBKM clustering analysis algorithm—is proposed, which overcomes the shortcomings of the traditional clustering analysis algorithm and demonstrates the effectiveness and superiority of the algorithm are *d* through theoretical proof and experimental verification.

(3) The improved clustering analysis algorithm is applied to the embedded online intelligent teaching platform to realize the personalized, innovative learning system of the embedded online smart teaching platform. It reflects the individualized and brilliant teaching concept and dramatically enhances the intelligence of the embedded online intelligent teaching platform. The application of the system also proves the effectiveness and practicability of the GBKM algorithm. It optimized the teaching mode of international news communication.

Data Availability

The dataset can be accessed upon request.

Conflicts of Interest

The authors declare that they have no conflicts of interest.

References

[1] H. S. Da and S. J. Shin, "Implementation of algorithmic to write articles by stock robot," *The International Journal of Advanced smart Convergence*, vol. 5, no. 4, pp. 40–47, 2016.

[2] H. Natali, "Policy Implications From Algorithmic Profiling and the Changing Relationship Between Newsreaders and the Media," *Javnost The Public*, vol. 23, pp. 188–203, 2016.

[3] M. M. E. Bishouty, K. Saito, T. Chang, and S. Graf, "Teaching improvement technologies for adaptive and personalized learning environments," *Learning Environments and Technologies*, pp. 225–242, Springer, Berlin, Heidelberg, 2015.

[4] F. R. D. Melo, E. L. Flôres, S. D. D. Carvalho, R. A. D. Teixeira, L. F. Loja, and R. D. S. Gomide, "Computational organization of didactic contents for personalized virtual learning

environments," *Computers & Education*, vol. 79, pp. 126–137, 2014.

[5] C. K. Hsu, G. J. Hwang, and C. K. Chang, "A Personalized Recommendation-Based mobile Learning Approach to Improving the reading Performance of EFL students," *Computers & education*, vol. 63, pp. 327–336, 2013.

[6] R. Knauf, Y. Sakurai, K. Takada, and S. Tsuruta, "A case study on using personalized data mining for university curricula," in *Proceedings of the 2012 IEEE International Conference on Systems, Man, and Cybernetics (SMC)*, Seoul, Korea (South), October 2012.

[7] S. Kausar, X. Huahu, I. Hussain, Z. Wenhao, and M. Zahid, "Integration of data mining clustering Approach in the personalized E-learning system," *IEEE Access*, vol. 6, Article ID 72724, 2018.

[8] K. Sreenath and G. Jeyakumar, "Evolutionary Algorithm Based Rule(s) Generation for Personalized Courseware Construction in Educational Data Mining," in *Proceedings of the 2016 IEEE International Conference on Computational Intelligence and Computing Research (ICCIC)*, pp. 1–7, Chennai, India, December 2016.

[9] Y. Yamamoto, R. Knauf, Y. Miyazawa, and S. Tsuruta, "Increasing the sensitivity of a personalized educational data mining method for curriculum composition," *Emerging Issues in Smart Learning*, pp. 201–208, Springer, Berlin, Heidelberg, 2015.

[10] W. V. Ch and S. L. Mora, "Analysis of Data Mining Techniques Applied to LMS for Personalized Education," in *Proceedings of the 2017 IEEE World Engineering Education Conference (EDUNINE)*, pp. 85–89, Santos, Brazil, March 2017.

[11] J. L. Castejón, R. Gilar, P. Minano, and M. Gonzalez, "Latent class cluster analysis in exploring different profiles of gifted and talented students," *Learning and Individual Differences*, vol. 50, pp. 166–174, 2016.

[12] K. R. Galloway and S. L. Bretz, "Using cluster analysis to characterize meaningful learning in a first-year university chemistry laboratory course," *Chemistry Education: Research and Practice*, vol. 16, no. 4, pp. 879–892, 2015.

[13] J. Y. K. Chan and C. F. Bauer, "Identifying at-risk students in general chemistry via cluster analysis of affective characteristics," *Journal of Chemical Education*, vol. 91, no. 9, pp. 1417–1425, 2014.

[14] E. Yukselturk and E. Top, "Exploring the link among entry characteristics, participation behaviors and course outcomes of online learners: an examination of learner profile using cluster analysis," *British Journal of Educational Technology*, vol. 44, no. 5, pp. 716–728, 2013.

[15] A. M. F. Yousef, M. A. Chatti, M. Wosnitza, and U. Schroeder, "A cluster analysis of MOOC stakeholder perspectives," *RUSC. Universities and Knowledge Society Journal*, vol. 12, no. 1, pp. 74–90, 2015.

[16] M. Durairaj and C. Vijitha, "Educational data mining for prediction of student performance using clustering algorithms," *International Journal of Computer Science and Information Technologies*, vol. 5, no. 4, pp. 5987–5991, 2014.

[17] A. Stes and P. V. Petegem, "Profiling approaches to teaching in higher education: a cluster-analytic study," *Studies in Higher Education*, vol. 39, no. 4, pp. 644–658, 2014.

Hindawi
Scientific Programming
Volume 2022, Article ID 5779130, 9 pages
https://doi.org/10.1155/2022/5779130

Research Article

Effect Evaluation and Student Behavior Design Method of Moral Education in Colleges and Universities under the Environment of Deep Learning

Yeqing Zhang, Tianji Liu, and Bao Ru

North China University of Science and Technology, Hebei, Tangshan 063210, China

Correspondence should be addressed to Yeqing Zhang; zhangyq@ncst.edu.cn

Received 28 June 2022; Revised 31 July 2022; Accepted 3 August 2022; Published 29 August 2022

Academic Editor: Lianhui Li

The traditional ideological and moral education evaluation mechanism in colleges and universities faces many challenges. Among them, the traditional ideological and political theory course evaluation mechanism is difficult to solve the contradiction between the teaching content of the ideological and political theory course and the ideological knowledge of the educated, and the test scores of the ideological and political theory course are difficult to measure the level of students' ideological awareness that has become a prominent problem. The evaluation mechanism of ideological and political education in colleges and universities based on deep learning technology can play a role in the formative evaluation and consequential evaluation of courses, thus forming a new mechanism for evaluating ideological and political education in colleges and universities, and further improving the effectiveness of ideological and political education.

1. Introduction

In 2017, the Ministry of Education issued the "Ideological and Political Work Quality Improvement Project Implementation Outline in Colleges and Universities" [1]. The "Outline" proposed: "Improve the quality evaluation mechanism of ideological and political education in colleges and universities, and study and formulate the evaluation index system of ideological and political work in colleges and universities." This marks the national optimization and innovation of the quality evaluation mechanism of ideological and political education work in colleges and universities has been brought to a new height. There are three main areas of quality assessment of ideological and political education work in colleges and universities: supply side assessment, demand-side assessment, and management assessment [2]. In general, "supply-side" and "demand-side" are economic concepts. In the quality evaluation system of ideological and political education work, supply side evaluation and demand-side evaluation refer to the evaluation of the educational content of educators and the evaluation of educated people, respectively. Assessment of learning outcomes. Under the new historical conditions, both educators and educated people have undergone profound changes, and the incompatibility of the traditional ideological and political education work quality evaluation system has become increasingly obvious [3]. Only by establishing new ideas and borrowing new technologies can we realize the optimization and innovation of the quality evaluation system of ideological and political education. In view of this, this paper is mainly based on deep learning technology, one of the core technologies of artificial intelligence, to provide optimization ideas for the evaluation system of ideological and political theory courses in colleges and universities.

The effectiveness of ideological and political theory courses has always been an important concern of ideological educators in colleges and universities because the effectiveness of courses is related to the quality of ideological and political theory courses [4]. In order to maximize the effectiveness of ideological and political theory courses, it is necessary to deal with the contradictions in the teaching of ideological and political theory courses. First of all, the

content to be taught by educators in ideological and political theory courses and the ideological conditions of the educated are a pair of contradictions in the teaching work of ideological and political theory courses [5]. The content taught by ideological and political theory educators is the principles of Marxism and the theoretical achievements of the Sinicization of Marxism, which are scientific theories proved by practice; and the educated are college students, who grew up in a society with diverse values, and they themselves bring There is a diverse knowledge background, and their ideas and concepts are not yet stable, and it is easy to change [6, 7]. To adjust such a pair of contradictions, the designers of ideological and political theory courses must not only ensure the scientific and advanced nature of the content taught by educators but also maintain continuous evaluation of the learning effects of educated people's ideological and political theory courses to ensure Within a certain period of time, the content of the curriculum education will keep pace with the ideological level of the educated. Such "synchronization" requires advanced evaluation mechanisms to assist.

Second, the examination results of the educated ideological and political theory course and the actual behavior of the educated in real life are another pair of contradictions in the teaching work of the ideological and political theory course in colleges and universities. Nowadays, the assessment of ideological and political theory courses is mainly based on the final written examination. Educated students can still obtain high scores by memorizing knowledge points in such an assessment, but such high scores are not the main purpose of ideological and political theory courses. The main educational purpose of the ideological and political theory course is to enable the educated to make correct value judgments in real social practice through the teaching of Marxist theory. However, the fact that an educated person has achieved excellent results in the examination of the ideological and political theory course does not mean that he will also practice the advanced ideas advocated by the ideological and political theory course in social life. Students who achieve excellent grades in the assessment will not necessarily demonstrate the corresponding political and moral qualities in their actual behaviors, nor will they necessarily be able to convert the same excellent grades into positive and positive behaviors in long-term social activities [8, 9]. The key to improving the effectiveness of ideological and political theory courses is to ensure that the educated have achieved a certain ideological change and bring this ideological change into their daily life [10]. This requires educators to grasp the ideological transformation of the educated in the course of teaching ideological and political theory courses and to use the evaluation mechanism to complete the measurement of the level of ideological development. However, "the construction of the evaluation system of ideological and political education in colleges and universities is not perfect, and the evaluation methods and methods are relatively lagging behind." The current traditional evaluation system of ideological and political education in colleges and universities cannot effectively solve the above contradictions [11].

Deep learning is a new technology in the field of artificial intelligence. This concept was proposed by British artificial intelligence expert Professor Hinton and others. It mainly refers to "using the multi-layer abstraction mechanism of the human brain to stimulate the learning process of the human brain through a neural network, so as to realize the abstract expression of a large amount of data in the real world." What's more, "practice has proved that deep learning can capture the underlying essential features or rules within data such as natural images, videos, speech, and music with potentially complex structural rules" [12]. From this point of view, deep learning technology has a technical support function for ideological and political education theory courses. In practice, we can explore the innovation of ideological and political education evaluation according to the evaluation needs of ideological and political courses and the corresponding model of deep learning technology. This paper mainly selects the formative evaluation and the consequential evaluation of the ideological and political theory course as two evaluation methods for model construction.

2. Related Works

Intelligence refers to the ability of people to understand the objective world and use knowledge to solve practical problems. It is concentrated on the depth, accuracy, and completeness of reflecting objective things, as well as the speed and quality of applying knowledge to solve problems. Judgment, association, and creation are manifested. Turing, the "father of artificial intelligence," once conducted an experiment called the Turing test to test whether a computer could not be detected when it communicated with people. Artificial intelligence expert Wisniewski believes that the intelligence of artificial intelligence is reflected in "machines have the ability to learn and understand things, deal with problems and make decisions." Artificial intelligence is a computer program that imitates human intelligence. It relies on massive data and precise algorithms to achieve intelligent applications. For example, Microsoft's machine Xiaoice, Google's AlphaGo, can express its intelligence through image perception, semantic understanding, knowledge expression, and reasoning calculus.

Deep learning provides artificial intelligence with a smarter algorithm, and machines can learn by themselves by optimizing rules and models through data. The earliest research on artificial intelligence can be traced back to 1956, during which it experienced several slumps. An important reason is the lack of data and computing power. Deep learning was proposed by Hinton et al. in 2006, and more advanced algorithms that support artificial intelligence have subsequently emerged. Unlike humans, the second generation of artificial intelligence relies on logical analysis of the causal relationship between things to make decisions and judgments, and discover the correlation between things through deep learning supported by big data. The method it takes is not to analyze the sample survey data, but to analyze the whole data, so as to find the correlation between two or more groups of data [6]. For intelligent robots, the most

important thing is big data and intelligent algorithms. The more and more complete the data, the more accurate and less error-prone decision-making and judgment will be. The cognitive development of machines has made significant progress. For example, machines can look at millions of pictures a day and complete deep learning, while humans have strong intuition and reasoning abilities, and only need to browse and learn a few pictures to grasp the rules [10]. The combination of the machine's deep learning and human reasoning ability is the symbiosis and integration of two types of intelligence, which is the future communion intelligence. The advantages of robots are reflected in speed, accuracy, load-bearing capacity, repetition consistency and operation time, etc., while human capabilities are reflected in thinking and logical reasoning, learning and skill progression, experience and real-time decision-making, interactive collaboration, safety, etc. The combination of the advantages of both humans and robots will exceed the capabilities of a pure human or robot [11]. For example, the expert system in distance education can use its own knowledge reserves to answer students' questions, record, evaluate, and diagnose students' daily learning situations, find problems and errors in students' learning process, and realize individualized teaching. The spiral rise of the SOLO level reflects the development process of individual learning resulting from quantitative change to qualitative change and understanding level from shallow to deep. Pursuit coincides with deep learning. Therefore, from the perspective of the quality level and understanding level of learning, the SOLO taxonomy is related to shallow learning and deep learning. Figure 1 shows an illustration of machine learning and deep learning.

In the field of artificial intelligence, swarm intelligence originally originated from the research on the behavior of many social insect biological groups. Simple individuals, through mutual cooperation and cooperation, emerge such a feature of higher intelligent behavior, which is called swarm intelligence [12]. What is the intrinsic connection between swarm intelligence and artificial intelligence? Classical artificial intelligence represented by symbolic logic and expert systems is rule-driven deterministic intelligence, while artificial intelligence represented by neural networks and deep learning is data-driven uncertainty intelligence [4]. Swarm intelligence is an artificial intelligence composed of two interactive bits of intelligence. The intelligence of our social groups is also driven by interaction to form a joint force to achieve innovation and development. Swarm intelligence can gather human knowledge and wisdom in a wider range than any previous technology, and promote the development of human history.

Deep learning technology obscures the effectiveness of school moral education. On the one hand, technology has brought new measurement standards, which makes it more difficult to measure the effectiveness of moral education content. For example, the emergence of smartphones has changed the relationship between people and changed the individual's perception of the world and self-awareness. McLuhan believes that "the impact of any medium (any extension of man) on individuals and society is due to new scales; any extension (or any new technology) of our to introduce a new scale into things" [13]. The new scale brought by artificial intelligence technology has become a new standard for measuring the effectiveness of moral education. Therefore, under the background of new technologies, student morality has new development characteristics and laws. However, if schools only emphasize the traditional moral education goals, they ignore the students in the actual technical environment, students will not be able to perceive the real situation of students moral growth, and will not be able to understand the real effectiveness of moral education, thus falling into a passive situation. On the other hand, the complexity of moral education content increases the difficulty of measuring the effectiveness of moral education. On the platform provided by artificial intelligence, students can obtain moral education resources that they care about, and discuss and exchange values with others. Artificial intelligence technology supplements the lack of time and space to teach moral education content in schools and makes up for the actual needs of students. However, in the context of artificial intelligence technology, whether the huge content of moral education is too broad, whether it is in line with the characteristics of children, and how effective is it? It is not easy to observe concretely.

3. Evaluation and Analysis of Moral Education Achievements under Deep Learning

This study defines the meaning of classroom teaching effectiveness as follows: The judgment of classroom teaching effectiveness is not only based on the actual development of students but more importantly, whether students' development level meets the requirements of the curriculum objectives, that is, the achievement of curriculum objectives. Figure 2 shows the relationship between efficiency and benefit in teaching effectiveness.

This research mainly adopts the connotation definition of deep learning defined by scholar Zhang Hao, deep learning is "learners master unstructured deep knowledge and carry out critical higher-order thinking, active knowledge construction, effective transfer application and real problem solving, and then realize the development of higher-order abilities such as problem-solving ability, critical thinking, creative thinking, and meta-cognitive ability." The definition of this meaning can be understood from the following two aspects: First, deep learning is an integral part of students' learning process and a specific way of learning. Deep learning requires students not only to memorize and understand relevant knowledge but also to think critically about the knowledge they have learned and to actively construct and transform it, so as to finally transfer knowledge to real life and solve complex problems question. Second, focus on the development of higher-order abilities and thinking. Through deep learning, the development of higher-order abilities such as problem-solving ability, critical thinking, creative thinking, and meta-cognitive ability can be realized. These abilities can correspond to the four "application, analysis, synthesis, and evaluation" in Bloom's educational goal taxonomy higher cognitive levels. It can be

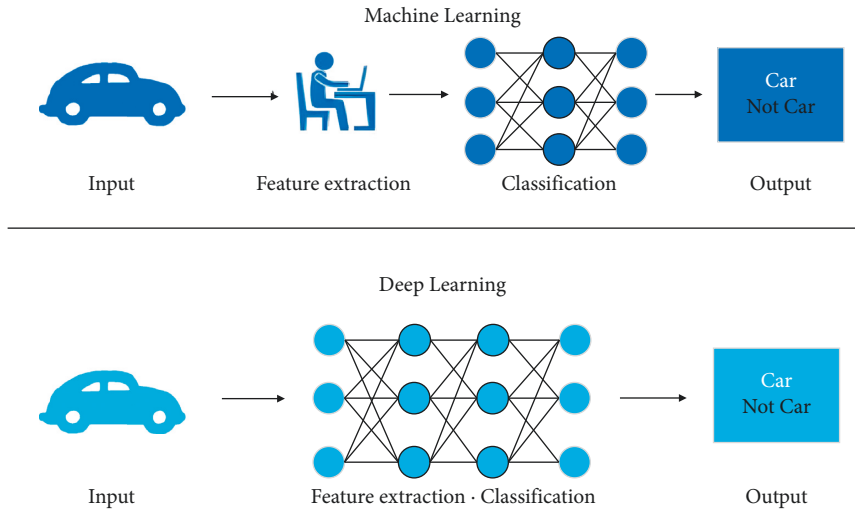

Figure 1: Illustration of machine learning and deep learning.

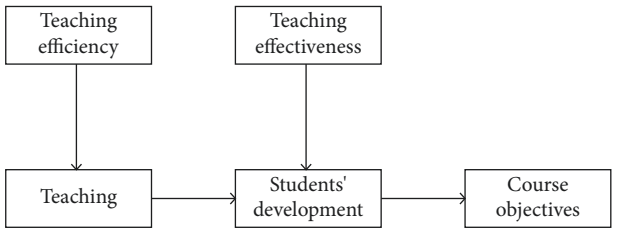

Figure 2: The relationship between efficiency and benefit in teaching effectiveness.

seen that deep learning is oriented toward the acquisition of advanced cognitive skills and involves higher-order thinking activities.

3.1. Deep Learning Features. According to the learners' understanding and mastery of knowledge, we can divide learning methods into deep learning and shallow learning. However, deep learning and shallow learning are not separated but interpenetrated. From the perspective of students' learning process, deep learning starts from simple learning with low emotional and behavioral input and gradually turns to advanced learning with high emotional and behavioral input. Therefore, when many scholars in the domestic academic circle express the characteristics of deep learning, they often compare them with shallow learning in the statement and then draw the characteristics of deep learning. For example, Professor Li Jiahou compared the characteristics of deep learning and shallow learning and concluded that the characteristics of deep learning are manifested in three aspects: "understanding and criticism, connection and construction, migration and application." The author uses Li Jiahou's comparative framework for deep learning characteristics. Based on the deep learning characteristics supplemented by other researchers, we select the memory methods, cognitive results, learning motivation, learning behavior, learning effectiveness, reflective state, thinking ability, and cognition of learners in deep learning and shallow learning. Differences in skills, etc., are compared in more detail.

Through the comparison in Table 1, deep learning emphasizes comprehension memory in terms of memory methods and focuses on the construction and transformation of knowledge in terms of cognitive results. In terms of learning behavior, it is a mixed behavior with high emotion and high behavioral investment. Conduct critical thinking and self-reflection in behavior, focus on transferring the knowledge to memorization life in cognitive skills, show learning as a strong endogenous motivation in learning motivation, and emphasize high effect in learning effect, high efficiency, and high level, focusing on the advanced thinking level in the thinking level, and highlighting the student learning as the center in teaching.

3.2. The Understanding and Transformation of Knowledge Must Go through Deep Learning. In the course of ideological and political theory courses in colleges and universities, college students should first memorize the concepts and knowledge of the basic viewpoints of socialism with Chinese characteristics [13–15]; the second is the consolidation and transformation of knowledge. When college students complete the memorization of this viewpoint of socialism with Chinese characteristics, they will assimilate or adapt this knowledge to clearly repeat the knowledge they have learned; again, it is the transfer and application of knowledge. When asked about the content of basic viewpoint of socialism with Chinese characteristics, college students can quickly retrieve the relevant knowledge to answer. To sum up, through the above three stages, the students' knowledge learning process of the basic viewpoints of socialism with Chinese characteristics is explained. This learning process focuses on understanding and transformation to help students better learn relevant knowledge [16]. Understanding and transformation are high-level cognitive processing and one of the main features of deep learning. Therefore, it can be

Table 1: Comparison of deep learning and shallow learning features.

	Deep learning	Shallow learning
Memory	Memorizing on the basis of understanding	Rote memorization
Cognitive results	Build exercises between knowledge and make conceptual changes	Learning scattered or isolated
Learning behavior	Complex activities with high emotional and behavioral input	Simple activities with low emotional and behavioral input
Reflect on state	Critical thinking, self-reflection	Lack of critical thinking and self-reflection
Cognitive skills	Transfer what you learn to your life	Unable to use knowledge flexibly
Thinking level	Higher level of thinking	Lower levels of thinking
Learning motivation	Internal understanding drives learning	Learning driven by external pressure
Learning effect	High effect, high efficiency and high-level	Low effect, low efficiency, low level
Teaching methods	Focus on student learning	Take the teacher's teaching as the center

said that the understanding and transformation of relevant knowledge must go through deep learning. Figure 3 shows generalized knowledge learning stage and classification model.

3.3. The Acquisition of Abilities and Skills Must Go through Deep Learning. In the cognitive stage, first of all, by observing the actions of others using Marxist theory to analyze and solve practical problems, to stimulate situational awareness to form an internal action image as a reference for actual analysis and problem-solving; second, when forming After the image, students combine their own abilities and experience to form operational level expectations, that is, they have self-awareness of whether they can skillfully use Marxist viewpoints to analyze and solve problems. In the connection stage, when students face complex problems, they will know how to use the worldview of Marxist theory to analyze the problem, and at the same time, they will use the Marxist methodology to solve the problem. In turn, the connections that students form in problem-solving become a new round of stimulation.

To sum up, the above three stages explain the acquisition process of students' ability to analyze and solve problems by using the Marxist world outlook and methodology, which is essentially the process of internalizing knowledge into ability. This process focuses on the transfer and application of knowledge, emphasizing the application of the learned knowledge to real life. And this process is one of the main characteristics of deep learning, so it can be said that the acquisition of students' abilities and skills must be carried out by deep learning.

3.4. The Formation of "Three Views" Must Go through Deep Learning

First, know "choices"—make the right choices when faced with situations that conflict with existing values. Various values and cultural ideologies in modern society collide, exclude, and merge with each other, which leads to college students often entering a choice situation premised on moral conflict, and the choice situation is opposite and incompatible. How to make the right choice is a difficult challenge for college students. Therefore, it is required to teach students to make choices, and to do so when making choices: first, know how to make free choices according to their own values; second, when faced with multiple choices, know how to weigh the pros and cons of these choices; Choose consequences for analysis and thinking in order to make correct and sensible choices [17].

Second, learn to "value"—value your choices and feel content. Many college students have different performances from their predecessors, on and off-campus. From a psychological point of view, this is essential because college students are unwilling to be responsible for behaviors that are not of their own will and without emotional intervention. According to Ruths, he believes that "value comes from the choices we are willing to make," in other words, only on the basis of careful thinking and cherish the results of their choices, college students will be responsible for their choices with words and deeds. Therefore, at this stage, students are required to: first, learn to be satisfied with the choice they have made, and affirm their choice with sufficient reasons; second, be willing to publicly admit this choice.

Finally, put into action, act on that choice, and repeat it as a way of life. College students make rational choices and cherish them when faced with choices, but these cannot make college students form correct values. Laths believes that in order for students to establish a true value system, "the cherished choice must be put into action, so that the action reflects the chosen value orientation." Based on this, at this stage, students are required to: first, put the cherished choices into actions, so that the actions reflect the correct value orientation; a way of life [18]. To sum up, Laths believes that through choice, cherishing, and action, students' value issues have been evaluated and clarified, resulting in correct values. Although the value clarification theory is a Western value education theory, because values are universal in human society, the education methods of values also have certain commonalities, which are the "three views" for middle school students in the ideological and political theory courses in our country's colleges and universities. The formation provides realistic operability.

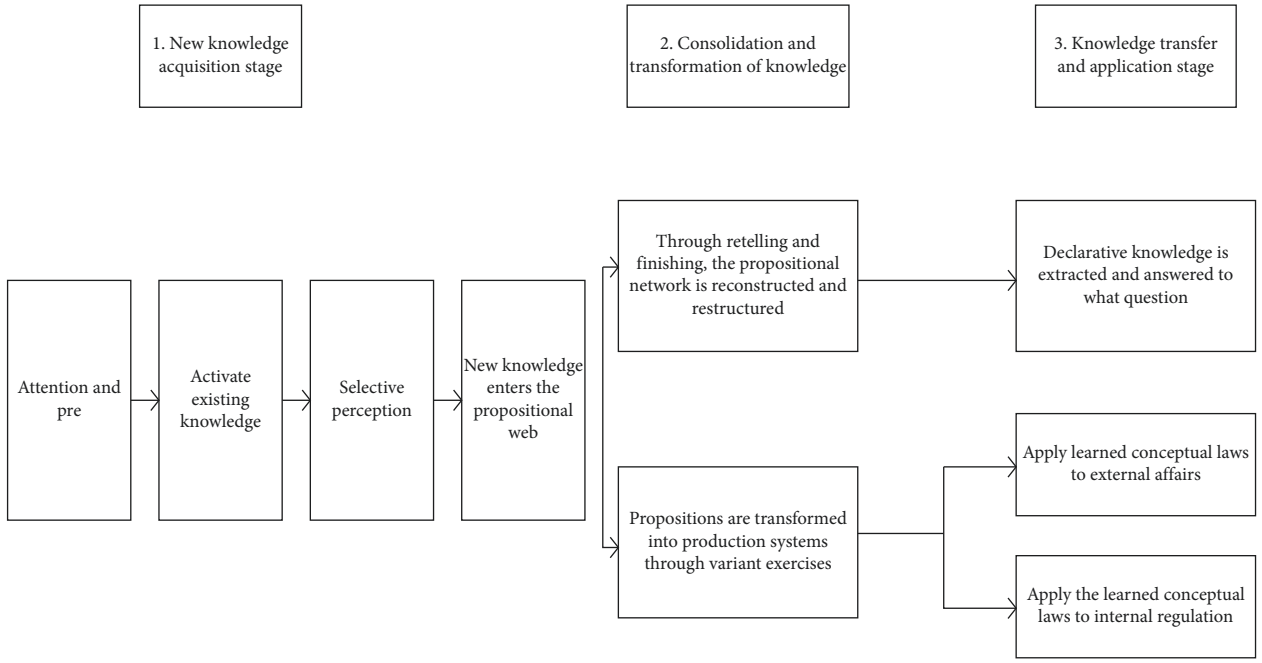

Figure 3: Generalized knowledge learning stage and classification model.

4. Survey Design and Implementation

4.1. Investigation Plan Design. Investigating the status quo of the effectiveness of classroom teaching of ideological and political theory courses in colleges and universities is convenient for analyzing the difference between the actual state and the state of classroom teaching of ideological and political theory courses in colleges and universities from the perspective of deep learning, which is the real basis for follow-up countermeasures [19]. In other words, we need to understand the subject and object of the ideological and political theory of classroom teaching behavior in colleges and universities, that is, the teaching and learning behavior of teachers and students, and analyze whether their behavior can contribute to the effectiveness of ideological and political theory classroom teaching. From the perspective of deep learning, we believe that the mark of teachers and students achieving the effectiveness of classroom teaching in ideological and political theory courses is that students have the characteristics of deep learning in the learning behavior of ideological and political theory courses and that teachers can inspire students' deep learning behaviors [20].

Therefore, this study conducted a sample questionnaire survey on teachers and college students of ideological and political theory courses in colleges and universities. To investigate the current situation of classroom teaching in ideological and political theory courses in colleges and universities for teachers of ideological and political theory courses, we mainly understand the occurrence of teaching behaviors that stimulate students' deep learning in the teaching process. The teachers of ideological and political theory courses in colleges and universities are mainly composed of full-time teachers and ideological and political counselors, so the questionnaire survey objects for teachers are also taken from these two groups [21]. In addition, a survey of the current situation of ideological and political theory courses in colleges and universities was conducted for the students from freshman to senior year, in order to understand the in-depth study of students' ideological and political theory courses. The questionnaire is conducted at the end of the school year, so even the first-year students have already taken part in the ideological and political theory course, which meets the needs of the sample.

Regarding the analysis of survey data, the descriptive statistics function of SPSS software is used to analyze the teaching behavior of college teachers in ideological and political theory courses and the deep learning behavior of students, and use independent sample T-test and one-way analysis of variance to understand the group differences of the above behaviors. Table 2 shows a list of the content design of student questionnaires.

After statistics, a total of 135 questionnaires were distributed for teachers, 135 were recovered, 134 were valid, the recovery rate was 100%, and the effective rate was 99.3%; a total of 1,300 questionnaires were distributed for students, 1,254 were recovered, 1,221 were valid, and the recovery rate was 96.5%, the effective rate is 93.9%. The basic information of the samples of the teacher questionnaire and the student questionnaire are shown in Tables 3 and 4, respectively.

Through investigation and analysis, it is found that the learning behavior of college students in ideological and political theory courses basically does not have the characteristics of deep learning behavior. It is mainly manifested in the lack of interest in learning ideological and political theory courses, the basic lack of high-level information

Table 2: List of content design of student questionnaires.

Research topic	Survey content	Observation point	Question id
Overall learning	Students' judgment of their overall learning status	Self-judgment of students' overall learning status and academic performance	*Q*1, *Q*2
Learn drive	Students' judgment of their own motivation and strength in ideological and political theory courses	Whether the students have the desire to learn the ideological and political theory course and study interest	*Q*3, *Q*4, *Q*5, *Q*6, *Q*7
High-level information processing	Students' judgment of their own high-level knowledge processing in the course of ideological and political theory learning	Whether students have the learning characteristics of high-level information processing in the learning process of ideological and political theory courses, and whether teachers have the elements to urge students' deep learning behavior in the course homework arrangement and course examination implementation from the perspective of students	*Q*8, *Q*9, *Q*10, *Q*11, *Q*12, *Q*13, *Q*14, *Q*15, *Q*16
Comprehensive application of knowledge	Students' judgment on their comprehensive use of ideological and political theory courses	The situation of college students' comprehensive use of knowledge in ideological and political theory class teaching and the situation of teachers guiding students to use comprehensive knowledge	*Q*17, *Q*18, *Q*19, *Q*20, *Q*21, *Q*22

Table 3: The basic situation of the questionnaire survey sample of the current situation of classroom teaching of ideological and political theory courses in colleges and universities.

	Teacher group		Seniority					Master course				
	Full-time teachers	Counselor	Less than 1 year	1–3 years	4–6 years	7–25 years	26–33 years	Think repair	Outline	Netherlands	Wool	Policies
Frequency (person)	70	64	23	42	33	30	6	70	24	17	19	4
Proportion (%)	52.2	47.8	17.2	31.3	24.6	22.4	4.5	52.2	17.9	12.7	14.2	3.0

processing in the course of ideological and political theory courses, and the lack of comprehensive application of knowledge [22]. See Figure 4 for a horizontal comparison of the mean values of each survey content.

There are also some group differences in the above situation. Whether it is the learning drive of ideological and political theory courses or the level of information processing, girls are worse than boys, and science and engineering students are worse than liberal arts students. From the analysis of the differences in different grades, the first-year students' ideological and political theory courses are slightly better than those of other grades.

By analyzing the current situation of classroom teaching of ideological and political theory courses in colleges and universities, it is found that the classroom teaching behaviors of ideological and political theory teachers are not ideal enough to stimulate students' deep learning [23]. When designing curriculum objectives, teachers do not fully realize the important role they should play in the realization of advanced curriculum objectives; although teachers have adopted some teaching methods to promote deep learning, the effect is not good; the teacher-student relationship cannot promote information teachers cannot fully and accurately understand the difficulties encountered by students in the learning process of ideological and political theory courses, and it is difficult for students to understand the purpose of teachers to encourage them to conduct classroom discussions; lack of understanding, it is difficult for the course examination to give feedback on the real situation of students' deep learning; the classroom teaching atmosphere of ideological and political theory is not ideal. See Figure 5 for a horizontal comparison of the mean values of each survey content.

Depth learning is the purpose of ideological and political classroom teaching in the new era that emphasizes autonomy, inquiry, and cooperative learning. In order to guide students to learn independently, teachers should change their role as knowledge imparters, and at the same time be a learning theme designers and learning process guidance.

Table 4: The basic situation of the questionnaire survey on the current situation of college students in the ideological and political theory course in colleges and universities.

	Gender		Colleges and universities			Professional class		Grade			
	Man	Woman	Synthesis class	Liberal arts classes	Engineering	Liberal arts	In science and engineering	Freshman	Sophomore	Junior	Senior
Frequency (person)	713	508	433	399	389	490	731	366	215	363	277
Proportion (%)	58.4	41.6	35.5	32.7	31.9	40.1	59.9	30	17.6	29.7	22.7

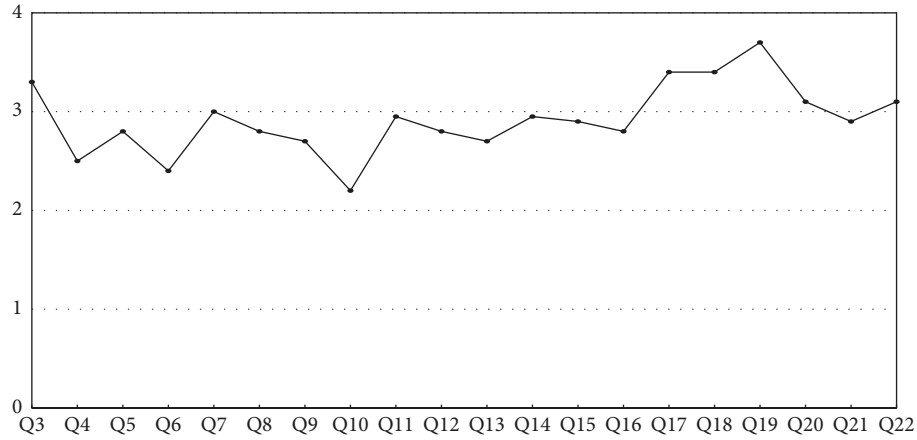

Figure 4: Mean values of each item in the student questionnaire.

Figure 5: The mean value of each item in the teacher questionnaire.

5. Conclusion

On the basis of analyzing and summarizing the characteristics of deep learning, combined with the current problems in the teaching process of moral education in colleges and universities, this paper proposes a teaching strategy for high school ideological and political classrooms from the perspective of deep learning [24]. In the teaching process of high school ideological and political courses from the perspective of deep learning, under the guidance of teachers, students not only deepen their understanding, grasp, construct, create, transfer and apply the knowledge they have learned through reflection on the process and results of their own learning activities, but also achieve the knowledge goal of deep learning; it also promotes the development and improvement of related skills, transfers application and problem solving, and achieves the skill goal of deep learning [25].

Data Availability

The dataset can be accessed upon request.

Conflicts of Interest

The authors declare that they have no conflicts of interest.

References

[1] Y. Zheng, "Challenges facing college moral education in the new era and coping strategies," *Learning & Education*, vol. 10, no. 2, p. 146, 2021.

[2] C. Yao, *Commercial Colleges' Moral Education Practice Mode*, pp. 249–252, Editorial Board of "Northeast Asia Academic Forum" of Harbin University of Commerce, 2015.

[3] H. Wang and Y. Xiang, "New situations and approaches of college moral education in the mobile internet era[J]," *Higher Education of Social Science*, vol. 9, no. 2, 2015.

[4] X. Zhu, "Optimization of college moral education based on big data[P]," in *Proceedings of the 8th International Conference on Education Management, Information and Management Society (EMIM 2018)*, Dordrecht, August 2018.

[5] Yu Lei and C. Wang, "Research on the college moral education reform and the mechanism of practice based on the cultivation of the innovative spirit[C]," *Proceedings of 2013 3rd International Conference on Social Sciences and Society(ICSSS 2013*, vol. 40, pp. 79–83, 2013.

[6] Y. Xi, "College moral education decision system designing based on web mining[C]," *Proceedings of the 2012 IEEE 19th International Conference on Industrial Engineering and Engineering Management(IE&EM 2012)*, pp. 2259–2261, Institute of Electrical and Electronics Engineers, Berlin, Heidelberg, 2012.

[7] J. Luo and X Wen, "Establishment of network platform of virtuai teaching laboratories in colleges and universities based on JSP technology[J]," *Advanced Engineering Forum*, vol. 1837, no. 4-4, 2012.

[8] L. I. Wei and T. I. A. N. Jian-Lin, "The construction of moral education mode in colleges based on hidden education," in *Proceedings of the 3rd Annual International Conference on Modern Education and Social Science (MESS 2017)*, Nanjing, China, April 2017.

[9] B. Lei, "Optimize the carrier of "internet + moral education" to improve the effectiveness of college moral education practice[P]," *2021 2nd International Seminar on Advances in Education, Teaching and E-learning*, Lisbon, Portugal, 2021.

[10] X. Fang and X. Sun, "The index system establishment and demonstration of management performance evaluation in college moral education[J]," *International Journal of Advancements in Computing Technology*, vol. 4, no. 2, 2012.

[11] Li Gao, "A brief analysis on college moral education in the epoch of network," *Asian Social Science*, vol. 6, no. 10, 2010.

[12] P. A. R. K. Yn-Hui, "Educational philosophy and college moral education: is college moral education possible?" *Journal of European Economy*, vol. 5, 1996.

[13] L. Ding, "Analysis of course ideology and politics in public finance teaching in applied undergraduate universities[J]," *Scientific Journal of Economics and Management Research*, vol. 4, no. 2, 2022.

[14] Y. Zhang, "Exploration of ideological and political construction of software testing course," *Scientific Journal of Technology*, vol. 4, no. 7, pp. 78–83, 2022.

[15] G. Shen, "Exploration and practice on the construction of curriculum ideological and political education for English majors[J]," *Advances in Vocational and Technical Education*, vol. 3, no. 3, 2021.

[16] Y. Jiang, "Exploration on the teaching reform of the course ideology and politics into the circuit course[J]," *Lifelong Education*, vol. 10, no. 1, 2021.

[17] J. Zhang, "Exploration and practice of teaching reform of engineering cost integrated with ideological and political concept[J]," *Lifelong Education*, vol. 10, no. 1, 2021.

[18] X. Yu, X. Dong, S. Liu, L. Hao, and Y. Zhang, "Research on the teaching reform of "curriculum ideology and politics" for engineering postgraduates[J]," *International Journal of Social Science and Education Research*, vol. 4, no. 11, 2021.

[19] Y. Li, "Teaching research of middle school English classroom ideology and politics under the background of "suspension of classes and non-stop school"," *International Journal of Social Science and Education Research*, vol. 4, no. 11, 2021.

[20] L. Ji, "Research on the essence of interaction relationship of ideological and political education based on spiritual communication in the era of big data[J]," *International Journal of Higher Education Teaching Theory*, vol. 2, no. 4, 2021.

[21] J. Wu and D. Wang, "The cultivation path of college students' moral education from the perspective of curriculum ideology and politics[J]," *Adult and Higher Education*, vol. 3, no. 2, 2021.

[22] H. Zhu, Z. Zhang, and Y. Hua, "Teaching exploration and practice of advanced mathematics based on curriculum ideology and politics[J]," *Curriculum and Teaching Methodology*, vol. 4, no. 4, 2021.

[23] X. Ou and H. Chen, "The permeation of curriculum ideology and politics in college teaching[J]," *Curriculum and Teaching Methodology*, vol. 4, no. 4, 2021.

[24] H. Cen, "Research on adult public English teaching based on new media information technology with curriculum ideological and political characteristics[J]," *Higher Education of Social Science*, vol. 21, no. 1, 2021.

[25] J. Wang and M. Zhu, "Research on the construction of college English reading courses based on ideology and politics curriculum," *Scientific and Social Research*, vol. 4, no. 1, pp. 182–186, 2022.

Hindawi
Scientific Programming
Volume 2022, Article ID 1458003, 8 pages
https://doi.org/10.1155/2022/1458003

Research Article

Research on the Optimization Technology of Mechanical Product Design Plan Based on Fuzzy Comprehensive Evaluation Analysis Method

Zhijie Wang, Yan Cao, Hu Qiao, Yujia Wu, and Miao Liu

School of Mechatronic Engineering, Xi'an Technological University, No. 2 Xuefu Middle Road, Weiyang District, Xi'an 710021, China

Correspondence should be addressed to Yan Cao; caoyan@xatu.edu.cn

Received 9 June 2022; Accepted 16 July 2022; Published 29 August 2022

Academic Editor: Lianhui Li

In the scheme design stage of mechanical products, several design solutions need to be evaluated so that the best design solution can be selected from them. Because the evaluation of mechanical product scheme design is a multilevel, multiattribute and contains many fuzzy models, fuzzy comprehensive evaluation becomes an advantageous model for the evaluation of mechanical product scheme design. In this article, a fuzzy comprehensive evaluation method is constructed, and a combination of the subjectivity of determining weights by hierarchical analysis method and the objectivity of determining weights by entropy value method is used to calculate the weights of evaluation indexes, and a combined assignment method is established to improve the reliability of the evaluation method. Then, the best solution is selected by calculating the comprehensive evaluation value of each product design solution. Finally, the validity, reasonableness, and feasibility of the evaluation model are verified through the evaluation and selection of three design solutions for a gearbox reducer, which also provides a new method for the evaluation and selection of other product design solutions.

1. Introduction

In the conceptual design phase of mechanical products, schematic design is a key aspect of product design, and the quality of the product design scheme directly affects the final product. The product solution design stage is a complex, fully defined, and innovative design reasoning process [1–4]. According to the product demand information, there may be a variety of product solutions designed, and the evaluation of the scheme often involves a variety of technical indicators. How to consider the impact of various uncertainty factors on the weight of the indicators, it is necessary to establish a perfect product design program evaluation model, and comprehensively evaluate many technical indicators. Thus, it can obtain the optimal mechanical product design scheme, which is also the key to ensuring product performance and further design [5–8]. A comprehensive evaluation of mechanical product design solutions can effectively ensure the quality of the design and also enable the designer to preferably select the best solution among many design solutions that meet the target requirements in all aspects of performance [9–11].

There are various evaluation methods commonly used in product solution design, such as data envelopment analysis (DEA) [12], robust design [13], analytical hierarchy process (AHP) [14], grey correlation analysis [15], artificial neural network [16], analytic network process [17], etc. Chen et al. [18] developed a decision model that combines the design criteria of IF World Design Guidelines and multiattribute decision methods, which can help decision-makers to systematically evaluate and improve the performance of product designs. Yuan et al. [19] proposed a new fuzzy integrated evaluation method for configuration solutions integrating customer requirements based on fuzzy set theory. Li and Zhang [20] proposed a method combining the Kano model (KM), hierarchical analysis method (AHP), and quality function unfolding (QFD) method with intuitionistic fuzzy sets (IFS) to solve the design decision problem of new

product development, and finally the reliability and scientificity of the method were verified by examples. Xu et al. [21] described the evaluation problem of the overall mechanical product design solution as an incomplete multiparameter decision problem and established a decision method for the evaluation of mechanical product solution design by information entropy and ordered weighted average operator. Yumoto [22] established an AHP-based product selection based on the decision rules of a rough set of qualitative evaluation decision support system. Du et al. [23] proposed an improved approach to the traditional quantitative Kano model that facilitates the personalization of products for heterogeneous customer classification groups and can realize accurate marketing. At present, most of the research on the evaluation methods of mechanical product design solutions is done by applying fuzzy theory, fuzzy processing of qualitative indicators, and using methods such as expert scoring to rank the overall evaluation value of design solutions. In the evaluation process, the setting of indicator weights mostly uses empirical methods, which has a strong subjectivity. In this article, the characteristics of technical indicators of mechanical product design solutions are analyzed, hierarchical analysis and information entropy are introduced to describe the uncertainty of indicator weights, the comprehensive evaluation value of design solutions is applied, a preferential model and solution method are constructed for the evaluation of product design solutions, and finally the effectiveness of the method is verified through the evaluation of a gearbox reducer design solution as an example. This evaluation method can not only improve the efficiency by fully scientific design evaluation but also reduce the design cost.

2. Construction of Fuzzy Comprehensive Evaluation Analysis Method

2.1. Fuzzy Comprehensive Evaluation System. Fuzzy hierarchical analysis is an evaluation method formed by integrating fuzzy mathematics and hierarchical analysis. The complexity of the objective world and the ever-changing nature of eternal motion give the world a random uncertainty and a more general uncertainty, that is fuzziness. Therefore, based on the affiliation theory of fuzzy mathematics, qualitative evaluation is transformed into quantitative evaluation, that is, fuzzy mathematics is used to make an overall evaluation of things or objects that are subject to multiple factors [24]. This method can effectively improve the objectivity and scientific nature of the design evaluation, and the specific evaluation process is:

(1) Determining the set of evaluation indicators U

In order to facilitate weight allocation and evaluation, the evaluation indicators can be divided into m subsets according to the attributes of the evaluation indicators, and each category is regarded as a single evaluation indicator and called the first-level evaluation indicator. The first-level evaluation index can set the subordinate second-level evaluation index, and the second-level evaluation index can set the subordinate third-level evaluation index, and so on. Denoted as $U_1, U_2, \ldots, U_s$, it should satisfy:

$$\begin{aligned} U &= U_1 \cup U_2 \cup \ldots \cup U_s \\ U_i \cap U_j &= \varnothing \, (i \neq j, i, j = 1, 2, \ldots, s). \end{aligned} \tag{1}$$

(2) Determining the rubric set V of evaluation indicators

The set of rubrics $V = \{v_1, v_2, \ldots, v_n\}$ is the evaluation grade standard and the set of rubric grades is composed of the total evaluation results that the evaluator may make to the evaluated object. In this article, the rubric set V is divided into five levels: good, better, average, qualified, and unqualified, and its level score corresponds to 90, 70, 50, 30, and 10.

(3) Determining the weight vector of evaluation indicators

The weight is a quantitative value that compares and weighs the relative importance of the factors in the evaluated thing as a whole. In the fuzzy comprehensive evaluation, the weights will have a great influence on the final evaluation results, and different weights will sometimes get completely different conclusions.

(4) Establishing the fuzzy comprehensive evaluation matrix **R**

The fuzzy comprehensive evaluation matrix composed of the affiliation degree of each evaluation index relative to the evaluation set is:

$$R = \begin{pmatrix} r_{11} & r_{12} & \cdots & r_{1n} \\ r_{21} & r_{22} & \cdots & r_{2n} \\ \vdots & \vdots & \ddots & \vdots \\ r_{m1} & r_{m2} & \cdots & r_{mn} \end{pmatrix} \quad \left(0 \leq r_{ij} \leq 1\right). \tag{2}$$

(5) Calculating the evaluation vector **B** of the product design solution

After determining the weights of each evaluation index, the evaluation vector B of the product design solution is obtained by synthesizing the resulting weight vector W of each evaluation index with the evaluation matrix R of the corresponding evaluation indicators.

$$\begin{aligned} B = W \bullet R &= (\omega_1, \omega_2, \cdots, \omega_n) \begin{pmatrix} r_{11} & r_{12} & \cdots & r_{1n} \\ r_{21} & r_{22} & \cdots & r_{2n} \\ \vdots & \vdots & \ddots & \vdots \\ r_{m1} & r_{m2} & \cdots & r_{mn} \end{pmatrix} \\ &= (b_1, b_2, \cdots, b_n). \end{aligned} \tag{3}$$

(6) Calculating the comprehensive evaluation value **K** of product design solutions

The fuzzy comprehensive evaluation matrix **B** is transformed into a comprehensive evaluation value K, and different solutions are selected according to their **K** values.

$$K = B \cdot V^T. \tag{4}$$

After getting the evaluation value, a comparison of multiple solutions will give an intuitive and quantitative understanding.

2.2. Calculation of Integrated Weights. The methods for calculating the weights of product design evaluation indicators are mainly divided into subjective and objective methods. The final results obtained when applying the subjective method are highly subjective, while the objective method is a method that uses attribute indicators to determine the weights. In order to get more objective and reliable weights of product design evaluation indexes, this article combines subjective and objective methods and proposes a combined weighting method. The subjective method applies the hierarchical analysis method and the objective method applies the entropy value method, then the weights obtained from both are combined, and then the comprehensive weights are derived to provide reliable calculated weights for the subsequent evaluation of product design solutions.

2.2.1. Analytical Hierarchy Analysis to Determine the Weights. In the early 1970s, American operations researcher Professor Saaty proposed the analytical hierarchy process (AHP) [25]. After years of development, this method is now a more mature combination of qualitative and quantitative analysis of multi-criteria decision-making methods. AHP is easy to use, reliable, and practical. It has been widely used at home and abroad after years of development. The principle of AHP is similar to the process of thinking and judging when deciding; when analyzing a problem, the decision-maker has to establish a hierarchical recursive system structure for the influencing factors of the constraint object, so that the decision-maker can rationalize the complex problem.

(1) Construct Decision-Making Indicator System. The establishment of decision indicators is generally determined according to the professional knowledge or engineering practice experience of the evaluator, but the indicators selected in this way are somewhat arbitrary, and the number of decision indicators usually selected is too large, with a serious overlap of information between them and poor representativeness. Therefore, it is necessary to select decision indicators in accordance with the principles of completeness and coordination, scientificity and mutual exclusivity, feasibility and sensitivity, the combination of dynamic and static, the combination of qualitative and quantitative principles, and the decision indicator system of the final constructed product design scheme.

(2) Constructing Judgment Matrix. After the recursive hierarchy has been established, the affiliation between the upper and lower elements is determined. The next step is to determine the weights of the elements at each level. The relative importance of the different indicators is determined by a two-by-two comparison of the indicators at the next level that affects the indicators at the upper level. In this article, the 1 to 9 scale method of hierarchical analysis [26] (Table 1) is used to construct a judgment matrix by comparing each evaluation index in the evaluation system between two so as to calculate the weights corresponding to the evaluation indexes at the criterion level and each subcriterion level.

(3) Consistency Test of Judgment Matrix. The judgment matrix constructed by a two-by-two comparison does not necessarily have consistency, and a consistency test is required to control the deviation generated by the judgment matrix within a certain range before proceeding to calculate the weights. At present, the maximum characteristic root $\lambda_{\max}$ of the judgment matrix is generally applied to test the consistency of the judgment. The consistency index is calculated according to the following expression:

$$CI = \frac{\lambda_{\max} - m}{m - 1}, \tag{5}$$

where CI is the consistency index of the judgment matrix, $\lambda_{\max}$ is the maximum eigenvalue of the judgment matrix **A**, and m is the order of the judgment matrix ***A***.

The average random consistency index RI is introduced to measure the allowable range of inconsistency of judgment matrices of different orders. The RI values of judgment matrices of order 1 to 9 are shown in Table 2.

Determining the allowable range of inconsistency and calculating the inconsistency ratio CR test formula for the judgment matrix **A** is performed according to the following expression:

$$CR = \frac{CI}{RI}, \tag{6}$$

where CR is the consistency ratio and RI is the random consistency index.

When the calculated $\mathbf{CR} \leq 0.1$, the judgment matrix can be considered consistent, indicating a reasonable weight assignment.

(4) Calculation of Weights. There are many methods to calculate the final weight vector for hierarchical analysis, among which the easiest and most commonly used method is the eigenvector method; so in this article, we choose the eigenvector as the method to calculate the weight vector and has Perron's theorem [27] as its theoretical basis.

Perron's theorem: If $A = (a_{ij})_{n \times n}$ is a positive matrix and $\rho(A)$ is its spectral radius, then the following conditions are satisfied.

(1) The largest eigenvalue $\lambda_{\max}$ of A exists, is unique, and $\lambda_{\max} = \rho(A)$;

Table 1: Scale value table.

Scale value	The value of a_{ji}
1	Evaluation indicator A is the same importance as B
2	Evaluation indicator A is slightly important than B
3	Evaluation indicator A is slightly important than B
4	Evaluation indicator A is more important than B
5	Evaluation indicator A is obviously important than B
6	Evaluation indicator A is very important than B
7	Evaluation indicator A is fiercely important than B
8	Evaluation indicator A is more fiercely important than B
9	Evaluation indicator A is fiercely important than B

Table 2: *RI* values of high-order average random consistency index.

m	1	2	3	4	5	6	7	8	9	10
RI	0.00	0.00	0.58	0.90	1.12	1.24	1.32	1.41	1.45	1.48

(2) The normalized eigenvector $\lambda_{\max}$ corresponding to $\omega = (W_1, W_2, \ldots, W_n)^T$ is a positive vector, that is every element of ω is greater than zero.

The relative importance weight vector ω is first obtained by solving the eigenequation of matrix A in terms of the largest eigenvalue $\lambda_{\max}$ and its corresponding eigenvector and normalizing it.

The eigenvectors are obtained by solving the eigenvalues of matrix **A** and their corresponding eigenvectors $\lambda_{\max}$ and then normalizing them to obtain the relative importance weight vector ω.

$$(A - \lambda_{\max} I)\omega = 0. \tag{7}$$

The eigenvector corresponding to λ is

$$\omega = (\omega_1, \omega_2, \ldots, \omega_n)^T. \tag{8}$$

The feature vector ω corresponding to the maximum eigenvalue $\lambda_{\max}$ is the weight vector of the scheme set.

(5) Multilevel Indicator Weights. The calculation method of the weight vector in the comprehensive evaluation can obtain the weight of each decision indicator to the upper decision factor layer, the weight of each indicator to the total decision target is needed in the decision, and the weight of the decision factor to the total decision target can be calculated by AHP. Let there be a total of s decision indicators in the decision factor layer and the weight D of the indicators in the factor layer obtained by AHP, then the weight of the final decision indicator on the total decision objective is equal to the product of the weight of the corresponding decision indicator and the weight of the upper decision factor, which is denoted as:

$$\omega_j = \omega_j^e \bullet \omega_j^z, \ (j = 1, 2, \ldots, s), \tag{9}$$

where ω_j^e is the weight of the decision factor C corresponding to the indicator C_j, ω_j^z is the weight of decision factor C to the overall objective of the decision, ω_j is the weight of indicator C_j on the total objective of the decision.

2.2.2. Entropy Evaluation Method for Determining Weights. In information theory, entropy is a measure of uncertainty. The greater the amount of information, the smaller the uncertainty and the smaller the entropy; conversely, the greater the entropy [28]. According to the properties of entropy, the randomness and the degree of disorder of a scheme can be judged by calculating the entropy value. The entropy evaluation method (EEM) is an objective assignment method, which determines the index weights according to the size of the information provided by the observations of each index and can reduce the influence of the subjectivity that exists in the hierarchical analysis method on the analysis results [29].

(1) Constructing the indicator matrix

Assuming that there are n evaluation levels and m evaluation indicators, the evaluation indicators are scored according to the expert opinions, which constitute an $n \times m$ indicator matrix **A**.

$$A = \begin{bmatrix} a_{11} & a_{12} & \cdots & a_{1m} \\ a_{21} & a_{22} & \cdots & \cdots \\ \cdots & \cdots & \cdots & \cdots \\ a_{n1} & a_{n2} & \cdots & a_{nm} \end{bmatrix}, \tag{10}$$

where a_{ij} is the value of the jth indicator of the ith program.

(2) Normalizing the indicator matrix

Since the units of measurement of each indicator are not uniform, it is necessary to standardize them before using them to calculate the composite indicators so as to solve the problem of homogenization of the different qualitative indicator values. The indicator matrix **A** is normalized to obtain the normalization matrix **P**.

$$P = \begin{bmatrix} p_{11} & p_{12} & \cdots & p_{1m} \\ p_{21} & p_{22} & \cdots & p_{2m} \\ \vdots & \vdots & \ddots & \vdots \\ p_{n1} & p_{n2} & \cdots & p_{nm} \end{bmatrix}$$

$$p_{ij} = \frac{q_{ij}}{\sum_{i=1}^{n} q_{ij}} \tag{11}$$

$$\text{positive indicators} \quad q_{ij} = \frac{a_{ij} - a_{\min}}{a_{\max} - a_{\min}}$$

$$\text{positive indicators} \quad q_{ij} = \frac{a_{\max} - a_{ij}}{a_{\max} - a_{\min}}$$

$$i = 1, \ldots, n, \ j = 1, \ldots m$$

(3) Calculating the information entropy value $\mathbf{E_j}$ of the jth indicator

$$E_j = -\frac{1}{\ln(n)} \sum_{i=1}^{n} p_{ij} \ln\left(p_{ij}\right) \ (i = 1, \ldots, n, j = 1, \ldots, m), \tag{12}$$

where: $0 \le \mathbf{E_j} \le 1$.

(4) Calculating the information entropy redundancy $\mathbf{D_j}$

$$D_j = 1 - E_j. \tag{13}$$

(5) Calculating the entropy weight of each indicator

$$\omega_j = \frac{D_j}{\sum_{j=1}^{m} D_j}. \tag{14}$$

2.2.3. Determining the Comprehensive Weights of Indicators. The hierarchical analysis method and entropy value method have obtained subjective weights and objective weights, respectively, and it is necessary to recombine the subjective and objective weights to get more accurate comprehensive weights. Then the comprehensive weight of each evaluation index is calculated by the following formula [30].

$$\begin{aligned} W_j &= \frac{\omega_j^{(a)} \cdot \omega_j^{(e)}}{\sum_{j=1}^{m} \omega_j^{(a)} \cdot \omega_j^{(e)}} \\ AHP\text{: } \omega_a &= \left(\omega_1^{(a)}, \omega_1^{(a)}, \ldots, \omega_m^{(a)}\right) \\ EEM\text{: } \omega_e &= \left(\omega_1^{(e)}, \omega_1^{(e)}, \ldots, \omega_m^{(e)}\right). \end{aligned} \tag{15}$$

3. Fuzzy Comprehensive Evaluation Based on Mechanical Product Design Scheme Optimization

3.1. Establishment of Fuzzy Comprehensive Evaluation System. The article takes the evaluation of a gearbox reducer design scheme as an example, and three preliminary design options are available [31].

(1) A two-stage reduction: this scheme can make full use of space to reduce the center distance, but it is bound to increase the supporting devices such as shafts, gears, and bearings for the first-stage drive.

(2) Single-stage transmission, with the clutch arranged in the middle end and the box components divided into two large parts, namely the box and the front cover; the pinion is hollow-set on the long shaft, and the input power is transmitted to the pinion through the long shaft and the clutch closure on it.

(3) Single-stage transmission, the structure of scheme (2) is partially adjusted: the input shaft adopts torsion shaft transmission, the pinion gear is empty set on the torsion shaft, which makes the reducer have the characteristics of small size; the clutch is arranged at the rear end, the box combination surface is changed from longitudinal section to transverse section, which improves the assembly and disassembly performance of the clutch parts and output shaft parts; however, the process is more difficult.

By reviewing the information, a total of 2 principles of technical indicators T and economic indicators E were identified as the first-level indicators of the evaluation index system. Performance indicator $T1$, processability indicator $T2$, and service-oriented indicator $T3$ constitute the secondary indicators of technical indicator T, and labor cost $E1$ and time cost $E2$ constitute the secondary indicators of economic indicator E. And center distance $T11$ and weight $T12$ constitute the tertiary indicators of performance indicator $T1$, ease of installation $T21$ and ease of processing $T22$ constitute the tertiary indicators of processability indicator $T2$, and ease of maintenance $T31$ constitutes the tertiary indicators of serviceability indicator $T3$. The processing cost $E11$ and material cost $E12$ are the tertiary indicators of labor cost, and the time of trial production and production start-up $E21$ and design progress $E11$ are the tertiary indicators of time cost [31] (Figure 1).

3.2. Method of Calculating the Comprehensive Weights of the Evaluation Indexes of the Design Scheme

(1) AHP method to determine the evaluation index weights of gearbox reducer design scheme

For gearbox product development, according to historical data and the experience of relevant engineering designers, two comparisons are made using the 1–9 scale method to construct the judgment matrix of evaluation indicators at all levels, calculate the weights under a single criterion based on the work formulas (5)–(8), and conduct consistency tests on the judgment matrix of order $n > 2$ (Table 3).

(2) EEM to determine the weight of gearbox reducer design evaluation index

By inviting experts to make a two-by-two comparison of the evaluation indexes at each level of the gearbox reducer design evaluation system shown in Figure 1 using the 1 to 9 scale method, the judgment matrix A of the evaluation indexes at each level is constructed.

$$A = \begin{bmatrix} 1 & 1/7 & 2 & 1/2 & 1 & 1 & 1/2 & 3 & 3 \\ 7 & 1 & 8 & 4 & 7 & 7 & 4 & 9 & 9 \\ 1/2 & 1/8 & 1 & 1/3 & 1/2 & 1/2 & 1/5 & 1 & 1 \\ 2 & 1/4 & 3 & 1 & 2 & 2 & 1 & 5 & 5 \\ 1 & 1/7 & 2 & 1/2 & 1 & 1 & 1/2 & 3 & 3 \\ 1 & 1/7 & 2 & 1/2 & 1 & 1 & 1/2 & 3 & 3 \\ 2 & 1/4 & 5 & 1 & 2 & 2 & 1 & 7 & 7 \\ 1/3 & 1/9 & 1 & 1/5 & 1/3 & 1/3 & 1/7 & 1 & 1 \\ 1/3 & 1/9 & 1 & 1/5 & 1/3 & 1/3 & 1/7 & 1 & 1 \end{bmatrix}. \tag{16}$$

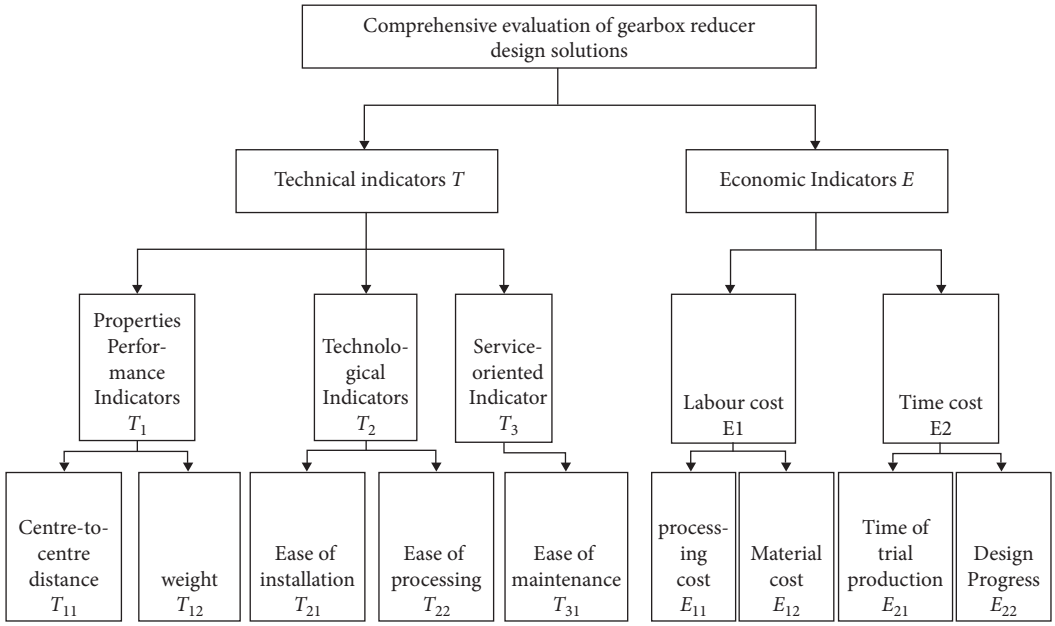

Figure 1: Gearbox reducer design scheme evaluation index system.

Table 3: Indicator weights and consistency test.

Tertiary level indicator weight and consistency test			
Evaluation indicators	Weight vector	CR	Consistency check
$T1$	(0.125, 0.875)	—	—
$T2$	(0.25, 0.75)	—	—
$T3$	—	—	—
$E1$	(0.25, 0.75)	—	—
$E2$	(0.5, 0.5)	—	—
Secondary level indicator weight and consistency test			
Evaluation indicators	Weight vector	CR	Consistency check
T	(0.73, 0.19, 0.08)	0.058	Pass
E	(0.83, 0.17)	—	—
Primary level indicator weight and consistency test			
Evaluation indicators	Weight vector	CR	Consistency check
Overall solution	(0.75, 0.25)	—	—
Final weight vector			
$W = (0.068, 0.480, 0.036, 0.107, 0.060, 0.052, 0.155, 0.021, 0.021)$			

The entropy and entropy weights of each three-level index under the gearbox reducer design scheme can be obtained by equations (10)–(13) (Table 4).

(3) Comprehensive weight determination of evaluation indicators

The comprehensive weight vector of security principle evaluation indexes can be derived from equation (14) as

$$\mathbf{W}_1 = (0.090, 0.320, 0.069, 0.115, 0.086, 0.082, 0.136, 0.051, 0.051). \quad (17)$$

3.3. Determining the Affiliation Matrix R of the Product Design Solution. In this article, the affiliation matrix of the literature [32] on the three design options of the gearbox reducer is directly chosen as shown in Table 5.

3.4. Determining the Evaluation Matrix B of the Product Design Solution. The evaluation matrix **B** for each gearbox reducer design option can be calculated according to (3).

Scheme 1:

$$\mathbf{B}_1 = \mathbf{W} \bullet \mathbf{R}_1 = (0.1870, 0.0996, 0.0342, 0.3142, 0.3650). \quad (18)$$

Scheme 2:

$$\mathbf{B}_2 = \mathbf{W} \bullet \mathbf{R}_2 = (0.1620, 0.2172, 0.3190, 0.2206, 0.0812). \quad (19)$$

Scheme 3:

$$\mathbf{B}_3 = \mathbf{W} \bullet \mathbf{R}_3 = (0.0966, 0.2934, 0.3606, 0.2494, 0). \quad (20)$$

3.5. Determining the Comprehensive Evaluation Value of the Product Design Solution K. According to (5), the evaluation score **K** can be calculated for each gearbox reducer design solution.

Scheme 1:

$$\mathbf{K}_1 = \mathbf{B}_1 \bullet \mathbf{V}^{\mathbf{T}} = (0.1870, 0.0996, 0.0342, 0.3142, 0.3650)(90, 70, 50, 30, 10)^T = 38.588. \quad (21)$$

Scheme 2:

Table 4: Entropy and entropy weight of the third-level indicator.

Entropy	(0.642, 0.482, 0.677, 0.609, 0.642, 0.642, 0.616, 0.743, 0.743)
Entropy weights	(0.112, 0.162, 0.101, 0.122, 0.112, 0.112, 0.119, 0.080, 0.080)

Table 5: The affiliation matrix of each design solution.

Scheme	Affiliation matrix R
Scheme 1	$R_1 = \begin{bmatrix} 1 & 0 & 0 & 0 & 0 \\ 0 & 0 & 0 & 0.2 & 0.8 \\ 0 & 0 & 0.2 & 0.6 & 0.2 \\ 0.4 & 0.6 & 0 & 0 & 0 \\ 0 & 0 & 0 & 0.4 & 0.6 \\ 0 & 0 & 0 & 0.8 & 0.2 \\ 0 & 0 & 0 & 0.8 & 0.2 \\ 0.2 & 0.4 & 0.4 & 0 & 0 \\ 0.8 & 0.2 & 0 & 0 & 0 \end{bmatrix}$
Scheme 2	$R_2 = \begin{bmatrix} 0.2 & 0.6 & 0.2 & 0 & 0.2 \\ 0 & 0 & 0.4 & 0.4 & 0.2 \\ 0 & 0.2 & 0.6 & 0.2 & 0 \\ 0.4 & 0.6 & 0 & 0 & 0 \\ 0 & 0 & 0.2 & 0.6 & 0.2 \\ 0.2 & 0.4 & 0.4 & 0 & 0 \\ 0 & 0.2 & 0.6 & 0.2 & 0 \\ 0.8 & 0.2 & 0 & 0 & 0 \\ 0.8 & 0.2 & 0 & 0 & 0 \end{bmatrix}$
Scheme 3	$R_3 = \begin{bmatrix} 0.4 & 0.6 & 0 & 0 & 0 \\ 0 & 0 & 0.4 & 0.6 & 0 \\ 0 & 0.2 & 0.6 & 0.2 & 0 \\ 0.2 & 0.4 & 0.4 & 0 & 0 \\ 0.2 & 0.6 & 0.2 & 0 & 0 \\ 0 & 0.4 & 0.4 & 0.2 & 0 \\ 0 & 0.4 & 0.4 & 0.2 & 0 \\ 0.2 & 0.4 & 0.4 & 0 & 0 \\ 0.2 & 0.4 & 0.4 & 0 & 0 \end{bmatrix}$

$$\mathbf{K}_2 = \mathbf{B}_2 \bullet \mathbf{V}^{\mathbf{T}} = (0.1620, 0.2172, 0.3190, 0.2206, 0.0812)$$

$$(90, 70, 50, 30, 10)^T = 53.146. \quad (22)$$

Scheme 3:

$$\mathbf{K}_3 = \mathbf{B}_3 \bullet \mathbf{V}^{\mathbf{T}} = (0.0966, 0.2934, 0.3606, 0.2494, 0)$$

$$(90, 70, 50, 30, 10)^T = 54.744. \quad (23)$$

The final rating results of the gearbox reducer design scheme calculated by the above method are $\mathbf{K}_3 > \mathbf{K}_2 > \mathbf{K}_1$, with scheme 3 being the best, scheme 2 the second best, and scheme 1 the worst. This is consistent with the evaluation results of literature [32, 33], and from the actual analysis, scheme 1 uses two-stage reduction, which requires an additional level of transmission system supporting device, while scheme 2 uses a single-stage transmission and scheme 3 is an improved design based on scheme 2, so the evaluation results are also consistent with the actual situation.

4. Conclusions

Evaluation decision plays a crucial role in the design process, and its effectiveness directly affects the direction and results of the design progress. In the decision-making process, when determining the weights of each evaluation index, combining the subjectivity of the hierarchical analysis method to determine the weights and the objectivity of the entropy weight method to determine the weights, the decision-makers can evaluate the design solutions more scientifically and accurately and improve the reliability of the design solution evaluation. The final design scheme, Scheme 3, was preferentially selected after evaluating three designs for a gearbox reducer, which is not only consistent with the literature evaluation results [28, 29] but is also in line with the actual analysis results. This method confirms its scientificity, validity, and reliability, thereby reducing the product development cycle and improving its quality.

Data Availability

The data used to support the finding of this study can be obtained from the corresponding author upon request.

Conflicts of Interest

The authors declare that they have no conflicts of interest.

Acknowledgments

This research was supported by Xi'an Science and Technology Project (Grant 2020KJRC0032), Research on the development of practical skills of professional degree students of the Chinese Society for Degree and Postgraduate Education (2020ZDB89), Innovation Capability Support Program of Shaanxi Province (2018TD-036), and Research and Practice Project on Comprehensive Reform of Postgraduate Education in Shaanxi Province in 2020.

References

[1] J. C. L. López, J. S. Noriega, and O. A. Valenzuela, "A preference choice model for the new product design problem," *Operational Research*, vol. 2021, pp. 1–32, 2021.

[2] M. Pozatti, M. M. e S. Bernardes, D. R. Vieira, and M. C. Chain, "Frame conditions for implementing design methods in the product development industry," *International Journal of Product Development*, vol. 24, no. 4, p. 297, 2020.

[3] M. Cantamessa, F. Montagna, S. Altavilla, and A. Casagrande-Seretti, "Data-driven design: the new challenges of digitalization on product design and development," *Design Science*, vol. 6, no. e27, p. e27, 2020.

[4] F. Tao, F. Sui, A. Liu et al., "Digital twin-driven product design framework," *International Journal of Production Research*, vol. 57, no. 12, pp. 3935–3953, 2019.

[5] X. Q Yan, Y. Li, J. Chen, W Li, and Y. Xiong, "A method of implementing formalized multidisciplinary collaboration in product conceptual design process," *Proceedings of the Institution of Mechanical Engineers Part C: Journal of Mechanical Engineering Science*, vol. 231, no. 18, pp. 3342–3357, 2017.

[6] Y. Chen, Z. Zhang, Y. Xie, and M. Zhao, "A new model of conceptual design based on Scientific Ontology and intentionality theory. Part I: the conceptual foundation," *Design Studies*, vol. 37, pp. 12–36, 2015.

[7] D. C. Eddy, S. Krishnamurty, I. R. Grosse, and M. Steudel, "Early design stage selection of best manufacturing process," *Journal of Engineering Design*, vol. 31, no. 1, pp. 1–36, 2019.

[8] Y. Feng, "Research on computer-aided product innovation design based on TRIZ," *Journal of Computational and Theoretical Nanoscience*, vol. 13, no. 12, pp. 9876–9881, 2016.

[9] J. Ma and G. E. O. Kremer, "A systematic literature review of modular product design (MPD) from the perspective of sustainability," *International Journal of Advanced Manufacturing Technology*, vol. 86, no. 5-8, pp. 1509–1539, 2016.

[10] J. W. Chen, H. J. Yang, J. J. Cui, and J. S. Zhang, "Concept semantics driven computer aided product innovation design," *Journal of Computational Methods in Science and Engineering*, vol. 16, no. 3, pp. 575–590, 2016.

[11] W. Wei, Z. Tian, C. Peng, A. Liu, and Z. Zhang, "Product family flexibility design method based on hybrid adaptive ant colony algorithm," *Soft Computing*, vol. 23, no. 20, pp. 10509–10520, 2018.

[12] H. C. Zhang, Y. F. Yang, A. M. Yang, and L. N. Shi, "Data envelopment analysis model of mechanical product design," *Applied Mechanics and Materials*, vol. 443, pp. 58–61, 2013.

[13] X. C. Lu and H. X. Zhang, "Product evaluation in stages based on Robust design," *Applied Mechanics and Materials*, vol. 215-216, pp. 489–492, 2012.

[14] S. Yu, "GP-based optimisation of product parameters of design alternatives to support life cycle design," *International Journal of Environmental Technology and Management*, vol. 14, no. 5/6, p. 417, 2011.

[15] W. M. Wang, G. F. Wang, and Y. G. Feng, "Optimal Grey model for multi-attribute decision making with triangular fuzzy numbers and its application in evaluating of engineering design schemes," *Mathematics in Practice and Theory*, vol. 42, no. 12, pp. 21–27, 2012.

[16] Z. Rui, G. Li, and L. Ju, "Optimization design of pump motor based on genetic algorithm and neural network," *Industrial Electronics & Applications. IEEE*, vol. 2016, pp. 38–42, 2016.

[17] X. B. Chen, "A comprehensive decision-making model for risk management of supply chain," *Expert Systems with Applications*, vol. 42, no. 12, pp. 21–27, 2011.

[18] T. L. Chen, C. C. Chen, Y. C. Chuang, and J. J. H. Liou, "A hybrid MADM model for product design evaluation and improvement," *Sustainability*, vol. 12, no. 17, Article ID 6743, 6743 pages, 2020.

[19] C. Yuan, W. Wang, Y. Lin, and Y. Chen, "A novel fuzzy comprehensive evaluation method for product configuration design integrated customer requirements," *Advanced Science Letters*, vol. 6, no. 1, pp. 774–778, 2012.

[20] M. Li and J. Zhang, "Integrating Kano model, AHP, and QFD methods for new product development based on text mining, intuitionistic fuzzy sets, and customers satisfaction," *Mathematical Problems in Engineering*, vol. 2021, no. 5, pp. 1–17, 2021.

[21] X. H. Xu, J. Feng, and B. S. Tong, "An evaluation method for schemes of mechanical product conceptual design with incomplete multi-technique-parameters," *Journal of Engineering Graphics*, vol. 2006, no. 2, pp. 27–31, 2006.

[22] M. Yumoto, "Development of decision support system for product selection based on AHP, using the decision rule of rough set for qualitative evaluation," *IEEJ Transactions on Electronics, Information and Systems*, vol. 139, no. 9, pp. 1080–1091, 2019.

[23] L. H. Du, H. Chen, Y. D. Fang et al., "Research on the method of acquiring customer individual demand based on the quantitative Kano model," *Computational Intelligence and Neuroscience*, vol. 1, Article ID 505271, 12 pages, 2022.

[24] L. A. Zadeh, "Fuzzy sets as a basis for a theory of possibility," *Fuzzy Sets and Systems*, vol. 1, no. 1, pp. 3–28, 1978.

[25] T. L. Saaty, "Decision making, new information, ranking and structure," *Mathematical Modelling*, vol. 8, no. 6, pp. 125–132, 1987.

[26] Y. Ren, "Evaluation system for interactive asset performance management based on 1-9 scaling method," *Experimental Technology and Management*, vol. 34, no. 11, pp. 259–262, 2017.

[27] M. Bernasconi, C. Choirat, and R. Seri, "A re-examination of the algebraic properties of the AHP as a ratio-scaling technique," *Journal of Mathematical Psychology*, vol. 55, no. 2, pp. 152–165, 2011.

[28] B. Liu, "Some research problems in uncertainty theory," *Journal of Uncertain Systems*, vol. 3, no. 1, pp. 3–10, 2009.

[29] D. L. Mon, C. H. Cheng, and J. C. Lin, "Evaluating weapon system using fuzzy analytic hierarchy process based on entropy weight," *Fuzzy Sets and Systems*, vol. 62, no. 2, pp. 127–134, 1994.

[30] S. Hu and J. Liu, "Application of fuzzy comprehensive evaluation method in product design scheme decision," *Journal of Machine Design*, vol. 37, no. 01, pp. 135–139, 2020.

[31] Qi. Gao, *Study on Strategy and Method of Design for Quality*, Zhejiang University, 1998.

[32] K. Liu, Q. Zhao, and S. Zhou, "Fuzzy comprehensive evaluation for conceptual design of mechanic product based on new membership conversion," *Journal of Mechanical Engineering*, vol. 45, no. 12, p. 162, 2009.

[33] G. Huang, Z. Yu, and Z. Wu, "A method of comprehensive evaluation with subjective and objective information based on evidential reasoning and rough set theory," *China Mechanical Engineering*, vol. 2001, no. 8, pp. 90–94+7, 2001.

Hindawi
Scientific Programming
Volume 2023, Article ID 9783524, 1 page
https://doi.org/10.1155/2023/9783524

Retraction

Retracted: An Auxiliary Teaching System for Spoken English Based on Speech Recognition Technology

Scientific Programming

Received 18 July 2023; Accepted 18 July 2023; Published 19 July 2023

This article has been retracted by Hindawi following an investigation undertaken by the publisher [1]. This investigation has uncovered evidence of one or more of the following indicators of systematic manipulation of the publication process:

(1) Discrepancies in scope
(2) Discrepancies in the description of the research reported
(3) Discrepancies between the availability of data and the research described
(4) Inappropriate citations
(5) Incoherent, meaningless and/or irrelevant content included in the article
(6) Peer-review manipulation

The presence of these indicators undermines our confidence in the integrity of the article's content and we cannot, therefore, vouch for its reliability. Please note that this notice is intended solely to alert readers that the content of this article is unreliable. We have not investigated whether authors were aware of or involved in the systematic manipulation of the publication process.

Wiley and Hindawi regrets that the usual quality checks did not identify these issues before publication and have since put additional measures in place to safeguard research integrity.

We wish to credit our own Research Integrity and Research Publishing teams and anonymous and named external researchers and research integrity experts for contributing to this investigation.

The corresponding author, as the representative of all authors, has been given the opportunity to register their agreement or disagreement to this retraction. We have kept a record of any response received.

References

[1] L. Bao and J. Lv, "An Auxiliary Teaching System for Spoken English Based on Speech Recognition Technology," *Scientific Programming*, vol. 2022, Article ID 6519228, 11 pages, 2022.

Hindawi
Scientific Programming
Volume 2022, Article ID 6519228, 11 pages
https://doi.org/10.1155/2022/6519228

Research Article

An Auxiliary Teaching System for Spoken English Based on Speech Recognition Technology

Lei Bao[1] **and Jing Lv**[2]

[1]*Oxbridge College, Kunming University of Science and Technology, Kunming, China*
[2]*Sichuan Normal University, Chengdu, China*

Correspondence should be addressed to Lei Bao; leibao_kmust@yeah.net

Received 28 June 2022; Revised 16 July 2022; Accepted 22 July 2022; Published 28 August 2022

Academic Editor: Lianhui Li

Because the English language has always been inaccurate and seemed difficult to correct errors, this development has created a reputation based on improvements to the DWJ algorithm and HMM speech scores and correction mistake. In this paper, different signal characteristics are used using the DWJ algorithm: the Mel frequency cepstrum coefficient compares the standard speech library and the distance between the speech sample and the sample message received. The conversation deciphered the Viterbi code according to the HMM model, which was recognized and evaluated by posteriori probabilities. Finally, the professional data were used to fix the wrong phone to determine, score, and make repair mistakes. The results of the experiments show that the tests used in this article are reliable. The results of the experiment show that the standard English language proficiency in this article is reliable, which can provide students with timely, accurate, and objective assessment and teaching feedback, improving English language proficiency.

1. Introduction

As the most widely used language in the world, it is important to learn and master English. However, learning English has always affected Chinese. Learning, reading, listening, and speaking English on a daily basis is the hardest part. With the advancement of computer science and technology, training, and education, the use of computer-assisted speech technology allows for solving this problem. Technology can transform existing instructional patterns and learning environments and transform information into text by doing, analyzing, recognizing, and understanding them. In combination with other language skills such as fluency, speech technology, and machine translation. English language proficiency systems have been developed to help students correct non-verbal cues on time and without repetition. This will greatly benefit students' English language learning experience and result in significant community and business benefits.

2. Literature Review

The basis of telephone calls is knowledge of speech and speech measurement. Speech recognition technology, or Automatic Speech Recognition (ASR), is the technology of translating information into commands or texts by using automatic recognition and comprehension technology (many are computers) to use interactive communication between man and machine. Thus, speech skills have become a hot topic in recent years [1, 2]. The demands of high-end software, hardware, and procedures for speech signal processing work are due to changes in speech, data signal frequency, volume of speech, in particular, multiple acknowledgments and measures. From the classical dynamic time distortion (DTW) algorithm to the hidden Markov simplified model (HMM) and then to the latent inertia device (ANN), speech recognition has become the norm. *Unprecedented Difficulties*. As a result, it is difficult to improve its accuracy and speed, making it difficult to make a significant impact on knowledge of speech, material, and industry [3].

For the classic speech recognition algorithm, DTW solves the problem of different call length patterns based on dynamic programming ideas. DTW is the easiest and most effective way to identify personal information, as it is virtually no longer included in training. However, it has many shortcomings, especially the ability to recognize an independent speaker, speak fluently, and speak with large words. The main reason is that there is no efficiency for training using statistical procedures, and it is not easy to use simple and advanced instructions for algorithms.

HMM creates a set number of models of speech signal time. The HMM model describes the acoustic model of speech in an appropriate way and uses training techniques in organically blended low-pitched and upper-level speech patterns in cognitive exploration algorithm so a better effect can be obtained. However, HMM also has some limitations [4]. First, the HMM-based approach does not consider the impact of perception. Secondly, large-scale speech corpora need to be collected to train HMM templates of standard speech to obtain robust HMM. Moreover, since call is an aid to second language learning, it involves more nonnative speech recognition. When recognizing nonnative speech, the recognition performance of HMM trained by native speech will be greatly reduced, so it is necessary to carry out self-adaptive nonnative speech recognition. Even so, it is still difficult for the adaptive HMM to achieve good results in nonnative speech recognition. In addition, HMM also has the following problems: the prior statistical knowledge of speech signals is required, the classification decision-making ability is weak, and the Viterbi recognition algorithm has a large amount of computation and Gaussian mixture probability calculation. These shortcomings make it difficult to further improve the performance of HMM model. For English speech recognition with large amount of data and complex pronunciation changes, HMM has more obvious shortcomings, which makes the speech recognition time longer. Therefore, the HMM-based speech recognition method has encountered a major development bottleneck [5].

3. Improved DWT Algorithm

3.1. Speech Recognition Principle. The main idea of knowledge of technology is to bring speech into a product of learning, translating practical information into text that is conveyed through the processes of machine knowledge and understand, and allow the machine to control speech. Speech recognition can illustrate the principle of acceptance as shown in Figure 1. The most important module of speech recognition is to eliminate speech and modify speech patterns.

3.2. Voice Signal Preprocessing. The first step in speaking skills is before the speaking process. The advancement of speech characters is not only the basis of speaking skills, but also an important factor in the development of the characteristics of speech. Only at the prespeaking stage of the speech signal is it possible to subtract the features that

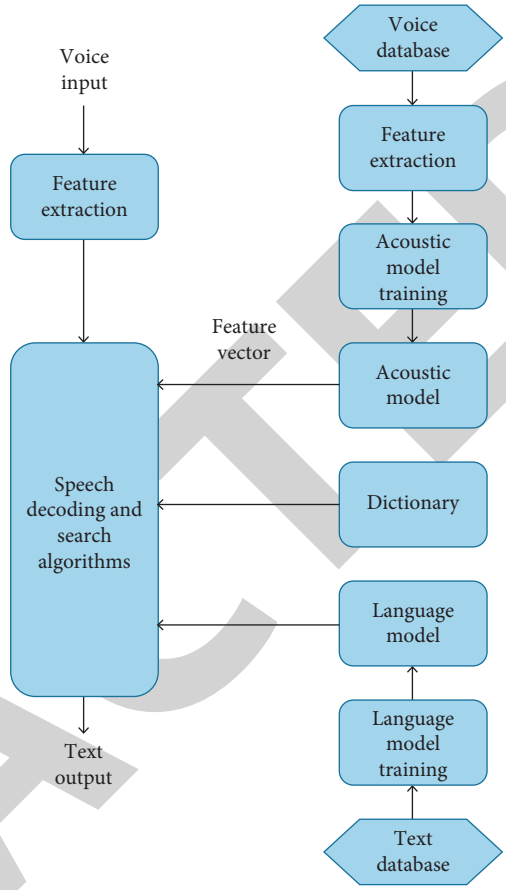

Figure 1: Principle of speech recognition.

indicate the speech and then carry out the comparison with the sample to get the result related similarities. The audible signal preprocessing module typically has five steps: digitizing the audible signal, endpoint detection, enclosing, windowing, and preemphasis[6].

3.2.1. Speech Signal Digitization. A loudspeaker signal is a type of clock-changing wave and is an analog signal. However, since computers only receive digital signals, if a computer wants to make a speech sound, it must digitize the speech signal. The process of digitizing spoken characters involves comparisons and quantification. After sampling and quantization, the speech signal becomes a digital signal.

3.2.2. Preemphasis. The first task is to improve the signal frequency, eliminate the frequency signal in the speech signal, and smooth the signal spectrum. In the spectrum of speech signals, the higher the frequency, the lower the amplitude. When the frequency of a speech signal is doubled, its amplitude of the energy spectrum decreases by 6 dB. In order to balance the signal spectrum and facilitate the analysis of the spectrum and other characteristics, it is first necessary to see that the signal is speech signal. High-frequency speech signals and low-frequency speech signals are difficult to obtain. Special attention is paid to solving this

problem. One indicator is the use of digital audio signals through filters with enhanced 6Db/8 frequency characteristics. This is a first-class digital filter, as shown in the following equation:

$$H(z) = 1 - \mu * z^{-1}. \quad (1)$$

If expressed in time domain, the preaccentuated signal S_2(n) is

$$S_2(n) = S(n) -^{*} S(n-1), \quad (2)$$

where μ is 0.9375.

3.2.3. Framing and Windowing. Generally, speech symbols are considered infinite and change over time. However, in the short term, such as l0 ms–25 ms, there is a slight change in the characteristics of the speech signal. We can define this short-term problem as a stable signal, and the characteristics of the speech at this time can be considered as constant [7]. Therefore, it can describe the speech signal using a short time; that is, the speech signal is segmented parallel to the time axis. To achieve the purpose of speech comparison, we subtract the speech signal characteristics for each speech segment and compare them with the segmented speech characteristics. At the same time, the overlap of the frames should be facilitated by the transition of the line adjacent to the speech signal and the continuity of the signal. This overlap is often called the transformation, and the data contained in a ton of speech is called a long line [8].

3.2.4. Endpoint Detection. There is no way to determine the end. Different search processes can be used in different systems. In this form, the system uses a combination of short-term zero interference velocity and short-term momentum to capture the final points. Both methods are time-consuming and the results are reliable and accurate.

The short-term energy is a reflection of the law of change in terms of volume over time. Assume that the long-range magnitude of the X range of the nth energy of the speech signal is indicated by E. then its calculation formula is shown as follows (where N is the frame length):

$$En = \sum_{m=0}^{N-1} x_n^2(m), \quad 0 \le m \le N-1. \quad (3)$$

We can tell the difference between speech and voice by analyzing the signal strength. The distance between the speaker signal and the pickup will indicate more. Short power consumption, speech signal, and noise can be easily seen in the example of signal-to-noise ratio. However, in a low- to high-pitched environment, the short-wave energy does not exactly distinguish the melody [9].

The short-time zero intersection signal is the number of short-time signals transmitted across the x-axis in the range. The signal recording time for a continuous speech signal is the number of times it crosses over the time axis of the zero intersection reported. If the two values of an example of a discrete signal are different, it means that they pass through the time axis at once. Therefore, a zero-intersection value can be calculated. We define the short-time zero-crossing rate of speech signal as follows:

$$Z_n = \frac{1}{2} \sum_{m=0}^{N-1} \left| \operatorname{sgn}[x_n(m)] - \operatorname{sgn}[x_n(m-1)] \right|, \quad (4)$$

where sgn[x] is a symbolic function, as follows:

$$\operatorname{sgn}[x] = \begin{cases} 1 & (x \ge 0) \\ -1 & (x \le 0). \end{cases} \quad (5)$$

Low-energy sound tones have a low cross-sectional area, while high-energy sound tones have a high cross-sectional area. In general, by identifying the zero-crossing speed, it can be seen that the speech segment has a stable zero-crossing speed, but the volume is not the case. Therefore, we can filter the end of the conversation by short-term zero intersection [10].

3.3. Feature Extraction of Speech Signal. Decomposing speech signal features for improved speech reduces system storage capacity, shortens run time, and effectively improves comparison efficiency [11].

Now, after the speech signal has been completed, several measures have been selected for the following characteristics: linear estimated coefficient (LPC), linear hypothesis cepstrum coefficient (LPCC), and Mel cepstrum coefficient (MFCC). These measurements can determine the characteristics of the speech signal. The Mel cepstrum coefficient (MFCC) is stronger for noise operation and more stable than the linear frequency (LPC). Using three negative traits (MFCC, tone, and size) to measure English proficiency, the final experiment showed that MFCC had the highest accuracy [12].

The relationship between Mel scale and frequency can be illustrated by the following equation (where f is the truth rate of the signal):

$$f_{\text{mel}} = 2595 \operatorname{long}_{10}\left(1 + \frac{f}{700}\right), \quad (6)$$

where f is the unit of actual frequency in Hz. MFCC parameter extraction principle's block diagram is shown in Figure 2.

3.4. Dynamic Time Warping (DTW) Recognition Algorithm. Dynamic time distortion is best associated with the principle of dynamic programming by performing time differences between the design and the experimental model. This bends two sentences connected to different clocks on the time axis so that the two points speak better. There are two time series, m and N, and their lengths are h and K. M sequence is the design, n is a sequence model, and the values of each point in the system are the same indicating the value of each column of temporary speech. For example, the sentence of m speech contains the whole H number. The characteristic value of the

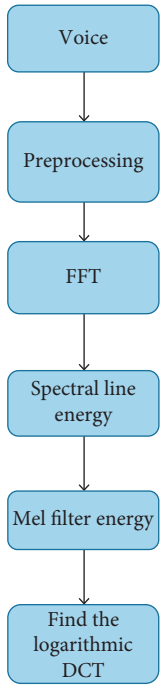

Figure 2: Schematic block diagram of MFCC feature parameter extraction.

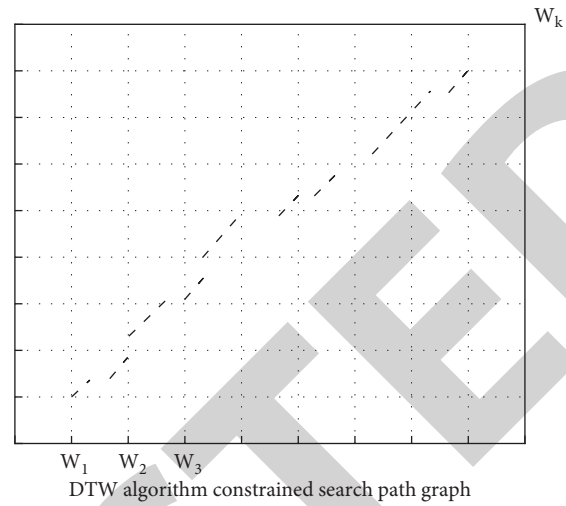

Figure 3: DTW algorithm constraint search path diagram.

i-th frame is mi. The Figure 3 shows data formula (7) of the two sequences:

$$M = m_1, m_2, \ldots, m_i, \ldots, m_h;$$
$$N = n_1, n_2, \ldots, n_j, \ldots, n_k; \quad (7)$$

In order to better compare the two speech periods, we need to compare the two periods and create a network of $h * k$ matrices as shown in the figure below. We draw each model audible signal frame on the horizontal axis of the rectangle joint and then draw each sample audible signal frame on the vertical axis of the rectangle joint. The diagrams below are drawn with data from two categories. The intersection of each grid in the figure shows that the distance between m_i and n_j can be marked w_i; that is, the similarity of each point in m is temporary and each point in n is temporary. The smaller the distance, the higher the similarity. Euclidean sites are usually used. Each term of the matrix (i, j) represents a comparison of the terms mi and n_j. The DTW algorithm can be scaled down to see the way through multiple points in this network. Content across the network is a parallel content that counts in two sections. The two sequences can be represented in Figure 3 by the two combinations.

From the above analysis, we can define the passage through the lines in the figure according to the method of exploration with the time difference of W. The k-th definition of W indicates drawings of m and n.

From the above analysis, we can determine the way in which the lines in the figure become the means of exploration with time change, shown as W. Conclusion k-th of W is defined as the formula, indicating the sequences M and N. So we have the following formula:

$$W = w_1, w_2, \ldots, w_{k-i}, \ldots, w_k; \max(m, n) \le k \le m + n - 1. \quad (8)$$

3.5. Improved DTW Algorithm. In the previous section, the DTW algorithm always uses all words as the basis of training and recognition and does not consider the distribution of words. Due to the low slope limit during modification, many points in the network cannot be reached. As shown in Figure 4, it is not necessary to calculate the appropriate frame spacing for the diamond layer mesh content [13]. In addition, it is not necessary to keep the matrix parallelism of all the frames and the matrix components, because only three networks of the previous line are used in the calculation counts for each network point in each row. The combined use of these two functions can reduce computing and storage space [14].

Adjusting multiple lines of the research matrix can affect the required speed. We can control the search area by adjusting the two slopes. If the search is too small, the search speed will be better, more useable methods will be lost, and the comparison will be inaccurate. Changing the search facilities too much may quickly affect competition [15]. Finally, the development of DTW exploration after the experiment did not explore the whole of the matrix data in the figure, but reduced the area of the surrounding parallelogram by two lines with 2/3 and 3/2 slopes. It is the last point that works. A field is a parallelogram called an exploration figure. A field is a parallelogram called an exploration figure. In the origin and endpoint of the parallelogram (top right) and the parallelogram formed by the two edges 2/3 and 3/2, the following two points Send and Xb finally counted. In such areas, rapid and similar searches are the best options [16]. Improvements to traditional DTW algorithms are aimed at improving the performance of comparison speech. Figure 4 shows the research method for improving the DTW algorithm.

In Figure 4, the actual dynamic bending is divided into three sections: $(1, x_a)$, $(x_{a+1}\ x_b)(x_{b+1}N)(1, x_a)$, $(x_{a+1}\ x_b)$ $(x_{b+1}N)$, as shown in

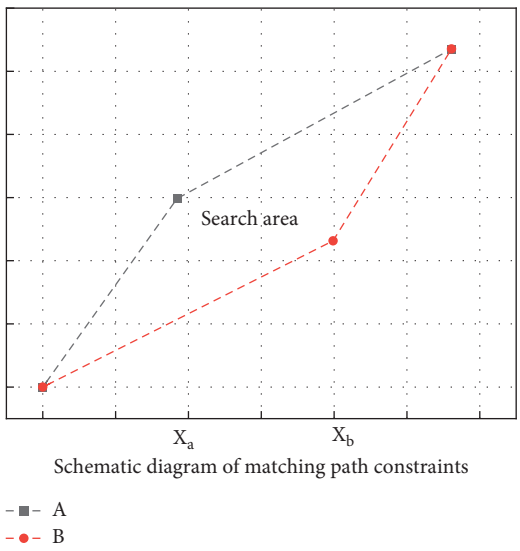

Figure 4: Schematic diagram of matching path constraint.

$$\begin{cases} x_a = \dfrac{1}{3}(2M - N) \\ \\ x_b = \dfrac{2}{3}(2N - M) \end{cases}, \tag{9}$$

where x_a and x_b both take the nearest integer; thus, the limiting condition formula (10) for the length of M and N is also obtained:

$$\begin{cases} 2M - N \geq 3 \\ 2N - M \geq 2. \end{cases} \tag{10}$$

If the above conditions are not met, the difference between the two is considered to be very good for dynamic bending modification.

It is not necessary to compare each pole on the x-axis with every pole on the y-axis, except the pole on the y-axis. The calculations for ymin and ymax are as follows:

$$y_{\min} \begin{cases} \left(\dfrac{1}{2}\right)x, & 0 \leq x \leq x_b \\ \\ 2x + (M - 2N), & x_b \leq x \leq N \end{cases}, \tag{11}$$

$$y_{\min} \begin{cases} 2x, & 0 \leq x \leq x_a \\ \\ \left(\dfrac{1}{2}\right)x + \left(M - \left(\dfrac{1}{2}\right)(1/2)N\right), & x_a \leq x \leq N. \end{cases} \tag{12}$$

The connecting parts of our three bends are >case. For each front frame of the x-axis, the y-axis ratio is different, but the bending properties are the same, and the distance change is made by the following model:

$$\begin{aligned} D(x, y) = d(x, y) + \min[&D(x - 1, y), \\ &D(x - 1, y - 1), D(x - 1, y - 2)]. \end{aligned} \tag{13}$$

For each front column of the x-axis, only the storage space of the previous column is required. Therefore, instead of storing the entire distance matrix as a whole, only vectors D and D of the two lines should store the storage space of the previous line and count the storage space of the line now, which has been modified for all forward and post. According to the above model, the storage area D of the previous line and the relative $D(X, v)$ of all the frames of the current line are stored in vector D by calculating the storage location of the current pole and then assigning the new D position to D as the new location stored in the next row. In this way, it goes to the end line of the x-axis, and M meaning of vector D is the parallel to the dynamic curve of the two models.

4. Voice Scoring and Error Correction

4.1. Similarity Comparison Method DTW. At present, there are many methods to measure the pronunciation quality. Our requirements for the scoring algorithm are as follows: high reliability and consistency with experts' scoring only reflect the learners' ability to pronounce Chinese and do not pursue the best similarity with standard pronunciation individuals. Following this study, the HMM-based phoneme probability algorithm was stable and not easily altered due to changes in the learner's behavior or voice channel, indicating similarities between learners' speech and speech patterns.

In speech processing, we cannot simply compare input features with templates directly, because speech signals have considerable randomness. Even if the same person reads the same sentence aloud, it is impossible to have exactly the same length of time. For example, with the faster phonation speed, the length of the vowel stable part will be shortened, while the length of the consonant or transitional part will remain basically the same. Therefore, time regulation is essential. Dynamic time warping is a nonlinear warping technique that combines time warping with distance measure computation. Suppose that the feature vector sequence of the reference template is $a_1, a_2, a_3, \ldots, a_m, \ldots a_M$, the feature vector sequence of the input speech is $b_1, b_2, b_3, \ldots, b_n, \ldots b_N$, and $M \neq N$. Then, the dynamic regularization is to find a time regularization function $m = w(n)$ and map the time axis n nonlinearly to the time axis m of the reference template, so that

$$D(n, w) \min_{w(n)} \sum_{n-1}^{N} d[n, w(n)], \tag{14}$$

where $d[n, w(n)]$ represents the distance between the nth and input eigenvectors and the $w(n)$ reference template vector. Obviously, $w(n)$ should be a nondecreasing function. Dynamic time warping aligns the input features with the reference template features in time to eliminate the nonessential differences between them. Figures 5 to 9 show the schematic diagram of the distortion between the two modes in the case of direct matching, linear matching, and nonlinear matching. It can be seen from the figures that when the nonlinear matching method is adopted, it is possible to minimize the nonessential difference between the two modes.

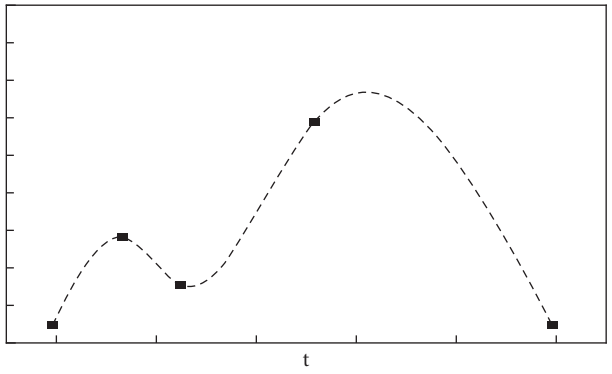

Figure 5: Direct matching.

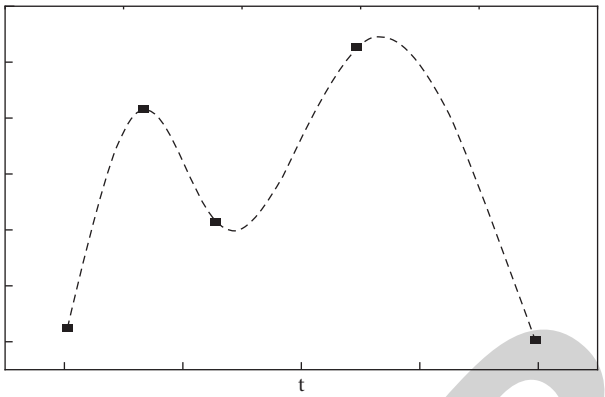

Figure 6: Linear matching.

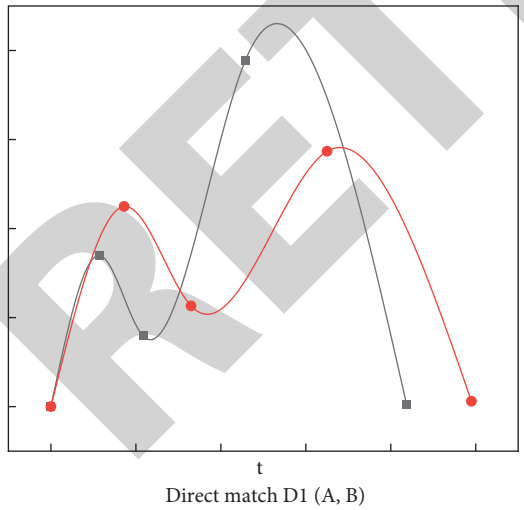

Figure 7: Direct matching D1.

Dynamic time warping is an optimization problem. Dynamic programming technology is often used to solve this problem. The concept that local optimization can lead to global optimization is used. The purpose of the solution is to find the optimal time warping function $w(n)$ and the corresponding $D(n, w)$. Recursive formulas (15) and (16) can be derived as follows:

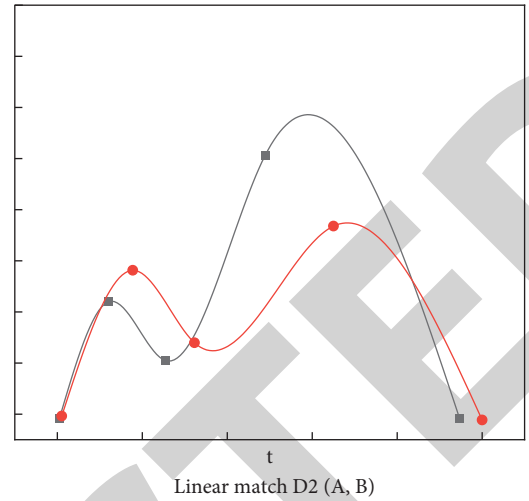

Figure 8: Linear matching diagram (D2).

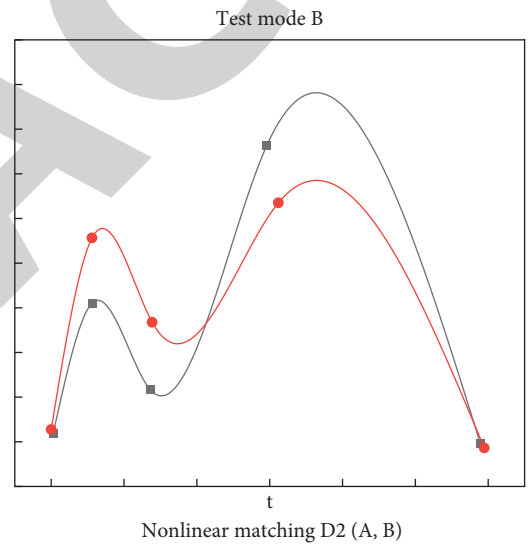

Figure 9: Nonlinear matching (D2).

$$D(n+1,m) = d[n+1,m] + \min[D(n,m)g(n,m) \\ D(n,m-1), D(n,m-2)], \tag{15}$$

$$g(n,m) = \begin{cases} 1, & w(n) \neq w(n-1) \\ \infty, & w(n) = w(n-1). \end{cases} \tag{16}$$

Since the calculation of each point $D(n+1, m)$ requires the calculation of all three points D values on the n column, it is very time-consuming to calculate the time regularity using the dynamic programming technique. In pattern recognition, it is often necessary to calculate the distance between features. In speech recognition, the similarity between the reference mode and the input mode is determined by the distortion measure between the two frames [17]. It is a measure that reflects the difference between signal features and is represented by $D(x, y)$. In the calculation of DTW distance, the absolute value average distance equation is used as follows:

$$D(x, y) = \frac{\sum_{i=1}^{N} |x_i - y_i|}{N}. \quad (17)$$

DTW distance cannot be directly used as pronunciation score. We need to find a suitable guide to score from a distance. It is considered a relationship of distance and interest:

$$\text{score} = \frac{100}{1 + a(\text{dist})^b}. \quad (18)$$

Obviously, this formula can map the distance to the score range of 0100. To solve the unknown parameters a and B in the formula, we need to know some pairs of fractions and distances. The above parameters can be solved from the scores and DTW distances of some experts in the experiment. Using the formula in this paper, even if the distance is larger or smaller than that in the test, the score can be reasonably converted to the interval of 100 to 0 [18]. As two characteristic parameters are actually used, the actual score estimation formula is slightly more complex than the above formula, and the final score is shown in the following weighted sum formula of the two:

$$\text{score} = w_1 * \frac{100}{1 + a_1(\text{dist}_1)^{b1}} + w_2 * \frac{100}{1 + a_2(\text{dist}_2)^{b2}}. \quad (19)$$

The unknown parameters in the formula meet certain restrictions: $a_1, a_2, b_1, b_2 > 0$, $w_1 + w_2 = 1$. a_1, a_2, b_1, b_2 are the parameters of converting distance into fraction, and w_1, w_2 are the weights of three features.

4.2. HMM-Based Scoring Method. The competition using the HMM speech model is another alternative to speech competition, starting with voice, and hoping to see the difference between the experimental speech and the acoustic structure and the music and score words accordingly [19].

The flow of the scoring system is shown in Figure 10. Preprepared acoustic modeling and music modeling are used as the answer model using speech recognition technology, and the differences in speech test and models are identified and scored, working with the scoring mechanism [20–28].

The most common method based on the HMM model is to provide telephony. Procedures include logistics scores and postevent scores. Compared to comparison scores, the type of approach for some shows the learner's ability to speak rather than the data that influences the differences between learners and speakers. Its definition is as follows:

$$Si = \sum_{t=\tau_i}^{\tau_{i+1}-1} \lg[P(q_t|q_{t-1})P(o_t|q_t)], \quad (20)$$

where O_t and q_t are the analysis vectors of phase t and state of HMM. The definition of a model is, then, the result of a change state; that is, A in the HMM model is the resultant distribution of the probe vector, which is B in HMM.

Scoring method for sentences is as follows:

$$s = \frac{\sum W_i S_i}{\sum W_i}, \quad (21)$$

where S is the sentence score, S_i is the sound score, and W_i is the weight song. The advantages of registration do not apply to data. After combining the advantages and disadvantages of the various dialing algorithms, the system uses an HMM-based phoneme-based probability algorithm as a call measurement method.

HMM Back Probability-Based Score: since speaking of sentences for elementary English students is also slow, speech speed should be increased as a significant impact on speech scores. Finally, the score of phoneme duration can be defined as follows:

$$D = \frac{1}{N} \sum_{i=1}^{N} \lg[p(f(d_i|q_i))], \quad (22)$$

where d_i is the duration of segment i corresponding to phoneme q_i and $f(d_i)$ is the normalization function. Considering the independence of text and speaker, the speech duration is normalized by the measurement of speech rate (ROS). ROS is the number of phonemes per unit time in a sentence or in all utterances of a speaker. Generally, $f(d_i) = \text{ROS}*^{d_i}$ is taken.

4.3. Error Detection. After the recognition and scoring process of forced association of phonemes, MFCC eigenvalues get the corresponding associated phoneme string, phoneme start time and end time, and score. On the basis of these results, we began to detect phoneme errors. According to the results of the most phoneme like judgment, we can roughly divide phoneme reading errors into three categories: misreading, missing reading, and adding phonemes. Define the most phoneme like phoneme as the phoneme formula with maximum HMM likelihood:

$$q_i' = \text{argMax}[L_i(q)]. \quad (23)$$

$L_i(q)$ is the likelihood formula of any factor q in time period i:

$$L_i(q) = P(q|Q_i) = \sum_{t=\sigma_i}^{\sigma_{i+1}-1} [P(s_t|s_{t-1})P(o_t|s_t)]. \quad (24)$$

Missed phoneme: q_i is not pronounced, as in the following formula:

$$q_i = \begin{cases} q_{i-1} \\ q_{i+1} \\ \text{SIL} \end{cases}. \quad (25)$$

Mispronunciation element: the pronunciation of q_i is so wrong that it sounds more like another pronunciation. It is expressed as q_{i+1}, and it is not a missed phoneme error. At the same time, it is believed that q_i is misread as q_i.

Adding phoneme: there are redundant phonemes in the phoneme recognition result.

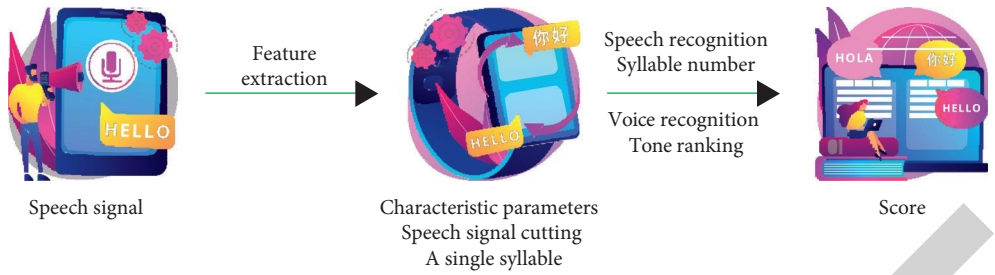

Figure 10: Flowchart of scoring system.

The results obtained by the correlator cannot distinguish the three errors. The error detection module can only locate the wrong phoneme according to the phoneme score. If it wants to go further, it needs to get the phoneme recognition results through the recognition process to determine which error it belongs to. Two error detection methods can be designed to meet the above different requirements.

If it is not required to detect the error type, the correlator can first evaluate the phoneme level correlation score of the speech and set the threshold value. When the corresponding phoneme score is lower than the threshold value, the phoneme will be classified as the wrong phoneme. If you need to detect specific types of errors, you need to add a phoneme recognition process.

4.4. Experimental Simulation and Result Analysis

4.4.1. Data Source. These lines use Arabic-language digital data installed in the UCI machine training library developed by the Automatic Alarm Laboratory of Baji-Mokhtar University. This data is called an Arabic number after the MFCC has resolved 13 conflicts in a total of 8800 dialog boxes (88 callers, 10 Arabic numerals, each number repeated 10 times). The call was made by 44 men and 44 women ages 16–40.

The content of this article is about 24 undergraduate students of our college, including 15 boys and 9 girls. The content is recorded using a 16 kHz, 16-bit encoding sampling program, CoolEdit. There are 10 written sentences, which are usually in English.

4.4.2. Recognition Rate Test. Acknowledgment level is the fact that the platform can accept user feedback. This is especially important because it is one of the most important measures in the performance of cognitive skills. On the platform, only the speech test module uses the speech experience. Therefore, only a test run of these models was conducted here to ensure that the training platform was able to recognize the English characters that had been developed in the past. In addition, the ambient noise makes it difficult to get the sound at the time. To perform the test, a sample library of recorded sounds was used in the experiment, namely, 3 true and 3 unrecorded sounds. To reduce the impact of ambient noise, a quiet room is the best place for this experiment. Table 1 provides information on platform level testing.

In the text above, 1 is true and 0 is incorrect. The above tips check if you know the phonetic symbols in English. In terms of acknowledgment, verbal analysis is a great way to measure the accuracy of speech and then learn the English depth of symbols combined with other functions of the platform. Therefore, based on the benefits of the accreditation level of speech screening, we can achieve the training benefits mentioned in this paper.

4.5. Speech Evaluation Experiment. In this paper, the correlation coefficient and the Pearson correlation coefficient are used to illustrate the relationship between the measurement technology and the measurement book.

Depending on the speech characteristics of college students who have different levels of English proficiency, we have different measures (movement, speed, tone, and music) and measured widely, as recommended by English experts. Levels of detailed information and related assessment models are shown in Table 2.

This book was reviewed by two college English teachers. They assessed 10 sentences of English speaking written by 24 high school students one by one, including 4 marks in music, fast, melodic, vocal music, and general measurement. Pearson correlation coefficient is used in this paper to evaluate the reliability of the book review results, because the content of the teachers during the book review will affect evaluation results.

To make it easier to calculate, the levels A, B, C, and D of the scale were changed to 4, 3, 2, and 1, respectively. Pearson's relationship analysis (two experiments) found that the scores of four measures, namely, noise, velocity, noise, and tone, were correlated ($r > 0, P < 0.05$) for each group, regardless of total scores. This suggests that both instructors can follow the same measurement standards during the test and measure the reliability of the test data.

In addition, the results of the two teacher evaluations were averaged (e.g., the average of students' scores on different sentences). The score is the end of the measurement book.

4.6. Inspection of Evaluation Indicators. The procedure described in this paper can measure volume, speed, and intonation of 240 samples in 10 sentences of 24 students. Test results are found in Tables 3 and 4.

Table 1: Speech recognition test results.

Test result	Test 1 Correct	Test 2 Correct	Test 3 Correct	Test 4 Error	Test 5 Error	Test 6 Error	Accuracy
i	1	1	1	1	1	0	0.98
u	1	1	1	1	1	1	1
a	1	0	0	1	1	1	0.56
e	0	0	1	0	1	1	0.73

Table 2: Artificial evaluation grade and evaluation standard.

Grade	Intonation	Speed of speech	Rhythm	Intonation	Population
A	Complete and correct content, clear and fluent pronunciation, no obvious pronunciation error	Moderate speaking speed	Accurate accent pronunciation, strong sense of rhythm	Accurate and natural intonation	Excellent pronunciation
B	Relatively complete and accurate content, relatively clear and fluent pronunciation, no serious pronunciation error	Speak a little fast (slow)	More accurate accent pronunciation, with a good sense of rhythm	Accurate and natural intonation	Good pronunciation
C	Basically complete and correct content, basically clear and fluent pronunciation, pronunciation errors that affect understanding	Speaking fast (slow)	Ordinary accent pronunciation, with a certain sense of rhythm	Basically accurate intonation, but not natural enough	General grasp of pronunciation
D	Incomplete and accurate content, pronunciation not clear and fluent, and serious pronunciation errors that affect understanding	Speaking too fast (slow)	Accent pronunciation error, too many (less) accents, poor sense of rhythm	Inaccurate and unnatural tone of voice	Poor overall pronunciation

Table 3: Evaluation index test results: number of samples.

Index number of samples	Consistent	One-level difference	Two-level difference	Three-level difference
Intonation	206	32	2	0
Speed of speech	197	43	0	0
Rhythm	204	33	3	0
Intonation	193	45	4	1

Table 4: Evaluation index experimental results: statistical index.

Index difference level	Consistency rate (%)	Adjacent consistency rate (%)	Pearson
Intonation	87.25	99.58	0.7
Speed of speech	82.08	100	0.493
Rhythm	85.00	98.75	0.543
Intonation	81.00	98.34	0.627

For intonation testing, there were only 207 models with the same level of measurement technology, manual measurement, one-level difference, two-level difference, and no three-level difference. This shows that the machine and manual ratios have a correlation of 87.25%, the adjacent coefficient is up to 99.58%, and the Pearson correlation coefficient is 0.7, indicating that the method in this article is reliable.

For speech speed measurement, there were 197 models at the same level of measurement technology and manual test, 43 models with one-level difference, and two or three with different levels. This shows that the machine and manual speed correlation coefficient are 82.08%, the correlation coefficient is up to 100%, and the Pearson correlation coefficient is 0.493, indicating the reliability of the velocity measurement.

In terms of test results, there were 204 models of the same stage of machine testing and test manual, 33 models with one-stage difference, and only 3 models with two stages difference, without three-stage difference. This means that the accuracy levels of the machine and manual assembly are as high as 85%, the relative safety rating is as high as 98.75%, and the Pearson correlation coefficient is 0.543, indicating that the measure of consistency is reliable.

For sound analysis, there were 192 models of the same level of measurement machine and manual test, 44 models

with one-level difference, and only 4 models with two-level difference, no three-level difference. This shows that the machine and the manual correlation coefficient are 81%, the cohesive position is 98.34%, and the Pearson correlation coefficient is 0.627, indicating that the correction of this is reliable. In conclusion, the language, speed, atherosclerosis, and intonation assessment methods used in this article are reliable and can be used to improve the English language standard.

5. Conclusion

According to the English pronunciation habits of Chinese people, this paper studies and establishes a targeted corpus. Combined with the needs of Chinese speaking learners, it explains and compares the relevant technologies at each stage in the processing of users' voice. In the speech endpoint detection phase, this paper uses a combination of short-time zero-crossing rate and short-time energy to detect the endpoint of speech. In the speech comparison phase, this paper uses the improved DTW algorithm to recognize the speech similarity. Compared with the traditional DTW algorithm, it speeds up the recognition time and speed, and the recognition effect is better.

The HMM-based phoneme probability algorithm is ideal. It is not easy to change due to changes in students' personal characteristics or sounds and better to show similarities between students' words and speech patterns. HMM-style speech recognition technology is used to determine Viterbi's language, and acknowledgment scores are made with subsequent results. Speech scores based on comparisons and patterns will appear to be studied using techniques such as decomposition of feature parameters, forced coupling, and dynamic distortion time, and some scores mechanisms were studied and their numbers were included in the experiment.

This paper examines the English-speaking skills of college students in China as educational materials, improves the process of measuring the computer English proficiency, and measures various elements such as music, pace, and melody. We performed speed measurement according to the time of speech of the different characteristics of the frequency, noise measurement as a measure of the energy of the short time and the combination, and sound measurement according to the basic frequency. The results of the experiment show that the melody, tempo, rhythms, and musical measurements used in this article are reliable. In addition, taking into account the weight of the above measurements, the retrospective measurement has developed a model for the appropriate measurement and objective of the quality of the quotation. The results of the experiment show that the standard English proficiency test in this article is reliable. It provides students with timely, accurate, and objective analysis and instructional strategies and assists students in identifying differences in their speech and speech patterns, correcting their mispronunciation, and improving the effectiveness of teaching English.

Data Availability

The dataset can be accessed upon request.

Conflicts of Interest

The authors declare that they have no conflicts of interest.

Acknowledgments

This work was supported by the Scientific Research Fund Project of Yunnan Provincial Department of Education: "Research on the Construction of Effective Paths for English Language Acquisition of Yunnan College Students Affected by Dialect Transfer" (Project no. 2022J1088).

References

[1] S. V. Ushie and J. A. Basake, "Teaching method as solution to students performance in oral English in secondary education," *The International Journal of Humanities & Social Studies*, vol. 9, no. 2, 2021.

[2] X. Li and Y. Xie, "Application of virtual reality technology in oral English teaching for college English majors," *Journal of Physics: Conference Series*, vol. 1820, no. 1, Article ID 12148, 5 pages, 2021.

[3] W. Huang, "Strategies to reduce students' oral English anxiety," *Journal of Higher Education Research*, vol. 3, no. 2, pp. 191–193, 2022.

[4] V. O. Falola and S. B. Jolayemi, "Impact of Multimedia Technology on the Teaching and Learning of Oral English in Osun State Secondary Schools, nigeria," *Durban University of Technology*, vol. 2, no. 1, 2020.

[5] G. Xiashi and Y. Lin, "Impact of language ego, the native language effect on oral English learning of high school students," *International Journal of English and Cultural Studies*, vol. 3, no. 1, p. 33, 2020.

[6] Y. Song, "The influence of background music teaching on accuracy and fluency of freshmen 's oral English in China," *International Journal for Innovation Education and Research*, vol. 8, no. 11, pp. 265–275, 2020.

[7] L. Nos and S. Dongi, "Pedagogical conditions of using the game activities in the development of oral English speech of primary school students," *Young Scientist*, vol. 10, no. 86, pp. 409–415, 2020.

[8] H. Tan and Z. Xie, "Exploring the relationship between foreign language anxiety, gender, years of learning English and learners' oral English achievement amongst Chinese college students," *English Language and Literature Studies*, vol. 10, no. 3, p. 31, 2020.

[9] S. Zhou, Y. Zhang, X. Liu, Y. Wang, and X. Shen, "Empirical research of oral English teaching in primary school based on 4c/id model," *Journal of Higher Education Research*, vol. 1, no. 4, 2020.

[10] Y. Lin and Q. Ji, "Analysis of college oral English class design from the perspective of tblt—taking "read all about it" as an example," *OALib*, vol. 7, no. 11, pp. 1–9, 2020.

[11] J. Wang, "The enlightenment of second language ego to oral English teaching in senior high school," *Theory and Practice in Language Studies*, vol. 10, no. 10, p. 1310, 2020.

[12] J. Wang, "Speech recognition of oral English teaching based on deep belief network," *International Journal of Emerging Technologies in Learning (iJET)*, vol. 15, no. 10, p. 100, 2020.

Hindawi
Scientific Programming
Volume 2022, Article ID 2772665, 9 pages
https://doi.org/10.1155/2022/2772665

Research Article

Building a Smart City Planning System Integrating Multidimensional Spatiotemporal Features

Jing Lu

Yunnan Municipal Construction Engineering Consulting Co., LTD, Yunnan Kunming 650228, China

Correspondence should be addressed to Jing Lu; 20212138026@stu.kust.edu.cn

Received 18 July 2022; Revised 8 August 2022; Accepted 11 August 2022; Published 28 August 2022

Academic Editor: Lianhui Li

With the development of mobile communication technology and the popularization of mobile devices, the connection between people has become increasingly close, the data circulating between them have increased rapidly, and the multidimensional space-time characteristics have gradually entered the stage of the times. The proposal of the basic smart city system is a revolution in the concept of urban construction. A smart city is both an opportunity and a challenge for the urbanization process. By analyzing the multidimensional spatiotemporal feature engineering, this paper studies the development trend of smart cities and discusses how multidimensional spatiotemporal features play a fundamental role in the smart city system.

1. Introduction

The rapid development of today's science and technology, the popularization of the Internet, and the introduction of the Internet of Things have greatly increased people's demand for data transmission. At the same time, the construction of the mobile Internet has increased the number and scale of data transmission. With the development of information technology, the pace of urban informatization has been accelerated, and the level of urbanization has been further improved. Subsequently, urban problems such as environmental pollution, low urban management efficiency, unreasonable industrial structure, and traffic congestion have emerged. In order to solve the increasingly serious urban problems, the construction of smart cities has long been put on the agenda, and it is the application of multidimensional spatiotemporal features that provide the basic conditions [1]. This paper briefly introduces the smart city system and describes the application of multidimensional spatiotemporal features in smart cities with the help of examples. The purpose of multidimensional space-time feature engineering is to develop new or comprehensively utilize existing technologies to process multidimensional space-time features, so as to carry out planning, construction, and operation management of multidimensional space-time features. The research on multidimensional spatiotemporal characteristics is divided into processing analysis and secondary development. By analyzing this huge amount of data, a lot of hidden information can be discovered, and deep-level information can be mined, so as to propose a processing plan that adapts to the actual situation; dimensional spatiotemporal features carry out operations similar to businesses accepting consumer feedback, adjusting products, and engaging in operation management, so as to achieve their goals. The basis of smart city systems is multidimensional spatiotemporal feature engineering. The development of multidimensional spatiotemporal features affects the construction, development, and operation of smart city systems [2].

There is no doubt that man is wise. Let the city, an inanimate body, be as intelligent as a human being and be able to solve urban problems by itself. This is the construction of a smart city. The construction of a smart city includes many aspects such as government affairs, transportation, medical care, and security. It requires the support of various information technologies such as multidimensional space-time features, cloud computing, and artificial intelligence. It also requires the construction and improvement of infrastructure [3]. A smart city is a new form of urban development in contemporary society, which is of

great significance for improving the government's service and management capabilities, promoting the upgrading of industrial structure and the gathering of knowledge-based talents. The new smart city is characterized by openness, co-construction, and sharing and is committed to achieving equalization of services, eliminating the information gap, and promoting the construction of urban characteristics. The construction and development of smart cities revolves around multidimensional spatiotemporal characteristics. A "smart" city is like a smart person. On the premise of having a complete infrastructure, it should extensively collect information and resources from all aspects of society and analyze and process them, so as to form various complete databases. On the basis of perfect data resources, through the use of advanced information technologies such as the Internet of Things, cloud computing, and multidimensional space-time features, various application platform systems are built to achieve effective prediction and monitoring of economic and social affairs and to assist leaders in making scientific decision-making and improve the management level of the city, so as to provide the public with more intelligent services [4]. During the whole operation process of the city, new data resources will be generated and perceived by the city, which will further promote the improvement of the database and the improvement of processing capacity, thus forming a closed virtuous circle. It can be seen that multidimensional spatiotemporal features play a fundamental role in the construction of smart cities. The building equipment monitoring system is an important part of the intelligent system of the smart community. As the name suggests, the building equipment monitoring system is built for the unified management and monitoring of different equipment in the building, including electrical equipment, HVAC equipment, water supply, drainage equipment, and special equipment [5].

The working principle of the system is as follows: data information is received from various sensors, so that the property can comprehensively and intuitively understand and grasp the operation status of different equipment in the building. For example, according to the pictures taken and transmitted by the camera, we can know whether anyone needs to use the public entertainment area and judge whether the lighting equipment in the area needs to be turned off or whether the temperature of the central air conditioner needs to be adjusted; with the information, judge the actual operation of the power transformation and distribution system and make adjustments in time; and according to the repair and maintenance dates of the equipment in the building, the property management can make appointments for professionals in time. After the system is completed, the information collection, centralized management, and control of all equipment in the building can be realized through the system. Such equipment management and control mode are conducive to the rational allocation of human, material, and other resources and can also save community public resources, thereby improving the energy conservation and environmental protection of smart communities. At the same time, the building equipment monitoring system can be used to realize the timely and accurate understanding and mastery of the energy consumption of different equipment in the building and provide effective reference information for the reasonable formulation of property energy use indicators and employee KPI indicators [6]. In the smart community, the video intercom system can provide voice and video transmission services for properties and residents, residents and visitors, and visitors and properties. At present, the video intercom system has been used more and more in the construction of smart communities. Many video intercom systems can not only transmit signals to the property owner but also connect with gas alarms, smoke alarms, etc., so that even when the resident is not at home, the property owner can timely discover the hidden safety hazards in the house and realize correctly. Effective control of the risk of household property loss is also conducive to simplifying the property management process and improving the quality of property services. When planning and designing the video intercom system, the property terminal should be installed at the property, the household terminal should be connected to each household, and the visitor terminal should be installed at the public entrance of each residential building [7].

2. Research Method Design

The design of this research method is divided into four parts: data analysis and acquisition, data cleaning and screening, multidimensional big data information fusion, and smart city flow spatiotemporal distribution design. The research technology roadmap is shown in Figure 1.

2.1. Data Acquisition. Frequently used software applications were found through offline questionnaire surveys, such as Weibo check-in, Douyin location sharing, and Mafengwo travel notes, and then the data were divided according to the software characteristics, such as the Weibo check-in data structure contains a user ID, check-in time, check-in location, and other information. Finally, use web crawlers to collect the information generated by tourists using popular software functions near POIID according to keywords, and form an initial data set according to the divided data structure standards for several months [8].

2.2. Data Cleaning. Since the initial data set consists of comprehensive and noncustomized data, which contains a lot of useless data, in order to ensure the scientificity and accuracy of the results, the initial data set needs to be fully cleaned before it can be applied to subsequent analysis [9]. In the data cleaning and screening stage, the deletion method, regression method, mean smoothing method, etc. can be used to preprocess the data first. On the one hand, it can solve the problem of missing data, and on the other hand, it can remove the noise in the initial data. First, data cleaning and screening standards were formulated, then many parameters were obtained through small-scale on-the-spot investigation, and a statistical model was established to perform data mining on the spatiotemporal information in the data and identify tourist groups. Then, according to the

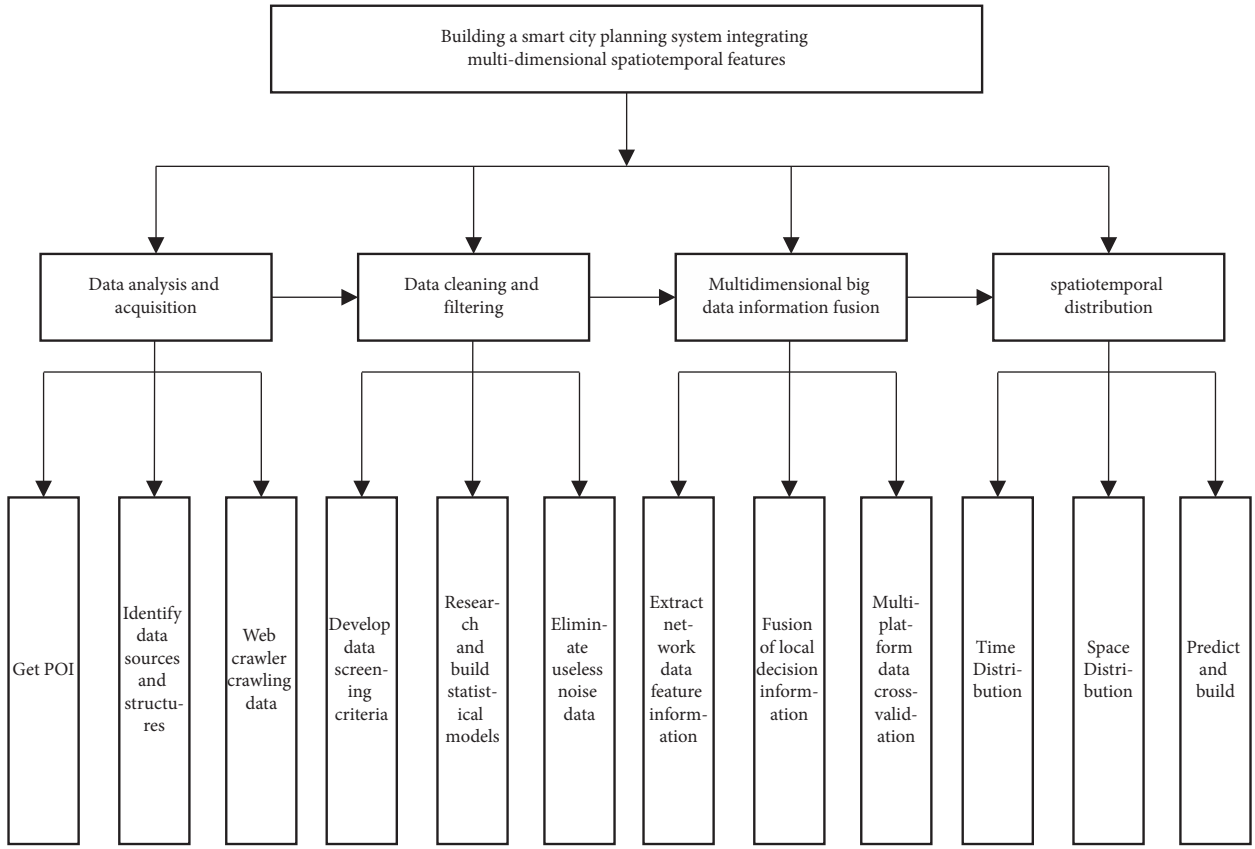

Figure 1: Technology roadmap.

user attribute characteristics, unclear geographical source, incomplete information, and the months with incomplete data or fewer data are excluded, and the final remaining data are used as the data basis of this study [10].

2.3. Multidimensional Big Data Information Fusion. Multidimensional big data information fusion has very important value and significance in the era of big data. In the study of smart city flow, there are often more than one factor that affects the spatiotemporal distribution characteristics of smart city flow, so using different data sources can provide important information from different sides and improve the accuracy of data and the reliability of results [11]. D–S or evidence theory, neural network, and other algorithms can be used to integrate and analyze the characteristic information extracted from the data of Weibo, Douyin, and other network platforms and further evaluate or infer the local decision information obtained by further mining the value of the data in order to enhance the role of information and, finally, conduct interactive verification of data on different platforms to exclude abnormal points, improve the confidence of data results, and prevent decision-making mistakes [12].

2.4. Space-Time Distribution Design. This method first integrates the information based on multidimensional big data and uses the time stratification method and software frequency index to analyze the seasonal, intra-month, intra-week, and intra-day time distribution characteristics of urban smart cities in the flow; then using GIS spatial analysis and kernel density methods, the spatial distribution characteristics of urban smart city flow, such as the "seasonal change" map of urban smart city flow core density and the smart city flow core density map of different attributes, were visualized. A statistical model was established for the analysis of spatial and temporal distribution characteristics of urban smart city flow and a general smart city flow research model to help researchers, city governments, or smart city enterprises re-understand the source market, develop smart city resources in a targeted manner, and design smart city products and smart city lines [13].

3. System Model Construction of Smart City

Models are the most important and most basic tools for studying systems. In order to express the characteristics, properties, or laws of motion of a certain aspect of the entity, the model abstracts the characteristics of the entity at a certain level and expresses them in a certain structural form, so as to help people better understand the characteristics of the object, predict changes, and control the operation or structural design. A system model is a description of the essential properties of a certain aspect of a system, which provides knowledge about the system in a certain form (such as words, symbols, diagrams, and mathematical formulas). A

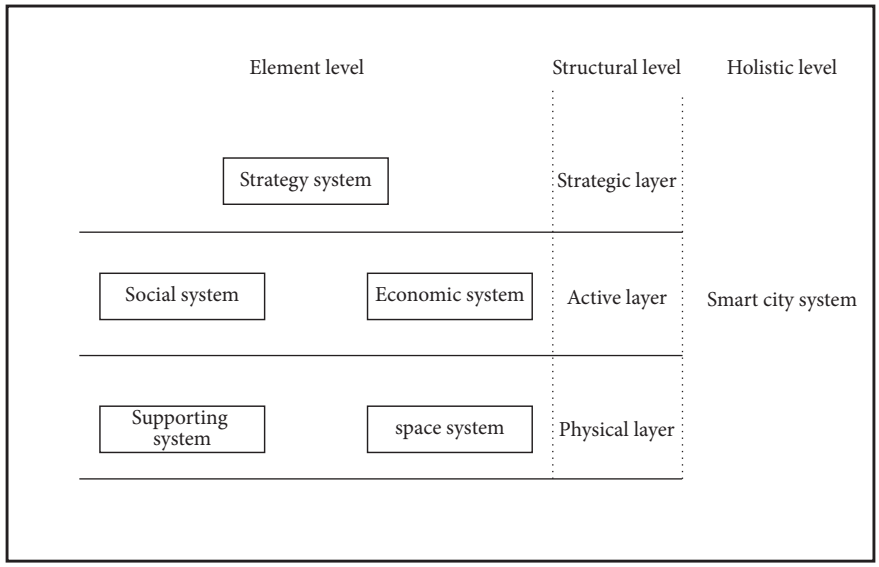

Figure 2: Schematic diagram of the elements and structures of the smart city system.

system model is a description, imitation, and abstraction of a real system. It consists of main factors that reflect the nature or characteristics of the system, and it embodies the relationship between these main factors [14]. This part will build a system model of a smart city based on the relevant theories of complex systems, combined with the previous analysis of the elements and structures of the smart city system.

3.1. Smart City System Based on Communication and Control Laws of Complex Open Systems. It can be seen from the above analysis that the smart city system is composed of five subsystems—strategic system, social system, economic system, support system, and space system—as well as three layers—strategic layer, activity layer, and physical layer. From the perspective of the hierarchy of the system, the five subsystems have different degrees of complexity, and the corresponding relationship between the five subsystems and the three levels is shown in Figure 2. As can be seen from the figure, from the structural level, the smart city system is composed of three complex levels: the physical layer, activity layer, and strategic layer; and from the element level, the support system and spatial system of the smart city system are located in the physical layer, the social system and the economic system are located in the activity layer, and the strategy system is located in the strategic layer.

This is how, in the smart city system, the three layers and the five subsystems are organized and connected.

The communication and control rules of the system are important mechanisms for maintaining complex open systems to withstand environmental shocks. In complex systems theory, another group of concepts equally important as the classification and hierarchy of the system is the communication and control of the system, i.e. the maintenance of the system level requires a series of information exchange processes for regulation or control. In other words, a hierarchy of open systems must require communication and control processes if the system is to survive the shocks dictated by the environment. In a complex system, control is an active action of the controlling subject on the controlled object. The controlling subject obtains, processes, or uses the information to make the controlled object act according to the predetermined purpose of the controlling subject and guide the object to the predetermined purpose [15]. In the control theory of complex systems, according to Ashby's Law of Necessary Diversity, the diversity of controllers must be equal to or greater than the diversity of controlled persons, that is, the diversity and complexity of the "organizational management" performed by the controlling subject must be equal to or greater than the "operational activities" carried out by the controlling subject to achieve the purpose, and the diversity and complexity of "operations" must be equal to or greater than the "objective environment" represented by the controlled object [16].

Corresponding to the smart city system, in order to achieve the purpose of building a smart city by smart city builders, the development strategy and the implementation measures formulated by the builders (control subjects) must be more complex and advanced than the activities of people in the smart city system. The material environment, likewise, the complexity, and the advanced level of human activities must be greater than the material environment faced by the smart city system, so as to effectively realize the transformation of the material environment. At the same time, in order to cope with the diverse changes in the environment, human activities at the active layer also need to play the greatest active role in a certain autonomous way. If the strategic layer restricts the diversity of people's activities in the active layer too much, it will make it difficult for the smart city system to adapt. If the changes in the environment are not well controlled, the development of the system will go with the flow, and the goal of smart city construction will not be achieved [17]. Based on the above analysis, the corresponding relationship between the three levels of the

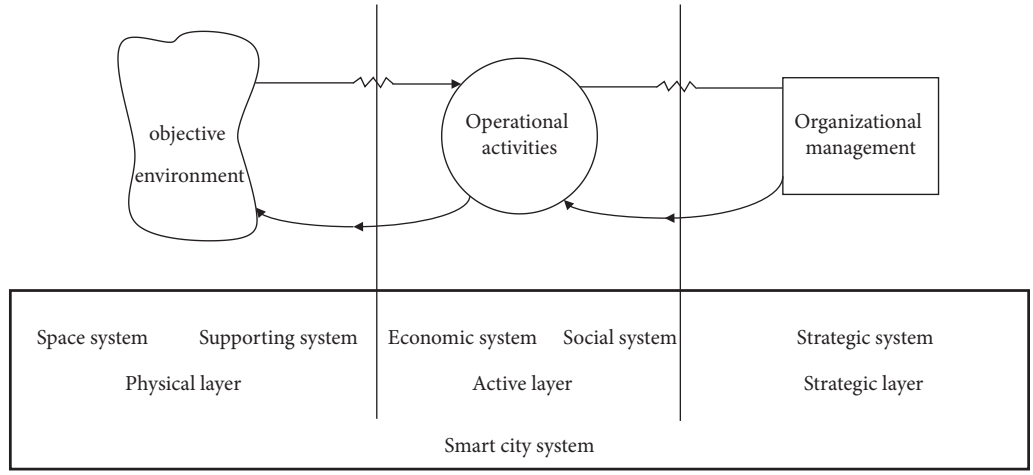

Figure 3: Relationship between the elements and structures of the smart city system and the communication and control of the complex system.

smart city system and the control and communication of the complex system is shown in Figure 3.

3.2. Smart City System Based on Viable System Model. The communication and control relationship between the three levels and five subsystems of the smart city system can be further analyzed using the viable system model (VSM).

In order to further understand the survival principle governing complex organizational behavior, Bill established a living system model formed by five subsystems connected according to certain communication and control laws, as shown in Figure 4. The model connects the five subsystems through a composite of information and control loops. The survival system model composed of the five subsystems through interconnection and interaction shows various control laws and conditions that are necessary to support the healthy operation of a complex system [18].

In the smart city system, the vital system model reveals the communication and control laws of different subsystems and different system levels of the smart city system.

There is a specific connection between the five subsystems and the three levels of the smart city system and the five subsystems of the living system model and the environment in which the five subsystems act:

(1) The external environment that is "System 1" in the living system model acts on correspondence to the physical layer of the smart city system. The "overall environment" in the physical layer is the space system of the smart city, which is the accommodation place for people to carry out various activities, has certain physical characteristics, and is reflected in the smart city as an intelligent flow space [19]. The "local environment" in the physical layer is the support system of the smart city. It builds corresponding to smart application systems in different functional areas of the city with emerging information and communication technologies and information infrastructure within a certain spatial range. In a smart city, these intelligent application systems have become the material and technical carriers that people rely on to carry out various smart forms of economic and social activities. At the same time, in the physical layer, it is precisely because of the extensive application of a large number of intelligent application systems established in the support system that the "overall environment" of the original material from in the space system begins to become intelligent and fluid. The flow space of urban space has brought the decentralized and network development of the physical form of urban space [20].

(2) "System 1" in the living system model, as well as the adjustment activities of "System 2" and the management and audit activities of "System 3," which are related to the implementation and operation activities of "System 1" themselves, all correspond to the smart city system's active layer. In a smart city, according to the different types of people's activities, the implementation and operation activities of "System 1" can be mainly divided into seven major activities: social and cultural activities, public administration activities, social interaction activities, production activities, circulation activities, consumption activities, and innovation activities. These different types of activities are guided, constrained, and controlled by the corresponding aspects of strategy execution and implementation from the strategy layer. The implementation of the strategy at the strategic level, on the one hand, in accordance with the planning and content of the strategic plan, combined with relevant resources such as funds and talents, organizes and manages the development of the above activities in seven aspects, provides necessary services, and conducts regular assessments to ensure verification of the degree of the intellectual development of different types of activities; on the other hand, it regulates and constrains people's

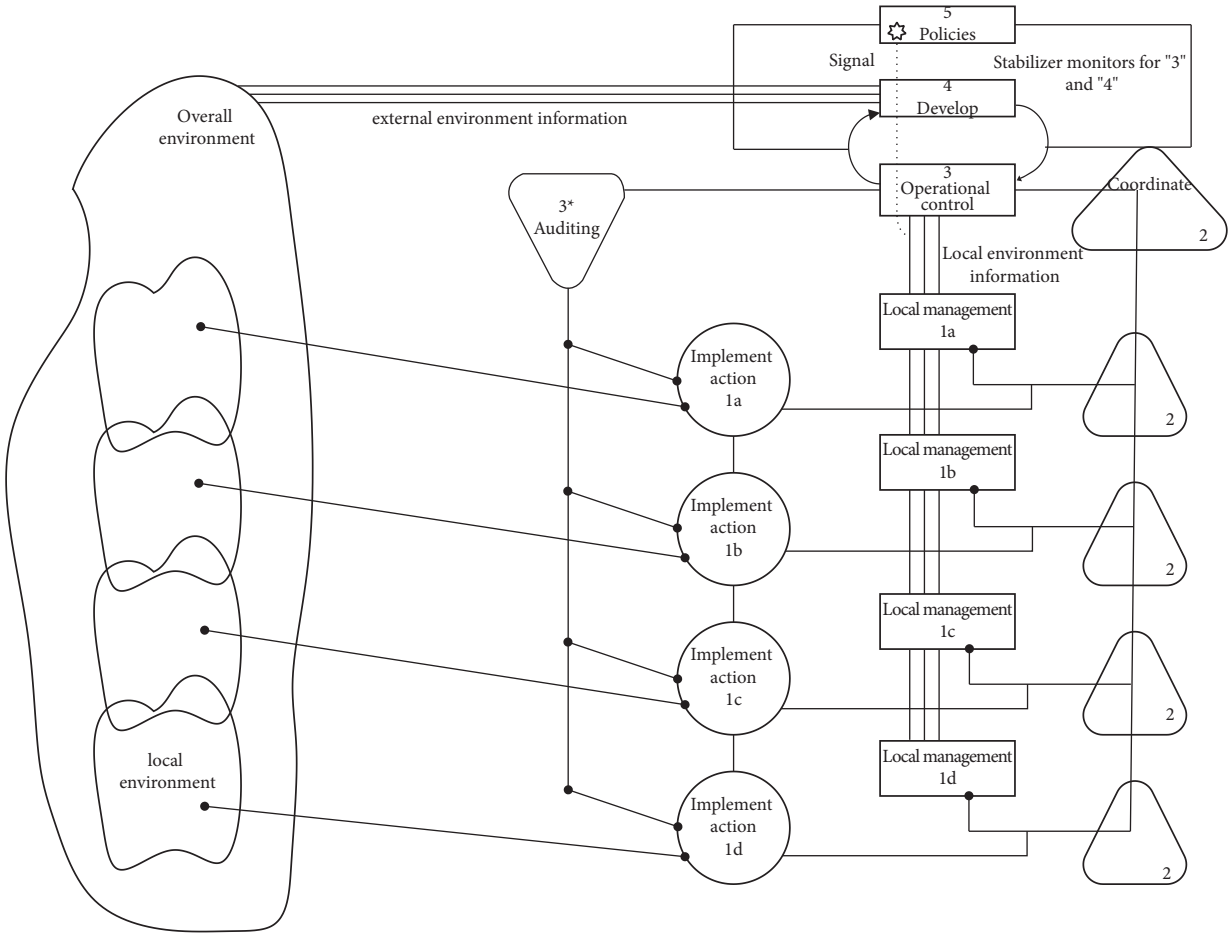

Figure 4: Living system model.

various economic and social activities through the supporting policies and regulations, technical standards and specifications, information security requirements and institutional innovation rules in the implementation of strategic planning, so as to ensure that each coordination of class activities. The above seven types of social and cultural activities are integrated with the guidance, restraint, and control from the implementation of the strategy to form a social and cultural system, public administration system, social relationship system, production system, circulation system, consumption system, innovation system. The corresponding economic and social subsystems such as the system, and the corresponding subsystems are further combined to form a social system and an economic system [21].

(3) "System 2," "System 3," "System 4," and "System 5" in the VSM together correspond to the strategic layer of the smart city system. Among them, "System 2" and "System 3" correspond to the "strategic implementation" of the smart city system strategic layer, "System 4" corresponds to the "strategic research" of the smart city system strategic layer, and "System 5" corresponds to the smart city system "strategic planning" at the strategic level. The strategy implementation that exerts the control function of "System 3" is connected with the strategic plan corresponding to "System 5." On the one hand, it is accepting and interpreting the basic plan for smart city development in the strategic plan, and on the other hand, it is related to the economic and social situation of the people in the activities. Activities are connected to guide, control, and constrain people's economic and social activities in accordance with the requirements of strategic planning. "System 2" is also an integral part of strategic implementation. As mentioned above, it regulates people's economic and social activities in accordance with policies and regulations, technical standards and specifications, information security requirements, and institutional innovation rules that support and guarantee the implementation of strategic planning. "System 3" jointly ensures the implementation of the strategic plan. The strategic research that exerts the development function of "System 4" fully analyzes the internal and external environment faced by the development of the smart city system through relevant basic research, special research, and case studies and provides necessary information support for the strategic planning and implementation of the

smart city. The strategic planning that exerts the policy function of "System 5" indicates the direction and path for the development of the smart city system by describing the strategic vision of smart city development, formulating strategic goals and strategic tasks for smart city construction, and clarifying the strategic focus of smart city construction, so as to ensure that the smart city system can develop into a city system with "smart" characteristics [22]. It can be seen that the strategic layer and the strategic system are the core of the smart city system, which establish the communication and control mechanism of the entire smart city system and promote the city system to continuously move towards a "smart" city system.

It can be seen that the living system model realizes that different parts of the organization and the entire organization operate according to their own goals through appropriate information flow and communication chain. The operation and development of smart city systems also follow these communication and control laws.

3.3. System Model Description of Smart City

3.3.1. Corresponding Relationship between the Elements and Structures of the Smart City System and the Conceptual Connotation of the Smart City System. The smart city system is an urban system with the characteristics of "smart" formed by the coupling and effect of the intelligence of information technology and the intelligence of people and the urban system. From the analysis of the conceptual connotation of the smart city system above, it can be seen that in the formation and operation of the smart city system, the first is the combination of emerging information technology and the city subsystem to build an intelligent city subsystem, and then the human wisdom and intelligence. The intelligent urban subsystem is combined to form a smart urban subsystem. Finally, human wisdom is combined with various intelligent urban subsystems and smart urban subsystems to build a smart urban system. At the same time, it can be seen from the previous analysis that the smart city system is composed of five subsystems: strategic system, social system, economic system, support system, and space system and also how they reflect the wisdom of people in the smart city system and the intelligent city subsystem and the connection and combination of smart city subsystems.

From the relevant analysis of the elements and structures of the smart city system, it can be seen that the smart city system is composed of three layers: the strategic layer, the activity layer, and the physical layer, and five subsystems: strategic system, social system, economic system, support system, and space system, which are interconnected, interact, and jointly build a smart city system with "smart" characteristics. In the smart city system, the support system and the space system are located at the physical layer, which is the result of the intelligent transformation of the original urban material elements and material forms by emerging information and communication technologies. They are all intelligent cities with intelligent application systems as the core subsystem. Therefore, the support system and the space system correspond to the intelligent urban subsystems in the smart city system. The social system and the economic system are located in the activity layer, which mainly reflects the intelligent form of people's economic and social activities. They are constructed by people with the ability to "cognition, judgment, analysis, and action" using information technology under the support of the support system and the space system. Various forms of activities carried out by the intelligent application system and related activities are integrated into the intelligent city subsystem. Therefore, the social system and the economic system correspond to the smart city subsystems in the smart city system. The strategic system is located at the strategic layer. It formulates smart strategic planning with human "insight, foresight, and wise response," and plans, organizes, guides, and coordinates the construction of smart city subsystems and the development of smart city subsystems. In turn, a more scientific and reasonable development model emerges in the entire smart city system to realize the "smart" development of the entire city [23]. Therefore, the strategic system corresponds to a good combination of human intelligence, intelligent city subsystem, and smart city subsystem in the smart city system.

3.3.2. System Model Design of Smart City. The system model of the smart city is the description, imitation, and abstraction of the smart city system, and it describes the relationship between the elements of the smart city system in a certain structural form. According to the three levels of the smart city system structure and the relationship between the five subsystems, this paper constructs the smart city system model shown in Figure 5. It can be seen from the figure that the system model of a smart city is composed of three layers: strategic layer, activity layer, and physical layer, and five subsystems: strategic system, social system, economic system, support system, and space system. The strategic system is located at the strategic layer, which is at the highest level of the smart city system; the social system and economic system are at the activity layer that is at the middle of the smart city system, and the support system and space system are at the physical layer that is at the bottom of the smart city system. At the same time, the strategic system, social system, economic system, support system, and space system are all interrelated, interactive, and interdependent [24].

The formation, operation, and development of the smart city system are revealed through the interconnection and interaction between the five subsystems in the three layers. Specifically, the formation, operation, and development of the smart city system are realized by the relationship and function of the five subsystems from high to low complexity [25]. Among them, the strategic system is the soul and core of promoting the entire smart city system to present "wisdom": the construction of information network infrastructure, intelligent application system, and public information platform in the system; the formation of highly intelligent flow space and scientific and rational spatial development pattern in the

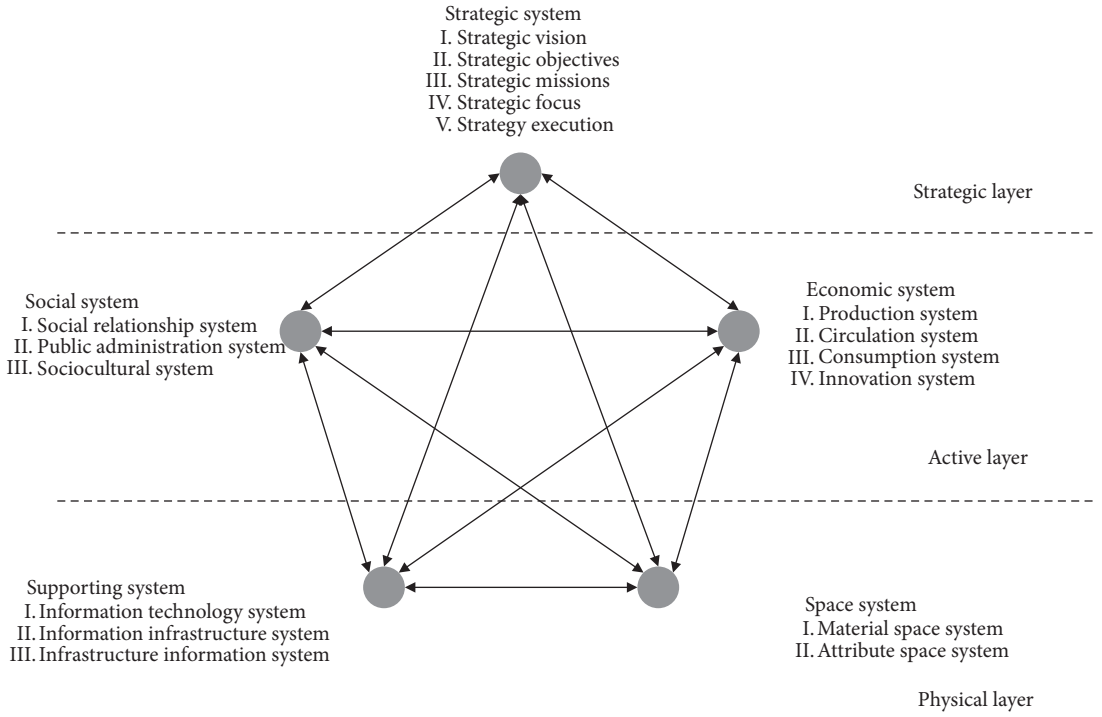

Figure 5: Schematic diagram of the system model of a smart city.

space system; and the social environment in the social system that is more in line with the needs of modern people's survival and development. On the other hand, the strategic system realizes the social system, economic system, support system, and spatial system through its restraint, control, and adjustment functions; coordinates and balances development; and then promotes the continuous optimization of the entire urban system. The social system and the economic system are closely related to human activities, and they are the most dynamic and creative system components in the smart city system. Under the guidance and regulation of the strategic system, as well as the support of the support system and the space system, the social system creates a good social environment and conditions to promote the all-round development of human beings. The economic system lays a solid material foundation for the all-round development of human beings by creating more diverse and rich material living conditions and environments, thus creating a social and economic environment in the city that is more in line with the development needs of modern people. The support system and the space system are closely related to the material elements in the city. They are formed in the deployment and implementation of the strategic system and provide the material basis and support place for people's economic and social activities in the smart city. Social activities provide technical and material support, and the space system provides resources, environment, and support sites for people's economic and social activities. It can be seen that the support system and the space system jointly build the basic conditions that are more in line with the needs of modern urban operation and development.

4. Conclusion

In this rapidly developing information age, opportunities and challenges coexist. The combination of informatization and urbanization is inevitable, and so is the construction of a smart city system. Firmly grasp the technical foundation of "multidimensional space-time characteristics" and reasonably solve the problems of security and privacy are of great importance to the construction of smart city systems. In terms of building a smart city, my country has lagged behind for a period of time, with insufficient infrastructure construction, and is competing with many developed countries. It must vigorously develop multidimensional space-time characteristics to solve difficulties and come first. My country's smart city construction should be designed and planned according to local conditions, combined with its own original characteristics, based on multidimensional space-time characteristics, comprehensive use of various science and technology, and strong strategic support to bring urban construction to a new height.

Data Availability

The data set can be accessed upon request.

Conflicts of Interest

The author declares that there are no conflicts of interest.

References

[1] G. Anthopoulos Leonidas, P. Zohreh, L. Kristina, S. Tobias, N. Bjoern, and N. Ioannis, "Smart cities as hubs: Connect, collect and control city flows," *Cities*, vol. 125, 2022.

[2] K. Saini Dinesh, H. Saini, P. Gupta, and Mabrouk Anouar Ben, "Prediction of malicious objects using prey-predator model in Internet of Things (IoT) for smart cities [J]," *Computers & Industrial Engineering*, vol. 168, 2022.
[3] Smart Data, "Smart cities" 2022[J]," *Photogrammetric Record*, vol. 37, no. 177, 2022.
[4] Q. Guo, Y. Wang, and X. Dong, "Effects of smart city construction on energy saving and CO2 emission reduction: evidence from china[J]," *Applied Energy*, vol. 313, 2022.
[5] R. Sharma and R. Arya, "UAV based long range environment monitoring system with Industry 5.0 perspectives for smart city infrastructure[J]," *Computers & Industrial Engineering*, vol. 168, 2022.
[6] S. Ketu and P. K. Mishra, *A Contemporary Survey on IoT Based Smart Cities: Architecture, Applications, and Open Issues[J]*, Wireless Personal Communications, (prepublish), 2022.
[7] C. Maestosi Paola, "Smart cities and positive energy districts: urban perspectives in 2020[J]," *Energies*, vol. 15, no. 6, 2022.
[8] A. Kokkala and V. Marinos, *An Engineering Geological Database for Managing, Planning and Protecting Intelligent Cities: The Case of Thessaloniki City in Northern Greece[J]*, Engineering Geology, (prepublish), 2022.
[9] K. Tian, H. Chai, Y. Liu, and B. Liu, "Edge intelligence empowered dynamic offloading and resource management of MEC for smart city Internet of Things," *Electronics*, vol. 11, no. 6, p. 879, 2022.
[10] *Smart Cities Market Set to Register Huge 25% CAGR to 2030 [J]*, M2 Presswire, 2022.
[11] M. Giehrl, *Erst die Bürger öffnen das Tor zur Smart City[J]*, Wirtschaftsinformatik & Management, (prepublish), 2022.
[12] J. Mario, M. Tea, and Ć. Maja, "End-user approach to evaluating costs and benefits of smart city applications[J]," *International Journal of E-Services and Mobile Applications*, vol. 14, no. 1, 2022.
[13] D. Orejon Sanchez Rami, C. Garcia David, and R. Andres Diaz Jose, G. Calderon Alfonso, Smart cities' development in spain: a comparison of technical and social indicators with reference to european cities," *Sustainable Cities and Society*, vol. 86, 2022 (prepublish).
[14] M. Qonita and S. R. Giyarsih, "Smart city assessment using the boyd cohen smart city wheel in salatiga, indonesia[J]," *GeoJournal*, vol. 351, 2022 (prepublish).
[15] E. M. Leclercq and E. A. Rijshouwer, "Enabling citizens' Right to the Smart City through the co-creation of digital platforms," *Urban Transformations*, vol. 4, no. 1, p. 2, 2022.
[16] K. Koundinya, D. Anushka, S. Gupta, D. Amit, C. Pooja, and R. Shailendra, "ConvXSS: a deep learning-based smart ICT framework against code injection attacks for HTML5 web applications in sustainable smart city infrastructure[J]," *Sustainable Cities and Society*, vol. 80, 2022.
[17] H. Zhu, L. Shen, and Y. Ren, "How can smart city shape a happier life? The mechanism for developing a Happiness Driven Smart City[J]," *Sustainable Cities and Society*, vol. 80, 2022.
[18] S. Blasi, A. Ganzaroli, and I. De Noni, "Smartening sustainable development in cities: strengthening the theoretical linkage between smart cities and SDGs[J]," *Sustainable Cities and Society*, vol. 80, 2022.
[19] X. Chen, "Machine learning approach for a circular economy with waste recycling in smart cities," *Energy Reports*, vol. 8, pp. 3127–3140, 2022.
[20] Y. Chen, P. Liang, L. Fu et al., "Using 5G in smart cities: a systematic mapping study[J]," *Intelligent Systems with Applications*, vol. 14, 2022.
[21] R. Armin, G. Amirhossein, M. Maral et al., "An investigation of the policies and crucial sectors of smart cities based on IoT application[J]," *Applied Sciences*, vol. 12, no. 5, 2022.
[22] K. Sachin, S. Kumar Tarun, and S. Singh, "Fate of ai for smart city services in India: a qualitative study[J]," *International Journal of Electronic Government Research*, vol. 18, no. 2, 2022.
[23] S. Ioannis, P. Ilyas, Ntalampiras Stavros, I. Konstantaras Antonios, and N. Antonidakis Emmanuel, "Edge computing for vision-based, urban-insects traps in the context of smart cities[J]," *Sensors*, vol. 22, no. 5, 2022.
[24] J. H. Kim and J. Y. Kim, "How should the structure of smart cities change to predict and overcome a pandemic?" *Sustainability*, vol. 14, no. 5, p. 2981, 2022.
[25] A. Muna, "Internet of medical Things and edge computing for improving healthcare in smart cities[J]," *Mathematical Problems in Engineering*, vol. 2022, Article ID 5776954, 10 pages, 2022.

Hindawi
Scientific Programming
Volume 2022, Article ID 4663213, 7 pages
https://doi.org/10.1155/2022/4663213

Research Article

Automatic Cutting System Design of Robot Hand Based on Stereo Vision

Hongbiao Mei,[1] **Zhongping Li**,[2] **and Chunhong Zou**[1]

[1]*Department of Mechanical and Electrical Engineering, Gannan University of Science and Technology, Ganzhou 341000, China*
[2]*National Furniture Product Quality Inspection and Testing Center (Jiangxi), Ganzhou 341000, China*

Correspondence should be addressed to Hongbiao Mei; meihongbiao@gnust.edu.cn

Received 19 June 2022; Revised 21 July 2022; Accepted 25 July 2022; Published 27 August 2022

Academic Editor: Jie Liu

At present, the pouring riser of valve castings is mainly removed by manual cutting, polluting the environment and causing harm to the human body with a low efficiency. Therefore, an automatic cutting pouring riser method using the stereo vision system and manipulator is proposed. The relative position of the valve casting and the end of the manipulator is obtained through the position transformation of the valve casting coordinate system, the manipulator end of the coordinate system, and the camera coordinate system. The spatial motion trajectory of the manipulator is planned, implementing automatic pouring riser cutting of the same valve casting with the same pose. The experimental results show that the position deviation and the angle deviation of the repetitive positioning accuracy and the random positioning accuracy of the visual system are within ±1 mm and ±1°; in the pouring riser cutting test, the maximum deviation between the actual cutting trajectory and the theoretical cutting trajectory is 3 mm. In summary, the method shows a good reliability and could meet the requirements of cutting accuracy.

1. Introduction

As a control unit to control medium flow in the pipeline conveying system, the valve which is widely used in petroleum industry, chemical industry, metallurgy, electric power industry, etc., can change the channel section and medium direction to realize the diversion, globe, throttle, check, or the overflow pressure relief, and other functions. Because of the complexity of its internal structure, the major part of valve blank is manufactured by casting [1–4]. The pouring riser which is inevitable in the cast process should be cut out as "excess" for subsequent machining. At present, the pouring riser is cut with a hand-held abrasive cutting machine basically which has high labor intensity and low efficiency [5–7]. Large amounts of metal dust and smoke from cutting process float in the air and cause environmental pollution. In addition, the cutting staff who breathe these kinds of dust is likely to suffer from occupational diseases, such as pneumoconiosis, and this has a negative influence on the social image of enterprises [8–12]. Therefore, it has become an urgent problem for the valve manufacturers to develop an automatic cutting method and equipment for cutting pouring riser.

With the development and advancement of the industrial robot technology, the robot is gradually used to cut the pouring riser of the valve and other castings. At present, the common way is to clamp the casting onto the mechanism. Cutting tools, such as cutting disc and flame cutter, are installed at the end of the robot. The cutting trajectory is determined by teaching; then, the robot is controlled to move to finish the cutting according to the teaching trajectory. The advantage of this method is that one teaching track could be called for cutting the same casting theoretically. However, in practice, due to the complex shape of blank parts, it is difficult to determine a coarse datum to improve positional accuracy, resulting in overcutting or undercutting. In addition, enterprises would bear a huge manufacturing cost of positioning and clamping devices for different castings. Thus, large time cost for track teaching causes a lower efficiency and cannot meet the production requirements of enterprises.

In summary, developing a universal positioning method and fixture for valve casting is of great significance. Furthermore, the positioning device of valve casting should meet the following two requirements: (1) for different types of valve castings, the same positioning method and device can be fixed on the same positioning clamping device, and (2) for the same valve castings fixed on the clamping device in the same position and attitude, the pouring riser cutting will be completed using the same teaching program after track teaching.

This paper discusses the positioning method and system for automatic cutting pouring riser of valve castings by an integration of machine vision, robot, network communications, artificial intelligence, and information processing technology [13–16], to achieve the same body in the same position, and the posture is clamped on the automatic cutting equipment, with the same program to complete the same valve pouring riser cutting, which laid a foundation for automatic cutting of the pouring riser and solved the urgent problems faced by enterprises. The research and development work has broad application prospects, which can significantly improve the economic benefits of foundry enterprises and achieve good social benefits.

2. Positioning System Composition

The positioning system mainly includes the following: 6-dOF industrial robot, 4 high-precision industrial infrared cameras, computer, positioning disc, and flange. Robots, industrial cameras, and computers are connected to switches to form industrial Ethernet, which uses the TCP/IP protocol for communication.

The positioning disc is positioned and mounted to the end of the robot with the flange. The end of the robot is a flange structure, the end face has a pin hole and a stopper, users can achieve their own process equipment or precise positioning between the actuator and the robot by the pin hole and fixing structure; in addition, there are 8 bolt holes on the end face to facilitate the user to install and fasten the positioning fixture to the robot. The corresponding pin hole and convex platform are designed on the flange plate, the convex platform is loaded into the stopper, and then the pin is installed into the pin hole of the flange and at the end face of the robot to position the flange precisely on the robot. Another pin hole is processed in the center of the flange, and then there are two pin holes on the flange. The positioning plate is processed with two pin holes which are corresponding to the flange plate, and four bolt holes are processed in the circumferential direction and installed on the flange plate after positioning.

When the system is working, we place the body casting into the work space at first and then place three marker balls on the circular convex platform; an infrared camera would measure the coordinates of the marker ball in the camera coordinate system, and a computer would calculate the motion parameters of the robot according to the coordinates of the three marked balls; the robot takes the positioning plate and moves to the top of the body casting according to the parameters (for the same valve castings, the position and attitude relationship between the positioning plate and valve body should be fixed. In this way, the positioning clamping device on automatic cutting equipment can be ensured with the same position and attitude). After positioning, the operator connects the body casting to the positioning plate by the welding steel for its subsequent installation and positioning on the cutting equipment.

The crucial problem is to solve the motion parameters of the robot according to the position and attitude of the valve casting, to ensure that the position and attitude between the positioning plate and the valve are within the specified deviation range after the same valve robot moves. In this paper, coordinate transformation is used to solve this problem. More detail about the principle of positioning and the method of solving robot motion parameters will be presented in subsequent paragraphs.

3. Positioning Principle and Algorithm

Four coordinate systems ((C), (R), (V), and (P)) are, respectively, fixated on the camera, robot, valve casting, and positioning plate. The main function of the system is to drive the positioning plate from the initial position to move to the upper part of the body and keep it in a fixed attitude relationship with the valve. For the coordinate system, we make the xoy plane of the positioning plate coordinate (P) parallel to the xoy plane of the valve coordinate system (V), the z-axis must coincide, and the origins differ by an adjustable height H. In order to calculate the robot motion parameters to achieve the position and attitude relationship, the transformation relationship between the body coordinate system and the robot coordinate system needs to be established. The following describes how to achieve this principle and model by establishing the transformation relationship between coordinate systems to calculate the motion parameters of the robot.

3.1. Establishment of the Camera Coordinate System (C). The camera system is a multicamera stereo vision system [17–29] composed of 4 infrared cameras, which can measure the object's coordinates in 3D space. Calibration software and calibration devices are provided by the manufacturer. After the camera is installed and the working space is determined, the establishment of camera coordinate system (C) can be quickly completed according to the manufacturer's instructions and software. The establishment process will not be described in detail in this paper. The camera coordinate system (C) is the bridge to link other coordinate systems, the establishment and the transformation relationship of the other coordinate systems are realized by establishing the transformation relationship between the body casting coordinate systems (V) and (C), the transformation relationship between the robot coordinates (R) and (C), and the transformation relationship between the location plate coordinates (P) and (C). The motion parameters of the robot are calculated according to these transformation relations.

3.2. Transformation Relationship between the Body Casting Coordinate System (V) and the Camera Coordinate System (C). Three circular convex platforms are casted according to design reference, on which are placed the reflective marking balls A, B, and C; the midpoint of the connection between A and B is O_V, and we make sure that $CO_v \perp AB$ when casting. The coordinates of the three reflective marker balls in camera coordinates were obtained by camera shooting, which were, respectively, denoted as

$$A = \begin{bmatrix} x_A^C \\ y_A^C \\ z_A^C \end{bmatrix} B = \begin{bmatrix} x_B^C \\ y_B^C \\ z_B^C \end{bmatrix} C = \begin{bmatrix} x_C^C \\ y_C^C \\ z_C^C \end{bmatrix}. \tag{1}$$

When the valve casting coordinate system (V) is established, O_V is the origin of coordinates, vector $\vec{AB}$ is the x-axis, the normal vector of the plane formed by A, B, and C is z-axis, and the y-axis is determined according to the right-hand rule.

The body casting coordinate system (V) can be regarded as the coordinate system which coincides with the camera coordinate system (C) after rotation and translation. Rotation is the change of attitude, which can be represented by a 3×3 rotation matrix, denoted by ${}_V^C R$; translation is the change of the origin, which is represented by a vector of 3×1, and the origin of the valve casting coordinate system (V) is O_V, which is denoted as O_{CV} in the camera coordinate system (C); then,

$${}^C\mathbf{O_V} = \begin{bmatrix} \frac{\left(x_A^C + x_B^C\right)}{2} \\ \frac{\left(y_A^C + y_B^C\right)}{2} \\ \frac{\left(z_A^C + z_B^C\right)}{2} \end{bmatrix}. \tag{2}$$

The unit vector on the x-axis of the body casting coordinate system (V) is denoted by e_{Vx}^C in (C); then,

$$e_{Vx}^C = \frac{\vec{AB}}{\vec{AB}}. \tag{3}$$

We connect CA and CB in the camera coordinate system (C) to construct vectors $\vec{CA}$ and $\vec{CB}$; then, the vector corresponding to z-axis of the body casting coordinate system (V) in the camera coordinate system (C) is the cross-product of these two vectors, and the unit vector of the z-axis of the body casting coordinate system (V)is denoted by e_{Vz}^C in the camera coordinate system (C); then,

$$e_{Vz}^C = \frac{\vec{CA} \times \vec{CB}}{\vec{CA} \times \vec{CB}}. \tag{4}$$

The unit vector of the y-axis of the body casting coordinate system (V) is denoted by e_{Vy}^C in the camera coordinate system (C); then, e_{Vy}^C is the cross product between the two unit vectors, which are the x-axis and the z-axis of the body casting coordinate system (V) in the camera coordinate system (C) vector; then,

$$e_{Vy}^C = e_{Vz}^C \times e_{Vx}^C. \tag{5}$$

In the camera coordinate system, the unit vector of x, y, and z-axis can be expressed as

$$e_{Cx} = \begin{bmatrix} 1 \\ 0 \\ 0 \end{bmatrix} e_{Cy} = \begin{bmatrix} 0 \\ 1 \\ 0 \end{bmatrix} e_{Cz} = \begin{bmatrix} 0 \\ 0 \\ 1 \end{bmatrix}. \tag{6}$$

Then, the elements in the rotation matrix ${}_V^C R$ can be represented by the dot product between unit vectors e_{Vx}^C, e_{Vy}^C, and e_{Vz}^C and unit vectors e_{Cx}, e_{Cy}, and e_{Cz}, when e_{Vx}^C, e_{Vy}^C, and e_{Vz}^C are the unit vectors of x, y, and z-axis of the body casting coordinate system (V) in the camera coordinate system (C) and e_{Cx}, e_{Cy}, and e_{Cz} are unit vectors of the x, y, and z-axis of the camera coordinate system; then,

$${}_V^C R = \begin{bmatrix} e_{Cx} \cdot e_{Vx}^C & e_{Cx} \cdot e_{Vy}^C & e_{Cx} \cdot e_{Vz}^C \\ e_{Cy} \cdot e_{Vx}^C & e_{Cy} \cdot e_{Vy}^C & e_{Cy} \cdot e_{Vz}^C \\ e_{Cz} \cdot e_{Vx}^C & e_{Cz} \cdot e_{Vy}^C & e_{Cz} \cdot e_{Vz}^C \end{bmatrix}. \tag{7}$$

3.3. Transformation Relationship between Robot Tool Coordinate System (R) and Camera Coordinate System (C). The tool coordinate system (R) is at the end of the robot which is formulated by the robot manufacturer. A positioning pin hole and a positioning stopper are at the end of robot, origin of coordinates is the center of the stopper, x-axis is the line between the center of the pin hole and the center of the stopper whose direction is from the center of the pin hole to the center of the stopper, z-axis is the axis direction, and y-axis is determined by the right-hand rule as aforementioned. The robot can be accurately positioned through the convex platform and the positioning pin hole of the flange.

In the stereo vision system, the traditional method to determine the coordinate transformation relationship between the robot and the camera is complicated and difficult to implement; therefore, this paper will adopt the following methods to establish this relationship. A T-type calibration rod is processed and manufactured, the corresponding T-groove, the positioning pin hole, and the thread hole are processed along the x and y-axis of the tool coordinates on the positioning flange. Two marking balls D and E are placed on the T-type calibration rod along the x-axis direction, to ensure that D and E are symmetrically arranged on both sides of the origin of the robot coordinates, and two marking balls are placed along the y-axis. The coordinates of marking balls D, E, F, and G in the camera coordinate system can be obtained with the camera; the transformation relationship between the tool coordinate system (R) and the camera coordinate system (C) is established according to the similar method in Section 3.2.

The robot coordinate system (R) is obtained from the camera coordinate system (C) after rotation and translation. It represents the change of attitude, which can be represented by a 3×3 rotation matrix, denoted by ${}^{C}_{R}R$. Translation is the change of origin, denoted by a 3×1 vector, and the coordinates of the origin O_R of the robot tool coordinate system (R) are ${}^{C}\mathbf{O_R}$ in the camera coordinate system (C).

The midpoints of D and E are taken as the coordinate origin O_R of the robot tool coordinate system (R), and the coordinate of O_R in the camera coordinate system (C) is O_{CR}; then,

$$ {}^{C}\mathbf{O_R} = \begin{bmatrix} \frac{\left(x_D^C + x_E^C\right)}{2} \\ \frac{\left(y_D^C + y_E^C\right)}{2} \\ \frac{\left(z_D^C + z_E^C\right)}{2} \end{bmatrix}. \tag{8} $$

The unit vector on the x-axis of the robot coordinate system (R) is indicated in the camera coordinate system (C) as

$$ e_{Rx}^C = \frac{\vec{DE}}{\vec{DE}}. \tag{9} $$

The unit vector on the y-axis of the robot coordinate system (R) is indicated in the camera coordinate system (C) as

$$ e_{Ry}^C = \frac{\vec{FG}}{\vec{FG}}. \tag{10} $$

The unit vector on the z-axis of the robot coordinate system (R) is e_{Rz}^C in the camera coordinate system (C); it can be obtained from the cross product of e_{Rx}^C and e_{Ry}^C; then,

$$ e_{Rz}^C = e_{Ry}^C \times e_{Rx}^C. \tag{11} $$

Elements in the rotation matrix ${}^{C}_{V}R$ is the dot product between two unit vectors, in which one is the unit vector of each coordinate axis of the robot tool coordinate system (R) in the camera coordinate system (C) denoted by e_{Rx}^C, e_{Ry}^C, and e_{Rz}^C and another is the unit vector of the x, y, and z axes of the camera coordinate denoted by e_{Cx}, e_{Cy}, and e_{Cz}; then,

$$ {}^{C}_{R}R = \begin{bmatrix} e_{Cx} \cdot e_{Rx}^C & e_{Cx} \cdot e_{Ry}^C & e_{Cx} \cdot e_{Rz}^C \\ e_{Cy} \cdot e_{Rx}^C & e_{Cy} \cdot e_{Ry}^C & e_{Cy} \cdot e_{Rz}^C \\ e_{Cz} \cdot e_{Rx}^C & e_{Cz} \cdot e_{Ry}^C & e_{Cz} \cdot e_{Rz}^C \end{bmatrix}. \tag{12} $$

3.4. Transformation Relationship between the Positioning Plate Coordinate System (P) and Robot Tool Coordinate System (R). The positioning plate is positioned on the flange through two pin holes; in this way, the position and attitude between the positioning plate and the robot are fixed. We establish the coordinate system (P) of the positioning disk and take the line between the center of the two pin holes of the positioning disk as the x-axis, the vertical orientation of the positioning plate is the z-axis, the y-axis is determined according to the right-hand rule, and the center of the positioning plate is taken as the origin of the coordinates O_P. When the coordinate system of the positioning plate is established in this way, its x and y axes are parallel to the x and y axes of the robot tool coordinate system and their z-axis overlaps. There is only translation between the positioning plate coordinate system (P) and the robot tool coordinate system (R), and there is no rotation of the coordinate axis. The rotation transformation matrix is an identity matrix, denoted by

$$ {}^{R}_{P}R = \begin{bmatrix} 1 & 0 & 0 \\ 0 & 1 & 0 \\ 0 & 0 & 1 \end{bmatrix}. \tag{13} $$

When the thickness of the position plate is h_p and the thickness of the flange plate is h_f, the coordinates of the origin of the positioning plate coordinate system (P) in the robot tool coordinate system (R) can be denoted by

$$ O_P^R = \begin{bmatrix} 0 \\ 0 \\ -\left(h_p + h_f\right) \end{bmatrix}. \tag{14} $$

3.5. Transformation Relationship between the Robot Tool Coordinate System (R) and the Valve Coordinate System (V). The function of the positioning system is to make the robot drive the positioning plate to move from the initial position to the upper side of the valve. At this time, the xoy plane of the positioning plate coordinate (P) is parallel to the xoy plane of the valve coordinate (V), and the Z axis coincides. The distance of the origins of the coordinates is H, in which $H = h + f$. Then, the translational motion of the robot can be regarded as moving from its initial position to $H + h_p + h_f$ on the z-axis of the body frame (V). Then, only the transformation relationship between the camera coordinate system (C), valve coordinate system (V), and the robot coordinate system (R) needs to be considered.

The robot coordinate (R) overlaps with the camera coordinate system after rotation and translation and then moves again to the origin of the robot coordinate (R) to the point P; its Z axis coincides with the z-axis of the body coordinate system; its x-axis and y-axis are, respectively, parallel to the x-axis and y-axis of the body coordinate system (V), and the x-axis and y-axis are parallel to the x-axis and y-axis of the valve coordinate system (V).Then, the transformation relation between the robot coordinate system (R) and the valve coordinate system (V) can be established.

Table 1: The repeat positioning accuracy test.

Times	1	2	3	4	5	6	7	8	9	10
$\mathbf{OO}'$ (mm)	0.5	−0.6	1.9	0.4	1.3	1.6	−1.1	−1.2	−0.9	0.2
θ (℃)	0.1	−0.12	0.4	0.08	0.26	0.32	−0.23	−0.25	−0.18	0.04

The rotation transformation matrix between the valve coordinate system (V) and the robot coordinate system (R) is denoted by ${}^{R}_{V}R$; then,

$$ {}^{R}_{V}R = {}^{R}_{C}R \times {}^{C}_{V}R = {}^{C}_{R}R^{T} \times {}^{C}_{V}R. \tag{15} $$

The coordinate of P in the valve coordinate system {**V**} is ${}^{\mathbf{V}}\mathbf{P}$; then,

$$ {}^{\mathbf{V}}\mathbf{P} = \begin{bmatrix} 0 \\ 0 \\ \mathbf{H} + \mathbf{h_p} + \mathbf{h_f} \end{bmatrix}. \tag{16} $$

The coordinate of P in the camera coordinate system {**C**} is ${}^{\mathbf{R}}\mathbf{P}$; then,

$$ {}^{\mathbf{C}}\mathbf{P} = {}^{\mathbf{C}}_{\mathbf{V}}\mathbf{R}\,{}^{\mathbf{V}}\mathbf{P} + {}^{\mathbf{C}}\mathbf{O}_{\mathbf{V}}. \tag{17} $$

The coordinate of P in the robot coordinate system {**R**} is ${}^{\mathbf{R}}\mathbf{P}$; then,

$$ {}^{\mathbf{R}}\mathbf{P} = {}^{\mathbf{C}}_{\mathbf{R}}\mathbf{R}^{\mathbf{T}}\left({}^{\mathbf{C}}\mathbf{P} - {}^{\mathbf{C}}\mathbf{O}_{\mathbf{R}}\right). \tag{18} $$

By substituting equation (17) into equation (18), we get

$$ {}^{\mathbf{R}}\mathbf{P} = {}^{\mathbf{C}}_{\mathbf{R}}\mathbf{R}^{\mathbf{T}}\left({}^{\mathbf{C}}_{\mathbf{V}}\mathbf{R}\,{}^{\mathbf{V}}\mathbf{P} + {}^{\mathbf{C}}\mathbf{O}_{\mathbf{V}} - {}^{\mathbf{C}}\mathbf{O}_{\mathbf{R}}\right). \tag{19} $$

4. Calculation of the Robot Motion Parameters

According to the transformation relationship between the robot tool coordinate system (R) and the valve coordinate system (V), the motion parameters of the robot from the initial position and attitude adjusting to the same position and attitude with the valve can be calculated.

The adjustment of robot attitude is achieved by rotation angles γ, β, and α around x_R, y_R, and z_R of the robot tool coordinate system; then, positioning between the positioning disc and the valve can be calculated as

$$ \begin{aligned} \gamma &= A\tan 2\left[{}^{R}_{V}R(3,2), {}^{R}_{V}R\ (3,3)\right], \\ \beta &= A\tan 2\left\{-{}^{R}_{V}R(3,1), \sqrt{\left[{}^{R}_{V}R(1,1)\right]^{2} + \left[{}^{R}_{V}R(2,1)\right]^{2}}\right\}, \\ \alpha &= A\tan 2\left[{}^{R}_{V}R(2,1), {}^{R}_{V}R(1,1)\right]. \end{aligned} \tag{20} $$

The robot's translation of x_R, y_R, and z_R along the tool coordinate system (R) is , $\Delta x, \Delta y, \Delta z$.

$$ \Delta\mathbf{x} = {}^{\mathbf{R}}\mathbf{P}\ (1), \qquad \Delta\mathbf{y} = {}^{\mathbf{R}}\mathbf{P}(2), \qquad \Delta\mathbf{z} = {}^{\mathbf{R}}\mathbf{P}(3). \tag{21} $$

After calculation, the motion parameters of the robot are sent to the robot controller through industrial Ethernet and the positioning between the positioning disc and the valve can be realized according to the motion parameters.

5. Practical Application of the Positioning System

The positioning system is established, including 4 infrared cameras, Kawasaki robot, and computer. As a lot of matrix calculations are involved in the positioning algorithm, MATLAB 2017 software is installed on the computer to realize the positioning algorithm and provide a human-computer interaction environment.

The operation process is as follows: Click "static calibration" button to realize automatic calculation of the rotation matrix ${}^{C}_{R}R$ and the translation vector P_{RC} between the robot tool coordinate system (R) and the camera coordinate system (C). During the positioning operation, enter the valve code and the height difference H between the locating disc and the corresponding valve; thickness h_p and flange thickness h_f are automatically retrieved from the Excel table by the system. The "Start" button is used to start the positioning system to read coordinates from the camera, calculate the movement parameters of the robot, and control the robot move to the upper side of the valve to achieve positioning. The "Reset" button is used to reset the robot to its initial position and attitude. Parameters of the new valve or modified parameters of the old valve can be saved into the Excel sheet by clicking "Save" button, and click the "Save" button.

In order to verify the accuracy of the positioning method, a cross laser is installed on the positioning disk and the experiments are as follows: (1) the repeat positioning accuracy test: fix the valve in a certain position, repeat the positioning process for 10 times, and observe the center position of the cross cursor and the deflection angle of the cross line; (2) the random positioning accuracy test: move the valve randomly, change its position and attitude, change the position and attitude of the valve, and observe the center position of the cross cursor and the deflection of the cross line in every motion.

6. The Error Evaluation Method

In order to evaluate the precision of repeat, after the first position, mark the center and the projection line of cross laser on the valve castings (solid lines x and y and point O). The deviation of the projection line and the center (dotted lines $\hat{x}'$ and $\hat{y}'$ and point O') from the first projection line and center was compared in the subsequent positioning.

In the deviation between the cross laser, the translation error is evaluated by the distance OO' and the angle positioning error is evaluated by θ. According to the geometric relationship, it can be calculated as

Table 2: The random positioning accuracy test.

Times	1	2	3	4	5	6	7	8	9	10
$\mathbf{OO}'$ (mm)	−2.4	−0.06	−1.84	2.37	−2.41	−2.7	0.341	1.6	−1.12	−1.92
θ (℃)	−0.49	−0.01	−0.38	0.48	−0.49	−0.51	0.07	0.33	−0.23	−0.39

$$\theta = \tan^{-1}\left(\frac{OO'}{OO_R}\right), \tag{22}$$

where $OO_R = H + h_p + h_f$.

In the test, the thickness of the positioning plate is $h_p = 40mm$, the thickness of the flange is $h_f = 40mm$, and the positioning height is $H = 200mm$, and then $OO_R = H + h_p + h_f = 280mm$.

The data of the repeat positioning accuracy test are shown in Table 1, and the experimental data of the random positioning accuracy test are shown in Table 2.

The test results show the following: (1) in the repeat positioning accuracy test, the position error is within ±2 mm and the angle positioning error is within ±0.5°C; (2) in the random positioning accuracy test, the position error is also controlled within ±3 mm and the angle positioning error is controlled within ±1°C. The results show that the positioning method is effective.

7. Conclusion

To solve the problem of locating the valve on cutting equipment in automatic cutting of pouring riser after valve casting, a positioning system integrating stereo vision, robot, and information processing technology for automatic pouring riser cutting of valve casting was designed, using the principle and method of coordinate transformation. We establish a coordinate relationship between the rotation and translation by fixing the coordinate system of the valve castings, positioning plate, robot, and camera. We calculated the motion parameters of robot in the working space and realized that the positioning plate can be positioned to the upper side of the same type valve casting with the same position and attitude. The experimental results and the actual cutting show that the proposed positioning method has high positioning accuracy, satisfies the cutting accuracy requirements of valve castings, and has a wide application prospect.

Data Availability

The experimental data used to support the findings of this study are available from the corresponding author upon request.

Conflicts of Interest

The authors declare that they have no conflicts of interest regarding this work.

Acknowledgments

This study was supported by the Natural Science Foundation of Jiangxi Provincial Education, Department Study on Vulnerability Model of Geological Disaster System in Southern Rare Earth Ore (GJJ171498), and Innovator Plan Project of Ganzhou City Science and Technology Bureau, Study on Vulnerability Prediction and Evaluation Model of Disaster System in Ionic Rare Earth Ore (2018-150).

References

[1] P. X. Fu, X. H. Kang, Y. C. Ma, K. Liu, D. Li, and Y Li, "Centrifugal casting of TiAl exhaust valves," *Intermetallics*, vol. 16, no. 2, pp. 130–138, 2008.

[2] I. Gali, K. Vukovi, Z. Tonkovi, and I. Čular, "Numerical simulation of initiation and crack growth on cast valve body," *Engineering Failure Analysis*, vol. 117, Article ID 104793, 2020.

[3] K. Liu, Y. C. Ma, M. Gao et al., "Single step centrifugal casting TiAl automotive valves," *Intermetallics*, vol. 13, no. 9, pp. 925–928, 2005.

[4] B. Han, L. Luo, X. Meng, and X. Xue, "Generation Reason and Elimination of Blowhole in Vacuum Suction Cast TiAl-Based Alloy Exhaust Valve," *Rare Metal Materials and Engineering*, vol. 1, 2018.

[5] E. N. Eremin, G. N. Minnekhanov, and R. G. Minnekhanov, "Improving the Quality of Cast Metal of Pipeline Valves by Modification of Nanodispersed Refractory Particles," *AIP Conference Proceeding*, vol. 2007, Article ID 5051933, 2007.

[6] M. Çöl, F. Kahrıman, M. Uygun, and S. Adişen, "Examinations of casting cracks in a high alloy steel valve," *Materialpruefung: werkstoffe und Bauteile*, vol. 58, no. 9, pp. 731–734, 2016.

[7] J. Fourie, J. Lelito, P. Żak, P. Krajewski, and W Wolczynski, "Numerical optimization of the gating system for an inlet valve casting made of titanium alloy," *Archives of Metallurgy and Materials*, vol. 60, no. 3, pp. 2437–2446, 2015.

[8] M. Pang, W. He, C. Z. Liu, X. L. Wang, and X. B. Kang, "Surface hardening of a vermicular cast iron used for integral molding valve seat by high power laser[J]," *Applied Mechanics and Materials*, vol. 456, pp. 474–477, 2014.

[9] C. Xiong, Y. Ma, C. Bo, and K. LIU, "Water modeling of mould filling during suction casting process of automotive exhaust valves of γ-TiAl based alloys[J]," *Acta Metallurgica Sinica -Chinese Edition-*, vol. 47, no. 11, pp. 1408–1417, 2011.

[10] H. P. Li, C. Y. Liang, L. H. Wang, and H. S. Wang, "Numerical simulation of casting process for gray iron butterfly valve," *Advanced Materials Research*, vol. 189-193, pp. 260–264, 2011.

[11] W. B. Sheng, C. X. Ma, and W. L. Gu, "Properties and ca4ge-engine test of TiAl-based alloy valves by permanent mold casting," *Advanced Materials Research*, vol. 139-141, pp. 557–560, 2010.

[12] B. Valentan, I. Drstvensek, T. Brajlih, P. Sever, S. Brezovnik, and J. Balic, "Additive fabrication in metallurgy - case study of grey cast iron valve production[J]," *Strojarstvo*, vol. 52, no. 1, pp. 69–74, 2010.
[13] C. Yu and H. Pei, "Face recognition framework based on effective computing and adversarial neural network and its implementation in machine vision for social robots," *Computers & Electrical Engineering*, vol. 92, no. 1, Article ID 107128, 2021.
[14] S. Opiyo, C. Okinda, J. Zhou, E. Mwangi, and N Makange, "Medial axis-based machine-vision system for orchard robot navigation," *Computers and Electronics in Agriculture*, vol. 185, Article ID 106153, 2021.
[15] D. Zhang and Z. Guo, "Mobile sentry robot for laboratory safety inspection based on machine vision and infrared thermal imaging detection," *Security and Communication Networks*, vol. 2021, no. 1, pp. 1–16, 2021.
[16] Z. Song, J. Yao, and H. Hao, "Design and implementation of video processing controller for pipeline robot based on embedded machine vision," *Neural Computing & Applications*, vol. 34, no. 4, pp. 2707–2718, 2021.
[17] X. Zhang, W. Gong, and X. Xu, "Magnetic ring multi-defect stereo detection system based on multi-camera vision technology," *Sensors*, vol. 20, no. 2, p. 392, 2020.
[18] J. Ren, F. Guan, T. Wang et al., "High Precision Calibration Algorithm for Binocular Stereo Vision Camera Using Deep Reinforcement Learning," *Computational Intelligence and Neuroscience*, vol. 2022, 2022.
[19] H. Chen, "Target Positioning and Grasping of NAO Robot Based on Monocular Stereo Vision," *Mobile Information Systems*, vol. 2022, 2022.
[20] L. Li and C. Mao, "Big data supported PSS evaluation decision in service-oriented manufacturing," *IEEE Access*, vol. 8, no. 99, pp. 154663–154670, 2020.
[21] S. Tao, "Big data system for dragon boat rowing action training based on multidimensional stereo vision," *Mathematical Problems in Engineering*, vol. 1, 8 pages, 2022.
[22] Y.-H. Jin, K.-W. Ko, and W.-H. Lee, "An indoor location-based positioning system using stereo vision with the drone camera," *Mobile Information Systems*, vol. 2018, 2018.
[23] C.-S. Wang, Ko-C. Chen, T. H. Lee, and K.-S. Hsu, "Development and application of the stereo vision tracking system with virtual reality," *Mathematical Problems in Engineering*, vol. 2015, pp. 1–5, Article ID 545498, 2015.
[24] L. Li, B. Lei, and C. Mao, "Digital twin in smart manufacturing," *Journal of Industrial Information Integration*, vol. 26, no. 9, Article ID 100289, 2022.
[25] T. Xue, X. Lin, and L. Yang, "Measurement of circumferential liquid film based on LIF and virtual stereo vision sensor," *Journal of Sensors*, vol. 2016, pp. 1–5, Article ID 2872947, 2016.
[26] L. Li, T. Qu, Y. Liu et al., "Sustainability assessment of intelligent manufacturing supported by digital twin," *IEEE Access*, vol. 8, pp. 174988–175008, 2020.
[27] M.-J. Lee and S.-Y. Park, "Refinement of inverse depth plane in textureless and occluded regions in a multiview stereo matching scheme," *Journal of Sensors*, vol. 2022, pp. 1–13, Article ID 7181445, 2022.
[28] L. Li, C. Mao, H. Sun, Y. Yuan, and B. Lei, "Digital twin driven green performance evaluation methodology of intelligent manufacturing: hybrid model based on fuzzy rough-sets AHP, multistage weight synthesis, and PROMETHEE II," *Complexity*, vol. 2020, no. 6, pp. 1–24, Article ID 3853925, 2020.
[29] Q. Zou, J. Yu, H. Fang, J. Qin, J. Zhang, and S. Liu, "Group-Based atrous convolution stereo matching network," *Wireless Communications and Mobile Computing*, vol. 2021, Article ID 7386280, 11 pages, 2021.

Hindawi
Scientific Programming
Volume 2022, Article ID 4755519, 8 pages
https://doi.org/10.1155/2022/4755519

Research Article

Short-Term Power Load Forecasting Model Design Based on EMD-PSO-GRU

Weihao Zhang[1] **and Ting Wang**[2]

[1]*School of International Education, Henan University, Zhengzhou 65292, Henan, China*
[2]*State Grid Hubei Electric Power Co, Ltd, Jingzhou Power Supply Company Power Dispatching Control Center, Jingzhou, Hubei, China*

Correspondence should be addressed to Weihao Zhang; 1924030003@henu.edu.cn

Received 7 July 2022; Revised 31 July 2022; Accepted 3 August 2022; Published 26 August 2022

Academic Editor: Lianhui Li

Aiming at the nonlinear, nonstationary, and time series characteristics of power load, this study proposes a load forecasting method based on empirical mode decomposition and particle swarm optimization of the gated recurrent unit neural network. First, the original power load data are decomposed into a limited number of modal components and a residual component by using empirical modal decomposition to reduce the nonstationarity and complexity of the load sequence and decrease the association between different IMFs. The subsequences build prediction models based on the gated recurrent unit neural network, respectively, and use the particle swarm algorithm to optimize the network-related hyperparameters to increase the parameter accuracy of the model; finally, superimpose the prediction results of each subsequence to obtain the final load prediction value. The results of the case study show that compared with the traditional forecasting algorithm, the proposed EMD-PSO-GRU forecasting model method can better dig the trend information of forecasting, fit the load curve better, and have higher forecasting accuracy.

1. Introduction

Accurate load forecasting is an important guarantee for stable operation of power grids, scheduling optimization, and reducing operating costs [1]. Smart grid provides a high-quality and massive database for load forecasting. With the rapid evolution of the energy Internet [2], it is more urgent and important to study algorithms with the ability to process big data and high forecasting accuracy. The accuracy of the model has important significance and high engineering application value [3, 4].

In terms of load forecasting, traditional forecasting models such as autoregression (AR), although fast in operation, have high data requirements and lack the ability to adapt and predict. The robustness is poor, and it is difficult to meet the requirements of load forecasting [5]. In recent years, the development of artificial intelligence technology has provided ideas for solving these problems, but some new problems are still derived. Xiangyu et al. [6] used a deep belief network to quickly analyze complex influencing factors, which improves the prediction accuracy, but it only targets regional loads and lacks adaptability. Wu et al. [7] used a parallelized multicore support vector machine (SVM) for load prediction, and the prediction error is reduced to a certain extent compared with a single-core SVM, but it lacks the consideration of the correlation between time series data. Shi and Zhang [8] considered the training differences of different algorithms and proposed a stacking load forecasting model embedded with various machine learning algorithms. This model ensures good accuracy in forecasting, but the cost of model integration is too high and the time is long. With the growing development of deep learning, the gated recurrent unit network as a kind of the special RNN model [9, 10] is widely used to predict events in time series due to the introduction of modules with "memory function" in its structure [11], but it has two deficiencies, namely, the

model learning rate and the number of neurons in the hidden layer, which are difficult to determine. Among them, the learning rate determines the training effect of the model, and the number of neurons in the hidden layer affects the fitting effect of the model. Usually, these parameters are determined by experience and are uncertain, which leads to a decrease in the accuracy of the model.

Similar to other neural networks, GRU's model parameters often need to be selected by human experience, and the fitting ability, training speed, and prediction effect of different model parameters are quite different. In order to more reasonably determine the model parameters of GRU and improve the stability of power load forecasting, a method is proposed based on EMD-PSO to optimize GRU network hyperparameters. Through example analysis, the prediction results verify the effectiveness of the proposed model.

2. Model Theory

2.1. Empirical Mode Decomposition. EMD is a decomposition method, which can decompose the signal according to the specific time scale features of the data and adaptively decompose the local feature signals on different time scales to obtain IMF and residual signals with different characteristics. Each IMF component obtained by decomposition has a certain physical meaning. It represents the variable components of various time scales contained in the raw load data, and the residual term represents the basic trend of the load sequence. The specific EMD steps for a given original time series $x(t)$ are as follows [12, 13]:

(1) Identify maximum and minimum points in the original sequence $x(t)$, use the cubic spline interpolation method to respectively fit $x_{up}(t)$ and $x_{low}(t)$, and calculate the mean $m(t)$ of the upper and lower envelopes.

$$m(t) = \frac{\left[x_{\text{up}}(t) + x_{\text{low}}(t)\right]}{2}. \tag{1}$$

(2) Calculate the difference between the original sequence $x(t)$ and the envelope mean $m(t)$, denoted as $h(t)$.

$$h(t) = x(t) - m(t). \tag{2}$$

(3) Determine whether $h(t)$ satisfies the IMF constraints; if not, use it as a new input sequence, and repeat steps (1) to (2) until the constraints are met; if so, $h(t)$ is the first IMF component, denoted as $c_1(t) = h(t)$, and separates $c_1(t)$ from the original sequence $x(t)$ to obtain $r_1(t)$.

$$r_1(t) = x(t) - c_1(t). \tag{3}$$

(4) $r_1(t)$ is regarded as a new original sequence, and the abovementioned smoothing steps are repeated to obtain the remaining IMF components and one remaining component. The final result of EMD can be expressed as

$$x(t) = \sum_{i=1}^{n} c_i(t) + r_n(t). \tag{4}$$

In the formula: $c_i(t)$ is the i-th intrinsic mode function component; $r_n(t)$ is the residual component, representing the trend term of the original series.

By using the empirical mode decomposition method, different components can be decomposed from the load time series to form a series of subsequence components [14]. Compared with the original series, the subsequence has stronger stationarity to improve accuracy.

2.2. Gated Recurrent Unit Neural Network. The GRU network optimizes LSTM's three gate functions, integrates oblivion gates and input gates into one update gate [15–17], and mixes neuronal and hidden states simultaneously. This can effectively mitigate the following problems: GRU addresses the "vanishing gradient" of RNN networks and reduces the training time of the model. GRU network basic structure is shown in Figure 1.

The calculation formula of the internal structure is

$$\begin{aligned} r_t &= \sigma\left(W_{\text{r}} \cdot \left[h_{t-1}, x_t\right]\right), \\ z_t &= \sigma\left(W_{\text{z}} \cdot \left[h_{t-1}, x_t\right]\right), \\ \widetilde{h}_t &= \phi\left(W_{\widetilde{h}} \cdot \left[r_t \times h_{t-1}, x_t\right]\right), \\ h_t &= \left(\text{I} - z_t\right) \times h_{t-1} + z_t \times \widetilde{h}_t, \\ y_t &= \sigma\left(W_{\text{o}} \cdot h_t\right). \end{aligned} \tag{5}$$

x_t, h_{t-1}, r_t, z_t, $\widetilde{h}_t$, and y_t, respectively, represent the input vector, the state memory variable at the previous moment, the state of the reset gate, the state of the update gate, e-th state of the current candidate set, and the output vector; W_{r}, W_{z}, $W_{\widetilde{h}}$, and W_{o} are the weight parameters; I represents identity matrix; [ ] represents vector connection; · represents matrix dot product; × represents matrix product; σ represents sigmoid activation function; and ϕ represents tanh activation function. The mathematical description of σ and ϕ is as follows:

$$\begin{aligned} \sigma(x) &= \frac{1}{1 + \text{e}^{-x}}, \\ \phi(x) &= \frac{\text{e}^{x} - \text{e}^{-x}}{\text{e}^{x} + \text{e}^{-x}}. \end{aligned} \tag{6}$$

GRU networks use update gates and reset gates as core modules. x_t and h_{t-1} at the previous moment is input into the update gate after the sigmoid nonlinear transformation to determine the state of the previous moment. The reset gate controls the amount of information written to the candidate set, stores the information at the previous moment through h_{t-1} times $\text{I} - z_t$, and records the information at the current moment through $\widetilde{h}_t$ times z_t.

2.3. Particle Swarm Optimization Algorithm. In PSO, each particle has an initial velocity and position, and the fitness value of the particle is determined by the fitness function

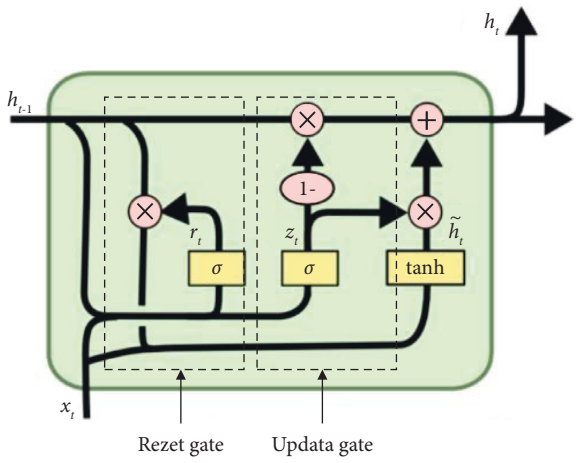

Figure 1: GRU network structure.

[18]. In the iteration, each particle can store the searched optimal position, and its velocity determines the direction and distance of flight [19]. The particles update their speed and position by comparing the fitness values, the optimal value detected by the particle itself is the individual extremum, and the optimal solution detected by the entire population is the global extremum [20]:

$$\begin{aligned} v_i(t+1) &= \omega v_i(t) + c_1 R_1 \left[R_i^b(t) - x_i(t)\right] \\ &\quad + c_2 R_2 \left[R_g^b(t) - x_i(t)\right], \\ x_i(t+1) &= x_i(t) + v_i(t+1). \end{aligned} \tag{7}$$

In the formula, t is the number of iterations; $v_i(t)$ is the speed of the i-th particle in t iterations; ω is the inertia weight; c_1, c_2 are the cognitive coefficients; R_1, R_2 are uniformly distributed random numbers; $Rb/i(t)$ is the individual historical optimal position of a particle i; $Rb/g(t)$ is the historical optimal position of the group; $x_i(t)$ is the position of the particle in t iterations.

The inertia weight ω is an important parameter of PSO. The larger the weight, the stronger the global search ability of the algorithm; the smaller the weight, the stronger the local search ability of the algorithm [21, 22]. The dynamic adjustment of the inertial weight is adopted.

$$\omega(n) = \omega_{\max} - (\omega_{\max} - \omega_{\min})\left(\frac{n}{n_{\max}}\right), \tag{8}$$

where ω_{max} represents the maximum weight, ω_{min} represents the minimum weight, and n_{max} is the maximum number of iterations.

3. EMD-PSO Optimizes the Prediction Model of GRU Hyperparameters

3.1. PSO Optimizes the GRU Hyperparameter Model. The PSO algorithm is a random search and parallel optimization algorithm, which has the characteristics of simplicity, good robustness, and fast convergence speed, and has a high probability of finding the global optimal solution to the problem [23]. The algorithm optimizes the hyperparameters of the GRU and establishes a load forecasting model with higher accuracy. In the GRU model, two hyperparameters have a positive effect on the prediction performance of the model, namely, the number of GRU neurons and the learning rate. Taking these two key parameters as the characteristics of particle optimization, the PSO algorithm is used to adjust and optimize the GRU model. The flowchart of the PSO-GRU load forecasting model is shown in Figure 2.

3.2. EMD-PSO-GRU (EPG) Load Forecasting Model. The load sequence is complex and nonstationary. The decomposed components are input to the GRU model and the PSO algorithm is used to optimize the GRU model hyperparameters. Finally, superimpose the prediction results of each component to get the final prediction value. To improve prediction accuracy, this study proposes the EMD-PSO-GRU hybrid prediction model architecture shown in Figure 3.

The specific steps for building a model are as follows.

(1) The original load time series is divided into several subsequences by EMD

(2) Divide each subsequence into a training set and a validation set and normalize the dataset. Since the GRU model is highly sensitive to the data scale, the original data have a large difference in the order of magnitude; in order to avoid that the change of larger value will cover the change in smaller value, it is necessary to constrain the input data to a similar order of magnitude to avoid affecting the effect of power load forecasting due to the large individual input value. The dataset is between [0, 1] to reinforce the convergence speed of GRU.

(3) Learn the complex relationship between input and output variables in each subsequence by building a GRU network and through the PSO algorithm to determine the optimal GRU network hyperparameters

(4) Use the trained GRU network to predict the subsequence and deformalize the prediction result to obtain the real prediction value

(5) Add the prediction results of each subsequence to obtain the final result of the load

3.3. Model Evaluation Metrics. To evaluate the performance of the prediction model, MAPE and RMSE are used as evaluation indicators [24–33], which are defined as follows:

$$\begin{aligned} y_{MAPE} &= \frac{1}{n}\sum_{i=1}^{n}\frac{\left|y_i - \hat{y}_i\right|}{y_i} \times 100\%, \\ y_{RMSE} &= \sqrt{\frac{\sum_{i=1}^{n}\left(y_i - \hat{y}_i\right)^2}{n}}, \end{aligned} \tag{9}$$

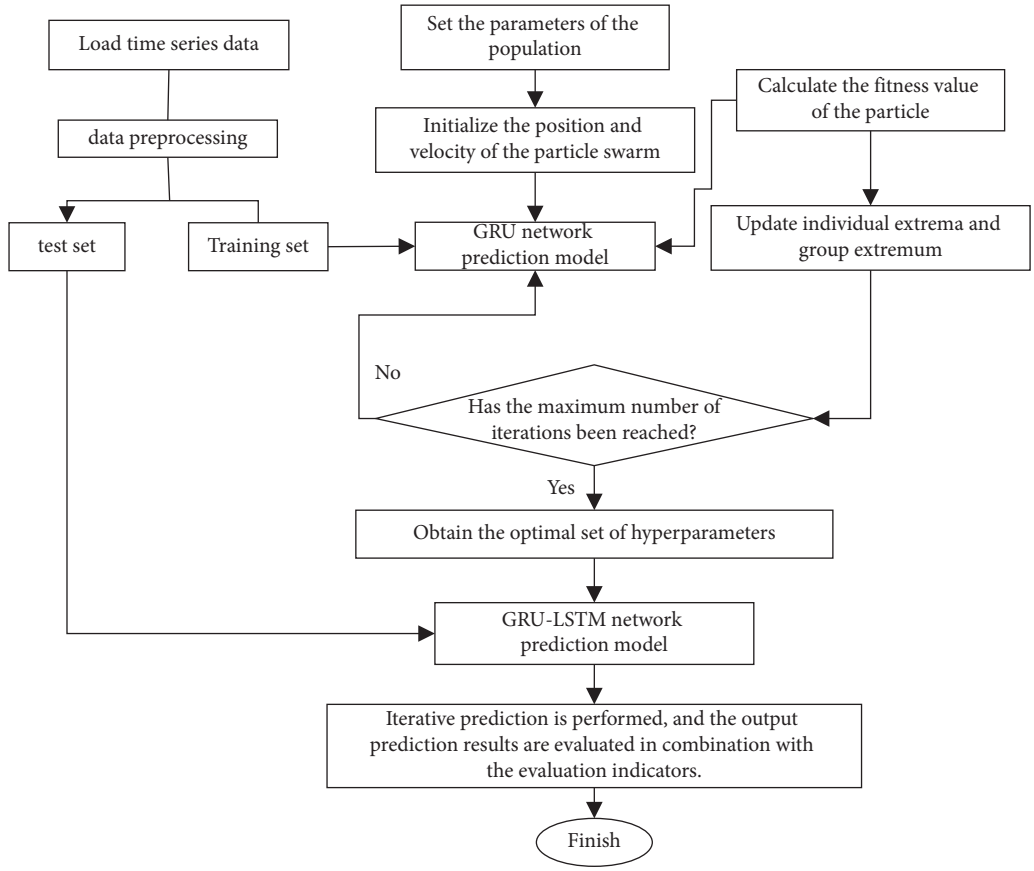

Figure 2: Flowchart of the PSO-LSTM load prediction model.

where y_i is the actual load value on the i-th day; $\hat{y}_i$ is the load forecast value on the i-th day; n is the number of samples in the test set.

4. EMD-PSO Optimizes the Prediction Model of GRU Hyperparameters

To verify the scientificity and reliability of the load forecasting model based on EMD-PSO-GRU proposed in this study, the power load data of a specific area from January 1, 2016, to May 8, 2020, are used. Figure 4 shows the raw data of the average daily load, with a total of 1588 data samples divided into a training set and test set with a ratio of 9 : 1, in which the training set data has 1430 data and the test set has 158 data.

4.1. EMD Decomposition. The load data are decomposed by EMD, and it is decomposed step by step from high frequency to low frequency into 9 IMF components and a residual component. The decomposition result is shown in Figure 5. Compared with the original power load sequence, the decomposed components become more stable in turn. The nine IMF components, respectively, reflect the influence of different influencing factors on the load data at different scales, and the residual component represents the long-term change trend of the load sequence.

4.2. Model Parameter Settings. The number of PSO population sizes is set to 8, the dimension of population optimization is set to 2, the maximum number of iterations is set to 10, the learning factors $c_1 = 2$, $c_2 = 2$, and the inertia weights are set to $w_{\max} = 1.2$, $w_{\min} = 0.8$. The range of the number of neurons is set to [1, 60], and the range of the learning rate is set to [0.001, 0.01].

4.3. Hyperparameter Optimization Results. The predictive performance of a GRU network depends on the choice of parameters for building the network, such as the learning rate and the number of hidden layer nodes. The learning rate and the number of hidden layer nodes in the GRU network are determined by the PSO optimization. Table 1 shows the optimal learning rate and optimal number of hidden layer nodes for the GRU network for each IMF.

In order to verify the superiority of the EMD-PSO-GRU hybrid prediction model, PSO-GRU, GRU, SVM, and RNN models were established under the same prediction process for comparative analysis.

4.4. Load Forecasting Result Analysis. Each model is trained with the data of the training set, the prediction results are compared and verified with the data of the test set, and the MAPE and RMSE evaluation indicators are selected to evaluate the accuracy of the prediction model. The

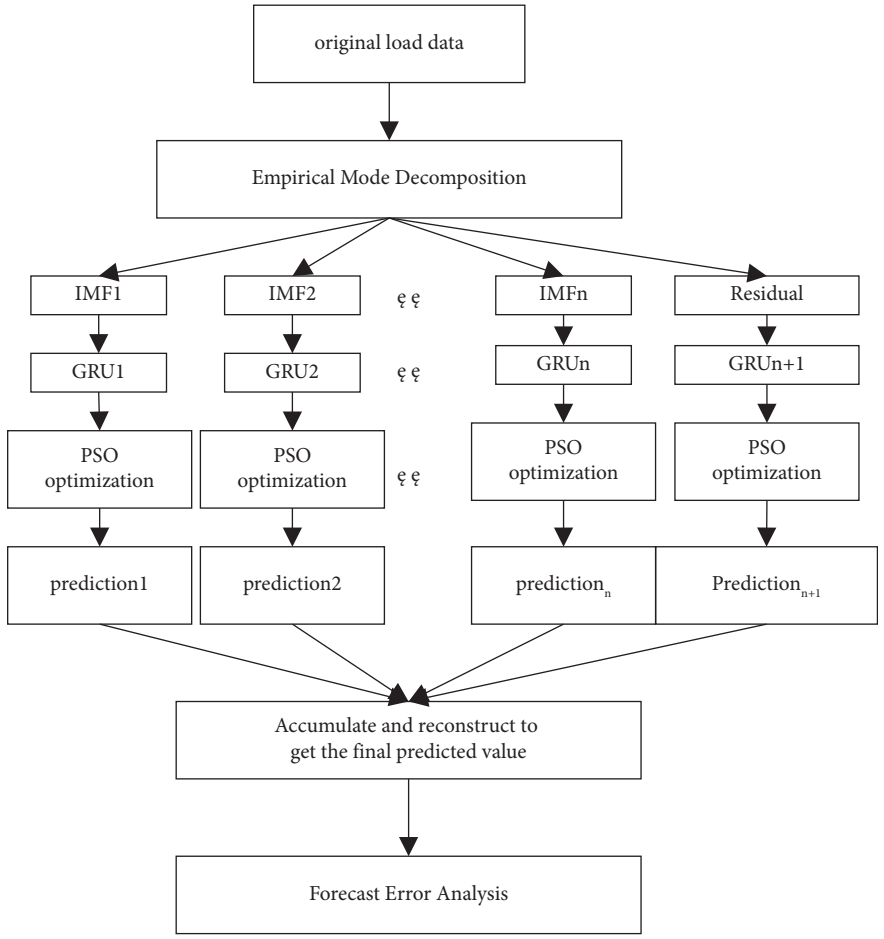

Figure 3: EMD-PSO-GRU combined prediction flowchart.

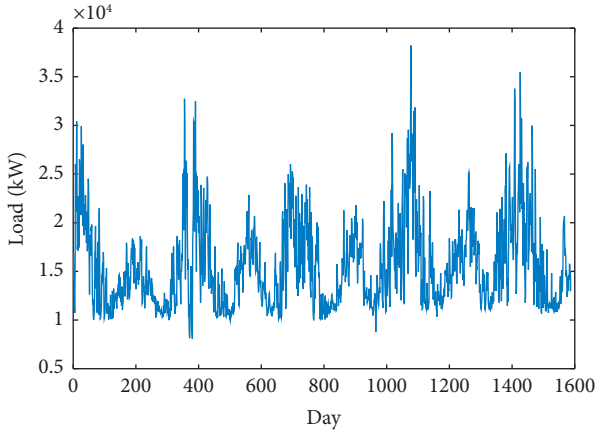

Figure 4: Load raw data.

comparison results of the test set are shown in Figure 6. In order to more clearly see the prediction performance of each model, the error rates of the last two months on the test set are selected for comparison, and the comparison chart is shown in Figure 7. It can be seen from Figures 6 and 7 that among the five models of EMD-PSO-GRU, PSO-GRU, GRU, SVM, and RNN, the overall fitting effect of the EMD-PSO-GRU model and the fitting effect at the peaks and troughs of the waves, The combined effect is better, and the error rate is obviously smaller. It can be seen that the empirical mode decomposition can stabilize the data with strong volatility and then predict it, which can effectively improve the prediction accuracy of the model.

The prediction accuracy evaluation results of each model are shown in Figure 8, and the quantitative indicators of each evaluation result are shown in Table 2. The accuracy evaluation results of the evaluation indicators of the EMD-PSO-GRU model are the best, and the prediction effect of the SVM model is the worst. The MAPE index of the EMD-PSO-GRU model is 1.678%, and the RMSE index is 259.32. Compared with the PSO-GRU prediction model, the MAPE is reduced by 24.92%, and the RMSE is reduced by 28.85%. Strong data stabilization before prediction can effectively improve the prediction accuracy of the model. The MAPE of PSO-GRU is 2.235%, and the RMSE is 364.48. Compared with the GRU model, its MAPE is reduced by 19.78%, and the RMSE is reduced by 25.60%. Due to the influence of experience, adaptively finding the optimal solution of hyperparameters is very important to improve the prediction performance of GRU, which can better improve the prediction accuracy.

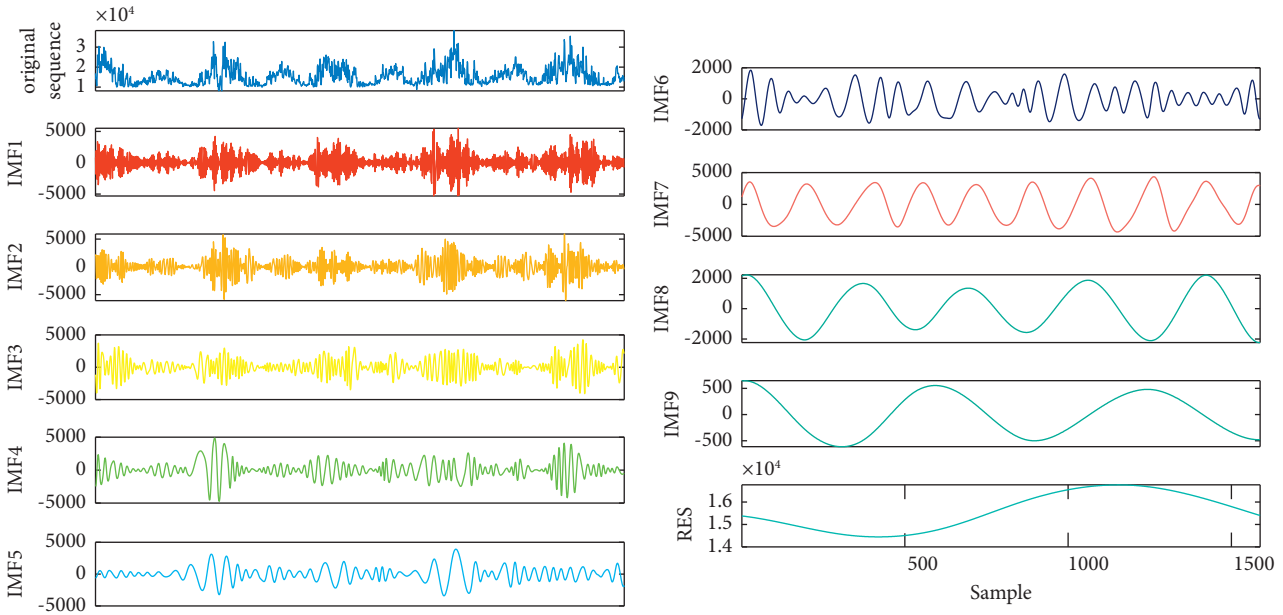

Figure 5: EMD exploded view.

Table 1: Hyperparameter optimization results for each IMF.

Sequence components	The number of neurons in the hidden layer	Learning rate
IMF1	36	0.0092
IMF2	52	0.0082
IMF3	42	0.0063
IMF4	38	0.0086
IMF5	40	0.0055
IMF6	55	0.0037
IMF7	56	0.0036
IMF8	38	0.0035
IMF9	53	0.0086
RES	38	0.0065

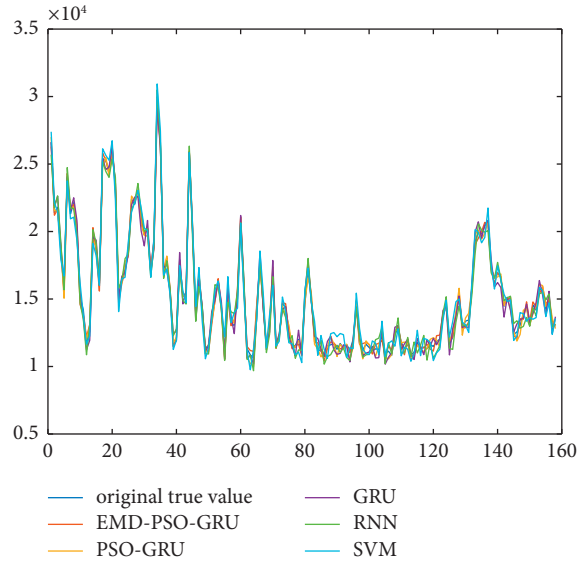

Figure 6: Comparison of prediction results of each model.

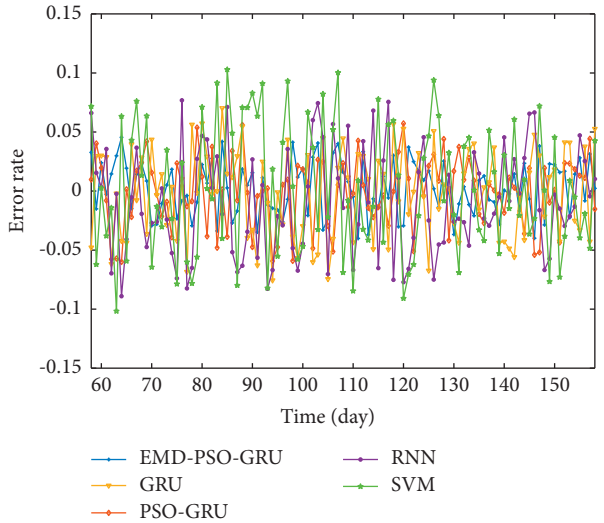

Figure 7: Comparison of the prediction results error rates of each model in the last two months on the test set.

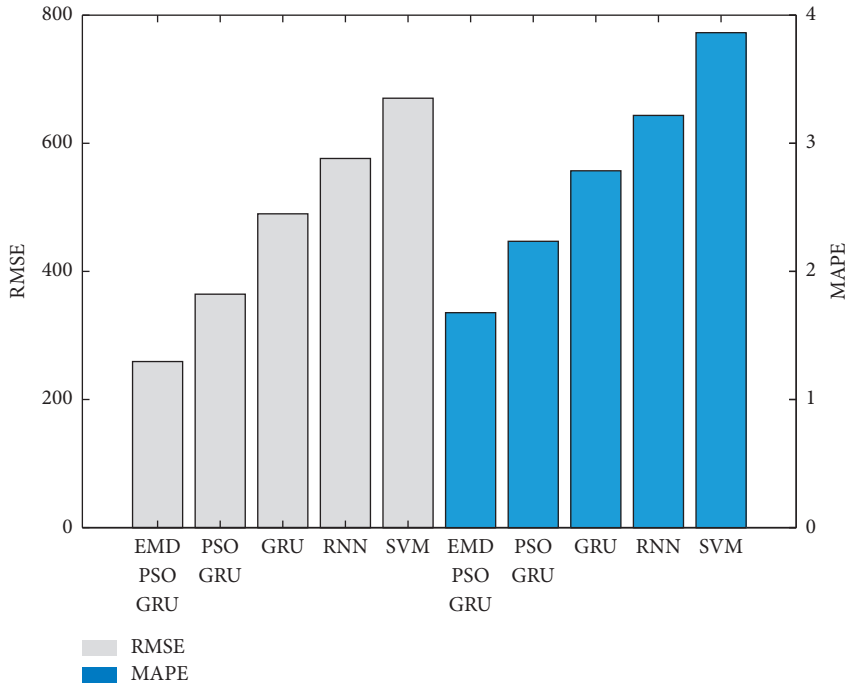

Figure 8: Comparison of prediction performance of each model.

Table 2: Evaluation indicators of the prediction performance of each prediction model.

Model	RMSE	MAPE/%
EMD-PSO-GRU	259.32	1.678
PSO-GRU	364.48	2.235
GRU	489.92	2.786
RNN	576.32	3.218
SVM	670.38	3.864

5. Conclusions

A load forecasting method based on the EMD-PSO-GRU is proposed. First, the data are subjected to variational modal decomposition, preprocessing, and division of the sample dataset, and then, a GRU neural network forecasting model is established for each subsequence. The PSO algorithm is used to optimize the hyperparameters of the GRU neural network, and finally, the respective sequence prediction results are accumulated to obtain the final load prediction value. The method proposed has the following merits:

(1) The EMD decomposition method can well mine the essential features such as cycles and trends in the sequence

(2) Show good advantages of the GRU network in the field of data mining. The GRU network has a unique network structure and strong learning ability for time series data.

(3) The PSO algorithm has stronger global optimization ability and convergence speed by adding nonlinearly changing inertia weights, avoiding the drawbacks of traditional manual selection of hyperparameters, and can independently optimize the hyperparameters of the network model

(4) The prediction accuracy of the "decomposition-prediction-reconstruction" method is higher. The proposed method demonstrates better prediction accuracy compared with the existing artificial intelligence prediction methods.

Data Availability

The data used to support the findings of this study are included within the article.

Conflicts of Interest

The authors declare that they have no conflicts of interest.

Acknowledgments

The authors gratefully acknowledge the support of Henan University and the authors of the literature cited in the paper.

References

[1] Z. Ruicheng, G. U. Jie, and J. Zhijian, "Research on short-term load forecasting variable selection based on fusion of data driven method and forecast error driven method," *Proceedings of the CSEE*, vol. 40, no. (2), pp. 487–500, 2020.

[2] I. K. Nti, M. Teimeh, O. Nyarko-Boateng, and A. F. Adekoya, "Electricity load forecasting: a systematic review," *Journal of Electrical Systems and Information Technology*, vol. 7, no. 1, pp. 1–19, 2020.

[3] A. Al Mamun, M. Sohel, N. Mohammad, M. d. S. H. Sunny, D. R. Dipta, and A. E. Hossain, "comprehensive review of the

load forecasting techniques using single and hybrid predictive models," *IEEE Access*, vol. 8, pp. 134911–134939, 2020.

[4] J. Zhang, Y. M. Wei, D. Li, Z. Tan, and J. Zhou, "Short term electricity load forecasting using a hybrid model," *Energy*, vol. 158, pp. 774–781, 2018.

[5] Z. Wang, Z. H. A. O. Bing, and J. I. Weijia, "Short-term load forecasting method based on GRU-NN model," *Automation of Electric Power Systems*, vol. 43, no. 5, pp. 53–58, 2019.

[6] K. Xiangyu, Z. Feng, and E. Zhijun, "Short-term load forecasting based on deep belief network," *Automation of Electric Power Systems*, vol. 42, no. 5, pp. 133–139, 2018.

[7] Q. Wu, J. Gao, G. S. Hou, B. Han, and K. Y. Wang, "Short-term load forecasting support vector machine algorithm based on multi-source heterogeneous fusion of load factors," *Automation of Electric Power Systems*, vol. 40, no. 15, pp. 67–72, 2016.

[8] J. Shi and J. Zhang, "Load forecasting based on multi-model by stacking ensemble learning," *Proceedings of the CSEE*, vol. 39, no. 14, pp. 4032–4042, 2019.

[9] T. Li, Y. Xu, J. Luo, J. He, and S. Lin, "A Method of Amino Acid Terahertz Spectrum Recognition Based on the Convolutional Neural Network and Bidirectional Gated Recurrent Network model," *Scientific Programming*, vol. 2021, 2021.

[10] Y. Gao, R. Wang, and E. Zhou, "Stock Prediction Based on Optimized LSTM and GRU Models," *Scientific Programming*, vol. 2021, 2021.

[11] X. Wang, W. Li, and Q. Li, "A New Embedded Estimation Model for Soil Temperature prediction," *Scientific Programming*, vol. 2021, 2021.

[12] A. J. Quinn, V. Lopes-dos-Santos, D. Dupret, A. C. Nobre, and M. W. Woolrich, "EMD: empirical mode decomposition and Hilbert-Huang spectral analyses in Python," *Journal of open source software*, vol. 6, no. 59, 2021.

[13] J. J. Ruiz-Aguilar, I. Turias, J. González-Enrique, D. Urda, and D. Elizondo, "A permutation entropy-based EMD–ANN forecasting ensemble approach for wind speed prediction," *Neural Computing & Applications*, vol. 33, no. 7, pp. 2369–2391, 2021.

[14] D. Han, N. Zhao, and P. Shi, "Gear fault feature extraction and diagnosis method under different load excitation based on EMD, PSO-SVM and fractal box dimension[J]," *Journal of Mechanical Science and Technology*, vol. 33, no. 2, pp. 487–494, 2019.

[15] Y. Zhang, T. Zhou, X. Huang, L. Cao, and Q. Zhou, "Fault diagnosis of rotating machinery based on recurrent neural networks," *Measurement*, vol. 171, Article ID 108774, 2021.

[16] Y. Suo, W. Chen, C. Claramunt, and S. Yang, "A ship trajectory prediction framework based on a recurrent neural network," *Sensors*, vol. 20, no. 18, p. 5133, 2020.

[17] S. Yang, X. Yu, and Y. Zhou, "Lstm and gru neural network performance comparison study: taking yelp review dataset as an example," in *Proceedings of the 2020 International workshop on electronic communication and artificial intelligence (IWECAI)*, pp. 98–101, Shanghai, China, June2020.

[18] W. Deng, J. Xu, H. Zhao, and Y. Song, "A Novel Gate Resource Allocation Method Using Improved PSO-Based QEA," *IEEE Transactions on Intelligent Transportation Systems*, vol. 23, no. 3, pp. 1737–1745, 2020.

[19] X. Ren, S. Liu, X. Yu, and X. Dong, "A method for state-of-charge estimation of lithium-ion batteries based on PSO-LSTM," *Energy*, vol. 234, Article ID 121236, 2021.

[20] Y. Zhu, G. Li, R. Wang, S. Tang, H. Su, and K. Cao, "Intelligent fault diagnosis of hydraulic piston pump combining improved LeNet-5 and PSO hyperparameter optimization," *Applied Acoustics*, vol. 183, Article ID 108336, 2021.

[21] W. Zhu, H. N. Rad, and M. Hasanipanah, "A chaos recurrent ANFIS optimized by PSO to predict ground vibration generated in rock blasting[J]," *Applied Soft Computing*, vol. 108, Article ID 107434, 2021.

[22] S. S. Band, S. Janizadeh, S. Chandra Pal et al., "Novel ensemble approach of deep learning neural network (DLNN) model and particle swarm optimization (PSO) algorithm for prediction of gully erosion susceptibility," *Sensors*, vol. 20, no. 19, p. 5609, 2020.

[23] L. T. Le, H. Nguyen, J. Dou, and J. Zhou, "A comparative study of PSO-ANN, GA-ANN, ICA-ANN, and ABC-ANN in estimating the heating load of buildings' energy efficiency for smart city planning," *Applied Sciences*, vol. 9, no. 13, p. 2630, 2019.

[24] H. Eskandari, M. Imani, and M. P. Moghaddam, "Convolutional and recurrent neural network based model for short-term load forecasting," *Electric Power Systems Research*, vol. 195, Article ID 107173, 2021.

[25] L. Yin and J. Xie, "Multi-temporal-spatial-scale temporal convolution network for short-term load forecasting of power systems," *Applied Energy*, vol. 283, 2021.

[26] R. Zhang, S. Chen, Z. Zhang, and W. Zhu, "Genetic Algorithm in Multimedia Dynamic Prediction of Groundwater in Open-Pit Mine," *Computational Intelligence and Neuroscience*, vol. 2022, 2022.

[27] L. Li, C. Mao, H. Sun, Y. Yuan, and B. b. Lei, "Digital twin driven green performance evaluation methodology of intelligent manufacturing: hybrid model based on fuzzy rough-sets AHP, multistage weight synthesis, and PROMETHEE II," *Complexity*, vol. 2020, no. 6, pp. 1–24, 2020.

[28] E. Pekel, M. Gul, E. Celik, and S. Yousefi, "Metaheuristic approaches integrated with ANN in forecasting daily emergency department visits," *Mathematical Problems in Engineering*, vol. 2021, p. 2021.

[29] L. Li and C. Mao, "Big data supported PSS evaluation decision in service-oriented manufacturing," *IEEE Access*, vol. 8, pp. 154663–154670, 2020.

[30] R. Kafieh, R. Arian, N. Saeedizadeh et al., "COVID-19 in Iran: forecasting pandemic using deep learning," *Computational and Mathematical Methods in Medicine*, vol. 2021, 2021.

[31] L. Li, T. Qu, Y. Liu et al., "Sustainability assessment of intelligent manufacturing supported by digital twin," *IEEE Access*, vol. 8, pp. 174988–175008, 2020.

[32] L. Li, B. Lei, and C. Mao, "Digital twin in smart manufacturing," *Journal of Industrial Information Integration. January*, vol. 26, no. 9, 2022.

[33] Y. Mai, Z. Sheng, H. Shi, and Q. Liao, "Using improved XGBoost algorithm to obtain modified atmospheric refractive index," *International Journal of Antennas and Propagation*, vol. 2021, 2021.

Hindawi
Scientific Programming
Volume 2022, Article ID 2647749, 8 pages
https://doi.org/10.1155/2022/2647749

Research Article

Refinement Evaluation Method of Financial Management Quality of Listed Companies Based on the ERP Model

Ling Chen and Haijun Kang

School of Finance and Accounting, Fuzhou University of International Studies and Trade, Fuzhou 350200, Fujian, China

Correspondence should be addressed to Haijun Kang; kanghaijun@fzfu.edu.cn

Received 26 June 2022; Revised 29 July 2022; Accepted 4 August 2022; Published 26 August 2022

Academic Editor: Lianhui Li

With the development of economic globalization, the trend of internationalization and alliance of large enterprises is becoming more and more obvious, and the competition and cooperation among enterprises are still continuing. In this new historical stage, it is very necessary to ensure the smooth implementation of financial management and coordination with other systems, in line with the times, to establish, improve, and ensure a scientific and reasonable enterprise financial management model and prove its effectiveness. However, the existing research on the specific implementation of the integrated financial management model based on the theory and case studies is not specific enough, the process tracking is not detailed enough, the implementation effect evaluation theory lacks scientificity and integrity in the establishment of the index system, and the evaluation methods are relatively simple. In view of the above problems, this paper proposes the specific implementation steps and problems that need to be paid attention based on the financial management model for large listed companies, establishes the evaluation index system of enterprise implementation by using the method, and quantifies the listed companies before and after the implementation of integrated financial management. The comparisons give credible results. This paper is of great significance for improving the existing performance evaluation system, responding to national policies, promoting the development of enterprise informatization, and improving the success rate and competitiveness of enterprise integrated financial management implementation.

1. Introduction

With the advent of the digital information age, digital transformation of enterprises is an inevitable choice to adapt to the development of the times, and information technology is an important means to help enterprises achieve digital transformation. Digital management can not only realize the integration of enterprise management information, but also help enterprises to achieve a qualitative leap in their management level. As a tool set beyond the scope of management, the ERP system plays a role in driving the efficient operation of the internal processes of the enterprise and revitalizing the enterprise resources, thereby helping the enterprise to successfully realize the digital transformation [1]. In order to adapt to the development of the digital age, many enterprises have begun to improve their daily operation and management levels by building their own ERP systems and fully implementing ERP systems. When most enterprises go online with ERP systems, due to the limited management foundation and human resources, they choose to launch ERP subsystems one by one to smoothly realize the transformation of information management. As the most important economic management activity of an enterprise, corporate financial management is essentially a work of organizing corporate financial activities and dealing with corporate financial relations, covering all aspects of the company's economic business. Because the management efficiency and operation effect of the company's daily business are closely related to the overall level of the company's financial management system, therefore, enterprises will choose to launch the ERP financial management system first [2].

During the implementation of the ERP financial management system, the advantages of the ERP financial management system cannot be brought into full play because the internal business processes of the enterprise cannot

be fully integrated with the ERP financial management system, which eventually leads to the failure of the ERP financial management system. According to an Accenture research report, nearly 80% of ERP systems have not achieved the expected results after going online. It shows that the implementation of ERP financial management system cannot be accomplished overnight and the system should be upgraded through continuous evaluation and optimization, so that it is possible to enjoy the benefits brought by information integration [3]. However, most enterprises tend to ignore this point when they build their own ERP systems and fully implement ERP systems. There is often a situation of "emphasizing the system, neglecting evaluation and weak optimization," which goes against the original intention of enterprises to use the ERP system to improve the efficiency of operation and management. Therefore, it is necessary to discuss whether ERP can be better applied to the financial management model, so that the logistics, information flow, and capital flow can be effectively integrated, and it is necessary to study whether the integrated financial management based on ERP can be successfully implemented, what is the effect of the implementation, and whether it can improve the financial management level of enterprises and meet the requirements of rapid development of enterprises. On the basis of discussing the relevant theories, this paper deeply studies the financial management mode and effect of enterprises based on ERP and establishes the financial management evaluation index system. Quantitative evaluation was carried out, and a practical research was carried out on the refined evaluation method of financial management quality of listed companies based on ERP model.

2. Research Status of ERP Financial Management Evaluation Methods at Home and Abroad

Enterprise Resource Planning, referred to as ERP system, refers to the digitalization of enterprise management through the combination of modern information technology and advanced enterprise management concepts. ERP is essentially a thinking mode of enterprise management, which uses the internal and external resources of the enterprise to provide the optimal solution for the daily operation activities of the enterprise, thereby helping the enterprise to achieve the operation and management goals and improve the actual management level of the enterprise [4, 5]. To evaluate the implementation effect of ERP financial management system, it is necessary to identify the relevant factors that affect the implementation effect of ERP financial management system.

Domestic scholars started late to study the factors affecting the ERP financial management system. Zhang et al. summarized the influencing factors that affect the implementation of ERP systems in enterprises as changes in financial organizations, integration of financial systems, optimization of core financial processes, and a perfect evaluation system [6]. Chen Hu collects relevant information by means of a questionnaire survey and summarizes the factors that affect the implementation of the financial management system into four factors: business process management, system quality, business standardization, and personnel management. Martin assumed the influencing factors of the ERP financial management system, designed a questionnaire, and used a regression model to verify the correlation between the hypothesized influencing factors [7, 8]. He et al. based on the perspective of process reengineering, take the enterprises that implement financial management systems in China as samples and establish an analysis model of influencing factors. Through empirical methods, it is verified that the factors affecting the financial management system of Chinese enterprises include strategic planning, business process management, and organizational structure design [9–11]. In terms of performance, Miao built the performance evaluation system of the enterprise ERP financial management system, hoping to improve the management level of the enterprise through the construction of the performance evaluation system, so that the enterprise can occupy a favorable position in the fierce market competition [12]. In order to evaluate the performance of the ERP system, Liu optimizes the internal process of the ERP, improves the existing information system, and at the same time improves the efficiency of enterprise management and enhances the competitiveness of the enterprise. By introducing the financial management theory of the balanced scorecard, we can obtain which aspects of the enterprise need to be optimized [13]. Zhang et al. also constructed an ERP system evaluation system based on the balanced scorecard to evaluate and analyze the implementation performance of China Unicom's ERP system and put forward optimization suggestions after calculating the membership of each evaluation index [14]. Pan used the grey fuzzy correlation method based on the balanced scorecard to analyze the difference in the effect of enterprises before and after the implementation of the ERP system [15]. In terms of influencing factors, after analyzing the main influencing factors of the enterprise ERP financial management system, Li evaluated the situation of the ERP financial management system during the use period and weighted the obtained evaluation results, so as to obtain the time to get the weighted evaluation results. Then, the contribution is evaluated by introducing weights, and finally the financial management system is evaluated based on the dynamic weighted evaluation sequence [16]. Huang et al. built an index system composed of three dimensions: ERP basic operation, comprehensive benefits, and personnel training and growth and used the evaluation system to evaluate the application effect of the ERP system of supply chain enterprises, so as to improve the evaluation ability of supply chain enterprises to the ERP system [17].

In the 1980s, foreign scholars' research on ERP financial management system gradually deepened. Three scholars including Mudimigh et al. discussed ERP system, financial management, and system integration, respectively, and proposed the fact that ERP financial management system should be based on ERP software in the construction process. Based on the financial data as the core, the integration advantages of the ERP system can be realized [18]. On the

basis of decision support theory, Elisabeth emphasized that the ERP financial management system should meet the process-oriented characteristics and further put forward the view that the system process should be optimized when improving the function of the financial management system [19]. Based on three theories: the urgency of the foundation, the state capability of the national implementation plan, and the technical cooperation between tasks, Trkman proposed the fact that enterprises should continuously improve and optimize the cooperation between business process tasks and management cycles, so as to make the business management reach the best state [20]. In order to make ERP effectively implemented after the introduction, Rajan CA uses TAM (Technical Acceptance Model) to analyze the factors affecting ERP implementation and also tries to analyze the impact of ERP system on performance and work efficiency [21]. Through investigation and research on the types and characteristics of enterprise financial management systems, Zhi proposes how to build an enterprise ERP financial management system based on the ERP environment and the importance attached by senior managers to the construction of ERP financial management systems to promote the development of enterprise financial management. Basic requirements and other viewpoints are found in [22]. Lin analyzes the ERP financial management system in the shipping industry, proposes how to build the ERP-based financial management information management system for shipping companies, and designs its business process in detail. Finally, the designed system is tested [23]. The evaluation of ERP abroad has formed a relatively mature theoretical system, mainly including the ABCD evaluation system and the evaluation of the three parts of the ERP system use purpose, ERP operation problem handling, and factors affecting the success of ERP implementation formulated by the American standardization organization system. ABCD evaluation system mainly includes five research areas: strategic planning, continuous optimization of system quality, development of new products, plan execution, and control. By elaborating the content of each part in detail, explaining the problems involved in this part and the differences in its characteristic attributes between different levels of A, B, C, and D, a more comprehensive problem is drawn, and the questions raised will be discussed and broken down into several components. For example, taking the strategic planning section, first, grade each subquestion of the strategic planning; then divide the strategic planning into four different levels, A, B, C, and D. Level A: strategic planning development and implementation is an ongoing process that drives people's decisions and actions, reflecting a "customer first" perspective. Whether all employees of the company can clearly express the company's purpose, long-term planning and strategic goals is as question. Level B: the formulation and implementation of the strategic plan are a formal matter that should be developed by the company's senior decision makers and middle managers and should be carried out at least once a year. When making decisions based on a strategic plan, the company should enable employees to understand the company's basic purpose and long-term planning. Level C: even though the company seldom formulates and uses strategic planning to make decisions, it can still smoothly make decisions related to the direction of the company's operations. Level D: the company has never developed a strategic plan. And put forward comprehensive questions to judge whether the enterprise has achieved the expected effect after implementing the ERP financial management system; finally, evaluate each comprehensive problem. The evaluation result here is not the average score for each small problem, but it is to provide the basis for the comprehensive score [24].

From the above research results, it is found that domestic and foreign scholars have carried out certain research on the ERP financial management system and the evaluation and optimization of the ERP financial management system. And it can be found that domestic and foreign scholars' research on ERP financial management system is mostly based on the analysis of its internal structure and how to achieve coordination between systems. Conduct research and develop a relatively complete evaluation system to meet the evaluation needs. However, in the selection of research objects, most of them are large enterprises in developed countries, which generally have the characteristics of large scale, clear process, and standardized management. However, domestic scholars started late, and so far they have not formed an authoritative, systematic ERP financial management evaluation system that can meet the needs of enterprises. Most of the researchers' research on the evaluation system is only in the initial stage. By summarizing the research results of ERP financial management optimization at home and abroad, it is found that foreign researchers pay more attention to explore the reasons for the low success rate of system application and try to formulate scientific and effective solutions from a macroperspective to realize the optimization of ERP system. However, domestic scholars mostly explore the optimization of ERP financial management system from the microperspective of the enterprise level. By analyzing the application status of the system and proposing solutions for the existing problems to achieve system optimization, the solution is more practical.

3. Implementation Analysis of ERP Integrated Financial Management System

ERP financial management system: as far as listed companies are concerned, the accounting module used to integrate financial data is the basis for the normal operation of the financial management system, the fund management module is an important part of the operation of financial management, and budget management is the basis for enterprises to carry out financial management and also is an important means of financial management. In a word, the accounting module, fund management module, and budget management module not only connect the beginning and end of the enterprise financial management work, but also run through the most important components in the ERP financial management system of listed companies: accounting module, capital management module, and the application status of the comprehensive budget management module which is described [25]. Generally, the accounting

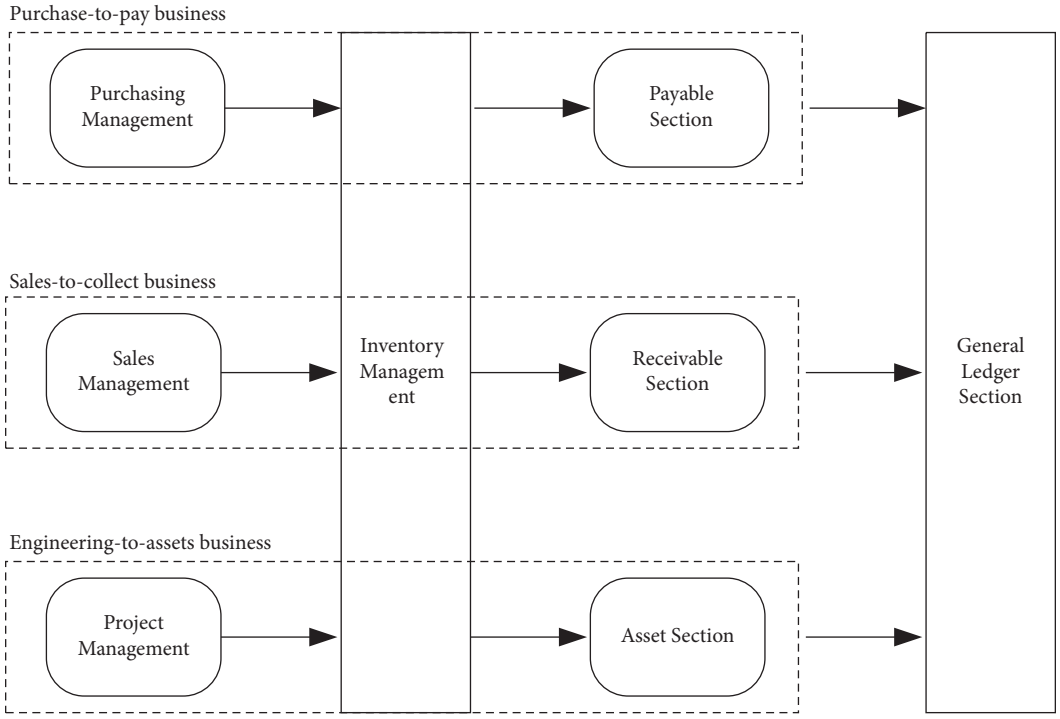

Figure 1: Integration diagram of the general ledger section of the accounting module composition.

module of listed companies uses the Oracle suite, which realizes the integration between the module components and the functional upgrade of some blocks. The accounting module includes general ledger, accounts receivable, accounts payable, assets, purchases, and projects. The relationship between these components and the general ledger blocks is shown in Figure 1.

(1) General ledger section: the general ledger section is the core of the accounting module. Basic elements such as accounting subjects, accounting periods, currency, and book sets in the system are set in the general ledger section. Each submodule will transfer the generated accounting entries to the general ledger block during business processing, generate journals, and update account balances to generate subsidiary ledgers, general ledgers, and various financial statements. Since the financial information of the enterprise will be automatically posted to the general ledger section through the system, and other submodules will also share data with the general ledger section, the general ledger section should be the best platform for querying company information.

(2) Accounts receivable segment: the accounts receivable section is mainly used to manage the customer's current business, business collection, and settlement business, including the management and preservation of customer data and information, the issuance of sales invoices integrated with the BOSS system, and the management of customer accounts receivable and payment collection information, recording receipt vouchers and controlling the aging of customer arrears. At the same time, the accounts receivable section can automatically import the data of the business daily report interface provided by the BOSS system into the business accounts receivable invoice and import the bank receipt information into the accounts receivable section through this interface and then batch verification of invoices received.

(3) Accounts payable segment: for listed companies, dealing with suppliers is a very important business activity for the company. The payable section is used to manage the business dealings with suppliers. The section contains basic information about suppliers such as supplier locations, contacts, and bank accounts. For the invoice management of the business transactions of the enterprise, the invoice needs to be paid after a strict approval process. The payment method can choose single payment or batch payment.

(4) Assets sector: it is mainly used to manage and account for various assets of the enterprise and is specifically used to process various businesses in the process of enterprise asset management in batches, such as processing the increase and decrease of assets, depreciation and amortization, and provision for impairment. In each accounting period, as long as the financial staff submits the asset processing request, the asset section will automatically accrue depreciation or amortization, transmit the relevant entries to the general ledger section, and automatically update the asset account balance sheet. The asset section is integrated with the accounts payable section and the project section. In the asset section, users can find asset information at any time, such as

the original value of the asset, accumulated depreciation in use, asset age, remaining life, storage location, custodian, and asset status, and can update asset information.

4. Refinement Evaluation Method of EPR Integrated Financial Management Quality Based on ISM-ANP

Because of its unique practicality, the integrated financial management based on EPR has gradually attracted the attention of relevant institutions all over the world and has carried out extensive research. There are few studies on the evaluation of ERP integrated financial management implementation, but it is very important. This paper combines the integrated financial management mode to bring changes to the enterprise compared with the traditional financial management mode, extracts the relevant performance factors, establishes the enterprise implementation evaluation index system, and carries out the weight calculation, trying to quantify the implementation effect of the integrated financial management based on ERP.

4.1. Establishment of ERP Implementation Evaluation Index System. According to the industry situation of electronic manufacturing, after consulting relevant experts and implementing ERP-based integrated financial management, the following indicators of the industry will be greatly affected:

(1) *Management Benefits.* (1) After the implementation of integrated financial management, the network and software are used to standardize the management of the enterprise, straighten out the management process of the enterprise, and make the inventory cost of the enterprise drop significantly. Through effective daily supervision, the purpose of reducing inventory costs and saving funds has been basically achieved. At the same time, due to the constraints of the network and software, the occurrence of enterprise violations and illegal acts has been effectively prevented, and the work efficiency of employees has been greatly improved, thereby increasing management benefits. (2) The information and data in the system can be used to continuously adjust the ratio of inventory to funds, increase the turnover frequency of products as much as possible, increase the turnover rate of funds, and improve the efficiency of the use of funds. And the credit control module of the system can be used to monitor the accounts receivable and accounts payable in real time, strengthen the analysis of information, prevent the occurrence of "bad debts," and improve the credit of the enterprise. (3) With the development of the project, especially the continuous improvement of the process, it overcomes the randomness of the management behavior of the managers and prompts the employees to gradually change the logic of dealing with things that they used to think in the past and understand that the work they do is not only about the existing operations. When the process is moved into the system, it is more important to find the unreasonable part of the original work and to integrate the advanced management ideas and methods into the future process. It helps to improve the team awareness of employees and makes the whole company form an excellent management team.

(2) *Economic Benefits.* (1) After using the system, the entire production process of the enterprise is organically combined, so that the enterprise can effectively reduce the inventory, ensure stable logistics to support normal production, improve efficiency, reduce the enterprise's inventory investment, improve the inventory turnover rate, and effectively reduce capital occupation. (2) Reduce the phenomenon of delayed delivery and improve the level of on-time delivery. From the beginning of the product sales plan, it manages and counts various pieces of information about its sales products, sales areas, and sales customers and makes a comprehensive analysis of sales volume, amount, profit, performance, and customer service. The inventory is steadily reduced, the service level of the enterprise is greatly improved, and the delay rate is reduced, thereby greatly improving the credibility of the enterprise. (3) The procurement lead time is effectively shortened. With timely and accurate production plan information, purchasing personnel can concentrate on value analysis, source selection, study negotiation strategies, understand production problems, can determine reasonable order quantities, excellent suppliers, and maintain the best safety reserves. Provide ordering and acceptance information, track and urge materials purchased or outsourced for processing, and ensure the timely arrival of goods. This shortens the procurement time and saves procurement costs.

After the implementation of ERP-based integrated financial management is completed, the evaluation before and after the implementation is carried out, and the evaluation factors proposed before are comprehensively analyzed, the main indicators are extracted, and a comprehensive performance evaluation system is established. The evaluation factors mainly include capital turnover, work efficiency, management Informatization level, employee quality, customer satisfaction, corporate image, reduction of downtime, shortened procurement lead time, reduction of delayed delivery, reduction of inventory, reduction of management personnel, management benefits, growth benefits, customer benefits, economic benefits, and enterprise integration benefits.

4.2. Implementation Effect Evaluation Based on ISM-ANP. Set up an IMS evaluation structure team, according to the calculation requirements, after expert discussion, the final

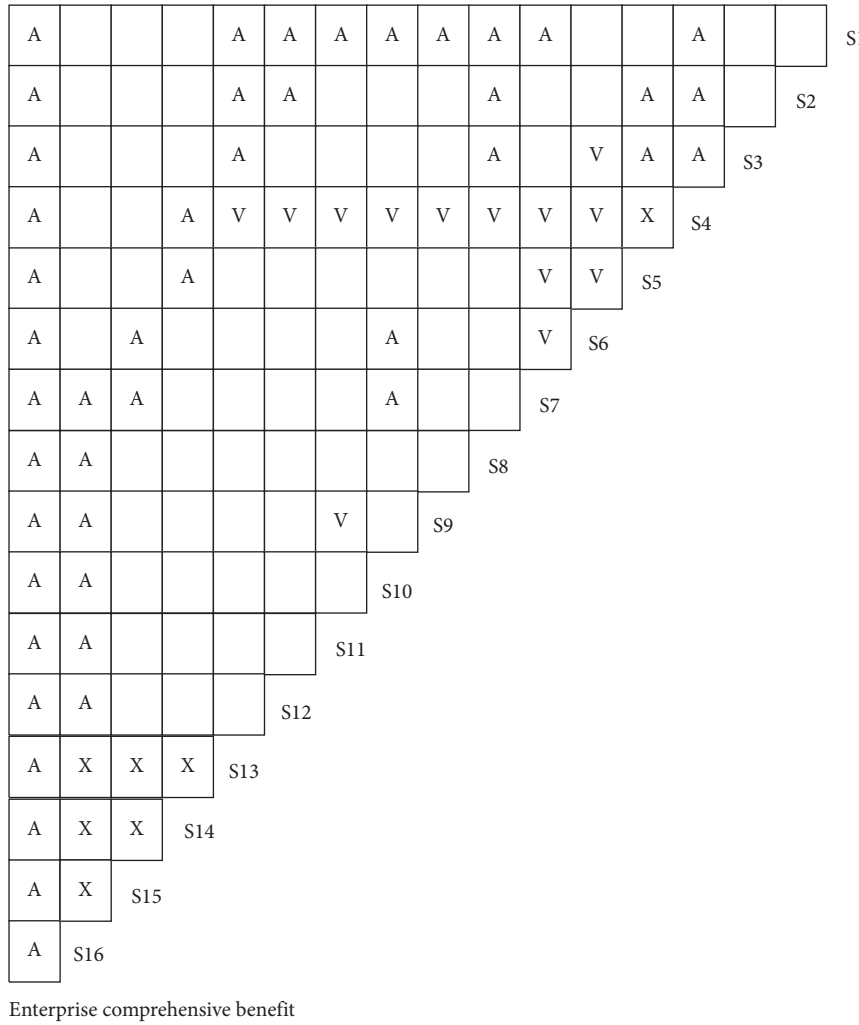

Figure 2: Integration diagram of the general ledger section of the accounting module composition.

indicators will be listed as follows: S_1 capital turnover, S_2 work efficiency, S_3 production capacity, S_4 management information level, S_5 staff quality, S_6 customer satisfaction Degree, S_7 corporate image, S_8 reduce downtime, S_9 shorten procurement lead time, S_{10} reduce backorder, S_{11} reduce inventory, S_{12} reduce management personnel, S_{13} management benefits, S_{14} growth benefits, S_{15} customer benefits, and S_{16} economic benefits and enterprises overall benefit.

According to the suggestions of experts, establish the relationship diagram of the mutual influence of various indicators, as shown in Figure 2. "V" means that the row factor has a direct or indirect influence on the column factor, "A" means that the column factor has a direct or indirect influence on the row factor, "X" means that the row and column influence each other, and blank means that there is no mutual influence between the row factor and the column factor.

Calculating the logical relationship of the mutual influence factors of the enterprise comprehensive evaluation index of the reachability matrix R and L, the adjacency matrix A can be obtained. Let $A_1 = A + 1$, $A_2 = (A + 1)^2$, . . ., $A_r = (A + 1)^t$. Then, after the Boolean algebra operation rules, $R = A_2$ is obtained, the row and column factors of the reachable matrix R are the same, and it is a 17th-order square matrix; the arrangement order is S_1, S_2, . . ., S_{17}. The element corresponding to 1 in the new array indicates that the factor of the row has an influence on the factor of the column and the element of 0 means that the factor of the row has no influence on the factor of the column.

The evaluation model is obtained by ISM-ANP method, MATLAB programming, and SD software, S_1 capital turnover, S_2 work efficiency, S_3 production capacity, S_4 management informatization level, S_5 staff quality, S_6 customer satisfaction, S_7 corporate image, S_8 reducing downtime and waiting for materials, S_9 shortening procurement lead time, S_{10} reducing delayed delivery, S_{11} reducing inventory, S_{12} reducing management personnel, S_{13} management benefits, S_{14} growth benefits, S_{15} customer benefits, S_{16} economic benefits, and S_{17} various indicators of comprehensive enterprise benefits. The weights are shown in Table 1.

After the implementation of the integrated financial management model based on the increase of each indicator: $J = R * \omega = 0.3409 = 34.09\%$.

R = (10%, 50%, 30%, 10%, 80%, 50%, 10%, 30%, 50%, 50%, 60%, and 30%); ω = (0.1776, 0.0959, 0.0763, 0.1216,

Table 1: ERO implementation evaluation model of the final weight of each index.

Name	Normalized by cluster	Limiting
Production capacity	0.50774	0.177629
Work efficiency	0.27419	0.095924
Capital turnover	0.21806	0.076286
Employee quality	0.48486	0.121581
Management informatization level	0.51514	0.129172
Corporate image	0.71118	0.026877
Customer satisfaction	0.28882	0.010915
Management personnel cost	0.17364	0.062792
Inventory cost	0.25569	0.092463
Backorder cost	0.12497	0.045192
Procurement lead time	0.14627	0.052894
Downtime cost	0.18506	0.066920
Manufacturing cost	0.11436	0.041355

0.1292, 0.0269, 0.0109, 0.0628, 0.0925, 0.0452, 0.0529, 0.0669, and 0.041). It can be seen from the above calculation that, after the refined evaluation method of financial management quality based on the ERP model, the comprehensive performance of the enterprise is improved compared with that before the implementation of the model. Factors and the dependence and feedback relationship between factors can be considered, and the effect of implementation can be more clearly defined.

5. Conclusion and Outlook

This paper mainly expounds the basic theory of ERP integrated financial management implementation, the necessity of implementation, the implementation process and safeguard measures, etc., and puts forward the important factors that affect enterprise performance after the implementation of ERP integrated financial management. According to these factors, the evaluation index system is designed, the rationality and scientificity of the index design are verified by MATLAB software, the weight of the evaluation index system is calculated by the ISN-ANP method, and the index is explained and analyzed in detail. Finally, taking a listed company as an example, through the research on the implementation process of the integrated financial management based on the company, it analyzes the existing problems, the process of implementation, and the results of the implementation before the company does not implement it and finally draws the conclusion that the integrated financial management is based on the company's refined assessment method of financial management quality. The experimental results show that the comprehensive performance of the enterprise after implementing the integrated financial management quality refined evaluation method is 34.09% higher than that before the model is not implemented.

5.1. Summary

(1) The process and safeguard measures for the implementation of integrated financial management are proposed. On the basis of summarizing the theories of EPR and integrated financial management, this paper expounds the concept and characteristics of ERP-based financial management. These theories will lay a good foundation for the successful implementation of ERP projects.

(2) ISM-ANP method is used to solve the problem of establishing the effect evaluation system of ERP integrated financial management implementation.

This paper introduces the ISM-ANP method and applies it to the ERP implementation effect evaluation index system. The combination of ISM and ANP can comprehensively consider various clear or unclear factors that affect enterprise performance and can consider the dependence and feedback relationship between factors, which can better solve the problem of ERP implementation effect. In this paper, referring to the industry situation and according to the suggestions of experts, the ISM-ANP method is applied to establish the implementation effect evaluation index system suitable for the electronic manufacturing industry. The use of MATLAB software and SD software for calculation saves time is beneficial to the ISM-ANP analysis method. Further promotion and application provide a reference index system for the relevant listed companies on the refined evaluation method of ERP financial management quality.

5.2. Prospect. Due to the authors' lack of practical experience and limitations of various conditions, although this paper has carried out research in terms of method and empirical analysis, there are still many deficiencies in the implementation process model and implementation evaluation index system of Chen Company, which need to be studied by other scholars' conduct further research.

(1) Since the factors affecting enterprise performance after the implementation of ERP are quite complex, there are a large number of qualitative indicators, which makes the artificial selection of indicators not particularly objective, and the analysis of the factors related to the implementation effect is relatively superficial, so the evaluation of such indicators is not very objective. Whether the selection can accurately evaluate the implementation effect still needs further research and analysis.

(2) The evaluation model and data sources need to be further improved. This paper adopts the Delphi method to assign the relationship between the indicators and the relative importance assignment by experts, which may have a certain degree of subjectivity, the reliability of the collected data is not high, and there are defects of subjective factors, which requires follow-up completely.

Data Availability

The dataset can be obtained from the corresponding author upon request.

Conflicts of Interest

The authors declare that they have no conflicts of interest.

References

[1] Y. Y. Chen and S. F. Pei, "Brief analysis of modern accounting information system in ERP system," *Financial Economy*, vol. 444, no. 18, pp. 167–169, 2016.

[2] J. Y. Ren, "Construction and optimization of enterprise financial management informatization under cloud computing environment," *Accounting Newsletter*, vol. 13, no. 705, pp. 109–111, 2016.

[3] Y. Liu, "Construction of enterprise ERP information system based on financial business process reengineering—taking tongda refractory group as an example," *Accounting Newsletter*, vol. 1, no. 2, pp. 85–89, 2017.

[4] J. Y. Teng, "The application and function of ERP system in enterprise financial accounting," *Chinese Business Theory*, vol. 1, no. 29, pp. 135-136, 2018.

[5] S. J. Huang, "Design of intelligent ERP system based on big data," *Modern Electronic Technology*, vol. 41, no. 24, pp. 94–97, 2018.

[6] R. J. Zhang, Y. J. Zhang, and H. Chen, "Research on the key factors of process reengineering of financial shared services of enterprise groups—based on the management practice of ZTE corporation," *Accounting Research*, vol. 1, no. 7, pp. 57–64, 2010.

[7] W. Martin, "Critical success factors of shared service projects-results of an empirical study," *Advancesin Management*, vol. 1, no. 5, pp. 21–26, 2012.

[8] H. Haken and M. Synergetics, "Introduction and advanced topics," *Spring*, vol. 67, no. 3, pp. 773-774, 2004.

[9] Y. He and F. Zhou, "An empirical study on the key factors of my country's enterprise groups implementing financial shared services," *Accounting Research*, vol. 1, no. 10, pp. 59–66, 2013.

[10] F. Z. Chen and W. W. Chen, "Analysis and research of financial management demand based on ERP," *fFriends of Accounting*, vol. 1, no. 8, pp. 36–38, 2010.

[11] X. D. Mai, "Design and implementation of enterprise accounting information system from the perspective of ERP," *Accounting Newsletter, Canada.*vol. 654, no. 34, pp. 93–95, 2014.

[12] X. Y. Miao, "Talking about the construction of enterprise performance evaluation system under the background of ERP system," *Modern Commerce*, vol. 1, no. 5, pp. 118-119, 2011.

[13] X. Y. Liu, "ERP project performance evaluation based on balanced scorecard," *Accounting Monthly*, vol. 1, no. 12, pp. 99–102, 2015.

[14] H. Zhang, L. S. Chang, and Q. X. Guan, "Shaanxi Unicom ERP implementation performance evaluation," *Journal of Xi'an University of Posts and Telecommunications*, vol. 20, no. 6, pp. 106–111, 2015.

[15] Y. Y. Pan, "An ERP performance evaluation model based on grey fuzzy iterative algorithm," *Computer and Digital Engineering*, vol. 12, no. 1, pp. 103-104, 2014.

[16] M. Li, "TOPSIS evaluation method of financial management system based on dynamic weighted sequence," *Statistics & Decisions*, vol. 1, no. 21, pp. 171–173, 2016.

[17] H. L. Huang, Q. Mei, and Y. P. Shi, "Evaluation of supply chain level ERP operational performance in "internet +" environment," *Accounting Monthly*, vol. 798, no. 14, pp. 44–50, 2017.

[18] A. Mudimigh, M. Zairi, and M. Mashari, *European Journal of Information Systemse*, vol. 10, 2001.

[19] J. Elisabeth, "Enterprise resource planning: implementation procedures and critical success factors [J]," *European Journal of Operational Research*, vol. 146, no. 2, pp. 1–6, 2003.

[20] P. Trkman, "The critical success factors of business process management," *International Journal of Information Management*, vol. 30, no. 2, pp. 125–134, 2010.

[21] C. A. Rajan and R. Baral, "Factors affecting the user acceptance of ERP and the impact on the individuals: a conceptual model," *Modern Foreign Language*, vol. 1, no. 11, pp. 324–356, 2014.

[22] J. Zhi, "The construction of financial management system of enterprises based on ERP," *Agro Food Industry Hi-Tech*, vol. 28, no. 1, pp. 1420–1424, 2017.

[23] P. Lin, "Design and implementation of financial accounting information management system of shipping companies based on ERP," *Journal of Coastal Research*, vol. 94, no. sp1, pp. 470–472, 2019.

[24] M. Haddara and A. Elragal, "ERP adoption cost factors identification and classification: a study in SMEs," *International Journal of Information Systems and Project Management*, vol. 1, no. 2, pp. 5–21, 2022.

[25] W. Gao, "Research on the optimization of financial management module of enterprises under ERP environment," *Chinese and Foreign Entrepreneurs*, vol. 1, no. 33, pp. 65–67, 2019.

Hindawi
Scientific Programming
Volume 2023, Article ID 9847362, 1 page
https://doi.org/10.1155/2023/9847362

Retraction

Retracted: Innovation and Practical Methods of Music Education Path in Colleges and Universities under the Popularization of the 5G Network

Scientific Programming

Received 18 July 2023; Accepted 18 July 2023; Published 19 July 2023

This article has been retracted by Hindawi following an investigation undertaken by the publisher [1]. This investigation has uncovered evidence of one or more of the following indicators of systematic manipulation of the publication process:

(1) Discrepancies in scope
(2) Discrepancies in the description of the research reported
(3) Discrepancies between the availability of data and the research described
(4) Inappropriate citations
(5) Incoherent, meaningless and/or irrelevant content included in the article
(6) Peer-review manipulation

The presence of these indicators undermines our confidence in the integrity of the article's content and we cannot, therefore, vouch for its reliability. Please note that this notice is intended solely to alert readers that the content of this article is unreliable. We have not investigated whether authors were aware of or involved in the systematic manipulation of the publication process.

Wiley and Hindawi regrets that the usual quality checks did not identify these issues before publication and have since put additional measures in place to safeguard research integrity.

We wish to credit our own Research Integrity and Research Publishing teams and anonymous and named external researchers and research integrity experts for contributing to this investigation.

The corresponding author, as the representative of all authors, has been given the opportunity to register their agreement or disagreement to this retraction. We have kept a record of any response received.

References

[1] Y. Sun and H. Jin, "Innovation and Practical Methods of Music Education Path in Colleges and Universities under the Popularization of the 5G Network," *Scientific Programming*, vol. 2022, Article ID 1536911, 7 pages, 2022.

Hindawi
Scientific Programming
Volume 2022, Article ID 1536911, 7 pages
https://doi.org/10.1155/2022/1536911

Research Article

Innovation and Practical Methods of Music Education Path in Colleges and Universities under the Popularization of the 5G Network

Ying Sun and Honglian Jin

School of Arts and Design, Yanshan University, Qin Huangdao, Hebei 066200, China

Correspondence should be addressed to Ying Sun; sunying@ysu.edu.cn

Received 5 July 2022; Revised 29 July 2022; Accepted 2 August 2022; Published 25 August 2022

Academic Editor: Lianhui Li

In the era of the 4G network, the scale and pattern of online music education have been formed, and its necessity and educational achievements have emerged. The 5G network era is coming, and online music education is once again facing new challenges, and it is imperative to make necessary changes. This paper, by expounding on the changes brought about by the 5G network era, combined with the characteristics of online music education in colleges and universities, will summarize and analyze the current work status and problems faced. Improve the level of work and make online music education reach a new height.

1. Introduction

In recent years, my country's higher music education has developed rapidly[1]. The latest data from the Ministry of Education show that the total number of students in various types of higher education in China is nearly 37.8 million. Among them, music education in colleges and universities, as one of the priorities in higher education, has always been highly valued by the party and the state [2, 3]. With the widespread use of 4G network technology, music education has also broken through the traditional single face-to-face mode, gradually introducing new technologies, broadening work ideas, and opening up new positions for online music education, attracting more college students to learn theory and education through online media. The results are remarkable. Recently, with the rapid development of network technology, the 5G network after 4G has achieved trial networking, and a faster and more convenient network era is coming. Under the new situation, the online music education work in colleges and universities will inevitably face new challenges, and the work ideas and methods will also face new changes [4].

The rapid development of network technology and the continuous progress of new media technology have brought about great changes in people's daily life. Smartphones that can be connected to the Internet have become an important item for everyone to travel. As long as there is a mobile phone, reading and learning, shopping and driving, information query, and even identity verification can be realized. 4G network technology has truly changed people's daily life habits. Traffic and Wi-Fi have become the channel tools for modern people to exchange information with others. Among them, the emergence of new network media has expanded the channels for people to obtain information on a daily basis from newspaper publications and television broadcasts to network news terminals. Text, pictures, audio, and video, as information carriers, are constantly combined on new online media and become links and pushes. No matter at home or abroad, no matter the size of the news, just take out your mobile phone and can know what is going on in the world. The dividends brought by the 4G network era are obvious, the technological innovation is faster than expected, and the 5G network is coming to everyone [5]. In 2014, the transmission network based on 5G technology was interviewed for the first time. After several years of research and development, at the end of 2017, the 5G-phased full-featured standardization was completed. My country also

authorized the three major domestic operators to carry out system experiments in 2018. The technical principles of 5G networks do not need to be repeated, but the changes it will bring cannot be ignored. First, the data transmission speed in the 5G era has increased. The data transmission speed of the 5G network can exceed 1 Gb per second, and the theoretical peak value can reach tens of Gb per second. Compared with the 4G network, the data transmission speed is greatly improved. Second, in the 5G era, more devices and terminals can access the network. In addition to mobile phones, computers, and a small number of other devices, the current devices that can access the network will add more access devices and everyone will also have more smart devices that can access the network. Third, the 5G era will promote the development of big data technology. With more devices connected to the network, more data will be formed. Some scholars say that this will bring about a tsunami and blowout of data. The previous sampling data analysis technology cannot meet the demand, and it is inevitable that more big data technology that can analyze the whole data will be used. The explosive growth of data also puts more demands on big data technology, and the further development of big data technology is in line with the arrival of the 5G era. Traditional music and musical traditions are constantly changing with the evolution of social life, not fixed [6–8]. The relationship between Chinese and Western music has gone through different stages since its birth, and the situation and people's mentality reflected in each stage are different. The research in this area really goes from the analysis and explanation of the abstract idea to the concrete and detailed explanation. In music teaching, when affirming the excellence of traditional Chinese music, it is undeniable that the introduction of Western music has had a historical impact on the development of music in our country. The introduction of music forms does not equal the introduction of culture. The surface form of music culture is very important. It is easy to teach and accept [9, 10], and its psychological form has a deep relationship with a nation's way of life, behavior, and aesthetics in the deep level. What is more important now is to do research on the psychology of music culture. As far as my country's national music culture is concerned, from the point of view of being passed down from generation to generation and having characteristics, traditional music is not only regarded as traditional music in our era but also as traditional music in all dynasties [11]. In addition to historical inheritance, traditional music is especially important for its expressive and developmental nature, and the historical penetrating power that any tradition must have. After generations in the process of historical evolution, it still maintains its vitality and maintains its existence. This requires that the tradition must have the ability to recreate and the internal mechanism of recreation, and have the vigor of continuous reconstruction.

College students are more likely to accept the traditional education model, which requires face-to-face communication between teachers and students, which is conducive to the interaction between teachers and students, and the effect is obviously irreplaceable. The current college students are thoughtful, energetic, and have a strong ability to accept new things. It is the group characteristics of college students. It has become a reality that college students are proficient in using mobile phones and computers to access information online. In the process of music education, using new media tools such as WeChat, Weibo, and various teaching APPs to communicate ideas with students through the Internet and transmit positive energy will inevitably make college students more receptive and more willing to accept. The network music work has also passed the initial stage of testing the water and has further developed to a mature and high-level stage. The content is more abundant [12]. The rapid development of network technology has profoundly affected people's daily life, and basic needs such as food, clothing, housing, and transportation can be solved by using the network. Among them, obtaining information through the Internet has become the behavioral habit of many people, especially college students, and it is not uncommon to have problems with "Baidu look" and "Zhihu look." Network technology also provides technical support for music education, and the emergence of new network media provides content and platform support for music education. The massive information on the Internet has become an important resource information base for music education [13], and the form of expression is more intuitive. WeChat, QQ, Weibo, etc. are commonly used information interaction platforms. College students are willing to obtain rich music through new online media. The use of the Internet and new media has further improved the effect of music education. Data from December 2018 show that the usage rates of WeChat Moments, Qzone, and Weibo are 83.4%, 58.8%, and 42.3%, respectively. As a group with more access to the Internet, college students often use various social media tools such as WeChat, QQ, and Weibo. Using new media tools and the convenience of the Internet, Si music education can be integrated into all aspects of daily life, which is convenient to create a good campus cultural environment, and is no longer limited by a fixed location and time. Through the effective use of life bits and fragmented time, as an effective supplement to the traditional education model, it is close to the needs and preferences of college students, easy to stimulate their enthusiasm and interest in learning, and increases the diversity of music education work methods. It is easier to achieve the ideal results of smooth acceptance, hydration, and noiselessness [14, 15].

2. Current Situations and Problems

For a long time, in the educational practice of our country, emphasis is placed on science and engineering, ignoring humanities, utilitarianism, ignoring quality, focusing on majors, ignoring foundations, focusing on books, and ignoring practice. The understanding of music education in ordinary colleges and universities is superficial, and the cultivation of college students' aesthetic education emotions has been neglected. However, some leaders in charge of music education in colleges and universities do not pay enough attention to music education. They mistakenly believe that music education is just simple singing and dancing, and think that holding some competitions and cultural

performances is the whole of music education, which leads to the teaching practice of music education in colleges and universities. It is not valued in music, and it is only in form and appearance, so college students' musical aesthetic ability cannot be truly improved and developed. Society lacks a profound understanding of the essence of music education, coupled with the fact that music education cannot bring direct economic benefits, and its role cannot be seen in the short term, to a certain extent, some people despise it and only regard it as a kind of embellishment or decoration, without knowing its value in essence. Therefore, society, schools, or families have given enough attention to music education. In this way, both educators and educated people bury in their hearts the subconscious thought that music education is not important, and its educational effect can be imagined. At present, most of the public music teachers in many colleges and universities come from professional music academies (departments), and their majors are vocal music, instrumental music, or theoretical composition during their studies. Therefore, they only focus on technical teaching in the teaching process, so that students have a good understanding of music. Compared with students majoring in music, students of other majors in colleges and universities have different foundations, different specialties, and different interests and hobbies. Although the teaching object and teaching purpose of the two are different, the teaching content is similar. The music curriculum is very random, the curriculum is scattered, and the phenomenon of people setting up courses can be seen everywhere. In addition, the teaching materials for general music courses in most colleges and universities are very limited, and there are only a few teaching materials recommended by the music education associations of colleges and universities. Compared with the situation where there are dozens of general comprehensive teaching materials for other disciplines and majors, there is a world of difference. The teaching content is separated from the actual needs of ordinary college students in colleges and universities. The public music textbooks are not included in the textbook management system uniformly ordered and distributed by the school. The textbooks used in the teaching are all searched and purchased by the teachers themselves. Therefore, it is difficult to guarantee quality. It can be seen from the survey data and the information inquired that the current situation of music education in ordinary colleges and universities has been greatly improved, but it is not as optimistic as we imagined. It seems that its situation is still dispensable. It is very strong, and some people regard it only as a kind of decoration, which is still in form and appearance and has not been paid any attention fundamentally. "Art education is important in talking, secondary in doing, not in busy." The phenomenon is still widespread. Furthermore, the development of music education in ordinary colleges and universities in my country is still unbalanced. Although a few schools have achieved good results, most of them still have many problems, such as the management organization of music education is not perfect, the teaching management is not perfect; the general lack of teachers and the low level of teachers; insufficient funding; and single teaching materials, teaching content, and teaching forms; the reasons for all these phenomena are complex. Obviously, some problems cannot be solved by individuals, but only by the government and schools before they can be gradually solved and implemented. This article only analyzes and discusses the problems existing in music education in ordinary colleges and universities, hoping to find out the crux of the existing theory and practice.

(1) More attention but still insufficient. At present, various colleges and universities have realized the powerful function and importance of the Internet, and many kinds of music teaching workers have also carried out educational and teaching activities through various network media tools, so that the working interface of music education is not only offline but also extended to online and established a solid educational position on the Internet [16]. The emphasis on online music education in colleges and universities has definitely increased, but the degree of emphasis is still insufficient [17]. There are still many websites and web pages and WeChat public platforms in colleges and universities, but the quality is not high. They pay attention to the form of content and despise the connotative value of content. The resource investment in online music education is still not enough. If you only think that online music is just a mechanical transfer of offline music education to the network, or that online music education only needs a few computers connected to the network, it proves that online music education is not enough. There is also a biased understanding [18].

(2) Rich in content but different in quality. On the network platforms of colleges and departments, especially the WeChat public platform, information is released quickly, and the content covers a wide range of categories. However, there are still actual phenomena of uneven quality of some content published on different platforms or on the same platform. Too much emphasis on whether the title is eye-catching, the number of clicks on a single article, etc., and the lack of strict control of the quality of the content, the phenomenon of fried rice, and stereotypes still occur, and teachers in professional fields use online platforms and new media tools to conduct professional There are still fewer lectures.

(3) The use of media tools tends to be skilled but the form lacks innovation. After the development in recent years, the number of university network platforms has reached a certain scale, with corresponding influence, and outsiders also know school information mainly through network media. There are more and more teachers and students in colleges and universities who are familiar with the use of new media tools. The website pushes a beautiful and professional layout and has accumulated a lot of operating experience. Information is released quickly, and news information can be released on the same day, which is much faster than traditional

paper media. However, with skill and speed, the atmosphere of music education through new online media is not strong, and most of them are information transmission, which fails to effectively combine music education and information. The newly generated network tools cannot be understood and used in time, which makes the innovation of music education work form insufficient. Figure 1 shows the relationship between music innovation education disciplines.

(4) In quality education, music quality teaching is very important [19]. As an important part of art education, music education has a very high aesthetic education value. It is the most direct university aesthetic education and plays an irreplaceable role in the full implementation of quality education. Pursuing the comprehensive and balanced development of college students' personalities is the basic concept of music education in colleges and universities.

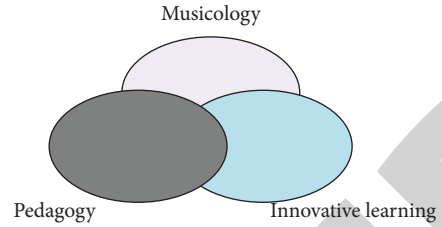

Figure 1: The relationship between music innovation education disciplines.

3. Ideas for Music Education Work under 5G

(1) Establish the awareness of full participation in online music education in the 5G era. With the advent of the 5G network era, the impact of new technologies and the emergence of massive data will inevitably bring about new changes in the network music work pattern in colleges and universities [20, 21]. In colleges and universities, student education is not only the task of teachers but also the work responsibility of student staff, class tutors, and related staff. Similarly, the basic idea of educating people by all staff is bound to apply to the field of ideological and political work. All kinds of people can integrate music education into it based on their own work, form music education into work habits, and reflect music education with practical actions. In the 5G era, the network will pervade life, and the music education work examples of all kinds of people will become valuable materials for online music education, and everyone will become a participant in online music education. Through online sharing and reporting, narration, and guidance, online and offline linkages are formed to create an organic working system for online music education in the 5G era. Colleges and universities should help every worker to establish an important awareness of full participation in online music education through educational guidance and policy support.

(2) Strengthen the construction of online music educators in the 5G era. Online music education requires a professional workforce [22]. In the 5G era, the emergence of new technologies and the new changes in the network landscape have put forward more and higher job requirements for online music educators. Most colleges and universities have not established a full-time network music education team, and many workers still undertake a lot of other work. The new job requirements will bring more work tasks, and the establishment of a full-time team will ensure full input of work energy to meet the new challenges. At the same time, the resource investment in the workforce should continue to increase, and the professional quality of the workforce should be improved through the training of theoretical literacy, media technology, educational methods, and frequent exchanges in the Internet industry, media industry, and education industry. In the full-time work team, the theoretical talent team will be further enriched, and finally, a team of network music educators in the 5G era with strong ideas, outstanding abilities, and a combination of full-time and part-time jobs will be formed. The full-time work team combined with the actual work of full participation in online music education will help colleges and universities to ensure the work effect of online music education in the 5G era [23].

(3) Open up a new frontier for online music education in the 5G era. In the 5G era, network transmission is faster and traffic costs may be lower. Coupled with the emergence of various technologies, the impact is no less than the 4G era. Among the online tools currently used by college students, WeChat, QQ, and Weibo are no longer new, and more media apps such as Douyin and Zhihu have also become online gathering places for college students. Online music education cannot only be satisfied with WeChat, Weibo, and other tools but should quickly adjust to emerging platforms to work. In the future, if the traffic cost is further reduced, the traditional text and pictures may also lose their advantages, and the audio and video will have more room for development. The focus of online music education can also gradually shift from text and pictures to audio and video, using audio and video to share news information and convey correct ideas. At the same time, try to introduce VR technology, big data analysis technology, etc. in online music education, through new technological innovation work mode, data analysis to understand the current state of mind of college students, understand the different needs, and provide a reliable basis for future work design.

Constructive music teaching is a teaching mode based on constructivism theory. The teaching mode of constructivism is "student-centered, teachers play the roles of organizers, guides, helpers, and facilitators in the whole teaching process, and use the learning environment elements such as situation, collaboration, and conversation to give full play to students' initiative, enthusiasm and initiative, and ultimately achieve the purpose of enabling students to effectively realize the meaning construction of the current knowledge." In this model, students are the active constructors of the meaning of knowledge, and teachers are the organizers, guides, helpers, and facilitators of meaning construction; the knowledge provided by textbooks is no longer the content taught by teachers, but students actively construct the object of meaning; the media is no longer a means and method to help teachers impart knowledge, but a cognitive tool for students to actively study and explore collaboratively. The more mature teaching methods that have been developed so far include scaffolding, throwing, and random access (also known as random access). These theoretical frameworks are fully applicable to the music teaching process and can be used innovatively.

(1) Scaffolding music teaching. The scaffold originally refers to the scaffolding used in the construction industry. It is used here to vividly describe a teaching method, that is, students are regarded as a building, and students' "learning" is a process of actively constructing themselves, while teachers' "Teaching" is a necessary scaffolding that supports students to continuously construct themselves and develop new problem-solving skills. Taking the Xiangjiao version of the music textbook "Let the World Be Full of Love" as an example, teachers can show students the structure diagram of the whole class (see the figure below) by writing on the blackboard before class, so that students can clarify their learning ideas and goals [24]. On this basis, fill in the detailed content of the section one by one in groups. In the whole teaching, teachers only teach songs through various media and guide students to promote teaching progress one section at a time, while more time is reserved for students to use section thinking to construct to make the world full of love as the theme. The system of emotion and knowledge can achieve the purpose of aesthetic and emotional education for students. Figure 2 shows making the world full of love.

(2) Throwing-out music teaching. This teaching mode requires that it be established on the basis of contagious real events or real problems. The real events or problems are vividly likened to "sketches," because once the event or problem is determined, the entire teaching content and teaching process are also confirmed, just like the ship is wrongly fixed. For the music class "Let the world be full of love," "pin" is "to fill the world with love," which not only includes the song "Let the world be full of love" but also guides students on how to understand and feel "love." Love

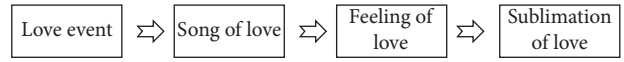

Figure 2: Making the world full of love.

"includes human affection and human love (see the picture below)." After the teacher "breaks down," the rest of the time needs to be more for teachers to participate in students' discussions on an equal footing and for students to communicate and share with each other. Different individual students have different understandings of "love" and different feelings about the song. Sharing their experiences of enjoying or feeling "love" in communication can enrich students' in-depth and diverse understanding of "love," and deepen emotional cognition. Figure 3 shows understanding and feeling of "love."

Creative music activity is complex, which requires the fusion of music logic with more left-brain activities and musical intuition with more right-brain activities, so that music innovation education and brain science are linked together, interacting, influencing, and promoting each other. Figure 4 shows the relationship between music creation and brain function.

In the creative music teaching practice, the creative teaching method is the main method, the game teaching method and the technology intervention method are supplemented, and the interactive method, the telling method, and the guiding method are also used comprehensively. The teaching concept basically involves three major music teaching systems, such as letting students create rhythm with rhythm and melody, using Colvin gestures to create melody, and using Orff instruments to improvise an accompaniment. The teaching theme of "Cultivating Musical Ability by Participating in Creative Music Games" is to integrate games into the process of music learning, improve students' interest in music creation, and encourage creative performance; the teaching target is eighth-grade students who have never been exposed to songwriting. The content is the development and extension of the typical Spanish-style flamenco dance rhythm [25]. First, divide all the students into four groups, namely, rhythm group, transmission group, rhythm group, and singing group; secondly, collectively learn and practice knowledge about rhythm patterns, transmission objects, rhythm, and pitch; and third, groups will cooperate to display the music knowledge they have learned; fourth, creative teaching, requiring students to improvise specific and incomplete melodies, and show their achievements through the students' creative work session. The teaching steps are as follows: first, import through collective momentum and rhythm imitation games; second, sound creation learning through the students' understanding of the regular staff, create music for the displayed graphic spectrum. Figure 5 is an example of a graph spectrum.

The arrival of the 5G network is just around the corner, and people's life will be more convenient. The online music work in colleges and universities will also usher in new changes accordingly, adapt to technological changes, combined with the new work situation, establish a music work

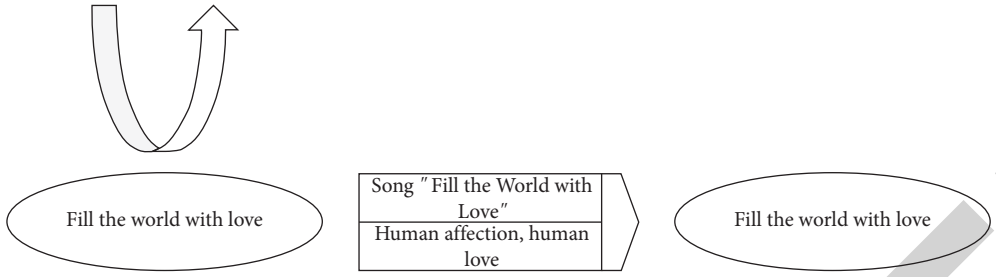

Figure 3: Understanding and feeling "love."

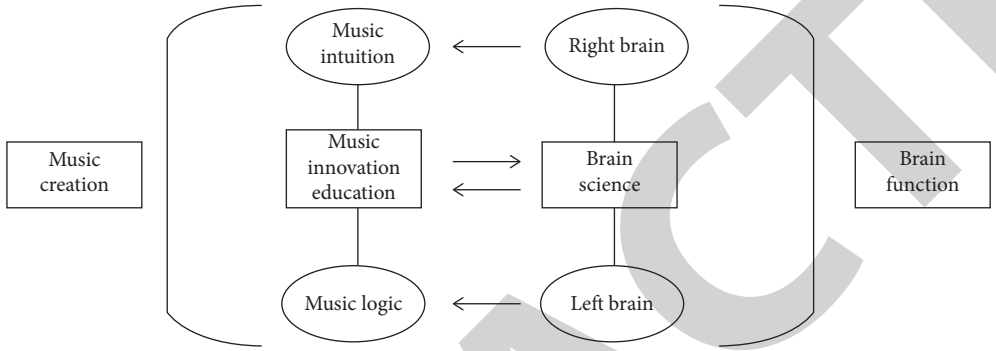

Figure 4: The relationship between music creation and brain function.

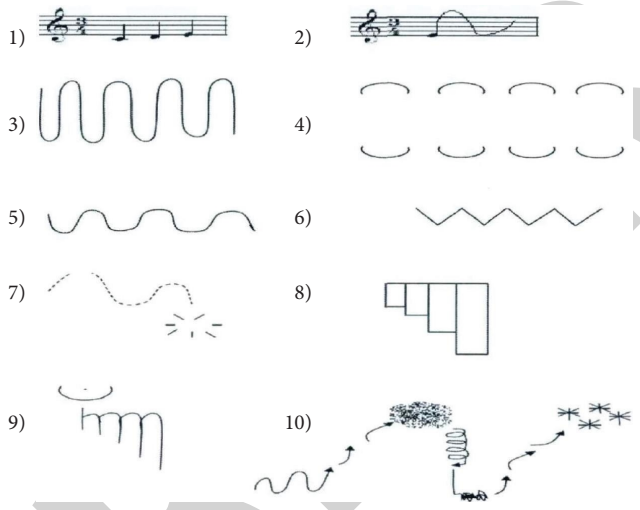

Figure 5: Example of a graph spectrum.

awareness in line with the new era of the Internet, constantly broaden work ideas, innovate work methods, and improve content quality by improving content quality, innovating the form of content expression, and introducing new technologies will surely once again enhance the work level of online music education.

4. Conclusion

In short, under the impact of the Internet in today's society, traditional statistical services have been unable to keep up with the times. While the Internet has provided great help, it has also put forward new requirements for traditional statistical services. The complex and difficult statistical service system will definitely be replaced by the electronic information-based statistical service system. Therefore, it is an inevitable trend in the new era to establish an electronic information-based statistical service file system in the statistical service department. Following the trend, increasing the information management efficiency of statistical services, and establishing an electronic information-based statistical service system in the new era is a major way for our statistical service industry to contribute to society. It is also the technical basis for promoting the comprehensive management of statistical services. Therefore, statistical service departments should fully realize the importance of informatization construction of statistical services, improve the statistical service system, improve the professional quality of statistical service personnel, and promote the informatization construction of statistical services.

Data Availability

The dataset can be accessed upon request.

Conflicts of Interest

The authors declare that they have no conflicts of interest.

References

[1] W. Jing, K. Marimuthu, and A. Prathik, "College music education and teaching based on AI techniques," *Computers & Electrical Engineering*, vol. 100, 2022.

[2] D. Huang, "Analysis on the present situation and reform ways of music education in colleges and universities," *Advances in Educational Technology and Psychology*, vol. 5, no. 12, 2021.

Hindawi
Scientific Programming
Volume 2022, Article ID 2334108, 7 pages
https://doi.org/10.1155/2022/2334108

Research Article

The Comfort Analysis Model Design of the Ground Light Environment of a Dome Reflective Badminton Court in a University

Xiujuan Ding,[1] Lichao Wang ,[2] and Chao Wu[3]

[1]*Physical and Health Education, Shanghai Business School, Shanghai 201400, China*
[2]*School of Physical Education, Xi'an University of Architecture and Technology, Xi'an 710000, China*
[3]*Shanghai Vocational College of Agriculture and Forestry, Shanghai 201699, China*

Correspondence should be addressed to Lichao Wang; 466159012@xauat.edu.cn

Received 12 July 2022; Revised 26 July 2022; Accepted 1 August 2022; Published 25 August 2022

Academic Editor: Lianhui Li

School sports is an important part of sports. The participants are mainly school students. Students play an important role in the development of the country. The development of campus sports is particularly important for the future development of the country. With the continuous improvement of the level of sports technology, to achieve higher, faster, and stronger sports goals, the requirements for sports venues continue to increase. To study whether the environment of the school's badminton court meets the requirements of the school's teachers and students to exercise and whether it can achieve the purpose of improving their own sports skills, the above problems are studied. Through the analysis of the light environment in the school grounds, to judge some problems existing in the badminton field of the school, improvement measures are put forward through research, and feasibility analysis of the improvement measures is carried out.

1. Introduction

The light environment is an important indicator that affects the comfort of the badminton court, so a suitable light environment affects the performance of athletes to a certain extent [1]. The impact of the light environment on athletes is mainly manifested as glare, due to inappropriate distribution or range of brightness, or too strong contrast, causing discomfort or visual conditions that reduce the ability to distinguish details or objects. According to the degree of glare's impact on vision, it can be divided into disability glare and discomfort glare. Disabling glare can cause a decline in visual ergonomics, while discomfort glare affects people's visual comfort [2–5]. Generally speaking, the presence of glare in badminton courts is uncomfortable glare. Uncomfortable glare will weaken visual function to a certain extent, affect visual performance and work efficiency, and cause safety hazards in important visual workplaces. Long-term effects will cause psychological damage, discomfort, and visual fatigue, which in turn lead to physical discomforts such as irritability, inability to concentrate, migraine, and eye diseases. Therefore, uncomfortable glare is an important indicator in lighting design, which is usually evaluated by the UGR system (unified glare value) [6–9]. In addition, there are the VCP method, the cutoff angle method, and the CIBSE LG3 method for reflected glare. The physical term for the light environment is called light intensity, abbreviated as illuminance, and the unit is lux or lx.

2. Experimental Investigation

2.1. Experimental Objects and Instruments. In the badminton court of a university gymnasium, a student was selected as the experimental object, and the serving test was performed in 3 different illumination time periods. An experimental subject is picked, and the skin temperature, heart rate, etc., are recorded before the test, so that the heart

rate is stable, and then, the ball is served in sequence in 7 fields. Make sure that the test subjects are tested when their heart rate is basically stable. The test subjects serve on the side of the court, and then, the data are recorded. The experimental equipment used mainly includes thermometers, black ball thermometers, sports watches, and hula hoops.

2.2. Experimental Method. This study investigates the badminton court in a university gymnasium and mainly analyzes the problems existing in the light environment of the badminton court in the gymnasium of the university. The research methods mainly include survey method, literature research method, simulation method, qualitative analysis method, and experimental summary method.

2.3. Experimental Scheme. The university arranged a total of 7 indoor badminton courts side by side. 7 courts were used as the control group, and only the light environment of these 7 courts was studied. The light environment experiment is mainly divided into two parts. The first part is to test the illumination of each area of the badminton court in the gymnasium of the school. Since each field is large, each field is divided into 12 areas to test the badminton field in groups and test the illuminance of each area of each site. Figure 1 shows the division of badminton test area.

The lighting of the school's gymnasium badminton court consists of two lighting modes: natural light sources and lamps. There are windows on the north and south sides of the venue and a ribbon-shaped skylight on the top. The illuminance test is to test the illuminance of the site at different times, record the illuminance of each site area under different light environments, and conduct statistical sorting and analysis. According to the use time of the venue, the illumination data of each venue will be obtained in six time periods: 9 : 00, 11 : 00, 13 : 00, 15 : 00, 18 : 00, and 21 : 00. The test content includes glare in each area and direct illumination in each area. The second part of the light environment experiment is to analyze whether the light environment of the school's gymnasium badminton court has an impact on sports through experiments.

3. Results Analysis

3.1. Thermal Environment-Related Indicators. In photometry, "luminosity" is the density of luminous intensity in a specified direction, but is often misunderstood as illuminance. The international unit of luminosity is the light received per square meter (called candela in mainland China, Hong Kong, and Macau). Light intensity has a great influence on the photosynthesis of organisms. It can be measured by a light meter [10–15].

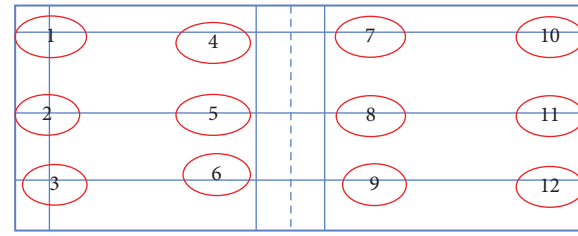

Figure 1: Division of badminton test area.

3.1.1. Calculation Formula.

$$\text{Average illuminance (Eav)} = \frac{\text{total luminous flux of light source } (N * \Phi) * \text{utilization factor (CU)} * \text{maintenance factor (MF)}}{\text{area area}\left(m^2\right)}. \quad (1)$$

(Note: applicable to indoor or stadium lighting calculations).

Utilization coefficient: 0.4 for general indoor use and 0.3 for sports.

Maintenance coefficient: generally, 0.7 ~ 0.8 is taken.

3.1.2. Standard Value. The average illuminance on the work surface or reference plane is maintained, and the average illuminance on the specified surface shall not be lower than this value. It is the average illuminance on a specified surface at the moment when the lighting installation must be maintained, which is the illuminance required to ensure visual safety and visual efficacy at work. The national standard of the People's Republic of China "Architectural Lighting Design Standards" GB50034-2013 specifies the general illuminance standard values for new, renovated, and expanded residential, public, and industrial buildings.

3.2. Illumination Data Analysis of Each Area of the Badminton Court. During the investigation, it was found that the lighting methods of the school's gymnasium badminton court mainly include complete natural lighting, combination of natural lighting and artificial lighting, and complete artificial lighting [16–19]. In most cases, the badminton court in the gymnasium of our school only relies on natural lighting and artificial lighting. In the case of the combination of the two lighting modes, it only exists in the morning and evening with natural light sources but cannot meet indoor lighting. The time is relatively short. This experimental investigation mainly studies the illuminance of indoor lighting under natural light and when the lights are turned on without natural light. In the case of sufficient natural light sources, it can be divided into two situations: curtains drawn and curtains not drawn. Therefore, this survey mainly studies various time periods of natural light, including 9 : 00, 11 : 00, 13 : 00, 15 : 00, 18 : 00, and 21 : 00. According to the illuminance of each area in six time periods, the following

statistical table is obtained according to the calculation formula of average illuminance (Eav) (Table 1).

It can be seen from Table 1 that the illuminance value of the badminton court varies with time, and there are obvious differences in the illuminance of each venue in different time periods. The comfort of the venue is judged by the illuminance value of each venue.

From Figure 2, it can be seen from the broken line graph of the illuminance of the badminton court that the illuminance changes in each venue in different time periods and the illuminance of the draw is also different for different venues in the same time period according to different distribution positions. Combining the statistical table of illuminance values of each venue at different times in Table 1 and the two graphs of the broken line chart of illuminance of the badminton court in Figure 2, it can be clearly found that the illuminance of the venue increases from both sides to the middle under natural light sources, while the illuminance of each area is relatively stable when the lights are turned on. The reason for affecting the illuminance is the use of lamps and lanterns. The survey test tested six time periods, namely, the illuminance of the site under three relatively typical lighting conditions under the condition of sufficient natural light source on sunny days, without drawing the curtain, pulling the curtain under the condition of sufficient natural light source, and turning on the light under the condition of insufficient natural light source. Among them, the test is 9 : 00, 11 : 00, 13 : 00, and 18 : 00. The four time periods are the data when the curtain is not drawn under the condition of sufficient natural light source, and 15 : 00 is the area of the venue after the curtain is drawn under the condition of sufficient natural light source. The data of 21 : 00 are the illuminance of each venue area under the condition that the natural light source is insufficient at night and the lights must be turned on at night. It can be seen from the test that the illumination of each area in the room is the highest when the curtains are not drawn under the condition of sufficient natural light source, followed by the curtains drawn with sufficient natural light source, and the illumination of each site is the lowest under the condition of artificial lighting. Among them, the illuminance is higher at 11 : 00 and 13 : 00 in the four time periods when the curtains are not drawn under the natural light source, followed by the time periods of 9 : 00 and 18 : 00, and the indoor curtains are shading at 15 : 00, but the illuminance inside the site is still higher than that in the morning and evening. From the experimental data, it can be seen that the lighting conditions of each site are also different in the same time period, because the installation of indoor windows is asymmetric on the north and south sides, and the installation positions of the windows are different, so the lighting conditions are not the same. The average illuminance on the north side with windows on both sides is higher than that on the south side. Because there are windows on the south side of Nos. 3 and 4, the lighting conditions are good, and there are pillars on the north side of Nos. 3 and 4 to block the light. The southern site is higher than the northern site under lighting conditions. Due to the location of the windows, the north and south sides of Site 1 and Site 7 are walls, so the illuminance under natural lighting is the lowest in the entire site. There are no windows on the west side of the No. 2 field, but there are windows on the east side. Therefore, the illuminance of 1, 4, 7, and 10 areas of No. 2 field is lower than that of 3, 6, 9, and 12 areas. According to the illuminance test data when the lights are turned on under the condition of insufficient natural lighting, it is found that the average illuminance of each area is between 250 lux and 350 lux under the condition of turning on the lights. There is a malfunction for some reason, resulting in the failure of normal lighting. Among them, the faulty lights have the first light and the second light on the north side of the east row in the middle of Nos. 3 and 4; the lights on the northwest side between No. 4 and No. 5 are faulty; the two lights on the south side of the row on the side were faulty; the two lights on the southernmost side of the west column between sites 5 and 6 were faulty, and the lights on the east side between sites 5 and 6 were faulty; a row of lights were in the middle of venues 6 and 7. Therefore, the illuminance of some areas is lower than the average value of this time, which leads to areas 2, 3, 7, 8, 9, 10, 11, and 12 of No. 4, areas 1, 2, and 3 of No. 5, and the entire No. 6 illumination in areas 1, 4, 7, 10, and 11 of the site; Site 7 will be affected.

Table 1: Statistical table of the average value of illuminance at different times in each site. Unit: lux/m^2.

Numbering	Time					
	9 : 00	11 : 00	13 : 00	15 : 00	18 : 00	21 : 00
Venue 1	495	627	655	542	558	271
Venue 2	571	678	708	596	609	308
Venue 3	788	895	925	736	827	304
Venue 4	730	977	867	838	772	218
Venue 5	729	1008	866	820	711	255
Venue 6	716	931	851	761	752	131
Venue 7	611	714	744	714	645	243

3.3. Analysis of the Experimental Data of the Ground Light Environment of the Badminton Court. There is a control experiment in this experiment. To verify the influence of the light environment on the exercising population, other environmental factors and the personal factors of the experimental subjects should be basically controlled to avoid affecting the experimental results. Their heart rate and skin temperature are tested before each experiment to ensure that the heart rate of each experiment is basically the same, so as to avoid the testers' own physical conditions affecting the experimental results. The different time periods of the experimental illumination are divided into six groups. The illumination conditions in the six groups are the same as the conditions in the illumination experimental data. Each group of experiments is divided into seven times, and seven sites are tested. Test data of badminton court ground illumination environment (Table 1). The variable in the data is the time period of the test, and the ambient temperature in the test will be different due to the different control time period. Therefore, the ambient temperature is also used as a control variable, and both horizontal and vertical analysis are required to avoid as much as possible. Experimental bias:

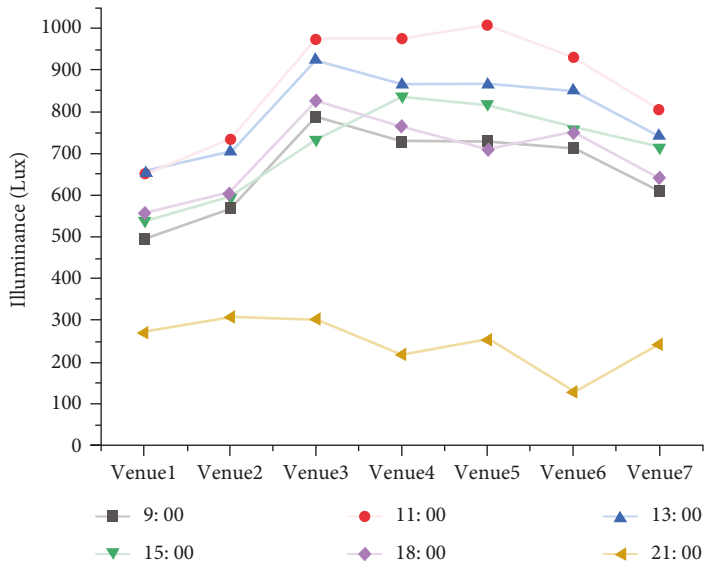

Figure 2: Badminton court field illuminance line chart.

To more intuitively see the influence of different temperatures and illuminance on the experimental results in this experiment, the bar graph of the ground light environment test data of the badminton court in Figure 3 is drawn according to the experimental data.

Figure 3 is a bar chart of the ground light environment test data of the badminton court, which can visually display the scores of each venue at different temperatures in different time periods and the scores of each venue at the same temperature in the same time period. Comparing the illumination environment scores of the same venue in different time periods, we can find the impact of different illumination in different time periods on sports performance. Through the difference in the scores of different venues in the same time period, it can be found that the impact of illumination in different venues on sports performance. The bar chart mainly shows the score of each field, and the main influencing factor is the different illumination of each field under different conditions during the test period. According to the experimental data of the badminton light environment, it can be seen that the illumination in each test period is different, so the final experimental result score data will also be different. The temperature during the experiment is also one of the influencing factors of the experimental results. Therefore, to visually see the score data under the influence of the two environmental factors, temperature and illuminance, the origin data analysis software is used to draw a 3D scatter diagram as shown in Figure 3. The three-dimensional scatter diagram is drawn from the test data of the ground light environment of the badminton court, and the three-dimensional scatter diagram obtained by the test data of the ground light environment of the badminton court. In Figure 2, we can see the scores of the experimental objects under the two experimental conditions of X-axis ambient temperature and Y-axis field illumination. Through the line chart and the three-dimensional scatter chart, it can be seen that the badminton court in the school gymnasium has different effects on sports under different time and light conditions. From the line graph of the ground light environment experiment data of the badminton court in Figure 1, it can be seen that in the six time periods, in these groups of experiments at 9 : 00, 18 : 00, and 15 : 00, the scores of each venue are higher than other time periods; in the experiment at 21 : 00 (insufficient natural light source, turn on the lights), the low scores of each venue were lower than other time periods. By analyzing the experimental data under the conditions of light and temperature, using the temperature as a quantitative measure, and analyzing the data of the experiment under the same or similar temperature conditions, we can know that for sports, the light intensity needs to be within an appropriate range, and people can exercise to achieve intended purpose, when the illumination is too high or too low is not conducive to physical exercise. The three time periods with the highest scores, 9 : 00, 15 : 00, and 18 : 00, are basically between 500 lux and 800 lux. The experiment shows that when the illumination is between 500 lux and 800 lux, athletes will achieve the best performance.

4. Discussion

4.1. Influence of Light Environment on Motion. Lighting mainly affects the illuminance and glare in the light environment [20–22]. When the illuminance is not enough, it will affect the judgment of the sports people on badminton and causes visual damage. Through the illumination test experiment and the analysis of the light environment experiment, it can be seen that there are many problems in the badminton court in the gymnasium of the school. First of all, the illumination of the indoor badminton court of the school is uneven and there is glare. According to the national standard, the illumination of the badminton court is not less than 300 lux, while the illumination of our school's indoor badminton court is only about 200 lux when the natural light source is insufficient, which is not up to 300 lux. Illumination standard: in the experiment, No. 4 field

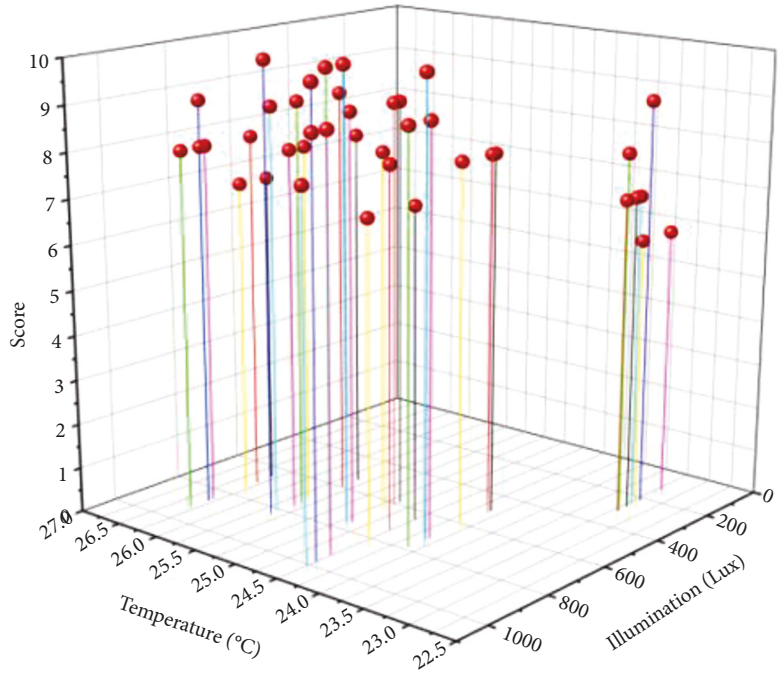

Figure 3: 3D scatter plot of the experimental data of the ground light environment of the badminton court.

scored the highest, and No. 4 field had medium illumination in each experiment, neither the highest nor the lowest. In the three experiments, the site with the lowest score data was the site with the highest or lowest illumination during the test during that time period. From the three-dimensional scatter diagram of the ground light environment test data of the badminton court in Figure 2, it can be found that both the illumination and temperature of the environment have a certain influence on the exercise performance, and there is also a standard value when the temperature and illumination affect exercise. In the influence process, it can be found that the influence of light on the movement is mainly in two cases, the illumination is too high or the illumination is too low. When the illuminance reaches a certain range, it is the most comfortable illuminance for exercise. Under this and illuminance conditions, people who are exercising will neither be unable to judge the movement situation because the illumination is too low, nor will they cause glare because the illumination is too high. Through this experiment, it can be found that the most suitable illumination range is in the range of 500 lux to 800 lux, so the final improvement of the stadium badminton court should also reach this illumination range. From the above data analysis, it can be concluded that the illumination has a certain influence on the badminton movement, and the optimal illumination required for the exercise is between a certain value. When the illumination is too high or too low, it is not conducive to sports.

4.2. Improvement Measures for Badminton Court. Through the above experiments and data analysis, it can be found that the problems to be improved in the badminton court in the gymnasium of the school mainly include insufficient lighting and glare [23–25]. Regarding the problem, we will improve the badminton court in the school's gymnasium. For the problem of insufficient light illumination, higher-power lamps can be selected, and the existing damaged lamps can be repaired, to achieve the effect of increasing the illumination. For the glare problem, the illumination mode of the lamps can be changed and the illumination angle can be adjusted. Aiming at the problem of field illumination, the DIALux lamp modeling software is used for analysis. First, the spatial structure diagram of the badminton court in the gymnasium of the school as shown in Figure 4 is established to carry out the overall simulation analysis.

Figure 4 is a model based on the overall structure of the badminton court in the gymnasium of our school to restore the existing structure of the badminton court of the school, including all doors and windows. In this way, the interior lighting of the venue and the illumination of each area can be simulated under the condition of sufficient natural light sources. Then, the simulated environment is combined and arranged according to the installation method of the existing lamps. After the arrangement is completed, the DIALux software is used for lighting analysis.

As shown in Figure 5, the lighting of the badminton court in the gymnasium of the school is basically arranged around the lamps in the absence of natural light sources at night. The illuminance of the places illuminated by the lamps in a straight line is higher and then gradually decreases to the places where the lamps cannot illuminate. The calculation results show that the average illuminance on the ground of the badminton court in the entire gymnasium is about 150 lux, the maximum illuminance is 230 lux, and the minimum illuminance is 62 lux. The illuminance distribution is not uniform, and the illuminance values are quite

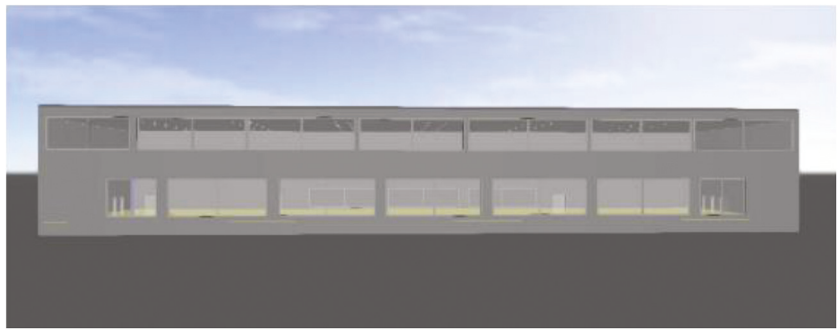

Figure 4: Construction of the badminton court model of the gymnasium.

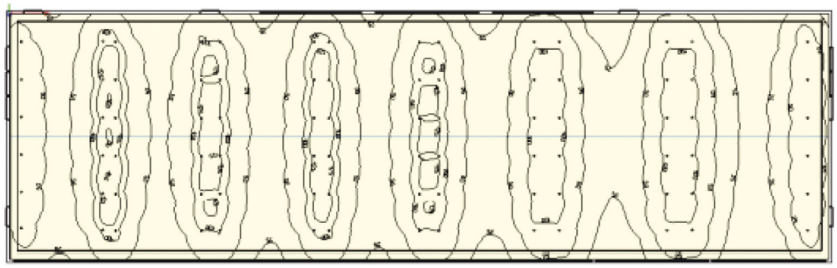

Figure 5: Simulation calculation result of the lighting tube of the badminton court in the gymnasium of the school.

different. However, considering that the light distribution method of the badminton court in the school gymnasium is mainly distributed on both sides of each badminton court, the light is irradiated to the middle of the badminton court by playing against each other on both sides, so that although the overall illumination is not uniform, exercising on the badminton court. The area can have good lighting. Therefore, although some areas have low illumination, they are basically dead ends of the movement and do not affect the overall badminton movement.

5. Conclusion

Although the venue as a whole meets the standards, some parts need to be improved. Compared with the standard facilities of the venue, the overall feeling of the sports crowd is also extremely important. Improving sports skills requires not only standard venue facilities but also the subjective feelings of sports people. Through the illumination experiment, it can be found that the illuminance of the badminton court in the gymnasium of the school is different under different illumination conditions and in different areas of the venue. The factors that affect the illumination include the light source and the building structure. Therefore, venue lighting not only needs to consider the selection of lamps but also allocates reasonably according to different venues and arranges lamps reasonably to achieve the desired effect. The ground light environment experiment of the badminton court found that among the lighting factors affecting the sports crowd, the school's badminton court illuminance has a suitable range. When the illuminance is between 500 lux and 800 lux, it is the most comfortable for the sports crowd, and when the illumination is too low, it will affect the sports. It will affect people's visual effects in badminton, and when the illumination is too high, it is easy to produce glare, so the improvement of the venue should be based on the illumination standard between 500 lux and 800 lux.

Data Availability

The dataset can be accessed upon request.

Conflicts of Interest

The authors declare that they have no conflicts of interest.

References

[1] L. Ye, "Discussion on lighting design of stadiums," *Building Electric*, vol. 39, no. 9, pp. 109–118, 2020.

[2] L. Ge, "Research on various glare evaluation parameters," *China Lighting*, vol. 28, no. 12, pp. 35–38, 2018.

[3] D. Yang, *Natural Light Glare Evaluation Method and its Application Research*, Tianjin University, Tianjin, China, 2018.

[4] Y. Lin, J. Qiu, and Y. Liu, "Current situation and progress of uncomfortable glare research at home and abroad," *Chinese Journal of Lighting Engineering*, vol. 27, no. 2, pp. 7–13, 2016.

[5] X. Guan and H. Zhao, "Measurement and analysis of lighting in Shenzhen university gymnasium," *Light Source and Lighting*, vol. 52, no. 2, pp. 31–33, 2010.

[6] X. Bai, *Research on the Evaluation index System of Light Environment in the Main Space of university Gymnasium*, Jilin University of Architecture, Jilin, China, 2018.

[7] S. Wang, Li Xian, and F. Hua, "Investigation and prediction model of the lighting environment of college gymnasiums based on visual fatigue: taking Hebei Province as an example," *Architecture and Culture*, vol. 80, no. 8, pp. 192-193, 2021.

[8] H. Tian, Z. Hong, H. Tiantian, and H. Zhang, "Research on indoor lighting glare measurement method based on digital

camera images," *Advances in Laser and Optoelectronics*, vol. 56, no. 02, pp. 199–206, 2019.

[9] J. Li and L. Huang, "Anti-glare design based on indoor flat lighting fixtures [J]," *Chinese Journal of Lighting Engineering*, vol. 31, no. 1, pp. 59–63, 2020.

[10] T. Uchida and R. Araya, "Applications of the atmospheric transport and diffusion of les Modeling to the spread and dissipation of COVID-19 aerosol particles inside and outside the Japan national stadium (tokyo olympic stadium)," *Modelling and Simulation in Engineering*, vol. 2021, Article ID 8822548, 19 pages, 2021.

[11] L. Li and C. Mao, "Big data supported PSS evaluation decision in service-oriented manufacturing," *IEEE Access*, vol. 8, Article ID 154663, 2020.

[12] I. Meta, F. Serra-Burriel, J. C. Carrasco-Jiménez et al., "The camp nou stadium as a testbed for city physiology: a modular framework for urban digital twins," *Complexity*, vol. 2021, Article ID 9731180, 15 pages, 2021.

[13] L. Li, C. Mao, H. Sun, Y. Yuan, and B. Lei, "Digital twin driven green performance evaluation methodology of intelligent manufacturing: hybrid model based on fuzzy rough-sets AHP, multistage weight synthesis, and PROMETHEE II," *Complexity*, vol. 2020, no. 6, pp. 1–24, Article ID 3853925, 2020.

[14] L. Geng, "Adaptive Gaussian Incremental Expectation Stadium Parameter Estimation Algorithm for Sports Video Analysis," *Complexity*, vol. 2021, Article ID 9963246, 10 pages, 2021.

[15] Z. Dang, S. Liu, T. Li, and L. Gao, "Analysis of Stadium Operation Risk Warning Model Based on Deep Confidence Neural Network Algorithm," *Computational Intelligence and Neuroscience*, vol. 2021, Article ID 3715116, 10 pages, 2021.

[16] L. Li, B. Lei, and C. Mao, "Digital twin in smart manufacturing," *Journal of Industrial Information Integration*, vol. 26, no. 9, Article ID 100289, 2022.

[17] Y. Shen, P. Yang, P. Zhang et al., "Development of a multitype wireless sensor network for the large-scale structure of the national stadium in China," *International Journal of Distributed Sensor Networks*, vol. 2013, 2013.

[18] L. Li, T. Qu, Y. Liu et al., "Sustainability assessment of intelligent manufacturing supported by digital twin," *IEEE Access*, vol. 8, Article ID 174988, 2020.

[19] J. Kou, S. Xiong, Z. Fang, X. Zong, and Z. Chen, "Multi-objective Optimization of Evacuation Routes in Stadium Using Superposed Potential Field Network Based ACO," *Computational Intelligence and Neuroscience*, vol. 2013, 2013.

[20] L.-C. Zhu, Z. Gao, J.-M. Zhu, and D. Zhang, "Construction of the Evaluation System of Sustainable Utilization of Large Stadiums Based on the AHP Method," *Mathematical Problems in Engineering*, vol. 2020, p. 12, 2020.

[21] L. H. Li, J. C. Hang, Y. Gao, and C. Y. Mu, "Using an integrated group decision method based on SVM, TFN-RS-AHP, and TOPSIS-CD for cloud service supplier selection," *Mathematical Problems in Engineering*, vol. 2017, Article ID 3143502, 14 pages, 2017.

[22] L. H. Li, J. C. Hang, H. X. Sun, and L. Wang, "A conjunctive multiple-criteria decision-making approach for cloud service supplier selection of manufacturing enterprise," *Advances in Mechanical Engineering*, vol. 9, no. 3, Article ID 168781401668626, 2017.

[23] Y. Guo, "Moving target localization in sports image sequence based on optimized particle filter hybrid tracking algorithm," *Complexity*, vol. 2021, Article ID 2643690, 11 pages, 2021.

[24] J. Yang, "Sports Video Athlete Detection Based on Associative Memory Neural Network," *Computational Intelligence and Neuroscience*, vol. 2022, Article ID 6986831, 9 pages, 2022.

[25] Y. Ge, X. Yu, M. Chen, C. Yu, Y. Liu, and G. Zhang, "Monitoring dynamic deformation of building using unmanned aerial vehicle," *Mathematical Problems in Engineering*, vol. 2021, p. 11, 2021.

Hindawi
Scientific Programming
Volume 2022, Article ID 1620540, 9 pages
https://doi.org/10.1155/2022/1620540

Research Article

Smart Home Design Based on Computer Intelligent Simulation Analysis

Wenbo Zhang and Si Li

Nanchang University, College of Science and Technology, Jiangxi, Nanchang 330022, China

Correspondence should be addressed to Wenbo Zhang; 2018030600032@jlxy.nju.edu.cn

Received 15 June 2022; Revised 9 July 2022; Accepted 13 July 2022; Published 25 August 2022

Academic Editor: Lianhui Li

With the continuous development of the social economy, people from all walks of life attach great importance to the smart home design of artificial intelligence technology. In the context of the information age, people's requirements for the quality of life are also gradually upgrading, and the requirements for home furnishing have also been upgraded from the traditional requirements of only living places to the expectation that a more intelligent, convenient, smart home has gradually been brought into life by people. The smart home system can integrate all control terminals into one system and implement on-site or remote control of home equipment using the computer terminal and mobile phone terminal, to realize the function of managing home equipment more conveniently and flexibly. Artificial intelligence technology as one of the important links adopts a structured design scheme to control and complete the design of the smart home system. Compared with most smart home systems on the market, this system also focuses on the safety precautions of the residential environment. It adopts infrared detectors for doors and windows and gravity sensing devices for indoor floors. The space-time barriers between home systems optimize and enhance the user's living experience. The article first analyzes the architecture, mainstream technology, and characteristics of computer technology and then discusses the design and implementation of my country's smart home system, providing strong support for subsequent research.

1. Introduction

With the rapid progress of computer technology and the continuous reduction in hardware costs [1, 2], virtual reality (VR) technology has ushered in a new wave of development, and many companies have begun to participate in the research and development of VR technology. Google of the United States developed the Google Cardboard product, Samsung of South Korea developed the Gear VR headset, and Sony of Japan developed the PlayStation headset. However, while the hardware equipment is booming, the lack of content seriously restricts the development and popularization of VR technology. At present, most companies try to expand the research direction and development prospects of VR technology by combining existing experience and new technical theories, especially the application of VR technology in the field of home improvement. The smart home is a new living concept based on the combination of many technologies [3–5]. As the pursuit of spiritual quality is becoming more and more personalized, the traditional two-dimensional design concept can no longer meet the needs of modern people. Smart home products [6–9] are relatively expensive equipment and show functional characteristics through specific physical objects, which are expensive and difficult to adapt to the individual needs of customers.

The traditional home display method usually uses 3D renderings for visual simulation display [10], but this display method cannot realize the preview of the whole scene, which easily leads to the finished product being less than the customer's psychological expectation. Therefore, more and more people begin to apply VR technology [11] to the home simulation display system. This display method can not only provide users with an immersive home experience but also realize the self-service design of home details such as floors, floor tiles, and wallpaper patterns [9]. In addition, the traditional home display method has a complex design and

low drawing efficiency, while the home display method based on VR technology can be operated in batches, thereby improving work efficiency. To improve the display effect of home simulation [3] and realize immersive home display, this study proposes a home simulation display system based on virtual reality. The system is developed and designed based on HTC Vive VR equipment, fully considering the interaction between home display and users, and realizes personalized home decoration design. The simulation design and implementation results show that the proposed home display system can not only provide users with an immersive home experience but also can carry out modular design to improve the development efficiency.

The basic principle of a smart home [12, 13] is to allow human beings to experience the progress and development of technology and bring convenience to human life. Firstly, the application scenarios of a smart home are analyzed, how the intelligent functions in the home are realized intelligently, and the virtual reality technology is used to express intelligence [14, 15]. Therefore, this simulation system combines 3D modeling, from the user's point of view, and uses virtual reality technology to achieve a 3D demonstration of some functions of the smart home [16] control system. When the user clicks the relevant button, the simulation system will make a corresponding control response. Relying on ordinary residential quarters, this study takes the real simulation of the surrounding environment as the premise, fully excavates the basic needs of the residents as the criterion, fully demonstrates the convenience brought by the home to human beings, and completes a virtual simulation of a smart home with basic function demonstration system [17]. There are also many personalized smart home control methods, and the demonstration platform can be customized according to the user's DIY.

This study uses three-dimensional modeling technology, taking residential quarters as an example, to study the technology of a home simulation system. By collecting data and using SketchUp software to build and optimize the model of the simulation system, a realistic home scene model is constructed. The comprehensive use of the Unity3D rendering engine, combined with the virtual simulation system technology, realizes the intelligent simulation of the internal functions of the home, allowing users to feel the convenience brought by real smart home control on the computer [18]. The simulation system is easy to carry and provides convenience for smart home publicity, and at the same time, compared with the previous home control physical equipment, the simulation system costs less. This simulation system gives full play to the interactivity and autonomy of the 3D visual simulation technology in virtual reality and makes full use of the Unity3D rendering engine combined with the built-in ShaderLab shading language to further improve the rendering effect, creating a more realistic day, night, and indoor and outdoor effects. It improves the user's sense of immersion and simulates various intelligent control functions in the home.

Our work mainly studies the design of the smart home system, by analyzing the architecture of computer technology and the main features of its technology.

2. Overall Function Design of the System

2.1. Simulation System Function Design. To realize the personalized home design, the choice of various types of units, and hardcover rooms, this study proposes a home simulation display system based on virtual reality. The system realizes the roaming display, UI interaction, and scene switching of the rough house and DIY design, as shown in Figure 1. For DIY design, personalized home design can be achieved by implementing functions such as home object interaction, handle prompts, furniture placement, and floor material switching. The establishment of the smart home virtual simulation system [19, 20] has three macroscopic tasks: (1) the planning and construction of the entire scene environment; (2) the interactive realization of indoor scenes; and (3) the interactive realization of outdoor scenes. The 3D scene model is realized by modeling software; the 3D engine design realizes the interactive roaming of indoor and outdoor scenes and the demonstration of indoor home functions. The design of the entire simulation system follows the waterfall model, which is gradually refined from top to bottom. Figure 1 shows the overall functional architecture of the system.

The specific function design of each module is as follows: (1) the basic unit type module realizes the roaming display, UI interaction, and multi-scene switching of the home, and the user can realize the roaming by operating the handle. The purpose of this function is to achieve a global view of the layout of the house and use the UI menu to interact with the details of the home. (2) The self-service design module realizes the functions of personalized home design and user-independent switching of furniture and floor materials, object highlight display, and teleportation. As can be seen from the above figure, the simulation system mainly designs and realizes core functions such as intelligent simulation of internal components of the home in the virtual home scene, interactive roaming of the virtual scene, and dynamic simulation of the work of the housing pipeline.

2.2. Technical Process of Simulation System Implementation. The entire scene technical process mainly consists of three modules: data acquisition, SketchUp modeling, and Unity3D rendering. Firstly, the collected data are abstracted, the scene is set and planned, the house base map is made in AutoCAD, and the scene model is constructed using virtual modeling technology, material, and texture. After that, the construction of the simulation scene is improved in Unity3D, the required special effects are added to the environment, the virtual roaming of the scene is realized, and the program design simulation of the simulation system production is carried out for the functional demonstration in the home, and finally, the real-time rendering of the virtual environment is realized to complete the whole process. Figure 2 is a block diagram of the system technology roadmap.

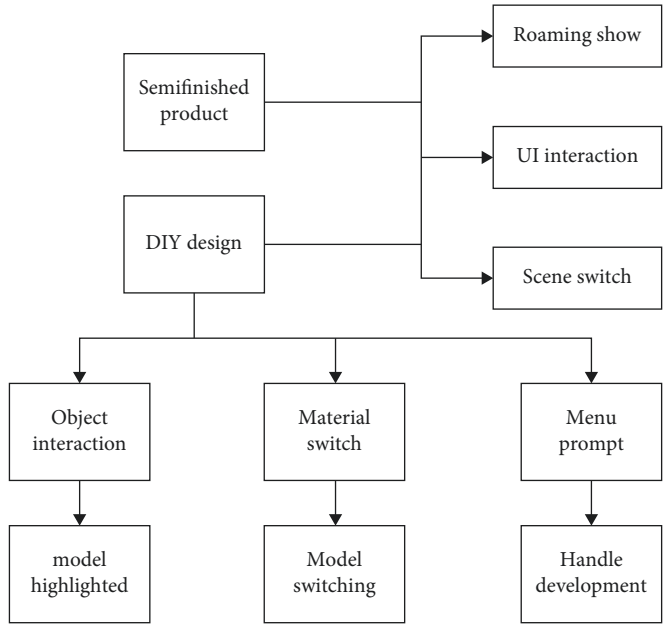

Figure 1: Overall functional architecture of the system.

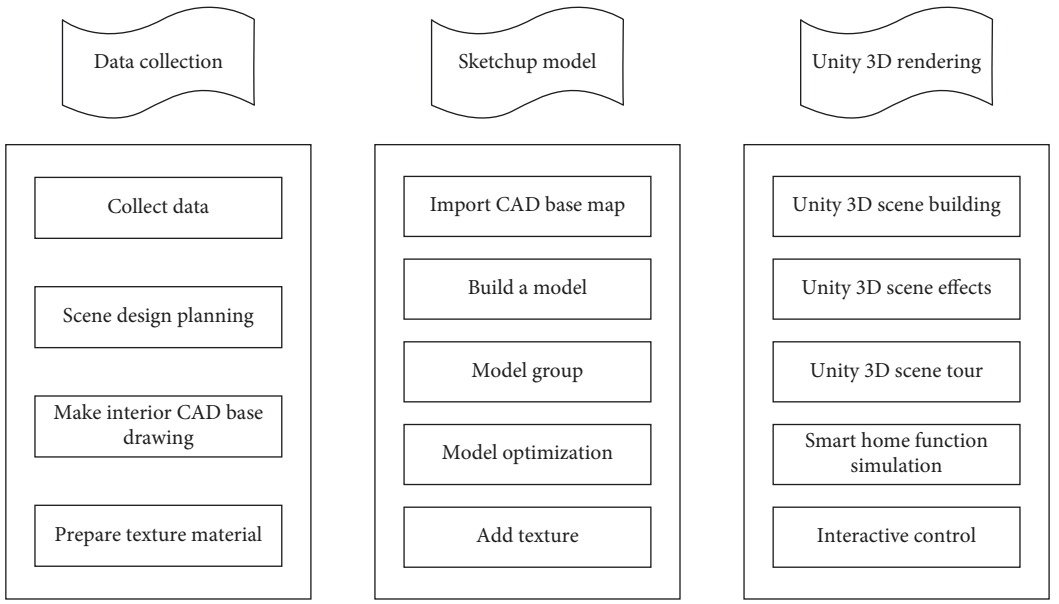

Figure 2: System technology roadblock diagram.

The technical route of design and implementation of a smart home virtual simulation system is as follows:

(1) Carrying out the overall design and planning of the scene, building indoor and outdoor virtual environment models, and determining the scale, implementation route, and development tools of the simulation system development scene

(2) Planning the area of the terrain; dividing the terrain area, the road interval, the number of street lamps, and the interval between the lamps; and setting the placement position of the home

(3) The construction of the entire scene, the setting of light effects, the simulation of the natural environment, the construction of indoor object models, etc

(4) The optimization, grouping, importing, and exporting preprocessing of 3D model to realize roaming interactive system

(5) Adding sky effects, light sources, trees, fountains, fallen leaves, sun halo, and other environmental special effects to the virtual scene in the Unity3D engine; setting the roaming mode; and realizing the interactive control operation of the home and indoor household facilities

2.3. Selection of System Development Tools. The basis for the establishment of the entire simulation system is the model, and the quality of the model will affect the efficiency of the entire simulation system, so the establishment of the model is very important. At present, in the 3D simulation system, macroscopically, the modeling methods can be divided into two types: preprocessing modeling and real-time modeling. Microscopically, it can be divided into three types: the first is to use 3D software to model; the second is to measure and model through instruments and equipment; and the third is to use images or videos to model.

(1) Using 3D Software to Model. You can see many excellent modeling software packages in the market, and the more well-known ones are 3D Max, SketchUp, Maya, and AutoCAD. The basic operations are to construct complex geometric scenes by rotating, extruding, stretching, or doing Boolean operations on the solid model. Using modeling software to build 3D models mainly includes geometric modeling, kinematic modeling, physical modeling, object behavior, and model segmentation.

(2) Modeling with Instruments. 3D scanner is also known as 3D digitizer. It is a device used to analyze a real-world object or environment to gather data on its shape and possibly its appearance (e.g., color). The collected real stereo color data will be used to convert into digital signals that can be recognized by computers, which can then be used to build digital 3D models.

(3) Modeling Based on Images or Videos. Image-based modeling and rendering (IBMR), referred to as IBMR, is a super-active research field in the current computer graphics community. Using IBMR technology, the information provided by the image is expressed by a three-dimensional model, which makes the entire transformation process convenient and fast.

2.3.1. Selection of Modeling Software

(1) SketchUp. The elegance and ease of traditional pencil sketches and the speed and flexibility of modern digital technology are perfectly combined by SketchUp Master. Master Sketcher is completely different from how we usually let the design process match the software too much, and it was specially developed to match our design process. In the design process, we are usually used to start from an inaccurate scale and proportion to start the overall thinking and continue to add details as the thinking progresses. Of course, if you need to, you can easily and quickly make precise drawings. Unlike CAD, which is difficult to modify, Sketch Master allows us to easily solve various modifications that occur throughout the design process according to design goals. Figure 3 shows SketchUp modeling example diagram.

(2) Blender. Blender is a free and open-source 3D graphics and image software that provides a series of animated short film production solutions from modeling, animation, material, and rendering, to audio processing, video editing, etc. Blender has a variety of user interfaces that are easy to use in different jobs and has built-in advanced film and television solutions such as green screen keying, camera reverse tracking, mask processing, and post-junction compositing. Figure 4 is the logo of blender.

Figure 3: SketchUp modeling example diagram.

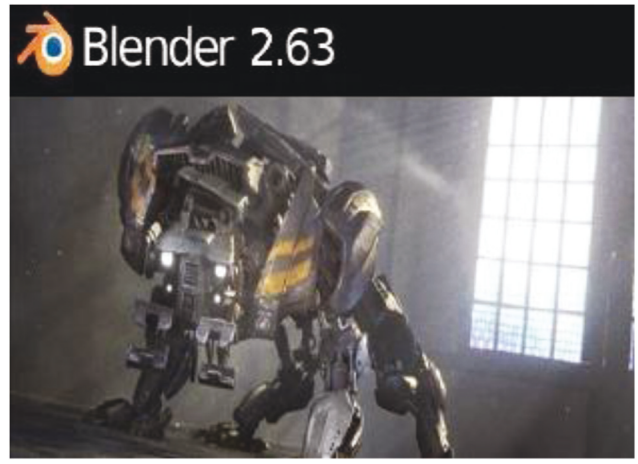

Figure 4: Logo of blender.

2.4. Realization of Function Display of Custom Home. To achieve an immersive user experience effect, this study uses HTC Vive equipment to build a workstation and combines VR technology to realize the basic unit module and DIY design module. The specific implementation process includes four stages: resource collection and production, environment deployment, application development, and release testing. The specific operation details of each stage are shown in Figure 5.

3. Design and Implementation of the System Model

3.1. System Design. The design of smart home system [21] is mainly composed of security protection function, intelligent control of household appliances, and network communication. Various system operations are carried out by the

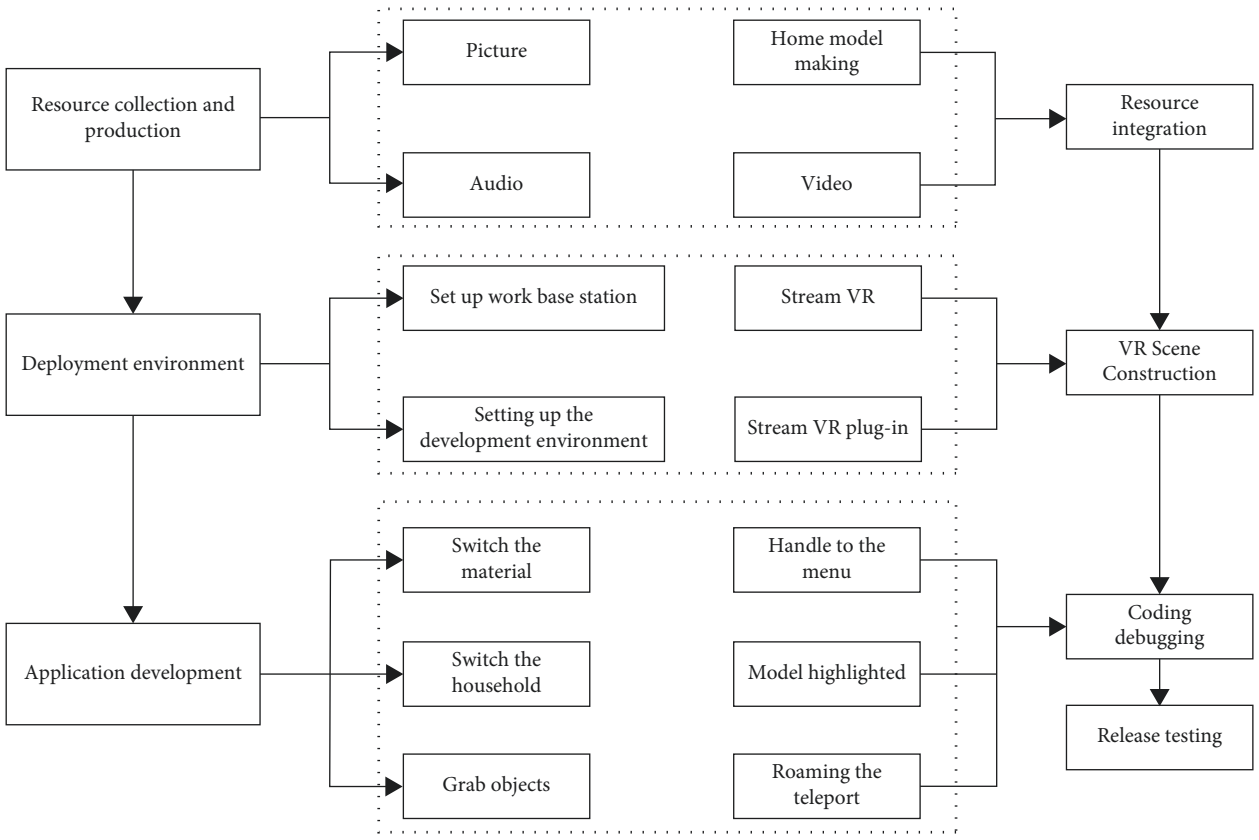

Figure 5: System implementation details.

intelligent security module, equipment control module, and wireless transmission module, respectively. The network communication is based on the wireless transmission module. Through the AP mode, the computer, mobile phone, and other devices can control the current mode. The intelligent control of home appliances is to use voice recognition to issue professional instructions to the system first and then control the operation of each system through the matrix keyboard. In terms of safety precautions, technologies such as video capture and human body detection are applied. When a human body passes by, the human body detection template will run immediately, turn on the camera, monitor the behavior and movements of people in the house at all times, save the data information, and transfer the picture to the mobile phone for mobile terminal.

3.1.1. System Hardware Design. In terms of system hardware design, the STM32 development platform is used as the core control of the system, the cloud platform provided by China Mobile and the wireless communication Wi-Fi technology is used as the communication medium, and temperature and humidity, flame sensors, and photosensitive sensors are mainly used in sensing nodes, smoke sensors, and other devices, collecting home environment information in real time, and displaying relevant data through display devices; at the same time, the system controls and links home devices through multiple relays.

The system adopts STM32F103 chip as the main controller, and its minimum system consists of power supply circuit, reset circuit, and crystal oscillator circuit. For the reset circuit, when the system is powered on, due to the existence of the capacitor, the NRST is at a low level. When the capacitor is fully charged, the reset pin (NRST) is at a high level, and the system works normally. After this pin is grounded, the system forms a manual reset. For the crystal oscillator circuit, the internal and external crystal oscillators can be switched, and the system is connected to an external 8 MHz crystal oscillator and a 32.768 kHz crystal oscillator, and the highest frequency multiplier of the system is 72 MHz.

Considering that the system hardware devices are relatively complex and the number is large, this article only introduces some of the hardware. In the display terminal, the hardware design method of the IIC protocol is adopted. Compared with the design of the SPI protocol, this design method reduces the general IO ports of the system and saves hardware resources; in the control terminal, considering that the operating voltage of the system is inconsistent with the operating voltage of hardware devices such as relays. A level converter is designed through the LM393 chip to solve the misjudgment phenomenon caused by inconsistent levels between devices; at the sensing terminal, each sensor node retains direct output (0-1) and analog output The interface is convenient for system calls; in the transmission terminal, the Wi-Fi module of the ATK-ESP8266 model is chosen,

which has fast transmission speed and stable network and only needs to keep two data interfaces and two power interfaces to work.

3.1.2. System Software Design. In the software design of this system, it is mainly divided into sensor information collection at the perception layer, information transmission at the network layer, and multichannel relay control and data display at the application layer. Finally, the data obtained by the system are processed through a normalization algorithm.

In the design of the main program of the system, the sensor module, display module, control module, communication module, etc., used in the system are first initialized. After the initialization is completed, it is connected to the cloud platform. When connected to the cloud platform, the system will sense that the data of the layer are uploaded to the cloud platform in real time and judged. If there is an abnormality, the system will activate the alarm function. At the same time, the user can issue commands through the cloud platform to control the home equipment and upload the status of the home equipment in real time.

In the wireless communication node, the Wi-Fi module is mainly to perform related mode initialization settings. After the settings are completed, a TCP connection is established with the cloud platform. When the system is connected to the cloud platform, operations such as data uploading and command issuance can be performed.

After the data processing completes the collection of monitoring information, the collected information is preprocessed and classified, and finally, the processed information is learned, the most suitable processing method is calculated, and the data are sent to the user through the PTZ. According to the characteristics of smart home diversity, the data are monitored in a direct and normalized way.

The collected data are classified and processed by MATLAB software, various types of data are represented by graphs, and the size of the collected data and whether it is abnormal can be seen intuitively. At the same time, to ensure that abnormal information can be monitored and pushed to users, the data are analyzed through a normalization algorithm inside the system.

3.2. System Implementation. Nowadays, computer technology and 5G technology are becoming more and more mature, and high technology has gradually been integrated into people's daily life. As an important way to implement computer technology, smart home system is mainly reflected in the three aspects of upper computer, lower computer, and terminal control, as shown in Figure 6.

3.2.1. Host Computer Level. The host computer level includes data interaction, front-end control, Web page control module, and app control module. The back-end Django technology and the front-end Vue.js technology are used to complete Web page development. Being able to produce API objects helps to reduce the complexity of background management. Window + Frame + Html code is used to implement control, and finally, the communication between the server and API.Ajax is realized, and the information is transmitted to the cloud SVN/GIT server.

3.2.2. Lower Computer Level. The lower computer is composed of a wireless transmission module, manual control module, voice playback module, backup power module, and other components. The single-chip system module is mainly implemented by the STM32F103VET6 single-chip microcomputer, and the voice playback module is completed by the most advanced iFLYTEK module, which constitutes the XFS5152-TTS voice synthesis module. The voice system is controlled. The speech recognition module is based on the Micro Snow LD3320 speech recognition module. The chip used is produced and designed by a specific company. This chip can run independently without the help of other chips. The equipment control module can reasonably control items such as doors and curtains. The driving stepper motor is very different from the voice recognition system. It uses the TB6600HG chip. The construction process of this chip is very complicated, and the current can reach 5 A. The driver has 5 subdivision modes, such as 1/16, 1/81, and 1/1, which can work stably in any environment. The manual control module uses matrix keys, and the keyboard module is mainly based on the 4×4 scale of external expansion and in-line keys, which is more stable than other keys.

3.2.3. Terminal Control. The terminal control module consists of a TFT LCD. It is the main project of ALIENTEK. It has the characteristics of wide viewing angle and low consumption. It can work at ultralow temperature. It can also collect humidity data, light intensity, and air quality in the air through the display camera, which is conducive to user perception.

The system selects the XFS5152-TTS voice module, which can synthesize Chinese and English voices, as well as play and record functions. The stepper motor is driven by a PWM constant current bipolar sine wave micro-stepper motor to drive a single chip, which has a reset function and a standby function, which can protect the parts due to built-in overheating in time. AP mode is like a mobile phone hotspot function, any Wi-Fi-related device can be connected, and it has a lot in common with the network bottom device mode. In this system, ESP8266 mainly uses the USART3 carrier to maintain communication with the microcontroller. It can also use the SSID mode and UDP broadcast mode of the mobile phone Wi-Fi terminal to broadcast. The broadcast uses the ESP8266 module, which can be directly connected to the router to keep the entire network unobstructed, which is conducive to remote control through mobile phones. In addition, the system has upgraded the sensitivity control system and safety protection system. In terms of energy, a backup power supply is added, which is usually used to save data and instructions that have not been saved in time when an unexpected power failure occurs. In terms of antitheft prevention, it not

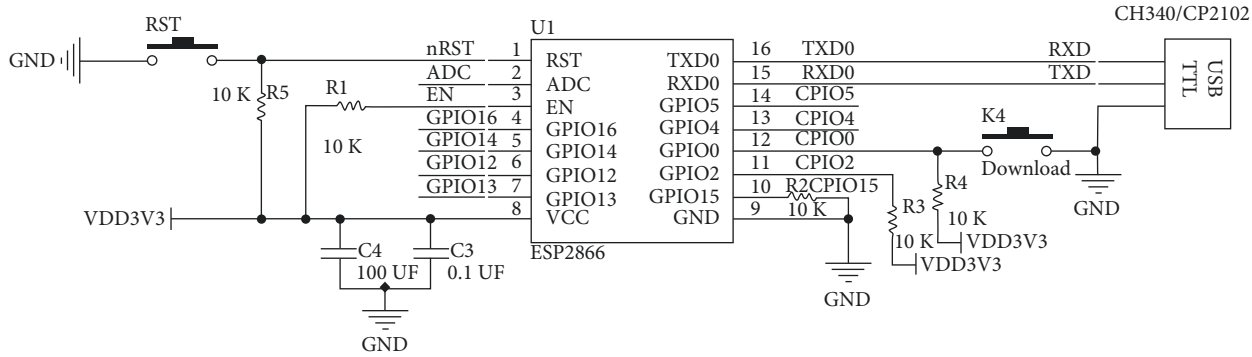

Figure 6: Schematic diagram of remote control template.

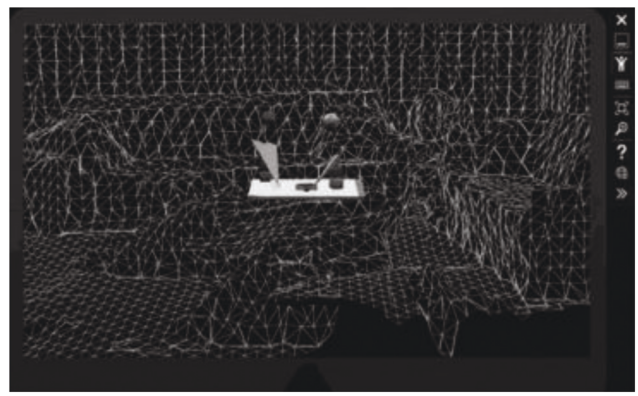

Figure 7: Point cloud data collected by the device.

only designs traditional image monitoring technology but also incorporates the latest infrared detection technology and gravity sensing technology. All residential door locks are equipped with face recognition technology, which is convenient for users to enter while saving the traditional key to open the door. In addition, an infrared receiving module and an infrared transmitting module are set above the door panel and on the top ceiling. These two modules are directly connected to the door lock switch. When the door lock is normally opened, the infrared detector will be turned off for a period of time. It will not be activated until the resident reenters, and then, it will enter a state of 24/7 persistent monitoring. If nonresident personnel enter, it is illegal entry, and then, the two infrared modules will not be closed normally. When the door panel is pushed open by an external force, it will directly trigger the security system and issue a special alarm to remind the residents. At the exposed windows of the residence, an infrared detection module is also set up and connected to the alarm system. In addition to the infrared technology in the doors and windows, a gravity sensing system is also placed on the indoor floor to form an all-around protection for the house. When a serious change in gravity is detected, the alarm system will be automatically triggered. The wireless technology module can control the communication Web page in a remote way and can realize remote control on the intelligent terminal.

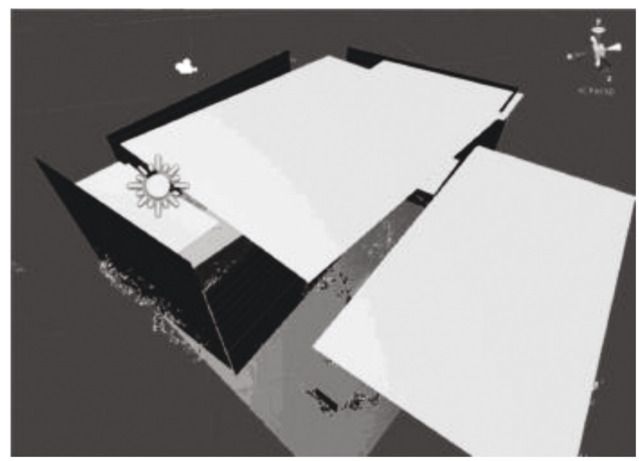

Figure 8: Modeling results.

4. System Implementation and Testing

Since the VR-based virtual reality home simulation system has certain requirements on software and hardware, this article uses HTC Vive equipment to build a workstation and uses the following development environment and tools to realize the functions of each module of the system. The system environment is as follows: Windows 10, 64-bit system, Nvidia GeForce GTX 1080 GPU, and Intel®

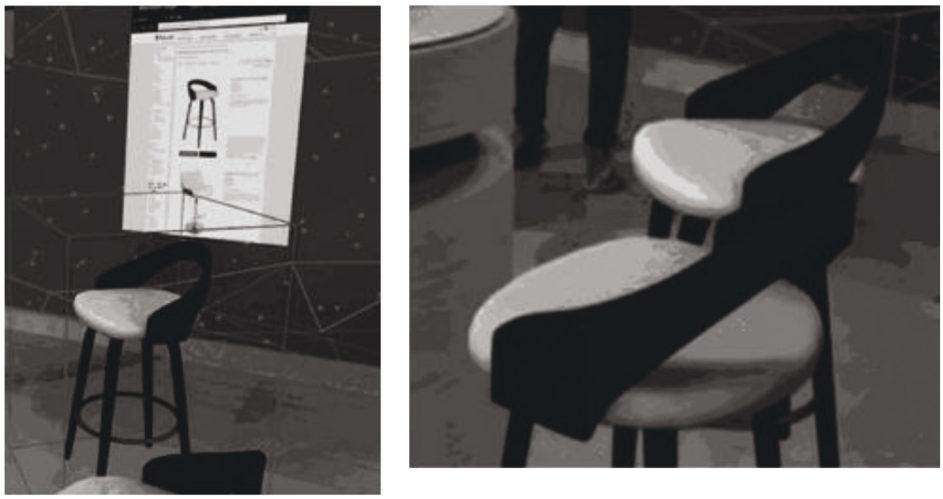

(a) (b)

Figure 9: User interaction results.

Table 1: Comparison of computational events and memory occupied by algorithms before and after optimization of different models.

Number	Model	Memory footprint (MB)	Elapsed time (s)
1	Before optimization	548	1.62
	After optimization	417	1.05
2	Before optimization	433	1.24
	After optimization	359	0.87
3	Before optimization	845	1.97
	After optimization	766	1.84

Core(TM) i7-7700 CPU, VR development kit is DOTween (HOTween v2) 1.1.640, Virtual Reality Toolkit 3.2.1, and SteamVR Plugin 1.2.3.

Figure 7 is a visual display of the point cloud data collected by the device in this study. Figure 8 shows the results obtained after modeling the set of point cloud data.

This study also implements user-defined interactive operations and implementation effects, as shown in Figure 9. Users can interact with the movement, zoom, and holographic projection of the modeling results.

To verify the effectiveness of the model optimization in this study, Table 1 shows the computation time and memory occupied by the algorithm before and after model optimization. As can be seen from Table 1, the optimization can significantly save memory and reduce computation time.

5. Conclusion

This study proposes a computer-based smart home [21] simulation display system to achieve personalized home design, diverse unit types, and decoration choices. The system uses the interface function module to realize the interaction between the system and the user and adopts the basic apartment type roaming module to realize the apartment type roaming function, and the hardcover model room display module provides the user's self-service design function. The scene rendering function, handle prompt, home placement, and floor material switching based on HTC Vive show that the home display method designed in this study can not only provide users with an immersive virtual home effect experience but also has high drawing efficiency and operational low-cost advantage. To sum up, with the continuous popularization of information technology, computer technology has a huge space for development. It can connect with different items in an intelligent way and finally realize intelligent management and control. At the same time, the complete application of computer technology in smart homes can not only improve the safety of smart homes [22, 23] but also improve people's quality of life. It completely breaks the space and time constraints of traditional home management, better improves the intelligent level of home life, and allows people to enjoy it more comfortably [24, 25].

Data Availability

The dataset can be accessed upon request.

Conflicts of Interest

The authors declare that there are no conflicts of interest.

Acknowledgments

The authors thank Science and Technology Research Project of Jiangxi Provincial Department of Education, Research on Green Ecological Furniture Design Practice Based on Ergonomic Data Analysis (No. GJJ217803).

References

[1] R. Raz Kamaran, "Smart home design flexibility as an enabler of sustainability and the reception in Sulaiymaniah, Kurdistan Region-Iraq [J]," *Journal of Building Pathology and Rehabilitation*, vol. 5, no. 1, 2020.

[2] Software and Systems Research, "New Findings on Software and Systems Research Described by Investigators at University of Bari (Supporting End Users to Control Their Smart Home: Design Implications from a Literature Review and an Empirical Investigation) [J]," *Computer Weekly News*, 2019.

[3] Ze Fu, "Research on innovative smart home design based on user experience [C]," in *Proceedings of the 4th International Symposium on Social Science (ISSS 2018)*, pp. 642–645, Atlantis Press, Amsterdam, Noord-Holland, The Netherlands, May 2018.

[4] C. Cheng, "Discussions on the pattern development of smart home design [C]," in *Proceedings of the 2018 International Conference on Social Sciences, Education and Management (SOCSEM 2018)*, pp. 656–661, Shaanxi Province, China, October 2018.

[5] Lennar Selects Baldwin Hardware, *Kwikset for Wi-Fi Certified Smart Home Design Program [J]*, Wireless News, 2017.

[6] L. Ruihua, S. Changqing, and S Changqing, "Smart home design based on cloud computing and internet of things," *Journal of Computational and Theoretical Nanoscience*, vol. 13, no. 11, pp. 8075–8080, 2016.

[7] F. Valiyullah Khan, N. S. Teja, A. L. Aaqib Parvez, and R. R Das, "Low cost smart home design," *Indian Journal of Science and Technology*, vol. 8, no. S2, p. 295, 2015.

[8] T. Xu, Z. H. Hu, J. J. Wang, and H. H. Song, "Smart home design based on wireless transmission technology [J]," *Applied Mechanics and Materials*, vol. 2279, pp. 291–294, 2013.

[9] K.-Ah Jeong, G. Salvendy, and R. W. Proctor, "Smart home design and operation preferences of Americans and Koreans," *Ergonomics*, vol. 53, no. 5, pp. 636–660, 2010.

[10] Ji-W. Song, "Smart home design guidelines based on a real home life case study [J]," *Journal of Integrated Design Research*, vol. 7, no. 1, 2008.

[11] D. E. N. G. Jin-wen, X.-jun Zhang, W. A. N. G. Yue, and Mu-jun Liu, *A Smart Home Design and Implementation Based on Kinect[P]*, DEStech Transactions on Computer Science and Engineering, 2018.

[12] D. Caivano, D. Fogli, R. Lanzilotti, A. Piccinno, and F. Cassano, "Supporting end users to control their smart home: design implications from a literature review and an empirical investigation [J]," *Journal of Systems and Software*, vol. 144, 2018.

[13] O. Sihombing, N. Zendrato, Y. Laia et al., "Smart home design for electronic devices monitoring based wireless gateway network using cisco packet tracer," *Journal of Physics: Conference Series*, vol. 1007, no. 1, Article ID 012021, 2018.

[14] Ji-E. Lee, "A study on smart home design incorporating ubiquitous healthcare services [J]," *Computer Technology and Application*, vol. 4, no. 7, 2013.

[15] A. Bardell, "Digital and the modern smart home," *ITNOW*, vol. 63, no. 4, pp. 16-17, 2022.

[16] M. Basheer Al-Somaidai, "LabVIEW based SNMP proxy agent for smart home design," *American Journal of Networks and Communications*, vol. 5, no. 4, p. 73, 2016.

[17] J.-H. Hwang, "An analysis of the research and policy on the smart home design for the elderly based on the U-healthcare," *JOURNAL OF THE ARCHITECTURAL INSTITUTE OF KOREA Planning & Design*, vol. 31, no. 4, pp. 53–60, 2015.

[18] H. Ali, M. Adda, M. Atieh, and W. Fahs, *Smart Home Design for Disabled People based on Neural Networks [J]*, Procedia Computer Science, vol. 37, , 2014.

[19] *IDC Reports on the Worldwide Smart Home Devices Market [J]*, Manufacturing Close - Up, 2021.

[20] *Big Changes Imminent for Smart home Camera market [J]*, M2 Presswire, 2021.

[21] G. Xiao, "Machine learning in smart home energy monitoring system," *IOP Conference Series: Earth and Environmental Science*, vol. 769, no. 4, p. 042035, 2021.

[22] Anonymous, "Top smart home integration questions [j]," *Kitchen and Bath Business*, vol. 68, no. 3, 2021.

[23] C. Zhou, T. Huang, S. Liang, X. Yuan, and M. Elhoseny, "Smart home R&D system based on virtual reality," *Journal of Intelligent and Fuzzy Systems*, vol. 40, no. 2, pp. 3045–3054, 2021.

[24] L. Corporation, *Lennar Launches World's First Wi-Fi CERTIFIED Smart Home Designs with Amazon Alexa [J]*, Telecommunications Weekly, 2017.

[25] A. Muhammad, D. Kumar Saini, Kashif Zia, and M. Ali, "Fekihal. Educational aspects of service orientation: smart home design issues and technologies [J]," *TEM Journal*, vol. 6, no. 2, 2017.

Hindawi
Scientific Programming
Volume 2022, Article ID 2352676, 9 pages
https://doi.org/10.1155/2022/2352676

Review Article

The Application Method of Big Data of Data Mining Algorithm in College Basketball Teaching

Yu OuYang,[1] YanHong Zhang ,[1,2] and Youliang Li[1]

[1]*School of Physical Education, Nanchang Institute of Science and Technology, Jiangxi, Nanchang 330108, China*
[2]*Shaanxi Normal University, Shaanxi, Xi'an 710062, China*

Correspondence should be addressed to YanHong Zhang; zhangyanhong@peihua.edu.cn

Received 7 June 2022; Revised 29 June 2022; Accepted 5 July 2022; Published 23 August 2022

Academic Editor: Lianhui Li

The teaching quality monitoring and evaluation system in colleges and universities gives the scientific and objective evaluation of school teaching work and effectively optimizes and adjusts the important system of teaching work under the condition of deep excavation of the problems. However, the data on the teaching quality of colleges and universities in the state of static storage has seriously affected the value of data existence and the mining of laws. This paper mainly analyzes the application types of data mining technology in the college basketball teaching quality monitoring and evaluation system and discusses the data mining implementation method in the college basketball teaching quality and evaluation system, hoping to have a certain reference for relevant personnel.

1. Introduction

Today is an era of informatization, and also an era of the knowledge economy. As one of the most active and important factors, talents should be highly valued. As a base for cultivating high-quality talents, colleges and universities should pay more attention to the quality of talent training, provide high-quality talents for various constructions of our society, and realize the high-quality development of my country's economy [1]. In addition, the competition among countries is becoming more and more fierce. The essence of the competition is the competition of talents. If my country wants to occupy a more favorable position in the world, it needs to strengthen the training of talents. The cultivation of talents depends on education, and the quality of basketball teaching is of great significance to the quality of talent cultivation. Colleges and universities should fully recognize the importance of basketball teaching quality, not only to take effective measures to improve the teaching quality but also to take effective methods to monitor and evaluate the teaching quality [2–4], to ensure that the teaching quality of colleges and universities meet the needs of students development requirements.

With the continuous popularization of the Internet, basketball news information, and basketball events have been widely disseminated on the network platform, and the public's enthusiasm for basketball is rising. College basketball teaching is facing many challenges and opportunities. In the online teaching platform, teachers can integrate and disseminate rich teaching resources, exchange and share teaching experiences with other experienced teachers, and even communicate with distant teachers through remote interaction to improve teachers' teaching levels. Under the background of big data, the assessment and management of basketball teaching are more professional and informative, which standardizes the evaluation model of basketball teaching and training, and improves the effectiveness of basketball teaching; colleges and universities can also use digital assessment and management to improve basketball training and teaching. Carry out assessment and management, change the traditional and vague evaluation methods, and continuously optimize the relevant standards and norms of basketball training and teaching, so that basketball learning can achieve the goal of skill, professionalism, and healthy exercise.

There are many methods for monitoring and evaluating the quality of basketball teaching in colleges and universities,

among which data mining technology [5, 6] is a more effective method and has strong practical value. Relevant personnel should conduct in-depth research on data mining technology [7] so that it can play a greater role in the monitoring and evaluation system of basketball teaching quality in colleges and universities so that colleges and universities in our country can cultivate higher-quality talents. The guiding role of data mining [8] in basketball teaching is shown in Figure 1.

Data mining technology can perform data classification and prediction, cluster analysis and association analysis, etc., and can conduct deep data mining, which is an important research field to improve analysis and decision-making capabilities [9–11]. The introduction of data mining technology into teaching quality monitoring, objective analysis of existing performance data, and mining of valuable information will undoubtedly help improve teaching measures and improve teaching quality. At present, there have been related research on the application of data mining technology to teaching management [12]. For example, the literature studies the course association classification model and student achievement prediction algorithm based on frequent pattern spectral clustering; the literature proposes a K-nearest neighbor based local optimal The reconstructed incomplete data imputation method combined with the random forest model realizes the prediction of grades; the literature studies how to use the undergraduate grade data to infer the students' performance during the postgraduate period by means of various prediction and statistical methods. On the basis of learning from previous research experience, this paper uses factor analysis to comprehensively evaluate and analyze the performance of students majoring in computer science and proposes an improved decision tree method to predict student performance. A detailed comparative analysis was carried out, and a method that could better promote the monitoring of teaching quality was found.

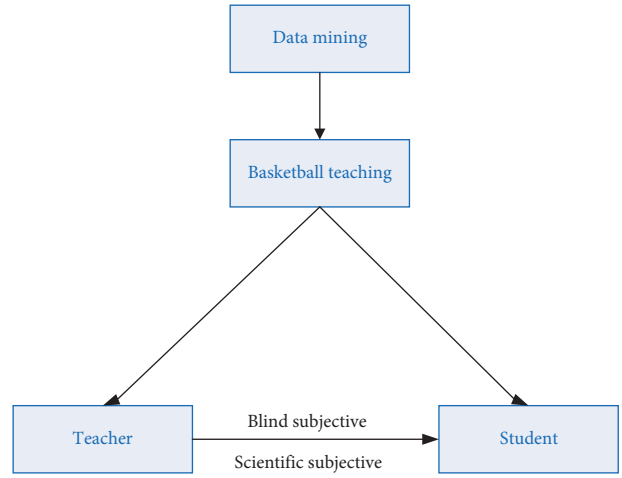

Figure 1: The role of data mining in basketball teaching.

2. Related Work

2.1. Data Mining and Knowledge Discovery. The superficial meaning of data mining technology means that when faced with a pile of data [13], it can be well processed, analyzed, and screened over and over again among these many data to select the most useful data. Databases are generally very complex. In this complex database, resources are continuously utilized. Through the study and mastery of data mining technology, the long-term accumulated data can be processed, and some data are random. If it is processed manually, it may increase the difficulty of the work of the staff and make the data cluttered. Users must learn to extract the data so that the data can be better used in people's lives. In the process of learning data mining technology, it is necessary to continuously learn new knowledge, discover new knowledge, follow the local characteristics and rules of different systems, and the data can be updated in time, and the knowledge in the database must be analyzed in detail; this requires A lot of information, the patterns or concepts and laws of this kind of information are different, each has its own level, has a future prediction direction for the data, and makes decisions at the same time; another point is that data mining technology should be based on different The information of the students should be updated in a timely manner, and the information of the students should be understood in time, so as to have a good guiding effect on the course.

Knowledge discovery (KDD): knowledge discovery is a broader term for the so-called "data mining," which is to obtain knowledge according to different needs from information represented by various media. The purpose of knowledge discovery is to shield users from the tedious details of the original data, extract meaningful and concise knowledge from the original data, and report directly to the users. There is still confusion between database-based knowledge discovery (KDD) and data mining [14], and the two terms are often used interchangeably. KDD represents the entire process of transforming low-level data into high-level knowledge. KDD can be simply defined as KDD is the specific process of identifying valid, novel, potentially useful, and basically understandable patterns in data. Data mining, on the other hand, can be thought of as the extraction of patterns or models from observational data, which is a general interpretation of data mining. Although data mining is at the heart of the knowledge discovery process, it is usually only a part of KDD (roughly 15% to 25%). Therefore, data mining is only one step of the whole KDD process, and there is no exact definition of how many steps and which steps must be included in the KDD process. However, a general process should accept raw data input, select significant data items, reduce, preprocess, and enrich data sets, transform data into appropriate formats, find patterns in data, and evaluate and interpret findings.

Because the quality of the data mining algorithm [15, 16] will directly affect the accuracy of the knowledge found by KDD, and most of the current KDD research focuses on data mining algorithms and applied technologies, people often do not strictly distinguish between data mining andknowledge discovery in databases both use each other. Generally, it is

called KDD in the field of scientific research, and it is called data mining in the field of engineering [17].

2.2. Data Mining Process. The KDD process is shown in Figure 2. The KDD process can be summarized into three parts: data preprocessing, data mining, and interpretation and evaluation of results.

2.2.1. Data Preprocessing. Data preprocessing refers to the set of techniques implemented on a database to remove noise, and missing and inconsistent data. The different data preprocessing techniques involved in data mining are data cleaning, data integration, data reduction, and data transformation. The need for data preprocessing stems from the fact that real-time data and many times database data are often incomplete and inconsistent, which can lead to incorrect and inaccurate data mining results [18]. Therefore, in order to improve the quality of the data to be observed and analyzed, it can be processed through these four steps of data preprocessing. The more data you improve, the more accurate observations and predictions will be. Figure 3 shows the steps of data preprocessing.

2.2.2. Data Mining. Data mining technology refers to a process of automatically retrieving from a large amount of complex data and automatically sorting out relevant information. To be precise, data mining is the "eye" for discovering knowledge base data, that is, to regularly search for chaotic data in massive data, so as to sort out the information that people need in an orderly manner. In fact, the process of data mining is fully automated, but many experts point out that only 80% of the time and experience in the data mining process is spent in the preprocessing stage. According to objective facts, many preparations need to be done before data mining technology. Even so, data mining technology is very convenient and can maximize work efficiency in practical applications [19]. In particular, teaching quality management using data mining technology in colleges and universities can assist teachers and college administrators in teaching analysis and other work, continuously develop and improve teaching systems and mechanisms, and promote the scientific development of schools. Accelerate the modernization of higher education with Chinese characteristics in the new era.

2.2.3. Interpretation and Evaluation of Results. The patterns discovered in the data mining stage may have redundant or irrelevant patterns after evaluation, and then they need to be eliminated; it is also possible that the patterns do not meet the user's requirements, then it is necessary to fall back to the previous stage of the discovery process, such as reselecting. The data adopts new data transformation methods, sets new parameter values, and even changes a mining algorithm. Also, since KDD is ultimately intended for human users, it may be necessary to visualize the patterns found, or convert the results into another representation, that is, understandable to the user. Data mining is just one step in the overall process. The quality of data mining has two influence factors: one is the effectiveness of the data mining techniques used, and the other is the quality and quantity of the data used for mining (the size of the data). If the wrong data or inappropriate attributes are selected, or the data is inappropriately transformed, the mining results will not be good [20]. The whole mining process is a continuous feedback process. For example, the user found that the selected data was not very good during the mining process. Or the mining technique used.

2.3. Methods and Technologies of Data Mining. There are many ways to operate data mining technology. First of all, the genetic algorithm will be introduced. This method is based on the laws of nature, survival of the fittest, survival the fittest, combining different data, evolving, and finally merging together so that it becomes new data information, and the newly established data still needs to have the ability to select the overall situation, integrate the data, and finally become a data system, and then use the data, so that it will be very convenient to use [21]. It makes the arrangement of information more convenient; the second method is a decision tree, which is to first organize and summarize all the data, and then classify the data, organize the data information for branch processing, and search from the middle. The most valuable information, and then clean up the data that does not meet the conditions, because this process is like the process of growing a sapling, so it is called a decision tree. The biggest advantage of this method is that the operation is very simple, The process is also very smooth, and the most important thing is that the work efficiency is very high. This method is very suitable for a large amount of data, which will reduce the pressure and burden on the staff.

The first method is to clarify the management and decision-making problems. If there are problems in the process of education and teaching management, we must constantly summarize and summarize the emergence of such decision-making management problems, and at the same time identify them. Established in time, so that specific data can be turned into goals so that it can be redefined; the second method is to extract the original data, and the data can be managed and customized according to different goals, and because the teaching management information system The establishment of the database and other related teaching functions require the support of a lot of data [22]. In the process of extracting from the database, the noise data must be excluded, and it cannot be interfered with by the vacant data. These data are integrated and transformed for accurate processing; the third point is to design data and continuously mine data. Because of the different goals, for the completion of data mining tasks, various data algorithms should be used to establish a data algorithm. Processing model; the fourth is the refinement of data. With the huge database and the screening of value metrics, this data will have a corresponding mining mode, and at the same time, it must be processed and integrated according to different teaching management needs.

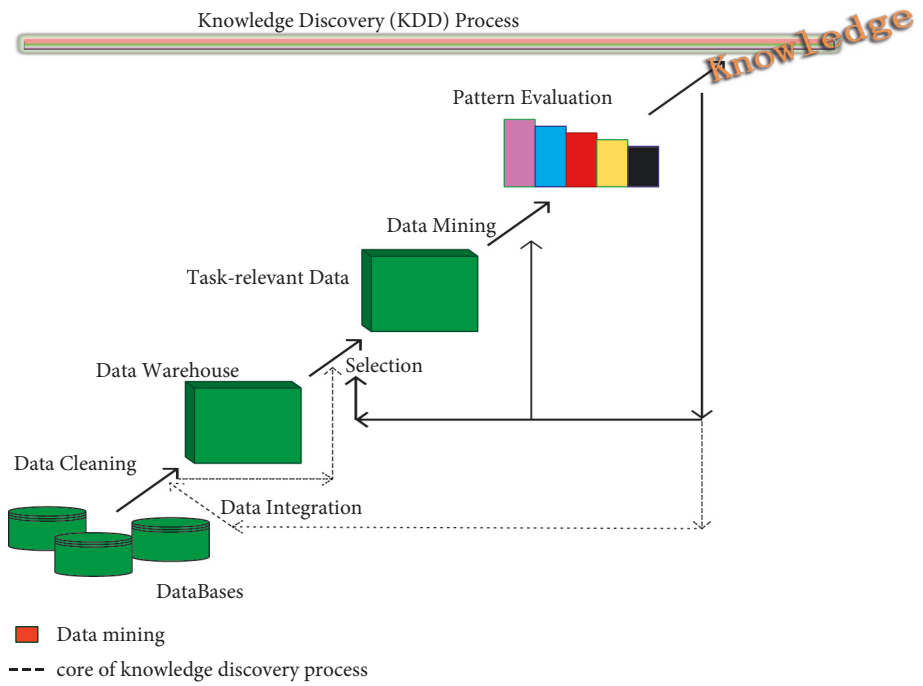

Figure 2: KDD process diagram.

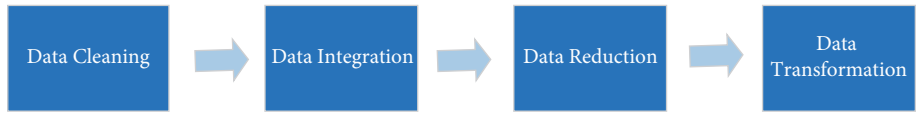

Figure 3: Data preprocessing steps.

3. Explore the Application of Data Mining Technology in College Basketball Teaching

This chapter mainly explores the application of data mining classification technology in college basketball teaching, puts forward the implementation plan of data mining technology in college basketball teaching application, and introduces the implementation process of the plan by taking the analysis of students' performance in college basketball teaching as an example.

3.1. The Implementation Process of Classification Mining. Data mining is a decision support process and a deep-level data information analysis method. It is undoubtedly very beneficial to apply data mining techniques to the evaluation of teaching. It can comprehensively analyze the hidden internal relationship between test results and various factors connection. For example, through the analysis of the school's student performance-related database system, data mining tools can answer similar questions such as "what factors may have an impact on students' academic performance," which cannot be achieved by traditional evaluation methods? Through data mining and analysis, the evaluation results can bring unprecedented gains and surprises to teaching.

In the past, the database query method was usually used to process a large amount of data information in the teaching process. Here, the author proposes a classification algorithm in data mining, which can convert a large amount of data into classification rules, so as to better analyze these data. Figure 4 is a flow chart of classification implementation.

3.2. Data Collection. In this example, the author can discuss the basic learning situation of students (such as knowledge base, classroom learning effect, students' interest in the course, homework completion, time spent after class, and learning methods used), what factors have an impact on academic performance, and what are the reasons why students' academic performance is excellent or their academic performance is unsatisfactory, and expect to use the obtained analysis results to guide future teaching work [23].

Student achievement analysis is all about finding functional relationships between two or more attributes. To analyze the causes of students' academic performance, we need data from the following aspects:

3.2.1. Basic Information about Students. The data structure is as follows: student number, name, gender, place of origin, department, major, and class. This information is available through the school's student management information system.

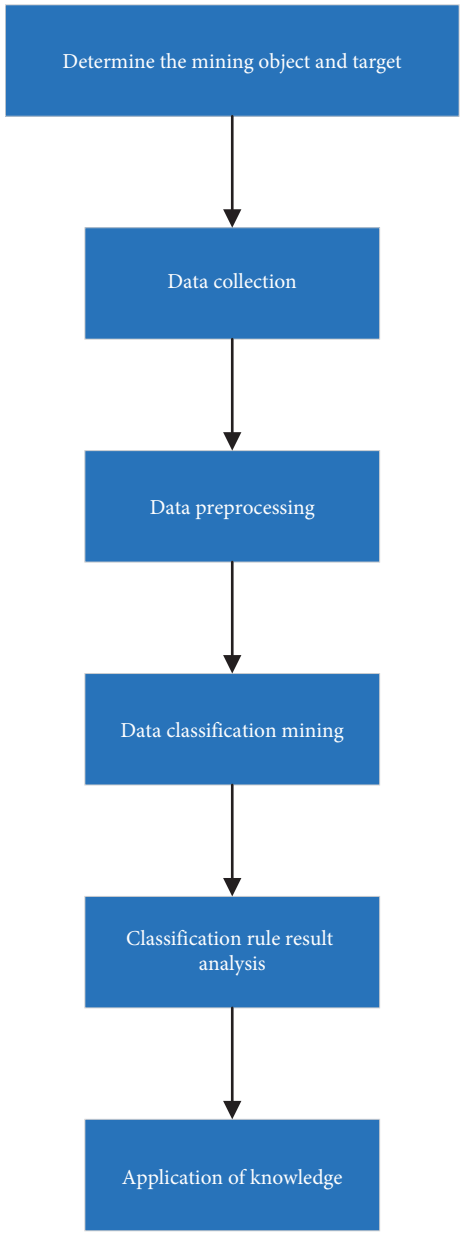

Figure 4: The implementation process of classification mining.

3.2.2. Student Survey Information. The content includes the degree of love for the major, the course, the mastery of preschool knowledge, the effect of classroom learning, and learning methods [24]. This information is mainly generated by students filling out surveys.

In the past, these tasks usually required the production of questionnaires. After students filled out the questionnaires, teachers spent a lot of time and energy collecting these data. Because this work is very tedious, it will take up a lot of time. Therefore, many teachers are reluctant to do this work, thus making it impossible to complete the very important work of mastering the basic information of students.

3.2.3. Grade Database. The score database includes students' usual homework scores and course test scores. This database is generated by teachers during the teaching process.

In this example, the method adopted by the author is: that all assignments require students to upload the written examinations to the submission system in the form of electronic documents in the prescribed format and prescribed file name [25]. The basketball movement standard test is conducted in accordance with the prescribed movements and prescribed methods, and the results are registered.

3.3. Data Pre-Processing

3.3.1. Data Integration. It is merging data from multiple data sources together. In this study, the multiple database files obtained by data collection are used to generate the basic database of student achievement analysis by database technology, as shown in Figure 5.

3.3.2. Data Cleaning. The main job of data cleaning is to fill in missing data values.

In the basic database of student achievement analysis, we see that there are some attributes that we are interested in missing attribute values. For these vacancies, data cleaning techniques can be used to fill them.

For these vacancies, data cleansing techniques can be used to fill them. There are many ways to fill in blank values for properties:

(1) Ignore tuples: this is usually done when the class label is missing or the tuple has multiple attributes with missing values.

(2) Fill in missing values manually: generally speaking, this method is time-consuming and may not work when the dataset is large and many values are missing.

(3) Fill in the missing value with a global constant: replace the missing property value with the same constant (e.g., "Unknown"). But if the missing values are all replaced with "Unknown," the mining program might mistake them for an interesting concept, since they all have the same value—"Unknown." Therefore, although the method is simple, it is not recommended here.

(4) Fill in the empty values with the average value of the attribute.

(5) Use the mean of all samples that belong to the same class as the given tuple.

(6) Fill gaps with the most probable values which can be determined by regression methods, Bayesian methods, or decision tree induction.

In this example, the method of ignoring tuples is used to delete records that have not taken the test or that have a large number of vacancies in the online survey data filled out by students. For other individual vacancies, because the total number of records is not too many, and the vacancy values are few, other individual vacancies are filled manually. The filling principle is to use other attribute values of the record as filter conditions to filter in

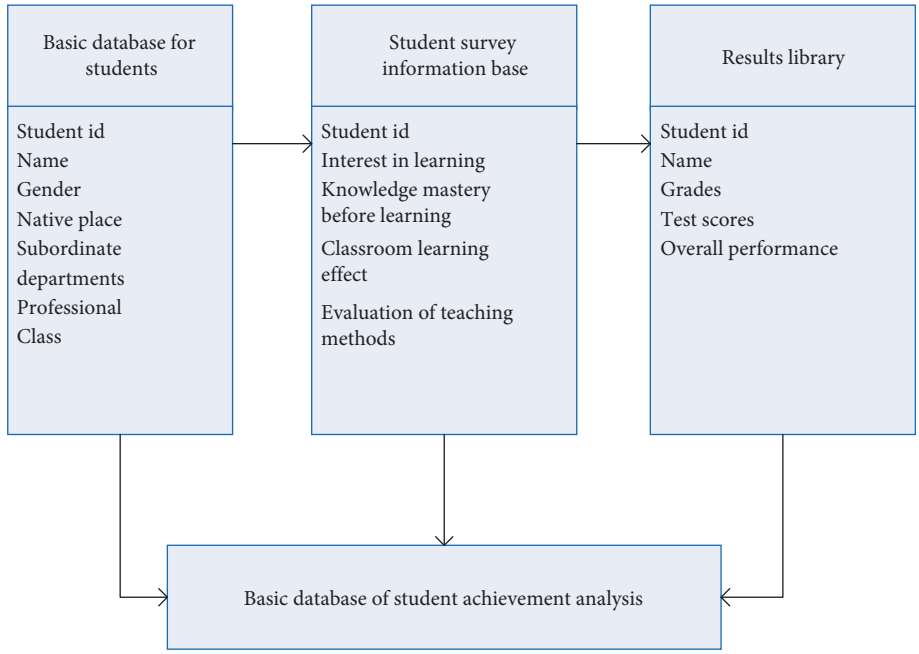

Figure 5: Establishment of the basic database for student achievement analysis.

the database. After filtering, use most of the attribute values to fill the vacancy.

3.3.3. Data Conversion. Data transformation is mainly to normalize the data.

This paper uses the concept stratification technique, Continuous-valued attributes can be converted to discrete-valued attributes (i.e., discretized). Histogram analysis is a relatively simple discretization method, which is divided into two categories: equal-width binning and equal-depth binning. Equal-width binning divides attribute values into equal parts or intervals. In equal-depth bins, the values are divided so that each part contains as many samples as possible. Here, using equal-depth binning for discretization, all values of the usual grade attribute are divided into three categories: the grades from 0 to 70 belong to "poor," 70 to 85 belong to "average," and above 85 belong to "good."

3.3.4. Data Reduction. The purpose of data reduction is to reduce the size of the data to be mined, but it will not affect (or basically not affect) the final mining results. Here, the method of dimensionality reduction is adopted, that is, the really useful feature attributes are found from the initial feature attributes to reduce the number of feature attributes or variables to be considered in data mining.

Since there are many attribute fields in the student information table, in order to facilitate the establishment of the decision tree model, this paper selects the after-school practice time, the degree of understanding of the course before learning, the classroom learning situation, and the usual practice situation. The total grade attribute is used as the basis for establishing the total grade classification decision tree model to analyze the student's learning situation.

3.4. Data Classification Mining. The purpose of classification mining is to establish a decision tree model for performance analysis.

Based on the characteristics of the dataset, in this classification mining research, in order to make the generated rules easy to understand, the decision tree method is chosen. Since the training set is not too large, you can choose the GongD3 or C4.5 algorithm for classification and mining, and here the Gong3 algorithm is selected for classification.

3.4.1. ID3 Algorithm. The most famous algorithm in the decision tree algorithm is the ID3 algorithm proposed by Quinlan. The ID3 algorithm starts with all training samples at the root node of the tree, selects an attribute to distinguish these samples, and produces a branch for each value of the attribute. Move the corresponding sample subset of branch attribute values onto the newly generated child nodes. This algorithm is applied recursively to each child node until all samples on a node are assigned to a certain class. ID3 algorithm is a greedy algorithm. It uses a top-down, divide-by-recursive approach to construct a decision tree.

Let S be a set containing s data samples, and the category attribute can take m different values, corresponding to m different categories C $(1 = 1' \ldots' m)$. Suppose s1 is the number of samples in category C_i; then, the amount of information required to classify a given data object is

$$I(s_1, s_2, \ldots, s_m) = -\sum_{i=1}^{m} p_i \log_2(p_i). \quad (1)$$

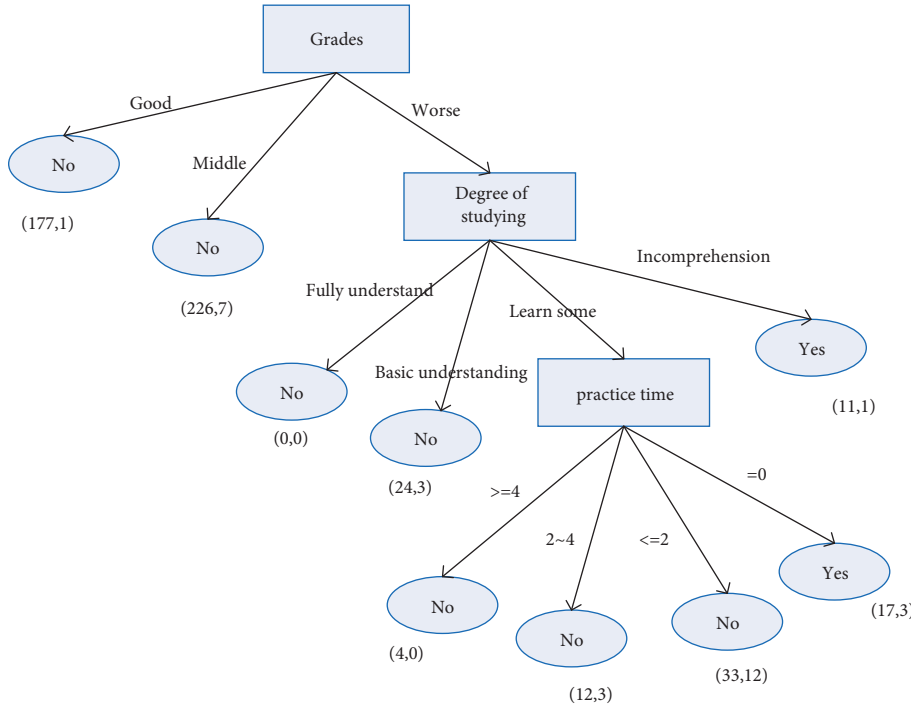

Figure 6: Decision tree of whether the grades after pruning fail.

where p_i is the probability that any data object belongs to a category C_i.

Let an attribute A take V different values $\{a_1`a_2`\ldots`a_v`\}$. Using the attribute A, the set S can be divided into v subsets $\{s_1`s_2`\ldots`s_v`\}$. Among them, s_j contains the data samples, whose attribute A in the S set takes the value of a_j. If attribute A is selected as a test attribute (i.e., attribute A is used to divide the current sample set), let s_{ij} be the number of samples belonging to category c_i in subset s_j. Then the information required to divide the current sample set by attribute A (the direct descendant) can be calculated according to the following formula:

$$E(A) = \sum_{i=1}^{v} \frac{S_{1j} + \cdots + S_{mj}}{S} I\left(S_{1j} + \cdots + S_{mj}\right). \quad (2)$$

In this way, the information gain obtained by using attribute A to divide the corresponding sample set of the current branch node is

$$\text{Gain}(A) = I(S_1, S_2 \cdots, S_m) - E(A). \quad (3)$$

The information gain of each attribute is calculated by the above formula. Select the attribute with the highest information gain as the test attribute for the given set S, create a node, mark it with this attribute, create a branch for each value of the attribute, and perform sample division.

3.4.2. Using the ID3 Algorithm to Generate a Decision Tree Model. Since there are many attribute fields in the student information table, when establishing a decision tree model for whether the grades are good or not, this paper selects the after-class computer time, the degree of understanding of the course before learning, and the classroom learning situation. The attribute field of normal work status, whether the attribute is good or not is used as a category attribute. When establishing the decision tree model of whether the grade is failed or not, the attribute of failing or not is used as the category attribute.

3.4.3. Decision Tree Pruning. When a decision tree is just established since many branches are constructed from abnormal data in the training sample set (due to noise and other reasons), the decision tree is too "blooming," which reduces the comprehensibility of the tree At the same time, it also increases the dependence of the decision tree itself on historical data, that is to say, this decision tree may be very accurate for this historical data, but the accuracy drops sharply once it is applied to new data. The condition is called overtraining. In order to make the rules contained in the obtained decision tree have a general meaning, the decision tree must be modified. The task of branch pruning is mainly to delete one or more branches and replace these branches with leaves to simplify the decision tree, so as to improve the speed of classification and recognition in the future and the ability to classify and recognition of new data.

There are usually two methods for pruning branches, which are

(l) *Prepruning Method.* The method is realized by stopping the branch generation process in advance, that is, by judging whether it is necessary to continue to divide the training sample set contained in the node on the current node. Once the branch is stopped, the current node becomes a leaf node. The leaf node may contain multiple training samples of

different categories. Since this pruning is done before branching, it is called prepruning.

(2) *Postpruning Method*. This approach addresses the problem of overtraining from another angle. On the basis of allowing the decision tree to grow most fully, it cuts off those leaf nodes or branches that are not generally represented in the decision tree according to certain rules. After pruning, the pruned branch node becomes a leaf node, and it is marked as the category with the largest number of categories in the samples it contains.

Prepruning requires more computation time, but the resulting decision tree is more reliable. In this paper, the method of postpruning is adopted. First, the error rate of a fully grown decision tree is calculated, and a maximum allowable error rate is specified by the user. When the pruning reaches a certain depth and the calculated error rate is higher than the maximum allowable value, stop pruning immediately, otherwise, continue pruning. Figure 6 is a decision tree for the classification of failing grades after pruning.

4. Conclusion

Under the background of the increasing development of science and technology in our country, the combination of science and technology with higher education, the application, and research of intelligent information systems, is more conducive to promoting the modernization of colleges and universities. Through the application of data mining technology in the quality evaluation of basketball teaching in colleges and universities, the limitations of traditional basketball teaching management can be effectively improved, and various unfavorable factors that hinder teaching management can be found in time. In the school's teaching, the use of data mining technology in basketball teaching can reasonably collect, analyze and summarize the relevant data of colleges and universities, and then find and solve problems in time, which not only reduces teaching accidents but also makes all aspects of colleges and universities. Management Metropolis eliminates drawbacks, coordinates the overall construction of the school, comprehensively cultivates high-quality talents and innovative ability levels, and promotes the construction of modern teaching in colleges and universities on the basis of improving the quality of teaching, laying a solid precondition for cultivating high-quality talents, and for the realization of lay the foundation for the construction of world-class universities and first-class disciplines [18–26].

Data Availability

The dataset can be accessed upon request.

Conflicts of Interest

The authors declare that there are no conflicts of interest.

References

[1] Y. Fan and J. Fan, "Construction of OBE concept autonomous learning mode in university teaching based on the Internet [J]," *Journal of Cases on Information Technology*, vol. 24, no. 5, 2022.

[2] H. Shen, "Discussion on the professional construction of college teaching management team[J]," *Learning & Education*, vol. 10, no. 4, 2021.

[3] k. y. Kim, h. r. Min, m. w. Nam, j. w. Woo, and ja. Kim, "A study on the current status and needs assessment of the center for teaching and learning in the universit," *Korean Educational Research Association*, vol. 56, no. 3, pp. 227–257, 2018.

[4] J. V. Iyengar, "The potential of computer assisted instruction in college teaching[J]," *Journal of Computer Information Systems*, vol. 36, no. 4, 2016.

[5] M. C. Massi, F. Ieva, and E. Lettieri, "Data mining application to healthcare fraud detection: a two-step unsupervised clustering method for outlier detection with administrative databases," *BMC Medical Informatics and Decision Making*, vol. 20, no. 1, p. 160, 2020.

[6] Information Technology, "Data Mining; Data from iran university of science and technology advance knowledge in data mining (application of data mining techniques for the investigation of track geometry and stiffness variation)[J]," *Information Technology Newsweekly*, 2020.

[7] Artificial Intelligence, "Studies from china medical university describe new findings in artificial intelligence (research on data mining application of orthopedic rehabilitation information for smart medical)[J]," *Journal of Robotics & Machine Learning*, 2020.

[8] N. Saraf Sandhu, A. K Upadhyay, and S. Sharma, "Data mining application in process control of smart material manufacturing[J]," *International Journal of Recent Technology and Engineering*, vol. 8, no. 5, 2020.

[9] J. Wessel, A. Turetskyy, O. Wojahn, C. Herrmann, and S. Thiede, "Tracking and tracing for data mining application in the lithium-ion battery production[J]," *Procedia CIRP*, vol. 93, 2020.

[10] Information Technology, "Data Mining; Reports from University of Petra Describe Recent Advances in Data Mining (Application of Data Mining Algorithms for Improving Stress Prediction of Automobile Drivers: A Case Study in Jordan) [J]," *News of Science*, 2019.

[11] S. Koteeswaran, N. Malarvizhi, E. Kannan, S. Sasikala, and S. Geetha, "Data mining application on aviation accident data for predicting topmost causes for accidents," *Cluster Computing*, vol. 22, no. S5, pp. 11379–11399, 2019.

[12] Information Technology, "Data Mining; Research Conducted at Technical University Has provided New Information about Data Mining (Data Mining Application in Assessment of Weather-Based Influent Scenarios for a Wwtp: Getting the Most Out of Plant Historical Data)[J]," *Computers, Networks & Communications*, 2019.

[13] G. Venkatesh, M. Lawanyashri, and V. Sai Saraswathi, "DATA mining application towards adverse effects of anti-diabetic drugs[J]," *International Journal of Innovative Technology and Exploring Engineering*, vol. 8, no. 7, 2019.

[14] Information Technology, "Data Mining; Researchers from Shandong University of Science and Technology Report on Findings in Data Mining (Application of Data Mining in an Intelligent Early Warning System for Rock Bursts)[J]," *Information Technology Newsweekly*, 2019.

[15] S. Padma Priya and D. Usha, "Data mining application for credit card fraud detection system[J]," *International Journal of Managment, IT and Engineering*, vol. 8, no. 11, 2018.
[16] J. Reynaldo and D. B. Tonara, "Data Mining Application Using Association Rule Mining ECLAT Algorithm Based on SPMF[J]," *MATEC Web of Conferences*, p. 164, 2018.
[17] H. Huanxiang and N. Jan, "An English online homework tutoring system supported by Internet database[J]," *Journal of Mathematics*, vol. 2021, Article ID 5960185, 12 pages, 2021.
[18] Y.-C. Wang, J.-J. Tsai, and X. Chen, "Data mining: application of EGARCH dynamic model on the volatility of high-frequency exchange rate data[J]," *Journal of Physics: Conference Series*, vol. 2021, no. 1, 1941 pages, 2021.
[19] S. Zhang, J. Chen, W. Zhang, Q. Xu, and J. Shi, "Education data mining application for predicting students' achievements of Portuguese using ensemble model," *Science Journal of Education*, vol. 9, no. 2, p. 58, 2021.
[20] Ka R. Grimes, S. Park, A. McClelland et al., "Effectiveness of a numeracy intelligent tutoring system in kindergarten: a conceptual replication," *Journal of Numerical Cognition*, vol. 7, no. 3, pp. 388–410, 2021.
[21] P. Sharma and M. Harkishan, "Designing an intelligent tutoring system for computer programing in the pacific[J]," *Education and Information Technologies*, vol. 27, 2022 (prepublish).
[22] O. Sychev, N. Penskoy, A. Anikin, M. Denisov, and A. Prokudin, "Improving comprehension: intelligent tutoring system explaining the domain rules when students break them," *Education Sciences*, vol. 11, no. 11, p. 719, 2021.
[23] T. Xu, X. Wang, J. Wang, and Y. Zhou, "From textbook to teacher: an adaptive intelligent tutoring system based on BCI.[J]," in *Proceedings of the Annual International Conference of the IEEE Engineering in Medicine and Biology Society*, p. 2021, IEEE Engineering in Medicine and Biology Society, Glasgow, UK, 2021.
[24] C. Uddagiri and K. Neelu, "An intelligent tutoring system for new student model using fuzzy soft set-based hybrid optimization algorithm[J]," *Soft Computing*, vol. 25, no. 24, 2021.
[25] D. Shin, "Teaching mathematics integrating intelligent tutoring systems: investigating prospective teachers' concerns and TPACK[J]," *International Journal of Science and Mathematics Education*, (prepublish), 2021.
[26] S. Qian, "Design and implementation of computer aided instruction system based on Web[J]," *Insight - Information*, vol. 3, no. 3, 2021.

Hindawi
Scientific Programming
Volume 2022, Article ID 4189148, 7 pages
https://doi.org/10.1155/2022/4189148

Research Article

An Improved Privacy Protection Algorithm for Multimodal Data Fusion

Z. F. Chen,[1] **J. J. Shuai**,[1] **F. J. Tian**,[2] **W. Y. Li**,[1] **S. H. Zang**,[1] **and X. Z. Zhang**[1]

[1]*School of Computer Science and Technology, Changchun University of Science and Technology, Changchun 130022, China*
[2]*Mandarin Training and Testing Center of Jilin Province, Changchun 130022, China*

Correspondence should be addressed to Z. F. Chen; chenzhanfang@cust.edu.cn

Received 30 May 2022; Revised 8 July 2022; Accepted 25 July 2022; Published 23 August 2022

Academic Editor: Lianhui Li

With the rapid development of Internet technology, the use and sharing of data have brought great opportunities and challenges to mankind. On the one hand, the development of data sharing and analysis technology has promoted the improvement of economic and social benefits. On the other hand, protecting private information has become an urgent issue in the Internet era. In addition, the amount and type of information data are also increasing. At present, most algorithms can only encrypt a single type of small-scale data, which cannot meet the current data environment. Therefore, it is very necessary to study the privacy protection algorithm of multimodal data fusion. To improve the security of privacy protection algorithm, combined with the idea of multimode, this paper combines the improved traditional spatial steganography algorithm LSB matching method and the improved traditional transform domain steganography algorithm DCT with AES encryption algorithm after modifying the S-box and then combines it with image stitching technology, so as to realize a safe and reliable privacy protection algorithm of multimode information fusion. The algorithm completes the hidden communication of private information, which not only ensures that the receiver can accurately recover private information in the process of information transmission but also greatly improves the security of private information transmission.

1. Introduction

With the rapid development of Internet technology, the use and sharing of data have brought great opportunities and challenges to mankind. Nowadays, people pay more and more attention to their private information. The college entrance examination registration and voluntary filling system provide services to more than 10 million candidates across the country. These candidates' personal information is stored in the college entrance examination registration and voluntary filling system; the national social security system is more about the pension, medical care, employment, and other information of hundreds of millions of people across the country. The development of data sharing and analysis technology has promoted the improvement of economic and social benefits. At the same time, the protection of private information has become an urgent problem in the Internet era. At present, the amount of information is increasing, and there are more and more types. Most algorithms can only encrypt a single type of small-scale data, which cannot meet the current data environment. Therefore, it is necessary to study the privacy protection algorithm of multimodal data fusion.

In recent years, pin academics have achieved a series of results on traditional modified/embedded information hiding. Literature [1] proposed a data hiding/protection strategy combining PVD (pixel value difference), LSB, and MPE (modification of prediction error) to improve steganographic capacity and resistance to RS steganalysis. The literature [2] uses MSB (most significant bit) to select the best embedding point and combines the AES encryption algorithm to embed the ciphertext in the lowest significant bit of that point. Literature [3] implements a digital watermarking technique based on hybrid multibit multiplication rules by secret key control from the DWT domain.

Meanwhile, the concept of reversible data hiding (RDH) has been proposed from the perspective of whether the original carrier image can be recovered. Reversible data hiding refers to embedding secret information into the "reversible domain" of the original carrier image so that the image can be recovered without distortion after extracting the secret information. This technique is widely used in military, medical, and legal forensic fields. Literature [4] proposes embeddable pixel pairs (EPP, embeddable pixels pairs) as the embedding unit of secret information and achieves reversible information hiding through secret bit extraction and carrier recovery. Although the focus of reversible information hiding is on the lossless recovery of the carrier, the encryption process also inevitably makes modifications to the original carrier.

Zero-hiding techniques guide the change of steganography from embedding to nonembedding. The multilayer partially homomorphic textual information steganography based on zero-hiding proposed in literature [5] achieves a better balance in terms of robustness, security, and capacity. However, in the image domain, zero-hiding follows that although it achieves no modification of the image carrier, it generates other necessary information as the secret key for decoding by the receiver, such as associated documents and secret message extraction files, thus causing additional channel occupation.

At present, the traditional "coding/mapping" approach is more mature, and the evaluation scheme has been established by the academic community in recent years. In [6], the image grid is divided and the image SIFT features are combined with hash sequences to quantize and encode the feature sequences and build an image library, which can be used for indexing. The literature [7] adopts the idea of carrier-free information hiding and uses the brightness features of the material molecular structure for encoding to establish the mapping relationship between binary sequences and image carriers. The literature [8] focuses on image global features, quantization coding the gray gradient coeval matrix to achieve carrier-free information hiding and constructing a high-secure satellite communication model. The classical transformation methods in information hiding are discrete cosine transform (DCT), discrete wavelet transform (DWT) [9], and discrete Fourier transform (DFT) [10]. The literature [11] proposes carrier-free information hiding based on DCT (discrete cosine transform) and LDA (latent Dirichlet allocation, document topic generation model) models.

In summary, information hiding algorithms have been progressing in the process of exploration, and different steganography methods have different focuses on performance evaluation. However, on the issue of "how to hide," many existing steganographic methods always revolve around the three existing frameworks, while combining various technologies to jointly promote the development of information hiding.

Based on the traditional steganography embedding algorithm, this paper improves the spatial domain steganography algorithm and transforms the domain steganography algorithm to improve the embedding capacity and antisteganalysis ability of the algorithm. Combined with image stitching technology, the mapping capacity of the noncarrier information hiding algorithm is improved, and the large capacity noncarrier information hiding algorithm is used to hide the key. Joint information encryption method is to achieve multimodal data fusion privacy protection system. The system improves the diversity and security of the system by using the key control steganography algorithm.

2. Multimodal Data Fusion Privacy Protection Algorithm

2.1. Improved Spatial Domain Steganography Algorithm. However, the disadvantage of the traditional LSB algorithm is that when the embedded message is large, it takes a long time, and it can only deal with simple stream format files. So, in this paper, based on the traditional LSB matching algorithm, according to the texture characteristics of the image, the texture complex region is selected to embed the private information into the carrier image with complementary embedding rules. The embedding capacity of the traditional LSB matching algorithm is improved. The traditional LSB matching algorithm is to embed secret information into gray images randomly. At present, color images are generally used in network transmission. Therefore, this paper first divides them into RGB layers, selects regions with complex image textures to embed private information, and embeds them into different color layers in different regions of the carrier image in a complementary, so as to improve the embedding capacity and undetectability of the spatial domain steganography algorithm.

2.1.1. RGB Layered. The color image has RGB three color channels, and the three-channel component diagram is different. When the secret image is hidden in different layers, it is different from the original carrier image. The secret image is hidden in the image carrier of each layer of R, G, and B. In this paper, the R channel and G channel are used as complementary channels to embed private information, which can achieve better results in this respect and better resists statistical analysis. In this way, embedding private information in two layers can improve the embedding capacity and reduce the change of the statistical characteristics of the original carrier image caused by private information embedding, which improves the capacity and undetectability of information hiding.

2.1.2. Image Grayscale Cooccurrence Matrix. The image gray level cooccurrence matrix can be used to describe the texture features of the image, and the ciphertext is embedded into the complex area of the texture features of the image. The effective steganography of the ciphertext is completed by using the redundant space of the image [12].

In this paper, four parameters (energy, entropy, dissimilarity, and correlation) are derived to describe the texture characteristics of the image gray level cooccurrence matrix in image texture analysis.

$$\text{Energy} = \sum_{i=0}^{L-1}\sum_{j=0}^{L-1} P(i,j)^2, \tag{1}$$

$$\text{Entropy} = \sum_{i=0}^{L-1}\sum_{j=0}^{L-1} P(i,j)\log_2 P(i,j), \tag{2}$$

$$\text{Inertia} = \sum_{i=0}^{L-1}\sum_{j=0}^{L-1} |i-j| p(i,j), \tag{3}$$

$$\text{Coherence} = \frac{\sum_{i=0}^{L-1}\sum_{j=0}^{L-1}(i+1)(j+1)p(i,j) - \mu_1\mu_2}{\delta_1\delta_2}. \tag{4}$$

These four features respectively reflect the characteristics of the gray distribution of the image, including uniformity, the thickness of the capacity texture of the carrier image, and the similarity of the elements in the matrix. The matrix is formed by these four features, $T\ (4) = \{\text{Energy, Entropy, Inertia, Coherence}\}$. Then, the embedding region is determined by selecting parameters.

2.1.3. Embedding of Secret Information. The spatial domain steganography algorithm first extracts the texturally complex subblocks of the original color carrier image. The ciphertext is divided into two groups and the carrier image subblock texture features are used to obtain the embedding position. A set of ciphertext is embedded in the R channel in +1 form and a set of ciphertext is embedded in the G channel in −1 form, and the channels are combined to obtain a color image containing the cipher.

2.2. Improved Transform Domain Steganography Algorithm. Based on the traditional modified message hiding transform domain steganography algorithm, this paper divides the color image into three channels of RGB for embedding the ciphertext to increase the embedding capacity. The ciphertext is grouped into two bits and embedded into the more stable intermediate frequency region after the DCT transform. Because digital images are DCT-transformed, the low and medium frequency signals have the highest energy, but the private information embedded in the low and medium frequency signals can easily be observed directly by the human eye; in the high-frequency part, the energy is low and unstable, so the intermediate frequency region after DCT transform is selected for private information embedding. This region can better meet the imperceptibility and robustness of the steganography algorithm.

2.3. Large Capacity Carrier-Free Information Hiding Algorithm. The traditional mapped carrier-free information hiding algorithm has the problem of low steganographic capacity. In this paper, multiple mapped images are reorganized and stitched into one image using image stitching technology to improve the steganographic capacity of the carrier-free information hiding algorithm and realize the secure mapped steganographic writing of keys and some private information.

By using the features of the image for binary encoding, a binary sequence can be derived without any modification to the image. In this way, the image can form a mapping relationship with the corresponding private information. This mapping relationship requires a one-to-one correspondence between the private information and the images in the image library. That is, if the length of the binary sequence of private messages is n, the image library must have at least 2^n images. The value of n has to be chosen appropriately for the possibility of implementation and the security of mapping hidden information.

The steganographic capacity of carrier-less information mapping is low, and image stitching technology is used to improve the steganographic capacity of the algorithm. Multiple images are similarly spliced to form a complete key image and sent to the receiver. Taking the 2×2 modes as an example, the splicing combination process is shown in Figure 1.

2.4. Multimodal Data Fusion Privacy Protection Algorithm Design. The multimodal data fusion privacy protection algorithm uses two images to steganography the ciphertext (private information encrypted to form the ciphertext) and the key, one using a spatial domain steganography algorithm or a transform domain steganography algorithm to steganography the ciphertext, with the key controlling the choice of the specific algorithm, and the other using a carrier-free information hiding algorithm to steganography the key in a mapped fashion. This design can ensure the safe transmission of private information so that any image cannot be decoded after being illegally intercepted. Even if the two images are intercepted, the interceptor does not know the operation mode of the system and cannot crack the contains secret images.

The information transmitted by the multimodal data fusion steganography system consists of two parts: the ciphered image and the key-mapped image. Due to the long length of the AES encryption key, a 6×6 stitching mode is used and the private information is encrypted by the message encryption technique (AES encryption algorithm after modifying the S-box), and then the ciphertext is embedded in the chosen ciphertext steganography algorithm, where an improved spatial domain steganography algorithm and a transform domain steganography algorithm can be chosen to form the ciphered image. Keymapping image mainly implements mapped hiding of the key; the key consists of two parts, $\text{key} = \{\text{keychoose, keyencryption}\}$; these two parts are, in order, the ciphertext steganography flag bit and the encryption algorithm key. The coverless information hiding technique uses a 6×6 pattern to stitch the submap into a complete carrier image to form a key mapping image. After receiving the key image, the receiver splits and then deciphers the type of ciphertext steganography algorithm used and the key of the encryption algorithm, respectively. The effect of the secret image is shown in Figure 2. The cryptographic image and the key mapped

Figure 1: Splicing assembly process.

(a) (b)

Figure 2: (a) Secret images. (b) Keymapping images.

image are transmitted, and then the receiver gets the private information in a specific way.

As shown in Figure 2, after receiving the key-mapped image and the cryptographic image, the receiver needs to first segment the key-mapped image according to the rules to obtain 36 subimages. The subgraphs are decrypted separately in mapped form, and the decrypted results are combined in stitching order to obtain the key for the complete encryption algorithm and to determine the type of steganography algorithm using the first-bit flag bit, with the spatial domain steganography selected if the first bit is 0, and the transform domain steganography is selected if it is 1. The ciphertext is decrypted by the corresponding steganographic algorithm on the cryptographic image, and the ciphertext is decrypted by the encryption algorithm key obtained from the key-mapped image to obtain the plaintext.

The process of implementing the multimodal data fusion privacy protection algorithm is shown in Figure 3, where the private information and the key of the encryption algorithm are first encrypted to obtain the ciphertext. The spatial domain steganography algorithm or transform domain steganography algorithm is selected to embed the ciphertext, and the modified embedding algorithm is selected to embed the ciphertext. The secret key containing the type symbol of the ciphertext steganography algorithm and the information encryption key is obtained. The secret key is mapped by the noncarrier information hiding mapping algorithm, and the encrypted image and the key mapping image are generated.

When decrypting, the key mapping image is first segmented and then decrypted by the carrier-free information hiding algorithm. The codes corresponding to the 36 subgraphs are decoded according to the carrier-free information hiding technique; the codes are combined and processed to obtain the key of the encryption algorithm and the ciphertext steganography algorithm type flag. The cryptographic image is then decrypted according to a determined steganographic algorithm to produce the ciphertext. Finally, based on the previously derived key, the private message is decrypted by an encryption algorithm.

3. Algorithm Implementation

3.1. System Implementation. The multimodal data fusion privacy protection algorithm consists of several application forms, the core of which is the data fusion steganography. Click on the image fusion steganography, there are two links for the sender and the receiver, and select the sender. There are three inputs on the transmitter side: the plaintext before processing, the encryption key, and the carrier image selection path. One input, the selection of the ciphertext steganography algorithm, is used to implement the selection of the spatial domain steganography algorithm or the transform domain steganography algorithm. There are 3 output items: the encrypted ciphertext, the mapped image 1, and the encrypted image 2. There are six additional function buttons: Encryption, Key Mapping, Browse, Ciphertext Steganography, Save, and Send. A brief description of each function button is given follows (Figure 4):

(1) Encryption: encryption of the input plaintext and a key of a specific length to obtain the ciphertext using the AES encryption algorithm with a modified *S*-box;

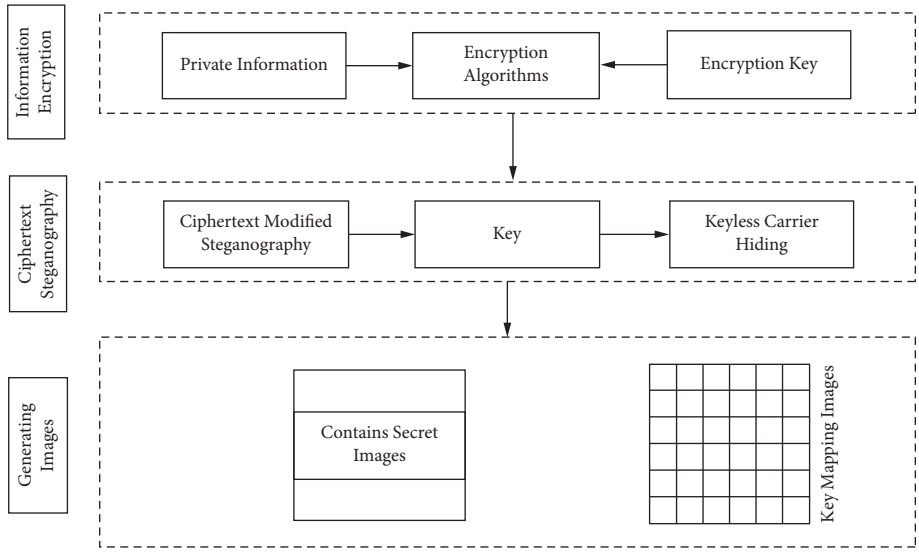

Figure 3: The encryption process of multimodal data fusion privacy protection algorithm.

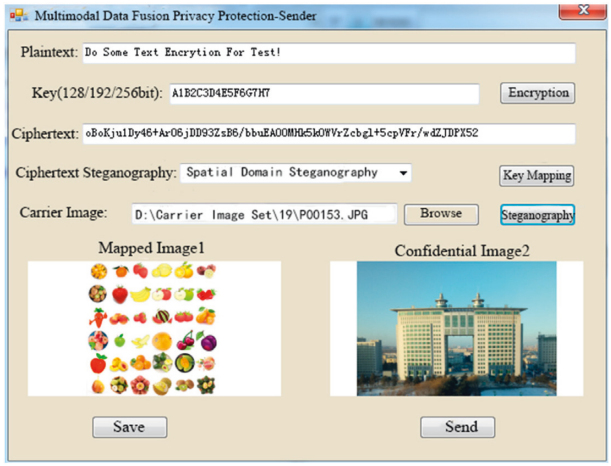

Figure 4: Sender-side steganography-spatial domain steganography.

(2) Key Mapping: based on the chosen ciphertext steganography algorithm and the encryption algorithm key, a carrier-free information hiding mapping steganography is performed to obtain mapped image 1;

(3) Browse: jump to the image selection page and select the appropriate carrier image for ciphertext steganography;

(4) Ciphertext steganography: the ciphertext obtained in (1) is steganographically written to the carrier image in (3) according to the selected ciphertext steganography method, and the sender selects the spatial domain steganography algorithm to complete the steganographic effect as shown in Figure 4;

(5) Save: jump to the image, save the page, and select the save path option to save the mapped image 1 and the encrypted image 2 locally;

(6) Send: jump to the send page, fill in the recipient's details, and transmit two coded images to the sender.

The multimodal data fusion privacy-preserving-receiver side is shown in Figure 5, with a total of one input item being the path selection of the image containing the secret. The three output items are the mapped image 1, the coded image 2, and the plaintext (private message). Five function buttons are included, namely, Browse, Get Mapped Image 1, Get Confidential Image 2, Decrypt, and Clear buttons. A brief description of each function button is given as follows:

(1) Browse: it obtains the path to the folder containing the key-mapped image and the ciphertext steganography image;

(2) Get Mapped Image 1: the system reads the key mapping image in the specified folder and segments the key mapping image, storing the 36 subimages in the order in the program directory;

(3) Obtaining a Confidential Image 2: the system reads the ciphertext steganography image under the specified folder and displays it in the system interface;

(4) Declassify: the subgraph obtained from (2) is decrypted by the carrier-free information hiding algorithm mapping, combined, and processed to obtain the ciphertext steganography flag and the encryption algorithm key, the corresponding steganography decryption algorithm is performed on the carrier image 2 to obtain the ciphertext, and the ciphertext is decrypted according to the AES decryption algorithm after modifying the S-box, resulting in the plaintext, and displayed;

(5) Clear: it clears the cryptographic image selection, the mapped image, the encrypted image, and the plaintext and deletes the split subimage of the key-mapped image stored in the program directory, clears the system cache image, and restores the receiver page to the initial page.

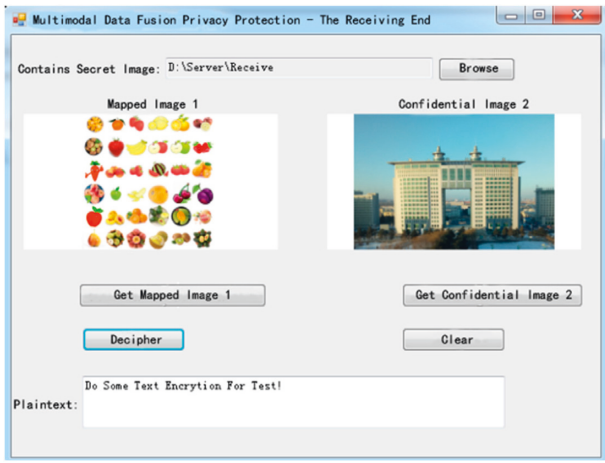

Figure 5: Decryption completion page on the receiving end.

As can be seen from the above, this system implements a multimodal data fusion privacy protection algorithm, which encrypts private information by modifying the AES encryption algorithm after the S-box and completes the steganography of the ciphertext and key after the information hiding algorithm (improved spatial domain steganography, improved transform domain steganography, and carrier-free information hiding algorithm). The receiver decrypts the key and the ciphertext according to the two steganographic images in turn and then performs the message decryption operation to recover the private message accurately.

3.2. Non-detectability Analysis. Multimodal data fusion privacy protection algorithms are implemented by three types of algorithms: information encryption algorithms, modified steganography algorithms (improved spatial domain steganography and improved transform domain steganography), and high-capacity carrier-free information hiding algorithms. The proper fusion of these algorithms makes the multimodal data fusion privacy protection algorithm highly secure. The following analysis addresses the undetectability of key-mapped images and ciphertext images in the multimodal data fusion privacy protection algorithm.

The undetectability of the multimodal data fusion privacy protection algorithm is objectively evaluated from the perspective of mathematical-statistical analysis. The key-mapped images before and after steganography are evaluated using root mean square error and peak signal-to-noise ratio, with the root mean square error calculated as shown in equation (5) and the peak signal-to-noise ratio shown in (6).

$$\mathrm{MSE} = \frac{\sum_{x=0}^{N_x} \sum_{y=0}^{N_y - 1} [S'(x,y) - S(x,y)]^2}{N_x \times N_y}, \tag{5}$$

$$\begin{aligned} \mathrm{PSNR} &= 10\lg\left(\frac{(\max S(s,y))^2}{\mathrm{MSE}}\right) \\ &= 20\lg\left(\frac{\max S(s,y)}{\mathrm{MSE}}\right), \end{aligned} \tag{6}$$

Table 1: Test results.

Spatial domain steganography ratio	Transformation field steganography ratio	JSTEG detection ratio
0.1	0.1	0
0.2	0.2	0
0.3	0.3	0
0.4	0.4	0
0.5	0.5	0

where S (x, y) is the gray value of the sampled points of the key-mapped images and S (x, y) is the gray value of the sampled points of the stitched original images. The smaller the MSE value, the smaller the image distinction, and similarly, the larger the PSNR value, the smaller the image distinction. The key-mapped images in this paper are not different from the original images, and the root mean square error and peak signal-to-noise ratio are calculated as shown in the following equations:

$$\mathrm{MSE} = 0, \tag{7}$$

$$\mathrm{PSNR} = \infty. \tag{8}$$

Based on the mathematical-statistical analysis, it can be concluded that the key mapping image of the multimodal data fusion privacy protection algorithm is completely undetectable; in other words, none of the existing steganalysis algorithms can detect the key information in the key mapping image.

The JSTEG method was used to detect the embedding rate of cryptographic images and to verify the undetectability of the steganography algorithm. The detection of the 600×400 pixel cipher laden image was performed using the JSTEG method, which is an information hiding algorithm based on JPEG images, with the steganography ratio incremented from 0.1 to 0.5, and the detection results were obtained as shown in Table 1.

From Table 1, it can be concluded that the detection result of the JSTEG algorithm is 0 for both spatial domain steganography algorithm and transform domain steganography algorithm, JSTEG cannot effectively detect the ciphertext steganography method used in this paper, and ciphertext steganography with multimodal data fusion privacy protection has good effect in resisting dedicated steganography analysis algorithm.

4. Conclusions

This paper designs and implements a multimodal data fusion privacy protection algorithm based on image steganography, joint information encryption algorithms, steganography of encrypted ciphertext by two modified embedding steganography algorithms (spatial domain steganography and transform domain steganography), and mapped steganography of key according to the carrier-free information hiding algorithm. The algorithm has proved through experiments to be a great guarantee of the security of private information.

Future attempts can be made to combine it with deep learning of artificial intelligence technology to further improve the efficiency and algorithmic diversity of the algorithm. In the mentioned image fusion encryption, this paper has not considered the fusion in multiple modes, which needs further research.

Data Availability

The data used to support the findings of this study are available from the corresponding author upon request.

Conflicts of Interest

The authors declare that there are no conflicts of interest regarding the publication of this paper.

Acknowledgments

This work was supported by the Science and Technology Research Program of Jilin Province, China (Nos. 20190201267JC and 20200703003ZP).

References

[1] M. Hussain, A. W. A. Wahab, N. Javed, and K. H. Jung, "Recursive information hiding scheme through LSB,PVD shift, and MPE," *IETE Technical Review*, vol. 35, no. 1, 2018.

[2] Z. Sultana, F. Jannat, S. S. Saumik, N. Roy, N. K. Datta, and M. N. Islam, "A new approach to hide data in color image using LSB steganography technique," in *Proceedings of the IEEE International Conference on Electrical Information & Communication Technology*, Khulna, Bangladesh, December 2017.

[3] J. B. Wu, X. X. Fei, and N. F. Wang, "Research on image zero hiding algorithm based on chaotic sequence and DCT transform," *Electronic Measurement Technology*, vol. 40, no. 5, pp. 174–179, 2017.

[4] J. L. Wang, X. Sun, and X. Q. Feng, "Adaptive reversible information hiding using pixel permutation," *Chinese Journal of Graphical Graphics*, vol. 23, no. 1, pp. 1–8, 2018.

[5] N. Naqvi, A. T. Abbasi, R. Hussain, M. A. Khan, and B. Ahmad, "Multilayer partially homomorphic encryption text steganography (MLPHE-TS):A zero steganography approach," *Wireless Personal Communications*, vol. 103, 2018.

[6] S. Zheng, L. Wang, B. Ling, and D. Hu, "Coverless information hiding based on robust image hashing," *Intelligent Computing Methodologies*, Springer, vol. 10363, pp. 536–547, Heidelberg, Germany, 2017.

[7] Y. Cao, Z. Zhou, X. Sun, and C. Gao, "Coverless information hiding based on the molecular structure images of material," *Computers, Materials & Continua*, vol. 54, no. 2, pp. 197–207, 2018.

[8] J. B. Wu, Y. W. Liu, Z. W. Kang, S. RahbarJia, and Y. Jia, "A coverless information hiding algorithm based on grayscale gradient Co-occurrence matrix," *IETE Technical Review*, vol. 35, no. 1, pp. 23–33, 2018.

[9] S. Roy and A. K. Pal, "A hybrid domain color image watermarking based on DWT-SVD," *Iranian Journal of Science and Technology, Transactions of Electrical Engineering*, vol. 43, no. 2, pp. 201–217, 2019.

[10] X. T. Zhang, Q. T. Su, Z. H. Yuvan, and D. Liu, "An efficient blind color image watermarking algorithm in spatial domain combining discrete Fourier transform," *Optik-International Journal for Light and Electron Optics*, vol. 219, no. 2, Article ID 165272, 2020.

[11] X. Zhang, F. Peng, and M. Long, "Robust coverless image steganography based on DCT and LDA topic classification," *IEEE Transactions on Multimedia*, vol. 20, no. 12, pp. 3223–3238, 2018.

[12] T. D. Denemark, M. Boroumand, and J. Fridrich, "Steganalysis features for content-adaptive JPEG stegano- graphy," *IEEE Transactions on Information Forensics and Security*, vol. 11, 2016.

Hindawi
Scientific Programming
Volume 2022, Article ID 2183093, 8 pages
https://doi.org/10.1155/2022/2183093

Research Article

Cost Management and Forecasting Method for the Whole Life Cycle of Water Conservancy Projects Based on Multiple Regression Analysis

Sha Li

College of Hydraulic Engineering, Zhejiang Tongji Vocational College of Science and Technology, Hangzhou, Zhejiang 311231, China

Correspondence should be addressed to Sha Li; z20220070902@zjtongji.edu.cn

Received 3 June 2022; Revised 4 July 2022; Accepted 12 July 2022; Published 23 August 2022

Academic Editor: Lianhui Li

The water conservancy project is an important livelihood engineering project, and it is also an important factor to ensure the living water supply, power supply stability, and economic development of the regional population. Therefore, the management of water conservancy projects is particularly important. The core management content is cost control, which can maximize the benefits of the project and avoid the waste of investors' funds. This study studies the whole process control of water conservancy project cost, explains the problems existing in the current domestic water conservancy project cost control, and finally expounds on the whole process control measures, in order to provide a reference for related work. In this study, SPSS software is mainly used to establish a multiple linear regression model to analyze the influencing factors of water conservancy projects. Through the method of model solving, the relationship between hydraulic engineering and various variables is analyzed, and the multi-linear verification is improved, so as to further test the model, optimize the model, and finally manage and predict it accurately.

1. Introduction

In recent years, with the rapid development of my country's water conservancy project construction. Due to the long construction period of water conservancy projects [1], large investment, and many cooperative departments, it is greatly affected by natural resources, topography, geology, hydrometeorological conditions, as well as local economic development level, transportation, and other resource market conditions [2, 3]. Personality is very prominent. In terms of pricing, water conservancy projects have the characteristics of a single piece, multiple times, diversity of methods, and complexity of basis [4, 5]. These characteristics determine the unique problems in the cost management of water conservancy projects that are different from other construction projects [6, 7].

At present, the cost management mode of water conservancy projects in my country is divided into stages and units, that is, the cost control in the project decision-making and design stage is completed by the cost professionals of the design unit, and the cost control in the contracting stage is carried out by the project owner who can bid by himself or can bid. The cost consulting unit with the agency qualification is completed, the cost control in the construction phase is completed by the cost professionals of the supervision unit, and the cost control in the completion and post-evaluation phases is completed by the cost consulting unit with the qualification for a price review. Project decision-making and design stage are important stages of cost management. Therefore, doing a good job in the management of water conservancy projects can ensure the daily life of the people [8], and the requirements for project cost management are the highest.

Project cost is an important part of project construction. A scientific and reasonable project cost [9, 10] plays an important role in the construction of the entire project. The construction of a project, obtaining a standard and reasonable project cost, has already made a good start and can

invest in the preliminary project that has a good investment standard. The economic expenditure can be kept within a controllable range so that the construction of the project can be completed quickly and well. In the construction of water conservancy projects, the cost management of the whole process can not only measure the investment in the life cycle of the construction project but also grasp the investment as a whole [11]. In the process of project management, the influencing factors of project cost mainly include financing methods, construction plans and exploration, and other factors [12, 13]. The analysis of all quotation management in the process of water conservancy project construction can make water conservancy projects in the process of construction [14]. As a major construction project in modern society, the water conservancy project needs to pay enough attention to the cost management of the whole process, so as to ensure that the water conservancy project construction achieves the rationalization of capital utilization in the whole process of construction. It also needs to promote the completion of high-quality and high-efficiency water conservancy project construction, and improve the benefits of project construction [15, 16].

The necessity of investment control in the whole life cycle of water conservancy projects: The reason for constructing the investment control mechanism for the whole life cycle of water conservancy projects is to improve the corresponding work at each stage and link the construction system, and effectively implement the staged supervision mode because different stages have unique characteristics. Therefore, only by improving the procedural supervision and management model can the integrity of the management process and the comprehensive level of investment control be improved. The most important thing is to integrate the static control mechanism, dynamic control mechanism, deviation analysis mechanism, and remedial adjustment mechanism in the investment control structure of the whole life cycle of water conservancy projects, so as to establish a really good supervision mode and comprehensive supervision system [17]. In the whole life cycle management of water conservancy projects, to a certain extent, relies on the computer software system of integrated information [18]. The application of BIM (Building Information Modeling) technology (see Figure 1) can fully reflect the physical and geometric characteristics of water conservancy buildings, display project appearance, location, and environmental information in three-dimensional space, and integrate various engineering information of buildings, including progress, material information, and cost information. In the BIM model, all information is provided by a unified data source, and the engineering information is independent, logically related, and consistent.

2. Existing Problems

We mainly use SPSS software to establish a multiple linear regression model to analyze the factors that affect hydraulic engineering. Through the method of model solving, the relationship between hydraulic engineering and various variables is analyzed, and the verification of multi-linearity is improved. This is to further test the model, optimize the model, and finally carry out accurate management and prediction.

2.1. Problems in the Decision-Making Stage. Judging from the construction situation of water conservancy projects in recent years, some projects have not been completed in strict accordance with the construction period, which means that the investment costs that investors need to bear also need to rise, resulting in the inability to better control the cost of water conservancy projects [19]. The problem that caused this situation is that the basis for the cost estimation in the decision-making stage of the water conservancy project is not sufficient, and it is not considered according to the actual situation, and the construction plan is formulated only after the theoretical approval.

2.2. Design Phase Issues. Engineering design is a prerequisite for the construction of all construction projects. At present, many design institutes have fallen into a misunderstanding when designing water conservancy projects, that is, they think that as long as the quality is strictly controlled, the design scheme can be optimized, resulting in the neglect of engineering costs, to design the overall cost-effectiveness of the program is generally low. Although quality is the core criterion for determining the service life and value of a project, it does not mean that cost is unimportant. Simply considering an influencing factor will lead to deviations in the design scheme and make cost control difficult.

2.3. Project Quotation Problem. The project list quotation method is a cost control method after the construction of most projects in the world. At present, only a few economically developed areas in China use this method, and most areas have not yet implemented it. When using the bill of quantities for quotation, the company chooses the industry quota as the reference value, which makes the cost involved in the bill of quantities only the social average, and does not reflect the actual cost control of the construction unit, resulting in this kind of cost. The means of control cannot be implemented.

2.4. Issues in the Implementation Phase. The main problem affecting project cost management in the implementation stage is the modification of the construction design. At present, in many domestic water conservancy projects [20], investors and constructors randomly modify the construction design, which can directly lead to an increase in project costs. At the same time, there is no domestic law or regulation that is completely aimed at the management of construction costs, which makes the construction contract have many loopholes in the process of signing so that the construction party can make use of loopholes to modify the project quantity, which will seriously affect the water conservancy project and the cost control.

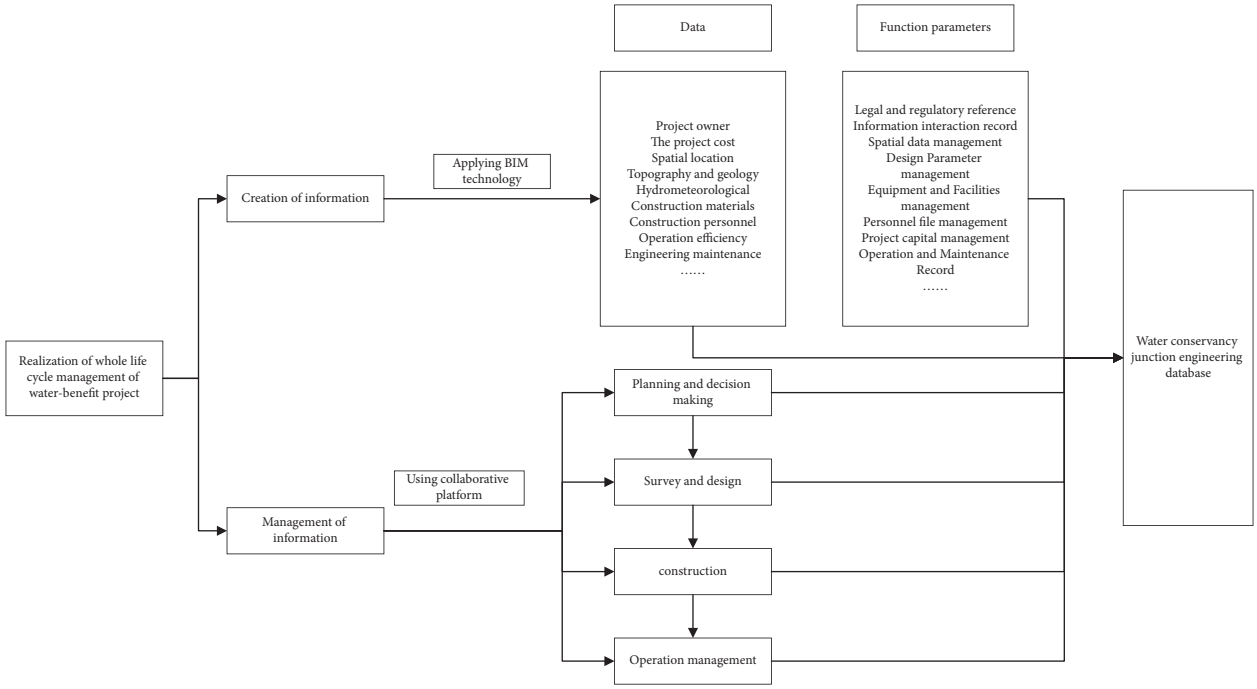

Figure 1: Full life cycle management of water conservancy projects.

2.5. Issues in the Settlement Phase. There may also be some loopholes in the formulation and signing of water conservancy project contracts, which leads to the situation that the investor and the construction party shirk each other when the project is settled. It is mainly manifested in the fact that the construction party increases the amount of the project cost in the settlement by falsely reporting the construction volume; while the investor bargains with the construction party under the loopholes in the contract clauses, and some construction parties try to avoid this "malicious" bargaining behavior. Therefore, there will be a situation of falsely reporting the project cost. Both parties did not strictly follow the contract settlement method, which made the cost control of the water conservancy project more difficult to carry out, and even could not be settled, so the project could not be put into use, increasing the additional cost in the later period.

3. Number of Control and Management Measures in the Whole Process of Water Conservancy Project Cost

3.1. Water Conservancy Project Cost Process. The control of water conservancy project cost is different in different stages such as project proposal, feasibility study report, initial design, bidding and construction, and complete acceptance. The construction of water conservancy projects uses a lot of manpower, material resources, and financial resources. In the process of project implementation, the implementation of good management and control of the whole process of construction cost can save a lot of cost for my country's economic construction and ensure that the project has good quality and profit. First, have a clear understanding of the concept of water conservancy project cost control and management, and then explain the management and control involved in water conservancy construction before, during, and after the event, so as to draw powerful measures for water conservancy construction project control and management, and in order to provide effective reference and basis for the management and control of engineering cost of water conservancy construction projects in my country in the future. Therefore, the corresponding preparations should be done in the early stage of the construction project, and the funds should be controlled in the reserved cost and stage coefficient in the investment decision-making stage. The following processes are usually required in the cost of water conservancy construction projects, as shown in Figure 2.

3.2. Cost Control Measures in the Decision-Making Stage. In the decision-making stage of a water conservancy project, the investor should communicate with the auditors in the early stage and conduct a comprehensive evaluation of the water conservancy project to be invested in. During the evaluation process, it is necessary to conduct a comprehensive survey of the market and analyze the geological exploration data of the construction site to make the construction period and early cost evaluation results more accurate.

3.3. Cost Control Measures in the Design Stage

(1) The design institute needs to optimize the design scheme according to the requirements of the investor. The premise of optimization includes not only the quality of the project but also the cost of the project. The design work is carried out on the

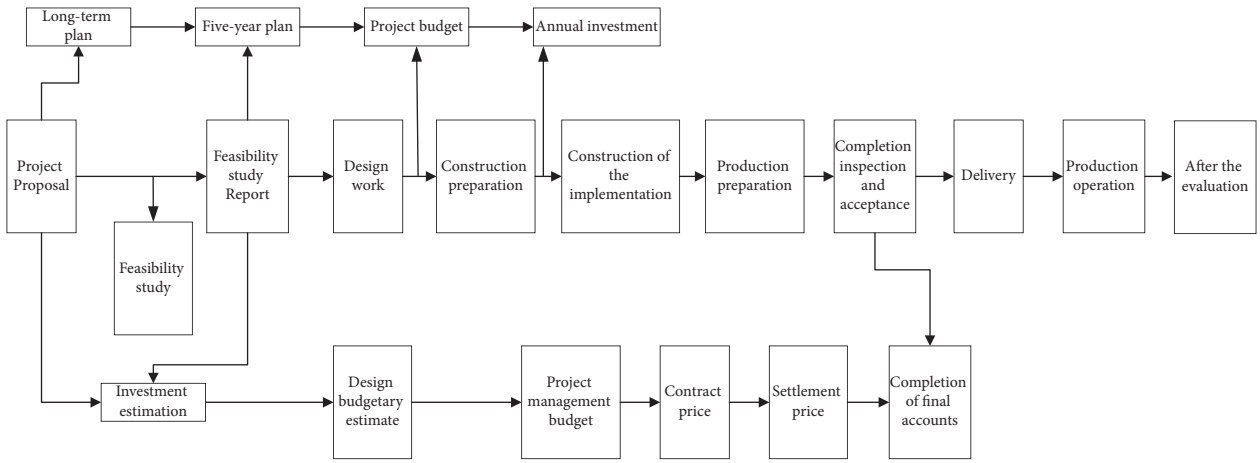

Figure 2: Construction flowchart.

premise of engineering quality, and then the economic credibility of the design scheme is evaluated, and at the same time, it is studied whether the architectural function of the design scheme meets the needs of the investor. In addition, the method of limit design can also be adopted, and the investor can directly control the estimated cost of the project within a certain range when communicating with the design institute.

(2) During the design process, it is necessary to consider the design changes in the construction stage. Designers should comprehensively consider the correlation between design changes and the impact of construction costs. Usually, the earlier design changes occur in the construction stage, the smaller the impact on the overall cost. Therefore, it is necessary to conduct a comprehensive study of the influencing factors immediately after the design is completed, so as to minimize the change in the design scheme.

3.4. Cost Control Measures in the Construction Stage. First of all, it is necessary to formulate a dynamic and static cost control plan in the construction stage. The static control plan is mainly to be discussed by the construction party, the investor, and the design institute before the start of construction. Modify the process links that the construction unit cannot meet in the plan. At the same time, the investor and the builder should sign a cost pre-limited contract, that is, to formulate a scope of approval for the fluctuation of the project cost, and stipulate the conditions that can affect the cost of the project, and the additional cost caused by other conditions will not be paid. Dynamic cost control refers to the review and compensation management of cost changes caused by modification of the construction design during the entire construction stage, and the reasons for changes in the construction process and the design changes are reported to the cost management department for review. The changes within the scope are approved for revision, while those beyond the contract limit need to be negotiated by the investor and the construction party for related compensation issues. It should be noted that the limited terms in the contract shall not be arbitrarily changed during the construction stage. If a party unilaterally changes the contract, it shall bear all the additional costs. In the construction stage, where investment mainly occurs, construction site management should be done well, and corresponding management and control should be done to reduce costs and eliminate waste. They should pay attention to the following aspects: 1. Do a good job in investment tracking management. Through effective tracking management, the corresponding problems can be found in a timely and effective manner, and the quality of the project can be effectively grasped in terms of quality, progress, and cost, so as to reasonably save costs and solve problems. Identify the control basis, such as project management budget and the project contract price, etc., through project measurement, control of project changes, etc., according to the actual workload completed by the contractor, and strictly determine the actual project costs incurred during the construction stage. 2. Strictly review the construction organization design. During the construction process, the construction plan that is technically feasible and economically reasonable should be selected as far as possible. According to the nature and scale of the project, the length of the construction period, the number of workers, mechanical equipment, material supply, transportation, geological, climatic conditions, and other specific technical and economic conditions, the construction organization design, construction plan, The construction schedule is optimized, and finally, the most rational use of manpower, material resources, financial resources, and resources is selected. Correctly handle the dialectical and unified relationship between project cost, construction period, and quality, and improve the comprehensive economic benefits of project construction. 3. Control engineering changes. If the corresponding project quantity is changed, it will bring a lot of unnecessary trouble to the original budget investment. In engineering contracting, many common phenomena will occur, due to factors such as construction site conditions, climate changes, changes in construction progress, and

changes, differences, and delays in contract terms, specifications, standard documents, and construction drawings, which will inevitably lead to engineering contracting. Claims arise, which in turn lead to changes in the investment in the project.

3.5. Cost Control Measures at the Completion Stage. The completion settlement report is the most direct data reflecting the actual cost of the water conservancy project, and it is also the core reference data for investors to consider the projected income. In order to control the project cost at the time of completion and settlement, it is necessary to conduct a comprehensive review of the actual construction volume of the water conservancy project, compare the early design drawings, revised drawings, and as-built drawings, and cooperate with auditors to inspect all construction links. Carefully check whether there is any false report of construction volume. At the same time, it is also necessary to refer to the limited terms in the contract when completing the settlement to avoid the problem of "malicious" price reduction by the investor and ensure the economic benefits of the construction party, so as to avoid their fraudulent behavior and make the whole process of cost work more complete and accurate.

4. Multiple Regression Analysis Models

4.1. Introduction to Multiple Regression Models. Multiple regression analysis [21, 22] refers to the establishment of a linear or nonlinear mathematical model between multiple variables by considering one variable as a dependent variable and one or more other variables as independent variables. Statistical analysis methods use quantitative relationships and use sample data for analysis. In addition, there is also a multiple regression analysis that discusses the linear dependence of multiple independent variables and multiple dependent variables, which is called the multiple multiple regression analysis models (or simply many-to-many regression) [23]. Usually, multiple factors affect the dependent variable, and the problem that multiple independent variables affect one dependent variable can be solved by multiple regression analysis [24]. For example, economic knowledge tells us that in addition to commodity price P, commodity demand Q is also affected by factors such as the price of substitutes, the price of complementary products, and consumer income, and even includes the quality variable of commodity brand (Brand Quality variables cannot be measured numerically, and dummy variables need to be introduced into the model). Multiple regression analysis has a wider range of applications. Since linear regression analysis is relatively simple and common, the following first introduces multiple linear regression [25, 26]. On the basis of linear analysis, dummy variable regression and a class of curve regression models that can be transformed into linear regression are gradually introduced.

One of the more famous multiple regression models is principal component analysis, which we use in this article. When using statistical analysis methods to study multivariate subjects, too many variables will increase the complexity of the subject. People naturally want to get more information with fewer variables. In many cases, there is a certain correlation between variables. When there is a certain correlation between two variables, it can be interpreted that the information of the two variables reflecting the subject overlaps to a certain extent. Principal component analysis is to delete the redundant variables (closely related variables) for all the variables originally proposed, and establish as few new variables as possible so that these new variables are uncorrelated, and these new variables reflect. The information on the subject should be kept as original as possible. The principal component analysis is the basic mathematical analysis method, and its practical application is very wide, such in demographics, quantitative geography, molecular dynamics simulation, mathematical modeling, mathematical analysis, and other disciplines. Analytical method is that the component analysis is a multivariate statistical method that examines the correlation between multiple variables. It studies how to reveal the internal structure of multiple variables through a few principal components, that is, derive a few principal components from the original variables so that they can be as fully as possible. It is possible to retain a lot of information about the original variables, and they are not related to each other. Usually, the mathematical processing is to linearly combine the original P indicators as a new comprehensive indicator.

The most classic way is to use the variance of F1 (the first linear combination selected, that is, the first comprehensive indicator) to express, that is, the larger the Var(F1), the more information F1 contains. Therefore, F1 selected in all linear combinations should have the largest variance, so F1 is called the first principal component. If the first principal component is not enough to represent the information of the original P indicators, then consider selecting F2 to select the second linear combination. In order to effectively reflect the original information, the existing information of F1 does not need to appear in F2 again, which is called F2, is the second principal component, and so on, and this way the third, fourth, ..., P-th principal components can be constructed.

4.2. Statistics of Data. Due to its public welfare nature, the construction funds of water conservancy projects are mostly invested by the government. The policies and financial levels of different provinces affect the decision-making of water conservancy project construction. In addition, engineering projects of different times and scales also have a greater impact on decision-making. The author counted a total of 20 initial approvals as samples, from which 17 samples were selected to estimate the regression model, and the remaining 3 samples were used for model testing.

4.3. Data Analysis. The multiple regression function is

$$E(y) = \beta_0 + \beta_1 x_1 + \beta_2 x_2 + \cdots + \beta_k x_k. \quad (1)$$

It can be seen from formula (1) that the value of the dependent variable in the model is composed of the linear

function of the independent variable and the random variable of the error term, and the model parameters determine the specific form of the linear relationship between the dependent variable and the independent variable. The key point of using multiple regression analysis is to determine the specific values of the model parameters, then determine the specific form of the multiple linear regression model, and analyze the results according to the results. It is the mean or expected value and zero, and obeys the normal distribution, and it is independent.

The least-squares method is used to obtain the estimator of the regression coefficient, and the normal equation is as follows:

$$\begin{aligned}
&\widehat{\beta}_0 n + \widehat{\beta}_1 \sum_{i=1}^{n} x_{i1} + \cdots + \widehat{\beta}_k \sum_{i=1}^{n} x_{ik} = \sum_{i=1}^{n} y_i,\\
&\widehat{\beta}_0 \sum_{i=1}^{n} x_{i1} + \widehat{\beta}_1 \sum_{i=1}^{n} x_{i1}^2 + \cdots + \widehat{\beta}_k \sum_{i=1}^{n} x_{i1} x_{ik} = \sum_{i=1}^{n} x_{i1} y_i,\\
&\widehat{\beta}_0 \sum_{i=1}^{n} x_{ik} + \widehat{\beta}_1 \sum_{i=1}^{n} x_{ik} x_{i1} + \cdots + \widehat{\beta}_k \sum_{i=1}^{n} x_{ik}^2 = \sum_{i=1}^{n} x_{ik} y_i,
\end{aligned} \tag{2}$$

The dependent variable is the total static investment of the project, and the independent variables are the storage capacity, the irrigation surface, and the dam height. With the help of SPSS software, the estimated quantities of the regression coefficients are: $\widehat{\beta}_0 = 51281.672$, $\widehat{\beta}_1 = 10.797$, $\widehat{\beta}_3 = 1420.701$, $\widehat{\beta}_4 = -315.564$.

So the empirical regression equation between static total investment and storage capacity, irrigation surface, and dam height is: $y' = 51281.672 + 10.797x_1 + 1420.701x_1 - 315.564x_3$.

Where y' means Static total investment (ten thousand yuan), x_1 means Reservoir storage capacity (ten thousand m^3), x_2 *means* Irrigated area (ten thousand mu), and x_3 means reservoir dam height (m).

The accuracy of the estimation depends on how well the regression equation fits the sample data. Usually, the multiple determination coefficient R^2 is used to evaluate the goodness of fit of the empirical equation of the multiple regression model. In order to avoid increasing the independent variable and overestimating R^2, this study adopts the modified multiple determination coefficient, and its calculation formula is

$$\left(R^2 = 1 - \frac{n-1}{n-k-1}\right)\left(1 - R^2\right), \tag{3}$$

where R^2 means modified multiple determination coefficient, n means sample size, and k means the number of parameters in the model.

The regression coefficient of determination is $R^2 = 0.948$ and modified multiple determination coefficient is $R^2 = 0.936$, which show that the goodness of fit of the empirical equation of the multiple linear regression model is good. The histograms and standard P-P plots of regression standardized residuals are shown in Figures 3 and 4, respectively.

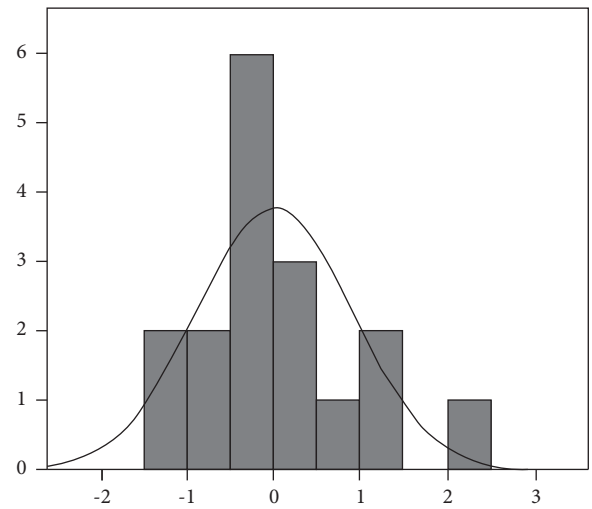

Figure 3: Histogram of regression standardized residuals.

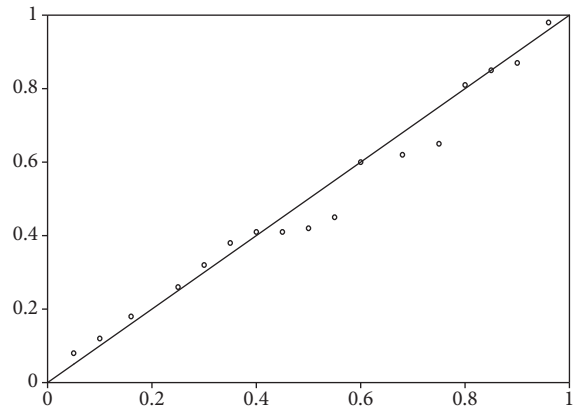

Figure 4: Standard P-P plot of regression standardized residuals.

Figure 5: Logo of SPSS.

4.4. SPSS Software Application Analysis. Using SPSS software (Figure 5) analysis, the following can be obtained (Tables 1, 2, 3).

The data used in this study is tested by multiple regression estimation models, and through the multiple regression analyses of SPSS software, the regression equation is summarized as $Y = -587.209 + 0.115 + 103.464$.

Table 1: Table data obtained after multiple regression analysis.

Model	R	R Part	Adjusted R squared	Errors in standard estimates
1	0.976[a]	0.953	0.947	388.04391
2	0.987[b]	0.975	0.967	304.74013

Note: a. Predictor variables: (constant), total floor area; b. Predictor variables: (constant), total floor area, number of floors; c. Dependent variable: total project cost. At this time, the = 0.967 obtained by the regression analysis is relatively close to 1, so the reliability of this regression model is considered acceptable.

Table 2: Excluded variables.

Model		Enter beta	t	Significant	Partial correlation	Collinear statistical tolerance
1	Construction layer	0.472b	2.444	0.045	0.678	0.097
	Building height	0.298b	1.849	0.107	0.573	0.174
	Time limit for a project	−0.478b	−0.879	0.408	−0.315	0.020
2	Building height	−0.592c	−1.113	0.308	−0.414	0.012
	Time limit for a project	−0.217c	−0.467	0.657	−0.187	0.019

Note: a. Dependent variable: total project cost; b. Predictors in the model: (constant), gross floor area; c. Predictors in the model: (constant), gross floor area, The number of building floors thus obtain a regression equation: $Y = -587.209 + 0.115 + 103.464$.

Table 3: Coefficients.

Model		Unnormalized coefficient		Normalization coefficient	t	Significant
		B	Standard error	Beta		
1	(Constant)	96.677	300.262		0.322	0.756
	Gross floor area	0.213	0.017	0.976	12.730	0.000
2	(Constant)	−587.209	365.957		−1.605	0.153
	Gross floor area	0.115	0.042	0.528	2.732	0.029
	Construction layer	103.464	42.339	0.472	2.444	0.045

The meaning of this equation is that the total cost of recent engineering projects is greatly affected by the total construction area of the project and the number of building layers.

5. Conclusion

The cost control and management of water conservancy projects should run through the whole process, including engineering decision-making, design, construction, completion settlement, and other stages. Among them, cost control in the engineering design and construction stages is particularly important. In the design stage, the project quality and cost should be used as reference standards to design the optimal water conservancy project plan. The technical and economic demonstration and comparison are an important part of the project evaluation and selection in the feasibility study stage. In this study, the key contents considered in the design of the slope reinforcement scheme are analyzed in detail, and the multiple linear regression is carried out on the important parameter samples that affect the cost. After comparing with the real cost, the model accuracy meets the estimation requirements, and each parameter is easy to obtain in the feasibility study stage, and the model is easy to use. Therefore, this model has strong applicability to the economic comparison and selection of slope reinforcement schemes in the feasibility study stage.

Data Availability

The dataset can be accessed upon request.

Conflicts of Interest

The author declares that there are no conflicts of interest.

Acknowledgments

The authors thank Basic Scientific Research Funds Provincial and Ministerial Level Cultivation Projects; Research on water conservancy Project cost Management Technology System based on the view of the whole life cycle (No. FRF22PY001).

References

[1] S. Li, Y. Wang, and Yu Zeng, "The standardization system of water conservancy project cost management under the EPC general contract mode," *IOP Conference Series: Earth and Environmental Science*, vol. 787, no. 1, Article ID 012118, 2021.

[2] M. Liu, "Simulation of mathematical model to estimate the cost of large-scale hydraulic engineering[J]," *Applied Mechanics and Materials*, vol. 3365, pp. 602–605, 2014.

[3] Y. Song, D Wu, L. Yuan, and B Chao, "Impact analysis of replacing business tax with value-added tax on water conservancy project cost[P]," in *Proceedings of the 4th Annual International Conference on Material Engineering and Application (ICMEA 2017)*, 2018.

[4] X. Ni and X. Hou, "Application of big data technology in water conservancy project informatization construction," *IOP Conference Series: Earth and Environmental Science*, vol. 768, no. 1, Article ID 012113, 2021.

[5] Q Lu and J. Huang, "Study on water conservancy project construction and sustainable development planning[J]," *Basic and Clinical Pharmacology and Toxicology*, vol. 128, 2021.

[6] F. Fang, "Numerical and data-driven modelling in coastal, hydrological and hydraulic engineering," *Water*, vol. 13, no. 4, p. 509, 2021.

[7] S. Zhang, "Application of information entropy and TOPSIS coupling model in impervious design of hydraulic engineering," *E3S Web of Conferences*, vol. 248, Article ID 03022, 2021.

[8] R. Yang, "Research on settlement prediction of small water conservancy project based on ELM model optimized by genetic algorithm[J]," *E3S Web of Conferences*, vol. 248, 2021.

[9] A. Wahab and J. Wang, "Factors-driven comparison between BIM-based and traditional 2D quantity takeoff in construction cost estimation," *Engineering Construction and Architectural Management*, vol. 29, no. 2, pp. 702–715, 2022.

[10] R. Wang, A. Vahid, C. Clara Man, H. Shu-Chien, and C.-J. Lee, "Assessing effects of economic factors on construction cost estimation using deep neural networks[J]," *Automation in Construction*, vol. 134, 2022.

[11] S. Jana, M. . Peter, and K. Katarína, "Innovative cost estimation methods for building production[J]," *Selected Scientific Papers - Journal of Civil Engineering*, vol. 16, no. 2, 2021.

[12] R. Damiano and B. Mariusz, "Guaranteed cost estimation and control for a class of nonlinear systems subject to actuator saturation[J]," *European Journal of Control*, vol. 61, 2021.

[13] S. Muhammad Wajid, A. Asad, A. Muhammad, U. Ghulam Moeen, C. Tariq Nawaz, and U. Asad, "Design and cost estimation of solar powered reverse osmosis desalination system [J]," *Advances in Mechanical Engineering*, vol. 13, no. 6, 2021.

[14] W. Zang, A. Zecchin, and J. J. Gong, "Engineering - hydraulic engineering; findings from university of adelaide in hydraulic engineering reported (inverse wave reflectometry method for hydraulic transient-based pipeline condition assessment)[J]," *Journal of Engineering*, vol. 146, no. 8, Article ID 04020056, 2020.

[15] J. Zhang, D. Du, D. Ji, Y. Bai, and W. Jiang, "Multivariate analysis of soil salinity in a semi-humid irrigated district of China: concern about a recent water project," *Water*, vol. 12, no. 8, p. 2104, 2020.

[16] Q. Qin, W. Liu, K. Jin et al., "Cloud platform-based real-time supervision to safety inspection of hydraulic engineering metallic structures and equipments," *IOP Conference Series: Earth and Environmental Science*, vol. 525, no. 1, Article ID 012056, 2020.

[17] D. C. yan, X. J. qiang, Ge Hua, and L. Rui, "Application of mathematical model in water conservancy project at confluence section[J]," *IOP Conference Series: Earth and Environmental Science*, vol. 510, no. 4, 2020.

[18] J. Wu, S. Qian, Y. Wang, and Y. Zhou, "Engineering - hydraulic engineering; investigators from hohai university report new data on hydraulic engineering (residual energy on ski-jump-step and stepped spillways with various step configurations)[J]," *Journal of Engineering*, vol. 146, no. 4, Article ID 0602002, 2020.

[19] "The uMkhomazi water project[J]," *IMIESA*, vol. 44, no. 10, 2019.

[20] X. Sun, S. He, Yi Guo, W. Sima, W. Liu, and Y. Wang, "Comprehensive evaluation of the impact of the water conservancy project in on the ecosystem of the yangtze river basin," *Journal of Coastal Research*, vol. 94, no. sp1, p. 758, 2019.

[21] X. Chen, L. Pan, and N. Xiu, "Solution sets of three sparse optimization problems for multivariate regression[J]," *Journal of Global Optimization*, vol. 137, 2022 (prepublish).

[22] X. Chen, R. Tu, Li Ming, and Y. Xu, "Prediction models of air outlet states of desiccant wheels using multiple regression and artificial neural network methods based on criterion numbers [J]," *Applied Thermal Engineering*, vol. 204, 2022.

[23] S. Nakayama, S. Sekine, and Y. Nagata, "A study of MT systems applied to multivariate regression," *Total Quality Science*, vol. 7, no. 1, pp. 10–22, 2021.

[24] J. O. Adegbite, H. Belhaj, and A. Bera, "Investigations on the relationship among the porosity, permeability and pore throat size of transition zone samples in carbonate reservoirs using multiple regression analysis, artificial neural network and adaptive neuro-fuzzy interface system," *Petroleum Research*, vol. 6, no. 4, pp. 321–332, 2021.

[25] M. Sharma, H. Agrawal, and B. S. Choudhary, "Multivariate regression and genetic programming for prediction of backbreak in open-pit blasting," *Neural Computing & Applications*, vol. 34, no. 3, pp. 2103–2114, 2021.

[26] S. Kang, W. Nam, W. Zhou, I. Kim, and P. J. Vikesland, "Nanostructured Au-based surface-enhanced Raman scattering substrates and multivariate regression for pH sensing," *ACS Applied Nano Materials*, vol. 4, no. 6, pp. 5768–5777, 2021.

Hindawi
Scientific Programming
Volume 2022, Article ID 9193454, 8 pages
https://doi.org/10.1155/2022/9193454

Research Article

Research on Scoring of Business English Oral Training Based on Deep Neural Network

Wei Duan

School of International Studies, Chengdu Jincheng College, Chengdu 611731, Sichuan, China

Correspondence should be addressed to Wei Duan; duanwei@cdjcc.edu.cn

Received 16 May 2022; Revised 28 June 2022; Accepted 9 July 2022; Published 22 August 2022

Academic Editor: Lianhui Li

A scoring approach of business English oral training based on a deep neural network is put forward. Based on speech recognition technology, automatic correction technology, deep learning technology, machine learning technology, and the scoring data of business English oral training generated by the general computerized examination platform system, this paper uses the audio data of students' oral expression questions collected by the existing general computerized examination platform, and studies artificial intelligence technology, deep learning technology, and machine learning technology to train the intelligent scoring system, it realizes the intelligent scoring of oral expression questions, which plays a positive role in language training guidance and correction. Finally, the accuracy of the intelligent scoring system is verified by the correlation between the score of the intelligent scoring system and the manual score of teachers. The higher the correlation with manual scoring, the higher the scoring accuracy of the intelligent scoring system.

1. Introduction

With the rise of AI [1–3] to the national strategic level, AI technology has become more and more popular, and AI + education is also the key research direction of educational technology [3–8]. How to combine artificial intelligence technology [9, 10], deep learning technology [11, 12], machine learning technology [13] and education is a problem worthy of research in the field of educational technology [12–15]. English is a very important subject in the field of education. If artificial intelligence and business English skill training can be combined, it will be of great help to improve students' interest in learning English, correct students' English pronunciation, evaluate students' academic performance, and guide students' learning. Artificial intelligence technology developed to a research climax as early as the 1990s. Recently, with the release of Google's deep learning engine TensorFlow and artificial intelligence technology, it became more popular after alpha dog defeated Li Shishi, which is also expected [16]. TensorFlow brings convenience and ease of use to deep learning and training, and this game also shows that artificial intelligence can still perform well in this scenario [17–19]. Business English speaking training score plays an important role in Business English teaching. Under the background of artificial intelligence, it is very urgent and necessary to research the scoring of business English oral training based on a deep neural network.

2. Current Situation and Problems of Oral Business English Training

With the rapid development of the Internet, "Internet + education" has become a trend [20–22]. The business English oral skills training system trains and evaluates English through online learning, so that students have made great progress in all aspects of English listening, speaking, reading, and writing. After years of accumulation, a large number of valuable teaching data are stored in the system. These source data provide a basis for our work. The current situation of oral business English teaching and training is deeply analyzed from four aspects: teaching objectives, content, implementation, and assessment.

(1) Teaching objectives

At present, the formulation of oral English curriculum standards for business English Majors in most colleges and universities is dominated by teaching materials and focused on knowledge. The listed objectives include pronunciation rules, intonation, word quantity, and expressions commonly used in daily life and social life.

(2) Teaching content

Due to the limitations of employing foreign teachers or professional teachers without a business background in China, the teaching content is mainly based on the English teaching content itself, and there is no subject matter of oral English practice for business application background.

(3) Teaching implementation

Due to the reasons of teachers and teaching resources, business English mostly adopts large class teaching, and the number of people in each class is between 35 and 45. In terms of curriculum, oral English is a professional basic course, which is generally set up in the first and second semesters, with 4 class hours per week. Interviews and questionnaires with teachers and professional students in many colleges and universities show that the current teaching methods are mainly teachers' explanation and demonstration (accounting for about 40% of the classroom time) and student group practice (accounting for 50%), with additional personal practice (accounting for 10%). At the same time, the per capita time of students' special oral practice after the class is less than 20 minutes per week.

(4) Teaching evaluation

In Teacher-centered courses, students perform less alone and lack quantitative process records. At the end of the semester, the final assessment will be conducted only in the form of one-to-one oral daily dialogue, question and answer, and monologue.

According to the current situation of oral English teaching and training, combined with the training needs of business English talents, this paper analyzes the main problems existing in the current oral English teaching and training, including (1) the application of teaching objectives is not high; (2) the teaching content is not contemporary enough; (3) lack of pertinence in teaching implementation; (4) the process of teaching evaluation is not strong.

3. Design of Intelligent Scoring System

Oral Business English training includes two parts, English learning and English examination. English learning refers to that students can use the system to conduct self-test and practice relevant English topics when learning English at ordinary times. English test is organized by teachers. Students are evaluated before, during, and at the end of each semester. After the examination, the students will participate in the questionnaire, which includes learning interests, whether they pass CET-4 or CET-6, the difficulty of the topic, their satisfaction with the examination system, etc. The oral business English training system will collect students' test data, in which the objective question system can directly give scores through the standard answers set in advance, and the subjective questions need to be corrected manually by teachers. This puts forward higher requirements for teachers' energy. The purpose of this study is to save teachers' energy and make subjective questions score automatically.

The topic types of business English oral training include single choice, multiple choice, cloze, oral expression, and English writing. Among them, subjective questions include oral expression questions and English writing questions. English writing can be corrected according to the automatic correction system. The intelligent correction of oral expression questions realizes the automatic scoring of the business English oral training system.

Through the interview with English teachers, the needs for an intelligent scoring system are determined. There are two main aspects of demand as follows:

(1) Accuracy

Since it is automatic scoring, if the accuracy of scoring is not high enough to meet the expectations of teachers, the scoring work will lose its significance. The total score of oral expression questions is 10 points. Compared with the manual score of teachers, the error of no more than 1 point is acceptable and the total score of the whole English test is 100, so the error for the total English score is less than 1%, which can meet the expectations of teachers.

(2) Time consuming

If the time of the intelligent scoring system is too long, which is longer than the time of teachers' manual correction system, it will consume teachers' time longer and lose the significance of saving teachers' time and energy. It takes no more than one minute to batch correct the oral expression questions of about 30 students in a class, which is the ideal automatic correction time for teachers.

3.1. Data Preparation Design. Based on the above demand analysis, the overall design of the intelligent scoring system is shown in Figure 1.

First, the audio data is processed. The corresponding features are extracted from it, then input into the neural network or linear regression model, and finally, the score is output. The language used for all processes is mainly python.

The python language has now become the mainstream language for machine learning programming. This language is more superficial than Java, C++, and C#. It also acts as a "glue" language to "glue" together functional modules written in other languages. Python has a rich software library, which is very helpful for machine learning. NumPy is an essential library in python, which provides some

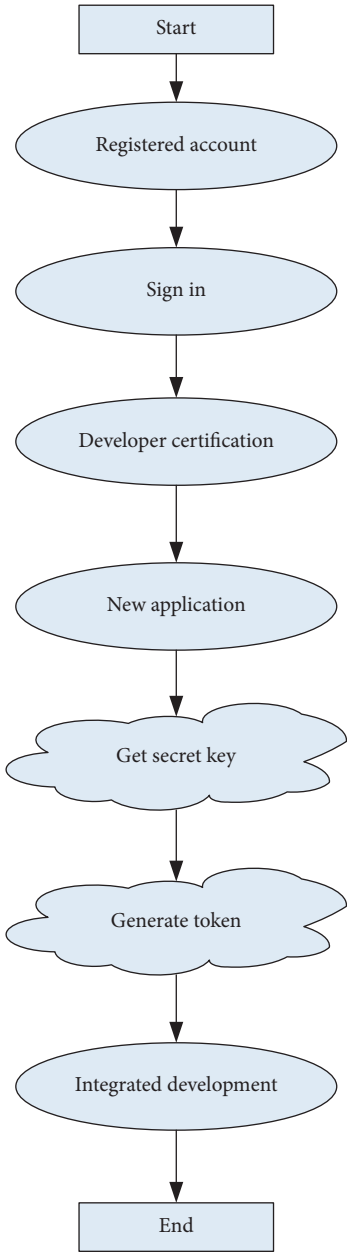

Figure 1: The overall design of the intelligent scoring system.

commonly used functions and standard libraries for data calculation. For example, operations related to matrices and arrays can be done using NumPy, and the code is simple and easy to maintain.

3.1.1. Data Processing. The data processing is divided into two parts. One part is processing the oral expression questions answers (audio data), and the other part is processing the data in the system (including student learning data and test data).

(1) Audio data processing

First, the audio data is recognized by speech recognition, and then the text is corrected according to the requirements of composition correction according to the automatic correction scheme. Natural language processing includes text segmentation, sentence segmentation, construction of dictionaries, and word frequency statistics. The processed data is then subjected to data cleaning in preparation for the subsequent feature extraction. The flowchart of audio data processing is shown in Figure 2.

The flow of natural language processing is shown in Figure 3. The text recognized by the audio is firstly segmented and sentenced through speech recognition, the function words that have no real meaning, such as a and an, are removed, and only actual words such as nouns and adjectives are left. Then, a dictionary is constructed to count the frequency of each word.

(2) System data processing

The system data processing of the college English skill training system is divided into two parts as follows: learning data processing and examination data processing. After the data is extracted, the data needs to be cleaned because the extracted data will have a lot of dirty data and empty data, and these data need to be cleaned so as not to affect the results of subsequent model training. The system data processing is shown in Figure 4.

3.1.2. Feature Extraction. After the feature is extracted, too many features will lead to a complex model. Moreover, some features have little correlation with the target variable, so it is necessary to use the methods of feature transformation and feature selection to extract features.

Feature transformation methods are divided into normalization, discretization, and dimensionality reduction. Feature selection includes filtering, encapsulation, and integration. The definition of feature selection is to select a suitable feature set from many features, making the model make the evaluation index higher in the evaluation stage; that is, the model is more accurate, and the quality is better.

(a) The first is the filtering method. The filtering method can assign a weight to the feature through some common statistical methods, such as the chi-square test, T-test, information entropy and information gain, correlation coefficient, and covariance. This weight means that the more significant the correlation between the feature and the output result, the greater the impact on the result; the smaller the correlation, the less the effect on the result.

(b) The encapsulation method refers to selecting different feature subsets among many features. Some features can be excluded according to human experience and combined to achieve different effects. Then, according to different features, the effect to be predicted, the features of each combination of each group are evaluated, and the feature with the best effect is selected. In this way, a subset of features with

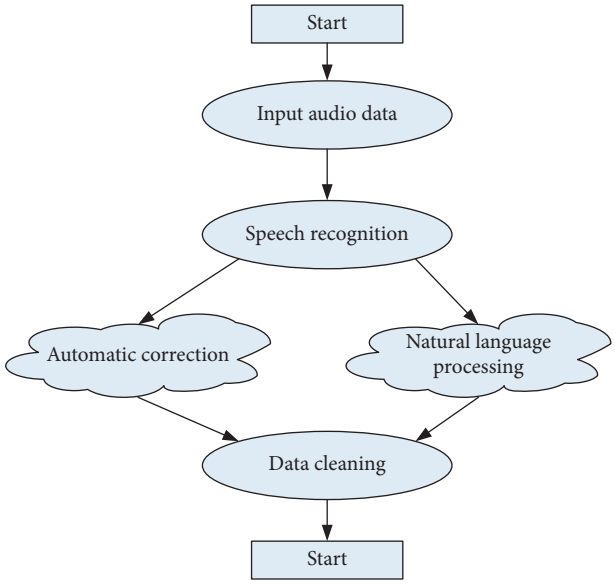

Figure 2: Audio data processing.

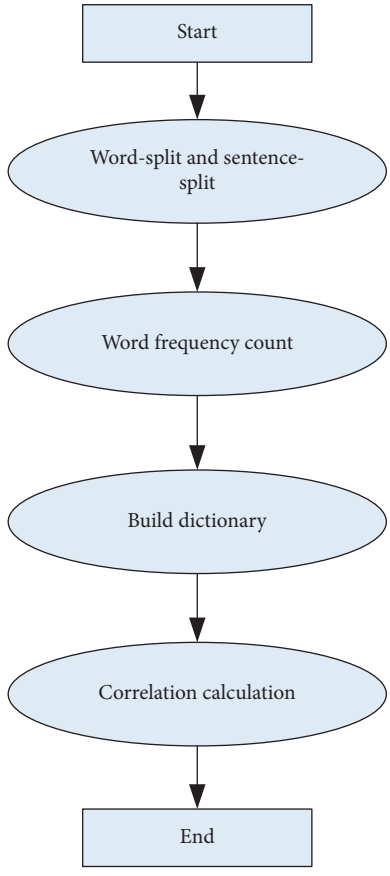

Figure 3: Natural language data processing.

better effects can be selected; that is, some irrelevant features are excluded, or features that have less influence on the target result.

(c) The inheritance method refers to the premise that the model has been trained. Then, the data information is trained through this model to learn the characteristics that make the model accuracy the best. For example, the logistic regression model in the machine learning model can determine the weight of each input feature according to the model to determine the importance of the impact of each feature on the target variable; in this way, the importance of the features can be obtained, and the features can be filtered. The method of feature processing is shown in Figure 5.

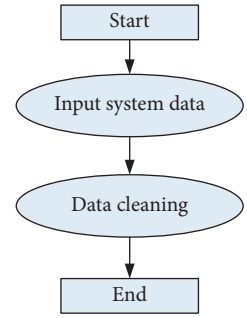

Figure 4: System data processing.

The design of the correlation calculation model is shown in Figure 6.

3.2. Intelligent Scoring System Design. The dataset was randomly divided into training and test sets using Python's random method. The training set accounted for 80%, with a total of 3,122 samples, and the test set accounted for 20%, with a total of 781 samples.

3.2.1. Linear Regression Model Design. According to the principle and usage scenarios of linear regression, experiments were carried out using the linear regression model [23–26] as shown in Figure 7.

3.2.2. Deep Neural Network Model Design. There are many mainstream deep learning open source tools on the market [27–29]. TensorFlow was developed by Google and has been widely used in recent years. On GitHub, you can see that TensorFlow has considerable attention and collection. Other deep learning tools such as Caffe and Torch do not have as much attention as TensorFlow, which shows that TensorFlow plays a pivotal role in the minds of deep learning developers and researchers. Many researchers study the training effect of these deep learning tools. Generally speaking, it is not objective. Each deep learning tool has its advantages and disadvantages. The specific situation needs to be analyzed in detail. This research mainly uses TensorFlow to train the neural network model.

The name of TensorFlow has already explained its two most essential components, Tensor and Flow. These two words are translated into Chinese as tensor and flow, respectively, which are explained from the perspective of the data model and calculation model. Tensor represents multidimensional data, that is, the data model. Flow refers to the

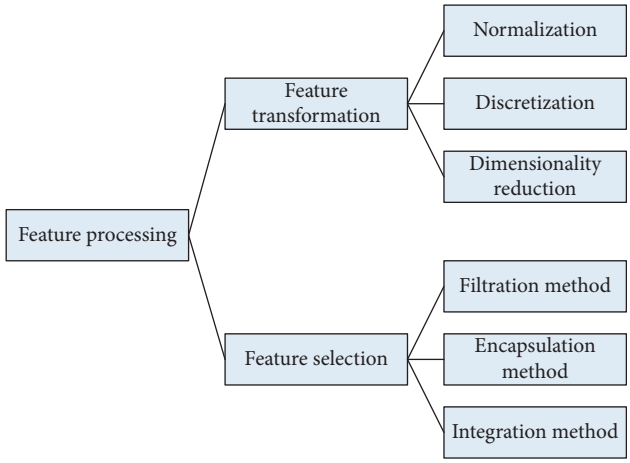

Figure 5: Feature processing.

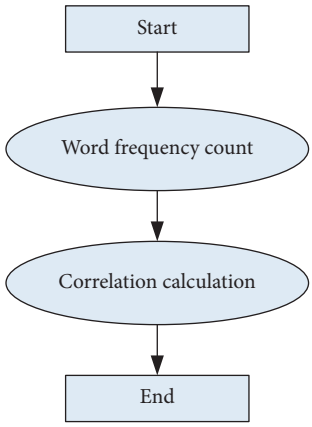

Figure 6: Correlation calculation model.

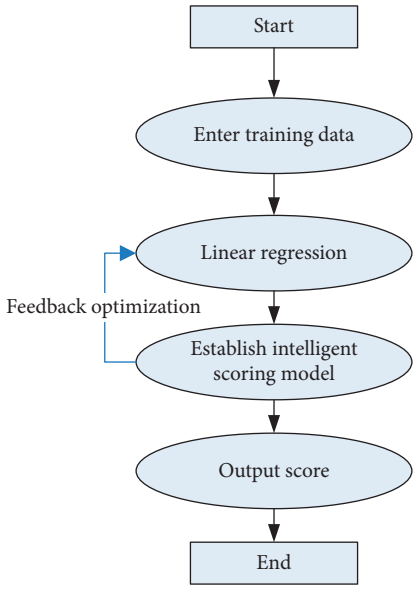

Figure 7: Linear regression model.

flow computing performed by tensor Tensor, which means the computing model. Each calculation in TensorFlow is a node on the graph, and the edges between nodes describe the dependencies between nodes.

In Python, "import TensorFlow as tf" is generally used to load TensorFlow. Tf can use TensorFlow more easily in programming. The TensorFlow program is divided into two parts, the first part needs to define all the calculations in the calculation graph, and the second part is to perform calculations.

There are many ways to install TensorFlow, which can be installed using Docker, installing using Pip, or compiled from source code. TensorFlow is divided into CPU version and GPU version. I installed the CPU version; the method used is Pip installation. The following is a detailed introduction to my installation method.

Pip is a small tool for Python that can easily and conveniently install and manage Python packages. Install TensorFlow using Pip - a three-step process. The first step is to install Pip. Select the appropriate version of Pip for your operating system to install. The second step is to find the proper installation package for TensorFlow. Because TensorFlow is divided into CPU and GPU versions, the GPU version requires the computer to support CUDA (Compute Unified Device Archive, a computing platform); I installed the CPU version. Currently, GPU installation still has specific restrictions on the environment. After the first two steps are completed, you can proceed to the third step, install TensorFlow through Pip. During installation, the commands installed will vary slightly depending on the version of Python. The steps of the deep neural network model are shown in Figure 8.

The steps of the deep neural network model (Figure 8) are as follows: input the training data into the neural network, and then use the neural network to train an intelligent scoring model continuously, and then input the test data into the intelligent scoring model to obtain the preliminary results of the intelligent scoring, compare this result with the teacher's score, and then feedback and optimize the model, improve the model, and finally determine the intelligent scoring model; then input the test data into the intelligent scoring model and finally determine the score and then output it.

3.2.3. Fusion Design of Linear Regression Model and Deep Neural Network Model. The linear regression model and the deep neural network model are respectively assigned a weight and then summed to calculate the fused value. The final weighted prediction results in the experiment are $p = Lr\_model * \alpha + dnn\_model * \beta$, $\alpha + \beta = 1$, of which Lr_model and dnn_model are the results of the linear regression model and the deep neural network model, respectively. The values of α and β change dynamically during each training and are related to relevant parameters and datasets.

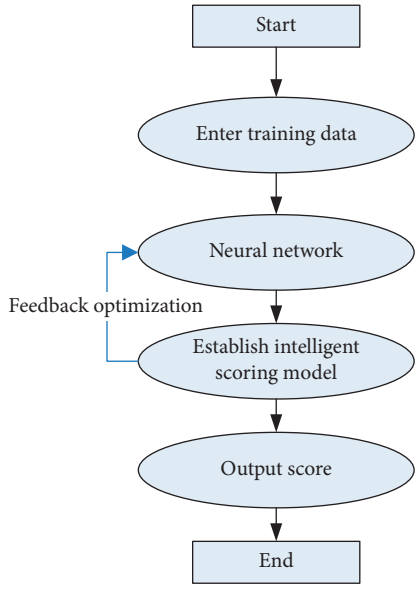

Figure 8: Deep neural network model.

3.3. Experimental Results of the Intelligent Scoring System

3.3.1. Model Evaluation. The weight value results of the linear regression model are shown in Table 1.

The result of the weight value of the deep network is shown in Table 2.

The weight value results after the linear regression model-neural network model fusion are shown in Table 3.

The dataset is randomly divided into a training set and test set, of which the training set accounts for 80%, with a total of 3,122 samples, and the test set accounts for 20%, with a total of 781 samples. The random sampling is divided into five categories, and the five categories are marked as *A*, *B*, *C*, *D*, and *E*, respectively.

There are three models as follows: the linear regression model (lr), the deep neural network model (DNN), and the model after the fusion of the two models (lr_DNN). We calculate the respective Recall and Precision to evaluate the model; the results are shown in Table 4. It can be seen from the table that the Recall and Precision after the fusion of the linear regression model and the deep neural network model are significantly better than the deep neural network model and the linear regression model.

3.3.2. Evaluation of Scoring Accuracy. The dataset was randomly divided into a training set and test set, of which the training set accounted for 80%, with a total of 3,122 samples, and the test set accounted for 20%, with a total of 781 samples. The method for judging whether the score is accurate or not is shown in Figure 9.

Among the 781 samples, 711 samples were predicted correctly, and 70 samples were predicted wrong. Therefore, the calculated accuracy rate is 91.04%, and the formula for calculating the accuracy rate is as follows:

Accuracy rate = (accurate number of scores/total number of scores) $*$ 100% = 91.04%

Table 1: Linear regression model weight values.

Feature	Weights
Automatically correct total score	0.4910
Total test score	0.4343
Relativity	0.4286
Content related	0.3698
Sentence	0.3591
Vocabulary	0.3275
English training times	0.3251
English interest level	0.3240
Objective test score	0.3132
Homework completion	0.3018
Chapter structure	0.2993
College English test 4 and 6	0.2744
Passed college English test 4 and 6	0.2058
Gender	0.1932

Table 2: Deep neural network weight values.

Feature	Weights
Automatically correct total score	0.4796
Total test score	0.4479
Relativity	0.3990
Sentence	0.3797
Content related	0.3690
English interest level	0.3291
English training times	0.3291
Objective test score	0.3195
Vocabulary	0.3110
Homework completion	0.3089
Chapter structure	0.2996
College English test 4 and 6	0.2493
Passed college English test 4 and 6	0.2633
Gender	0.1446

Table 3: Weight values after model fusion.

Feature	Weights
Automatically correct total score	0.4898
Total test score	0.4330
Relativity	0.3846
Sentence	0.3797
Content related	0.3879
English interest level	0.3248
English training times	0.3189
Objective test score	0.3195
Vocabulary	0.3110
Homework completion	0.3089
Chapter structure	0.2996
College English test 4 and 6	0.2687
Passed college English test 4 and 6	0.2384
Gender	0.1878

The main reason for the accuracy of the predicted samples is that the established intelligent scoring model can objectively describe the students' verbal expression ability, and teachers' scores are relatively concentrated, generally ranging from 7 to 9 (10-point scale). The main reason for the inaccuracy of the predicted samples is that the usual grades of some students cannot reflect their learning situation. For

Table 4: Evaluation of three models.

	lr_DNN (%)		DNN (%)		lr (%)	
	Recall	Precision	Recall	Precision	Recall	Precision
A	91.23	93.52	89.12	88.09	84.16	87.03
B	92.43	92.41	87.35	86.21	83.88	86.97
C	90.69	91.90	89.31	90.75	85.54	88.74
D	92.34	92.28	88.81	84.90	88.90	85.10
E	91.83	90.31	91.04	89.34	89.91	85.74

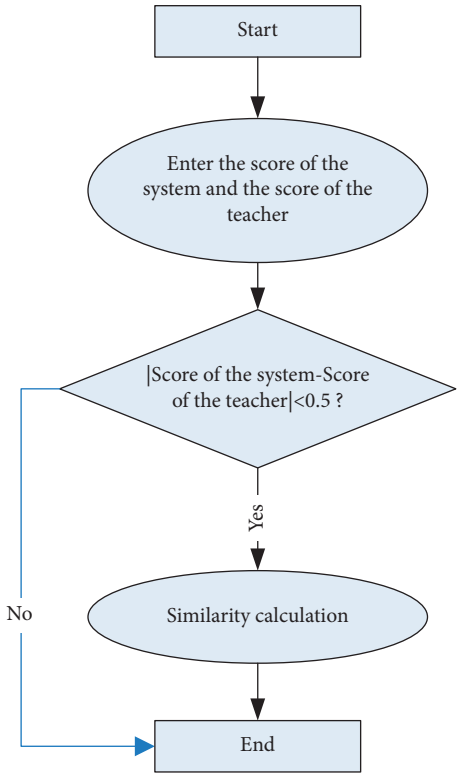

Figure 9: Evaluation of scoring accuracy.

example, student A is not interested in English but has a higher score on the oral English expression question. It is usual for the prediction results to have a certain error. Due to the diversity of samples, it is acceptable for the accuracy of a certain model to have the error within a reasonable range.

4. Conclusions

With the deepening of China's opening to the outside world, business English majors put forward higher requirements for oral application ability. Making full use of various educational information technologies to promote the normalization, informatization, and networking of oral teaching and training is an important measure to improve the oral application ability of business applications. Based on the analysis of the current situation of applied oral English teaching and training, this paper combs the prominent problems in the current teaching, such as low application of objectives, insufficient timeliness of the content, insufficient pertinence of implementation, and weak evaluation process, and puts forward a scoring method of business English oral English training based on deep neural network.

This paper explores a new teaching mode. Focusing on business application, this model promotes the transformation of teaching objectives from knowledge to ability, introduces scene application and other rich teaching contents, promotes the implementation of "online and offline" hybrid teaching, and implements curriculum formative assessment and evaluation, so as to promote student-centered teaching reform and improve students' oral application ability. After one academic year's pilot application in many business English application courses, the new model has better results in classroom effect, student investment, performance assessment, innovative practice, and practice.

Although it is based on the student's oral test data in the business English oral skill training system for speech recognition, automatic correction, machine learning modeling, and neural network modeling, there will still be many problems in the actual operation process. The limitations of this study are as follows: inaccurate speech recognition results, inaccurate oral score, and limitations of the deep learning model.

(1) Although speech recognition has been claimed to have an accuracy of more than 95% in the official documents, in the actual process, the output results of speech recognition will be affected by the examination environment, the influence of surrounding students, and the noise nearby. If the speech recognition result is not accurate, it will have a certain impact on the oral score.

(2) At present, most oral evaluation still adopts the subjective evaluation of teachers, and the oral evaluation itself is a difficult problem to overcome. Different teachers have different scoring standards, and there are differences in the scores between teachers. Most of them take the form of average scores to calculate the student's scores. Therefore, in the process of automatic recognition of oral scoring, there will be a difference between the system scoring standard and the teacher scoring standard. In short, it is difficult to quantify teachers' scoring standards, and it is difficult to reach an agreement between the scoring standards of the automatic correction system and teachers' scoring standards.

(3) The following research can optimize the scoring model and select the most appropriate model with the in-depth study of neural networks. Moreover, with the gradual increase of the computing power of CPU and GPU, the model can be more complex. In this way, even if the complexity of the model is increased and the amount of calculation becomes larger, the results can be calculated quickly.

Data Availability

The dataset can be accessed upon request.

Conflicts of Interest

The authors declare that they have no conflicts of interest.

References

[1] X Cheng, K. Liu, and K. Liu, "Application of multimedia networks in business English teaching in vocational college," *Journal of Healthcare Engineering*, vol. 2021, Article ID 5519472, 9 pages, 2021.

[2] Y. Xin, "Analyzing the Quality of Business English Teaching Using Multimedia Data Mining," *Mobile Information Systems*, vol. 2021, Article ID 9912460, 8 pages, 2021.

[3] Y. Shi and H. Shi, "Construction of an Assessment System for Business English Linguistics Based on RNN Multidimensional Models," *Mathematical Problems in Engineering*, vol. 2022, Article ID 8446281, 8 pages, 2022.

[4] Y. Chen, "Business English translation model based on BP neural network optimized by genetic algorithm," *Computational Intelligence and Neuroscience*, pp. 2021–10, Article ID 2837584, 2021.

[5] X. Zhang, "The influencing factors of business English intercultural communication based on data mining," *Lecture Notes on Data Engineering and Communications Technologies*, vol. 85, pp. 173–181, 2022.

[6] L. Li and C. Mao, "Big data supported PSS evaluation decision in service-oriented manufacturing," *IEEE Access*, vol. 8, no. 99, Article ID 154670, 2020.

[7] J. Zhang and F. Li, "Blended teaching of business English based on semantic combination and visualization technology," *Lecture Notes on Data Engineering and Communications Technologies*, vol. 81, pp. 535–540, 2021.

[8] L. Li, B. Lei, and C. Mao, "Digital twin in smart manufacturing," *Journal of Industrial Information Integration*, vol. 26, no. 9, Article ID 100289, 2022.

[9] W. Kuang, "Business English online classroom teaching based on ESP demand analysis technology," *Lecture Notes on Data Engineering and Communications Technologies*, vol. 102, pp. 1119–1128, 2022.

[10] X. Qin, "Business English visualization system based on video surveillance and the internet of things," *Microprocessors and Microsystems*, vol. 80, Article ID 103639, 2021.

[11] L. Li, C. Mao, H. Sun, Y. Yuan, and B. Lei, "Digital twin driven green performance evaluation methodology of intelligent manufacturing: hybrid model based on fuzzy rough-sets AHP, multistage weight synthesis, and PROMETHEE II," *Complexity*, vol. 2020, 24 pages, 2020.

[12] J. F. Chen, C. A. Warden, D. Wen-Shung Tai, F. S. Chen, and C. Y. Chao, "Level of abstraction and feelings of presence in virtual space: business English negotiation in Open Wonderland," *Computers & Education*, vol. 57, no. 3, pp. 2126–2134, 2011.

[13] R. Han and Y. Yin, "Application of web embedded system and machine learning in English corpus vocabulary recognition," *Microprocessors and Microsystems*, vol. 80, Article ID 103634, 2021.

[14] L. Li, T. Qu, Y. Liu et al., "Sustainability assessment of intelligent manufacturing supported by digital twin," *IEEE Access*, vol. 8, Article ID 175008, 2020.

[15] L. Niessen and N. M. P. Bocken, "How can businesses drive sufficiency? The business for sufficiency framework," *Sustainable Production and Consumption*, vol. 28, pp. 1090–1103, 2021.

[16] P. Henz, "The alpha dog in the human-AI team," *Steel Times International*, vol. 44, no. 1, pp. 29–32, 2020.

[17] H. Wang, J. Zhao, B. Wang, and L. Tong, "A quantum approximate optimization algorithm with metalearning for maxcut problem and its simulation via tensorflow quantum," *Mathematical Problems in Engineering*, vol. 2021, Article ID 6655455, 11 pages, 2021.

[18] Bo Liu, Q. Wu, Y. Zhang, Q. Cao, and X. Xu, "Exploiting the Relationship between Pruning Ratio and Compression Effect for Neural Network Model Based on TensorFlow," *Security and Communication Networks*, vol. 2020, Article ID 5218612, 8 pages, 2020.

[19] Y. Du, S. Sun, S. Qiu, S. Li, M. Pan, and C.-H. Chen, "Intelligent recognition system based on contour accentuation for navigation marks," *Wireless Communications and Mobile Computing*, vol. 2021, Article ID 6631074, 11 pages, 2021.

[20] W. Lv and Q. Zhong, "Design and Optimization of Children's Education Online Monitoring System Based on 5G and Internet of Things," *Scientific Programming*, vol. 2022, Article ID 5336786, 18 pages, 2022.

[21] Y. Ding, N. Zhang, and Y. Li, "College Physical Education Course Management System Based on Internet of Things," *Mobile Information Systems*, vol. 2021, Article ID 587439, 10 pages, 2021.

[22] H. Yu, "Application analysis of new internet multimedia technology in optimizing the ideological and political education system of college students," *Wireless Communications and Mobile Computing*, vol. 2021, Article ID 557343, 12 pages, 2021.

[23] M. Suhail, I. Babar, Y. A. Khan, M. Imran, and Z. Nawaz, "Quantile-Based Estimation of Liu Parameter in the Linear Regression Model: Applications to Portland Cement and US Crime Data," *Mathematical Problems in Engineering*, vol. 2021, Article ID 1772328, 11 pages, 2021.

[24] H. Mokhort, "Multiple linear regression model of meningococcal disease in Ukraine: 1992-2015," *Computational and Mathematical Methods in Medicine*, vol. 2020, Article ID 5105120, 7 pages, 2020.

[25] A. F. Lukman, B. M. G. Kibria, K. Ayinde, and S. L. Jegede, "Modified one-parameter liu estimator for the linear regression model," *Modelling and Simulation in Engineering*, vol. 2020, Article ID 9574304, 17 pages, 2020.

[26] Y. O. Ouma, C. O. Okuku, and E. N. Njau, "Use of Artificial Neural Networks and Multiple Linear Regression Model for the Prediction of Dissolved Oxygen in Rivers: Case Study of Hydrographic Basin of River Nyando, Kenya," *Complexity*, vol. 2020, Article ID 9570789, 23 pages, 2020.

[27] T. Yao, B. Zhang, J. Peng et al., "Defect Prediction Technology of Aerospace Software Based on Deep Neural Network and Process Measurement," *Mathematical Problems in Engineering*, vol. 2022, Article ID 1276830, 8 pages, 2022.

[28] W. Zhang, Y. Li, X. Li et al., "Deep Neural Network-Based SQL Injection Detection Method," *Security and Communication Networks*, vol. 2022, Article ID 4836289, 9 pages, 2022.

[29] S. Yang and S. Yang, "Research on E-commerce oral English blended teaching," in *Proceedings of the - 2nd International Conference on E-Commerce and Internet Technology, ECIT*, pp. 36–39, Hangzhou, China, March 2021.

Hindawi
Scientific Programming
Volume 2022, Article ID 2076633, 13 pages
https://doi.org/10.1155/2022/2076633

Research Article

Remote-Sensing Inversion Method for Evapotranspiration by Fusing Knowledge and Multisource Data

Jingui Wang,[1] **Dongjuan Cheng**,[1] **Lihui Wu**,[2] **and Xueyuan Yu**[3]

[1]*School of Water Conservancy and Hydroelectric Power, Hebei University of Engineering, Hebei, Handan 05600, China*
[2]*Handan Design and Research Institute of Water Conservancy and Hydropower, Hebei, Handan 056001, China*
[3]*HeBei Gal Xiang Geographic Information Technology Service Co., Ltd, Hebei, Handan 056001, China*

Correspondence should be addressed to Jingui Wang; wangjingui@hebeu.edu.cn

Received 8 June 2022; Revised 14 July 2022; Accepted 20 July 2022; Published 22 August 2022

Academic Editor: Lianhui Li

Evapotranspiration (ET) is the main process parameter of the land surface heat and water balance. Evapotranspiration remote-sensing inversion can be divided into two types of methods, process-driven and data-driven, according to the model power. This paper presents a comprehensive and systematic review of the research progress of data-driven ET remote-sensing inversion methods and their products; reviews the basic principles, advantages, and disadvantages of related methods/products from three perspectives: empirical regression, machine learning, and data fusion; and finally indicates the development direction of data-driven ET remote-sensing inversion research.

1. Introduction

Evapotranspiration (ET) is the process by which surface water is transferred to the atmosphere, including evaporation of water trapped from water bodies, soils, and vegetation surfaces and transpiration by plants. As an important vehicle for water transfer and energy conversion in the land-air system, accurate estimates of evapotranspiration are essential for understanding global climate change, ecological and environmental issues, water cycle, and hydrological processes, as well as for mixing and irrigation of water for agriculture, monitoring agricultural droughts, and improving agricultural water use efficiency. To obtain complete spatial and temporal information on land surface ecosystems, two different scales of research tools are needed, namely ground-based observations and remote sensing. Currently, more than 400 stations and 2,000 ground-based flux observation sites have been constructed worldwide. In China, a network of 45 stations has been initially built to cover the major ecosystem types in Central Park. To capture the spatial heterogeneity, scale effects, and uncertainties of surface evapotranspiration and to provide ground truth measurements at scale for developing and validating remote-sensing estimation models of evapotranspiration, the Integrated Heihe River Basin Ecological/Hydrological Processes Remote-Sensing Experiment constructed a dense three-dimensional flux observation matrix consisting of vorticity correlators, large-aperture scintillators, and automatic weather stations. However, the above observations are all station-scale based, and the spatial heterogeneity of large scale and nonuniformity of hydrothermal transport lead to the poor spatial representation of station-based observations, while intensive observations at large scale with multiple stations are usually time-consuming and laborious. Remote sensing, due to its macroscopic nature and large observation range, can overcome the spatial scale scaling problem involved in station-based observations, and a series of remote-sensing-based ET inversion models have been constructed [1]. Due to the low spatial resolution of geosynchronous satellites, which is difficult to meet the realistic demand, data from polar-orbiting satellites are usually used, and the time coverage period of polar-orbiting satellites is generally one week (e.g., Landsat at around 10: 00 a.m., MODIS Terra at around 10: 30 a.m., and Aqua at around 13: 30 p.m.), and the ET estimated based on these data is instantaneous ET. Daily, monthly, yearly, or even annual time

series of evapotranspiration are more useful than instantaneous evapotranspiration. For example, daily evapotranspiration is needed for meteorology, hydrology, and global atmospheric modeling; the dynamics of water consumption in agricultural fields during the growing season require estimation of the corresponding time-series evapotranspiration, and watershed water balance studies require estimation of time-series evapotranspiration. Therefore, it is necessary to explore the expansion of the time scale of remote-sensing inversion evapotranspiration and derive the cumulative daily to monthly values from the instantaneous values at the time of satellite transit to meet the research and application needs in the fields of climate, ecology, hydrology, and agriculture. With the development of satellite remote-sensing technology, surface parameters closely related to surface water and heat fluxes such as surface temperature, vegetation index, and soil moisture can be obtained by remote-sensing inversion, and remote-sensing inversion of evapotranspiration has become an effective method to obtain the spatial and temporal distribution of evapotranspiration at regional and global scales with high accuracy and timeliness. Due to the spatial heterogeneity of the subsurface surface, complex near-surface meteorological conditions, and the dynamics of hydrothermal transport processes, the spatial and temporal variability of surface evapotranspiration varies greatly, and the accurate estimation at the regional scale still faces great challenges [2].

Existing methods for remote-sensing inversion of evapotranspiration can be classified into conductivity-based and temperature-based methods according to the principle mechanism [3] and into methods based on shortwave band data, thermal infrared band data, and microwave band data according to the driving data. In this paper, we classify them into two major categories according to the model drivers: process-driven physical inversion methods, such as energy balance residual methods and methods based on Penman–Monteith or Priestley–Taylor formulas; and data-driven inversion methods, including empirical regression methods, machine learning methods, and data fusion methods. Process-driven methods are based on theories and assumptions of photosynthesis, canopy conductance, and respiration in the biosphere and use simplified ecosystem processes and components to form established model structures that simulate the carbon-water-energy exchange of ecosystems. This type of approach has a better physical basis and can achieve high estimation accuracy when high-precision input data are available. However, regional surface heterogeneity, complexity of impedance parameterization, and cumulative data errors make the process-based physical methods complex and limited in their estimation results when applied to regions, and their regional extension is limited by the lack of high-quality input data, making it difficult to obtain the desired regional estimation accuracy.

The data-driven remote-sensing inversion method for evapotranspiration is a method to obtain evapotranspiration estimates by establishing the relationship between evapotranspiration-driven data (observed fluxes or existing evapotranspiration products) and their closely related characteristic parameters. In this paper, we classify the data-driven methods into empirical regression methods, machine learning methods, and data fusion methods (Figure 1). Empirical regression methods and machine learning methods estimate actual evapotranspiration by directly constructing empirical relationships between remote sensing, meteorological and hydrological variables, and ET reference true values (e.g., observed fluxes), while data fusion methods improve ET accuracy or spatial and temporal resolution by fusing ET products with the same or different spatial and temporal resolutions. Related studies have found that complex physical and analytical methods do not necessarily have higher accuracy than simple empirical and statistical methods, while the diffusion and application of machine learning methods have greatly improved the accuracy of surface parameter estimation. The advantage of data-driven methods lies in the ability to capture data relationships sensitively and to construct well-fitting regression relationships with low errors to estimate steam emanation by relying on data alone. Unlike the traditional physical model, it does not need to predict the physical mechanisms of evapotranspiration processes or to obtain all variables that have an influence on them. It is only necessary to construct relationships between the obtained remote sensing, meteorological and observational flux data to obtain highly accurate estimation results.

With the development of the global flux observation network, more and more flux observation data have been shared and acquired, and data-driven methods have been developed rapidly. This paper presents a comprehensive and systematic review of the research progress of data-driven remote-sensing inversion methods and products at home and abroad; summarizes the basic principles, advantages, and shortcomings of related methods/products from three aspects: empirical regression, machine learning, and data fusion; and finally indicates the future development direction of data-driven remote-sensing inversion of evapotranspiration.

2. Data-Driven Inversion Method for Remote Sensing of Evapotranspiration

2.1. Experience Regression Method. Early empirical regression methods estimated surface evapotranspiration using a non-linear relationship between ground gas temperature difference and evapotranspiration and net radiation. With the long-term and continuous acquisition of observation data, the empirical regression method no longer relied only on the difference in ground gas temperature but estimated evapotranspiration by directly constructing linear or non-linear relationships between evapotranspiration and various climate or remotely sensed invertible parameters that are closely related to it. Later, in order to construct empirical models with higher applicability and accuracy, it was gradually developed to combine physical models and construct empirical regression relationships using globally distributed multisite flux observations.

Since the 1970s, with the advent of handheld infrared radiometers, researchers have begun to study the relationship between crop canopy temperature and plant

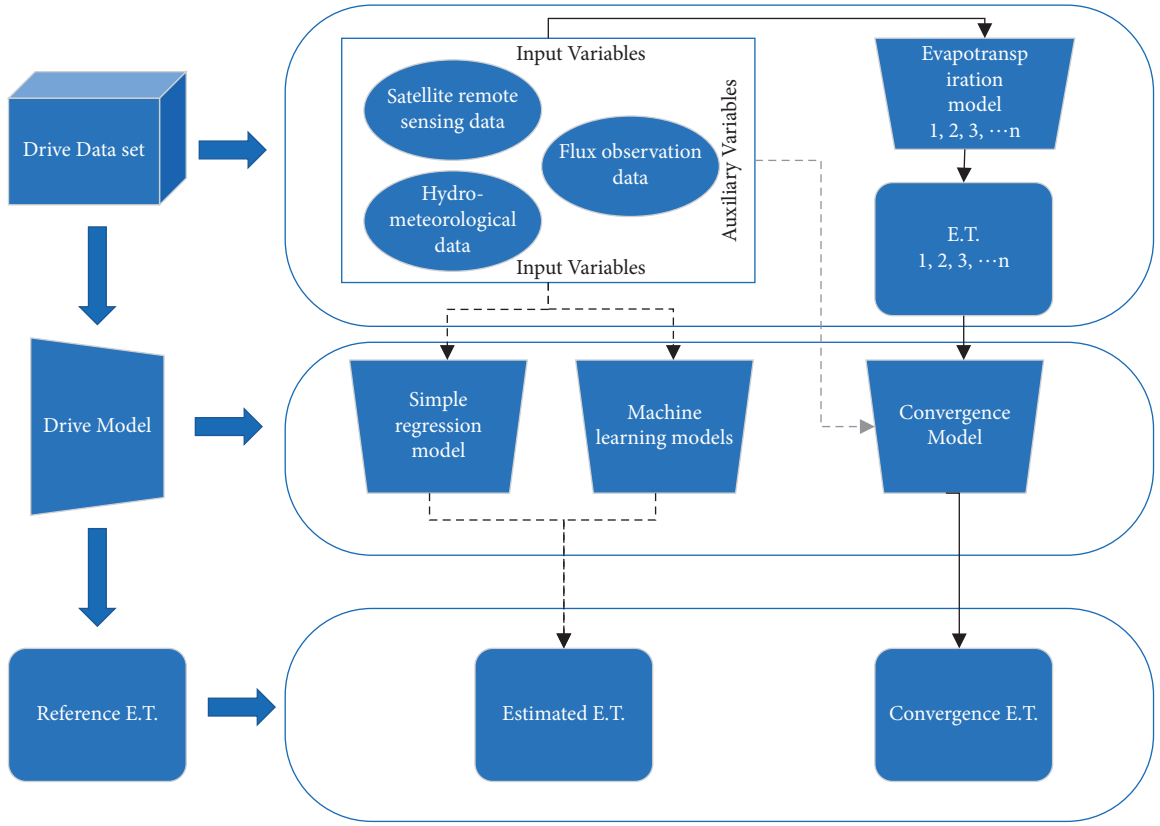

Figure 1: Integral flowchart of the data-driven remote inversion method for evapotranspiration (ET).

evapotranspiration. Jackson et al. [4] constructed an empirical model based on the relationship between instantaneous surface temperature at noon and the temperature difference between the reference altitude and daily evapotranspiration. The development of remote-sensing satellite detection technology, such as the early TIROS satellites (Television and Infrared Observing Satellite), NOAA satellites (National Oceanic and Atmospheric Administration), and HCMM satellites (meteorological satellite), has made it possible to estimate evapotranspiration on a large scale. With the progress in understanding and the availability of more satellite data, a series of time-scale extension methods have been proposed by different scholars. The idea of these methods is to obtain the daily evaporation by temporally extending the instantaneous latent heat flux based on parameters that remain constant with time or vary with a certain pattern. Interpolation and data assimilation methods are used to obtain connected long time series of evapotranspiration. Currently, some representative time-scale expansion methods include empirical model, sinusoidal relationship method, evaporation ratio method, reference evaporation ratio method, surface impedance method, astronomical radiation ratio method, and data assimilation method.

Empirical models (also known as statistical models) determine daily evapotranspiration by fitting latent heat LE, sensible heat H, net solar radiation R, and soil heat flux G under certain assumptions using instantaneous remotely sensed observations and ground truth values. This method was first proposed by Jackson et al. and has since been widely adopted [5]. Jackson et al. calculated daily evapotranspiration from the difference between daily net radiation and instantaneous remotely sensed land surface temperature (LST) and surface air temperature during daytime (usually at 13:30–14:00), as shown in the equation in Table 1. Seguin and Itier [6] found that daily evapotranspiration was also related to vegetation cover, surface roughness, wind speed, temperature stratification, and atmospheric stability and changed the above equation to an exponential form as shown in the equation in Table 1. Subsequently, Carlson [5] found that B and n vary with wind speed and surface roughness but are more sensitive to NDVI (normalized difference-vegetation index) and vegetation and proposed a simple method, as shown in the equation in Table 1. The method uses the difference between the LST at the time of satellite transit and the air temperature at 50 m height above the ground to calculate the daily evapotranspiration. The method is relatively simple and practical, but the coefficients B and n vary with the vegetation cover, introducing some cumulative error to the calculation results. Rivas and Caselles [7] estimated regional reference evapotranspiration based on LST and local meteorological data at the time of satellite transit, as shown in the equation in Table 1. The advantage of this method is that it has few parameters and high accuracy, and the disadvantage is that it is not universal and requires refitting the values of a and b with the PM equations based on local meteorological data when the regions are different.

Table 1: Summary of commonly applied empirical regression methods.

Methods	Parameter meaning	References	Remark
$LE_d = R_{n,d} - G_d - B_1(T_{1s} - T_{1a})$	LE_d is daily evapotranspiration, mm· d^{-1} $R_{n,d}$ is daily net radiation flux, MJ· m^{-2}· d^{-1} G_d is daily soil heat flux, MJ· m^{-2}· d^{-1} T_{1s} and T_{1a} are ground surface temperature and the temperature at 1.5 meters above the ground surface, at 13:30–14:00 local time, ˚C B_1 is lysimeter empirical parameters for regression of observed data	Jackson et al. [4]	(1)
$LE_d = R_{n,d} - B_2T(rad13 - T_{a13})^{n_1}$	T_{rad13} and T_{a13} are radiated ground surface temperature and the temperature at 2 meters above the ground surface, at 13:00 local time, ˚C B_2 and n_1 are calibration parameters based on surface roughness and atmospheric stability	Seguin et al.[5]	(2)
$LE_d = R_{n,d} - B_3(T_{rad} - T_{a50})^{n_2}$	T_{rad} and T_{a50} are radiated ground surface temperature and the temperature at 50 meters above ground surface, at 13:00 local time, ˚C B_2 is average overall conductivity of daily apparent heat flux n_1 is correction parameters for non-neutral static stability	Carlson et al.[6]	(3)
$ET_{r,d} = \mathrm{a} - T_{rad} + b$	$ET_{r,d}$ is daily reference evapotranspiration, mm· d^{-1}a, b are parameters fitted using the PM formula based on local meteorological data	Rivas and Caselles [7]	(4)

The empirical model can obtain high-precision evapotranspiration throughout the day by remote-sensing observation of LST, temperature, and net daily radiation only once a day at noon under the condition of sufficient moisture supply and relatively stable surface atmosphere, which is very convenient for large-scale remote-sensing applications and can be of great use in irrigation management and crop yield estimation. The evapotranspiration during the rainy period needs to be obtained by interpolating the evapotranspiration of consecutive sunny days. The parameters B and n for different regions need to be determined by empirical regression and are not universal.

Solar radiation provides the energy source required for evaporation; soil moisture can directly provide water for soil evaporation, and its deficiency has a coercive effect on evaporation; surface temperature difference (difference between surface temperature and near-surface air temperature) is the temperature condition that allows evaporation process to occur, and surface temperature can indicate information such as surface soil moisture condition. Wind speed, vegetation index, vegetation cover, leaf area index, and so on can provide information about the heterogeneous condition of the ground, such as roughness and impedance, which can influence the evapotranspiration process [8, 9]. The estimation of evapotranspiration can be considered as a complex non-linear regression analysis of several meteorological and remotely sensed variables, and its general form can be summarized in thefollowing equation, in conjunction with the equations provided in Table 1:

$$ET = f(R_n, R_s, T_s, T_a, VI, WS, RH_{da}, dVP_i \ldots), \quad (1)$$

where R_n represents net surface radiation, R_s represents incident shortwave radiation, T_s represents surface temperature, T_a represents air temperature, VI represents vegetation index, WS represents wind speed, RH_{da} represents daily average relative humidity, and dVP_i represents water vapor pressure inverse difference.

In the twentieth century, when remote-sensing inversion theory and ET research were less mature, such methods played an important role in estimating ET over small areas and could provide reliable information for moisture availability in practical applications [6]. Due to its dependence on ground-based observations, it is difficult to be applied to ET estimation over large areas.

Eddy covariance systems (EC) allow for more accurate ground-based flux observations, and with the establishment of a flux observation network based on eddy correlation (EC) system, long-term and continuous large-scale acquisition of observation data becomes possible. In particular, the sharing of open data from projects such as Fluxnet and ARM, have let to the emergence of regression statistics methods in various manifestations, and the combination of remote-sensing products, meteorological data, and flux observations to invert vapor combining remote-sensing products, meteorological data, and flux observations to invert the vapor has been well developed [10]. The empirical regression method no longer relies solely on the difference in ground temperature but estimates evapotranspiration by directly constructing linear relationships between evapotranspiration and its various closely related meteorological or remotely sensed reversible parameters. It was found that in the absence of a large number of meteorological observations, the evapotranspiration of image elements can be estimated from only a small number of remotely sensed reversible parameters, such as surface temperature, vegetation index, and surface albedo. However, the regression relationships constructed using meteorological and flux observation data from a few stations have large uncertainties in regional transplantation and require re-evaluation of empirical coefficients, while it is relatively difficult to construct empirical models with high applicability and accuracy. For this reason, research on empirical regression methods has been gradually developed to construct empirical regression relationships based on physical models using globally distributed multistation flux observation data [11]. Wang et al. [9] divided surface evapotranspiration into radiative and aerodynamic terms, introduced wind speed to calculate aerodynamic impedance, and combined ground

observation data, meteorological, and remote-sensing data to propose an empirical regression relationship based on the Penman–Monteith equation-based empirical regression relationship with certain physical significance for various surface types and confirmed that the accuracy of the empirical algorithm should be higher than that of the general model algorithm by re-fitting the coefficients for different land types separately, as shown in Figure 2. Yao et al. [12] proposed a simple hybrid empirical evapotranspiration estimation model based on a two-source model and validated by ground observations, which can be used for global surface evapotranspiration estimation. Yao et al. [13, 14] established an empirical estimation method based on Priestley–Taylor equation using 240 Fluxnet sites worldwide and determined the coefficients for different land classes. The empirical coefficients of the Priestley–Taylor equation were re-parameterized by replacing the available energy at the surface with the more readily available incident shortwave radiation.

Because thermal infrared surface temperatures are affected by clouds, simple regression methods applicable to large regions or the globe tend to use more readily available air temperatures as model inputs, Table 2, with calculated root mean squared error (RMSE).

There is also a trapezoidal eigenspace method based on the CWSI (crop water stress index) water deficit index for estimating regional surface evapotranspiration, as shown in Figure 3.

Based on the concept of CWSI (crop water stress index), Moran et al. [15] introduced the water deficit index (WDI), defined as the ratio of actual evapotranspiration to potential evapotranspiration, based on the Ts-VI trapezoidal space to estimate regional surface evapotranspiration and water deficit, and extended the CWSI applied in the total vegetation cover area to the partial-vegetation cover area. The CWSI applied in all-vegetation areas was extended to partial-vegetation areas. The input of surface observations for the trapezoidal method includes water vapor pressure, air temperature, wind speed, and maximum and minimum stomatal impedance. The trapezoidal method assumes that Ts-Ta on the wet and dry edges varies linearly with vegetation cover. To calculate the WDI at each image point in the trapezoidal space, the values of the four vertices of the trapezoid are obtained by combining the CWSI theory with the Penman–Monteith equation, that is, (1) the top of full vegetation cover with good moisture, (2) the top of full vegetation cover under water deficit, (3) the top of saturated bare soil, and (4) the dry bare soil.

2.2. Machine Learning Method. From constructing empirical relationships with observations from a few stations to constructing empirical relationships with observations from globally distributed stations, simple empirical statistical methods are becoming increasingly difficult to meet the high-precision needs of practical applications. Due to the excellent classification and regression prediction capabilities, machine learning methods are beginning to be used in studies of evapotranspiration estimation. Machine learning methods construct empirical models based on patterns contained in data without specifying any functional form; have good data adaptability [16]; can significantly improve regression prediction accuracy; can also mine new information from data to facilitate the generation of understanding of new mechanisms [17]; and have been widely used in geological fields, such as surface parameter inversion, groundwater studies, downscaling, remote-sensing image fusion, and so on [18]. The results have been widely used in the field of geology, such as surface parameter inversion, groundwater studies, downscaling, and remote-sensing image fusion [18].

A study by Genaidy et al. [19] was one of the first studies that received wide attention on the use of neural networks for evapotranspiration estimation. Yang et al.[20] used a support vector machine approach to successfully estimate the evapotranspiration for the contiguous United States at 8 d using surface temperature, enhanced vegetation index, and surface cover in combination with incident shortwave radiation based on remotely sensed data and observations from 22 AmeriFlux sites. Jung et al. [21] used a support vector machine approach to estimate the evapotranspiration at 8 d scale evapotranspiration. The study by Jung et al. [21] published in *Nature* is one of the most influential studies in recent years using machine algorithms to estimate evapotranspiration, which used the model tree ensemble (MTE) approach to integrate surface meteorological data, remote-sensing data, and flux site data to assess monthly evapotranspiration at the global scale. Since then, especially in the past 5 years, a large number of related studies based on machine learning have emerged. Although these studies mainly focus on the comparative evaluation of different machine learning algorithms, the estimation results of different machine learning methods do not differ much, as confirmed by the study [22]. The accuracy of the estimation results between different machine learning methods is comparable after adjusting the parameters to obtain the optimal parameters [23]. The advantage of machine algorithms is that the model construction incorporates observed data, similar to encapsulated complex empirical algorithms, and high model simulation accuracy, and the disadvantage is that the model accuracy depends on the data, including data quality, data processing methods, data representativeness, and data scale issues. The focus of this paper is to summarize the application of machine learning methods to the inversion of evapotranspiration rather than to present the principles of each machine learning method, and information about the methods can be found in the above references.

The existing studies on regional evapotranspiration estimation based on various machine learning methods are summarized, and the existing studies are divided into two categories: one is the estimation of regional image-scale evapotranspiration through site-liter scale expansion, and the other is the estimation of regional image-scale evapotranspiration through image or watershed scale expansion.

(1) The regional evapotranspiration model is constructed with in situ observed flux data as the image element true value, combined with remote-sensing products and climate information. Depending on the source of the driving data,

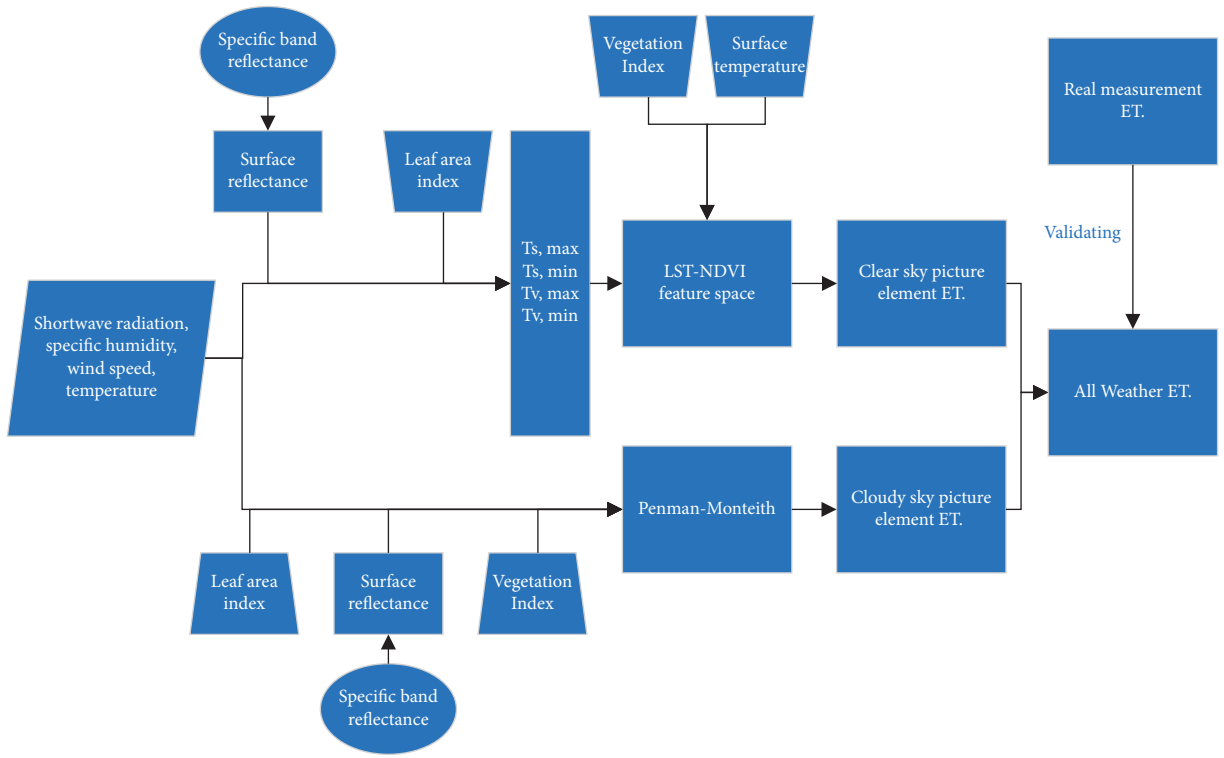

Figure 2: Flow chart of the all-weather ET inversion method.

Table 2: Imperial regression methods for the large region or global application.

Reference	Input	Time span	Station	Time scale	Results
Wang and Liang [8]	$VI, WS, R_s, RH_{da}, dVP_i$	1982–2002	International 64 flux observation sites	16 days	$R^2 = 0.94$; RMSE = 17 W/m^2
Yao et al. [12]	R_n, T_a, VI	2000–2008	12 ARM sites, 7 Fluxnet sites, 3 China flux observation sites	16 days	$R^2 = 0.84$; RMSE = 14.74 W/m^2
Yao et al. [13]	$VI, T_a, R_n, RH_{da}, dVP_i$	2000–2009	240 Fluxnet sites	1 day	Daily: $R^2 = 0.68 - 0.87$; RMSE = 11.5 − 20.9 W/m^{2}Monthly: $R^2 = 0.80 - 0.96$; RMSE = 4.3 − 18.1W/m^2
Yao et al. [14]	R_s, VI, RH_{da}	2000–2009	100 Fluxnet sites	1 day	Daily: $R^2 = 0.42 - 0.81$; RMSE = 15.8 − 28.2 W/m^{2}Monthly: $R^2 = 0.58 - 0.86$; RMSE = 11.7 − 23.9 W/m^2

two types of models can be built: one is to combine the ground frame flux observation data with all-remote-sensing products as the model driver; the other is to combine the ground frame flux observation data with climate and weather information and remote-sensing products as the model driver. The method effectively utilizes the observation data of the global flux observation network, gives full play to the powerful regression prediction capability of machine learning technology, fuses the accuracy error of the driven data, and improves the accuracy of remote-sensing inversion of surface evapotranspiration. The method effectively utilizes the observation data of the global flux observation network, gives full play to the strong regression prediction ability of machine learning technology, and fuses the accuracy error of the driving data to improve the accuracy of remote-sensing inversion of surface evaporation. However, most studies ignore the spatial scale differences between the source area of flux observations and gridded gas data or moderate resolution remote-sensing products. Such methods use in situ observed flux data as image element true values to construct models and combine remote-sensing products with climatological and meteorological information to obtain regional evapotranspiration. Various machine learning methods, such as neural networks, kernel function methods, and tree

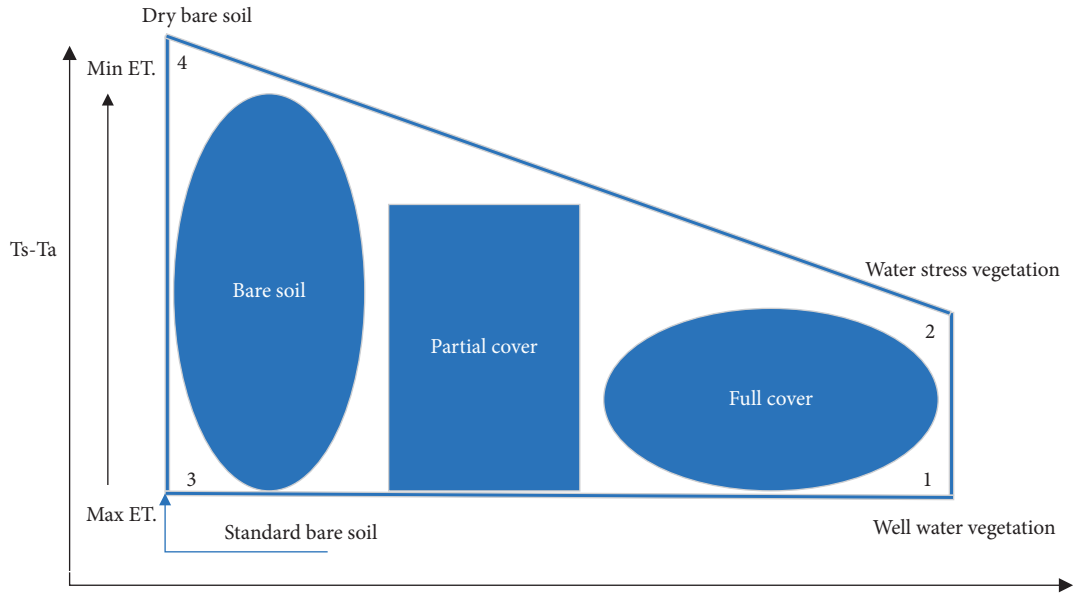

Figure 3: Schematic diagram of the terrestrial temperature difference-vegetation cover trapezoid relationship.

models, are used to obtain the spatial and temporal distribution of evapotranspiration at high scales in the observed regions and even globally. Depending on the source of the driving data, they can be divided into two categories. (i) Combination of ground-based observations and all-remote-sensing products as model drivers. Based on Moderate Resolution Imaging Spectroradiometer (MODIS) surface products, or in combination with Global Land Surface Satellite (GLASS), Global Energy and Water Exchanges-Surface Radiation Budget (GEWEX-SRB), Cloud and Earth Radiation Energy System (CERES), or the Japan Aerospace Exploration Agency (JAXA), researchers can use multiple remote sensing metrics as driving data to invert regional surface evapotranspiration through machine learning upgraded models [17, 20, 22]. (ii) Combining ground observation data with meteorological and climate information and remote-sensing products as model-driven data. Regional meteorological indicators are obtained from meteorological reanalysis data or weather station interpolation, and the combination of MODIS and GLASS remote sensing can invert surface parameters to drive model upscaling and estimate regional surface evapotranspiration [16, 22]. Comparing these two types of methods, the uncertainty of remote sensing combined with meteorological data-driven models is greater than the uncertainty of all-remote sensing as a data-driven model due to the inherent uncertainty of meteorologically driven data sets [22]. The advantage of remote sensing combined with meteorological data-driven models is that the input of meteorological data makes it possible to invert to obtain spatiotemporally continuous daily surface evapotranspiration, but it also reduces the spatial resolution of the inversion results. Meanwhile, its low spatial resolution cannot effectively take into account the spatial scale differences between the source area of site flux observations and gridded meteorological data or medium-resolution remote-sensing products, which reduces the inversion accuracy.

In addition, surface temperature and ground temperature difference, which are important parameters in traditional physical models for evapotranspiration estimation, are less applied in machine learning methods (Figure 4). Only a few studies have considered the effect of thermal infrared surface temperature as a driving factor in global applications [24, 25]. Thermal infrared surface temperature can provide valuable information such as surface soil moisture status for estimating evapotranspiration [26], and Jimenez [24] showed that the sensible and latent heat flux accuracy is significantly reduced when there is no thermal infrared surface temperature input. Although there are still some shortcomings, under the existing conditions, the site upscaling approach effectively utilizes the observed data from the global flux observation network, takes full advantage of the machine learning technology with powerful regression prediction capability, incorporates the accuracy error of the driving data, and improves the accuracy of remote-sensing inversion of surface evapotranspiration.

(2) Combine the existing shelf model flux products or reanalysis products to construct the relationship between remote-sensing variables and fluxes at image scale to obtain regional evapotranspiration directly or construct the relationship between watershed variables and watershed evapotranspiration to obtain evapotranspiration at image scale by downscaling. These methods can effectively solve the problem of matching spatial scales. However, the model construction of the image-scale scaling method uses the land surface model flux products or re-analysis products as the real values, and there is no set of products with fully reliable accuracy, so there is great uncertainty in the regional evapotranspiration obtained using this method. The Global Soil Wetness Project-2 (GSWP-2) compared global evapotranspiration estimates from 15 models and found global annual evapotranspiration variability ranging from 272 to 441 mm/a [27]. By comparing 41 global surface evapotranspiration (GSE) product data sets from 1985 to 1995, the

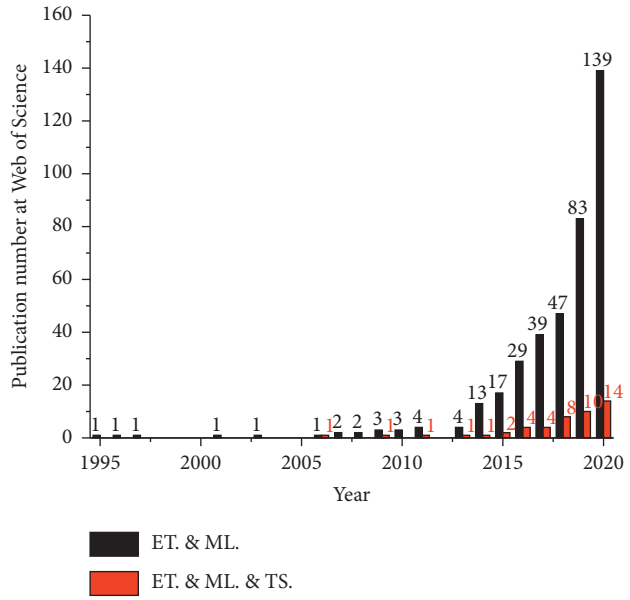

Figure 4: Number of articles published in 1995–2020 on topics that include evapotranspiration and machine learning (ET and ML) and evapotranspiration, machine learning, and surface temperature (ET and ML and TS; based on a web of science platform).

study found that the global average annual surface evapotranspiration was about 1.59 ± 0.19 mm/d (46 ± 5 W/m^2). Simulated values are lower than the reference data set as of IPCC AR4 (IPCC Fourth Assessment Report), whose standard deviation is 0.16 mm/d (4.6 W/m^2), while the standard deviation of 0.12 mm/d (3.6 W/m^2) for the GSWP LSMs (the Global Soil Wetness Project land surface models) dataset is even lower than the standard deviation of IPCC AR4 [28].

There is also a method for estimating regional evapotranspiration at the watershed downscale. This method is to construct the relationship between basin variables and basin evapotranspiration in combination with basin evapotranspiration, downscaling to get like meta-scale evapotranspiration. Lappen and Schumacher [29] based on surface water balance method from rainfall data from rain barrel observatory, river runoff from the hydrological observatory, combined with gravity recovery and climate experiment (GRACE) and Terrestrial Water Storage Anomaly (TWSA) data to obtain monthly-scale evapotranspiration from 95 watersheds worldwide, and used a model tree integration approach to relate variables such as radiation, temperature, rainfall, wind speed, and vegetation index to monthly-scale watershed evapotranspiration to estimate monthly-scale using spatialized meteorological and satellite data global evapotranspiration using spatialized meteorological and satellite data. This method effectively solves the spatial scale matching problem and can obtain high-precision basin-scale monthly evapotranspiration, but it cannot describe the spatial and temporal (e.g., between different days and between different grids) heterogeneity of evapotranspiration in the basin and cannot accurately obtain high-precision daily evapotranspiration.

2.3. Data Fusion Method. ET estimation based on data fusion can be divided into two categories, that is, fusion with the same spatial and temporal resolution and fusion with different spatial and temporal resolutions.

(1) Same spatial and temporal resolution fusion is the fusion of ET obtained from models with multiple spatial and temporal resolutions with flux observations or ET products as reference true values to obtain higher accuracy ET estimates. This approach combines the advantages of physical models with solid physical mechanisms and data-driven methods with strong regression prediction capabilities, combining the advantages and disadvantages of various algorithms. The problem is that the fusion accuracy is limited by the accuracy of the individual model being fused. The fusion accuracy is limited by the accuracy of the individual models being fused. Depending on whether the fused ET models and the fusion method used can be explicitly expressed, they can be subdivided into two types: multimodel ET explicit fusion and multimodel ET implicit fusion.

Considering that different algorithms have their own advantages and disadvantages, the study of multialgorithm fusion has become a new trend in the study of quantitative remote sensing of vapor distribution in order to improve the accuracy of vapor emission. For example, models such as simple averaging, Bayesian averaging, empirical orthogonal function method, Taylor fusion model, and machine learning methods have been applied to multimodel ET fusion studies of evapotranspiration [30, 31]. The data-driven multimodel ET fusion method combines the advantages of physical models with solid physical mechanisms and data-driven methods with powerful regression prediction capabilities and combines the advantages and disadvantages of various algorithms to directly fuse the observed data, avoiding the problems of missing physical mechanism or low accuracy caused by using only data-driven methods to invert ET. It avoids the problem of missing physical mechanism or low accuracy caused by inversion of evapotranspiration using only physical models and can obtain more reliable evapotranspiration estimation results, while the estimation accuracy is improved to some extent.

Explicit multimodel ET fusion means that both the ET model to be fused and the fusion method used can be explicitly expressed. As the name implies, explicit fusion is characterized by the fact that the fusion model (including the model to be fused and the fusion method) can be expressed in an explicit formula that is easy to manipulate and replicate. The fusion of process-based physical models and data-driven empirical regression models using simple averaging, Bayesian averaging, or simple Taylor's method is currently a common approach for the explicit fusion of multiple models [30]. Bayesian averaging or simple Taylor fusion is essentially a weighted average method, where the scores of the different models to be fused are weighted according to the evaluated Bayesian or simple Taylor models. Its general expression is as follows:

$$ET = w_1 ET_1 + w_2 ET_2 + \cdots + w_n ET_n, \tag{2}$$

$$ET_n = f_n(v_{n1}, v_{n2}, \ldots, v_{ni}, \ldots, v_{nm}), \tag{3}$$

where w_n denotes the weight of the n-th model to be fused, ET_n is the nth model to be fused, f_n denotes the equation expression of the n-th model to be fused, and v_{ni} denotes the i-th model driver of the nth model to be fused. When using this approach for multimodel fusion, the selection of multiple models is more important, and a balance is needed to select the number of over- and underestimated models. The advantage of this approach is that it can balance the overestimation and underestimation of different algorithms, reduce their overestimation or underestimation, and improve the accuracy of the algorithm; the disadvantage is that the fusion accuracy is highly dependent on the accuracy of the fusion models themselves, and the uncertainty of the weight ratio of the fusion models inherently limits its wide application.

Implicit fusion of multimodel ET means that the fused ET model or the fusion method used cannot be expressed explicitly, that is, the fused model includes estimation methods that cannot be expressed in explicit formulas (e.g., machine learning methods, assimilation methods, pattern methods, etc.) [14, 32] or methods that cannot be expressed in explicit formulas (e.g., machine learning methods, etc.) as fusion methods for process-based multimodel fusion studies of physical or empirical regression models [31], or neither the model being fused nor the fusion method can be expressed explicitly. The essence of multimodel implicit fusion is product fusion, that is, multiple models to be fused need to be used to obtain their respective ET values, and then fusion methods are used to fuse site or regional products. The general expression is as follows:

$$ET = f\left(ET_1, ET_2, \ldots, ET_n\right), \tag{4}$$

where ET_n is the n-th model to be fused estimation result and f denotes the fusion method. Compared with the traditional physical model and display fusion, the implicit fusion method improves the estimation accuracy; compared with the empirical regression method and machine learning method, this type of method is more reliable than the empirical regression method and machine learning method when the area is scaled, especially in the area where the observed data are lacking or difficult to obtain. Meanwhile, the model fusion approach can still obtain reliable ET estimates with good accuracy for regions where vegetation cover is poor and it is difficult to obtain reliable and high-precision ET estimates using machine learning site upscaling alone. The shortcomings of this method are similar to the multimodel ET explicit fusion; the fusion accuracy is still limited by the accuracy of the fused algorithm itself and the dissimilarity between the selected models; and the complex structure of the fused model also affects its computational efficiency.

(2) The fusion of different spatial and temporal resolutions refers to the data-driven approach to establish the linkage between data to achieve spatial and temporal fusion or downscaling of evapotranspiration products to obtain ET products with high spatial and temporal resolutions, so as to effectively solve the problem of not being able to directly obtain high spatial and temporal resolution surface evapotranspiration from single-source remote-sensing data under the existing conditions. The disadvantage is that the fusion accuracy is highly dependent on the accuracy of the low-resolution ET products. Without a high accuracy single-source remote-sensing ET product, the uncertainty of data-driven spatiotemporal fusion or downscaling ET results will be directly increased. Spatiotemporal fusion and downscaling processes are similar [33], both of which are centered on establishing connections between data, and the advantage of the data-driven approach is that it can better capture and construct the relationships between data.

ET spatiotemporal fusion is the fusion of ET products with high temporal resolution and low spatial resolution and ET products with high spatial resolution and low temporal resolution to obtain ET products with high spatiotemporal resolution (Figure 5(a)). At this stage, there are few studies that directly fuse surface evapotranspiration products with different spatial and temporal resolutions; unlike slowly changing parameters such as surface reflectance, surface evapotranspiration is dynamically changing and its spatial and temporal fusion is difficult [34]. Data-driven ET downscaling research uses specific methods to elevate the high spatial resolution drivers to coarser scales; uses data-driven methods (e.g., machine learning methods) to establish a non-linear relationship between evapotranspiration at coarse scales, that is, low spatial resolution, and the drivers; and then applies this non-linear relationship to the high spatial resolution drivers to obtain the high spatial resolution evapotranspiration.

ET downscaling is to establish the relationship between the high spatial resolution process parameters and the low spatial resolution ET products and then downscale to obtain the high spatial resolution ET products (Figure 5(b)). Ke et al. [35] combined spatiotemporal fusion methods and machine learning downscaling methods to construct three spatiotemporal downscaling method schemes to obtain the actual evapotranspiration products of 30 m for 8 days. The three methods are (1) the Landsat-scale vegetation index at moment t2 is obtained by the fusion of Landsat, MODIS at moment t1, and MODIS surface reflectance at t2. We obtained the Landsat surface temperature at moment t2 by combining fusing Landsat, MODIS at time t1, and MODIS surface temperature at t2.And combine with the MOD16 ET product, the evapotranspiration at Landsat scale at t2 moment is obtained by machine learning downscaling method. (2) The Landsat-scale vegetation index at moment $t2$ is obtained by fusing the Landsat-scale vegetation index at moment $t2$ after inversion of Landsat, MODIS, and MODIS surface reflectance at different resolutions at moment $t1$ and moment $t2$, respectively, and the rest of the steps are the same as (1). (3) The vegetation index and surface temperature at moment $t1$ are obtained by inversion of Landsat at moment $t1$; the MOD16 evapotranspiration product at moment $t1$ is obtained; the Landsat-scale evapotranspiration at moment $t1$ is obtained by using the machine learning downscaling method; and then the Landsat-scale evapotranspiration at moment $t2$ is obtained by combining the MOD16 evapotranspiration products at moment $t1$ and moment $t2$.

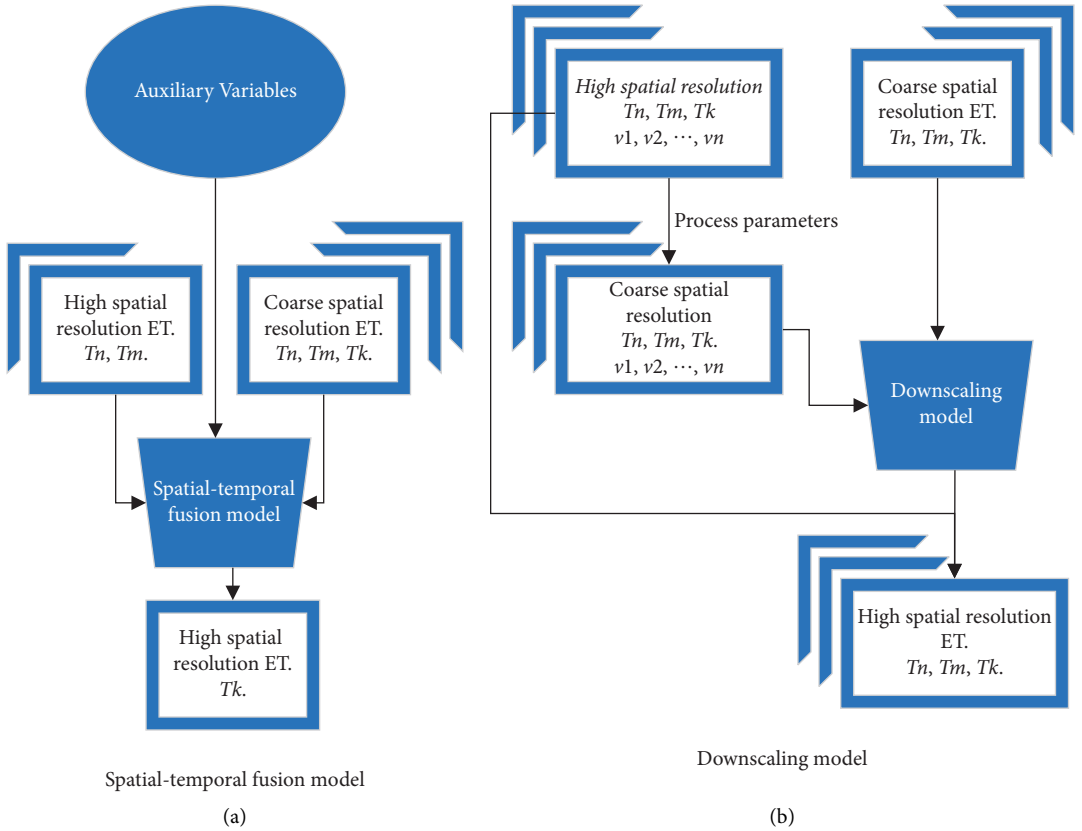

Figure 5: Schematic diagram of the principle of fusion of evapotranspiration (ET) data with different spatial and temporal resolutions: (a) spatialtemporal fusion model and (b) downscaling model.

2.4. ET Products Based on Data Fusion. The GLASS ET product is a spatially continuous latent heat flux remote-sensing product covering the global land surface, generated based on a Bayesian multimodel fusion approach, combining AVHRR, MODIS, and MERRA reanalysis data. Reference [30] used Bayesian averaging for different land surface coverage types, fusing two Penman–Monteith-based process models, two Priestley–Taylor-based process models, and a data-driven semiempirical model as the formal algorithm for the GLASS product land surface evapotranspiration. The product has a temporal resolution of 8 d, a maximum spatial resolution of 0.05° for the AVHRR-based product, and a maximum spatial resolution of 1 km for the MODIS-based product. Compared to the five fused evapotranspiration algorithms, the accuracy of the GLASS evapotranspiration product is significantly improved by the fusion of different ground classes and is closer to the ground truth. Compared with the machine learning-based product, the advantage of this product is that the fusion model has a physical mechanism and is relatively reliable in areas without flux observations; the disadvantage is that the fusion accuracy is limited by the accuracy of the fusion algorithm.

Hi-GLASS ET product is a high spatial resolution global land surface latent heat flux remote-sensing product based on the Taylor capability weight fusion method, combined with Landsat and MERRA reanalysis data. Yao et al. [36] used the Taylor capability weight approach, fusing a Penman–Monteith-based process model, a dual-source model, two Priestley–Taylor-based process models, and a data-driven empirical model, as the formal algorithm for land surface evaporation flux generation for the Hi-GLASS product. The product has a temporal resolution of 16 d and a spatial resolution of 30 m. The accuracy of the Hi-GLASS evapotranspiration product is better than that of the fused single algorithm. The advantages and disadvantages of this product are similar to those of the GLASS algorithm.

Synthesis ET product, is a monthly-scale, 1 km resolution remote-sensing combination data set produced by the simple averaging plus combination approach. Elnashar et al. [37] selected 12 sets of evapotranspiration products and constructed an evaluation matrix for ground validation of the selected products using eddy-related observations from 645 flux observation sites worldwide and sort selection based on accuracy.. The remote-sensing model with the best performance in terms of accuracy was selected for simple averaging and product combination. Finally, the NTSG product (downscaled to 1 km by nearest neighbor resampling) was selected for 1982–2000 (Table 3); MOD16A2 (V105) and NTSG products were simply averaged and selected for 2001–2002; 2003–2017,; simple averaging of the PML product (upscaled to 1 km by image element averaging) and the SSEBop product, with the SSEBop product were selected for 2018–2019. Combine them together to constitute the final Synthesis ET product. This product combines the

Table 3: Existing multimodel fusion products for global evapotranspiration.

Product	Reference	Methods	Accuracy	Temporal resolution	Spatial resolution	Time span (year)
GLASS ET	Yao et al. [14]	Bayesian	$R^2 = 0.72$ RMSE: 42.2 W/m^2	8 d	1 km	2000–2018
Hi-GLASS ET	Yao et al. [36]	Taylor skill fusion	$R^2 = 0.65$ RMSE: 23.8 W/m^2	16 d	30 m	2013–2018
SynthesisET	Elnashar et al. [37]	Simple average and combination	RMSE: 20.95–20.12 mm/month	1 month	1 km	1982–2019

advantages of several integrated products and provides users with a set of integrated products with relatively reliable accuracy that can be used directly without comparison; however, the products with different spatial resolutions have different spatial scales represented by their image elements, and the accuracy ranking by direct verification comparison without considering the flux observation source area lacks rationality.

3. Discussion and Conclusion

Although the data-driven methods have become more and more diverse in the past decade, from the initial non-linear relationship with temperature difference and net radiation to estimate surface evapotranspiration, to the construction of semiempirical regression relationships based on physical models with a large amount of observation data, to the widespread use of machine learning and deep learning methods, the data-driven methods have become more and more diverse, and the accuracy of data-driven evapotranspiration inversion has been gradually improved, and a variety of data-driven global evapotranspiration products have emerged, but there are still some urgent problems to be solved.

(1) Lack of evaporation products with high spatial and temporal resolution. The existing data-driven products are difficult to combine both high temporal and high spatial resolution features: for the full remote-sensing-driven inversion method, there is a lack of accessible remote-sensing data with high spatial and temporal resolution and spatial and temporal continuity; for the products that rely on gas data, the existing reanalysis products have a coarse resolution. The existing data-driven products have difficulty in combining both high temporal and high spatial resolution features; only the yet-to-be-released Hi-GLASS-ET product has a high spatial resolution (30 m) but a low temporal resolution (16 d), while the product with the high temporal resolution has a coarse spatial resolution (0.5°), and most of the remaining products have a coarse spatial and temporal resolution (8 d 0.05° and above). For the all-remote sensing-driven inversion methods, there is a lack of accessible remote-sensing data with high spatial and temporal resolution and spatial and temporal continuity; for products relying on meteorological data, the coarse resolution of existing global reanalysis products reduces the spatial resolution of estimation results; the variability of different meteorological data and the uncertainty of regional meteorological data also increase the uncertainty of estimation accuracy.

(2) The problem of spatial scale mismatch. The spatial scale difference between the source area of site observation and satellite image elements reduces the inversion accuracy. Most of the existing studies are based on EC observation data and establish the relationship between observation flux and meteorological observation or medium-resolution remote-sensing products to obtain national or global scale evapotranspiration. The low spatial resolution of remote-sensing and meteorological driven data makes it impossible to effectively consider the spatial scale difference between the source area of site flux observation and gridded meteorological data or medium-resolution remote-sensing products.

(3) Physical mechanisms are inadequate and spatial scalability is limited. Due to global climate differences, topographic relief, and surface heterogeneity, a limited number of stations cannot represent all surface conditions globally. For example, the estimation accuracy cannot be guaranteed in regions where there is a lack of observation data such as deserts and wetlands. Empirical methods or machine learning methods construct models based on a limited number (several hundred) of station observations, and the accuracy is better in regions where observation data are available, but the lack of data representativeness limits the generalization of the model, making its spatial scalability to be investigated.

(4) The important drivers of evapotranspiration, such as surface temperature and soil moisture, are not sufficiently considered. The existing methods mostly consider moisture input factors such as water pressure deficit and relative humidity and mostly use remote-sensing variables such as vegetation index, which can better reflect long-term changes in evapotranspiration but cannot monitor short-term changes. The thermal infrared surface temperature can provide valuable information such as surface soil moisture state for estimating evapotranspiration, and can better indicate the spatial and temporal

heterogeneity of evapotranspiration. Microwave remote sensing can provide soil moisture information directly. Existing methods mostly consider moisture input factors such as water vapor pressure deficit and relative humidity and do not effectively consider soil moisture information that has a direct impact on evapotranspiration.

(5) Observation data quality problem. The data-driven approach mostly uses flux observation data to drive the model, and the global application of the flux of EC observations has the problem of energy nonconfinement. It is still controversial whether energy balance closure correction is needed when using data-driven methods to invert ET.

(6) Lack of data-based evapotranspiration separation methods. The separation of soil evapotranspiration and vegetation evapotranspiration is more scientifically relevant and useful than the global approach, but there is still a lack of data-driven evapotranspiration separation methods.

This paper summarizes the advantages and problems of existing data-driven remote-sensing inversion methods for evapotranspiration in terms of both methods and available global products, from empirical regression, to the wide application of machine learning, to data fusion and downscaling. In today's big data era, where information is being collected much faster than we can understand, extracting and interpreting information is the challenge of the moment, and data-driven methods based on data are the opportunity within the challenge. Although data-driven inversion models can obtain high accuracy of vapor emission, they cannot replace physical models. Some physical models are more sensitive to specific input parameters than data-driven models, and it is more difficult to obtain high-precision input parameters on a global scale, which makes it difficult for physical models to surpass data-driven methods in terms of estimation accuracy. Compared with physical models, most data-driven methods lack the ability to explain the evapotranspiration process, which makes the analysis of estimation results limited in terms of interpretability. Ultimately, the core problem of data-driven inversion of remotely sensed evapotranspiration is still a problem of data. On the one hand, due to the powerful regression capability of data-driven (machine learning) methods, good accuracy estimation results can be obtained even if the driving data are wrong; on the other hand, when the spatial and temporal representativeness of the data is extremely limited, it is difficult for a clever woman to cook without rice. Considering that data-driven (machine learning) based methods can substantially improve the regression prediction accuracy, an important development direction is the deep integration of data-driven methods with physical models, which is severely lacking in the existing data-driven methods. Although existing data-driven fusion methods for evapotranspiration with the same spatial and temporal resolution have been combined with physical models to conduct multimodel fusion studies, the strength is still insufficient, mainly from the external combination, that is, using machine learning methods as fusion models to integrate physical methods, and lack of internal combination, that is, using machine learning methods to estimate input parameters that are difficult to obtain in vapor dispersion physical models and improving the accuracy of physical models by improving the estimation accuracy of complex parameters (e.g., surface roughness) in physical models.

Under the current situation of scarcity of high-precision and high spatial and temporal resolution driving data, data-driven methods and physical models should be closely combined to complement and promote each other so that mechanism and high-precision can coexist and jointly improve the accuracy of evapotranspiration remote-sensing inversion to obtain evapotranspiration remote-sensing products with high accuracy and good scalability.

Data Availability

The data set can be accessed upon request.

Conflicts of Interest

The authors declare that they have no conflicts of interest.

Acknowledgments

This study was supported by the Hebei Funding Project of Postgraduate Student Innovation Ability Training (no. CXZZBS2021019) and Handan Science and Technology, Bureau Municipal Science and Technology R & D Project (no. 21422012250).

References

[1] Z. L. Li, R. Tang, Z. Wan et al., "A review of current methodologies for regional Evapotranspiration estimation from remotely sensed data," *Sensors*, vol. 9, no. 5, pp. 3801–3853, 2009.

[2] S. Liu, Z. Xu, L. Song et al., "Upscaling evapotranspiration measurements from multi-site to the satellite pixel scale over heterogeneous land surfaces," *Agricultural and Forest Meteorology*, vol. 230-231, pp. 97–113, 2016.

[3] J. M. Chen and J. Liu, "Evolution of evapotranspiration models using thermal and shortwave remote sensing data," *Remote Sensing of Environment*, vol. 237, Article ID 111594, 2020.

[4] R. D. Jackson, R. J. Reginato, and S. B. Idso, "Wheat canopy temperature: a practical tool for evaluating water requirements," *Water Resources Research*, vol. 13, no. 3, pp. 651–656, 1977.

[5] B. Seguin and B. Itier, "Using midday surface temperature to estimate daily evaporation from satellite thermal IR data," *International Journal of Remote Sensing*, vol. 4, no. 2, pp. 371–383, 1983.

[6] T. N. Carlson, W. J. Capehart, and R. R. Gillies, "A new look at the simplified method for remote sensing of daily

evapotranspiration," *Remote Sensing of Environment*, vol. 54, no. 2, pp. 161–167, 1995.

[7] R. Rivas and V. Caselles, "A simplified equation to estimate spatial reference evaporation from remote sensing-based surface temperature and local meteorological data," *Remote Sensing of Environment*, vol. 93, no. 1–2, pp. 68–76, 2004.

[8] K. Wang and S. Liang, "An improved method for estimating global evapotranspiration based on satellite determination of surface net radiation, vegetation index, temperature, and soil moisture," *Journal of Hydrometeorology*, vol. 9, no. 4, pp. 712–727, 2008.

[9] K. Wang, R. E. Dickinson, M. Wild, and S. Liang, "Evidence for decadal variation in global terrestrial evapotranspiration between 1982 and 2002: 1. Model development," *Journal of Geophysical Research*, vol. 115, no. D20, Article ID D20112, 2010.

[10] K. Wang and R. E. Dickinson, "A review of global terrestrial evapotranspiration: observation, modeling, climatology, and climatic variability," *Review of Geophysics*, vol. 50, no. 2, 2012.

[11] P. L. Nagler, J. Cleverly, E. Glenn, D. Lampkin, A. Huete, and Z. Wan, "Predicting riparian evapotranspiration from MODIS vegetation indices and meteorological data," *Remote Sensing of Environment*, vol. 94, no. 1, pp. 17–30, 2005.

[12] Y. Yao, S. Liang, Q. Qin, K. Wang, and S. Zhao, "Monitoring global land surface drought based on a hybrid evapotranspiration model," *International Journal of Applied Earth Observation and Geoinformation*, vol. 13, no. 3, pp. 447–457, 2011.

[13] Y. Yao, S. Liang, X. Li et al., "A satellite-based hybrid algorithm to determine the Priestley-Taylor parameter for global terrestrial latent heat flux estimation across multiple biomes," *Remote Sensing of Environment*, vol. 165, pp. 216–233, 2015.

[14] Y. Yao, Z. Di, Z. Xie et al., "Simplified priestley–taylor model to estimate land-surface latent heat of evapotranspiration from incident shortwave radiation, satellite vegetation index, and air relative humidity," *Remote Sensing*, vol. 13, no. 5, p. 902, 2021.

[15] M. S. Moran, T. R. Clarke, Y. Inoue, and A. Vidal, "Estimating crop water deficit using the relation between surface-air temperature and spectral vegetation index," *Remote Sensing of Environment*, vol. 49, no. 3, pp. 246–263, 1994.

[16] M. Jung, M. Reichstein, H. A. Margolis et al., "Global patterns of land-atmosphere fluxes of carbon dioxide, latent heat, and sensible heat derived from eddy covariance, satellite, and meteorological observations," *Journal of Geophysical Research*, vol. 116, no. 3, Article ID G00J07, 2011.

[17] M. Reichstein, G. Camps-Valls, B. Stevens et al., "Deep learning and process understanding for data-driven Earth system science," *Nature*, vol. 566, no. 7743, pp. 195–204, 2019.

[18] W. Zhao, S. B. Duan, A. Li, and G. Yin, "A practical method for reducing terrain effect on land surface temperature using random forest regression," *Remote Sensing of Environment*, vol. 221, pp. 635–649, 2018.

[19] M. A. Genaidy, "Estimating of evapotranspiration using artificial neural network," *Misr Journal of Agricultural Engineering*, vol. 37, no. 1, pp. 81–94, 2020.

[20] F. Yang, M. White, A. Michaelis et al., "Prediction of continental-scale evapotranspiration by combining MODIS and AmeriFlux data through support vector machine," *IEEE Transactions on Geoscience and Remote Sensing*, vol. 44, no. 11, pp. 3452–3461, 2006.

[21] M. Jung, M. Reichstein, P. Ciais et al., "Recent decline in the global land evapotranspiration trend due to limited moisture supply," *Nature*, vol. 467, no. 7318, pp. 951–954, 2010.

[22] M. Jung, S. Koirala, U. Weber et al., "The FLUXCOM ensemble of global land-atmosphere energy fluxes," *Scientific Data*, vol. 6, no. 1, p. 74, 2019.

[23] H. Wu and W. Ying, "Benchmarking machine learning algorithms for instantaneous net surface shortwave radiation retrieval using remote sensing data," *Remote Sensing*, vol. 11, p. 2520, 2019.

[24] C. Jiménez, C. Prigent, and F. Aires, "Toward an estimation of global land surface heat fluxes from multisatellite observations," *Journal of Geophysical Research*, vol. 114, no. D6, Article ID D06305, 2009.

[25] G. Tramontana, M. Jung, C. R. Schwalm et al., "Predicting carbon dioxide and energy fluxes across global FLUXNET sites with regression algorithms," *Biogeosciences*, vol. 13, no. 14, pp. 4291–4313, 2016.

[26] M. C. Anderson, W. P. Kustas, J. M. Norman et al., "Mapping daily evapotranspiration at field to continental scales using geostationary and polar orbiting satellite imagery," *Hydrology and Earth System Sciences*, vol. 15, no. 1, pp. 223–239, 2011.

[27] P. A. Dirmeyer, X. Gao, M. Zhao, Z. Guo, T. Oki, and N. Hanasaki, "GSWP-2: multimodel analysis and implications for our perception of the land surface," *Bulletin of the American Meteorological Society*, vol. 87, no. 10, pp. 1381–1398, 2006.

[28] B. Mueller, S. I. Seneviratne, C. Jimenez et al., "Evaluation of global observations based evapotranspiration datasets and IPCC AR4 simulations," *Geophysical Research Letters*, vol. 38, no. 6, 2011.

[29] C.-L. Lappen and C. Schumacher, "The role of tilted heating in the evolution of the MJO," *Journal of Geophysical Research: Atmospheres*, vol. 119, no. 6, pp. 2966–2989, 2014.

[30] Y. Yao, S. Liang, X. Li et al., "Bayesian multimodel estimation of global terrestrial latent heat flux from eddy covariance, meteorological, and satellite observations," *Journal of Geophysical Research: Atmospheres*, vol. 119, no. 8, pp. 4521–4545, 2014.

[31] Y. Bai, S. Zhang, N. Bhattarai et al., "On the use of machine learning based ensemble approaches to improve evapotranspiration estimates from croplands across a wide environmental gradient," *Agricultural and Forest Meteorology*, vol. 298-299, no. 299, Article ID 108308, 2021.

[32] Y. Chen, W. Yuan, J. Xia et al., "Using Bayesian model averaging to estimate terrestrial evapotranspiration in China," *Journal of Hydrology*, vol. 528, pp. 537–549, 2015.

[33] Q. Yuan, H. Shen, T. Li et al., "Deep learning in environmental remote sensing: achievements and challenges," *Remote Sensing of Environment*, vol. 241, Article ID 111716, 2020.

[34] T. Wang, R. Tang, Z.-L. Li, Y. Jiang, M. Liu, and L. Niu, "An improved spatio-temporal adaptive data fusion algorithm for evapotranspiration mapping," *Remote Sensing*, vol. 11, no. 7, p. 761, 2019.

[35] Y. Ke, J. Im, S. Park, and H. Gong, "Downscaling of MODIS one kilometer evapotranspiration using landsat-8 data and machine learning approaches," *Remote Sensing*, vol. 8, no. 3, p. 215, 2016.

[36] Y. Yao, S. Liang, X. Li et al., "Estimation of high-resolution terrestrial evapotranspiration from Landsat data using a simple Taylor skill fusion method," *Journal of Hydrology*, vol. 553, pp. 508–526, 2017.

[37] A. Elnashar, L. Wang, B. Wu, W. Zhu, and H. Zeng, "Synthesis of global actual evapotranspiration from 1982 to 2019," *Earth System Science Data*, vol. 13, no. 2, pp. 447–480, 2021.

Hindawi
Scientific Programming
Volume 2022, Article ID 8372929, 11 pages
https://doi.org/10.1155/2022/8372929

Research Article

Active Control for Marine Engine Room Noise Using an FXLMS Algorithm

Qianqian Yu[1] and Erming Cao[2]

[1]*School of Law, Shanghai Maritime University, No. 1550, Haigang Avenue, Shanghai, China*
[2]*College of Power and Energy Engineering, Harbin Engineering University, No. 145, Nantong Street, Nangang District, Harbin, China*

Correspondence should be addressed to Erming Cao; cem@hrbeu.edu.cn

Received 16 June 2022; Revised 15 July 2022; Accepted 22 July 2022; Published 18 August 2022

Academic Editor: Lianhui Li

The noise in the marine engine room has always been a major cause of disturbance and damage to sailors' physical and mental health; however, the antinoise countermeasures were being ignored by the industry. To further reduce the noise in the marine engine room, the system structure of active noise control (ANC) and the theoretical basis of the least mean square (LMS) and filtered *X* least mean square (FXLMS) algorithm are studied. Based on the FXLMS algorithm ANC system, the simulation study of active noise control in the marine engine room of a multigas carrier is carried out. According to the simulation results by the diagrams plotted on the time domain and spectrum, the ANC systems with the FXLMS algorithm can effectively reduce the noise in the marine engine room by about 20 dB, especially for the peak low-frequency range of 20–500 Hz with a large antinoise effect.

1. Introduction

To deal with the global energy crisis and fulfill the demand for "low-carbon," the global power engine has set off a wave of electrification. This electric engine is not only a little more efficient than the traditional internal combustion engine, but also has the advantages of zero pollutant emissions and low noise. But ocean-going ships, which are the main vehicle for global trade, are still far away from real electrification. It means that the internal combustion engine will remain the main driving engine or generator for ships. Although the internal combustion engine has the advantages of high efficiency and high reliability, its noise has been troubling the physical and mental health of the crew, reducing the safety and comfort of the ship. Some studies have pointed out that a crew exposed to high noise for a long time is more likely to feel tired, also can easily lead to inattention and reduce work efficiency even lead to safety accidents [1, 2]. What is more serious, it may be deleterious to cardiovascular, endocrine, and nervous systems, and it is associated with neuropsychiatric disorders [3, 4]. To keep the crew away from heavy noise on board, the 90th meeting of the International Maritime Safety Committee (MSC) in May 2012 approved the draft revision of the Noise Level Rules, which set higher requirements for the noise reduction performance of ships [5]. The shipbuilder and class should take reasonable means to control the cabin noise of ships.

Traditional noise control solutions are focused on passive noise reduction methods. Zhu indicates that semiactive mufflers can control exhaust noise effectively [6]. Liu studied the flow and noise control performance of a compressor silencer [7]. Liang concluded the floating floor of the vessel's engine room can reduce the vibration and noise [8]. Some researchers studied the fuel injection and control strategy from the perspective of the combustion side to reduce the combustion noise of engines [9, 10] while the speed and frequency variations challenge to passive noise reduction. Researchers pay more attention to controllable magnetorheological damping with linear or nonlinear system control methods for better vibration and noise control [11–13].

Because of the huge cost and less controllable flexibility of passive vibration and noise control methods, more and

more industries are starting to use active noise control methods in specific regions [14–16]; those applications indicate the good potential of the active noise control method. The active noise controller recognized the reference noise frequency and then output the opposite amplitude to achieve the effect of reducing the noise. For different kinds of noise resources and applications, lots of different algorithms and solutions of ANC systems have been studied and applied during the past decades [17, 18]. Zeb simulates the improvement of active noise control for the vehicle by the filtered-input recursive least squares (FxRLS) algorithm [18]. Jiang evaluated the performance of the modified hybrid active noise control system (HANC) which combines the strengths of narrowband ANC and broadband ANC systems on vehicle noise reduction [19]. Even though many ANC solutions have been adopted for small space room applications, the studies of active noise control on large vessel engine rooms have almost not been reported before. Due to the good convergence and stabilities of the FXLMS algorithm, it has been adopted in this article to design the active noise controller for marine engine room noise control. Hence, the noise in the marine engine room has been identified, and the preliminary results of ANC control were reported in this article. The research in this article will provide some beneficial foreshadowing for further ANC applications applied on the vessel.

2. Materials and Methods

Active noise control is a noise control method that adds noise reduction by a control signal which is released by a secondary sound source during the initial noise signal propagation route. The interference theory of sound waves shows that two sound waves with the same frequency and opposite phase overlap each other in the propagation path to produce the interference phenomenon so that the acoustic amplitude of the original noise signal cancels each other. The active noise control achieves the purpose of controlling the noise by achieving the attenuation of the sound energy by interfering with the acoustic wave. In the interference phenomenon of sound waves, the phase and amplitude of two columns of interfering sound waves are two key factors that determine whether the sound energy can decay. In practical application, the reverse phase offset acoustic wave can be auxiliary generated by matching the adaptive digital processor and the electroacoustic device, and the effective suppression of primary noise can be realized. Figure 1 shows the schematic diagram of the noise signal superposition principle.

Primary noise is the original noise signal, and secondary noise is the noise generated by the speaker which is used to offset the original noise. When the system works normally, the output signal of the speaker interferes with the original noise signal in a specific space. To form a stable interference, the two-column waves need to meet the following three conditions: (1) the propagation direction is the same, (2) the phase difference remains constant, and (3) the vibration frequency is the same.

Analysis from the perspective of mass point displacement: Let the noise signal be represented by equation (1), the cancellation signal be represented by equation (2), and the signal superimposed in the specified noise reduction area be represented by equation (3).

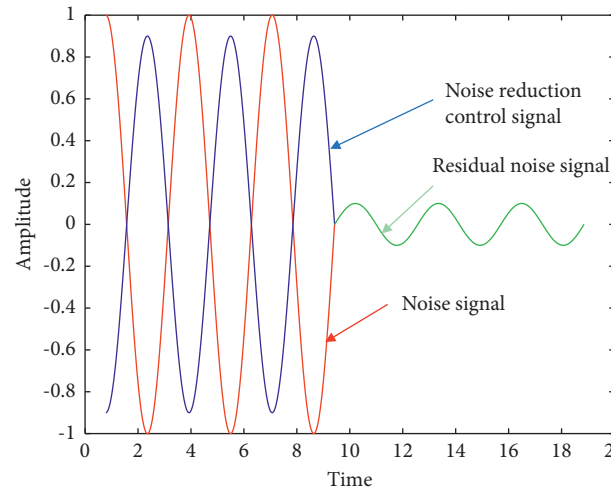

Figure 1: Schematic diagram of noise signal superposition principle.

$$E1 = A_1 \sin(\omega_1 t + \varphi_1), \tag{1}$$

$$E2 = A_2 \sin(\omega_2 t + \varphi_2), \tag{2}$$

$$E3 = E1 + E2 = A_1 \sin(\omega_1 t + \varphi_1) + A_2 \sin(\omega_2 t + \varphi_2). \tag{3}$$

The superimposed waveform stability is poor when the frequency ω_1 is not equal to ω_2. When the difference between the amplitude of A_1 and A_2 is large, the superimposed waveform amplitude cannot reduce the final noise compared with the original noise signal. When ω_1 is equal to ω_2,

$$E_3 = A * \left|2 + 2\cos(\varphi_2 - \varphi_1)\right| * \sin(\omega_1 t + \varphi_1). \tag{4}$$

For the positive noise reduction effect, the phase difference of φ_1 and φ_2 should be in the order of $[2n\pi + 3/3\pi, 2n\pi + 4/3\pi]$, or the interference phase length phenomenon will occur; therefore, the noise reduction system cannot play a noise reduction effect in this condition. The adaptive process of the ANC noise reduction system is to adjust the initial phase of the cancellation signal to meet the phase requirements of the system. In the active control of noise, due to the time-change of the noise signal and environmental factors, an adaptive controller is needed to effectively control the accurate tracking of noise signal under the premise of system stability. The filter in the adaptive control system realizes the real-time signal processing function by adapting to the environmental changes of the adaptive algorithm. The adaptive controller consists of a digital filter and a corresponding adaptive algorithm for adjusting the filter parameters, which are the main focus of the controller design work. The objective of the adaptive algorithm is to set an objective function, which is to make the result approach a target value by constant iterative computation.

2.1. Active Noise Control System. The active noise control system usually consists of sensors, controllers, and speakers. The sensor can be divided into a reference signal sensor and an error sensor. The acoustic sensor, speed sensor, or acceleration sensor can be used as input signals. The controller mainly includes the signal processing hardware and the control function of the software programs.

The active noise control system is divided into a feedback system and a feedforward system. The feedforward system usually selects the noise signal to collect the noise source in the reference signal selection, and the controller sends out the control signal after processing the input reference signal. The feedback system is often used when the control system cannot collect the initial reference signal.

2.1.1. Feedforward Active Control System. The system equivalent diagram is shown in Figure 2. In the figure, $p(n)$ is the noise signal, $W(z)$ is the controller, $H_1(z)$ is the primary path transmission function, and $H_2(z)$ is the secondary path transmission function.

The reference signal sensor picked up the signal $x(n)$ which was released by the noise source, and then the speaker played the control signal $y(n)$ which was processed by the controller algorithm. The error sensor picks up the error signal $e(n)$ after interfering with the noise source noise and the control signal emitted by the secondary sound source interferes and transmits it to the controller. The controller adjusted the weight coefficient by using the design algorithm to reduce the error signal until the system has become stable.

2.1.2. Feedback Active Control System. The controller responds to the signal feedback by the error sensor when the feedback system processes the noise signal. Because the signal is picked up by the feedback control system through the error sensor and then used as the controller input, it is easy to be disturbed by other noise and reduces the stability of the system, which has a certain impact on the system noise reduction effect. In the feedback active noise control system, the signal processing takes an error signal as its input signal. The equivalent control system diagram is displayed in Figure 3. Compared with the feedforward active noise system, its noise reduction performance is poor and rarely used.

The symbol definitions in Figure 3 are omitted here as the same symbols were used in Figure 2.

2.2. LMS and FXLMS Algorithms for ANC System. Because of the time-varying characteristics of the noise signal, it is difficult to predict in advance and makes the noise difficult to be tracked in real time. ANC technology requires tracking the time-varying noise signal by adjusting the controller to make the generated secondary noise signal minimize the original noise signal. An adaptive filter can track the time-varying signals well and continuously by adjusting the required control signals to produce them through some optimization error criterion.

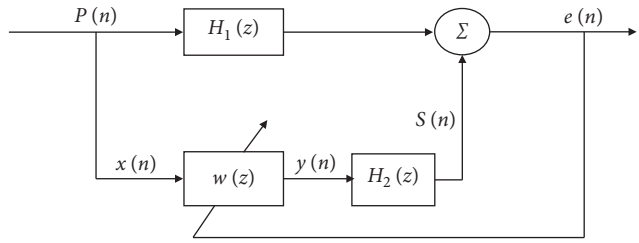

Figure 2: Feedforward active control system equivalent diagram.

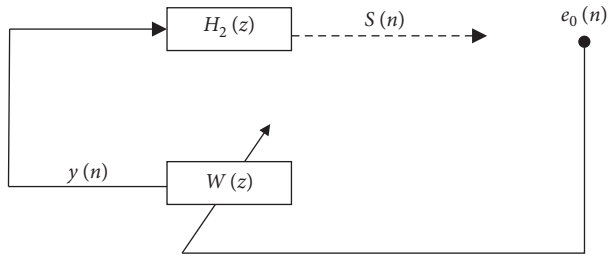

Figure 3: Feedback active control system equivalent diagram.

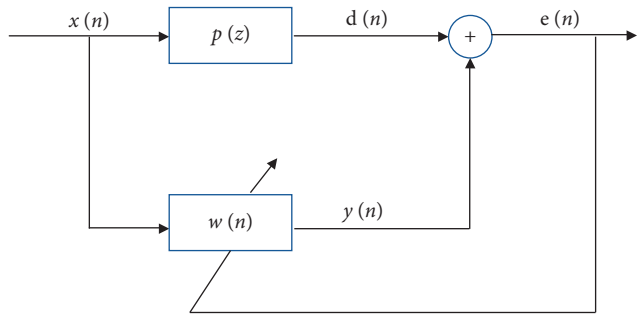

Figure 4: Block diagram of noise LMS algorithm active control system.

This optimization error criterion belongs to the ANC algorithm. The adaptive LMS algorithm and FXLMS algorithm are widely used.

2.2.1. LMS Algorithm. The equivalent diagram of the LMS algorithm is shown in Figure 4.

The noise signal $x(n)$ is processed by the primary path transmission function $P(z)$ and then becomes as the primary noise signal $d(n)$. The noise signal $x(n)$ and the error signal $e(n)$ are transmitted to the adaptive filter to update the weight coefficient, and the adaptive filter outputs $y(n)$ making the error signal $e(n)$ gradually reduce.

Symbol definition: $x(n)$: noise signal; $P(z)$: primary sound source transmission path; $d(n)$: initial noise signal of the error sensor; $e(n)$: error signal; $w(n)$: the LMS adaptive filter; and $y(n)$: output signal of the LMS adaptive filter.

The input signal at time n gets a response by a filter of order L:

$$X(n) = [x(n), x(n-1), \ldots\ldots, x(n-l+1)]^T. \quad (5)$$

The vector of the filtered weight coefficient at time n is expressed as

$$W(n) = [w_1(n), w_2(n), \ldots\ldots w_L(n)]^T. \quad (6)$$

The filter output signal $y(n)$ can be expressed as

$$y(n) = X^T(n)W(n) = W^T(n)X(n) = \sum_{i=1}^{L} w_i(n)x(n-l+1). \quad (7)$$

The error signal at time n is

$$e(n) = d(n) - y(n) = d(n) - w^T(n)x(n). \quad (8)$$

Using the minimum mean-variance error optimization criterion,

$$\begin{aligned} J(n) &= E\left[e^2(n)\right] = E\left[\left(d(n) - w^T(n)x(n)\right)^2\right] \\ &= E\left[d^2(n)\right] - 2W^T(n)E[d(n)X(n)] \\ &\quad + W^T(n)E\left[X(n)X^T(n)\right]W(n), \end{aligned} \quad (9)$$

delimit R and P as the equations below.

$$\begin{aligned} R &= E\left(X(n)X^T(n)\right), \\ P &= E(d(n)X(n)). \end{aligned} \quad (10)$$

R is the autocorrelation matrix of the reference signal and P is the intercorrelation matrix between the expected signal and the reference signal.

Then formula (9) is reduced to

$$J(n) = E\left[d^2(n)\right] - 2W^T(n)P + W^T(n)RW(n). \quad (11)$$

$J(n)$ is the quadratic function about W, and to realize the minimum error signal, the gradient obtained by equation (11) is indicated by

$$\begin{aligned} \nabla(n) &= \frac{\partial J(n)}{\partial W}\Big|_{W=W(n)} = \left[\frac{\partial J(n)}{\partial W_1}, \frac{\partial J(n)}{\partial W_2}, \ldots\ldots, \frac{\partial J(n)}{\partial W_L}\right] \\ &= 2RW(n) - 2P. \end{aligned} \quad (12)$$

The above equation is made equal to 0, and then the filtering coefficient W_0 for the minimum error signal is obtained, namely, the Wiener solution.

$$W_0 = R^{-1}P. \quad (13)$$

Returning to the formula (11),

$$\begin{aligned} J\min &= E\left[d^2(n)\right] - 2P^TR^{-1}P + \left[R^{-1}P\right]^T RR^{-1}P \\ &= E\left[d^2(n)\right] - P^TW_0, \\ J(n) &= J\min + \left[W(n) - W_0\right]^T R\left[W(n) - W_0\right]. \end{aligned} \quad (14)$$

When the autocorrelation matrices R and P are known, the adaptive filter algorithm can calculate the W_0, that is, it only needs to know the autocorrelation matrix R and the intercorrelation matrix P to obtain the best filter weight coefficient. In practice, P and R are not necessarily certain; however, the minimum mean square algorithm does not require an autocorrelation matrix, it still can obtain the best-filtered weight coefficient through the steepest descent method.

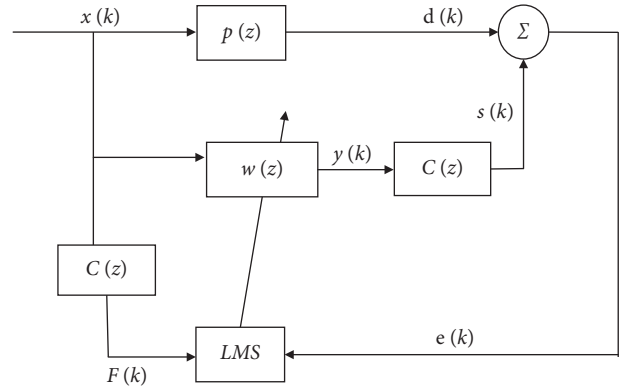

Figure 5: Block diagram of noise FXLMS algorithm active control system.

From the steepest descent theory, the filter weight vector at the next moment can be expressed as $w(n+1)$.

$$W(n+1) = W(n) - \mu\nabla(n). \quad (15)$$

In the equation (15), μ is the convergence step and $\nabla(n)$ is the gradient of the n-th iteration.

Taking the gradient in the LMS algorithm from the square root of the error signal as an unbiased estimate of $\nabla(n)$,

$$\widehat{\nabla} = \frac{\partial e^2(n)}{\partial W} = -2e(n)X(n), \quad (16)$$

$$W(n+1) = W(n) + 2\mu e(n)X(n). \quad (17)$$

2.2.2. FXLMS Algorithm. The FXLMS equivalent diagram of the active noise control system is shown in Figure 5.

In practice, the LMS algorithm ignores the existence of the secondary path $C(z)$, that is, the control signal $y(k)$ from the speaker can bring the error signal close to zero, but the signal $y(k)$ after passing through the secondary path $C(z)$ does not necessarily make the error signal close to zero. Because the electrical signal emitted by the speaker transmits through a series of digital-analog conversions to the microphone, there is a certain time difference with the reference signal, which can easily lead to the instability of the system. Based on this, Morgan [20] proposes to place the same filter in the reference signal path to realize the weight update of the LMS algorithm, thus realizing FXLMS's algorithm. $C'(z)$ can estimate the statute of $C(z)$ precisely which is required in the algorithm, and the two are approximately equal. Adding the estimation $C'(z)$ of the secondary path transmission function improves the LMS algorithm and indeed becomes the essential difference between FXLMS and LMS algorithms [21–30].

Symbols definition: $x(k)$: noise signal; $P(z)$: primary sound source transmission path; $P(k)$: primary path transmission function; $d(k)$: initial noise signal of the error sensor; $C(z)$: secondary sound source transmission path;

$C(k)$: secondary path transmission function; $e(k)$: error signal; $w(z)$: self-adapting filter; $y(k)$: output signal of the adaptive filter; $s(k)$: secondary noise signal passing through the secondary path; $C'(z)$: estimated secondary path; and $F(k)$: noise signal generated through the estimated secondary path.

The desired signal is transmitted through the primary path and can be represented as a convolution of the reference signal with the primary path transmission function.

$$d(k) = x(k) * P(k). \tag{18}$$

Similarly, the secondary noise signal emitted by the speaker may be expressed as

$$s(k) = y(k) * C(k). \tag{19}$$

The filter weight coefficient and the algorithm input signal vector are

$$\begin{aligned} W(k) &= [w_1(k), w_1(k), \ldots\ldots, w_L(k)]^T, \\ F(k) &= [f(k), f(k-1), \ldots\ldots, f(k-l+1)]^T = X(k)C(k). \end{aligned} \tag{20}$$

The output of the filter of L order at time k in the FXLMS algorithm is

$$y(k) = X^T(k)W(k) = W^T(k)F(k) = \sum_{l=1}^{L} w_l(k) f(k-l+1). \tag{21}$$

To delimit $r(k)$ as the filtered signal, which is the convolution of the reference signal and the secondary path transmission function can be expressed as

$$r(k) = X(k) * C(k). \tag{22}$$

The derived error signal is

$$e(k) = d(k) + s(k) = d(k) + r^T(k)W(k). \tag{23}$$

The relation of the filter weight can be derived by equation (17).

$$W(k+1) = W(k) - 2\mu e(k) r(k). \tag{24}$$

R is defined as the autocorrelation matrix of the reference signal, by which its orthogonal matrix can be expressed as Q.

$$R = Q\Lambda Q^T. \tag{25}$$

Λ is the diagonal matrix composed of the eigenvalues of the R,

$$\begin{aligned} \Lambda &= \operatorname{diag}(\lambda_1, \lambda_2, \ldots, \lambda_L), \\ W(n+1) &= \left[\mathrm{I} - 2\mu Q\Lambda Q^T\right] W(n) + 2\mu P, \\ E[W(n+1)] &= Q[\mathrm{I} - 2\mu\Lambda]^{n+1} Q^{-1} E[W(0)] + 2\mu P. \end{aligned} \tag{26}$$

In the above formula, $W(0)$ is the initial value of the filter weight; thus, the convergence conditions of the above formula are

Table 1: Engine parameter for sampling noise signal in the marine engine room.

Items	Unit	Value
Bore	mm	400
Stroke	mm	1770
Speed	rpm	125
Cylinder number	—	6
Power	kW	4950
Firing order	—	1-6-2-4-3-5

$$\left|1 - 2\mu\lambda_{\max}\right| < 1. \tag{27}$$

Equation (27) can be transformed as

$$0 < \mu < 1/\lambda_{\max}. \tag{28}$$

$\lambda_{\max}$ is the maximum eigenvalue of the positive definite matrix R, and the adaptive filtering weights converge when the convergence step size factor μ satisfies equation (28). Usually, the autocorrelation matrix R is unknown but the reference signal is available, and the mean square value of the reference signal and the autocorrelation matrix R satisfy the following relationship:

$$\begin{aligned} Tr[R] &= \sum_{i=0}^{N} \lambda_i = \sum_{n=1}^{L} E\left[x^2(n)\right], \\ \lambda_{\max} &< Tr[R]. \end{aligned} \tag{29}$$

Therefore, the convergence step length μ satisfies the following relationship:

$$0 < \mu < \frac{1}{\sum_{n=1}^{L} E\left[x^2(n)\right]}. \tag{30}$$

The sum mean square of the reference signal is known, and the value range of the convergence steps can be prejudged by the reference signal.

3. Results

3.1. Noise Sampling. This article collects the cabin noise as a reference noise signal on a multigas carrier. The noise source of the marine engine room is mainly derived from the noise of a 6-cylinder two-stroke low-speed engine, and its main parameters are shown in Table 1.

Usually, for a certain type of engine, the engine room noise is greatly affected by the engine speed and power. The higher the speed, the greater the power, and the more obvious the corresponding noise. The position of the microphone of the noise reference signal is located on the top of a 1 m distance of the exhaust manifolder between cylinder 3 and cylinder 4. The sampling frequency of the reference signal collection is 8 kHz, under the condition that the engine speed of 125 rpm, the power is 3715 kW, which corresponds to a 75% load operating condition. All the generators are stopped, and the electric power consumption on the vessel is provided by the main engine shaft belt generator. Figure 6 shows the actual drawing of the low-speed engine in the engine room. The main noise in the

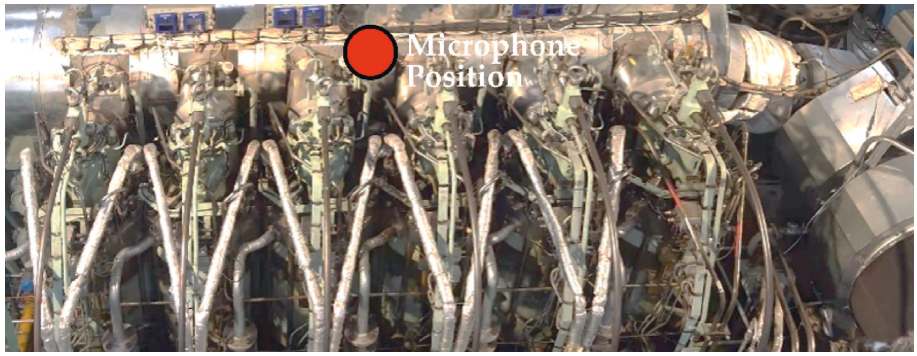

Figure 6: Schematic diagram of reference noise signal picking up position in the marine engine room.

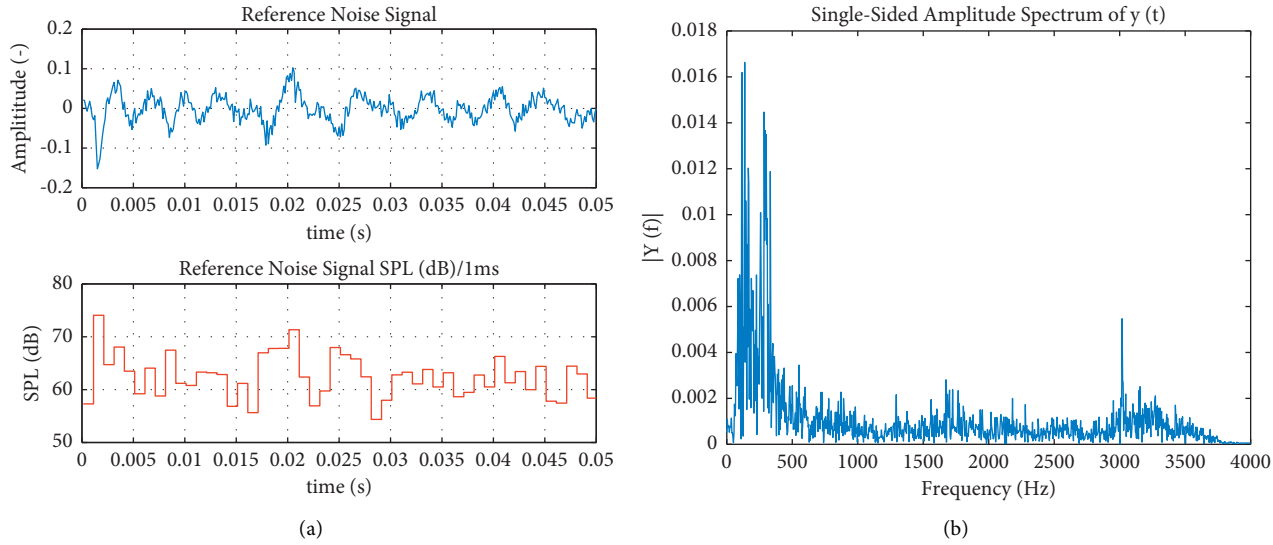

Figure 7: Characteristics of the noise signal in the marine engine room. (a) The time domain diagram of reference noise signal; (b) the spectrum diagram of reference noise signal by fast Fourier transform (FFT).

engine room comes from the friction, vibration, air transmission, and combustion noise of the two-stroke engine.

3.2. Signal Processing and Modeling. Figure 7 is the characteristics of the noise signal in the marine engine room. Figure 7(a) shows the time domain map of the reference signal after being analyzed. The engine running noise in the engine room shows obvious periodicity, so the acquisition signal within 50 ms is selected as an input, and the analytical spectrum map shows that the frequency at the peak noise is concentrated between 80 and 400 Hz, which is displayed on Figure 7(b). These low-frequency noises are difficult to eliminate by the passive noise reduction method.

The active noise reduction calculation model of engine cabin noise with the FXLMS algorithm has been established on the MATLAB platform. White noise is used as an excitation to identify the secondary path transmission function $C'(z)$ offline. It is assumed that the characteristics of $C'(z)$ are variable and unknown at the first. The offline estimation method can be used to identify the secondary path transmission function, and the identification coefficient of $C'(z)$

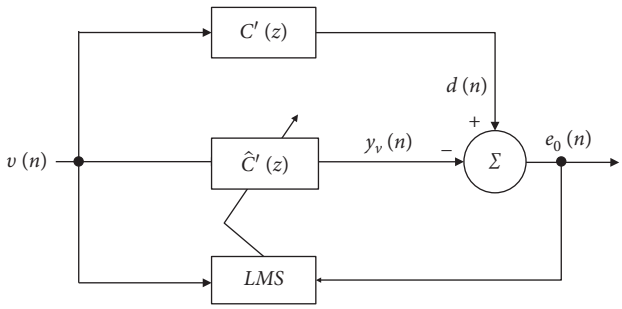

Figure 8: The block diagram of offline identification for secondary transmission path function.

is used as the fixed coefficient of the FXLMS algorithm. The steps of offline identification are shown in Figure 8.

A white noise signal in the n moment is $v(n)$, the secondary path output value is $d(n)$, $y_v(n)$ is the value of the white noise through the secondary path identification, and $e_0(n)$ is the error value between the secondary path output value and secondary path identification value. It can be considered that the secondary path identification function

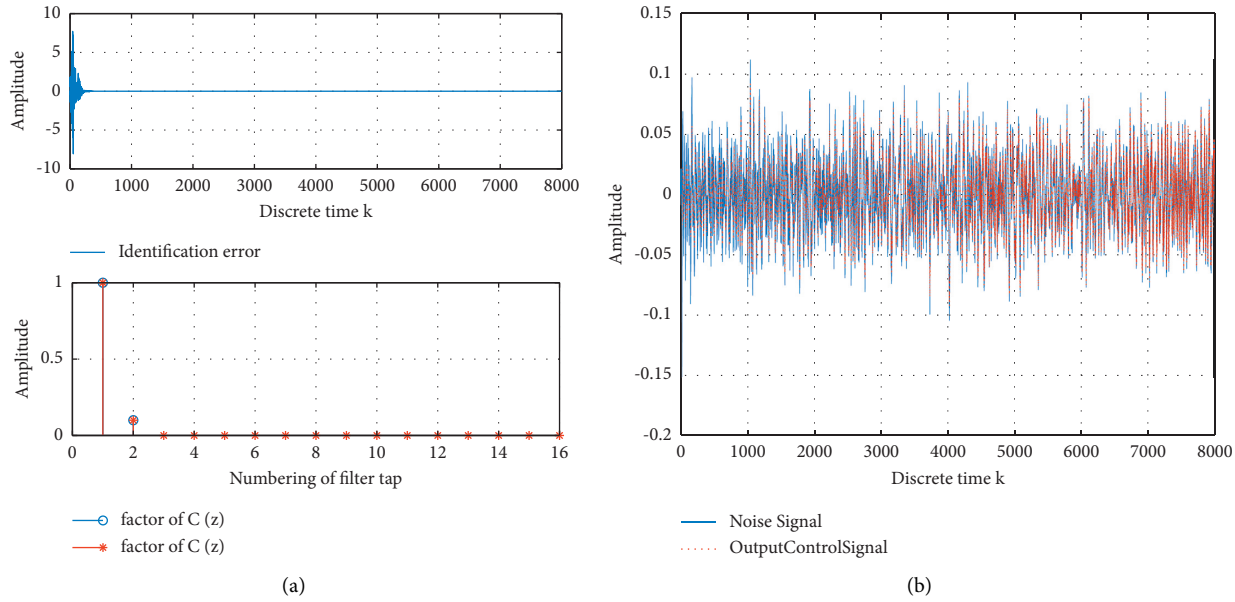

Figure 9: Offline identification results for secondary path transmission function and output control signal. (a) The simulation results of offline identification by LMS algorithm; (b) the output control signal of FXLMS ANC systems.

$\widehat{C}'(z)$ is closer to the secondary path function $C'(z)$ when the error value $e_0(n)$ is close to zero through the LMS algorithm's constantly iterative update.

Offline identification is a system identification independently separated from the ANC system, which will not increase the operation burden of the ANC system, and also will not damage the robustness of the ANC system. If the secondary path transmission function of the ANC system remains unchanged, offline identification has certain advantages.

During the simulation tests, the primary and secondary transmission functions are set as equations (31) and (32).

$$p(z) = z^{-1} - 0.07z^{-3} + 0.006z^{-4}, \tag{31}$$

$$C(z) = \frac{1}{(z + 0.1)}. \tag{32}$$

The filter order of the FXLMS algorithm N was set as 16, the convergence step factor μ was 0.1, the sampling frequency was 8000 Hz, the total simulation discrete sampling data was 8000, and the whole simulation time was set within one second.

3.3. Disclosed Results. Figure 9 shows offline identification results for the secondary path transmission function and output control signal. The offline identification error and the iteration coefficient of the secondary path transmission function are shown in Figure 9(a). After the two-order iteration and the simulation discrete step length of 600, the offline system identification error tends to be zero. It shows that the LMS algorithm is accurate and efficient for the offline identification of the secondary path transmission function. As shown in the simulation calculation results in Figure 9(b), the control signal of the adaptive output of the speaker agrees well with the reference noise signal after 4000 iteration steps.

The residual noise continuously drops under the action of the active noise reduction system quickly, and gradually stabilizes to a low error value of 0.01 after 5000 steps, and no divergence phenomenon occurs. Comparing the signal amplitude and sound pressure level on the time domain diagram, the blue curve in Figure 10 is the original noise reference signal, and the red curve is the error signal processed by the FXLMS algorithm ANC noise reduction system, indicating that the ANC system significantly reduces the active noise reduction of marine engine room noise. From the perspective of SPL degrees, it shows that the maximum SPL is reduced by about 20 dB at the end of the simulation.

The noise reduction effect was evaluated from the perspective of power, and Spectrum Analyzer was used to analyze the input noise signal and the output error signal by frequency spectrum. The analysis results are shown in Figure 11. As can be seen from Figure 11, the error signal which is colored in blue is generally lower than the input noise signal which is colored in yellow in the full frequency range, and the noise reduction effect at the peak frequency of 125 Hz and 300 Hz is about 20 dB. It is obviously noticed that the ANC system has a better noise reduction effect in the low-frequency range of 20-500 Hz. The ANC system based on the FXLMS algorithm has a good active control effect on the cabin noise of the periodic, low-frequency, and high-intensity noise signal.

When considering the impacts of the different convergence step factors μ, three sets of different μ have been studied. The noise reduction performance is shown in Figure 12 for $\mu = 0.1$, 0.5, and 0.9, respectively.

The results show that the noise reduction performance is linearly improving with the decreasing with the convergence step factor μ. In Figures 12(a) and 12(b), when $\mu = 0.9$, the maximum SPL decrease is about 10 dB, not also a large

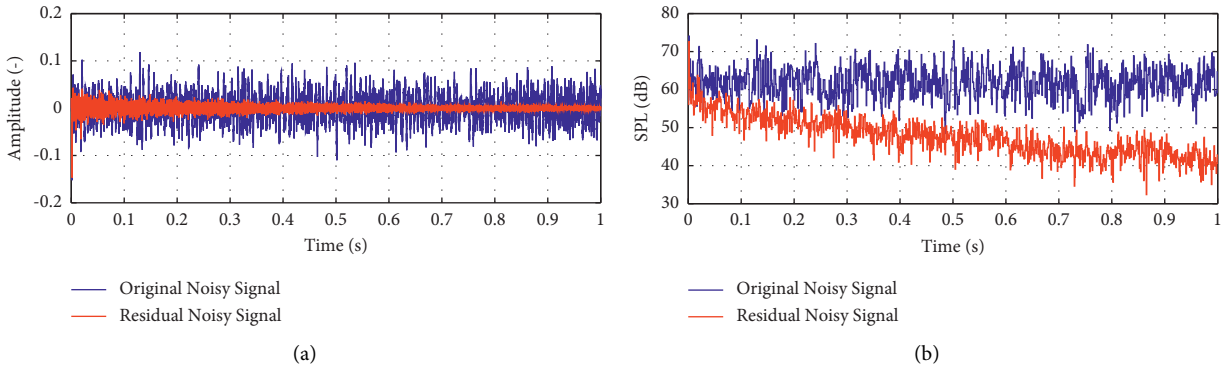

(a) (b)

Figure 10: The time domain collation map diagram of the amplitude and SPL between reference noise signal and residual noise signal by FXLMS ANC system. (a) Amplitude comparison. (b) Reference noisy signal SPL (dB) 1 ms.

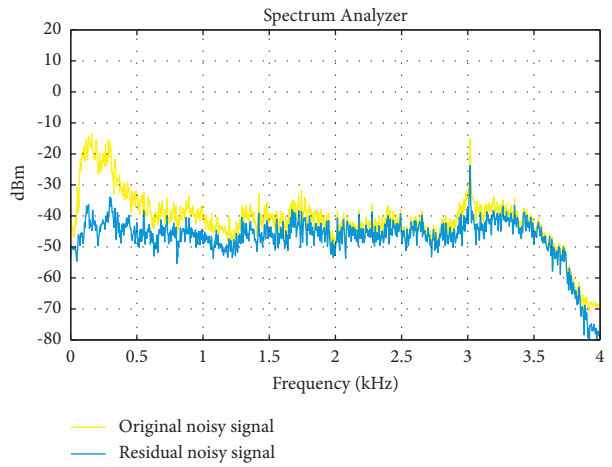

Figure 11: The spectrum analyzer between reference noise signal and residual noise signal by FXLMS ANC system.

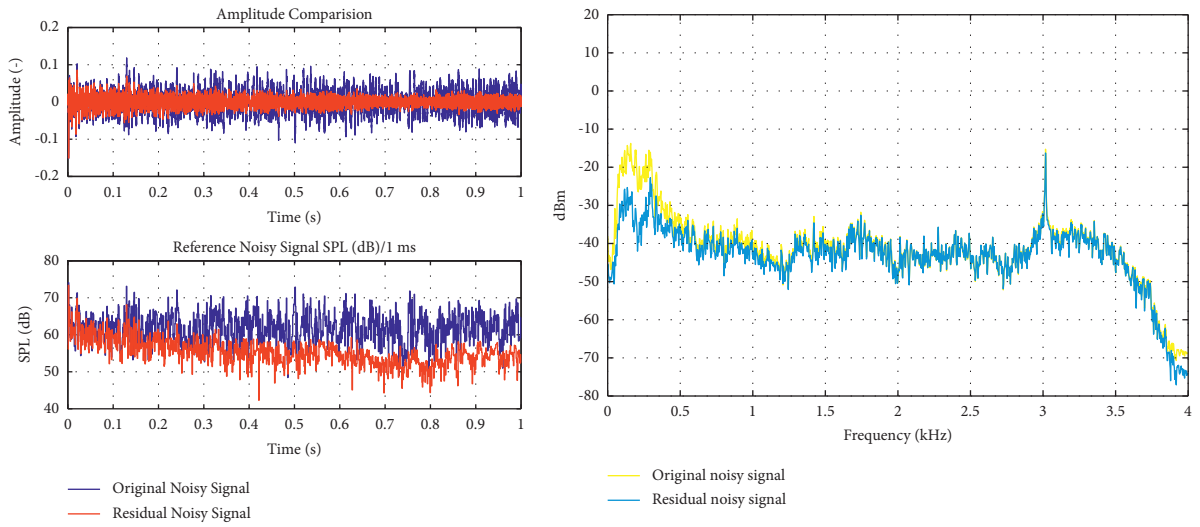

(a) (b)

Figure 12: Continued.

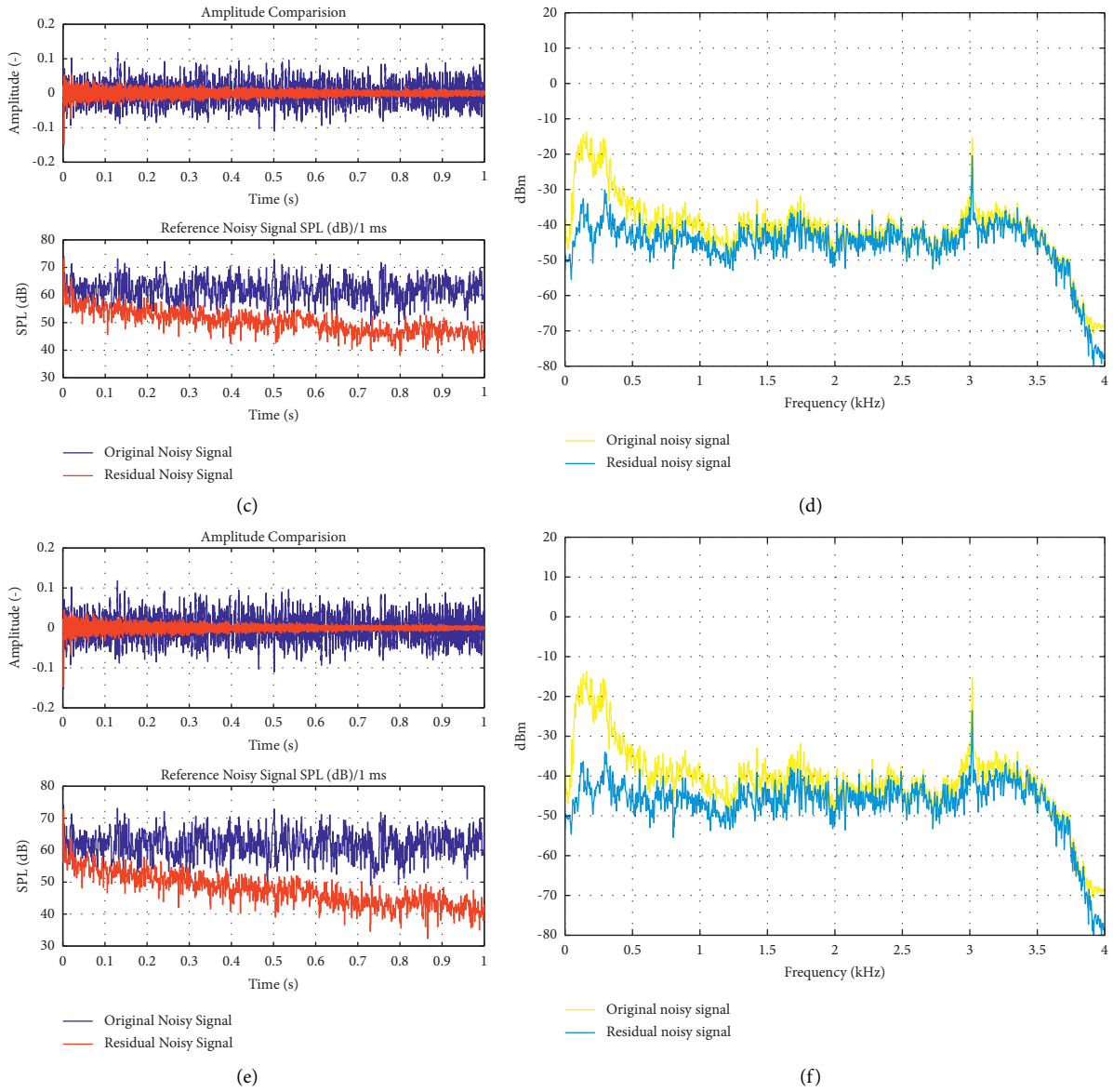

FIGURE 12: Noise reduction performance for different convergence step factors μ. (a) The time domain diagram for $u = 0.9$; (b) the spectrum analyzer diagram for $u = 0.9$; (c) the time domain diagram for $u = 0.5$; (d) spectrum analyzer diagram for $u = 0.5$; (e) the time domain diagram for $u = 0.1$; (f) spectrum analyzer diagram for $u = 0.1$.

fluctuation for the final residual noise signal but also a weak or even bad noise reduction performance for the frequency range of 1.5-4 kHz are observed. As a comparison for $\mu = 0.5$, the results in Figures 12(c) and 12(d) show a better noise reduction performance, the maximum SPL decrease is about 15 dB; for $\mu = 0.1$, the results in Figures 12(e) and 12(f) show the maximum SPL decrease is about 20 dB. The results show that the convergence step factor has great importance for the ANC workings.

4. Discussion

This article studied the significant noise reduction performance in the marine engine room for ANC systems with the FXLMS algorithm. The first part of the article explained the composition of active noise reduction systems and the modeling theory basis of LMS and FXLMS algorithms. The latter part of the article introduced the simulation conditions, ANC modeling, as well as the disclosed results. In detail, the reference marine engine room noise signal from a gas carrier has been imported and analyzed, which indicated that periodic and peak low frequency are the main characteristics of the noise signal. An ANC system with an FXLMS algorithm was designed to control the sample noise. The model calculation shows that the ANC system based on the FXLMS algorithm significantly suppressed the marine engine room noise. During the entire one-second simulation time, the residual marine engine room noise signal after active control is significantly lower than the input noise signal, as well as the SPL drops by about 20 dB. The controlled marine

engine room noise is generally improved over the input noise over the full frequency range, especially a drop of SPL by about 20 dB for the peak low frequency at 125 Hz and 300 Hz which can be concluded on the spectrum analyzer diagram. While the noise reduction performance for ANC system with FXLMS algorithm has important variations on the convergence step factor. The residual signal error increases linearly with the convergence step factor when compared to the results for different convergence step factors 0.1, 0.5, and 0.9. It shows some limitations in the performance of ANC systems with FXLMS algorithms. When considered, the engine room noise is always stable and can even continue throughout the ship's life cycle; the limitations can be minimized by the initial optimum for the convergence step factor. Further research will focus on multipath ANC systems design and variable convergence step factor optimum for ANC systems [31].

Data Availability

The data used to support the findings of this study are available from the corresponding author upon request.

Consent

Not applicable.

Disclosure

The funders had no role in the design of the study; in the collection, analyses, or interpretation of data; in the writing of the manuscript, or in the decision to publish the results.

Conflicts of Interest

The authors declare no conflicts of interest.

Acknowledgments

The understanding of the background laws and regulations for seafarers was highly supported by Professor Cao Yanchun at Shanghai Maritime University; the sampling noise signal was provided by China Shipbuilding Power Engineering Institute Co., Ltd.

References

[1] S. A. Girard, M. Picard, A. C. Davis et al., "Multiple work-related accidents: tracing the role of hearing status and noise exposure," *Occupational and Environmental Medicine*, vol. 66, no. 5, pp. 319–324, 2009.

[2] K. Irgens-Hansen, H. Gundersen, E. Sunde et al., "Noise exposure and cognitive performance: a study on personnel on board Royal Norwegian Navy vessels," *Noise and Health*, vol. 17, no. 78, pp. 320–327, 2015.

[3] X. D. Li, Z. Y. Song, T. Wang, Y. Zheng, and X. Ning, "Health impacts of construction noise on workers: a quantitative assessment model based on exposure measurement," *Journal of Cleaner Production*, vol. 135, pp. 721–731, 2016.

[4] G. Frenzilli, L. Ryskalin, M. Ferrucci et al., "Loud noise exposure produces DNA, neurotransmitter and morphological damage within specific brain areas," *Frontiers in Neuroanatomy*, vol. 11, p. 49, 2017.

[5] International Marine Organization (Imo), "Code on noise levels on board ships," *IMO Resolution MSC*, vol. 337, p. 91, 2012.

[6] Y. W. Zhu, F. W. Zhu, Y. S. Zhang, and Q. G. Wei, "The research on semi-active muffler device of controlling the exhaust pipe's low-frequency noise," *Applied Acoustics*, vol. 116, pp. 9–13, 2017.

[7] C. Liu, Y. P. Cao, Y. Liu, W. Zhang, P. Ming, and S. Ding, "Numerical and experimental analyses of intake silencer and its effects on turbocharger compressor performance," *Advances in Mechanical Engineering*, vol. 11, Article ID 168781401982667, 2019.

[8] B. N. Liang, H. L. Yu, and Y. N. Cai, "Prediction and control on vibro-acoustic environment of vessel engine room floating cabins," *Journal of Vibroengineering*, vol. 16, pp. 3052–3063, 2014.

[9] Z. X. He, T. M. Xuan, Z. C. Jiang, and Y. Yan, "Study on effect of fuel injection strategy on combustion noise and exhaust emission of diesel engine," *Thermal Science*, vol. 17, no. 1, pp. 81–90, 2013.

[10] S. B. Al-Omari, M. Y. E. Selim, and A. A. J. Al-Aseery, "Control of noise and exhaust emissions from dual fuel engines," *Journal of Renewable and Sustainable Energy*, vol. 3, no. 4, Article ID 43103, 2011.

[11] Z. X. Deng, Q. H. Yang, S. Zhao, and H. B. Wei, "Multi-objective optimization of magneto-rheological mount structure based on vehicle vibration control," *Journal of Intelligent Material Systems and Structures*, vol. 32, no. 11, pp. 1155–1166, 2021.

[12] H. J. Song, S. B. Choi, and K. S. Kim, "Control performance of ER engine mount subjected to temperature variations," *International Journal of Modern Physics B*, vol. 19, no. 7n09, pp. 1675–1681, 2005.

[13] Q. J. Liu, W. Chen, H. S. Hu, Q. Y. Zhu, and Z. X. Xie, "An optimal NARX neural network identification model for a magnetorheological damper with force-distortion behavior," *Frontiers in Materials*, vol. 7, p. 10, 2020.

[14] K. Mazur, S. Wrona, and M. Pawelczyk, "Performance evaluation of active noise control for a real device casing," *Applied Sciences*, vol. 10, no. 1, p. 377, 2020.

[15] K. Ye, J. C. Ji, and S. Han, "Semi-active noise control for a hermetic digital scroll compressor," *Journal of Low Frequency Noise, Vibration and Active Control*, vol. 39, no. 4, pp. 1204–1215, 2020.

[16] E. Noh, S. Woo, D. J. Lee et al., "Active control of low-frequency noise in bubbly water-filled pipes," *Journal of Mechanical Science and Technology*, vol. 33, no. 7, pp. 3127–3135, 2019.

[17] A. Mirza, A. Zeb, M. Yasir Umair, D. Ilyas, and S. A. Sheikh, "Less complex solutions for active noise control of impulsive noise," *Analog Integrated Circuits and Signal Processing*, vol. 102, no. 3, pp. 507–521, 2020.

[18] Y. Jiang, S. M. Chen, F. H. Gu, H. Meng, and Y. Cao, "A modified feedforward hybrid active noise control system for vehicle," *Applied Acoustics*, vol. 175, Article ID 107816, 2021.

[19] A. Zeb, A. Mirza, Q. U. Khan, and S. A. Sheikh, "Improving performance of FxRLS algorithm for active noise control of impulsive noise," *Applied Acoustics*, vol. 116, pp. 364–374, 2017.

[20] D. R. Morgan, "History, applications, and subsequent development of the FXLMS Algorithm [DSP History]," *IEEE Signal Processing Magazine*, vol. 30, no. 3, pp. 172–176, 2013.

[21] Y. Cheng, B. Li, J. Wang, and H. Li, "Research on PSD replication for multiaxial hydraulic vibration test system based on FXLMS algorithms," *Shock and Vibration*, vol. 2021, Article ID 6610817, 9 pages, 2021.
[22] L. Li and C. Mao, "Big data supported PSS evaluation decision in service-oriented manufacturing," *IEEE Access*, vol. 8, Article ID 154663, 2020.
[23] Y.-Y. Wang, Yi-N. Li, W. Sun, C. Yang, and G. H. Xu, "FxLMS method for suppressing in-wheel switched reluctance motor vertical force based on vehicle active suspension system," *Journal of Control Science and Engineering*, vol. 2014, Article ID 486140, 16 pages, 2014.
[24] L. Li, B. Lei, and C. Mao, "Digital twin in smart manufacturing," *Journal of Industrial Information Integration*, vol. 26, no. 9, Article ID 100289, January 2022.
[25] M. C. Huynh and C.-Y. Chang, "Nonlinear neural system for active noise controller to reduce narrowband noise," *Mathematical Problems in Engineering*, vol. 2021, Article ID 5555054, 10 pages, 2021.
[26] L. Li, T. Qu, Y. Liu et al., "Sustainability assessment of intelligent manufacturing supported by digital twin," *IEEE Access*, vol. 8, Article ID 174988, 2020.
[27] S. Ryu and Y.-S. Lee, "Characteristics of relocated quiet zones using virtual microphone algorithm in an active headrest system," *Journal of Sensors*, vol. 2016, Article ID 5185242, 9 pages, 2016.
[28] S. Yan, X. Luo, X. Sun, J. Xiao, and J. Jingyue, "Indoor acoustic signals enhanced algorithm and visualization analysis," *Computational Intelligence and Neuroscience*, vol. 2021, Article ID 7592064, 13 pages, 2021.
[29] L. Li, C. Mao, H. Sun, Y. Yuan, and B. Lei, "Digital twin driven green performance evaluation methodology of intelligent manufacturing: hybrid model based on fuzzy rough-sets AHP, multistage weight synthesis, and PROMETHEE II," *Complexity*, vol. 2020, no. 6, 24 pages, Article ID 3853925, 2020.
[30] X. Zhang, S. Yang, Y. Liu, and W. Zhao, "IMproved variable step size least mean square algorithm for pipeline noise," *Scientific Programming*, vol. 2022, Article ID 3294674, 16 pages, 2022.
[31] D. Y. Shi, W. S. Gan, B. Lam, and S. L. Wen, "Feedforward selective fixed-filter active noise control: algorithm and implementation," *IEEE-ACM Transactions on Audio Speech and Language Processing*, vol. 28, pp. 1–1492, 2020.

Hindawi
Scientific Programming
Volume 2022, Article ID 5178538, 10 pages
https://doi.org/10.1155/2022/5178538

Research Article

Chinese Commodity Price Evidence Study for COVID-19 Shock and Price Stickiness Model Design

Jie Qin,[1] **Jiawei Wang**,[1] **and Tiandan Zheng**[2]

[1]*School of Business, Renmin University of China, Beijing, China*
[2]*School of Business, Nanjing University of Information Science & Technology, Nanjing, China*

Correspondence should be addressed to Jie Qin; qinjie010@ruc.edu.cn

Received 30 June 2022; Revised 21 July 2022; Accepted 28 July 2022; Published 18 August 2022

Academic Editor: Lianhui Li

Based on the high-frequency price data, this article estimates the extent of price stickiness, identifies the pricing model, and applies the micro-results to analyze the dynamic characteristics of inflation. The results show that the price moves downward steadily during the COVID-19 epidemic. Secondly, the commodity price displays low stickiness, and the pricing model shows the time-dependent pricing (TDP) model in general. Finally, the inflation inertia is negative, indicating the macro-control is effective on COVID-19 epidemic and has the feature of contradiction to the economic cycle. And inflation inertia mainly comes from food commodities, which means that the anchoring object of the policy should be food commodities during the COVID-19 pandemic.

1. Introduction

In recent years, epidemics have affected human health and social stability. The COVID-19 epidemic that outbroke at the end of 2019 posed a great challenge to economic and social development. It has broken the original balance between supply and demand and directly affected macroeconomic stability. Therefore, it is increasingly important to ensure effective macro-control measures when we face the impact of the outbreak.

Price stickiness refers to the fact that price does not react to market in time, making price sticky [1]. Price stickiness is usually observed in daily life. However, it is not individual commercial price stickiness but aggregate price patterns and inflation that affect the macroeconomic operation [2], which lead to discussions on the pricing model and the relationship between price stickiness and inflation. Previous studies have shown that price stickiness is closely related to price adjustment [3–5]. At present, price adjustment mainly falls into two models: One is the time-dependent pricing (TDP) model, that is merchants adjust the price in a fixed time which price changes are exogenous. The other is the state-dependent pricing (SDP) model, that is the adjustment of commodity prices by merchants depends on the market. The price changes are endogenous.

There have been abundant researches on price stickiness. In the early stage, due to the difficulty in obtaining price data, they mainly focused on specific categories of commodities. Based on this, scholars concluded that commodity prices had high price stickiness [6, 7]. Moreover, menu cost [8, 9], sticky information [10], and consumer sentiment [11] were the main causes of price stickiness. With the development of e-commerce, the sample range was expanded. Bils and Klenow found that price changes were frequent, and the price lasted less than 4.3 months when they investigated 350 sorts of goods price from the Bureau of Labor Statistics [12]. Similarly, Klenow and Kryvtsov detected that the price lasted 3.8 months, and the pricing model adopted the time-dependent pricing (TDP) model on the basis of the data from BLS from 1988 to 2003. The web crawler technology further enriched the commodity category and frequency [13]. Cavallo held that the pricing model was the combination of SDP and TDP by capturing daily online commodity data of five countries [14]. Jiang et al. supported this view. They also found that the price lasted 2 months or less, and the price

adjustment model was the combination of SDP and TDP by the data from China's high-frequency goods price [15].

Some research on price stickiness found that it was related to inflation inertia. Lunnemann and Matha studied the price data of 15 EU countries and found that the price stickiness of service price and regulated service was positively correlated with the inertia of service price inflation [16]. Mato reached the same conclusion based on Brazilian commodity prices [17]. In contrast, Cecchetti and Debelle found that the higher the price stickiness, the lower the inflation inertia [6].

It can be seen that price stickiness is closely related to the pricing model, and there are differences in price setting behavior, resulting in changing the inflation inertia. Moreover, there is no unified conclusion about the relationship between price stickiness and inflation inertia. At the same time, empirical research on price stickiness under the outbreak is still very scarce. Therefore, this article uses online high-frequency price data to study the price stickiness during COVID-19, observes the pricing model and inflation inertia, and provides more reliable empirical evidence for macroeconomic models.

The purpose of this article is to investigate the price stickiness during COVID-19. Compared with the previous literature, the contributions are mainly as follows: Firstly, we use web crawling technology to get the daily commodity prices on COVID-19. The micro-results are used to analyze inflation inertia for the first time, which effectively connects the micro-basis with the macro-application. Secondly, we attempt to measure the price stickiness when the epidemic outbroke. At the same time, the variance decomposition method is used to judge the pricing mode. This article finds that price performs low stickiness, and the pricing model is state-dependent pricing on COVID-19. Finally, we construct an AR model to analyze the inflation inertia and find that inflation inertia is negative, which means the effectiveness of macro-management during the outbreak. And inflation inertia mainly comes from food commodities, which means that the anchoring object of the policy should be food commodities on COVID-19.

The rest of the article is organized as follows: Section 2 introduces data acquisition and data processing; Section 3 shows the measurement results of price stickiness; Section 4 analyzes inflation inertia based on the results of price stickiness; and Section 5 obtains conclusions.

2. Data

2.1. Data Collection. This article collects the commodity price from Taobao platform with the web crawling technology [18, 19]. The data acquisition process is as follows: The first step is to access the Taobao platform with Python to obtain information such as product names, classification, links, and others and store the commodity information in the MySQL database. The second step is to retrieve the product links from the database and matched them on a price comparison website to acquire the historical prices of commodities. The final step is to process the price data with Python and measure the price stickiness to further analyze the inflation.

Table 1: Data sources.

Observations	7712415
Product number	48073
Date	2019/12/16–2020/8/22
Product information	Brand, ID, selling price, product link
Retailer information	Name, ID, location

Compared with offline data, online data are used to study price changes with certain advantages. Firstly, online data increase the frequency of price analysis, and daily data could reflect the price changes more flexibly. Secondly, more enterprises select online sales as an alternative to offline sales when they consider the segmented domestic market. Thirdly, online and offline data are the same about 72% of the time, and online data have a good representation.

2.2. Data Source. The data collected in this article covers 48,073 sorts of commodity information on Taobao from December 2019 to August 2020, with a total of 7,712,415 observations. We match the commodities with eight categories that are divided by State Statistics Bureau (NBS) to facilitate the subsequent analysis. We divided the goods category into food; clothing; residence; household equipment; transport, post, and telecommunication; culture, education, and recreation; medicine and health care; and other goods and services. The data description of commodity is shown in Table 1.

2.3. Data Preprocessing. This article refers to the existing literature and preprocesses the original data in combination with the characteristics of online price as follows:

2.3.1. Missing Value Processing. This article uses daily price data to analyze price stickiness. Some random factors (i.e., software problems, message interrupt, etc.) might result in the missing of price information on a certain day or period, which is required to add the missing information. Therefore, we use the price of missing values in the previous period to replace the missing price until the new price appears [19, 20].

2.3.2. Outlier Processing. The abnormal fluctuations in price will affect the measurement of price stickiness and interferes with the price changes. This article defines the values that the price increased by over 500% or the price decreased by over 90% as outlier value, according to the former research [21]. We choose to eliminate the outlier value to ensure the reliability of results, considering a small number of abnormal values in the dataset.

2.3.3. Period Processing. The sample period referred to the time span from the first appearance of the price to its last time [22]. This article gets rid of the sample periods of less than 7 days to warranty the measurement feasibility.

This article ultimately selects 47,219 commodities and 7,709,816 observations by processing the missing value, abnormal value, and sample period.

3. Measurement of Price Stickiness

3.1. Price Index. The price index is an index that reflects price changes. This article measures the price index by indexing the commodity price obtained by Taobao. We use the Jevons geometric index formula to calculate the commodity price index.

Firstly, we calculate the relative price of each commodity i in period t, pcr_{ti}

$$pcr_{ti} = \frac{p_{ti}}{p_{t-1i}}, \tag{1}$$

where p_{ti} is the price of commodity i at day t, and p_{t-1i} is the price of commodity i at day t-1.

Secondly, the relative prices of all commodities are geometrically averaged in period t, pcg_{tz}

$$pcg_t = \sqrt[n]{pcr_{t1} * pcr_{t2} * \cdots * pcr_{tn}}. \tag{2}$$

Finally, using equation (2), the first day of the sample period is set to 100 to obtain the commodity price index, pci_t

$$pci_t = pcg_t * pcg_{t-1} * \cdots * pcg_1 * 100. \tag{3}$$

Figure 1 shows the trend of commodity price index, in which the green dotted line indicates the outbreak time of COVID-19 in China: January 20, 2020. We can see that the price moves downward steadily during the COVID-19 epidemic.

In order to further study the changes of commodity prices on COVID-19, we analyze eight categories of commodities that are divided by NBS. The results are shown in Figure 2.

3.2. Descriptive Statistics. This section makes the descriptive statistics of price changes. The statistical results are reported in Table 2. We find that 81.24% of the commodities generally change price during the sample period, price adjustments of a commodity are 15.70 times, and commodity price shows low price stickiness. In the meantime, commodities of price increased account for 34.65%, while the decreased goods are 65.35%. It can be drawn that the majority of commodity price is changed and the price moves downward during COVID-19. Then we further classify the commodities into eight categories, and the results are similar to the above.

3.3. Frequency and Period. This section evaluates the price stickiness by calculating the frequency and period of price changes. On the one hand, the price frequency refers to the number of price changes during the sample period. We figure up the price frequency based on the methods of Gopinath and Rigobon (GR methods) [23]. The detailed methods are as follows:

We calculate the price frequency of commodity i in category $d$freq$_{di}$:

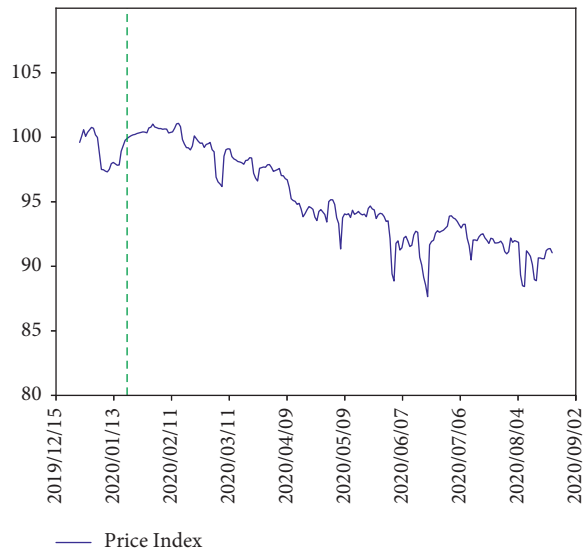

Figure 1: Price index.

$$\text{freq}_{di} = \frac{npc_{di}}{obs_{di}}, \tag{4}$$

where npc_{di} is the price change times of commodity i in category d. obs_{di} denotes the numbers of observations. Using (4), we divide the commodities into eight categories that are provided by NBS and calculate the price frequency of each category by using the median method, freq$_d$:

$$\text{freq}_d = \text{median}(\text{freq}_{di}). \tag{5}$$

In order to get the overall price frequency, we calculate the change frequency of eight categories of commodities by the weighted average method where the weight of eight categories of goods is based on the method of He [24]. The overall price frequency is:

$$\text{freq} = \sum w_d * \text{freq}_d, \tag{6}$$

where w_d is the relative weight of goods i. In order to ensure the robustness of the results, we adopt the BK method to measure the price adjustment frequency. The BK method was used by Bils and Klenow. They calculated the arithmetic mean of each category of goods based on a single good price frequency and got the overall price frequency by the weighted average method. On the other hand, price period refers to the duration of the price until it changes. We obtain the price period according to the method of Jin et al. (4), which is

$$\text{period} = -\frac{1}{\ln(1 - \text{freq})}. \tag{7}$$

It can be seen that there is a negative relationship between price frequency and period, that is to say, the higher the price frequency, the shorter the price period, indicating that the price stickiness is higher. The specific results of price frequency and period are shown in Table 3.

The price stickiness is low during the COVID-19 epidemic as shown in Table 3. According to the GR method and BK method, the overall price frequency is 7.85% and 9.65%,

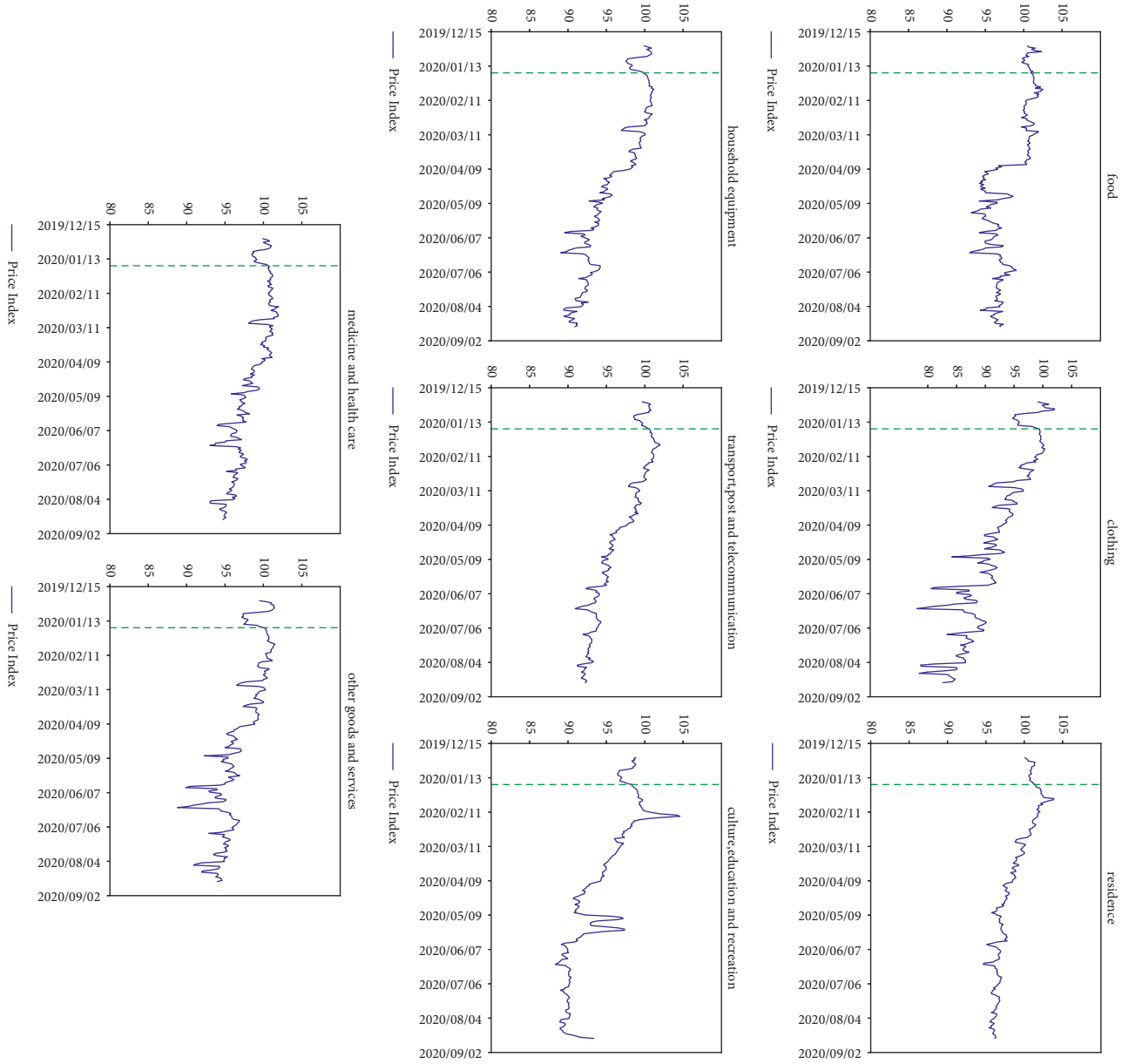

Figure 2: Price index of eight categories.

respectively, and the overall price period is 12.23 days and 9.86 days. The extent of price stickiness is far lower than the result of existing studies. Jiang et al. (2020) discovered that the price frequency is 2.24% (GR method) and 3.39% (BK method). As shown in Table 3, the results show that the price period is shorter and price adjustment is more frequent during COVID-19.

We find that there are differences in the price frequency and period among eight main categories. The extent of price stickiness is ranked from low to high: clothing; other goods and services; household equipment; transport, post, and telecommunication; culture, education, and recreation; medicine and health care; food; and residence. It can be drawn that clothing goods have the lowest price stickiness, whose price frequency is 13.50% and the price period is 6.90 days. The results explain that the commodities that change the price make up 13.50% and price adjustment cycle is 6.90 days. Residence goods have the highest price stickiness. Its price frequency is 4.17% and the price period is 23.48 days, which prove that commodities of clothing are best sold during the COVID-19 epidemic. The results are similar to the findings of Jin (2013).

3.4. Price Size. The preceding section discovers that the price stickiness is low during the COVID-19 epidemic by estimating the price stickiness in terms of price frequency and period. In order to further observe the price stickiness, this section measures the size of price changes. The detailed processes are as follows:

Table 2: Statistical description of price change.

Index	(1) Price change (%)	(2) Adjustment time	(3) Price rise (%)	(4) Price down (%)
All	81.24	15.70	34.65	65.35
Food	75.03	12.63	46.49	53.51
Clothing	80.14	16.96	28.88	71.12
Residence	34.24	5.41	43.93	56.07
Household equipment	84.79	17.32	30.86	69.14
Transport, post, and telecommunication	79.64	12.50	33.35	66.65
Culture, education, and recreation	84.71	15.32	38.72	61.28
Medicine and health care	74.45	11.26	39.03	60.97
Other goods and services	83.10	18.75	35.55	64.45

Notes: Column 1 shows the percentage of observations that have changed prices. Column 2 is the number of price adjustments. Column 3 has the percentage of observations that price is increased during the sample period. Column 4 shows the percentage of observations that price is decreased during the sample period.

Table 3: Price frequency and period.

Index	GR		BK	
	(1) Price frequency (%)	(2) Price period (day)	(3) Price frequency (%)	(4) Price period (day)
All	7.85	12.23	9.65	9.86
Food	7.92	12.12	10.18	9.32
Clothing	13.50	6.90	14.79	6.25
Residence	4.17	23.48	5.56	17.49
Household equipment	10.00	9.49	11.64	8.08
Transport, post, and telecommunication	9.09	10.49	10.90	8.67
Culture, education, and recreation	8.75	10.92	9.91	9.59
Medicine and health care	8.75	10.92	11.21	8.41
Other goods and services	12.08	7.77	13.49	6.90

Notes: Columns 1 and 2 match the price frequency and price period by the BR method. Similarly, Columns 3 and 4 report the results by the BK method.

We calculate the price size of commodity i at t in category d, size_{di}:

$$\text{size}_{di} = \left|\frac{\text{p}_{dit}}{\text{p}_{dit-1}}\right|, \tag{8}$$

where p_{dit} is the price of commodity i at day t in category d. p_{dit-1} denotes the price of commodity i at day t-1 in category d. Using (7), we divide the commodities into eight categories that are provided by NBS and calculate the price size of each category by using the GR method and the BK method, sizem_d and sizea_d are

$$\text{sizem}_d = \text{median}\left(\text{size}_{di}\right), \tag{9}$$

$$\text{sizea}_d = \text{mean}\left(\text{size}_{di}\right). \tag{10}$$

In order to get the overall size of price change, we calculate the size of eight categories of commodities by the weighted average method. The overall price frequencies based on eq (9) and (10) are

$$\begin{aligned} \text{sizem} &= \sum w_d * \text{sizem}_d, \\ \text{sizea} &= \sum w_d * \text{sizea}_d. \end{aligned} \tag{11}$$

Based on the results of Table 4, during the COVID-19 epidemic, the scale of price change was small, and the difference between the scale of price increase and price decrease was not obvious. The size of price changes is 13.62% and 13.18% by calculating separately with the GR and BK methods, which is less than the results of previous studies. Jin found that the price adjustment range was 24.90%. Jiang et al. found that the median of commodity price adjustment is 19.49% and the arithmetic average is 20.07%. Meanwhile, we find that the difference between the price size increased and that decreased is 0.04%, indicating that the price change is symmetrical during COVID-19. Combined with the results in Table 1, we find that the times of price reduction are greater than that of price raise. Therefore, we obtain that the price moves downward steadily during the COVID-19 epidemic. One cause is that the pricing behavior of merchants will consider consumer sentiment in accordance with fair pricing theory. The abnormal fluctuation of prices causes the consumers' negative emotion, which would influence the partnership between merchants and consumers [25, 26]. Therefore, merchants do not arbitrarily change price during the epidemic, when they will consider the consumer feelings that merchants should deliver the altruism to consumers.

We find that there are differences in the price size among eight categories of goods which are divided by NBS. The size of price change is ranked from low to high: residence; other goods and service; household equipment; transport, post, and telecommunication; medicine and health care; culture, education, and recreation; food; and clothing. The commodity of clothing has the maximum difference in the price increase and decrease, which is 1.06%. Residence goods have the minimum difference, which is 0.06%. The size of price changes among

Table 4: Price size.

Index	GR			BK		
	Size change (%)	Size rise (%)	Size down (%)	Size change (%)	Size rise (%)	Size down (%)
All	12.79	13.62	13.18	20.17	24.58	18.09
Food	16.44	18.43	17.47	23.37	28.95	22.05
Clothing	14.99	15.52	16.58	18.73	21.06	19.66
Residence	9.96	9.69	9.75	21.03	25.79	16.77
Household equipment	13.26	14.11	14.02	19.37	23.46	18.09
Transport, post, and telecommunication	8.53	8.70	8.47	14.43	17.15	12.85
Culture, education, and recreation	10.99	11.70	11.11	15.88	19.20	14.14
Medicine and health care	14.70	15.98	15.61	22.27	27.39	20.50
Other goods and services	10.06	10.52	10.60	13.88	15.85	13.49

Note. Columns 1, 2, and 3 match the size of price change, size of price increase, and size of price decrease, respectively, by the GR method. Columns 4, 5, and 6 report the results by the BK method.

eight main categories of commodities has no significant difference, explaining that the price changes are relatively symmetrical. Thus, this article discovers that the prices of eight categories of commodities move downward stably.

3.5. Pricing Model. Based on the price frequency and size, this article finds that the price moves downward steadily during the COVID-19 epidemic. We inspect the pricing model with the variance decomposition method (short for KK method) proposed by Klenow and Kryvtsov in order to further analyze the source of price fluctuations. KK method decomposes the variance of price changes into time-dependent pricing (TDP) terms and state-dependent pricing (SDP) term and compares the variance contribution rate between the two, so as to obtain the pricing model. The details are as follows:

Let I_{it} represents an indicator of a price change for commodity i in day t:

$$I_{it} = \begin{cases} 1, & p_{it} \neq p_{it-1}, \\ 0, & p_{it} = p_{it-1}, \end{cases} \tag{12}$$

where p_{it} denotes the log of price of commodity i in day t. We use the following equation for aggregate inflation, π_t:=

$$\begin{aligned} \pi_t &= \sum_{i=1}^{N} w_{it} \left(p_{it} - p_{it-1}\right) \\ &= \left(\sum_{i=1}^{N} w_{it} I_{it}\right) * \left(\frac{\sum_{i=1}^{N} w_{it} \left(p_{it} - p_{it-1}\right)}{\sum_{i=1}^{N} w_{it} I_{it}}\right) \\ &= fr_t * dp_t. \end{aligned} \tag{13}$$

As shown, eq (13) represents that the aggregate inflation can be expressed as extensive margin and intensive margin. fr_t is the fraction of the commodities' changing price changes in day t, that is the numbers of merchants adjusting price when inflation occurs. dp_t signifies the weighted-average magnitude of adjusting price in day t, that is the magnitude of price changes by merchants when inflation occurs. According to the model of Klenow and Krystov, the external environment could influence the pricing behaviors of merchants when inflation (π_t) is relevant to fraction (fr_t). Instead, pricing behavior cannot be influenced when inflation (π_t) is irrelevant to fraction (fr_t). Therefore, we reach that the pricing model is the time-dependent pricing (TDP) model if inflation (π_t) is uncorrelated with fraction (fr_t). When inflation rate (π_t) is relevant to magnitude (dp_t) and fraction (fr_t), the pricing model is the state-dependent pricing (SDP) model. The results are shown in Table 5.

We find that coefficients of π_t is negative and small in Table 5, indicating that there exists low inflation phenomenon on COVID-19. Meanwhile, the overall inflation decomposition result of all commodities price displays that π_t and dp_t have a higher relevance degree where the correlation coefficient is 0.601, and the regression coefficient of dp_t is significant at 1% level. The correlation coefficient of π_t and fr_t is 0.095, and the regression coefficient of fr_t is not significant. The results show that the pricing model fits the time-dependent pricing (TDP) model during the COVID-19 epidemic, which explain that most merchants can flexibly change price based on the market environment. In addition, we get that the pricing models of eight categories of commodities are heterogeneous. The correlation coefficient of clothing goods is 0.286. At the same time, the regression coefficient of fr_t is significant. It indicates that the pricing model of clothing goods is state-dependent pricing (SDP) model where fr_t and dp_t are highly related to π_t and regression results are significant. However, the pricing model of other category goods is time-dependent pricing(TDP) model where regression between π_t and fr_t is not significant at the 1% level. It shows that the price changes of these commodities are limited during the COVID-19 epidemic.

Then, the variance decomposition of the inflation (π_t) is made to clarify the contributions of time-dependent pricing (TDP) term and state-dependent pricing (SDP) term. The first-order Taylor expression is carried out on (13):

Table 5: Correlations and regression results.

Index		(1) Correlation	(2) Coefficient	(2) P value
All	π	1.00	—	—
	fr_t	0.095	0.718	0.171
	dp_t	0.601	6.861	0.001
Food	π	1.00	—	—
	fr_t	0.135	0.846	0.042
	dp_t	0.778	7.280	0.001
Clothing	π	1.00	—	—
	fr_t	0.286	0.072	0.001
	dp_t	0.806	0.199	0.001
Residence	π	1.00	—	—
	fr_t	−0.029	−0.413	0.538
	dp_t	0.5214	23.782	0.001
Household equipment	π	1.00	—	—
	fr_t	0.000	−0.074	0.904
	dp_t	0.779	5.701	0.001
Transport, post, and telecommunication	π	1.00	—	—
	fr_t	−0.045	−0.415	0.598
	dp_t	0.756	8.319	0.001
Culture, education, and recreation	π	1.00	—	—
	fr_t	−0.032	−0.148	0.767
	dp_t	0.879	8.218	0.001
Medicine and health care	π	1.00	—	—
	fr_t	0.032	0.122	0.777
	dp_t	0.540	8.143	0.001
Other goods and services	π	1.00	—	—
	fr_t	0.132	0.944	0.064
	dp_t	0.800	4.001	0.001

Notes: Column 1 shows correlation coefficient between inflation (π_t), fraction (fr_t), and magnitude (dp_t). Column 2 is the regression coefficient and p-value that inflation (π_t) regress on fraction (fr_t) and magnitude (dp_t).

$$\mathrm{var}(\pi_t) \approx \underbrace{\mathrm{var}(dp_t) * \overline{fr_t}^2}_{\text{TDP term}} + \underbrace{\mathrm{var}(fr_t) * \overline{dp_t^2} + 2 * \overline{fr_t} * \overline{dp_t} * \mathrm{cov}(fr_t, dp_t)}_{\text{SDP term}}, \tag{14}$$

where fr_t denotes extensive margin, and dp_t represents intensive margin. When the TDP model is dominant, $\mathrm{var}(fr_t)$ and $\mathrm{cov}(fr_t, dp_t)$ are equal to 0 that the inflation variance is decided by the TDP term. However, when the SDP model is dominant, $\mathrm{var}(fr_t)$ is not equal to 0, that is the SDP term has an influence on the inflation variance. The results of the inflation variance decomposition are shown in Table 6.

The variance decomposition results are reported in Table 6. We discover that proportion of TDP term is far more than that of SDP terms, which verify the results in Table 5. However. TDP terms of clothing goods exceed 100%. The reason might be that the mean of fr_t raises the TDP term and the variance of fr_t lowers the SDP term when we consider the high frequency of price changes during the COVID-19 epidemic.

As we know, commodity prices move downward steadily; meanwhile, the low inflation phenomenon exists during the COVID-19 epidemic. The overall pricing model is time-dependent pricing model, and the pricing models of categorized commodities are heterogeneous. The results led to problems that whether macro-policies should respond to price changes during COVID-19. If so, what commodities should policy anchor? An analysis of the dynamic characteristics of inflation is required to answer these questions. Zhang (2008) supposed that the key to understand the dynamic characteristics of inflation was to identify the inertial characteristics, namely inflation inertia [27]. The next section analyzes the dynamic process of inflation by measuring the inflation inertia.

4. Inflation Inertia

4.1. AR Model. Inflation inertia refers to the duration which inflation deviated from the equilibrium state due to being disturbed by random factors [28]. As a general rule, the greater inflation inertia is, the more obvious hysteresis effect of policies is. Therefore, it is of great significance to policy regulation by accurately measuring the inflation inertia. By referring to the existing literature on the measurement of inflation inertia [27, 29], we evaluate the inflation inertia by making use of the sum coefficients in the AR model. The AR model is as follows:

Table 6: Variance decomposition.

Index	(1) cov(fr, dp)	(2) TDP term (%)	(3) SDP term (%)
All	−0.000667	85.64	14.36
Food	−0.000363	97.86	2.14
Clothing	0.000516	101.69	−1.69
Residence	−0.000757	58.28	41.72
Household equipment	−0.000762	87.05	12.95
Transport, post, and telecommunication	−0.000456	79.91	20.09
Culture, education, and recreation	−0.000373	94.95	5.05
Medicine and health care	−0.00118	86.91	13.09
Other goods and services	−0.000302	98.84	1.16

Notes: Column 1 shows the covariance between fr_t and dp_t. Column 2 is the changes in the intensive margin, which account for all of the variation in inflation in staggered TDP models. Column 3 shows changes in the extensive margin, which only contribute in SDP models.

Table 7: Inflation inertia.

Index	Model	(1) MUE	(2) OLS
All	AR(3)	−0.198	−0.199
Food	AR(6)	−0.664	−0.691
Clothing	AR(3)	−0.311	−0.313
Residence	AR(2)	0.069	0.064
Household equipment	AR(2)	−0.106	−0.103
Transport, post, and telecommunication	AR(3)	−0.188	0.156
Culture, education, and recreation	AR(4)	0.149	−0.296
Medicine and health care	AR(3)	−0.296	−0.141
Other goods and services	AR(2)	−0.152	−0.199

Notes: Column 1 shows inflation inertia coefficient using median unbias method to estimate the AR model. Column 2 is inflation inertia coefficient using least square method to estimate the AR model.

$$\pi_t = c + \sum_{i=1}^{n} \rho_i \pi_{t-i} + \varepsilon_t, \tag{15}$$

where π_t is the inflation rate, and $\sum \rho_i$ represents the sum of coefficients in the AR model, which measures the inflation inertia. Considering the collinearity caused by the lag of explanatory variable, OLS will result in deviations of estimated results [30]. Therefore, this article takes the median unbias estimation that was proposed by Roy and Fuller [31] in order to ensure the robustness of the results.

4.2. Empirical Results. The estimated results are reported in Table 7. It can be seen that the overall inflation inertia is less than 0. The main reason is that the economy is at the low inflation state during the COVID-19 epidemic. We use the Jevons geometric index formula to process price index according to the method of Guo [32]. The overall commodity price index is 96.83, which contribute that the inflation inertia is reversal. The results are similar to the research of Chen [33]. It illustrates that macroeconomic policies are featured by going against the economic cycle, and macro-management is effective [34]. Food commodities has a higher inflation inertia than non-food commodities. It can be sure that the inflation inertia mainly comes from food commodities during the COVID-19 epidemic. The reasons may include that food commodities have the largest weight that reach nearly 1/3 among the eight categories of commodities, and the proportion of food expenditure is relatively high that achieves 30.16%. The fluctuation of food price caused by the COVID-19 epidemic will directly affect the dynamic characteristics of inflation.

Further, the impact of COVID-19 may cause the structural mutation of model estimation. When the outbreak happened at the initial stage, people would be in a greater demand for some commodities that improves the price of these commodities. With the outbreak is to be gradually brought under control, the demand for commodities will weaken. The commodity price will go through a significant adjustment, bringing out the structural mutation of the AR model during COVID-19. On this account, we conduct a structural breakpoint test by referring the method of Zivot and Andrews [35]. As shown in Table 8, commodities of clothing and culture, education, and recreation did not have obvious structural mutations, while the other commodities have significant structural breakpoints. In order to get more accurate estimation results, we divided the time series into two stages based on the structural breakpoint and held that commodities of food still have great inflation where coefficients are −0.208 and −0.684%, respectively. Meanwhile, this article discovers that there is a great difference among commodities of food, residence, household equipment, and medicine and health care.

The above results show that the demand for commodities of food, residence, supplies and services, and medical services greatly increase during the early period of the COVID-19 epidemic and the price of that is increased. However, with the gradual control of COVID-19, the demand for such

Table 8: Structural mutation of inflation inertia.

Index	Model	(1) Inflation inertia	(2) Breakpoint	(3) t-value
All	AR(3)	−0.198	07 April 2020	−5.319
All-before	AR(4)	−0.114	—	—
All-after	AR(3)	−0.282	—	—
Food	AR(6)	−0.664	07 April 2020	−6.845
Food-before	AR(1)	−0.208	—	—
Food-after	AR(6)	−0.684	—	—
Clothing	AR(3)	−0.311	24 June 2020	−5.330
Clothing-before	—	−0.322	—	—
Clothing-after	—	−0.301	—	—
Residence	AR(2)	0.069	21 June 2020	−4.802
Residence-before	AR(2)	−0.071	—	—
Residence-after	AR(3)	−0.008	—	—
Household equipment	AR(2)	−0.106	11 April 2020	−4.969
Household equipment-before	AR(4)	0.053	—	—
Household equipment-after	AR(2)	−0.373	—	—
Transport, post, and telecommunication	AR(3)	−0.188	08 April 2020	−5.031
Transport, post, and telecommunication-before	AR(5)	−0.057	—	—
Transport, post, and telecommunication-after	AR(3)	−0.112	—	—
Culture, education, and recreation	AR(4)	0.149	19 March 2020	−2.948
Culture, education, and recreation-before	—	—	—	—
Culture, education, and recreation-after	—	—	—	—
Medicine and health care	AR(3)	−0.296	05 May 2020	−4.636
Medicine and health care-before	AR(4)	−0.225	—	—
Medicine and health care-after	AR(3)	−0.404	—	—
Other goods and services	AR(2)	−0.152	11 April 2020	−6.169
Other goods and services-before	AR(4)	−0.119	—	—
Other goods and services-after	AR(2)	−0.24	—	—

Notes: Column 1 shows inflation inertia coefficient using median unbias method to estimate the AR model. Column 2 is the date of structural mutation in AR model. Column 3 is the P value that test the structural mutation.

commodities is reduced, and the accumulation of commodity supply makes the inflation inertia larger.

5. Conclusions

Based on the online high-frequency price data, this article measures the price stickiness of commodities during the COVID-19 epidemic and analyzes pricing models and inflation inertia, which provide the micro-basis for macropolicy. The main conclusions are as follows:

Firstly, the commodity price moves downward steadily during the COVID-19 epidemic. On the whole, most commodities of price shows a downward trend during the sample period. In the meantime, the commodities of price has a minor change size, and the difference between the size increased and that decreased is not obvious. The price of eight categories of goods is similar to the aggregate price performance. The reason lies in that merchant will formulate pricing strategy based on consumer sentiment. The abnormal fluctuations of prices cause the consumers' negative emotion, which would influence the partnership between merchants and consumers. Therefore, price moves downward steadily under the consumer sentiment.

Secondly, the commodity price displays the low stickiness, and the pricing model shows time-dependent pricing (TDP) model in general. We find that most commodities show a time-dependent pattern through eight commodity classification and only clothing commodity belongs to state-dependent pricing (SDP) model. The results show that the price adjustment of most commodities is limited during the COVID-19 period.

Thirdly, we construct AR model to estimate inflation inertia and clarify the dynamic characteristics of inflation. The results show that the inflation inertia is negative, which means that the macro-control is effective during the COVID-19 epidemic and has the characteristics of going against the economic cycle. It indirectly indicates that COVID-19 is a short-term market shock, and inflation inertia mainly comes from commodities of food, which means that government should regulate the inflation by aiming at food goods during the COVID-19 epidemic.

This article affirms the price stickiness of commodities during the COVID-19 epidemic and thus has practical significance. However, there are still some limitations that need to be further studied. Firstly, we just consider the price stickiness during the COVID-19 epidemic, ignoring the control of other emergencies and limiting the scope of application of our conclusions. Secondly, the data have not been fully mined, and the processing method of high-frequency data still needs to be further improved. Thirdly, the sample data need to be expanded. For example, Amazon and JD can be added as research objects, but it is difficult to obtain and match cross platform commodity information. This is a key issue that needs to be solved in subsequent studies.

Data Availability

The dataset that support the findings of this study can be accessed upon request.

Conflicts of Interest

The authors declare that they have no conflicts of interest.

References

[1] S. N. Qu, L. X. Wu, and J. C. Xia, "The Fluctuations of China's consumer price: sticky price, price Setting and policy experiments," *Economic Research Journal*, vol. 47, no. 11, pp. 88–102, 2012.

[2] Z. F. Su and C. N. Chen, "China's consumer price stickiness and sector inflation inertia," *Economic Perspectives*, vol. 49, no. 2, pp. 265–292, 2002.

[3] A. M. Sbordone, "Prices and unit labor costs: a new test of price stickiness," *Journal of Monetary Economics*, vol. 49, no. 2, pp. 265–292, 2002.

[4] L. Li, B. Lei, and C. Mao, "Digital twin in smart manufacturing," *Journal of Industrial Information Integration*, vol. 26, no. 9, Article ID 100289, January 2022.

[5] C. Douglas and A. M. Herrera, "Why are gasoline prices sticky? A test of alternative models of price adjustment," *Journal of Applied Econometrics*, vol. 25, no. 6, pp. 903–928, 2010.

[6] S. G. Cecchetti, "The frequency of price adjustment: a study of the newsstand prices of magazines," *Journal of Econometrics*, vol. 31, no. 3, pp. 255–274, 1986.

[7] L. Li, T. Qu, Y. Liu et al., "Sustainability assessment of intelligent manufacturing supported by digital twin," *IEEE Access*, vol. 8, Article ID 174988, 2020.

[8] D. Levy, M. Bergen, S. Dutta, and R. Venable, "The magnitude of menu costs: direct evidence from large U. S. Supermarket chains," *Quarterly Journal of Economics*, vol. 112, no. 3, pp. 791–824, 1997.

[9] L. Li, C. Mao, H. Sun, Y. Yuan, and B. Lei, "Digital twin driven green performance evaluation methodology of intelligent manufacturing: hybrid model based on fuzzy rough-sets AHP, multistage weight synthesis, and PROMETHEE II," *Complexity*, vol. 2020, no. 6, 24 pages, Article ID 3853925, 2020.

[10] G. A. Calvo, "Staggered prices in a utility-maximizing framework," *Journal of Monetary Economics*, vol. 12, no. 3, pp. 383–398, 1983.

[11] L. Li and C. Mao, "Big data supported PSS evaluation decision in service-oriented manufacturing," *IEEE Access*, vol. 8, no. 99, Article ID 154663, 2020.

[12] M. Bils and P. J. Klenow, "Some evidence on the importance of sticky prices," *Journal of Political Economy*, vol. 112, no. 5, pp. 947–985, 2004.

[13] P. J. Klenow and O. Kryvtsov, "State-dependent or time-dependent pricing: does it matter for recent US inflation?" *Quarterly Journal of Economics*, vol. 123, no. 3, pp. 863–904, 2008.

[14] A. Cavallo, "Scraped data and sticky prices," *The Review of Economics and Statistics*, vol. 100, no. 1, pp. 105–119, 2018.

[15] T. F. Jiang, K. Tang, and T. X. Liu, "The stickiness of online prices in China," *Economic Research Journal*, vol. 55, no. 6, pp. 56–72, 2020.

[16] P. Lunnemann and T. Y. Mathä, "Regulated and services' prices and inflation persistence," 2005, https://ssrn.com/abstract=691862.

[17] S. Matos, "Reconciling the Micro Evidence on price Stickiness and Inflation Persistence Using Brazilian CPI," in *Proceedings of the 32 Meeting of the Brazilian Econometric Society*, Salvador, BA, USA, December 2010.

[18] S. Z. Ma and C. Fang, "Does offline market segmentation promote firms' online selling:an explanation for China's E-commerce expansion," *Economic Research Journal*, vol. 55, no. 7, pp. 123–139, 2020.

[19] A. Cavallo, "Are online and offline prices similar? Evidence from large multi-channel retailers," *The American Economic Review*, vol. 107, no. 1, pp. 283–303, 2017.

[20] T. Huang and X. J. Jin, "Lucky number preference, mantissa pricing and price stickiness: evidence from the internet prices," *Finance & Trade Economics*, no. 12, pp. 121–132, 2014.

[21] E. Cavallo, A. Powell, and O. Becerra, "Estimating the direct economic damages of the earthquake in Haiti," *The Economic Journal*, vol. 120, no. 546, pp. 298–312, 2010.

[22] X. J. Jin, T. Huang, and Y. Zhu, "An estimate of the degree of nominal price stickiness in China," *Economic Research Journal*, vol. 48, no. 9, pp. 85–98, 2013.

[23] G. Gopinath and R. Rigobon, "Sticky borders," *Quarterly Journal of Economics*, vol. 123, no. 2, pp. 531–575, 2008.

[24] XH. He, "Accurately understand key concepts in the dispute over CPI," *Macroeconomics*, no. 3, pp. 3–7+13, 2011.

[25] J. Qin, C. H. Li, and S. W. Zhuang, "The impact of novel coronavirus pneumonia on commodity price," *Journal of Business Economics*, no. 12, pp. 19–36, 2021.

[26] E. T. Anderson and D. I. Simester, "Price stickiness and customer antagonism," *Quarterly Journal of Economics*, vol. 125, no. 2, pp. 729–765, 2010.

[27] CS. Zhang, "The nature of inflation inertia in China and its implications on monetary policy," *Economic Research Journal*, no. 2, pp. 33–43, 2008.

[28] J. Fuhrer and G. Moore, "Inflation persistence," *Quarterly Journal of Economics*, vol. 110, no. 1, pp. 127–159, 1995.

[29] J. B. Taylor, "Low inflation, pass-through, and the pricing power of firms," *European Economic Review*, vol. 44, no. 7, pp. 1389–1408, 2000.

[30] D. W. K. Andrews and H. Y. Chen, "Approximately median-unbiased estimation of autoregressive models," *Journal of Business & Economic Statistics*, vol. 12, no. 2, pp. 187–204, 1994.

[31] A. Roy and W. A. Fuller, "Estimation for autoregressive time series with a root near 1," *Journal of Business & Economic Statistics*, vol. 19, no. 4, pp. 482–493, 2001.

[32] S. Guo, "Survival analysis of a stochastic cooperation system with functional response in a polluted environment," *Advances in Difference Equations*, vol. 2020, no. 1, pp. 354–419, 2020.

[33] YB. Chen, "Research on New Keynesian Phillips curve in China," *Economic Research Journal*, vol. 43, no. 12, pp. 50–64, 2008.

[34] Z. C. Bian and H. Q. Hu, "Sticky prices, sticky information and Chinese Phillips curve," *The Journal of World Economy*, vol. 39, no. 4, pp. 22–43, 2016.

[35] E. Zivot and D. W. K. Andrews, "Further evidence on the great crash, the oil-price shock, and the unit-root hypothesis," *Journal of Business & Economic Statistics*, vol. 10, no. 3, pp. 251–344, 1992.

Hindawi
Scientific Programming
Volume 2022, Article ID 5423927, 8 pages
https://doi.org/10.1155/2022/5423927

Research Article

Design and Application of Spatial Experience System for Urban Village Reconstruction Based on GIS

Weiwei Chen

Art College, South China Agricultural University, Guangzhou, Guangdong 510642, China

Correspondence should be addressed to Weiwei Chen; freevv125@scau.edu.cn

Received 28 June 2022; Revised 30 July 2022; Accepted 3 August 2022; Published 18 August 2022

Academic Editor: Lianhui Li

This paper takes the village in the city as a case study, through the investigation of the basic information of the village in the city, such as housing construction, construction quality, property rights characteristics, and so on. We use GIS technology to evaluate the construction and reconstruction cost of the plot. This paper puts forward different transformation schemes and explores the application of GIS technology in the transformation planning of urban villages. Finally, this paper designs a GIS-based spatial experience system for micro-transformation of urban villages.

1. Introduction

At present, urbanization is an inevitable trend of social and economic development in the world [1–5]. With the strong impetus of reform and opening up and the development of the market economy, China's urbanization process continues to accelerate. In 1978, China's urbanization rate was 17.9%. In 2011, it reached 51.27% and exceeded 50%. In 2017, China's urbanization rate reached 58.52%. From the perspective of urbanization development laws in the world, when the urbanization rate exceeds 50%, it means that urbanization has entered a rapid development stage, which will inevitably lead to profound social changes. What follows is that the urban spatial structure, industrial positioning, urban planning, urban management, and other aspects will face new development. However, in the process of China's rapid urbanization, a universal and unique phenomenon—village in city has emerged. The village in the city is the product of urbanization under the urban-rural dual system in China and has developed into a typical problem gathering place in the process of the evolution of the urban-rural dual system to the unification. At present, the focus of China's reform and development is to reform the urban-rural dual system. Among them, dealing with the problem of villages in cities is an important content related to the overall development of China's urban and rural areas and the formation of a new pattern of urban-rural integration. It is also the key to solving the urban-rural dual system.

The essence of urbanization in developing countries is the process of constantly breaking the urban-rural dual structure and gradually realizing urban-rural integration [6, 7]. China's urban-rural dual system was formed in the planned economy era. It is undeniable that in that special historical period, this economic system played an important role in China's economic and social development at that time. However, with the development of the times, China has turned from a planned economy to a market economy. The progress of industrialization has accelerated the development of urbanization. The urban-rural dual system, which once played a role in promoting China's economic and social development, has not only become a stumbling block to the development of urbanization. At the same time, it has also become one of the adverse factors restricting the development of the whole society and has been intensively reflected in the villages in the city. Under China's urban-rural dual management system, although urban villages have already belonged to cities and towns within the geographical scope, they are still rural systems and rural organizational systems in terms of the management system. Although the villagers in urban villages no longer engage in agricultural

production, they cannot enjoy the same social security as urban residents in terms of education, medical treatment, and health care. Nowadays, a series of environmental, social, and economic problems caused by villages in cities have not only become one of the most difficult problems in urban transformation and urban governance in large and medium-sized cities in China, but also become a bottleneck restricting urban development. It can be said that the emergence of urban villages is an inseparable knot in the process of urbanization. Most Chinese cities, large and small, are facing the problem of urban villages. The transformation of urban villages has become a major event that the local government must pay attention to. However, in the actual process of urban village reconstruction, no matter which city or place in China has encountered great challenges, such as insufficient funds for urban village reconstruction and the inability to guarantee the legitimate interests of villagers in the process of reconstruction.

The village in the city is the form of urban material space in the process of urbanization in China. It is the product of the imbalance between urban and rural areas and has deep and complex social problems. From big cities to small- and medium-sized cities, there are many urban village problems involving economy, society, environment, and so on, which has become a chronic disease that seriously puzzles the healthy, harmonious, and sustainable development of cities. In order to promote the healthy development of China's urbanization and improve the quality of urbanization and urban quality, we must take reasonable and effective control measures to transform villages into cities and actively promote the healthy development of urbanization.

At present, the phenomenon, existing problems, and formation mechanism of the village in the city have been thoroughly revealed by the academic circles, and the idea of the transformation of the village in the city has gradually become clear, but the implementation effect of the case study and planning scheme of the transformation is not very ideal. The research on urban village reconstruction planning mainly involves two aspects: system reform and material space transformation. In the process of promoting the transformation of urban villages, many places first adopted the reform of the administrative management system, and the research also relatively focused on the contents of registered residence, land, management, grass-roots organizations, and the operation of the village collective economy. On the one hand, the research on the transformation of material space is a theoretical discussion, involving transformation ideas, operation modes, technical schemes, demolition compensation and resettlement, economic analysis, social analysis, system and policy support, etc. On the other hand, it is the empirical study of transformation planning, which is mainly manifested in the planning and design scheme of urban villages. Although the scientificity and operability of the planning scheme are closely related to the complexity of the transformation of urban villages, the lack of in-depth research on the basic situation of urban villages and insufficient application of technical methods in the planning process are also important reasons for the lack of feasibility of the planning scheme. The application of GIS technology [8–13] can establish a detailed basic database. Through the statistical analysis function of GIS, planners, and reconstruction implementers can clearly grasp the difficulty of reconstruction of urban villages, the reasonable sequence of reconstruction, the arrangement of demolition and resettlement, etc. The application of GIS technology will provide a powerful technical guarantee for the reconstruction planning of villages in cities.

2. Related Work

2.1. Urban Village. Village in the city is a special phenomenon in the process of rapid urbanization under the urban-rural dual system in China. Compared with China, the phenomenon of urban villages in some developed countries is relatively rare. In addition, urban villages appeared relatively late. Therefore, scholars have not conducted much special research on urban villages in China. However, urban problems similar to the characteristics of "village in city" have also appeared in the urbanization process of some developed countries, especially the urban sprawl in the United States after 1950, and the slums in Latin America, Asia, and other developing countries in the process of rapid urbanization and excessive urbanization. Although the formation mechanism of these phenomena in some developed countries is different from that in China, the theoretical basis for the transformation of urban villages in China can be found from the western urbanization theory and the research on urban fringe. The scholar who first proposed and used the concept of urbanization was a serda, who defined the concept of urbanization in the book basic principles of urbanization published in 1867 [14]. In the mid-eighteenth century, the rise of the industrial revolution accelerated the pace of urbanization. With Britain as the representative, under the influence of the industrial revolution, France, Germany, the United States, and other countries have successfully completed the industrial revolution. With the substantial improvement of labor productivity and productivity, the industry of these countries has developed rapidly, while the development of industrialization has also led to the rapid development of Urbanization in these countries, and emerging cities continue to appear.

The industrial revolution not only promoted the development of industrialization, but also prompted more and more rural people to gather in cities. With the continuous expansion of urban scale, coupled with the lack of scientific and reasonable urban planning, urban spatial layout was disordered, and social security and residents' living standards were getting lower and lower. In the mid-nineteenth century, some western industrial cities represented by London, England had different problems one after another. The emergence of this phenomenon has attracted more and more western scholars' attention to the direction of urban development. During the discussion on the direction of urban development, two completely different views were formed. One was represented by the British scholar Howard, who advocated that the future direction of urban development should be an idyllic city [15]. The other is represented

by Le Corbusier, who advocates that the future direction of urban development should be modern cities [16]. Compared with the view of developing modern cities, although the idea of developing garden cities is somewhat idealistic, the idea of urbanization that garden cities focus on pursuing low density in regional space and advocating that life should return to green nature provides a certain theoretical reference for China's sustainable urban development and effective land use. The modern urban theory put forward by Le Corbusier argues that cities must be concentrated if they want to develop. Only when cities are concentrated can they bring power to urban development. Cities also need to build a large number of high-rise buildings to make the population concentrated in the city, and the traffic, housing, environment, and other problems caused by population concentration can be solved by other technical means. Le Corbusier's modern urban thoughtfully embodies the concept of intensive land use and advocates that the expansion of urban scale should take the road of connotation development.

Scholars began to systematically study the urban internal spatial structure very early. For example, in 1826, von Thunen, a German economist, published the book "the relationship between agriculture and national economy in isolated countries," in which he put forward the famous agricultural location theory. The theory points out that the level of economic development and its productivity determine the type of agricultural land use and the degree of intensification of agricultural land use, and further points out that the distance between agricultural production land and the agricultural product market has a greater impact on the type of agricultural land use and the degree of intensification of agricultural land use. In 1909, the German economist Weber put forward the famous Weber's industrial location theory in his book on industrial location. The theory chooses the industrial production activities of the three basic links of production, circulation, and consumption as the research object, scientifically analyzes and accurately calculates the relationship between factors such as transportation and labor agglomeration, and puts forward the principle of minimum cost, that is, for industrial products, the lowest point of production cost is the most ideal location for industrial enterprises. From the development of location theory, the early location theory did play a positive role in the scientific and rational use of land, but this theory also has its limitations, such as single research object, pure theoretical derivation, and lack of practicality. After that, with the proposal of concentric circle theory, fan theory, and multicore theory, the location theory has been further developed. These three theories profoundly reveal the general laws of urban land use and functional zoning and emphasize the leading role of CBD in urban development and functional zoning, which has a positive guiding significance for the planning and construction of Chinese cities.

Urban fringe and urban village have different meanings, but they are closely related. From a regional perspective, the urban fringe is a transitional zone between the periphery of the urban built-up area and the rural area. Its boundary is not very obvious, and it also has dynamic characteristics. The village in the city is a construction area within the urban built-up area and the fringe, and it is a "point" of the urban fringe. From the aspects of land use, economic characteristics, and social structure, the two have certain similarities. They are both in the process of obvious transformation from rural to urban. Compared with the urban fringe, the urban village has more urban characteristics. Therefore, the research theories and methods on the urban fringe can be used for reference in the study of villages in cities in China. The first scholar to put forward the concept of "urban fringe" is German geographer L. Louis. At the same time, his explanation of this concept has also been widely recognized by scholars all over the world. In 1936, Herbert Louis studied Berlin, a large European city, from the perspective of morphology. In his study of the regional structure of Berlin, he found that some areas that were originally located on the edge of the city were gradually surrounded with the continuous expansion of the city and eventually became part of the urban area. Herbert Louis called this surrounded area the urban fringe.

Since the 1970s, there have been more and more studies on the urban fringe in some developed countries, and most of them focus on the rapid development of urbanization. The research content has also changed from the initial spatial form to the research on the development law, influencing factors, and dynamic mechanism of the urban fringe. In the research on the characteristics of regional structure, Golledge believes that there are seven differences between the urban fringe and the rural and urban areas. They are a small amount of agriculture in the urban fringe, intensive crop production, flexible and changeable population, medium density, rapid expansion of new residential areas, and widespread provision of incomplete services, public facilities, and speculative housing. In the study of suburban characteristics, R.E. Boll discussed from a sociological point of view that the urban fringe has the suburban characteristics of living tendency according to class, selective immigration, frequent commuting, weakened geography, and social hierarchy. Adedayo Adesina takes Nigeria as the research object, analyzes the social structure characteristics of urban-rural fringe in developing countries, and points out the potential impact of informal economic activities on government policies. In the study of urban-rural integration, he emphasized the concept of continuous unity between urban and rural areas, analyzed the relationship between changes in real estate structure, land use structure, agricultural structure, and social and community structure, and found that there were environmental differences in the process of such regional transformation between different cities. In the study of land use difference, the urban fringe is divided into inner edge zone and outer edge zone according to the nature and intensity of land use. The inner edge area means that the land use has been in the advanced stage from rural to urban. The outer edge area refers to the agricultural land use as the main landscape, but the land use has obvious suburban characteristics.

In developing countries, slums generally refer to informal settlements, where urban poverty is most evident. Although there are different names, different land tenure

systems and different building structures, overcrowding, unsafe living conditions and the lack of clean water, electricity, sanitation, and other basic living services are common characteristics of slums. The rapid growth of urban and rural migrants, growing poverty, and unsafe land tenure have led to the continuous emergence of slums, and the most important factor is the large-scale migration of the rural population to cities. Since the 1950s, the rural population in developing countries has decreased by an average of 25%. Compared with a large number of rural to urban migrants, the construction of urban planning and urban management system has been slow, which has accelerated the formation of slums and led to the growing scale of slums. Some experiences and lessons can be learned from the practice of slum reconstruction in some developed countries.

2.2. GIS Technology. With the development of computer technology, it has been applied in various fields [17–20]. In the process of using GIS spatial data, better analysis ability can be obtained [10–13]. With the assistance of GIS spatial data, it can ensure that the planning and design personnel can simulate the current planning scheme, and make an objective evaluation of the scheme content under the condition of reasonable screening, so as to obtain better planning decision-making content. Under the support of GIS spatial data, the buffer area can also be superimposed in the form of layer superposition, and the best planning path can be selected in the form of automatic matching. Based on this form of spatial analysis, the perfection of the planning area setting is guaranteed from many different levels, such as residential area, Park Square, public facilities location, pedestrian and vehicle route selection, and the best arrangement, and gradually replaced the traditional form of planning and design methods. In addition, in the process of using the GIS system, it can comprehensively consider the social development, economic growth, natural conditions, and other factors within the scope of the urban planning area. In the case of multiple factor superposition analysis, it ensures the comprehensiveness and objectivity of the prediction and evaluation and further makes an accurate prediction of the economic development trend within the planning area on the basis of the planned urban land grade. The application of GIS technology in the field of urban planning industry can not only improve the overall design efficiency in the process of planning and design, but also obtain better planning and design results and improve the implementation quality of urban planning and design under the condition of shortening the design cycle. In the process of managing data information with the help of GIS technology, it can not only expand the storage capacity of data information, but also improve the data maintenance and updating ability of the system with the help of a variety of different types of spatial data, provide convenient support for the display of data query, superposition, clustering, network proximity, spatial information, and other functions, and make the urban planning and design scheme gradually transform toward the rational direction.

In the process of using GIS to carry out management work, it is necessary to comprehensively analyze the specific application requirements of urban planning and design, so as to ensure that in the process of using traditional surveying and mapping technology, it can avoid the impact of other interference factors and reduce the adverse effects on urban planning and design. The system operation mode based on GIS technology needs to take the satellite system as the basic support within a specific range. In the subsequent use process, the detection work should be carried out for the satellite data information system to ensure the convenience of the detection work. Due to the special nature of relevant external factors, it is necessary to take effective application measures through the rational use of GIS technology in various regions to ensure the visual characteristics of measurement links and provide support for the update of Surveying and mapping technology.

In the process of accelerating urbanization construction, higher requirements are put forward for software surveying and mapping management, which needs to be based on the concept of strictness and rigor, in the form of manual measurement and with the help of the actual utility of measuring instruments, to ensure the accuracy of the finally measured data information, so as to ensure the timeliness of data information update. In addition, there are relatively many types of interference factors caused by the degree of measurement results, which puts forward higher requirements for the traditional surveying and mapping work, and it is necessary to ensure the perfection of the satellite detection process setting. It is necessary to take GIS technology as the basic guarantee to ensure the effectiveness of satellite detection after the completion of satellite detection. In the implementation stage of the actual measurement work, it is necessary to process the collected information to ensure the timeliness of information processing, set the range according to the existing value, and reduce it to the minimum within a limited time. In addition, during the implementation of measurement, the main purpose is to ensure the accuracy of data information, ensure the accuracy of satellite positioning, and enable it to operate stably in orbit 120 km away from the Earth.

When surveying and mapping the ground area based on GIS, it is necessary to strictly follow the specific requirements of signal reception, so as to preset and process the relevant devices, and adjust and evaluate the relevant technical information based on the fully automatic observation form. In addition, in the process of introducing relevant surveying and mapping instruments, it is necessary to ensure the effectiveness of the use of instruments, take this aspect as the focus of the surveying and mapping link, strengthen the management of various types of instruments and equipment, lay a good foundation for the sustainable development of surveying and mapping operations, ensure that the actually obtained surveying and mapping information has the characteristics of detail, and draw the topographic map in an intuitive form. It can not only reduce the use of labor costs, but also ensure the feasibility and operability of GIS mapping mode on the basis of improving work efficiency. Comparing the GIS surveying and mapping

technology with the traditional human light surveying and mapping method, it can be seen that in the process of using GIS technology to carry out surveying and mapping work, it can effectively improve the actual surveying and mapping efficiency and can be used under complex environmental conditions. In full combination with the actual situation, it ensures the effective implementation of Surveying and mapping work and management work and meets the specific requirements of urban planning and design work.

3. Research on the Application of Urban Village Reconstruction Scheme

3.1. Research Framework. The working process of urban village reconstruction planning is as follows: (1) investigation and analysis of the basic situation. Through the on-the-spot survey, questionnaire survey, personal interview, literature reading, and other means, we mainly understand the basic information of urban villages, such as population, housing and land income, policies, and systems. (2) Collection and analysis of basic data. Establish GIS analysis database to collect basic data including land cadastre (topographic map, house cadastre data, etc.), house conditions (structure base area, floor height, house property right, building quality, etc.), and social and economic factors (house cost, demolition cost, population, etc.). (3) Analysis and evaluation of transformation ideas. Through GIS technology, this paper studies the scheme of urban village reconstruction, the method of demolition and resettlement, and the sequence arrangement of reconstruction and reconstruction. (4) Form a preliminary plan and ideas. Through communication and coordination with villagers, local managers and reconstruction implementers, the reconstruction scheme is revised. (5) Preparation of planning scheme (as shown in Figure 1).

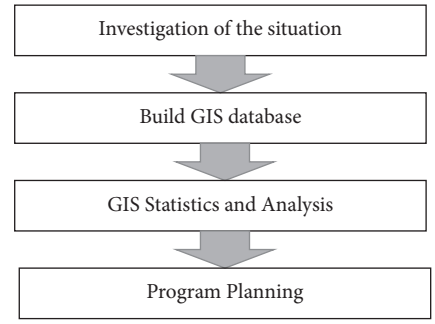

Figure 1: Preparation of the planning scheme.

3.2. Data Collection. The data collection of the GIS database is mainly based on the following sources: (1) the topographic map is imported to form the GIS base map, which digitizes the basic information such as roads, river waters, and houses, including the house base range and area, floating platform range and area, floor height, and other house information. (2) According to the house cadastre and property rights data of the Housing Administration Bureau, confirm the property right information of all houses in the reconstruction area and enter it into the attribute of the house object in the GIS database. (3) The construction quality of all houses is determined through on-site investigation, which is divided into four grades: A, B, C, and D. At the same time, the buildings with historical protection value shall be determined.

3.3. Evaluation and Classification of Existing Buildings. In general, three different technical schemes can be adopted for the transformation of Urban Villages: first, overall transformation, which refers to the comprehensive transformation from the overall pattern to individual buildings, but some historical buildings may also be retained, mainly for urban villages with poor overall human settlements. Second, local transformation refers to the key transformation of local areas and key elements without major adjustment of the overall pattern, mainly aiming at the villages in the city where the problems are not prominent. The third is to retain the renovation, which means that the internal environment of urban villages is renovated without adjustment of the overall pattern, mainly for urban villages with mild problems and good living environment. What kind of transformation plan should be adopted for the transformation of urban villages? Not only the living environment of urban villages, but also the economic feasibility of the transformation should be considered. The reconstruction of urban villages involves the demolition compensation of the original houses and the relocation and resettlement of the original residents after the reconstruction, which increases the cost of house demolition and resettlement compared with the general real estate development. Therefore, the economic cost and investment income of the transformation should be considered in the selection of the transformation scheme of urban villages. Therefore, it is necessary to evaluate the plot ratio, building quality, property rights, and rental benefits of urban villages. Figure 2 presents the research idea map.

3.3.1. Plot Division. There are obvious differences between the buildings in the East and the west of the village in the city, so it is necessary to adopt different transformation strategies according to local conditions. Firstly, according to the natural geographical environment (such as ponds and rivers), road conditions, and architectural characteristics, the village in the city is divided into 17 plots of similar size.

3.3.2. Statistical Analysis. By using the statistical analysis function of GIS, the basic building conditions of each plot are obtained.

3.3.3. Cluster Analysis. According to the building conditions of each plot, the index values that can best reflect the building characteristics, such as building area, building floor area ratio, average floors, and building quality index, are selected as variables for hierarchical cluster analysis. After testing, the method of sum of squares of Wald's deviation is the best for classification and can analyze the building conditions of each group:

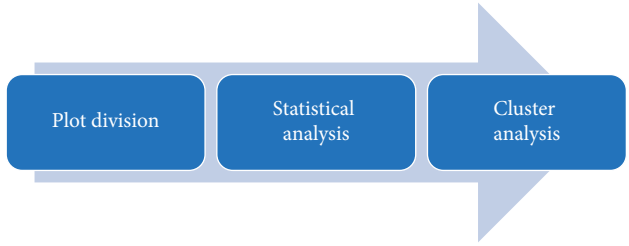

Figure 2: Research idea map.

The first group is a low-density building area. The main feature is that the natural landscape in the plot is good, there are large ponds and waters, and the building density, building floor area ratio, and the average number of floors are relatively low. It is a low-cost or high-efficiency reconstruction area. However, the building quality of each plot varies greatly. The plots with a good living environment should be retained and renovated, while the plots with a poor living environment should be listed as key reconstruction areas.

The second group is a medium-density building area, which belongs to a typical traditional rural settlement type. The main characteristics are that the building density in the plot is high, the living environment is relatively poor, and the building quality, floor height, and floor area ratio are general. It is an area in urgent need of reconstruction.

The third group is high-density building areas. The main features are that the average number of floors of buildings in the plot is relatively high, the building quality is relatively good, the building plot ratio is relatively high, and the reconstruction cost is large. It belongs to a local reconstruction area.

3.4. Establishment of Thematic Map and Analysis of Influencing Factors. The above statistical analysis is aimed at the economic evaluation of the amount of housing reconstruction and demolition, which provides a fundamental basis for the determination of the reconstruction scheme. However, it still stays at the level of the mathematical analysis method, and more objective factors must be considered in determining the transformation plan. With the application of GIS technology, the planning can establish thematic maps according to these factors for analysis, and finally achieve the purpose of comprehensive consideration.

Because the original rural planning and management system is not perfect and the villagers' legal meaning is weak, illegal buildings in urban villages are quite common. Therefore, for the houses that have been planned and legally built, the planning should be retained as far as possible. The vast majority of houses in Dongxifang, a village in the city, have incomplete formalities. The main purpose of urban village reconstruction is to improve the environment of urban village. Therefore, the quality of housing construction and the overall construction landscape should become the main evaluation factors of urban village reconstruction.

4. System Design and Application Platform Based on GIS Architecture

With the putting forward of the GIS concept, GIS application terminal is developing toward miniaturization and mobility. GIS Server is developing toward a cross-platform and service-oriented architecture and supports minicomputer, mainframe, cluster, and other applications. The new generation t-c-v three-tier software architecture (terminal cloud virtual), a GIS application model for cloud services proposed by MAPGIS, a large domestic GIS manufacturer, provides users with a cloud GIS basic platform suitable for geographic information services. T-c-v architecture is a loosely coupled software architecture [21–23]. The three layers refer to the terminal application layer, cloud computing layer, and virtual device layer, respectively. Based on the concept of service orientation, each layer is connected by standard service interfaces to provide all-round sharing of data, functions, and services, as well as aggregation and migration of services; replace the current small and medium-sized computing mode with the super large-scale computing mode. The framework can solve the problems of isolated services and difficult integration, make data integration and mining easier, improved data storage organization and management capabilities, and provided users with fast, convenient, and broader information service capabilities. The terminal application layer provides users or developers with standard interfaces to access, so as to facilitate the construction of various terminal applications. Table 1 presents the T-C-V three-layer software architecture.

4.1. Virtual Device Layer (V Layer). The virtual device layer refers to the organization of software and hardware devices such as computers, network facilities, storage devices, and large databases at the bottom based on virtualization technology, shielding the heterogeneity of different computers, networks, and storage devices, managing all software and hardware resources in an integrated manner, virtualizing them into corresponding logical resource pools, and providing a unified and efficient operating environment for cloud computing layer applications. The virtual device layer is the foundation to support cloud computing and cloud GIS services. Users can use various terminal devices to obtain GIS services at any place and at any time.

4.2. Cloud Computing Layer (C Layer). The cloud computing layer combines the current cutting-edge cloud computing technology and the characteristics of geospatial information to establish a framework for massive geographic information data, functions, resource management, and service system. On the basis of supporting super large-scale and virtualized hardware architecture, a massive GIS data, function and resource management, and service system framework are established, and services are established according to the idea of "plug and play" and the concept of aggregated services. The cloud computing layer deploys the cloud GIS services provided by GIS application developers and end users. Among them, basic GIS platform developers can

Table 1: T-C-V three-layer software architecture.

Layer	Specific structure
V layer	Virtual device layer
C layer	Cloud production center Cloud service warehouse Cloud management center
T layer	Terminal application layer

provide basic GIS function services, GIS application software developers, and other end users from all walks of life can provide GIS function services of different granularity that can form various applications. The energy source of the cloud computing layer constantly generates new resources and expands the cloud, while ensuring that other resources can be smoothly connected to the cloud. The cloud service warehouse is mainly used to manage various cloud GIS services. The cloud management center is used to manage the registration, discovery, scheduling, and security of all services in the cloud and ensures the normal operation of online transactions of cloud services.

4.2.1. Cloud Production Center. One of the important roles of the cloud computing layer is to generate various cloud resources for users to customize. In order to ensure that all cloud resources can be connected to the cloud for global users and that these resources can be aggregated and reconstructed. Map GIS 10 has launched the development mode of "framework + plug-in." All applications in this development mode are composed of frameworks and plug-ins. These frameworks and plug-ins are independent of each other. They are connected through certain standards and specifications. As long as the frameworks and plug-ins contained in applications that meet the same standards and specifications can be freely aggregated and reconstructed. At the same time, MAPGIS 10 provides powerful runtime support and can easily access third-party applications. Users can directly customize, aggregate, and reconstruct the application system based on the rich kernel resources provided by MAPGIS 10 and use the existing framework and plug-in resources. They can also customize the development functions based on unified development standards and development processes based on various end application development runtime and API resources provided by MAPGIS 10 to form cloud service resources.

4.2.2. Cloud Service Warehouse. The cloud computing layer is also the cloud GIS Service Center, and the cloud service warehouse is the window to share cloud GIS services to various users. All cloud services managed in the cloud service warehouse are built based on unified service standards, which ensures that third parties can make arbitrary calls according to the unified call standards, so as to facilitate the global sharing of cloud services. MAPGIS 10 adopts a floating flexible architecture and uses a function warehouse and a data warehouse to manage function services and data services respectively, so as to ensure that functions and data can be completely separated, thus ensuring the "drift, aggregation and reconstruction" characteristics of cloud services.

4.2.3. Cloud Management Center. The cloud computing layer is also the cloud management center, providing the whole process management and monitoring of cloud GIS services from discovery, registration, and invocation; unified management of all resources of cloud environment operation, including management of cloud online use, delivery, security, and other contents. According to the cloud business model, it restricts the online transaction and payment, security, as well as the registration, discovery, and invocation of cloud services, so as to provide a good operating environment for the cloud.

4.3. Terminal Application Layer (T Layer). The terminal application layer provides users with standard access interfaces, and users can build various terminal applications. It allows users to access the cloud and obtain resources through various terminal devices such as PC computers, intelligent terminals, various monitoring devices, and various application software with distinctive applications running on these devices. Through the cloud services provided in layer C, terminal applications can be freely scalable, customized, expanded, and developed to meet various public and private cloud applications from individuals, groups, enterprises, the public, the government, and so on.

5. Conclusion

GIS technology provides an effective analysis tool for data and graphics processing for urban research. It is widely used in urban planning management, urban information system, and other fields and is mostly combined with transportation research, land use, and other research. At present, the domestic GIS technology mainly focuses on the macro problems of physical space, while some developed countries begin to pay attention to the micro-level analysis of social, economic, and psychological factors, which has been widely used in the reconstruction of old cities. The task of urban village reconstruction in many cities in China is urgent. However, due to the lack of collection of basic data and the application of advanced technical methods, the urban village reconstruction schemes are often lack scientificity and operability. As a means of quantification and visualization, GIS analysis is a good tool for observing and analyzing the construction of urban villages. It is helpful to establish a data database for transformation analysis and to help planners analyze and study the social and economic factors of urban villages. In the future, it can be seen that the application of GIS in urban village reconstruction project provides strong analytical support for the determination of the reconstruction scheme, the implementation of the reconstruction sequence, and the evaluation of investment income.

Data Availability

The dataset can be accessed upon request.

Conflicts of Interest

The author declares that there are no conflicts of interest.

Acknowledgments

The author thanks the Youth Project of Humanities and Social Sciences of The Ministry of Education, Research on Micro-Transformation Strategy of Urban Villages from the Perspective of Cultural Inheritance (no. 18YJC760008).

References

[1] D. Vlahov and S. Galea, "Urbanization, urbanicity, and health," *Journal of Urban Health: Bulletin of the New York Academy of Medicine*, vol. 79, pp. S1–S12, Article ID 90001, 2002.

[2] H. Ritchie and M. Roser, "Urbanization," *Our world in data*, 2018.

[3] H. Tisdale, "The process of urbanization," *Social Forces*, vol. 20, no. 3, p. 311, 1942.

[4] J. G. Williamson, "Migration and urbanization," *Handbook of Development Economics*, vol. 1, pp. 425–465, 1988.

[5] L. Bertinelli and D. Black, "Urbanization and growth," *Journal of Urban Economics*, vol. 56, no. 1, pp. 80–96, 2004.

[6] J. V. Henderson, "Urbanization in a developing country: city size and population composition," *Journal of Development Economics*, vol. 22, no. 2, pp. 269–293, 1986.

[7] M. Ravallion, "On the urbanization of poverty," *Journal of Development Economics*, vol. 68, no. 2, pp. 435–442, 2002.

[8] Z. Nedović-Budić, "The impact of GIS technology," *Environment and Planning B: Planning and Design*, vol. 25, no. 5, pp. 681–692, 1998.

[9] D. J. Maguire, "An overview and definition of GIS," *Geographical information systems: Principles and applications*, vol. 1, no. 1, pp. 9–20, 1991.

[10] S. M. Fletcher-Lartey and G. Caprarelli, "Application of GIS technology in public health: successes and challenges," *Parasitology*, vol. 143, no. 4, pp. 401–415, 2016.

[11] Z. Nedovic-Budic, "Evaluating the effects of GIS technology: review of methods," *Journal of Planning Literature*, vol. 13, no. 3, pp. 284–295, 1999.

[12] A. Carrara, M. Cardinali, and F. Guzzetti, "GIS technology in mapping landslide hazard," *Geographical Information Systems in Assessing Natural Hazards*, pp. 135–175, Springer, Dordrecht, 1995.

[13] A. Carrara, F. Guzzetti, M. Cardinali, and P. Reichenbach, "Use of GIS technology in the prediction and monitoring of landslide hazard," *Natural Hazards*, vol. 20, no. 2/3, pp. 117–135, 1999.

[14] J. Yao, P. Xu, and Z. Huang, "Impact of urbanization on ecological efficiency in China: an empirical analysis based on provincial panel data," *Ecological Indicators*, vol. 129, Article ID 107827, 2021.

[15] E. Howard, *Garden Cities of Tomorrow*, Faber, London, UK, 1946.

[16] N. Katsikis, "On the geographical organization of world urbanization," *MONU-Geographical Urbanism*, vol. 20, pp. 4–11, 2014.

[17] Z. Jia, Y. Lin, J. Wang et al., "Multi-view spatial-temporal graph convolutional networks with domain generalization for sleep stage classification," *IEEE Transactions on Neural Systems and Rehabilitation Engineering*, vol. 29, pp. 1977–1986, 2021.

[18] Z. Jia, X. Cai, Y. Hu, J. Ji, and Z. Jiao, "Delay propagation network in air transport systems based on refined nonlinear Granger causality," *Transportation Business: Transport Dynamics*, vol. 10, pp. 586–598, 2022.

[19] Z. Jia, Ji Junyu, and X. Zhou, "Hybrid spiking neural network for sleep EEG encoding," *Science China Information Sciences*, vol. 4, 2022.

[20] Z. Jia, X. Cai, and Z. Jiao, "Multi-modal physiological signals based squeeze-and-excitation network with domain adversarial learning for sleep staging," *IEEE Sensors Journal*, vol. 22, no. 4, pp. 3464–3471, 2022.

[21] H. Lu, X. Zhong, and L. Xian-gang, "Construction of service-oriented regional geo-hazards meteorological early warning model base," in *Proceedings of the 2015 International Conference on Industrial Informatics-Computing Technology, Intelligent Technology, Industrial Information Integration*, pp. 93–96, IEEE, Wuhan, China, December 2015.

[22] W. Kefeng and Y. F. Yue, "Design and construction of the virtual cloud platform for the laboratory," *International Journal of Smart Home*, vol. 9, no. 11, pp. 235–262, 2015.

[23] G. Cho and S. H. Lee, "Cloud-based virtual port-container terminal establishment and operation analysis," *Electronics*, vol. 9, no. 10, p. 1615, 2020.

Hindawi
Scientific Programming
Volume 2022, Article ID 2378535, 10 pages
https://doi.org/10.1155/2022/2378535

Research Article

Knowledge Sharing Efficiency Analysis Model Design of Internet Open Innovation Community

Song Wang[1] **and Jingjing Nie**[2]

[1]*School of Humanities, Arts and Digital Media, Hangzhou Dianzi University, Hangzhou 310018, Zhejiang, China*
[2]*School of Economics, Hangzhou Dianzi University, Hangzhou 310018, Zhejiang, China*

Correspondence should be addressed to Song Wang; wangsong@hdu.edu.cn

Received 14 July 2022; Revised 25 July 2022; Accepted 30 July 2022; Published 18 August 2022

Academic Editor: Lianhui Li

The emergence of Internet technology has changed the technological innovation path and knowledge acquisition paradigm of enterprises and promoted the construction of digital technology, digital platform, and digital infrastructure. A large number of companies have begun to create brand communities and obtain suggestions for product improvement and innovation from the communities. However, obtaining innovative opinions and inspiration through the community to the final realization is not achieved overnight. It needs to go through the process of knowledge sharing to user interaction, from user interaction to knowledge creation and discovery and from knowledge discovery to innovation contribution. To study the efficiency of Internet community innovation, it is necessary to decompose the innovation process into two parts: problem adoption and problem solution, and then analyze them separately to get the influence combination and path. Taking Xiaomi (one of the world's largest mobile phone manufacturers) online community as an example, this article decomposes the process of issue solution into adoption stage and solution stage by crawling the relevant data of posts through web crawlers, takes the adoption efficiency and problem-solving efficiency as antecedents, and uses fuzzy set qualitative comparative analysis method to analyze the combination of conditions that affect the former two. It is of great significance to improve the knowledge sharing and innovation research of the open innovation community.

1. Introduction

With the increase in the number of manufacturers and the types of goods in the market, consumers have higher requirements for purchasing products. In order to cope with the changes in the market, enterprises maintain the original market by improving the shortcomings of their products and constantly carry out technological and product innovation, expecting to expand the market scale. The emergence of new and powerful Internet technology promotes the construction of digital technology, digital platform, and digital infrastructure, and changes the path of technological innovation and knowledge acquisition paradigm of enterprises to a great extent, so that enterprises cannot carry out closed innovation as in the past. They should refer to external ideas while seeking technological progress. Chesbrough calls this new model open innovation. NASA, Toyota, P&G, IBM, Xiaomi, Starbucks, Haier, and other enterprises have realized the importance of open innovation, and began to put the technical problems encountered by enterprises on the platform, hoping that third-party personnel can provide solutions; or absorb users' product opinions on the platform, and constantly improve old products and develop new products that meet users' preferences. Therefore, at the moment when open innovation is widely used, the efficiency of adopting and solving the opinions provided by users of the research platform plays an important role in improving products, accelerating innovation, and developing products that meet the needs of consumers.

2. Literature Review

Digital technology and tools have penetrated into modern business, and have been applied in a variety of companies [1]. The use of digital technology has a significant impact on

the innovation process, redefining the creation of products and services [2]. Chesbrough proposed that companies in the new century should not innovate in a vacuum, but should carry out open innovation, and can refer to external opinions when seeking technological progress [3]. With the rapid advancement of information technology, Internet-based user-generated content continues to emerge, providing sufficient knowledge resources for enterprises' open innovation. In order to make full use of user-generated content to improve corporate innovation capabilities and maintain competitive advantages, more and more companies have begun to create and use Internet-based user-generated content platforms, that is, open innovation communities, and have gradually become an important platform for companies to gather innovative resources. At present, innovation platforms with relatively mature systems have been established at home and abroad. InnoCentive platform in the United States is the world's top place for discussion and solutions to problems. Toyota, P&G, and NASA have launched research and development problems on this platform. Starbucks' mystarbucks idea platform has accumulated 150,000 ideas from users in 5 years [4]; one-third of the R&D innovation of Xiaomi company comes from fans, and 80% of the modification opinions of MIUI system come from users of Xiaomi community [5]; Haier has realized significant financial and innovation benefits through open innovation through the hope platform [6]. Therefore, it is necessary for enterprises to carry out open innovation.

At present, the research on open innovation platform includes the following aspects:

(1) Research on the connotation of open innovation communities: in 2003, Chesbrough introduced the concept of closed and open innovation platform, which defined open innovation as a model. In the open new era, enterprises can use external ideas when seeking technological progress, and combine internal and external ideas into an architecture and system according to the needs of business model [3]. Open innovation community has become an important platform for enterprises to gather innovation resources. Many enterprises relied on the Internet to build a content production and release platform to attract users to directly or indirectly participate in innovation-related activities such as the creativity, R&D, and promotion of enterprise internal products, and carried out high-quality user-generated content creation [7]. Obviously, open innovation community is a platform concept, and its most important constituent element is "knowledge." Through the combination of external knowledge and internal knowledge, new knowledge is generated, and then enterprise science and technology innovation can be accelerated [8]. In addition, some scholars believe that innovation elements are not only limited to knowledge, but also include a variety of innovation resources. For example, Laursen and Salter [9] believe that the important point of open innovation community is to connect internal and external innovation resources of enterprises, and "user" is also one of the important elements of knowledge collaborative innovation in the open innovation community. The process of technological innovation is no longer completed by enterprises alone. The enterprise can guide users to participate in the innovation of products or services, and promote the innovation of products or services through sharing among users [10].

(2) Through the perspective of social network and social capital, some scholars studied the behavior and motivation of platform users. For example, some scholars have studied the relationship between open innovation network structure and social network caused by user interaction. Starting from the structural dimension, relationship dimension, and cognitive dimension, there is an article that attempted to explore the relationship between three dimensions of social network and its impact on the user innovation participation behavior, and then analyzed its impact on the utilization of enterprise innovation knowledge points, and constructed a relationship model of user participation in innovation and enterprise innovation performance based on social network [11]. From the perspective of social networks, there was an article taking innovation community members as the research object, incorporating them into the social network analysis framework, and describing customer participation in the context of innovation communities from the three dimensions of network characteristics, network behavior, and network capabilities [12].

(3) Research on the main body of open innovation platform. Some scholars have studied that the construction of an open innovation platform for small and medium-sized enterprises under the Internet+ should rely on the external environment and professional management and operation teams, and make full use of the resources of large enterprises [13]. Z.Zhenggang and J.Silong [14] studied the construction of innovation platforms for industrial clusters and classified the platforms according to the role played by the government in the process of platform construction and operation. In the context of digital and open innovation, the most significant change in innovation network is that "customer" or "consumer" has become one of the main bodies of the innovation network. These consumers form clusters, surpassing enterprises, universities, and scientific research institutes, and they provide more and more extensive elements for innovation [15].

(4) Research on platform user behavior. Some scholars analyzed the influencing factors of users' continuous knowledge-sharing behavior in the open innovation community. It showed that the degree of users' self-presentation, available social learning opportunities, recognition of enterprises, and recognition of users

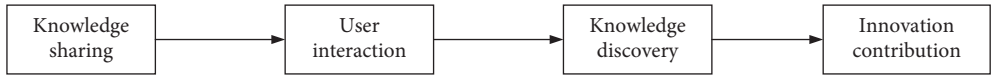

Figure 1: The process of internet open innovation.

with creative sharing experiences had a significant positive impact on users' continuous creative sharing behavior [16]. Some scholars used data mining to obtain platform data and studied the impact of quantity, quality, and emotion on individual innovation contribution in the open innovation community [17]. Li et al. [18] conducted theoretical research on the characteristics of leading users in open innovation communities, and proposed three characteristics: demand leadership, active expression, and community influence. Then based on the improved weblog method, the qualitative weblog and quantitative data analysis were combined to construct theoretical steps to identify leading users.

(5) Research on platform knowledge sharing and collaborative innovation. The latest research progress in this area has examined how the factors of platform users' collective or community level affect the actions and decisions of individuals and enterprises in different ways and under different backgrounds. Verstegen et al. [19] combined the analysis of the individual and collective levels of the use of digital technology within the platform, and explained how collective promotion (i.e., the possibility of target-oriented action by multiple members of the group) is implemented by a group of heterogeneous participants. Zhou et al. [20] studied the influencing factors of user knowledge sharing in the open innovation community, and believed that innovation self-efficacy, result expectation, social identity, and community influence have significant positive effects on user knowledge-sharing behavior. Ren [21] and others have studied the factors influencing innovative users' knowledge sharing in the community under the open innovation paradigm, and explored the development path of their knowledge sharing. These studies indicate that by examining the interaction between individual-level factors and community- (or collective-) level factors, it is expected to have a more detailed understanding of the innovation process of digital platform.

As shown in Figure 1, the Internet open innovation is a process from knowledge sharing to user interaction, from user interaction to knowledge creation and discovery, and from knowledge discovery to innovation contribution.

The current research mainly focuses on the first half of the knowledge innovation process, focusing more on the motivation and behavior of knowledge sharing, the influencing factors of knowledge discovery and user behavior, etc. The research framework and the selected influencing factors and indicators mainly point to the behavior and motivation of users participating in knowledge sharing, and the research on the efficiency of problem-solving in the open innovation community is very limited.

However, it is of great significance for innovation platforms and communities to discover problems from the final solution of problems in products. Only when users get feedback on problems and convey their opinions to enterprises through the platform, the role of innovation communities can form a closed loop, enabling users to play a role in product design and upgrade the final effects. Therefore, the main research work of this article is to analyze the combination of factors affecting the efficiency of problem-solving in the open innovation community, identify the combination of factors contributing to the current efficiency in different situations, and put forward suggestions to improve the efficiency of problem-solving.

3. Research Design

3.1. Research Objects and Data Acquisition. This article chooses Xiaomi community as the research object. Xiaomi Company was founded in April 2010. In only 1 year, its annual income has exceeded 100 billion yuan. In the rapid rise of Xiaomi Company, its unique business model has played an important role. One year after the company was founded, Xiaomi community began to build. In the early days of its establishment, the influence of Xiaomi community was limited, but with the increase of content and functions, it began to play a role in product development, new product promotion, paid rush purchases, and other activities, and became an important bridge connecting companies, products, and users. It is a typical and successful open innovation platform. The crawler is used to crawl the post data in the Xiaomi community forum. The crawled data content includes post type, number of replies, number of approvals, number of views, time of issue creation, time of issue establishment, time of issue development, and time of issue optimization. The time of data extraction is December 2020. After preliminary integration, this article chooses to crawl the relatively complete content of notebook circle, mobile phone manager, router, Redminote88pro, network signal, cloud service, control center, super power saving, Xiaomi health, Xiaomi Bluetooth headset, and Xiaomi extreme 10 data for analysis.

3.2. Path Identification Method and Variable Setting. This article chooses the fuzzy set qualitative comparative analysis method to identify the combination of conditions that affect the efficiency of the problem being adopted and solved. At first, we introduce the process of the issue solution as shown in Figure 2.

Qualitative comparative analysis first appeared in Ragin's book "Comparative Methods." As a case-oriented research, this method is based on mathematical theories such as sets and Boolean algebra, and it realizes an organic combination of quantitative and directional optimal characteristics [22].

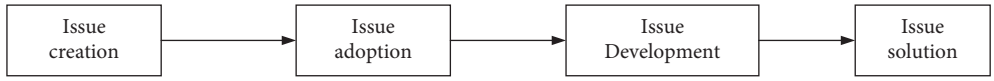

Figure 2: The process of issue solution in Xiaomi Community.

Qualitative comparative analysis methods include multivalue set, clear set, and fuzzy set. According to the theory of fuzzy sets, the relationship between sets in reality is not as clear as that in the traditional set theory [23]. According to the concept of fuzzy set, the membership score of a set may be any number between 0 and 1. In a fuzzy set qualitative comparative analysis, each case is regarded as a combination of attributes [24], abandoning the net effect of a single variable, and looking at the problem from the overall perspective and configuration thinking. Different attribute combinations correspond to the results.

After the users put forward questions, only a part of the issues can be adopted by the platform and put on file for settlement, and the settlement time of different issues on file is not the same. Therefore, the fuzzy set qualitative comparative analysis method is used to scientifically reveal the combination of conditions that affect the efficiency of the adoption and settlement of issues, and to deeply analyze under what circumstances the issues will be first adopted and put on file, and what are the characteristics of issues that need less time to solve. Table 1 shows the variable setting of issue adoption efficiency.

As shown in Table 1, issue adoption efficiency is measured by the time difference between question creation and project establishment as the result variable of the analysis; the antecedent variables include the number of dynamics in the circle, the number of employees stationed in the circle, the number of answer groups composed of platform users, the type of post, the number of posts, the number of approvals, and the number of views. There are two types of posts: help and suggestions. The number of posts refers to the number of posts that users reply to in the question posts that have been adopted for filing. The number of approval and the number of views, respectively, indicate the data of approval and views of the adopted issues.

As shown in Table 2, problem-solving efficiency refers to the difference between the time of question creation and the time of solution. When problem-solving efficiency is analyzed as a result variable, the adoption efficiency of the issue needs to be increased in the antecedent variables. The shorter time for the issue to be adopted, the more attention the enterprise pays to the issues, and it will inevitably give relatively more human resources and material resources to improve and solve the issue. Therefore, when we analyze the combination of conditions that affect the efficiency of the issue solution, it is necessary to consider the adoption efficiency put into the antecedent variable.

Table 1: Variable setting of issue adoption efficiency.

Variable type	Variable name
The result variable	Issue adoption efficiency
The antecedent variable	The number of dynamics in the circle
	The number of employees stationed in the circle
	The number of answer groups composed of platform users
	The type of post
	The number of posts
	The number of approvals
	The number of views

Table 2: Variable setting of issue solution efficiency.

Variable type	Variable name
The result variable	Issue solution efficiency
The antecedent variable	The number of dynamics in the circle
	The number of employees stationed in the circle
	The number of answer groups composed of platform users
	The type of post
	The number of posts
	The number of approvals
	The number of views
	Issue adoption efficiency

4. Data Processing

4.1. Descriptive Statistical Analysis. Before in-depth analysis of the data, in order to understand the distribution of the data, the descriptive statistical analysis is carried out first as shown in Table 3.

From the results of descriptive statistical analysis, it can be seen that the dispersion degree of dynamic variables is the highest, the communities where popular products are located usually have more dynamic, while the dynamic number of products with small audience is limited, so the dynamic will be less. And the standard deviation of other variables is not different, which indicates that the data distribution of these variables is relatively concentrated and the range of change is small.

In this article, the post type variable is treated as a 0–1 dichotomous variable, in which 1 corresponds to the help post and 0 corresponds to the suggestion post. The descriptive statistical analysis of the dichotomous variable is of little significance. Through simple statistics, it is found that the vast majority of post types are help type, and a small part are suggestion type.

4.2. Data Calibration. The calibration reported below and the set relation analysis was performed using the fuzzy set/QCA 3.0 program [25]. Data calibration is to set up three critical points: complete membership point, cross membership point, and complete nonmembership point, and use fsQCA software to convert the data to 0–1. When selecting the critical point, according to the existing theory and knowledge, combined with the data and quantile points, this

Table 3: Descriptive statistical analysis of variables.

Variable name	Mean	Std	Min	Max
The number of dynamics in the circle	27038	1591.72	1132	84000
The number of employees stationed in the circle	38	3.01	11	135
The number of answer groups composed of platform users	74	3.30	17	155
The number of posts	81	14.39	1	1334
The number of approvals	29	18.92	0	3933
The number of views	189	22.00	1	1560
Issue adoption efficiency	19	2.96	0	327
Issue solution efficiency	31	3.55	0	332

Table 4: Data calibration.

Variable name	Complete	Cross	Complete non
The number of dynamics in the circle	1132	20000	63000
The number of employees stationed in the circle	11	17	135
The number of answer groups composed of platform users	17	79	155
The number of posts	1	8	541.4
The number of approvals	0	2	42.6
The number of views	1	48	941.6
Issue adoption efficiency	0	4	114.4
Issue solution efficiency	1	11	139.8

article refers to the calibration methods of Wei et al. [26] and Fiss [27], and defines 95% as the full membership point, 50% as the cross membership point, and 5% as the complete nonmembership point.

4.3. Necessity Analysis. Since the post type is a dichotomous variable, the data itself is already between 0 and 1 (Table 4), so it is not necessary to calibrate the data, so it can be used directly [28].

After the data calibration, the data need to be checked for necessity. If a necessary condition appears in the antecedent variable, the parsimonious solution obtained by software processing data will eliminate the necessary condition, but only when the condition appears in the condition combination, the result will occur. Therefore, the necessity of checking variables is an essential step. Generally speaking, if the consistency is greater than 0.9, it is considered as a necessary condition.

4.3.1. Necessity Analysis of Adopting Efficiency as an Antecedent Variable. As shown in Table 5, for the results of the necessity of adoption efficiency, it is found that the consistency of post type is as high as 0.97, which indicates that the type of help or suggestion has a significant impact on whether the topic is adopted. Therefore, it is necessary to eliminate the necessary condition of post types in the subsequent data processing.

4.3.2. Necessity Analysis of Solution Efficiency as an Antecedent Variable. As shown in Table 6, for the results of the necessity of solution efficiency, it is found that the consistency of post types is as high as 0.98, which indicates that whether the post is a help or a suggestion type also has a significant impact on whether the issue is implemented. Therefore, it is necessary to eliminate the post type in the subsequent data processing.

4.4. Sufficiency Analysis. Sufficiency analysis is needed after the necessity test. Different from the above necessary condition analysis, configuration analysis attempts to reveal the sufficiency analysis of the results caused by different configurations composed of multiple conditions [29], that is, to discuss whether the set composed of multiple antecedent conditions is a subset of the result set. The same as the necessity test is that it is necessary to set a minimum consistency threshold to check the sufficiency. The minimum recommended threshold of consistency is 0.75. The previous articles on the qualitative comparison of Fuzzy Sets set different thresholds for consistency, Zhang Ming sets the threshold value to 0.76; Zhao sets the threshold value to 0.75; and Zhang Weiguo sets the threshold value to 0.8. After the analysis of the test threshold, 0.85 is selected as the consistency threshold, and the case threshold is set to 1 [28, 30, 31].

Through the qualitative comparative analysis of fuzzy sets, we can get the parsimonious solution, intermediate solution, and complex solution. The parsimonious solution includes all the logical remainder, but does not consider whether the logical remainder is reasonable, so the parsimonious solution often deviates from the fact; the complex solution does not include any logical remainder, only observes the solution formed by the case data; and the intermediate solution includes the theoretical remainder which is in line with the expectation of the theoretical direction and verified evidence. Some articles choose different solutions to analyze the results. Wan and Wang chose to analyze the complex solutions; Zhang reported the intermediate solutions supplemented by the simplified solutions; Wen and Fiss [27, 28] choose to analyze the intermediate solutions. Due to a large number of paths, in order to better

Table 5: Necessity analysis of adopting efficiency.

The result variable: issue adoption efficiency		
Variable name	Consistency	Coverage
The number of dynamics in the circle	0.588207	0.678658
~The number of dynamics in the circle	0.655170	0.797542
The number of employees stationed in the circle	0.642569	0.688506
~The number of employees stationed in the circle	0.632391	0.837685
The number of answer groups composed of platform users	0.612197	0.648111
~The number of answer groups composed of platform users	0.612601	0.823811
The number of posts	0.755574	0.709604
~The number of posts	0.501858	0.805001
The number of approvals	0.751858	0.740199
~The number of approval	0.491438	0.730810
The number of views	0.729483	0.716633
~The number of views	0.483037	0.720655
The type of post	0.967852	0.605151
~The type of post	0.032149	0.361818

Table 6: Necessity analysis of solution efficiency.

The result variable issue solution efficiency		
Variable name	Consistency	Coverage
The number of dynamics in the circle	0.549777	0.621715
~The number of dynamics in the circle	0.670431	0.799902
The number of employees stationed in the circle	0.612906	0.643673
~The number of employees stationed in the circle	0.642163	0.833726
The number of answer groups composed of platform users	0.549118	0.569779
~The number of answer groups composed of platform users	0.642163	0.833726
The number of posts	0.746003	0.686694
~The number of posts	0.500494	0.786862
The number of approvals	0.764876	0.738052
~The number of approval	0.469095	0.683723
The number of views	0.735784	0.708459
~The number of views	0.479891	0.701735
The type of post	0.975853	0.598030
~The type of post	0.024147	0.266364
Issue adoption efficiency	0.729108	0.714621
~Issue adoption efficiency	0.535438	0.762559

analyze the characteristics of each path and the relationship between paths, we choose to interpret only the intermediate solution.

4.4.1. Sufficiency Analysis of Adopting Efficiency as an Antecedent Variable. As shown in Table 7, for the sufficiency analysis [32–38], the abbreviation of the variable will be used below. We use DY (dynamics) to replace the number of dynamics in the circle, use ES (employees stationed) to replace the number of employees stationed in the circle, use GOA (group of answer) to replace the number of answer groups composed of platform users, use PO (posts) to replace the number of posts, use AP (approval) to replace the number of approval, and use VI (views) to replace the number of views.

Since the variables of dynamic, employees stationed, and answer group are platform-level variables, and the variables of post number, the number of approval, and views are issue-level variables, different paths can be classified and analyzed according to the level of function. It can be seen from the Table 7 that the overall consistency of the obtained path is 0.834, which is greater than the set threshold, indicating that the antecedent condition of the corresponding case composition is the sufficient condition for the occurrence of issue adoption. The overall coverage rate of the path is 0.785, which shows that the results of this article can explain 78.5% of the cases.

There are only two ways to act through the issue level. Among them, the core function is the number of views and posts, which measures the user's attention to the problem. Even if the platform variable does not play a significant role, the more likely the problem will be adopted as long as there are enough customers who pay attention to the issue and the number of views on the topic reaches a certain scale. If the general and significant defects of the products cause a lot of attention, the possibility of the issue being adopted will increase.

There are two paths that work through the platform level. The core variable in the first path is the answer group, and the core variable combination in the second path is dynamic and employees stationed. From the comparison of the two

Table 7: Sufficiency analysis of adoption efficiency.

Function level	Conditional combination	Raw coverage	Consistency
None	~DY*~ES*~AP	0.357	0.902
Issue	~DY*~ES*VI	0.480	0.886
	~DY*~ES*~GOA*PO	0.403	0.937
Platform	~ES*GOA*~AP*~VI	0.223	0.958
	DY*ES*~GOA*~PO*~AP*~VI	0.121	0.978
Issue + platform	DY*ES*GOA*~AP*VI	0.222	0.852
	DY*ES*GOA*~PO*AP	0.204	0.859
	DY*ES*GOA*AP*~VI	0.232	0.850
	DY*ES*~GOA*AP*VI	0.237	0.957
	DY*~ES*GOA*PO	0.234	0.956
	~DY*GOA*PO*~AP	0.242	0.927
Solution coverage		0.785	
Solution consistency		0.834	

Table 8: Sufficiency analysis of solution efficiency.

Function level	Conditional combination	Raw coverage	Consistency
Issue	~DY*~ES*~PO*VI	0.330	0.905
	~DY*~ES*~PO*~AP*AD	0.222	0.889
	~DY*~ES*~GOA*PO*AD	0.362	0.955
	~ES*~GOA*~PO*VI*~AD	0.220	0.918
	~DY*~ES*~GOA*PO*AP*~VI	0.254	0.968
	~DY*~ES*AP*VI*AD	0.372	0.939
Platform	DY*ES*~GOA*~PO*~AP*~VI*~AD	0.113	0.972
Issue + platform	DY*ES*GOA*AP*~AD	0.276	0.844
	DY*GOA*PO*AP*~AD	0.265	0.857
	DY*ES*~GOA*AP*VI	0.247	0.980
	~DY*ES*GOA*PO*~AP*~VI	0.207	0.951
	DY*~ES*GOA*~AP*~VI*AD	0.146	0.967
	DY*ES*GOA*~PO*~VI*~AD	0.177	0.850
	~DY*GOA*PO*~AP*~AD	0.195	0.909
Solution coverage		0.735	
Solution consistency		0.859	

paths, it can be concluded that when the issue-level variables do not play a role, the interpretation group variables and dynamics, and the variable combinations of employees stationed can replace each other to improve the efficiency of topic adoption. This path is suitable for companies that already have obvious improvement directions and optimization plans for their products, and file a case after a small number of customers have put forward optimization requirements.

Through the dual level of platform and issue, there are six paths, of which five paths have more than or equal to two core variables at the platform level, and three paths have all variables at the platform level, which shows that the factors at the platform level can more affect the adoption of problems. In the combination with platform variables, the approval number appears three times, the number of posts appears two times, and the number of views appears one time. The approval number and the number of posts often have clear optimization and improvement needs, which can promote the adoption of problems better than the number of views. This path describes that the enterprise itself has the intention of optimization. After a large number of customers have clear optimization requirements for a product at the same time, it promotes the platform to pay attention to the problem and take optimization actions.

4.4.2. Sufficiency Analysis of Solution Efficiency as an Antecedent Variable. Table 8 shows the results of the sufficiency analysis [39–45] when the solution efficiency is taken as an antecedent variable. Using the same classification method, the results are divided into three categories. It can be seen from Table 7 that the overall consistency of the obtained path is 0.859, which is greater than the set threshold, indicating that the antecedent conditions of the corresponding case composition are sufficient conditions for the occurrence of issue adoption. The overall coverage rate of the path is 0.735, which shows that the results of this article can explain 73.5% of the cases.

Among the six paths at the issue level, the core variable combinations of the two paths with higher coverage are adoption efficiency, the number of posts, adoption efficiency,

and the number of views. At the same time, the adoption variable appears three times, the number of views appears three times, the number of approval appears two times, and the number of posts appears two times in these six paths. From the summary of the characteristics of the path: whether the topic is adopted or not is the key to whether the problem can be solved. Therefore, the company pays attention to the issue, and the issues that are filed will definitely respond later; meanwhile, the characteristics of path variables are the same as those in the adoption stage, and the number of views and posts are high-frequency variables, which indicates that the attention of a large number of users not only improves the enterprise's attention from the beginning of the problem establishment, but also promotes the platform interaction. In the process of problem-solving, continuous attention can also supervise the efficiency of enterprise problem-solving. This path corresponds to the implementation of the problem that has been filed by the enterprise and has a large number of views.

In one path at the platform level, dynamic and employees stationed are its core variables, which play a significant role in promoting the implementation of issues. However, the coverage rate of this path is relatively low, indicating that most of the problems in reality cannot be solved by platform alone.

There are seven paths formed under the dual effects of platforms and issue, and the number is slightly more than the first type. At this level, the highest frequency of platform variables is the answer group, which refers to the group of question-answering users in the circle. The larger the size of the answer group, the more likely the problem is to be solved. The second highest frequency variable is dynamic, which refers to the active state of users in the circle. A circle with more dynamics indicates to a certain extent that the number of users who use the product and follow the product is large. The variables that appear more frequently in the issue level are the number of approval and the number of posts. Users can convey clear modification opinions through posting or expressing opinions. Therefore, this group of paths describes the situation that has been concerned by a large number of users, and the problems that have put forward clear opinions or have been concerned by a large number of users, and in the circle where the questions are located, the larger scale of the answer group are executed more efficiently.

4.5. Robustness Test. Robustness testing can be done from two perspectives: set theory and statistical theory. From the perspective of set theory, the robustness test is realized by changing the calibration threshold and increasing or decreasing variables; from the perspective of statistical theory, the robustness test is realized by changing the data time span and other methods. In this article, the robustness test is carried out from the perspective of set theory. After changing the threshold of the adequacy test to 0.86, the path is basically consistent, which proves that the results are robust.

5. Research Conclusions and Prospects

5.1. Research Conclusion. By collecting various data on posts in the Xiaomi community, the fuzzy set qualitative comparative analysis method is used to identify the combination of conditions that affect the efficiency of issue adoption and solution.

First of all, in the necessary analysis, the consistency of post type is as high as 0.97, which is the necessity index. So, we need to delete this variable in the sufficiency analysis. In this article, when processing the data, the assignment of the post type for help is 1, and the suggested assignment is 0. Usually, when users have found that the product has problems hindering their use, the help-seeking type of post appears and users will seek help from enterprises through the platform. While the suggestion type of post is often that the product itself does not have problems hindering the use, and users hope to get a better sense of use by improving a certain aspect of the product for more convenient use. When the product is improved, it is generally updated on the basis of the normal use of the product, so the help type post will have higher efficiency in adoption and implementation than the suggestion type post.

Secondly, from the path analysis of adoption efficiency and solution efficiency, we can see that the most common path is the combination of platform-level variables and issue-level variables. This shows that in the whole process from the emergence of problems to the solution, what we need is the cooperation of the platform and the users. Only when the users actively raise problems and the platform actively cooperates to deal with problems, can we more effectively promote the problem solution. We can find that there are two paths through the issue level, two paths of the platform level, and six paths of the platforms and issue level when adoption efficiency is an antecedent variable. There are six paths through the issue level, one path of platform level, and seven paths for the two-layer interaction of issues and platforms when solution efficiency is an antecedent variable. From the adoption stage to the solution stage, the number of paths through the role of the issue-level increases significantly, and a single issue level variable as the core variable can become a path of the solution stage, which indicates that the fluctuation of the issue-level variable can significantly affect the process of the issue implementation.

Thirdly, in general, the coverage of paths with fewer core variables is higher than that with more core variables. The greater the number of core variables, the higher the requirements for corresponding cases, and the fewer cases corresponding to them.

5.2. Shortcomings and Prospects. In this article, the data obtained from the Xiaomi community is limited. At present, the data only includes the platform level and the issue level. If we can increase the personal information data of platform users and the related data of different circles, we can establish a more reasonable structure. We can analyze the influencing factors of problem adoption and problem solution from the three levels of platform, circle, and issue, and carry out more in-depth research. If we can get more relevant data about the appropriateness of problem solution methods, we can also study the combination of variables to promote the generating of high appropriateness solutions.

Data Availability

The dataset can be accessed upon request.

Conflicts of Interest

The authors declare that they have no conflicts of interest.

Acknowledgments

This research was supported by the Key Project of Zhejiang Soft Science Research Program "Digital Transformation of Enterprise Technological Innovation Empirical Research Based on Internet Open Innovation Platform," Project No. 2021C25029.

References

[1] Y. Yoo, R. J. Boland, K. Lyytinen, and A. Majchrzak, "Organizing for innovation in the digitized world," *Organization Science*, vol. 23, no. 5, pp. 1398–1408, 2012.

[2] S. Nambisan, K. Lyytinen, A. Majchrzak, and M. Song, "Digital innovation management: reinventing innovation management research in a digital world," *MIS Quarterly*, vol. 41, no. 1, pp. 223–238, 2017.

[3] H. W. Chesbrough, *Open Innovation: The New Imperative for Creating and Profiting fromTechnology*, Harvard Business Press, Boston, MA, USA, 2003.

[4] G. Meiling and B. Xinhua, "Key factors identification of open innovation community knowledge collaboration in mobile environment-based on the knowledge ecological perspective," *Library and Information Service*, vol. 61, no. 13, pp. 99–107, 2017.

[5] B. Yanzhuang, G. Lei, and Y. Hongchun, "Research on the growth mechanism of proprietary intellectual property rights brand driven by entrepreneurship:the case of Xiaomi technology Co.Ltd," *Science & Technology Progress and Policy*, vol. 32, no. 12, pp. 79–85, 2015.

[6] Sohu, "Haier's 2017 market innovation Report," http://www.sohu.com/a/215351977_708421.

[7] Z. Keyong, "Research on Knowledge Sharing in Open Innovation Commiunty," Jilin University, Jllin, China, Doctor, 2017.

[8] P. M. Di Gangi and M. Wasko, "Steal my idea! Organizational adoption of user innovations from a user innovation community: a case study of Dell IdeaStorm," *Decision Support Systems*, vol. 48, no. 1, pp. 303–312, 2009.

[9] K. Laursen and A. Salter, "Open for innovation: the role of openness in explaining innovation performance among UK manufacturing firms," *Strategic Management Journal*, vol. 27, no. 2, pp. 131–150, 2006.

[10] C. Qiaolian, Y. Liguo, S. Yongchuan, and L. Junnan, "Construction of enterprise-oriented innovation community from the perspective of open innovation," *Science Research Management*, vol. 38, no. S1, pp. 487–493, 2017.

[11] L. Jingyan, W. Yu, and L. Li, "The impact of user innovation behavior on enterprise innovation performance under OIC-the perspective of social network," *Science & Technology Progress and Policy*, vol. 37, no. 6, pp. 128–136, 2020.

[12] L. Yigang, L. Haigang, and Z. Xiaoguo, "A research on the relationship betweenmembers' participation behavior and organizational adoption in innovation communities from the social network perspective," *Science Research Management*, vol. 37, no. S1, pp. 309–317, 2016.

[13] W. Fang, "The practice of open innovation platform construction under Internet plus-based on the view of small and medium enterprises," *Science & Technology Progress and Policy*, vol. 33, no. 15, pp. 15–21, 2016.

[14] Z. Zhengang and J. Shilong, "Compar ative study on mode of generic technology innovation terr ace of industrial clusters in China," *Science & Technology Progress and Policy*, vol. 7, pp. 79–82, 2008.

[15] L. Ruoyu, Z. Yang, D. Yiwen, Z. Dongme, and F. Xu, "Enterprise innovation network: tracing, evolution and research prospect," *Management World*, vol. 37, no. 1, pp. 217–233, 2021.

[16] S. Nambisan, M. Wright, and M. Feldman, "The digital transformation of innovation and entrepreneurship: progress, challenges and key themes," *Research Policy*, vol. 48, no. 8, Article ID 103773, 2019.

[17] G. Meiling, C. Ming, and H. Jieping, "Research on the impact of open innovative community governance mechanism on user knowledge contribution behavior-based on the mediating effect of virtual community sense," *Science & Technology Progress and Policy*, vol. 36, no. 20, pp. 30–37, 2019.

[18] W. Li, L. Qinfang, and M. Yunlong, "Identifying lead users in open innovation community based on extended netnography," *Science Research Management*, vol. 40, no. 10, pp. 259–267, 2019.

[19] L. Verstegen, W. Houkes, and I. Reymen, "Configuring collective digital-technology usage in dynamic and complex design practices," *Research Policy*, vol. 48, no. 8, Article ID 103696, 2019.

[20] T. Zhou, H. Lianzi, and D. Shengli, "Research on the factors affecting users' knowledge sharing in open innovation communities," *Journal of Modern Information*, vol. 40, no. 3, pp. 58–64, 2020.

[21] L. Ren, "Influencing factors and development approaches of knowledge sharing in online open innovation community," *Information Science*, vol. 37, no. 9, pp. 48–53, 2019.

[22] C. C. Ragin, *The Comparative Method: Moving beyond Qualitative and Quantitative Strategies*, University of California Press, California, CA, USA, 1987.

[23] H. Junzhi, "Fuzzy-set methods in comparative political analysis," *Journal of Social Sciences*, vol. 5, pp. 30–38, 2013.

[24] C. C. Ragin, *Redesigning Social Inquiry:Fuzzy Sets and beyond*, University of Chicago Press, Chicago, IL, USA, 2008.

[25] C. C. Ragin, K. A. Drass, and S. Davey, *Fuzzy-set/Qualitative Comparative Analysis 3.0*, University of California, Irvine, CA, USA, 2017.

[26] G. Wei, G. Jian, and L. Jizhen, "Effect route of entrepreneurship policy on city entrepreneurship:A research based on fuzzy set qualitative comparative analysis," *Journal of Technology Economics*, vol. 37, no. 4, pp. 68–75, 2018.

[27] P. C. Fiss, "Building better causal theories : a fuzzy set approach to typologies in organization research," *Academy of Management Journal*, vol. 54, no. 2, pp. 393–420, 2011.

[28] Z. Wen, L. Yuejiao, and Z. Huihui, "Can government R&D subsidies improve the innovation efficiency of enterprises?——a study based on fsQCA," *R & D Management*, vol. 32, no. 2, pp. 37–47, 2020.

[29] Z. Ming, C. Weihong, and L. Hailin, "Why do Chinese enterprises completely acquire foreign high-tech enterprises—— a fuzzy set qualitative comparative analysis (fsQCA) based on 94 cases," *China Industrial Economics*, vol. 4, pp. 117–135, 2019.

[30] C. C. Ragin, "Set relations in social research : evaluating their consistency and coverage," *Political Analysis*, vol. 14, no. 3, pp. 291–310, 2006.
[31] Z. Ming and D. Yunzhou, "Qualitative comparative analysis (QCA) in management and organization research:position, tactics, and directions," *Chinese Journal of Management*, vol. 16, no. 9, pp. 1312–1323, 2019.
[32] Y. Li, X. Liu, and G. Xu, "Robustness Analysis of a Type of Iterative Algorithm for R-L Fractional Nonlinear Control Systems in the Sense of Lp Norm," *Mathematical Problems in Engineering*, vol. 2021, Article ID 6661543, 9 pages, 2021.
[33] L. H. Li, J. C. Hang, H. X. Sun, and L. Wang, "A conjunctive multiple-criteria decision-making approach for cloud service supplier selection of manufacturing enterprise," *Advances in Mechanical Engineering*, vol. 9, no. 3, 2017.
[34] B. Zeng, Y. Zheng, P. Wu et al., "Simulation Analysis of Combined Mechanics of the Thrust Rotary Guide Drill," *Scientific Programming*, vol. 2022, Article ID 4639555, 9 pages, 2022.
[35] L. Chen, P. Zhan, L. Cao, and X. Li, "Discrimination and Correlation Analysis of Multiview SAR Images with Application to Target Recognition," *Scientific Programming*, vol. 2021, Article ID 6646388, 2021.
[36] L. Li and C. Mao, "Big data supported PSS evaluation decision in service-oriented manufacturing," *IEEE Access*, vol. 8, no. 99, 2020.
[37] F. Alhaidari, N. A. Shaib, M. Alsafi et al., "ZeVigilante: Detecting Zero-Day Malware Using Machine Learning and Sandboxing Analysis Techniques," *Computational Intelligence and Neuroscience*, vol. 2022, Article ID 1615528, 15 pages, 2022.
[38] L. Li, C. Mao, H. Sun, Y. Yuan, and B. Lei, "Digital twin driven green performance evaluation methodology of intelligent manufacturing: hybrid model based on fuzzy rough-sets AHP, multistage weight synthesis, and PROMETHEE II," *Complexity*, vol. 2020, no. 6, 24 pages, Article ID 3853925, 2020.
[39] L. H. Li, J. C. Hang, Y. Gao, and C. Y. Mu, "Using an integrated group decision method based on SVM, TFN-RS-AHP, and TOPSIS-CD for cloud service supplier selection," *Mathematical Problems in Engineering*, vol. 2017, Article ID 3143502, 14 pages, 2017.
[40] M. S. Ali, M. Hymavathi, H. Alsulami, T. Saeed, and B. Ahmad, "Passivity analysis of fractional-order neutral-type fuzzy cellular BAM neural networks with time-varying delays," *Mathematical Problems in Engineering*, vol. 2022, Article ID 9035736, 18 pages, 2022.
[41] X. Liu and S. Gao, "Stochastic stability analysis for stochastic coupled oscillator networks with bidirectional cross-dispersal," *Computational Intelligence and Neuroscience*, vol. 2022, Article ID 2742414, 6 pages, 2022.
[42] L. Li, T. Qu, Y. Liu et al., "Sustainability assessment of intelligent manufacturing supported by digital twin," *IEEE Access*, vol. 8, Article ID 174988, 2020.
[43] H. Zhang, H. Shi, J. Hou, Q. Xiong, and D. Ji, "Image Sentiment Analysis via Active Sample Refinement and Cluster Correlation Mining," *Computational Intelligence and Neuroscience*, vol. 2022, Article ID 2477605, 15 pages, 2022.
[44] L. Li, B. Lei, and C. Mao, "Digital twin in smart manufacturing," *Journal of Industrial Information Integration*, vol. 26, no. 9, Article ID 100289, 2022.
[45] Z. Liu, F. Ni, R. Li et al., "Persistent homology-based topological analysis on the gestalt patterns during human brain cognition process," *Journal of Healthcare Engineering*, vol. 2021, Article ID 2334332, 11 pages, 2021.

Hindawi
Scientific Programming
Volume 2022, Article ID 7838269, 7 pages
https://doi.org/10.1155/2022/7838269

Research Article

Research on Data-Driven Distribution Network Planning Method

Xingdong Liu,[1] Daolin Xu,[2] Hui Peng,[2] XiaoChuan Xu,[1] HuiDeng Liu,[1] and Xin Zhang[3]

[1]*Chongqing Urban Power Supply Branch, State Grid Chongqing Electric Power Company, Chongqing 400010, China*
[2]*State Grid Chongqing Electric Power Company, Chongqing 400014, China*
[3]*School of Electrical Engineering, Chongqing University, Chongqing 400044, China*

Correspondence should be addressed to Xin Zhang; 202011131181@cqu.edu.cn

Received 27 May 2022; Revised 14 June 2022; Accepted 20 July 2022; Published 16 August 2022

Academic Editor: Lianhui Li

With the development of the intelligent and interactive power system, the elements of distribution network planning continue to increase. The distribution network connects the transmission system and individuals, directly affects the individual's power consumption experience, and is a key link in the power system. A reasonable planning scheme can not only improve the power supply capacity and reliability of the distribution network but also fully apply the data of each system in the distribution network to realize the optimal planning of the medium-voltage distribution network driven by data. Firstly, this paper constructs the CIM model and the distribution network topology model and establishes the wiring pattern recognition feature library. The network reconstruction and planning method research was carried out for the target line, and a typical operation scenario of the distribution network was generated. At the same time, based on the time period network loss index, the distribution network reconfiguration optimization model and distribution network expansion planning model are established, and the solution method of the distribution network reconstruction and expansion planning model is expounded. A reconstruction optimization scheme with the best overall network loss performance is in the network operation scenario. The experimental results of the final example show that based on the proposed time period network loss index, the overall operation loss of the distribution network in a period can be calculated more accurately, and the optimized planning scheme is more suitable for the load power consumption characteristics of the region, and the method has certain feasibility.

1. Introduction

Since the reform and opening up, my country's economy has matured rapidly, people's living criteria have been constantly heightened, and the demand for electric energy has continued to rise. With the continuous acceleration of my country's socialist modernization handle, electricity plays an increasingly important role in all fields of society. Electricity supply and safety have become the basis for national, social, and economic development and are related to national security issues. With the rapid construction of modern allocation net and the construction of power big data platform, the informatization and automation level of allocation net have been greatly improved. The wide application of allocation net GIS system, production management system, operation management system, and allocation net automation system makes the data analysis between different systems of the allocation net easier, and provides a solid foundation for the application of big data to the planning and optimization of the allocation net. Base. In 2016, my country's electricity "13th Five-Year Plan" clearly stated that it is necessary to increase the construction of the allocation net. The "13th Five-Year Plan" period, a modern allocation net that is compatible with a well-off society, will be basically built [1]. The implementation of the "13th Five-Year Plan" for electric power has significantly accelerated the transformation and construction of my country's allocation net system, and the power supply capacity, safety, and reliable of the allocation net have been greatly improved. However, there are still many problems in the current allocation net operation, such as the speed of social development is too fast and the load is not balanced, resulting in heavy overload problems in allocation net lines and station areas [2]. Therefore, the optimization plan and structure of the

allocation net still need to be improved. The 10 kV medium-voltage allocation net is the core component of the allocation net, which directly affects the individual's power experience and is also a key link in the power system. A suitable allocation net grid planning optimization scheme should not only have good performance in uncertain scenarios but also improve the power supply capacity, reliability, and equipment utilization of the network, which is more conducive to social and economic development [3]. If there are defects in the planning and optimization scheme of the allocation net grid, it may lead to unstable network operation, poor power supply capacity and reliability, and even detrimental to the long-term development of society [4]. Therefore, it is necessary to study the optimization planning method of 10 kV medium-voltage allocation net.

The identification of the wiring pattern of the allocation net feeder is an important part of the distribution planning and optimization work. This work mode, which mainly relies on the manual judgment of planning staff to screen and integrate different system data and problems, and then propose corresponding planning and construction projects based on experience, and then carry out corresponding calculation and analysis and comparison, not only has a huge workload but also because of the data. The lack of calculation and analysis tools leads to the remediation plan relying more on manual experience and lack of rigorous calculation and analysis. In the previous allocation net optimization planning work, extreme situations are often considered, which may not match the actual situation. So as to make the allocation net optimization planning scheme more suitable for the actual allocation net, it is more necessary to consider the actual operation scenarios of the regional allocation net. With the gradual deepening of the construction of the big data platform, the allocation net planning has the opportunity to obtain more sufficient operation data than before, so that based on the data-driven idea, according to the allocation net GIS system, production management system, allocation net automation system, and operation comprehensive analysis of data from various systems such as management systems. We realize the analysis and simulation of the typical operation scene of the allocation net under the data drive. By considering typical operation scenarios, combined with the existing structural requirements of the power grid, the network can be more reasonably optimized to improve the network operation performance and better arrange the investment of capital resources. With the more and more extensive application of artificial intelligence algorithms in practical work, the work that could only be done manually in the past can be realized through intelligent discrimination and analysis of computers.

2. Research Status of Optimization Planning Methods for Distribution Network at Home and Abroad

With the rapid construction of the modern allocation net and the construction of the power big data platform, the informatization and automation level of the allocation net have been greatly improved, and the wide application of GIS systems, production management systems, power marketing systems, and allocation net automation systems makes the data analysis of the allocation net easier and lays a solid foundation for the data-driven optimization planning of the allocation net. With the more and more extensive application of artificial intelligence algorithms in practical work, the work that could only be done manually in the past can be realized through intelligent discrimination and analysis of computers. In the actual allocation net optimization planning work, the export and comprehensive analysis of the allocation net historical data are mainly done manually, and the comparison of the implementation effects of different planning schemes requires a lot of manual calculations. This work mode, which mainly relies on the manual judgment of planning staff to screen and integrate different system data and problems, and then propose corresponding planning and construction projects based on experience, and then carry out corresponding calculation and analysis and comparison, not only has a huge workload but also because of the data. The lack of calculation and analysis tools leads to the remediation plan relying more on manual experience and lack of rigorous calculation and analysis.

2.1. Research on Optimization and Reconfiguration of Distribution Network. Distribution network reconfiguration is an allocation net optimization method that enables the allocation net to achieve the optimal operation mode by changing the opening and closing states of the segment and tie switches in the allocation net, on the premise that the allocation net is connected and radiated. The optimization goals of allocation net reconfiguration usually include balancing the load, reducing network losses, and improving power supply reliability [5–7]. On the time scale, we aimed at optimizing the network structure for the manipulation of the allocation net, while dynamic reconfiguration takes into account the time scale, and reconfigures and optimizes the manipulate of the allocation net within a period of time. Static reconstruction generally takes the typical load of a certain period as the object to optimize the allocation net structure, and the research focuses on the improvement of the optimization algorithm [8, 9]. In the literature [10], the inertia weight is introduced into the traditional firefly algorithm, and chaos is used. Theoretical adjustment of algorithm parameters, and the addition of an elite retention strategy to solve the problem of reconfiguration of allocation net with DG, improves the calculation speed and global performance of the algorithm. Dynamic reconstruction studies the real-time and dynamic optimization of the network structure during the manipulation of the allocation net. Usually, the specific operation modes of each time period are reconstructed, respectively [11, 12]. Reference [13] uses the interval number to DG and continuous load forecasting, uses the improved FCM (Fuzzy c-means) algorithm to divide the time period of the reconstruction, and uses the decimal particle swarm algorithm to solve the static reconstruction problem to achieve dynamic reconfiguration of allocation net.

The main problem of static refactoring is that refactoring in the face of a single typical operating scenario does not necessarily guarantee the optimal refactoring target for the entire period. The traditional typical scenario construction handle lacks scientificity and is often formed by using the maximum operation mode of the allocation net or the distribution transformer capacity combined with the load coefficient. Therefore, allocation net reconstruction scheme makes it to perform the best in the entire action period of allocation net. Strictly speaking, traditional allocation net reconfiguration belongs to the category of operation optimization. However, in recent years, power grid companies have put forward indicators of capital utilization efficiency and equipment utilization, and more reasonable arrangements for planning funds and planning project progress have become one of the very important considerations for planning departments. Due to the limitation of investment scale and project construction period, through reasonable transformation of distribution network, the power supply capacity of existing distribution network framework is fully explored, load distribution is balanced, network loss is reduced, and voltage level is improved. It is effective in the utilization rate of funds with equipment utilization to solve the weak links of the existing power grid.

2.2. Research on Distribution Network Planning. The research on distribution network planning develops with the development of society. The early research on allocation net planning is mainly about the location and capacity of power supply and the planning method of grid. From the perspective of time, load considerations can be divided into static load planning and dynamic load planning. From the perspective of planning objects [14–16], planning can be divided into subsystem planning and overall system planning [17–19]. Static load planning regards the load of the network as constant and considers the network planning in a relatively single scenario; dynamic load planning considers the load changes of the network and usually divides the planning into multistage planning. Subsystem planning is the planning for a single system of the allocation net, which can usually be divided into power subsystem planning and grid planning. The overall system planning is the planning for the overall system of the allocation net. The relationship is between the power supply and the grid. In the static programming model, the literature [20] used the 0, 1 mixed integer model for the first time in the circuit planning of the allocation net. In the dynamic programming model, reference [21] uses the dynamic load planning model to plan the allocation net substation, and the model solves the problems of the capacity, location, and construction time of the substation. In addition, the current allocation net planning model research includes economic model, reliability model, comprehensive model, and research on practical engineering application of allocation net planning. Reference [22] established a planning model with the goal of maximizing the annual comprehensive income of DG operators, the smallest annual comprehensive cost of power distribution companies, and the largest annual comprehensive income of individuals participating in demand-side response. Reference [23] added reliability cost calculation to the established multistage planning model and considered constraints such as energy storage charging and discharging constraints and extreme load scenarios. Reference [24] is oriented to the allocation net problem and designs a method for automatically generating planning schemes for solutions to different problems in the allocation net, and quantitatively forms an automatic generation method for various typical problems. The planning method is based on the established planning model. In terms of planning algorithms, the use of allocation net optimization planning algorithms can be roughly divided into mathematical optimization algorithms and heuristic algorithms. Because there are usually a large number of integer decision variables in the allocation net planning problem, there are often linear and nonlinear objective functions and constraints in the planning model. When solving large-scale system decision-making combinations, mathematical optimization algorithms are prone to the "curse of dimensionality" problem, so it is difficult to use traditional mathematical optimization methods to solve them directly. By contrast, heuristic algorithms are now also called artificial intelligence algorithms, which solve problems by simulating the evolution and development of things in life.

3. Building a Data-Driven Distribution Network Operation Scenario Method

A large amount of historical load data of the distribution network records the load operation characteristics of the allocation net. If an allocation net optimization planning scheme that is more in line with the regional load power consumption characteristics is required, the operating feature of the allocation net should fully considered. In this paper, the generation method of typical operation scenarios is introduced. Based on this, a period network loss exponent is put forward to assess the overall network operation wear and tear manifestation of the scheme in the whole scheduled time. The not-alike load amalgamation and each node of the allocation net are called the operation scenarios of the allocation net. Because the load points in the allocation net are different, the load type operation scenes of the allocation net are very large. Directly taking the node load value as the node load feature is able to rashly write the action scene of the allocation net at a fixed time hint, no more than its troublesome to depict the operation scene of the allocation net in a fixed time hint interval. To fully consider the historical operational site of the allocation net and reduce amount of calculation, this paper proposes a period network abrasion index in light of the typical operating scenarios obtained by clustering and the proportion of the duration of the scenarios, to achieve a practical overall evaluation of the reconstruction scheme. The allocation net is divided into several types of typical operation scenarios and their time proportions in a period of time. A network loss evaluation index is established as follows:

$$H_i = f_{si}(x)t_{si}, \tag{1}$$

$$H = \sum_{i=1}^{K} H_i. \tag{2}$$

In formulas (1) and (2), f_{si} is the network fray count function in the i typical operating script, which originates from the propulsion spread calculation equation, x is the allocation net reconstruction scheme, the switching condition vector, t_{si} is the time occupation the i operational site ratio, K is the quantity of representative scene, H_i is the network loss index of the i scenario, and H is the network loss index of the entire period, all in power units.

Since the calculation of the time period network loss index requires the calculation of the network loss index of each typical scenario, the accuracy of the network loss index of each scene is the premise of the validity of the time period network loss index. To verify the validity of the proposed network loss index during the period, the load data of an allocation net for 30 days is analyzed and calculated in the scenario. The network loss of all actual scenarios in various scenarios is used as a comparison, and the calculation results are shown in Table 1.

The actual network loss in the scenario in Table 1 is the precise network loss obtained after the power flow calculation for all the monitoring sections classified in the typical scenario, which requires a large amount of calculation. The scenario network loss index comprehensively considers the network loss and its time proportion corresponding to typical scenarios, which is different from the network loss. However, the data in the table show that the use of the time-scenario network loss index can correctly characterize different scenarios while reducing the calculation scale. The relationship between the sizes of the network loss shows the effectiveness of the index to characterize the network loss of the allocation net.

4. Reconstruction of Distribution Network and Model Planning

Based on the idea of comprehensive analysis of distribution network representative scene, combined with time period network abrasion index, a mathematical model of allocation net reconfiguration optimization and planning is established. Due to the high global requirements of the algorithm to solve the model, a relatively mature genetic algorithm was selected to optimize the model. The algorithm coding method and the method of judging the effective solution were introduced, and the feasibility of the method was verified by an example analysis.

4.1. Distribution Network Reconstruction and Planning Based on Operation Scenario Analysis. The flow chart of distribution network expansion planning in this paper is shown in Figure 1. Through the work in the previous chapters, the current status information data of the allocation net have been obtained, including the topology structure of the allocation net and the historical load of the allocation net. On this basis, according to the installation information reported by individuals, the analysis and construction of the future allocation net are carried out, and feasible lines are pre-established. A planning model with the lowest comprehensive cost is established, and the genetic algorithm is finally used for optimization. Allocation net expansion planning refers to the reasonable expansion and optimization of lines and substations under the premise of satisfying regional development and current operation to further improve the power supply capacity and reliability of the network [25].

To improve the efficiency, the cost of the planning scheme should be reduced as much as possible while meeting the requirements of the expansion plan. In actual projects, the cost of allocation net expansion planning mainly includes the cost of new lines and the cost of operating losses after the lines are built. The goal of the allocation net expansion planning in this paper is to reduce the cost of new lines and operating losses, and establish a mathematical model with the lowest comprehensive cost as the planning optimization goal.

4.2. Genetic Algorithm for Distribution Network Reconfiguration and Planning. The distribution network reconstruction problem is a large-scale nonlinear mixed integer programming problem. It is easy to converge to the local optimum when solving so that the algorithm jumps out of the local optimum and calculates to the global optimum solution hot spot. The methods for solving nonlinear optimization problems can generally be divided into mathematical optimization algorithms and heuristic algorithms. Among them, the mathematical optimization algorithm is prone to the "curse of dimensionality" problem when solving larger system decision-making combinations. Therefore, the heuristic algorithm is more widely used in comparison, such as the use of the following algorithms: the experimental design of the three groups: the allocation net reconstruction modus in the light of the used to gain reconstruction scheme 1 as group 1, an average load scenario is established, and the reconstruction scheme 2 is solved as group 2 and is used for comparison as group 3. We calculate the period network loss index of each group of reconstruction schemes and the homologous equivalence net wear and tear power calculation, the homologous equivalence net wear, and tear power calculation under the power. The obtained reconstruction optimization scheme and corresponding index calculation are shown in Table 2.

The calculation results of the total network loss of each group of schemes are shown in Table 3.

The average voltage in the node period of the allocation net under each scheme is shown in Figure 2.

It can be seen from Figure 2 that the reconfiguration optimization scheme obtained by the method proposed in this paper makes the average voltage of each node more balanced during the period, and the network operation is improved. Table 3 shows that the reconstruction scheme 1 has taken many by optimizing the network loss index of the scheme period. Compared with the reconstruction scheme 2,

Table 1: Comparison of network loss scenarios.

Scenes	Scenario duration	Duration ratio (%)	Scenario network loss	Scenario network loss index	Scenario actual network loss amount
1	161	22.36	127.96	28.61	20.86
2	147	20.42	591.66	120.80	87.49
3	159	22.08	40.49	8.94	6.56
4	147	20.42	201.85	41.21	29.85
5	106	14.72	358.51	52.78	38.32
Sum	720	100	1320.47	252.34	183.08

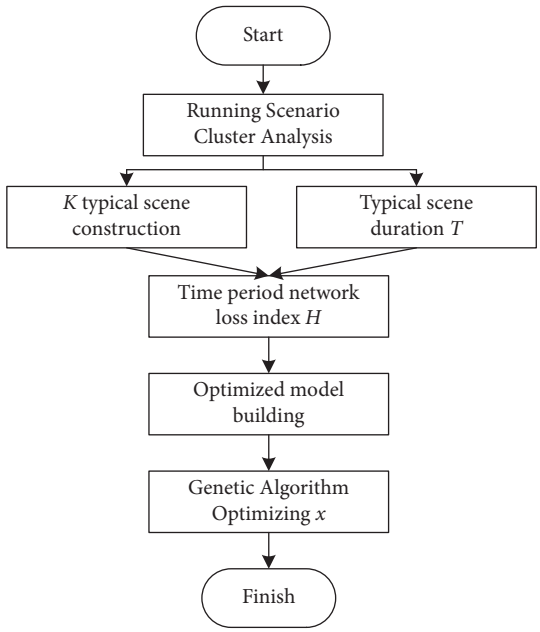

Figure 1: Process of allocation net reconfiguration.

Table 2: Reconfiguration solutions and corresponding performance.

Group	1	2	3
Reconstruction plan	9,14,28,33,36	7,9,14,28,32	33,34,35,36,37
Network loss index H during the plan period	154.76	173.8	307.93
Network loss P under the average load scenario	146.67	139.98	246.84

Table 3: Calculation results of total network loss of each solution.

Group	1	2	3
Quarterly actual total network loss	343.95	386.49	685.37
Equivalent total network loss for scenario analysis	341.71	383.75	679.91
Calculation error	2.24	2.74	5.46
Equivalent total network loss for average load scenarios	323.85	309.08	545.02
Calculation error	20.1	77.41	140.35

the performance is better in the whole period, and the actual quarterly total compared with scheme 2, the network loss is decreased by 42.54 MWh. Compared with scheme 3 without the optimization of allocation net reconstruction, the grid power scheme 2 is decreased by 298.88 MWh. From the calculation of the indicators of each scheme in Table 2, scheme 1 also shows simply using a single average load value. Instead of load characteristics, it is impossible to obtain the optimal reconstruction scheme within the allocation net. The simulation of the example verifies the feasibility of the allocation net reconstruction and planning method based on the analysis of the operation scenario. The lack of calculation and analysis tools leads to the remediation plan relying more on manual experience and lack of rigorous calculation and analysis. The results of the example show that the reconstruction and planning scheme considering the regional

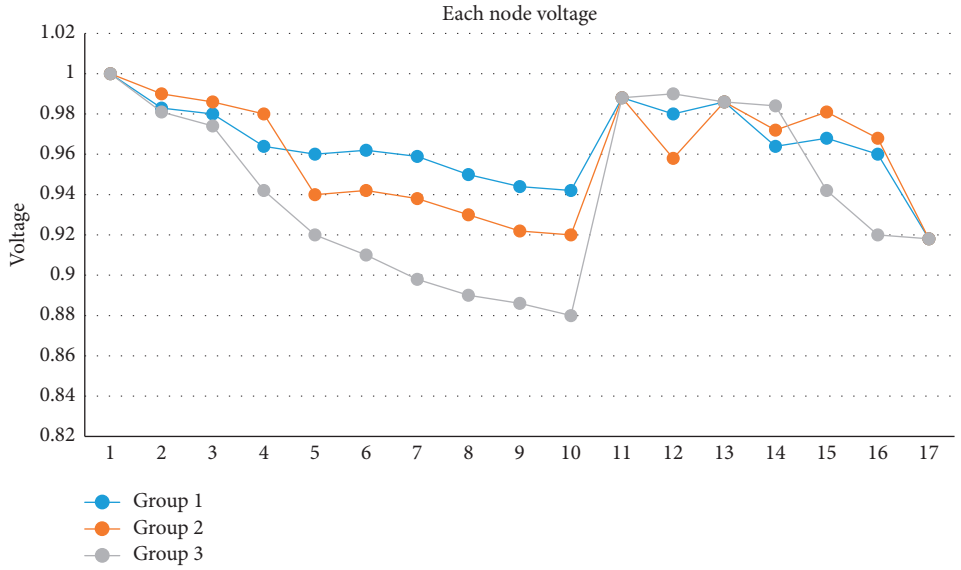

Figure 2: Node voltage under each solution.

allocation net operation scenario can be more effective than considering a single operation scenario. It fits the load power consumption characteristics of the region, and the overall performance is better.

5. Conclusion and Outlook

This paper mainly studies and applies the data of each system in the allocation net, and carries out the research on the optimization planning of the medium-voltage allocation net, including the identification of the wiring pattern of the medium-voltage allocation net and the optimization and expansion planning of the network frame reconstruction. The data of the method study come from the allocation net GIS system, production management system, operation management system, metering system, and allocation net automation system, based on the CIM model obtained by each system, regional historical load data, load increase, and decrease report data research. The topology analysis and wiring pattern recognition of allocation net based on CIM are realized.

5.1. Summary. Aiming at the related problems in the optimization and planning of allocation net reconfiguration, an allocation net data-driven allocation net operation scenario generation method is introduced. The typical operation scenarios of allocation net reconstruction are generated. In the region and the information of industrial expansion and installation, the planning scene of the allocation net is generated, and the effectiveness of the scene generation is analyzed. The mathematical model and solution method of allocation net reconfiguration and planning are introduced, and the mathematical model of allocation net reconfiguration and planning for operation scenario analysis is established based on the time period network loss index. Since the mathematical model has high requirements on the global convergence ability, a relatively mature genetic algorithm with strong as algorithm, and coding method of the genetic algorithm and the effective solution judgment method are introduced. The data-driven allocation net optimization planning method is as follows. Through the allocation net topology analysis and wiring pattern recognition, the wiring to be optimized with heavy overload problems is found, and the reconstruction optimization solution is given priority. We make expansion plans. The simulation of the example verifies the feasibility of the allocation net reconstruction and planning method based on the analysis of the operation scenario. The results of the example show that the reconstruction and planning scheme considering the regional allocation net operation scenario can be more effective than considering a single operation scenario. It fits the load power consumption characteristics of the region, and the overall performance is better.

5.2. Prospect. Although the research has achieved certain results, there are still many problems that need to be improved. The research prospects are as follows:

(1) The historical load data from the allocation net and how to make full use of the historical load data to construct a more realistic operation scenario can still be deeply considered and studied, in the planning research of this paper; although a certain load margin is reserved in the setting of the allocation net planning requirements, there are still many uncertain factors in the actual allocation net operation, such as the uncertainty of the future load. The research considerations such as the uncertainty of electricity prices and electricity prices are still not in-depth enough.

(2) In the proposed method for optimization, reconstruction, and expansion planning of allocation net operation, the optimization algorithm used is the

widely used genetic algorithm, but when applied to large-scale networks, local optimal results may still occur. Improvements in use can still be studied.

Data Availability

The dataset can be accessed upon request.

Conflicts of Interest

The authors declare that there are no conflicts of interest.

Acknowledgments

The authors thank Yudian technology 13, provincial- and municipal-level research, and application of distribution grid planning technology based on data sharing.

References

[1] Y. R. Lin, *Research on a Theoretical Line Loss Analysis Method of Distribution Network Planning State [D]*, Guangdong University of Technology, Guangdong, 2017.

[2] D. K. Chen, "Research on the "14th Five-Year" planning and development thinking of distribution network [J]," *Intelligent Building and Construction Machinery*, vol. 1, no. 7, pp. 108-109, 2019.

[3] J. T. Shi, F. Xue, and Y. J. Li, "Low-carbon target grid planning of active distribution network based on immune binary firefly algorithm [J]," *Journal of Tianjin University*, vol. 50, no. 5, pp. 507–513, 2017.

[4] R. A. Jabr, "Polyhedral formulations and loop elimination constraints for distribution network expansion planning," *IEEE Transactions on Power Systems*, vol. 28, no. 2, pp. 1888–1897, 2013.

[5] J. R. Zhu, H. Leng, and G. H. Tang, "A survey of network reconfiguration algorithms for smart distribution networks [J]," *Hunan Electric Power*, vol. 35, no. 6, pp. 1–5, 2015.

[6] W. X. Zhai, G. J. Yu, and H. L. Li, "Research on the optimization of urban distribution network based on the principle of load balancing [J]," *Power Supply*, vol. 34, no. 7, pp. 67–70, 2017.

[7] J. J. Tu, J. B. Liao, and Z. A. Wang, "Optimal reconfiguration of intelligent distribution network considering power supply reliability [J]," *Journal of Shanghai Electric Power University*, vol. 33, no. 3, pp. 239–243, 2017.

[8] J. G. Liu, Q. Wang, and L. Z. Shan, "Fault recovery of distribution network based on adaptive ant colony algorithm [J]," *Guangdong Electric Power*, vol. 31, no. 5, pp. 134–139, 2018.

[9] D. W. Wang and Z. L. Piao, "Multi-objective distribution network reconstruction based on sequential optimization and fuzzy ant colony algorithm [J]," *Grid and Clean Energy*, vol. 32, no. 9, pp. 44–49, 2016.

[10] Z. Xu, J. S. Pan, and S. X. Fan, "Reconfiguration method of distribution network with DG based on improved firefly algorithm [J]," *Power System Protection and Control*, vol. 46, no. 14, pp. 26–32, 2018.

[11] W. Y. Tan, M. Liu, and Y. P. Luo, "A review of research on dynamic reconfiguration algorithms and time division of distribution networks [J]," *Electricity and Instrumentation*, vol. 57, no. 11, pp. 63–67, 2020.

[12] X. G. Chen, B. Yu, and R. Long, "Dynamic reconfiguration of distribution network based on PAM period division [J]," *Power System Protection and Control*, vol. 47, no. 7, pp. 99–105, 2019.

[13] Z. H. Dong and L. X. Lin, "Dynamic reconfiguration of distribution network based on improved fuzzy C-means clustering period division [J]," *Grid Technology*, vol. 43, no. 7, pp. 2299–2305, 2019.

[14] D. M. Crawford and S. B. Holt, "A mathematical optimization technique for locating and sizing distribution substations, and deriving their optimal service areas," *IEEE Transactions on Power Apparatus and Systems*, vol. 94, no. 2, pp. 230–235, 1975.

[15] R. N. Adams and M. A. Laughton, "Optimal planning of power networks using mixed-integer programming. Part 1: static and time-phased network synthesis [J]," *Electrical Engineers Proceedings of the Institution*, vol. 121, no. 2, pp. 139–147, 2016.

[16] T. Gonen and B. L. Foote, "Distribution-system planning using mixed-integer programming," *IEE Proceedings C Generation, Transmission and Distribution*, vol. 128, no. 2, p. 70, 1981.

[17] J. E. D. Northcote-Green, A. B. Cummings, and D. L. Wall, "Classifier and feature set ensembles for web page classification [J]," *Journal of Information Science*, vol. 42, no. 2, pp. 150–165, 2016.

[18] H. K. Temraz and V. H. Quintana, "Distribution System Expansion Planning Models: An Overview [J]," *Electric Power Systems Research*, vol. 12, 1993.

[19] B. J. D. Sitompul, O. S. Sitompul, and P. Sihombing, "Enhancement clustering evaluation result of davies-bouldin index with determining initial centroid of K-means algorithm [J]," *Journal of Physics: Conference Series*, vol. 1235, no. 1, pp. 12–15, 2019.

[20] H. K. Temraz and M. M. A. Salama, "A planning model for siting, sizing and timing of distribution substations and defining the associated service area," *Electric Power Systems Research*, vol. 62, no. 2, pp. 145–151, 2002.

[21] Z. Y. Li, X. Lei, and S. Y. Qiu, "Active distribution network coordination planning considering the interests of "source-grid-load" tripartite [J]," *Grid technology*, vol. 1, no. 2, pp. 378–386, 2017.

[22] S. Y. Wang and C. S. Wang, "Urban medium voltage distribution network planning based on multi-objective model [J]," *China Power*, no. 11, pp. 46–50, 2006.

[23] X. Shen, M. Shahidehpour, and Y. Han, "Expansion Planning of Active Distribution Networks with Centralized and Distributed Energy Storage Systems," *IEEE Power & Energy Society General Meeting (PESGM)*, vol. 8, IEEE, 2018.

[24] C. Gao, Y. Q. Zhao, and J. X. Zhang, "Research on automatic planning method of distribution network oriented to solve the current grid problems [J]," *Power System Protection and Control*, vol. 46, no. 15, pp. 85–92, 2018.

[25] Y. H. Liu, Y. F. Li, and L. Li, "Overview of individual coding of genetic algorithms for distribution network reconfiguration [J]," *Computer Applications and Software*, vol. 35, no. 10, pp. 33–37, 2018.

Hindawi
Scientific Programming
Volume 2022, Article ID 2243891, 9 pages
https://doi.org/10.1155/2022/2243891

Research Article

Visual Memory Neural Network for Artistic Graphic Design

Yuchuan Zheng

School of Arts, Shanxi Normal University, Taiyuan, Shanxi 030031, China

Correspondence should be addressed to Yuchuan Zheng; 322092@sxnu.edu.cn

Received 6 June 2022; Revised 11 July 2022; Accepted 15 July 2022; Published 16 August 2022

Academic Editor: Lianhui Li

Artistic graphic design is the aesthetic result of the designer's fusion of various elements, with a high degree of independence. Considering the lack of significant visual design scope and aesthetic indicators of graphic design, our research aims to build an upgraded network model that can categorize different types of artistic graphics with labels and realize the free combination of graphic solutions. We realize the scheme reorganization of artistic graphic design from the perspective of computer vision and propose the artistic graphic design method based on memory neural network. We built a computer vision environment and reconstructed the computer vision network to set up an independent deep camera vision range calculation law. Considering the artistic graphic region segmentation problem, we propose the self-attentive mechanism, which can quantitatively segment different artistic graphic regions according to temporal features, before arranging them in a sequence to obtain the graphic region feature vector. We also add the LSTM structure based on the attention mechanism to match with the self-attention features of the graphical region segmentation module and pass the matched attention feature vector to the LSTM network to extract the labeled text feature information of the graphs. To test the effectiveness of our method, we build a database of artistic graphics and set up an adaptive training process. We also compared deep learning methods of the same type, and the experimental results proved that our method outperformed other deep methods in artistic graphic design by keeping the scheme reorganization accuracy and quantitative evaluation of artistic models above 90%.

1. Introduction

The most critical purpose of art graphic design is to solve the positioning solution and emergency plan of the product in the complete solution. During the establishment of the final solution of the product, different design processes and emergency measures need to be presented in visual communication in real time [1, 2]. Based on the artistic design needs of the client's feedback, the appearance and approach are reconstructed in terms of appearance, methodological improvement, and style review on different levels such as screen, space, structure, and logic. In the field of visual design, textual language is active in another way in the coordination of solutions. Professional artists and design will communicate textual elements to the audience in visual form according to the client's perception of the product, and this creative design style is the key point of figuration of artistic graphic design [3]. The representation of artistic graphics is shown in Figure 1.

The elements of art graphic design consist of both static and dynamic, and for all artistic design, graphic design applies to a range of disciplines such as painting, sculpture, and drawing. Graphic design as a basic discipline is widely used in various art industries and is also used in industry. Selecting independent design elements, building perceptual logic models, and constructing visual environments according to different design principles are all part of artistic graphic design. Considering the high professional requirements of artistic graphic design for manual labor, many researchers started to study automatic combination systems for artistic graphic design [4–7]. This research requires the integration of an artistic graphics database, computer vision unit, deep learning algorithm unit, data preprocessing unit, etc. Many researchers have already started their work accordingly.

Artistic graphic design solutions generate many unstable situational factors when it comes to human-environment communication scenarios. When dealing with image key

Figure 1: Expression of artistic graphics.

issues feature extraction, most researchers take the approach of fusion of different algorithms. Behavior recognition algorithms are mainly justified for personal graphic design, and image recognition algorithms are mainly utilized for environmental static buildings [8, 9]. Combining the two algorithms, dynamic features of the person and static features of the environment can be obtained separately, and matching the appropriate classifier can subdivide the person's action features and map them with static features. Most researchers in artistic graphic designers prefer to use deep learning methods in the experimental phase [10–14]. Deep neural networks can capture different types of graphical features, and in artistic scene construction, different levels of combinations can be generated in the design scheme depending on the database coverage of the graphics. Each combination has independent network training parameters with generalizability. In the early visual communication research, researchers tried to construct 3D scenes using deep cameras, using deep learning algorithms to learn pixel elements in the scenes, and embedding the trained models into the artistic graphic design system, which can automatically match different scene combinations according to the customer's needs. Customers can choose the corresponding graphic design solutions according to their needs. The application of deep learning accelerates the speed of scenario design and reduces the complexity of scenario design. In convolutional neural network weight screening, the training parameters and weights can be specified within a specified threshold according to the complexity of the original graphic data, and the model with the best graphic design is used in the test results.

The current character recognition algorithms cannot achieve nodal feature connection at the temporal level, resulting in missing longitudinal features between nodes at the time of acquisition. In the process of predicting behavior, artistic graphic design requires the dynamic coexistence of character features and environmental features, but the spatial information error is impossible to compensate for at the temporal level, which causes the problems of time consuming, inefficient, and low accuracy in image design solution generation [15–17]. To meet the special needs of different artistic graphic designs, some researchers have adopted 3D scanners for scene reconstruction and then used motion capture methods to reconstruct characters and environments on demand. Such an approach enables directed scene reconstruction for different graphic design projects, and researchers who adopt this method mostly use RGB images in the selection of behavior recognition data. Although this method has high timeliness and low experimental cost, it is the preferred method for most researchers. However, the method requires a certain experimental environment, and the graphical design scheme can be miscombined in the case of unstable nonstructural factors. To solve this problem, some researchers have used an approximate linear method to optimize the data minimization problem and extracted to generate predefined templates on the scene reconstruction combination problem to prevent combination errors that lead to system whiteout [18, 19].

Considering that the graphic design contains skeletal information of each node in the character model reconstruction, there is a directional problem between the normalization of skeletal information and vector information transfer, which reduces the generalization of the character graphic design. The extraction of temporal level behavioral features from skeletal information becomes exceptionally difficult under the dual effect of nonstructural factors [20]. To solve this problem, some researchers strictly control the input of experimental conditions to reduce the influence of nonstructural factors. The depth camera is used as the only channel for depth information extraction, and the correlation between temporal convolution features and behavioral labels is obtained by matching the data video frame rate with the temporal convolution layer. In the matching of skeletal points with skeletal joints, some researchers try to create multiple spatial dimensions to match from different measures as a way to obtain the maximum match. The results of reasonable graphical design tests can be filtered according to the set range of criterion values [21–24]. When setting the graphic windows dynamically, all the dynamic windows are set to a uniform size to avoid the problem of inconsistent output features, and it is the deep neural network that can flexibly identify multiple skeleton sequences when receiving skeletal point feature data to increase the robustness of the model. We analyzed the visual effects and principles of composition of artistic graphic design. Considering the differences and independence of art graphic design, we realize the scheme reorganization of artistic graphic design from the perspective of computer vision and propose a memory neural network-based artistic graphic design method.

The rest of this study is organized as follows. Section 2 presents the history of research and research results on the intelligent design of artistic graphics. Section 3 describes in

detail the principles and implementation process related to visual memory neural network-based art graphics design. Section 4 shows the related experimental setup, the experimental data set, and the analysis of the experimental results. Finally, Section 5 summarizes our research and reveals some further research work.

2. Related Work

In the process of character graphic design, artists and technicians have different requirements for the effect of the dynamic presentation of characters, and there is a gap between the overall retention effect of graphics and the effect achieved by deep neural network models. To balance the requirements of both artistic design and technical processing, some researchers try to use RGB graphic data as the input of the scheme combination, and for the requirement of optical flow information in the scheme, graphic design artists require full traversal of still life appearance and dynamic character features. Some of the node-tracking information is often lost in the implementation process of technicians, and the behavioral linear resolution cannot be completed for dynamic character features. Therefore, some researchers have treated the above features separately, with the study in literature [25] oriented toward still life contour feature acquisition and the study in literature [26] oriented toward dynamic character skeletal point optical flow information feature capture. In addition, researchers in the literature [27] proposed a dense trajectory extraction algorithm for still life feature classification, which is based on the SVM algorithm and classified by feature association, and the efficiency of this classification method is experimentally proven to be excellent. Researchers in the literature [28] optimized the former study based on the addition of RGB cameras to capture optical flow features and optimize the bad trajectory data by matching the trajectory information co-generated by optical flow features with dense trajectories. Traditional RGB algorithms require manual labeling of behavior types and preprocessing management of data labels to prevent behavior label overlap. The biggest drawback of the RGB algorithm is that it relies too much on manual label classification design, and cannot freely combine solutions according to feature types in the graphical design combination scheme.

Traditional graphic design solution combination methods do not perform well at the level of accuracy and speed, and the graphic solution classification and frame rate processing effects cannot achieve real-time results. Some researchers have tried to optimize the visual graphic design solution combination using deep learning methods. Deep neural networks for graphic design can process the visual effects brought by graphic design solutions from the pixel level, and different visual presentation effects are easier to achieve at the pixel level according to the specific needs of the customer. Researchers in the literature [29] proposed a two-layer CNN algorithm when dealing with graphic design optical flow features, and the method can obtain deep pixel features between combinations of graphic schemes. Researchers in the literature [30] optimized based on dual-stream neural networks and proposed an independent frame feature fusion convolution algorithm, which was designed to achieve feature optimization and compensation in the deep convolution of graphic features in the first and second layers, and the experimental final output of the graphic design model was tested with better efficiency.

A convolutional neural network, as the most basic network structure for image recognition, is more relevant for video data with continuous frames. Compared with single-frame data processing, graphic contextual feature information is more easily linked. If a series of natural language processing neural networks are to be adopted for graphic sequences, they will be more closely related to the integration requirements of data sequences. Recurrent neural networks were the initial adaptive training model used in this study to complete the pretraining of primary combinatorial solutions for graphic design. As graphic design became more demanding at the artistic level, the researcher gradually focused his research on the complementarity of the strengths between different neural networks. In the literature [31], a recurrent neural network and a memory unit network were fused in dealing with the graphic design sequence problem, and an ordered graphic sequence integration was accomplished with the assistance of attention mechanisms. The literature [32] utilized computer vision to complete the directed graphical visual scene reconstruction in advance, and the method was also directly cited as a template by subsequent studies, which reduced the time cost and experimental cost and improved the efficiency of visual reconstruction. The literature [33] proposed a two-layer network nesting structure, where the authors selectively arranged some structures of RNN and LSTM algorithms in a spatial network in a flashback manner, and the graphical input was also RGB data. Researchers in the literature [34], on the other hand, proposed a new and improved LSTM approach, where the authors proposed the model for dense graphical target labeling and segmentation, where the input and output times are automatically ordered according to the matched image sequences in the design of the attention mechanism. To address the influence of unstructured factors, some researchers try to represent the graphical design in 3D space with RGB three channels as the width of feature extraction, and the method is experimentally proven to work better in the face of graphical design schemes with depth information. Some researchers extract interference information in the original graphic data and realize label mapping linkage through interference information and unstructured factors, which can directly filter out most unstructured factors during the model training process. The method works better in subsequent experimental demonstrations but is more dependent on manual processing of the raw data, which is more workload.

3. Method

3.1. Computer Vision Reconstruction. In graphic reconstruction design, the mapping relationship between pixel distances and realistic distances of graphic designs is usually determined from a two-dimensional graphic pixel

coordinate system. To ensure the accuracy, most researchers use the camera calibration method, through which the graphic elements under the pixel coordinate system can be converted to the world coordinate system by the camera calibration operation. The system of automatic combination of schemes for artistic graphic design is to realize automatic extraction of artistic graphic features, an automatic combination of schemes, etc. For this purpose, we designed a computer vision reconstruction mathematical equation as follows:

$$\begin{aligned} x'_{ti} &= f_1\left(x'_{ij}\right), \\ y'_{ti} &= f_2\left(y'_{ij}\right), \end{aligned} \tag{1}$$

where f represents the mapping association between real coordinates and pixel coordinates, and the automatic transformation of the projection matrix can be done given the predetermined pixel coordinates.

According to the art graphic design requirements, the corresponding heights and nodes of different design patterns can be obtained according to the camera calibration. For irregular geometric art graphics, we can zone the graphics and subdivide them into rectangles, squares, triangles, and so on. Rectangles and squares are relatively easy to calculate and can be directly brought into the mathematical equation. For triangular clusters, trigonometric functions need to be added to the original equation to calculate the node distances and feature vector information of the art figure. The computer vision system is built as shown in Figure 2.

For a given graphic design target, dimensional mapping and pixel coordinate positioning can be done within the first line of action. In a real scene, the dynamic movement distance can be accurately measured in the projection and camera angle as long as the range of the graphic design target is within the range limit. The area between the first action line and the second action line belongs to the maximum distance where the depth information of the depth camera acts, and within this area, it can be used for 3D graphic design, and the spatial information of each graphic node can be accurately recorded in the detailed vector information due. Those beyond the second action line belong to the invalid region. According to the calculation equation of the triangle function, we can get the information of camera angle, action line angle, action range angle, and the angle of nodes inside the graphical target. The mathematical equation of the clip angle calculation is shown below.

$$\alpha = \arccos\left(\frac{d_{aj}^2 + d_{ak}^2 - d_{jk}^2}{2d_{aj} \times d_{aj}}\right) - \arcsin\left(\frac{d_{jd} \times \sin \angle ajk}{d_{ad}}\right) - \arcsin\left(\frac{d_{ek} \times \sin \angle ajk}{d_{ae}}\right). \tag{2}$$

3.2. Self-Attentive Based Neural Network for Artistic Graphic Design. We refer to many literature on the construction of neural networks for graph design, and according to our need

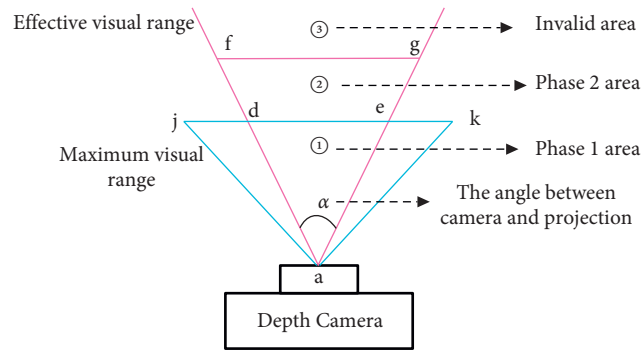

Figure 2: Computer vision system construction.

for graph design solutions with only combinations, we use the partial structure of convolutional neural networks and temporal convolutional networks. In the temporal convolutional network part, we divide the graphics into different regions, all of which will be arranged in a certain order, assuming that the input sequence is $X = (x_1, x_2, \ldots, x_n)$, n represents the number of graphic design time regions division, and xi represents the pattern node data in the ith feature acquisition stage of the art graphics, which is represented as a projection matrix with dimensions $T \times M \times D$ dimensions, where D represents the graphic design dimension, T represents the temporal label of the region, and M represents the number of graphic nodes. In the structural design of the temporal convolution layer, we use a $3 \times 3 \times t$ filter as the initial feature extraction, set the pooling layer to $3 \times 3 \times 1$, and the rest of the initial convolution layer dimensions are set to $3 \times 3 \times 3$. The last graphical temporal convolution result will come with the temporal depth information of all the previous convolution layers, and according to the temporal depth range obtained from the test, the best temporal convolution result can be retained for each feature [35].

We segment the art graph into regions and then combine the node vector features of each region into different sequences, each sequence will also be subjected to pooling operation and batch normalization after the initial convolution calculation. Finally, n feature vectors of different time regions of the art graphics at the time level will be obtained. Each set of sequences represents a combination of art graphics in an independent period. The scale of each graphical feature is $X \in R^{N \times M \times K}$, where K represents the feature dimension of each time region node. On top of this, we add an attention mechanism to weight the weighted features of each art-graphic region. To migrate the self-attentive weighted features to the original art graphics, we reshape the region nodes in the attention network. Assuming that the expression of the region node X after reshaping is $Y = [y_1, y_2, \ldots, y_m]$, where $y_i \in R^{NK}$, by forwarding propagation network we define the self-attention weighting calculation a_i as the following equation:

$$a_i = \sigma\left(W^a \times y_i + b_i^a\right), \; i = 1, 2, \ldots, m, \tag{3}$$

where W^a and b_i^a denote the self-attentive parameters with matrix bias and $\sigma(*)$ represents the activation function. We denote the mathematical equations of the self-attentive

model as $s_{att} = [s_1, s_2, \ldots, s_m]$ in the artistic graph input matching $X \in R^{N\times M\times K}$. To ensure the generalization of the input graphics in, we denote the attention graph as $A \in R^{N\times M\times K}$, where K represents the artistic graphics features after K feature extractions. Finally, we weight all the previously obtained features for conversion, and the mathematical equation is as follows:

$$\begin{aligned} f_n &= A \cdot X, \\ f_n^{(1)} &= \left(FNN\left(\text{MultiHead}\left(f_n^{(0)}, f_n^{(0)}, f_n^{(0)}\right)\right)\right), \end{aligned} \tag{4}$$

FNN stands for feed-forward neural network and $f_n^{(1)}$ features of node sequences in art graphics regions.

3.3. Attention-Based LSTM. To facilitate the traversal and association of temporal convolutional features, we used the LSTM algorithm as an association network, and to the LSTM, we added an attention mechanism to associate with the self-attention layer in the temporal convolutional network. Our proposed visual memory neural-based art graphics design network is shown in Figure 3.

In the above figure, γ represents the comprehensive fusion output of the attention feature vector, and ρ represents the average weight fusion output of the attention feature vector. During the reorganization of the art graphic design scheme, we assigned a different focus of attention mechanism to each graphic area. In the face of different art styles, each art style was evaluated under the artist's assessment with multiple indicator scores according to the differences in expression. For example, the difference between color art and rule art, color art mainly emphasizes RGB pixel intensity and establishes the assignment point of color art attention mechanism based on the local pixel threshold response. The contour intensity is mainly used as the threshold response for rule art, and the attention mechanism assigns weights based on the response threshold. In each period, the improved LSTM network can extract feature vectors of the same dimension from the same attention mechanisms. In this way, different dimensional features are extracted in batches, and finally, the global graphic combination scheme features are obtained in the final class.

Suppose the art graphics data has N feature sets $f = [f_1, f_2, \ldots, f_n]$, each of which is obtained in the dual association role of temporal convolutional network and long short-term memory network. When the feature sets are used as input, the inverse network of the temporal convolutional layer receives only one fused feature graph at a time, and the first half of the network can output a high-level feature graph at any time under the action of the LSTM network, and the outputs of the different dimensional attention mechanisms are calculated as shown below.

$$\begin{aligned} h_i &= g\left(f_i\right), i \in (1, n), \\ Q &= \left[h_1, h_2, \ldots, h_n\right], \\ \alpha &= \text{softmax}\left(w^T \tanh\left(Q\right)\right), \\ r &= Q\alpha^T, \end{aligned} \tag{5}$$

where g denotes the extraction method of LSTM network in artistic graphic region features. Q represents the combination of temporal features in different dimensional outputs. If the feature outputs in the same dimension are used as local feature sequence inputs, the forgetting gate will not be able to filter useful features due to the existence of blank features between periods. α denotes the attention of n features in the predicted output of the memory network unit. r denotes the weighted sum of attention of all time dimensions. To solve the problem of the inconsistent combination of multiple artistic graphics schemes and uncoordinated input dimensions, we also propose a graphics feature compression method based on variable pooling operations. This method can compress the attention of different dimensions according to uniform dimensions and decompress the uniform features at the graphical design combination network layer, and each network layer has a built-in data preprocessing layer to avoid the problem of confusing data formats. The variable pooling feature compression network is shown in Figure 4.

4. Experiment

4.1. Training. Artistic graphic scheme free combination model for scheme requires huge graphic database support. For the creation of the database, the database classification can perceive the differences in art graphics in drawing style, color, and contour, to extract the different features of each type in the deep neural network. We map the depth information in the depth camera to the pixel coordinates, to obtain the representation of the contour nodes in space according to the graphic contour extraction algorithm. The pixel coordinates and depth information will produce information mapping in two different data sequences, and to check whether the graph and combination classification are unified, we set independent region thresholds. It has an excellent scheme combination effect for still life graphics. In the model training process, we plan a reasonable training process according to the demand for artistic graphics combinations, as shown in Figure 5.

4.2. Data set. At the initial stage of the art graphics database creation, we invited professional art aestheticians to evaluate art graphics for aesthetic indicators, object emphasis, color harmony, balance elements, motion blur, and other indicators and developed an independent evaluation system. In the art graphics design data collection, we manually labeled the art graphics that have generated economic benefits, and the labeled information contains graphic size, artistic category, combination direction, etc. For the database sequence classification, we adopted the rule of thirds and experimentally reconstructed a quantitative evaluation model. In the quantitative evaluation model, the art graphics' ease of use, aesthetics, balance, and contrast remain the performance evaluation benchmarks for the automatic art graphics combination model. In all art graphics data sets, we set 80% of the training set and 20% of the test set. In the experimental implementation of the art graphics data set, we defined only

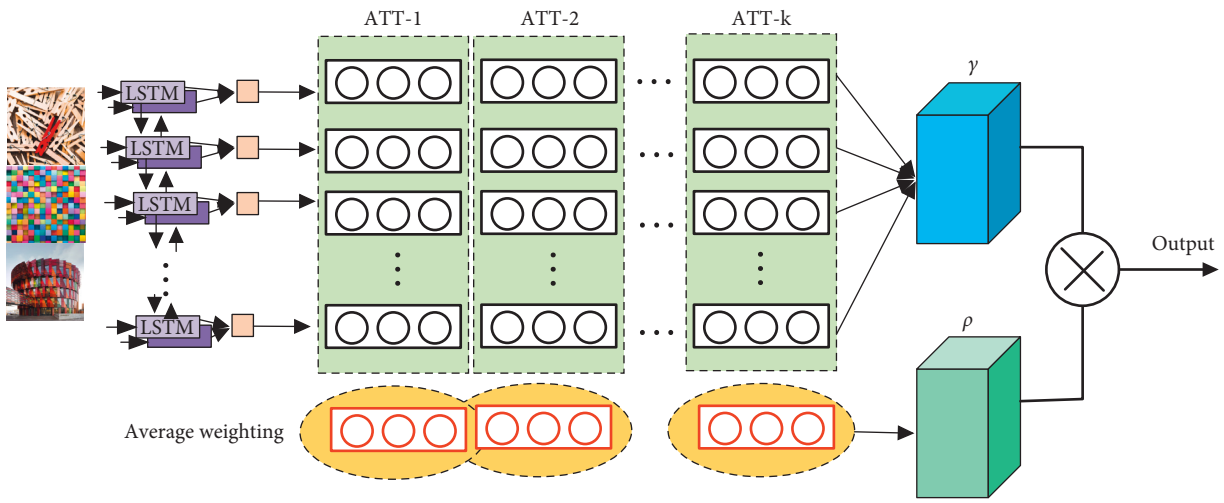

Figure 3: Visual memory neural network.

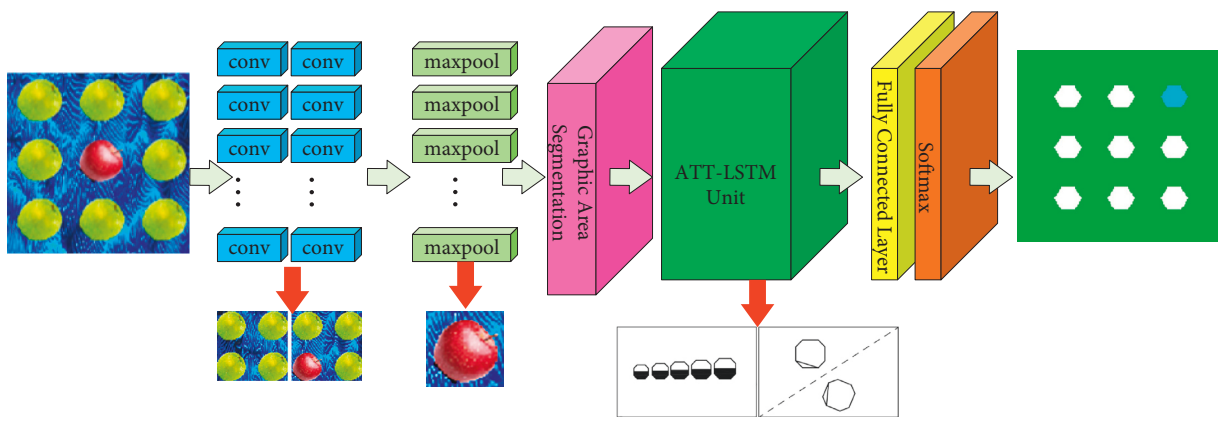

Figure 4: The variable pooling feature compression network.

three categories of artistic graphics at the beginning of the study, namely color category, regular combination category, and multiple arrangement category. The details of the art graphics data set are shown in Table 1.

4.3. Analysis. In the prior experiments, we found in the method validation experiments that machine learning methods have poor accuracy in the visual communication of artistic graphics and cannot achieve real-time requirements. Deep learning methods perform better in the scheme combination of artistic graphics; therefore, in the later experiments, we use deep learning methods as the base reference. In the first stage of experiments, we compare the effect of three methods, CNN [36], RNN [37], and LSTM [38], on the combination of artistic graphics. The first phase experiments are evaluated in terms of precision (P) and recall (R). The experimental results are shown in Table 2.

According to the experimental data in Table 2, it is clear that the combination of artistic graphic design solutions performs better in the image-based deep learning approach. However, the image-based deep neural network method cannot access the information contained inside the artistic graphic labels and cannot achieve the fusion and generalization of data features at the textual level. The accuracy of CNN-like methods stays around 80% in the three types of artistic graphic scheme combinations. Our method incorporates not only CNN methods but also LSTM methods. The structure of the dual network makes up for the model's feature capture of textual information of art graphics, and the joint mapping of pixel features and textual features can effectively compensate for the shortcomings of the pure image-like methods. Therefore, the experiment proves that our method can keep the accuracy above 90% in all the art graphics combinations, which is significantly better than other methods.

In the second phase of the experiment, we validated the artistic graphic aesthetic index. Based on the opinions of professional art aestheticians, we chose three important indicators for validation: Balance Element (BE), Color Harmony (CH), and Object Emphasis (OE). The balance element is to verify the visual balance of art graphics after reconstruction. Color Harmony is to verify that the artistic graphic features are fully captured at the pixel level. Object Emphasis is to highlight the art graphics in similar combination schemes. The results of the experiments are shown in Table 3.

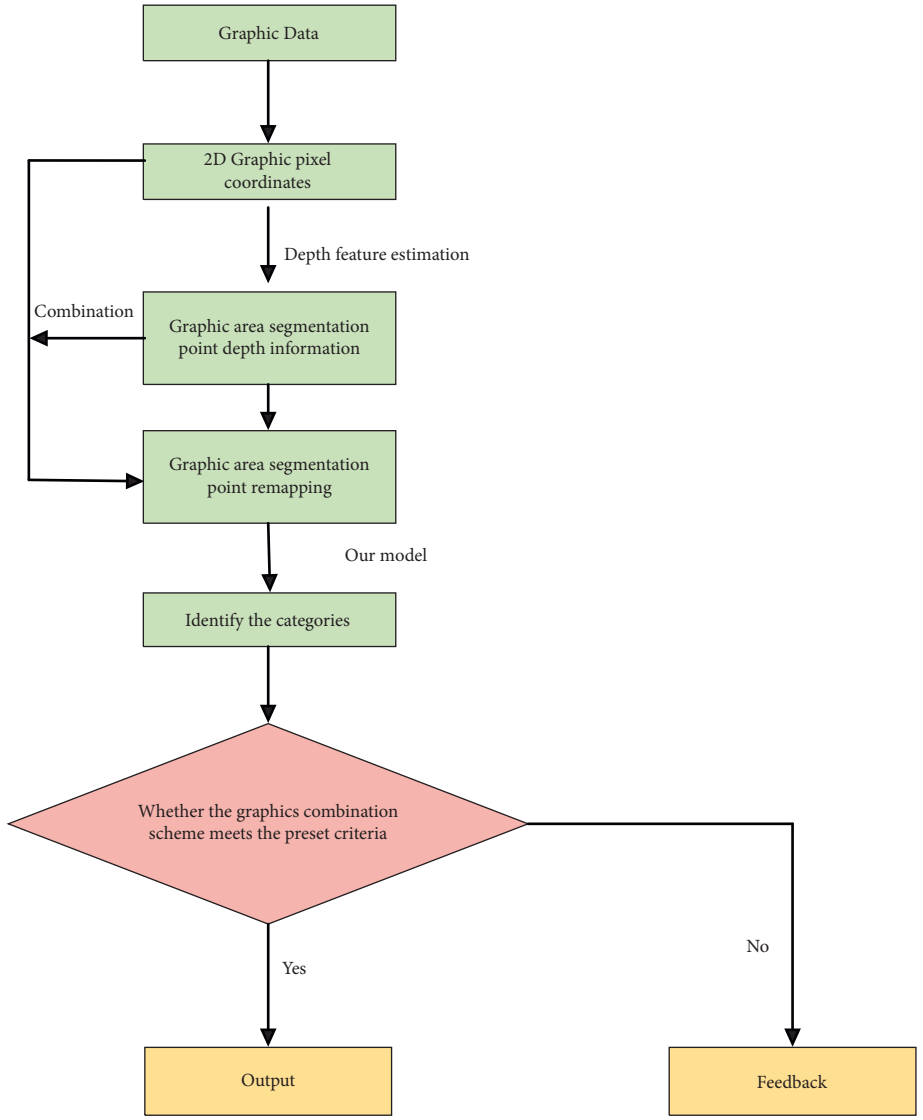

Figure 5: Art graphic design model training process.

Table 1: The detail of art graphics data sets.

	Data sets		
	Color	Regular combination	Multiple arrangement
Train	42880	34880	53040
Test	10720	8720	13260
Total	53600	43600	66300

Table 2: Experimental results of combining the accuracy of different art graphics schemes.

	Color		Regular combination		Multiple arrangement	
	P (%)	R (%)	P (%)	R (%)	P (%)	R (%)
CNN	73	83	85	86	80	83
RNN	66	75	61	74	69	76
LSTM	77	76	79	77	71	79
Ours	93	89	95	90	90	89

Table 3: Experimental results of the accuracy of aesthetic indicators of art graphics.

	Color	Regular combination	Multiple arrangement
Balance element	0.89	0.87	0.92
Color harmony	0.96	0.81	0.90
Object emphasis	0.92	0.96	0.95

The experimental data in Table 3 shows that the best performing type of art graphics among the balanced elements is the multiple arrangement art graphics, which is more advantageous when evaluating the balanced elements because of the multiple arrangement graphics with different combinations of elements. In the color harmony, the best effect is in the color art graphics, and the color harmony index is not good enough because the regular combination and multiple arrangements pay more attention to the outline and space planning. Target emphasis performs well in all

Table 4: Experimental results of different methods of quantitative evaluation model.

	CNN	RNN	LSTM	Ours
Graphics design ease of use	0.7	0.7	0.8	0.9
Graphic combination balance	0.7	0.8	0.8	0.9
Graphic category aesthetics	0.8	0.7	0.8	0.9

three art types. This shows that we should fully consider the role of color harmony and balance elements when classifying database categories. Our method maintains an accuracy rate of 80% in both evaluation indexes, and the experimental data are more accurate in the actual test, thus showing the high efficiency of our method in the experiment.

In the third phase of the experiment, we validated the art graphics quantitative evaluation model, and we tested the experimental performance in the three phases according to the three aspects of art graphics design ease of use, graphic combination balance, and graphic category aesthetics, and the experimental results are shown in Table 4.

From the above experimental results, it can be seen that CNN and RNN methods are not stable enough in the quantitative evaluation model. The LSTM method keeps above 0.8 in the quantitative evaluation model, and due to the memory units embedded in the LSTM network, the under-conditioned feature vectors can be selectively screened in the quantitative evaluation model through the forgetting gate. Our method achieves 0.9 in the quantitative evaluation model, which shows that our method outperforms other deep learning methods and proves the superiority of our method.

5. Conclusion

In this study, we analyze the visual effects and principles of composition of artistic graphic design. Considering the differences and independence of artistic graphic design, we realize the scheme reorganization of art graphic design from the perspective of computer vision and propose the method of art graphic design based on memory neural network. Referring to numerous deep learning methods such as CNN, RNN, and LSTM, we experimentally validated each method and finally designed a two-layer network structure based on CNN and LSTM networks. We built a computer vision environment and reconstructed the computer vision network to set up an independent deep camera vision range computation law. Considering the artistic graphic region segmentation problem, we proposed a self-attentive mechanism, which can quantitatively segment different artistic graphic regions based on temporal features, after arranging them in a sequence to obtain the graphic region feature vector. In the last part of the network structure, we propose the LSTM structure based on the attention mechanism to match with the self-attention features of the graphic region segmentation module and pass the matched attention feature vector to the LSTM network to extract the labeled text feature information of the graphics. To test the effectiveness of our method, we build a database of artistic graphics and set up an adaptive training process. We also compare deep learning methods of the same type, and the experimental results demonstrate that our method outperforms other deep methods in artistic graphic design in terms of scheme reorganization accuracy and quantitative evaluation of artistic models.

Intelligent design of art graphics is a very complex study, where visual scene construction and graphic area segmentation are key point technologies. In the research of this paper, we only choose three simple art categories as research, in fact, there are more complex art categories. In future research, we will try more art types and use the two-layer LSTM algorithm to enhance the feature capture range of the model and improve the generalization of the model.

Data Availability

The data set can be accessed upon request.

Conflicts of Interest

The author declares that there are no conflicts of interest.

Acknowledgments

The author thanks the General Project of Philosophy and Social Science Research in Colleges and Universities of Shanxi Provincial Education Department (no. 2013228).

References

[1] G. Kress and T. Van Leeuwen, *Reading Images: The Grammar of Visual design*, Routledge, vol. 33, no. 6, Oxfordshire, England, UK, 2020.

[2] R. Hirsch, *Light and Lens: Photography in the Digital age*, Routledge, Oxfordshire, England, UK, 2012.

[3] B. Peterson, *Using Design Basics to Get Creative results*, Adams Media, Avon, MA USA, 1996.

[4] S. Bell, *Elements of Visual Design in the landscape*, Routledge, Oxfordshire, England, UK, 2019.

[5] J. Lin, "Development of scales for the measurement of principles of design," *International Journal of Human-Computer Studies*, vol. 71, no. 12, pp. 1112–1123, 2013.

[6] W. Rawat and Z. Wang, "Deep convolutional neural networks for image classification: a comprehensive review," *Neural Computation*, vol. 29, no. 9, pp. 2352–2449, 2017.

[7] A. Carballal, A. Santos, J. Romero, P. Machado, J. Correia, and L. Castro, "Distinguishing paintings from photographs by complexity estimates," *Neural Computing & Applications*, vol. 30, no. 6, pp. 1957–1969, 2018.

[8] R. G. Condorovici, R. Vrânceanu, and C. Vertan, "Saliency map retrieval for artistic paintings inspired from human understanding[J]," *Proceedings of the SPAMEC*, 2011.

[9] C. H. Bock, J. G. A. Barbedo, and E. Del Ponte, "From visual estimates to fully automated sensor-based measurements of plant disease severity: status and challenges for improving accuracy," *Phytopathology Research*, vol. 2, no. 1, pp. 1–30, 2020.

[10] P. Machado, J. Romero, M. Nadal, A. Santos, J. Correia, and A Carballal, "Computerized measures of visual complexity," *Acta Psychologica*, vol. 160, pp. 43–57, 2015.

[11] X. Guo, Y. Qian, L. Li, and A. Asano, "Assessment model for perceived visual complexity of painting images," *Knowledge-Based Systems*, vol. 159, pp. 110–119, 2018.

[12] E. Cetinic, T. Lipic, and S. Grgic, "Learning the principles of art history with convolutional neural networks," *Pattern Recognition Letters*, vol. 129, pp. 56–62, 2020.

[13] L. Liu, E. A. Silva, C. Wu, and H. Wang, "A machine learning-based method for the large-scale evaluation of the qualities of the urban environment," *Computers, Environment and Urban Systems*, vol. 65, pp. 113–125, 2017.

[14] Y. Wu, W. AbdAlmageed, and P. Natarajan, "Mantra-net: manipulation tracing network for detection and localization of image forgeries with anomalous features," *Proceedings of the IEEE/CVF Conference on Computer Vision and Pattern Recognition*, pp. 9543–9552, 2019.

[15] A. Tomé, M. Kuipers, T. Pinheiro, M. Nunes, and T Heitor, "Space-use analysis through computer vision," *Automation in Construction*, vol. 57, pp. 80–97, 2015.

[16] W. Huang and H. Zheng, "Architectural Drawings Recognition and Generation through Machine learning[J]," in *Proceedings of the 38th Annual Conference of the Association for Computer Aided Design in Architecture (ACADIA)*, ACADIA, Mexico City, 2018.

[17] D. Karimi, H. Dou, and S. K. Warfield, "Deep learning with noisy labels: Exploring techniques and remedies in medical image analysis," *Medical Image Analysis*, vol. 65, 2020.

[18] D. Moussazadeh and A. Aytug, "The concept of the aesthetic features in architectural structures of the museums[J]," *International Journal of Architectural and Environmental Engineering*, vol. 12, no. 12, pp. 1142–1150, 2018.

[19] M. Balzani, F. Maietti, and B. M. Mugayar Kühl, "Point cloud analysis for conservation and enhancement of modernist architecture," *The International Archives of the Photogrammetry, Remote Sensing and Spatial Information Sciences*, vol. 1XLII-2/W3, pp. 71–77, 2017.

[20] C. Belém, L. Santos, and A. Leitão, "On the Impact of Machine Learning: Architecture without Architects? in CAAD Futures," *On the Impact of Machine Learning in Architecture*, 2019.

[21] S. Stabinger and A. Rodriguez-Sanchez, "Evaluation of deep learning on an abstract image classification dataset," in *Proceedings of the IEEE International Conference on Computer Vision Workshops*, pp. 2767–2772, IEEE, 2017.

[22] Y. C. Tang, J. J. Huang, M. T. Yao et al., "A review of design intelligence: progress, problems, and challenges," *Frontiers of Information Technology & Electronic Engineering*, vol. 20, no. 12, pp. 1595–1617, 2019.

[23] Y. K. Yi, Y. Zhang, and J. Myung, "House style recognition using deep convolutional neural network," *Automation in Construction*, vol. 118, Article ID 103307, 2020.

[24] L. Lettry, M. Perdoch, and K. Vanhoey, "Repeated Pattern Detection Using CNN activations," in *Proceedings of the 2017 IEEE Winter Conference on Applications of Computer Vision (WACV)*, pp. 47–55, IEEE, Santa Rosa, CA, USA, 2017.

[25] C. Yan, Z. Li, and Y. Zhang, "Depth image denoising using nuclear norm and learning graph model, ACM Transactions on Multimedia Computing," *Communications, and Applications (TOMM)*, vol. 16, no. 4, pp. 1–17, 2020.

[26] M. Li, J. Lv, and C. Tang, "Aesthetic assessment of paintings based on visual balance," *IET Image Processing*, vol. 13, no. 14, pp. 2821–2828, 2019.

[27] H. Wang, A. Kläser, C. Schmid, and C. L. Liu, "Dense trajectories and motion boundary descriptors for action recognition," *International Journal of Computer Vision*, vol. 103, no. 1, pp. 60–79, 2013.

[28] F. Perronnin and C. Dance, "Fisher kernels on visual vocabularies for image categorization[C]," in *Proceedings of the 2007 IEEE conference on computer vision and pattern recognition*, pp. 1–8, IEEE, Minneapolis, MN, USA, 2007.

[29] K. Simonyan and A. Zisserman, "Two-stream convolutional networks for action recognition in videos[J]," *Advances in Neural Information Processing Systems*, vol. 27, 2014.

[30] K. Thömmes and R. Hübner, "Instagram likes for architectural photos can Be predicted by quantitative balance measures and curvature," *Frontiers in Psychology*, vol. 9, Article ID 1050, 2018.

[31] C. C. S. Liem and A. Panichella, "Oracle issues in machine learning and where to find them," in *Proceedings of the IEEE/ACM 42nd International Conference on Software Engineering Workshops*, pp. 483–488, IEEE, New York, NY, USA, 2020.

[32] N. Murray, L. Marchesotti, and F. Perronnin, "AVA: a large-scale database for aesthetic visual analysis," in *Proceedings of the 2012 IEEE conference on computer vision and pattern recognition*, pp. 2408–2415, IEEE, New York, NY, USA, 2012.

[33] A. Lecoutre, B. Negrevergne, and F. Yger, "Recognizing Art Style Automatically in Painting with Deep learning[C]," in *Proceedings of the Asian Conference on Machine Learning*, pp. 327–342, PMLR, 2017.

[34] J. Llamas, P. M Lerones, R. Medina, E. Zalama, and J Gómez-García-Bermejo, "Classification of architectural heritage images using deep learning techniques," *Applied Sciences*, vol. 7, no. 10, p. 992, 2017.

[35] K. He, X. Zhang, and S. Ren, "Deep Residual Learning for Image recognition," in *Proceedings of the IEEE Conference on Computer Vision and Pattern Recognition*, pp. 770–778, IEEE, Las Vegas, NV, USA, 2016.

[36] J. Gu, Z. Wang, J. Kuen et al., "Recent advances in convolutional neural networks," *Pattern Recognition*, vol. 77, pp. 354–377, 2018.

[37] W. Zaremba, I. Sutskever, and O. Vinyals, "Recurrent neural network regularization," *arXiv preprint arXiv*, vol. 1409, p. 2329, 2014.

[38] S. Hochreiter and J. Schmidhuber, "Long short-term memory," *Neural Computation*, vol. 9, no. 8, pp. 1735–1780, 1997.

Hindawi
Scientific Programming
Volume 2022, Article ID 5159027, 8 pages
https://doi.org/10.1155/2022/5159027

Research Article

An Empirical Study on the Training Characteristics of Weekly Load of Calisthenics Teaching and Training Based on Deep Learning Algorithm

Hao Xu,[1] **Huiying Feng**,[2] **and Zhangrong Liu**[2]

[1]*Department of Physical Education, Fujian Forestry Vocational and Technical College, 353000 Nanping, China*
[2]*Fujian Forestry Vocational and Technical College, 353000 Nanping, China*

Correspondence should be addressed to Hao Xu; xuhao@sg.edu.vn

Received 25 May 2022; Revised 18 June 2022; Accepted 28 June 2022; Published 16 August 2022

Academic Editor: Lianhui Li

Load training is an important part of the daily training of aerobics athletes. Therefore, the research on the characteristics of aerobics movement of athletes in load training has been paid extensive attention by teaching units. Deep learning algorithm in artificial intelligence algorithm is used to study the characteristics of calisthenics teaching and training, which is a beneficial exploration to improve the scientific of calisthenics training programs. The basic principles of the neural network algorithm and implementation process are described. After the basic structure and characteristics of the network are analyzed, a comprehensive solution to optimize and improve the regularized deep belief network algorithm is proposed. The results show that compared with other learning algorithms, the feature classification error rate of the optimized regularized deep belief network algorithm is 6% lower than that of other algorithms. Although the training speed of the model decreases, the convergence period of the deep neural network algorithm can better achieve the extraction accuracy of abstract features of training data when the deep learning period increases. Being less affected by input parameters, the algorithm will have better stability and be more conducive to extracting the features favorable to classification. In the field of deep learning, the advantages of the deep neural networks can effectively classify the training characteristics of aerobics athletes and provide scientific decision-making basis for subsequent teaching and training.

1. Introduction

Artificial intelligence algorithms supported by machine learning, deep learning, and other theories, with the help of computer-aided platforms, better realize accurate and efficient rule classification and feature mining of large amounts of data. In the training of aerobics, a lot of functional training is needed, so it is necessary to effectively improve the level of aerobics skills. In the past, the research on feature data of functional training mainly relied on artificial means, and the analysis period was often long and the analysis effect was not very ideal. In this paper, the deep neural network is introduced to carry out feature classification research on the load characteristics of aerobics teaching and training, aiming to find out the movement characteristics of athletes' functional aerobics training accurately and to provide scientific and accurate data support for the optimization of subsequent training programs. The main direction of this research is to discuss the feasibility of neural network algorithms in deep learning theory by analyzing the basic theory of artificial neural networks. Based on the deep belief model, the regularized deep belief network algorithm with batch normalization is constructed. The simulation results show that the optimized regularized deep belief network algorithm has advantages in the accuracy of feature classification and algorithm iteration.

A deep neural network plays a very good supporting role in feature extraction, pattern recognition, and other aspects. The principle of a feature extraction algorithm based on a deep neural network is to select important feature information from research data by simulating the information characteristics of the biological nervous system. In this

paper, the study focuses on the neural network algorithm, pays attention to the latest achievements in the field of in-depth learning, analyses the basic modules, model structure, and implementation process of the in-depth neural network, explores how to better improve the advantages of the indepth neural network algorithm, and helps to effectively classify the characteristics of athletes' load training in Aerobics Teaching and training.

The deep learning theory is introduced to the basic artificial algorithm. Based on the need of extracting load training features, which are optimized to improve the accuracy and robustness of the deep neural network in mining training features. For the analysis technology of the basic principle and process of the artificial neural network, insufficient training of traditional deep belief network, combined with batch normalization algorithm, a batch orthodoxy classification method is proposed, and the modified optimization algorithm is applied to the classification of aerobics load training characteristics. Experiments show that the optimized deep belief network effectively enhances the classification and mining of large-scale and complex training data by the neural network algorithm and provides real and reliable data support for the subsequent optimization of the aerobics teaching program.

The main contents of this paper are as follows: Section 1 discusses the advantages of deep neural network algorithm in data feature classification and how the artificial intelligence algorithm based on computer technology can effectively and accurately analyze complex data. Section 2 describes the principle and advantages of the deep neural network algorithm and puts forward the original intention of this paper. The principles and implementation process are described. Section 3 gives the design flow of the deep neural network algorithm. The reliability of the batch normalization algorithm of the basic depth confidence network algorithm for data feature classification is introduced. Section 4 introduces the optimization strategy and performance characteristics of the hybrid algorithm which combines the batch normalization algorithm and the depth neural network algorithm. Section 5 summarizes the research content of the optimized depth neural network algorithm and analyses the future research direction of aerobics teaching classification and training data mining.

2. Related Work

Research on neural networks by scholars at home and abroad have been well applied in many industries and fields. In the research on GPS positioning, Sun et al. proposed a hybrid algorithm to improve the selection of optimal satellite combinations. The accuracy of satellite positioning is improved by improving the accuracy of geometric dilution. [1]. In Wozniak and Giabbanelli's research on forest data recognition, the way to improve the accuracy of recognition and classification by BP neural network is discussed. The clustering algorithm is introduced to optimize the BP neural network, which makes up for the slow convergence of the BP neural network algorithm [2]. Tian et al. introduced an optimized BP neural network to solve the reliability problem of excessive noise data by using a new executive [3]. In the application of gesture recognition, Li et al. discussed how to improve the BP neural network algorithm to search for local minima. By introducing the chaos principle, a hybrid algorithm model of genetic algorithm and BP neural network is constructed, which improves the quality of the optimal solution of the algorithm [4]. Wang and Jeong discussed the feasibility of optimizing the BP neural network by using wavelet transform theory and discussed back propagation characteristics [5]. Li et al. explored the application of optimization in the comprehensive error compensation of multiaxis machine tools. By updating both the read factor and amplification factor, the convergence effect of the algorithm is improved. In practical application, an error prediction model of machine tool processing accuracy is constructed [6]. In Song et al.'s study on forest data recognition, the way to improve the accuracy of BP neural network recognition and classification is discussed. The clustering algorithm is introduced to optimize the BP neural network, which makes up for the slow convergence of the BP neural network algorithm [7].

In academic research in recent years, Liu explored how to use visualization tools to help users better interpret depth models in recent years [8]. By developing and deploying an interactive visualization system based on improved ActiVis and constructing multiple coordinated views, the results of deep neural network models at various levels, such as instances and subexample, can be studied [9]. Ahn et al. studied how to classify driver's head data using a depth neural network, and proposed a multitask learning depth neural network based on the small gray images. The multitask learning to monitor accurately by using the multiview pictures transmitted by sensors under different environmental conditions such as illumination, vehicle vibration, driver's posture change, and external occlusion [10]. Sharma et al. focused on how to reduce the operating bandwidth and maintain the classification accuracy of the algorithm. By constructing a bit-level processing element array, the operating bandwidth of the deep neural network is dynamically fused, so that the accuracy of the algorithm is not affected under the finest granularity computing conditions [11]. Lubbers et al. introduced a layered interactive particle deep neural network to study the molecular characteristics of two-character computational data sets. The deep neural network achieves the most advanced prediction performance on organic molecular data sets. It can also identify the uncertain regions of the model while realizing the limited and accurate prediction of energy [12]. Zhu et al. explore how to effectively apply depth neural network in image classification. By constructing a training model using features, the performance of the algorithm is effectively improved [13]. Groene al. studied the variance of human behavior and brain measurement interpretation by building three feature models. Among them, the deep neural network was used to simulate the advanced visual features of human eyes. Experiments show that the depth neural network can effectively classify scenes, which is very similar to the function of the human eyes [14]. In the research of computer single-layer scanning data, You et al. explored the use of denoising model

by the deep neural network, to improve the effective classification of images. Experiments show that this scheme can improve the reliability of information retrieval and has a good application prospect in clinical medicine [15].

Through the analysis and application of artificial neural networks and depth neural networks, it can be seen that there are many good results of intelligent algorithms in image classification, prediction models, image retrieval and positioning, real-time picture monitoring, and other applications. However, under the support of current big data, it is still a worthwhile research area to improve the intelligence level of aerobics teaching and training by studying the characteristic data of aerobics symbol load training. Therefore, in this paper, the deep neural network algorithm will be optimized, and it will be explored how the optimization algorithm model can provide strong data support for feature classification in aerobics load training [16].

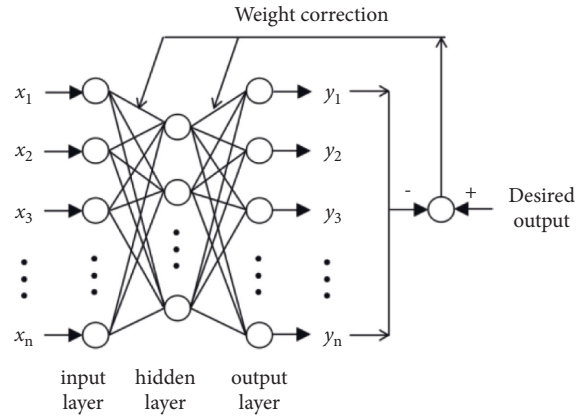

Figure 1: Structure of BP neural network.

3. Methodology

3.1. Neural Network Algorithms. To solve the problem of nonlinear separability, multilayer functional neurons need to be used. Therefore, one or more hidden layers are usually added between the input layer and the output layer. Both hidden layers and output layers are functional neurons with activation function and threshold. More generally, the common neural network is the hierarchical structure shown in Figure 1. There is no same-layer connection or cross-layer connection between neurons. Such neural networks are usually called multilayer feedforward neural networks. BP algorithm is a typical learning algorithm with tutor guidance. The basic idea is to learn a certain number of sample pairs (input and expected output), that is, the input of the sample is transmitted to each neuron of the network input layer. After being calculated by the hidden layer and output layer, each neuron of the output layer outputs the corresponding expected value [17]. If the error accuracy between the expected value and the expected output does not meet the requirements, the error is propagated back from the output layer (note that the error is propagated) and modified through the modification formula of weight and threshold, so that the error between the output of the whole network and the expected output is continuously reduced until the accuracy is met. In other words, the BP network attributes the error between the network output and the expected output to the fault of weight and threshold. Backpropagation apportions the error to each functional neuron. The adjustment of weight and threshold should also be adjusted along the direction of the negative gradient, which is the fastest decline of the error function.

The learning and training of the BP neural network mainly include two processes: forward propagation and error backpropagation. In the forward propagation process, the external data variables are input from the input layer, processed by the neural nodes of each hidden layer, then transformed nonlinearly, and finally output information from the output layer [18]. In this paper, an output error prediction model of a parallel mechanism based on virtual experiments and a BP neural network is constructed. A fast prediction method for output error of parallel robot mechanism is proposed. Considering the hinge installation error and hinge axis error of the parallel mechanism, a virtual prototype model containing the above input errors is established. The output error of the mechanism is solved by virtual experiment simulation. It is assumed that the errors of mechanical components in mass production obey normal distribution and multiple groups of input error data subject to normal distribution are constructed [19]. Then, the BP neural network prediction model of the mechanism is established. If the actual output result of the output layer deviates greatly from the expected target value, the error backpropagation is carried out. In this process, the error will be backpropagated to each layer of BP neural structure one by one, and the error value will be shared with all neural nodes. Each neural node takes this information as information to continuously and repeatedly adjust the connection weight between the input layer and the hidden layer, the connection weight, and threshold between the hidden layer and the output layer. Until the error is reduced to an acceptable level or until the preset number of learning times. Its structure is shown in Figure 1.

From the above knowledge, the perceptron has only one layer of functional neurons (the so-called functional neurons are neurons with a threshold, and the input layer has no threshold). It has poor learning ability and can only solve linear problems, or even nonlinear separable problems such as XOR.

To solve the problem of nonlinear separability, multilayer functional neurons need to be used. Therefore, one or more hidden layers are usually added between the input layer and the output layer. Both hidden layers and output layers are functional neurons with activation function and threshold. More generally, the common neural network is the hierarchical structure shown in Figure 2. There is no same-layer connection or cross-layer connection between neurons. Such a neural network is usually called multilayer feedforward neural network. The BP neural network learning algorithm flow is shown in Figure 2.

The convergence speed is affected by the variety of error surface distribution in two-dimensional space. The factors

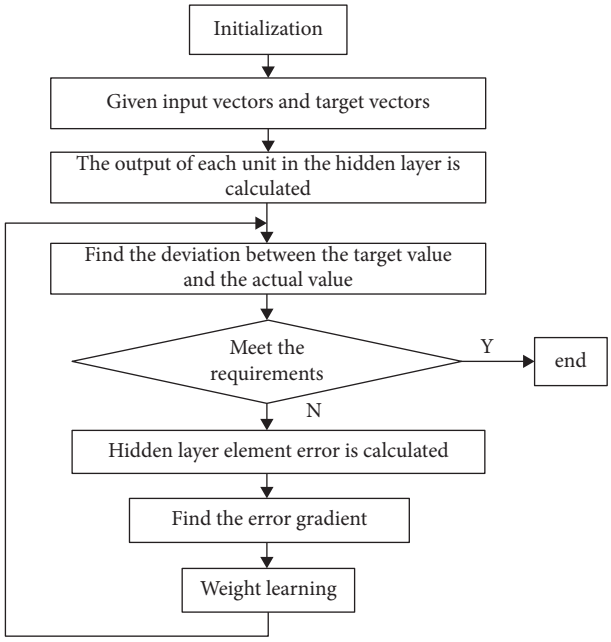

Figure 2: Algorithm flow chart.

that affect the stability and speed of nonlinear convergence are mainly related to the model—mainly the structural stiffness. For some structures, from a conceptual point of view, it can be considered as a geometrically invariant stable system. However, if the stiffness of several main members with similar structures is very different, it may lead to large errors in numerical calculation. The gridding method is essentially a method of using known point values for dimensional space interpolation. The main differences between different methods are the range of sampling points and the weight of known points. The difference in sampling point range is global interpolation and local interpolation, and the difference in known point weight lies in the difference in weight function (basis function). Because the multiple regression method is a trend surface mapping method, and the local polynomial interpolation method can also be regarded as the local trend surface method, that is, using a surface to fit the known data can adopt different powers, which is mainly used to distinguish the regional field from the local field, so the method itself plays a role in removing the fine structure. Although the number of hidden layers can enhance the network's ability to deal with negative linearity, it will also bring too complex technical problems. It is not right that the more the hidden layer is, the better the situation will be. After it exceeds a certain number, the number of hidden layers needs to be determined by experiments (Figure 3).

3.2. Deep Neural Network Algorithms and Their Optimizing Strategies. The deep learning here mainly comes from the deep learning model theory. It is to understand the number of nonlinear operation combinations obtained in the neural network learning from the level of multilayer flying linear function relations. The common shallow structure of the neural network and deep structure of neural network often use fewer neurons to get better generalization performance. Figure 4 is a deep neural network structure with three hidden layers. Deep learning makes good use of the learning characteristics of deep neural networks. At present, there are three main structures of deep neural networks. The first is the generative depth structure, which is used to describe the joint probability distribution of the research object and the high-order correlation characteristics of the data. The second is the discriminatory depth structure, which is to discriminate and judge the pattern classification and describe the posterior distribution of the data. The third is a hybrid structure, which is a combination of generative and discriminatory structures, which can effectively distinguish data.

It is a deep neural network superposed by a restricted Boltzmann machine (RBM). Because of its multilayer structure, it has advantages in obtaining compression coding of data sets. Figure 5 is the construction process diagram of the deep belief network. In the pretraining stage, a greedy unsupervised learning algorithm is used to train each RBM from bottom to top, so that an unsupervised deep belief network can be obtained through repeated iterative training. The gap between the output structure of the money box transmission and the label data can be obtained. In another word, supervised learning from top to bottom is used to fine-tune the deep belief network of unsupervised learning.

The output of the previous RBM in the figure is the input of the latter RBM. If the deep belief network contains one hidden layer, the joint probability distribution of the model can be shown in formula (1). Here, when h_{i+1} is known, which is the probability distribution of the deep belief network,

$$\begin{aligned} P(v, h_1, h_2, \ldots, h_l) &= P(v \mid h_1) P(h_1 \mid h_2), \ldots, P(h_{i-2} \mid h_{i-1}) P(h_{i-1} \mid h_i) \\ &= P(v \mid h_1) \left(\prod_{i=1}^{i-2} P(h_1 \mid h_{i+1}) \right) P(h_{i=1}, h_i). \end{aligned} \tag{1}$$

In practical applications, deep belief networks are often undertrained. Therefore, the BN is a deep belief network. The batch regularization algorithm uses an independent regularization method to process the scalar features, which is the batch processing of input data samples. In the fine-tuning of traditional deep belief networks, the distribution of input data at each level is affected by the variation of

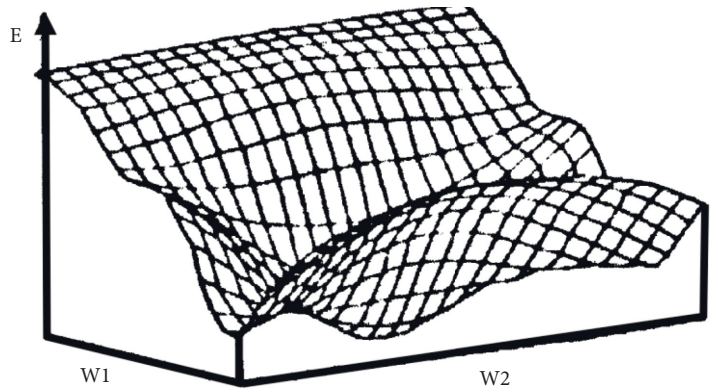

Figure 3: Distribution in two-dimensional space.

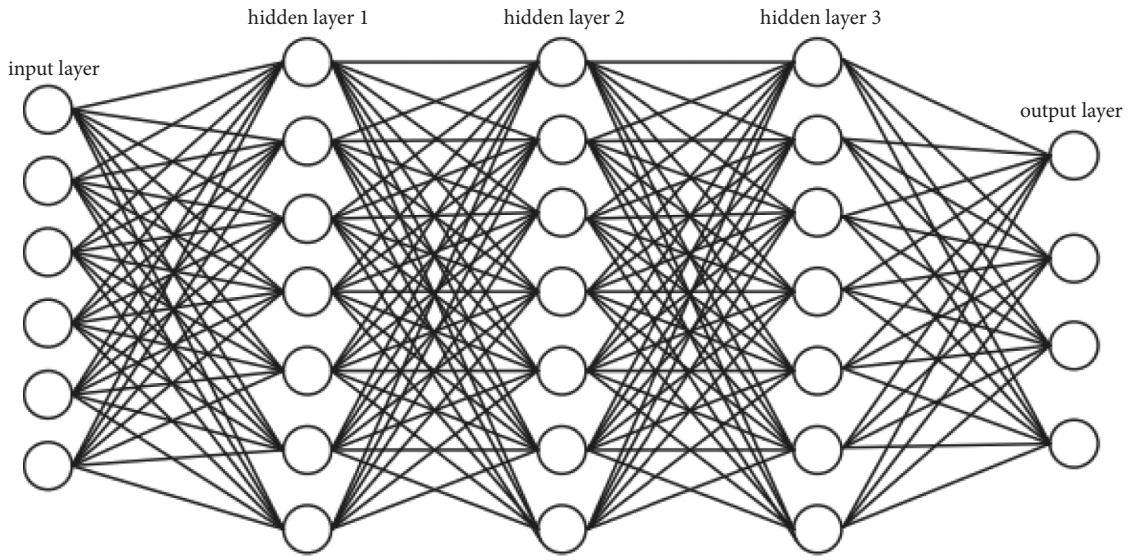

Figure 4: Deep neural network structure diagram with three hidden layers.

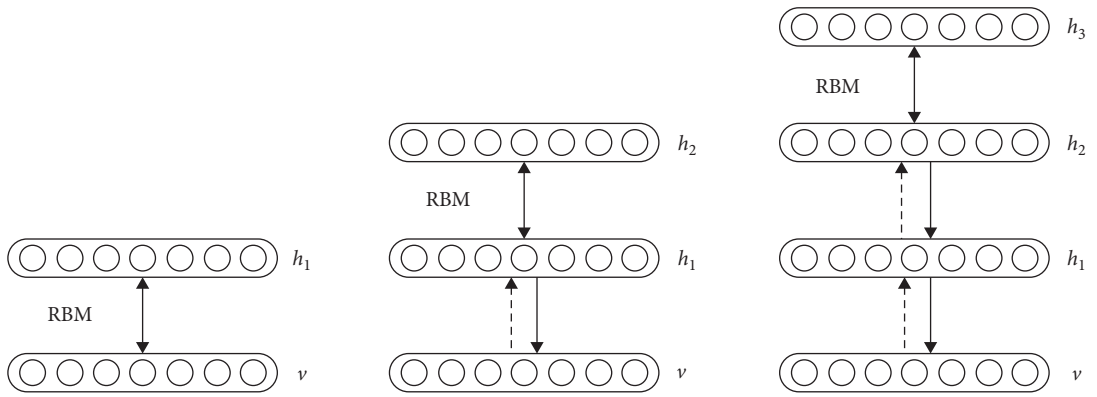

Figure 5: The construction process diagram of deep belief network.

parameters. Under this condition, the complexity of networks is very high. If the activation function is used to map the output value as the input data to the latter layer, the distribution of the input data will not change significantly in the training. In another word, the optimization goal of making the deep belief network run more stable can be achieved. Based on this optimization idea, the batch regularization is in the fine-tuning stage. The structure of the

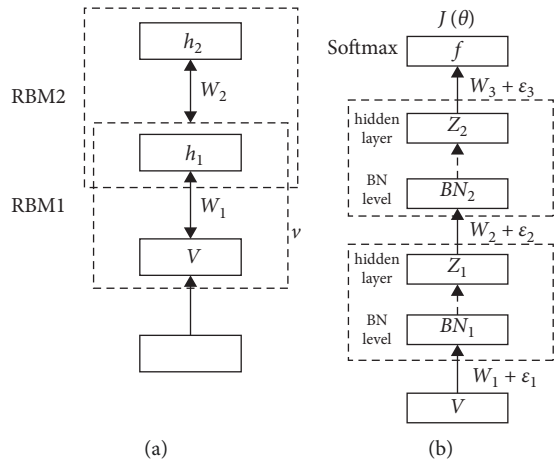

Figure 6: BN-DBN structural drawing. (a) Pretraining. (b) Further optimization.

batch regularized depth belief network (BN-DBN) is shown in Figure 6.

Figure 6(b) uses the batch regularization algorithm to process the input features of the batch regularization algorithm (BN) layer and then deactivate the function layer as the input value. In BU processing of a deep neural network with hidden layer l, formulas (2)–(4) will be used. Each batch of training samples is $D\{x_1, \ldots, x_m\}$. The input value of a k dimension x is expressed by $x^{(k)}$. The sample set is D, the mean is μ_B, and the variance is σ_B^2. Each dimension of the input value x is regularized with $\hat{x}_i$.

$$\mu_D^{(l)} = \frac{1}{m}\sum_{i=1}^{m} x_i^{(l)}, \tag{2}$$

$$\sigma_D^{(l)^2} = \frac{1}{m}\sum_{i=1}^{m}\left(x_i^{(l)} - \mu_D^{(l)}\right)^2, \tag{3}$$

$$\hat{x}^{(l)} = \frac{x_i^{(l)} - \mu_D^{(l)}}{\sigma_D^{(l)}} = \frac{x_i^{(l)} - 1/m\sum_{i=1}^{m} x_i^{(l)}}{\sqrt{1/m\sum_{i=1}^{m}\left(x_i^{(l)} - \mu_D^{(l)}\right)^2}}. \tag{4}$$

Batch regularized deep belief network (BN-DBN) mainly uses scale transformation and translation transformation parameters to make the model more expressive. In this way, the gradient propagation of the deep belief network will not be affected if some layer of the network has parameters to be transformed. When the weights of new parameters are too large, the gradient of the whole model will be reduced by using scale transformation. This method can realize that the whole batch regularized depth belief network (BN-DBN) is always in a stable state during parameter training.

4. Batch Regularized Deep Belief Network (BN-DBN) Performance Experiments

4.1. Experimental Conditions and Parameters. The hardware condition of this test is Windows 10 operating system, with 4.00 GB memory and MATLAB R2014a tool. The database used in the experiment is the characteristic database of the aerobics training team of M University in 2017. It contains 50,000 training samples and 12,000 test samples. The experimental data collected in this database are randomly obtained, using 5000 training samples and 1500 test samples. The parameters selected in the experiment are based on the parameters obtained after a large number of experiments. In the unsupervised learning stage, without considering the batch regularization algorithm (BN), the number of hidden dangerous layers of the network is 2, and there are 100 neuron nodes in each layer. The batch size is 120. When the number of iterations exceeds 10, the momentum parameter is set to 0.85. When the number of iterations is less than 10, the momentum parameter is set to 0.65. The maximum number of iterations is 200. The initial learning rate of the supervised stage is set to 0.05, and the maximum initial value of fine-tuning times is 100. In the experiment, the batch regularized deep belief network is compared with the original model, and the performance advantages are discussed. The experiment adopts the contrast method. The other feature extraction algorithms are basic depth belief network (DBN) of an automatic encoder (AE) and dropout-DBN.

4.2. Stability Experiment of the BN-DBN Algorithm. The setting of the initial learning rate in traditional DBN will directly affect the stable operation and convergence speed of the algorithm. It often needs a lot of practical experiments to select the appropriate learning rate. In the experiment, it is needed to verify the stability of the BN-DBN algorithm. When other parameters are fixed, the learning rate should change between 0.0005 and 0.05. Based on the characteristic data set of aerobics athletes' weekly load training in 2017, the BN-DBN algorithm was compared with ANN, K-nearest neighbor algorithm (KNN), basic depth belief network (DBN), and dropout-DBN. The results are shown in Figure 7. Under the curve operation of BN-DBN and other algorithms, the classification error rate is 0.6% lower than that of the dropout-DBN algorithm. The results show that the algorithm has high stability.

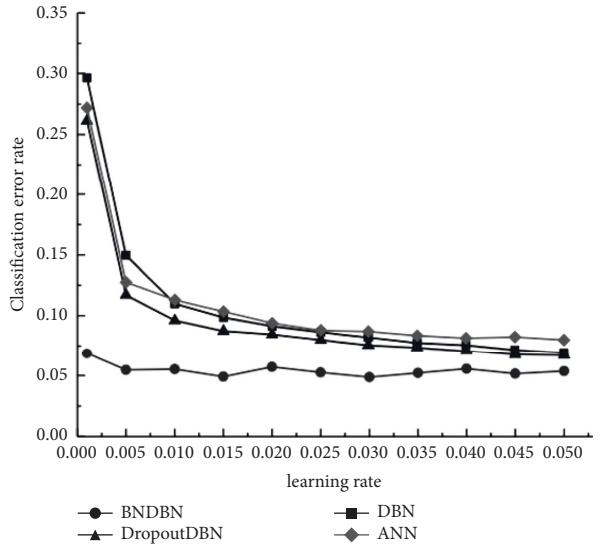

Figure 7: Comparison of classification error rates of four algorithms under different learning rates.

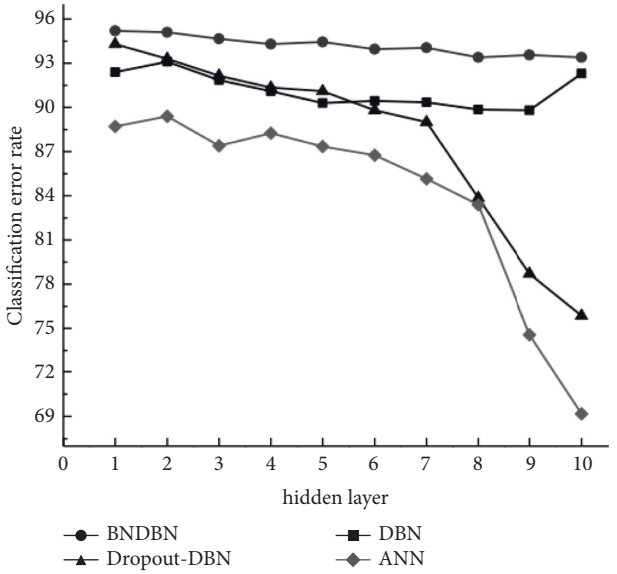

Figure 8: Comparison of classification accuracy of four algorithms with different numbers of hidden layers.

4.3. Performance Experiment of BN-DBN Algorithm. Compared with traditional neural network algorithms, the greatest advantage is depth. The algorithm is more likely to exhibit overfitting phenomenon. To verify the performance of the BN-DBN algorithm proposed in this paper on a deeper level, it is needed to assume that other parameters are fixed, which will increase slowly, up to 10 hidden layers, or to use aerobics training data as experimental data. This is the performance of the classification accuracy of the BN-DBN algorithm and other algorithms under the change of hidden layer (Figure 8).

The experimental data above show that, in the training of feature extraction, the statement that the performance of the network will be better if the number of hidden layers increases is not right. With the same data scale, if the number of hidden layers increases continuously, the classification curves of the four algorithms are in a downward trend. This is mainly because the hidden layer has to extract sample features at different levels in each different layer. The more the number of hidden layers is, the richer the concept of feature expression will be, which will reduce the classification. But the abstraction effect of the BNBDN algorithm is better, which means that although the parameters will change constantly, BNBDN runs well and is more suitable for feature extraction.

5. Conclusion

ANN is an artificial intelligence algorithm that simulates the neural structure of the human brain to reproduce the thinking ability. It has a good application prospect in the research of prediction, classification, and feature extraction. The general deep learning process refers to inputting the feature vector into the neural network. After the operation of the internal code, the neural network outputs the results we need. Different from ordinary programs, the scale of the neural networks is larger, and it can process a large amount of data and get results more quickly. To achieve what a single program cannot do, the premise of the use of the neural networks needs a lot of data for training, that is, it takes longer to create a neural network. A deep belief network algorithm is proposed, and the algorithm is optimized and updated according to the need for aerobics load training feature classification. BN is introduced to optimize the deep belief network. The algorithm and the scalar features of each layer in the neural network are processed by the independent regularization method of the batch regularization algorithm, which is the batch processing of input data samples. This paper has a 0.6% lower classification error rate than dropout-DBN when it is optimized. The BN-DBN can extract the characteristics of data more accurately, and the algorithm has high stability. The abstraction effect of BNBDN algorithm is better, and it is more suitable for feature extraction. However, the study still has some limitations. BN-BDN algorithm still has room for improvement, so building a hybrid model structure is the direction of future research.

Data Availability

The experimental data used to support the findings of this study are available from the corresponding author upon request.

Conflicts of Interest

The authors declare that they have no conflicts of interest regarding this work.

References

[1] M. Sun, Y. Wang, S. Xu, H. Yang, and K. Zhang, "Indoor geomagnetic positioning using the enhanced genetic algorithm-based extreme learning machine," *IEEE Transactions on Instrumentation and Measurement*, vol. 70, pp. 1–11, 2021.

[2] M. K. Wozniak and P. J. Giabbanelli, "Comparing implementations of cellular automata as images: a novel approach to verification by combining image processing and machine learning," in *Proceedings of the 2021 ACM SIGSIM Conference on Principles of Advanced Discrete Simulation*, vol. 11, pp. 13–25, New York, NY, USA, May 2021.

[3] W. Tian, Y. Bao, and W. Liu, "Wind power forecasting by the BP neural network with the support of machine learning," *Mathematical Problems in Engineering*, vol. 2022, pp. 1–10, Article ID 7952860, 2022.

[4] D. J. Li, Y. Y. Li, J. X. Li, and Y. Fu, "Gesture recognition based on BP neural network improved by chaotic genetic algorithm," *International Journal of Automation and Computing*, vol. 15, no. 3, pp. 267–276, 2018.

[5] J. Wang and J. Jeong, "Wavelet-content-adaptive BP neural network-based deinterlacing algorithm," *Soft Computing*, vol. 22, no. 5, pp. 1595–1601, 2018.

[6] Z. Li, B. Zhu, Y. Dai, W. Zhu, Q. Wang, and B. Wang, "Research on thermal error modeling of motorized spindle based on BP neural network optimized by beetle antennae search algorithm," *Machines*, vol. 9, no. 11, p. 286, 2021.

[7] S. Song, X. Xiong, X. Wu, and Z. Xue, "Modeling the SOFC by BP neural network algorithm," *International Journal of Hydrogen Energy*, vol. 46, no. 38, pp. 20065–20077, 2021.

[8] M. Liu, "Retracted article: optimization of marine biological sediment and aerobics training mode based on SVM," *Arabian Journal of Geosciences*, vol. 14, no. 15, p. 1503, 2021.

[9] D. Bertucci, M. M. Hamid, Y. Anand et al., "Visual exploration of large-scale image datasets for machine learning with treemaps," 2022, https://arxiv.org/abs/2205.06935.

[10] B. Ahn, D. G. Choi, J. Park, and I. S. Kweon, "Real-time head pose estimation using multi-task deep neural network," *Robotics and Autonomous Systems*, vol. 103, pp. 1–12, 2018.

[11] H. Sharma, J. Park, N. Suda et al., "Bit fusion: bit-level dynamically composable architecture for accelerating deep neural network,"vol. 6, pp. 764–775, in *Proceedings of the 2018 ACM/IEEE 45th Annual International Symposium on Computer Architecture (ISCA)*, vol. 6, IEEE, Los Angeles, CA, USA, May 2018.

[12] N. Lubbers, J. S. Smith, and K. Barros, "Hierarchical modeling of molecular energies using a deep neural network," *The Journal of Chemical Physics*, vol. 148, no. 24, Article ID 241715, 2018.

[13] H. Zhu, A. Mohamed, B. Zheng et al., "Benchmarking and analyzing deep neural network training,"vol. 3, pp. 88–100, in *Proceedings of the 2018 IEEE International Symposium on Workload Characterization (IISWC)*, vol. 3, IEEE, Raleigh, NC, USA, September 2018.

[14] I. I. Groen, M. R. Greene, C. Baldassano, Li Fei-Fei, D. M. Beck, and C. I. Baker, "Distinct contributions of functional and deep neural network features to representational similarity of scenes in human brain and behavior," *Elife*, vol. 7, Article ID e32962, 2018.

[15] C. You, W. Cong, G. Wang et al., "Structurally-sensitive multi-scale deep neural network for low-dose CT denoising," *IEEE Access*, vol. 6, pp. 41839–41855, 2018.

[16] A. L. Persiyanova-Dubrova, T. V. Marphina, and N. G. Badalov, "Water aerobics training: selection and control of the exercise intensity using the Borg scale," *Voprosy Kurortologii, Fizioterapii, i Lechebnoi Fizicheskoi Kultury*, vol. 98, no. 2, p. 39, 2021.

[17] M. Zhao, B. Tang, L. Deng, and M. Pecht, "Multiple wavelet regularized deep residual networks for fault diagnosis," *Measurement*, vol. 152, Article ID 107331, 2020.

[18] X. Yan, Y. Liu, and M. Jia, "Multiscale cascading deep belief network for fault identification of rotating machinery under various working conditions," *Knowledge-Based Systems*, vol. 193, Article ID 105484, 2020.

[19] G. Pan, Y. Wu, M. Yu, L. Fu, and H. Li, "Inverse modeling for filters using a regularized deep neural network approach," *IEEE Microwave and Wireless Components Letters*, vol. 30, no. 5, pp. 457–460, 2020.

Hindawi
Scientific Programming
Volume 2022, Article ID 8729731, 12 pages
https://doi.org/10.1155/2022/8729731

Research Article

Automation Design and Organization Innovation of Manufacturing Enterprises Based on the Internet of Things

Wang Qilin[1] **and Zhao Yue**[2]

[1]*Dalian Polytechnic University, School of Information Science and Engineering, Dalian 116034, Liaoning, China*
[2]*Liaoning Normal University, School of Chinese Language and Literature, Dalian 116021, Liaoning, China*

Correspondence should be addressed to Wang Qilin; wangql@dlpu.edu.cn

Received 3 July 2022; Revised 16 July 2022; Accepted 21 July 2022; Published 16 August 2022

Academic Editor: Lianhui Li

The Internet of Things manufacturing technology is an important symbol for measuring the level of a country's scientific and technological development. Enterprises that apply the Internet of Things manufacturing technology represent the level of a country's industrial development to a large extent. However, the introduction of IoT manufacturing technology will not automatically generate benefits. It needs to be matched with a suitable organizational structure to maximize the advantages of IoT manufacturing technology. The enterprise organization structure has always been the focus of enterprise organization research and management research. From the linear system to the network organization, the innovation of enterprise organizational structure has never stopped. Therefore, the research on the organizational structure innovation of IoT manufacturing technology enterprises has strong theoretical and practical significance. This study conducted an empirical study on the impact of organizational innovation climate and individual innovation behavior on organizational structure innovation in IoT manufacturing technology enterprises in the form of a questionnaire survey. The structural equation model of organizational innovation climate and personal innovation behavior is proposed, the data and questionnaires are statistically and factorially analyzed by software such as SPSS 18.0 and AMOS 7.0, and the hypothesized structural equation model is verified.

1. Introduction

Since Schumpeter put forward the theory of technological innovation in 1912, innovation research has been a hot topic in academic circles. Early research on innovation was mainly carried out from a macro perspective, looking at innovation from a highly macro and abstract perspective, viewing enterprises as participants in the economic system, and focusing on the output of the economic system rather than the performance of the enterprise. With the change in environment and the rise of organizational theory, organizational structure innovation has become a research topic. In the late 1980s and early 1990s, the American manufacturing industry first proposed the concept of IoT manufacturing technology to enhance its own competitiveness and promote national economic growth based on the opportunities and challenges it faced. In the following years, there was a wave of applying IoT manufacturing technology around the world. New industrial countries such as Europe, America, Japan, and China have listed IoT manufacturing technology as a national high-tech and key development project. Manufacturing is the pillar industry of China's national economy. About a quarter of the population is engaged in this industry, creating great material wealth. Therefore, it is the core of China's national economy and the driving force of industrialization. China has introduced the Internet of Things manufacturing technology for more than 20 years, which has played a good role in promoting its economic growth because the theory of organizational innovation at home and abroad is not very unified and perfect. In addition, with the gradual formation of the global economic integration development model, for enterprises applying IoT manufacturing technology, the challenges faced by organizations in their operation are becoming more complex and

diverse, which inevitably requires organizational theory. Keep up with the times. In particular, the global financial crisis in 2008 had a great impact on our country. The downward pressure on the domestic economy was increasing. The state proposed to strengthen technological transformation, accelerate the industrial adjustment of technological innovation, and put forward higher requirements for the application of Internet of Things manufacturing technology [1–5].

This paper studies and analyzes the dynamic system of enterprise organizational innovation applying IoT manufacturing technology, describes the entire emergent process of IoT manufacturing technology enterprise organizational innovation, and proposes an organizational innovation process model with adaptive robust control links according to the emergent characteristics. At the same time, a questionnaire survey was carried out on the employees of enterprises applying the Internet of Things manufacturing technology to investigate the organizational innovation atmosphere and personal innovation behavior, and empirical data were obtained. SPSS 18.0 was used to conduct a statistical analysis of the data and questionnaires. By using AMOS7.0 to verify the hypothetical structural equation model of organizational innovation climate and individual innovation behavior, the relationship between the two is obtained, which is a useful tool for IoT manufacturing technology enterprises. Achieving a higher degree of organizational structure innovation provides a valuable reference.

2. Related Work

At the end of the twentieth century, with the emergence of the new economy and the development of the theory of enterprise innovation, the theory of organizational innovation began to appear. There is no unified definition and classification of organizational innovation, and the similarities and differences between it and organizational structure innovation are unclear. For example, many scholars define organizational innovation as the organization adopting a new idea or behavior, where innovation refers to a new product, a new service, a new technology, or a new management practice. Alasoinni defined organizational innovation as a change in the division of labor and interactions within functions, between functions, and between organizations. Knight divided organizational innovation into four categories: product or service innovation, production process innovation, structural innovation, and people innovation. Michael Hammer and James Champy put forward the theory of process reengineering and enterprise reengineering. BPR became a new method of business organization that emerged in the United States in the early 1990s. They gave a precise definition of BPR: BPR is a fundamental rethinking of business processes and a complete overhaul to achieve dramatic improvements in business performance measures such as cost, quality, service, and speed. This definition contains four keywords: radical, thorough, dramatic, and flow. At the same time, Peter Senge, a professor at the Massachusetts Institute of Technology in the United States and a famous management scientist, pointed out the management concept of Learning Organization, stating that today's society has entered the information age, and enterprises must remain in the social reform and market economy tide. Invincibly, becoming a learning enterprise organization is a development trend. Based on the basic principles of system dynamics, he specifically conceived some basic characteristics of future enterprises, including flat organizational structure, organizational informatization, more open organization, and the relationship between employees and managers gradually shifting from subordination to work. Correspondingly, for IoT manufacturing technology, in the 1960s, Joan Woodward studied the impact of technology on organizational structure. Lee and Leonard found that self-guided trolleys changed the nature of employees' work in a low-volume manufacturing environment; scholars such as Samson believed that the successful implementation of IoT manufacturing technology should carefully consider organizational and human resource issues such as responsibilities, recognition of changes, positions, and skills. Ghani et al. proposed that necessary organizational changes must be made in the application of IoT manufacturing technology to obtain higher performance. Saraph and Sebastian reviewed numerous studies and concluded that the failure of IoT manufacturing technology is mainly due to the neglect of key human resource factors. Gerwin and Kolodny believed that IoT manufacturing technology has led to many changes in human resource management and practice and further suggested that human resource development should be integrated with the design of new technologies in manufacturing companies. Scholars such as Mital proposed that the purpose of enterprise application of IoT manufacturing technology is to enhance the reliability and flexibility of production and improve product quality and economy, pointing out that the key to the successful implementation of IoT manufacturing technology lies in the human factor. Mohammed Zhari published the paper "The Role of Total Quality Management on Organizational Innovation," which provided new ideas for organizational structure innovation [6–11].

3. The Characteristics and Process of the Innovation Power of the Organizational Structure of the Internet of Things Manufacturing Technology Enterprises

3.1. IOT Manufacturing Technology Enterprise Organizational Structure Innovation Power Mode and Relationship. Foreign scholars attribute the power source of enterprise organizational structure innovation to technology power source, market power source, government power source, and transaction cost source. Chinese scholar Zhang Gang drew on the viewpoints of other scholars at home and abroad and summarized the main contents of six aspects of the dynamic mechanism of enterprise organizational structure innovation, that is, six possible main sources of power for organizational structure innovation: the introduction of new technologies in enterprises and the orientation of enterprise strategies. Changes in corporate value orientation and the

company's own development needs are the triggers for social, political, and economic changes. This paper believes in the innovation of enterprise organizational structure as a new organizational form for enterprises to adapt to environmental changes and productivity development requirements based on advanced manufacturing technology (Internet of Things manufacturing technology). The core innovation power of enterprises can be roughly divided into three modes. (1) Technology is the driving force of the organizational structure innovation model of the induced enterprise. From the perspective of the power source of innovation, the driving force of the technology-induced organizational structure innovation mainly comes from the development of new technologies for the enterprise. For enterprises in the fast "high-tech" industry, they have no choice but to innovate because to achieve market leadership, only continuous innovation and daring to take risks will enable enterprises to have better development opportunities. Therefore, the technology-induced enterprise organizational structure innovation model is the most important driving force for the organizational structure innovation of advanced manufacturing technology enterprises [12]. (2) The innovative power of the strategic-oriented organizational structure mainly comes from the change in the strategic orientation of the enterprise. For example, the senior leaders or managers of the enterprise make advance judgments on the changes in the internal and surrounding environment of the enterprise or make quick responses according to the existing changes. The specific performance is that according to the actual situation of the external environment and internal conditions, the corresponding material and organizational resources are concentrated to determine the organizational vision, clarify the goal of planning, adjust product structure, and realize strategic innovation. Subsequently, structural and cultural innovations are started along with strategic innovation and proceed simultaneously to realize the dynamic matching of the enterprise's strategic, cultural, and structural innovation and achieve the purpose of promoting enterprise organizational structure innovation [13]. (3) The driving force of market pressure-oriented organizational structure innovation mainly comes from the pressure of market competition. The increasingly fierce competition environment pressure in the market makes enterprises have to consider innovative changes to deal with the problems of survival and development. The competition with competitors, the competition of products or services, the competition of product quality, the competition of capital strength, the competition of marketing and public relations require enterprises to use new technologies to develop and improve products and, at the same time, adjust their organizational structure to achieve the purpose of reducing enterprise costs and enhancing competitiveness [14].

Therefore, the market competition is more intense. Companies are more inclined to adopt new technologies and restructure efficient organizations to build competitive advantage. The development of new products and changes in organizational structure and systems, among others, aim to continuously provide high-quality goods and customer service. The combined effect of the three innovation power modes brings continuous power support to the innovation of organizational structure. The pulling effect caused by their interaction also provides favorable support and traction for their respective innovation models. Enterprises integrate the industrial structure through technological induction and accordingly need to adjust the department setting, resource allocation, and responsibility structure in the enterprise structure. The change in structure will inevitably lead to the innovation of structure, which will lead to the subtle change of corporate culture, that is, the change of corporate values and behavioral norms. Gradual changes in structure and culture, in turn, induce further changes in corporate strategy. Therefore, the innovation of the organizational structure of enterprises driven by technological induction is through structural innovation to cultural innovation and finally affects strategic innovation. The market pressure-type organizational structure innovation mainly promotes the change in enterprise strategy through changes in the external environment, thereby affecting the adjustment of the industrial structure of the enterprise or directly inducing the enterprise to enhance its competitiveness by introducing new technologies. It can also be seen from the innovation of strategic-led organizational structure that the changes in corporate culture and structure are carried out simultaneously and appear interactively under each innovation mode. Therefore, under specific circumstances, the various modes are mutually reinforcing and mutually inducing relationships, as shown in Figure 1.

3.2. General Innovation Process Model of IoT Manufacturing Technology Enterprise Organizational Structure

3.2.1. Process Model of General Organizational Structure Innovation. As an important content of modern enterprise management, organizational structure innovation is carried out based on the process. Lewin proposed a three-stage model of the organizational innovation process of unfreezing-change-refreezing. On the basis of Lewin's three-stage model, Koter proposed an eight-stage model of the organizational innovation process (establishing crisis awareness, forming a guiding team, creating a vision, communicating between leaders and organizational members, empowering relevant personnel to make changes, planning goals to create short-term effects, consolidate achievements and deepen reforms, and institutionalize new achievements and new methods). Scheinti put forward the "adaptation cycle" theory of the organizational innovation process. He believed that organizational innovation is a continuous cycle process (insight into changes in the environment, research changes, implementation of changes, stability of changes measures, output changes results). The specific performance of organizational innovation activities is the orderly progress of each stage or the effective connection of each link. In other words, each stage and each link can fully explain that organizational innovation is a process composed of a series of activities with corresponding functions. Based on the

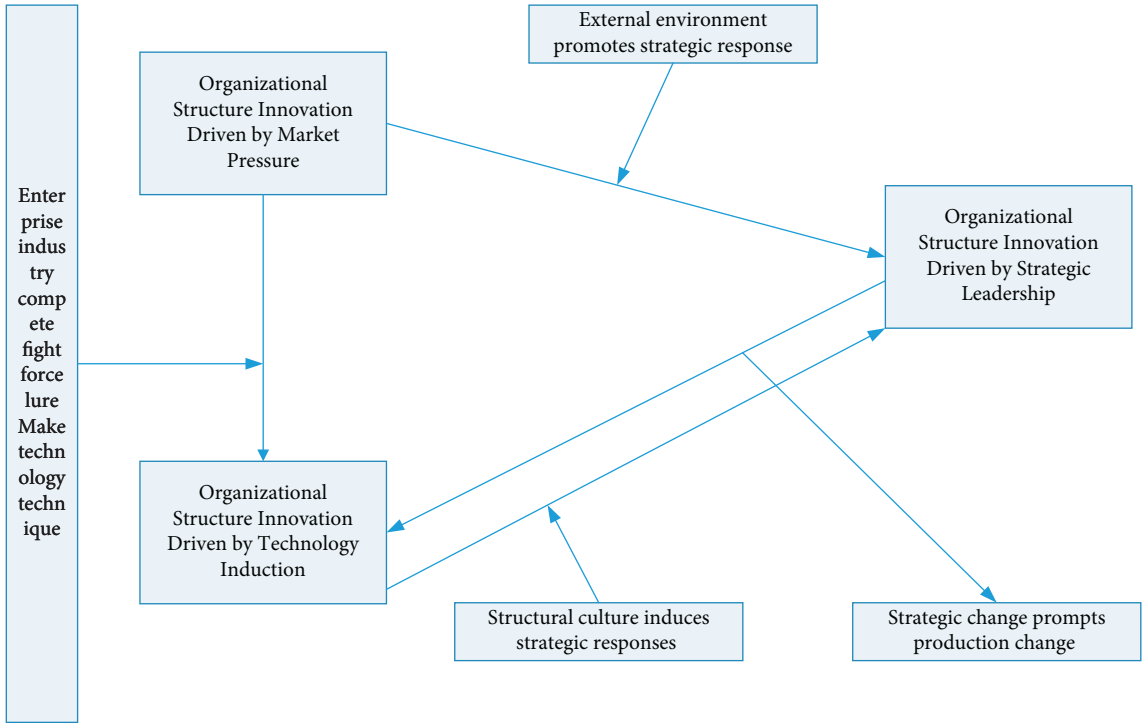

Figure 1: Interrelationships among the three innovation dynamic models.

viewpoints of scholars at home and abroad, we generally divide the specific implementation process of organizational structure innovation activities into two major stages. Action to make a choice the second stage is the organization implementation stage, which puts the selected action plan into practice to guide the organization and individual behavior [15]. The specific links included in these two stages are as follows: Figure 2.

(1) Organizational structure innovation formulation stage. (1) The occurrence and determination of problems: at this stage, the managers of the organization need to consider the development and changing trends of the internal and external environment of the organization and find out the problems that the organization faces or will face at this stage according to the actual situation of the organization. For example, strong market pressure or the mismatch between organizational structure and product structure, according to which the goal of enterprise organizational structure innovation is formulated. (2) The problem is included in the organizational agenda. This stage is the feasibility analysis and demonstration stage of the innovation goal of the enterprise organizational structure. For all activities with the process, the process must be carried out under restricted conditions, so the process of organizational structure innovation must also be carried out in a specific organizational structure innovation environment. The problem that enterprises should consider is whether the goal of organizational structure innovation can be successfully achieved under the existing environmental conditions of the organization. If the result of the demonstration is that the goal of enterprise organizational structure innovation cannot be achieved under the existing organizational environment of the enterprise, then the enterprise needs to redefine the goal of organizational structure innovation according to the demonstration situation. Many enterprise organizational structure innovations end in failure, most of which are due to the lack of feasibility demonstrations of organizational structure innovation, which leads to the establishment of organizational structure innovation goals that are out of the actual situation of enterprises and organizations, resulting in increased risks of organizational structure innovation. (3) Organizational planning and preassessment: this stage is the design and selection stage of the company's organizational structure innovation plan. Enterprises design several alternative organizational structure innovation plans according to the established organizational structure innovation goals and inherent resource conditions of the organization. Enterprise decision-makers select the best plan for implementation through a comprehensive evaluation of the

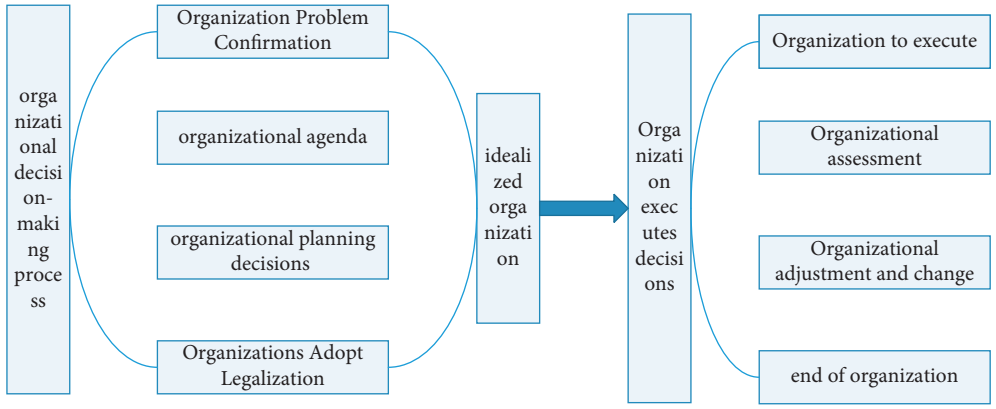

Figure 2: Organizational structure innovation process.

alternative plans. In addition, the value tendency and risk preference of organizational decision-makers, the actual resource conditions possessed by the enterprise organization, and the coordination of various interests within the organization are also important factors that affect the choice of innovative plans for enterprise organizational structure.

(2) Organization and implementation stage. (1) Organizational execution: the implementation of organizational structure innovation by the enterprise is the final confirmation of the innovation plan by the entire organization and is transferred to a controlled release. The specific content includes the acquisition of resources, the preparation of relevant documentation and manuals, and the training of organizational members. The final and crucial step is implementation because no matter how excellent an organization structure innovation plan an enterprise chooses, the implementation of the innovation plan largely determines whether the plan can achieve the ideal goal of organizational structure innovation. (2) Organizational evaluation: this stage evaluates the innovation effect of enterprise organizational structure. Enterprises need to generate a complete and effective evaluation index system according to the ultimate goal of organizational structure innovation, use this as a standard to make accurate value judgments on the effect evaluation of the organizational structure innovation process of enterprises, and provide feedback information according to the judgment for future improvement. The evaluation content in this process mainly includes the following aspects: suitability of organizational goals; input-output efficiency of organizational structure innovation; adequacy of organizational performance; actual performance of organizational structure innovation; resource input quality and allocation; the evaluation of the situation; the fairness of the organization's formulation and implementation; the coordination of the internal interests of the organization; and the impact on the overall development of the enterprise. (3) Organization adjustment and improvement: this stage is the consolidation and adjustment of the innovation process of the enterprise organizational structure. Consolidate and adjust the organizational structure innovation of the enterprise according to the evaluation of the organizational structure innovation effect. If the effect of the organizational structure innovation is more significant and achieves the corporate organizational structure innovation goal set in advance, then the existing innovation achievements will be consolidated. If the organizational structure innovation effect is not very good, then the organizational structure innovation plan must be carried out. Improve and adjust, and then implement the improved and adjusted program. If the final organizational structure innovation result is far from the original target, it is impossible to achieve the goal of organizational structure innovation through timely improvement and adjustment of the organizational structure innovation plan. Implement new innovation activities under the newly formulated organizational structure innovation goals. (4) The end of the organization means the end of organizational structure innovation activities. To sum up, the general organizational structure innovation is divided into two stages, and each stage has four subprocesses. The first is the decision-maker's process on what action to take for the organizational problem, which includes four subprocesses in the first stage: the occurrence and identification of the problem; the problem included in the organizational agenda; organizational planning and change; and organizational adoption and legalization change. Then, an idealized organizational structure innovation is formed through organizational formulation; then, it is transferred to the organizational execution stage of organizational structure innovation. The four subprocesses of this stage are organizational implementation, organizational evaluation, organizational adjustment and change, and organizational termination. The specific process is shown in Figure 2.

3.2.2. Characteristics of Organizational Structure Innovation Process. Through the general process model of organizational structure innovation, we can see that organizational structure innovation is a cycle with dynamic, systematic uncertainty and regular changes in the process of risk. Therefore, the process of organizational structure innovation has the following characteristics: (1) organizational structure innovation is a reciprocating and cyclical process. The organizational structure innovation process is different from the previous production process. It is often through repeated cycles between several steps in the innovation process to finally achieve the goal of improving organizational efficiency that the enterprise expects. (2) The process of organizational structure innovation is dynamic and systematic. The process of enterprise organizational structure innovation is dynamic and changes with time. Enterprises in different life cycle stages have different organizational characteristics. In different life cycle stages, the innovation of enterprise organizational structure needs to be adjusted accordingly. In addition, in the process of organizational structure innovation, members of the organization organically combine a series of resources in the enterprise and the organization to achieve the purpose of preorganizational structure innovation. This involves all aspects of the enterprise coorganization system. The process of structural innovation is an uncompromising complex system engineering. (3) The process of organizational structure innovation is uncertain and risky. Because, in most cases, the environment of organizational structure innovation is not static and there are many uncontrollable factors within the enterprise organization, such as the way of thinking and code of conduct of the people inside the organization, and because people's cognitive ability to things is limited, we cannot fully understand and recognize the innovation process and cannot fully and effectively solve various problems in the innovation process. It has also been affected to varying degrees [16].

The process of organizational structure innovation is not only a simple change in the organizational structure or organizational procedures of an enterprise, but a reasonable and stable arrangement of human, material, and financial resources and their structure in the enterprise or organization, which means the combination of enterprise resources. The change of the method requires breaking the internal balance of the original organization, and the breaking of this balance can easily lead to the loss of control of enterprise management, coupled with the uncertainty of the process of organizational structure innovation itself, which means that the process of organizational structure innovation is full of risks for businesses.

4. An Empirical Study on the Impact of IoT Manufacturing Technology Companies on Organizational Structure Innovation

4.1. Study Design and Research Methods. This study used the empirical research method of a questionnaire survey. The content of the questionnaire is the organizational innovation climate scale and the personal innovation behavior scale. The organizational innovation climate scale is mainly based on the KEY scale of amabile and borrowed from the revision of the KEY scale based on the Chinese background by Jian Qiu Haozheng, Sun Rui, and Liu Yun, among others. The personal innovation behavior scale was designed based on Scott and Bruce's three-stage model of innovation behavior and Janssen's scale on innovation behavior. Questionnaire scores of the two scales are through the summary, induction, sorting, testing, item analysis, exploratory factor analysis, and confirmatory factor analysis. Among them, the organizational innovation climate scale contains six dimensions and 24 items, and the personal innovation behavior scale contains eight items. The formal measurement items passed the reliability and validity test, which proved that the organizational innovation climate in the background of advanced manufacturing technology enterprises could be improved by colleagues support (CS), supervisor support (SS), organizational philosophy (OV), resource provision (RS), task characteristics (TC), knowledge support (KS), and other six aspects are measured and evaluated. The personal innovation behavior of employees in IoT manufacturing technology enterprises can be measured and evaluated in two aspects: the generation of innovative ideas ($F1$) and the implementation of innovative ideas ($F2$). The research questionnaire showed good reliability and validity. Both the organizational innovation climate questionnaire and the personal innovation behavior questionnaire are designed in the form of a five-point Likert scale because, in most cases, the five-point scale is the most reliable, and if the options exceed five points, it is difficult for ordinary people to distinguish enough. The three-point scale limits the expression of moderate and strong opinions, and the five-point scale can express the difference between moderate and strong opinions. The respondents choose according to their actual situation in the enterprise and the degree of agreement for each item. In the innovation climate questionnaire, "1" means strongly disagree, "5" means strongly agree, "1" in the innovation behavior questionnaire means never innovating, and "5" means very frequent innovation. At the same time, the questionnaire adopts the method of filling in the blanks and selection and also collects the personal background information of the respondents, including age, gender, education, position, and tenure of service.

4.1.1. Sample Selection and Data Sources and Distribution. The research object of this research is knowledge workers in enterprises applying advanced manufacturing technology. According to the principle of improving the efficiency of questionnaire recovery as much as possible and meeting the required samples, the formal questionnaire survey was conducted by two methods. One is to distribute questionnaires to colleagues through familiar students working in companies that apply advanced manufacturing technology. Good relationships among colleagues and ease of contact ensured high questionnaire recovery rates and questionnaire validity. The second method is to collect questionnaires by sending web-mails to enterprises applying advanced manufacturing technology. This method is inefficient and

has poor recovery. The validity of the questionnaire is also high. The questionnaire survey was carried out from August to September 2010. A total of 200 questionnaires were distributed by the first method, and 175 valid questionnaires were recovered. The effective recovery rate of the questionnaire was 87.5%. A total of 100 questionnaires were distributed by the second method, 34 valid questionnaires were recovered, and the effective recovery rate of the questionnaires was 34%. A total of 300 questionnaires were distributed, and 209 valid questionnaires were recovered, and the effective recovery rate was 70%.

4.1.2. Questionnaire Test Method

(1) Correlation Analysis of questionnaire items: each variable measurement item in this paper reflects related constructs and concepts, so item scores should be moderately related to each other. If an item has a very low correlation coefficient with all or most other items (often with < 0.03 as the criterion), then the item cannot be part of the scale. If one item is highly correlated with most other items (often by > 0.70), then it is questionable as an independent measure of the scale (Tang, 1999). In this study, 0.70 was used as the criterion for selecting topics. Item-total correlation analysis (Corrected Item-Total Correlation, CITC for short) is one of the methods to purify measurement questions. The CITC analysis follows the following principles: all the items whose CITC is less than 0.40 and which can increase Cronbach's alpha coefficient should be deleted (Tian, Bearden, and Hunter, 2001). Therefore, we use 0.40 as the critical criterion to decide the choice of measurement items.

(2) Reliability analysis of questionnaire items: the commonly used information test method in the Likert attitude scale is Cronbach's alpha coefficient method. For item selection, the internal reliability of each subscale is mainly measured by the degree of change of the α coefficient before and after item deletion to test whether the items are really the theoretical constructs that are intended to measure the design and to what extent are all items that measure the same constructs internally consistent. The larger the Cronbach's alpha value, the better the correlation between the questionnaire items and the higher the reliability of internal consistency. In general, Cronbach's alpha values greater than 0.8 indicate excellent internal consistency, values between 0.6 and 0.8 indicate good internal consistency, and values below 0.6 indicate poor internal consistency. The scholar Gay (1992) believed that the reliability coefficient of any test or scale above 0.90 means the reliability is very good. Scholars have different opinions on the acceptable minimum reliability coefficient, such as 0.70 (De Vellis, 1991; Nunnally, 1978) and 0.80 (Bryman and Cramer, 1997). However, most believe that if the reliability is below 0.60, it is appropriate to revise the research tool. In this study, the standard of Cronbach's alpha was set to 0.70.

(3) Exploratory factor analysis of questionnaire items: exploratory factor analysis is to test whether all items theoretically belonging to the same dimension can clearly form a common factor with the largest extraction variance ratio so that the connotation of this dimension can be expressed and conceptualized. In this study, the KMO (Kaiser–Meyer–Olkin) measure and Bartlett's sphericity test were used to judge whether the samples were suitable for factor analysis. The KMO value is used to judge the standard as shown in table 1, and the Bartlett sphericity test generally only needs to reach a significant level. Then, the principal component analysis method and the maximum variance method are used to rotate and solve the common factor, the eigenvalue is greater than 1, the gravel diagram determines the number of factor extractions, the factor loading is less than 0.50 as the topic selection scale, and the cumulative variance explanation rate of the extracted factors is not less than 50%. At the same time, the item with cross-factor loading exceeding 0.40 (Gorsuch, 1983) is not allowed. Otherwise, the item will be deleted, as shown in Table 1.

(4) Questionnaire item validity analysis: the construct validity of the questionnaire was analyzed by confirmatory factor analysis. It can test the stability of a scale structure and can also simplify the items obtained by exploratory factor analysis. Judging whether a model and data are well fitted is usually judged by combining absolute fitting indicators and relative fitting indicators. Absolute fitting indicators include x^2/df, GFI, AGFI, NCP, ECVI, RMR, and RMSEA; relative fitting indicators include CFI, NFI, IFI, TLI, and RFI. In this study, the indicators of x^2/df, RMSEA, IFI, TLI, CFI, and GFI will be combined to judge the degree of model fit [17–20].

(1) x^2/df (view fit index): the fit index x^2/df value refers to a statistic that directly tests the similarity between the sample covariance matrix and the estimated covariance matrix and can be used to measure the overall fit of the model and try to correct the model with a low degree of fit. It is generally believed that when $x^2/df < 3$, the model fits better; the closer the x^2/df value is to 1, the better the model fits, $x^2/df > 2$ is an ideal result, $2 < x^2/df < 5$ indicates that the overall model is acceptable; $x^2/df > 5$ indicates that the observed data do not fit the model well, $x^2/df > 10$ indicates that the observed data does not fit the model, and the model is very poor.

(2) Root Mean Square Error of Approximation (RMSEA) is more sensitive to the error model and easily explains the quality of the model; the RMSEA index is less affected by the sample size and is a widely used fitting index in recent years

Table 1: KMO indicator standards.

KMO value	>0.90	0.80–0.90	0.70–0.80	0.60–0.70	0.50–0.60	<0.50
Standard	Very suitable	Suitable	Generally	Barely fit	Not suitable	Unacceptable

one. The variation interval of RMSEA is between 0 and 1, and it is generally believed that the closer to 0, the better. When RMSEA is less than 0.05, it indicates that the model fits very well; if it is greater than 0.05 and less than 0.08, it indicates that the model fits well; and if it is greater than 0.08 and less than 0.1, the model is acceptable.

(3) Incremental Fit Index (IFI) is generally in the range of 0 to 1, and the closer to 1, the better the fit. It is generally believed that greater than 0.9 indicates a good fit, and if IFI is greater than 0.8, the model is considered acceptable.

(4) Tucker–Lewis index (TLI), a nonstandard fitting index, is generally in the range of 0 to 1. The closer TLI is to 1, the better the fitting degree is. It is generally considered that a TLI greater than 0.9 indicates a good fit, and a TLI greater than 0.8 indicates that the model is acceptable.

(5) Comparative Fit Index (CFI): the variation range of CFI is between 0 and 1. The closer it is to 1, the better the degree of fit is. If the CFI is greater than 0.9, it is considered that the model has a good fit. When the CFI is greater than 0.8, the model is considered acceptable.

(6) Goodness of Fit Index (GFI): the variation interval of GFI is between 0 and 1. The closer it is to 1, the better the degree of fit is. If the GFI is greater than 0.9, it is considered that the model has obtained better results. If the GFI is greater than 0.8, the model is considered acceptable.

4.1.3. Structural Equation Model of Organizational Innovation Climate and Individual Innovation Behavior. Most studies believe that organizational innovation climate has a positive predictive effect on individual innovation behavior, whereas some studies believe that organizational innovation climate has no relationship with organizational innovation behavior. This paper focuses on the organizational innovation climate and organizational innovation behavior of IoT manufacturing technology enterprises. The relationship is further explored, and the following assumptions are made:

Hypothesis 1. Colleague support has a positive impact on individual innovative ideas.

Hypothesis 2. Colleague support has a positive effect on the implementation of individual innovative ideas.

Hypothesis 3. Supervisor support has a positive impact on individual innovative ideas.

Hypothesis 4. Supervisor support has a positive effect on the implementation of individual innovative ideas.

Hypothesis 5. Organizational philosophy has a positive impact on individual innovative ideas.

Hypothesis 6. Organizational philosophy has a positive impact on the implementation of individual innovative ideas.

Hypothesis 7. Resource supply has a positive impact on individual innovative ideas.

Hypothesis 8. Resource supply has a positive impact on the implementation of individual innovative ideas.

Hypothesis 9. Task characteristics have a positive impact on individual innovative ideas.

Hypothesis 10. Task characteristics have a positive impact on the implementation of individual innovative ideas.

Hypothesis 11. Knowledge support has a positive impact on individual innovative ideas.

Hypothesis 12. Knowledge support has a positive impact on the implementation of individual innovative ideas. By combining the above 12 assumptions, the structural equation model of the two groups of variables can be shown in Figure 3.

4.2. Questionnaire Test Results

4.2.1. Construct Validity Analysis of Organizational Innovation Climate Scale. According to the output results of the AMOS fitting model analysis, we summarize the main indicators in the validity analysis as shown in Table 2. The structural validity of the organizational innovation climate questionnaire is acceptable.

As shown in the results, after the confirmatory factor analysis of the factor structure model, the fitting indexes all reach the ideal level. Therefore, goal orientation can be divided into six clear dimensions: peer support, supervisor support, organizational philosophy, resource supply, task characteristics, and knowledge support, as shown in Figure 4.

4.2.2. Analysis of the Construct Validity of the Personal Innovation Behavior Atmosphere Scale. According to the output results of the AMOS fitting model analysis, we summarize the main indicators in the validity analysis as shown in Table 3. According to the above-mentioned main indicators and each indicator judgment standard, the

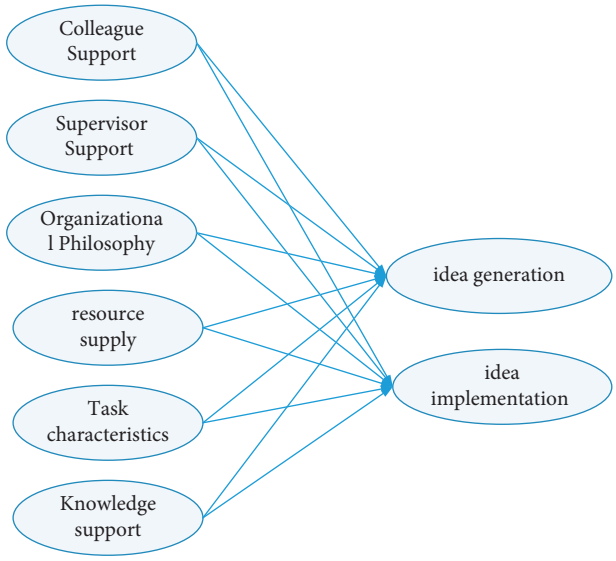

Figure 3: Hypothetical model.

Table 2: Confirmatory factor analysis of organizational innovation climate.

Variable	Fit metrics					
	x^2/df	RNSEA	IFI	TLI	CFI	GFI
Six-factor structure	1.617	0.064	0.862	0.834	0.875	0.821

RNSEA value reaches 0.100, and the minimum requirement is the personal innovation behavior questionnaire. Construct validity is okay.

As shown in the results, after the confirmatory factor analysis of the factor structure model, each fitting index has reached the ideal level. Therefore, goal orientation can be divided into two clear dimensions: the generation of innovative ideas and the implementation of innovative ideas, as shown in Figure 5.

4.3. Verification of the Organizational Innovation Atmosphere and Individual Innovation Relationship Structure Model of IoT Manufacturing Technology Enterprises. Based on the previous analysis, we use AMOS 7.0 to verify the hypothesis model of the relationship between organizational innovation climate and individual innovation behavior, as shown in Figure 6. The fitting index of the model is shown in Table 4. From the fitting index, it is assumed that the fitting degree of the model is good.

According to the verification results of the hypothesis structural equation model by the AMOS 7.0 software, as shown in Figure 6, in the IoT manufacturing technology enterprise, for hypothesis 1, the nonstandard regression coefficients of CS and $F1$ are 0.52, indicating that the support level of each colleague is 0.52. With an increase of one unit, the generation of individual innovative ideas will increase by 0.52 units; for hypothesis 2, when the nonstandard regression coefficients of parameters CS and $F2$ are 0.47, it indicates that for each unit increase in the support level of colleagues, the implementation of individual innovative ideas will increase by 0.47 units; for hypothesis 3, the nonstandard regression coefficients of parameters SS and $F1$ is 0.38, indicating that for each unit of supervisor support, the generation of individual innovative ideas will increase by 0.38 units; for hypothesis 4, the nonstandard regression coefficients of parameters SS and $F2$ are 0.25, indicating that each unit of supervisor support will increase individual innovative idea implementation students by 0.25 units; for hypothesis 5, the nonstandard regression coefficients of OV and $F1$ are 0.44, the generation of individual innovative ideas will increase by 0.44 units; for hypothesis 6, the standard regression coefficients of OV and $F1$ are 0.32, indicating that, for each unit increase in organizational concept level, the implementation of individual innovative ideas will increase by 0.32 units; for assuming hypothesis 7, the nonstandard regression coefficients of RS and $F1$ are 0.48, indicating that, for each unit increase in resource supply level, the generation of individual innovative ideas will increase by 0.48 units; for hypothesis 8, the nonstandard regression coefficients of RS and $F2$ is 0.50, indicating that, for each unit increase in resource supply level, the implementation of individual innovative ideas will increase by 0.50 units; for hypothesis 9, the nonstandard regression coefficients of TC and $F1$ are 0.43, indicating that, for each unit increase in task characteristic level, the generation of innovative ideas will increase by 0.43 units; for hypothesis 10, the nonstandard regression coefficients of TC and $F2$ are 0.52, indicating that, for each unit increase in the task characteristic level, the implementation of individual innovative ideas will increase by 0.52 units; for hypothesis 11, the nonstandard regression coefficients of KS and $F1$ are 0.40, indicating that, for each unit of knowledge support, the generation of individual innovative ideas will increase by 0.40 units; and for hypothesis 12, the nonstandard regression coefficients of KS and $F2$ are 0.36, indicating that, for each additional unit of knowledge support, the implementation of individual innovative ideas will increase by 0.36 units. [21–24].

To sum up, the organizational innovation climate has a significant positive impact on the innovation behavior of individuals in the organization. All 12 hypotheses have been verified, indicating that, in IoT manufacturing technology enterprises, people who are the main body of innovation, regardless of the factors that affect innovation in the organization, will have a certain impact on their innovation behavior. In particular, the stimulation, encouragement, and support of individuals' innovative behaviors by enterprises, to a large extent, determines whether the organization can successfully develop its innovative ability and dynamic adaptability. Therefore, the higher the organizational innovation atmosphere, the greater the promotion of individual innovation behavior, and the improvement of individual innovation ability has a positive effect on organizational structure innovation through the function of seeking maximum consistency in organizational management. The greater the promotion effect, the more conducive to improving the organizational structure innovation of IoT manufacturing technology enterprises.

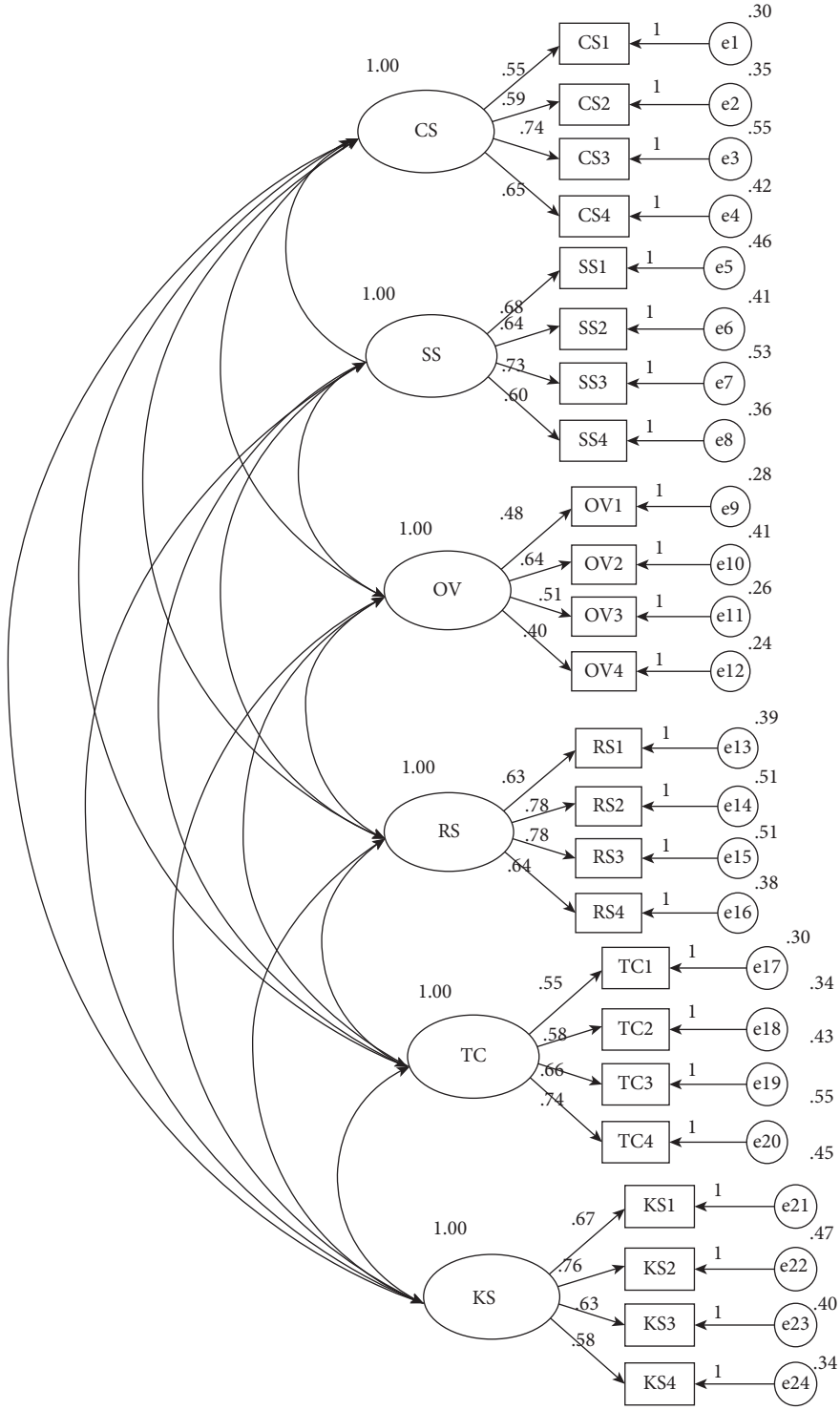

Figure 4: First-order six-factor structural model.

Table 3: Confirmatory factor analysis of personal innovation behavior.

Variable	Fit metrics					
	x^2/df	RNSEA	IFI	TLI	CFI	GFI
Two-factor structure	2.554	0.100	0.839	0.751	0.831	0.919

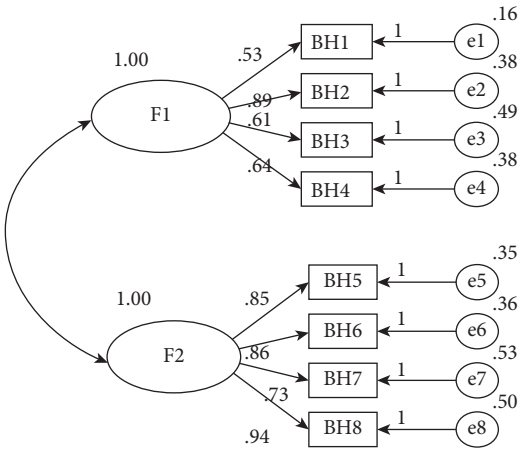

Figure 5: First-order two-factor structural model.

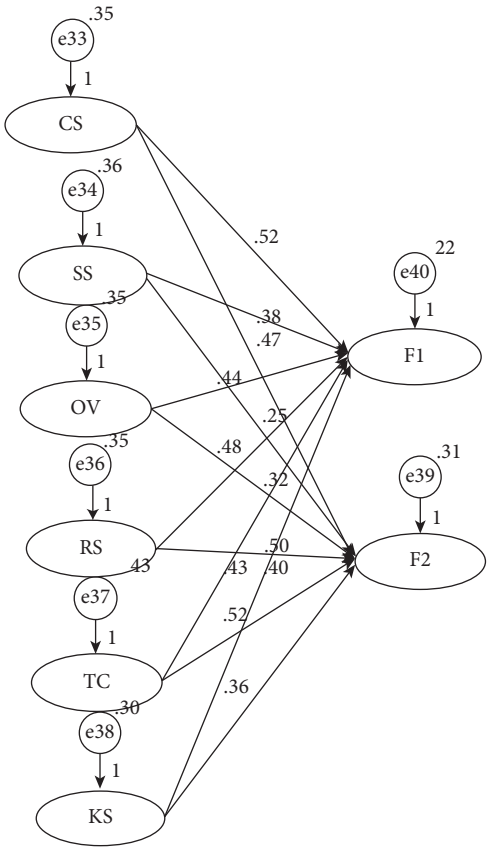

Figure 6: Hypothetical structural equation model.

Table 4: Hypothetical model fit metrics.

x^2/df	RNSEA	IFI	TLI	CFI	GFI
2.526	0.081	0.803	0.826	0.897	0.853

5. Conclusion

In recent years, there has been a wave of research and application of advanced manufacturing technology around the world. With the wide application of advanced manufacturing technology in China, many enterprises have obtained better benefits. However, many enterprises still fail when implementing IoT manufacturing technologies. The fundamental reason is that the traditional organizational management model of Chinese enterprises cannot well match the manufacturing technology of the Internet of Things, which restricts the development of the manufacturing technology of the Internet of Things. In order to maximize the benefits brought by IoT manufacturing technology, enterprises must learn to transform the traditional organizational management structure to adapt to the production requirements of advanced manufacturing technology. It is imperative to innovate the organizational structure of IoT manufacturing technology enterprises. The research of this paper not only has important theoretical significance for the development and enrichment of the theory of organizational innovation power and process theory of IoT manufacturing technology enterprises but also provides information on factors such as organizational innovation atmosphere and innovative behavior with others that affect the organizational innovation of IoT manufacturing technology enterprises. Empirical analysis research has strong practical application value. It provides a theoretical basis and useful reference for the organizational innovation practice activities of IoT manufacturing technology enterprises. The main points and conclusions are as follows.

This research conducted a questionnaire survey on the innovation atmosphere of enterprise organizations and individual innovation behavior among employees of enterprises applying advanced manufacturing technology, obtained empirical data, and used SPSS 18.0 to conduct statistical analysis on the data and questionnaire. Exploratory factor analysis, reliability analysis, and confirmatory factor analysis are mainly used to analyze the factor structure of the questionnaire, and each factor structure has good reliability and validity. Using AMOS 7.0 to verify the structural equation model of the hypothetical corporate organizational innovation climate and individual innovation behavior, it is concluded that the corporate organizational innovation climate has a significant positive impact on people's innovation behavior in IoT manufacturing technology enterprises. Organizational innovation climate plays a role in organizational structure innovation through the positive influence of individual innovation behaviors in an organization. The positive relationship between organizational innovation climate and individual innovation behaviors means that IoT manufacturing technology enterprises can achieve a higher degree of organizational structure. Innovation provides a valuable reference.

Data Availability

The dataset can be accessed upon request.

Conflicts of Interest

The authors declare that they have no conflicts of interest.

References

[1] R. E. Hoskisson, L. Eden, C. M. Lau, and M. Wright, "Strategy in emerging economies," *Academy of Management Journal*, vol. 43, no. 3, pp. 249–267, 2000.

[2] P. Junni, R. M. Sarala, V. Taras, and S. Y. Tarba, "Organizational ambidexterity and performance: a meta-analysis," *Academy of Management Perspectives*, vol. 27, no. 4, pp. 299–312, 2013.

[3] V. Parida, M. Westerberg, and J. Frishammar, "Inbound open innovation activities in high-tech SMEs: the impact on innovation performance," *Journal of Small Business Management*, vol. 50, no. 2, pp. 283–309, 2012.

[4] J. L. Hervas-Oliver, F. Sempere-Ripoll, and C. Boronat-Moll, "Process innovation strategy in SMEs, organizational innovation and performance: a misleading debate?[J]," *Small Business Economics*, vol. 43, no. 4, pp. 873–886, 2014.

[5] T. Takalo, T. Tanayama, and O. Toivanen, "Estimating the benefits of targeted R&D subsidies," *The Review of Economics and Statistics*, vol. 95, no. 1, pp. 255–272, 2013.

[6] P. Saariluoma, E. Kannisto, and T. Kujala, "Analysing micro-innovation processes:universities and enterprises collaboration[J]," *Communications of the IBIMA*, vol. 9, no. 3, pp. 19–23, 2009.

[7] C. Yu and A. Matta, "A statistical framework of data-driven bottleneck identification in manufacturing systems," *International Journal of Production Research*, vol. 54, no. 21, pp. 6317–6332, 2016.

[8] M. Reid, E. J. Hultink, T. Marion, and G Barczak, "The impact of the frequency of usage of IT artifacts on predevelopment performance in the NPD process," *Information & Management*, vol. 53, no. 4, pp. 422–434, 2016.

[9] T. Mauerhoefer, S. Strese, and M. Brettel, "The impact of information technology on new product development performance," *Journal of Product Innovation Management*, vol. 34, no. 6, pp. 719–738, 2017.

[10] M. T. Akcura and Z. D. Ozdemir, "Data-driven manufacturer-retailer collaboration under competition," *Enterprise Information Systems*, vol. 13, no. 3, pp. 303–328, 2019.

[11] H. S. Ismail and H. Sharifi, "A balanced approach to building agile supply chains," *International Journal of Physical Distribution & Logistics Management*, vol. 36, no. 6, pp. 431–444, 2006.

[12] V. Sambamurthy and B. V. Grover, "Grover shaping agility through digital options: reconceptualizing the role of information technology in contemporary firms," *MIS Quarterly*, vol. 27, no. 2, pp. 237–263, 2003.

[13] W. D. Hoyer, R. Chandy, M. Dorotic, M. Krafft, and S. S Singh, "Consumer cocreation in new product development," *Journal of Service Research*, vol. 13, no. 3, pp. 283–296, 2010.

[14] P. Pisano, M. Pironti, and A. Rieple, "Identify innovative business models: can innovative business models enable players to react to ongoing or unpredictable trends?" *Entrepreneurship Research Journal*, vol. 5, no. 3, pp. 81–99, 2015.

[15] T. H. Davenport, "How strategists use 'big data' to support internal business decisions, discovery and production[J]," *Strategy & Leadership*, vol. 42, no. 4, pp. 45–50, 2014.

[16] G. Troilo, L. M. De Luca, and P. Guenzi, "Linking data-rich environments with service innovation in incumbent firms: a conceptual framework and research propositions," *Journal of Product Innovation Management*, vol. 34, no. 5, pp. 617–639, 2017.

[17] P. M. Hartmann, M. Zaki, N. Feldmann, and A Neely, "Capturing value from big data – a taxonomy of data-driven business models used by start-up firms," *International Journal of Operations & Production Management*, vol. 36, no. 10, pp. 1382–1406, 2016.

[18] B. Baldassarre, G. Calabretta, N. M. P. Bocken, and T Jaskiewicz, "Bridging sustainable business model innovation and user-driven innovation: a process for sustainable value proposition design," *Journal of Cleaner Production*, vol. 147, no. 1, pp. 175–186, 2017.

[19] M. L. Markus, "New games, new rules, new scoreboards: the potential consequences of big data," *Journal of Information Technology*, vol. 30, no. 1, pp. 58-59, 2015.

[20] S. Lenka, V. Parida, and J. Wincent, "Digitalization capabilities as enablers of value Co-creation in servitizing firms," *Psychology and Marketing*, vol. 34, no. 1, pp. 92–100, 2017.

[21] R. B. Duncan, "the ambidextrous organization: designing dual structures forinnovation[J]," *Management of Organization Design*, pp. 167–188, 1976.

[22] J. G. March, "Exploration and exploitation in organizational learning," *Organization Science*, vol. 2, no. 1, pp. 71–87, 1991.

[23] C. Andriopoulos and M. W. Lewis, "Exploitation-exploration tensions and organizational ambidexterity: managing paradoxes of innovation," *Organization Science*, vol. 20, no. 4, pp. 696–717, 2009.

[24] M. L. Tushman and C. A. O'Reilly, *Winning through innovation[M]*, p. 23, Harvard Business School Press, Boston, 1997.

Hindawi
Scientific Programming
Volume 2023, Article ID 9787612, 1 page
https://doi.org/10.1155/2023/9787612

Retraction

Retracted: Impact of Carbon Information on Enterprise Value: Analysis Model Design Based on Big Data

Scientific Programming

Received 18 July 2023; Accepted 18 July 2023; Published 19 July 2023

This article has been retracted by Hindawi following an investigation undertaken by the publisher [1]. This investigation has uncovered evidence of one or more of the following indicators of systematic manipulation of the publication process:

(1) Discrepancies in scope
(2) Discrepancies in the description of the research reported
(3) Discrepancies between the availability of data and the research described
(4) Inappropriate citations
(5) Incoherent, meaningless and/or irrelevant content included in the article
(6) Peer-review manipulation

The presence of these indicators undermines our confidence in the integrity of the article's content and we cannot, therefore, vouch for its reliability. Please note that this notice is intended solely to alert readers that the content of this article is unreliable. We have not investigated whether authors were aware of or involved in the systematic manipulation of the publication process.

Wiley and Hindawi regrets that the usual quality checks did not identify these issues before publication and have since put additional measures in place to safeguard research integrity.

We wish to credit our own Research Integrity and Research Publishing teams and anonymous and named external researchers and research integrity experts for contributing to this investigation.

The corresponding author, as the representative of all authors, has been given the opportunity to register their agreement or disagreement to this retraction. We have kept a record of any response received.

References

[1] C. Kong and Y. Zhao, "Impact of Carbon Information on Enterprise Value: Analysis Model Design Based on Big Data," *Scientific Programming*, vol. 2022, Article ID 6180988, 8 pages, 2022.

Hindawi
Scientific Programming
Volume 2022, Article ID 6180988, 8 pages
https://doi.org/10.1155/2022/6180988

Research Article

Impact of Carbon Information on Enterprise Value: Analysis Model Design Based on Big Data

Cong Kong[1,2] and Yu Zhao[3]

[1]*School of Earth Sciences and Resources, China University of Geosciences Beijing, 29 Xueyuan Road, Beijing 100083, China*
[2]*CITIC Metal Co., Ltd., No.6 Xinyuan South Road, Beijing 100004, China*
[3]*China Center for Information Industry Development, Beijing, China*

Correspondence should be addressed to Yu Zhao; zhaoyu@ccidthinktank.com

Received 26 June 2022; Revised 9 July 2022; Accepted 13 July 2022; Published 9 August 2022

Academic Editor: Lianhui Li

Investors pay more and more attention to the issue of climate change information disclosure of listed companies. Whether the company can effectively deal with the impact of climate change on its own operations and make reasonable information disclosure will undoubtedly affect the value of the enterprise. Aiming at this, an analysis model based on big data is designed for the impact of carbon information on enterprise value. This study selects the sample stocks of the Shanghai Stock Exchange responsibility index every year as the research sample, counts the carbon information through the social responsibility reports of listed companies, and uses the index method to score the carbon information of each company to measure the quality of carbon information disclosure. Firstly, it analyzes the situation of carbon information disclosure in China through descriptive statistics and then constructs relevant models to conduct an empirical analysis on the impact of carbon information disclosure on enterprise value.

1. Introduction

Enterprise environmental information includes many aspects, and carbon information is also an important aspect, including enterprise carbon emission reduction strategy, carbon emission accounting standards and methods, and so on. The carbon disclosure project (hereinafter referred to as CDP) is an independent nonprofit organization, which aims to open up a special disclosure channel for climate change and provide information support for investors, nongovernmental organizations, and policymakers [1–4]. Among the enterprises that have accepted the CDP questionnaire and disclosed carbon information to them, the enterprises in Europe and the United States have always been in the leading position, and their carbon information disclosure in the CDP questionnaire is more specific and perfect, and the degree of disclosure is relatively high [1–5].

The high-quality carbon information disclosure of these foreign enterprises has been actively promoted by investors and local laws and regulations [6, 7]. The US government promulgated the mandatory greenhouse gas reporting system in 2009, which stipulates that certain special industries and companies that emit more than 25000 tons of greenhouse gas per year must report to the EPA. In the UK, regulations related to mandatory information disclosure are also under discussion. Japanese government departments, Canada, and Australia began to implement the system of reporting greenhouse gas emissions to relevant departments in 2004 and 2007, respectively [8–10]. Based on the above information, we can see that the government continues to put forward and improve the management system to continuously improve the information disclosure level of enterprises, and at the same time, the business risk of enterprises will also increase [11–15]. This situation will not only affect the specific response measures for enterprise emission reduction but also affect the enterprise value and future development path.

People pay more attention to climate change and have a deeper awareness of environmental protection [16]. Investors and stakeholders have begun to pay attention to whether

the products and services of enterprises are low-carbon, the company's carbon footprint, carbon trading, etc. The regulatory risks, product risks, technical risks, and physical risks related to climate change will have an impact on the company's asset portfolio and cost level [17–19]. The global economy is slowly changing into a low-carbon form, which will have a great impact on the competitiveness and long-term valuation of enterprises, which is gradually realized by people in the capital market. After disclosing carbon information to the public, the company will send a signal to the capital market, representing that the company will carry out management activities related to carbon emissions, which will have an impact on the value of the enterprise. After experiencing this series of situations, the resources in the market will be redistributed among the successful and neglected enterprises.

At this stage, the level of carbon information disclosure of Chinese companies is not high, and it is still in the initial stage. Among all the listed companies, there are not many companies that disclose carbon information. Even among the enterprises that disclose carbon information, the disclosure content lacks standardization and comprehensiveness. The research of this article can make enterprises aware of the significance of carbon information disclosure so as to improve the level and quality of carbon information disclosure in Chinese enterprises. In this way, the company's image has been well packaged, and the international competitiveness and social status of Chinese enterprises have also been strengthened. The research content of this article can provide suggestions on carbon information disclosure for government regulators and relevant policymakers. By analyzing the current situation of carbon information disclosure in China, this article puts forward some suggestions that the carbon information disclosure of Listed Companies in China can be integrated with the mainstream reports and formulates relevant laws and regulations to improve the content and form of carbon information disclosure, which can make carbon information disclosure more standardized and decision-making more effective.

2. Analysis Model Design

2.1. Sample Selection and Data Sources. This article selects A shares listed on the Shanghai Stock Exchange (SSE), uses the constituent stocks of the Shanghai Stock Exchange Social Responsibility Index each year as a research sample, and retrieves their social responsibility reports disclosed in 2012–2015. The SSE Social Responsibility Index takes the stocks of companies listed on the Shanghai Stock Exchange that have performed better in social responsibility in the corporate governance sector as constituent stocks, then the index thus compiled. In the research process, this article conducts the following screening on the research samples:

(1) Excluding the financial industry.

(2) The sample companies in this study require complete data in all aspects, so companies with incomplete disclosure data are excluded.

After screening, a total of 337 pieces of eligible data were found. The annual composition of the sample companies is shown in Table 1.

The sample data are from CSMAR and WIND, and the social responsibility report is searched and downloaded from https://www.cninfo.com.cn. The explanatory variable carbon information disclosure index (CDI) is scored manually from the social responsibility reports downloaded by each sample company.

2.2. Variable Selections

2.2.1. Explained Variables: Enterprise Value. Many indicators can measure enterprise value, and the key is to divide them into accounting and market indicators. Since enterprise value is a long-term dynamic concept. However, accounting indicators are only historical indicators, and the reflected information is not comprehensive. If accounting indicators are used to measure the value of an enterprise. It is easy to produce short-sighted situations, and it is easy to make inaccurate estimates of the future risks and development status of enterprises. Accounting indicators are relatively unstable, easily manipulated, and easily affected by relevant accounting data. Judging from the above situations, the accounting indicators cannot accurately and comprehensively reflect the real operating conditions of the enterprise. Therefore, it is not suitable as an indicator to accurately reflect an enterprise value.

As a market indicator, Tobin's Q reflects the relative value of an enterprise [20, 21]. Tobin's Q is not easy to manipulate and avoids fluctuating stock prices. EVA, which is also a market indicator, also needs to be calculated, which is relatively complicated and relatively difficult to determine.

2.2.2. Explanatory Variable: Carbon Information Disclosure Index. When designing the CDI score table, this study takes the stakeholder theory as the theoretical basis, combined with previous scholars' research on environmental information disclosure and the content of carbon information disclosure in the CDP questionnaire. At the same time, combined with the actual situation of my country's listed companies, a carbon information disclosure evaluation system suitable for Chinese enterprises is constructed.

Most scholars use the index method when studying environmental information disclosure. It was indicated that the index method could more accurately describe and evaluate social responsibility information. And many foreign scholars have used this method in their studies. The main point of attention in using the index method is first to classify the information to be studied, divide it into several major categories, and then subdivide each significant category into multiple subitems. Then you can start to score each item specifically. After each item has been scored, the sum of all scores is the variable indicator to be studied.

CDP China's questionnaire is an important reference for this article. In CDP China's questionnaire, carbon information disclosure is divided into three categories: strategic management, risks and opportunities, and greenhouse gas

Table 1: Annual composition of sample companies.

Year	Number of sample companies	The same number of companies as in the previous year
2012	85	
2013	85	77
2014	86	74
2015	82	72

emissions. Then, under these three categories, we continue to distinguish 12 subindicators such as risks and opportunities brought by climate change and strategic management of carbon emission reduction. The CDI scoring table in this article combines the actual situation of Chinese enterprises and the situation of carbon information disclosure in the corporate social responsibility report. Some deletions and additions are made to the contents of the CDP questionnaire to make it more in line with the actual situation of listed companies in my country. The carbon information disclosure in this article is divided into four categories: strategies for addressing climate change, climate change governance systems and policies, carbon emission reduction measures and actions, and carbon accounting emissions. Then each category is refined and subdivided into 17 small projects, such as corporate emission reduction strategies, and some projects can be divided into qualitative disclosure and quantitative disclosure. Each item is scored against the corporate social responsibility report, with 2 scores for quantitative disclosure, 1 score for qualitative disclosure, and 0 for no disclosure. The total score for the 17 items is 27 scores. After scoring, the total score of each item is CDI. The CDI score judges the detailed level of carbon information disclosure.

After scoring, some scholars will also consider the weight of information and assign different scores to corresponding information according to the different degrees of importance of the information. This study argues that although there may be some differences in the importance of different information, there is also a lot of subjectivity when assigning weights. In this way, the score may be subjectively influenced by the scorer to a large extent. Therefore, the following research did not consider the weight problem but directly added up the scores.

The CDI score table of this study is shown in Table 2:

2.3. Control Variables. According to the previous research of many scholars at home and abroad, it can be learned that many aspects may impact carbon information disclosure. In the following empirical research, we will consider controlling some factors, which will help reflect the impact of carbon information disclosure on corporate value to a greater extent.

2.3.1. Company Size. Social public pressure refers to attracting too much attention from the public, which will bring pressure on oneself. And this pressure is very likely to be affected by the company's expansion. If the company expands, the enterprise scale will be more significant. Therefore, the larger the company expands, the greater the pressure on the public to bear because the more significant the scale of the company, the easier it is to attract attention from all walks of life.

After a series of scientific studies has proved that a series of consequences of climate change will adversely affect enterprises and individuals because it will lead to problems such as resource shortage and air pollution. With the public's attention to this issue, the company began participating in related low-carbon activities. This article's research uses the degree of enterprise development to represent the pressure mentioned above. Because the bigger the company is, the more people related to its interests and other aspects are, and the easier it is to receive attention from the outside world. Therefore, this article believes that the larger the enterprise develops, the more willing to disclose its carbon information to the outside world.

Company size is a variable often used by domestic and foreign scholars to study enterprise value. This article uses the natural logarithm of the company's total assets at the end of the year to measure the company's size. It takes the company's size as a control variable that affects its value, denoted as SIZE.

2.3.2. Ownership Concentration. So far, the academic community has not reached a clear conclusion on whether the impact of equity on enterprise value is positive or negative. This article selects the sum of the top ten shareholders' shareholding ratios in the corresponding annual reports each year to measure the shareholding concentration and control the impact of the shareholding structure on the enterprise value.

2.3.3. Profit Capacity. Investors pay attention to a company's profit capacity before investing in a business. A company's profit capacity also affects many aspects of the business, such as asset liquidity. Based on the existing research, this article regards ROE as a control variable at the end of each year and adds it to the regression model for the calculation to represent profit capacity.

2.3.4. Company Growth. The ability of a company to grow is conducive to enhancing its value. For investors, a company's growth is an essential basis for their investment decisions. The higher the company's growth, the better the future development prospects. In this way, the company's investors will have a good expectation for the company's future stock price. It can be seen from this that the stronger the company's growth, the higher the value of the company in general. Many indicators can measure the company's growth. Combined with some previous studies by scholars, this article uses the operating income growth rate to measure the company's growth.

2.3.5. Industry Attributes. The public expects industries with high-carbon emissions to fulfill more social responsibilities. The nature of the industry to which the company belongs is

Table 2: Carbon information disclosure index (CDI) score.

	Carbon information disclosure project	Introduction
Climate change strategy	(1) Identification of opportunities and risks related to climate change	1 score for disclosure, no score for nondisclosure
	(2) Integrating low-carbon development into business strategies	1 score for disclosure, no score for nondisclosure
	(3) Proposing the concept of low-carbon development	1 score for disclosure, no score for nondisclosure
	(4) Enterprise emission reduction strategy	2 scores for quantitative disclosure, 1 score for disclosure, and no score for nondisclosure
	(5) Responsibility for climate change	1 score for disclosure, no score for nondisclosure
Climate change governance and policy	(6) Setting up a management organization	1 score for disclosure, no score for nondisclosure
	(7) Establishing a reward and punishment incentive mechanism	1 score for disclosure, no score for nondisclosure
Carbon reduction measures and action	(8) Carbon reduction targets	2 scores for quantitative disclosure, 1 score for disclosure, and no score for nondisclosure
	(9) Participation in carbon trading	2 scores for quantitative disclosure, 1 score for disclosure, and no score for nondisclosure
	(10) Publicity and training on carbon emission reduction	2 scores for quantitative disclosure, 1 score for disclosure, and no score for nondisclosure
	(11) Use of low-carbon products and services	1 score for disclosure, no score for nondisclosure
	(12) Enterprises use new technologies to reduce carbon emissions	2 scores for quantitative disclosure, 1 score for disclosure, and no score for nondisclosure
Carbon accounting and emissions	(13) Standard and method of carbon emission surface calculation	2 scores for quantitative disclosure, 1 score for disclosure, and no score for nondisclosure
	(14) Carbon emission performance (emission history, emission intensity, emission reduction)	2 scores for quantitative disclosure, 1 score for disclosure, and no score for nondisclosure
	(15) Energy consumption (energy consumption energy saving, and energy intensity (energy consumption per unit of output value))	2 scores for quantitative disclosure, 1 score for disclosure, and no score for nondisclosure
	(16) Rewards and punishments received by the environmental protection department	2 scores for quantitative disclosure, 1 score for disclosure, and no score for nondisclosure
	(17) Carbon emission reduction costs	2 scores for quantitative disclosure, 1 score for disclosure, and no score for nondisclosure

different, and the level of carbon information disclosure is different. At the same time, the industry attribute may impact the relationship between carbon information disclosure and corporate value. In addition, industry differences may affect the level of carbon information disclosure of enterprises.

According to the list of carbon emissions released by the Chinese Academy of Sciences, the top five industries with carbon emissions are defined as high-carbon emission industries, and the remaining industries are low-carbon emission industries. In this study, the industry attributes are assigned a value of 1 for companies in industries with high-carbon emissions and 0 for companies in industries with low-carbon emissions.

2.3.6. Nature of Ownership. Generally speaking, there is a relatively close relationship between state-owned enterprises and the government. Because of such a relationship, the public believes that state-owned enterprises should shoulder more environmental responsibilities than nonstate-owned enterprises. Our country's state-owned enterprises are different. Compared with other enterprises, they may fulfill more energy conservation and emission reduction responsibilities, and the disclosure of carbon information will be more comprehensive. This study uses the ownership nature of the firm as a control variable. If the state controls the company, then set this item to 1. Otherwise, it is 0; see Table 3.

2.4. Model Construction. This article uses a linear regression equation in an empirical study to examine the impact of a company's carbon disclosure on corporate value. The model used in this article is as follows: in the research, some frequently used variables are selected as control variables in the empirical analysis, such as enterprise size and ownership concentration, using CDI as an independent variable in the model results from scoring the carbon information disclosure index. Tobin's Q was used as the dependent variable in the study [20, 21]. Model 1 is constructed to study the impact of carbon information disclosure on corporate value.

Table 3: Description of research variables.

Variable type	Variable type	Variable symbol	Metrics	Calculation method
Explained variable	Corporation value	Q	Tobin's Q	Tobin's Q value = market capitalization at the end of the year/total assets at the end of the year
Explanatory variables	Carbon information disclosure level	CDI	Carbon disclosure index	Score table
	Company size	SIZE	Total assets	Company size = logarithm of total assets at the end of the year
	Ownership concentration	OCN	Shareholdings of the top ten shareholders	Ownership concentration = the sum of the shareholding ratios of the top ten shareholders
	Profit capacity	ROE	Return on equity	Return on equity = profit after tax/Owner's equity
	Company growth	GROWTH	Operating income growth rate	Company growth = (operating income at the end of the current period – operating income at the end of the previous period)/operating income at the end of the previous period
Control variable	Industry attributes	IND	Virtual variable, whether it is a high-carbon emission industry	According to the list of carbon emissions released by the Chinese Academy of Sciences, the top five industries with carbon emissions are defined as high-carbon emission industries, and the remaining industries are low-carbon emission industries. Companies in industries with high-carbon emissions are given a value of 1, and those with low-carbon emissions are given a value of 0
	Nature of ownership	STATE	Virtual variable, whether state-owned	1 for state, 0 for nonstate
	Year	YEAR	Virtual variable, set by year	In 2012, 2013, and 2014, set Y1, Y2, and Y3, respectively, set the current year to 1, and set the rest to 0

Model 1.

$$Q = \beta_0 + \beta_1 \mathrm{CDI} + \beta_2 \mathrm{SIZE} + \beta_3 \mathrm{OCN} + \beta_4 \mathrm{ROE} + \beta_5 \mathrm{GROWTH} + \beta_6 \mathrm{STATE} + \beta_7 \mathrm{YEAR} + \varepsilon. \quad (1)$$

At the same time, the model more deeply verifies whether the industry in which the company operates will have an impact on the relationship between the two. Therefore, the factor of IND is added to the interaction term of CDI.

Model 2.

$$Q = \beta_0 + \beta_1 \mathrm{CDI} + \beta_2 \mathrm{CDI} * \mathrm{IND} + \beta_3 \mathrm{SIZE} + \beta_4 \mathrm{OCN} + \beta_5 \mathrm{ROE} + \beta_6 \mathrm{GROWTH} + \beta_7 \mathrm{STATE} + \beta_8 \mathrm{YEAR} + \varepsilon, \quad (2)$$

where β_0 is the constant term in the regression equation, β_i is the coefficient evaluated for each explanatory variable, and ε is the random disturbance item.

3. Empirical Analysis

3.1. Correlation Analysis. To eliminate the influence of individual effects on the correlation between variables, the average value of each variable is calculated with the company as the unit. Then the correlation analysis is carried out. In this article, SPSS 19.0 [22, 23] is used to test the correlation of each variable in the model, and the test results are shown in Table 4.

From the correlation test, we can see a correlation between enterprise value and other variables, but the correlation between the respective variables is not exceptionally high.

3.2. Multiple Linear Regression Analysis. Since the sample companies from 2012 to 2015 are not the same, and the short time is only four years, the four-year sample is aggregated as cross-sectional data for regression analysis. Table 5 shows the multiple regression [24–29] results of the impact of carbon information disclosure on corporate value. It can be seen from Table 5 that the overall fitting degree is 0.336, indicating that the selection of explanatory variables in the model is reasonable. The variance inflation factor VIF of each variable is less than 2, meaning no multicollinearity problem among the variables.

Analysis of the regression coefficient shows that the correlation coefficient between the CDI and the enterprise value is 0.035, the significance is 0.037, and it is significantly positively correlated at the 5% level, which verifies that carbon information disclosure has a positive effect on corporate value. The correlation coefficient between the interaction term CDI * IND and corporate value is 0.086, with a significance of 0.002. It is also significantly positively correlated at the 5% level, indicating that industry factors can significantly impact the relationship between carbon information disclosure and corporate value.

In addition, enterprise value and company size are significantly negatively correlated. It shows that the expansion of the company's scale in this study is not

Table 4: Correlation test of each variable.

	Q	CDI	CDIND	SIZE	OCN	ROE	GROWTH	STATE
Q	1							
CDI	−0.063	1						
CDIND	0.142*	0.161**	1					
SIZE	−0.438*	0.467**	0.076	1				
OCN	0.077	0.382**	0.142**	0.359**	1			
ROE	0.204*	−0.016	−0.044	0.031	0.057	1		
GROWTH	0.083	−0.092	−0.052	0.063	−0.042	0.312**	1	
STATE	−0.166*	0.108	0.072	0.232**	0.151**	−0.190**	−0.207	1

Table 5: Multiple regression results of the impact of carbon information disclosure on corporate value.

	Unstandardized coefficients		Standardized coefficient			
	B	Standard error	Beta	T	Significance	VIF
Constant	10.247	0.094		11.367	0	
CDI	0.035	0.017	0.107	2.058	0.037	1.407
CDIND	0.086	0.027	0.151	3.265	0.002	1.04
SIZE	−0.439	0.043	−0.575	−10.795	0	1.417
OCN	0.013	0.003	0.222	4.457	0	1.257
ROE	2.542	0.683	0.182	3.727	0	1.166
GROWTH	0.007	0.005	0.089	1.81	0.073	1.137
STATE	−0.14	0.12	−0.057	−1.137	0.254	1.115
R-squared	0.338					
Adjusted R-squared	0.323					
F value	23.764					

Table 6: The impact of carbon information disclosure levels in different industries on corporate value.

	Group of high-carbon emission industries			Group of low-carbon emission industries		
	Beta	T	Sig	Beta	T	Sig
Constant	8.403	2.109	0.045	10.429	11.294	0
CDI	0.259	3.948	0	0.025	1.189	0.237
SIZE	−0.402	−2.264	0.032	−0.447	−10.666	0
OCN	0.013	0.916	0.365	0.016	4.697	0
ROE	3.26	2.225	0.035	2.243	2.842	0.007
GROWTH	0.002	0.303	0.762	0.004	1.706	0.088
STATE	0.045	0.103	0.919	−0.145	−1.143	0.253
Adjusted R-squared		0.313			0.335	
F value		3.864			25.755	

necessarily conducive to improving corporate value. On the contrary, the larger the company's scale is, the more likely it is to be exposed to risks and the more likely it is to be pressured by the outside world, which is not conducive to the growth of corporate value. The equity concentration and enterprise value are positively correlated at the level of 1%, indicating that increasing the equity concentration is conducive to the centralized management of enterprises and has a positive effect on enterprise value; enterprise value and profit capacity ROE are significantly positively correlated at the level of 1%, indicating that the higher the profit capacity of the enterprise, the greater the enterprise value.

3.3. Comparative Analysis by Industry. In this article, through group regression [28], the sample data of the high-carbon emission industry group and the low-carbon emission industry group are, respectively, substituted into Model 1 to examine the impact of carbon information disclosure in different industries on corporate value. The regression results are shown in Table 6.

It can be seen from Table 6 that the regression coefficient of the carbon information disclosure index and an enterprise value of high-carbon emission industries is 0.259, which is significantly positively correlated at the level of 1%. Still, the correlation coefficient between the level of carbon information disclosure and enterprise value in low-carbon emission industries is 0.025. The significance is 0.237, which is greater than the significance level, indicating that the CDI [30–33] of the sample of low-carbon emission industries does not correlate with the enterprise value.

The empirical analysis results show that the carbon information disclosure index of the overall sample enterprises is significantly positively correlated with the enterprise value. The same conclusion was drawn from the analysis of high-carbon emission sample enterprises. However, the

analysis results of low-carbon emission sample enterprises show no correlation between the two, which can indicate that industry factors impact the relationship between carbon information disclosure and enterprise value. Compared with low-carbon emission industries, the positive correlation between carbon information disclosure and enterprise value in high-carbon emission industries is more significant.

4. Conclusions

This study creatively combines the legitimacy theory, the effectiveness theory of the capital market, and other related theories with carbon information disclosure and takes these classical theories as the basis to study the impact of carbon information disclosure on enterprise value, which provides a reference for China's research on carbon information disclosure and a new idea for researchers' in-depth research in this field. First of all, it makes a descriptive analysis of the relevant quantitative characteristics of carbon information disclosure and analyzes the quality of carbon information disclosure between different years and different industries. Then, we carry out multiple linear regression to analyze the impact of carbon information disclosure on enterprise value. Then, the industry factors are added to the regression to verify whether the carbon information disclosure of high-carbon emission industries has a greater impact on enterprise value than that of low-carbon emission industries by setting the carbon information disclosure level and the industry multiplier.

Globally, the problems caused by the deterioration of the climate and ecological environment are becoming more and more serious. Therefore, energy conservation and emission reduction are currently a very important task for both relevant government departments and individuals in the society because this environment is closely related to and inseparable from everyone. The company is a major emitter of greenhouse gases, so it should bear more responsibility for energy conservation and emission reduction. There are many ways to strengthen the awareness of enterprise carbon information disclosure, such as low-carbon publicity and training of internal employees on low-carbon development. Let enterprises take the initiative to disclose carbon information to promote green and low-carbon development. Nowadays, China is facing severe ecological and environmental problems, so it is very important to disclose carbon information on time and comprehensively. The government has many tasks to shoulder. It needs to find ways to improve the awareness of carbon information disclosure of enterprises and give clear rewards or punishments to relevant enterprises. Only in this way can the overall situation of carbon information disclosure in China be improved.

Data Availability

The dataset can be accessed upon request.

Conflicts of Interest

The authors declare that they have no conflicts of interest.

References

[1] R. He, M. D. Zhou, and Q. Yang, "The influence of academic independent directors and confucianism on carbon information disclosure: evidence from China," *Complexity*, vol. 2021, Article ID 6646345, 14 pages, 2021.

[2] L. Yang, J. N. Ji, and C. S. Zheng, "Impact of asymmetric carbon information on supply chain decisions under low-carbon policies," *Discrete Dynamics in Nature and Society*, vol. 2016, Article ID 1369589, 16 pages, 2016.

[3] H. Xu, M. G. Wang, and W. G. Yang, "Information linkage between carbon and energy markets: multiplex recurrence network approach," *Complexity*, vol. 2020, Article ID 5841609, 12 pages, 2020.

[4] G. X. Wei, X. Zhang, and B. Bary, "Operational strategy for low-carbon supply chain under asymmetric information of fairness concerns," *Discrete Dynamics in Nature and Society*, vol. 2022, Article ID 7655745, 22 pages, 2022.

[5] H. Xu and M. G. Wang, "A novel carbon price fluctuation trend prediction method based on complex network and classification algorithm," *Complexity*, vol. 2021, Article ID 3052041, 19 pages, 2021.

[6] Q. Sun, L. W. Jiang, and H. T. Xu, "A double-layer combination algorithm for real-time information-sharing network design problem," *Complexity*, vol. 2021, Article ID 4856593, 18 pages, 2021.

[7] R. He, M. D. Zhou, and Q. Yang, "Female directors and carbon information disclosure: evidence from China," *Discrete Dynamics in Nature and Society*, vol. 2021, Article ID 7772601, 16 pages, 2021.

[8] X. Chen and X. Y. Chen, "Data visualization in smart grid and low-carbon energy systems: a review," *International Transactions on Electrical Energy Systems*, vol. 31, no. 7, 2021.

[9] L. Li, C. Mao, H. Sun, Y. Yuan, and B. Lei, "Digital twin driven green performance evaluation methodology of intelligent manufacturing: hybrid model based on fuzzy rough-sets AHP, multistage weight synthesis, and PROMETHEE II," *Complexity*, vol. 2020, 24 pages, 2020.

[10] M. Yu and T. Li, "Information sharing in a supply chain under cap-and-trade regulation," *Mathematical Problems in Engineering*, vol. 2018, Article ID 4573919, 18 pages, 2018.

[11] L. Mao and C. Mao, "Big data supported PSS evaluation decision in service-oriented manufacturing," *IEEE Access*, vol. 8, Article ID 154670, 2020.

[12] X. Cao, Z. Y. Xing, and S. Yin, "A novel dynamic multicriteria decision-making approach for low-carbon supplier selection of low-carbon buildings based on interval-valued triangular fuzzy numbers," *Advances in Civil Engineering*, vol. 2018, Article ID 7456830, 16 pages, 2018.

[13] Y. Zhang, "Research on China's regional carbon emission quota allocation in 2030 under the constraint of carbon intensity," *Mathematical Problems in Engineering*, vol. 2020, Article ID 8851062, 15 pages, 2020.

[14] C. Che, Z. H. Zhang, and Y. Chen, "Two-stage pricing decision for low-carbon products based on consumer strategic behaviour," *Complexity*, vol. 2021, Article ID 6633893, 12 pages, 2021.

[15] L. Qu, T. Liu, Y. Zhong et al., "Sustainability assessment of intelligent manufacturing supported by digital twin," *IEEE Access*, vol. 8, Article ID 175008, 2020.

[16] Z. Liu, B. Hu, and Y. J. Zhao, "Decision optimization of low-carbon dual-channel supply chain of auto parts based on smart city architecture," *Complexity*, vol. 2020, Article ID 2145951, 14 pages, 2020.

Hindawi
Scientific Programming
Volume 2022, Article ID 7899180, 7 pages
https://doi.org/10.1155/2022/7899180

Research Article

Practical Research on Primary Mathematics Teaching Based on Deep Learning

Xiuling Tian,[1] Jianan Zhao ,[1] and Kevin T. Nguyen [2]

[1]*Baoding Preschool Teachers College, Baoding, Hebei 072750, China*
[2]*Saigon University, Hochiminh City, Vietnam*

Correspondence should be addressed to Jianan Zhao; zhaojianan@stu.cpu.edu.cn

Received 30 June 2022; Revised 9 July 2022; Accepted 16 July 2022; Published 9 August 2022

Academic Editor: Lianhui Li

With the rapid development of the knowledge economy, learning that stays at a shallow level is no longer able to meet the challenges of the times and deep learning has come into being. The key to deep learning is to develop students' critical thinking, information integration, communication and collaboration, and constructive reflection skills, which can be cultivated in the process of problem solving. By exploring the theories of deep learning and problem solving, the basic elements of deep learning theory are incorporated into the design system of problem-solving teaching, and the problem-solving teaching model based on deep learning is proposed in conjunction with the content of elementary school mathematics, so that students can further develop their core literacy based on acquiring deep learning skills.

1. Introduction

The concept of deep learning was proposed by American psychologists Ference Marton and Roger Saljo in the mid-1950s, and in 2005, Professor Li Jiahou's research team introduced the concept of deep learning in a more systematic way for the first time [1, 2]. The concept of deep learning advocates that when building resources, we should pay attention to both explicit subject knowledge and implicit thought and culture, which highlights the cultural characteristics in deep learning and shows that deep learning is indeed intrinsically related to teaching subject culture. At present, the more concentrated research areas are mainly deep learning teaching (learning) model and strategy research, environment design research, and resource construction research. Among them, there are fewer research results on microscopic deep learning strategies and deep learning research focusing on classroom context recreation, which have certain limitations in guiding the teaching of front-line teachers and the learning of students in primary and secondary schools. Deep learning is a new integration and growth point for mathematical culture classroom teaching [3, 4]. This paper intends to explore the structure of elementary school mathematics classroom teaching from a new perspective based on microscopic deep learning strategies, resource development, and classroom context recreation, in an attempt to contribute their own new thinking on the cultivation of moral and core literacy in mathematics subjects.

2. Introduction to Deep Neural Networks

2.1. Deep Learning Model. The deep learning model, also known as the deep neural network model, is a classical nonlinear machine learning model whose design is inspired by the neural networks in the biological brain [5, 6]. During the continuous exploration of the biological brain, it was found that the basic unit of the biological mechanism of the brain is the neuronal cell. The basic structure of neuronal cells is shown in Figure 1, and each neuronal cell differentiates upstream and downstream into dendritic and axonal structures, respectively. When a nerve signal is transmitted, a chemical is released from the upstream neuron cell, which is captured by the dendritic structure as an input signal, processed by itself, and then transmitted to the downstream neuron cell through the axon by releasing

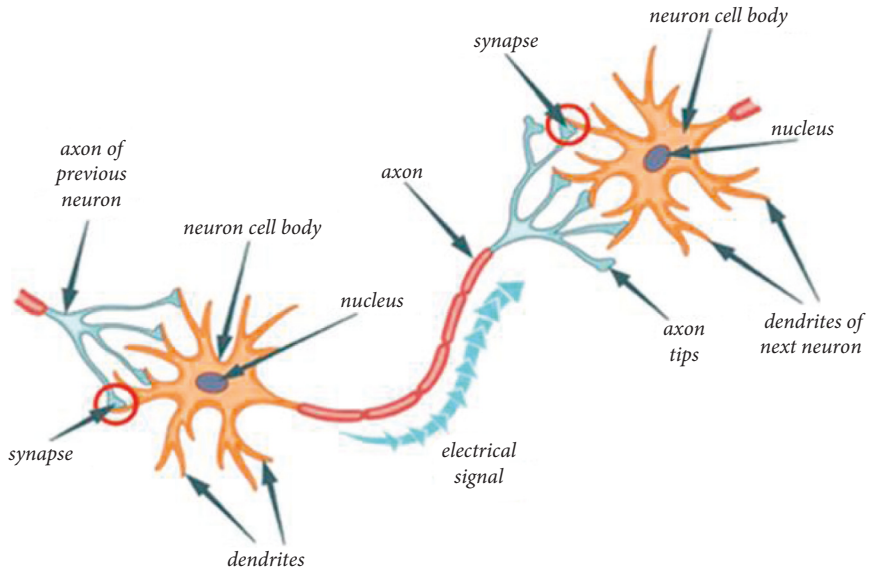

Figure 1: Neuronal cells.

the chemical. The neuronal cells release output signals that require the sum of the received input signals to reach a certain strength in order to be activated.

In Figure 2, the input of the j-th output neuron is $\beta_j = \sum_{i=1}^{p} w_{hj} b_h$; the input to the h-th hidden layer neurons is $a_h = \sum_{i=1}^{a} v_{ih} x_i$. In Figure 2, the neuron model is divided into three levels: "input layer," "hidden layer," and "output layer." Each "circle" represents a neuron, and the neuron in the "input layer" has only axon endings, the neuron in the "output layer" has only dendrites, while the neuron in the "hidden layer" has both dendrites and axon endings. The neurons in the "hidden layer" have both dendritic and axonal endings, and the lines between neurons represent the transmission of information [7, 8]. It is easy to see that the neuronal model perfectly simulates the process of biological understanding of the world: first, $x_i (i = 1, \ldots, d)$ in Figure 2 represents a number of input data, which is also the data to be transmitted from the "input layer" to the "hidden layer." Second, $v_{ih} (i = 1, \ldots, d; h = 1, \ldots, q)$ represents the "weight" of the information transmitted from the i-th neuron in the "input layer" to the h-th neuron in the "hidden layer." "Third, $b_k (k = 1, \ldots, d)$ denotes the data obtained by the k-th neuron in the "hidden layer." If this data reaches a preset "threshold," the neuron will be activated and the b_k data can continue to be transmitted to the "output layer"; if the "threshold" is not reached, the b_k will not be transmitted to the "output layer." If the "threshold" is not reached, kb will not be transmitted to the "output layer"; fourth, similarly, w_{hj} and $y_i (j = 1, \ldots, l)$ can be understood. In an ordinary neural network model, the input data $x_i (j = 1, \ldots, l)$ and the output data $y_i (j = 1, \ldots, l)$ are known, and a large amount of training data is used to determine the "weights" between the layers. Once all the "weights" are obtained, the artificial neural network model is built, through which the machine can simulate the human way of understanding the world to perform clustering, recognition, and optimization. When the "hidden layer" has multiple layers of neurons, a "deep learning" model in computer science is obtained (Figure 3).

2.2. Deep Learning in Education. If deep learning in computer science is to achieve intelligence by activating neurons and calculating weights among neurons, deep learning in education is to achieve teaching goals by activating students' knowledge and clarifying the relationship between old and new knowledge in teaching practice [9, 10]. It is clear that the "model" of deep learning in computer science corresponds to the teaching process based on deep learning in pedagogy, and there is a clear correspondence in terms of objectives, methods, and focus (see Table 1).

From the abovementioned correspondence between the two fields of deep learning, differences can be obtained [11, 12]. These are mainly reflected in the following aspects.

Firstly, machines do not have the ability to build models on their own, while one of the goals of deep learning in pedagogy is to enable students to explore the connections between knowledge on their own, which is the most essential difference between "human" and "machine."

Secondly, for machines, the modeling is roughly the same for the same input and output. However, for teaching, each student often has different knowledge constructs in the face of new knowledge, and the activated knowledge may be different.

Finally, although the implementation process of deep learning in these two fields is roughly the same, in computer science, deep learning requires the use of "sea of problems" and a large amount of data to get the model; while in pedagogy, teachers should pay more attention to the activation of students' knowledge and should not give students too much practice.

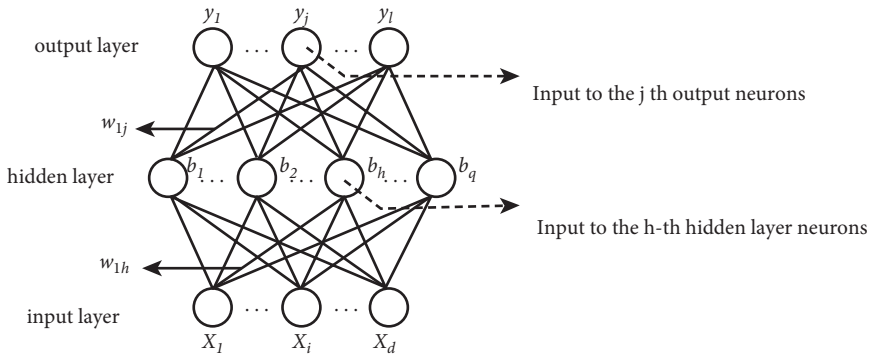

Figure 2: Neuronal model.

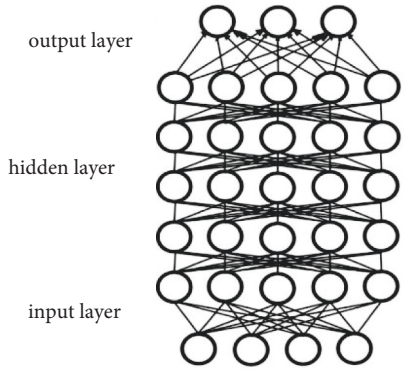

Figure 3: The deep learning models with multiple hidden layers.

3. Teaching Practices of Elementary School Mathematics Based on Deep Learning

The teaching practice of deep learning revolves around the core content of the subject, which requires teachers to create contexts suitable for deep learning so as to promote the overall development of students [13, 14]. Based on the understanding of the meaning of deep learning, the teaching process of deep learning should include setting learning tasks, actively exploring and activating knowledge elements, acquiring the essence of mathematics, consolidating the connections between knowledge elements, and summarizing the learning process.

3.1. Assigning Learning Tasks. The purpose of assigning learning tasks is to enable learners to carry out independent learning with the tasks. The learning tasks should be chosen to meet the requirements of the teaching objectives but also to be appropriately challenging for the students. These tasks can be mathematical knowledge itself or can be derived from real life, rich and complex teaching contexts created by the teacher.

3.2. Active Inquiry and Activation of Knowledge Elements. This component refers to students' deep inquiry into the learning tasks set by teachers and their active construction of their own problem-solving approaches and methods [15, 16]. The core content of a subject is the carrier for carrying out deep learning, a class of core content is composed of several learning units, a learning unit is composed of several knowledge points, and these basic constituent elements can be called knowledge elements. The process of active inquiry is student-oriented, and students are expected to make connections between new knowledge and old knowledge and activate as many existing knowledge elements in their cognitive structure as possible. The more knowledge elements students activate, the more likely they are to approach the essence of mathematics.

Take the process of proving the "butterfly theorem" for an arbitrary quadrilateral as an example. As shown in Figure 4, the main content of the "butterfly theorem" is for any quadrilateral, there is S_1: S_2= S_4: S_3 or S_1, S_2, S_3, S_4 (where S_1, S_2, S_3, and S_4 are the areas of four triangles).

The proof of this theorem is as follows: first, the magnitudes of the areas of the four triangles are $S_1 = 1/2$ OD·h_1, $S_2 = 1/2$ OB· h_1, $S_3 = 1/2$ OB· h_2, and $S_4 = 1/2$ OD· h_2. Second, it can be observed that △AOD and △AOB are two triangles of the same height, and their area ratios are S_1: S_2 = OD: OB. △COD and △BOC are also two triangles of the same height, and their area ratios are S_4: S_3 = OD: OB. Finally, the two equations are equivalently substituted, i.e., S_1: S_2=S_4: S_3 or $S_1 \times S_3$=$S_2 \times S_4$.

In fact, the proof of "butterfly theorem" is not very difficult, but there are many knowledge elements that need to be activated in the process of proof, such as ratio and proportion, calculation of triangle area, letters for numbers, simple equations, and equivalent substitution, which are all knowledge elements that students may activate in the process of learning the lesson. Only by activating the knowledge elements behind the "butterfly theorem" can students successfully acquire the essence of mathematics [17, 18].

3.3. Acquiring the Essence of Mathematics. This is the part where students are guided by the teacher to use the activated knowledge elements to acquire the essence of mathematics. If students cannot complete the deep learning through independent inquiry, the teacher can guide appropriately by prompting students which knowledge elements the task is related to and then allowing students to activate them,

Table 1: The correspondence of deep learning in the two domains.

	Deep learning in computers	Deep learning in teaching science
Model	Input layer (initial data) Hidden layer (transmitting between neurons in the brain, processing information, contains multiple layers of neurons) Output layer (output-processed information) Inspection model	Challenging learning tasks The existing knowledge in the cognitive structure The essence of mathematics Persistent evaluation
Goal	Get the machine to be able to learn	Promote students to have the ability of deep learning, independently explore the connection between knowledge, from "learn" to "learn" can "learn"
Method	Use a large amount of training data to determine the model	Under the guidance of teachers, students complete tasks, activate more knowledge elements, and independently explore the relationship between knowledge elements
Keynote	Training process, neuronal activation, and determination of the weights	Students' thinking process, the activation of knowledge element and the relationship between knowledge element

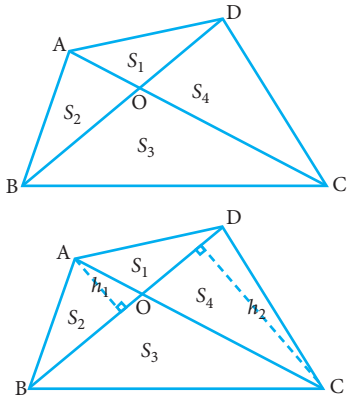

Figure 4: Butterfly theorem for arbitrary parallelograms.

unifying student independent inquiry and teacher guidance. This process is teacher-led and is intended to help students acquire the true essence of mathematics. Take the proof of the butterfly theorem as an example [19, 20]. For elementary school students, the mathematical essence of the theorem can be summarized as follows: one is the use of letters to represent unknown quantities and the use of letters to perform operations; the other is the use of the formula for the area of a triangle to convert the ratio of the area to the ratio of the "base." Therefore, teachers can guide students from these two aspects in the actual teaching process, prompting them to activate the relevant knowledge elements and then letting them use the activated knowledge elements to obtain the essence of mathematics.

3.4. Consolidating the Connections between Knowledge Elements. This component can also be called "continuous assessment," i.e., multiple assessments to determine whether students have "learned" something [21, 22]. Scientific continuous evaluation can improve teachers' teaching and professional development; it can optimize students' in-depth learning and promote their overall development. The assessment can be done by practicing postlesson exercises, taking unit tests, etc. For the proof of the butterfly theorem for any quadrilateral, the teacher can ask students to complete the following task after the proof is completed.

For example, the diagonal AC of quadrangle ABCD compares to BD compared to point O.

If the area of the triangle ABD is equal to 1/3 of the area of the triangle BCD, and it is AO = 2 and DO = 3, then how many times the length of the CO is the length of the DO (Figure 5).

The problem is the ratio of CO and DO. Since AO and DO are known quantities, the ratio of CO and DO can be converted to the ratio of AO and CO. From the diagram, we can see that AO and CO are in two triangles with the same base, which is in line with the essence of the butterfly theorem. Through the above example, teachers can guide students to further understand the process of proving the butterfly theorem, and let them apply the theorem to solve problems, consolidate the connection between knowledge elements, and finally achieve the purpose of in-depth learning.

3.5. Summarizing the Learning Process. Summarizing the learning process means that students can review the meaningful learning process they have participated in [23, 24]. Teachers can determine whether students have integrated new knowledge with old knowledge based on their summaries, which simply means that they "know how to learn." The deeper goal is to prepare students for learning new knowledge, encourage them to develop the habit of summarizing the learning process, and take the initiative to learn in depth, hoping that they will achieve the goal of "knowing how to learn." The above teaching practices correspond to the process of deep learning in computer science as shown in Table 2.

4. Teaching Strategies for Elementary School Mathematics Based on Deep Learning

4.1. Stimulating Positive Emotional Experiences and Cultivating Interest in Mathematics Learning. Teachers cause empathy between teachers and students through effective and positive communication with them in the teaching process. Give full play to the positive role of emotional

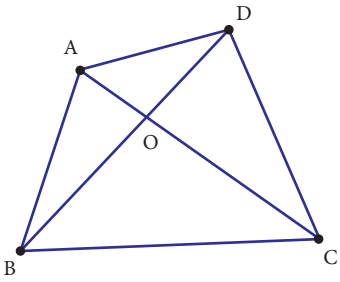

Figure 5: Any quadrangle "butterfly theorem" exercise diagram.

Table 2: Computer science summarizes the implementation process comparison of deep learning and deep learning teaching practice.

The implementation process of deep learning in computer science	Deep learning teaching practice
Determine the input initial data	Assign learning tasks, and lead to the main content of classroom teaching
Determine the neurons of the "hidden layer"	Actively explore and activate the knowledge meta
Through the training data, the weights and the activated neurons were determined	Get the essence of mathematics and guide students to recall the learned knowledge
By evaluating the model, by verifying the data	Consolidate the connection between knowledge yuan, test whether students firmly grasp knowledge
Finally determine the model	Summarize the learning process, and gradually form a good learning habits

factors in teaching activities, so as to promote teaching with emotion, teaching with emotion [25, 26]. With the help of multimedia to make mathematics teaching more intuitive and visual, to break the students' fear of mathematics and gradually cultivate students' interest in learning mathematics. Teachers try to connect the knowledge points learned in class with students' life, so that students can feel the existence and charm of mathematics in real life. Connecting mathematics with real life creates a lively, relaxed and interesting learning atmosphere so that students really love mathematics and take the initiative to learn mathematics.

4.2. Students Fully Participate in Teaching and Learning to Achieve Depth of Thinking. Master the laws of mathematics in a hands-on way. Piaget's cognitive development stage theory that children between the ages of 7 and 12 years old are in the concrete operation stage, the children of this stage of concrete operation thinking cannot leave the support of concrete things, has not yet formed the ability to abstract thinking. Psychological research shows that the more senses involved in collecting information, the more information is obtained, and the more solid knowledge is learned [27, 28]. Therefore, for students who are still in the concrete arithmetic stage, the use of multiple senses is conducive to the mastery of mathematical laws and the deepening of mathematical knowledge.

The development of mathematical thinking is promoted in cooperative learning. The exchange of ideas with each other produces two or even more ideas. This is also true in elementary school mathematics. In the process of learning knowledge, each student has a different way of thinking when faced with the same problem because of their individual differences and motivational characteristics, as well as their life environment and emotional and attitudinal differences. Through group discussion, each member of the group has the opportunity to express his or her own views and to exchange experiences and emotions with other members. Through group discussions, students incorporate the experiences and knowledge structures of others into their own knowledge structures and continuously promote self-reflection so that their own knowledge spirals upward and in the process students' mathematical thinking develops and deepens.

4.3. Breaking the Boundaries of Disciplines to Integrate Learning and Building a Mathematical Way of Thinking. In today's world, it is difficult to rely on the knowledge of a single discipline when students need to mobilize a wide range of knowledge, abilities, and methods to solve the complex problems of tomorrow's society [29]. Therefore, it is important to integrate the knowledge of other disciplines in the teaching and learning process of mathematics and to develop interdisciplinary thematic learning, not only to deepen students' understanding of mathematics and promote deeper learning of mathematics but also and more importantly, to develop students' comprehensive thinking skills and the ability to transfer knowledge, which is an important ability to solve complex problems across disciplines. Teachers break the limitations of their own subject knowledge in the mathematics teaching process and collaborate with teachers of other disciplines to create an integrated, multidisciplinary curriculum that fosters students' ability to think in multiple, holistic, and innovative ways and promotes the transfer of knowledge and skills.

4.4. Timely and Positive Assessment to Develop Students' Self-Confidence in Mathematics. Learning assessment is an essential part of teaching and learning activities [30–38]. For

students at the elementary school level, affirmative and positive assessment from teachers can stimulate students' intrinsic motivation to learn. The logical and abstract nature of mathematics makes it a subject that is not easy for students to master. In the process of learning, students will inevitably make mistakes, even some simple mistakes that teachers often emphasize, and when students make mistakes, they should not speak harshly, but should be "kind" to them. We should find out the weaknesses of students' knowledge and provide them with targeted individual counseling.

5. Conclusion

Deep learning is a hot topic of research and practice in the field of learning science, and it is important for understanding how people learn and how learning is best achieved. The ultimate goal of deep learning is to enable students to learn basic mathematical knowledge, explore the connection between related knowledge and understand the essence of mathematics, and finally move from "learning" to "knowing." As front-line teachers, they need to design challenging learning topics under the guidance of deep learning theory, so as to create good conditions for students to realize deep learning. According to the above discussion, teachers should pay attention to the following aspects.

First, the need for students to engage in deep learning is determined by mathematical knowledge itself. When mathematical knowledge is limited, the teaching process is much like the implementation of an artificial neural network, with few meta-connections in the "hidden layers" of knowledge. However, as students learn more mathematics, the teaching process should be based on the implementation of deep learning in computer science, and the connections of knowledge elements in the "hidden layer" become more and more complex. For example, in the lesson "position and direction," rays, angles, measures, number pairs, etc., are all knowledge elements in the "hidden layer," and their connections should be understood by students during the lesson.

Second, students' ability to learn in depth is not a task of one lesson, but a long-term process. In the middle and lower grades, teacher guidance may play a key role, as teachers can take the initiative in guiding connections to what students have already learned, but they should also give students as much time as possible to think on their own. In the upper grades, the key role should gradually shift to students, emphasizing interknowledge connections, multiple solutions to problems, and adequate communication.

Third, teachers should try to let students construct their own knowledge system and form the habit of independent learning during the teaching process. When summarizing the results of a lesson, students should not only be asked "what they have learned," but also "what they have used," so that they can recall the learning process. Only in this way can students gradually "learn" mathematics.

Data Availability

The dataset can be accessed upon request to the corresponding author.

Conflicts of Interest

The authors declare that they have no conflicts of interest.

References

[1] Q. Zhou and Z. Lu, "The design of in-depth learning in elementary school mathematics based on core literacy in mathematics," *Old District Construction*, no. 12, pp. 87–90, 2019.

[2] M. Cheng, "Research on teaching strategies of "deep learning" in elementary school mathematics," *Journal of Mathematics Education*, vol. 28, no. 4, pp. 66–70, 2019.

[3] X. Ma, "Exploring the effective path of carrying out deep learning in elementary school mathematics," *Science and technology wind*, no. 34, p. 31, 2019.

[4] Z. Qian and Q. Yang, "The front-end of elementary school mathematics teaching "three discriminations"--Thinking based on promoting students' deep learning," *Primary and secondary school teacher training*, no. 12, pp. 63–66, 2019.

[5] J. He and A. Xi, "Dimensions and attention to the overall design of elementary school mathematics units in the perspective of deep learning," *Journal of Hengshui Normal College*, vol. 18, no. 4, pp. 365–368, 2019.

[6] S. Zeng, S. Qiu, F. Tang, S. Chen, and F. Huang, "A study on the development of microteaching design for elementary school mathematics for AI generalist teachers: the example of "The sum of interior angles of triangles"," *Journal of Guangdong Second Normal College*, vol. 39, no. 6, pp. 21–30, 2019.

[7] Y. Chen, "Problem-driven teaching of elementary school mathematics in the context of deep learning: an example of "graph and geometry"," *Western Quality Education*, vol. 6, no. 1, pp. 232-233, 2020.

[8] H. Tian, "An analysis of teaching strategies of elementary school mathematics based on deep learning," *Journal of Yanbian College of Education*, vol. 33, no. 6, pp. 164-165+168, 2019.

[9] Y. Yang, P. Liang, C. Yang, and F. Liu, "An investigation of the teaching structure of deep learning in elementary school mathematics: the example of "multiplication and distribution law"," *Education and Teaching Research*, vol. 34, no. 7, pp. 31–40, 2020.

[10] S. Xia, "Deep learning and better growth--a study on deep learning in elementary school mathematics that points to students' good development," *Huaxia Teacher*, no. 21, pp. 36-37, 2020.

[11] M. Fang, "Deep learning: reconstructing elementary school mathematics classroom based on the perspective of "learning"," *Educational Science Forum*, no. 26, pp. 3–6, 2020.

[12] G. Zhu, "The essence and practice of teaching based on deep learning," *Shanghai Educational Research*, no. 12, pp. 89–92, 2020.

[13] R. Han and L Xiao, "On the deep learning process pointing to the core literacy of elementary school mathematics: the example of "The initial understanding of fractions" in the Human Education version," *Journal of the Corps of Education*, vol. 30, no. 6, pp. 71–75, 2020.

[14] R. Yu and S. Zhao, "The connotation and teaching practice of deep learning--a case study of elementary school mathematics," *Journal of Mathematics Education*, vol. 30, no. 1, pp. 68–73, 2021.

[15] G. Peng, "Implementation strategies of deep learning in elementary school mathematics," *Teaching and Management*, no. 17, pp. 56–58, 2020.
[16] G. H. Yu, "Teaching knowledge that points to deep learning: the case of elementary school mathematics," *Basic Education Curriculum*, no. 11, pp. 38–44, 2020.
[17] N. Yang and M. Luo, "How "scaffolding" becomes a "stumbling block"-a study of the graphical barriers in elementary school mathematics," *Journal of Computerized Education Research*, vol. 42, no. 7, pp. 114–121, 2021.
[18] Y. Ma, "A model of understanding and practice of deep learning--a case study of elementary school mathematics Curriculum. Teaching materials," *Teaching method*, vol. 37, no. 4, pp. 60–67, 2017.
[19] Y. Lin, "Design and implementation of unit learning activities in the context of deep learning," *Shanghai Educational Research*, no. 1, pp. 89–92, 2022.
[20] X. Wang, "A study on the practice of teaching application problems in elementary school mathematics pointing to deep learning," *Journal of Science Education*, no. 6, pp. 132–134, 2022.
[21] Q. Su, "Towards deep learning of metric teaching in elementary school mathematics [J]," *Teaching and Management*, no. 2, pp. 39–41, 2022.
[22] E. Teng, "Problem-driven teaching of elementary school mathematics in the context of deep learning: an example of "graph and geometry"," *Western Quality Education*, vol. 7, no. 23, pp. 184–186, 2021.
[23] X. Li, W. Li, and D. Zheng, "Researching children from the "heart"-a questionnaire survey report on the construction of elementary school mathematics wisdom classroom based on deep learning," *Educational Science Forum*, no. 10, pp. 56–58, 2022.
[24] F. Liu, "The design of school-based assignments in elementary school mathematics," *Science and Education Wenhui(Zhongjun)*, no. 4, pp. 145-146, 2020.
[25] X. Tan and X Ren, "A preliminary investigation of problem solving teaching mode based on deep learning in elementary school mathematics," *Journal of Guizhou Normal College*, vol. 35, no. 12, pp. 75–80, 2019.
[26] Q. Lin, "Deep learning of elementary school mathematics in digital environment," *Huaxia Teacher*, no. 20, pp. 52-53, 2020.
[27] L. Zhu and Y. Ma, "The analysis and consideration of "division", "fraction" and "ratio" in elementary school mathematics," *Journal of Mathematics Education*, vol. 29, no. 5, pp. 32–35, 2020.
[28] D. Zhu, "Teaching design of elementary school mathematics to promote the occurrence of deep learning," *Educational Theory and Practice*, vol. 40, no. 29, pp. 56–58, 2020.
[29] C. Chen, "A comparative study on the influence of different teaching strategies on deep learning: a case study of teaching "recurring decimals" in elementary school," *Shanghai Educational Research*, no. 11, pp. 85–87+67, 2020.
[30] L. Li, B. Lei, and C. Mao, "Digital twin in smart manufacturing," *Journal of Industrial Information Integration*, vol. 26, no. 9, p. 100289, 2022.
[31] L. Li, T. Qu, Y. Liu et al., "Sustainability assessment of intelligent manufacturing supported by digital twin," *IEEE Access*, vol. 8, pp. 174988–175008, 2020.
[32] L. Li and C. Mao, "Big data supported PSS evaluation decision in service-oriented manufacturing," *IEEE Access*, vol. 8, pp. 154663–154670, 2020.
[33] L. Li, C. Mao, H. Sun, Y. Yuan, and B. Lei, "Digital twin driven green performance evaluation methodology of intelligent manufacturing: hybrid model based on fuzzy rough-sets AHP, multistage weight synthesis, and PROMETHEE II," *Complexity*, vol. 2020, no. 6, pp. 1–24, Article ID 3853925, 2020.
[34] L. Song, "Exploring effective strategies for in-depth learning of elementary school mathematics under the concept of core literacy," *Modern Communication*, no. 21, pp. 180–182, 2020.
[35] X. Zhang, X. Zhang, and D. T. Jasni-Bin, "Intelligent Classroom Teaching Assessment System Based on Deep Learning Model Face Recognition Technology," *Scientific Programming*, vol. 2022, Article ID 1851409, 10 pages, 2022.
[36] L. Sun, K. M. Siddique, L. Wang, and S. J. Li, "Mixing characteristics of a bubble mixing microfluidic chip for genomic DNA extraction based on magnetophoresis: CFD simulation and experiment," *Electrophoresis*, vol. 42, no. 21-22, pp. 2365–2374, 2021.
[37] H. Fang, "Validity Analysis Based on Multidimensional Pattern Analysis and Machine Learning Theory in Educational Teaching Assessment," *Wireless Communications and Mobile Computing*, vol. 2022, Article ID 7395202, 7 pages, 2022.
[38] C. Tan, "Quality Assessment of Physical Education Teaching in Colleges and Universities Based on Joint Neural Network," *Mobile Information Systems*, vol. 2022, Article ID 2658327, 6 pages, 2022.

Hindawi
Scientific Programming
Volume 2022, Article ID 3744086, 13 pages
https://doi.org/10.1155/2022/3744086

Research Article

AOMC: An Adaptive Point Cloud Clustering Approach for Feature Extraction

Zhengyu Zhang and Mengdi Jin

Beijing University of Posts and Telecommunications, Beijing, China

Correspondence should be addressed to Zhengyu Zhang; 1534271067@xzyz.edu.cn

Received 13 June 2022; Revised 9 July 2022; Accepted 13 July 2022; Published 8 August 2022

Academic Editor: Lianhui Li

Point cloud local feature extraction places an important part of point cloud deep learning neural networks. Accurate extraction of point cloud features is still a challenge for deep learning networks. Oversampling and feature loss of point cloud model are important problems in the accuracy of image point cloud deep learning network. In this paper, we propose an adaptive clustering method for point cloud feature extraction—adaptive optimal means clustering (AOMC)—and apply it to point cloud deep learning network tasks. This method solves the problem of determining the number of clustering centers in the process of point cloud feature extraction so that the feature points contain the whole point cloud model and avoid the problem of losing detail features. Specifically, according to the loss characteristics of point cloud clustering, AOMC selects a different number of clustering centers for various models. Moreover, in light of the density distribution of the point cloud, the radius of the clustering subset is determined. This method effectively improves the accuracy of the point cloud deep learning network on object classification and parts segmentation. Our method reaches demand on Modelnet10 and shapenetcore_partanno_segmentation_benchmark datasets. In terms of deep learning network optimization, it has good performance. Additionally, our method has high accuracy and low algorithm complexity.

1. Introduction

With the rapid development of point cloud intelligence, researchers have paid much attention to the application of deep learning networks in point cloud recognition [1–3]. Moreover, machine learning algorithms are gradually being applied to improve the performance of point cloud recognition. Point cloud intelligence is widely used in surveying mapping, machine recognition, model design, virtual reality, and other fields [4–8].

Point cloud intelligence algorithm based on a deep learning network mainly focuses on object classification, object detection, parts segmentation, and semantic segmentation [9, 10]. Point cloud deep learning networks gather different functions in the same network to realize the integration of various tasks [11–15]. Figure 1 shows the main task and processing flow of the point cloud deep learning network, which includes two main parts: point cloud feature extraction and deep learning computing. The aim of point cloud feature extraction is to extract effective features from the point cloud model. The extracted features are used for analysis to meet different task requirements. The deep learning network is composed of different convolution kernels. The purpose of convolution is to use features to optimize the loss function, so as to realize the segmentation and classification of the point cloud model.

For the shape analysis task based on the point cloud, it is a fundamental problem to realize the effective representation of local shape features (normal, curvature, etc.). The representation of local shape features is affected by many interference factors, including noise, dynamic sampling density, complex geometric details, and defective parts. These interference factors undoubtedly affect the local shape feature representation of the point cloud and then affect the performance of related applications. To solve this problem, we usually use the local neighborhood estimation of each point in the point cloud to establish an implicit surface representation to realize the simulation of local features.

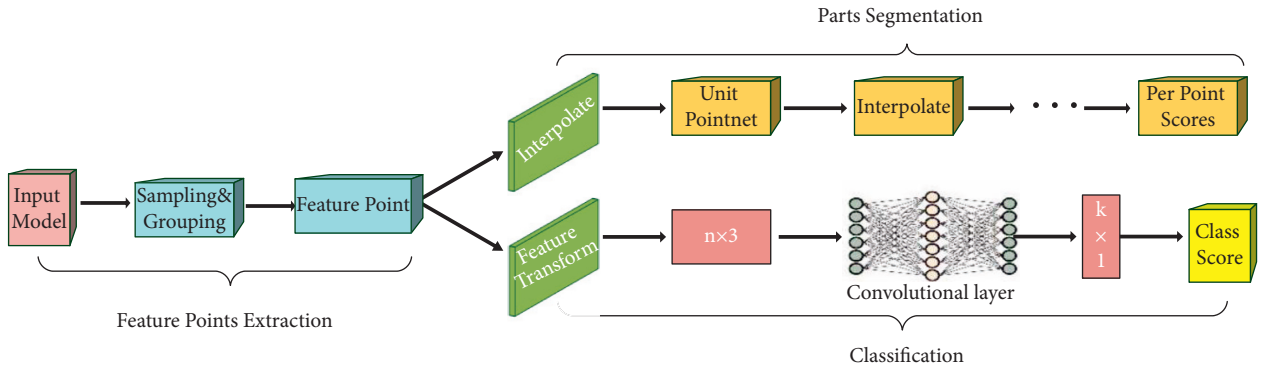

Figure 1: The architecture of point cloud deep learning network.

Because point cloud is of disordered and irregular data structure, unlike 2D data, it is impossible to simply use convolutional neural networks (CNN) for feature extraction. Before deep neural networks were envisioned, three-dimensional operators were commonly used to achieve point cloud parts segmentation [16, 17]. To capture finer structures and more accurate boundaries, numerous refinement strategies have been proposed. In 2015, the VoxNet model was presented based on the voxelization model [8]. At the same time, a multiview convolutional neural network (MV-CNN) was proposed based on the multiview sampling method [18]. However, none of these methods can directly act on point cloud data to extract the features of the point cloud.

Clustering is a typical unsupervised learning algorithm. The main idea is to divide the data set into different subsets according to the different attribute features of the undetermined data [3]. The main way to evaluate the clustering effect is to see if objects of the same category are classified into the correct subcategory. Compared with objects between groups, objects within groups have a high degree of similarity, while objects between different groups are very different. For 2D and 3D data, a clustering algorithm can realize effective segmentation of objects, which includes segmentation between different categories and segmentation of parts within objects.

Figure 2 shows the process of feature extraction of the 3D point cloud deep learning network. Firstly, the feature center of the point cloud is carried out. Then, taking the feature center as the center of the sphere and selecting the radius to extract the hierarchical feature points of the point cloud, the purpose is to obtain the local features of the point cloud model. Finally, the extracted feature points are input into the deep learning network to realize the task of point cloud classification and parts segmentation.

Figure 3 shows the process of point cloud feature extraction; if the feature center is not selected reasonably, it will lead to the loss of local features of the point cloud, which will affect the accuracy of the point cloud deep learning network [19, 20]. In practice, supervised learning and unsupervised learning can be used to select feature points of the point cloud [21–23]. However, the time complexity of some methods is high, and the accuracy of other methods is too low. Moreover, the algorithm parameters are not reasonable for the point cloud category, which leads to the waste of computing resources [24, 25]. Therefore, it is very important to propose a point cloud feature extraction method with low computational complexity, high accuracy, and adaptability for the optimization of the point cloud deep learning network.

In this paper, we primarily consider point cloud classification and parts segmentation, two model tasks in the point cloud processing world. We propose a feature extraction method based on unsupervised learning. The number and radius of clustering are determined according to different cloud types by statistical method. The adaptive feature extraction of the point cloud is realized by parallel optimization. This method not only can ensure the complete coverage of the point cloud range but also can avoid the occurrence of repeated sampling and missing sampling. Moreover, compared with the traditional adaptive clustering method, this algorithm has lower algorithm complexity and higher practicality in parameter settings.

This method includes the process of determining the number of clustering centers and feature points extraction of the point cloud model. The purpose is to achieve accurate feature extraction of the point cloud model and avoid the loss of detail feature points. And we apply the feature points in the training process of the point cloud deep learning network, improving the training speed and accuracy of the network.

Compared with the existing clustering methods, this method has some advantages. We also compare the convergence speed of the deep learning network during the training process to evaluate the effect of how this algorithm improved the process of network training. Experimental results show that this method has a certain effect on the optimization of the point cloud deep learning neural network. In summary, our major contributions are as follows:

(i) We propose a point cloud feature extraction method based on clustering and adaptive optimization. When extracting the feature points of point cloud models, it not only can keep details of the local feature but also can reduce the complexity of the algorithm.

(ii) Our method sets different sampling centers and sampling radii for different point cloud types. The

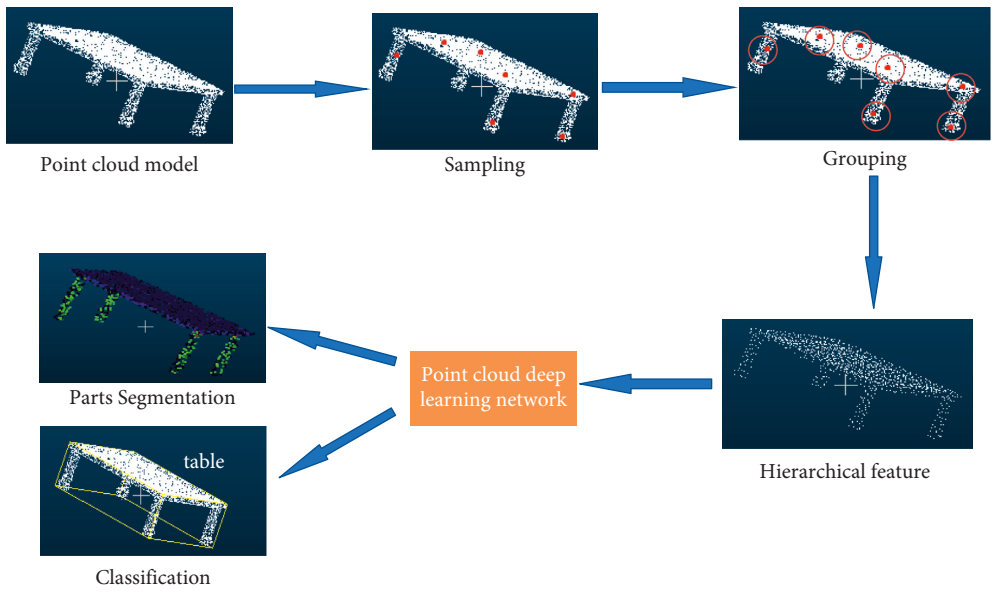

Figure 2: Hierarchical feature extraction process of point cloud deep learning.

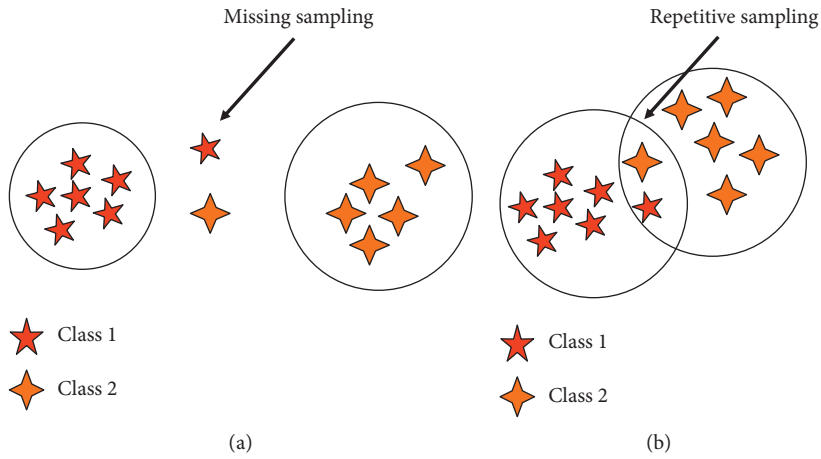

Figure 3: Problems in hierarchical feature learning of point cloud: (a) the sampling area does not cover the whole point cloud model and (b) the overlapping of sampling space leads to repeated feature extraction.

purpose is not only to cover the whole range of the point cloud and avoid missing detection but also to ensure that the overlapping part of the clustering subregion is small and prevent resampling.

(iii) We conduct comprehensive experiments on several benchmark data sets: Modelnet10 [26] and shapenetcore_partanno_segmentation benchmark [27], to validate the effectiveness and efficiency of our proposed method for point cloud classification and parts segmentation tasks. In the point cloud deep learning network optimization, it has a significant effect.

This paper is organized as follows. In Section 2, we provide an overview of the literature on point cloud feature extraction. We propose an adaptive point cloud clustering method in detail in Section 3. Section 4 shows the detailed experimental results. Finally, Section 5 concludes this paper.

2. Related Work

In the process of point cloud feature extraction, machine learning algorithms, including supervised learning [1, 2, 28, 29] and unsupervised learning [3, 30, 31], are widely applied. And the feature points are used to train deep learning networks [27, 32]. Point cloud feature extraction affects the performance of the deep learning network.

2.1. Supervised Learning. Supervised learning is to adjust the parameters of the classifier according to the class label of the sample space. Typical supervised learning includes SVM, naive Bayesian model (NBM), decision tree, and so on. In three-dimensional space, supervised learning determines the classification plane according to the category of the point cloud, so as to ensure the generalization ability of the classifier [28, 29].

Yu and Yang proposed a point cloud sampling method based on the k-nearest neighbor algorithm (k-NN) [1]. The k-NN algorithm determines the center of the sampling based on the category of point cloud data and calculates the radius of the sampling area. The algorithm fully considers the category attributes of each point in the point cloud and makes full use of the distribution of points in the point cloud.

But, for not categorized point cloud data, the k-NN algorithm cannot be used. At the same time, the amount of point cloud data collected by point cloud acquisition devices such as LiDAR is very large [12–14], and the amount of input data for training deep learning networks is also very large. Therefore, it is impossible to label the category of each point. Besides, the algorithm ignores the sparse degree of point cloud distribution, lacking certain self-adaptability. In addition, for point cloud models with more complex distributions, this algorithm increases the number of sampling points that increases the computational complexity of the deep learning network.

2.2. Unsupervised Learning. Unsupervised learning is an algorithm that divides the classification space without prior knowledge. Typical supervised learning includes PCA [30], agglomerative clustering, density-based spatial clustering of applications with noise (DBSCAN), and so on [31]. In the three-dimensional space, the clustering method can divide and extract the target of the point cloud without knowing the classification of the point cloud.

Han studied the point cloud clustering segmentation algorithm based on k-means [3]. This method is implemented based on a certain number of cluster centers, which lacks self-adaptability for different types of point clouds. At the same time, the k-means algorithm needs to initialize the cluster center number before clustering. Therefore, if the cluster center is not well selected, it will have a great impact on the k-means algorithm, which will lead to negative effects such as poor clustering or slow convergence speed.

There is a problem with unsupervised learning. Without knowing the exact number of samples, it is impossible to select the best number of clustering centers. If the number of feature points is too small, the feature information of the point cloud will be lost [33], and the task of point cloud recognition is impossible. If the number of feature points is too large, the complexity of the network will be too high, and the computing resources will be wasted [34, 35].

The unsupervised learning clustering algorithm has some limitations for unknown data. If the initial point of clustering is not selected well, it may affect the convergence effect of the clustering algorithm [9, 16]. Therefore, it is very important to select the initial points, which can cover the whole point cloud model for point cloud feature extraction [8, 10].

At the same time, for different point cloud categories, the value of the cluster subset number is different [1]. For the point cloud model with simple distribution, fewer clustering centers can cover the whole point cloud model. For the point cloud model with complex density distribution and more detailed features, uniform feature extraction is needed to achieve effective feature extraction.

Although DBSCAN clustering algorithm can determine the number of clusters center according to the classification of point cloud [36, 37], in practical application, it is necessary to determine the distance between core points and the minimum number of sample points (MinPts) in the classification subset. Sometimes, due to the accuracy of point cloud computing, the actual application effect of the DBSCAN algorithm needs to be improved. And DBSCAN algorithm has high complexity.

2.3. Point Cloud Deep Learning Network. In 2017, Qi et al. proposed a network model: PointNet [28], which directly targets disordered point clouds. At the same time, in order to obtain hierarchical features such as the CNN model and extract the local features of the point cloud, Qi et al. then proposed a point cloud deep learning network using hierarchical feature learning: PointNet++ [29]. PointNet++ network uses the farthest point sampling and ball query method, which fully covers all the points in the point cloud to avoid outliers in the sampling process. An array of improved algorithms are gradually applied to a deep learning network [38–41] in the past several years. Their main thought is to improve the effect of point cloud feature extraction for developing the performance of a deep learning network.

In the basic PointNet++ network, point cloud feature extraction uses the farthest point sampling and the ball query method, which has a certain degree of randomness and ignores the distribution features of the point cloud. Therefore, the feature clustering method is used here to extract and sample the feature of the point cloud. And the time complexity ($O(N^2)$) of farthest point sampling is high. At the same time, due to the random selection of sampling centers, there may be overlap between different sampling points areas, causing repeated sampling. In addition, the sampling radius of the basic algorithm is of fixed value, which will cause the lack of self-adaptability of sampling, and it is impossible to sample reasonably according to the specific situation of the point cloud distribution.

3. Our Method

We propose a novel point cloud sampling method based on unsupervised learning: adaptive optimal means clustering for point cloud feature extraction (AOMC), which improves the clustering effect of nonmeans clustering. It can be roughly divided into two steps: cluster center number determination and adaptive optimal cluster. Figure 4 shows the process of AOMC.

Firstly, our method determines the number of clustering centers for different categories of point cloud according to the change of the within-cluster sum of squared errors (SSE), raising the adaptability between the selection of the number of cluster centers and the point cloud category. The density of point cloud distribution is different among point cloud models. And various objects have different details, so it is a significant way to select suitable clustering center numbers for each of the point cloud models. Then, adaptive clustering

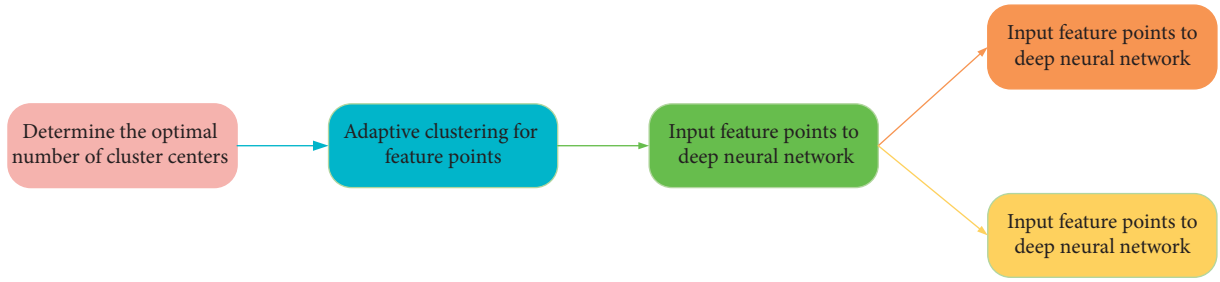

Figure 4: Adaptive optimal means clustering for neural networks.

is carried out. The requirement of clustering is not only to realize the uniform distribution of feature points in the point cloud model but also to avoid the loss of detail feature points. At the same time, AOMC avoids the repeated sampling caused by the excessive overlap of each subclass. AOMC makes the clustering centers reasonably and evenly distributed in the point cloud model, so as to improve the clustering effect. After sampling feature points, we input them into the deep learning network. CNN-based deep learning network can learn hierarchical features to achieve the parts segmentation and object detection tasks for point cloud models. The method is applied to the PointNet++ network. By the point cloud classification accuracy and parts segmentation tasks, the degree of improvement of the point cloud deep learning network by this algorithm is analyzed.

Figure 5(a) reflects the effect of common point cloud feature extraction. Because the number of clustering centers is uncertain, the position of the clustering center is unreasonable. Meanwhile, the cluster radius of different cluster subsets is the same, which leads to repeating sampling and missing sampling. The above factors will lead to the loss of point cloud features, which will affect the performance of the deep learning network.

Figure 5(b) is the result of adaptive point cloud feature extraction. Points are divided into two categories according to their distribution position. Each category has its own clustering center. According to the distance from the cluster center to the farthest point of the cluster subset, the radius of each cluster range is determined. It can be seen from Figure 4 that the adaptive clustering algorithm can effectively reflect the distribution features of the point cloud model. Therefore, the point cloud feature extraction through clustering can effectively reflect the structural features and distribution features of the point cloud. The loss of detailed features of the point cloud caused by randomness is avoided. The method we proposed is to use adaptive clustering to improve the performance of the deep learning network.

3.1. Number of Cluster Centers Generation. The error of the cluster algorithm is measured by *SSE*, where $\mu^{(j)}$ is the center point of the cluster j ($j \in \{1, 2, \ldots, k\}$). It is generally considered that the clustering solution process is a problem of optimization (minimization) of the SSE. We set the number of clustering samples as n. If the sample $x^{(i)}$ ($i \in \{1, 2, \ldots, n\}$) belongs to the j_{th} cluster, then $w^{(i,j)} = 1$; otherwise, $w^{(i,j)} = 0$.

$$SSE = \sum_{i=1}^{n} \sum_{j=1}^{k} w^{(i,j)} = \left\| x^{(i)} - \mu^{(j)} \right\|_2^2. \quad (1)$$

Based on the visualization tool of SSE, the optimal number of cluster centers is estimated for a given task. The basic method to determine the elbow point is to find the parameter of the cluster center when the clustering deviation increases abruptly. If the curve attenuation is gentle and there is no obvious elbow point, is the best sampling value when the SSE is set to be a threshold, usually less than 300.

We can draw the clustering deviation diagram with different values of the cluster center and observe the position of the elbow point.

Figure 6 is an image in which the SSE of the clustering changes with the number of cluster centers. It can be seen that the SSE decreases with the increase of cluster center number. When the number of cluster centers is three, the curve of Figure 6(b) presents an obvious elbow shape, which is called the elbow point. Therefore, three is a better choice for this set of data in Figure 6(a). The selection of elbow points should not only consider the degree of error change but also consider the absolute size of the error. If the error changes more gently with the increase of cluster centers or the elbow point appears in the place with a large error, the number of cluster centers with a small error should be selected as the best parameter.

3.2. Adaptive Optimal Clustering. After obtaining the optimal clustering center of each point cloud model, we then determine the location of the cluster center and divide the point cloud model into different subsets.

The main idea of AOMC is that the mutual distance between the initial cluster centers is as far apart as possible. We set the point cloud model as a set x. Our aim is to obtain a set of clustering results x_{cluster}. Initially, the point cloud model is a set of n sample points. We take μ to record each selected cluster center point.

We set an empty set M to record the selected cluster center points, then randomly select the first center point $\mu^{(1)}$ from the input sample, and add it to the set M.

For each sample point $x^{(i)}$ ($i \in \{1, 2, \ldots, n-1\}$) outside the set M, we calculate the shortest Euclidean distance $d(x^{(i)}, M)^2$ between each sample point and the current cluster center set M. According to the distance, the probability distribution $d(x^{(i)}, M)^2 / \sum_i d(x^{(i)}, M)^2$ is constructed.

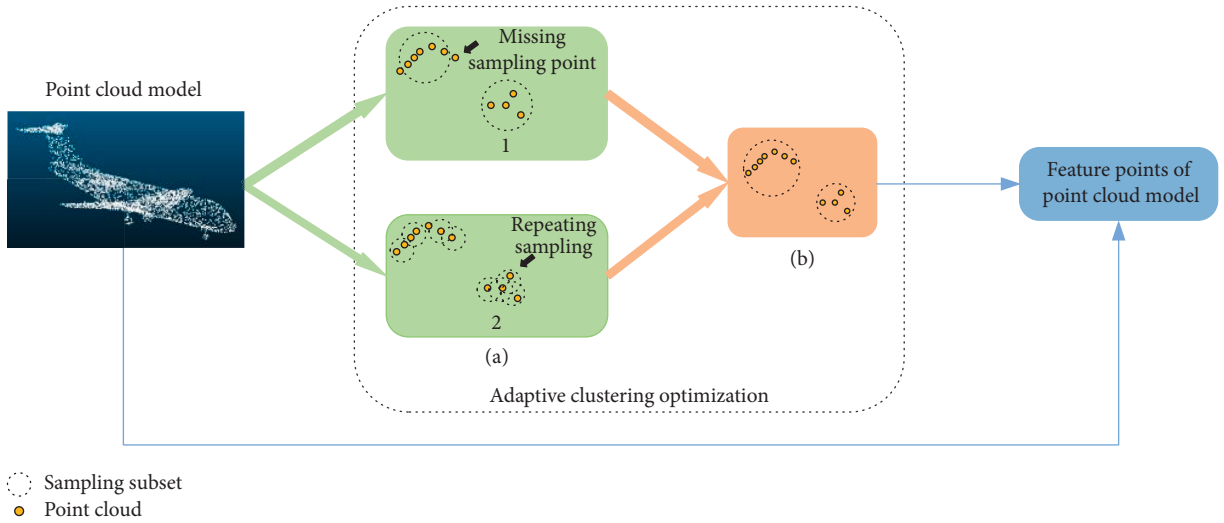

Figure 5: Comparison between common feature extraction and adaptive feature extraction: (a) common point cloud feature extraction and (b) adaptive point cloud feature extraction.

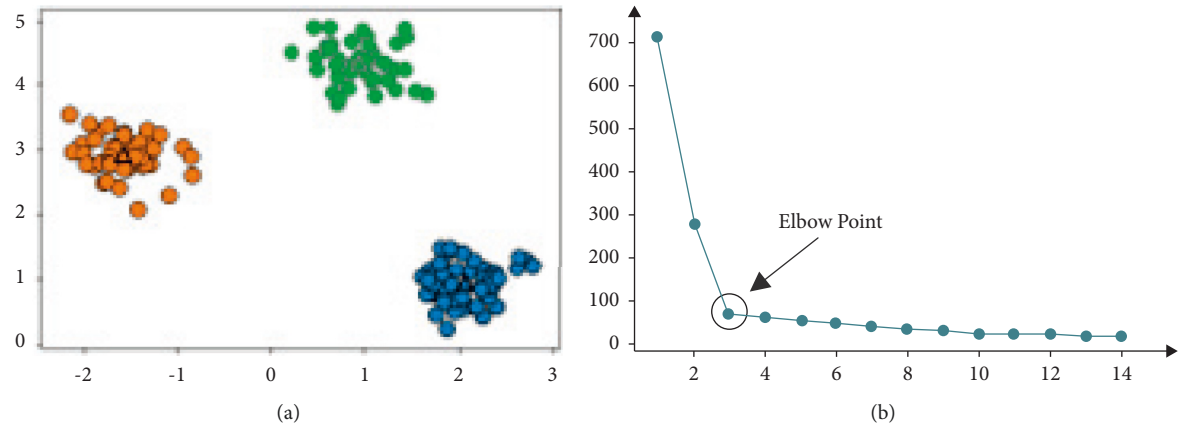

Figure 6: Elbow point selection schematic: (a) two dimensional of three cluster centers and (b) the relationship between the change of clustering number centers and SSE in (a). When the number of cluster centers is 3, the curve appears obvious "elbow point."

Then, based on the weighted distribution of distance, generate a probability value p between 0 and 1 and select the next central point $\mu^{(p)}$ from $x^{(i)}$ to M. In light of the probability distribution, the point in a set of $x^{(i)}$ farther away from M is more likely to be selected as the next cluster center $\mu^{(p)}$. This ensures the uniform distribution of the initial cluster centers in the point cloud model.

By repeating the above steps, the initial adaptive cluster centers are obtained. Compared with the random selection of initial cluster centers, the AOMC method ensures that the distance between the initial cluster center points is longer, and the distribution is uniform in the point cloud model.

The remaining points of x are classified into the cluster subsets corresponding to the cluster centers in M and initialize the SSE value of M. Then, set a threshold value for SSE. Based on the distribution of the points in the subset, the sample center of the subset is updated as the new cluster center in M. Update the current SSE of the point cloud model clustering result. Finally, when SSE is less than the threshold, we get the cluster result x_{cluster}.

The adaptive optimal means clustering (AOMC) algorithm is summarized in Algorithm 1:

3.3. Determination of Feature Points and Loss Function. After dividing the point cloud model into different adaptive clustering subsets, we then sample the data points of each subset. Sampling radius and loss function are defined as follows:

Sampling radius. We carry out cluster sampling of point clouds according to different types of point clouds. First, in order to prevent the occurrence of outliers, the maximum coverage is the entire sample space. The sampling radius is defined from the center point to the farthest point in the class:

$$r_j = \sqrt{\left\| x_{jf} - \mu_j \right\|_2^2} \quad j \in \{1, \ldots, k\}. \tag{2}$$

Loss function. In the point cloud deep learning network, the maximum cross-entropy function is used as the

Input: Point cloud model x
Output: Clustering results x_{cluster}
(1) $M \leftarrow \mu^{(1)}$
(2) **for** 1 to k do
(3) Compute $d(x^{(i)}, M)^2$
(4) Generate a value $p \in [0, 1]$
(5) **if** $p \in d(x^{(i)}, M)^2 / \sum_i d(x^{(i)}, M)^2$
(6) $M \leftarrow x^{(i)}$
(7) **end if**
(8) **end for**
(9) Initialize SSE for M
(10) **for** SSE > threshold do
(11) $x_{\text{cluster}}^{(j)} \longrightarrow SSE,\ j \in \{1, \ldots, k\}$
(12) Update M to the sample centers
(13) Update x_{cluster}
(14) Update SSE
(15) **end for**
(16) **return** x_{cluster}

Algorithm 1: AOMC: adaptive optimal means clustering for point cloud feature extraction.

measurement of the loss function. As shown in formula (3), it is the maximum cross-entropy function.

First of all, the input class of the neural network is normalized here, which is defined as follows:

$$L_S = \frac{e^{S_i}}{\sum_{i=1}^{k} e^{S_i}}, \tag{3}$$

where S_i denotes the output value of the multilayer perceptron for each point cloud class and k represents the number of point cloud classes in the sample. This operation is equivalent to the softmax layer function and $\cdots_S$ is output as a vector form. Next, the cross-entropy calculation is carried out between the output and the label, which is defined as follows:

$$L = -\frac{1}{k} \sum_{i=1}^{k} y_i \ln\left(L_{S_i}\right), \tag{4}$$

where y_i is the actual label of each point cloud class; the label of each point cloud class is multiplied by the natural logarithmic form output by the normalization layer, and finally, the mean loss of the point cloud class is calculated by means of the mean value as the loss function of the deep learning network.

4. Experiments

4.1. Data Sets. We conduct the experiments on two benchmark data sets. ModelNet10 contains 4,899 meshed CAD models from 10 categories. Each point cloud contains 10,000 coordinate points. Each point consists of three-dimensional position coordinate information (x, y, and z) and normal vector information (N_x, N_y, and N_z).

Shapenetcore_partanno_segmentation_benchmark data set includes 16,846 point cloud models from 19 types. Each point cloud contains about 2,500 coordinate points. Each point consists of three-dimensional position coordinate information and part segmentation information, whose purpose is to compare the prediction results of a deep learning network with real value.

Figure 7 is the example of the point cloud model in this research. As can be seen from Figure 7, the point cloud model has a large amount of data, and features need to be refined; otherwise, the processing algorithm will be time-consuming. Point cloud data is measurable. It can directly obtain three-dimensional coordinates, distance, azimuth, and surface normal vector on the point cloud and can also calculate the surface area and volume of the target expressed by the point cloud. Due to the limited laser penetration, the point cloud obtained by LiDAR scanning basically reflects the surface condition of the target, and there is almost no internal information about the target.

4.2. Evaluation Metrics. We use shapenetcore_partanno_segmentation_benchmark data set to test the network performance, randomly select 10 point cloud classes from them, and carry out parts segmentation analysis. We use mean intersection over union (mIoU) to evaluate the effect of a deep learning network on parts segmentation of point clouds [20–22].

$$mIoU = \frac{1}{k+1} \sum_{i=0}^{k} \frac{p_{ii}}{\sum_{j=0}^{k} p_{ij} + \sum_{j=0}^{k} p_{ji} - p_{ii}}, \tag{5}$$

where i represents the real value, j is the predicted value, p_{ij} is the probability that i is predicted to be j, and k is the number of categories in the sample. The larger the mIoU is, the more parts that prove that the predicted value coincides with the real value, the better the effect of network segmentation.

In order to verify the classification effect of this algorithm, the mean class accuracy ($m\ A\ P$) is used to evaluate the overall performance of network classification:

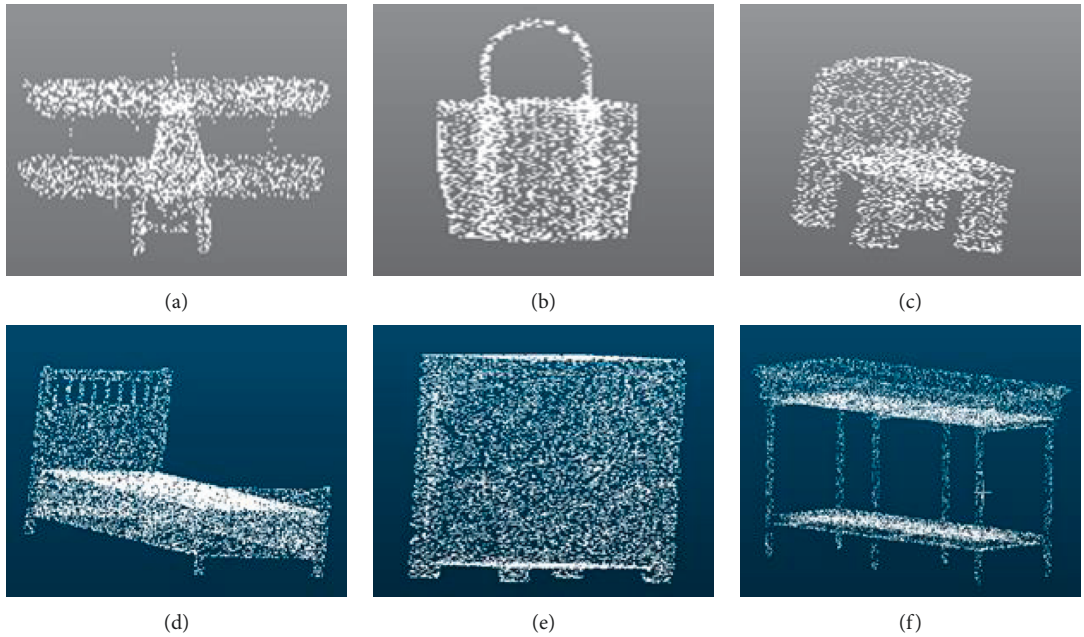

Figure 7: Examples of our point cloud model (top: shapenetcore_partanno_segmentation_benchmark and bottom: Modelnet10): (a) airplane, (b) bag, (c) chair, (d) bed, (e) dresser, and (f) table.

$$mAP = \frac{1}{k}\sum_{i=1}^{k} AP_i, \tag{6}$$

where k represents the number of point cloud classes and AP is the classification accuracy of each point cloud class.

4.3. Evaluation of Feature Point Extraction. The first two parts have already introduced the flow of the AOMC algorithm. Next, we use these methods to extract feature points from different types of point clouds. We use the Modelnet10 data set for analysis.

As shown in Table 1, the "elbow point method" is used to select the best clustering center number for 10 different types of the point cloud model in the data set.

Figure 8 illustrates the point cloud feature sampling using the AOMC algorithm, compared with the random feature sampling method, and the AOMC point cloud sampling points are more evenly distributed and can better capture local feature information, which achieves the purpose of improving the accuracy of point cloud deep learning network.

4.4. Overall Performance and Parameter Analysis of the Proposed Method. To better explain the benefits of the proposed AOMC clustering method, we make a comprehensive analysis from run time (time complexity), mAP, and mIoU. We compare and analyze the AOMC algorithm and other cluster methods, including farthest selection [27], random selection [34], DBSCAN [42], k-means [3], and agglomerative clustering [43]. Table 2 shows the performance of the combination of time complexity. What's more, Table 3 indicates the mIoU of each method on every point cloud model. Table 4 displays the comparison of mAP of various methods.

We evaluate the run-time performance of our method with a GTX 2080TI GPU, Core i9-9900K CPU, and 32 GB memory.

4.4.1. Run-Time Comparison. Run time is an important measure of algorithm complexity. Here, we calculate the run time of different point cloud feature extraction algorithms. In the Modelnet10 data set, there are 4,899 point cloud models. Each cloud model consists of 10,000 points. We set different feature points to comprehensively analyze and compare the time complexity of different feature extraction algorithms.

As can be seen from the data in Table 2, compared with the farthest selection, the algorithm complexity of AOMC is relatively low. In the actual experiment, due to the uneven density and dense arrangement of point cloud samples, it is difficult to adjust the parameters of the DBSCAN ($O(N * Eps)$, where Eps means the spending time finding each neighborhood point) algorithm, and the actual application effect is limited. The algorithm complexity of agglomerative clustering ($O(N^3)$) is the highest among them. Random selection has the highest sampling speed ($O(1)$), but it has a large loss of local characteristics of the point cloud. In practice, the time complexity of AOMC is slightly longer than that of k-means ($O(N * \log(N))$). The main reason is the determination of the number of cluster centers.

4.4.2. mIoU Comparison. Next, we analyze the performance of the feature extraction algorithm in parts segmentation tasks by comparing the mIoU of different point cloud models.

Table 1: Selection of cluster number of different point clouds based on "elbow point method."

Class	Bathtub	Bed	Chair	Desk	Dresser	Monitor	Nightstand	Sofa	Table	Toilet
Number of cluster centers	17	13	9	11	12	12	15	11	11	16

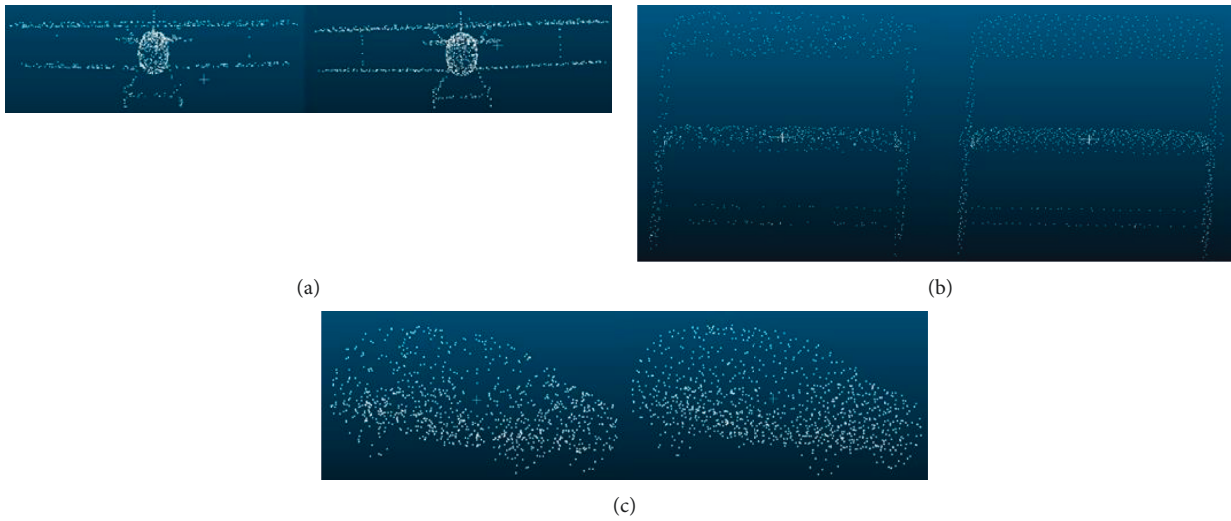

Figure 8: Comparison of point cloud feature sampling point between AOMC and random sampling. A total of 10m24 feature points are collected for each point cloud model; the left is random sampling; and the right is using AOMC to sample feature points. (a) Details of the wing are lost by random sampling. (b) and (c) Point cloud distribution of AOMC is more uniform than random sampling. (a) Airplane, (b) chair, and (c) car.

Table 2: Comparison of run time on local feature point extraction.

Feature points number	1,024	1,536	2,048
Farthest selection	1.51 s	3.56 s	5.83 s
Random selection	7×10^{-4} s	1.11×10^{-3} s	15×10^{-3} s
DBSCAN	0.07 s	0.08 s	1.01 s
k-means ($k = 10$)	0.32 s	0.36 s	0.47 s
Agglomerative clustering ($n = 10$)	2.91 s	2.96 s	3.01 s
Ours	0.55 s	0.58 s	0.64 s

Table 3: Comparison of mIoU on parts segmentation task. The best and the second-best methods are highlighted in red and green colors, respectively.

Method	Mean intersection over union (mIoU)										
	Avg (%)	Airplane (%)	Bag (%)	Chair (%)	Laptop (%)	Knife (%)	Mug (%)	Rocket (%)	Cap (%)	Table (%)	Earphone (%)
Farthest selection	81.60	82.40	81.10	90.70	90.60	86.10	95.10	54.50	89.90	82	68.50
Random selection	78.80	80.30	80	91	89	83.10	90.10	51.40	87.70	73	62
DBSCAN	79.70	79.20	78	89	90	83	95	56	82	80	65
k-means ($k = 10$)	80.70	83.10	74	88	91	84	87	57	90.10	81	72
Agglomerative clustering	79.30	81.40	73	83	84	83.40	91	59	88.40	80.40	69.40
Ours	83	84	79	91.70	89.40	89.90	94.30	61	83	84	74

It can be seen from Table 3 that AOMC, the method we proposed based on adaptive point cloud clustering feature extraction, is applied in the task of point cloud model parts segmentation. The mIoU of some point cloud models parts segmentation is improved.

We can see that AOMC obtains an average of 1.4% improvement over the second-best method: farthest selection. Compared with the random selection sampling method, AOMC has the best relative performance, which is about 4.2% enhancement. Although agglomerative clustering has the highest time complexity, its performance of parts segmentation is not better.

As shown in Figure 9, it is the effect of point cloud parts segmentation. The interior of the point cloud model is

Table 4: Comparison of the map on the classification task. The best and the second-best methods are highlighted in red and green colors, respectively.

Method	Mean intersection over union (mIoU)										
	Avg (%)	Airplane (%)	Bag (%)	Chair (%)	Laptop (%)	Knife (%)	Mug (%)	Rocket (%)	Cap (%)	Table (%)	Earphone (%)
Farthest selection	81.60	82.40	81.10	90.70	90.60	86.10	95.10	54.50	89.90	82	68.50
Random selection	78.80	80.30	80	91	89	83.10	90.10	51.40	87.70	73	62
DBSCAN	79.70	79.20	78	89	90	83	95	56	82	80	65
k-means ($k = 10$)	80.70	83.10	74	88	91	84	87	57	90.10	81	72
Agglomerative clustering	79.30	81.40	73	83	84	83.40	91	59	88.40	80.40	69.40
Ours	83	84	79	91.70	89.40	89.90	94.30	61	83	84	74

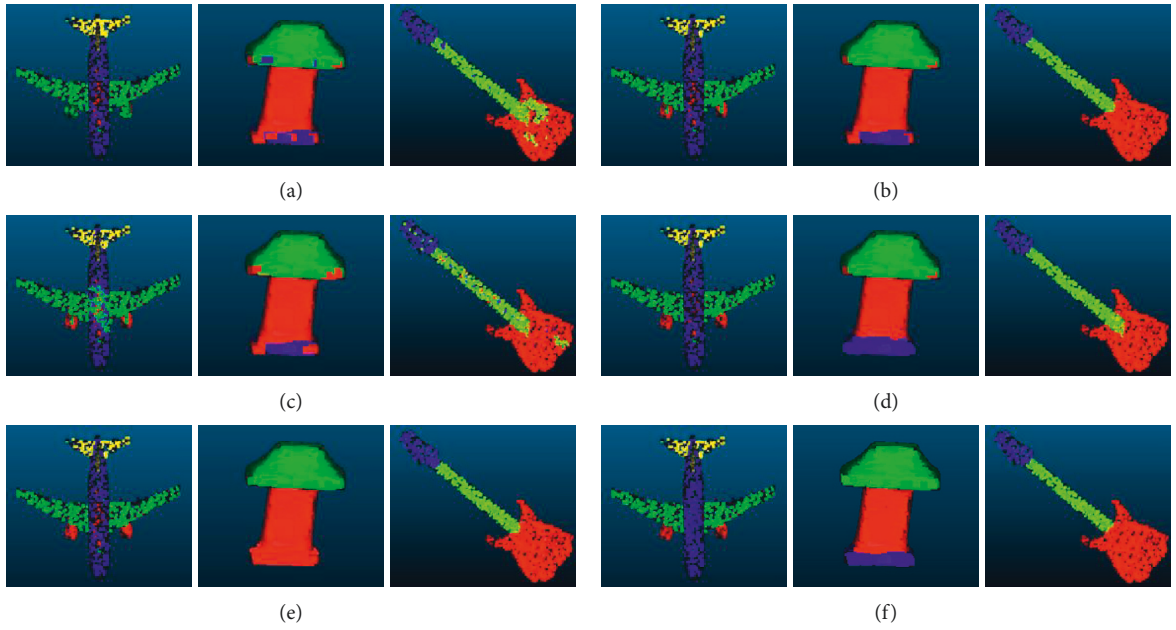

Figure 9: Point cloud parts segmentation example diagram. The point cloud model is divided according to the internal category (left: airplane, middle: lamp, and right: guitar). (a) random selection, (b) farthest selection, (c) DBSCAN, (d) k-means, (e) agglomerative clustering, and (f) ours.

divided into several parts. Random selection leads to a large number of point cloud classification errors, and it loses an array of model details. The engine of an airplane is almost confused with the wing. The parts of the guitar are not well differentiated.

The same problem exists in the DBSCAN sample method. In the airplane model, part of the fuselage point cloud is mistaken for the wing. And, of the lamp model, the base is confused with a lampshade. There are some classification errors on the guitar. In agglomerative clustering models, the lamp is only divided into two parts, and there are a few classification errors on the aircraft fuselage.

Although k-means and farthest selection has better segmentation effect, there are still a few mistakes. Compared with the above method, our method performs well in these point cloud models. The base, middle part, and shade of the lamp are clearly divided into three parts, and there is no error on the fuselage of an airplane. We can find that the point cloud deep learning network enables to capture better semantic information by adaptive clustering with parts segmentation task. This strategy suppresses the noises of redundant local details and brings significant improvement to the edge performance.

4.4.3. Accuracy Analysis. Feature extraction plays an important role in the optimization process of a deep learning network. Among them, it has a great influence on the accuracy of network classification. We calculate the classification accuracy of each point cloud model and then analyze the influence of feature extraction on network accuracy by average value.

It can be seen from Table 4 that the point cloud feature extraction method based on adaptive clustering has achieved good results in some point cloud models. The average mAP is 89.09%, which is the best performance among these feature extraction methods. Similar to the performance on parts segmentation, the AOMC clustering method has a 0.84% benefit over the second-best clustering algorithm.

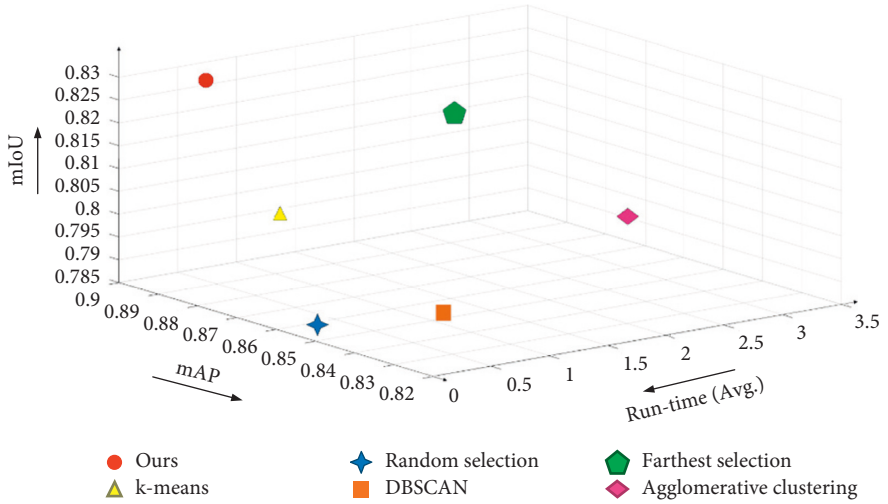

Figure 10: Comprehensive comparison of our method with other cluster feature extraction methods.

What's more, DBSCAN still performs not well in classification; the proposed method has a 6.67% advantage over that. Because of the inaccurate extraction of detailed information, the random selection method cannot accomplish the tasks of a deep learning network well.

Figure 10 shows the visual comprehensive comparison of different cluster feature extraction methods. From the comparison results, it can be seen that our method has high real-time performance. In the task of point cloud segmentation, the performance of this algorithm is the best. However, in the classification task, the comprehensive performance of this algorithm is not good, and it only performs well in several point cloud models. The comprehensive performance of the AOMC algorithm is better than that of other models. We can choose different scale point cloud densities according to different task requirements, which makes the algorithm more flexible.

As can be seen from Figure 11, the point cloud feature extraction method based on adaptive unsupervised learning makes the loss function optimization speed of the deep learning network faster and the loss value smaller. The main reason is that the adaptive clustering method can extract more detailed information, thus increasing the classification gap between hierarchical learning features of point cloud categories. At the same time, due to the high complexity of the farthest selection point sampling algorithm, the network convergence rate is slow. Because of the neglect of more detailed information in point cloud models, the random selection method has the lowest overall accuracy and the biggest loss value among all experimental methods.

It can be seen from Figure 12 that when the number of training times reaches a certain number, the accuracy of the deep learning network using the adaptive clustering method is higher than that of the other point cloud feature extraction methods. It is proved that the deep learning network using an adaptive clustering algorithm has a relatively high optimization speed. At the same time, the deep learning network used for feature extraction has higher accuracy. Compared with some point cloud feature extraction methods, the adaptive point cloud feature extraction method obtains more detailed targets, to improve the hierarchical feature learning effect.

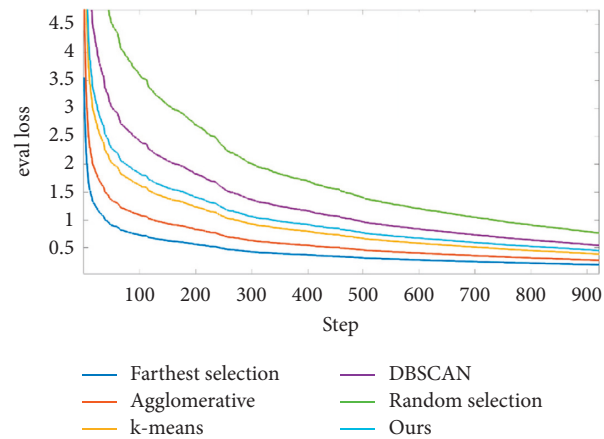

Figure 11: Training loss curve of the classified network.

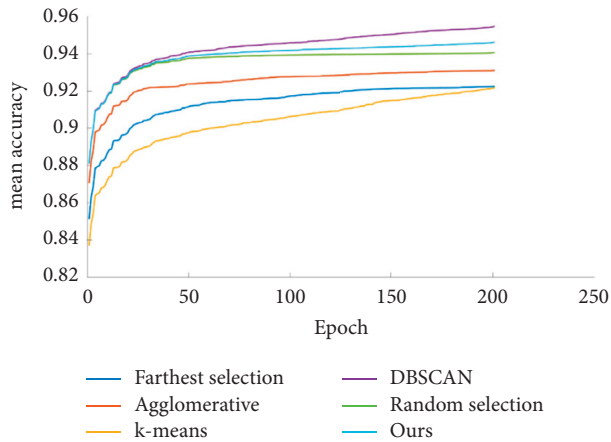

Figure 12: Training accuracy curve of classification network.

The experiments provide strong evidence for the advantages of adaptive unsupervised clustering for point cloud feature extraction. Adaptive point cloud clustering feature extraction method obtains better performance in time complexity. The reason is that the algorithm we proposed

avoids the overall traversal of the point cloud model and reduces the amount of calculation. In the point cloud deep learning task, the adaptive point cloud feature extraction method obtains higher accuracy of point cloud classification and parts segmentation. In the training process of the point cloud deep learning network, an adaptive feature extraction algorithm can improve the convergence rate of the network. Compared with the random selection method, the point cloud deep learning network achieves higher mean accuracy.

5. Conclusion

In this paper, we propose a novel point cloud feature extraction method based on unsupervised learning and adaptive optimization. AOMC point cloud feature extraction method consists of the cluster centers' number generation, adaptive clustering, and the applying tasks of the deep learning network. The accuracy and speed of the deep learning network are improved effectively. The performance of classification and parts segmentation is better.

Comparison results demonstrate the efficacy of the proposed methods. As can be seen from the experimental results, the method we proposed improves the effect of point cloud feature extraction and achieves the purpose of point cloud hierarchical feature learning. The accuracy of the point cloud deep learning network is improved. AOMC clustering algorithm improves the accuracy of the initial point of the clustering center, so as to improve the convergence rate and accuracy of the clustering processing. In the meantime, the method of selecting the best clustering center number by quantization SSE is put forward so that the point cloud clustering number and the point cloud category can be adapted to each other, and the fixed value method is no longer used to determine the amount of clustering center. As a result, it improves the rationality and accuracy of the point cloud deep learning. What is also worth noticing is that our clustering method realizes the purpose of improving the classification accuracy, parts segmentation accuracy, and convergence rate of the deep learning network.

The proposed method still has some drawbacks. It does not achieve the best performance in all point cloud models. And the steps of the algorithm are complicated. In the future, we plan to simplify the algorithm steps of AOMC. And improve accuracy for all models.

Data Availability

The data used to support the findings of this study are included within the article.

Conflicts of Interest

The authors declare that they have no conflicts of interest.

References

[1] T. Yu and J. Yang, "3d model recognition and classification based on k-nearest neighbor convolutional neural network," *Laser & Optoelec-tronics Progress*, vol. 27, no. 669, pp. 355–363, 2020.

[2] J. Zhang, X. Zhao, and Z. Chen, "A review of semantic segmentation of point cloud based on deep learning," *Las Optoelect Prog*, vol. 57, pp. 28–46, 2020.

[3] H. Han, *Research on Semantic Segmentation of 3d point cloud*, University of Electronic Science and Technology of China, Chengdu, China, 2020.

[4] M. K. Hasan, L. Dahal, P. N. Samarakoon, F. I. Tushar, and R Martí, "DSNet: automatic dermoscopic skin lesion segmentation," *Computers in Biology and Medicine*, vol. 120, Article ID 103738, 2020.

[5] W. You, A. Hao, S. Li, Y. Wang, and B. Xia, "Deep learning-based dental plaque detection on primary teeth: a comparison with clinical assessments," *BMC Oral Health*, vol. 20, no. 1, pp. 141–147, 2020.

[6] L. Wang, F. Liu, and J. Xu, "A semantic segmentation and edge detection model based on edge information constraint training," *Journal of Physics: Conference Series*, vol. 1518, no. 1, Article ID 012046, 2020.

[7] J. Masci, D. Boscaini, and M. Bronstein, "Geodesic convolutional neural networks on riemannian manifolds," in *Proceedings of the IEEE International Conference on Computer Vision Workshops*, pp. 37–45, Santiago, Chile, December, 2015.

[8] D. Maturana and S. Scherer, "Voxnet: a 3d convolutional neural network for real-time object recognition," in *Proceedings of the 2015 IEEE/RSJ International Conference on Intelligent Robots and Systems (IROS)*, pp. 922–928, IEEE, Hamburg, Germany, October, 2015.

[9] Y. Bisheng and D. Zhen, "Progress and perspective of point cloud intelligence," *Acta Geodaetica et Cartographica Sinica*, vol. 48, no. 12, p. 1575, 2019.

[10] J. Zhuangwei, G. Haiyan, and Z. Yufu, "Survey of point cloud semantic segmentation based on deep learning," *Journal of Frontiers of Computer Science & Technology*, vol. 15, no. 1, pp. 1–26, 2021.

[11] K. Lai, L. Bo, and D. Fox, "Unsupervised feature learning for 3d scene labeling," in *Proceedings of the 2014 IEEE International Conference on Robotics and Automation (ICRA)*, pp. 3050–3057, IEEE, Hong Kong, China, June, 2014.

[12] A. Golovinskiy, V. G. Kim, and T. Funkhouser, "Shape-based recognition of 3D point clouds in urban environments," in *Proceedings of the 2009 IEEE 12th International Conference on Computer Vision*, pp. 2154–2161, IEEE, Kyoto, Japan, October, 2009.

[13] R. B. Rusu and S. Cousins, "3d is here: point cloud library (pcl)," in *Proceedings of the 2011 IEEE International Conference on Robotics and Automation*, pp. 1–4, IEEE, Shanghai, China, May, 2011.

[14] S. Nowok, S. Kueppers, and H. Cetinkaya, "Millimeter wave radar for high resolution 3D near field imaging for robotics and security scans," in *Proceedings of the 2017 18th International Radar Symposium (IRS)*, pp. 1–10, IEEE, Prague, Czech Republic, June, 2017.

[15] R. B. Rusu, N. Blodow, and Z. C. Marton, "Aligning point cloud views using persistent feature histograms," in *Proceedings of the 2008 IEEE/RSJ International Conference on Intelligent Robots and Systems*, pp. 3384–3391, IEEE, Nice, France, September, 2008.

[16] C. Jing, *Semantic Segmentation of 3d point Clouds Based on Deep learning*, Xidian University, Xi'an, China, 2019.

[17] L. Li, Z. Li, S. Liu, and H. Li, "Occupancy-map-based rate distortion optimization and partition for video-based point cloud compression," *IEEE Transactions on Circuits and Systems for Video Technology*, vol. 31, no. 1, pp. 326–338, 2021.

[18] H. Su, S. Maji, and E. Kalogerakis, "Multi-view convolutional neural networks for 3d shape recognition," in *Proceedings of the IEEE International Conference on Computer Vision*, pp. 945–953, Boston, MA, USA, June, 2015.

[19] S. Ioffe and C. Szegedy, "Batch normalization: accelerating deep network training by reducing internal covariate shift," in *Proceedings of the International Conference on Machine Learning*, pp. 448–456, PMLR, Dehradun, India, July, 2015.

[20] M. Jaderberg, K. Simonyan, and A. Zisserman, "Spatial transformer networks," *Advances in Neural Information Processing Systems*, vol. 28, Article ID 02025, 2015.

[21] R. B. Rusu, N. Blodow, and M. Beetz, "Fast point feature histograms (FPFH) for 3D registration," in *Proceedings of the 2009 IEEE International Conference on Robotics and Automation*, pp. 3212–3217, IEEE, Kobe, Japan, May, 2009.

[22] R. B. Rusu, G. Bradski, and R. Thibaux, "Fast 3d recognition and pose using the viewpoint feature histogram," in *Proceedings of the 2010 IEEE/RSJ International Conference on Intelligent Robots and Systems*, pp. 2155–2162, IEEE, Taipei, Taiwan, October, 2010.

[23] A. Frome, D. Huber, R. Kolluri, T. Bülow, and J. Malik, "Recognizing objects in range data using regional point descriptors," in *Proceedings of the European Conference on Computer Vision*, pp. 224–237, Springer, Munich, Germany, September, 2004.

[24] S. Belongie, J. Malik, and J. Puzicha, "Shape matching and object recognition using shape contexts," *IEEE Transactions on Pattern Analysis and Machine Intelligence*, vol. 24, no. 4, pp. 509–522, 2002.

[25] F. Tombari, S. Salti, and L. Di Stefano, "Unique shape context for 3D data description[C]," in *Proceedings of the ACM Workshop on 3D Object Retrieval*, pp. 57–62, Firenze Italy, October, 2010.

[26] Z. Wu, S. Song, and A. Khosla, "3d shapenets: a deep representation for volumetric shapes," in *Proceedings of the IEEE Conference on Computer Vision and Pattern Recognition*, pp. 1912–1920, Seattle, WA, USA, June, 2015.

[27] C. R. Qi, L. Yi, and H. Su, "Pointnet++: deep hierarchical feature learning on point sets in a metric space," *Advances in Neural Information Processing Systems*, vol. 30, 2017.

[28] H. Rahmanifard, P. Maroufi, H. Alimohamadi, T. Plaksina, and I. Gates, "The application of supervised machine learning techniques for multivariate modelling of gas component viscosity: a comparative study," *Fuel*, vol. 285, Article ID 119146, 2021.

[29] M. Shibata, K. Okamura, K. Yura, and A. Umezawa, "High-precision multiclass cell classification by supervised machine learning on lectin microarray data," *Regenerative Therapy*, vol. 15, pp. 195–201, 2020.

[30] A. Yassine, L. Mohamed, and M. Al Achhab, "Intelligent recommender system based on unsupervised machine learning and demographic attributes," *Simulation Modelling Practice and Theory*, vol. 107, Article ID 102198, 2021.

[31] A. H. Aljemely, J. Xuan, F. K. J. Jawad, O. Al-Azzawi, and A. S Alhumaima, "A novel unsupervised learning method for intelligent fault diagnosis of rolling element bearings based on deep functional auto-encoder," *Journal of Mechanical Science and Technology*, vol. 34, no. 11, pp. 4367–4381, 2020.

[32] C. R. Qi, H. Su, and K. Mo, "Pointnet: deep learning on point sets for 3d classification and segmentation," in *Proceedings of the IEEE Conference on Computer Vision and Pattern Recognition*, pp. 652–660, Honolulu, HI, USA, June, 2017.

[33] G. Hetzel, B. Leibe, and P. Levi, "3D object recognition from range images using local feature histograms," in *Proceedings of the 2001 IEEE Computer Society Conference on Computer Vision and Pattern Recognition*, IEEE, Kauai, HI, USA, December, 2001.

[34] J. Guan and W. Pan, "Ground point cloud extraction algorithm based on multi region ransac," *Electronic Technology and Software Engineering*, vol. 14, pp. 176-177, 2020.

[35] Y. Zhu, R. Urtasun, and R. Salakhutdinov, "Segdeepm: exploiting segmentation and context in deep neural networks for object detection," in *Proceedings of the IEEE Conference on Computer Vision and Pattern Recognition*, pp. 4703–4711, Boston, MA, USA, July, 2015.

[36] X. Han, C. Armenakis, and M. Jadidi, "Dbscan optimization for improving marine trajectory clustering and anomaly detection," *The International Archives of the Photogrammetry, Remote Sensing and Spatial Information Sciences*, vol. XLIII-B4-2020, pp. 455–461, 2020.

[37] K. Indira and M. K. Kavitha Devi, "Multi cloud based service recommendation system using DBSCAN algorithm," *Wireless Personal Communications*, vol. 115, no. 2, pp. 1019–1034, 2020.

[38] Z. C. Marton, D. Pangercic, N. Blodow, and M Beetz, "Combined 2D-3D categorization and classification for multimodal perception systems," *The International Journal of Robotics Research*, vol. 30, no. 11, pp. 1378–1402, 2011.

[39] A. E. Johnson, *Spin-images: A Representation for 3-D Surface matching*, PhD Thesis, 1997.

[40] A. Aldoma, M. Vincze, and N. Blodow, "CAD-model recognition and 6DOF pose estimation using 3D cues," in *Proceedings of the 2011 IEEE International Conference on Computer Vision Workshops (ICCV Workshops)*, pp. 585–592, IEEE, Barcelona, Spain, November, 2011.

[41] A. Kirillov, K. He, and R. Girshick, "Panoptic segmentation," in *Proceedings of the IEEE/CVF Conference on Computer Vision and Pattern Recognition*, pp. 9404–9413, Long Beach, CA, USA, June, 2019.

[42] Y. Yang and M. Li, "A point cloud denoising method based on a hybrid filtering and density clustering algorithm," *Metrology & Measurement Technique*, vol. 47, no. 4, pp. 24–27, 2020.

[43] A. Zhu, J. Yang, and L. Wang, "A spatial non-cooperative target reconstruction technology based on hierarchical clustering," *Aerospace Control and Application*, vol. 46, no. 6, pp. 69–72, 2020.

Hindawi
Scientific Programming
Volume 2023, Article ID 9793108, 1 page
https://doi.org/10.1155/2023/9793108

Retraction

Retracted: The Method of Graphic Design Using 3D Virtual Vision Technology

Scientific Programming

Received 18 July 2023; Accepted 18 July 2023; Published 19 July 2023

This article has been retracted by Hindawi following an investigation undertaken by the publisher [1]. This investigation has uncovered evidence of one or more of the following indicators of systematic manipulation of the publication process:

(1) Discrepancies in scope
(2) Discrepancies in the description of the research reported
(3) Discrepancies between the availability of data and the research described
(4) Inappropriate citations
(5) Incoherent, meaningless and/or irrelevant content included in the article
(6) Peer-review manipulation

The presence of these indicators undermines our confidence in the integrity of the article's content and we cannot, therefore, vouch for its reliability. Please note that this notice is intended solely to alert readers that the content of this article is unreliable. We have not investigated whether authors were aware of or involved in the systematic manipulation of the publication process.

Wiley and Hindawi regrets that the usual quality checks did not identify these issues before publication and have since put additional measures in place to safeguard research integrity.

We wish to credit our own Research Integrity and Research Publishing teams and anonymous and named external researchers and research integrity experts for contributing to this investigation.

The corresponding author, as the representative of all authors, has been given the opportunity to register their agreement or disagreement to this retraction. We have kept a record of any response received.

References

[1] L. Li, "The Method of Graphic Design Using 3D Virtual Vision Technology," *Scientific Programming*, vol. 2022, Article ID 4135519, 9 pages, 2022.

Hindawi
Scientific Programming
Volume 2022, Article ID 4135519, 9 pages
https://doi.org/10.1155/2022/4135519

Research Article

The Method of Graphic Design Using 3D Virtual Vision Technology

Lin Li

Shanxi Vocational University of Engineering Science and Technology, Datong 030619, Shanxi, China

Correspondence should be addressed to Lin Li; lilin5@sxgkd.edu.cn

Received 18 May 2022; Revised 25 June 2022; Accepted 14 July 2022; Published 4 August 2022

Academic Editor: Lianhui Li

The traditional template scheduling method provides designers with design materials that do not reflect the real intention of designers, and a plane method based on three-dimensional virtual vision technology is proposed. In the given development environment, the mouse uses hand drawing, and the handwriting is formed by the obtained point sequence. The hand drawing adopts the method of smoothing noise to eliminate the noise, and the hand drawing stroke adopts two loops. The virtual model is drawn into 3D manually to realize the graphic design. After establishing the three-dimensional graphic design model, the visual effect is improved by using color mapping. The experiments show that this method can effectively realize the three-dimensional virtual model based on manual drawing, make the three-dimensional effect more real, meet the requirements of designers, and help designers show the real intention of design.

1. Introduction

As the market of practical design becomes bigger and bigger, the requirements for graphic design become higher and higher. For designers, the most important thing is "creativity," which is the key to differentiate designers from craftsmen [1]. Designers must form their own style of creation. Graphic design cannot be separated from the development of productivity and material civilization and even more so from the promotion of economic development [2]. Design works should put practicality in the first place and then take into account its artistry.

Grobius believed that the creation of beauty and industrialized production could be perfectly unified. He pointed out the following. "History shows that the idea of beauty changes with the progress of ideas and technology. Whoever thinks he has discovered eternal beauty is bound to fall into imitation and stagnation." Clothing design works such as those inspired by the traditional Chinese art of paper-cutting are loved by international and domestic fashion darlings, and many international high-end private custom clothing brands have absorbed a large number of traditional Chinese crafts such as embroidery [3], tassels, batik, blue and white ceramics, and so on to design a large number of classic works, as can be seen from the traditional Chinese elements absorbed in large quantities in the 2016 Veep lingerie; when tradition and innovation collide, the graphic design charm is remembered and recognized by the public, which improves the practicality of design works [4]. As the market for practical design becomes larger and larger, the requirements for graphic design become higher and higher, and for designers, the most important thing is "creativity," which is the key to differentiate designers from craftsmen. In the traditional logo design, the logo is just a simple trademark or logo, but now the logo design, in addition to the role of trademark or logo, carries more modeling, decoration, composition, and other roles, such as the trademark of CHANEL (Chanel) [5]. For example, our design works can be used in different positions of different products to meet people's aesthetics and achieve the dual effect of aesthetics and practicality [6].

In the process of graphic design, textual elements are mainly divided into various forms, such as advertising slogans, theme words, and supplementary descriptions. As an extension of graphic design and the main carrier of information dissemination, the text elements in graphic

design should not only focus on the functionality of text information but also need to take into account its cultural expression [7]. In addition, designers need to combine the artistic form of graphic image to design the text elements in graphic design, so as to bring people a refreshing feeling [8].

In graphic design, picture elements can be divided into painting elements, photography elements, and graphic elements, which not only contain the expression of image language and graphic language but also have the characteristics of enhancing the visual recognition and memory of the visual language of graphic design [9]. Among them, painting elements can express different visual languages by using various painting tools and styles selected by designers. Photography elements can greatly enhance the persuasion of graphic images, and graphic elements have the intuitive effect of simplifying abstraction [10]. The rational use of graphic elements enables graphic works to better express visual language. Therefore, based on the three-dimensional virtual vision technology, this paper realizes the high autonomy of planners through the 3D modeling of manual operation.

In this paper, the hand drawing adopts the method of smoothing noise to eliminate the noise, and the hand drawing stroke adopts two loops. The virtual model is drawn into 3D manually to realize the graphic design. After establishing the three-dimensional graphic design model, the visual effect is improved by using color mapping.

2. Related Work

Graphic design cannot be separated from the development of productivity and material civilization, and even more so from the promotion of economic development, design works should put practicality in the first place and then take into account its artistry [12]. Many of the world's high-end brands are fine-tuning their trademarks and advertising slogans with the development of the times, including car brands, food brands, clothing brands, daily-use brands, and so on. This highlights the fact that the market positioning of graphic design is not static, and its practicality is the first and artistry is the second in the role of marketing [13].

In the visual language of graphic design, visual recognition refers to the image that has certain color, size, shape, or structure and can attract people's attention from the visual aspect. The amount of information that people can obtain is greatly increased, which not only makes people's awareness of information greatly enhanced but also makes it difficult for people to focus on the visual aspect. Therefore, in order to attract people's attention to graphic design from the visual aspect, it is necessary for graphic design to start with image design and effectively attract the public's attention through special and distinctive design images, which is the centralized embodiment of the visual language of graphic design [14, 15]. The visual language of graphic design is further enhanced. It is believed that with the continuous development of visual art, more and more novel visual expressions will appear in graphic design, and the visual language of visual recognition will be further enhanced.

In the process of graphic design, in addition to using bright colors and creative shapes to attract people's attention, designers also need to integrate some information into the visual language of graphic design, so that people can read the information in the process of watching the graphic design content, so as to achieve the communication and dissemination of information, and this is the readability of the visual language of graphic design. In order to make the visual language of graphic design have certain readability, designers usually need to give certain spiritual and cultural connotation to the graphic design image in the process of graphic design, so that the visual language of graphic design image can be understood by people [16, 17]. Therefore, designers need to strengthen the coherence of the visual language in the graphic design image when designing, so that the graphic design can successfully realize the communication and dissemination of information.

In addition to the need to communicate and express information through the visual language of graphic design, graphic design designers also need to make people leave a long-term impression of the graphic design image, and when they think of the impression of the graphic design, they can recall the information that the graphic design works want to convey, and this is the memorability of the visual language. In the visual language expression of graphic design, the memorability of visual language is dependent on the visual recognition characteristics of visual language because graphic design with strong visual recognition characteristics has more innovative and unique graphic design image, which can cause strong stimulation to people's visual senses and trigger the resonance in people's heart, so that people can maintain a deep memory of the image of graphic design [18]. In the visual language of graphic design, the harmony and proportion of graphic images can make people find a unique attraction and charm in the process of viewing graphic design, which in turn forms a conditioned reflex in people's mind and stores their visual impression of graphic design for a long time [19]. If we can control the memorability of visual language in the process of graphic design, we can make graphic design further develop into an innovative and unique art form.

3. Methodology

The overall structure of the 3D simulation system for floor plan design was designed using virtual vision technology to provide services to each application system so that each heterogeneous system can easily access data-level services. The 3D simulation technology was used for distributed 3D floor plan design, and the interior space hierarchical layout was realized on the basis of modeling software. The operating system is Win7, and 3D simulation is used as a 3D program development tool, and the OpenGL graphics library is used to provide more point, line, and surface drawing functions in the modeling process. The configuration is shown in Figure 1.

Based on the overall design architecture, the system is modularized and functionalized to provide executable real-time 3D application files for 3D graphic design through virtual vision technology. The application loading mode of the 3D graphic design process is dynamically changed using virtual vision technology. To make the designed software

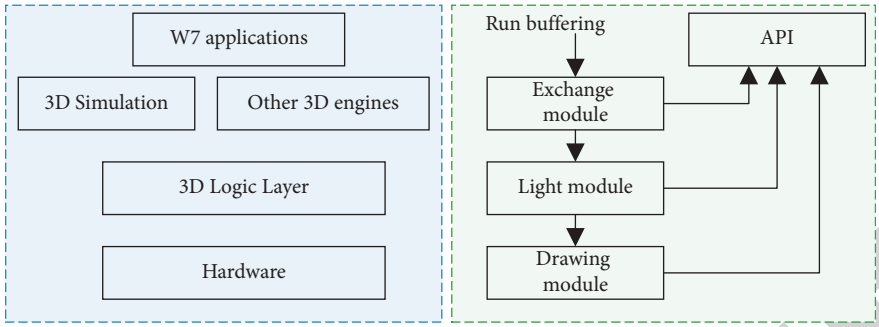

Figure 1: Overall structure of the 3D simulation system for graphic design.

functions more reasonable, 3DMAX 7.0 software is adopted as the 3D model making tool [20].

The 3D image virtual reconstruction system is mainly composed of three parts: sensor module, upper computer 3D imaging module, and circuit module, and its specific structure is shown in Figure 2.

It can be seen from Figure 2 that the system architecture consists of hardware structure, interaction of data and instructions, and management of system coordination. The main control chip is the core of the system, which can realize three-dimensional image reconstruction by combining microcontroller, Gigabit Ethernet, and other devices.

Based on the stereo sensors and display technology in 3D virtual reality technology to design the vision module, the module is mainly composed of multiple stereo vision sensors, mainly through the deployment of stereo vision sensors to the design of the indoor environment for three-dimensional imaging display. The specific model of the stereo vision sensor is Xtion ASUS, and its specific technical parameters are given in Table 1.

The data processing module consists of a PC and a GPU. The PC is mainly used for core data processing, and its specific parameters are given in Table 2.

The GPU is mainly used for image data processing, and the model chosen is Quadro Nvidia 3000M GPU, whose specific parameters are given in Table 3.

Establishing a good 3D virtual model requires corresponding technologies and tools. Firstly, the acquisition process of hand drawing is introduced: hand drawing with the mouse and forming a pattern with a given sequence of points R describes a sequence of ordered points

$$H(\alpha_i, \beta_i, \chi_i, U_m), \tag{1}$$

where q_i indicates the points in the display. The speed of each point is set, i.e., $v_i = |\overrightarrow{q_i q_{i+1}}|$; the faster the plotting speed is, the more dispersed the points are and the faster the points are collected.

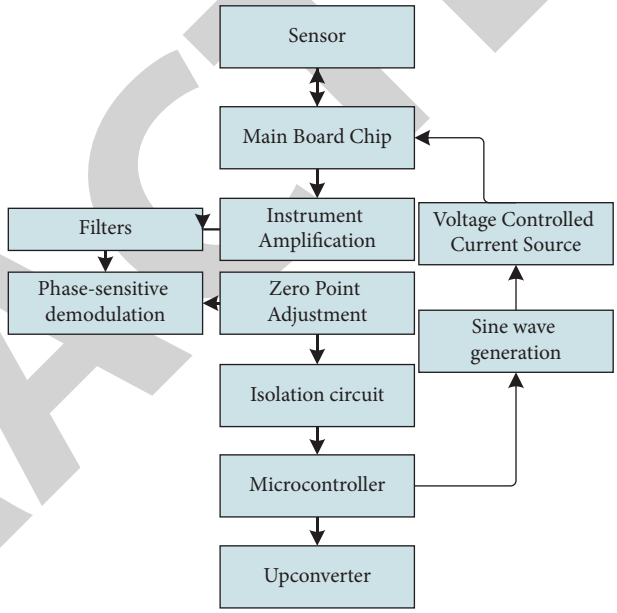

Figure 2: Diagram of the overall system structure.

When drawing with the mouse, the handshake will make a noise. In addition, there will be some errors when converting the input data into coordinate points on the display. The lower the resolution of the display, the greater the error. This section uses noise smoothing. The basic idea of smoothing noise is to adjust the value of the current point according to the value of adjacent points. Thus, we have

$$R^* = \{q_i^* \mid 0 \le i \le M - 1\},$$
$$q_i^* = \sum_{j=i-N}^{i+N} \omega_j q_j. \tag{2}$$

Table 1: Specific technical parameters of stereo vision sensor.

Serial number	Technical index	Specific parameters
1	Model	Xtion ASUS PRO
2	Size	5 × 3.5 × 18 cm
6	Viewable angle	Vertical angle: 57.5°, horizontal angle: 45°
7	Detection distance	0.9~4.6 m
8	Supported operating system	Win10, Vista

Table 2: Specific parameters of PC.

Serial number	Technical index	Specific parameters
1	CPU	Intel Core i5-0773M
2	Main frequency	4.0 GHz
3	Memory	16 GB
4	Graphics card model	Radeon AMD HD 0574

Table 3: Specific parameters of GPU.

Serial number	Technical index	Specific parameters
1	Base model	3000 MB
2	Number of CUDA cores	1772
3	Specific type of memory	GDDR4
4	Maximum memory capacity	9182 MB
5	Memory bit width	334 bit
6	Power consumption	240W
7	Resolution	2260 × 4186

In this section, manually draw the second-order curve corresponding to B, which is controlled by the shape of the multi-control point curve described in the following equation:

$$G(w) = \sum_{n=0}^{m} g_n f_{n,l}(w), \tag{3}$$

where $f_{n,l}(w)$ is used to describe the B-sample mixed basis function.

From (3), the points $G(w)$ on the fitted curve are mainly determined by the control points g_n. The inverse subdivision method is used to reduce the noise to ensure that it has equally spaced control points, where

$$A = [a_0, a_1, a_2, \cdots, a_m]^{\mathrm{T}}; B = [b_0, b_1, b_2, \cdots, b_n]^{\mathrm{T}}; S = \begin{bmatrix} \mathbf{X} \\ \mathbf{Y} \\ \mathbf{Z} \end{bmatrix},$$

$$X = \begin{bmatrix} 1 & 0 & 0 & 0 & 0 & 0 & 0 & \cdots \\ \frac{1}{2} & \frac{3}{4} & 1 & \frac{1}{2} & 0 & 0 & 0 & \cdots \end{bmatrix},$$

$$Y = \begin{bmatrix} 0 & 0 & \frac{1}{2} & -\frac{1}{4} & \frac{3}{4} & 0 & 0 & \cdots \\ 0 & 0 & 1 & \frac{1}{2} & -\frac{1}{2} & \frac{1}{4} & \frac{3}{4} & \cdots \\ \vdots & \vdots & \vdots & \vdots & \vdots & \vdots & \vdots & \ddots \end{bmatrix},$$

$$Z = \begin{bmatrix} \cdots & 0 & 0 & 0 & \frac{3}{4} & \frac{1}{2} & 1 & \frac{1}{4} \\ \cdots & 0 & 0 & 0 & 0 & 0 & 0 & 1 \end{bmatrix}. \tag{4}$$

Because the translation is carried out in the way of analysis and smoothing, the control points can be obtained only by the inverse division of a point sequence, so the adjusted curve corresponds to the initial input.

Through the combination of curves, the uniform distribution of points and the adaptive correction of points are realized, which is convenient for the control and operation of 3D model mesh obtained in graphic design.

After acquiring and preprocessing hand-drawn strokes, 3D virtual modeling is performed to realize the graphic design. For multi-stroke input, the input stroke information is saved by quaternions $H(\alpha_i, \beta_i, \chi_i, \delta_i) \longrightarrow U_i(D_i)$, and all elements are saved by means of a class library. Among them, $\alpha$is used to describe the recognized stroke information, β is used to describe the spatial location, χ is used to describe the topological information of the input strokes, and δ is used to describe the stroke characteristics. The stroke information obtained after processing is described by U_i, and the constraints that meet the design conditions are described by D_i. Stroke spatial location and topological information are mainly obtained through the stroke recognition process. The information of strokes designed by the designer is saved, and the angles of the planes in which different strokes are located are derived to obtain the spatial positions among the strokes. The three-dimensional modeling process of the designer's hand-drawn work is as follows.

After obtaining and preprocessing handwritten patterns, 3D virtual simulation is carried out to realize graphic design. To input multiple strokes, input and save stroke information through four elements, all of which are stored in the class library. In particular, the identification data used to describe the spatial position and the topological data used to describe the input stroke and the stroke features are described. After processing, the stroke information obtained is described in the description that meets the project conditions. The spatial position and topological information of handwriting are mainly obtained through the process of handwriting recognition. Save the designer's design information and export different angles to the plane, so as to obtain the spatial position between strokes. The constructor draws the hand-drawn work as follows.

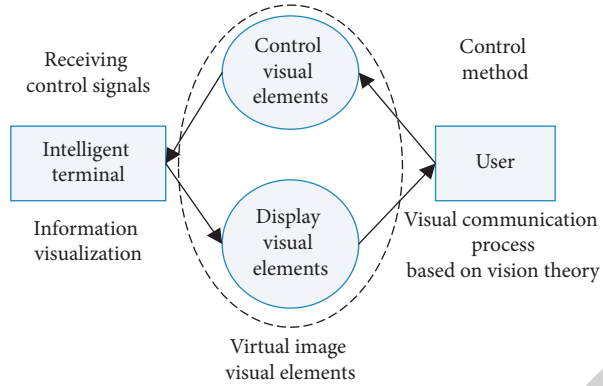

Figure 3: Virtual image visual interaction process.

(1) Initialize the input information $H(\alpha_i, \beta_i, \chi_i, \delta_i)$.

(2) Identify the strokes drawn by the designer: $H(\alpha_i, \beta_i, \chi_i, \delta_i) \longrightarrow U_i(D_i)$, and output the result if it is a single stroke; if not, proceed to the next step.

(3) Reasoning about the combined condition constraints of the design work.

$$D_m(U_i \wedge U_{i-1} \wedge \ldots \wedge U_1) \longrightarrow U_m\left(U_j(D_k), \ldots, U_n(D_l), D_m\right). \tag{5}$$

(4) Judge whether U_m belongs to the known model; if it does, insert it into the model and realize the 3D model construction; otherwise, repeat step (1).

In the process described above, step (2) aims to identify the input manual drawing, form the basic information of the image, and determine whether the modeling process is single or multiple. Otherwise, the next step will be to achieve matching by forcing the solution to obtain the 3D model.

After establishing the 3D planning work model, this section needs to show their real perception ability to improve the visual effect. The color effect can be obtained by three-dimensional simulation. To perform color mapping, you must set a set of colors and vertex colors for all vertices:

$$k[i][j] = \frac{b_{oc} + (t_{oc} - b_{oc})}{j \times i}. \tag{6}$$

After the information data are collected through the above steps, the virtual reconstruction of the 3D image is completed by using the visual interaction technology in visual communication, whose visual elements are mainly composed of display visual elements as well as control visual elements, as shown in Figure 3.

In Figure 3, the visual communication technology is applied to the virtual reconstruction, and the user sends the operation signal through the intelligent terminal, and after the internal processing and storage of the system, the display visual elements are fed back to the 3D image. The user completes the virtual graphic design of the 3D image through the feedback information data.

4. Experiments

In the range of 20–30 elements, the indoor environment is simulated by environmental interior design, interior design technology based on 3D virtual reality, system design based on environmental factors, and optimal indoor configuration system design, as shown in Table 4. It can be seen that within the range of 20–30 elements, the indoor design time simulation of the indoor design scene of the environmental interior design system based on 3D virtual reality is less than that of the indoor environment optimization based on environmental factors and layout optimization.

The comparison results of the time spent on indoor environment modeling are shown in Table 5.

It can be seen that within the range of 30–40 indoor environment design elements, the indoor environment design technology of scene simulation system based on 3D virtual reality takes less time than the simulation based on environmental factors and the optimization of indoor environment system [21, 22].

First, the designer who draws the objects manually starts and then carries out three-dimensional virtual simulation. The three-dimensional virtual simulation results shown in Figure 4(a)are shown in Figure 4(b). The diagram manually displays the three-dimensional virtual simulation results as shown in Figures 5(a) and 5(b).

The analysis of Figures 4 and 5 shows that this method can effectively realize the three-dimensional virtual simulation based on manual drawing, make the three-dimensional effect more realistic, and help the designer to show the

Table 4: Comparison results of indoor scene simulation time data.

Interior environmental design elements/pc	3D virtual reality technology system	Environmental factor system	Layout optimization system
20	12522	15585	16987
21	12565	15125	16582
22	12355	15022	16687
23	12265	15013	16263
24	12542	15456	16602
25	12088	15447	16155
26	12355	15006	16155
27	12022	15859	16659
28	12987	15988	16468
29	12020	15232	16022
30	12002	15146	16588

Table 5: Results of indoor scene simulation time data.

Interior environmental design elements/pc	3D virtual reality technology system	Environmental factor system	Layout optimization system
31	13458	16259	18652
32	13155	16569	18597
33	13235	16115	18462
34	13021	16467	18472
35	13126	16487	18321
36	13458	16497	18168
37	13489	16153	18021
38	13022	13155	18567
39	13529	16789	18129
40	13157	16168	18022

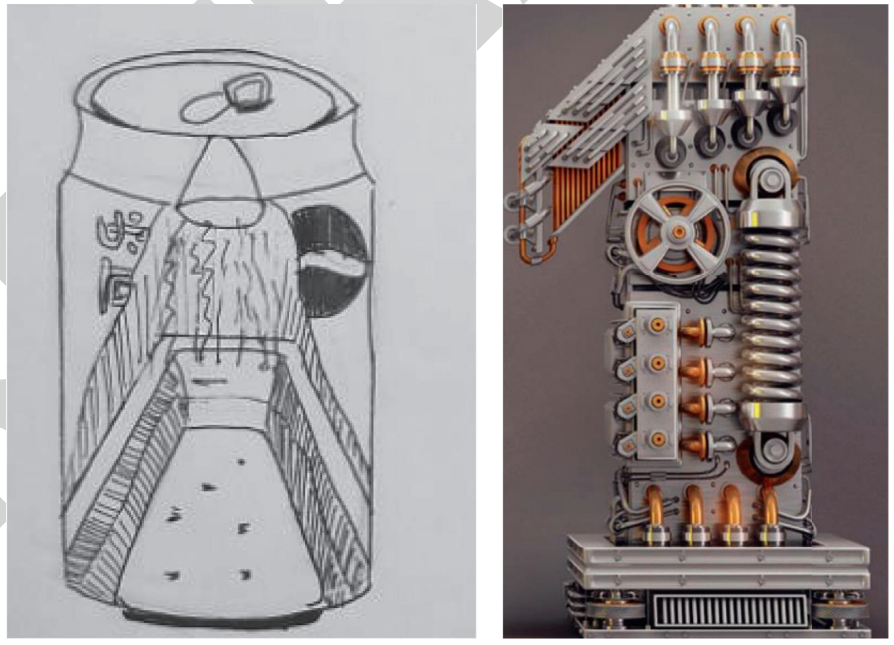

(a) (b)

Figure 4: Design results with the proposed method. (a) Hand drawing. (b) 3D virtual modeling.

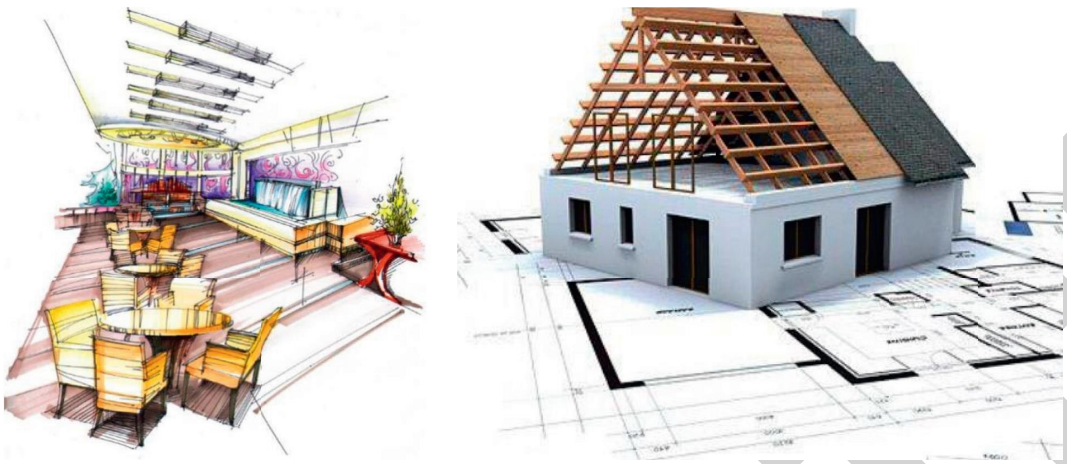

(a) (b)

Figure 5: Design results with the proposed method. (a) Hand drawing. (b) 3D virtual modeling.

Table 6: Scoring form.

Conformity		Very dissatisfied (1)	Dissatisfied (2)	Generally satisfied (3)	Satisfied (4)	Very satisfied (5)
Conformity	Completely (6)					√
	Basic (5)			√		
	A little (2)				√	
Does not meet	A little (2)		√			
	Basic (1)	√				
	Completely (0)					

Table 7: Comparison of evaluation results with three methods.

Evaluation metrics	Our method	Approach S	Machine vision method
Number of very unsatisfactory cases	0	4	2
Number of unsatisfied cases	3	5	5
Number of generally satisfied cases	3	11	15
More satisfied cases	13	18	19
Very satisfied cases	35	11	4
Average score	4.57	3.55	3.41

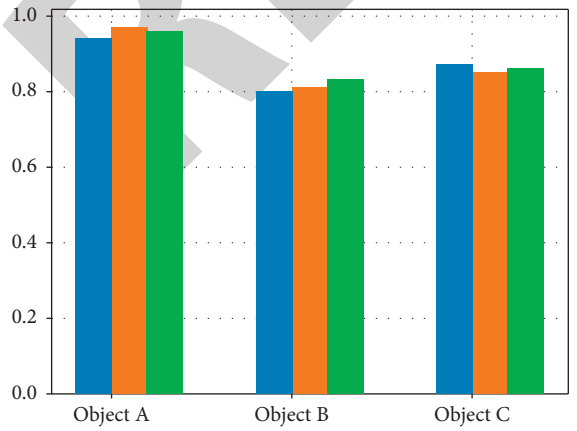

Figure 6: Design accuracy comparison results.

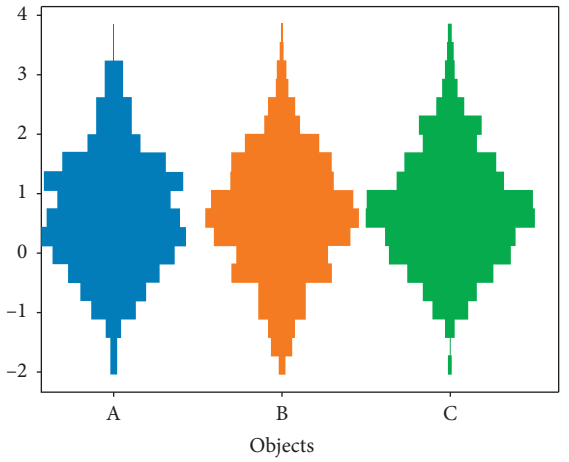

Figure 7: Comparison results on different design objects.

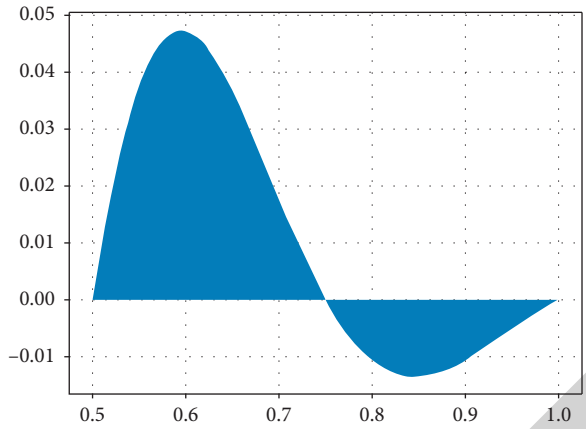

Figure 8: Changes in design fit.

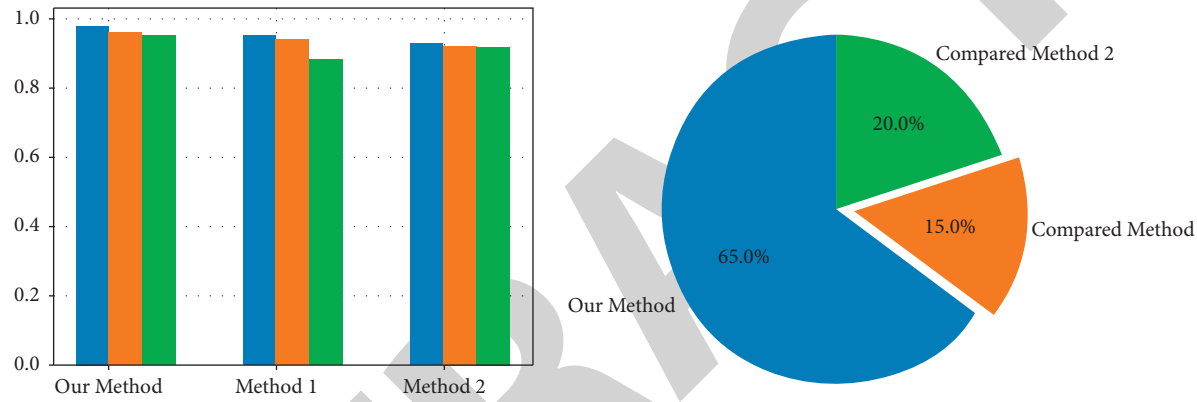

Figure 9: Comparison results of user satisfaction.

real intention. Planning and design is an uncertain process, so this section adopts the fuzzy planning evaluation method. The fuzzy evaluation method has been applied to psychology to quantify fuzzy problems [23].

When evaluating planning and design methods, it is not determined which type they belong to. Generally speaking, appraisers prefer one evaluation level, but there are other evaluation levels that cannot accurately evaluate their results.

The evaluation levels on both sides of the most satisfying level are compared in terms of their degree of conformity. The confidence level is assigned, and then the remaining levels are evaluated. If the participant thinks that the actual feeling matches the leftmost rank, the evaluation is performed in the order from left to right; otherwise, the evaluation is performed in the order from right to left.

The analysis of Tables 6 and 7 shows that no users are satisfied with the method, only two users are dissatisfied with the method, and all other users are satisfied with the method, of which 34 users are satisfied with the method. In contrast, 9 users were dissatisfied with the compressed sensing method and machine vision, only 10 users were satisfied with the compressed sensing method, and 6 users were satisfied with machine vision.

This paper systematically compares various planning methods based on 3D virtual technology and establishes three image types to be designed. In order to verify the design effect of three systems in three images, the results are shown in Figure 6.

For different design objects, we have compared the design effects of our model in detail. The specific results are shown in Figure 7. Further, we show the changes of our model in the design fit in Figure 8, and we can see that it has a good design fit.

From Figure 9, the user's evaluation of this method is 0.65 on average, which is significantly higher than that of the compressed sensing method and machine vision method with 0.2 and 0.15, which shows that this method meets the design requirements and verifies its effectiveness.

5. Conclusion

In graphic design, the main thinking and creativity of planners can be enhanced through visual expression so as to promote graphic design works to be more beautiful. A scheduling method based on 3D virtual vision technology is proposed. In order to create conditions, the acquisition and preprocessing of handwritten patterns are introduced. On this basis, a 3D virtual template with brush image and color is established. Experiments show that this method meets the requirements of designers and helps them show their real intention.

Hindawi
Scientific Programming
Volume 2022, Article ID 2839834, 9 pages
https://doi.org/10.1155/2022/2839834

Research Article

Construction and Risk Analysis of Marketing System Based on AI

Changcheng Zhu

Zhengzhou Sias College, Zhengzhou, Henan 451150, China

Correspondence should be addressed to Changcheng Zhu; 11609@sias.edu.cn

Received 2 June 2022; Revised 9 July 2022; Accepted 13 July 2022; Published 3 August 2022

Academic Editor: Lianhui Li

AI technology is rapidly changing traditional industries by using the technologies of big data, machine learning, and deep learning in AI technology. This study transforms and constructs the links of market research, market strategy, marketing strategy, and marketing activities in the marketing system. The use of AI can help companies to understand customer needs more comprehensively, find market opportunities more quickly, establish business goals more accurately, and achieve smart marketing and precision marketing in the true sense. AI technology also brings new challenges to the development of enterprises. This study analyzes the data risk, payment risk, ethical risk, and decision-making risk in the marketing system and puts forward the solutions.

1. Introduction

With the rapid development of science and technology, the knowledge economy system has gradually taken shape. The emerging high-tech industry represented by AI (Artificial Intelligence), as a powerful engine to stimulate social development, is imperceptibly affecting people's production and lifestyle [1, 2]. AI, a part of computer science, actually attempts to create a new type of intelligent machine. Such machines can respond to external stimuli like real humans. Large domestic and foreign Internet companies and venture capital institutions have set their sights on this industry [3].

In recent years, AI technology has developed rapidly with the strong support of national policies. AI is a technology that studies and develops to simulate, extend, and expand human intelligence, including big data, machine learning, deep learning, natural language understanding, image recognition[4, 5]. In case many traditional industries still do not use AI technology to improve the level of intelligence and complete the upgrading of the traditional system, they might be replaced by AI in the future.

Marketing is a very important link in traditional economic life, mainly around customers. At present, the global economy is in a period of decline, and business operations are facing great difficulties. How to expand the scale of operations and reduce operating costs have become important issues for enterprises to consider [6]. The use of AI can help enterprises to more comprehensively understand customer needs and find market opportunities more quickly. To establish business objectives more accurately, it is very necessary to study the application prospects of AI technology in marketing. This study uses AI technology to discuss the methods of transforming and constructing the traditional marketing system, analyzes and studies the possible risks of AI, and puts forward the solutions at the end.

2. Relevant Overview and Application of AI in Marketing

2.1. AI. AI is one of the most emerging fields of science and engineering. It was proposed by scientists such as McCarthy, Minsky, Rochester, and Shennong at the Dartmouth conference in 1956 [7]. In the subsequent development, different scholars have given different definitions of four different dimensions: human-like thinking, human-like action, rational thinking, and rational action. The relevant definitions are shown in Table 1.

Combining the viewpoints of different scholars, AI belongs to a branch of computer science. It is a technology to study and develop theories, methods, technologies, and application systems for simulating, extending, and expanding human intelligence. It tries to understand the

Table 1: Definitions of AI in four dimensions.

Dimension	Definitions	Representative scholar
Human-like thinking	AI has spontaneous behaviors related to human thinking and activities, such as decision-making, problem-solving, and learning.	Richard Bellman
Humanoid action	AI is the art of creating machines that enable them to exhibit human-like intelligence.	Ray Kurzweil
Rational thinking	AI is a subject that studies how to make computers perceive, reason, and act.	Patrick Winston
Rational action	AI is concerned with the intelligent behavior in artificial products.	Nils Nilsson

nature of intelligence, imitates human intelligence, and produces machines that are similar to human intelligence.

In other words, AI is a technical science that studies human thinking patterns and applies human thinking to machines, so that machines have human thoughts and behaviors, thereby replacing humans to complete certain tasks. As a new technical science, AI is different from general computer code programming. Its core idea is to use specific algorithms to judge and summarize events, so as to quickly complete the predetermined settings and operations [8]. This is inseparable from a large amount of data analysis, deductive inference, and calculation. After more than 60 years of development, AI has become an interdisciplinary frontier science covering multiple fields and multiple disciplines.

2.2. Marketing. Marketing is an activity or action. As for the concept of marketing, Philip Kotler believes that marketing is the management process of exchanging the products produced by individuals or organizations with others, so as to meet people's practical needs [9].

The American Marketing Association proposed that marketing is an activity process of disseminating valuable market supply. In fact, it is the process of realizing a function and a series of creation and communication, and then influencing this value on customers and realizing profits in this process. Many experts and scholars have defined marketing and have their own views.

In short, the market is a starting point and a destination in commodity marketing activities. In fact, marketing is not only a function but also a way to create, communicate, and deliver customer value to realize self-interest. Products can be delivered to consumers and partners through marketing. Marketing is not only an activity but also a process of sales behavior and art of creating and meeting customers.

2.3. Intelligent Marketing

2.3.1. Connotation of Intelligent Marketing. The traditional marketing model is crafted mainly through apps and offline and online advertising, or local promotion through bank outlets. These methods have the characteristics of high cost and low efficiency. Intelligent marketing uses AI technology to obtain customers through multi-dimensional online and offline intelligence and makes intelligent analyses based on big data information processing technology [10].

You can see the product needs of customers through user portraits, so as to achieve an accurate match between products and customer needs. This method greatly improves the efficiency and reduces the cost. It can not only improve customer satisfaction with products but also indirectly enhance the market competitiveness of banks, as shown in Table 2.

Intelligent marketing is mainly divided into two steps. The first step is personalized recommendation and intelligent customer acquisition. In order to attract customers, customer groups are divided according to customers' different consumption preferences. The second step is differentiated classification and precision marketing to develop differentiated marketing strategies for different products and different customers to achieve personalized precision marketing.

Personalized recommendations and intelligent customer acquisition are based on multi-channel data. Using big data, AI, and other technologies to deeply mine the relevant information of customers in multiple dimensions, analyze the daily behavior characteristics of customers, accurately identify customer needs, and achieve accurate portraits of customers. Differentiated classification and precision marketing are precision marketing after mining customers and screening customer needs through AI [11]. Formulate differentiated marketing strategies for different customer groups, personalize products to meet their needs, save marketing costs, improve marketing efficiency, and improve customer experience.

2.3.2. Technical Foundation of Intelligent Marketing. The rise of AI marketing is inseparable from the support of technology. According to the research of previous literature, the technical basis of the development of AI marketing can be roughly divided into three aspects:

(1) Mobile Internet and 5g technology provide the guarantee of massive data sources for the development of intelligent marketing. The important foundation of intelligent marketing development is data. Continuous and reliable data acquisition is one of the core technologies required by intelligent marketing. With the development of mobile Internet and 5G technology, marketing activities have widely penetrated consumers' daily behaviors such as work, entertainment, life, and consumption with the help of virtual reality technology, simulation technology, and artificial bio-intelligence technology, and comprehensively recorded consumers [12, 13]. The behavior data provided by intelligent marketing provides a massive source of data information for the

Table 2: Comparison of traditional marketing and intelligent marketing.

	Traditional marketing	Intelligent marketing
Customer acquisition mode	Offline physical outlets, mobile apps, etc.	Offline promotion, online drainage, the introduction of third-party platforms, with the help of partners' traffic channels and scene resources, expand customer contact business scenarios, and acquire customers through multiple channels.
Marketing mode	Lack of customer demand and product matching mechanism, and failure to recommend differentiated products and services based on customer characteristics.	Automatically generate customer portraits and labels based on AI analysis, and intelligently recommend products based on customers' age, risk appetite, income, and other levels to improve marketing efficiency.

follow-up analysis and processing of intelligent marketing.

(2) Cloud computing helps intelligent marketing complete complex data calculation and processing analysis. In the era of the mobile Internet, the development of big data has caused the exponential growth of network data. How to calculate, process, and analyze these massive data has become an important problem that must be solved in the development of intelligent marketing. With its powerful data computing ability, cloud computing technology solves the problem of massive data processing in the application of AI technology. The interconnection of all things is realized through the connection of multidimensional data, which makes the interactive experience between consumers and intelligent devices much better. The marketing scenario is also more intelligent due to timely and accurate data analysis [14].

(3) The commercial application technology of AI provides a network application environment for the development of intelligent marketing. The development environment of AI commercialization and the support of AI commercialization application technology have created a good external network application environment for the development of intelligent marketing.

2.4. Problems of the Traditional Marketing Model

2.4.1. Marketing Effect Is Not Ideal. In short, each product has a relative consumer group. However, the traditional marketing model only focuses on the promotion of products and providing corresponding services to consumers, and does not carry out personalized marketing for specific consumer groups. With the development of the times, it only chooses the traditional marketing model. That is, it cannot be promoted to the corresponding consumers according to the special properties of the product and the corresponding scope of application. It will lead to the retention of a large number of products and seriously affect the development of the enterprise itself. Therefore, in the current social development process, enterprises should promote products according to their own scope of use and unique attributes of products, and recommend products to corresponding audience groups in a targeted manner.

2.4.2. The Pattern Is Monotonous and Not Rich. Most of the traditional marketing models carry out product promotion and marketing through traditional media such as newspapers, TV, and magazines. However, these traditional marketing methods are relatively single and cannot cover all consumer groups. Information sources of current consumer groups are not limited to newspapers, TV, and magazines, and most consumer groups are doing shopping on the Internet environment. Therefore, if only the traditional marketing model is adopted, the long-term development of the enterprise itself cannot be promoted.

2.4.3. Traditional Marketing Costs Are Too High. Cost consumption is a very important factor in the production and marketing process of enterprises. In the process of using the traditional marketing model to promote product brands, there are many promotion processes and links, which further increases the cost of consumption. In the traditional marketing model, the communication between enterprise sales staff and consumers is prone to problems [15]. If the enterprise does not take corresponding adjustment measures, it will greatly increase the marketing cost of the enterprise, and even seriously affect the actual marketing effect of the enterprise's own brand products. In a word, in the marketing process of enterprise products, the relationship between cost and output is the biggest influencing factor.

2.5. Application of AI in Marketing

2.5.1. Marketing Characteristics of AI

(1) Cross Time and Space Marketing. Using the marketing method of AI, we can quickly obtain all the information of network users, who come from all over the country and even the world. AI can accurately screen their daily browsing records and push them with marketing information in line with users' preferences. This was something that could not be done in the past. The previous marketing was only manual marketing for the local area and a small area. Now, the use of AI can expand the scope of marketing to the whole country and even the world, so that more people can see the marketing copy and advertisements of enterprises.

(2) Multimedia Marketing. Now is an era of rapid technological development, and people can obtain information in various forms on the Internet. The use of AI for marketing is

in line with this characteristic. AI can convert the marketing scheme into various forms and appear on the user's push page. Users can use the network to further understand the products in various forms such as video, pictures, and text [16]. The characteristics of multimedia can enable AI to accurately understand the effect of marketing and collect the reactions of various users when they see advertisements and the reading volume of advertisements. It makes it easier to determine the customer group, and it can also better accumulate the experience for the future marketing of the enterprise.

(3) Growth. A very big benefit of using AI is that marketing can be kept growing. Most of the people who use smart products and the Internet are teenagers and middle-aged people. Middle-aged people now have enough economic strength, so their purchasing power is also very strong. Although teenagers have insufficient purchasing power now, marketing to their group can effectively cultivate potential customers for the future market. Therefore, using AI for marketing is a growing marketing method.

(4) Interactive Quality. The progress of traditional offline marketing is very slow, and the interaction is also very poor. Most users are office workers and they do not have time to specifically evaluate the marketing effect. With the use of AI marketing methods, it is possible to conduct surveys on marketing objects through the release of questionnaires on online platforms. Or you can put forward some suggestions for improvement, and constantly enrich the content of AI marketing so that they can better meet the needs of users and achieve the purpose of marketing.

(5) Hommization. Nowadays, many young people are reluctant to communicate with people directly, they like an independent life, and AI marketing is very suitable for users' needs. Users can learn the detailed introduction of the product through online marketing, and they can also communicate with the product and customer service through the online platform, and make purchases according to their own wishes. The offline marketing methods are somewhat forced marketing. It is possible that users do not need this product. Forced marketing will make them feel oppressed and have a bad impression of the product.

2.5.2. Application Status. With the popularity of the Internet, using computers and mobile phones to browse websites or application software is also known as a basic activity in people's daily life. During browsing the web, people often find that advertisements pop up, which is actually the "precision positioning marketing" of intelligent marketing. Based on the big data system and combined with the consumer behavior data provided by the demand-side platform, merchants can accurately grasp consumer preferences and demand information, so as to place advertisements in a targeted manner.

The application of AI in marketing can be summarized from the development history, logic principles, and practical effects of platforms such as demand-side platforms (DSP), data management platforms (DMP), real-time bidding (RTB), supply-side platforms (SSP), and other platforms [17].

In the first stage, thanks to the acquisition of consumer behavior data, precision marketing has achieved good marketing results in a short period of time. In addition to the lack of consumer information protection in China, intelligent precision marketing can obtain a large amount of consumer behavior data and preference data—and DSP, DMP, RTB, and other platforms have developed rapidly.

In the second stage, with the cooperation of major e-commerce platforms, major commercial databases have realized technology connection, resource sharing and data exchange, and the breadth and depth of intelligent precision marketing have been better developed.

In the third stage, intelligent precision marketing is widely used by major e-commerce platforms, search engines, and various web pages. Various industries imitate this marketing model, resulting in consumers' misunderstanding of precision marketing. For example, consumers constantly pop up marketing advertising pages when browsing the web, which affects consumers' normal life and work and hinders the development of intelligent marketing.

2.5.3. Existing Problems

(1) Lack of AI Talents. If enterprises want to improve their marketing competitiveness, they must keep up with the pace of social development, pay attention to the application of AI and use the network for more extensive marketing. In the process of application, there may be some problems. The use of AI in marketing is rising in recent years, so the gap between AI talents is very large. Many enterprises lack AI talents and can not effectively use AI for marketing.

(2) Improper Management Methods. Some enterprises use AI to establish platform-related websites, but there is no special management department to manage them, so the role of AI can not be brought into play. Enterprises do not know much about AI, so they should hire professionals to operate and help enterprises carry out effective marketing. Some enterprises will invite professional technicians to operate, but some of them cannot manage well because of a lack of experience and lack of experience in online marketing.

(3) Lack of Innovation Consciousness. The use of AI can speed up work efficiency to a great extent. However, due to the low innovation consciousness of enterprises, they do not pay attention to the combination of AI and market demand, and only use AI to put targeted advertising, which will lead to the lack of competitiveness in enterprises and the failure of marketing. Therefore, enterprises should cultivate their

awareness of innovation, use AI to collect information and data, and come up with some novel marketing means.

3. Construction of the Marketing System Based on AI

According to the traditional marketing system, based on the characteristics of market research, market strategy, marketing strategy, marketing activities, and other links, combined with various technical means of AI, a new system diagram based on AI has been established.

3.1. Market Research

3.1.1. Market Environment. Through data mining, data sharing, web crawler, and other technical means, we can more accurately understand and perceive the changes in the market environment. Seize the huge opportunities brought by market demand to enterprises in time to avoid the negative impact on enterprises due to changes in market conditions.

In terms of macro environment, AI can comprehensively analyze the impact of multiple indicators on industrial development, so as to realize the visualization of analysis results [18]. In terms of the perception of the microenvironment, the microenvironment model is established by using the micro marketing channels, enterprises, customers, competitors and other indicators, and through the deep learning algorithm, which can be dynamically observed at any time.

3.1.2. Consumer Behavior. Part of consumer behavioral data can be collected by conducting extensive market research and industry research. More importantly, through cooperation with Taobao, Pinduoduo, and other large e-commerce and offline stores, we can obtain massive consumer consumption data. On this basis, machine learning algorithms and natural language understanding technologies are used to conduct an in-depth analysis of data, accurately understand consumers' consumption needs, and predict consumers' future consumption behavior.

3.2. Market Strategy

3.2.1. Market Segmentation. The data mining algorithm is used to comprehensively analyze the consumers in the market, design the prediction algorithm, determine the market segmentation standard, and divide the consumers into several potential customer groups. It overcomes the biggest "expensive" problem of market segmentation without manual intervention. It has the characteristics of low cost and good effect.

The use of AI technology can even achieve complete market segmentation, and each consumer in the market constitutes an independent sub-market. Enterprises produce different products for each consumer according to their different needs, as well as comprehensive standard segmentation, and subdivide the whole market from multiple angles.

If we consider technologies in China, Baidu is one of the most powerful AI companies in China, and it has achieved leaps in many market segments. For example, opening Baidu Maps can realize automatic navigation only through manual dialogue; opening Xiaodu smart speakers can realize intelligent and visual control of all home appliances; and through AI fundus screening all-in-one machine, the diagnosis of ophthalmic diseases can be realized; using EasyDL customization Image recognition tools can be used to identify genuine and fake jadeite, fake and inferior traditional Chinese medicine, etc.

3.2.2. Target Market. On the basis of market segmentation, the deep learning algorithm is used to learn the laws from a large number of market data, identify and judge, determine the target market, and meet the needs of some sub-markets with corresponding products and services. Using the powerful data analysis means of AI, while refining and specializing the products, it can even achieve complete market coverage in theory and maximize the profits of enterprises [19]. Data mining technology has great potential for finding the target market. For example, someone once used the association algorithm in data mining technology to find the accurate relationship between power consumption and consumer products.

3.2.3. Market Positioning. Master the market status of similar products by means of big data analysis, integrate their own product attributes, and determine their unique market positioning. Create a distinctive and distinctive image for enterprise products. Leave a deep impression on customers, occupy their own position in the market, and enhance the vitality and pertinence of products. For example, in the Taobao interface, due to the different historical data consumed by each user and the different interfaces presented, the products sold on Taobao are more targeted and more attractive to consumers. In fact, relying on its technical service advantages in Taobao, Alipay, and Alibaba cloud, Alibaba has deeply integrated AI technology, and has formed an industrial layout in retail, automobile, finance, and other aspects.

3.3. Marketing Strategy

3.3.1. Marketing Mix. Deepen the analysis of marketing data and accurately grasp the market demand through big data algorithms. Through the deep learning algorithm, determine the marketing strategy, realize the marketing strategy combination model, optimize the marketing effect, and realize real precision marketing. For example, Xiaomi company has launched a marketing 1.0 solution based on AI,

including data linkage and media linkage. Through intelligent algorithms, we can have a deeper insight into the needs of users and deliver the right advertisements to accurate users more accurately.

3.3.2. Marketing Budget. The marketing budget is closely related to the company's production, supply, finance, R&D, etc. Using the data mining technology of AI, it can accurately determine the various resources required by each department to achieve the marketing objectives, and reasonably adjust the marketing budget. This will greatly improve the efficiency of the budget, improve the management level of enterprises, and optimize the input-output ratio of enterprises.

3.3.3. Precise Screening Push. There are many ways of marketing communication, but the push of selected content in the mobile client. The banner advertisements at the end of the tweets on the official account are unique products in this information age, and this is due to the addition of AI.

AI can intelligently analyze big data and mine the potential behavior activities behind these behavior data by recording the behavior of each user. The operation mode of Taobao we commonly use is a typical example. It will make a targeted push for your Taobao home page products according to your search keywords and historical consumption records. This is why when we enter the Taobao interface, we will find that each user's interface is different.

3.3.4. Online Service. Today, online shopping has become an indispensable part of people's life, and AI customer service is gradually replacing traditional artificial customer service. AI customer service can collect past customer service consultation records, analyze and summarize the problems mentioned more frequently, and answer most of the doubts for customers in a timely and accurate manner.

On this basis, the intelligent chat system will also extract effective keywords from the messages you launch, analyze the click-through rate and click times of users on relevant products, predict consumers' preferences, better guess consumers' real ideas, quickly respond intelligently through natural interaction, and recommend more suitable products faster and more standardized. This approach not only greatly reduces the waiting time of customers, but also greatly improves the sales efficiency and establishes stronger contact with customers.

3.3.5. Customer Follow-Up Management. Customers are the most important resources of enterprises. Making good use of customer autonomy can help enterprises improve their core competitiveness and ultimately greatly improve the company's profit margin. In the past, in order to improve customer loyalty, enterprises would set up special departments to carry out follow-up management of customers.

In 1999, Inc proposed the concept of Customer Relationship Management (CRM). The goal of CRM is to reduce the cost of the enterprise by improving the business process management of the enterprise in all aspects [20]. If the element of AI is introduced, it will surely attract more new customers while retaining old customers with the advantage of providing faster and more professional services. Such a new type of customer follow-up management mechanism has greatly improved the relationship between customers and enterprises, achieved continuous contribution to customer value, and comprehensively improved the profitability of enterprises.

3.3.6. Marketing After-Sales. After-sales service is an important part of marketing. It is also a means of promotion. Good after-sales service will bring a better reputation to enterprises and brands. Conversely, if major brands want to occupy an advantage in the market for a long time and improve customer stickiness and satisfaction, high-quality after-sales service is an indispensable part, which is mainly divided into after-sales service and after-sales follow-up. Good after-sales service can make customers think they have made the right decision, while high-quality after-sales follow-up can prevent returns and transfer them to other customers.

For example, in the past, small and micro enterprises had insufficient human resources and it was difficult to ensure good after-sales. Large brands continued to occupy the market with resource advantages, resulting in a vicious circle of growing large enterprises and declining small and medium-sized enterprises, and serious market polarization. But now, through the use of AI, this situation will be reversed to a great extent. By mining and optimizing relevant data, it can better meet the different needs of consumers and save material and human resources.

3.4. Marketing Activities

3.4.1. Marketing Plan. When determining a specific marketing plan, through in-depth mining and understanding of market data, the use of AI technology can better and accurately analyze the situation, and clarify the product status, market status, competition status, and macro environment. It can also better predict opportunity risks, assist marketing planners, determine marketing goals, understand financial risks, achieve closed-loop and complete control of the entire marketing plan, and adjust plan deficiencies in a timely manner according to external changes.

3.4.2. Marketing Organization. AI reduces the size of the marketing organization and also enhances the management capabilities of the marketing organization. It can make full use of the wireless, network, and mobile tools, such as mobile apps, WeChat applets, to improve the efficiency of the marketing organization, and realize intelligent management and intelligent presentation in the true sense. At present, the more common software in mobile phones includes Taobao, Pinduoduo, and JD.com. AI algorithms are used without exception. Every consumer's consumption behavior and consumption records affect the marketing organization behavior of the enterprise and ensure the realization of the marketing effect.

3.4.3. Marketing Control and Execution. Even if companies in the same industry adopt the same marketing strategy, the effects are sometimes quite different. The main reason is that there are differences in the control and execution capabilities of marketing organizations. Through AI technology, every link of marketing activities can be tracked and evaluated to ensure marketing effectiveness. Using big data, algorithms can also clean and standardize data such as annual plans, profitability, and work efficiency, and then mine and present them. Assist managers to improve the efficiency of marketing control and execution.

4. Risk Analysis and Solutions

4.1. Risk Analysis

4.1.1. Data Risk. The integrity and quality of source data will have a great impact on AI algorithms and applications, but objectively speaking, the data standards of marketing are different and the circulation efficiency is very low, which greatly reduces the value of analysis. Data leakage accidents occur frequently and lack effective data supervision, resulting in a grey industrial chain and undermining the fair market environment [3, 21]. Failure to monitor data quality may lead to the decline of enterprise operation efficiency, especially the lack of core data may lead to wrong judgment. Hackers' attacks and modification of data may bring unpredictable risks to the whole system, and in serious cases, it can lead to the collapse of the whole marketing system.

4.1.2. Payment Risk. In marketing activities, online payment is often required. As one of the most popular technologies, biometrics, such as face recognition, has inherent loopholes, which may lead to security failure. At this time, the face is biological information that can be obtained without personnel cooperation. Attackers can obtain photos through social networks, copy facial features, generate dynamic portraits using 3D technology, and train "blink/speak/shake your head" and other contents, which may successfully pass the security system. Intelligent speech technology also has the problems of weak recognition ability and low recognition rate. Hackers can hide malicious instructions in white noise or "dolphin attack" through ultrasound.

4.1.3. Ethical Risk. In the process of marketing, with the continuous progress of AI algorithms, humanoid performance will be more obvious, which brings new challenges to social governance and supervision. Do humans recognize the subject rights and prediction functions of AI in marketing systems?

In the market environment, fairness is one of the most important criteria. But the sources of AI algorithms are algorithm designers and software developers. In their work, they have their own subjective attitude and even bias and will write this bias into intelligent algorithms consciously or unconsciously. At the same time, the market research data to be processed may also have problems such as different data standards, which will lead to discriminatory follow-up operations.

4.1.4. Decision Risk. The basic process of AI deep learning can be divided into training and inference, that is, training the deep neural network model on the basis of big data, and then inferring the data and drawing a conclusion on the basis of training. Obviously, if there is a problem with the market-oriented data, it may not only lead to the problem of the trained network model but also get the wrong decision-making results. This will produce destructive results for the whole marketing system.

4.2. Corresponding Solutions. The marketing system involves all aspects of society and plays an important role in economic construction. To avoid the above problems, first of all, we should pay attention to the cultivation of senior talents of AI [22]. In particular, we should pay attention to cultivating their ideology to ensure that they can correctly recognize their subconscious attitudes toward inequality and even discrimination. Ensure the fairness of AI algorithm, protect the fairness and justice of the economic market, and ensure the long-term stability of economic construction.

Second, accelerate the development of AI algorithm frameworks with my country's independent intellectual property rights, eliminate the potential negative impact of foreign AI algorithm frameworks on economic development under the background of trade wars, and ensure that AI technology can finally be truly applied in my country's economic construction, establish a good platform, and lay a solid technical foundation.

Finally, it is necessary to support the development of AI chips with China's independent intellectual property rights. In the field of marketing, the core role is the intelligent processing of marketing data. Only by grasping the initiative in the development of AI chips and improving the technical level of chips, we can avoid the entire marketing system and even the national economy being controlled by others. At present, Baidu has developed the AI chip "Kunlun" in China, and large companies such as Huawei and Alibaba have followed suit and developed the latest AI chip products. This has greatly promoted the development of the smart chip industry.

4.3. Challenges Faced. The application of AI technology in the field of marketing has brought great convenience to enterprises and consumers, but technology has two sides. We must treat AI technology rationally and face up to the problems in the application of AI. According to the research of previous literature, we can understand the challenges faced by marketing in the era of AI from the following aspects.

One is the lack of compound marketing talents under the background of AI, which brings about the further connection between technology and marketing. At present, a

significant problem in the field of intelligent marketing is the further in-depth connection between technology and marketing. The lack of compound talents who understand the technology and the market makes enterprises face great obstacles in the process of applying AI.

The second is the data privacy protection and traffic fraud exposed in the process of AI marketing. The exposure of various data privacy news cases has made more and more users highly sensitive to the use of new technologies. A large number of illegal monitoring and interpretation of data without the consent of users seriously interfere with consumers' daily life. Some enterprises even use intelligent technology to predict and analyze users' personal information to obtain users' privacy.

The third is the psychological burnout of consumers in the all-around AI marketing environment. AI technology can recommend various personalized information to consumers, but this kind of continuous and accurate recommendation based on consumers' use traces is difficult to prevent consumers from getting bored [13, 19]. Ad recommendation anytime and anywhere, no ad interception across screens, and tracking recommendation of user browsing records have become more automatic and frequent driven by intelligent technology. Although AI technology can help enterprises accurately analyze user data, the data cannot fully reflect the hearts of consumers. Enterprises should avoid blindly following intelligent technology to prevent consumers from getting bored.

5. Conclusion

In the era of AI, marketing practitioners should make full use of the technical means of AI. Change the current situation of the marketing industry, improve the efficiency and pertinence of traditional marketing activities, realize the customized and intelligent design of products, and realize personalized and accurate marketing to customers. Fundamentally improve the economic benefits of enterprises and improve the vitality of products. The application of AI in the field of marketing is still in the initial stage of development. Enterprises must treat AI technology rationally when applying AI technology. We should not only see the convenience of data analysis and accurate identification brought by AI to enterprise marketing but also see the technical traps, user privacy, and other problems brought by AI applications. Of course, the application of AI technology in the field of marketing will have further development in the future, and enterprises should also carry out exploration and research in time.

Data Availability

*The dataset can be accessed upon request to the author.

Conflicts of Interest

The author declares no conflicts of interest.

References

[1] T. D. Nguyen, A. Paswan, and A. J. Dubinsky, "Allocation of salespeople's resources for generating new sales opportunities across four types of customers," *Industrial Marketing Management*, vol. 68, pp. 114–131, 2018.

[2] T. Liu, Z. Yuan, L. Wu, and B. Badami, "An optimal brain tumor detection by convolutional neural network and enhanced sparrow search algorithm," *Proceedings of the Institution of Mechanical Engineers - Part H: Journal of Engineering in Medicine*, vol. 235, no. 4, pp. 459–469, 2021.

[3] Q. Zhang, J. Lu, and Y. Jin, "Artificial intelligence in recommender systems," *Complex & Intelligent Systems*, vol. 7, no. 1, pp. 439–457, 2021.

[4] M. Jahanbakht, W. Xiang, L. Hanzo, and M. Rahimi Azghadi, "Internet of underwater things and big marine data analytics–a comprehensive survey," *IEEE Communications Surveys & Tutorials*, vol. 23, no. 2, pp. 904–956, 2021.

[5] Y. Yu, "Research on the evaluation algorithm of social capital influence of enterprise network marketing," *Security and Communication Networks*, vol. 2021, Article ID 7711322, 8 pages, 2021.

[6] H. Hwangbo, Y. S. Kim, and K. J. Cha, "Use of the smart store for persuasive marketing and immersive customer experiences: a case study of Korean Apparel Enterprise," *Mobile Information Systems*, vol. 2017, Article ID 4738340, 17 pages, 2017.

[7] X. Li, H. Jianmin, B. Hou, and P. Zhang, "Exploring the innovation modes and evolution of the cloud-based service using the activity theory on the basis of big data," *Cluster Computing*, vol. 21, no. 1, pp. 907–922, 2018.

[8] A. Fahmi and N. U. Amin, "Group decision-making based on bipolar neutrosophic fuzzy prioritized muirhead mean weighted averaging operator," *Soft Computing*, vol. 25, no. 15, pp. 10019–10036, 2021.

[9] J. He, L. Yu, and Y. Liu, "The multiple attribute association decision-making method to make online advertisements using influential users in social network," in *Proceedings of the 2016 IEEE First International Conference on Data Science in Cyberspace (DSC)*, pp. 406–411, IEEE, Changsha, China, June 2016.

[10] S. Kosasi and I. D. A. E. Yuliani, "Improving organizational agility of micro, small, and medium enterprises through digital marketing strategy," in *Proceedings of the 2017 2nd International Conferences on Information Technology, Information Systems and Electrical Engineering (ICITISEE)*, pp. 68–72, IEEE, Yogyakarta, Indonesia, November 2017.

[11] C. C. Sun, "Assessing the relative efficiency and productivity growth of the taiwan LED industry: DEA and malmquist indices application," *Mathematical Problems in Engineering*, vol. 2014, Article ID 816801, 13 pages, 2014.

[12] V. Devang, S. Chintan, S. Chintan, T. Gunjan, and R. Krupa, "Applications of artificial intelligence in marketing," *Annals of Dunarea de Jos University of Galati. Fascicle I. Economics and Applied Informatics*, vol. 25, no. 1, pp. 28–36, 2019.

[13] H. Wu, H. Han, X. Wang, and S. Sun, "Research on artificial intelligence enhancing Internet of things security: a survey," *IEEE Access*, vol. 8, pp. 153826–153848, 2020.

[14] D. Lee and S. N. Yoon, "Application of artificial intelligence-based technologies in the healthcare industry: opportunities and challenges," *International Journal of Environmental Research and Public Health*, vol. 18, no. 1, p. 271, 2021.

[15] M. D. Seckeler, B. M. Gordon, D. A. Williams, and B. H. Goldstein, "Use of smart technology for remote

consultation in the pediatric cardiac catheterization laboratory," *Congenital Heart Disease*, vol. 10, no. 6, pp. E288–E294, 2015.

[16] X. Yang, H. Li, L. Ni, and T. Li, "Application of artificial intelligence in precision marketing," *Journal of Organizational and End User Computing*, vol. 33, no. 4, pp. 209–219, 2021.

[17] F. Jiang, Y. Jiang, H. Zhi et al., "Artificial intelligence in healthcare: past, present and future," *Stroke and Vascular Neurology*, vol. 2, no. 4, pp. 230–243, 2017.

[18] C. Cath, S. Wachter, B. Mittelstadt, M. Taddeo, and L. Floridi, "Artificial intelligence and the "good society": the US, EU, and UK approach," *Science and Engineering Ethics*, vol. 24, no. 2, pp. 505–528, 2018.

[19] A. Abid, P. Harrigan, and S. K. Roy, "Online relationship marketing through content creation and curation," *Marketing Intelligence & Planning*, vol. 38, no. 6, pp. 699–712, 2019.

[20] S. Silva, P. Duarte, J. C. Machado, and C. Martins, "Cause-related marketing in online environment: the role of brand-cause fit, perceived value, and trust," *International Review on Public and Nonprofit Marketing*, vol. 20, no. 2, pp. 17–36, 2020.

[21] Y. Lu, "Artificial intelligence: a survey on evolution, models, applications and future trends," *Journal of Management Analytics*, vol. 6, no. 1, pp. 1–29, 2019.

[22] D. Schiff, "Out of the laboratory and into the classroom: the future of artificial intelligence in education," *AI & Society*, vol. 36, no. 1, pp. 331–348, 2021.

Hindawi
Scientific Programming
Volume 2022, Article ID 2742557, 8 pages
https://doi.org/10.1155/2022/2742557

Research Article

GIS-Based Medical Resource Evaluation Method

Xiao Yu

Division of Human Geography, Graduate School of Life and Environmental Sciences, University of Tsukuba, 305-0006, Tsukuba, Japan

Correspondence should be addressed to Xiao Yu; s1630225@u.tsukuba.ac.jp

Received 11 April 2022; Revised 30 May 2022; Accepted 6 June 2022; Published 3 August 2022

Academic Editor: Lianhui Li

As one of the public service resources, medical and health care has a great guarantee for people's healthy life and life safety and is an important part of ensuring the normal and orderly operation of urban functions. This paper takes the spatial pattern of urban medical resources in Hohhot as the research object and collects three types of urban medical resources, including clinics (health centers), specialized hospitals, and general hospitals, a total of 1300 sample points, based on GIS spatial analysis methods, using the average nearest neighbor, kernel density estimation method, standard deviation ellipse method, and accessibility measure to analyze the spatial distribution of medical resources. The results show that the medical resources in the urban area of Hohhot are all in a state of agglomeration, but due to the different functions of different types of medical resources, their distribution ranges and distribution directions also show different characteristics. Saihan District, Yuquan District in the southwest, has fewer medical facilities resources, and the distribution of the accessibility of the three types of medical facilities is quite different. Therefore, the spatial balance of comprehensive medical resources in the urban area of Hohhot needs to be further improved. The results of this paper have implications for the layout of medical facilities and planning has important reference significance.

1. Introduction

As the largest developing country, China is in a stage of rapid development. With the continuous development of the social economy, people's income level is continuously improved, living conditions are continuously improved, the demand for a better life is increasing day by day, and material life has been greatly satisfied at the same time [1–4]. The demand for various public service resources has also increased. During the "Twelfth Five-Year Plan" period, the state proposed to accelerate the establishment of a sound basic public service system, adhere to the people-oriented approach, improve the level of basic public services in cities, and strive to promote the balance of basic public services [5, 6]. Therefore, the spatial layout of public service facilities is related to people's quality of life and social justice [7–10]. The rational and scientific allocation of medical resources is related to whether residents can enjoy the various functions and services of urban medical resources conveniently and equally and is an important foundation for realizing the harmony and unity of the three pillars of economic development, social equity, and environmental friendliness [11–13]. In the past, the evaluation methods of medical resource allocation were mostly based on traditional databases to establish information systems and quantitatively evaluate medical resource allocation capabilities by using indicators such as the balance of medical resource supply and demand, the professional skills of medical staff, and medical technicians with a population of 1,000 [14–16]. However, the traditional database lacks spatial expression ability, which limits its ability to provide decision-makers with information on the spatial distribution of medical resources and decision support [17–20].

Basic public services include basic education, social employment, social security, and medical and health care. As one of the public service resources, medical and health care has a great guarantee for people's healthy life and life safety and is an important part of ensuring the normal and orderly operation of urban functions [21–23]. The research focus of foreign scholars on medical resources has shifted from the selection and layout of locations to the research on the fairness and accessibility of medical resources and then

gradually shifted to the spatial distribution and formation mechanism of medical resources. However, Chinese scholars have used the quantitative measurement method to study the fairness of hospital medical resource allocation from the number of hospitals and the number of doctors and have also conducted research on site selection, accessibility, and layout evaluation. At the end of 2019, a sudden outbreak of COVID-19 plunged the whole of China into a disaster. All cities responded quickly and set up designated isolation hospitals to fully guarantee the people's medical problems. However, in areas with severe epidemics, it is still difficult to find a bed, so the spatial distribution of medical resources will directly affect the time efficiency of patient treatment when the disease occurs [24–30].

As a part of urban public service facilities, medical service facilities also occupy an important position in the city's resource allocation. In the "Planning and Design Standards for Urban Residential Areas" (GB50180-2018), it is also mentioned that health centers and outpatient departments should be configured within the 15-minute living circle, which reflects the state's emphasis on the layout and distribution of medical service facilities. Studying the accessibility of medical service facilities and analyzing and evaluating the distribution of urban residents, it can not only improve the convenience and fairness of residents' access to medical service resources but also help optimize the layout of urban medical service facilities and improve medical services.

In China, many scholars have studied the accessibility and spatial distribution characteristics of medical facilities. Scholars in the field of geography mainly focus on the spatial distribution characteristics of facilities. Zeng Wen et al. took Nanjing City as an example to analyze the spatial pattern and causes of its medical service facilities. Mingji Quan took the Yanbian area as a sample, compared the spatial layout of medical facilities in the Yanbian area from 2007 to 2019, and summarized the evolution characteristics of medical facilities. Such studies are mostly theoretical explorations and lack planning advice to guide practical operations. Scholars in the field of planning focus more on evaluating the service level of facilities and exploring the spatial distribution mechanism. Taking the Hong Kong Special Administrative Region as an example, Ma Qiwei et al. analyzed the spatial layout and functional differences of medical service facilities, analyzed their influencing factors, and put forward suggestions for the path transformation suitable for the mainland on this basis. Taking Nanjing as an example, Cao Yang et al. comprehensively evaluated the service level of medical facilities from the perspective of residents' activities and put forward suggestions for improving the function of medical resources and optimizing the layout. Taking Hefei City as an example, Li Zao et al. analyzed the distribution pattern of its medical facilities and made a suitable aging analysis. However, from the perspective of the research scope, such research mostly focuses on a single urban or rural area and lacks thinking from the perspective of urban-rural integrated development.

Therefore, based on GIS spatial analysis methods, this paper uses the average nearest neighbor, kernel density estimation method, standard deviation ellipse method, and accessibility measure to analyze the spatial distribution of medical resources in the urban area of Hohhot. On this basis, its spatial pattern is evaluated and the deficiencies in the current model are found out.

2. Overview of the Study Area

Located in the Inner Mongolia Autonomous Region, Hohhot is the political, economic, and cultural center of the Inner Mongolia Autonomous Region approved by the State Council and an important central city in the northern border areas of my country. The city has a total of 4 municipal districts, 4 counties, and 1 flag. The city has a total area of 17,200 square kilometers, of which the built-up area is 260 square kilometers. The total population of Hohhot by the end of 2020 was 2.52 million. Among them, 439,575 people were in Xincheng District, 238,970 people were in Huimin District, 208,694 people were in Yuquan District, 563,712 people were in Saihan District, 359,107 people were in Tumutzuo Banner, 199,763 people were in Tuoketuo County, 203,893 people were in Helinger County, and 139,297 people were in Qingshuihe County. There are 167,023 people in Wuchuan County. A schematic diagram of the administrative divisions and population distribution of the study area is shown in Figure 1.

The acquisition method of medical resource data involved in this study is network survey, mainly from AutoNavi electronic map, and the data vector files of each region are from the resource and environment data cloud platform. The number of medical resources collected in the urban area of Hohhot includes a total of 1,176 clinics (health centers), a total of 23 specialized hospitals, and a total of 136 general hospitals. There are 13,760 beds in health institutions, including 3,505 in Xincheng District, 4,461 in Huimin District, and 2,696 in Yuquan District. There are 33,805 technicians in medical institutions, including 6,688 in Xincheng District, 5,768 in Huimin District, and 5,489 in Yuquan District. A more intuitive distribution of medical resources is shown in Figure 2.

3. Research Method

3.1. Average Nearest Neighbor. Average Nearest Neighbor refers to the average of the closest distances between points. The spatial pattern is judged by comparing the calculated average distance of the nearest neighbor point pair with the average distance of the nearest neighbor point pair in the random distribution pattern. It can be expressed as follows:

$$D_{ANN} = \frac{\overline{r_i}}{\overline{r_E}} = 2\sqrt{d}, \tag{1}$$

$$\overline{r_E} = \frac{1}{2\sqrt{n/A}} = \frac{1}{2\sqrt{D}}. \tag{2}$$

Formulas (1) and (2) refer to the actual nearest neighbor distance, in m, that is, the average distance between each hospital in the main urban area of Hohhot and its nearest hospital; $\overline{r_E}$ is the theoretical nearest

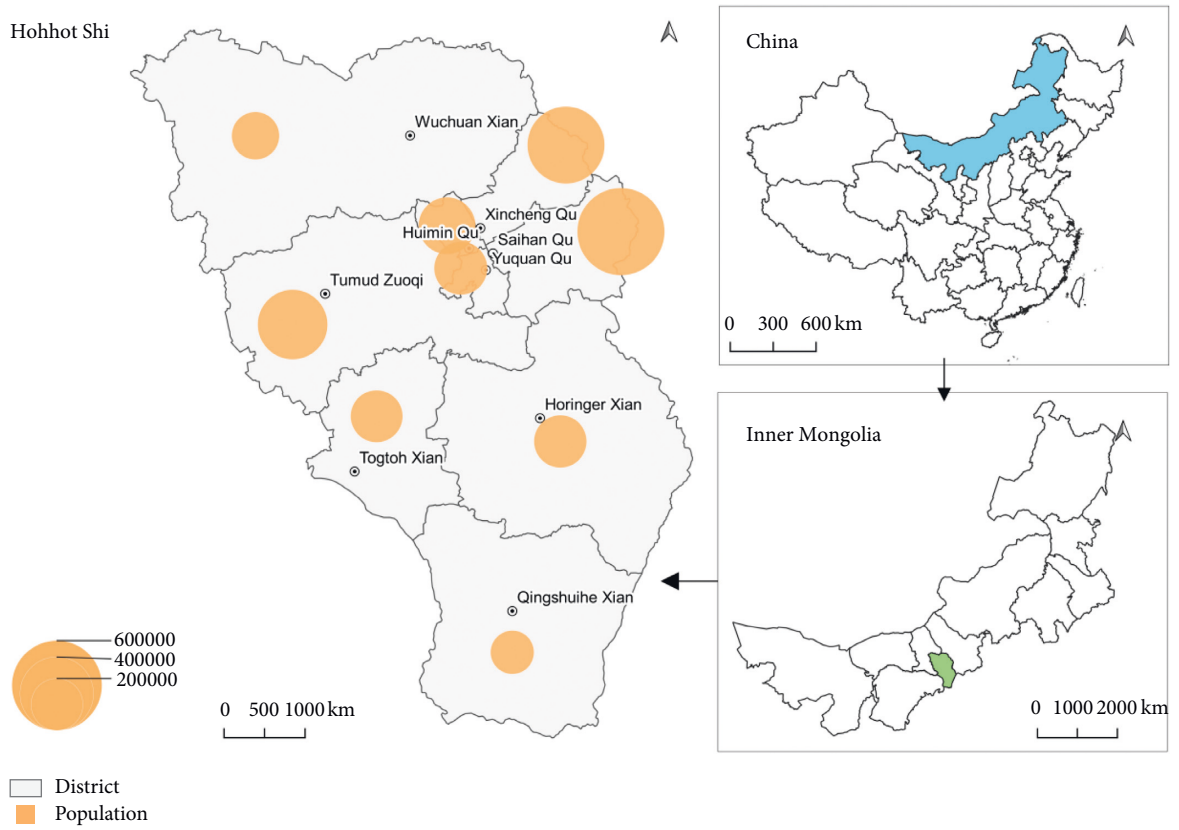

Figure 1: Schematic diagram of the administrative division and population distribution of the study area.

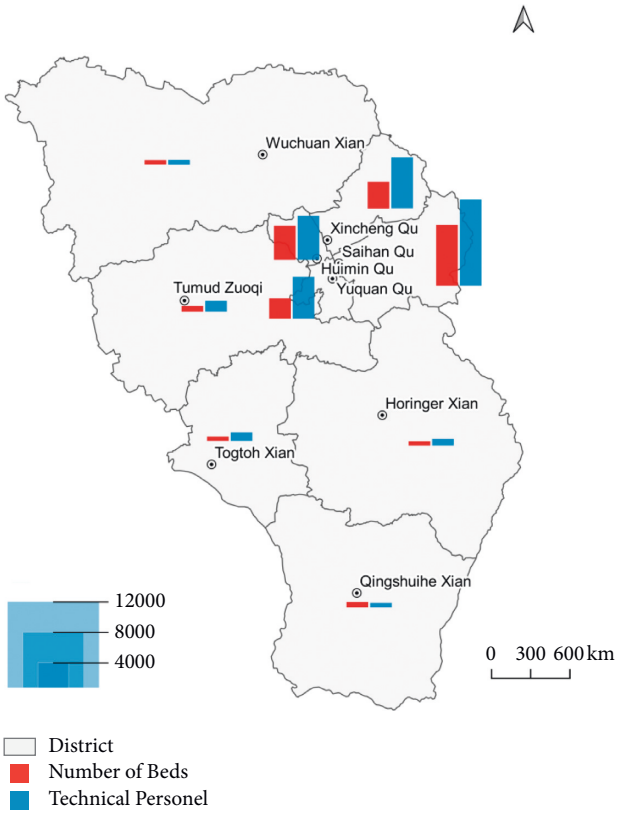

Figure 2: Distribution map of medical resources in Hohhot.

neighbor distance, in m, that is, the expected average distance between hospitals under random distribution mode, in m; n is the total number of hospitals; A is the total area of the main urban area of Hohhot City, in m^2; D is the main urban area intrahospital point density; and D_{ANN} is the nearest neighbor index. When $D_{ANN} = 1$, the hospital distribution state is random distribution; when $D_{ANN} < 1$, the hospital distribution state is an agglomerative state; and when $D_{ANN} > 1$, the hospital distribution state is discrete.

3.2. Kernel Density Method. The kernel density method is a density function used to estimate unknowns in probability theory. According to the estimation of known medical resource data points, the spatial aggregation degree of elements is analyzed. Information is effectively visualized. Its formula is as follows:

$$K(x) = \frac{1}{nd}\sum_{i=1}^{n} a\left(\frac{x - X_i}{d}\right). \tag{3}$$

In the formula, $a(x - X_i/d)$ is the kernel density function; $d(d > 0)$ is the distance from the hospital point to the time point X_i; and $K_{(x)}$ is the estimated value of the kernel density. Using the kernel density method, the spatial distribution information of clinics (health centers), specialized hospitals, and general hospitals is visually expressed by the

graphical method, and its spatial distribution characteristics are explored.

3.3. Standard Deviation Ellipse. The standard deviation ellipse method refers to analyzing the spatial distribution characteristics of medical resources from the center, distribution range, shape, and direction of the ellipse by constructing a standard deviation ellipse. It is an important method to study the distribution direction and characteristics of spatial points, and it is also one of the most commonly used methods in spatial pattern analysis. Its formula is as follows:

$$\begin{aligned} \mathrm{SDE}_x &= \sqrt{\frac{\sum_{i=1}^{n}\left(x_i-\overline{X}\right)^2}{n}}, \\ \mathrm{SDE}_y &= \sqrt{\frac{\sum_{i=1}^{n}\left(y_i-\overline{Y}\right)^2}{n}}. \end{aligned} \tag{4}$$

In the formula, x_i and y_i represent the coordinates of medical resource data points i; $\{\overline{X}, \overline{Y}\}$ represents the average center of medical resource data points; and n represents the total number of study areas.

3.4. Accessibility Measure. At present, the measurement methods of the accessibility of medical service facilities are mainly divided into two categories in the macroscopic view as follows: one is the potential model and the other is the two-step mobile search method. The two models can effectively measure the accessibility of service facilities by combining relevant evaluation factors such as medical population and hospital level with different calculation methods. This paper mainly uses the GIS-based network analysis method combined with the improved potential model to measure and evaluate the accessibility of medical service facilities in the main urban area of Hohhot City.

(1) *Potential Model.* Mainly derived from the law of universal gravitation in physics, it was first proposed by the French scholar Lagrange and later cited by geography, adding various influencing factors such as region, grade, and economy, and deformed and developed into a potential model. Today, the potential model has developed into a classic model for studying the interaction of social and economic spaces.

$$A_i = \sum_{j=1}^{n} \frac{S_j}{D_{ij}}. \tag{5}$$

Potential is the gravitational force that one object exerts on another object. In the formula, A_i is the potential of facility i to facility type j; it is the facility scale of facility j..

(2) *Improved Potential Model.* At present, for the research and development of the accessibility of urban medical facilities, factors such as the population of residential areas, the service capacity of public facilities, and the attenuation of the spatial distance between residential areas and medical service facilities are integrated into the basis of the potential model. It is also possible to set different influencing factors and other factors for different types of medical service facilities, such as service capacity, residents, city types, and resident types reachability for a more scientific explanation.

$$A_i = \sum_{j=1}^{n} \frac{S_j}{V_j D_{ij}^{\beta}}, \tag{6}$$

$$V_j = \sum_{i=1}^{n} \frac{P_i}{D_{ij}^{\beta}}. \tag{7}$$

In formula(7), A_i is the accessibility index of a certain settlement i to all medical service facilities j in the area; S_j is the facility scale of a medical service facility j. In this paper, the hospital or health center mainly includes the following: the beds represents the number of patients that can be carriedD_{ij} represents the distance from settlement i to the medical service facility j. The data in this part are mainly calculated by the OD travel table obtained from the analysis of the GIS network data. In formula (8), V_j is the service capacity of facility j; P_i is the population of a settlement i; and β is represented as the travel friction coefficient. After scholars' research on it, the value range of β is mainly between [0.9–2.29]; β, as an influencing factor that can reflect residents' willingness to travel, should have different values in different types of medical facilities. After comparative research, the friction coefficient β in this paper is 1 in general hospitals. Since the single statistical accessibility is not obvious to the data, we used the dispersion standardization method to process the data on the accessibility data from residential areas to various medical service facilities in Hohhot City. Rationality analysis is carried out using the interpolation analysis diagram of the property. The standardization of dispersion is a linear transformation of the original data so that the result falls into the [0, 1] interval. The conversion function is shown in the formula, where max is the maximum value of the sample data and min is the minimum value of the sample data.

$$X_j = \frac{A_i - \min_{1\le j\le n}\left(A_j\right)}{\max_{1\le j\le n}A_j - \min_{1\le j\le n}\left(A_j\right)}. \tag{8}$$

In the formula, X_j is the normalized value and A_i is the original value.

4. Results and Analysis

4.1. Spatial Aggregation Analysis of Medical Resources. To study the spatial pattern of medical resources in the main urban area of Hohhot City, it is first necessary to determine the relationship between these medical resources and whether the spatial distribution of these medical resources is random, agglomerated, or divergent. Therefore, based on the GIS spatial analysis method and ArcGIS software, the

average nearest neighbor analysis was performed on the three types of medical resources in the main urban area of Hohhot: clinics (health centers), specialized hospitals, and general hospitals, and the nearest neighbor ratio, Z score, and P were calculated. The nearest neighbor ratio was used as the basis for the spatial distribution and agglomeration degree of medical resources in the main urban area of Hohhot City, and the Z score and P value were used to test the significance of the results. The calculation results are shown in Table 1.

4.2. Spatial Structure Analysis of Medical Resources. Through the calculation of the nearest neighbor ratio D_{ANN} for the medical resources in the urban area of Hohhot, it can be seen that within this range, the spatial distribution of the three types of medical resources is in a state of aggregation. In order to observe the scope and size of each type of medical resource agglomeration more intuitively and understand its spatial structure, the nuclear density method is used to detect the state of medical resource agglomeration. The density of medical resources gradually decreases from the southwest high-density area to the Yuquan area, and its spatial pattern is mainly concentrated in the central and northeastern regions. The distribution of residents' medical resource needs is shown in Figure 3.

4.3. Spatial Analysis of Accessibility of Medical Resources

4.3.1. Accessibility from Residential Areas to General Hospitals. The layout of general hospitals in the central urban area of Hohhot is relatively concentrated. Large general hospitals with more than 500 beds are roughly distributed at the junction of the three urban areas, and the junction is also the center of the city's first development. There are a large number of residential areas and groups. The main road has a superior geographical location, so the accessibility from the residential area in the center to the general hospital is at the most advantageous level. In response to the trend of urban development, for Saihan District in the east, there are corresponding large-scale general hospitals, and the economic and technological development situation is relatively good. Most of the new urban areas are located in the central and northern parts of the city, so its residents have access to general hospitals in a relatively favorable position. In the southwestern region, due to development problems, the population agglomeration is relatively low, and most of the general hospitals allocated have low service capacity, resulting in the low accessibility of residents in the western and southern urban areas to general hospitals.

The accessibility standardized statistics are shown in Figure 4. The serial number on the horizontal axis in the figure represents the range of the standardization value of accessibility, and the corresponding relationship is shown in Table 2. According to the standardized statistics of accessibility, most of the values are between 0.1 and 0.6, accounting for more than 85% of the total number of residential areas, and the distribution in each value segment is relatively uniform, indicating that the number of residents from residential areas to general hospitals is relatively uniform. The accessibility is distributed in each numerical segment, and there is no obvious area where the numerical values are agglomerated.

4.3.2. Accessibility from Residential Areas to Specialist Hospitals. As the distribution of specialized hospitals is relatively scattered, the scale is small, and most of the geographical locations are at the boundary of the coverage of general hospitals, and the relatively advantageous location is at the junction junction of general hospital and specialist hospital services. Most of these types of areas have moderate-sized residential areas, dense populations, and relatively convenient transportation. In addition to the farmer's area in the west and the recreational area in the south, the main areas where residents have insufficient accessibility to specialized hospitals also added more peripheral areas in the northeast and east. There are fewer specialized hospitals in these areas, which are affected by distance factors, resulting in reduced accessibility.

The standardized statistics of the accessibility data are shown in Figure 5. The serial number of the horizontal axis in the figure represents the range of standardized accessibility values, and the corresponding relationship is shown in Table 3. A large number of standardized data are concentrated between 0 and 0.1, accounting for more than 80% of the overall data. Most of the numerical areas in this concentration are clusters with low accessibility, indicating that the accessibility from residential areas to specialized hospitals is local.

4.3.3. Accessibility from Residential Areas to Health Centers. Since most of the health centers use their surrounding communities or residential communities as their service units, the accessibility coverage of residents in Hohhot to the health centers is relatively balanced, and the more advantageous locations are mostly around large-scale community health centers, or adjacent to. There are many areas where small clinics are concentrated. However, most of the central urban areas are within the relatively good accessibility range, and even residents in the relative leisure and underdeveloped areas in the southwest of the city can have relatively average accessibility to health centers.

The standardized statistics of accessibility data are shown in Figure 6. The serial number on the horizontal axis in the figure represents the range of standardized accessibility values, and the corresponding relationship is shown in Table 4. The standardized numerical distribution of the accessibility of residential areas to health centers is concentrated between 0 and 0.2, and there is also a relatively scattered data distribution between the values of 0 and 1. Based on the analysis in Figure 5, most of the residential areas in the data concentration area are located within the service scope of the health center, so the entire data analysis shows that the level of accessibility from the residential area to the health center is relatively balanced.

Table 1: Average nearest neighbor parameters of the spatial distribution of medical resources in Hohhot.

Medical resources	Number of hospitals	Nearest neighbor ratio/ANN	Z score	P value
Clinic	1192	0.358	−41.16	0
Specialist hospital	140	0.422	−12.65	0
General hospital	168	0.481	−13.11	0

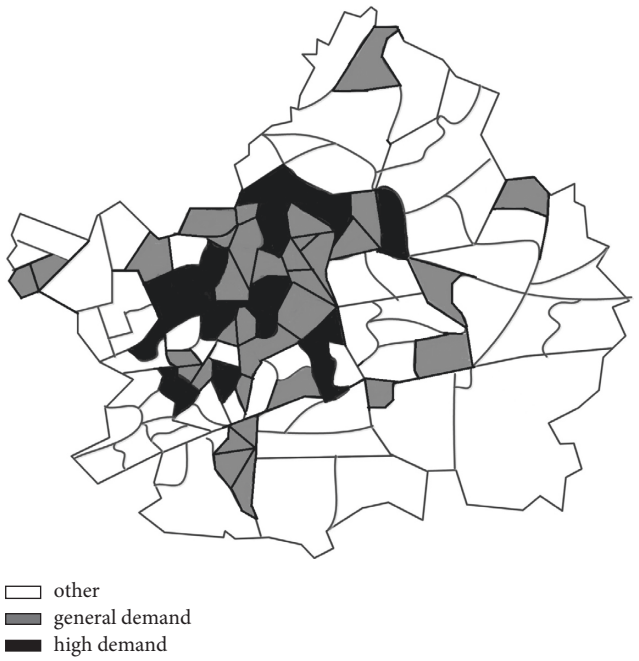

Figure 3: Distribution map of residents' medical resource needs.

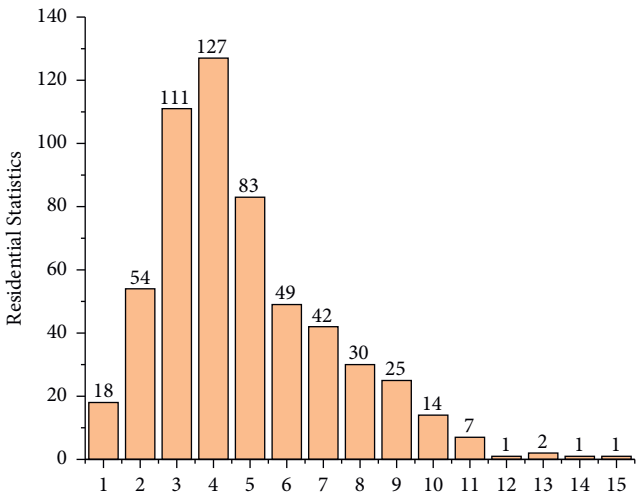

Figure 4: Standardized statistical chart of accessibility from residential areas to hospitals.

5. Conclusion

This research quantitatively studies the spatial distribution characteristics and accessibility of medical service facilities through quantitative models such as GIS spatial autocorrelation and network analysis. The three types of medical resources in the urban area of Hohhot all showed a state of

Table 2: Standardized numerical ranges for accessibility.

Serial number	Accessibility normalized values
1	[0.00, 0.07]
2	[0.07, 0.13]
3	[0.13, 0.20]
4	[0.20, 0.27]
5	[0.27, 0.34]
6	[0.34, 0.40]
7	[0.40, 0.47]
8	[0.47, 0.54]
9	[0.54, 0.60]
10	[0.60, 0.67]
11	[0.67, 0.74]
12	[0.74, 0.80]
13	[0.80, 0.87]
14	[0.87, 0.94]
15	[0.94, 1.01]

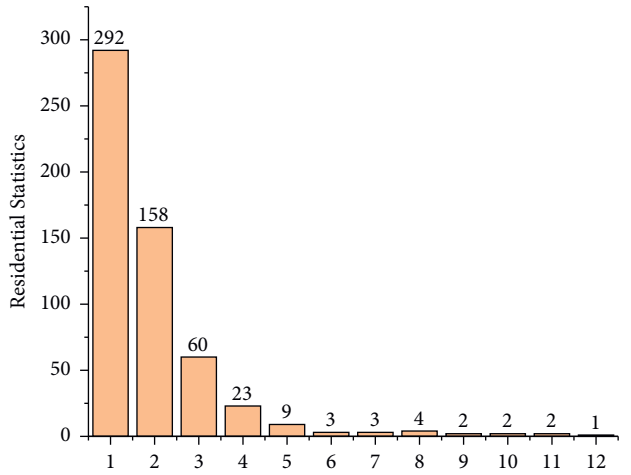

Figure 5: Standardized statistics on accessibility from residential areas to specialized hospitals.

Table 3: Standardized value ranges for accessibility.

Serial number	Accessibility normalized values
1	[0.00, 0.05]
2	[0.05, 0.10]
3	[0.10, 0.14]
4	[0.14, 0.20]
5	[0.27, 0.32]
6	[0.36, 0.41]
7	[0.45, 0.50]
8	[0.54, 0.59]
9	[0.63, 0.68]
10	[0.72, 0.77]
11	[0.81, 0.86]
12	[0.90, 0.95]

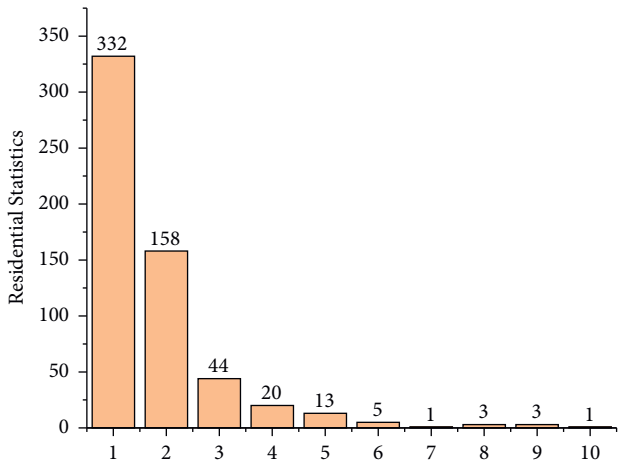

Figure 6: Standardized statistics on accessibility from residential areas to health centers.

Table 4: Standardized value ranges for accessibility.

Serial number	Accessibility normalized values
1	[0.00, 0.05]
2	[0.05, 0.10]
3	[0.10, 0.15]
4	[0.25, 0.30]
5	[0.35, 0.40]
6	[0.45, 0.50]
7	[0.55, 0.60]
8	[0.65, 0.70]
9	[0.75, 0.80]
10	[0.85, 0.90]

agglomeration and distribution, showing a high degree of agglomeration. As the settlement of urban population, the main urban area has a large demand for medical resources. Therefore, the agglomeration of medical resources provides great convenience for residents to live healthy life.

The accessibility of residents in general hospitals, specialized hospitals, and health centers in the central urban area of Hohhot was analyzed using the improved potential model and variance-normalized data. From the analysis results, it can be concluded that even in the urban area of Hohhot under the measurement of the accessibility of three different types of medical facilities, the accessibility of medical service facilities in the urban center and the more developed central and northeastern urban areas is better. However, the accessibility of medical resources in less developed areas such as southwestern urban areas is relatively weak. After comprehensively comparing the accessibility of different types of medical facilities, it can be seen that the medical resources of general hospitals and specialized hospitals are complementary in some locations in the urban area. Residents in the outer circle have limited medical resources. As a community-based medical service facility, although the accessibility performance of the western and southern urban areas is slightly weaker, the health center can still provide urban residents with a relatively balanced index of medical resource accessibility. Combined with the urban development planning of Hohhot, the following optimizations can be provided:

(1) Integrate medical resources in central urban areas with relatively abundant medical resources to avoid resource waste caused by high aggregation.

(2) In the southwest of the city, the existing specialized hospitals can be used to appropriately increase their scale, improve their service capabilities, and enhance the willingness of surrounding residents to seek medical treatment.

(3) Leisure and farmer areas in the east and north of the city can improve the scale and medical level of small general hospitals in their areas, and large-scale health centers can be established in their areas to provide basic medical services to residents.

(4) The scale of the research in this paper is relatively small, and the scope is mostly the central area of the city. The research method is relatively simple. In future work, the Gini coefficient and spatial correlation analysis can also be used to make reasonable analyses, improve the analysis system, and provide more reasonable advice.

Data Availability

The dataset can be accessed upon request.

Conflicts of Interest

The author declares that there are no conflicts of interest.

References

[1] X. Zong, X. Ding, and Z. Zhou, "Health level classification by fusing medical evaluation from multiple social networks," *Future Generation Computer Systems*, vol. 114, pp. 574–580, 2021.

[2] E. L. Antonsen, R. A. Mulcahy, D. Rubin, R. S. Blue, M. A. Canga, and R. Shah, "Prototype development of a tradespace analysis tool for spaceflight medical resources," *Aerospace Medicine and Human Performance*, vol. 89, no. 2, pp. 108–114, 2018.

[3] P. Manimegalai and U. S. Ragupathy, "Medical evaluation of improved label fusion based haematoma segmentation in traumatic brain injury images," *International Journal of Soft Computing and Engineering*, vol. 7, no. 6, 2018.

[4] W. Li, L. Deng, and J. Wang, "The medical resources allocation problem based on an improved SEIR model with sharing behavior," *Modern Physics Letters B*, vol. 35, no. 34, 2021.

[5] H. Li, D. Mu, P. Wang, Y. Li, and D. Wang, "Prediction of obstetric patient flow and horizontal allocation of medical resources based on time series analysis," *Frontiers in Public Health*, vol. 9, p. 646157, 2021.

[6] T. Wen, Z. Zhang, M. Qiu, Q. Wu, and C. Li, "A multi-objective optimization method for emergency medical resources allocation," *Journal of Medical Imaging and Health Informatics*, vol. 7, no. 2, pp. 393–399, 2017.

[7] S. Wan, Y. Chen, Y. Xiao, Q. Zhao, M. Li, and S. Wu, "Spatial analysis and evaluation of medical resource allocation in

China based on geographic big data," *BMC Health Services Research*, vol. 21, no. 1, p. 1084, 2021.

[8] A. Shi, X. Zhou, Z. Xie, H. Mou, Q. Ouyang, and D. Wang, "Internet plus health care's role in reducing the inequality of high-quality medical resources in China," *Asia-Pacific Journal of Public Health*, vol. 33, no. 8, pp. 997-998, 2021.

[9] M. Liu and Y. Xiao, "Optimal scheduling of logistical support for medical resource with demand information updating," *Mathematical Problems in Engineering*, vol. 2015, no. Pt.5, pp. 1–12, Article ID 765098, 2015.

[10] T. Sarkar, D. Sarkar, and P. Mondal, "Road network accessibility analysis using graph theory and GIS technology: a study of the villages of English Bazar Block, India," *Spatial Information Research*, vol. 29, pp. 405–415, 2020.

[11] F. Sun, J. Su, Y. Hu, and L. Zhou, "The prediction of new medical resources in China during COVID-19 epidemic period based on artificial neural network model optimized by genetic algorithm," *Journal of Physics: Conference Series*, vol. 1815, no. 1, pp. 20-21, 2021.

[12] Q. Huang, T. Zhu, and B. Lu, "Study on competitive power of medical resources of 31 provinces and cities in China based on factor and cluster analysis," *Basic and Clinical Pharmacology and Toxicology*, vol. 2021, p. 128, 2021.

[13] B. Ethel, M. Hunadi, C. Green, and M. Gerbrand, "Evaluating public ambulance service levels by applying a GIS based accessibility analysis approach," *South African Journal of Geology*, vol. 6, no. 2, 2017.

[14] B. Smaranda, B. Silviu, and C. Hariton, "An artificial immune system Approach for a multi-compartment queuing model for improving medical resources and inpatient bed occupancy in pandemics," *Advances in Electrical and Computer Engineering*, vol. 20, no. 3, p. 2341, 2020.

[15] Y. Meng, Y. Li, H. Liu, and Y. Huang, "Study on evaluation of urban and rural high-quality living space based on accessibility analysis——taking shahe city, hebei province as an example," *IOP Conference Series: Earth and Environmental Science*, vol. 769, no. 2, Article ID 022075, 2021.

[16] F. Gong and S. Tang, "Internet intervention system for elderly hypertensive patients based on hospital community family edge network and personal medical resources optimization," *Journal of Medical Systems*, vol. 44, no. 5, 2020.

[17] L. Zhu, S. Zhong, W. Tu et al., "Assessing spatial accessibility to medical resources at the community level in shenzhen, China," *International Journal of Environmental Research and Public Health*, vol. 16, no. 2, p. 242, 2019.

[18] H. Papadopoulos and A. Korakis, "Predicting medical resources required to be dispatched after earthquake and flood, using historical data and machine learning techniques: the COncORDE emergency medical service use case[J]," *International Journal of Interactive Communication Systems and Technologies (IJICST)*, vol. 8, no. 2, pp. 13–35, 2018.

[19] C. Zhao, X. Chunliang, and G. Yu, "FedEx and UPS network structure and accessibility analysis based on complex network theory," *Complexity*, vol. 2021, Article ID 6682670, 2021.

[20] H. C. Wu, M. H. Tseng, and C. C. Lin, "Assessment on distributional fairness of physical rehabilitation resource allocation: geographic accessibility analysis integrating google rating mechanism," *International Journal of Environmental Research and Public Health*, vol. 17, no. 20, p. 7576, 2020.

[21] Z. Zhang, S. Fan, and H. Zhang, "Park accessibility analysis based on location information and GIS: take shanghai hongkou district as an example," *IOP Conference Series: Materials Science and Engineering*, vol. 825, no. 1, p. 012028, 2020.

[22] T. Ala-Hulkko, O. Kotavaara, J. Alahuhta, M. Kesälä, and J. Hjort, "Accessibility analysis in evaluating exposure risk to an ecosystem disservice," *Applied Geography*, vol. 113, no. C, p. 102098, 2019.

[23] R. Shanmathi Rekha, S. Wajid, N. Radhakrishnan, and S. Mathew, *Accessibility Analysis of Health care facility using Geospatial Techniques Transportation Research Procedia*, vol. 27, pp. 1163–1170, 2017.

[24] S. Saikia and B. Gogoi, "GIS based accessibility analysis: a study on health care services in Jorhat district of Assam," *The Clarion- International Multidisciplinary Journal*, vol. 6, no. 1, p. 83, 2017.

[25] A. C. Ford, S. Barr, R. Dawson, and P. James, "Transport accessibility analysis using GIS: assessing sustainable transport in london," *ISPRS International Journal of Geo-Information*, vol. 4, no. 1, pp. 124–149, 2015.

[26] Z. Jia, Y. Lin, J. Wang et al., "Multi-view spatial-temporal graph convolutional networks with domain generalization for sleep stage classification," *IEEE Transactions on Neural Systems and Rehabilitation Engineering*, vol. 29, pp. 1977–1986, 2021.

[27] Z. Jia, J. Junyu, X. Zhou, and Y. Zhou, "Hybrid spiking neural network for sleep EEG encoding," *Science China Information Sciences*, vol. 65, no. 4, 2022.

[28] H. Li, X. Niu, and B. Wang, "Prediction of ecosystem service function of grain for green project based on ensemble learning," *Forests*, vol. 12, no. 5, p. 537, 2021.

[29] Z. Jia, X. Cai, and Z. Jiao, "Multi-modal physiological signals based squeeze-and-excitation network with domain adversarial learning for sleep staging," *IEEE Sensors Journal*, vol. 22, no. 4, pp. 3464–3471, 2022.

[30] Z. Jia, X. Cai, Y. Hu, H. Ji, and Z. Jiao, "Delay propagation network in air transport systems based on refined nonlinear Granger causality," *Transportation Business: Transport Dynamics*, vol. 10, pp. 1–13, 2022.

Hindawi
Scientific Programming
Volume 2022, Article ID 5460234, 8 pages
https://doi.org/10.1155/2022/5460234

Research Article

Financial Operation Revenue Management Method from the Perspective of Big Data

Yamin Si and Yufang Xu

Shanghai University of Finance and Economics Zhengjiang College, Jinhua, Zhejiang 321013, China

Correspondence should be addressed to Yufang Xu; z2017101@shufe-zj.edu.cn

Received 6 June 2022; Revised 4 July 2022; Accepted 8 July 2022; Published 2 August 2022

Academic Editor: Lianhui Li

With the rapid development of science and technology, information has become the theme of the 21st century. The development of network-based e-commerce has changed the global economic model, business management model, and people's work, life, and consumption patterns, forming a global information economy. As the core part of enterprise management, financial management has been strongly impacted by the management environment, application of technical methods to function execution, and management concepts. Under the background of big data, how to manage financial affairs of enterprises has become a problem worth exploring. This paper mainly discusses the financial operation revenue management from the perspective of big data, briefly discusses the big data and financial operation revenue management, and analyzes the relevant strategies for the effective development of financial operation revenue management combined with case studies.

1. Introduction

In the perspective of my country's rapid economic development, the cost control of enterprises is becoming more and more important. Only by doing well in cost control can enterprises benefit and consolidate their market position, which is conducive to the long-term development of enterprises. At present, there are many problems in the financial operation [1, 2] and cost control of enterprises, which need to be intervened and solved in time, so that the financial operation [3, 4] and cost control of enterprises will develop in a scientific and rational direction [5–8].

The object of enterprise financial operation [9–12] is the total funds flowing in the enterprise, and the efficiency of enterprise financial operation refers to the efficiency of the enterprise's working capital. The profit of a company often refers to the profit in operation, which shows the importance of the financial operation of a company. A good corporate financial operation not only invests effort in reaping profits [13], but also improves the layout of the company's debt repayment and analyzes market conditions and capital use risks, which can provide a reliable reference for corporate investors and creditors.

Cost control refers to the measures taken by enterprises to prevent and control production-consumption in order to achieve profitability. This can not only allow enterprises to successfully complete the set goals, but also retain costs as much as possible to maximize profits. Language is an effective help to achieve long-term development. Cost control involves many aspects, such as the cost control of raw material purchase in the early stage of production, and also includes the cost control of manpower and material resources in the production process. The expenses incurred by the enterprise department in the management process should also be included in the scope of cost control. What is more, the transportation and sales expenses incurred after the production is completed also need to be included in the content of cost control. It can be said that cost control covers all aspects of enterprise operation and management and is the key to enhancing enterprise profitability.

Although there are not a lot of financial management personnel in many enterprises [14–16], the quality of

financial management personnel is uneven [17], resulting in a low overall level of financial management [18]. Here, it is particularly important to pay attention to the financial personnel who are in line with international affairs [19], communicate, and contact. Since many enterprises are currently paying great attention to economic development, there is a situation in which scientific and technological personnel despise financial management personnel. Although financial management personnel have higher authority and rank in some enterprises [20], their work still revolves around transactional work, a huge amount of work. Pressure and complicated management matters have caused many financial managers to fail to take the time to learn management knowledge and improve management skills [21]. This is also the root cause of the generally low quality of financial managers in many enterprises [22]. In order to make the financial operation and management cost control of the enterprise return to the right path and play an active role, it is necessary for the enterprise to strengthen its attention. It is necessary not only to conduct regular reviews and inquiries on financial management [23], but also to go deep into the financial interior to explore the progress of financial management [24] and actively assist the financial management department to solve the problems encountered. In addition, it can also increase the investment and support for the financial department, which can be manpower support or capital investment, so as to effectively strengthen the position of financial management in enterprise operation management.

In addition, we must pay close attention to the control of cost stages, including preproduction control, in-production control, and circulation control, and set up a "one-to-one" supervision team for these three stages of cost control to effectively implement raw material purchase, product packaging, publicity, and planning, as shown in Figure 1. Infiltrate the supervision function in multiple links such as long-distance transportation, effectively control the cost expenditure, do a good job in the cost budget of each stage, reasonably divide the cost consumption ratio, and effectively control the overall operating cost of the enterprise within the planning scope.

2. Current Status of Corporate Financial Management

2.1. The Traditional Concept Has Not Changed. In the context of the rapid development of the Internet, big data is the main development direction at present, and the application of big data in work and life will become more and more common. The most significant feature of big data is the integration of resources to facilitate financial management. At the same time, big data also has strong data analysis and computing capabilities. Since there are still some problems in the process of financial enterprise management informatization construction in my country, it has caused certain obstacles to the construction of accounting informatization, thus limiting the value of big data services to play their due value. The method of financial management generally includes five basic links: financial analysis,

Figure 1: Planned scenario.

financial forecasting, financial decision-making, financial budgeting, and financial control. Each link has professional business methods and mathematical models; for example, the capital asset pricing model, accounts receivable turnover rate, capital structure, leverage principle, etc. are all important methods in financial management. At present, many enterprises still focus their financial management on fund management, and their work is limited to the settlement of accounts [25]. Enterprise financial management in the information age should first change the thinking of financial personnel, letting them clarify their responsibilities, not only limited to the statistics and comparison of accounts, but they should also focus on asset management, investment management, and financing management throughout the economic activities of enterprises.

In the case of technical limitations, the overall development level of big data services in my country is relatively low, the service methods provided by big data service providers are relatively simple, and the software service functions are relatively small. For the construction of enterprise financial management informatization, the services provided by big data are still difficult to meet the diversified needs of their own construction. At this stage, there are relatively few service providers providing big data in the Chinese market, and the main target groups of these providers are e-commerce companies, and they mainly provide financial management services for e-commerce companies. From this perspective, the research and development of big data in my country are simply optimized and upgraded according to the relevant needs of financial management, so as to meet the daily financial management needs of e-commerce companies. Since the content of big data services cannot fully meet the needs of e-commerce companies' financial management informatization construction, e-commerce companies should not rely too much on big data in the construction process; otherwise, it will limit the integration of e-commerce companies and hinder e-commerce companies. The development of financial management reduces the efficiency of financial management of e-commerce enterprises.

2.2. Provide Good Service for Enterprise Decision-Making. Although computers have been used in the financial management of enterprises, they have not played an important

role. In the past, financial work focused on statistical billing, bookkeeping, and bookkeeping and did not pay attention to the decision-making of the enterprise. The relevant staff of the enterprise did not pay much attention to the impact of the accounting statements on the future development of the enterprise and could not provide good services for the enterprise's decision-making.

2.3. Lack of Support for Management Information. When many enterprises carry out information-based financial management activities, they do not carry out overall planning and do not have a complete management system. In the past, financial management used specific financial software, and there was almost no communication with other departments. The accounting department had no business dealings with other departments. The only beneficiary of informatization in financial management was the accounting department, which could not effectively improve the efficiency of the entire enterprise.

Big data financial accounting information security can be divided into physical equipment security, network security, and business data security. Among them, physical equipment security refers to whether online accounting services are unblocked; network security refers to the protection of hardware, software, and data in the network system; commercial data security refers to whether it can provide timely and accurate services to customers, whether e-commerce enterprises and commercial information resources will be tampered with and leaked, etc. Therefore, in the field of information technology, the mentioned security is a relative concept, and absolute information technology security does not exist yet. In addition, big data platforms, data, etc. are managed by big data service providers, and these data are transmitted between users and the cloud, which is very likely to face risks such as interception or destruction by third parties. At the same time, due to the complex configuration of big data equipment and systems, and a large amount of data storage, once a risk occurs, it will cause irreparable losses. Therefore, in the construction of financial enterprise management informatization, the most important point is to ensure the security of financial information, which is of great significance to the long-term development of the enterprise. Under the background of big data, the scope of financial calculation is extremely wide, and if financial calculation cannot be combined with management, it will affect the transformation from accounting to enterprise management.

Accountants are the main participants in the construction of enterprise financial management informatization, and to a certain extent, the security awareness of accountants will have an impact on the security of accounting information. Because some accountants associate the effect of accounting work with managers and believe that the security of information depends on managers, accounting practitioners are not fully aware of accounting informatization. When the security awareness of accounting practitioners is weak, or the cognition of accounting informatization is lacking, accounting information loss events will occur frequently. Although big data services can provide convenience for e-commerce enterprises' financial management informatization construction, it is also difficult to avoid security problems.

In addition, in the construction of enterprise management informatization, there is a lack of effective application of new technologies, which leads to problems in the enterprise's informatization risk early warning mechanism. Due to the lack of an information-based risk early warning mechanism, the security of corporate financial data has been adversely affected. Restricted by factors such as low technical level and insufficient professional quality of staff, various technical problems are faced in the process of big data application. Therefore, it is of great significance to build an information-based risk early warning mechanism.

3. The Impact of Big Data on Financial Management

3.1. Informatization Promotes Business Process Reorganization in Financial Management. Although traditional financial management also uses computers, it only records the accounts and simply applies the computer. The financial work is separated from other work, the financial work efficiency is not high, and the waste of funds is serious. The informatization of financial management is to eliminate the information isolation of various departments and realize the integrated management of finance. Therefore, financial management must undergo a thorough change. The new financial management is different from the traditional financial management [25]. It conducts a comprehensive and in-depth analysis of financial work, improves the key links of financial management, and realizes the reorganization of business processes. Financial management in the traditional sense cannot adapt to today's economic development situation, so we are urgently required to improve the business process of financial management. We need to analyze every link in the business process. Accounting after the fact is a major feature of traditional financial management. This method is not conducive to taking advantage of computers and cannot preprocess finances. Therefore, it is necessary to change this model of traditional financial management and strengthen the connection between the financial department and other departments. Financial personnel have changed from former information processors to administrators of business work. Relying on information technology, they focus on business process processing and finally achieve the goal of enterprise management. In addition, the big data platform has certain limitations in network transmission. Frequent data access and massive data exchange will lead to network congestion and data delay, and the weak network transmission capacity limits the development of financial enterprise management informatization. Figure 2 shows the trend chart of financial management informatization.

Judging from the financial management work of Chinese enterprises, although many enterprises have recognized the importance of big data application and have also

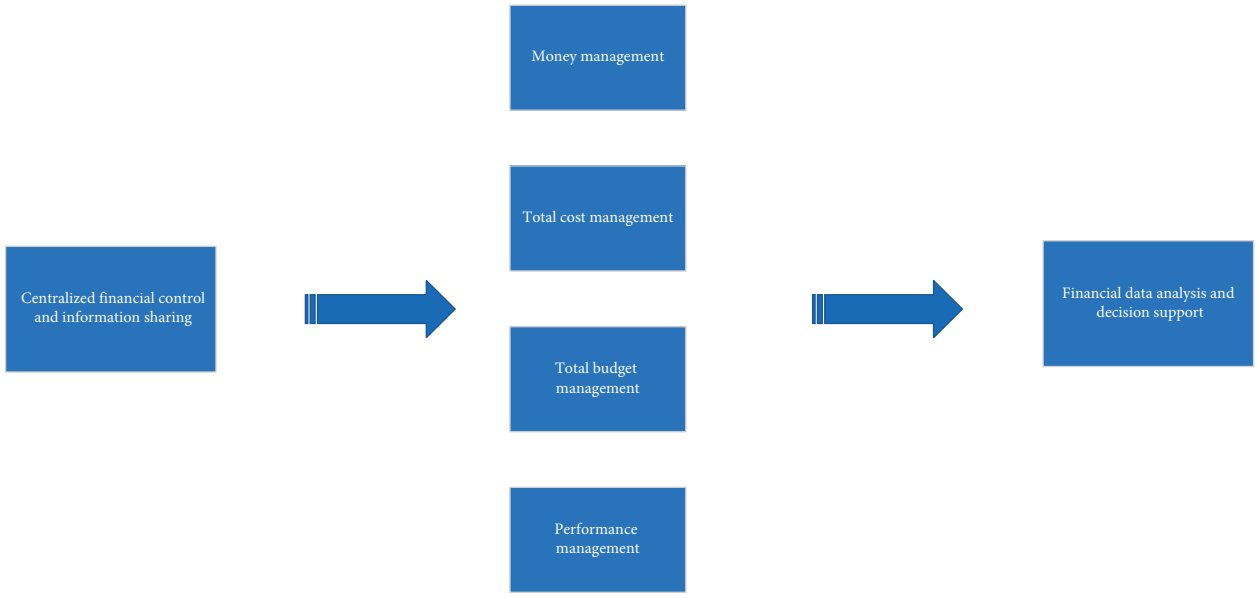

Figure 2: Trend chart of financial management informatization.

begun to actively explore specific countermeasures for the application of big data in the construction of financial enterprise management informatization, due to the lack of various mature technologies, the overall level of financial enterprise management informatization construction is relatively low. At the same time, due to the limitations of capital and technology, the service scope of big data is relatively small. In recent years, my country's scientific information technology has developed rapidly. As a new type of network technology, big data technology has entered the public's field of vision. Most e-commerce enterprise managers have limited awareness of big data, so they choose big data. There is certain blindness in data service providers, and it is difficult to correctly view big data service providers. Many business managers believe that the big data service provider with the largest number of users is the best. In addition, big data is still in the processing and development stage; further, development is still required, and a lot of costs must be invested in this process, which will limit the development of big data to a certain extent, but also increase the development of big data. risks faced. Compared with Western countries, my country's scientific research capabilities and financial support are relatively weak, resulting in the relatively weak competitiveness of my country's big data.

3.2. Informatization Promotes Internal Control of Financial Management. The internal control of financial management is to strengthen the protection of the funds of the enterprise, ensure the integrity of financial-related information, ensure the smooth implementation of relevant policies, improve the efficiency of financial management, effectively reduce the risk of financial management, and promote the realization of financial goals. The informatization of financial management has changed the traditional concept of financial management and expanded the scope of financial management. The use of informatization has led to internal changes in financial management, providing opportunities for further improvement of financial management, but also bringing risks. Information-based financial management is the comprehensive control and overall control of the enterprise. With the large-scale use of the network in life, people are paying more and more attention to the application of the network in financial management. Practice shows that the use of information technology solves the problems that cannot be solved by the traditional management model but increases the data risk of financial management. Therefore, it is necessary to strengthen the training of financial-related staff, accelerate the integration of financial management and information technology, focus on solving problems that arise, establish a financial management model that is compatible with social development, meet the development needs of enterprises, and bring more benefits to enterprises.

3.3. Informatization Increases the Risk of Investment. Information is the most important factor of production in today's era and an indispensable part of the operation of an enterprise. Information occupies a dominant position in enterprises, and investment in intangible assets is favored by business leaders. The proportion of an enterprise's intangible assets determines its position in the market. The development cost of information products is extremely high, which increases the business risk of enterprises. Market instability and changes in financial structure result in the variability and diversity of financial risks. There is a certain amount of uncertainty when developing information resources. Therefore, enterprises should strengthen the identification of risks and adopt reasonable control strategies. Figure 3 shows risks of Informatization Investment.

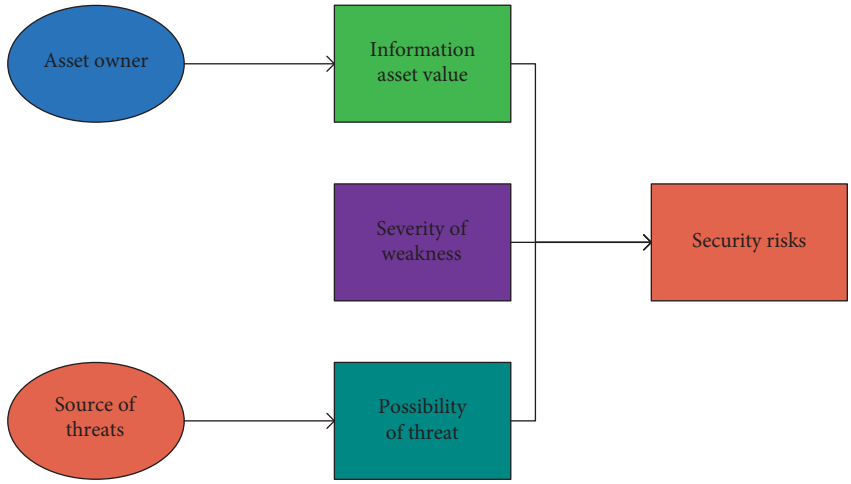

Figure 3: Risks of informatization investment.

4. Management Strategies of Enterprise Financial Operation Revenue from the Perspective of Big Data

4.1. Increase Capital Investment and Build a Big Data Platform. Adequate funds are an important guarantee for the research and development of big data technology, which can promote the development of big data technology. Therefore, from the national level, further improving the development level of big data technology can improve the comprehensive strength of the country. In this context, government departments need to give full play to their guiding role, actively deal with the problems of capital and technology of national big data technology research enterprises, comprehensively integrate the country's human, technical and financial resources, and promote complementary advantages between enterprises, achieve common development, and solve the problems of the insufficient national technology and insufficient funds. In addition, government departments can also consider establishing domestic demonstration projects for building big data platforms independently, guiding and regulating the research and development of big data platforms, and strengthening network construction to improve network transmission speed and efficiency. Figure 4 shows financial operation model from the perspective of big data.

4.2. Increase Service Content and Provide Rich Big Data Services. Providing rich big data services is the main direction of big data development in the future. Especially with the rapid development of science and technology, the healthy and sustainable development of various fields requires the technical support of big data. First of all, big data service providers need to fully understand the various needs of enterprises to ensure that each field can realize the construction of enterprise management informatization. In the process of developing and researching big data, big data suppliers need to maintain close contact with various industries, take meeting the actual needs of users as the guide, and improve the existing service content, so as to ensure that the big data service content can be more complete and more diversified service functions and fully meet the diversified needs of enterprise financial management informatization construction. For example, the analysis of financial statements and information decision-making can more comprehensively integrate all the management work of the enterprise, thereby helping the enterprise achieve the goal of informatization construction. Secondly, big data suppliers also need to provide customized services for enterprises, so as to meet the individual needs of enterprise financial management informatization construction and promote the sustainable and healthy development of enterprises.

4.3. Improve the Security of Big Data Services. The security of financial information has a direct impact on the development of enterprises. In this regard, enterprises must attach great importance to the processing and storage of financial information, and this is also an important factor affecting enterprise data security. In the process of enterprise financial management informatization construction, it is particularly necessary to pay attention to the security of big data services. Specifically, we can start from the following aspects. First, improve the technical level and strengthen the flexible application of various security technologies, so as to ensure the reliability and security of big data at the technical level, especially to solve the problem of data storage. For example, enterprises can develop various protection software to ensure the security of accounting data and information, and design-related usage protocols to ensure that various accounting information and data are more comprehensively protected to avoid threats to data security caused by hackers or viruses. Second, in the process of selecting a big data service provider, we must fully consider our own needs and try to choose a supplier with high quality in terms of reputation, so as to provide a stronger security guarantee for the construction of enterprise financial management

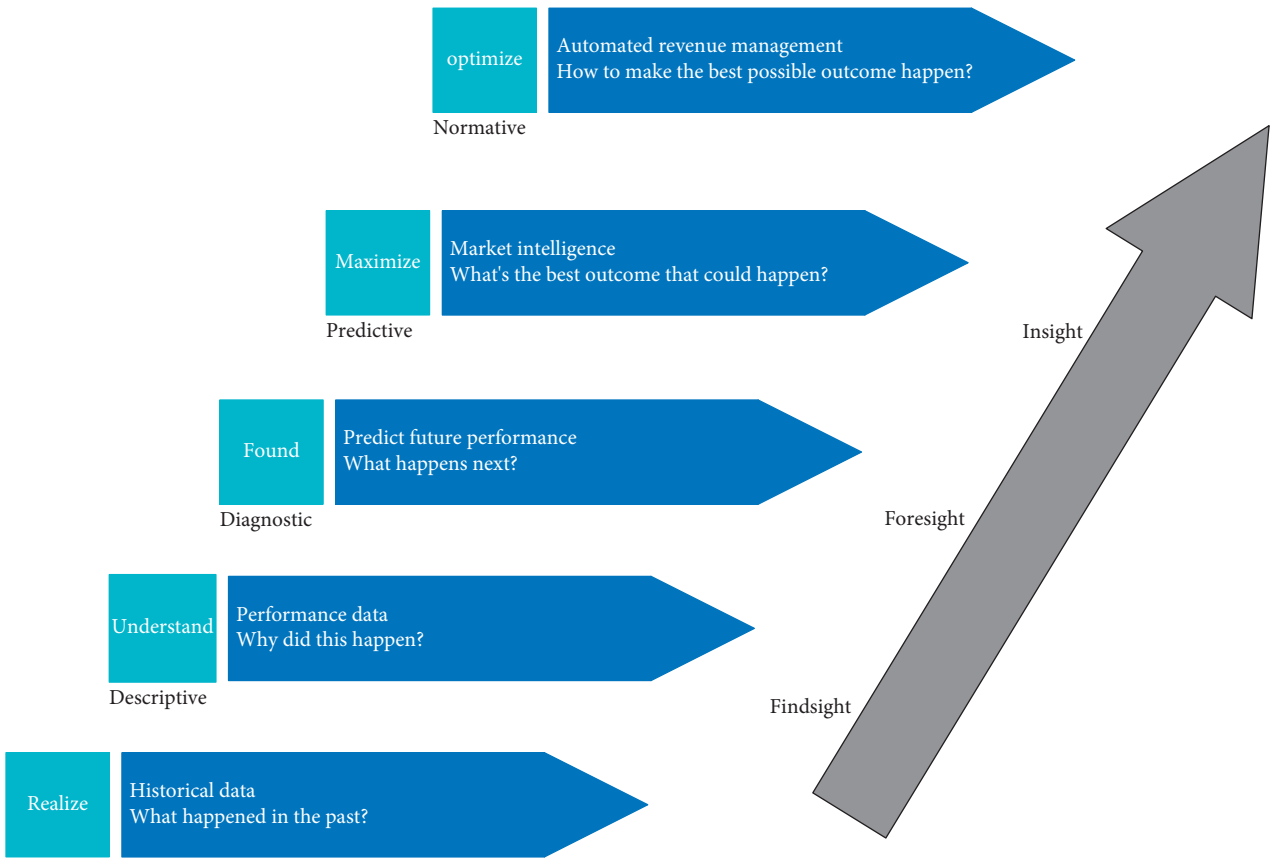

Figure 4: Financial operation model from the perspective of big data.

informatization. Third, from a legal perspective, protect big data services. The state needs to introduce corresponding policies and measures to further standardize the big data service market and create a good environment to ensure the security of corporate financial information.

4.4. Strengthen Safety Awareness and Improve Safety Management. In the process of informatization construction of financial enterprise management, it is necessary to strengthen the safety awareness of relevant staff, which is an important prerequisite for informatization construction. First of all, enterprises can establish an information security publicity and education platform to ensure that every accounting practitioner can recognize the importance of information security and apply this awareness to future work to avoid accounting information leakage. Secondly, government departments need to attach great importance to and strengthen the interaction with relevant technical departments, increase the introduction of big data technology-related guarantee resources, actively learn advanced cloud technology experience, and provide strong support for the application of big data in the construction of accounting informatization. Finally, big data service providers need to increase the construction of industrial parks, demonstration projects, and other projects under the guidance of advanced technical means, so as to improve the security level of big data services.

4.5. Optimize the Current Management System of E-Commerce Enterprises. In the context of the era of big data, in order to effectively exert the advantages of big data, we should pay attention to the rational use of management software systems and optimize and improve the actual needs of enterprise development. In addition, enterprises should pay attention to the introduction of advanced technology, which can ensure that the management system is further improved and can also ensure the work effect, thereby minimizing the operating cost of e-commerce enterprises.

5. Innovations in Financial Management Technology Methods from the Perspective of Big Data

In the network economy society, traditional financial management methods and methods are facing new challenges, and some new financial management technical methods have emerged as the times require.

(1) Network financial management. It is the enterprise that uses the network to realize the financial management function. Enterprises apply network technology to financial management, so as to solve a series of problems that cannot be solved by the current financial activities, such as cross-regional financial data transmission, accounting statement consolidation, and dynamic analysis of financial and

resource status, forming a brand-new financial management system. Network financial management relies on network financial software to complete the implementation, and network financial software will complete the collaborative management of finance and business, online management, and management of e-commerce. Through the network financial software, dynamic accounting and online economic resource management can be realized, and remote financial management, material management, and remote control behaviors such as remote reporting, accounting, auditing, and auditing of branches can be realized.

(2) Flexible financial management (as shown in Figure 5). In order to enhance survivability in the unpredictable and changeable environment in the network age, enterprises must implement flexible management and launch new products and personalized products to meet the dynamic and continuous innovation of the network economy. The flexible management of enterprises includes the management of production, personnel, information, and other aspects. The flexible management of finance is to realize the optimization of financial information resources through network technology from the perspective of financial accounting, planning, control, and analysis. Flexibility, in order to promote enterprises to improve the degree to which various financial information resources are used in a variety of ways, thereby promotes the comprehensive management of enterprises.

(3) Financial regeneration management. Business process regeneration is a new idea put forward by the American management scholars Michael and Hamer in the early 1990s. The goal of enterprise process regeneration management is to revive the vitality of the enterprise, rebuild the organizational structure and strategic planning, and restart the new life. Financial regeneration management is the revolutionary adjustment of financial activities and financial relations and the reallocation of financial resources; the purpose is to adapt to the needs of enterprises inside and outside and to adapt to the goals of enterprise management. Financial regeneration management is an important financial strategy to assist enterprises in their efforts to reduce product costs and improve economic efficiency. The development of electronic commerce and the development of network financial software make it necessary and possible for enterprise financial regeneration management. Enterprise financial regeneration management not only reduces labor costs and improves work efficiency, but also brings a series of new changes to enterprise management, such as customer orientation of values, employees implementing self-management, and the measurement of performance being transformed into the measurement of group results. Financial regeneration

Figure 5: Smart factory.

management brings new opportunities and challenges to enterprise management and also highlights the status of financial management.

(4) Financial virtual management. Virtual financial management must be implemented for virtual enterprises based on e-commerce. A virtual enterprise is a dynamic short-term strategic alliance consisting of several companies with common goals and cooperation agreements. Relying on the network, virtual enterprises break through the physical boundaries of enterprises. Although there are functions such as production, marketing, design, and finance on the surface, there is no organization within the enterprise to perform these functions. In the case of limited resources, in order to gain an advantageous position in the competition, the enterprise only masters the core functions; that is, the high value-added part that is highly dependent on enterprise knowledge and technology is in its own hands, and other low value-added departments are virtualized. Financial virtual management is to take the core functions of the enterprise as the center of financial management and to carry out centralized and coordinated financial management for each virtualized functional department. The supervising and coordinating functions of the middle managers of virtual enterprises are replaced by computer networks, and the organizational structure of enterprises tends to be flat. Financial virtual management is horizontal management that adapts to it, which can remove many intermediate links and enable the generation and confirmation of value. Financial virtual management also includes the management of virtual operations through the network, financial information, and other information generated by virtual transactions. Financial virtual management is a comprehensive and innovative financial management strategy based on a network technology to realize the optimization of financial information resources.

6. Conclusion

To sum up, as the process of economic globalization is gradually accelerating, under such an economic background, the competition of enterprises is becoming more and more

fierce, and the financial operation and cost control of enterprises will play a crucial role in helping enterprises to improve their competitiveness to enable enterprises to emerge suddenly and gain an advantage in the market. In view of this, enterprises should pay attention to cost control and control costs from all aspects, so as to improve the economic benefits of enterprises. This paper focuses on financial operation revenue management from the perspective of big data, hoping to make some achievements in financial operation management.

Data Availability

The dataset can be obtained from the corresponding author upon request.

Conflicts of Interest

The authors declare that there are no conflicts of interest.

References

[1] Wireless News, *Institute of Financial Operations New England Chapter Appoints Relyco's VP of E-Payment Solutions Johnson as Communications and Membership Officer*, Wireless News, 2012.

[2] Atlas Roofing Corp, *Atlas Roofing Standardizes on Oracle's PeopleSoft Financials and Supply Chain Management 9.1 to Support Changing Business Needs*M2 Presswire, Coventry, UK, 2012.

[3] J. K. Dugan, "ICD-10: from assessment to remediation to strategic opportunity," *Healthcare Financial Management: Journal of the Healthcare Financial Management Association*, vol. 66, no. 2, pp. 84–89, 2012.

[4] T. Affigne and R. Smith, "APSA treasurer's report 2007: another year of growth and innovation in APSA's financial operations," *PS: Political Science & Politics*, vol. 40, no. 4, pp. 842–847, 2007.

[5] M. Ran, "China's economic and financial operation and related policy analysis," *International Journal of Education and Economics*, vol. 4, no. 2, 2021.

[6] K. Fenstermacher and D. L. Gilmore, "Audit readiness is everybody's business: a partnership for audit success - the department of the navy's office of financial operations and naval audit service," *Armed Forces Comptroller*, vol. 62, no. 3, 2017.

[7] P. Amundson, "A financial analyst's development ... How the corporate management development program is supporting OCONUS financial operations," *Newsletter - United States Navy Supply Corps*, vol. 76, no. 4, 2013.

[8] T. Kathleen and C. Regina, "APSA's financial operations 2012-2013," *PS: Political Science and Politics*, vol. 47, no. 1, 2014.

[9] H. D. Putney, "Financial operation of the multiple-funded institute for cancer research," *Cancer*, vol. 29, no. 4, pp. 876–879, 1972.

[10] Y. Zhao, X. Deng, and Z. Shen, "The analysis of flipped classroom mode of CIMA financial operation course," in *Proceedings of the 6th International Conference on Electronic, Mechanical, Information and Management Society*, Shenyang, China, April 2016.

[11] L. Zhou, "Discussion on Financial Operation Mode of Agricultural Supply Chain in Hubei Province under the Background of Internet+," in *Proceedings of the 3rd International Conference on Social Science and Technology Education (ICSSTE 2017)*, Sanya, China, May 2017.

[12] A. DechasaSeifu, "Financial operating performance and challenges of omo and wisdom microfinance institutions in dilla town, Ethiopia," *International Journal of Advanced Research*, vol. 6, no. 2, 2018.

[13] Wiley Online Library, "C: financial operations and services," *World Banking Abstracts*, vol. 38, no. 6, 2022.

[14] S. Vezenkoska, I. Zdravkoski, P. Nikolovski, M. Blazhekovich, V. Nolcheska, and M. Kimovska, "Internal audit of financial operations," *International Journal of Sciences: Basic and Applied Research*, vol. 36, no. 3, 2017.

[15] Museum Store Association, "Museum store association retail industry report," *Financial, Operations, Salary, and Best Practices Information for the Nonprofit Retail Industry*, Taylor & Francis, Oxfordshire, UK, 2014.

[16] Indiegogo, *New Financial Management App Launches Indiegogo Campaign*, M2 Presswire, Coventry, UK, 2022.

[17] Z. Ma, M. Yuan, and Y. Song, "Analysis of the accounting and financial management of enterprises under the international trade environment improvement strategy," *Scientific Journal Of Humanities and Social Sciences*, vol. 4, no. 2, 2022.

[18] Wiley Online Library, "Issue information: European financial management 1/2022," *European Financial Management*, vol. 28, no. 1, 2022.

[19] C. C. Rosario, E. Olapane, M. P. Cataluňa, and L. C. Buenviaje, "Financial management capabilities among personnel in a state university in the Philippines," *Journal of Economics, Finance and Accounting Studies*, vol. 3, no. 2, pp. 158–168, 2021.

[20] X. Chen, "The influence of the big data era on the financial management of small and micro enterprises and the countermeasures," *Scientific Journal of Economics and Management Research*, vol. 3, no. 12, 2021.

[21] J. Huang, "Retraction Note: the characteristics of urban soil deposition and financial management of state-owned assets based on big data system," *Arabian Journal of Geosciences*, vol. 14, no. 22, p. 2422, 2021.

[22] H. Sun, "Reform and practice of teaching mode of financial management course from the perspective of college students' innovation and entrepreneurship," *Scientific Journal of Economics and Management Research*, vol. 3, no. 11, 2021.

[23] Y. Tang, "Corporate finance management in the age of ARTIFICIAL intelligence," *International Journal of Frontiers in Sociology*, vol. 3, 2021.

[24] X. Mao and X. Ma, "Challenges and countermeasures of enterprise financial management refinement in the intelligent age," *Journal of Global Economy, Business and Finance*, vol. 3, no. 8, 2021.

[25] O. Ogunlade, G. T. A. Oyebiyi, O. A. Babalola, and O. O. Fasesin, "Financial management and organizational culture as a hybrid for SMEs' performance in Nigeria," *Asian Journal of Education and Social Studies*, 2021.

Hindawi
Scientific Programming
Volume 2022, Article ID 4927610, 9 pages
https://doi.org/10.1155/2022/4927610

Research Article

Analysis Model Design on the Influencing Factors and Countermeasures of China's International Trade Facing the Belt and Road

Hao Cui

School of Institute for Research on Portuguese-Speaking Countries, City University of Macau, Taipa 999078, Macau

Correspondence should be addressed to Hao Cui; a19092105151@cityu.mo

Received 19 June 2022; Revised 4 July 2022; Accepted 8 July 2022; Published 2 August 2022

Academic Editor: Lianhui Li

Since the "Belt and Road" Initiative was put forward in 2013, it has attracted more and more attention. Many countries along the Belt and Road have participated in it, which has further deepened regional economic integration. Complex network analysis is an interdisciplinary method, which has a perfect overall perspective and data indicators that can quantify the relationship. More and more scholars have begun to pay attention to it and use it to carry out research. Based on the perspective of complex networks, this paper constructs the "Belt and Road" directed weighted network, respectively, according to the import and export trade data of countries and international organizations that have signed cooperation documents, and then studies the characteristics of the "Belt and Road" trade network by using a variety of network topology attribute analysis methods and node centric indicators.

1. Introduction

At the end of the 20th century, the establishment of WTO, G20, APEC, and other international trade organizations promoted the flow of production factors in various countries, adjusted the distribution of means of production in various countries, promoted the optimization of global industrial structure, and had a far-reaching impact on the development of the world economy [1, 2]. Since the beginning of the 21st century, similar regional cooperation cases have sprung up.

The "Belt and Road" Initiative takes peace and cooperation, openness and inclusiveness, mutual learning, and mutual benefit as the core spirit, adheres to the principles of joint consultation, joint construction, and sharing, and sends invitations to all countries and international organizations around the world to jointly address global economic issues, seek new development opportunities, and achieve mutual complementarity of strengths among countries, mutual benefit, and win-win results [3–8]. Since the Belt and Road Initiative was put forward, it has attracted wide attention, and more and more countries have participated in it. By the end of January 2020, 138 countries and regions have signed cooperation documents with China to jointly build the Belt and Road. At present, domestic economic development has entered the new normal, and the downward pressure on the economy is great. Expanding foreign cooperation has become an important way to promote the rapid transformation and development of the domestic economy. China has problems such as irrational industrial structure and large regional economic development gap [9–12]. The proposal of the "Belt and Road" Initiative will help to transfer the excess capacity in the eastern coastal areas to the central and Western regions and overseas so as to optimize the industrial structure and narrow the gap between the rich and the poor.

At present, domestic and foreign scholars' research on the trade of "the Belt and Road" is mostly from the perspective of the two countries participating in the cooperation and carries out empirical analysis on the economic and trade reciprocity brought about by the "Belt and Road" Initiative. However, this kind of analysis lacks a discussion on the overall pattern of trade among the Belt and Road cooperative countries, and there are few studies on quantitative analysis

of the interaction of trade among the Belt and Road countries through complex network analysis (CNA). Considering the interaction among multilateral countries, this paper constructs a trade network based on the bilateral import and export trade data of the "Belt and Road," explores the attribute characteristics of the "Belt and Road" trade from the perspective of a complex network, as well as the changes in the topology of the trade network since the "Belt and Road" Initiative, and puts forward and analyzed the deep-seated reasons affecting the changes in the pattern of the "Belt and Road" trade network, which has strong theoretical significance. The Belt and Road Initiative takes into account the needs of countries along the Belt and Road in economic development and trade cooperation and is conducive to promoting economic and trade exchanges between regions and countries.

Based on the import and export trade data of countries along the Belt and Road from 2009 to 2017, this paper uses the complex network analysis method to build the "Belt and Road" trade network, discuss the overall topology of the network and important trading countries, explore the changing trend of the trade network and the division of communities, discuss the main factors affecting the trade cooperation of countries along the Belt and Road, and then put forward some suggestions on the development of China's "the Belt and Road" cooperation, which has strong practical significance.

2. Construction of Trade Network

Nodes and edges between nodes are two essential elements for building complex networks [13]. In "the Belt and Road," trade, countries, and economies act as nodes, and trade relations act as links, forming a network structure. However, such a simple undirected, weightless network is challenging to describe the direction and scale of trade flow, and the network's topology is abstracted too simply, which will cause much information to be ignored and be quite different from the real trade network. Generally speaking, trade activities are bidirectional, including import and export. Scholars often combine import and export data into a network to conduct research. Import and export trade have significantly different meanings for a country: import reflects the inflow of goods and the country's demand for consumer goods, while export shows more of the country's resource output capability and manufacturing level. This paper constructs "the Belt and Road" import and export trade network and compares and analyzes the differences between national nodes in the two networks.

As of the end of January 2020, our country has signed 200 cooperation documents on the joint construction of the "Belt and Road" with 138 governments and 30 international organizations. The trade data of various countries in this paper are selected from the United Nations Trade Database (UNComtrade Database), and the bilateral trade data of the countries cooperating with the "Belt and Road" Initiative from 2009 to 2017 are extracted [14–16]. Specifically, this paper only studies commodity trade but does not include service industries. The customs HS code (Harmonized System) of trade data selects the latest version according to the data year, and trade data consists of all commodity codes (Commodity Codes), namely, AG1–AG6. The scale of the "Belt and Road" trade data is vast, the trade volume between countries is very different, and some countries have the phenomenon of missing trade data. Taking into account these factors may have an impact on the analysis of the network topology, setting a threshold of $1 billion for trade volume. Mainly analyze the trade network composed of significant import and export member countries. These countries' import and export trade volume accounts for 84.9% and 83.5% of the total import and export trade volume of the "Belt and Road," which is sufficiently illustrative and representative. After data preprocessing, the "Belt and Road" import trade network in 2017 included 93 nodes and 507 edges, and the export trade network had 101 nodes and 484 edges, excluding self-loops. Table 1 shows the number of nodes in the network.

We build "the Belt and Road" trade network through the adjacency matrix. In the import trade network, the trade volume of country i imported from country j is m, and we write as

$$w_{ji}^{\text{in}} = m. \tag{1}$$

The export volume of country i to country j is n, denoted as

$$w_{ij}^{\text{out}} = n. \tag{2}$$

Through the visualization processing of Gephi software, the "Belt and Road" import and export trade network in 2017 can be obtained.

3. Topological Structure Analysis of the Trade Network

3.1. Basic Characteristic Indicators of the Network. In complex network analysis, the degree is the most direct and important concept to describe the characteristics of nodes [17]. In an undirected network, the degree k_i of node i equals the number of edges directly connected to this node. For directed networks such as the "Belt and Road" trade network, we can introduce the concepts of in-degree and out-degree to expand: in-degree refers to the number of edges pointing from other nodes to this node, and out-degree refers to the number of edges from this node to other nodes. The average degree of all nodes in the network is the average degree of the network (AverageDegree) [18–20]. On average, each country in the "Belt and Road" trade network has import trade with 5 other countries and export trade with 5 other countries. In contrast, import trade is more extensive than export trade. Table 2 shows the average degree of import and export network.

From a statistical point of view, the number of all nodes with a degree of a certain value can be compared to the total number of nodes in the network as the probability of the degree value appearing. Thereby, the degree distribution of network nodes is obtained. The most common data distribution in daily life and study research is the normal

Table 1: Number of nodes in the network.

	Import trade network	Export trade network
Number of nodes before processing	145	145
Number of connected edges before processing	12133	10542
Number of nodes after processing	92	103
Number of corresponding edges after processing	509	488

Table 2: Average degree of import and export network.

	Import trade network	Export trade network
Average in-degree	5.48	4.81
Average out-degree	5.48	4.81

Table 3: Import and export network assortativity coefficient.

	Import trade network	Export trade network
Assortativity coefficient	−0.39	−0.40

distribution (Gaussian distribution). In economics research, many data distributions are often very different from normal distributions. Such distributions do not have a single characteristic scale and are also called "scale-free" distributions.

In 2017, the "Belt and Road" import and export trade network all obeyed such high-degree nodes, which accounted for a minority. And nodes with small-degrees account for the vast majority of "long-tailed distributions" (a type of "scale-free" distribution). In the import and export networks, 57% and 60% of the nodes have degrees less than or equal to 5, respectively. This shows that, in "the Belt and Road" trade cooperation, the trade connections of most countries are still relatively limited, and the network structure is not balanced.

Another dimension to studying the total nature of the BRI trade network is the degree of correlation. The correlation of degree considers the correlation of degree attributes between each node in the network. If the correlation is positive, it means that a node with a large degree is more inclined to connect to other nodes with a large degree. Such a network is called a "homologous network"; otherwise, it is called a "heterogeneous network." The "assortativity coefficient" is an important indicator to quantify the network's assortativity. It is defined as follows:

$$r = \frac{1}{\sigma_q^2} \sum_{j,k} jk\left(e_{jk} - q_j q_k\right), \tag{3}$$

where σ_q^2 is the variance of the redundancy distribution q_k.

After calculation, $r_{2017\text{import trade}} = -0.39$, and $r_{2017\text{export trade}} = -0.40$. Table 3 shows the import and export network assortativity coefficient. It shows that the import and export trade networks of "the Belt and Road" are all heterogeneous networks. Those countries with many trading partners are more willing to establish economic and trade connections with countries with few trading partners. There are trade connections between various countries, and the right to speak in trade not only is in the hands of big countries but also shows the pursuit of equality and win-win cooperation among countries along the "Belt and Road."

3.2. Centrality of Network Nodes. In complex networks, the location of a node determines its importance. Various centrality indicators can analyze the location of nodes in the network from different sides and then measure the importance of nodes placed in the network. The nodal centrality indicators studied in this paper mainly include degree centrality, betweenness centrality, closeness centrality, and eigenvector centrality.

3.2.1. Degree Centrality. Degree centrality is to use the degree of a node as a criterion for measuring the importance of its location. The larger the degree, the more important the node in the network:

$$DC_i = \frac{k_i}{N-1}. \tag{4}$$

Among them, N is the number of nodes in the network, and k_i is the degree of node i. Considering the influence of trade scale, the trade volume between the two countries is used as the weight of the connected edges, and for the directed weighted network, there are

$$\begin{aligned} DC_i^{\text{in}} &= \sum_{j=1} w_{ji}, \\ DC_i^{\text{out}} &= \sum_{j=1}^{N} w_{ij}. \end{aligned} \tag{5}$$

Table 4 shows the weighted in/out-degree of import and export network. By comparing the top ten countries with weighted in-degree and weighted out-degree in 2017, it is found that our country has the most extensive connections and the most significant trade volume in the import and export trade network. South Korea and Russia ranked second and third, respectively, and other countries with large trade volumes were mainly concentrated in Southeast Asia and the Middle East.

3.2.2. Betweenness Centrality. Bridges are often the only way to connect two places. In the trade network, if the connection between node A and node B must pass through node C, then C is such a node that acts as a bridge intermediary.

Table 4: Weighted in/out-degree of import and export network.

ID	Import trade network countries	Import trade network weighted in-degree	Export trade network countries	Export trade network weighted out-degree
1	China	$8.74E+11$	China	$8.26E+11$
2	South Korea	$3.32E+11$	South Korea	$2.99E+11$
3	Russia	$1.97E+11$	Russia	$2.09E+11$
4	Italy	$1.66E+11$	Singapore	$1.98E+11$
5	Malaysia	$1.34E+11$	Italy	$1.62E+11$
6	Thailand	$1.13E+11$	Malaysia	$1.07E+11$
7	Vietnam	$1.09E+11$	Vietnam	$8.62E+10$
8	Singapore	$1.08E+11$	United Arab Emirates	$8.58E+10$
9	Saudi Arabia	$1.08E+11$	Indonesia	$8.18E+10$
10	United Arab Emirates	$8.81E+10$	Poland	$7.01E+10$

The topological index that measures this characteristic of a node is called betweenness centrality, which is specifically defined as

$$BC_m = \sum_{s \neq m \neq t} \frac{n_{st}^m}{g_{st}}, \tag{6}$$

where g_{st} is the number of shortest paths from node s to node t and n_{st}^m is the number of shortest paths from node s to node t through node m.

From the perspective of the ability to control trade cooperation, countries with higher betweenness centrality have a more vital ability to influence trade activities, and excluding these countries will also have a more significant impact on the trade network.

Table 5 shows the betweenness centrality of countries in the "Belt and Road" trade in 2017. It can be seen from the above table that our country has played a very important role in connecting the "Belt and Road" import and export trade network. Betweenness centrality is nearly twice as high as the second. In addition to China, countries such as Italy, Russia, South Korea, the United Arab Emirates, South Africa, and Turkey also play a key "trade bridge" role. In fact, Italy, Russia, South Korea, the United Arab Emirates, and South Africa are the core trade countries in Western Europe, Eastern Europe, East Asia, the Middle East, and Africa, respectively. Each intraregional node realizes cross-regional trade by connecting with these countries.

3.2.3. Closeness Centrality. Another metric based on the shortest path between nodes is closeness centrality. If betweenness measures a country's ability to control a trade network, closeness quantifies the centrality of the country's topological position in the network. Closeness centrality is the average length of the shortest path from each node to other nodes. For a node, the closer it is to other nodes in the network, the higher the closeness centrality is:

$$CC_i = \frac{1}{\mathrm{d}_i} = \frac{N}{\sum_{j=1}^{N} \mathrm{d}_{ij}}. \tag{7}$$

Table 6 shows the closeness centrality of countries in the "Belt and Road" trade in 2017. Similar to betweenness centrality, the closeness centrality of China, Italy, Russia, South Korea, the United Arab Emirates, and Turkey is also at a high level in the network. It shows that these countries are not only trade bridges but also trade centers of various regions. The comparison of import and export networks shows that the imported network is closer, the connectivity between nodes is more robust, and its closeness centrality is generally higher than that of the export trade network.

3.2.4. Eigenvector Centrality. The importance of a node in the network is not only determined by the number of other nodes it is connected to but also closely related to the significance of these connected neighbor nodes. Imagine that node A is connected to several "network edge" nodes, and node B is connected to a small number of nodes with large betweenness. Although the degree of node B may be equal to or even smaller than that of A, the position of B in the network is much more important than that of A because it is also very likely to be an important "bridge" in the network. Based on this idea, the eigenvector centrality is defined as

$$x_i = c \sum_{j=1}^{N} a_{ij} x_j, \tag{8}$$

where C is a proportional constant, x_i is the important measure of node i, and a_{ij} is the network's adjacency matrix.

It can be obtained by iterative calculation:

$$x = \lambda_1^{-1} A x, \tag{9}$$

where λ_1 is the characteristic single root with the largest modulus of matrix A and x is the main eigenvector corresponding to λ_1.

Table 7 shows that the countries with high eigenvector centrality are mainly concentrated in East Asia and Southeast Asia. These countries are often the origin of raw materials for industrial production and are located on the "Belt and Road" shipping routes with convenient transportation. Most of the countries that trade with them are countries with a high degree of weight or betweenness.

Combining the above four different network centrality indicators, it can be found that our country has a pivotal position in the "Belt and Road" trade network. Specifically, our country's weighted in-degree and weighted out-degree are ranked first, and it is the largest import and export trade

Table 5: The betweenness centrality of countries in the "Belt and Road" trade in 2017.

ID	Import trade network countries	Import trade network betweenness centrality	Export trade network countries	Export trade network betweenness centrality
1	China	0.27	China	0.23
2	Italy	0.14	Italy	0.15
3	United Arab Emirates	0.08	South Korea	0.10
4	Russia	0.07	Turkey	0.09
5	South Africa	0.07	Russia	0.07
6	South Korea	0.06	United Arab Emirates	0.06
7	Turkey	0.06	South Africa	0.06
8	Poland	0.05	Uzbekistan	0.05
9	Saudi Arabia	0.05	Malaysia	0.04
10	Bulgaria	0.04	Ukraine	0.04

Table 6: The closeness centrality of countries in the "Belt and Road" trade in 2017.

ID	Import trade network countries	Import trade network betweenness centrality	Export trade network countries	Export trade network betweenness centrality
1	China	0.71	China	0.42
2	Italy	0.55	Italy	0.37
3	Russia	0.52	Turkey	0.34
4	South Korea	0.49	United Arab Emirates	0.33
5	Thailand	0.47	South Korea	0.33
6	Turkey	0.46	Russia	0.32
7	Saudi Arabia	0.46	Singapore	0.31
8	United Arab Emirates	0.46	Poland	0.29
9	Vietnam	0.45	Egypt	0.29
10	Malaysia	0.43	Austria	0.29

country. Our country's closeness centrality is the highest, which means that our country is at the center of the trade network. At the same time, our country also plays a powerful bridge intermediary role, strengthening economic and trade exchanges between regions.

3.3. Small-World Network Features. "Small-world network" is a representative class of complex networks. In such a network, many nodes are not directly connected but can be reached from any other node in the network via a small number of countable paths. The topological metrics that best describe this property are "average path length" and "clustering coefficient." The path in the network that connects the fewest edges between two nodes is the shortest between two points. The average path length is defined as the average of the geodesic distance between any two points in the network:

$$L = \frac{\sum_{s,t\in V} \mathrm{d}(s,t)}{n(n-1)}, \tag{10}$$

where V is the set of nodes in the network, $\mathrm{d}(s,t)$ is the shortest distance from s to t, and n is the number of nodes in the network.

The average path length reflects the closeness between nodes in the network, while the clustering coefficient reflects the "structure" of the network. It depicts the probability that nodes B and C connected to node A are also connected. E_i is the number of edges between all adjacent nodes of node i.

$$C_i = \frac{E_i}{(k_i(k_i-1))/2} = \frac{2E_i}{k_i(k_i-1)}. \tag{11}$$

The small-world network is a "transition type" between the fully regular nearest neighbor network and the random ER random network. The nodes in the former network have high clustering and long average distance, while the latter is the opposite. Small-world networks can be generated by adding randomness to the regular network. The small-world characteristics of the network can be measured using the Sigma parameter and the Omega parameter, which are defined as follows:

$$\mathrm{Sigma} = \frac{C/C_r}{L/L_r}, \tag{12}$$

where C and L are the average clustering coefficient and average shortest path length of the network, respectively. C_r and L_r are the average clustering coefficient and shortest path length of the equivalent random graph. If Sigma >1, the network is generally considered to have small-world properties.

The small-world coefficient (Omega) is between −1 and 1. The value close to 0 represents that the network has small-world features. The value close to −1 represents that the network is a lattice shape, and the value close to 1 represents that the network is a random graph by calculating the Sigma, Omega coefficients, and related indicators of the "Belt and Road" trade network in 2017 as shown in Table 8.

The Sigma coefficients of the "Belt and Road" import and export trade network are all greater than 1, and the Omega

Table 7: The eigenvector centrality of countries in the "Belt and Road" trade in 2017.

ID	Import trade network countries	Import trade network betweenness centrality	Export trade network countries	Export trade network betweenness centrality
1	China	0.73	China	0.61
2	South Korea	0.53	South Korea	0.43
3	Malaysia	0.19	Vietnam	0.36
4	Vietnam	0.18	Singapore	0.24
5	Thailand	0.15	Malaysia	0.23
6	Russia	0.14	Vietnam	0.19
7	Singapore	0.12	Indonesia	0.18
8	United Arab Emirates	0.12	Russia	0.17
9	Indonesia	0.11	Philippine	0.14
10	Italy	0.09	Italy	0.14

Table 8: "Small-world" indicators of the "Belt and Road" trade network in 2017.

	Import trade network	Export trade network
Sigma	1.13	1.15
Omega	−0.04	−0.02
Average path length	1.38	1.27
Average path length (weighted)	$3.42E+9$	$3.08E+9$
Average clustering coefficient	0.52	0.53

coefficient is close to 0. It shows that these two trade networks align with the characteristics of the small-world network. The Omega coefficients of the import and export trade network are all less than zero, and they tend to be random networks. The average path length of the export trade network is shorter. It shows that the export trade between countries along the "Belt and Road" is closer.

According to the phenomenon of "small-world" and trade networks, a trade network with the characteristics of "small-world" has unique advantages in terms of transaction efficiency. Because of its robust network connectivity, it can realize the overall situation Pareto Improvement of Networks.

4. Evolution of Node Importance

The previous section discussed the importance of nodes in the "Belt and Road" trade network in 2017 from different dimensions by analyzing various node centrality indicators. To study the changes in node attributes in the import and export trade network in the past nine years, the author first uses the PageRank algorithm to extract the top ten important nodes in the trade network in 2017 and then discusses the degree centrality, betweenness centrality, and closeness centrality of these core countries.

4.1. Network Core Node Selection. The PageRank algorithm [21–23] is a well-known key technology for web page ranking. It gave birth to the emergence and development of the Google search engine. The algorithm's starting point is that a node's importance depends on the number and quality of nodes pointing to it.

From this point of view, the PageRank algorithm can be regarded as a generalization of eigenvector centrality on directed graphs. The PageRank algorithm is divided into three steps. The initial step will equally divide the total PR value among all nodes, and then

$$\sum_{i=1}^{N} PR_i(0) = 1. \tag{14}$$

In the second step, the PR value of each node in step $K-1$ is equally divided by the nodes it points to, and the new PR value of each node is the sum of the PR values it has obtained. The third step is to reduce the scale factor s to keep the total PR value of the network at 1, and then

$$PR_i(k) = s\sum_{j=1}^{N} \overline{a}_{ji} PR_j(k-1) + (1-s)\frac{1}{N}. \tag{15}$$

Through calculation, the top ten core node countries with the average PageRank score of the "Belt and Road" import and export trade network in the past nine years are extracted, as shown in Tables 9 and 10.

The top ten countries in the PageRank score of the "Belt and Road" import trade network include China, South Korea, Russia, Italy, Saudi Arabia, Malaysia, the United Arab Emirates, Singapore, Thailand, and Indonesia. Among them, our country has always maintained first place in PR worth and is much higher than second South Korea. In the past 9 years, the fluctuation of our country's PR value has been slight, and the overall trend has maintained an upward trend, indicating that our country's position in the "Belt and Road" import trade network is improving. Except for Saudi Arabia and the United Arab Emirates, two Middle Eastern countries, two European countries, Italy and Russia, and other core countries are mainly located in Southeast Asia, which shows that the import trade of the "Maritime Silk Road" is more active.

Table 9: Top 10 countries in the "Belt and Road" import trade network PageRank value.

Country	2009	2010	2011	2012	2013	2014	2015	2016	2017
China	0.2001	0.2079	0.1981	0.2019	0.2101	0.2199	0.2471	0.2329	0.2371
South Korea	0.0738	0.0763	0.0708	0.0653	0.0738	0.0733	0.0788	0.0873	0.0728
Russia	0.0613	0.0542	0.0563	0.0562	0.0533	0.0572	0.0493	0.0452	0.0533
Italy	0.0591	0.0519	0.0481	0.0439	0.0471	0.0469	0.0471	0.0499	0.0511
Saudi Arabia	0.0338	0.0383	0.0408	0.0403	0.0408	0.0383	0.0318	0.0293	0.0268
Malaysia	0.0353	0.0392	0.0343	0.0312	0.0303	0.0282	0.0333	0.0352	0.0283
United Arab Emirates	0.0271	0.0399	0.0391	0.0329	0.0411	0.0369	0.0261	0.0279	0.0281
Singapore	0.0368	0.0373	0.0318	0.0353	0.0298	0.0303	0.0318	0.0303	0.0258
Thailand	0.0293	0.0332	0.0303	0.0272	0.0273	0.0262	0.0323	0.0362	0.0273
Indonesia	0.0241	0.0249	0.0251	0.0219	0.0211	0.0189	0.0221	0.0229	0.0211

Table 10: Top 10 countries in the "Belt and Road" export trade network PageRank value.

Country	2009	2010	2011	2012	2013	2014	2015	2016	2017
China	0.1031	0.1099	0.1081	0.1029	0.1231	0.1179	0.1131	0.1079	0.1171
Italy	0.0728	0.0693	0.0648	0.0563	0.0568	0.0673	0.0668	0.0723	0.0708
Russia	0.0393	0.0372	0.0423	0.0412	0.0423	0.0442	0.0333	0.0332	0.0383
South Korea	0.0361	0.0389	0.0401	0.0359	0.0401	0.0389	0.0351	0.0339	0.0351
Singapore	0.0318	0.0323	0.0288	0.0293	0.0298	0.0313	0.0288	0.0273	0.0218
United Arab Emirates	0.0233	0.0232	0.0213	0.0282	0.0273	0.0262	0.0303	0.0342	0.0333
Turkey	0.0201	0.0189	0.0241	0.0219	0.0251	0.0319	0.0331	0.0309	0.0351
Malaysia	0.0228	0.0223	0.0198	0.0223	0.0228	0.0233	0.0218	0.0203	0.0168
Poland	0.0193	0.0182	0.0183	0.0172	0.0173	0.0232	0.0253	0.0262	0.0273
Saudi Arabia	0.0141	0.0179	0.0181	0.0209	0.0201	0.0219	0.0301	0.0199	0.0221

The top ten countries in the PageRank score of the "Belt and Road" export trade network include China, Italy, Russia, South Korea, Singapore, the United Arab Emirates, Turkey, Malaysia, Poland, and Saudi Arabia. Comparing the two networks, our country's advantages in export trade are not as obvious as those in import networks. It shows that our country still has development potential in export trade, and the other node members in the two networks have not changed much.

Through screening the core nodes of PageRank, the countries in the "Belt and Road" trade network can be divided into import, export, and two-way trade, as shown in Table 11. Among them, import-oriented countries are represented by Thailand and Indonesia, and Poland and Turkey represent export-oriented countries. China, Italy, Russia, South Korea, Singapore, and the United Arab Emirates are all at the core of the import and export network and are two-way trade countries.

4.2. Changes in the Degree Centrality of Core Nodes. For the above representative important nodes, combined with the analysis methods of nodal degree centrality, betweenness centrality, and closeness centrality in the previous chapter, we further study the changes in the topological structure of the import and export trade network in 9 years.

According to the degree centrality, both networks can be divided into three echelons. Our country is in the first echelon, Italy, Russia, and South Korea are in the second echelon, and other core node countries form the third echelon. Overall, the degree centrality of the two network core nodes fluctuated relatively minor, and there was no obvious improvement around 2014. Except for China, the in-degree value of the imported network and the out-degree value of the export network are concentrated between 0.1 and 0.4. Our country's inbound and outbound centrality is ahead of other countries and maintains a steady growth trend. Compared with import trade, more countries have trade connections with our country in the export network, reaching 80. It accounts for 79% of the total number of exporting countries in the "Belt and Road."

In the import trade network, Italy, Russia, and South Korea are ranked after our country. Italy and South Korea have very similar in-degree curves, with fewer import partners in 2011 and 2012. In addition, affected by the sharp drop in international crude oil futures prices and Western economic sanctions, the financial crisis in Russia in 2014 and 2015 caused its import and export trade to enter an "ice period." The remaining core nodes are Southeast Asian countries, and their trade connections are mainly distributed along the "Maritime Silk Road." The Italian economy was affected by the European debt crisis in the export trade network. Before 2013, the export trade volume was less than 1 billion US dollars. It then increased in 2014 and remained around 0.4. South Korea, which ranks second in the centrality of out-degree, has been very active in export trade in recent years, and the average out-degree has increased by 25% compared with the average in-degree. In 2017, 33 countries became their export trading partners. In contrast, Russia's import and export trade is more balanced, including 25 partner countries.

4.3. Changes in Betweenness Centrality of Core Nodes. Compared with degree centrality, the betweenness variation of the two networks fluctuates greatly, and there is no

Table 11: Types of "the Belt and Road" trade countries.

Import trade country	Export trade country	Two-way trade country
Thailand and Indonesia	Poland and Turkey	China, Italy, and Russia South Korea and Singapore United Arab Emirates

obvious echelon division. Same as the degree centrality, in the two networks, our country's betweenness also ranks first, and the import betweenness is generally higher than the export betweenness, indicating that our country's role as a bridge in import trade is more prominent. In 2012 and 2015, due to the strengthening of import trade with Belarus, Sudan, Romania, Nigeria, and other countries, our country's betweenness showed a stepwise increase. Affected by the financial crisis, our country's export betweenness dropped from 0.31 in 2009 to 0.17 in 2011 and then remained relatively stable at around 0.2.

In the import trade network, in addition to China, the betweenness of Russia, the United Arab Emirates, and Indonesia also increased significantly in 2012. Among them, Russia and Indonesia have strengthened their import cooperation with the United Arab Emirates, Ecuador, and other Middle East and South American countries. But the increase in the betweenness of the UAE is due to the significant reduction in the import trade between Turkey, which has a strong trade connection, and the large betweenness countries such as Singapore and South Africa. On the other hand, it is due to the increase in the import trade volume between the UAE and regional representative node countries such as South Africa and Indonesia. In the export trade network, the value of Italian exports to Ukraine and South Africa nearly tripled. So, from 2014 to 2016, its export betweenness increased rapidly. However, Austria, Latvia, Slovenia, and other European countries reduced their export trade to South Korea, Russia, and the United Arab Emirates; the three countries' exports declined between 2013 and 2015.

4.4. Discussions. Through the above two centrality analyses on the core nodes of the "Belt and Road" import and export network, it was found that the proposal of the "Belt and Road" Initiative has a more significant impact on the export network than the imported network. The specific performance is that, after 2013, the export trade links between regions along the "Belt and Road" have become very close, and the overall export network has shown a trend of "decentralized" coordinated development. Affected by the external macroeconomic environment, the betweenness centrality of countries in the past nine years has been relatively sensitive and fluctuated wildly. As the only country in the EU that has signed a memorandum of understanding, Italy's influence on the trade network is gradually increasing. The UAE does not have the most significant number of trade connections in the import and export network. Still, its betweenness centrality is prominent, which shows that the UAE has a powerful ability to control trade in the Middle East. On the one hand, the top-level strategy of "the Belt and Road" has extensively promoted our country's foreign export trade. On the other hand, as a bridge of the trade network center, our country has strengthened the trade links between regions and countries along the "Belt and Road."

5. Conclusions

The "Belt and Road" trade network is a typical complex network. There are few pieces of authoritative literature at home and abroad that apply the complex network analysis method to the "Belt and Road" trade. This study has some innovations in terms of angle and method. This paper studies the trade networks of countries along the "Belt and Road" from the perspective of complex networks. This perspective is different from the model of taking a single country as the research object in most "the Belt and Road" trade studies but comprehensively analyzes the multilateral trade relations of countries along the "Belt and Road" and desalinates the impact of countries' own attribute differences on trade characteristics.

This research has certain characteristics of theoretical research and practical guidance. The theoretical characteristics are as follows. Although the practice of applying complex network technology to the research of international trade networks has been adopted by some scholars, most of the current research and analysis dimensions related to trade networks are one-sided. For example, only the topological structure of the network is analyzed and elaborated, and the influence factors of time and trade networks are not considered. In addition, through the application of analysis software, the network can be visually presented, which is more intuitive and convenient for further understanding and analysis. On the other hand, the research ideas and methods of this paper can also be extended to the trade network research of other regional or economic organizations, such as APEC, WTO, and G20, which provides a certain theoretical and methodological reference for subsequent related research. The characteristics of practice guidance are as follows: the research scope of this paper is the "Belt and Road" trade network. The node is composed of 138 cooperative countries. Compared with other global trade networks, it is more specific and focuses on the regional economy. The research results provide a theoretical basis and policy suggestions for guiding China to cope with the changes in the "Belt and Road" trade network.

Data Availability

The dataset can be accessed upon request.

Conflicts of Interest

The author declares no conflicts of interest.

References

[1] Y. Liu and S.-B. Tsai, "Dynamic evolution of service trade network structure and influence mechanism in countries along the "belt and road" with big data analysis," *Mathematical Problems in Engineering*, vol. 2022, Article ID 8378137, 13 pages, 2022.

[2] F.-J. Xie, R.-C. Feng, and X.-Y. Zhou, "Research on the optimization of cross-border logistics paths of the "belt and road" in the inland regions," *Journal of Advanced Transportation*, vol. 202214 pages, Article ID 5776334, 2022.

[3] Y. Wang, "Evaluation of the effects of the belt and road initiative on the unified economic and environmental efficiency of transportation infrastructure in China based on range-adjusted measure model and difference in difference model," *Complexity*, vol. 2021, Article ID 5277083, 20 pages, 2021.

[4] Z. Yang, Q. Meng, and C. Li, "Selecting the strategic port of "the belt and road" based on the global network," *Complexity*, vol. 2021, Article ID 9967773, 17 pages, 2021.

[5] J. Liu, S. Lin, M. Wu, and W. Lyu, "Winning and losing relationship: a new method of university ranking in the case of countries along the belt and road," *Complexity*, vol. 2021, Article ID 8811668, 13 pages, 2021.

[6] X.-F. Xu, M. Liu, Li Ma, and Y. Li, "Energy investment potential and strategic layout in countries along the "belt and road" based on principal component analysis," *Complexity*, vol. 2021, Article ID 5525844, 10 pages, 2021.

[7] G. Sui, J. Zou, S. Wu, and D Tang, "Comparative studies on trade and value-added trade along the "belt and road": a network analysis," *Complexity*, vol. 2021, Article ID 3994004, 12 pages, 2021.

[8] L. Zhang, Y. Zhao, D. Chen, and X. Zhang, "Analysis of network robustness in weighted and unweighted approaches: a case study of the air transport network in the belt and road region (open access)," *Journal of Advanced Transportation*, vol. 2021, Article ID 8810254, 13 pages, 2021.

[9] H. Zhang, Y. Li, Q. Zhang, and D. Chen, "Route selection of multimodal transport based on China railway transportation," *Journal of Advanced Transportation*, vol. 2021, Article ID 9984659, 12 pages, 2021.

[10] Lu Zhang, Y. Zhao, B. Dessein, D. Maeyer, and N. Philippe, "Determinants of Intercity Air-Passenger Flows in the "belt and road" region," *Complexity*, vol. 2021, Article ID 5514135, 14 pages, 2021.

[11] Y. Yang, W. Liu, K. Li, Y. Jin, and S. Liang, "Evaluation of Chinese transport infrastructure investment performance in countries along the belt and road initiative," *Mathematical Problems in Engineering*, vol. 2021, Article ID 8357939, 12 pages, 2021.

[12] J. Xu, X. Yang, and A. Razzaq, "Understanding the role of humanistic factors in trade network evolution across the belt and road initiative countries using the exponential random graph model," *Complexity*, vol. 2021, Article ID 1961061, 15 pages, 2021.

[13] X. Li and L. Fuzhou, "A dynamic econometric analysis of urbanization and ecological environment in silk road economic belt," *Scientific Programming*, vol. 2022, Article ID 4895213, 8 pages, 2022.

[14] R. Qiang and J. Yang, "Influential spreader identification in complex networks based on network connectivity and efficiency," *Wireless Communications and Mobile Computing*, pp. 1–8, Article ID 7896380, 2022.

[15] Li Yi, W. Fang, W. Zhang, W. Gao, and B. Li, "Game-Based Trust in Complex Networks: Past, Present, and Future," *Complexity*, vol. 2021, Article ID 6614941, 2021.

[16] A. Boutiara, M. K. A. Kaabar, Z. Siri, M. E. Samei, X. G. Yue, and X.-G. Yue, "Investigation of the generalized proportional Langevin and sturm-liouville fractional differential equations via variable coefficients and antiperiodic boundary conditions with a control theory application arising from complex networks," *Mathematical Problems in Engineering*, vol. 2022, pp. 1–21, Article ID 7018170, 2022.

[17] L. Li, C. Mao, H. Sun, Y. Yuan, and B. Lei, "Digital twin driven green performance evaluation methodology of intelligent manufacturing: hybrid model based on fuzzy rough-sets AHP, multistage weight synthesis, and PROMETHEE II," *Complexity*, vol. 2020, no. 6, pp. 1–24, Article ID 3853925, 2020.

[18] Yu Li and P. Liu, "Artificial Intelligence-Based Real-Time Signal Sample and Analysis of Multiperson Dragon Boat Race in Complex Networks," *Complexity*, vol. 2022, Article ID 4915973, 2022.

[19] L. Li, T. Qu, Y. Liu et al., "Sustainability assessment of intelligent manufacturing supported by digital twin," *IEEE Access*, vol. 8, pp. 174988–175008, 2020.

[20] L. Li and C. Mao, "Big data supported PSS evaluation decision in service-oriented manufacturing," *IEEE Access*, vol. 8, no. 99, pp. 154663–154670, 2020.

[21] Z. Zhu, Z. Huang, J. Chen, and L. Guo, "Topology-aware bus routing in complex networks of very-large-scale integration with nonuniform track configurations and obstacles," *Complexity*, vol. 2021, Article ID 8843271, 12 pages, 2021.

[22] L. Li, B. Lei, and C. Mao, "Digital twin in smart manufacturing," *Journal of Industrial Information Integration*, vol. 26, no. 9, Article ID 100289, 2022.

[23] M. Syed Ali, M. Usha, Q. Zhu, and S. Shanmugam, "Synchronization analysis for stochastic T-S fuzzy complex networks with markovian jumping parameters and mixed time-varying delays via impulsive control," *Mathematical Problems in Engineering*, vol. 2020, pp. 1–27, Article ID 9739876, 2020.

Hindawi
Scientific Programming
Volume 2022, Article ID 7113312, 10 pages
https://doi.org/10.1155/2022/7113312

Research Article

Data Mining Algorithm for College Students' Mental Health Questionnaire Based on Semisupervised Deep Learning Method

Maoning Li

Xi'an Jiaotong University City College, Shaanxi, Xi'an 710018, China

Correspondence should be addressed to Maoning Li; limaoning@stu.xjtu.edu.cn

Received 18 May 2022; Revised 20 June 2022; Accepted 23 June 2022; Published 1 August 2022

Academic Editor: Lianhui Li

In recent years, there are many cases of college students who have psychological problems affecting their studies, dropping out of school, and even committing suicide. College students, as a part of high-level talents, have always been regarded as outstanding members of society. They default to have strong psychological qualities, but the reality is disappointing. Various pressures such as academics, social relations, and employment make college students the mental exhaustion has led to many bloody tragedies. The timely detection of psychologically abnormal students has become one of the most concerned and thorny issues in major universities. By constructing a mental health state perception model for college students and optimizing the model parameters, it can be seen that the f score of the internal and external tendency model has increased by 3.3%, the f score of the depression binary model has increased by 2.5%, and the anxiety binary model of the f score has increased by 2.5%. The score increased by 8%. The established model has an obvious effect and can quickly analyze the difference between the behaviors of psychologically abnormal students and normal students in school and also provide a management decision-making basis for college student managers and psychological counselors.

1. Introduction

The frequent dropout and suicide incidents in recent years have proved that many students have more or less psychological problems, and these psychological problems have aroused widespread concern in society. At the same time, at all stages of life, people may have psychological problems due to various complex reasons. Early detection of these psychological problems can play a huge role in protecting personal safety. Because of the rapid development of disciplines such as computer science and mathematics, technologies such as deep learning, data mining, and big data are also making rapid progress and are increasingly integrated into people's daily lives. More and more algorithms are emerging in the field of computer science to solve certain problems and in many ways outperform traditional methods. For example, traditionally, people use indicators such as degree centrality and edge betweenness to analyze social networks, which can better describe some characteristics of social networks but usually only express part of the information in social networks and may contain more noise, and network representation learning based on deep learning solves this problem very well, which usually captures more information in the network for more detailed analysis and identification. This research uses network science, deep learning, network representation learning, other technologies, and students' social network data to identify students who are more likely to have psychological problems. Accurate identification can give families and schools the opportunity to intervene in students as early as possible and prescribe the right medicine to solve students' problems. Helping psychologists provide psychological counseling can largely avoid the deterioration of students' psychological problems; reduce school dropout, suicide, and other incidents; and reduce social tragedies. At the same time, a new way to efficiently utilize multiview network data is proposed; more potential social information between views is preserved; and the problem of label imbalance that is common in such data is proposed. It is proposed to identify students' psychological problems through deep learning technology,

which also provides a direction for the identification and research of students' psychological problems in the future [1–7].

2. Related Work

In recent years, many experts and scholars have realized the importance of educational big data. They have used data mining technology to analyze and mine the data generated by students in school and have achieved remarkable results. They have put the data mining results into education and teaching. A person's psychological characteristics are often expressed through daily life behaviors and routines. Therefore, recently, researchers have begun to try to dig out information that can reflect their mental health status from the daily behavior data of college students. Several studies have shown a strong relationship between mental health status and online behavior. DongNie et al. explored the relationship between search behavior and personality traits and further attempted to determine how search behavior can be used to identify personality. They collected two data sets: one from a questionnaire on 16 personality factors and the other from web access logs from Internet gateways. By calculating the correlation coefficient between individuals' search behavior and personality, some interesting patterns were found; there are several specific behaviors that have a strong correlation with personality, such as directory index search, knowledge search, dwell time, keyword usage, click habits, and so on. Through regression analysis, most personality dimensions can be predicted by search engine behavior. AngLi et al. propose an algorithm for predicting mental health problems through network usage behavior. They recruited 102 college students and used the SCL-90 questionnaire to conduct a psychological survey. Through the results of the questionnaire, they obtained the mental health level of college students (10 dimensions) and conducted statistical analysis on the online behavior of college students. Based on web usage behavior, a computational model for predicting the scores of each dimension of SCL-90 is established. The results show that the fluctuation range of the Pearson correlation coefficient between the predicted score and the actual score of each dimension is between 0.49 and 0.65, and the fluctuation range of the relative absolute error is between 75% and 89%. Zangane and Hariri et al. explore the role of emotional factors in doctoral students' online information retrieval. Their study sample, 50 PhD students, aggregated information by observing user facial expression records, Morae software log files, and pre- and postsearch questionnaires. The findings suggest that there is a significant relationship between emotional expression and the individual characteristics of searchers. Searcher satisfaction with search results, Internet search frequency, search experience, interest in search tasks, and familiarity with similar searches were associated with increased happiness. An examination of user emotions during search shows that users with happy emotions spend a lot of time searching for and viewing search solutions. ChangyeZhu and BaobinLi et al. proposed a new method to detect depression through time-frequency analysis of network behavior. They recruited 728 graduate students, obtained their depression scores through the Zung self-rating depression scale (SDS), and then collected digital records of their online behavior. Through time-frequency analysis, they built a classification model to distinguish between high and low SDS groups, and a predictive model that more accurately identified the mental state of the depressed group. The experimental results show that both the classification model and the prediction model can better reflect the change in mental health, and the time-frequency feature can better reflect the change in mental health. The research at this stage is mainly limited to the behavior analysis of a certain type of specific group and the psychological analysis and interpretation of the influencing factors. However, the continuous update and iteration of data mining technology have provided a great boost to the research work in psychology. Driven by data mining technology, the construction of university informatization platforms has become more perfect. The use of mathematical models in machine learning makes it possible to predict the psychological state of students. Based on the main research contents of the above research scholars, the analysis of college education data has always been a research hotspot in the field of data mining. Through the data mining of students' in-school education, the researchers use data mining technology and analysis theory to draw conclusions about students' academic performance, social relations, and poor students and provide data support and data support for the construction of college informatization and smart campuses. The theoretical basis also provides valuable guidance and suggestions for college administrators [8–14].

3. Related Technical Methods

3.1. Data Processing Technology

3.1.1. Data Filtering. Although data mining is a method for massive data analysis, it does not mean that we need to use all the collected data because, when collecting data in the early stage, we did not specifically consider the use of these data in the future. However, the value density of these data is very low, which is not conducive to later data analysis. Therefore, when there are specific research goals, only the data that are useful for target analysis need to be selected. For the research purpose of this study, the original data are the records of students' online behavior in school collected through the network system. The key information in the records are the student ID, the website visited, the type of website visited, the time of visiting the website, and so on. The rest of the information cannot be used, such as some parameters and codes designed by the log system to ensure security, which are useless for our analysis.

3.1.2. Data Cleaning. Data cleaning is mainly to solve the problem of poor data quality caused by some accidental factors for some useful data after data screening. The main means are as follows:

Missing value processing: when the data set with missing data accounts for a relatively low proportion of the whole

data set and the data volume of the sample is relatively large, in this case, it can be processed through the deletion method, that is, the data items with missing values can be directly discarded. Another common processing method is the filling method. This method is used to fill in the data according to the average value of the data near the dimension where the missing value is located when the data volume itself is not particularly large and there are many missing samples.

Outlier processing: it is also called outlier processing or error value processing. If the value of one dimension in a data item is far greater than or less than the value of other data items in the sample, the data item with the outlier is called an outlier. In the case of outlier data, it cannot be discarded directly. It is necessary to analyze it to judge whether it is reasonable and then decide on the processing strategy. For example, in real life, the age range of people is greater than 0 and less than 150. When the value in the data item exceeds this range, it can be regarded as an abnormal value. This method is a simple analysis method.

When the data is considered to have the same meaning as the addition and subtraction of several dimensions, they can represent the same meaning. Eliminating duplicate data dimensions plays a certain role in data downsizing and model burden reduction. It ensures the uniqueness and representativeness of data dimensions.

Noise data processing: the random error or variance of the measured data caused by some reasons is the so-called noise, which is the interference to the data. The commonly used methods are the box division method and regression method. The box division method forms a small group of nearby ordered values, namely "box," and then smoothes these ordered data values with the mean, median, or boundary of the data in the box to make these data locally smooth. The regression rule is to use a regression function to fit these noisy data and play the role of smoothing data denoising [15].

3.1.3. Data Conversion. Data conversion processing can also be called data mapping processing, which generally has three cases. One is the encoding conversion of text data. Since the computer cannot directly process text data, such as calculating the distance between two data, it is necessary to numerically encode the text. For example, in the gender type, the male is coded as 1, and the female is coded as 0; common encoding methods include one-hot encoding and so on. The second is format conversion. For example, date data need to be converted into a unified format type to facilitate subsequent analysis and processing. The third is the mathematical processing of numerical data. For example, when it is found that the numerical value of a certain dimension encountered changes in the form of an exponential, the exponentially changing data can be quickly converted into decimal numerical data, which is convenient for observation and analysis through the following formula [16]:

$$y = \log_m (x + k). \tag{1}$$

In the same way, when the data changes in the form of a power function, it can be processed by the method of opening the n^{th} power, and it can be converted into small numerical data that is easier to observe by formula (2), where y is the converted value and x is the value obtained before conversion.

$$y = \sqrt[n]{x}. \tag{2}$$

3.1.4. Data Integration. The student's on-campus network behavior data are recorded in the log system and saved in log format, while some basic information data of the student are saved in the student management system. During data analysis and model training, it is cumbersome and error-prone to operate the data in each system, so a data integration method is needed to extract these data and save them in the same environment for processing.

3.2. Data Analysis Technology. The biggest difference between logistic regression analysis and linear regression analysis is that the data types of the variables Y analyzed are different. Logistic regression analysis can analyze discrete categorical data, while linear regression analysis can only analyze continuous data types [17].

3.2.1. Logistic Regression Distribution

Definition 1 (Logistics). Let x be a continuous random variable, when x has the following distribution function and density function; then x is said to obey the logistic regression distribution.

$$\begin{aligned} F(x) &= P(X \le x) = \frac{1}{1 + e^{-(x-\mu/\gamma)}}, \\ f(x) &= F'(X \le x) = \frac{e^{-(x-\mu/\gamma)}}{\gamma\left(1 + e^{-(x-\mu/\gamma)}\right)^2}. \end{aligned} \tag{3}$$

The distribution function and density function plots are shown in Figure 1.

3.2.2. Binary Logistic Regression Analysis. Binomial logistic regression is suitable for dealing with the situation when the value of the dependent variable y has only two categories, which is essentially a prediction model of classification probability. The value of the variable x is a real number. When the value of the dependent variable y is 1, the probability model is shown in equations 4 and 5, and when it is 0, it is shown in the following equations:

$$P(Y = 1|x) = \frac{\exp(\omega \cdot x + b)}{1 + \exp(\omega \cdot x + b)}, \tag{4}$$

$$P(Y = 0|x) = \frac{1}{1 + \exp(\omega \cdot x + b)}, \tag{5}$$

where $x \in R^n$ is the input value of the model, $y \in 0,1$ is the output value of the model, $\omega \in R^n$ is the parameter, ω is called the weight vector, b is called the bias, and $\cdot x$ is the inner

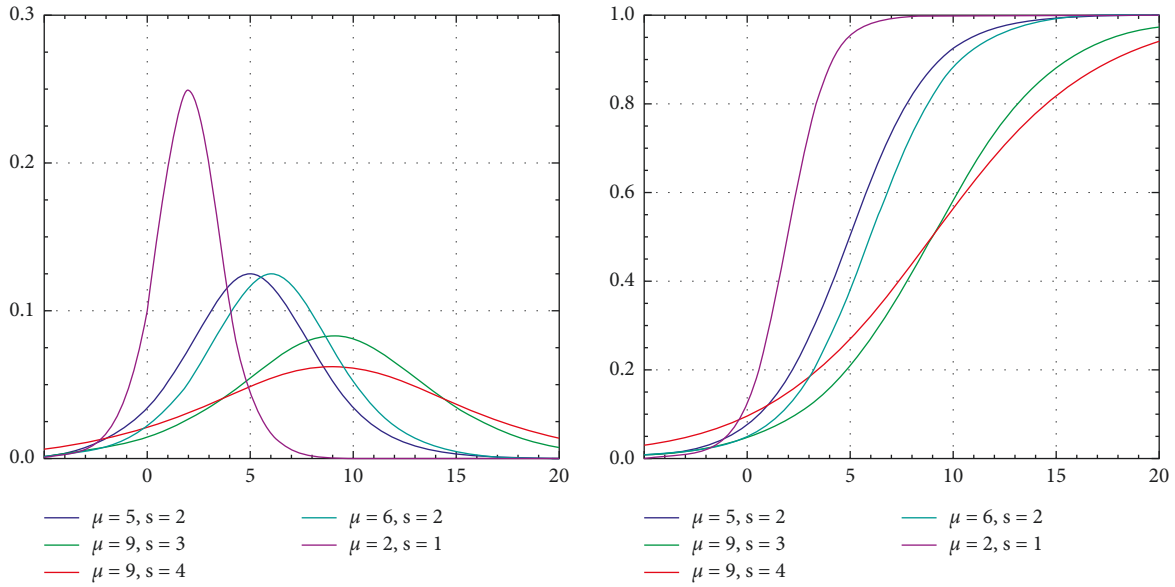

Figure 1: Distribution function and density function.

product of ω and x. Assuming a given input vector $x = (x_1, x_2, x_3, \cdots, x_n)$, the logistic regression analysis model can separately calculate $p\ (y = 0|x_n)$ and $p\ (y = 1|x_n)$ for each dimension x of the input vector value. The concept of event probability and logarithm is introduced here. Let P be the probability of occurrence of an event, and $1 - P$ corresponds to the probability that it does not occur. The probability of an event can be expressed by the ratio between the two, that is, $P/(1 - P)$; on this basis, the logarithmic probability of the event can be obtained by taking the logarithm. The formula is shown in (7). The odds can be given by the following equation [18]:

$$\text{logit}(p) = \log \frac{p}{1-p}, \tag{6}$$

$$\text{logit}(p) = \log \frac{p(Y=1|x)}{1-p(Y=1|x)} = \omega \cdot x + b. \tag{7}$$

It can be seen from formula (7) that when the value of the dependent variable y is 1, the calculation formula of the logarithmic probability of logistic regression analysis is actually a linear function. The logistic regression analysis is essentially fitting this linear function so that this linear function can distinguish the two categories of the original data as much as possible. The larger the value of the linear function, the greater the log probability of the logistic regression, the closer the classification type is to class 1, and vice versa; it is closer to class 0.

3.3. Data Mining Technology

3.3.1. Classification Algorithm. The essence of a classification algorithm is to train a classifier on a labeled data set so that it can divide a new data set. The process of evaluating the results of the classification algorithm is inseparable from the existence of a confusion matrix, which is a computing tool often used in classification algorithms. Figure 2 shows the composition of the confusion matrix [19]. Then the basic elements of classification problems are as follows: training data, that is, the sample data set used to learn the model; feature, that is, the attribute used to describe data and the basis of classification; model, that is, the external framework of classifier; algorithm, that is, the method of constructing classification rules; and evaluation, that is, the final evaluation of the effect of the model. The purpose of the classification algorithm is to mine the hidden rules in label data, so as to divide the data set in feature dimension space.

There are four parameters in the confusion matrix, which are as follows:

TP (true positive): true examples, which refer to the positive tuples correctly classified by the classifier

TN (true negative): true negative, which refers to the negative tuples correctly classified by the classifier

FP (false positive): false positive, which refers to negative tuples that are misclassified as positive tuples by the classifier

FN (false negative): false negative, which refers to the evaluation index of the positive tuple classification model that is misclassified as a negative tuple by the classifier can be calculated by the four parameters of the above confusion matrix:

Accuracy rate: also known as overall recognition rate, it generally measures how well the classification model can correctly identify various data sets:

$$\text{accuracy} = \frac{(\text{TP} + \text{TN})}{(P + N)}. \tag{8}$$

Precision: it reflects the proportion of correct classification in the classification results of the classification model for each category, that is, the accuracy of the model when judging each category.

$$\text{precision} = \frac{\text{TP}}{(\text{TP} + \text{FP})}. \tag{9}$$

		Predictive classification +	Predictive classification −	Total
Actual classification	+	TP (true positives)	FN (false negatives) Type II error	TP+FN (Actual positive)
	−	FP (false positives) Type I error	TN (true negatives)	TP+FN (Actual negative)
	total	TP+FP (Predicted positive)	FN+TN (Predicted positive)	TP+FP+FN+TN

Figure 2: Confusion matrix.

Recall rate: also known as sensitivity, it can reflect the sensitivity of the classification model to each category of data set, that is, the proportion of a certain type of data that can be correctly identified by the model.

$$\text{recall} = \frac{\text{TP}}{(\text{TP} + \text{FN})} = \text{sensitivity}. \tag{10}$$

F score: since the above two indicators are negatively correlated, in order to measure the comprehensive performance of the model on the two indicators, their harmonic mean is used as a new indicator, and the value of this indicator ranges from 0 to 1. The larger the value, the better the effect of the model.

$$F_1 = \frac{2 \times \text{precision} \times \text{recall}}{\text{precision} + \text{recall}}. \tag{11}$$

3.3.2. Integration Algorithm. There is no perfect algorithm model in the field of data mining. The idea of an integrated algorithm is to combine different types of algorithm models through a certain strategy, so as to improve the overall model's ability to classify data sets. There are two main strategies for ensemble learning algorithms: bagging and boosting. The main idea of the bagging strategy is to combine the results of each base classifier and then determine the final classification result of the overall model by voting, which can effectively increase the stability of the classification. When training the base classifier, a part of the data of the sample is extracted by the method of bootstrap to construct the training data set of the base classifier. This kind of "incomplete learning" is to reduce the difference between each base classifier.

4. Feature Construction of a Mental Health State Perception Model Based on Deep Learning

4.1. Data Preprocessing. The network log data mainly comes from a dedicated network log collection server. Through the user's application to access the network, the link data accessed by the user is collected, so as to obtain the user's network log information. The main content of the log information is: "A record of a user accessing a certain network type at a certain point in time." A sample of log information is shown in Table 1 [20].

Table 1: Sample table of log information.

Property name	Numerical value
Student ID	2021**********
Gender	Male
Age	Twenty-one
Point in time	2021-11-15, 00:00:00
Website name	Taobao
Site type	Shopping

Compared with the website type, the attribute of the website name is too careful and narrow, and it obviously belongs to the category of shopping. There is no need to distinguish the two. Therefore, when extracting feature dimensions from log information, the website name is not a required item. For the point-in-time information, in order to facilitate the processing of data at a point in time, it is divided into two parts: the part of year-month-day is used as "date," and the part of hour:minute:second is used as "time." The finally extracted feature dimensions are student ID, gender, age, date, time, and website type; the format is shown in Table 2 [21].

4.2. Static Variable Analysis Based on Binary Logistic Regression. As shown in Table 2, there are two static variables in this research, gender variable and age variable. Static variables are property variables that are basically unchanged or unchanged for a long time. Firstly, the univariate binary logistic regression analysis was performed on the gender variable and the age variable. The dependent variable was divided into three groups. The extroverted "1" and the introverted "0" were the one group, and the depression "1" and the asymptomatic "0" were the one group.

Next, a multivariate binary logistic regression analysis was performed with the combination of gender and age as the dependent variable, and the results are shown in Table 3.

It can be seen from the results in Table 3 that the results of logistic regression are the same as those of univariate analysis. Combining the results of the two analyses, it can be concluded that the gender and age factors are not statistically significant for the psychological state indicators and can be ignored.

4.3. Feature Construction Based on Information Entropy. This study proposes two concepts for the design and construction of features. These two concepts are regularity

Table 2: Network log feature dimension table.

Student ID	Gender	Age	Date	Time	Site type
2018*******	Male	Twenty-one	2018-11-15	00:00:00	Shopping

Table 3: Logistic regression results of gender and age variables.

	Regression coefficients	Standard error	$P > \|z\|$
Dependent variable: extroversion			
Sex	−0.0628	0.063	0.316
Age	−0.0497	0.101	0.626
Dependent variable: depression			
Sex	−0.0007	0.001	0.502
Age	0.4027	0.405	0.322
Dependent variable: anxiety			
Sex	−0.1113	0.257	0.665
Age	−0.1583	0.090	0.078

of surfing behavior and degree of dependence of surfing behavior. The regularity of surfing behavior is a measure of the regularity of students' surfing behavior of visiting different types of web pages within a period of time. The design of this regularity is based on the concept of Shannon's information entropy. According to the information entropy, the order and purity of a data set can be measured. Therefore, combined with the theory of information entropy, a method for calculating the regularity of students' online behavior is designed. Method. For example, for online shopping behavior, let Shopping Regularity be SR, set shopping times to different intervals, and the shopping frequency interval is [0, 5], [6, 11], [12, 25], [26, ...), according to the number of times of shopping per day to determine which interval it belongs to, and finally we will get the frequency distribution corresponding to these n intervals as C = {C1, C2, ..., Cn}, and the probability corresponding to each interval is p, and the calculation formula is as follows:

$$p_i = \frac{c_i}{s}, \quad i = 1, 2, \ldots, n, \quad S = \sum_{i=1}^{n} c_i. \tag{12}$$

Then the calculation formula of shopping regularity SR is

$$SR = -\sum_{i=1}^{n} p_i \log p_i. \tag{13}$$

The method of interval probability is also used to calculate the degree of dependence on online behavior. As shown above, the number of visits of a certain type of Internet access in the day is divided into intervals, and then the frequency of occurrence of this type in which interval is calculated in the statistical period. If the interval is the highest, then it is determined that the interval is dependent on this type of network behavior. If the interval is a low-order partition, the degree of dependence is light, and if it is a high-order partition, the degree of dependence is higher. This research transforms mild dependence into number "1," moderate dependence into number "2," and high dependence as "3." When defining the interval division of the degree of dependence, two cases are considered. When accessing data of social platform type, such as when processing microblog data, it is divided into two types: browsing microblogs and publishing microblogs. The interval can be divided into [0, 30] times as a low degree of dependence interval, [31, 60] times as a medium degree of dependence interval, and more than 60 times as a high degree of dependence interval. The dependence degree interval for publishing microblogs can be divided into [0, 10] times as a low dependence degree interval, [10, 19] times as a medium dependence degree interval, and more than 20 times as a high dependence degree interval. The feature dimensions of the final constructed sample data set are shown in Table 4.

4.4. Feature Selection Based on Genetic Algorithm. After removing the uncorrelated static variables, the regularity and degree of dependence of various network types and the existence of the student ID are left in the sample data set. For each pair of labels, not all types of network behavior data are helpful for model training, and redundant data participating in the training will reduce the accuracy of the model. Therefore, this study uses the adaptive iterative ability of the genetic algorithm to perform feature selection and uses it to perform feature selection according to different label states. The iterative graph of the feature dimension obtained by the genetic algorithm is as follows: the horizontal axis is the number of feature combinations, and the vertical axis is the fitness function score, as shown in Figure 3.

When based on the internal and external trend tags, the extracted feature dimensions are 8, and the effect is the best.

Table 4: Sample data set example table.

Student ID	Gender	Age	Shopping regularity	Shopping dependence	Browsing Weibo regularity
*******	1	Twenty-one	2.35	2	3.25

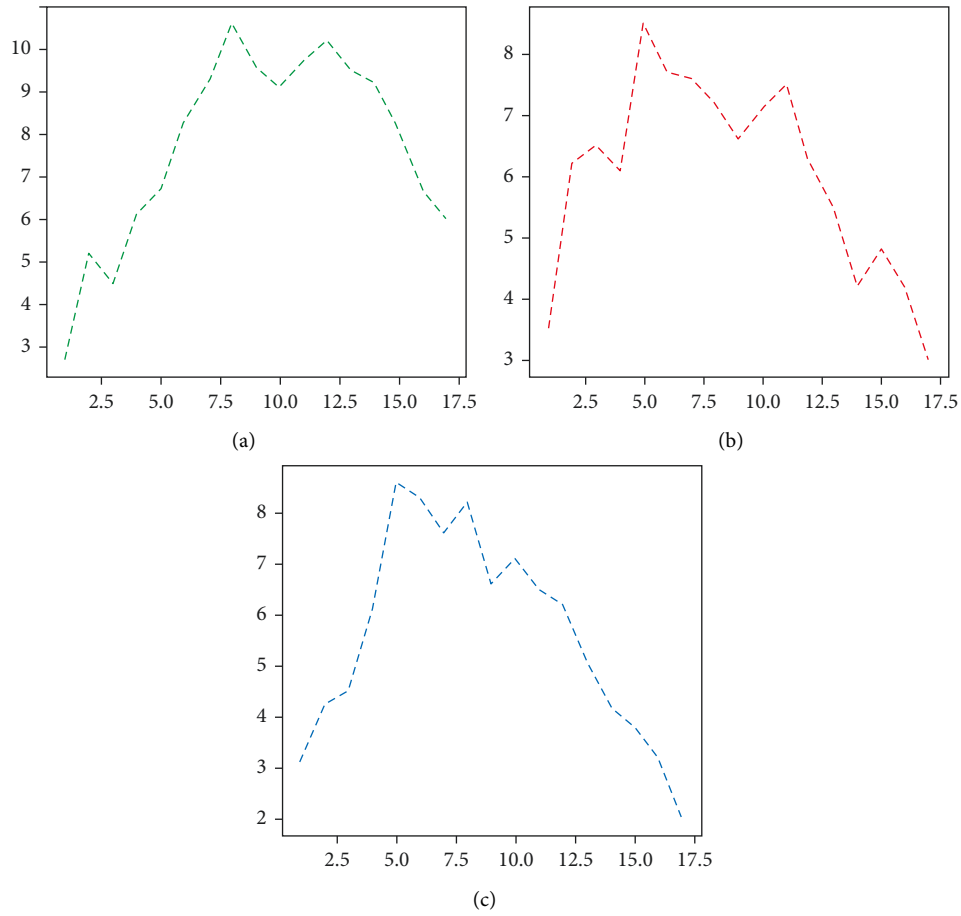

Figure 3: Iterative diagram of genetic algorithm.

These feature dimensions are WeChat regularity, WeChat dependence, WeChat posting regularity, Weibo regularity, video Watching regularity, video viewing regulation dependence degree, reading regularity, and reading dependence degree.

Based on the label of depression or not, the effect is best when the extracted feature dimensions are 5. These feature dimensions are shopping dependence, listening to music, WeChat dependence, map website regularity, and game dependence. Based on the anxiety label, the extracted feature dimension is 5, and the effect is the best. These feature dimensions are short video website dependence degree, information website dependence degree, music listening regularity, game regularity, and shopping regularity.

5. Experiment and Result Analysis

5.1. Experimental Environment. The experimental environment and related parameters are shown in Table 5.

Table 5: Experimental environment and configuration.

Lab environment	Environment configuration
Operating system	Windows 10
CPU	Intel(R) Core(TM) i5-6500 3.2 GHz
RAM	32G
Programming language	Python
Programming tools	Jupyter notebook

5.2. Data Preparation. The data used in this experiment comes from two parts, which are divided into two parts: label data and feature dimension data. The processing of these two parts of data is as follows: label data processing: when labeling the psychological state information of internal and external tendency, the data with external tendency score are classified as label "1," and the data with internal tendency score are classified as label "0." For the pair of labels with or without depressive symptoms, the score 4 is taken as the threshold. The data less than the threshold are classified as the label with no depressive symptoms "0," and the data

Table 6: Sample data set example table.

Student ID	Shopping regularity	Shopping dependence	Weibo regularity	...	Label 1	Label 2	Label 3
*******	3.25	2	2.35	...	0	1	1

greater than the threshold are classified as the label with depressive symptoms "1." Similarly, for the treatment of the pair of labels with or without anxiety symptoms, the score 4 is also used as the threshold. The data less than the threshold are classified as the label without anxiety symptoms "0," and the data greater than the threshold are classified as the label with anxiety symptoms "1." Examples of specific sample data sets are shown in Table 6.

5.3. Comparison and Analysis of Model Experiment Results. The optimal model of the three mental state models is the random forest model, which does have a strong role in the field of classification. The parameter adjustment and optimization of the random forest model is mainly carried out through the grid search method. The parameter adjustment of the random forest mainly involves the following parameters: (1) n_estimators: the maximum number of iterations or the number of weak learners. If n_estimators is too small, it is easy to underfit, and if n_estimators is too large, overfitting will occur, so a suitable value for n_estimators is very important. (2) min_samples_split: the minimum number of samples required for internal node subdivision 3, min_samples_leaf: the minimum number of samples for leaf nodes 4, and max_depth: the maximum depth of the decision tree. Taking the GA-RF model of the two-category depression as an example, the process of parameter adjustment is as follows: in the first step, take n_estimators as the variable; the initial value is 10, and the interval is 10; and the output result is shown in Figure 4.

In the second step, (min_samples_split, max_depth) is used as the parameter combination; the starting value of min_samples_split is set to 100, and each change is 200; and the starting value of max_depth is set to 3, and each change is 2, and the output result is shown in Figure 5.

In the third step, take (min_samples_split, min_samples_leaf) as the parameter combination; the starting value of min_samples_split is set to 20, and each change is 10; and the starting value of min_samples_leaf is set to 60, and the output results are shown in Figure 6.

After comprehensively considering the above three steps, the optimal parameter combination of the depression model is obtained: n_estimators = 50, min_samples_split = 150, max_depth = 7, and min_samples_leaf = 25. Follow this step for the optimal parameters of the other two models and bring these parameters into the model. The f value of the model is shown in Table 7.

It can be seen from Table 7 that after the optimization of the model parameters, the f score of the model has been improved. For the internal and external tendency model, the f score increased from 0.765 to 0.79, an increase of 3.3%. For the depression binary model, the score of F increased from the original 0.81 to 0.83, an increase of 2.5%. For the anxiety

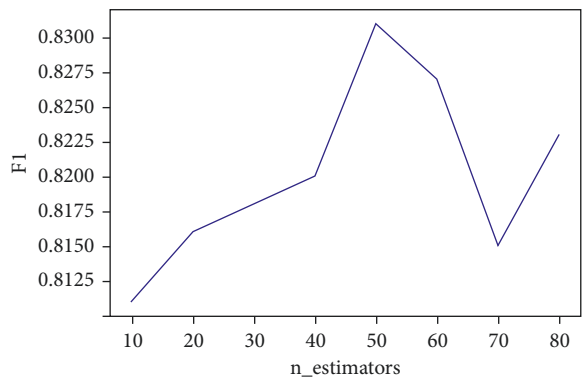

Figure 4: $F1$ values of GA-RF under different iterations.

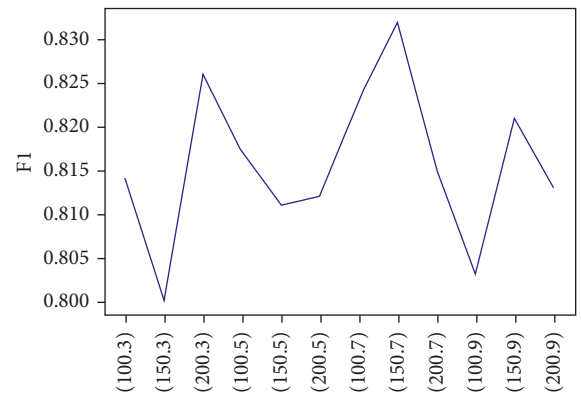

Figure 5: $F1$ values of GA-RF under different parameter combinations (min_samples_split and max_depth).

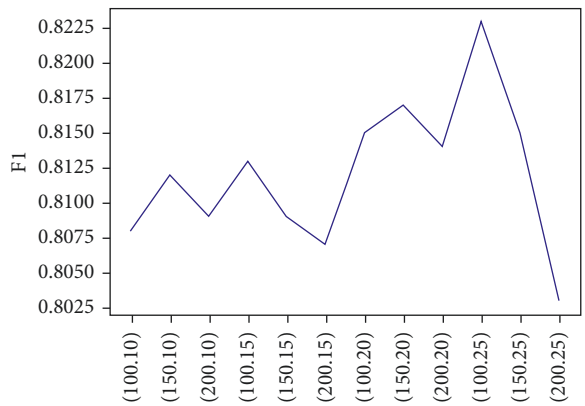

Figure 6: $F1$ values of GA-RF under different parameter combinations (min_samples_split and min_samples_leaf).

Table 7: Model output values under optimal parameters.

Model	n_estimators	min_samples_split	max_depth	min_samples_leaf	$F1$ value
Internal and external tendencies	70	300	13	50	0.79
Depression	50	150	7	25	0.83
Anxiety	55	100	7	30	0.81

binary classification model, the score of f increased from the original 0.75 to 0.81, an increase of 8%.

6. Conclusion

Nowadays, the topic of students' mental health has attracted more and more attention from society. For example, the incidents of college students committing crimes and committing suicide caused by the abnormal psychology of college students have also often caused heated discussions in public opinion. At present, most of the students have insufficient understanding of mental illness or even have an attitude of neglecting and not paying attention, so these students with mental abnormalities cannot be found and treated effectively in time. These students and conducting interventions are a top priority in student management efforts. With the development of data mining technology, the construction of the data analysis model has been solved for us in terms of model analysis. This paper is based on the research on the psychological state prediction model that is used to capture students' psychological state information based on the students' online data collected on the university campus and the psychological assessment scale indicators. This research is based on the deep learning theory. The model is constructed, analyzed, and adjusted, aiming to grasp the psychological state information of students more comprehensively and accurately through the network behavior data of students in school. The results of the model experiments show that the f scores of the three models have improved. The models used in this study are only classification models in the field of machine learning, and the more popular deep learning models are not used. The next step will use deep learning. The network structure model of the aspect is used for model experiments to compare the operation of the two models.

Data Availability

The data set can be accessed upon request.

Conflicts of Interest

The author declares that there are no conflicts of interest.

Acknowledgments

The author would like to thank 2018 Shaanxi Provincial Social Science Fund Project, Research and Practice of Research Evaluation System of Higher Vocational Colleges Based on Need Level Theory (no. 2018Q09).

References

[1] J. Park, D. S. Lee, and H. Shablack, "When perceptions defy reality: the relationships between depression and actual and perceived Facebook social support," *Journal of Affective Disorders*, vol. 200, pp. 37–44, 2016.

[2] L. A. Jelenchick, J. C. Eickhoff, and M. A. Moreno, "Facebook depression?" social networking site use and depression in Older adolescents[J]," *Journal of Adolescent Health : Official Publication of the Society for Adolescent Medicine*, vol. 52, no. 1, pp. 128–130, 2013.

[3] K. C. Fernandez, C. A. Levinson, and T. L. Rodebaugh, "Profiling: predicting social anxiety from facebook profiles," *Social Psychological & Personality Science*, vol. 3, no. 6, pp. 706–713, 2012.

[4] Y. Bengü and üzer Ahmet, "The Relationship between Internet Addiction, Social Anxiety, Impulsivity, Self-Esteem, and Depression in a Sample of Turkish Undergraduate-Medical-Students," *Psychiatry-Research*, vol. 1, Article ID S0165178118306127, 2018.

[5] C.-C. Lin, "The relationships among gratitude, self-esteem, depression, and suicidal ideation among undergraduate students," *Scandinavian Journal of Psychology*, vol. 56, no. 6, pp. 700–707, 2015.

[6] S. D. Amarasuriya, A. F. Jorm, and N. J. Reavley, "Predicting intentions to seek help for depression among undergraduates in Sri Lanka," *BMC Psychiatry*, vol. 18, no. 1, p. 122, 2018.

[7] K. e. ZHANG, "Four Changes of Modern Universities from the Perspective of "4V" of Big Data," *Canadian Social Science*, vol. 11, 2015.

[8] M. I. Jordan and D. E. Rumelhart, "Forward models: supervised learning with a distal teacher[J]," *Cognitive Science*, vol. 16, no. 3, 1992.

[9] T. Dietterich, "Approximate statistical tests for comparing supervised classification learning algorithms," *Neural computation*, vol. 10, no. 7, pp. 1895–1923, 1998.

[10] S. Kotsiantis, "Supervised Machine Learning: A Review of Classification Techniques," *Informatica*, vol. 31, 2007.

[11] H. B. Barlow, "Unsupervised learning," *Neural Computation*, vol. 1, no. 3, pp. 295–311, 1989.

[12] T. Hofmann, "Unsupervised learning by probabilistic latent semantic analysis," *Machine Learning*, vol. 42, no. 1-2, pp. 177–196, 2001.

[13] X. Zhu and A. B. Goldberg, "Introduction to semi-supervised learning," *Synthesis Lectures on Artificial Intelligence and Machine Learning*, vol. 3, no. 1, p. 130, 2009.

[14] M. F. A. Hady and F. Schwenker, "Semi-supervised learning," *Intelligent Systems Reference Library*, vol. 49, no. 2, pp. 215–239, 2013.

[15] A. G. B. Rs Sutton, "Reinforcement Learning," *A bradford book*, vol. 15, no. 7, pp. 665–685, 1998.

[16] L. K. Pack, M. L. Littman, and A. W. Moore, "Reinforcement learning: an introduction," *Ieee Transactions on Neural Networks*, vol. 16, no. 1, pp. 285-286, 2005.

[17] T. Joachims, "Making large-scale SVM learning practical," *Advances in Kernel Methods Support Vector Learning*, 1998.
[18] S. R. Safavian and D. Landgrebe, "A survey of decision tree classifier methodology," *IEEE Transactions on Systems Man & Cybernetics*, vol. 21, no. 3, pp. 660–674, 1991.
[19] V. Vladimir and Y. Svetnik, "Random Forest A Classification and Regression Tool for Compound Classification and QSAR Modeling," *Journal of Chemical Information & Modeling*, vol. 43, 2003.
[20] G. Ratsch, "Soft margins for adaboost," *Machine Learning*, vol. 42, no. 3, pp. 287–320, 2001.
[21] M. Collins, R. E. Schapire, and Y. Singer, "Logistic regression, AdaBoost and bregman distances," *Machine Learning*, vol. 48, no. 1/2/3, pp. 253–285, 2002.

Hindawi
Scientific Programming
Volume 2022, Article ID 9083154, 9 pages
https://doi.org/10.1155/2022/9083154

Research Article

Chinese Cross-Language Definition Recognition Method Based on DE-BP Model

Yanxia Shen,[1] **Yi Zhang**,[2] **and Mingwei Zhu**[3]

[1]*College of Liberal Arts and International Education, Xi'an Peihua University, Xi'an, Shaanxi 710125, China*
[2]*College of Liberal Arts, Huaibei Normal University, Huaibei, Anhui 235000, China*
[3]*College of Computer Science and Technology, Xi'an University of Technology, Xi'an, Shaanxi 710054, China*

Correspondence should be addressed to Yanxia Shen; shenshen@peihua.edu.cn

Received 22 May 2022; Revised 27 June 2022; Accepted 1 July 2022; Published 1 August 2022

Academic Editor: Lianhui Li

As an important linguistic phenomenon in verbal communication, relayed speech exists in a large number of news texts and is also one of the most prominent features of the Chinese language. However, at present, there are few systematic comparative studies on the recognition of the relayed problems in Chinese language crossover, and the existing methods are highly subjective. This paper makes a qualitative comparative analysis of the reported speech in the Chinese language by the DE-BP model, which combines differential evolution (DE) algorithm and BP (backpropagation) neural network to recognize the Chinese cross-language paraphrase. After that, we obtained some meaningful findings as follows. In the Chinese language, the frequency of indirect paraphrase is the highest, followed by direct paraphrase, while other categories, namely, free indirect paraphrase, free direct paraphrase, and narrative paraphrase of speech acts, are relatively rare. Through the identification and manual labeling of reported verbs and then the word frequency statistics, it is found that the number of reported verbs in English newspapers is dominant in general, and there is a significant difference between them.

1. Introduction

Relaying speech is a basic form of human language. When people want to convey what has happened in the past, what is happening now, or what may happen in the future, either in their own words or in the mouths of others, they need to communicate through relaying speech [1]. Only in this way has human civilization survived; without speech, language has been reduced to mere communication tools. The most basic feature of reported speech is reflexivity (i.e., people use language to refer to language itself). People report not only what others say but also what others comment, criticize, and so on. Accordingly, the definition of relayed speech generally involves two features, namely, reflexive feature and two-layer structure [2]. The reported speech is defined as the speech of the words, words of words, and also the words of the words and words about words. The uniqueness is embodied in paraphrased words. Two different contexts or styles can also appear in a single syntactic structure and in the process of interaction between speakers and hearers [3].

Paraphrased words have common features in all human languages. Now, we know that all languages have been paraphrased in one way or another; even those innate configurations of bad language also have their own paraphrased way and sometimes may have to rely on contextual characteristics; paraphrased words have a certain universality in human behavior. Most languages have their own paraphrased way; as said, paraphrased words as a kind of double-layer structure in the process of the formation and development of human language are indispensable and play an important role. Every conversation is filled with numerous paraphrases and interpretations of what others have said. According to this line of thinking, every speech is actually a free translation because every speech is a patchwork of quotes, assimilation, and conversion of others' words [4, 5].

As for the terms of paraphrased speech, the usage is more complicated. For the paraphrased speech (perhaps the most well-known term so far), there is no unified opinion, and there is no consistent view among the various expressions of the verbal paraphrase phenomenon. By telling a story,

considering the ability of human memory and expression, most of the words may not be original but transferred from other people or other media [6].

The research on the recognition of Chinese language paraphrase will further enrich the research on paraphrase, which is a common phenomenon in communication, no matter in daily conversation or written discourse, which is full of a large number of other speeches. On the one hand, it can explain the ideographic meaning of public discourse, and on the other hand, it can deepen the understanding of the discourse reported by people in the news. As a language form, reported speech not only contains two speech forms and contexts but also reflects the system and essence of social communication and cognition. Analysis of relayed speech helps to show the conversational nature of language: constructive studies of dialogue, especially of relayed forms, because they reveal the basic and constant active acceptance of other speakers that constitutes the essential feature of dialogue. Human personality is only a part of the society as a whole, which is realistic from the perspective of history but productive from the perspective of culture [7, 8]. The study of reported speech is helpful to further understand the sociological essence behind these phenomena. In addition, the study of reported speech also helps to reveal the complex cognitive mechanism of human beings, including perception, storage, memory, and verbal expression, and can further enrich the different perspectives on paraphrased speech [9].

It can further verify the feasibility of the critical linguistics and corpus-combined technology. Critical discourse analysis has made great achievements in revealing the relationship between language and ideology, but criticism and doubts about it have been constantly heard. Although many scholars put forward criticisms, they also put forward many constructive suggestions, such as proposing that only reliable conclusions can be drawn based on a large corpus to strengthen critical discourse analysis. Contrastive analysis is an important means of language research [10]. It is of great academic and practical value to reveal the common and special laws between one's own language and other's language by studying other languages or by contrastive analysis of different languages. This research is faced with two main difficulties: First, the research on free translation of Chinese is not enough, and there is still a big gap in theory and category. Second, there are few direct references. Because of the above difficulties, it is of great significance to strengthen the research on the recognition methods of Chinese free translation [11].

From the perspective of application, it will help improve the level of Chinese journalists' news reporting, distinguish foreign news pitfalls, maintain the national image, improve the ability of critical thinking and reading, and enlighten the field of foreign language teaching and translation to a certain extent. From the point of communication, the success of external publicity is largely determined by the effect of information dissemination. In fact, China's current external communication capacity is far from satisfying the image of a rapidly rising power. This study is helpful in enhancing the mutual understanding between China and foreign countries, improving the effectiveness of communication, and avoiding misunderstanding and has a strong realistic and contemporary significance [12, 13]. It gives a qualitative comparative analysis of the reported speech in the Chinese language from the types of reported speech by the DE-BP model and obtains some meaningful findings.

This section mainly introduces the research topics of discourse paraphrase in existing literature, the related research on Chinese language paraphrase recognition, and the specific application of recognition methods in news discourse, summarizes the achievements and shortcomings of previous studies, and determines the direction of this research. Discourse paraphrase is a universal phenomenon in human speech communication, which has been widely concerned by linguists, philosophers, and literary critics. Various terms have appeared successively, including quotation and paraphrase [14]. The study of language expression has always been troubled by the confusion of terms and concepts. Different terms represent different aspects of the process of language translation, and different theoretical perspectives reflect the complexity and diversity of discourse translation itself [15].

Quotation is widely used in literature, reflecting scholars' discussions on the reflexivity of language and the nature of paraphrase. In semantic and philosophical studies, quotation is a general term, and its classification is mainly based on the use and mention of language [16, 17]. From the perspective of projection structure, the juxtaposition is a quotation, while the subject-subordinate is a report. Thus, it can be seen that quotation is not very clear in terms of conceptual significance. Sometimes it refers to the quotation of abstract language expression, and sometimes it only refers to the direct quotation of concrete discourse. Quoted speech is a term widely used in linguistic research of speech paraphrase, mainly used to refer to different ways of paraphrasing another speech. It mainly focuses on the grammatical characteristics of different types of relayed speech and the rules of phase five conversion [18]. Most of the researches on discourse relayed use direct speech and indirect speech to refer to relayed speech. A relatively general term is used when discussing paraphrasing in various styles. According to the stylistic attributes of the original discourse, three direct forms of discourse are distinguished: direct speech, direct thinking, and direct writing. Thus, relayed speech is a term mainly used in linguistic research of discourse relaying [19].

As far as English is concerned, the differences between direct and indirect discourse lie in tenses, person, and the form of expression of the original discourse. In terms of morphology, direct discourse retains the original tense of the verb, while indirect discourse needs to refer to the time in the clause to move the time of the relayed discourse. Textual free translation mainly focuses on various free translations in literary works, especially the analysis of the relationship between direct speech and indirect speech. In addition to direct speech and indirect speech, there are also free direct speech, free indirect speech, and narrative paraphrase of speech act in the Chinese language [20, 21]. Direct speech has two features that can show the presence of the narrator:

quotes and paraphrases clauses; free direct speech is to remove one or two of these characteristics; The narration of speech act only conveys the occurrence of the act, but does not convey the content and form of speech, so the content of speech is not so important in this form [22].

The pragmatic study of discourse retransmission tends to explore the mode and function of discourse retransmission in context. Speech connects two discourse events. The main term used is relayed speech, and direct speech and indirect speech are used when referring to various types of relayed speech. From the perspective of linguistic function, the paraphrase is referred to as the signal sound in the text: if the speaker or writer in some way signals the presence of another voice in the text, then any paragraph derived from that voice [23, 24]. Free translation is a misleading term that means that one can freely translate the words of another while retaining the nature of the original speech. The term used is constructed dialogue: framing discourse as dialogue is not paraphrasing but a recontextualization of words within the current discourse [25]. In the study of discourse free translation, free translation is a topic that scholars pay most attention to. The early studies mainly describe the grammatical characteristics of various types of reporting and the rules of conversion from direct speech to indirect speech under the influence of structuralism. When people want to paraphrase what they have said before or what someone else has said, there are two ways: give the exact expression of direct speech used by the original speaker; modify indirect discourse according to the relayed context [26].

The function of discourse retransmission is closely related to various ways of discourse retransmission [27]. This section mainly introduces the attitude of the narrator and the pragmatic functions of discourse retransmission in the specific discourse. In the sequence of relayed speech, direct speech is the conventional pattern, and from direct speech to the right, the sense of freedom gradually strengthened. Free indirect speech is on the more indirect side of the speech expression gradient, allowing the narrator to take two perspectives, creating a distance between the reader and the character's words and inserting the author's voice, resulting in a satirical effect. The sound effect of direct speech is a kind of guidance and quotation, not indirect speech with direct speech mixed with narrative language. It provides the narrator with a summary of the character's language, and can speed up the contrast between the narrator's direct speech and the interrogative speech and control the dialogue [28].

The narrative of speech act has the function of highly checking and concealing and turning the human and object discourse into speech act to narrate, and the author exercises the biggest intervention right. The recognition of discourse paraphrase focuses on the stylistic effects of various paraphrase types in literary works, and its advantage lies in that these categories are regarded as a conscious paraphrase of any words or thoughts by the author through the choice of structure. Attitude refers to the current relayed on the original information or speaker evaluation, including neutral, positive, and negative [29]. Therefore, no matter how precise the paraphrased words may be and no matter how pure the motives of the paraphrase may be, removing a passage from its original context and recontextualizing it in a new network of relationships are bound to interfere with its original effect [30]. Functional research of discourse paraphrase is reflected in two aspects: the intervention and paraphrase of the relayed discourse and the pragmatic functions of discourse in the whole discourse. Stylistics studies have shown that different ways of paraphrases and narrator paraphrases are related to the degree of involvement as reported speech. Recent empirical studies have fully demonstrated that discourse paraphrasing appears in different types of discourse and has multiple functions. On the one hand, citing the discourse of others can provide an objective basis for the current discourse. And different free translation methods reflect the differences between subjects. From the perspective of the existing research on speech paraphrase, the research on speech paraphrase recognition has gradually moved from static grammatical description to dynamic pragmatic study, and significant findings have been obtained [31].

This paper mainly uses the DE-BP method to study the recognition problem of Chinese cross-language paraphrase, which is beneficial to verbal communication. This research mainly consists of four parts. The first part introduces the research background and significance of comments on the framework of this paper. The second part mainly introduces the DE-BP-based Chinese cross-language paraphrase recognition. The third part introduces the experimental results and analysis. The fourth part is the summary part of this research.

Based on the above analysis, the main contributions of the paper are shown as follows:

(1) It makes a qualitative comparative analysis of the reported speech in the Chinese language by the DE-BP model

(2) It is found that other categories, namely, free indirect paraphrase, free direct paraphrase, and narrative paraphrase of speech acts, are relatively rare

(3) It is found that the number of reported verbs in English newspapers is absolutely dominant in general, and there is a significant difference between them

2. DE-BP-Based Chinese Cross-Language Paraphrase Recognition

2.1. Chinese Cross-Language Paraphrase Recognition. Chinese cross-language paraphrase recognition is the restriction of the various contextual factors, making it impossible to accurately reproduce the original discourse, and this research fully reveals that the speech paraphrased the complex characteristics of a speech act; however, the research on fidelity of speech transmission is also lacking of detailed description, because the specific forms of speech reporting are closely related to fidelity. In a specific context (e.g., news context), what is the similarity or arbitrariness between the paraphrase and the original discourse? In addition, the relationship between various forms of retransmission and the authenticity of the content of retransmission needs further investigation. The typical Chinese cross-

language paraphrase recognition process is given in Figure 1, in which the meaning A is interpreted from the end of the original sentence and assigned the corresponding importance weight, finally obtaining the cross-language interpretive awareness.

As can be seen from the figure, the research trend of discourse paraphrase has shifted from static description to pragmatic function of discourse paraphrase in a specific context, revealing the essential characteristics of discourse paraphrase and the contextual factors that influence the choice of discourse paraphrase. Words can be seen from a sentence input, paraphrasing words is essentially a process of the project, and another word is a token of the characterization and again is weaker than the restatement of the literal type, factors influencing the discourse context of conveying including before the words and the words of the various factors, especially the restriction role of conveying paraphrased context of discourse.

2.2. DE-BP Model. Based on the above discussion, the BP (backpropagation) neural network is used here to solve the problem.] By simulating the neural function of the human brain, the data samples are learned, and the link weights and thresholds between units are established to deal with complex nonlinear problems without specific functional forms. According to the error between the actual value and the expected value, from the output layer through the hidden layer to the input layer, the link weight between each layer is revised layer by layer. By iteratively correcting the weights, the gap between the observer and the predicted value becomes smaller and smaller, and the model performance becomes better and better. When the error is less than a certain value, it indicates that the network training is completed.

$$E = \sum_{i=1}^{m} (x_i - c_i)^2. \tag{1}$$

Then, we expand the above error definition to the hidden layer:

$$E = \frac{1}{2}\sum_{k=1}^{l}\left[d_k - f(net_k)\right]^2 = \frac{1}{2}\sum_{k=1}^{l} d_k - f\left(\sum_{j=0}^{m}\omega_{jk}y_{jk}\right)^2. \tag{2}$$

We expand further to the input layer; there is

$$\begin{aligned} E &= \frac{1}{2}\sum_{k=1}^{l} d_k - f\left[\sum_{j=0}^{m}\omega_{jk} f\left(net_j\right)\right] \\ &= \frac{1}{2}\sum_{k=1}^{l} d_k - f\left[\sum_{j=0}^{m}\omega_{jk} f\left(\sum_{j=0}^{n} v_{ij}\chi_i\right)\right]^2. \end{aligned} \tag{3}$$

It can be seen from the above formula that the network input error is a function of the weights of each layer, so the error can be changed by adjusting the weights. Obviously, the principle of adjusting weights is to reduce errors continuously, so the weights should be proportional to the gradient descent of errors:

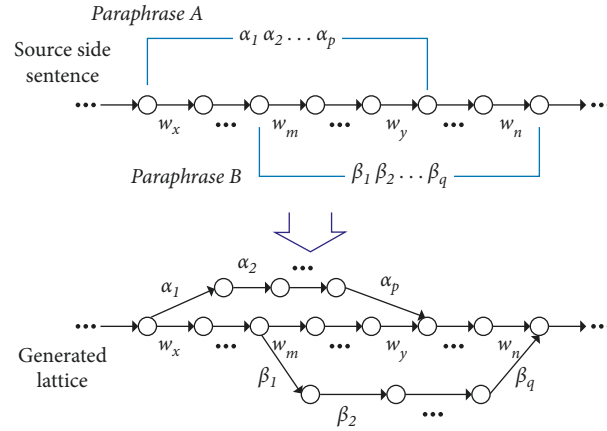

Figure 1: The typical Chinese cross-language paraphrase recognition process for an input sentence.

$$\begin{aligned} \Delta\omega_{jk} &= -\eta\frac{\partial E}{\partial \omega_{jk}},\ j = 0, 1, 2, \ldots, m; k = 1, 2, \ldots, \ell, \\ \Delta v_{ij} &= -\eta\frac{\partial E\ \partial}{v_{ij}},\ i = 0, 1, 2, \ldots, n; j = 1, 2, \ldots, m. \end{aligned} \tag{4}$$

Then, the weight adjustment formula of each layer is

$$\Delta\omega_{jk}^{h+1} = \eta\delta_{h+1}^{k} y_j^h = n(d_k - o_k)o_k. \tag{5}$$

According to the above rule layer-by-layer analogy, the weight adjustment formula of the first hidden layer is as follows:

$$\Delta\omega_{pq}^{1} = \eta\delta_q^1\chi_p = \eta\left(\sum_{r=1}^{m_2}\delta_r^2\omega_{qr}^2\right)y_q^1. \tag{6}$$

There are some problems such as slow convergence speed, poor performance, uncertain learning rate, and easy to fall into local minimum. A proposed optimization algorithm for the traditional BP neural network, in the whole calculation process, generally exists in the local extremely small convergence speed and sometimes even oscillation and divergence problems to overcome its limitations in the traditional BP neural network. The differential evolution (DE) algorithm is introduced into the neural network to optimize the initial weights and thresholds of the network, which shows better nonlinear mapping ability and improves its prediction accuracy. Population initialization is as follows:

$$x_{i,1} = x_i^L + \text{rand}\left(x_i^U - x_i^L\right), i - 1, 2, \cdots, NP. \tag{7}$$

The mutation operation formula is as follows:

$$v_{i,G+1} = x_{r1,G} + F\left(x_{r2,G} - x_{r3,G}\right). \tag{8}$$

Then the interlace operation is as follows:

$$u_{ji,G+1} = \begin{cases} v_{ji,G+1}, & r_j \le CR \text{ or } j = \text{rand}(i), \\ x_{ji,G}, & r_j \ge CR \text{ or } j \ne \text{rand}(i). \end{cases} \tag{9}$$

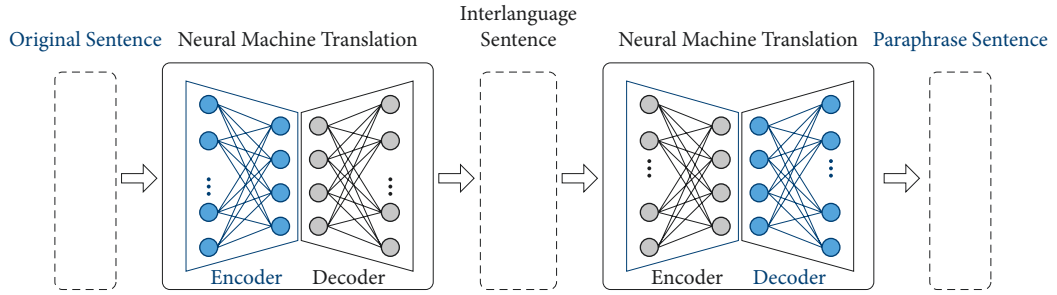

Figure 2: DE-BP-based Chinese cross-language paraphrase recognition frame.

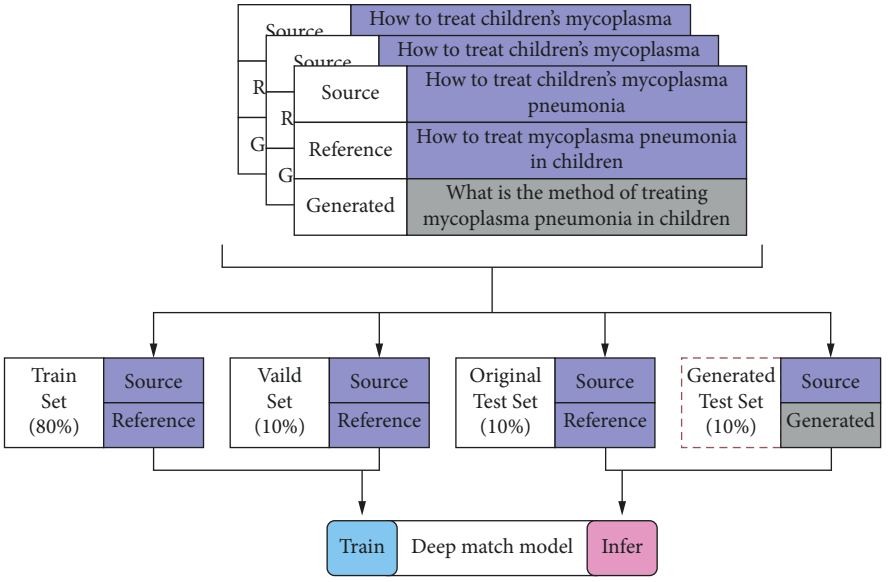

Figure 3: The process of similarity calculation.

Formulas (7)–(9) mainly study the mutation operation formula and interlace operation.

Accordingly, the selection operations are as follows:

$$x_{i,G+1} = \begin{cases} u_{i,G+1}, & f\left(u_{i,G+1}\right) \le f\left(x_{i,G}\right), \\ x_{iG}, & f\left(u_{i,G+1}\right) > f\left(x_{i,G}\right). \end{cases} \tag{10}$$

The fitness function is

$$f(X) = \sqrt{\frac{1}{N}\sum_{i=1}^{N}\left(Y_i^0 - Y_i\right)^2}. \tag{11}$$

Based on (1)–(11), Figure 2 gives DE-BP-based Chinese cross-language paraphrase recognition proposed in this paper, which mainly includes the original sentence, the neural machine translation, the interlanguage sentence, the neural translation, and the paraphrase sentence.

3. Experimental Results and Analysis

3.1. Introduction to Experimental Dataset. This study mainly adopts the method of corpus research and combines quantitative statistics with qualitative analysis. First of all, we collected news texts from People's Daily for consecutive months and established a large database. Then, according to the research purposes of different chapters, we extracted samples from the main corpus and built a secondary corpus. For some chapters, we also classified and collected them according to the subject needs. Then, we sorted all the

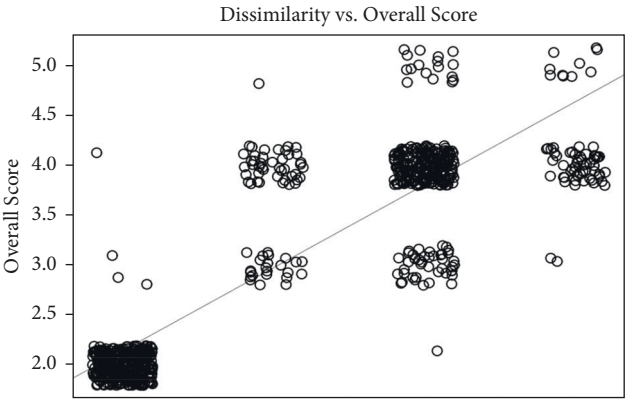

Figure 4: The relationship between Chinese paraphrase accuracy and corpus similarity.

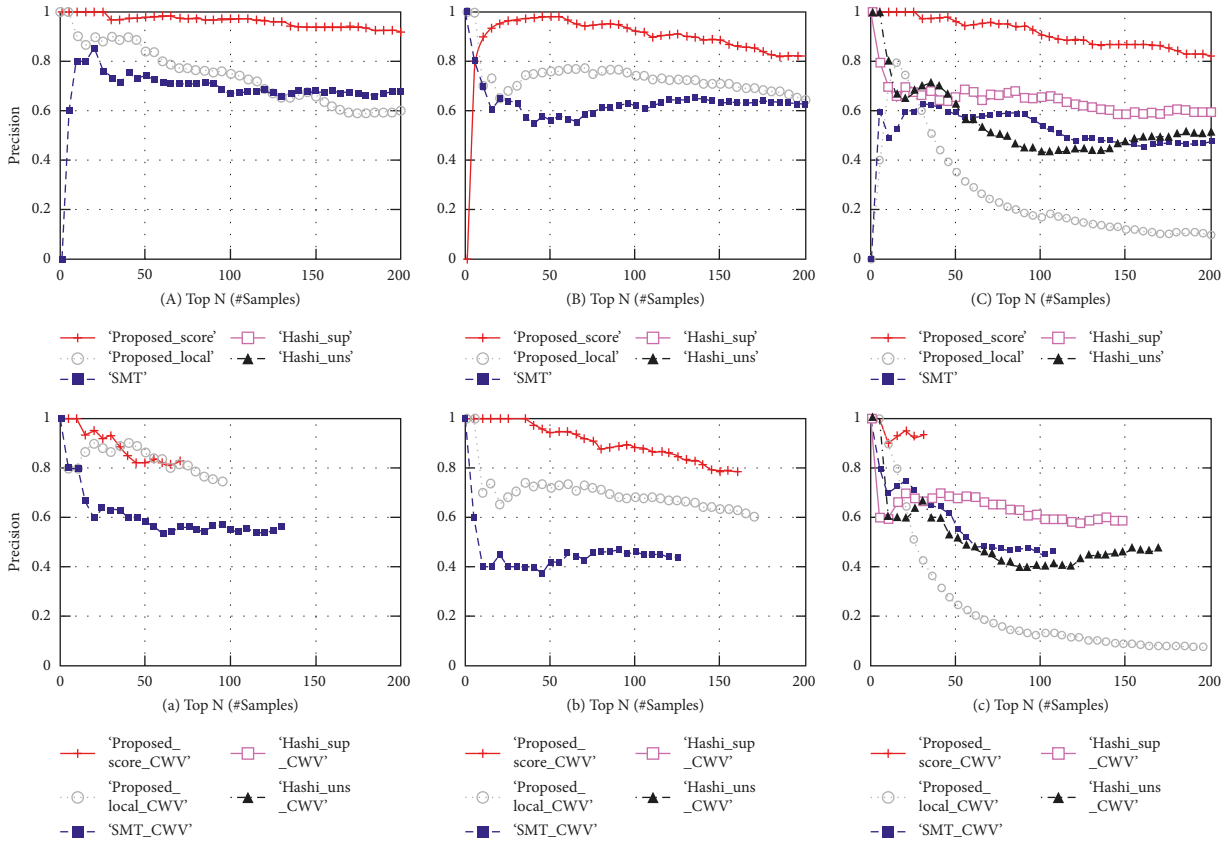

Figure 5: The recognition accuracy: English (a), Chinese (b), and Japanese (c).

subcorpora in each chapter of the newspaper into text documents to establish a pair of subcorpora.

In corpus collection, we mainly consider the following issues: the collected newspaper texts are all issued in years to reflect the recent situation. The establishment of the Chinese newspaper corpus should not only pursue the size but also consider whether it can fully explain and fit the research objectives of this paper.

3.2. Experimental Result Analysis. After establishing the cross-language recognition method based on the DE-BP algorithm, the established method is verified based on the data of 3.1. The specific simulation results are described as follows: after the corpus is established, we will mark the corpus of each section. Indirect reporting is judged by the absence of quotation marks and the use of the third person; free direct paraphrase is mainly in quotes without leading sentences. Among them, the indirect paraphrase is the residual form of indirect speech, which needs to be judged according to the specific context.

The main characteristic of narrative paraphrase of speech act is that it usually centers on a paraphrase verb or is used alone or forms a verb-object structure to indicate who performs a speech act. The specific results of similarity calculation between corpus are shown in Figure 3. The main purpose of the results of the graph is for the subsequent Chinese language paraphrase recognition service.

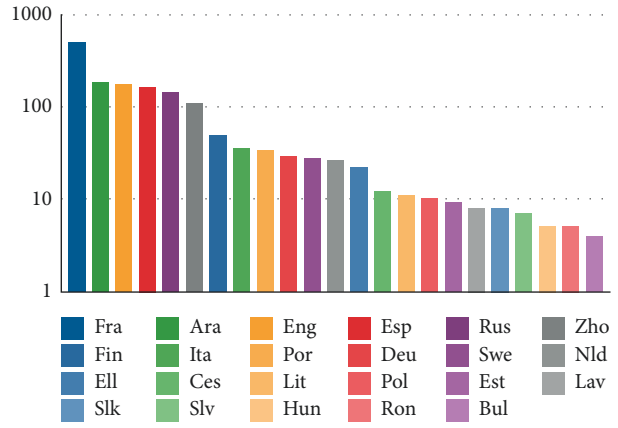

Figure 6: A graphical representation of the size of the set of definitions for each language.

Finally, we use two sets of classification models to analyze the sources of information: the former takes the proper nouns and pronouns that appear in the discourse to represent people or organizations as the judging criteria. According to the categorization of definite degree, the definite source of information generally has a surname or a given name, uses a definite noun phrase, or uses a definite anaphora or anaphora pronoun. Ambiguous sources are represented by indefinite noun phrases or by coreferential pronouns with no definite identity in the context. Sources

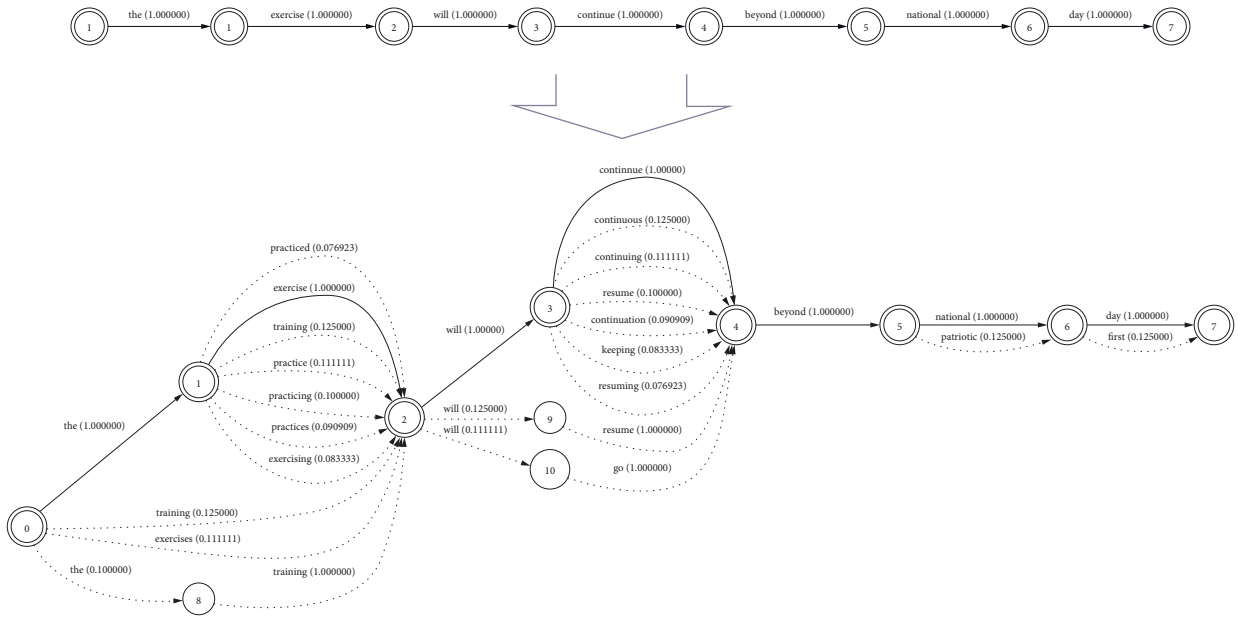

Figure 7: The example of a paraphrase process for an input Chinese sentence.

that cannot be identified are more complex, use the passive voice of the hidden actor, or use an unidentifiable noun structure, prepositional phrase construction that conceals the source, or some other vague expressions. Since the similarity is calculated in Figure 1, based on the obtained similarity, the relationship between Chinese paraphrase accuracy and corpus similarity is shown in Figure 4, as can be seen from the figure above. The higher the similarity is, the higher the recognition accuracy will be, and vice versa.

The recognition accuracy of Chinese cross-language paraphrase by different algorithms is shown in Figure 5. The curves are drawn from 2,000 samples, with each dot representing 50 samples. Then, we analyze the extent to which all methods of free translation are related to content word variation extraction. The bottom half of Figure 5 shows the results of the evaluation (curves labeled with CWV). PosedScore's sample size was significantly reduced compared to English and Japanese, but accuracy remained high. This is mainly due to the linguistic crossover caused by globalization.

In addition, the graphical representation of the size of the set of definitions for each language is shown in Figure 6. It can be seen from the figure that we extracted a significantly different number of identifying definitions for each language. The number of free translations generally varies greatly in size from the collection of French, Arabic, and Chinese free translations and other free translations used to extract free translations for that language. This is because we used a relatively large bilingual corpus for these three languages and a smaller recognition scale for the other languages, resulting in similar recognition results.

In the traditional sense, indirect speech is characterized by the use of the third person as the subject of the introductory sentence, and then the related sentence usually uses an object clause, as well as the moving of the verb tense, such as the present tense to the past tense. In addition, the words and phrases about time and place should be changed accordingly, such as today to yesterday. In addition, it should be pointed out that those paralinguistic features originally directly reported are also lost; for example, pronunciation and intonation, omission of address forms, and gestures and expressions are simplified or lost. Because individual words are separated from the original discourse, they have been broken away from the original grammatical structure and lost the original context, and the semantics have changed, or even the opposite.

Figure 7 gives the example of a paraphrase process for an input Chinese sentence. Figure 2 shows nodes (double circles) and edges (solid lines) from the input sentence by the original word, and at the bottom, Figure 2 shows the last lattice of new nodes (single-line circles) and new edges (dashed lines) from the paraphrase. It can be seen that the proposed method increases the diversity of source phrases and thus provides more flexible translation options in the decoding process.

4. Conclusions

The use of various paraphrasing strategies shows that the news paraphrase controls and manipulates the paraphrase; even if the paraphrase is highly similar to the original language, it will deviate from the original speaker's intention in a specific context.

On the whole, it is the way in which the Chinese language paraphrases behavior. The diversity of choice of diction and its influence on similarity reflects the conventional choice of paraphrase under the constraints of institutional context. However, the strategic regulation of news relaying behavior in the process of original discourse event itself (such as the adjustment of information type, information state, and amount of information) and relaying expression fully reflects the active choice of the relaying behavior under the influence of various institutional context factors. On the one

hand, it reflects the adaptability of news discourse reporting behavior, and on the other hand, it also reflects the subjectivity of news discourse reporting behavior. However, the research in this paper is only limited to small Chinese language paraphrases data. Big data and multiple kinds of data will be the focus of future research [32].

Data Availability

The dataset can be accessed upon request.

Conflicts of Interest

The authors declare that there are no conflicts of interest.

References

[1] H. Asghari, O. Fatemi, S. Mohtaj, and P. FailiRosso, "On the use of word embedding for cross language plagiarism detection," *Intelligent Data Analysis*, vol. 23, no. 3, pp. 661–680, 2019.

[2] L. Li, B. B. Lai, and J. P. Huang, "Paraphrase identification based on interpretable mechanism," in *Procedings of the 2021 3rd international conference on artificial intelligence and advanced manufacture (AIAM). IEEE*, pp. 416–421, Manchester, United Kingdom, October 2021.

[3] B. Sun, F. Zhang, J. Yuan, Z. Wei, and S. Ting, "Chinese medical paraphrase generation: based on neural machine translation," *Journal of European Economy*, vol. 47, no. 1, pp. 1–6, 2021.

[4] B. Sun, Y. Wu, Y. Zhao, Z. Hao, L. Yu, and J. He, "Cross-language multimodal scene semantic guidance and leap sampling for video captioning," *The Visual Computer*, pp. 1–17, 2022.

[5] V. Kumar, A. Verma, and N. Mittal, *Anatomy of preprocessing of big data for monolingual corpora paraphrase extraction: source language sentence selection//Emerging Advances in Intelligent Systems and Computing*, vol. 5pp. 495–505, Springer, Singapore Springer 2019.

[6] Y. Wang, M. Liu, Y. Zhang, Z. u. Jin'an, and C. Yufeng, "Research on the construction and application of paraphrase parallel corpus," *Beijing Da Xue Xue Bao*, vol. 57, no. 1, pp. 68–74, 2021.

[7] Y. Zhai, P. Safari, G. Illouz, A. Allauzen, and A. Vilnat, "Towards Recognizing Phrase Translation Processes: Experiments on English-French," 2019, http://arxiv.org/abs/1904.12213.

[8] M. Nagata, C. Katsuki, and M. Nishino, "A Supervised Word Alignment Method Based on Cross-Language Span Prediction Using Multilingual BERT," 2020, http://arxiv.org/abs/2004.14516.

[9] X. I. N. Bin and G. A. O. Xiaoli, *Reported Speech in Chinese and English Newspapers: Textual and Pragmatic Functions*, Routledge, England, 2021.

[10] J. Li, Z. L. Zha, and A. Wulamu, *International Journal of Legal Medicine*, vol. 135, no. 2, pp. 455-456, 2021.

[11] C. Mi, L. Xie, and Y. Zhang, "Improving data augmentation for low resource speech-to-text translation with diverse paraphrasing," *Neural Networks*, vol. 148, pp. 194–205, 2022.

[12] C. Federmann, O. Elachqar, and C. Quirk, *Multilingual Whispers: Generating Paraphrases with translation*, W-NUT, in *Proceedings of the 5th Workshop on Noisy User-Generated Text*, pp. 17–26, W-NUT, Hong Kong, November 2019.

[13] L. Shi and Y. Dong, "Chinese graduate students paraphrasing in English and Chinese contexts," *Journal of English for Academic Purposes*, vol. 34, pp. 46–56, 2018.

[14] G. Li, F. Liu, A. Sharma et al., "Research on the natural language recognition method based on cluster analysis using neural network," *Mathematical Problems in Engineering*, vol. 105, no. 2, pp. 583–597, 2021.

[15] P. Zhu, D. Cheng, F. Yang et al., "Improving Chinese named entity recognition by large-scale syntactic dependency graph," *IEEE/ACM Transactions on Audio, Speech, and Language Processing*, vol. 12, no. 5, pp. 55–68, 2022.

[16] M. Ilyas, N. Malik, A. Bilal, and S. Razzaq, "Plagiarism detection using natural language processing techniques," *Technical Journal*, vol. 26, no. 01, pp. 90–101, 2021.

[17] J. Jun, "Paraphrasing Chinese idioms: paraphrase acquisition, rewording and scoring[J]," *Turkish Journal of Computer and Mathematics Education (TURCOMAT)*, vol. 12, no. 3, pp. 1999–2005, 2021.

[18] G. Rocha and H. Lopes Cardoso, "Recognizing textual entailment: challenges in the Portuguese language," *Information*, vol. 9, no. 4, p. 76, 2018.

[19] H. Le, L. Vial, J. Frej et al., "Flaubert: Unsupervised language model pre-training for french," 2019, http://arxiv.org/pdf/1912.05372.

[20] X. Jia, J. Wang, Z. Zhang, N. Cheng, and J. Xiao, "Large-scale Transfer Learning for Low-Resource Spoken Language understanding," 2021, http://arxiv.org/pdf/2008.05671.

[21] N. T. T. Thuy, N. X. Bach, and T. M. Phuong, "Cross-language Aspect Extraction for Opinion mining," in *Proceedings of the 2018 10th International Conference on Knowledge and Systems Engineering (KSE)*, pp. 67–72, IEEE, Ho Chi Minh City, Vietnam, November 2018.

[22] M. Abdelhamid, F. Azouaou, and S. Batata, *A Survey of Plagiarism Detection Systems: Case of Use with English, French and Arabic Languages[J]*, arXiv preprint arXiv:2201.03423, 2022.

[23] L. Feng, J. Yu, D. Cai, S. Liu, H. Zheng, and Y. Wang, "ASR-GLUE: A New Multi-Task Benchmark for ASR-Robust Natural Language Understanding," 2021, http://arxiv.org/pdf/2108.13048.

[24] J. P. Corbeil and H. A. Ghadivel, "Bet: A Backtranslation Approach for Easy Data Augmentation in Transformer-Based Paraphrase Identification context," 2020, http://arxiv.org/abs/2009.12452.

[25] S. Alzahrani and H. Aljuaid, "Identifying cross-lingual plagiarism using rich semantic features and deep neural networks: a study on Arabic-English plagiarism cases," *Journal of King Saud University-Computer and Information Sciences*, vol. 3, no. 3, pp. 15–29, 2021.

[26] J. W. Lin and R. G. Chang, "Chinese story generation of sentence format control based on multi-channel word embedding and novel data format," *Soft Computing*, vol. 26, no. 5, pp. 2179–2196, 2022.

[27] J. A. Alzubi, R. Jain, A. Kathuria, and A. KhandelwalSaxenaSingh, "Paraphrase identification using collaborative adversarial networks," *Journal of Intelligent and Fuzzy Systems*, vol. 39, no. 1, pp. 1021–1032, 2020.

[28] L. Shi, "Application of big data language recognition technology and GPU parallel computing in English teaching visualization system," *International Journal of Speech Technology*, vol. 12, pp. 452–462, 2021.

[29] B. Thompson and M. Post, "Paraphrase Generation as Zero-Shot Multilingual Translation: Disentangling Semantic

Similarity from Lexical and Syntactic diversity," arXiv preprint arXiv:2008.04935, 2020.

[30] M. Zhang, L. Tan, Z. Tu et al., "Don't change me! User-controllable selective paraphrase generation," vol. 28, no. 107, pp. 3667–3676, 09290, arxiv.org/abs/2008.10064.

[31] Q. Du and Y. Liu, "Foregrounding learner voice: Chinese undergraduate students' understanding of paraphrasing and source use conventions for English research paper writing," *Language Teaching Research*, Article ID 136216882110270, 2021.

[32] H. Inaguma, T. Kawahara, and S. Watanabe, "Source and Target Bidirectional Knowledge Distillation for End-To-End Speech translation," 2021, http://arxiv.org/pdf/2104.06457.

Hindawi
Scientific Programming
Volume 2022, Article ID 6559155, 10 pages
https://doi.org/10.1155/2022/6559155

Research Article

Three-Dimensional Animation Space Design Based on Virtual Reality

Rongxue Zhang

Shenyang Institute of Engineering, Shenyang 110000, Liaoning, China

Correspondence should be addressed to Rongxue Zhang; zhangrx@sie.edu.cn

Received 22 May 2022; Revised 25 June 2022; Accepted 28 June 2022; Published 1 August 2022

Academic Editor: Lianhui Li

3D animation stereo space design is to process and analyze the collected target image information on the computer and finally obtain a 3D model that can represent the corresponding structure. As a branch of computer vision, 3D animation stereo space design is an important part of realizing the key technology of environment perception. What humans see in the three-dimensional world is a two-dimensional picture. Combined with the visual mechanism and the prior information of the object, it can realize the perception of the environment and promote the convenience of life and production. Games, movies, virtual humans, and any product that uses 3D technology require 3D engine support. The 3D engine encapsulates hardware operations and graphics algorithms and can manage a large number of texture and model resources to construct complex 3D scenes. In order to facilitate the research related to virtual human, in this paper, through the research and study of graphics-related mathematical knowledge and related technologies of engine architecture, an intelligent virtual animation generation engine based on DirectX12 is realized, and three-dimensional characters are controlled through related components, and the function of each module is tested and guaranteed. Test cases were designed to test the various functions of the engine and finally showed that the design goals in the demand analysis have been completed, and a lightweight three-dimensional animation three-dimensional space model has been realized.

1. Introduction

The emergence of digital technology has widened the expression space of animation art with its own advantages. It has brought new opportunities to animation art and scene design. According to the current research situation of scene design, in the conception method of animation scene design, people have formed thinking methods such as establishing the overall modeling consciousness, grasping the theme, determining the tone, and exploring unique and appropriate modeling forms. In terms of the expression of space in the scene, there are some specific methods for the elements and classification of animation scene and the methods of shaping the scene, such as using the sense of gravity, strengthening the depth of field, and using character scheduling. In the traditional scene design, there is also a certain theoretical basis for the light and shadow modeling and color creation in the scene. Light and shadow play an important role in animation film scene design, such as shaping space, creating atmosphere, and creating suspense. Nowadays, in the animation scene design, the design and research of furnishings and props are also an important aspect. In the film, they play an important role in explaining the character's identity, shaping the psychological space, depicting the task character, and setting off the task emotion. With the rapid development of the animation industry, the term "scene design" is gradually known to people, but from the previous development, film and television animation scene design is often ignored in the animation industry and animation theory circle. From the perspective of professional training and theoretical research, it is basically in its infancy. For digital scene design, in terms of the research on the characteristics and performance methods of scene design, there is still room for further research. There are only a few books on scene design in the market, which often elaborate scene design from the perspective of two-dimensional animation

or basic theory, without involving some characteristics of digital level. This paper attempts to build a lightweight 3D rendering platform that can quickly combine some intelligent algorithms with character control through the intelligent control framework to realize the interactive 3D animation space based on the natural user interaction interface [1–9].

2. Related Works

Since the 1970s, foreign countries have carried out a lot of research on graphics and engines. After half a century of development, a number of very excellent 3D software companies have been born. They include Discreet (later merged by Autodesk), Epic Games, Unity Technologies, Id Software, etc. These companies have played a great role in the development of computer graphics and the promotion of 3D engines and have produced rendering engines such as 3 ds Max, Maya, Unreal, Unity, and Blender. These engines are widely used to this day. Later, more special 3D engines were born. Zbrush developed by Pixologic is a 3D engine for sculpting modeling, Houdini developed by Side Effects Software focuses on special effects design and terrain editing, Substance Painter and Substance Designer developed by Allegorithmic are mainly used for texture material design, Marvelous Designer developed by Foundry Video Effects Company realizes clothing tailoring and cloth simulation, and Daz 3D produced by Daz Production Company can edit high-quality character models. The current hot direction in the generation of 3D human animation is to reduce the cost and increase the restoration degree of animation. Abroad, Ryo et al. proposed a method to create a spatial 3D model using the Kinect sensor. The 3D information of the space is obtained from the Kinect sensor, and the 3D model is created by synthesizing the images and the obtained 3D information. Kunlin et al. parameterized the standard model according to anthropometric parameters. Then, the Kinect depth map of the human body model was optimized by processing and matching the point cloud data by using the PCL library. Quick integration with the PCL library yields a realistic human model. A new method for 3D human modeling based on a single Kinect was obtained by using an iterative closest point algorithm to register the captured upper human 3D point cloud data with standard reference human data. Zhang et al. proposed a highly personalized human modeling analysis method based on a single Kinect. First, a high-precision human positioning point cloud based on a single Kinect is obtained, and then, on the basis of ensuring the accuracy of the head of the point cloud, the point cloud information is preprocessed. Finally, by using hierarchical compactness to support radial basis functions (CS-RBFs), a 3D human body model is obtained by fitting the sampled point cloud to the existing human body. At present, there are few related papers on directx12 and Vulkan. Some articles have a clear description of the modules of the 3D engine. Compared with the above research, this research is more inclined to extend from the 3D animation design, from the basic data structure design to the implementation of related technologies [10–19].

3. Key Technologies of 3D Animation Stereo Space

3.1. Scenario Management Technology. 3D characters and their environments can be collectively referred to as 3D scenes. The 3D engine needs to fully describe the scene and each object in it in order to integrate various model data and present them on the computer screen. According to different application requirements, the scene management technology in the engine can be divided into two categories:

(1) Scene management based on space division: this technology includes a variety of space conversion and division algorithms, including quadtree, octree, and Bsp tree. The core is to establish a hierarchical structure according to the spatial distribution relationship of objects, and the nodes in the tree represent an area of space where objects are stored on leaf nodes. This type of scene management mainly uses the tree structure to quickly locate scene objects, optimize collision detection, and view frustum culling [20].

(2) Scene management based on parent-child relationship: this management technology is also called "scene graph." The core is to establish a hierarchical tree structure based on the parent-child affiliation of objects. The nodes in the tree are objects with local transformation attributes, and the world transformation is obtained by passing the local transformation between the parent and the child. This type of scene management mainly records the transformation transfer direction through a tree structure, so as to perform the overall transformation of multicomponent objects. In the space partitioning technology, nonleaf nodes represent a space region and are mainly used for the efficiency optimization of internal computing.

In the scene graph, nodes represent objects with local transformation properties, which is convenient for batch manipulation of scene objects. After many 3D software tests, scene graph technology is very suitable for developers to create and design 3D scenes. Since this article focuses on the display of 3D characters and their environments, this article will focus on the technical details of the latter.

3.2. Character Animation Technology. 3D animation is one of the core technologies of virtual characters. Excellent animation performance can not only increase the authenticity of the characters but also enrich the interactivity of the characters. Animation technology has undergone a long history of evolution, but currently the most widely used animation technologies are mainly in the following two categories:

(1) Vertex animation and vertex animation texture technology (VAT): vertex animation directly records the spatial position of each vertex of the model mesh, which can simulate very complex animation

scenarios. This animation technology is often used to simulate some very real object systems such as cloth and fluid. However, in the early stage, due to the large storage space required for vertex animation and the difficulty of mixing and reusing, it was rarely used in real-time systems. With the development of GPU hardware, the vertex animation texture (VAT) technology was born. For an animation with n vertices and a time length of f, the coordinates of the vertices at each moment are stored in a texture of size $n * f$: animation texture sampling is performed in the vertex shader, and the pose transformation of the vertices is performed. The animation texture technology is often used for thousands of identical animated objects in the picture. It can greatly improve the efficiency of animation operation [21].

(2) Skeletal animation consists of two parts of data: the skinned mesh and the skeleton. The skinned mesh records the index of the bones affecting the vertices, and the skeleton records the parent-child relationship between the bones, as well as the local coordinate transformation curve of each bone. Through the local coordinate system transfer technology in the scene graph, the bone pose at a specific moment is calculated, and then the bone animation is mixed according to the bone index recorded by the vertices of the skinned mesh to obtain the final vertex coordinates, specifically as shown in Figure 1.

In the binding pose, set the palm bone world transformation matrix to $\mathrm{WorldMa}_{\mathrm{tBind\_Bone}}$ and the thumb mesh world transformation to $\mathrm{WorldMat}_{\mathrm{Bind\_Finger}}$; the offset matrix formula is as follows:

$$\mathrm{WorldMat}_{\mathrm{Bind\_Bon}} = \mathrm{Worldmat}_{\mathrm{Bind\_Finger}}\mathrm{WorldMat}-_{1\mathrm{Bind\_Bone}}. \tag{1}$$

The original coordinates of the mesh vertices are multiplied by the offset matrix to obtain the mesh vertex coordinates under the bone coordinate system and then multiplied by the skeletal animation matrix at a certain time to obtain the mesh vertex coordinates under the world coordinate system. The formula is as follows:

$$\mathrm{WorldMat}_{\mathrm{Anim\_Finger}} = \mathrm{OffsetMat}_{\mathrm{Finger2Bone}}\mathrm{WorldMat}_{\mathrm{Anim\_Bone}}. \tag{2}$$

3.3. Rendering Technology. The quality and efficiency of 3D rendering are closely related to the effect and fluency of character display. For the choice of rendering technology, it is necessary to consider satisfying complex materials and enriching the content of the picture and also consider maintaining the frame rate as much as possible in some extreme cases. Today's rendering technologies are mainly divided into two categories:

(1) Ray tracing\path tracing rendering technology: the core idea of ray tracing rendering technology is to shoot multiple rays from the camera toward the screen pixels, use the scene management based on space division, accelerate the intersection and reflection of scene objects, and calculate the direct light source, the contribution of the indirect light source to the pixel, and finally the actual brightness.

(2) Rasterization rendering technology: rasterization technology mainly maps the triangle surface transformation in all mesh models to the screen space through perspective projection and then disassembles them into pixels and obtains the actual brightness of pixel coloring according to the scene lighting information. Ray tracing technology is a rendering framework that can solve global illumination and can bring quite realistic lighting effects, but due to the need for a large number of ray calculations, it is often only suitable for offline rendering areas. For real-time rendering, most engines still use rasterization rendering architecture. In order to improve the real-time performance of interactive characters, this article will also use rasterization rendering technology as the rendering core. According to the different processes of rasterization rendering, it can be divided into the following two categories: forward rendering and deferred rendering.

3.4. Interactive Technology. Interactive intelligent characters are often able to respond to external input, as shown in Figure 2.

The technology in which machines process external input and feedback response is called human-computer interaction. Human-computer interaction technology can be divided into the following three categories according to the development period:

(1) Input interaction based on command line interface (CLI): command line input interaction is the earliest human-computer interaction technology. The user inputs instructions through the keyboard, and the computer processes and feeds the results back.

(2) Input interaction based on graphical interface (GUI): GUI is the most common interaction mode today, and most 3D games and interactive videos use graphic interaction technology.

(3) The input interaction based on natural user (NUI) is more natural and humanized than the previous two interaction methods. The user can control or interact with the virtual character through body movements and voice information. Restricted by hardware devices, in this way, the interaction between virtual characters and real users is more natural and harmonious. as shown in Figure 2.

4. Design of 3D Animation Three-Dimensional Space Model Based on Virtual Reality

4.1. Component System Design. The core of the traditional component system is as follows:

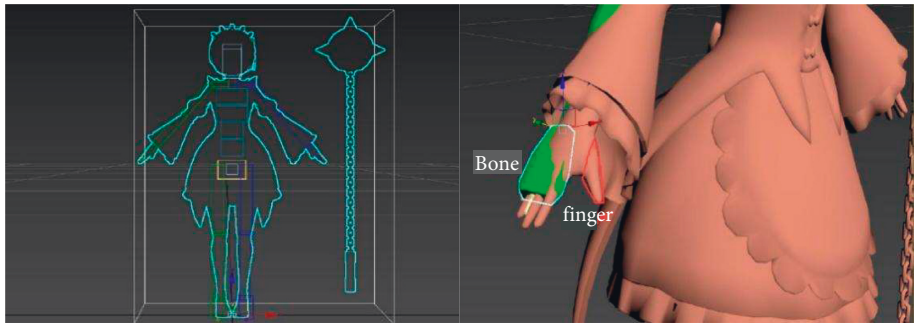

Figure 1: Bounding box view of the rig in 3 ds max.

Figure 2: The virtual human receives external input.

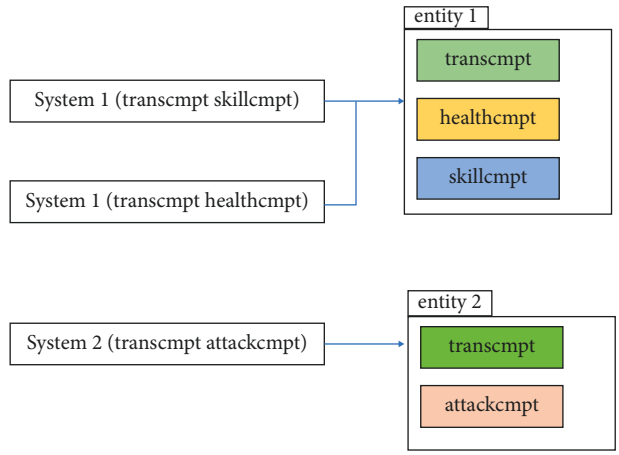

Figure 3: List of components in the system access entity.

(1) Each component inherits from a component base class and implements the Update function in the base class.

(2) There is a component list inside the entity class, which directly stores the base class component pointer. If the entity of the traditional component system is accessed through the System, the System will traverse the component list in the entity to determine whether it has all the required components, as shown in Figure 3.

In this working mode, the component data pointed to by the pointer is discrete. When the System operates a large number of entities, the Cache hit rate is not high, causing frequent page replacement and even page "jitter." In order to store component data in contiguous space as much as possible, all components of all entities are placed in a contiguous memory block. In this version, the data between entities is discrete, which will reduce the Cache hit efficiency when operating a large number of entities. Since the separation of data and operation functions is achieved, the data should be stored continuously, as shown in Figure 4.

As shown in Figure 4, the same components of all entities are stored together, but, for example, Entity2 does not contain the HealthCmpt component, while Entity1 and Entity3 do not contain the AttackCmpt component. When all the entity components are stored together, there will be gaps, making the entity and the corresponding component data. Location relationships are not easy to manage. Therefore, a better method is to put the component data of entities with "similar components" in an Archetype, as shown in Figure 4. Entity is only used as an index pointing to the Archetype to indicate the location of the data contained in the entity in memory. There is a memory pool implementation in Archetype, and each block of memory is divided into a fixed size, which is convenient for memory alignment and improves the efficiency of continuous data reading, specifically as shown in Figure 5.

Component addition or deletion is an important function of ECS. The operation process design is shown in Figure 6.

4.2. Local Coordinate System Transfer Design. Many 3D animation engines, including 3 ds Max, Unity, and Unreal, build scenes through SceneGraph. SceneGraph is a multifork tree that records the parent-child relationship between scene nodes. In the engine, the transform of the parent node property changes that affect child nodes is called parent-child pose transfer. The effect of the translation operation on subsequent nodes is very intuitive. Only the translation transformation of the parent node is directly applied to the child nodes, as shown in Figure 7.

But when it comes to the rotation and scaling of the parent and child classes, the child class will appear in an unbelievable shape, as shown in Figure 8.

It can be seen that the scaling of the parent class is not directly used for the subclass objects but produces "nonequal

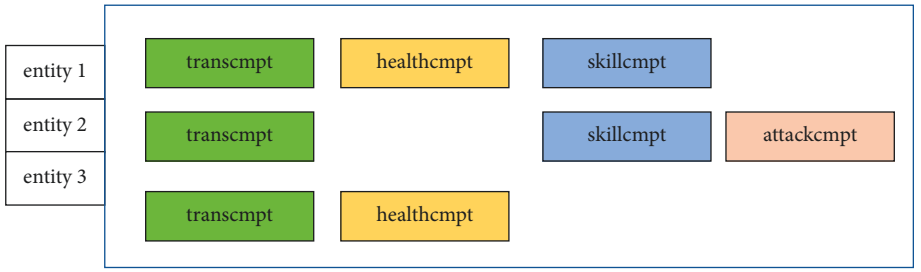

Figure 4: Contiguous storage of components.

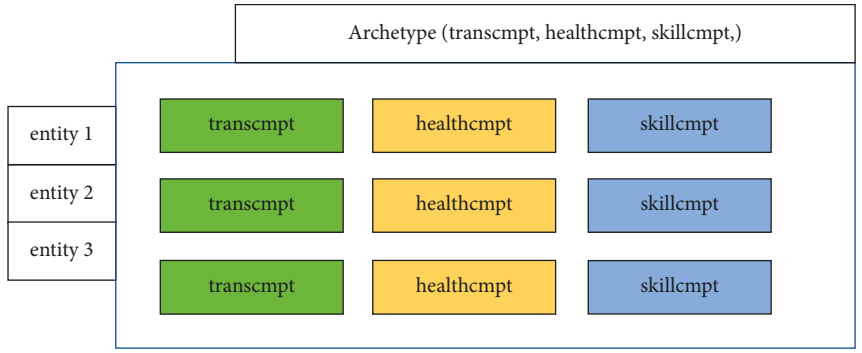

Figure 5: Centralized storage of entity with the same components.

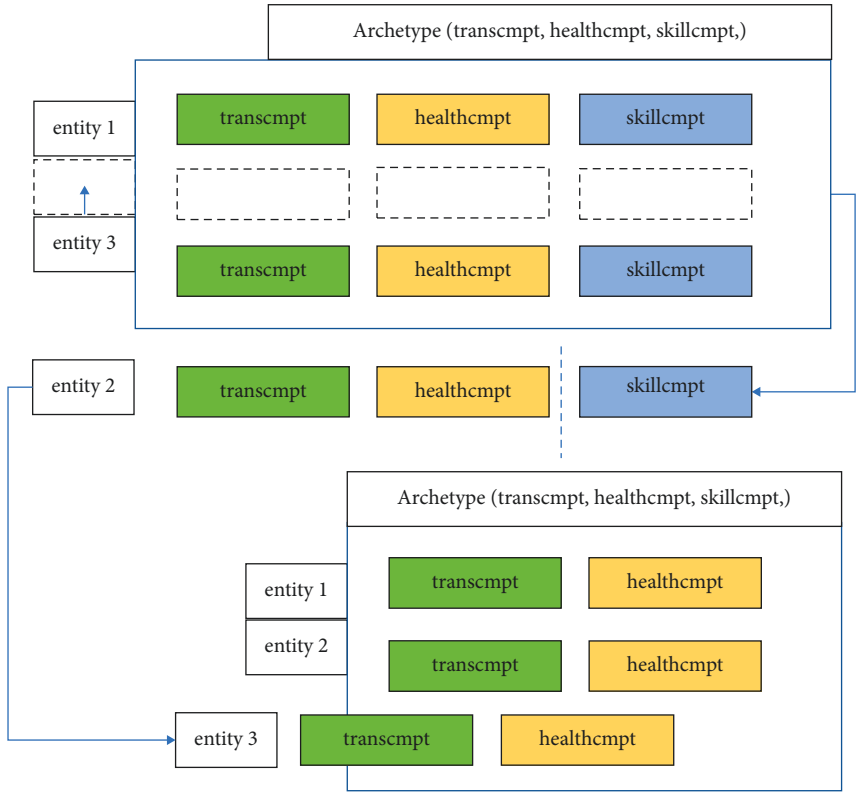

Figure 6: Component deletion process.

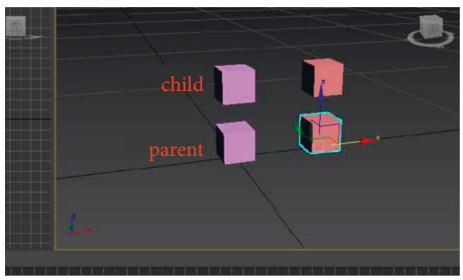

Figure 7: The effect of translation operation on parent and child nodes.

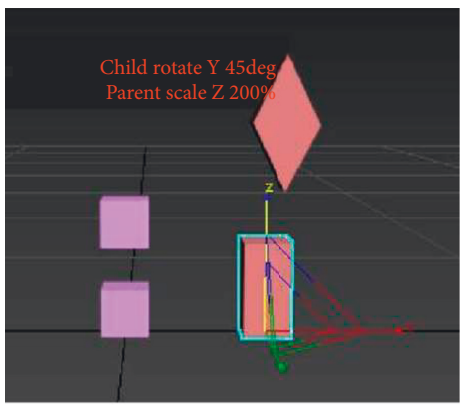

Figure 8: The effect of rotation and scaling on parent and child nodes.

scaling with angles" according to the rotation of the subclass. Nonequal scaling with an angle can be used as an example with a cube, as shown in the figure below. Double scaling with an angle of 45 degrees will result in what is shown in Figure 9.

Unequal scaling with angles can be split into two rotations and one scaling. For example, double scaling with a 45-degree angle is equivalent to the following: first rotate the coordinate system counterclockwise by 45 degrees to get the blue color shown in Figures 5–13, extend the new coordinate system to double the Y-axis direction, and then rotate the coordinate system 45 degrees clockwise to return to the original black coordinate system.

In order to store and load the scene, the basic data needs to be serialized and deserialized. Serialization and deserialization mean that all types of data are uniformly converted into binary and then stored in binary form or transmitted over the network. Relatively, when the file is read and the network is received, it is written according to the binary. The order of input is restored to the corresponding data structure.

A large amount of continuous data of the same type such as grids and animations can be read and written in binary using traditional data structures such as Vector. But sometimes it is necessary to record not only the value of the data, but also the dependencies between the data. The SceneGraph that represents the scene structure is this kind of data with dependencies, including the parent-child relationship between scene nodes and the mount relationship between entity and component. This kind of dependency obviously cannot be recorded with traditional data structures.

The data structure relationship designed in this paper is shown in Figure 10. This kind of inclusion relationship is very suitable for storing with JSON. JSON is a typical data structure that can be nested. It is very suitable for recording complex hierarchical data relationships. Many games in the market use JSON to store complex character attributes and level progress. Similarly, JSON can also be used to store the hierarchical relationship of SceneGraph. Another advantage of the JSON data structure is that it is convenient to add properties to JsonNode in the form of Key-Value, which is just suitable for storing resource indexes in material components and mesh components. There are many C++ JSON open-source libraries on GitHub. This article will use the cJSON open-source library to JSONize the scene structure. JSON data will change size according to the depth of SceneGraph, and it is also dynamic data, similar to Vector and String formats. When serializing JSON data, size is also required for reading and writing.

Through the serialization of static data and dynamic data, this study designs the following binary file structure. By storing and reading the binary file of this structure, the storage and restoration of 3D rendering scenes are basically realized, as shown in Figure 11.

4.3. Graphic Rendering Design

4.3.1. GBuffer Design. The first texture of the GBuffer can be used to record the normal information of the object. The normal may be the built-in normal of the object vertex, or the sampled normal calculated by the normal map and the surface tangent. The three-dimensional normal vector can be obtained through the text. The mentioned "normal compression formula" compresses the normal information into two dimensions. The second texture of the GBuffer can be used for the diffuse reflection color of the object. The diffuse reflection color will be obtained by sampling the diffuse reflection texture of the object material in the shader of the GBuffer. The first three channels of the four channels of RGBA are occupied, and the remaining one channel can be used to store other data. The third texture of GBuffer can be used to store special rendering information, such as Roughness (Roughness), Metalness (Metal), and masking (Ao) that may be statically baked for PBR material rendering. The last channel is used to store the RenderType, and the subsequent lighting processing stage will decide which lighting model to call for rendering based on the RenderType of the vertex. Since an object is basically not rendered by two different lighting models at the same time, the meaning of each channel will change with the RenderType. For example, when performing NPR rendering, it may be written into the MetalRoughAo texture, Emmisive, Shadow, equal coefficient. The sizes of the Gbuffer parts are as follows, totaling 80 bytes, as shown in Table 1.

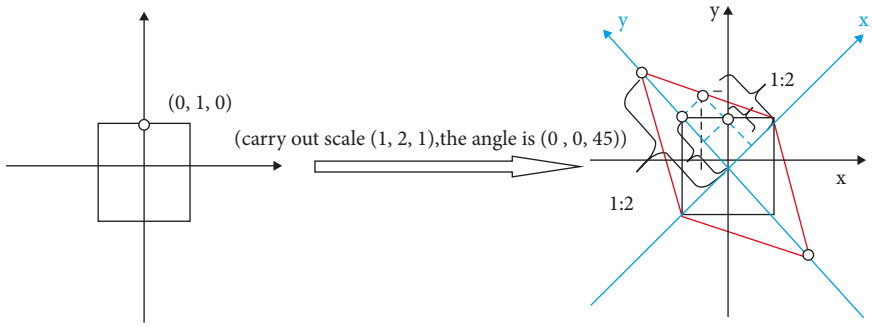

Figure 9: Unequal scaling with angles.

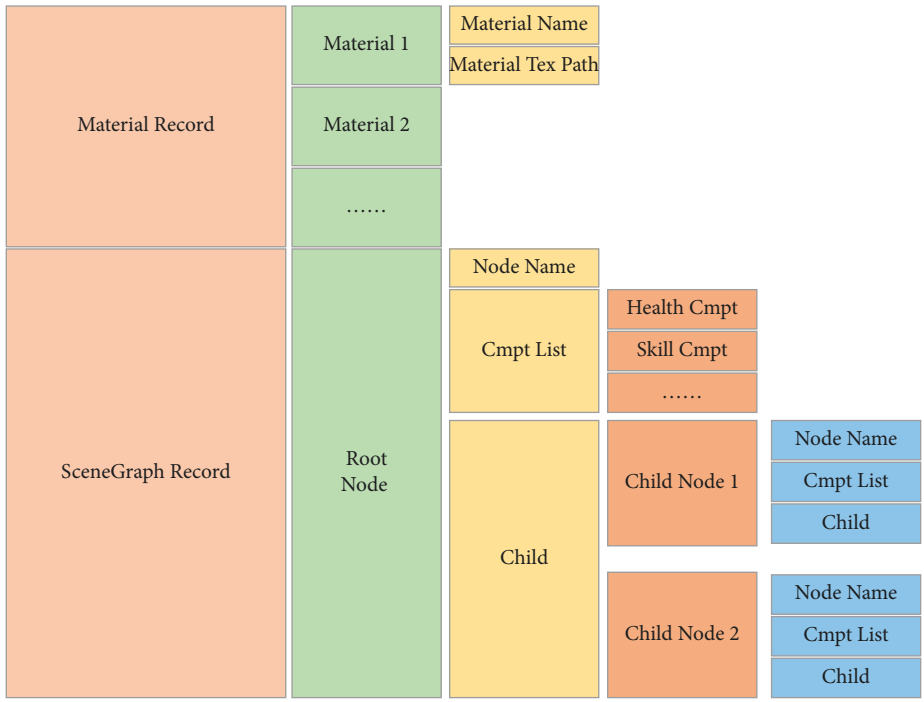

Figure 10: Inclusion relationship of scene data.

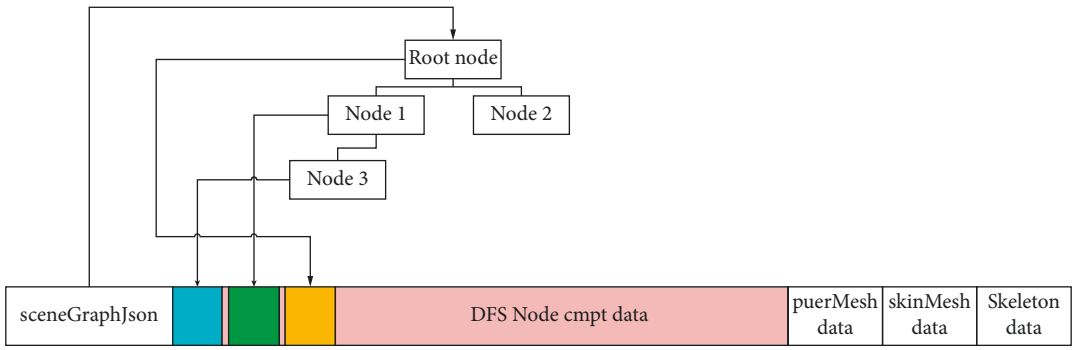

Figure 11: Data structure of binary archive.

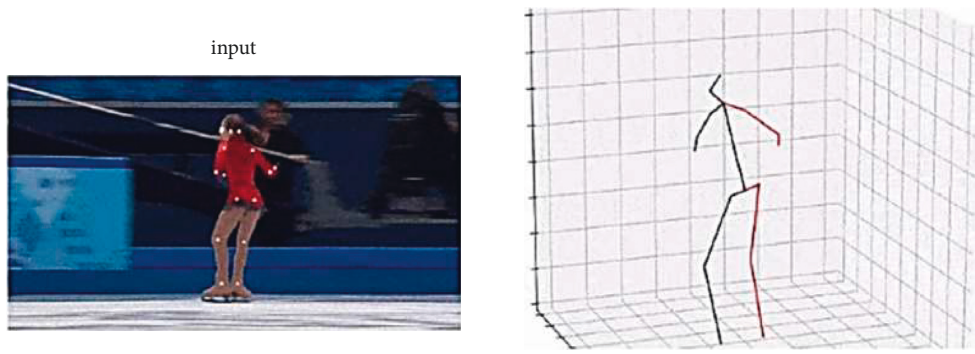

Figure 12: VideoPose3d recognition renderings (officially provided).

Figure 13: Test sample FBX file.

Table 1: GBuffer structure diagram.

4Byte	4Byte	4Byte	4Byte
Normal.X	Normal.Y	—	—
Albedo.R	Albedo.G	Albedo.B	Padding
Metal	Roughness	Occlusion	RenderType

4.3.2. Construction of Deferred Rendering Pipeline. First, we set the rendering target as a screen-sized texture, judge the lighting rendering model to be called according to the A channel data RenderType stored in the GBuffer, read other required parameters from the GBuffer, and perform lighting calculations. Subsequent forward rendering image post-processing can be performed to process some objects with transparency, but obviously, transparent objects cannot be rendered between front objects, which is even the disadvantage of delayed rendering [22].

4.4. Animation System Design. VideoPose3d is an open-source video input 3D pose estimation library, which is different from using the depth camera Kinect for 3D pose estimation. The library only needs the video data provided by the nondepth camera and processes the input video through a neural network to obtain coordinate estimation of 3D joint points. This chapter attempts to combine this neural network with 3D character animation, so that 3D characters have the interactive ability of action simulation.

The VideoPose3d model was presented as a paper at Facebook's 2019 Conference on Computer Vision in Pattern Recognition (CVPR). It has been open sourced on GitHub. Different from the traditional learning model based on joint point detection, this model uses the two-dimensional key points of the video frame as the input stream to perform time series convolution, so as to train to recognize the three-dimensional pose in the video, validated on the Human36 m dataset with good results. Another reason for choosing VideoPose3d is because the model provides a semi-supervised learning method for unlabeled video, by predicting the 2D key points of the unlabeled video, then estimating the 3D pose, and projecting the 3D pose to the 2D pose in reverse by passing in the camera parameters.

5. Analysis of Experimental Results

5.1. Test Environment and Tools. This article uses Windows 10 as the test operating system and uses Microsoft's C++ development environment Visual Studio 2019 for engine development. Vs 2019 provides a wealth of extension plug-ins, and you can download the HLSL syntax highlighting tool to improve the efficiency of Shader programming. In order to use the DirectX12 graphics development interface, the DirectX12 SDK needs to be installed, but most of the current Windows 10 SDK integrates the DirectX12 development environment. If the operating system includes it, you can write code directly without additional configuration. Part of the interface is written by Qt5.12.2. Qt's.ui file needs to be precompiled by Qt's built-in compiler, so the computer must install the corresponding version of Qt. The entire project is compiled and built through CMake, which is convenient to adapt to different versions of the Vs development environment.

5.2. 3D Animation Stereo Space Test. Take the FBX file below as a test example and refer to the running action around frame 180. Next, we will import the FBX into the engine for testing.

Figure 14: The test sample FBX file is imported into the engine of this subject and assigned to the material.

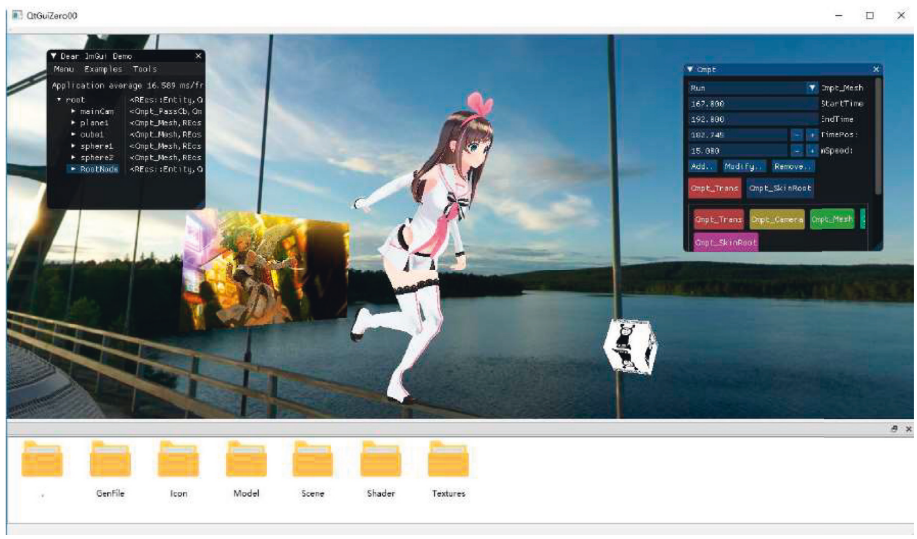

Figure 15: Comparison of running actions of the same keyframes in the engine.

The running action of about 180 frames imports the FBX into the engine and sets the material to paste the texture on the model. The effect is as shown in Figure 13.

Comparing Figures 13 and 14, it is shown that the engine basically uses the material function to restore the character image. Next, adjust the time axis of the Cmpt_SkinRoot component of the color correction root node to around 180 frames, and the following effects can be obtained.

It can be seen from Figure 15 that the FBX animation data analysis of the animation system in this study shows that the transformation of the local coordinate system of the bones is normal, and the simultaneous animation effect in 3 ds Max is restored. The end result is a demonstration of skeletal skinning techniques and a reproduction of the same animation system as 3dx Max's internal poses.

6. Conclusion

The advent of the digital age has had varying degrees of impact on all aspects of our lives. It has also had a great impact on art and even animation scene design. From the many breathtaking special effects in TV films and digital 3D animations that rely entirely on digital media, the powerful influence of digital technology is vividly displayed. The core purpose of this paper is to build a 3D character display platform based on DirectX12. In order to realize the display of 3D characters, the basic data required for 3D character display is firstly displayed, and then the related programming of DirectX12 is carried out around the acquisition and conversion of these data. In the development of the engine, the functions and architectures of many existing engines and open-source engines were referenced to design the various modules of the engine.

Data Availability

The dataset can be accessed upon request.

Conflicts of Interest

The authors declare that they have no conflicts of interest.

References

[1] M. Speicher, S. Cucerca, and A. Krüger, "VRShop," *Proceedings of the ACM on Interactive, Mobile, Wearable and Ubiquitous Technologies*, vol. 1, no. 3, pp. 1–31, 2017.

[2] T. Raffaillac and S. Huot, "Polyphony: programming interfaces and interactions with theEntity-component-system model," in *Proceedings of the ACM on Human-Computer-Interaction*, HAL, Valencia, Spain, June 2019.

[3] H. C. Park and N. Baek, "Design of selfengine: a lightweight game engine," *InformationScience and Applications*, Springer, New York, NY, USA, 2019.

[4] A. Razzaq, Z. Wu, M. Zhou, S. Ali, and K. Iqbal, "Automatic conversion of human mesh into skeleton animation by using Kinect motion," *International Journal of Computer Theory and Engineering*, vol. 7, no. 6, pp. 482–488, 2015.

[5] F. Bogo, A. Kanazawa, C. Lassner, P. Gehler, J. Romero, and M. J. Black, "Keep it SMPL: automatic estimation of 3D human pose and shape from a single image," in *Proceedings of the European ConferenceComputer Vision - ECCV*, pp. 561–578, Springer, Amsterdam, The Netherlands, October 2016.

[6] M. R. I. Hossain and J. J. Little, "Exploiting temporal information for 3d pose estimation," in *Proceedings of the European Conference on Computer Vision (ECCV)*, Springer, Germany, UK, August 2018.

[7] S. Park and N. Baek, "A shader-based ray tracing engine," *Applied Sciences*, vol. 11, no. 7, p. 3264, 2021.

[8] R. A. Pavlik, *Enabling Natural Interaction for Virtual Reality*, Iowa State University, Ames, US, 2014.

[9] J. Tompson, R. Goroshin, A. Jain, Y. Lecun, and C. Bregler, "Efficient object localization using ConvolutionalNetworks," in *Proceedings of the 2015 IEEE Conference on Computer Vision and Pattern Recognition (CVPR)*, IEEE, Boston, MA, USA, June 7- 12 2015.

[10] F. Kistler, B. Endrass, I. Damian, C. T. Dang, and E. André, "Natural interaction with culturally adaptive virtual characters," *Journal on Multimodal User Interfaces*, vol. 6, no. 1-2, pp. 39–47, 2012.

[11] P. Varcholik, *Real-Time 3D Rendering with DirectX and HLSL*, Addison-WesleyProfessional, Boston, MA, USA, 2014.

[12] W. Culbertson, *3ds Max Basics for Modeling Mideo game Assets:Volume 2: Model, Rigand Animate Characters for Export to Unity or Other Game Engines*, CRCPress, Boca Raton, FL, USA, 2021.

[13] C. Rudolph, *A Framework for Example-Based Synthesis of Materials for Physically BasedRendering*, Technische Universitat chemintz, Chemnitz, Germany, 2019.

[14] T. Pfister, J. Charles, and A. Zisserman, "Flowing ConvNets for Human Pose Estimation inVideos," *Computer Vision and Pattern Recognition*, vol. V2, Article ID 02897, 2016.

[15] D. Pavllo, C. Feichtenhofer, D. Grangier, and A. Michale, "3D human pose estimation in video withtemporal convolutions and semi-supervised training," in *Proceedings of the IEEE/CVF Conference on Computer Vision and Pattern Recognition (CVPR)*, CVF, Long Beach, CA, USA, June 2019.

[16] M. D. McIllroy, "Mass produced software components," in *Proceedings of the NATO Conference in Software Engineering*, Scientific Research, Rome, Italy, October 1969.

[17] J. Gubata, *Process Design Requirements -- Research Starters Business*, vol. 16, no. 11-12, pp. 1–13, 2008.

[18] S. Corsaro and J. Clifford, *Parrott. Hollywood 2D Digital Animation: The New Flash Production Revolution*, Course Technology PTR, Boston United States, 2004.

[19] P. Ratner, *3-D Human Modeling and Animation*, Wiley, Hoboken, NJ, USA, 3rd edition, 2009.

[20] B. Burns, *Manufacturing Systems Design -- Research Starters Business*, OAK Ridge National Laboratory, OAK Ridge, TN, USA, 2008.

[21] E. Michael and B. Erbschloe, *Reconfigurable Agile Manufacturing -- Research Starters Business*, Boston, MA, USA, 2009.

[22] A. Wienclaw Ruth, *Engineering Statistics for Manufacturing Systems -- Research Starters Business*, Cranfield University, Cranfield, England, 2008.

Hindawi
Scientific Programming
Volume 2022, Article ID 5747974, 13 pages
https://doi.org/10.1155/2022/5747974

Research Article

Quantitative Inversion Model Design of Mine Water Characteristic Ions Based on Hyperspectral Technology

Yunbo Li [1,2]

[1]*State Key Laboratory of the Gas Disaster Detecting, Preventing and Emergency Controlling, Chongqing 400037, China*
[2]*China Coal Technology and Engineering Group Chongqing Research Institute, Chongqing 400039, China*

Correspondence should be addressed to Yunbo Li; liyunbo@cqccteg.com

Received 4 June 2022; Revised 7 July 2022; Accepted 11 July 2022; Published 1 August 2022

Academic Editor: Lianhui Li

In view of the problems of low measurement accuracy and repeated calibration during the use of coal mine water quality analysis, the hyperspectral reflection noncontact measurement technology was proposed to solve the existing problems. KCl, NaCl, pH, $NaHCO_3$, and $CaCl_2$were used to indicate the characteristic ion information of Na^+, K^+, Ca^{2+}, Cl^-, HCO_3^-, and pH mine water in the laboratory, and 2220 spectral data were obtained by spectral determination. Savitzky–Golay convolution smoothing was used to smooth and denoise the original spectral data of each ion, and the relationship between the spectrum and the concentration of each reagent was obvious after smoothing and denoising pretreatment. The principal component regression method was used to build the inversion model of each ion content, and through the modeling study, the prediction set of KCl was found: the coefficient R^2 reaches 0.907, RPD is up to 2.7; the prediction set of NaCl was found: the coefficient R^2 reaches 0.957, RPD is up to 3.1; the PH prediction set was found: the coefficient R^2 reaches 0.785, RPD is up to 2.1; the prediction set of NaHCO3 was found: the coefficient R^2 reaches 0.137, RPD is up to 1.2; the prediction set of CaCl2 was found: the coefficient R^2 reaches 0.622, and RPD is up to 1.7. The results show that the hyperspectral method can play a better role in the extraction of K^+, Cl^-, Na^+, Ca^{2+}, and pH. It is difficult to extract HCO_3^- ions.

1. Introduction

Water hazard is one of the main threats to the safety of coal mine production, which causes serious loss of life and property. The prevention and control of water disaster in coal mines take water filling channel, water filling source, and water filling intensity as the main objects and take exploration, prevention, blocking, dredging, drainage, interception, and monitoring as the main means. Water samples are collected after water inrush or water gushing occurs in a mine, and the source of the water inrush or water gushing is judged by using the chemical composition of the water. It is a method widely used by technicians of geological survey and water control engineering in coal mines.

In foreign countries, the rock mass structure of coal seam floor and the prevention and drainage technology have been studied in depth, and a lot of experience has been accumulated in the mechanism of water inrush and the identification of water hazards. In the book Hydrogeochemistry written by Clevers et al., the application of groundwater pollution and chemical evaluation in hydrochemical analysis is systematically discussed from the perspective of hydrogeochemistry [1–4]. Clevers et al. obtained it by using the 3D edge detection seismic attribute method [1–4]. Clevers et al. used hydrological observation and a tracer test to test the effect of the tunnel drainage system [1–4]. However, there is little research work on the application of mine water chemistry and the identification of mine water inrush sources.

The main method of discriminating the source of water inrush in coal mines in China is the conventional hydrochemical discrimination method. By measuring the eight most widely distributed ions in groundwater, such as Ca^{2+}, Mg^{2+}, K^+, Na^+, $CO3^{2-}$, HCO_3^-, $SO4^{2-}$, and Cl^-. Its concentration accounts for more than 90% of the total ion concentration in groundwater, as well as the characteristic ion ratio, hardness, temperature, TDS index, and pH value [5–10]. The mine water chemical data of Taoyuan Coal Mine

was processed by using Piper's three-line diagram [5–7]. The hydrochemical characteristics of each aquifer in the Xuzhou mining area were introduced [8, 9]. Conventional hydrochemical methods were used to carry out hydrogeochemical analysis of underground aquifers in a mine in Xuzhou [10–12]. The conventional hydrochemistry of four water-bearing subsystems in Yaoqiao Mine, Xuzhou, was studied [13–16]. A systematic study on the hydrochemical characteristics of groundwater in the Ordovician karst aquifer in the middle part of the Taihang Mountains was made [17–20]. The Chongqing Research Institute of China Coal Science and Technology Group, Beijing Huaan Auto, and Wuhan Dida Huarui have carried out relevant research on water quality analysis technology and equipment and have applied it in various coal mine groups [21–29].

However, there are still some problems in the current underground ion electrode monitoring, such as inaccurate measurement and repeated calibration during use, which cannot meet the needs of online identification of water sources. It is urgent to develop a new type of online water quality analysis sensors.

2. Hyperspectral Experimental Determination of Common Ions in Mine Water

The purpose of the experimental test is to find the hyperspectral characteristic band of the liquid related to the coal mine. The experimental spectral acquisition equipment is a self-made spectral probe, and the experimental measurement process is composed of three parts of spectrometer calibration, standard solution production, spectral measurement, and accuracy evaluation [30].

Five reagents, NaCl, KCl, $CaCl_2$, $NaHCO_3$, and pH buffer, were measured to indicate Na^+, K^+, Ca^{2+}, Cl^-, HCO_3^-, and pH ion information, wherein the potassium ion and the chloride ion are indicated by KCl standard solution for a set of data (see Table 1 for details) [31–33]. Before measurement, the mother liquor is diluted with deionized water, and according to the test requirements, the sodium ion, potassium ion, chloride ion, and calcium ion dilution levels are 10, 50, 100, 500, 1000, and 10000 mg/L, the carbonate dilution levels are 0.44, 2.2, 4.4, 22, 44, and 440 mg/L, and the pH dilution levels are 4, 6.86, and 9.18. According to the order of KCl, NaCl, pH, $NaHCO_3$, $CaCl_2$, pure water, empty barrel, and green plants, 8 kinds of targets were measured, totaling 2220 hyperspectral data. Figure 1 shows the number of spectra of various standard solutions.

3. Ion Hyperspectral Data Preprocessing and Sensitive Band Selection

We carry out spectral quality evaluation on all obtained spectral data and select qualified spectral data [34–37]. At the same time, due to the influence of the external environment, there are many "burr" noises on the spectral curve, so it is necessary to reduce the noise on the spectral curve after smoothing and filtering. In this study, Savitzky–Golay convolution smoothing was used to smooth and denoise the original spectral data of each ion. The value of the spectrum after Savitzky–Golay smoothing at wavelength I is

$$x_{i,\text{Savitzky–Golay}} = \frac{\sum_{j=-m}^{m} c_j x_{i+j}}{N}. \quad (1)$$

In the formula, $x_{i,\text{Savitzky–Golay}}$ is the smoothed value at the wavelength I, x is the value before smoothing, m is the number of smoothing windows on the wavelength side, N is the normalization index, and $\sum_{j=-m}^{m} c_j$ is the smoothing coefficient, which can be obtained by polynomial fitting.

After smooth denoising pretreatment, the relationship between the spectrum and the concentration of each reagent is evident. Compared with the spectral data of "pure water + gradient" concentration, KCl, NaCl, pH, $NaHCO_3$, and $CaCl_2$ have obvious sensitive bands and rules. The higher the concentration of KCl, NaCl, and $CaCl_2$, the lower the overall reflectivity, which should be the mechanism under the action of Cl^-. The pH data show that the reflectivity of pure water and acidic liquid is in the middle. The reflectivity of neutral liquid is low and that of alkaline liquid is the highest. As a whole, the higher the concentration of $NaHCO_3$, the higher the reflectivity. Figure 2 shows the comparison of the KCl, NaCl, and pH spectral data before and after denoising, while Figure 3 shows the comparison of the spectral data of $NaHCO_3$, $CaCl_2$, and pure water before and after denoising.

4. Establishment of the Quantitative Inversion Prediction Model for Ion Hyperspectral Data

The mine water is a complex system composed of various chemical ions in the water. In this study, the principal component regression (PCR) method is used to establish the quantitative inversion model, which is based on principal component analysis (PCA) [38–46]. PCA is a multiple collinearity regression analysis method. The principle is that after the multicollinearity in the regression model is eliminated by the principal component analysis method, the principal component variables are used as independent variables for regression analysis, and then, the original variables are substituted back into the new model according to the score coefficient matrix.

The basic steps of PCA are as follows:

(1) The aim is to acquire a principal component of independent variable data through principal component analysis and select a principal component subset through standardized classification.

(2) The principal component obtained in step (1) is used as a new independent variable, and an estimated regression coefficient vector is obtained through linear regression analysis (the dimension is equal to the number of the selected principal components).

(3) We transform the regression coefficient vector into the proportion of the actual independent variables and use the selected PCA load (corresponding to the eigenvector of the selected principal component) to

Table 1: Standard solutions of five ions.

No Reagent	Sodium ion NaCl	Potassium ion KCl	Chloride ion	Calcium ion $CaCl_2$	Carbonate $NaHCO_3$	pH pH buffer
1	10	10	10	10	0.44	4
2	50	50	50	50	2.2	6.86
3	100	100	100	100	4.4	9.18
4	500	500	500	500	22	—
5	1000	1000	1000	1000	44	—
6	10000	10000	10000	10000	440	—

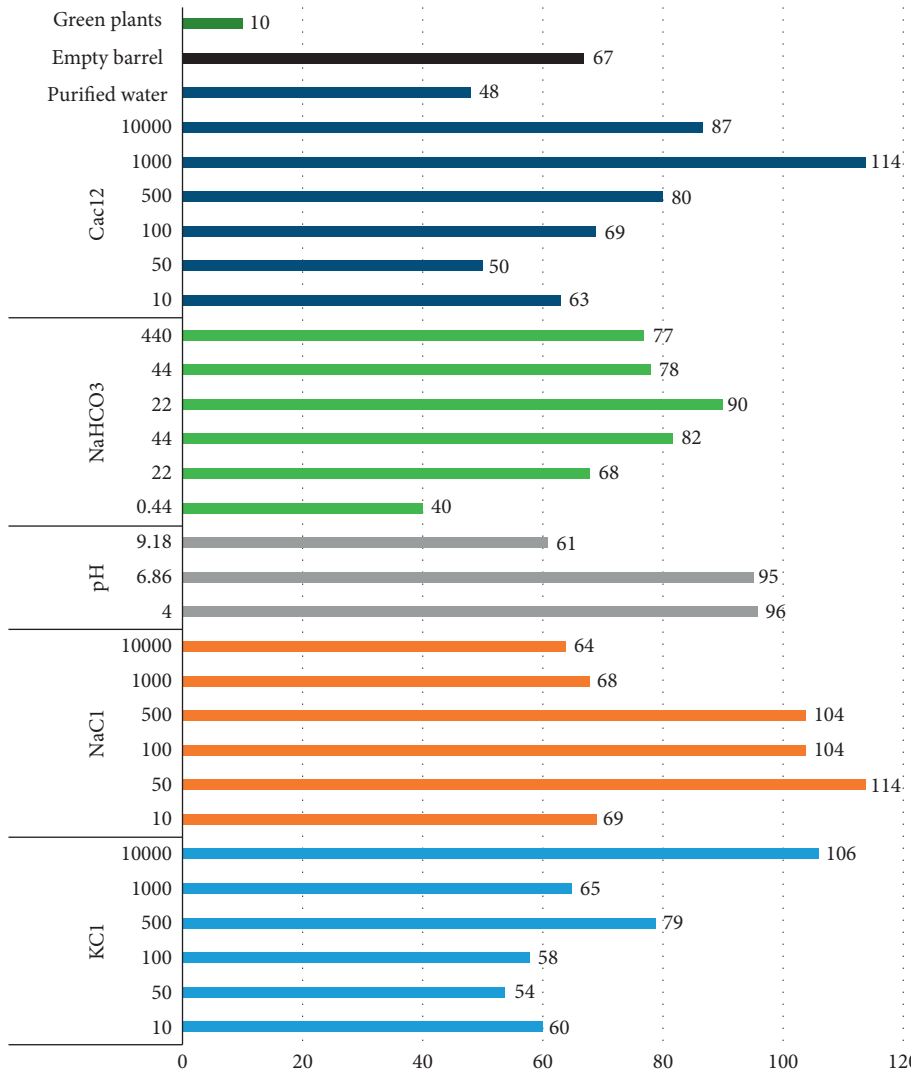

Figure 1: The number of spectra of various standard solutions.

obtain the final PCR estimator (dimension equal to the total number of independent variables) for estimating the regression coefficients.

For model evaluation, cross-validation was used to evaluate the model, and determination coefficients (R^2 and root mean of squared error (RMSE) were selected. The RMSE and relative percent deviation (RPD) were used as evaluation indexes. When the R^2 value of the calculated validation set is closer to 1, the RMSE value is lower, and when the RPD value is closer to 2, the model is more stable, the accuracy is higher, and the model is better. When R^2 is less than 0.50 and RPD is less than 1.40, the estimation ability of the model to the sample is poor, and the model is not available; $0.50 < R^2 < 0.75$ and $1.40 < \text{RPD} < 2.00$, the estimation ability of the model to the sample is improved, but only rough estimation can be made, and the model is available. When $R^2 > 0.75$ and $\text{RPD} > 2.00$, the model accuracy is high, the model is good, and the calculation formula is

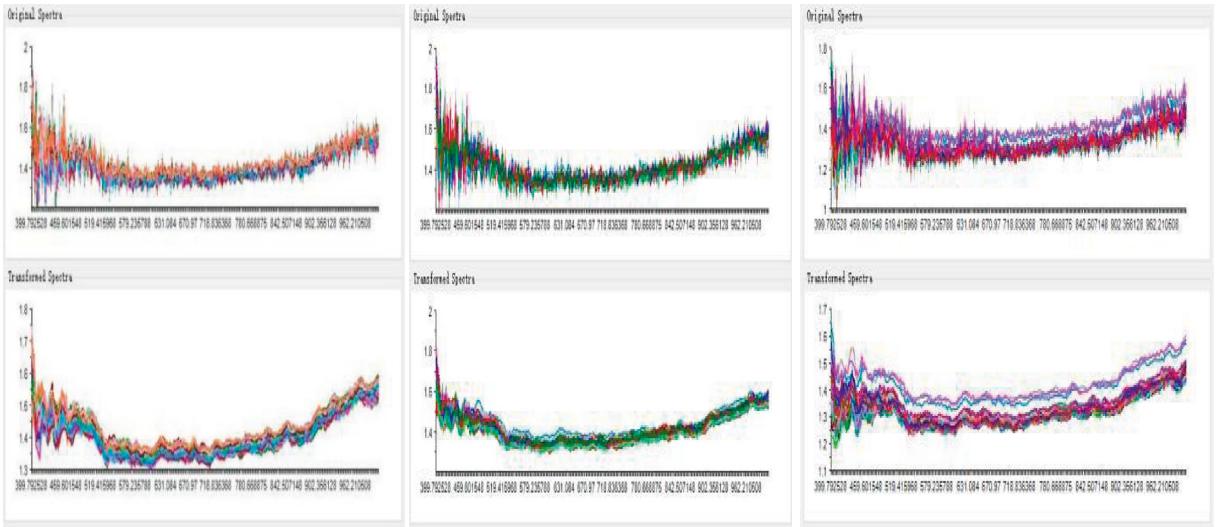

Figure 2: Comparison of the KCl, NaCl, and pH spectral data before and after denoising.

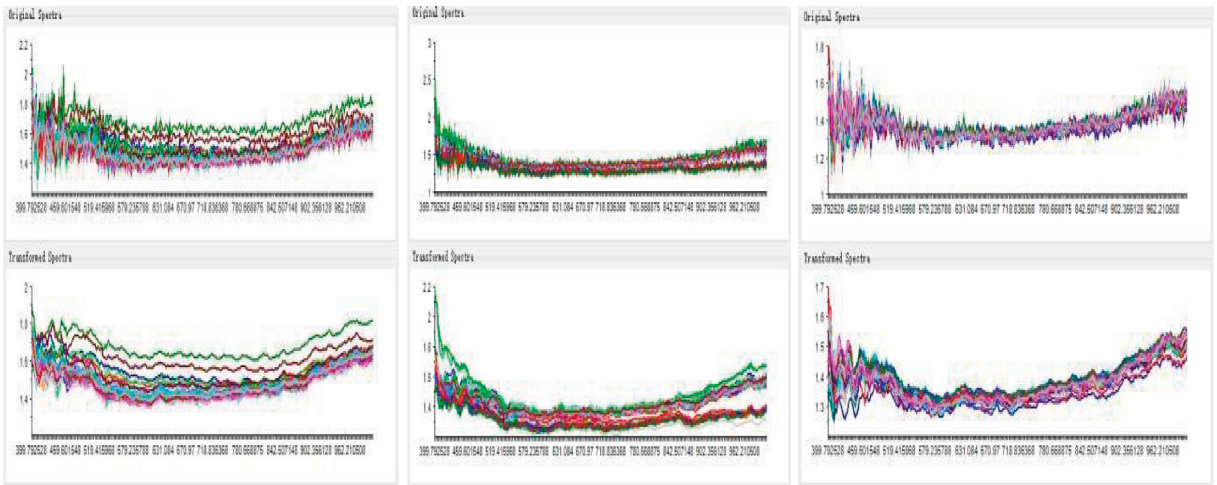

Figure 3: Comparison of the spectral data of $NaHCO_3$, $CaCl_2$, and pure water before and after denoising.

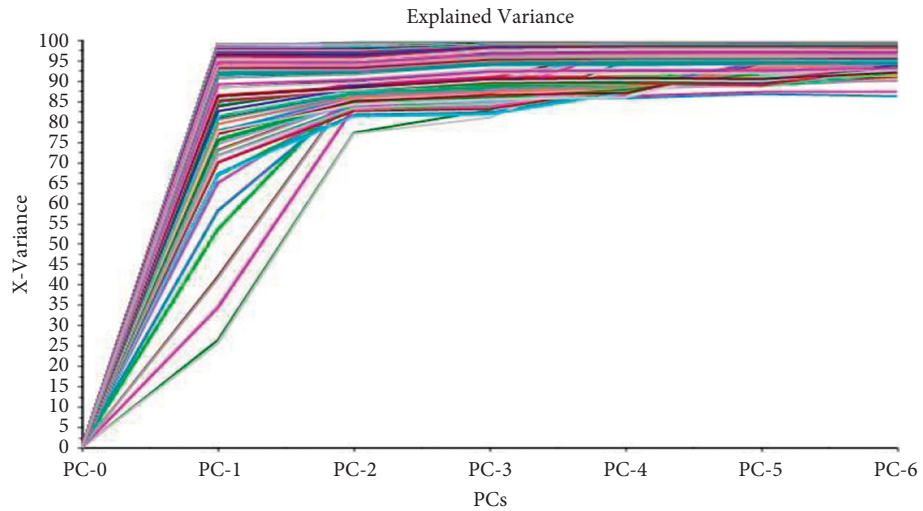

Figure 4: KCl principal component results.

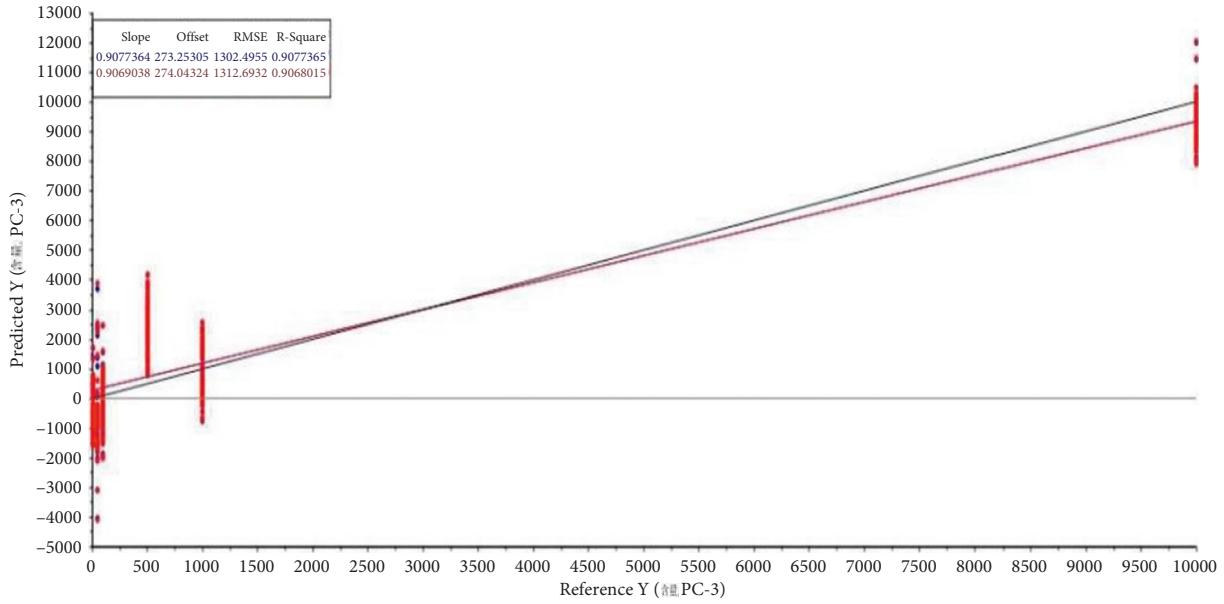

Figure 5: Comparison between the KCl actual measurement set and prediction sets.

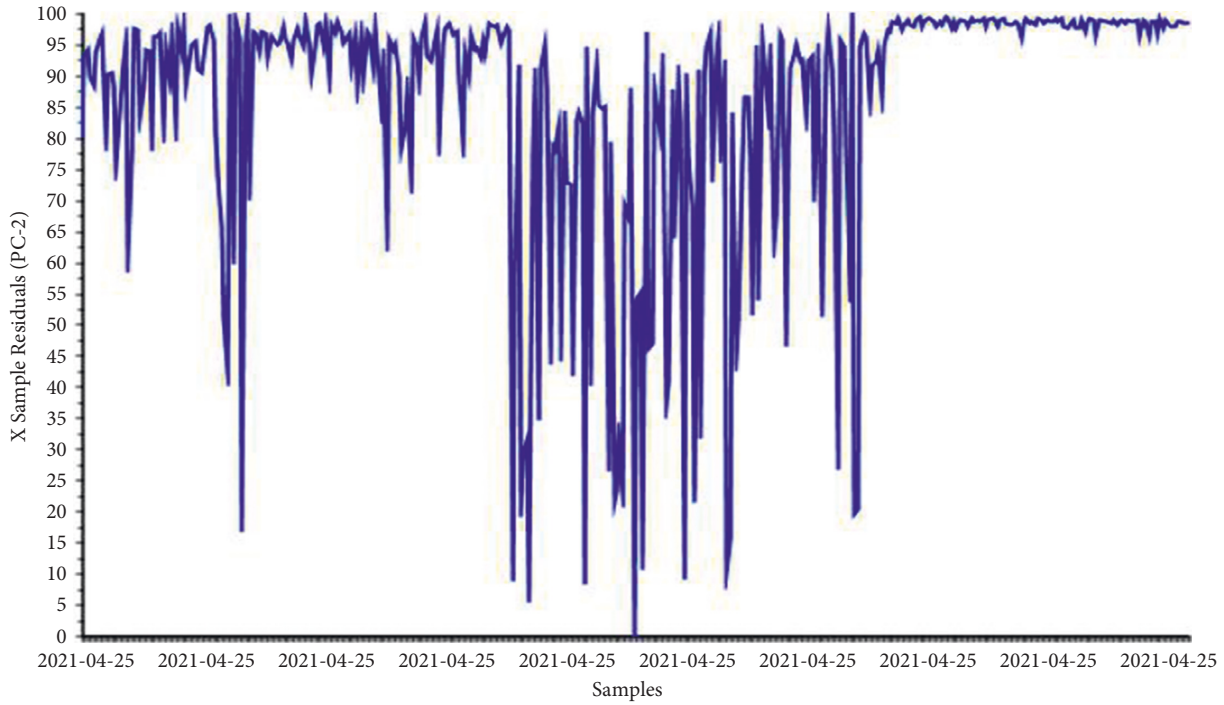

Figure 6: The role of sample points in the calculation of KCl content.

$$R^2 = 1 - \frac{\sum_{i=1}^{n} \left(y_i - y^{\Delta}\right)^2}{\sum_{i=1}^{n} \left(y_i - y^{-}\right)^2}, \tag{2}$$

$$\text{RMSE} = \sqrt{\frac{1}{n} \sum_{i=1}^{n} \left(y_i - y_i^{\Delta}\right)^2}, \tag{3}$$

$$\text{RPD} = \frac{SD}{\text{RMSE}}. \tag{4}$$

In the formula, y_i represents the measured value of the sample I, y_i^{Δ} represents the predicted value of the sample I, y^{-} represents the mean of all samples, n is the number of samples, and SD is the standard deviation of the measured values of the validation set samples.

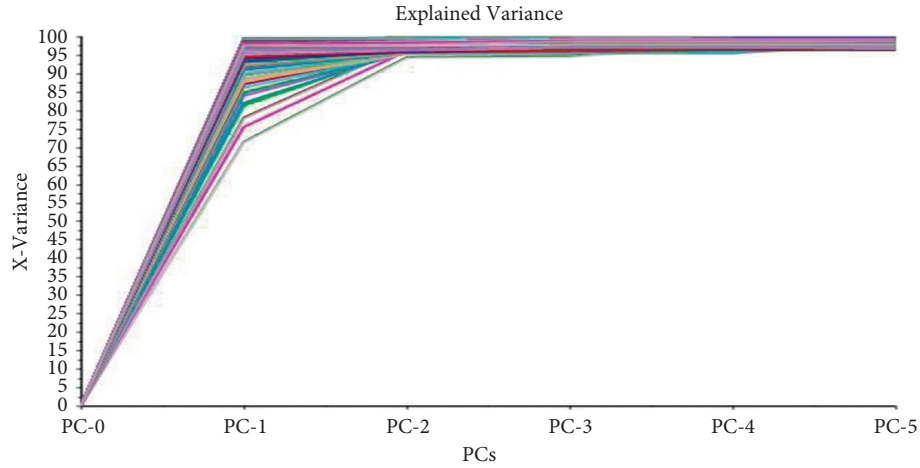

Figure 7: NaCl principal component results.

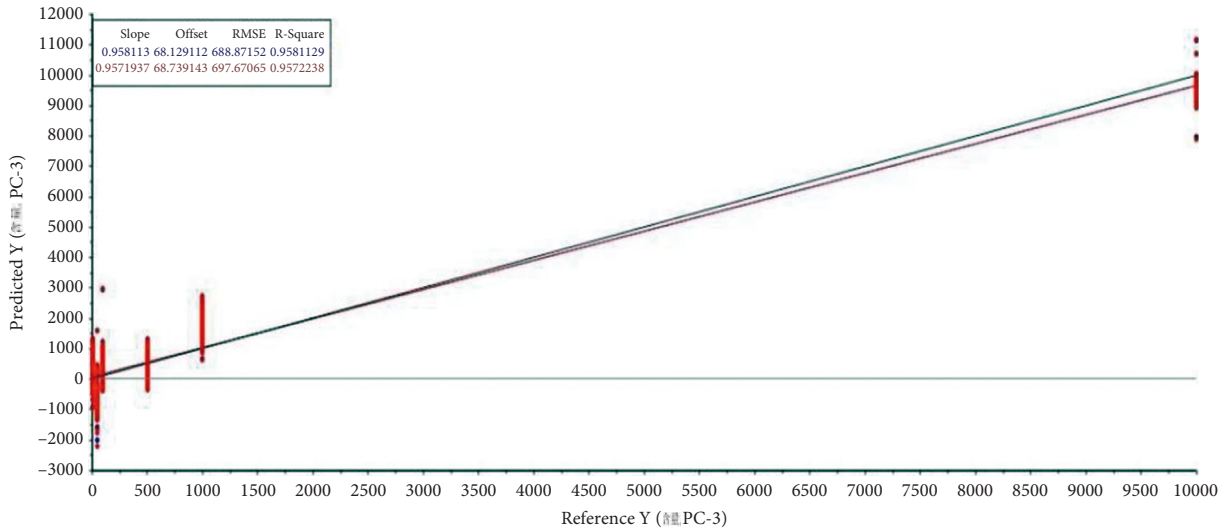

Figure 8: Comparison between measured and predicted NaCl sets.

4.1. KCl Content Spectral Prediction Modeling. 382 standard solution spectral data were selected, the largest 7 principal components were selected, and the weights were set equally [47–51]. CV prediction detection, cross-validation, and the principal component analysis model were established when the proportion of the validation set and modeling set was 0.70. The first three principal components can represent more than 80% of the content information. In the modeling set, the coefficient reaches R2 which reaches 0.908, and in the prediction set, the coefficient reaches R2 which reaches 0.907, and RPD is up to 2.7. In the process of computational modeling, the importance of all sample points and the samples collected in the middle section play a greater role. Figure 4 shows the KCl principal component results, Figure 5 shows the comparison between the KCl actual measurement set and prediction sets, and Figure 6 shows the role of sample points in the calculation of KCl content.

4.2. NaCl Content Spectral Prediction Modeling. Three hundred and ninety-nine standard solution spectral data were selected, the largest seven principal components were selected, and the weights were set equally [47–51]. CV prediction detection, cross-validation, and the principal component analysis model were established when the proportion of the validation set and the modeling set was 0.70. The first three principal components can represent more than 90% of the content information. In the modeling set, the coefficient reaches R2 which reaches 0.958, and in the prediction set, the coefficient reaches R2 which reaches 0.957, and RPD is up to 3.1. In the process of computational modeling, the importance of all sample points and the samples collected in the middle section play a greater role. Figure 7 shows the NaCl principal component results, Figure 8 shows the comparison between measured and predicted NaCl sets, and Figure 9 shows the role of sample points in the calculation of NaCl content.

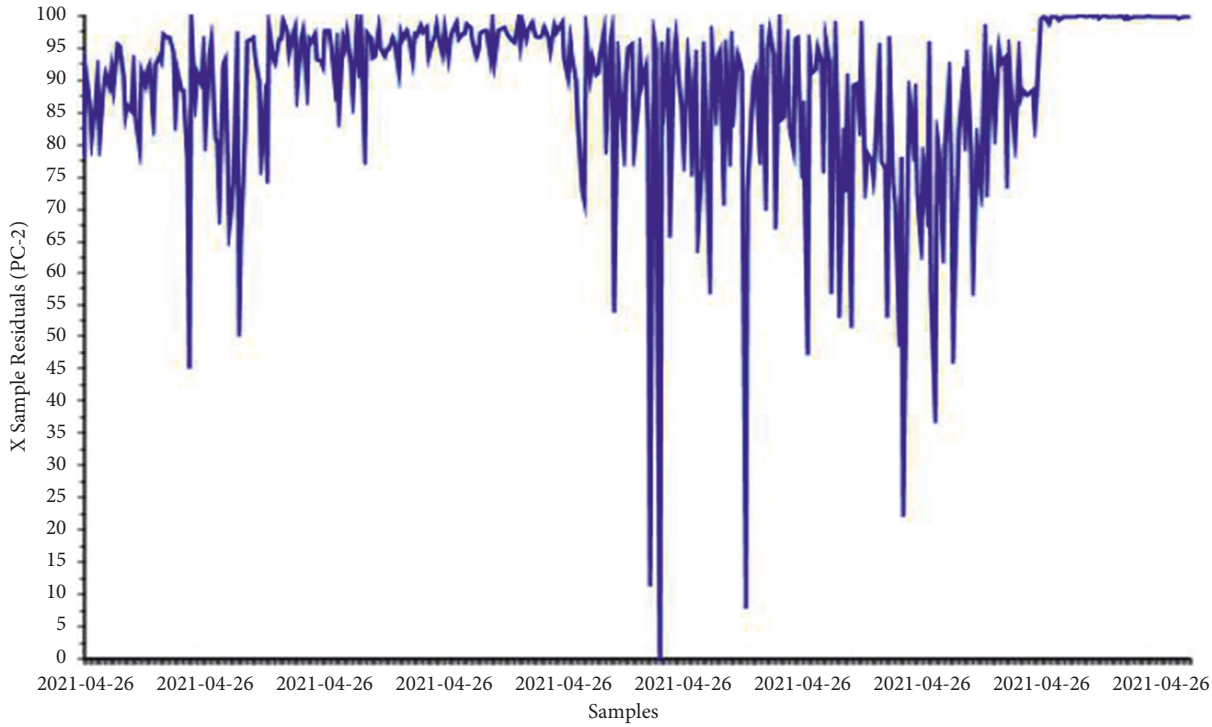

Figure 9: The role of sample points in the calculation of NaCl content.

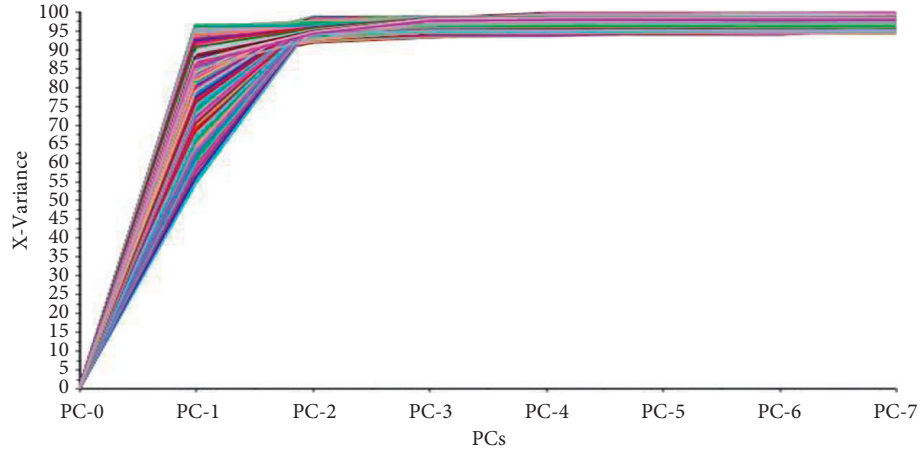

Figure 10: pH principal component results.

4.3. pH Content Spectral Prediction Modeling. 240 spectral data of standard solution were selected, the largest 7 principal components were selected, and the weights were set equally [47–51]. CV prediction detection, cross-validation, and the principal component analysis model were established when the proportion of the validation set and the modeling set was 0.70. The first three principal components can represent more than 85% of the content information. In the modeling set, the coefficient reaches R2 which reaches 0.791, and in the prediction set, the coefficient reaches R2 which reaches 0.785, and RPD is up to 2.1. In the process of calculation and modeling, the importance of all sample points and the samples collected in the previous section play a greater role. Figure 10 shows the pH principal component results, Figure 11 shows the comparison between measured and predicted pH sets, and Figure 12 shows the role of sample points in the calculation of pH content.

4.4. $NaHCO_3$ Content Spectral Prediction Modeling. 404 standard solution spectral data were selected, the largest 7 principal components were selected, and the weights were set equally [47–51]. CV prediction detection, cross-validation, and the principal component analysis model were established when the proportion of the validation set and the modeling set was 0.70. The first three principal

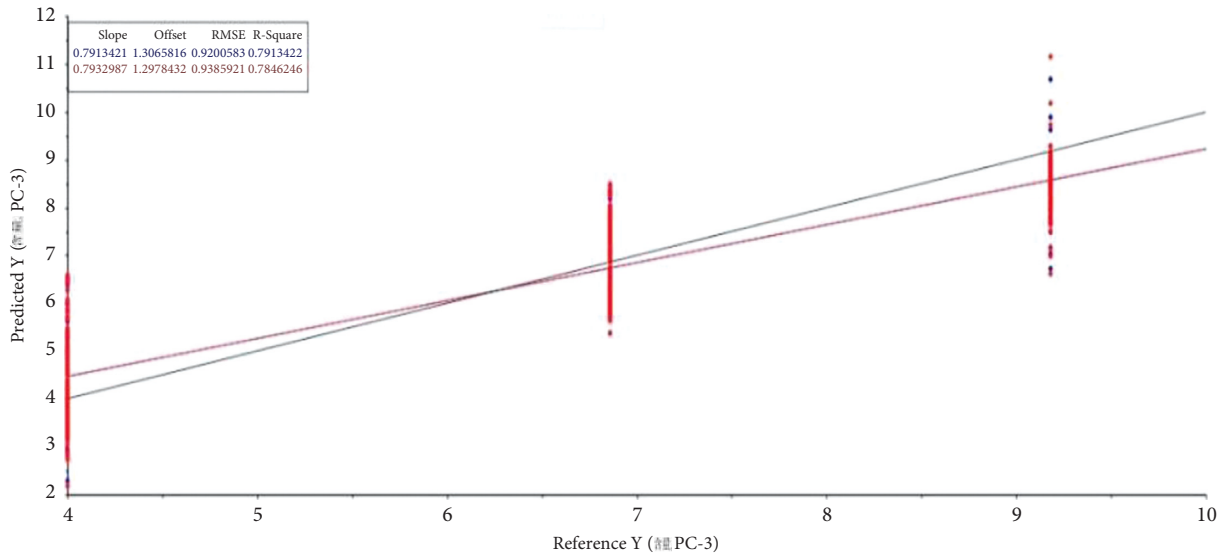

Figure 11: Comparison between measured and predicted pH sets.

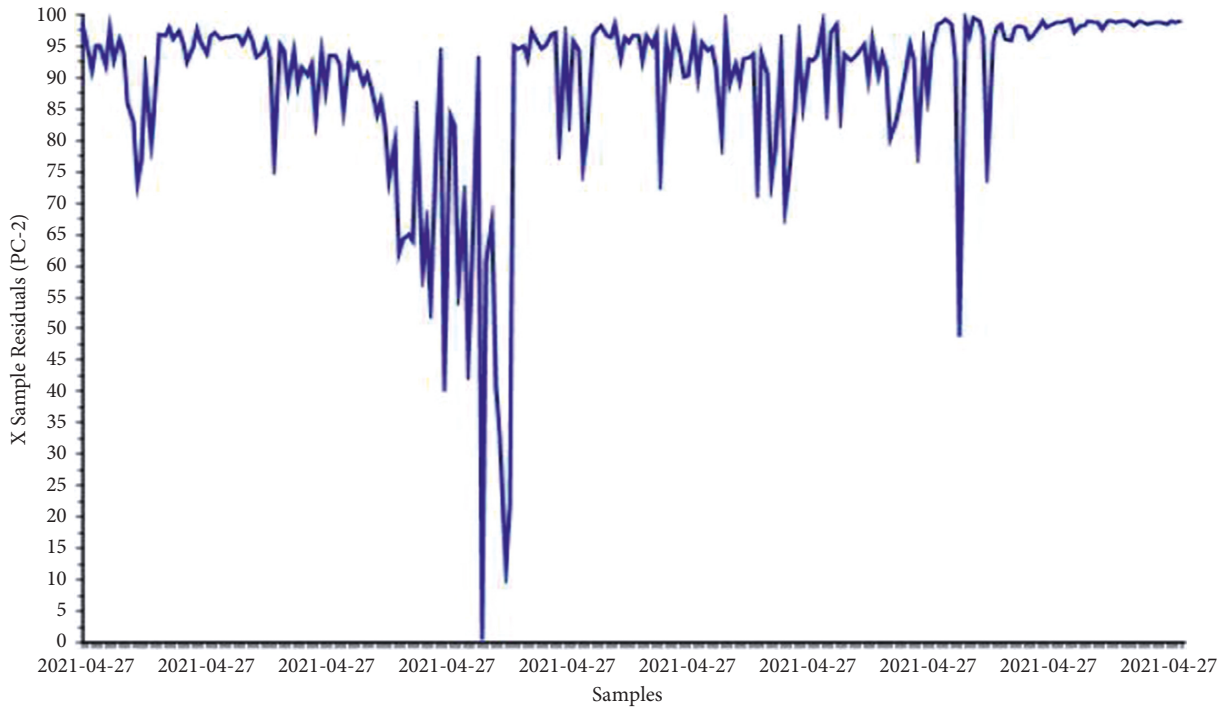

Figure 12: The role of sample points in the calculation of pH content.

components can represent more than 75% of the content information. In the modeling set, the coefficient reaches R2 which reaches 0.162, and in the prediction set, the coefficient reaches R2 which reaches 0.137, and RPD is up to 1.2. In the process of computational modeling, the importance of all sample points and the samples collected in the middle and back end play a greater role. Figure 13 shows the $NaHCO_3$ principal component results, Figure 14 shows the comparison between measured and predicted $NaHCO_3$ sets, and Figure 15 shows the role of sample points in the calculation of $NaHCO_3$ content.

4.5. $CaCl_2$ Content Spectrum Prediction Modeling. Four hundred and seventeen standard solution spectral data were selected, the largest seven principal components were selected, and the weights were set equally [47–51]. CV prediction detection, cross-validation, and the principal component analysis model were established when the proportion of the validation set and the modeling set was 0.70. The first three principal components can represent more than 55% of the content information. In the modeling set, the coefficient reaches R2 which reaches 0.630, and in the prediction set, the coefficient reaches R2 which reaches

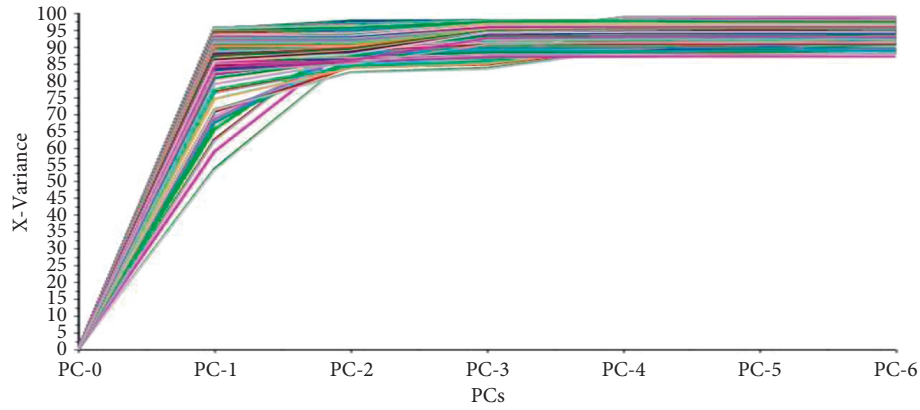

Figure 13: $NaHCO_3$ principal component results.

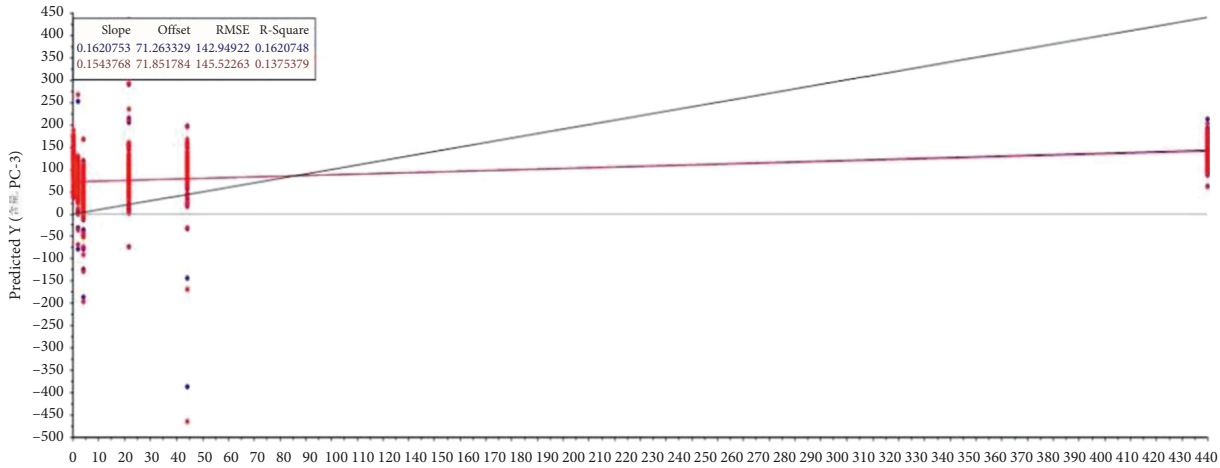

Figure 14: Comparison between measured and predicted $NaHCO_3$ sets.

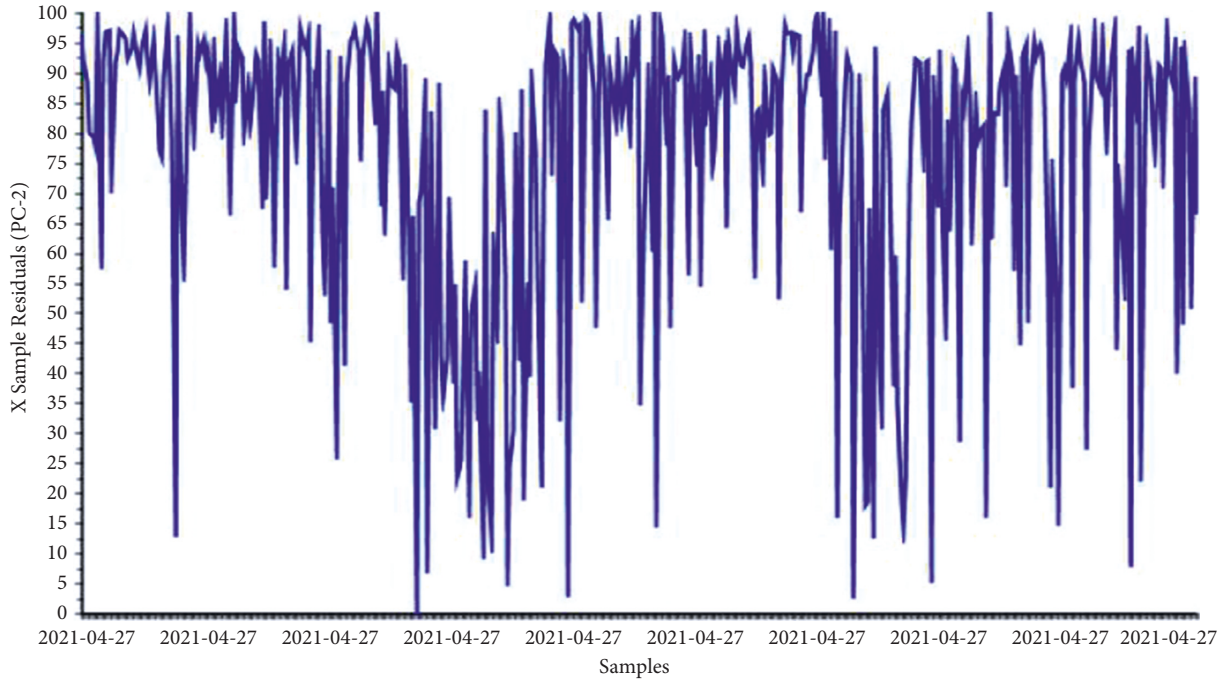

Figure 15: The role of sample points in the calculation of $NaHCO_3$ content.

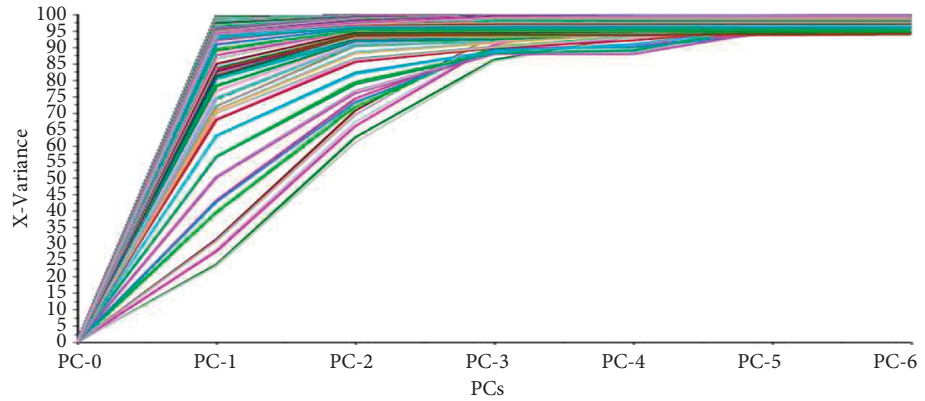

Figure 16: $CaCl_2$ principal component results.

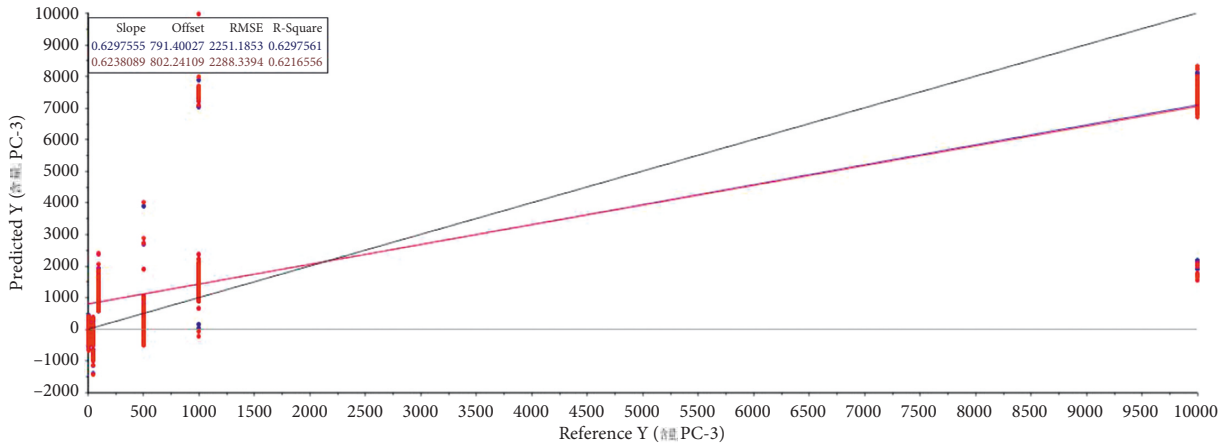

Figure 17: Comparison between measured and predicted sets of $CaCl_2$.

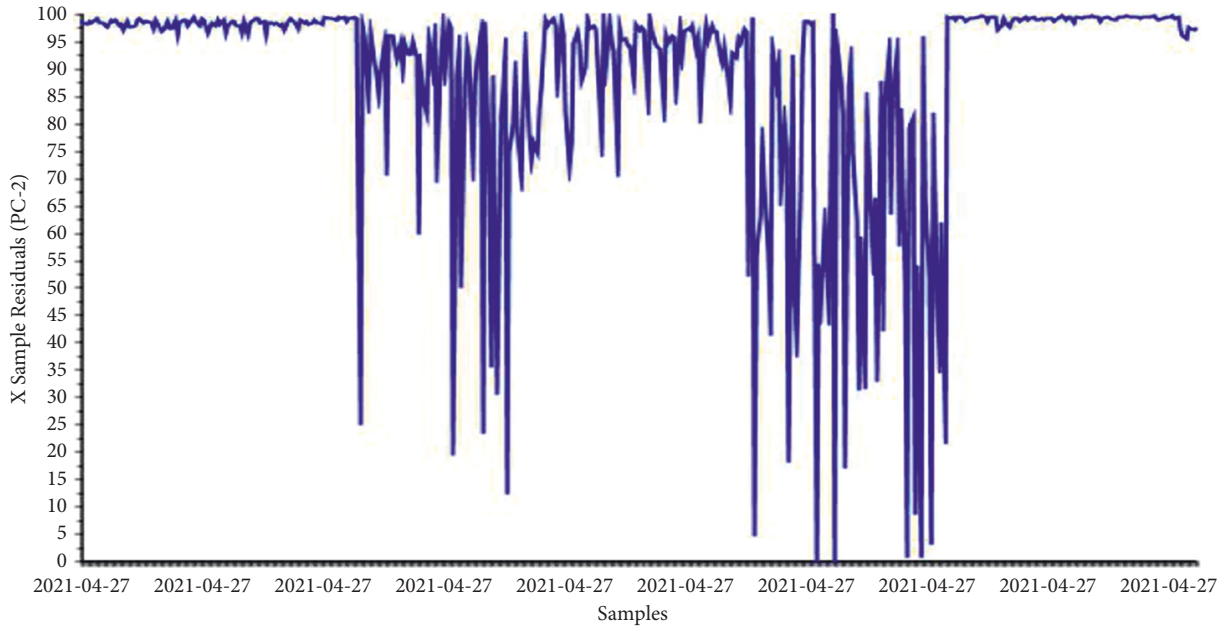

Figure 18: The role of sample points in the calculation of $CaCl_2$ content.

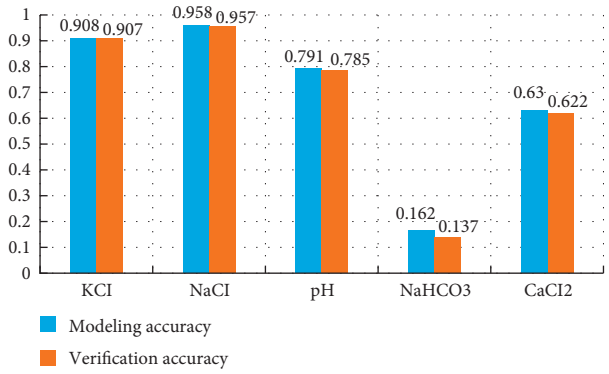

Figure 19: Comparison of extraction accuracy of various ions.

0.622, and RPD is up to 1.7. In the process of computational modeling, the importance of all sample points and the samples collected in the middle section play a greater role. Figure 16 shows the $CaCl_2$ principal component results, Figure 17 shows the comparison between measured and predicted sets of $CaCl_2$, Figure 18 shows the role of sample points in the calculation of $CaCl_2$ content, and Figure 19 shows the comparison of extraction accuracy of various ions.

5. Conclusion

Through the spectrum analysis of the characteristic ions of the mine water, the principal component regression method is used to carry out the quantitative inversion modeling of various ions, and the five standard solutions of KCl, NaCl, pH, $NaHCO_3$, and $CaCl_2$ indicate six ions (KCl includes K ions and Cl ions). The extraction precision of KCl and NaCl is higher than 0.9, followed by pH and $CaCl_2$, the precision is more than 0.6. The extraction precision of HCO_3 is the lowest, only 0.162. The results show that the hyperspectral method can play a better role in the extraction of K^+, Cl^-, Na^+, Ca^{2+}, and pH. It is difficult to extract HCO_3^- ions.

Data Availability

The dataset can be accessed from the corresponding author upon request.

Conflicts of Interest

The author declares no conflicts of interest.

Acknowledgments

The project was supported by the "Thirteenth Five-Year Plan," the Key National R&D Program (Online Dynamic Detection Technology and Equipment of Radio Wave Perspective in Mining Face, 2018YFC0807805).

References

[1] J. G. P. W. Clevers and L. Kooistra, "Using hyperspectral remote sensing data for Retrieving Canopy chlorophyll andNitrogen content," *Ieee Journal of Selected Topics in Applied Earth Observations and Remote Sensing*, vol. 5, no. 2, pp. 574–583, 2012.

[2] B. Bansod, R. Singh, and R. Thakur, "Analysis of water quality parameters by hyperspectral imaging in Ganges River," *Spatial Information Research*, vol. 26, no. 2, pp. 203–211, 2018.

[3] C. Giardino, V. E. Brando, P. Gege et al., "Imaging Spectrometry of Inland and coastal waters: State of the Art, Achievements and perspectives," *Surveys in Geophysics*, vol. 40, no. 3, pp. 401–429, 2018.

[4] K. Ryan and K Ali, "Application of a partial least-squares regression model to retrieve chlorophyll-a concentrations in coastal waters using hyper-spectral data," *Ocean Science Journal*, vol. 51, no. 2, pp. 209–221, 2016.

[5] W. Liu, Z. Zhao, H. Yuan, C. F. Song, and X. Y Li, "An optimal selection method of samples of calibration set and validation set for spectral multivariate analysis," *Spectroscopy and Spectral Analysis*, vol. 34, no. 4, pp. 947–951, 2014.

[6] X. Peng, W. Gao, and J. Wang, "Inversion of Soil parameters from hyperspectral based on Continuum Removal and partial least squares regression," *Geomatics and Information Science of Wuhan University*, vol. 39, no. 7, pp. 862–866, 2014.

[7] Z. Zhang, H. Wang, A. Karnieli, and J. Chen, "Inversion of Soil Moisture content from Hyperspectra based on ridge regression," *Transactions of the Chinese Society for Agricultural Machinery*, vol. 49, no. 5, pp. 240–248, 2018.

[8] X. Tang, J. Zhou, Na Zhang, and Q. Liu, "Nonlinear Internal model control system based on weighted Regularized Extreme learning machine," *Journal of University of Electronic Science and Technology of China*, vol. 45, no. l, pp. 96–101, 2016.

[9] Y. Zhang and L. I. Mei, "A Novel evaluation model of water quality based on PSO-ELM method," *Environmental Science & Technology*, vol. 39, no. 5, pp. 135–139, 2016.

[10] H. Yao, R. Huang, F. Gan, and Y. Liu, "Principal component analysis of the water quality evaluation in East lake," *Geomatics and Information Science of Wuhan University*, vol. 30, no. 8, pp. 732–735, 2005.

[11] H. Lin and Z. Du, "Some problems in Comprehensive evaluation in the principal component analysis," *Statistical Research*, vol. 30, no. 8, pp. 25–31, 2013.

[12] H. Zou, L. Jiang, and F. Li, "Water quality evaluation method based on principal component analysis," *Mathematics in Practice and Theory*, vol. 20, no. 8, pp. 85–90, 2008.

[13] G. B. Huang, Q. Y. Zhu, and C. K. Siew, "Extreme learning machine: a new learning scheme of feedforward neural networks," in *Proceedings of the 2004 IEEE International Joint Conference on IEEE*, pp. 985–990, IEEE, Budapest, Hungary, July 2004.

[14] M. A. Cho and A. K. Skidmore, "A new technique for extracting the red edge position from hyperspectral data: the linear extrapolation method," *Remote Sensing of Environment*, vol. 101, no. 2, pp. 181–193, 2006.

[15] P. Chen, D. Haboudane, N. Tremblay, J. Wang, P. Vigneault, and B. Li, "New spectral indicator assessing the efficiency of crop nitrogen treatment in corn and wheat," *Remote Sensing of Environment*, vol. 114, no. 9, pp. 1987–1997, 2010.

[16] K. Mcgwire, T. Minor, and L. Fenstermaker, "Hyperspectral Mixture modeling for Quantifying Sparse Vegetation Cover in Arid environments," *Remote Sensing of Environment*, vol. 72, no. 3, pp. 360–374, 2000.

[17] M. A. Vega-Rodríguez, C. J. Pérez, K. Reder, and M. Florke, "A Stage-based Approach to Allocating water quality monitoring Stations based on the WorldQual model: the Jubba river as a Case study," *Science of The Total Environment*, vol. 762, pp. 144–162, 2020.

[18] L. Wei, C. Huang, Z. Wang, Z. Wang, X. Zhou, and L. Cao, "Monitoring of Urban Black-Odor water based on Nemerow index and gradient Boosting Decision tree regression using UAV-Borne hyperspectral imagery," *Remote Sensing*, vol. 11, no. 20, p. 2402, 2019.

[19] K. Drnhfer and N. Oppelt, "Remote sensing for lake research and monitoring C Recent advances," *Ecological Indicators*, vol. 64, pp. 105–122, 2016.

[20] L. Feng, X. Hou, and Y. Zheng, "Monitoring and understanding the water transparency changes of fifty large lakes on the Yangtze Plain based on long-term MODIS observations," *Remote Sensing of Environment*, vol. 221, pp. 675–686, 2019.

[21] F. Baltacı, A. Kübra Onur, and S. Tahmiscioğlu, "Water quality monitoring studies of Turkey with present and probable future constraints and opportunities," *Desalination*, vol. 226, no. 1–3, pp. 321–327, 2008.

[22] M. M. Squires, L. F. W. Lesack, and D. Huebert, "The influence of water transparency on the distribution and abundance of macrophytes among lakes of the Mackenzie Delta, Western Canadian Arctic," *Freshwater Biology*, vol. 47, no. 11, pp. 2123–2135, 2002.

[23] E. S. Al-Kharusi, D. E. Tenenbaum, and H. Abdi, "Large-scale Retrieval of Coloured Dissolved Organic Matter in Northern lakes using Sentinel-2 data[J]," *Remote Sensing*, vol. 12, p. 157, 2020.

[24] L. Wei, C. Huang, Z. Wang, Z. Wang, X. Zhou, and L. Cao, "Monitoring of Urban Black-Odor water based on Nemerow index and gradient Boosting Decision tree regression using UAV-Borne hyperspectral imagery," *Remote Sensing*, vol. 11, no. 20, p. 2402, 2019.

[25] C. C. Trees, P. W. Bissettb, M. A. Molined et al., "Monitoring water transparency and diver visibility in ports and harbors using aircraft hyperspectral remote sensing," in *Proceedings of the Photonics for Port and Harbor Security*, pp. 91–98, SPIE, Orlando, Florida, United States, May 2005.

[26] X. He, D. Pan, and Z. Mao, "Water-transparency (Secchi depth) monitoring in the China Sea with the SeaWiFS satellite sensor," in *Proceedings of the Remote Sensing for Agriculture, Ecosystems, and Hydrology VI*, pp. 55–68, SPIE, Maspalomas, Canary Islands, Spain, October 2004.

[27] N. B. Chang, S. Imen, and B. Vannah, "Remote sensing for monitoring Surface water quality Status and Ecosystem state in relation to the Nutrient Cycle: a 40-Year perspective," *Critical Reviews in Environmental Science and Technology*, vol. 45, no. 2, pp. 101–166, 2015.

[28] Z. P. Lee, S. Shang, C. Hu et al., "Secchi disk depth: a new theory and mechanistic model for underwater visibility," *Remote Sensing of Environment*, vol. 169, pp. 139–149, 2015.

[29] J. F. Knight and M. L Voth, "Application of MODIS imagery for intra-annual water clarity assessment of Minnesota lakes," *Remote Sensing*, vol. 4, no. 7, pp. 2181–2198, 2012.

[30] V. Pedroso Curtarelli, C. Clemente Faria Barbosa, D. Andrade Maciel et al., "Diffuse Attenuation of Clear water Tropical Reservoir: a remote sensing Semi-Analytical Approach," *Remote Sensing*, vol. 12, no. 17, p. 2828, 2020.

[31] G. Rodrigues, M. Potes, M. J. Costa et al., "Temporal and Spatial Variations of Secchi depth and Diffuse Attenuation coefficient from Sentinel-2 MSI over a large Reservoir," *Remote Sensing*, vol. 12, no. 5, p. 768, 2020.

[32] F. Setiawan, B. Matsushita, R. Hamzah, D. Jiang, and T Fukushima, "Long-Term Change of the Secchi disk depth in lake Maninjau, Indonesia Shown by Landsat TM and ETM+ data," *Remote Sensing*, vol. 11, no. 23, p. 2875, 2019.

[33] W. Yang, B. Matsushita, J. Chen, K. Yoshimura, and T Fukushima, "Retrieval of Inherent Optical Properties for Turbid Inland waters from remote-sensing reflectance," *IEEE Transactions on Geoscience and Remote Sensing*, vol. 51, no. 6, pp. 3761–3773, 2013.

[34] D. Brzezinski and J Stefanowski, "Reacting to Different types of Concept Drift: the accuracy Updated Ensemble algorithm," *IEEE Transactions on Neural Networks and Learning Systems*, vol. 25, no. 1, pp. 81–94, 2014.

[35] Y. Zhang, J. Ma, S. Liang, X. Li, and M. Li, "An evaluation of eight machine learning regression algorithms for forest Aboveground Biomass estimation from multiple satellite data Products," *Remote Sensing*, vol. 12, no. 24, p. 4015, 2020.

[36] D. Raspopov and P. Belousov, "Development of methods and algorithms for identification of a type of electric energy consumers using artificial intelligence and machine learning models for Smart Grid Systems," *Procedia Computer Science*, vol. 169, pp. 597–605, 2020.

[37] W. Wang and Y. Lu, "Analysis of the mean Absolute Error (MAE) and the Root mean Square Error (RMSE) in assessing Rounding model," *IOP Conference Series: Materials Science and Engineering*, vol. 324, Article ID 012049, 2018.

[38] J. Liu, Z. Yu, and D. Ma, "An adaptive fuzzy min-max neural network classifier based on principle component analysis and adaptive genetic algorithm," *Mathematical Problems in Engineering*, vol. 2012, pp. 1–21, 2012.

[39] L. Li, B. Lei, and C. Mao, "Digital Twin in Smart Manufacturing," *Journal of Industrial Information Integration*, vol. 26, no. 9, Article ID 100289, 2022.

[40] X. Xu and C. Wen, "Fault Diagnosis method based on information Entropy and relative principal component analysis," *Journal of Control Science and Engineering*, vol. 2017, Article ID 2697297, 2017.

[41] L. Li, T. Qu, Y. Liu et al., "Sustainability assessment of Intelligent Manufacturing supported by Digital Twin," *IEEE Access*, vol. 8, pp. 174988–175008, 2020.

[42] Y. Li, "Research and Implementation of Emotional classification of Traditional Folk Songs based on Joint time-Frequency analysis," *Mobile Information Systems*, vol. 2022, Article ID 1224274, 2022.

[43] L. Li and C. Mao, "Big data supported PSS evaluation Decision in Service-Oriented Manufacturing," *IEEE Access*, vol. 8, no. 99, pp. 154663–154670, 2020.

[44] Z. Xun, "Monitoring and analysis of English Classroom Teaching quality based on Big data," *Security and Communication Networks*, vol. 2022, Article ID 5365807, 2022.

[45] L. Li, C. Mao, H. Sun, Y. Yuan, and B. Lei, "Digital Twin Driven green Performance evaluation methodology of Intelligent Manufacturing: Hybrid model based on fuzzy rough-sets AHP, Multistage weight Synthesis, and PROMETHEE II," *Complexity*, vol. 2020, no. 6, pp. 1–24, 2020.

[46] J. Cai, J. Zhao, K. Shen, J. Liu, X. Li, and Y. Ye, "Exploring Factors Affecting the Yellow-Light Running Behavior of electric Bike Riders at Urban Intersections in China," *Journal of Advanced Transportation*, vol. 2020, Article ID 8573232, 2020.

[47] Y. Ai, H. Ma, Xu Qu, Y. Qian, Y. Liu, and W. Zhang, "The cross-Scale life prediction for the high-Speed Train Gearbox Shell based on the three-Interval method," *Scientific Programming*, vol. 2022, Article ID 6439229, 2022.

[48] H. Sun, F. Kong, C. Xiu, W. Shen, and Y. Wang, "A Progressive Combined variable selection method for Near-Infrared spectral analysis based on three-step Hybrid Strategy," *Journal of Spectroscopy*, vol. 2022, Article ID 2190893, 2022.

[49] L. Sun, M. Siddique, L. Wang, and S. J. Li, "Mixing characteristics of a bubble mixing microfluidic chip for genomic DNA extraction based on magnetophoresis: CFD simulation and experiment," *Electrophoresis*, vol. 42, no. 21-22, pp. 2365–2374, 2021.

[50] J. Tian, X. Chen, Z. Liang et al., "Application of NIR spectral Standardization based on principal component score evaluation in wheat Flour Crude Protein model Sharing," *Journal of Food Quality*, vol. 2022, Article ID 9009756, 2022.

[51] S. Cang and A. Wang, "Research on hyperspectral image Reconstruction based on GISMT Compressed sensing and Interspectral prediction," *International Journal of Optics*, vol. 2020, Article ID 7160390, 2020.

Hindawi
Scientific Programming
Volume 2022, Article ID 7649256, 5 pages
https://doi.org/10.1155/2022/7649256

Research Article

Precise Asymptotics for the Uniform Empirical Process and the Uniform Sample Quantile Process

Youyou Chen [1] **and Zaichen Qian** [2]

[1]*School of Science, Zhejiang Sci-Tech University, Hangzhou 310000, China*
[2]*Ant Group, Hangzhou 310000, China*

Correspondence should be addressed to Zaichen Qian; cyyqzc385@163.com

Received 15 March 2022; Revised 11 April 2022; Accepted 17 June 2022; Published 31 July 2022

Academic Editor: Lianhui Li

One of the sources of "invariance principle" is that the limit properties of the uniform empirical process coincide with that of a Brownian bridge. The deep discussion of limit theorem of the uniform empirical process gathered wild interest of the researchers. In this paper, the precise convergence rate of the uniform empirical process is considered. As is well-known, when ε tends to 0, the precise asymptotic theorems can be demonstrated by referring to the classical method of Gut and Spătaru, by using some nice probability inequalities and so on. However, if ε tends to a positive constant, other powerful methods and tools are needed. The method of strong approximation is used in this paper. The main theorems are proved by using the Brownian bridge $B(t)$ to approximate the uniform empirical process $\alpha_n(t)$. The relevant results for the uniform sample quantile process are also presented.

1. Introduction and Main Results

Random phenomena exist in almost every branch of science and engineering and permeate every aspect of ordinary people's modern life [1, 2]. Probability theory is a subject that studies the quantitative regularity of random phenomena everywhere. Probability is a method of thinking about the world [3].

Probability limit theory is one of the main branches of probability theory [4, 5]. The famous probability scientists Kolmogorov and Gnedenko once said, "the epistemological value of probability theory can be revealed only through the limit theorem. Without the limit theorem, it is impossible to understand the real meaning of the basic concepts of probability theory." Probability limit theory is also an important basis of statistical large sample theory [4]. People are very concerned about whether the estimator approximates the real parameter when the sample size tends to infinity, that is, the so-called consistency in statistical large sample theory. Furthermore, we need to consider the speed at which the estimator approximates the real parameters and how to solve these statistical large sample problems. The solution of these problems must rely on the probability limit theorem.

Let $\{X, X_n; n \geq 1\}$ be a sequence of independent and identically distributed (i.i.d.) random variables with the common distribution function F, and set $S_n = \sum_{i=1}^{n} X_i$ for $n \geq 1$. Hsu and Robbins [6] introduced the following complete convergence.

$$\sum_{n=1}^{\infty} P\{|S_n| \geq \varepsilon n\} < \infty, \quad \varepsilon > 0, \tag{1}$$

This holds if $EX = 0$, and $EX^2 < \infty$. The converse part was proved by Erdös [7]. The complete convergence is stronger than the almost sure convergence. Obviously, the sum in (1) tends to infinity as $\varepsilon \searrow 0$.

The first result on the convergence rate of this kind was given by Heyde [8]. It is proved that

$$\lim_{\varepsilon \searrow 0} \varepsilon^2 \sum_{n=1}^{\infty} P\{|S_n| \geq \varepsilon n\} = EX^2, \tag{2}$$

if $EX = 0$, and $EX^2 < \infty$. Heyde [8], Alam [4] got general conclusions and termed them "precise asymptotics."

The precise asymptotics for "S_n" have been extensively studied. One can refer to Zhang [9], Huang [10], and so on. Now, we consider the relevant results for the uniform empirical process. Let $\{U_1, U_2, \cdots, U_n\}$ be a sequence of i.i.d. $U[0,1]-$ distributed random variables. Define the uniform empirical process as $\alpha_n(t) = n^{-1/2}\sum_{i=1}^{n}(I\{U_i \le t\} - t)$, $0 \le t \le 1$. Denote the norm of a function $f(t)$ on [0, 1] by $\|f\| = \sup_{0\le t\le 1}|f(t)|$, and $\log x = \ln(x \vee e)$. The following is one conclusion provided by Zhang and Yang [11].

Theorem 1. *Let $\{B(t); 0 \le t \le 1\}$ be a Brownian bridge, and for any $\delta > -1$, we have $\lim_{\varepsilon \searrow 0} \varepsilon^{2\delta+2}\sum_{n=1}^{\infty}(\log n)^{\delta}/nP\{\|\alpha_n\| \ge \varepsilon\sqrt{\log n}\} = E\|B\|^{2\delta+2}/\delta + 1$.*

The proof of Theorem 1 is based on the classical method introduced by Gut and Spătaru [12]. In this paper, we consider the situation "$\varepsilon \searrow c_0$" where c_0 is a positive constant, and the classical argument for the case of "$\varepsilon \searrow 0$" does not work anymore. We will use more powerful tools, such as strong approximation. Besides the uniform empirical process, we also consider the uniform sample quantile process. Let $0 = U_0^{(n)} \le U_1^{(n)} \le \cdots \le U_n^{(n)} \le U_{n+1}^{(n)} = 1$ denote the order statistics of the random sample $U_1, U_2, \ldots, U_n$, for each $n \ge 1$. Define the uniform quantile function as $U_n(y) = \begin{cases} U_k^{(n)} & \text{if } (k-1)/n < y \le k/n, k = 1, 2, \cdots, n \\ 0 & \text{if } y = 0 \end{cases}$. The uniform sample quantile process should be defined as $u_n(y) = n^{1/2}(U_n(y) - y)$, $0 \le y \le 1$. The following are our main results.

Theorem 2. *Let $a > -1$, $b > -1$, and $b_n(\varepsilon)$ be a function of ε such that $b_n(\varepsilon)\log n \longrightarrow \tau$ as $n \longrightarrow \infty, \varepsilon \searrow \sqrt{a+1}/2$. Then,*

$$\lim_{\varepsilon \searrow \sqrt{a+1}/2}\left[4\varepsilon^2 - (a+1)\right]^{b+1}\sum_{n=1}^{\infty} n^a(\log n)^b P\left\{\|\alpha_n\| \ge \sqrt{2\log n}\left(\varepsilon + b_n(\varepsilon)\right)\right\} = 2\exp\{-4\tau\sqrt{a+1}\}\Gamma(b+1), \tag{3}$$

and

$$\lim_{\varepsilon \searrow \sqrt{a+1}/2}\left[4\varepsilon^2 - (a+1)\right]^{b+1}\sum_{n=1}^{\infty} n^a(\log n)^b P\left\{\|u_n\| \ge \sqrt{2\log n}\left(\varepsilon + b_n(\varepsilon)\right)\right\} = 2\exp\{-4\tau\sqrt{a+1}\}\Gamma(b+1), \tag{4}$$

Theorem 3. *Let $a > -1$, $b > -1$, and $d_n(\varepsilon)$ be a function of ε such that $d_n(\varepsilon)\log\log n \longrightarrow \tau$ as $n \longrightarrow \infty, \varepsilon \searrow \sqrt{a+1}/2$. Then,*

$$\lim_{\varepsilon \searrow \sqrt{a+1}/2}\left[4\varepsilon^2 - (a+1)\right]^{b+1}\sum_{n=1}^{\infty} \frac{(\log n)^a(\log\ \log n)^b}{n} P\left\{\|\alpha_n\| \ge \sqrt{2\log\ \log n}\left(\varepsilon + d_n(\varepsilon)\right)\right\} = 2\exp\{-4\tau\sqrt{a+1}\}\Gamma(b+1), \tag{5}$$

and

$$\lim_{\varepsilon \searrow \sqrt{a+1}/2}\left[4\varepsilon^2 - (a+1)\right]^{b+1}\sum_{n=1}^{\infty} \frac{(\log n)^a(\log\ \log n)^b}{n} P\left\{\|u_n\| \ge \sqrt{2\log\ \log n}\left(\varepsilon + d_n(\varepsilon)\right)\right\} = 2\exp\{-4\tau\sqrt{a+1}\}\Gamma(b+1). \tag{6}$$

Remark 1. We define the general empirical process as $\beta_n(x) = \sqrt{n}(F_n(x) - F(x))$, $-\infty < x < \infty$, where $F_n(x) = 1/n\sum_{i=1}^{n} I_{(-\infty,x]}(X_i)$. If $F(\cdot)$ is a continuous distribution function since $\alpha_n(F(x)) = \beta_n(x)$, the results for $\beta_n(x)$ can be obtained immediately from the uniform case. But we cannot handle the quantile process in the same way.

2. Proofs

The starting point of this paper is the empirical distribution function. The empirical distribution function plays a very important role in statistics [13–18]. Although it is not a beautiful piecewise function, as a nonparametric estimation

of the distribution function, it is unbiased, consistent, and asymptotically obeys the normal distribution. The empirical process is constructed on the basis of the empirical distribution function. The uniform empirical process is a special and important one [19–21].

We lay out some lemmas which will be used in the proofs later. Lemma 1 is well known (cf. [22]). Lemma 2 and 3 are from Csörgó and Révész [23, 24].

Lemma 1. *Let $\{B(t); 0 \le t \le 1\}$ be a Brownian bridge. Then, for all $x > 0$,*

$$P\{\|B(t)\| \ge x\} = 2\sum_{k=1}^{\infty} (-1)^{k+1} e^{-2k^2x^2}. \tag{7}$$

In particular,

$$P\{\|B(t)\| \ge x\} \sim 2e^{-2x^2} \text{ as } x \longrightarrow +\infty. \tag{8}$$

Lemma 2. *There exists a sequence of Brownian bridges $\{B_n(t); 0 \le t \le 1\}$ such that for all n and x we have*

$$P\left\{\sup_{0\le t\le 1} \left|\alpha_n(t) - B_n(t)\right| > n^{-1/2}(K\log n + x)\right\} \le Le^{-\lambda x}, \tag{9}$$

where K, L, λ are positive absolute constants.

Lemma 3. *There exists a sequence of Brownian bridges $\{B_n(t); 0 \le t \le 1\}$ such that for each $n = 1, 2, \cdots$, and for all $|z| < c\sqrt{n}$ and $c > 0$, we have*

$$P\left\{\sup_{0\le t\le 1} \left|u_n(t) - B_n(t)\right| > n^{-1/2}(A\log n + z)\right\} \le Be^{-Cz}, \tag{10}$$

where A, B, C, c are positive absolute constants.

First, we obtain the conclusion for the Brownian bridge $\{B(t);\ 0 \le t \le 1\}$.

Proposition 1. *Let $a > -1$, $b > -1$, and $b_n(\varepsilon)$ be a function of ε such that*

$$b_n(\varepsilon)\log n \longrightarrow \tau \quad as \quad \varepsilon \searrow \frac{\sqrt{a+1}}{2}. \tag{11}$$

Then, $\lim_{\varepsilon\searrow\sqrt{a+1}/2}[4\varepsilon^2 - (a+1)]^{b+1}\sum_{n=1}^{\infty} n^a(\log n)^b P\{\|B\| \ge \sqrt{2\log n}\,(\varepsilon + b_n(\varepsilon))\} = 2\exp\{-4\tau\sqrt{a+1}\}\Gamma(b+1)$.

Proof. By Lemma 1 and (11), we have $P\{\|B\| \ge \sqrt{2\log n}\,(\varepsilon + b_n(\varepsilon))\} \sim 2\exp\{-4\log n\ (\varepsilon + b_n(\varepsilon))^2\} \sim 2\exp\{-4\varepsilon^2\log n\}\exp\{-8\varepsilon b_n(\varepsilon)\log n\}$ as $n \longrightarrow \infty$, uniformly in $\varepsilon \in (\sqrt{a+1}/2, \sqrt{a+1}/2 + \delta)$ for some $\delta > 0$. Therefore, for any $0 < \theta < 1$, there exist $\delta > 0$ and n_0 such that for all $n \ge n_0$ and $\varepsilon \in (\sqrt{a+1}/2, \sqrt{a+1}/2 + \delta)$,

$$\begin{aligned} &2\exp\left\{-4\varepsilon^2\log n\right\}\exp\left\{-4\sqrt{a+1}\,\tau - \theta\right\} \\ &\le P\left\{\|B\| \ge \sqrt{2\log n}\,(\varepsilon + b_n(\varepsilon))\right\} \\ &\le 2\exp\left\{-4\varepsilon^2\log n\right\}\exp\left\{-4\sqrt{a+1}\,\tau + \theta\right\}. \end{aligned} \tag{12}$$

We calculate that

$$\begin{aligned} &\lim_{\varepsilon\searrow\sqrt{a+1}/2}[4\varepsilon^2 - (a+1)]^{b+1}\sum_{n=1}^{\infty} n^a(\log n)^b \cdot \exp\left\{-4\varepsilon^2\log n\right\} \\ &= \lim_{\varepsilon\searrow\sqrt{a+1}/2}[4\varepsilon^2 - (a+1)]^{b+1}\int_e^{\infty} x^a(\log n)^b\exp\left\{-4\varepsilon^2\log x\right\}\mathrm{d}x \\ &= \lim_{\varepsilon\searrow\sqrt{a+1}/2}[4\varepsilon^2 - (a+1)]^{b+1}\int_1^{\infty} y^b\exp\left\{-[4\varepsilon^2 - (a+1)]y\right\}\mathrm{d}y \\ &= \lim_{\varepsilon\searrow\sqrt{a+1}/2}\int_{4\varepsilon^2-(a+1)}^{\infty} z^b e^{-z}\mathrm{d}z = \Gamma(b+1). \end{aligned}$$

From (12), and noting that θ is arbitrary, we get the proposition immediately. □

Proof of Theorem 2. Here, we only present the proof for (3) since the argument for (4) is similar. It is obvious, for $p < -1/2$,

$$\begin{aligned} &P\left\{\sup_{0\le t\le 1}|B(t)| \ge \sqrt{2\log n}\,(\varepsilon + b_n(\varepsilon)) + (\log n)^p\right\} \\ &\quad - P\left\{\sup_{0\le t\le 1}\left|\alpha_n(t) - B(t)\right| \ge (\log n)^p\right\} \\ &\quad \le P\left\{\sup_{0\le t\le 1}\left|\alpha_n(t)\right| \ge \sqrt{2\log n}\,(\varepsilon + b_n(\varepsilon))\right\} \\ &\quad \le P\left\{\sup_{0\le t\le 1}|B(t)| \ge \sqrt{2\log n}\,(\varepsilon + b_n(\varepsilon)) - (\log n)^p\right\} \\ &\quad + P\left\{\sup_{0\le t\le 1}\left|\alpha_n(t) - B(t)\right| \ge (\log n)^p\right\}. \end{aligned} \tag{13}$$

From Lemma 2, we have $P\{\sup_{0\le t\le 1}|\alpha_n(t) - B(t)| \ge (\log n)^p\} \le P\{\sup_{0\le t\le 1}|\alpha_n(t) - B(t)| \ge K\log n + (a+2)\log n/\lambda/\sqrt{n}\} \le Le^{-(a+2)\log n} = Ln^{-(a+2)}$, and then $\sum_{n=1}^{\infty} n^a(\log n)^b P\{\sup_{0\le t\le 1}|\alpha_n(t) - B(t)| \ge (\log n)^p\} \le L\sum_{n=1}^{\infty} n^{-2}(\log n)^b < \infty$. Furthermore, it follows

$$\lim_{\varepsilon\searrow\sqrt{a+1}/2}\left[4\varepsilon^2 - (a+1)\right]^{b+1}\sum_{n=1}^{\infty} n^a(\log n)^b P\left\{\sup_{0\le t\le 1}\left|\alpha_n(t) - B(t)\right| \ge (\log n)^p\right\} = 0. \tag{14}$$

On the other hand, since $p < -1/2$, we have $P\{\|B\| \ge \sqrt{2\log n}\,(\varepsilon + b_n(\varepsilon)) \pm (\log n)^p\} = P\{\|B\| \ge \sqrt{2\log n}\,(\varepsilon + b_n(\varepsilon) \pm 1/\sqrt{2}\,(\log n)^{p-1/2})\} \sim 2\exp\{-4\log n\,(\varepsilon + b_n(\varepsilon) \pm 1/\sqrt{2}\,(\log n)^{p-1/2})^2\} \sim 2\exp\{-4\varepsilon^2\log n\}\exp\{-8\varepsilon b_n(\varepsilon)\log n\} \sim P\{\|B\| \ge \sqrt{2\log n}\,(\varepsilon + b_n(\varepsilon))\}$, as. $n \longrightarrow \infty$

With Proposition 1, it follows

$$\lim_{\varepsilon\searrow\sqrt{a+1}/2}\left[4\varepsilon^2-(a+1)\right]^{b+1}\sum_{n=1}^{\infty}n^a(\log n)^b P\left\{\sup_{0\le t\le 1}|B(t)|\ge\sqrt{2\log n}\left(\varepsilon+b_n(\varepsilon)\right)\pm(\log n)^p\right\}=2\exp\{-4\tau\sqrt{a+1}\}\Gamma(b+1). \tag{15}$$

From (13) to (15), we get the result of Theorem 2. □

Proof of Theorem 3. In this part, we only present the outline of the proof for the uniform sample quantile process, so the arguments for Theorem 2 and 3 are mutually complementary.

Follow the proof of Proposition 1 closely, we can get the following conclusion. For any $0<\theta<1$, there exist $\delta>0$ and n_0 such that for all $n\ge n_0$ and $\varepsilon\in(\sqrt{a+1}/2, \sqrt{a+1}/2+\delta)$, $2\exp\{-4\varepsilon^2\log\log n\}\exp\{-4\tau\sqrt{a+1}-\theta\}\le P\{\|B\|\ge\sqrt{2\log\log n}(\varepsilon+d_n(\varepsilon))\}\le 2\exp\{-4\varepsilon^2\log\log n\}\exp\{-4\tau\sqrt{a+1}+\theta\}$

On the other hand, $\lim_{\varepsilon\searrow\sqrt{a+1}/2}[4\varepsilon^2-(a+1)]^{b+1}\sum_{n=1}^{\infty}(\log\log n)^a(\log\log n)^b/n\cdot\exp\{-4\varepsilon^2\log\log n\}=\Gamma(b+1)$.

Therefore, we have

$$\lim_{\varepsilon\searrow\sqrt{a+1}/2}\left[4\varepsilon^2-(a+1)\right]^{b+1}\sum_{n=1}^{\infty}\frac{(\log n)^a(\log\log n)^b}{n}P\left\{\|B\|\ge\sqrt{2\log\log n}\left(\varepsilon+d_n(\varepsilon)\right)\right\}=2\exp\{-4\tau\sqrt{a+1}\}\Gamma(b+1). \tag{16}$$

Like (13), we have. $P\{\sup_{0\le t\le 1}|B_n(t)|\ge\sqrt{2\log\log n}(\varepsilon+d_n(\varepsilon))+(\log\log n)^p\}-P\{\sup_{0\le t\le 1}|u_n(t)-B_n(t)|\ge(\log\log n)^p\}\le P\{\sup_{0\le t\le 1}|u_n(t)|\ge\sqrt{2\log\log n}(\varepsilon+d_n(\varepsilon))\}\le P\{\sup_{0\le t\le 1}|B_n(t)|\ge\sqrt{2\log\log n}(\varepsilon+d_n(\varepsilon))\}+P\{\sup_{0\le t\le 1}|u_n(t)-B_n(t)|\ge(\log\log n)^p\}$

By lemma 3, let $z=\log n/\lambda$, we can get. $\sum_{n=1}^{\infty}(\log n)^a(\log\log n)^b/nP\{\sup_{0\le t\le 1}|u_n(t)-B_n(t)|\ge(\log\log n)^p\}\le\sum_{n=1}^{\infty}(\log n)^a(\log\log n)^b/nP\{\sup_{0\le t\le 1}|u_n(t)-B_n(t)|\ge C\log n+\log n/\lambda/\sqrt{n}\}\le\sum_{n=1}^{\infty}(\log n)^a(\log\log n)^b/n\cdot Le^{-\log n}<\infty$

The rest of the proof is similar to Theorem 2 and is omitted here. □

3. Conclusion

The empirical process theory plays an important role in large sample theory in statistics. The researchers are very much interested in the large sample properties of the statistical estimator. As long as the sample size tends to infinity, the estimator converges to the true value of the parameter. In the procedure of demonstration of large sample properties, especially for the estimators in the semiparameter models, this study on convergence rates for the uniform empirical process and the uniform sample quantile process can provide a series of effective methods and tools.

The limitation of this study may lie in the lack of consideration of the exact asymptotic properties of uniform empirical processes; in addition, in the study of the convergence rate of the uniform empirical process and uniform sample quantile process, the influence of the exact asymptotic behavior of self-regularity and logarithmic law on the convergence rate should also be taken into account.

Due to the needs of practical applications, dependent random samples are often of more interest to statisticians. Positive and negative concomitants also widely exist in real life and engineering, such as reliability testing, statistical mechanics, and so on. The limit properties of the sequences of associated random variables, such as the law of iterated logarithm and the law of large numbers of the sequences of associated random variables, will be a hot topic in the future. In the future, the asymptotic properties of the test statistics of the model and parameters will be studied by parameter estimators.

Data Availability

The data set can be accessed upon request.

Conflicts of Interest

The author declares that there are no conflicts of interest.

Acknowledgments

This work was supported by the Natural Science Foundation of Zhejiang Province (Grant no. LQ18A010009).

References

[1] M. Li and W. ZhaoZhao, "Golden Ratio Phenomenon of random data obeying von Karman spectrum," *Mathematical Problems in Engineering*, vol. 2013, pp. 1–6, 2013.

[2] L. Li, B. Lei, and C. Mao, "Digital Twin in Smart Manufacturing," *Journal of Industrial Information Integration*, vol. 26, no. 9, p. 100289, Article ID 100289, 2022.

[3] L. Wang, J. X. Chen, G. Jiang, and B Zheng, "Robust spectrum sensing algorithm based on free probability theory," *Wireless Communications and Mobile Computing*, vol. 16, no. 13, pp. 1668–1679, 2016.
[4] I. Alam, "Limiting probability Measures," *JOURNAL OF LOGIC AND ANALYSIS*, vol. 12, 2019.
[5] W. Li and M. K. Ng, "On the limiting probability distribution of a transition probability tensor," *Linear and Multilinear Algebra*, vol. 62, no. 3, pp. 362–385, 2014.
[6] P. L. Hsu and H. Robbins, "Complete convergence and the law of large numbers," *Proceedings of the National Academy of Sciences*, vol. 33, no. 2, pp. 25–31, 1947.
[7] P. Erdos, "On a theorem of Hsu and Robbins," *The Annals of Mathematical Statistics*, vol. 20, no. 2, pp. 286–291, 1949.
[8] C. C. Heyde, "A supplement to the strong law of large numbers," *Journal of Applied Probability*, vol. 12, no. 01, pp. 173–175, 1975.
[9] L. X. Zhang, "Precise rates in the law of the iterated logarithm," 2001, https://arxiv.org/abs/math/0610519.
[10] W. Huang and L. X. Zhang, "Precise rates in the law of the logarithm in the Hilbert space," *Journal of Mathematical Analysis and Applications*, vol. 304, no. 2, pp. 734–758, 2005.
[11] Y. Zhang and X. Y. Yang, "Precise asymptotics in the law of the iterated logarithm and the complete convergence for uniform empirical process," *Statistics & Probability Letters*, vol. 78, no. 9, pp. 1051–1055, 2008.
[12] A. Gut and A. Spătaru, "Precise asymptotics in the Baum-Katz and Davis laws of large numbers," *Journal of Mathematical Analysis and Applications*, vol. 248, no. 1, pp. 233–246, 2000.
[13] J. A. Víšek, "Empirical distribution function under heteroscedasticity," *Statistics*, vol. 45, no. 5, pp. 497–508, 2011.
[14] D. Blanke and D. Bosq, "Polygonal smoothing of the empirical distribution function," *Statistical Inference for Stochastic Processes*, vol. 21, no. 2, pp. 263–287, 2018.
[15] G. Hesamian and S. M. Taheri, "Fuzzy empirical distribution function: properties and application," *Kybernetika*, vol. 49, no. 6, pp. 962–982, 2013.
[16] A. Munteanu and M. Wornowizki, "Correcting statistical models via empirical distribution functions," *Computational Statistics*, vol. 31, no. 2, pp. 465–495, 2016.
[17] G. G. Hu, S. S. Gao, Y. Zhong, and C. Gu, "Asymptotic properties of random Weighted empirical distribution function," *Communications in Statistics - Theory and Methods*, vol. 44, no. 18, pp. 3812–3824, 2015.
[18] N. Y. Li, Y. Li, and Y. Liu, "Empirical Bayes Inference for the parameter of power distribution based on Ranked set sampling," *Discrete Dynamics in Nature and Society*, vol. 2015, Article ID 760768, 2015.
[19] S. Tang, J. X. Zhang, and F. Q. Niu, "Spatial-temporal Evolution Characteristics and Countermeasures of Urban Innovation space distribution: an empirical study based on data of Nanjing High-Tech Enterprises," *Complexity*, vol. 2020, Article ID 2905482, 2020.
[20] G. Gao, G. T. Shi, H. Zou, and S. Zhou, "Characterizing the statistical properties of SAR Clutter by using an empirical distribution," *International Journal of Antennas and Propagation*, vol. 2013, pp. 1–8, 2013.
[21] C. S. Marange and Y. Qin, "A Simple empirical Likelihood Ratio test for Normality based on the Moment Constraints of a Half-normal distribution," *JOURNAL OF PROBABILITY AND STATISTICS*, vol. 10, pp. 1–10, 2018.
[22] P. Billingsley, *Convergence of Probability Measure*, Wiley, New York, 1968.
[23] M. Csörgó and P. Révéesz, *Strong Approximations in Probability and Statistics*, Academic Press, New York, San Francisco, London, 1981.
[24] Y. Chen and T. Li, "Moment convergence rates for the uniform empirical process and the uniform sample quantile process," *Communications in Statistics - Theory and Methods*, vol. 46, no. 18, pp. 9086–9091, 2017.

Hindawi
Scientific Programming
Volume 2022, Article ID 5828852, 7 pages
https://doi.org/10.1155/2022/5828852

Research Article

Innovation of Visual Communication Design of Interactive Packaging for Internet-Famous Food Based on Artificial Intelligence

Lina Wang

Department of Design Art, Taiyuan Institute of Technology, Taiyuan 030006, Shanxi, China

Correspondence should be addressed to Lina Wang; wangln@tit.edu.cn

Received 11 June 2022; Revised 7 July 2022; Accepted 11 July 2022; Published 31 July 2022

Academic Editor: Lianhui Li

The combination of visual communication design of food packaging and digital media art is the new trend. In this study, the visual communication design of interactive packaging of Internet-famous food is analyzed, and an innovative identification method of the interactive packaging visual communication design based on artificial intelligence is put forward. The weighted fusion rule of conjunction disjunction double operators is used to fuse the innovative evaluation information of multiple expert groups on interactive packaging, and finally, the innovative multigroup discrimination results of interactive packaging are obtained. Considering both the consistency of evaluation information and the contradiction of evaluation information, the weight factor is introduced to achieve the balance between conjunction operator and disjunction operator. The designed conjunctive disjunctive double operator weighted fusion rule can support the contradiction handling in the innovative discrimination of interactive packaging and has the advantages of convenient application and easy programming.

1. Introduction

Internet-famous food is a novel, popular snack food with distinctive cultural transmission characteristics with the emergence of new trends such as multimedia technology and webcast. It has the properties of both food and network information carrier. But food attribute is its essential attribute. Therefore, when carrying out the innovation of its interactive packaging visual communication design [1–9], we must first consider its food attributes.

Under the severe situation of increasingly fierce market demand, the food industry should not only work hard at the level of market demand and strict control of food quality and safety but also should further grasp the aesthetic characteristics of the public, use artistic advertising creative design to attract customers' attention, expand publicity and planning, and establish brand awareness, so as to promote the overall growth of food sales [10, 11]. Digital media art [12–16] has the comprehensive characteristics of "sound, image, form, and sound", which has a key practical significance for accelerating the dissemination of information content in the food industry and getting rid of the restrictions of food advertising on time and indoor space. Customers can use diversified digital media technology and Internet platforms to independently search for advertisements related to food enterprises, strengthen the promotion scope and resource sharing level of food advertising, and indirectly expand the scope of food advertising.

With the strong support of a series of digital media technologies, packaging designers show diversified performance effects according to the reasonable arrangement of the visual effect elements such as color, graphics, and text, and it also improves the intimate interaction with the public, mobilize enthusiasm, and creative thinking and meets the artistic needs of these people, and it further promotes the development trend of creative design of food packaging in the period of digital media technology [16]. Digital media art combines electronic information technology with media art to become a scientific and reasonable art with strong expressiveness and high scientific and technological content.

Taking this as an opportunity, this paper carries out the research on the visual communication design innovation of Internet-famous food interactive packaging based on artificial intelligence. Firstly, the visual communication design of interactive packaging of Internet-famous food is analyzed. Then, taking the interactive packaging design of an Internet-famous food as the object, using artificial intelligence algorithm, an innovativeness identification method of interactive packaging visual communication design is proposed.

2. Analysis of the Visual Communication Design of Interactive Packaging of Internet-Famous Food

The application of new media technology in food packaging design can not only improve and update the visual elements of the plan of food packaging materials but also introduces more practical sensory stimuli, so as to improve the competitiveness of products.

2.1. Communicating More Product Information to Consumers. The more basic function of food packaging is not only to store food commodities but also to display the basic information of food, including the name, production date, shelf life, origin, specification, and other basic information of the food. The digital media art plays a key role here, and Figure 1 shows several examples of the Internet-famous food packaging design enabled by digital media technology [17–20]. Many contemporary food packages are printed with two-dimensional codes and the application of the two-dimensional code technology is to make full use of the information content storage and expansion functions of digital media art. By scanning the QR code, customers can obtain more and more product-related information, so as to have a deeper understanding of the food categories. In fact, for example, the two-dimensional code displayed on the package of a well-known brand of milk containing beverage, and after scanning, consumers can immediately log in to the manufacturer's official website. The website presents the product variety, the surrounding environment of the production site, the natural environment of the production line, the natural environment of milk raw materials, etc., so that customers can have a deeper understanding of the manufacturer of milk containing beverage and cannot help thinking that the product will appear in similar transactions in the future.

At the same time, the two-dimensional code on the food packaging generally has various decorations such as animation elements, so the visual impact is more prominent, completing the unity of artistic beauty and practicality.

2.2. Building an Interactive Bridge between Products and Consumers. AR technology is a digital media technology commonly used in food packaging, especially in dairy packaging. It plays a key role in combining food visual effect elements to enhance the charm of food packaging. By using AR technology, customers can use mobile phones and other devices to scan the AR identification control module on food packaging to obtain the content of interaction and

Figure 1: Food packaging design enabled by digital media technology.

communication with AR, such as 3D display of the food origin [18]. Customers can visit the origin of food in a 720° panoramic view to obtain different visual effects of tourism experience.

It is not difficult to see that AR technology has built a bridge for the interaction between customers and virtual scenes, thus improving the interest and interactivity of food packaging materials and bringing more in-depth shopping experience to customers.

2.3. Realizing the Publicity and Marketing of Internet-Famous Food Products. No matter what kind of digital media art it may be, its application in food packaging is not rigid but expressive and harmonious [19]. For example, the food industry uses digital media art to apply various artistic creative patterns, such as various animation element pattern design, data element pattern design, and digital media technology content, such as H5 web page, WeChat public platform, and Sina Weibo post.

On the one hand, it conforms to the visual effect art aesthetics of the product packaging design, increases the visual effect art aesthetics of the food packaging, and attracts more customers' visual actual effect. On the other hand, it also makes use of food packaging materials more extensive. When customers appreciate this artistic creative pattern, it is easier for them to take the initiative to master the technical content of digital media in the pattern design, so as to achieve the expected publicity planning and promotion effect. In this way, food packaging reasonably connects the gap between the data world and the physical world and completes data marketing. The application of digital media art in food packaging materials has a certain inevitable trend, which is also the main countermeasure to improve the competitiveness of the food industry.

3. Innovativeness Identification Method of Interactive Packaging Visual Communication Design Based on Artificial Intelligence

For the Internet-famous food product, there are many feasible packaging design schemes in the process of

interactive packaging design. With the deepening and popularization of the innovative design in the food packaging industry, the key technical problem to be solved is how to distinguish the innovation of interactive packaging design, so as to provide basis for subsequent product promotion and marketing.

3.1. Evidence Theory. It is a feasible way to identify the innovation of interactive packaging design that experts belonging to multiple groups evaluate the innovation of interactive packaging design according to their own experience and wisdom and then integrate the evaluation information of the multiple groups [21–25]. However, they are affected by many complex factors, such as experts' knowledge background, practical experience, and the group interest they represent, and the evaluation information given by the experts from the multiple groups in the innovative evaluation of the interactive packaging design is also highly uncertain. The fusion of multigroup evaluation information is essentially an uncertain reasoning and decision-making process.

As an uncertain reasoning method, evidence theory has unique advantages in information fusion and has been widely used [26–34]. When the evaluation information of the multiple groups supports the proposition that "the innovation of interactive packaging design is the best," when these evidences are fused together, the fusion results should support this proposition to a greater extent. In other words, the fusion rules should be able to achieve "downward focus," that is, the focus from a subset with a larger cardinality to a subset with a smaller cardinality, so as to facilitate the decision-making and judgment. Sometimes, the evaluation information of some groups may be contradictory. For example, for a certain two groups, one may think that "the innovation of interactive packaging design is excellent" and the other may think that "the innovation of interactive packaging design is poor." At this time, the two groups have contradictory evaluation information on the innovation of interactive packaging design.

In this case, the conclusion is that "the innovation of interactive packaging design is excellent (the second group is not trusted)" or "the innovation of interactive packaging design is inferior (the first group is not trusted)" or "the innovation of interactive packaging design is excellent or inferior (it is impossible to judge which group is not trusted)" will be drawn. Therefore, when there are contradictions in the evaluation information, the fusion rules should be able to achieve "upward" processing, so as to delay the decision-making and avoid unreasonable conclusions in case of evidence contradictions. It can be seen that when there are contradictions in the evaluation information of multiple groups, using the traditional evidence fusion rules will produce a conclusion contrary to common sense. Therefore, there is an urgent need for an innovative identification method of interactive packaging design that can deal with this contradiction.

3.2. Technology Roadmap. An innovative identification method of interactive packaging visual communication design is proposed as shown in Figure 2.

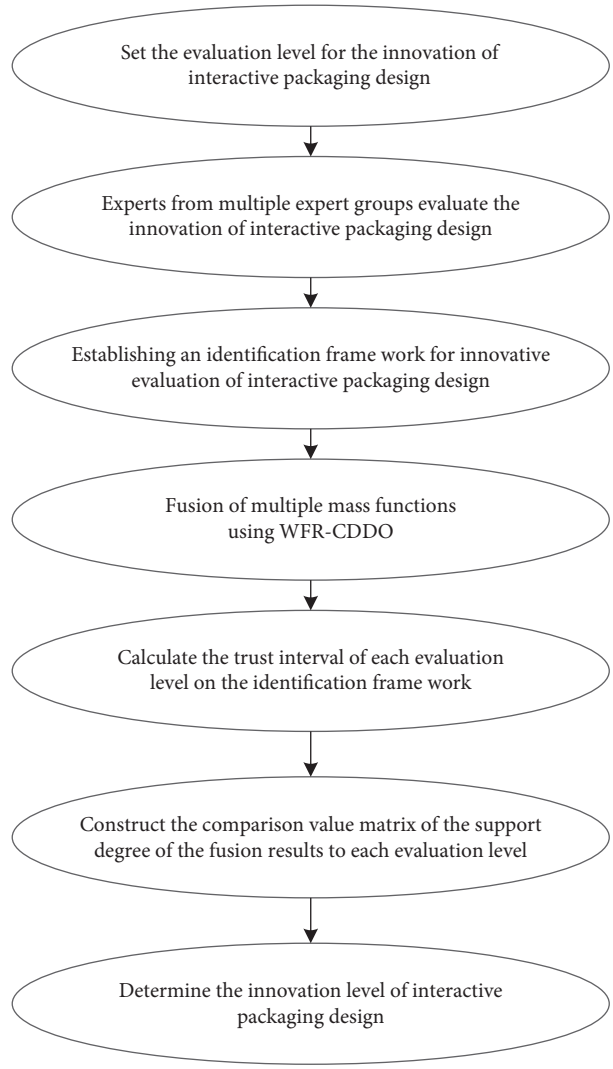

Figure 2: Innovativeness identification method of interactive packaging visual communication design.

Its steps are as follows.

Step 1. Set the innovativeness evaluation level of interactive packaging design as m levels : $S_1, S_2, ..., S_m$. From S_1 to S_m, the innovativenes decreases.

Step 2. Experts from n expert groups evaluate the innovativeness of interactive packaging design.

Here, there are ε_i experts in the i-th expert group, $i = 1, 2, ..., n$.

In the i-th expert group, the evaluation results of λ_i experts is that "the innovation of interactive packaging design definitely belongs to a certain level," where the number of experts who think the innovation of interactive packaging design belongs to $S_1, S_2, \ldots, S_m$" is $\varepsilon_{i1}, \varepsilon_{i2}, \ldots, \varepsilon_{im}$, where $\varepsilon_{i1} + \varepsilon_{i2} + \ldots + \varepsilon_{im} = \lambda_i$; the evaluation results of μ_i experts is "the innovation of interactive packaging design is vague and belongs to one of several levels," where the number of experts who think the innovation of interactive packaging design belongs to one level in $\{S_x, \ldots, S_y\}$ is

$\varepsilon_{i,(x,\ldots,y)}$, where $x = 1, 2, \ldots, m$, $y = 1, 2, \ldots, m$, $x \neq y$, and $\ldots + \varepsilon_{i,(x,\ldots,y)} + \ldots = \mu_i$, $\lambda_i + \mu_i = \varepsilon_i$.

Step 3. An identification framework for interactive packaging innovation evaluation is established as

$$\Theta = \{S_1, S_2, \ldots, S_m\}. \tag{1}$$

The evaluation information of n expert groups is regarded as evidence and further expressed as the basic probability assignment function under the identification framework $\Theta = \{S_1, S_2, \ldots, S_m\}$, which is expressed by mass. There are n mass functions $mass_1, mass_2, \ldots, mass_n$. For $mass_i$:

$$\begin{aligned} \mathrm{mass}_i(S_1) &= \frac{\varepsilon_{i1}}{\varepsilon_i}, \\ \mathrm{mass}_i(S_2) &= \frac{\varepsilon_{i2}}{\varepsilon_i}, \ldots, \\ \mathrm{mass}_i(S_m) &= \frac{\varepsilon_{im}}{\varepsilon_i}, \ldots, \\ \mathrm{mass}_i(\{S_x, \ldots, S_y\}) &= \frac{\varepsilon_{i,(x,\ldots,y)}}{\varepsilon_i}, \ldots. \end{aligned} \tag{2}$$

Step 4. Weighted fusion rules of conjunction disjunction double operators (WFR-CDDO) is adopted to realize the fusion of n mass functions $mass_1, mass_2, \ldots, mass_n$.

The expression of conjunction operator (CO) is

$$mass'(S) = \frac{1}{1-k} \sum_{S^p \cap S^q \cap \ldots \cap S^r = S} \mathrm{mass}_1(S^p)\mathrm{mass}_2(S^q)\ldots\mathrm{mass}_n(S^r), \tag{3}$$

where $mass'$ represents the mass function obtained by fusing n mass functions $\mathrm{mass}_1, \mathrm{mass}_2, \ldots, \mathrm{mass}_n$ with conjunction operator, $S^p, S^q, \ldots, S^r \subset \Theta$, $S = S_1, S_2, \ldots, S_m, \ldots, \{S_x, \ldots, S_y\}, \ldots$; $k = \sum_{S^p \cap S^q \cap \ldots \cap S^r = \varnothing} \mathrm{mass}_1(S^p)\mathrm{mass}_2(S^q)\ldots\mathrm{mass}_n(S^r)$ is a contradiction coefficient, reflecting the contradiction degree between N mass functions. If k is bigger, it means that the degree of contradiction among n mass functions $\mathrm{mass}_1, \mathrm{mass}_2, \ldots, \mathrm{mass}_n$ is higher.

The expression of the disjunction operator (DO) is

$$mass''(S) = \sum_{S^p \cup S^q \cup \ldots \cup S^r = S} \mathrm{mass}_1(S^p)\mathrm{mass}_2(S^q)\ldots\mathrm{mass}_n(S^r), \tag{4}$$

where $mass''$ represents the mass function obtained by fusing n mass functions $mass_1, mass_2, \ldots, mass_n$ with disjunction operator.

The expression of WFR-CDDO is

$$\begin{aligned} mass'''(S) &= \alpha \cdot mass'(S) + \beta \cdot mass''(S) \\ &= \alpha \frac{1}{1-k} \sum_{S^p \cap S^q \cap \ldots \cap S^r = S} mass_1(S^p)mass_2(S^q)\ldots mass_n(S^r) \\ &\quad + \beta \sum_{S^p \cup S^q \cup \ldots \cup S^r = S} mass_1(S^p)mass_2(S^q)\ldots mass_n(S^r), \end{aligned} \tag{5}$$

where α and β are the weighting factors of CO and DO, $\alpha \geq 0, \beta \geq 0$ and $\alpha + \beta = 1$. If we use k as the weighting factor of DO, that is, $\beta = k$, so $\alpha = 1 - k$.

WFR-CDDO is further expressed as

$$\begin{aligned} mass'''(S) &= \sum_{S^p \cap S^q \cap \ldots \cap S^r = S} mass_1(S^p)mass_2(S^q)\ldots mass_n(S^r) \\ &\quad + k \sum_{S^p \cup S^q \cup \ldots \cup S^r = S} mass_1(S^p)mass_2(S^q)\ldots mass_n(S^r). \end{aligned} \tag{6}$$

Then, n mass functions are fused through WFR-CDDO, and the fusion results are calculated in turn as $mass'''(S_1)$, $mass'''(S_2)$, ..., $mass'''(S_m)$, ..., $mass'''(\{S_x, \ldots, S_y\})$, ...

Step 5. Under the identification framework $\Theta = \{S_1, S_2, \ldots, S_m\}$, the belief function and plausibility function of level S_j are calculated as

$$Bel(S_j) = \sum_{S^p \subseteq S_j} mass'''(S^p), \tag{7}$$

$$Pl(S_j) = \sum_{S^p \cap S_j \neq \varnothing} mass'''(S^p). \tag{8}$$

They form the trust interval $[Bel(S_j), Pl(S_j)]$ of level S_j, where $j = 1, 2, \ldots, m$.

Step 6. Based on the trust intervals $[Bel(S_1), Pl(S_1)]$, $[Bel(S_2), Pl(S_2)]$, ..., $[Bel(S_m), Pl(S_m)]$ of $S_1, S_2, \ldots, S_m$, we calculate the matrix:

$$\Delta = (\Delta_{j,l})_{m \times m}, \tag{9}$$

where

$$\Delta_{j,l} = \frac{\max\{0, Pl(S_j) - Bel(S_l)\} - \max\{0, Bel(S_j) - Pl(S_l)\}}{Pl(S_j) - Bel(S_j) + Pl(S_l) - Bel(S_l)}. \tag{10}$$

It represents the comparison between the degree of support of the fusion result for "the innovation of interactive packaging belongs to S_j" and the degree of support of the fusion result for "the innovation of interactive packaging belongs to S_l," where $Bel(S_l)$ and $Pl(S_l)$ are the lower limit and upper limit of trust interval $[Bel(S_l), Pl(S_l)]$ of level S_l, respectively, and $l = 1, 2, \ldots, m$.

Step 7. According to $\Delta = (\Delta_{j,l})_{m \times m}$, if $\Delta_{j,l} > 0.5$, the degree of support of the fusion result for "the innovation of interactive packaging belongs to S_j" is higher than that of the fusion result for "the innovation of interactive packaging belongs to S_l," which is recorded as $S_j \succ S_l$. If $\Delta_{j,l} < 0.5$, the degree of support of the fusion result for "the innovation of interactive packaging belongs to S_j" is lower than that of the fusion result for "the innovation of interactive packaging belongs to S_l," which is recorded as $S_j \prec S_l$. If $\Delta_{j,l} = 0.5$, the degree of support of the fusion result for "the innovation of interactive packaging belongs to S_j" is equal to that of the fusion result

for "the innovation of interactive packaging belongs to S_l," which is recorded as $S_j \approx S_l$. After judgment in turn, the evaluation level with the highest degree of support is the innovation level of interactive packaging design.

4. Case Study

The shape, color, pattern, and material of packaging should be able to arouse people's favorite emotions because people's likes and dislikes play a very important role in buying impulse. Favors come from two aspects. The first is practical, that is, whether the packaging can meet the needs of consumers in all aspects and provide convenience, which involves the size, size, beauty, and other aspects of the packaging. The same skin care cream can be packaged in large bottles or small boxes. Consumers can choose it according to their habits; the same products with exquisite packaging are easy to be selected as gifts and those with poor packaging can only be used by themselves. When the packaging of the product provides convenience, it will naturally arouse consumers' favor. The interactive packaging design of a certain nut food is shown in Figure 3.

It is now necessary to identify the innovation of the interactive packaging visual Chuangda design. The implementation steps are as follows:

We set the innovative evaluation level of interactive packaging as level 3: S_1, S_2, S_3, which are superior, medium , and inferior in sequence. Experts from four expert groups evaluates the innovation of interactive packaging visual communication design. Here, the number of experts included in the four expert groups are as follows: ε_1 =25, ε_2 = 28 , ε_3 = 30 , and ε_4 = 27. The evaluation results of the fourexpert groups on theinnovation of interactivepackaging visual creative design are shown in Table 1–4, respectively.

Then, we construct the identification framework for the innovative evaluation of the interactive packaging visual creative design $\Theta = \{S_1, S_2, S_3\}$.

The evaluation information of the four expert groups is regarded as evidence and further expressed as the basic probability assignment function under the identification framework, which is expressed by $mass_1, mass_2, \ldots, mass_4$.

For $mass_1$, $mass_1(S_1) = 0.8000$, $mass_1(S_2) = 0.0400$, $mass_1(S_3) = 0.0400$, $mass_1(S_1, S_2) = 0.0400$, $mass_1(S_2, S_3) = 0.0400$, and $mass_1(S_1, S_3) = 0.0400$.

For $mass_2$, $mass_2(S_1) = 0.0357$, $mass_2(S_2) = 0.0714$, $mass_2(S_3) = 0.7500$, $mass_2(S_1, S_2) = 0.0357$, $mass_2(S_2, S_3) = 0.0357$, and $mass_2(S_1, S_3) = 0.0714$.

For $mass_3$, $mass_3(S_1) = 0.8333$, $mass_3(S_2) = 0.0333$, $mass_3(S_3) = 0.0333$, $mass_3(S_1, S_2) = 0.0333$, $mass_3(S_2, S_3) = 0.0333$, and $mass_3(S_1, S_3) = 0.0333$.

For $mass_4$, $mass_4(S_1) = 0.7778$, $mass_4(S_2) = 0.0370$, $mass_4(S_3) = 0.0370$, $mass_1(S_1, S_2) = 0.0741$, $mass_1(S_2, S_3) = 0.0370$, and $mass_1(S_1, S_3) = 0.0370$.

Based on WFR-CDDO, $mass_1, mass_2, \ldots, mass_4$ are fused.

CO is $\text{mass}'(S) = 1/1 - k\sum_{S^p \cap S^q \cap \ldots \cap S^r = S} \text{mass}_1(S^p)\ \text{mass}_2(S^q) \ldots \text{mass}_4(S^r)$, where $mass'$ represents the mass function obtained by fusing four mass functions with CO,

Figure 3: The interactive packaging design of a certain nut food.

Table 1: Evaluation results of the first expert group on the innovation of interactive packaging visual creative design.

	S_1	S_2	S_3	S_1, S_2	S_2, S_3	S_1, S_3
Number of experts	20	1	1	1	1	1

Table 2: Evaluation results of the second expert group on the innovation of interactive packaging visual creative design.

	S_1	S_2	S_3	S_1, S_2	S_2, S_3	S_1, S_3
Number of experts	1	2	21	1	1	2

Table 3: Evaluation results of the third expert group on the innovation of interactive packaging visual creative design.

	S_1	S_2	S_3	S_1, S_2	S_2, S_3	S_1, S_3
Number of experts	25	1	1	1	1	1

Table 4: Evaluation results of the fourth expert group on the innovation of interactive packaging visual creative design.

	S_1	S_2	S_3	S_1, S_2	S_2, S_3	S_1, S_3
Number of experts	21	1	1	2	1	1

$S^p, S^q, \ldots, S^r \subset \Theta$, $S = S_1, S_2, S_3, \ldots, \{S_x, \ldots, S_y\}, \ldots$; $k = \sum_{S^p \cap S^q \cap \ldots \cap S^r = \varnothing} \text{mass}_1(S^p)\text{mass}_2(S^q) \ldots \text{mass}_4(S^r)$.

DO is $\text{mass}''(S) = \sum_{S^p \cup S^q \cup \ldots \cup S^r = S} \text{mass}_1(S^p)\ \text{mass}_2(S^q) \ldots \text{mass}_4(S^r)$, where $mass''$ represents the mass function obtained by fusing four mass functions with DO.

The expression of WFR-CDDO is

$$\begin{aligned} mass'''(S) &= \alpha \cdot mass'(S) + \beta \cdot mass''(S) \\ &= \alpha \frac{1}{1-k} \sum_{S^p \cap S^q \cap \ldots \cap S^r = S} mass_1(S^p) mass_2(S^q) \ldots mass_4(S^r) \\ &\quad + \beta \sum_{S^p \cup S^q \cup \ldots \cup S^r = S} mass_1(S^p) mass_2(S^q) \ldots mass_4(S^r). \end{aligned} \tag{11}$$

It is further expressed as

$$mass^{'''}(S) = \sum_{S^p \cap S^q \cap \ldots \cap S^r = S} mass_1(S^p) mass_2(S^q) \ldots mass_4(S^r) + k \sum_{S^p \cup S^q \cup \ldots \cup S^r = S} mass_1(S^p) mass_2(S^q) \ldots mass_4(S^r). \quad (12)$$

According to WFR-CDDO, four *mass* functions $mass_1, mass_2, \ldots, mass_4$ are fused. We calculate the fusion results in turn: $mass^{'''}(S_1)$, $mass^{'''}(S_2)$, $mass^{'''}(S_3)$, $\ldots$, $mass^{'''}(\{S_x, \ldots, S_y\})$, $\ldots$:

(i) $mass^{'''}(S_1) = 0.7638$

(ii) $mass^{'''}(S_2) = 0.0141$

(iii) $mass^{'''}(S_3) = 0.1011$

(iv) $mass^{'''}(S_1, S_2) = 0.0422$

(v) $mass^{'''}(S_2, S_3) = 0.0309$

(vi) $mass^{'''}(S_1, S_3) = 0.0479$

Then, we calculate on identification framework $\Theta = \{S_1, S_2, S_3\}$.

The reliability function and plausibility function of S_1 are $Bel(S_1) = 0.7638$ and $Pl(S_1) = 0.8539$, which constitute the trust interval of S_1: $[Bel(S_1), Pl(S_1)] = [0.7638, 0.8539]$.

The reliability function and plausibility function of S_2 are $Bel(S_2) = 0.0141$ and $Pl(S_2) = 0.0872$, which constitute the trust interval of S_2: $[Bel(S_2), Pl(S_2)] = [0.0141, 0.0872]$.

The reliability function and plausibility function of S_3 are: $Bel(S_3) = 0.1011$ and $Pl(S_3) = 0.1799$, which constitute the trust interval of S_3: $[Bel(S_3), Pl(S_3)] = [0.1011, 0.1799]$.

Based on the trust intervals of S_1, S_2, S_3, we calculate

$$\Delta = \left(\Delta_{j,l}\right)_{3\times 3} = \begin{bmatrix} 0.5 & 1 & 1 \\ 0 & 0.5 & 0 \\ 0 & 1 & 0.5 \end{bmatrix}. \quad (13)$$

According to $\Delta = (\Delta_{j,l})_{3\times 3}$, $\Delta_{1,2} = 1 > 0.5$, so the degree of support of fusion results for "the innovation of interactive packaging visual communication design belongs to S_1" is higher than that of fusion results for "the innovation of interactive packaging visual communication design belongs to S_2," that is, $S_1 \succ S_2$.

$\Delta_{1,3} = 1 > 0.5$, so the degree of support of fusion results for "the innovation of interactive packaging visual communication design belongs to S_1" is higher than that of fusion results for "the innovation of interactive packaging visual communication design belongs to S_3," that is, $S_1 \succ S_3$.

$\Delta_{2,3} = 0 < 0.5$, so the degree of support of fusion results for "the innovation of interactive packaging visual communication design belongs to S_2" is lower than that of fusion results for "the innovation of interactive packaging visual communication design belongs to S_3," that is, $S_2 \prec S_3$.

Therefore, the evaluation grade with the highest degree of support for fusion results is S_1, and the innovation of interactive packaging visual communication design belongs to S_1.

5. Conclusions

As a comprehensive course across social sciences and humanities and social sciences, digital media art can be applied to the Internet-famous food packaging design, promote the reform and improvement of visual communication design of Internet-famous food packaging, make electronic information technology and news media technology organically combine with Internet-famous food packaging technology, and give new meaning to Internet-famous food packaging. When the evidence fusion rules in the classical evidence theory deal with the evidence contradiction in the innovative identification of interactive packaging visual communication design, they will get wrong results that are contrary to the common sense. Compared with the evidence fusion rules in the classical evidence theory, the conjunction disjunction double arithmetic weighted fusion rules provided in this study can support the contradiction processing in the innovative identification of interactive packaging visual communication design.

Data Availability

The dataset can be accessed upon request.

Conflicts of Interest

The authors declare that they have no conflicts of interest.

Acknowledgments

This work was supported by the Teaching Reform and Innovation Project of Colleges and Universities in Shanxi Province (J2019200) and Teaching Reform Research Project of Taiyuan Institute of Technology (2018YJ13).

References

[1] Yu. Chen, "Visual communication design based on 5G technology," *Wireless Communications and Mobile Computing*, vol. 2022, Article ID 1699213, 12 pages, 2022.

[2] J. Yang, X. LiLi, and X. Li, "Data-driven dynamic neural programming for network media nonlinear visual communication design," *Mathematical Problems in Engineering*, vol. 2022, p. 10, 2022.

[3] X. Liu, "Animation Special Effects Production Method and Art Color Research Based on Visual Communication Design," *Scientific Programming*, vol. 2022, Article ID 7835917, 13 pages, 2022.

[4] X. Guan and K. Wang, "Visual Communication Design Using Machine Vision and Digital Media Communication Technology," *Wireless Communications and Mobile Computing*, vol. 2022, Article ID 6235913, 11 pages, 2022.

[5] Y. Zhang, R. YuYu, X. ShiShi, K. HongHong, and K. Hong, "Visual communication design in print advertising under new media environment," *Wireless Communications and Mobile Computing*, vol. 2022, Article ID 7664127, 10 pages, 2022.

[6] Y. Gao, "Feature Extraction Technology-Guided Visual Communication Design for Folk Paper-Cutting," *Scientific Programming*, vol. 2022, Article ID 3210054, 9 pages, 2022.

[7] C. Ma and W. Chung, "Visual communication design based on collaborative wireless communication video transmission," *Journal of Sensors*, vol. 2022, Article ID 5348222, 11 pages, 2022.

[8] H. Zhang and C. Wu, "An analysis of computer-aided design software course teaching in visual communication design

major by integrating grey variable weight clustering evaluation model," *Advances in Multimedia*, vol. 2021, Article ID 6588734, 7 pages, 2021.

[9] W. Zhu, "A Study of Big-Data-Driven Data Visualization and Visual Communication Design Patterns," *Scientific Programming*, vol. 2021, Article ID 6704937, 11 pages, 2021.

[10] Z. Dong, L. Lu, Z. Liu, Y. Tang, and J. Wang, "Migration of toxic metals from ceramic food packaging materials into acid food Simulants," *Mathematical Problems in Engineering*, vol. 2014, Article ID 759018, 11 pages, 2014.

[11] E. Ghorbani, D. Moghaddam, A. Sharifan, and H. Kiani, "Emergency food product packaging by pectin-based antimicrobial coatings functionalized by pomegranate peel extracts," *Journal of Food Quality*, vol. 2021, Article ID 6631021, 10 pages, 2021.

[12] W. Ye and Y. Li, "Design and Research of Digital Media Art Display Based on Virtual Reality and Augmented Reality," *Mobile Information Systems*, vol. 2022, Article ID 6606885, 12 pages, 2022.

[13] Y. Li and W. Zhuge, "Application of Animation Control Technology Based on Internet Technology in Digital Media Art," *Mobile Information Systems*, vol. 2022, Article ID 4009053, 11 pages, 2022.

[14] M. Wang, J. Wang, and C. Zhang, "Visual Space System Design in Digital Media Art Design," *Scientific Programming*, vol. 2022, Article ID 3678090, 13 pages, 2022.

[15] P. Liu, C. Song, X. Ma, and T. Xuchao, "Visual Space Design of Digital Media Art Using Virtual Reality and Multidimensional Space," *Mobile Information Systems*, vol. 2022, Article ID 822057, 11 pages, 2022.

[16] H. Tian, "Application and Analysis of Artificial Intelligence Graphic Element Algorithm in Digital Media Art Design," *Mobile Information Systems*, vol. 2022, Article ID 6946616, 11 pages, 2022.

[17] Y. Liu, S. Wu, Qi Xu, and H. Liu, "Holographic Projection Technology in the Field of Digital Media Art," *Wireless Communications and Mobile Computing*, vol. 2021, Article ID 9997037, 12 pages, 2021.

[18] W. Ye and Y. Li, "Digital Media Art Display Design and Research under the Research of 3D Point Cloud Data Acquisition Technology Based on Sequence Images," *Mobile Information Systems*, vol. 2022, Article ID 7106900, 12 pages, 2022.

[19] X. Wu and Y. Li, "Experience Mode of Digital Media Art under Virtual Reality Technology," *Applied Bionics and Biomechanics*, vol. 2022, Article ID 5117150, 6 pages, 2022.

[20] T. Mao and X. Jiang, "The use of digital media art using UI and visual sensing image technology," *Journal of Sensors*, vol. 2021, Article ID 9280945, 11 pages, 2021.

[21] M. Liu, Y. Wang, J. Chen, and Y. Zhang, "Link Prediction Model for Weighted Networks Based on Evidence Theory and the Influence of Common Neighbours," *Complexity*, vol. 2022, Article ID 9151340, 16 pages, 2022.

[22] L. Li, B. Lei, and C. Mao, "Digital twin in smart manufacturing," *Journal of Industrial Information Integration*, vol. 26, no. 9, Article ID 100289, 2022.

[23] Y. Liu, T. Bao, H. Sang, and Z. Wei, "A novel method for conflict data fusion using an improved belief divergence measure in dempster-shafer evidence theory," *Mathematical Problems in Engineering*, vol. 2021, Article ID 6558843, 15 pages, 2021.

[24] L. Li, T. Qu, and Y. Liu, "Sustainability assessment of intelligent manufacturing supported by digital twin," *IEEE Access*, vol. 8, pp. 174988–175008, 2020.

[25] L. Li and C. Mao, "Big data supported PSS evaluation decision in service-oriented manufacturing," *IEEE Access*, vol. 8, no. 99, p. 1, 2020.

[26] J. Zhang, C. Wu, C. Ruan, R. Zhang, Z. Zhao, and X. Cheng, "ECG signal classification based on fusion of hybrid CNN and wavelet features by D-S evidence theory," *Journal of Healthcare Engineering*, vol. 2021, Article ID 4222881, 13 pages, 2021.

[27] L. Li, C. Mao, H. Sun, Y. Yuan, and L. Bingbing, "Digital twin driven green performance evaluation methodology of intelligent manufacturing: hybrid model based on fuzzy rough-sets AHP, multistage weight synthesis, and PROMETHEE II," *Complexity*, vol. 2020, no. 6, p. 24, 2020.

[28] Z.-Q. Liu, M.-C. Peng, and Y.-C. Sun, "Estimation of driver lane change intention based on the LSTM and dempster-shafer evidence theory," *Journal of Advanced Transportation*, vol. 2021, Article ID 8858902, 11 pages, 2021.

[29] Y.-L. Zhang and C.-Qv. Li, "Numerical characterizations of topological reductions of covering information systems in evidence theory," *Mathematical Problems in Engineering*, vol. 2021, Article ID 6648108, 9 pages, 2021.

[30] Z. Wan, M. Shi, F. Yang, and G. Zhu, "A novel pythagorean group decision-making method based on evidence theory and interactive power averaging operator," *Complexity*, vol. 2021, Article ID 9964422, 11 pages, 2021.

[31] C. Wang and H. G. Matthies, "Epistemic uncertainty-based reliability analysis for engineering system with hybrid evidence and fuzzy variables," *Computer Methods in Applied Mechanics and Engineering*, vol. 355, pp. 438–455, 2019.

[32] C. Wang and H. G. Matthies, "Evidence theory-based reliability optimization design using polynomial chaos expansion," *Computer Methods in Applied Mechanics and Engineering*, vol. 341, pp. 640–657, 2018.

[33] L. Sun, M. K. Siddique, L. Wang, and S. J. Li, "Mixing characteristics of a bubble mixing microfluidic chip for genomic DNA extraction based on magnetophoresis: CFD simulation and experiment," *Electrophoresis*, vol. 42, no. 21-22, pp. 2365–2374, 2021.

[34] Z. Wang, J. Jiang, and T. Wang, "Failure probability analysis and critical node determination for approximate circuits," *Integration*, vol. 68, pp. 122–128, 2019.

Hindawi
Scientific Programming
Volume 2022, Article ID 5333231, 9 pages
https://doi.org/10.1155/2022/5333231

Research Article

Urban Green Space Planning and Design for Sponge City

Hong Jiao and Jingliang Han

College of Landscape Architecture, Northeast Forestry University, Harbin, Heilongjiang 150000, China

Correspondence should be addressed to Jingliang Han; hanjingliang@nefu.edu.cn

Received 31 May 2022; Revised 17 June 2022; Accepted 20 June 2022; Published 30 July 2022

Academic Editor: Lianhui Li

Urban green space designed based on the concept of sponge city is an important sponge carrier. Guided by the theory of landscape ecology, this article introduces the artificial neural network (ANN) model and uses the research method of landscape pattern index to establish a model for the proportion of urban green space types and the characteristics and dynamic changes of landscape spatial pattern. Based on the optimal landscape pattern index, the theoretical value of the optimal proportion of ecological green space, community park, comprehensive park, roadside green space, protective green space, and strip green space is obtained through the model. Based on this proportion value, combined with the ANN model, the reasonable evaluation results of patch density and average perimeter area ratio, spread degree, and diversity index of planned green space are obtained. Then, according to the influence of various green spaces on each landscape index, the development trend of urban green space construction in the future is predicted.

1. Introduction

Due to global warming and the acceleration of urbanization, coupled with the increasingly prominent problem of natural resources, the environmental quality of urban development is also increasingly worrying. After meeting the needs of material and cultural life, modern people begin to put forward higher requirements for the living environment. People's longing for a better life includes people's hope to see blue sky, green grassland, and breathe fresh air. Therefore, it has become an urgent hope for modern people to change the current situation of the city and build a new ecological city more suitable for people's living. In this context, the concept of "building a sponge city with natural accumulation, natural infiltration, and natural purification" came into being [1–5].

The essence of sponge city is to establish an ecosystem in the city; use the power of nature for drainage; build a sponge city, make the rainwater of the city reach the natural accumulation, natural infiltration, and natural purification; make the city closer to nature; plan all kinds of resources as a whole; reduce the damage of development and construction to the original ecosystem; and realize the harmonious coexistence between mankind and nature.

As a recreational place for residents, urban green space has important value in the fields of ecological environment, society, and culture. In the construction of sponge city, urban green space, as an important carrier, can effectively play the "sponge" role of "infiltration, stagnation, storage, purification, utilization, and drainage" through the application of low-impact development engineering technology in the construction process [6–9]. However, the green space designed based on the concept of sponge city not only bears the inherent role of recreation, greening, and beautifying the environment, but also should play the role of sponge carrier in the face of water environment problems. If we can form an effective feedback mechanism for such green space from the perspective of users, it will promote the improvement of such sponge facilities and the effective play of sponge function.

From the perspective of land planning, environment, and ecology, urban green space refers to urban nonconstruction land dominated by natural and artificial vegetation. The main contents include two levels: one is the land used for greening within the scope of urban construction land, and the other is the area outside the scope of urban construction land, which plays a role in urban ecology, landscape, and

residents' leisure life and has a good greening environment. From the perspective of architecture, urban planning, and landscape architecture, urban green space refers to the area where green plants are planted within the scope of urban planning land, which can improve and maintain the ecological environment; beautify the city appearance; provide leisure and recreation sites; or have the functions of sanitation, safety, and protection. According to this definition, the production land of agriculture, forestry, and animal husbandry outside the urban regional planning and nature reserves do not belong to the category of green space. The definitions of urban green space obtained from different angles are different. Generally speaking, urban green space can be divided into broad and narrow concepts. In the narrow sense, it refers to the green land within the scope of urban land construction. In the broad sense, it generally refers to all areas covered by green plants. At present, the urban green space system we plan should be the combination of broad and narrow green space, so as to make a more reasonable analysis and discussion.

Urban environmental problems have always been a major problem restricting human survival and development [10–12]. In order to achieve sustainable development, we must act in accordance with the laws of nature. The proposal of the concept of sponge city is not only the process of constructing the rainwater system of urban low-impact development, but also the process of solving urban problems according to the laws of nature. As an important carrier of sponge city construction, park green space is expected to achieve the goal of "natural accumulation, natural infiltration, and natural purification" of sponge city while realizing the original function of urban park. In fact, after the completion of the sponge park green space, what is the realization of its sponge function? What is the feedback from park users? At present, there is still a lack of theoretical research in this field. Based on this, the purpose of this study is as follows:

(1) We need to comprehensively explore the relevant theories of green space planning and design based on the concept design of sponge city and the theory of post-use evaluation and seek a feasible method for post-use evaluation of the sponge park green space. (2) We hope to establish a feasible post-use evaluation system of the sponge park green space so that it can guide the post-use evaluation of the built sponge park green space. (3) After obtaining the results of post-use evaluation of practical cases, through the analysis of the results, we hope to promote the development and optimization of case green space and provide a reference for the construction and management of similar sponge green space in the future.

2. Overall Research Framework

Recently, the urban green space system planning in various parts of China has different methods, diverse technologies, and different quantitative indicators, so the planning has its own characteristics and has its rationality. However, how to evaluate its rationality, whether there are some deficiencies, and places that can be improved are the main starting point of this article. If problems are found in advance, it is not necessary to adjust the planning, but if we can be aware of the existing problems and consider them in the next round of planning, it will certainly help to promote the green space system planning in a more scientific and practical direction. For urban management departments, after the rapid development of urban construction, all localities will inevitably face the planning of new and old cities.

How to make the new town not completely "start a new stove" but reflect the urban characteristics; continue the green space layout, historical context, and other traditions of the old city; and whether the existing green space system planning is still applicable in the construction of new towns with policy tendencies are the breakthrough points of introducing artificial neural network (ANN) [13–16] to evaluate the existing green space system planning in this article.

ANN is an engineering system that simulates its structure and intelligent behavior based on the understanding of the organizational structure and operation mechanism of the human brain from the perspective of microstructure and function. It is a highly nonlinear processing system formed by the extensive interconnection of a large number of processing units (neurons), which is suitable for simulating complex systems. Human brain activity is a highly nonlinear dynamic system. Although the structure and function of several neurons are very simple, the behavior of the neural network composed of a large number of neurons is colorful and extremely complex. The nature of the overall activity is not equal to the simple addition of the activities of unit neurons.

The main contents of this study include: through the detailed study of the ANN principle, taking the method of landscape ecology as the intermediary, we interpret the feasibility of using the method to evaluate the urban green space system planning and construct the green space system planning evaluation system. According to the process of urban development, we thoroughly analyze the characteristics of the green space system in the urban green space system planning. On this basis, we divide three types of green space representing the "past, present, and future" of the study area and take the "present" green space as a sample to evaluate the rationality of "future" green space planning by establishing a simulation model. ANN is used to establish the relationship model between the proportion of green space types and landscape pattern index, predict the pattern changes of planned urban green space, and provide a reference basis for the overall evaluation of the existing urban green space system planning.

By compiling the network program, we use the artificial neural network model to model the green space data and landscape pattern index, simulate the internal relationship between various green space areas and landscape pattern index based on the existing data, predict the planning development trend, and optimize the green space system planning for sponge city. The technical route of this study is shown in Figure 1.

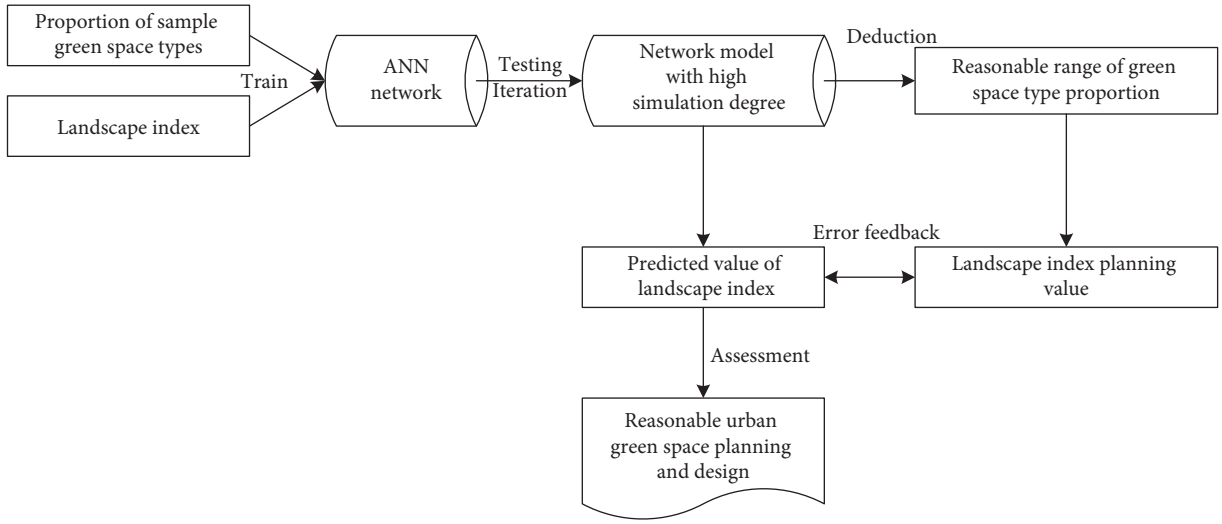

Figure 1: The technical route.

3. Methods

3.1. Evaluation System of the Green Space System Planning. Landscape ecological planning needs to select the influencing factors and calculate the weight of each factor to superimpose its effect. Similarly, the artificial neural network also needs to preselect the number of factors, that is the number of neurons in the hidden layer. The difference is that its factor characteristics are uncertain, which can only be identified within the network and cannot be truly expressed in language.

The most famous supervised algorithm is the error back propagation (BP) algorithm of a multilayer feedforward artificial neural network [17–20]. Structurally speaking, the network is composed of layers or layers above, that is the input layer, the hidden layer, and the output layer. Neurons in each layer form a full connection, while neurons in the same layer have no connection [21–25]. In the same network, there can be more than two hidden layers, as shown in Figure 2. The network with only one hidden layer is a basic network model.

For the BP network, there is a very important theorem, that is any continuous function in a closed interval can be approximated by a single hidden layer network, so a three-layer network can complete any dimension to dimension mapping. The selection of the number of neurons in the hidden layer is more complex. At present, it is mainly determined according to the previous experience and many experiments. So far, there is no ideal analytical formula to calculate. The number of hidden layers is not the more the better. It is directly related to the requirements of the problem and the number of input and output units. Too much number will lead to too long learning time, not necessarily the best error, poor tolerance, and unable to identify samples that have not been seen before. Therefore, there must be an optimal number of hidden units. The empirical formula can be used as a reference formula for selecting the best number of hidden layer neurons, or the number of hidden layer neurons can be determined by

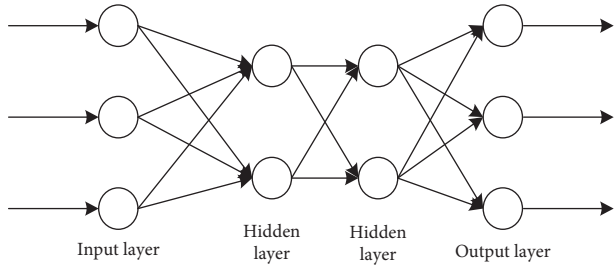

Figure 2: BP network.

experimental method without formula calculation. The process of this method is: initially put enough neurons and eliminate those that do not work through learning until they cannot contract; or start to put in fewer neurons. After learning a certain number of times, if it is unsuccessful, increase the number until it reaches a more reasonable number.

In the process of landscape ecological planning, between the current situation and planning, many factors need to participate in the planning process. Each factor has a corresponding weight proportion when it plays its role. The determination process of this weight is equivalent to the calculation process of the function, which is completed through the incentive function or transfer function. The relationship between the input layer and the output layer of the network is represented by a function as the carrier, which is the excitation function. The excitation function is an important weaving part of the network. It must be continuously differentiable so that it can be calculated by a gradient method.

3.2. Construction of Network

3.2.1. Input Layer. The selection principle of the input layer is to intuitively express the variables of research events. These variables should be measurable (e.g., distance and

length), searchable (e.g., quantity), or statistical. In relevant studies, elevation, slope, geomorphic zoning, population density, distance from the core landscape, and other indicators are mostly used as the input layer. Most of these indicators are objective or natural factors, which can reflect the impact of natural driving forces and human interference on the landscape to some extent and can better explain the significance of the network. In fact, in urban planning or green landscape planning, in addition to the basic ecological factors that need to be considered in urban construction, in more cases, the factors with practical guiding significance established based on these factors, or "secondary factors," such as land use punishment, population distribution, etc., or these basic "ecological sensitive factors" are often only used for reference without actual expression status.

In view of the above reasons, in the landscape ecological network of this article, the percentage of the area of various types of landscape is considered to be selected as the input variable, and multiple input variables composed of each sample together constitute the input layer matrix [21]. It is one of the basis to help us determine the dominant landscape elements in the landscape, and it is also an important factor to determine the ecosystem indicators such as biodiversity, dominant population, and quantity in the landscape. In fact, the process of forming the area percentage of various types of landscape in the city has integrated the repeated influence of all ecological, social, land use, and other factors. It can be said to be the "semi-finished product" of green space pattern. Researching on this basis may produce some errors, but this choice can directly adopt the existing achievements and strengthen the application and promotion ability of research, which has certain application value.

3.2.2. Output Layer. The data of the output layer are generally indicators that can reflect the essence or deep meaning of the event. These indicators have a logical connection with the data of the input layer that are not obvious but has a high internal correlation. At present, there are many kinds of landscape pattern indexes, and new indexes have been put forward by scholars. However, these indexes have a great correlation in essence, and the indexes do not meet the requirements of mutual independence [23, 24]. Therefore, using multiple indexes at the same time often cannot add "new" information. Naturally, using these indexes with great correlation to describe landscape pattern is not convincing enough. Theoretically, there must be an index system of landscape pattern, which is enough to describe the landscape pattern, but not redundant.

Therefore, the analysis of the mutual independence of landscape index has become an important research topic. Combined with the actual situation of this study, four landscape pattern indexes of patch density, Shannon diversity index, average perimeter area ratio, and spread degree are selected as the output layer of the network, as shown in Table 1. Based on the principle of landscape pattern index representing green space change and spatial allocation, it is expected to study the relevant characteristic process and change development trend of green space through these four indexes.

(1) Patch density, which is the number of patches per unit area, reflects the overall degree of patch differentiation or fragmentation of the landscape. The change of its value can reflect the intensity and direction of human interference. The high patch density indicates that there are many heterogeneous landscape elements in a certain area, with small patch size and high degree of fragmentation. For urban green space landscape, the degree of landscape fragmentation indicates the contribution and ability of urban green space landscape to biodiversity maintenance. Generally, under the condition of equal area, the higher the degree of fragmentation, the smaller the urban green space landscape patch unit, the simpler the function of the landscape unit, and the more unfavorable to biodiversity protection.

(2) Shannon diversity index indicates that the whole landscape is composed of only one patch. The increase of this index indicates that the patch types increase or the patch types are distributed in a balanced trend in the landscape. This index can reflect the landscape heterogeneity, especially sensitive to the unbalanced distribution of patch types in the landscape, that is it emphasizes the contribution of rare patch types.

(3) The average perimeter area ratio is one of the important indicators of the complexity of landscape spatial pattern. It represents the complexity of irregular objects and is used to measure the complexity of shapes. The lower the value is, the simpler the patch boundary is, and the less conducive to the maintenance of biodiversity.

(4) The spread degree, with a value of 0-1, is one of the most important indexes to describe the landscape pattern. This index describes the degree of agglomeration or extension trend of different patches in the landscape. Theoretically, a small value indicates that there are many small patches in the landscape. The landscape is a dense pattern with many elements. When the degree of fragmentation of the landscape is high, it indicates that some dominant patches in the landscape have formed good connectivity.

3.2.3. Network Training. "Network training" integrates two inseparable processes of learning and training. In principle, it is a process of looking for a set of useful weights and thresholds. The popular explanation is a process of learning and integrating the network into the network's own knowledge and experience through the existing data [21–25]. The connection weight is the knowledge reserve required by the neural network to solve practical problems. The training process of the network can be described as forward propagation of working signal and back propagation of error signal. First, training is to provide a training set, which is

Table 1: Landscape pattern indexes.

Index name	Patch density	Shannon diversity index	Average perimeter area ratio	Spread degree
Exponential space representation	Nonspatial component	Nonspatial component	Space configuration	Space configuration
Value range	>0	=0	>0	[0, 1]
Characteristic	Landscape fragmentation	Spatial heterogeneity	Landscape spatial structure	Optimal landscape pattern
Practical significance	It reflects human interference	Complexity of structure and function	Complexity of shape	Agglomeration degree or extension trend of different patch types

composed of several groups of input samples and the corresponding expected output. At the beginning of network construction, the ownership value and training value contained in the middle of the problem to be solved are unknown. Generally, the initial value of the network is randomly generated. Until the useful weight is found, the artificial neural network cannot represent this problem.

Step 1. The system randomly selects a learning sample; calculates the input of each neuron in the hidden layer with the input sample, initial weight, and threshold; and then calculates the output of each neuron in the hidden layer through the excitation function.

Step 2. The output of each neuron in the output layer is calculated by using the output matrix, initial weight, and boudoir value of the hidden layer, and then the response of each neuron in the output layer is calculated by the excitation function, that is the actual output of the sample.

Step 3. The generalization error of each neuron in the output layer is calculated by using the expected output of the sample and the actual output of the network. The generalization error of each unit in the hidden layer is calculated by using the initial weight of the hidden layer, the generalization error of the output layer, and the output of each neuron in the hidden layer.

Step 4. The generalized error is propagated back to the input layer, and the weights and thresholds of the input layer and the hidden layer are gradually corrected.

Step 5. The next learning sample is randomly selected and returned to the first step until all learning samples are trained.

Step 6. A group of input and output matrices is randomly selected from the learning samples again and returned to the first step until the global error of the network is less than a preset minimum, and the network training ends and reaches convergence.

From the above training process, it can be seen that the core of e-learning consists of four parts. First, the "signal forward propagation" of the input data from the input layer through the hidden layer to the output layer. Second, the error signal between the actual output and the expected output of the network is "error back propagation," which modifies the weight layer by layer from the output layer to the input layer through the hidden layer. Third, the network "memory training" process of repeated cycles of "signal forward propagation" and "error inverse propagation." Fourth, the global error of the network tends to the preset minimum, that is the process of network learning convergence.

4. Application of Urban Green Space Planning and Design Network

The trained network should also carry out a performance test. The test method is to select the test sample data and provide it to the network to test the correctness of the network's output. The test sample data should have a pattern similar to the learning data. These samples can be obtained by direct measurement or simulation. When the sample data are small or difficult to obtain, they can also be obtained by adding appropriate noise to the learning samples or interpolating according to certain rules. In order to better verify the generalization ability of the network, a good test sample set should not contain the same pattern as the learning sample.

When using ANN to simulate the existing urban green space system planning [26, 27], the omnidirectional expression of the landscape index should be considered on the whole green space landscape as far as possible and the index change should be evaluated after the construction of the network from the following aspects:

(1) Evaluate whether the type and proportion of planned green space are reasonable

The amount of green space reflects the level of urban green space, and the type proportion of green space can reflect the integrity and spatial structure of urban green space and will indirectly affect the function of green space.

(2) Evaluate whether the landscape fragmentation of the planned green space is reasonable

The size of patch density will directly reflect the degree of landscape fragmentation. The greater the patch density, the higher the degree of fragmentation. At the same time, it further reflects the living standard of urban residents, the quality of living environment, and the ecological level of the city.

(3) Evaluate whether the landscape diversity of planned green space is reasonable

The level of landscape diversity mainly depends on the number of landscape components and the

proportion of each landscape component. In the landscape system, the more the landscape components and the higher the degree of fragmentation, the greater the information content and uncertainty, the higher the landscape diversity index, and the higher the landscape heterogeneity.

(4) Evaluate whether the landscape fractal dimension of planned green space is reasonable

Landscape fractal dimension mainly measures the complexity of green space shape. The index selected in this study is the average perimeter area ratio. If the urban green space is greatly disturbed by human beings, the patch shape is regular and simple, and the landscape fractal dimension is low, which is unfavorable to the maintenance and construction of biodiversity. By evaluating the rationality of landscape fractal dimension, we can detect whether we pay too much attention to regular design and whether there are too heavy artificial carving traces in the process of green space design, so as to strengthen the attention to the naturalization, ecology, and diversification of green space.

To sum up, the type proportion of green space is related to the fragmentation and diversity of landscape, and there is a certain contradiction between fragmentation and diversity. In the process of evaluation and analysis, we must pay attention to this contradiction and comprehensively weigh and consider the value of landscape index.

5. Case Study

Based on the landscape ecological network, the network is constructed through the network command Newff built in MATLAB, and the hyperbolic tangent sigmoid (Tan-SIGMOD) function and linear function are selected as the excitation functions of the hidden layer and the output layer, respectively. In terms of performance setting, the maximum number of training is 6000, the learning rate is 0.01, and the preset expected error is 0.0001. The preset expectation error is too large and has no popularization value. The preset expected error cannot be set too small, because the number of samples is limited and the error setting is small, which will affect the generalization ability of the network, and there may be large errors in application.

According to the empirical formula of hidden layer design and the actual situation of this case, the number of hidden layer neurons in the network to solve this problem should be between 5 and 15. Therefore, it is necessary to design a network with a variable number of hidden layer neurons for debugging in advance and determine the optimal number of neurons through error comparison and trade-off consideration. In order to improve the training speed, set each index to a higher value during debugging, such as learning rate 0.05 and preset expected error 0.005, and the training error results are shown in Table 2.

It can be seen from Table 2 that in the error test with 5–15 as the number of hidden layer neurons, when the number of hidden layer neurons is less than 7, the network error is greater than 0.005, the preset target error value cannot be reached, and the network cannot converge. In the 6^{th} experiment, when the number of hidden layers reaches 10, the error reaches a lower value, and the error fluctuates with the increase of the number of neurons. In the 10^{th} training, that is when the number of hidden layers reaches 12, the error tends to a stable decline state, the training time is significantly shorter, and the training times are reduced. After less than 20 training, the error can reach the preset expected value. The network can converge without enough training, and the error is very small. Such a network can achieve high accuracy after training. However, when it comes to testing, it is likely to cause great errors, so its generalization ability is very poor and does not have generalization. To sum up, although the minimum error occurs in the network with 13 neurons in the hidden layer, its training time and times are too low and less than the number of samples. Therefore, it is more appropriate to select 10, which can not only ensure the training accuracy, but also improve the generalization ability of the network.

Table 2: Number of neurons in the hidden layer and its training error.

Training sequence	Number of neurons in the hidden layer	Error (10^{-3})
1	5	13.5056
2	6	8.4855
3	7	4.9513
4	8	4.3522
5	9	4.4355
6	10	1.9509
7	11	2.8112
8	12	4.4413
9	13	0.9422
10	14	2.6122
11	15	2.5234

After the network is created, it cannot be directly put into use. It can only be used as an urban green space model after training to meet the requirements. In neural network analysis, the sample data are generally divided into three parts: one part is used for network training, the other part is used as confirmation samples, and the other part is used as test samples. When using, the samples must be classified. According to their role in network analysis, they are divided into training samples (18 randomly selected), test samples (4), and simulation samples. In the selected samples, the protective green space and strip green space are evenly distributed, the roadside green space and community park are concentrated and scattered, and the ecological green space and comprehensive park are more concentrated in some samples. Training sample output layer data are shown in Table 3.

As can be seen from Table 3, the error of the network decreases sharply in the first 20 times of learning, and then gradually tends to be stable. After 135 times of learning, the network converges to reach the preset expected error value. There are two obvious fluctuation periods in the training process. The first occurs when the number of training times is times. At this time, all samples have just participated in a

Table 3: Training sample output layer data.

Sample number	Patch density	Shannon diversity index	Average perimeter area ratio	Spread degree
19	389.2528	1.0789	1105.3014	48.6681
16	320.1362	0.9112	1317.9503	55.0306
3	289.0374	1.1400	1043.5673	56.2471
22	215.1821	0.7293	1127.0597	62.1637
1	199.1799	1.2787	1121.1882	54.5327
12	153.1831	0.8915	1428.9752	60.9006
13	153.5420	1.0693	1086.6008	62.4801
2	184.4429	0.7671	1058.6464	63.1536
26	58.7127	0.5006	441.4895	73.4816
11	113.2049	0.6590	985.4602	68.8366
28	88.0661	0.6319	848.7701	68.0675
17	127.8780	0.9369	691.9037	66.5097
4	35.8730	1.0091	308.9164	65.1583
23	137.2126	1.5924	690.8689	52.7905
18	53.8462	1.3400	565.2578	52.7256
8	36.0435	1.3281	313.6877	52.9877
31	7.0275	1.2761	175.5812	55.1995
33	70.0896	1.0153	627.4805	51.8167
6	7.9927	1.0867	162.1879	51.9852
5	12.5912	0.9662	185.4276	56.3164
21	92.1729	0.8917	473.1836	59.4132
24	181.5919	0.7395	896.5168	49.0279

Table 4: Test sample input layer data.

Sample number	2	11	17	23
Protective green space	0.1024	0.0787	0.7189	0.3528
Roadside green space	0	0.3054	0.1126	0.0909
Ecological green space	0	0	0	0
Comprehensive park	0.7145	0	0	0.2822
Community park	0	0	0.1236	0.1551
Banded green space	0.1756	0.6312	0.0656	0.1378

Table 5: Test sample output layer data.

Sample number	2	11	17	23
Patch density	185.0742	153.0066	128.0687	135.0031
Shannon diversity index	0.8248	0.9235	0.9224	1.5398
Average perimeter area ratio	1059.0111	1428.0783	693.0627	691.0971
Spread degree	64.0777	61.0885	67.0027	53.0964

network training, and the substantial error adjustment is over. The second time occurs when the number of training times reaches 80, that is each sample has participated in the network correction for an average of 4 times. The network has adapted to the information contained in all samples. At this time, the network error no longer fluctuates, but decreases steadily until it reaches the set expected value.

After the network training, it must be tested to confirm its stability and popularization ability before it can be put into use. Its purpose is to determine whether the network meets the requirements of practical application. Test sample input layer data are shown in Table 4, and test sample output layer data are shown in Table 5.

We input the above data into the trained network, and the error is shown in Table 6.

As can be seen from Table 6, except that the diversity index error of samples 2 and 11 is large, the others maintain a high degree of coincidence, that is the network can better simulate the relationship between green space types and landscape pattern and has good popularization ability. The large error in the edge area of network data reflects the disadvantage of insufficient network samples. With the continuous increase of the number of samples, this error is bound to decrease gradually.

Table 6: Test sample error.

Sample number	2	11	17	23
Patch density	18.9952	−1.2040	−0.9760	0.0170
Shannon diversity index	−729.0094	307.9940	−0.1029	−0.5096
Average perimeter area ratio	−0.8021	0.0965	0.2189	−0.0088
Spread degree	−17.0065	3.9957	−0.2045	−0.0127

6. Conclusions

At present, the impact of green space on urban residents' life and urban environmental quality, urban characteristics, and historical and cultural preservation is becoming greater and greater. Urban green space has become a comprehensive function of urban residents' rest place, urban environmental maintenance, urban morphological structure guidance and control, and urban ecological security. The urban green space system planning, as a special planning of urban planning, has always been in a subordinate position of urban planning. In terms of preparation procedures, it is required

to further deepen the content of urban planning green space and put forward systematic and controlling planning points for urban green space construction, which is difficult to avoid the lag of planning.

The theories and methods of landscape ecology provide a theoretical basis for the study of urban green space spatial pattern. The application of GIS and artificial neural network in the analysis of landscape ecological pattern provides technical support for the study of urban green space layout. Through its learning ability, the artificial neural network can well simulate the relationship between urban green space composition and green space landscape pattern. After repeated training and testing of the network, a green space network with strong generalization and promotion ability can be obtained. On this basis, it can predict the quadrats of various green space proportions to judge whether it is in line with the actual situation of green space development in the study area.

Data Availability

The dataset can be obtained from the corresponding author upon request.

Conflicts of Interest

The authors declare that they have no conflicts of interest.

References

[1] Y. Chi, G. Bai, and H. Dong, "A new multicriteria decision-making method for the selection of sponge city schemes with Shapley-Choquet aggregation operators," *Mathematical Problems in Engineering*, vol. 2021, Article ID 6615709, 16 pages, 2021.

[2] K. Ding and Y. Zhang, "Practical research on the application of sponge city reconstruction in pocket parks based on the analytic hierarchy process," *Complexity*, vol. 2021, Article ID 5531935, 10 pages, 2021.

[3] H. Men, H. Lu, W. Jiang, and D. Xu, "Mathematical optimization method of low-impact development layout in the sponge city," *Mathematical Problems in Engineering*, vol. 2020, Article ID 6734081, 17 pages, 2020.

[4] X. Sun, "Study on engineering performance of green porous sponge ecological concrete," *Advances in Materials Science and Engineering*, vol. 2021, Article ID 8269053, 11 pages, 2021.

[5] T. Cheng, Z. Xu, S. Hong, and S. Song, "Flood risk zoning by using 2D hydrodynamic modeling: a case study in Jinan City," *Mathematical Problems in Engineering*, vol. 2017, Article ID 5659197, 8 pages, 2017.

[6] N.-D. Hoang and X.-L. Tran, "Remote sensing-based urban green space detection using marine predators algorithm optimized machine learning approach," *Mathematical Problems in Engineering*, vol. 2021, Article ID 5586913, 22 pages, 2021.

[7] Q. Xie and M. Lu, "Measures of Spatial and Demographic Disparities in Access to Urban green Space in Harbin," *China.Complexity*, vol. 2020, Article ID 8832343, 11 pages, 2020.

[8] R. Guo, X. Song, P. Li, G. Wu, and Z. Guo, "Large-scale and refined green space identification-based sustainable urban renewal mode assessment," *Mathematical Problems in Engineering*, vol. 2020, Article ID 2043019, 12 pages, 2020.

[9] J. Shan, Z. Huang, S. Chen, Y. Li, and W. Ji, "Green Space Planning and Landscape Sustainable Design in Smart Cities Considering Public Green Space Demands of Different Formats," *Complexity*, vol. 2021, Article ID 5086636, 10 pages, 2021.

[10] X. Feng, Y. Zhang, S. Qian, and L. Sun, "The traffic capacity variation of urban road network due to the policy of unblocking community," *Complexity*, vol. 2021, Article ID 9292389, 12 pages, 2021.

[11] L. Mei, K. Liu, and Bo-W. Zhu, "Enhancing the health and well-being of people with chronic diseases: assessment and sustainable development planning for therapeutic landscapes after urban expansion," *Journal of Healthcare Engineering*, vol. 2021, Article ID 2828141, 12 pages, 2021.

[12] H. Sun, H. Li, Y. Wang, and Y. Yang, "Intuitionistic fuzzy factorial analysis model for supplier selection of urban rail transit companies within a random environment," *Mathematical Problems in Engineering*, vol. 2021, pp. 1–13, 2021.

[13] H. Esfe, M Kamyab, M. Hassan, and D. Toghraie, "Statistical Review of Studies on the Estimation of Thermophysical Properties of Nanofluids Using Artificial Neural Network (ANN)," *Powder Technology*, vol. 400, 2022.

[14] F. Güleç, D. Pekaslan, O. Williams, and E. Lester, "Predictability of higher heating value of biomass feedstocks via proximate and ultimate analyses - a comprehensive study of artificial neural network applications," *Fuel*, vol. 320, Article ID 123944, 2022.

[15] R. Butola, R. M. Singari, Q. Murtaza, and L. Tyagi, "Comparison of response surface methodology with artificial neural network for prediction of the tensile properties of friction stir-processed surface composites," *Proceedings of the Institution of Mechanical Engineers - Part E: Journal of Process Mechanical Engineering*, vol. 236, no. 1, pp. 126–137, 2022.

[16] F. Mumali, "Artificial neural network-based decision support systems in manufacturing processes: a systematic literature review," *Computers & Industrial Engineering*, vol. 165, Article ID 107964, 2022.

[17] J.-X. Liang, J.-Fu Zhao, N. Sun, and B.-J. Shi, "Random forest feature selection and back propagation neural network to detect fire using video," *Journal of Sensors*, vol. 2022, Article ID 5160050, 10 pages, 2022.

[18] H. N. A. TuanTuan, N. D. X. Hai, and N. T. Thinh, "Shape prediction of nasal bones by digital 2D-photogrammetry of the nose based on convolution and back-propagation neural network," *Computational and Mathematical Methods in Medicine*, vol. 2022, Article ID 5938493, 18 pages, 2022.

[19] L. Li, C. Mao, H. Sun, and B. YuanLei, "Digital twin driven green performance evaluation methodology of intelligent manufacturing: hybrid model based on fuzzy rough-sets AHP, multistage weight synthesis, and PROMETHEE II," *Complexity*, vol. 2020, no. 6, 24 pages, Article ID 3853925, 2020.

[20] H. Zhang and J.-H. Mu, "A back propagation neural network-based method for intelligent decision-making," *Complexity*, vol. 2021, Article ID 6610797, 11 pages, 2021.

[21] L. Li and C. Mao, "Big data supported PSS evaluation decision in service-oriented manufacturing," *IEEE Access*, vol. 8, no. 99, pp. 154663–154670, 2020.

[22] X. Zhao, W. Gong, X. Li, W. Yang, D. Yang, and Z. Liu, "Back propagation neural network-based ultrasound image for diagnosis of cartilage lesions in knee osteoarthritis," *Journal of Healthcare Engineering*, vol. 2021, Article ID 2584291, 8 pages, 2021.

[23] L. Li, T. Qu, Y. Liu et al., "Sustainability assessment of intelligent manufacturing supported by digital twin," *IEEE Access*, vol. 8, pp. 174988–175008, 2020.

[24] G. Qi, J. Zhou, W. Jia, M. Liu, S. Zhang, and M. Xu, "Intrusion detection for network based on elite clone artificial bee colony and back propagation neural network," *Wireless Communications and Mobile Computing*, vol. 2021, Article ID 995637, 11 pages, 2021.

[25] L. Li, B. Lei, and C. Mao, "Digital twin in smart manufacturing," *Journal of Industrial Information Integration*, vol. 26, no. 9, Article ID 100289, 2022.

[26] S. Hua, "Back-propagation neural network and ARIMA algorithm for GDP trend analysis," *Wireless Communications and Mobile Computing*, vol. 2022, Article ID 1967607, 9 pages, 2022.

[27] Y. Hu, A. Sharma, G. Dhiman, and M. Shabaz, "The identification nanoparticle sensor using back propagation neural network optimized by genetic algorithm," *Journal of Sensors*, vol. 2021, Article ID 7548329, 12 pages, 2021.

Hindawi
Scientific Programming
Volume 2022, Article ID 9691331, 12 pages
https://doi.org/10.1155/2022/9691331

Research Article

Digital Recognition Methods Based on Deep Learning

Yuanbo Peng

School of Public Administration and Law, Hunan Agricultural University, No. 1, Nongda Road, Furong District, Changsha, Hunan Province 410128, China

Correspondence should be addressed to Yuanbo Peng; pengyuanbo@stu.hunau.edu.cn

Received 11 May 2022; Revised 25 May 2022; Accepted 7 June 2022; Published 25 July 2022

Academic Editor: Lianhui Li

In this paper, the K-nearest neighbor algorithm and the convolutional neural network will be used to train the handwritten digit recognition model, respectively. To establish a reasonable model structure, and through the training data, the model can learn to reflect ten different handwritten number features and finally give the probability of predicting number corresponding to the likelihood of each number. Taking the learning process of the handwritten numeral recognition algorithm based on deep learning as a clue, from deep learning to convolutional neural network, from simple to deep, the relevant basic concepts, model construction, and training process of deep learning are learned and understood. Finally, the deep learning framework uses MNIST as the training dataset to train a model with high recognition rate and then combines it with Open CV technology to realize the identification of handwritten numbers. A reasonable model structure is used to accurately identify the handwritten numbers in the test set. The neural network of deep learning is established with TensorFlow to realize the classification and recognition of handwritten numbers. Various deep learning methods such as CNN and KNN are learned and compared to complete the construction of deep learning architecture. The MNIST dataset was preprocessed, features extracted, and identified. The program is to complete the training of neural network and the recognition of numbers in the image, the recognition results of deep learning methods used are counted and analyzed, and the recognition rates of two different methods are compared to find ways to optimize these methods and improve the recognition rate.

1. Introduction

1.1. Research Background. With the rapid development of the current era and the great progress of the society, the machine gradually began to liberate people from the heavy work. With the progress of science and technology, people can no longer be satisfied with the artificial operation of machines and gradually move forward to learn the capable of artificial intelligence. Now, artificial intelligence is getting closer to people's lives. Machine learning, as the core of artificial intelligence technology, is a fundamental way to make computers intelligent. Deep learning is a new key technology and research direction in the field of machine learning, with high research price and application value. Deep learning [1, 2] enables machines to simulate human audio-visual, thinking, and other activities; solves many complex pattern recognition problems; and makes great progress in artificial intelligence-related technologies [3–5].

1.2. Research Meaning. With the development of computer technology and the advancement of information wave, how to input the massive digital information on paper into the computer has become a major research hotspot. For example, the manual input of bank bills, invoices, checks, tax bills, and other bills, often need to manually deal with a lot of information, will inevitably make mistakes, and there may be high labor cost, low efficiency, large workload, and other problems. The computer automatic identification input instead of manual input not only can complete the task in a high-precision way but also can liberate the relevant staff so that the workload can be greatly reduced. According to the different ways of digital sources, the current digital recognition problems can be divided into handwritten digital recognition, printed digital recognition, optical digital identification, and natural scene digital recognition, which has great practical value. For example, handwritten digit recognition can be applied to the recognition of bank money

order numbers, greatly reducing labor costs. Print digital identification can be applied to the automatic identification of postal codes. Optical digital recognition and natural scene digital recognition can be applied to license plate number identification in vehicle detection. Thus, it can be seen that the handwritten digital recognition technology has considerable application prospect and value. How to apply deep learning algorithms to the recognition of handwritten digits is a more popular research.

1.3. Domestic and Foreign Research. In recent years, the popularity of artificial intelligence has been greatly increased, and people's requirements for machine vision have become more and more demanding. Researchers around the world have devoted themselves to the research of handwritten digital recognition and made many achievements in this field.

1.3.1. Foreign Research. Liang uses 10 structural features, such as profile features, self-structure features, and curvature, combined with eight classifiers on the test set of CENPARMI, CEDAR, and MNIST databases and achieves a test identification rate of 99.58%. However, the calculation and storage costs of this method are high [6–9]. Guangbin et al applied existing biological vision to build a handwritten digital recognition model, which extracted linear separable features and reduced the error rate to 0.59% [10] in the MNIST training set. Guo et al proposed a method for integrating statistical and structural information on unconstrained handwritten digit recognition. The method improves the modeling of state time in conventional HMM by using state duration adaptive transition probability, using the macro states overcoming the difficulty [11] of HMM modeling pattern structure. There is a great improvement in speed and accuracy [12].

1.3.2. Domestic Research. Liu Gang and Zhang Honggang used the BP neural network based on handwritten digital recognition system designed by visual $C++6.0$ to verify the feasibility of BP neural network for handwritten digital recognition, with a good recognition rate of [13]. Wang proposed a new method, combining PCA (principal component analysis) and CNN method, and conducted experiments on the SVHN dataset, trying to improve the recognition rate of characters in natural scenes. Geng et al constructed and realized the handwritten digital recognition model based on Hopfield neural network, whose error identification rate and accuracy rate are more ideal [14, 15] than the identification method of BP network. However, due to the dependence of research on test samples, test images need to be similar to training images. With the gradual expansion of the scale of data collection, the requirements of test pictures and training pictures are gradually reduced, but the requirements of writing regularity are increased. In short, in this era, handwritten numeral recognition applications can replace manual writing in occasions with a high degree of standardization, such as bank checks [16].

1.4. Handwriting Number Identification Difficulties. Similar numeric distinction: However, only ten numbers are used, and the strokes are very simple, but different numbers can be written in the book, and there are significant regional characteristics. The writing method of a number is different, and people from different places are also different, so it is very difficult to create a universal high recognition digital recognition model [6–8].

The data are not large enough: seven billion people around the world in Arabic numbers, everyone has different writing habits, and existing any kind of dataset in the world cannot completely include everyone style handwritten digital pictures. Arabic digital user grow much faster than the dataset content, so the data are not big enough to handle this problem, which will become more obvious in the future [9–11].

1.5. Application of the Handwritten Digital Recognition System. Occasion 1: in the schools, students and teachers are senior intellectuals, writing Arabic numerals is very standard, and the handwritten number recognition system applied in the test paper results in summary can greatly reduce the workload of teachers [12].

Occasion 2: in the government, the government staff are high cultural literacy, writing Arabic numerals is very standard, and in the absence of handwritten digital recognition technology, the government office form is by artificial input, but this requires huge human input, and the emergence of handwritten digital recognition technology will liberate civil servants and improve the efficiency of government workers [17].

Occasion 3: in the banks, bank staff to deal with many checks every day, bills and forms of handwritten digital information, and long processing monotonous handwritten numbers will make bank workers to produce visual fatigue and greatly affect their work efficiency. The use of handwritten digital recognition technology will greatly reduce manpower and improve the efficiency and accuracy of bank workers [18].

2. Foundation and Model of Deep Learning

2.1. Introduction to Basic Principles

2.1.1. The Concept of Deep Learning. The concept of deep learning originated from the study of artificial neural networks. With the study of artificial neural networks, neural networks with multiple hidden layers have gradually entered people's vision. The deep learning based on the neural network training model with single output, multi hidden layers and single output structure has begun to attract scholars' attention [19–24]. The concept of deep learning was proposed by Hinton et al. in 2006. Its simplest deep learning model is shown in Figure 1.

$$\text{output} = x_1 w_1 + x_2 w_2 + x_3 w_3 + \cdots. \tag{1}$$

In the above formula, x_1, x_2, and x_3 represent the input; output represents the output; and w_1,w_2, and w_3 represent

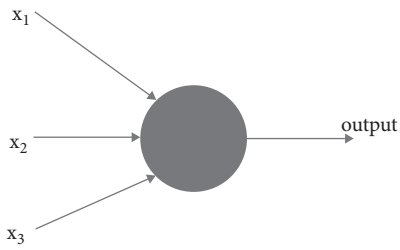

Figure 1: Monolayer neural network.

weights when delivered in the neural network, indicating the extent to which the input affects the output, which is more important. The larger w is (even over 1), the less important the input is, and the closer w tends to 0. In general, a typical deep learning model refers to a neural network with multihidden layers, representing more than three hidden layers, and deep learning models usually have eight or nine or more hidden layers. With more hidden layers, the corresponding neuronal connection weight parameters are more [25], [26]. This means that the deep learning model can automatically transfer many complex features, and the number of hidden layers can be transferred deeper on the neural network. A rigorous and mature neural network can realize complex functions and even realize mechanical intelligence, namely, artificial intelligence. The deep learning model diagram of the multihidden layer neural network is shown in Figure 2.

2.1.2. Deep Learning Algorithms—Classification of Neural Networks. In addition to the learning method, the deep learning algorithm is classified into networks containing only the encoder parts, networks containing only the decoder [6]parts, and networks with both the encoder and decoder parts. According to the application mode of technical structure, it is divided into differentiated depth structure, generative depth structure, and mixed structure. It can also be divided into a mentor network and a no-mentor network.

2.1.3. Sample Dataset for the Trained Neural Networks—MNIST Dataset. Flow chart of handwritten digital image recognition based on deep learning is shown in Figure 3.

In this graduation design, MNIST dataset is a widely used in the field of handwritten digital dataset because of small memory and easy to become the current learning handwritten number recognition students, so we use MNIST database for the experimental sample set to train the research method of the graduation design. The MNIST database serves as a standardized dataset with Arabic digital images of 0 to 9, all of which have been normalized and are aggregated into images of the same size and place numbers in the center. A uniform size of grayscale images is $28 * 28$, where the pixels range from 0 to 255. The representation of the data is expressed in the form of a vector, and in the TensorFlow, the pixel values of each pixel point can be viewed by the print corresponding array. The MNIST dataset contains 70000 handwritten digital images, of which 60000

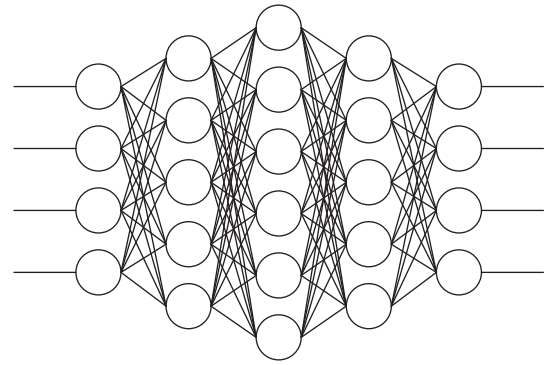

Figure 2: Multilayer neural network.

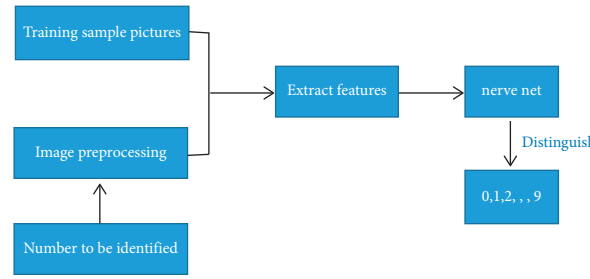

Figure 3: Flow chart of handwritten digit identification.

handwritten digital images are training sample sets and 10000 handwritten digital images are test sample sets.

Some images of the MNIST dataset are as shown in Figure 4.

The dataset stores common handwritten numbers, including the value of 0, 1, 2, 3, 4, 5, 6, 7, 8, and 9 and the Arabic numerals of 10. For each number, it contains a wide variety of strange forms. A lot of numbers are not the normal standard form of writing, so many images in the MNIST dataset are hard to identify, for example, the Arabic numeral "9," as shown in Figure 5 and 6. We can still see that the morphological difference of the same number in the entire MNIST database is quite large. It is precisely because there are so many different handwritten numeral images that MNIST data sets can have good recognition accuracy no matter how strange handwritten numerals are. However, this has also become a disadvantage of this recognition system and over-reliance on the big data of the dataset; once the picture is separated from the dataset, the accuracy is difficult to guarantee.

2.1.4. Working Framework for Deep Learning. With the gradual popularity of deep learning, scholars and research staff at home and abroad have developed a lot of deep learning work environment, such as Caffe, Torch, Theano, and TensorFlow; Caffe used to more applications in the field of image recognition, Torch and Theano used in programming and import process is slow, and TensorFlow used as the software, which become the most widely used deep learning framework. A large number of tedious handwritten data are transmitted into the artificial intelligence neural network, using the built neural network for research and

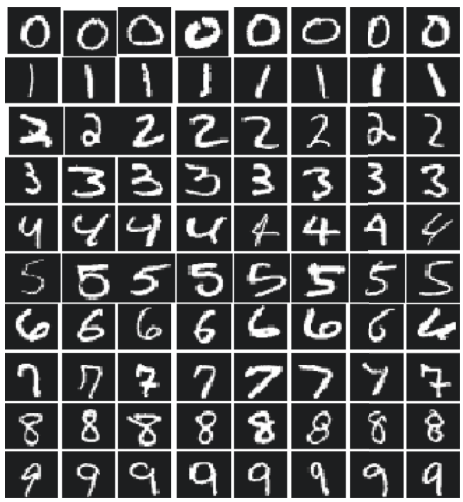

Figure 4: A part of the sample examples of the MNIST dataset.

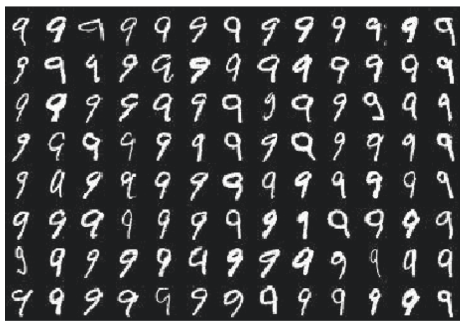

Figure 5: Training samples of 9 within the MNIST dataset.

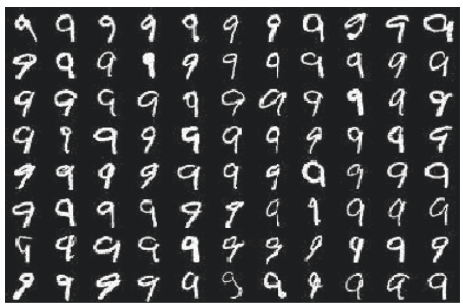

Figure 6: Test samples of 9 within the MNIST dataset.

processing, and finally get the output we want. TensorFlow was developed by Google in 2015 and attracted the attention of scholars all over the world once it was proposed. Just four years later, TensorFlow has become the most popular research and development software in the current era, and almost every deep learning lover is using TensorFlow.

Installation of the working frame

Step 1. Install the anaconda environment, log in to the anaconda official website, download the corresponding version of the anaconda installation package, and install it normally according to the prompts.

Step 2. Enter command line mode for the Windows system, enter [conda-version] to verify whether anaconda is successfully installed.

Step 3. Activate the TensorFlow environment and enter [pip install-upgrade--ignore-installed TensorFlow] in the command-line mode of the Windows system.

Step 4. In the TensorFlow environment, enter [python] and continue entering [import TensorFlow as tf]. If there is no error code reported, then the TensorFlow module is called successfully, which means that the installation is successful.

2.2. Handwritten Digital Image Recognition Based on the Convolutional Neural Network

2.2.1. Identification Principles of Convolutional Neural Networks. Convolutional neural network (CNN), as a class of feed-forward neural network with convolutional computing and deep structure, performs well in identifying handwritten numbers. The visual file convolution neural network includes convolution operation, pool operation (also known as down sampling) and full connection operation, the processed handwritten digital image, and the lenet-5 model in the handwritten digital feature sequence in the picture.

Convolution operation (Figure 7):

Green indicates the original image element value, red indicates the parameters in the convolution core, and yellow indicates the convolution core sliding on the original image. The right graph represents the feature map generated after the convolution operation. The results were calculated as the sum of each primary pixel value and the parameters in the convolutional kernel.

Pooling (*subsampling*) (Figure 8):

One pixel for pooling replaces a number of adjacent pixels on the original image, squeezing its size while retaining the feature map features. The effect of pooling can prevent the data explosion and save the operation amount and operation time, and it can be used to prevent overfitting and overlearning.

Full connection (Figure 9):

The final result is made based on the output of the full connection. There are generally two full connection layers for handwritten digit recognition.

Activation function ($y = f$) (Figure 10, *and* 11):

Linear function is as follows:

$$f(x) = k * x + c. \tag{2}$$

Ramp function is as follows:

$$f(x) = \begin{cases} T, x > c \\ k * x, |x| \le c \\ -T, x < -c. \end{cases} \tag{3}$$

Threshold function is as follows:

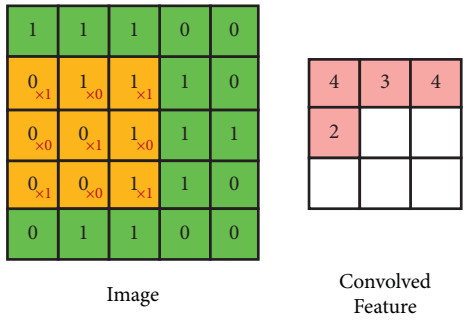

Figure 7: Schematic diagram of the convolution operations.

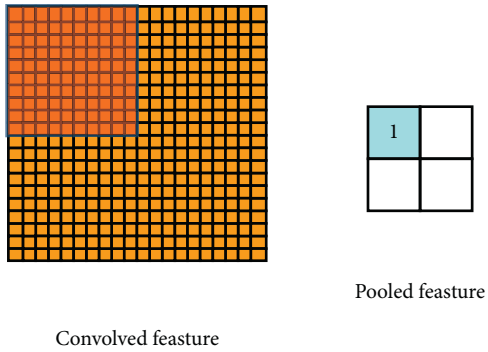

Figure 8: Schematic diagram of pooling.

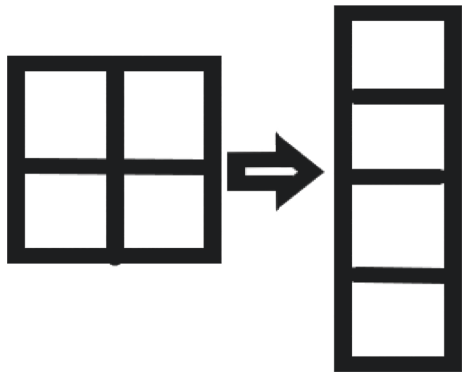

Figure 9: Schematic diagram of pooling.

$$f(x) = \begin{cases} 1, x \geq c \\ 0, x < c. \end{cases} \tag{4}$$

Type-S function is as follows:

$$f(x) = \frac{1}{1 + e^{-ax}} \ (0 < f(x) < 1),$$
$$f'(x) = \frac{ae^{-ax}}{\left(1 + e^{-ax}\right)^2} = af(x)[1 - f(x)]. \tag{5}$$

Bipolar S-type function is as follows:

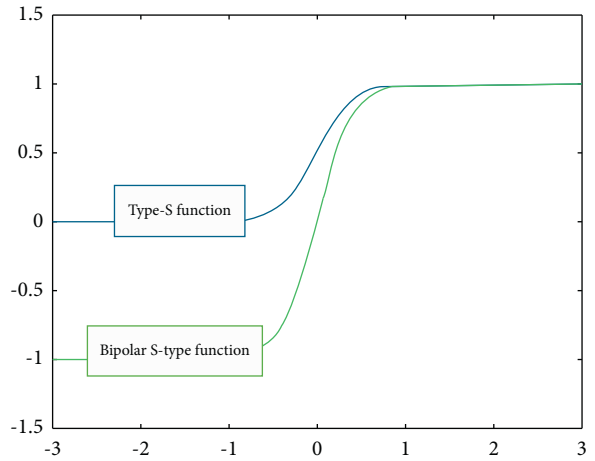

Figure 10: Function images of two functions.

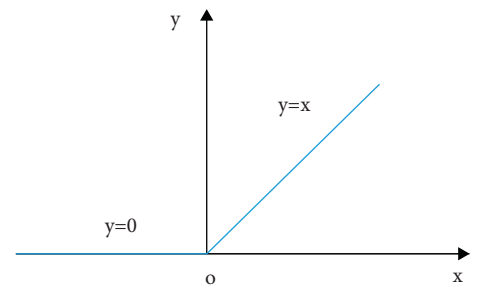

Figure 11: ReLU functional image.

$$f(x) = \frac{2}{1 + e^{-ax}} - 1 \ (-1 < f(x) < 1),$$
$$f'(x) = \frac{2ae^{-ax}}{\left(1 + e^{-ax}\right)^2} = \frac{a\left[1 - f(x)^2\right]}{2}. \tag{6}$$

ReLU function is as follows:

$$f(x) = \begin{cases} x, x > 0 \\ 0, x \leq 0, \end{cases}$$
$$f'(x) = \begin{cases} 1, x > 0 \\ 0, x \leq 0. \end{cases} \tag{7}$$

Considering the above algorithm and according to the LeNet-5 model, a complete CNN-based handwritten digit identification workflow is shown in Figure 12.

(i) Step 1. Handle write font picture conversion into a pixel matrix.

(ii) Step 2. The first layer of convolution of the pixel matrix is to generate six feature maps.

(iii) Step 3. Subsample each feature map to reduce the amount of data while retaining the feature maps. Six small graphs are generated, which look similar

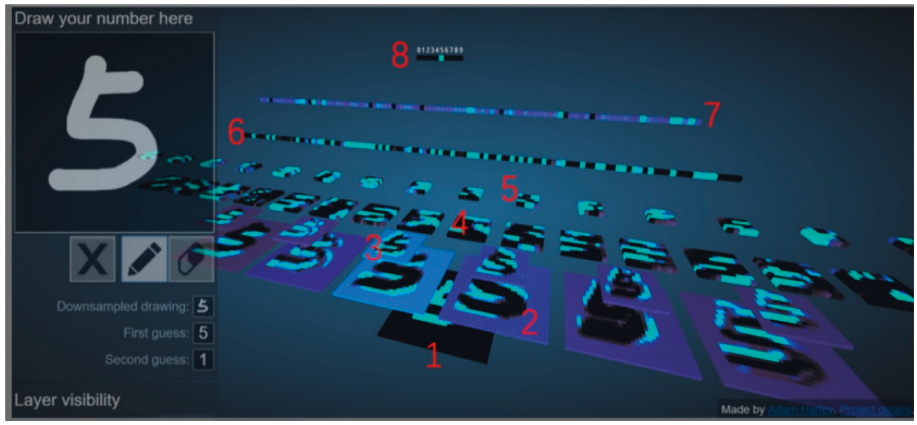

Figure 12: A visual interface for the complete workflow.

to the respective feature map of the previous layer, but are reduced in size.

(iv) Step 4. The second convolution of six small graphs is to generate more feature map s.

(v) Step 5. Subsample the feature map is generated by the second convolution.

(vi) Step 6. The first layer is a full connection layer.

(vii) Step 7. The second layer is a full connection layer.

(viii) Step 8. Gaussian connection layer to generate output results.

The CNN internal processing formula is as follows:

(i) Part 1: convolution formula

$$X_j^i = f\left(\sum_{i \in M_j} X_i^{l-1} * k_\theta^l + b\right). \tag{8}$$

(ii) In formula (8), X_i^{l-1} represents the element covered by j l-1 layer feature graph convolution; k_θ^l is the element in the l layer convolutional kernel; b refers to the offset; M_j is the region covered by the jth convolution core; $f(*)$ represents the activation function.

(iii) Part 2: pool formula

$$X_j^i = f\left(\mu_j^{l-1} + b\right). \tag{9}$$

(iv) In formula (9), μ_j^{l-1} is the output obtained after downsampling of l-1 layer image block; X_j^i is the output of l-1 layer and the input element of l layer.

(v) Part 3: full connection formula

$$Y^l = f\left(w^l X^{l-1} + b\right). \tag{10}$$

After convolution and pooling, the image output advanced features are weighted by the fully connected layer, and the final output is obtained through the activation function. For example, X^{l-1} is the output feature diagram of the previous layer and w^l is the weight coefficient of the fully connected layer.

2.2.2. Handwritten Digital Image Recognition Based on KNN. One of the simplest methods in the K-nearest neighbor classification algorithm (KNN), which is a data mining classification technology, is a theoretically mature method. The term K-nearest neighbor means that each sample can be represented by its nearest k neighbors. The core idea of the KNN algorithm is that if a sample has the k most adjacent samples in the feature space belong to a certain category, the sample also belongs to this category and has the characteristics of samples on this category. KNN is a commonly used opponent to write numbers to identify classification. A simple version of the algorithm is easily implemented by calculating the distance from the test examples to all stored examples, but it is massive for large training sets. Even for large datasets, the KNN is computationally tractable by using an approximate nearest neighbor search algorithm. Many more recent neighbor search algorithms have been proposed over the years. These are often designed to reduce the number of distance assessments actually performed. Euclidean distance, Manhattan distance, Minkowski distance, and cosine distance are as follows:

Part 1: Euclidean distance is as follows:

The Euclidean distance was taken as a distance measure, but this applies only for continuous variables

$$d = \sqrt{(x1 - y1)^2 + (x2 - y2)^2}. \tag{11}$$

Distance of the n-dimensional space is as follows:

$$\begin{aligned} d &= \sqrt{(x1 - y1)^2 + (x2 - y2)^2 + \cdots + (xn - yn)^2} \\ &= \sqrt{\sum_{i=1}^{n} (xi - yi)^2}. \end{aligned} \tag{12}$$

Part 2: Manhattan distance is

$$d = |x1 - y1| + |x2 - y2|. \tag{13}$$

Part 3: the Minkowski distance

For two points x and y in n-dimensional space, the Minkowski distance between two points x and y is as follows:

$$d = p\sqrt{\sum_{i=1}^{n}|xi - yi|^p}, \tag{14}$$

where p represents the dimension of the space, the Manhattan distance when $p = 1$, the Euclidean distance when $p = 2$, and the Chebyshev distance when p tends to infinity. Then, the Chebyshev distance between two points is the maximum of the absolute difference in the coordinate values between the two points

$$\max(|x1 - y1|, |x2 - y2|). \tag{15}$$

3. Design and Implementation

3.1. Install. OpenCV is a library file established by Intel in 1999. With the development of recent years, OpenCV has developed into an open source cross-platform computer vision library, with very good compatibility and perfectly compatible with Linux, Windows, and Mac OS operating systems. The OpenCV provides a transparent interface for the Intel. There is a special optimized processor APP library where OpenCV automatically loads some database during startup. After the anaconda environment is installed, the configured Anaconda Navigator has integrated various library files. OpenCV can use python as the programming language. After Anaconda Navigator installs the OpenCV library files, the call of OpenCV can be completed with anaconda built-in software. We open the anaconda built-in software Spyder or Jupyter Notebook (TensorFlow) and enter import cv2 as cv. No error code produced that the OpenCV installed successfully. Figure 13 is the Installed Anaconda Navigator interface diagram.

3.2. Programming Language—Python. The birth of Python language perfectly solves the deficiency of ABC language and also completes the function that ABC language does not have. It can be said that Python has developed from ABC, and countless ABC speakers have turned to the embrace of Python. Today, Python has developed into one of the most popular computer languages in the world. Even in some countries, Python language learning has joined the local primary school students, enough to show the popularity of Python. Using the Python has the following features:

(i) Concise and readability

(ii) Good scalability

(iii) Completely free

3.3. Handwritten Number Recognition System

3.3.1. KNN Handwritten Number Recognition Method. KNN is an instance-based learning, or local approximation and delayed learning, delaying all computations into classification. The K-nearest neighbor algorithm is one of the simplest machine learning algorithms.

3.3.2. CNN Handwritten Number Recognition Method. As a commonly used classical machine learning algorithm, CNN has been proposed and studied since forty years ago. Some experts have proposed the classical CNN architecture, demonstrated the potential of deep structure in feature extraction, and made major breakthroughs in image recognition tasks, setting off a wave of in-depth learning research boom. Convolutional neural network, as an existing deep structure with certain application cases, has also returned to people's vision for further research and application. Practice has proved that the accuracy of CNN network structure in handwriting digital recognition system is ideal and can basically meet the actual needs.

3.4. System Design and Implementation

3.4.1. System Construction. We install anaconda prompt in Anaconda Prompt, use Anaconda to create a virtual environment with Python version 3.6 by entering command line conda create-n TensorFlow python = 3.6, and install CPU version TensorFlow 2.0.0 with command line pip install TensorFlow 2.0.0. We will import all the modules required to train the model, wait for them to download and install the corresponding library, and test the TensorFlow with the following code to verify that the installation of the TensorFlow is successful, as shown in Figure 14.

Computational results.

This means that the TensorFlow environment has been successfully built. Code running diagram is shown in Figure 15.

The programming software used is Spyder, a cross-platform, scientific computing integrated development environment using Python language. Writing code with this editor has many advantages, and it is convenient to import libraries. This is a digital recognition task. Thus, there are 10 numbers (0 to 9) or 10 categories to be predicted. The prediction error is reported using Python.

3.4.2. Sample Selection. The sample is a simple and practical computer vision dataset, MNIST dataset, which contains the image set of handwritten numbers as shown in Figure 16.

Implementation with "mnist = input_data.read_data_sets ('MNIST_data',one_hot = True)" code.

A total of 60000 training data images in the MNIST dataset can be used to train the model, and 10000 test data images to test the recognition accuracy, each at 28 ∗ 28 pixel. Each pixel can be represented by a single grayscale value. The dataset was constructed from a number of scanned document datasets available from the National Institute of Standard Technology (NIST). This is where the dataset names originate, such as the modified NIST or MNIST datasets. Digital images are obtained from various scanned documents, standardized, and centered. This makes

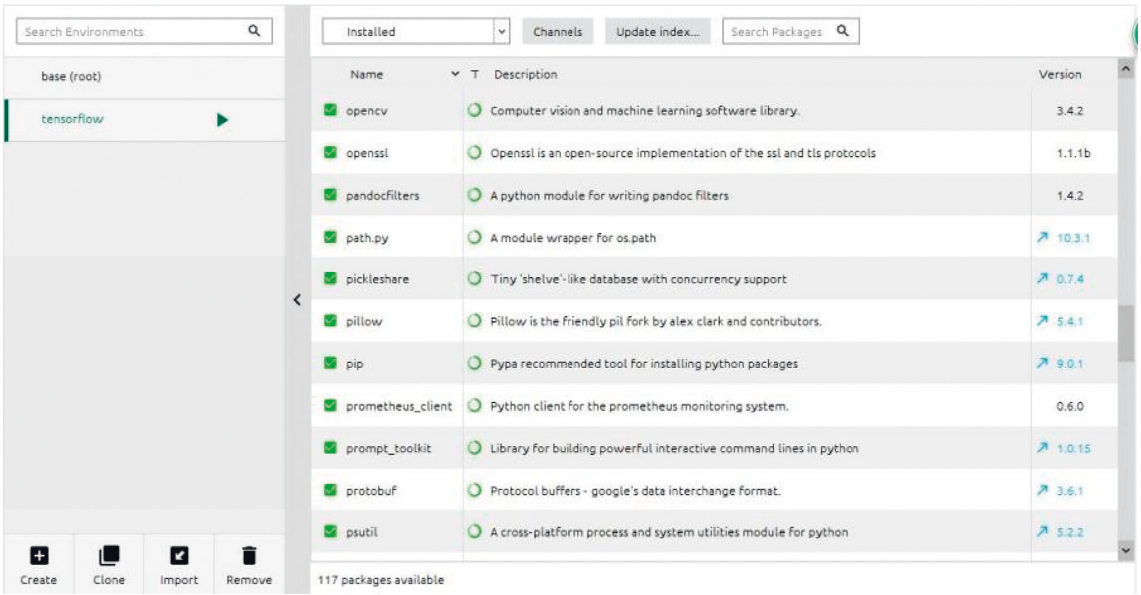

Figure 13: Installed Anaconda Navigator interface diagram.

```
import tensorflow as tf
tf.compat.v1.disable_eager_execution ()
hello = tf.constant ('hello, tensorflow')
sess= tf.compat.v1.Session ()
print (sess.run (hello))
```

Figure 14: Validation.

```
>>> import tensorflow as tf
>>> tf. compat. v1. disable_eager_execution ()
>>> hello = tf. constant ('hello, tensorflow')
>>> sess= tf. compat. v1. Session ()
>>> print (sess. run (hello))
b' hello, tensorflow'
```

Figure 15: Code running diagram.

```
Train-images-idx3-ubyte (Training data images-60000)
Train-labels-idx1-ubyte (Training data-label)
T10k-images-idx3-ubyte (Test data images-10000)
T10k-labels-idx1-ubyte (Test data -label)
```

Figure 16: Image set of handwritten figures.

it an excellent dataset for evaluating models, allowing developers to focus on machine learning with very little data cleaning or preparation. Each image is a square of 28 ∗ 28 pixel (total of 784 pixels). Standard partitioning of the dataset was used to evaluate and compare the models, where 60,000 images were used to train the model, while a separate set of 10,000 images was used to test the model.

3.4.3. Model Construction. KNN mode

The sample is a simple and practical computer vision dataset, MNIST dataset, which contains the image set of handwritten numbers:

(i) Step 1. Load data.

(ii) Step 2. Data preprocessing.

(iii) Step 3. Calculate the distance between the test data and each training data.

(iv) Step 4. Sort it by the increasing relationship of the distance.

(v) Step 5. Select the K points with the smallest distance.

(vi) Step 6. Determine the frequency of the previous K points.

(vii) Step 7. The most frequent category among the first K points was returned as the predictive classification of the test data.

CNN model

The model is constructed based on the basic architecture of the convolutional neural network. The convolutional layer is responsible for extracting features, the sampling layer is responsible for feature selection, and the fully connected layer is responsible for classification.

(i) Step 1. Load the data.

(ii) Step 2. Data preprocessing: dimension adjustment.

(iii) Step 3. Convolutional layer for convolution operation: the convolution kernel is generally initialized in the form of a random decimal matrix, and the convolution kernel will learn reasonable weights.

(iv) Step 4. Pooling layer: a single pixel is used to replace the neighboring multiple pixels on the original image to maximum sample the data and retaining features while greatly simplifying the complexity of the model and reducing the parameters of the model.

(v) Step 5. Full connection layer: we integrate the distributed features together and output them as a value, greatly reducing the impact of feature

location on classification. The fully connected data have its own weight, and the sum of their own weight product is the probability of the original image identification.

(vi) Step 6. Start the training, find the error between the output value and the target value when the error is greater than the expected value, send the error back to the network, successively to obtain the error of the full connection layer, low sampling layer, and convolution layer. The error of each layer can be understood as the total error of the network, how much the network should bear; when the cycle iteration reaches the set cycle after the training.

(vii) Step 7. Return the prediction results.

This chapter mainly introduces the library file OpenCV of image processing and then introduces Python, a language that can be invoked by OpenCV, and finally returns to the design requirements of this graduation design and describes the design and implementation of TensorFlow for the workflow of KNN and CNN.

4. Training Process and Results

4.1. Deep Learning and Training Process. KNN training process is shown in Figure 17.

KNN model first read test sample data, calculate the test data and the training data, sort the distance from small to large, select the smallest K points, determine the frequency of K point category, select the highest frequency category as prediction classification, and finally output classification results.

CNN training process is shown in Figure 18.

The CNN model first reads the test sample data; extracts the data features, updates the weight, convolutional layer, and pooling layer; and finally reaches the full connection layer. After judging the training cycle, it ends the training and finally outputs the classification results.

Training data for the CNN and KNN models are shown in Table 1.

Due to the low recognition rate of the convolutional and pooling layers, there are lag and crash phenomena due to the computer configuration problem. Therefore, in order to improve the recognition rate, it is decided to add a convolutional layer and a pooling layer into two convolutional layers and pooling layer. The training data are as shown in Table 3.

After adding a convolutional layer and a pooling layer, the program operation speed slowed down significantly. It took 20 minutes for cycle iteration and 30 cycles for cycle iteration for nearly two hours, but the recognition rate was significantly improved.

4.2. Realize the Whole Process

4.2.1. Training and Preserving the Model. After the convolutional neural network framework is built, the keeper saver is defined, and the trained model is saved with saver after the training completion.

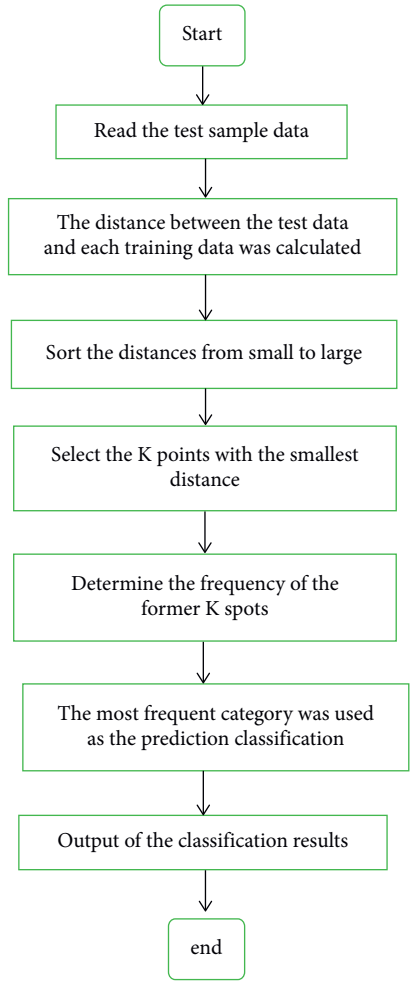

Figure 17: Flow chart of KNN algorithm training.

Definition:saver = tf.train.Saver()//saver.

saver.save(sess,'/home/XXX/learning_tensorflow/form/model.ckpt')//Save the model/Fill the save address of the model in quotes.

The model is obtained as shown in Figure 19.

4.2.2. Image Preprocessing.

(1) Step 1. Select the image

(2) Open the handwritten digital image of the computer, as shown in Figure 20.

(3) It can be seen from the above that the handwritten digital pictures that can input the convolutional neural network requires that the pixels of these pictures are 28 ∗ 28, while the pictures to be identified are often greater than 28 ∗ 28 pixels and do not meet the requirements, so appropriately reduce the images to be processed into the same format as the MINIST dataset.

(4) Step 2. Processing method

The imread function comes with grayscale image reading, and the imread function reads in grayscale image.

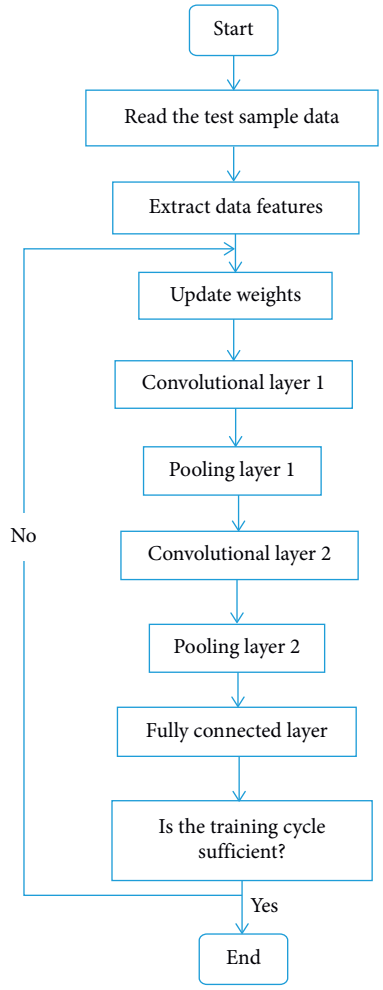

Figure 18: Flow chart of CNN algorithm training.

Table 1: Recognition rates at different K values and training set sizes.

K	2	3	4 (%)	5 (%)
5000 training images	89%	92%	88	92
10000 training images	91%	96%	94	94

The convolutional neural network training results with only one convolutional layer and one pooling layer are as shown in Table 2.

Table 2: Recognition rate at the different number of cycles of the CNN.

Cycle index	100 (%)	200 (%)
Discrimination	82	90

Table 3: Recognition rate at different cycles of CNN convolved by two layers.

Cycle index	5 (%)	30 (%)
Discrimination	88	99

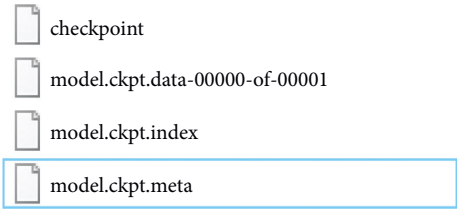

Figure 19: A well-trained model.

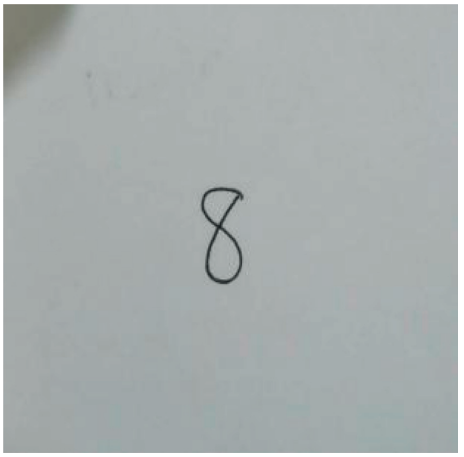

Figure 20: Images to be processed.

Figure 21: The processed image.

Counterphase grayscale diagram, reversing the black and white threshold with access pixel and processing pixel by pixel.

Using the threshold function, the reverse-phase binarization image is performed.

Use the rank scanning method to find out the digital border to determine the specific location of the number.

The filled pixels were resized to $28 * 28$ pixels and finally processed into the same format as the images in the MNIST dataset, as shown in Figure 21.

(5) Step 3. Adjusted model

[saver.restore(sess,"C:/Users/Desktop/demo/model.ckpt")//Call the trained model].

We import the handwritten digital pictures processed by OpenCV into the neural network model, run the test.py program, and identify the results. All the test pictures are shown in Table 4.

Table 4: Identification results of the ten handwritten digit pictures

Handwritten digital pictures	The number identified by the program	Result
	0	Correct
	1	Correct
	2	Correct
	3	Correct
	1	Error
	5	Correct
	6	Correct
	7	Correct
	8	Correct
	9	Correct

After the analysis, it was found that only the picture "4" in the above table was wrong, and all the others were correct, so that the task of this graduation design was successfully completed.

5. Conclusion

This graduation innovation point includes the following three parts:

(i) Part 1: The title of the graduation design is the handwritten digital picture research based on convolutional neural network, but the relatively simple KNN algorithm and CNN algorithm are easy to achieve, highlighting the advanced aspects of convolutional neural network. Learning deep learning from different angles can more intuitively understand the advantages of convolutional neural network in image recognition. Choosing KNN algorithm is to better understand the idea of K-nearest neighbor method. At the same time, several algorithms are also helpful to learn Python programming language.

(ii) Part 2: It really realizes the recognition of handwritten digital pictures, not just an accuracy, but the real identification of a written digital picture, the more practical graduation design requirements, can make students interested, and the boring accuracy is not intuitive and too theoretical.

(iii) Part 3: Really introduced OpenCV technology, with OpenCV to process pictures so that the measured pictures are not subject to $28 * 28$ pixels requirements, and any pictures after OpenCV processing can be imported into the built neural network framework [26].

Data Availability

The dataset can be accessed upon request.

Conflicts of Interest

The authors declared that they have no conflicts of interest.

References

[1] X. T. Huang, *Research and Application of Handwritten Digital Recognition Based on Deep Learning*, IEEE, New York, USA, 2018.

[2] L. Li, B. Lei, and C. Mao, "Digital twin in smart manufacturing," *Journal of Industrial Information Integration*, vol. 26, no. 9, Article ID 100289, 2022.

[3] L. Li, T. Qu, Y. Liu et al., "Sustainability assessment of intelligent manufacturing supported by digital twin," *IEEE Access*, vol. 8, pp. 174988–175008, 2020.

[4] L. Li and C. Mao, "Big data supported PSS evaluation decision in service-oriented manufacturing," *IEEE Access*, vol. 8, no. 99, pp. 154663–154670, 2020.

[5] L. Li, C. Mao, H. Sun, and B. YuanLei, "Digital twin driven green performance evaluation methodology of intelligent manufacturing: hybrid model based on fuzzy rough-sets AHP, multistage weight synthesis, and PROMETHEE II," *Complexity*, vol. 2020, no. 6, pp. 1–24, Article ID 3853925, 2020.

[6] J. Chen, "A free handwritten digital recognition algorithm for combined structural features," *Computer Engineering and Applications*, vol. 49, 2013.

[7] L. Huang, "A review of convolutional neural network research," *Journal of Computer Science*, vol. 40, no. 6, pp. 1229–1251, 2017.

[8] X. Wang, "Study on the recognition method of handwritten number based on BP neural network [J]," *Practice and knowledge of mathematics*, vol. 12, pp. 112–115, 2014.

[9] N. Liang, G. Huang, P. Saratchandran, and N. Sundararajan, "A fast and accurate online sequential learning algorithm for feedforward network," *IEEE Transactions on Neural Networks*, vol. 17, no. 6, pp. 1411–23, 2006.

[10] G. Huang, Q. Zhu, and C. K. Siew, "Extreme learning machine:Theory and applications," *Neurocomputing*, vol. 70, no. 1-3, pp. 489–501, 2006.

[11] Z. Guo and G. C. Fox, "Improving Map Reduce performance in heterogeneous network environments and resource utilization," in *Proceedings of the 12thIEEE/ACM International Symposium on Cluster,Cloud and Grid Computing*, pp. 714–716, IEEE, Ottawa, ON, Canada, May 2012.

[12] M. T. Hagan, H. B. Demuth, and M. H. Beale, *Neural network*Mechanical Machinery Industry Press, Beijing, 2018.

[13] G. Liu, H. Zhang, and J. Guo, "A Hidden Markov model for offline handwritten digit recognition," *Computer Research and Development*, vol. 9, no. 8, 2003.

[14] X. Geng, M. Zhang, and J. Shen, "Handwritten number recognition based on structural feature classification of BP networks," *Computer Technology and Development*, vol. 22, 2007.

[15] Z. Yu, Y. Feng, and Z. Luo, "Handwritten digital recognition method based on skeleton structural features," *Microcomputer Information*, vol. 16, 2010.

[16] S. Ogawa and K. Zhang, "Research on handwritten number recognition based on statistical and structural features," *Computer Engineering and Design*, vol. 15, 2012.

[17] Y. Bengio, *Learning Deep Architectures for AI(foundations and Trends in Machine Learning)*, Now Publishers, Hanover, MA, U.S.A, 2009.

[18] R. Parisi, E. D. D. Claudio, G. Lucarelli, and G. Orlandi, "Car plate recognition by neural networks and image processing," in *Proceedings of the 1998 IEEE International Symposium on Circuits and Systems (ISCAS)*, Monterey, CA, U.S.A, June 1998.

[19] J. Nash and U. Cessing, "Face recognition technology based on deep learning," *Proceedings of the IEEE International Symposium on Circuits and System*, vol. 5, no. 3, pp. 31–37, 2000.

[20] L. Zheng, J. Wu, Y. Chen, and M. Zhu, "Balanced k-Way partitioning for weighted graphs," *Journal of Computer Research and Development*, vol. 52, no. 3, pp. 769–776, 2015.

[21] G. P. Coelho, C. C. Barbante, L. Boccato, R. R. F. Attux, J. R. Oliveira, and F. J. V. Zuben, "Automatic feature selection for BCI:An analysis using the davies bouldin index and extreme," in *Proceedings of the Intemation Joint Conference on Nevral Networks*, no. 20, pp. 1–8, Brisbane, QLD, Australia, June 2012.

[22] Y. Qiao, *Study on Characteristic Extraction and Recognition of Offline Hand-Written Chinese Character Based on Process Neural Network*, Hefei University of Technology, Hefei, China, 2013.

[23] R. Liang, B. Pan, and S. Zheng, "A multilevel classifier design for handwritten numbers," *Modern Computer (Professional edition)*, vol. 20, pp. 155–157, 2009.

[24] Z. Yu, M. Zhang, and X. Geng, "Deep learning and its application in industry," in *Proceedings of the Computer technology and application progress based on BP network-17th national computer science and technology application (CACIS) academic conference (volume 1)*, vol. 11, no. 04, pp. 15–17, 2006.

[25] X. Wang, H. Zhang, and C. Wang, "Offline handwritten digital recognition method based on bijection transform," *Computer Engineering and Application*, vol. 49, no. 001, pp. 227–230, 2013.

[26] Z. Liu, P. Shi, and J. Guo, "Free handwritten digital neural network identification method based on the structural features of external concentric circles," *Chinese Informatics Journal*, vol. 11, no. 2, p. 7, 1997.

Hindawi
Scientific Programming
Volume 2022, Article ID 1351109, 9 pages
https://doi.org/10.1155/2022/1351109

Research Article

Analysis of the Deep Development Mechanism of College Education under the Field Theory

Qianqian Zhao and Yan Li

Cangzhou Normal University, Office of Academic Affairs, Cangzhou 061001, Hebei, China

Correspondence should be addressed to Qianqian Zhao; zhaoqq1991@caztc.edu.cn

Received 9 June 2022; Revised 23 June 2022; Accepted 28 June 2022; Published 21 July 2022

Academic Editor: Lianhui Li

Nowadays, the development of online college education is in full swing, and various online college education platforms have also sprung up. The development of technology has made these online platforms more and more powerful, escorting the continuous development of online education. Colleges and universities, as the main front for the cultivation of high-quality talents in my country, have already introduced large-scale online courses into education and teaching, enriching the teaching content, and expanding the teaching form. In the face of new technical means and abundant online education resources, the teaching quality of online classrooms in colleges and universities is so low, which deserves our further reflection. For a long time, the effect of online classroom teaching in colleges and universities has been closely concerned by the academic community, but most of them start from external factors, ignoring the internal relationship of online classrooms. Clarifying the complex relationships in the online classroom field of colleges and universities and clarifying the rules of habitus and capital operation in the online classroom field of colleges and universities are the intrinsic motivation and important source to stimulate the vitality of the online classroom field of colleges and universities and improve the quality of teaching. By grasping the essence of classroom teaching and analyzing the inherent characteristics of the online classroom field, this research intends to clarify the proper state of the online classroom field, and to explore the reasons why the current online classroom field function has not been fully realized, so as to find the depth of college education.

1. Related Introduction

The development of information technology has revolutionized the way and influence of information dissemination time and time again, and subsequently caused changes in social organization, management methods, economy, and industrial structure. These changes have a subtle impact on all aspects of people's lives. With the acceleration of the modernization of education, the application of online technology in the field of education has become more and more extensive. Colleges and universities are the main positions for talent training, and online classroom teaching has gradually become a new normal teaching method. However, many studies have shown that the teaching effect of online classrooms in colleges and universities is not satisfactory. There are still many problems. These series of problems are not only external factors but also internal factors that cannot be ignored. Therefore, using the field theory to analyze the problems existing in the online classroom field of colleges and universities from the perspective of internal relations is of great value to improve the teaching effect of online classrooms in colleges and universities and the quality of online education in colleges and universities.

As an existing form of classroom, online classroom is mainly characterized by breaking the time and space constraints of classroom teaching. The research and analysis of it has certain limitations. But in the sense of space, in the process of classroom teaching, teachers and students are in different positions of power due to the difference in the mastery of cultural knowledge between teachers and students, thus forming a complex relationship network, which

is not in line with the field theory. In this relational network, there are specific logical rules that both teachers and students should abide by. This logical rule aims to promote the flow and reproduction of cultural capital between teachers and students, which is exactly what the online classroom should be.

Field is a relational theory that aims to study the relational workings between actors within the field. In the normalized classroom field, teachers and students are in the same physical field, and the connection in the field is very easy to construct. Teachers can control the power in the classroom by virtue of their own cultural capital. Students because of their culture, the relative weakness of capital can only agree with the rules within the classroom field. In the process of classroom teaching, teachers can timely and accurately observe students' learning status, communicate and interact with students, and adjust teaching content and methods so as to attract students to "enter," supervise their "presence," and avoid students' "absence." At the same time, according to the view of situationism, learning activities cannot be separated from learning situations, and different learning situations will have different degrees of influence on the effect of teaching. In the normalized classroom field, students are in the same physical space, and their behaviors will definitely be influenced by other students around them and be driven into learning activities, so that most students can abide by the rules of the field and participate in cultural capital. The constraints of time and space are broken, teachers and students are in an abstract social space, and it is difficult for teachers to grasp the learning status of students in a timely and accurate manner. In the context of collective learning, it is also difficult to integrate into classroom learning; on the other hand, due to the abundance of online course resources, students have more power in the choice of knowledge, teachers' power in the classroom is also weakened, and students have the ability to learn independently [1–10].

However, due to the fact that the relationship between teachers and students and their respective roles in the online classroom field of colleges and universities cannot be timely transformed from the normalized education field, the teaching methods of teachers and the learning methods of students still maintain the normalized classroom field habit in. The unclear relationship between teachers and students and the mismatch of habitus and other factors have caused various problems in the online classroom field of colleges and universities, and the field cannot function normally, resulting in low quality of online classroom teaching. How to clarify the internal relationship of the online classroom field of colleges and universities, form a healthy online classroom field of colleges and universities, and make the functions of the online classroom field of colleges and universities really play, is the main problem to be solved in this research.

2. Related Work

In today's increasingly popular online teaching, due to the change of teaching mode, the teaching behavior of teachers in online teaching has undergone great changes compared with traditional teaching. On the basis of comparative analysis of teachers' teaching behavior in traditional teaching and teachers' teaching behavior in network teaching, Liu Fanhua found that traditional classroom teaching is teacher-centered, and teachers' teaching is the main way for students to acquire knowledge. In the process of classroom teaching, teachers control the rhythm of the entire classroom, and teachers supervise students' learning behaviors to ensure that students carry out learning activities under the guidance of teachers; however, in online teaching, due to the openness of online platforms and learning resources, students can choose the content of learning by themselves, build knowledge in advance through the addition of interest, become the protagonist in the classroom, and the teacher becomes the facilitator in the classroom, which is more in line with the current student-based education and quality education requirements. Francescucci conducted an experimental study on two modes of online video teaching and class teaching in 2013 and 2018, respectively. In the 2013 experiment, because students did not understand the online video teaching mode, one-third of the students said they were unwilling to do so. Learning is carried out online, but in the 2018 experiment, it was found that the effect of online video teaching and class teaching was equivalent, and there was no significant difference between students' participation and final grades. Faulconer set up four modes in one course for experimentation, which are class teaching, online asynchronous, online synchronous, and remote video. The test results show that the teaching effect is not much different, but the dropout rate of asynchronous online classroom is slightly higher than that of the other three forms. Skylar explored the teaching effect and student satisfaction of online teaching and face-to-face teaching, and found that students' grades in face-to-face teaching were slightly higher than online teaching, and nearly four-thirds of students also expressed a preference for face-to-face teaching [11–14].

Most of the existing studies take the field as the theoretical perspective and use the field habitus to analyze the specific problems in the online classroom, such as the interaction between teachers and students in the field of online teaching in colleges and universities, and the learning field of management flipped classroom. By sorting out related research studies in the field of online education, this study found that the above research mainly takes the specific form of online classroom as the research object. By grasping the essence of classroom teaching and analyzing the inherent characteristics of the online classroom field, this research intends to clarify the proper state of the online classroom field, and to explore the reasons why the current online classroom field function has not been fully realized so as to find an optimization path.

3. Behavioral Scenarios of Online Classrooms and Analysis of College Students' Demand Behaviors

3.1. Behavioral Scene Construction of Online Classroom. As well as the theory of embodied cognition based on Merleau-Ponty's embodied phenomenology, the theoretical sources of these two aspects become the theoretical support for the research on the online classroom user behavior model in this study. Through "scenario construction" to restore the user's real use scene or simulate the user's mentality, then in the field construction, it is to connect the original realm of the experience and the user's present, and finally make the immersive experience and meaning happen [15].

The realm of the online classroom is to build a private space of one's own, in which class tasks and thinking activities can be effectively completed. The inspiration of this study from Heidegger's field theory is to return to the original classroom environment, allowing users to complete the construction of experience and meaning in a focused situation, under the synthesis of their own apperception or body schema. Therefore, the first step of construction is to help him move towards the realm and connect the immersive scene. The second step is to help him focus on the task flow of the target interface through sensory design. Figure 1 shows the framework of the classroom behavioral scene model research.

3.2. Construction of Fielded Embodied Behavior Model in Online Classroom. On the one hand, the fielding theory puts forward the hypothesis of the learning experience model of "formal display-practice-comprehension." On the other hand, learning experience is both a learning cycle process and an experience cycle process. Users recognize and learn from experience. According to the observation and interview of classroom learning, and derived from the theory of embodiment, the process model of the fielded embodied behavior in the online classroom is finally determined, which are physical participation, experience meaning, reflection (self-examination) [1], situational motivation (motivation) [2],. physical participation [3], experience meaning [4], reflection (self-examination) [5], and cooperation [16].

3.3. The "SHDD" Positioning of Online Classroom Experience Based on the Phenomenological Perspective

3.3.1. Establishment of "SHDD" Positioning for Online Classroom Experience. "Outer experience" and "inner experience" together constitute "one experience." Dewey believed that "an experience" has no " dead center," that is, the "outer experience" and "inner experience" will not be suddenly interrupted. The user's combination of "external experience" and "internal experience" determines the quality of "one experience." This study proposes to use the ratio (qualitative) of "inner experience" to "outer experience" to locate a student's experience. Internal experience: external experience ≥1, indicating that the final experience is beyond expectations (full expectations); internal experience: external experience <1, indicating that the final experience is lower than expected (vacant expectations). On this basis, this study further proposes an experiential "SHDD" orientation. The two poles of the ordinate are "inner experience: outer experience ≥1" and "inner experience: outer experience <1." The abscissa is examined from the dimension of frequency, and the two poles are " Occasinally " and "Frequently," respectively. This results in four quadrants. When the user's internal experience: external experience ≥1 occurs for the first time, it brings a sense of surprise to the students and gains a trustworthy group of students. When the user's internal experience: external experience ≥1 often occurs, it brings students a sense of happiness and gains a loyal student group. When the user's internal experience: external experience <1 occurs for the first time, it will bring students a sense of disappointment and gain a tired student group. When the user's internal experience: external experience <1 often occurs, it brings students a sense of deception and gains a disgusting group of students. Trusting and loyal student groups will further lead to good teacher reviews, while bored and disgusting student groups may lead to bad teacher reviews, specifically as shown in Figure 2 [17].

3.3.2. Experience Containers in the Classroom. The simple process of predetermining a purpose-achieving a purpose does differentiate an "experience" from a piecemeal experience, but it is not a sufficient measure of the quality of purpose-completion, i.e., how good or bad it is. Taking "classing" as an example, the preset purpose of "classing" did not include key factors such as course content, whether to procrastinate in class, teacher attitude, etc., which led to the fact that although students completed the purpose of "classing," they felt this "one experience" is in short supply. In other words, there is no system for describing how good or bad "an experience" is. After all, the expected construction is multilayered, so it is necessary to re-examine "an experience" from the perspective of body metaphor. As "an experience" experience, like "substance" "event" "behavior" and " state " become the object of physical metaphor. Therefore, this study proposes to take experience as the object of body metaphor and construct a conceptual container with inner-outer orientation from the genetic level. This is an experience "container" with the behavior of entering the classroom as the turning point. The experience before entering the classroom is the experience outside the container, which is called the "external experience"; the experience after entering the classroom is the experience in the container, which is called the "internal experience" [18]. The "EEI model" divides the process of experience into three stages: expectation, event, and impact. It is essentially a time model that explores how the experience occurs in the time dimension and its follow-up. But all time models have their limitations. On the one hand, from the physical dimension, the time model cannot show the obscurity of the product or service to the user's final experience; on the other hand, from

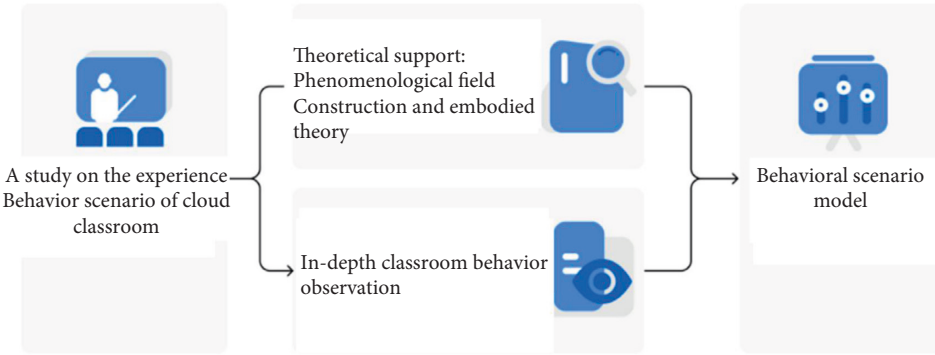

Figure 1: Research framework of classroom behavior scene model.

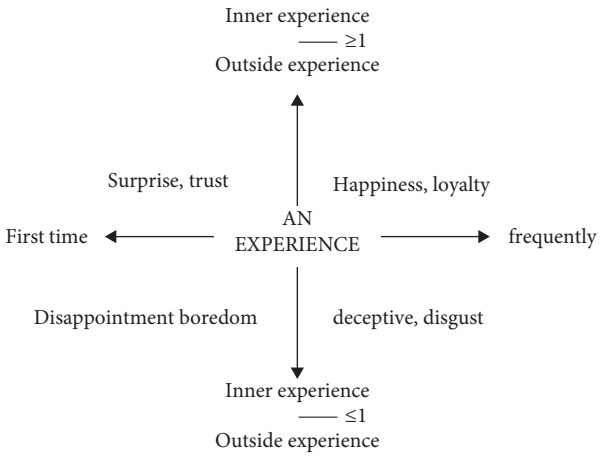

Figure 2: The "SHDD" orientation of a student's experience.

the philosophical dimension, any experience occurs in time and time. In the intuitive form of space, the "experience container" proposed in this study is not only based on time but also emphasizes the shielding effect of the spatiality of experience on people's intuition.

4. Design of Online Classroom Experience Based on Field Theory

4.1. Establishment of a Situation Description Swimlane Diagram. Swimlane diagram is a Unified Modeling Language (UML) activity diagram designed to show the activities of different characters at the same time. In 2007, Yvonne Shek of nForm Company modified the Unified Modeling Language activity and invented the Scenario Description Swimlanes [1]. Scenario description swimlane diagram describes the various behaviors of multiple participants (students, teachers, family members, etc.) in a series of activities in the online classroom, making the results more intuitive and clear, and this overall analysis is compared to the simple addition of each part better results. The swimlane diagram in the online classroom scenario includes storyboards, resources, user experience, target process, tool contact requirements, and pain points, as shown in Figure 3 [19].

According to the situation description swimlane diagram, the situation space of online classroom users is drawn, as shown in Figure 4.

4.2. Building a User Journey Map. The process of the traditional offline classroom is as follows: check the time and place of the class-on the way to the classroom-check in and punch in (or have)-find a seat-open textbooks, handouts and other school supplies-listen to the class-take notes-discuss with classmates between classes (or)-be called to answer questions (or yes)-record coursework-leave class-pack school supplies-leave the classroom. Among them, the classroom acts as a space medium that brings together teachers and students. For students and teachers, it is a temporary residence, and the bell of the get out of class will always ring. [20,21].

The class process of the existing online classroom products is as follows: the teacher notifies the class in the class group when the class will take place. When the time comes, the teacher will drop a Tencent conference meeting number or link to the group, or invite the whole class to join the live broadcast on the corporate WeChat. After the teacher entered the meeting, he shared his screen to explain the PPT for lesson preparation, and the students took notes while listening to the class. After the course is over, everyone will leave the conference live room. The students then communicate and collaborate with the classmates in the group on WeChat or other communication tools to complete the homework. This process is inconvenient. Everyone is distributed in different parts of the country. A collaborative tool group with online classrooms as the carrier becomes very necessary.

In the traditional service blueprint, the direct interface between products and services and users is called the operation interface. The interface not only refers to the human-computer interaction interface of the mobile phone screen or computer window in the narrow sense, but actually covers the direct or indirect contact between products and services and users. Mr. Dai Fupping proposed generalized interface and full-contact design thinking based on Husserl's spatial intuition. That is to say, the contact is not only performed on the specified contacts, but also contacts outside the specified contacts. Non-contacts also become contacts through

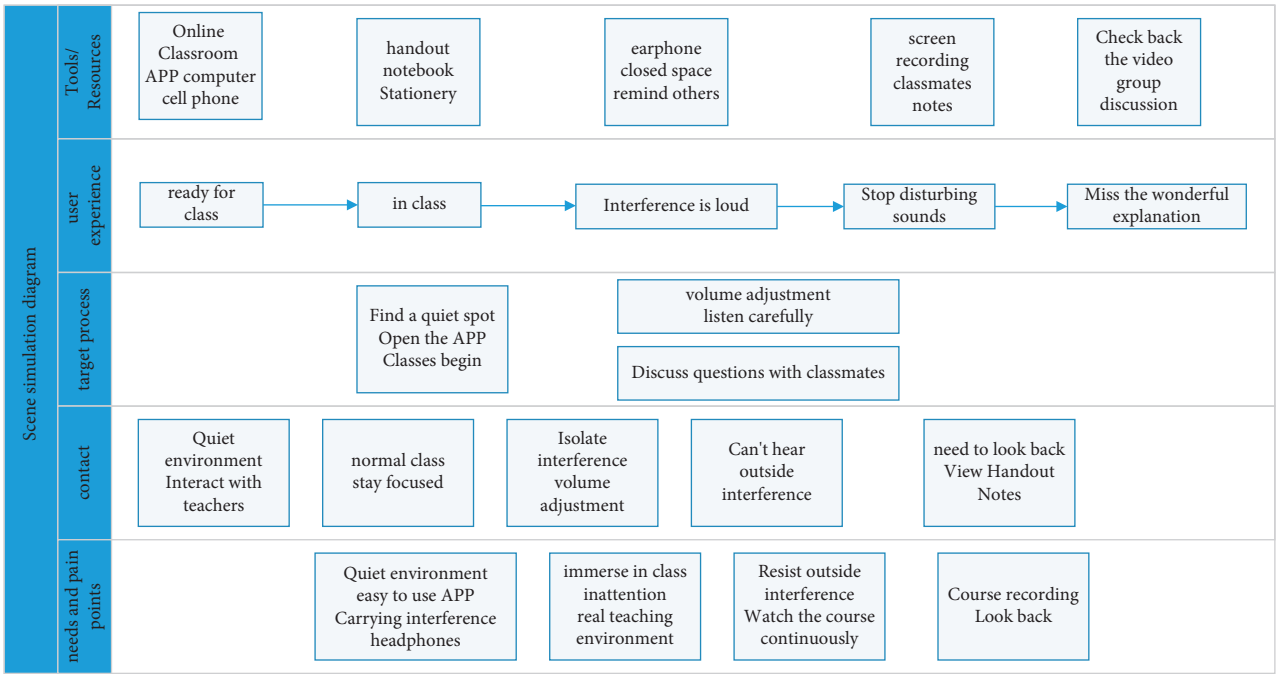

Figure 3: Scenario description swimlane diagram.

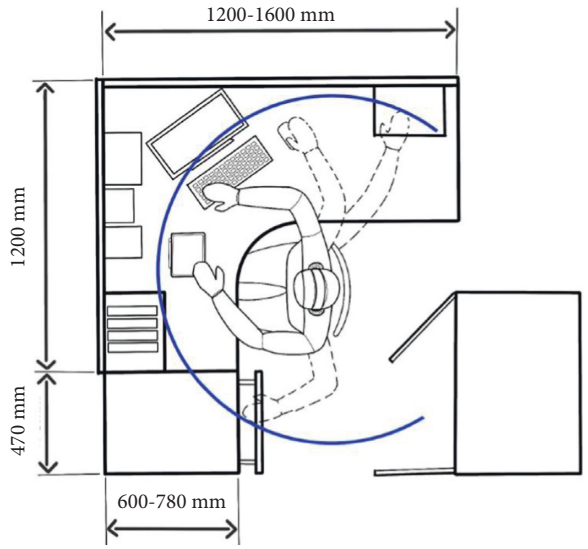

Figure 4: Online classroom user scenario space.

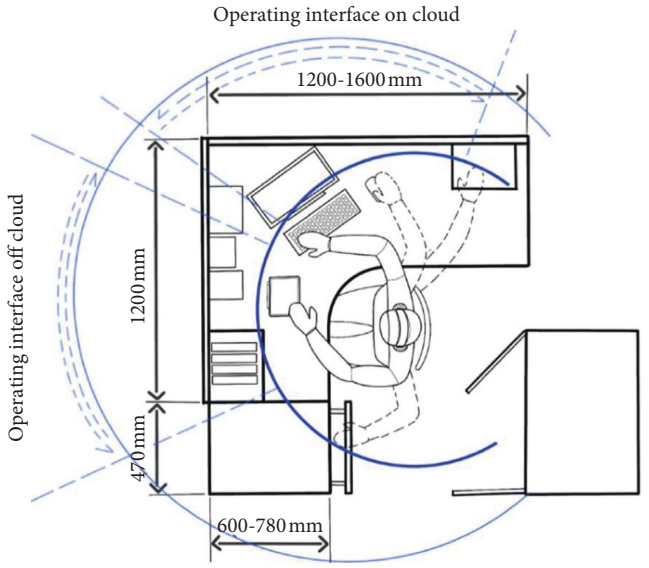

Figure 5: Online classroom user interface.

contact, so they are actually full contacts. This is actually because Mr. Dai Fuping took human freedom into consideration in the design at the philosophical level. The subjective initiative of human freedom cannot be ignored. Do not regard the user as a number or symbol in an equation, but consider that he is a person with essential intuitive ability. Therefore, in the apperception of this essential intuitive ability, non-contact points may also become contact points, as shown in Figure 5.

Restored to the specific online classroom scene, the apperception of this essential intuitive ability of people is reflected in the specific scene. The generalized interface includes not only the software interaction interface of the class but also the interface background or background interface formed by the desks and chairs in the space where it is located. Not only that, the head-mounted hardware in this design is in contact with the user's scalp to form a body interface, and the touch panel is adjusted to form an interactive interface with fingers. These interfaces will be composed of a series of experience touch points, such as the elasticity of the head beam, the texture, and agility of touch.

4.3. Building an All-Touch User-Other Interface. Turning to the other (derAndere), that is, the subject of the full-contact and generalized interface with other people in this space is

replaced, such as the user's parents, friends, and even pets. What potential touchpoints will they have with the product or target user in this common field ? These things that traditional designers choose to ignore can actually be taken into account, because we cannot design a person completely separated from his real-life scenes and characters. If the touch points of the people around the user can be taken into consideration, it will eventually bring about changes in the way people communicate with each other. The product as a carrier becomes a dual interface, which is the interface of "Möbius strip." Different people's interfaces can produce a meeting point, instead of connecting users with other people's space or resources through a product. Taken apart, this is an "onion" interface, as shown in Figure 6. The dual interface proposed in this study is to use the product as the medium to bring people in this space into the category of experience design. This is different from the previous contact points above, which are not only the contacts of a certain person, but the full-user, full-contact, or full-consciousness contact in the true sense. Improvements in the way people interact with each other in the spatial field can be achieved through this dual interface.

Under the guidance of the design thinking of all-consciousness and all-contact, this research integrates the potential interaction interface of family members and the target interaction interface of students into a system and at the same time as the object of experience design, forming a "student user as the main body of operation." "Online operation interface," "offline operation interface," and "other interface" with family members as the main body. In order to enable target users to obtain an immersive online and offline operating experience without being disturbed by others, it is necessary to study the behavioral scenarios of others and design the interface of others so that others can operate in this field. Get the feedback they should have, and then guide them to make the right behavior, as shown in Figure 7.

By establishing different behavioral scene models, the interface systems of different roles are not mechanically integrated so that the target users have an immersive class experience. According to the different types of touchpoints, this study divides the touchpoints into the following types: visual touchpoints, physical touchpoints, and interactive touchpoints. And incorporate different types of touchpoints into the appropriate interface.

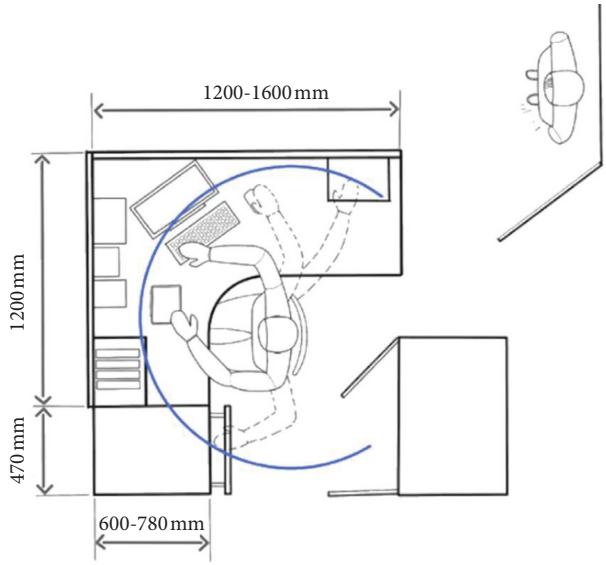

Figure 6: Family members in an online classroom scenario.

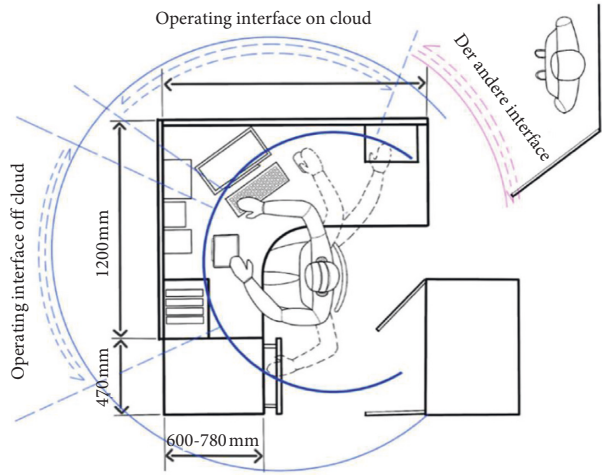

Figure 7: "Other interface" in online classroom space.

4.4. Main Product Modules and Experience Service System

4.4.1. Class Module. The class module includes three scenarios: before class, during class, and after class. Before class, students can learn the specific information of this course by entering the course details page, including course name, instructor, course label, course outline, teaching objectives, homework and discussion, and related training plans, and can also recommend this course to your classmates. During class, after students enter the class, the system automatically turns off the students' microphones and cameras. Students can manually turn on the microphone and camera, and can share the class ID to add classmates. In terms of hardware, students can enter the immersive classroom atmosphere by wearing professional online classroom headsets. The hardware has microvibration energy, and by taking a pat on the avatar, a private interaction is formed between students without affecting the classroom environment. There are class notes, drawing boards, and schedules in the classroom recording tool. You can cancel the acceptance of classmates' pats, and enable or disable the beauty function. One of the most distinctive designs on the student side is the curriculum. Clicking a course on the curriculum will jump to the course details page. If you are in class, you will directly jump to the class live page. The traditional curriculum only provides viewing; the curriculum designed in this study provides classroom entrance. Friends can view each other's class schedule and learn about each other's class time and common courses. After class, the

system will automatically generate class time for users, and a more detailed statistics will be formed every week, such as "You have completed 290 minutes of course study this week and participated in three courses, which is great !" which will push some short sentences about learning methods. The biggest difference between the class module on the teacher side and the student side is that the teacher can edit and design the course content, and has more authority to operate the classroom. For example, the "Take a pat" function can only allow the teacher to take pictures of the students, and the students cannot take pictures of the teacher.

4.4.2. Collaboration-Shared Modules. Compared with the traditional student work alone, the current student work advocates division of labor and cooperation. In this study, an online group module is designed on the student side of the online classroom, which is used for students to collaborate and discuss learning. The truth is always clearer and clearer, and the practice is always the best standard to verify the theory. This process is an effective supplement to the classroom time. Taking the design school where this institute is located as an example, all courses require teamwork to be completed, and design activities pay attention to team awareness and do not advocate fighting alone. In the existing online classroom products, there is a lack of collaborative design for college students. Interaction and vision overlapped for a period of time. At this time, visual students will first formulate visual specifications and components, and product students will also join the discussion. Group members can manage their own personal plans. Everyone's personal plan can be synchronized to the online end in real time and shared with team members. Each individual plan involves other team members, forming a positive cycle of mutual promotion. The relationship between classmates is not only a collaborative relationship but also a relationship of friends. In order to avoid strong work attributes, this study added some interesting designs to the online group, such as today's Whisper. This is an anonymous truth-talking area that can add a little fun to busy work and add some lubricant to task-driven and sometimes tense relationships, as shown in Figure 8.

4.4.3. Lesson Preparation and Preview Linkage Lesson Preparation Module. Existing mainstream online classroom products such as DingTalk, Enterprise WeChat, and Tencent Meetings do not have modules for teachers to prepare lessons. Their office attributes and tool attributes are relatively strong, and they attach importance to timely meeting capabilities in product design. In the design of online classes for college students, the teacher's lesson preparation is very important, which is related to the quality of the class. This is also designed under the guidance of all-touch design thinking. In the previous investigation, this study found that most of the online classes during the COVID-19 epidemic did not have syllabuses and had a strong temporary nature. This results in students not knowing what to expect before class, and therefore not knowing how to prepare. Some

Figure 8: Usability test results.

Figure 9: Software and hardware interaction.

difficult and systematic courses, such as advanced mathematics and physics, lack of preclass preparation is very unfriendly to students. In traditional classrooms, teachers have difficulty in grasping the basic situation of students during lesson preparation, and often fall into misunderstandings. The online classroom lesson preparation module designed in this research solves this problem well. Taking advantage of the timeliness of online and online sharing, while teachers are preparing lessons, they can be shared with class groups in a timely manner to form positive interactions with students and get feedback on lesson preparation. Teachers can do questionnaires, voting, and other activities in the group, and design courses in a "personalized" style, realizing " personalized courses" that cannot be achieved in traditional classrooms.

4.4.4. Software and Hardware Interaction Module. The software and hardware interaction module is based on the online classroom software and hardware parts. Why introduce hardware? Professional hardware is to create an immersive classroom space, to separate students and teachers from their environment, and devote themselves to classroom learning and teaching. In traditional classrooms, each course will be completed in an independent classroom. The function of the classroom is to isolate the classroom

from other environments and form a closed and immersive teaching environment. First of all, as a specialized device, the hardware can only be used on the online classroom APP, specifically as shown in Figure 9. This research draws on several market-proven professional equipment, such as iFLYTEK's professional voice recorder and Bose's "Sleep Bean." The hardware extracts students from the home environment through noise reduction technology and then uses sound technology to simulate the immersion brought by the sound space of the offline classroom.

5. Conclusion

Under the process of education modernization, the development of online education has become an inevitable trend. As the main front of talent training and the key implementation object of education modernization development plans, the teaching effect of online classrooms in colleges and universities is a problem that is generally concerned by the current society. It is particularly necessary to improve the teaching effect of online classrooms in colleges and universities through investigation and research. Therefore, through Bourdieu's field theory, this study analyzes various relationships in the online classroom field of colleges and universities from a microperspective, aiming to clarify the ideal state of the online classroom field of colleges and universities so as to find an optimization path and improve colleges and universities. Combining the theoretical research of Heidegger and Merleau-Ponty, this study proposes a "field-based embodied behavior model"; through the research on the characteristics of cloud classroom experience and the investigation of actual needs, it proposes a "new positioning of cloud classroom learning experience." At the level of experience design strategy, combining the field-based embodied behavior model and the specific design practice form, the "experience design strategy under the embodied scFene" is proposed; based on the new positioning of cloud classroom learning experience, "experience design for experience unmasking" is proposed.."

Data Availability

The dataset can be accessed upon request.

Conflicts of Interest

The authors declare that they have no conflicts of interest.

References

[1] C. J. Bonk, K. J. Kim, and T. Zeng, "Future directions of blended learning in higher education and workplace learning settings," in *Proceedings of the World Conference on Educational Multimedia,Hypermediaand Telecommunications*, pp. 3644–3649, Montreal, Canada, June 2005.

[2] D. T. Bourdeau, K. V. Griffith, J. C. Griffith, and J. C. Griffith, "An investigation of the relationshipbetween grades and learning mode in an English composition course," *Journal ofUniversity Teaching & Learning Practice*, vol. 15, no. 2, 2018.

[3] P. Bourdieu, "The forms of capital," in *Handbook of Theory and Research for the Sociology of Education*, J. Richardson, Ed., pp. 69–72, Greenwood Press, Santa Barbara, CA, USA, 1986.

[4] C. Clark, N. . Strudler, and K. Grove, "Comparing asynchronous and synchronous video vs.TextBased discussions in an online teacher education course," *Journal of AsynchronousLearning Net-work*, vol. 19, no. 3, pp. 84–96, 2015.

[5] D. H. Jonassen, *Learning to Solve Problems with Technology: AConstructivist Perspective*p. 256, 2nd edition, Prentice-Hall, Hoboken, NJ, USA, 2002.

[6] E. K. Faulconer, J. Griffith, B. Wood, S. Acharyya, and D. Roberts, "A comparison of online, video synchronous, and traditional learning modes for an introductory undergraduate physics course," *Journal of Science Education and Technology*, vol. 27, no. 5, pp. 404–411, 2018.

[7] A. Francescucci and M. Foster, "The VIRI (virtual, interactive, real-time, instructor-led) classroom: the impact of blended synchronous online courses on student performance, engagement, and satisfaction," *Canadian Journal of Higher Education*, vol. 43, no. 3, pp. 78–91, 2013.

[8] A. Francescucci and L. Rohani, "Exclusively synchronous online (VIRI) learning: the impact on student performance and engagement outcomes," *Journal of Marketing Education*, vol. 43, no. 3, pp. 78–91, 2018.

[9] D. Gedera, "SPStudents ' experiences of learning in a virtual classroom [J]," *International Journal of Education and Development Using Information and Communication Technology*, vol. 10, no. 4, pp. 93–101, 2014.

[10] A A. Skylar, "Comparison of asynchronous online text-based lectures and SynchronousInteractive web conferencing lectures," *Issues in Teacher Education*, vol. 18, no. 2, pp. 69–84, 2009.

[11] J. M. Spector, "Conceptualizing the emerging field of smart learning environments," *Smart Learning Environments*, vol. 1, no. 1, pp. 2–10, 2014.

[12] C. Quigley and J. Patrick, *Globalization's Contradictions; Geographies of Discipline,destruction and transformation*, Routledge, London, 2007.

[13] R. J. Pasco, *Capital and Opportunity: A Critical Ethnography of High School Students At-Risk*, University Press of America, Lanham, Maryland, 2003.

[14] D. W. Norton, "The strategic technical communicator: a critical action inquiry of information architecture," *Social Affairs*, vol. 24, no. 5, pp. 22-23, 2001.

[15] E. B. Weininger and A. Lareau, "Translating Bourdieu into the American context: the question of social class and family-school relations," *Poetics*, vol. 31, no. 5-6, pp. 375–402, 2003.

[16] M. Marinetto, "Who wants to be an active citizen?" *Sociology*, vol. 37, no. 1, pp. 103–120, 2003.

[17] C. Forde, S. Martin, and A. D. Galvin, "Children and young people's right to participate: national and local youth councils in Ireland," *The International Journal of Children's Rights*, vol. 24, no. 1, pp. 135–154, 2016.

[18] C. Quigley and J. Patrick, *Globalization's contradictions ; Geographies of discipline, destruction and transformation*, Routledge, vol. 97, no. 4, , pp. 802–804, London, 2007.

[19] M. Gerissdoerfer, P. Savaget, and S. Evans, "The Cambridge Business Model Innovation Process," *Procedia Manufacturing*, vol. 8, pp. 262–269, 2017.

[20] P. Zhou and Y. Zhang, "Analysis and Thinking on the Current Situation of Student Participation in Online Teaching Platforms," *Journal of Nanjing Radio and Television University*, vol. 33, no. 02, pp. 40–43+81, 2010.
[21] Q. Zhu and F. Li Lu, "The formation of media weakness and its rescue for vulnerable groups in the perspective "concept," *Social Sciences*, vol. 44, no. 6, 2005.
[22] Y. Zhu, X. Han, J. Yang, and J. Cheng, "Higher education with the help of online development has become an irreversible trend - a comprehensive analysis of the 11-year series of reports on online education in the United States and enlightenment," *Tsinghua University Education Research*, vol. 35, no. 04, pp. 92–100, 2014.

Hindawi
Scientific Programming
Volume 2022, Article ID 2944750, 12 pages
https://doi.org/10.1155/2022/2944750

Research Article

Design of 3D Display System for Intangible Cultural Heritage Based on Generative Adversarial Network

Jiachun Wang,[1] **Junkui Song**,[2] **Yizhe Zhang**,[3] **and Hao Chen**[4]

[1]*Jinling Institute of Science and Technology, Nanjing 211169, Jiangsu, China*
[2]*SangmyungUniversity, Cheonan 330-720, Republic of Korea*
[3]*School of Art, Pujiang College, Nanjing University of Technology, Nanjing 211200, Jiangsu, China*
[4]*College of Mechanical and Electrical Engineering, Jinling Institute of Technology, Nanjing 211169, Jiangsu, China*

Correspondence should be addressed to Jiachun Wang; wjch@jit.edu.cn

Received 18 May 2022; Revised 14 June 2022; Accepted 29 June 2022; Published 21 July 2022

Academic Editor: Lianhui Li

This paper designs a three-dimensional display system for intangible cultural heritage based on generative adversarial networks. The system function is realized through four modules: input module, data processing module, 3D model generation module, and model output module. Two 3D model reconstruction methods are used to realize the transformation from 2D images to 3D models. In the low-resolution Nuo surface 3D construction, multiresidual dense blocks are introduced and applied to the deep image super-resolution network. The experimental comparison results show that the quadratic optimization multifusion 3D construction model proposed in this paper can achieve considerable improvement and can improve the reconstruction accuracy by about 6.3%. In the high-resolution 3D construction of the Nuo surface, a generative adversarial network model is used to improve the generator, discriminator, and loss function of the original SRGAN model. Experimental results show that this method can generate super-resolution images with more realistic and natural depth maps. In addition, when it is used for high-resolution 3D Nuo surface sculpting, it can also generate 3D voxel Nuo surfaces with more details.

1. Introduction

At present, the development status of intangible cultural heritage projects and the protection of intangible cultural heritage need to be improved. The modern production and way of life have undergone great changes, and traditional handicrafts and artworks have been gradually replaced by industrial products, resulting in certain difficulties in the status quo of intangible cultural heritage projects and the life status of intangible cultural heritage inheritors. The biggest problem facing intangible cultural heritage is the lack of intangible cultural heritage. On the one hand, the intangible cultural heritage is complicated and difficult to learn; on the other hand, some of the intangible cultural heritage is mostly oral, and there is no specific learning carrier. To solve the problem of the decline of national culture caused by the reduction in intangible cultural heritage, it is urgent to use modern three-dimensional construction technology to reproduce the intangible cultural heritage.

The traditional 3D construction technology uses 3D reconstruction software to construct the target 3D, and the construction result has high accuracy, but the use of the software requires training of professionals and detailed data of the modeled objects. In addition, the multi-view geometric method can also be used for 3D construction [1, 2], using multiple views to complete the fusion of different information of the target, so as to complete the 3D construction of the target. However, the above methods are difficult to complete the three-dimensional reconstruction and display of intangible cultural heritage. Therefore, how to complete the 3D construction of a single RGB image quickly and with high quality is particularly important. With the deepening of deep learning research, deep learning models based on CAD databases have begun to be used for 3D

reconstruction of a single image. In 2015, Wu [3] started to propose the 3D ShapeNets model, which utilizes deep convolutional belief networks to learn the joint distribution of all 3D voxels in a data-driven manner. Their proposed model learns the distribution of complex 3D shapes across different object classes from raw CAD data, performing joint object recognition and shape reconstruction from 2.5D depth maps. Choy [4] proposed a new structure—3D recurrent reconstruction neural network in 2016, which avoids the prior matching problem existing in traditional methods, which is derived from a large number of A mapping of learning objects to their 3D shapes in synthetic data sets, using one or more images of real objects from any viewing angle as input and 3D voxels as output. In addition, taking advantage of the powerful ability of generative adversarial network in image generation [5–8], more and more scholars have begun to study the use of GAN for 3D model reconstruction. Generative adversarial networks proposed earlier use a game-like approach to generate images from random noise and refine them to approximate real images. Inspired by this, Wu et al. [9] extended the 2D generative adversarial network to 3D generative adversarial network in 2016. Gadelha et al. [10] proposed projective generative adversarial networks, which estimated the 3D shape and viewpoint, respectively, through the generator network to generate a binary projection image for the projection module and then used the discriminator network to judge true and false. Riegler et al. [11] proposed a learning-based deep fusion method, designed a 3D convolution model for octree network fusion, and used one or more depth maps as input to estimate the 3D space division, ranging from coarse to fine. The reconstruction resolution is increased to $128 \times 128 \times 128$ in three steps. The GAN-based idea uses the discriminator to judge the reconstructed high-resolution image and the ground truth image, which makes the generated high-resolution image closer to the real image as a whole, has more details, and is more in line with human visual perception.

Based on the 3D reconstruction technology of intangible cultural heritage based on generative adversarial network, this paper takes Guangxi Nuo surface as the research object and introduces in detail how to design the 3D display system of intangible cultural heritage. By establishing an intangible cultural heritage data set, a multifeature fusion method is used for low-resolution voxel 3D modeling, and a high-resolution 3D model of intangible cultural heritage is established based on a generative adversarial network.

2. Relevant Knowledge

2.1. Convolutional Neural Networks. A simple convolutional neural network is mainly composed of three types of network layers: convolutional layer with nonlinear activation function, pooling layer, and fully connected layer, and the basic structure is shown in Figure 1, where the small white box represents the size of the convolution kernel. Among them, the size of the convolution kernel can be any value smaller than the size of the input image, and the larger the convolution kernel, the larger the receptive field. Therefore, the more picture information is seen, the better the features are obtained. However, using an excessively large convolution kernel will lead to a dramatic increase in model computation, which is not conducive to increasing the depth of the neural network. In Figure 1, the input layer takes the pixels of the image as the feature node as input. During the forward propagation process, the convolution kernel slides along the width and height of the image and calculates the convolution kernel and the dot multiplication between inputs. Finally, the response of the input to the convolution kernel at each spatial position is obtained, which is called a feature map. To make the neural network have nonlinear fitting ability, a nonlinear activation function is usually added to the convolutional layer. Since the increase in the feature map after the convolution operation will lead to too many parameters of the neural network, the pooling layer is often used to reduce the spatial dimension of the feature map. Finally, outputting the results through a fully connected layer can accomplish tasks similar to handwritten digit recognition.

2.1.1. Convolutional Layer. In different image processing tasks, the input image can be subjected to convolution operation to extract different features for processing. Different features can be extracted using different convolution kernels, such as edges and contours. It is well known that the depth of the neural network can improve the performance of the model more than the width. In the convolutional layer, due to the local connection and weight sharing of the convolutional layer, the parameters that the neural network needs to learn are greatly reduced, which is also conducive to designing a larger neural network to handle more complex tasks. In a convolutional neural network, for an input image X, its convolution is defined as follows:

$$s(i, j) = (X * W)(i, j) = \sum_{m} \sum_{n} X(i + m, j + n) W(m, n). \quad (1)$$

Among them, W is the convolution kernel, X and W are both two-dimensional matrices, (i, j) represents the two-dimensional matrix coordinates, and $W(m, n)$ represents the weight at the convolution kernel (m, n). Figure 2 is a schematic diagram of a simple convolution. In Figure 2, the convolution kernel calculates the value of 9 pixels on the input image at a time, and then, the sliding step size moves one unit to the right or down, respectively. Finally, the convolution kernel traverses the entire input image to obtain a 2×2 output feature map.

2.1.2. Pooling Layer. The introduction of the pooling layer imitates the human visual system to reduce the dimension and abstract the input object, and the use of the pooling layer can retain the main features of the image and reduce the parameters of the model, which can also reduce the degree of overfitting of the model to a certain extent and improve the generalization ability of the model. In addition, the pooling layer can make the model pay more attention to a certain feature present in the image rather than the location of the feature.

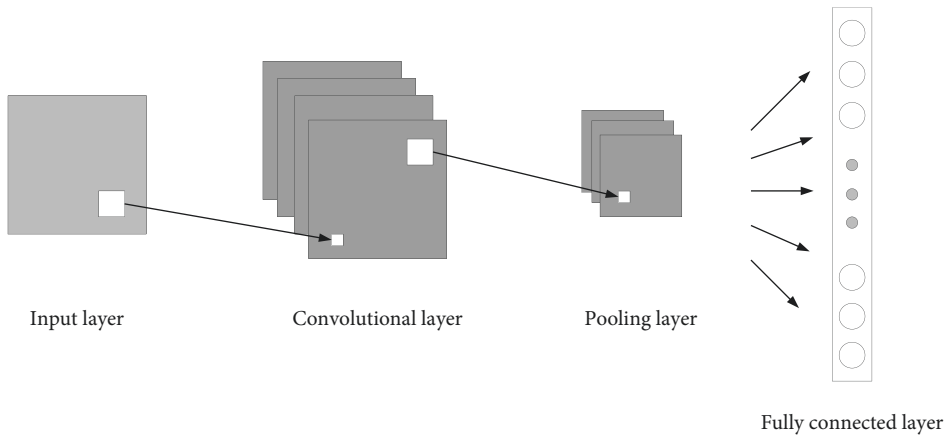

Figure 1: Basic structure of convolutional neural network.

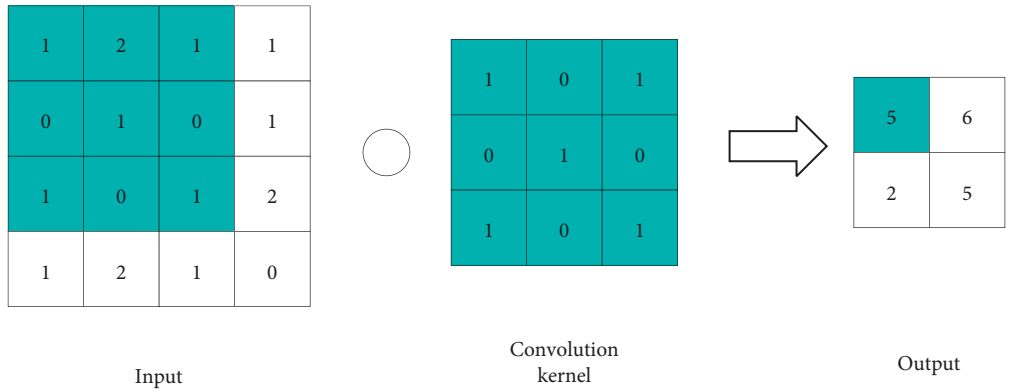

Figure 2: Two-dimensional convolution operation.

The max-pooling layer is one of the most commonly used nonlinear pooling functions. This pooling operation divides the input image pixels into multiple sub-pixel regions and then takes the maximum pixel value of each sub-pixel region as the output. Suppose the size of the convolution kernel W is $p \times q$, the stride is s, and the input x is an $m \times n$ matrix, and then, the maximum pooling layer is calculated as follows:

$$y(i, j) = \max[x(i \times s + r, j \times s + k)],$$
$$r = 0, 1, \cdots p - 1, \quad (2)$$
$$k = 0, 1, \cdots, q - 1, \frac{i \leq (m - p)}{s}, \frac{j \leq (n - q)}{s}.$$

The pooling operation is shown in Figure 3. In Figure 3, max pooling is computed using a filter of size 2×2 with a stride of 2. Comparing the calculation results with the input image, it can be seen that the data are reduced by 75% after the max-pooling layer.

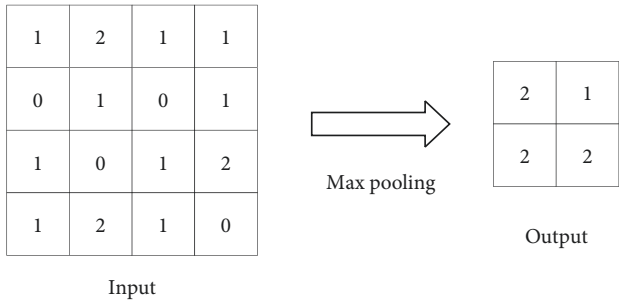

Figure 3: Max-pooling operation.

2.1.3. Fully Connected Layer. Each layer of the fully connected layer is composed of many neurons, and each neuron is connected with each neuron in the previous layer to integrate the previously extracted features. The essence of a fully connected layer is to transform one feature space into another feature space. To improve the performance of the neural network, the fully connected layer uses a nonlinear activation function. Due to its own characteristics, the use of fully connected layers can lead to a dramatic increase in the parameters of the model. Therefore, the general convolutional neural network model uses one or more fully connected layers after the convolutional layer and the pooling layer.

2.1.4. Activation Function. In neural networks, activation functions usually refer to functions that can achieve nonlinear mapping. The main function of the activation function

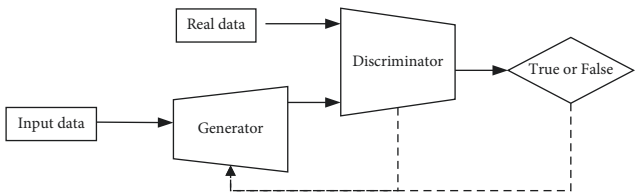

Figure 4: Basic model of generative adversarial network.

is to add nonlinear factors, so that the neural network can approximate any nonlinear function and solve the defect of insufficient expression ability of the linear model. Several commonly used nonlinear activation functions are as follows: sigmoid function, tanh function, ReLU function and its variants, and Swish function.

(1) Sigmoid Function. The sigmoid function is a common activation function, and its mathematical expression is as follows:

$$f(x) = \frac{1}{1 + e^{-x}}. \tag{3}$$

The sigmoid function can make the output smooth and continuously limited in the range of 0~1, which is close to linear in the region of the input near 0 and nonlinear in the region far from 0. The result tends to be 1 for large positive numbers and 0 for large negative numbers. It is precisely because of the existence of its saturation region that the gradient of the input at both ends of the function is almost 0, causing the gradient to disappear. In addition, because the output value of the sigmoid function is not centered at 0, the model convergence is prone to oscillation during back propagation.

(2) ReLU Function.

$$f(x) = \begin{cases} x, & x > 0 \\ 0, & x \le 0 \end{cases}. \tag{4}$$

The ReLU function is equivalent to $f(x) = \max(0, x)$, the output below the threshold is 0, and the output above the threshold is linearly invariant. Experimental results show that the ReLU function converges 6 times faster than the tanh function [12]. However, ReLU may update the weights to positions that are never activated again due to excessive gradients during training. Also, setting the learning rate too high may cause most of the neurons in the network to not be activated. To solve the possible vanishing gradient of the model due to the negative value problem in ReLU, a series of variants are proposed, such as leaky ReLU [13]. When $x < 0$, the input is multiplied by 0.01 as the output, and the mathematical formula is as follows:

$$f(x) = \begin{cases} x, & x > 0 \\ 0.01x, & x \le 0 \end{cases}. \tag{5}$$

2.2. Generative Adversarial Networks. Generative adversarial networks (GANs) were first proposed by Goodfellow et al. in 2014 [14]. The generative adversarial network is different from the traditional convolutional neural network. It uses two neural networks to play a game to train the neural network. GAN consists of a generator and a discriminator. The basic model is shown in Figure 4. First, the generator network generates the corresponding target data from the input data. Then, the discriminant network judges whether the data from the generator network are real or fake after learning the knowledge of the real data. To generate more realistic target data to deceive the discriminator, the generation network needs to continuously optimize its generation ability. The generation network and the discriminant network optimize each other in the process of continuous confrontation and finally make the whole network reach the Nash equilibrium. As the discriminator network approaches the optimal solution, the generator network also approaches the minimum.

Currently, GANs are commonly used in image generation tasks and 3D object reconstruction tasks. The standard GAN objective function can be described as follows:

$$\min_G \max_D V(D, G) = E_{x \sim p_{\text{data}}(x)}[\log D(x)] + E_{z \sim p_z(z)}[\log(1 - D(G(z)))]. \tag{6}$$

2.3. 3D Construction Based on Voxel Representation. At present, in the three-dimensional construction model of the image, the encoding-decoding architecture is generally used. The encoding stage in this architecture can use different encoders, and similarly, the decoding part in the decoding stage can also use different neural network-based decoders. In the decoder stage, the voxel-based 3D decoder decodes the feature vector to generate a A 3D shape represented by a voxel. Because of the regular 3D decoder, which needs to convolve each voxel position in the 3D volume, the network computation time and memory need to grow cubically as the resolution at which the 3D volume is generated increases, but the method is robust to input, enabling voxel-based 3D construction methods to reconstruct 3D shapes of arbitrary topologies. Deep learning is a type of representation learning, that is, generating useable representations from data. In the encoding-decoding architecture, the encoder can extract the main low-dimensional representation through learning, and the decoder can generate the required high-dimensional data through the low-dimensional representation. For the 3D construction model represented by voxels, it can be divided into a direct representation decoding model, an intermediate representation decoding model, and other decoding models. In this paper, the decoding model is directly represented, and the specific process is shown in Figure 5.

The network consists of a 2D encoder and a 3D decoder. In general, encoders use 2D convolutional neural networks, while decoders use 3D deconvolutional networks. In the encoding stage, the 2D encoder encodes the input 2D image into a low-dimensional latent vector for feature compression. This practice of compressing the input image from a high-dimensional space to a low-dimensional space is mainly to preserve the main features of the input image to a greater extent, which makes the model parameters

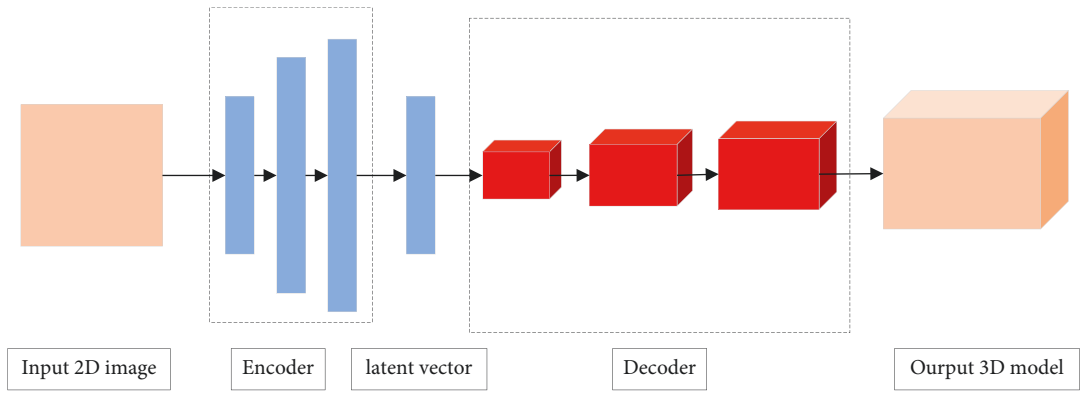

Figure 5: Direct representation decoding model.

significantly reduced to fit in the video memory. In the decoding stage, the decoder decodes the latent vectors to generate 3D shapes. Therefore, in short, the 3D construction process of this architecture is to design a 2D encoder to extract image features and then use a conventional voxel decoder to output a 3D shape.

3. System Design

To realize the 3D display system of intangible cultural heritage based on generative adversarial network, this section develops according to the development steps of software engineering standard. Firstly, a detailed demand analysis is carried out for the 3D display system, and then, according to the system design principle, the functional structure of the 3D display system is designed and analyzed, and finally, each functional module is designed in detail.

3.1. System Design Requirements. This paper aimed to complete the three-dimensional display of intangible cultural heritage and contribute to the inheritance and protection of intangible culture. In particular, it has the following significance.

(1) Digital Protection of Intangible Cultural Heritage. In this study, the artistic features of intangible cultural heritage are preserved in the form of three-dimensional digitalization, and the digital protection of intangible cultural heritage is realized.

(2) Cultural Heritage Display Application Design Strategy. There are many theoretical supports and research methods for the current research on client display applications, but these methods are usually generally applicable models. This study narrows the scope of the research and attempts to summarize the design strategies for cultural heritage display applications, for the purpose of this type of application. The design provides reasonable and scientific design ideas.

(3) Case Design of Three-Dimensional Display of Intangible Cultural Heritage. For the purpose of education, the sample case of intangible cultural heritage display application is realized, aiming to achieve a better user experience, users are enabled to have a systematic and comprehensive understanding of intangible cultural heritage, and users are allowed to have a stronger understanding of traditional cultural interest, to achieve better protection of traditional culture and improve the effect of cultural transmission.

3.2. System Design Principles. When designing the three-dimensional display system for intangible cultural heritage, we follow the following principles in system development.

The first is the abstract principle. Abstraction refers to the simplification of complex phenomena, which must be simplified to the extent that it is convenient for people to analyze and understand.

The second is the encapsulation principle. The encapsulation principle is a rule that developers must use when developing the system structure. Each individual program component needs to be encapsulated into a single and independent module, and the module's internal processing logic details are exposed as little as possible when defining a module. It is necessary to require that each module can be independently developed and tested, and the final complete program is assembled from a series of sub-module programs. The principle of encapsulation can greatly improve the modifiability, testability, and portability of the system.

The third principle is the principle of independence between modules. The independence between modules means that any relatively independent subsystem program is completed by an independent module, and the connection between this module and other modules must be achieved very simply. Two standards are commonly used in the industry to measure the independence between modules: cohesion and coupling. Cohesion is a measure of how closely each element is related to each other within each module. The coupling measures the degree of independence between each module, which mainly depends on the interface information type and interface complexity provided by each module and the way to call the module.

3.3. System Structure Design. The key to realizing the dance generation application based on generative adversarial network lies in the patch-based pixel generation in the

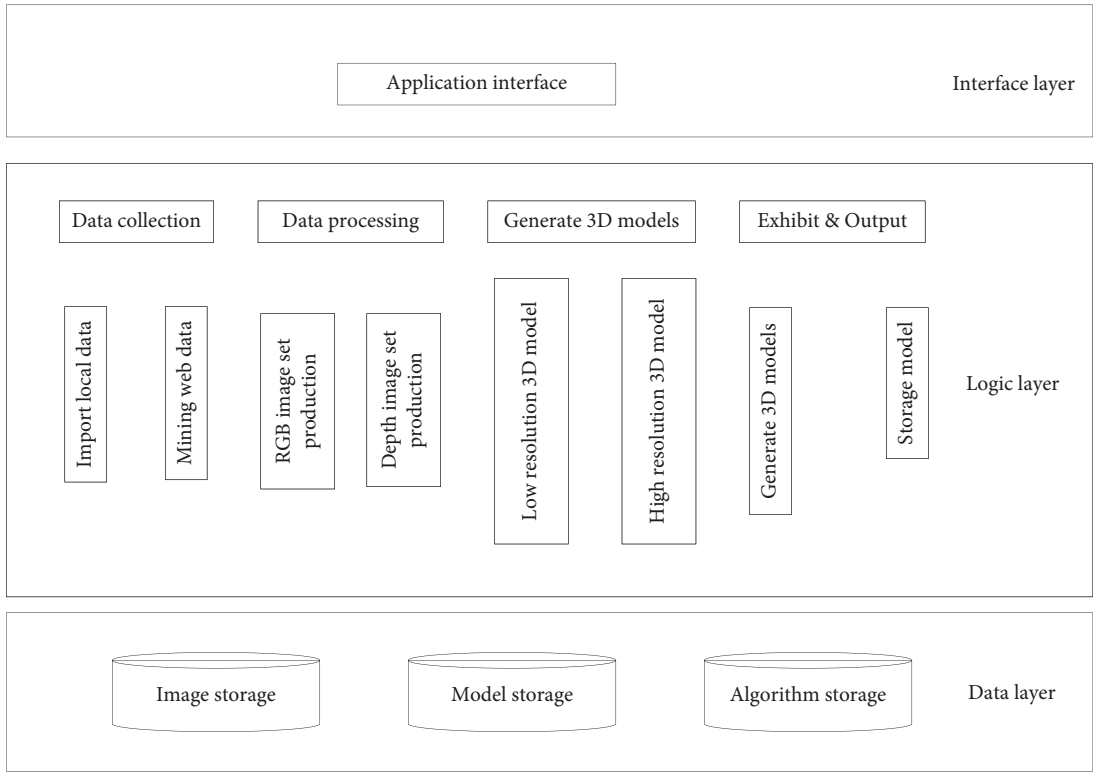

Figure 6: Overall structure of the three-dimensional display system of intangible cultural heritage.

generative network and the multiscale image discrimination in the discriminant network and the final loss function design. The overall structure of this application is shown in Figure 6.

3.3.1. Interface Layer. The interface layer is mainly used for the interaction between the user and the system, and all functions need to be as simple as possible. This application interface mainly includes various controls and view modules, such as select video button, display video view, generate dance button, and text prompt view. The application interface will directly display the original dance video and the generated dance video to the user, compare the synthesis effect, and generate corresponding indicator descriptions. Simple and elegant interface design will bring users a good user experience.

3.3.2. Logic Layer. The logic layer is often the core of the entire application system, including the realization of core functions and the connection between the upper and lower layers. The main functions include reading local images or mining data from Web pages. Collecting data are an essential function for generating models; in addition, the system needs to call other open-source projects to make RGB image sets and depth image sets; more importantly, inputting RGB images and depth images into the trained generative model to obtain the target 3D model is the core of the system application; finally, the system displays the generated 3D model to the user.

3.3.3. Data Layer. The data layer is mainly used to store and read data, including image storage, algorithm storage, and model storage.

3.4. System Function Design. This section mainly focuses on the module design of this application, including the overall module design of this application and the detailed design of each module. The functional structure diagram of the system is shown in Figure 7.

This application is mainly divided into four modules according to the system implementation framework, mainly including input module, data processing module, 3D model generation module, and model output module. This section focuses on the data processing module and the 3D model generation module.

3.4.1. Image Set Production Module. In the task of 3D reconstruction of images, one of the keys for deep learning to exert its powerful learning ability is to establish relevant data sets for training. The establishment of the data set is the basis for the 3D construction of the entire model. The data set in this paper mainly refers to the MVD method [15] in the production process. At present, there is no public 3D Nuo mask model of the Maonan people at home and abroad. The only way to solve the data set problem is to use a 3D scanner to collect scans in the field. A total of 36 Maonan Nuo masks were collected by visiting the Huanjiang Maonan Autonomous County Museum in Hechi, and a 3D voxel library and a 2D database were created by scanning.

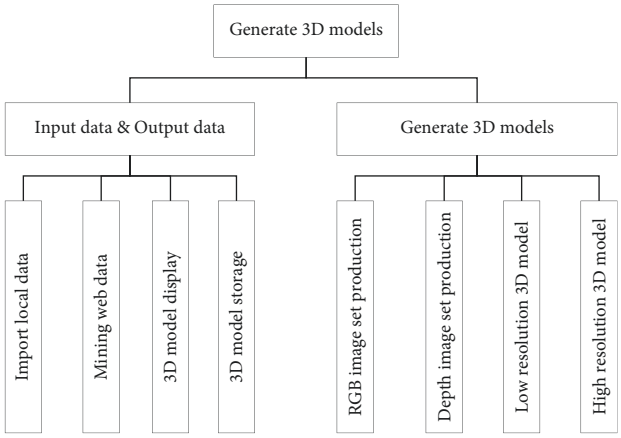

Figure 7: Functional module division.

3.4.2. Low-Resolution Reconstruction Module. This module adopts a multifeature fusion method, first generates a 3D model as the initial reconstruction result, and then optimizes the 3D encoding-decoding network to generate a low-resolution Nuo surface voxel 3D model.

(1) 3D model construction

(2) Loss function

To train the model to generate better 3D shapes, a suitable loss function is required. The loss function of the model is defined as the L_2 loss between the reconstructed 3D object and the real 3D object. The loss function can be defined as follows:

$$L_2 = \left\| \mathrm{Pred}_x - GT_y \right\|_2^2. \tag{7}$$

(3) Training method

This paper uses a 128×128 RGB image as input, and the final output resolution of the network is a voxelized 3D shape of $64 \times 64 \times 64$. This article implements a NVIDIA GTX 1080 with a Dell desktop as the hardware platform and 8G of GPU memory. In addition, the software platform installs TensorFlow on Ubuntu 16.04 and utilizes GPU acceleration to train the network. To fit into the GPU memory size, the training batch size of the single-shot network is 32. The training process uses the Adam optimizer with $\beta 1 = 0.5$ and $\beta 2 = 0.9$ in the optimization parameters. Meanwhile, the initial learning rate is set to 1 × 10–4, and the network is trained for 300 epochs. Then, training is fine-tuned for another 50 epochs. For the secondary optimization multifusion reconstruction model, the pretrained model first generates a 3D volumetric surface with a resolution of $32 \times 32 \times 32$, and then, the network model parameters are fixed and sent to the 3D encoding-decoding network for secondary optimization. A 3D Nuo surface with a resolution of $64 \times 64 \times 64$ is allowed. Other training parameters remain the same as other network training parameters.

3.4.3. High-Resolution Reconstruction. Module. This module uses a generative adversarial network to obtain a high-resolution Nuo surface voxel 3D model. The image super-resolution method based on the generative adversarial network can reconstruct a more natural super-resolution image, which is mainly due to the two networks adopting the idea of confrontation, that is, using the two opposing sides to play a game against each other. First, the low-resolution images are reconstructed into super-resolution images through a generator network. Then, the discriminator compares the input super-resolution image with true and false sexual judgments. Subsequently, the discriminated results are returned to the optimized generator network and discriminator network. Repeatedly, the final generator network and discriminator network complete self-optimization in mutual confrontation. Early SRGANs were implemented on the basis of standard generative adversarial networks (SGANs). The discriminator loss and generator loss of this network are as follows:

$$\begin{aligned} L_{\mathrm{SGAN\_}D} &= -\log\left(D\left(I^{HR}\right)\right) - \log\left(1 - D\left(G\left(I^{LR}\right)\right)\right), \\ L_{\mathrm{SGAN\_}G} &= -\log\left(D\left(I^{HR}\right)\right). \end{aligned} \tag{8}$$

The binary cross-entropy loss function adopted by the SGAN model has the property of unstable training. How to balance the training of the generator and the discriminator is a problem. To this end, some research works try to improve SGAN [16] with other loss functions, for example, relative GAN loss function. Inspired by these works, we also try to improve its network structure and loss function based on SRGAN. Next, we introduce an improved generative adversarial network image super-resolution model.

(1) Improved Generative Adversarial Network Super-Resolution Model. The improved generator network is shown in Figure 8. First, we replace the FEB in the feature extraction module (FEM) from the residual dense block of the SRGAN model to a multiresidual dense block. Through the improved multiresidual dense block, more features are reused in the image feature extraction stage and a deeper network is designed. After the features of the image are extracted, two sets of convolution and image sub-pixel convolution operations are performed to generate a fourfold super-resolution image. The multiresidual dense block with batch normalization layer is used.

The improved discriminator network is shown in Figure 9. Recent experiments [17] show that strided convolutional layers in the discriminator network lead to reduced resolution of the generated feature maps. Ultimately, this causes the super-resolution images generated by the model to lose details. Therefore, we adopt the same improvement and set the stride size to 1 for all strided convolutions. To make the model fit in memory for training, we change the number of output feature maps for each layer to the amount shown in Figure 9. The other

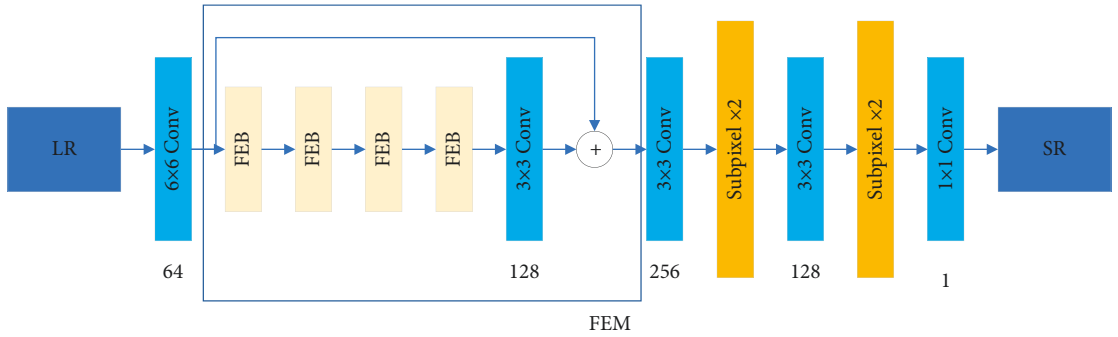

Figure 8: Improved generator network.

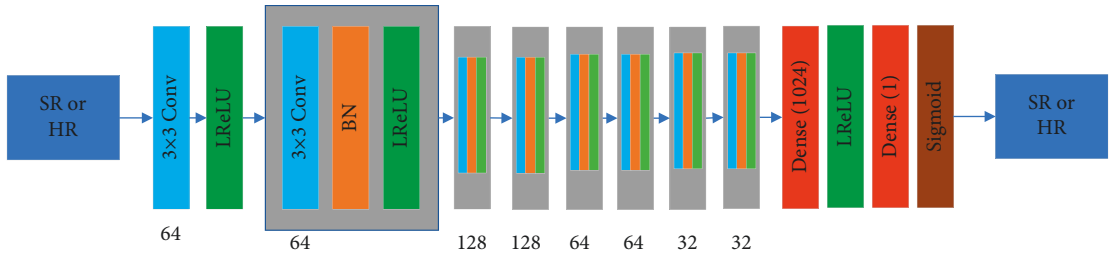

Figure 9: Improved discriminator network.

structures of the discriminator network remain unchanged from those in SRGAN.

(2) Loss function

The loss function of the generator consists of three parts: L_1 content loss, perceptual loss LVGG, and relative average adversarial loss LRa_G. The loss function can be expressed as follows:

$$L_G = \alpha L_1 + \beta L_{\mathrm{VGG}} + \gamma L_{Ra\_G}. \tag{9}$$

Among them, α, β, and γ represent the coefficients used to balance the overall loss, which are taken as 1, 10–3, and 2×10^{-6}, respectively, in the experiment. LVGG calculates the loss in the feature space of super-resolution images and high-resolution images. To ensure that the reconstructed image is structurally similar to the real image, we use pixel-based L_1 content loss. The L_1 loss computes the 1-norm distance between the generated super-resolution image G(ILR) and the true high-resolution image IHR. This loss function can be expressed as follows:

$$L_1 = G\left(I^{LR}\right) - I_1^{HR}. \tag{10}$$

In the SGAN training process, when training the generator, the real data samples are not used in the loss function, which means that the optimization of the entire generator is entirely guided by the discriminator. In the relative GAN, the loss function of the generator uses real data samples as a reference. Furthermore, in SGAN, the model is forced to recognize real samples as real and fake samples as fake. In the relative GAN, the real and fake samples are mixed and the discriminator is used to judge the real and the fake. This method is more stable for GAN training to a certain extent. In addition, it also has a faster advantage in training speed.

The generator loss function and discriminator loss function relative to GAN are expressed as follows:

$$\begin{aligned} L_{G\_Ra} &= -E_{I^{HR}}\left[\log\left(1 - D_{Ra}\left(I^{HR}, G\left(I^{LR}\right)\right)\right)\right] \\ &\quad - E_{I^{HR}}\left[\log\left(D_{Ra}\left(G\left(I^{LR}\right), I^{HR}\right)\right)\right], \\ L_{D\_Ra} &= -E_{I^{HR}}\left[\log\left(D_{Ra}\left(I^{HR}, G\left(I^{LR}\right)\right)\right)\right] \\ &\quad - E_{I^{LR}}\left[\log\left(1 - D_{Ra}\left(G\left(I^{LR}\right), I^{HR}\right)\right)\right]. \end{aligned} \tag{11}$$

4. System Implementation and Testing

4.1. System Development Environment. The training and generation of this application are run on the server, and the runtime development environment configuration is shown in Table 1. For the core algorithm, a large amount of video memory is required. This time, 8 Tesla P100 GPUs are used for training, and the training time is 5*24 hours. Since the system model needs to be trained for a long time, the displayed samples are all models trained in advance.

4.2. System Application Test

4.2.1. Low-Resolution Nuo Surface Voxel 3D Construction Based on Multifeature Fusion. The training details between the traditional 3D reconstruction model, the multi-fusion 3D reconstruction model, and the quadratic optimization multi-fusion 3D reconstruction model are set according to Section 4. By comparing the parameter sizes of different models, we can know the degree of GPU memory required by different models, which can determine whether the model can meet the hardware conditions to a certain extent. In

Table 1: System development operating environment.

Host parameters	OS: CentOS CPU: Inter E7 RAM : 128 GB GPU: Tesla P100*8 GPU RAM : 16 GB
Core algorithm development environment	PyTorch: 0.4 CUDA: 8.0 IDE: VIM Program language: Python 3
Application test development environment	CPU: Inter E7 PyTorch: 0.4 GPU: Tesla P100*8 GPU RAM : 16 GB Program language: Python 3 GUI : PyQt5

addition, the training time of different 3D reconstruction models is also an important indicator to measure the performance of a model. In Table 2, the single iteration time between different models and the parameter sizes of the models is listed. As can be seen from Table 2, the number of model parameters between the improved model and the traditional 3D reconstruction model is not much different, and the parameters of the multi-fusion feature fusion model are 0.1 M more. However, the multi-fusion 3D reconstruction model has greatly improved the single iteration time, and the speed is 1 time faster than that of the traditional 3D reconstruction model. The iteration time and model parameters of the secondary optimized multi-fusion 3D reconstruction model include the iteration time and model parameters of the pretrained multi-fusion 3D reconstruction model. The second optimization of the multi-fusion 3D reconstruction model in a single network training is not much different from other model parameters, but it is more time-consuming than other models in terms of iteration time. In the experiment, the traditional 3D reconstruction model takes 10 hours, while the improved multi-fusion 3D reconstruction model takes only a few hours. Using 3D deconvolution to generate a higher-resolution 3D object from a lower-resolution 3D object requires more computation time. However, rearranging multiple low-resolution 3D objects to form a higher-resolution 3D object will save computational overhead.

The rendered images in the test set are directly used as the input of the low-resolution Nuo surface 3D construction model, and a 3D Nuo surface with a resolution of $64 \times 64 \times 64$ is output. The 3D reconstruction results of different models are shown in Figure 10. Figure 10(b) is the low-resolution 3D shape generated by the traditional 3D reconstruction model, Figure 10(c) is the low-resolution 3D shape generated by the multifeature fusion 3D reconstruction model, and Figure 10(d)is the low-resolution 3D shape generated by the quadratic optimization of the multifeature fusion 3D reconstruction model. As can be seen from Figure 10, the overall reconstruction results on the rendered image in Figure 10(b) compared with Figure 10(c) and Figure 10(d) are not much different. However, due to the low reconstruction resolution, these reconstruction results cannot show the required details, and only rough contours can be reconstructed. Comparing the reconstruction results of different models with the real 3D structure shown in Figure 10(d), there is not much difference in appearance. However, in terms of details, the improved models proposed in this paper can achieve better visual effects than the traditional 3D construction models. The experimental results show that the proposed 3D construction model can preliminarily complete the generation of corresponding 3D shapes from a single Nuo surface image.

Using IoU as an evaluation metric is used to measure the quality of the generative model. IoU measures the degree of overlap (intersection-over-union ratio) between the reconstructed model and the real model and takes a value from 0 to 1. The higher the IoU calculation result, the closer the reconstructed model is to the real model. The IoU value was calculated on the test results of each model. The IoU is calculated as follows:

$$IoU = \frac{\sum_{i,j,k}\left[I\left(x_{(i,j,k)} > t\right)I\left(y_{(i,j,k)}\right)\right]}{\sum_{i,j,k}\left[I\left(x_{(i,j,k)} > t\right) + I\left(y_{(i,j,k)}\right)\right]}. \tag{12}$$

The results are shown in Table 3. The fully improved multifeature fusion 3D reconstruction model is better than the traditional 3D reconstruction model and can achieve better performance. From the perspective of model reconstruction accuracy, the quadratic optimization multi-fusion 3D construction model proposed in this paper can achieve considerable improvement and can increase the reconstruction accuracy rate by about 6.3%. Therefore, different comparative experiments show the superiority of the model proposed in this paper in 3D reconstruction of the Nuo surface.

4.2.2. 3D Construction of High-Resolution Nuo Surface Voxels Based on Generative Adversarial Networks. Low-Resolution Results from the Previous Module. The network training period is set to 100, and other parameter settings of the network are the same as above. The generator is pretrained with pixel-based loss. The pretraining method can ensure that the generator can obtain images with better visual quality from the beginning. This way of pretraining avoids the need for the discriminator to discriminate on irrelevant generated images at the beginning, but allows the discriminator to focus on the details of the reconstructed image. The comparison results of the depth map super-resolution experiment based on the GAN method are shown in Figure 11. GAN-based image super-resolution methods do not look visually different from multiresidual dense methods. This may be due to the fact that the reconstructed image is a depth map, and the differences between each local depth image are subtle and not obvious on the reconstructed depth image. However, the calculation results on the PI score show that the improved GAN-based image super-resolution

Table 2: Comparison of the single iteration time and model parameters of the improved 3D.

Model	Iteration time (s)	Model parameters (M)
Traditional 3D reconstruction model	0.4	27.0
Multi-fusion 3D reconstruction model	0.2	27.1
Secondary optimization multi-fusion 3D reconstruction model	0.49	54.3

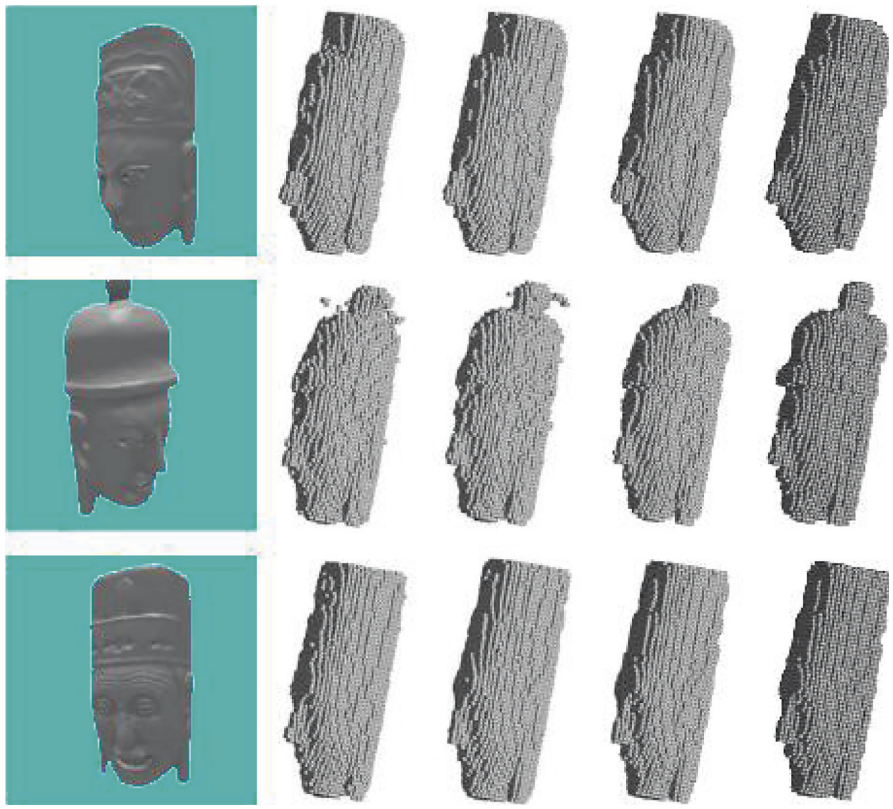

Figure 10: Comparison of reconstruction results on rendered images: (a) input image; (b) traditional method; (c) multifeature fusion method; (d) quadratic optimization multifeature fusion method; (e) real 3D shape.

Table 3: IoU result comparison of different methods.

Model	IoU
Traditional method	0.728
MFF-3D	0.734
ESPCN-3D	0.730
MFF + ESPCN-3D	0.736
MFF + ESPCN-3D_2	0.791

method can achieve lower perceptual scores. This shows that GAN-based methods are able to generate more realistic depth images overall. However, it also needs to be seen that there is still a big gap between the smaller details and the real depth image based on the GAN method.

Figure 12 shows the comparison results of the improved 3D Nuo surface high-resolution reconstruction results in this section and the quadratic optimization, multifusion, and multiresidual dense 3D Nuo surface high-resolution method proposed in Section 3. As can be seen in Figure 12, the GAN-based approach looks similar to the multiresidual dense approach overall. However, in terms of the local details of the generated Nuo surface depth map, the GAN-based method can reconstruct more Nuo surface details. In addition, it is also necessary to see that the multiresidual dense depth map super-resolution method adopts the mean square error loss function, and the depth map generated by this loss function is smooth on the whole. Therefore, the reconstructed 3D Nuo surface is smooth as a whole. However, the

Figure 11: GAN-based image super-resolution comparison results. (a) Real image. (b) Multiple residual dense. (c) SRGAN. (d) OUR-GAN.

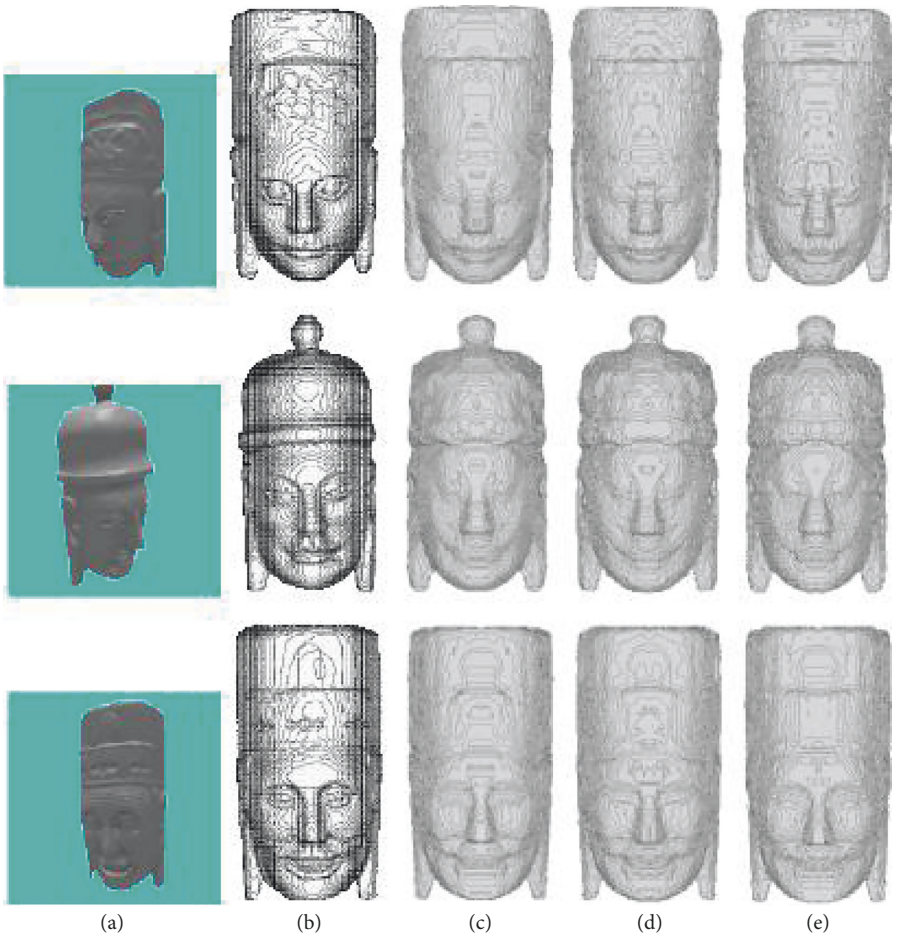

Figure 12: High-resolution comparison results of 3D Nuo masks based on GAN: (a) input; (b) real shape; (c) multiresidual dense method; (d) SRGAN method; (e) OUR-GAN method.

surface of the 3D Nuo surface generated by the GAN method is relatively rough, mainly because the super-resolution depth map generated by the GAN method is also prone to image artifacts when generating more realistic surface details.

5. Conclusion

The main research content of this paper is the design of a three-dimensional display system for intangible cultural heritage based on generative adversarial networks. The system function is realized through four modules: input module, data processing module, 3D model generation module, and model output module. Through two 3D model reconstructions, the three-dimensional display of intangible cultural heritage is realized.

This paper takes the Nuo surface as the research object and tests the function of the system. In the low-resolution 3D construction of the Nuo surface, the reconstructed Nuo surface is relatively rough due to the low resolution. This

makes it difficult to show the details of the reconstructed 3D Nuo surface in appearance. Multiresidual dense blocks are introduced and applied to the depth image super-resolution network. At the same time, a perceptual loss function is applied, which combines the advantages of residual blocks and dense blocks to make the output depth image more realistic. The experimental comparison results show that our proposed multiresidual dense high-resolution Nuo surface voxel 3D construction model can achieve better performance. The quadratic optimization multi-fusion 3D construction model proposed in this paper can achieve considerable improvement and can improve the reconstruction accuracy by about 6.3%.

Inspired by the SRGAN model's ability to generate images with more high-frequency details, we also use generative adversarial networks for high-resolution Nuo surface voxel 3D construction. To be able to further improve the performance of GAN-based image super-resolution, we improve its generator, discriminator, and loss function on the original SRGAN. Experimental results show that this method can generate super-resolution images with more realistic and natural depth maps. In addition, when it is used for high-resolution 3D Nuo surface sculpting, it can also generate 3D voxel Nuo surfaces with more details.

Data Availability

The data set can be obtained from the corresponding author upon request.

Conflicts of Interest

The authors declare that they have no conflicts of interest.

Acknowledgments

The authors thank major project of China/Mijia Social Science Foundation, integration and research of literature, images, and cultural relics of Chinese ancient wind instruments (no. 17ZDA245).

References

[1] R. Hartley and A. Zisserman, "Multiple view geometry in computer vision," *Kybernetes*, vol. 30, no. 9/10, pp. 1865–1872, 2008.

[2] C. Cadena, L. Carlone, H. Carrillo et al., "Past, present, and future of simultaneous localization and mapping: toward the robust-perception age," *IEEE Transactions on Robotics*, vol. 32, no. 6, pp. 1309–1332, 2016.

[3] Z. Wu, S. Song, A. Khosla et al., "3D shapenets: a deep representation for volumetric shapes," in *Proceedings of the IEEE Conference on Computer Vision and Pattern Recognition*, pp. 1912–1920, April 2015.

[4] C. B. Choy, D. Xu, J. Y. Gwak, K Chen, and S Savarese, "3D-r2n2: A Unified Approach for Single and Multi-View 3d Object reconstruction," in *Proceedings of the European Conference on Computer Vision*, pp. 628–644, 2016, https://arxiv.org/abs/1604.00449.

[5] X. Chen, Y. Duan, R. Houthooft, J. Schulman, I. Sutskever, and P. Abbeel, "Infogan: interpretable representation learning by information maximizing generative adversarial nets," in *Proceedings of the Conference and Workshop on Neural Information Processing Systems*, pp. 2172–2180, Barcelona, Spain, December 2016.

[6] X. Yan, J. Yang, K. Sohn, and H. Lee, "Attribute2image: Conditional Image Generation from Visual attributes," in *Proceedings of the European Conference on Computer Vision*, pp. 776–791, Amsterdam, The Netherlands, October 2016.

[7] M. Y. Liu and O. Tuzel, "Coupled Generative Adversarial networks," in *Proceedings of the Conference and Workshop on Neural Information Processing Systems*, pp. 469–477, Barcelona, Spain, December 2016.

[8] H. Zhang, T. Xu, H. Li et al., "StackGAN++: realistic image synthesis with stacked generative adversarial networks," *IEEE Transactions on Pattern Analysis and Machine Intelligence*, vol. 41, no. 8, pp. 1947–1962, 2019.

[9] J. Wu, C. Zhang, T. Xue, W. T. Freeman, and J. B. Tenenbaum, "Learning a probabilistic latent space of object shapes via 3d generative-adversarial modeling," in *Proceedings of the Conference and Workshop on Neural Information Processing Systems*, pp. 82–90, Spain, December 2016.

[10] M. Gadelha, S. Maji, and R. Wang, "3D shape induction from 2d views of multiple objects," in *Proceedings of the International Conference on 3D Vision*, pp. 402–411, Qingdao, China, October 2017.

[11] G. Riegler, A. O. Ulusoy, H. Bischof, and A. Geiger, "Octnetfusion: learning depth fusion from data," in *Proceedings of the International Conference on 3D Vision*, pp. 57–66, April 2017.

[12] A. Krizhevsky, I. Sutskever, and G. E. Hinton, "Imagenet classification with deep convolutional neural networks," in *Proceedings of the Conference and Workshop on Neural Information Processing Systems*, pp. 1097–1105, 2012.

[13] A. L. Maas, A. Y. Hannun, and Y. NgA, "Rectifier nonlinearities improve neural network acoustic models[C]," *International Conference on Machine Learning*, vol. 30, no. 1, p. 3, 2013.

[14] I. Goodfellow, J. Pouget-Abadie, M. Mirza et al., "Generative Adversarial nets," in *Proceedings of the Conference and Workshop on Neural Information Processing Systems*, pp. 2672–2680, Montreal, Canada, December 2014.

[15] E. Smith, S. Fujimoto, and D. Meger, "Multi-view silhouette and depth decomposition for high resolution 3d object representation[C]," *Conference and Workshop on Neural Information Processing Systems*, pp. 6478–6488, 2018.

[16] X. Wang, K. Yu, S. Wu et al., "Esrgan: Enhanced Super-resolution Generative Adversarial networks," in *Proceedings of the European Conference on Computer Vision*, pp. 63–79, Munich, Germany, September 2018.

[17] D. Lee, S. Lee, H. Lee, K. Lee, and H. J. Lee, "Resolution-preserving generative adversarial networks for image enhancement," *IEEE Access*, vol. 7, pp. 110344–110357, 2019.

Hindawi
Scientific Programming
Volume 2022, Article ID 4818985, 8 pages
https://doi.org/10.1155/2022/4818985

Research Article

Vegetation Coverage Monitoring Model Design Based on Deep Learning

Lilei Zhang,[1,2] Wenwen Wang,[3] Yujie Dong,[1] and Longliang Wu[4]

[1]*College of Architecture and Survey and Draw Engineering, Shanxi Datong University, Datong 037000, China*
[2]*Datong Key Laboratory of Mine Geohazard Prevention and Environment Recovery Shanxi, Datong 037000, China*
[3]*Key Laboratory of Coal Geological Geophysical Exploration Surveying & Mapping Institute of Shanxi Province, Jinzhong 030600, Shanxi, China*
[4]*bureau Public Works of Shenzhen Municipality, Shenzhen 518031, Guangdong, China*

Correspondence should be addressed to Longliang Wu; wulongliang@foxmail.com

Received 26 May 2022; Revised 9 June 2022; Accepted 13 June 2022; Published 21 July 2022

Academic Editor: Lianhui Li

Based on the medium-resolution Landsat TM and OLI satellite images in the study area, the deep learning ENVINet-5 model is adopted for vegetation coverage monitoring. By referring to the fusion image and Google Earth high-resolution satellite image, the training samples and verification samples are manually labeled, and the labels of four types of ground objects (desert, water body, cultivated land, and construction land) are made. Through the ENVI deep learning binary classification model, the labeled training samples are trained, and a large number of samples of desert, water, and cultivated land are extracted and transformed into corresponding label images. Then, a large number of training sample labels extracted from the model are combined with the manually made construction land sample labels and both of them are used as the training samples of the ENVI deep learning multiclassification model. According to the classification process of the deep learning model (creating label image, initializing training model, and training model and model classification), through the adjustment of various parameters, the four types of ground objects in the study area are finally classified. Finally, the classification results that meet the accuracy requirements are statistically analyzed. It is proved that the model classification results can meet the use requirements.

1. Introduction

Desertification is an important factor threatening human survival and sustainable development in the 21st century. How to effectively prevent and mitigate desertification is the focus and hotspot of current research [1–4]. Land desertification seriously reduces the carrying capacity of the ecological environment, and the area and degree of desertification land are rapidly expanding, which seriously restricts the sustainable development of society [5]. Monitoring vegetation coverage and rocky desertification and timely and accurate assessment of the current situation and changes in desertification will help to formulate global actions to prevent and eliminate desertification [6–8].

The traditional desertification research mainly adopts the artificial field mapping method, which has the disadvantages of time-consuming, laborious, and low efficiency in the implementation process [7]. With the emergence of remote sensing technology [9–11] and vigorous development of information technology [12–18], its macro-, objective, and economic advantages make up for the shortcomings of traditional desertification research to a certain extent, so it can better deal with environmental change monitoring [16–18]. On the other hand, with the development of computer technology, the machine learning method [19–21] is widely used in the classification and extraction of remote sensing images. It can better extract the ground features in the image. Especially in recent years, the emergence of deep learning has greatly improved the technical means of image processing. Rapid and accurate feature classification of a large amount of data can better adapt to the development of society and meet the needs of human production and life.

As a complex form of machine learning, deep learning can make the system automatically discover the feature expression of data. Compared with other machine learning types, it can continuously improve the prediction accuracy without external guidance or intervention, and draw conclusions through multilayer learning in neural networks. For the processing of remote sensing images, deep learning attempts to discover and use the spatial, spectral, and statistical features of remote sensing images. In view of this, a vegetation coverage and rocky desertification monitoring method is proposed based on deep learning in this study, so as to provide a scientific basis and data basis for ecological environment monitoring and sandy vegetation restoration in desertification areas.

2. Methods

2.1. Deep Learning Model Architecture. The ENVINet-5 model is developed based on TensorFlow deep learning framework. The model architecture is based on the improvement of the U-NET neural network, which is similar to the U-NET architecture. It is a mask-based and encoder-decoder architecture. Combined with the powerful remote sensing image processing software ENVI, researchers can directly use the deep learning network to process remote sensing images.

This study uses the ENVINet-5 deep learning module to classify the ground objects in Landsat medium-resolution satellite images in the study area [22, 23]. The ENVINet-5 model architecture has 5 levels and 27 convolution layers, and each level represents different pixel resolutions in the model. We input the original image into the model, slice it, and then use a 3×3 convolution layer to convolute the slice, so as to increase the number of image features. We use a 2×2 pooling layer to reduce the size of the image, so as to reduce the operation and retain most of the features of the image. The sampling process is divided into upsampling process and downsampling process. We recognize and classify many features generated in the downsampling process, so as to achieve the purpose of feature classification.

After the remote sensing image is loaded into the deep learning network, the convolution operation will be carried out after slicing. Convolution is essentially to extract the features in the image and generate feature images with different dimensions, which are often composed of multiple convolution kernels of different sizes. The size of the commonly used convolution kernel is 3×3 and 5×5. In this study, the convolution kernel size of a deep learning network is 3×3. In addition, the function of activation function is indispensable in convolution operation. The activation function can better solve the gradient disappearance problem, simplify the computational complexity, speed up the training speed, and reduce the burden of computer operation. In convolution operation, the rule activation function is often used. As a nonlinear activation function, it can better solve the problem of overfitting in training.

After the convolution operation, a large number of feature images will be generated. If the convolution operation is carried out again, the amount of operation will be greatly increased. Therefore, it is necessary to reduce the amount of computation and retain more feature information of the generated feature image. The appearance of the pooling layer solves this problem better. Common pooling methods include mean pooling and max pooling. In this study, max pooling is used, and the window size is 2×2. It can not only extract the main features but also reduce the amount of computation. After pooling, the feature image size is reduced to half of the original size.

In addition, the loss function is introduced into the deep learning network, which can map values to non-negative space. When the value of the loss function is smaller, it means that it is closer to the real value. Therefore, the classification effect of the model can be quantitatively evaluated and optimized. The commonly used loss functions include root mean square error, cross-entropy loss, and so on.

2.2. Deep Learning Model Parameters

2.2.1. Epochs and Batches. In order to make the training model achieve better classification results, the number of training iterations (epochs) needs to be adjusted. In ENVI deep learning, the number of iterations (epochs) represents that the model intelligently extracts the number of slices (batches) from the label image. Because there is bias judgment when extracting slices, an epoch refers to the number of slices trained before bias judgment adjustment.

The determination of the number of epochs and the number of extracted slices has certain randomness, which depends on the diversity of learning feature sets. In ENVI deep learning, the number of iterations is generally set between 16 and 32. For the number of patches per epoch, the number of slices extracted by each epoch determines the training amount of the model, which is usually set between 200 and 1000.

The model will use multiple slices at the same time in an iterative training. Batch refers to a group of slices read in an iterative training. Batches run in an iterative training and stop after reaching or exceeding the total number of slices. The number of slices in a group needs to be set according to the size of GPU video memory.

2.2.2. Class Weight and Loss Weight. The ENVI deep learning network uses the statistical technology of inverse transform sampling to train the model based on slice deviation selection. By introducing a deviation, the model can see the slices of highlighted feature pixels more often. In inverse transform sampling, the samples introduced into the model are directly proportional to their contribution to the probability density function. The deviation is controlled by the class weight parameter in the Train TensorFlow Mask Model tool. The value range of the class weight parameter is 0 to 2 (when the maximum value is set for the sparse training set, the valid range of the maximum value is 0 to 6).

The loss weight parameter is used for the deviation loss function, focusing on the correct identification of characteristic pixels and reducing the identification of background

pixels. Parameters are useful when the distribution of feature targets is sparse. A value of 0 indicates that the model treats the feature and background pixels equally. Increasing the value of the loss weight parameter will bias the loss function to find the characteristic pixels. The valid range of parameter values is 0 to 3.

2.2.3. Solid Distance and Blur Distance. In the process of model training, in addition to the weight of features and background pixels, the size and edge of features must also be considered. The solid distance parameter is often used to expand the size of linear or point features. The parameter value size represents the number of pixels around the marked ROI, which forms the target feature together with the ROI.

In deep learning, the setting of blur distance helps the model to obtain the sharp edge of the target. By setting the fuzzy edge and gradually reducing the fuzzy value in the model training, the model is close to the sharp feature of the target. In the ENVINet-5 model, the value range of blur distance is 0 to 70.

2.3. Deep Learning Model Extraction Process. The ENVINet-5 is defined by basic neural network parameters. To extract target, it is necessary to create a label raster that can indicate the target and then use the label sample to train the model. The label image can be created jointly with the tools ROIs and Deep Learning/Build Label Raster from ROI, and then, the label sample is used to train the model. The trained model can find targets with similar features in other images. The extraction result is a class activation map/raster, in which the DN value represents the probability that the pixel belongs to a certain ground object target. The deep learning training model involves the adjustment of parameters and has a certain degree of randomness. Due to the convergence mode of the algorithm, different models will be obtained even if the parameters in the training are the same. The extraction process is shown in Figure 1.

2.3.1. Create Label Image. For target recognition, label rasters need to be created to train the model. Based on the original image to be classified, through field investigation, sample site selection or, combined with a high-resolution image as reference, we establish proprietary identification marks for different ground objects, so as to create label images. In order to generate high-quality label images, representative samples of typical areas should be selected.

First, we select the object of interest in the typical area to create ROI. The ROI drawn should contain a variety of surface features such as shape, color, and texture, which is conducive to improving the classification accuracy of the model.

Finally, we use the Deep Learning/Build Label Raster from ROI tool in the ENVI toolbox to create label images. The tag image contains the original band and mask band of the input image. Different DN values of the mask band represent different types of ground objects.

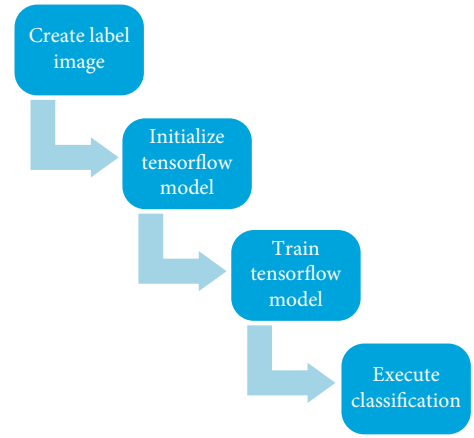

Figure 1: The extraction process.

2.3.2. Initialize TensorFlow Model. In ENVI, we select the Deep Learning/Train TensorFlow Mask Model tool. Before deep learning model training, it is needed to initialize or load a TensorFlow model. Model initialization needs to define model parameters, including patch size, number of bands used for training, and saving path.

2.3.3. Train TensorFlow Model. After model initialization, various parameters and weights need to be set in the train TensorFlow mask model to guide TensorFlow model to learn target features.

In the training process, the label image is repeatedly exposed to the model. The model learning converts the spectral and spatial information in the label image into a class activation gray image to highlight the extracted target. Through the loss function, the model can know the wrong random guess results. Through the adjustment of internal parameters or weights of the model, the model is more accurate. The trained TensorFlow model can find the same features in other images.

2.3.4. Execute Classification. We use the trained model to search for the same ground feature in other images and use TensorFlow Mask Classification tool to classify and extract remote sensing images.

2.4. Remote Sensing Monitoring of Vegetation Coverage. Vegetation coverage refers to the percentage of the vertical projection area of vegetation on the ground in the total area of the statistical area. It is of great practical significance to analyze and evaluate the regional ecological environment by obtaining the regional surface vegetation coverage and revealing the change and dynamic change trend of surface vegetation in the region. The vegetation index method has little dependence on surface measured data, has universal applicability, and can be extended to a wide range of areas. It is a reliable means to quantitatively monitor the change in vegetation cover.

The calculation formula for normalized vegetation index is as follows:

$$NDVI = \frac{(\mathrm{NIR} - \mathrm{RED})}{(\mathrm{NIR} + \mathrm{RED})}, \quad (1)$$

where NIR is the near-infrared reflectance of remote sensing image, and RED is the infrared reflectance of remote sensing image.

Vegetation coverage retrieved by normalized vegetation index is as follows:

$$VFC = \frac{(NDVI - NDVIs)}{(NDVIv - NDVIs)}, \quad (2)$$

where NDVIs is the NDVI value of bare soil or nonvegetation coverage area, and NDVIv is the NDVI value of pure vegetation pixel.

$$NDVIs = \frac{(VFC\max * NDVI\min - VFC\min * NDVIm\!ax)}{(VFC\ \max - VFC\ \min)},$$
$$\mathrm{N}DVIv = \frac{((1 - VFC\ \min) * NDVIm\!ax - (1 - VFC\ \max) * NDVI\min)}{(VFC\ \max - VFC\ \min)}, \quad (3)$$

where NDVImax and NDVImin are the maximum and minimum NDVI values in the study area. Because noise is inevitable, the value within a certain confidence interval is generally taken, and the confidence interval is determined according to the actual situation of the image.

Furthermore, it can be converted into the following:

$$VFC = \frac{(N\ DV\ I - N\ DV\ \mathrm{Imin})}{(N\ DV\ \mathrm{Im}ax - N\ DV\ \mathrm{Imin})}. \quad (4)$$

Therefore, the data of different vegetation coverage levels in each period of the study area can be obtained.

2.5. Deep Learning Model. Based on the U-shaped neural network structure, we use the means of jump connection to make the output UAV image features of each decoding layer in the decoder corresponding to the encoder (the image size is the same). Each decoding layer is an interworking structure, which makes full use of the image features extracted by all coding layers in the encoder. Compared with the traditional neural network deep learning model based on encoder-decoder, it can get more accurate results under a small amount of training data. The specific model framework is shown in Figure 2.

As can be seen from Figure 2, the encoder part of the model is designed with four coding layers and two convolution layers, and the decoder is composed of four decoding layers and one softmax layer, in which the activation function used by the model is ReLU function. The specific steps are as follows: input the remote sensing HD image data into the encoder, extract the features through the encoder, and output the feature images with the size of I/2, I/4, I/8, and I/16 (I represents the image size), with the numbers of 16, 32, 64, 128, and 256, respectively. Then, the feature images output by the encoder are analyzed by the decoder and the image segmentation results with the size of I are output, that is, the divided vegetation coverage area (the result output is white) and nonvegetation coverage area (the result output is black), so as to calculate the vegetation coverage of different typical sample plots.

3. Experiment and Analysis

This research mainly applies the computer to test. The computer system is Windows 1064 bit professional version, the processor model is Intel Core i7-9750h, the graphics card model is NVIDIA GeForce GTX 1050, the memory size of the solid-state disk is 512 g, and the memory size is 8 g. The computer is loaded with the remote sensing image processing software ENVI 5.5, in which the deep learning binary classification model and multiclassification model are installed for the binary classification and multiclassification of ground objects, respectively.

In the process of training model, the label image is needed to mark the training target so that the ground object categories can be distinguished in the neural network. We use the region of interest tool in ENVI to manually draw or import the existing vector data. At present, the deep learning two classification model supports single-class target extraction. In view of the need for a large number of training samples for deep learning, and according to the actual distribution of features in the study area, label images are made for deserts, water bodies, and cultivated land in the study area. After model extraction, a large number of samples can be provided for the deep learning multiclassification model.

The study selects the deep learning binary classification model in ENVI and uses ENVINet-5 to extract desert, water, and cultivated land from some label samples. Due to the small area occupied by the construction land, it is manually selected with reference to the high-score image. Then, the extracted three types of features and construction land are made into multiclassification label samples as the training and verification samples of the deep learning multiclassification model. Figure 3 shows a partial screenshot of the desert, water, and cultivated land label images.

After the image label is made, the model needs to be initialized. We need to define model parameters, including patch size, the number of bands used in training, and output path. The slice size of this test is set to 300×300 pixels, which cannot be greater than the number of pixels with the minimum side length of the cropped subregion, and the number of bands is set to the number of bands of the original

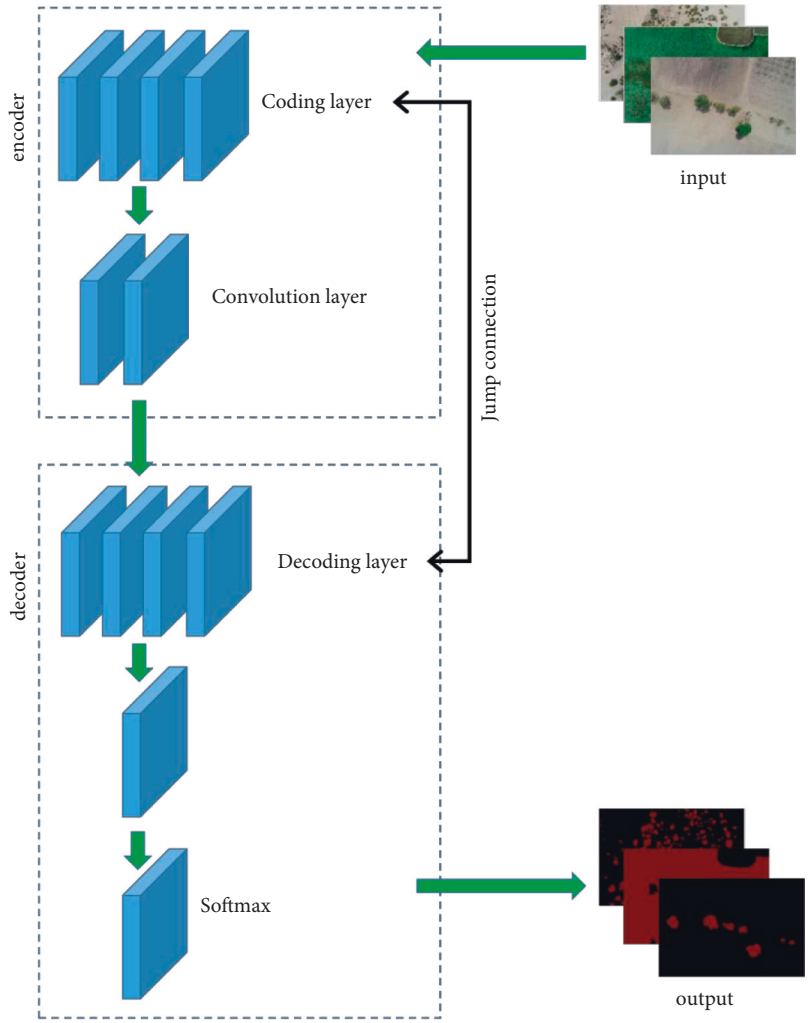

Figure 2: The deep learning model for vegetation coverage extraction.

Figure 3: A partial screenshot of the desert, water, and cultivated land label images.

image. After the initialization of the model, it is necessary to set the parameters of the training model (train TensorFlow mask model). For the number of iterations, we set the number of iterations to 30 according to the computing power of the computer processor and the size of GPU memory. The number of slices per epoch determines the training amount of the model. The number of slices is generally selected between 200 and 1000. We set the number of slices in iterative training to 300. The number of patches per batch is set to 4. The fixed distance and blur distance are mainly set according to the drawing of the label image. The classification weight has a minimum value of 0 and a maximum value of 2, and the loss weight ranges from 0 to 3. We adjust it according to the actual training effect.

After parameter adjustment, the final parameter is set as 20 iterations, 300 training slices per iteration, 4 reading slices per batch of training, 0.8 classification weight, and 0.6 loss weight. Considering the features of the study area, we do not set the fixed distance and fuzzy distance. The image extraction results are shown in Figure 4.

The desert, water body, and cultivated land extracted by the binary classification model are used to make the region

Figure 4: The image extraction results.

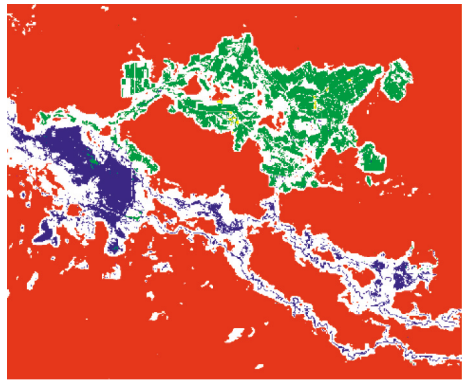

Figure 5: The area of interest.

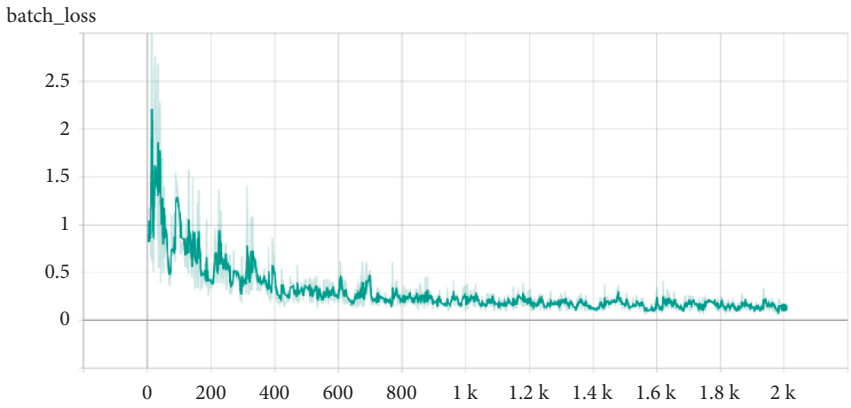

Figure 6: Loss function curve.

of interest based on the extraction results. Together with the manually drawn construction land, the area of interest is shown in Figure 5.

The training process of the multiclassification model is similar to that of the two classification models, with occasional differences. Only when initializing the output category of the training model, we can set it to 4 categories and set the number of slices to 304. The multiclassification depth model trained by samples is used to extract different features in the study area. The loss function curve and training accuracy curve in the training process are shown in Figures 6 and 7. The minimum loss value is 0.1483, and the maximum training accuracy is 0.9425.

After extraction, the classification map of desert, water body, cultivated land, and construction land is obtained, and then, the accuracy test is carried out in combination with the verification points selected by field investigation, fusion image, and Google Earth high-score image. A total of 43646 validation samples (20055 deserts, 9169 water bodies, 9407 cultivated land, and 5015 construction land) were used to calculate the producer accuracy, overall classification accuracy, and kappa coefficient of feature classification in combination with the transfer matrix to carry out the comprehensive evaluation model. The overall classification accuracy is equal to the sum of correctly classified pixels divided by the total number of pixels. Kappa coefficient represents the proportion of error reduction in the evaluated classification compared with completely random classification. We output the classification results that meet the precision requirements. The test results are shown in Table 1.

Based on the verification accuracy of the extraction results, we can see that the overall classification accuracy is

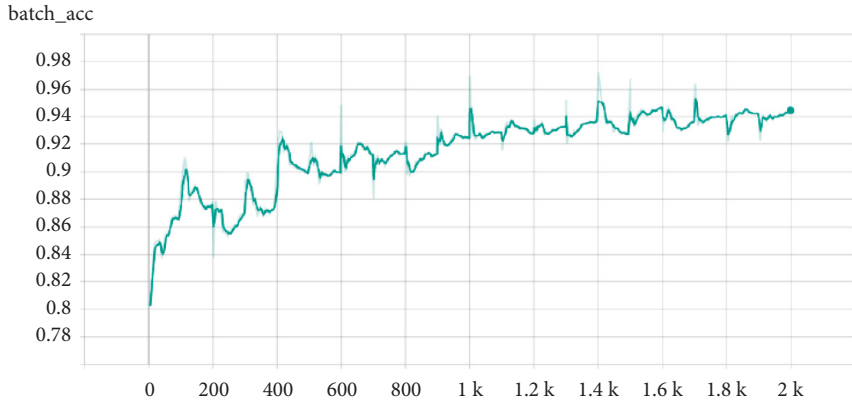

Figure 7: Training accuracy curve.

Table 1: The classification results.

	2000 year	2005 year	2010 year	2015 year	2018 year
Desert precision	87.11%	85.34%	85.04%	84.88%	86.87%
Water precision	86.23%	91.09%	88.02%	85.87%	85.66%
Cultivated land precision	85.66%	89.02%	90.11%	85.34%	90.00%
Construction land precision	88.19%	86.22%	92.22%	89.02%	89.02%
Overall precision	89.89%	85.88%	87.52%	87.76%	85.87%
Kappa coefficient	0.86	0.85	0.85	0.84	0.85

more than 85%, and the kappa coefficient is about 0.85. The model classification results can meet the use requirements.

4. Conclusions

In this study, we take the northwest region of China as the research area. Based on the Landsat medium-resolution remote sensing satellite images of five periods (2000, 2005, 2010, 2015, and 2018) in the study area, and based on ENVI 5.5, the remote sensing image software processing platform used for image preprocessing, the deep learning model is used to classify the features of desert, water body, construction land, and cultivated land in the study area in recent 19 years. The classification results satisfying the accuracy are obtained; furthermore, the annual change in desertification in the region is statistically analyzed by using the single land dynamic degree and land-use transfer matrix method, and the mutual transfer between desert and other features. Based on the above classification results, the desert area was extracted to obtain the normalized vegetation index (NDVI), and then, the vegetation coverage of the study area was obtained. Combined with the quantitative relationship between vegetation coverage and desertification, the classification results of desertification grades in different years in the study area were obtained, and the mutual transformation among severe, moderate, and mild desertification areas was analyzed by using the transfer matrix method. The results show that the main feature of the study area is the rocky desert, accounting for more than 80% of the area. In the past 19 years, it has reduced to 106.33 km^2, the average annual growth rate is −0.32%, and the rocky desertification continues to reverse. The results showed that the ecological environment in different research periods developed well as a whole.

Compared with traditional machine learning classification methods, the deep learning method used in this study can automatically extract the features of remote sensing images, so it can effectively avoid the complex work of manual extraction and feature selection, and has high operability.

There are many influencing factors of desertification. Due to the limitations of data source, time, economy, and technology, this study still has many deficiencies. The Landsat series remote sensing data used in this study do not have a high spatial resolution, and one pixel may contain a variety of ground objects. It is not conducive to the establishment of a pure feature sample set, which has certain errors in the training and verification of the model. The high spatial resolution remote sensing data greatly increase the probability of pure pixels, which is conducive to the better learning of samples by the deep learning model. In the model training of deep learning, the adjustment of parameters is subjective and tentative. After meeting the classification results, further experimental research was stopped. In the next step, the scientific parameter adjustment method can be used to obtain better classification results.

Data Availability

The dataset can be accessed upon request.

Conflicts of Interest

The authors declare that they have no conflicts of interest.

Acknowledgments

This work was financially supported by the College-Level Project of Shanxi Datong University (XJG2021223) and the Teaching Reform Project of Shanxi Datong University (2020K14).

References

[1] F. Bu and C. Zhong, "Remote sensing monitoring of land desertification in four counties of Bashang, Hebei based on Landsat-8," in *Proceedings of the SPIE - The International Society for Optical Engineering*, Article ID 1216237, Seventh Asia Pacific Conference on Optics Manufacture APCOM, Hong Kong, February 2022.

[2] N. Zerrouki, A. Dairi, F. Harrou, Y. Zerrouki, and Y. Sun, "Efficient land desertification detection using a deep learning-driven generative adversarial network approach: a case study," *Concurrency and Computation: Practice and Experience*, vol. 34, no. 4, 2022.

[3] Li Cui, "Analysis of Spatial and Temporal Distribution Characteristics of Land Desertification Based on GIS and Remote Sensing Images," *Scientific Programming*, vol. 2021, Article ID 7557175, 12 pages, 2021.

[4] Z. Guo, W. Wei, P. Shi et al., "Spatiotemporal changes of land desertification sensitivity in the arid region of Northwest China," *Dili Xuebao/Acta Geographica Sinica*, vol. 75, no. 9, pp. 46–68, 2021.

[5] D. Xu, X. You, and C. Xia, "Assessing the spatial-temporal pattern and evolution of areas sensitive to land desertification in North China," *Ecological Indicators*, vol. 97, pp. 150–158, 2019.

[6] M. He, "Evaluation of potential contribution of plant growth-promoting bacteria to land desertification," in *Procedding of the E3S Web of Conferences, 2nd International Conference on Civil Architecture and Energy Science*, vol. 165, Russia, CAES, May 2020.

[7] H. Yue, "Dynamic monitoring of land desertification in coal mining districts in the north of Shaanxi Province," in *Proceedings of the 2nd International Symposium on Land Reclamation and Ecological Restoration*, pp. 219–221, CRC Press, China, 2017.

[8] J. He, J. Xu, W. Kang, W. Xu, and X. Wang, "Evolution dynamic characteristics of land desertification in Zoige county, China," *Linye Kexue/Scientia Silvae Sinicae*, vol. 52, no. 1, pp. 159–165, 2016.

[9] W. Yang, H. Song, L. Du, S. Dai, and Y. Xu, "A Change Detection Method for Remote Sensing Images Based on Coupled Dictionary and Deep Learning," *Computational Intelligence and Neuroscience*, vol. 2022, Article ID 3404858, 14 pages, 2022.

[10] S. Cui, Z. Jiang, and P. Li, "Remote sensing image target recognition system based on heapsort," in *Proceedings of the 2021 International Conference on Big Data Analytics for Cyber-Physical System in Smart City*, vol. 102, pp. 1083–1092, Springer, Singapore, 2022.

[11] P. Yan, X. Liu, F. Wang, C. Yue, and X. Wang, "LOVD: land vehicle detection in complex scenes of optical remote sensing image," *IEEE Transactions on Geoscience and Remote Sensing*, vol. 60, Article ID 5615113, pp. 1–13, 2022.

[12] M. Thaller, "INFORMATION TECHNOLOGY, INFORMATION AND HISTORY," *Vestnik permskogo universiteta-istoriya-PERM UNIVERSITY HERALD-HISTORY*, vol. 46, no. 3, pp. 159–174, 2019.

[13] L. Li, B. Lei, and C. Mao, "Digital twin in smart manufacturing," *Journal of Industrial Information Integration*, vol. 26, no. 9, Article ID 100289, 2022.

[14] L. Li, T. Qu, Y. Liu et al., "Sustainability assessment of intelligent manufacturing supported by digital twin," *IEEE Access*, vol. 8, pp. 174988–175008, 2020.

[15] A. M. Titu and A. Stanciu, "Merging Operations Technology with Information Technology," in *Proceeding of the 12th International Conference on Electronics, Computers and Artificial Intelligence (ECAI)*, IEEE, Bucharest Romania, June 2020.

[16] L. Li and C. Mao, "Big data supported PSS evaluation decision in service-oriented manufacturing[J]," *IEEE Access*, vol. 8, no. 99, pp. 154663–154670, 2020.

[17] L. Li, C. Mao, H. Sun, Y. Yuan, and B. Lei, "Digital twin driven green performance evaluation methodology of intelligent manufacturing: hybrid model based on fuzzy rough-sets AHP, multistage weight synthesis, and PROMETHEE II," *Complexity*, vol. 2020, no. 6, 24 pages, Article ID 3853925, 2020.

[18] S. Okada, "From information technology to energy technology," *Electrochemistry*, vol. 87, no. 5, p. 246, 2019.

[19] M. J. Iqbal, M. M. Iqbal, I. Ahmad, M. O. Alassafi, A. S. Alfakeeh, and A. Alhomoud, "Real-Time Surveillance Using Deep Learning," *SECURITY AND COMMUNICATION NETWORKS*, vol. 2021, Article ID 6184756, 17 pages, 2021.

[20] C. Suxia, Z. Yu, W. Yonghui, and Z. Lujun, "Fish Detection Using Deep Learning," *Applied Computational Intelligence and Soft Computing*, vol. 2020, Article ID 3738108, 13 pages, 2020.

[21] C. N. Dang, M. N. Moreno-García, and F. De la Prieta, "Hybrid deep learning models for sentiment analysis," *Complexity*, vol. 2021, Article ID 9986920, 16 pages, 2021.

[22] H. B. Wang, J. J. Zhao, B. Wang, and L. Tong, "A quantum approximate optimization algorithm with metalearning for MaxCut problem and its simulation via TensorFlow quantum," *Mathematical Problems in Engineering*, vol. 2021, Article ID 6655455, 11 pages, 2021.

[23] B. Liu, Q. Wu, Y. Zhang, and Q. Cao, "Exploiting the Relationship between Pruning Ratio and Compression Effect for Neural Network Model Based on TensorFlow," *Security and Communication Networks*, vol. 2020, Article ID 5218612, 8 pages, 2020.

Hindawi
Scientific Programming
Volume 2022, Article ID 6913046, 8 pages
https://doi.org/10.1155/2022/6913046

Research Article

Innovative Design of Artificial Intelligence in Intangible Cultural Heritage

Jing Xie [1,2]

[1]*Yunnan Technology and Business University, Kunming 650000, Yunnan, China*
[2]*Jose Rizal University, 80 Shaw Blvd, Mandaluyong City, Metro Manila, Philippines*

Correspondence should be addressed to Jing Xie; 20080901001@ytbu.edu.cn

Received 20 May 2022; Revised 9 June 2022; Accepted 14 June 2022; Published 20 July 2022

Academic Editor: Lianhui Li

Driven by artificial intelligence technology, the research of intangible cultural heritage innovative design is carried out. Firstly, the appearance modeling characteristics, decorative element characteristics, and composition form characteristics of typical intangible cultural heritage products are analyzed. According to the collected relevant data of intangible cultural heritage products and existing products, combined with the regional cultural characteristics of intangible cultural heritage products and other factors, the analysis Atlas of intangible cultural heritage product innovation design is constructed. Based on perceptual engineering, the elements of intangible cultural heritage product innovation design for user participation are determined according to the needs and perceptual images of users. The shape grammar is used to extract the elements of intangible cultural heritage products, deduce and deform them, and finally generate the preliminary design scheme.

1. Introduction

Intangible cultural heritage refers to various traditional cultural expressions handed down from generation to generation by people of all ethnic groups and regarded as an integral part of their cultural heritage, as well as physical objects and places related to traditional cultural expressions. Intangible cultural heritage is an important symbol of the historical and cultural achievements of a country and nation and an important part of Chinese excellent traditional culture. "Intangible cultural heritage" is opposite to "material cultural heritage," which is collectively referred to as "cultural heritage." To some extent, intangible culture is a nation's unique cultural memory, and its inheritance value and application value are worthy of in-depth exploration. There are many kinds of intangible cultural heritage in China [1–6]. With the progress of domestic economic development and social development, many intangible cultural heritages began to appear in people's vision, but there are still a large number of intangible cultural heritage facing the dilemma of no inheritance [7–10]. Intangible cultural heritage may integrate with other industries, explore its market value with the help of the people, and regard it as an unattractive cultural element in the innovative design system, so as to lay a more solid foundation of traditional culture while promoting the progress of cultural design level. It is worth noting that the national cultural spirit behind the intangible cultural heritage can also become the power source to promote the progress of cultural and creative industries [11–14]. Modern innovative design can be based on material cultural heritage and traditional cultural spirit, fully reflect the important value of innovative thinking, and create cultural products that can better meet people's diversified needs with the help of more diversified forms of expression.

Intangible cultural heritage is different from static cultural relics displayed in museums [13, 14]. It is the inheritance and accumulation of culture and the continuation of living civilization with vitality. However, the current situation of China's intangible cultural heritage is not optimistic, as shown below.

(1) Insufficient attention to intangible cultural heritage: at present, for many people, intangible cultural heritage is a vague concept. The first reason is the

lack of regulations and measures and rescue and protection funds; second, the inheritance and dating of some intangible cultural heritage. Due to the impact of industrialized mass production, most of the intangible cultural heritages of technology type have complex production processes. Young people's unintentional learning leads to no successors and abandoned technology, which directly leads to the loss of many materials; third, the concept of intangible cultural heritage protection is backward, the technology and means are single, and there is no connection with new technologies and methods.

(2) A large number of intangible cultural heritage are disappearing. Intangible cultural heritage is a valuable spiritual wealth. It carries the cultural memory of national generations and is a cultural symbol of national diversity. However, these memories and symbols are easy to be ignored and forgotten over time, especially some oral cultural heritage. They will be trapped in remote and underdeveloped areas, which will make them more vulnerable and underdeveloped.

From the conceptual conception in the 1960s to the practical application today, artificial intelligence [15–19] has triggered three upsurges of development and application. Different from previous academic research, business demand is the primary factor leading this upsurge. The continuous expansion of application scope not only improves its application value and influence, but also realizes the organic integration of artificial intelligence technology and industrial chain. As the combination of human knowledge, skills, and aesthetic taste, traditional handicraft intangible cultural heritage belongs to an important part of the cultural industry. Artificial intelligence also brings new technical means and development space for its dissemination. As the continuation of human cognitive ability and emotional talent, the deep learning rate of artificial intelligence in the field of cognitive understanding is much higher than that of human beings. In the field of communication, artificial intelligence has strong practicability, such as natural language technology, real-time learning technology, cross screen recognition technology, and intelligent interaction technology. The embedding of digital technology makes virtual information coexist with tangible forms, and the accessibility and experience of intangible cultural heritage resources have been enhanced. Through technological empowerment, we can integrate the traditional intangible cultural form into the contemporary cultural ecology, make it survive and develop healthily, and continue to grow new cultural forms adapted to the times.

2. User Participatory Innovative Design

Under the development trend of experience economy, users are no longer satisfied with the ownership of a single commodity [20, 21]. On the basis of meeting the basic material needs, they begin to seek the creation of their own lifestyle and pursue their own products or services. User participatory design is to integrate users into the design, in which the status and power of all participants are equal. The concept of participatory design originated from Nordic countries. Its original intention is to add the "voice" of the public to the decision-making of public affairs. At this time, the Nordic trade union movement made the new law give new rights to enterprise employees, and employees have the right to decide and speak to change their working environment. User participatory design mainly emphasizes the participation of users, which is less related to design. Later, it was developed into a design method by American enterprises.

User participatory design method is a modern design method that takes the user as the center, integrates the user into the design process, and cooperates with each other on the premise of respecting the user's background, ability, and ideas. It is also a modern design method to meet the diversified needs of users and ensure the equality of design. Compared with the traditional design method (the difference between them is shown in Table 1), user participatory design method is more flexible and open, allowing users to participate in the design process to the greatest extent and enable users to get the best interactive experience. At present, participatory design has been applied to many research fields.

With the rapid development of social and economic level, users' demand for products is not only satisfied with functionality and practicability, but also the pursuit of spiritual enjoyment. This study proposes the design concept of "user participation." Its purpose is to open some design rights and production rights to users, so that nonrelic lovers, designers, and the general public can give full play to their advantages and characteristics and carry out independent innovation with the assistance of relevant personnel, truly participate in the design and production process of intangible cultural heritage innovative products, and improve users' participation and sense of experience, so as to better carry forward and inherit traditional culture.

User participation in design starts from user analysis and establishes user needs, such as interaction needs, self-realization needs, use needs, and cultural needs, by analyzing users' physiology, behavior, and psychology. Then, it analyzes user demand data, designs and develops product forms and decorative elements that meet users' needs, and allows users to give full play to their creativity through user participation in design. Finally, complete the product design and production. The user participation design process is shown in Figure 1.

The specific steps are as follows:

(1) User analysis: it mainly analyzes the physiological, behavioral, and psychological needs of target users, which helps designers better understand users and obtain characteristic needs. Products can only be accepted by users on the premise of truly grasping the needs of users. In the whole design process, the user is the main body to help designers more accurately obtain the real needs of users, so as to find a solution satisfactory to users. User analysis is the first step of user participatory design. The commonly

Table 1: The difference between user participatory design method and traditional design method.

	User right	Inclusiveness	Main output	Value goal	Main demands	Technical advantages	Difficulties in modeling and decoration
Traditional design method	Right of choice	None	Products	Low production cost	Rapid and mass production	Low cost, short production cycle, and high efficiency	It is up to the designer
User participatory design method	Right of choice, right of creation, and right of design	Inclusiveness (no set goals)	Experience	Meet creative needs	Open and independent creation	High yield, novel, unique, and diversified	Determined by user's design ability

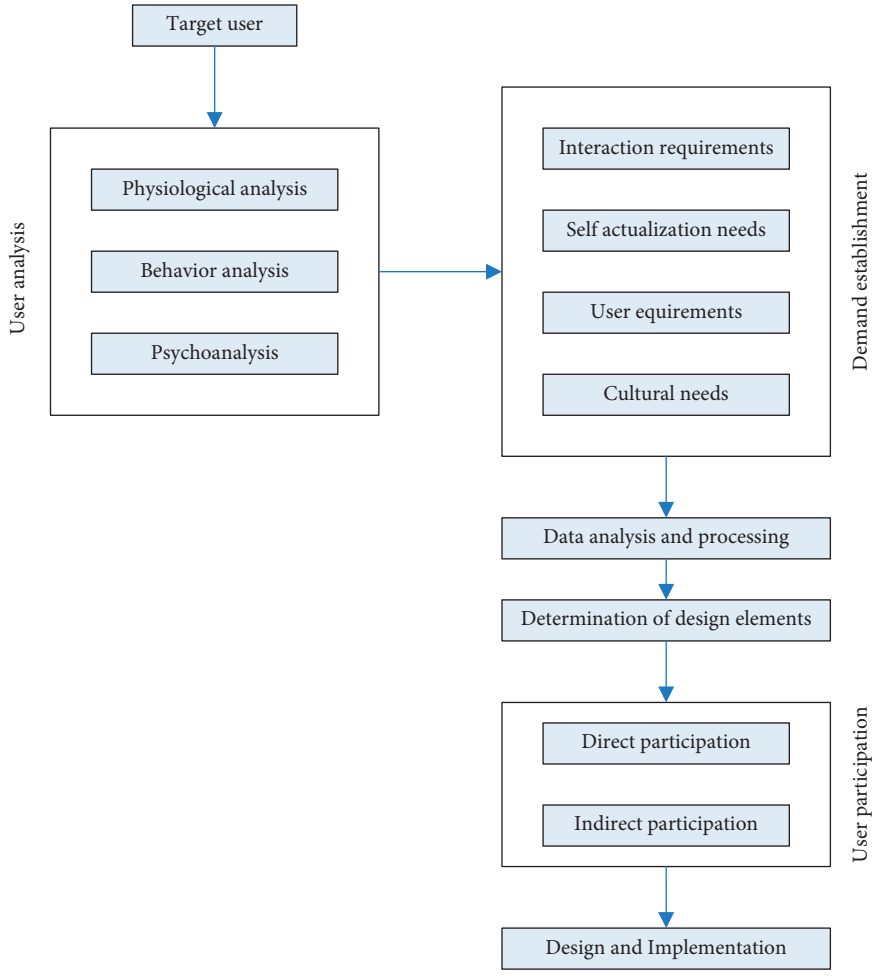

Figure 1: The user participation design process.

used methods include interview, accompanying observation and cultural analysis.

(2) Requirements acquisition: through field research, user interview, accompanying observation and cultural analysis, we can understand the user's life situation, behavior habits, cultural concepts, and expectations, so as to further improve the information needed for the research and prepare for relevant data analysis. We gradually insight and analyze the role of stakeholders in nonlegacy cultural and creative products and explore the service experience of users in the process of using products from multiple angles.

(3) User demand analysis: we obtain the relevant data information of users through questionnaires and other methods and finally establish the user needs according to the distribution characteristics of the data.

(4) Design element development and user participation: according to the needs of users, determine the shape,

decoration, and decorative style of products. Users can make their own choices and then directly or indirectly participate in the process of product design and production.

(5) Design and implementation: users design and choose under the guidance of designers or traditional craftsmen and finally complete the production of products.

3. Extraction and Reconstruction of Innovative Design Elements of Intangible Cultural Heritage Driven by Artificial Intelligence

3.1. Design Element Extraction. The innovative design elements of intangible cultural heritage are mainly extracted from intangible cultural heritage products, including ancient products and existing products, from which the characteristic factors such as appearance modeling, decorative elements, composition form, and color application are extracted, respectively. The feature factor extraction model of intangible cultural heritage innovative design is shown in Figure 2.

Through consulting relevant documents, visiting museums, and field investigation of intangible cultural heritage product factories, we collected a large number of cultural relics, pictures, documents, and other materials containing intangible cultural heritage innovative design factors, screened and sorted out the collected materials, mainly divided into ancient products and existing products, formed the characteristic analysis table of intangible cultural heritage products, and constructed the analysis Atlas of design elements.

3.2. Selection and Reconstruction of Design Elements. The intangible cultural heritage innovative design for user participation is mainly divided into five parts: selection of design elements, reconstruction of design elements, generation of design scheme, evaluation of design scheme, and participation in the production experience. The specific process is shown in Figure 3.

(1) Identify design elements. Based on perceptual engineering, collect relevant perceptual words according to the user's perceptual image, let the user score the sample, and determine the elements of intangible cultural heritage innovative design through the user's perceptual semantic word evaluation results and the target user's perceptual image words for intangible cultural heritage innovative design products.

(2) Design element refactoring. The shape grammar is used to deduce and deform the design elements selected by the user, generate new design elements, and reconstruct the design elements.

(3) Generate design scheme. According to the needs of users and the regenerated design elements, finally generate multiple sets of initial design schemes for users to choose and evaluate.

(4) Design scheme evaluation. The fuzzy comprehensive evaluation method is used to evaluate and score the generated multiple sets of design schemes and finally select several groups of schemes with high scores for refinement.

(5) Participate in the production experience. Users first choose their favorite product components through app, including the shape, decoration, style, and carcass of intangible cultural heritage innovative design products, and then participate in the post-production of products offline, under the guidance of relevant professionals, including carcass production, decoration, and polishing.

Perceptual engineering is guided by the needs of users and expresses perceptual problems qualitatively or quantitatively through mathematical analysis, so as to achieve the goal of guiding product design. We use perceptual engineering and shape grammar to guide the design of many similar modeling elements and decorative elements of intangible cultural heritage innovative products for users to choose independently. Firstly, through the comparative analysis of the characteristics of the collected intangible cultural heritage ancient products and existing products, such as appearance modeling, decorative elements, and composition forms, we can get the common design factors and select 10 typical samples from the collected samples of intangible cultural heritage products. We collect relevant perceptual words according to users' perceptual images, classify and sort out the collected semantic words, and finally get 63 semantic words. Then, we invite 30 typical users to rate the 63 perceptual semantic words collected, select words with similar semantics according to the score, and select "sharp-mellow," "complex-concise," "gorgeous-plain," "exaggerated-elegant," "simple-exquisite," "rough-smooth," "gorgeous-plain," and "dim-bright" 8 pairs of adjectives.

In order to further obtain the user's perception preference of intangible cultural heritage innovative design products, 10 samples were selected from the design element Atlas of intangible cultural heritage innovative products, and the perception survey was carried out by using the 7-order scale method. According to the semantic vocabulary correlation, they were divided into 7 levels: 3 points, −2 points, −1 point, 0 point, 1 point, 2 points, and 3 points, where "0" means consistent, "−2" and "2" mean average, and "−3" and "3" mean very high.

Finally, the distribution of users' perceptual semantic vocabulary evaluation results is obtained. By constructing a five-point psychological evaluation table and connecting the semantic vocabulary of each group of samples with broken lines, the semantic vocabulary description diagram of intangible cultural heritage innovation style features is obtained. According to the evaluation results and results of users' perceptual semantic words, the perceptual image words of target users for intangible cultural heritage innovative products are smooth, exquisite, mellow, elegant, bright, simple, and elegant.

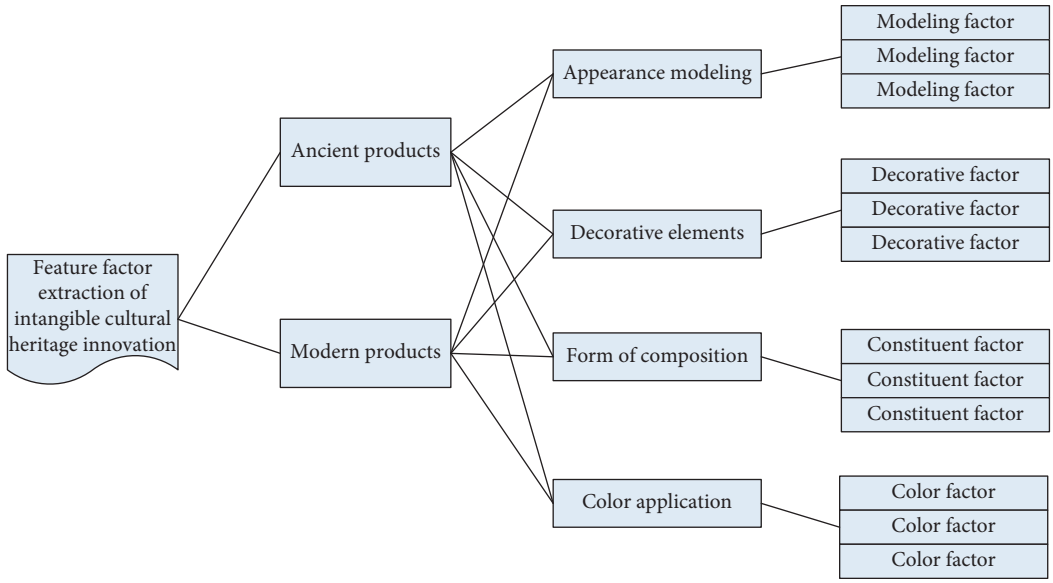

Figure 2: The feature factor extraction model of intangible cultural heritage innovative design.

According to the extraction method of design elements of intangible cultural heritage innovative products and based on the positioning needs of intangible cultural heritage innovative products, modeling elements, decorative elements, and color elements are selected, respectively. Based on the perceived image of the target user, determine the parent elements, and then determine the appearance modeling elements and color elements, so as to provide design element support for subsequent practice.

Based on the selected design elements of intangible cultural heritage innovative products, the shape grammar [22] is used to deduce and deform them, and finally new design elements are obtained. Shape grammar (SG) can be represented by

$$\mathrm{SG} = (S, L, R, I), \tag{1}$$

where "SG" is the shape set derived from "s" through translation, scaling, deformation, and mirroring, "L" represents the marker set, "R" is the reasoning rule set, and "I" is the original shape. According to the morphological deduction rules in the shape grammar theory, the seven rules of shape grammar are used to properly deform the original intangible cultural heritage innovative product design elements and then form new intangible cultural heritage innovative product design elements that meet the aesthetic needs of users by means of random arrangement and combination, replacement, addition and deletion, scaling, and staggered cutting. In the choice of color, black is generally selected as the main color, and red and yellow are the auxiliary colors.

3.3. Design Scheme Generation. Through the shape grammar deduction rules, the elements are deformed and redesigned to obtain new design elements. According to the needs of users, 6 sets of initial design schemes are finally generated. The preliminary design schemes can meet the basic needs of users. In order to further meet the diversified needs of users, this study selects the fuzzy comprehensive evaluation method [23–26] to evaluate the scheme generated by reasoning. With reference to the design elements of intangible cultural heritage innovative products, the evaluation index is set as

$$E = \{e_1, e_2, \ldots, e_n\}, \tag{2}$$

where $n = 5$.

According to the needs and satisfaction of users, the evaluation weight of each evaluation index of intangible cultural heritage innovative product design is determined by scoring method.

$$W = \{0.3, 0.3, 0.2, 0.1, 0.1\}, \tag{3}$$

where the highest weight given is 0.3 and the lowest is 0.1. e_5 is regarded as the basic demand in the evaluation index. We invite 100 users to evaluate the scheme. The evaluation and test criteria are shown in Table 2.

Finally, three schemes with high scores are selected for design optimization. Taking scheme 1 as an example, the evaluation and test results are shown in Table 3.

The fuzzy judgment matrix D of the design optimization solution is obtained from Table 4.

Then, the comprehensive evaluation model B is

$$B = W \times D. \tag{4}$$

That is, $B = \{0.224, 0.139, 0.185, 0.191, 0.261\}$.

The comprehensive evaluation results of the final 100 users on the six initial design schemes are shown in Table 5.

According to the evaluation results, it can be seen that 22.4% think scheme 1 is very good, 8.8% think scheme 2 is very good, 31.8% think scheme 3 is very good, 24.6% think scheme 4 is very good, 27.4% think scheme 5 is very good, and 21.8% think scheme 6 is very good. The top schemes are scheme 3, scheme 5, and scheme 4 in turn. Therefore, this

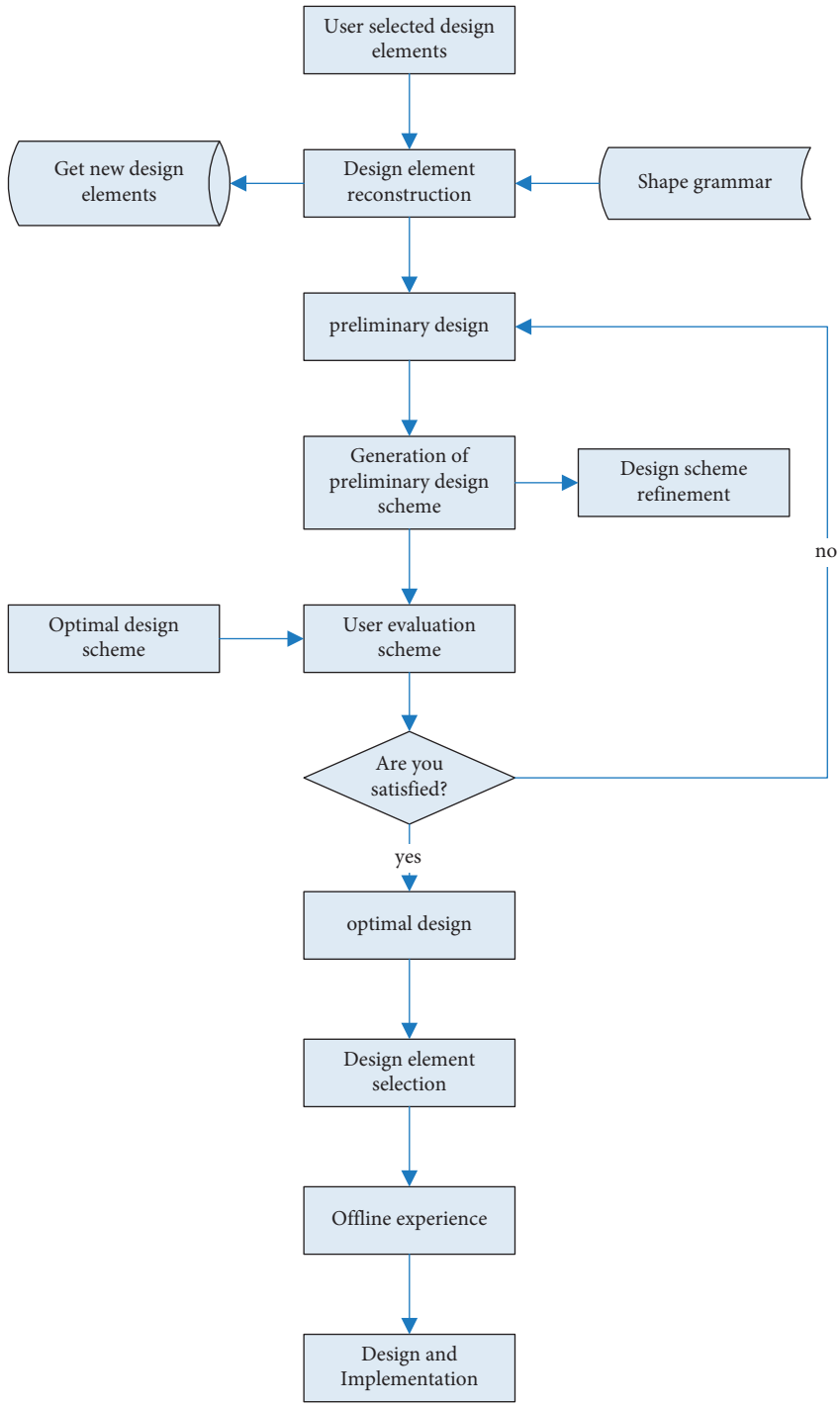

Figure 3: The intangible cultural heritage innovative design for user participation.

Table 2: The evaluation and test criteria.

Evaluation criterion	Gradation	Evaluation weight	Explanation
e_1	Extremely consistent (G_1)	0.3	Users can have space to give full play to their creativity.
e_2	Very consistent (G_2)	0.3	The product composition form can fully express the ideas of users.
e_3	Generally consistent (G_3)	0.2	The design style is fashionable, modern, and simple.
e_4	Basically consistent (G_4)	0.1	The overall design of the product is novel and unique.
e_5	Consistent (G_5)	0.1	The product has certain value and function.

Table 3: The evaluation and test results of scheme 1.

	G_1	G_2	G_3	G_4	G_5
e_1	35	12	16	17	20
e_2	17	15	20	21	27
e_3	23	12	6	20	39
e_4	16	5	30	32	17
e_5	6	29	35	5	25

Table 4: The fuzzy judgment matrix D.

	G_1	G_2	G_3	G_4	G_5
e_1	0.35	0.12	0.16	0.17	0.2
e_2	0.17	0.15	0.2	0.21	0.27
e_3	0.23	0.12	0.06	0.2	0.39
e_4	0.16	0.05	0.3	0.32	0.17
e_5	0.06	0.29	0.35	0.05	0.25

Table 5: The comprehensive evaluation results of the final 100 users.

Initial design scheme	G_1	G_2	G_3	G_4	G_5
1	0.224	0.139	0.185	0.191	0.261
2	0.088	0.117	0.383	0.251	0.161
3	0.318	0.114	0.083	0.182	0.303
4	0.246	0.211	0.131	0.127	0.285
5	0.274	0.273	0.157	0.073	0.223
6	0.218	0.057	0.123	0.380	0.222

study takes these three sets of schemes as the schemes for end users to participate in practice and carries out iterative optimization to get the final design scheme.

4. Conclusions

With the acceleration of market evolution, people's material life is becoming richer and richer, and their needs are becoming more and more diversified. The demand for products is no longer just functional, but also pays more attention to the feeling of spiritual level, and has higher requirements for the aesthetic value and cultural value of products themselves. This study comprehensively uses questionnaire survey, user interview, and user perception preference analysis to analyze and study the personal needs of users and the methods and processes of user participation in design. Finally, the theory is applied to practice to complete the research on the innovative design of artificial intelligence in intangible cultural heritage.

This study uses the Atlas analysis method to analyze and summarize the characteristics of intangible cultural heritage products, constructs the analysis Atlas of intangible cultural heritage products, determines the design elements of intangible cultural heritage innovative products according to the needs of users, deforms and reconstructs the design elements of intangible cultural heritage innovative products based on the shape grammar, deduces the deformation, obtains new design elements that meet the aesthetic needs of users, and generates the initial design scheme. The fuzzy comprehensive evaluation method is used to score and evaluate the generated design scheme, and the scheme with the highest user satisfaction is selected for iterative optimization to obtain the final design scheme. Secondly, through a series of design practices, it provides users with independent creative space and platform to meet the diversified needs of users. Finally, the design of intangible cultural heritage is verified by user-oriented design.

The main innovations of this study are as follows: (1) by combining traditional handicrafts with modern design ideas, the market transformation channels of intangible cultural heritage innovative design products are increased, and a user-oriented intangible cultural heritage innovative design model is established. (2) In view of the difficulties faced by intangible cultural heritage art, explore the needs of different users for intangible cultural heritage innovative products, let users participate in the design process of intangible cultural heritage innovative products, enable users to obtain the creative dominance of products, and improve users' consumption experience. (3) According to the needs of users, this paper puts forward the design scheme of intangible cultural heritage innovative products to meet the needs of user groups and promote the wide dissemination of intangible cultural heritage culture.

Data Availability

The dataset can be accessed upon request.

Conflicts of Interest

The author declares no conflicts of interest.

References

[1] Q. Li, "Intelligent intangible cultural heritage innovation platform under the background of big data and virtual systems," in *Proceedings of the 2nd International Conference on Artificial Intelligence and Smart Energy ICAIS*, pp. 560–563, Coimbatore India, February 2022.

[2] L. Zhang, "Digital protection of dance of intangible cultural heritage by motion capture technology," *Lecture Notes on Data Engineering and Communications Technologies*, vol. 85, pp. 429–436, 2022.

[3] Z. Chen, J. Huang, H. Dai, and J. Liu, "Development route analysis of intangible cultural heritage industry of China based on data mining," *Journal of Physics: Conference Series*, vol. 1848, no. 1.

[4] W. Zhang and M. Liu, "APP interface design of qiang people's silver jewlery based on user experience," in *Proceedings of the 3rd International Conference on Contemporary Education, social sciences and humanities*, vol. 4, pp. 686–690, Dublin, Ireland, August 2018.

[5] M. Liu and W. Zhang, "Form bionic design research based on product semantics, 2018International Conference on Contemporary Education," *Social Sciences and Ecological Studies*, vol. 12, pp. 607–612, 2018.

[6] Y. Feng, W. Zhang, P. Luan, and M. Liu, "Design of game style navigation APP interface based on user experience," in

Proceedings of the 3rd International Conference on Culture, Education and Economic Development of Modern Society, vol. 2, pp. 384–391, MoscowRussia, March 2019.

[7] H. Ding, "Digital Protection and Development of Intangible Cultural Heritage Relying on High-Performance Computing," *Computational Intelligence and Neuroscience*, vol. 2022, Article ID 4955380, 2022.

[8] L. Li, B. Lei, and C. Mao, "Digital twin in smart manufacturing," *Journal of Industrial Information Integration*, vol. 26, no. 9, 2022.

[9] I. Li, "Sustainability assessment of intelligent manufacturing supported by digital twin," *IEEE Access*, vol. 8, pp. 174988–175008, 2020.

[10] Z. Xu and D. Zou, "Big Data Analysis Research on the Deep Integration of Intangible Cultural Heritage Inheritance and Art Design Education in Colleges and Universities," *Mobile Information Systems*, vol. 2022, Article ID 1172405, 2022.

[11] L. Li and C. Mao, "Big data supported PSS evaluation decision in service-oriented manufacturing," *IEEE Access*, vol. 8, pp. 154663–154670, 2020.

[12] L. Li and C. Mao, "Digital twin driven green performance evaluation methodology of intelligent manufacturing: hybrid model based on fuzzy rough-sets AHP, multistage weight synthesis, and PROMETHEE II," *Complexity*, vol. 2020, p. 24, Article ID 3853925, 2020.

[13] L. Huang and Y. Song, "Intangible Cultural Heritage Management Using Machine Learning Model: A Case Study of Northwest Folk Song Huaer," *Scientific Programming*, vol. 2022, pp. 1–9, 2022.

[14] Xi. Deng, Il T. Kim, and C. Shen, "Research on convolutional neural network-based virtual reality platform framework for the intangible cultural heritage conservation of China hainan li nationality: boat-shaped house as an example," *Mathematical Problems in Engineering*, vol. 2021, pp. 1–16, 2021.

[15] B. C. Stahl, R. Rodrigues, N. Santiago, and K. Macnish, "A European Agency for Artificial Intelligence: protecting fundamental rights and ethical values," *Computer Law & Security Report*, vol. 45, July, 2022.

[16] M. Ashok, R. Madan, A. Joha, and U. Sivarajah, "Ethical framework for artificial intelligence and digital technologies," *International Journal of Information Management*, vol. 62, February, 2022.

[17] A. M. Oprescu, G. Miro, L. Garcii et al., "Towards a data collection methodology for Responsible Artificial Intelligence in health: a prospective and qualitative study in pregnancy," *Information Fusion*, vol. 83-84, pp. 53–78, July 2022.

[18] L. Chong, G. Zhang, K. Goucher-Lambert, K. Kotovsky, and J. Cagan, "Human confidence in artificial intelligence and in themselves: the evolution and impact of confidence on adoption of AI advice," *Computers in Human Behavior*, vol. 127, Article ID 1.

[19] W. Huo, G. Zheng, J. Yan, Le Sun, and L. Han, "Interacting with medical artificial intelligence: integrating self-responsibility attribution, human–computer trust, and personality," *Computers in Human Behavior*, vol. 132, Article ID 107253, July, 2022.

[20] Szykman, A. Greluk, A. L. Brandão, and J. P. Gois, "Development of a gesture-based game applying participatory design to reflect values of manual wheelchair users," *International Journal of Computer Games Technology*, vol. 2018, 2018.

[21] B. Danbjørg, Dorthe, L. Wagner, R. . Kristensen, Bjarne, and J. Clemensen, "Nurses' experience of using an application to support new parents after early discharge: an intervention study," *International Journal of Telemedicine and Applications*, vol. 2015, 2015.

[22] P. B. Silva, E. Eisemann, R. Bidarra, and A. Coelho, "Procedural content graphs for urban modeling," *International Journal of Computer Games Technology*, vol. 2015, 2015.

[23] D. Liu, "Fuzzy Comprehensive Evaluation Method of Ecological Environment Damage Compensation System and Management Based on Improved Association Rule Algorithm," *Mobile Information Systems*, vol. 2021, 2021.

[24] J. Zhou, A. Wang, X. Su, C. Zhang, and Kang, "Xusheng.Prediction and allocation of EDP based on gray model and fuzzy comprehensive evaluation," *Mathematical Problems in Engineering*, vol. 2021, 2021.

[25] Yi Lu, J. Zheng, C. Zhao, and G. Ren, "Risk assessment of a cryogenic globe valve by using combined group decision and fuzzy comprehensive evaluation," *Mathematical Problems in Engineering*, vol. 2021, 2021.

[26] Z. Zhu, J. Zhu, Y. Liu et al., "Parameter optimization of ultrafine comminution based on analytic hierarchy process: fuzzy comprehensive evaluation," *Journal of Control Science and Engineering*, vol. 2021, 2021.

Hindawi
Scientific Programming
Volume 2022, Article ID 1920933, 6 pages
https://doi.org/10.1155/2022/1920933

Research Article

Data Recovery Technology Based on Subspace Clustering

Li Sun and Bing Song

Department of Internet Security, Henan Police College, Zhengzhou 450046, Henan, China

Correspondence should be addressed to Li Sun; sl@hnp.edu.cn

Received 5 June 2022; Revised 17 June 2022; Accepted 20 June 2022; Published 20 July 2022

Academic Editor: Lianhui Li

High-dimensional data usually exist asymptotically in low-dimensional space. In this study, we mainly use tensor t-product as a tool to propose new algorithms in data clustering and recovery and verify them on classical data sets. This study defines the "singular values" of tensors, adopts a weighting strategy for the singular values, and proposes a tensor-weighted kernel norm minimization robust principal component analysis method, which is used to restore low-probability low-rank third-order tensor data. Experiments on synthetic data show that in the recovery of strictly low-rank data, the tensor method and weighting strategy can also obtain more accurate recovery when the rank is relatively large, which improves the volume of the rank. The proposed method combines the two and reflects its superiority through the restoration of 500 images under a small probability noise level.

1. Introduction

In recent years, the development of science and technology has been changing with each passing day, and at the same time, it has also brought complicated data [1–4]. With the development of the Internet and artificial intelligence [5–8], the data on education, medical treatment, e-commerce, transportation, and other industries show explosive growth. How to mine useful information from massive data has become a research hotspot. Due to the continuous improvement of people's ability to obtain data, the scale of data is becoming larger and larger, and the structure is becoming more and more complex, such as millions of frames of video, texts, and web pages carrying hundreds of millions of information.

Data recovery and clustering are of great significance to the analysis of high-dimensional data [9–14]. Many high-dimensional data usually exist approximately in low-dimensional subspaces, and the low rank prior of data becomes the key to effective data recovery [15–18]. In cluster analysis, many data are usually modeled as coming from multiple cluster subspaces. Based on this, the data are clustered and a popular subspace clustering algorithm is formed.

Analyzing these high-dimensional data not only occupies memory and takes time but also because the useful information of the data often only exists in the low-dimensional space, other redundant components will bring great interference to the analysis algorithm [19]. Noise or outliers due to the increase of information will also affect the performance of the algorithm. How to grasp and make use of the characteristics of data has become a breakthrough in the effective analysis of data. In the form of data processing, the traditional method of matrix decomposition usually needs to transform multi-level data samples into column vectors, which inevitably destroys the original structure of data and leads to information loss. While retaining the original form of the data, the tensor form will be used for decomposition. In recent years, in the field of practical application, the analysis of tensors has played an increasingly important role, so more and more scholars have paid attention to it. The forms of tensor operations are diversified with the in-depth exploration of the academic community.

2. Data Recovery of Low-Rank Third-Order Tensors under Small Probability Sparse Noise

Low rank exists widely in data. In algorithms applied to traditional matrix factorization, converting each multi-order data sample into a long column vector form is necessary

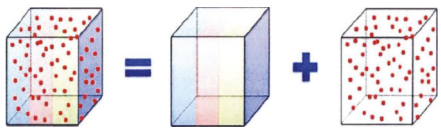

Figure 1: Schematic diagram of TRPCA decomposition.

[20]. A third-order tensor has a lower-rank structure than the corresponding matrix. Therefore, theoretically, from the perspective of low-rank recovery, the original structure of tensors has certain advantages.

Theorem 1. *For any tensor:*

$$\mathscr{A} \in \mathbb{R}^{n_1 \times n_2 \times n_3}. \tag{1}$$

We convert each of its side slice matrices into a column vector, the matrix $\mathscr{A}$ is formed by these column vectors, which is unfold ($\mathscr{A}$).

Then the average rank of $\mathscr{A}$ is less than or equal to the rank of $\mathscr{A}$, that is,

$$r_a(\mathscr{A}) \le r(\text{unfold}(\mathscr{A})). \tag{2}$$

Prove:

$$\text{bcirc}(\mathscr{A}) = \left[I_{n_1 n_3}, P, P^2, \ldots, P^{n_3-1}\right] \begin{bmatrix} A & & & \\ & A & & \\ & & \ddots & \\ & & & A \end{bmatrix}, \tag{3}$$

where P is the permutation matrix $\begin{bmatrix} O & \cdots & O & I_{n_1} \\ I_{n_1} & \cdots & O & O \\ \vdots & \ddots & \vdots & \vdots \\ O & \cdots & I_{n_1} & O \end{bmatrix} \in \mathbb{R}^{n_1 n_3 \times n_1 n_3}$.

Then,

$$r_a(\mathscr{A}) = \frac{1}{n_3} r(b\text{diag}(\mathscr{A})) = \frac{1}{n_3} r(\text{bcirc}(\mathscr{A})). \tag{4}$$

So,

$$r_a(\mathscr{A}) \le \frac{1}{n_3} r\left(\begin{bmatrix} A & & & \\ & A & & \\ & & \ddots & \\ & & & A \end{bmatrix}\right) = r(A). \tag{5}$$

2.1. Tensor Low-Rank Structure of RGB Images. An RGB image data itself is a third-order tensor, and the general image tensor has a low-rank structure, which will be explained from experiments in this section. Two-color pictures are randomly selected from the Berkeley Segmentation dataset [21], and the picture size is 321×481. Each picture's data (RGB picture) can be regarded as a third-order tensor (set as $\mathscr{A} \in \mathbb{R}^{m \times n \times 3}$). We perform tensor singular value decomposition for each image: $\mathscr{A} = \mathscr{U} * \mathscr{S} * \mathscr{V}^*$. Also, we calculate the singular value of $b\text{diag}(\mathscr{A})$. It can be seen that the general RGB image itself has a tensor low-rank structure.

Tensor low-rank representation (TLRR) [22] and tensor robust principal component analysis (TRPCA) [23] use the tensor low-rank structure to remove the sparse noise of the image. The decomposition of TRPCA is shown in Figure 1.

2.2. Tensor-Weighted Nuclear Norm Minimization Robust Principal Component Analysis Method. Perform singular value decomposition on a matrix of approximately low rank; the larger singular value corresponds to the "main structure" information of the matrix, such as larger edges and smooth parts in the image matrix. The small noise does not interfere much with the main structure of the matrix; therefore, in the denoising algorithm based on singular value shrinkage, different singular values should be treated differently. Based on this prior, weighted nuclear norm minimization (WNNM) [24] and weighted nuclear norm minimization-robust principal component analysis (WNNM-RPCA) [25] give a small degree of shrinkage to large singular values based on nuclear norm minimization (NNM) and robust principal component analysis (RPCA), respectively, and greatly improve the denoising effect.

The singular value of any tensor $\mathscr{A}$ is defined as the singular value of $b\text{diag}(\mathscr{A})$; then, the above analysis is also valid for tensor singular value decomposition. Referring to the weighting strategy in literature [26], we set the weight of each singular value σ_i of the tensor as

$$w_i^{t+1} = \frac{C}{\sigma_i\left(\mathscr{A}^t\right) + \epsilon}. \tag{6}$$

In this equation, σ_i represents the i-th singular value of $\mathscr{A}$, t represents the number of iterations, C is a normal number, and ε is a minimal number to prevent the denominator from being 0.

The $L1$ norm is often used to characterize random probability noise. For example, RPCA, etc. For the problem of removing small probability noises from third-order tensors, a tensor-weighted nuclear norm minimization robust principal component analysis method is proposed as

$$\min_{\mathscr{L},\mathscr{E}} \|\mathscr{L}\|_{w,*} + \|\mathscr{E}\|_1, s.t. x = \mathscr{L} + \varepsilon. \tag{7}$$

To deal with the equality constraint problem, the augmented lagrange multiplier method is used, that is,

$$\min_{\mathscr{L},\mathscr{E}} \|\mathscr{L}\|_{w,*} + \lambda\|\mathscr{E}\|_1 + \frac{\mu}{2}\|\mathscr{X} - \mathscr{L} - \mathscr{E}\|^2 + < y, X - \mathscr{L} - \mathscr{E} >. \tag{8}$$

We solve equation (8) by the alternating direction method of multipliers (ADMM) method. This is a supplementary explanation of the solution to the following model used to update $\mathscr{L}$.

Giving the tensor $Z \in \mathbb{R}^{n_1 \times n_2 \times n_3}$, the $\mathscr{L}$ of the following function is solved as

$$\min_{\mathscr{L}} \|\mathscr{L}\|_{w,*} + \frac{\mu}{2}\|\mathscr{L} - \mathscr{Z}\|^2. \tag{9}$$

This is equivalent to the following matrix model:

$$\min_{\mathscr{L}} \|b\text{diag}(\mathscr{L})\|_{w,*} + \frac{\mu}{2}\|b\text{diag}(\mathscr{L}) - b\text{diag}(\mathscr{Z})\|^2. \tag{10}$$

Let

$$b\text{diag}(\mathscr{L}) = \begin{bmatrix} L_1 & & \\ & L_2 & \\ & & \ddots \\ & & & L_{n_3} \end{bmatrix}, \quad b\text{diag}(\mathscr{Z}) = \begin{bmatrix} Z_1 & & \\ & Z_2 & \\ & & \ddots \\ & & & Z_{n_3} \end{bmatrix}, \tag{11}$$

where $L_i, Z_i \in \mathbb{R}^{n_1 \times n_2}$ $, i = 1, \ldots, n_3$.

Then, the model can be transformed into

$$\min_{L_i} L_{i,w,*} + \frac{\mu}{2}L_i - Z_i^2, \quad i = 1 \ldots, n_3. \tag{12}$$

It can be solved by applying Theorem 2.

Theorem 2 ([see 25]). *Suppose $Y \in \mathbb{R}^{m \times n}$, for the wavelet neural network prediction (WNNP) problem of the reweighted strategy:*

$$\min_X \|X\|_{w,*} + \|Y - X\|^2, \tag{13}$$

where $w_i^t = C/\sigma_i(X^t) + \epsilon$, C is a positive constant, ϵ satisfies $\epsilon < min(\sqrt{C}, C/\sigma_1(Y))$ and initializes $X^0 = Y$, then the problem has a closed-form solution.

We perform singular value decomposition on Y:

$$Y = U \sum V. \tag{14}$$

Then, the closed-form solution is

$$X^* = U \sum V^T, \tag{15}$$

where,

$$\sum = \begin{pmatrix} \text{diag}\left(\sigma_1(X^*), \widetilde{\sigma_2}(X^*), \ldots, \sigma_n(X^*)\right) \\ 0 \end{pmatrix},$$

$$\sigma_i(X^*) = \begin{cases} 0 & c_2 < 0, \\ \dfrac{c_1 + \sqrt{c_2}}{2} & c_2 \geq 0, \end{cases} \tag{16}$$

$$c_1 = \sigma_i(Y) - \epsilon, c_2 = \left(\sigma_i(Y) + \epsilon\right)^2 - 4C.$$

3. Experiments

It is assumed that the value range of each element in the low-rank tensor $\mathscr{A}$ is $[a, b]$, and the element with frequency p in $\mathscr{A}$ is disturbed by noise. This experiment mainly explores the accurate recovery of low-rank third-order tensor $\mathscr{A} \in \mathbb{R}^{n_1 \times n_2 \times n_3}$ under low-probability sparse noise by the proposed tensor-weighted nuclear norm minimization robust principal component analysis method.

The main comparison algorithms are RPCA [27], WNNM-RPCA [25], low-rank representation (LRR) [28], tensor robust principal component analysis (TRPCA) [23], and tensor low-rank representation (TLRR) [22]. Each positive slice matrix of the tensor is denoised separately when applying the matrix methods: WNNM-RPCA and LRR.

In addition to the parameters already set, set

$$C = 4p\sqrt{n_1 n_2}. \tag{17}$$

p value prior is needed here. Better results can be obtained without p prior value, but experiments show that setting the C value in this way is more effective.

3.1. Synthesis of Data. Firstly, the vector linearly produces a low-rank tensor. The steps of this experiment are:

(1) Generate a low-rank tensor:

$$\mathscr{A} = \text{fold}(\text{unfold}(\mathscr{B})C), \tag{18}$$

where $\mathscr{B} \in \mathbb{R}^{n_1 \times r \times n_3}, \mathscr{C} \in \mathbb{R}^{r \times n_2}$, all obey the normal distribution $\mathscr{N}(0, 1)$.

(2) Randomly select the element whose proportion frequency is p from $\mathscr{A}$ and set it as a large random value in the range of $[a, b]$. $[a, b]$ is set as the value range $[\min(\mathscr{A}), \max(\mathscr{A})]$ of $\mathscr{A}$.

(3) Use the corresponding algorithm to process separately to get the recovery value $\mathscr{A}^*$.

(4) Comparing the relative error,

$$\text{RF} = \frac{\mathscr{A} - \mathscr{A}^*}{\|\mathscr{A}\|}. \tag{19}$$

The restoration fails if the error is greater than 0.2.

Then, we fix $n_1 = 300$, $n_2 = 300$, $n_3 = 5$, $p = 0.15$ unchanged, set r to 5, 10, 15, 20, 40, 60, 80, respectively. Each group of experiments generates 10 noise data recovered by different algorithms (each row in the error result table uses the same group of data), and the average results are taken. A comparison of recovery errors for low-rank tensors produced by vector linearity is shown in Table 1.

Then, tensors linearly generate low-rank tensors. This experiment is different from the first experiment only in the method of generating low-rank tensors in step 1, which is changed to

$$A = B * C, \tag{20}$$

Table 1: Comparison of recovery errors for low-rank tensors produced by vector linearity.

r	RPCA	WNNM-RPCA	TRPCA	TWRPCA
5	$5.58e-11$	$3.86e-08$	$1.23e-08$	$1.01e-08$
10	$5.64e-11$	$4.70e-08$	$1.12e-08$	$1.08e-08$
15	$4.88e-11$	$5.65e-08$	$7.76e-09$	$1.04e-08$
20	$5.21e-11$	$6.26e-08$	$1.11e-08$	$9.44e-09$
40	$5.98e-11$	$1.01e-07$	$3.78e-04$	$9.23e-09$
60	0.13	$4.55e-04$	0.12	$1.55e-09$
80	—	—	—	—

"—" indicates that recovery failed.

Table 2: Comparison of recovery errors for low-rank tensors produced by tensor linearity.

r	RPCA	WNNM-RPCA	TRPCA	TWRPCA
5	$5.39e-11$	$7.69e-08$	$8.51e-09$	$6.21e-09$
10	0.012	$1.31e-07$	$6.84e-09$	$6.72e-09$
15	—	—	$7.22e-09$	$5.78e-09$
20	—	—	$4.24e-09$	$3.92e-09$
40	—	—	$1.04e-08$	$4.70e-09$
60	—	—	0.12	$6.72e-09$
80	—	—	—	$9.62e-09$

"—" indicates that recovery failed.

where $\mathscr{B} \in \mathbb{R}^{n_1 \times r \times n_3}$, $\mathscr{C} \in \mathbb{R}^{r \times n_2 \times n_3}$, all obey the normal distribution: $\mathcal{N}(0,1)$. The results are shown in Table 2.

From the above two experiments, we can draw the following conclusions: in the case of low-rank and low-noise level, the inpainting result of RPCA is the most accurate. This also verifies the theory described in [27]. From the perspective of "tolerance" to rank, both the tensor method and the weighting strategy make the original algorithm significantly improved. The improvement effect of the tensor method is particularly significant in the recovery of data generated by tensor linearity.

3.2. Image Restoration. This experiment uses 500 pictures from the Berkeley dataset [27–29] under different scenarios. For each test picture, the pixel value of $p = 3\% \sim 15\%$ is randomly selected and set to a random value of [0, 255], and different algorithms are applied to repair. When applying the proposed tensor weighted nuclear norm minimization robust principal component analysis method, the experiments show that the denoising results need to be performed twice by the proposed tensor weighted nuclear norm minimization robust principal component analysis method for better results. Taking mean square error (MSE) and peak signal to noise ratio (PSNR) values as evaluation indicators:

$$\begin{aligned} \mathrm{MSE} &= \frac{\|\mathscr{L} - X\|^2}{n_1 n_2 n_3}, \\ \mathrm{PSNR} &= 10\log_{10}\left(\frac{\|X\|_\infty^2}{\mathrm{MSE}}\right), \end{aligned} \tag{21}$$

where $\mathscr{L}$ is the recovery result for $\mathscr{X} \in \mathbb{R}^{n_1 \times n_2 \times n_3}$.

Under the noise level of $p = 9\%$, each algorithm recovers the data of four example images. The average processing time of the four images is shown in Figure 2. MATLABR 2020 is used in this experiment, the computer parameters are the operating system win10, CPU Inter(R) Core(TM) i5-3230M, CPU of 2.60 GHZ, and the memory of 8 GB.

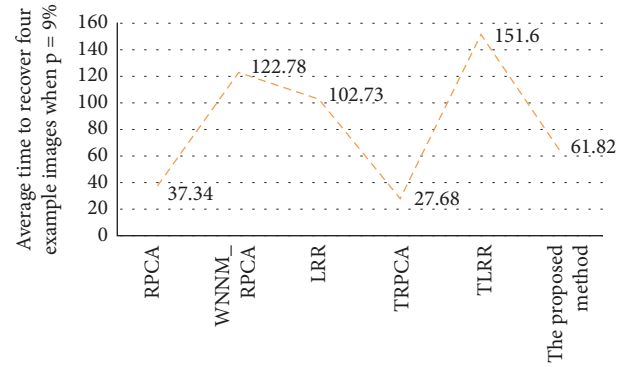

Figure 2: Average time to recover four example images when $p = 9\%$ (unit: seconds).

Under different noise levels, each algorithm restores 500 images, and the average MSE and PSNR values are shown in Tables 3 and 4, respectively (the best results are shown in bold).

It can be seen from Tables 3 and 4 that the repair results of the tensor method are better than the repair results of the matrix method; WNNM-RPCA and TWRPCA obtained by the weighted strategy perform better in similar methods, and the lower the noise level, the more pronounced the advantage of the weighted strategy.

As mentioned above, the larger part of the singular value of the data represents the "main structure" of the data itself. At the same time, the low noise level has less influence on the main structure of the data, and the weighting strategy uses this prior. The experimental results further verified this hypothesis.

Table 3: Average MSE value recovered from 500 pictures.

	$p = 3\%$	$p = 6\%$	$p = 9\%$	$p = 12\%$	$p = 15\%$
RPCA	199.78	214.66	226.93	242.23	260.63
LRR	174.63	186.30	196.63	215.69	241.02
WNNM-RPCA	72.10	115.63	171.23	220.28	266.78
TRPCA	65.78	78.62	88.52	101.08	118.52
TLRR	42.25	48.52	55.32	65.29	77.04
The proposed method	17.65	23.05	36.11	55.85	79.55

Table 4: Average PSNR value recovered from 500 pictures.

	$p = 3\%$	$p = 6\%$	$p = 9\%$	$p = 12\%$	$p = 15\%$
RPCA	24.55	25.74	25.44	25.71	25.00
LRR	26.21	25.96	25.63	25.63	24.25
WNNM-RPCA	30.66	27.85	26.50	25.21	24.30
TRPCA	30.25	30.10	29.66	28.61	27.96
TLRR	32.62	31.57	31.68	30.51	29.82
The proposed method	38.55	36.32	32.80	31.02	29.01

4. Conclusions

This study focuses on the data recovery of low-rank third-order tensors under small probability sparse noise. Tensor t-product is only one of many tensor operations. Although it has an excellent performance in some aspects, it can not achieve all aspects of transcendence. Tensor subspace has more "right shift" closeness than quantum space, but this property has not been further analyzed in combination with practice. In the face of practical problems, the theoretical analysis of this paper is relatively weak. It is hoped that there will be more in-depth theoretical research in the future, and there will be more perfect trade-off strategies for various forms of matrix or tensor operations.

In data recovery, although the tensor weighting strategy proposed in this paper has brought better results, the current experiments have only achieved better results under small probability noise. Relevant experiments show that the weighting parameters are also related to the image itself, and the image information should be taken into account when determining the weighting parameters. For example, images with more details (such as texture images) and smoother images should be treated differently; in addition, the RGB image itself is regarded as a third-order low-rank tensor, and the application of weighted low rank will make the image lose some detail information while denoising. We can use the prior of nonlocal approximation for reference to aggregate the similar blocks of the image to obtain a tensor with a lower rank, and then use the corresponding algorithm to denoise. However, because TRPCA, TLRR, TWRPCA, and other methods dealing with sparse noise do not have an explicit solution, it will consume memory and greatly increase the time cost. Therefore, it is hoped that there will be a denoising algorithm that considers the image information and can estimate the noise level in the future.

Data Availability

The dataset can be accessed upon request.

Conflicts of Interest

The authors declare that they have no conflicts of interest.

References

[1] Q. Chang, S. Nazir, and X. Li, "Decision-Making and Computational Modeling of Big Data for Sustaining Influential Usage," *Scientific Programming*, vol. 2022, Article ID 2099710, 2022.

[2] Z. Bai and X. Bai, "Sports Big Data: Management, Analysis, Applications, and Challenges," *Complexity*, vol. 2021, Article ID 6676297, 2021.

[3] W. Huang, "Research on the Revolution of Multidimensional Learning Space in the Big Data Environment," *Complexity*, vol. 2021, Article ID 6583491, 2021.

[4] Y. Gao, "Design of children's product packaging preference based on big data machine learning," *Wireless Communications and Mobile Computing*, vol. 2021, Article ID 8424939, 10 pages, 2021.

[5] L. Li, B. Lei, and C. Mao, "Digital twin in smart manufacturing," *Journal of Industrial Information Integration*, vol. 26, no. 9, Article ID 100289, 2022.

[6] L. Li, T. Qu, Y. Liu et al., "Sustainability assessment of intelligent manufacturing supported by digital twin," *IEEE Access*, vol. 8, pp. 174988–175008, 2020.

[7] L. Li and C. Mao, "Big data supported PSS evaluation decision in service-oriented manufacturing," *IEEE Access*, vol. 8, no. 99, pp. 154663–154670, 2020.

[8] L. Li, C. Mao, H. Sun, Y. Yuan, and B. Lei, "Digital twin driven green performance evaluation methodology of intelligent manufacturing: hybrid model based on fuzzy rough-sets AHP, multistage weight synthesis, and PROMETHEE II," *Complexity*, vol. 2020, no. 6, pp. 1–24, 2020.

[9] J. He and Y. Zhou, "Real-time data recovery in wireless sensor networks using spatiotemporal correlation based on sparse representation," *Wireless Communications and Mobile Computing*, pp. 1–7, 2019.

[10] J. Chen, Y. Yan, S. Guo, Y. Ren, and F. Qi, "A system for trusted recovery of data based on blockchain and coding techniques," *Wireless Communications and Mobile Computing*, pp. 1–12, 2022.

[11] J. He and J. Wen, "Analysis model of the impact of refined intervention in operating room on patients' recovery quality and complications after thoracic surgery based on deep neural network," *Journal of Healthcare Engineering*, pp. 2021–11, 2021.

[12] S. Ji, Y. Sun, and J. Shen, "A method of data recovery based on compressive sensing in wireless structural health monitoring," *Mathematical Problems in Engineering*, pp. 1–9, 2014.

[13] D. Chang, Li Li, Y. Chang, and Z. Qiao, "Cloud Computing Storage Backup and Recovery Strategy Based on Secure Iot and Spark," *Mobile Information Systems*, vol. 2021, Article ID 505249, 2021.

[14] X. Wang, Y. Chen, W. Ruan, Q. Gao, G. Ying, and Li Dong, "Intelligent Detection and Recovery of Missing Electric Load Data Based on Cascaded Convolutional Autoencoders," *Scientific Programming*, vol. 2020, Article ID 8828745, 2020.

[15] Y. Zhou, Yu Hu, J. Chen, Z. Huang, H. Huang, and Yi F. Zhang, "Identity-based designated-verifier proxy signature scheme with information recovery in telemedicine system," *Wireless Communications and Mobile Computing*, pp. 1–11, 2022.

[16] J. Lu, T. Tian, Y. Tang, and B. Tang, "Performance analysis of data transmission for joint radar and communication systems," *Mathematical Problems in Engineering*, pp. 2021–14, 2021.

[17] J. Zhang, J. Che, X. Sun, and W. Ren, "Clinical Application of Perioperative Anaesthesia Management Based on Enhanced Recovery after Surgery Concept to Elderly Patients Undergoing Total Knee Replacement," *Computational Intelligence and Neuroscience*, vol. 2022, Article ID 039358, 2022.

[18] P. Hu, J. Zhu, J. Gong et al., "Development of a Comprehensive Driving Cycle for Construction Machinery Used for Energy Recovery System Evaluation: A Case Study of Medium Hydraulic Excavators," *Mathematical Problems in Engineering*, vol. 2021, Article ID 8132878, 2021.

[19] Y. Li and H. Zhang, "Effect of joint use of external minifixator and titanium lockplate on total active motion range and hand function recovery in comminuted metacarpal and phalanx fracture patients," *Journal of Healthcare Engineering*, pp. 1–6, 2022.

[20] H. Tang, *Honey on Basketball Players' Physical Recovery and Nutritional Supplement*, , p. 2022, Computational Intelligence and Neuroscience, 2022.

[21] D. Martin, C. Fowlkes, D. Tal, and J. Malik, *A Database of Human Segmented Natural Images and its Application to Evaluating Segmentation Algorithms and Measuring Ecological statistics*, IEEE, in *Proceedings of the IEEE International Conference on Computer Vision*, August 2002.

[22] P. Zhou, C. Lu, J. Feng, Z. Lin, and S Yan, "Tensor low-rank representation for data recovery and clustering," *IEEE Transactions on Pattern Analysis and Machine Intelligence*, vol. 43, no. 5, pp. 1718–1732, 2021.

[23] C. Lu, J. Feng, Y. Chen, W. Liu, Z. Lin, and S. Yan, "Tensor robust principal component analysis: exact recovery of corrupted low-rank tensors via convex optimization," in *Proceedings of the IEEE Conference on Computer Vision and Pattern Recognition (CVPR)*, pp. 5249–5257, New York, NY, USA, May 2016.

[24] J. F. Cai, E. J. Candès, and Z. Shen, "A singular value thresholding algorithm for matrix completion," *SIAM Journal on Optimization*, vol. 20, no. 4, pp. 1956–1982, 2010.

[25] S. Gu, L. Zhang, W. Zuo, and X. Feng, "Weighted nuclear norm minimization with application to image denoising," in *Proceedings of the IEEE Conference on Computer Vision and Pattern Recognition*, pp. 2862–2869, Columbus, OH, USA, September 2014.

[26] S. Gu, Q. Xie, D. Meng, W. Zuo, X. Feng, and L Zhang, "Weighted nuclear norm minimization and its applications to low level vision," *International Journal of Computer Vision*, vol. 121, no. 2, pp. 183–208, 2017.

[27] E. J. Candes, M. B. Wakin, and S. P. Boyd, "Enhancing sparsity by reweighted ℓ 1 minimization," *Journal of Fourier Analysis and Applications*, vol. 14, no. 5-6, pp. 877–905, 2008.

[28] G. Liu, Z. Lin, S. Yan, J. Sun, Y. Yu, and Y Ma, "Robust recovery of subspace structures by low-rank representation," *IEEE Transactions on Pattern Analysis and Machine Intelligence*, vol. 35, no. 1, pp. 171–184, 2013.

[29] D. Martin, C. Fowlkes, J. Malik, and D. Tal, "A database of human segmented natural images and its application to evaluating segmentation algorithms and measuring ecological statistics," in *Proceedings of the IEEE International conference on computer vision*, vol. 3, p. 416, IEEE Computer Society, Los Alamitos, CA, USA, July 2001.

Hindawi
Scientific Programming
Volume 2022, Article ID 5882921, 10 pages
https://doi.org/10.1155/2022/5882921

Research Article

Design of a Multimodal Teaching Method for Business English in a Wireless Network Environment

Fen Liu and Laiying Deng

Guangzhou City Polytechnic, Guangzhou, Guangdong 510000, China

Correspondence should be addressed to Laiying Deng; denglaiying@gcp.edu.cn

Received 20 May 2022; Revised 15 June 2022; Accepted 29 June 2022; Published 20 July 2022

Academic Editor: Lianhui Li

In the background of the information age of "Internet+," the traditional teaching mode of business English has many drawbacks in terms of curriculum, teaching content, teaching methods, and teachers' backgrounds and cannot adapt to the needs of the times. Therefore, business English teaching should actively follow the trend of "Internet + education" and continue to innovate in a multimodal way. The multimodal teaching mode of "wireless network + business English" is in line with the background of "Internet+," optimizing teaching resources to the maximum extent and truly realizing the effective combination of Internet and business English teaching. The Internet-based multimodal innovation can be carried out in the four elements of business English teaching: environment, task, learner, and guide teaching. The specialization and modernization of business English teaching can be promoted through the optimization of O2O multisituational classroom, the application of multimodal tasks in three-dimensional teaching materials, the communication of diversified categories of students, and the configuration of multilevel teachers across fields.

1. Introduction

With the continuous innovation of information technology, we have entered the 2.0 era of Internet development [1]. On July 4, 2015, the State Council issued the "Guidance on actively promoting the 'Internet+' action." According to the Guidance, the "Internet+" is "the deep integration of Internet innovations with all areas of the economy and society. As the infrastructure and innovation factor, the "Internet+" is instrumental in promoting technological progress, efficiency improvement, and organizational change, enhancing the innovation and productivity of the real economy. This also indicates that "Internet+" has been incorporated into national strategy and will become an important form of social innovation and development in the future [2]. The profound influence of modern information technology represented by the Internet on all aspects of education is also being gradually reflected. The "Internet + education" is not a simple addition of the two but a kind of change and innovation, using information technology and the Internet platform to integrate the Internet with education in depth so that the Internet thinking really penetrates the teaching design, teaching content, teaching evaluation, and other aspects of the teaching process, resulting in new teaching forms and models. In this environment, the reform of the teaching mode of business English courses in colleges and universities is in urgent need of strengthening the integration with information technology to co-construct and share high-quality and effective educational resources [3].

The new industry of "Internet + traditional industry" provides new thinking and new opportunities for the innovative development of the education industry. With the development of wireless networks and smart terminals, multimodal communication methods, mainly pictures, text, audio, and video, are gradually replacing one-dimensional text and rapidly becoming the mainstream form of information transmission in education and communication activities. In multimodal information, language text and other hypertext social symbols such as images and videos jointly construct meaning and spread in real time through the

emerging mobile Internet media, greatly compensating for the disadvantages of traditional paper media, which are static and monotonous.

Business English, as an interdisciplinary cross-emerging major integrating business knowledge and skills and English language ability, still suffers from development problems such as lack of unified teaching objectives, weak teachers, lagging teaching methods, and single evaluation methods at this stage [4]. Therefore, starting from the four main elements of the teaching mode and using Internet thinking for the organic optimization and allocation of multimodal teaching resources, this paper focuses on analyzing how business English teaching can be multimodally innovated and updated at the level of environment, task, learner, and guide to promote the informational development of business English professional construction.

2. The Main Problems in Traditional Business English Teaching

With the development of global economic integration, the demand for business English professionals in China has been rising, especially the demand for talents with high quality, solid language foundation, and business knowledge. Therefore, many colleges and universities, especially those undergraduate colleges and universities in transition, have opened business English majors one after another [5]. However, due to the strong practicality and interdisciplinarity of business English, the traditional teaching mode in ordinary colleges and universities can no longer meet the requirements of society for business English talents, and its drawbacks are becoming more and more obvious. The shortcomings of the teaching mode are becoming more and more obvious.

2.1. The Curriculum Lacks Modernity. At present, the core courses of business English majors in colleges and universities are mainly set around traditional international trade activities, such as foreign trade correspondence, international marketing, business negotiation, and so on. However, with the vigorous development of information technology, the economic form has long been not only limited to a certain mode, such as the increasing growth of cross-border e-commerce with B2B and B2C as the main mode [6], which highlights the huge gap in the demand for related talents. But the corresponding business English talents in colleges and universities cannot really dovetail with each other, and the professional curriculum is obviously not forward-looking enough, without closely linking the business activities in the Internet era with the related teaching, and the related courses are very insufficient or even blank.

2.2. Lack of Practicality of Teaching Contents. Business English itself is a special-purpose English, and its practical teaching purpose is different from that of traditional English majors. However, due to the limitation of the speed of updating the teaching materials, when teachers teach business English courses, most of the teaching of professional business knowledge stays at the level of books, and it is difficult to combine the new terms, new terminology, or new business environment that emerge rapidly nowadays. As a result, when students graduate, as long as they work in related industries, they will obviously feel that their professional knowledge is lacking, or their professional background is incompatible with the employment environment, and the gap is obvious [7]. This makes the profession, which should have strong practical value, lack real practicality, and thus face an awkward situation in the job market.

2.3. Lack of Diversity in Teaching Methods. In today's rapid development of information technology, the application of multimedia technology and the Internet are both very common. And diversified teaching modes are also inseparable from these. However, in business English teaching, the teaching methods in many colleges and universities are still very single, and most of them still follow the teaching mode of English majors; the teacher is still the main body in the classroom; most of the time the teacher teaches the knowledge points; the students learn more passively; there are few or no links of teacher-student interaction and student-student interaction; and there are few courses that allow students to really participate in practical operations effectively [8]. The teaching process is heavy on theory indoctrination and light on practical operation phenomenon abounds. If students do not have timely and complete practical training, it is difficult for them to apply what they have learned in the future, which is very unfavorable to the cultivation of high-quality and application-oriented business English talents.

2.4. Lack of Professionalism in Teachers' Background. In colleges and universities, business English is a young and emerging major compared with other majors, but many teachers are purely English education majors who are not very familiar with business practice, or even if they have studied related professional knowledge, most of them only stay at the level of books, lacking practical experience and social practice ability itself. As a result, they cannot really integrate business ideas and practical methods into teaching and cannot fully realize the cultivation of students' core competence and professionalism. In Business English, English is only a tool, and business knowledge is the pillar. If the teacher's knowledge framework focuses on language rather than business or if the teacher accumulates personal corpus during teaching but does not share relevant professional knowledge in time, the knowledge structure is old and not up-to-date [9] and lacks professionalism he or she should have or he or she will not be able to meet the training needs of business English talents. Therefore, in order to evaluate the relationship between the number of business English courses and the teaching effect of business thinking and practical methods, the researchers obtained the internal relationship between the number of business English classes and business thinking through the statistical data of many colleges and universities. The mathematical relationship is as

follows. Figure 1 shows the relationship between the quality of business English talents, business knowledge, and pure English teaching. As can be seen from the figure, in addition to the English language itself, business knowledge plays an important role in the quality of business English talents.

$$N = \sum_{i=1}^{n} n_i,$$
$$E_n = \sum_{m=0}^{N-1} x_n^2(m), \quad (1)$$
$$M_n = \sum_{m=0}^{N-1} \left| x_n(m) \right|,$$

where N is the number of business English courses, E_n is the teaching effect of business ideas and practical methods, and M_n is the teaching effect of pure English education.

3. Feasibility of "Wireless Network + Business English" Teaching Mode

3.1. Opportunity of "Internet+" for Teaching. The Internet has the largest amount of information and resources in the world today, and these huge amounts of information are interconnected in an intricate form, and the direct or indirect resources that can be served and shared for teaching are inexhaustible. The Internet supported by big data also makes information collection more convenient for each learner, making mobile devices the carriers of virtual communities and virtual classrooms. In other words, in the context of "Internet+," the teaching mode is different from the traditional form, and the forms, channels, and media for teaching and learning have become more diversified and diverse. They can cut and reconstruct the knowledge system independently, and if they are truly integrated with the business English teaching process, they will make teaching more vivid, effective, and relevant, thus showing the humanity of teaching.

3.2. The Fit between Business English Teaching and Wireless Network. In the era of "Internet+," the traditional education model of one school, one teacher, and one classroom is fading; a wireless network and one mobile terminal, millions of students, schools, and teachers of your choice are emerging as the new education model, which is the charm of "Internet + education" [10]. The nature of the business English major determines that it is by no means only a simple language teaching but with the help of teaching English language knowledge to develop students' intercultural business communication skills. This major requires a high level of practical ability, and the teaching of business English must be combined with information technology, which is in line with the background and diversity of the "Internet+" era. Therefore, it is feasible and inevitable to rely on network information, deeply integrate various high-quality teaching resources, and explore the construction of the "Internet + business English" teaching mode.

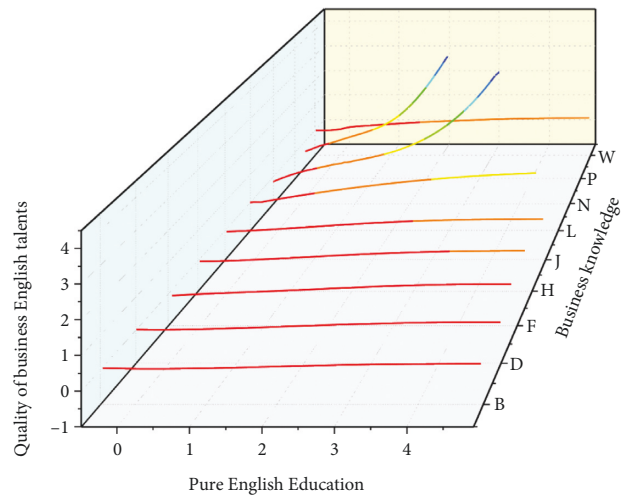

Figure 1: The relationship between the quality of business English talents, business knowledge, and pure English teaching.

4. The Construction of Multimodal Interactive Teaching Model of Business English

4.1. Analysis of Multimodal Interaction. Norris, a famous linguist, believes that multimodal interaction is universal [11]. Communication interaction forms social action through the mediation of various modalities. Norris points out that in communicative interaction, verbal and nonverbal modalities have different interactive effects depending on the context of interaction, and verbal modalities do not play a dominant role in all interactions. The choice of modality use needs to take into account the differences in communicative contexts. In addition, multimodal interaction should take into account the degree of interactional awareness and attention of the communicative subject and the participant and pay active attention to the feelings, thoughts, and feedback of the communicative subject and the participant and informed unity. Modal density and modal configuration are the key elements of multimodal interaction research. Modal density and modal intensity are proportional to each other, and the higher the modal intensity, the higher the modal density. Modal complexity refers to the number of modalities used in the construction of the action; the greater the number, the greater the modal complexity.

4.2. Multimodal Interactive Teaching Model. "Multimodality" refers to the inclusion of different symbolic modalities in a finished communication product or communication activity [12], as well as the various ways in which different symbolic resources are mobilized to construct meaning in a given text [13]. In the early twenty-first century, Stein proposed a multimodal pedagogy, which argues that course instruction and assessment should be centered on the modal characteristics of the learning environment centered on the development of all communicative activities in the classroom as multimodal [14]. As a pedagogical concept, multimodal teaching means that under the guidance of multimodal theory, teachers use a variety of teaching tools and diverse teaching channels, such as the

Internet, pictures, videos, and role-plays, to activate and engage learners' various senses, synergize, and construct them into the most effective way of meaningful expression and communication.

In the process of multimodal interactive teaching, learners' multiple abilities are stimulated and highlighted. The role of the teacher changes from "preaching, teaching, and solving" [15] to that of a collaborator, modality selector, and perceptual stimulator of students' learning, while the students perceive, decode, and store the multimodal input knowledge and then output it to form a positive interaction with the teacher and learners, thus realizing the deep transformation and internalization of knowledge. In business English teaching, teachers can make full use of the multimodal system to design teaching sessions, accumulate and build a multimodal corpus and curriculum resources with the help of multiple learning platforms on the Internet, activate students' sensory potential to the maximum extent, and provide a multimodal interactive teaching and learning environment for teachers and students, so as to collaborate students' multimodal understanding of relevant knowledge and complete their meaning construction [16]. Figure 2 shows the relationship between students' multimodal understanding of relevant knowledge and multimodal corpus, curriculum resources, and multimodal interactive teaching environment. As can be seen from the figure, there is a positive correlation between the three.

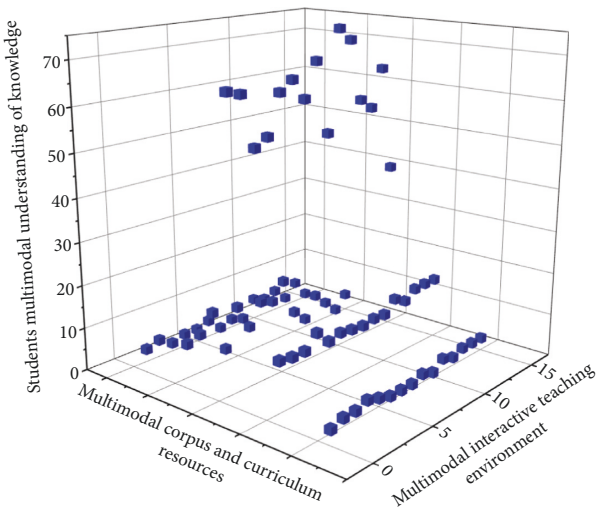

Figure 2: The relationship between students' multimodal understanding of relevant knowledge and multimodal corpus, curriculum resources, and multimodal interactive teaching environment.

4.3. "Wireless Network + Business English" Teaching Mode. In the era of the "Internet+," the openness and sharing of knowledge have brought great changes to the language service industry and new requirements to traditional teaching. However, the integration of the two is not a patchwork that can be achieved overnight. In the teaching of business English, teachers should fully reform and improve the teaching concept, teaching content, and teaching methods, so as to maximize the allocation and optimization of teaching resources and truly realize the effective combination of Internet and business English teaching.

4.3.1. Change of Teaching Concept. Teaching is not only the transmission of knowledge but also the conversion process of learners' internalization of knowledge. Therefore, in business English teaching, teachers should update their teaching concept, deeply understand the essence of business English as special-purpose English, emphasize the cognitive subject role of learners, and practice the teaching concept of "student-centered" [17]. Therefore, teachers should design teaching sessions that meet learners' learning requirements and enhance their practical skills, and let students actively participate in various practical activities, cooperate with each other, and give full play to students' initiative and enthusiasm when teaching according to learners' characteristics and the features of "Internet+." Teachers are transformed into instructors and collaborators of students in constructing knowledge, while students become real participants and constructors of learning.

4.3.2. Update of Teaching Contents. In the teaching practice of "wireless network + business English," the change of teaching content is the most important. Business English itself is different from general language teaching, so teachers should comply with the requirements of the "Internet+" era and add more real-life corpus as the course content. In the course "Cross-cultural Business Communication" [18], for example, teachers should not only introduce basic business etiquette and cross-cultural knowledge but also add real cases of cross-cultural business communication through online platforms or shared corpora, select typical cases of successful or unsuccessful communication for learners to analyze and dig into, and then let students give feedback on the learning effect to assess the students' construction of new business communication. The students will then give feedback on the learning effect to assess the validity of their new knowledge. In the context of "Internet+," there is a constant flow of resources shared on relevant online platforms. Therefore, the resources provided by teachers (e.g., authentic business texts) do not necessarily have to be in one form but can be multimodal, such as videos, images, text, or a combination of both or all three.

Multimodal interactive teaching models emphasize multiple inputs, and business activities are evolving rapidly. While "Internet+" provides teachers with diversified teaching resources, teachers should also, according to the latest development in business communication, make use of the advantages of multimedia, effectively select the best and most practical cases, actively establish a dynamic network resource database, update the data content at any time, and improve the authenticity and timeliness of teaching content. The data content is updated at any time to enhance the authenticity and

timeliness of teaching content and improve students' learning ability. The number of dynamic network resource databases is closely related to the diversification of teaching materials and business teaching cases. Through the statistical analysis of a large number of network resources and business teaching cases, scholars and experts try to find out the internal relationship between the capacity of teaching resources and students' learning ability. Based on the results of statistical analysis, a correlation between them is obtained. In order to quantitatively evaluate the relationship between the capacity of dynamic network resource base based on diversified teaching resources and students' learning ability, the mathematical expression are as follows:

$$\begin{aligned} D(X,Y) &= \sqrt{\sum_{i=1}^{n}(x_i - y_i)^2}, \\ D^n &= \sum_{i=1}^{j}\sum D\left(X, Y_i^{n-1}\right), \\ \delta^n &= \frac{\left|D^{n-1} - D^n\right|}{D^n}, \end{aligned} \tag{2}$$

where D is the volume of the dynamic network resource library, D^n is the updated data volume of network the resource library, δ^n is students' learning ability based on diversified teaching resources, and X and Y represent diversified teaching resources and business practical cases, respectively.

4.3.3. Breakthrough of Teaching Methods. The multimodal interactive teaching mode of "wireless network + business English" is based on a personalized teaching mode on the one hand and emphasizes the spirit of cooperation on the other hand, that is, while respecting the different learning characteristics and habits of individuals, it can collaborate with each other in learning according to the metacognitive ability of learners so that students can have targeted fragmented knowledge points but also allows them to actively interact, build on their strengths, internalize their knowledge, and acquire the most needed business communication skills.

In the precourse self-study stage, students no longer rely on books to simply prestudy the text content but instead learn the knowledge points in a targeted manner based on the learning applications and system modules provided by the relevant online platforms and multimodal teaching resources [19]. Online teaching methods such as catechism and microlearning allow students to preview the important knowledge and background information of the course by watching videos at any time and any place, according to their own learning habits and pace. Take the "Business Negotiation" course as an example where students can learn the background knowledge and negotiation process of a certain negotiation case first and summarize and analyze it by themselves so that they can discuss it in class. At this stage, "Internet+" teaching allows students to learn any knowledge point repeatedly without the limitation of time, place, and number of students, which breaks the traditional teaching method, makes full use of the time before class, and gives new vitality to the multimodal interactive teaching mode. In the classroom stage, the teacher-student relationship is a "two-way interaction" [20]. The role of the teacher has also changed dramatically. In the business English classroom, teachers should abandon the traditional teaching method of knowledge inculcation and carry out a flipped classroom based on the favorable resources of "Internet+" teaching. For example, in the course "Business English Translation," teachers can design a complete and clear teaching task, give a specific translation task online, and ask students to complete the translation practice in a project-oriented way. In this process, students can collaborate and discuss with each other in groups, while the teacher provides personalized guidance, observes and judges the teaching progress, and dynamically grasps the students' learning situation. The teacher is a facilitator and supervisor of student learning. In the flipped classroom, students complete the output of language knowledge and the internalization of business knowledge through the practice of real tasks or projects.

In the practical stage of teaching, we can strengthen the cooperation between schools and enterprises by means of "innovation and entrepreneurship" competitions, participation in projects, or internship in enterprises so that students can experience the foreign business process directly and effectively comprehend what they have learned in class so that they can apply what they have learned. For example, under the trend of "Internet+," the rise of cross-border e-commerce has completely overturned the traditional form of business transactions. To make students understand B2B and B2C business knowledge [21], teachers can use real cross-border e-commerce network platforms, such as sales, Amazon, eBay, or online virtual trading systems so that students can do practical work and find real problems. Teachers can realize teacher-student interaction online, help students solve problems in time, realize students' various business communication skills, and meet the urgent demand for high-quality applied business English talents in the "Internet+" era. In the business English talent market, it is often necessary to calculate the number of morning English talents to be accommodated according to the development of e-commerce platforms. The following formula can be used to evaluate the demand for business English talents on different e-commerce network platforms. And taking three cross-border e-commerce network platforms (Selling, Amazon, and eBay) as an example, Figure 3 shows the histogram of the proportion of business English talents in different cross-border e-commerce network platforms in different periods.

$$\begin{aligned} X &= \{X_1, X_2, \ldots, X_m\}, \\ X_i &= \{X_1, X_2, \ldots, X_n\}, \end{aligned} \tag{3}$$

where X is the demand for a cross-border e-commerce network platform for business English talents and X_i is the

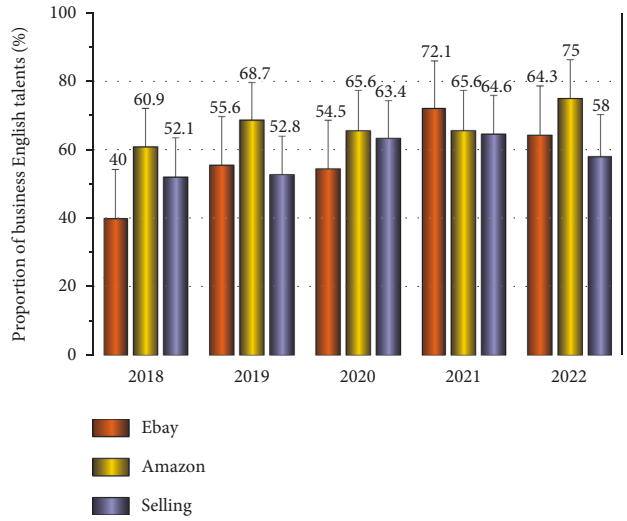

Figure 3: Histogram of the proportion of business English talents in different cross-border e-commerce network platforms in different periods.

demand for an e-commerce network platform for business English talents.

5. "Internet+" Multimodal Interactive Innovation from Four Elements of Teaching

5.1. Wireless Network + Environment: The Setting and Optimization of O2O Multisituational Classroom. The nature of the teaching environment is the decisive factor in the richness and density of teaching action modality. In the traditional business English teaching process, the environment mainly refers to the teaching classroom, where all teaching activities basically take place. The modalities used to construct interactive meanings in traditional classrooms are mainly visual modalities based on teacher-book-textbook and auditory modalities based on teacher lecture-student response. Students answer questions in a single form and limited content, and easy to form the inertia of students' participation motivation is not high, resulting in low teaching efficiency. The O2O (online-to-offline) business model in the new "Internet + economy" [22] has given profound inspiration to the education industry, thus giving rise to the emerging teaching model of the flipped classroom. The flipped classroom is a new form of "Internet + classroom" classroom, which greatly enriches the types of modalities and increases the complexity and intensity of modalities by adjusting the ratio of the number of modalities, thus enhancing the density of modalities and the construction of meaning in multimodal interactive behaviors.

With the development and popularity of smartphones and mobile networks, learners can download multimodal learning materials and conduct learning activities anytime and anywhere. Therefore, in the long run, schools need to consider updating the classroom format, including seat design and multimedia hardware equipment, to support and ensure the smooth implementation of the flipped classroom. The typical flipped classroom does not highlight the practical nature of business English teaching, so it needs to be contextualized and optimized. At present, many universities already have business English practice courses, but they are basically separate from the relevant theory courses, which is not conducive to the comprehensive development of theory and practice. The business English flipped classroom can be optimized from online and offline to form a new form of O2O classroom (as shown in Figure 4).

In addition to various user-based learning platforms, the online environment can also be increased to varying degrees by adding a high-simulation model with a scene layout as the foreground.

In addition to various user-based learning platforms, the online environment can also be enhanced to varying degrees with a high level of simulation modeling training platform that foregrounds the layout of scenes and various new media platforms that attract the attention of communicative subjects, such as WeChat, Weibo, QQ, and Blue Ink Cloud Class. The offline environment can be composed of multiple scenarios such as activity classrooms, practical training bases, and public markets. The activity classroom can be used for business activities such as negotiation, forum, and seminar; the practical training base jointly organized by the school and enterprises can be used for realistic business training, such as entering the simultaneous interpretation box for business translation courses to feel the real atmosphere, which can help mobilize the real emotions of the learning subjects for experiential teaching; the public market includes banks, courts, science and technology parks, ports, and other real communication places related to business English communication situations. The public market includes banks, courts, science and technology parks, ports, and other real communicative places related to business English communication situations, which can be used to conduct situational multimodal tasks such as field surveys, industry research, and sample interviews. Learners improve their ability to solve practical problems through the flipped mode of online simulation and offline field restoration of Business English O2O classroom, which first trains virtually and then operates realistically and helps colleges and universities cultivate composite business English talents who meet market demand [23].

5.2. Wireless Network + Tasks: Design and Use of Multimodal Tasks for Stereoscopic Teaching Materials. The task is the interface between learners and the guide, and it is the medium for learners to reflect on their learning ability and the guide to check the teaching situation, which can be divided into two parts: classroom materials and after-class tasks (as shown in Figure 5).

On the one hand, the multimodal innovation of the new three-dimensional business English teaching materials is carried out. The new three-dimensional textbook responds to the learning characteristics of today's learners of "multiple information, communicative images, and short attention span" and realizes the real-time connection between paper

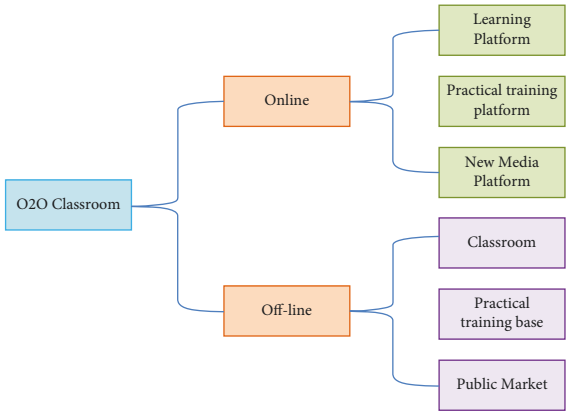

Figure 4: "Wireless network + environment": O2O new form of the classroom.

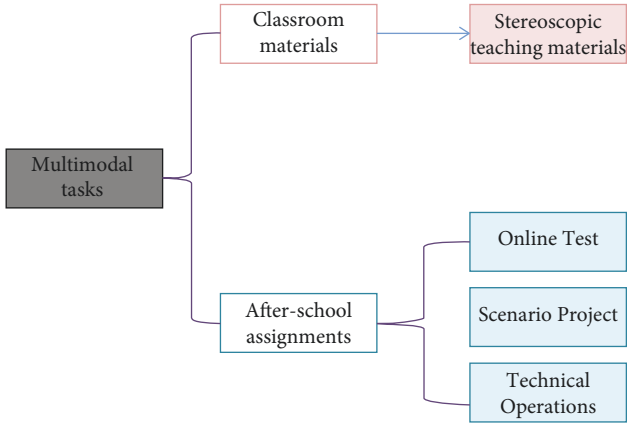

Figure 5: "Wireless network + tasks": three-dimensional multimodal tasks.

textbooks and digital resources through QR code links, forming a new three-dimensional textbook of "paper book + digital course + tablet version of the digital textbook." The new form of teaching material is three-dimensional and diverse. The use of new stereoscopic high-modal density and multimodal structured teaching materials that are based on the representational modality of print and supplemented by nonrepresentational modalities such as sound, video, and scene layout can increase students' attention as interactive communicators, stimulate their sense of active participation, and realize language and business learning in multimodal interactive communication, which will greatly enhance the contextualized experience of learning and lasting and profound learning effects.

On the other hand, the multimodal after-school tasks that accompany the three-dimensional teaching materials should also be designed in an integrated way. The multimodal after-school tasks in the "Internet+" mode can be divided into three forms: online tests, scenario-based projects, and technical assignments [24].

The online test refers to the digital input of traditional homework based on multiple choices, judgments, links, and short answers to questions, which is distributed to learners for practice on the learning platform or online push in the form of regular open test. Some of the objective questions in the digital online test can be reviewed and corrected in real time, which improves the interest and effectiveness of traditional practice.

Scenario-based projects are scenario-based integrated assignments implemented in specific real-life situations, such as market research, street interviews, and so on. The coordinated use of mobile Internet allows for real-time follow-up of project progress, tracking of respondents for dynamic feedback, and remote assignments from anywhere and anytime, enhancing the possibility and operability of scenario-based project implementation.

More novel is technical homework, which requires learners to have a high level of overall ability. It refers to learners' electronic presentation of learning results through the use of modern information technology, including short video production such as microfilm, PowerPoint presentation, business platform project development, and online store operation, as well as other multimodal tasks integrating business skills and information technology. In the field of e-commerce, business platform companies and customers often need to collect business platform projects to measure the learning effectiveness of information technology. Therefore, in order to quantitatively describe the relationship between e-display of learning results and project development of the business platform, the mathematical equation is as follows. Figure 6 shows the popularity of modern information technology on different e-commerce platforms. Technology assignments can also be used as an alternative to traditional assignments. For example, traditional unimodal paper assignments on business translation can be presented in the form of multimodal videos to increase the interest in the learning process and learners' sense of accomplishment. In addition, online tests, situational projects, and technical assignments can be personalized through new forms of teaching materials, and popular breakthrough models can be used to stimulate learners' enthusiasm for active learning.

$$\sigma(x) = \frac{1}{1 + e^{-x}},$$

$$\mathrm{RE}(x) = \max(0, x), \tag{4}$$

$$D = \frac{1}{a\sigma(x) + b},$$

where D represents an electronic display of learning achievements by modern information technology, x represents business platform project development, RE is the multimodal tasks, $\sigma(x)$ represents technical operation, and a and b are the relative parameters.

5.3. Wireless Network + Learners: Combining and Communicating with Diverse Categories of Students. Learners are the subject and the center of this communicative and interactive behavior of teaching activities, and they are the guide, the task, and the object of environmental services in the teaching process, and their learning and practice results are the only

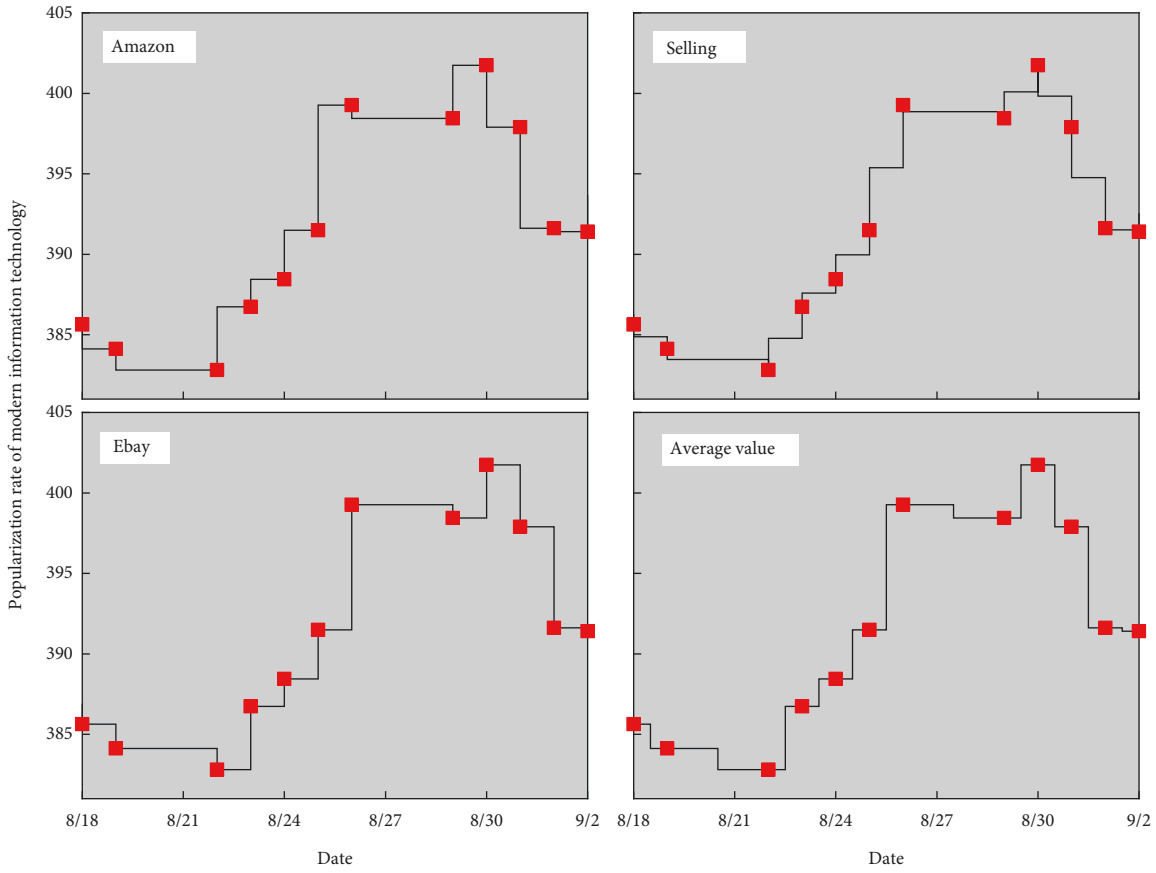

Figure 6: The popularity of modern information technology on different e-commerce platforms.

criteria to test the success of teaching activities [25]. Therefore, the multimodal interaction innovation of business English teaching should focus on the main role of learners, give full play to humanistic thinking, divide different types of learners according to their own and acquired learning characteristics, and selectively optimize the combination of learner groups according to different learning needs and teaching modes to achieve better learning interaction. According to the learners' innate environment, they can be divided into Chinese learners who are native Chinese speakers and foreign learners who are native English speakers or other foreign languages; according to the learners' habitual communication mode, they can be divided into traditional learners who are dominated by teachers' lectures and independent learners who are dominated by multichannel personalized learning resources; according to the learners' learning habits, they can be divided into unimodal learners who are text-based and multimodal learners who are dominated by pictures and videos. According to the learners' learning habits, they can be divided into text-based unimodal learners and picture-video-based multimodal learners; according to the learners' social status, they can be divided into student learners and social learners; according to the learners' geographical location, they can also be divided into learners from our school, learners from neighboring schools, learners from outside the province, learners from abroad, and so on (as shown in Figure 7). In teaching practice, if we can distinguish

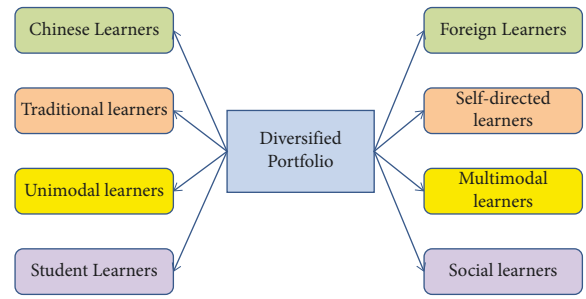

Figure 7: "Wireless network + learners": Diverse student combinations.

different combinations of learners according to different classroom modules and teach them according to their needs, the teaching effect will have a great breakthrough.

In a multimodal and innovative business English teaching interaction, different types of learners can be combined according to different course requirements. For example, in an offline intercultural classroom, a combination of foreign and Chinese students with different cultural backgrounds can lead to more authentic and effective results in both classroom discussions and group role-playing experiences. High-intensity modalities such as language, posture, and eyes that are highlighted in the classroom can be amplified and used more frequently, and the modal

density and complexity of the classroom will be increased to deepen students' impressions. The "wireless network + learners" model can break through the geographical boundaries of learners, enabling more off-campus, off-province, foreign, and social learners to share learning resources with our learners and interact with business English in multiple modalities. Different learner combinations can also prompt hidden frozen actions and contextualized actions to rise to the surface and become mid-scene or even foregrounded actions; for example, classes with foreign learners will highlight hidden cultural differences such as arrival time points and other hidden frozen actions, strengthening the communicative subject's sense of participation and attention.

5.4. Wireless Network + Guide: Configuration and Selection of Multilevel Teachers across Fields. In the new era of "Internet+," the dominant position of the teacher in the traditional sense gradually diminishes and then retreats as the guide of teaching activities. As the guide of teaching activities, the allocation and selection of teachers has a pivotal role in the curriculum. Business English is an interdisciplinary subject, and its professional nature requires that teachers should be equipped with cross-disciplinary and dual-teacher talents. Generally speaking, business English teachers should have "good ideological quality, teaching ability (including the ability to organize teaching, use teaching methods and implement teaching evaluation), and professional knowledge (English language skills + business knowledge)." In addition, the new era of "Internet+" also requires business English teachers to pay more attention to the use of new media and other online platforms to search for relevant real-time materials for business teaching in terms of teaching ability and to highlight the application of business practical knowledge and skills in terms of professional knowledge.

At present, teachers of business English in local universities are generally divided into four types as follows:

(1) Full-time teachers majoring in English linguistics and literature who serve after further study of relevant business courses

(2) Full-time teachers majoring in commerce and business with better English

(3) Part-time teachers who are elites from relevant enterprises or industries

(4) A very small number of teachers who have graduated with a master's or doctoral degree in business English

The potential problems of these four types of business English teachers are as follows: first, solid language skills but insufficient business knowledge; second, rich business knowledge but poor language skills; third, proficient business skills but systematic business English theory needs to be improved; and fourth, comprehensive business English skills but lack of practical experience.

It can be seen that there is still a big problem in the construction of business English teachers' teams. As an emerging profession, the number of graduates with a master's degree or above is relatively small, and the possibility of employing teachers with the right profession in all aspects is small. Therefore, in order to ensure the joint development of business, language, and practical skills, the above four types of teachers are needed to form the Business English faculty in stages. For the basic courses in freshman and sophomore years, English majors can be used to teach; for the business courses in junior and senior years, business majors need to be guided by teachers on staff; for the practical courses in senior years, especially during an internship, part-time teachers from outside companies can be used to guide them. The "wireless network + guide" model makes the external part-time teachers of business courses break through the limitation of time and space to a certain extent, from local enterprises to the whole country or even abroad. In addition, the new form of flipped class courses can be divided into modules of a multiteacher distribution system to teach, learn from the strengths of others, really improve the quality and effectiveness of classroom teaching, and realize the school-enterprise linkage and collaborative education.

6. Conclusion

The wireless network-based multimodal teaching mode of business English fragments theoretical knowledge in a multimodal way for students to personalize their learning, realizing teacher-student and student-student interaction and improving learning efficiency. However, the implementation of "Internet+" teaching is constantly challenging and requires continuous improvement so that learners can form the awareness of "Internet+" and actively use the "Internet+" learning. The Internet + learning platform should be used for learning.

Thus, the construction of business English discipline should keep pace with the times by developing "wireless network + environment," " wireless network + task," "wireless network + learner," and the new era model reform of "wireless network + environment," "wireless network + task," "wireless network + learner," and "wireless network + guide," combined with the new era development requirements of the O2O multisituational classroom settings and optimization, three-dimensional teaching materials and multimodal task design and use, the combination and communication of diversified categories of students, cross-field multilevel teacher configuration and selection of multimodal interactive innovation, focusing on teaching activities in the main position of learners in teaching activities, the use of multimodal scenarios to stimulate learners' active emotional factors, and more effective implementation of business English teaching practices. Business English teachers should respond to the needs of the times in terms of teaching philosophy, teaching content, and teaching methods so that students can spontaneously and actively use the "wireless network + business English" teaching mode to engage in learning.

Data Availability

The data set can be accessed upon request.

Conflicts of Interest

The authors declare that they have no conflicts of interest.

References

[1] L. Zhou, F. Li, S. Wu, and M. Zhou, ""School's out, but class's on", the largest online education in the world today: taking China's practical exploration during the COVID-19 epidemic prevention and control as an example," *Best evid chin edu*, vol. 4, no. 2, pp. 501–519, 2020.

[2] H. Aldowah, S. U. Rehman, S. Ghazal, and I. N. Umar, "Internet of Things in higher education: a study on future learning," *Journal of Physics: conference Series*, vol. 892, no. 1, Article ID 012017, 2017.

[3] Q. T. Liu, B. W. Liu, and Y. R. Lin, "The influence of prior knowledge and collaborative online learning environment on students' argumentation in descriptive and theoretical scientific concept," *International Journal of Science Education*, vol. 41, no. 2, pp. 165–187, 2019.

[4] D. J. Shernoff, S. Sinha, D. M. Bressler, and L. Ginsburg, "Assessing teacher education and professional development needs for the implementation of integrated approaches to STEM education," *International Journal of STEM Education*, vol. 4, no. 1, p. 13, 2017.

[5] K. Csizér and G. Tankó, "English majors' self-regulatory control strategy use in academic writing and its relation to L2 motivation," *Applied Linguistics*, vol. 38, no. 3, pp. 386–404, 2017.

[6] X. Wang, J. Xie, and Z. P. Fan, "B2C cross-border E-commerce logistics mode selection considering product returns," *International Journal of Production Research*, vol. 59, no. 13, pp. 3841–3860, 2021.

[7] S. P. Campbell, "Ethics of research in conflict environments," *Journal of Global Security Studies*, vol. 2, no. 1, pp. 89–101, 2017.

[8] N. S. Bidabadi, A. N. Isfahani, A. Rouhollahi, and R. Khalili, "Effective teaching methods in higher education: requirements and barriers," *Journal of advances in medical education & professionalism*, vol. 4, no. 4, p. 170, 2016.

[9] B. P. Pritchard, D. Altarawy, B. Didier, T. D. Gibson, and T. L. Windus, "New basis set exchange: an open, up-to-date resource for the molecular sciences community," *Journal of Chemical Information and Modeling*, vol. 59, no. 11, pp. 4814–4820, 2019.

[10] C. Xue, "Research on the future teacher quality cultivation innovation under the background of" Internet+ education"," *World Scientific Research Journal*, vol. 5, no. 12, pp. 210–214, 2019.

[11] S. Norris, *Analyzing Multimodal Interaction: A Methodological Framework*, Routledge, Oxfordshire, 2004.

[12] Y. Liu, "Research on flipped classroom teaching mode from the pm," *Theory and Practice in Language Studies*, vol. 11, no. 10, pp. 1258–1265, 2021.

[13] I. Literat and N. Kligler-Vilenchik, "Youth collective political expression on social media: the role of affordances and memetic dimensions for voicing political views," *New Media & Society*, vol. 21, no. 9, pp. 1988–2009, 2019.

[14] N. Wang, J. Chen, M. Tai, and J. Zhang, "Blended learning for Chinese university EFL learners: learning environment and learner perceptions," *Computer Assisted Language Learning*, vol. 34, no. 3, pp. 297–323, 2021.

[15] H. Serin, "Perspectives on the teaching of geometry: teaching and learning methods," *Journal of Education and Training*, vol. 5, no. 1, pp. 131–137, 2018.

[16] A. Ali, A. Liem, S. S. Isa, and S. S. Isa, "Investigating meaning-making process in design collaboration activities: designers interaction with objects," *Environment-Behaviour Proceedings Journal*, vol. 5, no. SI3, pp. 109–116, 2020.

[17] H. Serin, "A comparison of teacher-centered and student-centered approaches in educational settings," *International Journal of Social Sciences & Educational Studies*, vol. 5, no. 1, pp. 164–167, 2018.

[18] E. N. Malyuga, A. V. Krouglov, and B. Tomalin, "Linguo-cultural competence as a cornerstone of translators' performance in the domain of intercultural business communication," *XLinguae*, vol. 11, no. 2, pp. 566–582, 2018.

[19] W. Xu and Y. Zhou, "Course video recommendation with multimodal information in online learning platforms: a deep learning framework," *British Journal of Educational Technology*, vol. 51, no. 5, pp. 1734–1747, 2020.

[20] X. Lan and U. Moscardino, "Direct and interactive effects of perceived teacher-student relationship and grit on student wellbeing among stay-behind early adolescents in urban China," *Learning and Individual Differences*, vol. 69, pp. 129–137, 2019.

[21] G. L. Lilien, "The B2B knowledge gap," *International Journal of Research in Marketing*, vol. 33, no. 3, pp. 543–556, 2016.

[22] F. Wang, "Research on marketing mode based on the internet economy," *Financial Engineering and Risk Management*, vol. 4, no. 1, pp. 69–72, 2021.

[23] R. R. Damari, W. P. Rivers, R. D. Brecht, P. Gardner, C. Pulupa, and J. Robinson, "The demand for multilingual human capital in the U.S. Labor market," *Foreign Language Annals*, vol. 50, no. 1, pp. 13–37, 2017.

[24] S. Alyahya and M. Alsayyari, "Towards better c software testing process," *International Journal of Cooperative Information Systems*, vol. 29, no. 01n02, Article ID 2040009, 2020.

[25] C. Dichev and D. Dicheva, "Gamifying education: what is known, what is believed and what remains uncertain: a critical review," *International journal of educational technology in higher education*, vol. 14, no. 1, pp. 1–36, 2017.

Hindawi
Scientific Programming
Volume 2022, Article ID 6829386, 17 pages
https://doi.org/10.1155/2022/6829386

Research Article

Common Structure Mining of 3D Model Assembly Model Based on Frequent Subgraphs

Hu Qiao,[1] Xufan Wang,[1] Zihao Wang,[1] Liang Wang,[1] and Ying Xiang[2]

[1]*School of Mechatronic Engineering, Xi'an Technological University, Xi'an, Shaanxi 710021, China*
[2]*College of Mechanical and Electrical Engineering, Shaanxi University of Science and Technology, Xi'an, Shaanxi 710021, China*

Correspondence should be addressed to Ying Xiang; yingcara@hotmail.com

Received 20 May 2022; Accepted 21 June 2022; Published 19 July 2022

Academic Editor: Lianhui Li

As an important data source of complex product design and manufacturing, 3D assembly model has accumulated a large number of 3D assembly models in various manufacturing industries under the background of widely used digital design technology. In order to make better use of reusable common structure information about 3D assembly model, reduce repetitive labor, and shorten product development cycles, a common structure mining method of 3D assembly models was proposed. Firstly, based on the attribute neighbourhood diagram of individual parts of the 3D assembly model, the information of the assembly feature attributes is maintained and the nonassembly feature attributes are simplified to form an attributed assembly feature neighbourhood diagram; then, based on the assembly relationship between the parts of the 3D assembly model, the attributed assembly feature neighbourhood diagrams of the parts are combined to form a 3D assembly model attribute neighbourhood diagram. Secondly, the common structure of the 3D assembly model is extracted by the frequent subgraph mining algorithm. Finally, a set of fixture models is used to verify the results, which show that this 3D assembly model common structure mining method can accurately and effectively explore the common structure information of the product and has good results.

1. Introduction

With the development of information science and technology, as well as the development of knowledge related to product modelling, CAD model has a qualitative leap in its ability to describe information in terms of connotation or denotation. The human being as an individual has certain three-dimensional characteristics in his or her visual senses in life, thus allowing him or her to perceive the three-dimensional model in life and its surroundings and to obtain more information.

The 3D assembly model contains many structures, functions, attributes, and other reusable information that reflect the design intent. This paper proposes a 3D assembly model common structure mining method with the 3D model as the object, as shown in Figure 1. The common parts of the graphs that are frequently found and meet the reuse requirements, namely, common structures, are then discovered. The study of the common structure discovery and reuse method will provide a reference method for the designers to discover this valuable reuse information in the design and manufacture of products and provide a reference method for the analysis and reuse of 3D assembly models.

The representation of 3D assembly model information requires comprehensive expression of relevant information on 3D assembly model so as to provide information sources for subsequent related excavation and reuse work. Therefore, the representation of 3D assembly model information should include topological structure information that can express the structural resources related to the model, semantic information that can express the name, type and function as parts, and some characteristic information that can express the coordination relationship between parts.

Chakrabarty et al. [1] proposed the hierarchical structure model of 3D assembly model for complex 3D assembly model. Liu et al. [2] specifically divided product attributes, behaviours, and other information into product layer, feature layer, and other layers, and realized the connection

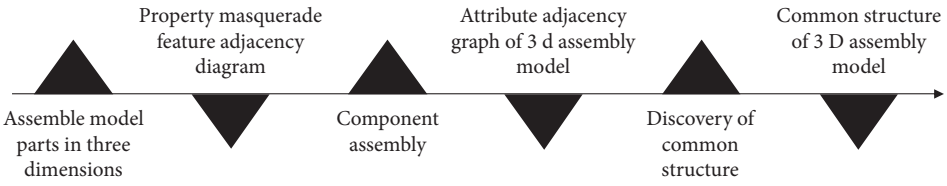

Figure 1: Schematic diagram of common structure method.

relationship between information layers on the basis of the hierarchical model. Based on the representation of hierarchical model, Mou [3] constructed human-machine collaborative quantification of the mutual assembly relations between parts of 3D assembly model so as to be used in assembly sequence planning of 3D assembly model. Li [4] constructed a reuse-oriented hierarchical model, such as the inclusion relationship of structural features and the morphological relationship of features, based on the correlation topological relationship and surface hierarchical division. Yang et al. [5] proposed a two-dimensional descriptor of process information oriented to 3D assembly instruction issuing, used an abstract matrix representation method to represent 3D process information, and established an assembly instruction issuing model.

Graph model representation is mainly composed of nodes and edges based on graph theory. Graph model can be used to describe the connection relation between structure and structure of 3D assembly model. The representation method of graph model is favoured by many scholars and applied in many research fields. Bourjault [6] expressed 3D assembly model based on graph structure. The model is a simple undirected graph, whose nodes correspond to the set of parts in the model, while edges correspond to the set of assembly relations between parts. On the basis of Bourjault's diagram model, Homem de Mello and Sanderson [7] added expressions of relevant functional attributes, thus establishing a graph model representation method of five-dimensional topology. Xiao et al. [8] proposed a single assembly interface 3D assembly model of information retrieval method: first, the preliminary model information retrieval is used, and then information is filtered according to the result of retrieval. Assembly model geometry retrieval can be converted to look for problems with the attribute adjacency graph. Finally, frequent subgraph mining algorithm is used with conjugate subgraph attribute adjacency graph search.

Zuo [9] took brake products as an example. First, the attribute connection graph expression specification is constructed, and then common design units are obtained based on clustering algorithm and frequent subgraph algorithm so as to realize assembly model information mining. Wu [10] took auto parts products as the research object, analysed the common information among products for objects at different levels, pointed out the key points to be dealt with in the reuse process, and proposed a reuse system suitable for products on this basis. Ma [11] expressed the assembly structure of products based on the number diagram of product structure and proposed the module division method of product cluster on the basis of frequent subgraph mining. Zhou et al. [12] proposed a local structure similarity analysis method of 3D assembly model based on subgraph isomorphism and case matching. Firstly, based on the attribute adjacency graph, the assembly relations between parts in 3D assembly model are transformed into corresponding elements in the graph. Secondly, the classification rules and preprocessing rules of the connection relation were defined, and similar 3D assembly model structures were matched based on the correlation algorithm. Han et al. [13] proposed a method to identify key assembly structures in complex mechanical assembly. Firstly, the model was represented by complex network, and then the key assembly functional parts were obtained based on the evaluation model. Finally, the key assembly structures were identified by heuristic algorithm. Wang et al. [14] constructed graphic descriptors to express the geometric and topological information of 3D assembly models and combined clustering algorithm and frequent subgraph mining algorithm to realize the mining of reusable models.

2. Materials and Methods

2.1. Representation of 3D Assembly Model Information. The representation of 3D assembly model information requires comprehensive expression of relevant information of 3D assembly model so as to provide information sources for subsequent related excavation and reuse work. Therefore, the representation of 3D assembly model information should include topological structure information that can express the structural resources related to the model, semantic information that can express the name, type, and function of parts, and some characteristic information that can express the coordination relationship between parts. In the representation of model information, attention should be paid to the accurate and comprehensive representation of model information. Secondly, the constructed method should be as simple, clear, and reasonable as possible, which can be applied to the subsequent related excavation and reuse work.

At present, attribute adjacency graph is used to build model, which has too much structure data and low application efficiency. Or take the whole part in the 3D assembly model as a single node and the connection relation between parts as the edge to construct the model attribute connection graph. Although these models have simple structure, they pay insufficient attention to the geometric shape information of the 3D assembly model itself. Therefore, in order to not only express important assembly information of 3D assembly model, but also improve application efficiency, this paper proposed a 3D assembly model information

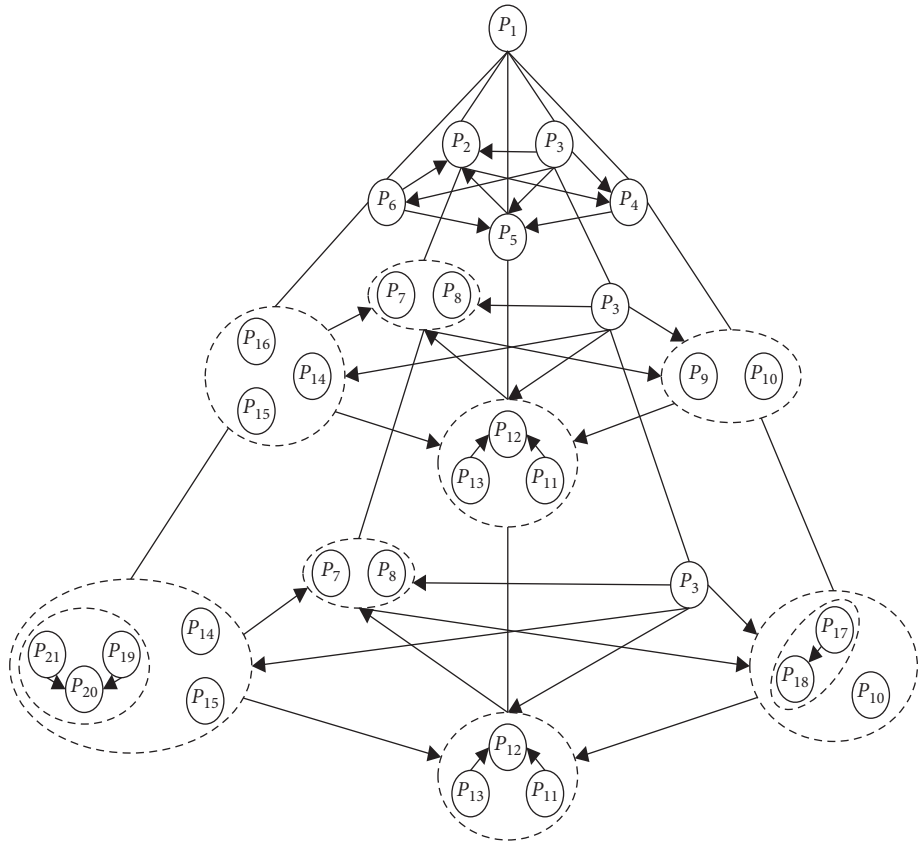

(a)

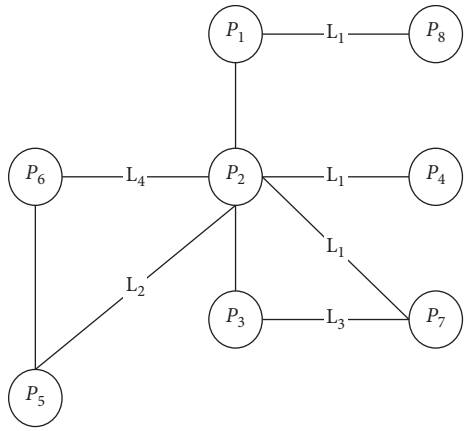

(b)

Figure 2: Continued.

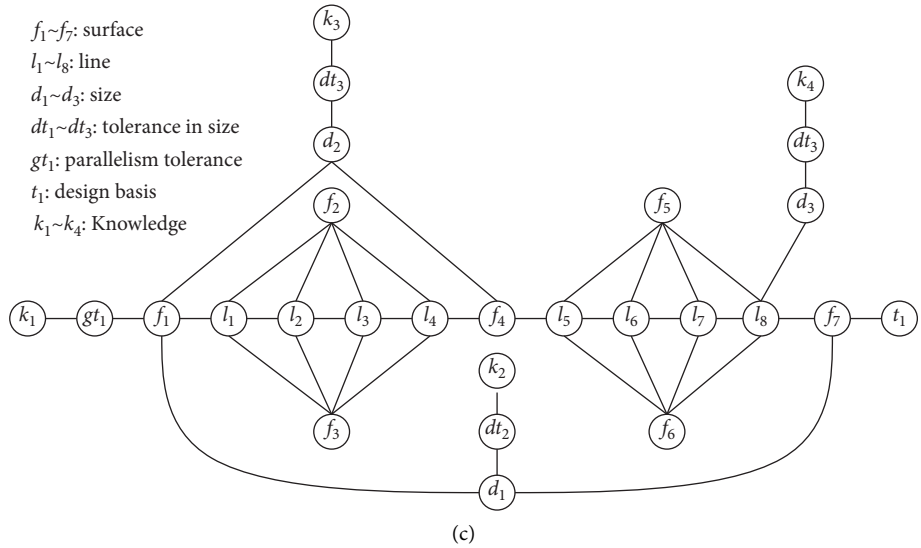

Figure 2: The model represents the sample diagram. (a) Hierarchical directed graphs represent sample graphs. (b) The property connection diagram represents the sample diagram. (c) Hybrid adjacency graphs represent sample graphs.

representation method based on assembly features. Firstly, on the basis of the attribute adjacency graph, the assembly features of each part in the 3D assembly model were retained, the nonassembly features were simplified, and the attribute assembly feature adjacency graph of the parts was constructed. Then, on this basis, the relationship between the parts in the 3D assembly model is analysed, and the assembly scheme is constructed based on this, and then the attribute adjacency graph of the 3D assembly model is established. Based on the above research, an effective way of information representation of 3D assembly model is presented.

2.1.1. The Definition of Attribute Adjacency Graph

Definition 1. Attribute adjacency graph: It is mainly a graph representation model in which the parts surface is the node and the adjacency relationship between the surfaces is the edge, so as $G = \{V, E, \alpha, \beta\}$ to express the topological relationship of the parts, where V represents the set of nodes, and any element v_i in the set meets the corresponding relationship with one side of the part; E represents the set of edges, is the adjacency relation of faces; any element in the set has a corresponding element, mainly including the geometric type of faces, the number of faces, and so on. β represents the set of attributes of an edge, and any element in the set has one element corresponding in E, mainly including the type of the edge and the position of the adjacent surface.

According to the current research, many scholars have proposed a variety of model representation methods. For example, shown in Figure 2(a) is the layered orientation graph model of [15] and shown in Figure 2(c) a mixture of adjacency graph model [16], respectively, the corresponding models of component assembly tolerance level, size, design, design standards, and other information in detail, and solve the problems of the corresponding field, but for the 3D assembly model related to discover. The structure is multifarious, time-consuming, and of low retrieval efficiency and high cost. The attribute connection graph model [17] as shown in Figure 2(b) is simple in form, but it ignores the geometric shape information of the model itself, resulting in low accuracy of excavation results and large differences among models.

To sum up, this paper divides the shape features of the model into assembly features and nonassembly features. Assembly features include assembly information in parts and are used to construct the body shape of parts, which plays a decisive role in the assembly process of 3D assembly models. Nonassembly features are auxiliary features in parts, which are local modifications of part information and play little role in the assembly process of 3D assembly model. In this paper, based on the attribute adjacency graph of 3D model, the assembly feature information in the part model is preserved first, and then the semantic node is used to replace the other information in the model so as to construct the attribute assembly feature adjacency graph of the part. Its definition is as follows.

Definition 2. Property masquerade feature adjacency diagram: It is a graphical representation that focuses on assembly features in part models and is represented by $G = \{V, E, \alpha, \beta, V_0\}$, where V represents the set of nodes, and any element v_i in the set corresponds to one side f_i in the assembly features of parts; E represents the set of edges, in which any element e_j corresponds to the side formed by adjacent surfaces f_n and f_m in the assembly features of parts; and α represents the attribute set of the node, which mainly includes the geometric type of the face and the number of sides of the face. β represents the set of edge attributes, including the type of edge and the position relation of adjacent surfaces. $V_0 = \{I_N, I_F, I_C\}$ represents the semantic node of this part, which is the semantic expression

Table 1: The class encoding of the connection type.

Serial number	Coding	Connection type
1	a	Soldering
2	b	Threaded connection
3	c	Pin seal
4	d	Contact connection
5	e	Other

Table 2: The class encoding of the connection type.

Serial number	Coding	Contact type of mating surface
1	0	Plane-plane contact
2	1	Plane-cylinder contact
3	2	Cylinder-cylinder contact
4	3	Other

of other information except assembly features in this part, including the semantic information of part name (I_N), function (I_F), and category (I_C).

2.1.2. Construction of Attribute Adjacency Graph for 3D Assembly Model. The 3D assembly model is essentially a set of information set, that is, a collection of entities modelled by the designer in 3D space and the representation of their properties. For two parts in a 3D assembly model that are in contact with each other, two types are distinguished: contact connections and assembly connections, by determining whether they have assembly requirements. A contact connection is where two parts are in contact but there is no requirement for assembly. Conversely, where there is a requirement for assembly, the connection is an assembly connection. Secondly, assembly connections can be subdivided into welded, threaded, and pinned connections, depending on how the two parts are connected. In the process of discovering and reusing the common structure of a model, the assembly model requires special attention to the assembly relationships between parts as opposed to the part model. In this paper, the types of connection relation between parts and the contact types of mating surfaces are classified and coded, respectively, and the results are shown in Table 1 and Table 2. For example, the code "b1" means that the connection relation between two parts is "pin connection" and the contact type of the mating surface is "plane-cylinder contact."

Taking the assembly process of the 3D assembly model shown (Figure 3) as an example, the 3D assembly model shown in Figure 3(c) is assembled by part A shown in (Figure 3(a)) and part B shown in (Figure 3(b)), respectively. By searching the assembly features corresponding to the model and related process documents, it can be obtained that the connection relation between parts is "threaded connection," and the contact type of mating surface is "cylinder-cylindrical contact"

Based on the adjacency graph construction steps of attribute make-up features described above, corresponding graph representations are made for part A and part B, respectively. The results are shown in Figure 4(a) and Figure 4(b). The nodes marked with shadows in the graph

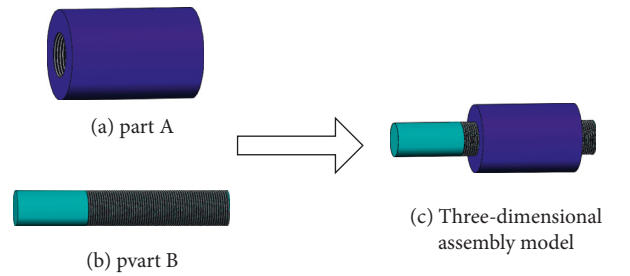

Figure 3: Assembly diagram of 3D assembly model. (a) Part A. (b) Part B. (c) Three-dimensional assembly model.

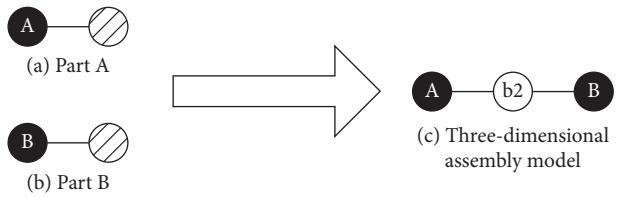

Figure 4: Schematic diagram of attribute adjacency graph construction of 3D assembly model. (a) Part A. (b) Part B. (c) Three-dimensional assembly model.

represent the mating surfaces of the parts. Then, based on the classification and coding specification of the connection relation, the mating surfaces are assembled into a node, which is named as the mating node, that is, the node marked with "B2" ("B" means thread connection; "2" means cylinder-cylindrical contact). Thus, the adjacency graph of model attributes is constructed, and the result is shown in Figure 4(c).

The structure of attribute adjacency graph constructed by this method is more concise, and the graph contains the related information of part name, category, function, and so on. The size of the constructed graph is much smaller than that of the traditional method. Compared with the traditional method, the graph size is too large due to too many parts, and the complexity of the attribute adjacency graph can be reduced to a large extent, and the effect is more obvious.

2.2. Common Structure Mining of 3D Assembly Model Based on Frequent Subgraph. The excavation of the common structure of 3D assembly model is not to discover the assembly model structure with identical structure, process, and function, but to find the model structure with similar structure and different local structure in the corresponding database. In fact, the process of discovering common structures is to integrate the design experience of similar model structures and accumulate relevant design advantages so as to effectively increase the reuse efficiency of 3D assembly models.

In this paper, simplified structural data information is used as input information to reduce the scale of attribute adjacency graph of 3D assembly model and reduce the complexity of common structure excavation. In addition, the semantic nodes and coordination nodes in the attribute adjacency graph of 3D assembly model are preprocessed to reduce the size of the attribute adjacency graph of 3D

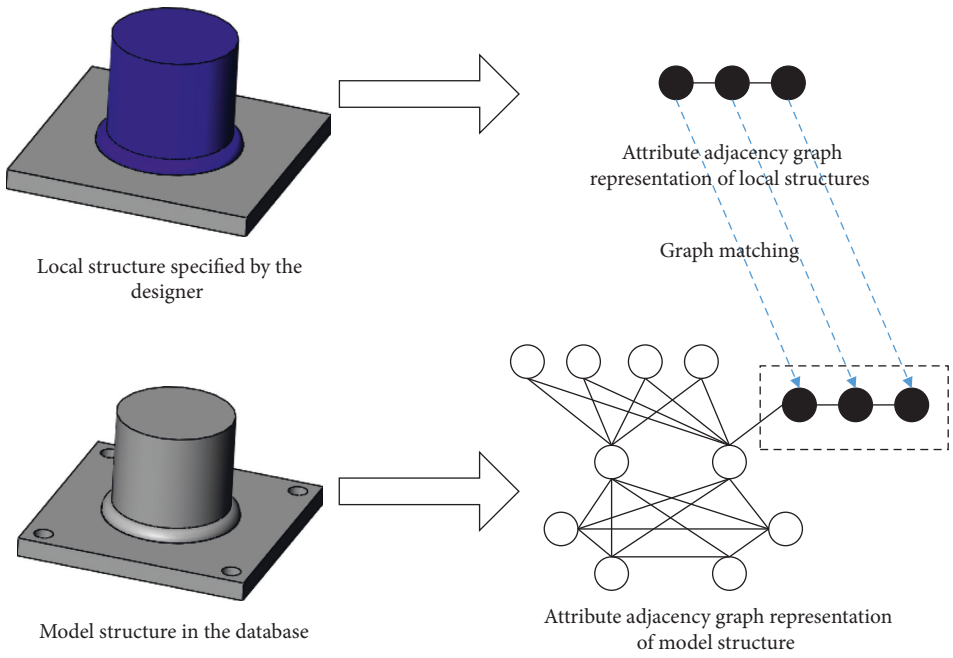

Figure 5: Isomorphism diagram of subgraph.

Table 3: Symbol definitions.

Symbol	Definition
V_0^a	Semantic node of part a
$V_{a,b}$	Mating nodes between parts a and b
Q	A collection of all attribute adjacency graphs
Q_P	All preprocessed Atlas
H^K	Set of K-order candidate frequent subgraphs
R^K	Set of frequent subgraphs of order K
T	Set of all frequent subgraphs, $T = \{R^1, R^2, \ldots, R^m\}$
id	In H^K or R^K, the address number corresponding to the subgraph
F	All vertex properties corresponding to the subgraph
M	The adjacency matrix corresponding to the property adjacency graph
C_{id}	In the construction of $K+1$ candidate subgraph, it is necessary to connect two k-order frequent subgraphs containing the same $K-1$-order frequent subgraph, C_{id} represents the address list of all $K-1$-order frequent subgraphs, and C_{id} is usually obtained when the candidate subgraph is generated
S_{id}	If there is a subgraph isomorphism between a subgraph and a graph in Q, S_{id} is used to store the address number of the graph in Q, and S_{id} is usually obtained when frequent subgraphs are generated

assembly model, which is the first screening of the frequent subgraph mining process, before the common structure is mined through frequent subgraph. Through this process, the matching range is effectively reduced, and the overall mining efficiency is improved.

2.2.1. Related Concepts and Definitions

Definition 3. Graph isomorphism: Given graphs $G_A = (V_A, E_A)$ and $G_B = (V_B, E_B)$, G_A and G_B are isomorphic if there is a mapping between the two graphs $f: V_A \longrightarrow V_B$ and $e_A = (v_A, v_A')$ is an edge in G_A, and if and only if $e_B = (v_B, v_B')$ is an edge in G_B.

Definition 4. Subgraph isomorphism: It is known that figures G_A and $G_B$and G_B' are a subgraph of G_B. If there are isomorphic relationship in G_B' and G_A, the subgraphs G_A and G_B are isomorphic.

The subgraph isomorphism process shown in Figure 5 is the graph isomorphism process of a subgraph of a graph and another graph. The judgment of isomorphism relation between two graphs is essentially the judgment of mapping relation between nodes in the graph, and the mapping relation under node mapping relation also satisfies the corresponding mapping relation. Among them, the left side of the two charts, respectively, as the design requirements of the model structure and database structure, the blue part is the design personnel designated by the local structure (i.e., the subgraph), two figures on the right side are, respectively, corresponding to the attribute adjacency graph, said black nodes mapping relationship of vertices, said two figures of subgraph isomorphism; namely, the dotted line represents the mapping relationship between vertices.

Definition 5. Frequency We know that Atlas $Q = \{q_1, q_2, \ldots, q_n\}$ and q are subgraphs. If q appears in q_i and $i \in n$, that is, q is isomorphic to q_i subgraph, then x_i is 1; otherwise, q is not isomorphic to any subgraph in q_i; then, x_i is 0. Based on formula $\lambda = \sum_{i=1}^{n} x_i/n$, λ is obtained, and λ is frequency ($\sum i = 1_n x_i$ is the sum of the number of graphs with isomorphism).

Definition 6. Frequent subgraph: The minimum frequency $\lambda_{\min}$ is known. If $\lambda_{\min} \le \lambda$ exists, q is called its frequent subgraph in the Atlas Q.

Definition 7. Generic structure: Given a 3D assembly model database, $D = \{d_1, d_2, \ldots, d_n\}$ represents its attribute adjacency graph set, d meets the condition of frequent subgraph and is the frequent subgraph of graph D. In the model database, the relevant structures of 3D assembly model corresponding to D are called common structures.

2.2.2. Discovery of Common Structure. Scholars at home and abroad often use frequent subgraph algorithm to solve common structure mining problems. Apriori algorithm has a strong influence on the mining of frequent subgraphs and is widely used [18–20]. This algorithm is a frequent item set algorithm [21, 22] that excavates and analyses association norms. The generation of frequent item sets mainly goes through the generation of candidate sets and candidate pruning and is solved through layer-by-layer search. In other words, it generates high-order item sets on the basis of low-order item sets. In addition, the generation and testing strategies are used to discover frequent item sets, and pruning operations are carried out according to the related properties of candidate pruning to obtain high-order candidate sets. Finally, the item sets that do not meet the minimum frequency are deleted through frequency judgment so as to generate high-order frequent item sets. Two classical frequent subgraph mining algorithms, AGM algorithm [23] and FSG algorithm [24], are evolved on the basis of Apriori algorithm. AGM algorithm is based on Apriori algorithm, which generates k-order candidate set by adding one node each time. Then, the graph isomorphism is used to judge whether there are identical $k-1$ candidate sets in k-order candidate sets. The algorithm needs to traverse the data set repeatedly. When the graph size increases, the running time of the algorithm will increase and the efficiency of the algorithm will decrease. The FSG algorithm generates k-order candidate sets by adding edges one at a time. In the attribute adjacency graph, there are more edges than nodes, resulting in more candidate sets. In order to optimize the efficiency of the algorithm, the intersection of the TID (Transaction ID) lists of all k-order candidate sets is calculated for frequency counting and candidate pruning. To sum up, this paper takes graph nodes as the object, combines the advantages of the two algorithms and optimization methods such as preprocessing to improve the efficiency of the algorithm, and then achieves the purpose of discovering the common structure of the model.

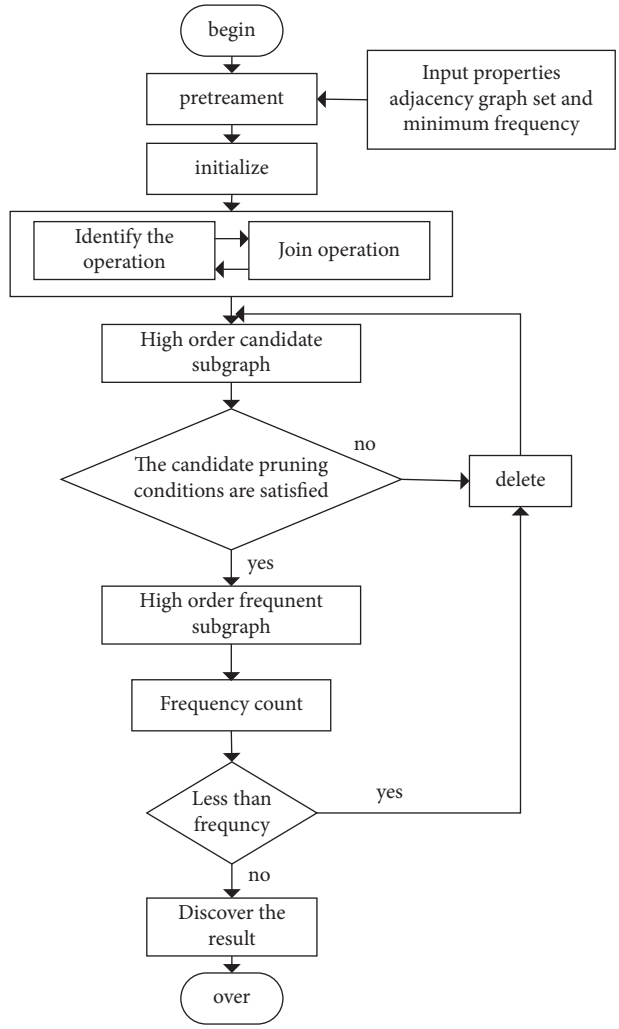

Figure 6: Flowchart of frequent subgraph algorithm.

To facilitate the description of the algorithm, the following symbols and data structures are defined, as shown in Table 3.

The algorithm steps are described as follows:

Step 1. Pretreatment.

Step 2. Initialize the first-order and second-order frequent subgraphs.

Step 3. Connect two K-order frequent subgraphs (including the same low-order frequent subgraphs) to form $K+1$-order candidate subgraphs.

Step 4. Prune the candidate subgraph of order.

Step 5. After $K+1$ candidate subgraph is generated, frequency counting is performed.

Step 6. Find and delete redundant structures in the candidate subgraph set.

Step 7. Cycle until no new frequent subset can be formed.

As can be seen from the above algorithm steps, frequent subgraph algorithm mainly includes preprocessing, initialization, generation of candidate set, candidate pruning,

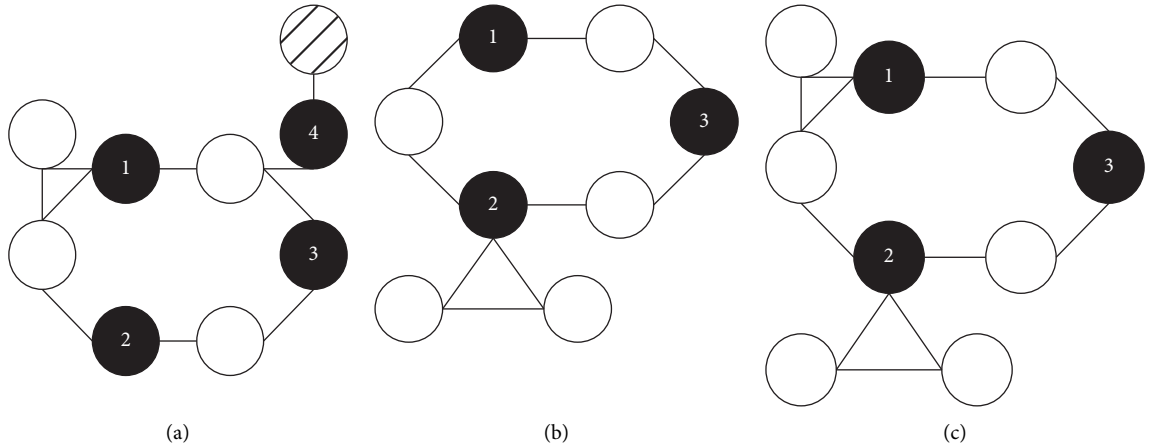

Figure 7: AAG of multi-assembly interface. (a) Property adjacency graph 1. (b) Property adjacency graph 2. (c) Property adjacency graph 3.

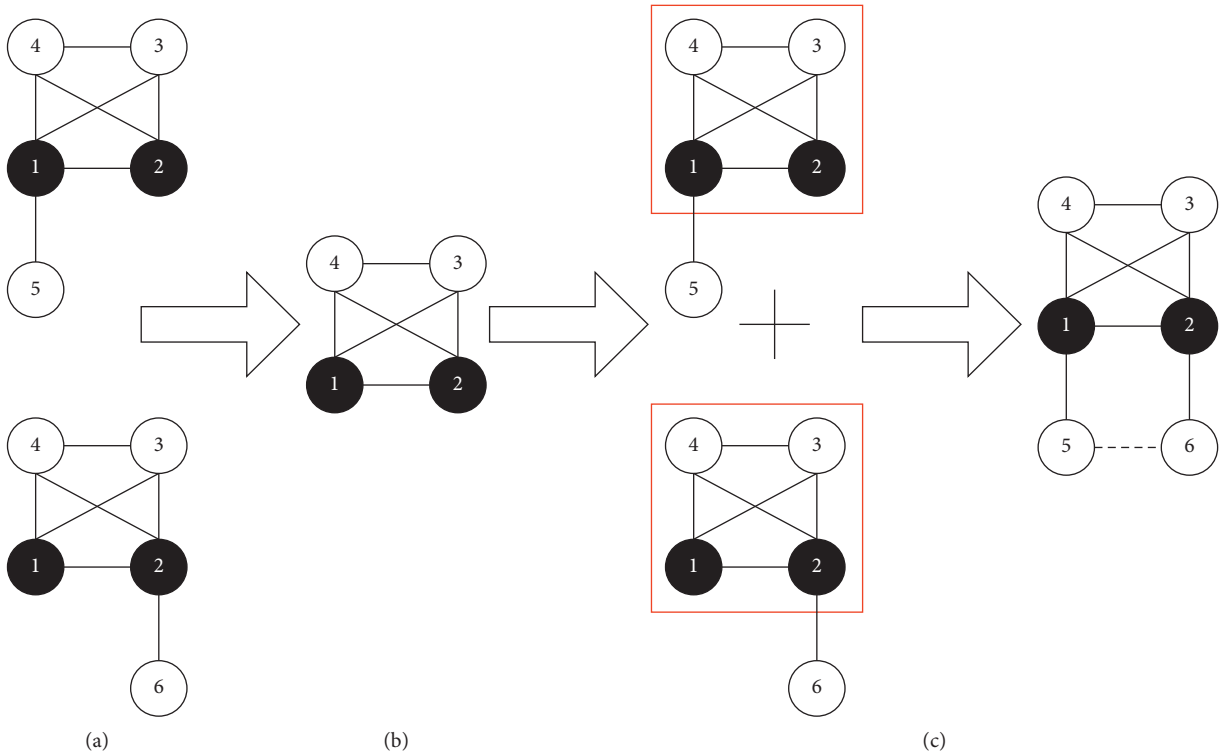

Figure 8: Sample graph of candidate set generation. (a) Property adjacency graph. (b) Subgraph recognition. (c) Subgraph connection.

frequency counting, redundancy screening, and other common structure excavation processes shown in Figure 6, showing the flowchart of the algorithm. Since all elements in the attribute adjacency graph have corresponding attributes, the similarity of corresponding attributes should be judged during excavation. This paper refers to the similarity calculation method of for judgment so as to obtain more accurate excavation results.

(1) Pretreatment. The preprocessing is carried out before frequent subgraph mining, mainly by removing the semantic nodes that appear independently in each attribute adjacency graph of the graph set and the coordination nodes that are only connected with this node. That is, semantic nodes that appear only in one graph and coordination nodes that are only connected to them do not appear in other graphs. The preprocessing process is the preliminary screening of common structure excavation so as to reduce the size of Atlas and the number of matching. The following definitions of semantic node frequency are given in this chapter.

Definition 8. Semantic node frequency: We have $Q = \{q_1, q_2, \ldots, q_n\}$ and V_0^a. If V_0^a occurs in q_j and satisfies $V_0^a \in q_i$, $i \in n$, $j \in n$, $j \neq i$, then l_i is 1; otherwise, l_i is 0. The semantic node frequency ζ is obtained by the formula $\zeta = \sum i = 1_n l_i/n$.

In Figure 7, attribute adjacency graphs corresponding to a group of 3D assembly models are used to demonstrate the

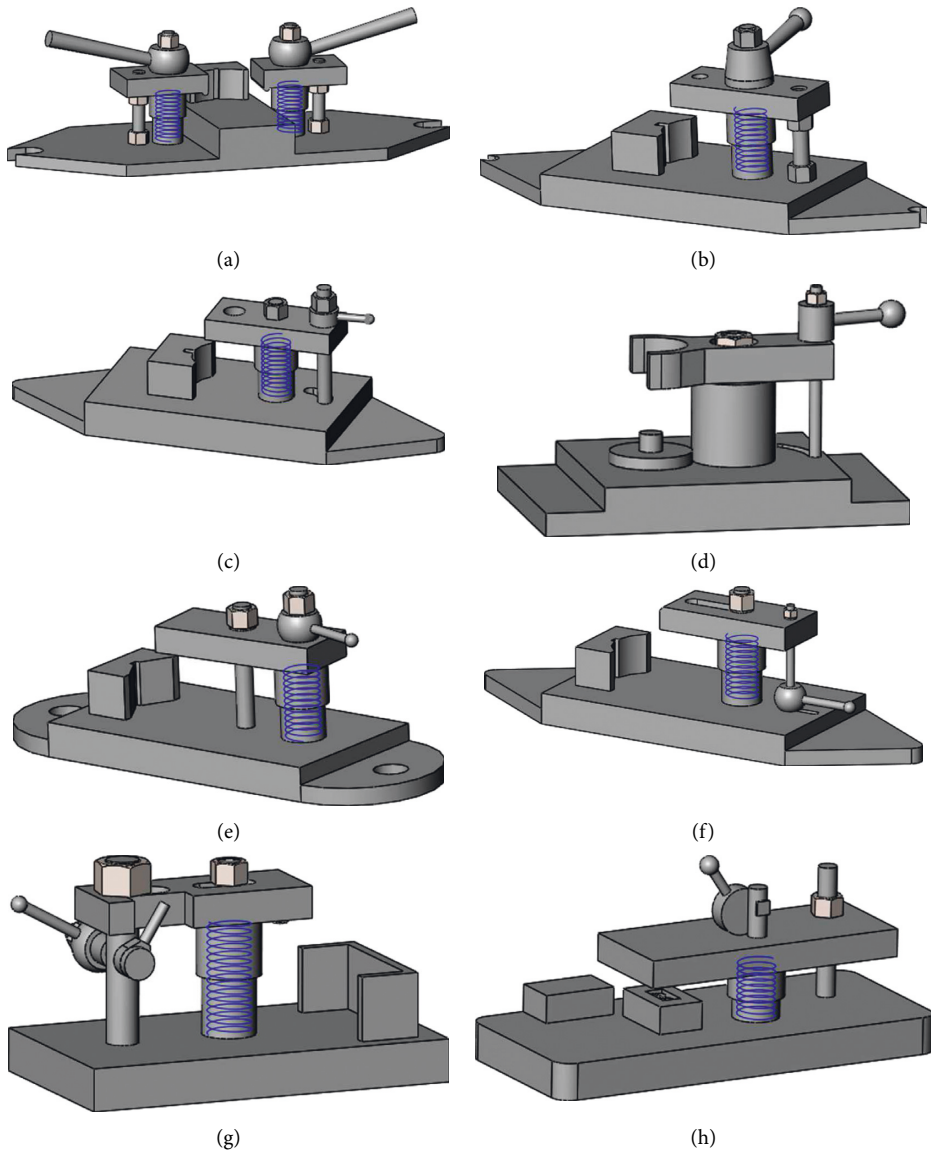

Figure 9: Three-dimensional assembly model of fixture. (a) Tongs 1, (b) tongs 2, (c) tongs 3, (d) tongs 4, (e) tongs 5, (f) tongs 6, (g) tongs 7, and (h) tongs 8.

pretreatment process. Black nodes are semantic nodes, and other nodes are coordination nodes. The preprocessing mainly traverses the adjacency graph of these 3D assembly model attributes. First, the semantic node is traversed. It can be observed from the figure that only the semantic node No. 4 in Figure 7(a) exists independently, and Figure 7(b) and Figure 7(c) do not contain the semantic node, so the semantic node will be deleted during the preprocessing. Then, the coordination nodes connected with the semantic node are judged. If a coordination node is only compatible with the semantic node, the coordination node will also be deleted in the preprocessing process, as shown in Figure 7(a), and the shaded part is the coordination node only connected with the semantic node. Until the traversal of all nodes is completed, the preprocessing process is finished, and the next step is entered.

In summary, the pseudocode describing the steps of the preprocessing Algorithm 1 is as follows.

Although the number of scanning Atlas increases in the pretreatment process, the number of scanning irrelevant nodes can be reduced to a large extent, the scan scale can be reduced, the matching loss can be reduced, and the excavation efficiency can be improved.

(2) Initialize. After preprocessing, the first-order frequent subgraph and second-order frequent subgraph need to be initialized. For the attribute adjacency graph of 3D assembly model, the first-order frequent subgraph can be easily obtained, which corresponds to nodes in the attribute adjacency graph, and connecting any two first-order frequent subgraphs is unique. The second-order frequent subgraph was obtained by traversing the attribute adjacency graph of

Input: Q and $\zeta_{\min}$.
Output: Q_P.
Step 1. Begin
Step 2. $a = 1$, $n = 1$
Step 3. while $q_n \neq \varnothing$ and $q_n \in Q$ do//A graph in a loop Atlas
Step 4. While $V_0^a \neq \varnothing$ and $V_0^a \in q_n$ do//Semantic nodes in a loop graph
Step 5. if $\zeta(V_0^a) < \zeta_{\min}$ then
Step 6. remove V_0^a, $V_{a,b}$ //Remove the relevant nodes whose frequency is less than the threshold
Step 7. end if
Step 8. $a = a + 1$
Step 9. end while
Step 10. $n = n + 1$
Step 11. end while
Step 12. return Q_P //Extract the preprocessed Atlas
Step 13. End

Algorithm 1: Preprocessing algorithm.

the 3D assembly model. In order to facilitate the later acquisition of high-order frequent subgraphs, the *id*, *F*, *M*, C_{id}, and S_{id} other data structures of second-order frequent subgraphs are stored accordingly.

(3) Generation of Candidate Sets. The core idea of candidate set generation is to generate high-order candidate subgraph on the basis of low-order frequent subgraph. That is to generate $K + 1$-order candidate subgraph through K-order frequent subgraph. The generation of candidate set needs to go through two processes: (1) identification, judging whether two K-order frequent subgraphs contain the same $K - 1$-order frequent subgraphs; (2) connection: two K-order frequent subgraphs that meet the recognition conditions are connected to form $K + 1$-order candidate subgraphs.

The first step of candidate set generation is recognition; that is, in the corresponding two K-order frequent subgraphs (large graphs), judge whether the $K - 1$-order frequent subgraphs (small graphs) are the same. If they are the same, the next step can be connected. Otherwise, the connection cannot be made.

The second step in candidate set generation is joining. After identifying two identical small graphs, it is necessary to connect the large graphs containing the small graphs to obtain $K + 1$-order candidate subgraphs. The joining process can be understood as the joining process of adjacency matrix, namely, $(K \times K) + (K \times K) \Rightarrow (K + 1) \times (K + 1)$.

Suppose that the adjacency matrix of two identical small graphs is $\mathbf{M}_{K-1}^0$, then the adjacency matrix of the two large graphs is $\mathbf{M}_K^a$ and $\mathbf{M}_K^b$, respectively, and the matrix form is shown in formulas (1) and (2). Connect the matrices $\mathbf{M}_K^a$ and $\mathbf{M}_K^b$ so as to obtain the corresponding candidate subgraph of $K + 1$ order, and its matrix form is shown in formula (3).

$$\mathbf{M}_{K+1}^a = \begin{bmatrix} \mathbf{M}_{K-1}^0 & a_1 \\ a_1^T & 0 \end{bmatrix}, \tag{1}$$

$$\mathbf{M}_{K+1}^b = \begin{bmatrix} \mathbf{M}_{K-1}^0 & b_1 \\ b_1^T & 0 \end{bmatrix}, \tag{2}$$

$$\mathbf{M}_{K+1}^c = \begin{bmatrix} \mathbf{M}_{K-1}^0 & a_1 & b_1 \\ a_1^T & 0 & c_{K,K+1} \\ b_1^T & c_{K+1,K} & 0 \end{bmatrix}, \tag{3}$$

where a_1 and b_1 represent column vectors of dimension, respectively.

$c_{K,K+1}$ represents the adjacency between a_1 and b_1. When the adjacency of a_1 and b_1 is different, the corresponding value of $c_{K,K+1}$ is also different.

$$c_{K,K+1} = \begin{cases} 1, & \mathrm{a_1 and\ b_1 have\ an\ adjacency,} \\ 0, & \mathrm{there\ is\ no\ adjacency\ between\ a_1 and\ b_1.} \end{cases} \tag{4}$$

The sample graph of candidate set generation is shown in Figure 8. The two attribute adjacency graphs shown in Figure 8(a) are mainly used to carry out corresponding subgraph recognition and connection process. The two attribute adjacency graphs shown in Figure 8(a) are composed of five different vertices, respectively. In order to connect them, the same low-order frequent subgraphs need to be identified first, and the result of subgraph recognition is shown in Figure 8(b). Based on the same low-order frequent subgraph after recognition, the two attribute adjacency graphs (Figure 8(a)) are connected to obtain the high-order candidate subgraph. The process of subgraph connection is shown in Figure 8(c), where the red line box is the same low-order frequent subgraph, and the dotted line is the adjacency relationship between vertices 5 and 6. If there is adjacency relationship between the two, the dotted line is transformed into a solid line. If no adjacency exists, delete the dotted line.

After the subgraph is connected, the generated $K + 1$-order candidate frequent subgraph is compared with the existing graph in R^{K+1}. If there is no such $K + 1$-order candidate frequent subgraph in R^{K+1}, it is added to R^{K+1}, and the low-order frequent subgraph *id* is added to C_{id} of the high-order candidate frequent subgraph C_{id}. Otherwise, the low-order frequent subgraph *id* is only added to C_{id} of the high-order candidate frequent subgraph, and then the repeated data is deleted.

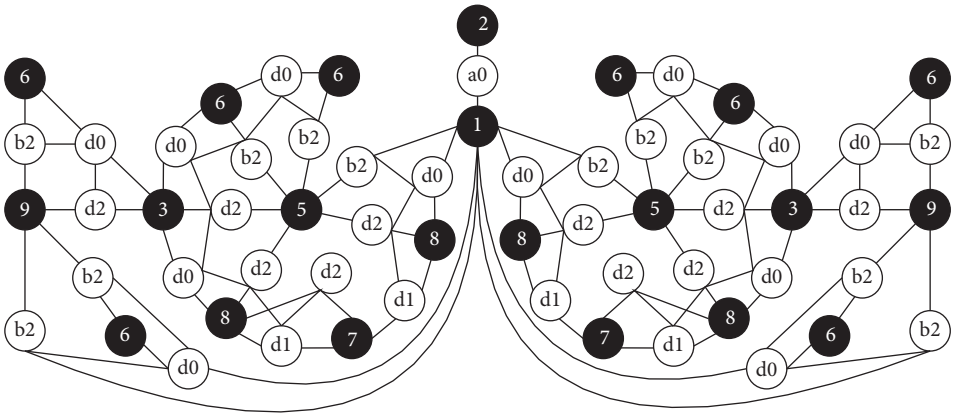

(a)

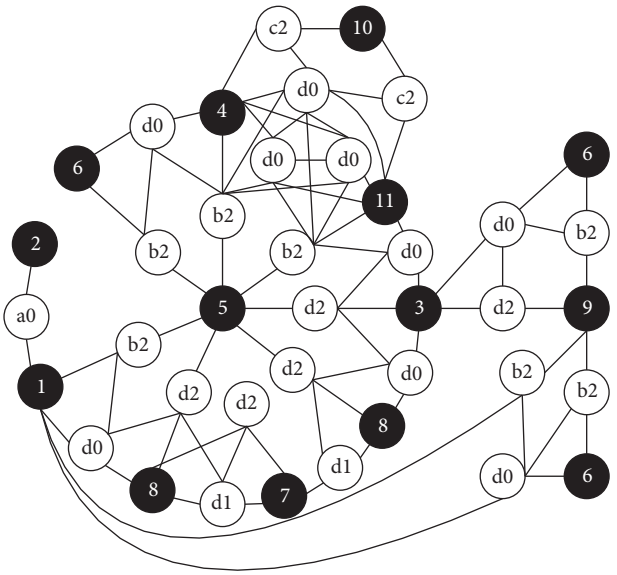

(b)

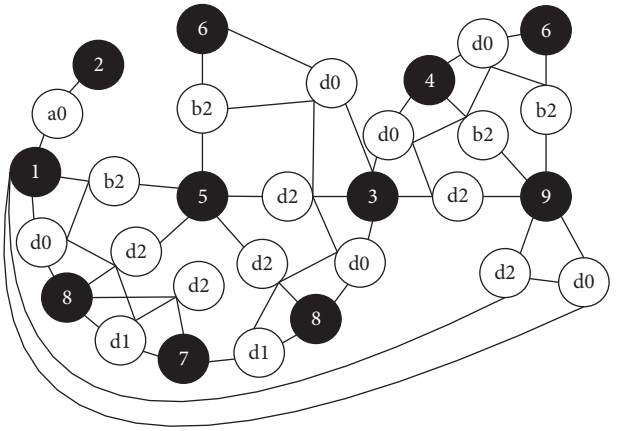

(c)

Figure 10: Continued.

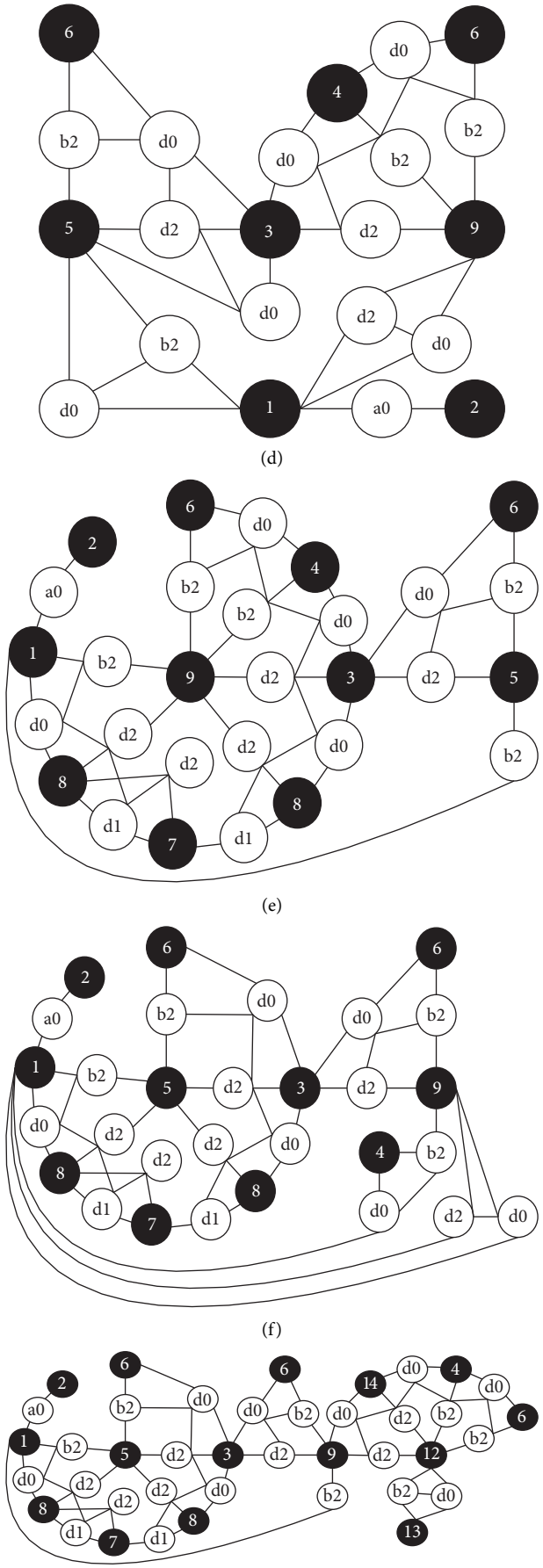

Figure 10: Continued.

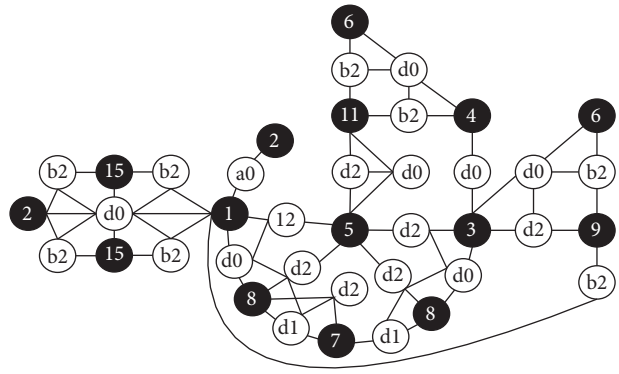

(h)

Figure 10: Fixture property adjacency diagram. (a) Tongs 1. (b) tongs 2. (c) tongs 3. (d) tongs 4. (e) tongs 5. (f) tongs 6. (g) tongs 7. (h) tongs 8. 1—base plate; 2—positioning block; 3—clamp; 4—the handle; 5—support 1; 6—nut; 7—spring; 8—spring protection sleeve; 9—support 2; 10—cylindrical pin; 11—rotating parts; 12—connecting rod; 13—swinging rod; 14—sleeve; and 15—screw.

(4) The Candidate Pruning. In the process of frequent subgraph mining, the following operations should be performed before the frequency counting of candidate subsets generated based on the generation of candidate sets:

(1) For $K + 1$-order candidate subgraphs, all of their K-order subgraphs are solved.

(2) On the basis of graph isomorphism, judge whether K-order frequent subgraphs contain K-order subgraphs.

(3) According to the related properties of candidate pruning, pruning was carried out. The related properties of candidate pruning are described as follows:

Given subgraph O, if O is frequent subgraph, then any subgraph $P(P \subseteq O)$ is frequent. If O is infrequent, then any subgraph $S(O \subseteq S)$ is infrequent.

Through the above operations, the number of candidate subgraphs with different structures and infrequent subgraphs is reduced, and the efficiency of frequency counting process is improved to a certain extent so as to improve the efficiency of frequent subgraph mining algorithm. However, once the number of isomorphic vertices increases, the corresponding retrieval efficiency will decrease. Therefore, this paper sets the number of frequent K-order subgraphs in C_{id} as a, and the number of all K-order subgraphs solved by $K + 1$-order candidate subgraphs as b. By comparing a and b, it can determine whether they meet the candidate pruning-related properties, when

$$n\begin{cases} < \lambda_{\min}, & \text{Delete it and prune it,} \\ \geq \lambda_{\min}, & \text{Isomorphism judgment is made on the graph in the intersection with the graph.} \end{cases} \tag{5}$$

The above two cases do not require a lot of subgraph isomorphism judgment, which greatly reduces the complexity of frequent subgraph algorithm and improves the retrieval efficiency of the algorithm.

(5) Redundancy Selection. On the basis of the Apriori algorithm, frequent subgraphs are often mined, and redundant candidate subgraphs are often generated. Since the formation of frequent subgraphs is based on the recognition and connection operation of low-order frequent subgraphs to construct high-order candidate subgraphs, the phenomenon of high-order including low-order subgraphs may occur. Therefore, this paper adopts the union of C_{id} table to realize, check whether there is the same item in the union set, if there is, remove the same item, and delete the corresponding subgraph in the frequent subgraph set. This avoids scanning the whole Atlas, reduces the workload, and improves the efficiency of the algorithm.

In summary, the pseudocode describing the frequent subgraph mining Algorithm 2 is as follows:

Through the process of preprocessing, initialization, candidate set generation, candidate pruning, frequency counting, and redundancy screening, a large number of frequent subgraphs with different frequency were obtained. Any frequent subgraph corresponds to the local model structure frequently appearing in the model, namely, the common structure, which contains a lot of information, such as the attribute information of corresponding parts in the 3D assembly model and the assembly relationship between parts.

3. Discussion

In order to validate the 3D assembly model based on graph theory in common structure is found feasible, based on the laboratory model of long-term accumulation, in resources, select one series machine tool fixture for 3D assembly model

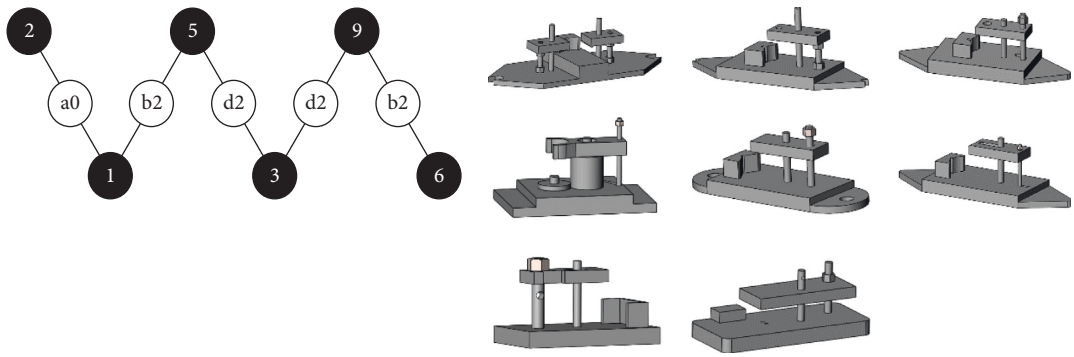

FIGURE 11: $\lambda_{min} = 1$ corresponds to frequent subgraph and 3D assembly model. (a) Frequent subgraph. (b) Three-dimensional assembly model.

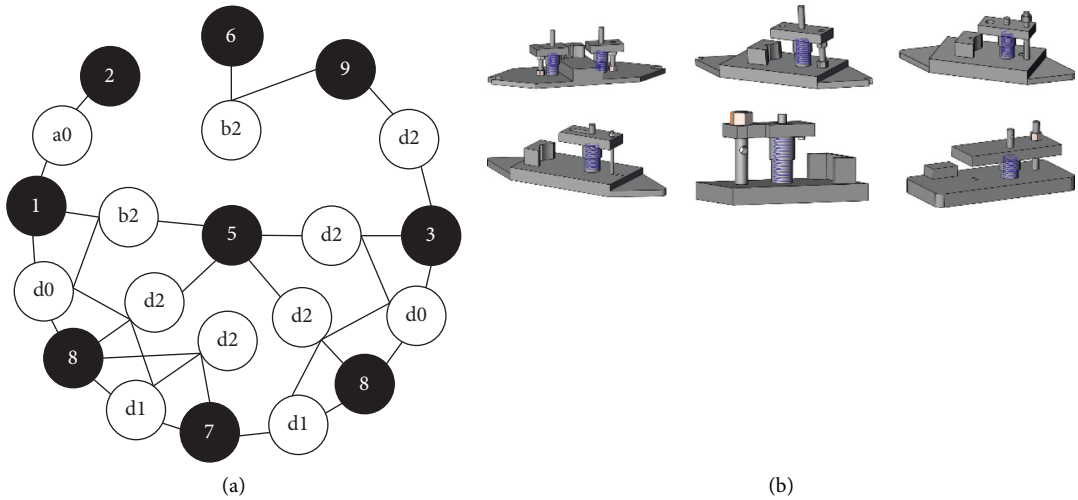

FIGURE 12: $\lambda_{min} = 0.75$ corresponds to frequent subgraph and 3D assembly model. (a) Frequent subgraph. (b) Three-dimensional assembly model.

as the research object, and use the method in this paper to describe concrete step in detail and validate the rationality and feasibility of relevant methods.

The 3D assembly model of a certain series of machine tools and fixtures as shown in Figure 9 is taken as the verification object, and the detailed example verification process is carried out through the representation of model information described in Section 2 and the excavation of common structures based on frequent subgraphs.

3.1. 3D Assembly Model Information Representation. Establishing a reasonable and effective 3D assembly model information representation is the key to subsequent correlation analysis. Therefore, based on the model representation method described in Chapter 2, the 3D fixture assembly model in Figure 9 is represented by an attribute adjacency graph.

3.1.1. Construction of Adjacency Graph of Attribute Configuration Feature. Firstly, according to the method described in Section 2.1.2, the relevant information of assembly features in the 3D assembly model is retained based on the attribute adjacency graph, and other information of parts is replaced by semantic nodes to construct the corresponding attribute assembly feature adjacency graph for all parts in the model. Fixture 2 as shown in Figure 9(b) is used in this paper for illustration. Relevant attribute information of parts can be obtained by searching for model structure tree, relevant design documents, national standards, industry standards, and other resources, and then the attribute assembly feature adjacency graph is expressed for all parts corresponding to Fixture 2. The results are shown in Table 4. In the table, the red part of the part model corresponds to the assembly feature part of the part. The black nodes in the attribute configuration adjacency graph correspond to the semantic nodes containing a lot of semantic information of the part.

3.1.2. Representation of 3D Assembly Model Information. Through the above steps, all parts in fixture 2 can get the corresponding attribute configuration feature adjacency diagram. Then, based on the attribute adjacency graph

input: Q and $\lambda_{\min}$
Output: T
Step 1. Begin
Step 2. Pretreatment
Step 3. Initialization H^1, H^2, $K = 2$
Step 4. While $H^K \neq \varnothing$ do
Step 5. $H^{K+1} \leftarrow \varnothing$
Step 6. $R^{K+1} \leftarrow \text{candidate}(H^K)$ //form candidate subgraphs
Step 7. For $\forall q^{K+1} \in R^{K+1}$ do//candidate pruning and frequency count
Step 8. If $\lambda(q^{K+1}) < \lambda_{\min}$ then
Step 9. remove q^{K+1} //remove subgraphs less than the frequency threshold
Step 10. end if
Step 11. end for
Step 12. $K = K + 1$
Step 13. end while//higher order subgraphs are generated in turn until no new subgraphs can be formed
Step 14. redundancy screening//screening of redundancy
Step 15. return T//gets frequent subatlas
Step 16. end

Algorithm 2: The frequent subgraph mining algorithm.

construction method in Section 2.1.3 and the second jig's 3D assembly model shown in Figure 9(b), the assembly relations between parts are found by searching the corresponding features and relevant documents available of the jig model. Next, this section combines the assembly relations to build the corresponding 3D assembly model attribute adjacency graph. The results are shown in Figure 10(b).

Through the above steps, the 3D assembly model attribute adjacency diagram of fixture 2 is created. By using Figure 10(b), it can be visually observed that the attribute adjacency diagram contains information related to the assembly features of each part, as well as semantic nodes containing a lot of semantic information about the part, and that the diagram representation scale is greatly reduced, suggesting an information representation idea that can be used for related design and manufacturing work. Similarly, by using the same method of constructing the attribute adjacency diagram for the 3D assembly model of fixture 2, a corresponding model representation of the other machine tool fixture models in Figure 9 was made, and the results are shown in Figure 10.

3.2. The Discovery of Common Structure. Based on the attribute adjacency graph of the machine tool fixture constructed above, the method described in Section 2.2.2 is adopted to explore the common structure of the fixture model. The common structure of 3D assembly models to vary from set frequency threshold, and the excavation results from any threshold are corresponding to the corresponding common structure. In the process of verification, in order to reflect the corresponding common structure of under different thresholds, as well as the actual situation and requirements, the minimum frequency threshold ($\lambda_{\min}$) is set to 1 and 0.75, respectively, in this paper. The two sets of thresholds are used to illustrate the corresponding experimental results as shown below.

When the frequency threshold is minimum (i.e., the common structures obtained by excavation are corresponding to all fixture models in this group), the frequency subgraph obtained under this threshold and the corresponding model structure of this frequency subgraph are shown in Figure 11.

Through observation and analysis of Figure 11, the basic composition of fixture model components in the common structure corresponding to the minimum frequency threshold $\lambda_{\min} = 1$ can be obtained, and the model structure of this series of machine tool fixtures can be preliminarily recognized and understood. Corresponding to the examples given in this paper, the common structure of this group of fixture models under the threshold value should at least include the pressure plate, bottom plate, support parts, nuts, positioning blocks, and other components. Parts are connected by welding, thread connection, contact connection, and so on.

When the minimum frequency threshold is $\lambda_{\min} = 0.75$ (i.e., in this group of models, the common structures obtained through excavation correspond to at least 6 fixture models), the frequent subgraph obtained under this threshold and the corresponding model structure of the frequent subgraph are shown in Figure 12.

Through observation and analysis of Figure 12, the common structure corresponding to the minimum frequency threshold $\lambda_{\min} = 0.75$ of this group of fixture models can be obtained, which should at least include pressing plate, bottom plate, support parts, spring, spring protective sleeve, nut, positioning block, and other parts. Parts are connected by welding, thread connection, contact connection, and so on.

To sum up, taking the attribute information and the assembly relation between all parts, this method can obtain the common structures which frequently appear and support the reuse demand. This method has certain reference value for the assembly relationship and parts in 3D assembly model topology similar common structure discovery and reuse. In the design and manufacture of products, designers

Table 4: The adjacency diagram of the attributes of the components in fixture 2.

Serial number	Part name	Parts model	Property masquerade feature adjacency diagram
1	Baseboard	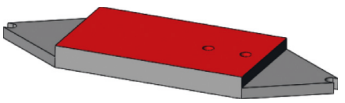	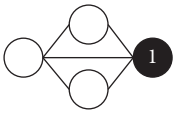
2	Set piece	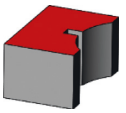	
3	Pressing plate	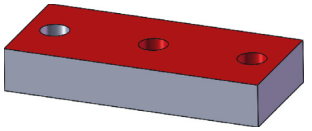	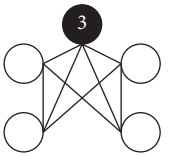
4	Handle		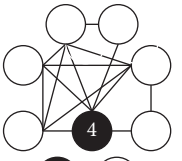
5	Strut member 1		
6	Screw nut	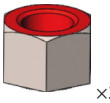 ×3	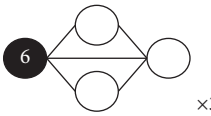 ×3
7	Spring	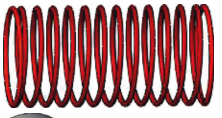	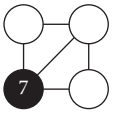
8	Spring sleeve	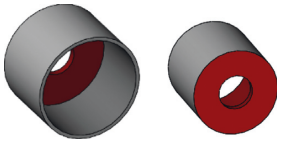	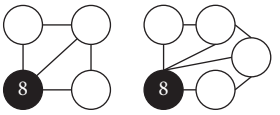
9	Strut member 2		
10	Straight pin		
11	Rotating part	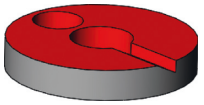	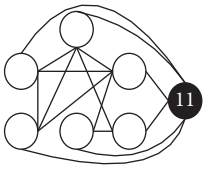

can set the corresponding minimum frequency threshold according to the personalized requirements of products, and then obtain the common structure that fits the design intention.

4. Conclusions

In this paper, a method for mining common structures of 3D assembly models is proposed. Firstly, the relevant information of the 3D model is extracted and represented by the attribute make-up feature adjacency graph. Then, the relationship between components in the 3D assembly model was analysed, and the isolated attribute assembly feature adjacency graph was combined to form the attribute adjacency graph of the 3D assembly model. Finally, frequent subgraph mining algorithm was used to discover the common structure of the 3D assembly model. The method can from 3D assembly model of product structure, the generality of the excavation support reuse to provide reference for related design work, improve the efficiency of product design and manufacture accuracy as well as design, increase the flexibility of the 3D assembly model information reuse, effectively improve product design and manufacturing enterprise of the reuse of exploring information resources.

4.1. Future Work

(1) In the process of graphical representation of model information, this paper mainly highlights the assembly features of the model and unifies the

nonassembly features in the semantic node representation. However, certain nonassembly features also contain important information about the 3D assembly model. Therefore, how to screen the useful structural features in the 3D assembly model and create a suitable information representation is one of the focuses of the subsequent research.

(2) In the design and manufacturing process of a product, there are many uncertainties in the many objective and subjective needs of designers for 3D assembly model information at different stages and under different conditions. Therefore, subsequent specific analysis of design intent can be carried out to summarise its composition characteristics and construct a more comprehensive and prominent semantic information expression standard for design personality, and this paper mainly focuses on similarity evaluation in design reuse, and the evaluation scope will be expanded subsequently.

Data Availability

The data used to support the finding of this study are available from the corresponding author upon request.

Conflicts of Interest

The authors declare that there are no conflicts of interest regarding the publication of this paper.

Acknowledgments

This project was supported by National Natural Science Foundation of China (Grant no. 51705392), Shaanxi Science and Technology Resources Open Sharing Platform (Grant no. 2021PT-006), Shaanxi Youth Science and Technology Rising Star Project (Grant no. 2020KJXX-071), and Shaanxi Provincial Department of Education Special Scientific Research Project (Grant no. 18JS043).

References

[1] S. Chakrabarty and J. Wolter, "A structure-oriented approach to assembly sequence planning," *IEEE Transactions on Robotics and Automation*, vol. 13, no. 1, pp. 14–29, 1997.

[2] Z. Y. Liu, J. R. Tian, and S. Y. Zhang, "Research on product level information representation for virtual assembly," *Journal of Computer Aided Design and Graphics*, vol. 13, no. 3, pp. 223–228, 2001.

[3] X. Y. Mou, *Method for Assembly Sequence Planning Based on Hierarchical Model and Human-Mputer Collaborative*, pp. 99–103, New Technology New Process, Beijing, China, 2015.

[4] Z. Li, *Research on Hierarchical Representation for Similarity Assessment and Reuse of 3D CAD Models*, Shanghai Jiao Tong University, Shanghai, China, 2015.

[5] G. Y. Yang, L. Tian, D. P. Zhao, and Y. Xin, "Two-dimensional description method of process information for 3D assembly instruction publishing," *Applied Mechanics and Materials*, vol. 602–605, pp. 3774–3777, 2014.

[6] A. Bourjault, *Contribution to a Methodological Approach of Automated Assembly: Automatic Generation of Assembly Sequence*, University de Franche-Comte, Besançon, 1984.

[7] L. S. Homem de Mello and A. C. Sanderson, "A correct and complete algorithm for the generation of mechanical assembly sequences," *IEEE Transactions on Robotics and Automation*, vol. 7, no. 2, pp. 228–240, 1991.

[8] H. Xiao, Y. Li, J. F. Yu, and Z. Jie, "CAD mesh model simplification with assembly features preservation," *Science China*, vol. 57, no. 3, pp. 1–11, 2014.

[9] M. Zuo, *A Method for Common Design Structure Discovery in 3D Assembly Models and Their Design Reuse*, Northwestern Polytechnical University, Xi'an, Shaanxi, China, 2016.

[10] S. F. Wu, *Design Reuse Method Research for Auto Parts*, Zhejiang University, Hangzhou, Zhejiang, China, 2009.

[11] T. Q. Ma, *Research on CAD Model Reuse Technologies Supporting Product Rapid Design*, Dalian University of Technology, Dalian, Liaoning, China, 2009.

[12] Y. Zhou and J. R. Zheng, "Local matching of assemblies based on subgraph isomorphism and case matching," *Journal of Computer-Aided Design & Computer Graphics*, vol. 22, no. 22, pp. 299–305, 2010.

[13] Z. Han, R. Mo, Z. Chang, L. Hao, and W. Niu, "Key assembly structure identification in complex mechanical assembly based on multi-source information," *Assembly Automation*, vol. vo37, no. 2, pp. 208–218, 2017.

[14] P. Wang, J. Zhang, Y. Li, and J. Yu, "Reuse-oriented common structure discovery in assembly models," *Journal of Mechanical Science and Technology*, vol. 31, no. 1, pp. 297–307, 2017.

[15] P. Liu, Y. Li, and K. F. Zhang, "Layered orientation graph modeling method for the assembly of complex products," *Journal of Machine Design*, vol. 24, no. 4, pp. 33–35, 2007.

[16] J. H. Liu and Y. Z. Hou, "MBD model parametric method based on hybrid-attributed adjacency graph," *Journal of Computer-Aided Design & Computer Graphics*, vol. 30, no. 07, pp. 155–160, 2018.

[17] A. Inokuchi, T. Washio, and H. Motoda, "An Apriori-Based Algorithm for Mining Frequent Substructures from Graph Data," in *European Conference on Principles of Data Mining and Knowledge Discovery*, D. A. Zighed, J. Komorowski, and J. Żytkow, Eds., pp. 13–23, Springer, Berlin, Heidelberg, 2000.

[18] J. F. Guo, W. Zhang, and R. Chai, *New Algorithm of Mining Frequent Subgraph, Computer Engineering*, vol. 30, no. 27, pp. 27–32, 2011.

[19] L. Yan, *Study on Steady Frequent Subgraph Mining Algorithm*, Liaoning University, Shenyang China, 2018.

[20] R. Agrawal, T. Imieliński, and A. Swami, "Mining association rules between sets of items in large database," in *Proceedings of the ACM SIGMOD International Conference on Management of Data*, vol. 22, pp. 207–216, ACM Press, Washington, D.C., USA, June 1993.

[21] R. Agrawal and R. Srikant, "Mining sequential patterns," in *Proceedings of the Eleventh International Conference on Data Engineering*, pp. 3–14, IEEE, Taipei, Taiwan, March 1995.

[22] Y. Z. Bao, *The Improvement of Apriori Algorithm on the Basis of Rough-Set Theory*, Shanghai Normal University, 2010.

[23] A. Inokuchi, T. Washio, and H. Motoda, "Complete mining of frequent patterns from graphs: mining graph data," *Machine Learning*, vol. 50, no. 3, pp. 321–354, 2003.

[24] M. Kuramochi and G. Karypis, "Frequent subgraph discovery," *Proceedings 2001 IEEE International Conference on Data Mining*, pp. 313–320, IEEE, San Jose, CA, USA, November 2001.

Hindawi
Scientific Programming
Volume 2022, Article ID 3199860, 9 pages
https://doi.org/10.1155/2022/3199860

Research Article

Construction and Optimization of Artificial Intelligence-Assisted Interactive College Music Performance Teaching System

Hanwen Zheng[1] **and Dandan Dai**[2]

[1]*Sichuan University of Culture and Arts, MianYang, Sichuan 621000, China*
[2]*NanChang JiaoTong Institute, NanChang, Jiangxi 330100, China*

Correspondence should be addressed to Dandan Dai; 06054@ncjti.edu.cn

Received 30 May 2022; Revised 25 June 2022; Accepted 28 June 2022; Published 19 July 2022

Academic Editor: Lianhui Li

This research focuses on the relationship between artificial intelligence technology and music performance in colleges and universities and explores the application of artificial intelligence technology in music teaching. At the same time, it explores the deficiencies of existing computer-assisted language learning software and systems through questionnaires and interviews and also proposes solutions, such as further understanding of theories, enhancing learners' confidence, and stimulating their interest in learning. The results of this research will help to improve the application of online intelligent human-computer systems in music teaching and provide dynamic support for improving the quality of music teaching and talent training in colleges and universities.

1. Introduction

The outstanding feature of the music performance major is performance. Whether students are studying vocal music or various instrumental music and dance, the core goal is to become a performer who can perform onstage. From the perspective of professional training goals and students' future career directions, the music performance major cultivates applied and compound talents. After graduation, students' main destination is social-cultural groups and relevant departments of enterprises and institutions. They are engaged in not only art performances but also the organization, guidance, planning, and implementation of art activities, which requires them to understand and be familiar with the characteristics, methods, procedures, details, etc., of music performances and related work, and also have the corresponding workability. Therefore, in the construction of the practical teaching system of this major, the first point is to firmly grasp the characteristics of the major and highlight the performative characteristics of practical teaching activities.

The fundamental purpose of music teaching in colleges and universities is to cultivate students' ability to perform music, but the level of music performance that students actually master at present cannot achieve the desired effect. With the rapid development of Chinese society and the continuous enhancement of international exchanges, skilled music performance has become particularly important, which has brought great challenges to music teaching in colleges and universities. In today's British music teaching, traditional teaching methods can no longer meet the needs of contemporary society for comprehensive talent training. In recent years, the rapid development of artificial intelligence technology has brought new opportunities for the modernization of music teaching, which provides new opportunities for the creation of an intelligent music teaching environment. At present, a consensus has been reached on the importance of artificial intelligence technology applied to teaching systems. Guided by the integration of information technology and curriculum, it is of great practical significance to conduct research on the application of artificial intelligence technology in college music teaching. Based on the above background, this paper needs to solve the following three problems: (1) What problems exist in the current music teaching in colleges and universities? (2) The interactive relationship between artificial intelligence and

music teaching; and (3) the specific practice of artificial intelligence in music teaching in colleges and universities.

For the above three questions, some scholars and education experts have already conducted research. For the first question, Huang et al. have preliminarily studied the advantages, disadvantages, and innovations of various college music teaching models [1]; Rebecca et al studied the problems existing in the teaching of music performance in colleges and universities in our country [2]. For the second question, Guoliang studied the relationship between artificial intelligence and music teaching [3]. For the third question, Kun et al. studied the application of artificial intelligence in the field of music teaching. This paper mainly studies the relationship between artificial intelligence and music teaching by discussing the current problems in music teaching in colleges and universities and improves the application of artificial intelligence in music teaching. These misconceptions have been in the consciousness of students and some teachers for a long time. With the development of artificial intelligence, scholars have begun to study how to use artificial intelligence to solve the problems encountered in music teaching. The application of artificial intelligence technology in music teaching starts from artificial intelligence and the problems it intends to solve and explores the application of artificial intelligence technology in music teaching around the relationship between artificial intelligence and music teaching. However, there are also many problems with artificial intelligence in university music teaching. Based on the research of the above scholars, the author believes that artificial intelligence can effectively solve the problems in music teaching, but at the same time, there are also some problems in the application of artificial intelligence in music teaching. This paper mainly aims at the shortcomings of artificial intelligence in music teaching and proposes solutions to improve the confidence of learners to stimulate their learning confidence and further improve the application of artificial intelligence in music teaching.

2. Related Work

In nature, living things live according to the principle of "survival of the fittest." In 1975, the random search algorithm proposed by Professor Holland from the United States used computers to solve intelligent analysis problems according to the survival law of nature which is the most effective method. The genetic algorithm (GA) was first proposed by John in the 1970s. The algorithm was designed and proposed according to the evolutionary laws of organisms in nature. It is a computational model of the biological evolution process that simulates the natural selection and genetic mechanism of Darwin's theory of biological evolution. It is a method to search for the optimal solution by simulating the natural evolution process. The algorithm converts the process of solving the problem into a process similar to the crossover and mutation of chromosomal genes in biological evolution through mathematical methods and computer simulation operations. When solving more complex combinatorial optimization problems, better optimization results can usually be obtained faster than some conventional optimization algorithms. Genetic algorithms have been widely used in combinatorial optimization, machine learning, signal processing, adaptive control, and artificial life. Each chromosome in the genetic algorithm corresponds to a solution of the genetic algorithm. Generally, we use the fitness function to measure the pros and cons of this solution. So the fitness from a genome to its solution forms a map. The process of the genetic algorithm can be regarded as a process of finding the optimal solution in a multivariate function. It can be imagined that there are countless "mountains" on this multidimensional surface, and these peaks correspond to the local optimal solution. And there will also be a "mountain" with the highest altitude, and then this is the global optimal solution. The task of the genetic algorithm is to try to climb to the highest peak, instead of falling into some small peaks. In addition, it is worth noting that the genetic algorithm does not have to find the "highest mountain." If the fitness evaluation of the problem is as small as possible, then the global optimal solution is the minimum value of the function. Correspondingly, what the genetic algorithm is looking for is "the deepest valley." The principle of the genetic algorithm is to express the set of problems to be solved as "groups." Before solving the operation, some of the "groups" are assumed to be the solution sets to be sought, and these initially identified solution sets are placed in the environment of the problem. Through the principle of survival of the fittest, new groups are continuously generated through operations such as combination, exclusion, and mutation, and they evolve continuously until the obtained "group" meets the expected value, that is, the optimal solution to the problem. The solution of the genetic algorithm starts from the initialization and randomly selects a subset from the whole population as the initial population. During the running process of the algorithm, the size of the population does not change all the time. An individual is each specific element in a population. Fitness is the degree of adaptation of the individual to the external environment. In order to measure the individual, the function of measuring the fitness is called the fitness function. According to this function, the survival law of nature is reflected. Coding is because the algorithm cannot directly process the parameters of the problem space, and it needs to be converted into a space set that the computer can recognize according to certain rules. The workflow of its algorithm is shown in Figure 1.

Among them, selection, crossover, and mutation are the genetic operators of the algorithm. Selection is to keep the individuals with strong adaptability in the group and eliminate the individuals with low adaptability; crossover is to replace a part of the structure of the individuals according to certain rules and then obtain new individuals; variation is performing a specific operation on a gene value in an individual to generate a new individual which is the most important means to improve the global search ability of the genetic algorithm.

3. Basic Baseline for System Construction

The basic idea of the construction of the practical teaching system of the music performance major according to the

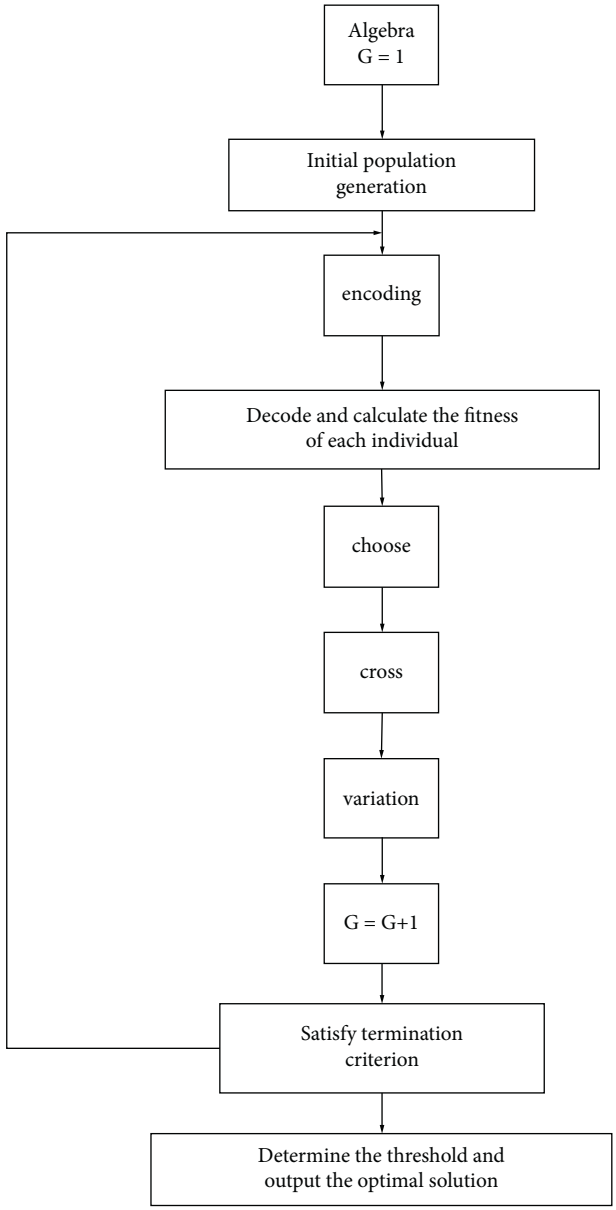

Figure 1: Steps of a genetic algorithm.

characteristics and training objectives of the music performance major, combined with the actual requirements of the society, the practical teaching system of this major should at least contain the following basic links:

(1) The practical link in the basic course: the most basic course in the music performance professional curriculum system is the professional basic course. The basic curriculum settings of each college include music theory, solfeggio, harmony, polyphony, musical analysis, Chinese music history, foreign music history, and national folk music. The teaching objectives of the basic courses of music performance should be the trinity of basic knowledge, basic theory, and basic skills. That is to say, the teaching tasks of these courses should not only enable students to master the basic knowledge and basic theory of music discipline but also carry out basic skills. Training and the organic combination of the three can lay a solid professional foundation for students. Among them, there is a flexible space for basic skills. From the perspective of the construction of the practical teaching system, these courses must become an integral part of the construction of the practical teaching system, and the development of the practical link should be strengthened in the curriculum planning. There are two main forms: one is exercise practice, that is, the relevant content in the course is repeatedly practiced through exercises so that students can form solid skills and skills on the basis of firmly grasping the relevant knowledge theory. For example, the music theory course, which involves the formation of intervals, mode tonal analysis, time value division, chord construction, etc., requires a large number of exercises to enable students to master relevant theories and knowledge and form basic skills for future music performance practice to lay the foundation. The second is the appreciation of works. Courses with a strong theoretical nature, such as Chinese music history and foreign music history, still need to expand the practical space. For example, some schools set the music history course as Chinese (foreign) music history and work appreciation, which is actually an organic combination of the practice of music appreciation in the teaching of music history courses. Even if the name of music appreciation is not clearly indicated in the course title, the practice of music appreciation should be combined with specific content in actual teaching.

(2) The practical link in the skill and skill course: in the course system of the music performance major, the core course is the skill and skill course, such as Chinese and foreign instrumental music, vocal music, piano, dance, ensemble, chorus, and piano accompaniment. In such courses, it is a practice-oriented course in itself, and the basic goal of its teaching is to enable students to master relevant skills and skills to perform complete musical works [4, 5]. And if it is not enough to stay at this level, the ultimate goal of mastering and using the corresponding skills and techniques should be implemented onstage performances. The setting of practical skills and skill courses also needs to be developed from two aspects, one is the penetration and strengthening of performance factors in the teaching of traditional skills and skills courses, and the other is the appropriate expansion of other related auxiliary skills and skills courses [6, 7]. From the perspective of cultivating students' practical ability, the teaching of traditional skills and skill courses requires the penetration of performance elements first and also to ensure the development and improvement of students' artistic practical ability to meet the needs of stage performances. This

requires strengthening the design training of facial expression language, body language, and emotional expression in the teaching process so as to enhance the admirability of the works in the process of interpretation so that they can achieve the effect of both form and spirit, touching people's hearts [8]. Second, it is necessary to create opportunities for students to practice practical exercises, such as regular professional reports, final professional examinations, and second classroom activities for practical demonstrations. The expansion of other auxiliary skills and skills courses is mainly to add some elective courses according to actual needs, such as makeup, program hosting, recitation, and pronunciation [9]. On the one hand, the setting of such courses can expand students' professional ability and enhance the adaptability of social work. On the other hand, it can effectively assist the study of other professional courses, and to a certain extent, it can help students' personality development [10].

(3) Independent practical links as practical teaching is getting more and more attention. Some schools generally set up independent practical teaching links in the process of formulating talent training programs for their majors, such as the second classroom activities of each semester, art practice weeks, professional apprenticeships, professional internships, and graduation reports (or graduation concerts). This link has a certain nature of comprehensive training, which plays a better role in cultivating students' professional practical ability [11–13]. The most critical part of this link is to strengthen the design and strengthen the implementation. The so-called strengthening design is to serialize, standardize, and even quantify the independent practice links. The second classroom activities should be carried out in close cooperation with the teaching of professional courses [14]. Art practice week should be arranged for at least one week per semester. They should run through the whole process of professional teaching, which requires overall planning and design to avoid randomness and randomness of activities. Low-level repetition ensures the scientific nature of practical training; the so-called strengthening implementation means strengthening the management and guidance of all practical teaching links and completing the corresponding practical training content according to plans and standards [15].

(4) Practical links in comprehensive art activities The so-called comprehensive art activities mainly refer to practical activities characterized by actual stage performances, which require students to mobilize all professional knowledge and abilities, and exercise and improve on the real stage of the campus and society. It is a professional practice activity as well as a social practice activity, and it is a bridge for students to go from the campus to the society. This should be a stage performance-type three-level practical activity system; that is, relying on the art stage, the three-level art practice activity system of professional basic practice, professional development practice, and professional improvement practice is unified. Professional basic practice art activities mainly refer to the art practice activities related to the teaching of professional courses [28]. For example, professional report concerts are held regularly, and professional examinations are held in the form of concerts every semester. The stage has become a platform for students to show their professional learning achievements, and the learning of single professional skills has become a comprehensive stage performance [16]. Using the skills and techniques learned in the classroom, we also need to carry out creative performance design, and preliminary stage practice accumulate corresponding stage experience and gradually improve stage adaptability. Professional development practice art activities mainly refer to the development of various types of practical performance activities [17–19]. This is an open stage space, which can carry out practical performance activities within the school, such as graduation concerts, large-scale comprehensive professional report concerts, and theatrical performances in major festivals or major events; it can also carry out interschool and even international art exchange activities. More importantly, we can vigorously carry out social art practice activities, such as performances in community culture construction, corporate culture construction, and performances in certain themed cultural activities carried out by local governments and local media. Such activities involve a wide range of activities, rich in content, high comprehensive level, and quality requirements, and truly achieve social integration, which is a comprehensive test and experience for students' professional level [20].

The artistic activities of professional improvement practice mainly refer to the practical activities of selecting some outstanding students to participate in high-level professional competitions. A unique advantage of the music performance major is that there are various art competitions in all walks of life every year, such as the annual national college student art exhibition activities, various art competitions held by the cultural department of the provincial education department, and media at all levels [21]. Professionally, it is a rare opportunity provided by the social stage for practical teaching work. It can be combined with such activities to carry out high-level artistic practice activities, such as holding trials.

The above are the basic construction ideas for the construction of the practical teaching system for the music performance major. The author tries to build a comprehensive and applicable professional practice teaching system through this design, which not only highlights the core professional characteristics of art performance but also includes other related work content; if the specific planning

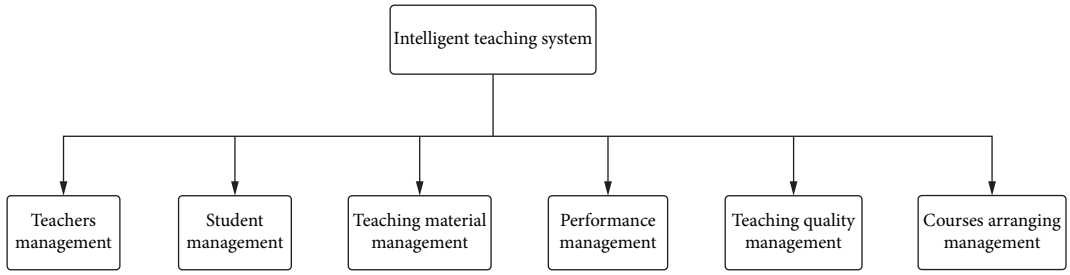

Figure 2: System functional structure diagram.

and implementation process can be scientifically designed and arranged reasonably and can fully mobilize the enthusiasm and initiative of students to carry out corresponding work in an all-round way and can strengthen management and assessment, then we will be able to achieve music. The performance major aims to cultivate applied and compound talents with a solid professional foundation, excellent basic skills, outstanding professional practical ability, and adapt to the needs of social and cultural development and construction [22].

4. System Design

4.1. Design Principles. The design of the teaching system should not only meet the needs of current school teaching but also be able to adapt to the needs of future development as the school expands over time.

(1) *Scalability*. The school is the cradle of cultivating talents for the country. With the continuous development of my country's economy and science and technology, society has put forward higher requirements for talents [23]. Therefore, schools have to keep changing with the needs of the society and put forward new requirements for the teaching system, which requires the teaching system to be continuously expanded in terms of functions to meet diverse needs.

(2) *Security Teaching Is a Very Serious Matter*. Students' teaching information, especially exam results, needs to be stored in student files, which raises higher requirements for the security of information storage and transmission in the teaching system.

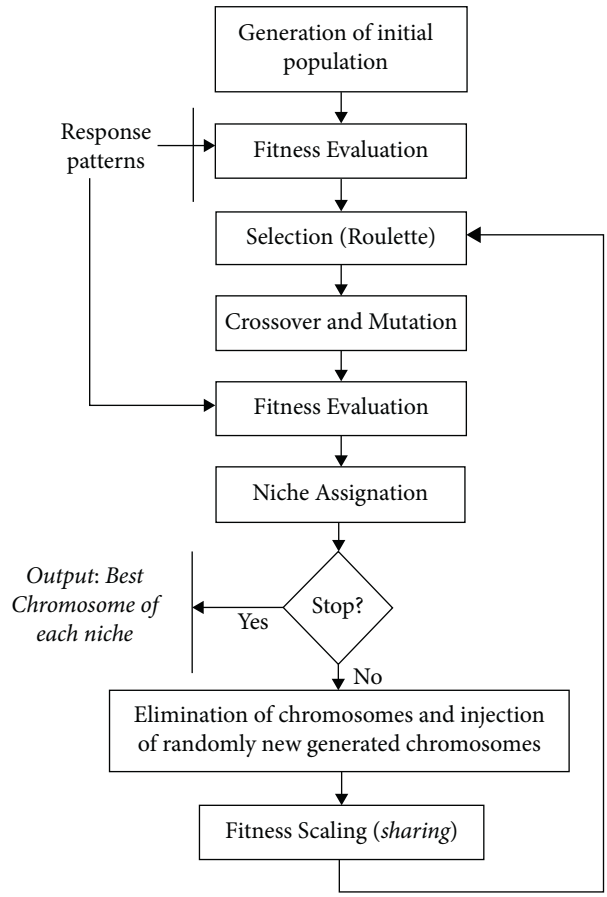

Figure 3: Diversity-enhanced genetic algorithm.

4.2. System Functions. For the entire teaching system, teachers and students, teaching materials, classes, grades, and evaluation form a complete teaching management process [24]. Therefore, the teaching management system mainly focuses on several elements of the teaching process. The developed intelligent teaching system mainly has the following modules. The specific functional structure is shown in Figure 2.

Among them, teacher management is mainly to manage and maintain teachers' basic information, scientific research, teaching, and other information; student management is to manage and maintain students' basic information, rewards, punishments, etc.; at the same time manage the information and maintenance [25]; performance management is the management and maintenance of students' test scores, reexamination scores, and other information; teaching quality management is a quality evaluation management system formed based on students' evaluations of teachers and expert evaluations; course management is that each teaching subject intelligently arranges courses according to its own teachers, students, teaching environment and other factors, so as to achieve the optimal allocation of teaching resources from the perspective of cultivating students' practical ability, the teaching of traditional skills, and skills courses [23]. First of all, the penetration of performance elements is needed to ensure that students' artistic practice ability can be developed and improved to meet the needs of stage performances. This

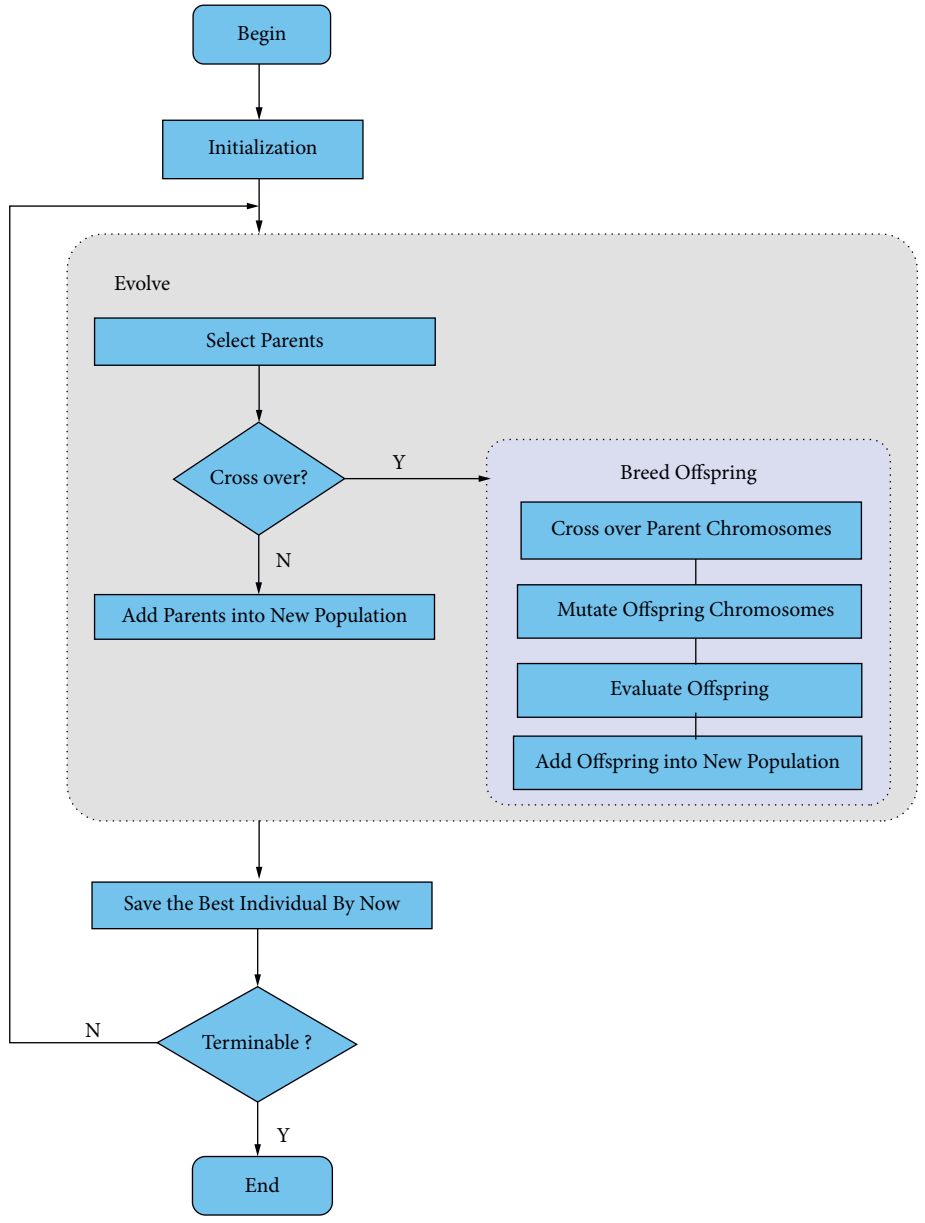

Figure 4: Simple genetic algorithm.

requires strengthening the design training of facial expression language, body language, emotional expression, etc. [26] in the teaching process, so as to enhance the admirability of the works in the process of interpretation, so that they can achieve the effect of both form and spirit and touch people's hearts. Second, it is necessary to create opportunities for students to practice practical exercises, such as regular professional reports, final professional examinations, and second classroom activities for practical demonstrations. The expansion of other auxiliary skills and skills courses is mainly to add some elective courses according to actual needs, such as makeup, program hosting, recitation, and pronunciation. On the one hand, the setting of such courses can expand students' professional ability and enhance the adaptability of social work. On the other hand, it can effectively assist the study of other professional courses, and to a certain extent, it can help students' personality development [26, 27]. There are many genetic algorithms, including diversity-enhanced genetic algorithms (Figure 3), simple genetic algorithms (Figure 4), and multiobjective genetic algorithms (Figure 5).

4.3. Database. The teaching management database is mainly used to store basic information such as teachers, students, grades, and textbooks. Some information appears repeatedly in different tables. In order to maintain the integrity and stability of the data information, the data items of the data table are designed. The main data items of each data table are as follows:

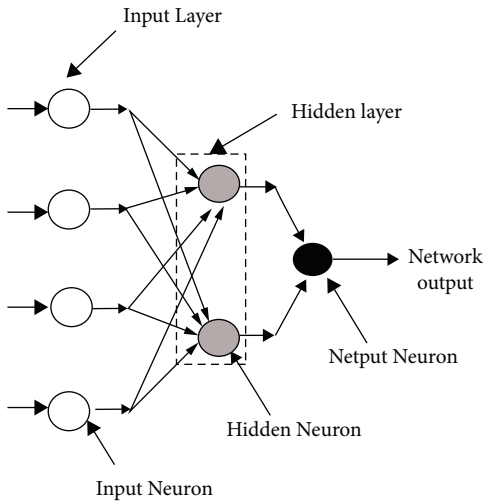

Figure 5: Multiobjective genetic algorithm.

(1) User basic information table: it is used to store login information, and the main contents are user login name, password, user authority, etc.

(2) Teacher information table: it is used to store the basic information of teachers. The main contents include the teacher's job number, name, gender, age, department title, telephone number, e-mail, QQ number, and home address.

(3) Student information table: it is used to store the basic information of students, the main contents are student number, name, gender, age, date of birth, home address, telephone, e-mail, QQ number, department, class number, and other contents.

(4) Classroom information table: it is used to store the information of different classrooms in the school. The main contents include classroom number, teaching building, classroom name, classroom capacity, classroom type, and so on. In addition to the above data tables, there are other data tables such as class basic information table, grade information table, course information table, teaching material information table, and class information table, which will not be described in detail here.

5. System Implementation

5.1. Course Scheduling Management. Class schedule is the top priority of a school. Schools should effectively integrate resources such as teachers, classrooms, classes, courses, and time to achieve the best configuration. The class schedule is to find the optimal combination problem under the condition of relatively limited resources. Regardless of the school, there are several constraints to avoid when scheduling classes.

(1) A teacher can only take one course at a certain time.

(2) A classroom can only arrange one course at a certain time.

(3) A class can only take one course at a certain time.

(4) The number of people in a certain class should be less than the capacity of the classroom. For the elements of class, course, classroom, time, and classroom, the mathematical formula is expressed as follows:

Class collection: $BJ = \{bj_1, bj_2, bj_3, ..., bj_a\}$;
Course collection: $KC = (kc_1, kc_2, kc_3, ..., kc_b)$
Classroom collection: $CR = \{(cr_1, cr_2, cr_3, ..., cr_c)$
Time collection: $SJ = (sj_1, sj_2, sj_3, ..., sj_d)$
Classroom collection: $JS = (js_1, js_2, js_3, ..., jd_e)$

The problem with the class schedule is the Cartesian product of the above five elements, $PK = BJ^* KC^* CR^* SJ^* JS$. It is necessary to find a set that satisfies the constraints in PK, that is, the result of the class schedule. Here, a genetic algorithm is used to solve the problem of course scheduling, and each individual in the PK set is regarded as a course scheduling scheme. All the course scheduling schemes are taken as the initial population, and the population is operated to get the optimal results.

5.2. Teacher Management. For the teacher module, not only the basic information of teachers is maintained but also the statistics of teachers' information, statistics on the workload of teachers in the school, analysis of the proportion of teachers with different professional titles in the school, statistics on the number of teachers of all ages in the school, and information on teachers' scientific research details. The teacher management module can help the teaching management department to analyze the information of teachers and provide first-hand information for the school to carry out teaching, professional title evaluation, and introduction of talents.

6. Conclusion

Using artificial intelligence technology to design and study the teaching system, we explain in detail how to use the genetic algorithm to manage the course arrangement. Functionally, the teaching system can meet the teaching needs of various types of colleges and universities. This paper studies the application of artificial intelligence in college music teaching. Traditional teaching methods are very fundamental, so teachers often spend most of their time explaining basic music theory while students are often busy taking notes. Teachers do not release various tasks to attract students' learning, resulting in a small number of students who are not interested in learning and remain silent in the classroom. Therefore, in order to change this phenomenon, teaching should adopt new teaching methods. The task-based teaching process is task design, warm-up, pretasks, tasks, reporting, and assessment. These tasks are often accomplished through interaction between students. In doing so, students can put what they have learned into practice. Combined with the definition and basic characteristics of artificial intelligence, use teaching methods to combine artificial intelligence with music classroom teaching, explore the benign relationship between music teaching and artificial intelligence, and promote teaching and talent training. As

the integration of information technology and music courses continues to accelerate, artificial intelligence has brought new opportunities for music teaching. In order for students to learn music well, we need to create a free environment. Our music class cannot be limited to the ordinary class mode to complete the learning. A relaxed and active atmosphere must be created. Rooting information technology such as artificial intelligence in music teaching practice, and giving full play to its technical advantages and cutting-edge features, can promote the quality of teaching and improve the level of talent training while achieving better development of artificial intelligence technology.

Data Availability

The dataset can be accessed upon request.

Conflicts of Interest

The authors declare that there are no conflicts of interest.

Acknowledgments

The authors thank Jiangxi Provincial Education Department, College Humanities and Social Science Research Project, Higher Vocational College Music Major Students Core Literacy Training Model Construction (no. 17YBA063).

References

[1] C. Huang and K. Yu, "Research on the innovation of college music teaching mode based on Artificial Intelligence," *Journal of Physics: Conference Series*, vol. 2, p. 1915, 2021.

[2] R. B. MacLeod, C. Blanton, J. Lewis, and D. Ortiz, "Near-peer mentorship: a model for private music instruction in an underserved community," *String Research Journal*, vol. 10, no. 1, pp. 45–60, 2020.

[3] G. Yang and L. Yang, "Exploration of vocal music teaching mode from the perspective of the age of artificial intelligence," *International Journal of Frontiers in Engineering Technology*, vol. 2, no. 1, 2020.

[4] K. Dr, L. Dr, A. Widyantoro, C. Boel, and M. Berendsen, "Developing an integrated music teaching model in Indonesia based on the Dutch music teaching model as the implementation of the 2013 CURRICULUM. Researchers world," *Journal of Arts, Science and Commerce*, vol. VIII, no. 2, 2017.

[5] K. Dong and Q. Li, "Multimedia pop music teaching model integrating semifinished teaching strategies," *Advances in Multimedia*, vol. 2022, Article ID 6200077, 2022.

[6] J. Liu, "The innovation of music teaching mode under the background of big data," *Journal of Physics: Conference Series*, vol. 3, p. 1852, 2021.

[7] "Innovation of college students' music teaching mode from the perspective of educational psychology," *The Journal*, vol. 33, no. S5, 2021.

[8] Li Lin, "Research on music teaching mode against the backdrop of "internet +"," in *Proceedings of 2019 International Conference on Management, Education Technology and Economics (ICMETE 2019)*, pp. 593–595, 2019.

[9] Y. He, "Children trusted music teaching mode based on uncertainty and individual music attributes," in *Proceedings of 2018 5th International Conference on Education Reform and Management Innovation (ERMI 2018)*, pp. 333–338, Guangzhou, China, December 2018.

[10] J. Han, "Development opportunity and development direction of vocal music teaching mode in diversified era," in *Proceedings of International Conference on Education Technology and Social Science*, pp. 357–360, Taiyuan, China, November 2014.

[11] Y. Qu, "Research on the teaching mode of music under the background of internet," in *Proceedings of the 2020 Annual Conference of Education Teaching and Learning*, Budapest, Hungary, December 2020.

[12] H. Lu, "Research on the reform of the teaching mode of accordion music in colleges and universities based on the diversified background," in *Proceedings of the 2020 2nd Asia-Pacific Conference on Advance in Education Learning and Teaching*, Guangzhou, China, December 2020.

[13] W. Yang, "Artificial Intelligence Education for Young Children: Why, what, and How in Curriculum Design and implementation[J]," . *Computers and Education: Artificial Intelligence*, vol. 3, Article ID 100061.

[14] S. Shin, "A study on the framework design of artificial intelligence thinking for artificial intelligence education," *International Journal of Information and Education Technology*, vol. 11, no. 9, pp. 392–397, 2021.

[15] E. Amy, H. Okada, and Y. Muto, "Contextualizing AI Education for K-12 Students to Enhance Their Learning of AI Literacy through Culturally Responsive Approaches," *Kunstliche intelligenz*, vol. 35, no. 2, pp. 153–161, 2021.

[16] P. Mu, "Research on Artificial Intelligence Education and its Value Orientation," in *Proceedings of the 2019 1st International Education Technology and Research Conference*, Taiyuan, China, September 2019.

[17] T. K. F. Chiu and C.-sing Chai, "Sustainable curriculum planning for artificial intelligence education: a self-determination theory perspective," *Sustainability*, vol. 12, no. 14, p. 5568, 2020.

[18] K. Kim, "An artificial intelligence education program development and application for elementary teachers," *Journal of The Korean Association of Information Education*, vol. 23, no. 6, pp. 629–637, 2019.

[19] S. Shin, "Designing the instructional framework and cognitive learning environment for artificial intelligence education through computational thinking," *Journal of The Korean Association of Information Education*, vol. 23, no. 6, pp. 639–653, 2019.

[20] J. Sandberg, Y. Barnard, and A. van der Hulst, "Interviews on AI education: kurt vanlehn and david merrill," *AI Communications*, vol. 5, no. 2, pp. 85–91, 1992.

[21] Y. Liu and J. Huang, "Practice and exploration of artificial intelligence education in universities of political science and law with Python," *Advances in Social Sciences* in *Proceedings of 2019 3rd international seminar on education, management and social sciences (ISEMSS 2019)*, vol. 345, pp. 550–554, Education and Humanities Research, Changsha, China, July 2019.

[22] T. W. Neller, "AI education matters," *AI Matters*, vol. 5, no. 2, pp. 8–10, 2019.

[23] M. Guerzhoy, "AI education matters," *AI Matters*, vol. 4, no. 3, pp. 14-15, 2018.

[24] Z. Dodds, L. G. Greenwald, A. M. Howard, S. Tejada, and B. Weinberg, "Components, curriculum, and community: robots and robotics in undergraduate AI education," *AI Magazine*, vol. 27, no. 1, 2006.

[25] K. Kim and Y. Park, "A development and application of the teaching and learning model of artificial intelligence education for elementary students," *Journal of The Korean Association of Information Education*, vol. 21, no. 1, pp. 137–147, 2017.

[26] E. Eaton, S. Koenig, C. Schulz et al., "Blue sky ideas in artificial intelligence education from the EAAI 2017 new and future AI educator program," *AI Matters*, vol. 3, no. 4, pp. 23–31, 2018.

[27] E. Esekhaigbe, E. N. Ekaka, and A. Musa, "Analysis of measures to further promote the application of "AI + education"," *Indian Journal of Public Health Research & Development*, vol. 3, no. 9, 2017.

Hindawi
Scientific Programming
Volume 2022, Article ID 5044858, 6 pages
https://doi.org/10.1155/2022/5044858

Research Article

Ion Current Simulation Model Design for a Spark-Ignited Engine

Zhanfeng Song, Chundong Liu, Zhanying Wang, Canguo Zhang, and Mingchao Geng

College of Mechanical Engineering, Hebei University of Architecture, Zhangjiakou, China

Correspondence should be addressed to Chundong Liu; lcd1104@hebiace.edu.cn

Received 13 May 2022; Revised 3 June 2022; Accepted 9 June 2022; Published 19 July 2022

Academic Editor: Lianhui Li

The use of ion current signals generated during the combustion process of mixed gas as a function of initial mixture composition, temperature and pressure to detect cylinder combustion states is the most recent approach in the design, development, and optimisation of automotive engine combustion control. This paper aims to design predictive identification and computationally fast and accurate ion current models for obtaining combustion information in the engine cylinder in real time. To build a more comprehensive ion current calculation model, the effect of the flame ionisation process, the geometry of the spark plugs, and the combustion pressure and temperature are considered in the new building ion current model. The simulation ion current waveform, which has a double-peak structure, is in good agreement with the experiment values; thus, the ion current model has the potential to be used for real-time control and optimisation of engine cylinder combustion.

1. Introduction

In recent years, the energy crisis and its long-term problem, as well as the challenge of CO_2 emissions, have increased concern for the development and design of new energy engines with clean energy, high efficiency, and low emissions. Developing new electronic engine control systems can improve the efficiency of combustion engines, achieve online monitoring of the combustion process, and obtain timely information about the mixture combustion state, allowing for low-carbon and high-efficiency combustion, which has drawn the attention of many researchers and has become an active area of engine combustion diagnostics and optimisation.

The ion current signals produced in the flame combustion process carry rich information about the engine combustion process, and the spark plug as an ion current detecting probe is robust and inexpensive to manufacture; it can be installed in spark-ignition engines to obtain combustion information, such as misfire detection, peak pressure position and in-cylinder pressure, and the total combustion heat release. Given the close relationship between the combustion process and the ions produced, the study discovered that the ion current waveform can reflect the characteristics of flame development, which has been divided into the ignition phase, the front phase, and the postflame phase. By analysing the ion current waveform's characteristic parameters, a researcher can gain a better understanding of the ion formation process in engines and develop a better control programme for engine performance and emissions [1–5].

In this paper, the new ion current computing model based on the combustion process is developed which considered the spark plug geometry, flame ionisation process, equivalence ratios, and engine model; the pressure model of the entire burning process is used in the simulation calculation, and the ignition energy is considered.

The objectives of this paper are to develop fast and robust tools for analysing the mixture gas combustion process in engine cylinders, which can aid in the design, analysis, and optimisation control of newer engine designs. The ion current comparison between model calculated values and experimental measured results validates the new building model. The ion current model may help in the rapid analysis of engine combustion performance and provide a new technology path for engine combustion performance optimisation control [4–7].

2. Flame Ion Current Theory and Formulation

2.1. The Ion Current in the Front Flame Phase. After the ignition system ignites the air-fuel mixture contained in the cylinder, the flame develops and ions are believed to be formed due to various chemical ionisation processes in the reaction zone of the propagating flame; the ion current is produced in one particular direction after the application of the electric field to ions. The reaction in equation (1) is considered a typical reaction in an internal combustion engine cylinder [8]:

$$C_3H_8 + 5O_2 \longrightarrow 3CO_2 + 4H_2O. \tag{1}$$

There are various flame ionisation mechanisms proposed for ion generation during the flame burning process [9], as shown in a comprehensive discussion of the feasibility of these mechanisms [7], with the chemi-ionisation reaction in the front flame phase being the dominant initiation ionisation reaction. Equation (2) shows the main elementary reactions that create ions [8] are

$$\begin{aligned} &CH + O \xrightarrow{k_1} = 5 \times 10^{-14} cm^3/s\ CHO^+ + e^-, CH\left(^2\Sigma^+\right) + O \longrightarrow CHO^+ + e^-, \\ &CHO^+ + H_2O \xrightarrow{k_2} = 7 \times 10^{-9} cm^3/s\ H_3O^+ + CO, H_3O^+ + e \xrightarrow{k_3} = 2.3 \times 10^{-9} cm^3/s\ H_2O + H. \end{aligned} \tag{2}$$

In above set of reactions, it is experimentally found that H^3O^+ is truly the dominant positive ion in hydrocarbon flames [10, 11] and the H^3O^+ ions are produced by proton transfer from CHO^+ to H_2O, which mostly contribute to the formation of the ion current [7–12].

The ionisation reaction rates (k_1, k_2, and k_3) are shown in Equation (2), which are given in reference [12]. As the ion species produced in the above reactions reached a steady-state concentration, the ion concentrations can be expressed as follows:

$$\begin{aligned} [CHO^+] &= \frac{k_1[CH][O]}{k_2[H_2O]}, \\ [H_3O^+] &= \frac{k_2[CHO^+][H_2O]}{k_3[e^-]} \frac{k_1[CH][O]}{k_3[e^-]_{\max}}. \end{aligned} \tag{3}$$

Based on the Saha equation, the local thermal equilibrium concentration is the function of temperature, as shown in the following equation:

$$\frac{n_i n_e}{n_{i-1}} = 2\left(\frac{2\pi m_e kT}{h^2}\right)^{3/2} \frac{B_i}{B_0} \exp\left[-\frac{E_i}{kT}\right]. \tag{4}$$

In Equation (4), T is the absolute temperature, h is Planck's constant, k is Boltzmann's constant, the n_i and $n_{i\text{-}1}$ are the number density of the ionised state i and i−1, respectively, n_e is the electron number density, m_e is the electron mass, E_i is the ionisation energy of the state I, and B_i is the internal partition function.

The electron drift velocity is a function of the mobility of electrons μ and the electrical field X, which is expressed as [10]

$$v_d = \mu X. \tag{5}$$

In classical physics, the particles mean free path length λ, the possibility of interaction between particles (which can be defined by their cross sections S), and the ion number density that passes through a volume can be expressed as follows:

$$\lambda = \frac{1}{n_{tot} S}, \tag{6}$$

$$n_{tot} = \sum_i x_i n_i, \tag{7}$$

where x_i is the species fraction and ρ_i is the number density of species, i.

The combustion temperature is the major contributor to the electron drift velocity in the combustion reaction, and the effect of the electrical field is relatively small [10]; the electron drift velocity expression is shown in the following equation:

$$\mu = \frac{e\lambda}{m_e v_T}, \tag{8}$$

$$v_T = \sqrt{\frac{8kT}{\pi m_e}}. \tag{9}$$

In the above equation, v_T is the mean random velocity of the electrons and m_e is the electron mass.

Since the combustion gas volume in the engine cylinder is cylindrical, the formula of the ion current can be expressed as follows:

$$I_1 = U \frac{\pi r^2 e^2}{Sd} \left(\frac{\pi^3 x_i}{8 m_e kT}\right)^{1/2} A, \tag{10}$$

$$A = \sqrt{\frac{\left(2\left(2\pi m_e kT\right)^{3/2}/h^3\right) B_i/B_0 \exp\left[-E_i/kT\right]}{n_{tot}}}. \tag{11}$$

In Equation (11), T is the combustion temperature, n_{tot} is the number density of total species, and x_i is the species fraction, where $n_{tot} = P/kT$ [6, 10].

2.2. The Ion Current in the Postflame Phase. The thermal NO formation mechanism is the so-called extended Zeldovich mechanism [10, 11], and the thermal NO formation

mechanisms consist of three elementary reactions in Equation (12) which were used for the estimation of the formation rate of NO from molecular nitrogen in near stoichiometric air-fuel mixtures.

$$\begin{aligned} O_2 + N_2 &\leftrightarrow NO + N, \\ N + O_2 &\leftrightarrow NO + O, \\ N + HO &\leftrightarrow NO + H. \end{aligned} \tag{12}$$

The NO formation rate is much slower than the combustion rate, and most of the NO formation takes place in the postflame regions. The concentration [NO] is defined as follows:

$$\frac{d[NO]}{dt} = 6 \times 10^{16} T^{-1/2} \exp\left[-\frac{69090}{T}\right] (O_2)_{eq}^{1/2} (N_2)_{eq}. \tag{13}$$

The eq subscript stands for equilibrated conditions and the unit is moles/cm^{3}sec. In the equation, the temperature and the amount of O_2 are strongly dependent on the rate of NO formation in the postflame phase. This finding suggests that thermal ionisation is the source of the ion current in the postflame region, and NO^+ dominating the ion current in the postflame region is consistent with much of the theory and experimental work in the thermal ionisation process [10, 11]. The ionisation ratio of NO is obtained from Saha's equation shown in Equation (4), and the electron drift velocity shown in Equation (5) can be calculated from basic gas kinetic theory. The result of the derivation, where the ion current is a function of temperature, has the following form:

$$I_2 = A\sqrt{\frac{\phi_s}{n_{\text{tot}}}} T^{1/4} \exp\left[-\frac{E_i}{2kT}\right]. \tag{14}$$

In the above formula, E_i is the ionisation energy of species s, n_{tot} is the total number density, and ϕ_s is the species fraction of species s. The symbol A is a constant which is shown in Equation (11).

So, because the total ion current includes the ion current produced by the chemical ionisation reaction as well as the ion current produced by the thermal ionisation reaction, the total ion current equation is as follows:

$$I_{tot} = I_1 + I_2. \tag{15}$$

2.3. Ion Current Measuring Circuit. The ion current in the combustion chamber is measured using a modified version of the spark plug inserted into the engine cylinder. The ion current measurement circuit is shown in Figure 1 [13, 14]. During the experiment, after the spark ignition is successful, the ion current generated during the combustion process is measured and the data are collected, and the combustion pressure data generated during the combustion process are collected using the ion current measurement circuit. The collection of the ion current data and combustion pressure data adopts the ADVANTECH 1710L data acquisition card, which holds an acquisition accuracy of ±2.48% [13, 14].

2.4. Engine Calculation Model. The engine geometry is taken into account in the calculation, and the relationship between the rotation of crank and engine cylinder volume is as follows:

$$V(\theta) = V_c + \frac{\pi B^2}{4}\left(l + a - a\cos(\theta) - \sqrt{l^2 - \left(a\sin(\theta)^2\right)}\right). \tag{16}$$

An analytic model for the combustion pressure is given in closed form, which is based on connection relations with components that are simple and convenient to measure and tune, and the model's advantage is that no ordinary differential equations must be numerically solved. The expression of the analytic model for the combustion pressure is

$$p(\theta) = \begin{cases} p_c(\theta) & \theta_{ivc} < \theta < \theta_{soc} \\ (1 - x_b)p_c(\theta) + x_b p_e(\theta) & \theta_{soc} < \theta < \theta_{evo} \end{cases} \tag{17}$$

The expression of the model is further decomposed as follows [4–6]:

$$\begin{aligned} p_c(\theta) &= p_{ivc}\left(\frac{V_{ivc}}{V(\theta)}\right)^{k_c}, \\ T_c(\theta) &= T_{ivc}\left(\frac{V_{ivc}}{V(\theta)}\right)^{k_c - 1}, \\ p_e(\theta) &= p_3\left(\frac{V(\theta)}{V(\theta)}\right)^{k_e}, \\ x_b(\theta) &= 1 - e^{-b\left(\theta - \theta_{soc}/\Delta\theta\right)^{m+1}}, \\ p_3 &= p_2\frac{T_3}{T_2}, \\ T_3 &= T_2 + \Delta T_{\text{comb}}, \\ \Delta T_{\text{comb}} &= \frac{\eta_c Q_{LHV}}{c_v}\frac{1}{1 + A/F}x_b, \\ p_2 &= p_c(\theta), \\ T_2 &= T_c(\theta), \\ \theta_c &= \Delta\theta_d + \frac{1}{2}\Delta\theta_b. \end{aligned} \tag{18}$$

2.4.1. Intake Valve Close to Start of the Compression Process. Using a polytropic compression model, pressure and temperature are calculated during the compression stroke from IVC to SOC and displayed as a function of the crank angle and the coefficient $k_c = 1.3$.

$$\begin{aligned} p_c(\theta) &= p_{ivc}\left(\frac{V_{ivc}}{V(\theta)}\right)^{k_c}, \\ T_c(\theta) &= T_{ivc}\left(\frac{V_{ivc}}{V(\theta)}\right)^{k_c - 1}. \end{aligned} \tag{19}$$

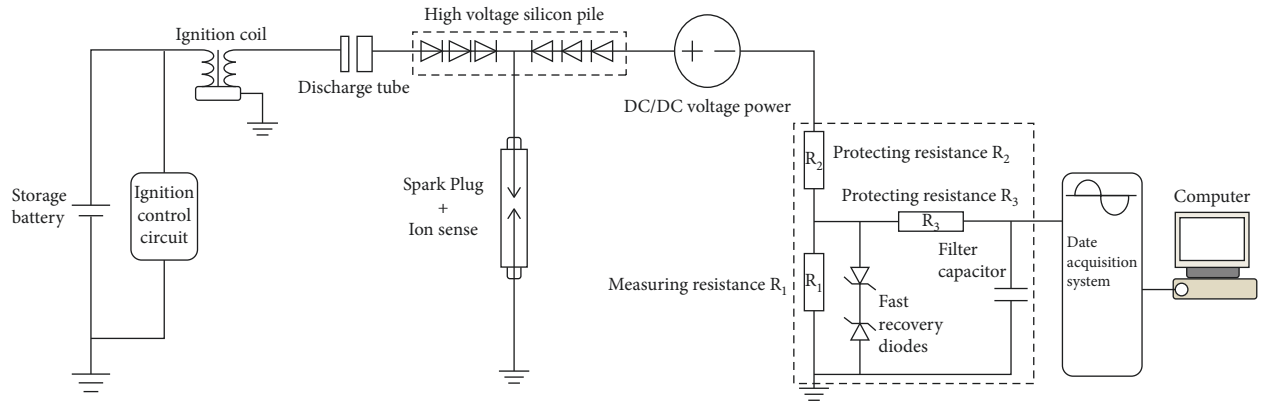

Figure 1: Ion current measuring circuit.

After to finish the compression stroke, the polytropic expansion stroke to begin, Equation (19) is performed to simulate the expansion stroke [4, 6, 8, 11, 12, 15].

2.4.2. Starting Combustion Process. After successful ignition, the combustion temperature rises in the cylinder due to the burning mixture, and the cylinder temperature is closely related to the LHV (low heating value) of the fuel, specific heat, A/F, and effective combustion efficiency.

$$T_3 = T_2 + \Delta T_{\text{comb}},$$
$$\Delta T_{\text{comb}} = \frac{\eta_c Q_{LHV}}{c_v} \frac{1}{1 + A/F} x_b. \tag{20}$$

The burned fraction of the combustible mixture in the cylinder is described by the Wiebe function combustion model, which is as follows:

$$x_b(\theta) = 1 - e^{-b\left(\frac{\theta - \theta_{soc}}{\Delta\theta}\right)^{m+1}}. \tag{21}$$

Where θ is the angle degree of crankshaft rotation, θ_{SOC} is the degree at the starting of combustion, $\Delta\theta$ is the duration degree of combustion, a and m are adjustable parameters of the Wiebe function which fitted to the values $b = 5$ and $m = 2$ to resemble actual mass fraction burned curves [4, 6, 11, 14–17].

2.4.3. Starting Expansion Process. After successful ignition, the combustion temperature rises in the cylinder due to the burning mixture.

During the expansion stroke (from SOC to EVO) process, the pressure and temperature are calculated using the polytropic expansion model, and the expression coefficient $k_e = 1.35$. The parameters of V_3, p_3, and T_3 in the following equation are related to the three-state in the ideal Otto cycle and described as follows [4, 6, 11, 16]:

$$T_c(\theta) = T_3\left(\frac{V_3}{V(\theta)}\right)^{k_e - 1},$$
$$p_e(\theta) = p_3\left(\frac{V(\theta_c)}{V(\theta)}\right)^{k_e},$$
$$p_3 = p_2\frac{T_3}{T_2},$$
$$p_2 = p_c(\theta),$$
$$T_2 = T_c(\theta). \tag{22}$$

Using the inverting the pressure ratio analysis (Matekunas, 1986, 1984, and 1983), the p_3 can be measured experimentally [17–20].

3. Simulation and Experimental Analysis

Based on the new building model, the ion current is calculated using the previously listed calculation formula, and the calculation parameters are shown in Table 1, 2, and 3.

The contribution of the major ionisation reaction and the species of charged ions to ion current generation are calculated. The parameters of several ion sources that dominate the ion current are as follows: the number of moles of H_2O is 0.125 and its ionisation energy $E_i = 12.6$ eV, the ionisation energy of CHO is $E_i = 9.88$ eV, the number of moles of N_2 is 0.75 and its ionisation energy $E_i = 15.5$ eV, and the ionisation energy of NO is $E_i = 9.27$ eV.

Figure 2 shows the calculated ion current results, the experiment measured ion current and the pressure change over the crank angle. Following a successful ignition, ion current signals are produced in the front flame during the chemi-ionisation process. The first peak of the ion current signal increases rapidly as the combustion reaction progresses; then, some of the generated ions are recombined quickly, and to produce more stabler new molecules, other ions have longer residential to the post-flame phase.

As shown in Figure 2, the calculated results and the experiment measured ion current signals have a double-peak structure, with the ion current decreasing after the first peak produced by the chemi-ionisation reaction until the second peak produced by the thermal ionisation.

Based on the chemi-ionisation theory and the derivation from formula (2) to (15), the first peak of the ion current

Table 1: The parameters of the model.

cv	Specific heat at the combustion
k_c	Polytropic coefficient for the compression pressure
k_e	Polytropic coefficient for the expansion pressure
Q_{LHV}	Heating value for the fuel
(A/F)	Stoichiometric air-fuel mass ratio
θ_{ivc}	Intake valve closing angle
θ_{evo}	Exhaust valve closing angle
p_{im}	Intake manifold pressure
T_{im}	Intake manifold temperature
$\Delta\theta_d$	Flame development angle
$\Delta\theta_b$	Fast burn angle
η_c	The fuel conversion efficiency

Table 2: Specification of ZS1100M-CNG engine characteristics and model parameters.

Cylinder diameter	100 (mm)
Piston stroke	115 (mm)
Connecting rod length	192 (mm)
Combustion efficiency	0.95
Rotate speed	1500 r/s
Polytropic compression exponent	1.335
Polytropic expansion exponent	1.35
LHV (MJ/kg)	44.5

produced is mainly due to the concentration of the H^3O^+ ion increase with combustion temperature. CHO^+ ions are produced firstly in the chemi-ionisation reaction; then, some protons transfer from CHO^+ to H_2O, and H^3O^+ is produced. The concentration of H^3O^+ ions will reach the maximum value at the first peak of ion current waveform timing along with the combustion going on, so the first peak of the ion current is mostly constituted of H^3O^+. Then, some CHO^+ are recombined quickly, and the ion current decreases. The pressure and temperature of the mixture combustion in the cylinder increase as the combustion reaction progresses; under high pressure and high-temperature conditions, NO^+, ions are the dominant ions generated by thermal ionisation reactions. When the ambient temperature is approximately 2000 K, the ionisation energy of the NO molecule is low: 9.26405 eV [21, 22]. At high temperatures, it easily ionises to NO^+, resulting in an increase in the rate of NO^+ production. As a result, the amplitude of the thermal ion current reaches its maximum, and the second peak of the ion current appears in the postflame combustion phase.

Figure 2 shows the change in cylinder pressure and ion current as the crank angle changes. The ion current waveform exhibits a double-peak structure as the combustion pressure changes; the ion current reaches the first peak before the TDC (top dead center), but the pressure reaches the peak after the TDC, and the second peak position of the ion current is consistent with that of the pressure peak position. Based on the ideal $PV = nRT$, the cylinder temperature and pressure are closely related, and the ion current signals produced ionisation reaction that depends on combustion temperature and pressure, revealing that the ion current characteristic curve in the combustion reaction

Table 3: The input parameters and the valve.

U	Spark gap voltage	80 V
r	Radius of the measurement cylinder	1 mm
d	Length of the measurement cylinder	1 mm
σ	Unit charge constant	0.1 Å^2
m_e	Electron mass	$9.31 \times 10^{-31} kg$
B_i/B_0	Internal partition function	1
k	Bolzmann's constant	1.38×10^{-23} J/K
h	Planck's constant	$6.63 \times 10^{-34} Js$
e	Unit charge constant	$1.6 \times 10^{-19} C$

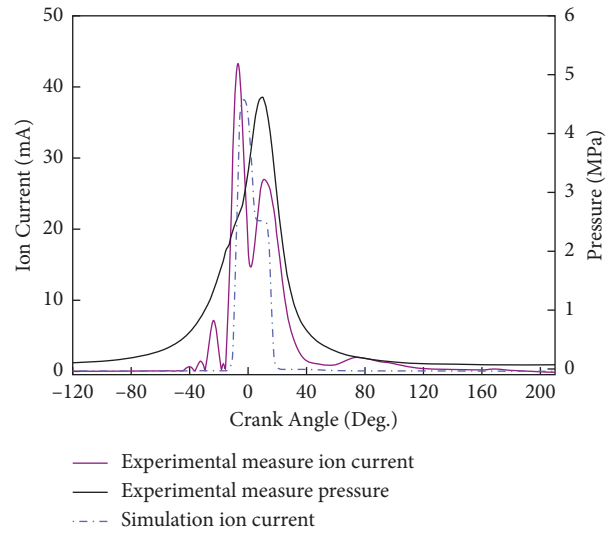

Figure 2: Ion current and the pressure variation versus the crank angle.

essentially reflects the intrinsic characteristics of the cylinder pressure and temperature during the combustion process.

Compared to the calculated and experimentally measured curve of the ion current in Figure 2, the calculated ion current follows the experimental ion current very closely; however, the peak and its width values of the calculated ion current are smaller than the experimental values, and the first peak timing are later than the experimental peak timing. The main cause of the above error is that the calculated model of the ion current primarily considers the predominant ionisation reaction mechanism and the predominant charged ions, resulting in calculated values of the ion current that are smaller and later than experimentally measured values.

4. Conclusion

This study developed the most recent model for predictive identification and computationally fast and accurate ion current for obtaining the combustion information in the engine cylinder in real time. The effect of the chemical ionisation and the thermal ionisation mechanisms, engine cylinder and spark plug geometry, and temperature and pressure of the entire combustion process are all considered in the model calculation formula to build a more comprehensive ion current calculation model. Because the

dominant function of the ionisation reaction mechanism and charged ion sources are emphatically considered in the calculations, the predicted peak value and the width of the ion current are smaller than the experimentally measured values. This model will be provided with a fast analytical method for considering the ion current as a function of the combustion flame ionisation reaction process, combustion pressure, and temperature; based on this model, a fast, robust tool for computing the ion current of the combustion process in the cylinder can greatly aid in the design, development, analysis, and control of new engine operating regimes.

Data Availability

The dataset can be accessed from the corresponding author upon request.

Conflicts of Interest

The authors declare that they have no conflicts of interest.

Acknowledgments

This work was supported by the Basic Research Foundation of Higher Education Institutions of Hebei Province (2022QNJS04), Doctor Scientific Research Foundation of Hebei University of Architecture (B-202002), and First-class Curriculum Construction Project of Automotive Engine and Transmission Virtual Simulation of Hebei University of Architecture (4070108).

References

[1] D. Zhu, J. Deng, R. Dewor, M. Wick, J. Andert, and L. Li, "Ion current-based homogeneous charge compression ignition combustion control using direct water injection," *International Journal of Engine Research*, vol. 22, no. 6, pp. 1825–1837, 2021.

[2] H. Xu, W. Fan, J. Feng, S. Qi, and R. Zhang, "Parameter Determination and ion current Improvement of the ion current sensor used for flame monitoring," *Sensors*, vol. 21, no. 3, p. 697, 2021.

[3] L. Li, B. Lei, and C. Mao, "Digital Twin in Smart manufacturing," *Journal of Industrial Information Integration*, vol. 26, no. 9, Article ID 100289, 2022.

[4] I. Andersson and L. Eriksson, "A Parametric model for ionization current in a four stroke SI engine," *Journal of Dynamic Systems, Measurement, and Control*, vol. 131, no. 2, Article ID 021001, 2009.

[5] L. Li, T. Qu, Y. Liu et al., "Sustainability Assessment of Intelligent manufacturing supported by Digital Twin," *IEEE Access*, vol. 8, pp. 174988–175008, 2020.

[6] I. Andersson, "Cylinder pressure and ionization current modeling for spark ignited engines[J]," vol. 581, p. 83, Linkopings Universitet, SE, 2002.

[7] H. F. Calcote, "Ion production and recombination in flames," *Symposium (International) on Combustion*, vol. 8, no. 1, pp. 184–199, 1961.

[8] Y. Shimasaki, M. Kanehiro, S. Baba, S. Maruyama, T. Hisaki, and S. Miyata, "Spark plug voltage analysis for monitoring combustion in an internal combustion engine (No. 930461)," SAE Technical Paper Series, 1993.

[9] P. Mehresh, R. W. Dibble, and D. Flowers, "EGR effect on ion signal in HCCI engines," SAE Paper 2005-01-2126, 2005.

[10] A. Saitzkoff, R. Reinmann, T. Berglind, and M. Glavmo, "An ionization equilibrium analysis of the spark plug as an ionization sensor[J]," , pp. 452–462, SAE transactions, 1996.

[11] G. A. Lavoie, J. B. Heywood, and J. C. Keck, "Experimental and Theoretical study of nitric Oxide formation in internal combustion engines," *Combustion Science and Technology*, vol. 1, no. 4, pp. 313–326, 1970.

[12] W. J. Miller, "Ionization in combustion processes[J]," *Oxidation and Combustion Reviews*, vol. 3, no. 2, p. 97, 1968.

[13] Z. Song, X. Zhang, Y. Wang, and Z. Hu, "Evaluation mass fraction burned obtained from the ion current signal fuelled with hydrogen/carbon dioxide and natural gas," *International Journal of Hydrogen Energy*, vol. 44, no. 46, pp. 25257–25264, 2019.

[14] Z. Song, X. Zhang, J. Zhang, and J. Cao, "Predicting the heat release rate of ion current combustion process fuelled with hydrogen/carbon dioxide and natural gas," *Journal of Energy Engineering*, vol. 145, no. 1, Article ID 04018068, 2019.

[15] A. Pundle, *Modeling and Analysis of the Formation of Oxides of Nitrogen and Formaldehyde in Large-Bore, Lean-Burn, Natural Gas Engines[D]*, University of Washington, Seattle, 2013.

[16] C. Pinca-Bretotean, S. Ratiu, and D. Stoica, "Mathematical model for cylinder pressure in a spark ignition engine[J]," *Annals of the Faculty of Engineering Hunedoara*, vol. 10, no. 3, p. 285, 2012.

[17] J. M. Rodrigues, A. Agneray, E. Domingues, X. Jaffrezic, and P. Vervisch, "Ionic current and flame electric potential measurements in a premixed laminar insulated flame[J]," , pp. 45-46, European Combust Meeting ECM, 2005.

[18] L. Eriksson, "CHEPP-a chemical equilibrium program package for matlab[R]," , pp. 730–741, SAE transactions, 2004.

[19] L. Eriksson and I. Andersson, "An analytic model for cylinder pressure in a four stroke SI engine[R]," , pp. 726–733, SAE Transactions, 2002.

[20] D. Yap, A. Megaritis, S. Peucheret, and M. L. Wyszynski, "Effect of hydrogen addition on natural gas HCCI combustion [R]," , pp. 1296–1305, SAE transactions, 2004.

[21] C. Kefa, Y. Qiang, and L. Zhongyang, "Combustion theory and pollution control[J]," Mechanical Industrial Publishing Company, Bei Jing, 2004.

[22] Z. Song, X. Zhang, and B. Zhang, "Study on the correlation between ion current integral signal and combustion pressure," *International Journal of Hydrogen Energy*, vol. 47, no. 12, pp. 8060–8070, 2022.

Hindawi
Scientific Programming
Volume 2022, Article ID 6173463, 10 pages
https://doi.org/10.1155/2022/6173463

Research Article

Text Reconstruction Method of College English Textbooks from the Perspective of Language Images

Xiaojuan Peng

Guilin University of Electronic Technology, Guilin 541004, China

Correspondence should be addressed to Xiaojuan Peng; deliapeng0826@guet.edu.cn

Received 21 April 2022; Accepted 18 May 2022; Published 18 July 2022

Academic Editor: Lianhui Li

With the continuous development of social economy, English learning plays an increasingly important role in daily communication. However, the update speed of English textbooks is far lower than the development speed of English. How to reconstruct the text of English textbooks in colleges and universities to improve the learning effect of college English has become an urgent problem to be solved. In order to solve this problem more effectively, this paper proposes a text reconstruction method for college English textbooks from the perspective of language images. First, this paper proposes a text reconstruction network model for college English textbooks, which includes two self-network models, namely, a text feature extraction network and an image feature extraction network. Second, text designs an English text feature reconstruction network to fuse image features and text features to guide the generation of new English texts according to the generated emotions. Finally, through a large number of experiments, it is proved that the text reconstruction method of college English textbooks from the perspective of language images can effectively generate new texts of college English textbooks, enhance the emotional color of college textbooks, and improve the effect of English learning.

1. Introduction

English plays an important role in the daily affairs of internationalization, but learning English [1, 2] is often a difficult problem. Usually, English learning requires teachers to reconcept and design the content of the text [3, 4], improve students' interest in learning in a reasonable way, turn boring learning into active learning, and deepen the understanding of the text content [5, 6]. The text reconstruction method of college English textbooks [7, 8] has gradually become an effective method to improve college students' English learning. Through the reconstruction of a variety of English knowledge in English textbooks and the use of diversified text forms, college students can improve the English learning methods and skills [9, 10] mastered by college students and deepen their understanding of the text content. The method of text reconstruction of English textbooks is widely used in various learning tasks such as English learning in primary and secondary schools, professional English training, and English reading teaching.

The teaching method of English textbooks is relatively simple. Traditional learning methods [11] often fail to stimulate students' desire to learn, limit students' imagination and comprehension ability, and cannot improve students' learning effect [12, 13]. Usually, teachers in colleges and universities will give a certain degree of guidance to study [14, 15] and reorganize [16, 17] the structure and content of college English textbooks, reconstruct the old-fashioned content in the text into lively cases, stimulate students' imagination, and improve students' learning effect. However, many teachers find some problems in the teaching process. First of all, each country has a certain degree of cultural difference [18, 19]. In order to improve students' ability to master English and improve their learning effect, students need to constantly feel the emotions [20, 21] and foreign cultures reflected in the text. Secondly, each teacher's teaching style [22, 23] is very different, and the understanding and reconstruction of the text content are very different. How to make students have a strong interest in the learning of English textbooks often requires teachers to pay a

lot of money, time, and energy [24, 25]. The difficulties in learning traditional college English textbooks are that the content of the text is relatively old-fashioned and lacks emotional color. College students will have a dull learning mood during learning, which will reduce the effect of learning.

With the continuous progress of science and technology, artificial intelligence methods represented by deep learning technology [26, 27] continue to solve the problems existing in real teaching. Deep learning technology is mainly divided into two aspects. One is the neural network method based on image processing [28, 29], which is mainly used to process image tasks and is widely used in vision-related tasks such as image recognition, image classification, and image segmentation. The second is the neural network method based on text processing [30, 31], which mainly deals with text tasks and is widely used in natural language processing tasks such as text emotion recognition, text emotion classification, and text prediction. In the task of text reconstruction of college English textbooks, it is mainly related to the content of the text and the images in the book. The text features and image features are extracted through neural networks, and new textbook texts with specific emotions can be generated by adding emotional factors and continuously improve students' learning interest and learning effect.

In order to allow college students to better master English and improve the effect of English learning, this paper proposes a text reconstruction method for college English textbooks from the perspective of language images. Firstly, this paper proposes a text feature extraction network based on college English textbooks. It mainly includes two subnetworks; the two subnetworks are the text feature extraction network and the image feature extraction network [32, 33]. Secondly, this paper designs an English text feature reconstruction network [34], which is mainly used to fuse image features and text features, reconstruct college English textbook texts according to the generated emotions, and generate texts with characteristic emotions. Finally, through a large number of experiments, it is proved that the text reconstruction method of college English textbooks based on the perspective of language images can effectively reconstruct the texts of college English textbooks, enhance the emotional color of college textbooks, and improve the English learning ability of college students' teaching burden. The main purpose of this paper is to solve the difficulty of learning English textbooks in colleges and universities, improve the learning effect of college students, and reduce the workload of teachers in schools.

2. Related Work

2.1. Image Feature Extraction. Image features exist widely in people's daily life and usually contain human emotional information, which is an effective way of emotional communication and communication between people. Human emotions are usually expressed through images, and this emotion representation method is widely used in intelligent monitoring, online learning, autonomous driving, and other fields.

Image emotional feature extraction is firstly to preprocess the input image, then use the convolutional neural network to extract the emotional information in the image, and then classify according to the extracted emotional information. Image emotion feature extraction is an indispensable link in neural network, and the effect of emotion feature extraction ultimately affects the effect of emotion classification. Convolutional neural networks can obtain higher-level and more abstract feature representations of images by directly extracting the features of images for learning, thus obtaining more essential features in images, and thus making deep learning features more accurate and general.

2.2. Text Feature Extraction. In recent years, text data has grown rapidly through the Internet, and a large amount of text data has been continuously accumulated. These massive data contain a lot of valuable information. Natural language processing is the main method to solve these pieces of text feature information. It uses the text to train a classifier model and then uses the trained network model to divide and supplement the new text.

Sentiment recognition of text content is also called sentiment analysis. It mainly divides the text into a variety of emotion types according to the meaning and emotional information expressed by the text, which is a multisentiment classification problem. By analyzing and researching these text data, important feature information is extracted, which can be used to analyze the public's attention to hot topics and emotional tendencies, which provides important research ideas for correctly guiding the direction of social public opinion.

With the continuous advancement and development of technology, multimodal data is still a very challenging task at present. In image and text multimodal data, the information contained in text and image is generally complementary. Compared with single-modal data of text or images, multimodal data contains more comprehensive information and can better display and explain the emotional characteristics used. First, the amount of information contained in data of different modalities is often different. Sentiment analysis of multimodal data requires effective understanding and extraction of emotional features of multimodal data. Compared with the traditional single-modal sentiment method, the multimodal sentiment analysis task needs to combine the effective information of multiple modalities to extract the feature interaction between the modal information and the multimodal information in a reasonable way.

2.3. English Text Reconstruction. It is often difficult to improve the English ability of college students through traditional English teaching methods, which are not conducive to students' good grasp of English syntax knowledge and enhance the effect of English learning. Therefore, on the basis of traditional college English textbook learning combined with English practical teaching activities, many teachers have proposed methods of text reconstruction of college English textbooks from the levels of syntactic

analysis, text sorting, title prediction, and textual analysis to improve English learning. The learning effect has a certain reference value.

English text prediction is a high-level idea of text reconstruction in English textbook learning. It requires readers to predict the unknown content of English textbooks based on existing information and personal understanding of textbook content. Mind map refers to presenting the text content in a more specific, vivid, and hierarchical organization based on the thematic events in English textbooks, using keywords, images, color changes, and other main branches. Based on the mind map of text content, it can help students have a deeper understanding of the content of English textbooks, splicing fragmentary knowledge, grasp the key points in learning, and understand English textbooks from a macrolevel. Reconstruction of text content is a common way of learning, which means that learners, from the perspective of the author, combine the knowledge and content they have learned and rewrite the text content, trends, trends, and so on on the basis of understanding and learning English textbooks. Reconstruction can deepen the understanding of the text content of the textbook and realize the process of learning, accumulating knowledge, and transforming the text content of college English textbooks. Text reconstruction can rearrange and understand the content of English textbooks, improve students' interest in learning, and deepen their understanding of the text in textbooks.

3. Methods of Text Reconstruction in College English Textbooks

In order to more effectively obtain the feature information of each modality and the interaction of feature information between modalities, this paper adopts a feature fusion model based on standard transformer structure to fuse the extracted image and text features and use it to generate emotional new text message in Figure 1. First, this paper proposes a text feature extraction network, which uses the LSTM network structure to encode temporally continuous text feature information, then uses the attention mechanism to obtain the text feature information that this paper pays more attention to, and finally generates text feature vectors for input into college English textbooks for text reconstruction in the network. Second, this paper proposes an image feature extraction network to input images from textbooks into the network structure. Its main function is to extract human emotional information through images, input the generated image feature vector into the text reconstruction network of college English textbooks, and add more emotional features to the newly generated text information. With two subnetworks and a backbone network, the text reconstruction method of college English textbooks proposed in this paper can generate new content with specific emotions through a generative method. Deep learning methods can generate various types of text reconstruction content, increase students' interest in learning, and greatly reduce the workload of school teachers.

3.1. Text Feature Extraction Network. The text feature extraction network proposed in this paper is improved on the basis of Att-CNN-BiGRU, which mainly consists of three aspects: text vectorization, text feature extraction, and feature vector generation, as shown in Figure 2. The first part is the vectorization of text features. The main function is to map each word in the input text to a vector representation, and the text vector is represented by the word vector.

Text vectorization is to map the text into a vector that can be recognized and processed by a computer. It is mainly to avoid the problems of one-hot encoding vector sparseness and dimension disaster. Generally speaking, text vectors are mainly composed of word vectors and position vectors. The word vector is to convert the words in the text into vectors that can express semantic information. Considering the meaning of the words and the influence between words, the semantic similarity of words is calculated. The position vector is to convert the position features of the words in the text into vectors and make it clear that the word in the sentence is the trigger word. The position feature is defined as the relative distance between the current word and the candidate word, which represents the relative position of the current word in the sentence.

$$\begin{aligned} S &= \{w_1, w_2, \ldots, w_n,\}, \\ X &= \{x_1, x_2, \ldots, x_n,\}, \\ x_i &= [e_i, pe_i], \quad d = d_w + d_p, \end{aligned} \tag{1}$$

where S represents the sentence, w_i represents the i-th value in the sentence, and n represents the length of the sentence. A similar method is used in this paper to map the word w_i to a real-valued vector x_i; usually, a sentence consists of multiple values.

The text feature extraction network model proposed in this paper is used to extract text features. Text features are divided into lexical-level features and sentence-level features. The lexical-level feature is to extract the background knowledge of the word, including the word's part of speech, semantic information, emotional information, and classification information. Sentence-level features are the contextual information of the entire sentence in the text, such as grammatical features, degree of association, and emotional expression. Convolution operations are used to extract lexical features in text, and BiLSTM and attention mechanism are used to extract sentence-level features.

Convolutional neural networks can only extract local feature information within the convolution window and cannot perform feature extraction and association on textual context information. In order to fully consider the lexical-level features and sentence-level features of each word and enhance the degree of association between words, this paper introduces a self-attention mechanism to obtain lexical-level features more comprehensively while avoiding lexical position information in the pooling operation of loss.

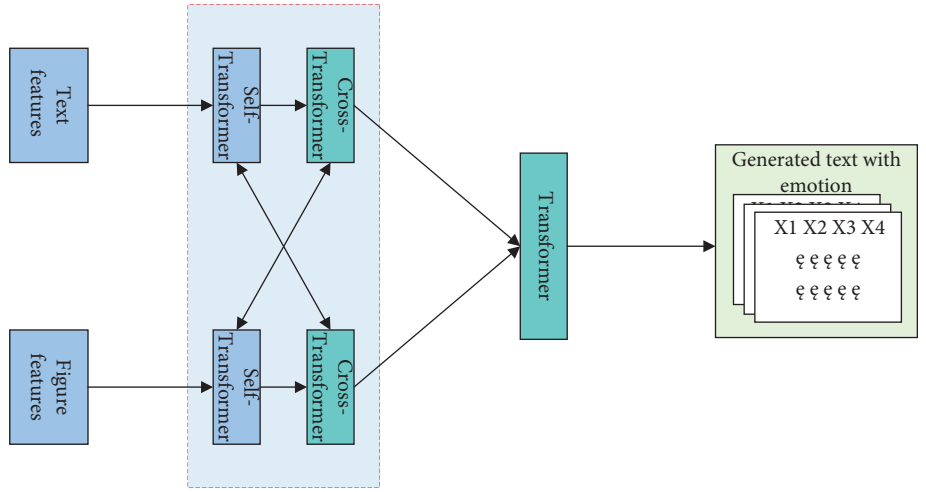

Figure 1: Structure diagram of the text reconstruction network of college English textbooks.

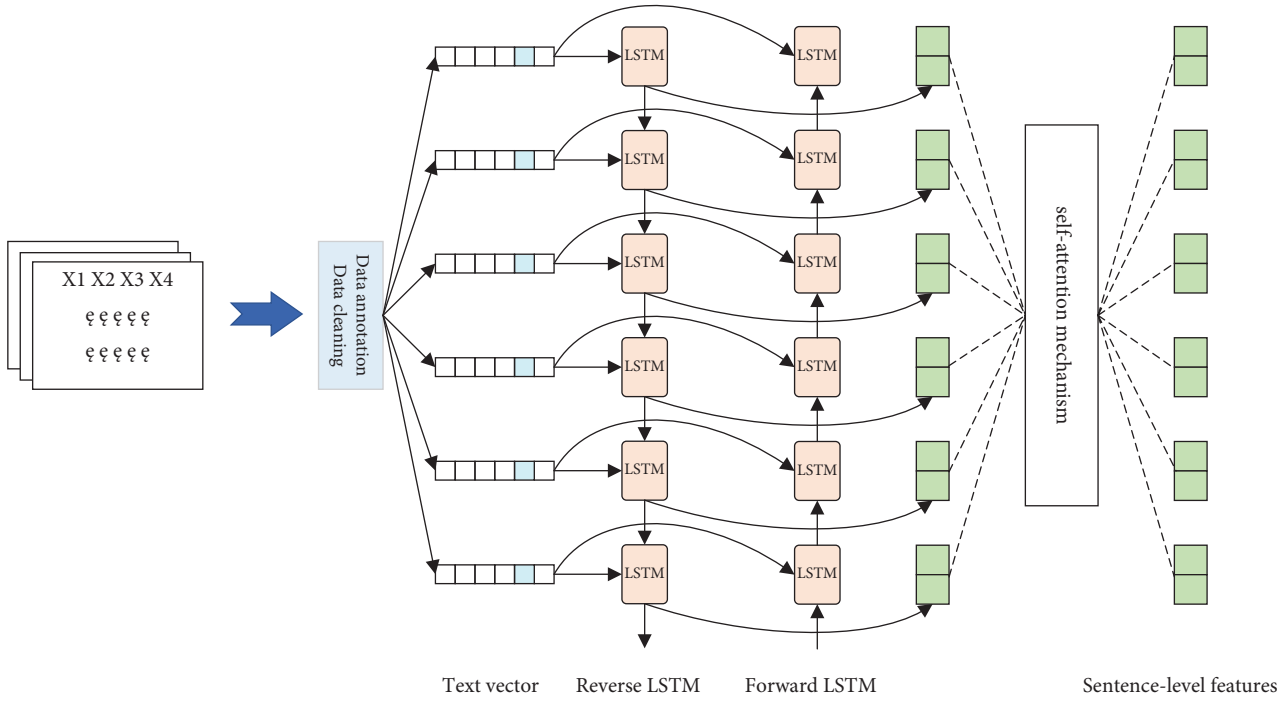

Figure 2: Network structure diagram of text feature extraction.

$$f_{att}(Q, K, V) = \text{softmax}\left(\frac{QK^T}{\sqrt{d_k}}\right)V, \quad Q \in R^{n\times d_k}, \quad K \in R^{n\times d_k}, V \in R^{n\times d_v}, \tag{2}$$

where T represents the transpose operation of the matrix and dividing by $\sqrt{d_k}$ is to prevent the inner product result from being too large in the experiment. The self-attention mechanism essentially reencodes the input matrix into a new matrix after considering the global feature information through the convolution operation of the matrix. The self-attention mechanism assigns different weights to different vocabulary-level features and considers the global information of the vocabulary and the relationship between related associations so as to obtain the corresponding vocabulary features or weights.

3.2. Image Feature Extraction Network. The AlexNet neural network is an 8-layer convolutional neural network with three hidden layers in Figure 3. Its basic structure includes an input layer, 5 convolutional layers, 3 pooling layers, 2 fully connected layers, and an output layer. The hidden layer consists of convolutional layers and pooling layers. Convolutional neural networks can obtain multidimensional features of images through convolution layers, and different

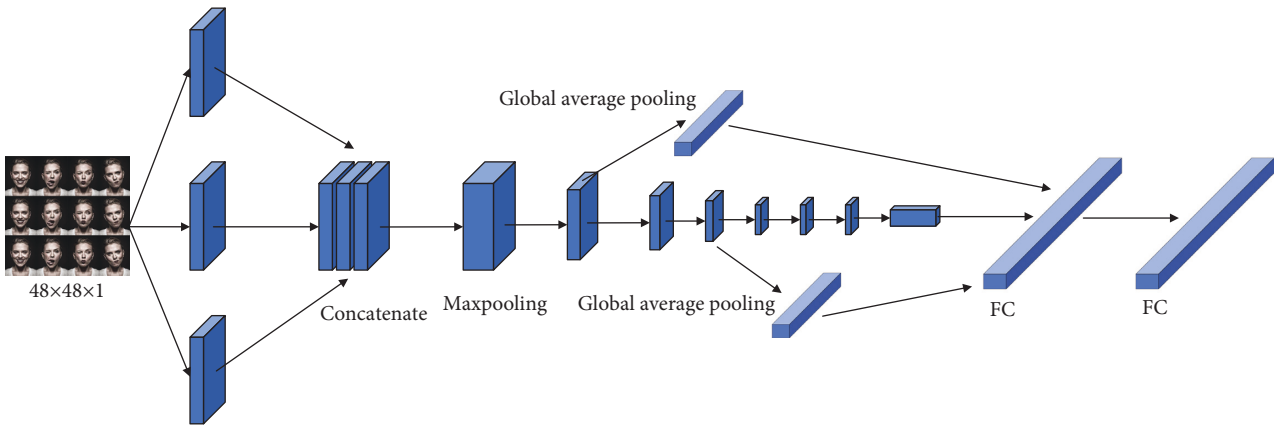

Figure 3: Network structure diagram of image feature extraction.

convolution kernels can extract different image features. For emotional images of faces, convolution kernels of different scales can be used for feature extraction, and feature information of different scales can be obtained. In this paper, various types of convolution kernels are used to obtain richer image features so that the feature information of the input data can be more accurately expressed.

The sizes of the multiscale convolution kernels in this paper are 1×1, 3×3, and 5×5, which extract features from the input image data, respectively, and add a BN layer at the end of the convolution layer to improve the multiscale convolution network. Finally, the obtained multidimensional expression features are connected and fused. This feature connection method ensures the richness of features. Among them, the 1×1 convolution kernel can organize information across channels, improve the expressive ability of the network model, and greatly enhance the nonlinear features while keeping the feature scale unchanged. At the same time, the channel can also be adjusted, the pixels on different channels are linearly combined, and then the nonlinear operation is performed to reduce the dimension and the number of parameters.

After cross-layer information fusion, the edge information is also enhanced while retaining the rich high-dimensional features of the feature map. In this paper, the first and second pooling layers of the network are connected to the fully connected layer, and the low-level feature information and high-level feature information are fused as the input of the softmax layer. It can effectively express the feature information of input data, alleviate the problem of gradient disappearance and explosion, enhance the propagation of features in different dimensions, and effectively utilize multidimensional feature information. Cross-layer connection fuses low-level features and high-level features to more accurately describe the feature information of the input data. However, too many parameters are generated in this way, which will cause parameter explosion and overfitting. There are many redundant features, which will reduce the training speed of the network and affect the accuracy of recognition. Therefore, a global average pooling layer is added at the end of the network model to average each feature map, and finally, the result is input to the softmax layer.

3.3. LSTM Neural Network. Because neural networks such as RNN retain previous data information when processing time-series-based data, the previous data will have less and less effect on the model with the subsequent data input; that is, there is a problem of long-distance dependence. In addition, some unimportant data will also be retained by neural network models such as RNN, resulting in data redundancy. In order to solve the above problems, this paper introduces the LSTM network structure. It has the characteristics of maintaining long-term memory and has good performance in processing time-series-based data. The network model structure is shown in Figure 4.

Equation (3) represents the forget gate of LSTM calculated from the input data and the hidden state. Equation (4) indicates that the input data and the weight of the forgetting gate are subjected to linear operation, and the output of the forgetting gate is obtained to represent the memory level of the long-term memory state. Equations (5) and (6) represent the input gate part of the LSTM.

$$C = \text{sigmoid}\left(W_1\left(x_{i-1}, h_{i-1}\right) + b_1\right), \tag{3}$$

$$C' = \text{sigmoid}\left(W_1\left(x_{i-1}, h_{i-1}\right) + b_1\right) \times c_i, \tag{4}$$

$$C_1'' = \text{sigmoid}\left(W_2\left(x_{i-1}, h_{i-1}\right) + b_2\right), \tag{5}$$

$$C_2'' = \text{sigmoid}\left(W_3\left(x_{i-1}, h_{i-1}\right) + b_3\right). \tag{6}$$

Through the calculation of the above formula, the LSTM network model can complete the update of the existing long-term memory elements, as shown in (7) and (8). Finally, the output gate, LSTM network model is improved. The LSTM network model comprehensively considers the influence of two aspects of the current long-term memory and the current input data elements in the output, as shown in formulas (9) and (10). Finally, the result of the long-term memory is activated by the tanh function, which finally represents the size and positive or negative of the actual output of the LSTM.

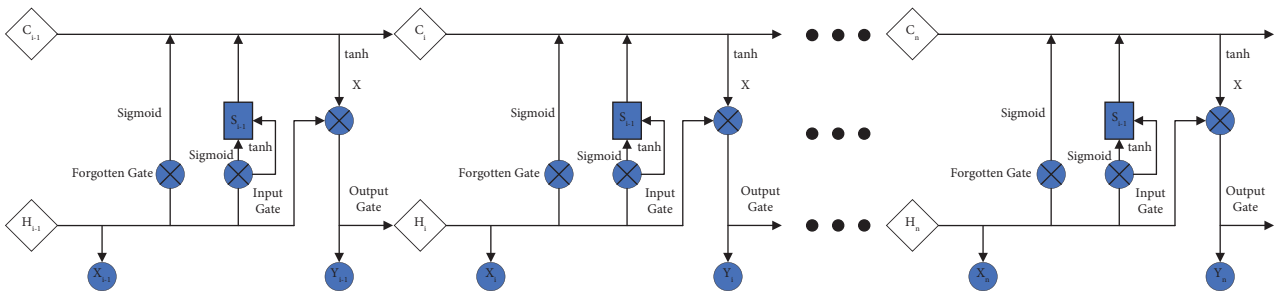

Figure 4: LSTM neural network structure diagram.

$$C'' = C_1'' \times C_2'', \tag{7}$$

$$c_i = C' \times C'', \tag{8}$$

$$y' = \text{sigmoid}\left(W_3\left(x_{i-1}, h_{i-1}\right) + b_3\right), \tag{9}$$

$$y_{i-1} = y' \times \tanh\left(c_i\right). \tag{10}$$

4. Experimental Results and Analysis

4.1. Experimental Setup. In terms of text feature extraction and processing, this paper uses the ACE2005 English prediction library as training data. It mainly annotates information such as event mentions, event trigger words, and event elements and is widely used in feature extraction tasks in English. It divides the dataset into training, validation, and test sets in a roughly 8 : 1 : 1 ratio. At the same time, the precision rate, recall rate, and $F1$ value are selected as important indicators for model performance evaluation.

In terms of image datasets, this paper uses the COCO large-scale dataset to train and test the network model. The main purpose of image training is to add emotional information to the newly generated text.

The text uses Adam optimizer to optimize the parameters of the neural network model. The initial learning rate is 10^{-3}, which is gradually reduced to 10^{-4} and 10^{-5}. By adjusting the learning rate, the loss function value of the network model is continuously reduced, and the prediction accuracy is continuously improved until a stable equilibrium state is reached.

There are many types of human emotions, and different datasets have different types. In order to prove the effectiveness of the proposed text reconstruction method for college English textbooks, this paper screened these emotion types. Both LSTM and GRU units are capable of processing sequences of events. In general, the LSTM prediction effect is better, and the GRU unit is actually more efficient. In this paper, more attention is paid to the generation effect of the text content, so the LSTM unit is adopted.

4.2. Evaluation Indicators. The loss function value is an important indicator for evaluating the actual performance of the model. When training a neural network, in order to improve the prediction effect of the network model, the loss function value is often reduced to a very low level in order to obtain more ideal network model parameters. The loss function is an important reference index to measure the performance of the neural network. Usually, the smaller the loss function value in the test set, the better the function model. For the text reconstruction task of college English textbooks, we use the MSE mean square loss function as the loss function in this paper to fit the regression problem of the predicted value.

$$\text{MSE} = \frac{1}{n}\sum_{i=0}^{n}\left(\hat{y}_i - y_i\right)^2. \tag{11}$$

Text or images based on time series usually contain hidden relationships. Through the training of neural network models, latent features between continuous data can be discovered to realize data prediction. In this paper, the MSE loss function is used to continuously adjust the parameters of the network model in reverse to improve the prediction effect of the network model.

In addition, in order to evaluate the prediction effect of the network model, this paper also adopts the MAE mean absolute error as the evaluation index of the model. MAE represents the mean absolute value of the error between the predicted value and the true value. Compared with MSE, MAE can directly reflect the difference with the original data. The smaller the MAE of the network model test data, the better the prediction result of the model.

$$\text{MAE} = \frac{1}{n}\sum_{i=1}^{n}\left|\hat{y}_i - y_i\right|. \tag{12}$$

4.3. Comparison and Analysis of Experimental Results. As shown in Figure 5, A–E represent the number of emotion categories in the image dataset in the subnetwork, which are angry, natural, fearful, happy, and sad, respectively. Correspondingly, the percentages in the figure represent the proportion of each type in the image dataset. From the figure, we can clearly see that the number of types B is the largest and the number of types E is the least. Natural and normal images make up the largest proportion of our dataset, and sad images make up the least. Image emotional feature extraction network is mainly trained on this dataset to extract emotional features in images.

Figure 6 shows the distribution of sentiment features in the text dataset. This paper mainly divides text sentiment features into two categories: one is positive sentiment, and

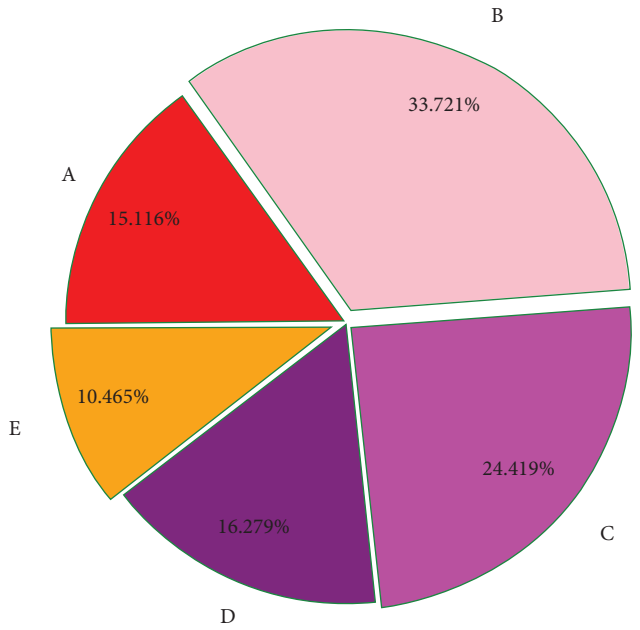

Figure 5: Proportion of emotion categories in image datasets.

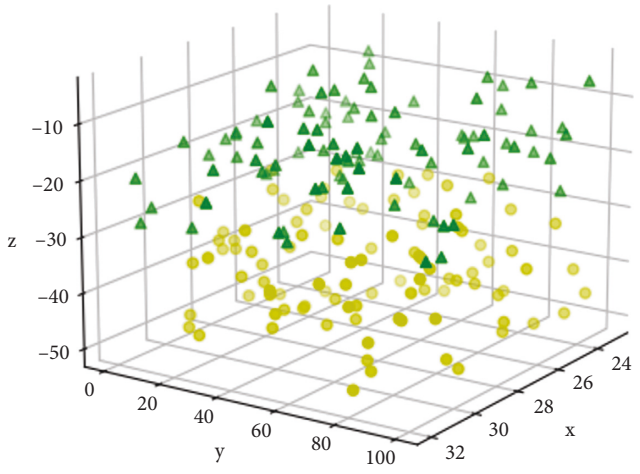

Figure 6: Sentiment dispersion in text datasets.

the other is negative sentiment. Positive emotions include joy, enthusiasm, and confidence, and negative emotions include anger, fear, and sadness. In the figure, we use green to represent positive sentiment in the text and yellow to represent negative sentiment in the text dataset. On the whole, the demarcation line between negative emotion and positive emotion is relatively clear, which is suitable for model training and testing.

Figure 7 shows the results of network model optimization learning. The two axes in the plane represent the model parameter settings of the image feature extraction and text feature extraction subnetworks. From the figure, we can see that the parameters of the network model can be optimized by setting some parameters in the image and text feature extraction subnetworks.

Figure 8 shows the learning effect of the image network model. The lighter the color value, the better the prediction effect of the model. From the above figure, we can clearly see

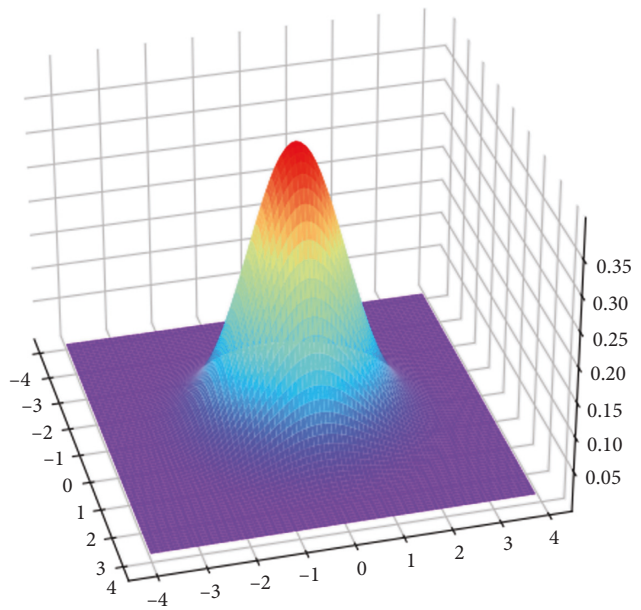

Figure 7: Network model optimization learning.

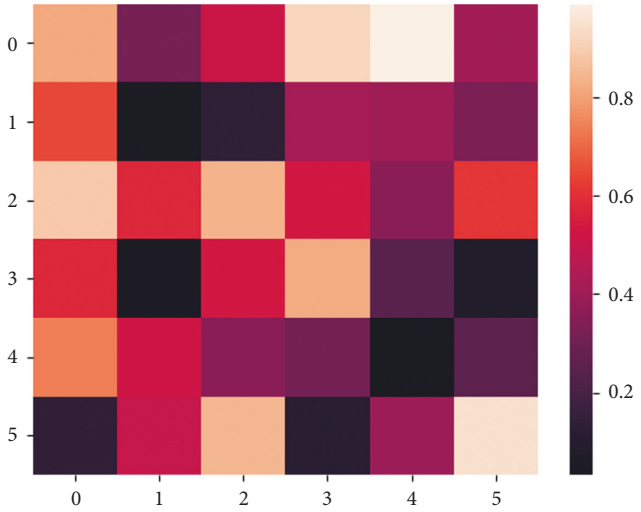

Figure 8: Confusion matrix for image network model learning.

that the network model in this paper has a certain accuracy in distinguishing emotion categories, which meets the requirements of image feature extraction.

Figure 9 shows the learning effect of the text feature extraction network. The deeper the red value of the color value, the worse the prediction effect, and the darker the blue value, the better the prediction effect. The text feature extraction network in this paper expands the category of emotion and has been able to classify 10 emotion types more accurately.

Figure 10 shows the learning effect of the backbone network model. The x-axis and y-axis, respectively, represent the number of iterations of the subnetwork model, which is the number of times of training in different data sets. The z-axis represents the effect of learning the backbone network model together with the two subnetwork models. From the

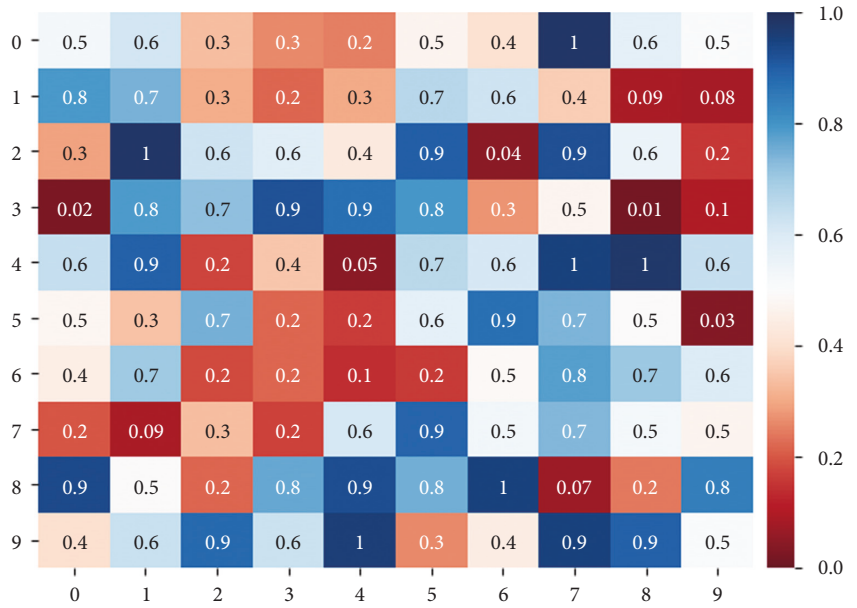

Figure 9: Prediction effect of text feature network model.

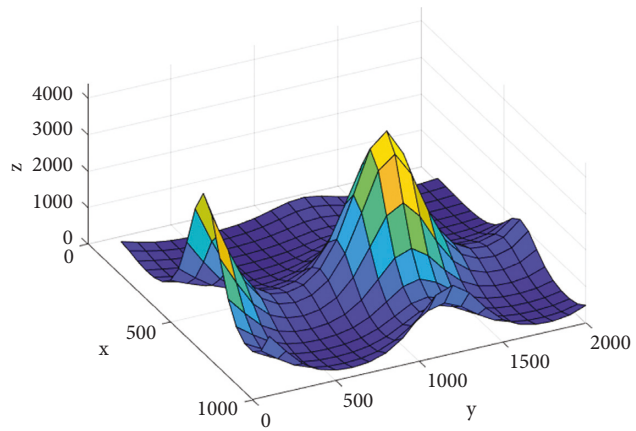

Figure 10: The learning effect of the backbone network model.

Figure 11: Comparison of various neural network models.

figure, we can see that multiple experiments and settings through multiple network models can effectively improve the generation effect of the entire network model.

This paper compares the methods of various neural network models, and the experimental results are shown in Figure 11. It should be noted that all experiments are trained and tested on the same test platform and only the structure of the network model is different. All experiments are trained from scratch with the same learning rate and optimizer. GT represents the real value of the data predicted by the network model, and other colors represent the experimental results obtained by CNN, RNN, transformer, and the method in this paper, respectively. From the data, we can clearly see that the method in this paper has a better prediction effect on the data and is closer to the true value.

5. Summary

In order to improve the learning effect of college English, this paper proposes a text reconstruction method for college English textbooks from the perspective of language images. In this paper, the text feature extraction network and image feature extraction network are used to obtain text features and image features, respectively. Then, this paper designs a multimodal feature fusion network and a college English text generation network, which mainly guides the reconstruction of new college English texts according to the emotional features in image texts, generates new texts of college English textbooks with emotions, and improves college English learning effect. Through a large number of experiments, it is proved that the reconstruction method of college English textbooks based on the perspective of language and images can improve the learning ability of college students and reduce the teaching burden of college teachers. The neural network model adopted by the text can handle multimodal data and can be extended to more data types in future work, such as audio data and video data.

Data Availability

The dataset can be obtained from the corresponding author upon request.

Conflicts of Interest

The author declares that there are no conflicts of interest.

References

[1] H. Dehghanzadeh, H. Fardanesh, J. Hatami, and O. TalaeeNoroozi, "Using gamification to support learning English as a second language: a systematic review," *Computer Assisted Language Learning*, vol. 34, no. 7, pp. 934–957, 2021.

[2] A. Hashemi and S. I. Kew, "The effects of using blended learning in teaching and learning English: a review of literature[J]," *The Eurasia Proceedings of Educational and Social Sciences*, vol. 18, pp. 173–179, 2020.

[3] F. Nappi and C. Spadaccio, "Keep fumbling around in the dark when it comes to infective endocarditis, or produce new, reliable data to redesign the guidelines?" *The Journal of Thoracic and Cardiovascular Surgery*, vol. 155, no. 1, pp. 75-76, 2018.

[4] D. J. Fremont, J. Chiu, D. D. Margineantu, D. Osipychev, and S. A. Seshia, *Formal Analysis and Redesign of a Neural Network-Based Aircraft Taxiing System with VerifAI[C]//International Conference on Computer Aided Verification*, Springer, Cham, pp. 122–134, 2020.

[5] K. Wijekumar, B. J. F. Meyer, P. Lei, and D. L. HernandezAugust, "Improving content area reading comprehension of Spanish speaking English learners in Grades 4 and 5 using web-based text structure instruction," *Reading and Writing*, vol. 31, no. 9, pp. 1969–1996, 2018.

[6] J. M. Vargas Vásquez and R. Zuñiga Coudin, "Graphic organizers as a teaching strategy for improved comprehension of argumentative texts in English[J]," *Actualidades Investigativas en Educación*, vol. 18, no. 2, pp. 32–54, 2018.

[7] B. Setyono and H. P. Widodo, "The representation of multicultural values in the Indonesian Ministry of Education and Culture-Endorsed EFL textbook: a critical discourse analysis," *Intercultural Education*, vol. 30, no. 4, pp. 383–397, 2019.

[8] H. P. Widodo, "A critical micro-semiotic analysis of values depicted in the Indonesian ministry of national education-endorsed secondary school English textbook," *Situating Moral and Cultural Values in ELT Materials*, Springer, Cham, pp. 131–152, 2018.

[9] M. Delphine, N. Sylvestre, N. Gabriel, and N. Wenceslas, "A psychometric analysis of the study skills questionnaire for university of Rwanda undergraduate students at national police college," *Creative Education*, vol. 13, no. 03, pp. 862–885, 2022.

[10] T. Bonsaksen, M. C. Småstuen, M. M. Thørrisen, and T. FongLimBrown, "Factor analysis of the Approaches and Study Skills Inventory for Students in a cross-cultural occupational therapy undergraduate student sample," *Australian Occupational Therapy Journal*, vol. 66, no. 1, pp. 33–43, 2019.

[11] I. A. Krishnan, G. D. Mello, S. A. Kok, and V. N. SabapathyMunianChingKandasamy RamalingamBaskaranKanan, "Challenges faced by hearing impairment students during COVID-19," *Malaysian Journal of Social Sciences and Humanities (MJSSH)*, vol. 5, no. 8, pp. 106–116, 2020.

[12] A. Syakur, L. Musyarofah, S. Sulistiyaningsih, and W. Wike, "The effect of project based learning (PjBL) continuing learning innovation on learning outcomes of English in higher education," *Budapest International Research and Critics in Linguistics and Education (BirLE) Journal*, vol. 3, no. 1, pp. 625–630, 2020.

[13] X. Wang, Y. Liu, and B. Ying, "The effect of learning adaptability on Chinese middle school students' English academic engagement: the chain mediating roles of foreign language anxiety and English learning self-efficacy[J]," *Current Psychology*, vol. 6, pp. 1–11, 2021.

[14] T. Xiong and Z. m Yuan, ""It was because I could speak English that I got the job": neoliberal discourse in a Chinese English textbook series," *Journal of Language, Identity and Education*, vol. 17, no. 2, pp. 103–117, 2018.

[15] A. Syakur, E. Junining, and M. K. Mubarok, "Developing English for specific purposes (ESP) textbook for pharmacy students using on-line teaching in higher education[J]," *Britain International of Linguistics Arts and Education (BIoLAE) Journal*, vol. 2, no. 1, pp. 467–474, 2020.

[16] H. Gong, Y. Sun, and X. Feng, "Tablegpt: few-shot table-to-text generation with table structure reconstruction and

content matching[C]," in *Proceedings of the 28th International Conference on Computational Linguistics*, pp. 1978–1988, Spain, 2020.

[17] T. M. Paixo, R. F. Berriel, M. C. S. Boeres et al., "Fast (er) reconstruction of shredded text documents via self-supervised deep asymmetric metric learning[C]," in *Proceedings of the IEEE/CVF Conference on Computer Vision and Pattern Recognition*, pp. 14343–14351, Seattle, WA, USA, 2020.

[18] M. Brunton and C. Cook, "Dis/Integrating cultural difference in practice and communication: a qualitative study of host and migrant Registered Nurse perspectives from New Zealand," *International Journal of Nursing Studies*, vol. 83, pp. 18–24, 2018.

[19] H. Forbes-Mewett, K. Hegarty, and R. Wickes, "Regional migration and the local multicultural imaginary: the uneasy governance of cultural difference in regional Australia," *Journal of Ethnic and Migration Studies*, vol. 6, pp. 1–18, 2021.

[20] I. W. Suryasa, I. N. Sudipa, I. A. M. Puspani, and I. M. Netra, "Translation procedure of happy emotion of English into Indonesian in kṛṣṇa text," *Journal of Language Teaching and Research*, vol. 10, no. 4, p. 738, 2019.

[21] W. Suryasa, I. N. Sudipa, and I. A. M. Puspani, "Towards a change of emotion in translation of kṛṣṇa text[J]," *Journal of Advanced Research in Dynamical and Control Systems. Special Issue on Social Sciences*, vol. 11, no. 2, pp. 1221–1231, 2019.

[22] B. Vermote, N. Aelterman, W. Beyers, and M. AperBuysschaertVansteenkiste, "The role of teachers' motivation and mindsets in predicting a (de)motivating teaching style in higher education: a circumplex approach," *Motivation and Emotion*, vol. 44, no. 2, pp. 270–294, 2020.

[23] K. J. Bartholomew, N. Ntoumanis, A. Mouratidis, and S. KatartziThøgersen-NtoumaniVlachopoulos, "Beware of your teaching style: a school-year long investigation of controlling teaching and student motivational experiences," *Learning and Instruction*, vol. 53, pp. 50–63, 2018.

[24] Y. Ding, D. Zeng, M. Li et al., "Towards efficient human-machine collaboration: real-time correction effort prediction for ultrasound data acquisition," *Medical Image Computing and Computer Assisted Intervention - MICCAI 2021*, Springer, in *Proceedings of the International Conference on Medical Image Computing and Computer-Assisted Intervention*, pp. 461–470, 2021.

[25] D. Goldmann, S. Schramm, and M. Galek, "Virtual double pulse tests to reduce measuring time and effort in semiconductor loss modeling[C]," in *Proceedings of the PCIM Europe 2019; International Exhibition and Conference for Power Electronics, Intelligent Motion*, pp. 1–7, Renewable Energy and Energy Management. VDE, 2019.

[26] S. Dargan, M. Kumar, M. R. Ayyagari, and G Kumar, "A survey of deep learning and its applications: a new paradigm to machine learning," *Archives of Computational Methods in Engineering*, vol. 27, no. 4, pp. 1071–1092, 2020.

[27] M. Veres and M. Moussa, "Deep learning for intelligent transportation systems: a survey of emerging trends," *IEEE Transactions on Intelligent Transportation Systems*, vol. 21, no. 8, pp. 3152–3168, 2020.

[28] A. A. Abdulrahman, M. Rasheed, and S. Shihab, "The analytic of image processing smoothing spaces using wavelet," *Journal of Physics: Conference Series*, vol. 1879, no. 2, 2021.

[29] K. Ding, K. Ma, S. Wang, and E. P. Simoncelli, "Comparison of full-reference image quality models for optimization of image processing systems," *International Journal of Computer Vision*, vol. 129, no. 4, pp. 1258–1281, 2021.

[30] P. Pandiarajaa, "A survey on machine learning and text processing for pesticides and fertilizer prediction[J]," *Turkish Journal of Computer and Mathematics Education (TURCOMAT)*, vol. 12, no. 2, pp. 2295–2302, 2021.

[31] T. O'Reilly, D. G. Feng, D. J. Sabatini, and D. J. WangGorin, "How do people read the passages during a reading comprehension test? The effect of reading purpose on text processing behavior," *Educational Assessment*, vol. 23, no. 4, pp. 277–295, 2018.

[32] L. Stappen, A. Baird, and L. Christ, "The MuSe 2021 multimodal sentiment analysis challenge: sentiment, emotion, physiological-emotion, and stress[M]," in *Proceedings of the 2nd on Multimodal Sentiment Analysis Challenge*, pp. 5–14, 2021.

[33] J. Tang, K. Li, and X. Jin, "CTFN: hierarchical learning for multimodal sentiment analysis using coupled-translation fusion network[C]," in *Proceedings of the 59th Annual Meeting of the Association for Computational Linguistics and the 11th International Joint Conference on Natural Language Processing*, vol. 1, pp. 5301–5311Long Papers, Thailand, 2021.

[34] B. Zhang, F. Yu, and Y. Gao, "Joint learning for relationship and interaction analysis in video with multimodal feature fusion[C]," in *Proceedings of the 29th ACM International Conference on Multimedia*, pp. 4848–4852, China, 2021.

Hindawi
Scientific Programming
Volume 2023, Article ID 9756367, 1 page
https://doi.org/10.1155/2023/9756367

Retraction

Retracted: Analysis of the Impact of Moral Education in Colleges and Universities Based on Short Video Technology

Scientific Programming

Received 18 July 2023; Accepted 18 July 2023; Published 19 July 2023

This article has been retracted by Hindawi following an investigation undertaken by the publisher [1]. This investigation has uncovered evidence of one or more of the following indicators of systematic manipulation of the publication process:

(1) Discrepancies in scope
(2) Discrepancies in the description of the research reported
(3) Discrepancies between the availability of data and the research described
(4) Inappropriate citations
(5) Incoherent, meaningless and/or irrelevant content included in the article
(6) Peer-review manipulation

The presence of these indicators undermines our confidence in the integrity of the article's content and we cannot, therefore, vouch for its reliability. Please note that this notice is intended solely to alert readers that the content of this article is unreliable. We have not investigated whether authors were aware of or involved in the systematic manipulation of the publication process.

Wiley and Hindawi regrets that the usual quality checks did not identify these issues before publication and have since put additional measures in place to safeguard research integrity.

We wish to credit our own Research Integrity and Research Publishing teams and anonymous and named external researchers and research integrity experts for contributing to this investigation.

The corresponding author, as the representative of all authors, has been given the opportunity to register their agreement or disagreement to this retraction. We have kept a record of any response received.

References

[1] Y. Jiang, "Analysis of the Impact of Moral Education in Colleges and Universities Based on Short Video Technology," *Scientific Programming*, vol. 2022, Article ID 3337606, 7 pages, 2022.

Hindawi
Scientific Programming
Volume 2022, Article ID 3337606, 7 pages
https://doi.org/10.1155/2022/3337606

Research Article

Analysis of the Impact of Moral Education in Colleges and Universities Based on Short Video Technology

Ying Jiang

Wuhan University of Communication, Wuhan, Hubei 430205, China

Correspondence should be addressed to Ying Jiang; jiangying@whmc.edu.cn

Received 18 May 2022; Revised 20 June 2022; Accepted 23 June 2022; Published 18 July 2022

Academic Editor: Lianhui Li

As the development of my country's mobile Internet continues to advance in depth, its related industries have also continued to rise and especially, the short video industry has ushered in a period of rapid development. In the past, the research on short videos mostly started from the perspectives of communication, sociology, culture, etc., mainly based on the discussion of the content and communication characteristics of Douyin short videos and analyzed the origins behind its rapid development. The relevant research on moral education in colleges and universities is relatively weak. Based on the relevant sample data collected from questionnaires and interviews, this paper focuses on analyzing the impact of short videos on moral education in colleges and universities from the perspective of pedagogy. The rapid popularization and wide application of short video applications have had a huge impact on the study habits and living habits of college students. College students' moral education educators must make good use of the short video application as a carrier, create new ideas for work, and enhance the attractiveness and influence of moral education work.

1. Introduction

In the era of convergent media, short videos are developing rapidly in cyberspace due to their immediacy, vividness, and audio-visual characteristics and have a broad market space [1–3]. The 46th "Statistical Report on the Development of China's Internet" pointed out that as of June 2020, the number of short video users in my country reached 818 million, accounting for 87% of the total Internet users. In 2020, the online video industry will be further improved and developed [4–7]. The dissemination advantage of video clips has become a hot spot in the development of the industry. College students, who are susceptible to new things, have become the main force of short videos. Both the number of netizens and the penetration rate have increased significantly compared with 2018 [8–12]. Under the background of the era when short videos are favored by college students, "high importance is attached to the construction and innovation of communication means", and choosing a discourse system and expression form that conforms to the characteristics of college students in the new era is an inevitable requirement for the development of modern college moral education. How to use the development advantages of college moral education for solving development problems is an important issue facing the current development of moral education in colleges and universities [13–15].

With the progress of the times and the development of the society, my country's Internet-related industries have grown rapidly in recent years and the development of the mobile Internet has made great progress, which has profoundly affected the current social format [16–20]. Among them, Douyin short videos are widely disseminated and popular among young people and have a great impact on the values, behavioral education, patriotism, and psychological intervention in the ideological and political education of young people [21, 22]. At present, with the widespread use of smartphones and the continuous development of related technologies, the related applications of short videos have become an integral part of most people's daily lives. According to the statistical report, as of March 2020, the number of mobile Internet users in my country was 897

million, accounting for 99.3% of the total Internet users. The per capita online time per week was 30.8 hours, with an increase of 3.2 hours from the end of 2018. According to the report, most people in my country habitually choose to use smartphones to surf the Internet, and the use of mobile Internet access and online video (short video) has maintained rapid growth [23–25].

At present, college education is faced with some problems, such as the single teaching form, and the teaching style is the most traditional teaching form and the most commonly used method in college teaching. However, there are problems such as monotonous content and boring teaching. The penetration of education will be restricted and limited, and it will lose its attractiveness to students over time; secondly, the imbalance of teaching resources is restricted by the differences in the development of education in various places, and the distribution of educational and teaching resources is also uneven. In particular, audio and video resources are far from being able to meet the needs of increasingly diversified, convenient, and autonomous education in traditional classroom teaching. Finally, teachers lack media literacy. At present, teachers only give students some abstract concepts. The teaching thinking is closed and conservative, and they follow the old rules. In the era of all media, new media technology represented by videos has rapidly penetrated into all fields of teaching, which has had a huge impact on teaching methods. The use of new media to innovate teaching methods is an inevitable choice for college teachers, and it also puts forward new requirements for the media literacy ability of teachers.

The rapid popularization and wide application of short video applications have had a huge impact on the study habits and living habits of college students. College students' moral education educators must make good use of the short video application as a carrier, create new ideas for work, and enhance the attractiveness and influence of moral education work.

2. Research Status of Short Videos in Moral Education

2.1. Short Video Application Research. In the context of the great development of the mobile Internet, online videos (short videos) have achieved rapid development by virtue of its own advantages and the short video is even reshaping the ecological pattern of mobile phone networks. According to the latest statistical report, the number of users of online videos (including short videos) in my country has reached 850 million, an increase of 126 million compared with 2018. Among them, short video users reached 773 million, accounting for 85.6% of the total netizens. The scale of short video users in my country and their utilization rates are shown in Table 1.

Douyin short videos were officially released in September 2016, and they have achieved rapid development with their unique algorithm advantages and marketing promotion. According to the information disclosed by the data portal "DataReportal," the number of users of Douyin short video has exceeded 800 million in January 2020 and it is expected that its number of users will soon exceed 1 billion and its market share is still increasing. It is already a leading company in the short video industry.

Table 1: Scale of short video users in my country and their utilization rate.

Time	The scale of short video users	Short video users (%)
2018.6	59320	74.5
2018.12	65008	79.2
2019.6	64748	75.7
2020.3	77362	85.9

In the research on short video content, a representative example is the Douyin Research Report jointly released by Miaozhen System and Haima Cloud Big Data in 2018. The report mainly divides short videos into four main types according to content creators: the first is actors and stars; the second is with a certain skill or expertise of the network red; the third is institutions and associations; the fourth is public hobbies. Deng Yongfang and Xie Jinpeng divided the video content on Douyin short videos into five main categories in "Seeing the Psychological Characteristics of Contemporary Young People from Popular Short Videos - Taking Douyin's App as an Example": handsome boys, beauties, cute babies, etc. The Yan Zhi group is represented by the Yan Zhi group; the creative group is represented by humor, dazzling skills, and eye-catching skills; the heart-moving group is represented by emotional expression; the intellectual group is represented by language teaching, skill teaching, makeup, food, etc. In the "Short Video Social Platform and Minor User Survey Report - Taking Douyin's Short Video as an Example," Hu Yuan divided its content into visual enjoyment, humor, knowledge popularization, creative skills, and talent show. There are six types of hot topics in current affairs.

2.2. Student Moral Education Research. In recent years, the user group of my country's mobile Internet has continued to expand from the middle to the two ends and the user group of Douyin short videos has extended to the lower age group especially. As shown in Figure 1, as of March 2020, the proportion of Internet users aged 10–19 years in my country reached an astonishing 19.3%. This age group is the scope of the vast majority of young people in my country.

Teenagers have strong self-awareness and curiosity and can easily accept new things. Douyin short videos on the mobile Internet are an important gathering place for current novelties. The improper use of Douyin short videos by teenagers can easily have an important impact on their values, patriotism, behavioral education, psychological intervention, etc. Similar cases also appear around us and in media reports from time to time. How to use short videos to spread positive information, effectively promote the ideological and political education of young people in my country, and prevent young people from being overly addicted.

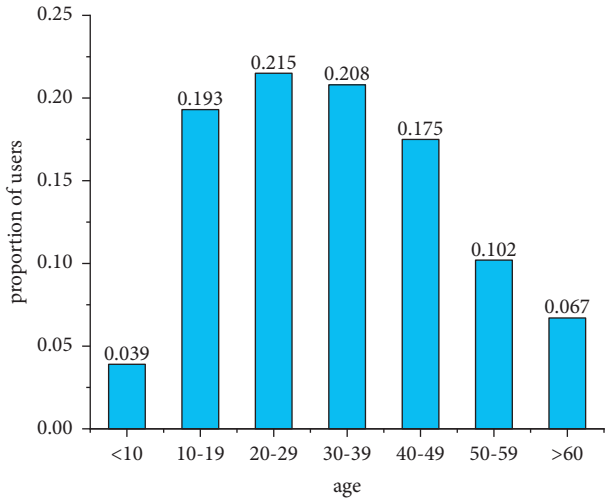

Figure 1: Age structure and proportion of netizens.

At present, there are few academic studies on the direct correlation between short videos and students' moral education. It is also a controversial topic whether the advantages outweigh the disadvantages or the disadvantages outweigh the advantages. Some scholars recognize its positive effects, some scholars have negative comments, and some scholars are neutral:

(1) Short videos have a good role in promoting moral education of students. Some researchers believe that short videos on Douyin can better promote the ideological and political education of young people and advocate active promotion and application. On the advantages of Douyin short video on ideological and political education of teenagers, it is believed that the user portrait design of Douyin can better meet the psychological expectations of teenagers; the supervision system enables young people's online ideological and political education to promote strengths and avoid weaknesses; the appeal of visual experience makes Douyin a carrier of ideological and political education, and it advocates to make full use of Douyin to promote ideological and political education of young people. In "Research on the Promotion Effect of Internet Media on Ideological and Political Education of Teenagers - Taking Learning Power Platforms and Douyin's Short Videos as Examples," Zhang Hanghang believes that Internet video platforms have gradually become the main way for young people to obtain entertainment and information Liu Tongguo and Du Xiaoyan pointed out in the article "Strategies for Strengthening Ideological and Political Education of Teenagers under the Background of the Popular Development of Short Videos" that short videos have become a favorite entertainment and leisure method for teenagers. With its pertinence and timeliness, it can also be expanded as an important tool for contemporary ideological and political education. Some researchers believe that the short video of Douyin plays a negative role in the ideological and political education of young people. A representative example is Lin Yirong's "Analysis of the Phenomenon of Moral Nihilism in Short Videos and Coping Strategies." It is observed that although short videos have a positive effect, at the same time, they contain a lot of moral nihilism. This phenomenon should be sorted out and criticized, to solve the problem of moral nihilism in short videos.

More researchers advocate a dialectical view of the role of Douyin short videos in students' moral education, and it is not appropriate to draw conclusions about the pros and cons. For example, Gao Pan analyzed the constantly developing short video platform and its impact on young people's thinking in the article "Thinking on the Ideological Education of Youth in the Short Video Era," focusing on the new changes in the ideological education environment for young people in the short video era. This article also proposes to optimize the platform environment of short videos to play a positive role in the ideological education of young people. In the article "Influence and Countermeasures of Mobile Short Videos on Teenagers' Moral Education," Hua Honglin analyzed the challenges brought by the tendency of pan-entertainment in mobile short videos to the moral education of adolescents and emphasized the use of mobile short videos to give full play to its role in moral education.

All in all, the research based on the dissemination of short videos and the psychological portraits of users has been relatively abundant, but the related research on the ideological and political education of young people, especially the ideological and political education of young people, encounters a relatively weak discussion of characteristics. Few studies have specifically focused on this special group of young people, based on ideological and political education, focusing on their self-presentation and self-description on the Douyin short video platform, and dialogue with society in a way they identify with. There is a lack of necessary intervention and guidance in the way young people contact new media such as Douyin short video, which makes it difficult to maintain the healthy growth of young people.

3. The Correlation between Short Videos and Moral Education in Colleges and Universities

3.1. Students Are an Important User Group for Short Videos. According to the latest statistical report of my country's CNNIC, as of March 2020, the number of short video users in my country was 773 million, accounting for 85.6% of the total number of netizens. The number of 19-year-old short video users is about 180 million. According to the results of my country's sixth census, it is not difficult to deduce the huge group of Douyin users of teenage. At the same time, according to the preliminary data of my country's seventh census, my country's population aged 0–14 is 253,383,938, accounting for 17.95% and the population aged 15–59 is 894,376,020, accounting for 63.35%. Compared with the sixth national census in 2010, the proportion of the population aged 0–14 increased by 1.35 percentage points.

Table 2: The weekly frequency of Douyin short videos used by teenagers.

Frequency	0 times	1–5 times	5–10 times	More than 10 times	Total
Dslbquantity	65	125	55	100	345
Proportion	18.8%	36.2%	15.9%	29.1%	100%

Table 3: The purpose of young people's exposure to Douyin short videos.

Options	Entertainment and relaxation	Enhancing learning	Making friends	Transferring positive energy	Others
Quantity	315	70	30	145	55
Proportion	91.3%	17.4%	8.7%	42%	15%

Combined with the data of short video users, it is not difficult to judge that the vast majority of young people in my country are actively or passively using or contacting media types such as Douyin short video media.

3.2. Short Video Is an Important Tool for Students' Moral Education. The development of the mobile Internet is the trend of the times, the short videos of Douyin are booming, and their social influence is obvious to all. Taking Chinese traditional culture as an example as an important part of contemporary youth ideological and political education, before relying on mobile short video dissemination, the education and promotion of excellent traditional culture have been in a tepid state and it has become more important in attracting the attention of young people. Unsatisfactorily, by incorporating Douyin short videos, breakthrough achievements have been made in its dissemination and influence. According to "Double Tradition: Research Report on Short Videos and Traditional Culture," as of the beginning of May 2019, there were more than 65 million short videos related to traditional culture released on the Douyin platform, which were played more than 16.4 billion times and liked 4.4 billion times.

Promoting excellent traditional culture itself is an important part of ideological and political education for young people. Some of the above projects are aimed at young people as the main target group, guiding them to love traditional culture, carry forward the quintessence of the country, and improve their ideological and political literacy. Through the above research, according to the proportion and calculation of the user group data of the Douyin short video platform, it can be seen that young people should have participated in it extensively and the educational effect achieved is even far beyond the traditional teaching method. Douyin short videos have become an important part for the ideological and political education of young people. At the same time, judging from the inner aspirations of young people, it is basically impossible to break away from the novelty of Douyin short videos. It is better to give full play to the advantages of Douyin short videos in combination with the characteristics of young people, develop them into an important platform for ideological and political education of young people, and gather the strengths of schools, society, families, and other parties to jointly promote the achievement of educational goals.

4. The Application of Short Video Technology in Moral Education in Colleges and Universities

4.1. A Survey on the Status Quo of Short Videos Affecting Moral Education in Colleges and Universities. This questionnaire survey was chosen to be distributed and implemented among the freshmen of a university. Most of the entire questionnaire survey process was conducted in an anonymous form, and a combination of online and offline questionnaires was adopted. Later, some students were randomly selected as the in-depth interview objects, in order to correct the questionnaire results. The distribution and collection of the entire questionnaire lasted for about two weeks. In order to display the results of the questionnaire more vividly, the results of the questionnaire are shown in Tables 2 and 3.

According to the questionnaire feedback on the purpose of young people's exposure to Douyin short videos, the vast majority of young people use Douyin short videos for entertainment, relaxation, and transmission of positive energy and a small number of young people said that it is to further strengthen their learning. From the perspective of the attractiveness of Douyin short videos, having nothing to do in free time and adding fun to life have become important factors for using Douyin short videos. At the same time, it is still not obvious that the youth group as the main body actively publishes short videos on Douyin. Most teenagers say that they have not done any publishing operations related to short videos of Douyin and more passively accept the relevant information on short videos of Douyin. Therefore, from the perspective of the time and behavioral characteristics of young people, it is feasible to use Douyin short videos to integrate the ideological and political education of young people, and young people themselves also have inherent demands in this regard.

4.2. The Positive Impact of Short Videos on Moral Education in Colleges and Universities

(1) It can resonate with students and provide rich materials. First of all, the natural characteristics of Douyin short videos make it easy to connect with daily life, and their content is more likely to resonate with students. The so-called "life is the best teacher." Traditional ideological and political education is

limited by various conditions, most of which are not closely related to life, so it is difficult for teachers to narrow the distance with students, and it is difficult to achieve learning in the environment. Douyin short videos are most closely related to daily life and even have a large amount of content based on daily life. For example, it can integrate relevant content of ideological and political education of young people in daily life and specific stories and match most of the boring theoretical knowledge. The music and scene effects are more likely to resonate with students, thus providing teachers with rich teaching materials.

Secondly, Douyin short videos can use modern Internet big data and other methods to provide rich materials for ideological and political education of young people. If teachers can reasonably use the short video content that is beneficial to the ideological and political education of young people in education, they can improve the effectiveness of ideological and political education for young people to a certain extent. The author has observed the relevant Douyin short videos of Zheng Qiang, a famous professor in my country. Professor Zheng Qiang combined his subject knowledge in many Douyin short videos to vigorously promote ideological and political education content such as patriotism. The playback volume of videos is often tens of millions, and it is obviously difficult for traditional teaching to achieve this effect.

In short, teachers can make good use of the advantages of Douyin short videos in all aspects to make them resonate with students in ideological and political education and enrich teaching materials. Judging from the relevant information observed and contacted by the author, this method has certain advantages in achieving educational effectiveness.

(2) It can optimize the way of communication and provide a new interactive space. In recent years, with the rise of online educational videos, the influence of Douyin's online educational short videos has also continued to expand. According to the official data of the Douyin platform, as of June 2019, there have been more than 5.47 million online educational short videos on the platform, with nearly 14.9 billion likes, more than 850 million forwarding and sharing, and more than 475.2 billion views. . At the same time, in order to better promote the combination and development of youth education and Douyin short videos, a number of educational institutions such as China Education Television and the Coordination Center of Communication University of China jointly launched the "Green Pepper Plan," which aims to promote the active participation of young people in Douyin. Audio and video online education are developing. At present, a large number of online education institutions have used Douyin to carry out various online education, which provides certain objective conditions for optimizing the dissemination of ideological and political education. As an effective supplement to after-school learning, online education is conducive to the optimization of the dissemination of ideological and political education for young people and provides a new interactive space.

(3) It can break through the limitations of time and space and provide convenient learning. The traditional ideological and political education for teenagers adopts class-based teaching, and both educators and teenagers need to conduct ideological and political education and teaching according to fixed course schedules and requirements. After extracurricular activities, teenagers have so far had few options on how to adjust their learning progress according to their own schedule. To a certain extent, the application of Douyin short videos can play a complementary and filling role. Teenagers can use a lot of leisure time to complete their studies, and they can also play the videos repeatedly for difficult problems to strengthen and consolidate.

The traditional ideological and political education for young people is confined to closed classrooms, and the fixed space makes it impossible for young people to accept and adapt to more teaching content and methods. The use of Douyin short videos by young people outside school or after school is conducive to improving their ideological and political literacy, moral sentiment, etc., and is also conducive to breaking through the limitations of learning space. The place for ideological and political education for young people is no longer limited to specific locations. Space units such as families, scenic spots, and historic sites can all become educational places.

In general, in view of the huge influence of Douyin short videos on the youth group, the relevant functions endowed by its platform can be used to break through the limitations of traditional teaching of ideological and political education, and to a certain extent, it is difficult to change the traditional teaching, which is difficult for students to resonate, and there is lack of materials, poor interaction, time and space confinement, and other issues. If we can make full use of the extra-school environment or after-school time, combined with the relevant advantages and characteristics of Douyin short videos, it will undoubtedly be of great significance to achieve the goals of ideological and political education for young people.

4.3. The Negative Impact of Short Videos on Moral Education in Colleges and Universities. In terms of ideological and political education for young people, although Douyin short videos have an important positive role, their negative impact is also prominent and some even tend to intensify. Analyzing the negative impact of Douyin short videos on the ideological and political education of young people is conducive to finding effective coping strategies, limiting the spread of negative factors to the greatest extent, and creating a good Internet ecological environment:

(1) Short videos impact the value judgment ability of young people. Value judgment is one of the important abilities of young people to understand and

judge the society. It is an integral part of the "Three Views" education and also affects the value orientation of young people's future life. During this period, the physical and mental development of young people is not perfect, they cannot form correct and independent judgments about external things, and their value judgment ability is easily affected by the external environment.

As shown in Figure 2, the survey results show that 49.28% of teenagers think that the impact is moderate, 14.49% think that it has no effect, and only 10.14% of the teenagers think that the impact is relatively large. It can be seen that most teenagers cannot make a clear value judgment on the impact of Douyin short videos. The questionnaire also confirms from the side that most adolescents in this period are still in the process of forming and developing their physical, mental, and critical thinking abilities and it is difficult to make clear value judgments on issues such as right and wrong, good and evil, and value standards.

(2) The pan-entertainment of short video dissemination increases the difficulty of ideological guidance. "Pan-entertainment" is a common phenomenon in today's online media. In a sense, Douyin short video is the representative force of "pan-entertainment" in contemporary online media. Its content is mostly humorous, with music, fashion, Internet celebrity trends, etc. This way of entertainment attracts people, especially the youth group. Under the influence of the idea of pan-entertainment, Douyin pushes many contents indiscriminately to a certain extent, which objectively increases the difficulty of ideological guidance of young people. Taking media reports as an example, Douyin has repeatedly ridiculed or insulted revolutionary martyrs with comics, funny videos, and other entertainment methods, which has been criticized by all walks of life, which is an important aspect of pan-entertainment. The widespread dissemination of similar negative information can easily lead to misleading, which in turn increases the difficulty of guiding young people's thoughts.

Taking the author's questionnaire as an example, the proportion of teenagers who choose to play Douyin short videos for entertainment and relaxation has reached an astonishing 91.3%, which means that entertainment and leisure are the ideological and behavioral motives for the vast majority of teenagers to use Douyin. At the same time, it also proves that the current pan-entertainment phenomenon of Douyin short videos has an increasingly prominent impact on young people. For example, common entertainment stars directly affect the idol selection of some teenagers, which can be seen from the pursuit of "little fresh meat" from time to time in the society; fast-food cultural entertainment and fragmented reading make some teenagers' cultural values superficial, lacking of the ability to speculate on cultural values; important historical "film and television tampering"

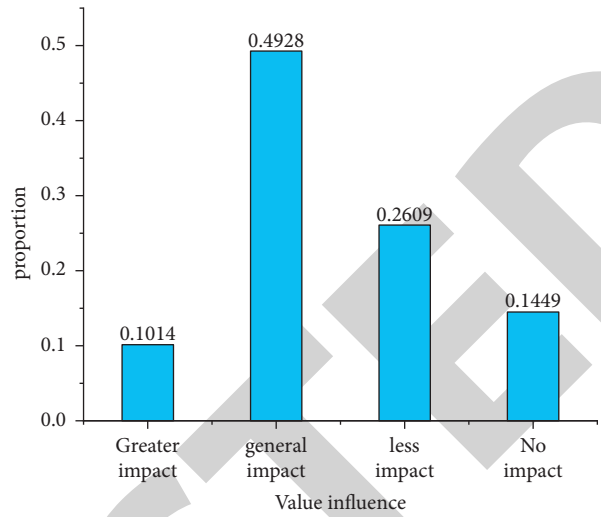

Figure 2: The impact of short videos on adolescents' value judgments.

and ideological and moral "joking and scolding" seriously affect young people's understanding of objective history and the improvement of ideological and moral quality. Similar pan-entertainment information is full of Douyin short videos, which cater to the public's preferences but increase the difficulty of guiding ideological and political education for young people.

5. Conclusion

In the context of new media, the popularization of short video applications such as Douyin and Kuaishou has had a huge impact on the ideas of college students. This makes the moral education workers in colleges and universities face new opportunities and challenges. The majority of moral education educators in colleges and universities should recognize the characteristics and advantages of a short video application, use the short video application platform, use new media technology, innovate moral education work methods, and cultivate outstanding technical talents with both political integrity and ability for the society. We explore the impact of the Internet media represented by Douyin short video on moral education in colleges and universities and finally form a feasible and practical coping strategy. The ultimate goal is to better protect the youth group and promote it to form a good value judgment, media literacy, and safety awareness, etc. In terms of discussing and solving this problem, it is impossible to rely on one side's efforts to solve it. It needs the concerted efforts of the government, society, schools, families, and other parties to promote it together for benign development. At the same time, it is impossible to achieve this overnight, and any method needs to be continuously verified by adolescents and social practice. Nowadays, with the progress and rapid changes in social science and technology, it is even more doomed that this is not a smooth road. However, in any case, we should not stop at the ideological and political education of young

Hindawi
Scientific Programming
Volume 2022, Article ID 8622419, 10 pages
https://doi.org/10.1155/2022/8622419

Research Article

Design of In-Depth Multi-intelligence Teaching System under the Mixed English Teaching Mode

Bin Kuai[1] **and Peihao Li**[2]

[1]*School of English, Xi'an Siyuan University, Shaanxi 710038, Xi'an, China*
[2]*University of Illinois Urbana-Champaign, Champaign 61820, IL, USA*

Correspondence should be addressed to Peihao Li; pzl0029@auburn.edu

Received 31 May 2022; Revised 18 June 2022; Accepted 26 June 2022; Published 18 July 2022

Academic Editor: Lianhui Li

After the implementation of the hybrid network-based English teaching system, a wide-ranging trial was carried out in schools. Although the trial time was not very long, according to the feedback given by the students, it is not difficult for us to find that the practicability of the English network teaching system is very strong, which is very suitable for current college students. The main goals of this research are the application development of the open source Moodle course management system and the practical design and realization of the English network teaching system based on in-depth research on the Moodle system and the secondary development technology. In view of the development of the existing English online teaching system in China and the current situation of domestic audio-visual information construction, it is planned that Moodle, an open source and free software system that fully complies with the CPL and GPL protocols, is used to teach the English language through in-depth research on the software support system. The software bottom layer supports the network teaching system and then uses PHP and web technology to expand and integrate system functions according to different needs and finally realize an English network teaching system suitable for college students at this stage.

1. Introduction

Blended learning is a relatively mature concept in the educational technology field, and it has been in a state of updating. In fact, in our previous teaching, blended teaching has been widely used, such as the combination of multiple teaching methods. The utilization of resources, the participation of various teaching media, etc. belong to blended teaching at a simple level. On the basis of traditional concepts, blended teaching in the information age includes online teaching and traditional classroom teaching. Online teaching is the usual teaching. The traditional classroom teaching is the teaching based on blackboard, chalk, and textbooks in the well-known real classroom. It is this advantage of blended teaching that makes higher education take a new direction. Traditional teaching can no longer meet the development needs of higher education. With the rise of the Internet, the combination of online teaching and traditional teaching has become deeper and deeper, and blended teaching has emerged as the times require. It has become the direction of higher education reform. In hybrid teaching, in order to play its role and advantages, network teaching must offer reasonable and effective online courses. In addition to media technology factors, it is necessary to rely on effective and reasonable network resources to design a complete teaching system as network teaching. At the same time, the irreplaceability of classroom teaching should also be avoided, and students should not be allowed to learn at will because of online teaching. Online teaching is only a necessary teaching method, and it has great potential, but it will never replace traditional classroom teaching. In view of the above analysis, we can give full play to the dual advantages of online teaching and classroom teaching, properly handle the relationship between the two, and further improve teaching efficiency [1–10]. This research clarifies the importance and necessity of English online teaching through

the analysis of different English teaching methods and combines the existing advantages of the Moodle system to construct a network system for English teaching. So the traditional education method is no longer the only way of English teaching, and more efficient English teaching is carried out through the network, so as to achieve the purpose of cultivating students' learning ability and English application ability.

2. Related Works

With the rapid development of information technology in the world, online education and traditional education are no longer two distinct fields, but they gradually present a situation of "you have me, I have you" and tend to the realm of mutual integration. "A ruler is short, an inch is strong," and combining the advantages of online education and traditional education will maximize the strengths and avoid weaknesses to achieve the best results. Currently, "E-learning" is gradually becoming a "Moodle online teaching system" internationally. At the end of the last century, various countries have put forward successful cases of blended teaching. Based on the online teaching system, many online courses of blended teaching have been developed, and more blended teaching models have been designed, especially in the United States and European countries. At present, the network teaching systems that support blended teaching widely used abroad include WebCT of the University of British Columbia, Learning Space of IBM, Blackboard of the United States, and OpenCourseWare (MIT OCW) of the Massachusetts Institute of Technology. In traditional American campuses, teachers have begun to break through the complete face-to-face teaching, and many teachers have begun to adopt the innovative teaching mode of blended learning. In the weekly teaching tasks, they take part of the class time to arrange the Moodle online teaching system, so that students can access the Internet in the dormitory or library. These teachers proposed to add the Moodle network teaching system to the course, which has many benefits in cultivating students' ability to acquire knowledge, analyze, and solve problems. The Moodle network teaching system has been actively introduced into school education, organically combined with and complementing the advantages of traditional classroom teaching, which is the so-called blended teaching. In the blended teaching, the Moodle network teaching system can give full play to not only its own advantages in classroom teaching, but also the advantages of traditional teaching, such as the efficient and centralized classroom teaching, the leading role of teachers, and the main role of students [11–16]. There are many open source teaching systems. Most of the teaching systems are integrated by CMS and components to form a community-based teaching system. Among them, the Moodle network teaching system based on open source is particularly extensively researched. Foreign research on teaching systems has gone deep into the combination of teaching mode and teaching system, how to integrate the system structure with the teaching mode, etc. Therefore, there are many secondary development technologies based on the Moodle system, through the integration of different plug-ins and modules, and addition and subtraction of functions to fit different teaching modes.

3. Related Theories and Technical Methods

3.1. Blended Teaching. Many scholars at home and abroad have different emphasis on the definition of the concept of blended teaching, and so far there is no more unified concept. Blended teaching can be divided into broad and narrow senses. In the broad sense, blended teaching includes teaching modes, teaching media, teaching resources, teaching theories, teaching methods, teaching evaluation, teaching space, teaching time, and other mixed senses. Blended teaching refers to a mix of offline and online teaching. In addition, becauseblended teaching and blended teaching are the most similar expressions, some scholars directly equate the concept of blended teaching with blended teaching. However, blended teaching and blended teaching are significantly different in focus and starting point. Blended teaching focuses on the main body of teaching—learning. Black believes that blended teaching combines face-to-face teaching and network-based teaching and then creates a teaching environment conducive to student teaching. Blended teaching starts from the dominant position of teachers and focuses on how to help students achieve optimal teaching results. Jennifer Hofmann proposed that blended teaching will use a concept as the basis. According to the characteristics of the teaching process, teachers can divide it into several stages. Professor G. Black defines "blended teaching" as a teaching form that combines the advantages of traditional teaching methods with the advantages of digital teaching or network teaching. Through the definition of blended teaching and the distinction between blended teaching and the concept of blended teaching, this study believes that blended teaching can be defined as a combination of traditional teaching methods and online teaching methods, giving full play to the role of teachers and students. The advantages of online and offline teaching methods are applied to teaching methods in blended teaching [17].

3.2. Moodle System

3.2.1. Moodle System Architecture. The Moodle system should have the following characteristics: it can run on a variety of systems; it is easy to install, learn, modify, upgrade, expand, integrate, etc. The architecture of the Moodle system is shown in Figure 1.

3.2.2. Moodle Business Logic Layer. As a perfect application of B/S mode, Moodle system should have a perfect business logic layer design, and some analysis of the core business logic in Moodle system is carried out here. In a general system, the first thing to pay attention to is the principle of authority allocation, so the judgment of authority is a core business logic in the Moodle system. The judgment of permissions in the Moodle system is done through a

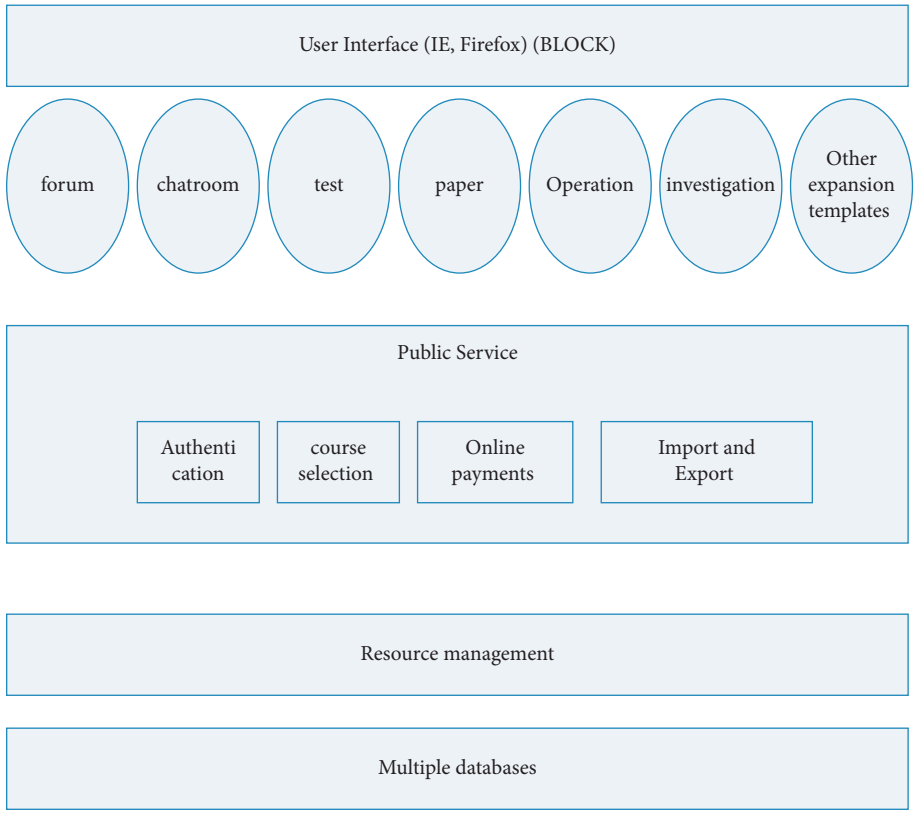

Figure 1: Moodle system architecture.

permission judgment function. In this function, the relevant permissions are judged through the acquisition of the context environment, and the code is shown as follows: [18].

```
$context = get_context_ instance (CONTEXT_SYSTEM);
require_capability ('moodle/site:config',$ context);
```

For an application, in addition to permissions, it also uses a security code to maintain the security of the application environment. It uses "if(!empty ($delete) and confirm_sesskey ()){}" to determine whether the logged in user is normal.

"print_error (' courserequestdisabled ');" is generally used to terminate the execution. Once an error occurs, the system will stop executing the remaining statements, and its function is similar to the exit statement.

3.3. Key Technologies of Secondary Development Based on Moodle System. This research aims to design and implement an English network teaching system based on Moodle. The system is aimed at college students who have preliminary teaching ability. In the process of systematic education, they have formed dependence on traditional education methods, and they have initially connected to and used the system. To implement teaching, we set up the English network teaching system on the Internet, based on the very popular B/S structure today, so that it can be promoted on a large scale and reduce the entry threshold. Because the secondary development of some modules is carried out on the basis of the original system, the system foundation should be the same. Although there are many systems that Moodle can set up, we chose the simple and cheap LAMP system: Linux, Apache, MySQL, and PHP. The four open source software components constitute the LAMP system that we are familiar with, and this basic development system is also a core key technology for secondary development. Using the object-oriented method in software engineering in the development process can make the system have the advantages of easy maintenance, high quality, high efficiency, and easy expansion.

3.3.1. Three-Tier B/S Architecture. B/S architecture is the structure of browser plus server, where B is the browser and S is the server. It is a supplement and improvement to the C/S structure. The biggest difference between it and the C/S structure is that the B/S structure does not need to install the client. The client's request will be sent through the browser, and the web server will receive the request after corresponding data processing is performed. During this period, the web server will also exchange data with the background server. Finally, the web server will send the processed data results back to the browser. In this structure, all the user interface is implemented through the browser, only a relatively small amount of transaction logic will be implemented in the front section, and most of the transaction logic will be implemented in the server side, which is the so-called three-tier structure. [19–21].

In the B/S three-tier structure system, because the server processes and implements almost all transaction logic, it has

the advantages of easy maintenance and upgrade. The software of the B/S architecture only needs to manage the server. No matter what modifications are made to the system, they can be modified at one point on the server side. The browser is just a tool for presenting the results of things. In this case, the usability of the system is further improved. However, because of this feature, the B/S architecture has some inevitable disadvantages. With the continuous upgrading of software and the continuous increase in the amount of information, the server will become more and more bloated, and the load on the server will also increase. It will become heavier and heavier, which is also a major test for the server on the server side and also increases the burden on the background maintenance personnel. However, with the development of science and technology, hardware devices are becoming more and more powerful, their processing capabilities are getting better and better, and most units using this architecture also have database storage servers for separate data backup, so B/S architecture is used. The construction and promotion of software are also an inevitable trend.

3.3.2. Ubuntu. In the design and implementation of the English online teaching system, the Linux system we use is Ubuntu. Although the Moodle system documentation recommends Unix as the best operating system, most of the Unix systems are not free. At the same time, the architecture of WAMP under the Windows system will be prone to instability, the system is overburdened, and the memory allocation is not enough, in addition to other various problems, which will eventually lead to system crashes. The operating system that is widely used in small companies has high stability, fast connection speed, and reasonable content distribution. Therefore, in the initial construction, considering the purpose of system stability and cost saving, the GNU/GPL-compliant Ubuntu was selected as the operating system.

3.3.3. Apache2. Apache is the abbreviation of Apache HTTP Server. It is one of the most popular web servers in the world. It is an open source software project belonging to the Apache Software Foundation. Apache has an absolute advantage over all kinds of existing web server software, far ahead of the second-place Microsoft IIS. Apache has various characteristics such as simplicity, fast speed, and stable performance, and it can run on almost all operating systems. The installation and configuration process of Apache is also very simple, and it is also very suitable for new developers. Its installation methods can be simply divided into two types: source code installation and binary package installation. These two installation methods have their own characteristics and are suitable for different user options. Since the Ubuntu system is used as the basic system in this study, we use the binary package installation method to install it. Just execute the following command in the terminal to automatically complete all the download and installation process: sudo apt-get install apache2. After the installation is complete, Apache2 will start automatically. If necessary, you can stop it by executing the command "sudo/etc/init.d/Apache2 stop" in the terminal; finally enter the command "sudo/etc/init.d/apache2 start"; and then start the Apache service once. There is an "apache2.conf" file in the "etc/Apache2" directory; we can modify Apache2 by modifying it. For example, modifying the "ports.conf" file can redirect the port and redirect the default port 80 to other nonconflicting ports, so that multiple sites can be established on one server, which is convenient for unified management. Under normal circumstances, the files that Apache2 will publish will be located in the "var/www" directory, which is the default value of Apache2. We can also modify the document root in the main configuration file to complete the redirection.

4. Design of a Hybrid English Teaching System Based on In-Depth Multi-intelligence

4.1. Development Tools and Environment. The English network teaching system is developed on the basis of the Moodle system. Therefore, the first step in the realization of the English network teaching system is to construct the operating environment and development environment of the whole system. Although PHP can be run without editing, the requirements for development software are not high. It can be developed using general web page editing software or even simple text editors such as Notepad. To improve the development speed and the accuracy of code writing, select PDT (Eclipse PHP development tools) as the preferred development environment. Eclipse can be used in several mainstream operating systems such as Windows, Linux, and macOS. It also belongs to an open source development system, so there is no need to pay extra fees to use it for program development. Although Eclipse is mainly developed for Java, among the many plug-ins of Eclipse, there are two specially developed for PHP. These customized plug-ins are Eclipse foundation and PHPEclipse, which are also open source software. After installing PDT in the large open source environment of LAMP, the corresponding PHP development can be carried out. At the same time, the official website of the Moodle system, which is also open source software, also recommends Eclipse in its development software, because its use is completely free without any additional development costs. After completing the installation of the operating system, you only need to enter the following command in the terminal of Ubuntu: sudo apt-get install Apache2 mysql-server-5.1 mysql-client-5.1 php5 libapache2-mod-php5phpmyadmin. You can set some accounts and other information during the installation process according to the prompts. When the LAMP environment is installed, it can be installed using Eclipse downloaded from the Eclipse official website. After everything is completed, the basic development environment construction of the English online teaching system is completed.

4.2. Implementation of System Database. There are many choices of databases, but due to the cost and the choice of the system construction environment made before, we choose MySQL as the database of the whole system. In the whole system, MySQL, as the underlying data support, can store all

user information, system parameters, login information, etc., to ensure that the system program can call data quickly and effectively. Code 1 of the student information database table establishment part is as follows:

4.3. Main Function Module Code and Implementation

4.3.1. Flowchart of the Overall Function of the System. The overall function flowchart of the system describes the general function realization process of the entire English network teaching system, which is particularly important for the entire English network teaching system. The identification of the user's identity and the subsequent behavior process are included in the overall function flowchart of the entire system, and the responses that should be made to operations in general are also included in the overall system function flowchart, as shown in Figure 2.

The overall function variables of the entire system can be set in the "config.php" file, and the different user-level key variables involved in the system can be set by controlling the same file and then detailed through the corresponding files. The source code of the "config.php" file is as follows:

4.3.2. Implementation of System Common Modules. There are many public modules in the English online teaching system, such as the login module and logout module. In these public modules, the corresponding process needs to be managed. We will take the login module as an example to understand how to realize it in the public module. In the login module, it is necessary to first judge the user's access situation and limit the user's login time. For example, within the valid time limit, you can log in by reading the session file to enter the account and password; otherwise, go back to the main login page to verify the user's account and password, which can ensure that the user does not need to repeatedly perform identity verification during the use process, and can also perform the role of identity confidentiality to a certain extent. After the user completes the identity verification, it will immediately return to the user's personal page. The interface is shown in Figure 3.

4.3.3. Course Content Management. In the English network teaching system, the course management should have a certain mode, which can enable all teachers to manage the course without special training. Course management must ensure the basic management functions while making the entire management process simple and easy to operate. For example, the basic adding and editing functions should be similar to or the same as Word document operations, so that teachers can adapt to the course content management functions faster. In the course content management page, the teaching content can also be classified and managed for the teaching of different skills in English listening, speaking, reading, writing, and translation. There are courses such as short reading comprehension and long reading, as well as composition training courses specially designed to exercise writing ability. Figure 4 is the interface diagram of the course management function.

In the course management function of the Moodle system itself, there is no function to time and manage the user's online time. In this study, related functions have been added for the first-years who have just entered the university. Since PHP is a scripting language, it will not be used in the long term. There are many problems in executing certain statements at the same time. Therefore, there is no perfect solution for using PHP to determine the user's online time. This study uses the method of inserting the user's exit time into the database and comparing it with the recorded user's login time. In order to improve the accurate timing online, the function of online timing is realized by formulating a program on the system server.

4.3.4. User Management. The user management function mainly exists for the unified management of all users in the English online teaching system by the administrator. Therefore, the following functions must be included in the user management function. First, there should be an individual user information management function. Each user in the English online teaching system can be managed individually with functions such as information, permissions, classes, and groups, followed by the batch user management function. The administrator should be able to manage a large number of users. Figure 5 shows the main interface of the user management function.

4.3.5. Job Management. In the English network teaching system, students' homework is submitted by uploading personal homework content or files. In the English online teaching system, students are the individual main unit, but students are put together to form a class, and the final homework will be stored in the database in a class as a unit. Students and teachers can log in to the English online teaching system for homework viewing, correction, etc. For example, students plan to get writing ability training after completing the corresponding course teaching. Students can click on the corresponding writing ability training course to enter the homework content. At that time, they can check and operate the homework they have completed again, such as downloading the voice for listening correction and so on. They can also view the specific content and requirements of the writing ability training they selected before, and after completion, they can upload the operation to complete the assignment submission. And they can view all their own homework in the student homework management process, in addition to performing download, upload, and other operations. Figure 6 shows the job management interface.

5. System Test

5.1. Interface Test. The interface plays the role of directly interacting with the user, and the user's first impression of the software basically depends on the interface. At the same time, whether the design of the interface is good also affects the user's ease of use of the software. The interface can help and guide the user to a certain extent. In the interface test, various windows existing in the interface should be tested. We conduct

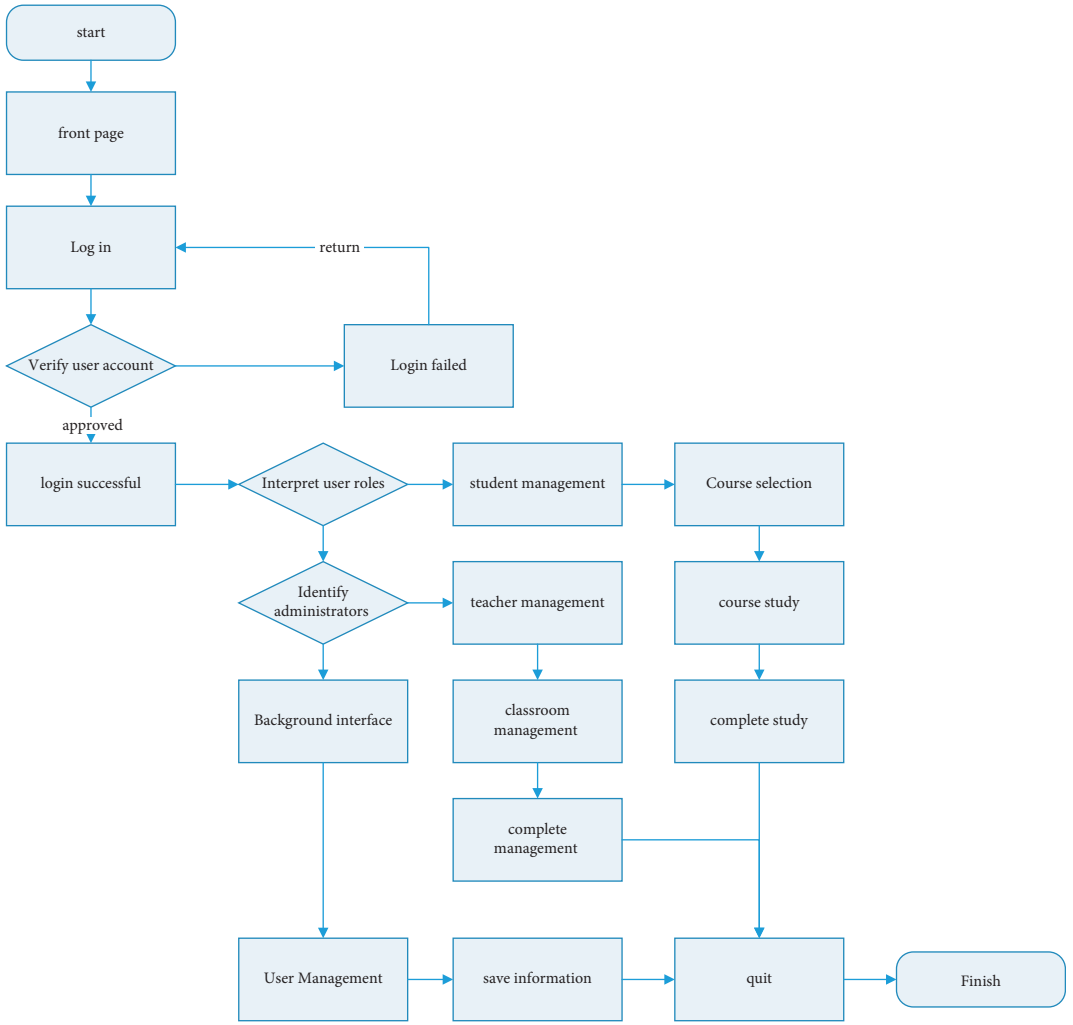

Figure 2: The overall function flowchart of the system.

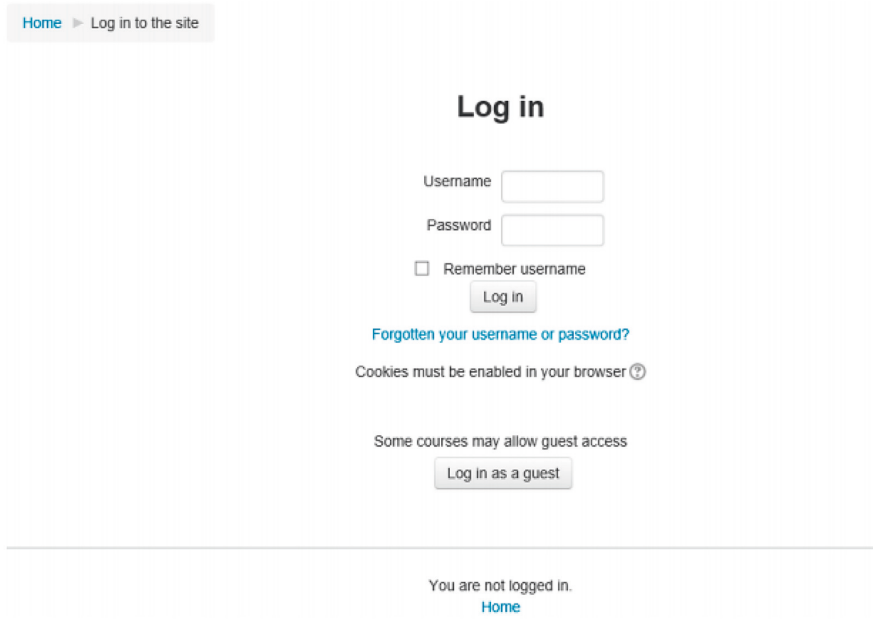

Figure 3: User login main interface.

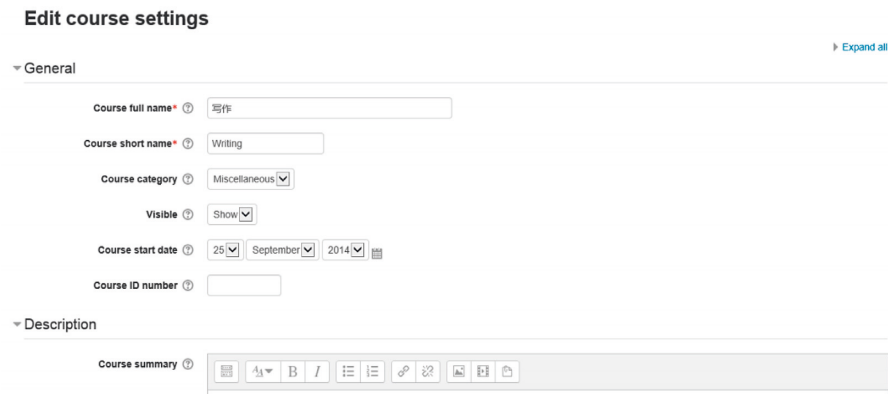

Figure 4: Course management function interface diagram.

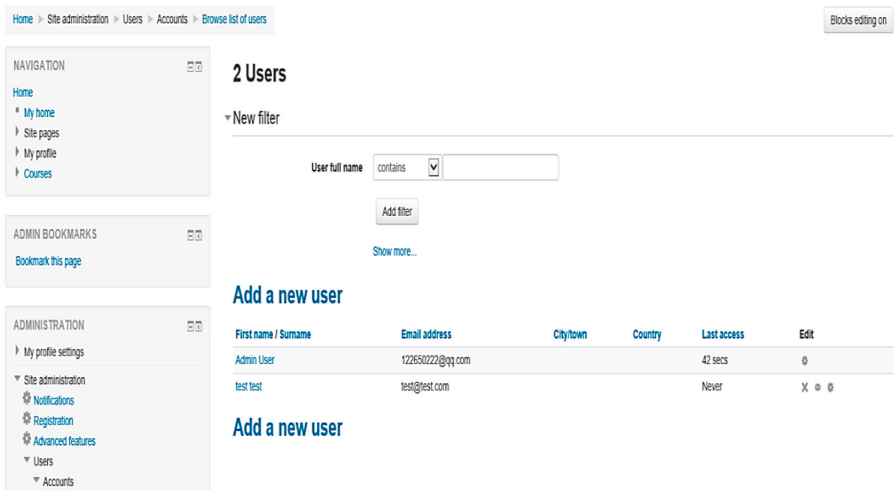

Figure 5: User management function diagram.

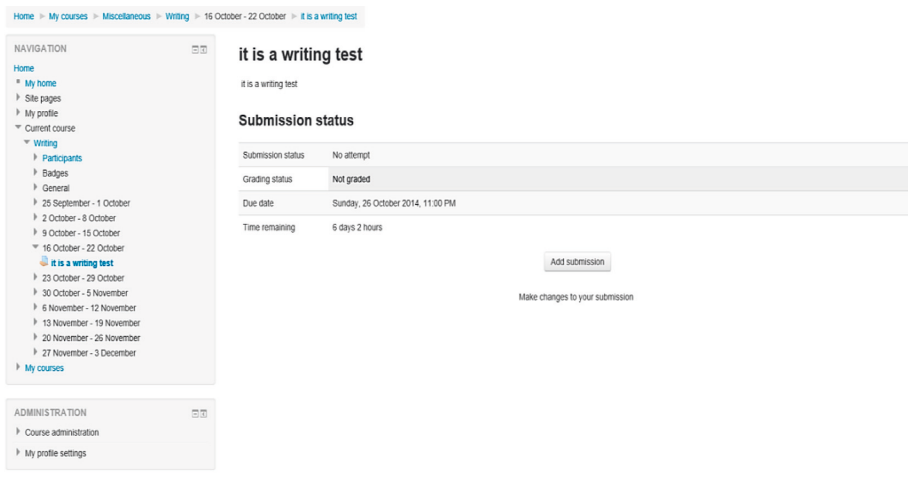

Figure 6: Job management interface.

individual tests to see if each UI meets the general usage expectations and whether the window objects and features conform to the standard. Because the English online teaching system is mainly used in the environment of domestic universities, it is inevitable that there will be a lot of Chinese and English content mixed in the interface, so the encoding of

Table 1: Test proportion distribution.

	Distributed type				
	Interface testing	Function testing	Security testing	Performance testing	Total
System test content	12	34	4	7	57
The proportion (%)	22	57	7	13	100

Chinese and English is particularly important. Errors will lead to garbled characters. At the same time, the typesetting methods of Chinese and English are different. If the same method is used for typesetting, this can easily cause irregularities in the interface, which will affect the cleanliness and beauty of the interface. Tests should also address both text encoding and typography.

5.2. Functional Testing. Functional testing can also be called black box testing. The testing method is to test the software according to the specifications and other documentation of the developed software. This testing method generally does not involve the working principle of the software content, so it is like a correct test for the tester. In functional testing, testers should observe the various output results of each function of the software from the perspective of ordinary users through various methods such as input and use, so as to discover the functional defects of the software.

5.3. Security Testing. The software responds to behaviors such as unauthorized user access or malicious damage by other users. In the security test, the testers use different identities of authorized users and non-authorized users to enforce different permission requirements of the system to test whether the permissions are normal and whether the data is normal.

5.4. Performance Test. The performance test is generally used to verify whether the performance of the software meets the requirements in the software demand environment and, at the same time, to confirm whether the repeated use can still meet the performance indicators. A total of 57 test cases were designed in this test, which involved interface testing, functional testing, security testing, and performance testing. The use case content distribution is shown in Table 1.

5.5. Analysis of Test Results

5.5.1. Interface Test Results. In addition to the necessary aesthetics, the interface of the English online teaching system should pay more attention to whether the function of the page is correct. All the functions of the software system based on the existence of the network rely on the existence of hyperlinks, so whether the hyperlinks are displayed correctly in the interface is particularly important, and each functional module should be expressed in a suitable size and clear way. The test results of this link are shown in Table 2.

5.5.2. Safety Test Results. After completing the basic functional test, corresponding security tests should be carried out for some common security vulnerabilities, including common functional modules that different user levels choose not to have, forced access to the corresponding content through the browser, and testing through the browser. The test results are shown in Table 3.

5.5.3. Performance Test Results. At the beginning of the design of the English network teaching system, it was hoped that it could be promoted on a large scale, so that more college students could enter the teaching mode of English teaching. Therefore, the system needs to handle a large number of users, and the performance should be tested in all aspects including concurrency and stability. User concurrency testing is the most important part of performance testing, including the process of load testing and stress testing. It mainly aims to gradually increase the number of users to increase the system burden until an unacceptable performance point or bottleneck occurs. Generally, it is necessary to test the concurrency of a normal number of users and the concurrency of users under a limit number.

Function: Users access the website from different regions at the same time to ensure that the website can be accessed normally.

Purpose: To test whether it is normal for 200 users to access the English online teaching system from different regions at the same time.

Method: Use the Apache bench test website that comes with the WAMP environment to access the website concurrently, test the usual time and bandwidth required for the visit, and analyze the website operation through the test data. The concurrent test results are as follows in Table 4:

Server performance testing is an important part of testing, including the process of load testing and stress testing. Mainly by simulating multiple users to use the system at the same time, until the system has insufficient performance or bottleneck, generally test the normal use and extreme use.

Function: Users use various functions to ensure normal functions.

Purpose: To test the ability of 200 users to simultaneously access the entire English online teaching system from different regions.

Is there a normal page?

Table 2: Interface test results.

Serial number	Test function	Testing method	Test results
1	Home navigation location	Client browser browsing	Normal
2	Interface function location	Browser	Correct
3	Content layout of the navigation bar	Browser	Correct
4	Interface text display	Browser	Normal
5	Interface being garbled	Browser	None
6	Interface text size	Browser	Normal
7	Interface text position	Browser	Normal
8	Hyperlink display method	Browser	Correct
9	Page layout	Browser	Normal
10	Browser compatibility	Browser	Normal

Table 3: Safety test results.

Serial number	Test function	Testing method	Test results
1	Wrong choice function	Selecting high-privilege user functions with low-level privilege users	This feature is not available
2	Forcing entry to content via URL	Directly entering the permission in the browser address bar without the content RUL address	Prompt for login information
3	Injection vulnerability	Using common injection vulnerabilities to gain advanced privileges	Cannot be injected

Table 4: Concurrency test results.

Number of concurrent clients	10	50	100	200
Average response time (s)	0.037	0.863	2.152	5.741
Denial of service rate (%)	0	0	1.3	2.9

Table 5: Server performance test results.

Number of concurrent clients	10	200	500	1000
Network utilization (%)	5	18	37	54
Average memory usage (%)	21	27	34	39
CPU usage (%)	7	15	39	57

Method: Use anychat to conduct high concurrent access to the website, test the CPU occupancy rate and memory occupancy rate of the server during the visit, and analyze the operation of the website through the test data. The concurrency test results are shown in Table 5.

6. Conclusion

Information-based teaching methods are developing through the efforts of a large number of educational practitioners, and the development and use of networked teaching systems are also an inevitable trend. For university teachers and students, the Internet has always been around, and the teaching classroom has also become an online classroom. The cramming method of knowledge instillation has gradually become rationalized, and it has become a teaching method in which students completely master the teaching subject. The English network teaching system is the connecting link in this key reform, and it is also the technical key for all ideas to become reality. The Moodle-based English online teaching system has finally realized the core functions of English online teaching, such as user login, teaching timing, course content management, user management, and homework management. From the operation situation and the feedback information of students, we can know that English online teaching is very suitable for today's college students. This teaching method effectively liberates students' teaching time and improves students' learning.

The English online teaching system is based on the secondary development of the Moodle system. Therefore, there are still many deficiencies in the localization customization of the Moodle system and the software compatibility of secondary development. In the future, we will continue to further develop the software and improve the English network teaching system, so as to improve the quality of the entire software teaching.

Data Availability

The dataset can be accessed upon request.

Conflicts of Interest

The authors declare that they have no conflicts of interest.

References

[1] T. Garcia and R. Pintrich, "The effects of autonomy on motivation and performance in the college classroom," *Contemporary Educational Psychology*, vol. 21, no. 4, pp. 477–486, 1996.

[2] M. Boekaerts, "Self-regulated learning: where we are today," *International Journal of Educational Research*, vol. 31, no. 6, pp. 445–457, 1999.

[3] S. A. Coutinho, "The relationship between the need for cognition, metacognition, and intellectual task performance,"

Educational Research and Reviews, vol. 1, no. 5, pp. 162–164, 2006.

[4] D. Thanasoulas, "What is learner autonomy and how can it be forstered?" *The Internet TESL*, vol. 10, no. 3, pp. 12–16, 2009.

[5] k. Chanock, "Autonomy and responsibility: same or different?" in *Proceedings of the Independent Learning Conference 2003*, Melbourne, Australia, September 2004.

[6] M. D. L. A. Clemente, "Teachers attitudes within a self-directed language learning scheme," *System*, vol. 29, no. 1, pp. 45–67, 2001.

[7] N. D. Yang, "Exploring a new role for teachers: promoting learner autonomy," *System*, vol. 26, no. 1, pp. 127–135, 1998.

[8] C. Barnum and W. Paarmann, "Bringing introduction to teacher:a blended learning model," *H.EJournal*, vol. 33, no. 2, pp. 56–64, 2002.

[9] P. Valiathan, "Blended learning models," *Encyclopedia of Information Science & Technology Second Edition*, vol. 30, pp. 33-34, 2002.

[10] M. B. Horn, *Heather Staker. Blended: Using Distrupive Innovation to Improve Schools*, John Wiley & Sons, Hoboken, NJ, USA, 2015.

[11] V. Demirer and I. Sahin, "Effect of blended learning environment on transfer of learning: an experimental study," *Journal of Computer Assisted Learning*, vol. 29, no. 6, pp. 518–529, 2013.

[12] J. H. Wu, R. D. Tennyson, and T. L. Hsia, "A study of student satisfaction in a blended e-learning system environment," *Computers & Education*, vol. 55, no. 1, pp. 155–164, 2010.

[13] H. Singh, "Building effective blended learning programs," *Educational Technology*, vol. 43, no. 6, pp. 51–54, 2003.

[14] B. Akkoyunlu and M. Y. Soylu, "A study of student's perceptions in ablended learning environment based on different learningstyles," *Educational Technology & Society*, vol. 11, no. 1, pp. 183–193, 2008.

[15] R. C. Shih, "Blended learning using video-based blogs: public speaking for English as a second language students," *Australasian Journal of Educational Technology*, vol. 26, no. 6, pp. 883–897, 2010.

[16] G. Black, "A Companison of traditional,online,and hybrid methods of course delivery," *Journal of Business Administration Online*, vol. 1, no. 1, pp. 67–73, 2002.

[17] J. Hofmann, "Blended learning case study," [EB/OL] http://www.leaming%20circuitor%202001/Apr2001/omann, 2008.

[18] H. Gardner, *Intelligence Refrained: Multiple Intelligences for the 21st century*, Basic Books, New York, NY, USA, 1999.

[19] H. Beetham and R. Shrpie, "An approach to learning activity design," in *Rethinking Pedagogy for a Digital Age: Designing and Delivering E-learning*, pp. 26–24, Routledge, London, UK, 2007.

[20] Y. Engeström, "Activity theory as a framework for analyzing and redesigning work," *Ergonomics*, vol. 43, no. 7, pp. 960–974, 2000.

[21] Y. Engeström, "Development as breaking away and opening up: a challenge to vygotsky and piaget," *Swiss Journal of Psychology*, vol. 55, no. 2/3, pp. 126–132, 1996.

Hindawi
Scientific Programming
Volume 2022, Article ID 1984979, 11 pages
https://doi.org/10.1155/2022/1984979

Research Article

3D Assembly Model Retrieval Method for a Multiassembly Interface

Hu Qiao,[1] Xufan Wang,[1] Tianhang Xu,[1] Zhenxing Wei,[1] and Ying Xiang[2]

[1]*School of Mechatronic Engineering, Xi'an Technological University, Xi'an 710021, Shaanxi, China*
[2]*College of Mechanical and Electrical Engineering, Shaanxi University of Science and Technology, Xi'an 710021, Shaanxi, China*

Correspondence should be addressed to Ying Xiang; yingcara@hotmail.com

Received 14 May 2022; Accepted 20 June 2022; Published 18 July 2022

Academic Editor: Lianhui Li

3D model retrieval is increasingly becoming a hot topic in today's research. The existing model retrieval methods are limited to the retrieval between similar models, while the matching retrieval for models with assembly relationships is neglected. They cannot realize the prediction of the virtual assembly and make the assemblers to spend extensive time detecting when there are assembly errors in the model. This work proposes a 3D assembly model retrieval method for multiassembly interface, which can retrieve the parts or subassemblies that can be assembled with the input model. In this work, a method for the reuse of the 3D assembly mode is also provided. The method here involves a series of steps, which includes an attribute adjacency graph to express the 3D assembly models, followed by the definition of a conjugated subgraph, and the serialization of the vertices of the graph for the Atlas of the assembly model. Finally, the frequent subgraph mining method is improved, and the 3D assembly model that satisfies the multiassembly interface is extracted. The article claims through the obtained results that this method not only allows the performance of the 3D assembly model retrieval of multiassembly interfaces but also the extraction of the 3D model required by designers, improving, at the same time, the product design efficiency.

1. Introduction

In today's digital design and manufacturing, most manufacturing enterprises modify existing products in the actual production process, and products designed from scratch almost do not exist [1–3]. The reuse of this model is particularly important. Especially in the aerospace, automotive, shipbuilding, and other fields produced more and more three-dimensional CAD models, and product design is based on the existing model above modification. The existing 3D model retrieval is more focused on the retrieval of parts themselves, and the technology is relatively mature, but in the practical application of enterprises, 3D CAD model mainly exists in the form of assembly, especially in manufacturing enterprises to achieve automatic workshop. This makes part model retrieval that cannot meet the actual needs of industry [4].

At present, the existing 3D model retrieval technology is based on model similarity retrieval. Firstly, the characteristic information of the model itself is marked, and then, the similarity retrieval is carried out in the model library. This method does not consider the topology structure of the assembly model, assembly connection, and other information, leading to the difficulty in the development of 3D model retrieval method. Although the intelligent retrieval of models can realize the retrieval of similar parts among models, it cannot realize the retrieval of models with matching relationship. In actual enterprise manufacturing, model retrieval is not limited to the retrieval between similar parts, but is more applied to the virtual assembly process of products. What users need is not the retrieval of a single similar model, but the matching model with the input model.

Most of the existing 3D model retrieval methods, such as 3D CAD model semantic retrieval based on sketch [5] and 3D model retrieval based on multilevel feature extraction [6], are based on assembly model granularity as the basis of reuse to retrieve the similarity of key semantic or geometric features. Most of these methods extract the features of 3D models, then compare the similarity based on the features, and finally achieve a purpose of retrieval.

In terms of part retrieval, Qin et al. [7] proposed a 3D CAD model retrieval approach that considers the speed, accuracy, and ease of use at the same time based on sketches and unsupervised learning. Hojoon and Lee [8] abstracted the features of the model as nodes and then calculated their similarity to finalize the retrieval. Zhou et al. [9] completed 3D model retrieval based on 2D image features. Li et al. [10] proposed a multiview diagram matching method for 3D model retrieval, which aimed at breaking down and integrating the complex multiview diagram similarity degree measurement into several single view diagram similarity degree measurement. Mcwherter et al. [11] carried out 3D model retrieval based on invariant topological vector (ITV) and composed vector by multiple topological invariants in entity connection graph as feature descriptor of entity model. The effectiveness of invariant topological vector in 3D model retrieval is verified by comparing with many feature descriptors. Bespalov et al. [12] proposed a model retrieval method based on scale-space decomposition in view of the difficulty in local feature extraction and matching of 3D models. Based on parametric decomposition, the network of 3D model is decomposed into several local engineering surfaces. Then, according to the correlation features between local surfaces, a binary tree containing the correlation features is constructed, and the adjacency graph of feature attributes is established. Finally, the similarity between 3D models is calculated based on the attribute adjacency graph. McWherter et al. [13, 14] proposed a 3D model retrieval method based on attribute adjacency graph, in which the vertices of attribute adjacency graph represent different faces of 3D model, and adjacent faces are connected by edges. Edges represent surface properties such as size and concavity. The attribute adjacency graph of the 3D model is shown in the figure below.

In terms of assembly retrieval, Dong and Xu [15] endowed the surface of assembly parts with the double attributes of function and structure and divided the surface into functional and nonfunctional surfaces so that it can account for the similarity of the part's shape and functional properties. Zhang et al. [16] used the similarity of 3D assembly model attributes to propose a method of discovering common design units to find reusable information in the model. Zhou et al. [17] analyzed the similarity of the local structure of the assembly on the basis of the subgraph isomorphism and matching of the items and provided a theoretical basis for the retrieval of the 3D assembly model. Wang et al. [18] used random walk and optimal matching theories to analyze the topological relations and comparative attribute characteristics of each part so that it can obtain the similarity of the assembly as a whole. Wu and Gao [19] proposed a 3D assembly model retrieval method based on the similarity of spatial structure, where the similarity of the assembly can be obtained by the attribute feature similarity of the product model and the similarity of the part's spatial position. Qiao et al. [20] proposed a single assembly interface 3D assembly model of information retrieval method, first using the preliminary model information retrieval, and then filtered according to the result of retrieval; assembly model geometry retrieval can be converted to look for problems with the attribute adjacency graph, finally using frequent subgraph mining algorithm with conjugate subgraph attribute adjacency graph search. In this paper, a three-dimensional assembly model with multiple assembly interfaces is studied.

However, the retrieval target models of these methods are similar to the input models and do not consider the retrieval of part or subassemblies that can be assembled with the input model. By contrast, the 3D assembly model is connected through the geometric interface between the parts. The geometric interface can be a single connection or be connected through multiple interfaces, which increase the difficulty for the 3D assembly model retrieval.

Considering the above problems, we take a multiassembly interface 3D assembly model as the object and study the 3D assembly model retrieval method. First, this method uses the attribute adjacency graph to express the graph of the 3D assembly model and builds the Atlas of the assembly model to establish the Atlas library. This method introduces the conjugated concept to define the conjugated subgraph between assembly parts. Then, the vertices of the graph are serialized for the Atlas of the assembly model, and the traversal times during the vertex matching process are reduced. On this basis, model retrieval is performed through the attribute adjacency graphs of parts, and it uses an improved frequent subgraph mining method to extract a 3D assembly model that satisfies multiple assembly interfaces. This article proposes a 3D assembly model retrieval method for the multiassembly interface, which can retrieve the parts or subassemblies that can be assembled with the input model, and it provides a method for the reuse of the 3D assembly model.

2. Materials and Methods

2.1. Representation of the 3D Assembly Model Based on Attribute Adjacency Graph and Definition of Conjugate Subgraph. There are many ways to represent the CAD model. Among them, the B-Rep model can easily obtain the geometric element information, topological relations, and attribute information of the model, so it is used by most commercial CAD systems. In the process of 3D model retrieval, the similarity degree of B-Rep model information needs to be compared, and how to express this information becomes the primary problem. The B-Rep can describe the modelled object more accurately. The B-Rep model not only describes the geometric information of all the geometric elements that constitute the modelling object but also describes the topological information of the object in detail. The topology information of a target object refers to the connections among all vertices, edges, and faces on the target. It can effectively improve the level of automation in the modelling process.

Attributed adjacency graph (AAG) [18] can express the geometric element information, topological relations, and attribute information of the model, and it is widely used.

2.1.1. Method for the Representation 3D Assembly Model Based on AAG. A 3D assembly model contains the relationship between parts, and its essence is a collection of information.

The points, lines, and surfaces contained in the part and the topological relationship between parts can be effectively expressed by the **AAG**'s nodes and their attributes and edges. The **AAG** of CAD model is represented by $G(V, E, \alpha(V), \beta(E))$:

(1) (V, E) is an undirected simple graph (without loops or heavy edges), V is the vertex set in the corresponding figure of the part, and $V = \{v_1, v_2, \ldots, v_i\}$, V_i represents the ith face of the part.

(2) E is the edge set in the corresponding figure of the part, and $E = \{e_1, e_2, \ldots, e_j\}$, E_j is the edge connecting the vertices v_a and v_b.

(3) $\alpha(V)$ represents the attribute set of the model's vertex and is used to represent the properties of the model surface, including the geometric information of the model surface and the number of edges of the surface;

(4) $\beta(E)$ represents the attribute set of the model's edge, including the type of edge, information on the concavity and convexity, and the positional relationship between the faces of the model. This study focuses on 3D assembly retrieval, focusing on the concavity and convexity of the side.

The cooperation relationship between the 3D assembly model parts can be converted into a certain attribute relationship between AAGs of part. A certain attribute relationship refers to the connection relationship and the type of contact surface between parts. The 3D assembly model can be represented by AAG's Atlas, expressed as $A = \{G, S, P\}$,

(1) $G = \{G_i, G_2, G_3, \ldots, G_i\}$ represents the AAG set of the assembly model part, and G_i represents the AAG of the ith part.

(2) $S = \{S_1, S_2, S_3, \ldots, S_m\}$ represents the set of part's connection type. The connection type can be divided into three categories, including threaded connection (screw connection, stud connection, nut connection, and special thread connection), keyway connection (round head flat key connection, flat head flat key connection, semicircular key connection, wedge key connection, and tangential key connection), and shaft hole connection (interference fit, clearance fit, and transition fit). m is the number of connections.

(3) $P = \{P_1, P_2, P_3, \ldots, P_n\}$ represents the set of a part's contact surface types. The contact surface types are plane and plane constraints (parallel on both sides, angled on both sides), plane and surface constraints (plane and cylinder tangent, and plane and sphere tangent), and surface and surface constraints, and coaxial constraints. n is the number of contact surfaces.

According to the above method of representation, an Atlas library of a 3D assembly model can be constructed. The Atlas contains the AAG of the part, the connection between the parts, and the type of contact surface between the parts. Different atlases have different attribute tags. When it retrieves a 3D assembly model, the computer can find the corresponding Atlas from the Atlas library according to the attribute tag.

2.1.2. Definition of Conjugated Subgraph. The assembly parts are connected by a geometric interface, and the conjugated relationship exists in the matching part of the geometric interface. That is, the topological connection of the mating parts is the same, but the concavity and convexity are opposite [21]. Therefore, through the AAG of the part, the 3D assembly model search can be transformed to find the AAG that satisfies the conjugate subgraph, to find the parts or subassemblies that can be assembled with the input model.

Definition 1. **Conjugated subgraph:** for the two AAGs to which the matching parts (assembly features) of the assembly parts correspond, their topological connection forms are the same, but their concavity and convexity are opposite, and they are called a conjugate subgraph. The conjugate subgraph features of assembly parts include the following: (1) the structure of the conjugate subgraph is the same; (2) the conjugate subgraph corresponds to the same vertex properties, the matching face has the opposite of the loss vector, and the matching area and radius of curvature are the same (nonessential conditions); and (3) the edge properties that the conjugate subgraph correspond to are the opposite.

For 3D assembly model retrieval of multiassembly interface, the input model has the features of multiple geometric interfaces, and its corresponding output model should also have multiple conjugate interfaces. As shown in Figure 1, the input model has two geometric interfaces, and the subassemblies that can be assembled with the input model also have two corresponding conjugate interfaces. The portion marked with a red circle in the figure is a conjugated subgraph with a matching relationship. They have the same topological structure, but the concavity and convexity are opposite.

2.2. Serialization of AAG. The model retrieval is based on AAG, which needs to perform judgment of subgraph isomorphism, and the definition of graph isomorphism and subgraph isomorphism are as follows:

Definition 2. **Graph isomorphism:** there are two graphs, $G_i = (V_i, E_i)$ and $G_j = (V_j, E_j)$. If there is a mapping relationship between them, f: $V_i \longrightarrow V_j$, and $e_i = (v_i, v_i')$ is one edge in G_i. If and only if $e_j = (v_j, v_j')$ is an edge of G_j, then G_i and G_j are isomorphic.

Definition 3. **Subgraph isomorphism:** for a given symbol graph G_i and G_j, if there is a G_j', then it is the subgraph of G_j and G_j', and if G_i are isomorphic, then G_i and G_j have subgraph isomorphism.

Subgraph isomorphism is a typical NP problem, which requires repeated traversal of the vertices of the graph. However, the vertices of the graph are unordered, which leads to a very large amount of computation for isomorphism judgment. In addition, the 3D assembly model retrieval of multiassembly interface extracts atlases, from the

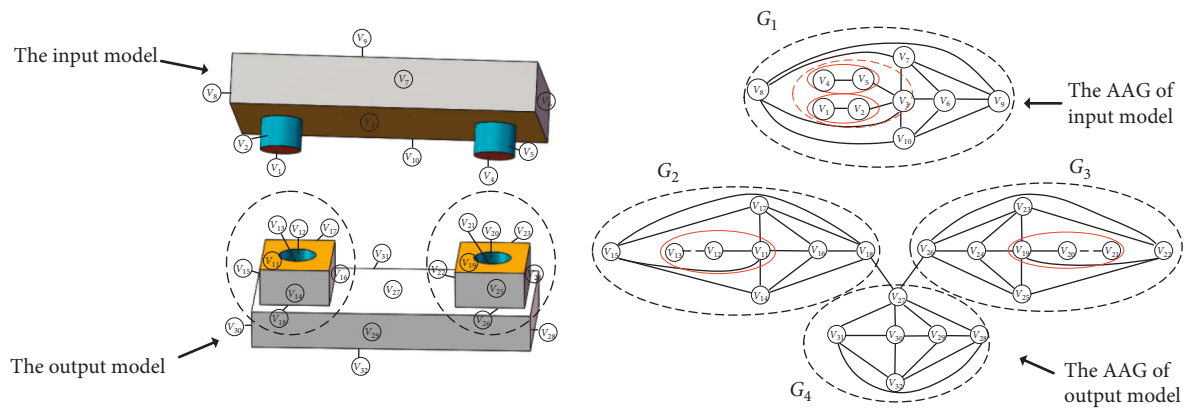

Figure 1: AAG of multiassembly interface.

Atlas library, that are similar to attribute information and topology of the input model. Then, it performs the judgment of isomorphism for each graph in the Atlas. There are multiple graphs in the Atlas, which also makes the calculation of graph isomorphism more difficult. Therefore, a method is needed to establish a unique sequence of vertices of graphs so that the judgment of graph isomorphism can reduce the amount of calculation.

Document [14] proposed that the sequence of the vertices of the AAG is determined according to the adjacency matrix M, and the adjacent vertices after serialization have adjacent edges in the graph. It defines the vector u as a sequence of vertex sets and satisfies

$$g(u) = \sum_{i=1}^{|V|-1} \sum_{k=1}^{|V|} (L(i,k) + L(i+1,k)) u_k^2, \tag{1}$$

where u_k is the k-th term of u and represents the sequence value of the k-th vertex of vertex set V. When u is the eigenvector corresponding to the largest eigenvalue of the adjacency matrix L, $g(u)$ can obtain the maximum value. In this study, after serializing vertices, the same type of vertices is guaranteed to have adjacent edges in the graph and satisfy the maximum aggregation of vertices of the same type. The specific steps of serialization are as follows:

The flow chart of the algorithm is shown in Figure 2.

Step 1. Define the linked list W. The starting point has the largest sequence value in the AAG, $W_0 = V_i$, $V_i = \max(u)$.

Step 2. Find W_{i-1} neighbors in AAG, $N_{W_{i-1}} = \{i | (W_0, V_i) \in E\}$.

Step 3. The ith point in the linked list W, $W_i = \{V_i | \max(u) \cap V \in N_{W_{i-1}}\}$.

Step 4. Get the serial number of the linked list W_i is $\max(u)-i$, and perform k-step iteration on the linked list and repeat step 2~step 3. The list length is $k+1$.

Step 5. Judge $k+1=n$, n is the number of vertices of AAG, if equal, the algorithm ends and the output is serialized. If not, it goes to the next step.

Step 6. Find the complement of vertex sets $C = \{i | V_i \notin W \cap V_i \in V\}$, and order AAG's new vertex set V=C. Then, go to step 2.

After all vertices of the AAG are accessed, the sorting result of the output is shown in Figure 3. The assembly interface can be summarized as "planar-plane," "square rib-groove," "circular pin-hole," "curved surface-curved surface," "dovetail rib-groove," and "square pin-hole" [20]. When these assembly interfaces are represented by AAG, the vertices of them always have the largest sequence value in AAG, and the vertices corresponding assembly interfaces are independent of other vertices. Therefore, the conjugate subgraph does not disappear owing to serialization.

The significance of serialization is to improve the computational efficiency of the algorithm. The 3D assembly model retrieval of multiassembly interface extracts atlases that are similar to the attribute information and topology relationship of input model from the Atlas library, and then, it performs a judgment of isomorphism on each graph in Atlas. There are multiple graphs in an Atlas, which increases the calculation of graph isomorphism judgment. This makes the entire algorithm more efficient.

2.3. 3D Assembly Model Retrieval Method. The output model of this paper's retrieval method is a part or the subassembly that can be assembled with the input model, and it has multiple geometric interfaces. The retrieval method needs to perform multiple isomorphism judgments of AAGs conforming to the conjugate subgraph; only when the conjugate subgraph of the target is greater than or equal to the input model, the corresponding Atlas can be selected, and then, the corresponding 3D assembly model can be extracted. On the basis of graph serialization, first, a method of efficient graph isomorphism judgment is used to judge the isomorphism of AAG that conforms to conjugate subgraph; then, on the basis of the method of graph isomorphism, the Atlas containing multiple conjugate subgraphs is selected by using the improved frequent subgraph mining algorithm so that the corresponding 3D assembly model is extracted. The overall algorithm flow is shown in Figure 4.

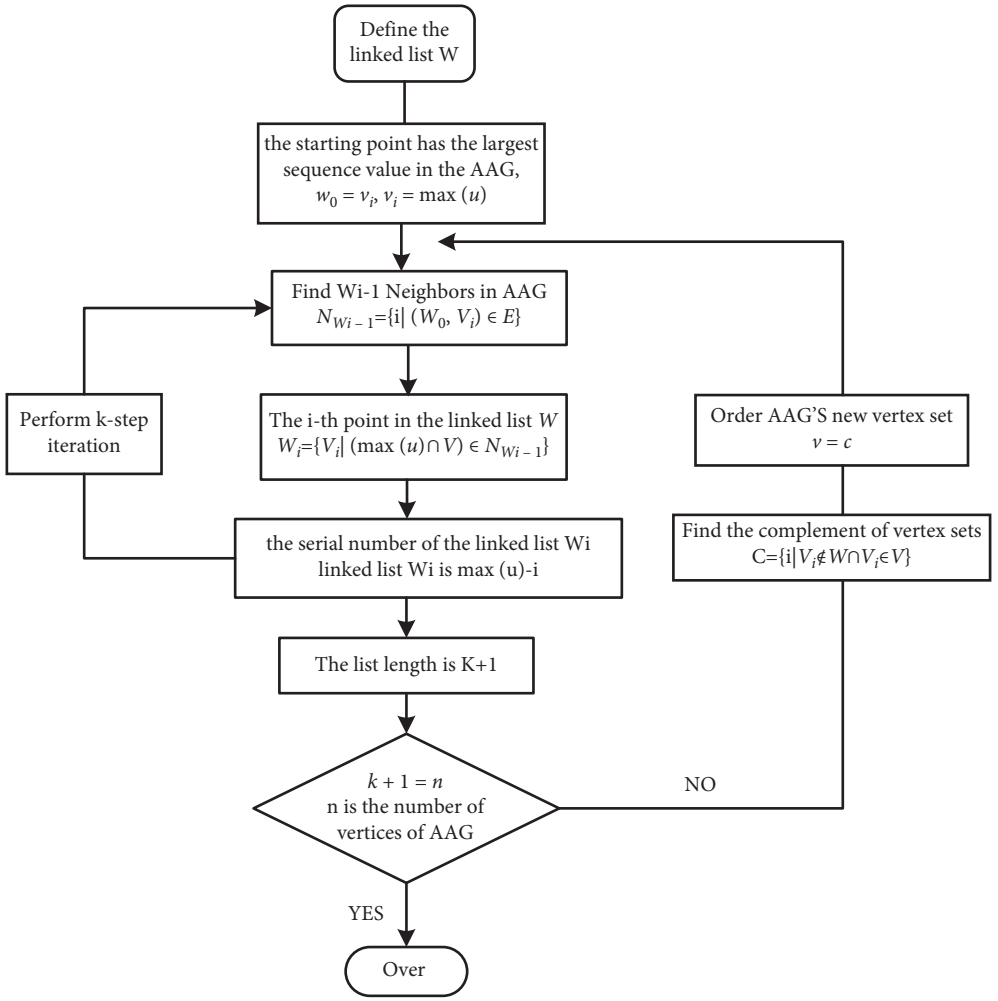

Figure 2: Serialization of AAG.

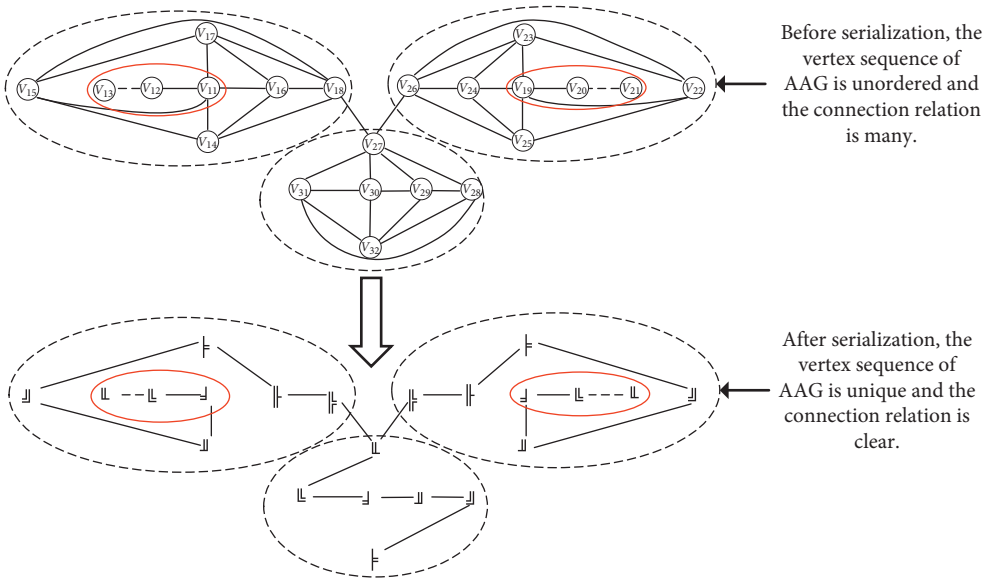

Figure 3: Result of AAG's serialization.

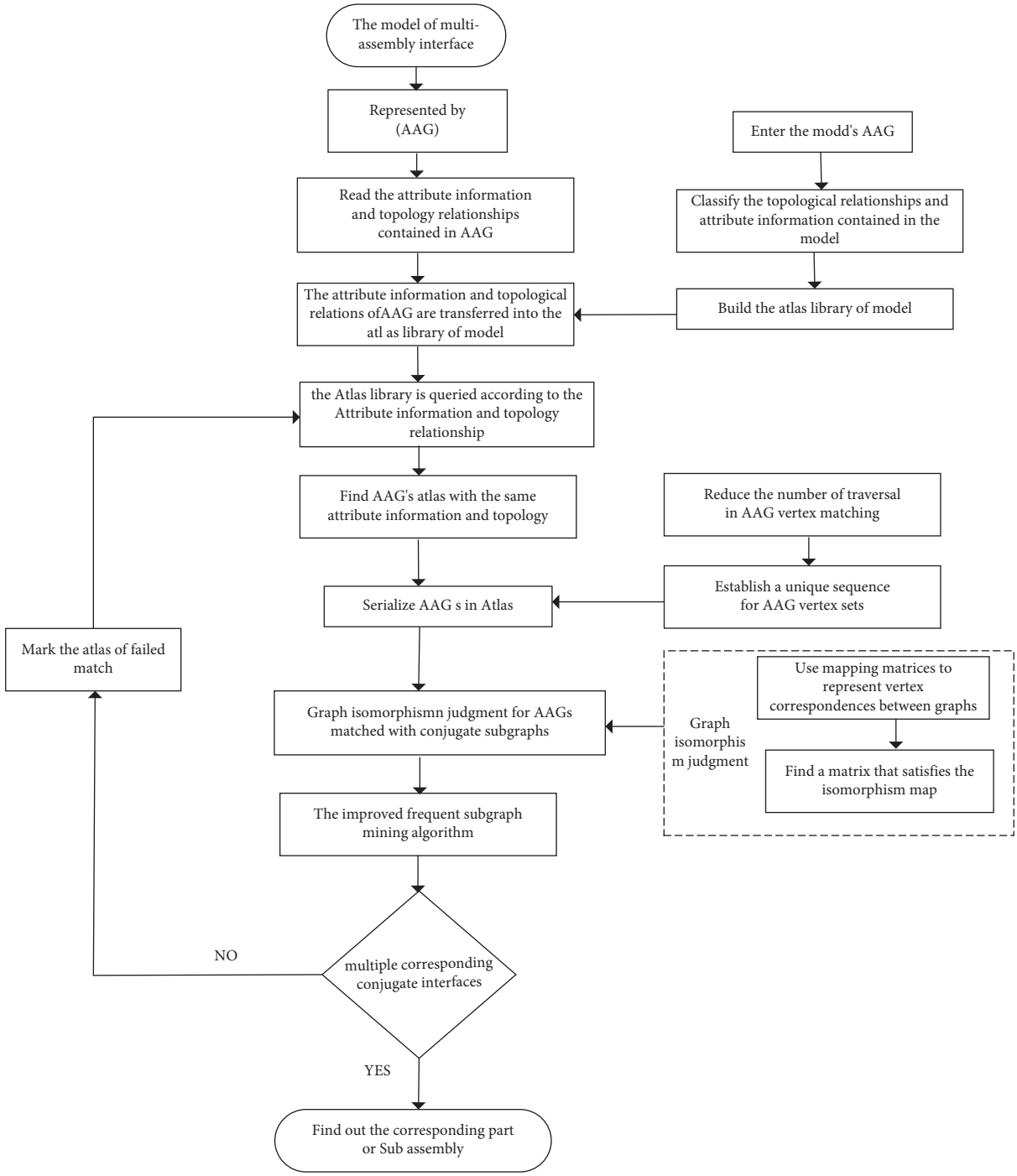

Figure 4: 3D assembly model retrieval method for multiassembly interface.

2.3.1. Method of Judgment of Graph Isomorphism. The 3D assembly model retrieval method based on AAG transforms the similarity analysis of the assembly parts model into the similarity analysis of the AAG with the conjugate subgraph. The graph similarity judgment is accomplished using the graph isomorphism judgment to determine whether two graphs are isomorphic; that is, it assesses whether there is a mapping relationship between two graph vertices. The mapping relationship between two graph vertices can infer the mapping relationship between two graph edges.

The computational complexity of subgraph isomorphism determination is an NP-complete problem. In this study, an efficient graph isomorphism determination method is used. We assume that we have G_1 and G_2, where G_1 is the target graph, and G_2 is the graph to be retrieved. The number of vertices of the vertex set V_1 of the graph G_1 is a, the number of vertices of the vertex set V_2 of the graph G_2 is b, and $a < b$. The mapping relationship of the vertices between the graphs G_1 and G_2 is represented by an $a \times b$ mapping matrix $M_{a\times b}$. m_{ij} is the i-row and j-column element in the mapping matrix M. If

V_1 and V_2 are related, then $m_{ij} = 1$; otherwise, $m_{ij} = 0$. For matrix $M_{a\times b}$, if there is a map with only one 1 per row and no more than one 1 per column, the matrix $M_{a\times b}$ represents the isomorphic mapping between G_1 and G_2.

The steps of the graph isomorphism matching algorithm are as follows:

Step 1. Initialize the mapping matrix M and set two empty sets V_1 and V_2. Use these sets to hold the vertices that have been matched by the two graphs during the retrieval.

Step 2. Retrieve from the first row of matrix M and look for columns with a value of 1 from left to right. For any ith row, if the value of the jth column is 1, and if the column is not occupied, it means that a possible vertex association is found.

Step 3. Add the two vertices of the previous step to sets V_1 and V_2.

Step 4. Determine whether the newly added vertices in V_1 and V_2 correspond to the matching vertex pairs in the final isomorphism graph.

If the newly added vertices in V_1 and V_2 correspond to the matching vertex pairs in the final isomorphism graph, the subgraphs that are composed of the set of vertices V_1 matched in G_1 and the set of vertices V_2 matched in G_2 are isomorphic. Thus, it can be judged that the subgraph formed by V_1 and the subgraph formed by V_2 are isomorphic.

2.3.2. Improved Frequent Subgraph Mining Algorithm. On the basis of the method of graph isomorphism matching, the frequent subgraph mining algorithm is improved. Frequent subgraph mining is actually a graph isomorphism matching process, which is used to judge the Atlas extracted from the Atlas library. From this, it can be concluded whether the Atlas contains conjugate subgraphs that conform to the features of the assembly interface, and the number of conjugate subgraphs can be determined. If the number of conjugate subgraphs in the graph set is greater than or equal to the number of geometric interfaces of the input model, then the corresponding 3D assembly model of the Atlas is extracted. Otherwise, the Atlas is marked as a failure.

The related definitions of frequent subgraph mining algorithms are as follows:

Definition 4. **Frequency:** there is a graph database $B = \{b_0, b_1, \ldots, b_n\}$ for subgraph b such that

$$\phi(b, b_i) = \begin{cases} 1, \text{if } b \text{ and the subgraph of bi are isomorphic} \\ 0, \text{if } b \text{ and the subgraph of bi are not isomorphic} \end{cases},$$

$$S = \frac{\sum \phi(b, b_i)}{|B|}, \tag{2}$$

$|B|$ represents the base of Atlas B, $\sum \phi(b, b_i)$ represents the total number of isomorphism of b and bi, $b_i \in B$, and S is the frequency.

Table 1: Symbolic meaning.

Symbol	Meaning
C^K	K-order candidate frequent subgraph sets
F^K	K-order frequent subgraph sets
F^F	All frequent subgraph sets, $FF = \{F^1, F^2, \ldots, F^n\}$

Definition 5. **Frequency subgraph:** for a given minimum frequency $S_{\min}$, if there is a subgraph b that satisfies $S \geq S_{\min}$, then b is called a frequent subgraph of the Atlas database B.

The simple steps of the frequent subgraph mining algorithm are as follows:

(1) Connect the K-order frequent subgraphs to generate $K+1$ candidate subgraphs;

(2) Clip the candidate $K+1$ order subgraph Atlas, and delete all $K+1$-order candidate subgraphs containing K-order infrequent subgraphs;

(3) Calculate the frequency of all subgraphs in the $K+1$-order candidate subgraph set;

(4) Delete candidate subgraphs with frequencies less than $S_{\min}$ in the $K+1$-order candidate subgraphs.

By solving the loop from $k = 0$ until it cannot generate higher-order frequent subgraphs, frequent subgraph mining is completed. Calculating the frequency of subgraphs is the process of graph isomorphism judgment. In extracting AAGs with conjugate subgraphs, the process needs to define some symbols to describe the algorithm. Table 1 lists some of these meanings.

The frequent subgraph Atlas generation algorithms are shown below. We start with Atlas B and frequency $S_{\min}$, and the output is the set F^K of the K-order frequent subgraph.

Frequent subgraph generation algorithm: (Algorithm 1)

Starting from $K = 0$, the above algorithm is cyclically named, and the set of all frequent subgraphs is obtained as $\mathrm{FF} = \{F^1, F^2, \ldots . F^n\}$.

The algorithm is based on the K-order frequent subgraphs to build $K+1$ candidate subgraphs. The $K+1$-order frequent subgraphs are obtained by using two K-order frequent subgraphs containing the same frequent subgraph of $K-1$ order. The two most important steps in this process are identifying two identical $K-1$-order subgraphs and connecting two K-order frequent subgraphs.

The recognition of two identical $K-1$-order subgraphs can record the IDs of all $K-1$-order frequent subgraphs in the K-order frequent subgraph properties. The same $K-1$-order frequent subgraph is obtained by the intersection of the two K-order frequent subgraph attribute values to avoid the judgment of subgraph isomorphism. The connection of two K-order frequent subgraphs can be seen as the process of generating the $(K+1\times K+1)$ adjacency matrix by combining two $(K\times K)$ adjacency matrices.

The importance of the retrieval method proposed in this paper lies in the following:

(1) The retrieval of assembly information improves the semantic consistency of the model's retrieval results from the perspective of assembly design intent.

(2) The search of the geometric structure adopts an efficient graph isomorphism decision method that is combined

(1) Begin
(2) $F^{K+1} \leftarrow \varnothing$, $C^{K+1} \leftarrow$ Candidate(F^k)//generate candidate subgraphs.
(3) For $\forall b^{K+1} \in C^{K+1}$ do//candidate sets downsizing and frequent count.
(4) If $\sigma(b^{K+1}) \geq S_{\min}$ then.
(5) $F^{K+1} \leftarrow F^{K+1} \cup \{b^{K+1}\}$
(6) End if
(7) End for
(8) Return F^K
(9) End

Algorithm 1: Frequent subgraph generation algorithm.

Table 2: Extraction results of attribute information and topology relation from Atlas library.

Retrieval target	Extraction result
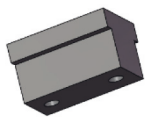 Input model 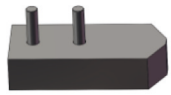 Output model Machine's jaws	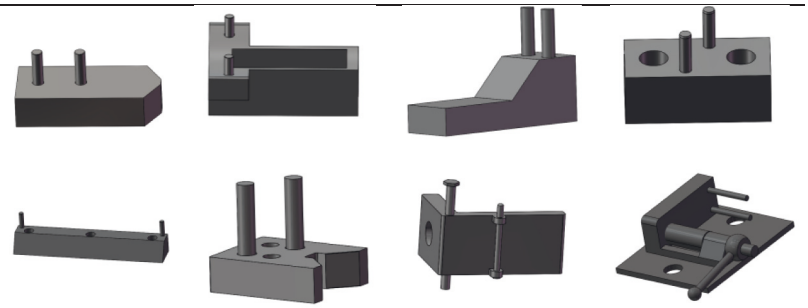
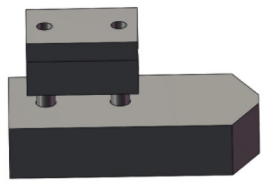 The assembly graph of machine's jaws	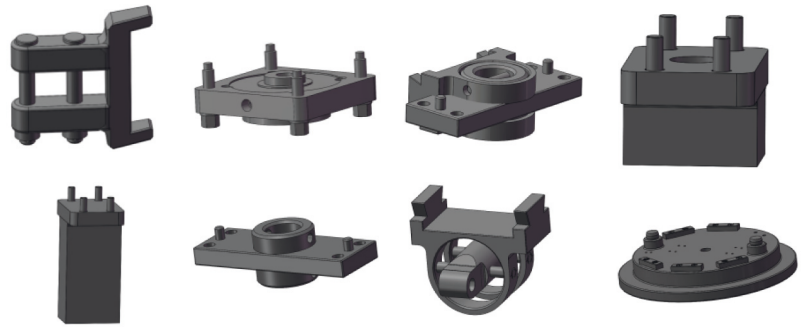

with frequent cartographic mining algorithms, thus improving the retrieval accuracy and retrieval efficiency.

The significance of the retrieval method proposed in this paper lies in the following: the graph that is extracted satisfies the conjugate subgraph with the features of the assembly interface and satisfies the set frequency. It can be used to judge the graph in the Atlas, resulting in a 3D assembly model with multiple conjugate interfaces.

3. Discussion

To verify the validity of this method, a CAD model library for machine tool fixtures and accessories was established. An experiment of 3D assembly model retrieval of multiassembly interface is performed using MATLAB software. The computer used was an Intel Core I7-8700K CPU with 4 GB of memory.

It takes the machine's jaws as the input model, which has two fixing holes. It needs to extract models that have conjugate features with the fixed holes in the model library, and there are two or more conjugate features.

In the retrieval process, first, the system reads the attribute information and topology of the input model. Then, it passes the reading input model information to the Atlas library of models, queries the Atlas library based on this information, and extracts the atlases whose attribute information and topology are similar to the input model. The corresponding 3D models of the retrieved atlases are listed in Table 2.

According to the table, the corresponding models of the Atlas are single assembly parts, and some are subassemblies. They all have the features of axial hole connection, plane and surface contact, or plane and plane contact.

After extracting the Atlas that is similar to the input model's attribute information and topology, the judgment of

Table 3: Retrieval of judgment of graph isomorphism.

S_{min} value	Retrieval result
S_{min}=1.00	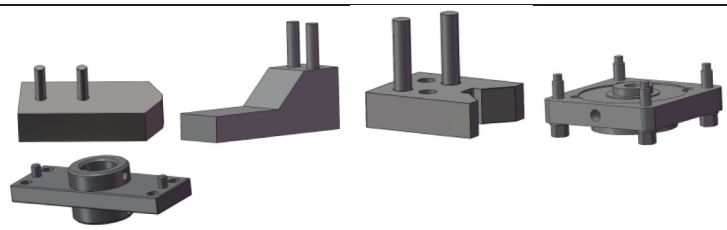
S_{min}=0.60	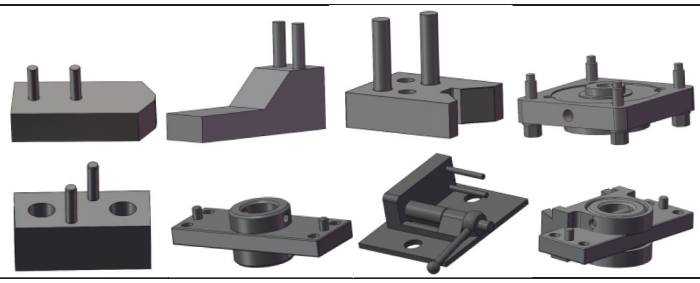

graph isomorphism is performed on the AAG of the Atlas. It judges whether the AAG in the Atlas contains conjugate subgraphs, and its number must be greater than or equal to the number of conjugate subgraphs of the input model. To verify the search conditions in the case of $S_{\min}$ with different frequency, experiments were performed with $S_{\min} = 1.00$ and $S_{\min} = 0.60$, respectively. The results of the retrieval are listed in Table 3.

After graph isomorphism judgment, the atlases of AAGs that do not conform to conjugate subgraphs are eliminated. Moreover, because the frequent subgraph mining algorithm is based on the idea of layer-by-layer iteration, the number of extracted atlases is reduced as the $S_{\min}$ increases. The meaning of changing $S_{\min}$ is that the scope of the output model can be set according to the designer's needs. When the design intent is clear, $S_{\min}$ can be increased to accurately output the model; when the design intent is ambiguous, $S_{\min}$ can be reduced to extend the range of the output model, which gives the designer more choices.

From Table 3, it can be seen that the retrieval method of judgment of graph isomorphism can accurately match the assembly interface of the 3D model. The Atlas of the model has similar attribute information and topological relations. Using the advantages that the AAG can express the topological structure of the 3D model, the model is retrieved from the shape structure, and the conjugate subgraph can retrieve the matching structure of the two models with the assembly relationship. Therefore, the matching 3D model of the assembly interface can be extracted through the judgment of graph isomorphism, which significantly improves the accuracy of model retrieval results.

Although the vertices of AAG are serialized and the number of vertices traversing in the judgment of graph isomorphism decreases, the calculation amount of judgment of AAG isomorphism in the Atlas is still large. Therefore, in order to verify the time efficiency of retrieval algorithm, the execution time of the algorithm under different $S_{\min}$ is verified. Experiments show that the larger $S_{\min}$ is, the shorter the execution time of the algorithm is. This is the result of the algorithm's iterative idea. The experimental results are shown Figure 5.

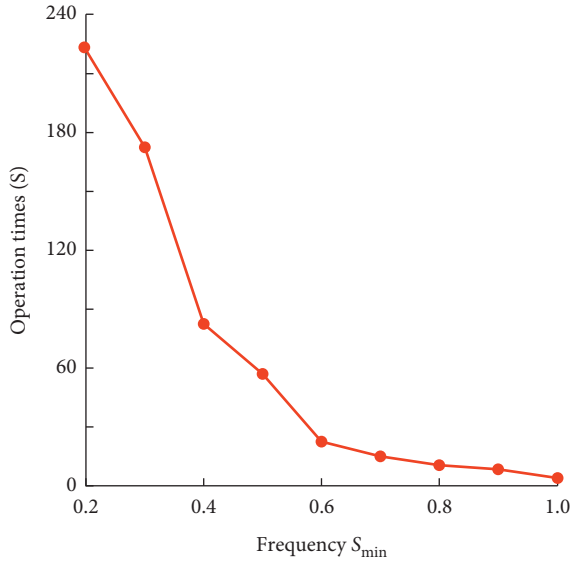

Figure 5: Operation of different $S_{\min}$.

4. Conclusions

In this paper, a 3D assembly model retrieval method for multiassembly interface is proposed. First, the 3D assembly model is represented by an attribute adjacency graph, and the definition of the conjugate subgraph is given according to the coordination relation between the assembly interfaces.

Then, the graph in the Atlas is serialized so that the vertex of the attribute adjacency graph has a unique sequence. Finally, through the method of efficient graph isomorphism judgment and the improvement of frequent subgraph mining algorithm, the attribute adjacency graph that conforms best to the assembly conjugate subgraph is judged in the Atlas, to extract the 3D assembly model of the multiassembly interface. Experimental results show that the method proposed in this paper can retrieve the parts or subassemblies that match the input model, and it provides a method to reuse the 3D assembly model.

4.1. Future Work. This paper proposes a 3D assembly model retrieval method incorporating assembly semantics, which is based on the existing 3D models of the subject group, whose semantic information has already been marked up, and the model information reflected is not perfect. In order to achieve a better 3D model retrieval system, further research can be done in terms of semantic annotation specification, similarity metric method, and 3D assembly model information subnetwork acquisition and pushing method.

(1) According to the different needs and influences of designers on 3D assembly model information in the early, middle, and late stages of design, the components of design intent in the time dimension are summarized and the semantic annotation specification of 3D assembly model information reflecting design intent is constructed.

(2) A design intent semantic information association mapping specification is constructed, and design intent information subnetworks of different sizes are formed according to different granularity of design intent. The similarity measure between the design intent information subnetwork and the subnetwork in the 3D assembly model information network is investigated, and the best matching subnetwork is searched for in the 3D assembly model information network.

Data Availability

The data used to support the finding of this study are available from the corresponding author upon request.

Conflicts of Interest

The authors declared that there are no conflicts of interest regarding the publication of this paper.

Acknowledgments

This project was supported by the National Natural Science Foundation of China (Grant no. 51705392), Shaanxi Science and Technology Resources Open Sharing Platform (Grant no. 2021PT-006), Key R & D plan of Shaanxi Province (Grant no. 2021NY-171), and Shaanxi Science and Technology New Star Project (Grant no. 2020KJXX-071).

References

[1] R. Jardim-Goncalves, J. Sarraipa, and C. Panetto, "Knowledge framework for intelligent manufacturing systems," *Journal of Intelligent Manufacturing*, vol. 22, no. 5, pp. 725–735, 2011.

[2] U. Soni, V. Jain, and S. Kumar, "Measuring supply chain resilience using a deterministic modeling approach," *Computers & Industrial Engineering*, vol. 22, no. 5, pp. 725–735, 2011.

[3] L. Monostori and J. Prohaszka, "A step towards intelligent manufacturing: modelling and monitoring of manufacturing pro-cesses through artificial neural networks," *CIRP Annals - Manufacturing Technology*, vol. 42, no. 1, pp. 485–488, 2015.

[4] R. An, "3D CAD model retrieval method based on hierarchical multi-features," Conference on International Conference on Graphic and Image Processing," *International Society for Optics and Photonics*, pp. 1–9, 2015.

[5] S. W. Kim, J. Yoon, S. Park, and J.-I. Won, "Shape-based retrieval in time-series databases," *Journal of Systems and Software*, vol. 79, no. 2, pp. 191–203, 2006.

[6] V. Jain and H. Zhang, "A spectral approach to shape-based retrieval of articulated 3D models," *Computer-Aided Design*, vol. 39, no. 5, pp. 398–407, 2007.

[7] F. Qin, S. Qiu, S. Gao, and B. Jing, "3D CAD model retrieval based on sketch and unsupervised variational autoencoder," *Advanced Engineering Informatics*, p. 51, 2022.

[8] S. Hojoon and S. H. Lee, "Three-dimensional model retrieval in single category geometry using local ontology created by object part segmentation through deep neural network," *Journal of Mechanical Science and Technology*, vol. 35, p. 11, 2021.

[9] Y. Zhou, Yu Liu, H. Zhou, and W. Li, "Wasserstein distance feature alignment learning for 2D image-based 3D model retrieval," *Journal of Visual Communication and Image Representation*, 2021.

[10] W. H. Li, W. Z. Nie, and An Liu, "Multi-view graph matching for 3D model retrieval," *ACM Transactions on Multimedia Computing, Communications, and Applications*, vol. 16, no. 3, 2020.

[11] D. Mcwherter, M. Peabody, W. C. Regli et al., "Solid model databases: techniques and empirical results," *Tanpakushitsu Kakusan Koso Protein Nucleic Acid Enzyme*, vol. 32, no. 10, pp. 1250–1269, 2001.

[12] D. Bespalov, W. C. Regli, and A. Shokoufandeh, "Local feature extraction and matching partial objects," *Computer-Aided Design*, vol. 38, no. 9, pp. 1020–1037, 2006.

[13] D. McWHERTER, M. Peabody, W. C. Regli, and A. shockoufandeh, "Transformation invariant shape similarity comparison of solid models," in *Proceedings of the ASME Design Engineering Technical Conference*, pp. 46–57, ACM Press, Germany, January 2001.

[14] D. McWHERTER, M. Peabody, A. C. Shokoufandeh et al., "Database techniques for archival of solid models[C]," in *Proceedings of the sixth ACM symposium on Solid modeling and applications*, pp. 78–87, ACM Press, Michigan, April 2001.

[15] Y. Dong and J. Xu, "Part 3D model retrieval method based on assembly structure similarity. Chin. J. Mech," *Computer Intergrated Manufacturing Systems*, vol. 394, no. 3, pp. 1177–1185, 2013.

[16] J. Zhang, M. Zuo, R. K. Yang et al., "Method to discover common design units from three-dimensional assembly models based on attribute similarity analysis," *Journal of Mechanical Engineering*, vol. 45, no. 4, pp. 273–280, 2009.

[17] W. Zhou, J. R. Zheng, and J. J. Yan, "Local matching of assemblies based on subgraph isomorphism and case matching," *Journal of Computer-Aided Design & Computer Graphics*, vol. 22, no. 2, pp. 299–305, 2010.

[18] Y. P. Wang, Y. Li, J. Zhang et al., "Similarity assessment of assemblies based on random walks and optimal matching," *Journal of Computer-Aided Design & Computer Graphics*, vol. 26, no. 3, pp. 401–410, 2014.

[19] Y. J. Wu and Q. Gao, "Spatial structure similarity retrieval of product assembly model," *Journal of Computer-Aided Design & Computer Graphics*, vol. 26, no. 1, pp. 113–120, 2014.

[20] H. Qiao et al., "A 3D assembly model retrieval method based on assembly information," *Assembly Automation*, vol. 39, no. 4, pp. 5556–5565, 2019.

[21] S. Joshi and T. Chang, "Graph-based heuristics for recognition of machined features from a 3D solid model," *Computer-Aided Design*, vol. 26, no. 1, pp. 58–66, 1988.

[22] H. Xiao, Y. Li, and J. F. Zhang, "CAD mesh model simplification with assembly features preservation," *Science China Information Sciences*, vol. 57, no. 3, pp. 1–11, 2014.

Hindawi
Scientific Programming
Volume 2022, Article ID 9471334, 10 pages
https://doi.org/10.1155/2022/9471334

Research Article

Improved Generative Adversarial Networks for Student Classroom Facial Expression Recognition

Chaoyi Wang

Aviation Institute, Jilin Communications Polytechnic, Changchun 130000, Jilin, China

Correspondence should be addressed to Chaoyi Wang; wchyi@jljy.edu.cn

Received 5 May 2022; Revised 5 June 2022; Accepted 28 June 2022; Published 16 July 2022

Academic Editor: Lianhui Li

To assess students' learning efficiency under different teaching modes, we used students' facial expressions in the classroom as a study point. An enhanced generative adversarial network is presented. We designed a generator as an automatic coding-decoding combination in a cascade structure with a discriminator configuration. It can retain different expression intensity features to the maximum extent. We also added a new auxiliary classifier, which can classify different intensity features and improve the model's recognition of detailed features of similar expressions, thus improving the comprehensive facial expression recognition accuracy. Our approach has a great advantage over the other facial expression recognition approaches on public datasets. Finally, we conduct experimental validation on the self-made student facial expression dataset in all cases. The experimental findings showed that our approach's recognition accuracy is superior to that of other methods, demonstrating the method's efficacy.

1. Introduction

In classroom teaching, what the teacher explains and what the students understand is not visually represented in the current assistive teaching systems. It is also a topic of debate which teaching style students would prefer between the traditional classroom teaching style and the modern smart classroom teaching style. The literature [1] then mentions that smart teaching and intelligent learning environments can give full play to students' cognitive abilities, greatly increase their interactivity, and provide better mastery of new knowledge. In terms of the current investigation, there is no intuitive system to measure students' acceptance of different teaching methods. For this reason, we will concentrate on this problem, we set out to identify facial expressions, and by obtaining the emotional expressions of the teacher and the facial expressions between students and then performing facial expression analysis, we can determine the students' acceptance and satisfaction with the teaching method. Our research, to some extent, provides some reference value for the quality of teaching and can respond to the effectiveness of teaching at the biotechnical level.

In human communication, facial expression is an important communication tool. It often adds different emotional factors to nonverbal communication, and it is crucial in the process of comprehending one another's emotional expression. With the advancement of biotechnology and computer science, facial expressions are used in various industries. The most common application area is privacy and security, which is most directly demonstrated by the face unlocking feature on cell phones and computers. Second, in the field of transportation, driver fatigue and drunken driving detection are also predicted by capturing facial expressions. Also, facial expression recognition technology is also frequently integrated into the fields of virtual reality, medical care, and service robotics [2–4]. Of course, the facial expression recognition technology is not so simple, and there are several technical difficulties to be broken. Different countries have different language and cultural backgrounds, and their meanings conveyed by facial expressions are more or less different. In addition, the results of facial expression recognition are not sufficient due to the objective influence of nonstructural conditions, such as occlusion, illumination, and focus problems. Recently, many researches have arisen

in the field of facial recognition to address these technical challenges, but the technological breakthroughs are all relatively limited [5].

The process of recording real-life student emotions is known as facial expression recognition, and the inner feelings can be mapped side by side from the fluctuations of emotions. The process is mainly based on video dynamic frames and still image sequences as the main recognition subject, and based on face recognition, it rises to a level to synthesize the linkage reaction among five senses, thus predicting facial expressions. The literature [3] starts the study from the simplest basic facial expressions, mainly the expressions of joy and sadness series. The authors, in order to obtain facial expressions accurately, first remove the noise from the images by preprocessing operations, followed by face detection to delineate the range of facial expression features. Then feature fusion is performed jointly with the linkage between the eyes, eyebrows, mouth, and cheeks, and finally, and facial expressions are predicted by matching with the training feature library.

To address the difficulties in facial expression recognition research, related researchers have made unremitting efforts. Some researchers have focused their research on manual features. For example, literature [6] proposed the use of Gabor filters to optimize manual features, and literature [7] proposed local binary patterns to break the limitations of manual features. The literature [8] proposed a gradient histogram method to extract features, which further enriched the artificial feature set. Some researchers put their research focus on deep neural networks. For example, the literature [9] innovatively improved the network structure in the approach using neural networks, and the authors picked to fine-tune the two-stage training algorithm to adapt the feature linkage between the five senses and enhance the expression recognition. The literature [10] both adopted generative adversarial networks, which further explored the intrinsic features of the face and eliminated the interference of nonsubjective factors. The literature [11], on the other hand, performed adaptive optimization on the constraint function and proposed island loss to determine the attribution problem between features by learning the connection between different expressions. The literature [12] places the research focus on the attention mechanism and proposes an adaptive regional attention network and validates the high efficiency of the network on the available dataset, and results proved that integrating the learnt model can increase the model's robustness.

However, facial emotion detection is not a simple work, so the previously mentioned studies ignore the direct connection between facial attributes and emotions, and the main reason for the poor recognition results is the inability to positively map the way of distortion among the five facial nodes, and the changes between specific locations cannot be responded. Some researchers have proposed setting up standard lines on the face for facial node calibration, and the literature [13] also mentions that using this approach can decrease the data variance and improve the stability of the model. The literature [14] also proposed model-aware flags for the automatic perception of facial position, and experiments demonstrated that this method not only reduces the workload but also preserves the robustness of the model. In the literature [15], it was unexpectedly found in the experiments that additional flagging of facial positions by predetermined trajectories could increase the recognition speed of the model without affecting the accuracy. All the above methods take an end-to-end form, and such methods also have certain limitations. Its recognition effect is limited by the quality of facial markers, and when facial expression features are captured, they can easily be incorporated into shallow features in a nonmaximal suppression operation.

To counteract the drawbacks of deep learning approaches, the literature [16] used a multitask learning strategy in neural network construction to enhance the primary task by shifting the learning number of different tasks. In addition, the literature [17, 18] added facial detection flags in the feature design of the facial action structure unit, which can aid in improving facial emotion recognition accuracy. In terms of multitask parameters, most of the previous studies launched optimization based on hard parameter sharing, but this approach limited the recognition efficiency of facial expressions to some extent. Nowadays, more soft parameters have started to be developed for sharing, such as the multitask convolutional partial sharing strategy in the literature [19] and the cross-stitch network proposed in the literature [20], which successfully break the efficiency limitation.

In our study, we consider various models comprehensively. We finally choose a generative adversarial network as the base method. To obtain the intensity features of different expressions hierarchically, we added a new auxiliary classifier and optimized the network structure. Finally, the effectiveness of our approach is demonstrated on both public and self-made datasets.

The rest of the study is arranged as follows. Section 2 presents the work related to different facial expression recognition methods. Section 3 introduces our adaptive improvement strategy and implementation process for generative adversarial networks. Section 4 presents the comparison of experimental databases and experimental methods. Finally, Section 5 presents research prospects and improvement directions.

2. Related Work

Traditional facial expression recognition research mainly relies on extracting geometric features, texture features, and hybrid features of the face as the basis [21]. The active shape model is the mostly used in facial expression recognition work and is the geometric feature method, which mainly uses facial feature points as a reference to construct geometric features and then localizes them. In practical application, the method is affected by lighting and occlusion and does not achieve better recognition results. The facial action unit is also a typical example of the geometric feature method. This method first divides the face into units and then compares them with the facial reference points by calculating the relative distance between units. However, this method requires intensive training in advance and has a very

high computational complexity at the time level [22]. Texture feature-based facial expression recognition methods are more common and usually have faster computational speed, but they are not effective for motion scenes such as Gabor filter and local orientation pattern methods. In the face of occlusion, the most effective method is the scale-invariant feature variation, which can automatically find the spatial extrema and extract their position, scale, and rotation invariants and can circumvent the effect of occlusion by local mapping, but this method is not effective for the target smoothed by edges.

In facial expression recognition work, the input video frames or image information are subjected to preprocessing operations and then input to convolutional layers of different scales for feature extraction, and then the facial features are transformed into independent vectors, and finally, the classification is completed by fully connected layers [23]. Different application scenarios have different structural requirements for convolutional neural networks [24], and to address the influence of nonstructural environmental factors, facial expression recognition work often requires specific preprocessing operations, such as the HOG feature method [25], the LBP method [26, 27], and the ROI method [28–30]. Different features have different extraction stages, resulting in multiple features in different dimensions, which cannot be unified at the time level and affect the convergence efficiency of neural networks. Besides, convolutional neural networks are often used by researchers as a basic network. According to different requirements for different tasks, convolutional neural networks are optimized and upgraded accordingly to the increase in the adaptability and performance of deep networks. Some researchers have designed cascade networks to enhance the efficiency of the localization of facial nodes [31]. Some researchers tried to add auxiliary modules to improve the robustness of the model [32]. Some researchers divided the network into parallel or tandem networks of small modules to achieve the inclusion of features at the decision level [33, 34]. All of the above research methods aim to improve the depth and parameter tuning of the network, which invariably increases the number of parameters. Considering the computational cost, some researchers have proposed recurrent neural networks [15], capsule networks [35], deep belief networks [36, 37], and so on.

For deep learning methods, the recognition accuracy is proportional to the volume of training data, and the richer the dataset, the higher the recognition accuracy. For facial emotion detection, building a database of facial expressions is undoubtedly a difficult and long-lasting task. The features of facial expressions are deeply related to different background cultures, and the process of data annotation usually requires the annotators to have a certain understanding of national culture and background. In addition, the optimization process of neural networks is often not transparent enough, and most researchers rely on constant repetition of experiments and experience to verify the optimal parameter sizes [38]. Therefore, the period and computational cost factors of the project need to be considered before adopting a deep learning approach. To circumvent complex parameter tuning strategies, the literature [39] proposed the multigranularity cascade forest method, an integrated neural network structure inspired by the cascade forest classification rule and the random forest rule. Compared with pure deep learning methods, this method has a smaller number of parameters and sets hidden layer hyperparameters to reduce the computational cost.

3. Method

3.1. Pipeline Overview. Researchers usually take an unsupervised approach to train the adversarial model, which belongs to the same deep neural network model and is divided into two parts in the phased design of the network. The generator part belongs to the front-end of the network and the discriminator belongs to the back-end. The generative adversarial network principle is simulated training at the neural network level, where different samples are iterated and generated in a random mode. The original samples are input at the input side, and the generator generates pseudosamples based on the original samples, and the usability of the generated samples is judged by comparing the difference between the original samples and the generated samples within a specified threshold of the pseudosamples. If the generated sample does not meet the standard value, by iterating this method, the pseudosamples can be approximated to the eigenvalues of the true samples in terms of eigenvalues. The structure of the generative adversarial network is shown in Figure 1.

In our study, face recognition systems can be made more robust by combining facial expression recognition with adversarial generating networks. Generative adversarial networks essentially play the facial expression details against each other by repeatedly updating iterations until the best facial expression features are obtained and then output to the terminal. Considering the facial expression details feature refinement, we define the classification of facial expressions to prevent the problem of increasing errors with different expression strengths.

3.2. Generator. The generator is in the front part of the adversarial network and its input is the real sample. After the real samples are input, the generator parses the real samples, divides the real samples into different feature nodes, and finally simulates the feature nodes to generate pseudosamples. The working process of the generator is shown in Figure 2.

We refer to the literature [40, 41] for an enhanced method to generative adversarial networks, where the generator is meant to work as an encoder and decoder in the tandem, which is a creative design. After several experimental verifications, we also apply the nested combination of encoding and decoding to the generator network. The encoder of the generator acquires different intensity facial expression features I^{low} by downsampling. Researchers in the literature [42] added a residual structure to the generator optimization to improve the efficiency of the generator encoding. We also verified the effectiveness of the method

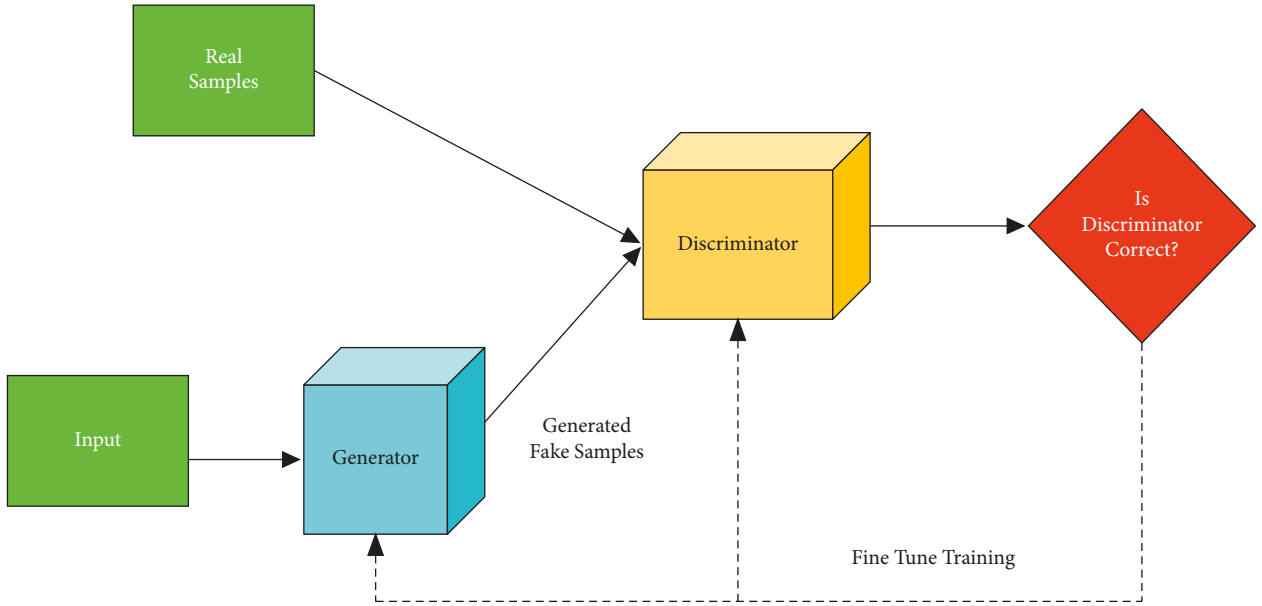

Figure 1: Generative adversarial network architecture.

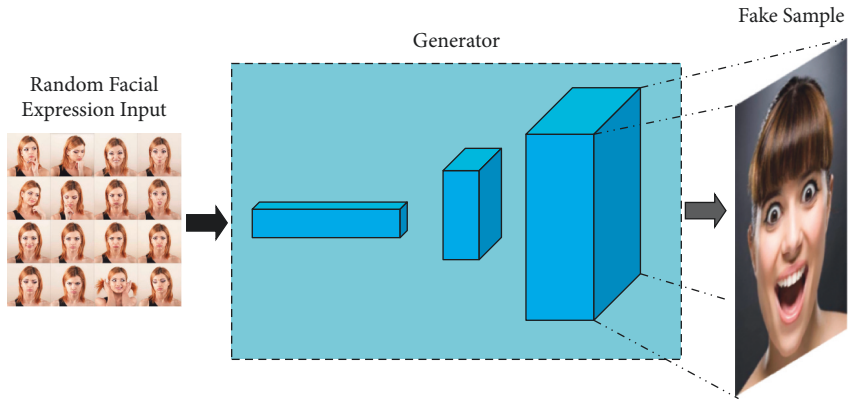

Figure 2: Facial expression generator process.

experimentally. In the decoder network layer, we use upsampling to transform the intensity features of facial expressions and then implement nonlinear activation by RELU. According to the decoder network optimization method in the literature [43], we implemented facial expression intensity figuration using the X-conv operator. Assuming the expression K input point $(p_1, p_2, ..., p_k)$, where K denotes the result of a multilayer perceptron of real samples, in a transformation matrix $X = MLP(p_1, p_2, ..., p_K)$ of dimension $K \times K$ is computed, and the summation between feature elements can be simplified to the commonly used convolution operator. When X is performing the computation of the transformation matrix, different facial expression nodes have different effects, and we define the mathematical equation of the X-conv operator as follows:

$$F_p = \text{X\_}conv(K, p, P, F),$$
$$\text{X\_}Conv(K, p, P, F) = Conv\left(K, MLP(P - p) \times \left[MLP_\delta(P - p), F\right]\right), \tag{1}$$

where p represents the facial expression feature node, K represents the facial expression traversal function, $P = (p_1, p_2, ..., p_k)^T$ represents the nodes within the neighborhood expression feature node with K nodes, and $F = (f_1, f_2, ..., f_K)$ represents the expression feature nodes in different domains. In the nonlinear connection of the X-conv operator, facial expressions of different intensities will have different feature expressions in the generator, and the details of the X-conv operator at each level are shown in Figure 3.

3.3. Discriminator. The discriminator network consists of a combination of fully connected and deconvolutional layers. The discriminator is at the output port of the generator. In the discriminator, different threshold ranges are set and the pseudosamples are marked as invalid if they are below the threshold range. The feature information of the invalid sample will be fed back to the generator with the simulation side of the real sample. All the feedback methods will pass the correct feature values in this back propagation way, and

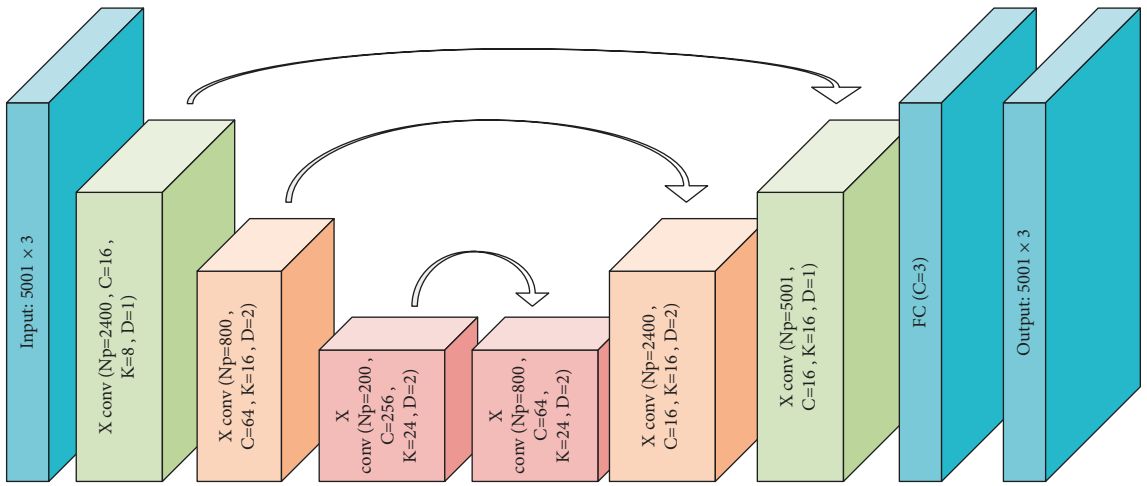

Figure 3: Detailed hierarchy of generators.

the generator will automatically correct the newly generated expression features based on the feedback feature values. The discriminator principle is shown in Figure 4.

The intensity of facial expression features was not consistent according to the differences in facial expression types. Low-intensity expression features are less demanding on the generator and only need to filter the facial contour data density. For high-intensity expression features, it is necessary to first decompose the high-intensity expression features and then convert them into low-intensity feature combinations. Researchers in the literature [44] will have used an alternating training model to optimize the discriminator with threshold discretization detection of pseudosamples. We define min-max as follows:

$$\min_{Gen}\max_{Dis} = \mathrm{E}_I^{high}\log\left(Dis\left(I^{high}\right)\right) + \mathrm{E}_I^{low}\log\left(1 - Dis\left(Gen\left(I^{low}\right)\right)\right), \quad (2)$$

where *Gen* denotes the twin sample of the generator and real sample and *Di s* denotes the threshold discrete detection of the discriminator and pseudosample. $\{I^{low}, I^{high}\}$ represents the feature intensity grading corresponding to facial expressions, and the generator *Gen* and discriminator *Di s* are distributed in a certain linear function, and the mathematical expression is as follows:

$$L_{G\_adv} = -\frac{1}{N}\sum_{n=1}^{N}\log\left(Dis\left(Gen\left(I_n^{low}\right)\right)\right),$$

$$L_{D\_adv} = -\frac{1}{N}\sum_{n=1}^{N}\left\{\log\left(Dis\left(I_n^{high}\right)\right) + \log\left(1 - Dis\left(Gen\left(I_n^{low}\right)\right)\right)\right\}, \quad (3)$$

where N represents the expression feature intensity. During the intensity feature convergence process, the pseudosample features can be ranked with respect to the degree of threshold discretization under the detection of the discriminator. The generator fine-tunes the new features at a later stage based on the feature discretization values fed by the discriminator. The different levels of discriminator network layers we constructed are shown in Figure 5.

3.4. Auxiliary Classifier and Loss Function. The intensity of facial expression features can cause feature loss in the middle transition layer of the network layer. For this reason, we add auxiliary classifiers in the middle layer, which can retain the facial expression feature information under different intensities. In the actual course scenario, facial expressions will have different levels of facial muscle expressions. In order to maintain a stable mapping relationship between expression changes and feature intensities, the adversarial loss function is utilized to guide the feature decomposition of real expressions. Adaptive linear fitting function is added to the auxiliary classifier network layer, and all samples are configured with low intensity features combined with low intensity features by default during the production of classifier pseudosamples. It prevents the problem of feature intensity confusion in the process of expression feature perception. The mathematical equations of feature perception added in the auxiliary classifier are shown below:

$$L_{perceptual} = \frac{1}{N}\sum_{n=1}^{N}\left\|\phi\left(G\left(I_n^{low}\right)\right) - \phi\left(I_n^{high}\right)\right\|, \quad (4)$$

where ϕ represents the expression feature intensity perceptron. In refining the pixel feature representation of 2-dimensional images of facial expressions, the high-intensity facial expression feature I^{high} and the linked expression feature $Gen(I^{low})$ generated by the generator take advantage of the point-by-point loss optimization to overcome the feature refinement and loss problems arising from the high-intensity feature decomposition. Researchers in the literature [45] performed experimental validation on the algorithm of point-by-point loss optimization, and the authors found that the L2 loss function is more stable. The mathematic functions are calculated as follows:

$$L_{pixel} = \frac{1}{N_{pixel}}\sum_{i=1}^{N_{pixel}}\left\|Gen\left(I^{low}\right)_i - I_i^{high}\right\|, \quad (5)$$

where N_{pixel} denotes the intensity expression of the facial expression at the two-dimensional level. According to the

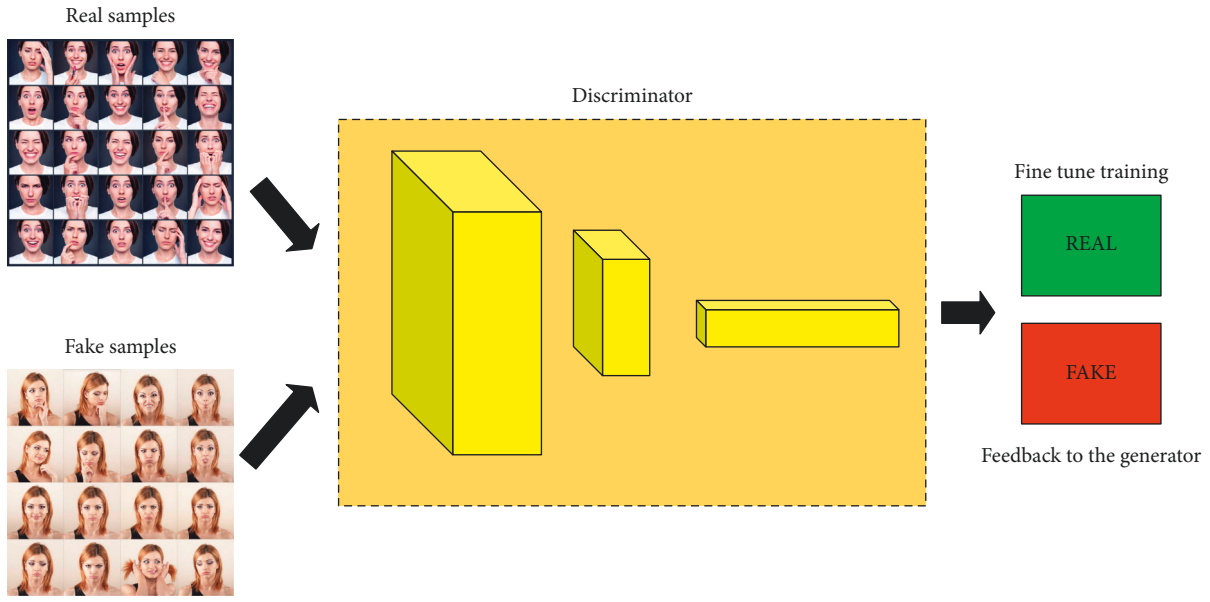

Figure 4: Facial expression discriminator process.

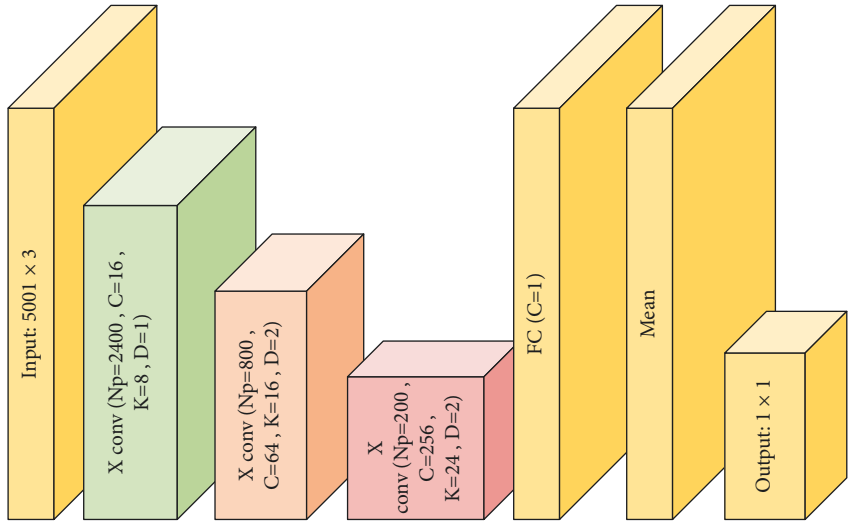

Figure 5: Detailed hierarchy of discriminator.

constraint effect of the loss function, we designed the new loss function has the following mathematical expression:

$$L = \omega_1 L_{G\_adv} + \omega_2 L_{pixel} + \omega_3 L_{perceptual}, \quad (6)$$

where ω_1, ω_2, and ω_3 denote the expression intensity feature weighting coefficients.

3.5. Improved Generative Adversarial Networks. In our study, to assess students' learning efficiency at the level of their facial expressions in the classroom, we present an enhanced generative adversarial network strategy for improving the accuracy of facial expression recognition models while also separating comparable expressions using feature intensity classification. The auxiliary classifier can provide feature generation guidelines and pseudosample feature discrimination to the generator and discriminator. At the pixel level, the auxiliary classifier middle layer neural network uses the X-conv operator to assist in synthesizing independent facial expression pseudofeatures, which are fed back in parallel with the generator in the joint output. The back propagation information from the discriminator will act as a filter in the auxiliary classifier to extract the feedback that aids in enhancing the effectiveness of the pseudofeatures into the real sample perception network. The facial expression detection network is shown in Figure 6.

4. Experiment

4.1. Datasets. We chose the well-known contemporary public facial expression datasets Oulu-CASIA (OC), Cohn–Kanade (CK+), and Facial multiview expression

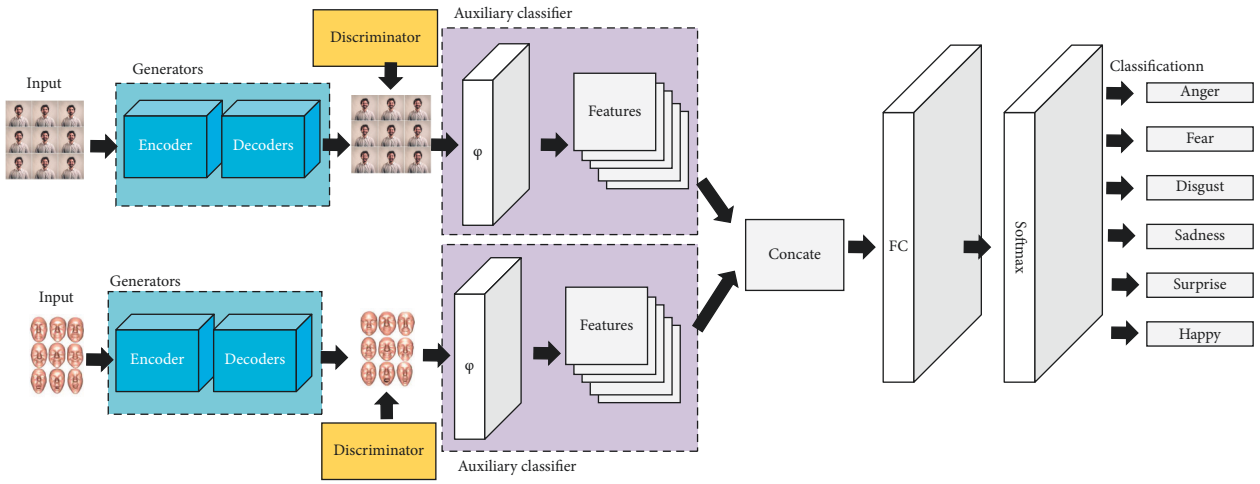

Figure 6: The structure of improved generative adversarial networks.

dataset with occlusion (FMEO) for the experimental test. Before performing expression classification operations on the above datasets, we collaborated with medical schools to manually standardize clear boundaries between expressions, and then we preprocessed all data to segment the images to specified sizes, with differences in the testing approach we took for different sizes of data.

The Oulu-CASIA dataset [46] contains a total of 2880 samples from the expression acquisition of 80 volunteers, which were captured using video recording and divided into visible light (VIS) series and near infrared (NIR) series according to the imaging system. Three different illumination methods were selected for the acquisition process to analyze the effect of detection methods on the structural environment. There are 480 videos of normal illumination samples, 60 videos of low illumination samples, and 15 videos of dark scenes. For the selection of the training set, we chose all the normal illumination video frame samples. The details of expression classification are shown in Table 1.

The Cohn–Kanade(CK+) dataset [47] contains a total of 593 video samples of facial expressions captured from 118 volunteers. Each piece of video is divided into 20–50 frames, and all video frame sequences are captured using a facial action coding system, which automatically classifies the expressions and labels them accordingly after the capture is completed. Its detailed facial expression classification information is shown in Table 2.

To evaluate the effectiveness of our strategy in complex situations such as occlusion, we chose FMEO to do the validation test. The dataset contains a total of 690 samples of data from 10 young volunteers, who were used in the experiment to collect facial expression samples by masking their faces with props, such as hats, glasses, and masks. The detailed classification of facial expressions in this dataset is shown in Table 3.

4.2. Experimental Settings. We trained the two-dimensional samples separately from the three-dimensional samples. The detailed parameter settings are shown in Table 4. In the validation process, we adopted the method mentioned in the literature [11]. For multitask learning training, to fairly compare random input expressions, we utilized a random search strategy with hyperparameter tuning.

4.3. Experimental Results. In the facial emotion detection work, we mainly analyze three metrics, such as accuracy (Acc), F1 score, and recall (R). To ensure that our method is effective, we conducted a test, and we choose traditional facial emotion detection approaches and a neural network series of facial emotion detection methods as control group experiments. We compared three methods, LBP_SVM, CNN, and LSTM. During the training and tuning phase, each network was trained independently without the recognition module to confirm the accuracy of each technique. The experimental results are shown in Table 5.

Table 5 proves the facial emotion detection effectiveness of our strategy. Considering the results of the experiments, CNN is the more commonly used method; however, it falls short of the LSTM approach in terms of facial expression recognition accuracy. This is mostly owing to the benefits provided by the LSTM's unique network topology, which can achieve local perception and maximize memory information fusion. Our method uses generative adversarial networks with a new CNN-based auxiliary classifier, which can recognize similar expressions hierarchically starting from the expression feature strength, further improving the accuracy of facial expression recognition while obtaining better robustness.

The experimental results show that the datasets OC and FEMO perform the best. Due to the computational cost, we mainly use the experimental results of datasets OC and FEMO as the main judging criteria. To test the efficiency of our approach for facial expression recognition in the classroom, we conducted experimental validation by self-made datasets. We collected classroom expression video data of 300 college students and manually labeled the homemade dataset according to the OC dataset labeling rules, and then tested it with the trained model. The results are shown in Table 6.

Table 1: Oulu-CASIA (OC) dataset facial expression classification.

	Anger	Fear	Disgust	Sadness	Surprise	Happy	Total
OC	799	790	765	794	768	784	4700
	Training set	3760		Test set	940		

Table 2: Cohn–Kanade (CK+) dataset facial expression classification.

	Anger	Fear	Disgust	Sadness	Surprise	Happy	Total
CK+	135	75	177	768	768	261	981
	Training set	785		Test set	196		

Table 3: FMEO dataset facial expression classification.

	Anger	Disgust	Happy	Sadness	Surprise	Total
FMEO	132	136	144	143	135	690
	Training set	552		Test set	138	

Table 4: Experimental parameter settings.

Parameter	Value
Initial learning rate	0.01
Decay rate	10
Weight decay	0.005
Epoch	80
Regularization	0.001
Margin loss discount	0.5
Dropout rate	0.1

Table 5: Results of text detection by different methods.

	OC			CK+			FMEO		
	Acc	R	F1	Acc	R	F1	Acc	R	F1
LBP_SVM	0.56	0.55	0.59	0.65	0.64	0.60	0.58	0.54	0.59
CNN	0.67	0.73	0.71	0.72	0.61	0.62	0.71	0.65	0.61
LSTM	0.75	0.82	0.80	0.76	0.72	0.73	0.81	0.77	076
Ours	0.89	0.94	0.83	0.86	0.81	0.83	0.89	0.95	0.93

Table 6: Results of text detection by different methods.

Method	Anger	Disgust	Happy	Sadness	Surprise
LBP_SVM	74.3	77.5	72.1	70.3	71.1
CNN	80.3	81.1	79.6	78.3	79.8
LSTM	85.3	86.4	82.1	84.3	81.8
Ours	95.3	96.3	93.1	92.7	93.6

In the students' facial expression recognition experiments, our improved generative adversarial network outperforms the others, and it further proves the effectiveness of our approach.

5. Conclusion

We offer a method for recognizing facial expressions based on an upgraded generative adversarial network. The method belongs to the deep training model, we divide the network into three stages. The front end of the network is the generator network layer, which relies on real sample features to generate pseudosamples. The middle of the network is the auxiliary classifier, which assists the generator in generating pseudosamples that are closer to the real samples. The end of the network is the discriminator network layer, which determines whether the pseudosamples satisfy the output conditions according to the degree of threshold discretization, and the pseudosamples that do not satisfy the conditions are fed back to the front layer for reconstruction. During the experiment, we test the efficiency of the strategy on the open-source datasets. In addition, we also test on the homemade student datasets. The experimental results prove that the facial expression detection accuracy of our method stays above 92%. Comprehensive performance of the model outperforms other methods.

Facial expressions are a very complex task to capture, and there are thousands of facial expressions in different scenes. In this paper, we tentatively select facial expressions with more prominent features as the study points. However, for many obscure expressions, our method still does not perform well. In further research, we are going to use a dual RNN framework to perceive the 3D features of facial expressions, and enhance the model's tolerance of high-intensity feature expressions.

Data Availability

The dataset can be accessed upon request.

Conflicts of Interest

The author declares that there are no conflicts of Interest.

Acknowledgments

The authors thank China Institute of Communications Education, The Fusion and Innovation of the Talent Training Model in International Cruise Service Professional Based on 1+x Certificate System (no. JTYB20-353).

References

[1] Z. T. Zhu, M. H. Yu, and P. Riezebos, "A research framework of smart education[J]," *Smart learning environments*, vol. 3, no. 1, pp. 1–17, 2016.

[2] G. R. Alexandre, J. M. Soares, and G. A. Pereira Thé, "Systematic review of 3D facial expression recognition methods," *Pattern Recognition*, vol. 100, Article ID 107108, 2020.

[3] S. A. Khan, A. Hussain, and M. Usman, "Facial expression recognition on real world face images using intelligent techniques: a survey[J]," *Optik*, vol. 127, no. 15, pp. 6195–6203, 2016.

[4] S. Li and W. Deng, "Deep facial expression recognition: a survey," *IEEE transactions on affective computing*, vol. 99, p. 1, 2020.

[5] Y. Miao, "Improved deep neural network for cross-media visual communication," *Computational Intelligence and Neuroscience*, vol. 2022, p. 1556352, Article ID 1556352, 2022.

[6] C. Chengjun Liu and H. Wechsler, "Gabor feature based classification using the enhanced Fisher linear discriminant model for face recognition," *IEEE Transactions on Image Processing*, vol. 11, no. 4, pp. 467–476, 2002.

[7] C. Shan, S. Gong, and P. W. McOwan, "Facial expression recognition based on Local Binary Patterns: a comprehensive study," *Image and Vision Computing*, vol. 27, no. 6, pp. 803–816, 2009.

[8] N. Dalal and B. Triggs, "Histograms of oriented gradients for human detection,"vol. 1, pp. 886–893, in *Proceedings of the 2005 IEEE computer society conference on computer vision and pattern recognition (CVPR'05)*, vol. 1, pp. 886–893, IEEE, San Diego, CA, USA, June 2005.

[9] H. Ding, S. K. Zhou, and R. Chellappa, "Facenet2expnet: regularizing a deep face recognition net for expression recognition," in *Proceedings of the 2017 12th IEEE International Conference on Automatic Face & Gesture Recognition (FG 2017)*, pp. 118–126, IEEE, May 2017.

[10] G. Ian, P. A. Jean, and M. Mehdi, "Generative adversarial nets," *Advances in Neural Information Processing Systems*, vol. 22, pp. 26772–32680, 2014.

[11] J. Cai, Z. Meng, A. S. Khan et al., "Island loss for learning discriminative features in facial expression recognition," in *Proceedings of the 2018 13th IEEE International Conference on Automatic Face & Gesture Recognition (FG 2018)*, pp. 302–309, IEEE, Columbia, USA, 2018.

[12] K. Wang, X. Peng, J. Yang, and Y MengQiao, "Region attention networks for pose and occlusion robust facial expression recognition," *IEEE Transactions on Image Processing*, vol. 29, pp. 4057–4069, 2020.

[13] Y. Wu and Q. Ji, "Facial landmark detection: a literature survey," *International Journal of Computer Vision*, vol. 127, no. 2, pp. 115–142, 2019.

[14] H. Jung, S. Lee, J. Yim et al., "Joint fine-tuning in deep neural networks for facial expression recognition," in *Proceedings of the IEEE international conference on computer vision*, pp. 2983–2991, IEEE, Santiago, Chile, December 2015.

[15] K. Zhang, Y. Huang, Y. Du, and L Wang, "Facial expression recognition based on deep evolutional spatial-temporal networks," *IEEE Transactions on Image Processing*, vol. 26, no. 9, pp. 4193–4203, 2017.

[16] Y. Zhang and Q. Yang, "A survey on multi-task learning," *IEEE Transactions on Knowledge and Data Engineering*, p. 1, 2021.

[17] G. Pons and D. Masip, "Multi-task, multi-label and multi-domain learning with residual convolutional networks for emotion recognition," 2018, http://arxiv.org/abs/1802.06664.

[18] E. Paul, *What the Face Reveals: Basic and Applied Studies of Spontaneous Expression Using the Facial Action Coding System (FACS)*, Oxford University Press, 2020.

[19] J. Cao, Y. Li, and Z. Zhang, "Partially shared multi-task convolutional neural network with local constraint for face attribute learning," in *Proceedings of the IEEE Conference on computer vision and pattern recognition*, pp. 4290–4299, IEEE, Salt Lake City, UT, USA, December 2018.

[20] I. Misra, A. Shrivastava, and A. Gupta, *Cross-stitch Networks for Multi-Task Learning*, in *Proceedings of the IEEE conference on computer vision and pattern recognition*, pp. 3994–4003, April 2016.

[21] T. Zhang, "Facial expression recognition based on deep learning: a survey," *Advances in Intelligent Systems and Computing*, Springer, in *Proceedings of the International conference on intelligent and interactive systems and applications*, pp. 345–352, 2017.

[22] S. Rajan, P. Chenniappan, S. Devaraj, and N Madian, "Facial expression recognition techniques: a comprehensive survey," *IET Image Processing*, vol. 13, no. 7, pp. 1031–1040, 2019.

[23] D. Canedo and A. J. R. Neves, "Facial expression recognition using computer vision: a systematic review," *Applied Sciences*, vol. 9, no. 21, p. 4678, 2019.

[24] N. Samadiani, G. Huang, B. Cai et al., "A review on automatic facial expression recognition systems assisted by multimodal sensor data," *Sensors*, vol. 19, no. 8, p. 1863, 2019.

[25] B. Sun, L. Li, and G. Zhou, "Combining multimodal features within a fusion network for emotion recognition in the wild," in *Proceedings of the 2015 ACM on International Conference on Multimodal Interaction*, pp. 497–502, ACM, WA, USA, November 2015.

[26] G. Levi and T. Hassner, "Emotion recognition in the wild via convolutional neural networks and mapped binary patterns," in *Proceedings of the 2015 ACM on international conference on multimodal interaction*, pp. 503–510, ACM, WA, USA, November 2015.

[27] M. M. Ghazi and H. K. Ekenel, "Automatic emotion recognition in the wild using an ensemble of static and dynamic representations," in *Proceedings of the 18th ACM International Conference on Multimodal Interaction*, pp. 514–521, ACM, Tokyo, Japan, November 2016.

[28] Z. Zhang, P. Luo, C. C. Loy, and X Tang, "From facial expression recognition to interpersonal relation prediction," *International Journal of Computer Vision*, vol. 126, no. 5, pp. 550–569, 2018.

[29] W. Hua, F. Dai, L. Huang, and G XiongGui, "HERO: human emotions recognition for realizing intelligent internet of things," *IEEE Access*, vol. 7, pp. 24321–24332, 2019.

[30] B. F. Wu and C. H. Lin, "Adaptive feature mapping for customizing deep learning based facial expression recognition model," *IEEE Access*, vol. 6, pp. 12451–12461, 2018.

[31] M. Liu, S. Li, S. Shan, and X Chen, "AU-Inspired deep networks for facial expression feature learning," *Neurocomputing*, vol. 159, pp. 126–136, 2015.

[32] A. Yao, D. Cai, and P. Hu, "HoloNet: towards robust emotion recognition in the wild," in *Proceedings of the 18th ACM international conference on multimodal interaction*, pp. 472–478, ACM, October 2016.

[33] B. K. Kim, S. Y. Dong, and J. Roh, "Fusing aligned and non-aligned face information for automatic affect recognition in the wild: a deep learning approach," in *Proceedings of the IEEE Conference on Computer Vision and Pattern Recognition Workshops*, pp. 48–57, IEEE, Las Vegas, NV, USA, June 2016.

[34] C. Pramerdorfer and M. Kampel, "Facial expression recognition using convolutional neural networks: state of the art," 2016, http://arxiv.org/abs/1612.02903.

[35] F. Zhang, T. Zhang, and Q. Mao, "Joint pose and expression modeling for facial expression recognition," in *Proceedings of the IEEE conference on computer vision and pattern recognition*, pp. 3359–3368, IEEE, Salt Lake City, UT, USA, June 2018.

[36] P. Liu, S. Han, and Z. Meng, "Facial expression recognition via a boosted deep belief network," in *Proceedings of the IEEE conference on computer vision and pattern recognition*, pp. 1805–1812, IEEE, Columbus, OH, USA, June 2014.

[37] D. Nguyen, K. Nguyen, and S. Sridharan, "Deep spatio-temporal features for multimodal emotion recognition," in *Proceedings of the 2017 IEEE winter conference on applications of computer vision (WACV)*, pp. 1215–1223, IEEE, Santa Rosa, CA, USA, March 2017.

[38] S. Khan and T. Yairi, "A review on the application of deep learning in system health management," *Mechanical Systems and Signal Processing*, vol. 107, pp. 241–265, 2018.

[39] Z. H. Zhou and J. Feng, "Deep forest," 2017, http://arxiv.org/abs/1702.08835.

[40] Y. H. Lai and S. H. Lai, "Emotion-preserving representation learning via generative adversarial network for multi-view facial expression recognition," in *Proceedings of the 2018 13th IEEE International Conference on Automatic Face & Gesture Recognition (FG 2018)*, pp. 263–270, IEEE, Xi'an, China, May 2018.

[41] H. Yang, U. Ciftci, and L. Yin, "Facial expression recognition by de-expression residue learning," in *Proceedings of the IEEE conference on computer vision and pattern recognition*, pp. 2168–2177, IEEE, UT, USA, June 2018.

[42] K. He, X. Zhang, and S. Ren, "Deep residual learning for image recognition," in *Proceedings of the IEEE conference on computer vision and pattern recognition*, pp. 770–778, IEEE, June 2016.

[43] Y. Li, R. Bu, and M. Sun, "Pointcnn: convolution on x-transformed points," *Advances in Neural Information Processing Systems*, p. 31, 2018.

[44] I. Goodfellow, J. Pouget-Abadie, M. Mirza et al., "Generative adversarial nets," *Advances in Neural Information Processing Systems*, vol. 27, 2014.

[45] R. Huang, S. Zhang, T. Li et al., "Beyond face rotation: global and local perception GAN for photorealistic and identity preserving frontal view synthesis," in *Proceedings of the IEEE international conference on computer vision*, pp. 2439–2448, IEEE, October 2017.

[46] G. Zhao, X. Huang, M. Taini, and M LiPietikäinen, "Facial expression recognition from near-infrared videos," *Image and Vision Computing*, vol. 29, no. 9, pp. 607–619, 2011.

[47] P. Lucey, J. F. Cohn, and T. Kanade, "The extended cohn-kanade dataset (ck+): a complete dataset for action unit and emotion-specified expression," in *Proceedings of the 2010 ieee computer society conference on computer vision and pattern recognition-workshops*, pp. 94–101, IEEE, San Francisco, CA, USA, June 2010.

Hindawi
Scientific Programming
Volume 2022, Article ID 9336561, 13 pages
https://doi.org/10.1155/2022/9336561

Research Article

Intelligent Control Strategy of Electrohydraulic Drive System for Raising Boring Power Head

Jun Zhang,[1,2,3] **Qinghua Liu**,[1,3] **Yun Chen**,[1,3] **Jiguo Wang**,[1,3] **Jinpu Feng**,[1,3] **Qingliang Meng**,[1,3] **Wei Cao**,[1,3] **Wei Tu**,[1,3] **and Xiaohui Gao**[4]

[1]*Ningxia Tiandi Benniu Industry Group Co., Ltd., Shizuishan 750000, China*
[2]*School of Mechanical and Transportation Engineering, Taiyuan University of Technology, Taiyuan 030024, China*
[3]*China Coal Science and Industry Group Co., Ltd., Beijing 100013, China*
[4]*School of Mechanical Engineering, Taiyuan University of Science and Technology, Taiyuan 030024, China*

Correspondence should be addressed to Jun Zhang; zhangjun07@tyut.edu.cn

Received 11 May 2022; Revised 5 June 2022; Accepted 15 June 2022; Published 15 July 2022

Academic Editor: Lianhui Li

The power head is the key part of the rock breaking work of the raise boring machine. Because the power head cannot adjust speed in time with the change in complex rock stratum, it leads to high failure rate, low work efficiency, and even accidents, so it is urgent to improve the controllability of the power head. In this paper, the electrohydraulic coupling mathematical model of the power head is established using the characteristic equations of dynamics and hydraulic components, and the control strategy of the fractional electrohydraulic drive system of the power head is proposed; genetic algorithm (GA), particle swarm optimization (PSO), and whale optimization algorithm (WOA) are used to adjust the parameters of FOPID, so as to improve the control effect of electrohydraulic system. The results show that the step response of WOA-FOPID control strategy is also better than that of genetic algorithm (GA) and particle swarm optimization (PSO). It can reach a stable state in 0.02 seconds, and the overshoot is only 0.12137%. The test verifies the correctness of the adaptive control and simulation results of the power head, which can effectively improve the adaptability of the power head to complex coal seams.

1. Introduction

Due to the advantages of the high safety, relatively low cost, and ensuring the safety of operators to the greatest extent, the reverse well drilling rig is widely used in underground roadway space, mine development, subway tunnel, and other projects, and the drilling technology is also a fundamental change technology for well hole drilling. In recent years, with the improvement of intelligent control technology of the drive system of the reverse well drilling rig, it has not only accelerated the speed of excavation but also greatly alleviated the labor intensity.

The power head is the key component of the reverse well drilling rig, and its control method and effect directly affect the safety and stability of the reverse well drilling rig in construction. At the same time, the intelligent control of the power head also has a positive role in promoting the intelligent construction of coal mines nationwide. Therefore, the intelligent control strategy of the electrohydraulic drive system of the power head has attracted the attention of the majority of scientific researchers at home and abroad. For example, Wang and Yang [1], and others studied the relationship between the four parameters of drill pipe tension, torque, rotational speed, and drilling speed in the power head control system. Shen and Liu [2] formulated the mathematical modeling and robust integral adaptive controller of the power head valve-controlled hydraulic motor based on Padde's theorem and the reverse step derivation method, which improved the accuracy and tracking speed of the system control. Yang [3] proposed a fuzzy PID control algorithm based on the problem of synchronization of four hydraulic motors in the power head device, which improved the synchronization accuracy of the motor. Cheng [4] used Amesim and MATLAB-Simulink to construct a joint

simulation model of the test bench drilling simulation system, and Cheng Lilin designed a fuzzy adaptive PID controller to analyze the control performance of the power head system. Zhang [5] used the method of co-simulation between Amesim and MATLAB-Simulink, the adaptability of different control algorithms of traditional PID fuzzy and feedback linear synovial membrane structure to the position tracking control of valve-controlled asymmetrical hydraulic cylinders is analyzed, and the problems of nonlinearity and low control accuracy of the electrohydraulic control system of the power head are solved. Foreign hydraulically driven reverse well drilling rig, power head drive using electrohydraulic proportional PID control technology, control unit using PLC or engineering controller [6–9], due to the introduction of computer control technology, and a variety of more complex control logic and PID control algorithms can be realized. The above literature research has made certain contributions to the intelligent control of the electrohydraulic drive system of the power head of the reverse well drilling rig and laid a certain foundation for the intelligent control algorithm of the power head. However, the research in the above articles is based on the traditional PID control algorithm. Especially in downhole operation, complex uncertainties such as surrounding rock parameters and downhole force of the drill will make the driving head of the drill unable to adjust the control parameters in time, resulting in low drilling efficiency, short service life of rock breaking hob, and even damage to the drill bit, sticking, etc. Under special working conditions, the traditional PID control effect is not ideal, even if the PID is re-parameter tuned, it still cannot achieve a good control effect, and it is essentially impossible to overcome the shortcomings of traditional PID control technology. Therefore, the complex system has a low control accuracy, reflecting the poor sensitivity and other issues, and it is difficult to explore the intelligent control principle of the electrohydraulic drive system of the power head from a deep level, and the parameter selection of the PID controller has a great impact on the control effect, the traditional parameter tuning method is still based on experience, and it is difficult to find a set of parameters with good control effect in a short period of time.

The fractional order FOPID controller has 5-bit adjustable parameters. Compared with other control laws, it has better dynamic performance, parameter adjustment flexibility, and control accuracy [10–12], and there is a great vacancy in the research and application of fractional order FOPID in the research of electrohydraulic system control method of raising boring. Based on the internal control principle of the reaming operation of the power head of the reverse well drilling rig, if the control effect is required to have good timeliness and reliability, the parameter adjustment research of the intelligent control algorithm is also indispensable, such as the particle swarm algorithm [13–15], the genetic algorithm [16], the gravity search algorithm [17], the neural network algorithm [18], the ILMI algorithm [19], and the whale optimization algorithm [20], which are all applied in the PID controller, improving the control effect of the traditional PID controller. The method of parameter tuning that relies on experience is got ridden.

Based on this, this paper establishes the electrohydraulic coupling model of the power head of raise boring machine from the dynamic principle, electrohydraulic coupling properties, and the characteristic equation of hydraulic components and puts forward the control method of the power head electrohydraulic drive system based on fractional FOPID. To further improve the control effect of the system, the genetic algorithm (GA), particle swarm algorithm (PSO), whale optimization algorithm (WOA), three groups of intelligent optimization algorithms are used to adjust the FOPID and PID controller parameters, and the influence of the above different combination algorithms on the control system is evaluated, to provide theoretical guidance for the reliability of the reaming operation of the reverse well drilling rig [21–24]. Finally, field experiments were conducted in Liuqiao Town, Suixi County, Anhui Province, to prove the effectiveness of WOA-FOPID control strategy in electrohydraulic drive control system. It further provides new theoretical guidance for the intelligent control strategy of the electrohydraulic drive system of the power head.

2. Mathematical Modeling

This article takes a deep well lane full-section test drilling rig (raising boring) as an example to study, which is the most widely used [25] and belongs to the lower lead upward expansion type. In order to apply intelligent drilling technology to raise boring machine, taking the power head as the research object, PLC and HMI are used to design the rock breaking control system. Four variable displacement piston pumps a11vlo130lrd are connected in series into two groups, which are driven by 132 kw motors to drive four mcr15a1500w80z32a0m2l4 2S 506u two-speed radial piston motors, and the hydraulic motor also controls the rotation of the power head [26, 27]. The overall idea of the structure composition, construction process, and control scheme of the reverse well drilling rig and the power head is shown in Figure 1.

To facilitate the theoretical modeling and analysis, the basic assumptions of hydraulic motor modeling are made. On this basis, the proportional amplifier, electrohydraulic proportional control valve, power head electrohydraulic coupling model, and the transfer function of power head hydraulic motor speed are established, respectively. The signal output by the controller is a voltage signal or a current signal, which is a component that amplifies its input signal and simplifies this model to a proportional link because of its input and output characteristics. Its transfer function is as follows:

$$G_i = \frac{I(s)}{U_i(s)} = K_b, \tag{1}$$

where K_b is the gain of the proportional amplifier.

The current signal output by the proportional link is based on dynamics and electromagnetic induction to drive the proportional solenoid movement, and then, the valve spool generates motion, thereby controlling the size of the

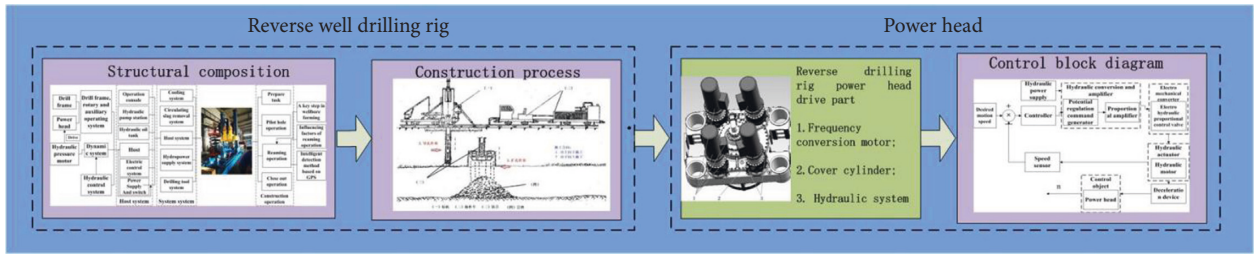

Figure 1: Overall train of thought block diagram.

valve opening and the direction of the liquid in and out. The working principle of the electrohydraulic proportional control valve is established, and the following expressions are established for the relationship between the coil current in the electromagnet, the driving force of the electromagnet, and the displacement of the valve core:

$$\begin{cases} u = L\dfrac{di}{dt} + \left(R_c + r_\rho\right)i, \\ F_d(t) = K_I U(t), \\ F_M(t) = m\dfrac{d^2x}{dt^2} + c\dfrac{dx}{dt} + k_s x. \end{cases} \tag{2}$$

The transfer function obtained by pulling the change of (2) is as follows:

$$G_2 = \frac{X(s)}{I(s)} = \frac{K_{xi}}{s^2 + 2\omega_n\xi s + \omega_n^2}. \tag{3}$$

In the formula, ω_n is the natural frequency of the spool, ξ is the damping ratio of the spool, and K_{xi} is the gain of the electrohydraulic proportional valve.

The electrohydraulic coupling model of the power head is composed of the hydraulic motor connected to the power head through the deceleration device, so the following relationship is established according to the flow continuity of the hydraulic motor valve, the static characteristic equation, the dynamic balance equation of the shaft, and C_d:

$$\begin{cases} q_L = C_d A x\sqrt{\dfrac{1}{\rho}\left(p_s - p_L\right)}, \\ q_L = D_m\dfrac{d\theta_m}{dt} + C_{tm}p_L + \dfrac{V_t}{4\beta_e}\dfrac{dp_L}{dt}, \\ T = D_m P_L = J\dfrac{d^2\theta_m}{dt} + B_m\dfrac{d\theta_m}{dt} + G\theta_m + T_f, \\ T_f = \dfrac{J_e s\omega_d(s) + B_e\omega_d(s) + T_d(s)}{i}. \end{cases} \tag{4}$$

As can be seen from Figure 1, the hydraulic motor and the power head are connected through the deceleration device, and the angular velocity exists: $\overrightarrow{r}$. A pull transform on equation (4) is performed to get the following equation:

$$\begin{aligned} T &= D_m P_L(s), \\ &= \left(iJ_1 + J_e\right)s\omega_d(s) + \left(iB_m + B_e\right)\omega_d + \frac{T_d(s)}{i}. \end{aligned} \tag{5}$$

From (5), it can be known that the equivalent inertia of the power head $J_d = iJ_1 + J_e$ is equivalent to viscous damping coefficient $B_d = iB_m + B_e$. The transfer function of the electrohydraulic coupling power head model under no-load state is sorted out:

$$G_{d1}(s) = \frac{\omega_d(s)}{U_i(s)} = \frac{K_d}{\left(s^2 + 2\omega_n\xi s + \omega_n^2\right)\left(s^2/\omega_d^2 + 2\xi_d/\omega_d s + 1\right)}, \tag{6}$$

where $K_d = K_\alpha K_{xi} K_q D_m / iD_m^2 + B_d(C_{tm} + K_c)$, $\omega_d = \sqrt{\beta_e[iD_m^2 + B_d(C_{tm} + K_c)]/V_t J_d}$, and $\xi_d = J_d\beta_e(C_{tm} + K_c) + B_d V/2\sqrt{\beta_e V_t J_d[iD_m^2 + B_d(C_{tm} + K_c)]}$.

Proportional amplifier, electrohydraulic proportional valve, and hydraulic motor-related parts of the parameters are as follows: the inertia of the motor shaft J is 67 kg·m^2, $\overrightarrow{r}$ is 0.4755 kg·m^2, the total volume V_t of the connecting pipe is 3×10^{-4} m^3, the elastic modulus of the system is 6.9×10^8 N/m^2, the flow gain K_q is 2.42 m^2/s, the motor displacement is 2.39×10^{-4} m^3/rad, the gear ratio of the reducer is i of 6.817, and the open-loop transmission function of the power displacement signal by calculating the angular velocity of the power head is as follows:

$$\begin{aligned} G_{d1}(s) &= \frac{\omega_d(s)}{U_i(s)} = \frac{K_d}{\left(s^2 + 2\omega_n\xi s + \omega_n^2\right)\left(s^2/\omega_d^2 + 2\xi_d/\omega_d s + 1\right)}, \\ &= \frac{8.476\times10^4}{5.487\times10^{-5}s^4 + 0.0252s^3 + 2.85s^2 + 432.59s + 10000}. \end{aligned} \tag{7}$$

By (7), we obtain the system without interference and control Bode diagram as shown in Figure 2.

From Figure 2, it can be seen that when the amplitude-frequency characteristics reach zero decibels, the phase-frequency characteristics are below −180° line, and the phase lag point has a negative stability margin at the 180° point, so there is a stability problem in the system, but due to the stability of the system itself and the dynamic characteristics, to make the system have a stable margin, it is necessary to add a controller to adjust to meet the stability requirements.

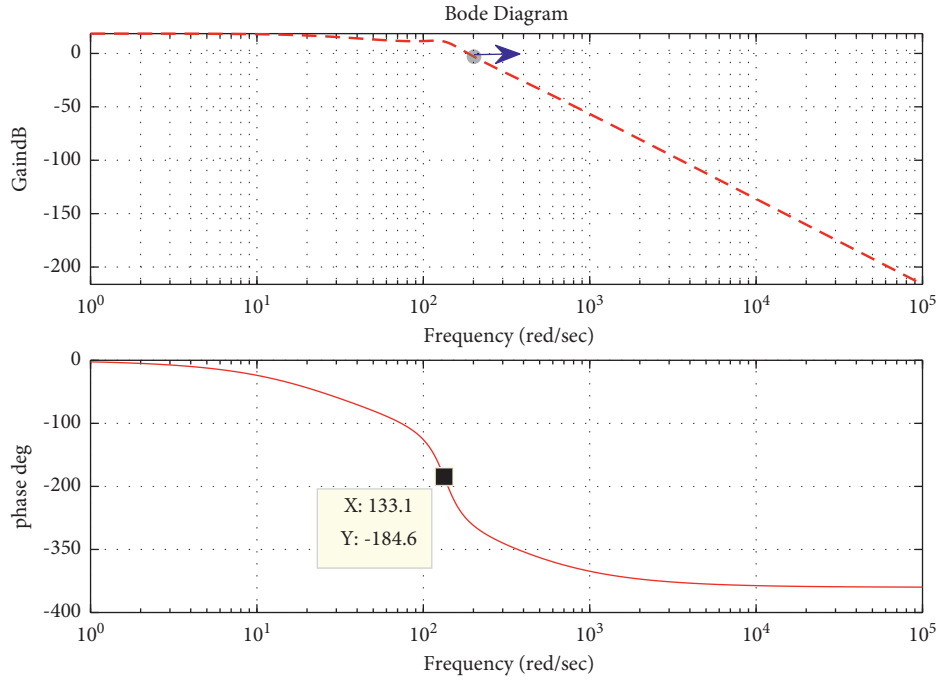

Figure 2: Open-loop Bode diagram of the system without interference and control.

3. Fractional Order FOPID Controller Design

As a branch of the control field, fractional order (FOPID) control has many advantages such as flexible and precise parameter adjustment, large system stability margin, and strong system robustness and has been widely used in different types of controller design [28–30]. Fractional order $PI^{\lambda}D^{\mu}$ control was first proposed by Igor Podlubny, and its superiority over traditional PID control was demonstrated through response analysis [28–30], [31-36]. Fractional order $PI^{\lambda}D^{\mu}$ controller of the order of parameters λ and μ can take any real number, in the $P-I-D$ plane, according to the different controller parameters to take the value; FOPID control system structure is shown in Figure 3. Compared with traditional PID control, fractional $PI^{\lambda}D^{\mu}$ control can more subtly reflect the transition process from proportional control to integral control and differential control, to achieve a control effect with higher accuracy, better stability, and stronger anti-interference ability.

The mathematical expression for the FOPID controller is as follows:

$$C(s) = \frac{U(s)}{R(s)} = K_p + \frac{K_i}{s^{\lambda}} + K_d s^{\mu}, \tag{8}$$

where K_p is the proportional gain, K_i is the integral gain, K_d is the differential gain, and λ and μ are the fractional and integral orders, respectively.

4. Whale Optimization Algorithm

Based on the advantages of fractional order PID control algorithm, this paper proposes a control strategy based on WOA-FOPID algorithm. There are many kinds of parameter tuning methods for FOPID. According to the regulation characteristics of the algorithm itself, it is mainly divided into traditional method tuning and intelligent optimization algorithm tuning, and the intelligent optimization algorithm is widely used because of its self-adaptability. In this paper, genetic algorithm (GA), particle swarm optimization (PSO), and whale optimization algorithm (WOA) are combined with FOPID control theory, respectively, and the above three intelligent optimization algorithms are used to set FOPID control parameters. The structure of intelligent control algorithm FOPID control system is shown in Figure 4.

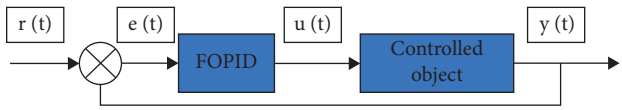

Figure 3: Structure of the FOPID control system.

To fully explore the advantages of genetic algorithm (GA), particle swarm optimization (PSO), and whale optimization algorithm (WOA), three intelligent optimization algorithms are combined with PID and FOPID, respectively, and the speed control effect of power motor is further analyzed through different control strategies. The flow chart of setting FOPID parameters by the developed intelligent optimization algorithm is shown in Figure 5.

5. Parameter Setting and Optimization Process of Real Analysis and Optimization Flow Simulation Analysis

There are many kinds of parameter tuning methods for FOPID. With the development of intelligent and control technology, according to the regulation characteristics of the algorithm itself, it is mainly divided into traditional method

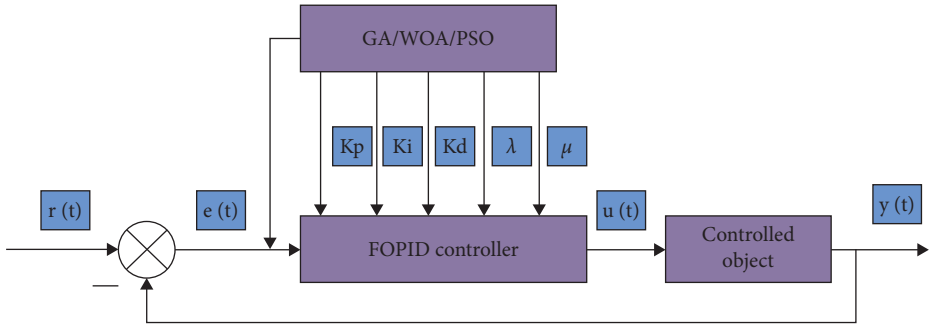

Figure 4: Structure diagram of the intelligent control algorithm FOPID control system.

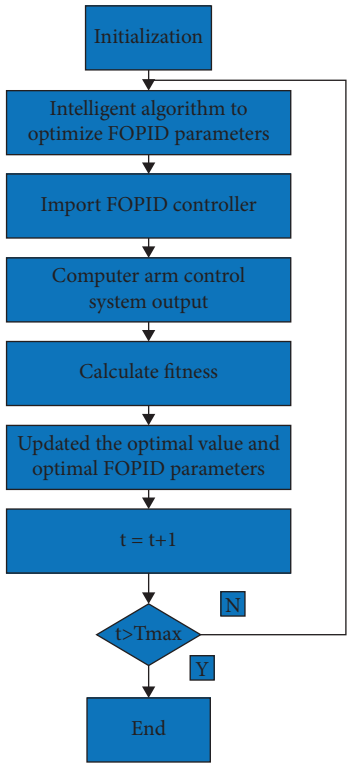

Figure 5: Flow chart of intelligent optimization algorithm for tuning FOPID parameters.

and intelligent optimization algorithm. The intelligent optimization algorithm is widely used because of its self-adaptability. The whale optimization algorithm (WOA) has been widely used because of its simple optimization mechanism and fast solution speed. The algorithm searches for the optimal solution by simulating the predation behavior of humpback whales [37–39] and solves the D-dimensional optimization problem in which f(x) is the optimization objective function:

$$Min\, f(x), s.t. 1 \le x \le u. \tag{9}$$

In servo control, the ITAE performance index weights the error so that the error signal converges to zero as soon as possible. The optimization objective function generates the objective function of control parameter optimization under the ITAE index, which is defined as follows:

$$fy = \sum_{t=0}^{N} L(t)|e(t)|. \tag{10}$$

Here, N is the number of search targets; $L(t)$ is the time series; and $e(t)$ is the error signal between the response frequency and the reference frequency. The smaller the Fy, the better the effect of dynamic response. As shown in Figure 6, the contents and steps of WOA are summarized.

In this paper, genetic algorithm (GA), particle swarm optimization (PSO), and whale optimization algorithm (WOA) are combined with PID and FOPID, respectively. Through different combined control strategies, the control effect of raising boring power head is further analyzed and compared. The specific parameter settings of each algorithm are shown in Table 1.

It can be seen in Table 2 for comparison of different combination strategies and control indicators, the dynamic response curve comparison diagram of each combination strategy of the regulation system is shown in Figure 7. Figure 7(a) is the step response diagram of each intelligent optimization algorithm and PID combination strategy, and Figure 7(b) is the step response diagram of each intelligent optimization algorithm and FOPID combination strategy; the comparison of PID and FOPID combined control strategies based on WOA is shown in Figure 8.

As can be seen in Figure 7, after adding PID and FOPID controllers, the system can quickly tend to a stable state. Comparing Figure 7(a) with Figure 7(b), in the control based on the same algorithm, the FOPID control is significantly better than the PID control in terms of response time and dynamic response; in Figure 7(a), the step response of WOA-FOPID control strategy is obviously better than the control strategy based on GA and PSO algorithm, and the overshoot is 8 35%, only 0.5%. Stable state is reached in 1 s; in Figure 7(b), the step response of WOA-FOPID control strategy is also better than the control strategy based on GA and PSO algorithm, at 0.5%. It reaches a stable state within 02 s, and the overshoot is only 0.5% 12137%. The simulation results in Figures 7(a) and 7(b) show that in the PID/FOPID combination strategy, the whale optimization algorithm (WOA) has more advantages than the genetic algorithm (GA) and particle swarm optimization algorithm (PSO) in the process of intelligent parameter adjustment.

Figure 8 compares the two controllers based on WOA. The results show that WOA-FOPID is more dominant, which further verifies the superiority of FOPID controller. In

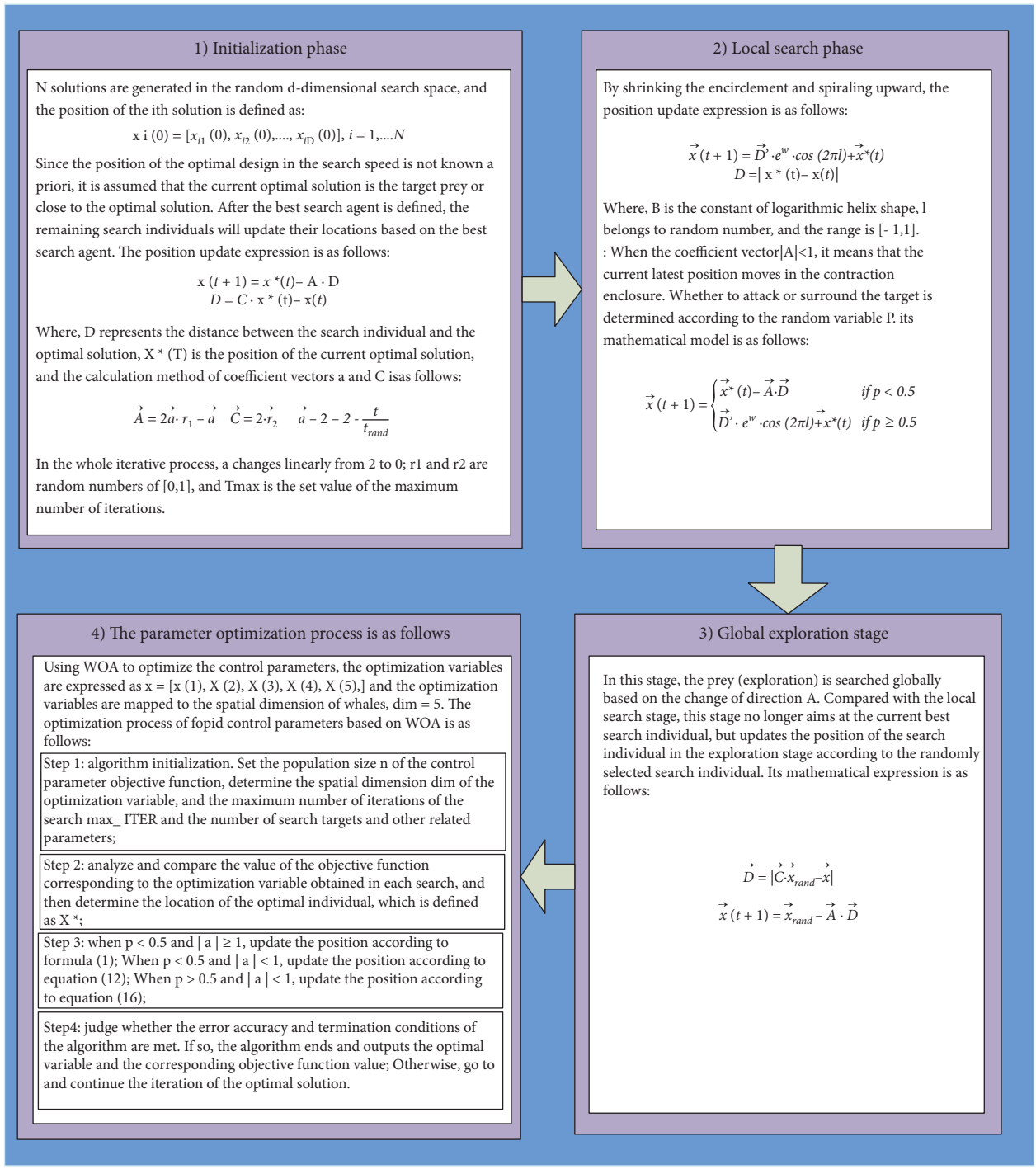

Figure 6: WOA steps and contents.

these combination strategies, it is concluded that the optimal controller is the FOPID controller based on WOA, and the parameters of the controller are as follows:

$$Gc = 15.2654 + 20s^{-1.0039} + 9.5963s^{1.1118}. \quad (11)$$

6. Experiment

To verify the correctness and effectiveness of WOA-FOPID control strategy in the electrohydraulic drive control system of the power head of raise boring machine, the performance test of the power head of raise boring machine was carried out in Liuqiao Town, Suixi County, Anhui Province. The on-site commissioning layout is shown in Figure 9.

To meet the normal operation of the rock breaking test rig, the rock breaking control system mainly adopts Siemens S7-1200 series PLC and its expansion module, combined with the control system designed by HMI to realize the start/stop action of the pump station motor, the forward/reverse action of the power head motor, the stepless speed regulation

Table 1: Specific parameter setting table of each algorithm.

	PSO	GA	WOA-FOPID	WOA-PID
Max_er	200	200	50	50
N	20	50	—	—
C1	1.49	—	—	—
C2	1.49	—	—	—
Variation parameters	—	0.8	—	—
Variation probability	—	0.75	—	—
Dim	—	—	5	3
Search agent no.	—	—	100	100

Table 2: Comparison of different combination strategies and control indicators.

Combination	Dynamic index		
	Standard variance	Overshoot (%)	Stabilization time (S)
PSO-PID	0.06309	30.1721	0.84
GA-PID	0.06309	30.1217	0.84
WOA-PID	0.03624	8.35	0.1
PSO-FOPID	0.06349	2.8197	0.51
GA-FOPID	0.03778	6.9309	0.16
WOA-FOPID	0.03535	0.12137	0.02

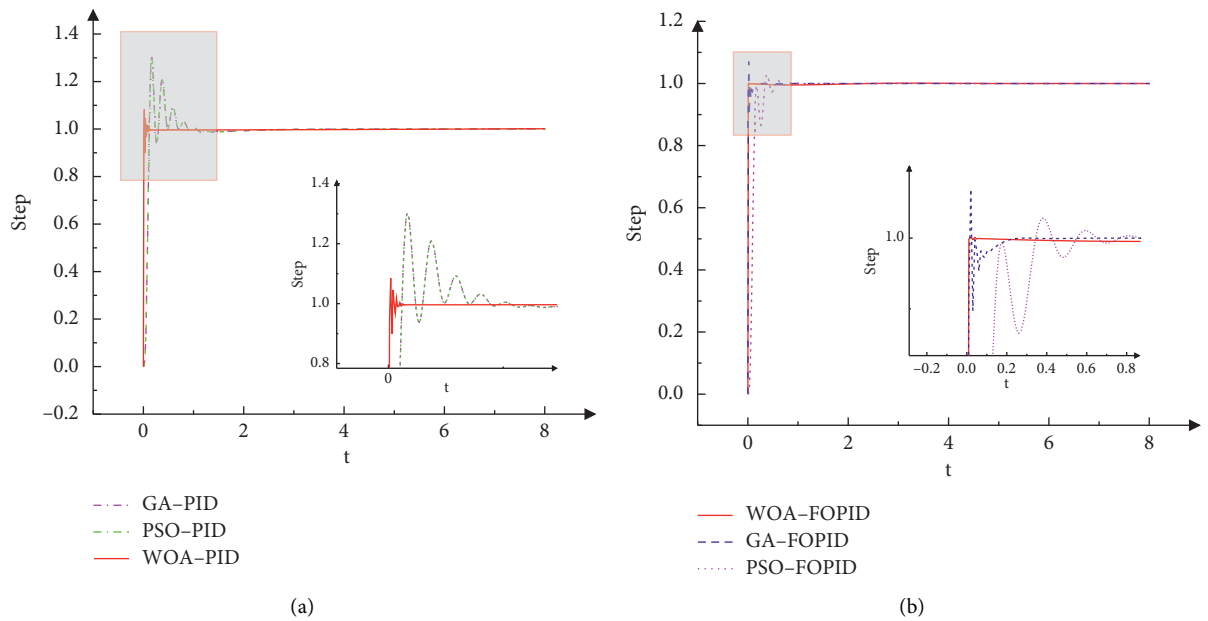

Figure 7: Comparison of dynamic response curves of each combination strategy of regulation system. (a) PID combination strategy. (b) FOPID combination strategy.

of the power head output shaft, the lifting/lowering action of the thrust cylinder, the pressure, displacement, stroke, constant pressure/constant torque drilling mode switching precise control of temperature control, and automatic operation of pump station. At the same time, the rock breaking control system is equipped with a remote control function to facilitate remote operation. S7-1200 series PLC and large screen display form the control core in the control cabinet, and each working condition monitoring and input/output drive unit cooperates with each other to ensure the stable operation of various control functions of the system. The general scheme of electric control system of raise boring machine is shown in Figure 10.

6.1. Power Head Speed Control Scheme. Power head speed regulation control model in the process of power head speed adjustment potentiometer from minimum to maximum adjusts the displacement of variable pump from 0 to 145 ml/R and variable motor from 215 to 65 ml/R in turn. That is, in the first half of the speed regulation process, the displacement of the motor remains unchanged, and only the

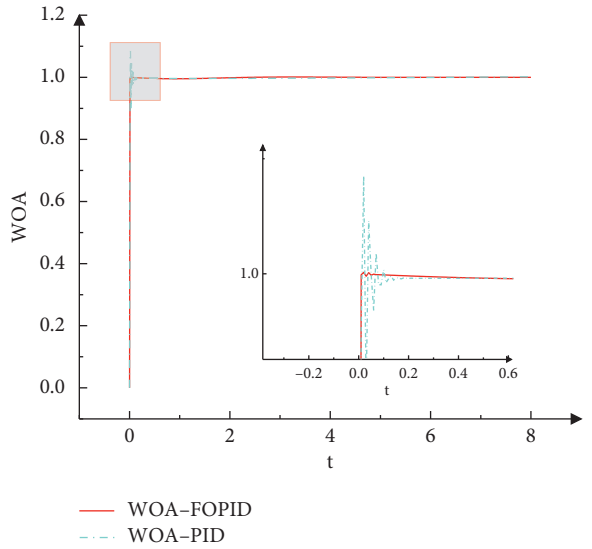

Figure 8: Comparison of control strategies based on WOA.

Figure 9: Site layout.

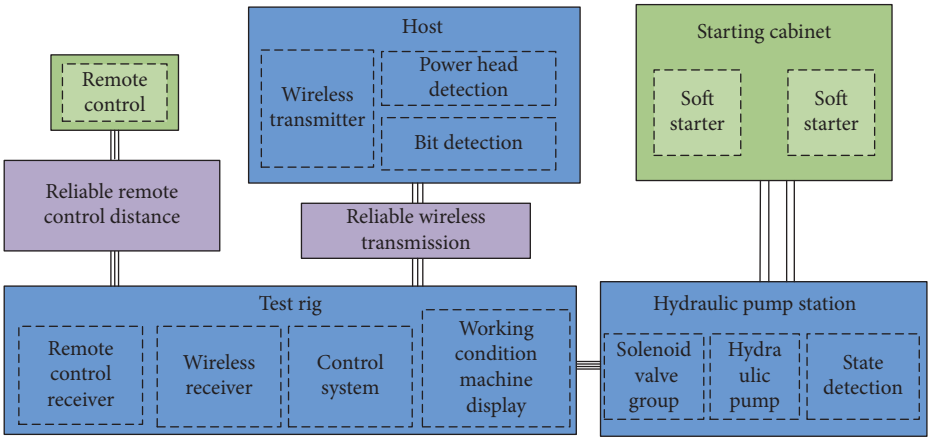

Figure 10: General scheme of the electric control system for raise boring rig.

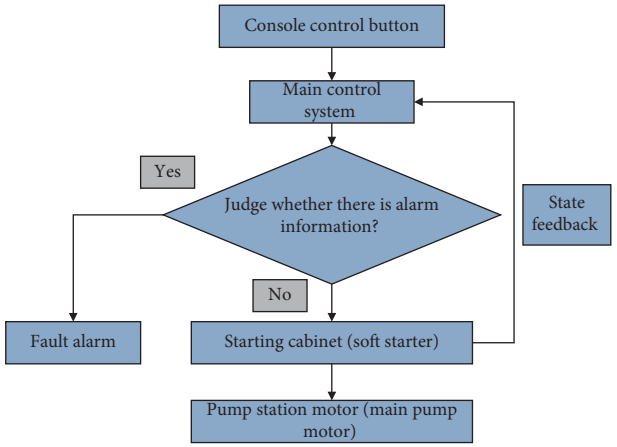

Figure 11: Control flow diagram of the main pump motor.

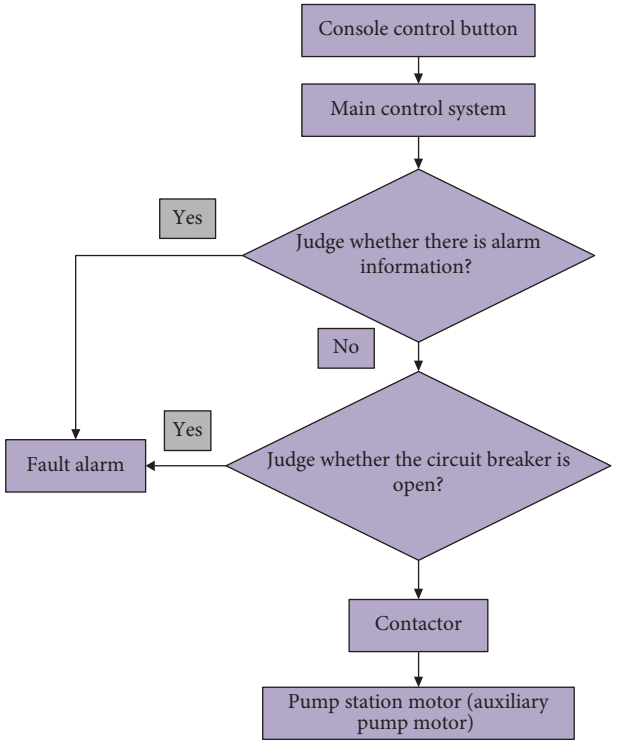

Figure 12: Control flow diagram of the auxiliary pump motor.

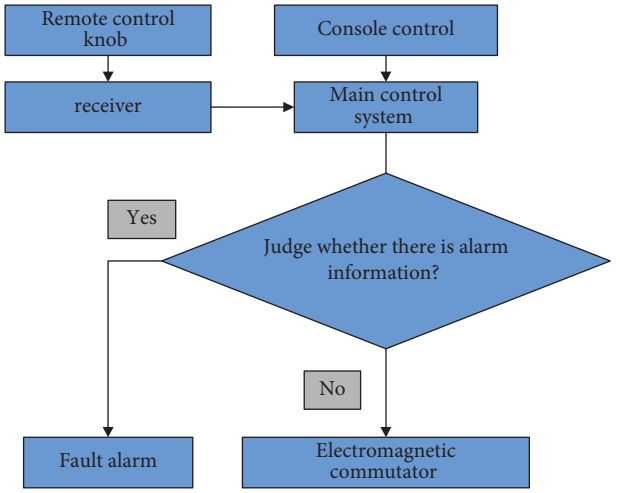

Figure 13: Flow chart of forward/reverse control of the power head.

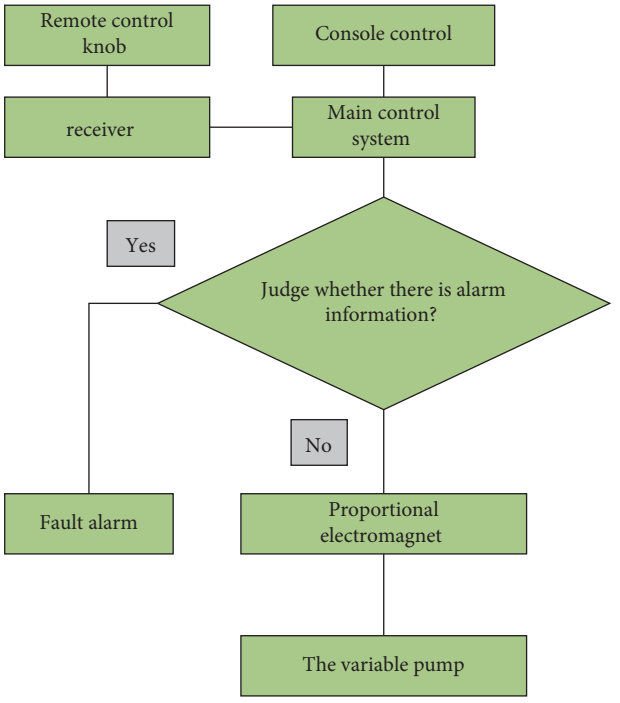

Figure 14: Flow chart of stepless speed regulation control of power head output shaft.

displacement of the variable pump is adjusted to meet the requirements of speed adjustment. In the second half, the maximum displacement output of the variable pump is maintained, and only the displacement of the variable motor is adjusted to meet the requirements of speed adjustment. In this way, no matter at any speed, the output torque is the maximum torque corresponding to the speed:

(1) *Remote Control and Valve Group Control of Hydraulic Pump Station.* Before the remote control of hydraulic pump station operates the control system, the pump station motor must be started first to make the pump station in working state. To avoid starting the pump station in another place, the system adds the start and stop button of the pump station motor on the control cabinet, and the start signal sent by the button acts on the soft starter remotely to realize the start and stop function of remote control motor.

Control Scheme. The main pump motor is started by soft starter, and the start/stop signal of soft starter is controlled through the console button to realize the start/stop control function of corresponding motor. Control process is in Figures 11 and 12.

The valve group control system sends the control command to PLC through the knob on the operation panel or the virtual button on HMI, and the output

Table 3: Experimental parameters (relationship between displacement and current of the power head motor).

Serial number	1	2
Electric current	200	600
Company	mA	mA
Displacement	216.5	0
Company	ml/r	ml/r
Maximum speed	2900	5500
Company	r/min	r/min

Table 4: Experimental parameters (relationship between pump displacement and current).

Serial number	1	2
Electric current	200	600
Company	mA	mA
Displacement	145	0
Company	ml/r	ml/r
Maximum speed	1450	1450
Company	r/min	r/min

Table 5: Experimental parameters (electromagnet at technical data EP1 and EP2).

Technical data electromagnets at EP1 and EP2			
Voltage		EP112 V (±20%)	EP212 V (±20%)
Control current (mA)	Initial control value at displacement $V_g$min	400	200
	Control termination value at displacement V_g max	1200	600

signal drives the corresponding solenoid valve action through the relay to realize the corresponding functions.

(2) The power head is driven by 160 ml/R variable pump and variable motor. To realize the adjustable steering and speed, the system designs a three-position knob to control the action of the electromagnetic directional valve, so as to realize the steering control of the power head. At the same time, the potentiometer is designed to input 0~5 V analog signal, and then, through the calculation of PLC speed regulation model, the first conductive signal of 0~10 V driving proportional amplifier is output, the proportional amplifier to output 200~600 mA current is controlled, and then the speed of power head is controlled.

Forward/Reverse Control Scheme of Power Head. Forward/reverse switching control is realized through three-position four-way solenoid directional valve. That is, the control of the electromagnetic directional valve is realized through the console knob or the remote controller knob, to realize the control of the forward/reverse switching function. Control flow is shown in Figure 13.

Stepless Speed Regulation Control Scheme of Power Head Output Shaft. The flow is adjusted by controlling the swing angle of variable pump, to realize the function of stepless speed regulation of power head output shaft. That is, the proportional electromagnet is controlled by the knob potentiometer, and then, the swing angle of the variable pump is controlled to realize the function of stepless speed regulation of the output shaft of the power head. Control flow is shown in Figure 14.

6.2. Implementation Plan. Field commissioning stage: This stage involves speed regulation of power head under shunt state. The experimental parameters are shown in Tables 3–5:

(1) Stage I: the displacement of the power head motor is kept unchanged, and the displacement of the hydraulic pump is adjusted from 0 ~ 145 (ml/r). At this time, the driving current of the power head motor is about 43 mA (the corresponding digital quantity is 2000). According to the driving characteristic curve, the maximum displacement of the power head motor is 216.5 ml/r.

(2) Stage II: the displacement of the power head motor is kept unchanged, the discharge of the hydraulic pump is adjusted to the maximum value of 145 ml/r (theoretical value), the actual control driving current is about 586 mA (corresponding to the digital quantity of 27000), and the flow of the corresponding pump is 140 ml/r. At this time, the displacement of the power head motor remains at the maximum value of 216.5 ml/r.

(3) Stage III: the maximum displacement of the hydraulic pump is kept unchanged at 145 ml/r, and the displacement of the power head motor is adjusted from 216.5 ml/r to $V_g$min. When the software controls the minimum displacement of the power head motor, the corresponding driving current is

Table 6: Meaning of each character in the text.

Symbol	Parameter meaning	Parameter value or unit
C_d	Flow coefficient of solenoid proportional directional valve	—
ρ	Hydraulic oil density	kg/m^3
A	Area of solenoid proportional directional valve port	m^2
p_s	Outlet oil supply pressure	MPa
x	Spool displacement of solenoid proportional directional valve	m
p_L	Outlet flow or load flow of solenoid proportional directional valve	m^3/s
C_{tm}	Total leakage coefficient of hydraulic motor	$C_{tm} = C_{im} + C_{em}/2$
V_t	Total volume of oil inlet chamber, oil return chamber, and connecting pipe of hydraulic motor	—
β_e	Effective bulk modulus of elasticity	—
D_m	Volume displacement per radian of hydraulic motor	—
θ_m	Angular displacement of output shaft of hydraulic motor	—
J_e	Equivalent inertia of reducer	—
B_e	Equivalent damping coefficient of reducer	—
U	Input voltage	—
F_d	Wire coil	—
i	Current in coil	—
R_c	Coil internal resistance	—
c	Damping coefficient of valve core armature assembly	—
r_p	Internal resistance of amplifier	—
K_I	Voltage force gain of proportional electromagnet	—
m	Quality of valve core armature assembly	—
L	Displacement of valve core	—
k_s	Spring stiffness of armature assembly	—
F_M	Current magnet driving force	—

about 526 mA, $V_g$min is 0.185 times, and V_g max = 216.5 ml/r × 0.185 = 40.0525 ml/r.

(4) Stage IV: the rotating speed of the power head is the maximum, and the Baote remains unchanged.

6.3. Empirical Conclusion

① Compared with "the power head parameter table of enhanced TD2000 drilling rig under shunting state and turning into working condition," there is an error in the maximum displacement control of hydraulic pump station, with an error of about 5 ml/r. There is still a little room for optimization, which can be optimized on-site.

② Compared with "the power head parameter table of enhanced TD2000 drilling rig under shunting condition and turning into working condition," the minimum displacement control of power head motor has error, and the error is about 2 ml/r, so the optimization needs to be careful (during plant commissioning, when the speed regulation exceeds a certain position, the speed of power head decreases instead).

③ In the whole speed regulation process, the trend is basically consistent with the table of power head parameters under shunting condition of enhanced TD2000 drilling rig, but there is a little error at the two end points. The error is as described in points ① and ② above. The position number described in the table is included in the whole speed regulation process and does not need to be corrected separately. Only the corresponding speed identification needs to be carried out on-site. The corresponding position is marked.

7. Conclusion

Aiming at the problem of whether the power head of raise boring machine can be driven in complex environment during reaming operation, using the fine-tuning characteristics of FOPID control to apply to the nonlinear control object, a method of adjusting FOPID control parameters based on whale optimization algorithm (WOA) is proposed. Through the establishment of the electrohydraulic coupling model of the power head of the raise boring machine and the simulation analysis in MATLAB software, the following conclusions are obtained (Table 6):

(1) From the simulation results of six different combined control strategies, it can be seen that the overall control effect of FOPID is much better than PID control in the overshoot and response time in the frequency response curve. In PID control, the overshoot is at least 8.35%, while the overshoot of FOPID control is at most 6.9309%. The results show that FOPID is more suitable for the electrohydraulic control of raising boring than PID, and the overall response time is shorter. It can adjust the angular speed of the power head in time and then control the fast and slow switching of the power head, which shows that FOPID control has a better application prospect in the electrohydraulic drive control of raising boring.

(2) Among the six combined control strategies, the combined strategy based on WOA has obvious

advantages in each control method. The overshoot of WOA-PID control strategy in PID control is at least 8.35% and takes 0.1 s; the overshoot of WOA-FOPID control strategy in FOPID control is at least 0.12137%, with a time of 0.02 s. From the numerical iteration process of WOA objective function, it can be found that WOA has good optimization ability and convergence performance, which verifies the excellent performance of WOA in control parameter tuning. The experimental data show that the WOA-FOPID combined control strategy studied in this paper can respond to the input in time, and the FOPID parameters are adjusted through WOA, which has a good effect on the optimization of control parameters and can effectively improve the control accuracy of FOPID.

(3) After the design of the control system is completed, it is debugged and applied on the raise boring rig. The control system realizes various functions including remote pump station start and stop control and single/double drive motor switching control and meets the requirements of process operation. Experiments show that the WOA-FOPID control strategy is effective in the electrohydraulic drive control system. The control strategy can make the electrohydraulic drive control have good real time, accuracy, and rapidity and can realize fast power head. Slow switching and high-precision control can be used as the exclusive control system of raise boring rig.

Data Availability

The dataset can be accessed upon request to the corresponding author.

Disclosure

An earlier version of this paper has been presented as preprint according to the following link: https://www.researchsquare.com/article/rs-1500559/v1 [39].

Conflicts of Interest

The authors declare that they have no conflicts of interest.

Authors' Contributions

Jun Zhang designed the overall research scheme, programmed and debugged the algorithm, and wrote the paper. Qinghua Liu, Yun Chen, and Jiguo Wang debugged the algorithm. Jinpu Feng, Qingliang Meng, and Wei Cao programmed the algorithm. Wei Tu and Xiaohui Gao checked the language of the paper.

Acknowledgments

The authors thank Youth Fund of National Natural Science Foundation of China, project name: research on uncertain motion characteristics and compound control mechanism of drilling and anchor manipulator based on Chebyshev interval algorithm, No. 52104165; Free Exploration General Fund of Shanxi Provincial Department of Science and Technology, project name: motion uncertainty analysis and closed-loop feedback control mechanism of drilling anchor manipulator, No. 20210302123123; and State Key Laboratory of Robotics and Systems, project name: research on motion uncertainty characteristics and compound control mechanism of manipulator of anchor drilling robot, No. SKLRS-2021-KF-16.

References

[1] H. Wang, "Hydraulic system design of raise boring machine using cartridge valve," *Mechanical design and manufacturing engineering*, vol. 48, no. 7, pp. 71–73, 2019.

[2] W. Shen and S. Liu, "Adaptive robust integral control of hydraulic motor servo position system based on network," *Journal of Shanghai University of technology*, vol. 43, no. 04, pp. 325–331, 2021.

[3] Y. Yang, *Research on Control Algorithm of Electro-Hydraulic Proportional Valve Controlled Four cylinder Synchronization*, Lanzhou University of technology, Lanzhou, China, 2019.

[4] L. Cheng, *Design and Research on Electro-Hydraulic Control System of Rotary Steering Drilling Tool Test Bench*, Xi'an University of petroleum, Xi'An, China, 2021.

[5] Y. Zhang, *Research On Key Technology of Performance Optimization of Electromechanical Hydraulic Integrated System of Drilling Rig*, General Coal Research Institute.

[6] X. Tong Research, *On Hydraulic Drive and Control System of Shield Cutterhead*, Zhejiang University, Zhejiang, China, 2008.

[7] L. Li, B. Lei, and C. Mao, "Digital twin in smart manufacturing," *Journal of Industrial Information Integration*, vol. 26, no. 9, Article ID 100289, 2022.

[8] D. Xue, "Zhao chunna design of fractional order PID controller for fractional order system," *Control theory and application*, no. 05, pp. 771–776, 2007.

[9] L. Li and C. Mao, "Big data supported PSS evaluation decision in service-oriented manufacturing," *IEEE Access*, vol. 8, no. 99, pp. 154663–154670, 2020.

[10] L. Li, T. Qu, Y. Liu et al., "Sustainability assessment of intelligent manufacturing supported by digital twin," *IEEE Access*, vol. 8, pp. 174988–175008, 2020.

[11] C. Yuan, J. Cai, and X. Wang, "Research on PID controller of vehicle suspension based on particle swarm optimization algorithm," *China Journal of agricultural machinery chemistry*, vol. 25, no. 5, p. 7, 2019.

[12] L. Li, C. Mao, H. Sun, Y. Yuan, and B. Lei, "Digital twin driven green performance evaluation methodology of intelligent manufacturing: hybrid model based on fuzzy rough-sets AHP, multistage weight synthesis, and PROMETHEE II," *Complexity*, vol. 2020, no. 6, pp. 1–24, 2020.

[13] J. Meng, H. Yang, and Q. Chen, "Simulation Research on PID control of automotive semi-active suspension based on genetic algorithm optimization," *Modern manufacturing engineering*, no. 6, p. 5, 2013.

[14] G. Wen, Xu Gong, Z. Li, and Z. Zhou, "Static output feedback control of vehicle semi-active suspension based on ILMI algorithm," *Automotive Engineering*, vol. 29, no. 6, p. 4, 2007.

[15] D. Xue, *Fractional Calculus and Fractional Control*, Science Press, Beijing, China, 2018.

[16] Z. Liu, C. song, S. Cheng et al., "Development history and current situation of drilling technology and equipment of raise boring rig in China," *Coal science and technology*, vol. 49, no. 01, pp. 32–65, 2021.

[17] F. Jingpu, C. Yun, K. Ma, and kuiwu Xu, "Tu Wei Design of electric control system for td2000/1200 top drive drilling rig," *Coal mining machinery*, vol. 42, no. 8, pp. 18–21, 2021.

[18] S. Mirjalili and A. Lewis, "The whale optimization algorithm," *Advances in Engineering Software*, vol. 95, no. 95, pp. 51–67, 2016.

[19] R. Li, B. Jc, C. Cx, and R. Manivannand, "Quasi-stability and quasi-synchronization control of quaternion-valued fractional-order discrete-time memristive neural networks," *Applied Mathematics and Computation*, vol. 395, Article ID 125851.

[20] M. Dalir and N. Bigdeli, "The design of a new hybrid controller for fractional-order uncertain chaotic systems with unknown time-varying delays," *Applied Soft Computing*, vol. 87, Article ID 106000.

[21] B. Sdna, D. Bao, and C. Sbc, "Smart dampers-based vibration control – Part 2: fractional-order sliding control for vehicle suspension system," *Mechanical Systems and Signal Processing*, vol. 148.

[22] S. Bushnaq, T. Saeed, D. Torres, and Z. Anwar, "Control of COVID-19 Dynamics through a Fractional-Order model," *Alexandria Engineering Journal*, vol. 60, no. 4, pp. 3587–3592, 2021.

[23] M. N. Musarrat and A. Fekih, "A fractional order sliding mode control-based topology to improve the transient stability of wind energy systems," *International Journal of Electrical Power & Energy Systems*, vol. 133, no. 107306, pp. 107306–107312, 2021.

[24] I. Podlubny, "Fractional-order systems and PI/sup/spl lambda//D/sup/spl mu//-controllers $\overrightarrow{r}$ controller," *IEEE Transactions on Automatic Control*, vol. 44, no. 1, pp. 208–214, 1999.

[25] X. Wu and Y. Huang, "Adaptive fractional-order non-singular terminal sliding mode control based on fuzzy wavelet neural networks for omnidirectional mobile robot manipulator - sciencedirect," *ISA Transactions*, vol. 121, pp. 258–267, 2021.

[26] H. M. Cuong, H. Q. Dong, P. V. Trieu, and L. A. Tuan, "Adaptive fractional-order terminal sliding mode control of rubber-tired gantry cranes with uncertainties and unknown disturbances," *Mechanical Systems and Signal Processing*, vol. 154, Article ID 107601, 2021.

[27] A. Sh, W. A. Jie, H. C. Chen et al., "A fixed-time fractional-order sliding mode control strategy for power quality enhancement of PMSG wind turbine," *International Journal of Electrical Power & Energy Systems*, vol. 134, Article ID 107354, 2022.

[28] D. Chu and H. Chen, "Wang Xuguang Whale optimization algorithm based on adaptive weight and simulated annealing," *Electronic news*, vol. 47, no. 5, pp. 992–999, 2019.

[29] D. Butti, S. K. Mangipudi, and S. R. Rayapudi, "An improved whale optimization algorithm for the design of multi-machine power system stabilizer," *International Transactions on Electrical Energy Systems*, vol. 30, no. 5, 2020.

[30] J. U. N. Zhang, C. F. Wang, and L. Wang, *Intelligent Control Strategy of Electro-Hydraulic Drive System for Raising Boring Power Head*, 2022, https://www.researchsquare.com/article/rs-1500559/v1A.

Hindawi
Scientific Programming
Volume 2022, Article ID 6972215, 9 pages
https://doi.org/10.1155/2022/6972215

Research Article

Comparing Middle School Students' Scientific Problem-Solving Behavior in Hands-On Manipulation Performance Assessment: Terms by Eye-Tracking Analysis

Shiyi Zang,[1,2] Pingting Lin,[1,2] Xinyu Chen,[1,2] Yi Bai,[1,2] and Huihua Deng [1,2]

[1]*Key Laboratory of Child Development and Learning Science of Ministry of Education, Southeast University, Nanjing, China*
[2]*Institute of Child Development and Education, Southeast University, Nanjing, China*

Correspondence should be addressed to Huihua Deng; 230208222@seu.edu.cn

Received 3 June 2022; Revised 16 June 2022; Accepted 20 June 2022; Published 14 July 2022

Academic Editor: Lianhui Li

This study specifically designed an eye-tracking supported scientific problem-solving assessment: hands-on manipulation task system to explore the differences in visual attention and cognitive processes between high and low science achievement groups. Thirteen students with high science achievement and fourteen students with low science achievement participated. Students needed to complete the hands-on manipulation assessment, consisting of three modules, including selecting experimental equipment, experimental design, and building the experimental model. Behavioral and eye movement data were collected during the process. The results showed that the high science achievement group allocated more visual attention to the hands-on manipulation task, acquired more information through visual fixation, and assigned more attention to the key area. In module three of the hands-on manipulation task, the high science achievement group transformed from a visual channel to a tactile channel, and they generated more hands-on behaviors depending on the experimental area. Furthermore, the results showed a high correlation between students' eye movement behavior and the performance of scientific problem-solving assessments. Eye movement behavior could predict students' performance in scientific problem-solving. The average fixation duration and the average fixation duration of the interest area were two significant determining parameters. The implications of the experimental results for front-line science education, curriculum designers, and science assessment were also discussed.

1. Introduction

China's educational reform in recent years emphasized the importance of cultivating students' ability to solve scientific problems. According to the Primary School Science Curriculum Standards issued by the Ministry of Education in 2017, primary school students should master the necessary scientific knowledge and scientific research methods, develop the ability to handle practical scientific problems, and participate in public affairs. In the face of increasingly complex scientific problems, the ability to quickly retrieve and integrate essential information to form practical scientific problems solving paths and take actions along a practical path is crucial [1]. In PCAP scientific academic assessment content framework, three competencies in students' continuous knowledge learning were mentioned: scientific inquiry, scientific reasoning, and problem-solving. Thinking skills that students need include creativity, critical thinking, problem-solving, and metacognition [2]. Problem-solving is the cognitive processing of transforming a known state into a goal state when the problem solver has no obvious solution [3]. Newell and Simon [4] believed that problem-solving began with information retrieval to construct the mental representation of external problems in well-structured problems. By comparing the difference between the target state and the known state, effective operations are performed to successfully transform the given state of the system into the target state. The OECD [1] proposed the framework for problem-solving that involves four main

processes: "exploration and understanding," "representing and formulating," "planning and executing," and "monitoring and reflecting." Traditional assessment measures like standardized tests are unsuitable for assessing multiple core competencies such as problem-solving competence. The following four methods are suggested for assessment: project assessment, performance assessment, group assessment, and portfolio assessment [5]. The reasoning could be strengthened when the relevant behavior is observed multiple times in multiple environments, and its performance takes into account cognitive, motivational, ethical, and emotional aspects [6]. Therefore, it is necessary to integrate evidence from various assessment sources. Redecke [7] stressed that, according to the core literacy to determine different evaluation ways, computer-based testing, online testing, simplified game, and electronic portfolio played a crucial role in the core literacy assessment. Meanwhile, the school curriculum evaluation should strengthen the technical development and application of authentic situation assessment. The Program for International Student Assessment (PISA) emphasized three characteristics of the problem-solving definition: "authentic situation" rather than the abstract problem. The "nonobvious" of scientific problem-solving reflected the nonroutine of problem solutions. The "interdisciplinary assessment" draws on a wide range of problem-solving knowledge [1].

The level description of problem-solving is not based on the specific thought process. It focuses on situational complexity, authenticity, and strategies. Authentic situation tasks require presenting situations that reflect real challenges in an individual's life and work, where students use scientific knowledge and skills, independent judgment, and creative collaboration to solve problems. The design of problem-solving tasks in [8] had carried out the computer management and human-computer interactive evaluation based on. An interactive task was added in which participants were designed to manipulate variables to determine the impact on the results [1]. NAEP has added interactive computer tasks and hands-on task sections since 2009. In hands-on tasks, students have to design scientific inquiry by themselves, select materials, and conduct an inquiry to solve problems and explain scientific phenomena [9]. Adopted the human-computer interaction mode, and the computer dynamically collected students' data to complete authentic situation tasks. However, as PISA tried to avoid repetition with other literacy evaluations when designing the assessment of problem-solving ability, thus such questions rarely involve the subject background knowledge, which restricted the practical application of problem-solving competency assessment. The "authenticity assessment" is always associated with performance assessment. The competency to use knowledge can only be assessed when completing a job in response to a specific task by using our knowledge and skills. This evaluation method can fully reflect students' competency, learning achievements, and extensive knowledge understanding [10]. According to the "authenticity evaluation" model, Chang [10] designed three different question forms to investigate students' scientific cognition level when studying ninth-grade students' scientific literacy. These studies found that the "authenticity evaluation" model with different question forms was an effective method to evaluate students' scientific literacy, among which "hands-on manipulation" significantly influences students' evaluation results. However, cultivating students' hands-on manipulation competency is often neglected due to time problems. Therefore, educators can improve their understanding of complex concepts by designing authentic situation models to reduce the gap between students' knowledge learning and real life.

The development of big data and information technology [11–14] provides a reliable supporting tool for this research. Many studies have found that some eye movement parameters [15–17], such as fixation duration, fixation duration percentage, fixation frequency, regression frequency, and average pupil diameter, provided critical evidence to explore the psychological process of students. Tai [18] compared the eye movement differences in problem-solving behaviors of participants with different professional backgrounds in scientific evaluation and found that the eye movement differences were related to the participant's professional level on a specific topic. Tsai et al. [19] investigated the eye movement differences of students with different professional backgrounds in PISA online assessment, and the study found that students majoring in science allocated more attention to critical areas and conducted deeper processing. Hu et al. [20] studied the information processing strategies of students in solving PISA interactive and analytical questions, which required self-discovery of information or provided a large amount of information in the questions. Students with good performance had a longer fixation duration in both questions. They tended to apply their previously constructed problem patterns to solve current problems, meanwhile adopting plan-driven forward reasoning to obtain more effective actions. Underperforming students switched their gaze points frequently between areas of interest and adopted "goal-result" backward reasoning, which required constant searching to reduce the difference between the current state and the target state. Krstić et al. [21] explored the students' eye movement patterns in PISA reading evaluation and found that students with high scores paid more attention to relevant information in texts and pictures, while students with low scores lingered in texts and pictures instead of extracting essential information. Kaller et al. [22] found evidence to distinguish the processes using eye-tracking technology. The study showed that the initial fixation change and fixation duration did not change with the problem structure, suggested that the early eye movements generate mental representations of the starting state and the target state, and compared the two states to determine structural differences. The problem structure did not affect the initial fixation change. The final gaze shifted before the problem structure affected the execution phase, suggesting that fine processing was related to the final fixation change. In recent studies, Mobile Eye Tracker (MET) has been conducted to compare the visual attention characteristics widely, people's cognitive process in authentic situation tasks allows participants to move their heads freely,

and their behaviors are not strictly restricted. For instance, participants can walk in the park [23] and complete the experimental task [24]. The applications of MET meet the needs of different topic formats in the evaluation, especially the hands-on evaluation format. In educational evaluation, using MET to study problem-solving helps reveal participants' strategies for acquiring information, making it possible for procedural evaluation. Bryan et al. [25] applied MET to the International Adult Competency Assessment (PIAAC). The study selected a computer-based technology assessment containing literacy, numeracy, and problem-solving modules, where participants may use a pen or calculator and interact verbally with the researcher. Off-screen eye movements were captured with MET to see how participants read and recognized information during problem-solving. In the experiment of physical concept learning, Chien et al. [24] proposed that hands-on manipulation was essential for laboratory learning. The previous studies showed the following: (1) More professional people showed more refined visual behaviors when performing tasks, paid more attention to areas related to actual tasks, and paid less attention to redundant areas [26]. (2) Studies on grouping participants according to their performance found that participants with higher achievement could not only effectively use previous knowledge [27] and identify task-related areas but also adopt more effective analysis strategies to gain relevant information [20]. (3) Eye movement indicators could predict students' evaluation performance. Studies have shown that successful problem solvers had smaller pupils on easy problems while larger pupils on complex problems [28]. Other studies have found that average fixation duration was the best predictor; students with longer average fixation duration showed deeper cognitive processing [27].

2. Purpose

This study designed a set of scientific problem-solving evaluation tasks in the authentic situation, including the paper evaluation and hands-on manipulation assessment. After completing the scientific knowledge task module presented on the computer, participants were required to complete three scientific problem-solving hands-on manipulation tasks. According to their scientific knowledge concept evaluation and previous comprehensive scores, the participants were divided into high and low groups. The differences in eye movement and cognitive process among different groups were explored. Eye movement tracking technology was used to record and collect the eye movement behavior of each participant, such as their average fixation time, fixation time percentage, average pupil diameter, fixation times in each task module, and the average fixation time and fixation time percentage in different areas of interest in each task module. The following research questions can be used as guidelines in pursuing this goal:

(1) Would the high science achievement group perform better than the low science achievement group in the hands-on manipulation assessment?

(2) When performing the hands-on manipulation assessment, would the high science achievement group allocate more visual attention than the low science achievement group?

(3) What is the relationship between students' scientific problem-solving performance and eye movement behavior?

(4) Could the eye movement behavior be used to predict students' performance in scientific problem-solving?

3. Methods

3.1. Participants. In this study, thirty-nine students from grade seven in Taicang No. 1 Middle School, Jiangsu Province, China, were randomly selected. The number of participants in the preliminary experiment was 7. The number of valid participants in the formal experiment was 27, and 5 were invalid participants, who were rejected because the rate of eye movement data did not reach 90%. There was no significant difference in age between the high and low science achievement groups ($n = 27$; between ages 12 and 13; M = 12.66; SD = 1.09; 15 males and 12 females). The students who participated in the assessment have studied the core science concepts covered. The scores of students' entrance science examination and core concept evaluation were weighted as the basis for grouping. The average score of 27 students was 56.78, and there was an extremely significant difference in the weighted average score between the two groups of students, $t_{(1,\ 25)} = 5.97$, $p < 0.001$. Twenty-seven students were divided into high and low science achievement groups based on their weighted average scores. There were 13 students in the high science achievement group but 14 students in the low science achievement group.

3.2. Design of Scientific Problem-Solving: Hands-On Manipulation Assessment. This study developed a science problem-solving assessment, "Energy Efficient House," to evaluate students' core science concept of "heat absorption and heat dissipation." Participants were required to make experimental hypotheses, build experimental platforms, obtain measured data, and form preliminary conclusions according to the experimental result. The hands-on manipulation assessment consisted of three task modules, which correspond to the problem-solving framework "exploration and understanding," "representing and formulating," and "planning and execution" proposed by OECD [1]. Students were required to read computer materials, learn assistance manuals, and operate experimental instruments.

Module one was the selection of experimental equipment, in which participants chose experimental equipment suitable according to the various equipment provided by the laboratory. Module two was the experimental design. Participants made the experimental hypothesis of the "relationship between color and heat absorption ability" and designed the experimental scheme based on the problem-solving orientation. Module three was to build the experimental model; after completing the preliminary

experimental design and equipment selection, participants needed to use experimental materials, sensors, and computer software to build an experimental model and then verify the hypothesis of "the relationship between object's color and heat absorption ability" by using the measured data.

The assessment was designed based on the ECD (Evidenced-Centered Design) model and explored the students' grasp of "heat energy" as the specific form of energy and conversion principle. Authoritative international science problem-solving assessments such as PISA, TIMSS, and NAP are based on paper or online text formats, while our research attempted to study hands-on science problem-solving processes.

The evaluation information presented on the computer was in well-constructed mixed text and composed of written web pages with paragraphs, tables, charts, and graphs organized in a mutually supportive and coherent manner. The computer was also equipped with experimental software adapted to the heat sensor, which was convenient for reading data from the sensor.

The experimental materials included a heating lamp, three metal heat absorption rods of the same material in different colors, an iron rack, a clamp, three-hole support, a pen, and a heat sensor. The usage of experimental equipment and sensors was described in the auxiliary manual, which was convenient for students to read. A team of four science education designers, consisting of two science teachers with master's degrees in science education, a science education researcher with a doctoral degree, and a science education professor, was responsible for designing the overall science problem-solving assessment.

The online scientific problem-solving evaluation assessment platform runs on the Linux server. The core of the scientific problem-solving evaluation system was programmed in PHP and MySQL to process large data sets and analytical programs efficiently.

3.3. The Encoding Process. The response of all participants in the scientific problem-solving assessment was recorded in the database for analysis. Meanwhile, the experimenter recorded participants' performance in the hands-on assessment for analysis. Three experimenters were all graduate students majoring in "educational technology" and "applied psychology." The experts' team developed a standard coding system and experimenter manual.

The coding system carried out detailed coding guidelines for the evaluation criteria of each question, such as how the principal tester scores the answers of each item and examples of answers that middle school students may have. Coding guidelines were developed according to the content of each module to ensure reliability and coding quality between encoders.

3.4. Eye Movement Analysis. Eye-tracking glasses 2 W were the instrument for participants to operate flexibly in computer-based scientific problem-solving assessment. The mobile tracking device designed and manufactured by the German company SMI recorded each student's eye movements at a 60 Hz sampling rate. It was a noninvasive system, as a standard pair of glasses weight 68 grams, with less impact on the psychological and physical burden of the students. The device was specially designed for the study of dynamic eye movement, and it provided maximum peripheral perception and binocular visual positioning to capture the natural gaze behavior of the students during the hands-on manipulation assessment. A standard three-point calibration and validation procedures were completed before the formal assessment. The following eye movement parameters were further analyzed from the original data to record participants' completion duration, total fixation duration (TFD), average fixation duration (AFD), fixation duration percentage (FDP), and Z score of pupil diameter (PDZ). BeGaze^{TM} software was used to analyze further each student's eye movement parameters in scientific problem-solving assessment. Division of AOI in hands-on manipulation assessment is shown in Figure 1.

4. Results

4.1. Different Hands-On Assessment Performance between High and Low Science Achievement Groups. The independent sample t-test result for the high and low groups of students showed that the high science achievement group students significantly outperformed the low science achievement group in the total score of the hands-on task, $t_{(1,\ 25)} = 5.97$, $p < 0.001$, the first module, $t_{(1,\ 25)} = 3.34$, $p < 0.01$, and the second module, $t_{(1,\ 25)} = 4.36$, $p < 0.001$. However, there was no significant difference in the score of the third module, $t_{(1,\ 25)} = 1.25$, $p > 0.05$.

4.2. Differences in Eye Movement Behavior between High and Low Science Achievement Groups in Hands-On Manipulation Assessment. Two-factor repeated measure ANOVA results among three modules in the assessment and the eye movement indexes furthermore conducted the simple effect analysis of the three modules and different scientific achievements, as shown in Tables 1–3. Tests of within-subjects effects on the module are shown in Table 1, and tests of between-subjects effects on group are shown in Table 2. The results of the simple effect analysis of different group students on FDP, AFD, and PDZ are shown in Table 3.

The main effect of the three modules on the FDP was highly significant, $F_{(2,\ 50)} = 11.11$, $p < 0.001$, $\eta^2 = 0.31$. The main effect of scientific literacy on FDP was significant, $F_{(1,\ 25)} = 7.95$, $p < 0.01$, $\eta^2 = 0.24$. The edge of interaction between scientific literacy level and hands-on assessment was significant, $F_{(2,\ 50)} = 2.53$, $p = 0.090$, $\eta^2 = 0.09$. During three modules of hands-on manipulation assessment, the result revealed that the high science achievement group allocated more visual attention to the task and more access to information through visual gaze than the low scientific achievement group, including $\mathrm{FDP}_{\mathrm{module1}}$, $F_{(1,\ 25)} = 1.87$, $p > 0.05$, $\mathrm{AFD}_{\mathrm{module1}}$, $F_{(1,\ 25)} = 1.32$, $p > 0.05$, $\mathrm{PDZ}_{\mathrm{module1}}$, $F_{(1,\ 25)} = 8.21$, $p < 0.01$. $\mathrm{FDP}_{\mathrm{module2}}$, $F_{(1,\ 25)} = 6.42$, $p < 0.05$, $\mathrm{AFD}_{\mathrm{module2}}$, $F_{(1,\ 25)} = 5.10$, $p < 0.05$, $\mathrm{PDZ}_{\mathrm{module2}}$, $F_{(1,\ 25)} = 6.99$, $p < 0.05$. $\mathrm{FDP}_{\mathrm{module3}}$, $F_{(1,\ 25)} = 6.92$, $p < 0.05$,

Figure 1: Division of AOI in hands-on manipulation assessment.

Table 1: Tests of within-subjects effects on the module.

	Source	Sum of squares	df	Mean square	F	η^2
FDP	Module	603.60	2	301.80	11.11***	0.31
	Module * group	137.64	2	77.58	2.53	0.09
	Error	1358.32	50	27.17		
AFD	Module	304559.91	1.36	224371.70	41.55***	0.62
	Module * group	20634.92	1.36	15201.91	2.82	0.10
	Error	183264.20	33.94	5400.49		
PDZ	Module	47.49	1.04	45.51	592.11***	0.96
	Module * group	0.58	1.04	0.56	7.26*	0.24
	Error	1.85	24	0.08		

Table 2: Tests of between-subjects effects on group.

	Source	Sum of squares	df	Mean square	F	η^2
FDP	Group	683.26	1	683.26	7.95**	0.24
	Error	2149.97	25	86.00		
AFD	Group	61848.75	1	61848.75	6.30*	0.20
	Error	245413.36	25	9816.53		
PDZ	Group	$1.03 * 10^{-12}$	1	1	0.16	0.01
	Error	$1.54 * 10^{-13}$	23	$0.03 * 10^{-12}$		

Table 3: Results of the simple effect analysis of different group students on FDP, AFD, and PDZ.

	AOI	Sum of squares	df	Mean square	F
FDP	Selection of experimental equipment	49.28	1	49.28	1.87
	Experimental design	214.91	1	214.91	6.42*
	Build the experimental model	556.70	1	556.70	6.92*
AFD	Selection of experimental equipment	1503.70	1	1503.70	1.32
	Experimental design	58363.37	1	58363.37	5.10*
	Build the experimental model	22616.60	1	22616.60	4.96*
PDZ	Selection of experimental equipment	0.25	1	0.25	8.21**
	Experimental design	0.33	1	0.33	6.99*
	Build the experimental model	0.01	1	0.01	1.89

$AFD_{module3}$, $F_{(1,\ 25)} = 4.96$, $p < 0.05$, and $PDZ_{module3}$, $F_{(1,\ 25)} = 1.89$, $p > 0.05$.

4.3. Differences of AOI in Eye Movement Behavior between High and Low Science Achievement Groups in Hands-On Manipulation Assessment. The two-factor repeated measurement ANOVA and multiple comparison test conducted on the FDP of AOI between the high and low groups and the key areas of each module were shown in Table 4. In module one, the FDP of the high group was significantly higher than the low group on the key auxiliary manual area, $F_{(1,\ 25)} = 10.02$, $p < 0.01$. In module two, the FDP of the high group was significantly higher than the low group on the key

Table 4: The key area of each module in hands-on manipulation assessment.

Stage of module	Auxiliary manual area	Worksheet area	Experimental area
Module one: Selection of experimental equipment	+		
Module two: Experimental design		+	
Module three: Build the experimental model			+

worksheet area, $F_{(1,\ 25)} = 7.40$, $p < 0.05$. In module three, the FDP of the high group was significantly higher than the low group on the key experimental area, $F_{(1,\ 25)} = 8.73$, $p < 0.01$.

4.4. The Correlation and Regression Analysis of Students' Eye Movement Behaviors and Scientific Problem-Solving Performance. The results of the Pearson correlation analysis, which was conducted to explore the correlation between students' eye movement behavior and scientific problem-solving performance, indicated that students' scientific problem-solving performance was highly correlated with their eye movement behavior, including cFDP ($r = 0.56$, $p < 0.01$), aAFD ($r = 0.77$, $p < 0.001$), cAFD ($r = 0.86$, $p < 0.001$), and bPDZ ($r = -0.97$, $p < 0.001$). In addition, a stepwise multiple regression analysis was used to assess which eye movement indicators could best predict students' scientific problem-solving performance. The results showed that aAFD and bAFD were the most significant predictors of eye movement when participants completed the scientific problem-solving task, as shown in Table 5, $T = -2.43$, $p < 0.05$, $\beta = -0.66$; $T = 2.31$, $p < 0.05$, $\beta = 0.48$.

The regression equation of Model one was

$$Y = 16.78 - 21.75\text{aPDZ} + 37.62\text{cPDZ} - 0.22\text{aAFD} + 0.05\text{bAFD} + 0.07\text{cAFD}. \quad (1)$$

The study compared the prediction result with students' hands-on manipulation performance; the prediction success rate for high science achievement students was 84.6%, but 78.6% for low science achievement students, and the total prediction success rate was 81.5%. In conclusion, the AFD and PDZ in the three modules of hands-on manipulation assessment could better predict the students' scientific performance. What is more, if the AFD of students was lower in module one but higher in module two, the student's scientific performance may be better.

4.5. The Correlation and Regression Analysis of AOI Index and Scientific Problem-Solving Performance of Students. The results of Pearson correlation analysis showed that students' AOI was highly correlated with their scientific problem-solving performance, including a2AFD($r = 0.81$, $p < 0.001$), b1AFD($r = 0.62$, $p < 0.001$), b3AFD($r = 0.63$, $p < 0.001$), and c3AFD($r = 0.7$, $p < 0.001$), as shown in Table 6. In addition, a stepwise multiple regression analysis was used to assess which AOI indicators could best predict students' science problem-solving performance. The results showed that b1AFD and c2AFD were the most significant predictors of AOI when participants completed the scientific problem-solving task, $T = 2.92$, $p < 0.01$, $\beta = 0.75$; $T = -2.60$, $p < 0.05$, $\beta = -0.60$.

Table 5: Standard multiple regression for eye movement indexes on scientific achievements.

Parameter	B	SE	β	T	Tolerance	VIF
Constant	16.78	37.60		0.45		
aPDZ	−21.75	13.20	−0.43	−1.65	0.40	2.52
cPDZ	37.62	26.73	0.37	1.41	0.40	2.47
aAFD	−0.22	0.09	−0.66	−2.43∗	0.36	2.75
bAFD	0.05	0.02	0.48	2.31∗	0.64	1.56
cAFD	0.07	0.04	0.43	1.70	0.43	2.32

∗a stands for module 1, b stands for module 2, and c stands for module 3.

Table 6: Standard multiple regression for AOI on scientific achievements.

Parameter	B	SE	β	T	Tolerance	VIF
Constant	82.36	18.60		4.43∗∗∗		
a1AFD	−0.08	0.05	−0.49	−1.68	0.27	3.67
a2AFD	−0.09	0.13	−0.23	−0.66	0.18	5.49
a3AFD	0	0.02	0	0.01	0.72	1.39
b1AFD	0.04	0.02	0.75	2.92∗∗	0.35	2.88
b2AFD	0.01	0.02	0.09	0.42	0.49	2.06
b3AFD	0.03	0.03	0.19	0.88	0.48	2.09
c1AFD	−0.01	0.02	−0.07	−0.37	0.59	1.70
c2AFD	−0.10	0.04	−0.60	−2.60∗	0.43	2.35
c3AFD	0.05	0.03	0.38	1.54	0.38	2.66

∗a1 stands for the auxiliary manual area in module 1, a2 stands for the worksheet area in module 1, a3 stands for the experimental area in module 1, and so on.

The regression equation of Model two was

$$Y = 82.36 - 0.08\text{a1AFD} - 0.09\text{a2AFD} + 0.04\text{b1AFD} + 0.01\text{b2AFD} + 0.03\text{b3AFD} - 0.01\text{c1AFD} - 0.10\text{c2AFD} + 0.05\text{c3AFD}. \quad (2)$$

The study compared the prediction results with students' hands-on manipulation performance; the prediction success rate of Model two for high science achievement students was 69.2%, but 92.9% for low science achievement students, and the total prediction success rate was 81.5%. Model two could explain 61% of the variability in student performance during the same overall success rate as Model one. Therefore, Model two could better predict the students' scientific performance. According to the significance index, if the AFD on the worksheet was higher in module two experimental design, while the AFD on the auxiliary manual was lower in module two experimental model building, the students' scientific performance may be better.

5. Discussion

The comparison of eye movement behavior between the high and low science achievement groups.

The study showed that the high science achievement group performed better than the low science achievement group in the hands-on manipulation performance, while eye movement behavior also showed that FDP and AFD were higher in the high science achievement group. One possible explanation was that high science achievement students allocated more visual attention in the hands-on manipulation assessment, more concentrated, and acquired information through visual gaze to a greater extent, while low science achievement students were more distracted by external factors when completing the task. Goldhammer et al. [29] pointed out that, in problem-solving tasks, the more time students spend on the task, the better they perform. In addition, they found the effect of time depended on the difficulty and intensity of the task, especially in the more difficult tasks; investing time in cognitive activities had a positive predictive effect on the successful completion of the task. The result of this study was consistent with previous studies that high science achievement students had higher fixation duration and were more concentrated.

The total fixation counts of high scientific achievement students were lower in module two experimental design and module three experimental model building. High science achievement students allocated more fixation duration and average fixation duration and fewer fixation counts in the cognitive processing, which were consistent with previous studies that students with longer average fixation duration tend to show deeper cognitive processing and better learning results. Students with high science achievement were more likely to be aware of the tasks' difficulties, especially representation, refinement, and execution. Thus, they took longer to think profoundly and achieve higher accuracy. These findings provided great support to several previous studies suggesting that high-level problem-solving students had deeper cognitive processing of task-related areas. They tended to apply their previously constructed mental models to solve problems, while low-level problem-solving students have not established a correct mental model due to their shallow cognitive processing of the critical areas in a problem-solving task. Thus, they reevaluated the consistency of the established model with the problem task by using the visual information of the auxiliary areas [30].

In the hands-on manipulation assessment, the high science achievement group had a higher PDZ than the low science achievement group, consistent with previous studies that individuals showed more significant pupil dilation when handling complex tasks [31]. Pupil dilation reflected individuals' continuous information processing, and challenging tasks would elicit more cognitive effort. In this study, the average pupil diameter of students was maximized in module three, which was the most challenging module. However, our results indicated no statistically significant difference between the high and low science achievement groups in module three, and one possible explanation was that students in both groups made more cognitive efforts in module three.

5.1. Comparison of AOI between High and Low Science Achievement Groups. The results showed that students with high science achievement assigned more visual attention to the auxiliary manual in module one, which was the key area of this module. Meanwhile, they allocated more attention to the key experimental area in module three, consistent with previous research that high-level students paid more attention to the task-related areas. In the hands-on manipulation assessment, the worksheet area and auxiliary manual area belong to the visual mode information of text or pictures, while the experimental area belongs to the tactile channel mode. The comparison between the two groups revealed that the high science achievement students had a statistically significant change in the problem-solving process from relying on visual channel mode to tactile channel mode. Particularly in module three, high science achievement students relied more on experimental areas and produced more hands-on behaviors.

The fixation sequence of the AOI revealed that high science achievement students showed more continuous cognitive processing in the key areas. In module three, the low scientific achievement students' gaze of interaction frequently switched between the key experimental area and auxiliary areas. The eye movement index reflected that the low science achievement students allocated more fixation duration in auxiliary manual area, which meant they could have recognition difficulty in experimental model building. The findings of students' cognitive processing were consistent with previous studies, and high-level problem solvers could deeper conduct cognitive processing of task-related areas [32].

5.2. Eye Movement Behavior Predicted Students' Scientific Problem-Solving Performance. The regression prediction model showed that the AFD and the AFD of AOI were the best indicators to predict students' performance in scientific problem-solving performance assessment. The finding added to previous evidence that eye movement was highly correlated with mental effort, reading processes, computer-based assessment of performance, and the construction of mental models. Students may perform better if they engage in deeper cognitive processing on relatively difficult tasks. In solving systematic experimental problems, if students could think profoundly and construct psychological models gradually, their evaluation performance may be better. These findings have implications for how eye-tracking-supported hands-on manipulation science problem-solving assessment could be used to improve science learning in junior high school students. In order to cultivate and improve students' scientific literacy, educators should pay more attention to students' cognitive process and deep thinking in science teaching and design high-level cognitive activities to achieve this goal. For instance, to establish a complete practice, encourage students to explore learning. The practice should

be set up as realistic as possible, regarded as solving problems in real life. When designing the practiced mask, we could start from the eight links of "asking questions, making assumptions, making plans, collecting evidence, processing information, drawing conclusions, expressing and communicating, and reflecting and evaluating."

In the practice of student inquiry, educators could use prominent hints to guide students to think deeply about key information and difficult problems rather than repeatedly thinking superficially. The guidance and intervention in practice would shape students' thinking and behavior patterns, relieve their anxiety when meeting practical problems, and improve students' problem-solving ability. However, solving practical problems depends not only on the ideas and skills of the problem solver but also on the difficulty of the problem itself. Therefore, the significance of setting up practical exploration lies in improving students' problem-solving ability on the one hand and guiding students to see the boundaries and limitations of problem-solving and recognize the future development direction of a specific field on the other hand, which has more excellent value in improving students' cognitive level and scientific literacy.

6. Conclusions

This study specifically designed an eye-tracking supported problem-solving assessment hands-on manipulation task system to further explore the differences in visual attention and cognitive progress between high and low science achievement groups in the scientific problem-solving process. The research combined synchronous computer and pupil 60 Hz tracking system technology with a hands-on manipulation assessment system to explore the students' cognitive processes in hands-on operation. The system included static concept evaluation problems and dynamic hands-on problems instead of being limited to reading and solving cognitive model exploration in static problems. These results are also very encouraging as they demonstrate some important findings. (1) Students in the high science achievement group performed better than those in the low science achievement group in solving scientific problems assessment, consistent with their eye movement behavior. (2) The results of ANOVA in eye movement indicator showed that, in the three modules of hands-on manipulation assessment, students with high science achievement had more fixation and concentration on the task and acquired more information through visual fixation. In contrast, students with low science achievement were more likely to be distracted by external factors when finishing the assessment. (3) ANOVA results in the AOI index showed that students with high science achievement paid more attention in key areas during different modules. In addition, students with high science achievement had a more noticeable change from relying on visual channel mode to relying on tactile channel mode in the problem-solving process. Particularly in module three, the execution phase of problem-solving, students with high science achievement paid more attention to the experimental area, which produced more operation behavior. These results were consistent with their eye movement behavior. (4) Eye movement behavior was highly correlated with scientific problem-solving performance. (5) Eye movement behavior could predict students' performance in scientific problem-solving. The AFD and the AFD of AOI were significant determining parameters.

The highlights of this work are summarized as follows:

(1) This study specifically designed an eye-tracking supported scientific problem-solving assessment: hands-on manipulation task system to explore the differences in visual attention and cognitive processes between high and low science achievement groups.

(2) The result showed that the high science achievement group allocated more visual attention to the hands-on manipulation task, acquired more information through visual fixation, and assigned more attention to the key area than the low science achievement groups.

(3) The study also found that the average fixation duration and the average fixation duration of the AOI were two significant determining parameters for predicting students' performance in scientific problem-solving. [33–39]

Data Availability

The dataset used to support the findings of the study can be obtained from the corresponding author upon request.

Conflicts of Interest

The authors declare that they have no conflicts of interest.

References

[1] N. J. Oecd Publishing, *PISA 2012 Assessment and Analytical Framework: Mathematics, reading, Science, Problem Solving and Financial Literacy*, p. 264, OECD Publishing (NJ3), Paris, 2013.

[2] S. E. Fahyan, "Assessment and teaching of 21st century skills," Edited by P. Griffin, B. McGaw, and E. Care, Eds., Springer, Cham, 2014.

[3] R. E. Mayer, "The promise of multimedia learning: using the same instructional design methods across different media," *Learning and Instruction*, vol. 13, no. 2, pp. 125–139, 2003.

[4] H. A. Simon and A. Newell, "Human problem solving: the state of the theory in 1970," *American Psychologist*, vol. 26, no. 2, pp. 145–159, 1971.

[5] M. Kalantzis, B. Cope, and A. Harvey, "Assessing multiliteracies and the new basics," *Assessment in Education: Principles, Policy & Practice*, vol. 10, no. 1, pp. 15–26, 2003.

[6] D. S. E. Rychen and L. H. E. Salganik, *Key Competencies for a Successful Life and Well-Functioning Society*, Hogrefe & huber, Cambridge, 2003.

[7] C. Redecker, "The use of ICT for the assessment of key competences," Publications Office of the European Union, Brussels, 2013.

[8] PISA results, *PISA 2012 Results: Creative Problem Solving*, Oecd, Paris, 2014.

[9] N. Board, *Science Framework for the 2011 National Assessment of Educational Progress*, National Assessment Governing Board, New York, 2014.

[10] S. N. Chang and M. H. Chiu, "The development of authentic assessments to investigate ninth graders? Scientific literacy: in the case of scientific cognition concerning the concepts of chemistry and physics," *International Journal of Science and Mathematics Education*, vol. 3, no. 1, pp. 117–140, 2005.

[11] L. Li, B. Lei, and C. Mao, "Digital twin in smart manufacturing," *Journal of Industrial Information Integration*, vol. 26, no. 9, Article ID 100289, 2022.

[12] L. Li, T. Qu, Y. Liu et al., "Sustainability assessment of intelligent manufacturing supported by digital twin," *IEEE Access*, vol. 8, pp. 174988–175008, 2020.

[13] L. Li and C. Mao, "Big data supported PSS evaluation decision in service-oriented manufacturing," *IEEE Access*, vol. 8, no. 99, pp. 154663–154670, 2020.

[14] L. Li, C. Mao, H. Sun, Y. Yuan, and B. Lei, "Digital twin driven green performance evaluation methodology of intelligent manufacturing: hybrid model based on fuzzy rough-sets AHP, multistage weight synthesis, and PROMETHEE II," *Complexity*, vol. 2020, no. 6, 24 pages, Article ID 3853925, 2020.

[15] Y. Tang and J. Su, "Eye movement prediction based on adaptive BP neural network," *Scientific Programming*, vol. 2021, Article ID 4977620, 9 pages, 2021.

[16] X. Li, Y. Zhou, and Y. He, "The fusion of eye movement and piezoelectric sensing technology assists ceramic art process optimization and mechanical characterization," *Journal of Sensors*, vol. 2021, Article ID 9748335, 11 pages, 2021.

[17] X. Jinjing, "Research on flipped classroom of university curriculum using eye movement analysis and LSTM neural network," *Wireless Communications and Mobile Computing*, vol. 2022, Article ID 2559864, 10 pages, 2022.

[18] R. H. Tai, J. F. Loehr, and F. J. Brigham, "An exploration of the use of eye-gaze tracking to study problem-solving on standardized science assessments," *International Journal of Research and Method in Education*, vol. 29, no. 2, pp. 185–208, 2006.

[19] P. Y. Tsai, T. T. Yang, and H. C. She, "Explore college students' cognitive processing during scientific literacy online assessments with the use of eye tracking technology," in *Proceedings of the 2015 IEEE International Conference on Advanced Learning Technologies*, pp. 303-304, Hualien, Taiwan, July 2015.

[20] Y. Hu, B. Wu, and X. Gu, "Learning analysis of k-12 students' online problem solving: a three-stage assessment approach," *Interactive Learning Environments*, vol. 25, no. 2, pp. 262–279, 2017.

[21] K. Krstić, A. Šoškić, V. Ković, and K. Holmqvist, "All good readers are the same, but every low-skilled reader is different: an eye-tracking study using PISA data," *European Journal of Psychology of Education*, vol. 33, no. 3, pp. 521–541, 2018.

[22] C. P. Kaller, B. Rahm, K. Bolkenius, and J. M. Unterrainer, "Eye movements and visuospatial problem solving: identifying separable phases of complex cognition," *Psychophysiology*, vol. 46, no. 4, pp. 818–830, 2010.

[23] F. Y. Yang, M. J. Tsai, and G. L. Chiou, "Instructional suggestions supporting science learning in digital environments based on a review of eye tracking studies," *Educational Technology & Society*, vol. 21, no. 2, pp. 28–45, 2018.

[24] K. P. Chien, C. Y. Tsai, H. L. Chen, W. H. Chang, and S. Chen, "Learning differences and eye fixation patterns in virtual and physical science laboratories," *Computers & Education*, vol. 82, pp. 191–201, 2015.

[25] M. Bryan, A. P. Bayliss, F. Piers, P. E. Engelhardt, E. S. Gareth, and B. Francesca, "Observing response processes with eye tracking in international large-scale assessments: evidence from the OECD PIAAC assessment," *European Journal of Psychology of Education*, vol. 33, no. 3, pp. 1–16, 2018.

[26] A. Gegenfurtner, E. Lehtinen, and R. Säljö, "Expertise differences in the comprehension of visualizations: a meta-analysis of eye-tracking research in professional domains," *Educational Psychology Review*, vol. 23, no. 4, pp. 523–552, 2011.

[27] S. C. Chen, H. C. She, M. H. Chuang, J. Y. Wu, J. L. Tsai, and T. P. Jung, "Eye movements predict students' computer-based assessment performance of physics concepts in different presentation modalities," *Computers & Education*, vol. 74, no. 3, pp. 61–72, 2014.

[28] C. J. Wu, C. Y. Liu, C. H. Yang, and Y. C. Jian, "Eye-movements reveal children's deliberative thinking and predict performance on arithmetic word problems," *European Journal of Psychology of Education*, vol. 36, no. 1, pp. 91–108, 2020.

[29] F. Goldhammer, J. Naumann, A. Stelter, K. Tóth, H. RölkeRölke, and E. Klieme, "The time on task effect in reading and problem solving is moderated by task difficulty and skill: insights from a computer-based large-scale assessment," *Journal of Educational Psychology*, vol. 106, no. 3, pp. 608–626, 2014.

[30] K. A. Ericsson and J. H. Moxley, "Experts' superior memory: from accumulation of chunks to building memory skills that mediate improved performance and learning," in *The SAGE handbook of applied memory*, pp. 404–420, Sage, Newcastle upon tyne, 2014.

[31] P. S. Huang and H. C. Chen, "Gender differences in eye movements in solving text-and-diagram science problems," *International Journal of Science and Mathematics Education*, vol. 14, no. S2, pp. 327–346, 2015.

[32] E. M. Reingold, N. Charness, M. Pomplun, and D. M. Stampe, "Visual span in expert chess players: evidence from eye movements," *Psychological Science*, vol. 12, no. 1, pp. 48–55, 2001.

[33] S. D. Newman and G. Pittman, "The tower of London: a study of the effect of problem structure on planning," *Journal of Clinical and Experimental Neuropsychology*, vol. 29, no. 3, pp. 333–342, 2007.

[34] T. Purpose and P. O. Pisa, *Beyond Pisa 2015: A Longer-Term Strategy Of Pisa*, Pisa, 2020.

[35] J. Rahm, H. C. Miller, L. Hartley, and J. C. Moore, "The value of an emergent notion of authenticity: examples from two student/teacher-scientist partnership programs," *Journal of Research in Science Teaching*, vol. 40, no. 8, pp. 737–756, 2003.

[36] N. Ruh, B. Rahm, J. M. Unterrainer, C. Weiller, and C. P. Kaller, "Dissociable stages of problem solving (ii): first evidence for process-contingent temporal order of activation in dorsolateral prefrontal cortex," *Brain and Cognition*, vol. 80, no. 1, pp. 170–176, 2012.

[37] M. A. Ruiz-Primo, "Informal formative assessment: the role of instructional dialogues in assessing students' learning," *Studies In Educational Evaluation*, vol. 37, no. 1, pp. 15–24, 2011.

[38] O. J. Solheim and P. H. Uppstad, "Eye-tracking as a tool in process-oriented reading test validation," *International Electronic Journal of Environmental Education*, vol. 4, no. 1, pp. 153–168, 2011.

[39] G. Wiggins, "Moving to modern assessments," *Phi Delta Kappan*, vol. 92, no. 7, p. 63, 2011.

Hindawi
Scientific Programming
Volume 2022, Article ID 1264160, 9 pages
https://doi.org/10.1155/2022/1264160

Research Article

Research on Regional Energy Visualization Based on Knowledge Graph

Zhongbo Li [1,2]

[1]*College of Energy Engineering, Zhejiang University, Hangzhou 310058, Zhejiang, China*
[2]*Beijing District Heating Group, Beijing 100028, China*

Correspondence should be addressed to Zhongbo Li; 11827107@zju.edu.cn

Received 31 May 2022; Revised 17 June 2022; Accepted 22 June 2022; Published 13 July 2022

Academic Editor: Lianhui Li

The equipment information in the regional energy system is difficult to retrieve and the amount of data is too large to realize intelligent application. In order to solve the problem, this paper proposes a regional energy visualization research method based on knowledge graph. Firstly, the collected regional energy information is classified. Secondly, the framework is defined for the unstructured data, which is difficult to be recognized by computer, and the hidden Markov model is used for word segmentation and labeling. Finally, the regional energy equipment information data are processed to construct the knowledge graph, the regional energy map structure information is represented by the ternary group graph structure, and the regional energy retrieval system is designed. The system can efficiently process and retrieve a large amount of natural language information in regional energy and realize the intelligence of regional energy equipment. It provides a strong guarantee for the efficient and stable operation of regional energy-related equipment and has a wide range of practical application and research value.

1. Introduction

District energy systems are local energy networks through which it is used to supply hot water, steam (district heating), cold water (district cooling), electricity (often called microgrids), or integrated supply to complex buildings. In the daily construction and operation of regional energy system, a large number of equipment parameters and operation data are accumulated, but the corresponding information is often idle in the system, which affects the data value discovery of regional energy system. With the increase of equipment information, how to retrieve equipment information efficiently is of great significance to the staff of regional energy system. However, the complexity of regional energy system equipment makes it difficult to accurately retrieve equipment information [1].

(1) The primary equipment information of the regional energy system is described in the form of natural language, which increases the difficulty for the computer to understand the equipment information, and the complexity of the equipment information causes great difficulties for the accurate retrieval of the information;

(2) The intelligence degree of the primary equipment information management is not enough and it cannot select useful information to utilization from a large number of monitoring data and historical data.

The continuous development of artificial intelligence technology, the Internet of Things, and other technologies provides a new direction for the intelligent management of regional energy system equipment information [2]. Natural language processing (NLP) is an intelligent and efficient text processing technology that can systematically analyze, understand, and extract key information from text data. As for the equipment information corpus of regional energy system, literature [3, 4] expresses the text by establishing semantic framework, but the semantic framework is difficult to adapt to the complex information situation of power equipment [5], and the framework relies on the definition of expert experience, so it is difficult to comprehensively

consider the complex expression mode of equipment of regional energy system. Literature [6, 7] uses machine learning algorithm to mine rules in corpus to represent features of corpus. However, the features selected by machine learning methods are basically limited to the occurrence of keywords [8] or the occurrence frequency of words [9]. These statistical features do not fully consider the internal logic of keywords in sentences, although they have certain regularity, they are easily limited to the textual features of defect records, which is not enough to explain. With the continuous development of intelligent regional energy system strategy, the equipment information of regional energy system increases exponentially, and the requirements for information storage and retrieval are higher and higher. As a kind of efficient database, knowledge graph can manage regional energy system equipment information effectively and provides a new way for regional energy equipment information management. Different from the traditional literature review [10–13], the literature knowledge graph can extract and screen structured knowledge sequences from a large number of literature data, then show the evolution process of research hotspots and map the cross-interaction between knowledge groups, so as to realize the mining of hot spots and emerging trends. At present, common mapping tools include CiteSpace [14], etc., which provides an efficient, repeatable, and rapidly applied analysis method for scholars and has application prospects in various fields.

Therefore, this paper tries to apply the knowledge graph method to the primary equipment information management of intelligent area energy system. Firstly, the data collected by the intelligent regional energy system information collection platform are classified. Secondly, considering that the unstructured data are difficult to be accurately recognized by the computer, the unstructured data extraction framework is defined, and the hidden Markov model is used to classify and annotate the collected data, providing data support for the construction of the primary equipment information knowledge map of the regional energy system. Finally, the knowledge graph of regional energy system is constructed on this basis, the regional energy system information is represented in the form of ternary group graph structure, and the primary equipment information retrieval system of regional energy system is designed. The system can effectively improve the retrieval efficiency of regional energy system equipment information and improve the intelligence level of regional energy system.

2. Regional Energy Data

2.1. Data Sources for Regional Energy Systems. Data sources of regional energy system mainly include original data, internal data of each automation system in the regional energy system, fault error recording information, and data obtained from monitoring of the surrounding environment [15]. The primary equipment of the regional energy system is directly connected to the high voltage grid of the power system and participates in the transformation, transmission, and distribution of power energy. There are many kinds of primary equipment in regional energy system, including transformer, circuit breaker, disconnecting switch, and other related equipment. Transformer is the main equipment for the conversion of AC power energy in the power system. It can realize the conversion of power energy between different voltage levels, so as to facilitate the connection of the power system and optimize the transmission of power energy. Transformer data not only include voltage, current, active power, reactive power, phase, and other data, but also include transformer online monitoring data, chromatographic data information, and also include the proportion of dissolved gas in power transformer insulation oil and gas production data information [16]. These data parameters constitute the main components of power transformer data.

The circuit breaker is an important piece of equipment to connect or disconnect the equipment of the power system. It is equipped with relatively perfect arc extinguishing device and has the ability to disconnect the current of the power system. The circuit breaker can change the connection relation of the power system and adjust the power flow according to the demand when the system is running normally. In the event of a system failure, a circuit breaker can disconnect the fault current and cut off the electrical connection between the faulty device and the system. The operation information of circuit breaker is important reference data for daily operation and management of regional energy system.

Switching equipment in regional energy system has the characteristics of high air tightness and good sensitivity, and many parameters such as moisture content and contact temperature of gas-insulated composite electrical equipment are important parameters that need to be monitored online. The GIS online monitoring system mainly monitors two types of data, one is the density of sulfur hexafluoride gas, the other is the water content generated when a small amount of water enters the monitoring system as SF6. The partial discharge monitoring system the of GIS online monitoring system can monitor the defects such as conducting small particles and some alien substances, conducting current, internal air gap, and blocked grounding brought into the equipment during manufacturing, installation, and maintenance. GIS real-time system can determine the location of hidden danger by collecting different location information. By using sensors to collect temperature information inside the equipment, GIS high-speed optical fiber temperature measuring instrument can quickly and accurately obtain the temperature information inside the equipment. The data generated by the common primary equipment in the area energy system, such as isolation switch, grounding switch, capacitor, reactor, and transformer, plays an important role in the maintenance and fault diagnosis of the area energy system.

Environmental monitoring data are also of great significance to intelligent regional energy system data. The micrometeorological monitoring system of the intelligent regional energy system can regularly collect environmental data around the intelligent regional energy system, including air humidity, haze information, and other data.

2.2. Regional Energy System Data Classification. In order to facilitate the operation of data collection and processing, it is necessary to classify and process the data of the smart district energy system. Among them, the data volume of primary equipment is huge and diverse, and the related similar data can be roughly divided into five types for cluster analysis, namely, basic data, online monitoring data, operation data, test data, and accident data.

(1) Basic data: basic data refer to the ledger and design parameters of the primary equipment. The data are usually complete and accurate. Including the basic parameters of power equipment information, such as rating, power, size, manufacturer, and date of production. These data are permanently stored in the power equipment database and the other data are the flow data of the equipment.

(2) Online monitoring data: online monitoring data are the continuous or periodic automatic monitoring and detection of regional energy system equipment. It has the characteristics of high monitoring frequency and large data volume and can reflect the electrical, mechanical, and chemical characteristics of related equipment, such as the insulation oil chromatographic analysis of transformers and dielectric loss of capacitance bushing.

(3) Operating data: operating data refer to written or electronic records obtained after a device is inspected according to the specified check content and period during a device running. Operation data reflect the specific operation of electrical equipment, such as current, voltage, active power, reactive power, and circuit breaker operation times.

(4) Test data: test data can reflect the electrical, mechanical, chemical, and other properties of the equipment data and their specific value through the use of professional instrument test. Usually, equipment test data are obtained by the experiment after equipment power outage, such as DC resistance and insulation resistance, but it also includes in the case of equipment without power outage, far away from the equipment body data test, such as oil pressure value.

(5) Accident data: when a fault occurs in the regional energy system, the accident data mainly refers to the data of the related equipment when the short-circuit accident occurs, such as the effective value and peak value of the short-circuit current and the waveform of the short-circuit current.

3. Regional Energy Information Processing Based on HMM Model

Vector representation of regional energy information is required before regional energy information processing. The common method is to use vector group form composed of 0 and 1 to represent regional energy information, but there are problems of dimensional disaster and data sparsity, and association information in the same statement cannot be represented, which lead to word isolation [17].

In order to effectively vectorizing the associated relationship among fault information, word vector representation based on deep learning is adopted in this paper. The word vector is determined by calculating the distance between words, and the model is shown in Figure 1.

This method introduces word vector to construct probability model, and the formula is as follows:

$$\begin{aligned} p(s) &= p(\omega) \\ &= p(\omega_1, \omega_2, \ldots, \omega_T) \\ &= \prod_{t=1}^{T} p(\omega_t | \text{context}). \end{aligned} \tag{1}$$

The words above are used to predict the words that may appear in the following paragraphs, and the hidden layer is used for nonlinear processing of the results. Finally, the corresponding probability value is obtained, and the maximum likelihood estimation is trained to obtain the word vector ω_t.

Variable regional energy information contains a large number of power system vocabularies but lacks the annotated corpus. Hidden Markov model (HMM) is used to process regional energy information. Each word in regional energy information has its own lexeme label. There are four kinds of morpheme labels in a sentence. B is the initial tag of the noun, M is the middle tag of the name, E is the end tag of the noun, and S is the single word tag. Each extracted information in the regional energy information record constitutes a corpus to be processed, and each word is labeled with lexeme. The word segmentation of regional energy information is summarized as A labeling problem. The word bit probability $\lambda = (\pi, A, B)$ of each word is obtained by HMM model, and the optimal labeling sequence is obtained by the Viterbi algorithm.

(1) State transition probability matrix: state probability of regional energy information word sequence.

Here, B, M, E, and S are the sequence of input words, and P is the probability of conversion between each state.

$$A = \begin{bmatrix} 0 & P\left(\frac{M}{B}\right) & P\left(\frac{E}{B}\right) & 0 \\ 0 & P\left(\frac{M}{M}\right) & P\left(\frac{E}{M}\right) & 0 \\ P\left(\frac{B}{E}\right) & 0 & 0 & P\left(\frac{S}{E}\right) \\ P\left(\frac{B}{S}\right) & 0 & 0 & P\left(\frac{S}{S}\right) \end{bmatrix}. \tag{2}$$

(2) Observation probability matrix: the probability of obtaining each observation value according to the current state.

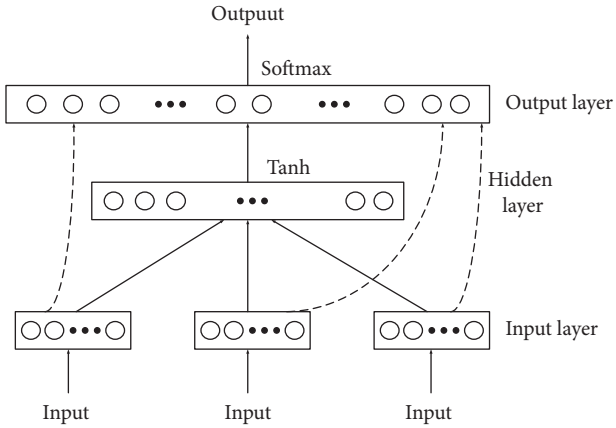

Figure 1: Word vector model.

Here, $P(o_n/Z)$ is the probability of the observed value, and o_n is the observed value.

$$B = \begin{bmatrix} P(o_1/B) & P(o_2/B) & \dots & P(o_nB) \\ P\left(\frac{o_1}{M}\right) & P\left(\frac{o_2}{M}\right) & \dots & P\left(\frac{o_n}{M}\right) \\ P\left(\frac{o_1}{E}\right) & P\left(\frac{o_2}{E}\right) & \dots & P\left(\frac{o_n}{E}\right) \\ P\left(\frac{o_1}{S}\right) & P\left(\frac{o_2}{S}\right) & \dots & P\left(\frac{o_n}{S}\right) \end{bmatrix}. \quad (3)$$

(3) State transition matrix: the probability of model transitions between states.

$$\begin{cases} S_t(i) = \max\limits_{1 \le j \le N} \left[S_{t-1}(j) a_{ij}\right] b_i(O_t), \\ \phi_t(i) = \arg \max\limits_{1 \le j \le N} \left[S_{t-1}(j) a_{ij}\right]. \end{cases} \quad (4)$$

(4) Optimal state sequence of energy information in the output region.

$$\begin{aligned} i_t^* &= \phi_{t+1}(i_{t+1}^*), \\ I^* &= (i_1^*, i_2^*, \dots, i_T^*). \end{aligned} \quad (5)$$

i_t^* represents the shortest path of regional energy information sequence, and I^* represents the optimal state sequence of regional energy information vocabulary.

4. Construction of Regional Energy Knowledge Map

Regional energy information has the characteristics of multidomain cross fusion and complexity. Knowledge graph is a structured semantic knowledge base, which extracts knowledge from text data in a structured way and forms the network knowledge structure of visual graph by connecting with each other [18]. Graph databases provide a unique perspective by focusing on the relational relationships between data. They can examine proprietary data from different perspectives and even connect it to external data resources to further reveal the underlying relationships. Using the node parallel mechanism of graph database can improve computing performance and, at the same time, storing data and knowledge in graph database to build knowledge map, which can help answer the data knowledge and query questions raised by people in natural language communication. In addition, semantic network is used to organically connect all the original regional energy data from different sources for deep mining, which can find the neglected or difficult to detect connections between different data [19].

The Neo4j graph database uses a high-performance engine to realize the visualization function, which can map entity-relationship-attribute to knowledge graph. This paper analyzes and stores the regional energy information through Neo4j graph database, finds the internal correlation of the information, and realizes the connection of equipment information.

The construction process of regional energy knowledge map is as follows:

(1) To identify and define the professional field according to the characteristics of the electric power field to build the main power.

(2) The regional energy corpus is processed by word segmentation. The security risk information is extracted and processed by word segmentation method. Then, the word segmentation results are tagged with part-of-speech tagging, and then the entities and attributes of each part are identified by naming. Due to the specialty and particularity of the words in the electric power field, the professional dictionary of the electric power industry is imported into the database as an auxiliary word segmentation tool. If the extracted entities and attributes match the words in the dictionary, the entities and attributes will be determined. In the specific field of regional energy, the knowledge graph of safety hazards belongs to the closed graph, so the entity disambiguation step is not required.

(3) Knowledge processing: it mainly extracts the basic elements of the knowledge graph contained in the regional energy data, namely entities, relations and attributes, and the inherent hazards of hidden dangers of power equipment. Besides the entity-entity and entity-attribute relationships, it also needs to extract attribute-attribute relationships. Through the dependency syntax analysis of "subject-verb-object," "definite form complement" and other dependency relations among entities and attributes, and through the manual selection of labeling types of safety risk relations, the terms related to electric power safety regulations are divided in detail in order to form a corpus of safety risk relations. After the extraction of relationships, to avoid redundancy, semantic similarity calculation is used to screen redundant relationships [7] to improve processing performance.

(4) Knowledge fusion: use Neo4j graph database [20, 21] to integrate the processed data, import entity-attribute-relation triplet of regional energy and load corpus, create relations and attribute matching among entities, form knowledge map of regional energy, and realize global index. Figure 2 shows the example of generating knowledge atlas of substation security risks. Then, the basic elements of the knowledge map are integrated, and the regional energy knowledge map is shown in Figure 3.

(5) Knowledge update: with the continuous advancement of power system construction and the continuous operation of power system, the knowledge map of regional energy should be updated and amended to ensure the accuracy and effectiveness of retrieval based on the accumulation of fault information. The construction process of the regional energy knowledge map is shown in Figure 4.

The architecture design of regional energy knowledge atlas search engine is shown in Figure 5, which is mainly composed of data warehouse, service module, and application module. Data warehouse includes distributed management of elastic-block hidden metadata, Chinese word segmentation, index management, and logstash batch file import. After processing, the hidden data are submitted to the service module, where the elastic search service provides all sorting and read access, the data-offer service provides new data entries, and the security service provides permission control and security management. Then, the application modules are introduced, including hidden danger information input, retrieval display, and regional energy knowledge map display. The process of regional energy visualization system based on knowledge graph search engine is shown in Figure 2. The design steps of the regional energy knowledge map engine are as follows:

(1) Build Django background processing framework, which is mainly used for page request forwarding and processing, as well as creating elastic search engine service module and HMM-VA word segmentation service module.

(2) A front-end display platform based on vue.js is built, which is mainly used for the front-end display of background processing content, including regional energy retrieval information display, regional energy knowledge map generation, and statistical analysis functions.

(3) Environment module is deployed on Ali Cloud. On CentOS system, Docker is used to deploy Django background, HMM-VA word segmentation service module, elastic search, Vue front end, and other requests, configure relevant parameters, and use them jointly.

According to the above steps, by inputting regional energy information and adding specific key information fields, such as "66 kV," "substation," "rainy day," and other keywords, the 66 kV regional energy knowledge map can be personalized and dynamically generated. The association search of the atlas can be used to analyze the types and causes of hidden dangers faced by all kinds of equipment, hazards after untreated results, possible treatment methods, violation of rules and regulations, prevention and control measures, etc.

5. Analysis of Experimental Examples

In this paper, regional energy data in recent three years are used as a data set to verify the effectiveness and practicability of the proposed method. The dataset contains information 1655 criteria. The hidden danger information is stored in the knowledge graph search engine by manual input and batch import. The proposed HMM word segmentation model is used for word segmentation processing of security hidden danger text. The validity of the proposed method is verified by the following four examples: comparison of regional energy data entity word segmentation methods; search engine information retrieval performance comparison; analysis of regional energy data cause knowledge atlas; and statistical analysis and prediction of regional energy data.

5.1. Comparison of Entity Segmentation Methods for Regional Energy Data. In this paper, the HMM model word segmentation steps, include corpus training, test set prediction, and word segmentation results. The power dictionary and regional energy data standard corpus of state grid corporation were used for pretraining, with a total of 150,000 words. The initial parameter information $\lambda=(\pi, A, B)$ was obtained by training the corpus in a supervised way instead of setting it as a fixed numerical parameter. The frequency of speech parts of energy data in each region was counted. The probability π can be calculated for the number of parts of speech and hidden speech of each region energy data and the corresponding words of the region energy data, and then the state transition probability matrix A and observation probability matrix B can be calculated.

Precision (P), recall (R), and F value, which are commonly used in entity word segmentation, were used as evaluation indexes to evaluate the word segmentation effect of regional energy data. Precision refers to the proportion of positive samples predicted by the model to positive samples in practice. The accuracy allows the classifier not to label negative sample errors as positive samples. Precision (P) is calculated in the following formula:

$$\text{precision} = \frac{TP}{TP + FP}, \tag{6}$$

where TP represents the number of entities in the test sample whose predicted category is positive and whose real category is positive. FP represents the number of entities whose prediction category is positive and real category is negative.

Recall rate refers to the proportion of positive samples that are predicted to be positive to positive samples that are actually positive. Recall rate can represent the ability of the

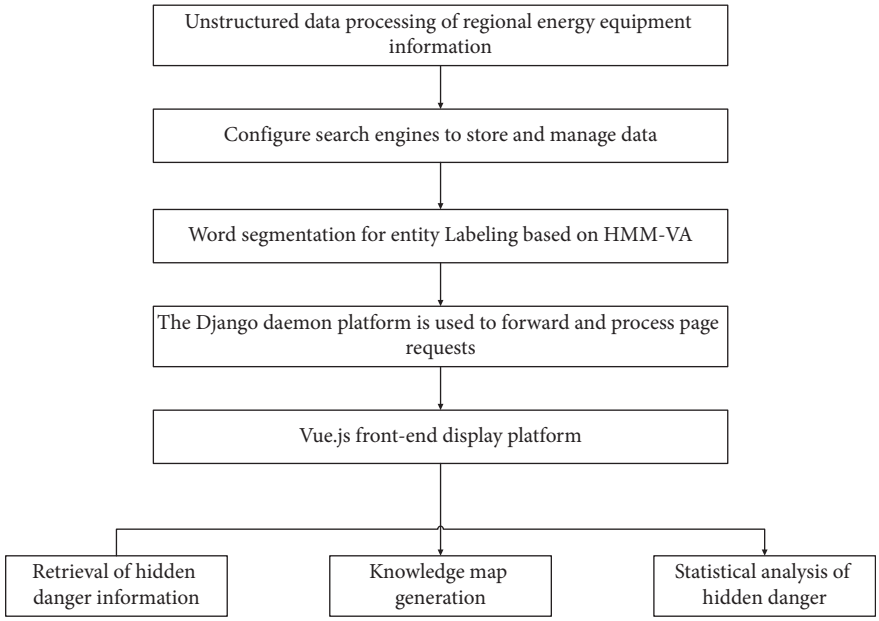

Figure 2: The process of regional energy visualization system based on knowledge graph search engine.

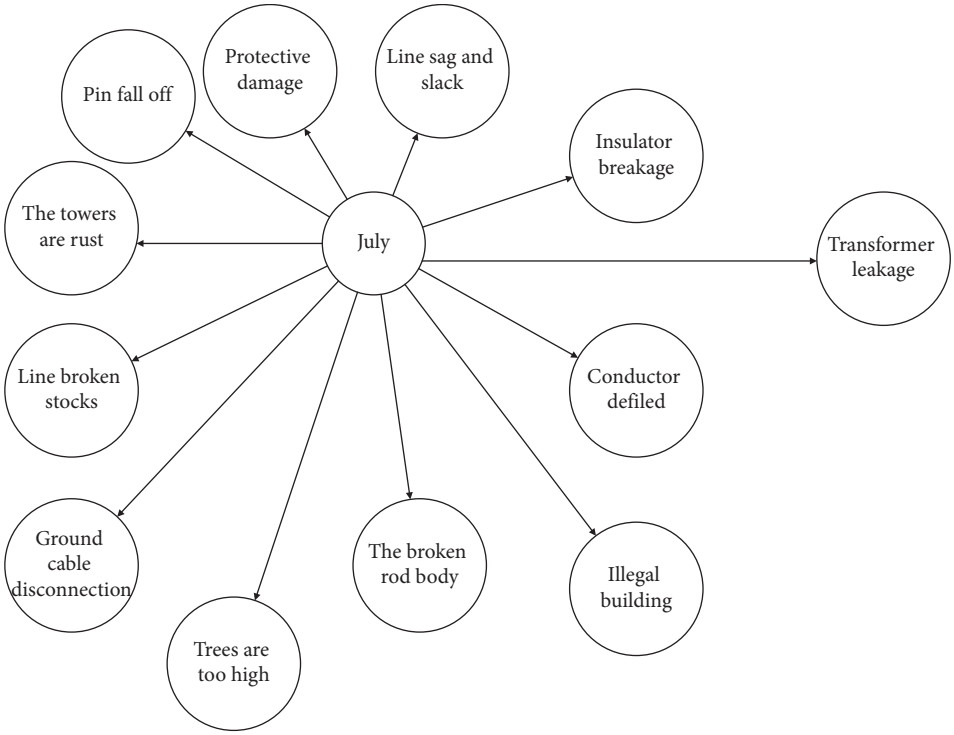

Figure 3: Knowledge Atlas of transformer Hidden dangers.

classifier to find all positive samples. The calculation of recall (R) is shown in the following formula:

$$\text{recall} = \frac{TP}{TP + FN}, \tag{7}$$

where FN is the number of entities whose prediction category is negative and real category is positive.

The harmonic mean of accuracy and recall is the F score. The specific calculation of F value is shown in the following formula:

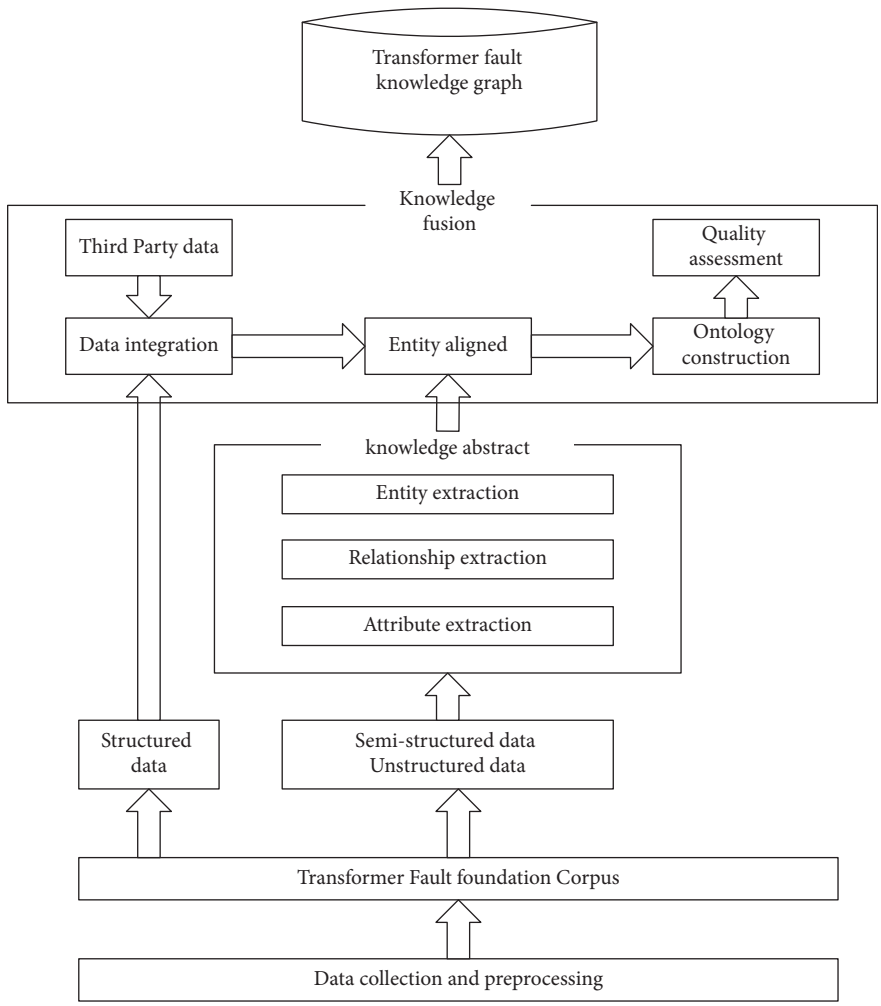

Figure 4: Knowledge graph construction process.

$$F = \frac{2 * \text{precision} * \text{recall}}{\text{precision} + \text{recall}}. \quad (8)$$

The comparison of different named entity word segmentation models is considered to verify the word segmentation effect of the proposed model. Models involved in the experiment include BM matching model [22], N-Gram word segmentation model [23], Jieba model [24], and HMM-VA model proposed in this paper. The above models were all carried out on the same training set and test set. Table 1 shows the comparison results of the test set in different named entity recognition models.

As can be seen from the experimental results in Table 1, the average performance of the HMM-VA regional energy data segmentation model proposed in this paper is 85.93%. Higher than Jieba model 5.81%, N-gram model 10.8%, and BM model 15.42%, respectively, and better than the other three entity word segmentation models in terms of accuracy, recall rate, and F value.

5.2. Information Retrieval Performance Comparison of Search Engines. The index performance of the system is measured by testing the index speed of standalone index [25], which is a standalone search engine using the default configuration of elastic search, and distributed index, which is a 12-node distributed search engine designed and configured for the system. The test results for index performance are shown in Table 2.

As shown in Table 2, the elastic distributed search engine designed and configured in this paper is obviously superior to the standalone search engine in index efficiency indexes, such as average data rate, central processing unit (CPU) occupancy, memory occupancy (mem), and read/write rate (Io) and load rate, indicating that the proposed method can effectively improve the real-time performance of regional energy data index. It also meets the requirements of quick disposal efficiency in the investigation of hidden dangers in actual substations.

As shown in Table 3, for the search of the four test keywords, the average response time of the single machine is 1295.05 ms, and the average response time of the search proposed in this paper is 110.75 ms, indicating that the response time of the engine is significantly lower than that of the original single machine, which fully proves the advantages of the search engine in this paper. In addition, with the increasing of data volume, the processing advantage of the search engine for regional energy data is very significant.

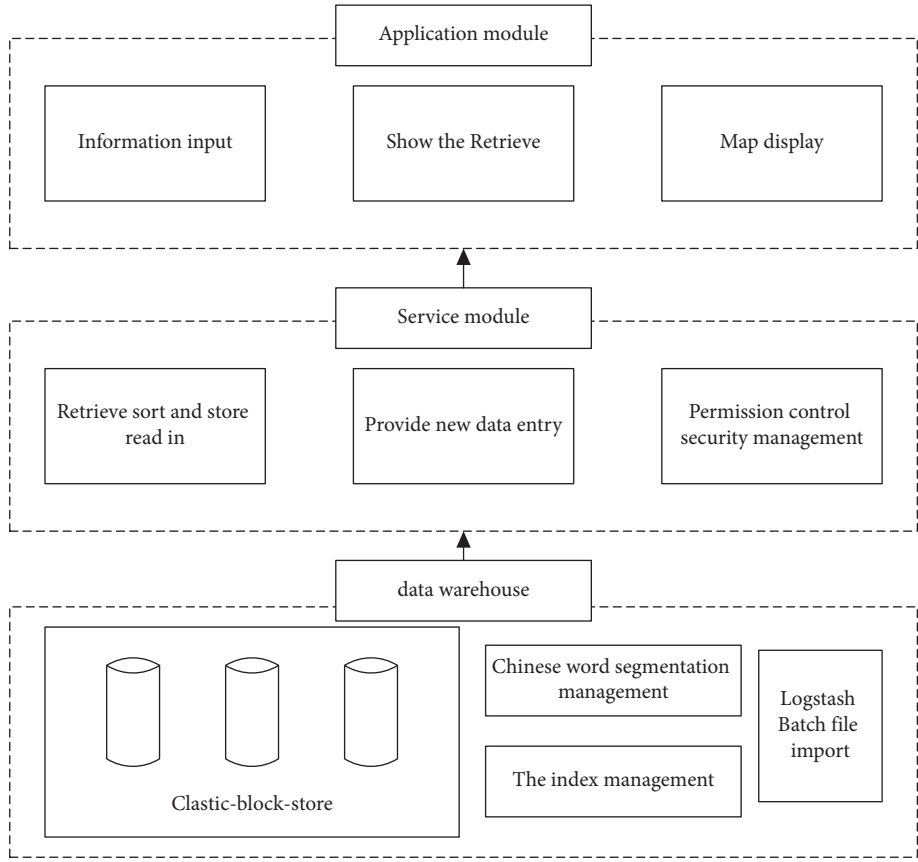

Figure 5: The architectural design of regional energy knowledge atlas search engine.

Table 1: Effect comparison of named entity recognition model.

Model	Precision (P) (%)	Recall (R) (%)	F score (F) (%)
BM matching	70.01	69.84	71.68
N-Gram word segmentation	76.77	74.27	74.35
Jieba model	81.52	80.31	78.54
HMM-VA	86.73	85.69	85.44

Table 2: Index test results.

	The average rate (thousand /SEC)	CPU (%)	Mem (%)	Io (%)	Load (%)
Single engine	6	57	63.6	90	43.1
The engine	39	14	16.5	41	18.7

Table 3: Search time test results.

Test key	Standalone search engine time (ms)	The system search response time (ms)
Substation	876	97
Rainy day	1438	161
Transformer	1389	84
Protection regulations	1479	101

6. Conclusion

This paper introduced technical knowledge map and flexible distributed search engine technology, this paper proposes a dynamic analysis method of regional energy data, through the research of regional energy data, distributed storage security hidden danger, to build knowledge map and analysis, has realized the knowledge map visualization display of search engine, and the safe hidden trouble efficiently retrieve and correlation analysis. It has good practical application value and promotion value. In the following research, more corpus features will be extracted in the relational extraction step to improve the accuracy of knowledge graph construction, so as to improve the analysis effect of regional energy data.

Data Availability

The dataset can be accessed upon request.

Conflicts of Interest

The author declares that there are no conflicts of interest.

References

[1] J. Lv, S. Zhang, H. Cheng et al., "A review of regional integrated energy system planning considering interconnection and interaction," *Proceedings of the csee*, vol. 41, no. 12, pp. 4001–4021, 2021.

[2] X. Zhang, W. Jing, and P. Wang, "Study on fault prediction method of high speed automata based on wavelet neural network," *Foreign electronic measurement technique*, vol. 39, no. 8, pp. 11–16, 2020.

[3] J. Cao, L. Chen, J. Qiu, and H. Wang, "Power grid defect text mining technology and its application based on semantic framework," *Power grid technology*, vol. 41, no. 02, pp. 637–643, 2017.

[4] G. Peng, Z. Zhou, and S. Tang, "Transformer fault prediction based on time series analysis and variable correction," *Electronic measurement technology*, vol. 41, no. 12, pp. 96–99, 2018.

[5] Y. Huang and X. Zhou, "Knowledge model for electric power big data based on ontology and semantic web," *CSEE Journal of Power and Energy Systems*, vol. 1, no. 1, pp. 19–27, 2015.

[6] Z. Wu, K. Bai, and L. Yang, "A review of text Mining for Electronic medical records," *Journal of Computer Research and Development*, vol. 58, no. 03, pp. 513–527, 2021.

[7] H. Tang, H. Huang, and Y. Tang, "Design of temperature and current measuring device for intelligent equipment," *Electric drive*, vol. 49, no. 05, pp. 93–96, 2019.

[8] Y. Wang, C. Peng, and Z. Wang, "Application of knowledge graph in power grid all-service unified data center," *Computer engineering and applications*, vol. 55, no. 15, pp. 104–109, 2019.

[9] J. Miao, J. Wang, and H. Zhang, "Research progress of uav fault diagnosis technology," *Chinese Journal of Scientific Instrument*, vol. 41, no. 09, pp. 56–69, 2020.

[10] Y. Fan, T. Ding, and Y. Sun, "Review and cogitation for worldwide spot market development to promote renewable energy accommodation," *Proceedings of the CSEE*, vol. 41, no. 5, pp. 1729–1752, 2021.

[11] Yi Ding, K. Xie, and Bo Pang, "Research on key issues of a unified national power market with Chinese characteristics (1): enlightenment, comparison and suggestions from foreign markets," *Power System Technology*, vol. 44, no. 7, pp. 2401–2410, 2020.

[12] Y. Song, M. Bao, and Yi Ding, "Summary of the key points of my country's power spot market construction under the new electricity reform and relevant suggestions," *Proceedings of the CSEE*, vol. 40, no. 10, pp. 3172–3187, 2020.

[13] Y. Xiao, X. Wang, and X. Wang, "Summary of research on electricity market facing high proportion of renewable energy," *Proceedings of the CSEE*, vol. 38, no. 3, pp. 663–674, 2018.

[14] C. Yue, C. Chen, Z. Liu, Z. Hu, and X. Wang, "Methodological function of CiteSpace knowledge graph," *Studies in Science of Science*, vol. 33, no. 2, pp. 242–253, 2015.

[15] W. Chen and H. Zhang, "Application of RF-LighTGBM algorithm in fan blade cracking fault prediction," *Electronic measurement technology*, vol. 43, no. 01, pp. 162–168, 2020.

[16] T. Liu, H. Chen, and G. Li, "Knowledge graph representation learning method for joint FOL rules," *Computer Engineering and Applications*, vol. 57, no. 4, pp. 100–107, 201.

[17] Li Mei-xuan, Y. Chun, and X. Jin, "Transformer fault diagnosis model based on combined prediction [J]," *Mathematical modeling and applications*, vol. 9, no. 4, pp. 49–56, 2020.

[18] X. Bian, L. Zhang, and Bo Zhou, "Based on knowledge atlas of the electric power market research both at home and abroad," *Journal of electrotechnics*, pp. 1–13, 2022.

[19] G. Liu, R. Dai, Yi Lu et al., "Power graph computing platform and its application in energy Internet," *Power Grid Technology*, vol. 45, no. 06, pp. 2051–2063, 201.

[20] Y. Ma and Z. Wu, "Modeling and analysis of power big data based on Neo4j," *New technology of electrical engineering and energy*, vol. 35, no. 02, pp. 24–30, 2016.

[21] H. Wang, Q. Zhang, and W. Cai, "Research on domain ontology storage based on Neo4j," *Application Research of Computers*, vol. 34, no. 08, pp. 2404–2407, 2017.

[22] Z. Yi, "Research on improved BM pattern matching algorithm based on network intrusion detection system," *Computer applications and software*, vol. 29, no. 11, pp. 193–195+207, 2012.

[23] F. Lizhou, G. Yang, and Xu Xue, "Based on N - "gramm bidirectional matching [J]," *Journal of Chinese word segmentation method of mathematical statistics and management*, vol. 33, pp. 633–643, 2020.

[24] P. Chen, X. Geng, M. Zou, and D. Tan, "Computer and Modernization," no. 3, pp. 77–81+92, 2020.

[25] D. Li and A. Madden, "Cascade embedding model for knowledge graph inference and retrieval," *Information Processing & Management*, vol. 56, no. 6, Article ID 102093, 2019.

Hindawi
Scientific Programming
Volume 2022, Article ID 8361251, 9 pages
https://doi.org/10.1155/2022/8361251

Research Article

Teaching Design and Practice of English Education under the Network Learning Space

Jing Shi and Junhui Zheng

Xi'an Siyuan University, Shaanxi, Xi'an 710038, China

Correspondence should be addressed to Junhui Zheng; zhengjunhui@xjtu.edu.cn

Received 30 May 2022; Revised 13 June 2022; Accepted 18 June 2022; Published 13 July 2022

Academic Editor: Lianhui Li

With the comprehensive coverage of the Internet in China, the online learning space can basically cover the whole country, but in terms of the use of online learning space in education, it has not been fully used. The basic application mode of the school, namely, autonomous learning, flipped classroom learning, collaborative learning, exchange, and discussion learning, and personalized learning mode, based on flipped classroom learning and relying on network learning space, design the corresponding English teaching process based on network learning space, according to the teaching process, the specific design of the platform, content, organization, implementation, and evaluation. From the research results, the students in the experimental class are more active and active in class than in the control class, their work scores are generally higher than those in the control class, and their interest in English has been significantly improved. The ability has also been significantly improved. After long-term practical research, it has been shown that the performance of the experimental class students in the online learning space has also been significantly improved. Therefore, it can be shown that the English course based on the network learning space has a certain positive influence and promotion effect on the teaching effect.

1. Introduction

With the continuous addition of new educational concepts and technologies, how to use modern information technology to provide services for learning and teaching has become the current focus. The continuous informatization and networking of high-quality resources has gradually increased the use of online teaching resources to assist teaching in junior high school English teaching. Rooted in the characteristics of junior high school English teaching, the use of online learning space in junior high school English teaching helps classroom teaching to show the superiority of modern educational methods. During the "Thirteenth Five-Year Plan" period, efforts will be made to promote the informatization of education, use modern information technology to complete the sharing of high-quality resources, focus on the breadth and depth of the application of online learning space, and gradually complete the concept of having a space for life and unique space for life. By 2022, the system will fully popularize the online learning space, integrate the use of information technology to solve practical puzzles in education and teaching, and complete the teaching application, management, and governance supported by the space, making it the norm. It will continuously promote teachers' use of online learning spaces, workshops, training communities, and other tools, use online resources, integrate offline discussions, complete the creation of "technological innovation classrooms," improve the use of information technology to analyze learning conditions, improve teaching, design, guidance on learning methods, and evaluation of academic performance and other diverse abilities and qualities, resolve difficulties in education and teaching, meet children's individual development needs, and help the school to carry out teaching innovation. From the perspective of teaching application, the deep integration of online learning space and English subject teaching has changed the traditional teaching mode. The use of online learning space in school education and home-school

coeducation helps to train talents' information literacy and promote educational information. To move forward, it is essential to strengthen and improve basic education informatization in junior high school English teaching and optimize its process. Therefore, with the support of online learning space, teachers and students have the opportunity to have a personalized online environment. Applying the online learning space to the real English subject teaching not only shows the idea of combining information technology with the subject but also becomes one of the important guides for applied research in the future [1–8]. This study takes English as the subject background. Through the analysis of the online learning space and the exploration of the online learning platform, it comprehensively considers how to integrate the diversified functions of the online learning space with the English teaching of junior high school and selects the appropriate teaching content. The junior high school English teaching based on the main functions of the online learning space is designed and implemented in the classroom. After that, interviews are conducted with students and teachers, and the results of the application are compared and analyzed according to the students' pre- and posttest scores in the experimental class in order to optimize the application of the online learning space in junior high school English teaching and provide support for its follow-up implementation in H Middle School, so that it can truly exert its advantages, effectively improve the quality of English education and teaching, and further promote the sharing of high-quality resources.

2. Related Works

There are foreign studies on the existence of online learning space to analyze. Regarding the current research situation abroad, in 2005, the design scheme of learning space and its technical configuration mentioned by American scholar Brown is very representative. Brown agrees that, compared with traditional learners, new learners pay more attention to interactivity and participation in experience. He encourages the design of corresponding learning modes and learning spaces based on the characteristics of learners themselves, and the design of the learning space and the configuration of technology should be considered according to the characteristics of new learners. After summarizing the relevant research on new learners, Brown proposed that they have characteristics such as "group activity tendency, goal and achievement orientation, multitask orientation, and high dependence on the network." Taking these characteristics as a reference, they provide a variety of corresponding learning. In 2010NETP (National Educational Technology Program), the United States mentioned the learning model assisted by technology support and the learners who use it. Having the construction paradigm existing in the personalized online learning space, which provides the information management, communication, and knowledge construction tools that learners need and integrates every learning participant into the space to form an online learning community, the University of Minnesota created an active classroom for the first time; in 2008, the British Joint Information Systems Committee issued the "21st Century Learning Space Design Guidelines" and said: "In order to meet the needs of two different teaching methods, teacher-centered and student-centered, building a technology-rich learning environment is an important research trend in learning space, and learning space must also be the focus of future research." In 2008, this framework focuses on how the virtual learning space supported by information technology plays a special role in teaching method reform and improving teaching efficiency. The first idea was proposed by the Norwegian University of Science and Technology; based on the problem-based learning model, Cindy divides the learning space into two types: problem space and related concept space. However, the above literature on learning spaces focuses on physical space design. The research on online learning space in foreign countries is gradually growing on the online learning platform, and the foreign online learning platform has become a universal and mature learning resource; especially in the United States, most schools have installed official learning websites, these websites can cover the whole school, and students and teachers within the school can learn through the network platform anytime, anywhere. [9–17].

3. Related Theories and Technical Methods

3.1. Vue.js Framework. Vue.js technology framework is a very convenient and powerful framework for front-end web design and development, and its essence is the JavaScript MVVM library. Vue.js is a lightweight front-end framework, Vue. The performance of js is very high, with fast data rendering speed. In addition, Vue.js technical framework provides many simple instructions and APIs for users to learn the front-end framework and can also efficiently build a relatively complete front-end page. Vue uses a simpler template for data rendering, which is closer to the native code mode. The development mode is also relatively simple and convenient, and it also provides tools for rapid development of projects, which is conducive to the analysis and analysis of later development personnel. Code maintenance and updates: the ViewModel of Vue is responsible for the two-way data binding and data monitoring of the database and the real DOM. The real DOM monitors the data at the ViewModel layer and transmits it to the database, and the data of the database monitors the monitored data in the view. The model layer performs two-way binding of data, passes it to the virtual DOM, and then obtains the real DOM to form a closed loop of DOM rendering [18]. The rendering process is shown in Figure 1.

In addition, the two-way data binding of Vue.js also plays an important role in the development of our project platform. Generally speaking, the data binding process of Vue.js is that the user enters data in the view interface. The view layer can bind data to both the view model layer and the model layer. After binding, the data is paired at the model layer. Data is bound to each other. This feature of Vue.js makes it easier for developers to run and maintain the system later, making the management of data state changes very simple and convenient [19]. The two-way data binding process is shown in Figure 2.

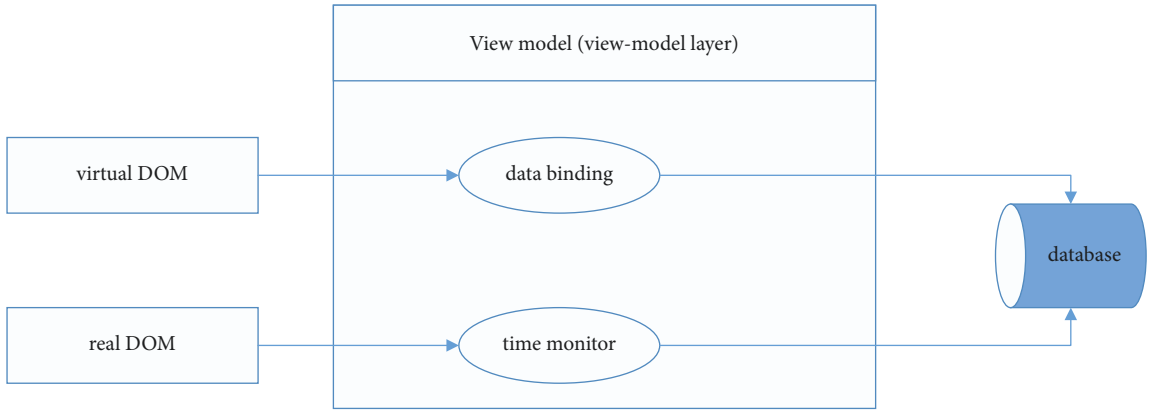

Figure 1: Rendering process.

The most prominent feature of Vue.js is that it has easy-to-manipulate components, and it is also the most used feature of the Vue.js framework. It can not only extend HTML but also encapsulate and reuse code to improve software development efficiency. Vue.js components come in four flavors, including global components, local components, nested components, and single components. Generally speaking, we most often use the form of global components. All global components in Vue can be used in all js instances, and the life cycle of use is relatively long. You can reuse the developed source code, develop new projects, expand the use of code, save development time, improve development efficiency, and save development costs.

3.2. Markdown Language. Markdown is a lightweight markup language that can easily and quickly write documents in various formats. Markdown is now a markup language commonly used by many international editors and writers. Compared with the HTML markup language, its language syntax is very simple, easy to learn, and the easiest to use. Editing various documents with markdown notation allows for very elegant and immersive recording. It pays more attention to the content, not the typography, because the editor or the platform can render the final typography of the article through markdown markup. The resulting effect is very simple and clear. On the other hand, the cost of learning markdown is not very high. As long as you understand this grammar rule, you can achieve the effect once and for all. It can also be used to write documents, which are saved in the software directory, and the file name is "README.md." In the English core literacy platform, we need to take notes or mark the chapters we read during the reading process. During the reading process, if you have any questions that you do not understand, you can leave a message to the teacher or ask questions on the forum. This process is inseparable from the language markdown. Markdown was originally primarily used for web writing. Later, after a series of development of the Internet, now markdown has been applied to more fields, and many extended grammars have also been generated. These grammars are based on the basic grammar. Functions such as tables, character lists, and fence codes are added. Another notable feature of markdown is that it has good compatibility. You can quickly open multiple editors, allowing you to write in one place and use it in many places. It works in any scenario where you can write. This is the solution for writing. This problem has been solved perfectly [20]. Markdown workflow is shown in Figure 3.

3.3. SQL Database. Structured Query Language, referred to as SQL, is a language in the database world. It uses query statements to query and modify data in the database. SQL is a relational database system in database classification and has all the features of relational databases. Databases can store large amounts of data, which are processed by computers to efficiently access collections of data. Structured Query Language can nest query data. Relational databases are managed by a database management system. Two-dimensional tables called database tables are used to manage data in relational databases. A database table consists of a column of data items and a row of data and is read and written in units of records. The most common system structure of relational database management system (RDBMS) is client/server type (C/S type), as shown in Figure 4 [21].

In the structure diagram of the relational database, the server is used to process requests from other programs. The client uses the SQL query statement of the program in the database to send a request to the server. The server receives the query statement and reads the data program to the database. The database performs logical judgment processing on the data request and responds to the requested program. The server responds to the received processed data to the client, and the user can get the processed data. It can also be sent to the relational database management system through SQL statements to change and obtain data.

4. Teaching Design of English Courses Based on Network Learning Space

4.1. Teaching Application Mode in Online Learning Space. For teaching based on the network learning space, this study proposes five basic modes suitable for teaching, namely, autonomous learning mode, collaborative learning mode,

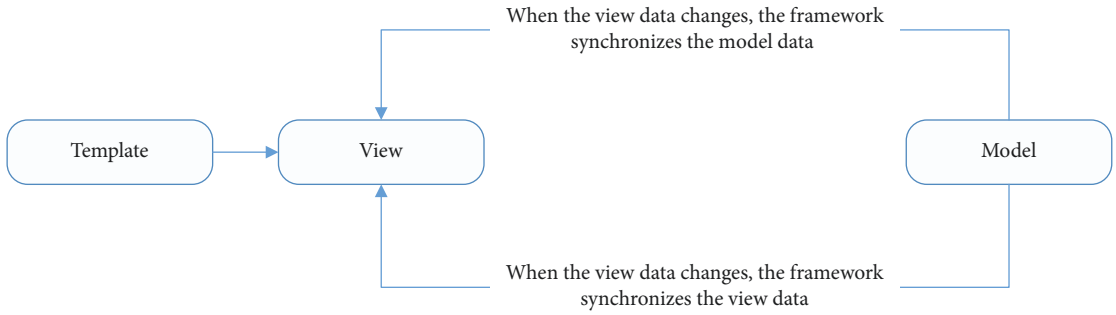

Figure 2: Two-way data binding.

Figure 3: Markdown workflow.

flipped classroom, communication and discussion mode, and personalized learning mode. One of the characteristics of the online learning space is that the students' autonomous learning ability can be developed. Therefore, the autonomous learning mode under the online learning space is one of the basic modes of the online learning space. The specific process is shown in Figure 5.

Students obtain tasks through the online learning space, then determine the learning goals, then conduct independent learning, and answer questions through self-learning methods such as searching for materials, viewing resources, and online communication learning and finally through self-examination to find insufficient and continue to learn mistakes. Collaborative learning mode under the network learning space collaborative learning is also one of the characteristics of the network learning space, so the collaborative learning mode under the network learning space is of great significance. The specific process is shown in Figure 6.

Collaborative learning is also one of the teaching methods commonly used by teachers. Collaborative learning in the online learning space has injected new vitality into teachers' classrooms, enabling collaborative groups to clarify learning goals and conduct targeted learning. The teaching process mainly takes place in the classroom. The teacher explains in the classroom, and the students practice after the class. The flipped classroom is the opposite. Students obtain teaching resources for learning before class, ask and solve problems in the classroom, and conduct summary evaluation and reflection after class. It can be seen that the flipped classroom mainly includes preclass learning and classroom inquiry. The flipped classroom learning mode in the online learning space is shown in Figure 7.

Communication and discussion mode in the online learning space mostly refers to the communication and discussion between students and students, and it is an important mode of informal learning to answer questions and solve doubts through discussions between classmates. The details are shown in Figure 8.

The communication and discussion mode in the online learning space breaks the traditional boundaries of time and space. Students' communication and discussion do not only happen in the classroom. A good online learning space creates an environment for students to communicate and discuss.

4.2. Teaching Process Based on Teaching Mode. According to the learning mode in the network learning space proposed above, this research constructs a teaching process based on the teaching mode, as shown in Figure 10.

From Figure 9, the teaching process based on the network learning space is mainly divided into three parts: before class, during class, and after class. Based on the flipped classroom, self-learning is carried out before class, and relevant knowledge is previewed; knowledge and skills are consolidated and strengthened through exchanges and discussions after class.

4.3. Teaching Design Based on Network Learning Space

4.3.1. Platform Selection Design. Teaching based on the network learning space requires the support of a specific teaching platform, and the teaching platform needs to include student space and teacher space. According to the research on each platform, this research chooses the "cloud class" education platform for teaching process practice. Cloud class has all the characteristics of online learning space, can share resources and communicate, can realize independent learning and collaborative learning, can track and give feedback on students' learning situation in time, and so on. It is a good online learning space.

4.3.2. Content Design. When choosing the teaching content of the online learning space, it is also necessary to consider the characteristics of its content:

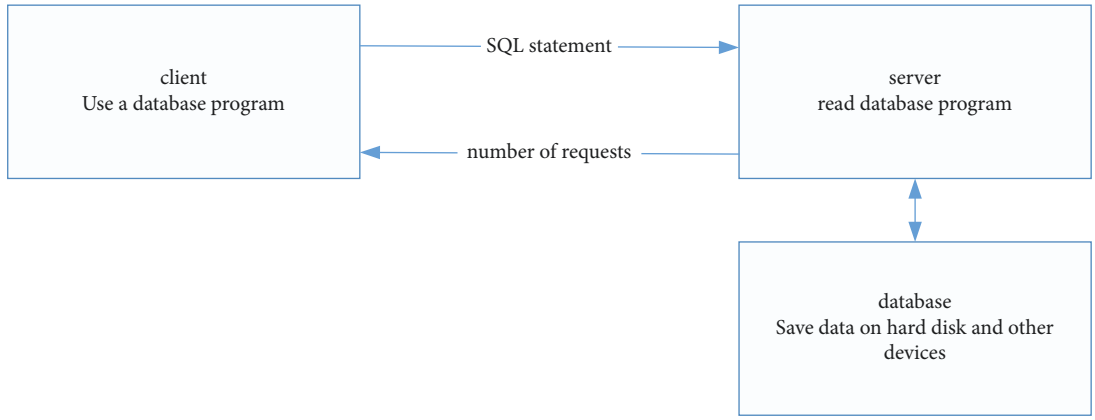

Figure 4: System structure of relational database.

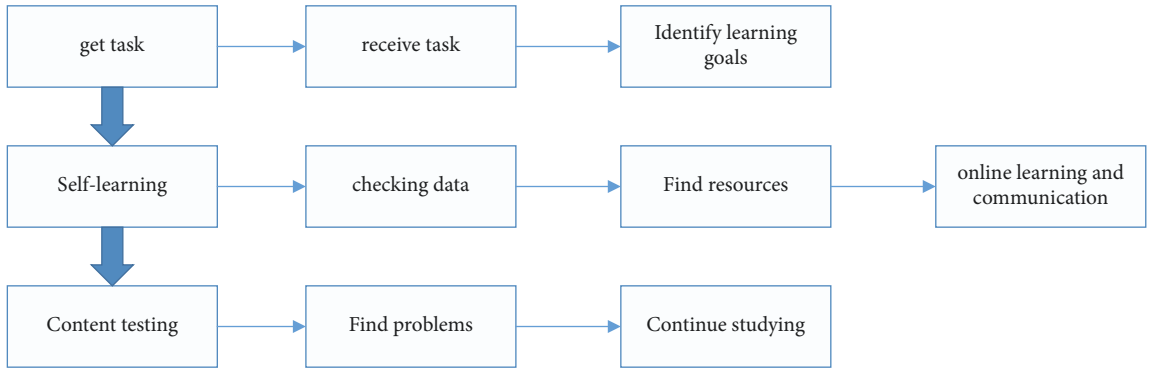

Figure 5: Self-directed learning mode in online learning space.

(1) *Challenging*. Generally, it refers to the degree of difficulty of learning content in the learning process. For students, the content of learning can neither be too easy nor too difficult. Students have basically mastered the simple content, and it is difficult to have the desire to communicate and discuss the content; too difficult learning content exceeds the students' own learning cognition and ability, which will also affect the effect of students' communication and cooperation.

(2) *Openness*. It generally means that there is no fixed answer to the content of learning, and the answer can be varied. In the process of students' learning, students get the best answer through mutual exchange and discussion and finally report according to the discussion process. Such learning content can further stimulate the enthusiasm of students to learn and communicate, obtain more different answers, and improve the learning effect.

(3) *Exploratory*. It generally means that students can learn knowledge independently in the process of inquiry and can use it to deal with practical problems at the same time. This type of learning content focuses on mobilizing students' autonomous learning, encouraging students to express their ideas bravely, and forming consensus answers among group members in group communication and discussion.

4.3.3. Implementation Design. The implementation design is a very important stage. It is mainly for teachers and students to cooperate with each other to carry out learning. In the implementation design stage, the first step, the teacher can introduce the problems of this class through some media, such as stories, audio, or video materials, to set up relevant scenarios so that students can understand the learning goals of this class through the platform. At the same time, you can also ask some questions so that students have some thinking before the class.

5. Application and Analysis of English Course Teaching Based on Network Learning Space

5.1. Design of the Experimental Study. For the purpose of the experiment, this research puts forward the following hypotheses. Hypothesis 1: using the English course teaching based on the network learning space, compared with the traditional teaching method, students can better grasp the relevant course knowledge, which is conducive to improving students' learning effect and level of learning. Verification method: after the experiment is over, professional information technology teachers are invited to

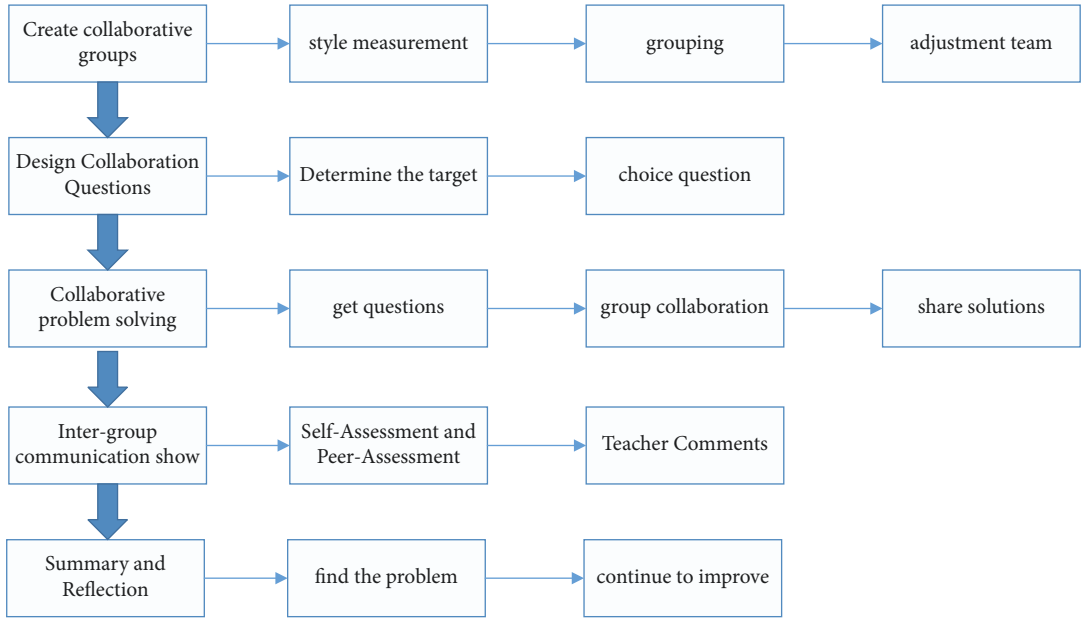

Figure 6: Collaborative learning mode in the online learning space.

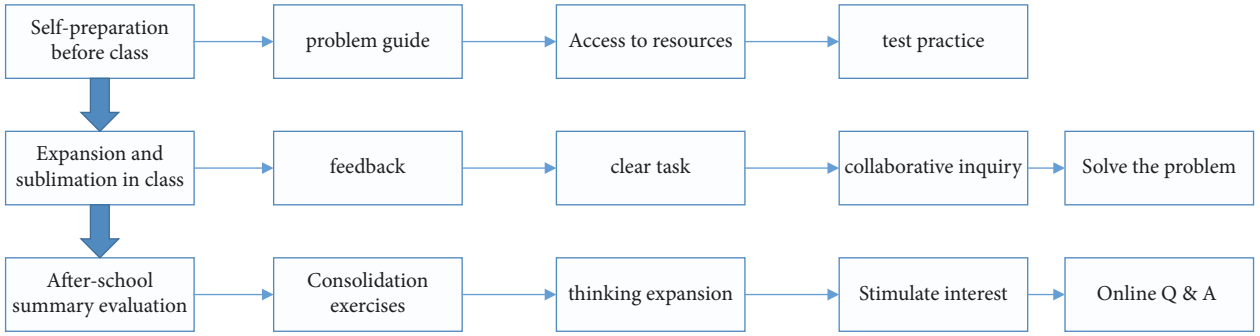

Figure 7: The flipped classroom learning mode in the online learning space.

make a score based on the classroom performance and the comparison of the works of the experimental class and the control class. Hypothesis 1 holds if the quality of the experimental class is better than that of the control class. Hypothesis 2: applying the teaching of English courses based on network learning space, students' collaborative learning ability and autonomous learning ability are improved. Verification method: after the experiment, verification is carried out through interviews and measurement methods. The students in the two classes were measured with the independent learning ability measurement table and the collaborative learning ability measurement table, and the independent sample t-test was carried out on the experimental data. If the measured data of the experimental class and the control class are significantly different and the scores of the experimental class are higher than those of the control class, then hypothesis 2 is established.

5.2. Experimental Procedure. During the experiment, students in the experimental class and the control class were observed in class. The experimental class adopted the English course teaching method based on the network learning space, and the control class adopted the traditional information technology classroom teaching mode. Through classroom observation, it is found that the students in the experimental class are more active in the classroom, have a higher degree of participation in the questions raised by teachers, and have more active discussions among group members and between groups. They can ask their own questions and take the initiative. If you ask your classmates and teachers for advice, the classroom has a good learning atmosphere, which is conducive to the cultivation and development of students' interests. Compared with the experimental class, the students in the control class were not active enough in class. Most of the students lacked interest in classroom activities. Only a few students could raise their hands to answer the teacher's questions. Practice time for things is not related to classroom learning. Moreover, the students in the control class were rarely able to ask questions to the teachers and classmates and solve the problems. There was less discussion time between the students and the teachers and students, and they basically practiced alone. Therefore, in terms of classroom activity and students'

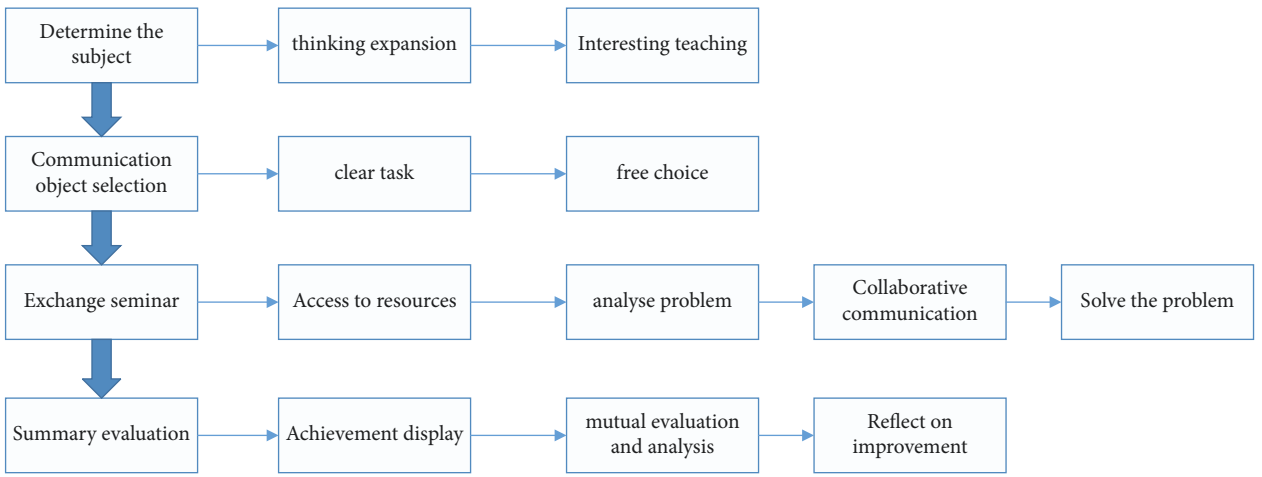

Figure 8: Communication and discussion mode in online learning space.

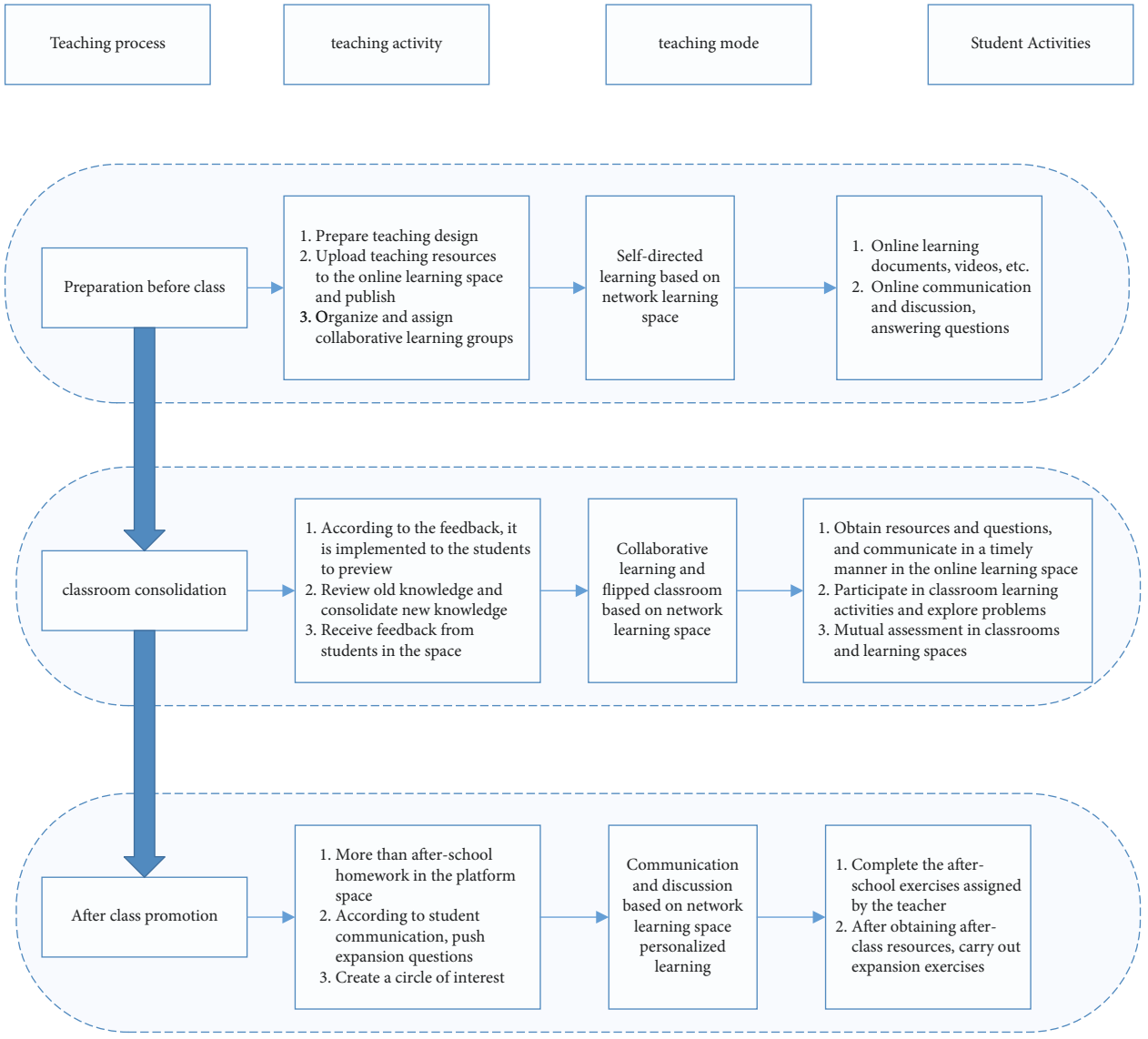

Figure 9: Teaching process based on Online learning space.

Table 1: Collaborative attitude group statistics.

	Grouping	N	J-means	Standard deviation
Total score	Test group	4 0	34.45	1.920
	Control group	4 0	33.12	1.343

Table 2: Independent sample t-test results for collaborative attitude.

Grouping	N	J-means	Standard deviation	Salience	Sig. (bilateral)
Test group	4 0	34.45	1.325	0.014	0.001
Control group	4 0	33.12			0.001

Table 3: Applications of online learning spaces.

Question	Very much in line (%)	Meet (%)	Basically meet (%)	Incompatible (%)	Very inconsistent (%)
1. You are using the online learning space because of a teacher's request	40	17.5	22.5	12.5	7.5
2. You are using the online learning space for your learning needs	10	15	25	35	1 5
3. Do you think the online learning space has made the course more interesting	75	15	7.5	2.5	0
4. Do you think the course resources in the online learning space are helpful for the learning of information technology courses	75	17.5	7.5	0	0
5. Your willingness to continue using the online learning space in the future	55	25	7.5	7.5	0

enthusiasm, the students in the experimental class performed better than those in the control class.

5.2.1. Analysis of Teaching Effect. This section mainly starts from the analysis of the results of the comparative experiment, compares the classroom performance, works, and achievements of the control class and the experimental class, and analyzes the teaching effect of English course teaching and traditional teaching based on the network learning space. Finally, the collaborative ability results are obtained.

After analyzing the experiment of this research, the collaborative learning ability of the two classes was measured again to find out whether there was a difference in the level of collaborative learning ability between the two classes after the experiment [1]. Analysis of the independent sample t-test results of "collaborative attitude" is shown in Tables 1 and 2.

From Table 1, it can be seen that the average value of the experimental class is 34.45, and the average value of the control class is 33.12. It can be seen that the average value of the experimental class is 1.325 higher than that of the control class. It can be seen from Table 2 that $p = 0.001$ and $p < 0.05$, indicating that the two classes cooperated after the experiment. Attitudes differ markedly. From the data level, it can be considered that the teaching process of this experimental study can improve the collaborative attitude of students.

5.2.2. Analysis of Learning Situation in Network Learning Space. The students' learning effect in the experimental class is investigated to understand the students' evaluation of the learning effect and the degree of satisfaction with the online learning space after the experiment. In order to understand the learning situation of students in the online learning space, this research made a scale based on excellent master's and doctoral dissertations. After filling in the data, the students imported the data into SPSS software and obtained an Alpha coefficient of $0.857 > 0.8$, with good reliability. The questionnaire divides the survey of the learning situation of the online learning space into two parts, namely, the survey and analysis of the application attitude and the application effect. (1) Results and analysis of application attitude for students' attitude towards the application of online learning space: this study set five questions, designed from the attitude and importance of online learning space, and the questionnaire design adopted a five-point Likert scale form from the data level to analyze the students' application attitude. The specific structure is shown in Table 3. According to the data obtained in Table 3, most of the students (80%) use the online learning space because of the teacher's request in the early stage of learning. This is in line with the current education situation in China. Students' cognition of learning comes from multiple sources. Due to the guidance of teachers and the fact that students in junior high school do not have the ability to find online learning spaces by themselves, teachers need to guide in the early stage of teaching; after the teaching practice based on online learning spaces, 90% of students believe that online learning spaces become more interesting, and interesting classes help attract students' attention; more than 90% of students believe that this way of teaching is helpful for course learning and can

improve classroom efficiency; 80% of classmates said that, in the future days, they will continue to use the online learning space. After teaching practice, students have a preliminary understanding of the online learning space, most students believe that the online learning space has a positive impact on their own learning, and most of the students have also recognized the importance of the online learning space and expressed that the online learning space will continue to be used in subsequent studies. (2) Application effect results and analysis: for the application effect of students on the online learning space, this study set five questions to analyze the learning effect of students in the online learning space. The specific investigation results are shown in Table 3.

6. Conclusion

Through the experimental data obtained from the experimental research of English course teaching based on the network learning space, the data is analyzed, processed, and summarized, and the following conclusions are initially obtained in this research. The teaching of English courses based on the network learning space can improve students' interest in learning to a certain extent and stimulate their passion for learning English courses, which can be reflected from the students' performance. The teaching based on the network learning space has the interest that the traditional classroom does not have. After the teaching method is changed, the autonomy of the students is improved, and the open network learning space provides a stage for the personalized development of the students. Through the classroom performance of the experimental class and the control class, the students in the experimental class are active in class and raise their hands positively, and the final performance evaluation is also better than that of the control class.

Data Availability

The dataset can be accessed upon request.

Conflicts of Interest

The authors declare that they have no conflicts of interest.

References

[1] G. D. Kuh, "What we're learning about student engagement from NSSE: benchmarks for effective educational practices," *Change: The Magazine of Higher Learning*, vol. 35, no. 2, pp. 24–32, 2003.

[2] K. S. Floyd, S. J. Harrington, and J. Santiago, "The effect of engagement and perceived course value on deep and surface learning strategies," *Informing Science: The International Journal of an Emerging Transdiscipline*, vol. 12, pp. 181–190, 2009.

[3] F. Marton and R. Säljö, "On qualitative differences in learning: I-outcome and process," *British Journal of Educational Psychology*, vol. 46, no. 1, pp. 4–11, 1976.

[4] J. Biggs, D. Kember, and D. Y. P. Leung, "The revised two-factor study process questionnaire: r-SPQ-2F," *British Journal of Educational Psychology*, vol. 71, no. 1, pp. 133–149, 2001.

[5] J. H. Flavell, "Metacognition and cognitive monitoring: a new area of cognitive developmental inquiry [J]," *American Psychologist*, vol. 34, no. 10, pp. 906–911, 1979.

[6] G. Geitz, D. J. T Brinke, and P. A. Kirschner, "Goal orientation, deep learning, and sustainable feedback in higher business education," *Journal of Teaching in International Business*, vol. 26, no. 4, pp. 273–292, 2015.

[7] D. Samuels-Peretz, L. Dvorkin Camiel, K. Teeley, and G. Banerjee, "Digitally inspired thinking: can social media lead to deep learning in higher education?" *College Teaching*, vol. 65, no. 1, pp. 32–39, 2017.

[8] M. A. Peters, "Deep learning, education and the final stage of automation," *Educational Philosophy and Theory*, vol. 20, no. 6-7, pp. 549–553, 2018.

[9] Y. Engeström, *From Teams to Knots: Activity-Theoretical Studies of Collaboration and Learning at Work*, Cambridge University Press, New York, USA, 2008.

[10] Y. Engeström, *Learning by Expanding: An Activity-Theoretical Approach to Developmental Research*, Cambridge University Press, New York, USA, 2015.

[11] Y. Engeström, "New forms of learning in co-configuration work," *Journal of Workplace Learning*, vol. 16, no. 1/2, pp. 11–21, 2004.

[12] Y. Engeström, *Studies in Expansive Learning: Learning what Is Not YetThere*, Cambridge University Press, New York, USA, 2016.

[13] Y. Engeström, A. Kajamaa, P. Lahtinen, and A. Sannino, "Toward a grammar of collaboration," *Mind, Culture and Activity*, vol. 22, no. 2, pp. 92–111, 2015.

[14] Y. Engeström, R. Miettinen, and R. Punamäki, *Perspectives on Activity Theory*, Cambridge University Press, New York, USA, 1999.

[15] Y. Engeström, J. Rantavuori, and H. Kerosuo, "Expansive learning in a library: actions, cycles and deviations from instructional intentions," *Vocations and Learning*, vol. 6, no. 1, pp. 81–106, 2013.

[16] Y. Engeström and A. Sannino, "Discursive manifestations of contradictions in organizational change efforts," *Journal of Organizational Change Management*, vol. 24, no. 3, pp. 368–387, 2011.

[17] Y. Engeström and A. Sannino, "Expansive learning on the move: insights from ongoing research/El aprendizaje expansivo en movimiento: aportaciones de la investigación en curso," *Infancia Y Aprendizaje*, vol. 39, no. 3, pp. 401–435, 2016.

[18] Y. Engeström and A. Sannino, "Studies of expansive learning: foundations, findings and future challenges," *Educational Research Review*, vol. 5, no. 1, pp. 1–24, 2010.

[19] A. Haapasaari, Y. Engeström, and H. Kerosuo, "The emergence of learners' transformative agency in a Change Laboratory intervention," *Journal of Education and Work*, vol. 29, no. 2, pp. 232–262, 2016.

[20] J. Hughes, N. Jewson, and L. Unwin, *Communities of Practice: CriticalPerspectives*, Routledge, London, United Kingdom, 2007.

[21] D. H. Jonassen and L. Rohrer-Murphy, "Activity theory as a framework for designing constructivist learning environments," *Educational Technology Research & Development*, vol. 47, no. 1, pp. 61–79, 1999.

Hindawi
Scientific Programming
Volume 2022, Article ID 4442374, 8 pages
https://doi.org/10.1155/2022/4442374

Research Article

Research on Software Vulnerability Detection Method Based on Improved CNN Model

Gao Qiang

Shandong Management University, School of Labor Relations, Jinan, Shandong 250357, China

Correspondence should be addressed to Gao Qiang; 14438120210041@sdmu.edu.cn

Received 16 April 2022; Revised 26 April 2022; Accepted 8 May 2022; Published 12 July 2022

Academic Editor: Jie Liu

A software construction detection algorithm based on improved CNN model is proposed. Firstly, extract the vulnerability characteristics of the software, extract the characteristics from the static code by using the program slicing technology, establish the vulnerability library, standardize the vulnerability language, and vectorize it as the input data. Gru model is used to optimize CNN neural network. The organic combination of the two can quickly process the feature data and retain the calling relationship between the codes. Compared with single CNN and RNN model, it has stronger vulnerability detection ability and higher detection accuracy. In contrast, the software algorithm of the improved CNN model has strong vulnerability detection ability and higher detection accuracy. In terms of training loss rate, the DNN + Gru model is 17.2% lower than the single RNN model, 10.5% lower than the single CNN model, and 7% lower than the VulDeePecker model.

1. Introduction

Software systems are widely used in various production and life fields. The primary issue to be considered in the development process is security. Software vulnerabilities will not only cause unnecessary consumption of resources, but also seriously damage the economic property of the application industry. Traditional vulnerability analysis is divided into three methods: static analysis, dynamic analysis, and combined dynamic and static analysis [1]. Xia [2] compared the static analysis method with other program analysis methods and found that the static analysis method has a higher degree of automation and faster speed in detecting software vulnerabilities, but the static analysis method generally has the problem of high false positive rate. Lu [3] proposes a vulnerability detection technology based on dynamic taint analysis, which realizes the taint propagation process based on control flow and data flow, but frequent taint mark detection takes up a lot of memory and reduces system performance. Pan and Zhou [4] propose a method of combining static code analysis of pollution propagation model and dynamic detection of purification units to discover vulnerabilities in web applications, but this method is only used for cross-site scripting attacks and is used to detect other vulnerabilities, such as poor ability. Perl et al. [5] proposed a tool VccFinder that uses SVM classifier to mark suspicious codes. Although this tool reduces the false positive rate, it needs to reextract features and perform model training every time when detecting codes in different languages. Li et al. [6] developed the VulPecker tool, which has a very low false positive rate when detecting vulnerabilities in code clones, but is not suitable for dealing with other types of vulnerabilities.

With the continuous development of the deep learning discipline, the use of machine learning to achieve software vulnerability detection has gradually emerged. A deep learning-based Android malicious application detection is proposed, and a recurrent neural network is used to detect Smali static code, but this method is only aimed at malicious application attack problems and cannot find vulnerabilities in the code itself [7]. Li et al. [8] proposed an improved long short-term memory network (LSTM) model, which is

applied to the vulnerability detection problem of open source code, but this model is only for C/C++ source code problems and can only handle API and library function calls question.

On the basis of the above method, this paper proposes a software vulnerability detection method of deformable convolutional neural network, relying on the activation function and residual unit to improve the stability of the training gradient, because the convolution kernel can be shared in the convolutional neural network, and the network depth determines the length of the back propagation path, so it can greatly reduce the algorithm's time when detecting software vulnerabilities memory consumption.

2. Software Code Feature Extraction

Feature extraction of software code is the key to vulnerability detection. Firstly, program slicing is performed with key points in the vulnerability library as entry points, and code fragments containing vulnerability features are extracted from open source code, and these code fragments are called "code unit sets" [7]. Secondly, the set of code units containing vulnerabilities is vectorized, and the features are represented in a vector form that can be processed by the deep learning model. The feature processing flow of open source code is shown in Figure 1.

2.1. Establish a Vulnerability Library. In order to ensure that the slicing tool can accurately locate the code part containing the vulnerability features, a vulnerability library needs to be designed, and the key points of program slicing are defined in the vulnerability library. Taking API misuse as an example, the calling function of the API in the program is the key point of API misuse in the vulnerability library. Using the calling function as the entry point, the parameters, statements, and expressions related to the key points in the code are extracted. Therefore, the design of open source software vulnerability library is an indispensable link in static code vulnerability detection.

The open source software vulnerability library designed in this paper is mainly based on the CVE vulnerability database. CVE is compatible with 28 communities and institutions and contains about 6,500 entries. It is currently the authoritative standard vulnerability library for vulnerability scanning and evaluation. In addition, this paper also combines other large vulnerability information bases, such as CWE, NVD, and CNNVD. Through comparative analysis, the vulnerability library is roughly divided into seven categories: input validation, buffer overflow, memory management, API misuse, error handling, information leakage, and cross-site scripting [9]. Some key points are shown in Table 1.

2.2. Program Slicing. Program slicing is used to implement static code vulnerability feature extraction and process static code into a code unit set containing features. In the slicing process, the key points in the vulnerability library are used as entry points, and the control flow graph and data flow graph

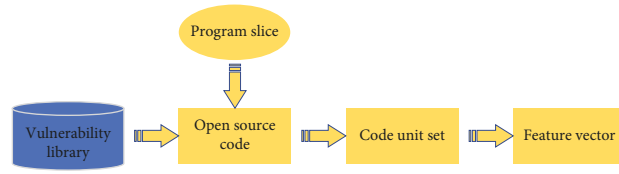

Figure 1: Feature code feature processing flow.

are constructed according to the order of mutual calls in the program and the flow of data parameters, so as to extract the expressions related to the key points. Formulas and statements and code statements and comments that are not related to features are removed [10]. There are many algorithms and tools related to program slicing. This paper uses LLVM to complete static code slicing.

2.3. Feature Vectorized Expression. After the program is sliced, a code unit set containing vulnerability features is obtained. The code unit set cannot be directly used as the input of the deep learning model and needs to be quantized into a fixed-length vector. In this paper, the word vectorization model word2vec is used to complete the vectorization of features. The word2vec model processes the code unit set by constructing a multilayer neural network. During the processing, the parameters of the neural network are continuously corrected and a series of linear and nonlinear operations are performed. Finally, we get the required word vectors. Before vectorizing the code unit set, the code unit set should be regularized, and the user-defined variables and function names in the code should be replaced with standard symbolic names in one-to-one correspondence. In this paper, the static analysis tool cppcheck is used to traverse line by line code and completes the substitution of user-defined variables and standardized names.

3. Improve the CNN Vulnerability Detection Model

3.1. CNN Model. The basic structure of CNN consists of an input layer, a convolution layer, a pooling layer, a fully connected layer, and an output layer. Generally, several convolution layers and pooling layers are used, and the convolution layers and pooling layers are alternately set; that is, one convolutional layer is connected to a pooling layer and so on. Since each neuron of the output feature surface in the convolutional layer is locally connected to its input, and the corresponding connection weights and local inputs are weighted and summed together with the bias value to get the input value of the neuron, this process is equivalent to the convolution process.

The convolution layer consists of multiple feature surfaces, each feature surface consists of multiple neurons, and each neuron is connected to the local area of the feature surface of the previous layer through a convolution kernel, which is a weight matrix (such as for two-dimensional avatars, it can be a 3×3 or 5×5 matrix) [11], the convolutional layer of CNN extracts input features through convolution operations, the first convolutional layer extracts

Table 1: Program vulnerabilities and key points.

Program vulnerabilities	Key points
Input validation problem	insect, create, select, alter, update, order, cookie, subject, system, command, open, close, getProperty, getRuntime
Buffer overflow problem	Strcpy, strlen, stract, strchr, scanf, sprintf, sterror, strcoll, sbumpc, strcnpy, cin, gets, fgets, getchat, getc,getpass, malloc, istream, printf
Misuse of API	Cin, gets, fgets, getchat, getc, getpass, memcpy, malloc, getParameter, equals, getProperty, read, gethostbyaddr
Content management issues	Malloc, calloc, realloc, alloca, free, new, delete, memcpy, memmove, memcmp, memchr, memset, mmap, munmap, memccpy, getpagesize
Error handling issues	-Alloca, catch, throw, EnterCriticalSection
Cross site scripting problem	URL, submit, cookie
Information leakage problem	Malloc, calloc, realloc, alloca, memcpy, memmove

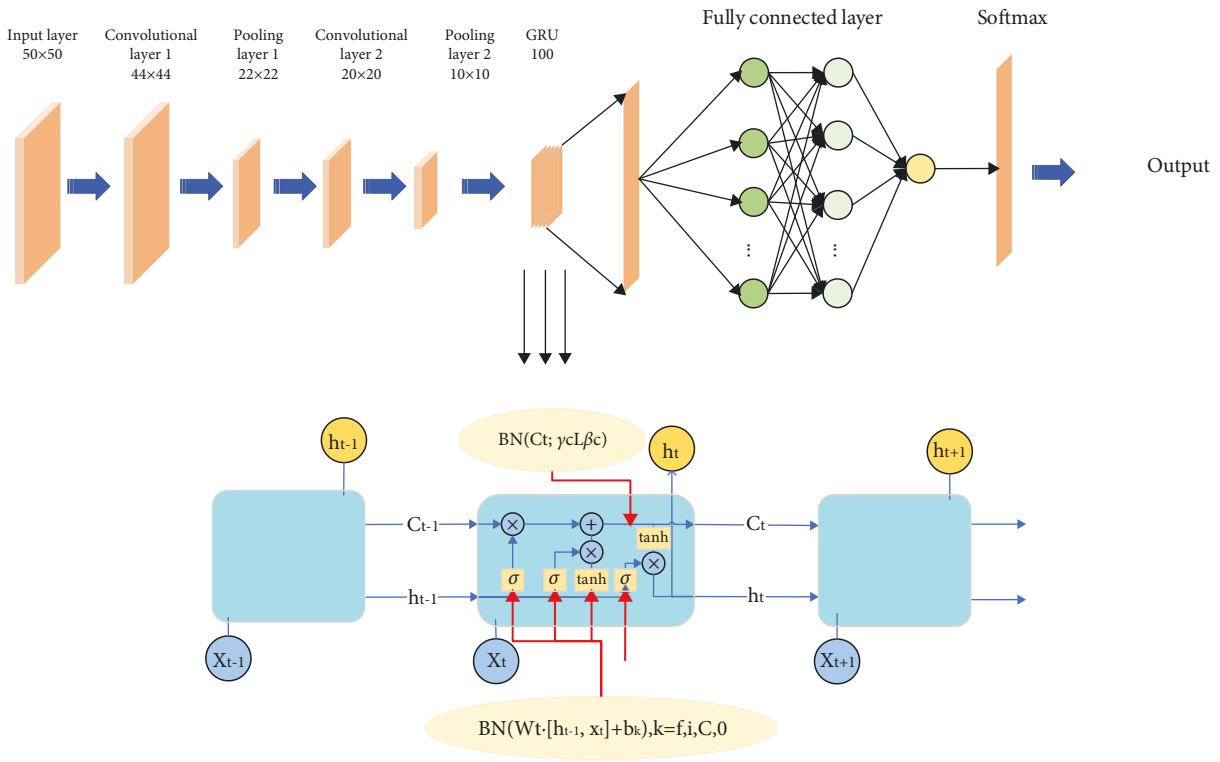

Figure 2: DNN + GRU model structure diagram.

low-level features, and the convolutional layer of higher layers extract higher-level features. Figure 2 shows a schematic diagram of the convolutional layer and pooling layer structure of a one-dimensional CNN.

The pooling layer follows the convolutional layer and is also composed of multiple feature surfaces, each of which uniquely corresponds to a feature surface of the previous layer and does not change the number of feature surfaces. As shown in Figure 2, the convolutional layer is the input layer of the pooling layer. A feature surface of the convolutional layer uniquely corresponds to a feature surface in the pooling layer, the neurons of the pooling layer are also connected to the local receptive field of the input layer, and the local receptive fields of different neurons do not overlap. The pooling layer aims to obtain spatially invariant features by reducing the resolution of feature surfaces [12].

The pooling layer plays the role of secondary feature extraction, and each neuron performs a pooling operation on the local receptive field. In the CNN structure, one or more fully connected layers are connected after multiple convolutional layers and pooling layers. Each neuron in the fully connected layer is fully connected to all neurons in the previous layer. The fully connected layer can integrate the class-discriminative local information in the convolutional layer or the pooling layer [13].

It can be seen from Figure 3 that the neurons of the convolution layer are tissue into each feature, and each neuron is connected to the local region of the upper layer, that is, the gland in the convolution layer. The feature in the input layer performs local connection [14]. The local connection weighted and passed to a nonlinear function such as the RELU function to obtain an output value of each neuron

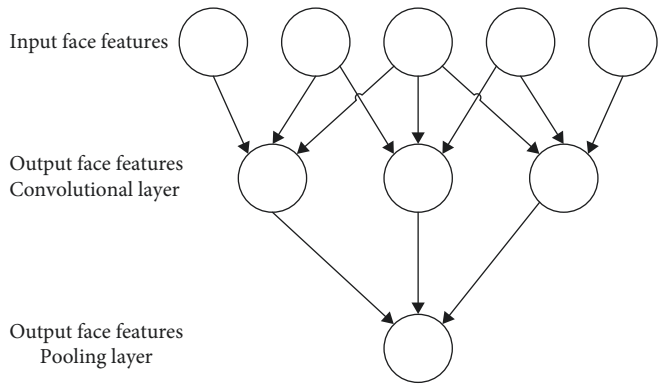

Figure 3: Schematic diagram of convolutional layer and pooling layer.

in the convolution layer. In the same input feature and the same output feature, the weight sharing of the CNN can reduce the model complexity by weight sharing, making the network easier to train.

3.2. CNN + GRU Model. Although CNN has good classification ability in vulnerability detection, it cannot well preserve the contextual relationship between code statements, and the overly complex neural network structure will have the problem of gradient disappearance as the number of layers increases [15]. RNN is often used to deal with time series problems and can better express the contextual calling relationship between codes, but RNN also has the problem of gradient disappearance. GRU is an effective variant of LSTM network. It has simpler structure and better effect than LSTM network. Therefore, it is also a very manifold network at present. Since Gru is a variant of LSTM, it can also solve the long dependency problem in RNN networks [16]. GRU introduces three gate functions into LSTM: input gate, forgetting gate, and output gate to control input value, memory value, and output value. In GRU model, there are only two doors: update door and reset door.

This paper proposes to combine CNN and GRU, organically integrate the advantages of the two models, and build a new model that is more suitable for open source software vulnerability detection. The CNN is used as the interface for interacting with the feature vector, and the GRU is used as the gating mechanism to deal with the relationship between the code statements, which constitutes the CNN + GRU model. The efficiency of CNN in processing data is higher and faster than GRU, and the automatic learning ability of convolution kernel is also stronger than GRU [17], and GRU model not only solves the problem of gradient disappearance in CNN, but also captures CNN Call information between code functions is ignored. The structure of the CNN + GRU model is shown in Figure 4.

In Figure 2, the first is the convolution and pooling processing of CNN. CNN can quickly process high-dimensional data and ensure the invariance of feature data to the greatest extent during dimensionality reduction [18]. Second, the GRU is embedded between the pooling layer and the fully connected layer, and the GRU is used to preserve the up-down calling

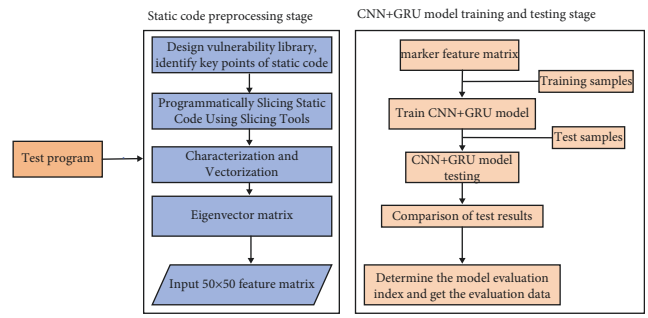

Figure 4: The process of CNN + GRU model detecting software vulnerabilities.

relationship between code data. Finally, the fully connected layer is used to complete the normalization process, and the processed output value is sent to the SoftMax classifier for classification and detection, and the classification result is obtained [19].

The input layer is a preprocessed 50×50-dimensional feature matrix. The red square in the figure represents the convolution kernel with a size of 7×7. The convolution kernel is the weight matrix in the perception field. The scan pitch for input data is set to 1. There may be out-of-bounds phenomenon when scanning to the boundary, the boundary needs to be expanded, and the value of the out-of-bounds part is set to 0. The input of the convolutional layer is the 50×50 feature matrix in the input layer, and the output matrix dimension is determined by

$$\begin{cases} \text{height}_{\text{out}} = \dfrac{\text{height}_{\text{in}} - \text{height}_{\text{kemel}} + 2 \times \text{padding}}{\text{stride}} + 1, \\ \text{width}_{\text{out}} = \dfrac{\text{width}_{\text{in}} - \text{width}_{\text{kemel}} + 2 \times \text{padding}}{\text{stride}} + 1. \end{cases} \tag{1}$$

In formula (1), height and width represent the length and width of the matrix, padding is the padding mode, and stride is the step size. To be precise, each convolution kernel also contains a bias parameter, but the formula omits bias. In the CNN + GRU model, padding is 0, stride is 1, and the length and width of the output matrix are $(50 - 7 + 2)/1 + 1 = 44$; that is, the input matrix of pooling layer 1 is 44×44

dimensions. The pooling layer is mainly to compress and reduce features and prevent overfitting. In pooling layer 1, a filter of size 2×2 is used, and the stride is chosen to be 2. It can be concluded that the output of pooling layer 1 is 22×22. The processing of convolutional layer 2 and pooling layer 2 is similar to convolutional layer 1 and pooling layer 1.

GRU is embedded between the pooling layer and the fully connected layer. Since CNN uses filters and windows of different sizes to process data, it often loses the up-down calling and transfer relationship between these code data. In addition, too many neural network layers will also have the problem of gradient disappearance, so it is necessary that GRU acts as a storage timing information and control gate in the whole model. In the GRU structure diagram, x is the input, h is the output, f_i is the forgotten part of the input information, and r_i is the memorized part of the input information. The calculation in GRU is shown in

$$\begin{cases} r_t = \sigma\left(W_r \times \left[h_{t-1}, x_t\right]\right), \\ f_t = \sigma\left(W_f \times \left[h_{t-1}, x_t\right]\right), \\ \widetilde{h}_t = \text{Relu}\left(W \times \left[f_t \times h_{t-1}, x_t\right]\right), \\ h_t = \left(1 - r_t\right) \times h_{t-1} + r_t \times \widetilde{h}_t. \end{cases} \tag{2}$$

In formula (2), w represents the weight, and relu is the activation function. In order to make CNN + GRU have nonlinear modeling ability, an activation function is added to GRU. The relu function, which is faster to calculate and can alleviate gradient disappearance, is selected as the activation function, as shown in

$$f(x) = \max(0, x), \tag{3}$$

where x is the input, $f(x)$ is the output, and relu can keep the gradient from decaying when $x > 0$, alleviating the problem of gradient disappearance.

The problem of program vulnerability detection is actually a two-category problem, with or without loopholes. So you need to add a fully connected layer and a SoftMax layer at the end of the model. The fully connected layer is responsible for further dimensionality reduction and purification of the features, and the classifier is responsible for whether the final sample contains vulnerabilities. Through filters (also called convolution kernels), the fully connected layer connects the input and output together, and the fully connected part is shown in

$$W * x + b = z. \tag{4}$$

Among them, $x = [x_0, x_1, x_2, \ldots, x_n]_T$ is the input vector; $y = [y_0, y_1, y_2, \ldots, y_n]_T$ is the output vector, then the filter part is a matrix of size $m \times n$, and b is a partial set of the term, $b = [b_0, b_1, b_2, \ldots, b_n]_T$.

SoftMax classifiers are widely used to solve multiclassification problems in various domains. The input feature of the SoftMax function is set to x, and the probability value is $p(y = j|x)$, assuming the function is as follows:

$$h_\theta(x) = \begin{bmatrix} p\left(y^{(i)} = 1|x^{(i)}; \theta\right) \\ p\left(y^{(i)} = 2|x^{(i)}; \theta\right) \\ \vdots \\ p\left(y^{(i)} = k|x^{(i)}; \theta\right) \end{bmatrix} = \frac{1}{\sum_{j=1}^{k} e^{\theta_j^T x(i)}} \begin{bmatrix} e^{\theta_1^T x(i)} \\ e^{\theta_2^T x(i)} \\ \vdots \\ e^{\theta_k^T x(i)} \end{bmatrix}. \tag{5}$$

The parameter θ is obtained through training, the setting of θ needs to minimize the regression cost function, k is the dimension of the vector, and the regression cost function of SoftMax is

$$J(\theta) = -\frac{1}{m}\left[\sum_{i=1}^{m}\sum_{j=1}^{k} 1\left\{y^{(i)} = j\right\} | b \frac{e^{\theta_j^T x(i)}}{\sum_{i=1}^{k} e^{\theta_j^T x(i)}}\right] + \frac{\lambda}{2}\sum_{i=1}^{k}\sum_{j=0}^{n}\theta_{ij}^2. \tag{6}$$

$(\lambda/2)\left(\sum_{i=1}^{k}\sum_{j=0}^{n}\theta_{ij}^2\right)$ is the weight failure; in order to minimize the value of $J(\theta)$, use iterative optimal algorithm. By seeking, gradient formulas can be obtained:

$$\nabla_{\theta_j} J(\theta) = -\frac{1}{m}\sum_{i=1}^{m}\left[1\left\{x_i\left(y_i = j\right\} - p\left(y_i = j|x_i; \theta\right)\right] + \lambda\theta_j. \tag{7}$$

$\nabla_{\theta_j} J(\theta)$ represents a vector, and a SoftMax model can be implemented by minimizing $J(\theta)$.

3.3. Model Assessment Indicator. Before training and testing models, you need to give an evaluation indicator of the vulnerability detection model, the accuracy (ACC), and the loss rate (LOSS), which is often used.

Refer to the mainstream assessment index system, according to the difference between the prediction results and the real results, divided into the following four cases [20]:

TP: the prediction result is positive and the real results are positive.

FP: the prediction result is positive, and the real results are negative.

FN: the forecast results are negative, and the real results are positive.

TN: the forecast results are negative, and the real results are negative. The calculation of the accuracy ACC is as shown in

$$\text{ACC} = \frac{\text{TP} + \text{TN}}{\text{TP} + \text{FP} + \text{FN} + \text{TN}}. \tag{8}$$

The loss rate of the CNN + GRU model is calculated by the cross-entropy loss function and reflects the gap between the prediction results and the real results by calculating the cross entropy. The collection of predicted results is used to represent the collection of real results, and the cross-entropy of the two sets can be defined as follows:

Table 2: Simulation experiment environment.

Name	Parameter
RAM	16 GB
HD	512 GB
CPU	Intel® Core™ i5-3515M
OS	64-bit Win10 physical machine
Python	3.7.1

$$H(p,r) = E_p[-|br] = H(p) + D_{KL}(pr). \quad (9)$$

$H(p)$ represents the entropy of P, and $D_{KL}(pr)$ is KL distance to measure the distance of two collections.

4. Simulation Experiment

When using the software vulnerability detection algorithm of the CNN model, the corresponding indicators are mainly the accuracy rate of training and the loss rate of training as the main basis for judging the detection of software vulnerabilities of the CNN model.

4.1. Experimental Environment. The training and testing environment of the vulnerability detection model is 16 GB memory, and the processor is Intel® Core™ i5-3515M, 64-bit Win10 physical machine. Open source data often have class imbalance problems; that is, most of the data are positive samples (samples without vulnerabilities), while the number of negative samples is low (samples with vulnerabilities). Such imbalance problems will affect the vulnerability detection model performance, causing vulnerability cases in the standard library. This dataset is preprocessed, including feature extraction, normalization, and vectorization of features. Finally, more than 300 samples were formed as experimental data (171 positive samples and 144 negative samples), and 215 samples were taken as training data (117 positive samples and 98 negative samples). The remaining 100 samples are used as test samples, 54 positive samples, and 46 negative samples, which are used to verify the vulnerability detection ability of the CNN + GRU model as shown in Table 2.

4.2. Detection Process. The vulnerability detection process can be divided into two stages: the static code preprocessing stage and the vulnerability detection model training and testing stage [21].

In the static code preprocessing stage, first of all, refer to the real vulnerability cases in CVE, extract the API functions with specific errors in the cases, divide the API functions into 7 categories to construct the open source software vulnerability library of this article, and use the API functions in the vulnerability library. It is the key point and the entry point of the program slice. Second, collect the data set, use LLVM to slice the data set program, extract key points from the data set code, and construct the control flow chart of the key point function. In the control flow graph, each node is a basic block. The variables and operations related to the key point function are found through each branch of the basic block. Finally, all the basic blocks related to the key point function are intercepted to form more than 300 code unit sets. In addition, it is necessary to standardize and vectorize the code unit set and use word2vec to vectorize more than 300 code unit sets in batches to obtain training samples. Use the same method to obtain test samples. Finally, normalize all the feature vectors, and process the feature vectors into a 50×50-dimensional feature matrix according to the size of the sample. The size of the ordinate is the dimension of the word vector, and the abscissa is the number of word vectors. If the word vector is less than 50, it is filled with 0. In the training and testing phases of the vulnerability detection model, the training model and the testing model need to be written, and the entire compilation process uses the python language. Add a label to the test sample, set the label of the sample containing the vulnerability to "0," and set the label of the sample without the vulnerability to "1." 215 samples were taken as training data. In the experiment, batch extraction was used to extract a fixed number of samples from the test samples each time, and the model was trained through multiple iterations. In the testing phase, use the trained CNN + GRU model for testing, compare whether the model test results are the same as the actual results, and test the detection ability of the CNN + GRU model. The overall process of the entire static code vulnerability detection is shown in Figure 4.

4.3. Analysis of Experimental Results. In the training phase, iterate 3000 training cycles, and use the minibatch gradient descent algorithm (MBGD) for batch extraction. Every 10 iterations, the current training accuracy rate (training ACC) and training loss rate (training loss) are output, and save the model document. The model document saves the weights that are adjusted and set when training the neural network, so that the model document can run directly. The detection results of part of the model during the training process are shown in Table 3.

During the training process, the accuracy and loss rate after 500 iterations are stable at 0.903 3 and 0.154 1. The weight values of the model at this time are saved in the ckft model document, and the parameters in the document are in the testing phase parameter to use. The changes in the accuracy and loss rates during training are shown in Figure 5.

As can be seen from Figure 5, when the number of iterations is less than 500, the accuracy of the whole curve is significantly improved; when the number of iterations is more than 500, the accuracy curve tends to be stable and remains at about 0.9. When the number of iterations is less than 500, the whole curve shows an obvious downward trend. When the number of iterations is greater than 500, the curve also tends to be stable and remains at about 0.15. After the model training is completed, the test samples are tested. By loading the model documents saved during the training, the model can be directly restored to the state at the end of the training. 100 samples are randomly selected from 315 test samples each time for 5 times. See Table 4 for test accuracy (test ACC) and test loss rate (test loss).

In order to further prove that the CNN + GRU model has high vulnerability detection ability, the CNN + GRU model

Table 3: CNN + GPU model training results.

Number of iterations	Training ACC	Training loss
10	0.3706	0.6635
20	0.6225	0.3782
30	0.8742	0.2375
60	0.9017	0.1581
90	0.9032	0.1543
120	0.9033	0.1541
150	0.9033	0.1541

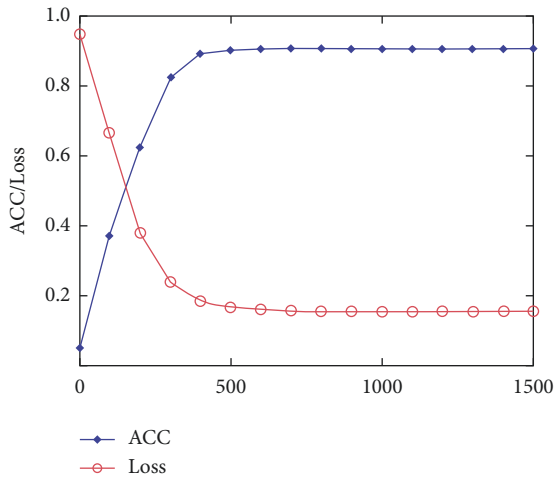

Figure 5: CNN + GRU model test results.

Table 4: CNN + GRU Model test results.

Sample	Test ACC	Test loss
1	0.8800	0.1617
2	0.8700	0.1674
3	0.8700	0.1707
4	0.8600	0.1972
5	0.8700	0.1591

Table 5: Data comparison of deep learning models.

Model	Training ACC	Training loss	Test ACC	Test loss
RNN	0.8372	0.1819	0.8000	0.2068
CNN	0.8810	0.1702	0.8400	0.1918
VulDeePecker	0.8791	0.1613	0.8300	0.1844
CNN + GPU	0.9033	0.1541	0.8700	0.1713

is compared with a single CNN, RNN, and the existing vulnerability detection model VulDeePecker [22]. The CNN, RNN, and VulDeePecker models were trained and tested using the same dataset, and the experimental results of the four models were compared. The specific results are shown in Table 5. The information in the table is the average of the training data and test data of the four models. It can be seen that the experimental results of CNN + GRU are the best.

The experimental results show that it is feasible to nest GRU into the pooling layer and fully connected layer of CNN. The CNN + GRU model proposed in this paper can not only ensure the invariance of feature vectors to the greatest extent during dimension reduction, but also preserve the invariance between codes. Call relationship has stronger vulnerability detection ability, and compared with CNN, RNN, and VulDeePecker models, CNN + GRU has higher accuracy and lower loss rate.

5. Conclusion

This paper proposes a software building detection algorithm based on an improved CNN model. Firstly, extract the vulnerability features of the software, use program slicing technology to extract features from static code, establish a vulnerability library, and standardize and vectorize the vulnerability library as input data. GRU model is used to optimize CNN neural network. The organic combination of the two can quickly process the feature data and retain the calling relationship between the codes. The improved CNN model is better than the single CNN and RNN model in vulnerability detection ability and detection accuracy. Compared with single CNN model and VulDeePecker model, the training loss rate is 4.25% higher. On the contrary, compared with single RNN model and VulDeePecker model, the training loss rate is 17.2% and 7% lower, respectively.

Compared with other single algorithms, the improved CNN algorithm has relatively high requirements for data and needs to be further optimized in the future.

Data Availability

The dataset can be accessed upon request.

Conflicts of Interest

The author declares that there are no conflicts of interest.

References

[1] H. Shahriar and M. Zulkernine, "Mitigating program security vulnerabilities," *ACM Computing Surveys*, vol. 44, no. 3, pp. 1–46, 2012.

[2] Y. Xia, "Research on security vulnerability detection technology based on static analysis," *Computer Science*, vol. 33, no. 10, pp. 279–282, 2006.

[3] K. Lu, *Research and Implementation of Vulnerability Attack Detection Technology Based on Dynamic Taint Analysis*, University of Electronic Science and Technology Press, Chengdu, China, 2013.

[4] G. Pan and Y. Zhou, "XSS vulnerability discovery based on static analysis and dynamic detection," *Computer Science*, vol. 39, no. s1, pp. 51–53, 2012.

[5] H. Perl, S. Dechand, and M. Smith, "VccFinder: finding potential vulnerabilities in opensource projects to assistcode audits," in *Proceedings of the 22nd ACM SIGSACConference on Computer and Communications Security*, pp. 426–437, Denver, CO, USA, October 12-16, 2015.

[6] Z. Li, D. Zou, and S. Xu, "VulPecker : an automated vulnerabilitydetection system based on code similarity analysis,"

in *Proceedings of the Conference on Computer Security Applications*, pp. 201–213, Angeles, CA, USA, December 2016.

[7] S. Chen, *Research and Implementation of Android Malicious Application Detection Technology Based on Deep Learning algorithm*, Beijing University of Posts and Telecommunications Press, Beijing, China, 2016.

[8] Z. Li, D. Zou, and S. Xu, "VulDeePecker: a deep learning-based system for vulnerability detection," in *Proceedings of the Network and Distributed Systems Security (NDSS) Symposium*, Diego, CA, USA, February 2018.

[9] Y. Shin, A. Meneely, L. Williams, and J. A. Osborne, "Evaluating complexity, code churn, and developer activity metrics as indicators of software vulnerabilities," *IEEE Transactions on Software Engineering*, vol. 37, no. 6, pp. 772–787, 2011.

[10] B. Chernis and R. Verma, "Machine learning methods for softwarevulnerability detection," in *Proceedings of the ACM International Workshop*, pp. 31–39, Tokyo, Japan, November 2018.

[11] R. Grosu and S. A. Smolka, *Monte Carlo Model checking// Tools and Algorithms Forthe Construction and Analysis of Systems*, Springer Berlin Heidelberg, Berlin, Germany, 2005.

[12] M. D. Zeiler and R. Fergus, "Stochastic pooling for regularzition of deep convolutional neural networks," 2013, https://arxiv.org/abs/1301.3557.

[13] Y.-L. Boureau, J. Ponce, and Y. LeCun, "A theoretical analusis of feature pooling in visual recognition," *International Conference on Machine Learning*, vol. 32, no. 4, pp. 111–118, 2010.

[14] D. Erhan, Y. Bengio, and A. Courville, "Why does unsupervised pre-training help deep learning?" *Journal of Machine Learning Research*, vol. 11, no. 3, pp. 625–660, 2010.

[15] J. Saxe and K. Berlin, "Xpose : a character-level convolutionalneural network with embeddings for detecting maliciousURLs, file paths and registry keys," 2017, https://www.arxiv-vanity.com/papers/1702.08568/.

[16] Z. Qu, L. Su, and X. Wang, "A unsupervised learningmethod of anomaly detection using GRU," in *Proceedings of the IEEE International Conference on Big Data & Smart Computing*, IEEE, Shanghai, China, January 2018.

[17] F. Wu, J. Wang, and J. Liu, "Vulnerability detection withdeep learning," in *Proceedings of the IEEE International Conference onComputer and Communications*, pp. 1298–1302, IEEE, Chengdu, China, December 2017.

[18] J. Su, Z. Tan, and D. Xiong, "Lattice-based recurrent neuralnetwork encoders for neural machine translation," in *Proceedings of the 31st AAAI Conference on ArtificialIntelligence*, pp. 3302–3308, February 2017.

[19] V. Nair, G. E. Hinton, and C. Farabet, "Rectified linear units implement restored boltzmann machines," in *Proceedings of the 27th International Conference on Machine Learning*, pp. 807–814, Haifa, Israel, July 2010.

[20] D. Silver, A. Huang, and C. J. Maddison, "Mastering the game of go with deep neural networks and tree search," *Nature*, vol. 529, no. 7587, pp. 484–489, 2016.

[21] S. Lawrence, C. L. Giles, A. C. Ah Chung Tsoi, and A. Back, "Face recognition: a convolutional neural-network approach," *IEEE Transactions on Neural Networks*, vol. 8, no. 1, pp. 98–113, 1997.

[22] C. Neubauer, "Evaluation of convolutional neural networks for visual regression," *IEEE Transactions on Neural Networks*, vol. 9, no. 4, pp. 685–696, 1998.

Hindawi
Scientific Programming
Volume 2022, Article ID 1044597, 11 pages
https://doi.org/10.1155/2022/1044597

Research Article

Leisure Sports Behavior Recognition Algorithm Based on Deep Residual Network

Zhen Chou

Changchun University of Science and Technology, Military Sports Department, Changchun 130022, Jilin, China

Correspondence should be addressed to Zhen Chou; chouzhen@cust.edu.cn

Received 25 April 2022; Revised 14 June 2022; Accepted 17 June 2022; Published 8 July 2022

Academic Editor: Lianhui Li

Aiming at the related problems existing in the field of leisure sports computing, in order to study the behavior recognition of leisure sports by deep residual network, based on the deep residual neural network theory, the behavior recognition algorithm and the corresponding robust model are used to analyze the leisure sports related samples, and the correlation model is used to predict and analyze the leisure sports related content. The results show that the change curves of Sig and Tanh functions can be divided into slow increasing stage, linear increasing stage, and stable stage. The y value corresponding to ReLU curve shows a linear change trend with the increase of x value. The Leaky function's corresponding curve can be divided into two stages. The function coincides with the ReLU function in the first quadrant and remains linear in the third quadrant. The activation function curves corresponding to layers 56 and 20 have a relatively large variation range, and both of them show an overall trend of gradual decline. On the whole, the curve value corresponding to layer 56 is higher than that corresponding to layer 20, indicating that the method of layer 20 is relatively good and the corresponding training error is relatively low. It can be seen from the robustness recognition rate of various methods under different training samples that F_l has the highest overall data recognition rate while S_c has relatively poor stability. However, the recognition rate of IDCC and DCC shows a relatively flat trend, indicating that these two methods have certain advantages in describing the robust recognition rate. The research results can provide theoretical support for the application of deep residual neural networks in other fields.

1. Introduction

Deep residual neural network has been widely applied in different fields: Aiming at the problems in the field of handwriting, a method based on deep residual network has been established, which can achieve higher accuracy [1]. In view of the problems existing in the accurate recognition of cancer lesions, deep learning technology can play a certain role in performing natural image segmentation, and this model has reasonable scale invariance and the ability to detect even small differences [2]. In view of the problems existing in the operation process of short-term load, a deep residual network short-term load prediction method based on adaptive method is proposed [3]. The accuracy and timeliness of neural network are considered in this method. A method using deep residual network to enhance image resolution was proposed. The method used behavior recognition algorithm and robustness analysis to calculate data and samples, and the results showed that the model could better reflect and describe images [4]. In order to better analyze and describe the characteristics of radar, an optimization model based on deep residual network is proposed. This model can not only analyze and verify the relevant data of radar, but also carry out predictive analysis of radar samples within a certain range, and the accuracy of this model has been verified by experiments [5]. The evaluation index of image quality is very important for image processing. Aiming at a series of problems existing in image research, an image evaluation model based on deep residual network and behavior algorithm is established. The model extracts relevant data for analysis, thus obtaining the corresponding model results, and the accuracy of the model has been verified through experiments [6]. Deep fuzzy neural network cannot well explain the behavior of nonlinear

dynamics. A new architecture based on deep residual neural network theory is established. In order to verify the superiority of the model, a large amount of data were used for verification, and the structure showed the accuracy of the model [7].

The above studies mainly analyzed the application of deep residual network in aspects other than leisure sports. Therefore, in order to better study related behavior recognition algorithms and other problems existing in leisure sports, deep residual neural network theory is adopted. Leisure sports are monitored and analyzed based on behavior recognition algorithm, and the correlation model is used to predict and analyze the sample data of leisure sports. The research results can provide support for the application of deep residual neural networks in other fields.

The scale of leisure sports is shown in Figure 1. From the scale of leisure sports, we can see that with the passage of time, the scale of sports shows a trend of gradual increase [8–10]. The scale of leisure sports increased by 5.7 times from 129 in 2011 to 731 in 2021, indicating that the scale of leisure sports is gradually increasing. In order to quantitatively analyze the change rule of leisure sports scale over time, the increment percentage of leisure sports scale at different times was plotted. It can be seen from the figure that the corresponding increment also shows a trend of gradual increase. In addition, it can be seen from the way of linear fitting that this law conforms to the quadratic function distribution. Through the above analysis, we can draw relevant conclusions: The scale of leisure sports increases gradually with the increase of time, and the increment proportion also shows an increasing trend. However, from 2019 to 2021, it can be seen that the increment of the size of leisure sports decreased, indicating that there are some problems in the development process of leisure sports scale, which has restricted the development of leisure sports scale to some extent.

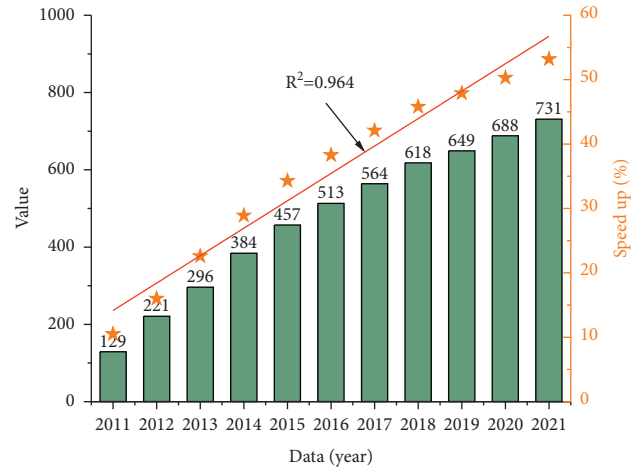

Figure 1: Leisure sports scale map.

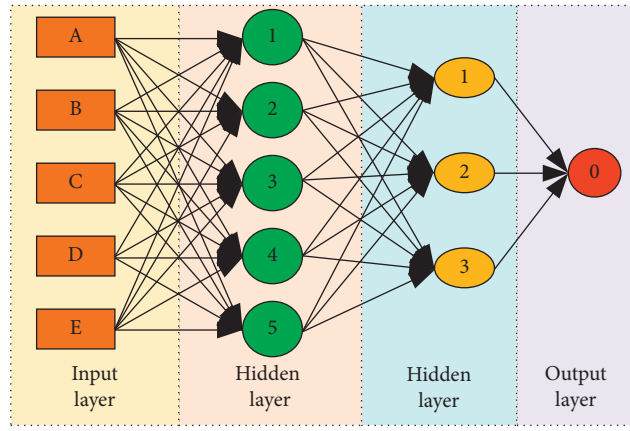

Figure 2: Fully connected neural network diagram.

2. Basic Theory of Deep Residual Networks

2.1. Convolutional Neural Network. Convolutional neural network (CNN) is the most representative deep learning algorithm, which has achieved great success in the field of computer vision [11, 12]. Compared with traditional fully connected neural networks, CNN has fewer training parameters and more flexible training methods and can deepen model layers through network optimization methods. When the network model trains image data, the original image to be processed or the preprocessed fuzzy image is first put into the input layer, and then the convolutional layer and pooling layer process the image of the input layer. The feature information is extracted to form the feature map, and then the activation layer performs nonlinear operation on the feature map to enlarge the image and reconstruct the final result. CNN uses convolution computation to propagate feedforward signals, and the corresponding fully connected neural network is shown in Figure 2.

Through the whole neural network diagram, we can see that neural network can be divided into three parts according to its different functions: input layer, hidden layer, and output layer. The specific data processing process is as follows: Firstly, the verification samples and data are imported into the input layer; the data is analyzed through the algorithm in the input layer; and then the analyzed data is imported into hidden layer 1. Further analysis and validation of the input data are carried out through the five units and modules in hidden layer 1, and the corresponding data is then exported. The data of the map is imported into hidden layer 2 again. In hidden layer 2, there are three variable elements that can verify the input data. After the above hidden layer analysis, the obtained data is output, so as to realize the description of the neural network.

In order to better analyze the computation process of convolutional neural network, an introduction neural network structure diagram is drawn, as shown in Figure 3. As can be seen from the convolutional neural network flow chart, convolutional neural network can be divided into five parts: convolution unit, upsampling, convolution, downsampling, and full connection. Firstly, the sample data is imported into the convolution part to extract the relevant features of the data. Then, the feature data is imported into the upsampling for further analysis, through a series of operations such as copying and pasting the data. Then, the pasted data is imported into the new convolution part again

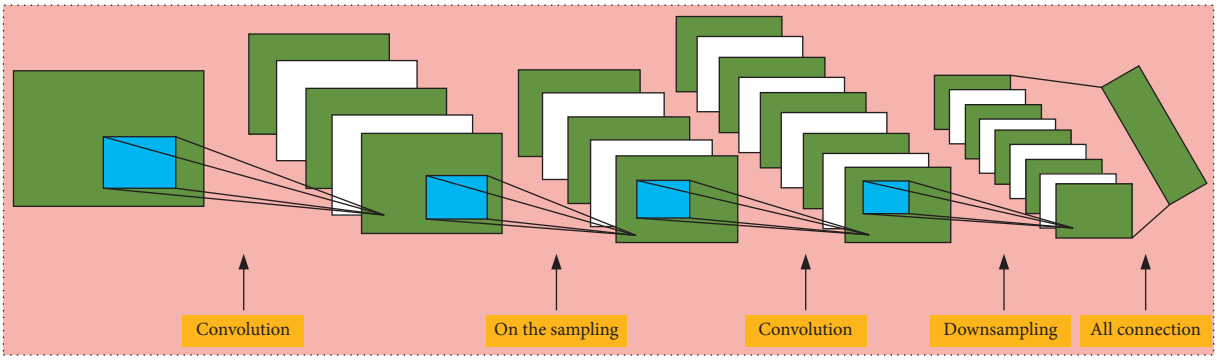

Figure 3: Convolutional neural network diagram.

for calculation. The newly obtained data is imported into the lower sampling for a new round of more accurate copy-and-paste operations. In this way, the obtained new data can be imported into the full connection operation. Through the full connection operation, the data sample can be analyzed and modified, and finally the relevant data can be exported.

Convolutional neural network mainly includes convolutional layer and corresponding activation function.

2.1.1. Convolutional Layer. The convolutional layer is the foundation of convolutional neural network and the most core component of the network. Through the combination analysis of the obtained local feature information, the global feature information is formed. The corresponding operation mode is as follows:

$$\mathrm{CONV}_{(ij)} = \sum_{i}^{m-1} \sum_{j}^{n-1} u_{ij} \times w + b, \quad (i = 1, 2 \ldots m-1; j = 1, 2 \ldots n-1), \tag{1}$$

where u_{ij} is the input image, m and n are the size of the input image, w is the size of the convolution kernel, and b is the bias constant of the convolution kernel. CONV(ij) is the characteristic graph output after convolution operation.

2.1.2. Activation Function. CNN adds an activation function layer to the network and analyzes the model better by adopting the feature mapping method of nonlinear function. The full name of ReLU function is modified linear unit. The function is one of the commonly used activation functions, which is characterized by low computational complexity and no exponential operation. The ReLU function can be expressed as follows:

$$f(x) = \max(0, x), = \begin{cases} x, & (x \geq 0), \\ 0, & (x < 0). \end{cases} \tag{2}$$

However, it is worth explaining that ReLU function has certain defects in the calculation process. When the data passes through the negative range of ReLU function, the output value is equal to 0. Under certain conditions, some neurons in the data network will no longer update parameters, thus reducing the expression ability of the network model. Based on the above problems, a Leaky-ReLU function is proposed to correct and optimize the ReLU function, which makes the output value not equal to 0 when the data passes through the negative range of the function. The Leaky-ReLU function can be expressed as follows:

$$f(x) = \begin{cases} x, & (x \geq 0), \\ \mathrm{ax}, & (x < 0). \end{cases} \tag{3}$$

The corresponding equations of Sig and Tanh are as follows:

$$\begin{cases} \mathrm{sig}(x) = \dfrac{1}{1 + \exp(-x)}, \\ \tanh(x) = \dfrac{\exp(x) - \exp(-x)}{\exp(x) + \exp(-x)}. \end{cases} \tag{4}$$

The graph of activation function corresponding to the above functions is shown in Figure 4. The y value of Sig function increases gradually with the increase of x, which can be divided into three parts: The first part belongs to the stable stage. In this stage, with the increase of x value, the corresponding y value shows a constant trend of change, and the value is near zero. In the next stage, with the increase of x value, y value shows the trend of the curve increasing in the last step, and the slope corresponding to the curve at this stage is approximately constant, indicating that the linear characteristics of the curve are obvious. After the second part, as the x value increases, and the curve recovers again, showing an approximately constant trend of change. However, compared with the first part, the y value corresponding to the constant phase in this part is relatively large. From the change curve of Tanh, this curve is basically consistent with the change trend of Sig curve, except that the corresponding y value is in a negative state in the stable stage of the first part. In the second stage, the curve still shows a linear trend of change, but compared with the Sig function, the slope of Tanh function in this stage is relatively larger. As the value of x increases further, the curve reaches the third stage and coincides with the corresponding curve of the Sig function at this stage.

From the ReLU curve, the corresponding y value shows a linear change trend with the increase of x value, and the

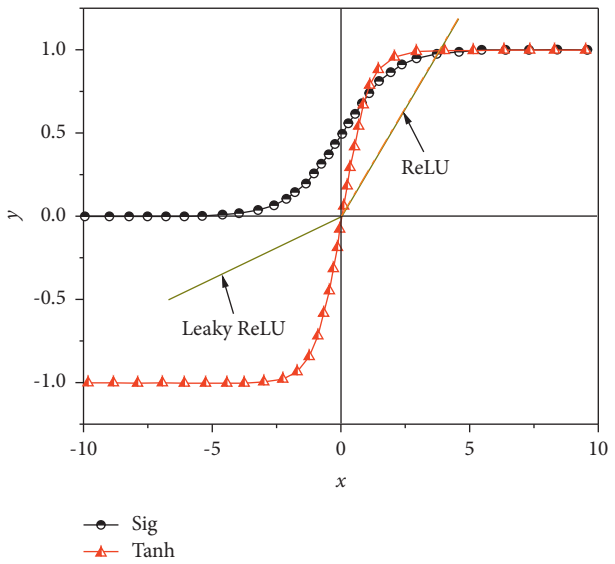

Figure 4: Activation function under convolutional neural network.

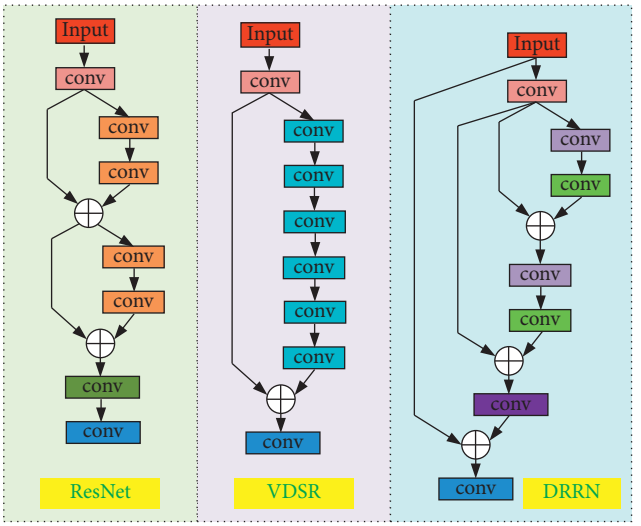

Figure 5: Comparison of several residual network structures.

slope of this linear curve is constant. In addition, the slope of ReLU curve is basically consistent with that of Sig function in the second stage. And, the curve corresponding to Leaky function can be divided into two stages, indicating that Leaky function belongs to a segmented function, which coincides with the curve of ReLU function in the first quadrant. In the third quadrant, it still shows a linear change rule, but the slope is relatively smaller than that in the first quadrant.

2.2. Basis of Residual Neural Network. Deep residual network has a good application effect in image classification, location task, and semantic segmentation and can effectively alleviate the related problems caused by the disappearance of gradient [13–15]. CNN convolution layer has the characteristics of local perception and weight sharing. Local perception means that the convolution layer only extracts local features during operation and then combines all local features into global features after operation. Weight sharing means that the weight parameters between the convolution kernels are shared and the features extracted by the convolution kernels with shared weight parameters are the same in any region of the neural network. These two characteristics enable CNN to have faster training speed and better network performance compared with traditional fully connected neural network. In order to better analyze the relevant calculation content of residual neural network, the structure diagram of different types of residual neural network is summarized, as shown in Figure 5.

In order to explore the structure differences of different residual neural networks, they can be divided into three structures according to the difference of their operation processes: ResNet structure, VDSR structure, and DRRN structure. It can be seen from the structure comparison diagram that the three structures are consistent in the initial data input and final data export, while there are great differences in the concrete computing part in the middle. The intermediate operation part of ResNet structure can include two identical data loop chains, which can make the data better for iteration and analysis and make the calculation results more targeted. In the VDSR structure, the data operation part is directly carried out without any cycle, which can ensure the fluency and authenticity of the data and make the data results more comparative. The running part in the middle of the DRRN structure belongs to the multi-iterative loop, and multiple iterative loops can make the analysis of experimental data more accurate thus making the derived structure more general.

The structure characteristics of several common residual neural networks are shown as follows [16–18]:

(1) VDSR: VDSR model is a new network structure that will add residual module into the deep neural network. Compared with SRCNN and other traditional super-resolution network models, the VDSR model has a faster training speed, and it can be found through calculation that the model can train image data of different sizes.

(2) DRRN: It adopts a deeper network structure, which makes better use of the residual network module. Each residual unit has two convolution layers, and the parameters at the corresponding positions between the convolution layers are shared. DRRN has faster computing speed and higher accuracy during training and can reconstruct higher-quality high-resolution images with less memory resources.

(3) ResNet: It refers to VGG19 network and is modified on its basis. Residual unit is added through short-circuit mechanism. The changes are mainly reflected in ResNet directly using convolutional samples for downsampling. In order to better analyze the influence of different layers on the training error of ResNet, the calculation results of ResNet under different layers are summarized, as shown in Figure 6.

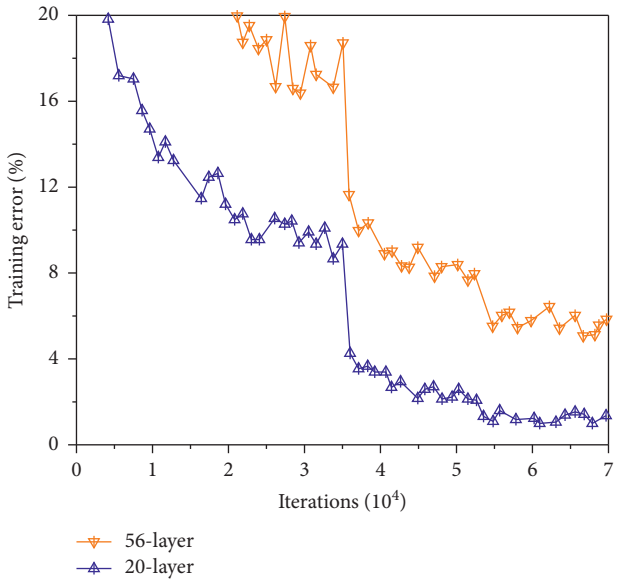

Figure 6: Activation function under residual neural network.

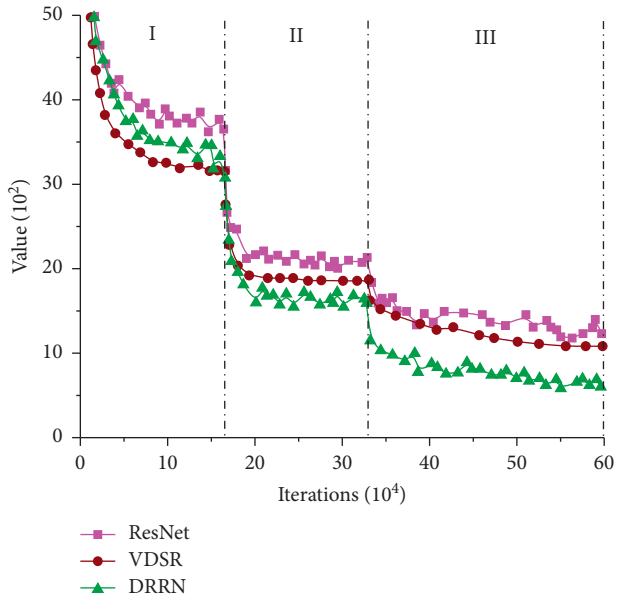

Figure 7: Comparison diagram of different residual network data.

The two activation functions of different types are shown in Figure 6. It can be seen from the figure that the curves corresponding to the 56th and 20th floors change in a relatively large range, and both of them show a trend of gradual decline on the whole. However, their different trends can be divided into two parts: In the first part, with the increase of the number of iterations, the two curves first show a trend of gradual decline, but in the process of change, there are still certain fluctuations in the data. This indicates that the training error corresponding to the activation function has a certain jump. When the number of iterations reaches 3.5×10^4, the curve suddenly drops rapidly and enters the second stage. The main reason for the rapid decline of the curve in this stage is that there is a certain jump in the relevant data, which leads to the rapid decline of the training error. In the second stage, the curve still shows an overall trend of gradual decline, but the corresponding data still have certain fluctuations. Compared with the first stage, the changes of the two curves are relatively small. On the whole, the curve value corresponding to the 56th layer is higher than that corresponding to the 20th layer, indicating that the training error corresponding to the 56th layer is higher than that of the 20th layer. At the same time, this also shows that the 20-layer method is relatively good and the corresponding training error is relatively low, which can better reflect the relevant properties of the activation function.

In order to better analyze the influence of structures corresponding to different residual neural networks on the calculation results, the calculation results of residual neural network structures of different types are summarized, as shown in Figure 7. As can be seen from the figure, different data structures show a trend of gradual decline on the whole. Their different trends can be divided into three stages on the whole: In the first stage, the residual neural network shows a trend of rapid decline and then slow decline. In the process of this change, the data of relevant structures fluctuated to some extent, indicating that the value of this data changed with the increase of the number of iterations. The overall performance is a certain degree of decline. With the further increase of the number of iterations, the data curve drops sharply, thus entering the second stage. At this stage, the data tended to be stable after experiencing a short rapid decline and remained stable all the time, indicating that the curve had good stability on the whole at this stage. As the number of iterations further increases, the data enters the third stage, and the curve shows a slow downward trend. The slope of the corresponding curve gradually approaches zero, indicating that the data has good stability after the first and second stages, and the data can be derived. The curves of different structures are basically the same. It can be seen that the curve values corresponding to ResNet structure are the largest. The values corresponding to the VDSR curve are the smallest in the first part, but only second to the ResNet structure in the second and third parts. The values of the corresponding DRRN structure are second only to ResNet in the first part, but lowest in the second and third parts, indicating that the stability of VDSR and DRRN structure is poor, while the stability of ResNet structure is relatively good.

2.3. Evaluation of Residual Networks. In order to better analyze the calculation results of the residual neural network, different analysis methods are adopted to analyze the deep residual network [19, 20]. The different evaluation indexes can be divided into subjective indexes and objective indexes.

2.3.1. Subjective Evaluation. Mean Opinion Score (MOS) is a subjective evaluation standard for residual network quality evaluation, and its definition is as follows:

$$\text{MOS} = \sum_{i=1}^{n} X_i, \tag{5}$$

where i represents the i-th sample to evaluate the residual network, and X_i is the score of the i-th sample to evaluate the residual network. MOS did not establish a rigorous mathematical model in the process of residual network quality evaluation. Considering the particularity of structural calculation, MOS was not used as the evaluation standard of residual network quality after reconstruction in this paper. The evaluation method of MOS is relatively fair and reasonable and is often used as an indicator of evaluation model algorithm. However, the results of MOS are also subject to subjective influence of participants. Different evaluators will have different views and opinions when comparing the same model, so there is a big gap in the evaluation results, leading to many uncertain factors.

The index of subjective evaluation is the range of scores, which is generally between 1 and 5: 5 means "very good evaluation," 4 means "good evaluation," 3 means "medium evaluation," 2 means "poor evaluation," and 1 means "poor evaluation."

2.3.2. Objective Evaluation. The principle of Mean-Square Error (MSE) is to evaluate the quality of the reconstructed network by analyzing the difference between the reconstructed residual network and the original neural network. It can be expressed as follows:

$$\mathrm{MSE}\frac{1}{\mathrm{mn}}\sum_{i=0}^{m-1}\sum_{j=0}^{n-1}\left(X_{ij}-Y_{ij}\right)^2, \tag{6}$$

where X_{ij} represents the reconstructed residual network with length and width of $m-1$ and $n-1$, and Y_{ij} represents the original neural network with length and width of $m-1$ and $n-1$.

Since the neural network will cause data changes in the process of computation and compression, it is more rigorous to use the Peak Signal-to-Noise Ratio (PSNR) to evaluate the quality of the reconstructed residual neural network.

The function of PSNR is to use data to reflect the advantages and disadvantages of each neural network algorithm, and its specific expression form is as follows:

$$\mathrm{PSNR} = 10\times\ \log_{10}\left(\frac{\mathrm{mn}\times(\mathrm{Max})^2}{\sum_{i=0}^{m-1}\sum_{j=0}^{n-1}\left(X_{ij}-Y_{ij}\right)^2}\right). \tag{7}$$

Max is the peak value of the model, which is 255 in general. If it is 1, it indicates that the model has been linearly normalized. Structural similarity is used to evaluate the similarity of residual neural network from the three aspects of contrast, brightness, and structure and is an index to measure the similarity of residual neural network. The evaluation method is more accurate and has a wider range than PSNR. The definition of structural similarity is as follows:

$$\mathrm{SSIM} = \frac{\left(2u_xu_{x1}+C_1\right)\left(2\delta_{xx1}+C_2\right)}{\left(u_x^2+u_{x1}^2+C_1\right)\left(\delta_x^2+\delta_{x1}^2+C_2\right)}, \tag{8}$$

where u_x represents the gray mean of the original neural network, δ_x represents the variance of the original neural network, u_{x1} represents the gray mean of the neural network after reconstruction, δ_{x1} represents the variance of the residual neural network after reconstruction, δ_{xx1} represents the covariance between x and x_1, and C_1 and C_2 are constants. Generally speaking, the closer SSIM is to 1, the higher the similarity is, and the better the computational quality of the model is. SSIM can evaluate the quality of models from three different aspects, better meeting the requirements of perceptual evaluation, so it is widely used in the field of super-resolution.

3. Behavior Recognition Algorithm

In order to better analyze the behavior recognition algorithm, a behavior recognition flow chart is drawn, as shown in Figure 8. As can be seen from Figure 8, the behavior recognition algorithm mainly includes acquisition end, information processing, feature extraction and behavior recognition. The specific calculation process is as follows: Firstly, the target and sample to be identified are imported to the collection end of the behavior recognition algorithm, and the samples are analyzed by feature extraction and behavior extraction in the collection end. Then, the parameters after feature extraction are input into the information processing module, corresponding to the extraction of morphological features and behavioral features. In order to better analyze the extracted data, the external morphological and behavioral features of the sample are fused through the feature extraction data plate. In this way, the corresponding analysis can be carried out by comprehensively considering the behavior of samples. Finally, the data are compared and verified with the data in the database of the corresponding object's morphological characteristics, so as to explain the relevant problems.

3.1. Basic Theory of Model. The path of behavior recognition algorithm is divided into two-stream recognition network model and class activation model [21–23].

3.1.1. Two-Flow Network Model. Image sequence and optical flow diagram can be regarded as two different modes of information, and the sampling sequence of each mode can be expressed as follows:

$$m_i = \left(m_{i1}, m_{i2}, \ldots, m_{iT}\right), \tag{9}$$

where T is the total number of video frames.

In the model corresponding to the behavior recognition algorithm, the modal features of the image sequence and the modal features of the light flow are average-pooled, and then the channel splicing and feature fusion are carried out, so that the final classification and prediction result of the network for the operation behavior in the video can be expressed as follows:

$$y = h\left(G\left(f_1\left(m_1\right)\right), G\left(f_2\left(m_2\right)\right)\right), \tag{10}$$

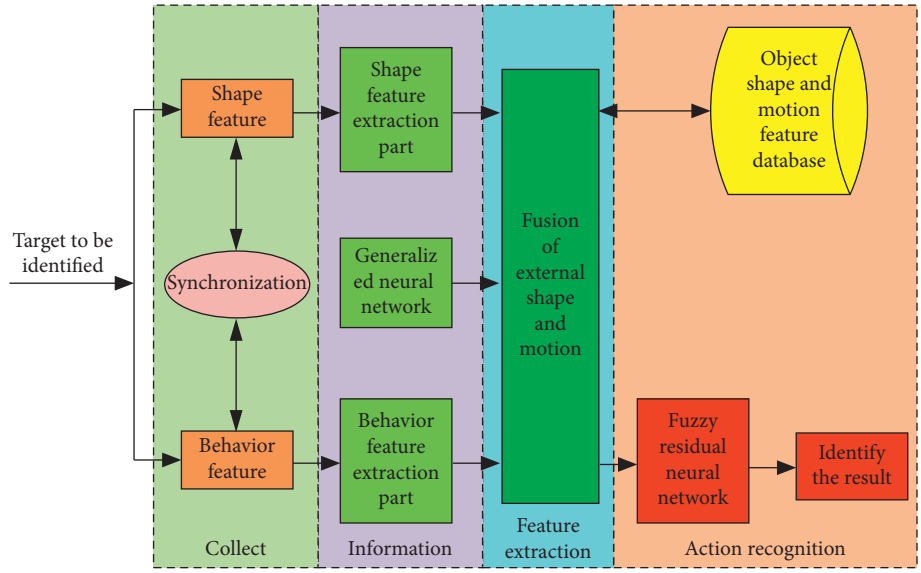

Figure 8: Behavior recognition flow chart.

where f_1 and f_2 are feature extractors of each mode, G is time aggregation function, h is multimode fusion function, and y is the predicted output of video.

3.1.2. Class Activation Model. Class activation model (CAM) is a salient feature model that generates specific categories using average-pooling layer in modern deep CNN network [24, 25]. The principle formula of CAM is derived as follows:

$$F_l = \sum_t f_l(i), \tag{11}$$

where $f_l(i)$ is set as the activation value of unit l at the spatial position i of the last convolutional layer of the network, and CNN network operation is performed on unit l to obtain F_l.

Softmax input for category c is as follows:

$$S_c = \sum_t w_l^c F_l, \tag{12}$$

where w_l^c is the weight.

Softmax output for category c is as follows:

$$P_c = \frac{\exp(S_c)}{\sum_t \exp(S_c)}. \tag{13}$$

For a given category c, its CAM can be expressed as follows:

$$M_c(i) = \sum_t w_l^c f_l(i). \tag{14}$$

Using the CAM generated by M_c, we can identify the image region considered by CNN when it classifies the image as class c. Therefore, if we use the highest probability categories corresponding to the results output by the Softmax function, the generated CAM will provide a saliency feature map of the image. Since the operation behavior in the first view focuses on the object being operated by the first person, CAM can be used to make the network focus on the area of the operation object in the image, so as to realize the spatial positioning of the operation object under weak supervision. In view of the differences among different algorithms in the class activation model, the calculation results of relevant parameters under different algorithms are summarized, as shown in Figure 9:

In order to better analyze the differences and connections of various methods under different training samples, their recognition rates are drawn, as shown in the figure. It can be seen from the figure that, with the gradual increase in the number of iterations, the training samples show different trends. Among them, the recognition rate of F_l data is the highest, and the overall variation range is between 80 and 90. The curve is relatively flat, indicating that the training method is relatively stable. The data of S_c curve was second only to that of F_l, which also showed relatively stable changes, with the overall change ranging from 70 to 89. On the other hand, the data of the corresponding identification methods P_c and M_c are relatively close on the whole, except that the number of iterations is relatively minimum when it is 10, and the range of other changes remains around 80. From the above analysis, we can see that the F_l and S_c methods have relatively high recognition rate, while the P_c and M_c methods have relatively low recognition rate.

3.2. Robust Analysis. Multiple samples are selected as robustness test data for the above algorithm [26–28]. Relevant studies show that the robustness recognition rate of class activation model is higher than that of other methods under different number of training samples [29–31].

Specifically, for each frame of the input image, CAM is firstly calculated using the category with the highest probability output by CNN network, and then Softmax operation is applied along the spatial dimension. The obtained CAM is transformed into a probability graph, which is a spatial attention diagram. Finally, it is multiplied by the output of

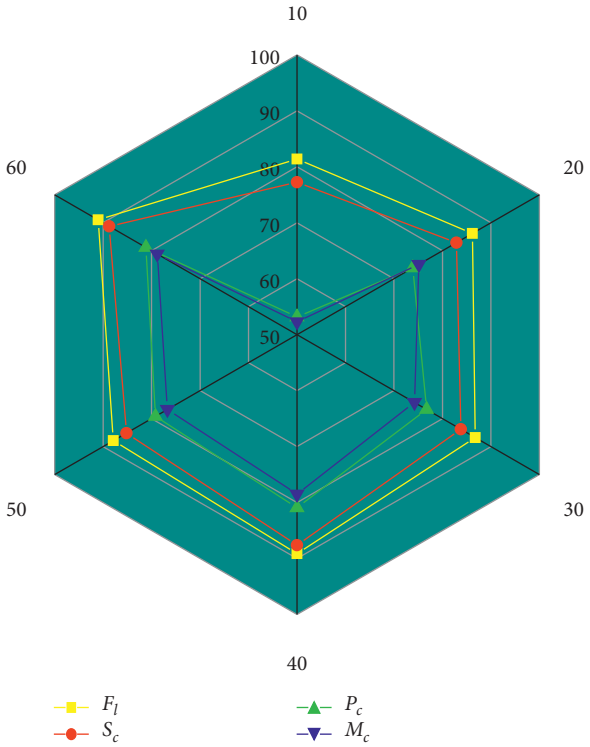

Figure 9: The recognition rates of various methods under different training samples.

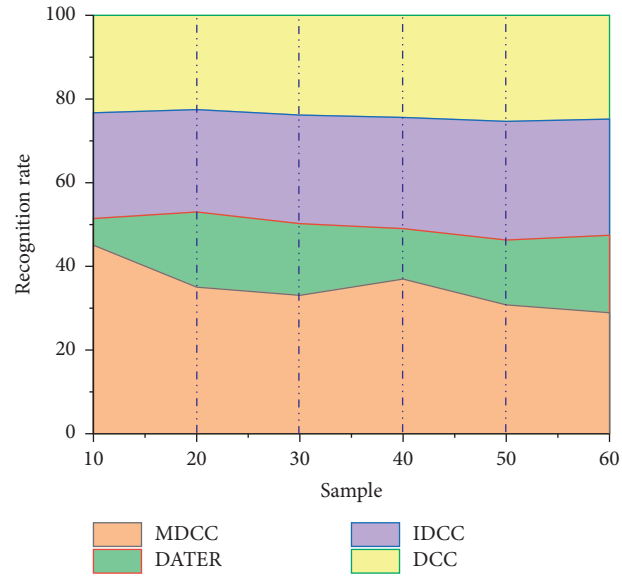

Figure 10: The robustness recognition rates of various methods under different training samples.

the last convolutional layer of CNN network to obtain a new image feature with spatial attention. For each image input frame, the class of CAMs with the highest probability needs to be output using the network. Firstly, the data are applied Softmax operations along the spatial dimension to transform the resulting CAMs into probability maps, and then the last layer of convolution is multiplied with the CNN network output to obtain new image features with spatial attention. The corresponding formula is as follows:

$$f_{\mathrm{SA}}(i) = f(i)\frac{\exp\left(M_c(i)\right)}{\sum_i \exp\left(M_c(i)\right)}, \tag{15}$$

where f_i is the feature graph output by the convolution layer at the spatial position i, $M_c(i)$ is the CAM obtained using the category c with the highest probability output by CNN network, $f_{\mathrm{SA}}(i)$ is the image feature obtained using spatial attention, and $\odot$ is the product of the corresponding elements.

The above methods have certain errors in the recognition of training samples. In order to better study the robustness recognition rates of various methods under different training samples, robustness analysis method is adopted to calculate the data, as shown in Figure 10. As can be seen from the figure, the overall recognition rate of F_l data is the highest, showing a trend of slow decline at first and then a gentle change. The identification trend corresponding to S_c identification method increases rapidly at first, then decreases slowly, and finally increases rapidly, indicating that the stability of this identification method is relatively poor. However, the recognition rate of IDCC and DCC shows a gentle trend of change on the whole, and the corresponding recognition rate is basically the same, indicating that these two methods have certain advantages in describing the robust recognition rate. Therefore, under different training methods, the order of the robustness recognition rate is F_l, P_c, M_c, and S_c.

4. Analysis of Leisure Sports Behavior Recognition Algorithm

4.1. Introduction to Leisure Sports. Leisure sports require people to choose their favorite sports to exercise after work, in order to achieve the goal of physical exercise and relaxation. Compared with traditional sports, leisure sports take fitness and entertainment as the main goals, assuming that all participants can participate in sports in a relaxed state of mind and body. In addition, recreational sports are not necessarily winners like traditional sports, but emphasize that all participants can get a sense of physical and mental pleasure and improve their physical quality, and play a certain role in enriching their spare time.

With the continuous development of the times, leisure sports have become an indispensable part of people's daily life. Leisure sports, as a new form of sports, are characterized by freedom, culture, nonutility, enthusiasm, and initiative. In order to better analyze the influence of different factors on leisure sports, the proportion chart of leisure sports under different impression factors is summarized, as shown in Figure 11. From the proportion of different factors, it can be seen that enthusiasm, as the most important influencing factor in leisure sports, accounts for 33.33% of the total. The proportion of nonutilitarian factors in leisure sports is about 23.33%. Culture, as an important influencing factor, accounts for about 20% of leisure sports. Free activities are one of the leisure sports pursued by people in today's environment, accounting for about 13.33. The lowest proportion

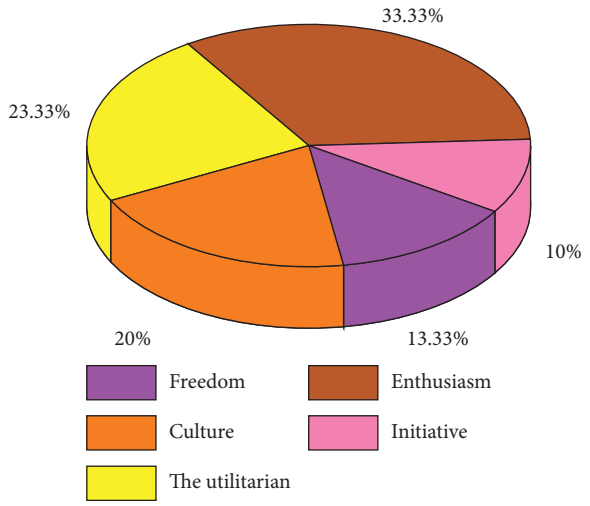

Figure 11: Proportion of main characteristics of leisure sports.

is that of the initiative factor, which is only 10%, indicating that initiative has the least influence on leisure sports.

4.2. Analysis of Leisure Sports Behavior Algorithm. On the basis of the above research, in order to better analyze and study the relevant content of leisure sports, based on the theory of deep residual neural network, behavior recognition algorithm is used to analyze the relevant data of leisure sports, so as to obtain the corresponding recognition algorithm of leisure sports. In order to more accurately describe the variation rule of the samples of the behavioral motion algorithm, the calculation results of different samples under the behavior recognition algorithm are summarized, as shown in Figure 12.

By using the above method to identify leisure sports under different samples, the corresponding sample analysis graph was obtained. It can be seen from the graph that, with the gradual increase of samples, the corresponding value showed a relatively fluctuating trend of change, which remained at about 40 on the whole. The variation trend is a series of fluctuation changes, which first slowly decreases, then gradually increases with the increase of samples, then slowly decreases, and finally slowly increases again. The values are relatively high when the sample size reaches about 52–56. Specifically, when the sample number was 54, the highest sample value (278) was reached.

In order to better analyze the impact of different models on leisure sports, different models are used to analyze relevant data, and the prediction curves of leisure sports under different models are obtained through iterative calculation, as shown in Figure 13. It can be seen from the figure that the calculated data of different models show different changing curve trends, which can be divided into three stages. From the perspective of the dual-flow model, the curve shows a rapid downward trend in the first stage, with a large drop range, indicating that the stability of the curve in this stage is poor. As the number of iterations increases, the curve enters the second stage. The overall performance of the curve is relatively flat, and the variation range is small, indicating that

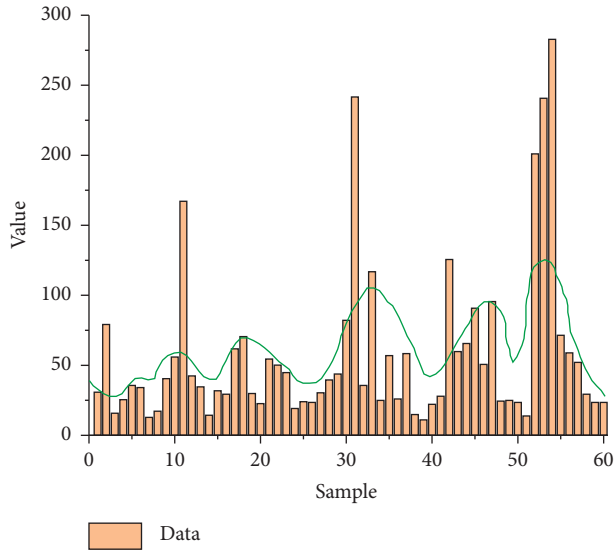

Figure 12: Sample diagram.

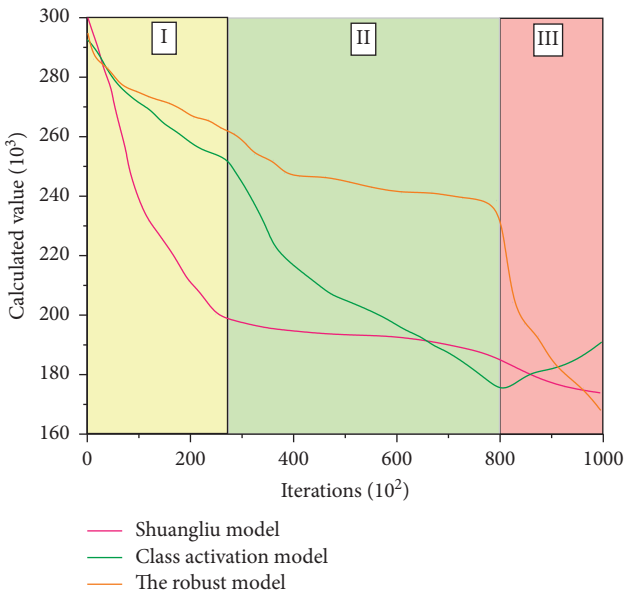

Figure 13: Prediction curves of leisure sports under different schemes.

the stability of the curve in this stage is relatively high. Finally, the curve enters the third stage, showing a slow downward trend. In the quasi-activation model, the curve shows a rapid downward trend in both the first and second stages, but the downward trend in the second stage is higher than that in the first stage. In the third stage, the curve shows an upward trend, indicating that the model increases to a certain extent when the number of iterations is high. In the robustness model, the curve drops slowly in the first stage, shows an approximately constant change trend when it reaches the second stage, and drops rapidly in the third stage. On the whole, the three models have basically the same overall range of variation. The robustness model has good stability in the first and second stages, while the dual-flow model has good stability in the third stage.

5. Conclusion

(1) As time goes by, the scale of sports shows a trend of gradual increase. The scale of leisure sports increases from 129 in 2011 to 731 in 2021, an increase of about 5.7 times. The scale of leisure sports increases gradually with the increase of time, and the increment proportion also shows an increasing trend.

(2) Activation curves of residual neural networks with different structures are basically the same, and the curve values corresponding to ResNet structure are the largest. The values corresponding to the VDSR curve are the smallest in the first part. The DRRN structure values are second only to ResNet in the first part, but lowest in the second and third parts. This indicates that the stability of VDSR and DRRN structures is poor, while the stability of ResNet structures is relatively good.

(3) The overall variation range of F_l data recognition rate is between 80 and 90, and the curve is relatively flat, indicating that the training method is relatively stable. The data of S_c curve was second only to F_l curve, which also showed relatively stable changes. However, the data of the corresponding P_c and M_c identification methods are relatively close, indicating that the recognition rates of P_c and M_c methods are relatively low.

(4) The calculated data of different models show different changing curve trends, which can be divided into three stages. On the whole, the three models have basically the same overall range of variation. The robustness model has good stability in the first and second stages, while the dual-flow model has good stability in the third stage.

Data Availability

The dataset can be accessed upon request.

Conflicts of Interest

The author declares that there are no conflicts of interest regarding the publication of this paper.

References

[1] G. Abosamra and H. Oqaibi, "An optimized deep residual network with a depth concatenated block for handwritten characters classification," *Computers, Materials & Continua*, vol. 68, no. 1, pp. 1–28, 2021.

[2] G. Bansal, V. Chamola, P. Narang, S. Kumar, and S. Raman, ""Deep residual network and morphological descriptor based framework for lung cancer classification and 3D segmentation," *IET Image Processing*, vol. 14, no. 7, pp. 1240–1247, 2020.

[3] W. Shen and X. Li, "Facial expression recognition based on bidirectional gated recurrent units within deep residual network," *International Journal of Intelligent Computing and Cybernetics*, vol. 13, no. 4, pp. 527–543, 2020.

[4] X. Gao, D. Qin, and J. Gao, "Resolution enhancement for inverse synthetic aperture radar images using a deep residual network," *Microwave and Optical Technology Letters*, vol. 62, no. 4, pp. 1588–1593, 2020.

[5] C. Ge, Q. Du, W. Sun, K. Wang, J. Li, and Y. Li, "Deep residual network-based fusion framework for hyperspectral and LiDAR data," *Ieee Journal of Selected Topics in Applied Earth Observations and Remote Sensing*, vol. 14, no. 99, pp. 2458–2472, 2021.

[6] H. Han, Z. Li, J. Jia, J. Zhang, and M. Wang, "Blind image quality assessment with channel attention based deep residual network and extended LargeVis dimensionality reduction," *Journal of Visual Communication and Image Representation*, vol. 80, no. 2, pp. 406–442, 2021.

[7] J. Li and Y. Chen, "A physics-constrained deep residual network for solving the sine-Gordon equation," *Communications in Theoretical Physics*, vol. 73, no. 1, pp. 150–169, 2021.

[8] Q. Li, H. Kang, R. Zhang, and Q. Guo, "Non-invasive precise staging of liver fibrosis using deep residual network model based on plain CT images," *International Journal of Computer Assisted Radiology and Surgery*, vol. 17, no. 4, pp. 627–637, 2022.

[9] Z. Li, X. Xu, and D. Zhang, "Cross-model hashing retrieval based on deep residual network," *Computer Systems Science and Engineering*, vol. 36, no. 2, pp. 383–405, 2021.

[10] J. Zhao, L. Hu, Y. Dong, L. Huang, S. Weng, and D. Zhang, "A combination method of stacked autoencoder and 3D deep residual network for hyperspectral image classification," *International Journal of Applied Earth Observation and Geoinformation*, vol. 102, no. 4, pp. 10245–10269, 2021.

[11] H. Pan, "Research on intelligent fault diagnosis of rolling bearing based on improved deep residual network," *Applied Sciences*, vol. 11, no. 15, pp. 436–457, 2021.

[12] P. M. Rajasree, A. Jatti, and D. Santosh, "An improved transfer learning approach towards breast cancer classification on deep residual network," *Indian Journal of Computer Science and Engineering*, vol. 12, no. 4, pp. 1136–1148, 2021.

[13] Q. Chen, W. Zhang, K. Zhu, D. Zhou, H. Dai, and Q. Wu, "A novel trilinear deep residual network with self-adaptive Dropout method for short-term load forecasting," *Expert Systems with Applications*, vol. 182, no. 12, pp. 115–142, 2021.

[14] S. Wei-Chung and C. Dar-Ren, "Classification of malignant tumors in breast ultrasound using a pretrained deep residual network model and support vector machine," *Computerized Medical Imaging and Graphics*, vol. 87, no. 12, pp. 10182–10199, 2021.

[15] S. S. Sobin and M. V. Celestin, "Feedback deer hunting optimization algorithm for intrusion detection in cloud based deep residual network," *International Journal of Modeling, Simulation, and Scientific Computing*, vol. 15, no. 106, pp. 726–745, 2021.

[16] H. Sun, A. Wang, W. Wang, and C. Liu, "An improved deep residual network prediction model for the early diagnosis of alzheimer's disease," *Sensors*, vol. 21, no. 12, pp. 4182–4196, 2021.

[17] W. Wang, Z. Zhou, H. Liu, and G. Xie, "MSDRN: pansharpening of multispectral images via multi-scale deep residual network," *Remote Sensing*, vol. 13, no. 6, pp. 120–142, 2021.

[18] L. Yan, J. Feng, T. Hang, and Y. Zhu, "Flow interval prediction based on deep residual network and lower and upper boundary estimation method," *Applied Soft Computing*, vol. 104, no. 11, pp. 1072–1088, 2021.

[19] H. Lin and J. Yang, "Light weight IBP deep residual network for image super resolution," *IEEE Access*, vol. 9, no. 19, pp. 52–69, 2021.
[20] S. Zhu, Q. Zhang, W. Zhai, and Z. Yuan, "Sensor deploying for damage identification of vibration isolator in floating-slab track using deep residual network," *Measurement*, vol. 183, no. 2, pp. 428–436, 2021.
[21] X. Chen and V. Dinavahi, "Group behavior pattern recognition algorithm based on spatio-temporal graph convolutional networks," *Scientific Programming*, vol. 2021, no. 15, Article ID 2934943, 57 pages, 2021.
[22] K. Arati, K. Ashish, and K. Manish, "Human activity recognition algorithm in video sequences based on integration of magnitude and orientation information of optical flow," *International Journal of Image and Graphics*, vol. 22, no. 1, pp. 596–612, 2021.
[23] P. Wang and Z. Xu, "A novel consumer purchase behavior recognition method using ensemble learning algorithm," *Mathematical Problems in Engineering*, vol. 2020, no. 16, Article ID 6673535, 745 pages, 2020.
[24] C. Pang, "Simulation of student classroom behavior recognition based on cluster analysis and random forest algorithm," *Journal of Intelligent and Fuzzy Systems*, vol. 40, no. 2, pp. 2421–2431, 2021.
[25] M. Sivarathinabala, S. Abirami, and R. Baskaran, "Abnormal gait recognition using exemplar based algorithm in healthcare applications," *International Journal of Communication Systems*, vol. 33, no. 4, pp. 365–379, 2020.
[26] T. Somoskoi, C. Vass, P. Jojart, P. Santha, and K. Osvay, "Development of a defect recognition algorithm for visual laser-induced damage detection," *Laser Physics*, vol. 30, no. 4, pp. 4602–4623, 2020.
[27] A. Takaoka, "A recognition algorithm for adjusted interval digraphs," *Discrete Applied Mathematics*, vol. 294, no. 3, pp. 253–256, 2021.
[28] R. Ma, Z. Zhang, and E. Chen, "Human motion gesture recognition algorithm in video based on convolutional neural features of training images," *Journal of Complexity*, vol. 21, no. 45, pp. 736–752, 2021.
[29] S. Wu, "Simulation of classroom student behavior recognition based on PSO-kNN algorithm and emotional image processing," *Journal of Intelligent and Fuzzy Systems*, vol. 40, no. 4, pp. 7273–7283, 2021.
[30] M. Zhou, L. Han, H. Lu, C. Fu, and D. An, "Cooperative malicious network behavior recognition algorithm in E-commerce," *Computers & Security*, vol. 95, no. 16, pp. 1018–1048, 2020.
[31] D. Zhang and H. J. Min, "A sport monitoring system based on the optimized adaptive fuzzy PID control algorithm in OneNet internet of things and cloud platform," *Computational Intelligence and Neuroscience*, vol. 2022, Article ID 8234066, 13 pages, 2022.

Hindawi
Scientific Programming
Volume 2022, Article ID 6355959, 11 pages
https://doi.org/10.1155/2022/6355959

Research Article

Dance Art Scene Classification Based on Convolutional Neural Networks

Le Li

College of Music, University of Sanya, Sanya 572000, China

Correspondence should be addressed to Le Li; 16461071021@stu.wzu.edu.cn

Received 24 May 2022; Revised 17 June 2022; Accepted 22 June 2022; Published 8 July 2022

Academic Editor: Lianhui Li

Digital multimedia resources have become an important part of people's daily cultural life. Automatic scene classification of a large number of dance art videos is the basis for scene semantic based video content retrieval. In order to improve the accuracy of scene classification, the videos are identified using a deep convolutional neural network based on differential evolution for dance art videos. First, the Canny operator is used in YCbCr colour space to detect the human silhouette in the key frames of the video. Then, the AdaBoost algorithm based on cascade structure is used to implement human target tracking and labelling, and the construction and updating of weak classifiers are analysed. Next, a differential evolution algorithm is used to optimise the structural parameters of the convolutional neural network, and an adaptive strategy is adopted for the scaling factor of the differential evolution algorithm to improve the optimisation solution accuracy. Finally, the improved deep convolutional neural network is used to train the classification of the labelled videos in order to obtain stable scene classification results. The experimental results show that by reasonably setting the crossover rate of differential evolution and the convolutional kernel size of the convolutional neural network, high scene classification performance can be obtained. The high accuracy and low root-mean-square error validate the applicability of the proposed method in dance art scene classification.

1. Introduction

Due to the accelerated pace of life today, many people are busy with work, resulting in not having enough time to rest. People want to enrich their spare time activities more in their leisure time, such as dancing. However, as dance learning usually requires attending professional classes offline, resulting in many people not having much time to learn. Therefore, it has become a trend to learn dance by searching and watching online videos [1–7]. The main means of expression in the art of dance is the flexible footwork and graceful movement of the human body. Dance expresses feelings and reflects social life through this art form. As society continues to develop, people's demand for quality of life continues to increase. The traditional offline dance learning method is no longer able to meet people's needs, and is still very limited. As more and more people want to learn dance, which creates the problem of limited resources in teaching dance teachers, the original face-to-face teaching method can no longer meet the actual needs. Online teaching has become more and more accepted and has become a new mode of teaching.

The online teaching and learning process requires students to access the knowledge they learn through the computer network. As online teaching not only maximises the sharing of information resources, it can also generate multiple forms of teaching and learning, helping to improve teaching efficiency and achieve sharing of teaching resources. At present, there is an explosive growth in the use of digital multimedia video. Along with the popularity of the Internet, massive amounts of dance art video data have appeared on various online media [8–10]. According to relevant statistical reports, online media around the world generate about tens of T of video data every day, which contains video data of movies, music and dance.

With so much dance video data available, only a fraction of it is of interest to each individual. So, how can one find the data one needs from this dance video data? This requires

effective scene classification of this dance video data. Classifying scenes from a large number of dance videos can be a very difficult task. The traditional method is to annotate and classify these videos manually, thus, forming a database of dance videos that can be indexed by keywords. However, with the huge amount of dance video data, it would take a lot of human resources, money, and time to use the manual annotation method [11–13]. This manual approach requires staff to face a large amount of dance video data every day, which is prone to visual errors, thus, leading to errors in video annotation and classification. Therefore, this traditional method has major drawbacks [14]. An alternative approach is to use computers to analyse these massive amounts of video data and eventually achieve an automated dance video scene classification system. In using computer technology to annotate, classify, and retrieve dance videos, an efficient algorithm needs to be designed to process them [15]. In recent years, the issues of video annotation, video scene classification, and video retrieval have become a hot research topic in the multimedia field. Numerous scholars and research institutions have conducted in-depth research on this problem.

Traditional video scene classification methods generally use manually designed features for modelling. Wei et al. [16] proposed a motion human tracking algorithm based on region segmentation contours with more accurate and stable performance in complex occlusion situations. Suganya et al. [17] proposed an AdaBoost-STC and random forest based human eye tracking and localisation algorithm. Wang et al. [18] proposed a target tracker based on likelihood graph and real-time AdaBoost cascade. Both methods are effective in improving tracking speed without degrading tracking accuracy. Ibrahim et al. [19] conducted a video classification study using video saliency features. They divided the RGB colour channel of each frame into three images, and then combined the grey-scale images to arrange these three images in temporal order to obtain three spatio-temporal container models. These spatio-temporal containers were then subjected to pyramidal degradation and the regions of significance in the containers were divided using mean clustering. Finally, a support vector machine is used to classify the video scenes. This algorithm has a more complex process and is not effective in video scene classification. Calvin et al. [20] mapped motion vectors into the unit circle and divided it into 8 regions. Each motion vector is mapped to the coordinate axes of the corresponding region, and the corresponding matrix is derived as features for the data on the axes. Finally, the SVM is used to classify the video. However, this method can only detect the corresponding moments taken as features, and finally, the video is classified using SVM. However, this method can only detect some motion patterns in the video, such as jumping, running, swimming, and some other specific events, and cannot determine the scene classification of the video. Lu et al. [21] classify the video by taking the comparative values of luminance between regions in the video as featured, and by using Hidden Markov Model (HMM). This method is able to eliminate the influence of factors such as illumination on the video, but can only perform the classification of different categories of videos, such as news, movie, and animation videos. In addition, the calculation of the parameters of the HMM requires a large number of videos for training, and the whole process is more complicated.

Semantic-based information processing has developed rapidly in recent years with the development of artificial intelligence and data mining techniques. Many researchers are conducting research in mapping from the underlying features of the video to the semantic information of the video. By mining the semantic information of videos and forming semantic rules according to certain algorithms, scene classification of video data can be achieved. Therefore, the use of semantic information to classify video is also a future trend in video classification. Deep learning abandons the complex operation process of the underlying features in the traditional algorithm, so it can effectively achieve the task of video semantic information mining based on computer vision. Convolutional neural network (CNN) [22–24], which emerged in the field of deep learning, first achieved great success in image recognition and image segmentation. Then, breakthroughs in typical network structures continued, such as recurrent neural network (RNN) [25, 26], deep belief network (DBN) [27], generative adversarial networks (GAN) [28], and other types of network structures. These network structures are capable of enhancing the feature extraction capability of models in a supervised learning manner. Compared to traditional machine learning methods, deep neural networks perform feature extraction at different scales on images, combining gradients to explore better strategies, and saving the tedious manual feature extraction process. As a result, deep neural networks only require a well-designed network structure. With the excellent image feature representation capability, deep neural networks have good robustness in dealing with scene classification problems of sports, news, and other videos. However, dance art videos are more diverse and involve human target tracking and labelling problems, so, the various types of network structures available in deep learning do not perform well enough for the scene classification task of dance videos.

The aim of this study is to automatically classify scenes from dance videos using deep convolutional neural networks and to further improve the accuracy of the model through structural parameter optimisation. The proposed method helps to implement a video content retrieval task based on scene semantics.

Key innovations and contributions to the video include the following:

(1) Both the contour model and the AdaBoost algorithm show some advantages in terms of robustness and accuracy of video target tracking. Therefore, a combination of both is proposed to solve the person tracking problem in dance art videos.

(2) A deep CNN based on differential evolution (DE) [29] was proposed to address the problem of unsatisfactory classification efficiency and stability of the traditional CNN structure in processing the classification of dance video scenes based on

semantic information. The DE algorithm was introduced to optimally solve the network parameters, and an adaptive strategy was adopted for the scaling factor of the DE algorithm to improve the accuracy of the optimal solution.

The rest of the paper is organized as follows: in Section 2, the target detection based on human silhouette model in dance video isstudied in detail, while Section 3 provides the human tracking based on the cascade structure AdaBoost algorithm. Section 4 provides the DE-CNN based dance video scene classification. Section 5 provides the experimental results and analysis. Finally, the paper is concluded in Section 6.

2. Target Detection Based on Human Silhouette Model in Dance Videos

In dance video data, the human body often rotates, translates, and stretches. However, the detection of human targets becomes difficult, when the body's pose is constantly changing. Therefore, the video uses a statistical learning model based on a human contour model to implement human body detection.

2.1. YCbCr Colour Model. First, the RGB colour model is converted into a YCbCr colour model in the 3D colour space, which is mainly used for edge detection and image segmentation in the digital video field, and its colour cube diagram is shown in Figure 1.

$$\begin{bmatrix} Y \\ Cb \\ Cr \end{bmatrix} = \begin{bmatrix} 16 \\ 128 \\ 128 \end{bmatrix} + \begin{bmatrix} 65.481 & 128.553 & 24.966 \\ -37.797 & -74.203 & 112 \\ 112 & -93.786 & -18.214 \end{bmatrix} \begin{bmatrix} R \\ G \\ B \end{bmatrix}, \quad (1)$$

where Y is the intensity information, Cb and Cr are the colour difference components of the colour image.

2.2. Canny Operator Edge Detection. The human body image is preprocessed by edge detection, in order to extract the human contour features. The first order derivative of the two-dimensional function $f(x, y)$ of the human body image is expressed as follows:

$$\nabla f(x, y) = \begin{bmatrix} \dfrac{\partial f}{\partial x} \\ \dfrac{\partial f}{\partial y} \end{bmatrix}. \quad (2)$$

The second order derivative of a two-dimensional function $f(x, y)$ is expressed as follows:

$$\nabla^2 f(x, y) = \frac{\partial^2 f(x, y)}{\partial x^2} + \frac{\partial^2 f(x, y)}{\partial y^2}. \quad (3)$$

The luminance region can be divided by finding the pixel points that satisfy $\nabla^2 f(x, y) = 0$. The video uses the Canny operator [30] to implement human edge detection. The edge direction of each pixel point is calculated by equation (4).

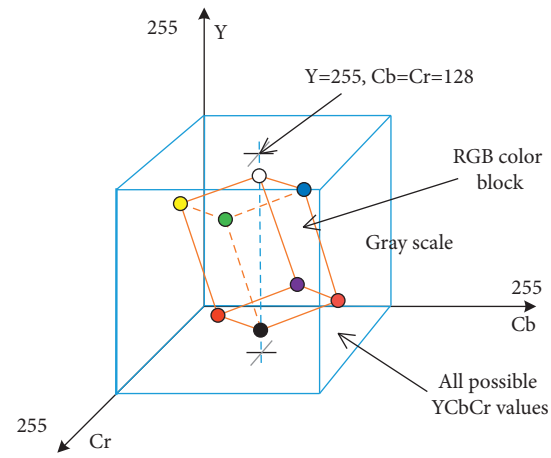

Figure 1: YCbCr colour model.

$$\alpha(x, y) = arc\ \tan\begin{bmatrix} \dfrac{\partial f}{\partial y} \\ \dfrac{\partial f}{\partial x} \end{bmatrix}. \quad (4)$$

The pixel point with the maximum pixel gradient is set as the edge pixel point. The pixel gradient is calculated as shown follows:

$$g(x, y) = \frac{1}{(\partial f/\partial x)^2 + (\partial f/\partial y)^2}. \quad (5)$$

3. Human Tracking Based on the Cascade Structure AdaBoost Algorithm

Recently, integrated methods like AdaBoost (adaptive boosting) have been successfully applied to many target tracking problems. AdaBoost classifier is a meta-algorithmic classifier and utilises the same base classifier (weak classifier). Based on the error rate of the classifier, the AdaBoost classifier can be assigned different weighting parameters. Finally, the integrated classifier outputs predictions occur by means of a summation operation of the weights.

3.1. Construction and Updating of Weak Classifiers. For each pixel in each image frame, the weak classifier is defined as follows:

$$h(x) = \text{sign}\left(h^T x\right), \quad (6)$$

where x is the sample and h is the adjusted segmentation hyperplane, calculated as follows:

$$h = \left(\mathbf{A}^T \mathbf{W} \mathbf{A}\right)^{-1} \mathbf{A}^T \mathbf{W} y, \quad (7)$$

where y is the sample label, $\mathbf{A}$ is a matrix, and $\mathbf{W}$ is a diagonal matrix of weights. The sample weights are updated as follows:

$$D_i = D_i e^{\alpha_t |h_t(x_i - y_i)}. \tag{8}$$

3.2. Description of the Algorithm Flow. The AdaBoost algorithm is an iterative algorithm. AdaBoost can aggregate multiple weak classifiers from the same training set to form a strong classifier. The main steps of the AdaBoost algorithm are shown as follows:

Step 1. Set the input be $\{(x_1, y_2), (x_2, y_2) \ldots (x_n, y_n)\}$ where, $x_i \in X$, $y_i \in \{-1, 1\}$ and the data set be X. Initialize the weights $D_1(i)$ is shown as follows:

$$D_1(i) = \frac{1}{n}, \quad i = 1, 2 \ldots n.t \tag{9}$$

Step 2. Find the weak classifier h_t: $X \longrightarrow \{-1, 1\}$, when $t = 1, 2 \ldots T$ and train a weak classifier h_j with each feature f_j, which gives a weighted error rate.

$$\epsilon_j = \sum_{t=1}^{n} D_t, h_t(x_i) \neq y_i. \tag{10}$$

Step 3. The classifier h_t with the smallest weighted error rate ϵ_j is selected and its smallest weighted error rate value is noted as ϵ_t. The weights of the weak classifier are then calculated as follows:

$$\alpha_t = \frac{1}{2}\ln\left(\frac{1 - \epsilon_t}{\epsilon_t}\right). \tag{11}$$

Step 4. The actual method used to update the sample weights is shown as follows:

$$D_{t+1}(i) = \frac{D_t(i)\exp[-\alpha_t y_i h_t(x_i)]}{Z_t}. \tag{12}$$

where Z_t denotes the normalisation parameter.

Step 5. Construct the final strong classifier using the following approach.

$$H(x) = \operatorname{sign}\left(\sum_{t=1}^{T} \alpha_t y_i h_t(x)\right). \tag{13}$$

4. DE-CNN Based Dance Video Scene Classification

4.1. Adaptive DE Algorithm. Let the population size be N, the attribute dimension be D, the differential scaling factor be F, the crossover rate be CR, and the value of each individual be $[U_{\min}, U_{\max}]$, then the j dimensional attribute [31] of the i-th individual can be shown as follows:

$$x_{ij} = U_{\min} + \text{rand} \times (U_{\max} - U_{\min}), \tag{14}$$

where $i = 1, 2, \cdots, N$, $j = 1, 2, \cdots, D$, rand are random numbers in (0, 1).

Individuals x_i^G, $(i = 1, 2, \ldots, N)$ of the G generation can obtain the $G + 1$ generation using the mutation operation.

$$v_i^{G+1} = x_{r_1}^G + F \times \left(x_{r_2}^G - x_{r_3}^G\right), \tag{15}$$

where r_1, r_2, and r_3 are three random individuals from the G generation. A common range of F values is $[0, 2]$.

The individual crossover method is shown as follows:

$$u_{ij}^{G+1} = \begin{cases} v_{ij}^{G+1}, & \text{rand}(0, 1) \leq CR, \\ x_{ij}^G, & \text{otherwise.} \end{cases} \tag{16}$$

Compare x_i^G with u_i^{G+1} and find the fitness value of each individual. Select the individual with the higher fitness value for the subsequent evolutionary process.

$$x_i^{G+1} = \begin{cases} u_i^{G+1}, f\left(u_i^{G+1}\right) > f\left(x_i^G\right), \\ x_i^G, f\left(u_i^{G+1}\right) \leq f\left(x_i^G\right), \end{cases} \tag{17}$$

where f represents the fitness function. The DE algorithm stops, when the maximum number of generations $G_{\max}$ is reached.

A common range of F values is $[0, 2]$. The optimisation process for DE is closely related to the F value. A wrong choice of F value will result in unsatisfactory optimisation performance of the differential evolution algorithm. Therefore, adaptive F values are introduced in the calculation. The value range of $F_{\min}$ and $F_{\max}$ is $[0, 2]$.

$$F = F_{\min} + \left(F_{\max} - F_{\min}\right) \times e^{1 - G_{\max}/G_{\max} - G + 1}. \tag{18}$$

The F value becomes progressively smaller as the evolutionary generation G changes. Early evolution pursues population diversification, while late evolution focuses on search ability, so that the DE algorithm is more likely to obtain optimal individuals.

4.2. CNN Model Design. Machine learning has played a huge role in computer vision processing techniques. Most of the traditional machine learning methods use shallow structures that deal with limited data operations. A large number of experiments have proven that the feature expressions learned from shallow structures, when dealing with complex classification problems, are difficult to meet the practical needs. In recent years, computer performance has continued to improve, providing a powerful support for deep learning. New deep learning models are constantly being proposed and successfully incorporated into application areas such as image recognition, speech recognition, and natural language processing.

Common deep learning models in image recognition include deep belief network (DBN), recurrent neural network (RNN), generative adversarial network (GAN), capsule network (CapsNet), restricted boltzmann machines (RBMs), and convolutional neural network (CNN). Based on the deep

convolution neural network, this paper selects the most representative dance video as the recognition object.

Originally designed, specifically to handle image recognition tasks, CNNs are multilayer neural networks and are currently the most classical and commonly used computational structure in the field of computer vision. The basic structure of a CNN consists of an input layer, an implicit layer and an output layer. The implicit layer is the core part of the convolutional neural network, which contains the convolutional layer, the pooling layer (also known as the downsampling layer), and the fully connected layer, as shown in Figure 2.

Pooling layers generally reduce the dimensionality of the input feature map between successive convolutional layers. The pooling layer effectively reduces the output feature vector of the convolution layer. This process uses a partially contiguous region of the image as the pooling region and translates the sliding window matrix of the pooling function within the region. The pooling size and step size control the sliding window size and translation rule respectively, as shown in Figure 3.

Let the set of dance video samples be $\mathbf{X} = (x_1, x_2, \ldots x_N)$. The m video attribute features are convolved through the l layer.

$$x_{lj} = f\left(\sum_{j\in m} x_{l-1} * k_{lj} + b_{lj}\right), \tag{19}$$

where k_{lj} and b_{lj} represent the weights and biases assigned to the features j by the l layer, respectively, and $*$ is the convolution.

$$f(z) = \frac{1}{1+e^{-z}}. \tag{20}$$

Convolution of m features is from N samples. Convolution kernel size $h \times w$:

$$g(x) = \max_{1\le k\le h\times w}(x_k). \tag{21}$$

Assuming $M = N/(h \times w)$, then the original sample $\mathbf{X} = (x_1, x_2, \ldots x_N)$ is reconstructed after convolution pooling as $\mathbf{X}' = (x_1, x_2, \ldots x_M)$. The conversion operation is then performed on $\mathbf{X}'$.

$$x_j^l = f\left(\sum_{i=1}^{M} a_{ij}\left(x_i^{l-1} * k_i^l\right) + b_j^l\right). \tag{22}$$

The restrictions are $\sum a_{ij} = 1, 0 \le a_{ij} \le 1$.

After obtaining all the connected layers of the CNN, the classifier is selected to predict the sample class. Let the training output and the actual value of the k-th node be y_k and d_k, respectively, and the error term be δ_k.

$$\delta_k = (d_k - y_k) y_k (1 - y_k). \tag{23}$$

Assuming that the l and $l+1$ layers contain L and P nodes, respectively, the error of node j in the l layer is δ_j.

$$\delta_j = h_j\left(1 - h_j\right)\sum_{k=1}^{P} \delta_k W_{jk}, \tag{24}$$

where h_j is the output and W_{jk} is the weight of the neuron j to the neuron k in the $l+1$ layer. The weights are updated as shown follows:

$$\Delta w_{jk}(n) = \frac{\eta}{1+N}\left(\Delta w_{jk}(n-1) + 1\right)\delta_k h_j, \tag{25}$$

where η is the learning rate.

The bias $\Delta b_k(n)$ is updated as follows:

$$\Delta b_k(n) = \frac{\alpha}{1+N}\left(\Delta b_k(n-1) + 1\right)\delta_k, \tag{26}$$

where α is the bias update step, typically $\alpha = 1$. The adjusted weights are shown as follows:

$$w_{jk}(n+1) = w_{jk}(n) + \Delta w_{jk}(n). \tag{27}$$

The adjusted offsets are shown as follows:

$$b_k(n+1) = b_k(n) + \Delta b_k(n). \tag{28}$$

The error for all nodes E is shown as follows:

$$E = \frac{1}{2}\sum_{k=1}^{M}(d_k - y_k)^2. \tag{29}$$

When E meets the set threshold, the iteration stops and a stable CNN model is obtained.

4.3. Classification Process Based on DE-CNN Model. Before the CNN can be applied to classify a video, the sample data to be classified first needs to be transformed, which is mainly to address the vectorisation process of the video attributes. The converted Skip-gram facilitates efficient input to the CNN. After the CNN video classification model is established, the random weights and biases are optimally solved by the DE algorithm. An adaptation function is established based on the video classification accuracy function. The optimal individuals of weights and biases are obtained by multigeneration evolution of DE. Finally, the video classification results are obtained using CNN for classification training, as shown in Figure 4.

5. Experimental Results and Analysis

5.1. Experimental Setup. In order to validate the performance of the DE-CNN model in dance video scene classification, simulation experiments were conducted on dance video sequences (resolution 640×480), with the length of 400 frames. Firstly, the performance of human target tracking was verified. Secondly, the performance was verified for different DE algorithm parameters. Then, the performance was verified for different convolutional kernel sizes. Finally, the performance of the DE-CNN model is compared with commonly used video scene classification algorithms.

The data sources for the video classification experiment were 11 large video websites. All videos were in MP4 format, and seven categories of dance videos were selected for the classification test: classical dance, ballet, folk dance, modern dance, tap dance, jazz dance, and Latin dance. The number of videos in each category is 500, so there are 3500 dance video sequences in the experimental video dataset. The

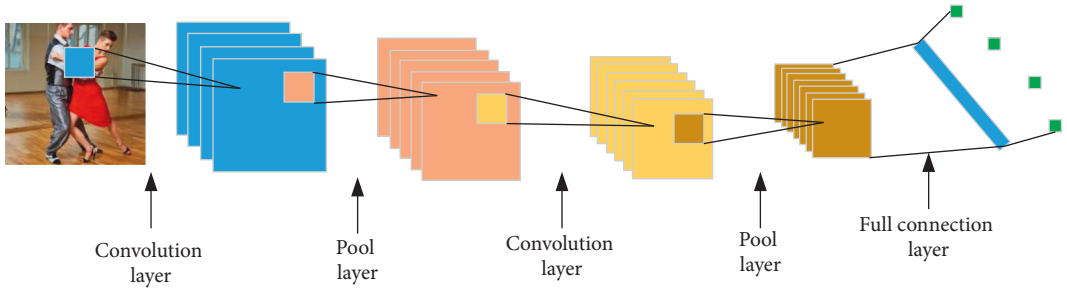

Figure 2: CNN network structure.

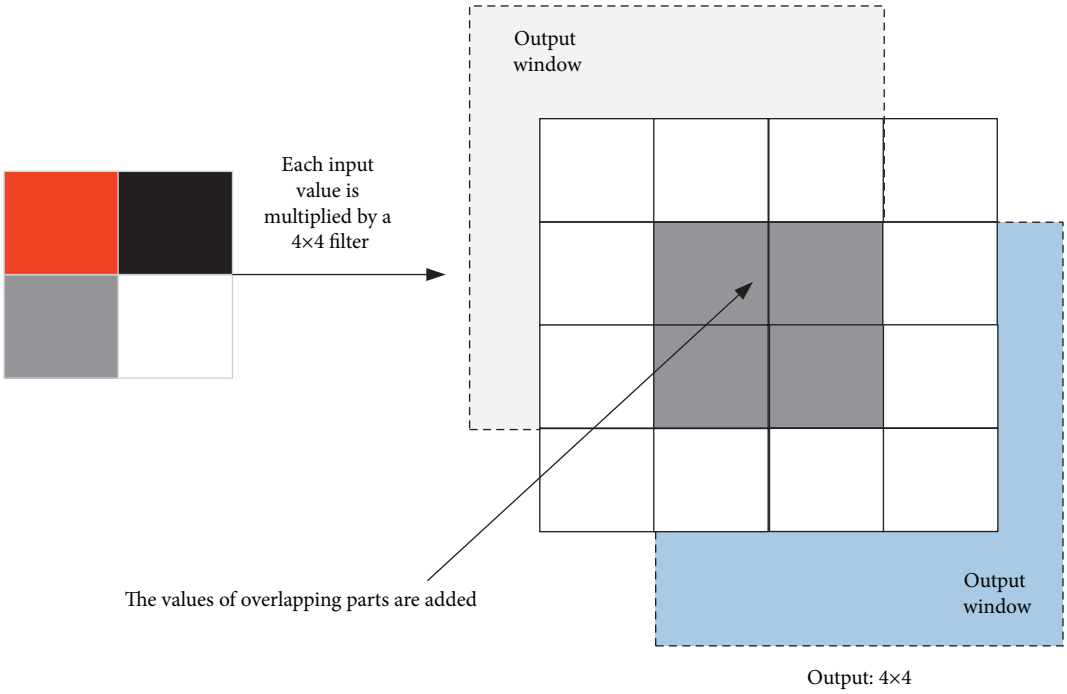

Figure 3: Pooling feature diagram.

length of each video sequence was 400 frames and the duration was 5 min. Some of the data of the dance video samples are shown in Figure 5.

The proposed method classifies the dance videos so that automatic scene recognition can be achieved. Information on the experimental video dataset is shown in Table 1.

The video from Table 1 was transformed using the Skip-gram structure, thus completing the video-to-attribute vector mapping. This allowed the video samples to be trained for CNN classification. During the experiments, the entire dance video sample set was trained and tested in a 7 : 3 ratio respectively. The experimental hardware environment is: CPU i7 3770 (3.4 Hz), 8 G RAM. The experimental software environment is: Windows 10 operating system, Matlab 7.0 simulation software. The initial values of DE algorithm settings are $F_{\min} = 0.2$, $F_{\max} = 0.9$, $CR = 0.1$, and $G_{\max} = 100$. CNN convolutional kernels are $2 * 2$ by default.

5.2. Human Target Tracking Performance. The effect of human target detection was first quantified in order to assess its robustness. The panning errors for human detection are shown in Figure 6. As can be seen from Figure 6, the human detection is good in the panning case with an average error of less than 10 pixels.

In addition, in order to quantitatively compare the tracking performance, the comparison experiments of the same video sequences are conducted by using hybrid algorithm, AdaBoost-STC algorithm, and adaptive EKF algorithm.

$$d = \sqrt{\sum_{i=1}^{N} (x_i - y_i)^2}, \tag{30}$$

where x_i is the centre of the trace result and y_i is the centre of the baseline result.

After repeating the experiment 100 times and taking statistical averages, the human tracking results for the three different algorithms on a 400-frame video sequence are shown in Figure 7.

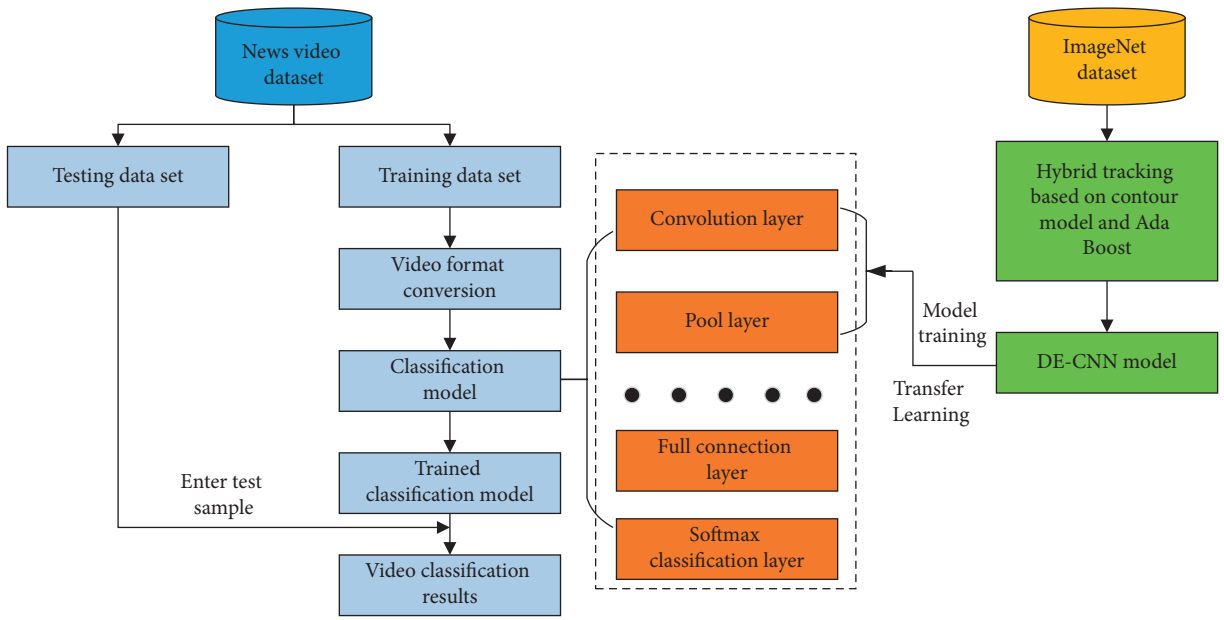

Figure 4: Flow of dance video scene classification based on DE-CNN model.

As can be seen in Figure 7, the difference in centroid pixel error between the three different algorithms is not very significant until 250 frames. However, as the tracking time increases, the hybrid tracking algorithm based on the contour model and AdaBoost shows a stronger advantage when it exceeds 250 frames. In other words, the hybrid tracking algorithms based on the contour model and AdaBoost are better in terms of stability and robustness under the same conditions.

5.3. Video Classification Performance with Different Convolution Sizes. CNN structures with different kernel sizes were used to test the experimental samples separately, and the results are shown in Table 2.

From Table 2, the best results were obtained when the convolutional kernel size of $3 * 3$ was chosen, and the classification accuracy of the dance video data samples came to 92.16%. When the size increases, the classification accuracy and standard deviation are decreasing. This is because the convolution size is too large, resulting in a larger convolutional granularity, which reduces the opportunity for the important attributes of the samples to participate in the convolution and transformation operations. The temporal performance of the DE-CNN algorithm on the dance video dataset, when the convolutional kernel size is $3 * 3$ is shown in Figure 8.

As can be seen from Figure 8, the classification time of the DE-CNN model was about 55 s at a convolutional kernel size of $3 * 3$. Ultimately, the classification accuracy of the DE-CNN model at convergence was all over 0.9.

5.4. Optimisation Performance of the DE Algorithm. In order to verify the optimisation performance of the DE algorithm for CNN, the performance of the test samples was simulated using the CNN algorithm and the DE-CNN algorithm, respectively.

As can be seen from Table 3, the DE-CNN algorithm showed better performance in the classification of dance video scenes. All three metrics of DE-CNN video classification exceeded 0.9. The maximum classification accuracy of DE-CNN was 93.18%, while the maximum classification accuracy of CNN was only 88.96%, so the accuracy of DE-CNN was significantly improved. This is mainly due to the fact that after weight optimisation by DE, the CNN obtains better weights and bias initial values, resulting in a more accurate video classification performance. The comparison of the convergence performance of the two algorithms will be continued below, as shown in Figure 9.

It can be seen that the convergence performance of DE-CNN is significantly superior compared to CNN. In the classification of dance video data samples, DE-CNN converges with an RMSE of about 0.18, while CNN converges with an RMSE value of about 2.5. Therefore, the DE-CNN algorithm has better classification stability compared to the CNN algorithm. In terms of convergence time, the CNN converges in about 5 s less than the DE-CNN. This may be due to the longer time taken by the DE algorithm to solve for the optimal weights and biases. However, in terms of the overall DE-CNN classification time, the DE algorithm consumes a small percentage of the time and has less impact on the video classification time.

5.5. Video Classification Performance of Different Algorithms. The commonly used plain Bayesian (NB) [32], BP neural network [33], LSTM neural network [34], and DE-CNN were used to compare and analyse the test dataset respectively, as shown in Figure 10.

In terms of classification accuracy of the videos, DE-CNN and LSTM algorithms have the highest classification accuracies. In terms of classification time, the LSTM

(a) (b) (c) (d) (e) (f)

Figure 5: Partial data presentation of the dance video sample. (a) Classical dance. (b) Ballet dance. (c) Folk dance. (d) Tap dance. (e) Jazz dance. (f) Latin dance.

Table 1: Information on the experimental video dataset.

Dance video category	Number	Video sources
Classical dance	500	Google videos, Baidu videos
Ballet	500	CCTV, movies, Microblog, Facebook
Folk dance	500	Youku App, Twitter, MetaCafe
Contemporary dance	500	Netflix, LiveLeak
Tap dance	500	Microblog, Google videos
Jazz dance	500	Facebook, LiveLeak
Latin dance	500	CCTV, Baidu videos, Twitter

algorithm consumes the longest time, followed by the DE-CNN algorithm, and the NB algorithm the least time.

The following continues to test the stability of the 4 algorithms in video scene classification. The RMSE performance of the 4 algorithms was verified and is shown in Figure 11.

It can be seen that the DE-CNN algorithm has the best RMSE values and the NB performs the worst. This also indicates that the classification RMSE values are more sensitive to the number of video categories. In summary, for scene classification of 3500 dance video sequences, the DE-CNN model still achieves good classification time and

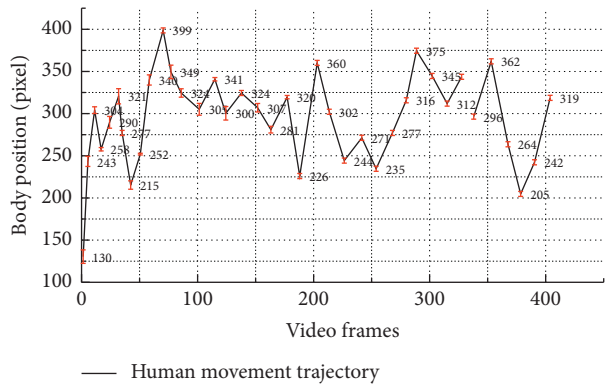

Figure 6: Translation error.

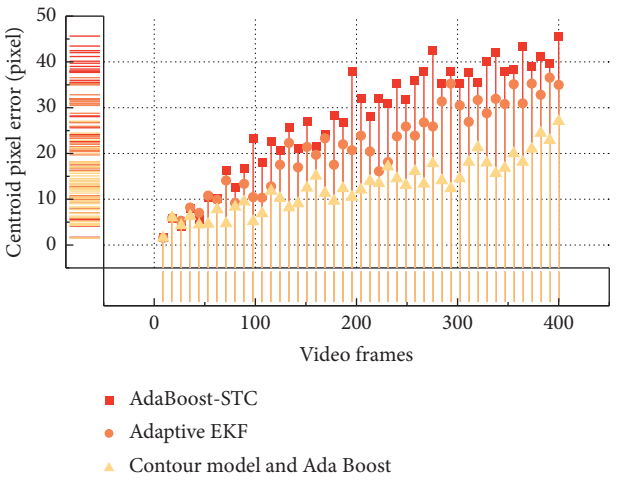

Figure 7: Tracking result of three algorithms.

Table 2: Classification accuracy.

Convolution kernel size	Number of categories	Accuracy	RMSE
2 * 2	7	0.9164	0.1862
3 * 3	7	0.9216	0.1847
4 * 4	7	85.1937	0.2334
5 * 5	7	68.6171	0.5219

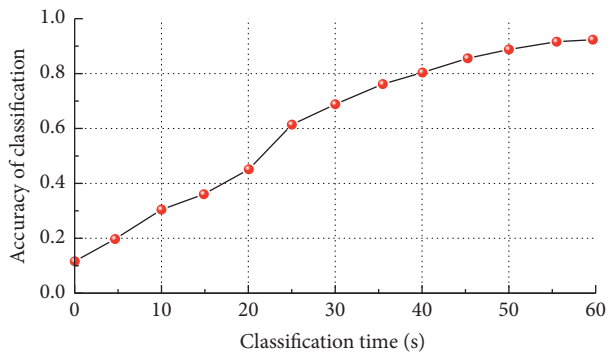

Figure 8: Classification accuracy (convolution kernel 3 * 3).

Table 3: Classification performance of CNN and DE-CNN algorithms.

Algorithms	Accuracy	Recall rate	F1 value
CNN	0.8646	0.8473	0.8064
DE-CNN	0.9275	0.9014	0.9012

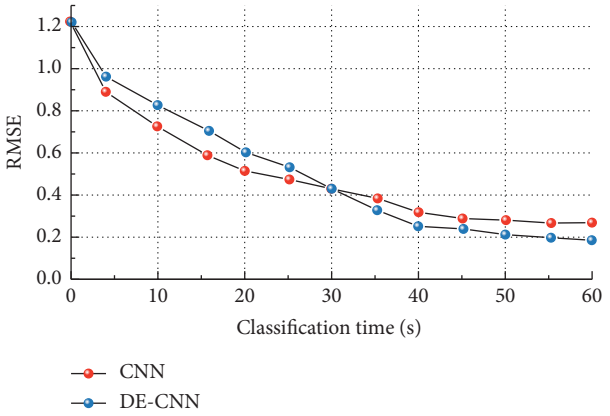

Figure 9: RMSE values of the two algorithms.

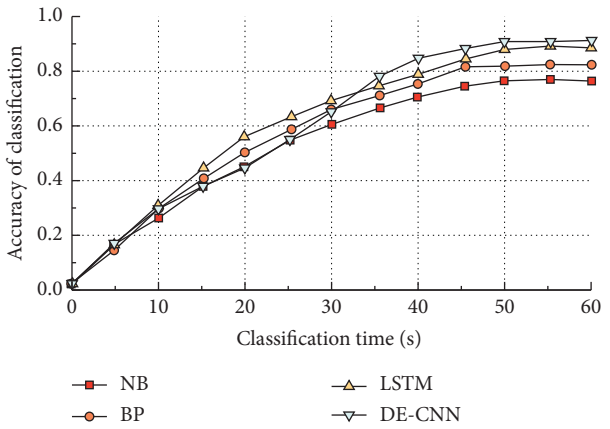

Figure 10: Classification accuracy of four algorithms.

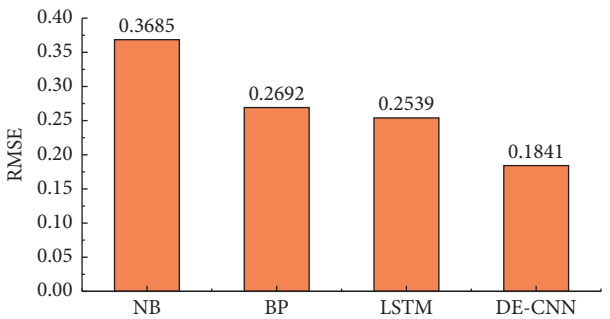

Figure 11: RMSE performance of different algorithms.

RMSE performance under the condition of obtaining high classification accuracy.

6. Conclusion

In this paper, a differential evolutionary convolutional neural network model is applied to scene classification of dance videos. A contour model-based detection approach is used to achieve human target detection, which effectively improves the robustness of human detection. The AdaBoost algorithm based on cascade structure is used to achieve human target tracking. The weight optimisation solution advantage of the differential evolution algorithm is used to improve the applicability of the convolutional neural network model in video scene classification. The following conclusions are drawn.

(1) The average error in human motion detection is less than 10 pixels, which indicates higher robustness.

(2) The proposed method has a smaller pixel error in the centroid of human movement than other methods and is suitable for a long tracking process.

(3) Compared with commonly used video classification algorithms, the proposed DE-CNN model has significant advantages in terms of classification accuracy and RMSE performance. Subsequent studies will further tune the differential evolution parameters to improve the video scene classification time performance.

Data Availability

The experimental data used to support the findings of this study are available from the corresponding author upon request.

Conflicts of Interest

The authors declare that they have no conflicts of interest to report regarding the present study.

References

[1] G. Gao, W. Zhang, Y. Wen, Z. Wang, and W. Zhu, "Towards cost-efficient video transcoding in media cloud: insights learned from user viewing patterns," *IEEE Transactions on Multimedia*, vol. 17, no. 8, pp. 1286–1296, 2015.

[2] S. Norazean, M. A. Mazli, and G. Faizul, "Students' perceptions on using different listening assessment methods: audio-only and video media," *English Language Teaching*, vol. 10, no. 8, pp. 93–97, 2017.

[3] K. K. Loh, B. Tan, and S. Lim, "Media multitasking predicts video-recorded lecture learning performance through mind wandering tendencies," *Computers in Human Behavior*, vol. 63, pp. 943–947, 2016.

[4] J. Adams, G. Christian, and T. Tarshis, "Managing media: reflections on media and video game use from a therapeutic perspective," *Journal of the American Academy of Child & Adolescent Psychiatry*, vol. 54, no. 5, pp. 341-342, 2015.

[5] I. Dewi and W. A. Ni, "The positive impact of teams games tournament learning model assisted with video media on students' mathematics learning outcomes," *Journal of Education Technology*, vol. 4, no. 3, pp. 367–371, 2020.

[6] Y. Hao, T. Mu, R. Hong, M. Wang, N. An, and J. Y. Goulermas, "Stochastic multiview hashing for large-scale near-duplicate video retrieval," *IEEE Transactions on Multimedia*, vol. 19, no. 1, pp. 1–14, 2017.

[7] R. Fernandez-Beltran and F. Pla, "Latent topics-based relevance feedback for video retrieval," *Pattern Recognition*, vol. 51, pp. 72–84, 2016.

[8] Y. Zhu, X. Huang, Q. Huang, and Q. Tian, "Large-scale video copy retrieval with temporal-concentration SIFT," *Neurocomputing*, vol. 187, no. 4, pp. 83–91, 2016.

[9] R. Harakawa, T. Ogawa, and M. Haseyama, "[Paper] accurate and efficient extraction of hierarchical structure ofWeb communities forWeb video retrieval," *ITE Transactions on Media Technology and Applications*, vol. 4, no. 1, pp. 49–59, 2016.

[10] L. Gu, J. Liu, and A. Qu, "Performance evaluation and scheme selection of shot boundary detection and keyframe extraction in content-based video retrieval," *International Journal of Digital Crime and Forensics*, vol. 9, no. 4, pp. 15–29, 2017.

[11] W. Feng, R. Liu, and Z. Zhu, "Fall detection for elderly person care in a vision-based home surveillance environment using a monocular camera," *Signal, Image and Video Processing*, vol. 8, no. 6, pp. 1129–1138, 2014.

[12] R. M. Bommisetty, A. Khare, M. Khare, M. Khare, and P. Palanisamy, "Content-based video retrieval using integration of curvelet transform and simple linear iterative clustering," *International Journal of Image and Graphics*, vol. 132, no. 16, pp. 6–9, 2021.

[13] S. Ren, K. He, R. Girshick, J. Sun, and R.-C. N. N. Faster, "Faster R-CNN: towards real-time object detection with region proposal networks," *IEEE Transactions on Pattern Analysis and Machine Intelligence*, vol. 39, no. 6, pp. 1137–1149, 2017.

[14] T. Roska and L. O. Chua, "The CNN universal machine: an analogic array computer," *IEEE Transactions on Circuits & Systems II Analog & Digital Signal Processing*, vol. 40, no. 3, pp. 163–173, 2015.

[15] Z. Zeng, T. Huang, and W. X. Zheng, "Multistability of recurrent neural networks with time-varying delays and the piecewise linear activation function," *Neurocomputing*, vol. 21, no. 8, pp. 1371–1377, 2016.

[16] Z. Wei, Z. Lin, H. Kim, Y. Kim, and J. Kim, "An improved object tracking algorithm based on camshift combined with active contour and kalman filter," *Journal of Information and Computational Science*, vol. 11, no. 6, pp. 1753–1764, 2014.

[17] E. Suganya and C. Rajan, "An AdaBoost-modified classifier using stochastic diffusion search model for data optimization in Internet of Things," *Soft Computing*, vol. 24, no. 14, pp. 10455–10465, 2020.

[18] Y. Wang and L. Feng, "Improved Adaboost algorithm for classification based on noise confidence degree and weighted feature selection," *IEEE Access*, vol. 8, pp. 153011–153026, 2020.

[19] Z. Ibrahim, M. Saab, and I. Sbeity, "VideoToVecs: a new video representation based on deep learning techniques for video classification and clustering," *SN Applied Sciences*, vol. 1, no. 6, pp. 1–7, 2019.

[20] J. M. Calvin, M. Hefter, and A. Herzwurm, "Adaptive approximation of the minimum of Brownian motion," *Journal of Complexity*, vol. 39, no. 4, pp. 17–37, 2017.

[21] Y. Lu, K. Gu, and Y. Cai, "Automatic lipreading based on optimized OLSDA and HMM," *Soft Computing*, vol. 26, no. 9, pp. 4141–4150, 2022.

[22] X. Sun, P. Wu, and S. Hoi, "Face detection using deep learning: an improved faster RCNN approach," *Neurocomputing*, vol. 299, no. 7, pp. 42–50, 2018.
[23] M. Frid-Adar, I. Diamant, E. Klang, A. Amitai, J. Goldberger, and H. Greenspan, "GAN-based synthetic medical image augmentation for increased CNN performance in liver lesion classification," *Neurocomputing*, vol. 321, no. 12, pp. 321–331, 2018.
[24] R. Andri, L. Cavigelli, D. Rossi, and L. Benini, "YodaNN: an architecture for ultralow power binary-weight CNN acceleration," *IEEE Transactions on Computer-Aided Design of Integrated Circuits and Systems*, vol. 37, no. 1, pp. 48–60, 2018.
[25] J. Wu, C. Hu, Y. Wang, X. Hu, and J. Zhu, "A hierarchical recurrent neural network for symbolic melody generation," *IEEE Transactions on Cybernetics*, vol. 50, no. 6, pp. 2749–2757, 2020.
[26] Z. Li and S. Li, "Kinematic control of manipulator with remote center of motion constraints synthesised by a simplified recurrent neural network," *Neural Processing Letters*, vol. 54, no. 2, pp. 1035–1054, 2022.
[27] G. Fu, "Deep belief network based ensemble approach for cooling load forecasting of air-conditioning system," *Energy*, vol. 148, no. 4, pp. 269–282, 2018.
[28] J. M. Wolterink, T. Leiner, M. A. Viergever, and I. Isgum, "Generative adversarial networks for noise reduction in low-dose CT," *IEEE Transactions on Medical Imaging*, vol. 36, no. 12, pp. 2536–2545, 2017.
[29] M. Ramadas, M. Pant, A. Abraham, and S. Kumar, "ssFPA/DE: an efficient hybrid differential evolution-flower pollination algorithm based approach," *International Journal of System Assurance Engineering and Management*, vol. 9, no. 1, pp. 216–229, 2018.
[30] M. A. Ingle and G. R. Talmale, "Respiratory mask selection and leakage detection system based on Canny edge detection operator," *Procedia Computer Science*, vol. 78, pp. 323–329, 2016.
[31] A. Roy, C. P. Dubey, and M. Prasad, "Gravity inversion for heterogeneous sedimentary basin with b-spline polynomial approximation using differential evolution algorithm," *Geophysics*, vol. 86, no. 3, pp. 1–63, 2021.
[32] S. H. Alizadeh, A. Hediehloo, and N. S. Harzevili, "Multi independent latent component extension of naive Bayes classifier," *Knowledge-Based Systems*, vol. 213, no. 2, Article ID 106646, 2021.
[33] G. Stuart, N. Spruston, B. Sakmann, and M. Häusser, "Action potential initiation and backpropagation in neurons of the mammalian CNS," *Trends in Neurosciences*, vol. 134, no. 3, pp. 440–444, 2016.
[34] N. Zhang, S. L. Shen, A. Zhou, and Y. F. Jin, "Application of LSTM approach for modelling stress-strain behaviour of soil," *Applied Soft Computing*, vol. 100, Article ID 106959, 2021.

Hindawi
Scientific Programming
Volume 2022, Article ID 8401395, 10 pages
https://doi.org/10.1155/2022/8401395

Research Article

Design and Application of Marketing Intelligent Platform Based on Big Data Technology

Xianfeng Chen

School of Business Administration, Henan University of Animal Husbandry and Economy, Henan, Zhengzhou 450044, China

Correspondence should be addressed to Xianfeng Chen; 81364@hnuahe.edu.cn

Received 23 May 2022; Revised 17 June 2022; Accepted 21 June 2022; Published 8 July 2022

Academic Editor: Lianhui Li

The progress of big data technology has promoted the development of intelligent marketing for education companies. The online course selection system on the official website of the education company can provide users with online course selection and purchase services. The early marketing conversion rate remained below 0.09% throughout the year. After the analysis of the marketing department, it is found that there are some problems on the official website, such as a low marketing conversion rate. To improve the marketing conversion rate of the official website, the marketing department puts forward business needs. The experiential marketing strategy has been formulated, and it is planned to implement experiential course purchase and secondary marketing on the official website. The IT R & D department has established a big data marketing intelligent recommendation system project to meet the business needs put forward by the marketing department. Firstly, use the big data real-time computing technology to collect the user behavior information of users screening courses on the official website. Real time analysis of user behavior information can predict the courses given to users, which is conducive to the purchase of courses. Then, use the big data machine learning technology to integrate the marketing activity opportunity data in each marketing activity opportunity management system and establish a user portrait. For users who have participated in online or offline marketing activities but have not purchased courses, offline predict the courses and classes that can be recommended to users to carry out secondary marketing for them. Finally, the information of recommendable courses and classes predicted in real time and offline is displayed in the display area of the official website, which makes the marketing conversion rate of the official website reach 0.20%, which is 125% higher than that of the original official website.

1. Introduction

In the era of big data, information overload is serious, and a large amount of information is generated on the internet all the time [1–4]. A large amount of information is presented in front of the users. It is more difficult for users to filter out the information that meets their wishes. At the same time, a large amount of information has great business value for enterprises. How to transform this information to help the operation and development of enterprises has also been a problem perplexing enterprises. It is difficult for users to find information that meets their wishes, and enterprises are trying to push the information beneficial to the operation of enterprises to users. The intelligent recommendation system has built an information bridge between users and enterprises. Users search or browse information on the enterprise website, which records the behavior of the users searching or browsing information. The intelligent recommendation system constructs the user portrait based on the above user behavior recorded on the website, analyzes the user preference information based on the data of the user portrait, and recommends the information that conforms to the user's search intention and the enterprise's marketing strategy to the user in combination with the enterprise's marketing strategy [5–8].

The internet e-commerce industry has rich practical experience in using the intelligent recommendation system to help enterprises operate, such as Amazon, Taobao, etc. The internet e-commerce industry recommends users to search or browse similar products according to the products

selected by users and in combination with the industry attributes of e-commerce enterprises, such as commodity inventory location, merchant advertising investment, etc. Each industry has its own industry-specific attributes. In the process of studying the implementation of the intelligent recommendation system in its own industry, it will be combined with its own industry-specific marketing attributes, and the education industry is no exception. In the field of education, the research and practice of big data intelligent recommendation are mostly in the fields of intelligent evaluation, educational law discovery, educational management and decision-making, online learning, and adaptive learning. As the basic theoretical and technical support of big data landing research in the field of education, the recommendation system selects user learning behavior data, such as courses, learning processes, and test evaluation. Combined with the relevant research of education big data, build the relevant big data intelligent recommendation application with the business nature of the education industry. Learning from the practical experience of the internet e-commerce industry recommendation system and combined with the unique business attributes of the education industry, various educational institutions are exploring and studying to build a unique recommendation system for the education industry [9, 10].

This paper takes the big data marketing intelligent recommendation system of Education Company H as the research object, which provides a reference for educational enterprises on how to use the big data intelligent recommendation system to realize user experience class purchase. Since its establishment, Education Company H has gradually developed into an institution with foreign language training and basic education as the core. Its teaching products span a wide range, covering various educational stages, such as preschool education, middle school education, university education, and overseas consultation. The campus covers many provinces in China and has many users, however, the company has many problems in its daily channel business activities. The online course selection system on the official website of Education Company H provides users with online course selection and purchase services. The online course selection system on the official website has more than 600,000 classes of thousands of courses for users to select and purchase courses online. User screening courses consume a lot of time and energy. The online course selection system on the official website does not integrate the business opportunity information of various marketing activities. It is still unknown which marketing activities promote users to buy courses, and it has lost the opportunity to carry out secondary marketing to users on the online course selection system on the official website. In response to the above problems, Education Company H investigated the successful big data intelligent recommendation system cases at home and abroad, referred to relevant technical and academic literature, and learned from the intelligent recommendation system models of well-known internet and e-commerce companies at home and abroad, such as Amazon predictive shopping and Taobao intelligent recommendation. Combined with the relevant theories of market research and prediction [11–13], consumer behavior [13–15], and user information behavior [16–18], the marketing department proposes to implement user experience course purchase in the online course selection system on the official website.

The IT R & D department has established a big data marketing intelligent recommendation system project to meet the business needs of the online course selection system on the official website to implement the user experience course purchase. Firstly, the big data marketing intelligent recommendation system uses the big data real-time computing technology to analyze the user behavior and predict the courses and classes that can be recommended to users by collecting the user's behavior of viewing the detailed information of courses and classes on the online course selection system on the official website. Then, the big data marketing intelligent recommendation system uses the big data machine learning technology [19–22] to integrate the marketing activity business opportunity data in each marketing activity business opportunity management system and mine the causal law between user behavior and user class purchase offline. Using the mining causal law, offline predict the recommended courses and classes for users who have participated in marketing activities but have not purchased courses. Finally, the online real-time predicted recommendable course class information and the offline big data predicted recommendable course class information are displayed in the "guess what you like" display area on the website of the online course selection system of the official website, which supports the online course selection system of the official website to implement the user experience course purchase and realize secondary marketing to users, and it improves the marketing conversion rate of the online course selection system of the official website.

Education Company H uses big data technology to enhance the enterprise's marketing ability, and it also provides a reference for relevant enterprises in the domestic education industry on how to apply big data technology to help enterprise operation. Although the field of big data recommendation in the field of internet e-commerce has been relatively mature, the education industry has many unique attributes in the field of education. It cannot fully learn from the big data application mode in the field of e-commerce. It can only develop a big data marketing recommendation system suitable for its own industry attributes in the field of education on the basis of reference. It is the application of domestic educational institutions in the field of big data, lack of relevant practice in the field of channel marketing, and lack of reference for successful practice cases.

2. Current Situation of Big Data Intelligent Recommendation System at Home and Abroad

The big data intelligent recommendation system originated from internet e-commerce. The most well-known foreign company that develops and applies the recommendation system is Amazon. Amazon applied predictive shopping

recommendations on its global e-commerce website in 2013. Amazon applies the famous item-to-item collaborative filtering recommendation algorithm [23–27] in predictive shopping. This algorithm records the user behavior data generated by users on the Amazon e-commerce platform, such as browsing goods, staying on the goods page, putting products into the shopping cart, and purchasing goods. Amazon uses the big data intelligent recommendation algorithm to calculate the goods users likes. It also predicts the goods that users may buy in the next stage.

The commodity recommendation ideas and rules of the internet e-commerce industry are not only applied to Amazon but also to Facebook, Walmart, and other companies. The application of big data personalized recommendation in the field of internet e-commerce greatly reduces the work of users screening goods, enhances users' shopping experience, and promotes the popularization of intelligent recommendation mode in various industries, including the education industry. The foreign education industry has widely used the big data intelligent recommendation technology in adaptive learning and other fields. The well-known product is the Knewton platform. The behavior of each student and the response to each content item can not only improve the system's understanding of a single learner and a single content item but also improve the understanding of all the contents in the system and all online students. At Arizona State University, more than 2000 students participated in the experiment of Knewton products in a two-semester course. The experimental results show that after students use the Knewton platform, the dropout rate of students decreased by 56%, and the passing rate of students increased from 64% to 75%. At the same time, 45% of students can complete the course four weeks in advance.

The Smartbook product is a personalized recommendation platform that supports thousands of McGraw-Hill courses, and it calculates the courses and fields that students should pay attention to based on their previous user behavior. Scootpad products identify the weaknesses of each student through diagnostic exercises to ensure that they receive personalized learning courses. At the same time, teachers can guide specific students by creating targeted homework. The successmaker product provides reading and mathematics software and personalized learning paths for students aged K-12. It was launched at Stanford in the 1960s as a joint project with IBM and Dr. Patrick supplies, a computer learning expert. The product mainly provides adaptive mathematics and reading guidance for primary school students. The perfect combination of the internet big data technology and education has promoted the development of educational science. The application of big data intelligent recommendation technology in the foreign education industry is worth learning from. The application of big data technology in the domestic education industry has just sprung up in recent years. While learning from the experience of internet e-commerce and big data in the foreign education industry, educational institutions have also made some breakthroughs in the field of big data application.

3. Business Requirements of Marketing Platform

3.1. Current Situation of Online Course Selection System on Official Website. The online course selection system on the official website of Education Company H provides users with online course selection and purchase services. The online course selection system on the official website has a low marketing conversion rate, which is maintained below 0.09% throughout the year. The marketing department sorted out the current situation of the online course selection system on the official website to find the reasons affecting the low marketing conversion rate of the official website.

3.1.1. Show the Course Screening Results from the Perspective of Community Characteristics. The online course selection system on the official website has more than 600,000 classes of thousands of courses for users to select and purchase courses online. The online course selection system on the official website provides the function of course screening, which is realized by keyword full-text retrieval technology (similar to Baidu search technology). In the process of course selection and purchase, the user selects and combines the screening course conditions to screen the course class information that meets the user's own purchase needs. The keywords for screening courses include the course subject, school, campus, class time, course class price range, etc. The course class information that meets the screening conditions is presented to the user in the form of a list. The information in the list can be sorted according to the course class price and class opening time. The results of course screening are displayed to users from the perspective of community characteristics, i.e., when the screening conditions of selection and combination are the same. We can see that the course class information after course screening is the same, the content and the sequence of content are unchanged, and the results sorted by price or class opening time are the same. The information of the displayed courses and classes is not differentiated, and there is a lack of content display of individual trait differentiation.

3.1.2. Business Opportunity Information of Various Marketing Activities to be Integrated. The online course selection system on the official website has not integrated the business opportunity information of various marketing activities, and it is unknown which marketing activities promote users to buy courses. In all kinds of marketing activities, Education Company H will collect the marketing activity opportunity information of users' purchase intention. The business opportunity information of marketing activities is stored in the business opportunity management system of various marketing activities. The marketing activity business opportunity management system refers to the marketing auxiliary IT system that provides users with consulting, evaluation, and participation in offline marketing activities and other services before users buy courses, such as offline customer service consulting business opportunity management system, CRM telephone customer service business

opportunity management system, OTS online evaluation business opportunity management system, offline marketing activity business opportunity management system, etc. Users who have the intention to purchase courses finally need to enter the online course selection system on the official website for online course selection and purchase. As the online course selection system on the official website does not integrate the marketing activity business opportunity data in the business opportunity management system of various marketing activities, it is not known which marketing activities promote users to buy courses.

3.2. Problems of Online Course Selection System on Official Website. After sorting out the current situation of the online course selection system on the official website, the marketing department found two problems affecting the conversion rate of the online course selection system on the official website.

3.2.1. Lack of Display of Individual Trait Differentiation Content. In the process of screening courses on the online course selection system on the official website, users select and combine the conditional keywords of the screening courses to screen the courses and classes that meet the users' needs for the course purchase. The filtering function realized by the keyword full-text retrieval technology cannot fully reflect the user's demand for course purchase in the user's behavior, push the course class information that does not meet the user's own demand for course purchase, and affect the user's experience of course selection and purchase. Learn from the relevant theories of market research and prediction and big data marketing theory, investigate and collect the user behavior-related data and information in the process of user screening courses, analyze the user behavior-related data and information from the perspective of individual characteristics, predict the courses that meet the user's purchase needs, recommend the courses that meet the user's purchase needs to users on the online course selection system on the official website, enable users to quickly find courses and classes that meet their own purchase intention, and promote users to purchase courses and improve the marketing conversion rate.

3.2.2. Lack of Secondary Marketing to Users. The online course selection system on the official website did not integrate, mine, and use the marketing activity business opportunity information of various marketing activities, and it lost the opportunity of secondary marketing to users. For example, the user calls the CRM call center and inquires about IELTS-related courses. Then, when the user enters the online course selection system on the official website, the system shows users IELTS-related courses for the first time. On the one hand, the user can no longer screen the courses. On the other hand, the user can conduct secondary marketing IELTS courses, which will certainly promote the improvement of the conversion rate of the official website. The user's intelligent behavior in the user information behavior theory points out that the user's behavior is related to a specific goal. Integrate, mine, and use the marketing activity business opportunity information of each marketing activity to analyze the relationship between users' participation in marketing activities and users' purchase of courses, and predict the courses that users may buy to carry out secondary marketing to users.

3.3. Practical Experience of User Experience Shopping in Internet E-Commerce Industry. The marketing department, after discovering the problems of Chu duo in the online course selection system on the official website, actively looked for ways to solve the problems. In the process of finding solutions to the problems, the marketing department found that the practical experience of the internet e-commerce industry in implementing user experience shopping on e-commerce websites and e-commerce apps is worth learning from. The marketing department summarized the practical experience of experiential shopping in the e-commerce industry as follows: (1) in the internet e-commerce industry, add commodity recommendation information to the page of the e-commerce website or e-commerce mobile app to recommend the same kind of commodity to users who have just viewed the commodity. For example, if users view commodity A on Taobao, Taobao will display the same kind of commodity to users in the "you may still like" commodity display area. (2) In the internet e-commerce industry, various information systems of e-commerce have realized the sharing of user behavior data. The user has viewed commodity A on the e-commerce website. When the user enters the e-commerce mobile app, he can see the recommendation information of commodities similar to commodity A. Similarly, the user has viewed product A on the e-commerce mobile app. When the user enters the e-commerce website, he can also see the recommendation information of products similar to product A. The second user of user marketing is thus realized.

3.4. Online Implementation of Experiential Marketing Business Needs on the Official Website. To solve the problems existing in the online course selection system on the official website and learn from the practical experience of user experiential shopping in the e-commerce industry, the marketing department plans to implement experiential course purchase in the online course selection system on the official website to promote the improvement of the conversion rate of the official website.

3.4.1. Online Real-Time Experiential Course Purchase Business Requirements. The online course selection system on the official website realizes the intelligent recommendation of online real-time marketing, recommends courses similar to the courses viewed by online users on the official website, and realizes the business needs of experiential course purchase. The specific business needs are as follows: (1) the display method of recommendation results: learn from the user experiential shopping practice method of the internet

e-commerce industry, and add the "guess you like" display area on the web page of the online course selection system on the official website. It is used to highlight the course class information recommended to users. (2) The formulation of online real-time marketing intelligent recommendation strategy: from the perspective of individual characteristics of users, the marketing department formulates the online real-time marketing intelligent recommendation strategy on the official website, which is used to clarify the business rules of online real-time recommending courses and classes to users on the official website. (3) Build an online real-time user portrait: investigate and collect the user behavior information of the course filtered and viewed by the user on the online course selection system on the official website, analyze the user behavior, and predict the course classes preferred by the user in real time. (4) The construction of the algorithm model and prediction: using an online real-time intelligent recommendation-related technologies, combined with user preferences and online real-time marketing intelligent recommendation strategy on the official website, calculate and obtain the course classes recommended to users and display the course class information recommended to users in real time in the "guess what you like" display area. Figure 1 presents the online real-time experiential course purchase business requirements.

3.4.2. Demand for Secondary Marketing Business of Offline Big Data. The online course selection system on the official website realizes the intelligent recommendation of offline big data marketing. Analyze the relationship between users' participation in marketing activities and users' purchase of courses using the business opportunity data of various marketing activities (business opportunity data, i.e., the information of users' intention to purchase courses collected in marketing activities). Predict the courses and classes that users may buy offline, and recommend the courses and classes predicted offline to users online on the official website to realize the business demand of secondary marketing for users. The specific business requirements are as follows: (1) build offline big data user portrait: investigate, collect, and integrate the marketing activity opportunity data in each marketing activity opportunity management system to build an offline big data user portrait. The marketing activity business opportunity management system is as follows: offline customer service consulting business opportunity management system, CRM telephone customer service business opportunity management system, OTS online evaluation business opportunity management system, and offline marketing activity business opportunity management system. (2) Build the algorithm model and prediction: based on the offline big data user portrait data, mine the causal law between users' participation in marketing activities and users' purchase of courses offline, and build an offline recommendation algorithm model. The offline recommendation algorithm model is used to predict the courses that may be purchased by users who have participated in online and offline activities but have not purchased courses on the official website. When users enter the official website, the courses that may be purchased by users predicted offline will be recommended to users on the official website. (3) The formulation of an intelligent recommendation strategy for offline big data marketing: the marketing department, based on the relevant theories of user behavior information, formulates an intelligent recommendation strategy for offline big data marketing, which is used to clarify the business rules of courses and classes that recommend offline prediction to users online on the official website. (4) Only provide offline big data marketing intelligent recommendation service to registered users: only provide offline big data marketing intelligent recommendation service to registered users who log in to the online course selection system on the official website with their mobile phone number, and do not provide offline big data marketing intelligent recommendation service to unregistered browsing users. Figure 2 presents the demand for secondary marketing business of offline big data.

4. Marketing Business Needs to Realize the Overall Design of IT System Architecture

4.1. Origin of Big Data Marketing Intelligent Recommendation System Project of Education Company H. The online course selection system on the official website of Education Company H has been in operation for many years. The online course selection system on the official website is now implemented with the B/s technology architecture. The R & D and realization of the user experiential course purchase business requirements of the online course selection system on the official website requires the use of the internet technology and big data technology. It greatly changes the technical architecture of the original online course selection system on the official website. After discussion between the IT R & D department and the marketing department, it was decided to establish a big data marketing intelligent recommendation system project in the form of a subsystem of the online course selection system on the official website to meet the business requirements related to the user experience course purchase of the online course selection system on the official website. The big data marketing intelligent recommendation system and the online course selection system on the official website work together to realize the user experience course purchase. The specific collaborative work content is shown in the figure below.

Figure 3 shows the collaborative work between the big data marketing intelligent recommendation system and the online course selection system on the official website. The description is as follows: (1) the online course selection system on the official website collects user behavior information and sends the user behavior information to the big data marketing intelligent recommendation system. (2) The big data marketing intelligent recommendation system realizes the user experience class purchase business requirements proposed by the marketing department, calculates the online real-time marketing intelligent recommendation and offline big data marketing intelligent recommendation, and stores the calculated recommendation results in the recommendation result information index of the ES search engine. (3) The big data marketing intelligent recommendation system provides

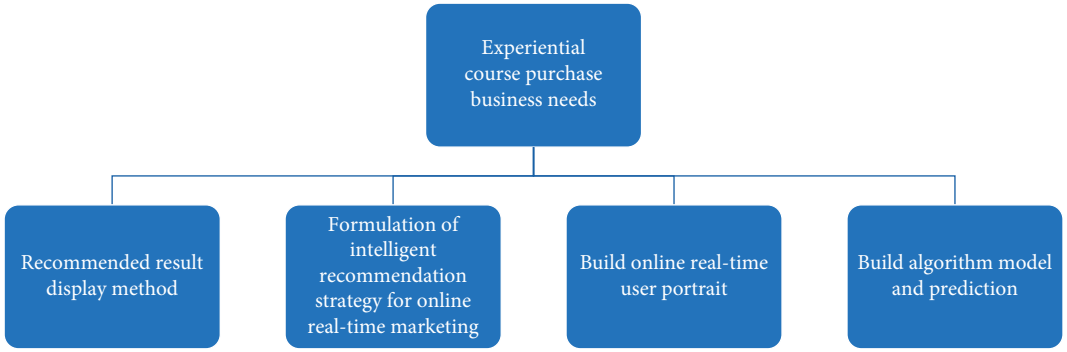

Figure 1: Online real-time experiential course purchase business requirements.

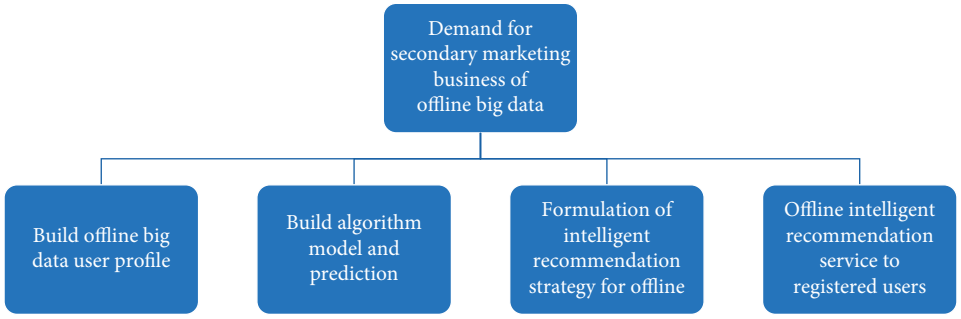

Figure 2: Demand for secondary marketing business of offline big data.

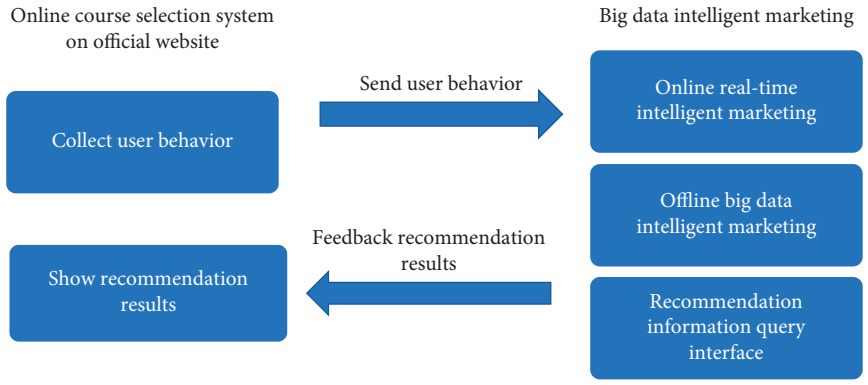

Figure 3: Collaborative work between big data marketing intelligent recommendation system and online course selection system on official website.

a recommendation information query service interface and recommendation information query service for the online course selection system on the official website. (4) The "guess what you like" display area is added to the web page of the online course selection system on the official website. When the "guess you like" display area of the online course selection system on the official website is displayed in the browser, call the recommendation information query service interface provided by the big data marketing intelligent recommendation system to obtain the recommendation information, and display the course information recommended for online users on the official website in the "guess you like" display area.

In the big data marketing intelligent recommendation system, to use IT technology to realize the marketing business needs, we first need to divide the functional modules to realize the business needs and specify the IT technology required by the functional modules. At the same time, we need to design and explain how each functional module cooperates with each other to complete the business needs, which is the problem to be solved in the overall design stage of IT system architecture.

4.2. Overall Design of Big Data Marketing Intelligent Recommendation System Architecture of Education Company H. The marketing business requirements of the online course selection system on the official website are mainly composed of the following two core business requirements: online real-time marketing intelligent recommendation and offline big

data marketing intelligent recommendation. The IT R & D department established the big data marketing intelligent recommendation system project after analyzing the feasibility of the demand realization of the marketing business demand of the online course selection system on the official website. Recommend courses on the official website and use the intelligent data system to recommend courses and provide users with big data service. The IT R & D department has carried out the overall design of the IT architecture of the big data marketing intelligent recommendation system.

According to the requirements of the online marketing recommendation system, the intelligent computing module can realize the two core functions of the online marketing recommendation system: (1) according to the requirements of the online marketing recommendation strategy, the intelligent computing module can realize the two core functions of the online marketing recommendation system and realize the real-time prediction of the business needs of online user preference courses. (2) Offline big data marketing intelligent recommendation calculation unit: according to the requirements of offline big data marketing intelligent recommendation strategy specification, excavate the causal law between user behavior and user course purchase in marketing activity business opportunities, and use this causal law to predict the courses that users who have participated in marketing activities but have not purchased courses may buy. At the same time, there are several functional modules to assist in the realization of marketing business needs, such as the following: each marketing activity business opportunity management system database, data extraction and synchronization program, ES data search engine, big data buffer middle layer, internet web service interface, etc. Online real-time marketing intelligent recommendation calculation unit, offline big data marketing intelligent recommendation calculation unit, and other functional modules are combined to form the overall architecture of big data marketing intelligent recommendation system, and they work together to meet the needs of marketing business. The following is a brief description of the functional design of each functional module cooperating with each other to realize business requirements. Table 1 presents the overall design of the big data marketing intelligent recommendation system architecture of Education Company H.

4.2.1. Design of Intelligent Recommendation Function for Online Real-Time Marketing. Online real-time marketing intelligent recommendation solves the business problem of recommending user-preferred courses and classes for online users on the official website in real time. In the overall architecture design of the big data marketing intelligent recommendation system, several functional modules are divided to realize the business requirements of online real-time marketing intelligent recommendation. The divided functional modules and how to cooperate with each other to complete the functional design of business requirements are briefly described as follows: (1) the official website online user behavior information receiving service interface: is used to receive the user behavior information sent by the official website online users to view the course details and forward the user behavior information directly to the "big data buffer layer." The user behavior information receiving service interface is implemented by the spring-cloud microservice technology. (2) Big data buffer layer: it is used to receive the online user behavior information on the official website forwarded by the "user behavior information receiving service interface," cache the user behavior information and wait for the "online real-time marketing intelligent recommendation computing unit" to read. The significance of the big data buffer layer is to smoothly transfer the user behavior data to the "online real-time marketing intelligent recommendation computing unit" during the peak access of the official website to prevent the computing unit from a system crash because of an excessive amount of calculation. The big data buffer layer is implemented by the flume and Ka & a technology. (3) Online marketing intelligent recommendation calculation unit: read the user behavior information in the "big data buffer layer," analyze the online user behavior, calculate and obtain the course classes and recommended scores recommended to online users according to the recommendation rules in the "online real-time marketing intelligent recommendation strategy specification," and store the calculated recommendation results and recommended scores in the "ES search engine." The online marketing intelligent recommendation computing unit is implemented by the storm real-time computing framework. (4) ES search engine: mainly used to store online real-time recommendation result information. The ES search engine is implemented by the Elasticsearch search framework. The use of Elasticsearch search engine technology to provide the storage and query of recommendation results is mainly because Elasticsearch has very fast and stable data writing and data query characteristics, which can solve the performance problems of a large number of recommendation result information data writing and data query during the peak of official website access.

4.2.2. Design of Intelligent Recommendation Function for Offline Big Data Marketing. The business problem of offline big data marketing intelligent recommendation is to mine the causal law between users' participation in marketing activities and users' purchase of courses and use this causal law to offline predict the courses that users who have participated in online or offline marketing activities but have not purchased courses may buy. In the overall architecture design of the big data marketing intelligent recommendation system, several functional modules are divided to realize the business requirements of offline big data marketing intelligent recommendation. The divided functional modules and how to cooperate with each other to complete the functional design of business requirements are briefly described as follows: mining the causal law of users' participation in marketing activities and users' purchase of courses in the business opportunity data of marketing activities. When the user enters the official website, recommend the courses that

Table 1: The overall design of the big data marketing intelligent recommendation system architecture.

The overall design of intelligent recommendation system architecture
Design of intelligent recommendation function for online real-time marketing
Design of intelligent recommendation function for offline big data marketing
Function design of replacing offline recommended courses with similar courses on the official website

may be purchased by the user predicted offline to the user on the official website. (1) Collect and extract marketing activity opportunity data from each marketing activity opportunity management system database. The marketing activity business opportunity management system database includes the following: CRM telephone customer service business opportunity management system database, OTS online evaluation business opportunity management system database, offline customer service consulting business opportunity management system database, offline marketing activity business opportunity management system database, course product database, and order database of online course selection system on the official website. The purpose of collecting and extracting marketing activity data is to analyze the causal law between user behavior and the user class purchase. Hence, data collection is divided into two steps: collecting "cause" data and collecting "result" data, which is as follows: the first step is to collect "cause" data. Extract the marketing activity business opportunity data from the CRM telephone customer service business opportunity management system database, OTS online evaluation business opportunity management system database, offline customer service consulting business opportunity management system database, and offline marketing activity business opportunity management system database. There is information about the user's intention to purchase courses in the business opportunity data of marketing activities, such as the user's call to the CRM call center, telephone consultation regarding IELTS-related courses, leaving information about the user's intention to purchase IELTS courses, etc. The second step is to collect "fruit" data. Extract the user's historical order information from the course purchase order database of the online course selection system on the official website. In the first and second steps above, the business opportunity data of marketing activities collected and extracted will be stored in the "big data storage system." At the same time, the time of data collection and extraction is 2 a.m. every day, because the business is relatively idle at this time. (2) Big data storage system: used to store the original marketing activity opportunity data in the collected marketing activity opportunity management system. (3) Big data user portrait: it consists of two types of user portraits: user portraits of purchased courses and user portraits of nonpurchased courses. Use Spark SQL and hive technology to extract, clean, and convert the original marketing activity business opportunity data stored in the big data storage system, and build the user portraits of purchased courses and nonpurchased courses. Analyze the data of user portraits of purchased courses, and use the big data machine learning algorithm to find the causal law between the user behavior and user purchase courses. This causal law is used to predict the course classes that users in the user portrait of nonpurchased courses may buy. (4) User preference course recommendation: it uses big data machine learning technology to predict the course products that users may buy. Using big data machine learning technology, train the algorithm model on the data of the user portraits of the purchased courses and find out the causal law between the user behavior and user purchase courses. The trained algorithm model is used to predict which courses and classes the users in the user portrait of nonpurchased courses may buy and the probability of possible purchase. If the course classes in the recommendation results of offline prediction have expired in the online course selection system on the official website and are no longer sold, replace the expired course classes with the similar course classes being sold in the online course selection system on the official website.

4.2.3. Function Design of Replacing Offline Recommended Courses with Online Similar Courses on the Official Website. The result of online real-time marketing intelligent recommendation is calculated based on the class data of the courses being sold. The results of offline big data marketing intelligent recommendation are calculated based on the historical business opportunity data of marketing activities and the historical data of the user course purchase. Therefore, the course classes in the offline big data recommendation results may have expired and will not be sold in the online course selection system on the official website. Therefore, before recommending offline predicted recommendation results to online users on the official website, it is necessary to replace the courses in the recommendation results with similar courses on the official website. By simulating the user behavior of the official website, convert the course class information in the offline big data recommendation results into user behavior information, take the converted user behavior information as the request parameter of the service interface, and call the online user behavior information receiving service interface of the official website to hand over the replacement of similar courses to the online real-time marketing intelligent recommendation module. The online real-time marketing intelligent recommendation module will convert the offline recommended course classes into similar course classes being sold online on the official website, and store the recommendation results after replacing the course class information in the ES search engine.

5. Conclusion and Prospect

With the advent of the internet big data era, information technology is developing by leaps and bounds, and the traditional enterprise operation and marketing mode is also

changing. The traditional market survey and prediction model has been replaced by information technology. By collecting user behavior and other information on Web pages or apps, we can understand users better than through questionnaires and interviews. The traditional commodity sales model gradually changes from the mode of users looking for commodities to the mode of products looking for users. It uses big data machine learning technology to predict users' preferred commodities and timely recommends commodities to users. The internet and big data are rapidly and quietly changing the world, the marketing mode of modern enterprises, and people's lifestyle. Education Company H, moving with the times and keeping up with the pace of the internet big data era, has developed a big data marketing intelligent recommendation system using the internet big data technology to support the online course selection system on the official website and realized user experience course purchase. After analysis and research, the conclusions drawn are as follows: (1) use the big data real-time computing technology to recommend user-preferred courses to users in real time to reduce the workload of user course screening. Firstly, collect the user behavior of users viewing the detailed information of courses and classes on the official website. Then, analyze the user behavior and predict the course class of user preference. Finally, the online real-time recommendation of the predicted user preference courses and classes to users improves the online marketing conversion rate of the official website. (2) Use the big data machine learning technology to integrate the business opportunity data of various marketing activities and realize secondary marketing on the official website. Firstly, collect the business opportunity data of various marketing activities from the business opportunity management database of various marketing activities. Then, use the big data machine learning technology to analyze the causal law between users' participation in marketing activities and users' purchase of courses. Finally, using the causal law obtained from the analysis, for users who have participated in marketing activities but have not purchased courses, offline predict the courses and classes that users may buy. When users log in to the official website, the system will recommend courses and courses that can be predicted offline to users at the first time. This way can realize the secondary marketing to users and improve the online marketing conversion rate of the official website.

In the future, more recommendation algorithm models will be implemented to improve the recommendation business and improve the accuracy of recommendation. The big data marketing intelligent recommendation system delivered in phase I realizes the real-time marketing recommendation strategy, which is mixed with the decision-making information from the perspective of enterprise marketing, such as recommended accommodation classes and VIP classes. It has not been able to completely solve the real purchase needs of users from the perspective of users' individual characteristics. In essence, the big data marketing intelligent recommendation system should look at and solve problems from the perspective of users' individual characteristics and provide users with courses that they really want to buy, and the marketing mode has shifted from traditional marketing products to marketing users. At present, only the decision tree algorithm is used for offline recommendation business. There are many similar algorithms in the field of machine learning, which can be used together to select the best algorithm model most suitable for business and improve the accuracy of recommendation. In the future, collaborative filtering or classification-related machine learning algorithms will be used to classify similar populations and recommend similar courses to similar populations; In the future, association rules and related algorithms will be used to analyze the historical data of course purchase, find the associated courses that are often purchased together, recommend the associated courses to users, and so on.

Data Availability

The dataset can be accessed upon request.

Conflicts of Interest

The author declares that there are no conflicts of interest.

Acknowledgments

The authors thank Special (Soft Science) General Project of Key R & D and Promotion in Henan, the realistic dilemma, action mechanism, and evolution path of regional brand of agricultural products in Henan to promote rural revitalization (no. 222400410540).

References

[1] L. Cai and Y. Zhu, "The challenges of data quality and data quality assessment in the big data era," *Data Science Journal*, vol. 14, p. 224, 2015.

[2] W. Xu, H. Zhou, N. Cheng et al., "Internet of vehicles in big data era," *IEEE/CAA Journal of Automatica Sinica*, vol. 5, no. 1, pp. 19–35, 2017.

[3] Y. Li, C. Huang, L. Ding, Z. Li, Y. Pan, and X. Gao, "Deep learning in bioinformatics: introduction, application, and perspective in the big data era," *Methods*, vol. 166, pp. 4–21, 2019.

[4] J. Yang, Y. Li, Q. Liu et al., "Brief introduction of medical database and data mining technology in big data era," *Journal of Evidence-Based Medicine*, vol. 13, no. 1, pp. 57–69, 2020.

[5] F. M. Hsu, Y. T. Lin, and T. K. Ho, "Design and implementation of an intelligent recommendation system for tourist attractions: the integration of EBM model, Bayesian network and Google Maps," *Expert Systems with Applications*, vol. 39, no. 3, pp. 3257–3264, 2012.

[6] K. Meehan, T. Lunney, K. Curran, and A. Mccaughey, "Context-aware intelligent recommendation system for tourism," in *Proceedings of the 2013 IEEE international conference on pervasive computing and communications workshops (PERCOM workshops)*, pp. 328–331, IEEE, San Diego, CA, USA, 18-22 March 2013.

[7] J. Borràs, A. Moreno, and A. Valls, "Intelligent tourism recommender systems: a survey," *Expert Systems with Applications*, vol. 41, no. 16, pp. 7370–7389, 2014.

[8] R. A. Hamid, A. S. Albahri, J. K. Alwan et al., "How smart is e-tourism? A systematic review of smart tourism

recommendation system applying data management," *Computer Science Review*, vol. 39, p. 100337, 2021.

[9] O. Stitini, S. Kaloun, and O. Bencharef, "The recommendation of a practical guide for doctoral students using recommendation system Algorithms in the education field," in *Proceedings of the Third International Conference on Smart City Applications*, pp. 240–254, Springer, Tetouan, Morocco, 11 October 2018.

[10] G. Punj and D. W. Stewart, "Cluster Analysis in marketing research: review and suggestions for application," *Journal of Marketing Research*, vol. 20, no. 2, pp. 134–148, 1983.

[11] D. McFadden, "The choice theory approach to market research," *Marketing Science*, vol. 5, no. 4, pp. 275–297, 1986.

[12] C. Fornell, "A second generation of multivariate analysis: classification of methods and implications for marketing research," *Marketing Research*, pp. 221–226, 1985.

[13] W. Raaij and K. Wandwossen, "Motivation-need theories and consumer behavior," *BEBR faculty working paper*, vol. 05, pp. 590–595, 1977.

[14] R. T. Michael and G. S. Becker, "On the new theory of consumer behavior," *The Swedish Journal of Economics*, vol. 75, no. 4, pp. 378–396, 1973.

[15] W. H. Cummings and M. Venkatesan, "Cognitive dissonance and consumer behavior: a review of the evidence," *Journal of Marketing Research*, vol. 13, no. 3, pp. 303–308, 1976.

[16] K. E. Pettigrew, R. Fidel, and H. Bruce, "Conceptual frameworks in information behavior," *Annual Review of Information Science & Technology*, vol. 35, pp. 43–78, 2001.

[17] D. Nahl, "A conceptual framework for explaining information behavior," *Simile: Studies in Media and Information Literacy Education*, vol. 1, no. 2, pp. 1–16, 2001.

[18] K. E. Fisher, S. Erdelez, and L. E. F. McKechnie, *Theories of Information Behavior*, p. 431 Information Today, Inc, New Jersey, USA, 2005.

[19] Z. Jia, X. Cai, Y. Hu, J. Ji, and Z. Jioa, "Delay propagation network in air transport systems based on refined nonlinear Granger causality," *Transportation Business: Transport Dynamics*, vol. 10, no. 1, pp. 586–598, 2022.

[20] Z. Jia, Y. Lin, and J. W. H. Wang, "Multi-view spatial-temporal graph convolutional networks with domain generalization for sleep stage classification," *IEEE Transactions on Neural Systems and Rehabilitation Engineering*, vol. 29, pp. 1977–1986, 2021.

[21] Z. Jia, J. Junyu, X. Zhou, and Y. Zhou, "Hybrid spiking neural network for sleep EEG encoding," *Science China Information Sciences*, vol. 65, no. 4, p. 33, 2022.

[22] Z. Jia, X. Cai, and Z. Jiao, "Multi-modal physiological signals based squeeze-and-excitation network with domain adversarial learning for sleep staging," *IEEE Sensors Journal*, vol. 22, no. 4, pp. 3464–3471, 2022.

[23] R. G. Crespo, O. S. Martínez, J. M. C. Lovelle, B. C. P. García-Bustelo, J. E. L. Gayo, and P. O. Pablos, "Recommendation System based on user interaction data applied to intelligent electronic books," *Computers in Human Behavior*, vol. 27, no. 4, pp. 1445–1449, 2011.

[24] S. Gong, "A collaborative filtering recommendation algorithm based on user clustering and item clustering," *Journal of Software*, vol. 5, no. 7, pp. 745–752, 2010.

[25] B. Sarwar, G. Karypis, J. Konstan, and J. Riedi, "Item-based collaborative filtering recommendation algorithms," in *Proceedings of the 10th international conference on World Wide Web*, pp. 285–295, May 1-5, 2001.

[26] L. Xiaojun, "An improved clustering-based collaborative filtering recommendation algorithm," *Cluster Computing*, vol. 20, no. 2, pp. 1281–1288, 2017.

[27] Z. Huang, D. Zeng, and H. Chen, "A comparison of collaborative-filtering recommendation algorithms for E-commerce," *IEEE Intelligent Systems*, vol. 22, no. 5, pp. 68–78, 2007.

Hindawi
Scientific Programming
Volume 2022, Article ID 4489430, 12 pages
https://doi.org/10.1155/2022/4489430

Research Article

Analysis Model Design on the Impact of Foreign Investment on China's Economic Growth

Lintao Zhang[1] **and Robin H. Xang**[2]

[1]*School of Economics, Hainan University, Haikou 570228, China*
[2]*International University, Vietnam National University Hochiminh City, Hochiminh, Vietnam*

Correspondence should be addressed to Lintao Zhang; zlintao@hainanu.edu.cn

Received 6 June 2022; Revised 17 June 2022; Accepted 20 June 2022; Published 8 July 2022

Academic Editor: Lianhui Li

This research mainly analyzes the influence of foreign investment in the era of big data on China's economic growth, in the process of analyzing the impact of foreign investment on the national economy, based on the analysis of the current situation of foreign investment and error-correction model, etc., through the correlation coefficient matrix to determine the variables data needed to fit the model; after fitting the model, the residual model is extracted, and the stationarity of the residual sequence is tested . On the basis of the above, this paper analyzes the difference of foreign direct investment in different regions, combined with the coastal areas and central region model and actual situation analysis, analyzes the two foreign direct investment (FDI) development speeds, base development speed, and average development speed, at the same time for the two regions in 2017; the specific direction of FDI do a detailed analysis. Finally, a series of conclusions are obtained.

1. Introduction

For China, since the reform and opening up in 1978, the economy of the eastern coastal areas has shown a trend of rapid development, while the economic development of the central and western regions is relatively slow compared with the coastal areas [1–5]. The impact of foreign direct investment on China is very far-reaching, but due to China's large and vast territory, the impact of foreign direct investment on different regions is different [6, 7]. For example, Jiangsu is located in the eastern coastal areas of China, and it has the advantage of the eastern coastal areas. From 1978 to 2017, Jiangsu's foreign direct investment quota was from $639915 million to $2513541 million; located in the central of Henan; foreign direct investment increased from $495.27 million to $1722428 million. Only from the surface data observation, we can find the foreign direct investment quota in t'e two regions [8–11]. This research is devoted to t7-he analysis model design of the impact of foreign investment on China's economic growth, so as to provide decision support for the formulation of macroeconomic policies and the management and control of microeconomic operation.

2. Analysis of the Impact of Foreign Investment on the National Economy

2.1. Current Utilization of Foreign Investment in China. Since the reform and opening up, the level of China's export-oriented economy has been continuously improved, the scale of introducing and utilizing foreign capital has been continuously expanding, the level has been continuously improved, and the number of domestic foreign-invested enterprises has also been continuously increasing [9–12]. Next, the statistical analysis of foreign direct investment will be conducted from the change of foreign investment quota, capital source, and industrial investment.

2.1.1. Current Situation of Foreign Direct Investment in Recent Years. Data on the actual utilization of foreign direct

investment and foreign investment from 2009 to 2018 and 1999 to 2018 are processed in Figures 1 and 2.

From Figure 1, we can see that in the decade from 2009 to 2018, both actual utilized foreign direct investment and actual utilized foreign capital showed an upward trend, but the growth trend of actual utilized foreign investment and actual utilized foreign investment between 2012 and 2018 is slower than before. The actual use of foreign investment includes two parts, one is large foreign direct investment and the other is another foreign investment. From Figure 2, we can see the actual use of foreign direct investment and the actual use of foreign investment during the 20 years from 1999–2018 [13]. This shows that in the actual use of foreign investment, the actual use of foreign investment proportion gradually decreased, reduced to 0 in recent years. For example, in 2015, the actual utilization of foreign investment and the actual utilized foreign direct investment were the US $1,26,267 million, in 2016, both were US $12,6001 million, in 2017, both were US $13,1035 million, and in 2018, both were US $13,49,666 million, indicating that the actual utilization of other foreign investment in recent years was 0.

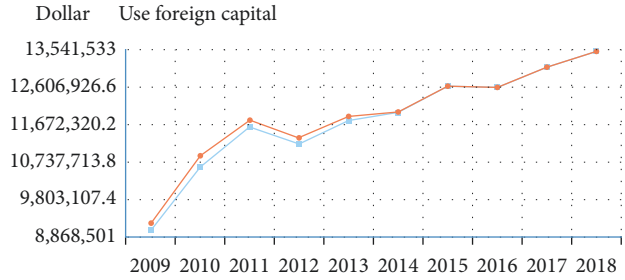

Figure 1: Actual use of foreign direct investment.

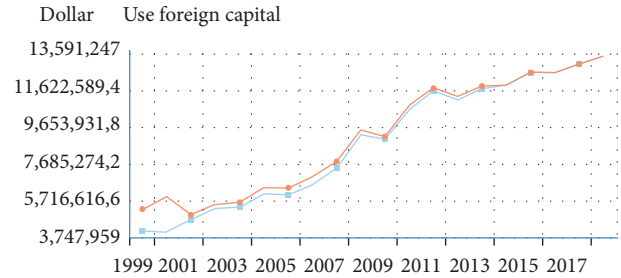

Figure 2: Data on the actual utilization of foreign capital.

2.1.2. Analysis of the Source Structure of Foreign Direct Investment. Under the background of the era of economic globalization, WTO was established on January 1, 1995, a total of 162 members, including a large part of the countries and regions in the world, can say the world economy roughly forms a whole, and the arrival of the electronic information age and transportation more and more convenient, our country and superior geographical location, rich resources attract all over the world to invest in our country [14–16]. China's foreign direct investment sources more areas, spread across five continents. Table 1 is the general situation of the sources of foreign direct investment in China from 2016 to 2018.

As can be seen from Table 1, China's foreign direct investment mainly comes from Asia, accounting for about 80%, while Hong Kong is the main source of foreign direct investment in China [17]. From the data, it can be concluded that more than half of China's foreign direct investment in China comes from Hong Kong, accounting for more than 60%. Among the five continents in the world, China's foreign direct investment from Africa is the least, which is less than 1%, which is directly related to the economic situation of Africa. Compared with Asia, the proportion of foreign direct investment from Europe, Oceania, and Latin America is also relatively small. From the above results, we can find that the source of a foreign direct investment structure is not reasonable, mainly foreign direct investment from Hong Kong. This phenomenon is related to the relationship between the mainland and Hong Kong; the transportation between China and Hong Kong region is very convenient, and for Hong Kong, the mainland also has various preferential policies. In addition, foreign direct investment is also directly related to the distance.

2.1.3. The General Situation of Foreign Direct Investment by Industry in China. This summary adopts the data of foreign direct investment in China in 2018 collected by the National Bureau of Statistics. Table 2 shows China's foreign direct investment in 2018 is roughly divided by industry (ten thousand dollars).

Taking out the largest amount of several industries from Table 2 into the pie chart, it is more convenient to see the specific direction of FDI in China (Figure 3).

It can be seen that China's foreign direct investment is mainly concentrated in the manufacturing, real estate, leasing, and business service industries, which account for about 62%. However, the FDI used for education, public management, and social organizations is particularly small, which shows that the introduction of FDI in China is extremely unbalanced in China, and the proportion of FDI varies greatly among various industries, which is also related to the main development of manufacturing and real estate industry in China.

2.2. Model Construction

2.2.1. Determination and Cointegration Test of the Sample Data. First of all, after inquiring about the database of the National Bureau of Statistics, the variables related to foreign direct investment ($X1$) include the number of contractual utilization of foreign investment projects ($X2$), the total import and export of foreign-invested enterprises (million US dollars) ($X3$) net foreign direct investment ($X4$), and the actual use of foreign direct investment ($X5$) [18–20]. Collect and collate data from 2009 to 2018 (incomplete data, so only 11 years). The correlation coefficient matrices were calculated between all the variables, such as in Table 3.

Table 1: Source structure of FDI in China (ten thousand dollars).

National	2016		2017		2018	
	Actual investment	Proportion	Actual investment	Proportion	Actual investment	Proportion
Summation	12600100	100%	13103500	100%	13496600	100%
Asia	9883103	78.44%	10919387	83.33%	10701310	79.29%
Hongkong	8146508	64.65%	9450901	72.13%	8991724	66.62%
Taiwan	196280	1.56%	177247	1.35%	139136	1.03%
Japan	309585	2.46%	326100	2.49%	379780	2.81%
Singapore	604668	4.80%	476318	3.64%	521021	3.86%
Korea	475112	3.77%	367253	2.80%	466688	3.46%
Africa	112720	0.89%	65746	0.50%	61042	0.45%
Europe	943439	7.49%	883619	6.74%	1119350	8.29%
Latin America	1221618	9.70%	636273	4.86%	902646	6.69%
North America	310421	2.46%	428552	3.27%	514789	3.81%
Oceania	126794	1.01%	160950	1.29%	190904	1.41%

Table 2: China's foreign direct investment in 2018 is roughly divided by industry (ten thousand dollars).

Index	Sum
Actual utilized amount of foreign direct investment	13496589
The amount of foreign direct investment actually utilized in agriculture, forestry, animal husbandry, and fishery	80131
The actual amount of foreign direct investment utilized in the mining industry	122841
The actual amount of foreign direct investment in the manufacturing industry	4117421
Actual utilization amount of foreign direct investment in the production and supply of electricity, gas, and water	442390
The amount of foreign direct investment actually utilized in the construction industry	148809
The actual amount of foreign direct investment in transportation, storage, and postal services	472737
Actual utilization amount of foreign direct investment in information transmission, computer services, and software industry	1166127
Actual utilization amount of foreign direct investment in the wholesale and retail industry	976689
The amount of foreign direct investment is actually utilized in the accommodation and catering industry	90107
The actual amount of foreign direct investment is utilized in the financial industry	870366
The actual amount of foreign direct investment is utilized in the real estate industry	2246740
The actual amount of foreign direct investment in leasing and business services	1887459
The amount of foreign direct investment actually utilized in scientific research, technical services, and the geological exploration industry	681298
The amount of foreign direct investment actually utilized by the water conservancy, environment, and public facilities management industry	47408
The amount of foreign direct investment actually utilized in residential services and other service industries	56166
The actual amount of foreign direct investment utilized in education	7420
The amount of foreign direct investment actually used in the health, social security, and social welfare industry	30178
The actual amount of foreign direct investment is utilized in the cultural, sports, and entertainment industries	52290
The amount of foreign direct investment actually utilized by public administration and social organizations	12

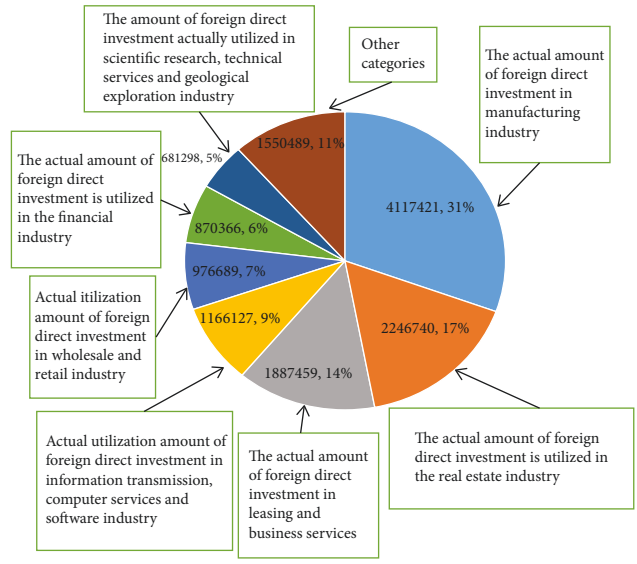

Figure 3: The proportion of FDI in various industries in China.

Table 3: Correlation coefficient matrix between the individual variables.

Covariance correlation	$X1$	$X2$	$X3$	$X4$	$X5$	Y
$X1$	$1.57E+12$ 1.000000					
$X2$	$7.92E+09$ 0.588991	$1.15E+08$ 1.000000				
$X3$	$2.10E+11$ 0.765397	$7.21E+08$ 0.306813	$4.79E+10$ 1.000000			
$X4$	$4.41E+12$ 0.825655	$1.56E+10$ 0.340532	$3.75E+11$ 0.401326	$1.82E+13$ 1.000000		
$X5$	$1.47E+12$ 0.998509	$7.51E+09$ 0.595392	$1.99E+11$ 0.775343	$4.04E+12$ 0.805613	$1.38E+12$ 1.000000	
Y	$2.03E+11$ 0.941857	$129E+09$ 0.696803	$2.31E+10$ 0.612225	$6.32E+11$ 0.860660	$1.88E+11$ 0.929698	$2.97E+10$ 1.000000

Table 3 shows that from 2009 to 2018, the correlation coefficient between FDI and actual FDI was 0.998509, indicating that the correlation between FDI and FDI is very high, and in the statistical Yearbook, some provinces have no data for FDI, so we can use foreign investment to measure FDI , and the correlation coefficient matrix can provide a theoretical basis for this. For the five variables with FDI, the correlation coefficient between foreign direct investment (X1) and the explained variables is the largest, indicating the strongest correlation between the two sets of data can be used as analyzed sample data.

Secondly, use Eviews to make a scatter map of China's GDP and foreign direct investment, as shown in Figure 4.

It can be seen from the figure that almost all points are evenly distributed on both sides of the line. GDP (Y) and F D of foreign direct investment I (X1) present a positive trend; combined with the correlation coefficient matrix, we can determine the two sets of time series as the analysis of the required data: economic growth is measured by GDP, recorded as Y: foreign direct investment with the actual use of foreign investment measured as an explanatory variable, recorded as FDI [21].

Next, the GDP (Y) and actual FDI from 2000 to 2019 will be taken as the sample data to analyze the problems. Table 4 shows China's GDP and FDI and its development speed.

Since both sets of GDP and actual FDI are time series, and the time-series data are often nonstable, the stability of GDPs and actual FDI is tested before analyzing the relationship between the two so as to prevent the phenomenon of false regression. After the first-order difference operation between GDP and actual foreign direct investment can pass the stability test of 95% confidence, so Y and FDI are the first-order single integral sequence, which belongs to the same order single integral variable, and may have a long-term stability relationship [22, 23]. Table 5 shows the unit root test results.

2.2.2. Sample Data Were Fitted. We take the GDP as the explanatory variable and the actual foreign direct investment as the explanatory variable. The model is set as follows:

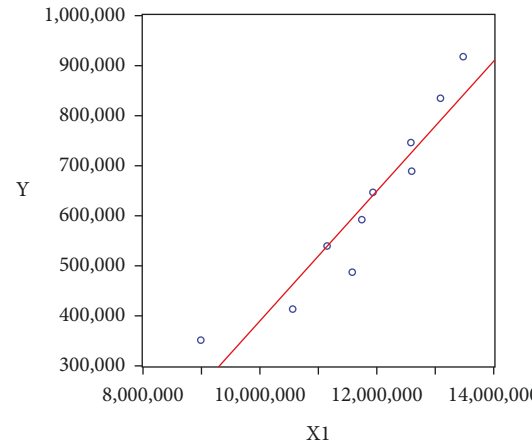

Figure 4: Scatter chart of China's GDP and foreign direct investment.

$$Y_t = C + \beta FDI_t + \mu_t. \tag{1}$$

The model is established by the least-squares method, and the results of the estimated parameters are shown in Table 6.

$$\begin{aligned} Y_t &= -331994 + 0.082954 FDI_t + \mu_t, \\ R^2 &= 0.916579\, F = 197.7735. \end{aligned} \tag{2}$$

Extract residuals:

$$\mu_t = Y_t + 331994 - 0.082954 FDI_t. \tag{3}$$

The residual stability (ADF) test is shown in Table 7.

The results show that the residual sequence is a nonsmooth sequence, which shows that there is no long-term stable relationship between Y and FDI, contradictory to the previous conclusion. Considering that the GDP unit is billions, and the actual foreign direct investment is dollars, the unit difference is particularly large, so the result may be the difference of units. So, the two groups of sample data measurement to eliminate the effect of the dimension take the logarithm of Y and FDI in Eviews 8.0. For the newly obtained data, Table 8 shows the stationarity test after taking the logarithm.

Table 4: China's GDP and FDI and its development speed.

Year	GDP/*a* hundred million	Month-on-month development speed	Foreign direct investment/ten thousand dollars	Month-on-month development speed
2000	100280.1	—	4071500	—
2001	110863.1	1.105534398	4687800	1.151369274
2002	121717.4	1.097907239	5274300	1.125111993
2003	137422.0	1.129025102	5350500	1.014447415
2004	161840.2	1.177687706	6063000	1.133165125
2005	187318.9	1.157431219	6032500	0.994969487
2006	219438.5	1.171470151	6582100	1.091106506
2007	270092.3	1.230833696	7476800	1.135929263
2008	319244.6	1.181983344	9239500	1.235755938
2009	348517.7	1.091694895	9003300	0.974435846
2010	412119.3	1.182491736	10573500	1.174402719
2011	487940.2	1.183978037	11601100	1.097186362
2012	538580.0	1.103782800	11171600	0.962977649
2013	592963.2	1.100975157	11758600	1.052543951
2014	643563.1	1.085333963	11956200	1.016804722
2015	688858.2	1.070381754	12626700	1.056079691
2016	746395.1	1.083525027	12600100	0.997893353
2017	832035.9	1.114739231	13103500	1.039952064
2018	919281.1	1.104857495	13496589	1.029998779
2019	990865.0	1.077869435	13810000	1.023221497

Table 5: Unit root test results.

Variable quantity	ADF	Type of inspection (c, t, n)	Critical value			Whether smooth
			1%	5%	10%	
Y	1.712258	(c, 0, 1)	−3.857386	−3.040391	−2.660551	No
DY	−5.478450	(c, 0, 1)	−3.920350	−3.065585	−2.673459	Yes
FDI	−0.801904	(c, 0, 1)	−3.886751	−3.052169	−2.666593	No
DFDI	−3.692204	(c, 0, 1)	−3.959148	−3.081002	−2.681330	Yes

Table 6: Regression results of Y versus FDI.

Variable	Coefficient	Std. Error	*t*-Statistic	Prob.
C	−3319941	58229.45	−5701480	0.0000
FDI	0.082954	0.005899	14.06319	0.0000
		Mean dependent var		
R- Squared	0.916579	S.D. dependent var		441466.8
Adjusted R-squared	0.911945	Akaike info criterion		2882374
S. E.of regression	85531.89			25.64581
Sum squared resid	1.32E+11	Schwarz criterion		25.74538
Log-likelihood	−254.4581	Hannan–Quinn criteria		25.66524
f-statistic	197.7735			0.315429
prob (F-statistic)	0.000000	Durbin–Watson stat		

Note. Data are obtained from the Eviews 8.0 regression results.

Set the model after eliminating the dimension to the following:

$$\ln Y_t = C + \alpha \ln FDI_t + \mu_t. \quad (4)$$

Then, Table 9 shows the results of the regression of lnY versus lnFDI.

Table 7: An ADF test for the extracted residuals.

		t-Statistic	Prob.*
Augmented dickey-fuller test statistic		−0.321640	0.9035
Test critical values:	1% level	−3.857386	
	5% level	−3.040391	
	10% level	−2.660551	

The results of the Granger causality test [9] show that the F value of $Y = 0.53843 < 0.80041$, which shows that gross domestic product (Y) is not the reason for FDI, and similarly, FDI is the reason for gross domestic product (Y).

2.3. Establishment of the Error-Correction Model. According to Granger's theorem, the error-correction model can be established with the cointegration relationship between the nonstationary variables, so we can establish the error-correction model between the above two variables. Table 10 shows the cointegration regression results of GDP and FDI.

The resulting error-correction model is as follows:

Table 8: The stationarity test after taking the logarithm.

Variable quantity	ADF	Type of inspection (c, t,n)	Critical value			Whether smooth
			1%	5%	10%	
lnY	−1.917836	(c, 0,1)	−3.857386	−3.040391	−2.660551	No
DlnY	−5.503037	(c, 0,1)	−3.920350	−3.065585	−2.673459	Yes
lnFDI	−2.114963	(c, 0,1)	−3.857386	−3.040391	−2.660551	No
DlnFDI	−5.704385	(c, 0,1)	−3.920350	−3.065585	−2.673459	Yes

Table 9: Results of the regression of lnY versus lnFDI.

Variable	Coefficient	Std. Error	t-Statistic	Prob.
C	−17.16385	1.095876	−15.66222	0.0000
LNFDI	1.872453	0.068567	27.30825	0.0000
R-squared	0.976432	Mean dependent var		12.75370
Adjusted R-squared	0.975122	S.D. dependent var		0.758087
S.E.of regression	0.119570	Akaike info criterion		−1315187
Sum squared resid	0.257347	Schwarz criterion		−1215613
Log-likelihood	15.15187	Hannan–Quinn criteria		–1.295749
F- Statistic	745.7405	Durbin–Watson stat		0.834389
Prob (F-statistic)	0.000000			

Note. Data are obtained from the Eviews 8.0 regression results.

Table 10: Cointegration regression results of GDP and FDI.

Variable	Coefficient	Std. Error	t-Statistic	Prob.
C	0.095734	0.011135	8.597814	0.0000
D (LNFDI)	0.457138	0.130286	3.508719	0.0043
ET (–1)	0.034950	0.124309	0.281156	0.7834
R-squared	0.513749	Mean dependent var		
Adjusted R-squared	0.432707	S.D. dependent var		
S.E.of regression	0.033125	Akaike info criterion		0.120798
Sum squared resid	0.013167	Schwarz criterion		0.043980–3.800180 -3.658570–3.801689
Log-likelihood	31.50135	Hannan–Quinn criteria		1.077134
G- Statistic	6.339296	Durbin–Watson stat		
Prob (F-statistic)	0.013218			

$$\Delta \ln \hat{Y}_t = 0.095734 + 0.457138\Delta \ln FDI_t + 0.034950 e_{t-1},$$
$$R^2 = 0.513749 DW = 1.077134. \tag{5}$$

The error-correction model $R^2 = 0.513749$is relatively bad, but P is far less than 0.05, so the model can be adopted.

2.4. Empirical Results Analysis. The empirical results show two aspects: (1) In the short term, FDI has a significant influence on GDP (i. *e*., economic growth). (2) In the long run, significant impact of FDI on GDP (i. e., economic growth). One percentage point change of FDI will cause a 0.46 percentage point change, and the large introduction of FDI will cause rapid growth of GDP.

2.5. Chapter Conclusion. In this section, the variable data needed to fit the model was first determined by the correlation coefficient matrix. After fitting the model, the residue is extracted, and the stationarity of the residue sequence is tested. Granger causality tests the model to find that FDI is the cause of Y. Finally, the model is corrected for error-correction and empirical analysis.

3. The Impact of Foreign Direct Investment on the Economy of Different Regions

3.1. Model Construction. When analyzing the impact of foreign direct investment on the economy of different regions, the factors with great impact on economic growth, such as consumption level, net export and labor force level (L), and domestic direct investment, should be combined [24, 25]. The sample data required for the analysis of the economic growth (Y) by FDI, consumption level (CPI), net export (NE), labor (L), (L), domestic investment (K), after the elimination of magnitude, the model can be set as follows:

$$\ln Y_t = \alpha_1 \ln FDI_t + \alpha_2 \ln NE_t + \alpha_3 \ln K_t + \alpha_4 \ln L_t + \alpha_5 \ln CPI_t + \mu_t. \tag{6}$$

3.1.1. Economic Growth Model of Coastal Areas (Jiangsu Province as an Example). Consumption level is measured by per capita consumption (CPI), labor (L) is employed, NE is expressed by the difference between exports and imports, and domestic investment (K) is measured by social fixed asset investment. Data of each variable in Jiangsu Province are collected as shown in Table 11.

Due to the inconsistent dimensions of each index, the influence of log-eliminating the dimensions and the sample data are all time-series data, so the stability needs to be tested. According to the results in Table 11, the first-order difference sequence is stationary [26–35], indicating a long-term relationship between these variables. Table 12 shows the test of the stationarity of the sample data.

The model can therefore be set to the following:

$$\ln Y_t = \alpha_1 \ln FDI_t + \alpha_2 \ln NE_t + \alpha_3 \ln K_t + \alpha_4 \ln L_t + \alpha_5 \ln CPI_t + \mu_t. \quad (7)$$

The results of fitting these variables at Eviews 8.0 are shown in Table 13.

The resulting fitted model is as follows:

$$\ln Y_t = 0.063049 \ln FDI_t + 0.045071 \ln NE_t + 0.490681 \ln K_t + 0.223155 \ln L_t + 0.268569 \ln CPI_t + \mu_t, \quad R^2 = 0.999152. \quad (8)$$

Table 14 shows the Stationarity test of the residuals. It can be seen that the fitting effect is good, and then the residuals of the model are proposed as follows:

$$\mu_t = \ln Y_t - 0.063049 \ln FDI_t - 0.04507 \ln NE_t - 0.490681 \ln K_t - 0.223155 \ln L_t - 0.268569 \ln CPI_t. \quad (9)$$

The results in Table 13 show that at the 5% significance level, the value of the t-test statistic is-3.629831, less than the cut-off of-3.052169, rejecting the null hypothesis that the residual root from the model and the residual sequence are a stationary sequence, and the long-term relationship between the explanatory variables and the explained variables can be learned.

3.1.2. Economic Growth Model of the Central Region (Henan Province as an Example). Data was collected first according to the coastal area operation method. The results obtained are as shown in Table 15.

All the data in Table 15 are done as in the previous section, and Table 16 shows the test of the stationarity of the sample data.

The model-fitting results are as follows:

$$\ln Y_t = 0.044262 \ln FDI_t + 0.042003 \ln NE_t + 0.526400 \ln K_t + 0.523185 \ln L_t - 0.040786 \ln CPI_t + \mu_t, \quad R^2 = 0.998457. \quad (10)$$

Extract residuals:

$$\mu_t = \ln Y_t - 0.044262 \ln FDI_t - 0.042003 \ln NE_t - 0.0526400 \ln K_t - 0.523185 \ln L_t + 0.040786 \ln CPI_t. \quad (11)$$

Table 17 is the Residual stationarity test. The results in Table 17 show that at the 5% significance level, the value of the t-test statistic is −3.748439, less than the cut-off of −3.052169. Thus, it rejects the null hypothesis that the residual roots from the model and the residual sequence are stationary sequences, and the long-term relationship between the explanatory variables and the explained variables can be learned.

3.2. The Differences Were Analyzed by Combining the Two Regional Models and the Actual Situation

3.2.1. Analysis of the Speed of FDI in the Two Regions. Taking the quota of foreign direct investment from 1999 to 2017 as the research object, the sequential development rate, fixed base development rate, and average development rate are calculated as shown in Table 18.

It can be seen from the calculation results in Table 18 that the month-on-month development rate of foreign direct investment in Jiangsu Province is basically stable between 0.84 and 1.15, while the floating range of the month-on-month development rate in Henan Province is between 0.66 and 1.67, which is slightly larger than that of Jiangsu Province.

The average development speed of FDI in Henan province and Jiangsu Province is calculated as follows:

$$\overline{x}_G = \sqrt[n]{x_1 x_2 \cdots x_n} = \sqrt[n]{R}. \quad (12)$$

According to the formula, the average development rate of FDI in Henan province is 1.20537, while the average development rate of FDI in Jiangsu Province is 1.07466. It can be seen that the average development rate of FDI in Henan province is higher than that of Jiangsu Province, but because its base is far smaller than that of Jiangsu Province, although it has grown too fast in the past 20 years, it is much different from Jiangsu Province.

3.2.2. Analysis of the Industrial Structure of Foreign Direct Investment in the Two Regions. The general situation of FDI by industry is as follows: the total foreign direct investment in 2017 was $2513541 million, of which FDI of manufacturing was $1118072 million, real estate $346007 million, leasing and business services $223912 million, electricity, heat, gas, and water production and supply $578.78 million, construction $2276.35 million, and other industries accumulated $540.34 million, as shown in Figure 5.

In 2017, FDI in Henan province showed a total FDI of $1722428 million, including manufacturing utilization FDI of $1034835 million, electricity, heat, gas, and water $2311.5 million, leasing and business services $8788.44 million, real estate $187056 million, construction $27.56 million, and $178,7.87 million in other industries. Figure 6 shows the portion of FDI industries in Henan Province.

Table 11: Data of each variable in Jiangsu Province.

Year	GDP(Y)/*a* hundred million	FDI/ten thousand dollars	Consumption per person (CPI)/ Yuan	Quantity of employment (L)/thousands of people	Social fixed assets investment(K)/*a* hundred million	Net export amount (NE)/ten thousand dollars
1999	7697.82	639915	3594	4390.71	2742.65	53.57
2000	8553.69	642358	3873	4418.14	2995.43	59.02
2001	9456.84	712201	4123	4436.45	3302.96	64.01
2002	10606.85	1036615	4708	4472.84	3849.24	66.55
2003	12442.87	1580214	5261	4499.97	5335.80	46.10
2004	15003.60	1213783	5913	4537.07	6827.59	41.37
2005	18598.69	1318339	7066	4578.75	8739.71	180.23
2006	21742.05	1743140	8182	4628.95	10071.24	368.42
2007	26018.48	2189206	9530	4677.88	12268.07	577.95
2008	30981.98	2512001	10882	4700.96	15060.45	838.04
2009	34457.30	2532289	11993	4726.54	18949.88	596.54
2010	41425.48	2849777	14035	4754.68	23184.28	753.08
2011	49110.27	3213173	17167	4758.23	26314.66	854.87
2012	54058.22	3575956	19452	4759.53	31706.58	1089.83
2013	59753.37	3325922	23585	4759.89	35982.52	1068.69
2014	65088.32	2817416	28316	4760.83	41552.75	1199.76
2015	70116.38	2427469	31682	4758.50	45905.17	1317.23
2016	77388.28	2454296	35875	4756.22	49370.85	1290.76
2017	85869.76	2513541	39796	4757.80	53000.21	1354.58

Table 12: Test of the stationarity of the sample data.

Variable quantity	ADF	Type of inspection (c, t, n)	Critical value			Whether smooth
			1%	5%	10%	
lnY	−1.650678	(c, 0, 1)	−3.886751	−3.052169	−2.666593	No
DlnY	−3.675515	(c, 0, 1)	−3.959148	−3.081002	−2.681330	Yes
lnFDI	−2.432745	(c, 0, 1)	−3.920350	−3.065585	−2.673459	No
DlnFDI	−5.173851	(c, 0, 1)	−3.920350	−3.065585	−2.673459	Yes
lnNE	−1.153147	(c, 0, 1)	−3.886751	−3.052169	−2.666593	No
DlnNE	−3.732355	(c, 0, 1)	−3.959148	−3.081002	−2.681330	Yes
lnK	−2.191837	(c, 0, 1)	−3.920350	−3.065585	−2.673459	No
DlnK	−6.132102	(c, 0, 1)	−3.920350	−3.065585	−2.673459	Yes
lnL	−2.104357	(c, 0, 1)	−3.886751	−3.052169	−2.666593	No
DlnL	−3.100355	(c, 0, 1)	−3.959148	−3.081002	−2.681330	Yes
lnCPI	0.304070	(c, 0, 1)	−3.886751	−3.052169	−2.666593	No
DlnCPI	−4.820446	(c, 0, 1)	−3.959148	−3.081002	−2.681330	Yes

Table 13: Fitting results of Jiangsu Province Economic Growth Model.

Variable	Coefficient	Std. Error	*t*-Statistic	Prob.
LNFDI	0.063049	0.043332	1.455021	0.1677
LNNE	0.045071	0.014036	3.211034	0.0063
LNK	0.490681	0.079267	6.190201	0.0000
LNL	0.223155	0.069220	3.223851	0.0061
LNCPI	0.268569	0.079660	3.371430	0.0046
	0.999152	Mean dependent var		1023329
	0.998910	S.D. dependent var		0.811391-
				4.180496-
R-squared adjusted R-squared S.E. of regression sum squared resid log-likelihood Durbin–Watson stat	0.026792	Akaike info criterion		3.931960- 4.138434
	0.010049	Schwarz criterion		
	44.71471	Hannan–Quinn criteria		
	1.600222			

Table 14: Stationarity test of the residuals.

		t-Statistic	Prob.*
Augmented Dickey–Fuller test statistic		−3.629831	−0.0166
Test critical values:	1% level	−3.886751	
	5% level	−3.052169	
	10% level	−2.666593	

Table 15: Data of each variable in Henan Province.

Year	GDP(Y)/*a* hundred million	FDI/ten thousand dollars	Consumption per person (CPI)/Yuan	Quantity of employment (L)/thousands of people	Social fixed assets investment(K)/*a* hundred million	Net export amount (NE)/ten thousand dollars
1999	4517.94	49527	1905	5205	1206.83	5.0734
2000	5052.99	53999	2215	5572	1377.74	7.1190
2001	5533.01	35861	2381	5517	1544.06	6.3840
2002	6035.48	45165	2553	5522	1725.93	10.3401
2003	6867.70	56149	3083	5536	2262.97	12.4442
2004	8553.79	87367	3625	5587	3099.38	17.3874
2005	10587.42	122960	4092	5662	4311.63	24.6582
2006	12362.79	184526	4530	5719	5904.71	34.7399
2007	15012.46	306162	5141	5773	8010.11	39.7798
2008	18018.53	403266	5877	5835	10490.64	39.5846
2009	19480.46	479858	6607	5949	13704.50	12.5457
2010	23092.36	624670	7837	6042	16585.86	32.7737
2011	26931.03	1008209	9171	6198	17768.95	58.3868
2012	29599.31	1211777	10380	6288	21450.00	76.0549
2013	32191.30	1345659	11820	6387	26087.46	120.1733
2014	34938.24	1492688	13078	6520	30782.17	137.3452
2015	37002.16	1608637	14507	6636	35660.35	123.4221
2016	40471.79	1699312	16043	6726	40415.09	144.4215
2017	44552.83	1722428	17842	6767	44496.93	164.4519

Table 16: Test of the stationarity of the sample data.

Variable quantity	ADF	Type of inspection (c, t, n)	Critical value			Whether smooth
			1%	5%	10%	
lnY	−1.385376	(c, 0, 1)	−3.886751	−3.052169	−2.666593	No
DlnY	−4.270420	(c, 0, 1)	−3.959148	−3.081002	−2.681330	Yes
lnFDI	−0.842845	(c, 0, 1)	−3.920350	−3.065585	−2.673459	No
DlnFDI	−3.119600	(c, 0, 1)	−3.920350	−3.065585	−2.673459	Yes
lnNE	−0.819215	(c, 0, 1)	−3.886751	−3.052169	−2.666593	No
DlnNE	−4.411203	(c, 0, 1)	−3.959148	−3.081002	−2.681330	Yes
lnK	−1.851008	(c, 0, 1)	−3.920350	−3.065585	−2.673459	No
DlnK	−2.754575	(c, 0, 1)	−3.920350	−3.065585	−2.673459	Yes
lnL	2.360425	(c, 0, 1)	−3.886751	−3.052169	−2.666593	No
DlnL	−3.633860	(c, 0, 1)	−3.959148	−3.081002	−2.681330	Yes
lnCPI	−0.236929	(c, 0, 1)	−3.886751	−3.052169	−2.666593	No
DlnCPI	−5.661558	(c, 0, 1)	−3.959148	−3.081002	−2.681330	Yes

Note. The data are obtained from Eviews 8.0.

Table 17: Residual stationarity test.

		t-Statistic	Prob.*
Augmented Dickey–Fuller test statistic		−3.748439	0.0131
Test critical values:	1%level	−3.886751	
	5%level	−3.052169	
	10%level	−2.666593	

3.2.3. Analysis of the Causes of the Difference. The economic growth model of Henan Province is as follows:

$$\begin{aligned}\ln Y_t = {} & 0.044262 \ln FDI_t + 0.042003 \ln NE_t \\ & + 0.526400 \ln K_t + 0.523185 \ln L_t \\ & - 0.040786 \ln CPI_t + \mu_t.\end{aligned} \tag{13}$$

Table 18: Speed of FDI development in both regions.

Year	Henan Province			Jiangsu Province		
	FDI	Month-on-month development speed	Determine the development speed of the foundation	FDI	Month-on-month development speed	Determine the development speed of the foundation
1999	49527	—	—	639915	—	—
2000	53999	1.09029	1.09029	642358	1.00382	1.00382
2001	35861	0.66410	0.72407	712201	1.10873	1.11296
2002	45165	1.25945	0.91193	1036615	1.45551	1.61993
2003	56149	1.24320	1.13370	1580214	1.52440	2.46941
2004	87367	1.55598	1.76403	1213783	0.76811	1.89679
2005	122960	1.40740	2.48269	1318339	1.08614	2.06018
2006	184526	1.50070	3.72577	1743140	1.32222	2.72402
2007	306162	1.65918	6.18172	2189206	1.25590	3.42109
2008	403266	1.31717	8.14235	2512001	1.14745	3.92552
2009	479858	1.18993	9.68882	2532289	1.00808	3.95723
2010	624670	1.30178	12.61272	2849777	1.12538	4.45337
2011	1008209	1.61399	20.35675	3213173	1.12752	5.02125
2012	1211777	1.20191	24.46700	3575956	1.11290	5.58817
2013	1345659	1.11048	27.17021	3325922	0.93008	5.19744
2014	1492688	1.10926	30.13887	2817416	0.84711	4.40280
2015	1608637	1.07768	32.48000	2427469	0.86159	3.79342
2016	1699312	1.05637	34.31082	2454296	1.01105	3.83535
2017	1722428	1.01360	34.77756	2513541	1.02414	3.92793

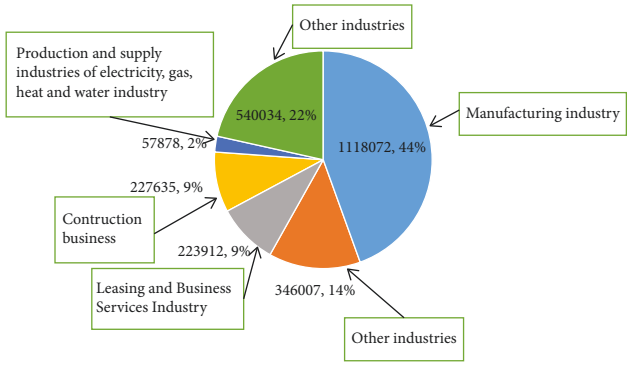

Figure 5: The portion of FDI industries in Jiangsu Province.

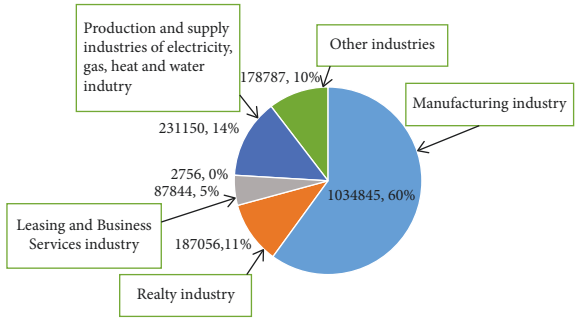

Figure 6: The portion of FDI industries in Henan Province.

The economic growth model of Jiangsu Province is as follows:

$$\ln Y_t = 0.063049 \ln FDI_t + 0.045071 \ln NE_t + 0.490681 \ln K_t + 0.223155 \ln L_t + 0.268569 \ln CPI_t + \mu_t. \quad (14)$$

It can be seen that when other variables remain unchanged, for every 1 percentage point of FDI growth, the GDP of Henan Province increased by 0.044262 percentage points, while Jiangsu Province increased by 0.063049 percentage points, and the difference between the two regions was 0.018787 percentage points. There are many reasons for this difference. From the analysis of this chapter, we can find some reasons: First of all, the distribution of FDI in Henan province is relatively uneven. FDI has been invested too much in the manufacturing industry, as high as 60%, while the manufacturing industry in Jiangsu Province is 44%, which is also due to the inconsistency between the leading industries in the two regions. Secondly, the construction industry is an important industry in promoting economic development. However, in terms of the construction industry, the FDI utilization in Jiangsu Province accounts for 9%, while the FDI introduced in the construction industry is only 0.0016%. Finally, although the growth rate of FDI introduced in Henan Province is very fast, its amount is far less than that of Jiangsu Province. Jiangsu Province has formed a relatively mature foreign joint venture, while the foreign investment in Henan Province is in the growth period, and the number of foreign direct investment cooperative enterprises is small.

4. Conclusion

Through the analysis of this paper, the study can obtain the following conclusions: First, China's FDI is mainly derived from the Hong Kong region. Second, foreign direct investment has a positive role in promoting China's economic growth but also increases China's domestic employment opportunities. Third, the distribution of foreign direct investment in various industries is very uneven, showing a situation dominated by manufacturing, leasing, and business services, and the real estate industry also accounts for a large proportion but relatively little foreign investment in education, public management, health, and social security. Fourth, in different regions, due to the regional economic law, development level is inconsistent, the introduction of FDI value is very different, and the introduction of the FDI economic benefits (i.e., GDP) because of different leading industries, so each industry introduced FDI also has different, but in each region are manufacturing most FDI. Manufacturing, leasing and business services and real estate are a large part of the FDI. These three major industries have contributed to economic growth after the introduction of FDI.

Data Availability

The dataset can be accessed upon request.

Conflicts of Interest

The authors declare that they have no conflicts of interest.

Acknowledgments

This work was sponsored in part by the Natural Science Foundation of Hainan Province: Research on the Evaluation System of Financial Opening of Free Trade Port with Chinese Characteristics (721RC523) and Philosophy and Social Science Research Base Subject of Hainan Province: Study on Effective Investment and its Efficiency in Hainan Province in the 14th Five-Year Plan (JD(ZC)20-13).

References

[1] X. Wang and X. Tian, "Foreign direct investment, digital inclusive finance and green Economy Development," *Business and Economic Research*, no. 07, pp. 168–171, 2022.

[2] S. Cao and T. Qi, "The Innovation and implementation of the Foreign Investment Law under the threshold of institutional opening," *Journal of Guizhou Normal University (Social Science edition)*, no. 06, pp. 145–156, 2021.

[3] Li Rui, Y. Ao, and Z. Li, "Quasi-natural experimental study on the influence of free trade Zone establishment on Foreign direct investment [J]," *World Economic Research*, no. 08), pp. 91–106, 2021.

[4] L. Huang and C. Wu, "Foreign investment, environmental regulation and urban green development efficiency of the Yangtze River Economic Belt [J]," *Reformation*, no. 03, pp. 94–110, 2021.

[5] L. Huang, Z. Wang, and X. Wang, "Research on the influence and mechanism of local economic growth target on foreign direct investment [J]," *International Economic and Trade Exploration*, vol. 37, no. 02, pp. 51–66, 2021.

[6] J. Zhou and Y. Zhang, "—— theory analysis of foreign direct investment, economic agglomeration and green economic efficiency," *International Economic and Trade exploration*, vol. 37, no. 01, pp. 66–82, 2021.

[7] X. Qiao and H. Liu, "The impact of foreign direct investment on economic growth," *Statistics and Decision-making*, vol. 36, no. 15, pp. 124–127, 2020.

[8] Y. Lv and B. Zhao, "Foreign direct investment, regional innovation and change of Industrial structure," *East China Economic Management*, vol. 34, no. 07, pp. 44–51, 2020.

[9] Z. Liu and C. Wen, "Innovation of foreign investment legislation under the background of a new round of opening up," *Journal of Xiamen University*, no. 03, pp. 127–139, 2020.

[10] Li Jian and X. C. Chong, "Economic growth effect and regional heterogeneity characteristics of Foreign direct investment," *Urban issues*, no. 04, pp. 51–61, 2020.

[11] G. Cai and H. Yang, "Can foreign direct investment improve China's factor market distortion [J]," *China's Industrial Economy*, no. 10, pp. 42–60, 2019.

[12] B. Sang, "Foreign direct investment motivation and changes in China's Business Environment," *International Economic Review*, no. 05, pp. 34–43, 2019, + 5.

[13] M. Lin and Z. Zhang, "Impact of competition policy on FDI in TFTA," *China Industrial economy*, no. 08, pp. 99–117, 2019.

[14] S. Tian, X. Li, and X. Wang, "Two-way direct investment and high-quality economic development of China," *Shanghai Economic Research*, no. 08, pp. 25–36, 2019.

[15] Li Chao, "Foreign investment, industrial structure and urban-rural income gap —— is based on state space model analysis," *Journal of Guizhou University of Finance and Economics*, no. 01, pp. 55–62, 2019.

[16] with H. Guang, Li Yu, and P. Duan, "Foreign direct investment, exchange rate screening and economic growth quality —— based on Chinese provincial samples," *Economic Science*, no. 02, pp. 59–73, 2017.

[17] X. Wang and Y. Huang, "Foreign direct investment and share of labor income: looting or icing on the cake," *China Industrial economy*, no. 04, pp. 135–154, 2017.

[18] Jiangshan, "On the legal construction of the national security review System for Chinese foreign investment," *Modern Law*, vol. 37, no. 05, pp. 85–95, 2015.

[19] H. Wang, P. Dong, Ke Qian, and Z. Yu, "Space-temporal relationship between foreign investment and regional economic development in Jiangsu province," *Economic Geography*, vol. 34, no. 01, pp. 22–27, 2014.

[20] M. Lai, Q. Bao, S. Peng, and X. Zhang, "FDI and technology spillover: research based on absorption capacity," *Economic Research*, no. 8, p. 11, 2005.

[21] K. Guo, "Study on the impact of foreign direct investment on Chinese industrial structure," *Economic research reference*, no. 21, pp. 18–20, 2000.

[22] J. Zhang and Y. Ouyang, "Empirical analysis of guangdong data by foreign direct investment, technology overlovers and economic growth," *Journal of Economics*, no. 11, pp. 10-11, 2003.

[23] L. Chen and J. Chen, "Experience research on the impact of foreign direct investment on China's economic growth," *The World Economy*, no. 6, pp. 7-8, 2002.

[24] L. Zhou and R. Ying, "Foreign direct investment and industrial pollution," *China's population Resources and Environment*, vol. 19, no. 2, pp. 9–11, 2009.

[25] L. Qi, "Discussion on the influence of foreign direct investment on manufacturing agglomeration," *Statistical Research*, no. 01, pp. 19-20, 2003.
[26] Z. Li and M. Lu, "Effectiveness analysis of preferential tax policies for Chinese foreign-invested enterprises," *The World Economy*, vol. 27, no. 10, p. 7, 2004.
[27] Z. Lu, "Financial asset risk measurement based on smart sensor big data security analysis and bayesian posterior probability model," *Wireless Communications and Mobile Computing*, pp. 1–12, 2022.
[28] L. Li, C. Mao, H. Sun, Y. Yuan, and B. Lei, "Digital twin driven green performance evaluation methodology of intelligent manufacturing: hybrid model based on fuzzy rough-sets AHP, multistage weight synthesis, and PROMETHEE II," *Complexity*, vol. 2020, no. 6, pp. 1–24, 2020.
[29] F. Du, "International trade balance algorithm based on the ownership principle of mobile edge computing," *Mathematical Problems in Engineering*, pp. 2021–11.
[30] L. Li and C. Mao, "Big data supported PSS evaluation decision in service-oriented manufacturing," *IEEE Access*, vol. 8, no. 99, pp. 154663–154670, 2020.
[31] Z. Lu, M. Li, and W. Zhao, "Stationarity testing of accumulated ethernet traffic," *Mathematical Problems in Engineering*, pp. 1–8, 2013.
[32] L. Li, T. Qu, Y. Liu et al., "Sustainability assessment of intelligent manufacturing supported by digital twin," *IEEE Access*, vol. 8, pp. 174988–175008, 2020.
[33] G. Li, Y. Wang, J. He, T. Hou, Le Du, and Hou, "Zhenhua. Fault forecasting of a machining center tool magazine based on health assessment," *Mathematical Problems in Engineering*, p. 2020, 2020.
[34] L. Li, B. Lei, and C. Mao, "Digital twin in smart manufacturing," *Journal of Industrial Information Integration*, vol. 26, no. 9, 2022.
[35] C. Liu, Z. Wang, H. Fu, and Y. Zhang, "A novel approach for nonstationary time series analysis with time-invariant correlation coefficient," *Mathematical Problems in Engineering*, pp. 1–12, 2014.

Hindawi
Scientific Programming
Volume 2022, Article ID 1489832, 10 pages
https://doi.org/10.1155/2022/1489832

Research Article

Analysis of Concentration in English Education Learning Based on CNN Model

Kun He[1] and Kun Gao[2]

[1]*Xi'an Siyuan University, Shaanxi, Xi'an 710038, China*
[2]*Xi'an Jiaotong University, Shaanxi, Xi'an 710048, China*

Correspondence should be addressed to Kun Gao; gaokun@mail.xjtu.edu.cn

Received 28 May 2022; Revised 14 June 2022; Accepted 18 June 2022; Published 8 July 2022

Academic Editor: Lianhui Li

Obtaining the learning behavior of terminal learners solves the problem of inability to understand students' concentration in class. When learners learn English, they can obtain learning concentration to understand learners' concentration, in order to analyze the influence coefficient of various learning behavior data on learning concentration. This paper will design and implement a terminal data acquisition tool to collect the device perception information in the learning environment of learners, and capture the learner's touch screen operation data based on the virtual simulation experiment, and then use the improved neural network to process the collected terminal sensor data for learning behavior. We identify and obtain the learner's learning activity state, and finally fit the learner's behavioral data weight through a linear regression equation, monitor the learner's learning state, and explore the influencing factors of learning concentration.

1. Introduction

In recent years, with the rapid changes in the era of intelligent information and the rapid development of the technological society, the trend of intelligentization has accelerated, and people's demand for intelligent life has gradually increased. Automated driving technology has entered the field of transportation, intelligent voice robots have entered the service industry, and intelligent sweeping robots have entered the field of home furnishing. In the context of education, it is on the agenda to develop intelligent applications suitable for English classroom education.

Concentration, also known as concentration, refers to the continuous and persistent listening state in the classroom and refers to the psychological state of a person when he is concentrating on a certain thing or activity. Due to their young age, primary and secondary school students do not have a strong sense of self-management, and their energy is easily dispersed by other things, resulting in insufficient energy invested in a relatively important thing. For example, when students are listening to a class, part of the time will be in a "slippage" state, which leads to many students' knowledge breakpoints, which directly affects the quality of the classroom. In addition, when the number of students in the class is large, it is difficult for English teachers to make real-time judgments on everyone's concentration while focusing on lectures. The low concentration of students leads to poor completion of homework after class, which will greatly increase the need for English teachers after class workload, and it is impossible to truly teach students in accordance with their aptitude. Therefore, the monitoring of students' concentration in English classroom is one of the most needed research directions. The traditional English classroom quality analysis is carried out by arranging lectures in the classroom, after-class questionnaires, etc., which is highly subjective, exposing the shortcomings of classroom real-time monitoring and analysis, and cannot meet people's expectations for high-quality English classroom teaching requirements and expectations. Therefore, it is most important to introduce intelligent education into the classroom, assist teachers in intelligent classroom management, and understand the listening status of each student anytime

and anywhere, so as to supervise English classrooms in a timely manner, and customize personalized English teaching plans in a timely manner after class one of the tasks. Research on a concentration monitoring and analysis system that can be applied to English classrooms has strong practicability and market space, and can also promote the development of English education in the direction of intelligence, comprehensiveness, and diversification, and has broad application prospects [1–10].

2. Related Work

Most scholars have done a lot of research on one aspect of mindfulness, attention, and put forward many insightful points, which provide a lot of thought reference for this research. To sum up, the relevant research on concentration is mainly carried out from the following three aspects: the first is the role of attention. It mainly conducts in-depth research on the phenomenon of inattentiveness in children, adolescents, athletes, etc.; the second is the research on the detection methods and evaluation standards of attention; and the third is the research on the cultivation of attention. The research on attention has a complete set of detection methods and evaluation standards. Although it is only a part of attention, it also provides many valuable references for the study of attention. Then, with the improvement of attention, the level of information technology, the research on the intelligent management, concentration monitoring, and analysis system of primary and middle school students' classrooms are moving toward the intelligent mode. In the 1850s, foreign scholar Aryamov made a statistical analysis of the attention of primary school students through the method of observation and recording, and believed that the attention span of primary school students aged 7–10 was about 20 minutes. This method does not have very good objectivity, has a strong subjective color, and also requires the observer to have the relevant ability. Later, the classroom teaching evaluation method appeared mainly by arranging different teachers to randomly listen to the class and record the lecture notes. This method cannot specifically reflect the concentration of each student during class. In recent years, the methods of monitoring students' classroom concentration have been studied in a more objective and convenient direction. The main methods of concentration monitoring include facial microexpression recognition; recognition and analysis of head posture information; and collection of physiological data such as brain waves (EEG), manual filling of questionnaires, and behavioral recognition of video images. However, the above methods have some problems more or less. Although the classroom expression evaluation system can identify most expressions of students in class, there will be certain errors due to the insufficient amount of existing data. A relatively complete classroom expression database is needed to train the model, and there is no such classroom expression database in the public libraries at home and abroad, and it cannot be completed in a short time if the collection is carried out. The above research shows that relying on a single dimension to monitor students' classroom concentration and analyze the results obtained is not accurate enough and unreliable. The advent of the era of intelligence has prompted the development of traditional classroom management in the direction of technology and informatization, and manual collection methods have gradually been replaced by automated operations. And at this stage, there is not much research on the concentration monitoring and analysis system of primary and secondary school classrooms that combines deep learning and multimodal integration, and there is a big gap, which is worth studying [11–16].

3. Relevant Theories and Technical Methods

3.1. Learning Behavior. Nowadays, with the widespread application of Internet devices such as networks and mobile terminals in all aspects of modern people's daily life, online learning has a positive impact on the progress of education in the field of higher education in my country. It not only breaks through the traditional teaching method and classroom model but also considered as a creative innovation of educational science and technology. By collecting and obtaining data about learners' learning behavior during online learning, it is possible to better understand and effectively optimize learning and the place where it occurs, discover information rules in learning behavior data, and apply them to realize its value. The process of learning behavior data acquisition includes the following three aspects, namely, data collection, data processing, and data analysis and presentation. The content of learning behavior data acquisition is shown in Figure 1 [17].

3.2. English Education Learning Behavior Concentration Recognition Technology

3.2.1. Classroom Attention Behavior Recognition Based on Long Short-Term Memory Network Model. Recurrent neural network (RNN) is a type of directed graph that combines the data connections between each neural node in the order of a corresponding time point, and RNN can be widely used in real-time processing. The input data of the corresponding spatial time series are extracted, and the network structure of the corresponding time-sequential objects of the output data with time-dependent characteristics is extracted. In the recurrent neural network, each node is connected to the next layer of neuron nodes through a one-way connection. During the network iteration process, each neuron contains its own previous information, and its output is affected by the previous neuron. Impact on its expanded unit is shown in Figure 2.

The structure of the RNN unit and its open structure in time are shown in Figure 2. In the figure, $x = (x_0, x_1, x_2, \ldots, x_t)$ represents the input sequence of the recurrent neural network, and $y = (y_0, y_1, y_2, \ldots, y_t)$ represents the output sequence of the recurrent neural network, and $h = (h_0, h_1, h_2, \ldots, h_t)$ represents the hidden state sequence of the recurrent neural network. The output state of each hidden layer of the recurrent neural network depends not only on the sequence t and x of the previous hidden input and output state layer of the current input neuron but also on the

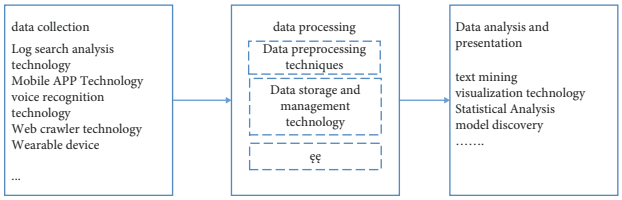

Figure 1: Learning behavior data acquisition process.

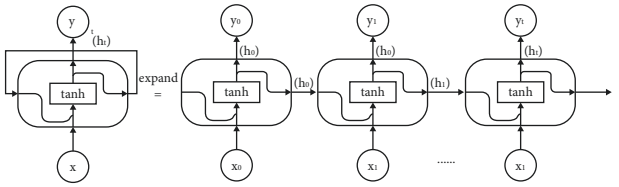

Figure 2: RNN unit expansion structure.

sequence of each hidden output state layer of the input neuron at the current moment h, and the expression of the calculation formula of the output layer at time t is as follows:

$$h_t = \tanh\left(w_{xh}x_t + w_{hh}h_{t-1} + b_h\right),$$
$$y_t = w_{hy}h_t + b_y. \tag{1}$$

Due to the limited amount of sequence historical data information that can be saved by samples in the hidden state of the recurrent neural network, problems such as gradient explosion or gradient disappearance may occur in the process of processing this long-term sequence of samples. Problems such as gradient explosion and disappearance will cause the recurrent neural network to be unstable and unable to converge to the optimal result, so the long short-term memory network (LSTM) with a strong feedback mechanism effectively solves the drawbacks of long-term dependence in the recurrent neural network. As a variant of the recurrent neural network, LSTM is composed of a self-connected memory data storage unit and three "gates" used to control the memory data information storage. The internal structure of the LSTM unit is shown in Figure 3 [18].

3.2.2. Recognition of English Education Learning Behavior Based on Convolutional Neural Network Model. A convolutional neural network system includes several layers of convolution, pooling, and fully connected layers. There is a huge technical difference between the point-to-layer structure of a convolutional neural network and the point-to-layer structure of a fully connected neural network. Each layer of neurons in a fully connected neural network must be arranged in a one-dimensional order, while each layer of a convolutional neural network must be arranged in a three-dimensional order. Compared with the fully connected neural network, the convolutional neural network has many basic characteristics such as multilayer local data connection, weight data sharing, and next-layer sampling. Local connection means that each neuron is no longer connected to all neurons in the previous layer, and weight sharing means that a group of neurons can share weights at the same

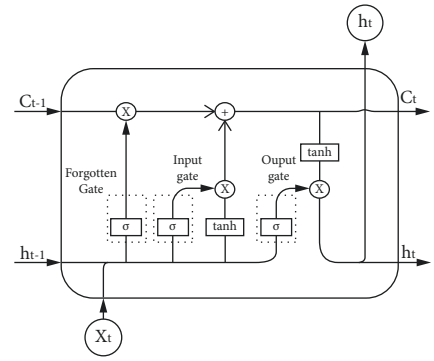

Figure 3: LSTM unit internal structure diagram.

position, not each connected neuron has its own positional weights. The downsampling method can greatly reduce the number of samples between each layer through the pooling layer, further greatly reduce the number of each parameter, and also greatly improve the robustness of the model. A schematic diagram of a convolutional neural network is shown in Figure 4.

The convolutional layer has the characteristics of realizing weight distribution and local links through the convolutional neural network. The convolutional layer performs feature extraction on the original input. The calculation formula is as follows:

$$a_{i,j} = f\left(\sum_{m=0}^{2}\sum_{n=0}^{2} w_{m,n}x_{i+m,j+n} + w_b\right). \tag{2}$$

In Formula 2 $w_{m,n}$ represents the weights of the functions in rows m and n, while x_{ij}-th row represents the elements of rows i, j. The element of row jth column w_b represents the bias term; f () represents the activation function; usually, the model construction selects the ReLU function as the activation function, and the definition of the ReLU function is as follows:

$$f(x) = \max(0, x). \tag{3}$$

Compared with the training process of the fully connected neural network, although the whole training method of the convolutional neural network is more complicated, the main workload and principle of the whole training are the same, mainly using a chain algorithm to obtain the derivation method, to recalculate the partial derivative coefficient of the weight function to the weight of each unit, and then update each weight according to the principle of reverse descent of the weight gradient. The process of training this algorithm requires a reverse weight propagation algorithm.

4. Establishment of Experimental Model of English Education Learning Concentration and Analysis of Experimental Results

4.1. Data Collection

4.1.1. Terminal Data Acquisition Framework. In the whole system, the design of the mobile terminal frame is very

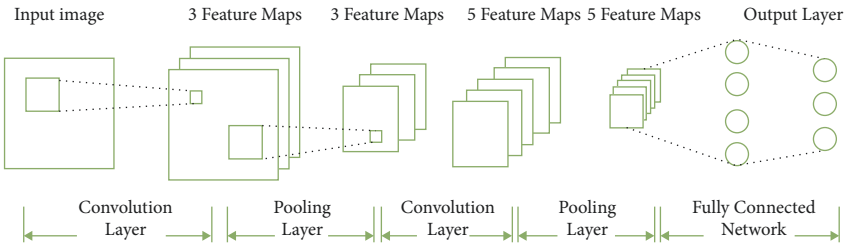

Figure 4: CNN neural network architecture.

important, and it is the cornerstone of the whole system. The functions completed in this design are shown in Figure 5. The terminal data, network data, and user usage data of learners ' English learning behavior are collected, stored, and uploaded, and the sensor data collected in real time are packaged in API and provided to the focus. Force recognition module is shown in Figure 6.

(1) Learner behavior data collection module. This module collects learning behavior data of a single terminal learner. The terminal data, network data, and user usage data of mobile terminal learners are collected to facilitate the calling and storage of other modules. The collected data are formed into a unified format "key-value" method in which the key is used as the unique identifier in the system, and the corresponding value saves the learner's learning behavior data in the form of a string.

(2) Local data storage module. This module receives and stores the collected mobile terminal learning behavior data. The collected data will be directly stored in the local server in the form of a database, providing sample data for subsequent model training.

(3) API calling module. This module provides the collected mobile terminal learning behavior data to the model in a standard format as sample data or to other models for calling. API (application programming interface) is an interface provided to the application program. After the system call is obtained, the API and the system call jointly complete the data access in the user mode and the kernel mode.

(4) Terminal behavior data upload module. This module stores the collected learning behavior data of English classroom teaching learners, uploads it, and sends it to the network side. The network side generates summary information according to the data uploaded by the terminal and sends the summary information to the terminal to visualize the results of the collected data.

(5) Learning concentration recognition module. This module is a research on learning concentration behavior recognition based on sensor data collected on terminal equipment. By building a model based on the LSTM model and integrating the convolutional neural network to improve the low-level processing unit to obtain the local saliency of the time series and the high-level processing unit to obtain the hidden feature of the time series, the classification of the learner's learning behavior and activity state are realized identify. When the terminal data acquisition system performs the startup operation, the application program is initialized, and the data for monitoring the terminal operation of the learner are set. We acquire terminal data information and network data information and return the data to the system; collect user usage data when the learner operation occurs, the corresponding device perception information is successfully captured by the system acquisition module; and store the acquired data in a standard format. We upload the acquired data to the server, and the operation flow of the terminal data acquisition framework is shown in Figure 6.

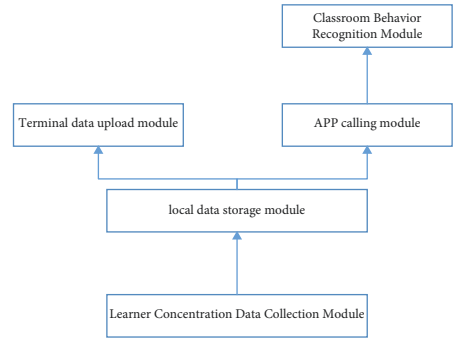

Figure 5: Logic diagram of terminal data acquisition framework.

4.1.2. Terminal Data Acquisition Development Platform and Tools. In this study, the Android system was selected as the development platform, and a set of learner terminal data acquisition system was implemented. Based on common technology architecture (MVC), Android Studio is used as the main development tool. Android Studio is an application editor developed by Google and specially developed for Android developers. The Android Studio development tool supports the flexible construction of the operating system based on Gradle and supports the automatic construction of multiple versions and the simultaneous generation of multiple APK files. Based on the above advantages, this paper uses Android Studio to develop and design the learner terminal data acquisition system.

4.1.3. Realization of Terminal Data Acquisition. The terminal data acquisition system frame includes three parts,

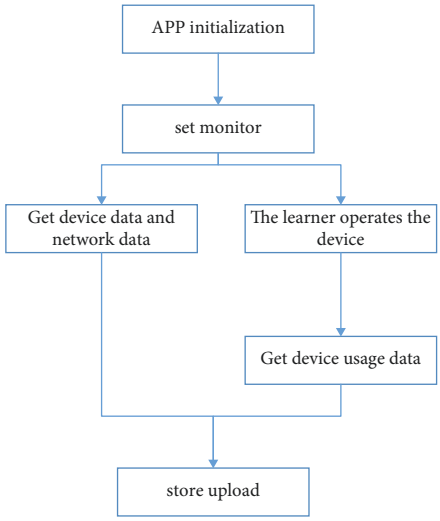

Figure 6: Operation flow chart of terminal data acquisition framework.

namely, terminal data, network data, and user usage data acquisition. The framework takes the sense controller class as the core, which combines the contents of device data (terminal data), network data (network data), and equipment usage data (user usage data) to work together. The core control class structure is shown in Figure 7.

(1) The realization of terminal equipment information acquisition is shown in Figure 7. The terminal device information acquisition is based on the digital serial number and DEVICE_ID dialing provided by the Android system to the mobile phone developer for acquiring the designated mobile terminal device name symbol.

(2) The realization of terminal power information acquisition, an information module about mobile phone power supply, is designed, and the mobile phone power supply is obtained in this way so that the learning behavior of learners on the mobile terminal can be better monitored and analyzed.

(3) As shown in Figure 8, the application "dataAcquisition," "rediobutton," "qqtest," and "Phone" are displayed as the list of APP usage in the virtual machine. The purpose of obtaining the usage of the APP is to obtain whether the learner has switched to other applications during English learning. During the learning process, multitasking is performed in parallel, which affects the concentration of learning.

(4) The realization of unlocking the screen event acquisition is shown in Figure 9. The purpose of acquiring the unlocking screen event is to analyze the behaviors of the English learners during the learning process. By analyzing the unlocking screen state, the learner-related learning information is obtained.

4.2. Human Behavior Recognition. In this study, a new neural network is designed: a two-layer convolutional neural

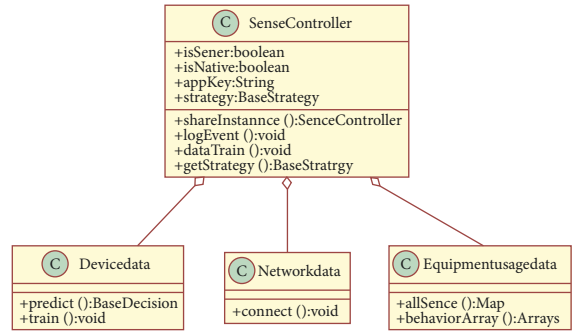

Figure 7: Core control class structure diagram.

network is integrated into the long short-term memory network. It only needs to send the preprocessed data to the network for training and does not need to manually extract the feature set.

The convolutional neural network plays a great role in identifying the concentration of English education learners. The low-level processing unit can obtain the local saliency of the time series, and the high-level processing unit can obtain the hidden features of the time series. In the face of time-series sensor data, convolutional neural networks need to perform convolution and pooling calculations along the time dimension, stack time-series sensor data into three-dimensional arrays, and extract time-series feature sets through convolution pooling. The long short-term memory network is a recurrent network that simulates the temporal correlation in time series problems through memory units, which can effectively obtain the temporal dependence of features.

4.2.1. Data Collection and Preprocessing. In order to obtain a form that is more conducive to learner feature extraction, the data should be preprocessed before feature extraction and model recognition. In order to fully mine the focus state information of English education learners, the data standardization is carried out by using the standard descriptive method, and the data are preprocessed by the sliding window technology of the sensor, and the data collected every second are used as a sample; that is, the sensor samples the learning behavior of the learner at a frequency of 50 Hz. When it is completed, all the collected data are sampled in a certain time dimension. When dividing, every 128 consecutive samples are taken as 1 sample. The distance between each sample and the starting position is 64 samples as a point, and each active window is described by 561 features. This study uses two-dimensional convolution operation to process time series, obtains the local dependency of sensor data time dimension, uses two-dimensional convolution to capture the spatial characteristics of English education learning behaviors, and obtains the two-dimensional matrix of learning action input according to the operation size, and the calculation formula of its dimension N is as follows:

$$N = \sqrt{m * 2 + \text{cell}(\sqrt{m})^2}, \tag{4}$$

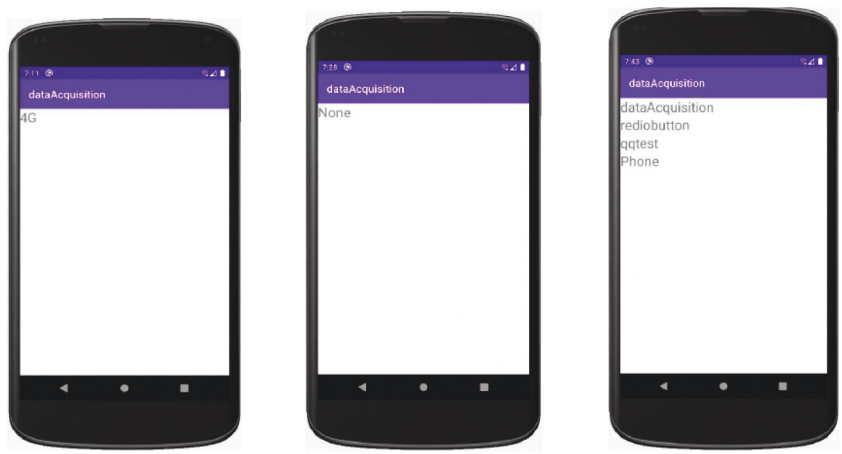

Figure 8: Access network type data.

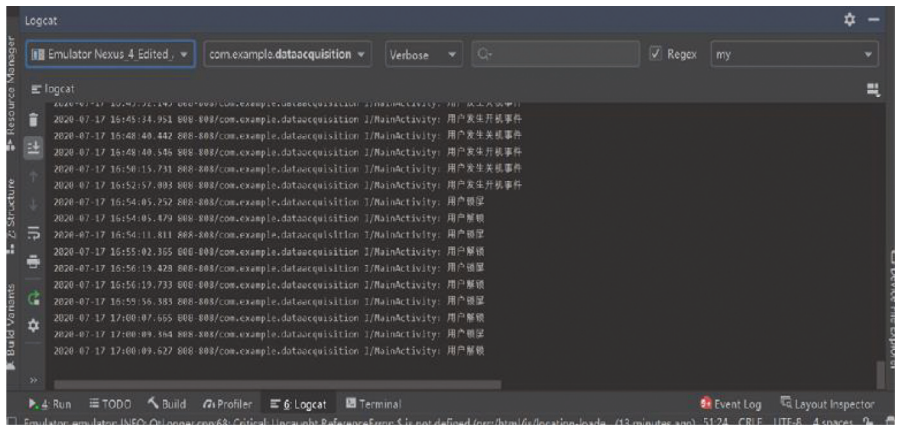

Figure 9: English learner learning behavior data.

where m is the number of collected data samples, and cell() is rounded up. The processed time-series data are input into the neural network for training, and the algorithm model is obtained. The output layer in the model is the softmax layer, and its output is a probability distribution, so the labels of the sample data also need to appear in the form of probability distributions.

4.2.2. Learner Learning Concentration Recognition Model. In this paper, the method of learner focus recognition is mainly based on the segmentation of various learning behaviors, and each learning behavior has a unique and refined action and category label.

Attention learning behavior recognition model takes human behavior, that is, multi-action sequence information as the input of the model, in which the multi-action output is used to predict the human behavior category of the model. The model mainly uses convolutional neural network and long short-term memory. The combined form of the network is used for human behavior recognition. The model is defined as the sequential Keras model, and a CNN model is defined with the Keras deep learning library. The network structure framework is shown in Figure 10. It mainly includes two one-dimensional convolutional layers, a dropout layer and a pooling layer. The training of the convolutional neural network model is very fast in which the dropout layer can slow down the learning process and make the final model better, and the pooling layer shortens the learned features to 1/4, so that it retains the most important elements. To better enable the model to learn features from the input data, we wrap the entire CNN model in a time distributed layer, allowing the same CNN model to be read in each of the four subsequences of the window. After the convolutional and pooling layers, the learned features are unrolled into a long vector, the extracted features are flattened and fed to the single-hidden layer LSTM model for reading, and the CNN-LSTM model will be in chunks. We read subsequences of the main sequence, allow the LSTM to interpret and extract features from each block, define dropout layers to reduce the model's overfitting to the training data, extract its own features before final classification of the activity, and finally, in turn, classify through fully connected layers and softmax layers.

4.2.3. Learning Behavior Recognition Model Training. In the process of fitting the CNN-LSTM model, no shuffle operation is performed on the sequence data, but the window of the input data is randomly adjusted during training, so the

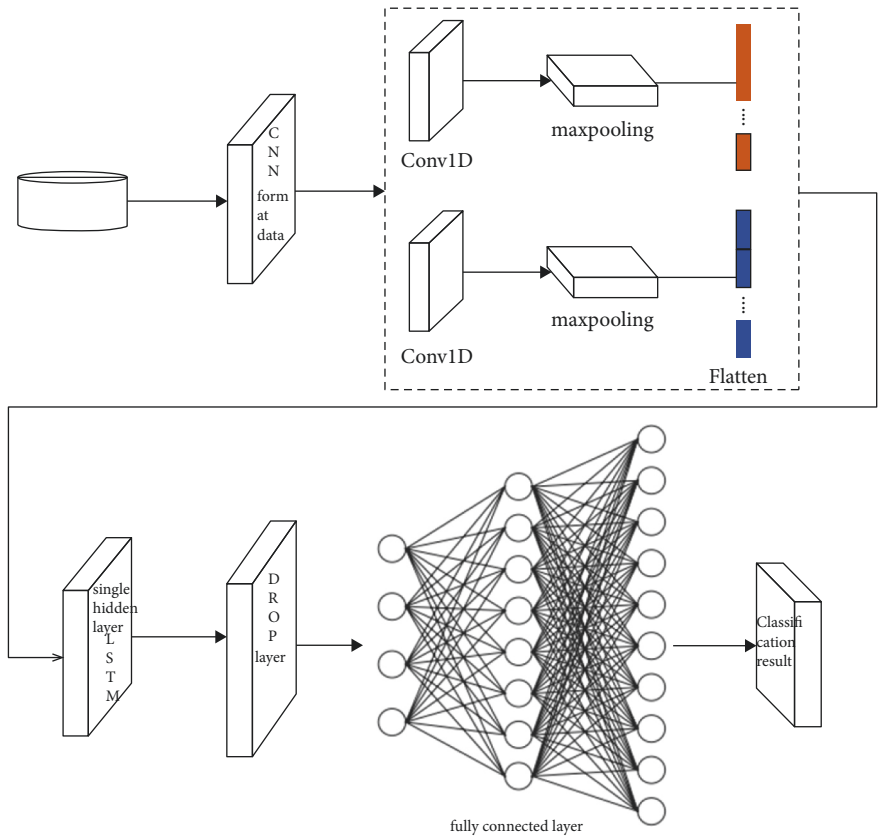

Figure 10: Building a neural network structure framework.

log information is not output to the standard output stream during model training. The number of iterations of the training model is 15, and the learning efficiency of the model is set to 0.1 to improve the generalization ability of the model. The Adam optimizer is used as the stochastic gradient descent algorithm to iteratively update the network weights for training data, providing a sparse stochastic gradient weight descent optimization algorithm that can effectively deal with the problem of network noise reduction. In the process of training the model, the optimization objective is set as the cross-entropy categorical_crossentropy to describe the accuracy of the model for human action recognition. Cross-entropy is defined as follows:

$$H_{y'}\, y = -\sum_{i=1}^{N} y_i' \log y_i. \tag{5}$$

Among them, y_i' and y_i represent the i-th ground-truth sample labels and the i-th predicted sample labels are the number of identified categories. After the weight matrix calculates the cross-entropy loss function, the weight matrix and the offset are corrected in turn. The neural network uses the gradient descent method to solve the minimum value of the loss function, which is defined as follows:

$$x_{\text{new}} = x_{\text{old}} - \varphi \frac{\partial f(x)}{\partial (x)}. \tag{6}$$

Among them, x_{new} and x_{old} represent the modified weight matrix and the uncorrected weight matrix, respectively, and $f(x)$ represent the learning rate, which is a hyperparameter of the neural network. The data features and labels of the test set are input into the evaluation function run_experiment respectively, and the accuracy of the model used for the test set data is calculated. By creating and evaluating models, debug information and a sample score are printed for each model.

4.2.4. Experimental Results and Analysis. The experimental results mainly compare and analyze the improved CNN-LSTM model proposed in this paper with the machine learning hierarchical hidden Markov model, machine learning algorithm, and LSTM model algorithm, in order to verify the accuracy of the model. First, some data sets used in the experiment, experimental environment, and parameter configuration in other experiments are briefly introduced, and then, the corresponding experiments are designed according to the needs and analyzed with the comparison results.

The data of the experiment come from the machine learning knowledge base of the public website UCI. The HAR data set collects sensor data on smartphones. The data set is recorded from 30 students, who collect six learning behaviors while wearing smartphones around their waists activity. They are dictation, reading, answering, discussion, thinking, and classroom practice. After the sampling work results are detected, all samples and data are divided according to the time dimension. The analysis results are

Table 1: UCI data sample distribution table.

	Dictation	Read	Answer	Discuss	Think	Classroom exercises	
Training set	1253	1307	1359	1355	1086	992	7352
Test set	491	537	532	496	471	420	2947
Total	1744	1844	1891	1851	1557	1412	10299

Table 2: Experimental parameter settings.

Parameter name	Parameter value
Length of time sample	128
Number of times to train the model	25
Number of batches per training	64
Time step	32
The number of neurons in the hidden layer	100
Learning rate	0.1
Dropout ratio	0.5

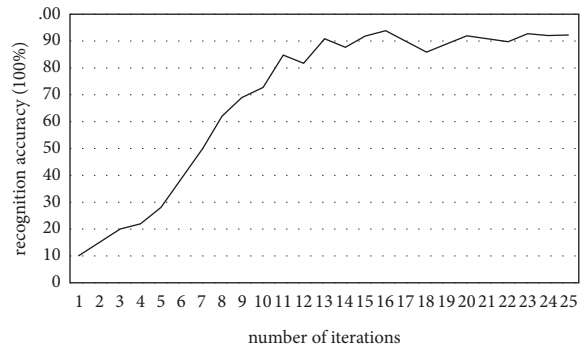

Figure 11: Variation curve of recognition accuracy of CNN-LSTM model training set.

2.56 seconds and a 50% overlapping fixed window for sampling. The segmentation of various learning behaviors is that every 128 consecutive samples are taken as a new sample, each sample data are 64 sampling points apart at its start and end positions, and each active window is described by 561 feature methods, and these data are analyzed. After normalization, the data values are between [−1, 1]. The entire sample set was redivided and split into two groups, with the behavioral data of 21 students as the training set and the behavioral data of 9 students as the test set. The entire UCI data set has a total of 10,299 data samples, and the specific sample distribution is shown in Table 1 [19–23].

Through the analysis of the data set, this paper continuously adjusts and tests the parameters, and obtains the optimal relevant parameters for the current training. The experiment is defined as a shallow-level CNN that extracts features from the input data, flattens the feature vector into a single-hidden-layer LSTM model, and adds a dropout layer that reduces the model's overfitting to the training data, and a dropout layer for classification. Softmax layer uses a fully connected layer to interpret the features extracted by the CNN-LSTM hidden layers before using the output layer for prediction. In the practice process of training the model, the method of stochastic gradient descent is used for training, and the optimization objective is set as the cross-entropy categorical_crossentropy to describe the accuracy of the model for classifying human actions. When performing the training operation iteratively, only a small part of the data is used for stochastic gradient descent each time, and 64 items are randomly selected from the training set as mini_batch; that is, the batch size is set to 64, and 64 data windows are inputs into the model before updating the model weights. In the CNN-LSTM model, the settings of parameters and matrix size are learned through model training, so 30% of the data set is selected as the training set to train the model to obtain the optimal parameters, and the remaining data are used as the test set to evaluate the performance of the model. The specific experimental parameter settings are shown in Table 2.

This experiment is a training test of the neural network model built based on the public data set of sensor data. In order to make the experimental results more accurate, the experiments are carried out under the weight parameter that obtains the highest accurate value, and the experimental results are compared with the hierarchical hidden Markov model, machine learning algorithm, and LSTM model. The recognition accuracy is used as an evaluation index for experimental comparison. The higher the accuracy, the better the performance of the model classifier.

When experimenting with the CNN-LSTM model, we set the experimental parameters. Figure 11 shows the change process of the recognition accuracy of the experimental training set based on the CNN-LSTM model. It can be seen that with the increase of the number of iterations, the recognition accuracy rate rises rapidly and remains above 0.92; the standard deviation is 0.373; and the recognition accuracy is accurate. The rate is about 92.499%.

Through the above experiments, the operation results based on the hierarchical hidden Markov model, machine learning algorithm, LSTM model, and CNN-LSTM model are obtained. The comprehensive recognition accuracy of the above experiments is summarized in Table 3. Compared with the existing research, it is found that the hierarchical hidden Markov model structure saves the storage space of the mobile phone and reduces the computational complexity, but the space complexity is expensive and the data overfitting phenomenon that may occur in the experimental classification process is not carried out. Processing. In the experiment based on machine learning algorithm, the data features selected manually after dimensionality reduction of the data by principal component analysis are still insufficient; when recognizing students' concentration behavior based on the LSTM model, the single-layer LSTM structure is used to process long-term sequences. There is a problem of taking too long to sample. Compared with the above three

Table 3: Comparison of experimental results.

Method	Recognition accuracy (%)
Hierarchical hidden Markov model	72.5
Machine learning algorithms	78.2
LSTM model	89.1
CNN-LSTM model	92.5

methods of human behavior recognition, the recognition accuracy of the CNN-LSTM model has increased, which indicates that the model has a higher accuracy rate and better effect in recognizing concentration behaviors in English classroom teaching.

By integrating the convolutional neural network on the basis of the LSTM model, the local saliency of the time series obtained by the low-level processing unit and the hidden features of the time series obtained by the high-level processing unit are improved. On the one hand, the model does not require manual feature extraction, which leads to deviations in the experimental results; on the other hand, the combination of convolutional neural network and long short-term memory network can make the model better learn features from the input data and achieve more effective results. *English learning concentration activity recognition*. Finally, the model is compared with the hierarchical hidden Markov model, machine learning algorithm, and LSTM model, and the models improve the recognition accuracy by nearly 19.99%, 14.29%, and 2.79%, respectively, thus verifying the effectiveness of the model.

5. Conclusion

This paper obtains learning behavior data based on the application scenario of mobile terminal learning, obtains the learning status device perception information of the learner by implementing a terminal data acquisition tool, captures the touch screen operation of the learner experiment based on the virtual simulation experiment, and then improves the CNN-LSTM by improving the CNN-LSTM. The collected terminal acceleration sensor data are processed for human behavior recognition, and the learning activity status of the learner is obtained. Finally, the influence of the learning behavior of the learner's mobile terminal on the learning concentration is analyzed by fitting the weights of various types of learner behavior data. The acquisition of learning behavior data of mobile terminal learners is the premise of analyzing the influence of learners' online learning concentration factors. The acquisition of learner behavior data provides experimental data sets for subsequent research modules such as intelligent learning guidance and personalized diagnosis.

Data Availability

The data set can be accessed upon request.

Conflicts of Interest

The authors declare that they have no conflicts of interest.

References

[1] C. Klonoff David, "New wearable computers move ahead: Google glass and smart wigs," *Journal of diabetes science and technology*, vol. 8, no. 1, 2014.

[2] N. Takashi, M. Daisuke, I. Hiroyuki, O. Yuki, and K. Ueda, "Application of Augmented Reality (AR) Technology to Locate the Cutaneous Perforator of Anterolateral Thigh Perforator Flap: A Case Report," *Microsurgery*, vol. 44, no. 18, pp. 15–18, 2021.

[3] C. A. Corneanu, M. O. Simon, J. F. Cohn, and S. E. Guerrero, "Survey on RGB, 3D, thermal, and multimodal approaches for facial expression recognition: history, trends, and affect-related applications," *IEEE Transactions on Pattern Analysis and Machine Intelligence*, vol. 38, no. 8, pp. 1548–1568, 2016.

[4] S. Neha and E. Sharma, Khular and K. Amita, Hybrid meta-heuristic algorithm based deep neural network for face recognition," *Journal of Computational Science*, vol. 30, no. 11, pp. 14-15, 2021.

[5] T. B. Moeslund, A. Hilton, V. Krüger, and L. Sigal, *Visual Analysis of Humans*, Springer, London, 2011.

[6] A. Kadkhodamohammadi, A. Gangi, M. De Mathelin, and P. Nicolas, "Articulated clinician detection using 3D pictorial structures on RGB-D data," *Medical Image Analysis*, vol. 35, 2017.

[7] D. Case, *Looking for Information: A Survey of Research on Information Seeking, Needs, and Behavior*, Academia Press, Amsterdam NL, 2002.

[8] Y. Lee and S. B. Cho, "Activity Recognition Using Hierarchical Hidden Markov Models on a Smartphone with 3D accelerometer," in *Proceedings of the International Conference on Hybrid Artificial Intelligence Systems*, pp. 460–467, Springer, Wroclaw, Poland, May 2011.

[9] F. Marton and R. Säljö, "On qualitative differences in learning: I-outcome and process," *British Journal of Educational Psychology*, vol. 46, no. 1, pp. 4–11, 1976.

[10] J. B. Biggs, "Student Approaches to Learning and Studying," *Australian: Australian Council for Educational*, vol. 1, pp. 8–19, 1987.

[11] T. W. Smith and S. A. Colby, "Teaching for deep learning," *The Clearing House: A Journal of Educational Strategies, Issues and Ideas*, vol. 80, no. 5, pp. 205–210, 2007.

[12] J. Biggs, Tang, and C. Teaching, *For Quality Learning at university: What the Student Does*pp. 214–220, Open University Press, Berkshire, UK, 3rd edition, 2007.

[13] H. Tüzün, M. Yılmaz-Soylu, T. Karakuş, Y. İnal, and G. Kızılkaya, "The effects of computer games on primary school students' achievement and motivation in geography learning," *Computers & Education*, vol. 52, no. 1, pp. 68–77, 2009.

[14] K. Kieser, H. Herbison, W. Waddell, K. Kardos, and I. Innes, "Learning in oral biology: a comparison between deep and surface approaches," *New Zealand Dental Journal*, vol. 102, no. 3, pp. 64–68, 2006.

[15] H. S. Barrows, "Problem-based learning in medicine and beyond: a brief overview," *New Directions for Teaching and Learning*, vol. 68, pp. 3–12, 1996.

[16] W. Hung, "The 9-step problem design process for problem-based learning: application of the 3C3R model," *Educational Research Review*, vol. 4, no. 2, pp. 118–141, 2009.

[17] A. Alrahlah, "How effective the problem-based learning (PBL) in dental education. A critical review," *The Saudi Dental Journal*, vol. 28, no. 4, pp. 155–161, 2016.

[18] B. Hoffman and D. Ritchie, "Using multimedia to overcome the problems with problem based learning," *Instructional Science*, vol. 25, no. 2, pp. 97–115, 1997.

[19] H. S. Barrows and M. Robyn, *Tamblyn Problem-Based Learning: An Approach to Medical Education Springer Publishing Company*, Springer, Berlin, Germany, 1980.

[20] J. R. Savery, "Overview of problem-based learning: definitions and distinctions," *Interdisciplinary Journal of Problem Based Learning*, vol. 1, no. 1, pp. 9–20, 2014.

[21] J. Biggs and C. Tang, *Teaching for Quality Learning at University*, McGraw-Hill, New York, NY, USA, 3rd edition, 2007.

[22] P. R. Pintrich, "The dynamic interplay of student motivation and cognition in the college classroom," in *Motivating Students: An Initial Attempt to Operationalize the Curiosity gap Model, Developments in Business Simulation and Experiential Learning*, J. G. Gentry, Ed., pp. 69–75, 2001.

[23] N. F. Harun, K. M. Yusof, M. Z. Jamaludin, and S. A. H. S. Hassan, "Motivation in problem-based learning implementation," *Procedia-Social and Behavioral Sciences*, vol. 56, pp. 233–242, 2012.

Hindawi
Scientific Programming
Volume 2022, Article ID 6896816, 7 pages
https://doi.org/10.1155/2022/6896816

Research Article

Research on the Relevance of Art Courses in Colleges and Universities Based on Data Mining

Chunxia Huang

Henan Vocational College of Economics and Trade, College of Art and Design, Zhengzhou, Henan 450000, China

Correspondence should be addressed to Chunxia Huang; hcxedu2021@henetc.edu.cn

Received 9 May 2022; Revised 30 May 2022; Accepted 7 June 2022; Published 7 July 2022

Academic Editor: Lianhui Li

With the development of educational informatization, the educational data of each school is increasing day by day. How to rationally use the existing information to make scientific teaching decisions is a problem that every educator is closely concerned about. This paper proposes a correlation analysis method for college art courses based on data mining technology. Through the study of association rules in data mining, the Apriori algorithm based on three-dimensional matrix is used to quickly mine student performance data, so as to obtain some reasonable and reliable courses. The results show that the method in this paper can find valuable information for curriculum setting from the actual teaching data, so as to reasonably optimize the curriculum, provide a decision-making basis for the revision of the art curriculum and syllabus in colleges and universities, and further improve the teaching effect and the quality of personnel training.

1. Introduction

With the development of various undertakings in the country, the society is required to cultivate more high-quality talents. As one of the most important talent training bases, the school has a long way to go. As far as the professional development of educational technology is concerned, there are common shortcomings in the school's professional construction, such as lack of characteristics, broad curriculum, and severe employment situation [1–5]. The school's curriculum setting directly affects the quality of teaching and the level of personnel training. The report shows that the factors restricting employment also include improper curriculum. Curriculum setting is not only related to the quality of talent training and student employment but also closely related to the development of disciplines. Therefore, it is particularly important to use existing data to reasonably set up courses in colleges and universities [6, 7].

In the course setting, the knowledge correlation of the course content itself is usually analyzed, and the course is set according to these correlations. This kind of correlation analysis based on course content and learning objectives solves problems such as course level and setting order, content connection, and credit hour allocation [8–11]. However, the curriculum is set simply by considering the relevance of the curriculum content without considering the actual situation of students' learning after the school offers such a course with valuable information [10, 12–14]. With the help of data to reflect the internal connection of courses and further research, we can set up courses more scientifically and reasonably, better optimize teaching management, and improve teaching quality [15].

With the vigorous development of education informatization, the data stored in the educational administration system, student employment system, and enrollment system of various schools is increasing rapidly. Faced with these massive data, how to extract effective information from it is a problem that every educator must think about. At this stage, the use of students' grade data in the educational administration system is only for query, statistics, and simple analysis, and no other information hidden behind the grades has been found in depth [16–19]. Data mining technology can analyze and process complex data. Using data mining technology, we can find the internal relationship between grades and find useful information, which is beneficial to improve the teaching management level and teaching quality

of colleges and universities. Therefore, the curriculum setting should not only consider the relevant course names on the surface of each course or the simple content of the courses, but should start more from the actual learning of students to find the learning effect that reflects the actual situation of the school curriculum [9, 20, 21].

Data mining technology is used to analyze the actual teaching data to find out the curriculum relevance reflected in it, but the relevance of the curriculum is not completely consistent with the relevance of the course content itself, and not only be obtained through a simple analysis of the course content, but it also reflects the actual situation of the school curriculum, the learning effect of the course, and the difference between the course setting, so how to use the real data generated in the actual teaching to more accurately find the existence of the course? Objective correlation is the problem to be solved in this study. In the above background and meaning, with the help of data mining technology, we can quantitatively analyze the course performance data in teaching practice, find the correlation between courses, and realize from the actual learning situation of students in our school to find the data reflected in the actual teaching. It can further optimize the curriculum construction and provide reference information for students' course selection, early warning of students' performance, and the formulation of training programs, thereby improving the quality of teaching. However, the use of data mining technology for course correlation analysis needs further research [14, 22]. Generally, researchers use the correlation between the academic performance of various subjects to reflect the correlation between courses, and the application of correlation analysis between courses is mainly reflected in three aspects: curriculum setting, grade warning, and student course selection. Sima Birong obtained the dependence relationship and degree of dependence between each course from the analysis results of students' course grades and could predict students' academic grades in subsequent courses; Ji Shunning used association rules and hierarchical association rules to analyze students' performance in school and the degree of dependence. Graduation data obtained the correlation between courses, core courses, and important skills and then constructed the curriculum system based on the project-based teaching mode of the major; Sun Yuehao used the association rule algorithm to analyze the course performance data of a major and found the curriculum and enterprise needs. Wang Hua et al. used the improved Apriori algorithm to analyze the learning effect of students to find the correlation between courses and used to early warning students' performance; Wu Haifeng et al. mainly focused on using data mining technology to build early warning models, respectively. Data statistics are used for low-level early warning, cluster analysis is used for landslide early warning, the correlation between courses is found through association rule analysis, and the association rule base is used to search to predict potential crises in the next semester's study and achieve the potential effect of early warning.

Therefore, this paper will use the three-dimensional matrix-based Apriori algorithm to mine the test scores of the four majors of painting, art design, photography, and animation in colleges and universities and find the dependencies and connections between the courses. The teaching reform provides scientific and reliable decision-making guidance.

2. Course Relevance Analysis

2.1. Correlation Analysis Overview. In the existing course setting, due to the mutual connection between the contents of each course, the content and arrangement of one course will have an impact on the learning of another course. The effect is called curriculum relevance in this study. Generally speaking, curriculum relevance includes the following two dimensions: one is the content dimension: that is, there are certain associations and connections between different curriculum contents; the other is the time dimension: that is, the temporal relevance of different courses and the different curriculum contents topic relevance when presented.

When there is not only a quantitative relationship between the things under study, but not a definite, stable, and one-to-one corresponding value like a functional relationship, this relationship is called a correlation relationship. Correlation is mainly used to describe the relationship between variables that cannot be represented by a functional relationship, but there is a dependent relationship. It uses appropriate statistical indicators to represent the strength and direction of the correlation between variables. Correlation is mainly used to study the covariant relationship between things and cannot directly reveal the internal causal relationship of things. Therefore, if it is necessary to judge whether the things that are related have a causal relationship at the same time, further analysis should be carried out according to the existing knowledge and experience.

Generally, r is used to represent the correlation coefficient, which reflects the change in direction and closeness of the correlation between things. Its value range is $0 \le |r| \le 1$, where the symbol of r indicates the direction of change between variables, and the "+" sign indicates that the changing trend between variables is consistent, increasing or decreasing, that is, positive correlation, "−" sign indicates that the direction of change is opposite, that is, negative correlation. The absolute value of r indicates the closeness of the connection between things. According to previous studies, several different degrees of correlation can be obtained according to the size of the correlation coefficient: $|r| \ge 0.8$, two variables are highly correlated, $0.5 \le |r| < 0.8$, two variables are significantly correlated, $0.3 \le |r| < 0.5$, the two variables are highly correlated, and $|r| < 0.3$, the two variables are not correlated. In practical problems, in addition to calculating the degree of correlation, a significance test must be completed, thereby reducing the random risk of sample data.

2.2. Quantitative Analysis of Course Relevance. Usually, the relevance of courses can be reflected in the categories, purposes, requirements, content, and types of hours of courses, etc., but the relevance of course purposes, requirements, and content is mostly qualitative analysis, and it is difficult to quantify it. Many researchers have begun to use

quantitative analysis of course performance to explore correlations between courses. For example, Gao Minghai et al. used the method of multiple linear regression to analyze the grade data and obtained the statistical relationship and rules between courses by constructing a data model; Liu Peng et al. used the correlation between a certain course and subsequent courses; Ji Lianen et al. obtained the correlation between courses by calculating the Pearson correlation coefficient of course performance data and combined interactive technology to design a multisubject-oriented student achievement visualization system; Yao Shuangliang used the improved Apriori algorithm after analyzing the students' grades in each course, and the association rules between courses were obtained; Li Ludan also used the simple correlation analysis method to calculate the correlation of the course grade data and then used the results of the course correlation to obtain the course setting optimization strategy.

Combining other researchers' analyses of the relevance of courses, this study also obtained the internal connection between courses by means of quantitative analysis of learning effect data. If the courses are highly relevant, further research on related courses can improve teaching to provide reference for the improvement of teaching quality. This study mainly takes an art major in a university as an example and explores the correlation between courses by mining the scores of each course in the teaching empirical data.

2.3. Curriculum Relevance Analysis Method

2.3.1. Simple Correlation Analysis. Simple correlation analysis is a method of analyzing the correlation between two variables. In course analysis, it is mainly used to analyze the correlation between different courses under the same type of course.

2.3.2. Canonical Correlation Analysis. Canonical correlation analysis is a method of analyzing the correlation between one set of data (X_1, X_2, X_3, . . ., X_m) and another set of data (Y_1, Y_2, Y_3, . . ., Y_n). In the course analysis, it is mainly used to analyze the overall correlation between different types of courses. The essence is to screen out several typical courses to comprehensively describe the relationship between the two types of courses.

2.3.3. Association Rule Analysis. Association rule analysis is used to find valuable associations in a large amount of data and obtain the association rules that describe the relationship between transactions, such as "if the antecedent is what, then what is the consequent" information to infer information about another transaction. In course analysis, it is mainly used to analyze the degree of mutual influence between courses.

3. Data Mining Algorithms

Data mining (DM) technology is an emerging technology that has emerged with the development of artificial intelligence and database technology in recent years. It is to screen out hidden, credible, novel, and effective data from a large amount of data. Association rules, also known as association patterns, were proposed by Agrawal et al. of BIM (Almaden research center) in 1993. Association rules refer to interesting associations or correlations between item sets in a large amount of data. The object discovered by association rules is mainly the transaction database, which is a knowledge model that describes the laws that are between items in a transaction at the same time. At present, there are many algorithms for association rules, and the Apriori algorithm is the most influential algorithm for mining frequent item sets of Boolean association rules. The algorithm uses an iterative method called layer-by-layer search. Its candidate generation-checking method significantly reduces the size of the candidate item set and leads to good performance. However, it has two disadvantages: one is that it may need to generate a large number of candidate item sets; the other is that it needs to scan the database repeatedly and check a large candidate set through pattern matching. Therefore, we use the improved Apriori algorithm based on the three-dimensional matrix to study art teaching in colleges and universities.

3.1. Algorithm Description

3.1.1. Related Definitions. Each transaction t used in mining association rules is stored in the data warehouse D, denoted as

$$D = \{t_1, t_2, \ldots, t_M\}. \tag{1}$$

In formula (1), each transaction t is composed of various attributes i, which can be expressed as

$$i = \{i_1, i_2, \ldots, i_N\}. \tag{2}$$

Define the association rule between attributes X and Y as X=>Y. The support of the association rule support is equal to the ratio of the number of transactions with attributes X and Y at the same time to the total number of transactions, which can be expressed as

$$\text{support}(X => Y) = \frac{\text{count}(X \cup Y)}{M}. \tag{3}$$

In formula (3), M is the total number of transactions and count $(X \cup Y)$ is the number of transactions, where attribute X and attribute Y appear at the same time. Confidence of the association rule is equal to the ratio of the support of the rule to the support of the attribute X itself, which can be expressed as

$$\text{confidence}(X => Y) = \frac{\text{support}(X => Y)}{\text{support}(X)}. \tag{4}$$

In formula (4), support(X) is the number of occurrences of attribute X. Data mining controls the minimum requirements that the resulting association rules need to meet by setting the minimum support and minimum confidence.

3.1.2. Algorithm Process. The traditional Apriori algorithm will generate a large number of candidate item sets when the amount of data is large and the analysis categories are many, especially when generating binomial sets and tri-item sets. And every time a higher level of frequent item sets are generated, the database needs to be rescanned, which will generate a lot of computational redundancy and low efficiency. Based on the Apriori algorithm, improvements are made to address these shortcomings of the traditional algorithm. The improved algorithm idea is as follows:

(1) First scan the database, and abstract the database into a two-dimensional matrix based on the attributes contained in all its transactions, which are used to store all the information in the database.

(2) Traverse each attribute of each transaction in the two-dimensional matrix. By reading two different attributes in the same transaction each time without repeating reading, the three-dimensional upper triangular attribute matrix Matrix (i, j, k) is established, and the coordinates are established according to the corresponding attributes. The coordinate intervals in the three dimensions are all $[1, N]$ (N is the largest attribute type). During the scanning process, each time the coordinates are repeated, the corresponding weight is increased by one, and the matrix can be expressed as

$$\text{Matrix}(i\ ,\ j\ ,\ k) = \text{Matrix}(i\ ,\ j\ ,\ k) + 1. \tag{5}$$

(3) Second, by reading the three-dimensional attribute matrix, we can directly obtain the frequent item set, frequent binomial set, and frequent tri-item set. The space diagonal of the first hexagram limit of the three-dimensional matrix is the support of frequent item sets. The coordinates (i, j, j) on the corresponding plane are the support of frequent binomial sets, and the coordinates (i, j, k) are the support degree of the corresponding three-item set.

(4) Because in transactions where the number of attributes is less than k, there must be no possibility of containing k item sets. Therefore, after getting the frequent three-item set, scan the database and delete the matters that contain no more than four attributes to simplify the database.

(5) Through the frequent three-item sets that have been obtained, the standard Apriori algorithm is used for subsequent calculations. The specific algorithm flow is shown in Figure 1.

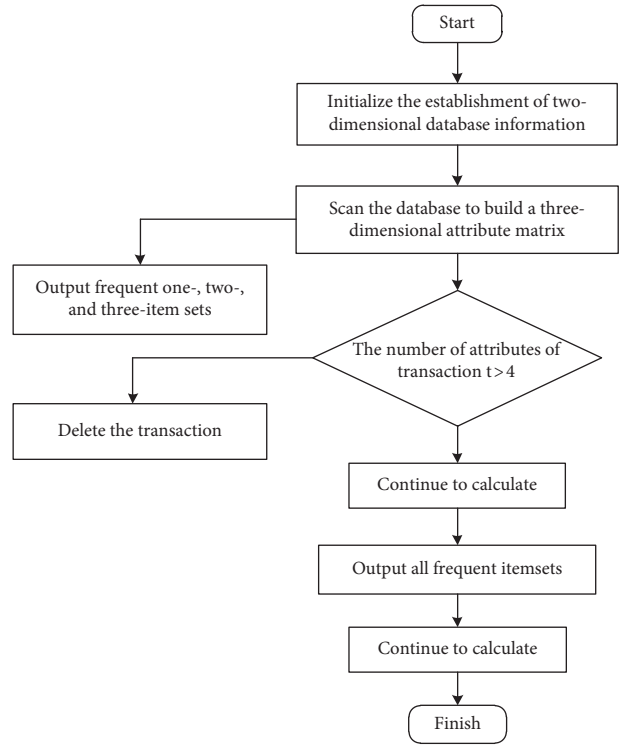

Figure 1: Three-dimensional matrix algorithm flow.

3.2. Algorithm Time Complexity Analysis. Suppose the number of transactions in the database is M, the average number of attributes of transactions is n, and the proportion of transactions with attributes less than 4 is b. The time complexity of the traditional Apriori algorithm is analyzed, and the time complexity of the two algorithms is compared. The time complexity is denoted by O. After the Apriori algorithm forms the frequent item set L_1, the time complexity of obtaining the candidate binomial set through the branch is expressed as

$$O\left[\frac{L_1(L_1-1)}{2}\right]. \tag{6}$$

Then, by scanning the database and calculating the support degree, the time complexity of frequent binomial set L_2 is expressed as

$$O\left[\frac{L_1(L_1-1)}{2}Mn\right]. \tag{7}$$

To obtain the frequent binomial set L_2 in the form of a three-dimensional matrix, it is only necessary to read the support of the corresponding coordinates (i, j, j) in the matrix one by one according to each candidate set (i, j) in the candidate binomial set. Candidate binomial sets are obtained from frequent one-item sets without pruning. The number of candidate binomial sets is $L_1L_1 - 1/2$. The time complexity of this process can be expressed as

$$O\left[\frac{L_1(L_1-1)}{2}\right]. \tag{8}$$

It can be seen that the complexity expressed by equation (8) is the same as that of equation (6), so in the process of calculating the frequent binomial set L_2, the time saved by the data mining algorithm based on the three-dimensional matrix is equation (6) + equation (7) − equation (8) = equation (7). It can be seen that the time saved in the process of calculating frequent binomial sets is related to M, n, and L_1, which can effectively save calculation time in larger data samples.

According to the frequent binomial set L_2, the time complexity of the candidate three-item set is obtained by linking and pruning, which can be expressed as

$$O[L_2(L_2-1)]. \tag{9}$$

Then, by scanning the database, the support degree is calculated to obtain the time complexity of the frequent three-item set C_3, which can be expressed as

$$O(C_3Mn). \tag{10}$$

Using the form of a three-dimensional matrix to obtain frequent trinomials, you only need to read the support of the corresponding coordinates in the matrix one by one according to each candidate set (i, j, k) in the candidate tri-lemma, and you can obtain the frequent tri-lemma. Its time complexity can be expressed as

$$O(C_3). \tag{11}$$

Then, the process of calculating frequent triplets, the data mining algorithm based on the three-dimensional matrix can save time as formula (9) + formula (10) – formula (11), which can be expressed as

$$O[L_2(L_2-1)+C_3(Mn-1)]. \tag{12}$$

Obviously, equation (12) is far greater than 0, and the time saved is related to M, n, L_2, and C_3. It can save a lot of calculation time when mining association rules with larger data sets. Before performing subsequent calculations, transactions with attributes less than 4 will be deleted. Therefore, each time the database is scanned, the maximum time complexity that can be reduced is

$$O(bM3). \tag{13}$$

The minimum time complexity that can be reduced is

$$O(bM). \tag{14}$$

The comparative analysis shows that the improved algorithm reduces the time complexity and improves the calculation efficiency compared with the traditional Apriori algorithm.

4. Relevance Mining of Art Classrooms in Colleges and Universities Based on Apriori Algorithm

4.1. Data Preprocessing. The nature of the four art undergraduate majors of the college is mainly divided into two categories: "compulsory" and "optional." Since the "compulsory" courses cover basic subjects and professional courses, the composition of the courses is relatively stable and the number of students in the required courses. At most, the level of grades can reflect the learning status of students to a greater extent, so choose the grades of "compulsory" courses for mining. The score assessment is mainly divided into usual scores + test scores and usual scores + work design. The usual results are subjective and unstable, so only the test results and work design are used for the results. Art courses have different assessment methods in different periods. Some grades use a 100-point system, and some grades use a grade system (excellent, good, medium, pass, and fail). The following methods are used to discretize the score system: 90 points or more (including 90 points) are rated as "excellent," represented by "A"; between 80 and 89 points are rated as "good," represented by "B"; 60 ~ A score of 79 is rated as "medium," represented by a "C"; a score of 60 is a pass, and a score of 60 or less is a "failed," and it is represented by an "E."

4.2. Transaction Representation. The Apriori algorithm requires the transaction database to adopt a horizontal structure, so it is necessary to convert the vertical structure of Table 1 (course information) to a horizontal structure with each student as a transaction, which includes the student's ID number and the score of each required course. We reorganize the data in Table 1 to obtain a data table structure that can be used for data mining, as shown in Table 2.

Each record in Table 2 represents student affairs. The student ID attribute can be regarded as the transaction identifier TID. The content of the latter attribute can indicate the item set of the transaction, that is, the grade of a certain professional course.

4.3. Mining Results. Table 3 lists some of the strong rules obtained by mining using the Apriori algorithm (only consider the course scores of students whose grades are A after discretization).

From the mining results in Table 3, it can be found that the probability that the color composition and photography exposure scores of the college's photography students are A is 27.5% and the probability that the color composition scores are A is 70.2%. It can be seen that the results of enhancing the color composition can significantly provide the results of photographic exposure. For art majors, the probability that both color and landscape sketching scores are A is 37.2%. It can be seen that the two courses have many similarities in the sense of color, and the students with a color score of A have the scores of landscape sketching. The probability of being A is as high as 78.3%, which further confirms the fact that strengthening the study of color courses can bring significant effects to the improvement of later landscape sketching. Based on the above results, it can be seen that the curriculum of the art major of the college is basically reasonable. Strengthening and consolidating the students' professional basic courses can bring significant teaching effects to the later professional courses. When revising the syllabus, it is necessary to ensure that the professional basic courses are included in the majors studied. The proportion of teachers who strengthen and consolidate students' professional basic courses in teaching can achieve a multiplier effect with half the effort.

Table 1: Course information of longitudinal structure.

Course no.	Course title	Course nature
2379	Art overview	Compulsory
2298	Color D	Compulsory
2247	Structure sketch	Compulsory
2317	Visual identity design	Compulsory
2137	Two-dimensional animation production	Compulsory
2161	Landscape sketch B	Compulsory

Table 2: The horizontal structure of student affairs transcripts.

Student ID	2379 2298 2247...2161
2018003564	A B B A...A
2018003572	A A A B...A
2018003578	B A C A...B
...	...
2018003812	A A B A...C

Table 3: Some strong rules obtained by association mining.

Rule precursor	Rule successor	Support	Confidence
...	...	...	...
Color composition A	Photographic exposure A	27.5	70.2
Plane composition A	Landscape photography A	31.2	66.9
Perspective principle A	Animated perspective A	25.4	71.3
Human anatomy A	Sketch human body A	21.8	69.6
Color A	Landscape sketch A	37.2	78.3
...	...	...	...

5. Conclusion

With the increasing number of students' information, how to use the existing information reasonably to improve the quality of personnel training is a problem that every educator is closely concerned about. Using data mining technology in the education industry, it is possible to find meaningful information from a large amount of data to provide decision support for educators. This paper mainly takes a large number of students' course data as the starting point, and with the help of data mining technology, it proposes a correlation analysis method for college art courses based on data mining technology. The examination results of each course of students majoring in painting, art design, photography, and animation in colleges and universities were quickly mined, and some reasonable and reliable course correlation rules were obtained. Valuable information, so as to rationally optimize the curriculum, provides a decision-making basis for the revision of the art curriculum and syllabus in colleges and universities, to further improve the teaching effect and improve the quality of personnel training. There are still some problems in this research, which is also the direction of future efforts [16]:

(1) Further research on the data mining algorithm, and by improving the algorithm, we can obtain a data score that is more suitable for our school's curriculum.

(2) Collect more extensive course-related data, and conduct further research on the laws to be studied as proposed in this paper.

(3) Introduce more data related to courses and students, and analyze the relevance of courses at a deeper level to more valuable information.

Data Availability

The dataset can be accessed upon request.

Conflicts of Interest

The author declares that there are no conflicts of interest.

References

[1] J. Xin, "Research on the integration of college art teaching and folk art resources," *Advances in Higher Education*, vol. 5, no. 2, 2021.

[2] X. Mo, "A preliminary study on the intervention of western oil painting creation imagery in college art teaching," *Learning &Education*, vol. 9, no. 4, 2020.

[3] L. Yang, "Research on the art classroom teaching with students as the main body," *International Journal of Educational Technology*, vol. 1, no. 3, 2020.

[4] H. Lu, "Application strategy of folk printing and dyeing technology in college art teaching," in *Proceedings of the 20214th International Conference on Arts, Linguistics, Literature and Humanities*, Milan, Italy, May 2021.

[5] X. Zhang, "On the applic ation of inquiry learning in college art teaching," *Curriculum and TeachingMethodology*, vol. 4, no. 5, 2021.

[6] X. Zhang, "Analysis on the cultivation strategy of creativity in college art teaching," *Journal of Sociology and Ethnology*, vol. 3, no. 6, 2021.

[7] T. Murray, "College art teaching tomorrow," *College Art Journal*, vol. 15, no. 3, 2015.

[8] D. Durst, "Artists and college art teaching," *College Art Journal*, vol. 16, no. 3, 2015.

[9] X. Mai, "Multimedia technology aids college art teaching research," *Journal of Physics: Conference Series*, vol. 1213, no. 4, Article ID 042010, 2019.

[10] R. Zhang, "The intervention and influence of contemporary art in college art teaching," *Lifelong Education*, vol. 9, no. 4, p. 271, 2020.

[11] Y. Chen, "Research on the application of art therapy into college art teaching in the context of COVID-19 prevention and control," *Journal of Education and'ulture Studies*, vol. 4, no. 2, 2020.

[12] Y. Zhao, "Innovative research on the teaching mode of art appreciation class based on multimedia technology," *International Journal ofIntelligent Information and Management Science*, vol. 10, no. 1, 2021.

[13] M. Jones and R. Nyland, "A case study in outcomes on open-source textbook adoption in an introduction to art class," *Frontiers in Education*, vol. 5, 2020.

[14] A. D. Singleton, "Data mining course choice sets and behaviours for target marketing of higher education," *Journal of Targeting, Measurement and Analysis for Marketing*, vol. 17, no. 3, pp. 157–170, 2009.

[15] C. Lin and L. Qun, "Discussion on the teaching of piano art appreciation course in colleges and universities," *Frontiers in Educational Research*, vol. 2, no. 4, 2019.

[16] E. Loder and R. Burch, "What can data mining teach us about triptan safety that we don't already know?" *Cephalalgia*, vol. 34, no. 1, pp. 3-4, 2014.

[17] Q. Zeng, L. Yuan, Z. Yi, Q. Du, and M. Cheng, "Research on active project -driven teaching practice and teaching reform of data mining course," *International Journal of Social Science and Education Research*, vol. 3, no. 9, 2020.

[18] T. Wang, W. Tan, and I. Xue, "A sudy on data mining course teaching based on fipped casroroedg of 1st itentional conference on education," *Economics and management research (ICEEMR 2017)*, vol. 95, pp. 23–26, 2017.

[19] S. Manaseer and A. Malibari, "Improve teaching method of data mining course," *International Journal of Modern Education and Computer Science*, vol. 4, no. 2, 2012.

[20] G. Lei and X. Chen, "Exploration and practice of data mining couue teaching oriented big data," in *Proceedings of the 2017 7th International Conference on Manufacturing Science and Engineering (ICMSE 2017)*, Xiamen , China, April 2017.

[21] X. Xing, B. Liu, and N. Hu, "Research and practice on bilingual teaching of data mining course for statistics postgraduates," in *Proceedings of the 7th International Conference on Education, Management, Information and Computer Science (ICEMC 2017)*, Xi'an, China, June 2016.

[22] Y. Chen, Y. Jiang, X. Zhang, L. Dong, D. Zhu, and N. Shu, "Correlation analysis of distribution network equipment decommissioning data based on three-dimensional matrix," in *Proceedings of the 2022 IEEE 6th Information Technology and Mechatronics Engineering Conference (ITOEC)*, pp. 1770–1774, Chongqing, China, March 2022.

Hindawi
Scientific Programming
Volume 2022, Article ID 7576521, 9 pages
https://doi.org/10.1155/2022/7576521

Research Article

Big Data Analysis Model for Vocational Education Employment Rate Prediction

Lili Wang

Yantai Vocational of Culture and Tourism, Yantai, Shandong 264199, China

Correspondence should be addressed to Lili Wang; wanglili@yvcct.edu.cn

Received 16 May 2022; Revised 14 June 2022; Accepted 17 June 2022; Published 7 July 2022

Academic Editor: Lianhui Li

Vocational education is an important means to promote the development of the national manufacturing industry. To correctly grasp the relationship between vocational education and the labor market, we start with the quality of vocational education and employment rate and study the interconnection between them. To this end, we propose a vocational education employment rate prediction method based on a big data model and build a vocational education quality assessment and employment rate prediction system. We draw on the big data cross-learning model to improve the model hyperparameters by using generalized intersection sets on the joint loss function to compensate for the shortcomings of dense vocational education datasets. We use the GSA algorithm to enhance the local features of different vocational education quality assessment index data series. To scientifically assess the recognition of vocational education, we evaluate the vocational education assessment indexes at the student level and the parent level to verify the reliability of the experiment. The experimental results prove that our method performs best in the prediction accuracy of vocational education quality assessment indicators, and the prediction accuracy rate stays above 91%. In the prediction of vocational education employment rate, the difference between the predicted and actual values of our method is the smallest, and the difference stays within 1%. Compared with other big data models, our method has higher prediction accuracy and better robustness.

1. Introduction

Vocational education is a powerful driver of manufacturing and plays an important role in the country's economic development. The integration of vocational education with secondary education can solve the contradiction of a single form of secondary school and provide more options for young people of school age. Diversified vocational education can not only improve the pressure for further education in the general education system but also address the pressure on employment rates in higher education [1, 2]. The more developed a city is, the more importance it places on vocational education, and the spread of vocational education can help rationalize the distribution of urban economies, can reduce youth unemployment, and is a necessary tool to guarantee skill acquisition for school-age youth [3]. For the general education system, vocational education offers multiple options for young students. Students with insufficient academic abilities can make voluntary choices about their future development according to their situation, fully guaranteeing their willingness to learn skills and advance to higher education [4].

Despite the important role of vocational education in socioeconomic mediation, the association between vocational education and employment rates is not supported by data. The feedback period of vocational education is long, and the linear correlation between economic feedback and the cost-effectiveness of vocational education is not strong enough for enterprises. After a large number of vocational education employment rate data analyses in which the employment rate of vocational education does not match the actual employment rate, the vocational education employment rate is in urgent need of a predictive model to enhance the economic benefits of vocational education [5]. The poor feedback on the economic benefits of vocational education has led society as a whole to hold a high and low opinion of vocational education. However, it is worth affirming that vocational education is by no means the only way out for

working-class people. Most studies on vocational education have discussed this issue, and the level of individual ability has a dominant role in the future development of students, followed by the financial background of the family. Statistics show that most students with strong family financial backgrounds do not choose vocational education because it is the immediate choice for students whose families do not have enough financial resources, and they do not represent a continuous low labor output after choosing vocational education. In fact, the vocational education system also provides reasonable promotion channels for students in the vocational job promotion system to prevent the occurrence of class differentiation problems [6, 7].

For capable vocational education students, they can also be promoted to engineering positions through their practical efforts, which is a reflection of the advantages of diversified vocational education [8, 9]. Vocational teaching was created as a powerful measure to balance the large differences in general learning in the financial background of families and to prevent class differentiation. Although the current economic feedback benefits of vocational education are influenced by several complex factors, students trained in vocational education occupy a significant employment advantage in terms of age, given the reduced labor market advantage due to aging [10, 11]. Some developed countries investigating the impact of vocational education have focused on the way the vocational education system is organized, for example, with a clearer division of labor and a specific vocational training model for different types of occupations. Vocational teaching schools will provide basic vocational theoretical and practical training in school and will also provide factory internships for corresponding jobs with one-on-one training and assessment by skilled workers in which those who pass the assessment can choose a variety of jobs [12, 13]. In addition, vocational education is based on the student development model in terms of curriculum, teaching mode, and teacher expertise. Although some studies have shown that there is some variation in the link between vocational education preparation models and the labor market, most studies can use data analysis and computer science methods to compensate for this variation.

Considering the differences between the vocational education system and the labor market, we refer to studies related to vocational education and find a compensatory relationship between selectivity bias, age effectiveness, and vocational education training model. Compared to the employment rate of general education students, the employment rate of vocational education students is oriented to different recruitment demands. However, according to the available data, the demand for vocational education jobs is much greater than the demand for jobs of general college graduates, which is a great advantage of the vocational education system. Depending on the length of the work cycle, vocational education students have a wider range of choices, with short-term company training, medium- and long-term factory practical work, and a long-term promotion system for engineers, giving vocational education students more room for development [14].

The rest of the paper is organized as follows. Section 2 presents the history and research results of vocational education quality research. Section 3 introduces the relevant principles and implementation details of the LSSVR-based vocational education quality and employment rate prediction model. Section 4 shows the experimental datasets and the analysis of the experimental results. Finally, Section 5 summarizes our research and reveals some further research work.

2. Related Work

Vocational education, which directly corresponds to manufacturing production jobs, can facilitate the renewal iteration of manufacturing and also maintain a steady increase in manufacturing output. Despite the poor feedback benefits of vocational education employment, the relationship between vocational education systems and socioeconomics is only a temporary mismatch in terms of macroeconomics [15–17]. The data on employment rates in vocational education are only temporarily inadequate, and with the intervention of scientific management and job planning tools, the vocational education system will become more relevant to students' situations in career training planning, employment rates will be more accurately predicted, and cooperation between companies and vocational education schools will increase substantially. Most economists, when considering the role of vocational education in the socioeconomy, give priority to the ability and substitutability between the vocational teaching system and manufacturing production jobs. The desired outcome of vocational education is the training of a pool of directly applicable skilled people for each skilled workplace, and the quality of vocational education training is indirectly reflected by the assessment of the competencies of skilled people at the firm level [18, 19]. The higher the quality of vocational education, the higher the economic benefits it generates for the company, which will indirectly increase the future employment rate of vocational education. This model of assessment in cooperation with companies tends to bring a more substantial employment rate increase than that of general higher education. In addition, researchers in the literature [20] argue that vocational education is an important measure to increase national manufacturing productivity, reduce youth unemployment, and reduce poverty. The literature [21, 22] in studies on vocational education found that vocational education is an important tool for national transformation and can achieve a smooth transition from developing to developed countries. Developing countries strongly advocate the training of industrialized and skilled personnel in vocational education to improve the vocational education system and promote the transformation of industrialized countries.

In labor market projections, some researchers have compared vocational education with general education in a hierarchical manner, taking into account the ability weights, cognitive weights, the ability to learn new knowledge among students, and other factors. However, in the data comparison of hands-on practical scores and efficiency of enterprise

rotations, vocational education students performed more superiorly. To equalize the differences in learning and cognitive abilities of vocational education students, some scholars have developed vocational education student development systems that aim to balance learning ability differences through skill acquisition for student ability prediction in employment rates [23, 24]. There are also researchers who have developed studies from students' family backgrounds, which provide great value for vocational education development based on students' family social status, family financial resources, family education, and family cohesion [25]. In addition, the development of students from different family backgrounds in the vocational education system strictly limits the development of student's abilities and indirectly predicts their future employment and development potential [26]. Some researchers started with the quality of vocational education, studied the distribution of vocational courses in different vocational schools, the strength of teachers, the arrangement of enterprise practice, and other key factors, and then established a prediction model for vocational education development system, which can effectively predict the development of students in different vocational education systems, providing a solid basis for the prediction of vocational education employment rate and providing detailed vocational training for enterprises that choose to cooperate with rules [27, 28].

Different countries have different planning systems and development orientations for vocational education. Compared to general higher education, the curriculum and delivery methods of the vocational education system are determined by the country's basic industrial model. Most industrially developed countries use a dual vocational education training system. For students who choose vocational education, vocational classroom studies and on-the-job training in companies Dei are alternatives to compulsory education, which is similar to the academic guidance courses offered by an academic education. In this case, researchers, to assess the educational quality and employment rate of vocational education, mostly use deep neural network models to capture the key influences from the multiple vocational education systems. The learning model of neural networks is used to integrate a large amount of vocational education data to effectively predict the trends of quality and employment rates of vocational education. For agricultural developing countries, which advocate vocational education similar to developed countries, but considering the weak industrial base due, the focus of vocational education training is more on theoretical education of vocational courses. In this case, to assess the quality and employment rate of vocational education, researchers mostly use data analysis and machine learning models due to the inability to capture a large amount of information on vocational education and employment rates in real time [29–31]. The data is limited, the trend of employment rate data can only be predicted by data analysis, and then machine learning is used to complete the learning of vocational education quality factors. The vocational education employment rate prediction results obtained in this way are less accurate and less preferable for the overall socioeconomic prediction.

3. Method

3.1. Mainstream Model. The demand for vocational education is closely related to employment rate and economic development, and we innovatively use vocational education employment rate and economic indicators as transition variables. We investigated the literature related to vocational education employment rate prediction research methods, among which the least square support vector regression (LSSVR) model performed the best in the research of employment rate prediction; therefore, we chose this model as our base network. To improve the employment rate prediction accuracy of the vocational education model, we proposed the gravitational search algorithm (GSA) to optimize the LSSVR model. The model contains three parts, as shown in Figure 1; the data preparation part represents the data input from various aspects of vocational education. The GSA part represents the additional part with the model parameters adjustment and the model structure optimization. LSSVR represents the backbone network of the vocational education employment rate prediction model.

3.2. LSSVR Mathematical Principles. In the literature research, it was found that the literature [32] proposed the support vector machine approach, which the authors applied to structural risk optimization with the main principle of statistical planning learning theory. In planning learning of large-scale data samples, the support vector machine causes the model to take a long time to process the data due to its complex structure. To solve the time-consuming problem, we take inspiration from the literature [33], and we use a nonlinear function $\varphi(y_t)$ based on the LSSVR model, assuming that the original data is y_t, and we try to map the original data into the high-level feature map by the nonlinear function. The linear regression is then performed on the mapping results, and the mathematical function relationship is shown as follows:

$$\overline{y_t} = w^T \varphi(y_t) + b, \tag{1}$$

where w represents the vocational education parameter weights and b represents the employment rate forecast bias. The values of these two parameters represent the prediction estimates with the least structural risk. The mathematics is calculated as follows:

$$\begin{aligned} &\text{Min} \frac{\left(w^T w\right)}{2} + \frac{\left(\gamma \sum_{t=1}^{T} e_t^2\right)}{2}, \\ &\text{s.t. } \overline{y_t} = w^T \varphi(y_t) + b + e_t, \ (t = 1, 2, \ldots, T), \end{aligned} \tag{2}$$

where γ represents the weight parameter and e_t represents the estimation error in time t. Based on the above solution equation function, to obtain the optimal solution to the optimization problem, we used the following mathematical equation to obtain the solution:

$$\overline{y} = \sum_{t=1}^{T} \alpha_t K(y, y_t) + b, \tag{3}$$

where $K(y, y_t) = \exp(-\|y - y_t\|^2/\sigma^2)$ is a kernel function with a Gaussian operator.

In the design of the network structure of LSSVR, we tried to set the parameter values of hyperparameters γ and σ^2 in advance by migration learning. After experimental tests, it was found that the parameter settings of migration learning could not reach the optimal values of data simulation, and for this reason, to enhance the similarity of data simulation, we borrowed the heuristic optimization algorithm proposed in the literature [34], and the GSA algorithm can achieve the optimization of large-scale data simulation with the assistance of the heuristic optimization algorithm, which takes the simulation of universal gravity as the main principle. The GSA algorithm is based on the main principle of simulating gravity, treating the search particles as a set of relative numbers in the universal gravity, and learning the gravitational optimal distance under the action of universal gravity by simulating the trajectory of this set of particles in space. The mutual attraction between particles follows the laws of dynamics, and the attraction between the host particles is positively related to their mass.

3.3. Model Optimization Principle. Assuming that there are N_a impact factors in the vocational education system, the data dimension of the i-th impact factor is defined as follows:

$$X_i = \left(x_i^1, \ldots, x_i^d, \ldots, x_i^n\right), \tag{4}$$

where n represents the dimensionality of the i-th vocational education quality factor and x_i^d represents the data mapping performance of the i-th vocational education quality factor in the d-th dimension, $i = 1, 2, \ldots, N_a$. The mathematical definition between the vocational education quality factors i and j in the d-th dimension at time t is as follows:

$$F_{ij}^d(t) = G(t)\frac{M_{pi}(t) \times M_{aj}(t)}{R_{ij}(t) + \varepsilon}\left(x_j^d(t) - x_i^d(t)\right), \tag{5}$$

where, at time t, $G(t)$ denotes the vocational education quality constant, $M_{pi}(t)$ denotes the i-th passive quality factor variable, $M_{aj}(t)$ denotes the j-th active quality factor variable, ε denotes a constant, and $R_{ij}(t)$ denotes the Euclidean distance between two employment rate variable factors i and j. The mathematical expressions are as follows:

$$R_{ij}(t) = \left\|X_i(t), X_j(t)\right\|_2. \tag{6}$$

The i-th employment rate variable factor in dimension d is defined as

$$F_i^d(t) = \sum_{j=1, j\neq i}^{N_a} \text{rand}_j F_{ij}^d(t), \tag{7}$$

where rand_j denotes a random variable whose data series are uniformly distributed within the ideal interval. Then, according to the gravitational acceleration formula of gravity, we migrate its mathematical expression to the vocational education employment rate prediction model. It is shown as follows:

$$a_i^d(t) = \frac{F_i^d(t)}{M_{ii}(t)}, \tag{8}$$

where $M_{ii}(t)$ denotes the i-th employment rate inertia quantity. Suppose $M_{ai}(t) = M_{pi}(t) = M_{ii}(t) = M_i(t)$. The mathematical expression of the i-th employment rate variable for the vocational education curriculum and practice factors at time t is as follows:

$$\begin{aligned} m_i(t) &= \frac{\text{fit}_i(t) - \text{worst}(t)}{\text{best}(t) - \text{worst}(t)}, \\ M_i(t) &= \frac{m_i(t)}{\sum_{j=1}^{N_a} m_j(t)}, \end{aligned} \tag{9}$$

where $\text{fit}_i(t)$ denotes the fitness value of the i-th employment rate variable factor at time t. To optimize the hyperparameters of the LSSVR model, we introduced the GSA algorithm, and to facilitate the experimental validation of hyperparameter ablation, we adopted a cross-validation grid search method for hyperparameter introduction.

3.4. Optimization Model. The GSA algorithm is mainly used to filter the best solution from the mixed trajectory by predefined data mixture search. To be able to get the best learning result, the algorithm is set up to automatically loop iteratively through the vocational education assessment range system, and the best predictor of employment rate is obtained by clustering algorithm during the iteration process. The main steps of GSA are shown in Figure 2.

The LSSVR model is used in the prediction of static samples of large data, the pretraining dataset is mainly used to determine the initial parameters of the predefined model in one stage, and the formal model training is performed after the initial parameters are determined. Finally, a test dataset is used for model evaluation.

To compare the predictive performance of the models, we used three metric items at the performance evaluation level. The root means square error (RMSE) is mainly used to measure the deviation between the predicted and true values and is more sensitive to outliers in the data. Mean absolute percentage error (MAPE) represents the relative error metric, which avoids positive and negative errors from canceling each other by absolute values. The Willmott's Index of Agreement (WIA) rated the accuracy and predictive power of the regression formulas, and the regression formulas for each parameter had good generalizability.

$$\begin{aligned} \text{RMSE} &= \sqrt{\sum_{t=1}^{N} \frac{(y_t - \overline{y}_t)^2}{N}}, \\ \text{MAPE} &= 100 \times \sum_{t=1}^{N} \frac{\left|1 - (\overline{y}_t / y_t)\right|}{N}, \\ \text{WIA} &= 1 - \frac{\sum_{t=1}^{N} (\overline{y}_t - \overline{\overline{y}})^2}{\sum_{t=1}^{N} \left(|\overline{y} - \overline{\overline{y}}| + |y_t - \overline{\overline{y}}|\right)^2}, \end{aligned} \tag{10}$$

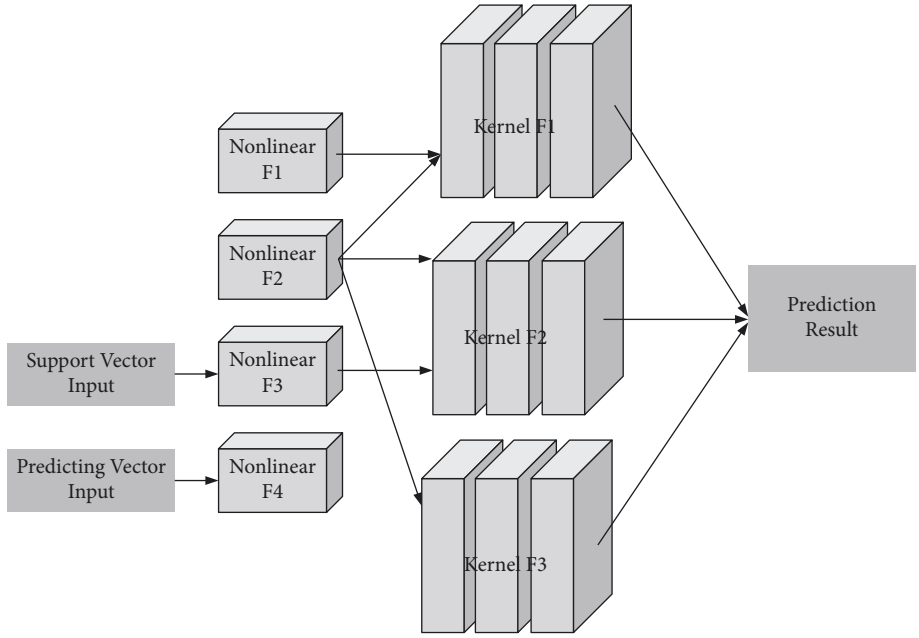

Figure 1: LSSVR model structural.

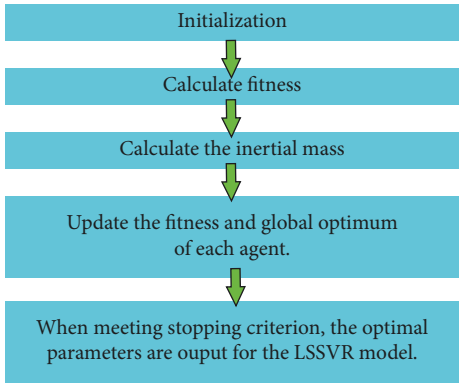

Figure 2: The main steps of GSA.

where N denotes the employment rate detection factor in the test set. In the assessment of vocational education employment rate prediction performance, RMSE and MAPE are used to predict the test accuracy. WIA is used to measure the peripheral prediction ability of the vocational education employment rate prediction model, so WIA is used to assess the generalization ability of the model. The Improved LSSVR for vocational education quality assessment and prediction system is shown in Figure 3.

4. Experiment

4.1. Data Preparation. Vocational education data collection was carried out with the support of professional data analysts. In the work of vocational education data collection, we referred to the data keyword collection methods mentioned in the literature [35–37]. We obtained data on vocational education in terms of curriculum data, faculty strength, training mode, and enterprise cooperation methods through keyword search on educational websites. For all the acquired data, we performed uniform preprocessing operations to integrate the data differences between mobile and PC to prevent the problem of training inapplicability due to data format mismatch during the model training. The data preprocessing process is shown in Figure 4.

To unify the orders of different types of vocational education data, we use the keyword of lag order $l\,(l = 0, 1, \ldots, L)$ to encode x, where the number of interrelationships between the vocational education quality series and the employment rate series y is calculated as follows:

$$r_l = \frac{\sum_{t=1}^{T-l}(x_t - \overline{x})(y_{t+l} - \overline{y})}{\sqrt{\sum_{t=1}^{T-l}(x_t - \overline{x})^2 \sum_{t=1}^{T-l}(y_{t+l} - \overline{y})^2}},$$
$$\overline{x} = \sum_{t=1}^{T-l} \frac{x_t}{(T-l)}, \overline{y} = \sum_{t=1}^{T-l} \frac{x_{t+l}}{(T-l)}, \tag{11}$$

where $l < T$. We set the number of interrelationships in the keyword search process to prevent the search from exceeding the bounded range and causing the problem of data inflation. After data collection, we added data cleaning and transformation work to match keywords as word labels relative to economic indicators and to build a vocational education database. The data details are shown in Table 1.

4.2. Preexperimental Evaluation. With the Ministry of Education's strong support for vocational education, the number of vocational teaching schools is increasing year by year, as shown in Figure 5. According to a large number of vocational education needs, the Ministry of Education sets up assessment norms for other types of vocational education by assessing successful vocational education models.

In the process of developing student training programs, vocational education usually refines the assessment

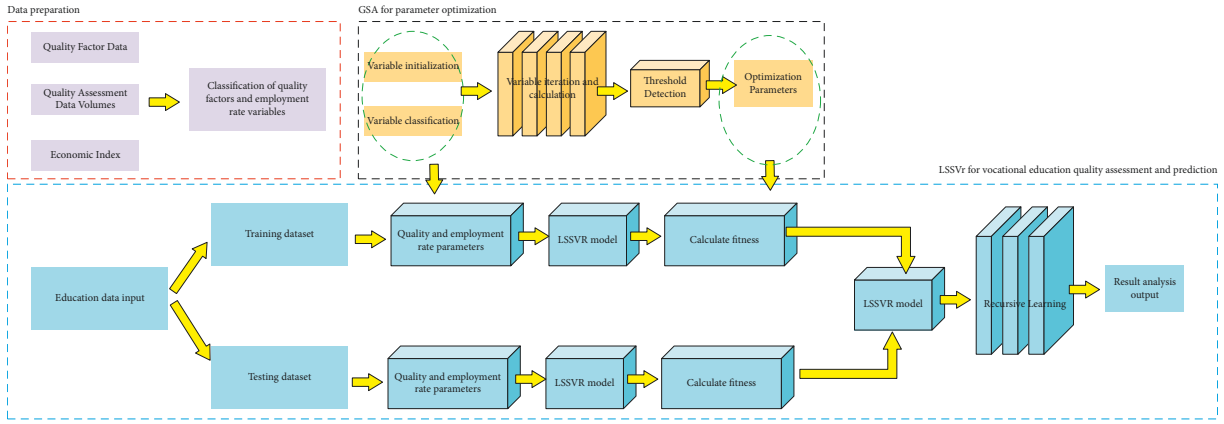

Figure 3: Improved LSSVR for vocational education quality assessment and prediction.

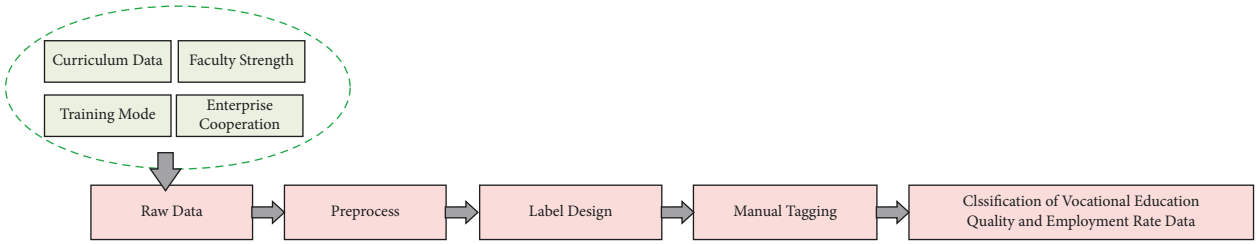

Figure 4: Data preprocessing process.

Table 1: Vocational education dataset classification and quantity.

	Train	Test	Total
Curriculum data	2981	1363	4344
Faculty strength	3635	2653	6288
Training mode	3453	1941	5394
Enterprise cooperation	3530	1696	5226

indicators to the purpose of vocational education (PVE), school enrollment (SE), professional settings (PS), education costs (EC), and employment rates (ER). To investigate the views of students and parents on the assessment indicators, we randomly interviewed 4 parents and 4 students, and each assessment indicator was evaluated with a score out of 100. The results of the survey are shown in Table 2. The quality construction of each assessment index helps to improve the employment rate of vocational education, which is a key aspect of vocational school construction.

From the above table, it can be seen that students and parents are more concerned about the details of the cost of vocational education among the assessment indicators stipulated by the Ministry of Education for vocational education. In the preliminary research, it was found that most of the students who choose vocational education have insufficient family financial resources; therefore, parents and students always rank first in terms of cost consideration for vocational education, and the cost-performance comparison between vocational education and general higher education is the key point to determine the enrollment volume. Besides, students and parents are most concerned about the employment rate of vocational education. The employment rate determines the stability of students' jobs after graduation, and for most students, the ultimate goal of choosing vocational education is to find a stable job. Employment rate data can directly reflect the economic benefits of vocational education in social development, and the higher the employment rate, the better the enrollment situation. The professional setting of vocational education is also the assessment index that students are more concerned about. The professional setting of vocational schools directly connects with social production, and different professional choices determine different employment positions. Therefore, for vocational schools, the broader the specialties set, the more choices students have, and the better their employment quality is.

4.3. Experimental Results. To verify the effectiveness of our vocational education employment rate forecasting system, we compared three different big data forecasting models. The autoregressive integrated moving average model (ARIMA) [38] is a well-known time series forecasting method, the main principle of which is to obtain a random series through time-lapse and then use a mathematical model to achieve an approximate description of this data series. The method is more widely used in a variety of economic segments and has a better effect on the prediction of economic trends. Backpropagation neural network (BPNN) [39] is based on a neural network and uses the principle of error backpropagation to apply supervised learning to batch data and finally generates a prediction model for trend prediction of characteristics among data. The BPNN model performs better in the prediction of economic risk control. The radial basis function (RBF) [40]

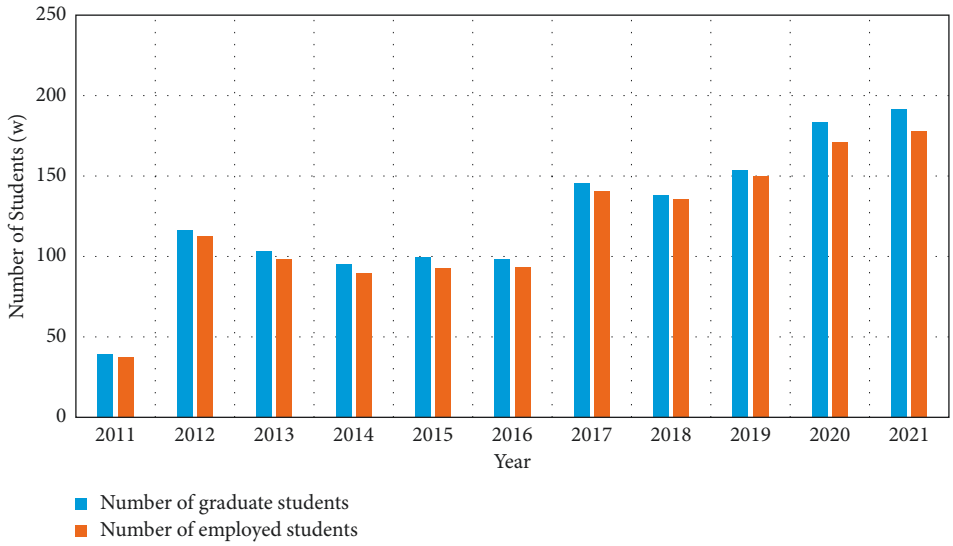

Figure 5: Number of graduates and employment over the years.

Table 2: Students and parents' evaluation of vocational education assessment indicators.

		PVE	SE	PS	EC	ER
Students	1	72	70	86	96	99
	2	76	74	85	94	98
	3	77	73	88	96	99
	4	71	71	89	93	99
Parents	1	78	72	85	98	96
	2	79	73	89	97	97
	3	75	72	90	92	96
	4	76	71	91	95	99

Table 3: Comparison of vocational education quality assessment of different methods.

Indicators	ARIMA (%)	BPNN (%)	RBF (%)	Ours (%)
Curriculum data	75	81	86	91
Faculty strength	73	83	85	92
Training mode	69	85	87	95
Enterprise cooperation	78	86	82	94

model works on the principle of mapping interoperability between low-dimensional data features in the hidden space and high-dimensional data features. The model is more commonly used in studies of predicting serial trajectories and data trends. To ensure independent validation relationships between the methods, five sets of experiments were conducted during the training process, and each set of methods was independently validated for different vocational education assessment indicators. The test results of each method were directly input to the statistical calculation part of the dataset, and the final evaluation results were obtained by balancing the total number and quality factors of the dataset. In the first stage of the experiment, we validated all vocational education quality feedback datasets and compared the efficiency of our methods with those of other methods. The experimental results are shown in Table 3.

From the experimental results in the above table, it can be seen that the ARIMA model does not perform well in the vocational education quality assessment index. Since the model is more suitable for predicting the trend direction of data in data prediction by hyperparameter addition, it is slightly insufficient in the accurate prediction of vocational education quality assessment indexes. The performance of BPNN and RBF models in the prediction accuracy of vocational education quality assessment indexes is not very different, maintaining around 85%. The overall prediction accuracy of our method stays above 90%, which is significantly better than other methods and proves the effectiveness of our method.

In the employment rate prediction experiment, we verified the proportion of different vocational education quality assessment indicators in the employment rate separately and subdivided the association between each vocational education quality assessment indicator and the employment rate. Before the start of the experiment, we performed preprocessing operations on vocational education feedback data to standardize the input format and sampling frequency of assessment index data to prevent the influence of data discrepancies on the experimental results. The results of the second phase of the experiment are shown in Table 4.

From the table above, we predict the employment rate of vocational education in the past five years and compare it with the actual employment rate. The experimental results found that the ARIMA model has a larger gap between the employment rate prediction and the actual employment rate. The BPNN model employment rate prediction is lower than the actual employment rate, but the difference between the predicted and actual values stays within 5%. The RBF model employment rate prediction is higher than the actual value because the mapping relationship between its implicit

Table 4: Comparison of predicted results of vocational education employment rates.

Years	Actual rate (%)	ARIMA (%)	BPNN (%)	RBF (%)	Ours (%)
2017	75	65	70	80	74
2018	86	78	80	88	85
2019	85	79	79	88	85
2020	70	63	66	75	71
2021	73	66	79	78	74

functions leads to a better match between the assessment indicators, so the predicted value is higher than the actual value, but the difference between both of them stays within 5%. The predicted employment rate of our model is closer to the actual value, and the difference between the predicted and actual values remains within 1%. This shows that our method is superior in vocational education employment rate prediction compared with other methods, which proves the effectiveness of our method.

5. Conclusion

In this paper, we propose a vocational education employment rate prediction method based on a big data model and build a vocational education quality assessment and employment rate prediction system. We draw on the big data cross-learning model to improve the model hyperparameters by using generalized intersection sets on the joint loss function to compensate for the shortcomings of dense vocational education datasets. We use the GSA algorithm to enhance the local features of different vocational education quality assessment index data series. In addition, we use the minimum outer matrix algorithm to extract the features of assessment index sequences of different dimensions to improve the accuracy of the model for vocational education quality index assessment. To scientifically assess the recognition of vocational education, we evaluate the vocational education assessment indexes at the student level and the parent level to verify the reliability of the experiment. The experimental results prove that our method performs best in the prediction accuracy of vocational education quality assessment indicators, and the prediction accuracy rate stays above 91%. In the prediction of vocational education employment rate, the difference between the predicted and actual values of our method is the smallest, and the difference stays within 1%. It proves that our method performs well in both vocational education quality assessment and employment rate prediction. Compared with other big data models, our method has higher prediction accuracy and better stability.

Although our method performs well in vocational education quality assessment and employment rate prediction, the number of assessment indicators of vocational education quality is huge, and only five assessment indicators are covered in our study. In our future research, we will try to add generative adversarial neural networks to the adversarial network as an auxiliary classification, optimize the reasonable segmentation of data sequences of different dimensions, and improve the model's inclusiveness of more vocational education quality assessment indexes.

Data Availability

The dataset can be accessed upon request.

Conflicts of Interest

The author declares that there are no conflicts of interest.

References

[1] G. Brunello, "On the Complementarity between Education and Training in Europe," *SSRN Electronic Journal*, vol. 11, p. 309, 2007.

[2] K. King and R. Palmer, *Technical and Vocational Skills Development: A DfID Briefing paper*, DFID, London, 2007.

[3] E. A. Hanushek, G. Schwerdt, L. Woessmann, and L. Zhang, "General education, vocational education, and labor-market outcomes over the lifecycle," *Journal of Human Resources*, vol. 52, no. 1, pp. 48–87, 2017.

[4] B. H. H. Golsteyn and A. Stenberg, "Earnings over the life course: general versus vocational education," *Journal of Human Capital*, vol. 11, no. 2, pp. 167–212, 2017.

[5] P. Ryan, "Is apprenticeship better? A review of the economic evidence," *Journal of Vocational Education and Training*, vol. 50, no. 2, pp. 289–325, 1998.

[6] S. Muryanto, "Evaluation on the automotive skill competency test through "discontinuity" model and the competency test management of vocational education school in Central Java, Indonesia[J]," *Heliyon*, vol. 8, no. 2, Article ID e08872, 2022.

[7] A. A. P. Cattaneo, C. Antonietti, and M. Rauseo, "How digitalised are vocational teachers? Assessing digital competence in vocational education and looking at its underlying factors," *Computers & Education*, vol. 176, Article ID 104358, 2022.

[8] J. Schueler, *Evaluation Framework Measuring Return on Investment (ROI) in TVET*, NCVER, Adelaide, 2016.

[9] S. Choi, "The impact of education levels and paths on labor market outcomes in South Korea: f," *Social Sciences & Humanities Open*, vol. 4, no. 1, Article ID 100152, 2021.

[10] D. van Dijk, J. ten Have, and M. Kotiso, "Opening the door of opportunities: h," *International Journal of Educational Research Open*, vol. 3, Article ID 100130, 2022.

[11] G. Brunello and L. Rocco, *The Effects of Vocational Education on Adult Skills and Wages: What Can We Learn from PIAAC?* French, 2015.

[12] W. Eichhorst, N. Rodríguez-Planas, R. Schmidl, and F. Zimmermann, "A roadmap to vocational education and training systems around the world," *Industrial and Labor Relations Review*, vol. 68, no. 2, pp. 314–337, 2013.

[13] E. Wildeman, M. Koopman, and D. Beijaard, "Fostering subject teachers' integrated language teaching in technical vocational education: results of a professional development program," *Teaching and Teacher Education*, vol. 112, Article ID 103626, 2022.

[14] M. E. Oswald-Egg and U. Renold, "No experience, no employment: the effect of vocational education and training work experience on labour market outcomes after higher education," *Economics of Education Review*, vol. 80, Article ID 102065, 2021.

[15] C. L. Baum, "The efffect of work interruptions on women's wages," *Labour*, vol. 16, no. 1, pp. 1–37, 2002.

[16] Y. Yu, X. Han, and L. Du, "Target part detection based on improved SSD algorithm," *Journal of Physics: Conference Series*, vol. 1486, no. 3, p. 5, Article ID 032024, 2020.
[17] T. Spielhofer and D. Sims, "Modern apprenticeships: hitting the target?" *Education + Training*, vol. 46, no. 3, pp. 112–118, 2004.
[18] C. Mupimpila and N. Narayana, "The role of vocational education and technical training in economic growth: a case of Botswana," *International Journal of Education Economics and Development*, vol. 1, no. 1, pp. 3–13, 2009.
[19] D. Guo and A. Wang, "Is vocational education a good alternative to low-performing students in China," *International Journal of Educational Development*, vol. 75, Article ID 102187, 2020.
[20] A. Nilsson, "Vocational education and training - an engine for economic growth and a vehicle for social inclusion?" *International Journal of Training and Development*, vol. 14, no. 4, pp. 251–272, 2010.
[21] Y. B. Park, M. H. Jang, H. J. Yoon, and D. S. Choi, "Historical overview and recent trends in secondary vocational education," in *The Present and Future of Secondary Vocational Education in Korea*, pp. 21–34, KRIVET, Seoul, 2014.
[22] K. W. Lee, D. H. Kim, and H. K. Lee, "Is the meister vocational high school more cost-effective?" *International Journal of Educational Development*, vol. 51, pp. 84–95, 2016.
[23] S. J. Choi, J. C. Jeong, and S. N. Kim, "Impact of vocational education and training on adult skills and employment: an applied multilevel analysis," *International Journal of Educational Development*, vol. 66, pp. 129–138, 2019.
[24] S. O. Chukwuedo, F. O. Mbagwu, and T. C. Ogbuanya, "Motivating academic engagement and lifelong learning among vocational and adult education students via self-direction in learning," *Learning and Motivation*, vol. 74, Article ID 101729, 2021.
[25] M. Koskenranta, H. Kuivila, M. Männistö, M. Kääriäinen, and K. Mikkonena, "Collegiality among social-and health care educators in higher education or vocational institutions: a mixed-method systematic," *Nurse Education Today*, Article ID 105389, 2022.
[26] L. M. Boonk, H. Ritzen, and H. Gijselaers, "Stimulating parental involvement in vocational education and training (VET): a case study based on learning histories of teachers, principals, students, and their parents," *Teaching and Teacher Education*, vol. 100, Article ID 103279, 2021.
[27] L. F. Ariyani, S. Widjaja, and H. Wahyono, "Vocational education phenomena research method," *MethodsX*, vol. 8, Article ID 101537, 2021.
[28] N. A. Pambudi and B. Harjanto, "Vocational education in Indonesia: history, development, opportunities, and challenges[J]," *Children and Youth Services Review*, vol. 115, Article ID 105092, 2020.
[29] K. Lindvig and H. Mathiasen, "Translating the learning factory model to a Danish vocational education setting," *Procedia Manufacturing*, vol. 45, pp. 90–95, 2020.
[30] M. Korber and D. Oesch, "Vocational versus general education: employment and earnings over the life course in Switzerland," *Advances in Life Course Research*, vol. 40, pp. 1–13, 2019.
[31] Q. Li, "Analysis and practice on the training of key ability of students majoring in electronic information in higher vocational education," *Procedia Computer Science*, vol. 183, pp. 791–793, 2021.
[32] V. Vapnik, *The Nature of Statistical Learning theory*, Springer science & business media, US, 1999.
[33] J. A. Suykens and J. Vandewalle, "Least squares support vector machine classifiers," *Neural Processing Letters*, vol. 9, no. 3, pp. 293–300, 1999.
[34] E. Rashedi, H. Nezamabadi-pour, and S. Saryazdi, "Gsa: a gravitational search algorithm," *Information Sciences*, vol. 179, no. 13, pp. 2232–2248, 2009.
[35] S. Park, J. Lee, and W. Song, "Short-term forecasting of Japanese tourist inflow to South Korea using Google trends data," *Journal of Travel & Tourism Marketing*, vol. 34, no. 3, pp. 357–368, 2017.
[36] X. Yang, B. Pan, J. A. Evans, and B. Lv, "Forecasting Chinese tourist volume with search engine data," *Tourism Management*, vol. 46, pp. 386–397, 2015.
[37] X. Li, B. Pan, R. Law, and X. Huang, "Forecasting tourism demand with composite search index," *Tourism Management*, vol. 59, pp. 57–66, 2017.
[38] G. E. P. Box and D. A. Pierce, "Distribution of residual autocorrelations in autoregressive-integrated moving average time series models," *Journal of the American Statistical Association*, vol. 65, no. 332, pp. 1509–1526, 1970.
[39] R. Hecht-nielsen, "Theory of the backpropagation neural Network Based on "nonindent" by robert hecht-nielsen, which appeared in proceedings of the international joint conference on neural networks 1, 593-611, june 1989. 1989 IEEE," *Neural Networks for Perception*, vol. 8, pp. 65–93, 1992.
[40] J. Park and I. W. Sandberg, "Approximation and radial-basis-function networks," *Neural Computation*, vol. 5, no. 2, pp. 305–316, 1993.

Hindawi
Scientific Programming
Volume 2022, Article ID 6554084, 8 pages
https://doi.org/10.1155/2022/6554084

Research Article

Evaluation Method of Ideological and Political Classroom Teaching Quality Based on Analytic Hierarchy Process

Peng Cheng

College of Art, Hubei Polytechnic University, Huangshi, Hubei 435000, China

Correspondence should be addressed to Peng Cheng; 205142@hbpu.edu.cn

Received 18 May 2022; Revised 14 June 2022; Accepted 21 June 2022; Published 6 July 2022

Academic Editor: Lianhui Li

Constructing a scientific evaluation system of curriculum education quality is an important content to improve the effectiveness of curriculum ideological and political education. Starting from the practical significance of exploring the effectiveness evaluation system of curriculum ideological and political education, supported by analytic hierarchy process, this paper constructs the evaluation model of curriculum educational quality through the five dimensions of curriculum design, teaching staff, student cognition, development evaluation, and system design, clarifies the hierarchical relationship between the implementation elements of curriculum ideological and political education from the micro level, and defines the basic responsibilities, in order to provide reference for curriculum teaching reform and educational quality evaluation.

1. Introduction

For a long time, there has been a phenomenon of "two skins" between ideological and political education and professional teaching in colleges and universities. Professional teachers "only teach but not educate people," and ideological and political education teachers (counselors) still fight alone. At the same time, according to the spirit of the National Conference on Ideological and Political Work in Colleges and Universities, classroom teaching, as the main channel and position for colleges and universities to carry out education, is the basic element and important carrier to implement the fundamental mission of "building morality and cultivating people." Therefore, in the curriculum reform, we should not only pay attention to the cultivation of students' professional knowledge and ability but also do a good job in shaping students' ideological guidance and values, so as to enhance knowledge in value guidance and strengthen value guidance in knowledge teaching.

At the National Conference on Ideological and Political Work in Colleges and universities, General Secretary Xi stressed that we should adhere to building morality and cultivating people as the central link, run the ideological and political work through the whole process of education and teaching, and realize the whole process and all-round education. However, for a long time, in terms of educational concept, we cannot correctly understand the relationship between knowledge transfer and value guidance, and the "whole curriculum education concept" has not been fully established. In terms of curriculum, we cannot correctly deal with the relationship between explicit curriculum and implicit curriculum. In terms of team building, the relationship between talent cultivation ability and moral cultivation ability cannot be handled as a whole. The reason is that, on the one hand, the evaluation system standard still stays in the traditional evaluation with knowledge, skills, and literacy as the core in the early years, and there is no reasonable design evaluation standard in the process of promoting the transformation of ideological and political curriculum to the three-dimensional education of curriculum ideological and political education [1]. On the other hand, in the current education and teaching reform of higher vocational colleges, it is rarely considered from the micro level such as classroom teaching. In the process of promoting the three-dimensional education of "curriculum thinking and politics," classroom teaching is a necessary place. How do teachers organize the curriculum teaching of "classroom thinking and politics" [2–5] and how to arouse and stimulate students' interest in

learning and how to improve the quality and efficiency of curriculum teaching are the key issues. Therefore, it is very necessary to carry out the monitoring, evaluation, and optimization of higher vocational classroom teaching quality under the background of "curriculum ideological and political" reform, optimize the methods of improvement, integrate the concept of "whole process and all-round education" into teaching evaluation and supervision, improve the evaluation criteria, and establish a richer teaching supervision team to diversify the evaluation personnel. It is timely to carry out the research on the quantitative evaluation of classroom teaching quality under the background of "curriculum ideological and political reform." The significance of the research lies in the following: First, it is conducive to the implementation of national education policies, the implementation of education and teaching laws and regulations, and the implementation of semester teaching plans. Ideological and political work is run through the whole process of education and teaching. Second, it is conducive to timely discover and summarize the deficiencies and advanced experience of classroom teaching under the background of "classroom ideological and political" reform and the quality of classroom teaching can be timely improved. Third, it is conducive to improve the scientificity, comprehensiveness, and timeliness of classroom teaching quality evaluation, increase the objectivity and fairness of evaluation effect, and stimulate teachers' enthusiasm to continuously improve classroom teaching quality.

2. Practical Significance of Curriculum Ideological and Political Evaluation

The effectiveness of curriculum refers to the degree to which educational activities achieve their preset goals. To evaluate the effectiveness of curriculum ideological and political education is to judge the actual or potential value of the implementation process and results of curriculum teaching as shown in Figure 1.

2.1. The Need of Innovation Theory Research Perspective. In recent years, many colleges and universities have made some positive explorations in the reform of curriculum ideological and political education and formed representative courses. In particular, the "Shanghai experience" first implemented and summarized by colleges and universities in Shanghai has become the standard bearer leading the teaching reform of ideological and political education in domestic higher education courses. Some scholars discussed the basic idea, connotation and composition of curriculum ideological politics, and curriculum ideological politics from different levels and summarized and analyzed the implementation path and logical relationship. Some scholars put forward good suggestions on the construction of evaluation indicators for the effectiveness of curriculum ideological and political education from the macro level [6–8]. It can be seen that scholars have made some achievements in the research of curriculum ideological and political effectiveness, but there is still a lack of technical research on the effectiveness

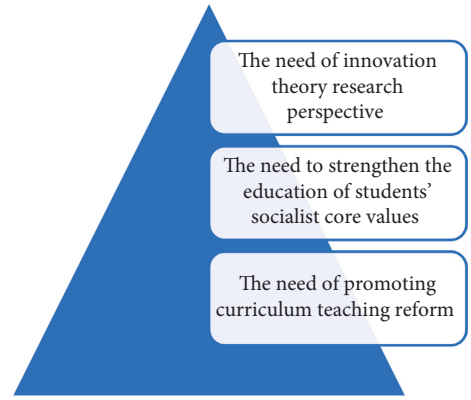

Figure 1: Practical significance of curriculum ideological and political evaluation.

evaluation system of curriculum ideological and political effectiveness, and there is also a lack of qualitative evaluation models and methods. Therefore, through qualitative analysis, this paper attempts to apply the analytic hierarchy process to the research on the quality evaluation of curriculum ideological and political education, build a multilevel and multifactor analysis model, and put forward the observation points of multidimensional evaluation from the micro level, so as to provide a theoretical basis for the research on educational evaluation of specific courses in the future.

2.2. The Need to Strengthen the Education of Students' Socialist Core Values. In the open information age, under the complex background of multiple social values and the interweaving and infiltration of a variety of social thoughts, the limitations of relying solely or excessively on ideological and political theory courses to guide the value of college students have become increasingly prominent. At the same time, with the promotion and implementation of the teaching reform of the credit system in domestic colleges and universities, in order to meet the personalized development needs of students, the school advocates more respect for the subject status of students, pays attention to the hierarchical and classified training of students, emphasizes the credit acquisition of students, and weakens the education follow-up and constraints on students in ethics, physical and mental health, professional quality, and so on. Students will also pay more attention to the pursuit of credits to meet the graduation requirements, pay attention to the improvement of their own knowledge and skills and the design of career development path, and despise the important value of Marxist basic principles and methodology and despise the study of socialist core values and the cultivation of ideological and moral character, which is easy to lead to weak personal ideals and beliefs and low political literacy. Therefore, by establishing the evaluation system of the effectiveness of curriculum ideological and political education, it is very necessary to urge all departments of the school to perform their basic responsibilities in promoting curriculum education from a multidimensional perspective.

2.3. The Need of Promoting Curriculum Teaching Reform. University courses are arranged based on the training objectives of various majors to a certain extent. The purposes of imparting curriculum knowledge are to promote students to better understand and love relevant majors (industries) or culture, constantly innovate knowledge through learning, promote the inheritance and promotion of industries or culture with practical actions, actively serve social development, and promote social progress and harmony. Promoting curriculum reform, starting the ideological and political mode of curriculum education, giving full play to the role of classroom teaching as the main channel and position of educating people, and realizing the collaborative education of various courses are the specific practice of implementing ideological and political education into the whole process of education and teaching. Scientifically construct the evaluation index system of curriculum education quality, clarify the evaluation dimensions and elements, guide the direction of curriculum ideological and political reform from the aspects of theory, action, and serving students' development, fully tap the ideological and political factors contained in relevant knowledge in the design of curriculum content, scientifically apply moral education means in the teaching process, and track and supervise the fixed-point and qualitative teaching process and make the teaching of ideological and political education theories and methods consistent with students' physical and mental health and personality development, in line with the national education policy and the development needs of the times.

3. Literature Review

In western countries, mainly represented by the United States and Britain, the evaluation of teaching quality of higher education has been very mature. The typical feature is the comprehensive evaluation of students' learning process and learning results. Different countries have different national conditions, and the evaluation methods cannot be completely copied. The early evaluation of higher education quality in China, which began in the 1980s, is essentially equivalent to the evaluation of classroom teachers' teaching quality. Teachers, as the object of evaluation, are generally students, experts, or peers and teaching supervisors. The common practice is to design indicators including "teaching attitude," "teaching method," and "teaching content" to quantitatively evaluate teaching attitude and the role of teaching contents and methods in improving teaching quality [9–11].

With the deepening of the research on the evaluation of teaching quality in colleges and universities, more and more scholars believe that the traditional evaluation of teaching quality (effect) is simplified to evaluate teachers' teaching activities. The main problems are as follows: paying attention to students' evaluation of teachers and neglecting teachers' self-evaluation, paying attention to summative evaluation and despising process evaluation, and attaching importance to the evaluation of teachers' teaching and despising the evaluation of students' learning. In recent years, the evaluation methods of some colleges and universities have been quietly changing from teachers to students. The research confirms that learning input has a significant positive correlation with learning harvest. It is suggested to promote the emotional connection between teachers and students through method guidance and value guidance, stimulate the internal driving force of students' learning, and comprehensively improve the learning quality [12–14]. In addition, researchers believe that students' autonomous learning is the main motivation to improve teaching quality and emphasize the stimulating effect of learning motivation and learning behavior on students' autonomous learning [15–17].

In addition to the "teaching" of teachers and the "learning" of students, such as the construction of school study style and examination style, school management and teaching guarantee play a vital role in mobilizing students' learning enthusiasm. The research shows that students' learning input is significantly positively correlated with curriculum requirements, college requirements, and support [18–20]. Some studies emphasize the influence of teaching media (such as teaching facilities) on improving classroom teaching effect. In addition to focusing on teachers and students, the improvement of teaching quality in colleges and universities is a comprehensive system, which needs the joint efforts of teachers, students, school leaders, families, society, alumni, and employers.

Indeed, the key place to improve the teaching quality of colleges and universities is in the classroom, and the key subject to improve the effect of classroom teaching is students. In the teaching process of teachers, this study mainly draws lessons from the indicators commonly used in the academic circles to reflect the teaching attitude, teaching content, and teaching methods. Different from previous studies, under the teaching requirements of "curriculum thinking and politics," the author believes the following: First, classroom teaching activities are a two-way interactive activity between teachers and students. The characteristics of teachers' appearance, personality, morality, professional quality, and behavior play a direct or indirect guiding role in students' values, outlook on life, and world outlook and ultimately affect the teaching effect. Second, the school's serious study style and examination style, strict teaching management and orderly teaching guarantee, and other logistics services also play a very important role in mobilizing students' learning enthusiasm. Third, the quality of classroom teaching includes not only the acquisition of theoretical knowledge but also the improvement of practical ability. With high-quality classroom teaching, students can not only thoroughly master theoretical knowledge and practical ability but also stimulate their interest in continuous learning and get happiness from autonomous learning. Such students can generally make career planning in advance and develop rapidly after graduation.

4. Construction of Analytic Hierarchy Process Model for Evaluation of Ideological and Political Effectiveness of Curriculum

4.1. Analytic Hierarchy Process. In recent years, with the development of data mining and deep learning, data analysis

technology has been developing in many fields [21–26]. Analytic hierarchy process (AHP), as a typical method of data analysis [27], was formally proposed in the mid-1970s. Analytic hierarchy process is a decision-making method that decomposes the elements always related to decision-making into objectives, criteria, schemes, and other levels and carries out qualitative and quantitative analysis on this basis. It is a comprehensive evaluation method of multiple attributes and multiple indexes. It is widely used in various fields related to decision-making. It is suitable for the target system with hierarchical and staggered evaluation indexes, and the target value is difficult to describe quantitatively. It is also one of the mainstream research directions of evaluation methods.

Curriculum education is a systematic activity. At the same time, it is affected by many factors, such as educational policy, professional environment, curriculum content, and teaching staff, which leads to many eigenvalues and complex levels of the effectiveness evaluation of curriculum ideological and political implementation. The analytic hierarchy process can provide a combination of qualitative and quantitative decision-making analysis methods to solve this problem by constructing the judgment matrix between factors. On the research path, we can form a scientific evaluation system by layering the educational factors involved in the process of curriculum education and teaching. For a specific course (major), the weight value of the evaluation index can be calculated and sorted in combination with the survey data. Finally, the fuzzy comprehensive evaluation method is used to obtain the comprehensive analysis data to complete the effectiveness evaluation of curriculum education.

4.2. Analytic Hierarchy Process Model. The quality evaluation model of effective ideological and political education in curriculum consists of three levels. According to the hierarchical construction method proposed by Professor Thomas SETI, since this stage considers the construction of evaluation system and does not involve decision-making, the scheme level is not described here. However, due to many index factors and complex relationships in the criterion layer, the criterion layer is further subdivided into subcriterion layers. First is the target level, that is, the evaluation results of scientific and effective curriculum education. Second is the criterion layer. Combined with the teaching characteristics and practical laws of ideological and political education, the criterion level is set as five dimensions: curriculum design, teaching staff, students' cognition, development evaluation, and system design.

4.3. Construction of Judgment Matrix. The judgment matrix is a key link in the application of analytic hierarchy process, which can show the relative importance of each index of the current level relative to a certain index of the previous level in the quality evaluation hierarchy model of Ideological and political education. According to the constructed curriculum education quality evaluation model, when evaluating the education effect of specific courses, the obtained evaluation data can be used to establish the judgment matrix of indicators at all levels, and then the appropriate calculation method can be used to calculate the relative weight of each element for a certain criterion level, conduct consistency test, and finally obtain effective evaluation data. Figure 2 presents the whole pipeline.

5. Hierarchical Relationship and Responsibilities among Various Executive Elements

Due to the many links and factors involved in the implementation of curriculum ideological and political education, if the responsibilities of various executive units or groups in colleges and universities are not fulfilled enough, this will lead to the lack of motivation for curriculum teaching reform, the uneven teaching effect, the different evaluation of students' recognition and sense of acquisition of the curriculum, and so on. Therefore, we sort out the implementation elements and responsibilities involved in the implementation process according to the established evaluation model.

5.1. The School Is a Top Designer. The school party committee should earnestly fulfill the main responsibility, put forward the overall requirements and objectives of curriculum ideological and political construction from the perspective of the national education development planning strategy, clarify the educational functions of each curriculum and the educational responsibilities of all teachers, issue the assessment and evaluation mechanism, and do a good job in supervision and implementation. All functional departments should jointly establish a curriculum evaluation and incentive mechanism guided by the effect of education and take the results of teachers' education as an important factor for teachers' post and grade determination. Through joint training with local schools and enterprises, we will build a collaborative and shared platform for ideological and political education resources.

5.2. College (Department) Is the Basic Executive Department. Colleges (departments) are the basic educational units of universities. First, we should do a good job in the selection of courses and teachers. Second, we should build a "great ideological and political" and "great coordination" education pattern, strengthen the exchanges between ideological and political discipline teachers and professional course teachers, front-line teachers, and ideological and political work team personnel, and do a good job in teacher education training. Third, we should introduce the specific implementation plan of curriculum ideological and political education, carry out the satisfaction evaluation of students' career development, and do a good job in the collection of evaluation data and result analysis. Fourth, we should do a good job in case summary, tap excellent teaching plans and educational models, and do a good job in experience promotion and case exchange.

5.3. Discipline (Curriculum Group) Is the Core Organization. Discipline (curriculum group) is the grass-roots organization to implement curriculum education. Disciplines such as

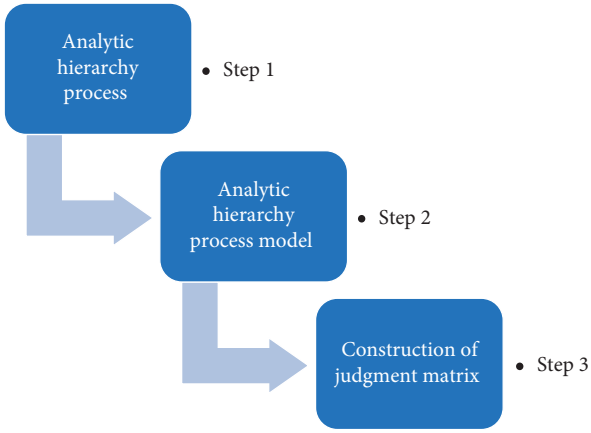

Figure 2: The whole steps of the experiment.

ideological and political education theory should actively assist teachers of other disciplines in the excavation of ideological and political education resources and the integration of teaching plans and actively advocate the all-round development of moral education. Other disciplines or curriculum groups should be driven by the students' curriculum selection and knowledge needs in the context of the new era, deeply explore the ideological and political education resources of various courses, and design the curriculum system and teaching scheme that can meet the students' personality characteristics and growth needs in the new era according to the training objectives and educational objectives of different majors, combined with the industry talent standards and learning from the OBE concept.

5.4. Teachers Are the Key Group to Implement Tasks. Teachers should really study curriculum thought and politics as a knowledge that can shape students' hearts and accurately locate the value orientation and teaching purpose of the curriculum in combination with the professional training objectives. First of all, we should establish the awareness of "interdisciplinary," do a good job in the excavation and introduction of ideological and political elements systematically and scientifically, and establish a multidimensional blending relationship between knowledge and life and social responsibility. Secondly, in the teaching process, pay attention to the attention and observation of students' ideological status, timely correct the inappropriate thoughts, views, and attitudes among students, and realize the organic combination of ideological and political education and professional course content. Thirdly, adhere to the unity of teaching by speech and teaching by example, take the lead in setting an example, become a mirror for students to behave and work, and become a banner for students to study and ask questions.

As the main way to implement the "three complete educations," curriculum education is a detailed and systematic project. In order to give full play to the role of the classroom as the main channel in educating people, colleges and universities must always adhere to the guidance of Marxist theory, promote the curriculum education reform with high standards and strict requirements, determine the direction and content of the curriculum reform, and clarify the main responsibilities and mutual relations of various implementation elements in the process of curriculum reform and education and teaching, so as to obtain a good evaluation path and effect of curriculum education quality and comprehensively form a vivid situation of collaborative education.

6. Suggestions on Classroom Teaching Quality

The main task of colleges and universities is to cultivate students into talents that play an important role in the society, and the evaluation of classroom teaching quality is an important aspect that directly reflects the quality of talents in colleges and universities. Under the guidance of the thought of "curriculum thought and politics," this paper puts forward targeted optimization strategies. Table 1 lists the suggestions on classroom teaching quality.

6.1. Change the Concept of Evaluation Purpose and Evaluation Content

6.1.1. Changing the Purpose Concept of Classroom Teaching Quality Evaluation. There is an inseparable relationship among education, society, and people. Classroom teaching is bound to be affected by various factors at the social level, especially the current social, economic, and cultural impact on college classrooms. Therefore, the evaluation of classroom quality also needs to be improved. Therefore, classroom teaching evaluation should change the traditional evaluation concept, abandon the traditional evaluation means and methods, and be under the guidance of curriculum ideology and politics, in line with the concept of modern talent training. Talents who meet social needs are important. Through the multidirectional evaluation of teachers' "teaching" and students' "learning" in classroom teaching evaluation, we need to pay attention not only to the results of classroom evaluation teaching but also to the evaluation of classroom teaching process, encourage teachers to actively participate in teaching evaluation, and finally improve teachers' teaching ability and the overall quality of teachers.

6.1.2. Enrich the Content of Classroom Teaching Quality Evaluation. The education of students in higher education mainly includes ideological education, skill training, scientific research, and social services, of which the most important are the ideological education and skill training of talents. Classroom teaching is the most important, direct, and fundamental way for colleges and universities to cultivate talents. Traditional classroom teaching activities only guide students to master scientific cultural knowledge according to teaching objectives, and this cultural knowledge is only a simple presentation of teaching materials, which restricts teachers' ability from being stimulated to a great extent. Under the traditional concept of teaching evaluation, the evaluation of classroom teaching mainly focuses on the selection of teachers' teaching methods and relevant

Table 1: The suggestions on classroom teaching quality.

Suggestion
Change the concept of evaluation purpose and evaluation content
Build a diversified evaluation subject
Establish effective feedback mechanism
Other recommendations

teaching materials, ignoring whether the curriculum content in teaching evaluation is in line with the current ideological development of college students and whether the curriculum content setting is reasonable. Therefore, the evaluation of classroom teaching quality changes the traditional evaluation concept of teachers' teaching behavior and teachers' curriculum setting. First is scientific and reasonable teaching content. According to the teaching objectives and teaching contents, teachers reasonably determine the role of teaching materials, determine the key points and difficulties of teaching contents, and guide students to effectively stimulate students' interest in learning while learning basic knowledge and skills, cultivate independent learning ability, enterprising innovation spirit and ability to solve practical problems, let alone ignore the cultivation of college students' humanistic quality, and actively study ideological courses. Second is implementing effective teaching methods. Teachers should be good at actively guiding students to participate in classroom teaching activities, actively play their due role in the classroom, and let students realize that they are the main body of the classroom. At the same time, teachers should pay attention to cultivating students' innovative spirit, cooperative spirit, and self-consciousness in the teaching process, which can not only cultivate students' ability to adapt to the society but also have the creative ability of independent thinking.

6.2. Building a Diversified Evaluation Subject. The traditional classroom evaluation in colleges and universities is mainly based on student evaluation, supplemented by peer evaluation, teaching supervision, and leading cadre evaluation, but, in practice, it gives great weight to student evaluation and ignores the importance of other evaluations. Therefore, we should build a diversified evaluation subject that encourages teachers to actively participate in evaluation and form a student evaluation and teacher self-evaluation as the main body, supplemented by peer evaluation and leading cadre evaluation.

6.2.1. Mainly Student Evaluation and Teacher Self-Evaluation. We should learn from the advanced experience of classroom teaching quality evaluation, combine the concept of advanced curriculum ideas and developmental teaching evaluation contents, and timely adjust the evaluation methods of teachers, which can help teachers constantly reflect on their teaching activities and teaching behaviors and make a comprehensive and intuitive evaluation of the teaching activities carried out in the classroom from multiple angles, levels, and directions, as well as helping teachers improve the quality of classroom teaching. At the same time, the evaluation subject can have diversified ways, which also means different evaluation methods. These evaluation methods can improve the process of classroom teaching and carry out comprehensive supervision and management.

6.2.2. Supplemented by Peer Evaluation and Evaluation of Leading Cadres. Classroom activities in colleges and universities are highly professional and different, so the classroom evaluation standards of different disciplines cannot use a unified way to judge the value. Compared with other evaluation subjects, peer evaluation has two advantages. The first advantage is that teachers with the same discipline background are very familiar with the teaching objectives, teaching contents, teaching structure, and teaching process of this discipline, so they can make very professional evaluation. The second advantage is that peers can conduct mutual evaluation after class and put forward problems and solve them, so as to comprehensively improve the quality of classroom teaching. The evaluation of leading cadres is generally divided into two levels: school and branch. More attention should be paid to the evaluation of leading cadres, while branch leaders are more familiar with professional courses, and the classroom teaching evaluation of all teachers in the middle and end of the period is checked, so as to promote the mutual communication of teaching methods among teachers.

6.3. Establish Effective Feedback Mechanism. Whether the results of classroom teaching quality evaluation are reasonable and effective and the use of evaluation results are the key to determine whether the whole evaluation process is effective. Reasonable evaluation can promote the improvement of classroom teaching quality; on the contrary, it is a mere formality. Establishing a perfect and effective feedback mechanism is an important measure to ensure that the evaluation results can be used in time. By establishing diversified and timely feedback forms, the evaluation results can be used more scientifically.

6.3.1. Timely and Diverse forms of Feedback. Improving the feedback mechanism is an effective bridge, which can timely and accurately deliver the evaluation results to teachers, help teachers improve their teaching behavior, and improve teachers' teaching level. However, the current feedback is unified feedback to teachers after counting the evaluation results of students, peers, and leading cadres through the teaching management part, which is not conducive to the timely improvement of teachers' teaching behavior in terms of time. Corresponding feedback forms should be set between the evaluation subjects, and the evaluation information of teaching supervisors and leaders on teachers should be delivered to teachers in time after the class. Teachers know the advantages and disadvantages in the teaching process through scoring results and personal opinions. Students' evaluation opinions should be delivered to teachers in time after collecting and sorting students'

information, The evaluation among peers should be released through the regular exchange seminars organized by the college. The person in charge of the branch specially organizes and requires each teacher to summarize their experience, make effective use of the evaluation results, and timely deliver the evaluation results to teachers after the classroom teaching quality evaluation, so as to effectively improve the efficiency of classroom teaching.

6.3.2. Effective Use of Evaluation Results. How to effectively summarize and apply the evaluation results and take them as an important basis to improve the teaching quality and the management department in charge of teaching in colleges and universities should change the traditional evaluation results, sort out the developmental teaching evaluation concept, and make an in-depth, detailed, and comprehensive analysis of the evaluation results. The Education department of colleges and universities should distribute the evaluation results to each department, timely urge the teaching secretary of the branch department to organize the evaluated teachers to discuss the evaluation results, and help teachers adjust the teaching contents and teaching methods in combination with the contents of the evaluation. At the same time, teachers should take the initiative to combine the new educational ideas and learn relevant professional knowledge, overcome many difficulties, constantly improve the classroom teaching behavior, constantly summarize, absorb, and improve the good evaluation results, pay attention to the poor evaluation results, maintain a good attitude, and make continuous improvement.

6.4. Other Recommendations. Teachers' teaching attitude and teaching content, teaching methods and professional quality, study style, examination style, and teaching guarantee have a common impact on students' knowledge acquisition and skill improvement. Students' own learning attitude is very important, which is basically consistent with the research conclusions of other scholars. Whether and how students learn plays a vital role in students' knowledge acquisition and skill improvement. Teachers' teaching attitude and teaching content cannot directly affect students' knowledge acquisition and skill improvement but can only play a small role in promoting through the school's study style, examination style, and teaching guarantee. Teachers' teaching methods and professional quality have the greatest impact on students' knowledge acquisition and skill improvement. They can not only promote directly but also have an indirect impact through the school's study style, examination style, and teaching guarantee. Therefore, under the background of "curriculum thinking and politics," the evaluation of classroom teaching quality in colleges and universities should go hand in hand with "teaching" and "learning" and "management."

6.4.1. Clarify the Learning Purpose and Correct the Learning Attitude. In the university, especially in the undergraduate stage, the courses learned are to a large extent to lay the foundation for future study and work. With the rapid development of science and technology and the accelerated replacement of new and old jobs, most people may have to engage in multiple types of work before retirement. Changing jobs is a very common and frequent thing. In the short term, a course seems to be of little help to one's postgraduate entrance examination and employment. It may come in handy when one changes his next job. It is necessary to urge students to take seriously the study of each course in the undergraduate stage with a long-term view, so as to meet the needs in the future.

6.4.2. Strengthen the Reform of Teaching Methods and Improve Teachers' Professional Quality. There is a close relationship between teaching methods and teaching contents. Teaching methods include both general teaching methods suitable for general courses and specific teaching methods according to the characteristics of specific courses. The teaching method to be adopted needs to be determined according to the specific courses and even the teaching objects of different majors. Experienced teachers focus on teaching methods and selected cases when they treat students of different majors in the same course, which puts forward higher requirements for teachers. Teachers' professional quality will also be fully demonstrated in the process of classroom teaching. Teachers with excellent professional quality are more attractive in classroom teaching, can stimulate students' learning potential, and significantly improve learning effect.

6.4.3. Strictly Enforce the Style of Study and Examination and Improve the Guarantee of Teaching. To sum up, if teachers' teaching attitude, teaching content, teaching methods, and professional quality can maximize the promotion of students' knowledge acquisition and skill improvement, the school's study style, examination style, and teaching guarantee play an important media role. Imagine that if the style of study and examination is not strict, students who usually do not study hard may get high scores by cheating, which will directly attack the enthusiasm of students who study hard. Through the construction of strict study style and examination style, maintain a fair examination environment and force students to study hard. Only in this way can teachers' teaching attitude, teaching content, teaching methods, and professional quality play a greater role in promoting students' learning knowledge and improving skills. Through the structural equation model, the author studies the influence of college teachers' teaching and professional quality, school style of study, examination style, and teaching guarantee on students' knowledge acquisition and skill improvement. There are far more factors affecting the effect of classroom teaching in colleges and universities; for example, how the social environment and employers affect the teaching effect needs further research.

7. Conclusion

The evaluation of classroom teaching quality is an important link in the teaching process. It is the key to measure the

quality of the whole teaching and plays a very important role in promoting and improving the teaching quality. The purpose of classroom teaching evaluation is to improve the improvement of classroom education quality and help teachers find the deficiencies in classroom teaching in time, as well as the mode of classroom teaching quality evaluation in colleges and universities. Methods and ideas need to be scientific, reasonable, and perfect in the future research and practice, so as to promote the reform of teaching classroom in colleges and universities. Our method is a general evaluation method, which can be applied to other fields in the future.

Data Availability

The dataset can be obtained from the author upon request.

Conflicts of Interest

The author declares that there are no conflicts of interest.

References

[1] J. J. Crowley and A. G. Hauser, "Evaluating whole school improvement models: creating meaningful and reasonable standards of review," *Journal of Education for Students Placed at Risk*, vol. 12, no. 1, pp. 37–58, 2007.

[2] P. Ur, *A Course in Language teaching[J]*, Cambridge University Press, Cambridge, England, UK, 1999.

[3] P. Ur, *A Course in English Language teaching[M]*, Cambridge University Press, Cambridge, England, UK, 2012.

[4] J. Biggs, "Aligning teaching and assessing to course objectives [J]," *Teaching and learning in higher education: New trends and innovations*, vol. 2, no. April, pp. 13–17, 2003.

[5] J. Yalden, *Principles of Course Design for Language teaching [M]*, Cambridge University Press, Cambridge, England, UK, 1987.

[6] D. Cantoni, Y. Chen, D. Y. Yang, N. Yuchtman, and Y. J. Zhang, "Curriculum and ideology," *Journal of Political Economy*, vol. 125, no. 2, pp. 338–392, 2017.

[7] P. Zheng, X. Wang, and J. Li, "Exploration and practice of curriculum ideological and Political Construction Reform --Take "information security" course as an example," *ASP Transactions on Computers*, vol. 1, no. 1, pp. 1–5, 2021.

[8] B. Zhang, V. Velmayil, and V. Sivakumar, "A deep learning model for innovative evaluation of ideological and political learning[J]," *Progress in Artificial Intelligence*, pp. 1–13, 2021.

[9] R. M. Felder and R. Brent, "How to improve teaching quality," *Quality Management Journal*, vol. 6, no. 2, pp. 9–21, 1999.

[10] D. Liston, H. Borko, and J. Whitcomb, "The teacher educator's role in enhancing teacher quality," *Journal of Teacher Education*, vol. 59, no. 2, pp. 111–116, 2008.

[11] S. E. Rimm-Kaufman and B. K. Hamre, "The role of psychological and developmental science in efforts to improve teacher quality," *Teachers College Record: The Voice of Scholarship in Education*, vol. 112, no. 12, pp. 2988–3023, 2010.

[12] J. Bai and H. Li, "Research on the demand-driven O2O & BIA blended interactive teaching mode," in *Proceedings of the 2020 International Conference on Information Science and Education (ICISE-IE)*, pp. 608–611, IEEE, Sanya, China, December 2020.

[13] H. Zhan, "Study on the cultivation of university teachers' ability of innovation and entrepreneurship education," in *Proceedings of the 4th International Conference on Culture, Education and Economic Development of Modern Society (ICCESE 2020)*, pp. 1209–1213, Atlantis Press, Moscow, Russia, March 2020.

[14] T. Bieber and K. Martens, "The OECD PISA study as a soft power in education? Lessons from Switzerland and the US," *European Journal of Education*, vol. 46, no. 1, pp. 101–116, 2011.

[15] K. Vaino, J. Holbrook, and M. Rannikmäe, "Stimulating students' intrinsic motivation for learning chemistry through the use of context-based learning modules," *Chemistry Education: Research and Practice*, vol. 13, no. 4, pp. 410–419, 2012.

[16] M. Shin and S. Bolkan, "Intellectually stimulating students' intrinsic motivation: the mediating influence of student engagement, self-efficacy, and student academic support," *Communication Education*, vol. 70, no. 2, pp. 146–164, 2021.

[17] R. A. Kusurkar, G. Croiset, and O. T. J. Ten Cate, "Twelve tips to stimulate intrinsic motivation in students through autonomy-supportive classroom teaching derived from Self-Determination Theory," *Medical Teacher*, vol. 33, no. 12, pp. 978–982, 2011.

[18] L. Darling-Hammond, "Teacher quality and student achievement: a review of state policy evidence[J]," *Education Policy Analysis Archives*, vol. 8, 1999.

[19] C. Masui, J. Broeckmans, and S. Doumen, A. Groenen, G. Molenberghs, Do diligent students perform better? Complex relations between student and course characteristics, study time, and academic performance in higher education," *Studies in Higher Education*, vol. 39, no. 4, pp. 621–643, 2014.

[20] S. M. Downing, "Validity: on the meaningful interpretation of assessment data," *Medical Education*, vol. 37, no. 9, pp. 830–837, 2003.

[21] Z. Jia, Y. Lin, J. Wang, X. Ning, Y. He, and R. Zhou, Y. Zhou, L. W. H. Lehman, Multi-view spatial-temporal graph convolutional networks with domain generalization for sleep stage classification," *IEEE Transactions on Neural Systems and Rehabilitation Engineering*, vol. 29, pp. 1977–1986, 2021.

[22] Z. Jia, Ji Junyu, X. Zhou, and Y. Zhou, "Hybrid Spiking Neural Network for Sleep EEG Encoding[J]," *Science China Information Sciences*, vol. 65, 2022.

[23] Z. Li, J. Wang, Z. Jia, and Y. Lin, "Learning space-time-frequency representation with two-stream attention based 3D network for motor imagery classification," *ICDM*, pp. 1124–1129, 2020.

[24] Z. Jia, X. Cai, and Z. Jiao, "Multi-modal physiological signals based squeeze-and-excitation network with domain adversarial learning for sleep staging[J]," *IEEE Sensors Journal*, 2022.

[25] Z. Jia, Y. Lin, Y. Liu, and J. Wang, "Refined nonuniform embedding for coupling detection in multivariate time series [J]," *Physical Review*, vol. 101, no. 6, Article ID 062113, 2020.

[26] Z. Jia, X. Cai, Y. Hu, and Z. Jiao, "Delay propagation network in air transport systems based on refined nonlinear Granger causality[J]," *Transportation Business: Transport Dynamics*, vol. 10, pp. 1–13, 2022.

[27] O. S. Vaidya and S. Kumar, "Analytic hierarchy process: an overview of applications," *European Journal of Operational Research*, vol. 169, no. 1, pp. 1–29, 2006.

Hindawi
Scientific Programming
Volume 2022, Article ID 5970188, 9 pages
https://doi.org/10.1155/2022/5970188

Research Article

A Method to Study Group Relationship of College Students Based on Predictive Social Network

Honggao Zhang,[1] Jie Zhang,[2] and Yu Shi[3]

[1]*School of Education, Linyi University, Linyi, Shandong 276000, China*
[2]*School of Pharmacy, Linyi University, Linyi, Shandong 276000, China*
[3]*Hebei Academy of Fine Arts, Shijiazhuang, Hebei 050700, China*

Correspondence should be addressed to Yu Shi; sy@hbafa.edu.cn

Received 18 May 2022; Revised 14 June 2022; Accepted 17 June 2022; Published 6 July 2022

Academic Editor: Lianhui Li

With the rise of social network platforms such as WeChat, Weibo, and TikTok, social networks have developed from simple social networks to complex social networks. Researchers have gradually found that the traditional data sampling methods can no longer meet the development needs of the complex social network structure. In order to save network resources, various methods of social relationship prediction have been proposed. In this paper, we propose a BTCS algorithm based on low sampling rate under cognitive model and conduct several sets of comparison experiments under different networks and different sampling rates, and the results show that the BTCS algorithm improves the prediction accuracy and reduces the prediction time under low sampling rate. To address the problems of poor stability and slow prediction speed of random sampling prediction methods, this paper proposes a CCS algorithm in colleges and universities using the characteristics of high awareness among nodes within the same college. It can effectively combine the cognitive characteristics of the nodes with the college attributes and apply them to the relationship prediction to realize the college-oriented relationship prediction. The simulation results show that the CCS algorithm is more stable than other random sampling prediction methods. The results make full use of the cognitive characteristics and college attributes of nodes in social networks; reduce the influence of multiple factors such as response time, data packet loss, and individual behavior on relationship prediction; and improve the efficiency of college student group relationship prediction, which has certain theoretical significance and application prospects.

1. Introduction

With the rapid development of information technology, e-commerce and social networking sites have become inseparable from people's daily life, coupled with the increasing networkedness and various data resources, the network has received wide attention as a new perspective for information analysis and management research. [1–6] Especially since entering the twenty-first century, Internet technology has been rapidly developed and people have rapidly entered the era of online Internet. With the rise of various social networking sites and communication software such as Weibo, WeChat, TikTok, Alipay, and QQ, they provide people with direct and quick platforms for online friendships and online shopping. [7–10] Network group is a collective form by individuals in the network with mobile devices or computers as the communication medium and information as the link. Its purpose is mainly study, interest, communication, or need, while college students' network group is an aggregation formed by college students on the network. The activities of college students on the Internet are not individual activities, but more interactive activities with others. Therefore, the communication behaviors of college students' netizens in the virtual space of the network constitute the group network of college students. The complex and changeable network environment brings abundant resources to college students and satisfies their pursuit of material and spiritual culture. However, the virtual network

world also changes the way of psychological activities of college students, making them show a variety of abnormal thinking or action in the network world. The popularity of these social networks and communication tools has revealed that data processing based on the attributes of the entities themselves ignores the information connections between entities and that such data processing methods cannot meet the needs of big data analysis and research. Therefore, in response to the ever-complex internode relationships, researchers have proposed a novel network, that is, social networks. In fact, social network not only refers to the scope of sociology but also includes various information networks, technology networks, and bio-information networks. [11–14] Of course, the most common social networks in daily life are social networks. For most online social networks, they often have thousands and tens of thousands of nodes, and the relationships between nodes are complex and may change in real time. Therefore, they have the same various properties of complex networks. These social networks with a large number of network nodes and complex relationships between nodes are called complex social networks, which is an important branch of complex networks. In recent years, due to the continuous improvement of the mathematical model of social networks, researchers have been studying complex social networks more and more deeply. [15–18] However, in the analysis of complex social networks, researchers have found that there are always nodes that cannot be directly sampled, and this part of node information plays an extremely important role in the overall study of the network. Therefore, the study of prediction methods for internode relationships in complex social networks is an important element of social network research. [19–21]

Social relationship prediction methods can solve the problem of difficult node information collection in interactive networks. In different social networks, they use different network models, so data collection under different models can have mutual effects. Social relationship prediction can provide a unified mechanism to predict out the relationship between nodes, which can realize the data analysis among interactive networks. College student group relationship prediction methods can achieve accurate prediction of internode relationships at low sampling rates. In the analysis of some specific networks, the sampling rate is often limited due to the influence of node response time and the properties of the nodes themselves. However, lower sampling rates can significantly reduce the accuracy of various analyses of social networks. It then needs to predict the topology of the network at low sampling rates. For the needs of these specific networks, the social relationship prediction method can accurately predict the topology of the overall network based on the information of the sampled nodes under the condition of sampling a small number of nodes, which plays an important role in the analysis of social networks at low sampling rates. The group relationship prediction method for college students has important practical applications. In practical applications, if researchers can make full use of the available data information, build accurate model structures, plan experiments rationally, and analyze and predict hidden relational information, then relational prediction methods will save time, improve efficiency, and produce accurate and valuable results for people. In social networking sites, friend recommendation is realized based on the information of friends' circle; in shopping sites, interest product recommendation is realized based on the kind of goods users browse; in biological information network, hidden species relationship is predicted based on experimental results, etc. [22–25] As an important tool of social network analysis, college student group relationship prediction plays an important role in the research of all fields of social networks. In recent years, researchers began to pay more and more attention to the study of social relationship prediction and proposed various college student group relationship prediction algorithms; especially, since the twenty-first century, researchers have combined college student group relationship prediction with the theoretical findings of psychology and searched for a new perspective on the integration of network structure prediction and individual perception: the social network cognitive model. [26]

The social network cognitive model is a network structure model that emphasizes the importance of network node perception on network structure prediction. It is an emerging mathematical model of social networks, whose core idea is to analyze the network structure by using the cognitive determination of individual nodes on the relationship between nodes of the whole network. As the field of network perception continues to develop, researchers have found that node perception capabilities can help node relationship prediction. Social relationship perception prediction has also gradually received the attention of social network researchers. Therefore, this paper addresses the research of social relationship prediction methods under the social network perception model with very significant scientific and practical significance.

2. BTCS Prediction Algorithm

2.1. Algorithm Improvement. In the prediction of relationships in complex social networks, most researchers find that network data collection is very difficult, especially in interactive networks, which can be affected by multiple factors such as response time, data packet loss, and individual behavior, resulting in unavailability of node information. However, traditional relational prediction methods are highly dependent on the sampling rate and response rate of nodes, and will directly affect the measurement results if the node information is lost or inaccessible. The flow chart of the traditional prediction method is shown in Figure 1. As can be seen from Figure 1, the sampling process of the traditional prediction method requires sampling all nodes in the network to obtain the internode relationship matrix. Then, according to the node relationship matrix, the senders and receivers in the network relationship are accessed and merged two by two. The network relationship exists only when both sender and receiver acknowledge the existence of the network relationship. If one party decides that the relationship does not exist, then the network relationship does not exist. Finally, the network topology matrix is obtained

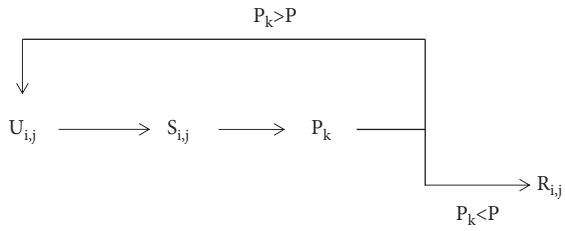

Figure 1: BTCS algorithm flow.

based on the merged results. However, in the traditional relational prediction method, it is affected by response time and sampling error, and data packet loss occurs. Therefore, the error analysis of the traditional method requires multiple repetitions of sampling. In the prediction of high-precision networks, the traditional method needs to complete multiple repetitions of sampling, which is very inefficient.

The BTCS algorithm achieves accurate prediction of social relationships at low sampling rates. The flow chart of the improved BTCS prediction algorithm is shown in Figure 2. Compared with traditional prediction methods, the BTCS algorithm is a randomized, low-sampling-rate relationship prediction method. It only needs to sample a small number of network nodes and obtain the cognitive determination information of the sampled nodes on the relationships among all nodes in the network, and then predict the social relationships among nodes based on the cognitive determination information without sampling all nodes. It adopts a threshold control method to adaptively control the node sampling error and avoid the duplicate sampling of data. Therefore, the BTCS algorithm can reduce the effects of response time, data packet loss, and individual behavior on node sampling and relationship prediction, and improve the efficiency of relationship prediction.

The BTCS prediction algorithm is a cognitive model-based relational prediction method, which is divided into three main steps: sampling, matrix merging, and fault-tolerant control process, as shown in the flow chart of the algorithm. The following section will introduce the specific process of each of the three steps of the BTCS algorithm.

2.2. Sampling Design. The data sampling process of BTCS prediction algorithm is different from the traditional relationship prediction method. In the traditional relationship prediction method, it needs to sample most of the network nodes and investigate to obtain the social relationships among the sampled members, while in the BTCS algorithm, it just samples a small number of nodes randomly, obtains the cognitive information of the sampled nodes on the social relationships among all network members, and records it in the form of a kind of three-dimensional 0–1 cognitive matrix set.

In the following example of the network (A, B, C, D, and E), Figure 3 represents the five cognitive matrices of members A, B, C, D, and E in the network (A, B, C, D, and E) in order. In each cognitive matrix, it records 20 social relationships among the members. In the sampling, the BTCS algorithm is randomly sampled in the sampling space n. In the network (A, B, C, D, and E), three nodes (A, D, and E) were randomly sampled when the sampling space n was 3, and the node sampling set m and the cognitive matrix set $R_{i,j,k}$ were obtained, where m = (1, 4, 5).

2.3. Matrix Design. There are three methods of matrix merging under the cognitive model: the cognitive slice method, the local summary structure method, and consistency structure dispel. Since these three methods merge the known and cognitive relationships of the sampled nodes equally in cognitive matrix merging, a new matrix merging method is proposed. According to the cognitive information of sampled nodes is divided into two categories of self-knowledge relationships and cognitive relationships, this paper divides the merging process into three cases: (1) merging self-knowledge relationships between sampled nodes; (2) merging cognitive relationship between sampled nodes; (3) merging known and cognitive relationship between sampled nodes. Merging rules are set according to these three cases.

We combine the known relationships between the sample nodes. In this paper, we use the merging local aggregation method, as in the following equation:

$$R_{i,j} = \left\{ R_{i,j,i} \cap R_{i,j,j} \right\}, \tag{1}$$

where $R_{i,j,i}$ and $R_{i,j,j}$ represent the known relationships in the cognitive matrix of sampled nodes i and j, respectively, and $R_{i,j}$ denotes the group relationship between node i and j. When both $R_{i,j,i}$ and $R_{i,j,j}$ are 1 and both the sender and receiver of the relationship determine that the relationship exists, then the relationship i to j is judged to exist and $R_{i,j}$ is 1.

Cognitive relationship merging between sampled nodes is as follows:

$$R_{i,j} = \begin{cases} 1, \sum_{m} R_{i,j,m} \geq K, \\ 0, \end{cases} \tag{2}$$

where $\sum_m R_{i,j,m}$ denotes the individual cognitive summary of all sampled nodes for the social relationship between i and j. K is a set threshold valve. When both sender i and receiver j of the relationship are not sampled, the summary value of cognitive information of the relationship is referred to all sampled nodes, and if the summary value is greater than or equal to K, then the relationship $R_{i,j}$ is determined to exist.

The known and perceived relationships between sampled nodes are merged.

$$R_{i,j} = \begin{cases} 1, \ R_{i,j} = 1 \sum_{m} R_{i,j,m} \geq K, \\ 0, \end{cases} \tag{3}$$

where $R_{i,j} = 1 \& \sum_m R_{i,j,m} \geq K$ denotes that when only one side of both sender i and receiver j of the relationship is sampled, then the known relationship of the sampled node is first considered to be 1. If the known relationship of the sampled node is 1 and the aggregated value is greater than or equal to K, then the relationship $R_{i,j}$ is determined to exist.

The final result θ is obtained by combining the three cases, $\theta = \alpha + \beta + \gamma$.

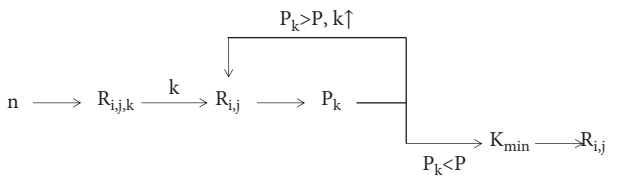

Figure 2: Upgraded BTCS algorithm flow.

Taking the network (A, B, C, D, and E) in Figure 3 as an example, the nodes (A, D, and E) are randomly sampled to obtain the sampling set (1, 4, and 5) and the cognitive matrix of A, D, and E. Then, the matrix merging is completed when the threshold value is 2, and the merging process and the merging results are obtained as shown in Figure 4. In Figure 4, α, β, and γ are the matrices obtained by merging in the first, second, and third cases, respectively; θ is the final result to obtain the real network matrix. The social relationship between the sampled nodes (A, D, and E) is obtained in α. For example, when analyzing the social relationship from E to D, by accessing the self-knowledge relationship of the cognitive matrix of D and E, we get $R_{E,D,D}$ and $R_{E,D,E}$ as 1. Then, we can decide that the social relationship from E to D exists, so we get $R_{E,D}$ =1 in α.

The social relationships between the unsampled nodes (B and C) are obtained in β. For example, in the analysis of the social relationships from B to C, the cognitive relationships of all sampled nodes are accessed and $\sum_m R_{B,C,m} = 2$, which is equal to the threshold K, so we get $R_{B,C}$ in x as 1. The social relationships between sampled nodes (A, D, and E) and unsampled nodes (B and C) are obtained in γ. For example, when analyzing the social relationship from A to C, the known information of the cognitive matrix of A is accessed first, and Ra is obtained as 1. Then, the cognitive relationships of all sampled nodes are accessed, and $\sum_m R_{A,C,m} = 2$, so $R_{A,C,A}$ is obtained in γ, and $R_{A,C}$ is 1.

The nodal relationship matrix θ is predicted by introducing the K-value merged 3D matrix $R_{i,j,m}$, and different prediction results θ are obtained under different K-values. The random partial sampling method under the social relationship cognitive model is a fast and efficient measurement method, and the prediction results are subject to error, which requires us to control the error within a tolerable range, so the error-tolerant control of the algorithm is important. Therefore, an error-tolerant control process with a threshold value is designed to adaptively regulate the value of K so that the prediction result θ is closest to the true result.

Firstly, we analyze the relationship between the sampling error rate and the threshold value as a function of P_K. These errors are divided into two categories: the first type of relationship error refers to the relationship does not exist in the real network, while the cognitive relationship is judged to exist; the second type of relationship error P_2 is the relationship exists in the real network, while the cognitive relationship is judged not to exist. In the dichotomous threshold algorithm, the threshold K is compared with the network recognition to determine whether the relationship holds, and the recognition is influenced by P_1, so P_1 is the main factor affecting the threshold reduction result, while P_2 will be gradually reduced in the reduction operation.

In Figure 4, the first type of error is generated by merging the cognitive matrices of sampled nodes A and D, which determine the nonexistence of the relationship A to D, while the cognitive determination exists in the cognitive matrix of E. In complex networks, P_1 increases as the network data increase, and the error P_1 can represent the network error rate P_k. Therefore, we need to analyze the relationship between the error P_1 and the threshold K.Therefore, this section analyzes the effect of the threshold K on θ by comparing the merged matrix θ and the cognitive matrix $R_{i,j,m}$ of the sampled nodes, and obtains the relationship between the value of K and the sampling error rate P_k.

$$P_k = \frac{V}{Q}, \tag{4}$$

where V is the number of errors present in the sampled nodes and Q is the number of possible errors in the sampled nodes.

Setting the fault-tolerance control condition. In this section, based on the maximum tolerable sampling error rate P' (0.1, 0.15, 0.2), an error-tolerant control process is established to find the smallest $K_{\min}$ value such that $P_k < P'$, and the matrix merging result is obtained when the output threshold K is $K_{\min}$, which is the closest to the real network. The prediction result is the closest to the real network.

A error-tolerant control process is designed. Through the above analysis, the relationship P_k between the error rate P and the threshold K is obtained. Therefore, according to the control theory and method, and the fault tolerance range, it can adaptively adjust the threshold K and control the error rate P_k within the fault tolerance rate P'. In words, in BTCS algorithm, fault-tolerant control process is an important part of the algorithm. Too large or too small K value will directly affect the accuracy of prediction results. BTCS algorithm mainly analyzes the direct relationship between K value and network sampling error, and designs the fault-tolerant control process of threshold value, which can adaptively control K value, find the best K value, minimize prediction error, and improve prediction accuracy.

2.4. Mathematical Model. The mathematical model of BTCS algorithm is divided into two parts: matrix dimension reduction model and fault-tolerant control model. In the matrix dimensionality reduction model, it combines the cognitive matrix according to the dimensionality reduction rules under the set K value. In the fault-tolerant control model, it analyzes the sampling error rate of the combined matrix, controls the error rate within the fault-tolerant range, and obtains the best threshold. Therefore, the mathematical model of BTCS algorithm is established step by step according to the matrix dimensionality reduction model and error-tolerant control model.

According to the matrix dimensionality reduction rules designed in the BTCS algorithm description, this subsection

A	A	B	C	D	E
A	0	0	1	0	1
B	0	0	1	0	0
C	1	1	0	0	0
D	0	0	0	0	0
E	1	0	0	0	0

A	A	B	C	D	E
A	0	1	0	0	0
B	1	0	0	0	1
C	0	1	0	0	1
D	0	0	0	0	0
E	0	0	0	0	0

A	A	B	C	D	E
A	0	0	0	0	0
B	1	0	1	0	0
C	1	1	0	0	0
D	0	0	0	0	0
E	0	0	0	0	0

A	A	B	C	D	E
A	0	0	1	0	1
B	0	0	1	1	0
C	1	1	0	0	0
D	0	1	0	0	0
E	1	0	0	0	0

A	A	B	C	D	E
A	0	0	0	1	0
B	0	0	0	0	1
C	0	0	0	0	0
D	1	0	0	0	1
E	0	1	0	1	0

Figure 3: 5 node awareness matrix.

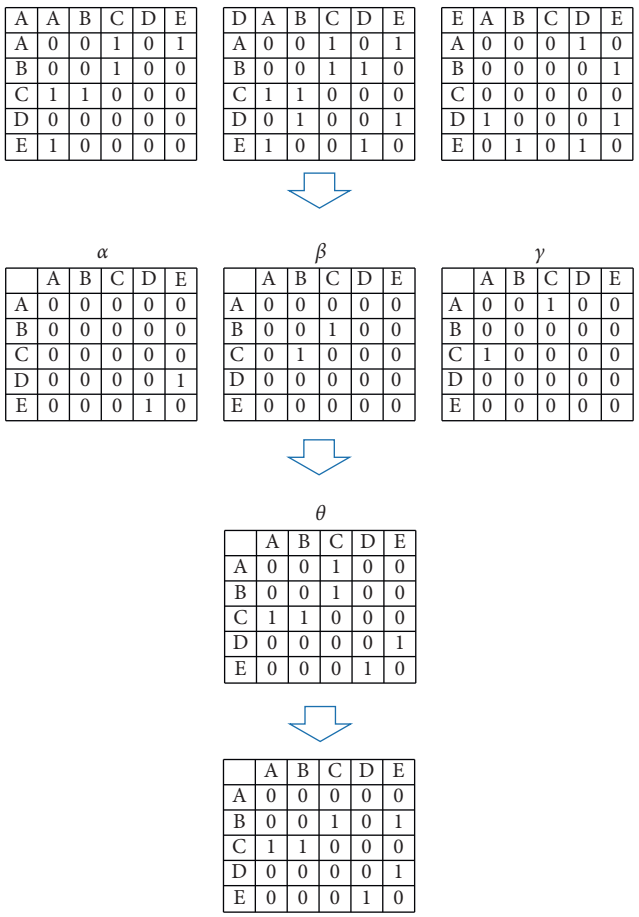

Figure 4: Merge matrix process.

first obtains the sampling set m, the cognitive matrix Y_i, and the set threshold K. Then, the valid information in the cognitive matrix is extracted in steps, and the mathematical matrix operations are obtained as follows:

(1) separate the cognitive matrix Yi to obtain the known relationship matrix $Y_{Z,i}$, and the cognitive relationship matrix $Y_{R,i}$.

Known relationship matrix:

$$Y_{Z,i} = i * Y. \tag{5}$$

Cognitive relationship matrix:

$$Y_{Z,i} = -i * Y_i. \tag{6}$$

Cognitive matrix:

$$Y_i = Y_{z,i} + Y_{R,i}. \tag{7}$$

Sampling node matrix and Z:

$$Z = \sum_{i=m} Y_{Z,i}. \tag{8}$$

Sampling node matrix and R:

$$R = \sum_{i=m} Y_{R,i}. \tag{9}$$

(2) The topological information among the sampled nodes is extracted from the cognitive relationship Z to obtain the matrix α.

Extraction matrix:

$$\begin{aligned} T &= m, \\ \alpha &= S_1 (T * Z). \end{aligned} \tag{10}$$

(3) extract the topological information of the cognitive relationship judgment to obtain β+γ.

2.5. Extraction Matrix

$$W = -m. \tag{11}$$

Cognitive information

$$\begin{aligned} P_1 &= W * Z, \\ P_2 &= W * R, \\ \beta + \gamma &= S_k (P_1 + P_2). \end{aligned} \tag{12}$$

The three cases are summed to obtain the reduced-dimensional merged matrix θ.

$$\theta = \alpha + \beta + \gamma. \tag{13}$$

2.6. Error-Tolerant Control Mathematical Model Implementation. According to the error-tolerant control process described by the BTCS algorithm, the sampling error rate P_k of the merged matrix under the set threshold K is analyzed and the mathematical model operation is obtained as follows:

(1) Calculate the number of errors W present in the sampled nodes.

$$W = S_k (T * R). \tag{14}$$

(2) Calculate the number of possible errors Q in the sampling nodes.

$$Q = T - \alpha. \tag{15}$$

(3) Sampling error rate P_k.

$$P_k = \frac{W}{Q}. \tag{16}$$

Finally, the sampling error rate P_k under the control of threshold K is obtained, and the dichotomous iteration method is used to find the optimal threshold value K that satisfies the fault tolerance condition.

3. CCS Relationship Prediction Method within Colleges and Universities

3.1. CCS Algorithm. In the social relationship cognitive model, the overall network random sampling prediction method ignores the different cognitive characteristics among nodes and ignores the high cognitive characteristics of nodes within the same college. Therefore, the stability of this relationship prediction method is poor. To address the shortcomings of the overall network random sampling prediction method, a relationship prediction method with random sampling in colleges and universities is proposed as the CCS prediction algorithm. [27] The CCS algorithm is applicable to networks where all college information is known and the college structures do not overlap. When a node belongs to more than one college at the same time, it is grouped into the college with the higher number of relationships among nodes.

The CCS algorithm takes advantage of the characteristics of high cognitive degree among nodes within the same college; firstly, the CCS algorithm assigns the sampled nodes to each college proportionally; then, the CCS algorithm completes the random sampling within the college according to the sampling space of each community to obtain the cognitive matrix of sampled nodes; finally, for the characteristics of high cognitive degree of nodes within the college, the CCS algorithm designs the matrix merging rules based on the college to get the final prediction results. Compared with other relationship prediction methods, the CCS prediction algorithm effectively combines the cognitive characteristics of nodes and college attributes.

The CCS prediction algorithm is a relationship prediction method in colleges and universities based on a social cognitive model. Figure 5 shows the flow chart of CCS prediction algorithm; in general, it is divided into three main steps: community-based sampling, intracollege node relationship merging, and inter-GA node relationship merging.

The community-based sampling is mainly to reasonably allocate the sampling nodes according to the network community structure and sampling space to obtain the sampling node cognitive matrix. In the community-based cognitive matrix merging, the sampled node cognitive matrix relationships are first classified into intracommunity

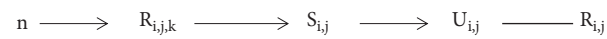

Figure 5: Flow chart of CCS prediction algorithm.

node relationships and intercommunity node relationships; then, the nodes are merged in steps according to the different intracommunity and intercommunity nodes to obtain the prediction results. In this section, four parts of community-based sampling process design, community-based node relationship classification, intracommunity node merging design, and intercommunity node merging design are introduced, respectively.

3.2. Sampling Process Design. In the data sampling process, the CCS prediction algorithm implements a community-based cognitive matrix data sampling, which combines cognitive information with college information. The community-based sampling characteristics of the CCS prediction algorithm are mainly reflected in the following three aspects.

The CCS prediction algorithm is a data sampling process based on a cognitive model. Like other relationship prediction methods under the cognitive model, the data obtained after sampling by the CCS prediction algorithm are also a kind of three-dimensional 0–1 cognitive matrix set $R_{i,j,k}$, where i represents the sender of the social relationship, j represents the receiver, and $R_{i,j,k}$ represents the observer of the social relationship between i and j. If K observes that the relationship from i to j exists, then $R_{i,j,k}$ indicates that it does not exist.

The CCS prediction algorithm is a data sampling process based on the node community structure. Based on the network community structure (C1, C2, ... CN), the CCS algorithm will allocate the sampling space to each community proportionally so that the sampling ratio within each community is the same. For communities with more nodes, the CCS algorithm allocates a correspondingly larger number of sampled nodes; while for communities with fewer nodes, the number of samples is correspondingly lowered to ensure an even number of sampled nodes within each community.

The CCS prediction algorithm is a data sampling process based on random sampling within communities. For each community, under the condition that the number of sampled nodes is determined, the CCS algorithm uses a random sampling method in which each node has the same probability of being sampled.

3.3. Stability Analysis. In this subsection, this paper analyzes the stability of the prediction algorithm under random sampling conditions. In order to analyze the stability of the prediction algorithm, multiple sets of experimental predictions were performed in this paper for different node sampling results under the same sampling space using the CCS algorithm, the Central Graph algorithm, and the LAS algorithm. In each set of experiments, 1000 random samples are performed for the same sampling space and 1000 prediction results are obtained, and the confidence interval (CI)

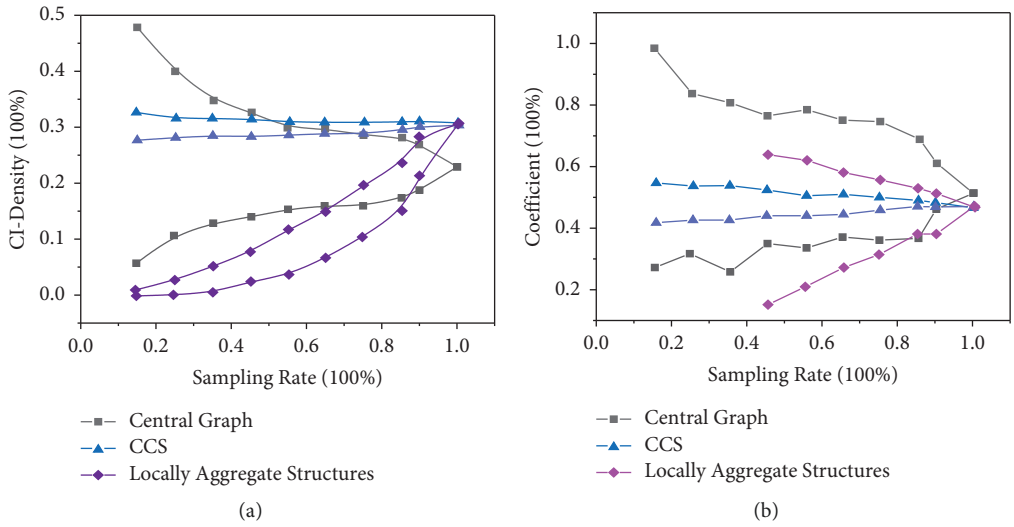

Figure 6: Density CI distribution (a) and clustering coefficient CI distribution (b).

numerical processing method is used to analyze the 1000 results.

In the confidence interval processing, this paper first ranks the performance parameters of 1000 prediction network results and then removes the first 2.5% and the last 2.5% to get the distribution curve of the performance parameters, and finally, this paper compares the confidence distribution of the performance parameters of the obtained prediction network results with the performance parameters of the real network results to analyze the stability of the algorithm under the random sampling conditions.

Figures 6(a) and Figure 6(b) show the density CI distribution curves and clustering coefficient CI distribution curves of the CCS algorithm, Central Graph algorithm, and LAS algorithm under different meter sample nodes at the same meter sample rate, respectively; where the horizontal coordinates indicate the sampling rate, the vertical coordinates indicate the network density values and clustering coefficient values of the predicted results, and the dashed lines indicate the performance parameters of the real network. From the analysis in Figures 6(a) and 6(b), it can be obtained that (1) the network density distribution and the clustering coefficient distribution of 1000 measurements at different sampling rates are within the confined curve range. (2) When the sampling space is small, the network density confidence interval distributions and the clustering coefficient confidence interval distributions of the 1000 random sampling prediction results of the CCS algorithm are smaller than those of the LAS algorithm and the Central Graph algorithm, and both are close to the performance parameters of the real network. (3) As the sampling rate increases, the network density confidence interval distribution and the clustering coefficient confidence interval distribution of the prediction results of the three prediction algorithms show convergence and gradually become smaller. However, compared with the other two algorithms, the network density confidence interval distribution and the clustering coefficient confidence interval distribution of the CCS algorithm are closer to the performance parameters of the real network. (4) When the sampling rate is larger, the CCS prediction algorithm outperforms the LAS algorithm and the Central Graph algorithm, and the CCS prediction algorithm predicts results that are close to the real network density. Therefore, the CCS algorithm is more stable than the other two algorithms, it is less volatile by the different sampling nodes and the stability of the algorithm is higher.

3.4. Prediction Accuracy Analysis. In terms of accuracy analysis of the prediction results, the mean square error of the three algorithms under different sampling rates is compared. In this paper, the CCS algorithm is compared with the Central Graph algorithm and the LAS (locally aggregates structures) algorithm.

To analyze the prediction accuracy of the CCS algorithm in communities, multiple sets of prediction experiments were conducted in the cognitive social network data package using the CCS algorithm with the Central Graph algorithm and the LAS algorithm, respectively, and network density MSE curves and average clustering coefficient MSE curves were obtained, as shown in Figures 7(a) and 7(b), where the horizontal coordinates denote the sampling rate, and the vertical coordinates indicate the MSE values of network density and clustering coefficients. From Figures 7(a) and 7(b), we can get that (1) the MSE values of CCS prediction algorithm fluctuate less than Central Graph algorithm and LAS algorithm at different sampling rates, and the prediction results of both CCS algorithms are very close to the real network. (2) When the sampling rate is small, the MSE values of Central Graph algorithm and LAS algorithm are larger, while the MSE values of CCS algorithm are smaller, and the prediction accuracy of CCS algorithm is still very high. (3) When the sampling rate is larger, the error value of the LAS algorithm gradually decreases and approaches the real network results, while the CCS algorithm still has a certain smaller error when the sampling rate is 1. Because in the sampling process of the CCS algorithm, it makes full use of the network community information and subcommunity

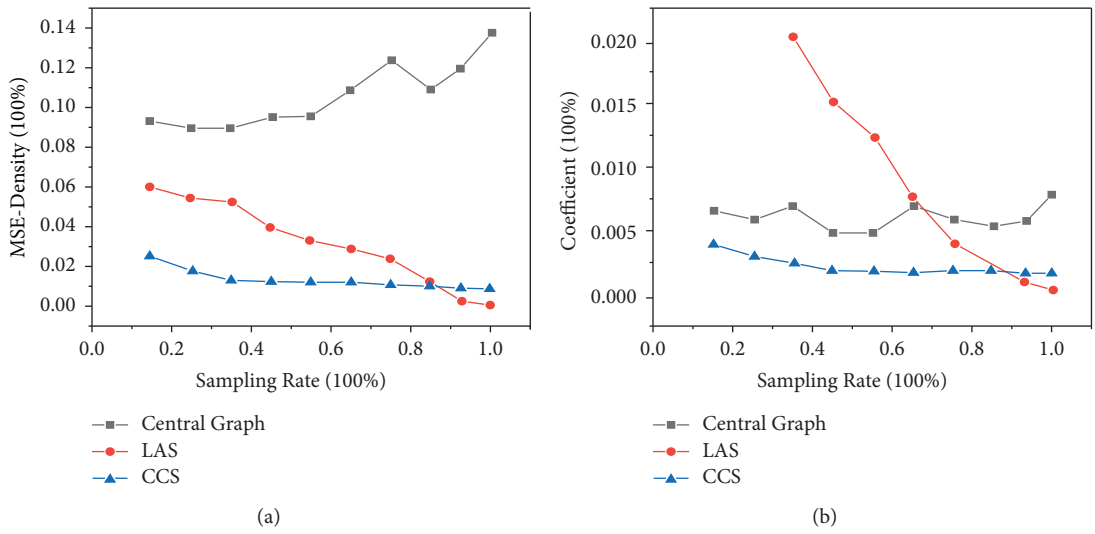

Figure 7: MSE of network density at different sampling rates (a) and MSE of clustering coefficients at different sampling rates (b).

random sampling to ensure the balance of the overall network cognition of the sampled nodes, it can always maintain a high prediction accuracy. When the sampling rate is 1, the community merging rule of CCS algorithm relies on the overall cognition of the community to complete the relationship determination instead of directly accessing the relationship sender and receiver, and thus, there is a small error even if all nodes are sampled.

The CCS prediction algorithm in the community is more stable, more accurate, and faster than other relationship prediction algorithms under cognitive models.

4. Conclusion

This paper addresses the relationship prediction method under the social network cognitive model. Based on the relationship prediction method under the cognitive model, a relationship prediction method under the cognitive model of college student group is proposed, that is, BTCS prediction algorithm. The cognitive nature of the nodes in the network is exploited, and the cognitive model of social relationships is combined with the relationship prediction technique to design a new method of cognitive matrix merging under the cognitive model of university student groups, which achieves the relationship prediction of complex social networks with low sampling rate and reduces the sampling time; secondly, two methods of threshold control and dichotomous lookup are introduced, and the interrelationship between threshold and network topological relationship error is analyzed, and the dichotomous lookup is used to optimize the measurement process. The method of dichotomous lookup is used to optimize the measurement process and improve the efficiency of threshold control. Based on the characteristics of high node awareness within the same college, a method for predicting college student group relationships in colleges and universities is proposed, that is, the CCS prediction algorithm. In social networks, network nodes not only have cognitive properties but also have social attributes. Due to the different social attributes among nodes, the closeness and cognitive degree among nodes are different. The group relationship prediction method for college students with random sampling under the cognitive model exploits the node cognitive characteristics to reduce the effects of response time, data packet loss, and individual behavior. Experimental results show that the CCS prediction algorithm in colleges and universities is more stable, more accurate, and faster than other group relationship prediction algorithms for college students under cognitive models.

Data Availability

The dataset can be accessed upon request.

Conflicts of Interest

The author declares that there are no conflicts of interest.

Acknowledgments

The authors thank the major commissioned project of Social Science Planning research of Shandong Province, Xi Jinping's Education Thought in the New Era (no. 18AWTJ51).

References

[1] G. H.-L. Cheng, P. Sung, A. Chan, S. Ma, and R. Malhotra, "Transitions between social network profiles and their relation with all-cause mortality among older adults," *Social Science & Medicine*, vol. 292, Article ID 114617, 2022.

[2] T. Hu, X. Zheng, X. Zhang, and D. D. Zeng, "ϵ-k anonymization and adversarial training of graph neural networks for privacy preservation in social networks," *Electronic Commerce Research and Applications*, vol. 50, Article ID 101105, 2021.

[3] Y.-J. Zhang, X.-l. Cai, H.-X. Hu et al., "Social brain network predicts real-world social network in individuals with social anhedonia," *Psychiatry Research: Neuroimaging*, vol. 317, Article ID 111390, 2021.

[4] J. E. Losee, G. D. Webster, and C. McCarty, "Social network connections and increased preparation intentions for a

disaster," *Journal of Environmental Psychology*, vol. 79, Article ID 101726, 2022.

[5] L. Chen, J. Chen, and C. Xia, "Social network behavior and public opinion manipulation," *Journal of Information Security and Applications*, vol. 64, Article ID 103060, 2022.

[6] D. Jeong, J. Kim, D. Choi, and E. Park, "Social networking services as new venue for public perceptions of energy issues: the case of Paris agreement," *Energy Strategy Reviews*, vol. 39, Article ID 100758, 2022.

[7] H. Suk and R. Grace, "Influence of social networks and opportunities for social support on evacuation destination decision-making," *Safety Science*, vol. 147, Article ID 105564, 2022.

[8] J. Gao, H. Hu, and H. He, "Household indebtedness and depressive symptoms among older adults in China: the moderating role of social network and anticipated support," *Journal of Affective Disorders*, vol. 298, pp. 173–181, 2022.

[9] J. Jabari Lotf, M. Abdollahi Azgomi, and M. R. Ebrahimi Dishabi, "An improved influence maximization method for social networks based on genetic algorithm," *Physica A: Statistical Mechanics and Its Applications*, vol. 586, Article ID 126480, 2022.

[10] J. Pulgar, "Classroom creativity and students' social networks: theoretical and practical implications," *Thinking Skills and Creativity*, vol. 42, Article ID 100942, 2021.

[11] C. K. Tanui, S. Karanth, P. M. K. Njage, J. Meng, and A. K. Pradhan, "Machine learning-based predictive modeling to identify genotypic traits associated with *Salmonella enterica* disease endpoints in isolates from ground chicken," *Lebensmittel-Wissenschaft & Technologie*, vol. 154, Article ID 112701, 2022.

[12] M. He, C. Li, Y. Kang, Y. Zuo, L. Duo, and W. Tang, "Clinical predictive model for the 1-year remission probability of IgA vasculitis nephritis," *International Immunopharmacology*, vol. 101, Article ID 108341, 2021.

[13] M. J. Wessel, P. Egger, and F. C. Hummel, "Predictive models for response to non-invasive brain stimulation in stroke: a critical review of opportunities and pitfalls," *Brain Stimulation*, vol. 14, no. 6, pp. 1456–1466, 2021.

[14] L. Wisnieski, D. E. Amrine, and D. G. Renter, "Predictive modeling of bovine respiratory disease outcomes in feedlot cattle: a narrative review," *Livestock Science*, vol. 251, Article ID 104666, 2021.

[15] J. Chu, Y. Wang, X. Liu, and Y. Liu, "Social network community analysis based large-scale group decision making approach with incomplete fuzzy preference relations," *Information Fusion*, vol. 60, pp. 98–120, 2020.

[16] Y. Muto, N. Awano, M. Inomata et al., "Predictive model for the development of critical coronavirus disease 2019 and its risk factors among patients in Japan," *Respiratory Investigation*, vol. 59, no. 6, pp. 804–809, 2021.

[17] H. Hesabi, M. Nourelfath, and A. Hajji, "A deep learning predictive model for selective maintenance optimization," *Reliability Engineering & System Safety*, vol. 219, Article ID 108191, 2022.

[18] R. S. Chavez, D. T. Tovar, M. S. Stendel, and T. D. Guthrie, "Generalizing effects of frontostriatal structural connectivity on self-esteem using predictive modeling," *Cortex*, vol. 146, pp. 66–73, 2022.

[19] R. Sandeepkumar, S. Rajendran, R. Mohan, and A. Pascoal, "A unified ship manoeuvring model with a nonlinear model predictive controller for path following in regular waves," *Ocean Engineering*, vol. 243, Article ID 110165, 2022.

[20] J. Casanelles-Abella, Y. Chauvier, F. Zellweger et al., "Applying predictive models to study the ecological properties of urban ecosystems: a case study in Zürich, Switzerland," *Landscape and Urban Planning*, vol. 214, Article ID 104137, 2021.

[21] X. Xu, Q. Zhang, and X. Chen, "Consensus-based non-cooperative behaviors management in large-group emergency decision-making considering experts' trust relations and preference risks," *Knowledge-Based Systems*, vol. 190, Article ID 105108, 2020.

[22] Y. J. Lee and E. M. Anderman, "Profiles of perfectionism and their relations to educational outcomes in college students: the moderating role of achievement goals," *Learning and Individual Differences*, vol. 77, Article ID 101813, 2020.

[23] D. Hadar-Shoval, M. Alon-Tirosh, and H. Morag, "Social relations between students from two groups in conflict: differences in stereotypes and perceived social distance between Jewish and Arab nursing students," *Nurse Education Today*, vol. 78, pp. 5–9, 2019.

[24] J. C. Rodil, A. Meca, K. K. Allison et al., "Measurement invariance testing for the United States identity scale (USIS) across non-hispanic black and white college students," *International Journal of Intercultural Relations*, vol. 86, pp. 134–144, 2022.

[25] J. Zhou, H. Scott, E. S. Huebner, and L. Tian, "Co-developmental trajectories of psychological need satisfactions at school: relations to mental health and academic functioning in Chinese elementary school students," *Learning and Instruction*, vol. 74, Article ID 101465, 2021.

[26] C. S. Song, C. Xu, E. A. Maloney et al., "Longitudinal relations between young students' feelings about mathematics and arithmetic performance," *Cognitive Development*, vol. 59, Article ID 101078, 2021.

[27] S. Du, Z. Chen, H. Wu, Y. Tang, and Y. Q. Li, "Image recommendation algorithm combined with deep neural network designed for social networks," *Complexity*, vol. 9, Article ID 5196190, 2021.

Hindawi
Scientific Programming
Volume 2023, Article ID 9831951, 1 page
https://doi.org/10.1155/2023/9831951

Retraction

Retracted: Intelligent Detection of Foreign Matter in Coal Mine Transportation Belt Based on Convolution Neural Network

Scientific Programming

Received 18 July 2023; Accepted 18 July 2023; Published 19 July 2023

This article has been retracted by Hindawi following an investigation undertaken by the publisher [1]. This investigation has uncovered evidence of one or more of the following indicators of systematic manipulation of the publication process:

(1) Discrepancies in scope
(2) Discrepancies in the description of the research reported
(3) Discrepancies between the availability of data and the research described
(4) Inappropriate citations
(5) Incoherent, meaningless and/or irrelevant content included in the article
(6) Peer-review manipulation

The presence of these indicators undermines our confidence in the integrity of the article's content and we cannot, therefore, vouch for its reliability. Please note that this notice is intended solely to alert readers that the content of this article is unreliable. We have not investigated whether authors were aware of or involved in the systematic manipulation of the publication process.

Wiley and Hindawi regrets that the usual quality checks did not identify these issues before publication and have since put additional measures in place to safeguard research integrity.

We wish to credit our own Research Integrity and Research Publishing teams and anonymous and named external researchers and research integrity experts for contributing to this investigation.

The corresponding author, as the representative of all authors, has been given the opportunity to register their agreement or disagreement to this retraction. We have kept a record of any response received.

References

[1] G. Ma, X. Wang, J. Liu et al., "Intelligent Detection of Foreign Matter in Coal Mine Transportation Belt Based on Convolution Neural Network," *Scientific Programming*, vol. 2022, Article ID 9740622, 10 pages, 2022.

Hindawi
Scientific Programming
Volume 2022, Article ID 9740622, 10 pages
https://doi.org/10.1155/2022/9740622

Research Article

Intelligent Detection of Foreign Matter in Coal Mine Transportation Belt Based on Convolution Neural Network

Guanchao Ma,[1] **Xisheng Wang**,[2] **Jianfeng Liu**,[1] **Weibiao Chen**,[1] **Qinghe Niu**,[1] **Yun Liu**,[2] **and Xiaocheng Gao**[1]

[1]*China Coal Shaanxi Yulin Daze Coal Industry Co., Ltd, Yulin City, Shaanxi 719000, China*
[2]*China Coal Information Technology (Beijing) Co., Ltd, Chaoyang District, Beijing 100120, China*

Correspondence should be addressed to Xisheng Wang; wangxis@chinacoal.com

Received 10 May 2022; Revised 3 June 2022; Accepted 6 June 2022; Published 5 July 2022

Academic Editor: Lianhui Li

This paper applies the CenterNet target detection algorithm to the foreign object detection of coal conveying belts in coal mines. Given the fast running speed of coal conveying belts and the influence of background and light sources on the objects to be inspected, an improved algorithm of CenterNet is proposed. First, the depth separable volume is introduced. The product replaces the standard convolution, which improves the detection efficiency. At the same time, the normalization method is optimized to reduce the consumption of computer memory. Finally, the weighted feature fusion method is added so that the features of each layer are fully utilized, and the detection accuracy is improved. The experimental results show that the improved algorithm has improved speed and accuracy compared with the original CenterNet algorithm. The foreign object detection algorithm proposed in this paper mainly detects coal gangue and can also detect iron tools such as bolts, drill bits, and channel steel. In the experimental environment, the average detection rate is about 20fps, which can meet the needs of real-time detection.

1. Introduction

As the main artery of coal mining and transportation, the working state of coal transportation belt directly affects the mining and transportation volume of coal. Foreign matters on the belt, such as large gangue and anchor bolt, are easy to cause problems such as scratch and tear of the belt and coal stacking and blocking at the coal chute during the high-speed operation of the belt. Therefore, the detection of large blocks, anchor bolts, and other foreign matters on the transportation belt can effectively ensure the safe production of the coal mine [1, 2].

Both target detection and image classification technology can realize the classification and recognition of belt foreign objects. However, target detection needs to locate the foreign object in the image before recognition, which increases the amount of calculation of the network to a certain extent, while image classification technology can directly identify the foreign object without locating the foreign object, and more computing resources can be used in fast foreign object recognition.

The complex environment of the mine makes the application of the existing image classification methods in the classification of foreign objects in coal conveying belt very challenging. Many scholars introduce machine vision technology into the image classification of foreign objects in the mine. Wang et al. [3] identified large foreign bodies of belt conveyor based on interframe difference method, threshold classification, and select-shape operator. He et al. [4] used the classification method of support vector machine to classify foreign objects in combination with the texture and gray features of foreign objects. Zhang [5] used multifeature fusion, combined with k-nearest neighbor algorithm and support vector machine for foreign object recognition. The above methods have achieved good results, but the image processing method combining feature extraction and classification algorithm has some problems, such as poor robustness and easy to be affected by illumination [6–9].

Convolution neural network uses convolution method for feature extraction, which has strong robustness and has

been widely used in many fields [10–13]. Some scholars also study the image classification network of mine foreign bodies. Pu et al. [14] established a foreign object recognition model based on vgg16 network and the idea of transfer learning, but the sample set was small, only 240 pieces. Su et al. [15] designed an improved LeNet-5 network and trained 20000 foreign object pictures in nonproduction environment, with a recognition rate of 95.88%. Ma [16], based on MobileNet network, optimized the network structure, improved the loss function, and further improved the recognition rate according to the characteristics of foreign object image. At this stage, the shortcomings of image classification of mine foreign bodies are as follows: (1). The sample collection is ideal without considering the actual working environment. (2). The network model has high complexity, large amount of parameters, low accuracy, and poor real-time performance.

Based on convolution neural network, in order to improve the adaptability of the algorithm for the detection of foreign matters in coal conveying belt under coal mine, this paper puts forward the corresponding improved method. In view of the low image quality caused by dark and uneven illumination in the underground, firstly, the dataset is preprocessed. Aiming at the problem of complex background of foreign object and large interference by coal block, the training data is correctly marked, the backbone network with good effect is adopted, and the weighted feature fusion of feature layers with different scales is introduced, which speeds up the convergence speed and reduces the amount of parameter calculation. Under the condition of ensuring the detection speed, the detection accuracy has been greatly improved.

2. Methods

2.1. Target Detection Algorithm. The CenterNet target detection method was proposed at the 2019 CVPR (Computer Vision and Pattern Recognition) conference [17–21]. The core idea of the algorithm is to regard the object to be detected as a point, that is, the center point of the target frame. Then, the center is found through the heat map and other attributes of the target object, such as the size information and pose information of the thing. The network structure of the CenterNet algorithm adopts ResNet-18, DLA-34, and Hourglass-104, three backbone networks for design and experiment. The three networks are complete encoding-decoding networks. The resolution of the final output feature map is subsampled 4 times compared to the original image, so that it can adapt to the detection of objects of various scales without multiscale design. The algorithm is based on anchor-free, so there is no need to set anchor boxes in advance, thereby avoiding the selection of related hyperparameters and eliminating the postprocessing process of NMS, which significantly reduces the computational load and training time of the network. The CenterNet object detection algorithm consists of three independent head structures: the center point prediction, the center point offset, and the target box's size, as shown in Figure 1.

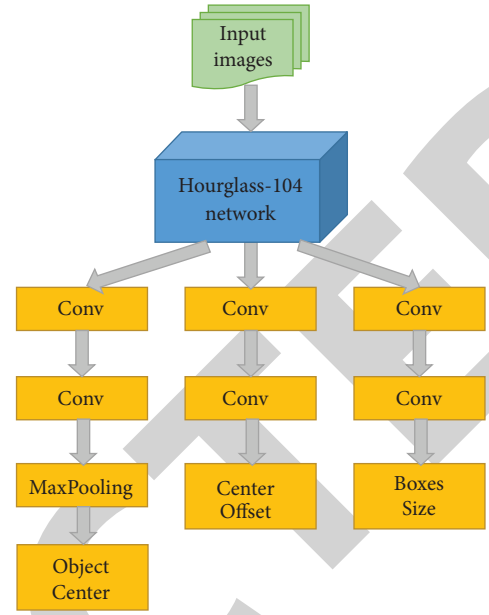

Figure 1: Algorithm structure.

Assuming that $I \in R^{W\times H\times 3}$ is the input image, where W and H represent the width and height of the image, respectively. After it is sent to the backbone network, a heat map containing the key will be generated.

$$Y \in [0,1]^{(W/R)\times(H/R)\times C}, \tag{1}$$

where R is the subsampled factor and C is the number of classes in the detection target.

If class c is detected at the position (x_i, y_i) of the heat map, $\hat{Y}_{x,y,c} = 1$; on the contrary, if there is no target object at the point, $\hat{Y}_{x,y,c} = 0$.

In the training phase, for an object, assuming that the coordinates of its real frame in the input image are $(x_1, y_1, x_2,$ and $y_2)$, the center point of the object can be expressed as $p = (x_1 + x_2)/2, (y_1 + y_2)/2$. After subsampled, the coordinates of the point are mapped to the heat map as $\tilde{p} = \lfloor p/R \rfloor$ and mapped it to the heat map $Y \in [0,1]^{W/R\times H/R\times C}$ through the Gaussian kernel transformation of the following formula:

$$y_{xyc} = \exp\left(-\frac{(x-\tilde{p}_x)^2 + (y-\tilde{p}_y)^2}{2\sigma_p^2}\right). \tag{2}$$

where σ_p is the standard deviation of the object size adaptation if the Gaussian kernels of two objects of the same category overlap, taking the one with the most value.

In the prediction stage, the most considerable eight-neighborhood value is first screened on the heat map, which is equivalent to performing an entire pooling operation with a kernel size of 3 on the heat map, and a total of 100 such values are selected. Assuming that P_c is the detected point, the coordinate of the i-th key point is (x_i, y_i) and using this point to regress, the calibration frame is

$$\left(x_i + \delta x_i - \frac{w_i}{2}, y_i + \delta y_i - \frac{h_i}{2}, x_i + \delta x_i + \frac{w_i}{2}, y_i + \delta y_i + \frac{h_i}{2}\right)s. \tag{3}$$

where $(\hat{x}_i, \hat{y}_i) = \hat{O}_{\hat{x}_i, \hat{y}_i}$ is the offset of the point in the heat map relative to the original image during the subsampled process and $(\hat{w}_i, \hat{h}_i) = \hat{S}_{\hat{x}_i, \hat{y}_i}$ is the length and width of the target corresponding to the current point measured.

$\hat{Y}_{x,y,c} = 0$ is used to represent the confidence of the point, that is, the probability of the existence of an object at the current center point. In this paper, the screening threshold is set to 0.3. For the 100 values selected above, it will be reserved as the final result if the predicted probability is greater than the threshold.

The Loss function of the CenterNet algorithm consists of three parts: the category loss function L_{cls}, the regression loss function L_{size}, and the bias loss function L_{off}, which are linear combinations of the three.

$$L_{\text{det}} = L_{\text{cls}} + \lambda_{\text{reg}} L_{\text{reg}} + \lambda_{\text{off}} L_{\text{off}}. \tag{4}$$

The category loss function is the Focal Loss function.

$$L_{cls} = -\frac{1}{N} \begin{cases} \left(1 - \hat{Y}_{xyc}\right)\log\left(\hat{Y}_{xyc}\right) Y_{xyc} = 1, \\ \left(1 - Y_{xyc}\right)^{\beta}\left(\hat{Y}_{xyc}\right)^{\alpha}\log\left(1 - \hat{Y}_{xyc}\right) \text{other}. \end{cases} \tag{5}$$

The target center bias loss function is

$$L_{\text{off}} = \frac{1}{N}\sum_{p}\left|\hat{O}_{\tilde{p}} - \left(\frac{p}{R} - \tilde{p}\right)\right|. \tag{6}$$

The regression loss function is

$$L_{\text{reg}} = \frac{1}{N}\sum_{k=1}^{N}\left|S_{p_k} - s_k\right|. \tag{7}$$

The relevant hyperparameters are chosen as $\lambda_{\text{reg}} = 0.1$, $\lambda_{\text{off}} = 0.1$, $\alpha = 2$, and $\beta = 4$.

2.2. Hourglass Network Improvements. In this paper, the Hourglass-104 network [22] is selected as the backbone network of the CenterNet algorithm to extract features and generate heat maps. The network consists of two Hourglass modules stacked, as shown in Figure 2.

For the first-order module shown in Figure 3, the network adopts a fully convolutional neural network structure in the form of encoding-decoding. The repeated use of bottom-up and top-down supervision mechanisms combined with intermediate results has achieved good results in keypoint detection.

The most basic network unit in the Hourglass-104 network is the residual module, as shown in Figure 4. Almost all the network computation is consumed in the convolution operation of the residual module. For the detection task in this paper, since the datasets are directly derived from video surveillance, the image resolution is vast, the training time is also very long, and the consumption of computer hardware facilities is also relatively high.

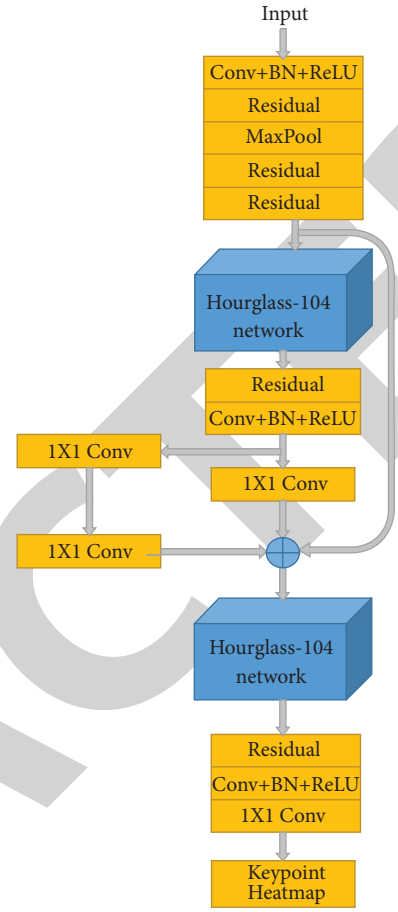

Figure 2: The structure of Hourglass-104 network.

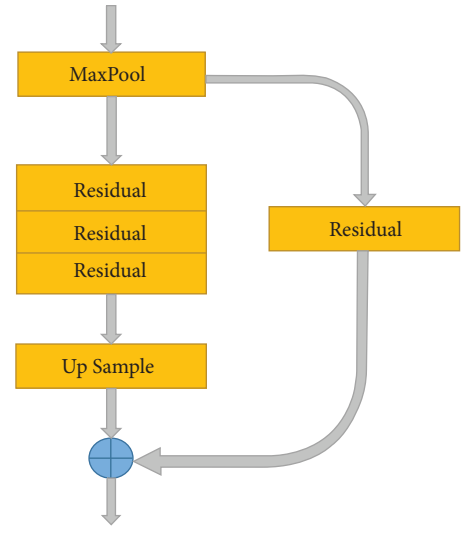

Figure 3: The first-order module.

To solve this problem, depthwise separable convolution (DSC) module is introduced. The DSC module is a lightweight network. In the processing process, the depthwise convolution of spatial relationship mapping is performed first, and then the point-by-point convolution of channel relationship mapping is performed. In the process of network

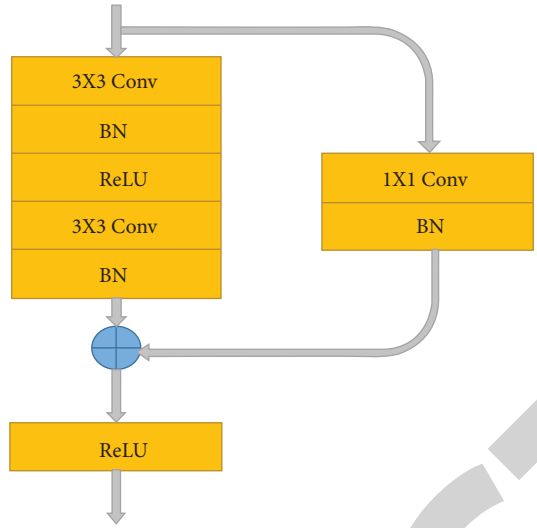

Figure 4: The residual module in the Hourglass-104 network.

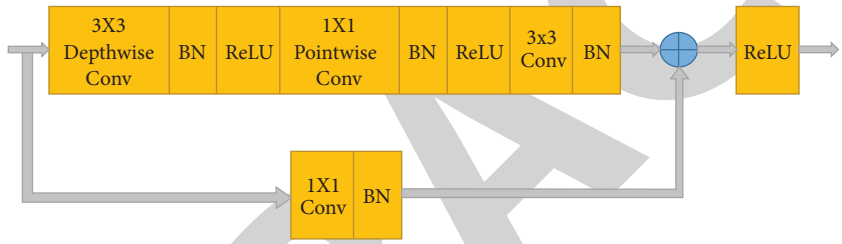

Figure 5: The residual module after introducing DSC.

training and detection, the calculation of parameters can be significantly reduced, which dramatically improves the network's work efficiency. The structure diagram of the residual module after introducing DSC is shown in Figure 5.

Assume that the input is (B, C, W, H) data, where B, C, W, and H are the size of the feature image batch size, the number of channels, width, and height, respectively. The convolution operation of $3 \times 3$is performed, and the calculation of standard convolution is as follows:

$$stc = B \times C \times W \times H \times 3 \times 3. \tag{8}$$

Depthwise separable convolution for calculation is used first, and then the depthwise convolution operation is performed, the calculation of the amount is as follows:

$$dw = C \times H \times W \times 3 \times 3. \tag{9}$$

Then, the pointwise convolution operation is performed, and the calculation of the amount is as follows:

$$pw = B \times C \times W \times H. \tag{10}$$

The total computational cost of depthwise separable convolution is the sum of the two.

$$dsc = dw + pw = (B + 3 \times 3) \times C \times W \times H. \tag{11}$$

The computational cost ratio of the standard convolution operation and the depthwise separable convolution operation is as follows:

$$\frac{ds\ c}{stc} = \frac{(B + 3 \times 3) \times C \times W \times H}{B \times C \times W \times H \times 3 \times 3} = \frac{1}{B} + \frac{1}{3 \times 3}. \tag{12}$$

When a lot of data are processed, the difference between the two calculation methods is more prominent.

2.3. Group Normalization Method. The calculation result of the BN layer depends on the data of the current batch. When the batch size is small, the mean and variance of the batch data are less representative, so the final result is also greatly affected. As shown in Figure 4, as the batch size becomes smaller and smaller, the reliability of the statistical information calculated by the BN layer becomes worse and worse, which will quickly lead to an increase in the final error rate. However, when the batch size is more significant, there is no noticeable difference. In target detection, segmentation, and video-related algorithms, the batch size is generally set relatively small due to large input images, diverse dimensions, and computer performance reasons. To weaken the influence of small-batch training on the detection results and make the CenterNet algorithm more flexibly applied to different hardware configuration environments, this paper improves the BN (batching normalization) in the backbone network to GN (grouping normalization).

Unlike BN, which normalizes channel by channel, GN groups channels and normalizes them in groups. First, the C channels are divided into G groups, and S_k=$\{c|[(c/G) = k]$, $c = 0, 1, \ldots, C\}$ is the channel number set composed of the

channel numbers that fall into the k-th channel group, where $k \in \{0, 1, \ldots, G-1\}$, let the i-th feature of the j-th sample of the current mini-batch sample set in the c-th channel be $x_i^{(j,c)}$, the result after normalization is $y_i^{(j,c)}$, and the corresponding calculation formula is as follows:

$$x_i^{(j,c)} = \frac{1}{\sigma_i^{(k)}}\left(x_i^{(j,c)} - \mu_i^{(k)}\right) \text{ and} \tag{13}$$

$$y_i^{(j,c)} = a\widehat{x}_i^{(j,c)} + b, \tag{14}$$

where sum is the mean and standard deviation of the i-th feature of each feature map of the k-th channel, respectively,

$$\mu_i^{(k)} = \frac{1}{m \cdot |S_k|} \sum_{j=1}^{m} \sum_{c \in S_k} x_i^{(j,c)} \text{ and} \tag{15}$$

$$\sigma_i^{(k)} = \sqrt{\frac{1}{m \cdot |S_k|} \sum_{j=1}^{m} \sum_{c \in S_k} \left(x_i^{(j,c)} - \mu_i^{(k)}\right)^2 + \varepsilon}. \tag{16}$$

The group-based normalization groups the feature map channels, making each channel's mean and standard deviation more stable, effectively weakening the influence of the number of samples in the small-batch sample set on the feature normalization, and at the same time, the learning efficiency of the model based on the gradient descent method under low memory capacity is improved.

2.4. Weighted Feature Map Fusion. In the CenterNet network structure, the input image is input into the Hourglass-104 network after being subsampled 4 times. After 8 times, 16 times, 32 times, 64 times, and 128 times of subsampled in turn, and then 2 times of upsampling in turn, only one feature map is output. The output feature map size is subsampled 4 times from the input image. It can be seen that only using the most extensive feature map for target detection will inevitably lose some features of the image.

To make full use of the feature map generated after the convolution operation, improve the detection ability of small-sized targets, and reduce the algorithm's complexity. In this paper, the input image is subsampled 2 times, and then sent to Hourglass, and then subsampled2 times, 4 times, 8 times, and 16 times in a turn, and output four feature maps, namely, P_1, P_2, P_3, and P_4, each feature's layer resolution is $(1/2^{i+1})$ times the input image, and multiple output feature maps are fused. Since each feature map contributes differently to the final fusion output, feature fusion cannot be performed directly. This paper uses a weighted method to fuse the features of each feature map; that is, when the feature map is fused, a learnable weight is assigned to each input feature map. During training, the network can learn to change the fusion weight of each feature map to change the importance of each feature map to the final detection result. To reduce the number of parameters and computation, the improved model directly uses short-circuit connections in the bypass convolution and instantly removes the convolution operation. The schematic diagram of feature fusion is shown in Figure 6. The feature maps from high-level to low-level are obtained after upsampling, and then added, and the final output has only one fused feature map p_{out}.

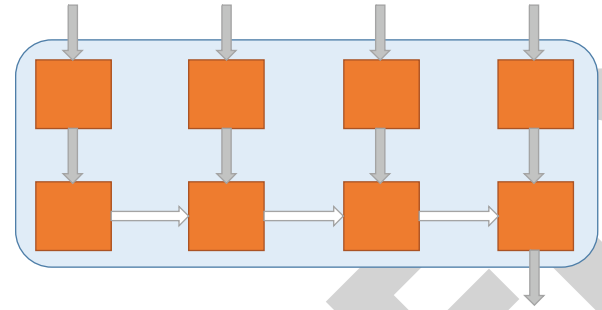

Figure 6: Feature fusion.

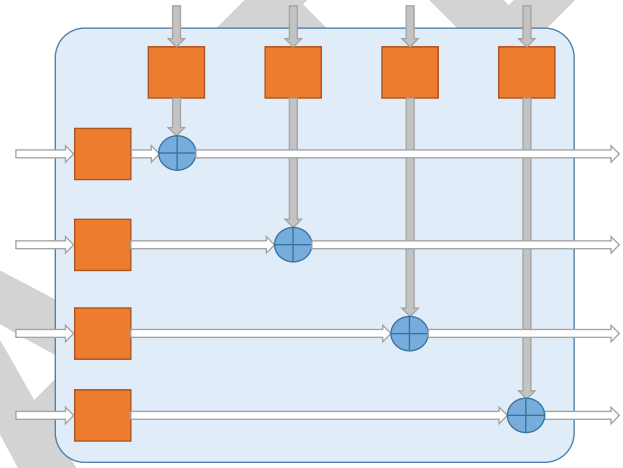

Figure 7: Weight fusion.

The calculation formula of feature fusion is

$$O = \sum_i \frac{\omega_i}{\varepsilon + \sum_j \omega_j} \cdot I_i, \tag{17}$$

where I_i is the input feature map, the fused feature map, and ω_i, $\omega_i \in [0, 1]$ is the corresponding weight. A minimum value $\varepsilon = 1e-4$ is set to avoid the situation where the denominator in the above formula is 0.

The fast normalized fusion method is also used for weight fusion of the feature maps output by the two Hourglasses, and the calculation formula is

$$P_{\text{out}} = \frac{\sum \omega_{ij} \cdot P_{ij}}{\sum \omega_{ij} + \varepsilon}. \tag{18}$$

The schematic diagram of weight fusion is shown in Figure 7.

The final improved CenterNet (Improve-CN) algorithm network structure is shown in Figure 8.

3. Experiments and Analysis

3.1. Data Preprocessing and Labeling. The dataset images in this paper include two types of gangue and iron. The gangue is mainly coal road gangue and washing gangue, and the iron

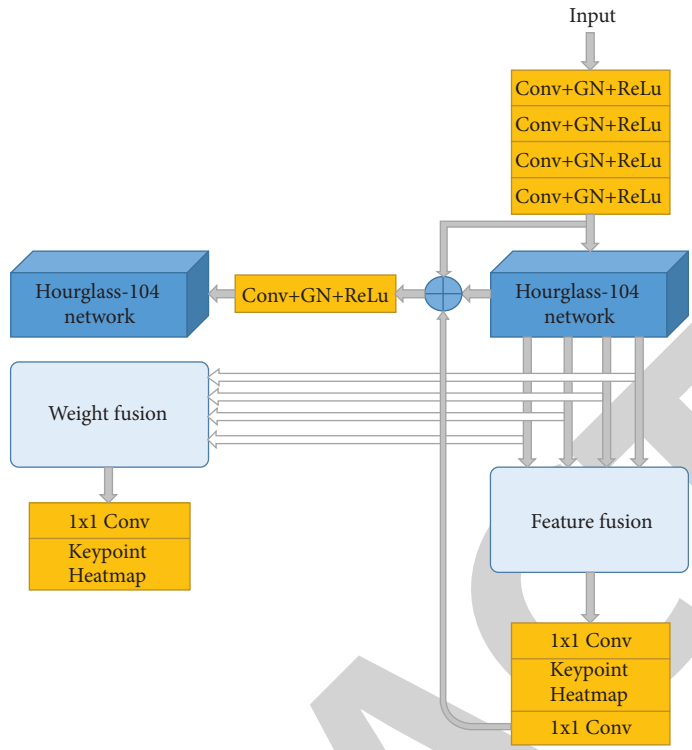

Figure 8: Improved CenterNet (Improve-CN) algorithm network structure.

includes bolts, drills, steel bars, and channel steel. The data is obtained through industrial infrared surveillance cameras. The foreign bodies obtained with this mounting type have the largest geometry. Detecting the foreign object early in entering the belt, effectively reducing the missed detection rate. There is no additional light source in the experiment, only the underground lighting source, and the possible miner's head-mounted lamp.

Due to low brightness in the coal mine and the uneven illumination caused by the irritating light source, the image quality obtained is poor. It is necessary to preprocess the directly acquired coal mine images to solve this problem. There is a lot of underground impulse noise in coal mines, so median filtering is performed first to eliminate the influence of noise and slight jitter. Although the effect of noise is eliminated, the contrast of the denoised image is still not high, and it is not easy to distinguish the foreground and background accurately. Therefore, the image continues to be enhanced. The method used is adaptive histogram equalization (AHE). AHE achieves the purpose of adjusting the image contrast by calculating the local histogram of the image and redistributing the brightness. The AHE algorithm improves the local contrast of the original image, makes the dark image brighter, suppresses the overbright area, and obtains more detailed information, which enhances the quality of the image.

Figure 9 compares the original image and the image after median filtering and adaptive histogram equalization.

The dataset in this paper is mainly composed of two classes, namely, "gangue" and "iron" (including channel steel, anchor rod, drill bit, and I-beam), which are marked with label software. After an image is observed, a file with the suffix "json" will be generated in the directory, which contains the name and ID of the marked image, the category label of the significant object, and the coordinates of the object frame. The coordinates are marked as the coordinates of the upper left corner and the lower right corner of the box. A total of 5,605 images of two types were collected in the dataset of this paper. Since the foreign objects in the coal conveyor belt are mainly gangue, the majority of gangue images are 3,421, and there are a total of 2,184 iron images. The pictures are divided in the dataset, 70% of which are used as the train set, 20% are used as a validation set, and the remaining 10% are used as the test set. The distribution of the datasets is shown in Table 1.

3.2. Network Training. Since the collected dataset pictures are few and cannot meet the training requirements of deep learning, the dataset needs to be augmented. In this paper, the dataset is augmented by random cropping, flipping, rotation, translation, and scaling. There are five types of scaling factors in augmentation (0.5,0.8,1,1.2, and1.5). During training, Batch size is set to 8, an epoch is 140, and the initial learning rate is 5×10^{-5}. At 90 rounds and 120 rounds, respectively, it is attenuated 10 times, and SGD is used for network optimization. The weight decay rate and momentum factor are designed to be 10^{-4} and 0.9, respectively, and the input image is uniformly scaled to 512×512 sizes. The experiments are all completed on Ubuntu18.04, Nvidia GTX1060 graphics card, E5-2650 v2 CPU, CUDA10.1, cudnn7.6.5, Pytorch1.2.0, and the

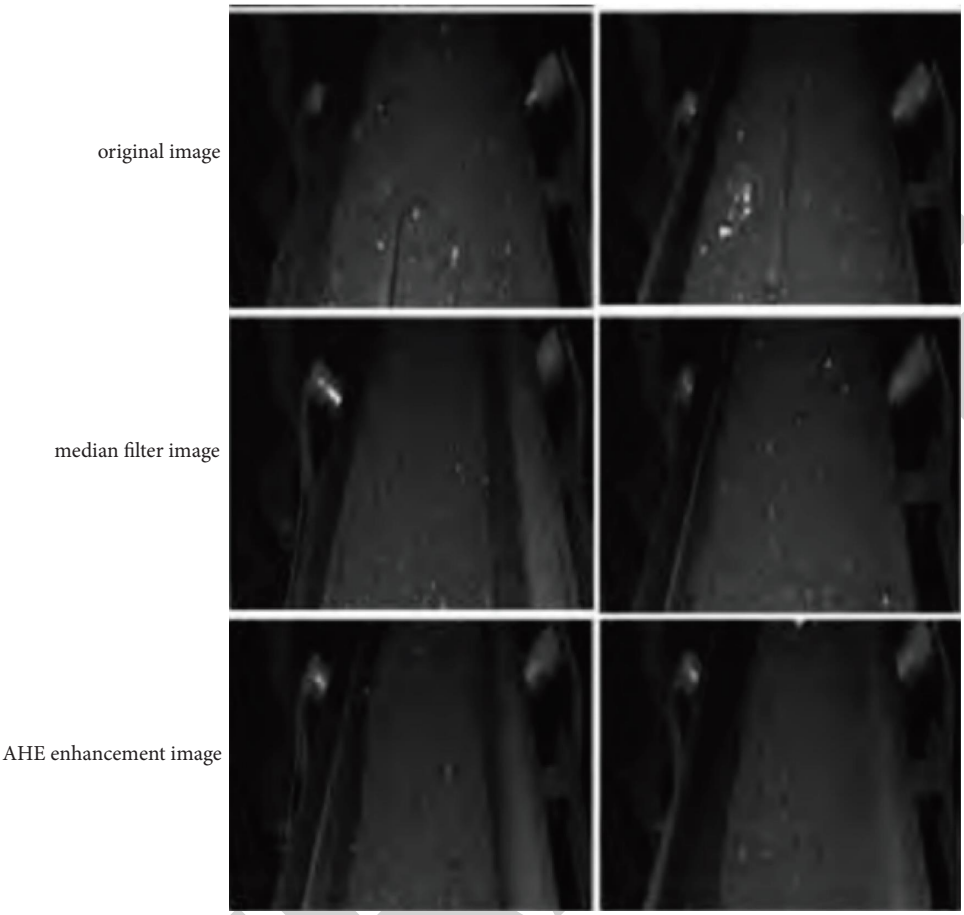

Figure 9: Comparison of the three images.

Table 1: Foreign object dataset in the coal belt.

Datasets	Gangue/piece	Iron/piece
Train set	2388	1545
Validation set	676	423
Test set	355	223

hyperparameters selection of each algorithm is completely consistent.

3.3. Experimental Results and Analysis. After about 100 rounds of training, the network converges. The loss function comparison between the improved algorithm and the original standard CenterNet algorithm is shown in Figures 10–13. The four figures are in order of total loss function curve, center point prediction loss function curve, target box regression loss function curve, and center point bias loss function curve. The abscissa is the number of training rounds, and the ordinate is loss change value. The blue line in the comparison image is the loss curve of the standard CenterNet algorithm and the orange line is the loss curve of the improved algorithm. It can be seen that the loss of the enhanced algorithm is reduced by about 0.3 compared with the original algorithm, and the original algorithm converges in about 120 rounds, that is, the improved algorithm speeds up the convergence speed. It can be seen from the loss function comparison curve that the improved algorithm has a smaller loss value than the original algorithm.

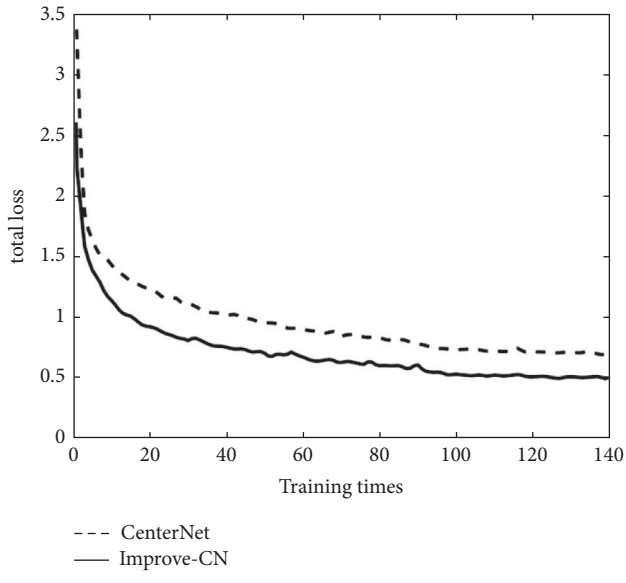

Figure 10: Total loss function curve.

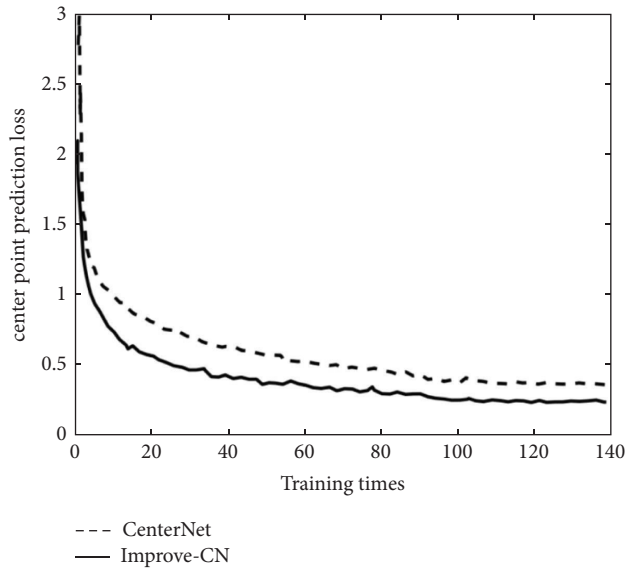

Figure 11: Center point prediction loss function curve.

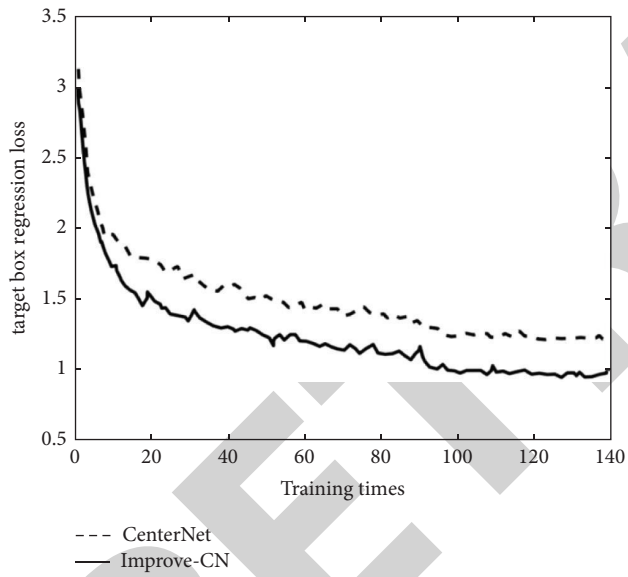

Figure 12: Target box regression loss function curve.

The quantitative comparison results of the two algorithms on the test set at 140 rounds are shown in Table 2. The main test indicators are average precision (AP) and average recall (AR), AP reflects the algorithm's accuracy and AR reflects the false detection level of the algorithm. The larger these two indicators are, the better the algorithm's performance is. AP_{50} and AP_{75} in Table 2 are the average accuracy rates when they are IOU ≥ 0.5 and IOU ≥ 0.75, respectively. AP_S, AP_M, and AP_L are the average accuracy indicators for small targets, medium targets, and large targets, respectively, and the AR indicators are marked in the same way.

It can be seen from Table 2 that the improved algorithm has a significant improvement in accuracy compared to the original algorithm, and the improved algorithm has

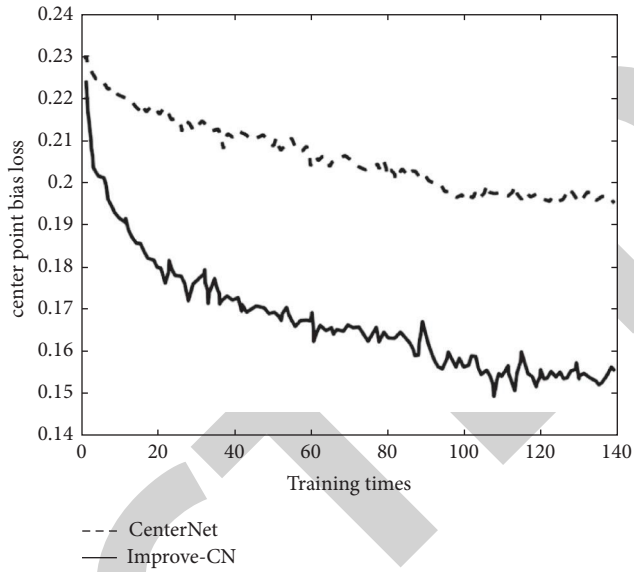

Figure 13: Center point bias loss function curve.

improved target accuracy and recalls for various scales, which is related to feature weighted fusion. By fusing the features at multiple scales, on the one hand, the rich semantic information of the high level can be fully utilized. On the other hand, the spatial location information of the low level can be obtained, which significantly improves the accuracy of the target detection.

Four test images are randomly selected from the test set and tested with the algorithm designed in this paper. The detection results are shown in Figure 14. It can be seen that the proposed algorithm can accurately detect targets of various scales, and the improved algorithm can also accurately detect slender "iron objects," especially those close to the edge of the conveyor belt and along with the movement direction distribution target.

Table 3 compares the detection results of different target detection algorithms in the test set after training under the same dataset. It can be seen that nearly 130 ms reduces the average detection time of the improved algorithm compared with the original algorithm, and the overall accuracy rate is improved by 6.9% or so. Compared with the two-stage faster R-CNN algorithm [23–26], the algorithm before and after the improvement significantly shortens the detection time, but the accuracy rate decreases because the improved algorithm only needs to predict the target's center point compared to the anchor frame. The computational complexity is significantly reduced, so the speed is improved. Still, many anchor boxes provide a greater possibility of correctly detecting the target, so the accuracy rate is higher, and the application can be used to monitor the same transmission belt through multiple cameras to offset this shortcoming. Compared with the one-stage detection algorithm YOLOv3, the detection speed and accuracy of the improved algorithm have been improved. The results show that the enhanced algorithm achieves a good balance between detection speed and accuracy.

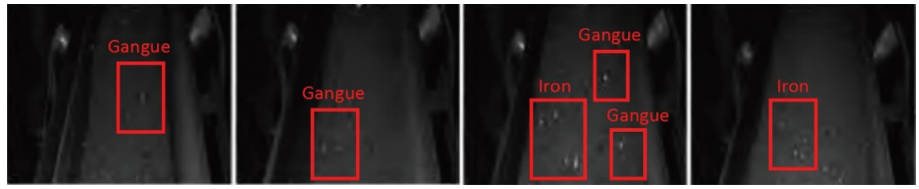

Figure 14: The foreign objects detection result with the proposed algorithm.

Table 2: Comparison between CenterNet and Improve-CN.

Evaluation indicators		CenterNet	Improve-CN
Average precision (AP)	AP_{50}	0.4822	0.5522
	AP_{75}	0.2669	0.3080
	AP_s	0.1056	0.1834
	AP_M	0.2778	0.3422
	AP_L	0.4531	0.4734
Average recall (AR)	AR_{50}	0.3888	0.5025
	AR_{75}	0.2522	0.3138
	AR_s	0.1835	0.3221
	AR_M	0.4341	0.5551
	AR_L	0.5012	0.5982

Table 3: The comparison among other objects detection algorithm.

Algorithm	Average detection Time/s	MAP
Faster R-CNN	4.1671	0.5877
YOLOv3	0.0943	0.4344
CenterNet	0.0626	0.4828
Improve-CN	0.0508	0.5521

4. Conclusion

As fixed-point monitoring by network cameras is gradually replacing manual inspection and becoming an essential underground monitoring method for coal mining enterprises, the proposed foreign object detection method can be directly deployed on this basis. As long as the host computer that meets the hardware requirements is configured, the noncoal foreign matter can be detected at the early stage when it enters the coal conveying belt, and an alarm response can be made. In the later stage, the robot can automatically sort the detected foreign objects to realize the integration of foreign object detection and grasping, which can improve work efficiency while protecting personal safety and further reducing potential safety hazards.

Data Availability

The dataset can be accessed upon request.

Conflicts of Interest

The authors declare that they have no conflicts of interest.

References

[1] J. Kan, P. Wang, and P. Wang, "Influencing factors of disturbance effects of blasting and driving of deep mine roadway groups," *Shock and Vibration*, vol. 2021, Article ID 8873826, 13 pages, 2021.

[2] K. Zheng, C. Du, J. Li, and B. Qiu, "Coal and gangue underground pneumatic separation effect evaluation influenced by different airflow directions," *Advances in Materials Science and Engineering*, vol. 2016, Article ID 6465983, 13 pages, 2016.

[3] Y. Wang, X. Guo, X. Liu, and Z. Zhao, "Design of visual detection system for large foreign body in belt conveyor," *Mechanical Science and Technology for Aerospace Engineering*, vol. 12, pp. 1–7, 2020.

[4] M. He, P. Wang, and H. Jiang, "Recognition of coal and stone based on SVM and texture," *Computer Engineering and Design*, vol. 33, no. 03, pp. 1117–1121, 2012.

[5] Y. Zhang, *Research on Gangue Identification Based on Video Processing*, pp. 1–99, China University of Mining and Technology, Xuzhou, 2018.

[6] F. Cen, X. Zhao, W. Li, and G. Wang, "Deep feature augmentation for occluded image classification," *Pattern Recognition*, vol. 111, Article ID 107737, 2021.

[7] G. Zhang, J. Yang, Y. Zheng, Z. Luo, and J. Zhang, "Optimal discriminative feature and dictionary learning for image set classification," *Information Sciences*, vol. 547, pp. 498–513, 2021.

[8] J. Fang, H. Liu, L. Zhang, J. Liu, and H. Liu, "Region-edge-based active contours driven by hybrid and local fuzzy region-based energy for image segmentation," *Information Sciences*, vol. 546, pp. 397–419, 2021.

[9] W. Wang, H. Zhang, Z. Zhang, L. Liu, and L. Shao, "Sparse graph based self-supervised hashing for scalable image retrieval," *Information Sciences*, vol. 547, pp. 622–640, 2021.

[10] D. Qiu, L. Zheng, J. Zhu, and D. Huang, "Multiple improved residual networks for medical image super-resolution," *Future Generation Computer Systems*, vol. 116, pp. 200–208, 2021.

[11] Z. Zhang, M. Huang, L. Shang, B. Xiao, and T. S. Durrani, "Fuzzy multilayer clustering and fuzzy label regularization for unsupervised person reidentification," *IEEE Transactions on Fuzzy Systems*, vol. 28, no. 07, pp. 1356–1368, 2020.

[12] D. Fernandes, A. Silva, R. Névoa et al., "Point-cloud based 3D object detection and classification methods for self-driving applications: a survey and taxonomy," *Information Fusion*, vol. 68, pp. 161–191, 2021.

[13] D. Cheng, L. Chen, Y. Cai, and L. Gao, "Image super-resolution reconstruction based on multi-dictionary and edge fusion," *Journal of China Coal Society*, vol. 43, no. 07, pp. 2084–2090, 2018.

[14] Y. Pu, D. B. Apel, A. Szmigiel, and J. Chen, "Image recognition of coal and coal gangue using a convolutional neural network and transfer learning," *Energies*, vol. 12, no. 9, pp. 1735–1746, 2019.

[15] L. Su, X. Cao, H. Ma, and Y. Li, "Research on Coal Gangue Identification by Using Convolutional Neural network," in *Proceedings of the 2018 2nd IEEE Advanced Information Management,Communicates, Electronic and Automation*

Hindawi
Scientific Programming
Volume 2022, Article ID 9260992, 12 pages
https://doi.org/10.1155/2022/9260992

Research Article

Research on Fault Diagnosis Technology of Industrial Robot Operation Based on Deep Belief Network

Yang Shuai

Jiangsu Vocational College of Electronics and Information, Huaian, Jiangsu 223003, China

Correspondence should be addressed to Yang Shuai; 044214@jsei.edu.cn

Received 14 April 2022; Revised 19 May 2022; Accepted 3 June 2022; Published 5 July 2022

Academic Editor: Lianhui Li

Fault diagnosis technology is the science of identifying the operating state of a machine or unit, and it studies the response of the change in the operating state of the machine or unit in the diagnostic information. It can give an early warning to the failure state of the machine and stop the machine before a major failure occurs so as to protect the life safety of the on-site staff and avoid huge economic losses to the enterprise. For mechanical equipment, fault diagnosis consists of three main links: fault detection; fault identification; and fault classification. Aiming at the problems that need to be solved in the fault diagnosis of industrial robots, this paper adopts a data-driven intelligent diagnosis method to establish a fault diagnosis model of industrial robots based on Deep Belief Network (DBN) and DSmT theory. Firstly, based on wavelet transform and information energy entropy correlation theory, the vibration signal of industrial robot is extracted, and the energy entropy normalized eigenvector is established. Then, the energy entropy normalized feature vector is divided into training set and test set to complete the creation of DBN network model. Finally, using DSmT theory to carry out decision-making fusion, a fault diagnosis model for industrial robots is established, and experiments are carried out on the K-R-R540 robot to verify the applicability of the established fault diagnosis model. It is proved by experiments that the industrial robot fault diagnosis model based on the deep belief network can meet the requirements of the recognition accuracy of robot faults, and the model will perform poorly when the faults coexist with multiple faults.

1. Introduction

The efficient production of industrial robots is the key to ensure the whole product production system of the enterprise. Therefore, enterprises and researchers pay attention to keeping industrial robots in an efficient working state. For enterprises, once the system of industrial robots breaks down, it will lead to the stagnation of the whole production line. If the faulty robot cannot be repaired in time, the robot fault may evolve into a huge production accident, and even threaten the life safety of enterprise staff. After the industrial robot is put into use, its application is under the artificial inspection and maintenance mechanism under strict regulations. The enterprise needs to invest a lot of human resources to complete the daily, weekly, and monthly inspection and maintenance of the industrial robot, and according to the inspection and maintenance record, the itinerary of the final equipment working state, and take this as the basis to form the equipment maintenance manual of the industrial robot and summarize the equipment parameters of the industrial robot in the fault state. After data analysis, the failure frequency of each equipment, as well as the failure law and failure cause, is obtained so as to accumulate practical experience for dealing with the failure in the future. This traditional industrial robot fault diagnosis has obvious disadvantages. It needs to consume a lot of human and material resources to complete, which is unbearable for ordinary small enterprises. Because they do not have a professional enterprise maintenance team to ensure production safety, they are finally banned in the fierce market competition. Moreover, with the continuous progress of production and the uncertainty and randomness of industrial robot fault itself, it is still unable to achieve timely early warning and fault isolation for unexplained faults, which is difficult to meet the efficient and safe requirements of industrial production.

Fault diagnosis is to identify and judge the early fault characteristics of the equipment through various monitoring methods based on the operation status of the equipment so as to formulate relevant maintenance plans. Based on the above research background, this paper will take industrial robot as the research object, based on signal processing knowledge and deep learning theory, and with the help of industrial robot fault simulation platform, study the application of deep confidence network in industrial robot fault diagnosis. From the perspective of practical considerations, when the industrial robot has faults or potential faults, the research in this paper can accurately identify the fault type and judge the fault degree, provide the basis for subsequent maintenance decisions, greatly reduce the downtime, and reduce the direct and indirect economic losses. From the perspective of theoretical research, it can enrich the content of industrial robot fault diagnosis methods and provide a certain theoretical reference and basis for the development of related research work [1–10].

2. Related Work

The widespread use of industrial robots requires researchers to monitor and evaluate their working status in real time. In order to achieve this goal, domestic and foreign scholars and experts have done a lot of research. Freeman et al. proposed that, by analyzing the robustness of the fault cause, the corresponding filter can be designed to eliminate strong interference, and the fault diagnosis of the underwater robot can be realized by calculating the residual error of the model. Saleh Ahmad et al. established a fault diagnosis system based on a reconfigurable robot model by applying additional force and torque sensors at the joints of the robot. This method requires additional sensors to be added to the structure of the robot, resulting in the failure of the robot hardware. *Additional Charges*. Hashimoto et al. established a fault diagnosis model based on Bayesian time series by analyzing the failure causes of the robot under working conditions, which can quickly identify the occurrence of robot faults and isolate them. This method requires a large number of system parameters of robot faults as prior conditions to guarantee the accuracy of the model. Verma et al. established a robot fault diagnosis method based on discrete-time observer by designing an observer method and completed the fault diagnosis of robot joints through the cooperation of detection and diagnosis observers. This method requires a large amount of joint sensor information. Jaber et al. analyzed the fault signals of the robot under various working conditions by collecting the vibration signal of the working state of the robot, using wavelet transform, time-frequency domain analysis, and other methods to realize the fault diagnosis of the robot. Ferreira et al. used the synovial observer to establish a robot fault diagnosis model and applied it to the fault diagnosis of the COMAU robot. The experiment proved that this method can achieve accurate diagnosis for a single fault, but it does not perform well in the diagnosis of robot fault states with multiple faults coexisting. The safe operation of industrial robots requires maintenance personnel to complete the processing of the faults that have occurred or will occur in time. The traditional fault diagnosis methods have been unable to adapt to the current production mode of enterprises. The establishment of a fault diagnosis model suitable for industrial robots is to solve this problem. Due to the complex structure of industrial robots, concurrent failures often occur. It is precisely because of the existence of this problem that a fault diagnosis method for industrial robots based on analytical thinking logic has been proposed. By using the idea of deep learning, it is possible to explore and identify the intrinsic relationship between various types of faults in industrial robots. So that when the robot fails, it can easily solve the failure problem in the operation of the industrial robot [11–15].

3. Related Theoretical Methods

3.1. Failure Analysis of Industrial Robots. The failure forms of industrial robots usually manifest as control system failures and drive system failures. Therefore, industrial robot failures can be divided into two categories: logical failures and physical failures. Logical faults are mainly caused by the failure of the industrial robot control system, and the robot cannot complete tasks according to the instructions, which is mainly manifested in the decline of performance indicators; physical faults are mainly due to the robot shutdown caused by the hardware failure of the industrial robot, including circuit aging or damage, motor failure, bearing wear, and reducer failure. Table 1 shows several common failure forms, failure characterizations, and failure causes of industrial robots. It can be seen from Table 1 that there is not a simple one-to-one correspondence between the failure forms of industrial robots, the failure representations, and the failure causes. Some more complex failure forms and failure representations correspond to multiple failure causes, and some failure causes will also occur. There are many different forms of failure characterization. Since the failure of industrial robots will be accompanied by changes in vibration signals, and it is precisely because of this unique feature, the easiest way to evaluate the current working state of industrial robots is to judge the vibration signals of industrial robots. According to the basis, as well as having good applicability, using vibration signal as the fault of industrial robot is also used as a main research method to study the fault of industrial robot [16].

3.2. Deep Belief Networks

3.2.1. Restricted Boltzmann Machines. Ordinary Boltzmann Machine (BM) is the predecessor of RBM. Each BM structure consists of two layers of networks, which are defined as the visible layer v and the hidden layer h, respectively. Figure 1 shows the BM structure. It can be found that the network structure of BM is fully connected by random neurons, so it has a strong ability to learn specific rules from complex data in an unsupervised form, but at the same time its disadvantages are also obvious. The fully connected structure makes the network. The training time is long, and the computational cost is high. The emergence of

Table 1: Several common failure forms, failure characterizations, and failure causes of industrial robots.

Failure form	Fault characterization	Cause of issue
Power system failure	The robot cannot be powered on	Power circuit failure
	Robot cannot move	Power chip failure
	The host computer restarts	Short circuited
Control system failure	Controller cannot be powered	Damaged control chip
	The control port is unstable	Control chip soldering
		Controller failure
	Robot out of control	Control program run away
		Damaged control chip
	Motor failure	Motor stuck
		Driver chip failure
		Motor overcurrent protection
Drive joint failure	Bearing failure	Bearing wear
		Bearing fracture
	Reducer failure	Damaged reducer
		Coupling loose

RBM is to improve the defects of BM network structure; it is a new unsupervised learning network structure model based on greedy learning. Except for the undirected nature of the interlayer connection, there is no difference from the general BM principle in terms of network definition of each layer, neuron output and representation, and neuron state value rules. Figure 2 shows the RBM structure organization. The energy model of RBM can be intuitively understood as follows: a small ball with a rough surface and an irregular shape is placed anywhere in a large bowl with a very rough surface. Affected by gravitational potential energy, generally speaking, when the state is stable, the probability of the ball staying at the bottom of the bowl is the greatest, and of course there is a certain possibility that it will stay at other positions in the bowl. In the theory of the energy model, the final stable stop position of the ball is defined as a state, each state corresponds to an energy, and this energy can be represented by an energy function. So, in a sense, the probability that the ball is in a certain state can be expressed by the energy of the ball in the current state [17].

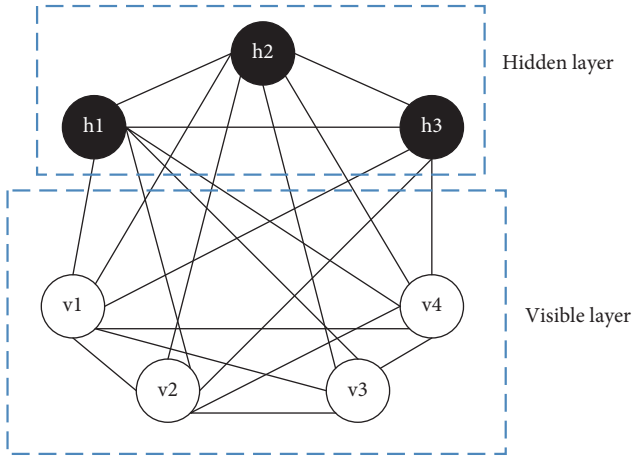

Figure 1: Schematic diagram of BM structure.

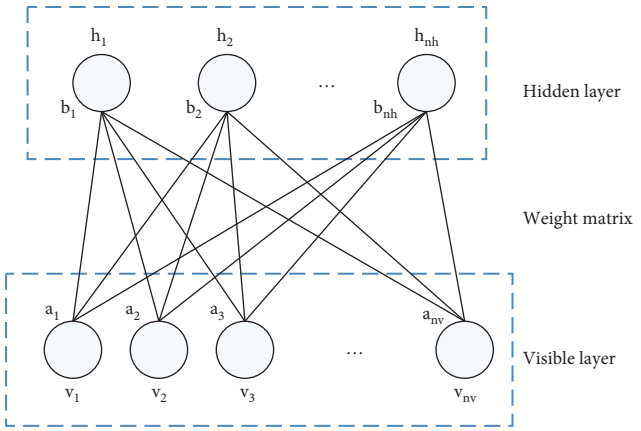

Figure 2: Basic structure of RBM.

3.2.2. Basic Structure of Deep Belief Network. RBM is an important foundation of DBN. From the macroscopic point of view, the network structure of DBN is mainly composed of several RBM stacks and a labeled classifier, as shown in Figure 3. As can be seen from Figure 3, this deep DBN network has four layers of hidden units, the input of the network is the sample data that meets the requirements, and the top is the label information corresponding to the input data. First, the prepared input sample data is assigned to each neuron in the visual layer of the first layer one by one, after a series of iterative training and learning (i.e., forward greedy learning and backward fine-tuning; the specific process will be introduced later), the weight matrix between each layer and the bias value of each neuron will reach a certain stable state, which can fit the training samples to the maximum extent. After the training is completed, when a test data sample is input, the trained network will automatically analyze and process the data and assign the possibility of each category according to the calculation result, and the sample will be included in the corresponding category with the highest probability. Inside the network, all feature data can share the entire network information together. This sharing mode makes it more convenient to extract the deep features of the data and can significantly enhance the memory capacity of the entire network. The

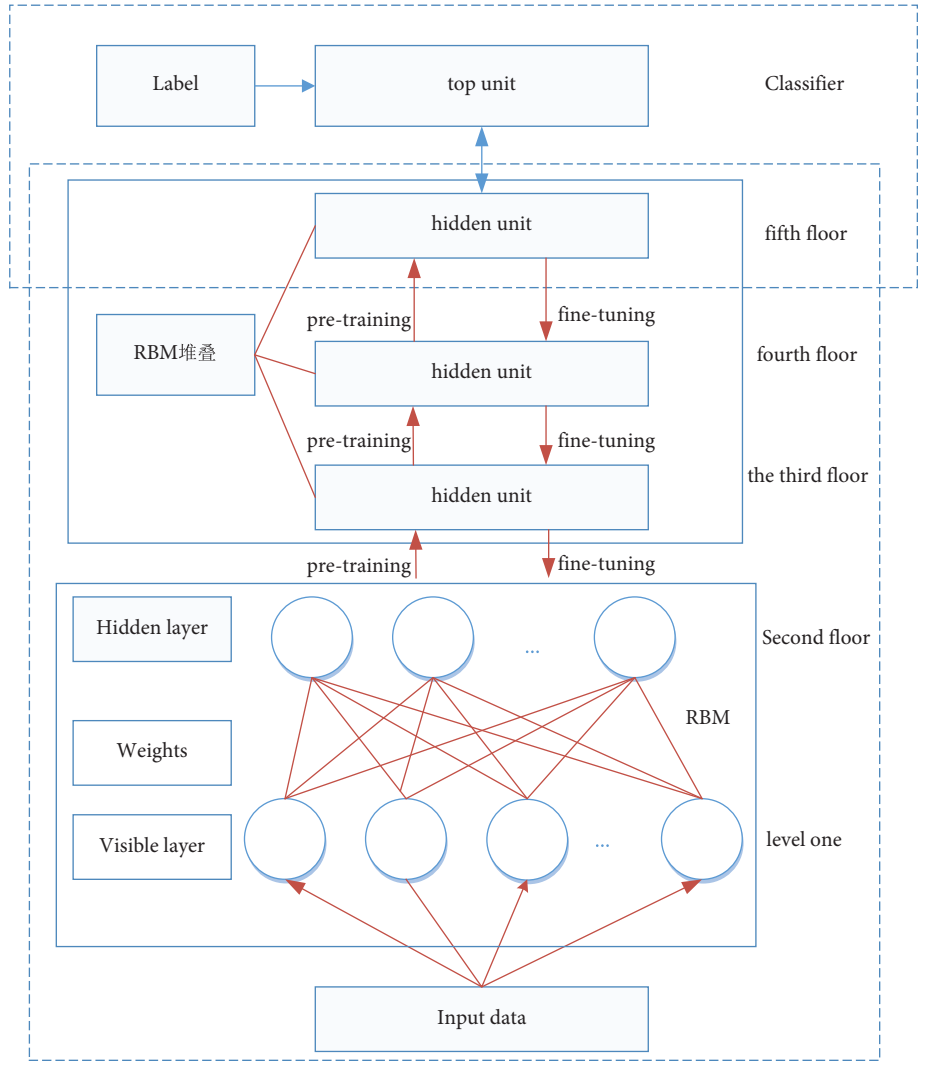

Figure 3: Schematic diagram of DBN network structure.

training process of DBN mainly includes two processes: forward greedy learning and backward fine-tuning. The greedy learning process of RBM is mainly to extract and mine the feature information of the input data layer by layer, and the backward fine-tuning process is to fine-tune the structural parameters of the entire DBN network through the known labels so as to adjust the parameters in the deep layer containing multiple hidden layer parameter vectors [18]. Through the neuron of the deep belief network and the ability to extract and mine the feature information of the input data layer by layer, it has a good application performance in industrial robot diagnosis.

3.2.3. Forward Greedy Learning. The forward greedy learning process is also called stacked RBM pretraining. In the whole process, the algorithm itself learns the data without the participation of label information, which belongs to a category of unsupervised learning. Before the DBN algorithm was proposed, one of the main bottlenecks encountered by the BP neural network was that when the number of network layers was too large, the problem of gradient dispersion would occur during the training process, resulting in a poor learning effect of the entire model. The proposed unsupervised greedy learning method solves this problem, it divides the deep network into multiple shallow network structures and restricts model training and parameter adjustment to this shallow network. It turns out that by adequately training these networks, good training results for the entire model can be achieved. The forward greedy learning process is shown in Figure 4. As can be seen from Figure 4, the training in each step is completed within a certain RBM. In the first step, the input data is assigned to the neurons of the visual layer, the data of the visual layer v is mapped to the hidden layer h_1 through greedy learning, and then the hidden layer h_1 is reconstructed through the CD-k algorithm to return to the hidden layer. View layer, and adjust the internal weights and biases after calculating the reconstruction error. On the basis of the first step, use the fully trained parameter vector to solve the hidden layer h_1, and use it as the input of the second RBM structure, and train the subsequent RBM structure in the same way until the training of the entire DBN network is completed [19–21].

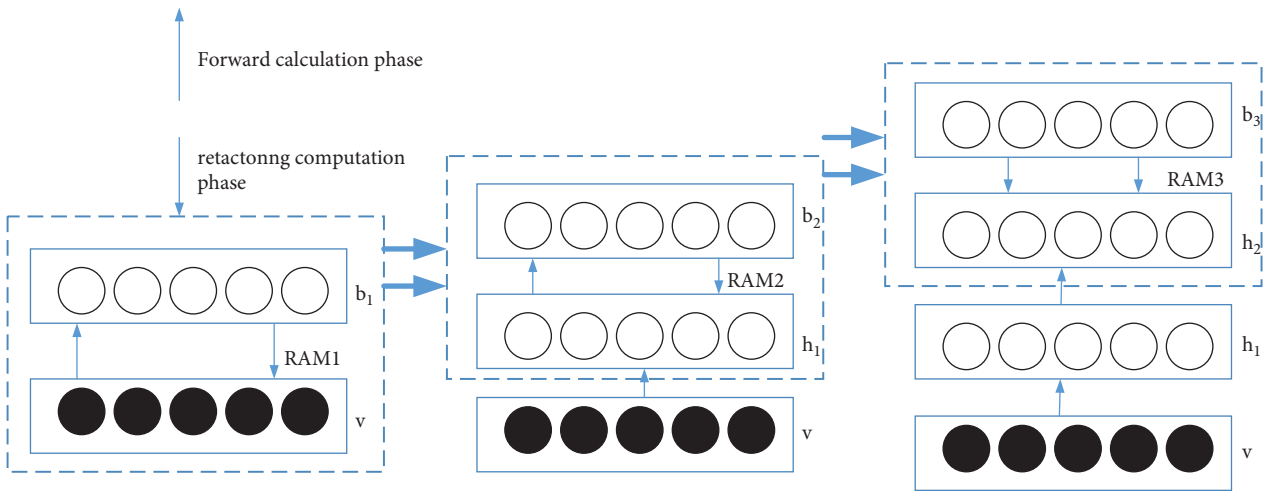

Figure 4: Greedy learning process before and after.

3.2.4. Backward Fine-Tuning. Forward greedy learning is a typical unsupervised training process, which can roughly capture information on the input vector, that is, obtain a solution set within a large range, and the corresponding internal parameter vector of each RBM is initially determined, but the model cannot be obtained. For a high-precision optimal solution, so it is necessary to use the backward fine-tuning strategy to find it from this large-scale solution set. Different from the forward greedy learning, the backward fine-tuning process is a supervised learning method. The pretrained parameters are used as initialization parameters, and the label information is used to further optimize each layer of the DBN network to improve the overall recognition rate and enhancement of the DBN network. *Robustness of the Model.* The principle of DBN's backward fine-tuning algorithm is similar to that of BP's reverse adjustment, mainly including fast gradient descent method and conjugate gradient descent method. Compared with the model obtained by the BP algorithm alone, the performance of the model after fine-tuning the network as a whole by using the gradient descent method combined with the label information tends to be better. Because the pretraining step has been performed before fine-tuning, it is now equivalent to only needing to do a local search within a specific parameter space, so it is relatively easier to converge, and it takes less time. The reverse fine-tuning process is shown in Figure 5.

4. The Establishment of Four Major Industrial Robot Fault Diagnosis Experimental Platforms

4.1. Introduction to the Experimental Platform

4.1.1. Experimental Equipment. The experimental platform is designed with the KR-3-R540 robot as the main equipment. The experimental equipment mainly includes KR-3-R540 robot, vibration exciter, several acceleration sensors, data acquisition and storage system, and data analysis system. Among them, the data acquisition and storage system and the data analysis system together constitute the experimental host computer, which can realize the calling and analysis of the vibration signal through the computer and obtain the experimental results; since the fault used in this chapter is described as the fault at the joint of the robot, the vibration excitation is used. The controller applies a preset continuous excitation at the robot joints, in this way to simulate the failure of the robot joints. The data analysis system is a computer equipped with Modal Genius software provided by Yiheng Company, the operating system is Windows 10, the CPU is Intel Core i7, and the running memory is 16 G.

4.1.2. Experimental Platform Function. In order to realize the acquisition of the vibration signal of the KR-3-R540 robot joint and the end effector, the main functions of the experimental platform designed in this chapter are as follows: (1) Acceleration sensor is used to collect the vibration signal of the acceleration sensor, of which a single acceleration sensor can only collect the vibration signal on the *Z*-axis; the three acceleration sensors can collect the vibration signal in the three directions of *XYZ* and store it in the data acquisition and storage system, which is convenient for the computer to retrieve the vibration data of the robot joints at any time. This system is Hangzhou Yiheng, the sensor data acquisition and storage system provided by the company. (2) Through the KR-3-R540 robot teach pendant, change the trajectory of the robot and the running speed of the robot (resp., 30%, 50%, and 70% of the maximum speed) so that the acceleration sensor can collect data at different speeds and different working trajectories. The robot vibration signal provides data support for model creation. (3) Through the modal analysis software, the modal analysis of the robot is carried out through the modal test. Through modal analysis, determine the cut-off frequency of the robot resonance frequency and vibration frequency. Provide data support for designing filter parameters in the next step. Figure 6 shows the sensor layout of the KR-3-R540 robot. A single acceleration sensor is applied from joint 1 to joint 5, corresponding to sensor 1 to sensor 5, respectively; because the structure of the end effector

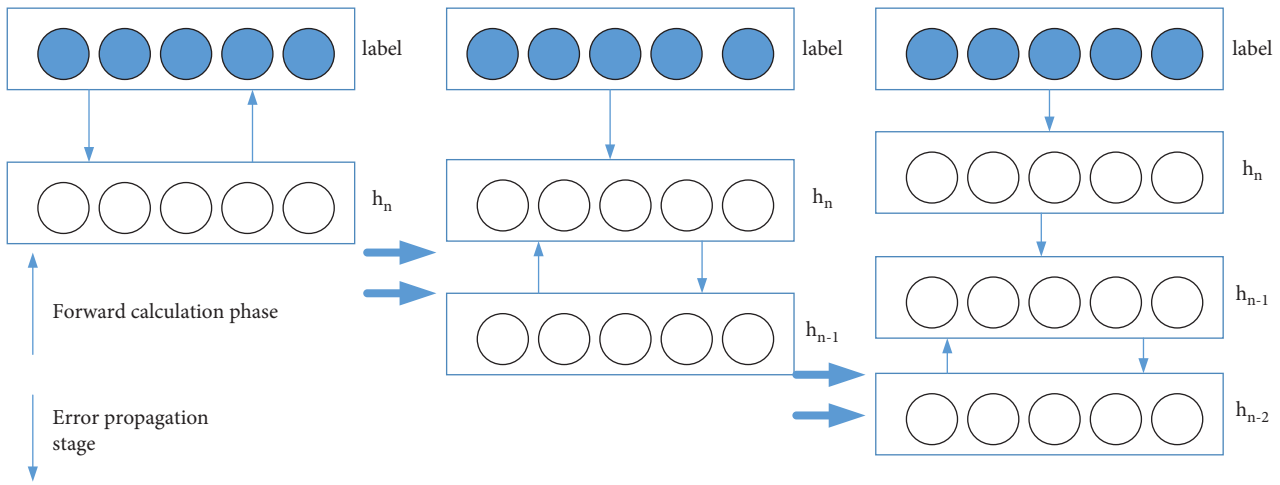

Figure 5: Background fine-tuning process.

and joint 6 is close, it is only at the end. Three acceleration sensors are applied to the actuator, corresponding to sensor 6, and no acceleration sensor is added to joint 6. Figure 6 shows the schematic diagram of the experimental platform. The vibration data is transmitted to the data acquisition and storage system through the single acceleration sensor applied to the robot joint and the three acceleration sensors of the end effector, and the subsequent analysis is performed by the computer.

4.2. Experiment Content and Data Collection

4.2.1. Experiment Content. Due to the interference of the motion frequency and resonance frequency of the robot, there is a large error in the original signal of the sensor. The range of the motion frequency and resonance frequency of the robot is obtained through the modal analysis experiment, and the signal is filtered by designing a filter. The time length is divided into experimental samples to obtain experimental data sets. In order to realize the creation of the robot fault diagnosis model, it is necessary to design experiments to collect the response joint vibration signals. Due to the limitation of technology and cost, the robot failure state used in this section is described as the robot's end pose deviation, which is not within the allowable range. The fault is a fault at the joint, and the fault is in the form of a simulated fault. The vibration exciter is set to continuously excite and interfere with the joint motion of the robot, resulting in the deviation of the robot's end pose beyond the allowable range. Set the robot running trajectory as a straight line in space. As shown in Figure 7, the vibration exciter interferes with the movement trajectory of the robot end effector before and after joint 1. In Figure 7(a), the movement trajectory of the robot end effector is in normal state; Figure 7(b) is the motion trajectory of the robot end effector after the vibration exciter interference (the point where the maximum deviation is intercepted is enlarged and displayed, and the different colors in the figure represent the repetitive motion trajectory of the robot). Since the error range of the robot's end effector is [0, 0.35 mm], comparing Figures 7(a)

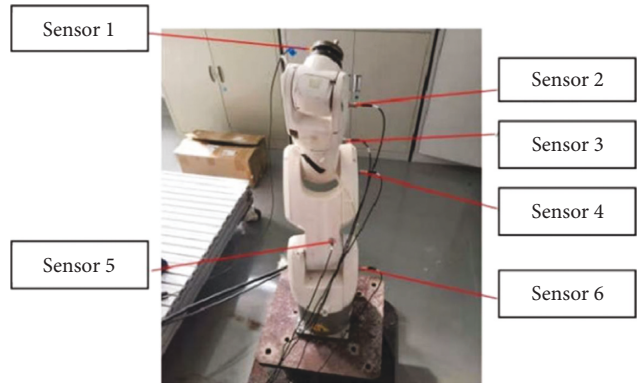

Figure 6: KR-3-R540 robot sensor layout.

and 7(b), it can be concluded that the pose accuracy of the robot's end effector is accurate after applying continuous excitation with the exciter. Serious deviation occurs. At this time, the robot state is regarded as a fault, and the specific fault is the fault at joint 1.

The specific content of the experiment includes the following steps: (1) Using the KR-3-R540 robot teach pendant, randomly set 10 closed-loop motion trajectories for the robot, and let the robot run at 30%, 50%, and 70% of the maximum speed. Complete the command movement, and the movement time is 20 s. (2) According to the above, set the robot joint fault; the fault status is divided into five categories; the first type of fault is expressed as no fault, the second type of fault is expressed as a joint fault, and the third type of fault is expressed as two joint faults, the fourth type of fault is represented as three joint faults, and the fifth type of fault is represented as four joint faults; the fault locations are set as joint 1, joint 2, joint 3, and joint 4. The detailed description of the fault is shown in Table 2. (3) Acceleration sensors are used to collect vibration signals of joints and end effectors in all working states of the robot. The sensors at the joints are single-term sensors, and the end-effectors are three-term sensors.

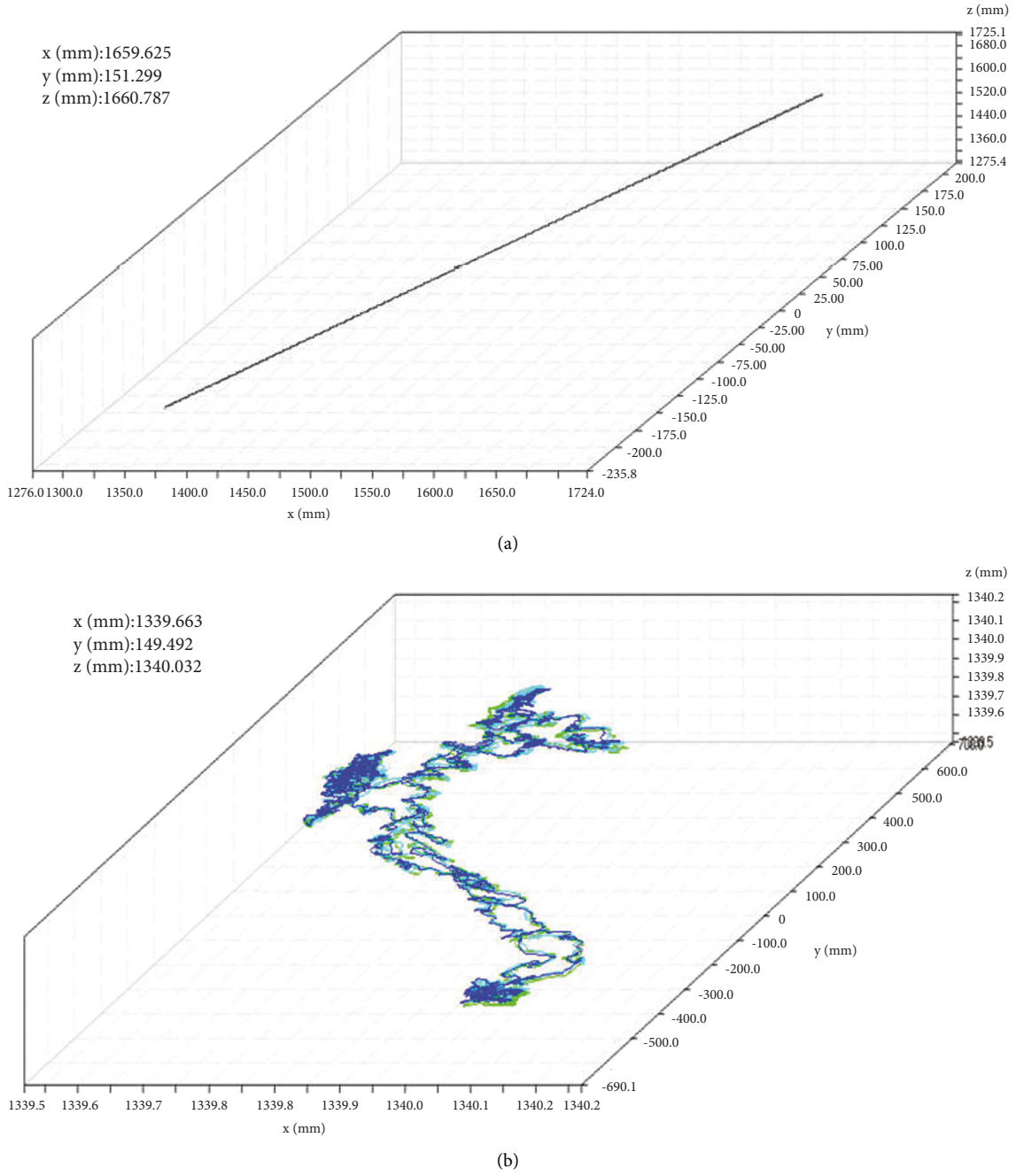

Figure 7: Comparison of the movement trajectories of the robot end effector before and after the exciter interference. (a) The motion trajectory of the robot end effector under normal conditions. (b) The exciter interferes with the movement trajectory of the robot end effector of joint 1.

4.2.2. Experimental Data. The joint vibration data of the robot is used to complete a series of steps to establish a fault diagnosis model suitable for the robot. Due to the limitation of technology and operation space, the acceleration sensor cannot be set inside the robot, but the sensor can only be set on the robot shell, which will inevitably collect the motion vibration signal and the robot resonance signal generated by the robot during the movement process. Filters need to be designed to eliminate these two interference signals. According to the modal analysis results, it can be known that the motion frequency of the robot is about 100 Hz; the resonance frequency is about 2200 Hz.

In this study, the vibration data acquisition system under the LabVIEW platform was designed, and experiments were carried out on the gear fault simulation test bench, and the gear fault diagnosis data set under different working conditions was obtained. After the vibration signal is collected under all working states of the industrial robot, the corresponding experimental data are obtained, and a total of 150 sets of different experimental source data are

Table 2: Robot fault description.

Fault description	Type 1 fault	Type 2 fault	Type 3 fault	Type 4 fault	Type 5 fault
Joint 1	0	1	1	1	1
Joint 2	0	0	1	1	1
Joint 3	0	0	0	1	1
Joint 4	0	0	0	0	1

Note. "0" means there is no fault at the joint; "1" means there is a fault at the joint.

obtained. Each group includes the vibration signals of each joint and the end effector, a total of 1200 sets of sensor source data. First, filter the source data, and set the filter parameters as follows: the low-pass filter frequency is 100 Hz, and the high-pass filter frequency is 2200 Hz. Then, 1200 sets of source data are divided with 0.1s as the sample length, and 240000 experimental samples are obtained, of which the number of experimental samples in normal state is 48000, and the number of experimental samples in all five fault states is 192000. The vibration signal dataset of the robot is shown in Table 3.

5. Fault Diagnosis of Industrial Robot Based on Deep Belief Network

5.1. Creation Process of Fault Diagnosis Model. This section creates an industrial robot fault diagnosis model based on a deep belief network (DBN). First, the wavelet transform is used to decompose and reconstruct the vibration signal of the industrial robot joint and the end effector. Then, the energy entropy normalized eigenvector of the wavelet reconstructed signal is constructed using the information energy entropy and normalization theory. Finally, the normalized feature vector is divided into a training set and a test set. The training set is used for forward layer-by-layer training and reverse fine-tuning of the basic parameters of the fault diagnosis model. The test set is used to test the accuracy of the fault diagnosis model.

5.2. Initialize DBN Network Parameters. In the process of establishing a fault diagnosis model, it is necessary to initialize the basic parameters of the DBN network, including the number of layers of the DBN network model, the dimension of the underlying input sample, the dimension of the upper output label, and the forward unsupervised layer-by-layer training learning rate, inverse fine-tuning learning rate, number of iterations, momentum factor, and weight matrix and bias. Among these basic parameters, the number of model layers and the number of iterations can be set according to experience, mainly based on model training time and model accuracy; the underlying input sample dimension is determined by the number of elements of the energy entropy normalized feature vector. The label dimension is determined by the fault category labels contained in the sample data; the weight matrix, bias, learning rate, and momentum factor can be determined according to the following rules. (1) Initial setting of the weight matrix and bias: the initial setting of the weight matrix directly affects the training speed of the model. If the initial setting of the connection weight is too large, the fault classification result will not meet the requirements, and the setting value is too small. This can lead to severely slow model training, neither of which is desirable. Usually, the initial setting of the weight should be a normal distribution conforming to N (0, 0.01), and the initial setting of the bias between the visible layer and the hidden layer can be 0. Because in the process of DBN network training, the weight matrix and bias will be continuously updated according to the update criterion, which can be initialized according to the empirical formula. The empirical formula is expressed as follows:

$$\begin{aligned} w &= 0.1 \times randn(n, m), \\ a &= zeros(1, n), \\ b &= zeros(1, m). \end{aligned} \tag{1}$$

In the formula, n is the number of input layer neuron units and m is the number of output layer neuron units.

(2) Initial setting of learning rate: the learning rate is a key parameter of the gradient descent algorithm, an important basic algorithm in the DBN network training process, which determines the gradient descent distance each time the algorithm is executed. If the initial set value of the learning rate is relatively small, it will cause the model to step too slowly towards the minimum loss function value, which will take extra time to complete the model training; if the initial set value is large, it will lead to DBN. The reconstruction error of the network is too large, which will seriously cause model training failure. The initial setting of the forward unsupervised layer-by-layer training learning rate of the DBN model is generally 0.1, and the initial setting of the reverse fine-tuning learning rate is generally 0.01.

(3) Initialization of momentum factor: the main role of momentum factor in DBN model training is to improve the antioscillation performance of the training process by introducing the estimated gradient value after the previous iteration into the algorithm so that the algorithm can converge quickly and stably to the allowable range.

$$\begin{aligned} \theta_{t+1} &= \theta_t + \Delta\theta_t, \\ \Delta\theta_t &= m_b \Delta\theta_{t-1} + \varepsilon \times \frac{\partial \ln L}{\partial \ln \theta}. \end{aligned} \tag{2}$$

In the formula, m_b is momentum factor; ε is learning rate; and $\partial lnL/\partial ln\theta$ is sample gradient.

The formula is the parameter update formula of the DBN network after adding the momentum factor. After the momentum factor is introduced, the update value of the DBN network parameter is calculated by the sample gradient

Table 3: Robot vibration signal dataset.

Running speed	Type 1 fault	Type 2 fault	Type 3 fault	Type 4 fault	Type 5 fault
30%	16000	16000	16000	16000	80000
50%	16000	16000	16000	16000	80000
70%	16000	16000	16000	16000	80000
Total	48000	48000	48000	48000	24000

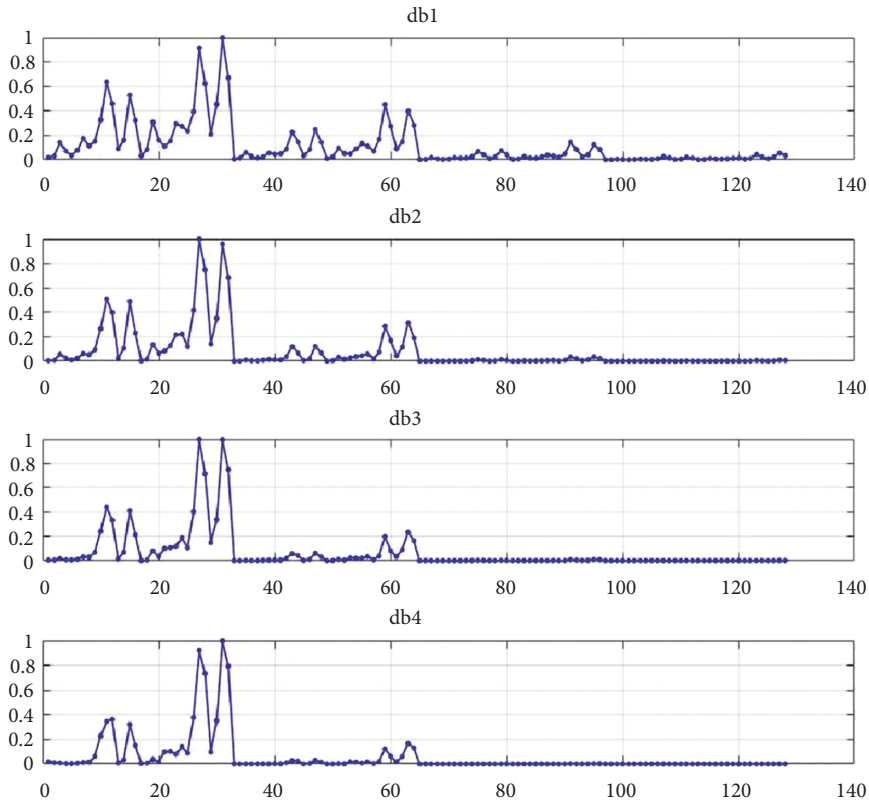

Figure 8: Node energy entropy under different wavelet bases. (a) db1. (b) db2. (c) db3. (d) db4.

and the correction value after the last iteration. The initial value of the momentum factor is generally set to [0.5, 0.9].

5.3. Model Accuracy Analysis. According to the analysis, it can be determined that the number of wavelet envelopes is 7. Figure 8 shows the energy entropy normalized eigenvectors corresponding to different wavelet base numbers. The abscissa is the wavelet packet decomposition node, and the ordinate is the element value in the energy entropy normalized eigenvector. It can be seen from the comparison in the figure that when the wavelet base is db1, there are still obvious differences after the 96th node, and the signal information is relatively complete; when the wavelet base is greater than db1, especially when the wavelet base is above db4, at 96. The normalized energy entropy of all nodes after the node is close to 0, the difference between the nodes is very small, and the signal information is seriously lost. In order to make the normalized energy entropy feature vector have a good representation and meet the requirements of the underlying input of the DBN model, the wavelet base is selected as db1 in this paper.

The software used in this section is MATLAB 2019b, the operating system is Windows 10, the CPU is Intel Core i7, the graphics card is NVIDIA 930 M, and the running memory is 8 G. Divide the sample data into training set and test set according to the ratio of 4 : 1. The training set includes 192,000 experimental samples (38,400 normal experimental samples and 38,400 each of 4 types of fault experimental samples); the test set contains 48,000 experimental samples (9,600 normal experimental samples and 9,600 each of 4 types of fault experimental samples). According to the decomposition level of 7 and the wavelet base of db1, the wavelet packet is decomposed and normalized. Each experimental sample can construct an energy entropy normalized feature vector containing 128 elements. The training set of the DBN network model is 192,000 input samples, and the test set is 48,000 input samples. The input layer item of the DBN network model is 128, the output layer is represented as the sample fault label, and the output layer item is 6. The basic parameters of the DBN model are shown in Table 4, and the sample labels corresponding to the output layer are shown in Table 5. The number of iterations of the

Table 4: DBN model parameters.

Parameter	Numerical value
Wavelet packet decomposition layers	7
Wavelet packet wavelet basis	db1
Initial bias	0
Initial weight	0.001
Learning rate	0.1
Momentum factor	0.9
Input layer item	128
Output layer project	6

Table 5: Sample labels corresponding to the output layer.

Sample description	Sample label					
Class I failure	0	0	0	0	0	0
Type II fault	1	0	0	0	0	0
Three types of faults	1	1	0	0	0	0
Four types of faults	1	1	1	0	0	0
Five types of faults	1	1	1	1	0	0

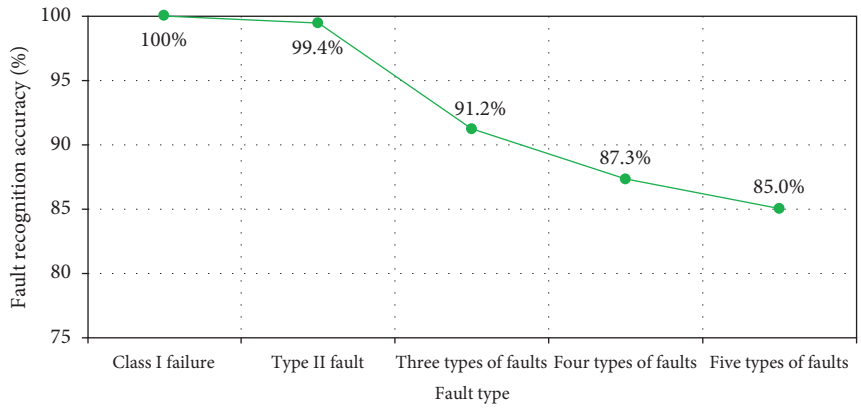

Figure 9: The fault identification accuracy of the fault diagnosis model based on DBN network when dealing with different fault states.

DBN model is set to 100, the number of inverse tuning times is preset to 100 and multiplied to 1000, and the learning rate and momentum factors are set to 0.1 and 0.9, respectively. Figure 9 shows the fault identification accuracy under different tuning times. It can be seen from Figure 9 that when the number of iterations reaches more than 900, the fault identification accuracy tends to a fixed value of 99.4%. It can be seen that the number of forward iterations of the DBN model used in this paper is 100 times, and the number of reverse tuning times is 100 times, should not be less than 900 times.

Figure 10 shows the fault identification accuracy of the fault diagnosis model based on DBN network when dealing with different fault states. It can be seen from the figure that the fault identification accuracy of the fault diagnosis model based on the DBN network can reach 99.4% when dealing with a single fault, and with the increase of the number of faults, the fault identification accuracy of the model also begins to decline, especially when dealing with the first fault. When there are five types of faults, the fault recognition accuracy is only about 85%. It is concluded that the fault diagnosis model based on DBN network used in this chapter is not good in dealing with the fault diagnosis of multiple faults coexisting, and the model needs to be further improved.

6. Conclusion

The status of industrial robots in industrial production is getting higher and higher, and its normal operation is directly related to production safety, and it is also particularly important for the fault diagnosis of industrial robots. In order to improve the fault recognition accuracy of the industrial robot fault diagnosis model, this paper is based on the DSmT theory, and the results of the DBN network model diagnosis are fused at the decision level to achieve the purpose of improving the fault recognition accuracy of the model. Taking the output layer of the fault diagnosis model of the DBN network as the fault evidence, the conflict between the pieces of evidence is analyzed, the fusion rules and decision rules of DSmT are selected, and the fault diagnosis model based on DBN and DSmT is established. According to the requirements of the model for the experimental sample data, an experimental platform is built, the basic

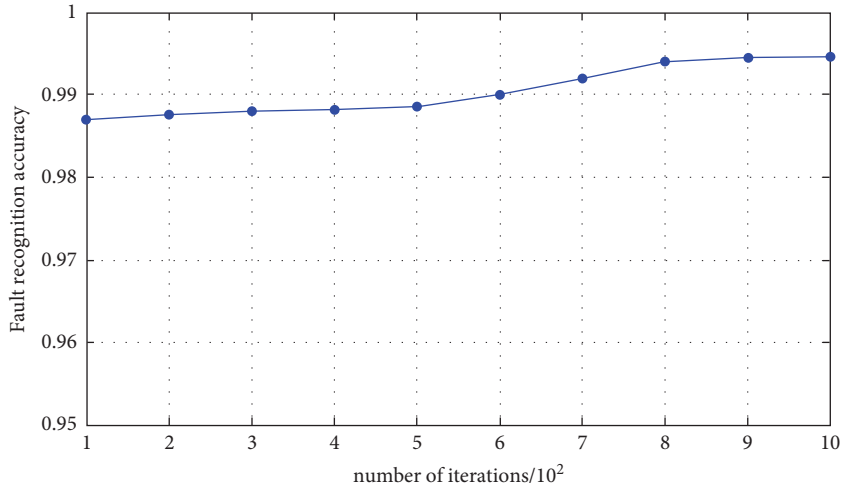

Figure 10: Fault recognition rate under different tuning times.

parameters of the DBN fault diagnosis model are determined through MATLAB programming, and a fault diagnosis model suitable for robots is established; finally, the fault diagnosis used in this experiment is verified by design experiments. The applicability of the model: It can be seen that the fault recognition accuracy of the industrial robot fault diagnosis model based on the DBN network can reach 99.4% when dealing with a single industrial robot fault. With the increase of the number of industrial robot faults, the industrial robot fault recognition accuracy of the model also begins to decline. Especially when dealing with the fifth type of fault, the accuracy of industrial robot fault recognition is only about 85%.

Data Availability

The dataset can be accessed upon request from the corresponding author.

Conflicts of Interest

The author declares that there are no conflicts of interest regarding the publication of this paper.

Acknowledgments

This work was financially supported by funding for the Sixth Phase of Jiangsu 333 Project High-Level Talent Training Plan and Huai'an Natural Science Foundation Project (HABZ201920).

References

[1] W. A C.B, H H.K, and T C.Y, "Use of an expert system shell to develop a power plant simulator for monitoring and fault diagnosis[J]," *Elsevier*, vol. 29, no. 1, pp. 27–33, 1994.

[2] M. Burth and D. Filbert, "fault diagnosis of universal motors during run-down by nonlinear signal processing," *IFAC Proceedings Volumes*, vol. 30, no. 18, pp. 411–416, 1997.

[3] A. Abdi, M. B. Tahoori, and E. S. Emamian, "fault diagnosis engineering of digital circuits can identify vulnerable molecules in complex cellular pathways[J]," *Science Signaling*, vol. 1, no. 42, p. 10, 2008.

[4] H. Çaliş, A. Çakir, and E. Dandil, "Artificial immunity-based induction motor bearing fault diagnosis[J]," *Turkish Journal of Electrical Engineering and Computer Sciences*, vol. 21, no. 1, pp. 1–25, 2013.

[5] P. Freeman, R. Pandita, N. Srivastava, and G. J. Balas, "Model-based and data-driven fault detection performance for a small UAV," *IEEE*, vol. 18, no. 4, pp. 1300–1309, 2013.

[6] S. G Liu, "Model-based fault detection of Modular and Reconfigurable Robots with joint torque sensing[J]," in *Proceedings of the 2013 IEEE/ASME International Conference on Advanced Intelligent Mechatronics*, vol. 1, pp. 134–139, Wollongong, NSW, Australia, 2013.

[7] T. N. S. W M H, "Study on model-based fault detection and diagnosis for mobile robot: fault diagnosis of internal sensor and robot-localization[C]," in *Proceedings of the JSME annual Conference on Robotics and Mechatronics (Robomec)*, vol. 1, pp. 255-256, 2003.

[8] A. K. S. Jardine, D. Lin, and D. Banjevic, "A review on machinery diagnostics and prognostics implementing condition-based maintenance," *Mechanical Systems and Signal Processing*, vol. 20, no. 7, pp. 1483–1510, 2006.

[9] R. Yan and R. X. Gao, "Harmonic wavelet-based data filtering for enhanced machine defect identification," *Journal of Sound and Vibration*, vol. 329, no. 15, pp. 3203–3217, 2010.

[10] Y. Lei, M. J. Zuo, Z. He, and Y. Zi, "A multidimensional hybrid intelligent method for gear fault diagnosis," *Expert Systems with Applications*, vol. 37, no. 2, pp. 1419–1430, 2010.

[11] K. He, X. Zhang, and S. Ren, "Deep residual learning for image recognition," in *Proceedings of the The IEEE Conference on Computer Vision and Pattern Recognition*, IEEE, Las Vegas, USA, 2016.

[12] A. Krizhevsky, I. Sutskever, and G. E. Hinton, "ImageNet classification with deep convolutional neural networks," *Communications of the ACM*, vol. 60, no. 6, pp. 84–90, New York, 2017.

[13] H. Shao, H. Jiang, F. Wang, and Y. Wang, "Rolling bearing fault diagnosis using adaptive deep belief network with dual-tree complex wavelet packet," *ISA Transactions*, vol. 69, pp. 187–201, 2017.

[14] M. Zhao, M. Kang, B. Tang, and M. Pecht, "Deep residual networks with dynamically weighted wavelet coefficients for fault diagnosis of planetary gearboxes," *IEEE Transactions on Industrial Electronics*, vol. 65, no. 5, pp. 4290–4300, 2018.

[15] W. Sun, B. Yao, N. Zeng et al., "An intelligent gear fault diagnosis methodology using a complex wavelet enhanced convolutional neural network," *Materials*, vol. 10, no. 7, p. 790, 2017.

[16] V. T. Tran, F. AlThobiani, and A. Ball, "An approach to fault diagnosis of reciprocating compressor valves using Teager-Kaiser energy operator and deep belief networks," *Expert Systems with Applications*, vol. 41, no. 9, pp. 4113–4122, 2014.

[17] F. Jia, Y. Lei, J. Lin, X. Zhou, and N. Lu, "Deep neural networks: a promising tool for fault characteristic mining and intelligent diagnosis of rotating machinery with massive data," *Mechanical Systems and Signal Processing*, vol. 72-73, pp. 303–315, 2016.

[18] H. Jeong, S. Park, S. Woo, and S. Lee, "Rotating machinery diagnostics using deep learning on orbit plot images," *Procedia Manufacturing*, vol. 5, pp. 1107–1118, 2016.

[19] O. Obst, "Distributed fault detection in sensor networks using a recurrent neural network," *Neural Processing Letters*, vol. 40, no. 3, pp. 261–273, 2014.

[20] O. Janssens, V. Slavkovikj, B. Vervisch et al., "Convolutional neural network based fault detection for rotating machinery," *Journal of Sound and Vibration*, vol. 377, pp. 331–345, 2016.

[21] A. M. Abdel-Zaher and A. M. Eldeib, "Breast cancer classification using deep belief networks," *Expert Systems with Applications*, vol. 46, pp. 139–144, 2016.

Hindawi
Scientific Programming
Volume 2022, Article ID 4870435, 11 pages
https://doi.org/10.1155/2022/4870435

Research Article

Design of a Public Cultural Service System for the Elderly Based on Intelligent Computing

Qing Zhou and Xiaofeng Xu

Art Design College of Zhejiang Gongshang University, Zhejiang, Hangzhou 310018, China

Correspondence should be addressed to Qing Zhou; zhouqing@mail.zjgsu.edu.cn

Received 18 May 2022; Revised 14 June 2022; Accepted 17 June 2022; Published 5 July 2022

Academic Editor: Lianhui Li

Public cultural services for the elderly are part of the government-led public services for society in order to meet the needs of people's spiritual and cultural life. As the global problem of ageing becomes increasingly serious, the problem of balancing the supply and demand of public cultural services for the elderly has become increasingly serious. How to realize a public cultural service system for the elderly with wide coverage and effective integration of resources has become a pressing problem to be solved. In order to solve the above problems, this article designs a public cultural service system for the elderly based on intelligent computing. Firstly, the problems that lead to the inefficient use of public cultural resources for the elderly are analyzed. Secondly, it attempts to introduce an advanced intelligent computing technology (Cuckoo Search) to build a three-dimensional public cultural resource sharing system for the elderly. Then, the standard Cuckoo algorithm is improved by using chaotic mapping and dynamic step size for the characteristics of public cultural services in order to improve the convergence speed and the accuracy of the search. The experimental results show that the designed system can effectively integrate the grassroots resources of cultural institutions such as libraries, cultural centres, and cultural service centres, verifying its effectiveness and feasibility.

1. Introduction

The right to culture is one of the fundamental rights of citizens. It is an important duty of governments to attach importance to and protect the basic public cultural rights of citizens. With the rapid development of the economy, the people have begun to pursue spiritual satisfaction after satisfying their material needs. People's demand for public cultural services is growing rapidly and is characterised by multilevel, differentiation and personalization. The ageing of the population is a major social issue in the twenty-first century and a major feature of human development in the twenty-first century. With the development of the country's economy and the improvement of people's living standards, the number of elderly people is increasing at an unprecedented rate [1–3]. Under the premise that material living conditions are basically satisfied, the spiritual and cultural needs of the elderly are receiving more and more attention.

The cultural industry for the elderly is an ageing business that aims to meet the spiritual and cultural needs of the elderly. The content of social security is divided into three levels: economic security, service security, and spiritual security [4–7]. Social security for the elderly is an important element of social security. Maslow's Hierarchy of Needs theory gives an incisive overview of the hierarchy of human needs. It is of great significance at this stage to organically combine public cultural services with the cause of the elderly so as to drive up the level of elderly services for the whole society. The construction and management of public cultural services is a process of gradual rise and improvement. Public cultural resources for the elderly are an important support to meet the growing cultural needs of the general public. In this context, it is of great practical importance to make a scientific analysis of the problems in using public cultural resources and to explore new ways of integrating resources.

With the growing differentiation in demand for public cultural services, a single cultural resource is no longer able

to meet the cultural needs of the majority of older people, and the integration of public cultural resources has begun to attract the attention of academics. Due to different research perspectives and local practices, researchers have conducted different studies on the integration of public cultural resources. After summarising, current research mainly discusses the integration of public cultural digital resources, the integration of public cultural resources, and the integration of public cultural resource paths [8–11]. The comprehensive use of various current advanced management methods and technologies to optimise the allocation of resources and to develop a reasonable integration plan are key elements in the design of public cultural service systems for the elderly. Currently, most of the public cultural resources management methods and integration schemes are still only in the original fixed manual mode. The low level of automation and informatization has resulted in a public cultural service system that is unable to meet the changing needs of older people. In other words, the existing public cultural service system for older people does not meet the time-sensitive requirements of changing needs. Therefore, the main objective of the design of public cultural services for older people is to optimise the allocation and path of the main resources according to the changing needs in real time.

At present, researchers have applied integer programming, linear programming, dynamic programming, and objective programming methods in operations research to solve a part of representative public cultural resources integration and optimisation problems. However, most of the public cultural resources integration and optimisation problems are NP-Hard problems, so the existing solution methods and strategies are not yet effective in solving the allocation of public cultural resources in real life. For example, the optimal solution algorithm can find the optimal solution to the scheduling problem in polynomial time for a specific optimisation objective, including the branch-and-bound method, mathematical planning method, and dynamic planning method. Kolpakov [12] used the branch-and-bound method to find the optimal solution to the small-scale problem with this objective based on the actual situation of production management with the objective of minimising time cost. For the feasible boundary problem along the positive direction of the gradient, Okon [13] proposed a multiobjective optimal solution for linear programming. Although the optimal solution algorithm can obtain an optimal solution, it requires an infinite exhaustion of the solution space of the problem and is therefore computationally too costly in terms of time. Based on knowledge and experience in solving scheduling problems, heuristic algorithms can obtain suboptimal solutions in a short time, such as goal tracking methods, linear relaxation methods, and domain search algorithms. For example, Güney [14] proposed a linear programming relaxation method for solving sequencing problems, implementing a 2-approximation algorithm based on three certainties. Although heuristic algorithms can construct problem solutions quickly, the quality of the solutions is poor. Heuristic algorithms often require a large number of iterative operations, and the solution efficiency and quality are greatly influenced by the structure of the algorithm and the choice of parameters.

Intelligent computing is a new type of algorithm developed by simulating natural organisms, with features such as self-organization, self-learning, and self-adaptation. The collective movement of groups of animals in nature is a very interesting phenomenon. Each member of a group of animals is an individual, yet all the individuals are able to form a whole. Intelligent computing mainly includes genetic algorithms, forbidden search algorithms, simulated annealing algorithms, particle swarm algorithms, and ant colony algorithms. Intelligent computing is easier than general heuristic algorithms to find suboptimal solutions close to the optimal solution of a problem. Gong et al. [15] proposed an ensemble genetic algorithm for solving interval multiobjective optimisation problems and demonstrated that intelligent computing has faster solution speed and better solution accuracy. Pan et al. [16] proposed a caching strategy for ethnic traditional sports video resources based on intelligent computing. Experimental results show that the ant colony simulated annealing algorithm can improve the hit rate of the content on mobile edge computing servers.

The most important issue in the design of public cultural services for older people is the optimisation of resource allocation and pathways. However, when the number of individual older people is large, the traditional method of manual resource integration consumes a lot of time and effort. In addition, the lack of adaptiveness of the traditional manual resource integration method leads to public cultural resources being restricted to a fixed path, which is inflexible and cannot meet the timeliness in real life. Therefore, in order to solve the above problems, this article proposes introducing intelligent computing [17–20] into the design of public cultural services for the elderly. By simulating the movement behaviour of a large-scale group of elderly people in real time, the optimal location and path of cultural resources can be planned. The Cuckoo Search (CS) algorithm [21–24] is an emerging type of group intelligence algorithm that can imitate the movement behaviour of a flock of birds searching for the best nest location, with strong local and global search capability and convergence speed. Therefore, the CS algorithm is used in this article to simulate the movement behaviour of groups of elderly people.

The main innovations and contributions of this article include the following:

(1) This article introduces advanced intelligent computing technology (Cuckoo Search) to build a three-dimensional system for sharing public cultural resources for the elderly.

(2) The standard CS algorithm is improved for the limited range of optional spaces in public cultural services using chaotic mapping and dynamic step size in order to improve the convergence speed and optimisation finding accuracy.

The rest of the article is organized as follows: in Section 2, the problems in the existing public cultural services system for older people are studied in detail, while Section 3

provides the problem statement and research ideas. Section 4 provides the public cultural service system for the elderly based on an improved CS algorithm. Section 5 provides the simulation results and analysis. Finally, the article is concluded in Section 6.

2. Problems in the Existing Public Cultural Services System for the Elderly

2.1. Inadequate Supply of Public Cultural Resources. Older people use public cultural facilities through cultural institutions such as libraries, cultural centres, and cultural service centres. A statistical survey was conducted on the public cultural resources for older people in a provincial capital city in China, for example. It was found that the service effectiveness of cultural institutions was unevenly distributed in most areas. For example, cultural service centres are too small and not well equipped. In addition, the number of mass cultural and sports activities organized by cultural institutions was less than 10 per year. Although public libraries and cultural centres at all levels have public electronic reading rooms and provide free access to the Internet, the speed of access to the Internet is unsatisfactory, and the facilities are not well equipped. However, the speed of access to the Internet is not satisfactory, and the resources available are very limited.

2.2. Public Cultural Resources Are Too Dispersed. For a long time, public cultural resources for the elderly have been scattered across a number of grassroots departments. Each department uses the public cultural resources it has in its own area to provide public cultural services for the elderly population. The constraints of the administrative system have created a situation where grassroots public cultural resources are too scattered to be effectively integrated, which is not conducive to the full utilisation of grassroots public cultural resources. In particular, the layout of grassroots public cultural facilities is unreasonable.

Firstly, the government deliberately pursues the agglomeration effect of public cultural facilities, resulting in many public facilities being concentrated around local administrative centres. This type of layout planning ignores the service radius of public cultural facilities, which makes it very inconvenient for the public to use public cultural facilities. Due to the rapid development of urbanisation, local administrative centres are located far away from the city centre. Secondly, due to the constraints of construction land conditions, many cultural centres or cultural service centres are built in the corners of cities, towns, and villages. Such a layout is also very unreasonable. It is not convenient for the masses to participate in activities, resulting in the marginalisation of cultural service institutions. In the long run, grassroots cultural service facilities have become ornamental, resulting in a great waste of cultural resources. Finally, the lack of communication and coordination between departments results in a poor layout. The lack of communication between the planning and construction departments of public cultural facilities and their users has led to deviations between the completed public cultural facilities and the needs of the public. This standardised construction planning ignores the actual needs of the users and, to a certain extent, also results in a waste of resources.

2.3. There Is Structural Waste in the Supply of Public Cultural Resources. The structural waste in the supply of grassroots public cultural resources refers, on the one hand, to the lack of coordinated planning resulting in the duplication of the construction of grassroots public cultural facilities; on the other hand, it refers to the inability to effectively match the supply of grassroots public cultural resources with the needs of the grassroots. Both of these aspects lead to low utilisation of grassroots public cultural resources, resulting in a waste of resources. Due to the administrative system, each department is responsible for the construction of public cultural facilities within its own area. This approach to resource planning is a "compartmentalised" construction model. The lack of coordination among all parties involved in the provision of public cultural services has led to the duplication of public cultural facilities and, to a certain extent, to a waste of resources. The imbalance between supply and demand leads to low utilisation of public cultural resources at the grassroots level. Public cultural resources are supplied in a single way, and there is a lack of feedback mechanisms on the needs of the public. The allocation of resources in public cultural institutions does not meet the needs of the public, which ultimately leads to low utilisation of public cultural resources at the grassroots level.

3. Problem Statement and Research Ideas

The group behaviour of animals shows consistency as a whole, but each member of the group is independent, i.e., having a certain freedom of behaviour. The behavioural trajectory of each individual is different. Therefore, due to this specificity of group behaviour, each individual's motor control is required to have certain random properties in order to make the final simulated group behaviour more natural.

The basic principle of the group intelligence algorithm is to simulate animal evolution and natural competitive behaviour, and it has strong advantages in solving process arrangement and route planning problems. The Cuckoo Search (CS) algorithm is an emerging kind of group intelligence algorithm [25–27] with strong local and global search ability and convergence speed. Therefore, in order to solve the most important problems of resource allocation optimisation in the design of public cultural services for the elderly, this article proposes introducing intelligent computing into the design of public cultural services for the elderly. By simulating the movement behaviour of a large-scale group of elderly people in real time, the optimal location of cultural resource subjects is planned. Collision detection is introduced in the generation of individual movement paths in order to solve the problem of collision between individuals. In addition, the standard CS algorithm is improved with chaotic mapping and dynamic step size in

order to increase the spatial range of group behaviour options and smoothly adjust the trajectory curve in order to improve the convergence speed and optimisation accuracy.

4. A Public Cultural Service System for the Elderly Based on an Improved CS Algorithm

4.1. Modelling of Individual Goals for Older People. The system designed simulates the public cultural services as a bird's nest and each individual elderly person as a cuckoo. By simulating the natural behavioural changes of the elderly population, the final birdhouse location is generated that best matches the actual needs. In order to provide a comprehensive view of the individual behaviour of the elderly, an RGB colour space model is used to represent the individual target characteristics of the group. The entropy of the individual image is first analyzed by RGB information $H(U)$.

$$H(U) = E[\log\ p_i] = -Ep_i \log\ p_i, \tag{1}$$

where p_i represents the probability of a single letter pixel occurring. The logarithm in the above equation generally takes the value of 2.

The colour degrees are calculated as follows:

$$\frac{1}{|\Omega|}\sum_{p\in\Omega}\left|R_p - G_p\right| + \left|G_p - b_p\right| + \left|B_p - R_p\right|, \tag{2}$$

where $|\Omega|$ is the individual size. R_p, G_p, and B_p are the RGB colour components.

The gradient distribution of individual targets in the population is then represented by a gradient histogram $g(p)$, which is calculated as follows:

$$g(p) = \min\left(\max\left(R_p, G_p, B_p\right), 1.1\right), \tag{3}$$

where 1.1 is the curve truncation value.

Finally, the texture features of individual targets in the population are represented using a grey-scale cooccurrence matrix $P(i, j)$, which is calculated as follows:

$$\begin{aligned} P(i,j) &= \#\{(x_1, y_1), (x_2, y_2) \in M \times N | f(x_1, y_1) \\ &= i, f(x_2, y_2) = j\}, \end{aligned} \tag{4}$$

where $f(x, y)$ represents the input population target of size $M \times N$ and $\#(x)$ represents the number of individuals in set x. i and j represent two different grey-scale values.

4.2. Basic CS Algorithm. A new global search algorithm, called the Cuckoo Search (CS) algorithm, was proposed in 2009 by modelling the behaviour of cuckoos searching for nests to lay their eggs [28]. In nature, cuckoos search for suitable nest locations to lay their eggs in a random way. To simulate the behaviour of the cuckoo in its nest search, first, three ideal states are set as follows:

(1) Each cuckoo lays one egg at a time and chooses a nest at random to incubate it.

(2) In a random selection process of nests, the best nest selected will be retained for the next generation.

(3) The number of available nests n is fixed and the probability of discovery by the nest owner is $p_a \in [0, 1]$.

Based on the three ideal states mentioned above, the updated formula for the optimal path and location of the bird's nest is shown as follows:

$$x_i^{t+1} = x_i^t + \alpha \oplus L(\lambda)\ (i = 1, 2, \ldots, n), \tag{5}$$

where x_i^t denotes the position of the nest of the i-th cuckoo in the t-th literation and a denotes the step parameter. S denotes the random walk step length. To facilitate the implementation of the algorithm, S in this article uses the vegetable dimensional flight formulation [29]:

$$S = \frac{\mu}{|\nu|^{(1/\beta)}}, \tag{6}$$

where the flight parameters μ and ν follow a normal distribution.

$$\mu N\left(0, \sigma_\mu^2\right), \nu N\left(0, \sigma_\nu^2\right), \tag{7}$$

$$\begin{aligned} \sigma_\mu &= \left\{\frac{\Gamma(1+\beta)\sin(\pi\beta/2)}{\Gamma[(1+\beta)/2]2^{(\beta-1)/2}\beta}\right\}^{(1/\beta)}, \\ \sigma_\nu &= 1. \end{aligned} \tag{8}$$

4.3. Improved CS Algorithm. Chaotic mapping [30–32] is the inherent characteristic of nonlinear dynamical system, which is a kind of random process with the certainty of the regular expression. Therefore, it is often used to improve the performance of intelligent algorithms to find the best performance. Therefore, in this paper, the standard CS algorithm will be improved using chaotic mappings. The logistic formulation of the standard chaotic mapping system is shown as follows:

$$y_{n+1} = 4y_n(1 - y_n), \tag{9}$$

where $n = 1, 2, \ldots$ is the state, y_n denotes a chaotic variable, and $y_n \in [0, 1]$.

In order to increase the range of optional spaces for group behaviour and improve global optimisation performance, the current optimal position of the bird's nest in the CS algorithm x_{best} is chaotically optimised:

$$y_1^k = \frac{x_{\text{best}} - x_{\min}^k}{x_{\max}^k - x_{\min}^k}. \tag{10}$$

The above equation is the process of mapping x_{best} to the defined interval [0, 1] of y_{n+1}. The chaotic sequence $y^k = (y_1^k, y_2^k, \ldots, y_T^k)$ is generated by performing T iterations on y_1^k according to equation (10):

$$y_{n+1}^k = 4y_n^k\left(1 - y_n^k\right). \tag{11}$$

Next, the chaotic sequence $y^k = (y_1^k, y_2^k, \ldots, y_T^k)$ is mapped back to the original space by the inverse of equation (11):

$$x_{\text{best},m}^{*k} = x_{\min}^{k} + \left(x_{\max}^{k} - x_{n}^{k}\right) y_{m}^{k}, \quad m = 1, 2, \ldots, T. \tag{12}$$

At each iteration, the adaptation value for each nest is calculated and the best location $x_{\text{best},m}^{*k}$ in each iteration will be selected. The best location $x_{\text{best},m}^{*k}$ is then used to replace a randomly selected nest location in the nest.

In the basic CS algorithm, Levy flight is used to generate a random step size. However, the variation of this step size is very unstable. During the search process, the larger the step size is, the easier it is for the CS algorithm to search for the global optimal solution; however, it reduces the search accuracy and even sometimes oscillates. The smaller the step size, the lower the search speed of the CS algorithm, but the local search ability is enhanced, which improves the solution accuracy. Therefore, the use of Levy flight to generate step size, although random, lacks adaptivity. To address this problem, the step size needs to be dynamically adjusted adaptively according to the search results at different stages, and the relationship between the global search ability and the search accuracy needs to be properly handled.

$$d_i = \frac{\left\| x_i^k - x_{\text{best},m}^k \right\|}{d_{\max}}, \tag{13}$$

where x_i^k is the location of the nest i at the iteration k and $d_{\max}$ is the maximum distance between the best nest location and the other nest locations in the group.

The specific dynamic step adjustment method is as follows:

$$\text{step}_i = \text{step}_{\min} + \left(\text{step}_{\max} - \text{step}_{\min}\right) d_i, \tag{14}$$

where $\text{step}_{\max}$ is the maximum step size and $\text{step}_{\min}$ is the minimum step size. Equations (13) and (14) allow for the automatic adjustment of the dynamic step size.

4.4. Collision Detection Based on NURBS Modelling. In order to prevent collisions between different individuals in a group, a group model was constructed by means of NURBS modelling and collision detection was introduced in order to solve the problem of collisions between individuals. The NURBS model is defined as follows:

$$C(t) = \frac{\sum_{i=0}^{n} \omega_i P_i N_{i,k}(t)}{\sum_{i=0}^{n} \omega_i N_{i,k}(t)}, \tag{15}$$

where P_i represents the position of the surface vertices of the target model, $N_{i,k}(t)$ represents the basis function of the nonuniform rational B spline curve, and ω_i represents the control adjustment weights. The method for collision detection is shown as follows:

$$\text{vel}\, j = \left[\sum_{i=1.i\neq j}^{n} \frac{1}{\text{dist}(i, j) \cdot n} \cdot \text{vel}\, j \right] \cdot S + \text{vel}\, j \cdot (1 - S), \tag{16}$$

where $\text{vel}\, j$ indicates the current speed of movement of the detected individual j and $S \in [0, 1]$ indicates the weight that controls the degree of aggregation of the group. $\text{dist}(i, j)$ denotes the distance between different individuals.

In order to keep the direction of each individual in the group consistent with that of other individuals, equation (16) only selects the average direction of the neighbouring individuals of the target individual.

$$\text{vel}\, j = \left[\sum_{i=1.i\neq j}^{n} \frac{1}{n} \cdot \text{vel}\, j \right] \cdot S + \text{vel}\, j \cdot (1 - S). \tag{17}$$

Finally, to complete the aggregation behaviour, to bring all individuals closer to the centre of the whole cluster, the final calculation of $\text{vel}\, j$ is shown as follows:

$$\text{vel}\, j = \left[\left(\sum_{i=1.i\neq j}^{n} \frac{\text{pos}i}{n} \right) - \text{pos}i \right] \cdot S + \text{vel}\, j \cdot (1 - S), \tag{18}$$

where pos$i$ represents the vector of cluster centres.

4.5. Steps for Planning the Best Cultural Resource Subject. An improved CS algorithm is used to simulate the movement behaviour of large groups of elderly people in real time so as to obtain the best locations for cultural resources. The aim of the planning is to obtain the best locations for cultural institutions, including libraries, cultural centres, and cultural service centres, so as to improve the coverage and utilisation rate of elderly public cultural service resources. The steps for the simulation of movement behaviour of elderly groups based on the improved cuckoo algorithm are as follows:

Step 1: set the number of individuals in the group, the nest location, the initial adaptation value, the maximum step size $\text{step}_{\max}$, and the maximum step size $\text{step}_{\min}$.

Step 2: calculate the fitness function value for each nest in order to obtain the current optimal nest location and optimal value. The individual fitness values fitness are calculated as follows:

$$\text{fitness} = \sqrt{(x - g_x)^2 + \left(y - g_y\right)^2 + (z - g_z)^2} - \text{rand}(t), \tag{19}$$

where (x, y, z) is the current position of the individual, (g_x, g_y, g_z) is the 3D coordinate of the cluster target location and $\text{rand}(t)$ is the threshold value. This threshold is needed for distance spacing because the individuals in the group cannot all gather to the final target point but rather surround it.

Step 3: perform chaotic mapping of the current optimal nest and a nest update process using equation (14) to produce a new generation of nest locations, such as cultural service centres.

Step 4: determine whether the stopping condition is met; if so, output the optimal location (e.g., cultural centres) and the optimal fitness value; otherwise, repeat step 3.

Step 5: after obtaining the optimal solution (the central position of the entire cluster, e.g., the library), the individuals in the population are collision detected with all other individuals, and if a collision occurs, then skip back to step 3 until no collision occurs.

5. Simulation Results and Analysis

5.1. Experimental Configuration Parameters. The experiments in this article are divided into two parts: (1) standard function testing and (2) simulation of the planning of public cultural resources. The environment used for the experiments is MATLAB R2016a, PC configuration of Intel 2.4 GHz, 8G RAM, Window 10 operating system. The basic parameters of the improved CS algorithm were set as follows: maximum step size is 1, minimum step size is 10^{-4}, variation probability is 0.5, crossover probability is 0.9, probability of the bird's egg being found by the host is 0.25, and population size is 50. The experiment was conducted to simulate the movement behaviour of a large group of elderly people in real time by the improved CS algorithm so as to obtain the best location and path of the cultural resource subject. The aim of the experiment is to obtain the best locations of cultural institutions, including libraries, cultural centres, and cultural service centres, so as to improve the coverage and utilisation of elderly public cultural service resources.

5.2. Standard Function Tests. The optimal solution performance of the improved CS algorithm was tested using six classical test functions, and the results obtained were compared with typical CS, ASCS [33], and DECS [34]. The maximum number of iterations in the tests was 1000, with 20 runs of each function and a dimension of 30. The variables of the six test functions took values in the range $[-5.12, 5.12]$. The six classical test functions were defined as follows:

(1) Sphere function:

$$f_1(x) = \sum_{i=1}^{n} x_i^2. \tag{20}$$

(2) Schwefel function:

$$f_2(x) = \sum_{i=1}^{n} |x_i| + \prod_{i=1}^{n} |x_i|. \tag{21}$$

(3) Rastrigin function:

$$f_3(x) = \sum_{i=1}^{n} \left[x_i^2 - 10\cos(2\pi x_i) + 10\right]. \tag{22}$$

(4) Griewank function:

$$f_4(x) = 1 + \frac{1}{4000}\sum_{i=1}^{n} x_i^2 - \prod_{i=1}^{n} \cos\left(\frac{x_i}{\sqrt{i}}\right). \tag{23}$$

(5) Ackley function:

$$f_5(x) = -20\exp\left(-0.2\sqrt{\frac{1}{n}\sum_{i=1}^{n} x_i^2}\right) - \exp\left(\frac{1}{n}\sum_{i=1}^{n}\cos(2\pi x_i)\right) + 20 + e. \tag{24}$$

(6) Quartic (noise) function:

$$f_6(x) = \sum_{i=1}^{n} i x_i^4 + \text{random}[0, 1), \tag{25}$$

where both $f_1(x)$ and $f_2(x)$ are a single-peaked function. The global optimal solution of $f_3(x)$ is within a steep canyon. $f_4(x)$ has numerous local optimum points. $f_5(x)$ and $f_6(x)$ are both complex multipeaked functions with a large number of local minima. The minimum, maximum, mean, and standard variance of each run were obtained. The results of the comparison of the six test functions are shown in Table 1.

As can be seen from Table 1, when the number of iterations is the same, the improved CS algorithm proposed in this article obtains results that are closer to the global optimal solution when solving for six functions than the other five algorithms. The average fitness value of the improved CS algorithm is improved by 10 orders of magnitude, and the variance is significantly reduced. In particular, for functions f_4 with an infinite number of local optima, both the minimum and average fitness values of the improved CS algorithm reach the theoretical optimum, while the CS algorithm falls into the local optimum. The Schwefel function is a complex single-peaked function and the Rastrigin function is a complex multipeaked function, and other existing algorithms are prone to produce local optimum solutions. The algorithm in this article enters the chaotic mapping and uses its ephemeral nature to improve the search range and accuracy.

In order to directly observe the optimisation-seeking effect of the improved CS algorithm and the typical CS algorithm on the six test functions, the evolutionary curves of the optimal fitness values of the two were compared, as shown in Figures 1–6. It can be seen that the improved CS algorithm has higher optimisation accuracy and faster convergence. In summary, the improved CS algorithm has improved in terms of convergence accuracy and convergence speed compared to CS. This is due to the use of a dynamic step size adjustment method, compared to a typical cuckoo algorithm with random step sizes, thus enhancing the search speed while ensuring global optimisation-seeking capability.

5.3. Modelling the Movement Behaviour of Large Groups of Older People. MATLAB programming was used to implement the improved CS algorithm based elderly group movement behaviour control, and the obtained path data was imported into NURBS software to simulate the crowd animation. The simulation of the elderly gathering group

Table 1: Comparison results of six test functions.

Function number	Algorithms	Minimum adaptation value	Maximum adaptation value	Average adaptation value	Variance
f_1	CS	$2.74E-08$	$1.21E-07$	$5.82E-08$	$5.93E-16$
	ASCS	$1.22E-17$	$7.09E-15$	$4.61E-16$	$1.48E-30$
	DECS	$9.22E-12$	$4.70E-11$	$1.91E-11$	$7.25E-23$
	Improved CS	$1.59E-20$	$9.33E-17$	$2.41E-18$	$1.71E-34$
f_2	CS	$2.32E-03$	$7.19E-03$	$3.91E-03$	$1.00E-6$
	ASCS	$9.32E-10$	$5.71E-09$	$2.22E-09$	$7.28E-19$
	DECS	$5.94E-06$	$7.84E-05$	$4.68E-05$	$2.01E-10$
	Improved CS	$1.45E-11$	$5.13E-10$	$6.47E-11$	$4.95E-21$
f_3	CS	0	$3.30E-26$	$1.07E-27$	$2.21E-53$
	ASCS	0	$1.97E-29$	$8.63E-31$	1.49EE – -61
	DECS	0	0	0	0
	Improved CS	0	0	0	0
f_4	CS	$1.22E-06$	$1.66E-03$	$1.85E-04$	$9.43E-08$
	ASCS	$2.95E-07$	$2.53E-03$	$1.21E-04$	$1.33E-07$
	DECS	$5.12E-13$	$5.14E-12$	$1.77E-12$	$9.97E-25$
	Improved CS	0	0	0	0
f_5	CS	$3.36E-03$	$5.76E-02$	$1.51E-02$	$1.35E-04$
	ASCS	$6.73E-09$	$3.46E-07$	$5.40E-08$	$5.08E-15$
	DECS	$1.94E-06$	$7.19E-06$	$4.04E-06$	$1.26E-12$
	Improved CS	$1.03E-10$	$6.48E-08$	$2.81E-09$	$1.38E-16$
f_5	CS	$3.67E-03$	$4.32E-02$	$2.22E-02$	$6.41E-05$
	ASCS	$3.47E-03$	$2.36E-02$	$1.13E-02$	$1.49E-05$
	DECS	$3.45E-06$	$1.91E-03$	$5.23E-04$	$2.05E-07$
	Improved CS	$7.88E-05$	$3.26E-03$	$8.44E-04$	$4.25E-07$

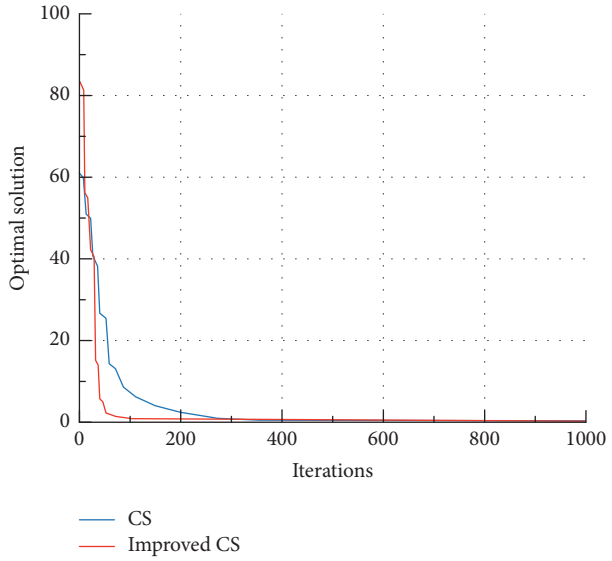

Figure 1: Iteration curve of function f_1.

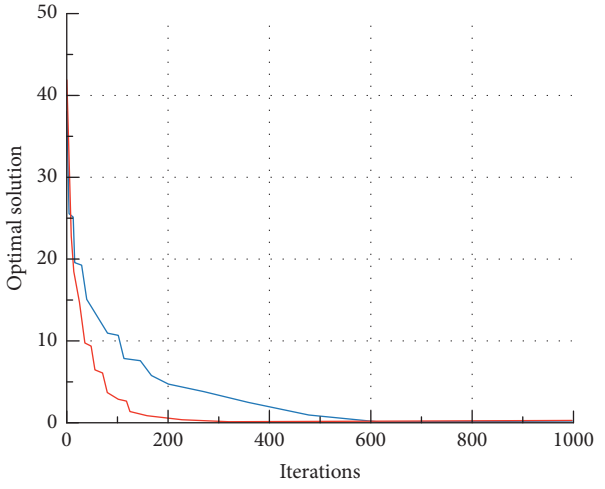

Figure 2: Iteration curve of function f_2.

movement behaviour based on the improved CS algorithm is shown in Figure 7, which verifies its feasibility.

5.4. Examples of Public Cultural Resources Planning. The essence of planning the public cultural resources is the Traveling Salesman Problem (TSP). This is the most basic route problem and a classical combinatorial optimisation problem. The feasible solution to the problem is the full permutation of all vertices. As the number of vertices increases, the corresponding number of feasible solutions increases accordingly. Therefore, public cultural resource planning is an NP-Hard problem. As shown above, the improved CS algorithm is very effective in finding the optimal solution to the continuous function problem. Next, the effectiveness of the improved CS algorithm in public cultural resource planning will be tested. The designed system modelled the public cultural service institution as a bird's

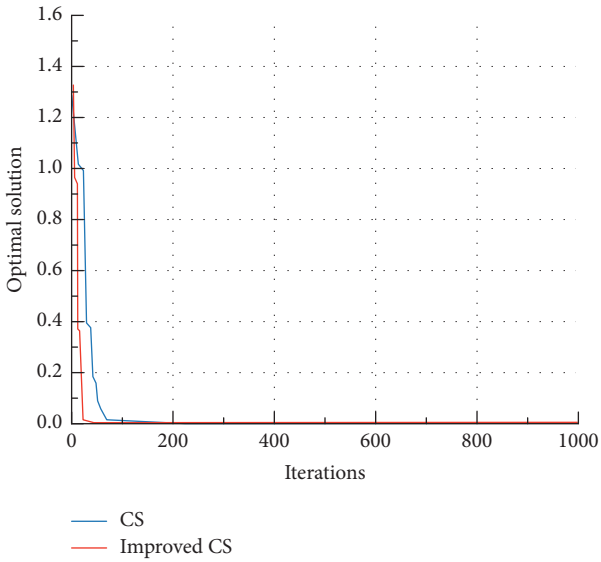

Figure 3: Iteration curve of function f_3.

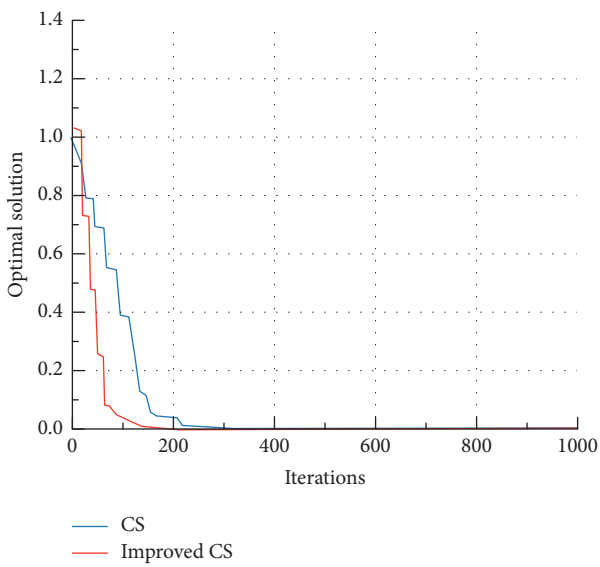

Figure 4: Iteration curve of function f_4.

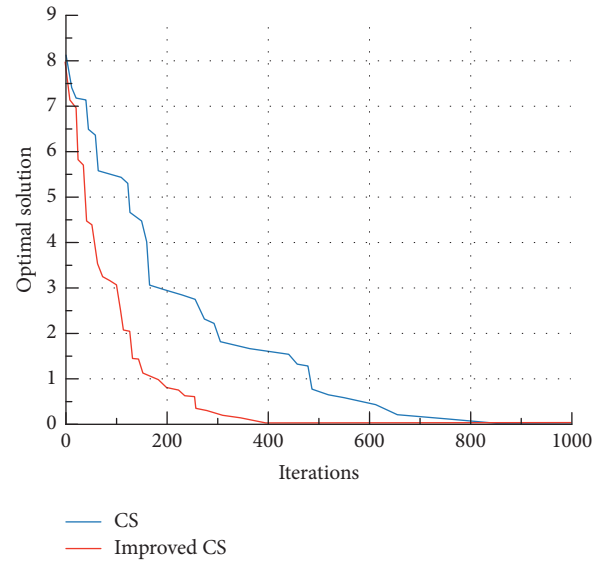

Figure 5: Iteration curve of function f_5.

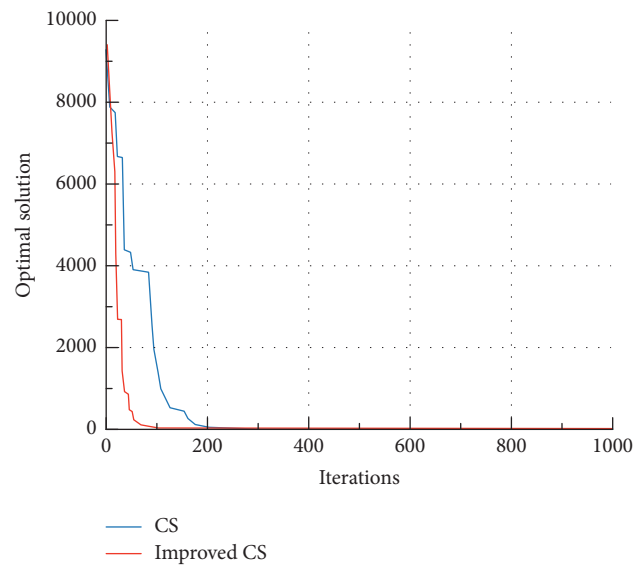

Figure 6: Iteration curve of function f_6.

nest and each individual elderly person as a cuckoo. The natural behavioural changes of the elderly population are simulated to ultimately produce the bird's nest location that best meets the actual needs. The location of the bird's nest location is the location of cultural institutions such as libraries, cultural centres, and cultural service centres.

The typical CS, ASCS, DECS, and improved CS algorithms were used to simulate the planning of public cultural resources for the elderly in each of the four cities, and a comparison of the simulation results is shown in Table 2. In City A, there are only 10 public cultural resources for the elderly. In City B, there are 30 public cultural resources for the elderly. In City C, there are 50 public cultural resources for the elderly. In City D, there are only 75 public cultural resources for the elderly.

As can be seen from Table 2, for the very-small-scale problem with 10 public cultural resources, all four algorithms can find the optimal solution. For the problem with 30 public cultural resources, the improved CS algorithm can find the optimal solution. For problems with 50 and 75 resources, the improved CS algorithm obtains optimal values that are closer to the optimal solutions compared to the other algorithms. It can be seen that the improved CS algorithm has better optimality finding accuracy. Finally, the coverage rate and utilisation rate of public cultural service resources for the elderly after using the designed system were counted in City D, and the results are shown in Figure 8.

As can be seen from Figure 8, the coverage and utilisation rate of public cultural service resources for the elderly in City D increased over time after using the designed

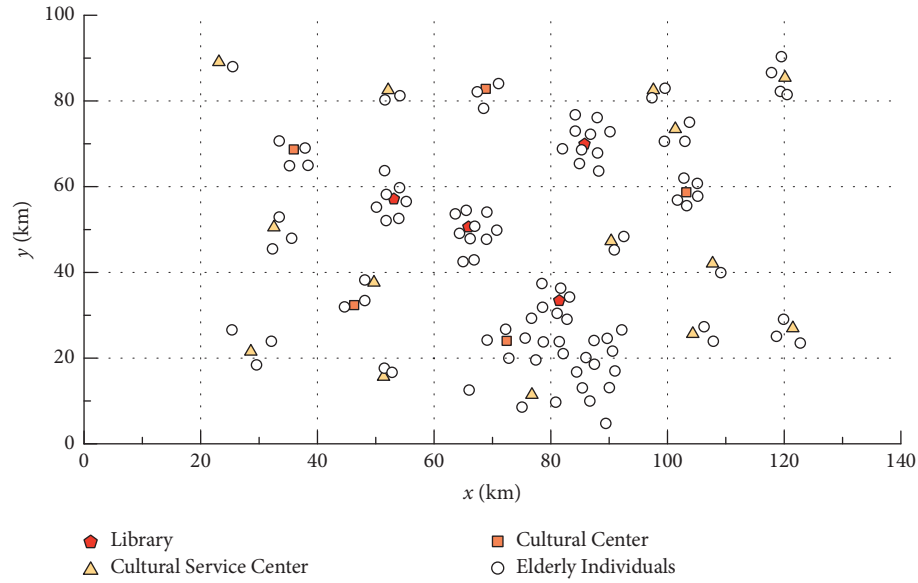

Figure 7: Simulation of movement behaviour of older people in congregate groups.

Table 2: Simulation comparison of public cultural resources planning.

City number	Optimum solution	Algorithms	Minimum adaptation value	Maximum adaptation value	Average adaptation value	Variance
A	2.6907	CS	2.6907	2.6907	2.6907	$1.43E-30$
		ASCS	2.6907	2.6907	2.6907	$5.23E-31$
		DECS	2.6907	2.6907	2.6907	$6.11E-31$
		Improved CS	2.6907	2.6907	2.6907	$5.82E-31$
B	423.741	CS	719.7529	787.0031	753.4504	442.0143
		ASCS	469.7712	782.6938	677.0514	8162.634
		DECS	499.4739	761.8066	607.7832	6354.7997
		Improved CS	423.741	720.4089	525.0658	6085.8082
C	427.855	CS	982.206	1018.3668	972.1053	564.1535
		ASCS	766.8296	1073.2126	981.7529	2517.9561
		DECS	635.8675	993.1679	904.5333	6125.7093
		Improved CS	510.5747	1040.1288	707.4548	13865.9908
D	594.18	CS	1664.7828	1815.353	1741.3225	1291.9662
		ASCS	1585.4851	1868.9838	1789.8069	2376.4924
		DECS	1568.5247	1775.9432	1707.7098	1795.046
		Improved CS	953.8732	1738.1591	1451.5683	25983.4133

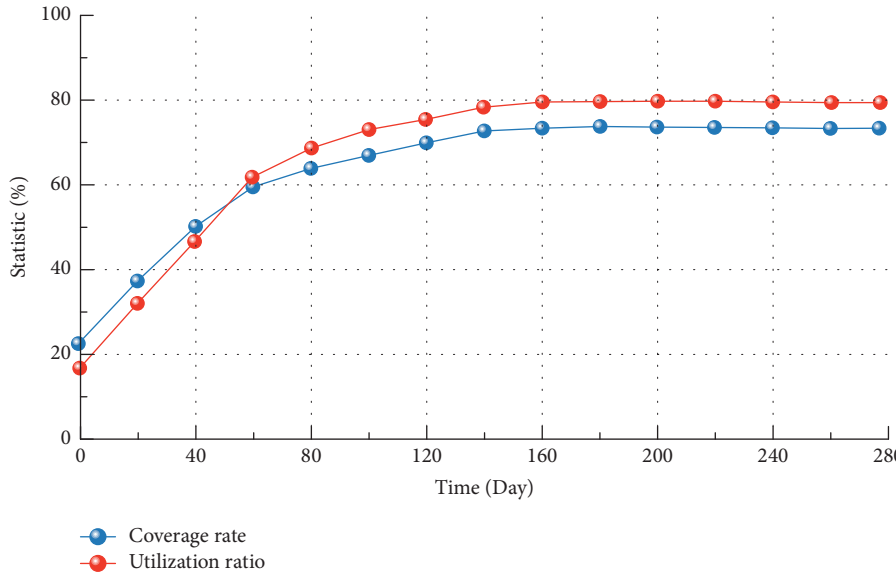

Figure 8: Variation curves of coverage and utilisation rate.

system. At 160 days, both the coverage and utilisation rates reached their highest values of 74.8% and 79.8%, respectively, verifying the effectiveness of the improved CS algorithm in the planning of public cultural resources for the elderly.

6. Conclusion

This article designs an intelligent computing-based public cultural service system for the elderly. Intelligent computing is introduced into the design of public cultural services for the elderly, thus solving the most important resource planning problem in the planning of public cultural services for the elderly. The CS algorithm is used to simulate the movement behaviour of large groups of elderly people in real time to plan the best location and path for cultural resource subjects. Collision detection is introduced in the generation of individual movement paths in order to solve the problem of collision between individuals. In addition, the standard CS algorithm is improved with chaotic mapping and dynamic step size in order to increase the spatial range of group behaviour options and to smoothly adjust the trajectory profile in order to improve the convergence speed and optimisation accuracy. Experimental results from six standard function tests show that the improved CS algorithm is very effective in finding the best for continuous function problems. The experimental results of the simulation with the planning of public cultural resources show that the coverage and utilisation rate of public cultural service resources for the elderly have been increasing with the improved CS algorithm, reaching 74.8% and 79.8%, respectively.

Data Availability

The experimental data used to support the findings of this study are available from the corresponding author upon request.

Conflicts of Interest

The authors declare that they have no conflicts of interest to report regarding the present study.

Acknowledgments

This work was supported by the Philosophy and Social Science Planning Project of Zhejiang Province, the double co-creating value of Matter & Spirit: The system structure of service design adapts to the elderly in the prospective community of Zhejiang (No. 22NDJC090YB).

References

[1] A. Bakhtiari, M. Hashemi, S. R. Hosseini, S. Omidvar, A. Bijani, and F. Khairkhah, "The Relationship between Depression and Metabolic Syndrome in the Elderly Population: The Cohort Aging Study," *Iranian Journal of Psychiatry*, vol. 13, no. 4, pp. 230–238, 2018.

[2] L. Ren, Y. Zheng, L. Wu et al., "Investigation of the prevalence of Cognitive Impairment and its risk factors within the elderly population in Shanghai, China," *Scientific Reports*, vol. 8, no. 1, p. 3575, 2018.

[3] T. Feng, Z. Feng, Q. Liu, L. Jiang, Q. Yu, and K. Liu, "Drinking habits and water sources with the incidence of cognitive impairment in Chinese elderly population: the Chinese Longitudinal Healthy Longevity Survey," *Journal of Affective Disorders*, vol. 281, no. 2, pp. 406–412, 2021.

[4] S. Liao, X. Yu, and Z. Luo, "Research on basic public cultural services in jiangxi Province of China: current situation, problems and countermeasures," *International Journal of Economic Behavior and Organization*, vol. 8, no. 3, p. 49, 2020.

[5] I. Aalders and N. Stanik, "Spatial units and scales for cultural ecosystem services: a comparison illustrated by cultural heritage and entertainment services in Scotland," *Landscape Ecology*, vol. 34, no. 7, pp. 1635–1651, 2019.

[6] A. Ecy, A. Mwb, and B. Kbh, "Influence of ecosystem services on management decisions by public land ranchers in the

intermountain west, United States," *Rangeland Ecology & Management*, vol. 72, no. 4, pp. 721–728, 2019.

[7] Y. Takase, A. A. Hadi, and K. Furuya, "The relationship between volunteer motivations and variation in frequency of participation in conservation activities," *Environmental Management*, vol. 63, no. 1, pp. 32–45, 2019.

[8] S. B. Morgan, A. Kestenbaum, M. Shields, and L. Dunn, "Understanding culture and diversity in spiritual care," *American Journal of Geriatric Psychiatry*, vol. 26, no. 3, pp. S81–S82, 2018.

[9] O. Roth-Cohen, S. Muralidharan, and C. La Ferle, "The importance of spiritual consumption, religious expression and subjective well-being among christians in the US during COVID-19," *Journal of Religion and Health*, vol. 61, no. 2, pp. 1719–1733, 2022.

[10] P. Barrett, J. Gaskins, and J. Haug, "Higher education under fire: implementing and assessing a culture change for sustainment," *Journal of Organizational Change Management*, vol. 32, no. 1, pp. 164–180, 2019.

[11] O. Woods, "Sonic spaces, spiritual bodies: the affective experience of the roots reggae soundsystem," *Transactions of the Institute of British Geographers*, vol. 44, no. 1, pp. 181–194, 2019.

[12] R. M. Kolpakov, "Optimal strategy for solving a special case of the knapsack problem by the branch and bound method," *Moscow University Mathematics Bulletin*, vol. 76, no. 3, pp. 97–106, 2021.

[13] E. E. Okon, "On technique for generating pareto optimal solutions of multi-objective linear programming problems [J]," *Science Journal of Applied Mathematics and Statistics*, vol. 7, no. 2, pp. 15–22, 2019.

[14] E. Güney, "An efficient linear programming based method for the influence maximization problem in social networks," *Information Sciences*, vol. 503, pp. 589–605, 2019.

[15] D. W. Gong, J. Sun, and Z. Miao, "A set-based genetic algorithm for interval many-objective optimization problems," *IEEE Transactions on Evolutionary Computation*, vol. 22, no. 1, pp. 47–60, 2018.

[16] W. Pan, B. Liu, and Z. Song, "Edge computing-induced caching strategy for national traditional sports video resources by considering unusual items," *International Journal of Distributed Systems and Technologies*, vol. 12, no. 2, pp. 1–12, 2021.

[17] X. Chen, Q. Shi, L. Yang, and J. T. Xu, "ThriftyEdge: resource-efficient edge computing for intelligent IoT applications," *IEEE Network*, vol. 32, no. 1, pp. 61–65, 2018.

[18] S. Garg, K. Kumar, N. Prabhakar, A. Ratan, and A. Trivedi, "Optical character recognition using artificial intelligence," *International Journal of Computer Application*, vol. 179, no. 31, pp. 14–20, 2018.

[19] M. Hossein and H. Sajad, "Artificial intelligence design charts for predicting friction capacity of driven pile in clay," *Neural Computing & Applications*, vol. 30, pp. 1–17, 2018.

[20] N. Liang, H. T. Zheng, J. Y. Chen, A. K. Sangaiah, and C. Z. Zhao, "TRSDL: tag-aware recommender system based on deep learning–intelligent computing systems," *Applied Sciences*, vol. 8, no. 5, p. 799, 2018.

[21] P. Civicioglu and E. Besdok, "A conceptual comparison of the Cuckoo-search, particle swarm optimization, differential evolution and artificial bee colony algorithms," *Artificial Intelligence Review*, vol. 39, no. 4, pp. 315–346, 2013.

[22] S. Walton, O. Hassan, K. Morgan, and M. Brown, "Modified cuckoo search: a new gradient free optimisation algorithm," *Chaos, Solitons & Fractals*, vol. 44, no. 9, pp. 710–718, 2011.

[23] D. D. Patil, R. P. Singh, and V. M. Thakare, "Analysis of ECG arrhythmia for heart disease detection using SVM and cuckoo search optimized neural network," *International Journal of Engineering & Technology*, vol. 7, no. 2, pp. 27–33, 2018.

[24] S. H. Gopalan, "ZHRP-DCSEI, a novel hybrid routing protocol for mobile ad-hoc networks to optimize energy using dynamic cuckoo search algorithm," *Wireless Personal Communications*, vol. 118, no. 4, pp. 3289–3301, 2021.

[25] P. Lakshminarayana and T. V. Sureshkumar, "Automatic generation and optimization of test case using hybrid cuckoo search and bee colony algorithm," *Journal of Intelligent Systems*, vol. 30, no. 1, pp. 59–72, 2020.

[26] Z. Bingul and O. Karahan, "A novel performance criterion approach to optimum design of PID controller using cuckoo search algorithm for AVR system," *Journal of the Franklin Institute*, vol. 355, no. 13, pp. 5534–5559, 2018.

[27] G. Sun, Y. Liu, Z. Chen, S. Liang, A. Wang, and Y. Zhang, "Radiation beam pattern synthesis of concentric circular antenna arrays using hybrid approach based on cuckoo search," *IEEE Transactions on Antennas and Propagation*, vol. 66, no. 9, pp. 4563–4576, 2018.

[28] D. Kumar, S. Ghosh, A. S. Kuar, and N. Maity, "Enhancement of laser transmission welds in acrylic and polypropylene copolymer (PPCP) using snap drift cuckoo search (SDCS) optimization," *Lasers in Engineering*, vol. 49, no. 4-6, pp. 205–225, 2021.

[29] S. S. Taheri, S. Seyedshenava, V. Mohadesi, and R. Esmaeilzadeh, "Improving operation indices of a microgrid by battery energy storage using multi objective cuckoo search algorithm," *International Journal on Electrical Engineering and Informatics*, vol. 13, no. 1, pp. 132–151, 2021.

[30] L. Meng, S. Yin, and C. Zhao, "An improved image encryption algorithm based on chaotic mapping and discrete wavelet transform domain," *International Journal on Network Security*, vol. 22, no. 1, pp. 155–160, 2020.

[31] S. Y. Li and K. R. Gu, "Smart fault-detection machine for ball-bearing system with chaotic mapping strategy," *Sensors*, vol. 19, no. 9, p. 2178, 2019.

[32] Q. Zhang, J. T. Han, and Y. T. Ye, "Image encryption algorithm based on image hashing, improved chaotic mapping and DNA coding," *IET Image Processing*, vol. 13, no. 14, pp. 2905–2915, 2019.

[33] M. A. Baset, Y. Zhou, and M. Ismail, "An improved cuckoo search algorithm for integer programming problems," *International Journal of Computing Science and Mathematics*, vol. 9, no. 1, p. 66, 2018.

[34] F. E. Ayo, O. Folorunso, F. T. Ibharalu, and I. A. Osinuga, "Hate speech detection in Twitter using hybrid embeddings and improved cuckoo search-based neural networks," *International Journal of Intelligent Computing and Cybernetics*, vol. 13, no. 4, pp. 485–525, 2020.

Hindawi
Scientific Programming
Volume 2022, Article ID 9147023, 8 pages
https://doi.org/10.1155/2022/9147023

Research Article

Analysis of Children's Sports Heuristic Teaching Based on Deep Learning

Xuesheng Wang,[1] **Xipeng Zhang**,[2] **and Feng Gao**[3]

[1]*Institute of Physical Education, University Huzhou, Zhejiang 313000, China*
[2]*Qingdao Huanghai University, Qingdao, Shandong 266000, China*
[3]*Jiaxing College Sports and Military Training Department, Jiaxing University, Jiaxing, Zhejiang 314000, China*

Correspondence should be addressed to Xuesheng Wang; 02088@zjhu.edu.cn

Received 28 April 2022; Revised 19 May 2022; Accepted 10 June 2022; Published 5 July 2022

Academic Editor: Lianhui Li

The "pursuit of deep learning" is mentioned among the recent trends driving the key trends driving educational technology in schools. "Deep learning" is widely used as a term, and classroom teaching has begun to focus more and more on deep learning. The heuristic teaching method is gradually accepted and used by educators all over the world with its scientific teaching mode and novel teaching methods. In today's children's physical education classroom, the heuristic teaching method has achieved certain results and effects, but in the process of trying, there is still room for development and improvement. Based on the deep learning model, this research will improve the existing heuristic teaching methods, through the experimental research on children's physical education classroom, observe the data results obtained by the deep learning-based children's physical education heuristic teaching, and analyze according to the results, so as to achieve the effect of heuristic teaching. A multilabel classification model ALSTM-LSTM is proposed according to the algorithm adaptation method in the multi-label learning method. The experimental results obtained an accuracy of 95.1%, which is higher than other deep learning models, and also reached the best in the evaluation indicators of precision, recall, and $F1$ score.

1. Introduction

With the continuous development of science and technology and the progress of society, the future society needs talents who can create high technology and new resources. Based on such a situation, it is urgent to deepen the reform of education. In the educational reform, heuristic teaching is a key point of the reform. Heuristic teaching emphasizes the combination of educators' follow-up guidance and students' thinking expansion, so that a class should not only learn the content of knowledge but also open up a new way of thinking for students, that is, independent inquiry learning. As the main body of education, students should actively participate in the curriculum and the process of knowledge exploration, so as to achieve the purpose of integrating knowledge. Educators should also respect students, fully mobilize students' interest in the inquiry process, care for students, not criticize students' wrong answers in class, give correct guidance, and encourage students to think. It can also improve students' self-confidence in mathematics learning. The multi-label analysis of posture in rope skipping refers to the use of the constructed deep learning model to judge which limb posture meets the standard and which limb posture needs to be corrected in the process of rope skipping. In artificial intelligence science, the multi-label limb posture analysis problem in children's physical education heuristic teaching can be transformed into multi-label learning problem. Based on the principle of deep learning, through the combination of multi-label limb posture analysis in children's sports heuristic teaching, this paper designs a heuristic teaching algorithm for children's sports, so as to solve the problems in the process of children's sports heuristic teaching [1–10].

2. Related Work

With the rapid development of Internet of Things technology, the combination of sports industry and emerging industries has become closer and closer. The first extension is based on reducing the subspace and swimming style information of possible posture configuration. The researchers have developed a class of label coding with spatial redundancy, which allows the network to learn the specific filter of swimming style. This principle is applicable to any form of activity information. The second extension focuses on the time of swimming video and proposes a two-step method, in which the initial pose estimation is refined in a fixed length sequence by an independent CNN module, and the experimental results show that the LSVM has reached the best first extension based on reduction possible. The second extension focuses on the time of swimming video, which proposes a two-step method in which the initial posture estimate is refined by a separate CNN module in a fixed length sequence. The experimental results show that the method has the ability to predict and improve the posture, which clearly improves the baseline CPM architecture, which provides help to attitude analysis during the player swimming. Extract human appearance characteristics and motion characteristics by using the OpenPose network model. Use supervisory machine learning to identify four activities categories, including sitting, standing, walking, and falling. The results show that the activity recognition method based on two-dimensional bone data can obtain better matching results as compared with the method based on three-dimensional bone data. Classification of KNN classifier is found by comparing the performance of K-nearest neighbor (KNN), support vector machine, Naive Bayes, linear discriminating formula (LDA), and feedforward reverse neural network (BPNN). The effect is best, and the overall accuracy is 98%. The robustness of the method also tests in two multi-camera view scenarios, and the results show that the CNN has better classification effect than other classifiers, and the classification results are 100%. From the current development of intelligent sports in the world, it has been gradually realized. This paper realizes the principle of intelligent sports in the heuristic teaching of children's sports, which involves many contents, mainly including the collection and processing of sports data and sports characteristics, the extraction of sports network model, the research on the development of the rope skipping action analysis system, etc., and the heuristic teaching experience research based on rope skipping in sports [11–15].

3. Related Theoretical Methods

3.1. Circulating Neural Network Model. The time series is a series of data accumulated in the time dimension, and many applications are analyzed in time series data. Assuming $1 = \{x,\ldots,x\}$, X_n is a time series of a length N, $X = \{X^1,\ldots,X^M\}$ consists of M different single-dimensional time series, and for each $1 \le i \le M$, the length of the time sequence is n. On the classification problem of the time series, the format of the data is usually as follows: dataset $D = \{(x_1, y_1), (x_2, y_2), \ldots, (x_N, y_N)\}$ indicating the time series and corresponding label, y_i is achieved by one-hot coding, and the length k indicates that there is K category. From a whole, in a network model based on a time series, the input is the corresponding classification probability of the continuous learning of the neural network in the middle of the time series. Because time data are complex and unstable, the depth learning method is not assumed to assume the basic mode of the data, which is more robust to noise, so the depth learning model is the preferred method in time series data analysis. Circulating neural networks are complex depth learning networks that can be remembered, so they are widely used in the processing of sequence data. The RNN unit is the backbone of the circulation network, and there are two incoming connections and two outgoing connections in the RNN. LSTM can select an input sequence area that contributes to class tags in the context vector by attention. Note that mechanisms are often used in natural language processing. In the machine translation, a set of context vectors C is conditioned in the target sequence y, and the context vector Ci depends on the annotation sequence $(h_1,\ldots,h_{Tx})$ that maps the input sequence to the encoder. In each comment, H_i contains information about the entire input sequence, and the model will focus on the part around the i-th word of the input sequence where c_{i} is weighted and calculated by h_{i} [16]:

$$c_i = \sum_{j=1}^{T_X} a_{ij} h_j. \tag{1}$$

Each comment a_{ij}'s weight hj is calculated as follows:

$$a_{ij} = \frac{\exp\left(e_{ij}\right)}{\sum_{k=1}^{T_x} \exp\left(e_{ik}\right)}, \tag{2}$$

where $e_{ij} = a(s_{i-1}, h_j)$ is the alignment model, which scores the matching degree of the input around the j position with the output at the i position. Bahdanau et al. parameterized the alignment model as a feedforward neural network that is co-trained with all other parts of the model, computing the soft alignment directly during the computation of the alignment model [17].

3.2. Heuristic Teaching Network Structure Based on OpenPose. In preschool physical education, OpenPose, an open source library for real-time multi-person pose estimation based on deep learning, is introduced. It can accurately estimate the pose of each person in the image in physical education teaching in real time, so as to realize the extraction of face, trunk, limbs, and hand bone points. It takes into account real-time performance and accuracy and has strong robustness. The core of this method is a bottom-up human pose estimation algorithm based on part affinity fields (PAFs), that is, to detect key points before acquiring the skeleton, which avoids the long calculation time in multi-person scenarios [18].

3.2.1. OpenPose Network Structure. Figure 1 shows the multi-level prediction network structure designed by

OpenPose. The framework is based on the VGG19 network model and converts the input image into image features F, $L(p)$, and $S(p)$ by stage prediction. $L(p)$ is the affinity vector field PAFs, and $S(p)$ represents the confidence of the key points in the skeleton. The structure divides the prediction into 6 stages, the first 4 stages predict the affinity vector field, and the last 2 stages predict the confidence. At each subsequent stage, the predictions from the previous stage are concatenated with the original image features as input to generate more refined predictions. After obtaining the confidence and affinity of the key points, the Hungarian algorithm is used to optimally match the adjacent key points to obtain the skeleton information of each person. OpenPose has good real-time performance and has designed a variety of model architectures to be compatible with different hardware configurations. It uses a monocular camera for reliable key point information without the need for a dedicated depth camera like Kinect. Parts that can be estimated are eyes, ears, nose, neck, shoulders, elbows, wrists, hips, knees, and ankles [19].

3.2.2. Confidence Map. In the human body pose estimation based on OpenPose, in order to obtain the coordinate information of the key points of the human body, the Gaussian modeling method is used to obtain the confidence map of the position of the key points, and the confidence map is used to represent the key points, wherein the value in the confidence map is expressed as a certain probability of key point locations. The confidence map of key point locations can be expressed as [20]

$$c_{j,k} = \exp\left(-\frac{\left\|p - x_{j,k}\right\|_2^2}{\delta^2}\right), \quad (3)$$

$$c_j(p) = \max S_k^{j,k}(P),$$

where j represents the joint point of the human body, k represents the kth target person in the image.

4. Action Analysis Algorithm in Heuristic Teaching Sports Scenario

Computer vision-based motion analysis during exercise is a complex problem, especially when analyzing vigorous sports. In order to achieve a detailed description of the body movements during the movement process, this paper uses deep learning to build a model of the network.

4.1. Problem Definition. The content of this paper is an implementation method of intelligent sports in the rope skipping motion analysis system, which involves many fields, including data collection and processing, feature extraction, data transmission, network model design, system implementation, etc. According to the flowchart, it can be clearly seen that the analysis of the swaying and jumping action mainly includes two modules: one module is used to obtain the key point information of the human body, and the other module is used to mathematically model the obtained key point information and build a multi-label classification network model [21].

The problem can be defined as given m groups of rope skipping records, preprocess m groups of sequence data to obtain a data sequence $D = (r1, r2, \ldots, rm)$, where rj, $i = 1, \ldots, m$ represent m sequence data, where the label set $L = (l1, l2, \ldots, ln)$, lj, $j = 1, \ldots, n$ represent the limb labels during the rope skipping process, and each record in D is associated with multiple labels in L. Multi-label pose analysis can be represented by a tuple (r_i, Y_i), where Y_i is contained in L. Our goal is to design and implement a label classification model that judges the limb labels Y_i during rope skipping based on the new pose dataset ri' [22–24].

4.2. Network Framework Design

4.2.1. MobileNetV2 Framework. Convolutional neural networks have made breakthroughs one after another in the field of computer vision, but the application of deep learning models on the mobile terminal is not wide enough. At present, the recognition effect of the lightweight network on the ImageNet dataset is based on top-1, which is improved compared with ResNet-34 and VGG19, and its accuracy is slightly lower than that of ResNet-50, which is lightweight. The high-level network model has a certain balance in real-time performance and accuracy. In order to train and apply the model in an environment with few resources and low hardware support, a lightweight network model is more needed in real scenarios. When obtaining the human body pose, the OpenPose network model first sends the image frame to VGG19 to obtain the set of image feature maps $F = (F1, F2, \ldots, Fx)$, where x represents the number of feature maps. However, VGG19 consumes more computing resources and will generate a lot of parameters during the training process, which will take up more memory. In view of the high performance and efficiency of MobileNetV2, this paper modified the original OpenPose method when extracting image feature maps.

The MobileNetV2 network is an improved version based on the MobileNet network. Its innovation is that an inverted residual structure is added to MobileNetV2. The inverted residual structure is different from the original residual structure.

4.2.2. ALSTM-LSTM Network Framework. In this paper, the human posture analysis problem in rope skipping obtained in physical education teaching is transformed into a multi-label classification problem according to the time order relationship. Because LSTM can play a role in global processing and storage unit, it can maintain good performance in time series. Attention mechanism is a global approach to processing. Applying attention mechanism to LSTM can improve the performance of LSTM. Therefore, inspired by LSTM and attention mechanism, this paper creatively proposes a method of applying attention mechanism in LSTM and combining a single LSTM for multi-label

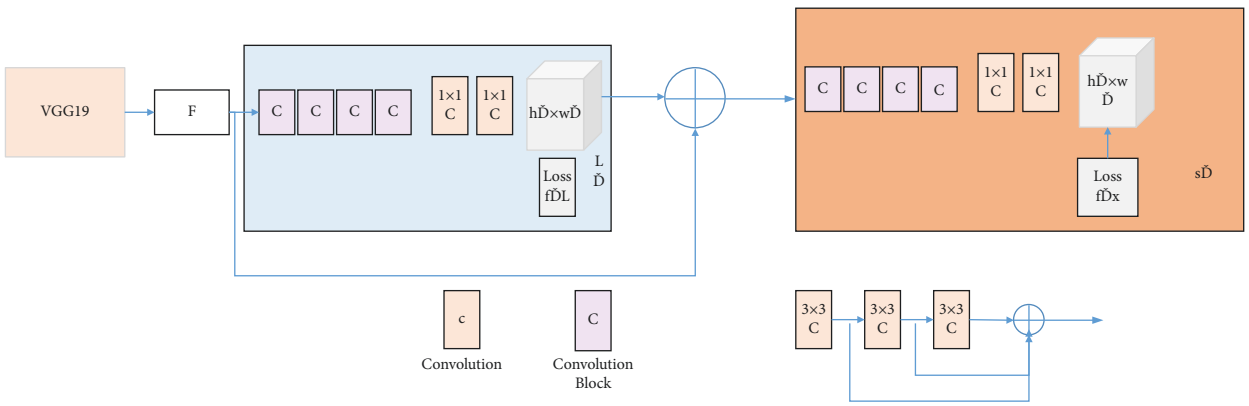

Figure 1: OpenPose network structure diagram.

classification. The network framework of ALSTM-LSTM is shown in Figure 2.

The most typical example in the breakthrough of the algorithm is the proposed batch normalization (BatchNorm) method. BatchNorm smoothes the solution space of related optimization problems, thereby ensuring more predictable gradients, which in turn allows the use of a wider range of learning rates for faster network convergence. This study demonstrates that adding a BatchNorm layer to a deep learning network model greatly improves the Lipschitzness of the loss function and gradient in the model. So, this article adds a BatchNormalization layer before using the LSTM and ALSTM layers. In addition, since this paper studies a multi-label classification problem, according to the multi-label algorithm transformation method, the activation function of the ALSTM-LSTM model in the last layer is set to the sigmoid activation function, and the loss function selects the binary cross-entropy loss function.

4.3. Attitude Estimation Optimization Algorithm. In the two branches of OpenPose, one branch is used to predict the confidence map (S) of the key point, that is, the probability value of this key point, and the other branch is used to predict the affinity field PAFs between the two key points (L).

$$f_s^t = \sum_{j=1}^{j} \sum_{p} w(p). \left\| S_j^t(p) - S_j^*(p) \right\|_2^2,$$
$$f_L^t = \sum_{j=1}^{C} \sum_{p} w(p). \left\| L_j^t(p) - L_j^*(p) \right\|_2^2. \tag{4}$$

The overall loss is the loss sum of each stage:

$$f = \sum_{t=1}^{T} \sum_{p} \left(f_s^t + f_L^t \right). \tag{5}$$

In order to further improve the generalization ability of the pose estimation algorithm and improve the accuracy of the algorithm, this paper introduces two weights and a penalty term into the total loss function:

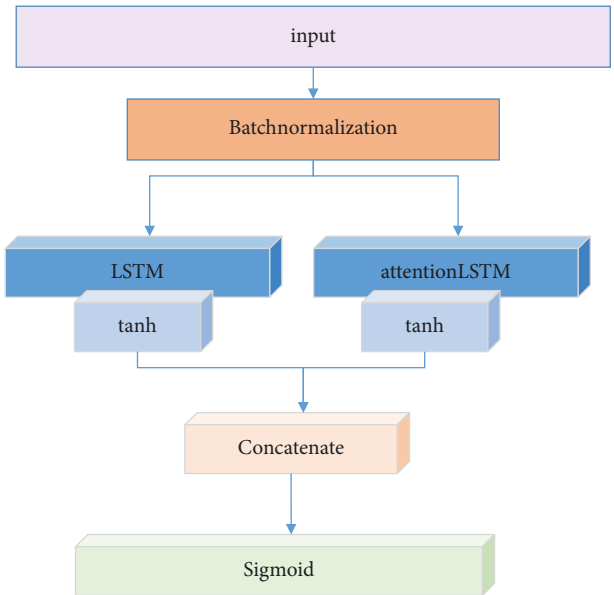

Figure 2: ALSTM-LSTM network framework.

$$f = \sum_{t=1}^{T} \left(\alpha f_s^t + \beta f_L^t + \theta \right). \tag{6}$$

By introducing weights, we analyze how much the losses in the two branches affect the results.

5. Design and Implementation of Heuristic Physical Education Teaching System

5.1. Overall Design of the System. The overall design of children's physical education teaching system determines which functions the system should realize according to the analysis of children's physical education teaching needs and generally explains how the system is realized. The overall design of children's physical education teaching is to introduce the functions of each module and the relationship between each other. The overall design of children's physical education teaching system includes the design of system function module and database table.

5.1.1. Functional Module Design. The function module design is to divide the smart rope skipping teaching system into several subsystems and then divide the subsystems into different modules according to their functions. The division of project modules can help developers simplify complex problems. The design of functional modules is a further refinement of the requirements. The appropriate division of functional modules can provide a detailed understanding of each function of the system, reduce the time for developers in the development process, and enhance the maintainability of the system. In this design, the Android-based smart rope skipping teaching system APP is implemented on the server side using the SSM framework and MySQL database. The SSM framework is a combination of three frameworks, namely, Spring Framework, SpringMVC, and MyBatis. At present, the SSM framework has been widely used in the development of websites and has become more and more popular in the development of commercial software. The APP client of this system adopts the basic mode of the current popular MVP (model view presenter), which is mainly composed of three major components: view, model, and presenter. The view is responsible for displaying the page, the model is responsible for providing data support for business processing, and the presenter is responsible for processing business logic. The entire system architecture is shown in Figure 3. The user transmits data through the mobile phone camera, the MySql database is responsible for storing the data, and the server accepts the user's data request, processes, and feeds the result back to the user.

5.1.2. Database Table Design. The design of infant physical education teaching database table further describes the infant physical education teaching data by relying on the conceptual structure design of infant physical education teaching database. The early childhood physical education teaching system includes four basic tables: personnel basic information table person, video information table video, information message table news, and rope skipping analysis results. The database table is established according to the relational schema as follows:

(1) User table: the user table is used to store the basic information of the user, including the user's id, user name, user's password, and user's authority. According to the user's authority, users can be divided into administrators and ordinary users. The structure of the user table is shown in Table 1.

(2) User video table: the user video table is used to store the id of the video uploaded by the user and the storage path of the video. The structure of the user video table is shown in Table 2.

(3) Message table: the message table is used to store the information and consultation related to the rope skipping test issued by the administrator, as well as some rope skipping skills. The message table contains the id of the message, the title of the message, and the content of the message. The structure of the message table is shown in Table 3.

(4) Analysis result table: analysis result table mainly stores the contents of the results of the analysis and analysis results. The analysis result surface structure is shown in Table 4.

5.2. Detailed Design and Implementation of the System

5.2.1. Environment Introduction. The development of the APP is carried out on the Android Studio platform. It is an Android integrated development environment that only supports Android development. It is a plug-in focused on Android development that Google excludes other functions from the IntelliJ IDEA Community Edition. It is equivalent to a weakened version of the IntelliJ IDEA which is different however. Before using Android Studio, you need to download Java JDK first. During use, Android Studio's prompt tool supports ProGuard and application signature. Android Studio's powerful layout editor can directly drag UI controls and preview the effect. There is also an Android emulator on Android Studio, which makes it easy to debug during the development of the APP. During the development of the software, the Android emulator was used and several models of mobile phones were used in the testing phase. On the server side, we use HUAWEI CLOUD server as data storage and model invocation and build the deep learning model on HUAWEI CLOUD server. The training process of deep learning is implemented through Python language, and SpringMVC is used to realize the controller layer of the server side. At the same time, it also realizes the communication interface between the server and the APP. Table 5 describes the environment used for the development of this system.

5.2.2. System Function Test. The goal of functional testing is to test each functional module of the system, determine whether each functional module is optimal, and make subsequent improvements based on the test results. According to demand analysis, the system is mainly divided into seven modules: system login registration module, model upload module, user management module, message release module, data upload module, and analysis report viewing module. According to the test, you can check whether each function can be carried out smoothly and optimize the interface according to the user experience. Test for each functional module is shown in Table 6. The purpose of the system registration login module test is to detect whether the user can jump normally when logging in, and whether the registered information is encrypted in the database.

The purpose of the model upload function test is to check whether the administrator can upload the newly trained model to the location specified by the server and ensure that the model can be called correctly, as shown in Table 7.

The purpose of the analysis report viewing function module test is to detect whether the server can return the results normally after the user uploads the one-minute rope skipping dataset to the server and correctly display it on the mobile phone page, as shown in Table 8.

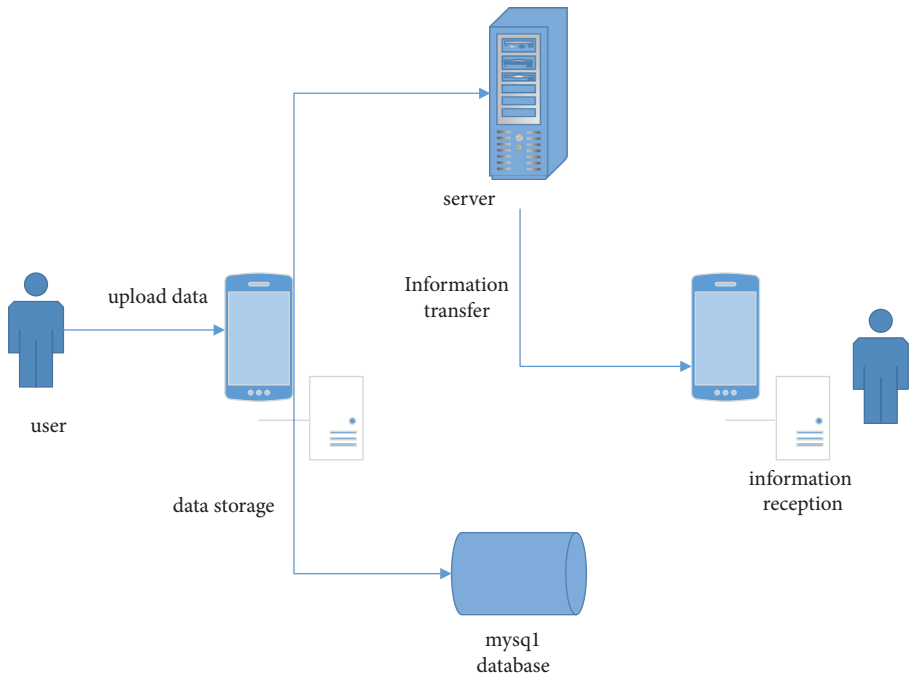

Figure 3: System architecture diagram.

Table 1: User information table.

Field name	Field type	Width	Primary key	Description
Person_id	Int	25	Yes	User unique ID, primary key
Person_name	Varchar	16		Username
Person_password	Varchar	16		User password
Person_power	Int	2		User rights

Table 2: User video table.

Field name	Field type	Width	Primary key	Description
Video_id	Int	25	Yes	Video unique identifier, primary key
Video_address	Varchar	100		Video address

Table 3: Message table.

Field name	Field type	Width	Primary key	Description
News_id	Int	25	Yes	Message unique identifier, primary key
News_title	Varchar	50		Message name
News_content	Varchar	500		Message content

Table 4: Result analysis table.

Field name	Field type	Width	Primary key	Description
Results_id	Int	25	Yes	Analysis result unique identification, primary key
Results_content	Varchar	500		The content of the analysis results

Table 5: System environment introduction.

Client	Android
Service terminal	Java
Deep learning model	Python 3.5
Database	MySql

Table 6: System registration and login function test case table.

Test module name	System registration login		
Condition	The user registers and logs in after the registration is successful. The password and account must meet the requirements.		
Serial number	Results required for needs analysis	Actual effect	Whether it is expected
1	RegisterLoginJump	Able to realize the jump of registration and login	Yes
2	The registration password needs to be encrypted	The registration password is encrypted in the database	Yes

Table 7: Model upload function test case table.

Test module name	Model upload		
Condition	Upload and train the new network model		
Serial number	Results required for needs analysis	Actual effect	Does it meet expectations
1	Upload the locally trained model to the server	Ability to upload and apply models	Yes

Table 8: Analysis report view functional test case table.

Test module name	Analysis report view		
Condition	The user uploads the rope skipping video to view the rope skipping analysis results		
Serial number	Results required for needs analysis	Actual effect	Does it meet expectations
1	User clicks the query report button query report	Correctly return query results and generate reports	Yes

Table 9: System performance test cases.

Serial number	Test performance name	Start event	End event	Time consumption (s)
1	Model upload	Click the model upload button	Model uploaded successfully	20.23
2	Analysis report query	Video upload	Analysis report query	75.23

5.2.3. System Performance Test. The performance of the system can directly affect the user's experience. In order to upload the model, the system performance is tested during the analysis report generation process. Its test is shown in Table 9.

6. Conclusion

Traditional teaching methods can play a certain role and effect in imparting knowledge and skills. It has the advantage of being able to popularize educational knowledge quickly, imparting knowledge to students under the circumstance of limited teaching environment, single teaching method, and tight teaching time. Combined with the literature, we can see that traditional teaching is derived from class-based teaching under specific social conditions. However, in the classroom of traditional teaching method, the shortcomings of this teaching method can be clearly found, including the lack of subjective initiative of students in learning, low learning interest, less interaction between teachers and students, and depressed classroom atmosphere. With the development of the times, predecessors have conducted more research on heuristic teaching, which has laid a solid foundation for the popularization of heuristic teaching in primary and secondary schools. Teaching research is rarely involved, and a set of elementary school basketball heuristic teaching experimental program has not been formed. Therefore, heuristic teaching is a new type of teaching method at present, which can be improved according to the inner development and actual needs of young children and is in line with the development needs of the current new era. In view of the current research hotspots for human behavior detection and recognition, this paper seldom studies the recognition of continuous actions in actual scenes, focusing on the improvement of the recognition rate and accuracy of motion actions, and is committed to solving traditional sports training equipment to realize the scientific, standardized, and unified management of children's sports training.

Data Availability

The dataset can be accessed upon request.

Conflicts of Interest

The authors declare that there are no conflicts of interest.

Acknowledgments

This paper is the research result of the scientific research project "Experimental research on the impact of skill sports on children's attention level (no. kx25064)" of Huzhou Normal University.

References

[1] B. L. M. Hernandez, D. Gober, D. Boatwright, and G. Strickland, "Jump rope skills for fun and fitness in grades K-12," *Journal of Physical Education, Recreation and Dance*, vol. 80, no. 7, pp. 15–41, 2009.

[2] Y. Wang, Yi Wang, and Z. Zhang, "Multi-label classification method of human behavior in rope skipping scene based on complexity graph," *Security and Communication Networks*, vol. 2022, Article ID 8202383, 7 pages, 2022.

[3] A. S. Ha, C. Lonsdale, J. Y. Y. Ng, and D. R. Lubans, "A school-based rope skipping program for adolescents: results of a randomized trial," *Preventive Medicine*, vol. 101, pp. 188–194, 2017.

[4] A. Subasi, D. H. Dammas, R. D. Alghamdi et al., "Sensor based human activity recognition using adaboost ensemble classifier," *Procedia Computer Science*, vol. 140, pp. 104–111, 2018.

[5] M. M. Hassan, M. Z. Uddin, A. Mohamed, and A. Almogren, "A robust human activity recognition system using smartphone sensors and deep learning," *Future Generation Computer Systems*, vol. 81, pp. 307–313, 2018.

[6] T. Li, D. Liu, and Y. Yang, "Phylogenetic supertree reveals detailed evolution of sars-cov-2," *Scientific reports*, vol. 10, no. 1, pp. 1–9, 2020.

[7] M. Kimura and T. Ohta, "On the stochastic model for estimation of mutational distance between homologous proteins," *Journal of Molecular Evolution*, vol. 2, no. 1, pp. 87–90, 1972.

[8] L. R. Foulds and R. L. Graham, "The steiner problem in phylogeny is NP-complete," *Advances in Applied Mathematics*, vol. 3, no. 1, pp. 43–49, 1982.

[9] L. L. Cavalli-Sforza and A. W. Edwards, "Phylogenetic analysis. Models and estimation procedures," *The American Journal of Human Genetics*, vol. 19, no. 3, pp. 233–257, 1967.

[10] R. Desper and O. Gascuel, "The minimum evolution distance-based approach of phylogenetic inference," *Mathematics of Evolution and Phylogeny*, Oxford University Press, Oxford, UK, 2007.

[11] N. Saitou and M. Nei, "The neighbor-joining method: a new method for reconstructing phylogenetic trees," *Molecular Biology and Evolution*, vol. 4, no. 4, pp. 406–425, 1987.

[12] P. H. Sneath and R. R. Sokal, "Unweighted Pair Group Method with Arithmetic mean," *Nu-merical Taxonomy*, vol. 1, pp. 230–234, 1973.

[13] M. N. Price, P. S. Dehal, and A. P. Arkin, "FastTree 2 - approximately maximum-likelihood trees for large alignments," *PLoS One*, vol. 5, no. 3, Article ID e9490, 2010.

[14] S. Guindon and O. Gascuel, "A simple, fast, and accurate algorithm to estimate large phylogenies by maximum likelihood," *Systematic Biology*, vol. 52, no. 5, pp. 696–704, 2003.

[15] A. Stamatakis, "RAxML version 8: a tool for phylogenetic analysis and post-analysis of large phylogenies," *Bioinformatics*, vol. 30, no. 9, pp. 1312-1313, 2014.

[16] R. Bouckaert, J. Heled, D. Kühnert et al., "Beast 2: a software platform for bayesian evolutionary analysis," *PLoS Computational Biology*, vol. 10, no. 4, Article ID e1003537, 2014.

[17] F. Ronquist, M. Teslenko, P. Van Der Mark et al., "MrBayes 3.2: efficient bayesian phylogenetic inference and model choice across a large model space," *Systematic Biology*, vol. 61, no. 3, pp. 539–542, 2012.

[18] J. Felsenstein, "Evolutionary trees from DNA sequences: a maximum likelihood approach," *Journal of Molecular Evolution*, vol. 17, no. 6, pp. 368–376, 1981.

[19] J. Felsenstein and J. Felenstein, *Inferring phylogenies*, Vol. 2, Sinauer associates Sunderland, MA, USA, 2004.

[20] Z. Yang, *Molecular Evolution: A Statistical approach*, Oxford University Press, Oxford, UK, 2014.

[21] B. Rannala and Z. Yang, "Probability distribution of molecular evolutionary trees: a new method of phylogenetic inference," *Journal of Molecular Evolution*, vol. 43, no. 3, pp. 304–311, 1996.

[22] B. Larget and D. L. Simon, "Markov chasin Monte Carlo algorithms for the bayesian analysis of phylogenetic trees," *Molecular Biology and Evolution*, vol. 16, no. 6, pp. 750–759, 1999.

[23] K. K. Kidd and L. A. Sgaramella-Zonta, "Phylogenetic analysis: concepts and methods," *The American Journal of Human Genetics*, vol. 23, no. 3, pp. 235–252, 1971.

[24] Y. Wang, Y. Zhang, L. J. Shen, and S. M. Wang, "Analysis and research on human movement in sports scene," *Hindawi Computational Intelligence and Neuroscience*, vol. 2021, Article ID 2376601, 12 pages.

Hindawi
Scientific Programming
Volume 2022, Article ID 6875192, 8 pages
https://doi.org/10.1155/2022/6875192

Research Article

Application of Traditional Chinese Elements in Visual Communication Design Based on Somatosensory Interaction Parameterisation

Jianjun Zhang[1] **and Jie Guo**[2]

[1]*Jinzhong University, Shanxi, Jinzhong 030619, China*
[2]*Shaanxi University of Science & Technology, Shaanxi, Xi'an 710000, China*

Correspondence should be addressed to Jie Guo; guojie@sust.edu.cn

Received 19 April 2022; Revised 24 May 2022; Accepted 7 June 2022; Published 4 July 2022

Academic Editor: Lianhui Li

In recent years, the interdisciplinary exploration of combining traditional visual communication design with somatosensory interaction technology has become a new form of artistic expression. In order to explore the feasibility of somatosensory interaction technology in visual communication design, this study proposes a 2D dynamic graphic generation method based on somatosensory interaction parameterisation and uses traditional Chinese elements as an example for specific applications in visual communication design. Firstly, the motion parameters recognised using the Kinect somatosensory interaction device are bound to the function variables used to generate the images in the development environment, thus enabling human somatosensory interaction with different characters in the scene. Secondly, a linear discriminant analysis based on kernel functions is used to reduce the dimensionality of the vector space, thus solving the problem of real-time and accurate capture of human movements. Then, using the skeletal parameter binding technique, the association between the motion parameters of the somatosensory interaction and the two-dimensional dynamic graphics is achieved. The experimental results show that the visual communication technique based on somatosensory interaction has a high recognition accuracy. Distinguished from traditional digital video, the proposed method can greatly enrich the visual representation of traditional Chinese elements.

1. Introduction

In recent years, there have been many points of convergence between the rapidly developing digital economy and the cultural industries. Science and art are beginning to merge in terms of technology and form. In today's cultural communication application scenarios, audiences increasingly need a good live experience. However, in the current presentation of design content, spatial interpretation is still usually done by means of printed posters or by showing offline videos [1–5]. As the design content itself is independent, the audience cannot communicate with the design content. To achieve real-time interaction between the design content and the audience, a fundamental change in the design approach is required. The interdisciplinary exploration of traditional visual communication design in combination with somatosensory interaction is a new solution to these problems.

In the landscape of museum exhibitions and tourism developments, designers prefer to use immersive interactive experiences to attract foot traffic. Unlike traditional interface interaction, somatosensory interaction emphasises the use of body movement responses to communicate with the product [6–8]. As a representative of Human-Computer Nature Interaction (HCI), somatosensory interaction is a new stage of technological development. With good immersion, low learning cost, and good user experience, somatosensory interaction has won wide application prospects and has received attention from scholars in various fields at home and abroad [9–12]. More advanced somatosensory interaction first appeared in 2007. During this period, Nintendo

combined somatosensory with gaming and introduced the concept of "health gaming." In 2010, Microsoft launched Kinect v1.0, which was released with the X-BOX console and won high reputation and sales. At this stage, Kinect v1.0 began to be used in the medical, fitness, and retail industries, with various leading-edge applications being attempted. As a noncontact means of interaction, somatosensory interaction has a natural advantage for scenario applications on immersive and large digital spaces. Currently, rapid advances in science and art are leading to increasing demands for spatial visual applications. The use of interactively updated visual information to improve spatial functionality is a future area for joint development across media.

In order to explore the feasibility of somatosensory interaction technology in visual communication design, this study proposes a 2D dynamic graphics generation method based on somatosensory interaction parameterisation and uses traditional Chinese elements as an example for specific applications in visual communication design. It is important to note that somatosensory interaction technology requires real-time and accurate capture and recognition of human movements. Therefore, this paper employs the latest Kinect v2.0 device and designs a method for action parameter feature extraction based on linear discriminant analysis.

2. Related Studies

Humans sometimes do not always speak the truth, but body language often expresses their truest emotions. Therefore, the recognition of human body movements has been an important research direction in the field of computer image recognition [13–16]. Currently, popular algorithms for body movement recognition include BP neural networks, decision trees, and Support Vector Machine (SVM), among others.

At this stage, the most commonly used hardware device for body movement recognition is the Kinect body sensor. For example, Ying et al. [17] proposed a human motion recognition method using the Kinect body sensor. Lai et al. [18] proposed a DSP-based portable human gesture action recognition system in real time, using a combination of spectral analysis and linear discriminant analysis (LDA) strategy. Although these two methods improve the accuracy and efficiency of action recognition, respectively, there are more types of actions in practical applications. At the same time, human actions are more complex in Kinect-based somatosensory interaction, resulting in real-time and high-dimensional action data, so the dimensionality of the vector space must be reduced as much as possible in order to recognise more action types in real time.

The main objective of this research is to visualise 2D motion graphics using the Kinect v2.0 device and apply it to visual communication design. When the body posture data obtained from the Kinect v2.0 device is used as a "parameter" in the 2D motion graphics, changes in body posture can trigger changes in the 2D motion graphics, creating an interaction between somatosensory and traditional Chinese elements. When a person walks across the screen, the Kinect sensor recognises the person's x-coordinates and maps them to the computer, which then projects the motion parameters onto the screen via a projector, causing the traditional Chinese elements in the 2D graphics to change dynamically by panning. The experimental results validate the effectiveness and accuracy of the proposed method.

Figure 1: Kinect v2.0.

The main innovations and contributions include the following: (1) This paper proposes an LDA-based feature extraction method for motion parameters in order to improve the recognition accuracy of the Kinect v2.0 device. (2) Using the binding technique of skeletal parameters, the association between somatosensory interaction motion parameters and 2D dynamic graphics is achieved.

3. Kinect v2.0-Based Parameterisation of Somatosensory Interaction

3.1. Key Technologies. Microsoft first announced Kinect in June 2009 [19, 20] with the hope that the hardware would merge motion with communication. The device was officially launched in November 2010, and in May 2013, Microsoft demonstrated the next generation Kinect v2.0, which allows developers to design based on the voice, gesture, and player sensory information sensed by Kinect v2.0, bringing users an unprecedented interactive experience. In this paper, we decided to use the Kinect 2.0 device as the base hardware for development.

The colour resolution of Kinect v2.0 has been dramatically increased from 640×480 to 1920×1080, enabling very beautiful images to be acquired. Kinect v2.0 can bone bind all 6 of the maximum number of identified users and identify 25 keys. The Kinect V2.0 will be able to bone bind all 6 users and identify 25 key nodes. Also, because of the increased resolution of the depth sensor, the user data can be separated from the person with a simple cut, and the detection range has been increased from 0.8–4 m to 0.5–4.5 m. It is important to note that the infrared sensor does not require light, i.e., it can still be used in dark or dark environments.

Kinect consists of a colour camera, an IR camera, and an IR projector with a microphone array underneath [21–23] as shown in Figure 1. The IR camera and IR projector work together to achieve the depth image function. The main hardware features of Kinect v2.0 are shown in Table 1.

The colour image is based on the data stream acquired by the colour camera on the far left of Kinect v2.0. The colour camera sensor is shown in Figure 2.

Depth image and skeleton tracking technology is the dominant technology in the Kinect device and is somewhat representative. It contains information about the distance of the current object from the camera's point of view in addition to the grey scale value. Each pixel has its own information, and when there are enough of them, they can form a point cloud that recreates the geometry of the object

Table 1: Kinect v2.0 key hardware features.

No.	Kinect key modules	Brief description of functions
1	Colour camera	Colour data streams are available and essentially all the functions of a normal camera can be achieved
2	IR projector	Emits infrared light into the external environment. Infrared light waves are picked up by the IR camera through scattering and provide a source of thermal energy
3	IR camera	Receives scattered infrared light and performs depth processing of the information to draw a depth image of the Kinect
4	Microphone array	Sound is collected from multiple microphones, filtered for ambient noise, complementary to the user's sound source, and can determine the user's location

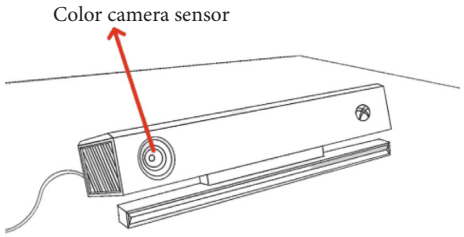

Figure 2: Colour camera sensor.

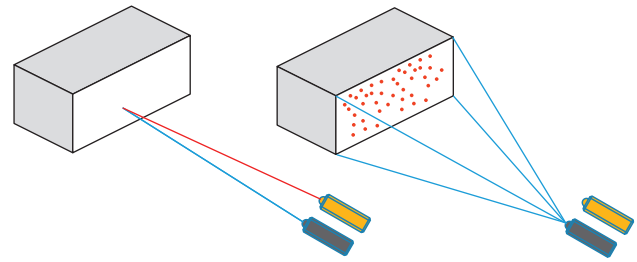

Figure 3: Imaging principle of TOF technology.

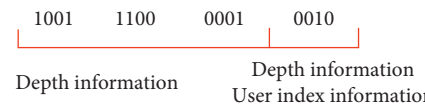

Figure 4: Depth image pixel information.

as well as its position and distance. The closer the object is, the darker the colour in the depth image, while the more distant the object is, the more white it tends to be. The TOF technique allows infrared light to be emitted and the attenuation of the light to be offset by phase detection, as shown in Figure 3.

The pixel information obtained from the depth image contains two parts, where the higher order 13 bits of information is the detected object pixel distance depth information. The Kinect sensor can detect the target human depth information in the valid range of 0.6 m to 4.5 m. The depth image pixel information is shown in Figure 4.

3.2. Feature Extraction and Recognition of Action Parameters. The motion data captured in Kinect-based somatosensory interaction is complex. In particular, when the types of actions to be recognised are large and variable, the action data can contain a large number of high-dimensional nonlinear features. Therefore, this paper uses linear discriminant analysis based on kernel functions to reduce the dimensionality of the vector space and thus solve the problem of capturing human actions accurately and in real time.

Due to the complexity and variability of human actions in VR scenes, it is not possible to extract some important high-dimensional nonlinear feature information hidden in the action data. Therefore, this paper introduces the kernel function in the LDA algorithm for nonlinear projection to extract the expression features.

In the Kinect captured human movement dataset, let $\mathbf{A}$ be the action matrix and $\mathbf{A}$ be the full rank matrix with class labels in the LDA algorithm [24, 25].

$$\mathbf{A} = [a_1 \dots a_n] = [B_1 \dots B_k] \in \mathbf{R}^{m \times n}, \tag{1}$$

where each $a_i\,(1 \le i \le n)$ is a data point in an m-dimensional space. Each block matrix $B_i \in \mathbf{R}^{m \times n}\,(1 \le i \le k)$ is the set of data items in class i. n_i is the size of class i, and the total number of data items in the data set $\mathbf{A}$ is n. Let N_i denote the index of the columns belonging to class i. The global centre c of $\mathbf{A}$ and the local centre c_i of each class $\mathbf{A}_i$ are denoted, respectively, as follows:

$$\begin{aligned} c &= \frac{1}{n} Ae, \\ C_i &= \frac{1}{n_i} B_i e_i, \quad i = 1, \dots, k. \end{aligned} \tag{2}$$

Suppose that the following settings are met:

$$\begin{aligned} S_b &= \sum_{i=1}^{k} n_i (c_i - c)(c_i - c)^T, \\ S_w &= \sum_{i=1}^{k} \sum_{j \in N_i} (a_j - c)(a_j - c)^T, \\ S_t &= \sum_{j=1}^{n} (a_j - c)(a_j - c)^T, \end{aligned} \tag{3}$$

where S_b, S_w, and S_t are referred to as the interclass scatter matrix, intraclass scatter matrix, and total scatter matrix, respectively.

$$S_t = S_b + S_w. \tag{4}$$

The standard LDA objective function can be shown as follows:

$$G = \arg\max_{G \in \mathbf{R}^{m\times 1}} \operatorname{trace}\left(\left(G^T S_t G\right)^{-1}\left(G^T S_b G\right)\right). \tag{5}$$

As the standard LDA algorithm uses a linear computational principle, it leads to less effective results in dealing with nonlinear problems and has a singularity problem. Therefore, kernel function-based LDA is used to reduce the dimensionality of the vector space and thus effectively extract the nonlinear features in human action data.

Set the kernel matrix is $\mathbf{K} = \phi(X)^T\phi(X) = [k_1^1, \ldots, k_i^j, \ldots, k_C^{N_C}]$, where $k_i^j = \phi(X)^T\phi(x_i^j)$. The Fisher criterion functions in H can be expressed as follows [26]:

$$J(w) = \frac{w^T \mathbf{S}_b^\phi w}{w^T \mathbf{S}_t^\phi w}, \tag{6}$$

where, w is the kernel space projection vector.

$$\begin{aligned} \mathbf{S}_w^\phi &= \sum_{i=1}^{C}\sum_{j=1}^{N_i}\left(\phi\left(x_i^j\right) - u_i\right) - \left(\phi\left(x_i^j\right) - u_i\right)^T, \\ \mathbf{S}_b^\phi &= \sum_{i=1}^{C} N_i\left(u_i - u\right)\left(u_i - u\right)^T, \end{aligned} \tag{7}$$

where u_i is the mean of the ith sample in H, u is the overall mean, and $\mathbf{S}_w^\phi$ is the intraclass scatter matrix w .This can be expressed as follows:

$$\mathbf{w} = \phi(X)\mathbf{a}, \tag{8}$$

where $\mathbf{a} = [\mathbf{a}_1, \ldots, \mathbf{a}_N]^T$. Equation (6) can be expressed as follows:

$$J(\mathbf{a}) = \frac{\mathbf{a}^T \mathbf{K}_b \mathbf{a}}{\mathbf{a}^T \mathbf{K}_t \mathbf{a}}, \tag{9}$$

where $\mathbf{K}_t$ denotes the overall scatter matrix of kernels and $\mathbf{K}_b$ denotes the scatter matrix between kernel classes [27].

$$\begin{aligned} \mathbf{K}_w &= \sum_{i=1}^{C}\sum_{j=1}^{N_i}\left(\mathbf{k}_i^j - \mathbf{m}_i\right)\left(\mathbf{k}_i^j - \mathbf{m}_i\right)^T, \\ \mathbf{K}_b &= \sum_{i=1}^{C} N_i\left(\mathbf{m}_i - \mathbf{m}\right)\left(\mathbf{m}_i - \mathbf{m}\right)^T, \\ \mathbf{K}_t &= \mathbf{K}_w + \mathbf{K}_b, \\ \mathbf{m}_i &= \frac{1}{N_i}\sum_{j=1}^{N_i}\mathbf{k}_i^j, \\ \mathbf{m} &= \frac{1}{N}\sum_{i=1}^{C}\sum_{j=1}^{N_i}\mathbf{k}_i^j, \end{aligned} \tag{10}$$

where $\mathbf{K}_w$ is a kernel intraclass scattering matrix. For any collected human action data point x, let $\mathbf{A}_{\text{opt}}$ denote a set of feature vectors of the optimal solution; then, we obtain the kernel space projection matrix [28, 29].

Figure 5: Live physical interaction in the Cleveland Museum of Art.

$$\begin{aligned} \mathbf{W}_{\text{opt}} &= \phi(X)\mathbf{A}_{\text{opt}}, \\ \mathbf{z} &= \mathbf{W}_{\text{opt}}^T\phi(x) = \mathbf{A}_{\text{opt}}^T\phi(X)\phi(x). \end{aligned} \tag{11}$$

Finally, an SVM classifier is used to implement the recognition of human actions. Combined with a SVM classifier, complex action classification recognition is finally achieved.

4. Two-Dimensional Motion Graphics in Visual Communication

4.1. Association of Movement Parameters with Two-Dimensional Dynamic Chinese Traditional Elements. Somatosensory is the perception of body posture, which can be achieved through a variety of sensors. Sensors can capture changes in our body posture, including the position of our head and individual joints, the speed and direction of movement, and even facial expressions, joint flexion of the hands, gestures, and so on. Essentially, these changes in body posture are changes in some data. Changes in the parameters of the posture data then cause changes in the generated graphics. When the body posture data obtained from somatosensory is used as a "parameter" in 2D dynamic graphics, changes in body posture can naturally lead to changes in 2D dynamic graphics. This creates an interaction between body sensing and 2D motion graphics, enabling the association of body sensing with 2D motion graphics. From a design and user experience perspective, this enables the user's behaviour to be involved in the design, resulting in a better user experience.

As shown in Figure 5, the Cleveland Museum of Art has developed a somatosensory interaction installation in Ohio, USA. In this installation, when a person approaches the screen, the image unfolds to form a Dunhuang fresco containing traditional Chinese elements. The Kinect body sensing device captures the movement signals of the audience and maps the recognised movement parameters to the traditional Chinese Figs on the mural. This interactive approach allows the audience to control the movement of a character in the image.

The motion of the character's arms, head, body, and legs in the motion graphics are motion-bound to the viewer's captured bone points, allowing the viewer to directly manipulate the character on-screen. This type of interaction

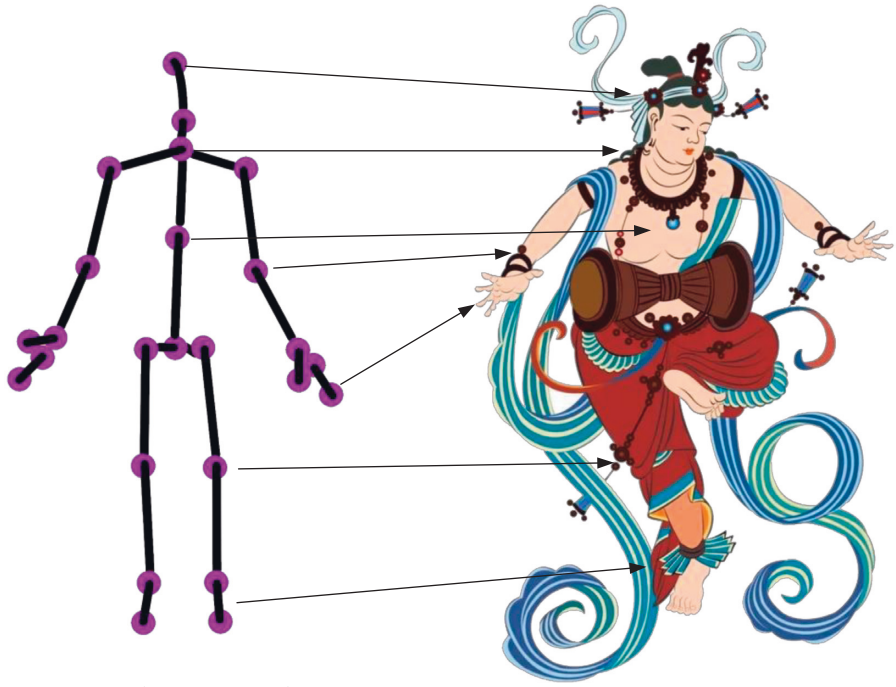

Figure 6: Correspondence between human bones recognised by Kinect and characters' bones in murals.

Table 2: Skeletal key point parameters.

Serial number	Bone point
1	SpineMid
2	Neck
3	Head
4	ShoulderLeft
5	ElbowLeft
6	WristLeft
7	HandLeft
8	ShoulderRight
9	ElbowRight
10	WristRight
11	HandRight
12	HipLeft
13	KneeLeft
14	AnkleLeft
15	FootLeft
16	HipRight
17	KneeRight
18	AnkleRight
19	FootRight
20	SpineShoulder
21	HandTipLeft
22	ThumbLeft
23	HandTipRight
24	ThumbRight
25	SpineBase

allows for a more fluid experience. The characters in the Dunhuang murals can be synchronised with the viewer's movements. By binding the motion parameters recognised by the Kinect interaction device to the function variables used to generate the images in the development environment, human interaction with the different characters in the murals can be achieved. The person can sense the motion graphics in different screens when they are in different areas.

Table 3: Experimental hardware configuration.

Configuration	Parameters
Processor	I9-9900 10 cores 20 threads
Memory	8 GB DDR4 3000 MHz
Video cards	AMD radeon pro WX 8G
Operating systems	Windows 10
USB interface	USB 3.0

4.2. Binding of Skeletal Parameters. The most resource-intensive part of the Kinect hardware is the bone tracking technology. The bone coordinate system is the most important part of the Kinect hardware, accounting for 50% of the resources of the entire Kinect system. Using this technology, 2D motion graphics applications based on somatosensory human-computer interaction can be developed. Kinect v2.0 can simultaneously identify the position information of six people and bind the user's pose to the coordinate information of key bone points. Bone data is also one of the most commonly utilised parts of action recognition based on Kinect hardware. The correspondence between the human skeleton recognised by Kinect and the character's bones in the mural is shown in Figure 6.

Each bone point is represented by a Joint. In Kinect v2.0, 5 new bone points have been added, as well as 20 bone points

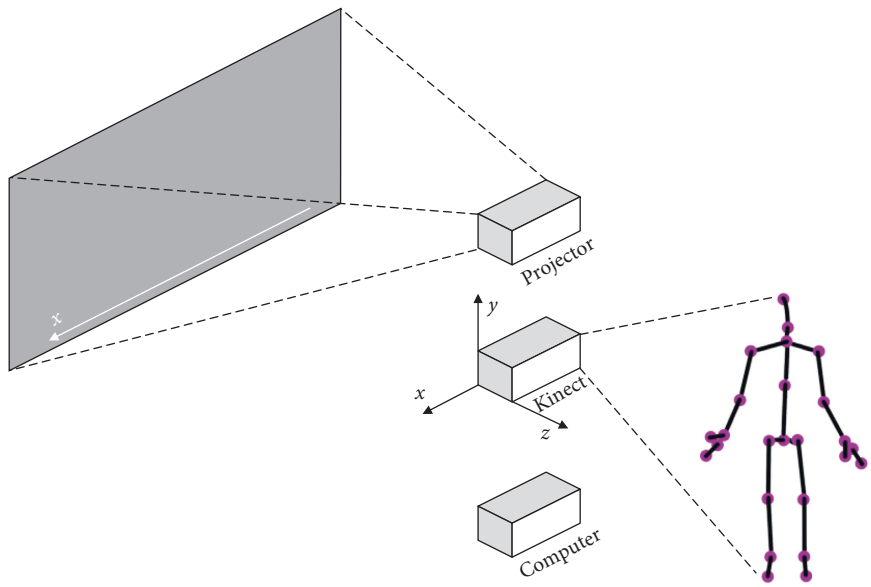

Figure 7: Experimental environment for somatosensory interaction.

in the previous version, all of which have corresponding names in the JointType, as shown in Table 2.

5. Experimental Results and Analysis

5.1. Experimental Setup. In order to implement the interactive features offered by the somatosensory device Kinect, the Kinect Development Kit needs to be installed before running the device. The main development software currently available is the official Microsoft SDK, which manages the colour images and depth information obtained by the Kinect camera through the SDK 2.0, sharing it with Unity 3D and writing language functions to control it. In the development environment configuration, the Kinect for Windows SDK 2.0 tool needs to be applied. The Kinect v2.0 device has a resolution of 1980×1080 and an FPS value of 30. The experiments were carried out using the official Kinect wrapper plugin. The experimental hardware configuration is shown in Table 3.

During the experiment, when a person walks across the screen, the Kinect sensor recognises the person's x-coordinates and maps them to the computer through arithmetic. The computer then projects the motion parameters onto the screen through a projector, causing the two-dimensional graphics in the mural to change dynamically in translation. The experimental environment for somatosensory interaction is shown in Figure 7.

5.2. Visual Communication Effects Based on Somatosensory Interaction. The Kinect recognition range is: 0.5–4.5 m, without special circumstances the whole body bone is generally selected for recognition and the full body sensory interaction is selected through subsequent program control. Kinect v2.0 device eliminates the generation of motors and the capture angle needs to be set manually. Therefore, after the capture angle has been determined, a horizontal plane distance conversion is performed for the farthest interaction distance threshold. The closest distance threshold is the horizontal plane distance at which the colour image just fully accommodates the user's entire body. In the absence of special requirements, the threshold can be contracted by 10% to ensure tracking stability. After the interaction range was set for the real environment, interaction capture detection was performed and the experimental results are shown in Table 4.

Table 4: Interaction range test.

Distance (m)	Number of tests	Number of times lost
0.5–0.55	30	4
0.55–1.0	30	0
1.0–1.5	30	0
1.5–2.0	30	0
2.0–2.5	30	0
2.5–3.0	30	0
3.0–3.5	30	0
3.5–4.0	30	0
4.0–4.05	30	0
4.05–4.5	30	0

Using the test data recognised by Kinect, the results and statistical analysis of the nine human movements were derived as shown in Figures 8 and 9 respectively.

As can be seen in Figures 8 and 9, the visual communication technology based on somatosensory interaction achieved 92.1% and 92.2% on the precision and accuracy metric averages, respectively. This indicates that the technology exhibits excellent performance across the nine action types. Unlike traditional digital video that does not have an interactive experience, somatosensory interaction associates a relationship between the person and the digital landscape. The viewer can assume that they are in the space depicted in the mural and can move freely. This allows the viewer and the digital work to break out of the binary spatial relationship

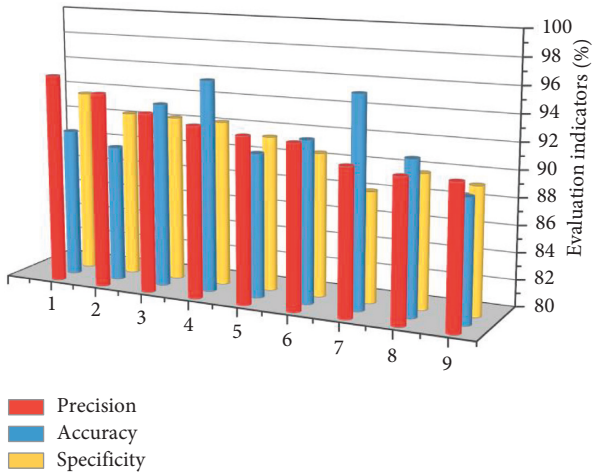

Figure 8: Experimental results of motion recognition.

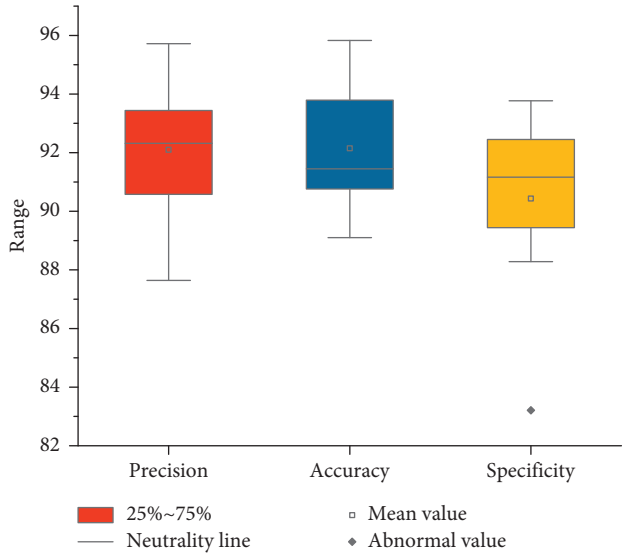

Figure 9: Statistical analysis.

and achieve a more multi-dimensional spatial expansion. The application of somatosensory interaction to the visualisation of two-dimensional motion graphics can greatly enrich the visual representation of traditional Chinese elements.

6. Conclusion

In order to explore the feasibility of somatosensory interaction technology in visual communication design, this study proposes a 2D motion graphics generation method based on somatosensory interaction parameterisation and uses traditional Chinese elements as an example for specific applications in visual communication design. The latest Kinect v2.0 device is used and an LDA-based feature extraction method for action parameters is designed in order to improve the recognition accuracy of the Kinect v2.0 device. Using the skeletal parameter binding technique between the human body and the characters in the graphics, the association between physical interaction action parameters and 2D dynamic graphics is realised, thus greatly enriching the visual representation of traditional Chinese elements.

Data Availability

The experimental data used to support the findings of this study are available from the corresponding author upon request.

Conflicts of Interest

The authors declare that they have no conflicts of interest to report regarding the present study.

Acknowledgments

This study was supported by Research on the Improvement of Jinzhong Intangible Cultural Heritage Technology and the Research and Development of "Jinzhong Gift" Cultural and Creative Design from the Perspective of Cultural Tourism Integration (No. jzwhlyj2021hx).

References

[1] K. E. Laver, S. George, S. Thomas, and G. Saposnik, "Virtual reality for stroke rehabilitation," *Physical Therapy*, vol. 2, no. 9, pp. 20-21, 2016.

[2] A. Rizzo, A. Hartholt, M. Grimani, A. Leeds, and M. Liewer, "Virtual reality exposure therapy for combat-related post-traumatic stress disorder," *Computer*, vol. 47, no. 7, pp. 31–37, 2014.

[3] P. H. Cosman, P. C. Cregan, and C. J. Martin, "Virtual reality simulators: current status in acquisition and assessment of surgical skills," *ANZ Journal of Surgery*, vol. 72, no. 1, pp. 30–34, 2015.

[4] Z. Merchant, E. T. Goetz, and L. Cifuentes, "Effectiveness of virtual reality-based instruction on students' learning outcomes in K-12 and higher education: a meta-analysis," *Computers & Education*, vol. 70, no. 1, pp. 29–40, 2014.

[5] B. Riecke, H. Veen, and H. Bülthoff, "Visual homing is possible without landmarks: a path integration study in virtual reality," *Presence*, vol. 11, no. 5, pp. 443–473, 2015.

[6] D Lloyd, "In touch with the future: the sense of touch from cognitive neuroscience to virtual reality," *Presence: Teleoperators and Virtual Environments*, vol. 23, no. 2, pp. 226-227, 2014.

[7] B. Zamani, A. Akbari, and B. Nasersharif, "Evolutionary combination of kernels for nonlinear feature transformation," *Information Sciences*, vol. 274, no. 274, pp. 95–107, 2014.

[8] A. Jindal, A. Dua, K. Kaur, M. Singh, N. Kumar, and S. Mishra, "Decision tree and SVM-based data analytics for theft detection in smart grid," *IEEE Transactions on Industrial Informatics*, vol. 12, no. 3, pp. 1005–1016, 2016.

[9] B. M. Aslahi-Shahri, R. Rahmani, M. Chizari, and A. Maralani, "A hybrid method consisting of GA and SVM for intrusion detection system," *Neural Computing & Applications*, vol. 27, no. 6, pp. 1–8, 2016.

[10] A. Rostami, M. Masoudi, and A. Ghaderi-Ardakani, "Effective thermal conductivity modeling of sandstones: SVM framework analysis," *International Journal of Thermophysics*, vol. 37, no. 6, p. 59, 2016.

[11] S. Narang, A. Best, A. Feng, and S. Kang, "Motion recognition of self and others on realistic 3D avatars," *Computer Animations and Virtual Worlds*, vol. 28, no. 3-4, 2017.

[12] B. O. Rothbaum, M. Price, T. Jovanovic et al., "A randomized, double-blind evaluation ofd-cycloserine or alprazolam combined with virtual reality exposure therapy for posttraumatic stress disorder in Iraq and Afghanistan war veterans," *American Journal of Psychiatry*, vol. 171, no. 6, pp. 640–648, 2014.

[13] Y. Chen, R. Chen, M. Liu, A. Xiao, D. Wu, and S. Zhao, "Indoor visual positioning aided by CNN-based image retrieval: training-free, 3D modeling-free," *Sensors*, vol. 18, no. 8, pp. 2692–2638, 2018.

[14] G. D. Fleishman, G. M. Nita, N. Kuroda, and S. Jia, "Revealing evolution of nonthermal electrons in solar flares using 3D modeling," *The Astrophysical Journal*, vol. 859, no. 1, pp. 112–129, 2018.

[15] R. Winzenrieth, M. S. Ominsky, Y. Wang, and L. Humbert, "Differential effects of abaloparatide and teriparatide on hip cortical volumetric BMD by DXA-based 3D modeling," *Osteoporosis International*, vol. 32, no. 6, pp. 33–45, 2021.

[16] F. Radicioni, A. Stoppini, and G. Tosi, "Necropolis of Palazzone in Perugia: geomatic data integration for 3D modeling and geomorphology of underground sites," *Transactions in GIS*, vol. 25, no. 5, pp. 149–160, 2021.

[17] S. Ying, C. Li, G. Li, G. Jiang, J. Du, and H. Liu, "Gesture recognition based on kinect and sEMG signal fusion," *Mobile Networks and Applications*, vol. 23, no. 4, pp. 797–805, 2018.

[18] H. Y. Lai, H. Y. Ke, and Y. C. Hsu, "Real-time hand gesture recognition system and application," *Sensors and Materials*, vol. 30, no. 4, pp. 869–884, 2018.

[19] C. Lee, J. Kim, S. Cho, J. Kim, and S. Kwon, "Development of real-time hand gesture recognition for tabletop holographic display interaction using azure kinect," *Sensors*, vol. 20, no. 16, pp. 311–319, 2020.

[20] I. Bulugu, "Sign language recognition using Kinect sensor based on color stream and skeleton points," *Tanzania Journal of Science*, vol. 47, no. 2, pp. 769–778, 2021.

[21] I. Ayed, A. Jaume-I-Capó, and P. Martínez-Bueso, "Balance measurement using Microsoft kinect v2: towards remote evaluation of patient with the functional reach test," *Applied Sciences*, vol. 11, no. 13, pp. 89–97, 2021.

[22] N. . Al, "Measuring the effectiveness of exergames among gen Z using kinect sensor and EEG," *Turkish Journal of Computer and Mathematics Education*, vol. 12, no. 3, pp. 1502–1508, 2021.

[23] M. Oudah, A. Al-Naji, and J. Chahl, "Elderly care based on hand gestures using kinect sensor," *Computers*, vol. 10, no. 1, pp. 5–13, 2021.

[24] F. Zhang, T. Y. Wu, J. S. Pan, G. Ding, and Z. Li, "Human motion recognition based on SVM in VR art media interaction environment," *Human-centric Computing and Information Sciences*, vol. 9, no. 1, pp. 40–48, 2019.

[25] L. Ding, W. Jiang, and Y. Zhou, "BIM-based task-level planning for robotic brick assembly through image-based 3D modeling," *Advanced Engineering Informatics*, vol. 43, no. 13, pp. 93–112, 2020.

[26] H. Huang, C. Lin, and D. Cai, "Enhancing the learning effect of virtual reality 3D modeling: a new model of learner's design collaboration and a comparison of its field system usability," *Universal Access in the Information Society*, vol. 20, no. 3, pp. 429–440, 2020.

[27] K Li, T. Wu, and Q. Liu, "Human contour extraction based on depth map and improved Canny algorithm," *Computer Technology and Development*, vol. 31, no. 5, pp. 6–12, 2021.

[28] W. Zhang, D. Kong, S. Wang, and Z. Wang, "3D human pose estimation from range images with depth difference and geodesic distance," *Journal of Visual Communication and Image Representation*, vol. 59, no. 2, pp. 272–282, 2019.

[29] K. Zou, L Ma, Rong, and C. Xu, "Image-based non-contact measurement method of human body parameters," *Computer Engineering and Design*, vol. 38, no. 2, pp. 6–11, 2017.

Hindawi
Scientific Programming
Volume 2022, Article ID 7582018, 11 pages
https://doi.org/10.1155/2022/7582018

Research Article

Analysis of the Influence of Economic Complexity on Regional Economic Management Based on Computer Informatization Model

Yu Fang and Wenyan Wang

Department of Economics and Management, Cangzhou Normal University, Cangzhou 061001, China

Correspondence should be addressed to Wenyan Wang; wangwenyan8805@caztc.edu.cn

Received 7 May 2022; Revised 23 May 2022; Accepted 30 May 2022; Published 1 July 2022

Academic Editor: Lianhui Li

This study adheres to the principle of combining empirical analysis and normative analysis and establishes an analytical framework according to the research ideas from theoretical analysis to empirical analysis to countermeasures. Suggestions for high-quality economic growth in my country and paths for promoting coordinated regional development were made. This study will take the data from 1993 to 2020 as a unit, taking into account factors such as education, consumption, investment, and labor costs and using SAR model, SEM model, and spatial panel data model to measure the degree of economic complexity in my country. For the research on the difference of regional economic growth in my country, this study is refined to the county level to measure the degree of regional economic development and compare and analyze the regional development differences, and we strive to use empirical evidence to scientifically analyze the degree of economic complexity and regional development differences, using the spatial panel model, SAR model, and SEM model to comprehensively consider the impact of my country's economic complexity on regional economic growth differences; finally, combined with theoretical analysis and empirical test results, based on the perspective of economic complexity, coordinated development provides countermeasures and provides corresponding suggestions for the high-quality development of my country's economy, the continuous optimization of industrial structure, and the establishment of regional cooperation mechanisms.

1. Related Introduction

The continuous upgrading of industrial structure, diversification of industrial types, and increasing economic complexity enable enterprises to formulate a reasonable development direction according to social needs. Finally, China encourages enterprises to take the path of green development, strengthen the content of science and technology, reduce resource consumption, actively realize the transformation of industrial structure, and make China's industrial structure scientific and reasonable. All this means that the stability of China's economic growth has been enhanced, and the diversity and complexity of the economy are also improving. With the continuous upgrading and optimization of industrial structure, industrial diversification, and the improvement of economic complexity, higher requirements are put forward for the measurement of economic development efficiency. More comprehensive, more specific, and more complex measurement indicators are indispensable for China's economic development in the construction of modern economic system. All regions pay more and more attention to the healthy development of market economy, actively explore regional cooperation and regional mutual assistance mechanisms, and pay more and more attention to the relationship between government and market. The current situation of China's regional economic development still has the problems of large regional economic differences and unbalanced regional social and economic development. In recent decades, most of the work of quantifying the complexity of socioeconomic systems and financial markets has been done by physicists. They help promote economic research by introducing Physics related

research methods and models into economic research. Although scholars have conducted a series of studies on economic development, international economic complexity, regional development balance, and other issues, under the background of China's economic growth from high speed to medium high speed, from high speed to high quality, based on the perspective of economic complexity, there is a lack of research on the level of economic development and regional development differences in China [1–10].

This study adopts a relatively novel nonmonetary index-economic complexity index as the measurement index of China's economic development and analyzes the differences of regional economic growth in China by subdividing counties. SEM model analyzes the impact of China's economic complexity on regional economic growth differences and improves the relevant theoretical research. Finally, based on a series of research evidence, this study attempts to put forward the countermeasures to control the dynamic and coordinated development of regional economy from the perspective of economic complexity, so as to provide some reference for broadening the research field of economic complexity and regional economy and growth differences.

2. Related Research Methods and Measurement Models

2.1. Theil Index. Theil entropy standard index calculates the inequality degree of regional or individual indicators through entropy, which is abbreviated as TL index in the article. The value of the TL index ranges from 0 to 1, with a coefficient approaching 0 indicating a small amount of difference, and a coefficient approaching 1 indicating a large developmental difference in the subject variable. And the Theil index has a decomposition property, which has a fine-grained role in the analysis of the difference properties of the measured subjects. The main formula of Theil index is as follows [11–15]:

$$T = \frac{1}{n}\sum_{i=1}^{n}\frac{y_i}{\overline{y}}\ln\left(\frac{y_i}{\overline{y}}\right). \tag{1}$$

The following formula is the application formula after data grouping:

$$T = \sum_{k=1}^{k} w_k \ln\left(\frac{w_k}{e_k}\right). \tag{2}$$

The good decomposability of the index can refine the research on the differences of the subjects and, more specifically, measure the degree of inequality of the measurement subjects. When the number of subject samples is large, it can be regarded as multiple group samples, and the disassembly of the main expression of Theil formula can analyze the contribution of the gap between sample groups and the gap within the group to the total gap specifically as follows:

$$\begin{aligned} T = T_b + T_w &= \sum_{k=1}^{k} y_k \ln\left(\frac{y_k}{n_k/n}\right) \\ &+ \sum_{k=1}^{k} y_k \ln\left(\sum_{i\in g_k}\frac{y_i}{y_k}\ln\frac{y_{i/}y_k}{1/n_k}\right). \end{aligned} \tag{3}$$

The difference between groups T_b is expressed as

$$T = \sum_{k=1}^{k} y_k \ln\left(\frac{y_k}{n_k/n}\right). \tag{4}$$

The intragroup gap T_w is expressed as follows:

$$T_w = \sum_{k=1}^{k} \mathrm{yk}\left(\sum_{i\in g_k}\frac{y_i}{y_k}\ln\frac{y_i/y_k}{1/n_k}\right). \tag{5}$$

T is the Theil index to measure inequality; k is the grouping sample value; y_i is the value of the individual; y_k is the variable value of the k group; e_k is the population proportion; n_k is the number of individuals in the k group g_k; w_k is the proportion of k groups of values to the total value. The sum of the within-group gaps of each group constitutes the within-group gap term, and the specific calculation methods are not very different.

2.2. Moran's I. Combine spatial data and variable data to analyze the characteristics of spatial data. The highlight of spatial measurement is that relatively common panel data or cross-sectional data take into account the effect of mutual distance to take into account the spatial effects and spatial dependencies between variables. Before constructing a spatial econometric model, it is necessary to consider the spatial relationship between regions and construct a spatial weighting matrix. In this paper, a geographic weight matrix W is constructed based on the geographic adjacency relationship. W contains the regional distance spatial matrix of 31 provinces and cities in my country (excluding Hong Kong, Macao, and Taiwan). Ordinary time series are only unidirectionally correlated, while spatial series have multidirectional correlations of variables, and there is the possibility of mutual influence. Before constructing a related spatial model, it is necessary to test the dependence and correlation of geographic space. For example, if Moran's I passes the test, a spatial econometric model can be used for analysis, and a spatial econometric model can be constructed for analysis. The correlation test shows that there is no spatial correlation in the tested area, so the time series model of Putin is suitable for analysis. Moran's I is actually the coefficient between the observed variable and the spatial lag, and the equation is expressed as

$$\mathrm{Moran's\,I} = \frac{\sum_{i=1}^{n}\sum_{j=1}^{n} W_{\mathrm{ij}}\left(x_i - \overline{x}\right)\left(x_j - \overline{x}\right)}{S^2\sum_{i=1}^{n}\sum_{j=1}^{n} W_{\mathrm{ij}}}. \tag{6}$$

The construction of Moran's index is based on the establishment of the spatial weight matrix W, i and j are expressed as the distance between regions, and S^2 is the sample variance, expressed as

$$S^2 = \frac{\sum_{i=1}^{n} (x_i - \overline{x})^2}{n}. \quad (7)$$

2.3. Spatial Lag Model (SAR). Spatial lag model SAR is a kind of spatial econometric model. The spatial lag model is also known as the spatial autoregressive model. The model lag process is an autoregressive process. There are many complex classifications of spatial econometric models, and there are higher-order and more complex situation settings in order. In view of the difficulty in estimating the spatial weight problem in the model, the current spatial econometric models are mostly based on the first-order model. The first-order autoregressive model and the first-order average moving model are set based on adding spatial weights to consider. The spatial lag model SAR reflects whether the correlation of the dependent variable affects the nearby area through a spatial mechanism. Formally, the space lag model is related to the ordinary time lag model, and there are similarities between the two, but the space lag model adds space factors to consider, and the multidirectionality of the space correlation makes the calculation of the space effect necessary. The expression of the spatial lag model SAR is as follows [16]: SAR model has a negative impact on my country's economic complexity and poor regional economic growth. Comprehensive consideration of the impact of different

$$y = \lambda W_y + X\beta + \varepsilon. \quad (8)$$

W is the established spatial matrix. There are various types of matrix, including geospatial weight matrix, economic distance spatial weight matrix or traffic weight matrix, etc. X is the data matrix, and λ is the spatial autoregressive coefficient, that is, the parameter of the lag term, the measurement. The significance of the influence of the spatial lag matrix on y is to measure the spatial multidirectional effect of each observation variable introduced into the model, β is the correlation coefficient, and ε is the white noise interference term.

2.4. Spatial Error Model (SEM). The spatial dependence of variables can also be represented by the error term. This model form reflects the effect that the regional spillover is a random outflow and is called the spatial error model SEM. The spatial error model expression is as follows:

$$y = X\beta + \mu = X\beta + (\mathrm{PMu} + \varepsilon), \quad \varepsilon \sim N\left(0, \sigma^2 I_n\right). \quad (9)$$

μ is the disturbance error term, and the regression value residual vector has spatial dependence; M is the spatial weight matrix; p is the autoregressive parameter, which means to measure the influence scale and degree of the variables in the local area on the surrounding area, etc. Spatial dependence: ε is the white noise interference term. This model is suitable for the measurement of the spatial relationship between the spatial dependence value and the variable due to the difference of the geographical relative position of the region in the presence of the spatial effect.

3. Spatial Econometric Analysis of the Impact of Economic Complexity on Regional Economic Growth Differences

3.1. Data Sources. In this experiment, the basic data of 31 provinces and cities in my country from 1993 to 2020 were selected for analysis. The reason why the study area does not include Hong Kong, Macao, and Taiwan is because the differences in the basic conditions of listing in various regions may lead to errors in model setting and parameter calculation. The data of this study come from "China Statistical Yearbook," "China County Statistical Yearbook," "China Financial Yearbook," "China Fixed Asset Investment Statistical Yearbook," "China Labor Statistics Yearbook," "China Science and Technology Statistical Yearbook," "China Education Statistical Yearbook," China Education Expenses Statistical Yearbook, China Price and Urban Residents Income and Expenditure Survey Statistical Yearbook, and provincial (municipal and autonomous region) statistical yearbooks and social statistical bulletins. The listed company data used to measure economic complexity in my country comes from the reset financial database. The selected dataset mainly uses the basic registration information and financial information of all listed companies on the Shanghai Stock Exchange and Beijing Stock Exchange since 1993 to 2020. The relevant experimental data in [17] can be viewed from the public official website, the data is authentic and reliable, and it has a certain representative significance. The relevant experimental data can be accessed from the public official website, and the data is authentic and reliable and has certain representative significance.

3.2. Spatial Autocorrelation Test of Regional Economic Growth Differences in My Country. The most common method to measure the spatial sequence and the spatial autocorrelation is Moran's I. Correlation: the Moran index I is between −1 and 0; that is, the measurement high-value area is adjacent to the low-value area. First of all, the article sets the spatial matrix of the 31 provinces and cities observed, and the 0-1 spatial weight matrix of 31×31 is used here. Table 1 shows the results of the global autocorrelation bilateral test on the Theil index of the explanatory variables in 31 provinces and cities. The global spatial autocorrelation index of my country's regional economic disparities, the Moran index, is all greater than 0, indicating that regional economic disparities have spatial correlations (Table 1). Except from 1993 to 1997 and 2004, the rest of the years passed the P test at the 5% level, and the test results are true and valid as a whole. This proves that the differences in regional economic growth in my country from 1993 to 2020 are spatially correlated, and the differences in economic growth between provinces and cities are interrelated and affect each other, rather than being single and independent [18].

Table 1: Spatial correlation test of regional economic differences from 1993 to 2020.

Years	Moran I	Z value	P value	Years	Moran I	Z value	P value
1993	0.039	2.07	0.07	2007	0.272	2.90	0.00
1994	0.039	3.07	0.07	2008	0.531	1.26	0.01
1995	0.001	2.33	0.07	2009	0.371	1.93	0.03
1996	0.039	2.06	0.07	2010	0.128	1.50	0.07
1997	0.007	3.37	0.06	2011	0.309	3.16	0.00
1998	0.038	3.06	0.05	2012	0.192	2.13	0.02
1999	0.055	3.81	0.02	2013	0.199	2.07	0.02
2000	0.055	2.20	0.04	2014	0.199	2.15	0.02
2001	0.061	2.86	0.02	2015	0.233	2.61	0.00
2002	0.064	2.91	0.02	2016	0.352	3.30	0.04
2003	0.028	1.57	0.03	2017	0.298	-2.86	0.02
2004	0.121	1.43	0.08	2018	0.179	1.99	0.02
2005	0.161	1.80	0.03	2019	0.228	3.48	0.02
2006	0.105	1.30	0.04	2020	0.164	1.93	0.03

According to the trend chart of Moran index drawn in Table 1, it can be found that, with the continuous development of the economy, the spatial relationship of regional economic growth differences in my country has shown a trend of fluctuation as a whole (Figure 1). The spatial correlation curve has been fluctuating and rising since 1993, reaching a peak in 2009, and then decreasing slightly. The curve change is relatively stable. This is because with the continuous development of social economy and the continuous improvement of transportation and communication construction, the connection in regional space has become closer, and the spatial correlation has been continuously strengthened. The economic development of a certain area will directly affect the economic situation radiating to the surrounding areas, coupled with population mobility and policy influence, resulting in a positive spatial correlation of economic growth differences.

3.3. The Spatial Impact of My Country's Economic Complexity on Regional Economic Growth Differences

3.3.1. Construction and Selection of the Spatial Econometric Model. In order to better construct a spatial econometric model and choose whether there is a spatial effect between the variables to be diagnosed. In order to conduct a more accurate spatial econometric analysis of my country's economic growth differences, it is necessary to perform a Lagrange multiplier test (LM test for short) on the estimated results of the spatial model to select a better spatial econometric model. After the spatial weight matrix is set, the reference items need to be tested for Spatial error and Spatial lag. The spatial effect test is set based on the ordinary linear model OLS test. Before the spatial effect test, it is assumed that there is no spatial autocorrelation in the level of economic growth differences between 31 provinces and cities in my country from 1993 to 2020. As can be seen from Table 2, among the three tests on spatial error, Moran's index, LM test, and RL test all rejected the hypothesis that there is no spatial autocorrelation in my country's economic development level, and the P values were all significant at the level of 0.05, and the statistical RL test was passed, and the LM test results were relatively good in the two tests after the space, and the above results all rejected that there is no space for the differences in economic growth levels of 31 provinces and cities in China from 1993 to 2020. The relevant null hypothesis shows that spatial econometric analysis is needed to measure the influencing factors of the differences in the level of economic development in my country (Table 2) [19, 20].

In the spatial econometric model, the spatial lag model (SAR) and the spatial error model (SEM) play an important role. Both of them take into account the spatial multidirectional effects between the variables in the model. The biggest difference between the two is the disturbance term constitute. The SAR model pays more attention to spatial dependence, and the key error items in the spatial error model are the product of the dependent variable and the corresponding spatial weight matrix. The SEM reflects the spatial dependence between variables through the error term. The components of the spatial lag item are the product of the corresponding spatial weight matrix and the error term. The SEM model lag term interprets the error term rather than the dependent variable of the model reference. In order to better explain the impact of my country's economic complexity on regional economic growth differences, the SAR model and the SEM model are now constructed to measure and analyze it.

3.3.2. Analysis of the Impact of My Country's Economic Complexity on Regional Economic Differences. In order to more accurately measure and evaluate the differences in my country's economic growth, it is necessary to conduct a comprehensive analysis of the geographic space of our city's Theil index. This paper divides my country's geographical space into eastern, central, western, and northeastern regions and analyzes the economic development and economic growth differences of cities located in different geographical locations. Specifically, each region has its own local economic characteristics, so the selected regions include both the eastern and central regions, as well as the western and northeastern regions.

The difference in economic growth in the eastern region of my country is generally high. As an important region for

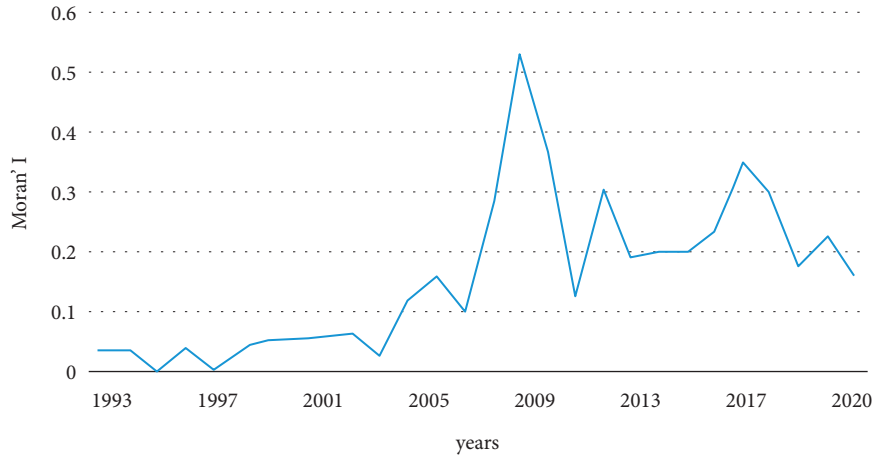

Figure 1: Spatial correlation test of regional economic differences from 1993 to 2020 (Moran I index).

Table 2: Spatial effect test of factors influencing my country's economic growth differences.

	Statistic	d*f*	*P*
Moran's I (spatial error)	6.403	1	0.02
Lagrange multiplier (error)	6.099	1	0.03
Robust Lagrange (error)	9.811	1	0.01
Lagrange multiplier (lag)	4.521	1	0.05
Robust Lagrange (lag)	7.233	1	0.02

my country's reform and opening up, the economic development level of the eastern region ranks high. In addition, the establishment of special economic zones has greatly promoted the social and economic development of the eastern region. As shown in Figure 2, Shijiazhuang, Shanghai, Fuzhou, Quanzhou, Huizhou, Shenzhen, Wenzhou, and other cities have relatively high Theil indices. These cities are the representatives of my country's economic and trade development and the development of the tertiary industry. Due to the successful transformation of foreign trade and some industries, the economic situation of some people in the city is good. At the same time, the social and economic developed areas are attractive to talents. Such areas are easy for most people to flow, and the quality and quantity of labor force are improved. It will counteract the development of the regional economy, strengthen the development of local industries, and add icing on the cake for the regional economy. The development of transportation and roads in such areas is convenient for the development of trade and the improvement of the economic level, but the rapid growth of economic development will accelerate the silence and elimination of other industries, causing outdated and technologically backward industries to stop developing and accelerate their elimination. However, the development of regions without excellent enterprises and convenient transportation is easy to be ignored, so that the economic growth rate of some regions is slow, and the economic development is lagging. Compared with some regions with ultra-high economic growth, the Theil coefficient increases, and the level of interregional economic development appears different. Compared with Shanghai and Shenzhen, the difference in economic growth in Beijing is not very high, first, because Beijing occupies a relatively small area in terms of geographical location; secondly, Beijing is the capital of my country, and its political significance is greater than its economic significance; Beijing pays attention to the grasp of macro-control. The eastern region is an important economic development region in my country and has made outstanding contributions to the high-quality social and economic development and industrial optimization and upgrading in China. Therefore, when formulating regional development strategies, it is more important to adjust measures to local conditions and formulate scientific development policies.

The economic growth differences in the western regions of my country are generally large, and the Theil index of some cities is more prominent. As can be seen in Figure 3, Lhasa, Nyingchi, Shigatse, Shannan, Yushu Tibetan Autonomous Prefecture, Xilingol League, Yulin, Zunyi, and other regions are regions with relatively unbalanced economic development and large differences in economic growth. There are many cities with unbalanced economic development in Tibet, Gansu, and Inner Mongolia, and there are some common reasons for the high Theil index in the western region: first, the provinces and cities in western my country generally have problems of being deep in the inland and difficult to build traffic roads; secondly, due to the geographical characteristics and development mode of the west, it is difficult to optimize and upgrade industries in some areas, and the backward productive forces cannot promote the improvement of social and economic levels; finally, due to the lack of education and the loss of talents, the

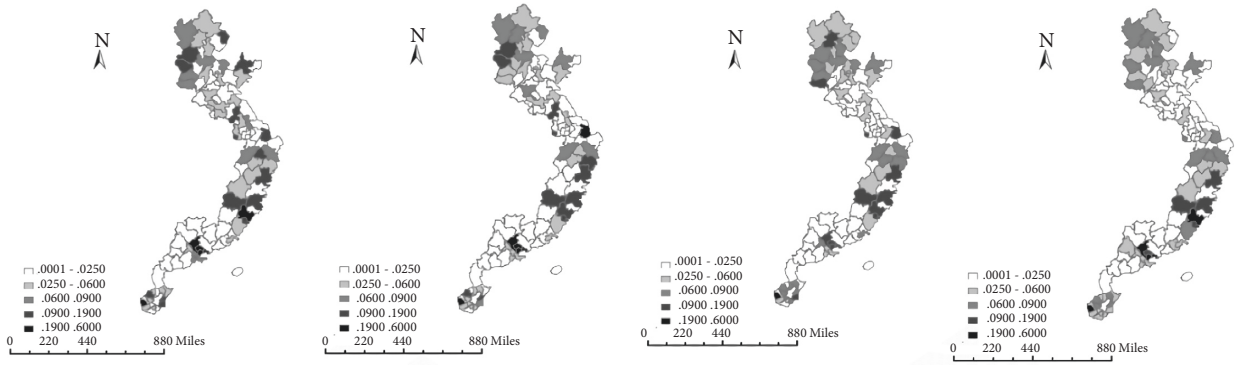

Figure 2: Differences in economic growth among cities in eastern region in 1993, 2002, 2011, and 2020.

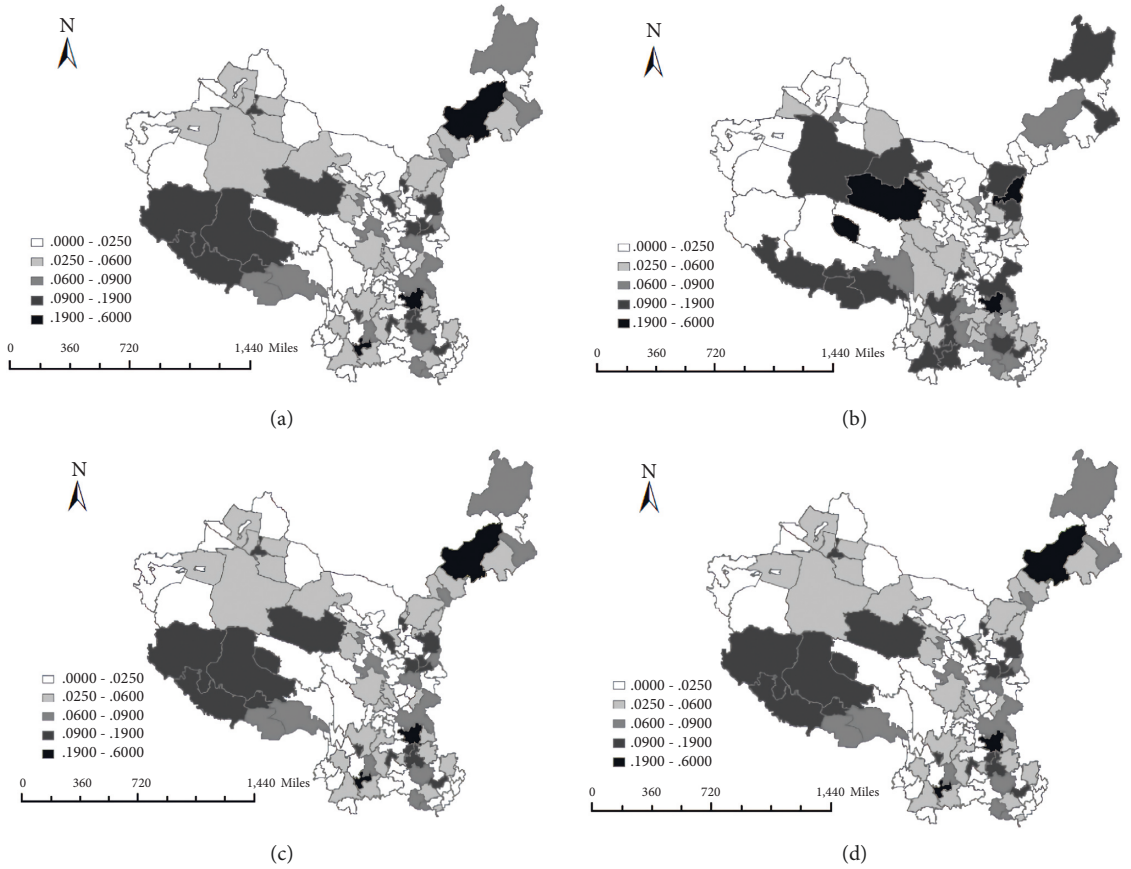

Figure 3: Differences in regional economic growth in western my country in 1993 (a), 2002 (b), 2011 (c), and 2020 (d).

speed of economic development is not easy to improve. There is a general problem in the west that productivity restricts the development of talent education, and the lack of high-quality labor will lead to a decline in social productivity. The western region has a wide geographical coverage, and the ecological environment in some regions is relatively fragile, which means that if the production mode of other regions is copied, the blind development of the primary and secondary industries will increase ecological pressure and pose a threat to green development. Within the western region, Xinjiang, Chongqing, and Guangxi do not have particularly prominent differences in economic growth among cities. Xinjiang, Inner Mongolia, Guangxi, and other regions are vast and sparsely populated, and their economic level is relatively average. Chongqing, as a municipality directly under the Central Government, has made some achievements in economic development, constantly strengthening foreign exchanges and industrial upgrading, and its social development level and per capita income are relatively considerable. The western region has a large area, uneven levels of economic development, a large number of poor people and regions, and an obvious gap between the

rich and the poor. This poses challenges and requirements for the government's scientific regulation and control policies. In formulating development strategies and economic development guidance, it is even more necessary. Adjust measures to local conditions and strengthen the grasp of regional economic and geographical features.

Compared with other regions, the difference in social and economic growth in the central region of my country is relatively small. Except for some provincial capital cities and transportation hub cities, the Theil index of other cities has little difference (Figure 4). Hefei, Nanchang, Changsha, and Wuhan, as provincial capitals, have a significantly higher degree of difference in economic growth compared with surrounding cities. This is due to the fact that such cities are the economic and political concentration points of a province, and the diversification of industries and scientific development of technology is more convenient. Provincial capital cities are more attractive to talents and labor, and at the same time, the infrastructure is more complete. As an important area connecting the north, south, and east of my country, the central provinces play an important role in transportation development. This is also the central urban area. We also explained one of the reasons for the relatively low Theil index. Jiujiang City, Yichang City, Zhuzhou City, Shiyan City, and other cities due to their excellent geographical location and traffic conditions have led to an increase in the economic development speed of some counties, and the difference in economic growth with the surrounding regions has increased, which shows that the city's Theil index is relatively high. The central region is linked to the whole country in terms of geographical location and has a vast territory; in terms of transportation development, water, land, and air transportation have huge innate development advantages, and the flat terrain and developed river channels can help speed up regional economic development; in terms of labor force, Henan, as the most populous province in my country, provides high-quality labor for regional development. Generally speaking, the development potential of the central region is huge. With the continuous construction of infrastructure and the continuous increase of investment, the economic development of the central region will continue to improve. However, in the process of development, it is still necessary to pay attention to the development caused by regional natural and human factors. With the steady improvement of the social economy, the economic growth differences between regions are continuously narrowed, and the social and economic development model is optimized.

Observing the differences in economic growth in Northeast China from 1993 to 2020 through Figure 5, it can be found that, except for Changchun City, Dalian City, Shenyang City, Daqing City, Anshan City, Yanbian Korean Autonomous Prefecture, and other cities, the economic growth of other regions as well as the growth differential is relatively stable, and the Theil index is on the small side. However, these regions with high Theil indices and large differences in economic growth often have their own characteristics and reasons for the differences in economic development levels.

Through a series of verification and consideration of the model, this study chooses to construct spatial lag model (SAR) and spatial error model (SEM) to analyze the spatial impact of China's economic complexity on the level of regional economic growth difference. Through the study of Table 3, it can be found that, in the spatial lag model, China's economic complexity is negatively correlated with the difference of regional economic growth, and the coefficient is −0.069. It shows that the improvement of China's economic complexity plays a catalytic role in narrowing the difference of regional economic growth. The economic complexity index can explain China's economic development. In the spatial lag model for studying the impact of China's economic complexity on regional economy, the Z value is −1.29, and the results pass the P test, which is significant at the level of 5%, indicating that the SAR coefficient is effective in the model results. The estimated value Rho of spatial autoregressive coefficient is 0.054, and the estimated value shows significant results at the level of 1%, indicating that there is a spatial effect on the impact of China's economic complexity on regional economic differences, and the model result is more significant. From the perspective of spatial measurement, Moran I index proves that there is spatial correlation between provinces and cities in China in terms of regional economic growth differences. The degree of regional economic growth difference in China does not exist independently but is closely related to the surrounding areas. Adding economic complexity to measure, through the spatial lag model, it can be concluded that if the economic complexity index of a province and city changes, the degree of economic growth difference between adjacent regions will also change, which is reflected in the good economic development and the improvement of economic complexity index, which will not only reduce the difference of regional economic growth, but also reduce the difference of economic growth in surrounding regions, and vice versa. This influence is bidirectional, even multidirectional. The result of the model means that when formulating the regional development strategy, the government needs to consider not only the actual development of the region, but also the policy implementation of surrounding provinces and cities and the actual situation of the region, so as to formulate strategies in line with the actual situation of the region. Science policy: by comparing the results of OLS panel regression test with those of SAR spatial lag model, it can be found that there are differences in variable regression coefficients between the two. The spatial error model is used to analyze the spatial characteristics of the impact of China's economic complexity on regional economic growth differences. Looking at Table 3, it can be found that the regression coefficient of SEM error term of spatial error model λ is shown as 0.049, and the regression coefficient is significant at the level of 1%. This shows that the spatial error model is reasonable, and the model results are true and effective. In the spatial error model, the spatial impact value of economic complexity index ECI on regional economic growth difference TL is −0.061, which is significant at the level of 5%. The Z value is −1.93, and the standard error is 0.05328. This result also verifies that there is a negative correlation between China's

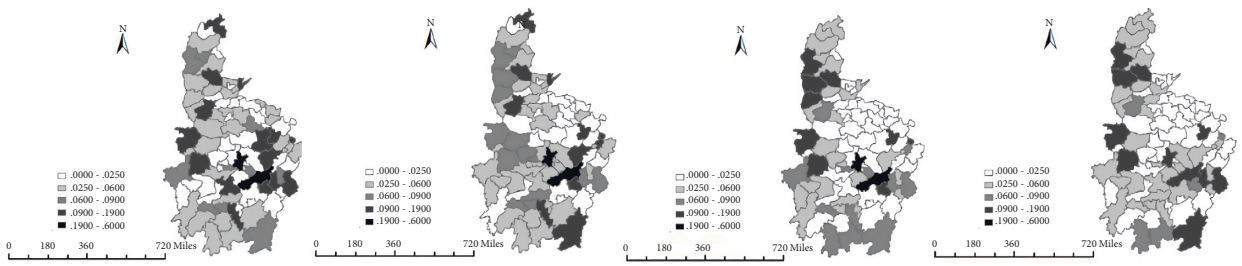

Figure 4: Differences in regional economic growth in central my country in 1993, 2002, 2011, and 2020.

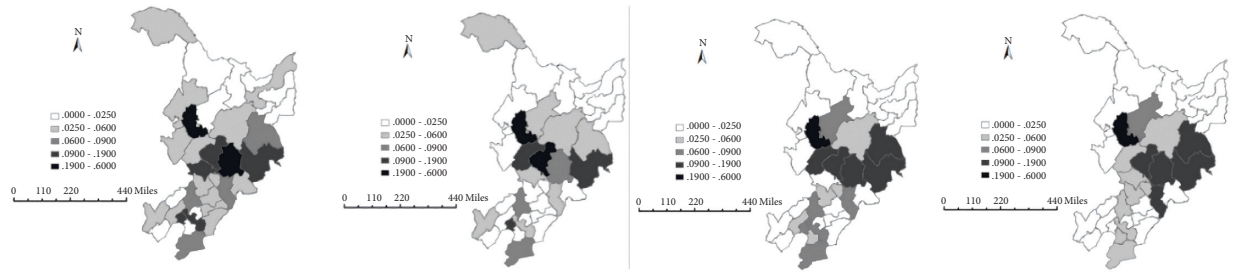

Figure 5: Differences in regional economic growth in northeastern region in 1993, 2002, 2011, and 2020.

Table 3: The impact of my country's economic complexity on regional economic growth differences—estimated results from spatial econometric models.

	Dependent variable L	
	SAR	SEM
ECI	−0.069*	−0.061*
	(−1.29)	(−1.93)
cons	0.021	0.211
n	868	868
Rho	0.054**	—
Lambda	—	0.049**

economic complexity index and regional economic growth differences. Improving the regional economic complexity index can reduce the difference of economic growth level, accelerate the balanced development of China's economy, promote the coordinated development of industrial development, and accelerate industrial transformation and upgrading.

3.4. Spatial Econometric Analysis of Other Factors Affecting My Country's Regional Economic Growth Differences. The differences in my country's economic development are not caused by a single reason, but different types of reasons of different natures lead to the differences in my country's economic development. In addition to my country's economic complexity index, the paper also adds other variables to measure and evaluates the impact of different factors on my country's regional economic growth differences through model analysis. The specific analysis results are shown in Table 4.

3.4.1. Analysis of the Impact of Investment Levels on Regional Economic Growth Differences. By observing the data of the IIFA terms in the SAM model, it can be found that the coefficients of IIFA are significant at the 1% level (Table 4). The investment level is represented by fixed asset investment here. The data shows that the improvement of the investment level has a reducing effect on the difference of regional economic growth in my country. If the regional investment is insufficient, it will lead to insufficient vitality of regional economic development and increase the difference of economic growth. At the same time, due to the correlation between different economic growth factors among different regions, the backward investment level will also lead to the slow development of the regional economy in the surrounding areas, which has an adverse effect on reducing the imbalance of regional economic development. Comparing the investment level parameters in the SEM model, the IIFA term coefficient in the SAM model is also significant at the 1% level (Table 4). The coefficient value in the SEM model is slightly higher than that of the investment level in the SAM model, but it also shows that the difference in my country's regional economic growth is affected by the investment level, and the improvement of the regional investment level is conducive to reducing the economic growth in the region and surrounding areas difference. This result shows that regional governments and enterprises should pay attention to the grasp of investment level and investment intensity

Table 4: Influencing factors of regional economic growth differences in my country—estimated results of spatial econometric model.

	Dependent variable: TL				
	(I)	(II)	(III)	(IV)	(V)
ECI (SAR)	−0.086** (−2.67)	−0.069* (−1.29)	−0.069* (−1.31)	−0.072* (−1.39)	−0.086* (−1.41)
ECI (SEM)	−0.041** (−1.76)	−0.061** (−1.93)	−0.056* (−1.59)	−0.06** (−1.69)	−0.055** (−1.71)
IIFA (SAR)	−0.179** (−2.54)		0.069** (1.72)		
IIFA (SEM)	−0.234** (−2.83)		0.087** (2.93)		
CPI (SAR)	−0.108** (−2.4)		−0.036* (−1.84)		
CPI (SEM)	−0.234** (−2.4)		0.087** (−1.88)		
EL (SAR)	0.118** (−2.57)			0.060** (−2.59)	
EL (SEM)	0.143** (2.69)			0.080 (2.57)	
HCS (SAR)	0.069 (0.93)			0.037* (1.13)	
HCS (SEM)	0.038 (0.79)			0.017* (1.08)	
IB (SAR)	0.309** (4.63)				1.172** (4.68)
IB (SEM)	0.352** (5.03)				0.228 (5.21)
n	868	868	868	868	868
Rho	0.051**	0.054**	0.049**	0.048**	0.056**
Lambda	0.584**	0.049**	0.047**	0.049**	0.594**

when formulating development strategies, strengthen the setting of scientific investment policies, and improve the high-quality development of regional economy through the introduction of investment [21–23].

3.4.2. Analysis of the Influence of Consumption Factors on Regional Economic Growth Differences. From the perspective of spatial measurement, with the continuous development of scientific and technological information and the continuous improvement of transportation facilities, the communication between populations in different regions has been enhanced, and the changes in people's lifestyles and consumption habits have led to the consumption level and consumption patterns in our country. The impact of social and economic development continues to increase. The consumption habits of the masses in a certain area will directly affect the economic growth difference index between this area and the surrounding areas. If the consumption level in this area declines, or there are differences in consumption patterns, it will directly lead to the expansion of the economic growth difference between this area and surrounding areas, and it is not conducive to regional economic development, and the opposite will have an impact on people's lives. The government should actively observe the characteristics of the market in a timely manner, guide the masses to develop healthy consumption habits, and continuously improve the consumption level of the people through the development of the social economy, and the improvement of the consumption level of the people will also promote the stable development of the social economy.

3.4.3. Analysis of the Impact of Educational Factors on Regional Economic Growth Differences. By analyzing the educational factors in Table 4, the results of the model show that the educational factors have a positive effect on the differences in regional economic growth in my country. Excessive cultural differences may cause regional economic growth differences to increase. In addition, there is a certain mobility of regional talents. Influenced by the treatment of regional talents, the impact of educational factors on the differences in my country's regional economy has spatial characteristics. Differences in education level and education level lead to differences in regional economic growth. The gathering of high-level talents will lead to the peak gathering of regional economies. However, if basic education is weak, regional economic differences will increase. The impact of educational factors on my country's economic differences is obvious. My country should pay attention to the development of education and the allocation of educational resources. It should not only pay attention to the development

of higher education, but also should not relax the construction of basic education. The development of education in areas with relatively weak economic development and the balanced development of education will play a role in reducing the gap in economic growth in my country [24, 25].

3.4.4. Analysis of the Impact of Human Capital on Regional Economic Growth Differences. This study measures the impact of human capital factors on regional economic growth differences and finds that the level of human capital has an impact on regional economic growth differences, but the impact is weaker than other factors. The level of economic development in the region and surrounding areas is rising; if the level of human capital declines, the difference in economic growth in this region will also be narrowed. It will have an impact on the level of human capital and regional economic development in the surrounding areas and will drive the level of human capital in the surrounding areas to decline and reduce the difference in regional economic growth. It should be noted that the representation vector of the level of human capital in the article is the proportion of the government's investment in education in GDP. It is necessary for my country to change from a country with a large population to a country with excellent human capital, but it also takes a certain amount of time. The improvement of the total amount of human resources, the rational distribution of human resources, and the rationalization of the structure of human resources can promote the continuous high-quality development of my country's economy. The continuous improvement of the human resources system is an issue that the society and enterprises have always paid attention to, only the continuous optimization and upgrading of human resources in order to better promote the economic and social benefits of enterprises.

3.4.5. Analysis of the Impact of Technological Innovation on Regional Economic Growth Differences. Whether it is the SAR model or the SEM model, the coefficient of technological innovation factor is the highest among all evaluation factors, which proves that, compared with other evaluation factors, the level of technological innovation in this model has the highest impact on the difference in economic growth in my country. And the level of technological innovation IB has a positive impact on the regional economic growth difference TL. Both the spatial lag model and the spatial error model show that, with the continuous increase of scientific and technological innovation in some regions, the economic value created by science and technology will increase significantly, which will cause the economic growth difference between the region and the surrounding regions to increase. Although regions with a low level of technological innovation can reduce the difference in economic growth between the region and surrounding regions, there may be a general lack of economic development momentum, which will affect the high-quality social and economic development. At the present stage, my country is in the historical intersection of industrial transformation and technological innovation revolution affecting the transformation of my country's economic development mode. The government and enterprises need to better grasp and control the technological innovation mode in a scientific way. While promoting the continuous development of industrial informatization and intelligence, we should also pay attention to the coordination of regional characteristics and different technological innovations, develop technological innovations according to local conditions, steadily improve my country's technological innovation capabilities, and drive new models of industrial systems with technological and intelligent production models. The construction of social production capacity and comprehensive national strength will be the key to narrowing the gap in economic growth in my country.

By analyzing the basic statistical data of 31 provinces and cities in my country from 1993 to 2020, the following conclusions are drawn:

First, the development of industries in my country is diverse, and there are regional differences in the diversity of industries. According to the measurement of industry indicators, the development of my country's regional economic industries can be divided into four types of regions, namely, regions with high industry diversity and low industry ubiquity, regions with low industry diversity and high industry ubiquity, and regions with low industry diversity and low industry ubiquity. Industry Prevalence Regions, High Industry Diversity, and High Industry Prevalence Regions.

Second, the time dimension of economic complexity in my country is not very different, but the economic complexity of regional spatial locations varies greatly. The economic complexity index is higher in the eastern region, such as Shanghai, Beijing, Tianjin, Guangdong, Fujian, and other regions. In the early stage of the western region, the economic complexity index was relatively low. In the later stage, due to the continuous development of the economy, the strengthening of the government's macro-control, and the construction of regional infrastructure, the types of industries in the region continued to increase, and the industry was upgraded. The index keeps rising.

Third, not only does the regional economic complexity index have a spatial impact on regional economic development, but also the levels of investment, household consumption, education, human capital, and technological innovation in the SAR model and SEM model also show that they are closely related to the regional economy. There is a spatial correlation of growth differences. The improvement of investment level has a reducing effect on the difference of regional economic growth in my country. If the regional investment is insufficient, it will lead to insufficient vitality of regional economic development and lead to the increase of the difference in economic growth.

4. Conclusion

This study combines my country's economic complexity with regional economic growth differences, puts the relevant basic data from 1993 to 2020 into a panel model for research, and uses the method of spatial econometrics to

comprehensively analyze my country's economic complexity and other factors. The impact of regional economic development was measured. The research highlights of the article lie in the nonmonetary indicators—the calculation of economic complexity, the measurement of regional economic growth differences refined to the county level, and the combination of economic complexity and regional economic growth differences. In general, the observation time span is long, the observation sample size is relatively abundant, and the results of each model are significant.

Data Availability

The dataset can be obtained from the corresponding author upon request.

Conflicts of Interest

The authors declare that there are no conflicts of interest.

References

[1] P. Aghion and P. Howitt, "A model of growth through creative destruction," *Econometrica*, vol. 60, no. 2, pp. 323–351, 1992.

[2] A. Tacchella, D. Mazzilli, and L. Pietronero, "A dynamical systems approach to gross domestic product forecasting," *Nature Physics*, vol. 60, no. 14, pp. 861–865, 2018.

[3] B. Balassa, "Trade liberalisation and "revealed" comparative advantage," *The Manchester School*, vol. 33, no. 2, pp. 99–123, 1965.

[4] R. A. Batchelor and J. S. Armstrong, "How useful are the forecasts of intergovernmental agencies? The IMF and OECD versus the consensus," *Applied Economics*, vol. 33, no. 2, pp. 225–235, 2001.

[5] C. Battiston and A. Tacchella, "How metrics for economic complexity are affected by noise," *ComplexEconomic Times*, vol. 41, no. 3, pp. 1–22, 2014.

[6] G. S. Becker and K. M. Murphy, "The division of Labor,-Coordination Costs,and knowledge," *Quarterly Journal of Economics*, vol. 107, no. 4, pp. 1137–1160, 1992.

[7] L. G. Calude, "The deluge of spurious correlations in big data," *Foundations of Science*, vol. 22, no. 3, pp. 595–612, 2017.

[8] F. Cecconi and M. Cencini, "Predicting the future from the past: an old problem from a modern perspective," *PLoS One*, vol. 80, no. 11, pp. 1001–1008, 2012.

[9] M. Cristelli, A. Gabrielli, A. Tacchella, G. Caldarelli, and L. Pietronero, "Measuring the intangibles: a metrics for the economic complexity of countries and products," *PLoS One*, vol. 32, no. 8, Article ID e70726, 2013.

[10] D. Clemente and C. Chiarotti, "Diversification versus specialization in complex ecosystems," *PLoS One*, vol. 31, no. 9, Article ID e112525, 2014.

[11] M. Dreher and J. R. Vreeland, "The political economy of IMF forecasts," *Public Choice*, vol. 137, pp. 145–171, 2008.

[12] M. Frenkel, J.-C. Rülke, and L. Zimmermann, "Do private sector forecasters chase after IMF or OECD forecasts?" *Journal of Macroeconomics*, vol. 37, no. 37, pp. 217–229, 2013.

[13] H. Hausmann, "The network structure of economic output," *Econ. Growth*, vol. 22, no. 16, pp. 309–342, 2011.

[14] J. Jarreau and S. Poncet, "Export sophistication and economic growth:evidence from China," *Journal of Development Economics*, vol. 97, no. 2, 2012.

[15] P. R. Krugman, "Increasing returns, monopolistic competition, and international trade," *Journal of International Economics*, vol. 9, no. 4, pp. 469–479, 1979.

[16] P. Krugman, "Increasing returns and economic geography," *Journal of Political Economy*, vol. 99, no. 3, 1991.

[17] E. Lorenz, "Atmospheric predictability as revealed by naturally occurring analogues," *Atmos. Sci*, vol. 26, no. 4, pp. 636–646, 1969.

[18] S. Zhu and R. Li, "Economic complexity, human capital and economic growth," *Applied Economics*, vol. 14, pp. 5–19, 2016.

[19] R. M. Solow, "Contribution to the theory of economic growth," *Economic Times*, vol. 70, no. 1, pp. 65–94, 1956.

[20] C. Tacchella and Caldarelli, "A new metrics for countries' fitness and products' complexity," *Sci. Rep*, vol. 2, no. 1, p. 723, 2012.

[21] C. Tacchella and Pietronero, "Economic complexity: conceptual grounding of a new metrics for global competitiveness," *Journal of Economic Dynamics and Control*, vol. 37, no. 8, pp. 1683–1691, 2013.

[22] Z. Wang and S. J. Wei, *What Accounts for the Rising Sophistication of China's Exports.China's Growing Role in World Trade*, University of Chicago Press, no. 1, , pp. 7–15, Chicago, IL, USA, 2010.

[23] Y. H. D. Wei, "Trajectories of ownership transformation in China:implications for uneven regional development," *Eurasian Geography and Economics*, vol. 45, no. 2, pp. 4–10, 2004.

[24] S. Yao, "Why are Chinese exports not so special?" *Chin & World Economy*, vol. 17, no. 1, 2009.

[25] H. Ye, "Equation-free mechanistic ecosystem forecasting using empirical dynamic modeling," *Proceedings of the National Academy of Sciences of the United States of America*, vol. 112, no. 13, pp. E1569–E1576, 2015.

Hindawi
Scientific Programming
Volume 2022, Article ID 7927659, 9 pages
https://doi.org/10.1155/2022/7927659

Research Article

Application and Research of the Image Segmentation Algorithm in Remote Sensing Image Buildings

Sichao Wu,[1] **Xiaoyu Huang**,[1] **and Juan Zhang**[2]

[1]*Xiamen Academy of Arts and Design, Fuzhou University, Xiamen 361000, Fujian, China*
[2]*Chengdu University, Chengdu 610000, Sichuan, China*

Correspondence should be addressed to Xiaoyu Huang; huangxiaoyu@fzu.edu.cn

Received 4 June 2022; Revised 13 June 2022; Accepted 20 June 2022; Published 1 July 2022

Academic Editor: Lianhui Li

Aiming at the problems of low building segmentation accuracy and blurred edges in high-resolution remote sensing images, an improved fully convolutional neural network is proposed based on the SegNet network. First, GELU, which performs well in deep learning tasks, is selected as the activation function to avoid neuron deactivation. Second, the improved residual bottleneck structure is used in the encoding network to extract more building features. Then, skip connections are used to fuse images The low-level and high-level semantic features are used to assist image reconstruction. Finally, an improved edge correction module is connected at the end of the decoding network to further correct the edge details of the building and improve the edge integrity of the building. Experiments are carried out on the Massachusetts building dataset, and the precision rate, recall rate, and $F1$ value reach 93.5%, 79.3%, and 81.9%, respectively, and the comprehensive evaluation index $F1$ value is improved by about 5% compared with the basic network.

1. Introduction

With the development of remote sensing technology, massive high-resolution remote sensing images provide data guarantee for research in the field of remote sensing [1, 2]. As the most important part of the national basic geographic database, buildings have very important research value in the fields of urban planning, change detection, and geographic information system construction. Building segmentation using high-resolution remote sensing images has always been the focus and difficulty of remote sensing research [3–5]. Traditional building segmentation methods are mostly based on traditional remote sensing image classification technology, but this method cannot achieve high-precision and fully automated segmentation. With the development of deep learning in the field of computer vision, Shao and Cai [6] proposed Fully Convolutional Networks (FCN) for image segmentation tasks, which overcome the shortcomings of traditional image segmentation methods and become the mainstream mode in image segmentation tasks. Subsequently, researchers have successively proposed image segmentation networks such as U-Net [7, 8] and SegNet [9, 10] on the basis of FCN. In order to improve the segmentation effect of buildings, many researchers in the field of remote sensing have made improvements on the basis of U-Net and SegNet networks. These methods either improve the feature extraction part of the network or compare the basic network with the classical structures in other networks. Combined, the segmentation accuracy of buildings is improved, but there is still the problem of edge blur caused by loss of details [11–13].

Therefore, based on the SegNet network, this paper designs a residual bottleneck structure that can extract multiscale features in parallel by modifying the activation function. Combined with the skip connection operation and the improved edge correction module, an improved deep semantic segmentation network RsBR-SegNet (Residual + Boundary Refinement-SegNet) is used to improve the accuracy and edge integrity of high-resolution remote sensing image building segmentation and provide a reference for the practical application of remote sensing image building segmentation.

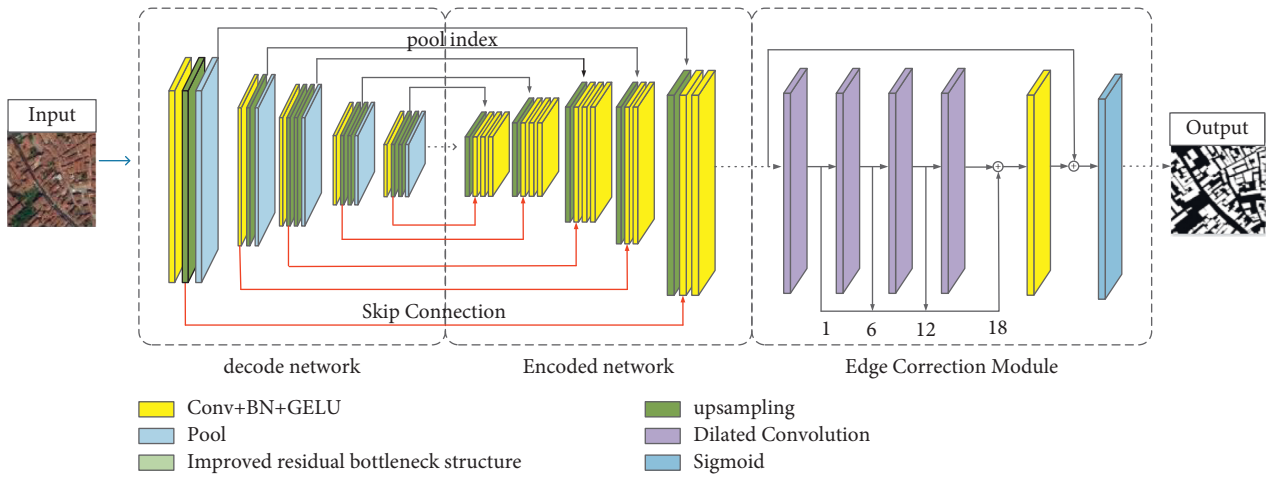

Figure 1: RsBR-SegNet model structure diagram.

2. Experimental Data

2.1. Introduction to Datasets. In order to verify the effectiveness and practicability of RsBR-SegNet in the task of building segmentation, experiments were carried out successively on the "Satellite dataset I (global cities)" [14] and the aerial remote sensing image dataset "Massachusetts Buildings Dataset" [15]. The "Satellite dataset I (global cities)" dataset contains 204 satellite remote sensing images of 512×512 pixels, with resolutions ranging from 0.3 m to 2.5 m. The "Massachusetts Buildings Dataset" dataset consists of 151 aerial remote sensing images in the Boston area, each image is 1500×1500 pixels in size, and the data are divided into 137 training sets, 10 testing sets, and 4 validation sets, with a resolution of 1 m.

2.2. Dataset Preprocessing and Expansion. In this paper, the "Satellite dataset I (global cities)" dataset is divided into the training set and test set according to 4:1, without any transformation, only to verify the effectiveness of the model in the task of building segmentation. Then, in order to prove the practicability of the network model in the field of remote sensing image building segmentation and considering the limited computing power of the computer, the "Massachusetts Buildings Dataset" dataset was cropped and expanded. First, each 1500×1500 image in the original training set is cropped into 9 images of 512×512 size, and then the training set is expanded to 12330 images through a series of data augmentation operations such as translation, mirroring, rotation, and random combination. We are required to crop the test set only and expand it to 90 images of size 512×512.

3. The Working Principle of the RsBR-SegNet Network Model

In order to improve the segmentation effect of buildings at the edges and details, this paper improves the SegNet network structure and builds a fully convolutional neural network RsBR-SegNet for building segmentation in remote sensing images. Its structure is shown in Figure 1. RsBR-SegNet preserves the upsampling way of the original SegNet, using GELU [16]. As an activation function, we are required to avoid neuron necrosis; retain the first layer of standard convolution in each convolution group in the encoding network to undertake the maximum pooling operation, and use the improved residual bottleneck structure to replace the remaining volumes in the encoding network. Layers are stacked to further extract image features, deepen the network depth, and improve the segmentation accuracy of buildings; use skip connections between the encoding network and the decoding network to fuse low-level features and high-level features between image channels to further retain the original detail information of buildings; the end of the decoding network is connected to an improved edge correction module to refine the edges of buildings and improve the integrity of building segmentation. The input of the network is a three-channel (red, green, and blue) remote sensing image of buildings, and the output is a single-channel segmentation result map, where the white pixels are the segmented buildings, and the black pixels are the background.

3.1. Activation Function. The original SegNet network uses ReLU (Rectified Linear Units) [17] as the activation function, but when the input value of the function is negative, the neuron will appear necrotic, which is an unavoidable defect of the ReLU function. For this reason, this paper selects GELU (Gaussian Error Linear Units, Gaussian Error Linear Units), which performs well in deep learning tasks, as the activation function in the RsBR-SegNet network because it is derivable at the origin and introduces the idea of random regularity. Therefore, the final activation transformation will establish a random connection with the input, avoiding the phenomenon of neuron necrosis and improving the speed and accuracy of learning. The function image is shown in Figure 2.

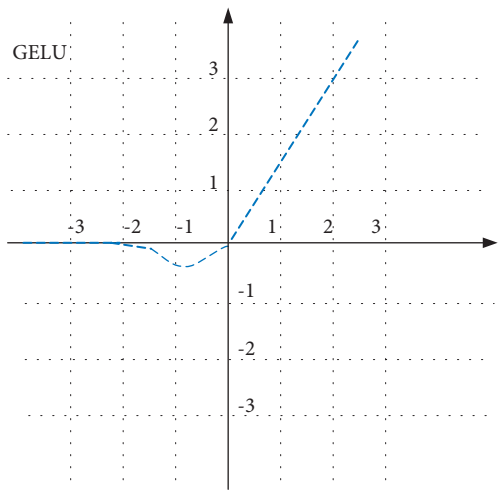

Figure 2: GELU activation function image.

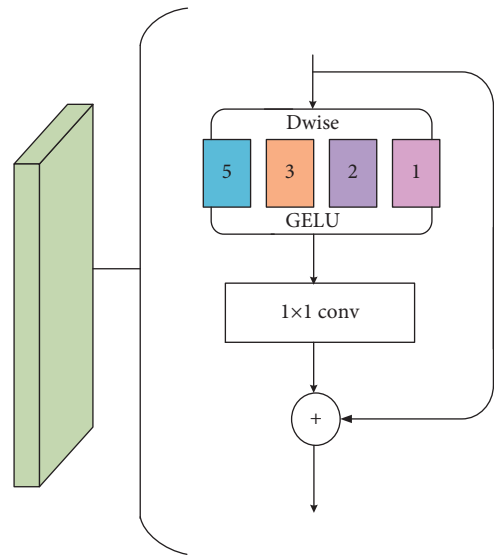

Figure 3: Improved residual bottleneck structure diagram.

3.2. Improve the Residual Bottleneck Structure. By increasing the network depth, the model can learn more complex detailed features, but the increase of the network depth will lead to problems such as gradient instability and network degradation during the training process. The residual bottleneck structure proposed in the ResNet network can alleviate this phenomenon. The MobileNetV2 network proposed by Guillermo et al. [18] is based on the original residual bottleneck structure and proposes a reverse residual bottleneck structure, which reverses the original channel dimension and uses depth-wise separable convolution for feature extraction, which improves segmentation speed and accuracy.

Although the depth-wise separable convolution used in the literature significantly reduces the number of weights, there is still room for improvement in segmentation performance. For this reason, this paper proposes an improved residual bottleneck structure to obtain more feature map information and improve the accuracy of building segmentation. First, in the improved residual bottleneck structure, the first layer adopts the convolution kernels of 5×5, 3×3, 2×2, and 1×1 for parallel calculation of channel-by-channel convolution, receives the feature maps of different receptive fields, concatenates the feature maps of each path together to obtain more features, and then uses point-by-point convolution to reduce the number of channels to the original input size, so that the improved residual bottleneck structure can effectively reduce the number of weights and improve segmentation performance. At the same time, the ReLU activation function will cause information loss due to neuron inactivation in low-dimensional input. GELU can effectively alleviate this phenomenon and improve performance. Therefore, GELU is also used as the activation function after the channel-by-channel convolution and the point-by-point convolution. After reducing the nonlinear transformation, the improved residual bottleneck structure is shown in Figure 3.

The improved residual bottleneck structure is influenced by the idea of the reverse residual bottleneck structure. In this structure, the channel dimension is also expanded and then contracted. By stacking depth-wise separable convolutions of different sizes, global features are further obtained and features improved. Extracting ability and reducing the occupation of running memory, the number of parameters is shown in equation (1). The number of parameters of the reverse residual bottleneck structure in the MobileNetV2 network is shown in equation (2).

$$\begin{aligned} P &= [5\times5+3\times3+2\times2+1\times1]\times M+4\times M\times1\times1\times N \\ &= (39+4\times N-N)\cdot M, \end{aligned} \tag{1}$$

$$\begin{aligned} P &= M\times1\times1\times6\times-M+6\times-M\times-3\times-3 \\ &\quad +6\cdot\times\cdot M\cdot\times1\times1\times-N=(54+6\times N+6\times M)\times M. \end{aligned} \tag{2}$$

In the above formula, P represents the number of parameters, M represents the number of input channels, and N represents the number of output channels.

The number of input channels of the residual bottleneck structure in the RsBR-SegNet network is equal to the number of output channels, so the number of parameters of the improved residual bottleneck structure is less than the number of parameters for the inverse residual bottleneck structure in the MobileNetV2 network.

3.3. Improve the Edge Correction Module. At present, most of the deep learning-based remote sensing image building segmentation methods generate building segmentation results in one step and do not make further corrections to the results. There is a large difference between the segmentation results and the ground truth [19–21]. In order to further correct the segmentation results, this paper proposes an improved edge correction module, which takes the single-channel probability map output by the model as input, automatically learns the residual between the input image and the corresponding real result during the training process, and further refines the input. Image for more accurate segmentation results. The original

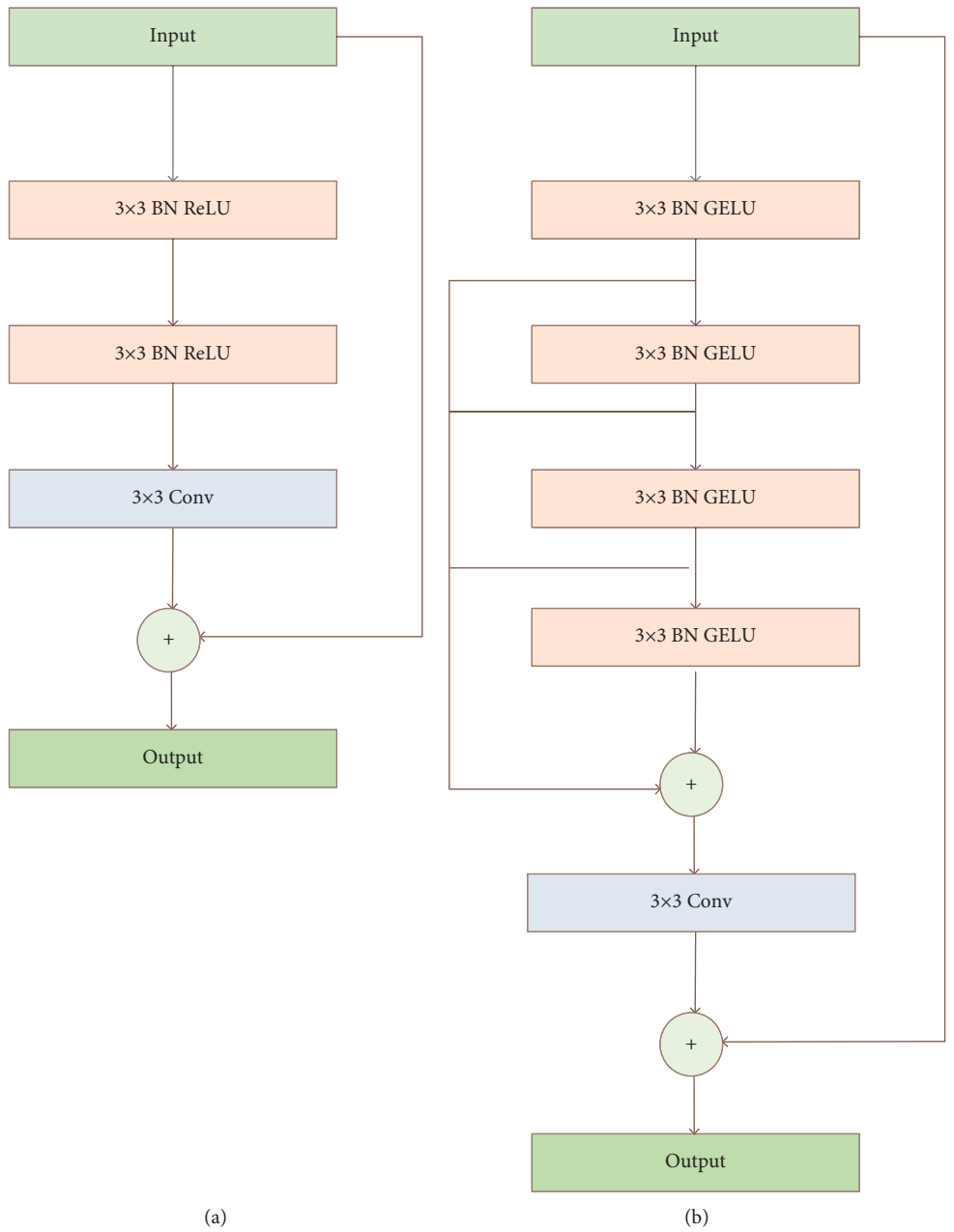

Figure 4: Comparison (a) of edge (b) correction modules.

edge correction module was originally proposed by Song et al. [22] to further refine the boundary information, and the structure is shown in Figure 4(a). Although this structure improves the segmentation accuracy of the boundary to a certain extent, due to the small number of network layers, the deeper features of the input image cannot be extracted. Therefore, an improved edge correction module is proposed, which corrects the original edge. On the basis of the module, the depth of the network layer and more receptive fields are increased, and its structure is shown in Figure 4(b).

In the improved edge correction module, four holes convolutions with expansion rates of 1, 6, 12, and 18 are used to extract image features, and then the extracted feature maps are superimposed. After each convolution operation, normalization, and in the activation operation, in order to avoid the phenomenon of neuron necrosis in ReLU [23–28], GELU is also selected as the activation function, and then the standard convolution of 3×3 is used to convert the number of feature map channels to 1, and then the obtained feature map is compared with the input image of this module. Fusion is performed to obtain the preliminary information of the prediction module, and finally, the fused feature map is classified by the Sigmoid function to obtain the final segmentation result map [29–33]. Compared with the original module, the improved edge correction module proposed in this paper has a deeper structure, and the extracted image features are richer. At the same time, the dilated convolution with different expansion rates can also

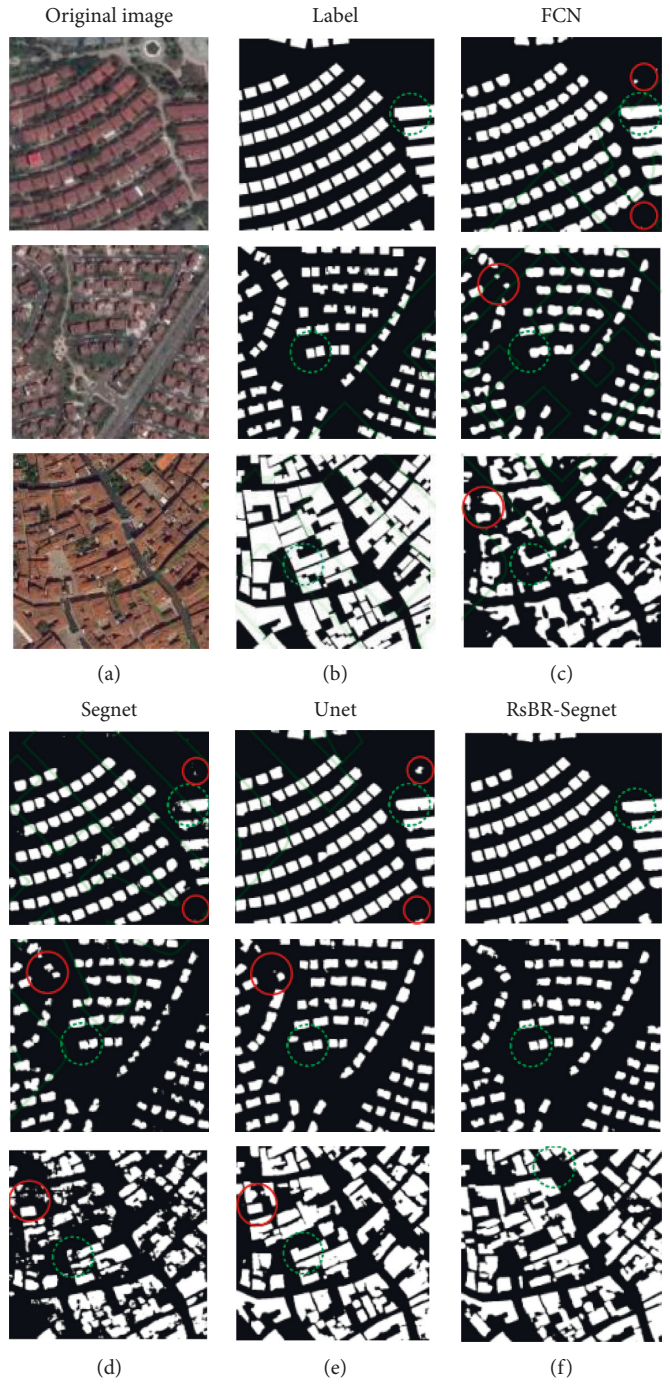

Figure 5: Comparison of segmentation results of satellite dataset I (global cities).

obtain more global information, which makes the final segmentation result of the building more accurate and complete.

4. Experimental Results and Analysis

The computer hardware configuration in this experiment is Intel Xeon(R) Gold 5215@2.5 GHz, 64 G memory, NVIDIA GeForce RTX 2080 Ti GPU. The operating system is 64-bit Ubuntu18.04, Cuda10.0 + Cudnn7.5, and the code is based on the PyTorch framework.

4.1. Evaluation Indicators. We use precision rate, recall rate, $F1$-score, and intersection over union (IoU) to evaluate and analyze the segmentation effect of remote sensing image buildings. The calculation formula is as follows:

$$\text{precision} = \frac{\sum tp}{\sum tp + \sum fp}, \tag{3}$$

$$\text{recall} = \frac{\sum tp}{\sum tp + \sum fn}, \tag{4}$$

Table 1: Evaluation of satellite dataset I (global cities).

Network name	Accuracy	Recall	$F1$ value	Cross-over
FCN	0.86315	0.69252	0.72543	0.57586
SegNet	0.83997	0.62044	0.66617	0.50669
U-net	0.86616	0.73194	0.73196	0.59867
RsBR-SegNet	0.87526	0.75458	0.75907	0.61834

$$F1 = \frac{2(\text{precision} * \text{recall})}{\text{precision} + \text{recall}}, \tag{5}$$

$$IoU = \frac{\sum tp}{\sum tp + \sum fp + \sum fn}. \tag{6}$$

Among them, tp indicates the pixels that correctly segment the building, fp represents the pixels that are wrongly classified as buildings, and fn represents the pixels that are buildings but not correctly segmented. The precision rate is used to measure the probability that the correctly predicted building samples account for all the predicted building samples in the prediction result. The larger the value, the more accurate the building segmentation is; the ratio is actual building samples, the larger the value, the more complete the segmentation of the buildings in the sample; the $F1$ value is used to integrate the two evaluation indicators of precision and recall, and the larger the value, the better the network model. The segmentation is more effective; IoU is used to evaluate the similarity between the identified building area and the ground truth area, and in IoU, a higher value indicates a higher correlation between the identified buildings and the ground truth.

4.2. Evaluation of Segmentation Results. In order to prove the effectiveness of the network in this paper, the classical semantic segmentation networks FCN, U-Net, SegNet, and the network in this paper are tested on the small sample dataset " Satellite dataset I (global cities)," and the experimental results are shown in Figure 5. Here, (a) is the original image, (b) is the label corresponding to the building in the original image, (c) is the segmentation result of the FCN network, (d) is the segmentation result of the SegNet network, (e) is the segmentation results of the U-Net network, and (f) is the segmentation result of the network RsBR-SegNet. In this paper, the area surrounded by the dotted frame is the comparison of segmentation details, and the area surrounded by the solid frame is the misclassification and omission in the segmentation results. It can be seen from the segmentation results that compared with other networks, the image scale change has less impact on the network in this paper, and there are fewer misclassifications and missed classifications in the segmentation results, and it performs better in the segmentation of small buildings. Edge recovery is also more complete. It can be seen from the first line of segmentation results that compared with other networks, RsBR-SegNet can effectively overcome the misclassification of buildings. From the second line of segmentation results, it can be seen that U-Net has a better segmentation effect on buildings than FCN and SegNet. RsBR-SegNet can further identify small buildings that U-Net misses and loses detailed information. The phenomenon has been effectively alleviated. The third row of segmentation results shows that for buildings interfered by vegetation and road shadows, RsBR-SegNet has a certain antiinterference ability, and the integrity of the building edge is higher.

Table 1 records the test results of each network model on the "Satellite dataset I (global cities)" dataset. As can be seen from the data in the table, compared with SegNet, the improved network has an increase of 3.5%, 13.4%, and 9.3% in evaluation indicators such as precision rate, recall rate, and $F1$ value, and an increase of 11.2% in IoU. It can be seen from the index comparison results that compared with SegNet and FCN, the improved network RsBR-SegNet achieves a significant improvement in the segmentation performance of buildings, and it also has certain improvement advantages compared with the U-Net network. A good segmentation effect can also be achieved on the dataset.

In order to prove the practicability of the network in this paper in the task of building segmentation, each network is tested on the expanded Massachusetts building dataset. The experimental results are shown in Figure 6. The meaning and legend of each column are consistent with Figure 5.

It can be seen from the segmentation results that the improved network has more advantages in the intensive small building segmentation task. The first line of segmentation results shows that compared with other networks, RsBR-SegNet has fewer misclassifications and missed classifications, and the edges of buildings are restored more completely. It can be seen from the segmentation results of the following lines that for small buildings that cannot be recognized by other networks in the figure, the improved network can still identify them effectively, and the overall segmentation effect of RsBR-SegNet is better than other comparison networks.

They are tested on the expanded Massachusetts building datase . Table 2 records the index evaluation results of each network. From the data in the table, it can be seen that in the large sample data set, the indicators of all networks have improved. Compared with SegNet, the improved network is improved by 1.7%, 6.1%, 5.0%, 6.7% in precision, recall, $F1$ value, and IoU, respectively. Compared with other classical semantic segmentation networks, the RsBR-SegNet network has improved various evaluation indicators, the accuracy rate reaches 93.503%, and the IoU reaches 69.746%, which fully proves the practicability of the improved network in the task of remote sensing image building segmentation.

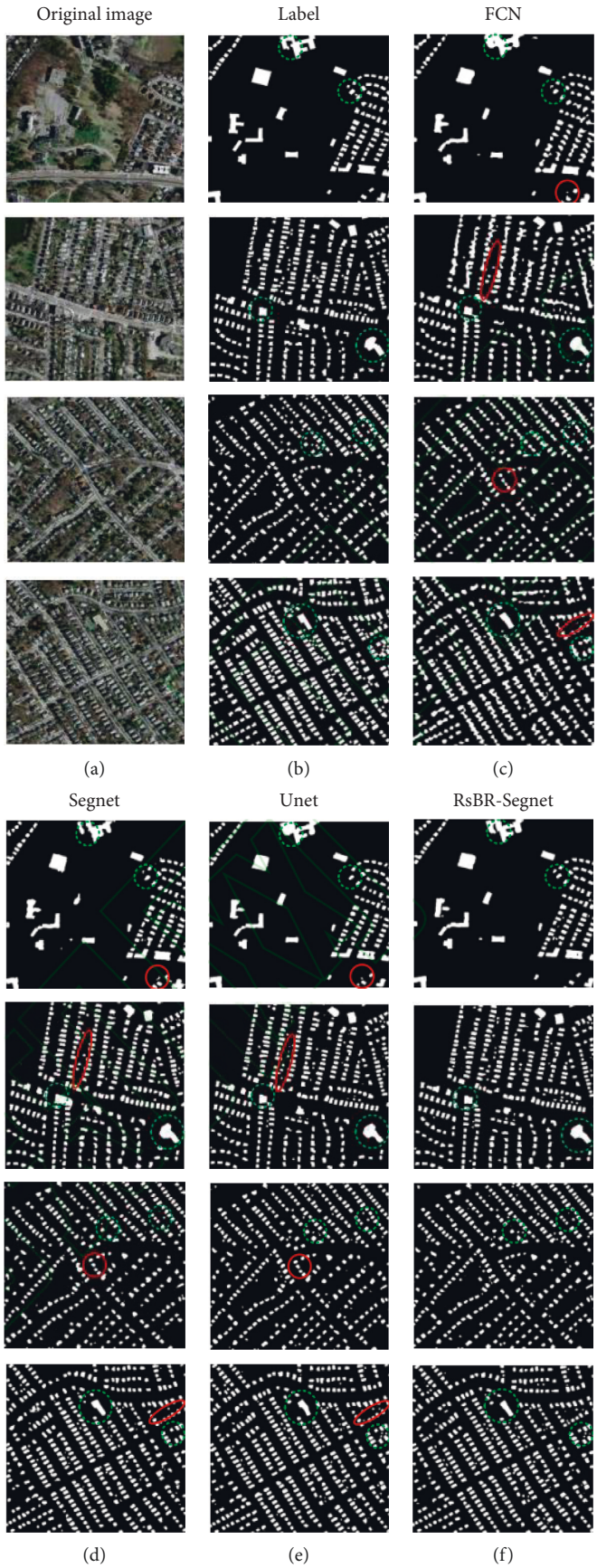

Figure 6: Comparison of Massachusetts building dataset segmentation results.

Table 2: Massachusetts building dataset evaluation.

Network name	Accuracy	Recall	$F1$ value	Cross-over
FCN	0.91789	0.73896	0.77118	0.63075
SegNet	0.91844	0.73145	0.77000	0.62998
U-net	0.92345	0.75802	0.79303	0.67429
RsBR - SegNet	0.93503	0.79288	0.81915	0.69746

5. Conclusion

This paper proposes a fully convolutional neural network RsBR-SegNet suitable for building segmentation. CELU as the activation function in the network has to be used to improve the learning ability of neurons, skip connections have to be used to fuse the low-level semantic features and high-level semantic features of the image, the phenomenon of loss of details needs to be alleviated, and the improved residual bottleneck structure and edge correction module are to be used to extract more buildings It can improve the segmentation accuracy and edge integrity of buildings. Experiments are carried out on satellite and aerial remote sensing image datasets, respectively, and the results show that the RsBR-SegNet network has more accurate segmentation results than the classical segmentation networks FCN, U-Net, and SegNet and effectively overcomes the edge blurring phenomenon. Compared with the evaluation indicators such as precision rate, recall rate, $F1$ value, and IoU, RsBR-SegNet has achieved the highest value, which is more suitable for remote sensing image building segmentation tasks.

Data Availability

The dataset can be accessed upon request.

Conflicts of Interest

The authors declare that they have no conflicts of interest.

Acknowledgments

The authors thank the project supported by Fujian Province Young and Middle-Aged Teachers' Education and Scientific Research Project Grant "Research on the Activation Design of Traditional Fujian Village Cultural Landscape" (Grant no. JAS21007) and project supported by the Fujian Province Social Science Planning "Fujian Folk Animation Research" (Grant no. FJ2021B195) support.

References

[1] A. Allbed and L. Kumar, "Soil salinity mapping and monitoring in arid and semi-arid regions using remote sensing technology: a review," *Advances in Remote Sensing*, vol. 2013, 2013.

[2] R. Kaur and P. Pandey, "A review on spectral indices for built-up area extraction using remote sensing technology," *Arabian Journal of Geosciences*, vol. 15, no. 5, pp. 1–22, 2022.

[3] G. Cheng, X. Xie, J. Han, L. Guo, and G.-S. Xia, "Remote sensing image scene classification meets deep learning: challenges, methods, benchmarks, and opportunities," *Ieee Journal of Selected Topics in Applied Earth Observations and Remote Sensing*, vol. 13, pp. 3735–3756, 2020.

[4] C. Liu, Z. X. Chen, S. Shao, J.-s. Chen, T. Hasi, and H.-z. Pan, "Research advances of SAR remote sensing for agriculture applications: a review," *Journal of Integrative Agriculture*, vol. 18, no. 3, pp. 506–525, 2019.

[5] S. C. Kulkarni and P. P. Rege, "Pixel level fusion techniques for SAR and optical images: a review," *Information Fusion*, vol. 59, pp. 13–29, 2020.

[6] Z. Shao and J. Cai, "Remote sensing image fusion with deep convolutional neural network," *Ieee Journal of Selected Topics in Applied Earth Observations and Remote Sensing*, vol. 11, no. 5, pp. 1656–1669, 2018.

[7] Z. Chen, C. Wang, J. Li, N. Xie, Y. Han, and J. Du, "Reconstruction bias U-Net for road extraction from optical remote sensing images," *Ieee Journal of Selected Topics in Applied Earth Observations and Remote Sensing*, vol. 14, pp. 2284–2294, 2021.

[8] Z. Chen, D. Li, W. Fan, H. Guan, C. Wang, and J. Li, "Self-attention in reconstruction bias U-Net for semantic segmentation of building rooftops in optical remote sensing images," *Remote Sensing*, vol. 13, no. 13, p. 2524, 2021.

[9] L. Weng, Y. Xu, M. Xia, Y. Zhang, J. Liu, and Y. Xu, "Water areas segmentation from remote sensing images using a separable residual segnet network," *ISPRS International Journal of Geo-Information*, vol. 9, no. 4, p. 256, 2020.

[10] M. Xue, B. Wei, and L. Yang, "Research on high resolution remote sensing image classification based on segnet semantic model improved by genetic algorithm," *The International Archives of the Photogrammetry, Remote Sensing and Spatial Information Sciences*, vol. XLII-3/W10, pp. 415–422, 2020.

[11] J. Lu, Y. Wang, Y. Zhu et al., "P_segnet and np_segnet: new neural network architectures for cloud recognition of remote sensing images," *IEEE Access*, vol. 7, pp. 87323–87333, 2019.

[12] J. Jiang, C. Lyu, S. Liu, Y. He, and X. Hao, "RWSNet: a semantic segmentation network based on SegNet combined with random walk for remote sensing," *International Journal of Remote Sensing*, vol. 41, no. 2, pp. 487–505, 2020.

[13] B. Cui, D. Fei, G. Shao, Y. Lu, and J. Chu, "Extracting raft aquaculture areas from remote sensing images via an improved U-net with a PSE structure," *Remote Sensing*, vol. 11, no. 17, p. 2053, 2019.

[14] Y. Yuan, X. Ma, G. Han, S. Li, and W. Gong, "Research on lightweight disaster classification based on high-resolution remote sensing images," *Remote Sensing*, vol. 14, no. 11, Article ID 2577, 2022.

[15] A. Khalel and M. El-Saban, "Automatic pixelwise object labeling for aerial imagery using stacked u-nets," 2018.

[16] Q. Zhang, C. Wang, and H. Wu, "GELU-Net: a globally encrypted, locally unencrypted deep neural network for privacy-preserved learning," pp. 3933–3939, 2018, IJCAI.

[17] A. F. Agarap, "Deep learning using rectified linear units (relu)," 2018.

[18] M. Guillermo, A. R. A. Pascua, and R. K. Billones, "COVID-19 risk assessment through multiple face mask detection using MobileNetV2 DNN," in *Proceedings of the 9th International Symposium on Computational Intelligence and Industrial Applications (ISCIIA2020)*, Beijing, China, 2020.

[19] D. Song, X. Tan, B. Wang, L. Zhang, X. Shan, and J. Cui, "Integration of super-pixel segmentation and deep-learning methods for evaluating earthquake-damaged buildings using single-phase remote sensing imagery," *International Journal of Remote Sensing*, vol. 41, no. 3, pp. 1040–1066, 2020.

[20] J. Hui, M. Du, and X. Ye, "Effective building extraction from high-resolution remote sensing images with multitask driven deep neural network," *IEEE Geoscience and Remote Sensing Letters*, vol. 16, no. 5, pp. 786–790, 2018.
[21] Y. Xu, L. Wu, Z. Xie, and Z. Chen, "Building extraction in very high resolution remote sensing imagery using deep learning and guided filters," *Remote Sensing*, vol. 10, no. 1, p. 144, 2018.
[22] S. Song, J. Liu, Y. Liu et al., "Intelligent object recognition of urban water bodies based on deep learning for multi-source and multi-temporal high spatial resolution remote sensing imagery," *Sensors*, vol. 20, no. 2, p. 397, 2020.
[23] Y. Sun, M. Dong, M. Yu et al., "Nonlinear all-optical diffractive deep neural network with 10.6 μ m wavelength for image classification," *International Journal of Optics, v*, vol. 2021, 2021.
[24] I. Uddin, D. A. Ramli, A. Khan et al., "Benchmark pashto handwritten character dataset and pashto object character recognition (OCR) using deep neural network with rule activation function," *Complexity*, vol. 2021, 2021.
[25] L. Li, B. Lei, and C. Mao, "Digital twin in smart manufacturing," *Journal of Industrial Information Integration*, vol. 26, no. 9, Article ID 100289, 2022.
[26] L. Li, T. Qu, Y. Liu et al., "Sustainability assessment of intelligent manufacturing supported by digital twin," *IEEE Access*, vol. 8, pp. 174988–175008, 2020.
[27] Z. Zhao, K. Hao, X. Ma et al., "SAI-YOLO: a lightweight network for real-time detection of driver mask-wearing specification on resource-constrained devices," *Computational Intelligence and Neuroscience*, vol. 2021, 2021.
[28] L. Li, C. Mao, H. Sun, Y. Yuan, and B. Lei, "Digital twin driven green performance evaluation methodology of intelligent manufacturing: hybrid model based on fuzzy rough-sets AHP, multistage weight synthesis, and PROMETHEE II," *Complexity*, vol. 2020, no. 6, pp. 1–24, 2020.
[29] W. Zhang, Y. Li, X. Li et al., "Deep neural network-based SQL injection detection method. Security and communication networks," vol. 2022, 2022.
[30] L. Li and C. Mao, "Big data supported PSS evaluation decision in service-oriented manufacturing," *IEEE Access*, no. 99, p. 1, 2020.
[31] Li Zhao, Y. Gao, and D. Kang, "Construction and simulation of market risk warning model based on deep learning," *Scientific Programming*, vol. 2022, 2022.
[32] J. Yang, "Personalized Song recommendation system based on vocal characteristics," *Mathematical Problems in Engineering*, vol. 2022, 2022.
[33] D. Liu, K. Huang, D. Wu, and S. Zhang, "A new method of identifying core designers and teams based on the importance and similarity of networks," *Computational Intelligence and Neuroscience*, vol. 2021, p. 3717733, 2021.

Hindawi
Scientific Programming
Volume 2022, Article ID 1291336, 8 pages
https://doi.org/10.1155/2022/1291336

Research Article

Methods of Improving and Optimizing English Education in Colleges and Universities Assisted by Microvideo Technology

Xiuhua Wang

Science and Technology College, Gannan Normal University, Gan Zhou 341000, Jiang Xi, China

Correspondence should be addressed to Xiuhua Wang; 2010008@gnnu.edu.cn

Received 27 April 2022; Revised 6 June 2022; Accepted 11 June 2022; Published 30 June 2022

Academic Editor: Lianhui Li

English teaching in general higher education is faced with great challenges. English teachers have to face a group of students from different regions, who have received different English teaching methods during middle school, and their English proficiency is uneven. At present, the teaching methods of most colleges and universities are backward, unable to make full use of modern information technology, and students have low interest in learning, poor independent learning ability, and low learning effect, especially in English. In order to comprehensively improve students' English level, English teaching methods in colleges and universities should be completely different from the traditional teaching methods in middle schools. This paper sorts out trial research, questionnaire survey, and data analysis method and combines some problems existing in college English teaching and the characteristics of microvideo, such as short, concise, sound, and text, to apply microvideo as a teaching resource in college English grammar teaching. A trial group was set up to study the effectiveness of microvideo teaching. No students in the trial group disliked the microvideo teaching and the average score of students in the trial group was 8.992 points higher than the average score of students in the traditional group. The results show that microvideo teaching can not only increase students' interest in learning English but also improve their English language skills.

1. Introduction

In recent years, with the continuous development of the network and modern education technology, the traditional teaching methods need to change correspondingly, and the teaching mode of microvideo has gradually entered the teaching stage. The integration of microvideo into English classroom teaching allows students to freely enter the situation created by the microvideo to learn independently, making the originally boring teaching process vivid and interesting. [1–5] Through rigorous design, microvideo can give students a large amount of information in a short time, which is suitable for students' cognitive characteristics such as short attention span. Microvideo can give different students different learning needs and meet their learning needs. In the case of intuitiveness and interest, students can complete their learning tasks more effectively and improve their self-confidence. [6, 7].

Through the application of microvideo in English classroom teaching, students can use microvideo to arrange and control their own learning according to their own situation in the English classroom, which can be carried out in a relaxed atmosphere, breaking the form of teacher singing a solo show in the original classroom. [8–12] Students can watch videos at their own pace, rather than closely following the pace of the teacher. What you have learned can be fast-forwarded, what you have not learned can be watched over and over again, or you can stop to think carefully or practice. In addition, you can also learn through group cooperation or with the help of the teacher. The teaching reform that combines microvideo with English classroom teaching truly focuses on learners, regards students as the main body of the teaching process, and respects students' individual differences and personalized needs. In China, in the present stage of higher education, the teaching of English subject is often valued as skills training, teaching form does not have novelty, could not keep up with the pace of The Times development, and English teachers are still in accordance with the "speak, play, and practice," the traditional teaching method of teaching, not giving full play to students'

various aspects and abilities. It is not conducive to the cultivation of information literacy. [13–16].

In the traditional teaching mode, there is less exploration in bring learners into the corresponding learning situation, which is generally explained step by step based on the examination content, which is insufficient to mobilize students' interest in learning. Based on constructivism theory, microlearning theory, situational teaching theory, and knowledge visualization theory, this paper deepens the unique advantages of microvideo teaching resources and applies them to English grammar teaching in colleges and universities through the integrated application of relevant theoretical concepts, in order to obtain better teaching effects and gradually form a teaching model, so as to enrich the theoretical research results of the application of microvideo in English grammar teaching. [17–21].

Microvideo teaching is helpful to enhance students' interest in Learning English and cultivating their independent learning ability. In order to change the monotonous and boring characteristics of traditional teaching and enhance students' interest and enthusiasm in learning English grammar, microvideo teaching should be applied in English grammar teaching in a timely and appropriate way to create a real and vivid language teaching situation. Meanwhile, with the help of microvideo, students can play the video unlimited times, anytime and anywhere, so that they can not only check and fill in the gaps of knowledge that they do not know but also review the old and learn the new, so as to cultivate students' ability of independent inquiry and learning. Microvideo can help teachers change teaching methods and improve classroom efficiency. Microvideo teaching is a new teaching method. In English grammar teaching, teachers can effectively integrate excellent microvideos and share resources, which can not only reduce the burden of teachers but also enable students to actively learn grammar knowledge, which is convenient to improve classroom efficiency and maximize classroom teaching. [22–25] Exploring the application of microvideo teaching in actual English grammar teaching, the microvideo teaching resources are applied to judge the ultimate impact of this teaching method on students' academic performance and to break through the key and difficult points. Based on the application of English grammar in colleges and universities, it is extended to all aspects of English listening, speaking, reading, and writing. [25–27].

Taking college English classroom teaching as an example, this paper analyzes the application ideas and status quo of conventional English teaching. According to the actual situation of college English classroom teaching, this paper tries to combine microvideo with classroom teaching to carry out classroom teaching reform, such as reasonable use of classroom time and improving teaching effect and efficiency.

2. Microvideo Theory

2.1. Microlearning Theory. The biggest characteristics of microvideo are short, fast, fine, and mass participation. Compared with traditional teaching resources, microvideo teaching resources have vivid images, stimulates the senses, make abstract knowledge interesting, short time, precise content, simplifies the classroom, improves classroom efficiency, and student participation.

Grammar is the basis of learning language subjects well. Languages are governed systems, and such rules are grammatical rules. Mastering grammar rules is the key to improve the language skills of listening, speaking, reading, and writing. Students not only need to master a variety of advanced vocabulary but also must master a variety of sentence patterns and tenses, which shows how difficult it is for college students to learn English grammar well. English grammar microvideo in higher education refers to the production of English grammar knowledge into short and concise video resources in accordance with English curriculum standards and students' cognition skills with the help of modern tools, so as to facilitate students' understanding and learning of grammar. We summarize the grammar contained in the textbook, download or record short videos of relevant grammar knowledge, and create a vivid and interesting micro-video teaching situation, thus causing a strong visual feast for students and motivating them. Meanwhile, we summarize and categorise the relevant grammar, simplify and systematise it in a piecemeal manner, so as to help students structure their grammar knowledge and build up their self-confidence in learning. The clear and convenient grammar tutorials provided by the grammar microvideo can meet the aim of some students to learn grammar when they want, where they want, and to consolidate their grammar knowledge whenever and wherever they want.

The concept of microlearning theory was first introduced in the early years of the 21st century and refers to learning activities that deal with relatively small learning units and focus on short periods of time. Microlearning also refers to "learning activities that break down knowledge into smaller learning units and that people can do in their daily communication and work", emphasising the convenience of microlearning. Microlearning is a learning activity supported by information technology with micromedia, microprocesses, and microresources based on the concept of ubiquity, connectivity, ecology, and uniqueness. Micromedia emphasise learning activities that involve learning to master smaller pieces of knowledge in a limited amount of time. Learners can learn whenever and wherever they need to, and the content knowledge learned is generally brief. The media provide many preprocessed knowledge modules or knowledge points, which are usually both interlinked and independent of each other.

2.2. Knowledge Visualization. Knowledge visualization is a new teaching idea and an important means to acquire knowledge in the era of graphic existence. Visual representation is the most effective form of knowledge visualization, including knowledge presentation, transmission, and acquisition. Knowledge visualization emphasizes the visualization of learning content and knowledge, and improves students' learning ability and knowledge construction ability

through visual organs. Knowledge visualization is a new requirement of teaching reform and development in the era of graphic survival. Knowledge visualization can not only externalize the tacit knowledge but also visualize, animate, and simplify the explicit knowledge, which can promote the dissemination and innovation of knowledge among groups. However, both visual design and visual application of knowledge are closely related to visual representation, which is an indispensable part of teaching. Therefore, visual representation is a crucial form to realize the value of knowledge visualization. In addition, based on graphic design and cognitive science, knowledge "transmission" and "innovation" can be promoted, such as concept map, mind map, and knowledge animation. Under the condition of information technology, numerous video websites have massive video resources, which provide great convenience for teaching. Figure 1 represents the transformation of dry knowledge into an easy-to-remember picture or video.

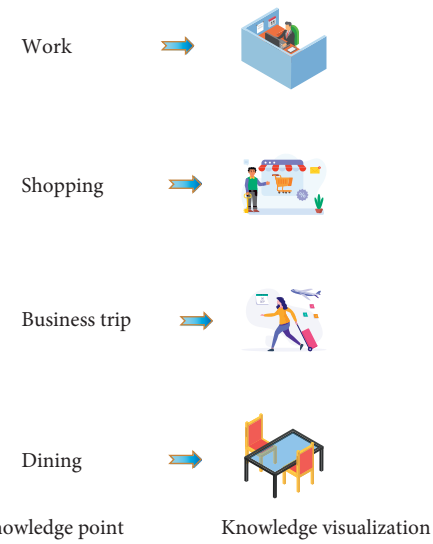

Figure 1: Visual transformation of knowledge points.

2.3. Immersion Teaching. Situational teaching is a kind of teaching mode which sets out from the angle of feeling and environment, feeling and speech, feeling and reason, and feeling and all-round development that creates the situation which is beneficial to students' study, stimulates students' interest, and combines emotional activities with cognitive activities. Video teaching in the foreign language classroom extends the teaching content by creating contexts, creating realistic and vivid language situations to arouse students' response to English, increase their enthusiasm for learning English, build their confidence in learning English, develop their ability to learn independently, form a good sense of English and intonation, and lay the foundation for them to communicate in English in their daily lives. The visualization process of teaching English increases the extent to which students remember points (Figure 2).

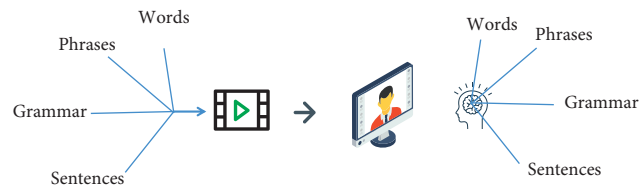

Figure 2: Visualizing the process of teaching English.

3. Feasibility of Microvideo Implementation

3.1. Features of English Language Teaching. Grammar is a combination of common patterns, types, and rules summarized from many complex grammar groups. Grammar has strong abstractness and generality. Grammar is a kind of language rules and is the key to master the language. Therefore, to learn a language, we must first understand its grammar rules, which is also true for English learning. English grammar is the expression of English language rules, which can be divided into five levels: sentence, clause, phrase, word, and morpheme. A good command of English grammar is very important for an English learner. The knowledge of English grammar includes not only verbs, adverbs, numerals, and other basic parts of speech but also difficult tenses, such as past continuous, present continuous, present perfect, and past perfect. English grammar content is such a large and complex collection, and it is scattered in English textbooks. In addition, the boring characteristics of grammar content itself make it even more difficult for non-native English learners to learn grammar well. However, after careful summarization, it is found that English grammar knowledge has potential stability and regularity. For the majority of college students, learning grammar is the most important thing to learn English well in the future. The short and concise feature of microvideo is combined with the systematic feature of English grammar. With the feature of both pictures and videos, students can better understand abstract grammar knowledge, master the rules of English grammar weaving, learn English language better, and improve English communication ability. Figure 3 shows the structure of the language.

3.2. Characteristics of English Teaching. In college, many students come from different regions and receive different education methods, so their learning ability and acceptance ability are at different levels. The traditional way of education is to teach according to one standard, which is difficult to meet the learning requirements of all people. At the same time, college students have more freedom in extracurricular activities, and it is more difficult to spend a lot of time previewing and reviewing lessons after class. Therefore, students must master more knowledge and memorize more knowledge points in class. At the same time, the use of more advanced teaching methods to increase students' independent learning ability, increase their personal interest. In teaching, teachers should grasp these characteristics of college students, timely and appropriate use of various teaching means, using new things to stimulate students' interest in learning. Only when students are full of fun and

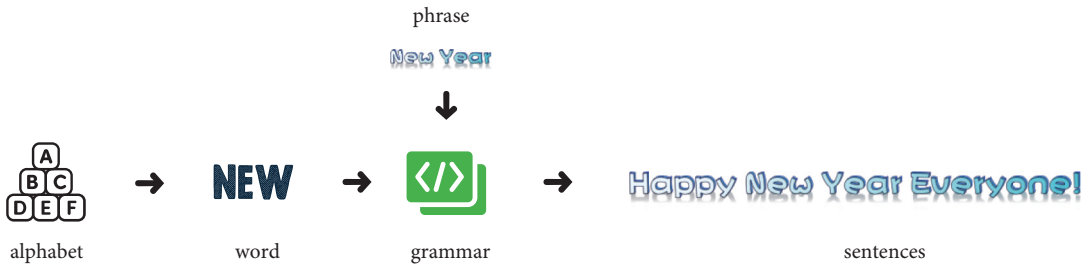

Figure 3: The structure of the language.

enthusiasm can they improve their learning efficiency and achieve twice the result with half the effort.

Microvideo teaching resources are generally set for a certain knowledge point or teaching link, and the length of time is generally limited to about five to eight minutes. Compared with traditional English grammar teaching, microvideos are more flexible and targeted, with clear themes and graphic features, which are more in line with the daily learning habits of college students. Combined with the characteristics of English textbooks and students' learning characteristics, the advantages of microvideo teaching resources in grammar teaching are found. Combining the "short and concise" characteristics of microvideo with the scattered and boring characteristics of language grammar, a microvideo teaching mode suitable for college students to learn English is created, which is conducive to students' mastering of grammar knowledge and improving their ability to use grammar, so as to study English more carefully and intently, and improve their English scores.

In traditional classroom teaching, teachers generally focus on the content of the books, with teachers talking and indoctrinating while students mechanically receive. The dryness and abstractness of English itself, as well as the teaching conditions and the characteristics of students, make it much harder for students to learn English well. The advantages of microvideo illustrations, short and concise, and the traditional classroom complement each other, making it possible to improve the quality of English teaching. The teaching context that the microvideo can create is more in line with students' cognitive needs and allows them to focus more on their English learning, thus stimulating their interest in learning English. The use of microvideo teaching in English language teaching is appropriate to create a language situation associated with the teaching content, so as to change the traditional teaching of a single boring mode and enhance students' interest and enthusiasm, and motivate them in learning English. Meanwhile, students can make use of the feature that microvideo can be played anytime and anywhere without restriction, so that they can not only check the content of knowledge that they do not understand but also learn new things from the past, thus developing students' ability and habit of independent inquiry into English language knowledge. Microvideo teaching is a new type of teaching method. By using the characteristics of storable and replayable microvideo teaching resources, teachers can effectively integrate and share resources of excellent microvideos in English teaching, which can not only reduce the burden of teachers but also make students actively participate in English classroom learning in order to improve the classroom efficiency of English learning. Therefore, the use of microvideos in English grammar learning is not only convenient for students but also for the teachers.

4. Implementation of Microvideo Teaching

4.1. Contrast Test Setup. In this trial, new students were divided into two groups of 100 each randomly assigned. The two groups were randomly selected. None of them had studied college English. One group followed the traditional teaching mode, while the other group adopted microvideo assistance in the normal teaching process. The trial lasted for a semester, and the effect of the trial was tested by comparing the scores at the end of the semester. At the same time, questionnaires were used to understand the application effect of microvideo in English teaching.

Design of the two groups of courses according to the first lesson of college English I, A New Start. The trial design is shown in Table 1.

4.1.1. Teaching Application Examples. Course: A New Start. Course focus analysis: this part of the course is the first lesson in the university and is about introducing people to each other and starting a new life. By watching a microvideo in which people are introduced to each other, it introduces what we are about to learn in this topic: A New Start. Students are able to recognise key vocabulary, key phrases, and important grammatical structures through the dialogue in the video. These points are then applied to the self-presentation through student interaction, and they are memorised without realising it. Figure 4 shows multiple scenarios of self-presentation.

The relevant microvideo is copied onto the electronic whiteboard in the trial class before the lesson and students are divided into established groups and assigned pre-watching tasks, which are completed through discussion and analysis among the group members. The exercises are then tested, explored, and summarized in class to further consolidate students' mastery of the new curriculum. This lesson uses microvideos to supplement the teaching of English and uses group competition and cooperation to complete the exercises, increasing students' motivation to participate.

Table 1: Trial design.

Teaching link	Microvideo teaching group	Traditional teaching group
1	Carry out microvideo guidance course	Learn according to books
2	Microvideo introduces new lessons, explains, and summarizes knowledge points	The teacher enters the new curriculum according to the textbook and summarizes the knowledge points orally
3	Microvideo consolidation exercises	Practice according to the exercises after class

Figure 4: Self-introduction microvideo.

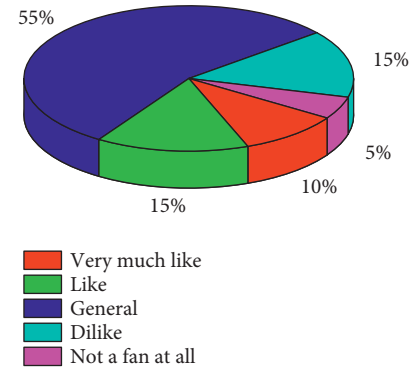

Figure 5: Level of enjoyment of the subject of English.

4.2. Effectiveness of Microvideo Teaching. The main purpose of this questionnaire is to find out students' attitudes and feelings towards the use of microvideo for English grammar teaching, feedback on its effectiveness, and whether they are willing to continue using it. The students' attitudes towards microvideo-assisted English teaching involved three main questions: Do you like English as a subject? Which aspect of English do you feel is the most difficult? In classroom teaching, do you like the teacher's use of microvideo for English teaching? The questionnaire was used to get a true picture of students' attitudes towards English as a subject, the difficulties in learning English, and how students really feel about the use of microvideo for English-assisted teaching in the classroom.

According to Figure 5, when it comes to whether students like English as a subject, 10% said they liked it a lot, 15% said they liked it, 55% said they liked it generally, 15% said they did not like it, and 5% said they did not like it at all. The above figures show that only 25% of the class enjoyed English. At the same time, 55% of the students expressed a general preference for English, which indicates that learning English is a major barrier to learning for most students. Therefore, it is imperative to increase the class participation rate and student enjoyment.

Figure 6 shows the results of the questionnaire survey on the most difficult part of English. As can be seen from Figure 6, 30% regard listening as the most difficult, 40% regard speaking as the most difficult, 10% regard reading as the most difficult, and 20% regard writing as the most difficult. As can be seen from the above data, oral English is considered the most difficult to learn by students. It can be seen that the output of English is the most difficult part of learning, and repeated input is needed to break through English learning. Repeated learning at difficult points can comprehensively improve oral English learning.

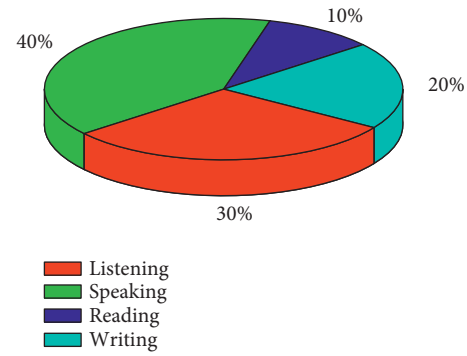

Figure 6: Most difficult part of English.

Figure 7 is a survey of students' liking for microvideo teaching. Figure 7 shows that 60% of the students like microvideos very much, 30% like them, and 10% like them generally. There is no student who does not like this teaching method. It can be seen from the data that all students can accept microvideo teaching, and 90% of students like teachers to use microvideo assisted teaching in English class. This shows that the microvideo teaching method is widely welcomed by students and is a successful attempt.

Figure 8 shows the research on how microvideo teaching helps English learning. As can be seen from Fig. 8, 21% of students think microvideo teaching is very helpful for English learning, 49% think it is helpful, 17% think it is a little helpful, and 13% think it is not helpful. It is worth noting that none of the students thought that microvideo teaching was useless for English learning. This shows that microvideo teaching can stimulate students' interest and enthusiasm in learning and make them like learning English more.

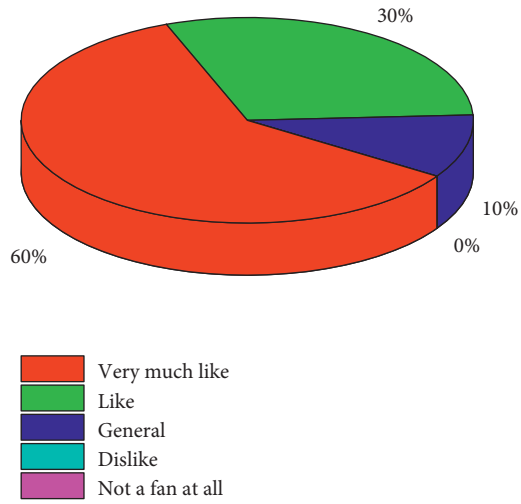

Figure 7: Level of liking microvideo.

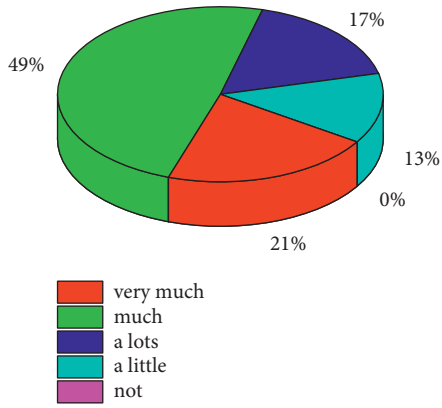

Figure 8: Results of microvideo teaching on the usefulness of learning.

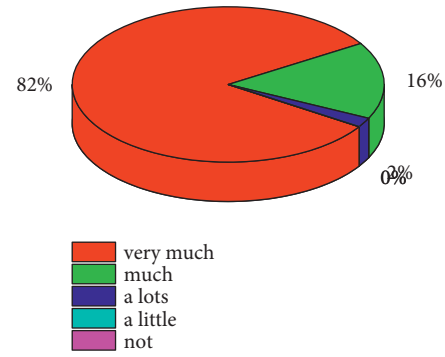

Figure 9: Results of the survey on whether students want to continue microvideo teaching.

The research in response to whether to continue with microvideo teaching is shown in Figure 9. As can be seen from Fig. 9, 82% of the students very much wanted to continue microvideo-assisted English teaching, 16% wanted to continue microvideo teaching, only 2% of the students generally wanted to continue microvideo teaching, and no students did not want to continue microvideo teaching. This reveals that all students hope to continue microvideo teaching, which is students' recognition of this teaching method.

4.3. Test Result Inspection. In this study, final tests were conducted on the trial group and the general group, and the results of the two groups were analyzed by sample Student-test, and the results obtained are shown in Table 2.

As can be seen from Table 2, the average score of the final exam of the trial group is 52.263, and that of the traditional group is 43.271. The average score of the trial group was 8.992 points higher than that of the traditional group, with a large gap between the two groups. The standard deviation of the final exam results of the trial group is 10.564, while that of the traditional group is 13.018, indicating that the distribution of the results of the traditional group was more discrete than that of the trial group, and there was a large difference among the students in the traditional group.

Table 2: Student-test analysis results of other grades of the two test groups.

Group	Sample size	Average	Standard deviation	Standard error
Microvideo	100	52.263	10.564	3.594
Traditional	100	43.271	13.018	4.171

As shown in Table 3, the P value of the independent sample test of scores was equal to 0.027 <0.05, indicating that the scores of the two groups were significantly different, and it was obvious that the scores of the trial group were higher than those of the traditional group.

Microvideo teaching resources are more in line with the preferences of contemporary university students than text and images. The classroom teaching involving microvideo

Table 3: Independent sample test form.

	Variance isotropy test		Mean isotropy student-test						
	F	Single tail significance	t	Degrees of freedom	Two-tailed significance	Average difference	Standard error difference	95% confidence upper bound	95% confidence lower bound
Assumed isovariance	1.825	0.257	1.951	97.534	0.027	6.578	3.952	−0.655	14.256
Nonassumed isovariance			1.951	94.554	0.027	6.578	3.952	−0.662	14.356

simplifies and vivifies students' English learning through dynamic pictures, lively situations, and brightly colored scenes, which has been praised by the majority of students. In English class, the introduction of microvideo English teaching timely and appropriately can not only attract students' attention but also mobilize students' enthusiasm in Learning English to a great extent and stimulate their enthusiasm for learning. Based on the above analysis of student questionnaire and performance test of microvideo English teaching, the teaching design of microvideo in the new English teaching in this study has injected vitality into classroom teaching to a certain extent. The vivid and lively scenes created by microvideos can well attract students' attention in class, improve students' motivation to learn or want to learn English, and improve classroom efficiency and English teaching effect.

5. Conclusion

In this paper, microvideo technology is applied to college English teaching. In the classroom teaching involving microvideo, students' English grammar learning is simplified and vivid through dynamic pictures, lively situations, and brightly colored scenes, which is highly praised by the majority of students. The success of microvideo in English teaching not only increases students' interest in English learning but also improves the level of college English teaching. The application of microvideo technology can well solve the problems of college English teaching and make students from different regions receive more appropriate teaching methods.

Data Availability

The data used to support the findings of this study are available from the author upon request.

Conflicts of Interest

The author declares no conflicts of interest.

References

[1] J. Guo, X. Nie, Y. Ma, K. Shaheed, I. Ullah, and Y. Yin, "Attention based consistent semantic learning for micro-video scene recognition," *Information Sciences*, vol. 543, pp. 504–516, 2021.

[2] Da Cao, L. Miao, H. Rong, Q. Qin, and L. Nie, "Hashtag our stories: hashtag recommendation for micro-videos via harnessing multiple modalities," *Knowledge-Based Systems*, vol. 203, p. 106114, 2020.

[3] H. Pan, L. Xie, Z. Wang, B. Liu, M. Yang, and J. Tao, "Review of micro-expression spotting and recognition in video sequences," *Virtual Reality & Intelligent Hardware*, vol. 3, no. 1, pp. 1–17, 2021.

[4] X. Gu, Lu Lu, S. Qiu, Q. Zou, and Z. Yang, "Sentiment key frame extraction in user-generated micro-videos via low-rank and sparse representation," *Neurocomputing*, vol. 410, pp. 441–453, 2020.

[5] M. Ramesh, L. S. Nair, T. R. Anoop, and T. N. Prakash, "Nearshore wave analysis from coastal video monitoring techniques at high energy micro tidal beach under sunlight dominance conditions: a case study from Valiathura beach in southwest coast of India," *Regional Studies in Marine Science*, vol. 51, p. 102205, 2022.

[6] M. Palmeira, "The interplay of micro-transaction type and amount of playing in video game evaluations," *Computers in Human Behavior*, vol. 115, p. 106609, 2021.

[7] T. A. Gavasheli, G. I. Mamniashvili, Z. G. Shermadini et al., "Investigation of the pinning and mobility of domain walls in cobalt micro- and nanowires by the nuclear spin echo method under the additional influence of a magnetic video pulse," *Journal of Magnetism and Magnetic Materials*, vol. 500, p. 166310, 2020.

[8] D. Dessì, G. Fenu, M. Marras, and D. ReforgiatoRecupero, "Bridging learning analytics and Cognitive Computing for Big Data classification in micro-learning video collections," *Computers in Human Behavior*, vol. 92, pp. 468–477, 2019.

[9] H. M. Fathi, M. W. Fawzy, I. I. Aboul-Eyon, A. H. I. Eldesouky, and N. N. Eesa, "Value of nail fold video capillaroscopy and carotid intima media thickness in assessment of micro and macro-vascular disease in systemic sclerosis patients," *The Egyptian Rheumatologist*, vol. 43, no. 4, pp. 275–280, 2021.

[10] S. T. Liong, J. See, and R. C. W. Phan, "Less is more: micro-expression recognition from video using apex frame," *Signal Processing: Image Communication*, vol. 62, pp. 82–92, 2018.

[11] S. Cojean and E. Jamet, "Facilitating information-seeking activity in instructional videos: the combined effects of micro- and macroscaffolding," *Computers in Human Behavior*, vol. 74, pp. 294–302, 2017.

[12] T. Schioppo, A. Orenti, P. Boracchi, O. De Lucia, A. Murgo, and F. Ingegnoli, "Evidence of macro- and micro-angiopathy in scleroderma: an integrated approach combining 22-MHz power Doppler ultrasonography and video-capillaroscopy," *Microvascular Research*, vol. 122, pp. 125–130, 2019.

[13] S. Abid, Z. Li, R. Li, and J. Waleed, "Anaglyph video smell presentation using micro-porous piezoelectric film olfactory display," *Displays*, vol. 39, pp. 55–67, 2015.

[14] S. Yagi, T. Ito, E. Ogawa et al., "Micro- and macro- borderless HBPT surgery using novel 3D-4K video system," *Journal of the American College of Surgeons*, vol. 227, no. 4-2, pp. e176–e177, 2018.

[15] X. Liu, B. He, S. Zhao, S. Hu, and L. Liu, "Comparative measurement of rainfall with a precipitation micro-physical

characteristics sensor, a 2D video disdrometer, an OTT PARSIVEL disdrometer, and a rain gauge," *Atmospheric Research*, vol. 229, pp. 100–114, 2019.

[16] X. Han, "Examining the college English teaching and listening based on English Proficiency Scale," *Aggression and Violent Behavior*, p. 101710, 2021.

[17] V. G. N. XiaoPang and S. Khapre, "Multimedia-based English teaching and practical system," *Aggression and Violent Behavior*, p. 101706, 2021.

[18] H. Zhang, R. Mervin, and B. S. Mohammed, "Core competence-based English major practical teaching system," *Aggression and Violent Behavior*, p. 101683, 2021.

[19] X. Pan and W. Zhong, "Teaching Spoken English for hospitality management major in China," *Journal of Hospitality, Leisure, Sports and Tourism Education*, vol. 30, p. 100375, 2022.

[20] Q. Cao, H. Hao, and V. Thanjai, "Occupational stress management of college English teachers under flipped classroom teaching model," *Aggression and Violent Behavior*, p. 101712, 2021.

[21] J. Ding, "Cloud computing database and remote system for real-time image acquisition application in English classroom teaching," *Microprocessors and Microsystems*, vol. 82, p. 103916, 2021.

[22] B. Labrador, "Word sketches of descriptive modifiers in children's short stories for teacher training in teaching English as a foreign language," *Linguistics and Education*, vol. 69, p. 101036, 2022.

[23] E. Bardone, A. Raudsep, and M. Eradze, "From expectations to generative uncertainties in teaching and learning activities. A case study of a high school English Teacher in the times of Covid19," *Teaching and Teacher Education*, vol. 103723, pp. 0742–051X, 2022.

[24] X. Ding, "College education and internal migration in China," *China Economic Review*, vol. 69, p. 101649, 2021.

[25] T. Kim, "Estimating pecuniary and non-Pecuniary returns to college education for academically marginal students: evidence from the college enrollment quota policy in South Korea," *Economics of Education Review*, vol. 83, p. 102142, 2021.

[26] A. Ajith, C. Temmen, D. Haynie, and K. Choi, "Association between adolescent smoking and subsequent college completion by parent education - a national longitudinal study," *Drug and Alcohol Dependence*, vol. 233, p. 109360, 2022.

[27] Y. Zhou and H. Zhou, "Research on the quality evaluation of innovation and entrepreneurship education of college students based on extenics," *Procedia Computer Science*, vol. 199, pp. 605–612, 2022.

Hindawi
Scientific Programming
Volume 2022, Article ID 7780816, 11 pages
https://doi.org/10.1155/2022/7780816

Research Article

A Method for Extracting Features of Modern Folk Opera Performance Art Based on Principal Component Analysis

Miao Yan, Xiaoyan Zhang, Zhengping Chen, Ying Yang, and Yang Zheng

College of Chinese-ASEAN Arts, Chengdu University, Sichuan, Chengdu 610106, China

Correspondence should be addressed to Miao Yan; yanmiao@cdu.edu.cn

Received 5 May 2022; Revised 29 May 2022; Accepted 2 June 2022; Published 29 June 2022

Academic Editor: Lianhui Li

With the continuous development of China's economy and society and the gradual reform of various industries, the modern folk opera performance art has received more and more attention, and through the excavation of features in the folk opera performance art, the modern folk opera performance level can be promoted. This paper proposes a generalised principal component analysis (PCA) feature extraction method, which first reorganizes the image matrix, constructs the overall scatter matrix based on the reorganized image matrix, and then finds the best projection vector for feature extraction. The proposed method is a further extension of the 2DPCA module, which can build a scatter matrix of arbitrary dimensions and obtain a projection vector of arbitrary dimensions. The results show that the best feature extraction is achieved by optimising the SVM with a principal component contribution of 50% and using the grid search algorithm. The smaller the dimension of the scatter matrix, the stronger the feature extraction ability of the generalised principal component analysis and the faster the feature extraction speed.

1. Introduction

1.1. Current Development of Modern Folk Opera Performing Arts. The analysis of the basic content and relevance of our vocal singing is of a certain systematic and complex nature. At the current stage of the world opera scene, all the operatic content of vocal singing is divided into two concepts: broad and narrow. Opera in the broadest sense of the word primarily means that there is no limit to the feelings expressed in opera and the way in which they are expressed. Opera performers who express relevant emotions in the course of their stage interpretations that are appropriate to the situation are singing opera in the broadest sense. Opera singing in the narrower sense, on the other hand, is primarily about the use of the stage performer's own characteristics. At the same time, playing to stage performers' own strengths in terms of speed or structure, they give a relatively delicate expression to the inner emotions of operatic characters, grasping their own emotions for operatic performances based on the understanding of the script and the actual situation of the characters. Such a vocal performance is called an operatic vocal performance in a relatively narrow sense.

Through comparison and analysis, we can see that both the broad sense of performance and the narrow sense of vocal performance in opera are closely related to the writer's creative state at the time. In the process of creating an opera, the writer's own state of mind and movements held at the time affect the overall opera and its expression. Considered in terms of scope, opera falls within the scope of the current phase of opera. At the same time, as opera continues to develop and grow, it has been able to inherit most of the commonalities and characteristics of the operatic form of expression and has become an art form rich in connotations. In the process of continuous development, opera mainly includes various forms of expression such as opera story, plot contradiction, and conflict.

However, the art of stage opera in China has expanded and developed rapidly since the founding of New China. During the past two decades, the art of opera in China has gained a great degree of enrichment, mainly in the form of folk opera. The main content of stage opera at this stage basically consisted of actors performing the roles of the main characters and singing on this basis, with the voice style possessing the characteristics of diversity and ethnicity. The

development of stage opera at this stage was mainly operatic in the narrower sense, mainly in the form of large lyrics sung by professional actors through their own unique accents and relatively specialized methods of expression. Generally in the performance of a stage opera, the singer can perform through different parts of the tone and characteristic tempo changes, thus creating a contrasting effect in the stage opera and thus reflecting the distinctive role of the main character and the emotional changes.

Through in-depth comparison and research and analysis, we can find that this stage of China's stage opera creation has made development and progress. The way in which different passages are sung in stage operas can already be contrasted in many ways in terms of content. However, it cannot be ignored that there are still some flaws and shortcomings in this stage of stage opera composition. The inability to compare partial passages or stanzas in minute detail has prevented a very strong sense of contrast in the artistic expression of opera during this period, a conclusion that can be drawn from a comparison of many classical cantatas. It is also clear from this analysis that a large part of the reason for remembering the classics is that the large passages are very significant and expressive, allowing for good expression in terms of pitch, quality, and timbre, but the operatic nature is not fully reflected.

There are two main reasons why the development of stage opera in China has struggled to reflect operaticism. The first is that the stage opera art form needs to rely on musical expression, but the attention of professional composers is often focused between passages and the comparative analysis of the levels of utterance rarely has an emotional element. The second is because the singing ability of professional actors in stage opera can have an impact on the artistic expression of stage opera, which requires professional actors to perform the main character's role freely.

However, through research and analysis, we can find that there is a large gap between the actors' own quality and the actual demands of role interpretation at this stage. After a certain degree of professional training, the performers may be able to sing with a certain degree of competence. At this stage, however, many folk opera programmes require a unique singing voice or talent, but many singers have a single tone or no contrasting characteristics in their interpretation. The operatic nature of vocal singing in folk opera performance art needs to be taken seriously.

1.2. Status of Research on Feature Extraction by PCA. Pattern recognition has long been a hot issue in research. Various methods have been proposed to extract the most effective discriminative features from patterns for pattern classification. PCA [1, 2], considered as a classical feature extraction [3] and data dimensionality reduction method, has been widely applied in the field of pattern recognition and computer vision. Sirovich and Kirby [4, 5] first used PCA to process face images and introduced the concept of eigenimages. Based on this, Turk and Pentland proposed an eigenface approach based on PCA [6]. Since then, PCA has been studied in depth and some new algorithms related to PCA have been proposed, such as ICA (Independent Component Analysis) and KPCA (Kernel Principal Component Analysis) [7].

Recently, Yang Jian et al. proposed 2DPCA [8] as a feature extraction method. On the basis of this, many scholars have conducted research [9, 10] and applications [11, 12], and the PCA method is applicable to the development of various industries [13]. Zhang et al. [14] proposed DPCA (Diagonal Principal Component Analysis). The module 2DPCA is the deformation and extension of 2DPCA, which is better than 2DPCA in terms of feature extraction performance.

By further extending the modular 2DPCA, a generalised PCA feature extraction method is proposed, which can be computed by building a scatter matrix of arbitrary dimensions when solving for the optimal projection vector, simplifying the operation process. The experimental results show that as the dimensionality of the scattering matrix decreases, the generalised PCA will have better feature extraction capability and faster processing speed. In this paper, a generalised PCA feature extraction method is proposed by applying the PCA method to modern folk opera performance art features extraction, in order to analyse the problems affecting the development of opera performance through the data and promote the improvement of modern folk opera performance.

2. PCA Theory

In order to fully reflect the information contained in modern folk opera performing arts images, multiple feature values need to be extracted for analysis. However, too many feature values can add to the burden of classification testing and have an impact on the analysis, so it is necessary to find the feature values that best reflect the differences in the images among the multidimensional feature values and reduce the multidimensional feature space to a lower dimensional feature space.

The basic idea of PCA is to reorganize the original data to obtain a new set of unrelated and independent data, in order to achieve the purpose of representing the information of the original data characteristics with less data [15, 16]. For a group of data with N indicator, after PCA, the new combination form is used to characterize the original data combination, and the combination with the largest variance $V_{ar}(N)$ among all linear combinations is called the first principal component, which is recorded as Q_1. When the principal component Q_1 is not enough to characterize the original data information, a new combination form is selected to complement the information of the original data, which is called the second principal component Q_2, and Q_2 should not overlap with the information of Q_1, Q_1, and Q_2 satisfy $\mathrm{COV}(Q_1, Q_2) = 0$, and so on until the number of principal components characterizes the original information feature. The steps of PCA are as follows:

(1) Suppose there is a set of samples noted as K. Firstly, the samples are standardized to obtain the standardized sample matrix R:

$$\mathbf{R}_{ij} = \frac{K_{ij} - (1/m)\sum_{m}^{i=1} K_{ij}}{\sqrt{1/m - 1\sum_{m}^{i=1}\left(K_{ij} - 1/m\sum_{m}^{i=1} K_{ij}\right)^2}}, \quad (1)$$

where $i = 1, 2, \ldots, m$; $j = 1, 2, \ldots, n$.

(2) Calculate the correlation coefficient matrix for the standardized sample B:

$$B = \frac{1}{m}\mathbf{R}^T\mathbf{R}. \quad (2)$$

(3) Let the eigenvalue be λ, then the characteristic equation of the correlation coefficient matrix B can be calculated, from which m characteristic roots can be obtained:

$$\left|B - \lambda I_m\right| = 0. \quad (3)$$

Based on the calculated eigenvalue $\lambda_i (i = 1, 2, 3, \ldots, m)$, the unit eigenvector $P_1, P_2, P_3, \ldots, P_m$ can be obtained.

The number of principal components, determined from the cumulative contribution of the principal components, is used to derive the covariance matrix and its eigenvalues for the data matrix and its matrix transpose matrix determined for each combination of principal components. The contribution of the principal components, the cumulative contribution can be determined from the following equations:

$$A_i = \frac{\lambda_i}{\sum_{m}^{i=1}\lambda_i}, \quad (4)$$

$$C_{(m)} = \frac{\sum_{p}^{i=1}\lambda_i}{\sum_{m}^{i=1}\lambda_i}, \quad (5)$$

where p is the number of eigenvalues to be determined.

(4) When the cumulative contribution of the principal components is greater than 90%, the first p combination of principal components can be considered here to include most of the characteristic information of the original data. The corresponding P is the first p principal components [17].

The flowchart of modern folk opera performing arts feature extraction using PCA in this paper is shown in Figure 1.

3. Principle of Feature Extraction

3.1. Image Recombination. Let $I_1, \ldots, I_N$ be a training set consisting of N n-dimensional image vectors, where $I_i = (I_1^i, \ldots, I_n^i)$. Each training sample is partitioned into one subvector of dimension k according to the same rules a_j^i and arranged according to equation (6) to form a new matrix sample A_i of size $1 \times k$. The number of vectors is $l = \text{ceil}(n/k)$, and if the last vector has less than k dimensions, it is padded with zeros:

$$A_i = \begin{bmatrix} a_1^i \\ \cdots \\ i \\ a_1 \end{bmatrix}. \quad (6)$$

3.2. Projection Vectors. Calculate the scatter matrix of the matrix sample $A_1, A_2, \ldots, A_N$, denoted as S_T:

$$S_T = \sum_{N}^{i=1}\left(A_i - \overline{A}\right)^T\left(A_i - \overline{A}\right). \quad (7)$$

Here, $\overline{A} = 1/N\sum_{N}^{i=1} A_i$, and since matrix S_T is a symmetric matrix, there must exist an orthogonal matrix $\Phi = (\varphi_1, \ldots, \varphi_n)$ such that S_T is diagonalised:

$$\begin{cases} \boldsymbol{\varphi}_i^T\boldsymbol{\varphi}_j = 1, & (i = j, i, j = 1, \ldots, n), \\ \boldsymbol{\varphi}_i^T\boldsymbol{\varphi}_j = 0, & (i \neq j, i, j = 1, \ldots, n). \end{cases} \quad (8)$$

The vector $\varphi_1, \ldots, \varphi_d$ corresponding to the first d largest eigenvalues of S_T is taken as the projection vector.

3.3. Feature Extraction. The sample F_i is divided into l subvectors b_j^i of dimension k according to the same partitioning rules and arranged according to the rules of equation (6) to form a matrix sample of size $1 \times k$, denoted as B_i. The number of vectors $l = \text{ceil}(n/k)$, when the last vector is less than k, is also filled with zeros. The matrix sample B_i is projected with the projection vector $\varphi_1, \ldots, \varphi_d$, and the eigenvalue matrix Y_i is extracted from B_i , and the elements of Y_i are the eigenvalues of the sample F_i to be tested:

$$Y_i = B_i(\varphi_1, \ldots, \varphi_d). \quad (9)$$

If sample I_i of eigenvalues needs to be extracted, then we have the following:

(1) When $k = m' \times n', l = 1$, the A_i obtained from image I_i is a vector of $1 \times m' \times n'$, which is the classical PCA feature extraction method.

(2) When $k = n', l = m'A_i$ is a matrix of $m' \times n'$, this is the 2DPCA feature extraction method.

(3) When $k = n'/z, l = zm'A_i$ is a matrix of $zm' \times n'/z$. This is the module 2DPCA feature extraction method. In fact, in the module 2DPCA algorithm, the dimensionality and specific values of the eigenvectors of the scattering matrix only vary with the chunking pattern in the row direction, independent of the chunking pattern in the column direction.

It can be seen that the generalised PCA feature extraction method proposed in this paper covers classical PCA, 2DPCA, and module 2DPCA. In addition, for images with a resolution of $m' \times n'$, k can be taken as an integer value in the range of $1 \leq k \leq m'n'$, which makes the algorithm more general and flexible.

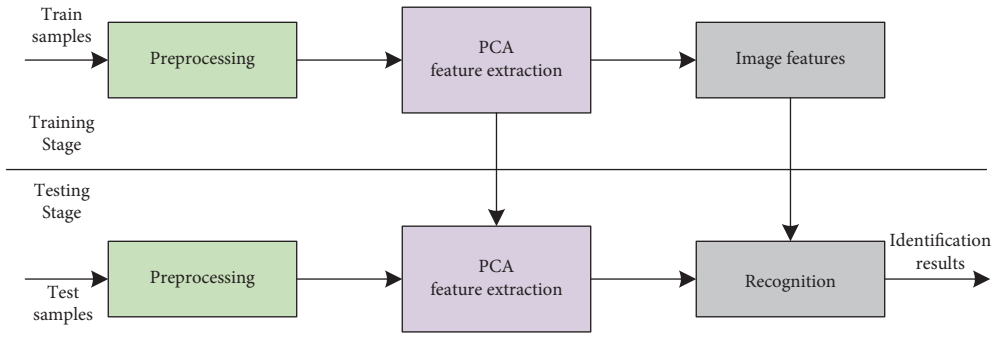

Figure 1: Flowchart of feature extraction by PCA.

3.4. Properties of the Algorithm. The generalised PCA feature extraction method has the following two important properties, which are the rationale behind the proposed generalised PCA:

(1) The scatter value of the sample set scatter matrix does not change depending on the dimensionality of the subvectors into which the samples are partitioned.

Let a vector sample I_i of dimension n be partitioned into a matrix sample A_i of dimension $1 \times k$ and the number of samples is N:

$$A_i = \begin{pmatrix} \mathrm{I}_1^i & \cdots & \mathrm{I}_k^i \\ \cdots & \cdots & \cdots \\ \mathrm{I}_{(l-1)k+1} & \cdots & \mathrm{I}_n^i \end{pmatrix}, \quad S_T = \sum_N^{i=1} (A_i - \overline{A})^T (A_i - \overline{A}). \tag{10}$$

The scatter between samples $tr(S_T)$ is then

$$\begin{aligned} tr(S_T) &= tr\left(\sum_N^{i=1} (A_i - A)^T (A_i - A)\right) \\ &= tr\left(\sum_N^{i=1} (A_i - A)(A_i - A)\right)^T \\ &= \sum_N^{i=1} \sum_1^{n=1} \sum_k^{j=1} \left(I^i_{(n-1)k+j} - I_{(n-1)k+j}\right)^2 \\ &= \sum_N^{i=1} \sum_d^{j=1} \left(I_j^i - I_j\right)^2. \end{aligned} \tag{11}$$

The final transformation of the scatter $\sum_N^{i=1} \sum_d^{j=1} (I_j^i - I_j)^2$ is independent of parameters k and l, which proves that the scatter between samples remains the same no matter how many dimensions the matrix is partitioned into and that the above conclusion holds true for $k = n$.

(2) The Euclidean distance between sample eigenvectors is equal to the Euclidean distance between the original sample vectors, regardless of the dimensionality of the vector sample split into matrix samples.

Let F_1 and be F_2 any two samples, which can be represented as l matrix samples B_1 and B_2 of dimension k:

$$B_i = \begin{pmatrix} F_1^i & \cdots & F_k^i \\ \cdots & \cdots & \cdots \\ F^i_{(l-1)k+1} & \cdots & F_n^i \end{pmatrix}. \tag{12}$$

Let the eigenvectors of F_1 be $B_1\Phi$, the eigenvectors of F_2 be $B_2\Phi$, and $\Phi = [\phi_1, \ldots, \phi_k]$ be the matrix consisting of all eigenvectors of the scattering matrix.

Similarly, the Euclidean distance $\mathrm{Dis}(B_1\Phi, B_2\Phi)$ between the eigenvectors of samples B_1 and B_2 of the split matrix is equal to the Euclidean distance $\mathrm{Dis}(F_1, F_2)$ between samples F_1 and F_2, and the same conclusion holds when $k = n$.

4. Experimental Results and Analysis

4.1. Experimental Data. The data set used in this paper was collected from the works of 40 modern folk opera artists, each consisting of 10 images with a resolution of 112×92. Some of the images were taken in different periods, with different degrees of variation in facial expressions and body movements. Among the 10 image samples of each person, the best ratio was selected according to the training model. Seven images from each person were randomly selected as the training set and the remaining three images as the test set, with the ratio of the total number of training and test samples for all people being 7 to 3. Each set of experiments was conducted five times, and the average of the five experiments was chosen as the final result.

4.2. Experiment 1. Each image is viewed as a 10,304 dimensional vector with a subvector dimension of k, taking a range of different values. The eigenvectors corresponding to the first seven largest eigenvalues of the scatter matrix are used as projection vectors to extract eigenvalues for classification with the nearest neighbour classifier, and the experimental data are shown in Table 1.

The comparison of recognition rate and time at different values of subvector dimension is shown in Figure 2. It can be seen that the recognition accuracy decreases as the subvector dimension increases, but the recognition time increases

Table 1: Experimental data for different values of subvector dimensions.

Subvector dimension k	12	23	46	92	184	368	736	1472
Recognition (%)	85	85	84	82	81.5	81.5	81	81.5
Time (s)	2.23	11.89	21.78	31.83	42.87	51.94	60.08	82.92

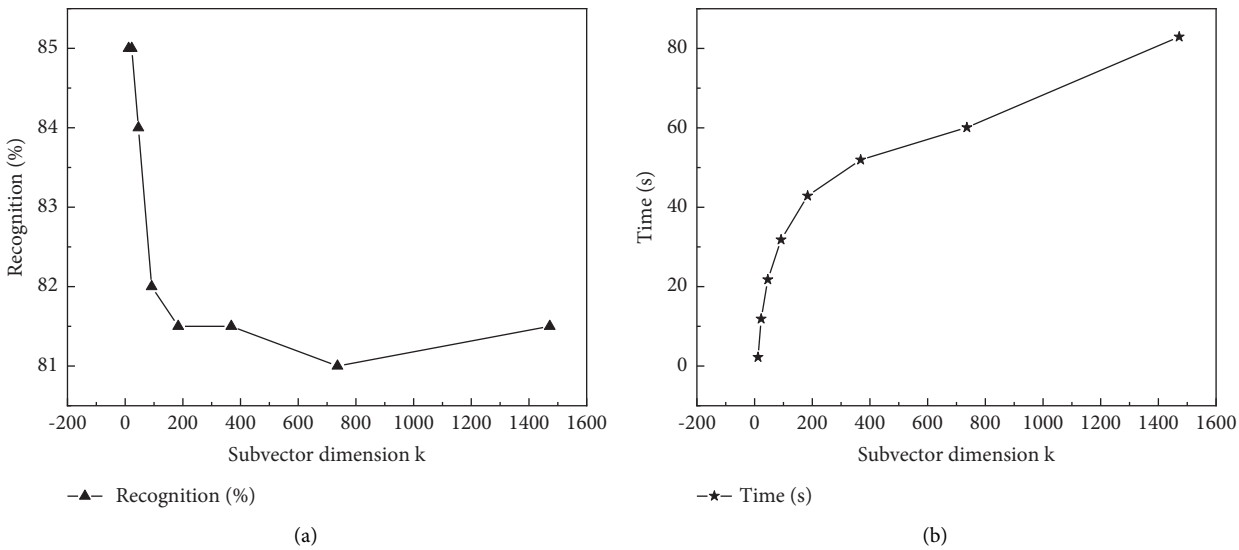

Figure 2: Comparison of data for different values of subvector dimensions: (a) recognition and (b) time.

gradually, which shows that the lower the subvector dimension, the better the experimental results.

The 2,240 eigenvalues were extracted from each image, and as the subvector dimension k increased, the number of projection vectors d was increased as the number of rows l of the matrix sample decreased, and vice versa, always making $l \times d = 2240$. The classification was performed with the nearest neighbour splitter, and the recognition rates are shown in Table 2.

The comparison between the recognition rate and the number of projection vectors d for the number of eigenvalues of 2240 is shown in Figure 3. From the figure, it can be seen that the recognition rate at different subvector dimensions is not very different, and the best recognition rate is achieved at dimension 23, and the number of projection vectors shows a positive proportional relationship with the number of projection vectors.

4.3. Experiment 2. In order to identify the influence of gender in the extraction of features in modern folk opera performance art, this study is then conducted. Twenty-two images of female opera artists were selected, and 11 colour images of 480×640 resolution each were used as experimental data. Due to the large size of the images, the images were converted to 120×160 grey scale before the experiment. Each image was considered as a 19 200-dimensional vector, and the first 5 images of each person were used as the training set, while the remaining 6 images were used as the test set. From each image, 1,200 feature values, i.e., $l \times d = 1200$, were extracted and classified using the nearest neighbour classifier, and Table 3 shows the experimental data.

The data comparison results for the projection vector d, recognition rate, and time consumed in this experiment are shown in Figure 4.

From Figure 3, it can be seen that the change in recognition rate is not very different, but the recognition time gradually becomes longer as the number of dimensions increases, and the projection dimension d also becomes larger as the number of k increases.

4.4. Experiment Comparison. The results of Experiment 1 and Experiment 2 show that the maximum recognition rate occurs when the number of projection vectors is the same or the number of extracted features is the same, but the value of k is smaller. The analysis shows that when the value of k is small, the scattering matrix is smaller and it is easier to extract the local features of the image. This is the real reason why 2DPCA is superior to PCA, and 2DPCA is superior to 2DPCA. Therefore, in practice, a smaller value of k is beneficial for the recognition rate.

The data in Tables 1 and 3 show that feature extraction takes less time when the value of k is small. Because the scatter matrix is small when the value of k is small, it takes less time to find the scatter matrix and projection vector, so the feature extraction of the image is faster. Therefore, in terms of speed, a smaller value of k is more effective in practice.

The number of image features in both experiments varies with the dimension of the subvector k as shown in Table 4.

Table 2: Comparison of recognition rates for a feature value of 2,240.

Subvector dimension k	23	46	92	184	368	736	1472
Number of projection vectors d	5	10	20	40	80	160	320
Number of image feature values	448 ∗ 5	224 ∗ 40	112 ∗ 20	56 ∗ 40	28 ∗ 80	14 ∗ 160	7 ∗ 320
Recognition (%)	85	85	84.5	84.5	84.5	83.5	83

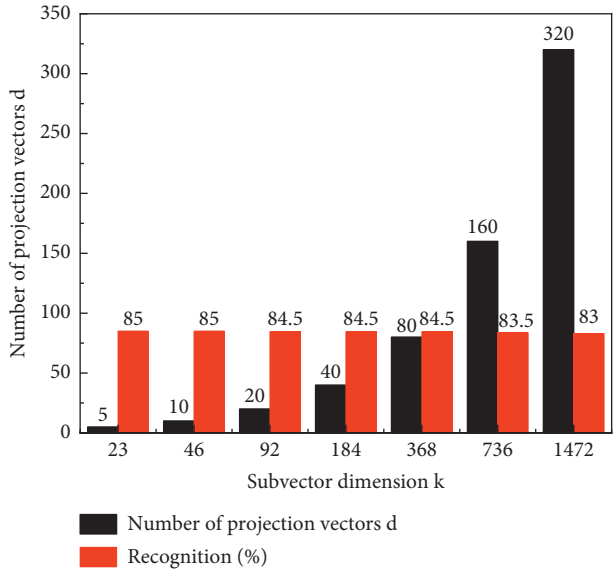

Figure 3: Comparison of data with an eigenvalue of 2240.

Table 3: Basic data set of Experiment 2.

Subvector dimension k	40	80	160	320	640	1280
Number of projection vectors d	2	4	8	16	32	64
Number of image feature values	480 ∗ 2	240 ∗ 4	120 ∗ 8	60 ∗ 16	30 ∗ 32	15 ∗ 64
Recognition (%)	78.8	77.3	76.5	76.5	76.2	76
Time (s)	1.95	12.38	23.16	38.31	42.85	85.26

A visual comparison of the number of image eigenvalues for the two experiments as a function of subvector dimension k is shown in Figure 5.

The larger the value of $k \times k$ and k, the larger the storage space required. When the value of k is taken as $m' \times n'$, the size of the scatter matrix is 10 304 × 10 304, which is difficult to achieve on a normal machine, while a smaller value of k is beneficial for saving storage space.

In summary, when k is taken as a small value, it is beneficial for the recognition rate, feature extraction speed, and storage space saving. Therefore, when the dimensionality of the vector sample is high, it is more beneficial to use a generalised PCA feature extraction method with a smaller value of k.

After fixing the value of k, the effect of the classifier on the effect of PCA on feature extraction is next considered. The experiments were conducted using the nearest neighbour classifier, followed by a support vector machine (SVM) [18, 19] to test the effect on feature extraction in modern folk opera performance art and to compare the experimental results with different principal component contribution rates, and finally, a grid search algorithm (GS) [20] is used to optimise the support vector machine parameters and thus improve the classification results.

The experiments are conducted on two datasets, Experiment 1 and Experiment 2, using the support vector machine instead of the nearest neighbour classifier, and each set of experiments is conducted five times, and the recognition results are shown in Table 5.

Comparing the data in Tables 1 and 3, it can be seen that the recognition results under SVM are higher than the nearest neighbour classifier in both experiments, which shows that SVM is more suitable for modern folk opera performing arts feature extraction. The visual comparison effect of the two experimental results is shown in Figure 6.

The data were dimensioned down using PCA to test the feature recognition results and classification time under different principal component contribution rates, as shown in Tables 6 and 7, and the comparison results are shown in Figure 7.

When using SVM for classification prediction, the relevant parameters (penalty parameter C and kernel function

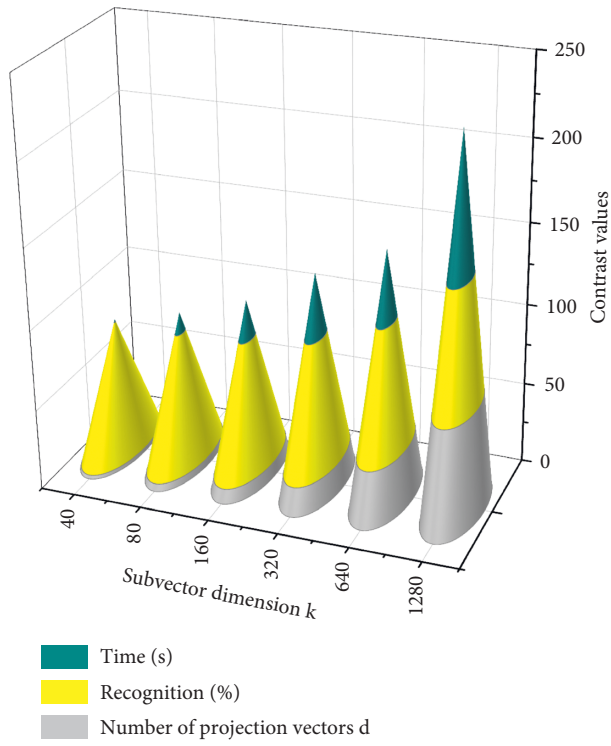

Figure 4: Comparison of data information from Experiment 2.

Table 4: Variation of the number of image features with subvector dimension k.

Subvector dimension k	12	23	46	92	184	368	736	1472
Experiment 1	4480	2240	1120	560	280	140	70	35
Experiment 2	960	960	960	960	960	960	960	960

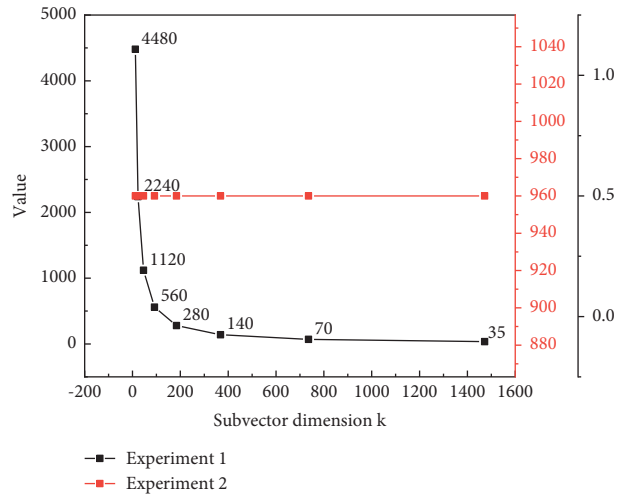

Figure 5: Comparison of image eigenvalue data from the two experiments.

parameter g) need to be adjusted to obtain the desired recognition accuracy. In this paper, a grid search algorithm is used to obtain the optimal model parameters. The grid search algorithm is an exhaustive search algorithm that finds the optimal hyperparameters of the model by combining all possible values of the parameters in a permutation by cross-validation. The combinations are then used for SVM training and the performance is evaluated using cross-validation to find the largest combination of parameters for the scoring pair and then returned to the model for training.

Table 5: Recognition results of the support vector machine.

Category	1 (%)	2 (%)	3 (%)	4 (%)	5 (%)
Experiment 1	86.5	87	86.5	87.5	87
Experiment 2	80	80.5	79.5	81	80.5

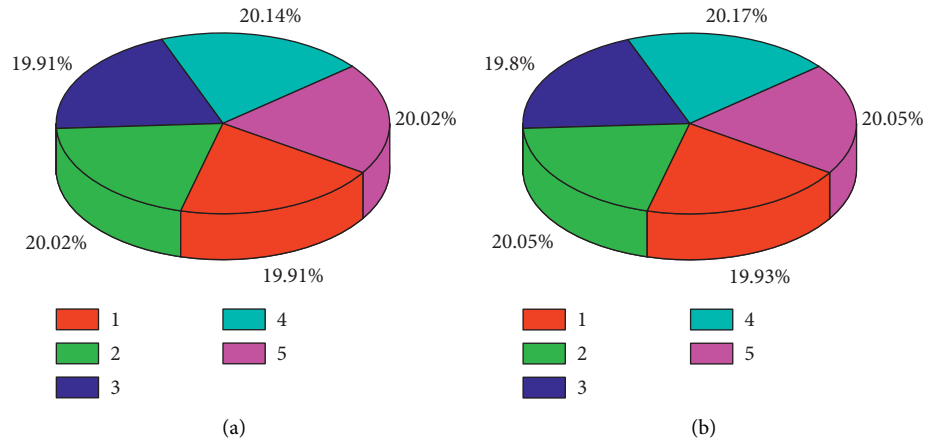

Figure 6: Pie chart of recognition results of support vector machine under two experiments: (a) Experiment 1 and (b) Experiment 2.

Table 6: Feature recognition results under different principal component contribution rates.

PCA	Recognition (%) Contribution of principal components		
Data	25%	50%	75%
Experiment 1	84	87	85
Experiment 2	78	81	80.5

Table 7: Feature identification time with different principal component contribution rates.

PCA	Time (s) Contribution of principal components		
Data	25%	50%	75%
Experiment 1	2.03	2.12	2.23
Experiment 2	1.81	1.89	1.95

As can be seen from Tables 6 and 7, feature identification results and time were improved when the principal component contribution was 50%, demonstrating the importance of the PCA method in feature extraction. Finally, the GS optimisation parameters were used and the classifier was noted as GS-SVM. When the k value was fixed and the principal component contribution was 50%, the experimental results for both classifiers are shown in Table 8.

A comparison of the accuracy of the recognition results of the two classifiers is shown in Figure 8.

From Figure 8, it can be seen that the recognition rate has improved significantly after using GS-optimised SVM, which shows that the feature extraction of modern folk opera performing arts is feasible after parameter optimisation. In summary, when the value of k is fixed and its value is small, the 2DPCA principal component contribution rate is 50%

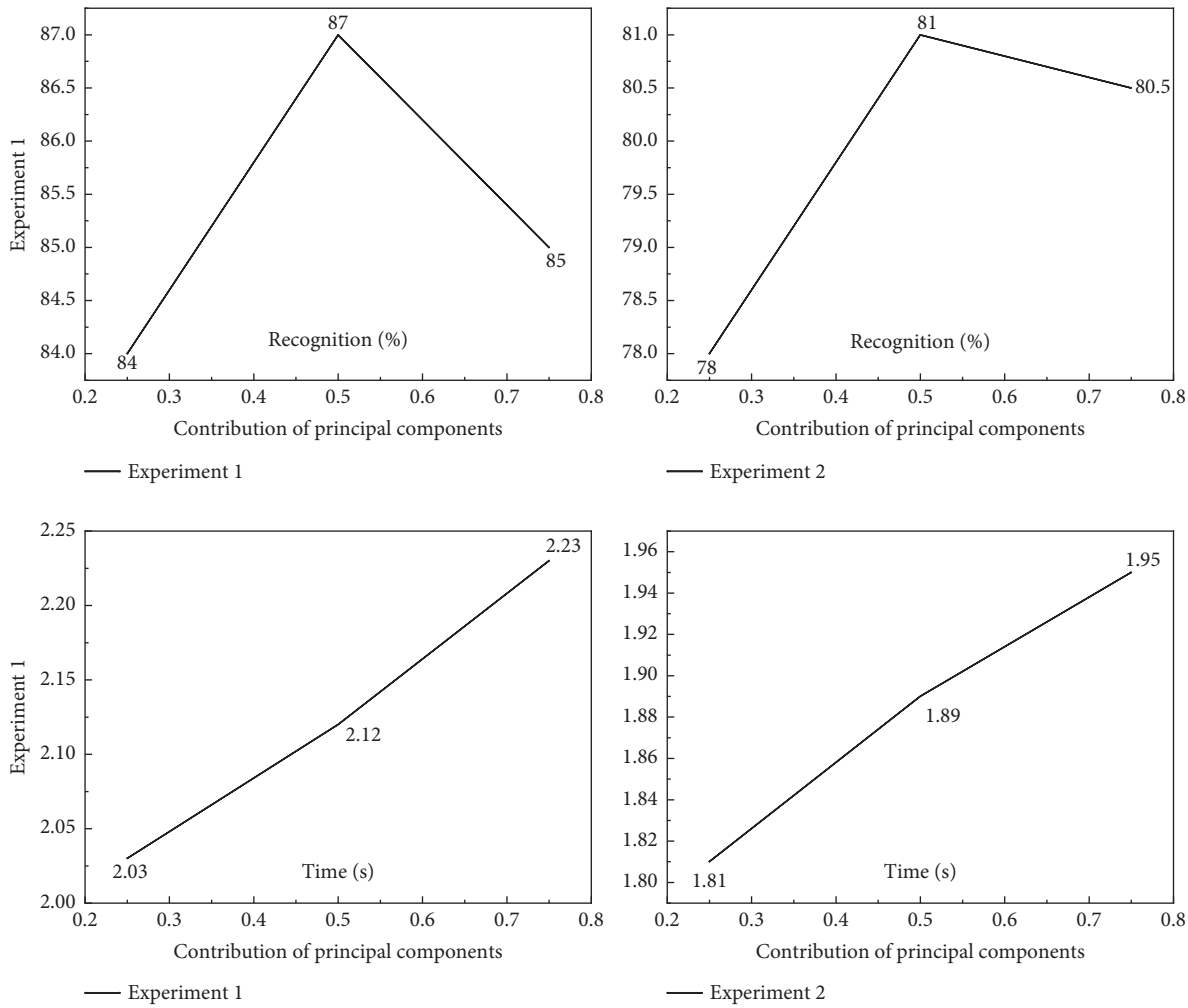

Figure 7: Comparison of feature identification results and classification time data for Experiment 1 and Experiment 2 with different principal component contribution rates.

Table 8: Grid search algorithm optimised recognition rate results.

Number of experiments	SVM (%)	GS-SVM (%)
1	87	89
2	86.5	87.5
3	87.5	90
4	87	89
5	86.5	88.5

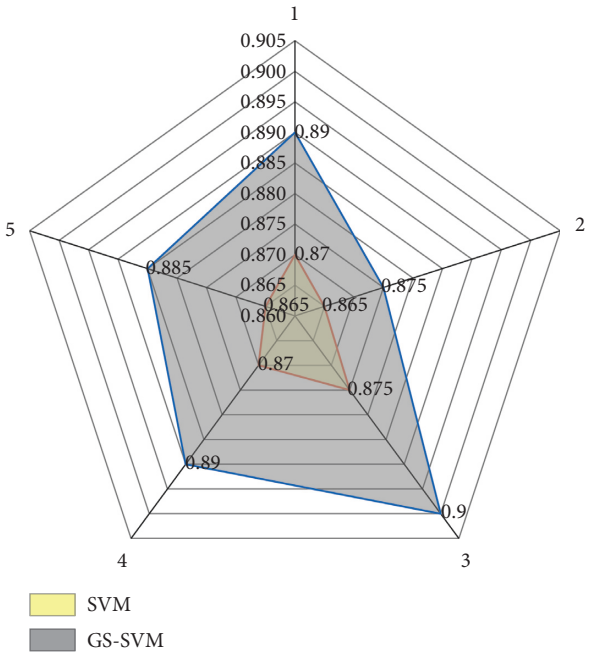

Figure 8: Comparison of the recognition rate of SVM and GS-SVM.

and the feature extraction effect using GS-SVM is the best, and the classification time reaches the shortest at this time.

5. Conclusion

In this paper, a generalised PCA feature extraction method is proposed for modern folk opera performing arts. The method consists of reorganising the image matrix, thereby reducing the dimensionality of the scatter matrix and improving the feature extraction capability of PCA, which incorporates classical PCA, 2DPCA, and module 2DPCA feature extraction methods. Experiments on both types of image data show that when subvector dimension k is small, the scatter matrix becomes smaller, requiring less storage space and less time, while the extracted feature values are more efficient and the recognition rate is higher. By comparing the effect of the nearest neighbour classifier and SVM on feature extraction, the experimental results show that the best feature extraction is achieved with a principal component contribution of 50% and the use of GS-optimised SVM, which improves the recognition rate by about 2%, demonstrating the important value of the proposed method. However, further research is needed to find out whether there is a specific rule when the dimension k of the subvectors in the image is taken as the best result.

Data Availability

The dataset can be accessed upon request.

Conflicts of Interest

The authors declare that there are no conflicts of interest.

Acknowledgments

The authors thank Research on the Interaction between Chinese National Opera Development and Audience (no. 2281921038).

References

[1] B. Mohamed, B. Rachid, and A. Hafid, "The use of principal component analysis for the prediction of double halide perovskites A2BX6," *Journal of Multiscale Modelling*, vol. 12, no. 2, pp. 56–59, 2021.

[2] W. Wang, "Performance evaluation of retail enterprises based on principal component analysis," *Modern Economy*, vol. 12, no. 2, pp. 293–302, 2021.

[3] K. Jinkwan and Y. Arakawa, "Classification of in situ reflection high energy electron diffraction images by principal component analysis," *Japanese Journal of Applied Physics*, vol. 60, no. SB, 2021.

[4] L. Sirovich and M. Kirby, "Low-dimensional procedure for characterization of human faces," *Optical Soc Am*, vol. 4, no. 1, pp. 519–524, 1987.

[5] M. Kirby and L. Sirovich, "Application of the Karhunen-Loeve procedure for the characterization of human faces," *IEEE Transactions on Pattern Analysis and Machine Intelligence*, vol. 12, no. 1, pp. 103–108, 1990.

[6] M. Turk and A. Pentland, "Eigenfaces for recognition," *Journal of Cognitive Neuroscience*, vol. 3, no. 1, pp. 71–86, 1991.

[7] B. Sch¨olkopf, A. Smola, and K. R. M¨uller, "Kernel principal component analysis[C]//Sch¨olkopf B, Burges C J C, Smola A J," *Advances in Kernel Methods- Support Vector Learning*, pp. 327–352, MIT Press, Cambridge, MA, USA, 1999.

[8] J. Jian Yang, D. Zhang, A. F. Frangi, and J.-Y. Yang, "Two-dimensional pca: a new approach to appearance-based face representation and recognition," *IEEE Transactions on Pattern Analysis and Machine Intelligence*, vol. 26, no. 1, pp. 131–137, 2004.

[9] M. N. Vo Dinh and S. Y. Lee, "Improvement on PCA and 2DPCA algorithms for face recognition," in *Proceedings of the The 4th International Conference on Image and Video Retrieval*, pp. 568–577, Singapore, July 2005.

[10] L.-W. Wang and X. Wang, "Is two - dimensional PCA a new tech-nique," *Acta Automatica Sinica*, vol. 31, no. 5, pp. 782–787, 2005.

[11] H. Kong, L. Wang, E. K. Teoh, X. Li, J. G. Wang, and R. Venkateswarlu, "Generalized 2D principal component analysis for face image representation and recognition," *Neural Networks: The Official Journal of the International Neural Network Society*, vol. 18, no. 1, pp. 585–94, 2005.

[12] R. M. Mutelo and L. C. Khor, "A novel Fisher discriminant for biometrics recognition: 2DPCA Plus 2DFLD," in *Proceedings of the International Symposium on Circuits and Systems (ISCAS'06)*, pp. 709–713, Kos, Greece, May 2006.

[13] P. Sanguansat and W. Asdornwised, "Two-dimensional linear discriminant analysis of principle component vectors for face recognition," *IEICE-Transactions on Info and Systems*, vol. E89-D, no. 7, pp. 2164–2170, 2006.

[14] D. Zhang, Z.-H. Zhou, and C. Songcan Chen, "Diagonal principal component analysis for face recognition," *Pattern Recognition*, vol. 39, no. 1, pp. 140–142, 2006.

[15] H. Zhang, M.-J. Li, W.-Z. Fang, D. Dan, Z.-Y. Li, and W.-Q. Tao, "A numerical study on the theoretical accuracy of film thermal conductivity using transient plane source

method," *Applied Thermal Engineering*, vol. 72, no. 1, pp. 62–69, 2014.

[16] L. L. Kerr, Y.-L. Pan, R. B. Dinwiddie, H. Wang, and R. C. Peterson, "Thermal conductivity of coated paper," *International Journal of Thermophysics*, vol. 30, no. 2, pp. 572–579, 2009.

[17] Y. He, "Rapid thermal conductivity measurement with ahot disk sensor," *Thermochimica Acta*, vol. 436, no. 1/2, pp. 122–129, 2005.

[18] Z. Sun, J. Santos, and C. Elsa, "Vision and support vector machine–based train classification using weigh-in-motion data," *Journal of Bridge Engineering*, vol. 27, no. 6, pp. 156–158, 2022.

[19] J. Li, Y. Lei, and S. Yang, "Mid-long term load forecasting model based on support vector machine optimized by improved sparrow search algorithm," *Energy Reports*, vol. 8, no. S5, pp. 491–497, 2022.

[20] W. Li, X. Xing, F. Liu, and Y. Zhang, "Application of improved grid search algorithm on SVM for classification of tumor gene," *International Journal of Multimedia and Ubiquitous Engineering*, vol. 9, no. 11, pp. 181–188, 2014.

Hindawi
Scientific Programming
Volume 2022, Article ID 4560613, 13 pages
https://doi.org/10.1155/2022/4560613

Research Article

Multisensor Human Resource Data Fusion and Its Application in Industrial Distribution

Sheng Jiang and ChuanZhen Zheng

School of Economics and Management, Tongji University of Shanghai, Shanghai 200092, China

Correspondence should be addressed to ChuanZhen Zheng; zcz2018@tongji.edu.cn

Received 25 April 2022; Accepted 30 May 2022; Published 28 June 2022

Academic Editor: Lianhui Li

Over the past 30 years of reform and opening up, China has undergone tremendous changes. With the continuous growth of China's economy, the core competitiveness of Chinese enterprises is also increasing day by day. After China joined the WTO in 2001, economic globalization hit Chinese enterprises. Under such circumstances, a large number of foreign multinational companies have entered China to establish factories, which has caused huge pressure on Chinese companies. Facing this unprecedented pressure, Chinese enterprises need to fundamentally improve management and operation problems. Companies need to change aggressively to respond to the shock of foreign companies. The development of multisensor technology has brought great changes to enterprise human resource management. The real-time changes in this technology allow the continuous optimization of human resource management. Human resource management technology also needs to adapt to the modern social environment and constantly improve and quickly existing enterprise employee management methods and methods. These technical contents need to be optimized, and the working methods need to be improved. At the current stage, enterprise human resource management has not fully understood multisensor technology. Enterprises have poor adaptability in the application of this technology, and have not carried out comprehensive planning and clear optimization of detailed rules from the macro level. On this basis, the company has also failed to establish a relatively excellent team of professional management talents. There are three issues involved in talent team management. This article firstly analyzes the effect of human resource management in contemporary enterprises based on multisensor technology. Enterprises need to improve their awareness and application of sensor technology. It also needs to establish the overall strategy of human resource management and specific means of implementation. Through the in-depth application of these technologies, enterprises can enhance the comprehensive capabilities of human resource management teams. The application of this technology also provides practical and effective help for modern enterprise human resource management.

1. Introduction

The key to improving the core competitiveness of an enterprise is to improve the ability of human resource management. The competition among enterprises in the 21st century is the competition among enterprise talents. For high-tech enterprises, the number of technical talents has become a symbol of enterprise strength. In this context, how to improve human resource management has become a topic of the times. Existing studies have carried out many new tentative studies on human resource management from the perspective of information. These studies combine human resource management with information to explore the efficiency and effect of strengthening human resource management in high-tech enterprises [1–3]. The existing research has conducted in-depth research on the basic theory of human resource management and information, and further summarized the general practice process of information management. Existing studies have systematically summarized the great changes brought about by information to human resource management. Many enterprises have gone through the process of transforming from manual human resource management to information-based human resource management. This method improves

the management efficiency of enterprises and realizes the management connection between Chinese enterprises and foreign enterprises [4–6]. This article systematically sorts out the existing relevant theories and optimizes the human resource management model of enterprises in the current environment. It also analyzes the combination of information technology and enterprise human resource management. Multisensor technology and enterprise human resource management: in the era of multisensor technology, the human resource management model of enterprises has also undergone tremendous changes, especially for the design of human resource management mode under multisensor technology. Enterprises need to improve the efficiency of enterprise management and human resource management from a more refined perspective. On this basis, from the perspective of high-tech enterprises, this article expounds the importance of knowledge workers and technical talents to high-tech enterprises. This article further sorts out the specific role of the e-HR software system in improving employee satisfaction and enthusiasm. It further analyzes the impact of mobile devices on human resource information. The purpose of this article is to improve the competitiveness of Chinese high-tech enterprises through the e-HR system. Through the improvement of its own competitiveness, the enterprise makes its own management more modern [7–10].

On this basis, this thesis analyzes the theory of human resource management information. The text analyzes the necessity of implementing human resource management information in high-tech enterprises. This article focuses on expounding the process of implementing human resource information in enterprises [11–13]. With the global economic integration and the arrival of the information age, human resources have become more important resources than material, financial, and information resources. Information resources are regarded as strategic resources for enterprises to gain a competitive advantage. In view of the problems such as insufficient effectiveness of the current enterprise human resources informatization construction, this study believes that enterprises need to adhere to the multisensor technology as the carrier to establish a perfect human resource management module. Enterprises need to provide a carrier platform for upgrading human resource management capabilities. On the one hand, enterprises adopt multisensor technology and can design a technical model suitable for business modules. The development and management of human resources in enterprises have gradually shifted from traditional personnel management to strategic human resource management. With the continuous optimization of enterprise functions, the management concepts and methods of enterprises need to make breakthroughs. Human resource management in China is still at the basic stage [14–16]. Chinese enterprises need to cope with the transformation of human resource management functions. The management concepts and methods of enterprises need to be broken through. However, China's human resource management work is far behind the world level in terms of theory and practice. This article systematically sorts out the domestic human resource management work. This article puts forward the specific content of enterprise human resources information management through systematic analysis. On this basis, through human resource information management, this article gives a specific method to quickly improve the operation efficiency of the enterprise. This article further analyzes and summarizes the methods commonly used in daily human resource management work in American and Japanese companies [17–19].

Through the positive and negative experiences and lessons, this article further analyzes and draws the main points of human resource management work. Guided by comprehensive strategy and corporate culture, this article ensures the correctness of the direction of human resource management work through a reasonable corporate development strategy. Enterprises can find the design of human resource management module that multisensor technology can be applied to the whole process of data resource collection, integration, and analysis. The technology can provide a scientific basis for the management of the human resources of enterprises. At the same time, enterprises also need to realize scientific planning of human resources under the guidance of multisensor technology. On this basis, this article promotes the continuous improvement of enterprise operation efficiency through systematic cultural management methods. In this article, the multisensor technology analysis method is adopted to make the management method of the enterprise continuously updated and optimized. In the specific research, this article subdivides the work of human resource management information. The specific information work is divided into the technical level and management level. Combined with the relevant research of existing scholars, this article believes that human resource information pays more attention to the management level [20]. This article further puts forward the specific ideas and measures for the development of enterprise human resources at different management levels. This technology can improve the management efficiency of human resources. Therefore, multisensor technology is of great help to the module design of enterprise human resource management. Different modules of an enterprise differ in their choice of strategy and corporate culture. Different enterprise development strategies produce different enterprise development ideas and practice models. At the technical level, companies focus on two issues. First, companies need to make forward-looking recommendations on the technical analysis of human resource management [21]. This technical analysis method can ensure that enterprises will not be eliminated for a long period. The choice of specific functions must be able to contribute to the realization of its own strategy. The development of an enterprise needs to match its own positioning and development needs. The flowchart of enterprise information management based on multisensor technology is shown in Figure 1.

2. The Research Progress on Information Management of Enterprise Human Resources

Enterprises need to deeply study the combination of information technology and human resource management.

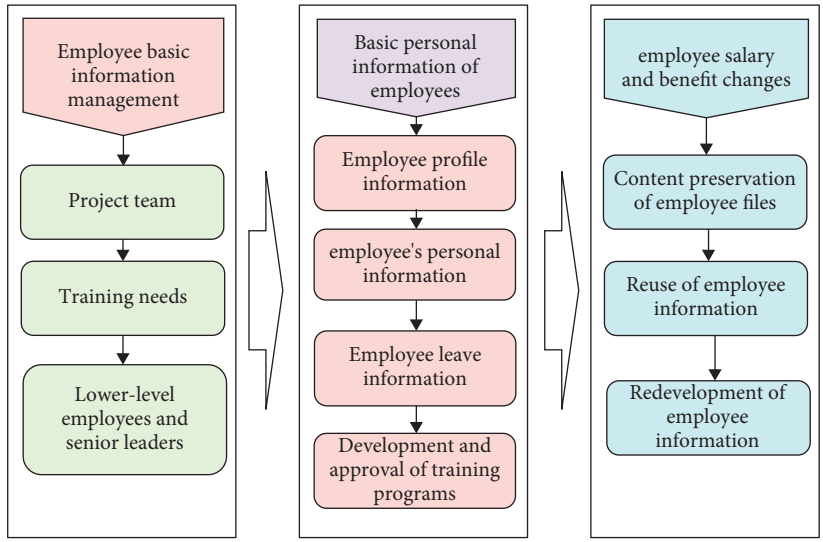

Figure 1: The flowchart of enterprise employee information management based on multisensor technology.

Information has become a new pillar supporting the development of our national economy. The information development of enterprises is also a new economic growth point worthy of our attention. The information industry has also received the attention of national leaders and governments. Under the background of economic globalization, information technology plays a very important role in the competition between enterprises.

2.1. The Main Achievements of Information Management of Enterprise Human Resources. The wave of information has a relatively large impact on traditional human resource management data. This kind of influence requires enterprises to abandon the original traditional concepts and take the initiative to add more information-based concepts. In the current environment, the network-based information environment has formed, and human resource management should change itself accordingly. In this case, the development of China's human resources information has entered a new era. The rapid development of information conforms to the needs of enterprise human resource management. Multisensor technology and human resource planning work: in the application of multisensor technology, the planning mode of human resources has changed. This technology provides a strong guarantee for the long-term and strategic nature of enterprise planning. In the process of continuous updating of multisensor technology, enterprise human resource management pays more attention to the actual situation. The 21st century is the era of the combination of knowledge and network, and the role of the knowledge economy is very important. In the environment of the knowledge economy, high-tech talents have become the main body of knowledge. People-oriented, knowledge-based, networked, and information-based developments are becoming more and more important. When enterprise management integrates information, human resources, as the most important factor, play a key role as a bridge. Traditional human resource management methods are often outdated, mainly sorting out resource data in a purely manual form. The method of personnel management is generally subjective, and the enterprise managers themselves mainly determine the standard of judgment.

The standards of performance appraisal of enterprises are generally relatively subjective. However, this relatively subjective performance appraisal model is inconsistent with the development demands of enterprises. With the advent of networking and information, computer and Internet technologies have been widely popularized in society. We must make full use of the convenience brought by information technology to our work and make human resource management more scientific. The human resources department is an ordinary department of an enterprise. In the overall development of the enterprise, it has not been deliberately elevated to a strategic level. The companies do not pay attention to human resources. Businesses only see people as tools to achieve business performance. In the information age, human resources have become an important resource for enterprises. Therefore, enterprises need to raise human resources to a strategic level. In this context, human resource management is very important. Enterprises need to abandon the traditional personnel management methods and make full use of information methods for human resource management. The organizational structure of the human resource planning function module based on multisensor technology is shown in Figure 2.

2.2. The Main Problems of Information Management of Enterprise Human Resources. In more than 30 years of reform and opening up, China's information technology has developed and changed faster and faster. It can be said that without information, there will be no modernization in China. Information technology is crucial to the development of China's economy, politics, and culture. In the process of China's transition from a planned economy to a socialist market economy, the market has also paid more and more attention to the management of human resources. Human

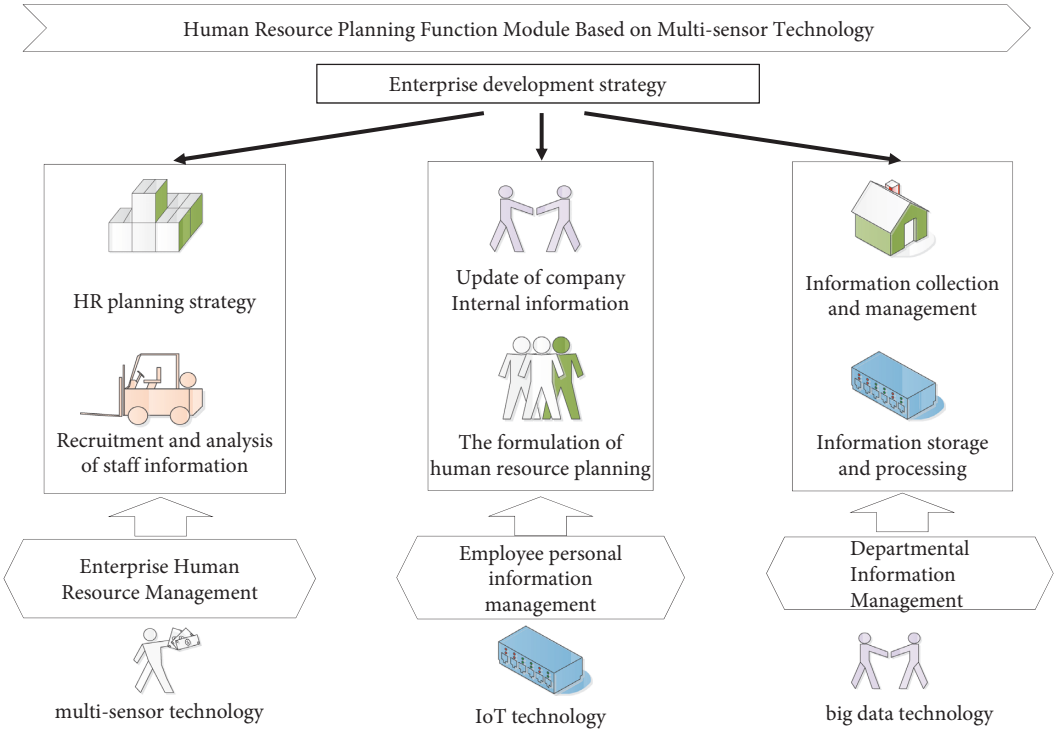

Figure 2: The organizational structure of the human resource planning function module based on multisensor technology.

resources have become an important resource and wealth of society. The management mode of human resources is in line with the country's people-oriented development concept. In the context of the rapid development of information technology, the combination of human resources and information has become an important part of enterprise development. The development of information technology can provide the high-speed operation of enterprises. Data integration and application in human resource management are key concerns of enterprises. The calculation formula for the information entropy of each node is as follows.

The calculation principle of local consistency is relatively simple, mainly using the Kendal Concorde coefficient, and the specific calculation formula is as follows:

$$W = \frac{\sum (R_i)^2 - n(\overline{R})^2}{1/12\mathrm{K}^2\left(n^3 - n\right)}. \tag{1}$$

The calculation formula of single-sample statistics is as follows:

$$t = \frac{\overline{X} - \mu}{\delta_x / \sqrt{n-1}}. \tag{2}$$

The calculation of the statistics of the hypothesis of the single-body sample is as follows:

$$t = \frac{\overline{X_1} - \overline{X_2}}{\sqrt{(n_1 - 1)S_1^2 + (n_2 - 1)S_2^2/n_1 + n_2 - 2(1/n_1 - 1/n_2)}}. \tag{3}$$

2.3. The Significance of Information Management of Enterprise Human Resources. This technology can be widely used in many industries. This technology has played a very important role in the management and operation of enterprises. Enterprise human resource management is a very practical technology. With the continuous development and update of multisensor technology, traditional human resource management methods are also facing a huge impact. With the innovation of technical methods, multisensor technology has also brought more opportunities for the development of enterprises. Human resource management plays an important role in the development of enterprises. The value of human resources reflects the comprehensive competitiveness of enterprises. A good human resource management method can build an optimistic and progressive work environment within the enterprise. The application of new technology can improve the enthusiasm and sense of responsibility of the company's employees. The specific calculation formulas are as follows.

Set two random sequences X and Y, the Pearson correlation coefficient between the two sequences is r, then

$$r = \frac{\operatorname{cov}(X, Y)}{\sqrt{\sigma_x^2}\sqrt{\sigma_y^2}} = \frac{\sum_{i=1}^{n}(x_i - \overline{x})(y_i - \overline{y})}{\sqrt{\sum_{i=1}^{n}(x_i - \overline{x})^2 (y_i - \overline{y})^2}}. \tag{4}$$

To ensure the accuracy of the results, this article uses two evaluation indexes, mean absolute error and root mean square error, to evaluate the optimization effect of the model. The specific calculation formulas are as follows:

$$\mathrm{MAE} = \frac{1}{s}\sum_{i=1}^{s}\left|\widehat{y}_i - y_i\right|, \tag{5}$$

$$\mathrm{RMSE} = \sqrt{\frac{1}{s}\sum_{i=1}^{s}\left[\widehat{y}_i - y_i\right]^2}, \tag{6}$$

$$\begin{aligned} J = &\sum_{i=1}^{N_p}\left\|y(k+i) - y_{ref}(k+i)\right\|_Q^2 \\ &+ \sum_{i=1}^{N_p}\|U(k+i)\|_R^2 + \sum_{i=1}^{N_p}\|\Delta U(k+i)\|_R^2. \end{aligned} \tag{7}$$

Considering the influence of the target vehicle's speed and penalty function on obstacle avoidance, the following obstacle avoidance function is selected:

$$J_{\mathrm{obs},i} = \frac{S_{\mathrm{obs}} v_i}{\left(x_i - x_o\right)^2 + \left(y_i - y_o\right)^2 + \varsigma}. \tag{8}$$

This technology helps to enhance the creativity of employees on the job. This technology can lay the foundation for the long-term and efficient development of the company. In the era of continuous innovation of multisensor technology, enterprise human resource management must be properly process optimized. Through refined human resource management, the enterprise guarantees the scientific validity of human resource planning. First, the enterprise adopts multisensor technology and builds a human resources multisensor technology library. This process optimization method can guide the reform and innovation of human resource management. This article needs to further strengthen the information construction of human resource management and uses multisensor technology to build a human resource management system with high accuracy, good predictability, and strong real time.

We treat each of the monomials as m input models in the original structure of the modeling network:

$$v_1 = a_0, v_2 = a_1 x_1, v_3 = a_2 x_2, \ldots, v_6 = a_5 x_1 x_2. \tag{9}$$

The final information $i_t \times C_t'$ is expressed as the value that can be obtained C_t from the output information of the joint forgetting gate:

$$C_t = f_t * C_{t-1} + i_t * C_t'. \tag{10}$$

The calculation method is:

$$O_t = \sigma\left(W_o \cdot \left[h_{t-1}, x_t\right] + b_o\right), \tag{11}$$

$$h_t = o_t * \tanh\left(C_C\right). \tag{12}$$

The use of this technology can effectively promote the long-term stable development of the company. On this basis, this article focuses on analyzing the impact of multisensor technology on enterprise human resource management. This article points out the dilemma faced by human resource management at this stage and proposes corresponding management methods. The conclusion of this article can effectively improve the effect of enterprise human resource management. The modular application framework of the e-HR system based on multisensing technology is shown in Figure 3.

3. The Influence of Multisensor Technology on Enterprise Human Resource Management

With the advent of the information age, multisensor technology has been widely used. Many enterprises have completed the analysis and integration of information through multisensor technology. Enterprises extract useful information from large-scale data, and integrate, analyze, and use it. The application of new technology promotes the close integration of enterprise management and information technology. Human resource management is an indispensable part of many management tasks of enterprises. Multisensor technology can reform and innovate the existing human resource management methods. This technology library facilitates accurate, granular analysis of multisensor technology. This technology helps to improve the planning efficiency of human resources to meet the data analysis needs of different types of structures. Then, human resource planning focuses on the systematic nature of resource management. Through this new technology and new method, the purpose, timeliness, and precision of human resource management can be strengthened. This new method can continuously improve the effect of enterprise human resource management and promote the development of enterprises in the direction of standardization and refinement. In the era of multisensor technology, enterprise human resource management is bound to closely link with information technology. Therefore, the human resources management personnel of enterprises need to have the professional ability and master certain information technology.

3.1. The Application Status of Multisensor Technology in Enterprise Human Resource Management. These enterprises need to gradually build a human resource management team with a high professional level and high level of information. In carrying out multisensor technology mining work, companies need to focus on strengthening their own level of innovation. Enterprises need to use the characteristics and advantages of multisensor technology to continuously improve and innovate the methods and paths of human resource management. Companies need to use multisensor technology to set a strategic direction for themselves. Businesses need to take advantage of multisensor technology for management. This technology can effectively promote the popularization of human resource management information. Enterprises need to build a system platform for human resource management with the support of multisensor technology. In the application of multisensor technology, enterprises need to continuously improve the management efficiency of human resources. The application of new technology provides a scientific basis for the scientific planning of human resources. In addition, the information work of enterprise human resources needs to establish a

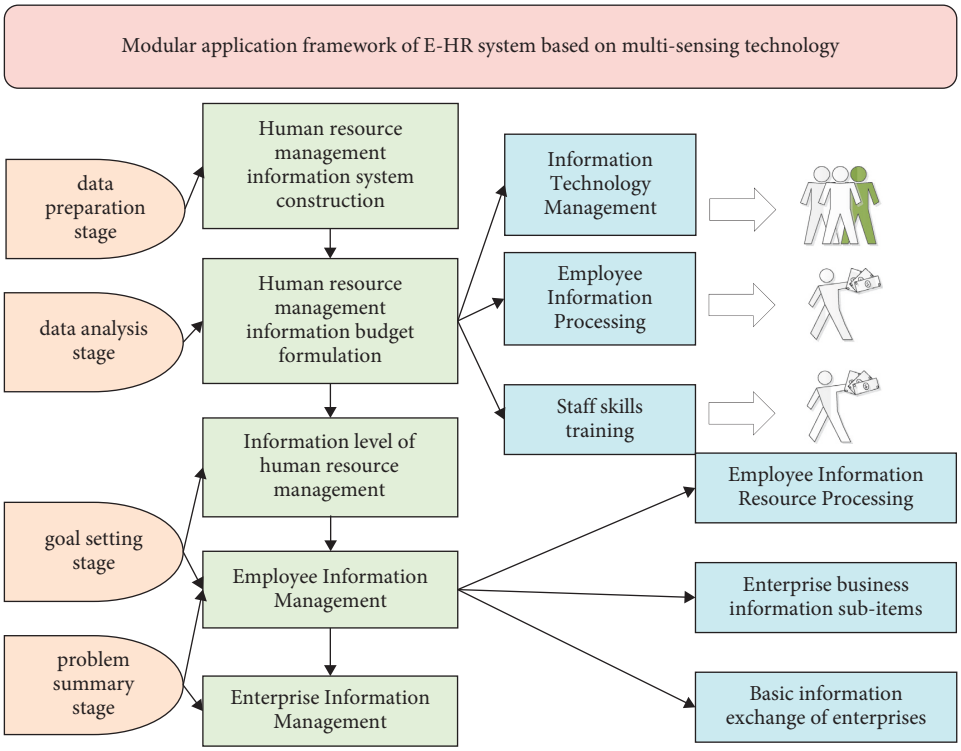

Figure 3: The modular application framework of the e-HR system based on multisensing technology.

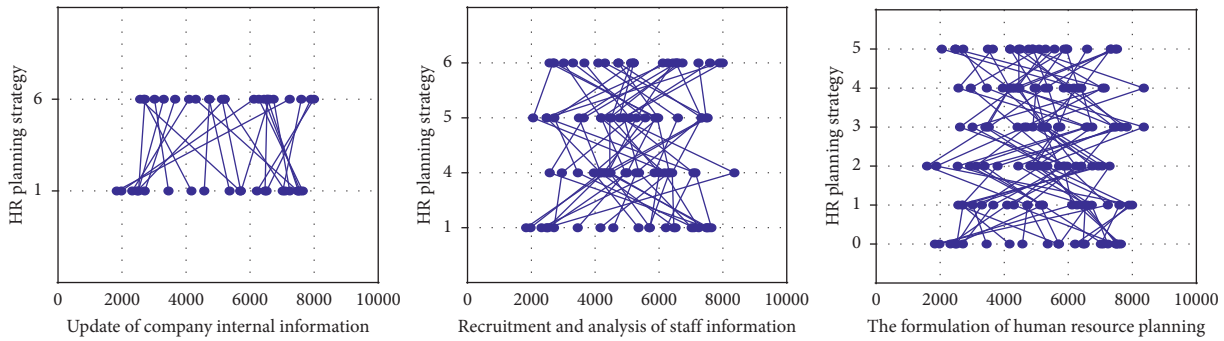

Figure 4: The comparison of different technologies applied in human resource management system construction.

good awareness of information confidentiality. This is because the personal information of employees, corporate information, and other contents are easily leaked on Internet data. Once the information is stolen, it will bring great loss to companies and individuals. This threatens the company's market position. Multi-sensor technology offers significant convenience. Enterprises will generate many data resources in the process of human resource management. Therefore, these massive data resources need reasonable extraction and analysis by human resource managers. These human resource managers need to identify the results of data analysis. This information can help managers obtain valuable data from a large amount of data and can also provide data support for the specific direction of human resource management. The comparison of different technologies applied in human resource management system construction is shown in Figure 4.

3.2. Enterprises Fail to Understand the Advantages of Multisensor Technology. Companies are less able to use new technologies in human resource management. The scientific nature of human resource management directly affects the long-term development of an enterprise. This situation also affects the making of important decisions within the enterprise such as multisensor technology and talent recruitment management. In the Internet era, enterprises need to use online recruitment technology as the main way to recruit talents. Through multisensor technology analysis, enterprises can understand and classify the basic data of applicants. Through basic data screening, enterprises realize the first-level check of talent recruitment. As the application of multisensor technology in enterprise human resource management continues to deepen, the influence of multisensor technology on human resource management is gradually increasing. This new technology has gradually

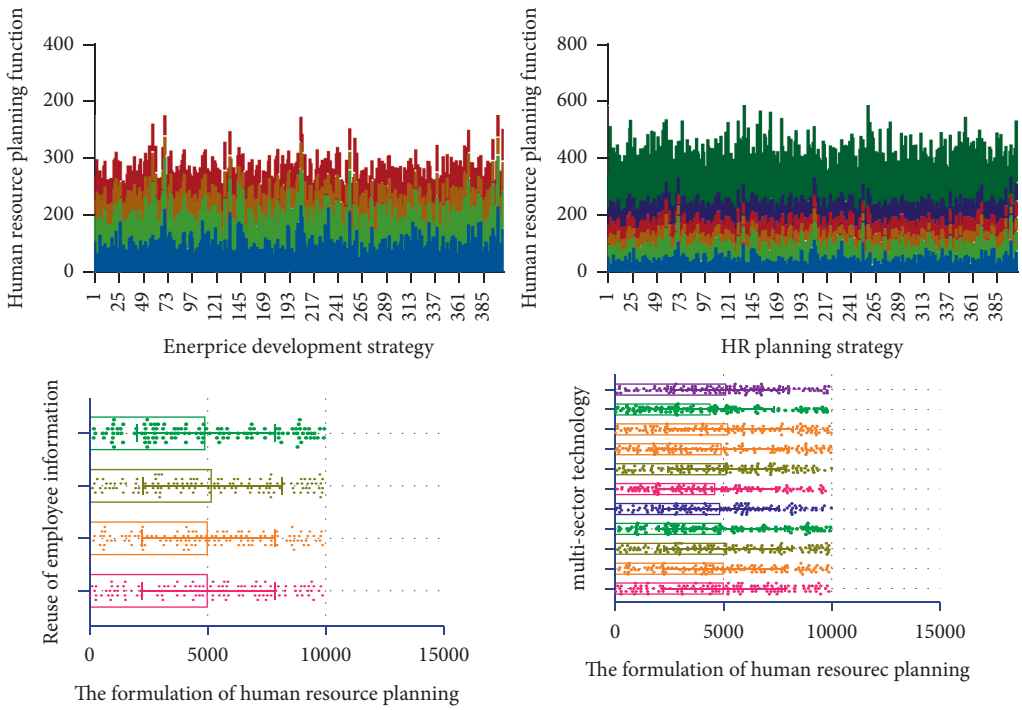

Figure 5: The comparison of human resource information construction in different scenarios.

applied to all aspects of human resource management. However, judging from the status quo of human resource management at this stage, the responsible personnel and managers of the enterprise have not been able to establish a scientific understanding of multisensor technology. Managers of enterprises have an insufficient understanding of the connotation of multisensor technology. Enterprises still lack attention to the innovation of human resource management systems. In addition, enterprises need to conduct directional analysis of capability data and development potential data. On this basis, the company compares the work experience, innovation, and development ability of the recruits and other information. Enterprises analyze employee information through multisensor technology. At present, the application of information technology by enterprises is still on the surface, and it cannot give full play to the advantages of information technology. In the process of human resource management, enterprises have not applied multisensor technology to manage decision-making. Enterprises are still stuck in the traditional thinking mode of human resource management. In addition, due to the long application time of traditional management concepts and methods, enterprise managers cannot give full play to the advantages of multisensor technology in practical work. Enterprise management lacks a long-term vision for the reform and development of the human resource management system. This lack of vision causes the human resource management system of enterprises still use traditional methods. The lack of application of this new technology affects the reform and development of the human resource management model. The comparison of human resource information construction in different scenarios are shown in Figure 5.

3.3. The Enterprise Did Not Carry Out Comprehensive Planning and Clarify the Optimization Rules. The improvement and optimization of enterprise human resource management should focus on the overall strategy of the enterprise. Enterprise managers need to clarify the direction and implementation plan of enterprise reform. In the era of continuous updating of multisensor technology, human resource managers of some enterprises do not consider enterprise development from the perspective of the overall strategy. Corporate managers themselves have not formulated detailed reform methods. At the same time, the strategic layout of many enterprises mainly continues the previous development model. These enterprises are neither connected to Internet technology nor fully integrated with multisensor technology. This situation has caused enterprises to encounter various difficulties in the process of the human resource management system. Enterprises have not established incentive systems and guarantee systems, and many reform measures cannot be implemented. The reform of the management system of human resources still needs to consider this from many aspects. In addition, the scope of work of human resource management is concentrated within the enterprise. Business leaders have not fully realized the importance of human resource management. This situation leads to difficulties in enterprise human resource management and personnel management. Enterprises cannot establish a comprehensive understanding of multisensor technology and cannot correctly predict the development direction of multisensor technology. Therefore, enterprises cannot formulate their own human resource management reform plans in combination with multisensor technology. The reform work of enterprises cannot be effectively implemented and the formalism is serious. The

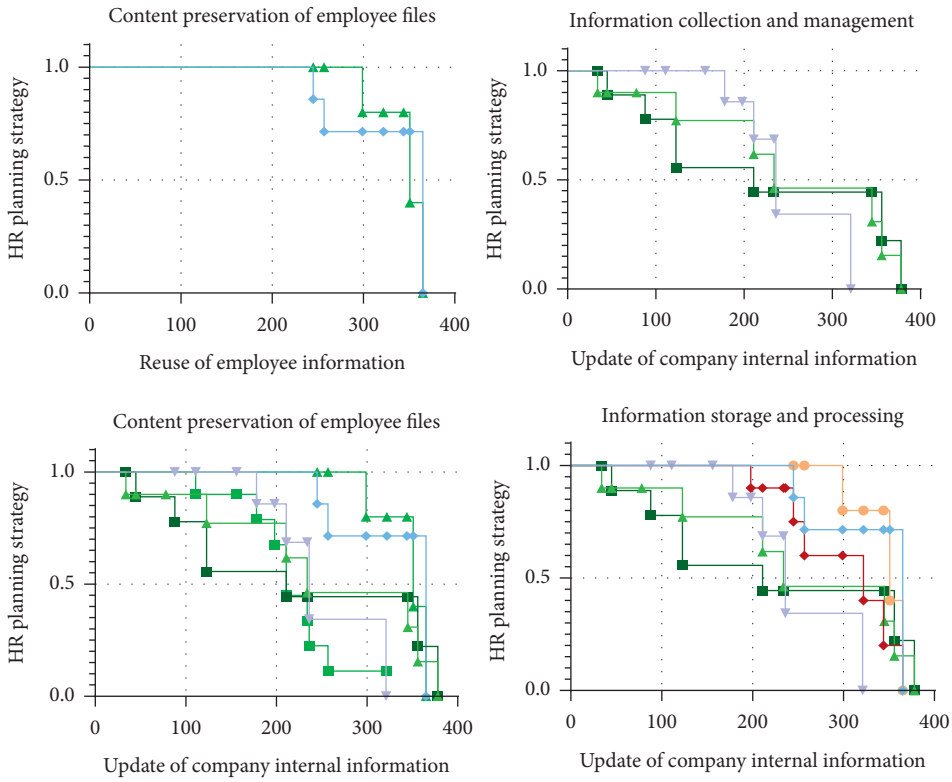

Figure 6: The comparison of the effect of information management within the enterprise among different departments.

comparison of the effect of information management within the enterprise among different departments is shown in Figure 6.

3.4. The Company Has Not Been Able to Build an Excellent Team of Professionals. China is in the era of the knowledge economy, and enterprises need to give full play to the value of talents. The value of talents is of great significance to the development of enterprises. In the era of multisensor technology, to achieve good results in human resource management, an excellent team of professionals must be established. Enterprises need to improve the comprehensive business level of the talent team. This analysis method can better meet the needs of the position and recruit talents that meet the needs of the enterprise. At the same time, enterprises also need to protect the value created by talents at work. Therefore, enterprises need actively carry out the application combination of multisensor technology and talent recruitment management. However, at this stage, the integration of human resource management and multisensor technology in most enterprises is not close enough. This integration is still in its infancy. In the composition of the human resource management team, only a very small number of workers have systematically learned too many sensor technologies and can flexibly use them. Enterprises need to analyze data of different characteristics, recruit high-quality talents for enterprises, and then achieve mutual benefit and win-win results. When carrying out the training of human resource managers, enterprises mainly conduct training in the traditional way. Enterprises rarely involve the knowledge points of multisensor technology in the training process. Even if the development of enterprises incorporates multi-sensor technical knowledge, it only stays on the surface. The application of technology by enterprises is mainly based on simple and common sense knowledge. Businesses cannot really improve managers' awareness of multi-sensor technology. This situation results in multisensor technology that cannot be fully integrated into the management of human resources. At the same time, the company did not pay attention to the introduction of management talents and did not formulate a reasonable salary system and incentive system. This situation also leads to a more serious brain drain, and enterprises cannot establish a comprehensive human resource management team.

4. The Introduction Strategy of Multisensor Technology in Enterprise Human Resource Management

4.1. Enterprises Need to Improve Their Awareness of Multisensor Technology. At the current stage, with the rapid development of the Internet and computer technology, the application scope of multisensor technology is becoming more and more extensive. Technology has had a major impact on various industry sectors. Enterprises pay more attention to the application of multisensor technology to human resource management. The application of new technology has become an important direction of the current reform of enterprise human resources management. Therefore, business leaders and human resource managers

must fully understand multisensor technology. Enterprises need to pay attention to the application of new technologies and continuously improve their business scenarios using multisensor technology. Multi-sensor technology and human resource development work. In the modern management system, the development of human resources is the core content of resource management. This kind of work is related to the important foundation of the strategic development of human resources of enterprises. In "multisensor technology," companies need to carry out multisensor technology analysis. Specifically, enterprises can work from the following two aspects. First, human resource managers should pay attention to the application of multisensor technology from an ideological point of view. Managers need to understand the important role of multisensor technology in human resource management. Managers need to change their management thinking and methods and understand multisensor technology as the focus of promoting human resource management reform. Enterprises need fully integrate multisensor technology in management methods, management concepts, and workflows. Businesses need to take advantage of multisensor technology.

Second, enterprises should combine multisensor technology to build a new human resource management platform. Enterprises need to further improve the actual effect of human resource management. The enterprise management department needs to further separate the work content of human resource management and personnel management. Enterprises need to gradually establish a human resource management method based on computer data. According to the characteristics of different employees, enterprises need to carry out a comparative analysis of multisensor technology. Enterprises carry out precise development of human resources according to the strengths and abilities of employees. At the same time, enterprises need to establish a comprehensive human resource management database according to their own conditions. Enterprises need to disclose the database within the company to realize the sharing and circulation of data information. Through this database, enterprises can better improve the efficiency of enterprise human resource management. Through this database, enterprises can keep an eye on the latest developments of employees at all levels. By establishing an information resource database, enterprises lay the foundation for future human resource management.

4.2. Enterprises Need to Clarify the Means of Implementing Human Resource Management. In the era of multisensor technology, the market environment has undergone tremendous changes. Changes in this market environment require constant innovation in human resource management. Enterprise management should constantly be reformed according to the external environment. Enterprises need to formulate a scientific human resource management strategy. At the same time, to ensure that the new management system can be fully implemented; enterprises also need to build a corresponding security system. In this way, we can improve the scientific and foresight of enterprise human resource management. Specifically, companies need to work from the following two aspects. First, enterprises should pay full attention to the application of multisensor technology in the process of human resource management. Enterprises need better tap the advantages of multisensor technology. Companies need to use multisensor technology accurately analyze their strategic goals.

On this basis, enterprises need to formulate a clear reform direction, implementation path, and ultimate goal; need to start from every detail to improve the recognition of organizational leaders and employees for human resource management. Enterprises need to change the traditional human resource development model and need to put more emphasis on the analysis of multisensor technology. It needs to scientifically realize the human resource development efficiency of "making the best use of their talents." Then, it should make full use of the advantages of multisensor technology and mobilize every employee to participate in human resource management. Enterprises need to divide the overall strategic layout into several branches according to their actual conditions. On this basis, let each employee undertake corresponding branch tasks. On the one hand, this management method can effectively stimulate the enthusiasm of employees, mobilize their subjective initiative of employees, and make employees feel their sense of responsibility and honor. On the other hand, this management method is also conducive to changing the main body of enterprise human resource management. Enterprises can rely on multisensor technology further extract valuable information in human resource management. Enterprises need to further share useful information internally to ensure the orderly progress of enterprise human resource management reform. The application comparison of multisensor technology in enterprise human resource management is shown in Figure 7.

4.3. Enterprises Need to Improve the Comprehensive Ability of Human Resource Management. Under the background of the modern knowledge economy, the stable development of enterprises cannot be separated from the support of excellent teams. Similarly, in enterprise human resource management work, an excellent team with strong professional ability is also very important. An excellent team is a carrier that promotes the continuous reform and innovation of human resource management. Therefore, enterprise leaders need correctly understand the important role of human resource management in enterprise development. Enterprises need to invest a certain amount of money to improve the comprehensive level of the human resource management team. In addition, enterprises need to carry out training courses and seminars on human resource management on a regular basis. In the process of learning, managers should improve their professional knowledge and skills in human resource management on the one hand. On the other hand, managers also need to learn more multisensor technology knowledge. Enterprises need to cultivate a team of compound talents with professional knowledge and multisensor technology knowledge. With the popularization

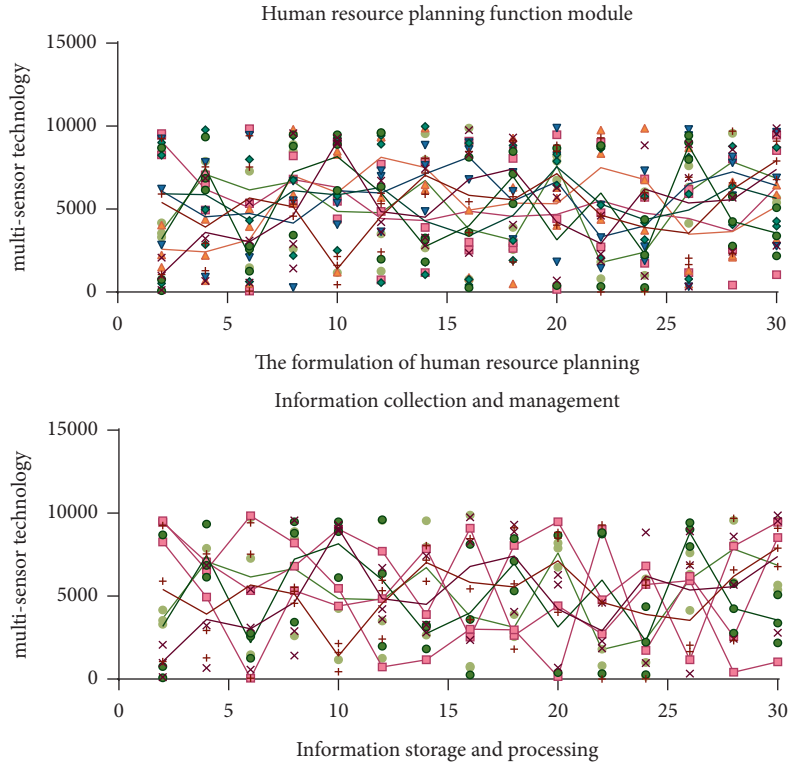

Figure 7: The application comparison of multisensor technology in enterprise human resource management.

of multisensor technology in human resource management, this technology will inevitably lead to changes in the human resource management system. At the same time, enterprises need simultaneously carry out reforms and innovations in talent incentives and salary management. Enterprises need to strengthen the introduction of talents in multisensor technology. Establish strategic cooperative relations with institutions of higher learning, scientific research institutions, and other institutions through the school-enterprise cooperation model. Enterprises need to introduce more multisensor technology professionals in human resource management. It needs to improve the deficiencies in human resource management work and promote the improvement of human resource management efficiency and quality.

5. Industrial Distribution of Human Resources

5.1. Personnel Configuration Module Design. In the existing human resources management system, though some daily personnel management work needed information input, register, statistics, and daily tasks, such as function modules, but all of these works are directly on the existing data processing, on the basis of no in-depth integrated use of the data mining analysis function. In particular, there are still some deficiencies in the design of human resource allocation based on data mining information.

By building a human resource allocation data mining analysis module in the system, combining indicator data of different description types, and using K-Means clustering algorithm for classification and analysis research, a unique human resource allocation analysis indicator system is proposed, which provides a method to improve the system's comprehensive human resource allocation analysis function.

5.2. Human Resource Allocation Needs. Before the design of the human resource allocation data mining function, we must first conduct a requirement analysis to clarify what basic functions need to be achieved by the mining function, which steps are necessary, the indicators that may be used, and the program language or program algorithm that needs to be used to achieve the function, etc., and then, we can carry out the specific function implementation program design.

According to the concept of modern human resources "personnel quality concept," human resources allocation is not simply a matter of increasing or decreasing the number of personnel, but more importantly, considering the comprehensive quality, work ability, work efficiency, work attitude, health condition and other factors of the personnel in the workforce. At present, before conducting staffing, human resource management departments usually give priority to the job responsibilities of each division, business characteristics, annual workload, and the number of personnel required to complete the tasks, according to the importance procedures of various factors, and conduct a comprehensive study to determine the staffing plan of the division according to whether the age structure, knowledge structure, gender structure, and ability of the existing personnel of the division can meet the needs of completing the tasks. Therefore, the analysis and study of human resource allocation tasks should not only analyze the issue of staffing

quantit but also analyze the structure and quality of the staffing of different divisions according to whether the divisional staffing is reasonable. In the past, when the human resource management department analyzed the basic quality configuration of the staff in the division, it was usually based on perceptual understanding, and there was a lack of in-depth data mining analysis tools and corresponding data analysis conclusions to support whether the configuration plan was reasonable, whether it could not meet the different needs of different divisions, and how to allocate human resources in a balanced manner when the number of existing staff structure could not be changed quickly.

This paper attempts to use the existing basic human resources data to cluster and analyze the basic quality of personnel, and visualize the basic quality of divisional personnel allocation through visual display so as to facilitate a more convenient judgment of whether the staffing is reasonable and provide a decision basis for the next human resources allocation adjustment.

5.3. Human Resource Allocation Data Mining Analysis Main Functions. Human resource allocation data mining is a new functional module in the original HR management system. According to the design plan of data mining analysis process and the need of data mining analysis task, this function module should have the following main functions: selection of data analysis index, entry display of data index, cleaning and modification of original data, construction of new data index, integration processing of data, selection of data mining algorithm, parameter setting and adjustment of data mining algorithm, realization of data mining algorithm, display of data mining, the display of results, backfill of data mining results, and graphical display of staffing situation. The functional design of the module combines some existing functional modules in the existing software, and at the same time extends it with the analysis needs. Among them, the selection and re-integration of analysis indicators can be done by using the original functions of the system, while the implementation of data mining algorithms and the presentation of results need to be redesigned to be realized.

5.4. Human Resource Allocation Module Data Mining Analysis Process. The general idea of the data mining process design of human resource allocation module is to use some basic functions of the existing human resource management information system and add algorithm analysis function and graphic display function; the main steps are as follows:

(1) Analysis of the data mining task. The initial analysis of the data mining task is carried out to clarify the main purpose of the mining task, the specific steps to be implemented, the main indicators involved, the overall effect you want to achieve, etc.

(2) Selection and construction of basic analysis index items. Based on the analysis results, the basic index items required for analysis are selected from the human resource information system, and a preliminary judgment is made as to whether the basic index items are complete. When there are incomplete indicator items, they are constructed by building new subtables and new indicator items as needed.

(3) Improvement of data of basic index items. The data of the basic index items are adjusted and improved; especially, the important data needed for analysis must be added and completed.

(4) Construction of personalized index items. Without changing the data of basic index items, new process index items are constructed through the system function, and the process index items are mainly processed in various forms such as merging, calculating, format converting, and intelligent fetching of basic index items to create personalized index items for data mining analysis in the next step.

(5) Human resource allocation analysis. Through the interface of human resource allocation analysis function module, K-Means clustering algorithm is used to cluster personnel. When analyzing, you need to select the analysis index items, set the number of clusters, the number of iterations, select the initial clustering center, and then cluster the personnel by K-Means clustering algorithm. After the clustering is finished, the clustering effect is judged whether it meets the expectation, if it meets the expectation, the result of clustering is backfilled into the basic index item; if it does not meet the expectation, the clustering is reclustered by adjusting the clustering parameters, initial centroid, or adjusting the clustering index until the clustering effect meets the expectation.

(6) Visualization display. According to the clustering results of backfill outputting the two-dimensional point diagram of divisional staff quality analysis, study and judge whether the staffing structure is reasonable, if it meets the task requirements, then end; if it does not meet the task requirements, then make appropriate staff adjustment, and then output the two-dimensional point diagram of divisional staff quality analysis to study whether it is reasonable.

Based on the analysis results and intuitive graphic display, management can more easily study and judge whether the staffing of each office is balanced and reasonable, and provide a basis for decision making on the staffing adjustment of the office at a later stage.

6. Conclusion

The theoretical significance of this study mainly includes the following aspects. First, the application of information technology has brought systematic innovation to the theory of human resource management. Information technology plays an important role in innovation and management practice. The combination of information technology and human resources fully meets the requirements of system management. This article takes high-tech enterprises as the research object and studies the information construction of human resource management. The article further sorts out and clarifies the specific solutions of human resource management. This study has practical significance in two aspects. On the one hand, the application of information technology can support enterprises in the comprehensive management of human resources. Information technology is very helpful for enterprises to carry out the information

construction of human management. Specifically, it can be reflected in management processes, functional design, training and compensation, and external consultation. On the other hand, information technology can provide relevant experience for other management work.

Especially for the management work related to human resources, the tools of information technology can bring good results. The application of information technology can provide a reference for the theoretical innovation of human resource management. In today's rapid development of the global economy, the competition between enterprises is the competition of talents. The importance of human resources has been valued by more and more enterprises. Under the background of rapid information iteration, enterprises need to make better use of talents to create a performance. The rapid development of enterprises also requires more professional talents and intellectual services. Enterprises need to use a variety of new technologies and new methods to efficiently manage talents. High-tech enterprises are the vanguards of enterprise reform and possess more knowledge-based talents. The management mode of human resources information of high-tech enterprises is also provided to other related industries for reference. The results of this study can drive the rapid development of Chinese enterprises as a whole. This article systematically sorts out the information problems of enterprise human resources, which helps to reduce enterprise human capital and improve enterprise management efficiency. The research in this article will help Chinese enterprises to develop as a whole and improve their international competitiveness. Therefore, this article has important practical significance to study the information work of enterprise human resources.

Under the background of the development of multisensor technology, enterprise leaders and managers must fully realize the application prospect of multisensor technology. In the work of human resource management, enterprises need to focus on strengthening the reform and innovation of human resource management technology. Enterprises need to improve the cognition and application level of multisensor technology and establish a strategic layout of human resource management. At the same time, enterprises need to set up an excellent compound human resource management team to lay the foundation for continuously improving the effect of enterprise human resource management.

Data Availability

The dataset can be accessed from the corresponding author upon request.

Conflicts of Interest

The authors declare that there are no conflicts of interest.

References

[1] M. T. Ballestar, A. García-Lazaro, J. Sainz, and I. Sanz, "Why is your company not robotic? The technology and human capital needed by firms to become robotic," *Journal of Business Research*, vol. 142, pp. 328–343, 2022.

[2] Y. Ramírez and N. Tejada, "University stakeholders' perceptions of the impact and benefits of, and barriers to, human resource information systems in Spanish universities," *International Review of Administrative Sciences*, vol. 88, no. 1, pp. 171–188, 2022.

[3] R. Kutieshat and P. Farmanesh, "The impact of new human resource management practices on innovation performance during the COVID 19 crisis: a new perception on enhancing the educational sector," *Sustainability*, vol. 14, p. 2872, 2022.

[4] A. Imamuddin, "An enterprise resource planning system solution for small-mid size enterprises: an information system development case study," *Information Technology and Management*, vol. 2, no. 1, pp. 160–168, 2021.

[5] T. M. Truong, L. S. Lê, E. Paja, and P. Giorgini, "A data-driven, goal-oriented framework for process-focused enterprise reengineering," *Information Systems and e-Business Management*, vol. 19, pp. 683–747, 2021.

[6] C. Atkinson, B. Lupton, A. Kynighou, and V. Antcliff, "Small firms, owner managers and (strategic?) human resource management," *Human Resource Management Journal*, vol. 32, no. 2, pp. 449–469, 2021.

[7] M. Kumar, J. B. Singh, R. Chandwani, and A. Gupta, "Context in healthcare information technology resistance: a systematic review of extant literature and agenda for future research," *International Journal of Information Management*, vol. 51, Article ID 102044, 2020.

[8] C. E. Oehlhorn, C. Maier, S. Laumer, and T. Weitzel, "Human resource management and its impact on strategic business-IT alignment: a literature review and avenues for future research," *The Journal of Strategic Information Systems*, vol. 29, no. 4, Article ID 101641, 2020.

[9] S. Jeon, I. Son, and J. Han, "Exploring the role of intrinsic motivation in issp compliance: enterprise digital rights management system case," *Information Technology & People*, vol. 34, no. 2, pp. 599–616, 2020.

[10] Z. Liu, S. Mei, and Y. Guo, "Green human resource management, green organization identity and organizational citizenship behavior for the environment: the moderating effect of environmental values," *Chinese Management Studies*, vol. 15, no. 2, pp. 290–304, 2020.

[11] H. Annabi and J. Locke, "A theoretical framework for investigating the context for creating employment success in information technology for individuals with autism," *Journal of Management & Organization*, vol. 25, no. 4, pp. 499–515, 2019.

[12] S. Choi, "Organizational knowledge and information technology: the key resources for improving customer service in call centers," *Information Systems and e-Business Management*, vol. 16, no. 1, pp. 187–203, 2018.

[13] Z. Peng, Y. Sun, and X. Guo, "Antecedents of employees' extended use of enterprise systems: an integrative view of person, environment, and technology," *International journal of information management*, vol. 39, pp. 104–120, 2018.

[14] J. C. Field and X. W. Chan, "Contemporary knowledge workers and the boundaryless work–life interface: implications for the human resource management of the knowledge workforce," *Frontiers in Psychology*, vol. 9, 2018.

[15] H. Liu, "Research on organizational change and its management under changing environment," *Human Resource Management Review*, vol. 2, pp. 1–21, 2018.

[16] F. Wang, "Analysis on the strategy of application of statisticalanalysis method in human resource management of

modem enterprise," *International Journal of Technology Management*, USA, 2017.

[17] N. Evans and J. Price, "Enterprise Information asset management: the roles and responsibilities of executive boards," *Knowledge Management Research & Practice*, vol. 14, no. 3, pp. 353–361, 2017.

[18] S. Slaughter and B. Cantwell, "Transatlantic moves to the market: the United States and the European Union," *Higher Education*, vol. 63, pp. 583–606, 2012.

[19] W. Wan and L. Liu, "Intrapreneurship in the digital era: driven by big data and human resource management?" *Chinese Management Studies*, vol. 15, no. 4, pp. 843–875, 2021.

[20] D. Choi, H. Lee, H. Y. Lee, and H. Y. Park, "The association between human resource investment in IT controls over financial reporting and investment efficiency," *International Journal of Accounting Information Systems*, vol. 43, Article ID 100534, 2021.

[21] C. Zhao, L. C. Fang, and Z. Wang, "Human resource management in China: what are the key issues confronting organizations and how can research help?" *Asia Pacific Journal of Human Resources*, vol. 59, no. 5, 2021.

Hindawi
Scientific Programming
Volume 2022, Article ID 7077261, 7 pages
https://doi.org/10.1155/2022/7077261

Research Article

Virtual Reality Design in Reading User Experience: 3D Data Visualization with Interaction in Digital Publication Figures

Tian Wei,[1] Yongkang Xing ,[2] Yushuo Wu,[3] and Ho Yan Kwan[4]

[1]*School of Creative Design, Dongguan City College, Dongguan 523419, China*
[2]*Center of Experimental Teaching, Guangdong University of Finance, Guangzhou 510521, China*
[3]*School of Internet Finance and Information Engineering, Guangdong University of Finance, Guangzhou 510521, China*
[4]*Software Engineering Institute of Guangzhou, Guangzhou 510980, China*

Correspondence should be addressed to Yongkang Xing; 70-173@gduf.edu.cn

Received 26 May 2022; Revised 7 June 2022; Accepted 9 June 2022; Published 27 June 2022

Academic Editor: Lianhui Li

With computer technology rapidly growing in recent years, there is a significant trend that virtual reality technologies turn into the public. The paper found that VR has a high potential to improve reading efficiency. The research discussed various figures, which is the key element for data visualization in digital publications. Furthermore, the research analyzes the characteristic of VR. The research divides the data into three types: Static Data, Dynamic Data, and Interactive Data. The research designs the framework to transfer the data into VR platforms. In order to evaluate the performance efficiency of the framework, we conducted performance evaluations and a user study with 20 participants. Compared with traditional 2D figures, the experimental results show that the 3D framework can be used as an effective visual tool for reading on VR platforms. The paper indicates the possible future view based on the design study.

1. Introduction

In recent years, virtual reality (VR) technology has developed rapidly in the entertainment, media, education, and medical industries [1]. Developers can use VR devices to integrate virtual content with natural scenes to combine various interaction methodologies. VR technologies mainly use headsets to interact with the virtual world using controllers or hand recognition [2, 3].

VR technology has two significant advantages as a communication medium. The first one is 'simulation' [4, 5]. The VR technologies can build a highly simulated environment [4, 5]. The second advantage is 'immersive' [4, 5]. The users explore the simulated environment with various interactive methodologies [4, 5].

Numerous studies show that the VR has a high potential to improve reading efficiency, considering the VR advantages. Baceviciute summarizes that reading in VR is found to be more cognitively effortful and less time-efficient by his user experiments [6]. Significantly, the reading is transferring from nonimmersive to immersive media [6, 7].

HTC Vive has released Vivepaper with VR digital publication in 2016 [8]. Vivepaper brings lives of pictures, videos, audio, and 3D models. Users can watch and listen to multimedia content in an innovative way by pointing fingers [8, 9]. However, Vivepaper only covers the tourism and fashion journey without a detailed content description. Besides, most VR digital publications only display the content in 2D panels in the 3D environment without considering redesigning its 3D User Interface (UI) layout [6, 10, 11].

We should consider how to use VR technologies as the carrier of digital publications in the era of digitization. The study aims to design a 3D data visualization framework in reading and optimize the VR reading user experience.

There are various types of publications globally. It is necessary to narrow the research scope into a specific aspect and analyze its related UI structure and design framework.

The social science publications include different figures and tables to illustrate the social research output to the public [12]. The figures provide convenience in reading and assist the reader in understanding the content. Suppose the

figures remain in 2D modes in VR platforms. In that case, it is significant that the 2D panel cannot improve the VR reading efficiency without applying VR features. Millais' research shows that 3D data visualization can lower the reading barrier and improve reading efficiency [13]. The research focuses on social sciences publications to build the initial design data visualization principle with fundamental VR characteristics. The research tries to provide a general and interactive UI framework to assist the social science publication transfer into the VR Reading field.

In this project, the research aims to design a general interactive data visualization framework. It covers various data figures from our research. It can improve the user experiences in VR reading. The proposed principle is based on VR interaction methodologies. The characteristics are as follows:

(1) The research uses the VR interaction features to build the data visualization principle and provide users with immersive exploratory experiences.

(2) The research balances the reading and VR characteristics. The research refers to 20 social science publications to conclude the general figure types. Meanwhile, 3D layout and gesture interaction are integrated with data visualization to enhance the user's immersive experiences.

(3) The research evaluates the performance efficiency of the framework. We conducted performance evaluations and a user study.

2. Related Works

The session investigates the related publication knowledge and describes how to build up the data visualization principles. The research designs a general 3D data visualization concept by dividing various figures.

The research uses Unreal 4(UE4) UX development tools to design data visualization prototypes based on VR devices. The research uses different publications' data to testify to the possibility of the principles. The prototype can display how the concept plan adapts to the VR environment and the existing social science publications.

2.1. Data Elements in Social Science Publications. Before designing the general data visualization framework, it is necessary to discuss the existing general data figure elements in social publications. The study uses 20 articles from various open-access social science journals including Sage Open, Sustainability, and Agribusiness. We use the articles as case study samples to investigate the general data elements. We summarize the data elements and analyze how the elements achieve usage in data visualization. With critical analysis, we believe that the study can help us better discuss the overall data visualization concept and build the framework.

Through the investigation, the histogram is the most general data element. 75% of articles have used column charts. The line chart occupies the second position which number is 65%. Some articles only use line charts and histograms [14, 15]. The flow chart is in the third position which number is 55%. The pie chart is in the fourth position with 30%. There are other specific charts with mixed types that occupy 20%. Besides, tables have appeared in 60% of articles.

By analyzing the above-given statistic, we can summarize the general data elements: column chart, line chart, flow chart, and pie chart. We should consider transforming them in the VR platforms.

2.2. Design Concept. The data and figure cannot directly transfer to VR platforms. Therefore, the digital publication should contain the data file and the VR system can read the data file when displaying the selected figure. The data visualization framework includes two significant functions: data loading and display, as shown in Figure 1. It is necessary to discuss how to load the data and display the data with immersive experiences.

In data loading, the study requires considering how to transfer the data from various data files to VR platforms. Therefore, it is necessary to customize the function library. The study uses Direct Excel, the plug-in to allow UE4 to load the data files from a specified path [16]. The study builds a customized function library to make reading the data more convenient through the functions provided by the plug-in. The customized function library can read the data of the table more flexibly. The library can read the specific data range and compare it with other ranges. It is beneficial to simplify the data visualization working process and improve efficiency [17–20].

Besides the loading, the framework should provide a suitable visualization in displaying the data. The study divides the data into three types: static data, dynamic data, and interactive data (Table 1).

The static data are the fundamental data visualization element. After loading the data, the static data display as a 3D layout without interaction and animation. Dynamic data does not only include the 3D perspective but also has an animation effect to display how the data transform and straightly to display the comparison trend. Interactive data can use most VR features, including 3D layout, animation, and gesture interaction. The data allows users to modify the data with gesture interaction and display the simulated result in a 3D environment.

3. Framework Overview

The framework [21, 22] contains three major sections: Static Data, Dynamic Data, and Interactive Data. The study sorts out different figures in these sessions and explains the working flow in the principles.

3.1. Static Data. Static Data displays the data in the 3D layout and provides the move manipulation with hand controllers. Static Data supposes to illustrate the data which is hard to use animation to display. By analyzing various figures, single-column charts, pie charts, and line charts can

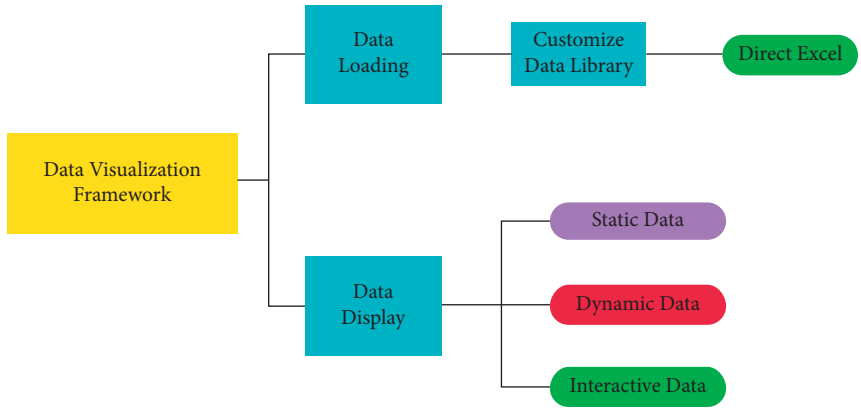

Figure 1: Framework overall structure.

Table 1: Data category.

	3D layout	Animation	Gesture interaction
Static Data	√	×	×
Dynamic Data	√	√	×
Interactive Data	√	√	√

be included with Static Data. The study aims to design the basic 3D visual effect to improve the above-given data figure.

We design the static column chart 3D layout plan as shown in Figure 2. The single-column chart has limited data and is clear to see the data, and the study uses the blue and red colors to highlight both sessions (Figure 2(a)). The single stacked column chart is the extended version of the single-column chart. The framework uses random colors with high contrast to highlight the data (Figure 2(b)). Both static column charts display the detailed percentage number in each session.

The static pie chart displays the pie in a 2D panel with 45-degree angles (Figure 3). The angles can provide the 3D perspective and the percentage number is beside each pie.

The 3D environment offers the line chart display with a three-axis (Figure 4). The line chart can straightly illustrate the trending in 3D mode and the position can display in the 3D environment.

3.2. Dynamic Data. Dynamic Data do not only provide the 3D layout but also allow us to play the trending with animation. The study aims to provide the convenience for users to analyze the dynamics trend. The study summarizes the chart which is suitable for animation. Dynamic Data includes regular column chart, pie chart, and line chart with a limited interaction in playing the animation.

Figure 5 displays the dynamic column chart 3D layout animation plan. The regular column chart has more data than the single-column chart. It usually contains data from multiple groups.

Using the animation can assist the user in contrasting the difference in groups (Figure 5(b)) and analyzing the growing trend (Figure 5(a)). The framework provides the horizontal and vertical columns in Figure 5.

Compared to the static pie chart, the dynamic pie chart uses the growing animation to represent the percentage (Figure 6). Each pie has a different height even though they have the same values. The percentage number is on the top of each pie. Different heights can assist the user in distinguishing the data belongs.

The dynamic line chart uses animation to represent the trend (Figure 7). The framework provides the key point highlight function. When the user marks the highlight option in the Excel file. It can display the key point value when the animation reaches the point.

3.3. Interactive Data. Compared to Dynamic Data, Interactive Data moves further, which focuses on interaction, animation, and 3D layout. The study aims to use interaction to lead the user to analyze the process and compare different groups' data conveniently. Therefore, "comparison" and "controlling" are the key features of Interactive Data.

Comparison figures usually compare different groups' data. Compared to regular column charts, the multiseries column chart has more information by lining different groups. Therefore, multiseries column charts should belong to the "comparison" group. However, different groups are usually hard to distinguish due to too many columns. Therefore, using interaction to display different states can improve the distinguishing result. The study designs the comparison interaction panel as shown in Figure 8. The panel provides the button to switch different groups. It also allows both groups are visible to compare. The user can easily distinguish the advantages of different groups.

A flow chart usually describes a complex working flow. A complex working flow has different conditions and results. It is hard to read due to various information and images. Therefore, it is necessary to provide the control flow

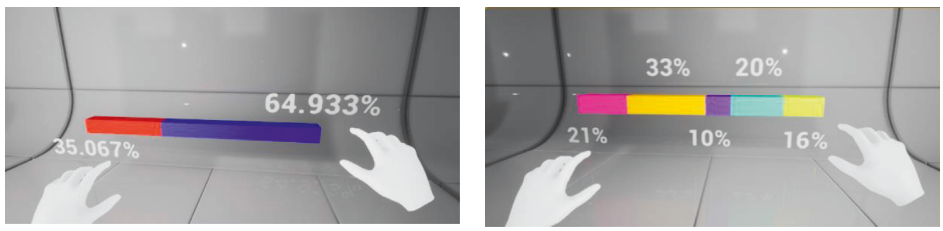

(a) (b)

Figure 2: Static Column Chart Overview in VR platform. (a) Single Column Chart; (b) single Stacked Column Chart.

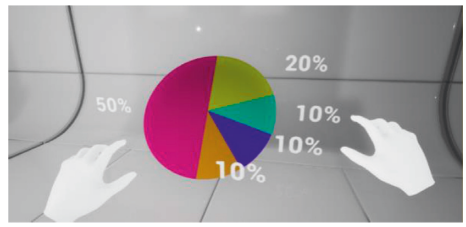

Figure 3: Static Pie Chart in VR platform.

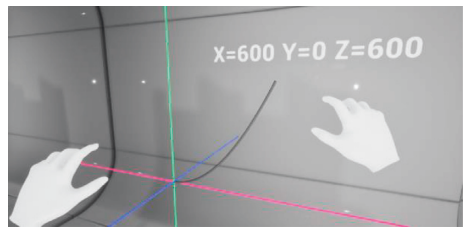

Figure 4: Static Line Chart in VR platform.

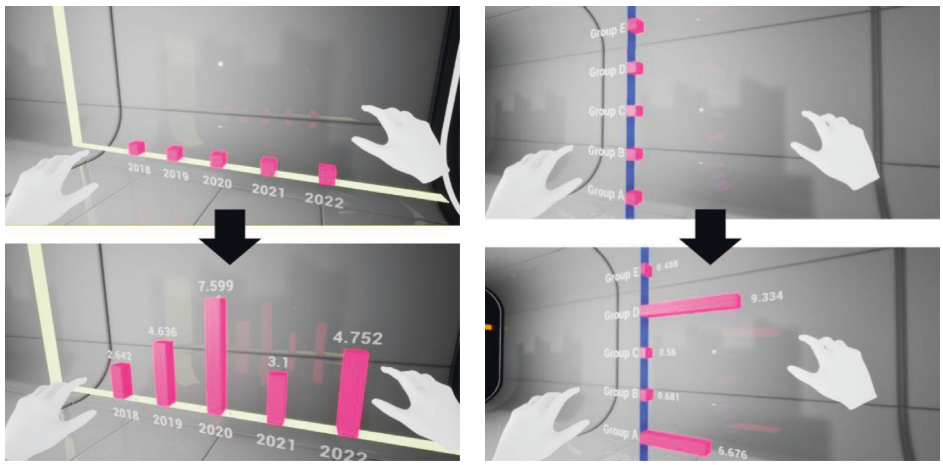

(a) (b)

Figure 5: Dynamic Column Chart Overview in VR platform. (a) Horizonal Column Chart; (b) Vertical Column Chart.

function. The 'controlling' can efficiently assist the user in checking different statuses.

Figure 9 displays the flow chart in Interactive Data. The interactive panel is in front of the chart. The user can select different statuses (previous and next) and results. The switching interaction can help the user to see how the research moves to the specific result by reducing other result information. Meanwhile, the user can check other statuses by switching the panel.

4. Evaluation

We conducted user studies to investigate the user experience in the VR reading through a questionnaire [23–26]. Formally, we have the following hypotheses: (1) our framework helps the users improve their reading efficiency in checking the figures. (2) Our framework helps increase users' immersive experience and engagement of the reading.

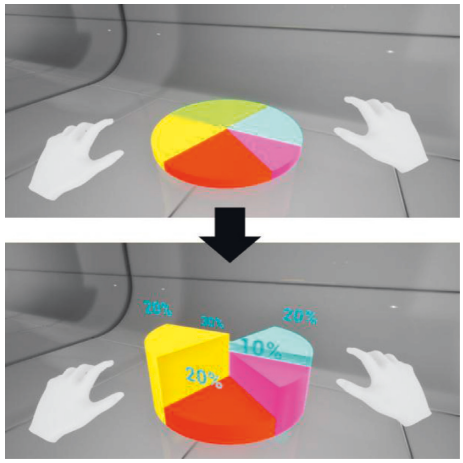

Figure 6: Dynamic Pie Chart in VR platform.

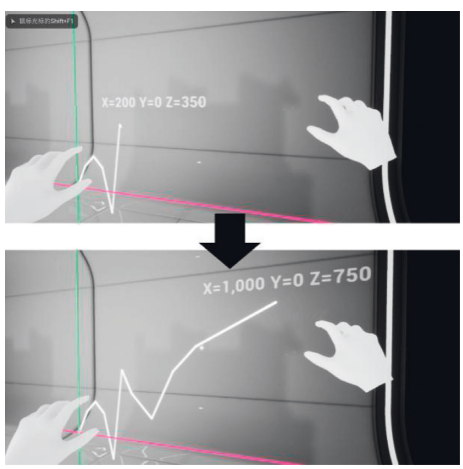

Figure 7: Dynamic Line Chart in VR platform.

4.1. Participants. Twenty participants (10 men, 10 women, aged 20–22 years old, $M = 21$) were recruited from Guangdong University of Finance to take part in this study. The study divides them into Group A and B. Group A and B are the experiment group. Group A uses VR devices (HoloLens (2) to interact with the 3D figures under our framework designed. Group B uses desktops to check the same data with traditional 2D reading mode.

4.2. Procedure. Group A participants took part in the interactive experiment. Figure 10 shows that the participants used HoloLens 2 to interact with the framework. Group B participants used desktops to explore the figures. Group A/B has 20 minutes time limitation to check 10 figures.

Table 2 displays the figures' distribution detail. All of Group B's figures are using the traditional 2D display. After the reading, participants were required to complete a brief questionnaire regarding the data information they watched. The questionnaire section includes five single choices and five judgments. The questionnaire covers the data information overview. The questionnaire asks for exact numbers

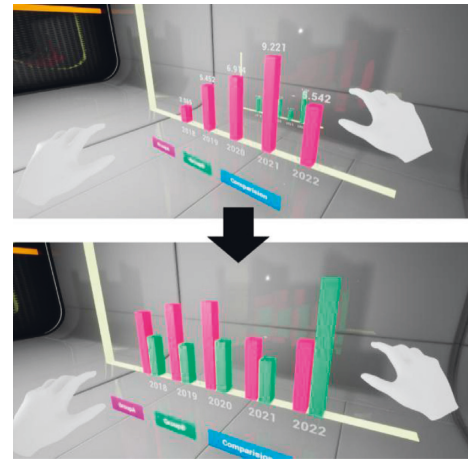

Figure 8: Multiseries column chart switching states in VR platform.

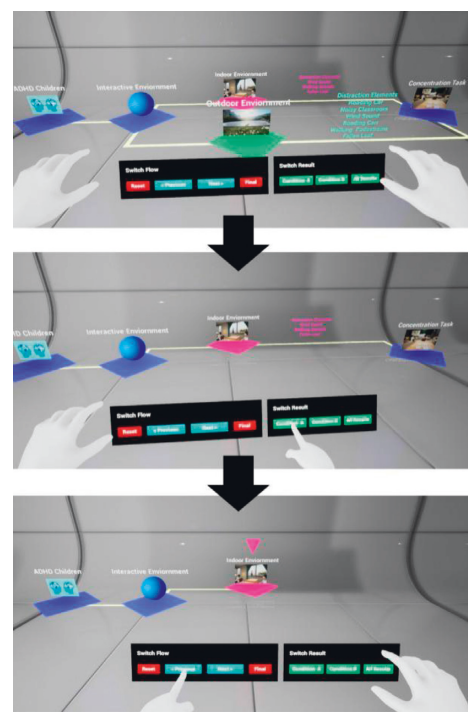

Figure 9: Interactive flow chart in VR platform.

such as maximum and minimum numbers. For instance, a question judges the trend in a dynamic line chart.

5. Results

The research collects the user score in two groups from questionnaire data. Figure 11 displays the user score distribution in each group. The research calculates the average and median score as shown in Table 3. For the data visualization framework, three trends are obtained as follows:

(1) It is encouraging that Group A has better performance in average and median score than Group B. But the superiority is very small which is only 3.07%.

Figure 10: Group a user test.

Table 2: User test Figures Distribution.

		Question numbers
Static Data	Static single column chart	1
	Static single stacked column chart	1
	Static pie chart	1
	Static line chart	1
Dynamic Data	Dynamic horizonal column chart	1
	Dynamic vertical column chart	1
	Dynamic pie chart	1
	Dynamic line chart	1
Interactive Data	Interactive flow chart	1
	Interactive column chart	1

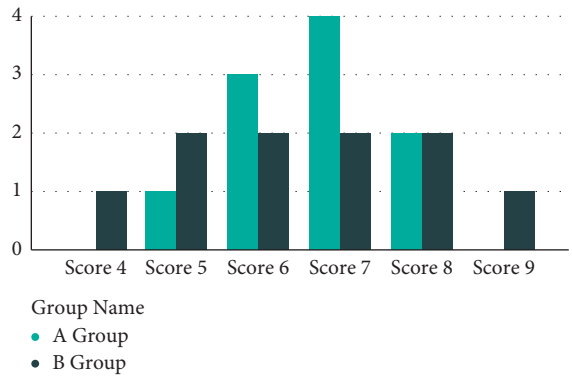

Figure 11: Group score distribution.

Table 3: User test score data.

	Group A (average score)	Group B (average score)
Static Data	2.4	2.7
Dynamic Data	2.8	2.9
Interactive Data	1.5	0.9
Total	6.7 7	6.5 6

(2) Group A has worse performance in Static Data. The average score is number is 11% lower than Group B.

(3) Group A has limited worse performance in Dynamic Data. The average score is number is 3.04% lower than Group B.

(4) Group A has better performance in Interactive Data. The average score is number is 66.67% higher than Group B.

Considering the above-given data, the data visualization framework can significantly improve performance efficiency, especially in Interactive Data. We conclude that the interaction can engage the user participant and remember the data. At the same time, the multiple-column chart and flow chart has more information than the Static and Dynamic Date Group. Therefore, it is significant that the VR interaction can assist with more complicated figures and information. The animation method can also provide similar experiences to the 2D reading. However, there are some existing issues. Significantly, the 3D figure without animation and interaction (Static Data) is worse than the traditional reading. We analysed that the Static Data contains simple figures which are easy to read. If we use the 3D display that may bring distraction due to the 3D environment and receive a negative effect. Therefore, we should consider that the simple figures do not fit with 3D reading.

Future research should optimize the Interactive and Dynamic Data. Furthermore, the controlling difficulty is another challenge for the users not familiar with VR applications. Therefore, the framework should provide more tutorial elements to decrease the difficulty. The study will consider the above data carefully and put forward the optimizing solution. The framework will continue to be optimized and contribute to the VR reading field.

6. Conclusion

In order to improve the reading user experience in VR platforms, the research aims to design a data visualization framework with VR characteristics. The paper finds that VR has a high potential to improve reading efficiency. The research discusses various figures, which is the key element for data visualization in social publications. A 3D data visualization framework is proposed to provide an immersive, explorative, and readable user experience. The framework divides data into three types: Static Data, Dynamic Data, and Interactive Data. The framework follows the VR features to provide a 3D visual effect and immersive interactive experiences. The research runs a comparative user test with 20 participants. The result shows that the framework is more attractive and efficient than reading the traditional 2D figures in VR platforms. Based on these evaluations, we believe that the proposed framework can be used as an effective reading tool for social science publications. The proposed

framework can improve user experience in the VR reading fields. Our research contains the VR reading field and uses VR interactive technology to improve user experiences. Future work continues to discuss data visualization and move to the VR text reading. We will use various statistical analysis methodologies such as mixed-ANOVA to measure the user experience after using the framework with pretest and post-test.

Data Availability

The data used to support the findings of this study are available from the corresponding author upon request.

Conflicts of Interest

The authors declare that they have no conflicts of interest.

Acknowledgments

This research was partly supported by the 14th Five-Year Planning Project for the Development of Philosophy and Social Sciences in Guangzhou (Grant no. 2022GZGJ290) and Department of Education of Guangdong Province and Guangdong University of Finance under Grant no. 2021WQNCX049.

References

[1] B. Arnaldi, P. Guitton, and G. Moreau, *Virtual Reality and Augmented Reality: Myths and Realities*, John Wiley & Sons, Hoboken, NJ, U.S.A, 2018.

[2] M. Speicher, B. D. Hall, and M. Nebeling, "What is mixed reality?" in *Proceedings of the 2019 CHI Conference on Human Factors in Computing Systems*, pp. 1–15, Glasgow, Scotland U.K, 2019.

[3] P. Milgram and F. Kishino, "A taxonomy of mixed reality visual displays," *IEICE - Transactions on Info and Systems*, vol. 7, no. 12, pp. 1321–1329, 1994.

[4] C. Flavián, S. Ibáñez-Sánchez, and C. Orús, "The impact of virtual, augmented and mixed reality technologies on the customer experience," *Journal of Business Research*, vol. 100, pp. 547–560, 2019.

[5] O. M. Zarka and Z. J. Shah, "Virtual Reality cinema: a study," *International Journal of Research and Analytical Reviews (IJRA)*, vol. 3, no. 2, pp. 62–66, 2016.

[6] S. Baceviciute, T. Terkildsen, and G. Makransky, "Remediating learning from non-immersive to immersive media: using EEG to investigate the effects of environmental embeddedness on reading in Virtual Reality," *Computers & Education*, vol. 164, Article ID 104122, 2021.

[7] P. L. P. Rau, J. Zheng, and Z. Guo, "Immersive reading in Virtual and Augmented Reality Environment," *Information and Learning Sciences*, vol. 122, 2021.

[8] VIVE Paper, "A new chapter of VR," 2021, http://www.vivepaper.com/en.html.

[9] Z. Zheng, B. Wang, Y. Wang et al., "Aristo: an augmented reality platform for immersion and interactivity," in *Proceedings of the 25th ACM international conference on Multimedia*, pp. 690–698, Mountain View, CA, U.S.A, October 2017.

[10] P.-L. P. Rau, J. Zheng, Z. Guo, and J. Li, "Speed reading on virtual reality and augmented reality," *Computers & Education*, vol. 125, pp. 240–245, 2018.

[11] F. Pianzola, K. Bálint, and J. Weller, "Virtual reality as a tool for promoting reading via enhanced narrative absorption and empathy," *Scientific Study of Literature*, vol. 9, no. 2, pp. 163–194, 2019.

[12] G. Thomas, "A typology for the case study in social science following a review of definition, discourse, and structure," *Qualitative Inquiry*, vol. 17, no. 6, pp. 511–521, 2011.

[13] P. Millais, S. L. Jones, and R. Kelly, "Exploring data in virtual reality: comparisons with 2D data visualizations," in *Proceedings of the Extended Abstracts of the 2018 CHI Conference on Human Factors in Computing Systems*, pp. 1–6, Montreal QC, Canada, April 2018.

[14] E. T. Njoya and A. M. Ragab, "Economic impacts of public air transport investment: a case study of Egypt," *Sustainability*, vol. 14, no. 5, p. 2651, 2022.

[15] R.-C. Jou and Y.-J. Day, "Application of revised importance-performance analysis to investigate critical service quality of hotel online booking," *Sustainability*, vol. 13, no. 4, p. 2043, 2021.

[16] Unreal Engine, "Driving gameplay with data from Excel," 2021, https://www.unrealengine.com/en-US/blog/driving-gameplay-with-data-from-excel?lang=en-US.

[17] L. Li, B. Lei, and C. Mao, "Digital twin in smart manufacturing," *Journal of Industrial Information Integration*, vol. 26, no. 9, Article ID 100289, 2022.

[18] Y. Wang and J. H. Sun, "Design and implementation of virtual reality interactive product software based on artificial intelligence deep learning algorithm," *ADVANCES IN MULTIMEDIA*, vol. 2022, Article ID 9104743, 7 pages, 2022.

[19] X. Zhang, "Virtual digital communication feature fusion based on virtual augmented reality," *Security and Communication Networks*, vol. 2022, Article ID 6345236, 7 pages, 2022.

[20] L. Li, T. Qu, Y. Liu et al., "Sustainability assessment of intelligent manufacturing supported by digital twin," *IEEE Access*, vol. 8, pp. 174988–175008, 2020.

[21] X. Ma, "Optimization of business English teaching based on the integration of interactive virtual reality genetic algorithm," *Journal of Electrical and Computer Engineering*, vol. 2022, Article ID 2455913, 9 pages, 2022.

[22] L. Li and C. Mao, "Big data supported PSS evaluation decision in service-oriented manufacturing," *IEEE Access*, vol. 8, no. 99, p. 1, 2020.

[23] P. Zheng, "The CAD digital automation analysis of costume designing based on immersive virtual reality models," *Advances in Multimedia*, vol. 2022, Article ID 3416273, 8 pages, 2022.

[24] Z. Tang, D. Zhang, and J. Q. Liu, "Investigation of fire-fighting evacuation indication system in industrial plants based on virtual reality technology," *Complexity*, vol. 2022, Article ID 2501869, 12 pages, 2022.

[25] L. Li, C. Mao, H. Sun, Y. Yuan, and B. Lei, "Digital twin driven green performance evaluation methodology of intelligent manufacturing: hybrid model based on fuzzy rough-sets AHP, multistage weight synthesis, and PROMETHEE II," *Complexity*, vol. 2020, no. 6, pp. 1–24, 2020.

[26] Y. Hong and Y. M. Ge, "Design and analysis of clothing catwalks taking into account unity's immersive virtual reality in an artificial intelligence environment," *Computational Intelligence and Neuroscience*, vol. 2022, Article ID 2861767, 12 pages, 2022.

Hindawi
Scientific Programming
Volume 2022, Article ID 1960038, 7 pages
https://doi.org/10.1155/2022/1960038

Research Article

The Application of 3D Printing Technology in Furniture Design

Shuguang Yang[1] and Peng Du[2]

[1]*School of Art and Design, Xuzhou Institute of Engineering, Xuzhou, Jiangsu 221000, China*
[2]*School of Art, Guangdong University of Foreign Studies, Guangzhou, Guangdong 510006, China*

Correspondence should be addressed to Peng Du; 10926@xzit.edu.cn

Received 11 May 2022; Revised 12 June 2022; Accepted 16 June 2022; Published 27 June 2022

Academic Editor: Lianhui Li

With the gradual deepening of the combination of 3D printing technology and the furniture manufacturing industry, the production of 3D printed furniture has begun to transition from experimental single furniture production to small batch furniture production, which will profoundly affect the manufacturing mode change of the furniture manufacturing industry in the future. This paper conducts a detailed study on the complex molding links, product development links, parts production links, and product body forming links of 3D printing technology in the furniture manufacturing industry. The design and printing process can provide practical reference for the manufacture of furniture products.

1. Introduction

In the context of the development of high-tech technologies, 3D printing technology has emerged as the times evolve. 3D printing technology has the advantages of digital and intelligent development and can be customized for specific products. 3D printing technology is a transformative digital additive manufacturing technology that manufactures three-dimensional objects through layer-by-layer superposition of materials influence. In recent years, with the development of this technology becoming more and more advanced, 3D printing technology has been widely used in aviation, transportation, manufacturing, and other fields [1–5]. 3D printing technology plays an important role in promoting the transformation of our country's manufacturing industry from the "Made in China" model at the low end of the industrial chain to the "Made in China" model, assisting the overall development of the manufacturing industry to upgrade from the downstream processing and assembly links to the upstream design and development links [6–8]. While the 3D printing technology continues to progress, promoting the combination of technology and specific industries is the only way to promote its long-term development [9, 10].

While the impact of 3D printing technology on the manufacturing industry has been deepening, the competition in our country's furniture manufacturing industry has become increasingly fierce [11–13]. How to correctly grasp the future development direction is a problem that most furniture manufacturers continue to explore. At present, in the overall development of the furniture manufacturing industry, enterprises continue to integrate, the market is constantly subdivided, and the professional division of labor is more clear. However, there are still serious product homogeneity, slow update speed, waste of resources, and serious pollution in the manufacturing process of furniture. It is difficult to meet consumers' needs for originality, diversity, and environmental protection of furniture products. Furniture manufacturing enterprises have an increasingly strong demand for the improvement of furniture manufacturing process and furniture modeling structure [14–17]. In addition, the intelligent upgrading of furniture products in the context of the development of intelligent manufacturing is also a gradually improved field in the furniture manufacturing industry. In recent years, the development of intelligent furniture has accelerated significantly [18–20]. In this situation of rapid changes in the furniture manufacturing industry, the rapid prototyping

characteristics of 3D printing technology and the superiority of solving complex technological processes have brought it into constant contact with the furniture manufacturing industry, and in the process of furniture production, technology plays an important role in the development of the industry. Increasingly, the mass customization trend of 3D printed furniture is taking shape. From the perspective of the development of 3D printing technology and the background of the furniture manufacturing industry, the application of 3D printing technology in the furniture manufacturing industry is an inevitable product for the continuous interaction between technological progress and market demands [2, 21–23].

With the advancement of 3D printing technology and the continuous decline of material manufacturing costs, the development of its technology research and equipment manufacturing has accelerated significantly, but the corresponding industrial applications are still facing a huge bottleneck period. Some domestic researchers in the field of 3D printing technology do not know enough about the specific industry needs, and there is a lack of specific industry support for research on 3D printing technology and materials, while the insiders in the furniture manufacturing industry also have less contact with 3D printing technology and have little understanding of new technologies. The lack of broad awareness of application methods and advantages has seriously hindered the further promotion of 3D printing technology in the furniture manufacturing industry. In the urgent need to open the communication channel of technological progress and industrial market, the research purpose of this paper is to analyze the application status of 3D printing technology in the furniture manufacturing industry and provide solutions to problems in the furniture manufacturing process through the application research of 3D printing technology.

2. 3D Printing Technology

3D printing technology is accurate in physical replication, and combined with scanning technology, more accurate replication effects can be obtained; there are various materials, and 3D printing technology can be used to print different materials to meet the needs of various fields; the printing speed is fast, which is comparable to traditional manufacturing. Compared with the process, it saves a variety of complex processing and improves the efficiency; the manufacturing cost is low, and compared with the traditional machine tool processing, it saves the cost of manufacturing materials and transportation, which can effectively reduce the cost; the degree of personalization can meet a variety of demands, wide range of manufacture, and fast delivery time. The emergence of new technologies has both advantages and disadvantages. 3D printing technology consumes a lot, which is more than 10 times that of the traditional manufacturing processes. Therefore, under the current social background that promotes green energy, 3D printing needs to be transformed to reduce the existing energy consumption; the combination of 3D printing technology and biotechnology will bring certain security risks to the society. If there is no restriction, there will be contradictions that are inconsistent with the development of technology; the emergence of 3D printing technology provides convenience for lawbreakers, and it is easy to cause certain threats to public security; at the same time, there are certain restrictions on the selection of material varieties. Today, with the rapid development of computer technology, it is easy to copy and transfer relying on 3D technology; equipment is expensive, and if it is to be widely promoted and applied, certain difficulties will be faced.

2.1. Basic Concepts of 3D Printing. The 3D printing technology is also known as rapid prototyping technology or additive manufacturing technology. 3D printing is based on three-dimensional models, using materials such as wires, powders, and liquids that can be melted and bonded by heating and layer-by-layer superimposition. However, the modern society is increasingly pursuing personalized customization, which is consistent with the advantages of 3D printing, such as short production cycles, small batch production, and convenient product shape change, so it brings space for 3D printing development.

2.2. Basic Types of 3D Printing

(1) Fused deposition type: this printing type of FDM is the most basic and elementary type of 3D printing. It mainly uses plastic filaments (ABS, PLA, nylon, etc.) to be heated and melted by the nozzle of the printer, and then, the materials are layered layer by layer. Extruded onto the printing platform, according to the slicing of the 3D model, the multilayer accumulation is carried out and finally the shaping of the solid model is completed. The overall process is similar to squeezing toothpaste, so this technology does not have high requirements on the printing environment and consumables and is relatively easy to use and control. It is generally used as an introduction to 3D printing and teaching.

(2) Selective laser sintering type: this printing type of SLS mainly uses powder (metal, ceramic, wax powder, plastic powder, etc.) as the material and is performed by sintering and bonding. During processing, the powder is first preheated to a temperature slightly below its melting point and then flattened under the action of a leveling stick; the laser beam is selectively sintered according to the layered cross section information under computer control. The molding method has the characteristics of simple manufacturing process, high flexibility, wide range of material selection, low material price, low cost, high material utilization rate, and fast molding speed. According to the above characteristics, the SLS method is mainly used in the foundry industry and can be used directly to make quick stencils.

(3) Light-curing three-dimensional molding: this printing type of SLA mainly uses liquid photosensitive resin and is cured by light. Light-curing

molding is the most widely used due to its high degree of automation in the molding process, good surface quality of prototypes, high dimensional accuracy, and the ability to achieve relatively fine dimensional molding.

2.3. Research Status of 3D Printing Technology. The time from theoretical research to practical application of foreign 3D printing technology is relatively early, and most of the fields involved are at the forefront of the development of the times, from 3D printing automobiles, aerospace parts, high-end medical models, and new concept architectural design to manufacturing and other applications. The 3D printing technology has also achieved leapfrog development in the field of foreign art design. Art design-related industries have made various cross-border attempts combined with the advantages of 3D printing technology. 3D printed shoes, clothes, accessories, etc., have appeared in world-class fashion for many times shows and art exhibitions. The new era has brought new opportunities for the application of 3D printing technology in indoor home furnishing. Foreign developed countries have carried out a lot of research and application in indoor interface modeling design and interior decoration construction. For example, in interior decoration products, Nervous System, a design firm from the United States, used generative algorithms to create the latest lamps made of nylon material. Nervous System is shown in Figure 1.

When the Nervous System light is turned on, the light will penetrate the hollow and divergent branch and leaf shells and project into the indoor space, making people feel like they are in a dream forest. In terms of interior furniture products, Dutch designer Drik Vander Kooij has designed "Endless Flowing" furniture, as shown in Figure 2.

By observing the chair, people will not realize that the Endless Flowing" chair is made of 3D printing. This is because Kooij uses a unique technology in 3D printing: Kooij 3D prints the chair, unlike most 3D printed furniture. When printing, the printer only moves back and forth. Instead, he allows his 3D printer to print in multiple directions to create a unique appearance.

Domestic research on 3D printing technology started relatively late, and there is insufficient research on 3D printing technology methods. Although there are individual units or individuals with advanced awareness about the use of 3D printing technology in China, they are not in-depth enough. The traditional domestic products in the home furnishing industry are relatively simple in shape and function, and the actual products manufactured cannot meet the original intention perfectly due to the limitations of craftsmanship. The application of domestic 3D printing technology is mainly at the architectural level and design level, and some cutting-edge technologies still have to be imported from abroad. Since most companies do not have a strong awareness of the application of 3D printing technology, they have not dig deeper or are skeptical of it and still design and manufacture household products in accordance with traditional concepts and processes. Facing the reform of new production methods and the "re-industrialization

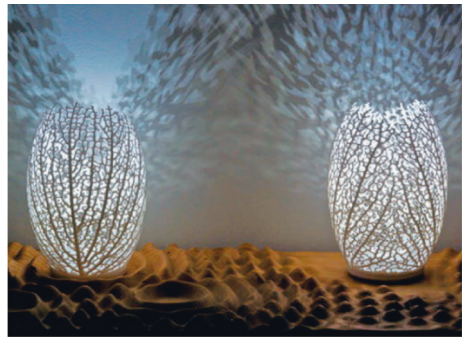

Figure 1: Vein lamps designed by Nervous System.

Figure 2: "Endless Flowing" furniture.

strategy" vigorously promoted by developed countries, the country attaches great importance to the R&D and industrialization of new digital manufacturing technologies such as 3D printing and intensifies personnel training, market cultivation, and application promotion. An example of the latest domestic experimental interior decoration works is the experimental villa of Shanghai Yingchuang Company's integrated printing of interior and exterior decoration and architecture, as shown in Figure 3.

With the development of the times, the new term "cross-border design" came into being. The innovative integration of craftsmanship is an important component of cross-border, and due to the requirements of new crafts and personalized design, 3D printing has become a tool that can concretize various personal tastes and materialized arts. The cooperation between interior decoration and 3D technology and convergence has become the inevitability of the times. The increasingly developed trend of 3D printing technology has greatly responded to people's claims of consumption and opened up a broader space for indoor home design. In the future, the application potential of 3D printing technology in indoor homes is huge, and it will better meet people's needs for personalized customization and modern smart home environment [15–17].

3. The Application of 3D Printing in Furniture Manufacturing

At present, the application scope of 3D printing technology in the furniture manufacturing industry is expanding, from

Figure 3: The world's tallest 3D printed building.

experimental single-piece furniture production to mold manufacturing, product development, parts production, and other manufacturing links. Its application mainly focuses on solving various complex problems such as shape complexity, material complexity, hierarchical complexity, and functional complexity in the production process. The 3D printing technology is closely related to the traditional furniture manufacturing process. The combination of new technology and traditional technology can cooperate to solve the problems of long R&D and production cycle and slow product update speed in the furniture manufacturing industry.

3.1. Application of 3D Printing Technology in Complex Furniture Molding. The application of 3D printing technology has promoted the current furniture manufacturing industry, which is firstly reflected in the simplification of the complex mold manufacturing process, which is used to solve the mold opening problem of some irregularly shaped furniture. In the prototype stage of furniture production such as upholstered furniture, metal furniture, and injection-molded furniture, some furniture or components need to be processed by plastic molding or metal casting and the furniture production is highly dependent on mold manufacturing.

Compared with traditional mold-opening methods, 3D printing technology is applied to the complex mold-making process of furniture products and its advantages are mainly reflected in the following aspects: first, it solves the rapid prototyping of complex shapes of molds and second, it saves the cost of furniture molding links. In the field of mold manufacturing, the application of 3D printing technology is also known as rapid mold manufacturing technology. This technology is used in conjunction with CNC machining centers, engraving machines, vacuum laminating machines, and other equipment to jointly provide rapid prototyping services for furniture molding. At present, the 3D printing technologies applied in the mold manufacturing process mainly include photocuring molding technology and selective laser sintering technology. The available printing materials include metal, plastic, ceramics, recycled paper, etc. When making molds with 3D printing technology, the shape of the mold is directly generated from computer graphics data, which can be adjusted at any time in the virtual model-making stage before the mold is printed.

3.2. The Application of 3D Printing Technology in the Research and Development of Furniture Products. At this stage, the application of 3D printing technology in the furniture manufacturing industry mainly focuses on the research and development of new furniture products and the printed furniture product prototypes are used for the appearance and structure verification of new products. The research and development stage of traditional furniture manufacturing usually requires multiple repeated communication processes such as product prototype design, mold making, and re-improving the prototype design. The one-time molding feature of 3D printing technology turns the repeated communication between furniture product design and mold production into direct printing of product prototypes, thereby simplifying the development process of furniture products as "furniture design-3D printing product prototypes-modifying product prototypes-reprinting and functional verification-final mold opening" process.

Specifically, the intervention of 3D printing technology is mainly to reduce the repeatability in the product development process through the following means:

(1) The performance of furniture products is pretested in the 3D model stage, and the process of determining the rationality of the design will be more concentrated in the stage of virtual model making and modification.

(2) The application of new technologies makes the design of furniture products take into account the satisfaction of product functions. The integrated molding of furniture products enables designers to obtain the prototype of furniture products more intuitively, better grasp the appearance and structure of furniture products, and improve the modeling accuracy. In the process of furniture design and modification, a variety of product prototypes can also be quickly printed, so that furniture product development can be upgraded from simple prototype trial production to conceptual model derivation, ergonomic analysis, visual analysis, form coordination and function testing, engineering comprehensive analysis of furniture products such as evaluation tests.

(3) We can concentrate on the product design department for mold making and small-scale trial production and reduce the time for docking with mold manufacturing enterprises, communication between company internal personnel, and product flow.

3.3. The Application of 3D Printing Technology in the Production of Furniture Parts. Since furniture products have high requirements on the structural strength and material adaptability of the connecting parts, the production of furniture parts mainly relies on standardized means to restrict the production of parts. In the assembly of traditional standardized connectors, the connectors are usually commissioned by furniture companies to produce parts manufacturers and complete the assembly in the furniture

assembly workshop. Although the standardized parts production process can meet the needs of various furniture connections, complex structural assembly processes are still required at the connections and furniture products exhibit obvious assembly characteristics. Therefore, furniture products are prone to wear and deformation of parts during use, and the service life is greatly affected by the firmness of the parts.

The application advantages of 3D printing technology in the production of furniture parts are as follows:

(1) The connectors are integrally formed by modular means, which reduces the use of screws and connecting hinges for furniture products, improves the degree of fit, and reduces the difficulty of parts production and assembly.

(2) In the mold-opening stage of traditional parts, a more concise mold shape is formed, so that the shape of the manufactured metal or plastic parts is more simplified, the structure is more reasonable, and it is beneficial to realize the simplified processing of complex structural parts.

(3) In addition to the initial process of applying 3D printing technology to furniture production, it can also exert its technical advantages in the process of secondary recycling of furniture, realize the processing of existing furniture incomplete parts, prolong the service life of furniture products, and obtain better quality products at a high environmental value.

3.4. The Application of 3D Printing Technology in the Molding of Furniture Main Body. In addition to the application in the auxiliary links of furniture production, the current industrial-grade 3D printers are mostly aimed at directly manufacturing molded products. The large-scale 3D printing equipment produced by some printer manufacturers specifically provides services for directly printing furniture products.

In the furniture main body forming process, the application advantages of 3D printing technology mainly include the following:

(1) 3D printing technology can reduce the time for auxiliary mold opening, parts production, assembly and splicing, and material consumption in furniture production, so that furniture products have the appearance characteristics of integral molding. 3D printing technology has successfully produced single furniture or small batch of furniture many times in the furniture manufacturing industry, and the products are mostly used for the manufacture and reproduction of high-end art furniture such as European-style or Chinese-style furniture.

(2) 3D printing technology can realize the one-time molding of the self-occlusal structure and cavity structure of the furniture. The printing of key parts of the furniture can remove the visual barriers of cumbersome mechanical parts and achieve a qualitative leap in functional innovation. The designer's consideration of the functionality of the work can be subtly realized through the modeling capabilities of computer modeling and 3D printing equipment. These structural features and plastic arts are usually difficult to achieve seamless assembly when they are made by cutting, molding, and other means.

(3) Manufacturers of 3D printing materials and equipment can conduct product research and development on nylon, wood-plastic, metal, resin, and other printing materials to obtain different textures of printing materials. These new printing materials realize the structural remodeling of traditional materials through the structural design of virtual three-dimensional models and provide new material choices for furniture production.

4. 3D Printing Furniture Product Model Practice

When the 3D printing equipment prints a single piece of furniture, its generalized manufacturing process consists of the following three parts: first, the acquisition of virtual 3D model data and format conversion are performed; second, the furniture is printed on the machine; finally, the post-processing after printing is performed.

4.1. Acquisition and Format Conversion of Virtual 3D Model Data. In the acquisition and format conversion of virtual 3D model data, there are mainly two steps as follows: first, acquisition of virtual 3D model data; second, model sorting and STL format conversion.

4.1.1. Acquisition of Virtual 3D Model Data. There are three main ways to obtain the virtual 3D data model of the furniture or parts to be printed: one is to establish 3D model data by means of traditional computer modeling software. The virtual 3D data modeling software that can be applied to 3D printing technology includes AutoCAD, Maya, 3DS MAX, Rhino3D, and other common commercial design software, and there are also relatively low-difficulty design software packages such as Blender, Sketch Up, and Tinkercad. At present, this method is the more commonly used modeling method. Through short-term learning, we can quickly grasp the modeling requirements of 3D printing furniture; the second is to establish 3D model data through parametric design software. Among the commonly used parametric design software, the mainstream application software is Pro/Engineer, UGNX, CATIA, and Solidworks. The modeling method of parametric design software can enable furniture products to establish various constraint relationships based on the parametric models, realize more intelligent programming design, and obtain the systematic and growing model effects so that furniture products can be standardized according to user requirements. With rapid customized modeling on the basis of products, this way of

building 3D data models is more in line with digital modeling thinking, so it can better utilize the advantages of 3D printing technology; the third is to obtain 3D models of existing furniture by using scanners and tactile devices After the furniture data is scanned by the 3D scanner, it needs to be converted into a triangular mesh model by a software. The advantage of this method is that it can realize the function of quickly copying the existing furniture products.

4.1.2. Model Sorting and STL Format Conversion. After acquiring the virtual 3D model data, it is necessary to scale and repair the model to adapt it to the size, model, and resolution of the printer used and then convert the data format of the furniture model after adjustment. After these virtual 3D models obtained by modeling or scanning are established, they need to be uniformly converted into a file format that can be read by the driver software of the 3D printer, usually into a printable multilateral network file, that is, a file in STL format. STL is one of the commonly used file formats for 3D printing. Specifically, small triangular patches in a large number of spaces are used to approximate the solid model, and the solid object is cut into digital cross sections or layers by software and divided into equal thicknesses along the Z axis. Slicing creates a two-dimensional image, which is transmitted to the machine according to the image information. Different materials are bonded and stacked layer by layer to form a three-dimensional entity, and then, the necessary code that can control the 3D printer hardware to construct the object is generated, which is stored in the database for future modification and use.

4.2. Printing Furniture on the Machine. After completing the processing of the 3D data model of the virtual space, the printing enters the specific manufacturing stage. When printing furniture, you need to choose a 3D printer that meets dimensional accuracy and structural strength to maintain continuous print jobs. The process steps are as follows.

4.2.1. Performing Layering and Support Settings. At present, the professional layering software mainly includes SLICER and SFACT. After the layering is completed, the generated GCODE file is transferred to the 3D printer. The thickness of each thin layer can be appropriately adjusted according to the type of printer and printing accuracy, generally in between tens to hundreds of microns. It is worth noting that the reasonable and accurate handling of complex models largely determines the success or failure of the printed product. The processed model needs to ensure that there are no overlapping triangles, and if there are overlaps and holes, the transcribed 3D model may break or the file may not be printed after transfer to the printer. For the problems of material consumption and printing time in large-volume solid virtual models, under the premise of ensuring the structural strength, the structure can be simplified and hollowed out to form a hollow shell-like object. This process needs to consider the following aspects: Firstly, the minimum wall thickness of the printing material needs to be met. Secondly, if it is a liquid printer, it is necessary to leave a minimum overflow hole when printing the model and finally set the width and height requirements of convex or concave detailed structures (such as yin and yang engraved characters) question.

4.2.2. Importing the Printer Program to Complete Printing. After finishing the previous link, the generated GCODE file is sent to the 3D printer for identification and printing, thus completing the acquisition and format conversion of the virtual 3D model data. In specific applications, printers of different molding methods and models are slightly different in receiving print data, which is embodied in differences in transmission speed, storage, and instruction set.

4.3. Postprocessing after Printing. After the main body of 3D printing furniture is completed, the key application difficulty is the postprocessing link. Like the furniture produced by the standardized production line, after the main body printing process of the furniture is completed, a series of postprocessing procedures such as grinding, polishing, and coloring of the furniture can be performed according to the requirements for the fineness of the molding surface and we can complete inspection and packaging of furniture products and finally complete furniture production.

At present, the postprocessing methods that can be used for 3D printing furniture mainly include the following: plastic, nylon, glass, and other parts. These are postprocessed by component splicing, sandpaper grinding, manual polishing, coloring, and steam smoothing; metal parts are processed by electroplating, oxidation, chemical conversion coating treatment, thermal processing, and other means for posttreatment. From the perspective of the entire production process, according to the structural characteristics and actual use of the product, various manufacturing modes such as printing first, processing after printing, processing while printing, and no processing after printing can be formed to complete large-scale, high-density, and high-quality products in a flexible and efficient way manufacturing of precision, complex products.

5. Conclusion

With the gradual deepening of the combination of 3D printing technology and the furniture manufacturing industry, the production of 3D printed furniture has begun to transition from experimental single furniture production to small batch furniture production, which will profoundly affect the manufacturing mode change of the furniture manufacturing industry in the future. This paper conducts a detailed study on the complex molding links, product development links, parts production links, and product main body forming links of 3D printing technology in the furniture manufacturing industry, as well as its general characteristics when using 3D printing equipment to print furniture products. The molding process, in the actual application process, needs to choose the appropriate printing

method according to the furniture production requirements and the characteristics of the printing equipment.

The application of 3D printing technology in the furniture manufacturing industry is a newborn calf compared to the current relatively mature furniture production technology. With the gradual expansion of the application depth in recent years, the state's support for this technology has also been unprecedentedly high. However, it is undeniable that due to the few examples of technology industry applications, the authors are still lacking in the ability to write papers and the research may be biased and not in-depth, such as statistical sorting of 3D printing technology data and specific cases in the argument. Analysis is not thorough enough. These reasons lead to the data legacy and some deficiencies in the research in this paper. These unresolved problems are also the key to the future development and application of 3D printing technology in the field of furniture manufacturing.

Data Availability

The dataset can be accessed upon request.

Conflicts of Interest

The authors declare that they have no conflicts of interest.

References

[1] Li Zhang, "Impact of 3D printing technology on the development of the industrial design[J]," *Applied Mechanics and Materials*, vol. 2773, no. 43 7-437, 2013.

[2] X. Li, D. Zhao, and J. Zhao, "A design case study: 3D printer software interface design based on home users preferences knowledge," *Proceedings of the Design Society: International Conference on Engineering Design*, vol. 1, no. 1, pp. 639–648, 2019.

[3] E. E. Petersen, R. W. Kidd, and J. M. Pearce, "Impact of DIY home manufacturing with 3D printing on the toy and game market," *Technologies*, vol. 5, no. 3, p. 45, 2017.

[4] M. Kocisko, M. Teliskova, J. Torok, and J. Petrus, "Postprocess Options for Home 3D Printers," *Procedia Engineering*, vol. 196, 2017.

[5] B. Donaldson, "CNC machining as a business strategy for 3D printing," *Modern Machine Shop*, vol. 93, no. 3, 2020.

[6] K. Peter, L. Rath, and H. Glor, "Building partnerships: using 3D printing to support take-home science activities," *Teacher Librarian*, vol. 47, no. 5, 2020.

[7] S.Da Guo, "Formative arts based on 3D printing technology," *Journal of Physics: Conference Series*, vol. 1533, no. 2, p. 022031, 2020.

[8] S.-H. Park, S.-B. Yi, and H.-M. Kim, "Developing guidance plan for problem-based learning utilizing 3D printing at the 'application of technology' area in Technology · Home economics subject at the junior high school level according to 2015 revision curriculum," *THE KOREAN JOURNAL OF TECHNOLOGY EDUCATION*, vol. 16, no. 2, 2016.

[9] Q. Wang, Xu Sun, S. Cobb, G. Lawson, and S. Sharples, "3D printing system: an innovation for small-scale manufacturing in home settings? – early adopters of 3D printing systems in China," *International Journal of Production Research*, vol. 54, no. 20, pp. 6017–6032, 2016.

[10] K. Shirin, E. Duffy, F. Smeaton Alan, and M. Aoife, "Monitoring of particulate matter emissions from 3D printing activity in the home setting," *Sensors*, vol. 21, no. 9, 2021.

[11] S. Bhattacharjya, L. A. Cavuoto, B. Reilly, W. Xu, H. Subryan, and J. Langan, "Usability, usefulness, and acceptance of a novel, portable rehabilitation system (mRehab) using smartphone and 3D printing technology: mixed methods study," *JMIR Human Factors*, vol. 8, no. 1, p. e21312, 2021.

[12] R. Whitwam, "The price of (Legally) 3D Printing Your Own Metal AR-15 rifle at home," *ExtremeTech.com*, 2014.

[13] C. Atwell, "3D print your home with cement," *Design News*, vol. 69, no. 8, 2014.

[14] P. K. Jain and P. K. Jain, "Use of 3D printing for home applications: a new generation concept," *Materials Today Proceedings*, vol. 43, no. P1, pp. 605–607, 2021.

[15] Anonymous, "3D printing company SQ4D prints three-bedroom home in 48 hours," *Design Cost Data*, vol. 64, no. 2, 2020.

[16] A. Developer, "Demonstrates speed, labor efficiency in 3D-printed home," *Concrete Products*, vol. 123, no. 2, 2020.

[17] A. Sika, "Celebrity architect BIG team on 3 D printing demonstration," *Concrete Products*, vol. 122, no. 9, 2019.

[18] S. Agarwala, G. Guo Liang, J. An et al., "Wearable bandage-based strain sensor for home healthcare: combining 3D aerosol jet printing and laser sintering," *ACS Sensors*, vol. 4, no. 1, pp. 218–226, 2019.

[19] Jeff Kerns Technology, "Recycle at home with 3D PRINTING," *Machine Design*, vol. 90, no. 8, 2018.

[20] K. Gábor, "3D printing at the highest quality in a home environment," *Journal of Applied Multimedia*, vol. 13, no. 2, 2018.

[21] T. Rayna and L. Striukova, "From rapid prototyping to home fabrication: how 3D printing is changing business model innovation," *Technological Forecasting and Social Change*, vol. 102, no. Jan, pp. 214–224, 2016.

[22] W. Wang, T. Y. Wang, Z. Yang et al., "Cost-effective printing of 3D objects with skin-frame structures," *ACM Transactions on Graphics*, vol. 32, no. 6, pp. 1–10, 2013.

[23] E. Zolfagharifard, "Home Makers: 3D Printing Has Helped Fuel a New Generation of DIY producers," *Engineer*, no. DEC, 2012.

Hindawi
Scientific Programming
Volume 2022, Article ID 8651415, 9 pages
https://doi.org/10.1155/2022/8651415

Research Article

Design and Application of the Piano Teaching System Integrating Videos and Images

Lina Li

Suzhou University Academy of Music, Anhui, Suzhou 234000, China

Correspondence should be addressed to Lina Li; lilinasj@ahszu.edu.cn

Received 18 May 2022; Revised 11 June 2022; Accepted 15 June 2022; Published 27 June 2022

Academic Editor: Lianhui Li

The art of piano playing has been continuously entering into people's life. However, with the continuous improvement of science and technology and living standards, the traditional teaching mode can no longer meet the piano teaching mode. The teaching of piano is different from traditional subjects, such as Chinese and mathematics. It requires students to experience the artistic characteristics and the live atmosphere of the players brought by the piano. This study integrates video and image teaching methods with piano teaching. Videos and images can more intuitively show the live atmosphere brought by piano players and musical artistic features brought by the piano. At the same time, this study uses the convolutional neural network (CNN) method to study the relevant features of videos and images of piano teaching. These features are mainly the characteristics of piano music, the behavior of players, and the basic knowledge of a piano. The research results show that the clustering method can effectively classify the features of videos and images in piano teaching, and the maximum classification error is only 1.89%. The CNN method also has high performance in predicting the relevant features of piano teaching videos and images. *Accuracy*. The largest prediction error is only 2.23%, and the linear correlation coefficient also exceeds 0.95. This set of the piano teaching mode that combines videos and images is beneficial to both teachers and students.

1. Introduction

The traditional teaching method is to use the blackboard or PPT to impart knowledge. With the continuous progress of computer-aided teaching methods and hardware equipment, the teaching mode has also undergone great changes [1]. Computers can help people with some tedious tasks. It can also display teaching content in the form of pictures or flow charts. It more intuitively shows teaching knowledge to the students. This is different from the traditional teaching mode. The piano teaching mode is different from the traditional methods of mathematics and Chinese subjects. Mathematics and Chinese teaching modes are knowledge and methods that need to be taught in textbooks. However, a piano is a teaching mode that needs to be understood [2, 3]. Piano art not only embodies the meaning of music itself but also embodies the humanistic feelings of the connotation of music. Therefore, the piano teaching mode is not a simple superposition of knowledge, it also requires students to experience the connotation of piano art. This requires the teaching mode of piano art to be improved. Traditional teaching methods can only allow students to learn the basics of piano, such as musical notation, musical notes, etc. It does not allow students to appreciate the humanities in it [4, 5]. The PPT method can allow students to learn piano knowledge in the form of pictures, but this method is far from enough. A piano is an artistic method that combines musical instruments and music, and it is also closely related to the emotional performance of the audience. The piano teaching classroom also requires students to combine the music scene and the form of the piano performance to carry out effective learning. The video method can record the ambient atmosphere, music atmosphere, and the content of the piano performance at the music scene, and it can effectively record the performance of the audience and the performer. Piano learners can learn more knowledge from piano-playing videos [6, 7]. The image can effectively record the key piano performance, it can capture the mood and

performance content of the piano player very well. However, the content of videos and images needs to be grasped and captured efficiently by the pianist, which requires big data technology to capture the key content of videos and images and relevant knowledge. This study intends to design a piano teaching mode by combining videos and images, which will better capture the content of the piano performance and the atmosphere of the scene. The research on the relationship between the content of videos and images and the content of the piano performance requires big data technology to analyze.

A convolutional neural network (CNN) can better extract the spatial features of data and it can also better map the relationship between input and output [8]. It has been widely used in many fields, such as image recognition and feature extraction. CNN can have higher efficiency and computing power than manual methods, so it can handle the relationship between large amounts of data very well. Video methods will contain many image features, and CNN can have better feature extraction capabilities in both videos and images [9, 10]. This research integrates videos and images to design a piano teaching mode, which mainly designs feature extraction. It also does not involve temporal features, so the CNN method was chosen in this study. The CNN method is also an intelligent algorithm that has developed rapidly in recent years, and many research objects have complex mapping relationships. However, there is relatively strong nonlinear correlation between these complex data. It is difficult for manual methods to deal with these problems with experience or professional knowledge. CNN methods can use these complex data to find correlations between data. At present, big data technology has produced algorithms related to spatial feature extraction or temporal feature extraction [11, 12]. There are relatively few temporal features involved in piano teaching videos and images recognition. Therefore, this study only selects the spatial features of piano teaching videos and images. CNN has relatively high requirements on computers and hardware devices. With the continuous advancement of science and technology, there will be huge amounts of data in every field. The larger the magnitude of the data, which requires deeper CNN to complete the feature extraction task [13, 14]. The birth of GPU technology makes it possible for CNN to develop to a deeper level. The computing power of GPU technology will be many orders of magnitude superior to the computing power of CPU. The piano video technology has more image features, and the GPU technology provides more technical support for the feature extraction of the video method.

This research will solve the shortcomings of the traditional piano teaching mode, it uses video and image methods to design a new teaching method for piano teaching. At the same time, CNN technology is used to extract spatial features existing in piano video and image teaching, and it can also be used to complete the extraction of nonlinear relationships. This set of an intelligent piano video and image teaching mode will not only effectively extract the piano player's behavior information and music and art content embodied by the piano but also improve students' learning efficiency and interest. Compared with the teaching mode of the blackboard or PPT, the teaching mode of videos and images will attract more students' attention. When students' learning attention and learning interest are improved, piano learners will gain more piano teaching knowledge.

In this study, a new piano teaching mode was designed using the form of videos and images. At the same time, this study uses the CNN method to extract the relevant features of piano video and image teaching. This study will be introduced from five aspects. Section 1 introduces and analyzes the defects of the piano teaching mode and the research significance of the CNN method in piano teaching. The research status of the mode of piano teaching is introduced in Section 2. The piano teaching mode and the CNN method combining videos and images are introduced in Section 3. Section 4 analyzes the feasibility and accuracy of CNN for feature extraction of videos and images in piano teaching mode, which is the core part of this research. Section 5 summarizes the full text.

2. Related Work

The piano is an art form that can reflect the art of music and humanistic feelings, and it can also integrate the audience and the performer into an art form. There is a big difference between piano teaching and the teaching mode of traditional subjects. Many researchers have conducted a lot of research on the teaching mode of a piano. Cui [15] uses augmented virtual reality technology AR to study the relevant skills of piano teaching. This study mainly proposes an online piano teaching mode. It selected a number of college students in Heilongjiang to study the relevant situation of the piano, which mainly includes the learners' subjective attitudes and personal learning progress. The results of the study found that 89% of students had a significant improvement in the learning of musical terminology, which was mainly in reading sheet music and using music materials. This online piano teaching mode provides a new teaching mode and development direction for piano teaching. Pi [16] believed that piano education can alleviate teaching fatigue and improve the teachers' happiness index. This study discusses the relationship between work fatigue and piano education. It mainly uses qualitative and quantitative methods to study the relationship between piano education and the teachers' happiness index. The results of the study show that piano teaching can improve work motivation and efficiency. At the same time, it found that the happiness index of most teachers in piano teaching is at a low level, and this research will help to improve the happiness index of piano teachers. Liu [17] has found that the current piano teaching mode lacks comprehensiveness and scientificity, and it has been unable to use the development of the piano teaching mode. This study uses BP neural network technology to establish a mode of the music signal and the piano teaching performance score. It selects well-known piano works as the test set to verify the effect of the mode. The research results show that this method can effectively verify the working level of the piano. It can accurately

provide players with a certain scoring reference. This method can not only improve the musical level of piano performance but it can also help to improve the talent of a piano. Xue and Jia [18] found that information technology has brought about tremendous changes in the development of all areas of life. However, the teaching and learning of music and musical instruments is a huge challenge for teachers and students in remote areas, and this artistic discipline is extremely disadvantageous to teachers and students in remote areas. This study uses the multi-information classification (MSC) algorithm of artificial intelligence technology to study the piano teaching mode in remote areas. This algorithm will be spread through the wireless network, it can effectively spread the teaching knowledge of a piano. This teaching mode can efficiently classify the piano information data. The research results show that this piano teaching mode is beneficial to teachers and students in remote areas. Li [19] found that deep learning technology and artificial intelligence technology will provide more technical support for the improvement of modern piano teaching quality. It studies note detection methods for piano teaching using convolutional neural networks. The input to the CNN neural network is the music signal for piano teaching. The results of the study show that the intelligent piano teaching method can improve students' interest in learning piano. This method will improve children's interest and efficiency in learning piano. Huang and Ding [20] proposed a back-propagation neural network piano teaching evaluation system. This can solve the problem that traditional note recognition methods are easily affected by noise. It used the optimized BPNN algorithm to accurately measure the pitch of the note and the time value of the note. The research results show that this mode can effectively correct the pitch problem in the piano teaching process, which is 5.21% higher than the traditional method. The optimized BPNN algorithm can significantly improve the error correction accuracy of the player's note and pitch, which is beneficial to improve the teaching quality of piano teaching. Guo et al. [21] used wireless network technology to realize the intelligent piano teaching mode. It uses the regression fitting algorithm and the Relief F weight algorithm to extract the characteristics of the piano teaching process. The results of the study found that the use of intelligent algorithms can quantitatively analyze the relevant characteristics of the piano teaching process. This is conducive to the reform of the piano teaching mode. Through the above literature review, it can be found that artificial intelligence technology has been applied in the process of piano teaching, and it is mainly used to identify signal features, such as notes. This study mainly uses CNN to identify the features in the teaching process of piano videos and images. This is an innovative study. Most of the studies mainly use neural network methods to study the timbre and note characteristics of piano teaching. However, this study utilizes the CNN method to perform feature extraction on videos and images of piano teaching.

3. Piano Video and Image Teaching Program, Design, and Algorithm Introduction

3.1. The Significance of the CNN Method for Piano Teaching. In order to solve the shortcomings of the traditional piano teaching mode, this research introduces video and image methods into the piano teaching classroom, which realizes a new piano teaching scheme. The CNN method will assist in the recognition of video and image features. There are huge data features in the videos and images in the piano teaching plan, and these features have relatively large correlation with the musical features of the piano and the behavioral features of players. It is difficult to teach these characteristics only by relying on teachers' professional knowledge and teaching experience. CNN methods can efficiently and accurately identify and extract these features. Then, the CNN method can also realize the mapping of piano teaching features to video and image information. These relevant information can be transmitted to piano learners through computer-aided systems. If the CNN method is not used to extract piano-related features in the piano teaching classroom plan, this will limit the display of piano features. Some music or player characteristics cannot be visually displayed through video and image methods. In short, the CNN method is more important for the piano teaching system, especially it involves the relevant information of the videos and images of the piano.

3.2. The Design and CNN of Piano Teaching Scheme Integrating Videos and Images. The goal of this research is to integrate video and image methods into a piano teaching method, and then it utilizes a CNN method to identify the relevant features of piano videos and images. The identified features will be visually displayed to the students or teachers through the computer-aided system. This will improve the learning interest and learning efficiency of piano learners. Figure 1 shows the piano teaching scheme and workflow that integrates videos and images. First, the features of the piano videos and images are processed into data between 0 and 255. These data will then be normalized to be between 0 and 1. It needs to feed piano-related video and image data into the CNN algorithm in the form of an input layer. However, these data need to be classified by a classification algorithm before being input into CNN, which is beneficial to improve the accuracy of prediction. The classification algorithm will perform effective classification processing according to set classification criteria. This research needs to map the feature relationships between piano videos, images and piano music features, player behavior features, and piano connotations. After these three features are processed, it will be visually displayed to teachers and students through a computer-aided system. Although this piano teaching method seems to be more complicated. However, once this teaching scheme is trained, it only takes a few seconds to achieve the mapping of relevant features. In an actual piano teaching session, this only takes a few seconds. This is also an efficient and accurate

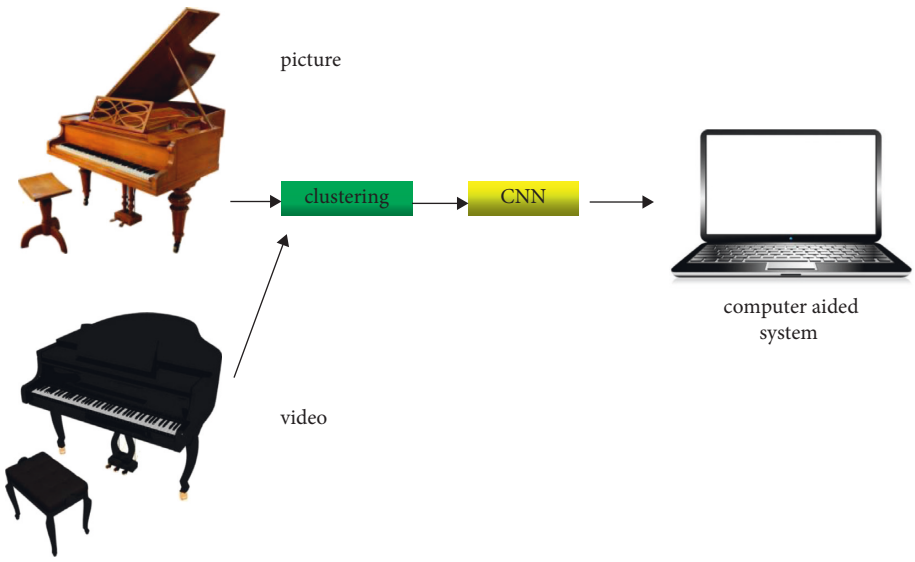

Figure 1: System design of piano teaching scheme integrating videos and images.

way from a time perspective. The computer-aided system will display the piano teaching features extracted by CNN to the students or teachers. Videos or images of piano teaching are also displayed to students or teachers through computer-aided systems.

The CNN method has great advantages in feature extraction and data mapping. It is also good at processing huge amounts of data and features. There is also a huge amount of data and associated features in the videos and images in piano teaching classes. These advantages of the CNN method are precisely to deal with the characteristics in piano teaching. Figure 2 shows the workflow of the CNN method. The CNN method has certain similarities with the fully connected neural network, which also utilizes the mechanism of forward propagation and back propagation. At the same time, its gradient descent is also carried out by means of derivation. However, it is more efficient than the fully connected neural network because it has a certain weight sharing mechanism. The weights of each layer are not connected to each other, it is selectively connected, which reduces the amount of parameter calculation. CNN can generally extract features with strong correlations. It will selectively filter features with weak correlation. CNN generally consists of multiple layers of convolutional layers, pooling layers, and activation functions. The process of feature filtering in CNN is carried out through the filters and strides of the convolutional layers. The output layer of CNN will perform error operation with the label data of piano teaching. The gradient descent method will calculate derivation based on the error between the predicted value and the actual value of the piano teaching. The step size used in this study is 1, and the number of filters is set to 64, which is a relatively common numerical range. Meanwhile, in order to fully exploit the features of piano videos and images, the learning rate is set to 0.0001.

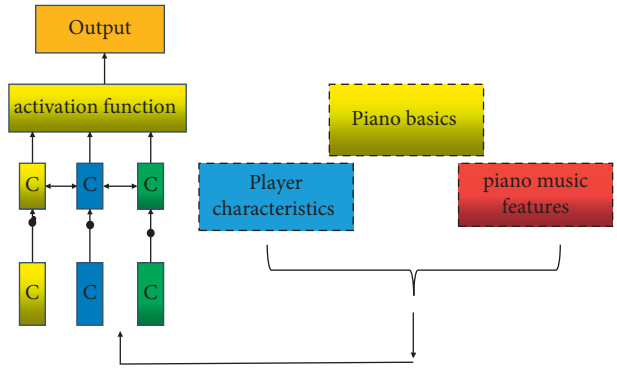

Figure 2: The workflow of the CNN method.

The difference between CNN and the fully connected neural network mainly reflects the existence of more hyperparameters, which are the source of feature selection and feature filtering. Different hyperparameter combinations will affect the accuracy and convergence of calculation results. Equation (1) shows the computational relationship that is satisfied between the hyperparameters. s represents the step size of feature selection. p represents the padding step size of the matrix. k represents the number of CNN filters.

$$w' = \frac{(w + 2p - k)}{s} + 1. \tag{1}$$

CNN is similar to other neural networks. It also has forward propagation mechanism and back propagation mechanism. These weights and biases are derived using automatic differentiation techniques. Equations (2) and (3) show the unfolded shape of weight derivative calculation at each layer. This is also the expanded form of loss function calculation.

$$E = \frac{1}{2}\sum_{k=1}^{m}\left[d_k - f\left(\text{net}w_k\right)\right]^2 = \frac{1}{2}\sum_{k=1}^{m}\left[d_k - f\left(\sum_{j=0}^{n}\omega_{jk}y_j\right)\right]^2, \tag{2}$$

$$E = \frac{1}{2}\sum_{k=1}^{m}\left[d_k - f\left(netw_k\right)\right]^2 = \frac{1}{2}\sum_{k=1}^{m}\left[d_k - f\left(\sum_{j=0}^{n}\omega_{jk}y_j\right)\right]^2 = \frac{1}{2}\sum_{k=1}^{m}\left[d_k - f\left[\left(\sum_{j=0}^{n}\omega_{jk}f\left(\sum_{j=0}^{q}u_{ij}\chi_i\right)\right)\right]\right]^2. \tag{3}$$

The derivation operation is a method to find optimal weights and optimal biases. Equations (4) and (5) show the calculation methods for the derivation of weights and biases. It can be seen that the gradient descent method is used here. Equation (6) shows the computation between each convolutional layer.

$$\Delta u_{ij} = -\eta\frac{\partial E\partial}{\partial u_{ij}}, \tag{4}$$

$$\Delta\omega_{ji} = -\eta\frac{\partial E}{\partial\omega_{ji}}, \tag{5}$$

$$\frac{\partial E}{\partial k_{ij}^{\zeta}} = \sum_{u,v}\left(\delta_j^{\zeta}\right)_{uv}\left(p_i^{\zeta-1}\right)_{uv}. \tag{6}$$

3.3. Introduction to Piano Feature Data Classification Algorithm. The video and image data in piano teaching differ greatly in magnitude and numerical size. If these data are fed into the CNN network layer together, this will lead to the problem of uneven weight distribution. The uneven distribution of weights leads to large errors in the results. Therefore, before feeding the video and image data of piano teaching into CNN, this data needs to be classified. The purpose of classification processing is to effectively classify different features. This allows the same type of features to have the same data distribution. Figure 3 shows the computational flow of the classification algorithm. It can be seen from Figure 3 that the classification algorithm can classify data with the same distribution characteristics together, and it can also separate different characteristics. In this study, the classification method of clustering was selected, which grouped the data of the same category into one category and processed different data separately. This classification method is processed according to the distance of data features.

When processing the data of piano teaching videos and images, the clustering method is mainly based on the distance of the data. Equation (7) shows the expression for the Euclidean distance, one of the commonly used distance

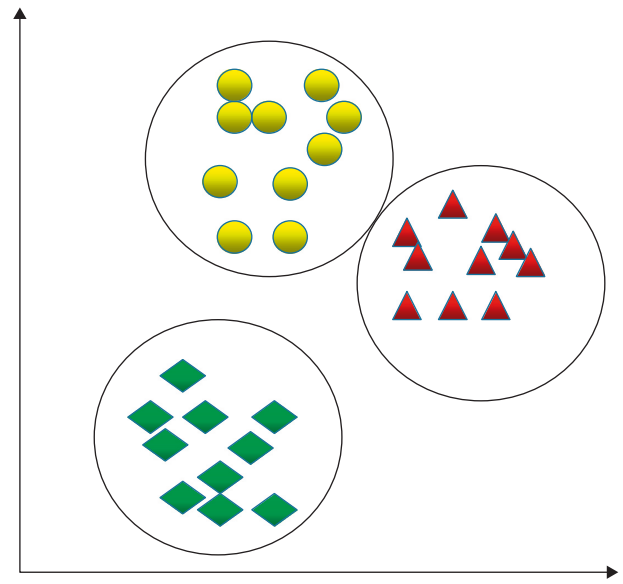

Figure 3: Clustering methods classification methods and principles.

measurements. Euclidean distance measures the distance between two points.

$$\text{dict}_{ed} = \sum_{k=1}^{m}\left(x_{ik} - x_{jk}\right)^2. \tag{7}$$

Equation (8) shows the Chebyshev distance measurement method. It measures the difference in distance between the coordinate values of points in space. Equation (9) shows the Minkowski's distance measurement method. This is also a variant of the Euclidean and Chebyshev distances. There is a p-value here, and when p takes different values, it represents a different distance measurement method.

$$\text{dict}_{cd} = \lim_{t\longrightarrow\infty}\left(\sum_{k=1}^{m}\left|x_{jk} - y_{ik}\right|^l\right)^{1/l}, \tag{8}$$

$$\text{dict}_{\min d} = \sqrt[p]{\sum_{k=1}^{m}\left|x_{ik} - y_{jk}\right|^p}. \tag{9}$$

Equation (10) shows the evaluation index of the external performance of classification. Among them, a, b, c, d represent different features of piano instruction videos and images. Equation (11) shows the Rand statistic, where P is the precision and R is the recall.

$$R = \frac{a+d}{a+b+c+d}. \tag{10}$$

$$F = \frac{\left(\beta^2+1\right)PR}{\beta^2 P + R}. \tag{11}$$

4. Result Analysis and Discussion

4.1. Classification and Prediction Error Analysis of Piano Videos and Images. The goal of this research is to use the

classification algorithm and the CNN algorithm to study the video and image features in the piano teaching process. In this study, video and image information of piano art courses in many colleges and universities in Hangzhou was selected as the research dataset. It will be divided into training set and test set. The test set is also a dataset derived from a college piano art course. This will ensure the reliability of algorithm verification.

In the piano teaching system integrating videos and images, the first step is to use the clustering algorithm to classify the related features of videos and images. The classification accuracy will affect the prediction accuracy of the CNN algorithm for videos and images in piano teaching. Figure 4 shows the classification errors of three features for videos and images of pianos. It can be seen from Figure 4 that the classification errors of the three related features of the piano are all within an acceptable range, and all the classification errors are within 2%. This is acceptable enough for teaching content with videos and images of the piano. The largest classification error is only 1.89%, and this part of the error mainly comes from the classification of the characteristics of piano players. The smallest classification error is only 1.23%, and this part of the error mainly comes from the classification of piano music features. This is mainly because there is a relatively large mutation in the characteristics of piano players. For the classification of the piano music feature method, this part of the error is only 1.52%. The classification errors of these three main features are all within 2%. This is a reliable error for both teachers and students of piano teaching.

After the three features of the piano videos and images are effectively classified, the CNN algorithm is required to predict the three features. This is a critical step for the piano teaching mode that combines videos and images. The video and image features of the piano predicted by CNN will be intuitively displayed to teachers and piano learners. The accuracy of the CNN algorithm in the piano teaching mode is also the key to the success of the fusion video and image piano teaching system. Figure 5 shows the prediction errors for three video and image features in the piano teaching mode. Overall, the CNN method has high feasibility and accuracy in predicting the characteristics of piano videos and images. This has high credibility for both teachers and students of piano lessons. All forecast errors are within 2.5%. The largest prediction error is only 2.23%, which mainly comes from the prediction of the characteristics of piano players. The characteristics of the pianist have a great relationship with the scene of the piano performance, and there is a great mutation in this part of characteristics. It is not just about the basics of the piano itself, so this part of the error is the biggest. Although this part of the error is the largest, it is also within a reasonable and acceptable range. The smallest error is also from the characteristics of piano music, and this part of the error is only 1.54%. The characteristics of piano music are closely related to the notes and spectrum of the piano. However, the mutation of this part of the characteristics is relatively small. This is because knowledge of the musical aspects of the piano is also less abrupt. The prediction error of CNN mainly comes from the

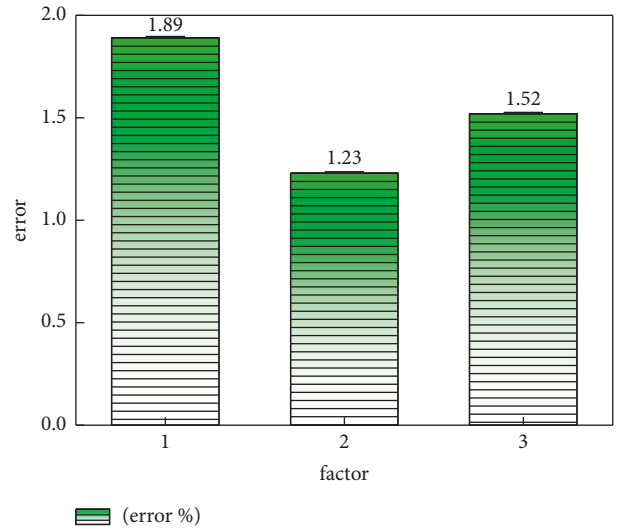

Figure 4: The classification errors of piano videos and images using clustering methods.

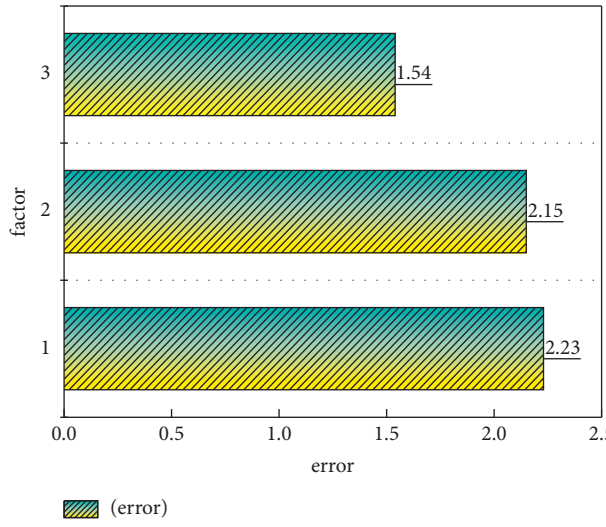

Figure 5: Three feature prediction errors of piano teaching mode using the CNN method.

error of the model and the error of the data. The reason for the relatively large error in this part is also that there is a certain cumulative error in the data when using the clustering method. In general, the CNN method can better complete the video and image prediction tasks in the piano teaching course.

4.2. Analysis of Three Characteristics of Piano Teaching Videos and Images. In this section, we discuss the piano music features, player behavior features, and basic piano features involved in videos and images in piano teaching. We selected 30 different sets of data to verify the accuracy and feasibility of CNN in predicting three features of piano teaching fusing videos and images. Figure 6 shows the distribution of predicted and actual values of musical features for piano teaching. In Figure 6, the green area represents the error of

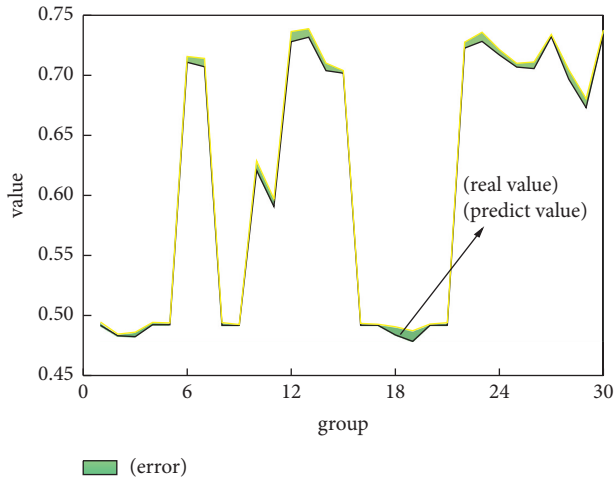

Figure 6: The predictive distribution of musical features in piano teaching.

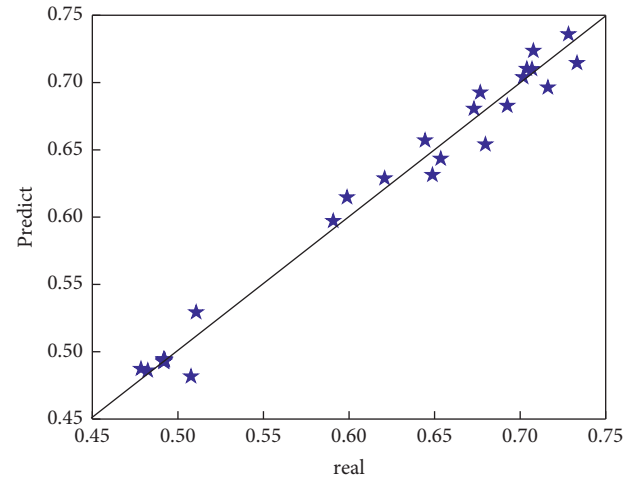

Figure 7: The correlation distribution of music feature prediction in piano teaching.

the predicted value of music features in piano teaching. The black lines represent the predicted values of the musical features of piano teaching. The yellow lines represent actual piano music characteristic values. In general, CNN can better capture the peaks and trends between different sets of data. Although there are many peaks and troughs in different groups of piano music characteristics, CNN can still capture the characteristics of these data as well. The green area represents the error between the predicted value and the actual value. It can be seen that the distribution of prediction errors for the musical characteristics of the piano is relatively small, and these prediction errors are relatively small. This further illustrates the feasibility and accuracy of CNN in predicting the characteristics of piano teaching music.

The linear correlation coefficient can further demonstrate the accuracy of CNN in predicting the characteristics of piano teaching music. If the linear correlation coefficient is closer to 1, it means that CNN has good performance in predicting the musical features of piano teaching. If the linear correlation coefficient is closer to both sides of the function $y = x$, it means that the linear correlation coefficient is closer to 1. Figure 7 shows the linear correlation coefficient distribution of the musical features of the piano teaching mode fused with videos and images. In general, all data points are relatively close to the linear function $y = x$, which means that the linear correlation coefficient exceeds 0.95. It can also indicate that the predicted value of the musical characteristics of piano teaching is relatively close to the actual value. In other words, the CNN method has been shown to be accurate in predicting the musical features of piano teaching fusing videos and images. This is an algorithm and the teaching system that students or teachers can trust.

The player's behavioral characteristics are also an important indicator in piano teaching. The player's behavioral characteristics can only be shown in the form of videos. It is difficult for traditional teaching models to capture the behavioral characteristics of performers. This shows that the piano teaching mode integrating videos and images designed

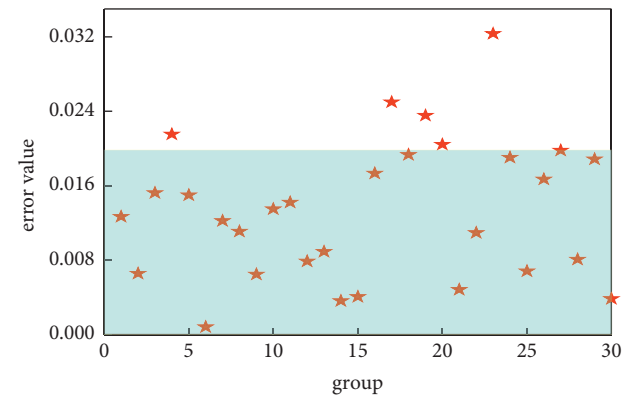

Figure 8: Scatter plot of player characteristics distribution in piano teaching.

in this study is innovative to a certain extent. Figure 8 shows the distribution of the prediction errors of the player's behavioral characteristics in the piano teaching mode. In Figure 8, the blue area represents data with prediction errors within 2%, a range where prediction effects can be distinguished. Overall, CNNs also have high reliability in predicting player behavior. Although the player's behavior information in the piano teaching mode has great volatility, it also has a great correlation with the piano performance scene. However, CNN has high reliability in predicting player behavior information for piano teaching. Most forecast errors are distributed within 2%. Only a small number of prediction errors exceed 3%. Basic knowledge of piano is also an important part of piano teaching. Figure 9 shows the distribution box plot of predicted and actual values for the basic knowledge of piano teaching. For the box plot, if the size of the box plot of the predicted value and the distribution of values are consistent with actual values, this indicates that the mode has a strong predictive ability. In general, the predicted value is basically the same as the actual value of the box, whether it is the size of the box or the distribution of the data. Basic knowledge of piano is

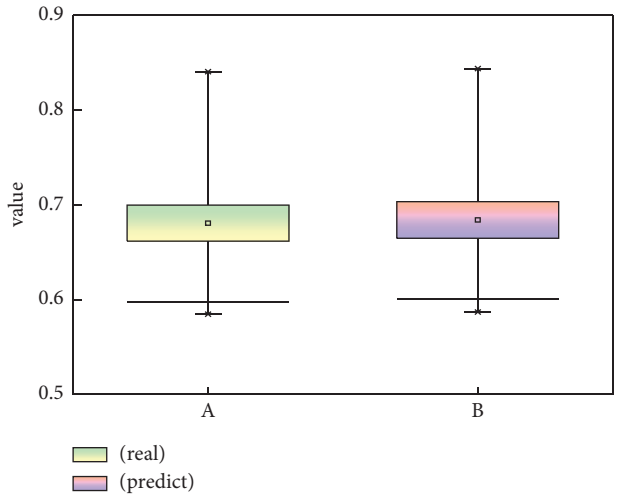

Figure 9: Predicted box distribution for the basics of piano teaching.

relatively easy to predict compared to the other two characteristics of piano teaching. CNN has basically reached a trustworthy level in predicting the basic knowledge of piano teaching.

5. Conclusion

With the advancement of technology and the improvement of living standards, the traditional teaching mode has limited the development of piano teaching. Piano teaching is a mode that is different from traditional subjects. It requires learners to experience the artistic information brought by piano. The player's on-the-spot performance will also have a certain impact on piano teaching.

This research introduces the teaching mode of videos and images into the teaching of piano, and it also uses CNN to predict the characteristics of piano music, player's behavior, and basic knowledge of piano in the piano teaching mode. Before using CNN prediction, this study also uses clustering methods to achieve the classification of piano video and image data. In terms of clustering, it shows certain feasibility in classifying relevant data of videos and images of piano teaching. The largest classification error is only 1.89%, and this part of the error comes from the relevant characteristic data of piano players. CNN also shows high accuracy in predicting the piano teaching features that fuse videos and images. The highest prediction error is only 2.23%, and this part of the prediction error also comes from the behavior characteristics of piano players. However, this part of the linear correlation coefficient exceeds 0.95. Overall, the design of this research is that the piano teaching mode that integrates videos and images will improve students' learning interest and efficiency, and CNN and clustering methods also show high accuracy in processing related features of piano videos and images.

Data Availability

The dataset is available upon request.

Conflicts of Interest

The authors declare that they have no conflicts of interest.

References

[1] A. Sepp, H. Ruismaki, and L. Hietanen, "Student teachers' and teacher educators' pedagogical reflections on piano courses in Finnish primary school teacher education," *Research Studies in Music Education*, vol. 4, no. 13, Article ID 221076997, 2022.

[2] A. Van and F. Villiers, "Psychological attributes of primary school piano learners preparing for regional and national music competitions in South Africa," *Muziki-Journal of Music Research in Africa*, vol. 18, no. 2, pp. 120–135, 2022.

[3] W. H. Luo and B. Ning, "Toward piano teaching evaluation based on neural network," *Scientific Programming*, vol. 2022, no. 5, Article ID 6328768, 2022.

[4] C. Lee and B. Leung, "Instrumental teaching as 'the noblest and the most under-praised job': multiple case studies of three Hong Kong instrumental teachers," *Music Education Research*, vol. 24, no. 1, pp. 42–55, 2021.

[5] Y. T. Niu, "Penetration of multimedia technology in piano teaching and performance based on complex network," *Mathematical Problems in Engineering*, vol. 11, no. 26, Article ID 8872227, 2021.

[6] Y. K. Yang, "Piano performance and music automatic notation algorithm teaching system based on artificial intelligence," *Mobile Information Systems*, vol. 4, no. 1, Article ID 3552822, 2021.

[7] Y. Zheng and B. Leung, "Perceptions of developing creativity in piano performance and pedagogy: an interview study from the Chinese perspective," *Research Studies in Music Education*, vol. 9, no. 25, Article ID 211033473, 2021.

[8] H. Z. Li, "Piano education of children using musical instrument recognition and deep learning technologies under the educational psychology," *Frontiers in Psychology*, vol. 12, no. 10, Article ID 7051116, 2021.

[9] J. F. Wang and F. F. Yang, "A fractional-order CNN hyperchaotic system for image encryption algorithm," *Physica Scripta*, vol. 96, no. 3, Article ID 035209, 2021.

[10] J. F. Zhao, X. Mao, and L. J. Chen, "Learning deep features to recognise speech emotion using merged deep CNN," *IET Signal Processing*, vol. 12, no. 6, pp. 713–721, 2018.

[11] T. Hsieh and J. Kiang, "Comparison of CNN algorithms on hyperspectral image classification in agricultural lands," *Sensors*, vol. 17, no. 6, Article ID 1724, 2020.

[12] Z. L. Hu, Q. Zhao, and J. Wang, "The prediction model of cotton yarn intensity based on the CNN-BP neural network," *Wireless Personal Communications*, vol. 102, no. 2, pp. 1905–1916, 2018.

[13] X. X. Jin, P. Peng, and Z. Huang, "Analysis of multi-level capital market linkage driven by artificial intelligence and deep learning methods," *Soft Computing*, vol. 24, no. 11, pp. 8011–8019, 2020.

[14] G. N. Li, X. W. Zhao, C. Fan, X. Fang, F. Li, and Y. Wu, "Assessment of long short-term memory and its modifications for enhanced short-term building energy predictions," *Journal of Building Engineering*, vol. 43, no. 9, Article ID 103182, 2021.

[15] K. X. Cui, "Artificial intelligence and creativity: piano teaching with augmented reality applications," *Interactive Learning Environments*, vol. 4, no. 13, Article ID 2059520, 2022.

[16] J. Pi, "Effect of ergonomics-based piano teaching on teachers' physical and mental health and the improvement of sense of

happiness," *Journal of healthcare engineering*, vol. 2022, no. 4, Article ID 9174441, 2022.

[17] X. Y. Liu, "Research on piano performance optimization based on big data and BP neural network technology," *Computational Intelligence and Neuroscience*, vol. 2022, no. 4, Article ID 1268303, 2022.

[18] X. M. Xue and Z. H. Jia, "The piano-assisted teaching system based on an artificial intelligent wireless network," *Wireless Communications and Mobile Computing*, vol. 4, no. 13, Article ID 5287172, 2022.

[19] W. Y. Li, "Analysis of piano performance characteristics by deep learning and artificial intelligence and its application in piano teaching," *Frontiers in Psychology*, vol. 12, no. 2, Article ID 751406, 2022.

[20] N. S. Huang and X. X. Ding, "Piano music teaching under the background of artificial intelligence," *Wireless Communications and Mobile Computing*, vol. 2022, no. 13, Article ID 5816453, 2022.

[21] R. Guo, J. N. Ding, and W. H. Zang, "Music online education reform and wireless network optimization using artificial intelligence piano teaching," *Wireless Communications and Mobile Computing*, vol. 4, no. 14, Article ID 6456734, 2021.

Hindawi
Scientific Programming
Volume 2022, Article ID 6802518, 9 pages
https://doi.org/10.1155/2022/6802518

Research Article

Analysis Model Design of the Intermediary Role of Psychological Expectation in Customer Value Proposition Driven Business Model Innovation against the Background of Big Data

Yong Wang [1,2]

[1]*School of Economics and Management, Southeast University, Nanjing 211189, China*
[2]*Zhejiang Business College, Hangzhou 310053, China*

Correspondence should be addressed to Yong Wang; 00334@zjbc.edu.cn

Received 29 April 2022; Revised 12 May 2022; Accepted 29 May 2022; Published 26 June 2022

Academic Editor: Lianhui Li

As the most important strategic resource of enterprises, big data has become the basic background of business model innovation. From the perspective of psychological contract, this paper discusses the mechanism of psychological contract in customer value proposition driven business model innovation and puts forward four research hypotheses. This paper adopts the confirmatory factor analysis method of structural equation to verify these four hypotheses. It is concluded that there is a significant positive relationship between customer value proposition and psychological contract; there is a significant positive correlation between psychological contract and business model innovation; and psychological contract has intermediary effect between value proposition and business model innovation. Furthermore, value proposition has a significant positive correlation with business model innovation, which has not been verified.

1. Introduction

Emerging information technologies and their applications have brought rapid growth in the amount of data, and the era of "big data" has come [1]. Big data is deeply affecting our life, work, and thinking [2, 3]. Big data has become the most important strategic resource for enterprises. Enterprises improve their competitiveness through the acquisition, cleaning, management, and processing of big data. Naturally, big data has also become an important driving force for business model innovation. Big data is affecting the business ecology of enterprises in various ways. It has become the basic background of business model innovation [4].

Big data represents a new way of life, which changes the demand content, demand structure, and demand mode of consumers [5–7]. Big data provides a new resource and capability and provides a new foundation and path for enterprises to discover value, create value, and solve problems. Big data is a new technology that provides basic conditions for the operation of the whole society. Big data is a way of thinking, which leads to the reconstruction of traditional concepts such as resources, value, structure, relationship, and boundary. Big data has the potential to be infinitely close to consumers and can provide accurate value proposition for enterprises [3, 8–10]. The application of big data technology helps us understand the real needs of consumers, accurately segment consumers, and then provide real-time and accurate products. As basic technical conditions and tools, big data resources have the energy to release and amplify the value of other resources. The key business and process innovation based on big data is the big data of enterprise business activities. The whole business process can be reengineered based on big data facilities and technology and data information flow. Big data is changing the resource environment, technology environment, and demand environment on which enterprises rely. Enterprises need to rethink the issues involved in the business model, such as who creates value, what value to be created, how to create value, and how to realize value.

In the era of big data, business enterprises have greatly increased their dependence on data. On the one hand, this will make the business model innovation based on data more convenient. On the other hand, this will also stifle the potential business model innovation without data support and greatly reduce the business model innovation not based on data. It can be seen that big data will bring changes in management rules and business model, thus bringing competitive advantages to enterprises. Big data has the potential to creatively destroy the business model [11].

Big data has become one of the driving forces of enterprise business model innovation. At the enterprise level, big data is used in many aspects of the business model, including customer value proposition innovation, key business and process innovation, revenue model innovation, external relationship network, and value network reconstruction [4]. Big data has the potential of creative destruction and promotes the transformation of the constituent elements and structure of the business model [12]. It is common to analyze the business model from the perspective of constituent elements and their relationship, which is also recognized by most researchers. Osterwalder et al. [13] proposed that enterprises can carry out business model innovation by changing the constituent elements in the business model system. Lindgadt et al. [14] proposed that there are two top-level elements of business model, namely, value proposition and operation mode, and believed that enterprises can choose one or several sub-elements to carry out innovation activities. Value proposition is an important component of business model and the starting point of business model innovation. It runs through the whole process of business model innovation and plays an important guiding role. It is very important to find a unique customer value proposition. In order to provide and realize customer value, enterprises must produce products or services with the help of corresponding resource capabilities and value networks, then transfer them to target customers, and obtain certain benefits. As Jiang and Liu [15] pointed out, business model includes value proposition, value creation, and value acquisition, which is the general framework of business model. This framework is systematic and dynamic.

In the context of big data, with the help of big data technology, enterprises can have in-depth insight into customer needs, timely respond to changes in customer needs, adjust the positioning of products or services, reduce transaction costs, reduce information asymmetry, enhance the emotional cognition between enterprises and customers and stakeholders, build psychological contracts, enhance trust relations, cultivate customer loyalty, and realize value creation and acquisition.

Since business model innovation is a systematic and dynamic work, it is a nonlinear process full of uncertainty from the proposition of customer value to the acquisition of customer value and enterprise value. The relationship between business model innovators, innovation teams, and business organizations; the relationship between stakeholders and business organizations; their psychological expectations and disappointments; and the relationship between rights and obligations are also constantly adjusted with the changes of business model innovation cycle. During this period, the formation, violation, and reconstruction of psychological contract will have a lot of impact on the effectiveness of business model innovation. However, there is a lack of research in this area.

Based on the above analysis, this paper intends to explore the intermediary role of psychological contract from the perspective of the general framework of customer value proposition driven business model innovation. Theoretically, it enriches the influence mechanism of psychological contract on business model innovation. In practice, it provides a reference for enterprises to implement business model innovation against the background of big data.

2. Conceptual Background

2.1. Business Model Innovation. Most scholars agree that changing the core elements of the business model or changing the relationship between the elements can realize the innovation of the original business model. Weill and Vitale [16] put forward the concept of atomic business model and believed that changing the combination mode of atomic business model can form a new business model. Yongbo [17] believes that business model innovation is the innovation of business model constituent elements and their combination, especially the innovation of the relationship between core value elements. Value proposition model innovation, value creation model innovation, value transmission model innovation, and value network model innovation are the main aspects of business model innovation. These four aspects play a role, leading to the continuous improvement of enterprise competitive advantage. In order to seek competitive advantage and fully explore the potential value of technological innovation or nontechnical service innovation, a set of continuous and dynamic logic to better realize the value proposition of consumers can be regarded as business model innovation [18].

Based on the above analysis, this paper believes that the business model innovation follows the construction logic, and the source of innovation is the customer value proposition. By establishing relations with different stakeholders, we can reach cognitive agreement and form a psychological contract, so as to obtain resources to create, transfer, and realize value.

2.2. Value Proposition. In the Internet era, against the background of big data, the internal and external environment change too fast, and the nonlinearity, uncertainty, and difficulty of prediction are becoming more and more obvious. Enterprises should constantly put forward new value propositions, constantly reflect, constantly improve, and innovate. The more complex it is, the more it is necessary to clarify the logic of development and find the pain points of customers. Among the components of business model innovation, the core element is customer value proposition. Business model innovation is a creative activity. From conception to formation, it is a continuous trial and

error exploration process. It is also the process from putting forward customer value proposition, perfecting customer value proposition, and implementing customer value proposition to realizing customer value proposition. All ideas and actions should focus on value proposition, constantly meet customer needs, and gradually cultivate customer loyalty. Customer value proposition is the core element of business model [19], the source of business model innovation, and the main line running through business model innovation.

Especially since 2000, with the advent of the Internet era, the development environment faced by enterprises has become more complex and full of uncertainty. The linear hypothesis is not tenable, product upgrading is accelerated, information transmission is convenient, big data plays a huge role, information exchange is almost cost-free, communication between manufacturers and customers is closer, and it is more common for customers to participate in enterprise design, interaction, and innovation. Business model innovation ushered in a new scene.

The emergence of a new customer value proposition is no longer a unilateral act of enterprises. Consumers have become "producers and consumers." Xiaomi mobile phone has created impressive performance. It is not so much product innovation as customer participation model innovation. It is the innovation of business model against the background of large data. It is a typical example of customer driven business model innovation, but also the deep participation of customers in the formation of customer value proposition, innovation of development, and perfection. Innovative customer value proposition drives the changes of other elements of the business model and changes the combination mode of the relationship between the elements of the business model. In a sense, it is an innovation in the construction of the relationship between the elements of the business model. The premise assumption of traditional value chain theory is that "industry" or "environment" factors are unchanged. However, this assumption obviously fails today. Modern business model innovation is to be good at changing value proposition, so as to reconstruct a microenvironment conducive to itself and create cross-border relationship combination [20]. Business model innovation is to reconstruct a new rule relationship [21]. The essence of business model is to continuously build a relationship combination across enterprise boundaries.

Building a new rule relationship is actually the shaping process of the new business model, which is a process of continuous trial and error, fault tolerance, and iteration. From the blueprint stage of customer value proposition to the conclusion of various cross-border relationships, it involves the cognitive problems of consumers, industries, and stakeholders, which is a process of psychological contract formation, violation, and reconstruction.

2.3. Psychological Contract. Psychological contract, which is also known as psychological contract, is a concept of social psychology. is a concept of social psychology. Its predecessor can be traced back to the interpersonal relationship theory in the early 1930s. In 1960, Chris Argyris, a famous American organizational psychologist, published understanding organizational behavior, in which psychological contract was first introduced into the field of management research from the field of social psychology, and the informal expectation relationship between factory employees and foremen was expressed as psychological work contract, which was considered to be the pioneer of psychological contract research in the field of management [22].

Robinson et al. [23] believe that psychological contract is the understanding of mutual obligations between employers and employees in the context of employment relationship, that is, employees' perception of the exchange relationship between explicit and implicit employee contributions and organizational incentives.

Early scholars tend to regard psychological contract as an invisible contract between organizations and individuals. There are two schools: unilateral psychological contract school and bilateral psychological contract school. The unilateral psychological contract school began in the 1980s, and its research focus is the individual level of the formation of psychological contract. Scholars who hold this view believe that psychological contract is essentially a subjective belief of reciprocal exchange and connection between individuals and organizations. This belief is based on the subjective understanding of commitment, but it is not necessarily realized by the organization or its agents [24].

There are many psychological contract schools on both sides: One is to define psychological contract as the sum of implicit and unwritten mutual expectations existing in the relationship between employees and employers. One view is that the cooperation mechanism exists between personal dedication and the acquisition of organizational desire. However, in essence, it is the mutual expectation relationship between employers and employees. It is the subjective feelings of both parties on each other's responsibilities and obligations, mainly including two levels: one is the employees' perception of mutual responsibility; the other is the perception of mutual responsibility, which is also known as the psychological contract school.

This paper holds that psychological contract is the perception of mutual responsibility between the organization and employees, including the stakeholders of employees and the organization. This is because, in the context of big data, the information asymmetry has been reduced unprecedentedly, the dynamic change process between psychological expectation and satisfaction will be more transparent, and the two-way nature of rights, responsibilities, and interests will be more obvious. Secondly, in the Internet era, the boundary of enterprises is blurred, the scope of organizations and employees participating in innovation activities is expanded, and even the organization is only a natural person and employees are not only employees of incumbent enterprises. As long as they contribute to innovation activities, they should be considered.

Li et al. [25] believe that psychological contract is mainly composed of three dimensions: transactional psychological contract, relational psychological contract, and management psychological contract.

Referring to the research of Robinson & Morrison, this paper divides psychological contract into three types: transaction contract, development contract, and relationship contract and discusses its relationship with business model innovation based on cognitive theory.

The formation of business model is a process of trial and error, and it is also a process of rule relationship. In this process, the change of the psychological contract of the business model innovation team is also dynamic, which needs to be transformed through formation, deconstruction, and reconstruction. In the initial stage of team formation‘ there is mistrust and uncertainty between the members and the team. The psychological contract of cooperation tends to be short-term and limited one. At this time, the model of psychological contract is economical. With the increase of cooperation time and cooperation opportunities among members of the team‘ members expect to have a good space for their own development. The team also hopes to obtain better output benefits with less human and material resources. Therefore, both the team and members have the motivation to promote the transformation of psychological contract to a developmental model. On this basis, the results of win-win cooperation will strengthen this sense of gain. This situation will gradually change to an open and collaborative mode, the organizational relationship will be more harmonious, the employees' sense of trust in the organization will be enhanced, and the team will have good output benefits. Employees also get a good space for their own development. At this time, a relatively stable relational psychological contract will be formed.

3. Research Hypothesis

Customer value proposition is a clear statement made by the enterprise on who to transfer benefits and what benefits to transfer [26]. Customer value proposition has strong trend and guidance, plays a good role in promoting the development of business model, and is the source of all business model innovation. The value orientation, value creation, and value acquisition in the value chain are realized through the value proposition of customers. For the characteristics of business model, it is an outward looking and creative exploration process, and all designs are based on customer value proposition. Johnson [27] pointed out that enterprises help target customers complete important tasks by providing a product or a service to meet their needs or solve problems. Target customers, supplies, and tasks to be completed are the three elements of value proposition. This concept emphasizes paying attention to the needs of target customers and the problem-solving degree of target customers, so as to provide products or services based on this. It is also the connotation of providing customers with value or service portfolio in the business model. Customer value proposition is the basis and source, the most active factor, and the soul of business model innovation [27, 28]. Reasonable value proposition is the premise of promoting business model innovation and creating value, which is the key for enterprises to obtaining competitiveness.

Based on the above analysis, this paper puts forward the first hypothesis.

Hypothesis 1. There is a significant positive correlation between customer value proposition and business model innovation.

Customer value proposition is the basis for customers to realize the delivered value and the starting point of enterprises' commitment to customers. Kotler [29] expounded customer value from the perspective of customer delivered value and believed that customer delivered value is the difference between total customer value and total customer cost. Gale Bradley [30] believes that customer value is the relative perceived quality of customers after the price of a product changes in the market. Holbrook [31] believes that customer value is created by goods through the process of customer experience. Whether the products or services provided by enterprises meet their needs or not, customers should perceive and evaluate the degree of satisfaction they have obtained. After comparing the expectation of the products provided by the manufacturer with the real gain, trust and satisfaction are generated, forming a psychological contract. It can be seen that customer value proposition is the basis for the formation of psychological contract between manufacturers and customers, and there is a positive correlation between them. Accordingly, this paper puts forward Hypothesis 2.

Hypothesis 2. There is a significant positive relationship between customer value proposition and psychological contract.

Most scholars believe that business model can be regarded as a structural template [32]. It can even be regarded as a configuration of measurement relationship [33]. Osterwalder [19] expressed the relationship in the business model as an abstract cooperative relationship between enterprises and stakeholders. Zott et al. [32] pointed out that the relationship between focus enterprises and stakeholders plays an important role in business model value creation. Due to the heterogeneity and dynamics of stakeholder relations and the diversity of value creation structure of business model, it will lead to the differentiation of value creation process and mechanism and the uncertainty of value creation results. However, in essence, the stakeholder relationship in the business model is also the subjective perception and comprehensive evaluation of stakeholders. Starting from the basic requirement of depicting the key and core characteristics of subjective perception, satisfaction, trust, and commitment can still be used as the basic dimensions of psychological contract between stakeholders [34]. Accordingly, this paper puts forward Hypothesis 3.

Hypothesis 3. There is a significant positive correlation between psychological contract and business model innovation.

The business model gradually realizes its logic of discovering, creating, transmitting, and obtaining value. In the logic of value creation, it involves the key business processes

of enterprises and the correlation mechanism between processes, including the operation mode of enterprises, consumers, upstream suppliers, potential entrants, and substitutes to create value in the competition. In the Internet era, new elements of business model are gradually taking shape. With the help of big data technology, the interaction between people becomes closer, and knowledge spillover and emotional communication become more frequent. The exchange of information between people and between people and organizations makes it easier to form psychological contracts, which promotes the continuous innovation of business models and the acceleration of the replacement of business models. This is also conducive to the effective coordination of value creation and business resources [32].

In this process of value creation, the psychological contract relationship between the individual members and the team in the organization implementing business model innovation reflects the unwritten mutual expectations between individuals and organizations and reflects the commitment and reciprocity of rights and obligations. If the content of organizational commitments and actions made by incumbent enterprises can stimulate the innovation spirit and team cohesion, the psychological contract relationship will be formed. Otherwise, there will be violation of the psychological contract relationship, degradation of innovation spirit, and lax team cohesion, which will inevitably affect the effectiveness of business model innovation. To stimulate the effectiveness of psychological contract in the context of big data, we should pay attention to the collective innovation, cognitive sharing, risk sharing, and cultivation of cooperative and enterprising awareness of business model innovation. Accordingly, this paper puts forward Hypothesis 4.

Hypothesis 4. Psychological contract has intermediary effect between value proposition and business model innovation.

4. Research Methods

4.1. Structural Equation Research Method. Social phenomena are complex, not as simple as natural phenomena. People and people, people and things, things and things are complex. Compared with general regression models, structural equation models are better for describing or fitting complex relationships and can be closer to objective reality. Structural equation model is mainly used to analyze and study the structural relationship between potential variables. Because potential variables cannot be measured directly, some measurable indicators are needed to reflect potential variables. These variables can be expressed in linear equations. This linear equation system is called structural equation modeling (SEM). SEM is suitable for the analysis of large samples. Generally speaking, the number of samples shall not be less than 100; otherwise, the software analysis is unstable.

SEM deals with the comparison of the overall model, so the indexes referred to mainly consider not a single parameter, but the coefficient of integration. At this time, whether individual indexes have specific statistical significance is not the focus of SEM analysis [35].

4.2. Questionnaire Design and Reliability Analysis

4.2.1. Questionnaire Design. Due to the fierce competition among enterprises, most enterprises pay attention to the confidentiality of their enterprise management information, especially the technological innovation and business know-how. It is difficult to conduct quantitative analysis in terms of business decision-making, partners, cooperation effect, and social benefits. Therefore, Likert quantitative scoring is often adopted in the study of enterprise business model. Ketokivi and Schroeder's research found that "although random errors and systematic deviations will cause some variation of measurement items, the perceived measurement of performance can still meet the requirements of reliability and validity." Whether from theoretical circles or business circles, people recognize the credibility of insiders' perception of the organization. Even without consulting financial data, they can have a basic judgment or even profound insight into the operation of the organization.

Based on the above considerations, the questionnaire is designed by Likert quantitative scoring. In order to design a high-quality questionnaire, the first draft of the questionnaire was completed on the basis of a large number of relevant references. After the first draft is completed, I invited colleagues and classmates with vice senior titles and doctorate degrees to help review and put forward suggestions. In addition, I also widely solicited the opinions of middle and senior managers of enterprises with whom I have contacts. In short, the questionnaire design widely mobilized contacts, solicited the opinions of experts and enterprise managers, and generated an open discussion at an academic seminar. Finally, these valuable opinions were classified and analyzed as an important reference for revision. The final questionnaire is targeted, readable, indirect, logical, and operable. In order to make the questionnaire conform to the reality and the purpose of the survey, at the beginning of the survey, the research team also interacted and modified based on the interview and the on-the-spot answers. Once there are questions about the meaning and measurement understanding, they will have in-depth communication and discuss how to improve the presentation together, so as to ensure the accuracy and clarity of the questionnaire. The questionnaire has been implemented for one year. The research team distributed it purposefully, even taking advantage of various opportunities such as business trips and family visits to distribute questionnaires. Through various channels such as training lectures for middle and senior managers of the enterprise, various seminars on economic management, on-site distribution, and interviews in the enterprise, a total of 160 questionnaires were distributed, and 155 were recovered, with a recovery rate of 96%. Excluding incomplete answers and similar and other unreliable questionnaires, the number of effective questionnaires was 150.

The final scale consists of 22 questions. Each option has five numbers: 1, 2, 3, 4, and 5. 1 means "very low," 2 means

Table 1: Corresponding table of model variables.

Latent variable	Connotation and item design basis	Measurable variable
Customer value proposition	Customer value proposition is to clearly state the interest combination to be provided to stakeholders, which should be attractive, differentiated, superior, and difficult for competitors to imitate [27, 36]	Q1 What is the social awareness of your products (services)? Q2 What is the degree of uniqueness of your products (services) relative to your competitors? Q3 Compared with peers and competitors, do you think your business model is different?
Psychological contract	Psychological contract is formed between employees and organizations as a variety of beliefs about each other's responsibilities and obligations [37]; the success of an enterprise requires teamwork [38]; consumer psychological contract is essentially a relationship of rights and obligations between enterprises and customers [39]	Q4 How satisfied are the partners with your business model? Q5 What is the degree of win-win benefits among the main partners of your business model? Q6 How stable is the relationship between your business model partners? Q7 How much knowledge is shared among your business model partners? Q8 How supportive are your business model partners?
Business model innovation	Whether it is a good business model depends on whether its performance exceeds the average level of the industry and whether it is sustainable, profitable, and expandable [40, 41]	Q9 What is the ability of your business model to attract key resources? Q10 How do you recognize the current market performance level of the enterprise? Q11 How confident are you that the current business model will shape the market performance of the enterprise in the next three years? Q12 How attractive is your business model to potential participants?

Table 2: Reliability test of latent variables.

Latent variable	Number of measurable variables	Cronbach's alpha
Customer value proposition	3	0.674
Psychological contract	5	0.884
Business model innovation	4	0.769
Total amount	12	0.916

"low," 3 means "general," 4 means "high," and 5 means "very high." The higher the score, the higher the recognition of the respondent for this option.

4.2.2. Setting of Latent and Measurable Variables of the Structural Equation Model (Table 1).

4.2.3. Reliability Analysis. Reliability is the degree of consistency or stability of measured data. Using SPSS version 22, Cronbach's test is carried out, and the coefficients obtained are shown in Table 2.

Generally speaking, the consistency of items is related to the measurement content. The larger the Cronbach α coefficient, the stronger the internal consistency. Previous studies have suggested that if Cronbach's α coefficient is greater than 0.7, it can be considered that the consistency between items is good.

Cronbach's coefficient value of Q1–Q3 items measuring customer value proposition in this study is 0.674, slightly lower than 0.7, and the values of the other items are more than 0.7, indicating that the corresponding items have high internal consistency. The overall Cronbach α coefficient value for the 12 items is 0.916, which has high consistency.

4.2.4. Model Design. The structural equation model shows [42–44] the standardized model (as shown in Figure 1). See Table 3 for the estimation results and test of business model innovation parameters by psychological contract, and Table 4 for the estimation results of standardization coefficient.

It can be seen from Table 3 that the CR values of all factor loads are much greater than 2. The probability that the parameters in the right column may be 0 P. Three asterisks, , indicate that the probability of 0 is less than 0.01. Therefore, all load coefficients are significantly nonzero at the significance level of 0.01. As can be seen from Table 4, the CR values of all variances are much greater than 2, so all variances are greater than 0.01 at the significance level of 0.01. It can be seen that the model estimation effect of psychological contract on the mechanism of business model innovation is good except BMI<---CVP.

4.2.5. Model Matching Analysis. It can be seen from Table 5 that the indexes meet the requirements when rounded, and the model fits well, indicating that the data matches the designed model. There is a significant positive correlation between value proposition and business model innovation, and Hypothesis 1 has not been verified.

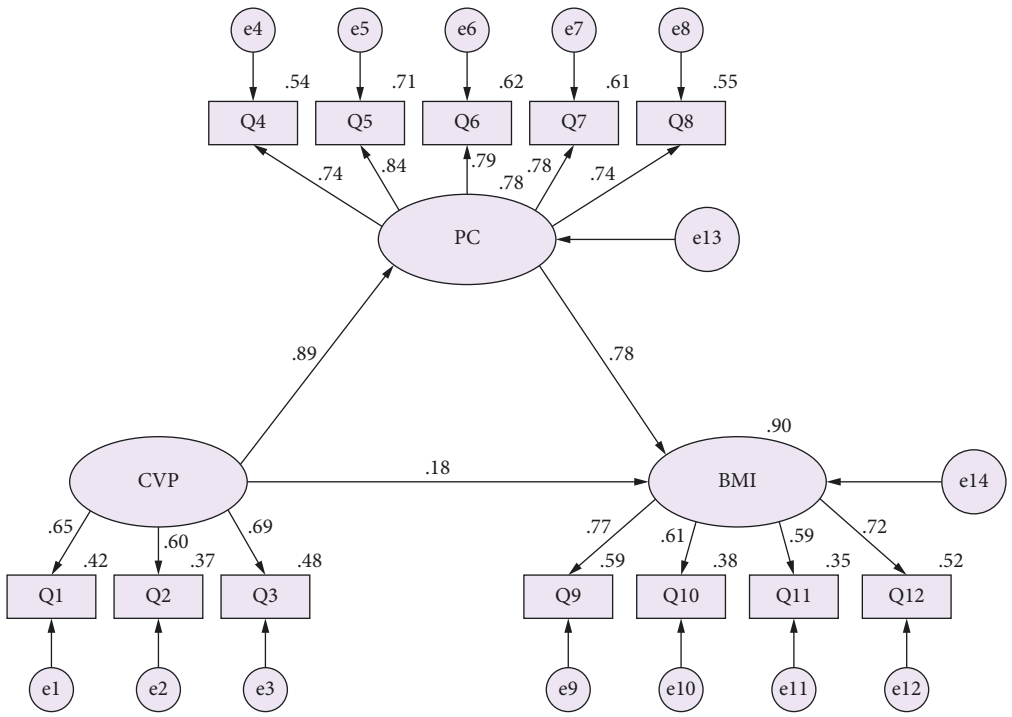

Figure 1: Structural equation model of the mechanism of psychological contract in business model innovation.

Table 3: Parameter estimation results.

			Estimate	SE	CR	*P*
PC	<---	CVP	0.917	0.154	5.943	***
BMI	<---	PC	0.801	0.248	3.230	0.001
BMI	<---	CVP	0.192	0.268	0.718	0.473
Q3	<---	CVP	1.000			
Q2	<---	CVP	0.852	0.144	5.919	***
Q1	<---	CVP	0.905	00.130	6.953	***
Q4	<---	PC	1.000			
Q5	<---	PC	1.249	0.123	10.140	***
Q6	<---	PC	1.167	0.123	9.451	***
Q7	<---	PC	1.187	0.128	9.255	***
Q8	<---	PC	1.092	0.120	9.068	***
Q12	<---	BMI	1.000			
Q11	<---	BMI	0.828	0.121	6.864	***
Q10	<---	BMI	0.844	0.120	7.009	***
Q9	<---	BMI	1.137	0.129	8.791	***

Table 4: Standardized regression weights.

			Estimate
PC	<---	CVP	0.885
BMI	<---	PC	0.784
BMI	<---	CVP	0.182
Q3	<---	CVP	0.692
Q2	<---	CVP	0.605
Q1	<---	CVP	0.646
Q4	<---	PC	0.738
Q5	<---	PC	0.845
Q6	<---	PC	0.785
Q7	<---	PC	0.778
Q8	<---	PC	0.741
Q12	<---	BMI	0.720
Q11	<---	BMI	0.593
Q10	<---	BMI	0.613
Q9	<---	BMI	0.766

Table 5: Fitting index.

Index name		Evaluation criterion	Index of this model
Absolute fitting index	CMIN/DF	<3	1.993
	GFI	>0.9	0.893
	RMR	<0.05	0.043
	RMSEA	<0.08	0.082
Relative fitting index	NFI	>0.9	0.892
	TLI	>0.9	0.925
	CFI	>0.9	0.942
Information index	AIC	The smaller, the better	155.644
	CAIC	The smaller, the better	155.644

Table 6: Standardized direct effects.

	Customer value proposition	Psychological contract	Business model innovation
Psychological contract	0.885	0.000	0.000
Business model innovation	0.182	0.784	0.000

Business model innovation <--- value proposition, $P = 0.472 > 0.05$.

Hypotheses 2 and 3 are verified. There is a significant positive relationship between customer value proposition and psychological contract. There is also a significant positive correlation between psychological contract and business model innovation.

The following is to analyze the intermediary role of psychological contract in customer value proposition and promoting business model innovation (see Table 6). The total utility is $0.182 + 0.885 * 0.784 = 0.876$. The intermediary effect is $0.885 * 0.784 = 0.694$. The proportion of intermediary utility in the total utility is $0.694/0.876 = 0.79$.

It can be seen that psychological contract plays a relatively large intermediary role in customer value proposition and promoting business model innovation, accounting for 79%. Hypothesis 4 is verified.

5. Conclusion and Discussion

Only three latent variables are selected in this paper, although there are many factors affecting business model innovation, which is a limitation of this research. In addition, there are only 150 samples, which is also a few number. In the future, in the context of big data, we should take external big data as a latent variable for in-depth research and discuss the impact of big data capability on psychological contract.

The policy enlightenment is that in the context of Internet big data, the implementation of business model innovation should pay attention to the role of relationship change and the research of psychological contract. In practice, we should strengthen the management of the psychological contract of employees and stakeholders; pay attention to the construction of system, culture, commitment, and trust; and constantly build a mood environment.

Data Availability

The dataset can be obtained from the author upon request.

Conflicts of Interest

The author declares that there are no conflicts of interest.

References

[1] M. Hilbert and P. López, "The world's technological capacity to store, communicate, and compute information," *Science (New York, N.Y.)*, vol. 332, no. 6025, pp. 60–5, 2011.

[2] V Mayer - Schonberger and K Chkie, *Big Data: A Revolution that Will Transform How We Live, Work, and Think*, Houghton Mifflin Harcourt, New York, 2012.

[3] L. Li and C. Mao, "Big data supported PSS evaluation decision in service-oriented manufacturing," *IEEE Access*, vol. 8, no. 99, p. 1, 2020.

[4] W. Li and J. Xia, "Business model innovation based on "big data"," *China industrial economy*, vol. 302, no. 5, pp. 83–95, 2013.

[5] Q. Chang, S. Nazir, and X. Li, "Decision-making and computational modeling of big data for sustaining influential usage," *Scientific Programming*, vol. 2022, 15 pages, 2022.

[6] L. Li, B. Lei, and C. Mao, "Digital twin in smart manufacturing," *Journal of Industrial Information Integration*, vol. 26, no. 9, Article ID 100289, 2022.

[7] Z. Bai and X. Bai, "Sports big data: management, analysis, applications, and challenges," *Complexity*, vol. 2021, Article ID 6676297, 11 pages, 2021.

[8] L. Li, T. Qu, Y. Liu et al., "Sustainability assessment of intelligent manufacturing supported by digital twin," *IEEE Access*, vol. 8, pp. 174988–175008, 2020.

[9] W. Huang, "Research on the revolution of multidimensional learning space in the big data environment," *Complexity*, vol. 2021, Article ID 6583491, 12 pages, 2021.

[10] Y. Gao, "Design of children's product packaging preference based on big data machine learning," *Wireless Communications and Mobile Computing*, vol. 2021, Article ID 8424939, 10 pages, 2021.

[11] Y. Jiang, *Analysis of eBay's business strategy in China based on dynamic competition theory*, Fudan University, Shanghai, 2013.

[12] H. Jing, "Research on business model innovation in the era of big data," *Scientific and technological progress and countermeasures*, vol. 31, no. 07, pp. 15–19, 2014.

[13] A. Osterwalder, Y. Pigneur, and C. L. Tucci, "Clarifying business models:origins,present,and future of the concept," *Communications of the Association for information systems*, vol. 16, 2005.

[14] Z. Lindgadt, M. Reeves, G. Stalk, and M. S. Deimler, "Business model innovation—When the game gets tough , change the game," *The Boston Consulting Group*, vol. 12, no. 9, pp. 1–8, 2009.

[15] W. Jiang and Y. Liu, "Connotation of business model and construction of research framework," *Scientific research management*, vol. 33, no. 5, pp. 107–114, 2012.

[16] P. Weill and M. R. Vitale, *Place to Space: Migrating to E-Business Models*, pp. 96–101, Harvard Business School Press, Boston, MA, 2001.

[17] S. Yongbo, "Business model innovation and competitive advantage," *Managing the world*, vol. 13, no. 7, pp. 182-183, 2011.

[18] H. Chesbrough and R. S. Rosenbloom, "The role of business model in capturing value from innovation evidence from Xerox corporation's technology spin—off companies," *Industrial and Corporate Change*, vol. 11, no. 3, pp. 529–555, 2002.

[19] A. Osterwalder, *The Business Model ontology—A Proposition in a Design Science Approach*, vol. 1, pp. 11–22, Universite de Lausanne, Écublens, Vaud, 2004.

[20] C. Zott and R. Amit, "The fit between product market strategy and business model:implications for firm performance," *Strategic Management Journal*, vol. 29, no. 1, pp. 1–26, 2008.

[21] L. Dong, X. Wang, X. Zhang, and X. Liu, "Research on rule-based business model -- function, structure and construction method," *China industrial economy*, vol. 16, no. 9, pp. 101–111, 2010.

[22] J. Zhang, Z. Yang, and Z. He, "Research on the loss control of knowledge workers from the perspective of psychological contract -- a case study of enterprises in Kunming," *Exploration of economic issues*, vol. 14, no. 12, pp. 152–158, 2009.

[23] S. L. Robinson, M. S. Kraatz, and D. M. Rousseau, "Changing obligations and the psychological contract: a longitudinal study," *Academy of Management Journal*, vol. 37, no. 1, pp. 137–152, 1994.

[24] F. Wei and W. Zhang, "New progress in the study of psychological contract theory abroad," *Foreign economy and management*, vol. 18, no. 2, p. 13, 2004.

[25] Y. Li, F. Wei, and S. Ren, "The impact of organizational psychological contract violation on managers' behavior," *Journal of management science*, vol. 22, no. 5, pp. 88–95, 2006.

[26] L. Dong and J. Su, "Technological revolution, institutional change and business model innovation -- on some major issues in the theory and practice of business model," *Journal of Southeast University: Philosophy and Social Sciences Edition*, vol. 13, no. 2, pp. 31–38, 2011.

[27] M. W. Johnson, C. M. Christensen, and H. Kagermann, "Reinventing your business model," *Harvard Business Review*, vol. 12, pp. 51–59, 2008.

[28] D. J. Teece, "Business models, business strategy and innovation," *Long Range Planning*, no. 43, pp. 172–194, 2010.

[29] P. Kotler, *Marketing Management*pp. 11-12, Tsinghua University Press, Beijing, 10 th ed edition, 2001.

[30] T. Gale Bradley, *Managing Customer value*, The Free, New York, 1994.

[31] M. B. Holbrook, "Customer value—a framework for analysis and research," *Advances in Consumer Research*, vol. 23, no. 1, pp. 138–142, 1996.

[32] C. Zott, R. Amit, and L. Massa, "The business model: recent developments and future research," *Journal of Management*, vol. 37, no. 4, pp. 1019–1042, 2011.

[33] M. Callon and F. Muniesa, "Economic markets as calculative collective devices," *Organization Studies*, vol. 26, no. 8, pp. 1229–1250, 2005.

[34] R. C. Runyana, B. STERNQUISTB, and J.-E. CHUNG, "Channel relationship factors in cross-cultural contexts: antecedents of satisfaction in a retail setting," *Journal of Business Research*, vol. 63, no. 11, pp. 1186–1195, 2010.

[35] R. Taisheng, *Amos and Research Methods Chongqing*, Vol. 08, Chongqing University Press, , Chongqing, 2010.

[36] M. Luo and L. Li, "Business model innovation in the Internet Era: from the perspective of value creation," *China industrial economy*, vol. 26, no. 01, pp. 95–107, 2015.

[37] R. Y. ShengtaiZhang, "Psychological contract breach, organizational commitment and employee performance," *Scientific research management*, vol. 32, no. 12, pp. 134–142, 2011.

[38] R. B. Reich, "Entrepreneurship reconsidered:the team as hero," *Harvard Business Review*, vol. 40, no. May-June, pp. 77–83, 1987.

[39] J. Shan, "Analysis on the impact of employees' Psychological Contract Violation on enterprises and its countermeasures," *Economic Research Guide*, vol. 31, no. 21, pp. 107–109, 2021.

[40] P. Timmers, "Business models for electronic markets," *Electronic Markets*, vol. 8, no. 2, pp. 3–8, 1998.

[41] X. Zhang, G. E. Hufei, Y. Zhao, and X. Liu, "Development and validity verification of typical business model characteristics scale," *Science of science and management of science and technology*, vol. 36, no. 03, pp. 56–66, 2015.

[42] R. Amit and C. Zott, "Value creation in e-business," *Strategic Management Journal*, vol. 22, no. 6/7, pp. 493–520, 2001.

[43] L. Li, C. Mao, H. Sun, Y. Yuan, and B. Lei, "Digital twin driven green performance evaluation methodology of intelligent manufacturing: hybrid model based on fuzzy rough-sets AHP, multistage weight synthesis, and PROMETHEE II," *Complexity*, vol. 2020, no. 6, 24 pages, Article ID 3853925, 2020.

[44] S. L. Rohinson and E. W. Morrison, "The development of psychological contract break and violation:a longitudinal study," *Journal of Organizational Behavior*, vol. 21, no. 5, pp. 525–546, 2000.

Hindawi
Scientific Programming
Volume 2022, Article ID 7129775, 10 pages
https://doi.org/10.1155/2022/7129775

Research Article

Design of Investment Potential Analysis Model of Integrated Energy Project Based on Deep Learning Neural Network

Rifu Huang,[1] **Tianyao Xu**,[1] **Chenkai Fan**,[1] **Xiaoyong Hu**,[1] **Wanyue Xu**,[1] **Panfei Li**,[1] **Kailing Lu**,[1] **Wei Liu**,[2] **Yakai Zhang**,[2] **Peitao Li**,[2] **and V.T. Pham**[3]

[1]*China Three Gorges Corporation, Wuhan 430010, Hubei, China*
[2]*Tianjin Tianda Qiushi Power New Technology Co., Ltd., Tianjin 300384, China*
[3]*Saigon University, Ho Chi Minh City, Vietnam*

Correspondence should be addressed to Rifu Huang; huang_rifu@ctg.com.cn

Received 20 April 2022; Revised 26 May 2022; Accepted 30 May 2022; Published 25 June 2022

Academic Editor: Lianhui Li

Under the background of energy conservation and emission reduction and large-scale promotion of electric energy substitution, fully exploring the complementary potential of various energy systems and realizing the optimization of comprehensive energy utilization are the most critical development goals of the current energy system. The key to achieving this goal is the investment potential analysis of integrated energy projects. In order to effectively solve the problems of difficult scientific determination of evaluation index weight and low accuracy of evaluation results in the analysis of investment potential of integrated energy projects, an investment potential analysis model of integrated energy project based on deep learning neural network is designed. The design process of the integrated energy project is summarized. The RBF-BP neural network model is established to obtain the correlation between the factors of the evaluation unit, further analyze and process the training results, and calculate the weight of the evaluation index. The obtained weight is substituted into the TOPSIS comprehensive evaluation model for the investment potential analysis of integrated energy projects. According to the investment potential analysis results, the investment potential analysis value of energy performance contracting (EPC) mode is 0.9122, which is the best operation mode. The results show that the analysis results reflect the investment potential of integrated energy projects more objectively and scientifically.

1. Introduction

Integrated energy system includes the production, use, and transmission of different types of energy, including many conventional energy subsystems, such as natural gas system and traditional power system, as well as new energy generation systems, such as geothermal power generation and wind power generation [1–5]. The integrated energy system can realize the comprehensive utilization of different types of energy, reduce the problems in energy supply, reduce the number of energy conversion, and reduce environmental pollution. It can not only meet people's demand for electricity, but also realize many other services, such as refrigeration and heating, so as to realize the cascade use of energy; improve energy efficiency; and promote the sustainable development of society, market economy, and energy [4]. However, there are many subsystems in the integrated energy system, and the operation mode and functional characteristics of these subsystems are also very different. The integrated energy system has rich levels, diversified structures, and nonlinear and multiple space-time characteristics, in which there are many problems to be solved. It is difficult to solve the problems only by using the traditional operation mode, control technology, and modeling and simulation technology [5].

The premise of investment potential analysis of integrated energy system is to realize system integration and optimization [6, 7]. The feasibility study, design, and operation mode optimization of integrated energy project need to be carried out on the basis of investment potential analysis. Therefore, the importance of investment potential analysis of integrated energy projects is extraordinary.

With the development of information technology [7–11], artificial intelligence technology has been gradually applied in various industries [12–16]. Because BP neural network [17–19] has strong learning ability and nonlinear fitting ability; it has been empirically applied to the field of investment potential analysis of integrated energy projects. In this paper, RBF-BP neural network is proposed and used to calculate the weight of investment potential evaluation index of integrated energy project. The example shows that this method not only makes full use of the advantages of fast approximation speed of RBF neural network, but also has the ability of BP neural network to better predict unknown samples and improve the evaluation accuracy.

The rest of this article is organized as follows. Section 1 introduces the engineering design of integrated energy project. The principle and algorithm design of RBF-BP neural network are described in Section 2. In Section 3, construction of index system and evaluation index weight solution based on RBF-BP neural network model are applied in a case, and finally the investment potential analysis result is obtained. The main contributions of this study are summarized and analyzed in Section 4.

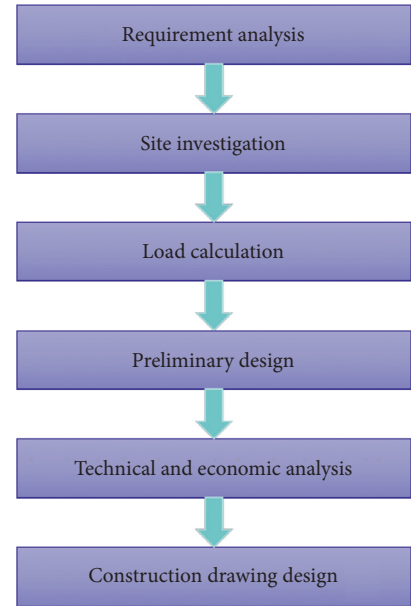

Figure 1: Technical scheme design process of integrated energy projects.

2. Engineering Design of Integrated Energy Project

According to different energy demands, integrated energy projects can be divided into solar energy and heat pump collaborative heating scheme; solar energy and low valley electric heat storage collaborative heating scheme; heat pump and low valley electric heat storage collaborative heating scheme; solar energy, heat pump, and low valley electric heat storage collaborative heating scheme. The collaborative controller is used to realize the collaborative regulation of different technologies. The standard of collaborative control is generally that the heat pump supplies the basic heat load. In the area with sufficient light, the solar heat collection is large, and the heat pump load is appropriately reduced. In areas with preferential valley price, electric boilers can be used to store heat in the valley to reduce the load of heat pump. Through the analysis and comparison of the investment potential of different technical schemes, the project technical scheme suitable for the industrial park is selected.

As shown in Figure 1, the technical scheme design process of integrated energy projects is divided into five steps:

(1) Requirement analysis: heating load demand of users in heating season, including design heat load, average heat load, and minimum heat load; annual heat load continuation diagram and analysis; hourly heat load calculation; annual average heat load simulation calculation and analysis, etc.

(2) Site investigation: understand the building system characteristics, energy structure around the building, climate resources, and other conditions in detail, and judge the applicable technology on site.

(3) Preliminary design: according to the analysis of users' heat load characteristics, determine the proportion and supply period of solar hot water heating. Combined with the heating load borne by solar energy and its time period, analyze whether it has the spatial and economic conditions for the implementation of electric heat storage. Comparative analysis of heat pump collaborative heating schemes is applied, especially for users with large-scale and stable needs of heating and refrigeration.

(4) Technical and economic analysis: determine the technical scheme and conduct technical and economic review on the scheme.

(5) Construction drawing design: issue detailed construction drawing design, and provide the list of materials, equipment, and project budget.

The main functions of the integrated energy project include the following:

(1) *Energy Monitoring.* From the perspective of the safe and stable operation of the energy network, the production and operation of energy subsystems such as electricity, cold/hot water, hot water, important energy production equipment in the park, and the energy consumption of buildings in the park are monitored through the three-dimensional visualization platform, so as to ensure the stable and safe operation of the park.

(2) *Energy Regulation.* With the help of a variety of technologies to complete the interaction between user load demand and energy production, such as optimizing the ratio, different energy amounts can be fully utilized.

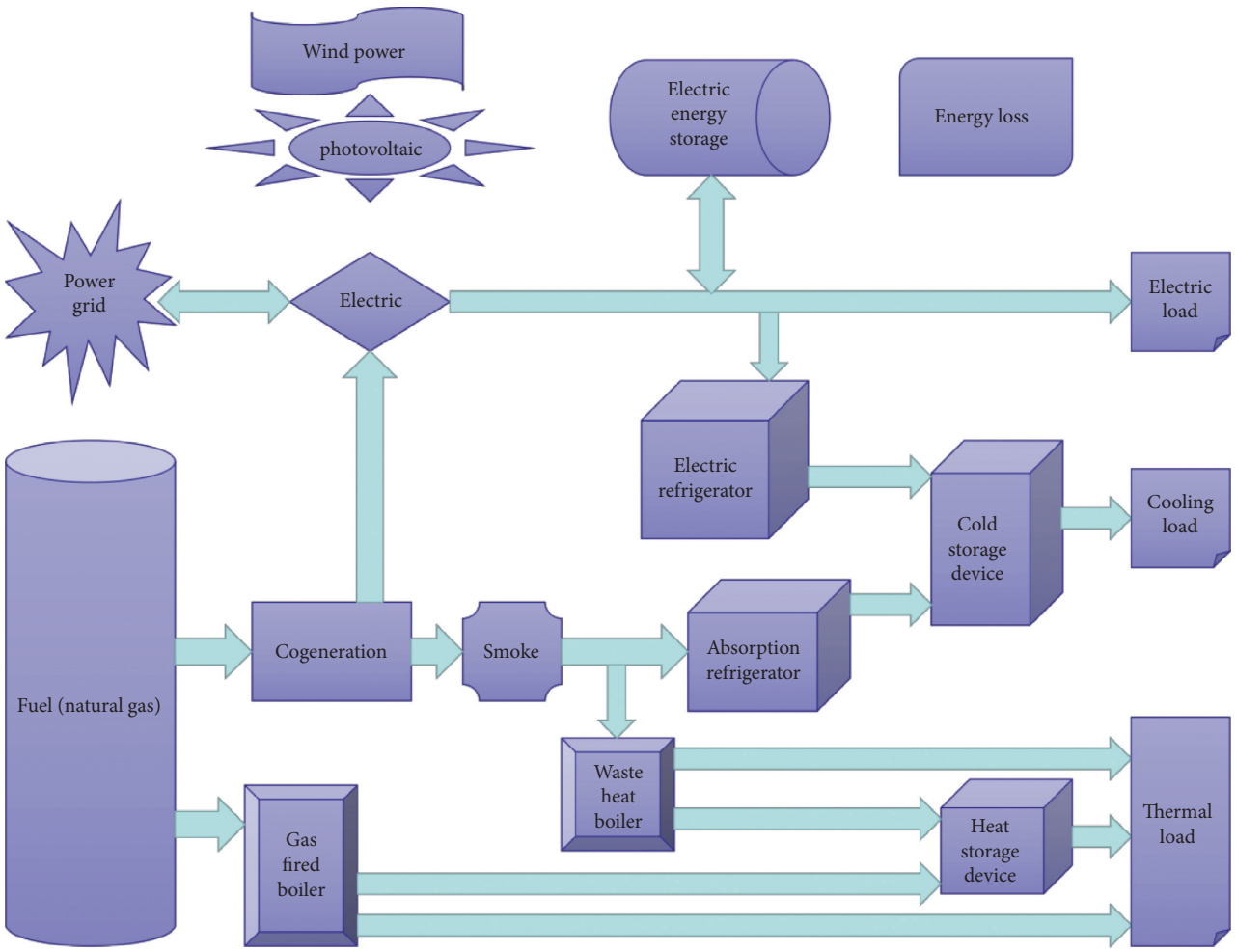

Figure 2: The energy flow of the integrated energy project.

(3) *Energy Analysis.* The interactive analysis of the power grid structure and the improvement of the power grid structure will provide the interactive support for the power grid decision-makers from the perspective of the visualization of the power grid structure and safety.

(4) *Asset Operation and Maintenance Management.* Through the management business of the whole life cycle of equipment in the park, intelligent patrol inspection business, digital maintenance business, and process three-line operation and maintenance business, realize the structured management, process standardization of the park, and provide information support for the information management of equipment inspection and maintenance in the park.

The energy flow of the integrated energy project is shown in Figure 2.

3. RBF-BP Neural Network Model

3.1. RBF and BP Neural Network Structure. BP neural network and RBF neural network are two commonly used neural network algorithms [20, 21]. As a global approximation network, BP neural network is a stable and reliable nonlinear function approximation method. However, it has the disadvantages of slow convergence speed and easy-to-trap local minimum, although the system is unstable and difficult to ensure that the learning result can reach the global minimum of mean square error. However, the system has good generalization performance. RBF neural network is a kind of optimal approximation network. If there are enough neurons in the hidden layer, it can approximate any continuous nonlinear function with arbitrary precision. RBF neural network has the advantages of simple training and fast learning convergence, overcoming local minimum problem, but having poor generalization ability. RBF-BP neural network combines the advantages of RBF neural network and BP neural network [20–26]. It consists of RBF subnet and BP subnet. Among them, a 4-layer neural network system includes input layer, two hidden layers, and output layer. The model structure is shown in Figure 3.

n, j, k, and m represent the number of neurons in input layer, first hidden layer, second hidden layer, and output layer, respectively. σ_j is the Gauss function width matrix. $C_{n,j}$ is the central vector matrix. $w_{k,j}$ is the weight matrix

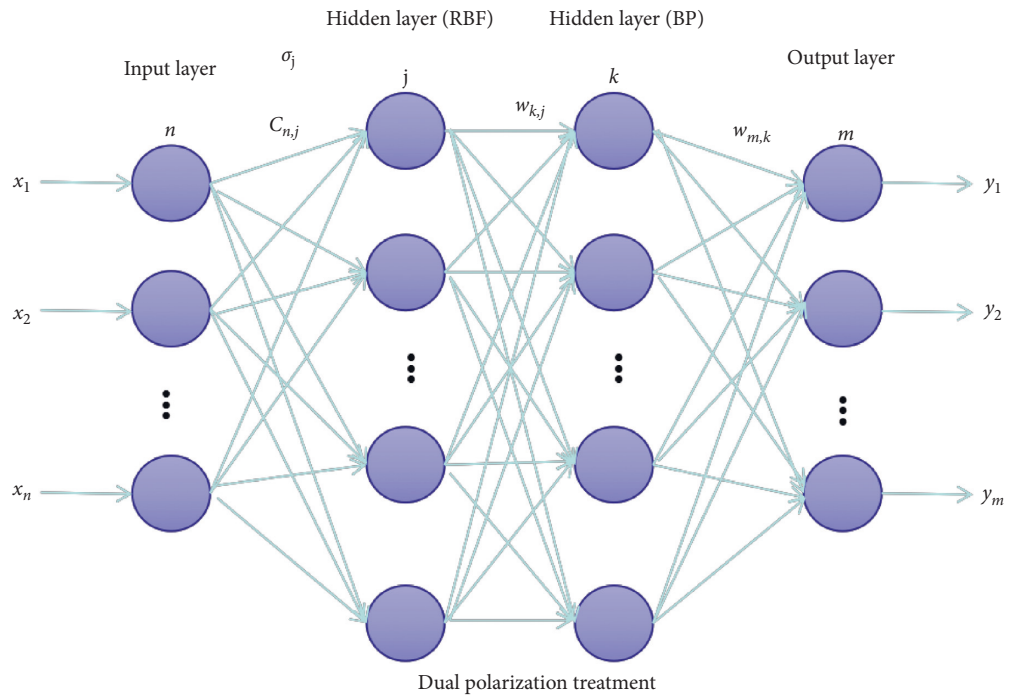

Figure 3: RBF-BP neural network structure.

between the second hidden layer and the second hidden layer. $w_{m,k}$ is the weight matrix between the second hidden layer and the output layer. The activation function of neurons in the first hidden layer is Gauss-type function. The activation function of neurons in the second hidden layer is Sigmoid-type function.

3.2. RBF and BP Neural Network Algorithm Design. According to the input training samples, through the RBF subnet preliminary training. After kernel mapping of the input sample by the hidden layer node of RBF subnet, the kernel mapping value needs to be double-polarized before it can be used as the input of BP network. The formula for $\varphi_j(x)$ dual polarization treatment is

$$\varphi_j(x) = 2.\varphi_j(x) - 1. \tag{1}$$

First the output of the hidden layer (i.e., input of BPNN) is as follows:

$$h_i = \sum_{j=1}^{N_2} w_{ij}\varphi_j(x),\ i = 1, 2, \cdots, N_3, \tag{2}$$

where N_3 is the number of nodes of the second hidden layer (BP) and w_{ij} is the weight between the two hidden layers.

Then, the output of RBF subnet is used as the input of BP subnet for strengthening training. Finally, BP subnet training results are obtained. It identifies and outputs results quantitatively. The algorithm flow is shown in Figure 4.

RBF and BP algorithm to realize the detailed steps are as follows.

Step 1. Initialize the weights and widths of each layer. Randomly set to the smaller number between [0,1]. Set parameters such as maximum training times, target accuracy, and learning rate.

Step 2. Calculate the center vector. Set the transfer function of RBF subnet hidden layer to Gauss function. It has the following form:

$$\varphi_j(x) = \exp\left(-\frac{x - C_j^{\,2}}{2b_j^2}\right), j = 1, 2, \cdots, N_3, \tag{3}$$

where φ is the output of RBF hidden layer node. N_2 is the number of nodes in the hidden layer. X is the input sample vector. C_j represents the center vector of the Gaussian kernel function. b_i represents the Gaussian kernel width of the JTH neuron ($b = d_{\max}/\sqrt{2N_2}$, $d_{\max}$ is the maximum value of each cluster center). $x - C_j$ is the Euclidean distance between x and C_j.

Step 3. Set the transfer function of BP subnet hidden layer as Sigmoid-type function:

$$F(h_i) = \frac{1}{1 + \exp(-h_i)},\ i = 1, 2, \cdots, N_3. \tag{4}$$

Step 4. Calculate the output value of node M at the output layer. Linear transfer function is adopted, which is expressed as

$$y(m) = \sum_{l=1}^{N_3} w_{lm}F(h_i), m = 1, 2, \cdots, N_4, \tag{5}$$

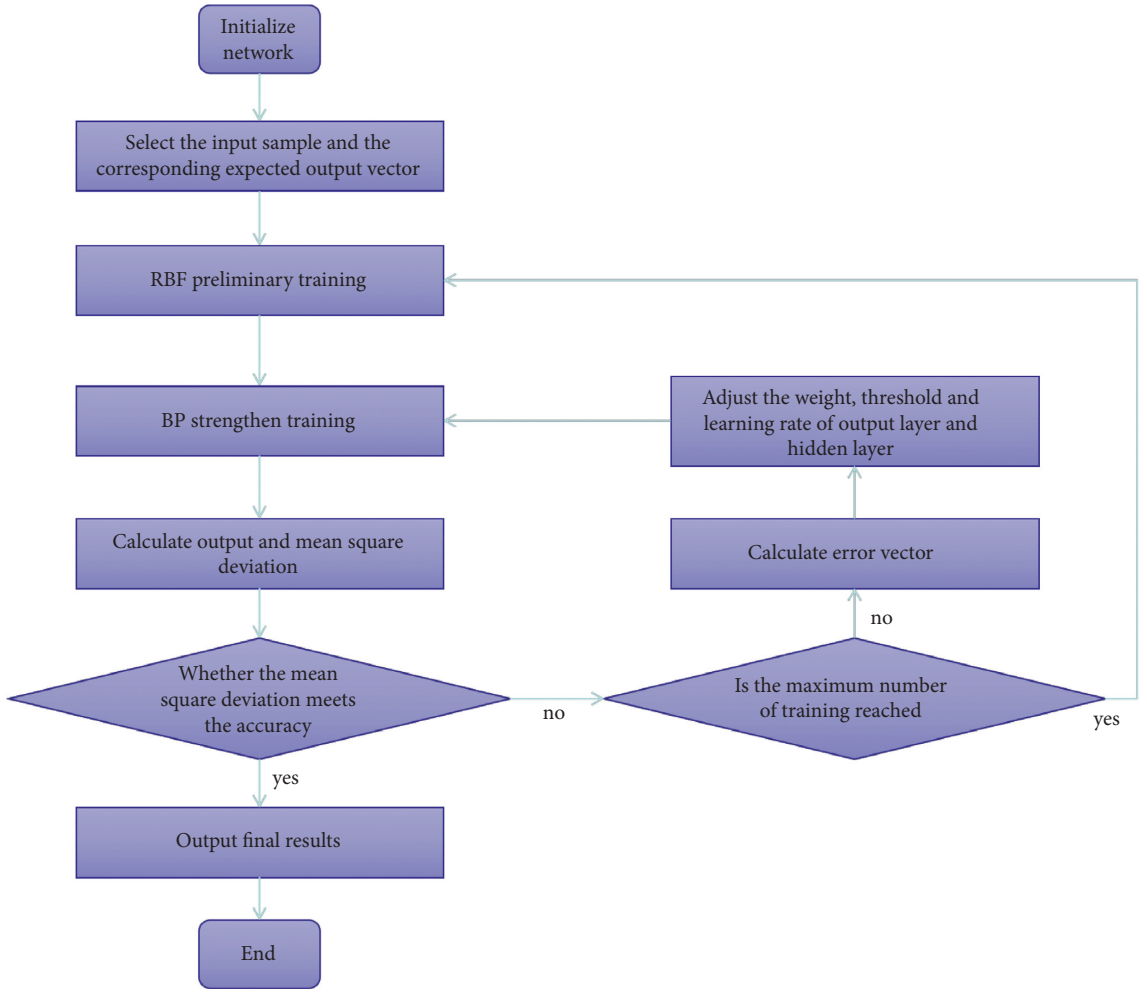

Figure 4: Algorithm flow.

where $y(m)$ is the output value of the m-th node in the output layer. N_4 indicates the number of output layers. w_{lm} represents the connection weight between neuron l of the full hidden layer and neuron m of the output layer.

$$E = \sum_{k=1}^{N_4} [d_k - y(m)]^2, \tag{6}$$

where d_k is the expected output value.

Step 6. Calculate the error vector of each neuron in the output layer:

$$\mathrm{ERR}_m = y(m)[1 - y(m)][d_k - y(m)]^2. \tag{7}$$

Step 7. Adjust the weight of each layer, rich value vector.

The weight coefficient w is adjusted according to the difference between the known output data d_j and the output data $y(j)$ calculated by formula (5). The formula of adjustment quantity is

$$\Delta w_{ij} = \eta \delta_j x_j, \tag{8}$$

where η is the learning rate (proportional coefficient) that can be adjusted adaptively. It is set to a value between [0,1] in the calculation. In network training, the value can be gradually increased until the satisfactory training speed can be achieved if the oscillation cannot be caused and the high precision can be ensured. x_j at the hidden node is the input of the whole network. In the output node, it is the output of the lower level (hidden layer) node ($j = 1, 2, \cdots, N_4$). δ_j is a value associated with output bias. For the output node,

$$\delta_j = \eta(1 - y(j))\big(d_j - y(j)\big). \tag{9}$$

For hidden layer nodes, the outputs are not comparable. Therefore, after reverse calculation, there are

$$\delta_j = x_j\big(1 - x_j\big)\sum_k \delta_k w_{jk}, \tag{10}$$

where k refers to traversing the upper (output layer) node. Error δ_j is calculated from the output layer backward layer by layer.

Each layer neuron weight is adjusted for

$$w_{ij}(t) = w_{ij}(t-1) + \Delta w_{ij}, \tag{11}$$

where t is the learning times. Each layer neuron weight is adjusted for

$$\theta_j = \theta_j + \eta.\mathrm{ERR}_j, \tag{12}$$

where η represents the learning rate.

In the process of running the program, when the training error of RBF-BP neural network is less than the set target accuracy, the training ends. At this point, it is converging. If the number of training selection times is greater than the maximum number of training times, it has not reached the target precision and the network structure does not converge. It returns to Step 2 and continues executing the program until the process converges.

4. Case Study

According to the field investigation and cooperation negotiation, there are three operation modes that can be applied to the comprehensive energy project in an industrial park: EPC mode, construction operation transfer (BOT) mode, and public-private partnership (PPP) mode. This section will build a comprehensive evaluation index system of investment potential of comprehensive energy department projects, use the model in Section 2 to solve the index weight, analyze the investment potential, and select the most suitable operation mode.

4.1. Construction of Index System. The key to the optimal planning and design of integrated energy service system is to determine the type and composition of equipment with long-term economy, energy conservation, and environmental protection according to the total cold, heat, and power demand of regional users and build a high-energy efficiency system. The construction of integrated evaluation index system is shown in Table 1.

Table 1: Integrated evaluation index system.

Index type	Index name
Economy feature	Annual comprehensive energy efficiency
Economy feature	Electricity charge savings
Energy saving feature	Total primary energy consumption
Energy saving feature	Annual electric energy substitution
Environmental protection feature	CO_2 emission reduction
Environmental protection feature	SO_2 emission reduction
Environmental protection feature	NO_x emission reduction

4.2. Evaluation Index Weight Solution Based on the RBF-BP Neural Network Model

4.2.1. Comprehensive Evaluation Model. In order to explain the investment potential level of an integrated energy project, the contribution and influence of the single factors in the above studies on the investment potential of integrated energy project are different. The contribution degree of each evaluation factor to the investment potential of integrated energy project in an industrial park was calculated by RBF-BP neural network. The calculation is as follows:

$$CI_i = \sum_{j=1}^{n} I_i w_{ij}, \tag{13}$$

where $I\ j$ is the j-th evaluation factor and w_{ij} is the weight of the j-th evaluation factor.

4.2.2. RBF and BP Neural Network Model Structure Determination. In order to obtain the weight of each evaluation index, it is necessary to standardize the value of the evaluation index. The reverse index and moderate index also need to do forward processing. This makes the values of all evaluation indicators between [0,1]. Positive indicators are standardized by maximum effect method (equation (14)). The minimum effect method is adopted to realize standardization of backward indicators (equation (15)). Moderate indicators are standardized by central effect method (equation (16)):

$$x_i' = 100 \times \frac{x_i - x_{\min}}{x_{\max} - x_{\min}}, \tag{14}$$

$$x_i' = 100 \times \frac{x_{\max} - x_i}{x_{\max} - x_{\min}}, \tag{15}$$

$$x_i' = \begin{cases} 100 \times \dfrac{x_i - x_{\min}}{k - x_{\min}}, & x_i < k, \\ 100 \times \dfrac{x_{\max} - x_i}{x_{\max} - k}, & x_i > k, \end{cases} \tag{16}$$

where x_i represents the actual value of the i-th lattice of this indicator. x_i' represents the forward normalized value. k is the most moderate value of this factor.

After standardized treatment, there is no difference in dimension, order of magnitude, and degree of variation among factors. Then, RBF-BP neural network model was used to solve the weight of each single factor.

Firstly, the number of neurons in each layer of RBF-BP neural network was determined, since the weight of four individual indicators was required in this study. Then, the number of input layer and output neural unit is set to 4. Forty groups of data were selected as training samples of neural network. Ten groups of data were used as test samples. Through continuous debugging, if the number of input layer neurons <the number of neurons in the hidden layer ≤ the principle of number of neurons in input layer + number of neurons in output layer, the number of neurons in the first hidden layer and the second hidden layer is set to 5. The network structure is shown in Figure 5.

The activation function of the first hidden layer adopts radbas( ) function. The activation function of the second hidden layer is tangent S-type transfer function tansig( ). The neuron transfer function of the output layer adopts the linear transfer function purelin( ). Network training algorithm uses

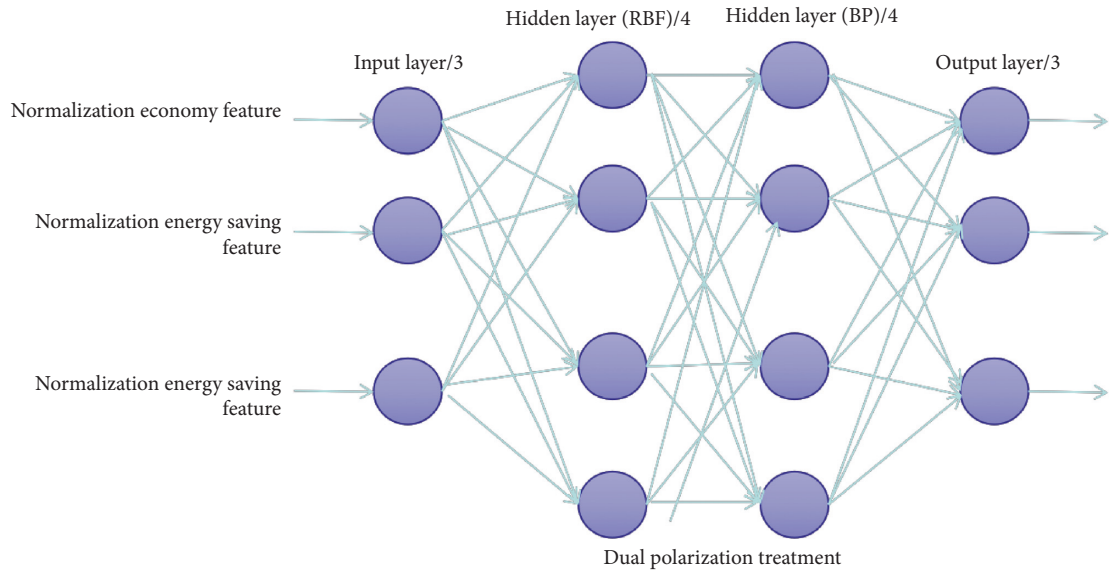

Figure 5: Network structure.

LM algorithm trainlm( ). Learning function uses gradient descent momentum learning function Learngdm( ).

We apply newff() to construct rBF-BP network: Net = newff(minmax(C), [S, 4, 4], {'radbas', 'tansig', 'logsig'},' trainlm}.

4.2.3. Network Training. According to the algorithm flow in Figure 4, the initial network training times were set as 100 times in parameter setting. The margin of error is set to 0.00001. The learning rate is set to 0.3. The simulated annealing algorithm was used to adjust the generation selection.

After the network is established, appropriate samples are determined according to the specific application and network size to train and learn network signals. This study establishes the characteristics and value range of evaluation indicators. 1500 samples were selected. After the normalization of the attribute values of each indicator. Partial data obtained are shown in Table 2.

MATLAB was used to select 40 groups of samples in the sample set for network training. The maximum number of training cycles is 150. Then, the entire sample is tested. After repeated network training, it is found that the network tends to converge when the number of selected generations reaches about 30 times. The convergence effect is shown in Figure 6. The final error is 0.7461×10^{-5}.

4.2.4. Model Training Results. The RBF-BP neural network model is used to train the normalized data of three evaluation factors (economy feature, energy saving feature, and environmental protection feature). The curve of mean square deviation is shown in Figure 7.

As can be seen from Figure 7, BP neural network achieves convergence after about 54 times of iterations. However, RBF-BP neural network model needs about 28 times to achieve convergence. It can be seen that RBF-BP neural network improves the convergence speed and the mean square error is always lower than BP neural network, indicating that RBF-BP neural network can improve the accuracy of the model.

Table 2: Sample data (part).

No.	Standardized economy feature	Standardized energy saving feature	Standardized environmental protection feature
1	0.1389	1	0.5832
2	0.2138	0.8201	0.8409
3	1	0.5106	0.4686
4	0.8511	0.6809	0.6395
5	0.7018	0.5328	0.7301
6	0.8202	1	0.7392
7	0.5457	1	1
8	0.2065	0.3540	0.6645
9	0.9708	1	0.6203
10	0.5145	0.5098	0.3642
11	1	0.6709	1
12	0.3955	0.3982	0.4084
13	0.7026	0.3453	0.8860
14	1	0.2529	1
15	0.8794	0.8135	0.8826

Figure 8 shows that although BP has a high evaluation accuracy (always higher than 80%), the evaluation accuracy of RBF-BP neural network is better than that of BP neural network. Statistical results show that in 40 groups of test data, the accuracy of training results of RBF-BP neural network model is greater than 90% and the accuracy of 22 groups was greater than 92%. This shows that the model has high approximation accuracy.

4.2.5. Solution of Index Weight. The results of neural network training only reflect the correlation between each neuron in the neural network. If it wants to get the weight of

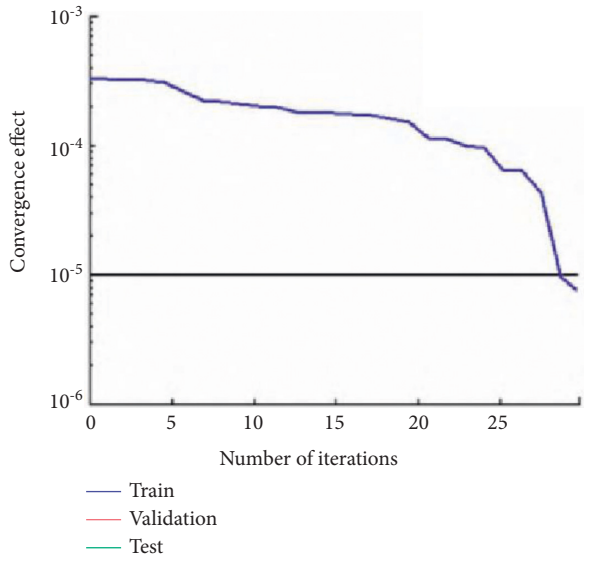

Figure 6: Network convergence.

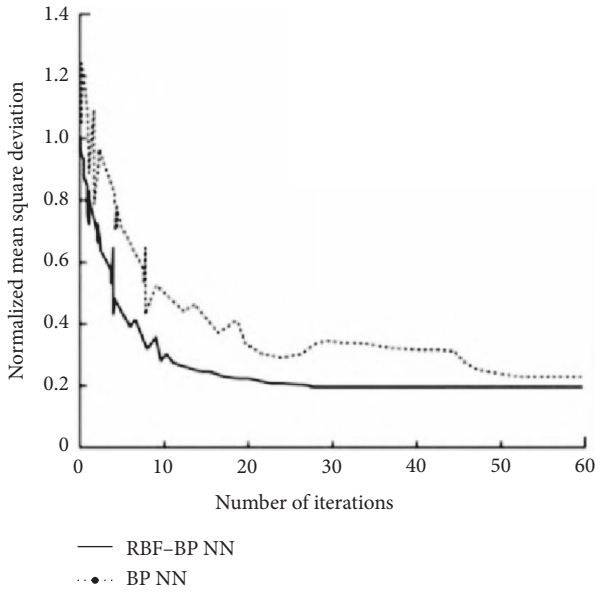

Figure 7: Normalized mean square deviation. The training accuracy of 40 groups of test samples is shown in Figure 8.

input factor to output factor, it needs to further analyze and process the weight of each neuron. In this paper, the following coefficients and indices are used to describe the relationship between input factor and output factor.

The relevant significant coefficient is

$$r_{ij} = \sum_{k=i}^{p} w_{ki} \frac{(1 - e^{-x})}{(1 + e^{-x})}, \tag{17}$$

$$x = W_{jk}, \tag{18}$$

The relevant index is

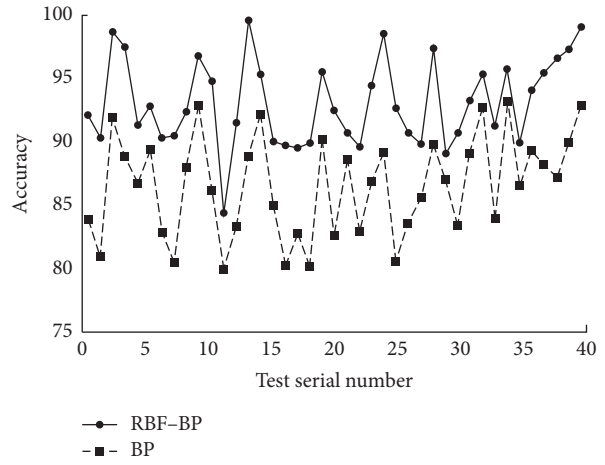

Figure 8: Training accuracy.

Table 3: Evaluation factor weight.

Evaluation factor	Weight
Economy feature	0.3082
Energy saving feature	0.3761
Environmental protection feature	0.3157

$$R_{ij} = \left| \frac{(1 - e^{-y})}{(1 + e^{-y})} \right|, \tag{19}$$

$$y = r_{ij}. \tag{20}$$

The absolute influence coefficient is

$$S_{ij} = \frac{R_{ij}}{\sum_{i=1}^{m} R_{ij}}, \tag{21}$$

where i is the RBF-BP neural network input unit, $i = 1..., m$. K is the hidden unit of neural network, $k = 1..., p$. J is the output unit of neural network, $j = 1..., n$. w_{ki} is the weight between input layer neuron I and hidden layer neuron K. w_{jk} is the same weight of output layer neuron and hidden layer neuron k.

Among the above three correlation coefficients, the absolute influence coefficient s_{ij} represents the weight of input layer neuron I to output layer neuron J.

Using equations (17)–(21), the weight of each evaluation index is concluded, as shown in Table 3.

4.2.6. Construction and Application of the Investment Potential Model. We will use TOPSIS method to comprehensively evaluate the investment potential of different operation modes. By substituting the index data into TOPSIS model for calculation, the Euclidean distance and investment potential analysis values of different operation modes can be obtained, as shown in Table 4.

According to the investment potential analysis results, the investment potential analysis value of EPC mode is 0.9122, which is the best operation mode, and the investment potential analysis value of BOT mode is 0.8076, which is second only to EPC mode. The comprehensive benefit value of PPP mode is the lowest, 0.4231.

Table 4: The Euclidean distance and investment potential analysis values of different operation modes.

	Euclidean distance to the best point	Euclidean distance to the worst point	Investment potential analysis value
EPC	0.1250	0.0143	0.9122
BOT	0.0944	0.0243	0.8076
PPP	0.0882	0.1451	0.4231

5. Conclusions

The integrated energy project can realize the organic integration and collaborative optimization among electricity, heat, gas, water, and other energy sources, mainly by using the coupling and complementarity of various energy sources in time and space. It can coordinate the energy supply and demand, effectively improve the utilization rate of renewable energy, and reduce the use of fossil energy as much as possible. It can also achieve the cascade use of energy and improve the comprehensive energy efficiency on the user side and supply side. Under the background of energy conservation and emission reduction and large-scale promotion of electric energy substitution, fully exploring the complementary potential of various energy systems and realizing the optimization of comprehensive energy utilization are the most critical development goals of the current energy system. The key means to achieve the above objectives is to improve environmental benefits, energy consumption, economic cost, and other factors through an integrated energy project.

An investment potential analysis model of integrated energy project based on deep learning neural network is designed. The case study results show that the analysis results are roughly consistent with the actual conditions. At the same time, it also shows that the model has high yield, fast learning speed, high fitting accuracy, and stronger generalization ability and can accurately and scientifically analyze the investment potential of integrated energy projects. RBF-BP neural network can combine the fast convergence speed and good stability of RBFNN with the strong reverse self-study ability and generalization ability of BPNN. The correlation training model of each factor based on RBF-BP neural network algorithm reflects the complex nonlinear relationship of each factor in the comprehensive evaluation results in the investment potential analysis of integrated energy projects. It can automatically adjust the correlation weight according to the influence of each index on the investment potential, abandon the subjective influence caused by artificial weight, and have good generalization ability. RBF-BP neural network can carry out nonlinear mapping of any continuous function and more accurately reflect the relationship between evaluation indexes and evaluation results.

Data Availability

The data used to support the findings of this study are available from the corresponding author upon reasonable request.

Conflicts of Interest

The authors declare that they have no conflicts of interest.

References

[1] D. Zhang, H. Zhu, H. Zhang, H. H. Goh, H. Liu, and T. Wu, "An optimized design of residential integrated energy system considering the power-to-gas technology with multi-functional characteristics," *Energy*, vol. 238, no. January 1, 2022.

[2] W. He, H. Lu, Y. Liu, G. Chen, and Z. Huang, "Rapid identification of economic indicators of integrated energy systems based on data analysis," *Mathematical Problems in Engineering*, vol. 2022, Article ID 9180774, 13 pages, 2022.

[3] R Dhaya, U. J Ujwal, T Sharma et al., "Energy-efficient resource allocation and migration in private cloud data centre," *Wireless Communications and Mobile Computing*, vol. 2022, Article ID 3174716, 13 pages, 2022.

[4] C. Yang, T. Hua, Y. Dai, G. Liu, X. Huang, and D. Zhang, "dongdong. Disturbance-Observer-Based adaptive fuzzy control for islanded distributed energy resource systems," *Mathematical Problems in Engineering*, vol. 2022, Article ID 1527705, 12 pages, 2022.

[5] Z. Hu and L. Zhou, "A data-driven approach for electric energy equipment using wireless sensing technology in the context of carbon neutrality," *Journal of Sensors*, vol. 2022, Article ID 3683723, 11 pages, 2022.

[6] S. Mohseni, A. C. Brent, S. Kelly, and W. N. Browne, "Demand response-integrated investment and operational planning of renewable and sustainable energy systems considering forecast uncertainties: a systematic review," *Renewable and Sustainable Energy Reviews*, vol. 158, April 2022.

[7] K. Ökten and B. Kurşun, "Thermo-economic assessment of a thermally integrated pumped thermal energy storage (TI-PTES) system combined with an absorption refrigeration cycle driven by low-grade heat source," *Journal of Energy Storage*, vol. 51, July 2022.

[8] L. Li, B. Lei, and C. Mao, "Digital twin in smart manufacturing," *Journal of Industrial Information Integration*, vol. 26, no. 9, Article ID 100289, 2022.

[9] L. Li, T. Qu, Y. Liu et al., "Sustainability assessment of intelligent manufacturing supported by digital twin," *IEEE Access*, vol. 8, pp. 174988–175008, 2020.

[10] L. Li and C. Mao, "Big data supported PSS evaluation decision in service-oriented manufacturing," *IEEE Access*, vol. 8, no. 99, p. 1, 2020.

[11] L. Li, C. Mao, H. Sun, Y. Yuan, and B. Lei, "Digital twin driven green performance evaluation methodology of intelligent manufacturing: hybrid model based on fuzzy rough-sets AHP, multistage weight synthesis, and PROMETHEE II," *Complexity*, vol. 2020, no. 6, pp. 1–24, Article ID 3853925, 2020.

[12] Y. Hu, J. Li, M. Hong, J. Ren, and Yi Man, "Industrial artificial intelligence based energy management system: integrated framework for electricity load forecasting and fault prediction," *Energy*, vol. 244, no. April 1, 2022.

[13] F Alassery, A Alzahrani, A.I Khan, K Irshad, and S Islam, "An artificial intelligence-based solar radiation prophesy model for green energy utilization in energy management system," *Sustainable Energy Technologies and Assessments*, vol. 52, August 2022.

[14] S. Sezer, F. Kartal, and U. . Özveren, "Artificial intelligence approach in gasification integrated solid oxide fuel cell cycle," *Fuel*, vol. 311, 2022.

[15] F. Khosrojerdi, O. Akhigbe, S. Gagnon, A. Ramirez, and G. Richards, "Integrating artificial intelligence and analytics in smart grids: a systematic literature review," *International Journal of Energy Sector Management*, vol. 16, no. 2, pp. 318–338, 2022.

[16] K. B. Letaief, Y. Shi, J. Lu, and J.. Lu, "Edge artificial intelligence for 6G: vision, enabling technologies, and applications," *IEEE Journal on Selected Areas in Communications*, vol. 40, no. n 1, pp. 5–36, 2022.

[17] S. Zheng, R. Yuan, L. Zhou, X. Yang, and H. Xiong, "Data security aggregation method of smart grid based on BP neural network," *Energy Systems*, vol. 20, 2022.

[18] B. Chen and Y. Wang, "Short-term electric load forecasting of integrated energy system considering nonlinear synergy between different loads," *IEEE Access*, vol. 9, pp. 43562–43573, 2021.

[19] F. Wu, R. Jing, X.-P. Zhang, F. Wang, and Y. Bao, "A combined method of improved grey BP neural network and MEEMD-ARIMA for day-ahead wave energy forecast," *IEEE Transactions on Sustainable Energy*, vol. 12, no. 4, pp. 2404–2412, October 2021.

[20] G. Liu, "A new method for fault diagnosis of building electrical system based on rbf-bp neural network," in *Proceedings of the - 2019 International Conference on Intelligent Computing, Automation and Systems, ICICAS*, pp. 470–474, Chongqing, China, December 2019.

[21] B. Ma, Y. Zhang, and L. Ma, "Research on the formation mechanism of MgO and Al2O3on composite calcium ferrite based on DA-RBF neural network," *Computational Intelligence and Neuroscience*, vol. 2022, Article ID 4327969, 12 pages, 2022.

[22] N. Liu, J. Zhang, S. Zhao, J. Xu, and Y. Wang, "A novel MPPT method based on large variance GA-RBF-BP," in *Proceedings of the 2017 Chinese Automation Congress*, Jinan, China, October 2017.

[23] X. Li, T. Zhang, Z. Deng, and J. Wang, "A recognition method of plate shape defect based on RBF-BP neural network optimized by genetic algorithm," in *Proceedings of the 26th Chinese Control and Decision Conference*, Changsha, China, June 2014.

[24] H. Wen, W. Xie, J. Pei, and L. Guan, "An incremental learning algorithm for the hybrid RBF-BP network classifier," *EURASIP Journal on Applied Signal Processing*, vol. 15, 2016.

[25] H. Hu, Y. Song, Pu Fan, C. Diao, and N. Cai, "A backstepping controller with the RBF neural network for folding-boom aerial work platform," *Complexity*, vol. 2022, Article ID 4289111, 9 pages, 2022.

[26] S. Zhang and C. Duan, "Clustering optimization algorithm for data mining based on artificial intelligence neural network," *Wireless Communications and Mobile Computing*, vol. 2022, Article ID 1304951, 16 pages, 2022.

Hindawi
Scientific Programming
Volume 2022, Article ID 2511825, 9 pages
https://doi.org/10.1155/2022/2511825

Research Article

Deep LSTM Network for Word-of-Mouth Management of Rural Tourism

Jun Wang

Changzhi Vocational and Technical College, Changzhi, Shanxi 046000, China

Correspondence should be addressed to Jun Wang; 18403078@masu.edu.cn

Received 7 May 2022; Revised 3 June 2022; Accepted 6 June 2022; Published 25 June 2022

Academic Editor: Lianhui Li

With the development of tourism, rural tourism as an industry with great development potential is gradually attracting urban consumers. Considering the differences between different types of rural tourism, I refine it at the visitor level to balance the differences in visitor groups of different types of rural tourism. I propose an improved LSTM framework for rural tourism theme feature extraction. I chose a deep neural network approach to decompose the diverse rural tourism word of mouth into different tourism themes. Then, through tourist feedback data preprocessing, destination theme detection, rural tourism type classification, and word-of-mouth management prediction network, I finally achieve an accurate grasp of rural tourism word-of-mouth features and develop corresponding tourism management strategies. To test the performance of our method, I established different types of rural tourism databases through field surveys for experimental validation. The experimental results show that our method achieves over 90% accuracy in review sentiment detection.

1. Introduction

With the dramatic expansion of the urban economy, urban space is constantly being compressed, and people's recreational space and park areas are decreasing. Along with the industrial development, the air quality within the city is decreasing, and more and more people are planning to travel to the countryside. Every holiday season, most people who work in the city choose to leave the city and travel to a distinctive countryside or town to experience the beauty, food, and culture of the countryside. Villages in different regions have different characteristics. Villages in coastal cities are themed around fishing villages, creating an all-around atmosphere of fishermen's life and allowing visitors to experience the fun of fishing. The villages in the inner mountainous areas are themed around hunting, with livestock kept in captivity in the mountain forests for visitors to simulate hunting, in addition to creating a paradise atmosphere for visitors to enjoy the tranquility of the countryside away from the hustle and bustle of the city [1, 2]. The countryside in the inland plains is dominated by herdsmen, creating original herdsmen's life projects to attract tourists to experience the details of herdsmen's life and make tourists have a different experience with the grassland culture being the cultural background. I cannot deny the siphon effect of big cities and tourist attractions. But, with the development of tourism, the demand for rural tourism has gradually increased. Different regions of rural tourism with a characteristic cultural background need to have a reasonable management model. From the deep level of the local cultural background, a reasonable strategic plan for rural tourism is formulated, together with computer-aided technology, to form a closed-loop system for rural tourism management [3–5].

To allow tourists to intuitively understand the cultural context of rural tourism, a weighting model with historical and cultural and landscape features should be built during the construction of tourism culture. In rural tourism destination selection, researchers in the literature [6] proposed five key points: destination image, life cycle, tourism experience, condition value, and destination quality. Of these, the destination image is the foundation of rural tourism, and a good destination image can add more appeal to the other key points and increase tourism expectations in the minds of

tourists. Researchers in the literature [7] have again demonstrated in a large number of studies that destination image is a decisive influence in tourism postmanagement and marketing. The destination image requires to be as simple and dynamic as possible. It gives more functionality to tourism activities in the process of building tourism culture and enhances tourists' sense of game experience and activity participation. Some tourism experts point out that tourists' image of the destination generates tourism word-of-mouth benefits, and excellent tourism word of mouth can enhance the chances of tourists' choice of tourist destinations and improve the value attributes of tourist destinations in tourists' minds [8]. In addition, good tourism word of mouth can bring a huge economic effect to rural tourism from souvenirs to food series.

The image of a tourism destination is directly proportional to the tourism word of mouth, so the image enhancement of rural tourism destinations is a key task in tourism management. The image of rural tourism is designed to convey the content, culture, and sense of the experience of rural tourism to the tourists. The tourists' understanding of the image of rural tourism needs to be combined with the actual tourism experience [9, 10]. Visitors' opinions and comments on rural tourism are the most important part of rural tourism word of mouth. Researchers in the literature [11, 12] have attempted to develop a mapping model between tourists' tourism experiences and tourism concepts for judging the conceptual differences in images between tourist destinations. The experimental results proved that heterogeneity exists between tourism purposes in terms of tourism word-of-mouth measures. Researchers in the literature [13] found that rural destinations with the tourism objective of discovering culture and history were more advantageous in the image assessment of rural destinations across geographic regions and that these rural destinations achieved an automatic closed-loop flow in terms of supply and demand pressure, which greatly reduced tourism development costs. Researchers in the literature [14] found that computer vision-based presentation of multidimensionality of tourism destination images can form a new concept for tourists and enhance the attractiveness of tourism destinations to tourists in terms of tourist numbers, cultural tourism definition, and tourist emotional variables for tourism word-of-mouth construction.

To enhance the impact of rural tourism, rural tourism uses optimal scheduling algorithms that play an active role in the rational allocation of resources [15, 16]. Diversification of rural tourism models is the most efficient means of enhancing the competitiveness of rural tourism. With the assistance of tourism agencies, rural tourism has introduced diversified experiences such as farmhouses, traditional culture experience villages, fishing villages, hunting grounds, and cultural and creative product villages. To save the development cost of rural tourism, the literature [17] proposes the construction and sharing of rural facilitation infrastructure and proposes a rural tourism organization to develop various comfort resources to revitalize citizens' rural tourism. In addition, rural tourism cultural product development and event planning are also important management tools for rural tourism to enhance the attractiveness of rural tourism to tourists and increase the network reputation of rural tourism. Researchers in the literature [18, 19] point out in the data analysis of rural tourism and the establishment of rural basic amenities that rural tourism, while preserving the local characteristics of resources, should take the construction of tourism culture as the main. In the analysis of data on rural tourism and the establishment of rural infrastructure facilities, the researchers pointed out that rural tourism, while preserving local resources, should focus on the construction of tourism culture as the main task and optimize tourism facilities by scientific means to reduce the uneven distribution of tourism resources such as vehicle congestion and accommodation shortage during the peak season. Reasonable expansion of tourist destinations to neighboring villages under the reasonable scope of tourism support construction not only can ease the pressure of tourism but also can create more economic benefits. The use of computer means for simulation and optimization is considered in the rational allocation of tourism resources to enhance the stability and sustainability of rural tourism [20].

The remainder of this paper is laid out as follows. Section 2 describes research related to rural tourism. Section 3 details the principles and implementation process related to the improved LSTM rural tourism word-of-mouth prediction network. Section 4 presents the relevant experimental datasets and an analysis of the results. Finally, Section 5 reviews our findings and reveals some additional research.

2. Related Work

The construction of rural tourism word-of-mouth should be judged on tourists' real experiences and tangible emotions, and the literature [21–24] has proposed a method of rational, and emotions were conceptually fused using images, and a cognitive evaluation method was proposed, which focused on testing three aspects of tourists' virtual impressions, real perceptions, and cultural knowledge of the tourist destination. Under the experimental conditions set by the authors, tourists' feelings are linearly correlated with the perceptions and perceptions of tourist destination images. The attributes of tourism word of mouth consist of tourism resources, tourism facilities construction, and tourism package completeness of the tourist destination, which also determine the relative excellence of the destination. Researchers in the literature [25] argue that different tourism cultures should have different assessment rules; therefore, the authors classify tourism destinations into four categories: natural landscapes, historical landscapes, cultural landscapes, and artificial parks. There are independent tourism word-of-mouth assessment models for different tourism destination categories, which make the construction of tourism word of mouth more balanced, detailed, and complete.

Researchers in the literature [26] have attempted to extract personal assessment opinions of tourist destinations from a list of representative attributes, using interval vectors with ordinal coding for automatic measurement of image

cognitive components. In addition, researchers in the literature [27] used a multidimensional scale's array mapping model, which was able to effectively discriminate polar emotions in the reviews of tourist destinations, and the efficiency of this array mapping model was experimentally demonstrated. Researchers in the literature [28] proposed a dyadic analysis applying nominal scales, where the authors compare the heterogeneity between different tourist destinations to obtain the values of tourism word-of-mouth attributes. Researchers in the literature [29] used an open-ended question model in the data processing of tourist feedback, starting from adjective and noun suggestions of tourist responses, to develop a tourism word-of-mouth assessment in a preliminary model.

Many researchers have attributed the influences of tourism word of mouth to tourists' intuitive feelings and emotional reactions to the destination. Researchers have assessed strategic images through tourists' feelings and emotions, and there are some tourists' opinions that contain the real situation of the destination, some tourists' opinions that are filled with a lot of subjective factors, and some tourists' opinions that contain a lot of constructible suggestions. The current tourism word-of-mouth assessment model does not correctly classify the mixed tourist opinions [30]. Although sentiment and word of mouth are directly related, it would certainly be unfair to travel platforms if they cannot screen out malicious comments from tourists. Tourism word of mouth is an objective opinion and emotion conveyed by tourists after they have personally experienced a tourist attraction, and the emotional dimension of tourism destination image should be based on tourists' objective feelings. Some researchers have proposed a Russel-based structure of tourists' emotional perceptions, which is mainly developed with a two-dimensional structure of emotional variables and a bipolar structure. Based on this, subsequent studies have gradually subdivided tourist feedback emotions such as boredom, pleasure, relaxation, depression, and so on. All emotions were coded in the same dimension on an interval scale, and the method was experimentally shown to be efficient in distinguishing tourists' polar emotions.

Several researchers have computer-modeled tourist destination images covering both the perceptual part and the affective image part. The data were then summarized in terms of image images, where the perceptual part images consisted of tourist cognitive data and the affective images consisted of tourist emotional data. There is a fixed linear relationship between cognition, emotion, and the overall image of the tourist destination. The emotional component can directly affect the overall image of the tourist destination, and the cognitive component affects one-fifth of the overall image of the tourist destination, but the cognitive component and the emotional component can be transformed under certain conditions [31]. For example, tourists' reasons for choosing a tourist destination, tourists' characteristics, tourists' travel habits, tourists' sources of tourist information, and so on are all part of the cognitive component. Such a linear relationship has been transformed into a destination image assessment model in later studies and has been widely used in many studies.

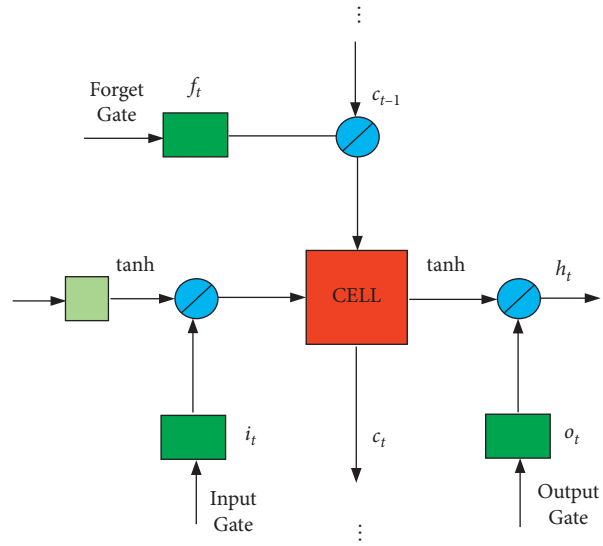

Figure 1: LSTM network.

3. Method

3.1. Travel Word-of-Mouth Feature Extraction Network. In the deep learning neural network model of traveler's word of mouth, I found that the long short-term memory network (LSTM) has extremely strong local perception ability in natural language processing, can learn traveler's word-of-mouth features with superhigh efficiency, and can store the relevant features in the short-term network to prevent the problem of information feature omission when learning new features subsequently. I found that some researchers also choose to use LSTM networks to parse tourist attraction text features and achieve good results. The structure of the LSTM network is shown in Figure 1. In this paper, I choose LSTM networks as the basic framework for rural tourism word-of-mouth feature extraction.

The semantic features of rural tourism word of mouth are input at the input side of the LSTM network, and all word-of-mouth semantic features form a feature sequence M before moving to the next stage with the following mathematical expressions:

$$M = [m_1, m_2, \ldots, m_t], \tag{1}$$

where t represents the length of the feature sequence M. Natural language processing was initially dominated by recurrent neural networks (RNN), and as natural language processing requirements became more stringent, RNNs were unable to provide complete features for global information due to the omission and loss of textual information due to the framework architecture. Therefore, the LSTM framework was formed based on the optimization of RNN, and the emergence of this method solves the problem of the sequential mapping of text features and also provides local features for global information continuously. The LSTM network has a total of four gates and one memory unit, which are an input gate i_t, forgetting gate f_t, output gate o_t, and a memory unit c_t for updating the hidden state h_t, as follows:

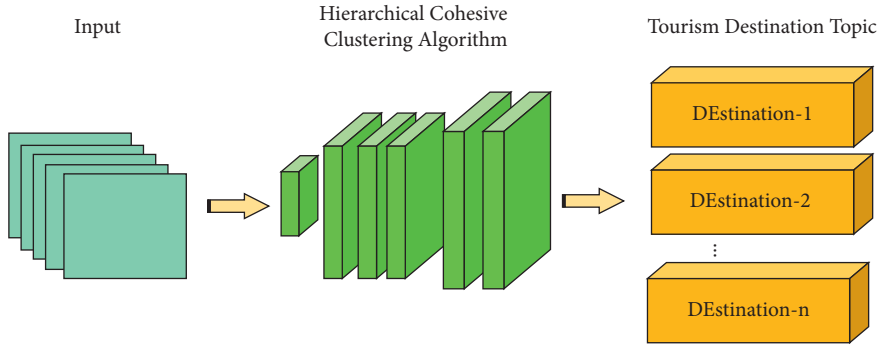

Figure 2: Tourism destination image topic detection network.

$$
\begin{aligned}
i_t &= \sigma\left(W_i x_t + V_i h_{t-1} + b_i\right),\\
f_t &= \sigma\left(W_f x_t + V_f h_{t-1} + b_f\right),\\
o_t &= \sigma\left(W_o x_t + V_o h_{t-1} + b_o\right),\\
c_t &= f_t \odot c_{t-1} + i_t \odot \tanh\left(W_c x_t + V_c h_{t-1} + b_c\right),\\
h_t &= o_t \odot \tanh\left(c_t\right),
\end{aligned}
\tag{2}
$$

where $\odot$ is a function similar to a multiplicative operation, V denotes the matrix associated with the weights, and b denotes the learning vector. In the process of natural language text information processing, LSTM needs to be trained in advance on the forgetting gate side of the semantic elements to obtain deeper text features and implicit features. Forward and reverse bidirectional semantic training allows for travel word-of-mouth character features to be completed ahead of feature replication and stored in hidden memory cells in a tandem combination before being passed to the next layer.

3.2. Tourism Destination Topic Detection. Tourism destination image theme detection is a fusion between text features and sentiment features, and character features between lexemes, words, sentences, and paragraphs can be fully mentioned in the text feature detection phase. To map each character feature to the set of sentiment features, I use a tagging approach. In the data preprocessing phase, I reset all text data sets to be trained and classify all text features in layers with the support of professional linguists. I classify text at four levels: lexemes, words, sentences, and paragraphs, and at each level, I manually annotate using different sentiment tags. Manual annotation is a huge project, and to reduce the workload and improve efficiency, I use the word root dispersion method, where I encode the same word roots and their similar texts predefined to the computer, to achieve automatic annotation of text data. Finally, this is used as the textual theme of the tourism destination image.

In the stage of tourism destination image theme assignment, I adopt the rule of sameness, that is, different text units share the same; tourism theme, which will not affect their tourism theme labels in the subsequent text decomplication. In special cases, I also follow the specified coding units, such as the annotation of keywords, technical terms, and new vocabulary, and I redesign the annotation process according to the actual situation. The details of tourism destination image theme detection are shown in Figure 2. In our design, each lexeme, word, sentence, and paragraph have a unique label, but this does not affect sentence-to-lexeme disassembly either. The disassembled labels change only at the text level, but their labels correspond to the text level and do not affect the labels at their next level.

To ensure the requirements of rural tourism destination management, I finally chose the hierarchical intraclustering clustering algorithm through extensive experimental validation [32]. I first segmented the text for tourism topics and then filtered the tourism features of word positions by different thresholds. The text clustering similarity was then used to determine the degree of matching between character features and textual tourism features by setting a criterion line and then adjusting the similarity of the extreme data according to the criterion line. The clustering of lexical positions and words can be done at once, while the clustering of sentences and paragraphs requires two to three cycles to satisfy the clustering requirements. The literature [33] proposes two evaluation metrics to determine the effectiveness of text tourism topic clustering in the same context. The mean value of word-level similarity discriminates whether the character features at the word level satisfy the feature mapping condition. The mean value of the maximum similarity between graphemes determines whether the mapping between grapheme features and tourism theme features is within the specified threshold. The mathematical equation of the above evaluation index is expressed as follows:

$$
\operatorname{sim}\left(T_1, T_2\right) = \frac{1}{2}\left(\begin{array}{l}
\dfrac{\sum_{w\in\{T_1\}}\left(\operatorname{maxsim}\left(w, T_2\right) * idf\left(w\right)\right)}{\sum_{w\in\{T_1\}} idf\left(w\right)}\\
\\
+\dfrac{\sum_{w\in\{T_2\}}\left(\operatorname{maxsim}\left(w, T_1\right) * idf\left(w\right)\right)}{\sum_{w\in\{T_2\}} idf\left(w\right)}
\end{array}\right),
\tag{3}
$$

where T_i represents a sentence and w represents a word contained in the sentence T_i. Considering that sentence- and paragraph-level clustering requires circular disambiguation and fairness of same-level clustering for bitwise N-dimensional character vectors, I additionally add cosine similarity as a weight.

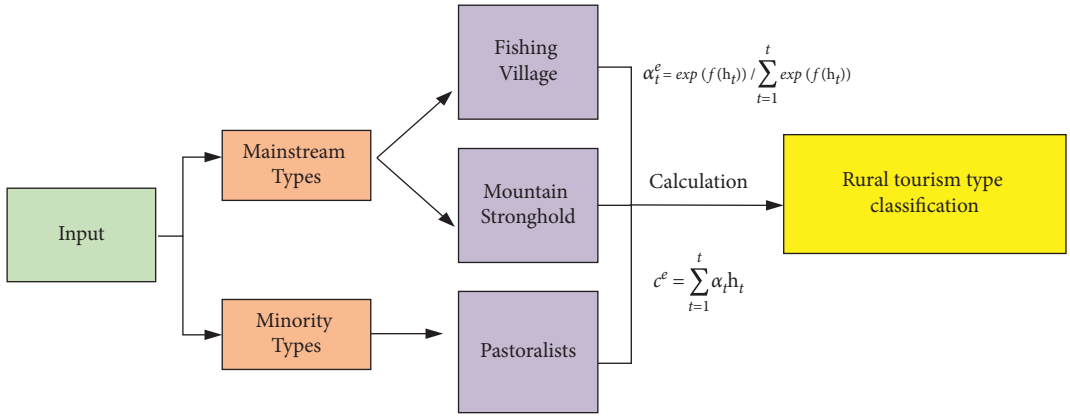

Figure 3: The rural tourism type classification network.

3.3. Rural Tourism Type Classification. Rural tourism type classification incorporates criteria of tourism themes and emotional characteristics of tourists. I need to classify the character hidden tourism theme features of lexemes, words, sentences, and paragraphs. Different character levels of hidden tourism theme features will have different responses. Considering the requirement of asynchronous homogeneity, I introduce an attention mechanism to monitor the abnormal states of different sequences and perform task control by classifier pointers so that the improved LSTM network can learn more character-level tourist sentiment features and improve the model's recognition accuracy of text sentiment features. Meanwhile, I add character sentiment tourism feature sharing in the improved LSTM network, and the weighted representation of the relevant feature sequences is $h_t = \sigma([\overrightarrow{h}_t, \overleftarrow{h}_t])$. Character sentiment features of different travel types correspond to different feature encoders, and I assume that the sequence of shared travel type features is $h_t = (h_1, h_2, \ldots, h_t)$, where t denotes the length of the sequence. I add an attention mechanism to the modified LSTM network to traverse the features α_t^e of the time sequence t. Each travel type corresponds to a weight h_t. The detailed mathematical expression is given below:

$$\alpha_t^e = \frac{\exp(f(h_t))}{\sum_{t=1}^{t} \exp(f(h_t))}, \tag{4}$$

where $f(h) = W^T h$, W represents the parameters that can be trained. c^e represents the weighted sum of the output sequences of the attention mechanism, and its weighting equation is as follows:

$$c^e = \sum_{t=1}^{t} \alpha_t h_t. \tag{5}$$

The travel type ordinary and hidden layers are interconnected, and the travel topic features are input to the next layer in the form of high-level semantic features c^e. The travel topic features are then classified. The rural tourism theme covers several categories of features, and to distinguish different tourism type features, I use a multimodal theme classifier. The rural tourism type classification network is shown in Figure 3. In this classifier, a total of 128 nodes are set in the fully connected layer based on the tourism features in the word element layer, and the activation function is chosen as ReLU for nonlinear activation. Before outputting to the next layer, I added a random deactivation layer to prevent the activation function from causing overfitting of the travel features. In the final output layer, I use softmax to activate the tourism theme features and then filter them according to the weights to get the text corresponding to the countryside tourism theme category.

3.4. Rural Tourism Word-of-Mouth Management Prediction Network. I developed the extraction of rural tourism word-of-mouth features via distributed vectors at the word position level using LSTM network processing in the initial stage. To complete the classification of multiple tourism theme features fed back by tourists, I manually constructed a rural tourism theme type database for detailed polar sentiment for each tourism category. Each character vector contains a set of tourism theme features, and all the character vectors are stacked to form a character vector matrix, and the matching of tourism theme features is obtained by mapping the unknown vectors to the categories in both directions. In the retrieval process, the index of tourism categories can be tracked in the projection layer by the rural tourism theme labels, and the tourism theme features are linked to the corresponding classification tables.

Considering that a large amount of tourist data is needed to support the pretraining of the rural tourism word-of-mouth prediction model. I pre-process tourist data from the restaurant, hotel, bar, and amusement park industries as data input for model pretraining. Considering the specificity of the embedding stage of tourism theme features, I split all tourism text features into characters for embedding, provided that such splitting does not affect the integrity of the text tourism type analysis. The detailed implementation network is shown in Figure 4. All the inputs are in the form of characters, starting from the left, and the thematic features of different tourism types are projected to the next layer through the bidirectional propagation and feedback of the network. The LSTM network can keep the number of features consistent in the process of text feature segmentation. I also used the CRFs method to ensure that the neighboring

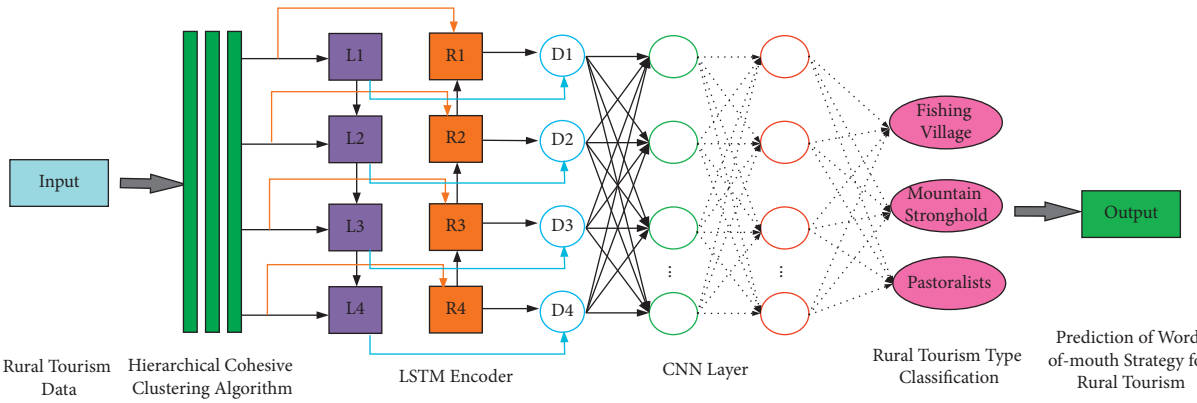

Figure 4: Rural tourism word-of-mouth management prediction network.

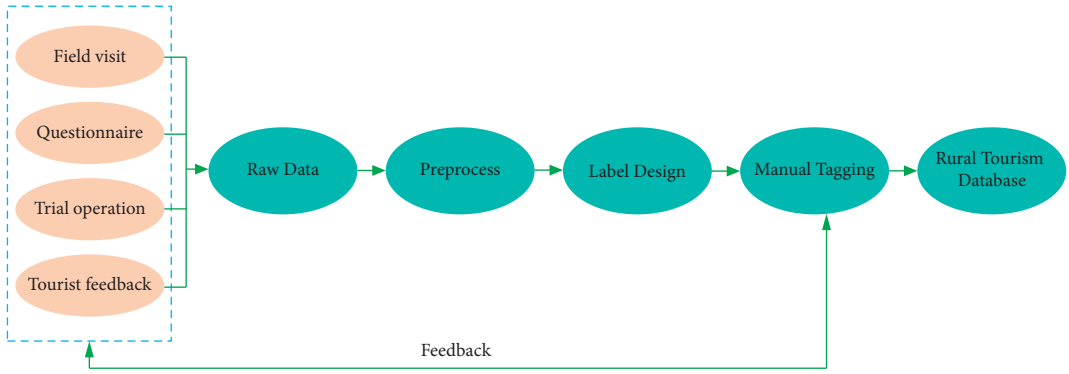

Figure 5: Rural tourism review data production process.

labels of each travel type do not affect the final predicted values. To refine the local information in long sentences, I added a CNN layer at the end to recursively feed the tour word-of-mouth features to ensure that the large-scale word-of-mouth features are fully controlled.

4. Experiment

4.1. Data Sets. Rural tourism is an emerging business in the tourism industry, with limited data on the same type of tourism industry, and there is no publicly available dataset on the Ib for rural tourism management. To validate the effectiveness of our method in rural tourism word-of-mouth management, I first collected feedback from rural tourism planning and trial operations in recent years on tourism websites and then visited some successful rural tourism cases in the field and recorded tourist satisfaction data of rural tourism. I used a splitting tool to preprocess each visitor's feedback data. Then I used the anomalous data detection system to screen out the anomalous data and obtained the preliminary polarity training set and test set by manual calibration. The data processing process is shown in Figure 5.

For different types of rural tourism, I categorized and outlined in the visitor feedback data so that rural tourism of the same type and scale is comparable, and rural tourism of different types and scales is only informative. For this purpose, I categorized different types of rural tourism data from field visits and finally obtained a homemade rural tourism dataset with details shown in Table 1. In the subsequent efficiency evaluation methods, I still use precision, recall, and $F1$ score to evaluate the effectiveness of rural tourism word-of-mouth prediction.

Table 1: The detail of data sets.

	Data sets classification		
	Fishing village	Pastoralists	Mountain stronghold
Train	4,932	3,966	4,261
Test	1,903	1,501	2,003
Total	6,835	5,467	6,264

Table 2: Accuracy of word-of-mouth prediction for different types of rural tourism.

	Fishing village (%)	Pastoralists (%)	Mountain stronghold (%)
RF	42	41	51
RNN	79	73	76
Ours	92	90	95

4.2. Experimental Results. To compare the efficiency of our approach in rural tourism word-of-mouth management, I

Table 3: Experimental reliability analysis results.

	Fishing village		Pastoralists		Mountain stronghold	
	Prediction	Actual	Prediction	Actual	Prediction	Actual
RF	0.94	0.88	0.91	0.85	0.96	0.88
RNN	0.95	0.91	0.92	0.88	0.95	0.90
Ours	0.94	0.93	0.94	0.93	0.95	0.95

conducted experiments based on three major rural tourism categories. I selected the random forest method (RF) and recurrent neural network (RNN) as the comparison algorithms. Each model maintains an independent running process during the training process. For the training parameter set, I used the migration learning method to reduce the computational cost. The experimental results are shown in Table 2.

As shown in Table 2, the accuracy of word-of-mouth prediction for different types of rural tourism industry remains above 90% for all categories of our method. Compared with the random forest method, the prediction accuracy is improved by up to 50 percentage points. This is at most 19 percentage points higher than the recurrent neural network method. The random forest method does not perform well in word-of-mouth prediction of rural tourism in the fishing village category. The random forest method, as a traditional machine learning method, relies too much on the construction and labeling of manual tourism text databases and is slow in processing when facing a large amount of tourist data. For unfamiliar tourist feedback, it is easy to generate misleading problems. This also leads to the poor word-of-mouth management results of the random forest method in our experiments. From the data, I can find that the accuracy of word-of-mouth detection of pastoralists is generally lower than in other categories of rural tourism. This is because pastoralists deal with a small base of tourists, and it is difficult to incorporate more tourism word-of-mouth feature vectors at the data learning level. Since fishing village and mountain stronghold are more sought after by tourists, more tourism word-of-mouth factors can be analyzed, and then the activation function is used to highlight their features, which improves the word-of-mouth prediction accuracy. Therefore, the word-of-mouth prediction accuracy of pastoralists is lower overall. To verify the credibility of our experiments, I supplemented the credibility verification experiments, in which I mainly compared the word-of-mouth prediction results with the actual results. The experimental results are shown in Table 3.

From the reliability analysis experiments in the table above, it is clear that the random forest method has the largest difference between the predicted and actual values, with a difference of about 0.06. Our method has the highest reliability, with only a 0.01 difference between the predicted and actual values. This shows the superiority of our method. To verify the effectiveness of our method in more detail, I conducted a comprehensive validation in terms of three metrics: recall (R), $F1$ score, and precision (P). Based on our preliminary study, I found that different types of rural tourism have different impacts on their word-of-mouth predictions due to different levels of popularity among tourists. Therefore, in the next experiments, I will analyze the categorized feedback data of tourists. Based on our previous work on the refinement of rural tourism themes, I again conducted a refinement of visitor categories. The experimental results are shown in Table 4.

Table 4: Comparison of prediction results of rural tourism word-of-mouth strategy.

	Fishing village			Pastoralists			Mountain stronghold		
	P	R	$F1$	P	R	$F1$	P	R	$F1$
RF	0.79	0.75	0.79	0.78	0.77	0.81	0.79	0.79	0.77
RNN	0.85	0.86	0.88	0.86	0.88	0.89	0.87	0.85	0.87
Ours	0.92	0.93	0.95	0.92	0.93	0.91	0.94	0.93	0.92

From the experimental results in the table above, it can be seen that our method performs better after visitor type refinement, as seen in the independent classification validation of different types of rural tourism. The experimental results are more objective and reliable and more responsive to the real feedback of the same type of tourists on rural tourism. From the accuracy and recall data, I can see that our method performs well. Our method can give word-of-mouth data management predictions for different types of rural tourism, and a weighted balance of this tourism theme features according to professional word-of-mouth evaluation agencies. Finally, rural tourism management strategies are developed based on the word-of-mouth prediction results. Such rural tourism word-of-mouth prediction results give tourists a detailed travel reference.

5. Conclusion

In this paper, I analyze the development and prospects of rural tourism and then discuss the links between rural tourism management and conventional tourism. Considering the differences between the different types of rural tourism, I refine them at the visitor level and balance the differences in the visitor base between the different types of rural tourism. Comparing various development factors of rural tourism, I propose an improved LSTM framework for rural tourism theme feature extraction. I discarded the traditional machine learning method and chose a deep neural network approach to decompose the diverse rural tourism word-of-mouth into different tourism themes for classification. Then, through visitor data preprocessing, destination theme detection, rural tourism type classification, and word-of-mouth management prediction network, I finally achieve an accurate grasp of rural tourism word-of-mouth features. To test the performance of our method, I built a database of different types of rural tourism through a field survey for experimental validation. The experimental results show that our method maintains over 90% accuracy in review sentiment detection, which is significantly better than other methods.

Since rural tourism is a new industry, the volume of data is too small. The performance of the deep neural network

model is proportional to the amount of training data. The amount of data I have is far from sufficient for the later study. For the optimization of the network, I will consider using bidirectional recurrent neural networks to process the feature sequences of different types of rural tourism word-of-mouth to achieve better accuracy of word-of-mouth prediction.

Data Availability

The data set can be accessed upon request.

Conflicts of Interest

The author declares that there are no conflicts of interest.

References

[1] S. Sotomayor, "Long-term benefits of field trip participation: young tourism management professionals share their stories," *Journal of Hospitality, Leisure, Sports and Tourism Education*, vol. 29, Article ID 100285, 2021.

[2] M. Sigala, S. Kumar, N. Donthu, R. Sureka, and Y. Joshi, "A bibliometric overview of the journal of hospitality and tourism management: research contributions and influence," *Journal of Hospitality and Tourism Management*, vol. 47, pp. 273–288, 2021.

[3] B. Taheri, G. Prayag, and B. Muskat, "Introduction to the special issue: consumer experience management and customer journeys in tourism, hospitality and events," *Tourism Management Perspectives*, vol. 40, Article ID 100877, 2021.

[4] N. Chambers and A. Cifter, "Working capital management and firm performance in the hospitality and tourism industry," *International Journal of Hospitality Management*, vol. 102, Article ID 103144, 2022.

[5] A. Mandić and J. Kennell, "Smart governance for heritage tourism destinations: contextual factors and destination management organization perspectives," *Tourism Management Perspectives*, vol. 39, Article ID 100862, 2021.

[6] A. V. Ruiz, R. Olarte, and V. Iglesias, *Evaluación de los destinos turísticos en función de su valor de marca*, pp. 427–450, Actas del XI Encuentro de Profesores Universitarios de Marketing, Valladolid, Spain, 1999.

[7] S. Baloglu and K. W. McCleary, "A model of destination image formation," *Annals of Tourism Research*, vol. 26, no. 4, pp. 868–897, 1999.

[8] J. D. Martín Santana and A. Beerli Palacio, *El proceso de formación de la imagen de los destinos turísticos: Una revisión teórica*, Estudios Turísticos, San Fernando, Spain, 2002.

[9] J. D. Martín Santana and A. Beerli Palacio, "Como influyen las fuentes de información en la imagen percibida de los destinos turísticos," *Revista española de investigación de marketing ESIC*, vol. 19, 2004.

[10] K. S. Chon, "The role of destination image in tourism: a review and discussion," *Tourist Review*, vol. 45, 1990.

[11] M. G. Gallarza, I. G. Saura, and H. C. Garcıa, "Destination image," *Annals of Tourism Research*, vol. 29, no. 1, pp. 56–78, 2002.

[12] N. Morgan and A. Pritchard, *Tourism Promotion and Power: Creating Images, Creating identities*, John Wiley & Sons, Hoboken, NJ, USA, 1998.

[13] A. Berbekova, M. Uysal, and A. G. Assaf, "A thematic analysis of crisis management in tourism: a theoretical perspective," *Tourism Management*, vol. 86, Article ID 104342, 2021.

[14] A. Leka, A. Lagarias, M. Panagiotopoulou, and A. Stratigea, "Development of a tourism carrying capacity index (TCCI) for sustainable management of coastal areas in mediterranean islands-case study naxos, Greece," *Ocean & Coastal Management*, vol. 216, Article ID 105978, 2022.

[15] T. J. Healy, N. J. Hill, A. Barnett, and A. Chin, "A global review of elasmobranch tourism activities, management and risk," *Marine Policy*, vol. 118, Article ID 103964, 2020.

[16] C. M. Echtner and J. R. B. Ritchie, "The meaning and measurement of destination image," *Journal of Tourism Studies*, vol. 2, no. 2, pp. 2–12, 1991.

[17] C. M. Echtner and J. R. B. Ritchie, "The measurement of destination image: an empirical assessment," *Journal of Travel Research*, vol. 31, no. 4, pp. 3–13, 1993.

[18] Y. Zhang, H. Yang, and G. Wang, "Monitoring and management of high-end tourism in protected areas based on 3D sensor image collection," *Displays*, vol. 70, Article ID 102089, 2021.

[19] G. Lukoseviciute and T. Panagopoulos, "Management priorities from tourists' perspectives and beach quality assessment as tools to support sustainable coastal tourism," *Ocean & Coastal Management*, vol. 208, Article ID 105646, 2021.

[20] N. J. Kim, "Policy orientations for rural tourism: a consideration of the rural amenity concept and components of tourism phenomenon," *Journal of Tourism Science*, vol. 28, no. 1, pp. 263–281, 2004.

[21] D. S. Kim and H. S. Choi, "Development of green-tourism potential evaluation method for rural villages considering amenity and human resources," *Journal of Korean Society of Rural Planning*, vol. 13, no. 2, pp. 7–16, 2007.

[22] Y. D. Kwon and J. S. Hong, "Economic analysis on rural amenity-based green tourism[J]," *Journal of Korean Society of Rural Planning*, vol. 9, no. 3, pp. 17–23, 2003.

[23] Y. G. Oh, J. Y. Choi, and S. J. Bae, "Evaluation of regional rural amenity values on living and tourism resource characteristics," *Journal of Korean society of rural planning*, vol. 14, no. 4, pp. 21–32, 2008.

[24] H. Erkuş-Öztürk and A. Eraydın, "Environmental governance for sustainable tourism development: collaborative networks and organisation building in the Antalya tourism region," *Tourism Management*, vol. 31, no. 1, pp. 113–124, 2010.

[25] M. Novelli, B. Schmitz, and T. Spencer, "Networks, clusters and innovation in tourism: a UK experience," *Tourism Management*, vol. 27, no. 6, pp. 1141–1152, 2006.

[26] H.-Y. Shih, "Network characteristics of drive tourism destinations: an application of network analysis in tourism," *Tourism Management*, vol. 27, no. 5, pp. 1029–1039, 2006.

[27] K. J. MacKay and D. R. Fesenmaier, "An exploration of cross-cultural destination image assessment," *Journal of Travel Research*, vol. 38, no. 4, pp. 417–423, 2000.

[28] A. Ghorbani, A. Danaei, S. M. Zargar, and H. Hematian, "Designing of smart tourism organization (STO) for tourism management: a case study of tourism organizations of South Khorasan province, Iran," *Helisyon*, vol. 5, no. 6, Article ID e01850, 2019.

[29] M. Koščak and T. O'Rourke, *Post-pandemic Sustainable Tourism Management: The New Reality of Managing Ethical and Responsible Tourism*, Routledge, England, UK, 2021.

[30] O. Pavlatos, "Drivers of management control systems in tourism start-ups firms," *International Journal of Hospitality Management*, vol. 92, Article ID 102746, 2021.

[31] R. A. Hamid, A. S. Albahri, J. K. Alwan et al., "How smart is e-tourism? A systematic review of smart tourism recommendation system applying data management," *Computer Science Review*, vol. 39, Article ID 100337, 2021.
[32] H. Schütze, C. D. Manning, and P. Raghavan, *Introduction to Information retrieval*, Cambridge University Press, Cambridge, UK, 2008.
[33] J. R. Shulcloper, "Reconocimiento lógico combinatorio de patrones: teoría y aplicaciones," Ph. D. Thesis, Universidad Central de Las Villas 'Marta Abreu', Santa Clara, Cuba, 2009.

Hindawi
Scientific Programming
Volume 2022, Article ID 3605987, 8 pages
https://doi.org/10.1155/2022/3605987

Research Article

Design Method of Product Concept Model Based on CAD Technology

Xiangbin Meng

School of Art and Design, Changzhou Institute of Technology, Jiangsu, Changzhou 213000, China

Correspondence should be addressed to Xiangbin Meng; mengxb@cit.edu.cn

Received 5 May 2022; Revised 28 May 2022; Accepted 8 June 2022; Published 24 June 2022

Academic Editor: Lianhui Li

With the comprehensive development of information technology, the continuous optimization of products can make enterprises stand in the market. Various industries are involved in the upsurge of computer-enabling products; computer-aided (CAD) technology has also been rapid development. CAD technology is composed of problem analysis, innovative method, problem transformation and problem-solving invention principle, standard solution, and so on. In this paper, the theoretical system, basic scheme, and solving algorithm of CAD technology are described in detail. Meanwhile, the content of value evaluation and root cause analysis is analyzed and solved to further illustrate the application process of CAD technology optimization products and gradually form a more perfect application method of CAD innovation technology so that its solution process is more scientific, operable, and universal.

1. Introduction

With the increasing development of the market economy and technology, all companies around the world are competing in the market, and the new products that are developed and successfully brought to market each year are the key to all companies' success in the competition [1, 2]. New products are the result of continuous technological innovation. An important part of product innovation is the creation of new concepts with marketability and realization possibilities that arise during the product concept design phase, a process that requires the support of knowledge. There are many problems that need to be solved in each stage of product innovation. Some of them can be solved according to experience, but they cannot solve difficult problems or invention problems, which form obstacles to product or process innovation. Inventing problem-solving theory can help corporate developers solve difficult problems, thereby removing obstacles [3–6]. The popularization and application in Chinese enterprises are of great significance to improve the independent innovation ability and market competitiveness. Since 2000, the former Soviet Union invention expert Akishule and a group of researchers, after years of efforts, put forward and create theory of the solution of inventive problems. The theory is proposed based on the analysis of a large number of high-level patents in the world. The core of the theory is to answer the problems of the process of invention problem-solving and support tools. Designers or problem solvers can solve current problems efficiently and conveniently on the basis of previous knowledge and experience in different fields of innovation. Achishuler argues that only patents are original, while the rest take advantage of existing ideas or concepts, plus novel methods. He firmly believed that the basic principles of solving invention problems existed objectively and could be organized into a complete theoretical system, which could be used to improve the success rate of invention, shorten the invention cycle, and make the solution of invention problems predictable [7–11]. After more than half a century of development and rapid explosive popularization and application in the past ten years, it has become an effective tool in the field of engineering technology to creatively solve the problems of product design and manufacturing process and has helped many well-known companies to achieve significant economic and social benefits [12].

The technology in the early stage of computer-aided innovation is only the application platform of electronic invention problem-solving theory. Due to the limited application scope of the early theory, it has high requirements on the user's knowledge level, thus greatly hindering the spread and promotion of technology [13]. Modern technology integrates innovation theory, innovation technology, and technology, and theory is no longer just a tool for experts to innovate, which greatly reduces the use of technology and promotes the spread and application of theory. With the rapid development of science and technology in recent decades, technology has become an important basic technology in the development of new industrial products. At present, computer-aided technology software is a powerful tool for designers to break the thinking pattern and broaden the ideas in the conceptual design stage of products in different fields and put forward effective design schemes with high quality [14–17]. Throughout the characteristics of these types of software, rich innovation knowledge base as important support, with the advantages of large storage, fast speed, stability, and reliability of the computer, reduces accidental factors and one-sidedness in the design process, so technology is more effective than conventional solutions in solving existing problems and innovation problems of products [18–22]. It should be emphasized that software relies on an innovation knowledge database and innovation problem-solving process to provide feasible ideas for design innovation, and the complete final scheme needs designers to refine and expand these ideas concretely. The development trend of software is to gradually integrate different innovation principles and thinking methods into software to strengthen its ability to assist designers in innovative ideas. Compared with the traditional innovation methods such as trial and error method and brainstorming method, it has distinct characteristics and advantages [23, 24]. It successfully reveals the inherent laws and principles of creation and invention and is committed to clarifying and emphasizing the contradictions existing in the system, rather than avoiding them. Its goal is to completely solve the contradictions and obtain the final ideal solution, rather than compromise. It studies the whole process of product design and development on the basis of the law of technological development and evolution so that innovative design is no longer a random behavior [25–27]. Computer-aided innovation systematically analysis problems can help the designers quickly find out the nature of the problem or contradiction, accurately position problem of direction, and break the conventional mode of thinking, in a different way of looking at problems and analysis, according to the law of evolution in technology to predict the future development trend and accelerate the process of the social innovation and high-quality products [28]-.

After years of development, it has become a knowledge-based, human-oriented systematic method for solving invention problems. Technology is a new and high technology integrating theory, ontology, modern design methodology, semantic processing technology, and computer software technology, providing natural language query technology based on semantic processing technology. Analyze the problem situation systematically, find the essence of the problem, and define the problem and conflict accurately to provide more reasonable solutions to innovative technical problems and technical contradictions. It can predict the future development trend based on the law of technological system evolution, which opens the way for making decisions and developing innovative products, and can effectively save the innovation results for future use.

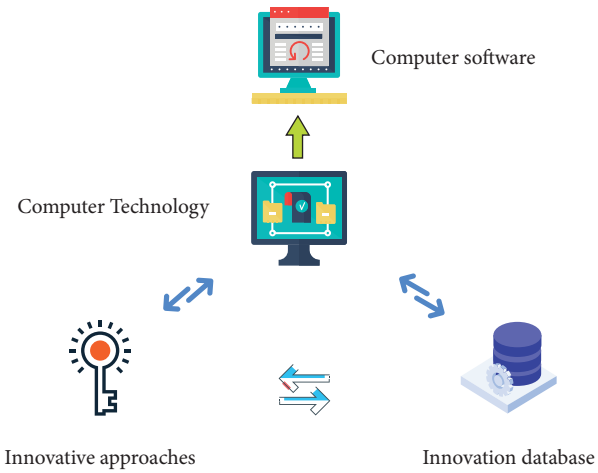

Figure 1: Computer-aided technology components.

2. Computer-Aided Technology

Computer-aided technology integrates modern design methods, invention and creation methods, knowledge of various engineering disciplines, and computer software technology and integrates scientific knowledge of multiple fields. Its system composition is shown in Figure 1. Technology provides technical support to designers at the stages of requirements analysis, concept design, solution design, and solution evaluation of new product development, assisting designers in broadening their thinking, guiding them to apply knowledge from various disciplines in an integrated and effective manner, gaining ground-breaking innovative thinking, and providing a constant stream of creative solutions for product design.

Analyzing the characteristics of innovative product design and the functional modules of the commonly used software mentioned in the previous section, the main functional modules of the current better software include project navigation, problem-solving tools such as innovation principles, technology forecasting, patent searching, solution evaluation, and knowledge management to help designers correctly analyze problems in technical systems, predict possible problems in the design phase, and explore the direction of innovative product development. Reasonable assessment of conceptual design options will reduce the probability of errors at this stage.

As can be seen in Figure 2, the designer can effectively use the built-in software in the field of multidisciplinary knowledge and the wisdom of predecessors, follow the rules of innovation, try to find the problems existing in the technical system, find innovative solutions to build their

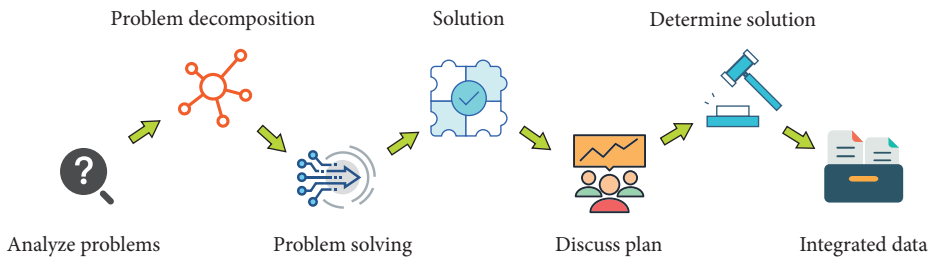

Figure 2: The logic of computer innovation technology.

own core technology and knowledge base, and help enterprises to effectively avoid the existing patent competition, into independent intellectual property rights.

2.1. Computer-Aided Innovative Design Platform. Pro/Innovator is a new generation of computer-aided innovative design tools combining TRIZ, ontology, modern design methodology, natural language processing technology, and computer software technology. With its powerful comprehensive analysis tools and innovative solution library created from the world's outstanding patents, technicians in different engineering fields can break the stereotype and broaden their thinking when facing each technical problem, analyze the problem with a new perspective and thinking, and quickly obtain operational and efficient solutions. Pro/Innovator problem-solving steps are divided into four stages: problem analysis, problem-solving, solution generation, and knowledge management.

2.1.1. Analyze Problems. The problem analysis stage consists of three modules: project navigation module, system analysis module, and problem decomposition module. Innovative design processes include project description, navigation module supporting project initiation, initial conditions and switching of each module, problem solution evaluation process, patent generation and project report generation. The system analysis module includes two parts: building component model and analyzing component value. Building component model mainly includes the interrelationship between functional analysis, role definition, flow analysis, and so on to help technical personnel from the perspective of system fully understand the problem system and its causation of the items constituting the system and subsystem effectively reveal the internal and external problems existing in the system and the weak link, so that the follow-up can be more accurate to describe the contradiction problem. The general improvement direction of the system model is further determined, which can also provide some reference for the subsequent system function evolution. After the completion of the system function analysis, the value analysis of each component of the system, first, determine the functional contribution value, problem, and cost allocation of each component. Then automatically calculate the ideal degree of each component of the system index, comprehensive analysis of each component of the initial problem of the degree of impact, and its contribution to the main function of the system value, and in order to locate the weak link in the system, clear system improvement direction. Component value analysis is based on the theory of value analysis in value engineering. The main idea of value analysis is to make certain product or certain operation have appropriate value at the lowest cost by analyzing the function and cost of the selected research object, that is, to realize the necessary function it has and improve the value of the object.

The problem decomposition module is a tool for the decomposition of surface problems, supporting the decomposition of initial problems and problems generated from the system analysis module. When describing the initial problem of a system, the root cause of the problem is often not found because the initial problem is not clearly and fully expressed at the beginning. Therefore, in order to dig out deeper causes, it is necessary to carry out a layer-by-layer analysis of the initial problem and its subproblems. The working principle of the problem analysis module is to use the triaxial analysis method to redefine the initial problems along the three axes of causality axis, operation axis, and subhypersystem axis and transform each subproblem into a triaxial diagram for analysis so that the root cause of the initial problems gradually emerges. In the process of problem decomposition, the causality of the problem is graphically expressed. In this process, other available resources in the system may be mined to analyze the actual causes of the existing resources.

The main working principle of problem decomposition module is based on the theory of root cause analysis and nine-screen method. The nine-screen method is one of the methods of system thinking, which can help people comprehensively and systematically analyze problems from multiple dimensions, such as structure, time, and causality, and find new ideas and solutions according to existing resources. Root cause analysis, also known as root cause analysis, is a process of analyzing problems in depth and finding out the mechanism or cause of failure. It is a simple and practical analysis tool for finding problems and locating causes. It helps to understand and explore the detailed causes behind the problems so that appropriate improvement and preventive measures can be taken. The root cause is determined and problem is fixed step by step. Root cause analysis is a systematic process of dealing with problems, including identifying and analyzing the causes of problems, finding solutions, and developing preventive measures.

2.1.2. Solve Problems. The tools in the problem-solving stage include the solution module, innovation principle module, and patent inquiry module. These three modules have their own knowledge base support, and appropriate modules can be selected according to the types of problems obtained in the previous step.

The solution module has a rich knowledge base of technical solutions, covering most engineering fields of manufacturing industry. The content of technical solutions is structured, refined, and supplemented by vivid, accurate, and professional animation demonstration and contains predefined solutions based on application examples of patent and innovation principles, as well as a library of technical solutions based on past experience of individuals or enterprises. It has a query tool based on ontology relationship, including functional query, structured query, and keyword query, and supports further expansion of query-related patents.

In the application of innovation principle module, the contradiction matrix is the basis of the tool, which supports the whole process of contradiction analysis and solution in the process of innovation problem-solving. It contains three ways to define contradictions: contradiction parameters, contradiction matrix, and contradiction definition wizard. After contradiction definition, the module will automatically give corresponding innovation principles to solve contradiction problems. Each innovation principle contains detailed subprinciples and is accompanied by animation demonstration to help users understand the connotation of innovation principles. The innovative thinking or breakthrough ideas obtained can be used as a reference to solve similar contradictory problems.

The patent query module contains multiple international patent databases and supports access to patent databases in China, the United States, Japan, and Europe. Patent query mode is an automatic extension function based on ontology relationship and function query. The module also has the ability to preview patent content through a web browser.

2.1.3. Form a Solution. In the process of solving contradictory problems, predefined solutions, alternatives, or analogical alternatives are generated based on some illuminating ideas. In order to obtain the best solution, these preliminary solutions need to be evaluated, and the final solution best suited to the initial problem can be selected based on the comprehensive evaluation results. The program evaluation module includes subjective evaluation and objective evaluation. Subjective evaluation includes a single expert program and a multiexpert program. The module provides an evaluation model and can also customize the evaluation model to set the weight of each expert according to the experience, background, or other factors of each expert. Objective evaluation refers to the evaluation based on the citation index of parametric patents. The evaluation results will be displayed in percentage format or bar chart format, and the predefined schemes or alternative schemes participating in the evaluation will also be ranked according to the comprehensive evaluation value.

2.1.4. Data Management. To improve the utilization rate and acquisition efficiency of knowledge, knowledge can be accumulated and shared by sorting out, summarizing, or adding knowledge to the user's knowledge base, and knowledge exchange and mutual learning between relevant personnel can be promoted. Knowledge management tools include project report generation, patent generation module, and knowledge sharing module. Software also has components, which can manage existing knowledge, obtain solutions to problems, and add them to the knowledge effect database of individuals or enterprises, so as to form a reference for similar problems that may occur in the future.

2.2. Value Analysis. Value analysis is a kind of thinking method and management technology to improve the value of the object of analysis. It is a thinking method and management technology to improve the value of the object of study by systematically analyzing the function and cost of the object of study through the cooperation of various related fields and constantly innovating. From the point of view of the purpose of carrying out value engineering activities, value engineering is through the analysis of the function and cost of the object of analysis, with the lowest life cycle cost of the object to reliably realize the necessary functions of the object of analysis, in order to obtain the best social and economic benefits. For products, it is necessary to improve their functions and reduce their life cycle costs through various means.

The main idea of value analysis is to make a product or an operation have appropriate value at the lowest cost by analyzing the function and cost of the selected research object, that is, to realize or create the necessary function it has and improve the value of the object. Value is the ratio of function and cost, which is inversely proportional to cost and directly proportional to function. That is, the higher the function, the lower the cost and the greater the value. Thus, the principle of value analysis is to improve product value to improve economic benefits by comparing product functions and costs.

In terms of the control scope of the product cost, value analysis considers product life cycle cost. Value analysis is to seek the lowest life cycle cost and to achieve the necessary function of the product as the goal and is committed to the study of the mutual interest between function and cost to overcome the one-sided consideration of a single aspect of blind practice. Value analysis is centered on function analysis. It is difficult to define product function accurately because there are many influencing factors, it is not easy to quantify abstract indicators, and people's evaluation methods of product function are different. Therefore, the analysis of product function can be considered the core of value analysis. Value analysis is an organized activity. Because the value analysis process runs through the whole life cycle of the product and involves a wide range of areas, it needs the cooperation of all units, departments, and professionals involved in the production of the product to accurately measure the cost of the product, function evaluation, and achieve the purpose of improving the efficiency of the unit cost of the product. Value analysis can reduce

product cost to the greatest extent. It can combine technology and economic problems organically and overcome the disjointed phenomenon of economy and technology in product design and manufacturing. Value analysis is a creative activity based on information. Value analysis is based on product cost, functional index, market demand, and other related information data, looking for the best solution for product innovation. In terms of the time spent on a product analysis, value analysis is carried out before product design and manufacture. Therefore, information is the basis of value analysis, and product innovation is the ultimate goal of value analysis.

2.2.1. Content of Value Analysis. The content of value engineering is the process of raising, analyzing, and solving problems according to the function and cost of products. The general working procedure of value engineering can be carried out in five stages: preparation stage, analysis stage, comprehensive stage, evaluation stage, and implementation stage. The specific working steps are shown in Figure 3.

The selection of value analysis object is the key step of value evaluation. The selection of objects mainly includes value coefficient analysis, cost proportion analysis, function evaluation coefficient analysis, and cost proportion analysis. The value coefficient is used to analyze the relationship between component function and cost, and the component whose cost does not adapt to function is taken as the key analysis object and the target of improvement. Value coefficient is determined by function coefficient and cost coefficient. Function importance coefficient refers to the proportion of part function to total product function, and cost coefficient refers to the proportion of part cost to total part cost.

$$\begin{aligned}\text{Value coefficient} &= \frac{\text{Function coefficient}}{\text{Cos coefficient}},\\ \text{Cost coefficient} &= \frac{\text{Cost of spare parts}}{\text{Total product cost}},\\ \text{Function coefficient} &= \frac{\text{Function of parts}}{\text{Product functions}}.\end{aligned} \tag{1}$$

The function coefficient of each component relative to the product is calculated according to the importance of the component in the whole component. A high value of the function coefficient indicates that the component has a great influence on the function of the component.

Cost-specific proportion analysis (ABC analysis method), a creation of Pareto, an Italian economist, is now widely used, especially in material cost analysis. It is a method that preferentially selects parts, processes, or other elements that account for a significant cost ratio as the object of value analysis.

Class A parts: the number of parts accounted for 10~20% of the total number of products, and the cost accounted for 70~80% of the total cost of products. Class C parts: the number of parts accounted for 70~80% of the total number of parts of the product, and the cost accounted for 10~20% of the total cost of products. Class B parts: the rest of the parts are called Class B, and the number of parts is proportional to the cost of the product. Using this classification method, we can find out the Class A parts which have the greatest impact on product cost as the main object of analysis and cost reduction. In practical application, the value coefficient analysis method is often combined with the ABC analysis method. Because A product often has many parts, it is relatively complicated to use the value coefficient analysis method for all parts. Generally, the ABC analysis method is adopted to select key parts, and then the value coefficient analysis method is applied to select specific objects based on the selected A or B categories.

Functional evaluation coefficient analysis method will queue up parts according to the size of functional requirements and preferentially select those with large functional coefficient as the value analysis object. And the cost proportion analysis method makes statistical analysis of various costs, and the largest one is the object of value analysis.

3. Root Cause Analysis

Root cause analysis is an analysis process of in-depth analysis of problems and finding out the mechanism or inducement of failure. It is a simple and practical analysis tool to find problems and locate causes, which can help to understand and dig out the detailed causes behind problems so as to take appropriate improvement and prevention measures. Root cause analysis is a systematic process to deal with problems, including identifying and analyzing the causes of problems, finding solutions, and developing preventive measures.

3.1. Root Cause Analysis Tool. The 5W2H method refers to the use of the five words "WHAT," "HOW," "WHY," "WHEN," "WHERE," "WHO," and "HOW MUCH" to ask questions in order to discover clues to solve problems, find ideas for inventions, and design ideas, so as to arrive at a comprehensive analysis of problems and ideas for solutions. The 5W2H method is shown in Figure 4.

In Figure 4, the process of asking and answering questions in the above seven areas provides some insight into the problematic events to be addressed and thus gets to the heart of the matter. The areas of the answers that are not at the desired level can then be improved in a more targeted way.

The system diagram lists the problems according to the order of occurrence and searches for all possible causes for each problem so as to get the root cause of the most likely problems. This is a way of describing an effect and all the possible causes that might affect it.

It can be seen from Figure 5 that the object of the tree diagram is a system, which is the relationship between a certain quality problem and its components. The graphic features are "layer-by-layer inclusive," just like a big tree. Therefore, a certain problem can be systematically decomposed into many components, and the logical and sequential relationship between them can be displayed. Through the description of the system, show the appearance of things to explore the most appropriate method to achieve the goal.

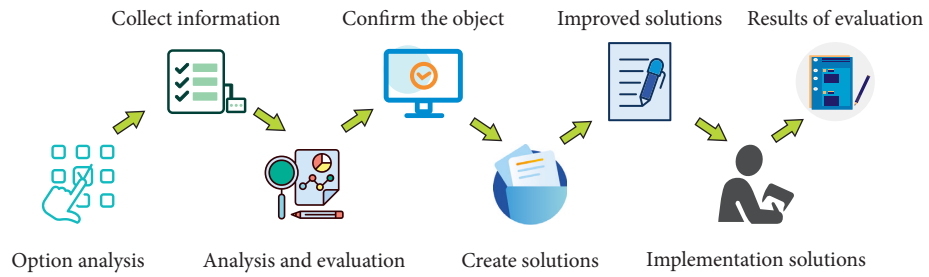

Figure 3: Process of value evaluation.

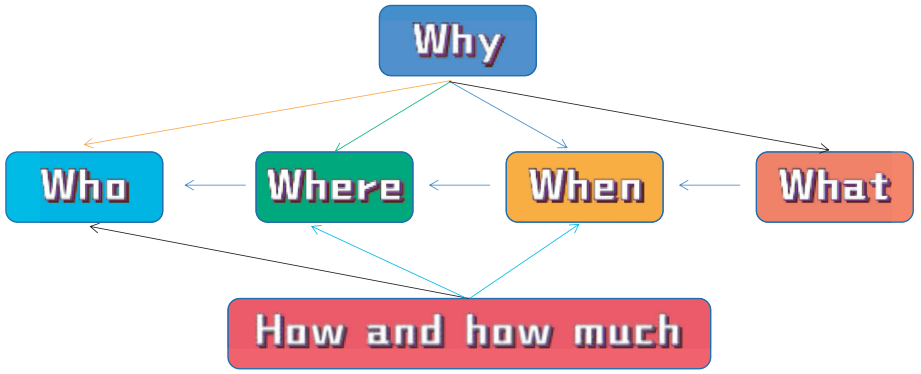

Figure 4: 5W2H method.

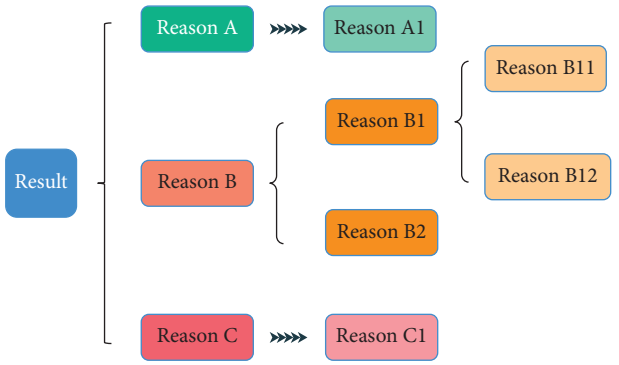

Figure 5: Structure of the system.

Figure 6: Root analysis process.

3.2. Application of Root Cause Analysis. The implementation of root cause analysis includes a series of logical processes, and its four key elements in solving problems are Define, Investigate, Verify, and Ensure. Based on the idea of Define, Investigate, Verify, and Ensure problem-solving tool, according to the characteristics of root cause analysis and the use of problem-oriented innovation strategy, the appropriate analysis method is selected and supported by a relevant knowledge base, and the prototype system structure is constructed, as shown in Figure 6.

The purpose of defining the problem phase is to set goals for improvement or solving the problem. Identify the conditions that are relevant to the problem and identify which factors may and may not be relevant to a particular problem. The purpose of the problem investigation stage is to find out the root and true cause of the problem. Through the analysis process, the basic situation of the problem is sorted out to lay a foundation for cause analysis and evaluation. It can be divided into two situations: when analyzing the problems of simplicity and inferiority, the "5 Why" analysis method can be given priority to gradually explore the root cause of the results through signs and find the root cause of the problem. In the analysis of complex problems, system diagram, and so on, in the design of manufacturing products, problems need to be analyzed from the machine, method, material, personnel, measurement, and environment in order to find the root cause of the problem. The

purpose of the problem identification and evaluation stage is to verify the validity of the root cause analysis. Analyze each cause with background information and data. The assessment identifies one or more most likely root causes. Verify and identify the cause of the problem through field tests or process descriptions that provide valid information to pinpoint the true cause. The stage of determining the best solution is to solve the root cause of the above three stages, use the invention of problem-solving-related tools and other methods to produce solutions, and then consider the feasibility of the solution from the perspective of time, cost, and resource utilization. Then the solutions are sorted out, the weight of each factor is set according to the existing common rules of the industry, the feasibility of the above schemes is evaluated by selecting appropriate evaluation criteria, and the best scheme is selected according to the comprehensive evaluation results. Finally, the effectiveness, reliability, and environmental adaptability of the scheme are verified by experiments.

In the problem decomposition module of Pro/Innovator, the subproblems of the initial problem were decomposed along the three axes of the causality axis, operation axis, and subhypersystem axis, and the subproblems were transformed into a three-axis diagram. The causal axis reflects the causal relationship between events that precede or follow the occurrence of the initial problem. This axis can be used to reveal the root cause and possible outcome of a problem, and the name of the causal axis node is Define Cause and Define Result. The action axis reflects the sequence of actions that represent all the actions experienced by the object in question. The hierarchy axis reflects how a subsystem or supersystem interacts with the technical system under consideration. The causality axis is the most commonly used and important decomposition axis for Pro/Innovator to solve problems. The layer-by-layer analysis of initial problems and subproblems along the causality axis by the problem decomposition module is actually the process of root analysis. Through the continuous decomposition of problems at the upper layer, the root causes of problems are gradually discovered. The graphical expression is similar to tree diagram or fishbone diagram. Pro/Innovator can automatically add analysis results to the project navigation and integrate them with subsequent problem-solving modules. When the problem decomposition module analysis does not reach ideal results, the solution process of root cause analysis can be used for deeper analysis.

The purpose of root cause analysis is to try to identify the contributing factors to a problem and analyze all the causes by repeatedly asking multiple whys and gradually digging deeper into the problem until the root cause is found. When exploring the root cause, try to evaluate each identified cause and try to give a solution, which will contribute to the overall improvement and improvement of the original problem. It should also be added that root cause analysis, as a general term, is not limited to the application process proposed in this chapter, but there are different structured approaches for solving specific problems.

4. Conclusion

CAD technology is an important auxiliary tool in the field of engineering. It benefits from the development of innovative methods and theories and the continuous integration with computer technology. The integration of technology innovation theory, value analysis, root analysis, and other theories makes the computer-aided innovation technology perfect day by day and consolidates its solid theoretical foundation. Computer-aided innovation technology supplements the limitations of traditional innovative design and technical improvement, and the integration of a variety of innovative methods can effectively help designers improve the efficiency of solving engineering design problems.

Data Availability

The dataset can be accessed upon request.

Conflicts of Interest

The author declares that there are no conflicts of interest.

Acknowledgments

The author acknowledges the Philosophical and Social Science Fund of Colleges and Universities in Jiangsu Province (no. 2016SJD760109) and the Education Reform Project of Changzhou Institute of Technology, Research and Practice of Digital Media Art Major Curriculum System and Content Based on Industry Standards (no. A3-3104-19-024).

References

[1] C. Wei, "Research on university laboratory management and maintenance framework based on computer aided technology," *Microprocessors and Microsystems*, vol. 6, Article ID 103617, 2020.

[2] Z. Wang, C.-H. Chen, X. Li, P. Zheng, and Li P. Khoo, "A context-aware concept evaluation approach based on user experiences for smart product-service systems design iteration," *Advanced Engineering Informatics*, vol. 50, Article ID 101394, 2021.

[3] G. Luo, Y. Guo, L. Wang, Na Li, and Y. Zou, "Application of computer simulation and high-precision visual matching technology in green city garden landscape design," *Environmental Technology & Innovation*, vol. 24, Article ID 101801, 2021.

[4] J. Luo, "Online design of green urban garden landscape based on machine learning and computer simulation technology," *Environmental Technology & Innovation*, vol. 24, Article ID 101819, 2021.

[5] Y. Zhou, M. Chen, Z. Tang, and Y. Zhao, "Simultaneous carbon storage in arable land and anthropogenic products (CSAAP): demonstrating an integrated concept towards well below 2°C, Resources," *Resources, Conservation and Recycling*, vol. 182, Article ID 106337, 2022.

[6] W. Chung, H. Lim, J. S. Lee et al., "Computer-aided identification and evaluation of technologies for sustainable carbon capture and utilization using a superstructure approach," *Journal of CO_2 Utilization*, vol. 61, Article ID 102032, 2022.

[7] E. Perez-Molina and C. Mejia, "Assessment of technology integration based on patent analysis — three archetypal case studies: computer generated animation, regenerative medicine and computer tomography," *World Patent Information*, vol. 66, Article ID 102058, 2021.

[8] Q. Liu, K. Wang, Y. Li, C. Chen, and W. Li, "A novel function-structure concept network construction and analysis method for a smart product design system," *Advanced Engineering Informatics*, vol. 51, Article ID 101502, 2022.

[9] C. Sasthav and G. Oladosu, "Environmental design of low-head run-of-river hydropower in the United States: a review of facility design models," *Renewable and Sustainable Energy Reviews*, vol. 160, Article ID 112312, 2022.

[10] B. H. W. Guo, Y. Zou, Y. Fang, M. Yang, P. X. W. Goh, and P. X. Zou, "Computer vision technologies for safety science and management in construction: a critical review and future research directions," *Safety Science*, vol. 135, Article ID 105130, 2021.

[11] S. Floryanzia, P. Ramesh, M. Mills et al., "Disintegration testing augmented by computer Vision technology," *International Journal of Pharmaceutics*, vol. 619, Article ID 121668, 2022.

[12] J. Yang, Y. Ma, M. Mao, P. Zhang, and H. Gao, "Application of regression model combined with computer technology in the construction of early warning model of sepsis infection in children," *Journal of Infection and Public Health*, vol. 13, no. 2, pp. 253–259, 2020.

[13] X. Zhu and S. Luo, "The influence of computer network technology on national income distribution under the background of social economy," *Computer Communications*, vol. 177, pp. 166–175, 2021.

[14] M. Ranjkesh Ghahnavieh, R. Kamgar, and H. Heidarzadeh, "A design-oriented model for FRP well-confined concrete cylinders under axial loading," *Structures*, vol. 38, pp. 1005–1017, 2022.

[15] Z. Ma, F. Xu, M. Wang, M. Zhang, and H. Zeng, "Design, fabrication, and dynamic testing of a large-scale outdoor aeroelastic model of a long-span cable-stayed bridge," *Engineering Structures*, vol. 256, Article ID 114012, 2022.

[16] D. Zhang, Xi Feng, C. Xu et al., "Rapid discrimination of Chinese dry-cured hams based on Tri-step infrared spectroscopy and computer vision technology," *Spectrochimica Acta Part A: Molecular and Biomolecular Spectroscopy*, vol. 228, Article ID 117842, 2020.

[17] G. Cao, Y. Sun, R. Tan, J. Zhang, and W. Liu, "A function-oriented biologically analogical approach for constructing the design concept of smart product in Industry 4.0," *Advanced Engineering Informatics*, vol. 49, Article ID 101352, 2021.

[18] L. R. Krol and T. O. Zander, "Chapter 2 - defining neuro-adaptive technology: the trouble with implicit human-computer interaction," in *Current Research in Neuroadaptive Technology*, s), S. H. Fairclough, and T. O. Zander, Eds., pp. 17–42, Academic Press, China, 2022.

[19] A. Raju Kulkarni, G. La Rocca, L. L. M. Veldhuis, and G. Eitelberg, "Sub-scale flight test model design: developments, challenges and opportunities," *Progress in Aerospace Sciences*, vol. 130, Article ID 100798, 2022.

[20] J. Chang, "Broadband technology opportunities program public computer center grants and residential broadband adoption," *Telecommunications Policy*, vol. 45, no. 8, Article ID 102147, 2021.

[21] K. P. Kusumo, K. Kuriyan, S. Vaidyaraman, S. García-Muñoz, N. Shah, and B. Chachuat, "Risk mitigation in model-based experiment design: a continuous-effort approach to optimal campaigns," *Computers & Chemical Engineering*, vol. 159, Article ID 107680, 2022.

[22] M. Scherz, E. Hoxha, H. Kreiner, A. Passer, and A. Vafadarnikjoo, "A hierarchical reference-based know-why model for design support of sustainable building envelopes," *Automation in Construction*, vol. 139, Article ID 104276, 2022.

[23] M. Kettler, H. Unterweger, and P. Zauchner, "Design model for the compressive strength of angle members including welded end-joints," *Thin-Walled Structures*, vol. 175, Article ID 109250, 2022.

[24] D. F. Andrade, J. P. Castro, J. A. Garcia, R. C. Machado, E. R. Pereira-Filho, and D. Amarasiriwardena, "Analytical and reclamation technologies for identification and recycling of precious materials from waste computer and mobile phones," *Chemosphere*, vol. 286, no. 2, Article ID 131739, 2022.

[25] K. Sharma and M. Giannakos, "Sensing technologies and child–computer interaction: opportunities, challenges and ethical considerations," *International Journal of Child-Computer Interaction*, vol. 30, Article ID 100331, 2021.

[26] S. S. Qarnain, S. Muthuvel, S. Bathrinath, and S. Saravanasankar, "Analyzing factors in emerging computer technologies favoring energy conservation of building sector," *Materials Today Proceedings*, vol. 45, no. 2, pp. 1290–1293, 2021.

[27] Jo-Yu Kuo, C.-H. Chen, S. Koyama, and D. Chang, "Investigating the relationship between users' eye movements and perceived product attributes in design concept evaluation," *Applied Ergonomics*, vol. 94, Article ID 103393, 2021.

[28] M. Meinel, T. T. Eismann, C. V. Baccarella, S. K. Fixson, and K. I. Voigt, "Does applying design thinking result in better new product concepts than a traditional innovation approach? An experimental comparison study," *European Management Journal*, vol. 38, no. 4, pp. 661–671, 2020.

Hindawi
Scientific Programming
Volume 2022, Article ID 9615461, 10 pages
https://doi.org/10.1155/2022/9615461

Research Article

Gated Recurrent Unit Framework for Ideological and Political Teaching System in Colleges

Yang Mu

Jinling Institute of Technology, Jiangsu, Nanjing 210000, China

Correspondence should be addressed to Yang Mu; my@jit.edu.cn

Received 9 May 2022; Revised 6 June 2022; Accepted 9 June 2022; Published 24 June 2022

Academic Editor: Lianhui Li

College ideological and political education has always been the primary content of national spiritual civilization construction. The current teaching methods are more flexible, resulting in the quality of ideological and political teaching not being reasonably assessed. To address this problem, we propose a method for assessing the quality of ideological and political teaching based on the gated recurrent unit (GRU) network and construct an automatic assessment system for ideological and political teaching. We draw on the migration learning model to improve the loss function by using the generalized intersection set over the joint loss function to compensate for the shortcoming of the small number of ideological and political teaching datasets. We use a masking algorithm to enhance the local features of teaching data sequences for different classes of ideological and political teaching quality assessment metrics. In addition, we use the minimum outer matrix algorithm to extract the sequence features of different assessment dimensions to improve the accuracy of the model for the quality assessment of ideological and political teaching. To meet the quality assessment conditions of ideological and political teaching, we compiled and produced ideological and political teaching datasets according to the teaching data coverage. The experimental results proved that our method performed best in comprehensive quality assessment accuracy in ideological and political teaching, with the assessment accuracy rate above 90%. Compared with traditional machine learning methods and deep learning methods, our method has higher accuracy and better robustness.

1. Introduction

College ideological and political education has always been the primary content of national spiritual civilization construction. In the process of cultivating talents in colleges and universities, cultivating talents requires not only professional skills but also noble ideological and moral cultivation. We advocate personality education as the foundation and ideological and political education as the bricks and mortar. Personality is the stable psychological foundation for the formation of life values, and the role of ideological and political education is to regulate bad moral habits and establish correct values. At present, colleges and universities have opened courses in ideological politics for college students. In addition to a positive theoretical explanation from the classroom level, school teachers also deepen ideological and political work from the psychological perspective of students, so that ideological and political education is implicitly integrated into the life values of college students [1]. Civic education is in full swing, but the quality of civic education is an unknown quantity. To study the quality of civic education, we referred to a large body of literature in the field of educational effectiveness research and drew on its educational quality validation methods [2–4]. One of the most mainstream educational validity testing methods is meta-analysis, and related research has shown that meta-analysis can extract student benefit factors at the student level, which can be converted into educational validity weights. Changes in student achievement, changes in life habits, and changes in learning attitudes can all be introduced into a multilevel statistical model. Some studies have directly matched the weights of classroom, school, student, and teacher to obtain different levels of educational grading, and the link between educational grading and learning outcomes can be used as a reference for educational effectiveness. For effective ideological and political education,

more perfect classroom performance in ideological and political courses, more enthusiastic teachers, more motivated students, and more interactive classrooms directly impact the quality of ideological and political education [5–7]. It has also been found that students' classroom performance also has a significant impact on the quality of ideological and political instruction, and the results of student thought quality tests administered during different academic years show that students' self-awareness in ideological and political courses has an indirect impact on the quality of ideological and political instruction [8, 9]. Currently, most researchers on the quality of ideological and political teaching and learning attempt to suggest a multidimensional assessment model that disperses assessment elements across the classroom and life, aiming to highlight the role of other influences on ideological and political teaching and learning in addition to mainstream civics.

In studies assessing the quality of ideological and political teaching, a large number of studies have attributed the factors that have the greatest impact on the quality of ideological and political teaching to the teachers themselves [10–12]. Some studies have indicated that teachers' teaching experience, educational height, and personality development all leave different impressions on students in the course, and the extent to which subject knowledge is imparted changes with students' impressions of the teacher. The degree of subject matter knowledge imparted also varies with students' impression of the teacher. In addition, students' learning methods and teachers' teaching methods have an indirect effect on the quality of teaching civics. This also reflects most of the classroom management problems of ideological and political teaching, teachers' teaching objectives development, and course structure planning reference. Issues such as students' performance in the classroom, the positive level of answering questions, the degree of completing assignments after class, and students' classroom feedback can reflect the quality of ideological and political teaching. The meta-analysis can synthesize teachers' teaching data to generate teachers' teaching effectiveness [13, 14]. For students, meta-analysis can also generate corresponding learning outcomes. Students' learning outcomes and teachers' teaching effectiveness are an important set of data for teaching quality assessment, and the results of a meta-analysis can provide feedback on the overall trend of teaching quality. The influencing factors of teaching quality evaluation are shown in Figure 1.

Teaching quality assessment is an important way to identify the effectiveness of education, and a variety of teaching quality assessment models have been studied in the field of educational effectiveness research, mainly using meta-analysis when it comes to teaching data analysis. All of these models cover multiple aspects of teaching and learning, including not only the interaction between students and teachers in the classroom, but also the teacher's preparation for the course, the teacher's mastery of the course, the student's completion of assignments at the end of the class, and the students' feedback on the course. Although different methods of assessing teaching quality use different data survey instruments, all teaching quality assessment models follow the following characteristics. Within the multivariate teaching quality framework, priority is given to the conceptual model of teaching quality, which also has limitations and is not comprehensive in its scope [15, 16]. Connections are established between scholars to integrate feedback on teaching quality with opinions among scholars to obtain recommendations on teaching quality weights.

The rest of the paper is organized as follows. Section 2 presents the history and research findings of teaching quality assessment research. Section 3 introduces the relevant principles and implementation details of the GRU-based ideological and political teaching quality assessment network. Section 4 shows the experimental datasets and the analysis of the experimental results. Finally, Section 5 summarizes our research and reveals some further research work.

2. Related Work

According to teaching effectiveness research, it was found that the model for assessing teaching quality is determined by multiple influencing factors. Researchers in the literature [17] have identified six inter-influential factors of teaching quality in teaching role assignment, which are course orientation, course structuring, classroom questioning, instructional modeling, instructional case application, and time management. The researchers also noted that the role of the teacher's teaching experience in the classroom directly influences the classroom learning environment and is a key indicator of classroom performance assessment. In the assessment of teaching quality in skill-based learning courses, the literature [18] suggests a more direct approach to assessing teaching effectiveness, such as structuring course instructional tests and theorizing skills assessment. Researchers in the literature [19] focused mainly on the degree of influence of the teaching model, and the authors framed the model for assessing teaching quality in terms of the ability of the teacher and students to interact and cooperate in the classroom. At the same time, the authors argue the interaction between different students and teachers in the same classroom as interrelated in terms of its contribution to the quality of teaching and learning in the whole course. To test this idea, researchers in the literature [20] adopted a control variable approach to verify the former idea based on the former. The experimental results showed that teaching quality was linearly associated with course instructional factors in stages and that efficient interaction between teachers and students during the effective teaching stage promotes the level of students' understanding of course knowledge.

Some researchers have defined five key indicators of instructional quality effectiveness: frequency, quality, stage, focus, and differentiation. These five indicators are derived from student feedback data from instructional assessments, teacher self-assessment data, and school ratings of classroom performance. Each of the five indicators corresponds to five dimensions of instructional effectiveness assessment, and each dimension can describe the function of an influencing factor in detail. For the quantitative characteristics

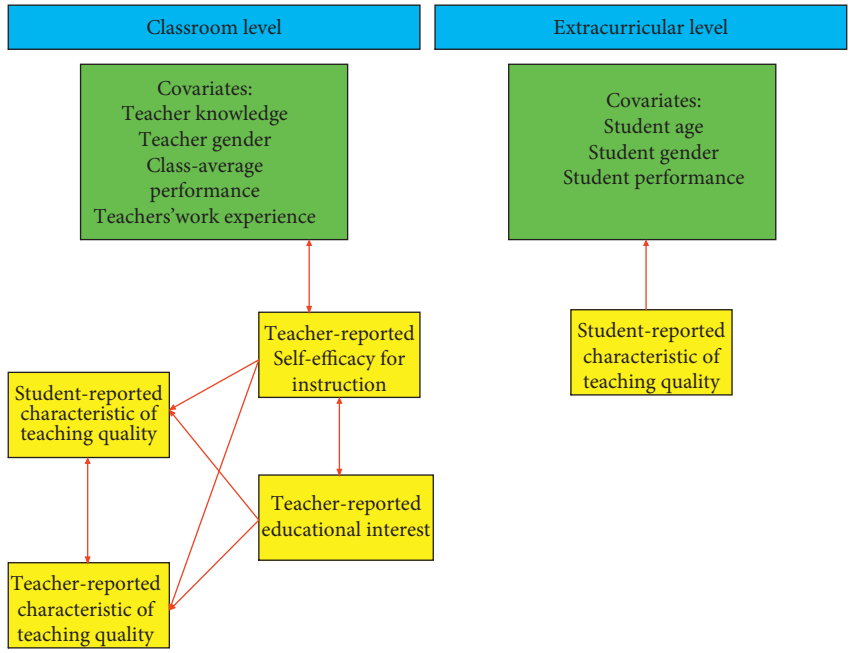

Figure 1: The influencing factors of teaching quality evaluation.

dimension, the authors chose frequency as the frequency of association between instructional effectiveness factors, thus achieving a quantitative role for each of the instructional effectiveness factors [21]. In matching individual instructional quality factors with the number of activities, it was found that cases of application of new knowledge were able to materialize the pedagogical theory and students were better able to understand this pedagogical approach. Such an approach can have a positive impact on the effectiveness of instructional quality. If too much time is spent on teaching examples of applications, it can create an illusion of a shift in the focus of learning for the students. That is why teachers need to structure the teaching phases. While grasping the course schedule, the course teaching methods should be reasonably arranged, and the centralized course model that pursues the course schedule should be avoided as much as possible, which will, on the contrary, produce negative effects on the classroom learning efficiency [22].

Most researchers have chosen the deep learning approach to evaluate teaching quality effectiveness research after comparing machine learning and deep learning approaches. Dynamic neural network models should be chosen as much as possible in the assessment models of teaching quality effectiveness, and dynamic neural network models can weigh the qualitative and nonqualitative characteristics of teaching quality factors. Researchers in the literature [23] found that for each neural network dimension of the instructional quality factors correspond to independent mathematical functional relationships, and for mapping associations between neural network dimensions and theories, dynamic neural network models can achieve single or multiple feature correspondences simultaneously. If all teaching quality assessment activities need to be completed according to expectations, the dynamic neural network model can generate corresponding teaching quality dimension assessment indicators at each stage, and according to the specific indicators, different neural network dimensions can be independently parameterized to obtain the expected values. Some researchers point out that the teaching quality assessment indexes of each neural network dimension are derived from a comprehensive functional assessment report, the index factors of each neural network dimension are independent of each other, the factors between dimensions do not influence each other, and the teaching quality factors of each neural network dimension will collaboratively govern the assessment trend of teaching quality according to the weight ratio when the overall teaching quality is assessed [24–26]. Each instructional quality assessment factor has a certain expectation of purpose fulfillment, and if an expectation corresponds to more than one purpose in an instructional course activity, the fulfillment rate of that expectation will decrease and the instructional quality assessment factor will be negatively affected [27, 28].

3. Method

3.1. Initial Structure. In the study of quality assessment of teaching of college and university civics, we conducted experiments between the machine learning model and the deep learning model, and the experimental results proved that the deep learning model was superior, so we finally chose the deep neural network model. We studied many neural network algorithms and conducted experimental validation, and finally we chose gated recurrent unit (GRU) as the network foundation. GRU is an upgrade of the RNN. GRU belongs to the algorithm of processing serial data, and in the quality assessment of college ideological and political teaching, GRU can obtain validity features from teaching data, also segment instances from the meta-analysis of

classroom performance and student feedback, and mask the target features with different thresholds. The GRU algorithm is a two-layer algorithm: the first layer is to scan the instructional sample data to generate the weight factors, and the second layer is to output the instructional validity factor mask on the recurrent neural network branch. In the mask decoding process, we adopt the separation method to decode each instructional validity factor independently and cover all instructional validity dimensions accurately.

The GRU algorithm is obtained by optimizing based on the recurrent neural network, which aims to mine more feature information from instructional data sequences, and the authors use instructional effectiveness factor feature regions to replace the sequential traversal of data sequences. To prevent over-stacking the network, the GRU network borrows from the VGG network proposed by Google, and the authors propose a local memory unit network based on the VGG network with adaptive improvements to the GRU network. The biggest advantage of this network is that it uses a series of short-term memory units instead of the iterations of long- and short-term memory networks. The structure of the GRU network is shown in Figure 2.

3.2. Mathematical Principles. RNN is a kind of feedforward neural network, which retains the advantages of a feedforward neural network and adds local feature processing network to efficiently identify data sequences of different lengths. Given a set of data sequences $x = (x_1, x_2, \ldots, x_T)$, the relationship between the front and back layers of the hidden layer state of the RNN has the following mathematical equation.

$$h_t = \begin{cases} 0, & t = 0, \\ \phi(h_{t-1}, x_t), & \text{otherwise}, \end{cases} \tag{1}$$

where ϕ denotes a nonlinear function. In the above mathematical equation, we use a combination of logistic sigmoid and affine transform to calculate ϕ, avoiding the problem of forwarding transmission difficulties due to data redundancy. Furthermore, assuming that the output of RNN is $y = (y_1, y_2, \ldots, y_T)$, and the length of this data sequence is also varied according to the input data sequence, then h_t has the following mathematical expression.

$$h_t = g(Wx_t + Uh_{t-1}), \tag{2}$$

where g represents the smoothed bounded function, and in the actual calculation, we adopt the hyperbolic tangent function as the bounded function. Assume that at the specified state h_t, the recurrent neural network outputs a new set of elements of the data sequence, the probability distribution of the elements can be represented according to the special symbols inside the model, the special symbols inside the model can be mapped to feature sequences at different lengths, and the matched sequence probabilities in the mapping have the following mathematical expressions.

$$p(x_1, \ldots, x_T) = p(x_1)p(x_2|x_1)p(x_3|x_1, x_2)\cdots p(x_T|x_1, \ldots, x_{T-1}). \tag{3}$$

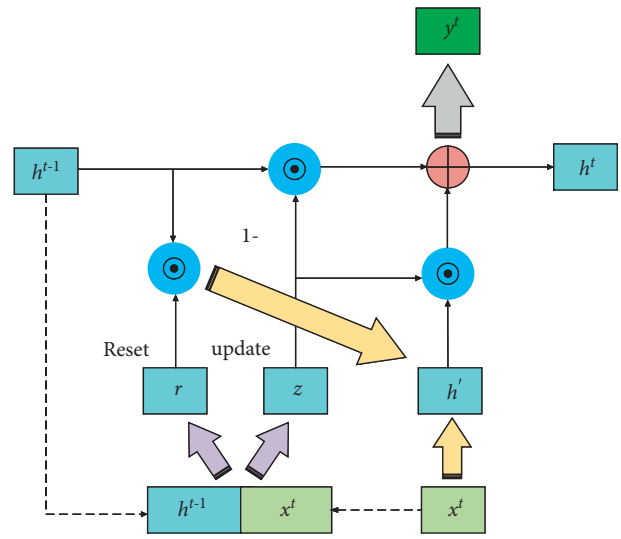

Figure 2: GRU network.

Each instructional effectiveness factor is modeled using a conditional probability distribution, where the final instructional effectiveness factor depends on the length of the sequence, and different sequence lengths correspond to different conditional probability distributions. The mathematical expression is as follows.

$$p(x_t|x_1, \ldots, x_{t-1}) = g(h_t). \tag{4}$$

In the literature [29], it was found during experiments that recurrent neural networks are prone to long-term dependencies in the process of training data sequences. Due to the specificity of the recurrent neural network structure, the problem of gradient disappearance often occurs during the training process, which makes the method less variable in gradient amplitude changes and more difficult to optimize the network structure. For data with a long sequence length, its long-term dependence on exponentially smaller is not conducive to the learning of new sequence features at a later stage. To solve this problem, some researchers try stochastic gradient descent to reduce the dependence on a gradient. Other researchers have used the gradient cropping method to circumvent the gradient disappearance problem. Some researchers have also used the second-order method to normalize the gradient vector to prevent the occurrence of gradient explosion and reduce the sensitivity of the network structure to the gradient method by using the same growth pattern of the second-order derivative as the first-order derivative [30]. The GRU algorithm is similar to the LSTM algorithm, but the structure of the two is significantly different, as shown in Figure 3.

An efficient activation function has been found in the approach of sequence feature capture optimization of recurrent neural networks. Researchers found a nonlinear implementation of affine transform and gated units that take local recurrent units or activation functions in an independent direction, called gated recurrent units. All gated cyclic units do not cause long-term dependencies when extracting features in sequences of variable length. In

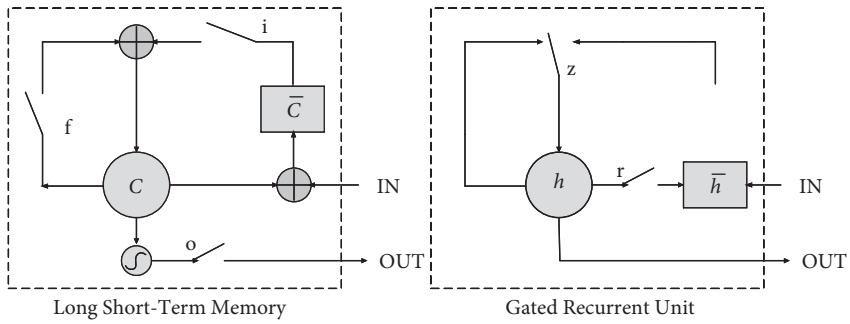

Figure 3: Structural differences between LSTM and GRU.

addition, GRU algorithms are often used in machine translation and speech recognition studies in addition to being able to process data sequences [31, 32].

3.3. Gated Recurrent Unit. Gated recurrent units (GRUs) were originally proposed by researchers in the literature [33]. The authors argued that each independent recurrent unit can correlate the dependencies between data sequences at different time scales during data sequence processing. Each cyclic unit is gated, and the gating method can regulate the flow of information within the unit on demand, and all gated units share a storage unit but do not share local feature information. During the processing of a whole data sequence, each gating unit acquires a segment of independent local sequence features, which will not overwrite the previous sequence features when new features are input, and the new features will be stored in the gating unit in parallel with the previous features. Suppose the GRU activation function is h_t^j at time t. The activation function of the previous layer is h_{t-1}^j, and the candidate activation layer is $\overline{h}_t^j$.

$$h_t^j = \left(1 - z_t^j\right)h_{t-1}^j + z_t^j\overline{h}_t^j, \tag{5}$$

where z_t^j represents an update gating unit that is capable of maintaining a superposition of activation function updates and stored sequences within the gating unit. The expression of the mathematical equation of the update gate is as follows.

$$z_t^j = \sigma\left(W_z x_t + U_z h_{t-1}\right)^j. \tag{6}$$

The processing means between the current state and the computed state of the new sequence is a linear summation operation, which is similar to the computation of the gating unit of the LSTM. All gating units in the GRU algorithm are in the visible state, and there is no unit controlling the hidden layer feature extraction in this algorithm structure, so the whole sequence processing is in the exposed state in this GRU algorithm unit. The mathematical principle between the features of the teaching data sequence is shown in Figure 4.

The expression of the $\overline{h}_t^j$ function for the candidate activation layer is shown below.

$$\overline{h}_t^j = \tanh\left(Wx_t + U\left(r_t \odot h_{t-1}\right)\right)^j, \tag{7}$$

where r_t denotes the reset gate and $\odot$ represents a multiplication operation. When the reset gate is closed, r_t^j is close to 0. The reset gate generates a special symbol for each sequence as it processes the sequence, and in addition, the reset gate is special in that the gating unit internally allows the previous sequence characteristics to be forgotten and new sequence characteristics to be stored. The mathematical expression of the reset gate r_t^j is shown below.

$$r_t^j = \sigma\left(W_r x_t + U_r h_{t-1}\right)^j. \tag{8}$$

3.4. Teaching Quality Assessment System. Referring to a large number of teaching quality effectiveness studies, we choose the GRU network as the base network. We introduced the GIOU loss function to enhance the generalized feature extraction ability of the model for teaching quality effectiveness factors, and we also chose Compute Unified Device Architecture to accelerate the computational power of the model. To improve the teaching quality assessment system, we added a classroom data recording tool as the data source for later teaching quality classroom assessments. Data preprocessing is performed on the teacher-side, student-side, and school-side teaching data samples, then the local gating unit feature layer is obtained by convolutional transportation, then-candidate regions are extracted on the feature layer, and the candidate regions are pooled and convolved to extract features. We introduce the GIOU loss function after the pooling layer and set 3 threshold criteria for the GIOU loss function, which is trained iteratively by teaching quality feature update and CUDA model acceleration. Finally, we obtain the grade features, grade matching features, and classroom teaching effect feedback features for teaching quality assessment.

Traditional machine learning methods in teaching quality effectiveness research are limited to the differences in available teaching feedback data, and no distinction can be made between staged and final teaching outcomes. This leads to a biased teaching quality assessment system, with the final teaching effectiveness accounting for the largest impact. To overcome this problem, we adopted a GRU gated unit-based recurrent neural network framework, which uses a masked gating structure that can reinforce the sequence features at the edges and can capture the local features of the sequences more comprehensively before storing them in each gating unit. Each sequence processing is divided into one stage, and the sequence features of each stage are stored in segments to avoid the loss of previous sequence features during the input

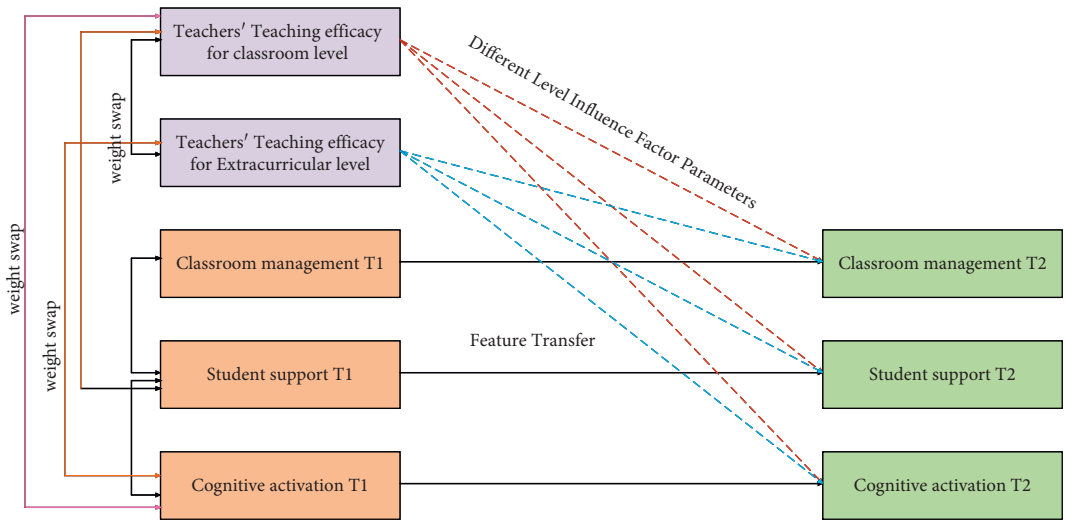

Figure 4: Structural differences between LSTM and GRU.

of new sequences. We also used the minimum external moment algorithm to accurately extract the sequence feature information of the teaching quality factor for independent segments. The detailed structure of the teaching quality assessment system is shown in Figure 5.

4. Experiment

4.1. Dataset. Current teaching effectiveness research does not have a systematic public dataset of teaching feedback. To validate our teaching quality assessment methods, we produced teaching quality feedback datasets supported by three dimensions: teacher, school, and student. To standardize the categories of teaching effectiveness assessment, we set up five main teaching quality assessment items in the early stage of teaching quality feedback dataset production, namely, teacher effectiveness (TE), student satisfaction (SS), classroom feedback (CF), course research (CR), and course size (CS). The detailed data preprocessing process is shown in Figure 6.

Teacher efficacy is the teacher's mastery of the course, the overall organization of the course, and the efficiency of the teacher's delivery, among other factors. Student satisfaction is only the level of satisfaction of the students who chose the course with the course and the instructor after taking the class. Classroom feedback refers to feedback and suggestions from students or the school about the problems of the course. Course research refers to the understanding and preparation of the course by the instructor before the course begins. Course size refers to the number of people who choose the course, which is often a direct indicator of the course's popularity and effectiveness. Different teaching effectiveness datasets were created according to the categories of teaching quality assessment indicators. Detailed information on the datasets is shown in Table 1.

4.2. Experimental Setting. To ensure the independence and stability of the ideological and political teaching quality assessment system, we configured an independent upper computer for the system, and all integrated systems were developed on the upper computer as the platform. In our experiments, we mainly configured the experimental environment of the Anaconda system. Considering the different requirements of the programming environment for the classroom interactive visual system and the teaching quality independent learning system, we configured multiple programming environments on the upper computer to suit different needs. In the construction of the ideological and political Teaching Quality Prediction Neural Network, we mainly use TensorFlow as the main framework. With the support of the powerful software community module, our teaching quality prediction network can be successfully built. The detailed training parameters are shown in Table 2.

4.3. Analysis of Experimental Results. To verify the effectiveness of our ideological and political teaching quality assessment system, we compared machine learning methods and deep learning methods. Among the machine learning methods, we chose the RF [34] algorithm, and among the deep learning algorithms, we chose the RNN algorithm [35] and the LSTM [36] algorithm. To ensure the independent validation relationship between methods, we conducted five sets of experiments during the training process and independently validated each group of methods for different teaching efficiency assessment metrics. The test results of each method were directly input into the statistical calculation part of the dataset, and the final evaluation results were obtained by balancing the total number and quality of the dataset. In the first phase of the experiment, we validated all teaching quality feedback datasets and compared the efficiency of our methods with those of other methods. For method testing efficiency metrics, we chose recall (R) and precision (P) as general evaluation metrics, where X_{TP} denotes the correctly assessed teaching quality data, X_{FN} denotes the teaching quality data without any features acquired, and X_{FP} denotes the incorrectly assessed teaching quality data. The experimental results are shown in Table 3.

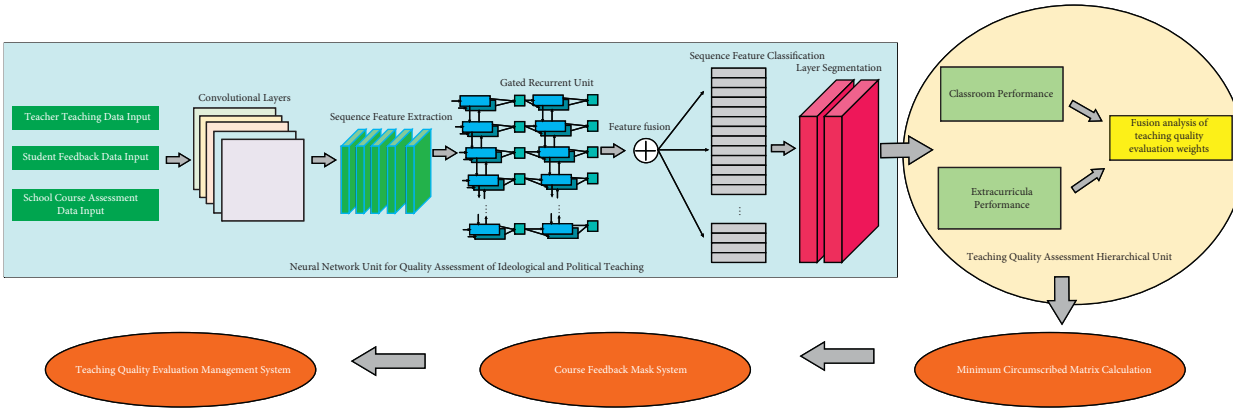

Figure 5: Ideological and political teaching quality evaluation system.

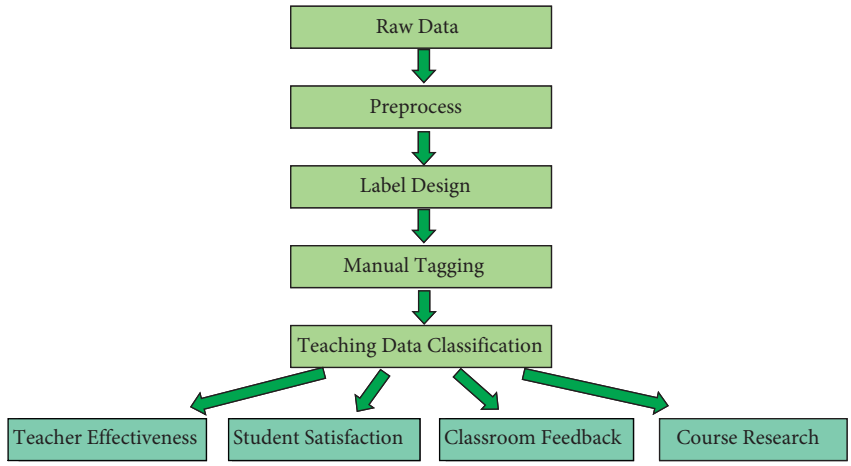

Figure 6: Data preprocessing process.

Table 1: Teaching effectiveness dataset classification and quantity.

	Train	Test	Total
TE	2993	1358	4351
SS	3651	2630	6281
CF	3412	1921	5333
CR	2978	1874	4852
CS	3021	1635	4656

Table 2: Experimental parameter settings.

Parameter	Value
Learning rate	0.001
Decay rate	0.001
Momentum	0.8
Epoch	130
Iterations	1000
Dropout rate	0.5

The X_{TP} in the experiment indicates the readiness rate for qualitative assessment per 500 samples of instructional feedback data. The experimental results in Table 3 show that the RF method has the highest number of instructional validity misclassifications, accounting for one-fifth of the total. The recall rate is only 64.1%, which is not very accurate.

Table 3: Comparison of teaching quality assessment of different methods.

Method	X_{TP}	X_{FP}	X_{FN}	R (%)	P (%)
RF	284	113	79	64.1	75.9
RNN	346	62	50	88.1	83.4
LSTM	373	31	30	91.1	92.5
Ours	434	5	4	98.1	98.5

The efficiency of teaching quality assessment is slightly better than RNN and LSTM methods, but there is still room for optimization. Our method has only five teaching effectiveness misclassification data, and the accuracy of teaching quality assessment reaches 98.5%. This is superior to other methods, which shows the superiority of our method in the first phase of experimental validation. In the second phase of the experiment, we verified the details of each teacher's teaching data separately. The highest student feedback score was 100, the highest expert rating was 10, and the highest workload was 25. Education represents the teacher's academic background, with higher scores representing higher education. Before the start of the experiment, we performed a preprocessing operation on the teaching quality feedback data to standardize the input format and sampling frequency of teaching quality data to prevent the influence of data

Table 4: Comparison of teaching quality data for teachers with different experiences.

Teacher (experience)	Workload	Leadership (%)	Student feedback	Expert score	Education
1(2)	8	72.3	85	7	8
2(4)	12	81.2	89	7	8
3(5)	14	89.8	91	8	7
4(8)	20	93.5	96	9	4

Table 5: Comparison of the accuracy of ideological and political teaching quality assessment by different methods.

	Classroom part (%)	Extracurricular part (%)
RF	64	71
RNN	73	75
LSTM	74	84
Ours	89	93

discrepancies on the experimental results. The results of the second phase of the experiment are shown in Table 4.

The results of the second phase of the experiment showed that teachers with more teaching experience had a heavier workload, and teachers with more years of experience held more positions in the school and had more work issues. At the leadership level, teachers with more years of work experience had stronger leadership skills, performed better in their courses, and had higher student feedback scores for their teachers. At the expert rating level, teachers with more work experience scored higher on the teaching quality assessment, and despite a less academic background, work experience became a major factor in improving teaching quality.

In the third stage of the experiment, the accuracy of the Civic Education Teaching Quality Assessment System is verified in assessing teachers' civic education performance and work assessment performance. We divided the ideological and political education into two categories: the classroom part and the extracurricular part, where the classroom part includes teaching progress and students' ideological and political performance, and the extracurricular part includes students' after-class homework. The experimental results are shown in Table 5.

The experimental results from the third stage show that all methods have higher assessment accuracy in the extracurricular part of ideological and political teaching than in the classroom part. The accuracy of the extracurricular part is higher than that of the classroom part because many assessment details cannot be implemented in the extracurricular part, so the highest scores are taken in many aspects. The RNN and LSTM methods still need to be improved in the work of meta-analysis of data outside the classroom. Our method performs best in the quality assessment of ideological and political teaching and learning, outperforming RNN and LSTM methods.

5. Conclusion

In this paper, we propose a method for assessing the quality of ideological and political teaching based on the gated recurrent unit (GRU) network and construct an automatic ideological and political teaching assessment system. We draw on the migration learning model to improve the loss function by using the generalized intersection set over the joint loss function to compensate for the shortcoming of the small number of ideological and political teaching datasets. We use a masking algorithm to enhance the local features of teaching data sequences for different classes of ideological and political teaching quality assessment metrics. In addition, we use the minimum outer matrix algorithm to extract the sequence features of different assessment dimensions to improve the accuracy of the model for the quality assessment of ideological and political teaching. To meet the quality assessment conditions of ideological and political teaching, with the support of ideological and political teachers, students, and school administration teachers, we compiled and produced ideological and political teaching datasets based on the teaching data coverage. The experimental results proved that our method performed best in comprehensive quality assessment accuracy in ideological and political teaching, with the assessment accuracy rate above 90%. The assessment accuracy rate is the best performance in teaching outside of class. It proves that our method performs well both inside and outside the ideological and political teaching classroom. Compared with traditional machine learning methods and deep learning methods, our method has higher assessment accuracy and better stability.

Although our method performs best in experiments inside and outside the ideological and political classroom, there is still much room for improvement in the accuracy of ideological and political teaching quality assessment. In future research, we will try to add generative adversarial neural networks to the adversarial network as an auxiliary classification to optimize the reasonable segmentation of teaching data sequences of different dimensions and improve the robustness and generalization of the network.

Data Availability

The dataset can be accessed upon request.

Conflicts of Interest

The author declares that there are no conflicts of interest.

Acknowledgments

The authors thank Ideological and Political Education in Colleges and Universities, "Social Science Application Research Project of Jiangsu Province" in 2021, Research on the "Integration of Six Aspects" Education System of Agricultural Majors in Colleges and Universities (no. 21sza-009).

References

[1] K. Sadeghi, F. Ghaderi, and Z. Abdollahpour, "Self-reported teaching effectiveness and job satisfaction among teachers: the role of subject matter and other demographic variables," *Heliyon*, vol. 7, no. 6, Article ID e07193, 2021.

[2] C. Chapman, D. Muijs, D. Reynolds, P. Sammons, and C. Teddlie, Eds., *The Routledge International Handbook of Educational Effectiveness and Improvement*, Routledge, England, UK, 2013.

[3] P. Antoniou, "A longitudinal study investigating relations between stages of effective teaching, teaching experience, and teacher professional development approaches[J]," *Journal of Classroom Interaction*, vol. 48, pp. 25–40, 2013.

[4] P. Sammons, "School effectiveness: coming of age in the 21st century," *Management in Education*, vol. 13, no. 5, pp. 10–13, 1999.

[5] J. Cilliers, B. Fleisch, J. Kotze, M. Mohohlwane, and S. Taylor, "The challenge of sustaining effective teaching: spillovers, fade-out, and the cost-effectiveness of teacher development programs," *Economics of Education Review*, vol. 87, Article ID 102215, 2022.

[6] B. Creemers and L. Kyriakides, *The Dynamics of Educational Effectiveness: A Contribution to Policy, Practice and Theory in Contemporary schools[M]*, Routledge, England, UK, 2007.

[7] K. J. Dickinson, B. L. Bass, E. A. Graviss, D. T. Nguyen, and K. Y. Pei, "How learning preferences and teaching styles influence effectiveness of surgical educators," *The American Journal of Surgery*, vol. 221, no. 2, pp. 256–260, 2021.

[8] L. Kyriakides, B. P. M. Creemers, A. Panayiotou, and E. Charalambous, *Quality and Equity in Education: Revisiting Theory and Research on Educational Effectiveness and improvement[M]*, Routledge, England, UK, 2020.

[9] P. Sammons, S. Davis, C. Day, and Q. Gu, "Using mixed methods to investigate school improvement and the role of leadership: an example of a longitudinal study in England[J]," *Journal of Educational Administration*, vol. 52, 2014.

[10] D. Muijs, L. Kyriakides, G. Van der Werf, B. Creemers, H. Timperley, and L. Earl, "State of the art-teacher effectiveness and professional learning," *School Effectiveness and School Improvement*, vol. 25, no. 2, pp. 231–256, 2014.

[11] J. Liu, R. Zhang, B. Geng et al., "Interplay between prior knowledge and communication mode on teaching effectiveness: interpersonal neural synchronization as a neural marker," *NeuroImage*, vol. 193, pp. 93–102, 2019.

[12] C.-M. Fernández-García, M. Rodríguez-Álvarez, and M.-P. Viñuela-Hernández, "University students and their perception of teaching effectiveness. Effects on students' engagement," *Revista de Psicodidáctica*, vol. 26, no. 1, pp. 62–69, 2021.

[13] S. K. Carpenter, A. E. Witherby, and S. K. Tauber, "On students' (mis)judgments of learning and teaching effectiveness," *Journal of Applied research in Memory and cognition*, vol. 9, no. 2, pp. 137–151, 2020.

[14] K. E. Brinkley-Etzkorn, "Learning to teach online: measuring the influence of faculty development training on teaching effectiveness through a TPACK lens," *The Internet and Higher Education*, vol. 38, pp. 28–35, 2018.

[15] C.-H. Sia, S. Ng, D. Hoon, J. Soong, J. Ignacio, and Y. Kowitlawakul, "The effectiveness of collaborative teaching in an introductory online radiology session for master of nursing students," *Nurse Education Today*, vol. 105, Article ID 105033, 2021.

[16] M. Liu, M. J. Gorgievski, J. Qi, and F. Paas, "Increasing teaching effectiveness in entrepreneurship education: course characteristics and student needs differences," *Learning and Individual Differences*, vol. 96, Article ID 102147, 2022.

[17] P. Sammons, *The Dynamics of Educational Effectiveness: A Contribution to Policy, Practice and Theory in Contemporary schools[J]*, Routledge, England, UK, 2009.

[18] B. Joyce, M. Weil, and E. Calhoun, *Models of Teaching*, Allyn & Bacon, Boston, MA, USA, 2000.

[19] M. Brekelmans, P. Sleegers, and B. Fraser, *Teaching for Active learning[M]*, pp. 227–242, Springer, Berlin, Germany, 2000.

[20] J. Baumert, M. Kunter, W. Blum et al., "Teachers' mathematical knowledge, cognitive activation in the classroom, and student progress," *American Educational Research Journal*, vol. 47, no. 1, pp. 133–180, 2010.

[21] B. P. M. Creemers and L. Kyriakides, *Improving Quality in Education: Dynamic Approaches to School improvement[M]*, Routledge, England, UK, 2013.

[22] C. V. Miguel, C. Moreira, M. A. Alves et al., "Developing a framework for assessing teaching effectiveness in higher education," *Education for Chemical Engineers*, vol. 29, pp. 21–28, 2019.

[23] M. E. Weiss, L. B. Piacentine, L. Candela, and K. L. Bobay, "Effectiveness of using a simulation combined with online learning approach to develop discharge teaching skills," *Nurse Education in Practice*, vol. 52, Article ID 103024, 2021.

[24] S. K. Veerabhadrappa, D. S. Ramalu, E. Y. S. Jin et al., "Effectiveness of online peer assisted learning as a teaching methodology for dental undergraduate students," *Educación Médica*, vol. 22, no. 6, pp. 320–324, 2021.

[25] Ö. Özbay and S. Çınar, "Effectiveness of flipped classroom teaching models in nursing education: a systematic review[J]," *Nurse Education Today*, vol. 102, Article ID 104922, 2021.

[26] N. T. Hendy, "The effectiveness of technology delivered instruction in teaching Human Resource Management," *International Journal of Management in Education*, vol. 19, no. 2, Article ID 100479, 2021.

[27] A. C. Carle, "Evaluating college students' evaluations of a professor's teaching effectiveness across time and instruction mode (online vs. face-to-face) using a multilevel growth modeling approach," *Computers & Education*, vol. 53, no. 2, pp. 429–435, 2009.

[28] E. G. İsmailoğlu, N. Orkun, İ. Eşer, and A. Zaybak, "Comparison of the effectiveness of the virtual simulator and video-assisted teaching on intravenous catheter insertion skills and self-confidence: a quasi-experimental study," *Nurse Education Today*, vol. 95, Article ID 104596, 2020.

[29] Y. Bengio, N. Boulanger-Lewandowski, and R. Pascanu, "Advances in optimizing recurrent networks[C]," in *Proceedings of the 2013 IEEE international conference on acoustics, speech and signal processing*, pp. 8624–8628, IEEE, Vancouver, BC, Canada, May 2013.

[30] R. Pascanu, T. Mikolov, and Y. Bengio, "On the difficulty of training recurrent neural networks[C]," in *Proceedings of the International conference on machine learning. PMLR*, pp. 1310–1318, Atlanta, GA USA, June 2013.

[31] A. Graves, A. Mohamed, and G. Hinton, "Speech recognition with deep recurrent neural networks[C]," in *Proceedings of the 2013 IEEE international conference on acoustics, speech and signal processing*, pp. 6645–6649, IEEE, Vancouver, BC, Canada, May 2013.

[32] D. Bahdanau, K. Cho, and Y. Bengio, "Neural machine translation by jointly learning to align and translate[J]," 2014, https://arxiv.org/abs/1409.0473.

[33] K. Cho, B. Van Merriënboer, D. Bahdanau, and Y. Bengio, "On the properties of neural machine translation: encoder-decoder approaches[J]," 2014, https://arxiv.org/abs/1409.1259.

[34] M. Belgiu and L. Drăguţ, "Random forest in remote sensing: a review of applications and future directions," *ISPRS Journal of Photogrammetry and Remote Sensing*, vol. 114, pp. 24–31, 2016.

[35] T. Mikolov, M. Karafiát, L. Burget, and J. Cernocký, "Recurrent neural network based language model[C]," in *Proceedings of the Interspeech 2010, 11th Annual Conference of the International Speech Communication Association*, pp. 1045–1048, Chiba, Japan, September 2010.

[36] S. Hochreiter and J. Schmidhuber, "Long short-term memory," *Neural Computation*, vol. 9, no. 8, pp. 1735–1780, 1997.

Hindawi
Scientific Programming
Volume 2022, Article ID 4194576, 8 pages
https://doi.org/10.1155/2022/4194576

Research Article

Construction of Artificial Intelligence Application Model for Supply Chain Financial Risk Assessment

Shutong Luo,[1] Min Xing,[1] and Jialu Zhao [2]

[1]*Changchun Finance College, Changchun 130000, Jilin, China*
[2]*Qiming Information Technology Co., Ltd., Changchun 130000, Jilin, China*

Correspondence should be addressed to Jialu Zhao; zhaojl693@nenu.edu.cn

Received 28 April 2022; Revised 14 May 2022; Accepted 30 May 2022; Published 23 June 2022

Academic Editor: Lianhui Li

An artificial intelligence integrated application model of supply chain financial risk assessment is constructed. Based on the financial data and supply chain data of listed companies in China's new energy electric vehicle industry, the supply chain financial credit risk evaluation index system is constructed. The data samples are preprocessed by PCA as the input data of the support vector machine, which effectively solves the problem of high-dimensional data in supply chain finance. By improving the inertia weight of particle swarm optimization and introducing mutation operation, a dynamic mutation particle swarm optimization algorithm is proposed to avoid the problem of particles falling into a local minimum in the process of optimization. Finally, the improved optimization algorithm is used to optimize the parameters of SVM and input AdaBoost integration as a weak classifier to build an integrated model with good performance in many aspects. The model has been successfully applied to the credit risk assessment of China's new energy vehicle supply chain finance. The comparison with other models shows that the constructed model has certain advantages in performance.

1. Introduction

Supply chain finance has become an emerging model to carry out comprehensive financial services for small and medium-sized enterprises [1–3]. The operation of the supply chain finance mode depends on the supply chain management activities of enterprises. Financial institutions provide financing design for the capital demander after an overall consideration of the capital flow, logistics, and information flow of the whole supply chain of the enterprise with financing demand. Supply chain finance is based on the good credit evaluation of core enterprises with a strong financial background in the supply chain [4–7]. At first, the financing model of supply chain finance appeared to solve the financing difficulties of small and medium-sized enterprises in the supply chain. Small and medium-sized enterprises operate on a small scale, and their assets and management capacity are limited. Moreover, small and medium-sized enterprises are generally in the situation of poor credit status, low degree of financial transparency, less or even no asset mortgage and guarantee. These factors lead to banks and other financial institutions unwilling to bear too many risks and inspection costs and provide loans for small and medium-sized enterprises, and the financing cost of small and medium-sized enterprises is often much higher than that of large enterprises. With the business exchanges between core enterprises and small and medium-sized enterprises, it improves their own commercial credit for small and medium-sized enterprises, making it easier for small and medium-sized enterprises to obtain loans from banks and other financial institutions.

Even after years of development, although supply chain finance is well known by more and more people, there are still many problems in practical operation, which need us to conduct more in-depth discussion and exploration [8–13]. Especially in terms of risk management and control, the risk management problems in supply chain finance deserve special attention. Risk management in supply chain finance emphasizes the antirisk ability of the

whole supply chain. Compared with the previous traditional financing model, the access scope of financial participants in the supply chain is extended to the whole supply chain, and the inspection standard is not limited to the financial indicators of an enterprise. Financial institutions implement closed credit to enterprises in the whole supply chain according to the real trade background and upstream and downstream credit strength of the enterprise, mainly based on the sales revenue of the enterprise or the determined future cash flow generated by trade. This is the advantage of supply chain finance. However, there are some risks in supply chain finance. There are many participating enterprises in a supply chain, and the mode of the supply chain will be different. This diversity and complexity may lead to the emergence of enterprises in a supply chain in the financing process with financial institutions. In order to obtain their own interests and maximize their own interests, it may threaten the interests of other cooperative enterprises in the supply chain to be damaged.

To study the risk problem in supply chain finance, for banks, from the uncontrollable risk of financing individual enterprises in the past to the controllable risk of financing enterprises as a whole in the supply chain, and by obtaining different information from each enterprise in the supply chain, firmly grasp the possible risks, keep them at the lowest level, and protect their own interests. For each subject in the supply chain, being able to control the risk of supply chain finance can not only ensure the stable operation of the supply chain system but also improve the efficiency and cooperation of the supply chain.

The vigorous development of information technology [14–17] has brought new opportunities to the financial risk assessment of the supply chain. Various advanced artificial intelligence methods, such as support vector machine (SVM) [18, 19], particle swarm optimization (PSO) algorithm [20, 21], and AdaBoost algorithm [22, 23], have been gradually applied in this field. This study is carried out under this background.

2. Credit Risk Evaluation Index System

Under the traditional financing model, there is a severe information asymmetry between the bank and the small and medium-sized enterprises applying for financing. It is difficult to make those small-scale, unsound financial systems, and their small and medium-sized enterprises that meet the requirements of bank guarantees or pledged assets are granted credit. Under the supply chain finance model, the evaluation indicators should consider the relationship between small and medium-sized enterprises and core enterprises and the overall situation of the entire supply chain to more comprehensively and accurately grasp the credit situation of financing enterprises. Therefore, based on the supply chain perspective, this paper considers the financial and nonfinancial status of financing enterprises and core enterprises and the overall operation status of the supply chain. The combination of qualitative and quantitative indicators has redesigned the credit risk evaluation index system to reflect the risk level of the whole chain, as shown in Figure 1.

3. Algorithm

Assuming a training sample set of n samples $\{(x_i, y_i), (i = 1, 2, \cdots, n)\}$, x_i is the first sample, $y_i \in \{1, -1\}$ is the classification hyperplane equation is $wx + b = 0$ (w is the normal vector of the hyperplane, b is the bias). It is assumed that the classification hyperplane can correctly classify samples into two categories, and the samples of the same category are placed on the same side of the hyperplane, that is, satisfying

$$\begin{cases} wx_i + b \geq 1, & y_i = 1 \\ wx_i + b \leq -1, & y_i = -1 \end{cases}, \quad (i = 1, 2, \cdots, n). \tag{1}$$

Then, we can get $y_i(w_i + b) \geqslant 1$.

The geometric distance between the sample point x_i and the classification hyperplane is $d_i = wx_i + b/\|w\|$, and then, the distance between the two types of samples is $2wx_i + b/\|w\|$, set $|wx_i + b| = 1, 2|wx_i + b|/\|w\| = 2/\|w\|$. The optimal hyperplane should maximize $2/\|w\|$, that is, minimize $\|w\|^2/2$. Adding penalty factor A and slack variable B to the above problem can be transformed into

$$\begin{cases} m\dfrac{\|w\|^2}{2} + C\sum_{i=1}^{n}\xi_i, \\ \\ s.t.\, y_i(w \cdot x_i + b) \geqslant 1 - \xi_i \, i = 1, 2, \cdots, n. \end{cases} \tag{2}$$

Lagrange function is built as

$$L(w, \xi, b, \alpha, \beta) = \frac{\|w\|^2}{2} + C\sum_{i=1}^{n}\xi_i - \sum_{i=1}^{n}\alpha_i\left[y_i(w \cdot x + b) - 1 + \xi_i\right] - \sum_{i=1}^{n}\beta_i\xi_i. \tag{3}$$

Due to the high-dimensional, nonlinear, and dynamic characteristics of supply chain financial evaluation indicators, SVM needs to introduce a kernel function $K(x_i, x_j) = \Phi(x_i)^T \cdot \Phi(x_j)$ to calculate the nonlinearity in high-dimensional space. The classification problem is transformed. Compared with several other SVM kernel functions, the radial basis (RBF) kernel function performs better in both linear and nonlinear data sets. Therefore, the radial basis kernel function is selected in this paper: $(x, x_i) = \exp(-\gamma\|x - x_i\|^2), \quad \gamma > 0$, is input to SVM.

According to equations (2) and (3), the original problem is transformed into a Lagrange dual problem:

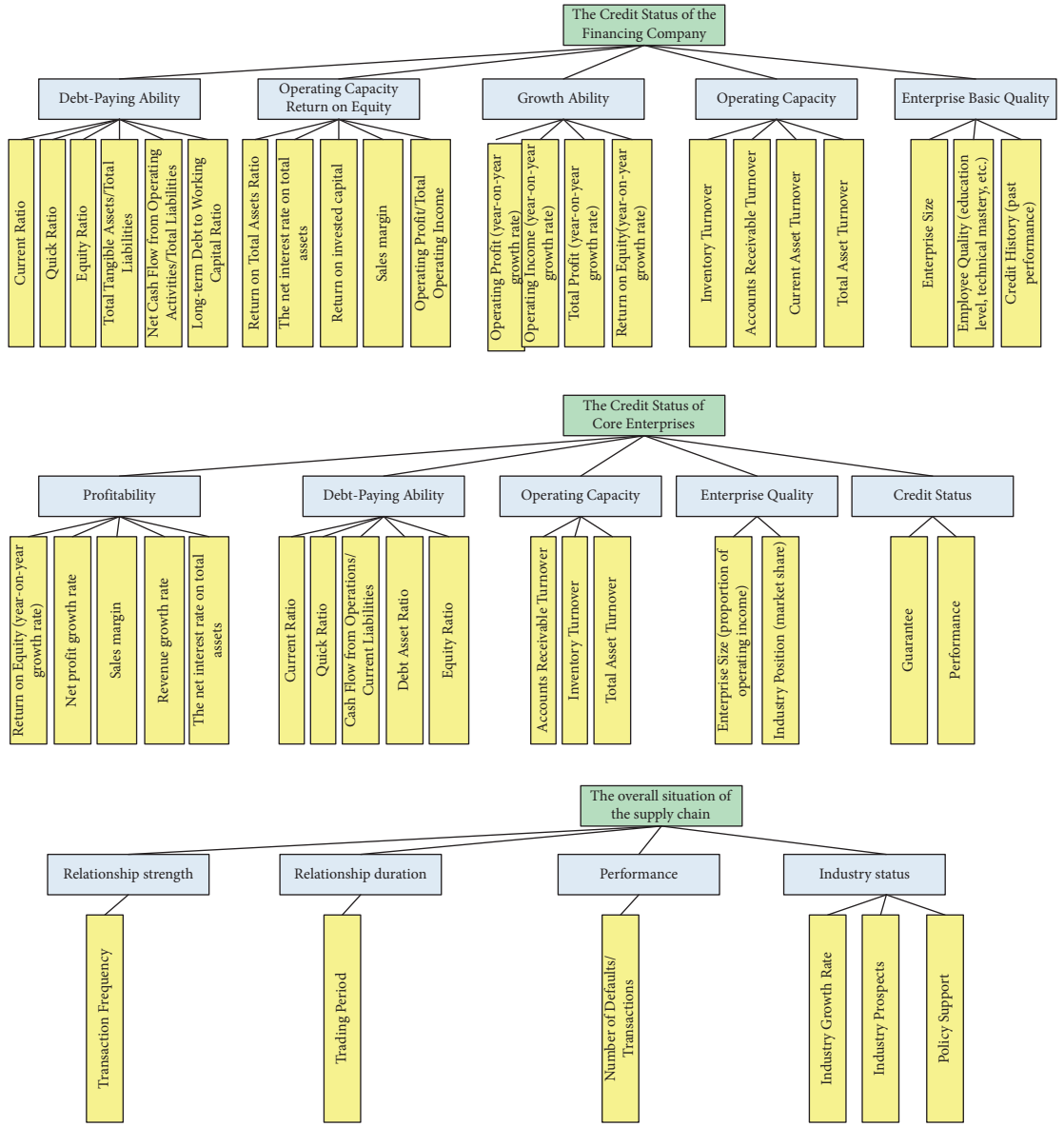

Figure 1: Credit risk evaluation index system.

$$\begin{cases} \max Q(\alpha) = L(w, \xi, b, \alpha, \beta) = \sum_{i=1}^{n} \alpha_i - \frac{1}{2}\alpha_i \alpha_j y_i y_j \left[\Phi(x_i)^T \cdot \Phi(x_j)\right] \\ \qquad\qquad = \sum_{i=1}^{n} \alpha_i - \frac{1}{2}\alpha_i \alpha_j y_i y_j K(x_i, x_j), \\ s.t. \sum_{i=1}^{n} \alpha_i y_i = 0, \alpha_i \geq 0, \ i = 1, 2, \cdots, n. \end{cases} \tag{4}$$

Set the optimal Lagrange multiplier $\alpha^* = (\alpha_1^*, \alpha_2^*, \cdots, \alpha_n^*)$, get $w^* = \sum_{i=1}^{n} \alpha_i^* y_i \Phi(x_i)$.

In summary, the optimal classification discriminant function is obtained.

$$f(x) = \operatorname{sgn}\left[w^* \Phi(x) + b^*\right] = \operatorname{sgn}\left[\sum_{i=1}^{n} \alpha_i^* y_i \Phi(x_i)^T \Phi(x) + b^*\right] = \operatorname{sgn}\left[\sum_{i=1}^{n} \alpha_i^* y_i K(x_i, x) + b^*\right]. \tag{5}$$

In the standard particle swarm optimization algorithm, the inertia weight ω is usually set to a fixed value, which is challenging to meet the dynamic requirements of the global search capability in the early stage of the algorithm iteration and the local search capability in the later stage. Based on the basic principles of particle swarm optimization, this paper considers the convergence accuracy and convergence speed of the algorithm. It uses the dynamic variation particle swarm optimization (DPSO) to optimize the parameters of the SVM, and the dynamic weights are as follows

$$\omega = \begin{cases} \omega_{\min} + \dfrac{(\omega_{\max} - \omega_{\min}) \times (f_i - f_{\min})}{f_{\text{avg}} - f_{\min}}, & f_i \leqslant f_{\text{avg}}, \\ \omega_{\max}, & f_i \rangle f_{\text{avg}}, \end{cases} \tag{6}$$

where $f_{\text{avg}} = 1/n \sum_1^n f_i$ represents the average fitness value of the particle.

$\omega_{\max}$ and $\omega_{\min}$ are the maximum and minimum weights, f_i is the fitness value of the current particle, f_{avg} and $f_{\min}$ represent the average fitness value and minimum fitness value of the particle $t-1$ generation, respectively.

For the particle with $f_i \rangle f_{\text{avg}}$, its ω value is $\omega_{\max}$. For the particle with $f_{\leqslant} f_{\text{avg}}$, when the particle fitness is the same, the ω value becomes larger. Otherwise, it becomes smaller. Drawing on the idea of genetic algorithm mutation, the mutation operation is introduced into the particle swarm algorithm. The particles jump out of the original area and enter other new areas to search to find a new group extreme value and cycle the mutation operation until the global optimum is found. The solution, the specific method is as follows.

Let the population fitness variance of the particle swarm be

$$\sigma^2 = \frac{1}{N} \sum_{i=1}^{n} \left(\frac{f_i - f_{\text{avg}}}{f}\right)^2, \tag{7}$$

where n is the number of particles in the particle swarm, and σ^2 represents the particle's degree of convergence. As σ^2 becomes smaller, the particle swarm gradually converges from a random search state. f represents the normalized scaling factor, and its values are as follows:

$$f = \begin{cases} m\left(\left|f_i - f_{\text{avg}}\right|\right), & \max\left|f_i - f_{\text{avg}}\right| \rangle 1, \\ 1, & \text{else}. \end{cases} \tag{8}$$

Let the aggregation degree of particles be α, and the calculation formula of t generation α is as follows:

$$\alpha = 1 - \frac{\sqrt{1/N \sum_{i=1}^{N} \left(f_i^c - f_{\text{avg}}^t\right)^2} - \sigma_{\min}}{\sigma_{\max} - \sigma_{\min}}. \tag{9}$$

$\sigma_{\max}$ and $\sigma_{\min}$ represent the maximum and minimum fitness values of the standard deviation of all particles, respectively. According to the definition of population aggregation degree, the formula for the mutation probability of t generation particles is set as follows:

$$P_{t+1} = \frac{\lambda \cdot \alpha}{\ln(N \cdot m)}. \tag{10}$$

P_{t+1} is proportional to the particle aggregation degree α, $\lambda \in [3, 5]$ is a fixed constant proportional gain, N represents the size of the population, and m represents the dimension of the optimization problem. The algorithm flow is shown in Figure 2.

AdaBoost (adaptive boosting) is an ensemble learning algorithm that strengthens weak learners by iterating over the weights of training samples. In this paper, AdaBoost is used to train the DPSO-SVM learner. The algorithm implementation steps are as follows:

Step 1. Input N initial learning and training sample sets:

$$D = \{(x_i, y_i)\}_{i=1}^{N}, \tag{11}$$

where x_i is the sample feature of the sample space, y_i is the category symbol of the category space.

Set the weight matrix of the initial training samples:

$$W_1 = (\omega_{11}, \omega_{12}, \cdots, \omega_{1i}, \cdots, \omega_{1N}). \tag{12}$$

Assuming that the weights of each training sample are equal; namely, $\omega_{1i} = 1/N$, $(i = 1, 2, \cdots, N)$.

Step 2. Use $W_t = (\omega_{t1}, \omega_{t2}, \cdots, \omega_{1i}, \cdots, \omega_{tN})$, training set data with weight distribution to learn, using DPSO-SVM as the base classifier

$$h_t(x_i)\colon x_i \longrightarrow \{-1, 1\}. \tag{13}$$

Step 3. Calculate the classification error of the base learner:

$$\varepsilon_t = \sum_{i=1}^{N} \omega_t(i) I\left[y_t \neq h_t(x_i)\right]. \tag{14}$$

If $|\varepsilon_t|$ is greater than the error setting value, go to Step 4; otherwise, the iteration is terminated.

Step 4. Calculate the weight of the DPSO-SVM classifier. Set

$$\alpha_t = \frac{\left\{\text{In}\left[(1 - \varepsilon_t)/\varepsilon_t\right]\right\}}{2}. \tag{15}$$

Update the weight of the training sample $\omega_{t+1}(i) = \omega_t(i) \exp\{-\alpha_t y_i h_t\}/C_t, C_t$, C_t is the normalization factor. Then,

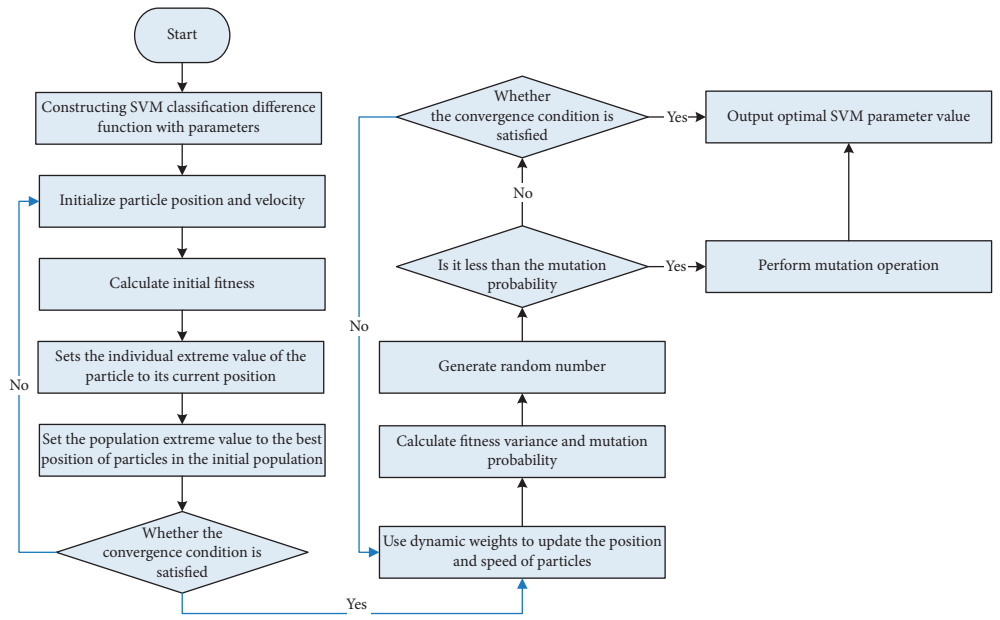

Figure 2: Algorithm flow.

$$C_t = \sum_{i=1}^{N} \omega_t(i) \exp\{-\alpha_t y_i h_t\}. \tag{16}$$

Return to Step 2 iteration.

Step 5. Combine each DPSO-SVM weak classifier:

$$f(x) = \sum_{t=1}^{T} \alpha_t h_t(x). \tag{17}$$

The final strong classifier model is obtained as

$$G(x) = \operatorname{sign}[f(x)] = \operatorname{sign}\left[\sum_{t=1}^{T} \alpha_t h_t(x)\right]. \tag{18}$$

4. Experiment

We select the relatively mature new energy vehicle supply chain in China's supply chain finance business as the research object. The financial and other relevant data of 60 domestic listed companies in the upstream and downstream of the chain in the past 5 years from 2016 to 2020, a total of 320 samples, excluding 52 samples with abnormal data, and the remaining 268 available samples, and released according to the annual 38 samples with "bad credit" were compared and screened out, and 230 samples with "good credit" were used as initial data.

Since the established evaluation index system has many variables and there is a certain correlation between each index, to simplify the data input to the model on the premise of ensuring the least loss of data information, principal component analysis (PCA) [24–26] is used to reduce the dimensionality of the collected data. Table 1 shows the eigenvalues and contribution rates of the principal components. It can be seen from Table 1 that the cumulative contribution rate of the first 12 principal components is 86.6680%, so the first 12 principal components are extracted.

Table 2 shows the 12 linearly independent principal components extracted after the principal component attribute reduction of the 46 supply chain financial risk evaluation indicators of the 268 original data samples. Inputting the dimensionality-reduced data into the evaluation model can significantly improve computational efficiency; it also avoids the problem that the support vector machine RBF kernel function is not good at dealing with dimensionally nonuniform datasets.

Taking the extracted 12 principal components as the input variables of the support vector machine, set 200 samples in the training set, 68 samples in the test set, the class label of bad samples is 1, and the class label of good samples is 0.

The improved particle swarm algorithm optimizes the penalty coefficient C and parameter g of the radial basis (RBF) kernel function. The parameters $C_1 = 1.5$、$C_2 = 1.7$, the population size is 30, and the maximum number of iterations is set to 300, the value range of SVM penalty coefficient C and kernel parameter g is set to $[0.001, 10]$, particle position $X_i \in [-6, 6]$, particle velocity $V \in [-10, 10]$.

After optimal selection, the parameters of the SVM kernel function are screened to obtain $C = 2.8284$, $g = 0.087936$, which is used as the basic parameter of the model.

Taking DP-SO-SVM as the base classifier, using AdaBoost to integrate DP-SO-SVM, the obtained classification results are compared with the single classifier SVM, PSO-SVM, and BP-AdaBoost. Table 3 compares classification results between different indicators of each model.

Accuracy reflects the ability of the classifier to classify and discriminate the overall samples, that is, the ability of the model to identify good and bad samples correctly. An

Table 1: PCA result.

Principal component	Initial eigenvalues		
	Eigenvalues	Variance (%)	Cumulative variance (%)
1	10.5091	22.8452	22.8452
2	8.5722	18.6343	41.4795
3	4.5007	9.7843	51.2638
4	3.2723	7.1132	58.3770
5	2.9594	6.4332	64.8102
6	2.2995	4.9983	69.8085
7	2.0413	4.4383	74.2468
8	1.3192	2.8662	77.1130
9	1.1995	2.6063	79.7193
10	1.1374	2.4723	82.1916
11	1.0532	2.2902	84.4818
12	1.0051	2.1862	86.6680

Table 2: Principal components of the 268 original data samples.

Code	F1	F2	F3	F4	F5	F6	F7	F8	F9	F10	F11	F12
1	−0.4976	−0.3612	−0.5216	−1.3382	−0.6266	1.2898	−0.5716	−0.0732	−0.5326	−0.4662	−0.1806	−0.2922
2	−0.4145	0.6247	0.1625	0.5927	0.1605	0.0617	0.9665	0.3117	0.0295	−0.2643	−0.3715	0.1287
3	−0.0836	−0.1382	−0.8316	−1.1692	0.2364	0.5518	−0.9906	−0.5682	−0.2296	0.2598	−0.7196	0.1488
4	−0.2025	0.1407	−0.5665	−0.0443	3.2635	−0.5633	−0.2875	−1.6223	−0.5925	−0.6943	−0.7085	0.1567
5	−0.2206	−0.4792	−0.3446	−0.3932	−0.0426	0.1488	−1.1766	−0.3362	−0.3526	0.4878	−0.6356	0.2628
6	−4.7765	−2.1403	1.7345	−2.5263	−1.9085	1.4337	5.8485	−4.3783	−4.3885	−1.5103	1.3355	−1.1613
7	−0.5156	−0.2272	−0.7406	−0.9292	0.0004	0.0948	−0.1606	−1.5692	−0.9626	−1.3952	−0.8866	−0.9332
...	...	...	...	...	...	...	...	...	...	...	...	...
268	0.5997	0.2912	−0.5793	0.6402	−1.3163	0.0212	−0.5273	−0.8408	0.4417	-0.2168	0.4357	0.3532

Table 3: Comparison of different results.

Algorithm	Accuracy	Recall	Precision	Specificity	G-means	F1-score	AUC
SVM	87.21	96.76	88.27	47.05	92.44	92.3	71.95
AdaBoost	89.72	98.41	89.69	52.96	93.93	93.87	75.64
PSO-SVM	92.34	96.99	91.21	58.81	95.52	95.37	79.44
DPSO-SVM	93.57	96.02	92.52	64.73	96.18	96.14	82.33
BP-AdaBoost	94.90	98.38	95.34	76.46	96.87	96.82	87.46
Ada-AMPSO-SVM	96.13	98.02	95.29	82.37	97.61	97.62	91.16

enterprise with good credit is evaluated as an enterprise with poor credit in the credit evaluation. For the credit institution, it is only the customer's future loan interest loss. Default risk of credit institutions will lead to irrecoverable loss of principal and interest of credit institutions. Therefore, compared with the Recall indicator, which represents the prediction accuracy rate in instances labeled as positive samples, this paper pays more attention to the size of the specificity indicator, which reflects the prediction accuracy rate in instances labeled as negative samples. Due to the specific sample data, the predicted value of the support vector machine for the test set is a single value, and the ROC curve is degraded. At this time, the AUC index cannot fully reflect the classifier's performance, so this paper uses F_1−Score, G− means, accuracy, and other indicators were used as the primary evaluation indicators. AUC was used as the auxiliary evaluation indicator.

The results in Table 3 show that all models can effectively classify the data collected in this paper, with the lowest classification accuracy of 87.21%. At the same time, it can be seen that the recognition error of negative samples is always higher than that of positive samples, so, in future research, more attention should be paid to the misclassification rate of bad samples.

Comparing different models, the performance of the PSO-SVM model is significantly improved based on SVM. Using an adaptive mutation particle swarm algorithm to optimize SVM, DPSO-SVM has a better classification effect than standard PSO-SVM. The accuracy of the test set samples is improved from 92.34% to 93.57%. The AdaBoost-DPSO-SVM model integrated with the AdaBoost algorithm has a significant improvement in various indicators, and the model accuracy reaches the highest, 96.13%. Compared with the BP-AdaBoost model, its classification performance is better.

The specificity index of the AdaBoost-DPSO-SVM model is the highest among the five models, indicating that it has the lowest error rate in identifying bad credit companies as good credit companies. The G-means and F1-score index values that comprehensively reflect the output effect of the

model are the highest, 97.63% and 97.62%, respectively, indicating that the AdaBoost-DPSO-SVM model proposed in this paper can be better applied to the assessment of supply chain financial credit risk.

5. Conclusions

The research on credit risk first appeared in the field of finance. It is one of the main risk types faced by credit subjects such as enterprises and financial institutions. Many domestic and foreign scholars study credit risk from different perspectives. In our research, we pay more attention to the evaluation of supply chain financial credit risk. The diffusion of credit risk among many subjects is the result of the joint action of internal and external factors such as the psychological and behavioral factors of credit risk holders, the network composed of credit risk holders as nodes, and the behavior of market regulators. The artificial intelligence integrated application model of supply chain financial risk assessment constructed in this paper provides a new perspective for accelerating the supply side structural reform in China's financial field, making finance better serve the real economy, and realizing high-quality economic development.

Data Availability

The dataset can be accessed upon request.

Conflicts of Interest

The authors declare that there are no conflicts of interest.

References

[1] X. Ren and X. Wang, "Research on optimization algorithm of digital supply chain finance in science and technology enterprises," *Lecture Notes on Data Engineering and Communications Technologies*, vol. 85, pp. 255–261, 2022.

[2] G. Soni, S. Kumar, R. V. Mahto, S. K. Mangla, M. L. Mittal, and W. M. Lim, "A decision-making framework for Industry 4.0 technology implementation: the case of FinTech and sustainable supply chain finance for SMEs," *Technological Forecasting and Social Change*, vol. 180, 2022.

[3] Y. Feng and Y. Wang, "Easing effect of supply chain finance constraints based on blockchain technology," in *Proceedings of the 2021 International Conference on Machine Learning and Big Data Analytics for IoT Security and Privacy*, vol. 97, pp. 961–968, Bangladesh, 2021.

[4] R. Jiang, Y. Kang, Y. Liu et al., "A trust transitivity model of small and medium-sized manufacturing enterprises under blockchain-based supply chain finance," *International Journal of Production Economics*, vol. 247, 2022.

[5] C. Wang, F. Yu, Z. Zhang, and J. Zhang, "Multiview Graph Learning for Small- and Medium-Sized Enterprises' Credit Risk Assessment in Supply Chain Finance," *Complexity*, vol. 2021, Article ID 6670873, 2021.

[6] Y. Hong, "New Model of Food Supply Chain Finance Based on the Internet of Things and Blockchain," *Mobile Information Systems*, vol. 2021, Article ID 7589964, 2021.

[7] R. Wang and Y. Wu, "Application of blockchain technology in supply chain finance of Beibu Gulf Region," *Mathematical Problems in Engineering*, vol. 2021, Article ID 5556424, 2021.

[8] Y. Wang, "Research on Supply Chain Financial Risk Assessment Based on Blockchain and Fuzzy Neural Networks," *Wireless Communications and Mobile Computing*, vol. 2021, Article ID 5565980, 2021.

[9] X. Huang, J. Sun, and Zhao Xiaoyun, "Credit Risk Assessment of Supply Chain Financing with a Grey Correlation Model: An Empirical Study on China's Home Appliance Industry," *Complexity*, vol. 2021, Article ID 9981019, 2021.

[10] J. Zhang, Z. Zhang, and Y. Liu, "Impact of interest rate risk on supply chain network under bank credit and trade credit financing," *Mathematical Problems in Engineering*, vol. 2021, Article ID 4718912, 2021.

[11] Q. Wei, X. Gou, T. Deng, and Bai Chunguang, "Restrain Price Collusion in Trade-Based Supply Chain Finance," *Complexity*, vol. 2021, Article ID 5554501, 2021.

[12] Q. Qu, C. Liu, and X. Bao, "E-commerce Enterprise Supply Chain Financing Risk Assessment Based on Linked Data Mining and Edge Computing," *Mobile Information Systems*, vol. 2021, Article ID 9938325, 2021.

[13] X. Xia and Y. Nan, "Pricing decision and financing approach selection of fund-deficient closed-loop supply chain under distributor's risk aversion," *Mathematical Problems in Engineering*, vol. 2022, Article ID 3077833, 2022.

[14] L. Li, B. Lei, and C. Mao, "Digital twin in smart manufacturing," *Journal of Industrial Information Integration*, vol. 26, no. 9, Article ID 100289, 2022.

[15] L. Li, T. Qu, Y. Liu et al., "Sustainability assessment of intelligent manufacturing supported by digital twin," *IEEE Access*, vol. 8, Article ID 174988, 2020.

[16] L. Li and C. Mao, "Big data supported PSS evaluation decision in service-oriented manufacturing," *IEEE Access*, vol. 8, no. 99, 1 page, 2020.

[17] L. Li, C. Mao, H. Sun, Y. Yuan, and B. Lei, "Digital twin driven green performance evaluation methodology of intelligent manufacturing: hybrid model based on fuzzy rough-sets AHP, multistage weight synthesis, and PROMETHEE II," *Complexity*, vol. 2020, no. 6, 24 pages, Article ID 3853925, 2020.

[18] X. Wang, Y. Li, J. Chen, and J. Yang, "Enhancing Personalized Recommendation by Transductive Support Vector Machine and Active Learning," *Security and Communication Networks*, vol. 2022, Article ID 1705527, 2022.

[19] S. Sun, "Shield Tunneling Parameters Matching Based on Support Vector Machine and Improved Particle Swarm Optimization," *Scientific Programming*, vol. 2022, Article ID 6782947, 2022.

[20] M. Yang, Y. Liu, and J. Yang, "A hybrid multi-objective particle swarm optimization with central control strategy," *Computational Intelligence and Neuroscience*, vol. 2022, 2022.

[21] Q. Zhu, "Classification and optimization of basketball players' training effect based on particle swarm optimization," *Journal of Healthcare Engineering*, vol. 2022, 2022.

[22] H. Bei, Y. Wang, Z. Ren, S. Jiang, K. Li, and Wang, "Wenyang. A statistical approach to cost-sensitive AdaBoost for imbalanced data classification," *Mathematical Problems in Engineering*, vol. 2021, Article ID 3165589, 2021.

[23] H. Zhou and G. Yu, "Research on Fast Pedestrian Detection Algorithm Based on Autoencoding Neural Network and Adaboost," *Complexity*, vol. 2021, 2021.
[24] C. Liu, Y. Huang, F. Huang, and J. Yu, "Multifeature Deep Cascaded Learning for PPG Biometric Recognition," *Scientific Programming*, vol. 2022, Article ID 7477746, 2022.
[25] X. Chen, "Social effect analysis of intelligent sports based on principal component analysis and fuzzy control," *Journal of Sensors*, vol. 2021, Article ID 4475448, 2021.
[26] H. Wu and X.-M. Gu, "Fuzzy Principal Component Analysis Model on Evaluating Innovation Service Capability," *Scientific Programming*, vol. 2020, 2020.

Hindawi
Scientific Programming
Volume 2022, Article ID 1219802, 12 pages
https://doi.org/10.1155/2022/1219802

Research Article

Deep Neural Network Model-Assisted Reconstruction and Optimization of Chinese Characters in Product Packaging Graphic Patterns and Visual Styling Design

Danjun Zhu and Gangtian Liu

Henan University of Science and Technology, Luoyang 471023, Henan, China

Correspondence should be addressed to Danjun Zhu; 9903680@haust.edu.cn

Received 20 March 2022; Revised 25 April 2022; Accepted 24 May 2022; Published 23 June 2022

Academic Editor: Jie Liu

Chinese character fonts not only carry the long history of Chinese civilization, but also burst out modern design art elements with distinctive Chinese characteristics. This article first analyzes the origin and writing form of several ancient Chinese characters and draws out the influence of the historical evolution of ancient Chinese characters on Chinese culture. In the basic theoretical structure of font design, traditional art elements and modern font design are integrated, and specific design cases are analyzed. A Chinese character packaging quality detection method combining machine vision and a lightweight convolutional neural network is proposed. First, the method based on threshold segmentation and affine transformation in machine vision is used to perform threshold processing on the image to be tested, and the Chinese character region is tilted and cropped; then, the network structure of the classification algorithm is designed according to the requirements of image features and defect recognition. The field images are produced, a dataset of Chinese character packaging defects is established, and then the proposed Chinese character packaging defect recognition network is verified and deployed to test the accuracy and detection speed of the algorithm deployed on the Jetson Nano embedded platform. Combined with theoretical research and case analysis, the design of packaging design series is practiced with the idea of combining Chinese character art design and classical culture.

1. Introduction

The birth of the written word symbolizes the progress of human society, and the culture of Chinese characters, which has undergone millennia of baptism, is the only ancient script that has survived and is still in use today [1, 2]. The study of the visual arts of Chinese characters has gradually become an important part of the design and is widely used in modern graphic design, such as poster design, packaging decoration and product description, book layout design, and media advertising communication. Packaging plays an increasingly important role in modern design trends, and more and more industries require product packaging design. For example, material products and other series of physical packaging belong to the traditional packaging design category, whereas film and media, advertising, and corporate image belong to the new modern packaging [3, 4]. Regardless of the modern and traditional packaging, all put words in the first place of design, and Chinese characters are an important member of font design. The design of Chinese characters in packaging design not only expresses the excellent Chinese civilization, but is also an outstanding representative of modern Chinese design. Through the study of the artistic expression of Chinese characters, it is possible to gain a deep understanding of the ideology and aesthetic flavour of Chinese civilization, to lay a good foundation for modern type design, to further explore the relationship between tradition and modernity, to promote a better breakthrough in the international development environment of modern art design of Chinese characters, and thus to better express the national spirit and Chinese style of packaging design. National cultural values and traditional art forms are the artistic sources of Chinese character font design. Especially in packaging design, the Chinese character

art form, with the modern design concept as the medium of packaging materials, conveys the connotation of Chinese character culture from the perspective of visual art, which has very important research significance and artistic value [5–7].

Chinese characters contain the long cultural history of our country and at the same time have a rich cultural heritage. It is not only a character, a language, but also a spirit, a heritage. Chinese characters have a wide variety of expressions, whether they are pictographs or morphological characters, and they have a unique charm that is much loved by Chinese children and even by people from overseas. Because of their plasticity, Chinese characters can have a strong visual effect in terms of shape, size, font, and meaning, conveying a message or even an aesthetic effect [8]. This feature of Chinese characters was discovered and explored by businessmen, so Chinese fonts began to appear in the design of product packaging, and this new form soon came to be noticed and loved by the public, and many businesses began to compete to imitate it, in order to give full play to the promotional role of Chinese fonts and to express the efficacy of the product vividly. Here we look at the linguistic expression of Chinese fonts in product packaging, and see the visual effect it plays [9].

The application of Chinese character font epigraphic decoration design in product packaging, from the text pen shape: the structure of Chinese characters is actually complex, different Chinese characters are composed of different strokes that make up the shape of the text, which is often referred to as the text pen shape. The brush shape is a type of Chinese character decoration and is used more often in product packaging [10].

The structural shape of the characters: different characters have different artistic shapes and are suitable for different product packaging designs. And some Chinese characters have a vivid image, which can give a good visual impact to a certain extent. We have just analyzed the characters from the perspective of strokes, and now we are talking about how to do a good job of decorating the characters from the point of view of the overall shape and the overall structure of the characters. Some Chinese characters have fewer strokes and the overall structure is simple and easy to understand, giving people a sense of simplicity and generosity. Such a Chinese character structure is combined with some novel and fun patterns, and then the text is processed through computer technology to enrich the image. Of course, different products have different packaging concepts and there is a great deal to be said for the choice of Chinese characters, which is something that packaging professionals should be aware of when they are working on the packaging [11, 12].

This article proposes a method for detecting the quality of Chinese character packaging by combining machine vision and lightweight convolutional neural networks. Firstly, a method based on threshold segmentation and affine transformation in machine vision is used for shareholding, skew correction, and cropping of the Chinese character region of the image to be measured; then, the network structure of the classification algorithm is designed according to the image characteristics and defect recognition requirements; finally, the production site images are collected to build a Chinese character packaging defect dataset, after which the proposed Chinese character packaging defect recognition network is validated and tested for the accuracy and speed of the algorithm deployed on the Jetson Nano embedded platform [13]. The accuracy and detection speed of the algorithm deployed on the Jetson Nano embedded platform was tested. Combining theoretical research and case studies, the design of the packaging design series is practiced with the idea of integrating Chinese character art design and classical culture. To sum up, we have a certain understanding of the visual language effect of Chinese character font design in product packaging. From the appearance, imagery, and overall calligraphy structure of Chinese characters, we explore how to integrate Chinese character fonts into packaging design, which can not only promote product promotion and the effect of sales, but also to meet people's aesthetic psychology. By analyzing the application of Chinese fonts in packaging design, the development of Chinese packaging is promoted.

2. Related Works

The study of Chinese fonts in packaging design, first of all, should cut into the subject from the perspective of philology, the process of development and evolution of Chinese fonts in the textual dimension is the mainstream academic argument of current textual research, by knowing the origin of civilization and the development of philology, to establish a theoretical basis for subsequent design practice [14].

Domestic research into the basic theory of packaging design is currently at a rapid stage of development, where the combination of theoretical literature and excellent design practice work has led to packaging having the role of an industry vane in the discipline of graphic design. Firstly, regarding the current status of the basic theory of packaging design, [15] makes a clear study of the relationship between packaging development and economic culture and provides a detailed overview of the essential functions of packaging, integrating the study of new materials and new design concepts into innovative design practice. In [16], the principles of visual communication design are systematically and clearly outlined, from conceptual theory to physiological activity, and sublimated through the study of visual perception into a perceptual account of visual art. In [17], a series of theories of packaging design is elaborated, including a complete theoretical study of the functional nature, cultural values, market positioning, design elements, and printing and manufacturing.

With the development of modern thinking of fashion and nationalism, packaging design is more dependent on the decoration of visual art design based on theoretical research, breaking through the traditional packaging forms and rules of design, which is the goal of the pursuit of market value. In [18], the visual language of packaging design such as text, colour, and graphics is studied separately to pursue a more suitable visual symbol design for the product, which is applied to design practice according to theoretical research.

In [19], the chronological evolution of packaging design is systematically studied, from the mid-19th century to the 1980s, a period of about 150 years of packaging design cases, with Europe and the United States as the main objects of study, revealing the history of economic culture and packaging design processes in developed Western countries or regions, allowing an intuitive understanding of the evolution and development of advanced design concepts abroad. It has a certain reference value for the innovation of modern packaging art and design forms in China. Reference [20] describes the rise of Japanese design after World War II and analyzes, from the perspective of reason and sensibility, the different senses of modern design for society, human beings, and nature, which is useful for the study of packaging design and consumer psychological appeal.

The packaging of Chinese characters is the final step in the process of testing the quality of Chinese characters before they are used as packaging to go to market. Compared to manual inspection, machine vision has great advantages in terms of speed and accuracy. Reference [21] used Blob Analysis on a smart camera to detect missing bottles and breaks in the packaging of specific colour Chinese characters; [22] used Speeded Up Robust Feature (SURF) with a support vector machine (SVM) to detect defects.

3. The Imagery of Chinese Fonts

The connotations of Chinese characters are rich and varied, and in addition to the use of representational decoration of Chinese characters as we have described earlier, the imagery of Chinese fonts can also be applied to the design of product packaging. What is the imagery of Chinese characters? The imagery of Chinese characters refers to the unique connotation of Chinese characters, combining this connotation with the essential features and practical functions of the product, enriching the expression of Chinese characters by implying meaning in form [23]. The imagery of Chinese characters can be divided into the morphological expression of the characters and the meaning of the characters. The morphological expression means finding the commonalities between the characters and the product and combining them with the meaning of the words in a comprehensive graphic art, which will produce unexpected design effects. The meaning of the word is to find the appearance or properties of the product and design the world by incorporating creative elements into the word, which can sometimes achieve a very good mood.

Whether we are talking about representations or imagery, in the end, it comes back to the calligraphic script and stylistic structure of the Chinese characters. The content of the text is important, as it introduces the product name, but if we focus on the content and structure of the art, the effect of the packaging will be doubled. The requirements for packaging are getting higher and higher, and the forms of packaging are becoming more and more diverse, with a series of new forms of expression such as images being discovered all the time. To continue to play the role of Chinese fonts in packaging design, we need to give more thought to the artistic and decorative quality of Chinese characters [24].

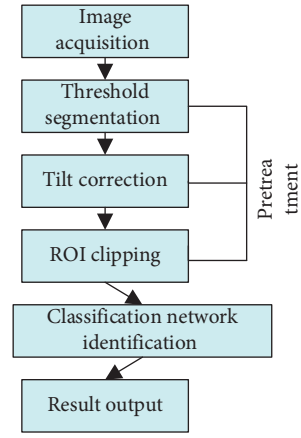

Figure 1: Flow of Chinese character packaging quality detection algorithm.

To sum up, we have a certain understanding of the visual language effect of Chinese character font design in product packaging, from the appearance, imagery, and overall calligraphic structure of Chinese characters to explore how to integrate Chinese fonts in packaging design, both to play the effect of product promotion and sales and to meet people's aesthetic psychology. Through the analysis of the use of Chinese fonts in packaging design, we will promote the development of Chinese packaging.

4. Programme of This Article

In order to meet the detection task of this article and to achieve low-cost deployment and improve production efficiency in a production environment, this article combines traditional image processing methods and designs a Chinese character packaging defect detection algorithm with reference to the Mobile Net series network structure. The first step is image acquisition, followed by preprocessing (threshold segmentation, tilt correction, ROI cropping) and recognition by the classification network, and finally the results are outputted. First, the original image captured by the industrial camera is preprocessed, including threshold segmentation, position correction, and region of interest (ROI) cropping [25], to obtain a single Chinese character region image; then the single Chinese character region images are fed into the packaging defect classification network in turn; finally, the category of each Chinese character region image is outputted (see Figure 1).

5. Image Preprocessing

The colour image was first grey-headed, that is each pixel in the image had equal component values in all three RGB channels. After grey-scale processing, the original image was cropped according to ROI based on the external trigger used by the camera and the relatively stable region of the Chinese character blister pallets in the image to reduce computational effort, and the region of interest image $f(x, y)$ was obtained, as shown in Figure 2(a). The blister tray in the grey-scale image is close to the grey value of a part of the

Figure 2: Image threshold process.

block in the background, and direct use of global shareholding cannot effectively separate out the tray. Figure 2(b) shows the result of the direct use of the maximum inter-class difference method (Otsu). Observing the ROI image shows that the edge distinction of the blister tray box background is obvious, so the edge information can be used to assist Otsu in shareholding [26].

In this article, the ROI image is first smoothed using a Gaussian filter, then the image edges are calculated using the Laplace operator [27], and then the Laplace image is thresholded using 99% of the absolute value of the Laplace image to specify a threshold non-negative T to obtain a sparse set of pixels $g_t(x, y)$, and the process can be expressed as:

$$g_t(x, y) = \begin{cases} 1, & |R(x, y)| \geq T, \\ 0, & \end{cases} \tag{1}$$

where $R(x, y)$ is the response of the filter template at the centre of its coverage area. The ROI image $f(x, y)$ is then multiplied by $g_t(x, y)$ to obtain $g(x, y)$:

$$g(x, y) = f(x, y) \times g_t(x, y). \tag{2}$$

Based on the histogram of non-zero pixels, the ROI image was minimized using the Otsu method [28], and the results are shown in Figure 2(c). Although a part of the interference region with similar grey scale is also segmented, the addition of edge information makes the blister tray and the interference region in the fruit segmented into mutually independent regions, and the threshold result is subjected to the connected domain operation, and then the regional area filtering is performed to obtain the complete blister tray segmentation image $I(x, y)$, as shown in Figure 2(d).

5.1. Chinese Character Packaging Defect Recognition Network. In this study, we use the Mobile Net series of networks as the basis for improvement. In the Chinese character packaging defect detection task, the image content of the Chinese character region after cropping and segmentation is relatively single, and there are few image categories, so there is no need for an overly deep network to extract features, and hence we can appropriately reduce the number of network layers and use continuous down sampling. The original MobileNetv2 network uses global average pooling after the last layer of convolution, but since the network in this article is a rectangular image input, the last layer of convolution produces a rectangular feature map, so the pooling layer is changed to adaptive average pooling [13].

The specific structure of the network is shown in Figure 3: two fully convolutional (FC) layers, five convolutional

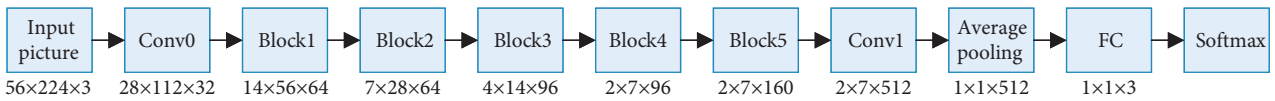

Figure 3: Defect classification network structure.

Figure 4: The imaginative representation of Chinese characters in the packaging design of "One Mountain, One Immortal."

blocks, an adaptive average pooling layer, a fully connected lawyer, and a Softmax classification function.

The first layer is a full convolutional layer with 32 3×3 convolutional kernels, Stride = 2, and the output is 32 $\times$ 28×112 feature maps; the second to sixth layers are five convolutional blocks (Blocks) in turn, and the internal expansion multiplier of the Blocks is 6, where Block1 ~ Block4 are set with a sliding step of 2 and successive down sampling, and the output feature map is $2 \times 7 \times 160$; the seventh layer is a full convolutional layer with 512 1×1 convolutional kernels, which is used for feature dimensioning; the eighth layer is an adaptive averaging pooling layer, which keeps the number of feature map channels unchanged and changes the feature map size to 1×1; the ninth layer is a fully connected full convolutional layer, which is used for feature dimensioning. ×The ninth layer is a fully connected layer, followed by a Softmax layer for classification. The batch normalization layer [14] is added after each network layer except the average pooling layer to speed up the training and improve the generalization ability of the model, and the ReLU6 activation function [15] is used after the batch normalization layer, and the dropout layer [16] is used after the fully connected layer to prevent the network from overfitting during training.

6. Case Studies

6.1. Visual Art Application of Chinese Characters in Packaging Design. With the continuous enrichment of technological design tools, the functional and stylistic design of packaging has significantly improved. On the basis of the design of elements such as text, colour, graphics, function, and shape, the research continues to address the artistic expression of Chinese characters in packaging design. The artistic value of Chinese characters in packaging design is studied from a psychological perspective, and the artistic expression of Chinese characters in packaging design is analyzed in terms of imagery, digitization, visualization, and the value demanded in contemporary social development.

The visual language of imagery in Chinese characters in packaging design is an exploration of abstract traditional cultural forms, a unique artistic expression of Chinese characters that can be applied to packaging design to enhance the overall aesthetic effect of the product's taste, mainly through the brushwork of calligraphy. The visual culture of calligraphy is the main source of inspiration for Chinese character elements in packaging design. The hieroglyphic strokes of calligraphy and the structure of the cloth and white contribute to the imaginative expression of the Chinese characters in a more classical Chinese context, which, combined with the post-modern classical design trend, has a positive impact on the artistic expression of Chinese characters in packaging design. The packaging design of "One Mountain, One Immortal" (Figure 4), designed by Hello Ocean Branding Studio, combines the character "mountain" with the shape of the product and the elegant classical aesthetic mood of the product, reflecting the beauty of the Chinese character imagery to the fullest (Figure 5). Moutai Town Wine's 2019 Year of the Hexi theme packaging uses calligraphic imagery to enhance the overall effect of the packaging.

Another trend in the artistic performance of Chinese characters in modern packaging design lies in following the pace of social economy, pursuing the power of science and technology, adding a more modern visual feel to the Chinese character font design, enabling consumers to quickly accept the design principles, conforming to the modern design atmosphere of consumers' personal lives, constantly strengthening

Figure 5: Imaginative representation of Chinese characters in Moutai town wine packaging design.

Figure 6: Digital representation of the Chinese character technology in the packaging design of the "Good Night Technology" Sleeping Drink.

the visual impact of science and technology, bringing the Chinese character elements of packaging design not only to inherit the tradition, but also to find the theme of Chinese characters in the modern environment. For example, Figure 6 is a display of the packaging design for Good Night Technology Sleeping Drink. The design combines the product's technological health theme with modern technological elements around the Good Night font. The design echoes the theme of the packaging design, which is a modern and minimalist aesthetic that makes consumers feel comfortable and healthy.

As shown in Figure 7, the application of Chinese characters in product packaging is based on the pictorial nature of Chinese characters, combining the beauty of the foot form and graphic design to show the specific image of the main idea to be expressed in the product packaging. The Chinese characters for the theme "Craftsmanship," the use of a labyrinth design and the shape of the Chinese gossip culture, express the main idea clearly, show the strong corporate culture of the product, and enhance the publicity of the product's high quality of hand brewing to win the trust of consumers.

Figure 7: The "artisanal creation" packaging design of snowflake beer in Chinese characters.

6.2. The Influence of Traditional Visual Art Elements on Packaging Design. Chinese traditional culture in packaging design art design elements, which are a representative of the Chinese national style, traditional visual culture of the people through society, national humanistic feelings, and the development of cultural industries, gradually formed the visual observation of artistic habits of life.

First of all, traditional graphics in packaging design are based on folk culture as the inspiration for creativity, with rich and varied styles and auspicious and simple meanings. The traditional elements of the "Fu Lu Shou Xi" and the "Tai Ji Ba Gua" and "Dragon and Phoenix Cloud" patterns are some of the more common visual cultural elements in modern packaging design (Figure 8). The visual cultural characteristics expressed in the example of Coca-Cola's product packaging show the unique creativity of the traditional Chinese visual culture.

Secondly, the literati's spiritual sentiment of ink and wash, the creative expression of traditional ink and wash in the artistic practice of packaging design, has a strong Chinese classical aesthetic connotation (Figure 9), visual culture packaging design of Taiwan Gaoshan tea, flower, bird, fish and insect ink painting, space extension, and clear meaning.

Thirdly, handicraft design elements of folk art provide creative inspiration for the traditional cultural and creative design of modern packaging. Folk art is a traditional art and culture passed down in the folklore, which is applied to the creative practice of modern packaging design, reflecting the representative literary style of national folk crafts (Figure 10). Also, it is a visual culture packaging designed and created by a new generation of Chinese designers, with a unique visual culture theme, expressing the creative aesthetics of local ethnic elements.

Fourthly, the paper-cutting technique breaks through the traditional new creative expression—new paper-cutting. The traditional paper-cutting technique is different from the traditional folk paper-cutting form of carving and uses a smooth and flowing cutting technique to present the beauty of life (Figure 11). The new paper-cutting packaging design by Mr Zhao Xigang, the creator of Modern Visual Culture's "New Paper-cutting," uses the graphic elements of "New Paper-cutting" to achieve a double harvest of professional art and ideology and culture.

7. Experiments and Analysis of Results

7.1. Preprocessing Algorithms. The preprocessing algorithm was tested using a total of 4,400 original images (five matches) constructed for the dataset. Since the threshold segmentation results determine the accuracy of the subsequent skew correction and ROI cropping, two control groups were set up in this article, using Otsu and global double shareholding as the shareholding methods in the preprocessing algorithm, respectively.

The preprocessing algorithm using the global double shareholding method was the fastest with an average time of 8.34 ms and an accuracy of 97.00%. As shown in Table 1, the main factor affecting the accuracy was the luminance fluctuation; the preprocessing algorithm using Otsu as the shareholding method had the lowest accuracy of 92.5%. The main factor affecting the accuracy was the difficulty in segmenting the pallet when it was close to a block with a similar grey level. The edge-assisted shareholding has good adaptability, with an accuracy of 100% and an average time of 15 ms for the preprocessing algorithm, which is a better overall performance.

Figure 8: Coca-cola's visual culture packaging design.

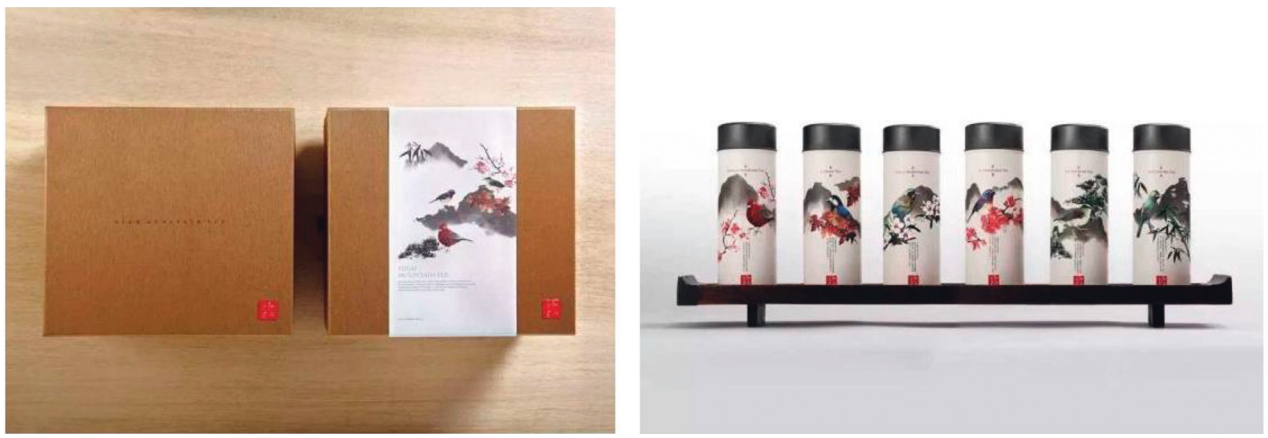

Figure 9: Taiwan high tea visual culture packaging design.

7.2. Identifying Networks. The proposed Chinese character packaging defect classification network (LocalNet) was trained and tested on the above constructed Chinese character packaging defect classification dataset, Nano compact deep learning module, and the Pytorch framework.

To compare the performance of this network with that of the reference network, two control groups were set up: one was the original MobileNetv2 with an input size of $224 \times 224 \times 3$, and the other was this network (LocalNet_224) with an input size of $224 \times 224 \times 3$. All three sets of experiments were trained using Stochastic Gradient Descent (SGD) [17], and the learning rate was adjusted using a cosine annealing strategy [18], as shown in Figure 12(a), with an initial learning rate of 0.1, a minimum learning rate of 1×10^{-8}, a momentum factor of 0.9, and a weight decay factor of 0.0003. The original MobileNetv2 network converged the fastest with a stable loss of 0.004, Local Net converged the second fastest with a stable loss of 0.005, and LocalNet_224 converged the slowest with a

Figure 10: Visual culture packaging design for the folklore "zaohuo faces."

Figure 11: Zhao Xigang's original "new paper cut" visual culture packaging design.

Table 1: Performance of preprocessing algorithms under different threshold methods.

Threshold method	ROI cutting accuracy (%)	Average time (ms)
Edge assist	100.00	15.00
Otsu	92.50	11.12
Global double threshold	97.00	8.34

stable loss of 0.035. Validation rates of the original MobileNetv2 and Local Net in Figure 12(c) were both 99.99%. The accuracy of both the original MobileNetv2 and Local Net in Figure 12(c) is 99.99%, and the accuracy of LocalNet_224 is 98.67%. From the experimental data, it can be seen that LocalNet_224 does not perform like MobileNetv2 in terms of training loss convergence and validation accuracy when using the input size of 224×224, while the training loss convergence and final training loss of Local Net with the input size of 56×224 are slightly lower than that of MobileNetv2. The validation accuracy is the same as that of MobileNetv2 and significantly better than that of LocalNet_224, which verifies the effectiveness of the proposed network structure design.

To verify the classification performance of the networks in this article, tests were evaluated on the test set constructed above, and a test control experimental group was also set up, including two lightweight networks—ShufflENetv2 [19] and Squeeze Net [20]—and two machine learning methods—Local Binary Pattern (LBP) [21] feature-based SVM and Extreme Learning Machine (ELM) [22]. The control group was pretrained on the training set.

Table 2 presents the performance comparison of different classification methods, including input size, number of parameters, accuracy, and the average time taken to detect a Chinese character region image using three different hardware conditions: GPU (NVIDIA Tesla V100), CPU (Xeon Gold 6148), and Jetson Nano. As shown in Table 2, in terms of the number of model parameters, the proposed model has 0.50×106 parameters, which are the lowest among the listed deep learning models. In terms of detection accuracy, ShuffleNetv2 has the highest accuracy of 99.99%, while the proposed network has 99.94%, with only 0.05 percentage points differences, and the LBP-ELM method has the lowest accuracy. In terms of detection time, the LBP-ELM method was the fastest due to the structural advantage of ELM, with 3.87 ms and 10.25 ms in the CPU environment of the computer and Jetson Nano,

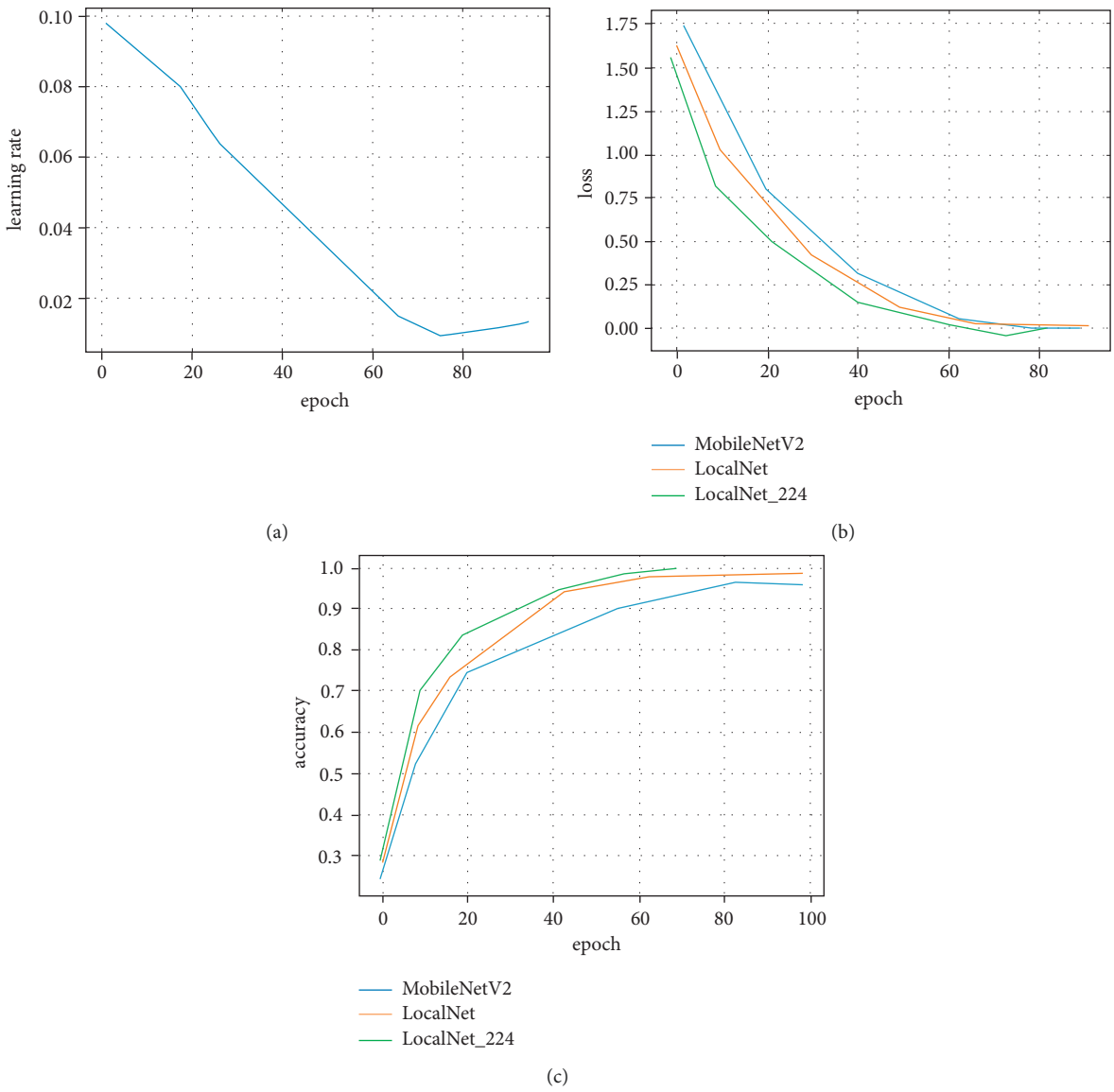

Figure 12: Experimental results. (a) Learning rate adjustment. (b) Loss. (c) Accuracy.

Table 2: Comparison of the performance of different classification methods.

Classification method	Enter size	Parameter quantity (10^6)	Accuracy (%)	Detection time (ms)		
				GPU	CPU	Jetson Nano
Squeeze Net	$224 \times 224 \times 3$	1.25	**97.63**	3.57	55.43	41.00
Shuffle Netv2	$224 \times 224 \times 3$	3.50	**99.99**	7.51	30.50	21.11
Mobile Netv2	$224 \times 224 \times 3$	3.50	**99.97**	6.20	31.15	20.51
LocalNet_224	$224 \times 224 \times 3$	0.5	**97.89**	2.23	18.17	13.45
Local Net	$56 \times 224 \times 3$	0.5	**99.94**	2.31	7.82	11.02
LBP-SVM	$56 \times 224 \times 3$	—	**91.10**	—	5.59	16.03
LBP-ELM	$56 \times 224 \times 3$	—	**87.96**	—	3.87	10.25

respectively; the detection time of the proposed network was the best among the deep learning models in the three hardware types, with 2.31 ms, 7.82 ms, and 11.02 ms, respectively. Although Squeeze Net has a small number of parameters, it still has a large number of conventional convolutional computations and therefore does not show any speed advantage. This shows that the proposed network is the best among the listed methods in terms of the number of parameters, accuracy, and detection speed. When the network is deployed on the Jetson Nano platform, for example, a box of five Chinese characters is preprocessed in 15 ms, and the overall detection time of the algorithm is

70.1 ms, which can reach 14 boxes/s and meet the requirement of real-time detection in the pipeline.

8. Conclusions

This study presents a Chinese character packaging quality inspection algorithm for a small computing platform (e.g., Jetson Nano), including a preprocessing algorithm for cropping images of Chinese character packaging areas and a recognition network, by analyzing images collected on a Chinese character packaging production line and borrowing ideas from the Mobile Net series of lightweight convolutional neural networks. Through experiments, the proposed preprocessing algorithm can accurately extract the image of the Chinese character packaging area, and the recognition network can achieve an inspection speed of 14 boxes per second on the Jetson Nano platform, which is much faster than the existing manual visual inspection speed of 1 box per second and achieves an accuracy rate of 99.94%. The deployment of this algorithm on a Chinese character packaging line significantly reduces the constraints of inspection speed on production line capacity and provides technical support for the automation upgrade of the packaging line. The next step is to carry out work related to algorithm optimization, model quantification, and hardware platform adaptation to further improve the speed and accuracy of the algorithm to meet the participation requirements.

Data Availability

The raw data supporting the conclusions of this article will be made available by the authors, without undue reservation.

Conflicts of Interest

The authors declared that they have no conflicts of interest regarding this work.

Acknowledgments

This article is the New Liberal Arts Research and Reform Practice Project of Henan Province: Research and Practice on Collaborative Education Mechanism of Integration of Industry and Education for Design Majors in Local Colleges under the Background of New Liberal Arts Construction Project (No. 2021JGLX046); Key Research and Popularization Project of Henan Province: Research on Key Technology of Modular Design of Intelligent Agricultural UAV Project funded by the Key Science and Technology Project of Henan Province (No. 2021-802).

References

[1] M. Bould, "The dreadful credibility of absurd things: a tendency in fantasy theory," *Historical Materialism*, vol. 10, no. 4, pp. 51–88, 2002.

[2] Z. Zhang, C. Zhang, H. Li, and T. Xie, "Multipath transmission selection algorithm based on immune connectivity model," *Journal of Computer Applications*, vol. 40, no. 12, 3571 pages, 2020.

[3] Y. Xiao, "Exploring the internal mechanism of evolution of Marxist philosophy," *Journal of Frontiers in Educational Research*, vol. 1, no. 1, pp. 4–7, 2021.

[4] M. Ding, "Application of visual elements in product paper packaging design: an example of the "squirrel" pattern," *Journal of Intelligent Systems*, vol. 31, no. 1, pp. 104–112, 2022.

[5] M. R. Klimchuk and S. A. Krasovec, *Packaging Design: Successful Product Branding from Concept to Shelf*, John Wiley & Sons, Hoboken, NJ, USA, 2013.

[6] L. Gong, M. Thota, M. Yu et al., "A novel unified deep neural networks methodology for use by date recognition in retail food package image," *Signal, Image and Video Processing*, vol. 15, no. 3, pp. 449–457, 2021.

[7] B. H. Schmitt, "Language and visual imagery: issues of corporate identity in East Asia," *The Columbia Journal of World Business*, vol. 30, no. 4, pp. 28–36, 1995.

[8] M. Thomas, "Evidence and circularity in multimodal discourse analysis," *Visual Communication*, vol. 13, no. 2, pp. 163–189, 2014.

[9] U. R. Orth and K. Malkewitz, "Holistic package design and consumer brand impressions," *Journal of Marketing*, vol. 72, no. 3, pp. 64–81, 2008.

[10] M. M. Gelici-Zeko, D. Lutters, R. ten Klooster, and P. L. G. Weijzen, "Studying the influence of packaging design on consumer perceptions (of dairy products) using categorizing and perceptual mapping," *Packaging Technology and Science*, vol. 26, no. 4, pp. 215–228, 2013.

[11] M. Flikkema, C. Castaldi, A.-P. de Man, and M. Seip, "Trademarks' relatedness to product and service innovation: a branding strategy approach," *Research Policy*, vol. 48, no. 6, pp. 1340–1353, 2019.

[12] M. Husić-Mehmedović, I. Omeragić, Z. Batagelj, and T. Kolar, "Seeing is not necessarily liking: advancing research on package design with eye-tracking," *Journal of Business Research*, vol. 80, pp. 145–154, 2017.

[13] P. Varela, L. Antúnez, R. Silva Cadena, A. Giménez, and G. Ares, "Attentional capture and importance of package attributes for consumers' perceived similarities and differences among products: a case study with breakfast cereal packages," *Food Research International*, vol. 64, pp. 701–710, 2014.

[14] J. Grobelny and R. Michalski, "The role of background color, interletter spacing, and font size on preferences in the digital presentation of a product," *Computers in Human Behavior*, vol. 43, pp. 85–100, 2015.

[15] S. Hussain, S. Ali, M. Ibrahim, A. Noreen, and S. F. Ahmad, "Impact of product packaging on consumer perception and purchase intention," *Journal of Marketing and Consumer Research*, vol. 10, no. 1, pp. 1–10, 2015.

[16] X. Tao, C. Zhang, and Y. Xu, "Collaborative parameter update based on average variance reduction of historical gradients," *Journal of Electronics and Information Technology*, vol. 43, no. 4, pp. 956–964, 2021.

[17] Z.-wan Zhang, Di Wu, and C.-jiong Zhang, "Study of cellular traffic prediction based on multi-channel sparse LSTM," *Computer Science*, vol. 48, no. 6, pp. 296–300, 2021.

[18] M. Rautela and S. Gopalakrishnan, "Ultrasonic guided wave based structural damage detection and localization using model assisted convolutional and recurrent neural networks," *Expert Systems with Applications*, vol. 167, Article ID 114189, 2021.

[19] M. M. Hafez, A. Fernández Vilas, R. P. D. Redondo, and H. O. Pazó, "Classification of retail products: from

probabilistic ranking to neural networks," *Applied Sciences*, vol. 11, no. 9, Article ID 4117, 2021.

[20] F. D. S. Ribeiro, L. Gong, F. Calivá et al., "An end-to-end deep neural architecture for optical character verification and recognition in retail food packaging," in *Proceedings of the 2018 25th IEEE International Conference on Image Processing (ICIP)*, pp. 2376–2380, IEEE, Athens, Greece, 2018 October.

[21] M. Malesa and P. Rajkiewicz, "Quality control of PET bottles caps with dedicated image calibration and deep neural networks," *Sensors*, vol. 21, no. 2, 501 pages, 2021.

[22] M. N. Örnek and H. Kahramanlı Örnek, "Developing a deep neural network model for predicting carrots volume," *Journal of Food Measurement and Characterization*, vol. 15, no. 4, pp. 3471–3479, 2021.

[23] X. Lin, J. Wu, S. Mumtaz, S. Garg, J. Li, and M. Guizani, "Blockchain-based on-demand computing resource trading in IoV-assisted smart city," *IEEE Transactions on Emerging Topics in Computing*, vol. 9, no. 3, pp. 1373–1385, 2021.

[24] J. Li, Z. Zhou, J. Wu et al., "Decentralized on-demand energy supply for blockchain in internet of things: a microgrids approach," *IEEE Transactions on Computational Social Systems*, vol. 6, no. 6, pp. 1395–1406, 2019.

[25] P. An, Z. Wang, and C. Zhang, "Ensemble unsupervised autoencoders and Gaussian mixture model for cyberattack detection," *Information Processing & Management*, vol. 59, no. 2, Article ID 102844, 2022.

[26] W. Duan, J. Gu, M. Wen, G. Zhang, Y. Ji, and S. Mumtaz, "Emerging technologies for 5G-IoV networks: applications, trends and opportunities," *IEEE Network*, vol. 34, no. 5, pp. 283–289, 2020.

[27] D. Jiang, F. Wang, Z. Lv et al., "QoE-aware efficient content distribution scheme for satellite-terrestrial networks," *IEEE Transactions on Mobile Computing*, vol. 15, no. 10, 1 page, 2021.

[28] G. Cai, Y. Fang, J. Wen, S. Mumtaz, Y. Song, and V. Frascolla, "Multi-carrier M-ary DCSK system with code index modulation: an efficient solution for chaotic communications," *IEEE Journal of Selected Topics in Signal Processing*, vol. 13, no. 6, pp. 1375–1386, 2019.

Hindawi
Scientific Programming
Volume 2022, Article ID 1191073, 9 pages
https://doi.org/10.1155/2022/1191073

Research Article

A Study of Artificial Intelligence-Based Poster Layout Design in Visual Communication

Huiyu Huo [1,2] **and Feng Wang** [1]

[1]*School of Design, Jiangnan University, Jiangsu, WuXi 214122, China*
[2]*College of Media and Art, Nanjing University of Posts and Telecommunications, Nanjing, Jiangsu 210023, China*

Correspondence should be addressed to Huiyu Huo; 7180306001@stu.jiangnan.edu.cn

Received 10 May 2022; Revised 27 May 2022; Accepted 1 June 2022; Published 22 June 2022

Academic Editor: Lianhui Li

In visual communication design, the basic design elements include four types of text, graphics, colour, and layout. While the first three can be called visual elements, layout design is the functional arrangement of visual elements. Layout design is as much about making the viewer receive visual information as it is about making them feel attractive. The combination of artificial intelligence and layout design has now become a popular direction in the field of visual communication design. However, the automatic layout design process achieved through an a priori design framework still requires human involvement and is a semi-intelligent application. To solve the above problems, this study proposes a poster layout design method based on artificial intelligence. The layout composition method consists of a learner and a generator. Firstly, the learner uses the spatial transformation network to learn the classification of layout composition elements and form the initial layout design templates for different composition cases. Secondly, the generator optimises the initial template based on the LeNet architecture using the golden ratio and trilateration parameters to produce multiple optimised templates. The templates are then stored in a library of corresponding templates according to their composition and framing style. The experimental results show that the proposed poster layout composition method achieves a higher accuracy rate than existing methods.

1. Introduction

Visual communication design, often also referred to as graphic design, is a creative act that encompasses graphics, text, colour, and layout. The purpose of visual communication design is to convey emotion and information [1–5]. In the Internet era, visual communication design has long since gone beyond the design laws of traditional graphic design. Cross-border integration of visual communication design has become an important development trend. In visual communication design, the basic design elements include four types of text, graphics, colour, and layout [6–8]. The first three can be called visual elements, while layout design is a relatively independent design art.

At the present stage, artificial intelligence (AI) has developed into an intersection of computer science, psychology, philosophy, art, and other technical sciences [9, 10]. With the development of deep learning and neural networks, AI has started to enter society, such as voice assistants and image recognition technology. How will artificial intelligence impact the field of design? In particular, design can be understood as a purposeful act of creation [11–13]. Artificial intelligence, on the other hand, can be understood as a tool with recognition functions for helping humans solve problems. Understood from this perspective, AI can be a kind of designer's aid. In recent years, more and more scholars are also exploring the combination of AI and design.

Currently, the combination of artificial intelligence and visual communication design has produced a number of intelligent applications [14–17], such as intelligent logo design, intelligent colour matching, and intelligent image search. In the case of magazine media, for example, intelligent automatic layout design has been implemented through an a priori design framework. However, this intelligent layout

design process still requires human participation and is a semi-intelligent application. Therefore, the core problem of this study is how to carry out automatic layout design through AI.

The first task in using AI for layout design is to make the computer understand the constituent elements of the layout. This research will use deep learning techniques to locate and identify the constituent elements of the layout in the target image. Machine learning is a discipline dedicated to the study of how computers can simulate the human brain [18–22]. Machine learning can use the empirical knowledge learned to continuously improve the performance of the system itself. With the continuous improvement of the computer hardware base (e.g., the rapid development of GPUs) and the large amount of data generated by various social networks, deep learning techniques have become a very important research direction in machine learning. Deep learning is a method for learning representations of data, with the advantage of replacing manual feature extraction with efficient hierarchical feature extraction. In recent years, many large Internet companies such as Microsoft, Google, Facebook, and Baidu have also set up relevant research teams. Deep learning has been widely used in various AI tasks such as speech recognition, computer vision, and natural language processing.

In traditional machine learning, the target image processing task is divided into two main steps. The first step relies on human experts to design the features manually. The second step is to provide the extracted features to a selected classifier for model training. This approach to image processing has been well used in practice in some respects. However, the process of manual feature extraction is time-consuming and labour-intensive and inevitably introduces some subjective differences due to differences in perception. It is difficult to fully standardise the execution criteria between different people or at different moments in time for the same person, which can easily result in the loss of feature information. This has limited the development of traditional machine learning to some extent. In recent years, image processing based on deep learning can solve the above problems very well. The biggest advantage is that no manual selection of extracted features is required.

Deep learning techniques can also significantly outperform traditional machine learning methods in terms of accuracy using convolutional neural network (CNN) models to autonomously learn appropriate image features. Andrearczyk et al. [23] proposed a convolutional neural network for processing handwritten digit recognition tasks. To solve large-scale computer vision recognition tasks, Zhang et al. [24] proposed an LeNet convolutional neural network model. The advantage of this network model is the use of ReLU as the activation function of the LeNet, which solves the problem of possible gradient dispersion in the sigmoid activation function in deeper network architectures. Wang et al. [25] proposed the dropout method, which effectively alleviates the problem of model overfitting during the training process of deep networks. The innovation of this method is that the neurons in the fully connected layer are inactivated with a certain probability (typically 0.5) during the training phase. The dropout method removes some of the neurons from the forward and backward parameter propagation, greatly reducing the interdependence between neurons and thus ensuring that mutually independent important features are extracted. Samir et al. [26] proposed a local response normalisation (LRN) to create a competitive mechanism for the activity of local neurons. LRN enhances the generalisation ability of the model by expanding the values of local neurons with larger responses and suppressing other neurons with smaller feedback. In addition to this, researchers have also tried to improve image processing accuracy through a number of conventional improvements. For example, the ReLU activation function has been modified into the very good fitting Maxout activation function, which not only inherits all the advantages of the ReLU activation function but also avoids the problem of "necrosis" of neurons due to negative gradients being set to zero.

Although all of these improvements improve the learning ability of the model to some extent, the AI-based layout design process involves more elements with greater spatial variation. For this problem, the above methods are obviously not effective solutions. Therefore, a layout composition method based on a learner and a generator is proposed. The main function of the learner is to use spatial transformer networks (STNs) [27] to classify layout composition elements and finally to realise the recognition and localisation of layout composition elements for learning the layout of selected poster cases and forming the initial layout template. Once the learning of the classification of the layout elements is completed, the element positions can be located. The main function of the generator is to optimise the initial template using the LeNet convolutional neural network. As the class, number, and position of the elements are already determined in the initial template, these parameters are only used to adjust the position of the elements. The final output of the generator is a parameter-optimised template, which is stored in a template library.

The main innovations and contributions of this study include the following:

(1) In this study, the popular LeNet convolutional neural network is used as the base network architecture and the STN is inserted in its input layer. The STN can be trained together with the LeNet and the original poster case can be automatically detected for spatial transformation during the training process, thus enabling the network model to extract more effective layout composition elements.

(2) There is a transition state in the spatial evolution process of the layout composition. To address this problem, an angular similarity softmax (A-softmax) loss function is used to replace the original softmax loss function of the LeNet architecture, which aims to make the intra-class distance between layout composition elements of the same category smaller and smaller, while the interclass distance between layout composition elements of different categories becomes larger and larger.

The rest of the study is organised as follows: in Section 2, the poster layout composition approach analysis is studied in

detail, while Section 3 provides the detailed layout composition method based on A-softmax convolutional neural network. Section 4 provides the experiments and analysis of results. Finally, the study is concluded in Section 5.

2. Poster Layout Composition Approach Analysis

2.1. Common Ways of Composing Poster Layouts. There is currently no unified view on the composition of posters in the academic community, so there are various classification methods. This study combines the existing classification methods and summarises the commonly used poster composition methods into the following three types, namely central composition, tilted composition, and three-part composition.

Center composition places the subject on the central axis of the layout. Posters with central composition, with the main body occupying the visual center, quickly attract the attention of the audience, concise layout, and a sense of stability. Three-part composition is to place the text and the main image according to the three-part line of the layout. In the three-part composition, the subject occupies two-thirds and the rest is the text. On the whole, the three-part composition has the effect of highlighting the main body and balancing the layout. In design examples, some poster works may be difficult to be classified into a certain composition method. Because of the disorder of free layout, it is difficult to summarise and define the characteristics of composition. Therefore, to simplify the analysis, this study only studies the layout design of a single composition mode.

2.2. Selection of Layout Adjustment Parameters. At present, the most commonly used layout design method is layout segmentation based on grid system, which is characterised by the use of mathematical calculation to divide the layout, thus guiding the layout of visual elements. In the development of modern design, grid-based layout segmentation is widely used in the field of poster design. Mathematical parameters commonly used in layout design include golden ratio, Fibonacci sequence [28], Vandergraff layout structure principle, and photography three-part method. The ratio of length to width in the golden ratio is about 0.618. In layout design, the most common use is to use golden rectangle to create grid. The three-part method is a composition technique used in photography. The photographer divides the length and width of the shot into three equal parts to form four intersection points and focuses the lens on the intersection points and near the three-point line.

In this study, the golden ratio and the three parts were chosen to optimise the layout template parameters. This is mainly because these two layout composition parameters have a more established and common use in guiding graphic layouts. In particular, when using the golden ratio division in poster layout design, the layout is first divided into golden ratio areas. Then, based on a reasonable reading order, the subject is placed at the visual focal point and the position and size of the elements are adjusted according to the golden ratio. When using the three parts, the position of the subject is first clarified, and the position of the text is used to determine the position of the subject to achieve different visual effects, such as the left and right placement of images and text, central placement, and diagonal placement.

3. Layout Composition Method Based on A-Softmax Convolutional Neural Network

Poster images present a wide variety of structures. Learning the classification of layout composition elements in poster images is the key to layout composition. However, due to the subjective nature of human extracted features, traditional machine learning methods cannot adequately characterise poster images, and complex layout composition elements are difficult to be fully described. In recent years, convolutional neural networks have been widely used in various image classification tasks due to their adaptive feature hierarchical learning capability. Compared with traditional machine learning methods, the process of feature extraction by convolutional neural networks is much simpler. The features extracted by convolutional neural networks are more capable of characterisation, and the classification accuracy has been substantially improved. Therefore, in this study, an improved LeNet architecture is proposed to achieve automatic classification learning of layout composition elements in poster images. In addition, several optimisation templates are output based on the trained classification network model.

The steps of the layout composition method based on A-softmax convolutional neural network are as follows: 1) the learner learns the layout composition elements categorically using STN to form the initial layout design templates for different composition cases and 2) the generator optimises the initial templates using the golden ratio and trilateration parameters on the basis of LeNet architecture to output multiple design solutions.

Due to the large spatial variation of layout composition elements in poster images, STN is embedded in the input layer of the LeNet as shown in Figure 1. Using STN, the whole network automatically learns more efficient layout composition elements during the training process. A-Softmax loss function is used to supervise the optimisation of the network model, forcing the network model to learn more discriminative layout composition elements and finally obtaining satisfactory classification learning results.

3.1. STN-Based Learner. As mentioned above, the proposed layout composition method is composed of a learner and a generator. The core function of the learner is to identify the classified layout composition elements. The STN is used for the recognition and classification learning of the layout composition elements. The aim is to locate and classify feature elements from an image and to obtain information on the position and size of the elements.

This study uses the popular LeNet convolutional neural network as the base network architecture and inserts an STN into its input layer, which can be trained together with the

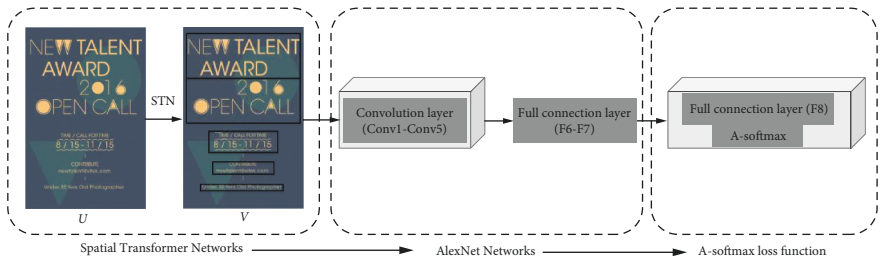

Figure 1: Layout composition method based on A-softmax convolutional neural network.

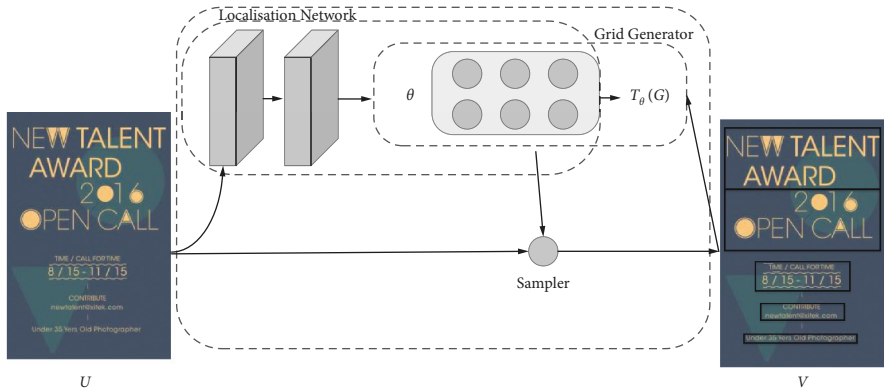

Figure 2: Spatial transform network model.

LeNet and can automatically detect the original poster case for spatial transformation during the training process, thus enabling the network model to extract more efficient layout composition elements. As shown in Figure 2, the STN can be divided into three parts.

As shown in Figure 2, the localisation network in the first part is a custom convolutional neural network architecture used to generate 2D affine transformation parameters. The input of learner is an initial set of poster images $U \in \mathbb{R}^{H\times W}$ with a width of H and a height of W . The output is a matrix transformation parameter θ of size $2 * 3$ obtained from the regression layer.

In the second section, the grid generator is used to solve for the mapping of each pixel coordinate with image V and initial image U. The mapping relationship between (x_i^t, y_i^t) and (x_i^s, y_i^s) is shown as follows:

$$\left(x_i^s, y_i^s\right) = T_\theta\left(G_i\right) = A_\theta\begin{pmatrix} x_i^t \\ y_i^t \\ 1 \end{pmatrix} = \begin{pmatrix} \theta_{11} & \theta_{12} & \theta_{13} \\ \theta_{21} & \theta_{22} & \theta_{23} \end{pmatrix}\begin{pmatrix} x_i^t \\ y_i^t \\ 1 \end{pmatrix}, \tag{1}$$

where T_θ represents the mapping matrix function, which is composed of the transformation parameters θ obtained in the first part. G_i denotes the mapping space grid coordinates. A_θ denotes the transformation matrix.

Finally, the sampler samples the pixel coordinates in the target image using the coordinate results obtained in the second part. Since some of the positions in the mapped initial image may be fractional, the sampling needs to be determined jointly by the other pixel values around that coordinate, hence the bilinear interpolation method used in this study.

$$V_i = \sum_n^H \sum_m^W U_{\mathrm{nm}} \max\left(0, 1 - \left|x_i^s - m\right|\right)\max\left(0, 1 - \left|y_i^s - n\right|\right), \tag{2}$$

where n and m denote the positions of the surrounding coordinates of the coordinates (x_i^s, y_i^s) in the initial image U, U_{nm} denotes the pixel value at a point in the initial image U, and V_i denotes the sampling value of the target image V at the ith pixel point. The above is the forward propagation process of the STN. Because the network can be trained to learn with a neural network model, the back propagation equation is shown as follows:

$$\frac{\partial V_i}{\partial U_{\mathrm{nm}}} = \sum_n^H \sum_m^W \max\left(0, 1 - \left|x_i^s - m\right|\right)\max\left(0, 1 - \left|y_i^s - n\right|\right). \tag{3}$$

$$\frac{\partial V_i}{\partial x_i^s} = \sum_n^H \sum_m^W U_{\mathrm{nm}} \max\left(0, 1 - \left|x_i^s - n\right|\right)\begin{cases} 0 & \left|m - x_i^s\right| \geq 1 \\ 1 & m \geq x_i^s \\ -1 & m < x_i^s \end{cases}. \tag{4}$$

Derivation of transformation parameters θ can be obtained as follows:

$$\frac{\partial V_i}{\partial \theta} = \begin{pmatrix} \dfrac{\partial V_i}{\partial x_i^s} \cdot \dfrac{\partial x_i^s}{\partial \theta} \\ \\ \dfrac{\partial V_i}{\partial y_i^s} \cdot \dfrac{\partial y_i^s}{\partial \theta} \end{pmatrix}. \tag{5}$$

The use of convolution and maximum pooling in traditional CNNs achieves some degree of translation invariance, but the artificially set transformation rules make the network overly dependent on a priori knowledge. As a result, CNNs are neither truly translation-invariant nor feature-invariant to non-artificial geometric transformations such as rotations and distortions. However, the STN with its derivative nature does not require redundant annotation and can adaptively learn how to transform the space for different data. STNs enable spatially invariant classification network models, which have been applied to tasks such as numerical recognition and face recognition.

3.2. LeNet-Based Generator. The final output of the learner is the original layout, while the generator optimises the original layout based on the corresponding optimisation parameters and produces several optimised layout templates. The generator optimises the initial template based on the LeNet architecture using the golden ratio and trilateration parameters to produce multiple optimised templates. The golden ratio is a strictly mathematical and artistic visual feature that is commonly used in layout design, sculpture, painting, and other fields. In layout design, the use of the golden ratio can often help to achieve harmony in the layout. The use of the golden ratio is divided into two main parts: firstly, it is used for the layout of visual elements to optimise their placement; secondly, it is used to adjust the size of text elements to create a logical reading hierarchy. The three-part method is a technique commonly used in painting and photography. The three-part method starts by dividing the image into three equal parts, then placing the focus of the image on the three-quarter line or its intersection, and setting the proportion of the object on the screen according to the different weights.

LeNet convolutional neural networks have powerful image characterisation capabilities and are widely used in many image classification tasks [29]. In this study, the LeNet is used as the base classification network architecture for feature learning of poster images. The network consists of one input layer (input), five convolutional layers (C1~C5), three maximum pooling layers (S1, S2, and S5), and three fully connected layers (F6, F7, and F8), as shown in Figure 3.

Convolution layers are convolved with different types of convolution kernels to extract different features. Three maximum pooling layers are located after C1, C2, and C5 to increase the nonlinearity between features and the spatial invariance of the features. The fully connected layers (F6 and F7) can be progressed to extract more refined features. The final layer (F8) is used to generate the category labels for the posters. In addition, ReLU activation functions are added after each convolutional and fully connected layer for solving the gradient dispersion problem when the network is deeper.

To prevent the network from overfitting during training, dropout layers were added after the two fully connected layers (F6 and F7) to randomly ignore a portion of the neurons. Also, during the training phase of the network, the original poster image with an input size of 256 ∗ ∗ 256 was

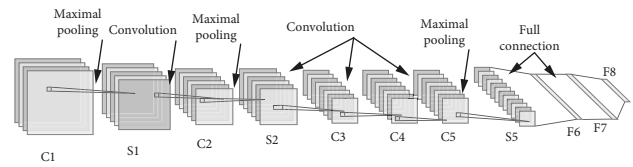

Figure 3: LeNet architecture.

randomly cropped (224 ∗ ∗ 224) in the input layer to enhance the complexity of the data. The network also places the LRN behind the activation functions in layers C1 and C2. The aim is to improve the speed of convergence of the classification network and to enhance the generalisation ability of the network model.

3.3. A-Softmax Loss Function. In machine learning, commonly used loss functions include contrastive loss and triple loss. These two loss functions can reduce the intra-class spacing and increase the interclass distance between classes to a certain extent. However, these two loss functions require a certain degree of selectivity in the training samples, and CNNs are usually used to train large datasets, which is undoubtedly an increased workload and time-consuming. In contrast, the softmax loss function is widely used in many convolutional neural network architectures due to its simplicity and strong classification accuracy.

The original softmax loss function cannot force the intra-class distance between the same classes to become smaller. To effectively address this problem, this study uses angular similarity to extend the softmax loss function to a more general A-softmax loss function. The A-softmax loss function enables smaller intra-class distances between the same classes and larger interclass distances between different classes. In general, when the category label of the ith input feature x_i is y_i, the definition of the loss function is shown as follows:

$$L = \frac{1}{N}\sum_i L_i = \frac{1}{N}\sum_i -\log\left(\frac{e^{f_{y_i}}}{\sum_j e^{f_j}}\right), \tag{6}$$

where N is the number of training samples and f_j is the score vector of the jth category. Since f is the product of the activation function output weight W and the input x_i, f_{y_j} can be written as follows: $f_{y_j} = W_{y_i}x_i$. When ignoring offsets, f_j can also be expressed as follows:

$$f_j = \left\|W_j\right\|\left\|x_i\right\|\cos\left(\theta_j\right), 0 \le \theta_j \le \pi, \tag{7}$$

where θ_j is the angle between the weight vector W and the input feature x_i . Thus, the softmax loss function can be expressed as follows:

$$L_i = -\log\left(\frac{e^{\left\|W_{y_i}\right\|\left\|x_i\right\|\psi\left(\theta_{y_i}\right)}}{\sum_j e^{\left\|W_j\right\|\left\|x_i\right\|\cos\left(\theta_j\right)}}\right). \tag{8}$$

For a binary classification problem, the original softmax loss function will generally satisfy the condition $\|W_1\|\|x\|\cos(\theta_1) > \|W_2\|\|x\|\cos(\theta_2)$, resulting in the correct

result for the input data x as category 1. However, the A-softmax loss function is motivated by the desire to constrain the above equation more tightly by adding a positive integer variable m. Such a constraint places a higher demand on the process by which the model learns the parameters W_1 and W_2, resulting in a wider categorical decision boundary between category 1 and category 2. Extending to the more general multiple category classification problem, the A-softmax loss function can be defined as follows:

$$L_i = -\log\left(\frac{e^{\left\|W_{y_i}\right\|\left\|x_i\right\|\psi\left(\theta_{y_i}\right)}}{e^{\left\|W_{y_i}\right\|\left\|x_i\right\|\psi\left(\theta_{y_i}\right)} + \sum_{j\neq y_i} e^{\left\|W_j\right\|\left\|x_i\right\|\cos\left(\theta_j\right)}}\right), \tag{9}$$

where $\psi(\theta)$ can be expressed as follows:

$$\psi(\theta) = \begin{cases} \cos(m\theta), & 0 < \theta \leq \dfrac{\pi}{m} \\ D(\theta), & \dfrac{\pi}{m} < \theta \leq \pi \end{cases}. \tag{10}$$

When $m = 1$, the expression of the A-softmax loss function (9) is equivalent to the expression of the original softmax loss function (8). When m is larger, the wider the decision boundary for classification, the more difficult it is for the model to learn. In equation (10), $D(\theta)$ is a monotonically decreasing function used to ensure that $\psi(\theta)$ is a continuous function. To simplify the forward and backward propagation of the A-softmax loss function during training, $\psi(\theta)$ is defined as follows:

$$\psi(\theta) = (-1)^k \cos(m\theta) - 2k, \theta \in \left[\frac{k\pi}{m}, \frac{(k+1)\pi}{m}\right], \tag{11}$$

where k is a positive integer.

To reveal the inherent distance distribution of the poster image data so as to reflect the proximity between features, feature extraction was carried out in this study using the fully connected layer (F7) with a more complete feature abstraction. A simple Euclidean distance formula was used to calculate the distance to the test data, resulting in a distance matrix of $2184 * 2184$. This distance matrix is sometimes referred to as the phase difference matrix and is used to reflect the relative confusion between features. The formula for the Euclidean distance is shown as follows:

$$D(x)_{ij} = \left(\sum_k \left(x_{ik} - x_{jk}\right)^2\right)^{1/2} \quad k \in [1, 4096], \tag{12}$$

where $D(x)_{ij}$ denotes the Euclidean distance between the ith image and the jth image feature in dataset x. k denotes a particular feature dimension for which the feature vector needs to be computed.

4. Experiments and Analysis of Results

4.1. Experimental Design and Evaluation Indicators. The aim of the experiment was to verify whether the proposed layout composition method could generate a useable design solution. The experimental design is based on the following idea: first, a product poster case that meets the relevant requirements is selected from the current poster template library of the AI design tool. Then, a learner is used to simulate the target detection model so as to locate the coordinates of the different elements. Secondly, the generator is used to generate output multiple optimised design solutions. Finally, the order of the designed posters is disordered and the simulated design results are left unmarked, allowing the tester to score the unmarked design solutions.

As mentioned above, the A-softmax loss function is used in this study to supervise a network model generated by combining STN and LeNet. The parameter weights are optimised by stochastic gradient descent (SGD) [30] and back propagation principles (BPPs) [31]. The initial learning rate was 0.00003, which was automatically reduced to 0.1 times the initial value after the network model was iterated 5000, 8000, and 12000 times, respectively. The momentum and weight decay were set to 0.9 and 0.0005, respectively. The PC used for the experiments had a 3.8 GHz AMD 5800X CPU, and the system was Windows 10.

Considering that the A-softmax loss function makes it difficult for the network model to converge during the training process, this study adds a decay factor to the learning strategy λ .

$$f_{y_i} = \frac{\lambda\left\|W_{y_i}\right\|\left\|x_i\right\|\cos\left(\theta_{y_i}\right) + \left\|W_{y_i}\right\|\left\|x_i\right\|\psi\left(\theta_{y_i}\right)}{1+\lambda}. \tag{13}$$

The decay factor λ is a large positive integer value at the beginning of the gradient descent. As the number of generations of the network model increases, the value of the decay factor λ decreases and stops at the minimum value. In the experiments in this study, the initial value of λ is 100000 and the minimum value is 15.

No experts or scholars have yet established evaluation criteria for the layout design of posters. To quantitatively analyse the experimental results, a seven-level Likert scale was chosen to obtain the results of five (overall comprehensive evaluation, readability of textual information, consistency of information perception weights, rationality of element placement relationships, and rationality of visual paths) evaluations. The main reason for this is that the Likert scale provides quick access to the test taker's level of agreement with a viewpoint or feeling and is the most commonly used subjective evaluation tool.

4.2. Example of Layout Composition. The posters that meet the filtering criteria are first selected from the poster template library. The filtering criteria include (1) the requirement that the elements do not block or overlap each other; (2) the composition of the poster is a central composition or a three-part composition; (3) the influence of other elements in the poster, such as colour, on the visual perception of the poster layout is as small as possible; and (4) the poster is a solid colour background or a textured background that is less intrusive to the identification of the elements. Although the layout composition method proposed in this study does not take into account the influence of colour elements,

Figure 4: Example of a central composition design and its initial template.

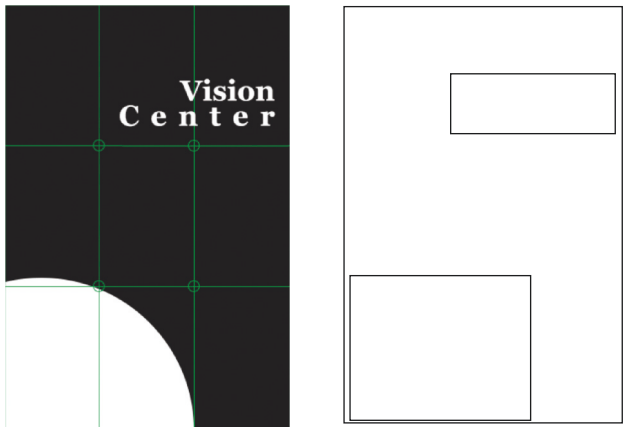

Figure 5: Example of a three-part composition design and its initial template.

colour can interfere more with the subjective evaluation of the audience when making an evaluation of the output design scheme. Therefore, the influence of this irrelevant variable on the experimental results should be minimised. Examples of the resulting layout composition are shown in Figures 4 and 5.

After completing the design of the experiment, the experiment used a seven-level Likert scale to obtain the evaluation results. Considering that the purpose of this experiment is to verify whether the output results of the model are useable or not. Therefore, the testers were required to have a certain foundation in design aesthetics, and factors such as the gender and occupation of the testers might have a large impact on the evaluation results, so the variables needed to be controlled reasonably. Ultimately, 55 students from art and design-related majors were selected for this experiment, of which the ratio of male to female was 1 : 1.

4.3. Analysis of Results. In the experiment, the posters will be presented to the testers randomly to reduce subjectivity. The average score of the 5 different indicator scores will be calculated through the experiment. Higher scores on the

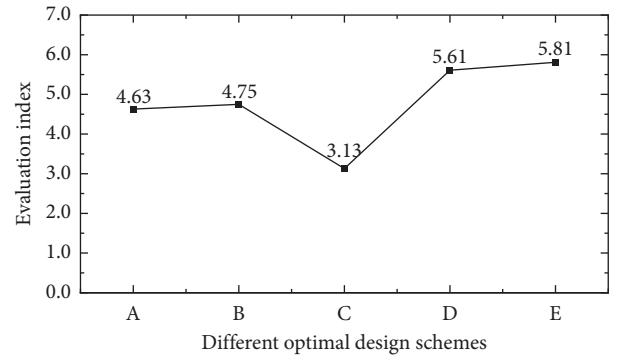

Figure 6: Score statistics for overall comprehensive evaluation.

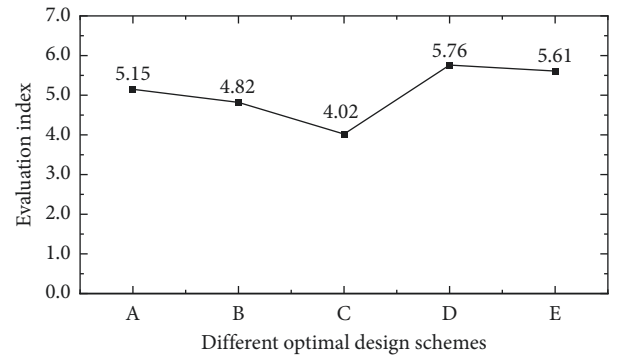

Figure 7: Score statistics for readability of textual information score statistics.

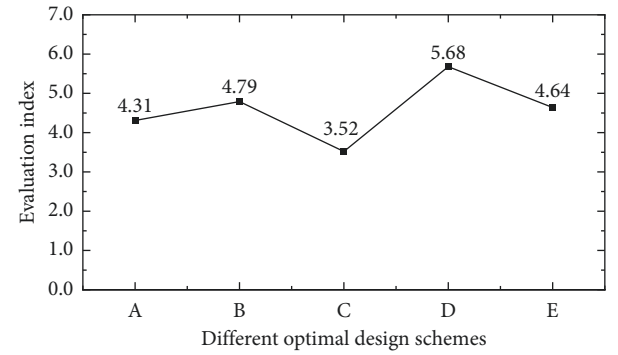

Figure 8: Score statistics for consistency of information perception weights.

indicators indicate a more positive evaluation, and lower scores indicate a more negative evaluation. The statistics of the scores for the five indicators are shown in Figure 6 to Figure 10.

As can be seen from Table 1, the A-softmax loss function successfully forces the network model to distinguish between more types of layout constituent elements than the original softmax loss function. As the value of m increases, the average correct rate increases, thus demonstrating the effectiveness of the supervised optimisation network model training with the A-softmax loss function in this study.

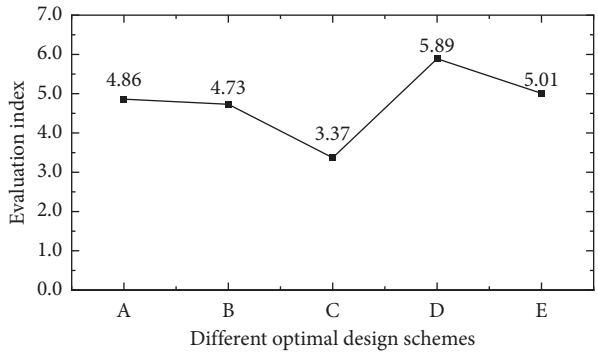

Figure 9: Score statistics for rationality of element placement relationships.

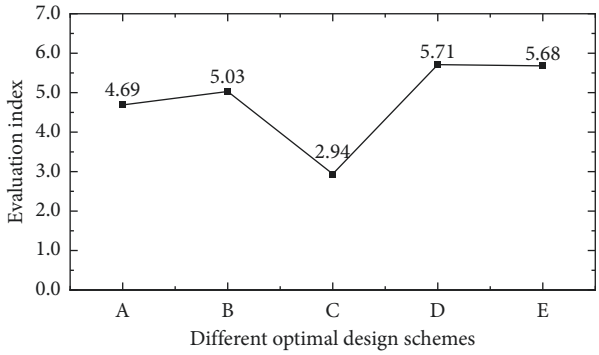

Figure 10: Score statistics for rationality of visual paths.

Table 1: Comparison of the precision the LeNet combined with the A-softmax loss.

Design solutions	$m = 1$	$m = 2$	$m = 3$	$m = 4$
A	0.984	0.994	0.996	0.997
B	0.938	0.949	0.955	0.949
C	0.836	0.856	0.88	0.888
D	0.83	0.838	0.834	0.834
E	0.841	0.834	0.851	0.858
Average	0.885	0.894	0.903	0.905

Table 2: Comparison of the precision of the LeNet combined with the STN and the A-softmax loss.

Design solutions	$m = 1$	$m = 2$	$m = 3$	$m = 4$
A	0.991	0.991	0.994	0.99
B	0.955	0.963	0.967	0.984
C	0.88	0.874	0.904	0.862
D	0.828	0.858	0.862	0.878
E	0.919	0.927	0.937	0.934
Average	0.914	0.922	0.932	0.929

As can be seen from Table 2, the average correct rates all improved considerably, proving that the STN was correctly trained to spatially transform the original images during the training process. Combining the STN with the LeNet can further improve the accuracy of the model. The proposed method at $m = 3$ achieved the best design results. At $m = 3$, the STN + LeNet + A-softmax model proposed in this study was compared with the LeNet, VGGNet [32], and Inception-v4 [33] network models, as shown in Table 3.

Table 3: Compared with existing methods.

Design solutions	STN + LeNet + A-softmax	LeNet	VGGNet	Inception-v4
A	0.994	0.984	0.998	0.976
B	0.967	0.938	0.908	0.85
C	0.904	0.836	0.812	0.706
D	0.862	0.83	0.824	0.83
E	0.937	0.904	0.895	0.851
Average	0.932	0.898	0.887	0.842

5. Conclusion

In this study, a poster layout composition method based on STN + LeNet + A-softmax is proposed. The layout composition method consists of a learner and a generator. The learner learns to classify the layout composition elements using STN and finally realises the recognition and localisation of the layout composition elements to form the initial layout template. The generator uses LeNet convolutional neural network to optimise the initial template, and the final output is the parameter-optimised template. The results show that the combination of the STN and the LeNet allows the network model to extract more effective layout components. At the same time, the A-softmax loss function guides the network model to learn the more discriminative layout elements. Compared with existing methods, STN + LeNet + A-softmax achieves better accuracy [34].

Data Availability

The experimental data used to support the findings of this study are available from the corresponding author upon request.

Conflicts of Interest

The authors declare that they have no conflicts of interest to report regarding this study.

References

[1] R. Chalfen, "A sociovidistic approach to children's filmmaking: the philadelphia project," *Studies in Visual Communication*, vol. 7, no. 1, pp. 3–32, 1981.

[2] L. M. Malmsheimer, ""Imitation white man": images of transformation at the carlisle Indian school," *Studies in Visual Communication*, vol. 11, no. 4, pp. 54–75, 1985.

[3] M. Schreiber, "Audiences, aesthetics and affordances analysing practices of visual communication on social media[J]," *Digital Culture & Society*, vol. 3, no. 2, pp. 89–94, 2018.

[4] Z. Zomay, B. Keskin, and C. Ahin, "Grsel letiim tasarm blümü rencilerinin sektrel logolardaki renk tercihleri - color preferences of visual communication design students in sectoral logos[J]," *OPUS Uluslararası Toplum Araştırmaları Dergisi*, vol. 17, no. 37, pp. 4181–4198, 2021.

[5] D. K. Kilgo and R. R. Mouro, "Protest coverage matters: how media framing and visual communication affects support for black civil rights protests[J]," *Mass Communication & Society*, vol. 8, no. 1, pp. 1169–1178, 2021.

[6] G. S. Dhanesh and N. Rahman, "Visual communication and public relations: visual frame building strategies in war and conflict stories[J]," *Public Relations Review*, vol. 47, no. 1, pp. 2511–2521, 2021.

[7] D. Shinar, "Art and communications in the west bank: visual dimensions of Palestinian nation building," *Studies in Visual Communication*, vol. 10, no. 2, pp. 2–15, 1984.

[8] J. Lin, "Research on the performance of impressionist painting color visual communication based on wireless communication and machine vision," *Security and Communication Networks*, vol. 15, no. 1, pp. 1–6, 2021.

[9] G. C. Liu and C. H. Ko, "Photoshop and illustrator use in instructional design: a case study of college visual communication course design," *The International Journal of Design Education*, vol. 15, no. 1, pp. 119–130, 2021.

[10] H. Li, "Visual communication design of digital media in digital advertising," *Journal of Contemporary Educational Research*, vol. 5, no. 7, pp. 36–39, 2021.

[11] R. Liu, B. Yang, E. Zio, and X Chen, "Artificial intelligence for fault diagnosis of rotating machinery: a review," *Mechanical Systems and Signal Processing*, vol. 108, no. 8, pp. 33–47, 2018.

[12] J. H. Thrall, X. Li, Q. Li et al., "Artificial intelligence and machine learning in radiology: opportunities, challenges, pitfalls, and criteria for success," *Journal of the American College of Radiology*, vol. 15, no. 3, pp. 504–508, 2018.

[13] E. J. Piedad, Y. T. Chen, H. C. Chang, and C. C. Kuo, "Frequency occurrence plot-based convolutional neural network for motor fault diagnosis," *Electronics*, vol. 9, no. 10, p. 1711, 2020.

[14] C. S. Wang, I. H. Kao, and J. W. Perng, "Fault diagnosis and fault frequency determination of permanent magnet synchronous motor based on deep learning," *Sensors*, vol. 21, no. 11, p. 3608, 2021.

[15] K. Satpathi, Y. M. Yeap, A. Ukil, and N Geddada, "Short-time fourier transform based transient analysis of VSC interfaced point-to-point DC system," *IEEE Transactions on Industrial Electronics*, vol. 65, no. 5, pp. 4080–4091, 2018.

[16] Y. Cheng, G. Zhang, C. Yu, P Bo, W Xuewei, and X Feng, "Application of short-time fourier transform in feeder fault detection of flexible multi-state switch[J]," *Journal of Physics: Conference Series*, vol. 1754, no. 1, pp. 149–160, 2021.

[17] E. Dupoux, "Cognitive science in the era of artificial intelligence: a roadmap for reverse-engineering the infant language-learner," *Cognition*, vol. 173, pp. 43–59, 2018.

[18] S. Garg, K. Kumar, N. Prabhakar, A. Ratan, and A Trivedi, "Optical character recognition using artificial intelligence," *International Journal of Computer Application*, vol. 179, no. 31, pp. 14–20, 2018.

[19] M. Hossein and H. Sajad, "Artificial intelligence design charts for predicting friction capacity of driven pile in clay[J]," *Neural Computing & Applications*, vol. 30, pp. 1–17, 2018.

[20] Y. F. Hu and Q. Li, "An adjusTab. envelope based EMD method for rolling bearing fault diagnosis[J]," *IOP Conference Series: Materials Science and Engineering*, vol. 1043, no. 3, pp. 327–339, 2021.

[21] G. R. Naik, S. E. Selvan, and H. T. Nguyen, "Single-channel EMG classification with ensemble-empirical-mode-decomposition-based ICA for diagnosing neuromuscular disorders," *IEEE Transactions on Neural Systems and Rehabilitation Engineering*, vol. 24, no. 7, pp. 734–743, 2016.

[22] Z. Qin, H. Chen, and J. Chang, "Signal-to-Noise ratio enhancement based on empirical mode decomposition in phase-sensitive optical time domain reflectometry systems," *Sensors*, vol. 17, no. 8, p. 1870, 2017.

[23] V. Andrearczyk and P. F. Whelan, "Using filter banks in Convolutional Neural Networks for texture classification," *Pattern Recognition Letters*, vol. 84, pp. 63–69, 2016.

[24] C. Zhang, X. Yue, R. Wang, N. Li, and Y. Ding, "Study on traffic sign recognition by optimized lenet-5 algorithm[J]," *International Journal of Pattern Recognition and Artificial Intelligence*, vol. 34, no. 1, pp. 1–21, 2020.

[25] H. Wang, W. Yang, Z. Zhao, T. Luo, J. Wang, and Y. Tang, "Rademacher dropout: an adaptive dropout for deep neural network via optimizing generalization gap," *Neurocomputing*, vol. 357, no. 9, pp. 177–187, 2019.

[26] S. Samir, E. Emary, K. El-Sayed, and H. Onsi, "Optimization of a pre-trained AlexNet model for detecting and localizing image forgeries," *Information*, vol. 11, no. 5, p. 275, 2020.

[27] H. M. Kasem, K. W. Hung, and J. Jiang, "Spatial transformer generative adversarial network for robust image super-resolution," *IEEE Access*, vol. 7, pp. 182993–183009, 2019.

[28] K. Naoki and U. Hiroshi, "A construction of simple and smaller-state real-time generator for exponential sequences [J]," *Artificial Life and Robotics*, vol. 25, no. 1, pp. 64–72, 2020.

[29] S. A. Wagle and R. Harikrishnan, "Comparison of plant leaf classification using modified AlexNet and support vector machine," *Traitement du Signal*, vol. 38, no. 1, pp. 79–87, 2021.

[30] T. Ye, M. Jian, L. Chen, and Z. Wang, "Rolling bearing fault diagnosis under variable conditions using LMD-SVD and extreme learning machine[J]," *Mechanism and Machine Theory*, vol. 90, pp. 175–186, 2015.

[31] H. X. Zhou, H. Li, T. Liu, T. Liu, and Q. Chen, "A weak fault feature extraction of rolling element bearing based on attenuated cosine dictionaries and sparse feature sign search," *ISA Transactions*, vol. 97, pp. 143–154, 2020.

[32] M. Jangra, S. K. Dhull, and K. K. Singh, "ECG arrhythmia classification using modified visual geometry group network (mVGGNet)," *Journal of Intelligent and Fuzzy Systems*, vol. 38, no. 3, pp. 3151–3165, 2020.

[33] D. B. Toan, J. Lee, and J. Shin, "Incorporated region detection and classification using deep convolutional networks for bone age assessment[J]," *Artificial Intelligence in Medicine*, vol. 97, pp. 1–8, 2019.

[34] D. J. Frey, A. Mishra, M. T. Hoque, M. Abdelguerfi, and T. Soniat, "A machine learning approach to determine oyster vessel behavior," *Machine Learning and Knowledge Extraction*, vol. 1, no. 1, pp. 64–74, 2018.

Hindawi
Scientific Programming
Volume 2022, Article ID 5902445, 16 pages
https://doi.org/10.1155/2022/5902445

Research Article

Simulation Model on Network Public Opinion Communication Model of Major Public Health Emergency and Management System Design

Lei Li,[1,2] **Yujue Wan**,[1,2] **D. Plewczynski**,[3] **and Mei Zhi**[1,2]

[1]*College of Safety Science and Engineering, Xi'an University of Science and Technology, Xi'an 710054, China*
[2]*Key Laboratory of Western Mines and Hazard Prevention, Ministry of Education of China, Xi'an 710054, China*
[3]*University of Warsaw, 02097 Warsaw, Poland*

Correspondence should be addressed to Lei Li; lilei_safety@xust.edu.cn

Received 26 April 2022; Revised 11 May 2022; Accepted 20 May 2022; Published 20 June 2022

Academic Editor: Lianhui Li

In order to identify the communication law of network public opinion in major public health emergency, a multifactor communication model based on multiagent modeling is proposed. Based on the SEIR model and NetLogo simulation analysis, the model integrates a variety of network public opinion communication characteristics and extends the existing single network public opinion communication model. Based on these studies, a network public opinion communication management system is designed and developed with Python tools. Case analysis and simulation results show that this model can better simulate the evolution trend of network public opinion communication in major public health emergency; the key communication channels of public opinion play an important role in the evolution of network public opinion, which can control and guide the network public opinion of major public health emergency from the three communication influencing factors of total number, initial number, and communication cycle. Communication cycle refers to the number of days in the process of network public opinion dissemination of major public health emergencies.

1. Introduction

At present, the number of netizens in my country accounts for 73.7% of the total population, and the Internet penetration rate exceeds 73% [1]. With the popularization and development of smart mobile terminals and mobile communication technologies, rich and diverse social media platforms have become netizens for information sharing and a gathering place for expressing opinions and emotional exchanges. When public health emergencies occur, public opinion on the Internet also arises, and it may bring serious negative effects. From the 2003 "SARS" virus to the H5N1 virus in 2005, the H1N1 flu in 2009, the H7N9 virus in 2013, and the new coronary pneumonia to today, the derivative accidents caused by public opinion brought about the incidents, reflecting the sudden public emergency in the context of the rapid development of the Internet. The importance of timely response to and disposal of public opinion on the Internet of health incidents is obvious.

In 2020, there was a large-scale outbreak of COVID-19 pneumonia in China. According to Baidu data, the average daily search frequency of the keyword "COVID-19 pneumonia" reached 300,000 times. As the enthusiasm of netizens gradually rises, there have been more than 700 million participations in public opinion discussions on the "COVID-19 pneumonia" on Internet platforms. In the context of public health emergencies, the facts have been focused, magnified, and distorted due to the failure of online public opinion to study and respond in time. At present, scholars' research on online public opinion on emergencies mainly focuses on natural disasters, major cases, and social hot spots. There are relatively few studies on Internet public opinion in the context of public health emergencies [2–6]. The analysis process of the functional resonance analysis method (FRAM) is applied to China's safety supervision

system to classify and evaluate government safety supervision functions [7] and explain the measures taken to reduce risks in the face of the current public health emergency COVID-19 outbreak [8]. After the outbreak of the epidemic, a large number of studies on treatment and response measures were quickly generated for the global pandemic of COVID-19 [9].

Based on this, how to understand and grasp the characteristics, laws, and development trends of public opinion communication of public health emergencies will help the regulatory authorities to study and judge the development trends of public opinions and take active and effective response measures in a timely manner, so as to improve the response to sudden public health emergencies, so as to improve the ability to deal with the network public opinion of major public health emergencies.

Therefore, taking the "COVID-19 pneumonia" as an example to visualize the spread of online public opinion in the context of public health emergencies, through intuitive and vivid data and images to analyze the trend and law of communication public opinion on public health emergencies, it can effectively reflect the law and characteristics of the spread of public opinion on the Internet of public health emergencies. In a quantitative way, the key nodes in the "COVID-19 pneumonia" online public opinion communication network were visually identified and analyzed, and suggestions for the management, control, and guidance of the online public opinion communication of public health emergencies were put forward.

2. Theoretical Basis

2.1. Simulation Platform

2.1.1. Gephi Visualization. Gephi provides for processing any network data that can be represented as nodes and edges and will be presented in the form of graphics images, such as data representing social relationships, information nodes, biology, ecology, physics, and other networks [10–13]. Gephi can not only process large-scale network data sets but also support mainstream network scientific algorithms. It can not only perform statistical analysis on network attributes at the node level but also use different layout algorithms to visualize the network, and it can also simulate dynamic network analysis.

2.1.2. NetLogo Simulation Platform. NetLogo is a multiagent modeling and simulation software, which is used for modeling and simulation of complex systems changing with time. NetLogo was developed by the Center for Connected Learning and Computer-Based Modeling (CCL) of Northwestern University. NetLogo simulation can provide a simple, convenient, and powerful computer tool for scientific research in various fields. Logo language is used to control and coordinate multiple disciplines to meet the needs of studying multidisciplinary laws. The simulation process is shown in Figure 1.

2.2. Online Public Opinion on Public Health Emergencies. In recent years, many public health emergencies have occurred all over the world. In order to efficiently and reasonably respond to public opinion on public health emergencies, scholars have combined public health incidents to obtain data through Twitter and Facebook and use model construction, empirical analysis, and other methods to carry out related research. Barbara Reynolds believes that public opinion on public health emergencies should be divided into a summary evaluation stage, a calming stage, a crisis stage, a precrisis stage, and an initial stage [14]. Wang et al. summarized the characteristics of online public opinion communication of public health emergencies through case analysis [15]. Haihong et al. proposed a multichannel and multicore model to study the development of online public opinion under public health emergencies [16]. Gaspar et al. believe that different types and stages of crisis response will be different, and the comments made by netizens do not fully represent their attitude [17]. Gomide et al. believe that the development trend of public health emergencies can be monitored through relevant public opinion information on the Twitter platform [18]. Pei et al. believe that, by monitoring the news media on the Weibo platform, it is possible to predict the spread of public health event news and identify early warning signals [19]. Signorini et al. believe that analyzing the content of Twitter users' posts can provide a basis for timely intervention in the development of public opinion on public health emergencies [20, 21]. The Center for Disease Control and Prevention of the University of Chicago and NORC conducted a network survey of state, regional, and local health departments and concluded that public health emergency preparedness and response to the cooperation of state and local health departments are the key links.

However, most domestic scholars in China choose Baidu Index and Weibo as data sources to conduct research from the perspectives of dividing communication stages, analyzing communication characteristics, and studying communication influencing factors. The "Regulations on Public Health Emergencies and Emergency Responses" believe that public health emergencies refer to infectious disease outbreaks and unexplained mass epidemics, major food poisoning, and occupational poisoning that occur suddenly and cause or may cause major losses to the public health and other public emergencies that endanger public health [22]. Cao and Lu believe that it has the three characteristics of emotional expression of netizens' opinions, diversified communication subjects, and self-interested media [23]. Teng believes that provinces with more netizens and higher levels of economic development have a higher degree of public opinion attention on public health emergencies [24]. An Lu et al. constructed a topic evolution model for various stakeholders of public health emergencies at different life cycle stages [25]. Lin et al. established a model of factors affecting the spread of public opinion in public health emergencies [26]. Zhou made an overview and analysis of the information problems exposed at each stage of the development of the new crown pneumonia epidemic and put forward countermeasures and suggestions from the perspective of the construction of emergency information management system [27].

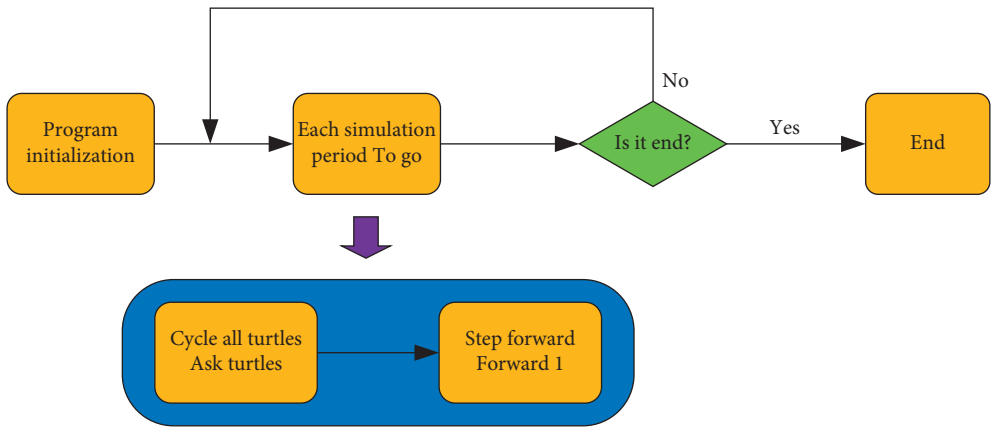

Figure 1: Simulation process.

Public opinion on public health emergencies is a form of public opinion on the Internet. On the basis of the scholars dividing the law of the spread of public opinion on the network of emergencies into three, four, or five stages [28, 29], based on the life cycle theory, six rules that conform to the law of spread of public opinion on the Internet of public health emergencies are proposed.

2.3. Influencing Factors of Network Public Opinion Communication

2.3.1. The Total Number of People Involved in Communication. The complexity of the network environment also makes it an influencing variable of public opinion communication. It is reflected not only in the process of personal information exchange but also in the process of emotional communication. Public opinion information communication is usually the product of emotional processing of most people in different cognitive stages. It represents the thoughts and attitudes of Internet users and has a strong cohesion to the related Internet users. Even if people together do not know each other, they may be involved in huge public opinion discussions. These pieces of unconfirmed public opinion information will spread on the network, and gradually spreading, more and more people will spread. Therefore, in the process of network public opinion communication, the more the total number of people involved, the faster the speed of public opinion information communication; the less the total number of people involved, the slower the speed of public opinion information communication. When the total number of people involved in the communication is less, the difficulty of information communication will be greater, so it is difficult to disseminate information. It is believed that public opinion information will not be disseminated, so public opinion will be controlled. Therefore, the total number of people involved in the communication is an important factor affecting the communication of network public opinion.

2.3.2. Number of Initial Spreaders. With the rapid development of network, network public opinion will produce a lot of public opinion information. Due to the diversity of content in the network environment, in the incubation period of public opinion, the initial communicators publish text, pictures, videos, and other pieces of related content through various social platforms, which will promote the rapid communication of public opinion information and be known by other Internet users. Therefore, the initial communicators of these pieces of public opinion information have strong communication, and in order to attract the attention to increase their own flow or click rate, they will continue to disseminate public opinion information related to major public health emergencies. Therefore, the number of initial communicators of public opinion information will have a certain impact on the process of public opinion communication.

2.3.3. Transmission Cycle. Public opinion communication cycle will also affect major public health emergency network public opinion communication. In the same space, the longer the cycle of public opinion communication, the wider the scope of its communication and the more the Internet users involved in the communication. In a long communication cycle, the heat of public opinion will grow higher and higher over time, and the development of public opinion will be difficult to control. Internet users can browse the news through the network social platform, quickly understand the relevant hot topics of public opinion according to forwarding and comments, and join the network public opinion dissemination. At this time, the network public opinion information will spread rapidly. This kind of communication phenomenon will greatly accelerate the scope of public opinion communication and at the same time make the cycle of public opinion survival in the network longer, resulting in greater difficulty in the control of public opinion.

2.4. SEIR Model. The SEIR model divides the total population into the following four categories: susceptibles, denoted as $S(t)$, indicating the number of people who are not infected but may be infected by virus at t time; exposed, denoted as $E(t)$, meaning the number of people who have been lurked after being infected at t; infectives, denoted as

$I(t)$, indicating the number of people who have been infected and become patients with infectious force at time t; recovered, denoted as $R(t)$, meaning the number of people who have recovered from the infected at t moment. If the total population is $P(t)$, then $P(t) = S(t) + I(t) + R(t)$ SEIR differential equation is

$$\begin{cases} \dfrac{\mathrm{d}S}{\mathrm{d}t} = -\left(\dfrac{r\beta IS}{N}\right), \\ \dfrac{\mathrm{d}E}{\mathrm{d}t} = \left(\dfrac{r\beta IS}{N}\right) - \alpha E, \\ \dfrac{\mathrm{d}I}{\mathrm{d}t} = \alpha E - \gamma I, \\ \dfrac{\mathrm{d}R}{\mathrm{d}t} = \gamma I. \end{cases} \tag{1}$$

In the above equation, α corresponds to the infection probability, β corresponds to the probability that the latent person is converted to an infected person, γ corresponds to the cure probability, and r is the number of people in contact.

The equation essentially reflects the changes of the number of unit time changes of susceptible $S(t)$ latent $E(t)$, infected $I(t)$, and rehabilitation $R(t)$ with time t, and they will affect each other.

3. Law of Network Public Opinion Communication Rules of Major Public Health Emergency

Taking the network public opinion of major public health emergency as the research object and taking "epidemic situation of new corona pneumonia in Wuhan City" as an example, the Gephi visualization tool and case analysis method are used for empirical research.

3.1. Review of Event Development. On December 30, 2019, influenza and related diseases were continuously monitored in Wuhan City, Hubei Province, China. Multiple viral pneumonia cases were found, and all were diagnosed as pneumonia cases with novel coronavirus infection. Since viral pneumonia was found in Wuhan in 2019, it was temporarily named "COVID-19" by the World Health Organization on January 12, 2020. The outbreak was released by WHO as a new coronavirus pneumonia epidemic for major public health emergency of international concern. Later, the Director-General of the World Health Organization, Thadsey, announced that the new coronavirus had become a global pandemic. Table 1 is the review of the epidemic development of "epidemic situation of new corona pneumonia in Wuhan City."

3.2. Data Source and Processing. Weibo has 212 million monthly active users and is the mainstream platform of China's social networking platform. This paper uses Sina Weibo as the data source and the development of online public opinion on the "COVID-19 pneumonia" epidemic as the research object. So far, according to the Baidu Index, Chinese netizens have participated in more than 800,000 daily discussions on public health emergencies, with an average spread of 5,238 items per hour. The daily search volume of high-frequency words such as "infectious disease," "resumption of work," "pneumonia," and "prevention and control" related to this public health emergency reached a total of 4.5 million times. It can be seen from this that the public health emergency of the new type of coronavirus pneumonia has caused great concern among Chinese netizens.

Quantitative analysis is carried out by dividing the important time period of the network communication of this public health emergency, identifying core nodes, and using Gephi to visually analyze the law of communication. Select the number of forwarding data posted by key bloggers on Weibo from December 31, 2019, to March 1, 2020. In the communication of online public opinion information, the higher the number of fans, the greater the influence. Therefore, the key bloggers are identified based on the number of fans, and the Weibo account with the highest number of fans participating in this public health emergency is selected as the key channel for this public opinion communication. Take 5–8 Weibo accounts as the research objects in each communication stage, search for relevant Weibo information according to important time periods and time sequence, and count all the reposts of each Weibo. As of March 1, 2020, a total of 66,000 Weibo accounts with varying degrees of influence, a total of 761,333 original Weibos on the topic of "COVID-19 pneumonia," and a total of 7,429,838 original Weibo forwarding data on key Weibo accounts have been obtained.Finally, organize the sample data table shown in Table 2. Due to the large amount of data collected in the experiment, after categorizing and counting the data, the Gephi tool is used for visual analysis, and the Gephi tool is used for visual analysis. During the drawing process, the "YifanHu" process is used for layout, and "ForceAtlas2" is used for focus.

3.3. Data Results and Discussion

3.3.1. Division of the Law of Communication Public Opinion on Public Health Emergencies on the Internet. According to the public opinion development process of "COVID-19 pneumonia" in public health emergencies, the forwarding volume of Weibo accounts in key channels of Weibo was selected as the data source, and the development trend of public opinion transmission of "COVID-19 pneumonia" was drawn in units of important time periods, as shown in Figure 1. On the whole, the public opinion of the public health emergency showed obvious stage characteristics, based on the life cycle theory combined with the time span of the public opinion of the public health emergency, the peak point, and many scholars in the early stage. On the basis of the stage division of public opinion, the redivision is in line with the current law of communication public opinion on

Table 1: Review of the development of the "COVID-19 pneumonia" epidemic.

Important time period (point)	Event content (situation)
2019.12.31–2020.01.15	On December 31, 2019, an unofficial network circulated a report that "patients with unexplained pneumonia were found"; on December 31, the Wuhan Health and Health Commission notified for the first time that "27 cases were confirmed, but the cause was not clear." On January 9, the official confirmation, the pathogen was identified as the "COVID-19."
2020.01.16–2020.01.26	The China centers for disease control and prevention were upgraded to the first-level emergency response (the highest level); subsequently, 30 provinces initiated the first-level response to major public health emergencies; Wuhan City was closed on January 23.
2020.01.27–2020.02.03	Various localities have successively issued notices on strengthening the standardized management of communities during the epidemic prevention and control period; there are too many suspected and confirmed patients, and Fangcang shelter hospitals and Huoshenshan hospitals have been established to treat patients. The WHO has listed the novel coronavirus epidemic as a public health emergency of international concern.
2020.02.04–2020.02.15	On the 11th, the World Health Organization officially named the pneumonia caused by the COVID-19 as COVID-19; Mi Feng, a spokesperson for the National Health Commission, said that, as of the 15th, the proportion of severe cases in Hubei and other provinces in the country has dropped significantly.
2020.02.16–2020.02.23	The epidemic situation in China has gradually improved, and countries outside Japan, South Korea, the United States, Italy, and other countries have begun to break out of COVID-19 pneumonia, causing domestic netizens to discuss again.
2020.02.24–2020.03.01	The new crown pneumonia epidemic has been under control, and China has lowered the emergency response level of the new crown pneumonia epidemic.

public health emergencies; that is, it is divided into six stages of latent, fermentation, outbreak, relief, repetition, and decline, as shown in Figure 2, and is verified through the "COVID-19 pneumonia" analysis.

Table 2: Sample data table of information communication of "COVID-19 pneumonia" Weibo during important time periods.

Period	Number of participating Weibo accounts	Number of original Weibos	Select the number of Weibo accounts	Weibo forwarding volume
2019.12.31–2020.01.15	6743	7186	7	172393
2020.01.16–2020.01.26	90183	152291	6	714913
2020.01.27–2020.02.03	100995	160421	7	2215159
2020.02.04–2020.02.15	122761	180074	5	1665850
2020.02.16–2020.02.23	106618	153423	7	1827211
2020.02.24–2020.03.01	76723	107938	8	834312

3.3.2. Visualized Analysis of the Law of Communication Public Opinion on the Internet of Public Health Emergencies. On the basis of the above-mentioned classification of public opinion transmission rules of public health emergencies, Gephi is used to visually analyze the "COVID-19 pneumonia."

During the incubation period of the first stage, the public is still in a state of understanding public health emergencies from unknown to understanding, and public opinion on the Internet has never occurred until it gradually ferments. At this time, public opinion begins to spread for the first time. After the unidentified pneumonia incident occurred in Wuhan, it can be seen from Figure 3(a) that it was reported as "Headline News," "People's Daily," "CCTV News," "CCS Open Class," "People's Daily Online," "Xinhua Viewpoint," Weibo accounts headed by "Xinhuanet" which are used as key communication channels, the communication network developed by using this as a core node is relatively sparse, and its influence at this stage is still relatively small.

In the second phase of the fermentation period, after the epidemic was identified as "COVID-19 pneumonia," as shown in Figure 3(b), it was reported as "CCTV News," "Headline News," "People's Daily," and "Beijing New." A large number of fans with scattered core nodes, led by Weibo accounts such as "Central Securities Public Courses" and "People's Daily Online," gradually received information. At this time, these Weibo accounts played a key role in attracting the attention of netizens and promoting the development of public opinion.

During the third stage of the outbreak, due to the initial transmission of Chinese netizens through the key communication channels of the previous stage, more netizens have learned about the occurrence of this public health emergency. At this time, the Weibo accounts of these key communication channels are playing a role. They have a great influence. As shown in Figure 3(c), the core nodes, such as "micro-blog secretary," "micro-blog administrator," "CCTV news," "People's Daily," "headline news," "Xinhua viewpoint," and "He Jiong," are rapidly expanding the

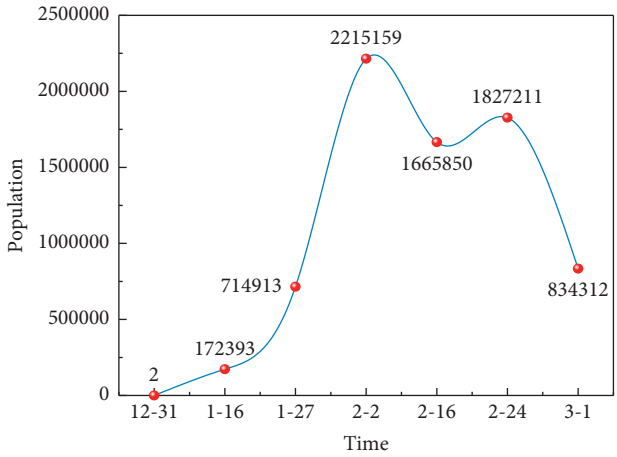

Figure 2: The communication trend of public opinion on the Weibo network of "COVID-19 pneumonia."

network of public opinion communication. The density of the network of the above core nodes is very high, and the number of microblog forwarding and fans increases sharply, resulting in the highest point of network public opinion in this major public health emergency. These key communication channels have exerted a huge influence and a wide range of influence at this stage, pushing the public opinion development of the "COVID-19 pneumonia" public health emergency to the climax.

In the remission period of the fourth stage, in view of the serious public opinion impact caused by the public health emergency "COVID-19 pneumonia," government departments have spoken out and conducted timely public opinion control, which reversed the perception of netizens. At this time, under the influence of these key communication channels, the development trend of online public opinion gradually stabilized. It can be seen from Figure 3(d) that the scope of the communication network composed of core nodes headed by "People's Daily," "Headline News," "CCTV News," "Xinhua Viewpoint," and "people's Daily Online" has gradually decreased, and the density of the communication network has also been reduced. Gradually decreasing, the public opinion of the "COVID-19 pneumonia" public health emergency at this stage has entered a stable period of remission.

In the fifth stage of the repetitive period, after the development of the previous stage, the development of public opinion should have stabilized. Due to the large number of rumors appearing and communication, under the influence of some key channel Weibo accounts, a large number of core nodes are connected. Fans are gradually increasing as secondary nodes, and the communication network is gradually becoming denser. Netizens' attention to this public health emergency has risen again. As shown in Figure 3(e), this stage is based on "People's Daily," "Headline News," "CCTV News," "Xinhua Viewpoint," and "People's Daily." The key communication channels led by "He Jiong" and "Ang Mi" have caused public opinion to show a trend of small climax.

In the sixth phase of the recession period, the heat for this public health emergency has been reduced to a relatively low level through the remission period. Therefore, the online public opinion of the "COVID-19 pneumonia" is about to enter recession and even die out. At this stage of the epidemic, as the epidemic was basically controlled, the panic of netizens was gradually eliminated, making public opinion tend to decline. Figure 3(f) shows that the microblogs are headed by "CCTV News," "People's Daily," "Headline News," "Xinhua Viewpoint," "People's Daily Online," "Xinhuanet," "Yao Chen," and "China News Weekly." As the core node of the blog account, the spread of public opinion has become smaller, and the density of the spread network has been significantly reduced. The public health emergency "COVID-19 pneumonia" network public opinion has entered a period of decline.

Based on Gephi visualization, it analyzes in detail the communication characteristics and rules of each stage of the public opinion communication network composed of some accounts of the key communication channels of Weibo as the core nodes and the amount of fan reposting as the secondary nodes and analyzes these key communication through visual graphics as shown in Figure 3. The role of channels in each stage of the process of public opinion communication is an empirical study of the proposed public opinion communication law of public health emergencies.

4. Construction of Network Public Opinion Communication Model of Major Public Health Emergency

4.1. Model Construction

4.1.1. SEIR Epidemic Model Hypothesis. When public opinion occurs, most Internet users (except witnesses) do not know about public opinion information, but they will soon obtain relevant information from various channels and make judgments on information. This paper will receive public opinion information that is easy to produce risk perception of Internet users called easy communicators; Internet users who receive public opinion information but are still suspicious of judgment and have not spread it are called carriers; when the perceived risk of public opinion information exceeds its own tolerance, the communication of public opinion information is called the communicator; otherwise the carrier state is maintained. Disseminators become immune under the influence of external factors such as truth or government intervention. With the continuous disclosure of the truth or the continuous emergence of rumors, immune people are affected by the evolution of public opinion and herd mentality and may be reintegrated into the communication of public opinion and become easy communicators.

Considering the complexity and uncertainty of public opinion communication after major public health emergency, the audience classification in the model is expanded and adjusted according to the interaction rules. The SEIR model is assumed as follows.

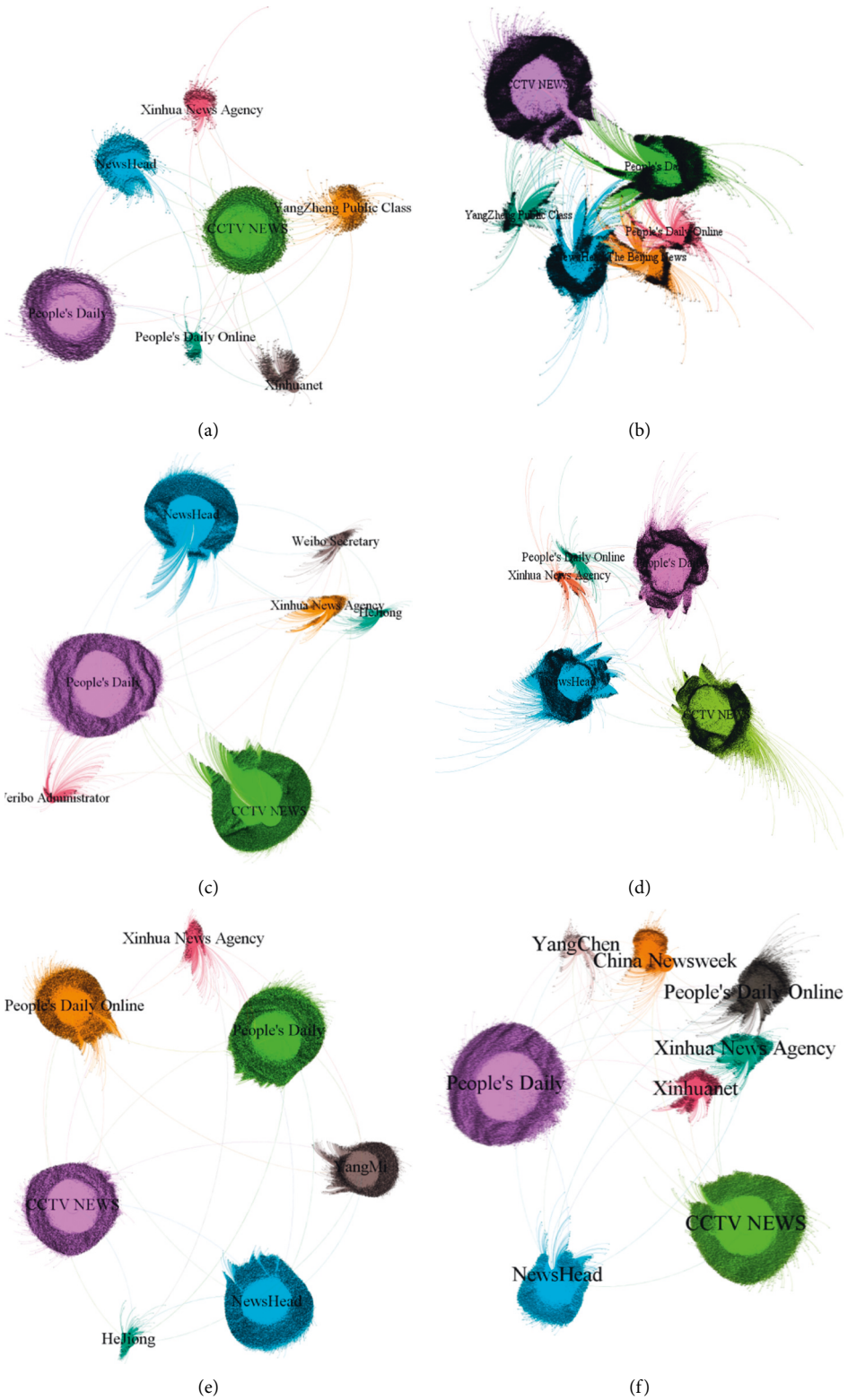

Figure 3: The law of the spread of public opinion on public health emergencies on the Internet. (a) Incubation period. (b) Fermentation period. (c) Outbreak period. (d) Remission period. (e) Recurrent period. (f) Decline period.

Hypothesis 1. Considering the long duration of major public health emergency and related information communication, the audience classification in the model is expanded, and the interaction rules are adjusted. The SEIR model is assumed as follows: the total number of people in the system remains unchanged during this period, and it is assumed to be 1. According to the spread of Internet users, the Internet users are divided into easy communicator S, latent E,

communicator I, and immune R. $S(t)$, $E(t)$, $I(t)$, and $R(t)$ are, respectively, used to represent the proportion of the four types of people in the total number at time t, which are denoted as S, E, I, and R and satisfy $S + E + I + R = 1$.

Hypothesis 2. Public opinion communication channels are not restricted, including online (network and media) channels and offline (interpersonal) channels.

Hypothesis 3. Each individual has several times of contact with information, but the transition rate between groups remains unchanged.

Hypothesis 4. In the whole communication region, only the behavior of the communicator will endanger the society, and the influence range of public opinion communication is positively correlated with the number of communicators.

4.1.2. Model Construction. According to the above infectious disease characteristics and assumptions of public opinion transmission after major public health emergency, an SEIR infectious disease model of public opinion transmission after major public health emergency is established, as shown in Figure 4.

SEIR differential equation is

$$\begin{cases} S_n = S_{n-1} - \dfrac{r\beta I_{n-1} S_{n-1}}{N}, \\ E_n = E_{n-1} + \dfrac{r\beta I_{n-1} S_{n-1}}{N} - \alpha E_{n-1}, \\ I_n = I_{n-1} + \alpha E_{n-1} - \gamma I_{n-1}, \\ R = nR_{n-1} + \gamma I_{n-1}. \end{cases} \tag{2}$$

In the formula, r is the person that every communicator can reach; α is the conversion rate from easy communicator to latent ones; β is the conversion rate from the latent person to the communicator; γ is the conversion rate from the transmitter to the immune.

4.1.3. Simulation Steps. The simulation software NetLogo is used to simulate the rumor communication model, observe the model trend diagram under different parameters, and analyze the influencing factors of public opinion communication, as shown in Figure 5.

The simulation steps are as follows: Step 1: initialize the parameters. Set a total number of initial communicators, transmission cycle, infection rate α, disease rate β, and cure rate γ. Step 2: click setup application parameters. Step 3: click Go, and then the model runs and continues to simulate. Step 4: observe the real-time curve. Record the "number-time" curve of vulnerable, latent, disseminator, and immune person. Step 5: end the simulation, data collation, and analysis. The simulated image changes in the simulation process are shown in Figure 6.

4.2. Analysis of Simulation Experiment

4.2.1. Factors Influencing Transmission

(1) The Total Number of People Involved in Communication. In general, it is believed that, in the same limited space, maintaining the same communication cycle, the more the people are, the faster the infection will be. In order to explore the influence of the total number of people involved in the communication of network public opinion in major public health emergency on information communication, we set the total number of people (population = 1000) as the control group and then set the total number of people (population = 2000, 3000, 4000) for the comparative study, so as to maintain the initial number of people and the communication cycle unchanged. The results are shown in Figure 7.

As shown in Figure 8, when $N = 1000$, the disseminator I approximates a horizontal line, which indicates that the number of disseminator I has not increased substantially in limited space, indicating that the number of public opinion disseminators is small, and controlling the development of public opinion is the best time. When $N = 4000$, disseminator I appeared at the earliest time, and this curve rose rapidly. This shows that the heat of public opinion in limited space has risen rapidly. When the relevant departments have not officially released confirmation news, most people have begun to spread information, and the scope of public opinion has begun to expand rapidly.

(2) Number of Initial Communicators. Similarly, in order to explore the influence of the number of initial communicators on the network public opinion communication of major public health emergency and to maintain the same total number of communicators involved and transmission cycle parameters, the number of the initial communicators is adjusted for simulation experiments. The results are shown in Figure 9.

(3) Transmission Cycle. Similarly, in order to explore the influence of communication cycle on the network public opinion communication of major public health emergency, the simulation experiments were carried out by adjusting the communication cycle to maintain the same parameters of the total number of people involved and the initial communicator. The results are shown in Figure 10.

4.2.2. Comparison between Real Cases and Simulation. After processing the data obtained by the crawler, the number of communicators in each stage of the real case is obtained. The number of communicators in the model simulation is the sum of the number of latent E and communicator I. After running NetLogo simulation software, the comparison between real case data and simulation results is shown in Figure 11.

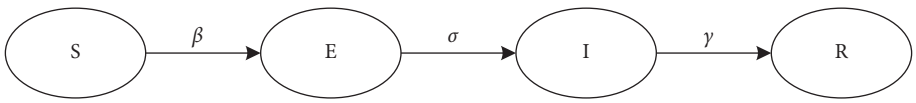

Figure 4: SEIR epidemic model of network public opinion transmission in major public health emergency.

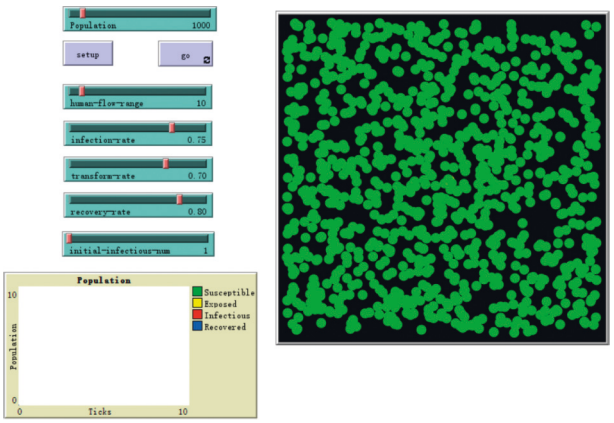

Figure 5: NetLogo simulation interface.

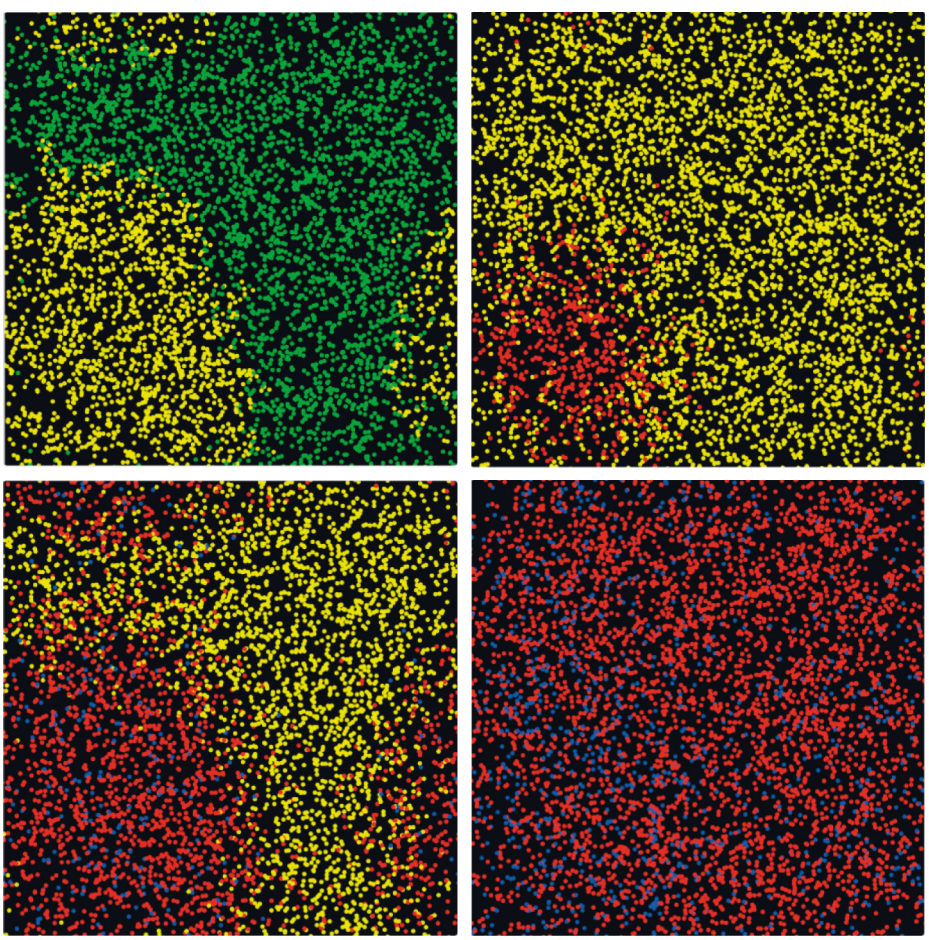

Figure 6: Simulation of image changes.

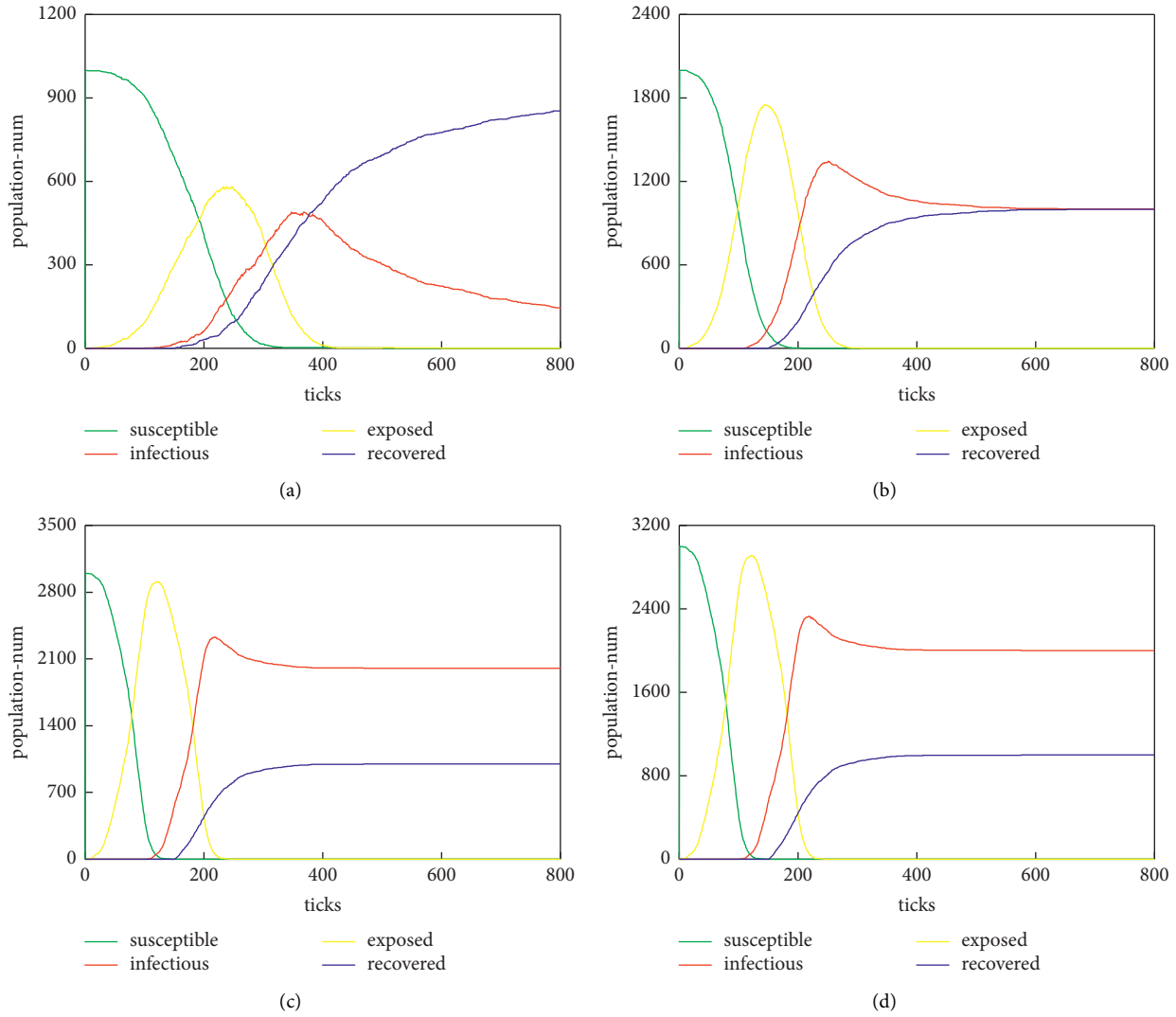

Figure 7: Impact of the total number of people involved in public opinion communication. (a) 1000. (b) 2000. (c) 3000. (d) 4000.

5. Network Public Opinion Communication Management System Design

The emergence of advanced information technology [30, 31] makes the design and development of network public opinion communication management system possible. Based on Python tools [32–35], the overall framework of the network public opinion communication management system is designed as shown in Figure 12.

5.1. Operation Process and System Architecture. Combined with the above research, we will design and implement the system. The modules of the system are divided into information collection module, public opinion content data preprocessing module, major public health emergency network public opinion monitoring module, and major public health emergency network public opinion evaluation module. The system operation logic diagram is shown in Figure 13.

The system architecture is shown in Figure 14.

As shown in Figure 14, the data collection layer adopts the theme crawler technology based on Python language and uses the third-party library Beautiful Soup and Urlib2 package to capture the data on the Weibo platform. The data storage layer adopts MySQL database to store the crawled data in the database. The algorithm execution layer uses Python's NumPy and JS language to bring the preprocessed data into the model established above and calculate the required results. The front-end display layer adopts HTML and CSS to realize the interaction of front-end pages, JS to realize the interaction function, AJAX technology to realize the data interaction with the server, and Ecarts to draw the front-end charts.

5.2. Development Environment. The development environment is as follows:

Experimental environment: Intel quad-core processor with 8G memory and 64-bit Windows 10 operating system.

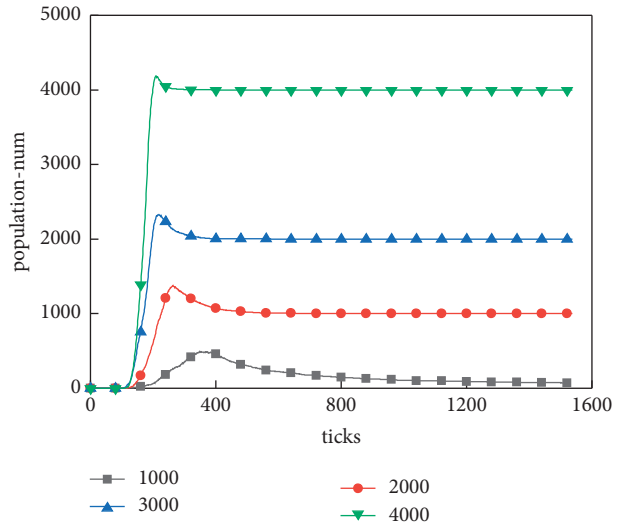

Figure 8: Changes in the I-curve of disseminator with different transmissions involving total numbers.

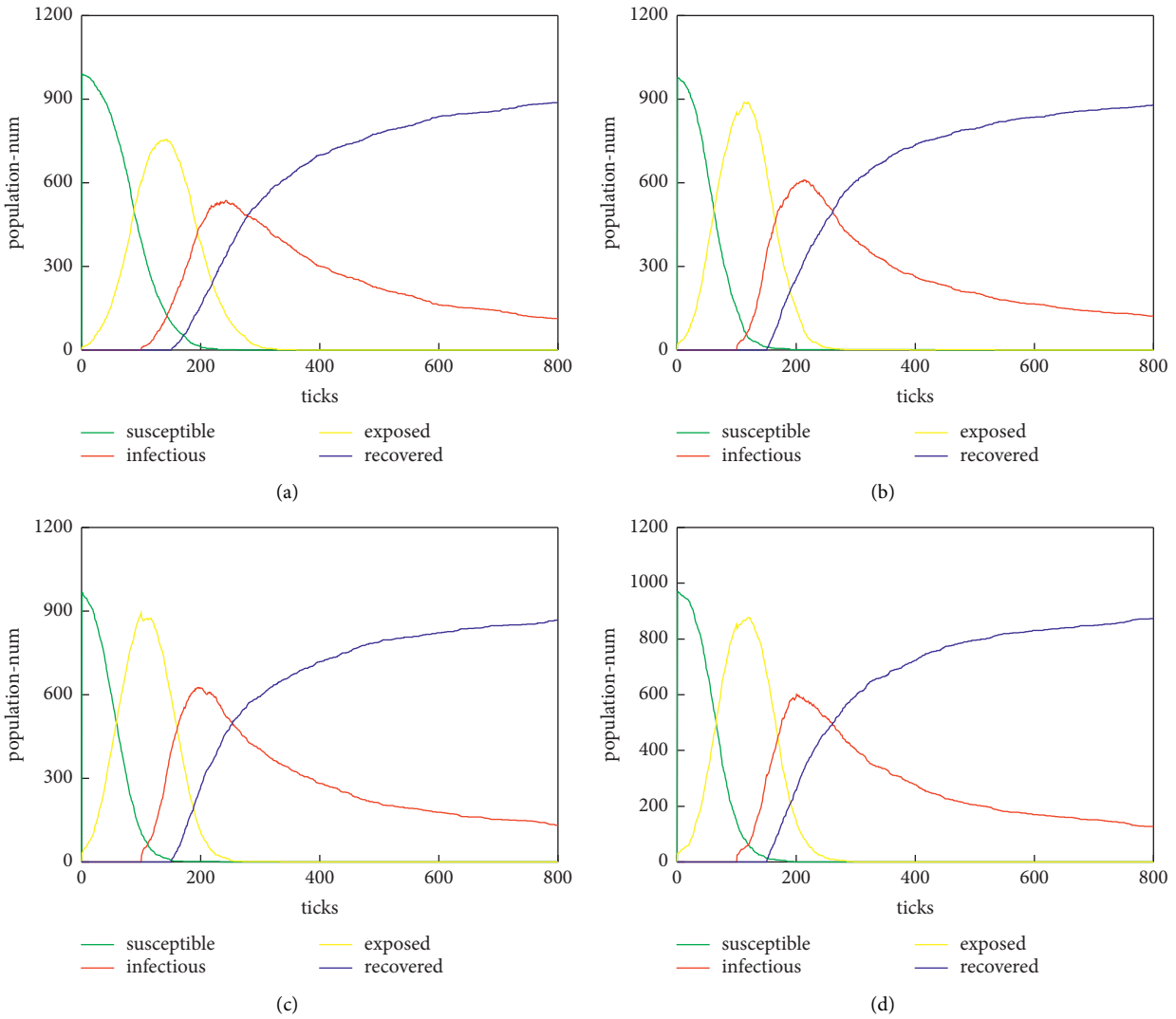

Figure 9: The impact of the initial number of communicators on public opinion communication. (a) 10. (b) 20. (c) 30. (d) 40.

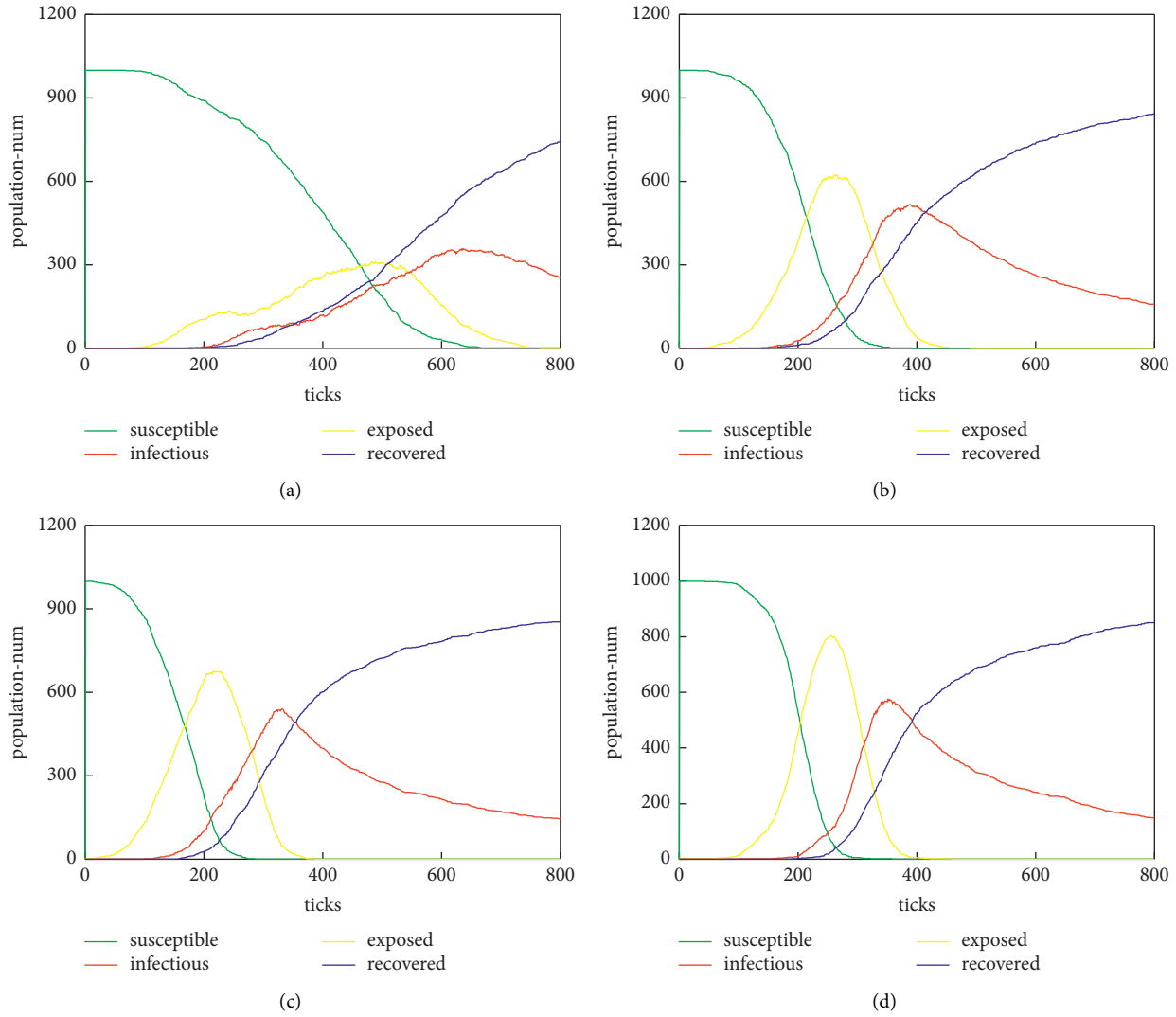

Figure 10: Influence of communication cycle on public opinion communication. (a) 5. (b) 10. (c) 15. (d) 20.

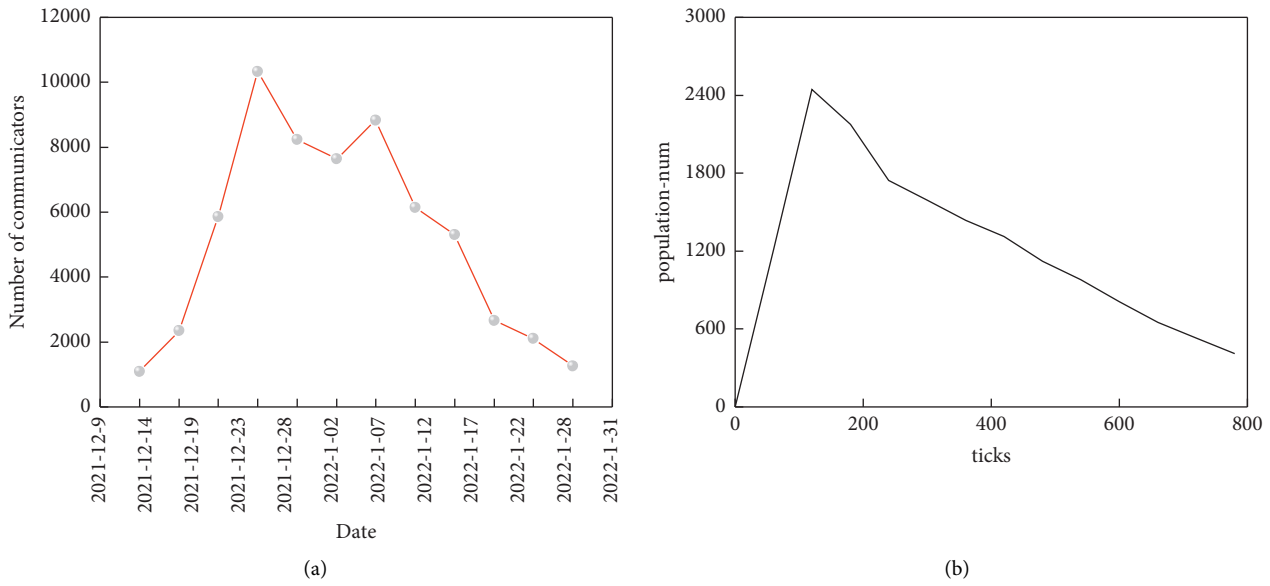

Figure 11: Comparison of real case data and model simulation data. (a) Trend of real case communicators. (b) Model simulation communicator trend.

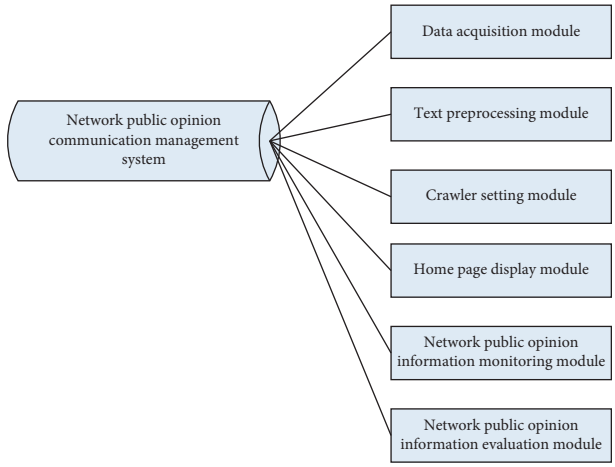

Figure 12: The overall framework of network public opinion communication management system.

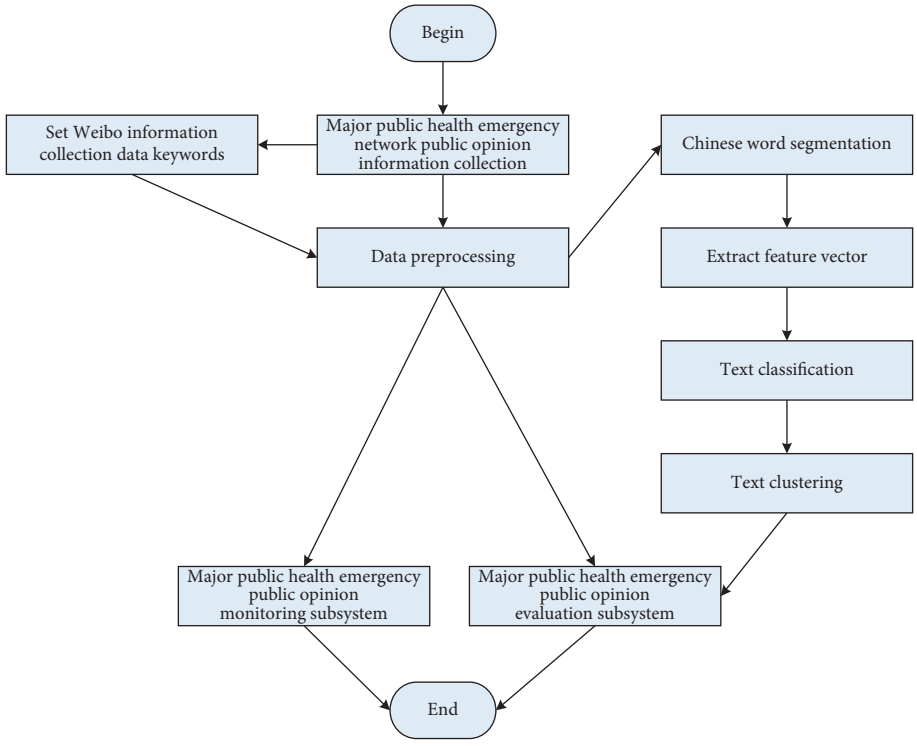

Figure 13: The system operation logic design.

Programming languages: Python, Java, HTML, CSS, and JavaScript.

Database: MySQL.

Development tools: PyCharm, Eclipse, and Sublime Text 3.

5.3. Database Design. For the data storage layer of the system, it is the design of the database. According to the above modeling analysis, crawled data, and preprocessed data, the database of the network public option communication management system is designed. The main data sheets are shown in Tables 3 and 4.

Table 3 is the crawler search major public health emergency history information table. Users can query and research the search history through this table.

After preprocessing the original data, the processed data is stored in the public opinion monitoring table after compiling the monitoring algorithm in the background. The public opinion monitoring table is shown in Table 4.

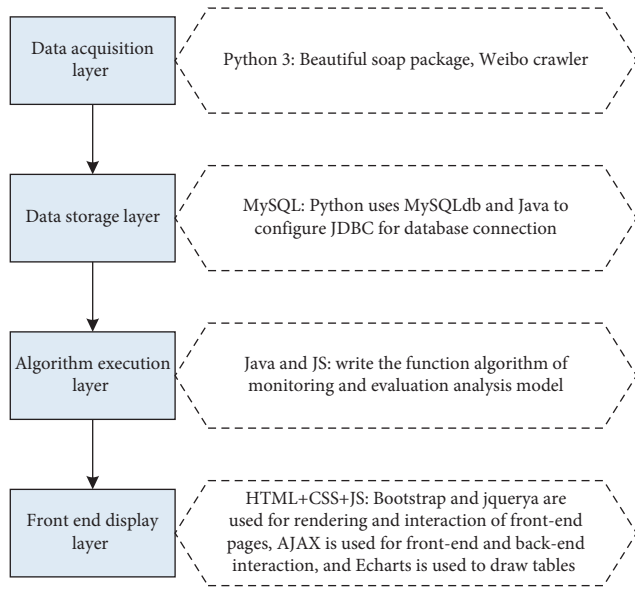

Figure 14: The system architecture design.

Table 3: The crawler search major public health emergency history information table.

Name	Type	Length	Decimal point	Nonempty	Remarks
ID	Int	11	0	Yes	Primary key identification
Topic	Varchar	50	0	No	Search topic
Count	Int	50	0	No	How many pieces of data did it crawl
Step	Int	50	0	No	Crawl interval
StartTime	Datetime	0	0	No	Start time
EndTime	Datetime	0	0	No	End time
CreateTime	Datetime	0	0	No	Record retrieval time

Table 4: The public opinion monitoring table.

Name	Type	Length	Decimal point	Nonempty	Remarks
ID	Int	11	0	Yes	Information ID
ParentID	Int	11	0	No	Original data sheet ID
TopicAtt	Float	50	0	No	Topic attention
TopicAttRate	Float	50	0	No	Change rate of topic attention
Topic	Varchar	200	0	No	Topic
StartTime	Datetime	0	0	No	Start time
EndTime	Datetime	0	0	No	End time

6. Conclusions and Suggestions

Taking "epidemic situation of new corona pneumonia in Wuhan City" as an example, using Gephi visual analysis, this paper makes an empirical study on the law of network public opinion transmission in line with the current major public health emergency. The specific conclusions are as follows:

(1) Put forward the law of network public opinion communication of major public health emergency. Based on the life cycle theory, taking the major public health emergency "COVID-19" as an example, and through Gephi visual analysis, the network public opinion communication law of major public health emergency is divided into six stages: latent, fermentation, outbreak, remission, recurrent, and decline. It provides a new idea for the regulatory authorities to grasp the development law of network public opinion of major public health emergency timely and accurately and judge the possible public opinion crisis.

(2) Construct a major public health emergency network public opinion communication model. Based on the SEIR model, taking the influencing factors of the network public opinion communication law of major public health emergency as the index, and through the NetLogo simulation, the results show that the total number of people involved in public opinion communication, the initial number of

people involved in public opinion communication, and the communication cycle are the three influencing factors of network public opinion, so as to construct the network public opinion communication law model of major public health emergency.

(3) Key communication channels play an important role in the development trend of network public opinion in major public health emergency. Among them, "People's Daily," "Headline News," and "CCTV News" are the three Weibo accounts with the largest number of forwarding, the highest number of fans, and the greatest influence. The common users connected with the three Weibo opinion leaders as the core nodes have the widest range of public opinion communication and have played a huge influence in the process of network public opinion communication of major public health emergency. Therefore, in order to prevent the negative impact of network public opinion on major public health emergency, it is necessary to intervene in key food transmission channels timely and effectively.

Epidemic development is the key to the development of network public opinion in major public health emergency. It has been found that the infection and treatment of COVID-19 pneumonia are the core to promote network public opinion. We should pay attention to and choose the appropriate time to intervene and guide the key communication channels with high influence. Through the control of public opinion, we can change the interaction between these key communication channels and Internet users' forwarding and comments, stop the spread of negative public opinion in time, reduce the spread of rumors, and guide public opinion to the positive.

Data Availability

The data that support the findings of this study are available from the corresponding author upon reasonable request.

Conflicts of Interest

The authors declare that they have no conflicts of interest.

Acknowledgments

This study was funded by the National Natural Science Foundation of China (52074214) and the Social Science Foundation of Shaanxi Province (2020M010). The authors sincerely thank the experts for their participation and valuable comments in the research process.

References

[1] Cnnic, "The 49th China Internet Report," *China Education Network*, vol. 2, no. 3, 2022.

[2] Y. Liu and H. Yang, "Network public opinion information monitoring platform for natural disaster events based on big data," *Disaster Science*, vol. 33, no. 4, pp. 13–17, 2018.

[3] C. Pan, "Huajuxiang. Internet public opinion survey based on workplace violence incidents suffered by nurses in a certain city of Jiangsu Province," *Medicine in Society*, vol. 29, no. 3, pp. 37–40, 2016.

[4] Y. Lan, "Construction of the security evaluation index system of network public opinion in emergencies," *Information Magazine*, vol. 30, no. 7, pp. 73–75, 2011.

[5] V. Santosh, N. Glen, H. Itai, and J. Yan, "Virtual Zika transmission after the first U.S.case: who said what and how it spread on Twitter," *American Journal of Infection Control*, vol. 46, pp. 549–557, 2018.

[6] A. Maria Popescu and M. Pennacchiotti, "Detecting controversial events from twitter," in *Proceedings of the 19th ACM International Conference on Information and Knowledge Management*, pp. 1873–1876, Association for Computing Machinery, NY,USA, October 2010.

[7] Y. Gao, Y. Fan, J. Wang, and D. Zhao, "Evaluation of Governmental Safety Regulatory Functions in Preventing Major Accidents in China," *Safety Science*, vol. 120, 2019.

[8] Y. Bruinen de Bruin, Anne-Sophie Lequarre, J. McCourt, C. Peter, and P. Filippo, "Initial Impacts of Global Risk Mitigation Measures Taken during the Combatting of the COVID-19 pandemic," *Safety Science*, vol. 128, 2020.

[9] H. Milad, C. J. Bliemer Michiel, G. Floris, and L. Jie, "The Scientific Literature on Coronaviruses, COVID-19 and its Associated Safety-Related Research Dimensions: A Scientometric Analysis and Scoping review," *Safety Science*, vol. 129, 2020.

[10] N. Aggrawal and A. Arora, "Visualization, Analysis and Structural Pattern Infusion of DBLP Co-authorship Network Using Gephi," in *Proceedings of the 2nd IEEE International Conference on Next Generation Computing Technologies (NGCT)*, Dehradun, India, October 2016.

[11] L. Li, B. Lei, and C. Mao, "Digital twin in smart manufacturing," *Journal of Industrial Information Integration*, vol. 26, no. 9, Article ID 100289, 2022.

[12] G. Sun, H. Z. Lv, and Z. Y. Guo, "Visualization analysis for business performance of Chinese listed companies based on Gephi," *CMC-computers materials & continua*, vol. 63, no. 2, pp. 959–977, 2020.

[13] L. Li, C. Mao, H. Sun, Y. Yuan, and B. Lei, "Digital twin driven green performance evaluation methodology of intelligent manufacturing: hybrid model based on fuzzy rough-sets AHP, multistage weight synthesis, and PROMETHEE II," *Complexity*, vol. 2020, no. 6, 24 pages, Article ID 3853925, 2020.

[14] B. Reynolds, *Crisis and Emergency Risk Communication: Pandemic Influenza*, pp. 109–154, Centers for Disease Control and Prevention, Atlanta, Georgia, 2006.

[15] J. Wang, M. Y. Guo, L. Zhang, L. Chen, and X Hou, "Research on dissemination rule of public opinion from SNA perspective: taking the vaccine safety event as an example," *Studies in Media and Communication*, no. 1, p. 42, 2017.

[16] E. Haihong, H. Yingxi, P. HaiPeng, Z. Wen, X. Siqi, and N. Peiqing, "Theme and sentiment analysis model of public opinion dissemination based on generative adversarial network," *Chaos, Solitons & Fractals*, vol. 121, pp. 160–167, 2019.

[17] R. Gaspar, C. Pedro, P. Panagiotopoulos, and B. Seibt, "Beyond positive or negative: qualitative sentiment analysis of social media reactions to unexpected stressful events," *Computers in Human Behavior*, vol. 56, pp. 179–191, 2016.

[18] J. Gomide, A. Veloso, M. Wagner et al., "Dengue Surveillance Based on A Computational Model of Spatio Temporal Locality of Twitter," in *Proceedings of the 3rd International Web Science Conference*, pp. 1–8, Association for Computing Machinery, NY,USA, June 2011.

[19] J. Pei, G. Yu, X. Tian, and M. Renee Donnelley, "A New Method for Early Detection of Mass Concern about public health issues," *Journal of Risk Research*, vol. 20, no. 4, pp. 516–532, 2017.

[20] A. Signorini, A. M. Segre, and M. Philip, "The use of twitter to track levels of disease activity and public concern in the U.S. During the influenza A H1N1 pandemic," *PLoS One*, vol. 6, no. 5, Article ID e19467, 2011.

[21] C. Chew and G. Eysenbach, "Pandemics in the age of twitter: content analysis of tweets during the 2009 H1N1 outbreak," *PLoS One*, vol. 5, no. 11, Article ID e14118, 2010.

[22] The State Council of the People's Republic of China, "Regulations on Public Health Emergencies," 2005, http://www.gov.cn/zwgk/2005-05/20/content_145.html.

[23] W. Cao and H. Lu, "The formation and guidance of public opinion in social media in the era of mobile internet—taking the WeChat dissemination of the "Shandong Vaccine Incident" as an example," *Southeast Communication*, vol. 6, pp. 56–58, 2016.

[24] W. Teng, "Research on the regional distribution of netizens' attention to public opinions on public health emergencies in public health," *Chinese Health Service Management*, vol. 32, no. 5, pp. 393–396, 2015.

[25] An Lu, T. Du, and G. Li, "etc. Stakeholders' concerns and evolutionary models of public health emergencies in social media," *Journal of Information*, vol. 37, no. 4, pp. 394–405, 2018.

[26] L. Wang, Ke Wang, and Wu Jiang, "The spread and evolution of public opinion on public health emergencies in social media: taking the vaccine incident in 2018 as an example," *Data Analysis and Knowledge Discovery*, vol. 3, no. 4, pp. 42–52, 2019.

[27] X. Zhou, "Research on emergency information management problems and countermeasures in the prevention and control of the new crown pneumonia epidemic," *Library and Information*, vol. 40, no. 1, pp. 51–57, 2020.

[28] S. H. Chaffee and M. J. Metzger, "The end of mass communication?" *Mass Communication & Society*, vol. 4, no. 4, pp. 365–379, 2001.

[29] R. Zeng, C. Wang, and Q. Chen, "Comparative research on the stages and models of network public opinion dissemination," *Journal of Information*, vol. 33, no. 5, pp. 119–124, 2014.

[30] L. Li and C. Mao, "Big data supported PSS evaluation decision in service-oriented manufacturing," *IEEE Access*, vol. 8, no. 99, pp. 154663–154670, 2020.

[31] L. Li, T. Qu, Y. Liu et al., "Sustainability assessment of intelligent manufacturing supported by digital twin," *IEEE Access*, vol. 8, pp. 174988–175008, 2020.

[32] Y. Fang, M. Xie, and C. Huang, "PBDT: Python Backdoor Detection Model Based on Combined Features," *Security and Communication Networks*, vol. 2021, Article ID 9923234, 2021.

[33] J. An, D. Peng, X. Zhou, J. Wu, and Zheng, "Penghua. Service-life study of polycarbonate outdoors using Python with incomplete data," *Modelling and Simulation in Engineering*, vol. 2020, Article ID 8909747, , 2020.

[34] V. Dolgopolovas, V. Dagiene, S. Minkevičius, and L. Sakalauskas, "Python for scientific computing education: modeling of queueing systems," *Scientific Programming*, vol. 22, no. 1, pp. 37–51, 2014.

[35] F. S. Bao, X. Liu, and C. Zhang, "PyEEG: An Open Source python Module for EEG/MEG Feature Extraction," *Computational Intelligence and Neuroscience*, vol. 2011, Article ID 406391, 2011.

Hindawi
Scientific Programming
Volume 2022, Article ID 8290106, 10 pages
https://doi.org/10.1155/2022/8290106

Research Article

ARM-Based Indoor RGB-LED Visible Light Communication System

Jingjing Bao, Qiang Mai, Zhangwen Fang, and Xiaowen Mao

School of Electronic Information, Dongguan Polytechnic, Guangdong, Dongguan 523808, China

Correspondence should be addressed to Jingjing Bao; baojj@dgpt.edu.cn

Received 21 April 2022; Revised 24 May 2022; Accepted 3 June 2022; Published 18 June 2022

Academic Editor: Lianhui Li

As a new green solid-state light source, semiconductor light-emitting diodes (LEDs) have the advantages of low power consumption, small size, long life, short response time, and good modulation performance. At the same time, the frequency band to which LED light sources belong does not require regulatory registration, thus alleviating the current problem of spectrum scarcity for wireless communications. However, white LED-based visible light communication (VLC) systems suffer from limited bandwidth and low energy efficiency. Therefore, an ARM-based indoor RGB-LED VLC system is proposed. Firstly, the three RGB colours are mixed into white light, thus obtaining a larger modulation bandwidth than normal white LEDs while illuminating normally. Secondly, the S3C6410 processor is used to modulate and demodulate the RGB-LEDs with biased light OFDM, thus obtaining a high spectrum utilisation while ensuring system transmission stability. Then, according to the characteristics of the light source of the VLC system, the leading and window functions used in the optical network transceiver module are designed to improve the communication energy efficiency of the system. Finally, functional tests were carried out on an ARM development board. The experimental results show that with a single RGB-LED light source, the maximum transmission distance is 5 cm, the maximum average delay is 68 ms, the maximum throughput is 25 Mbps, and the BER is controlled below 3.2×10^{-3}, which meets the basic communication requirements.

1. Introduction

With the advent of the 5G era, the demand for mobile data services is growing exponentially, and the available frequency band resources for RF communications are becoming increasingly scarce. As a result, the visible band, which has a huge bandwidth, is rapidly attracting widespread attention. Semiconductor light-emitting diodes (LEDs), as a new green solid-state light source, have the advantages of low power consumption, small size, long life, short response time, and good modulation performance [1–7]. By simply replacing conventional incandescent lamps with LEDs, the lighting can be transformed into a wireless network transmitter. Furthermore, with the development of conventional wireless communication, the limited radio spectrum resources are becoming increasingly prominent, leading to the issue of spectrum resource utilisation becoming very important.

The frequency band to which LED light sources belong does not require regulatory registration and can alleviate the current shortage of spectrum for wireless communication. Therefore, the use of white LED light sources for indoor lighting for VLC is a current research hotspot in the field of wireless communication at home and abroad. VLC is the use of specific modulation techniques to couple the data signals to be transmitted with light-emitting diodes [8–10]. At the same time, a high-speed modulated light wave signal from the LED device is used to transmit the information. The receiver generates an electrical signal based on the strength of the received light signal via a photodetector, and the signal is restored by the signal processing circuit.

LED-based VLC can greatly broaden the communication spectrum range and is one of the feasible solutions to alleviate the tight wireless spectrum resources. Its advantages are mainly reflected in these aspects [11–13]: (1) the data transmission speed is almost the same as that of optical fiber.

Under certain circumstances, it can transmit data at 1 Gbps. (2) VLC is not limited by spectrum. In contrast to RF wireless communication, VLC technology is able to allocate spectrum resources more scientifically. (3) VLC technology is green and environmentally friendly. VLC technology does not cause harm to the human eye and does not cause signal interference and impact on existing systems. (4) Good confidentiality: VLC technology is not easy to be listened to. (5) The cost is relatively low. VLC-related equipment and systems are very simple to deploy and are well compatible with current RF communication systems.

The above advantages show that if VLC technology can be applied to practical production and life, it will help completely solve the problems of spectrum resource constraint and signal interference. This shows that VLC technology has great potential for application. VLC technology can be perfectly integrated with the network access technology of today's homes. By using LED lighting in the average home as a kind of optical routing, it is possible to provide network access to the home.

VLC is a more energy-efficient and environmentally friendly way of accessing the Internet than mainstream Wi-Fi communication today. In addition, VLC can also be used for indoor positioning technology [14]. By collecting and transmitting the location information of indoor users through inherent indoor lighting devices, the precise positioning of moving people in indoor locations can be achieved. In some special spatial environments, such as aircraft, hospitals, and mines, there are a large number of electronic devices that are more sensitive to electromagnetic waves. In order to prevent serious consequences caused by electromagnetic wave interference, the use of electronic communication equipment in these situations is strictly limited. LED-based VLC is a good solution to these problems, as it does not generate electromagnetic interference.

ARM is a microprocessor with high performance and low power consumption and is favoured by the majority of terminal product manufacturers. The development of ARM terminals has become an important force in the development of information technology and the ARM platform has become the platform of choice for product development in people's lives. The implementation of visible light network access on ARM terminals will certainly greatly facilitate the exchange of information between people. Therefore, an ARM-based indoor VLC system is proposed.

2. Related Studies

VLC technology based on white LEDs is able to achieve both lighting and communication functions at a low cost and is suitable for various network access scenarios. Due to its advantages of being free of electromagnetic interference and green [15], VLC technology has attracted widespread attention and support worldwide.

Research work on VLCs first began in Japan. As early as 2000, Keio University in Japan proposed the feasibility of visible light as a light source for indoor lighting and communication [16]. In 2003, a large group of companies and research institutes formed the VLC Consortium (VLCC) with the aim of establishing a set of industry standards applicable to VLC. In 2008, the EU developed and implemented the OMEGA project, whose main objective was to study data applications for home access networks with transmission speeds exceeding 1 Gbis/s [17], which includes VLC.

At present, one of the key technologies for LED VLC is modulation, coding, and demodulation. Currently, most VLC systems use intensity modulation (IM) direct detection systems, and most of the coding methods are binary OOK (on-off keying) codes. Xiao et al. [18] proposed a real-time visible light transmission network based on non-return-to-zero on-off keying modulation (NRZ-OOK) with a transmission rate of 550 Mbit/s. Wang et al. [19] proposed a modulation technique based on phase shift Manchester coding (PS-Manchester) and mixed time-frequency equalisation, which used RGB-LED to achieve a higher transmission rate.

The light-emitting mechanism of white LEDs makes their bandwidth limited. As a result, the transmission rate of VLC networks is not very high in the currently implemented application scenarios. In visible communication systems, the core component of the transmitter module is the white LED, which can be divided into three main types: PC-LED, RGB-LED, and UV-LED. The RGB-LED light source is a monochromatic combination of red, green, and blue light in proportion to demand. As technology has evolved, the scope of RGB-LEDs has expanded to include more than just a mixture of red, green, and blue light, and RGB-LEDs can be used to produce the desired white light by combining multiple colours in the right proportions. For this reason, the majority of current research has focused on the use of PC-LEDs and RGB-LEDs as transmitters in VLCs. As the modulation bandwidth of RGB-LEDs is higher than that of PC-LEDs, RGB-LEDs are used in the network access scheme proposed in this paper.

In addition, because OFDM can effectively combat intersymbol interference caused by multipath propagation; its implementation complexity is much less than that of a single-carrier system using an equaliser. Therefore, the use of OFDM modulation technology has good prospects for development.

To meet the demand for green communication, current wireless communication technologies not only focus on improving transmission efficiency but also pay more attention to energy efficiency. Therefore, a lot of research work has been carried out on energy efficiency in VLC systems. Marshoud et al. [20] discussed the effect of different waveforms and modulation methods on LED energy efficiency in VLC systems. Ferreira et al. [21] came up with a new multiobjective optimisation method that allows flexible switching between energy efficiency and spectral efficiency functions. Chen et al. [22] derived a closed-form expression for the energy efficiency-spectral efficiency in VLC systems assuming that the LEDs operate in the linear region.

With its unique performance, VLC has great application prospects in the future. ARM is a microprocessor with the

advantages of high performance and low power consumption, so this paper attempts to combine ARM technology and VLC technology to study the feasibility of network access based on ARM terminals, bringing into play the advantages of both and providing a hardware implementation method for ARM-based VLC systems. This paper attempts to combine ARM technology and VLC technology to investigate the feasibility of network access based on ARM terminals, exploit the advantages of both, and provide a hardware implementation method for ARM-based VLC systems.

The main objective of this research is to increase the transmission bandwidth of VLC systems and improve LED energy efficiency. This paper proposes an ARM-based indoor RGB-LED VLC system. The main innovations and contributions include: (1) considering the large modulation bandwidth of RGB-LEDs compared to ordinary white LEDs and the advantages of OFDM modulation technology with its strong anti-interference capability and high spectrum utilisation, this study attempts to combine RGB-LEDs with OFDM technology in order to improve the system transmission bandwidth; (2) based on the characteristics of the light source of the OFDM-based VLC system, the leading and window functions used in the optical network transceiver module were designed to improve the communication energy efficiency of the system; and (3) an embedded ARM platform was built for OFDM modulation and demodulation to achieve low-cost network access for visible light systems.

3. VLC System Light Source Characteristics

3.1. Operating Principles and Characteristics of LEDs. The LED is a semiconductor structure with an internal PN junction that enables the conversion between electrical energy and light energy [23–25]. Therefore, like normal PN junctions, LEDs have physical characteristics such as forward conduction and reverse cut-off. When the PN junction is subjected to a forward voltage, the holes in the P region flow to the N region, while the electrons in the N region flow into the P region. In the process of flowing, when the electrons in high-energy state collide with holes, the excess energy is radiated out in the form of light. LED's light-emitting principle is shown in Figure 1. LED's light emission is spontaneous, so its directivity is poor. We can gather the light of LED by external devices to improve the received light power at the receiving end.

This paper uses the solid-state power amplifier (SSPA) model to describe the voltammetric characteristics of LEDs, which are PN junctions made of semiconductor materials and therefore have the same voltammetric characteristics as PN junctions. The forward voltammetric characteristics of LEDs can be expressed as follows:

$$I_F = I_s\left(\frac{qV_F}{enkT} - 1\right), \tag{1}$$

where I_s is the reverse saturation current, q is the electron charge, n is the constant, k is the Boltzmann constant, and T is the thermodynamic temperature.

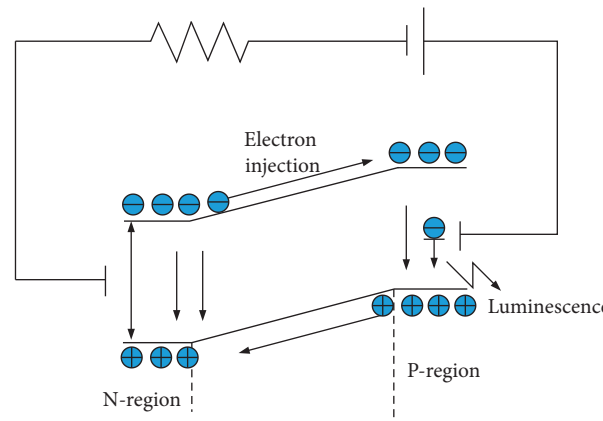

Figure 1: Principle of LED light emission.

The operating voltage of LEDs is divided into four regions, namely the reverse breakdown region, the cut-off region, the start-up region, and the operating region. The start and work zones are the positive zones and are the areas that the system design focuses on. The junction between the start and work zones is the LED turn-on voltage. When the forward voltage is applied to both ends of the LED and the working voltage is less than the starting voltage, the LED cannot normally emit light. At this point, the size of the current through the LED is zero. The working voltage of the LED is slowly increased. When the working voltage exceeds the starting voltage, the LED normally emits light. If we apply the reverse voltage to the LED, the LED is in the cut-off zone. If we continue to increase the reverse voltage, it is likely that the PN junction of the LED will be broken down by the reverse voltage. At this point, the critical voltage that breaks through the LED is called the breakdown voltage. When designing the transmitter circuit of a VLC system, we need to design the modulation circuit or signal coupling circuit according to the operating current of the LED.

3.2. Principle and Characteristics of the Receiving LED. For VLC receiver modules, the core device is the photodetector (PD). Photoelectric detection converts light signals into electrical signals by means of the photoelectric effect between substances. By using photodetection, the receiver can smoothly convert the received visible light signal into an electrical signal that can be recognised by the subsequent signal processing circuit. Currently, the most used photodetectors are positive-intrinsic-negative (PIN) photodiodes, avalanche photodiodes (APD), and image sensors [26].

In a multiuser scenario, each user needs a receiver to receive the signal. Although APDs are more sensitive and support a larger bandwidth, cost considerations led this study to use a PIN photodiode as the receiver. The photoreceiver used in the experiments is a silicon PIN photodiode S10784 from Hamamatsu, Japan. The S10784 has a peak wavelength of 660 nm or 780 nm, as well as a fast response time and high sensitivity. The detailed parameters of the silicon PIN S10784 are shown in Table 1.

Table 1: Silicon PIN S10784 parameters.

Parameters	Numerical values
Light-sensitive area	3.0 mm^2
Pixel count	1
Maximum reverse bias voltage	20 V
Spectral response range	340~1,040 nm
Peak wavelength	760 nm
Sensitivity	0.51 A/W
Dark current	1,000 pA
Cut-off frequency	250 MHz
Junction capacitance	4.5 pF

4. RGB-LED VLC Principle

4.1. Structure and Principle of RGB-LED. VLC technology uses high-speed signals emitted by LEDs to transmit data. This high-speed signal cannot be recognised by the human eye. On the transmitter side, the process of flashing light and dark LEDs at high speed is the process of sending the information. For example, "light" means "1," and "dark" means "0." At the receiving end, the light and dark signals are detected by a corresponding photoelectric detection device. After a series of amplification, filtering, shaping, and other processing, together with mathematical analysis and transformation methods, the information sent by the transmitter can be translated using decoding.

There are two general approaches to white LED formation [27]: PC-LED and RGB-LED. The basic structure of PC-LED is shown in Figure 2. RGB-LED produces the desired white light by mixing the various colours of light, as shown in Figure 3. By mixing the three colours of light at a certain power level, the white light perceived by the human eye is obtained. This method requires a certain electronic circuit to control the mixing ratio of these light colours. Although complex, this method provides the flexibility to obtain the desired light colour with high quantum efficiency.

The colour rendering and radiant luminous efficacy of the RGB-LED are influenced by the three lamps together. In order to make it as close to white as possible, $Ra > 80$ is required and the coordinates ($x = 0.33$ and $y = 0.33$) are satisfied. After several patchwork proportioning tests, the ratio of the three RGB colours was found to be 1:1.2:1. The specific proportioning data are shown in Table 2.

4.2. Solution Design for the Transmitter Side of RGB-LED VLC Systems. The transmitter side of the RGB-LED-based VLC system designed in this paper consists of an RGB-LED light source module, an RGB-LED driver module, a modulation module, and an adder-coupling module. The adder couples the RGB-LED DC drive voltage with the modulating voltage signal from the signal modulation module, which drives the RGB-LED light source module to emit a light signal loaded with useful information. A schematic diagram of the operation of the transmitter is shown in Figure 4.

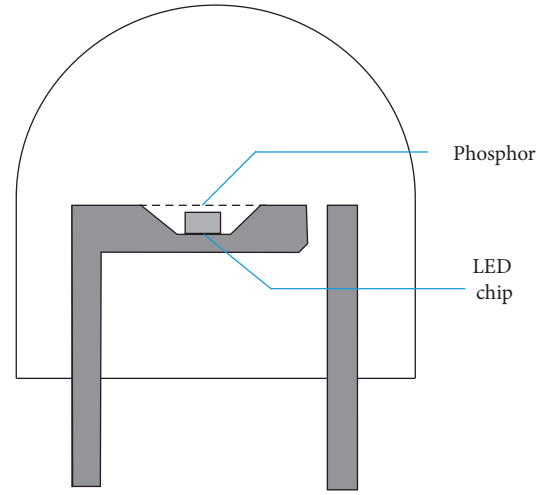

Figure 2: Basic structure of the PC-LED.

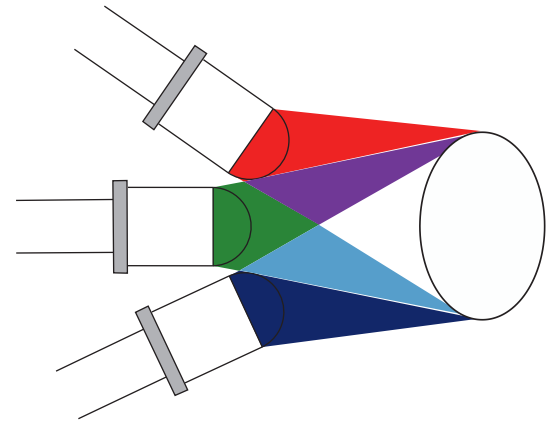

Figure 3: Basic structure of the RGB-LED.

5. ARM-Based Indoor RGB-LED VLC System Design

5.1. Geometric Model for Indoor VLC. Unlike traditional communication theory, the channel model in VLC is closely related to the light source, the channel, and the receiver. In this paper, only the direct line of sight (LOS) link between a single LED and a single PD is considered, and the geometrical scenarios for different layouts of indoor LEDs are considered, as shown in Figure 5. In a VLC system, the LOS optical channel can be well described by its DC gain. The channel DC gain g is defined as follows:

$$g = \frac{(m+1)A_{p\,d}}{2\pi d^2}\cos^m(\varphi)\cos(\theta)T(\theta)G(\theta), \quad (2)$$

where m is the Lambert emission coefficient, $A_{p\,d}$ represents the effective area of the PD, φ is the angle of light emission, θ is the angle of light incidence, and $T(\theta)$ and $G(\theta)$ represent the gain of the optical filter and concentrator, respectively.

5.2. Biased Optical OFDM Modulation Scheme. In this paper, the biased optical OFDM modulation technique is applied to a VLC system. Firstly, the input binary bit stream is

Table 2: RGB trichromatic white LED ratios.

LED	Wavelength (nm)	Spectral bandwidth	Radiant light effect	Energy (W)	Luminous flux
Red	614	20	311.6	1	311.6
Green	546	30	640.9	1.2	769.1
Blue	465	20	54.5	1	54.5

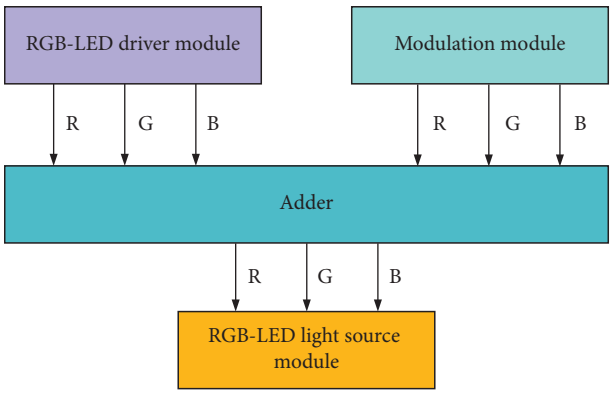

Figure 4: Diagram of the system on the sending end.

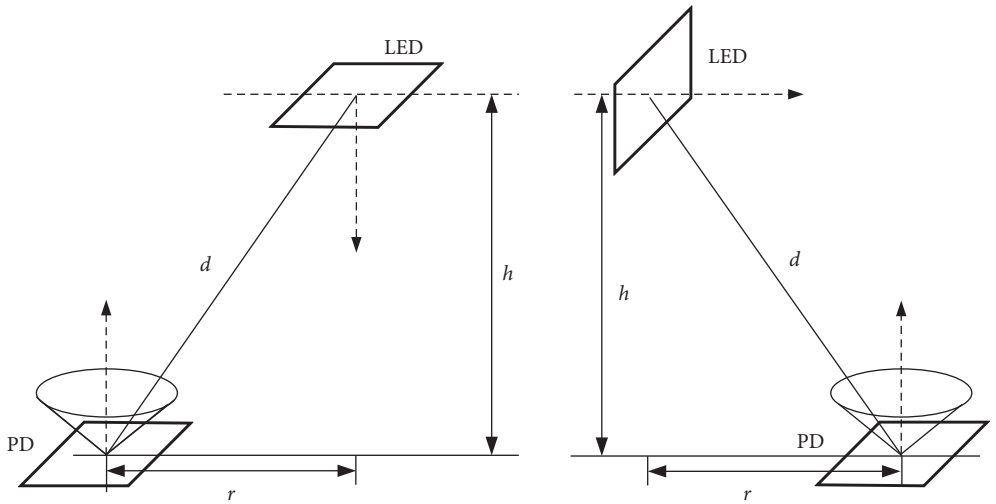

Figure 5: Geometric scene with different layouts of indoor LEDs.

modulated by QAM. Secondly, Hermitian symmetry is performed to obtain a frequency domain complex signal as follows:

$$X = \left[X_0, X_1, \cdots, X_{N/2-1}, X_{N/2}, X^*_{N/2-1}, \cdots, X^*_1\right]^T. \quad (3)$$

The Hermitian symmetry operation performed after QAM modulation is to ensure that the signal after the inverse fast Fourier transform (IFFT) operation is a real-valued signal. Without loss of generality, the real-valued OFDM symbol $x_u(n)$ can be expressed as follows:

$$x_u(n) = \sum_{k=0}^{N-1} \frac{X_k}{\sqrt{N}} e^{j2\pi nk/N}, \quad 0 < n < N-1, \quad (4)$$

where N is the total number of subcarriers.

In general, the DC bias voltage x_{DC} is defined as shown as follows [28]:

$$x_{DC} = \frac{U_{TOV} + U_{\max}}{2}, \quad (5)$$

where U_{TOV} is the LED turn-on voltage and $U_{\max}$ is the maximum DC voltage of the LED. After superimposing the DC bias voltage on $x_u(n)$, a positive real-valued signal $x(n)$ is obtained as follows:

$$x(n) = x_{\mathrm{u}}(n) + x_{\mathrm{DC}}. \quad (6)$$

The output signal via the LED $y(n)$ can be expressed as follows:

$$y(n) = \frac{f(v_{\mathrm{LED}})}{\left(1 + \left(f(v_{\mathrm{LED}})/i_{\max}\right)^{2t}\right)^{1/2t}}, \quad (7)$$

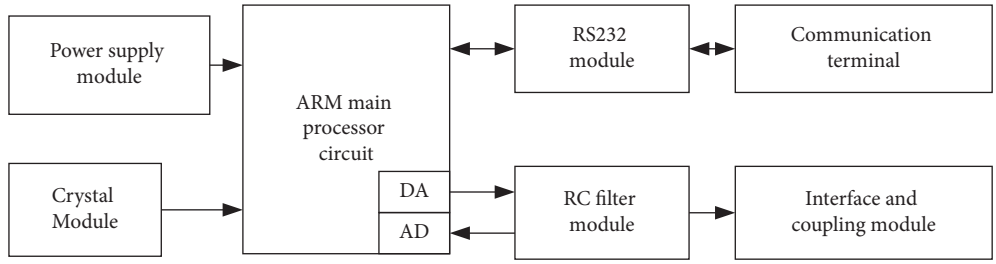

Figure 6: General block diagram of the system hardware.

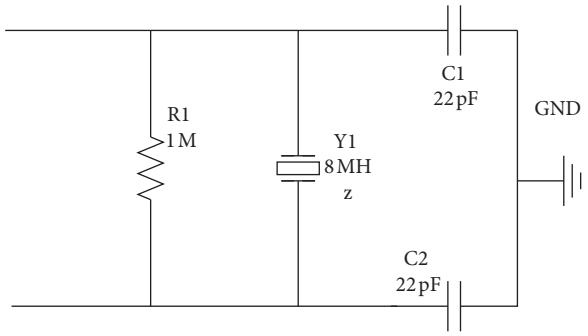

Figure 7: Crystal oscillator circuit of 8 M.

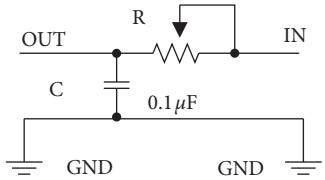

Figure 8: Low-pass RC filter circuit.

where v_{LED} denotes the DC voltage of the LED and $f(v_{\mathrm{LED}})$ denotes the DC voltammetric characteristic function of the LED. At the receiver end of a biased optical OFDM VLC system, the signal received by the photodetector PD can be expressed as follows:

$$r(n) = R_{\mathrm{PD}}\left[y(n) \otimes h_{\mathrm{c}}(n)\right] + z(n), \tag{8}$$

where R_{PD} is the responsiveness of the PD, $h_{\mathrm{c}}(n)$ is the equivalent VLC system channel gain, $\otimes$ represents the convolution operation, and $z(n)$ is the zero-mean additive white Gaussian noise (AWGN). At the receiver end of a biased optical OFDM VLC system, the photodetector PD converts the received optical signal into an electrical signal and then performs the opposite operation to the transmitter end, resulting in a binary signal.

5.3. Block Diagram of the Overall Hardware Architecture. In order to implement the functions of a biased optical OFDM VLC system, a high-performance processor is required for forward and inverse Fourier transform operations. The S3C6410 processor, based on the high-performance 32 bit ARM1176JZF-S core, was chosen after taking into account performance and cost factors. The ARM processor has lower power consumption and a rich peripheral interface, which is more suitable for OFDM system hardware implementation. The overall block diagram of the system hardware is shown in Figure 6.

5.4. Crystal Circuit Design. The system is powered directly by AC 220 V. In addition, to provide a stable 8 M frequency square wave output, the core S3C6410 processor has an external 8 M crystal oscillator as the clock signal, as shown in Figure 7.

5.5. Passive Low-Pass RC Filter Circuit Module. In order to perform the necessary noise filtering on the output signal of the system, a passive low-pass RC filter is externally connected to the DA/AD interface, and the modulated OFDM signal frequency f is expressed as follows:

$$f = \frac{1}{(2\pi RC)}, \tag{9}$$

where C indicates the capacitance in this circuit. C is set to 0.1 μF in this system. R indicates the resistor in this circuit. A potentiometer is used in this system so that it can be adjusted as required. The low-pass RC filter circuit is shown in Figure 8.

5.6. Design of Leading and Windowing Functions. Energy efficiency is an important indicator in optical communication systems and needs to be maximised wherever possible. Therefore, the improvement of energy efficiency has become a key issue in optical communication systems. Therefore, this paper attempts to design the lead and window functions used in the physical layer based on the biased optical OFDM VLC system to transmit signals only in the over-zero region, so as to improve the communication energy efficiency of the system as much as possible while ensuring the system bandwidth.

In this paper, we try to use only 1/3 of the band, that is, near the over-zero zone, for the transmission of the signal during the entire photoelectric conversion cycle. Because this zone has the lowest background noise and interference, it is the most desirable time slot for communication. Therefore, a constant envelope zero autocorrelation sequence is used as a leading code in order to shorten the frame length. Specifically, a Zadoff–Chu sequence was used, the expression of which is as follows:

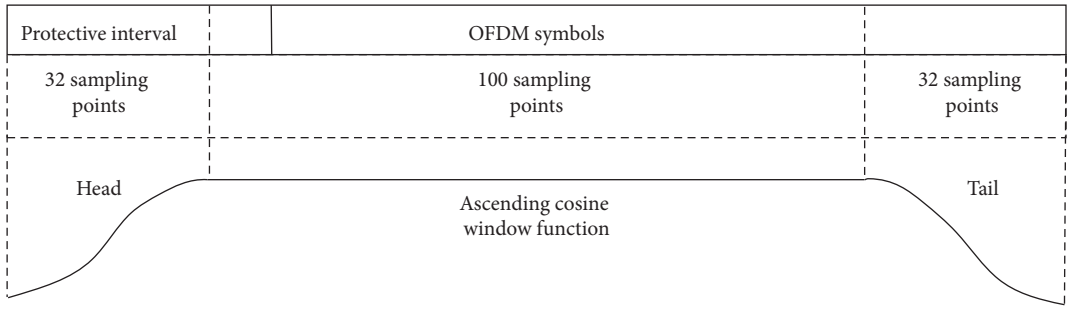

Figure 9: Time domain waveform of the window function.

$$a_k = \begin{cases} \exp\left[j2\pi \dfrac{M}{N}\left(\dfrac{k(k+1)}{2} + qk\right)\right], N \text{ is odd.} \\ \\ \exp\left[j2\pi \dfrac{M}{N}\left(\dfrac{k^2}{2} + qk\right)\right], N \text{ is even.} \end{cases}, \quad (10)$$

where $k = 0, 1, \ldots, N-1$, N denotes the length of the sequence, M is reciprocal to N, and q denotes a random integer.

The system was designed with a centre frequency of 421 kHz, and a Zadoff–Chu sequence ($N = 30$, $M = 29$, and $q = 15$) was chosen to meet the frame length parameters [29].

In order to window the OFDM signal with the aim of minimising spectral energy leakage, a rising cosine window is generally used, which is defined as follows:

$$w(t) = \begin{cases} 0.5 + 0.5 \cdot \cos\left(\dfrac{\pi + t\pi}{(\beta T_s)}\right) & 0 \le t \le \beta T_s \\ \\ 1.0 & \beta T_s \le t \le T_s \\ \\ 0.5 + 0.5 \cdot \cos\left(\dfrac{(t - T_s)\pi}{(\beta T_s)}\right) & T_s \le t \le (1+\beta) T_s \end{cases}, \quad (11)$$

where β indicates the roll-off factor of the added window and T_s indicates the cycle length of the symbol.

In this system, $T_s = 1{,}174$. The raised cosine window is calculated by discrete time.

$$w(n) = \begin{cases} 0.5 - 0.5 \cdot \cos\left(\dfrac{\pi \cdot n}{32}\right) & 0 \le n \le 31 \\ \\ 1 & 32 \le n \le 1141 \\ \\ 0.5 - 0.5 \cdot \cos\left(\dfrac{\pi \cdot (n - 1174)}{32}\right) & 1142 \le n \le 1173 \end{cases}. \quad (12)$$

Therefore, the time domain waveform diagram of the window function used in this system is shown in Figure 9.

DBPSK modulation is used to implement the subcarrier modulation, and the frame length of the system is defined as follows:

$$\begin{aligned} T_{\text{frame}} &= \frac{N_{\text{FFT}} \cdot N_{\text{pre}} + (N_{\text{FFT}} + N_{\text{CP}} - N_{\text{window}}) \cdot (N_{\text{FCH}} + N_{\text{DATA}})}{f_s} \\ &= [1024 \times 3 + (1024 + 120 - 32) \times 5] \div \left(2.0 \times 10^6\right) \\ &= 3.253\,(\text{ms}), \end{aligned} \quad (13)$$

where N_{DATA} indicates the length of the DATA field information, N_{CP} indicates the number of useful subcarriers, N_{window} indicates the number of window cover points, N_{FCH} indicates the number of frame control header symbols, N_{FFT} indicates the number of fast Fourier transform points, N_{pre} indicates the number of leading symbols, and f_s indicates the sampling frequency.

The results from equation (11) show that the frame length of the system is significantly reduced. Combined with the OFDM symbol power spectrogram after windowing, the planned over-zero zone signal transmission is accomplished, thus effectively improving the energy efficiency of data communication.

6. Experimental Results and Analysis

6.1. Experimental Setup. The commissioning process for the transmitter and receiver circuits of the RGB-LED VLC system is as follows:

(1) First of all, the mechanical performance of each module should be debugged and tested; check whether each module component is well connected to each other, especially whether the installed components are normal

(2) Check the component power supply and detect if the module is working properly

(3) Debugging program: burn the written software program into the microcontroller to see if the program makes each module perform the desired function

(4) Overall system debugging: debug the transmitter and receiver circuits and observe whether the output waveforms of each port meet the circuit requirements through an oscilloscope

After the selection and commissioning of the above system components, the prototype system was finally

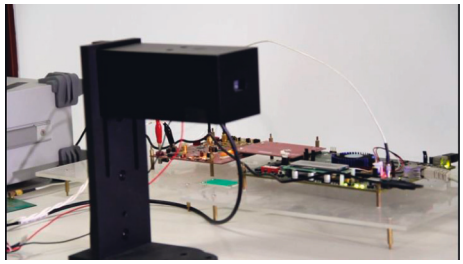

Figure 10: Indoor RGB-LED VLC system hardware.

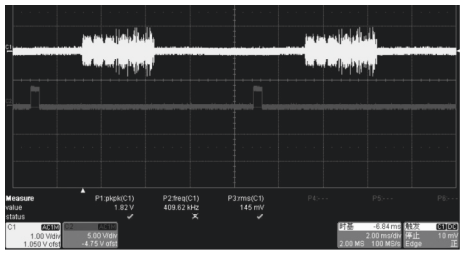

Figure 11: Time domain waveform of the frame signal.

Table 3: Relationship between voltage drop and light intensity.

LED voltage drop (V)	Light intensity (lux)
2.66	143
2.78	648
2.89	1,191
2.96	1,685
3.02	2,210
3.13	3,012
3.24	4,172
3.30	5,309

completed. The hardware of the indoor RGB-LED VLC system is shown in Figure 10.

6.2. Communication Trials and Performance Tests. Next, the system performance will be tested in terms of the driving voltage, communication distance, light intensity, and BER. As testing the three lights separately would be somewhat repetitive, a single RGB-LED light source is chosen for testing in this paper. The following experimental tests were carried out using blue light as an example. The time domain waveform of the received frame signal at the receiver side is shown in Figure 11. We can see that one frame of the oscilloscope represents 40 μs and the average period is 3 frames, so the signal frequency is 8.4 kHz.

The results of the drive voltage and light intensity tests are shown in Table 3. As can be seen from Table 3, the voltage drop of the LED is proportional to the light intensity. However, due to the limited carrying voltage of the LED, the maximum light intensity of the LED used in this system is 5,390 lux.

The relationship between the voltage intensity of the blue LED at different distances and the BER is shown in Table 4.

The BER is lowest when the light intensity at the transmitter is 3,370 lux, so the optimum communication

Table 4: Distance-light intensity-BER relationship.

Distance (cm)	Light intensity (lux)	BER ($\times 10^{-3}$)
1	4,220	5.2
1.5	3,370	4.8
2	2,830	5.1
2.5	2,520	5.4
3	1,952	6.1
3.5	1,392	6.7
4	1,342	6.7
4.5	976	8.6
5	811	9.8

Table 5: System throughput test results.

Distance (cm)	Uplink throughput (Mbps)	Downlink throughput (Mbps)
1	23	24
1.5	24	25
2	22	23
2.5	20	21
3	16	17
3.5	11	12
4	6	7
4.5	3	4
5	1	2

state for this system is a transmission distance of 1.5 cm and a light intensity of 3,370 1ux. The throughput of this system at distances from 1 to 5 cm was tested using a network tester, and the results are shown in Table 5.

With a packet size of 128 bytes and a throughput load of 80%, the system delay performance was tested using a network tester at different distances, and the results are shown in Table 6.

With a packet size of 128 bytes and a throughput load of 80%, the system delay performance was tested using a network tester at different distances, and the results are shown in Table 7.

As a key metric for communication systems, reliability verification is a necessary component of test validation. Using the Monte Carlo method, the ARM-based indoor RGB-LED VLC system was tested 20 times with a data transmission size of 500 frames each. The average BER results of the system are shown in Figure 12.

Overall, at a distance of 5 cm, the system has a packet loss rate of 0%, a maximum average delay of 36 ms, and a maximum throughput of 25 Mbps, all of which meet the actual broadband access requirements. In addition, Figure 12 shows that after −5 dB, the average BER of the system decreases significantly with the increase of the signal-to-noise ratio up to 4.8×10^{-3} level, which can effectively ensure the reliability of communication.

In terms of system energy efficiency, the maximum value of energy efficiency is obtained in the scenario of a horizontal LED layout when the horizontal distance $r = 1.5$ cm, which is in line with the above results (lowest BER). This is because at this position the LEDs are facing the PD and the PD can

Table 6: System delay test results.

Distance (cm)	Uplink delay (ms)	Downlink delay (ms)
1	11	9
1.5	15	13
2	21	18
2.5	27	25
3	36	34
3.5	41	42
4	48	49
4.5	57	56
5	68	65

Table 7: System packet loss rate test results.

Distance (cm)	Uplink delay (%) (ms)	Downlink delay (%) (ms)
1	0	0
1.5	0	0
2	0	0
2.5	0	0
3	0	0
3.5	0.01	0.01
4	0.01	0.01
4.5	0.01	0.01
5	0.01	0.01

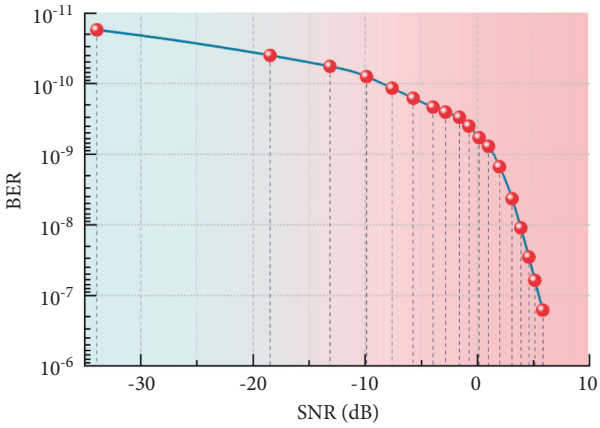

Figure 12: Average BER of the RGB-LED VLC system.

receive most of the light energy; therefore, the maximum system energy efficiency is obtained at this position. In practical system design, the horizontal distance r can be configured according to the requirements of the different layouts of the LEDs. It should be noted, however, that the smaller the horizontal distance r, the more difficult it is to implement a biased light OFDM system.

7. Conclusion

This paper presents an ARM-based indoor RGB-LED VLC system. RGB-LEDs are combined with OFDM technology to implement a VLC system in order to improve the system transmission bandwidth. Based on the characteristics of the light source of the OFDM-based VLC system, the leading and window functions used in the optical network transceiver module are designed to improve the communication energy efficiency of the system. In addition, an embedded ARM platform was built for OFDM modulation and demodulation to achieve low-cost network access for the visible light system. Experimental results verify the feasibility of the system. The maximum energy efficiency was obtained in the LED horizontal layout scenario when the horizontal distance $r = 1.5$ cm, and the BER was only 4.8×10^{-3}. Overall, at a distance of 5 cm, the system had a packet loss rate of 0%, a maximum average delay of 36 ms, and a maximum throughput of 25 Mbps, all of the above performance indicators meeting the actual broadband access requirements. Further research will be carried out on how to design good LED and PD arrays while increasing the transmission distance and ensuring system stability.

Data Availability

The experimental data used to support the findings of this study are available from the corresponding author upon request.

Conflicts of Interest

The authors declare that they have no conflicts of interest to report regarding the present study.

Acknowledgments

This work was supported by (1) Science and Technology Innovation Strategy Projects of Guangdong Province: Research on High Reliable Transmission Technology in an Indoor Visible Light Communication System (pdjh2022b1030) and Design of Full-Color Direct Display MiniLED Display Module Using Flip-Chip COB Package (pdjh2022b1026); (2) Special Projects in Key Fields of General Colleges and Universities of Guangdong Province: Design of Full-Color Direct Display MiniLED Display Module Using Flip-Chip COB Package (2020ZDZX3091) and Design and Research of Elevator Absolute Positioning System Based on Optical Communication and Artificial Neural Network (2021ZDZX1133); (3) Engineering Technology Research Center of General Colleges and Universities of Guangdong Province, Intelligent Terminal Application Engineering Technology Development Center (2021GCZX016); (4) Major Nature Science Projects of Guangdong Colleges and Universities: Study on Welding Process Control Based on the Morphology of Molten Pool (2019GZDXM016) and Intelligent Terminal and Intelligent Manufacturing Special Projects of Dongguan Vocational and Technical College: Scientific backbone (ZXE003); (5) SMT Component Placement Defect Recognition System Based on Deep Neural Network (ZXF005); and (6) Research of 5G Terminal OTA Performance Automatic Test System, Dongguan Science and Technology Commissioner Project (20201800500652).

References

[1] H. W. Chen, J. H. Lee, and B. Y. Lin, "Liquid crystal display and organic light-emitting diode display: present status and

future perspectives," *Light: Science & Applications*, vol. 7, no. 3, pp. 17–25, 2018.

[2] L. G. Langella, P. Silva, and L. Costa-Santos, "Photobiomodulation versus light-emitting diode (LED) therapy in the treatment of temporomandibular disorder: study protocol for a randomized, controlled clinical trial," *Trials*, vol. 19, no. 1, pp. 71–79, 2018.

[3] H. Zhong, T. Duan, H. Lan, M. Zhou, and G. Fei, "Review of low-cost photoacoustic sensing and imaging based on laser diode and light-emitting diode," *Sensors*, vol. 18, no. 7, pp. 2264–2278, 2018.

[4] J. Alexandersen, O. Sigmund, K. E. Meyer, and B. S. Lazarov, "Design of passive coolers for light-emitting diode lamps using topology optimisation," *International Journal of Heat and Mass Transfer*, vol. 122, pp. 138–149, 2018.

[5] C. Soeiro, D. Bitton, B. A. Maria, Z. L. Fernando, and N. A. Nikele, "Light Emitting Diode (LED) therapy reduces local pathological changes induced by *Bothrops asper* snake venom," *Toxicon*, vol. 152, pp. 95–102, 2018.

[6] W. Chen, Y. Zhuang, and W. Le, "Color-tunable and high-efficiency dye-encapsulated metal-Organic framework composites used for smart white-light-emitting diodes," *ACS Applied Materials & Interfaces*, vol. 10, no. 22, pp. 18910–18917, 2018.

[7] C. Qian, H. Zhang, J. Dai, Z. Shuang, and S. Wang, "Enhanced the Optical power of AlGaN-based deep ultraviolet light-emitting diode by optimizing mesa sidewall angle," *IEEE Photonics Journal*, vol. 10, pp. 1–7, 2018.

[8] H. L. Ji, H. C. Kang, and J. W. Jo, "Concentrated perovskite photovoltaics enable minimization of energy loss below 0.5 eV under artificial light-emitting diode illumination," *International Journal of Energy Research*, vol. 46, no. 4, pp. 5260–5268, 2022.

[9] A. E. Alexei, C. Hoepfner, and Panaccione, "Organic light emitting diode unit and method for manufacturing the same," *Metal Industries Research & Development Centre*, vol. 625, no. 5, pp. 135–148, 2018.

[10] G. S. Prasad and S. B. Kumar, "Shear bond strength of a bracket-bonding system cured with a light-emitting diode or halogen-based light-curing unit at various polymerization times," *Clinical, Cosmetic and Investigational Dentistry*, vol. 10, pp. 61–67, 2018.

[11] D. Xie, Y. L. Li, G. F. Wang, J. Jiang, and L. R. Sun, "Ultraviolet light-emitting diode irradiation induces reactive oxygen species production and mitochondrial membrane potential reduction in HL-60 cells," *Journal of International Medical Research*, vol. 49, no. 5, pp. 33–41, 2021.

[12] B. O. Rothbaum, M. Price, and T. Jovanovic, "A randomized, double-blind evaluation of D-cycloserine or alprazolam combined with virtual reality exposure therapy for post-traumatic stress disorder in Iraq and Afghanistan War veterans," *American Journal of Psychiatry*, vol. 171, no. 6, pp. 640–648, 2014.

[13] H. A. Elessawy, W. H. Borhan, and N. A. Ghozlan, "Effect of light-emitting diode irradiation on chronic nonhealed wound after below-knee amputation," *The International Journal of Lower Extremity Wounds*, vol. 20, no. 3, pp. 251–256, 2021.

[14] T. Grünbaum, S. Bange, J. Wei, and A. E. Leung, "Measuring the magnetic field amplitude of rf radiation by the quasistatic magnetic field effect in Organic light-emitting diodes," *Physical Review Applied*, vol. 15, no. 6, pp. 112–129, 2021.

[15] R. Winzenrieth, M. S. Ominsky, Y. Wang, and L. Humbert, "Differential effects of abaloparatide and teriparatide on hip cortical volumetric BMD by DXA-based 3D modeling," *Osteoporosis International*, vol. 32, no. 6, pp. 33–45, 2021.

[16] F. Radicioni, A. Stoppini, and G. Tosi, "Necropolis of Palazzone in Perugia: geomatic data integration for 3D modeling and geomorphology of underground sites," *Transactions in GIS*, vol. 25, no. 5, pp. 149–160, 2021.

[17] A. N. Kumar, V. Jadhav, R. Jawalekar, P. Akhare, and S. Gosavi, "Light emitting diode mediated photobiomodulation therapy in orthodontics - a review of contemporary literature," *Journal of Evolution of Medical and Dental Sciences*, vol. 10, no. 32, pp. 2672–2679, 2021.

[18] H. Xiao, R. Wang, G. He, Z. Lv, and K. Wang, "4 Mb/s under 3-m transmission distance using quantum dot light-emitting diode and NRZ-OOK modulation," *Optics Letters*, vol. 45, no. 6, pp. 83–92, 2020.

[19] Y. Wang, Y. Wang, N. Chi, J. Yu, and H. Shang, "Demonstration of 575-Mb/s downlink and 225-Mb/s uplink bi-directional SCM-WDM visible light communication using RGB LEDs and phosphor-based LEDs," *Optics Express*, vol. 21, no. 1, pp. 1203–1208, 2013.

[20] H. Marshoud, S. Muhaidat, and P. C. Sofotasios, "Optical non-orthogonal multiple access for visible light communication," *IEEE Wireless Communications*, vol. 25, no. 2, pp. 82–88, 2018.

[21] R. Ferreira, E. Xie, J. Mckendry, S. Rajbhandari, and H. Chun, "High bandwidth GaN-based micro-LEDs for multi-gb/s visible light communications," *IEEE Photonics Technology Letters*, vol. 28, no. 19, pp. 2023–2026, 2019.

[22] H. Chen, W. Guan, S. Li, and Y. Wu, "Indoor high precision three-dimensional positioning system based on visible light communication using modified genetic algorithm," *Optics Communications*, vol. 413, pp. 103–120, 2018.

[23] M. Fu, W. Zhu, and Z. Le, "Improved visible-light-communication positioning algorithm based on image sensor tilting at room corners," *IET Communications*, vol. 12, no. 10, pp. 1201–1206, 2018.

[24] N. Chi, *The Transmitter of the Visible Light Communication System*, 2018.

[25] J. Y. Wang, L. Cheng, J. B. Wang, Y. Wu, M. Lin, and J. Cheng, "Physical-layer security for indoor visible light communications: secrecy capacity analysis," *Communications, IEEE Transactions on*, vol. 66, no. 12, pp. 6423–6436, 2018.

[26] W. Guan, X. Chen, and M. Huang, "High-speed robust dynamic positioning and tracking method based on visual visible light communication using Optical flow detection and bayesian forecast," *IEEE Photonics Journal*, vol. 10, no. 3, pp. 1–22, 2018.

[27] W. Guan, Y. Wu, C. Xie, L. Fang, X. Liu, and Y. Chen, "Performance analysis and enhancement for visible light communication using CMOS sensors," *Optics Communications*, vol. 410, pp. 531–545, 2018.

[28] C. W. Chow, R. J. Shiu, and Y. C. Liu, "Non-flickering 100 m RGB visible light communication transmission based on a CMOS image sensor," *Optics Express*, vol. 26, no. 6, pp. 7079–7086, 2018.

[29] R. Ji, S. Wang, Q. Liu, and W. Lu, "High-speed visible light communications: enabling technologies and state of the art," *Applied Sciences*, vol. 8, no. 4, pp. 589–597, 2018.

Hindawi
Scientific Programming
Volume 2022, Article ID 4160821, 11 pages
https://doi.org/10.1155/2022/4160821

Research Article

Studying the Impact of Health Education on Student Knowledge and Behavior through Big Data and Cloud Computing

Zhilan liu[1] and Xiang Xu[2]

[1]*Department of Public Basic Education, Shanghai Civil Aviation Vocational and Technical College, Shanghai 200235, China*
[2]*School of Military Sports, Jiangxi Agricultural University, Jiangxi 330045, Nanchang, China*

Correspondence should be addressed to Xiang Xu; xuxiang@jxau.edu.cn

Received 25 April 2022; Revised 29 May 2022; Accepted 2 June 2022; Published 17 June 2022

Academic Editor: Lianhui Li

Artificial intelligence and big data, as emerging technologies that have attracted much attention in recent years, have broad application and development space in improving the development of intelligent and refined education in colleges and universities. The application of artificial intelligence and big data to the mental health education practice of college students has a very positive effect on accurately discovering and scientifically solving the mental health problems of college students. In order to combine big data and cloud computing platform organically, this paper introduces an intelligent algorithm based on multi-output support vector regression (MSVR) model and immune clone selection algorithm (ICSA). At the same time, we couple the two to obtain a new intelligent algorithm, namely, immune multiple output support vector regression (ICSA-MSVR) algorithm. Based on the prediction results of health education on students' knowledge and behavior by cloud computing platform, the necessary conditions for three intelligent algorithms to complete the task are summarized. Numerical experimental results show that ICSA-MSVR plays a role in both local search and global search, and is more effective in large-scale cloud computing task scheduling. In addition, in task scheduling, when the task completion time is short, ICSA-MSVR has a lower load imbalance than ICSA and MSVR, which can achieve better load balancing, and the load between virtual machines is closer. Finally, combined with the problems and the needs of students' health education, suggestions are put forward to deepen the application of technology in students' mental health education. This approach can provide corresponding ideas and reference methods for improving the scientificity, pertinence, and effectiveness of mental health education.

1. Introduction

Exercise and health education is an important part of students' knowledge and behavior, and it is an objective daily activity [1, 2]. With the development of technology, the ability to realize its value can be enhanced to a certain extent with the help of big data technology [3, 4]. How to dig, analyze, and use data in a scientific, efficient, and reasonable way, and explore the integration and development of traditional exercise and health education methods with modern information technology have become important means to release the value benefits of health education [5, 6]. In addition, the introduction of big data technology into the vision of health education can not only broaden the way of thinking of health education. This can also effectively integrate the universality of the use of big data and the specificity of health education, and improve the adaptability and realistic effectiveness of sports health education [7, 8].

Enhancing the applicability and effectiveness of sports health education is a realistic requirement under the new situation, new laws, and new scenarios. This situation is mainly manifested in two aspects.

(1) It is necessary to promote the renewal and reform of educational carriers here. These methods are aimed at profound changes taking place. Health education needs to strengthen the selection, update, and optimization channels of content resources and implementation methods on the basis of existing carriers, and conduct information dissemination

through normalized, personalized, and efficient carriers. This can effectively promote the achievement of the target effect.

(2) In addition, this method can optimize the predictive analysis capabilities of education. By combining artificial intelligence methods, we can maximize the advantages of health education.

Strengthening health education is the best path to implement the concept of health first and explore the integration of sports health education and big data, facing new situations, new laws, and new requirements. This is also a topic with outstanding strategic value in the post-epidemic era.

The post-epidemic era not only deepens the connotation of health education, but also puts forward more needs and requirements for it. The application of big data cannot be simply understood as a carrier innovation or technological innovation. The effective release of its series of value benefits requires the use of systematic thinking to make an overall plan for the two and to explore more measures to effectively integrate the two.

Big data is a new stage of informationization, digitalization, and intelligent development, which is both an objective external environment and an important technical carrier for health education. Relying on the new thinking and new concept of modern big data technology [9, 10], it is of distinctive significance and value to solve the methodological problems of health education under the new situation.

Although students entering university tend to be rational and mature in terms of knowledge and mind, due to the lack of deep understanding and experience of reality, they have certain vulnerability in terms of psychological and physical quality, which makes them easy to have mental and physical health problems due to some bad experiences. In the current situation where the pace of life and study pressure continue to increase, the issue of health education has obviously become a prominent problem among college students' groups. Therefore, more and more colleges and universities have incorporated health education into the education system of college students, hoping to enhance their knowledge behavior through professional and targeted health education.

However, the diversity of students' mental states and the lack of resources for health education teachers make it difficult to effectively meet students' individual physical and mental health education needs. This will result in health education often being reduced to a public knowledge curriculum [11, 12]. In such a situation, it is necessary to improve the ability of college teachers to screen, locate, and analyze the health education problems of college students with the help of technology. Artificial intelligence and big data, as the emerging technological content of computer science and technology innovation, can meet exactly this need.

In recent years, colleges and universities have gradually begun to explore the application of artificial intelligence and big data to the practice of college student health education, so as to enhance the relevance and effectiveness of mental health education [13, 14]. At present, the application of technology is still in the exploration stage, and no systematic and comprehensive application method has been formed.

In addition, in the field of school education, the value of focused data resources is extraordinary. However, due to the complexity of basic data resources, they do not directly serve educational activities, and their value can only be reproduced after certain processing, handling, and analysis. Only by focusing on the key points of exercise and health education and reproducing the value points can we synchronize and integrate the two to serve the educational activities. In other words, we can enhance the ability to achieve the goals of exercise and health education in a way that is driven by big data technology.

For a long time, the student population has shown a marked sensitivity to their psychological problems and is reluctant to talk about them too much. This makes it difficult to carry out mental health education for college students in an open and public way. Artificial intelligence and big data can rely on the functional advantages of the Internet platform, enabling universities and teachers to develop a personalized platform for college students' mental health education by using the Internet as a carrier. This allows students to log in to the system for content understanding and activity participation at any time and from any location on their own, truly eliminating the fear of health education for students.

Based on the above analysis, it is necessary to analyze the impact of health education on the knowledge and behavioral ability of students, especially contemporary college students, from the perspective of big data and cloud computing. This paper intends to introduce a novel big data combined with artificial intelligence approach [15, 16](based on immune multi-output support vector regression algorithm) and discuss the application of the novel approach in this field from the perspective of health education, in order to provide an idea for future applications of big data and cloud computing.

2. Immune-Based Multi-Output Support Vector Regression Algorithm

With the rapid development of science and technology, big data and cloud computing methods can be seen everywhere for different fields around the world. For example, the aerospace field often uses big data methods to detect tiny damage in equipment. For some nonlinear phenomena or some seemingly irregular situations, the use of big data analysis can often summarize the development trend of such problems and can have a better guiding role for future planning and development. This method is not only applied in the field of science and engineering, but also favored by researchers in the research process of social science. Taking the health education involved in this article as an example, the introduction of cloud computing and big data technology can to a certain extent liberate the traditional teaching mode that only relies on the teacher's name or urging mode. This method starts from the importance of

each student, and reasonably analyzes and predicts the trend of each variable, so that a corresponding teaching mode can be formulated for each individual, and the purpose of teaching students in accordance with their aptitude is truly achieved.

In fact, the realization of big data and cloud computing is also realized on the basis of artificial intelligence or intelligent algorithms. Although big data technology and cloud computing platform seem to be simple in application, the mathematical principles contained in them are very complex. Taking the BP neural network with the simplest principle and the most convenient operation as an example, the calculation of each neuron is obtained by iteration and inversion of a series of nonlinear functions. Although this calculation is complex, with the blessing of computer engineering technology, researchers can obtain a predictable network engineering through code programming. However, it is a huge project for us to turn an initial black box into a practical network project. This requires repeated verification and trial and error to be completed.

Fortunately, with the emergence of artificial intelligence technology, more and more intelligent algorithms are applied in various fields. Compared with the early stage of research, there is only one prediction system, BP neural network, and various optimization algorithms have been introduced. Genetic algorithm is considered to be an effective method to find the optimal solution. The neural network optimized by genetic algorithm improves the solution method of weights and thresholds in its original algorithm, making the whole calculation process more reasonable.

In the process of finding the optimal solution, particle swarm optimization is also applied. Compared with the genetic algorithm, the particle swarm optimization process does not need to set too many parameters in advance. However, before the algorithm is calculated, it requires the researcher to determine the fitness function first, which requires the researcher to have certain prior knowledge.

Compared with the above two optimization algorithms, support vector machine is a new type of calculation method. It shows many unique advantages in solving small sample, nonlinear, and high-dimensional pattern recognition. At the same time, this algorithm can also be extended to other machine learning problems such as function fitting.

In deep learning, support vector machines are supervised learning models related to related learning algorithms. This computational model can be used to analyze data and identify patterns. In addition, it can also be used for classification and regression analysis.

As an upgraded version of the genetic algorithm, the immune algorithm can make up for the shortcomings of the calculation principle inherent in the genetic algorithm. Under the premise of retaining the excellent characteristics of the genetic algorithm, this intelligent algorithm tries to selectively and purposefully use some characteristic information or knowledge in the problem to be solved to suppress the degradation phenomenon in the optimization process.

The immune algorithm simulates the immune process of the human body resisting external antigens through antibodies. It is a swarm intelligence search algorithm with an iterative process of generate and test. In the complex trial calculation process, this algorithm can maintain global convergence on the premise of retaining the best individuals of the previous generation. Therefore, this artificial intelligence algorithm has strong adaptability.

In the process of studying the influence of health education on students' knowledge behavior, this paper attempts to form a new type of prediction system by coupling support vector machine and immune cloning. In particular, we should focus on combining this coupling algorithm with big data technology and cloud computing platform, in order to make this prediction system more adaptable.

2.1. Multidimensional Output Support Vector Regression. The support vector machine [17, 18] learning method was proposed by Vapnik et al. based on the theory of statistical learning. For each regression computational problem, they can be represented as establishing a functional mapping relationship between the input and output quantities. Here, we assume that the function is $y(x) = \omega \cdot x + b$, $\{x_i, y_i\}$ $(i = 1, 2, \cdots, k), \{x_i, y_i\} \in R^d \times R^1$, and allow a certain amount of fitting error to exist by introducing a relaxation factor $\xi_i, \xi_i^* \geq 0$ in accordance with the structural risk minimization principle of statistical learning. In this way, the optimization problem mentioned in the text can be reduced to a minimization problem, and the optimization objective is established with the expression.

$$R(\omega, \xi_i, \xi_i^*) = \frac{1}{2}\|\omega\|^2 + C\sum_{i=1}^{k}(\xi_i + \xi_i^*), \tag{1}$$

where ω is the fit coefficient; $\xi_i, \xi_i{}^*$ is the relaxation factor; C is the penalty factor; and k is the sample size.

The Lagrange multiplier method [19, 20] is often used by researchers to solve optimization problems for this convex quadratic optimization problem. The Lagrange function can represent the expression as follows.

$$\begin{aligned} L(\omega, b, \xi_i, \xi_i{}^*, \alpha_i, \alpha_i{}^*, \gamma_i, \gamma_i{}^*) = {} & \frac{1}{2}\omega \times \omega + C\sum_{i=1}^{1}(\xi_i + \xi_i{}^*) \\ & - \sum_{i=1}^{1}\alpha_i[\xi_i + \varepsilon - y_i + f(x_i)] - \\ & \sum_{i=1}^{1}\alpha_i^*[\xi_i{}^* + \varepsilon + y_i - f(x_i)] \\ & - \sum_{i=1}^{1}(\xi_i\gamma_i + \xi_i{}^*\gamma_i{}^*), \end{aligned} \tag{2}$$

where $\alpha_i, \alpha_i{}^*, \gamma_i, \gamma_i^*$ is the Lagrange coefficient; $\alpha_i, \alpha_i{}^* \geq 0; \gamma_i, \gamma_i^* \geq 0; i = 1, 2, \cdots, k$.

According to the KKT condition, the expression of its pairwise form maximization function can be expressed as follows.

$$W(\alpha_i, \alpha_i^*) = -\frac{1}{2}\sum_{i,j=1}^{k}(\alpha_i - \alpha_i^*)(\alpha_j - \alpha_j^*)(x_i \cdot x_j) + \sum_{i=1}^{k}(\alpha_i - \alpha_i^*)y_i - \sum_{i=1}^{k}(\alpha_i + \alpha_i^*)\varepsilon, \tag{3}$$

where x is the i-th sample input value and x is the j-th sample input value.

Therefore, solving the optimization problem yields the support vector regression model can be expressed as follows.

$$f(x) = \sum_{i=1}^{k}(\alpha_i - \alpha_i^*)(x, x_i) + b, \tag{4}$$

where x is the input value of the sample to be predicted.

The above analysis is only applicable to linear regression problems. However, for nonlinear regression, many researchers need to introduce a feature space and use a nonlinear mapping to map the data to a high-dimensional feature space for linear regression. In addition, the implementation of this algorithm requires replacing the inner product operation in linear regression with a kernel function in the high-dimensional feature space. The kernel function is defined as follows.

$$K(x_i, x_j) = \phi(x_i) \cdot \phi(x_j), \tag{5}$$

where ϕ represents the nonlinear mapping function.

After the same derivation process as linear regression, we can finally obtain the support vector model fitting function as follows.

$$f(x) = \sum_{i=1}^{k}(\alpha_i - \alpha_i^*)K(x, x_i) + b. \tag{6}$$

The traditional support vector regression has a one-dimensional variable (SVR) as the output variable. This artificial intelligence algorithm makes its application scenarios limited. In some complex systems, we need to build multi-input-multi-output mapping system to solve the problem. The main reason for this difference is that a 1D SVR does not perform such tasks. Therefore, some research exists to extend the one-dimensional SVR to make it applicable to multidimensional output systems to solve more complex problems in practical engineering.

We extend the one-dimensional insensitive loss function to multiple dimensions. In addition, the loss function can be defined, and its expression is expressed as follows.

$$L(u_i) = \begin{cases} 0, & u_i < \varepsilon \\ (u_i - \varepsilon)^2, & u_i \geq \varepsilon, \end{cases} \tag{7}$$

where $u_i = \|e_i\| = \sqrt{e_i^T e_i}$; $e_i^T = y_i^T - \phi^T(x_i)W - b^t$; $W = [w^1, \cdots, w^Q]$; $b = [b^1, \cdots, b^Q]^T$, where ϕ is the nonlinear mapping kernel function; x is the sample input row vector; y_i is the sample output row vector $i = 1, \cdots, n$; n is the number of samples; and Q is the dimensionality of the output variable.

Based on the loss function shown in the above equation, we can construct the optimization objective function, whose expression can be expressed as follows.

$$L_P(W, b) = \frac{1}{2}\sum_{j=1}^{Q}\|\omega^j\|^2 + C\sum_{i=1}^{n}L(u_i). \tag{8}$$

To solve the mathematical optimization problem of multidimensional output support vector regression (MSVR) models, a large number of research results have proposed the use of iterative reweighted least squares (IRSL) to solve the problem.

In the optimization objective function of equation (8), we can approximate the loss function by replacing it with a first-order Taylor expansion.

$$L_P'(W,b) = \frac{1}{2}\sum_{j=1}^{Q}\|\omega^j\|^2 + C\left(\sum_{i=1}^{n}L(u_i^k) + \left.\frac{dL(u_i)}{du_i}\right|_{u_i^k}\frac{(e_i^k)^T}{u_i^k}\left[e_i - e_i^k\right]\right). \tag{9}$$

Meanwhile, we can construct a quadratic approximation of equation (9) instead of the original equation form. There are studies that confirm the approximate formula that can be used to represent the relationship between the independent variable and the response variable.

$$\begin{aligned} L_P''(W,b) &= \frac{1}{2}\sum_{j=1}^{Q}\|\omega^j\|^2 + C\left(\sum_{i=1}^{n}L(u_i^k) + \left.\frac{dL(u_i)}{du_i}\right|_{u_i^k}\frac{u_i^2 - (u_i^k)^2}{2u_i^k}\right) \\ &= \frac{1}{2}\sum_{j=1}^{Q}\|\omega^j\|^2 + \frac{1}{2}\sum_{i=1}^{n}a_i u_i^2 + CT. \end{aligned} \tag{10}$$

The main reason for using this approximate formulation is that W and b are decoupled in this formulation. This intelligent optimization solution does not require iteration, W and b; the approximate solutions of W and b can be calculated directly by taking the partial derivatives of W and b equal to 0. After the optimization objective is solved, the objective is to minimize the overall loss of W and b of the sample set. By the above operation, the multi-output support vector regression model is built.

2.2. Selection Algorithm Based on Immune Cloning. The biological immune system is a complex adaptive system. The human immune system is capable of recognizing pathogens and responding to them [21, 22]. The researchers used this mechanism to give this learning system some ability to learn, remember, and pattern recognize. Immune cloning systems can be used to describe the principles and mechanisms of information processing using computer algorithms to solve scientific and engineering problems.

Castro was the first to propose a clonal selection algorithm (ICSA). The algorithm is an intelligent method for solving complex problems inspired by the human immune system and simulating the function and mechanism of action of the biological immune system. It retains several

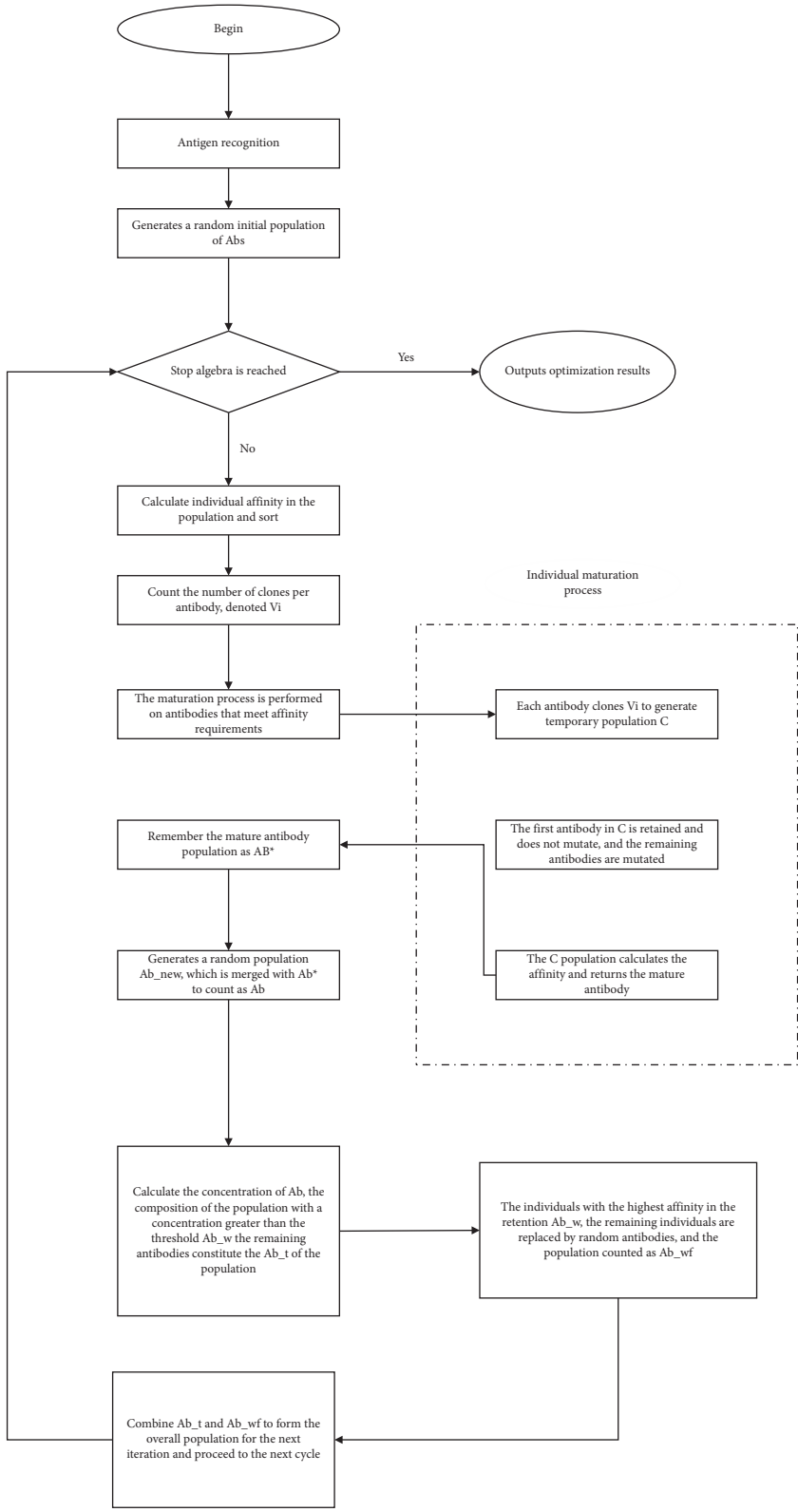

Figure 1: Flowchart of ICSA.

characteristics that are characteristic of the biological immune system. The advantages of this algorithm mainly include global search capability, diversity maintainer, extreme robustness, and parallel solving search process. Researchers can introduce this intelligent algorithm idea into the process of solving optimization problems.

The coupled algorithm introduced in this paper adds a population suppression process to the ICSA to control the

average concentration of the population and avoid premature convergence of the algorithm to a local optimal solution. This operation increases the global optimization capability of the artificial intelligence. The detailed process of the ICSA is shown in Figure 1.

The typical multi-peaked function Rosenbrock function (banana function) [24] is used to test the optimization ability of the improved ICSA. Such function expressions can be expressed as follows.

$$f(X) = \sum_{i=1}^{n-1}\left(100\left(x_{i+1} - x_i^2\right)^2 + \left(1 - x_i\right)^2\right), \tag{11}$$

where $X = [x_1, x_2, \ldots, x_n] \in \mathbb{R}^N$.

The global minimum point of the Rosenbrock function is obtained when all independent variables take the value of 1, and the minimum value of the function value is 0. We use the 10-element Rosenbrock function to test the optimization effect of the ICSA for multivariate functions. The search interval of the independent variable is $(-10, 10)$, and the algorithm parameters are set in Figure 2. As shown in the figure, NP denotes the number of antibody population sizes, G denotes the maximum number of cycles, and NC represents the number of clones.

We run the optimization algorithm 10 times and find the minimum value point of the function about 4 times. The results of these 10 times of optimization are shown in Figure 3. As shown in Figure 3, the ICSA has good optimization-seeking capability for multidimensional multipeak functions. This optimization algorithm can be applied to solve the optimization problem of MSVR model and the prediction performance of research health education based on the coupled ICSA-MSVR algorithm.

The main performance is that when the number of numerical experiments exceeds 5 times, the three algorithms show different prediction performances. When there are less than 5 experiments here, the prediction effects of the three algorithms are basically the same.

2.3. Inverse Analysis Method Based on ICSA-MSVR Coupling Algorithm. The values of the control parameters (penalty coefficients C, sensitivity coefficients ε, kernel function parameters σ) need to be specified artificially in the process of MSVR model building. In order to control the parameter values to achieve the minimum sample training error and the best generalization accuracy of the MSVR model, we propose to solve the parameters optimally by using the ICSA.

In the model training phase, the overall error function of the training sample set is defined as the optimization objective, and the error of individual samples is also adopted as the insensitive loss function. The training samples are divided into learning samples and testing samples, and we use the K-fold cross-validation method to calculate the overall sample error. This way the optimization objective function expression is expressed as follows.

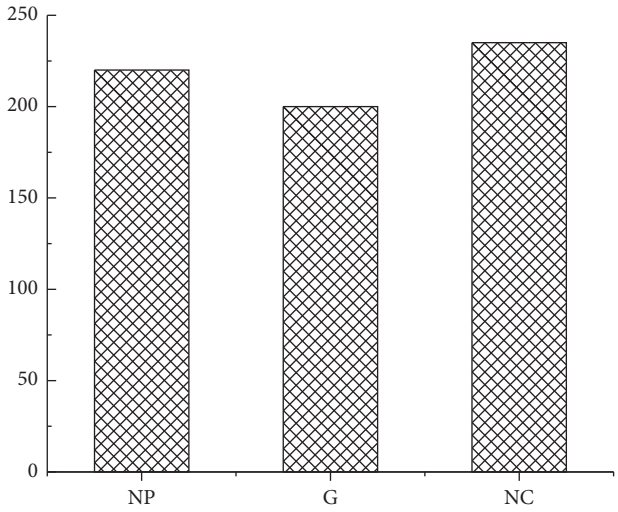

Figure 2: Specific application parameters of the ICSA.

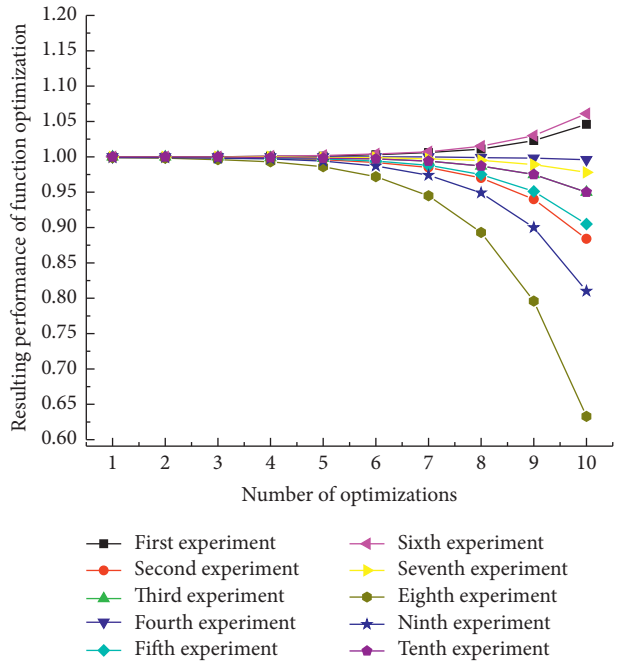

Figure 3: Rosenbrock function optimization results.

$$\begin{aligned}\left(C^*, \varepsilon^*, \sigma^*\right) &= \arg\min_{C,\varepsilon,\sigma} L_{\text{all}}(C, \varepsilon, \sigma),\\ L_{\text{all}}(C, \varepsilon, \sigma) &= \sum_{m=1}^{k}\sum_{i=1}^{k_m} L\left(u_i\right),\end{aligned} \tag{12}$$

where $L_{\text{all}}(C, \varepsilon, \sigma)$ denotes the overall training loss function; k denotes the number of sample aliquots; k_m denotes the number of training sample aliquots; and the superscript asterisk indicates the optimal parameter.

After the MSVR model is trained, i.e., the optimal MSVR model parameters are optimized by the ICSA. This completes the process of building the prediction model for the positive method inverse analysis process.

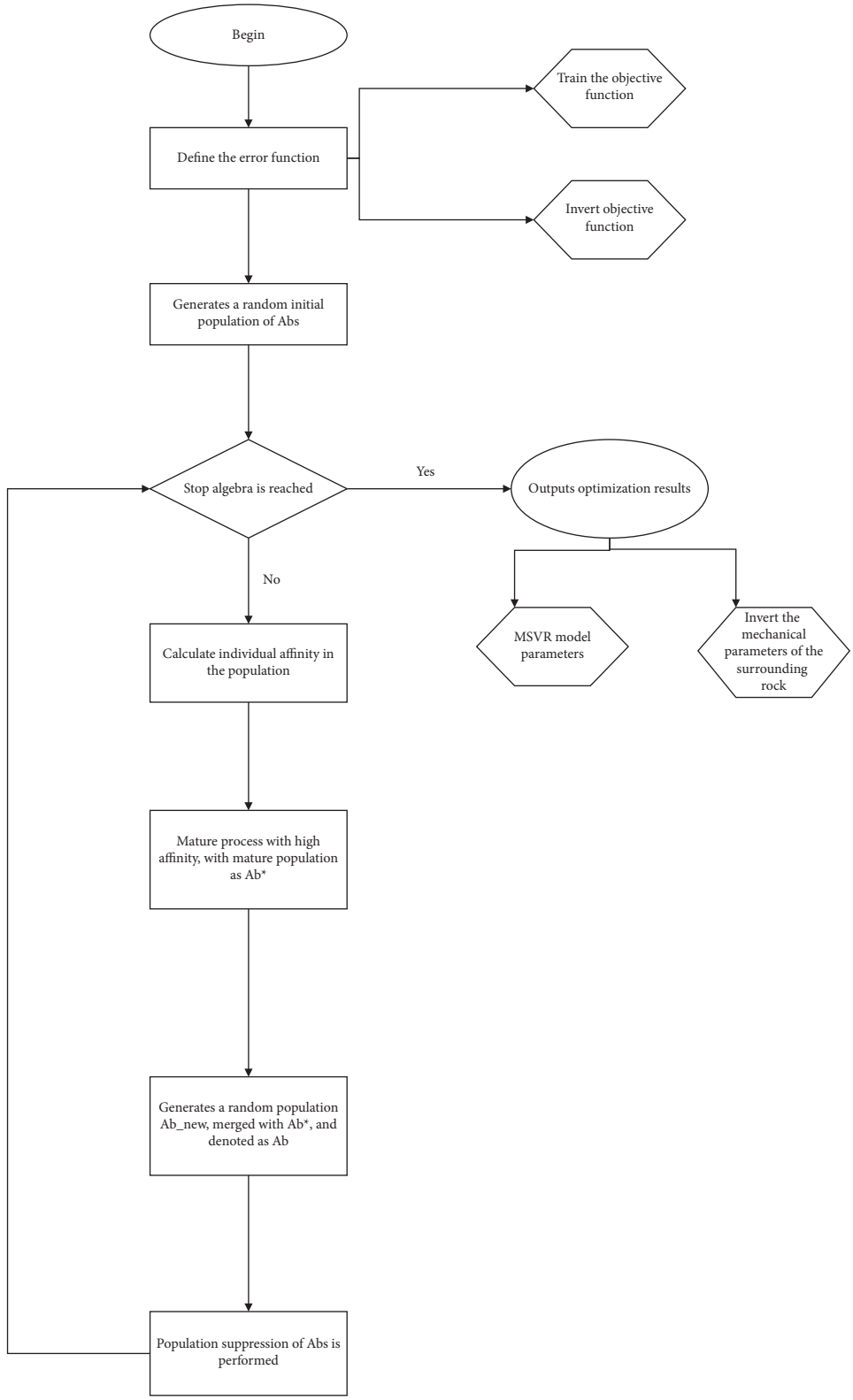

Figure 4: The calculation flow of the ICSA-MSVR coupling algorithm.

In the optimization process of the ICSA, in order to expand the search range of the parameters and the search efficiency, we mapped the parameters to be optimized exponentially; i.e., the range of values of the parameters in the population is the natural logarithm of the actual range of values. In addition, in the actual affinity calculation, the antibody individuals are mapped exponentially, and the calculation formula can be expressed as follows [23, 24].

$$P' = \exp(P). \tag{13}$$

The flow of the coupled ICSA-MSVR algorithm is shown in Figure 4. This newly introduced AI algorithm differs in the definition of the error function and the resultant output part of the model training process and the parameter identification process.

3. Simulation Results and Analysis

We take the results of a health education prediction for students' knowledge behaviors as an example and compare their task completion through the cloud computing platform. CloudSim is a cloud computing simulation platform jointly developed by the GridLab and Gridbus project at the University of Melbourne, Australia. It focuses on simulating cloud environments and testing the scheduling policies of different service models. To test the effectiveness of this paper's algorithm in cloud computing task scheduling, the CloudSim platform is used under Intel i5 processor, 12 GB RAM, and WINDOS10 operating system. In this subsection, we compare and analyze the improved algorithm (ICSA-MSVR), immune cloning algorithm (ICSA), and multidimensional output support vector machine (MSVR) introduced in this paper in three aspects: convergence speed, task completion time, and load imbalance of cloud computing task scheduling.

The strengths and weaknesses of the tested algorithms in terms of convergence speed are mainly reflected in the minimum number of steps to compute the iterations. At the scheduling scale of 200 cloud tasks and 10 VMs, we can compare the convergence speed of ICSA and ICSA by the relationship between the number of algorithm iterations and task completion time. In the analysis, we set the number of antibody population size to 220 and the number of clones to 235.

As shown in Figure 5, ICSA-MSVR converges better than ICSA, both ICSA-MSVR and ICSA converge quickly in the first 100 iterations, and ICSA-MSVR converges faster than ICSA. In addition, the ability of ICSA-MSVR algorithm to develop near the optimal solution is improved and the convergence speed of the algorithm is accelerated. Meanwhile, ICSA-MSVR gradually leveled off after 250 iterations, and the task completion time was less than that of ICSA.

The strengths and weaknesses of the tested algorithms in terms of cloud task completion time are directly reflected in the magnitude of task completion time. We set the number of virtual machines to 10 and the number of cloud tasks to 40, 80, 120, 160, and 200 [25], and then we can compare the task completion time of the three algorithms, ICSA-MSVR, ICSA, and MSVR, in cloud task scheduling and analyze them. The specific numerical experimental results are shown in Figure 6.

As can be seen in Figure 6, ICSA-MSVR takes less time for task completion and is better optimized than the other two algorithms. As the number of cloud tasks increases, the task completion time also increases. When the number of tasks is 40, the task completion time of ICSA-MSVR is 8s and 20s less than that of ICSA and MSVR, respectively. The

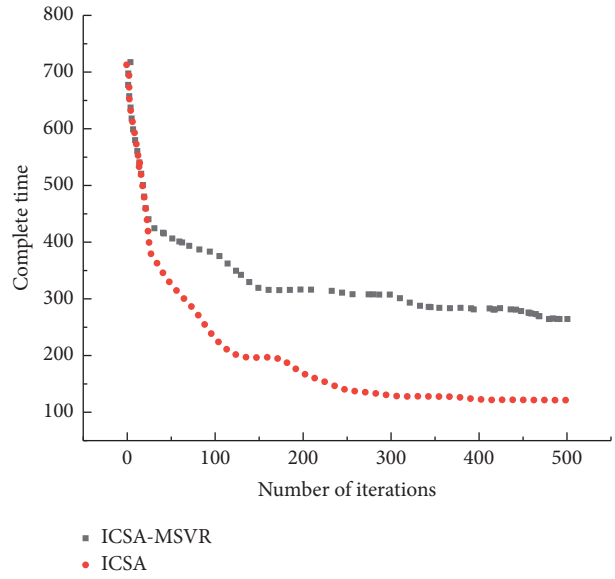

Figure 5: Convergence comparison of algorithms.

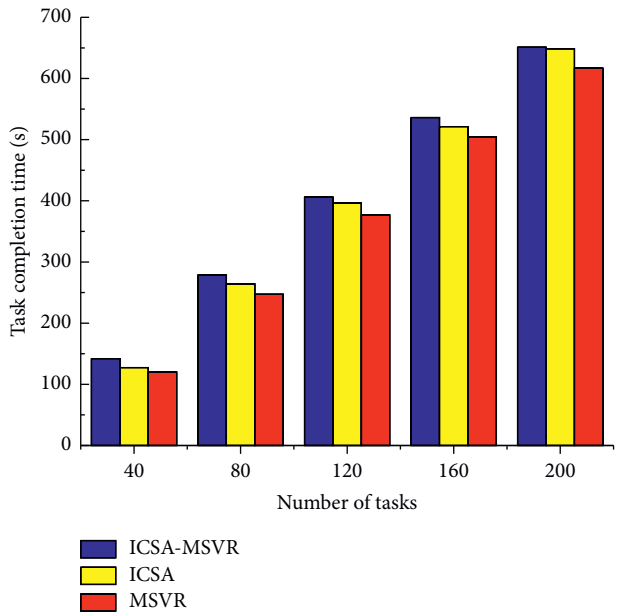

Figure 6: Comparison of task completion time.

number of tasks gradually increases, and the task completion time difference of each algorithm increases, and when the number of tasks reaches 200, the task completion time of ICSA-MSVR is 24s and 35s less than that of ICSA and MSVR, respectively, which decreases by 3.7% and 5.3%. The above analysis results prove that ICSA-MSVR works in both local search and global search, which is more effective on larger scale cloud computing task scheduling.

What we know is that the degree of load imbalance (DI) of the test algorithm is an important concept, and DI measures the degree of imbalance between virtual machines.

In this paper, we use the standard deviation to represent the imbalance DI. The smaller the DI value, the closer the amount of load among the virtual machines. The better the

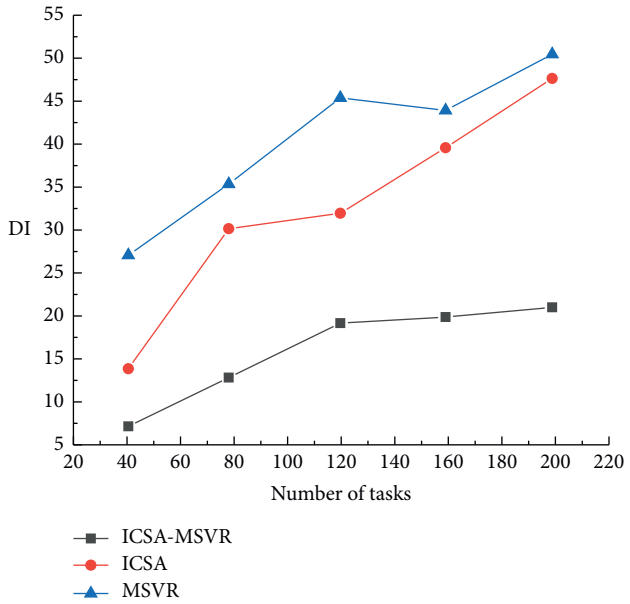

Figure 7: Comparison of DI values of the three algorithms.

load balance degree is, the more reasonable the scheduling policy is. The DI is expressed as follows.

$$DI = \sqrt{\frac{\sum_{j=1}^{n} (\text{Time} - AL)^2}{n}}, \tag{14}$$

where AL is the average load of the virtual machine and is the average task completion time of the virtual machine; Time is the load of the virtual machine; and n is the number of virtual machines.

When the number of cloud tasks is 40, 80, 120, 160, and 200, the load imbalance DI of the three algorithms, ICSA-MSVR, ICSA, and MSVR, is compared and analyzed as shown in Figure 7.

It can be seen from Figure 7 that the DI values of the three algorithms increase as the number of tasks increases, and the DI values of ICSA-MSVR are smaller than those of ICSA and MSVR. This situation indicates that in task scheduling with short task completion time, ICSA-MSVR has lower load imbalance than ICSA and MSVR, which can achieve better load balancing and closer load amount among virtual machines.

To further investigate the effectiveness of the three intelligent algorithms in the application of health education prediction of students' knowledge behavior, the next step is proposed by comparing the coefficient of determination (R^2) and the sum of squared residuals (SSE) of the three algorithms. It is well known that the closer the square of the correlation coefficient (R^2) is to 1, the smaller the sum of squared residuals (SSE) is, and the better the fit is. The R2 and SSE corresponding to the three algorithms are plotted in Figures 8 and 9.

As can be seen from Figures 8 to 9, compared with the three algorithms, ICSA-MSVR obtained the largest coefficient of determination and the smallest sum of squared

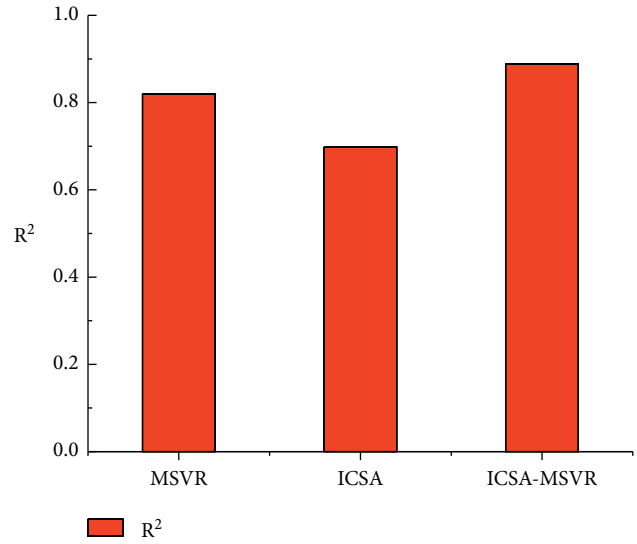

Figure 8: Comparison of the coefficients of determination of the three algorithms.

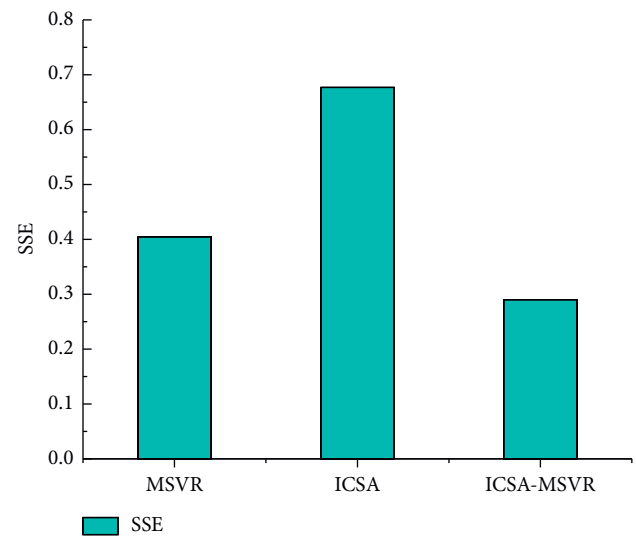

Figure 9: Comparison of the residual sum of squares of the three algorithms.

residuals, which can indicate that this method has the relatively best prediction performance.

In addition, we interpolated the predicted performance parameters of ICSA-MSVR for this case using the trajectory interpolation method. The processing results are shown in Figure 10. From Figure 10, we can see that the predicted performance indexes obtained by interpolation have good continuity after the optimization process of the coupled ICSA-MSVR algorithm. This method can provide some theoretical references for the subsequent analytical studies.

We can get from the above simulation case of health education analysis based on cloud computing that artificial intelligence and big data are technical contents that are emphasized and exploited in various fields in recent years, and applying them to mental health education of college

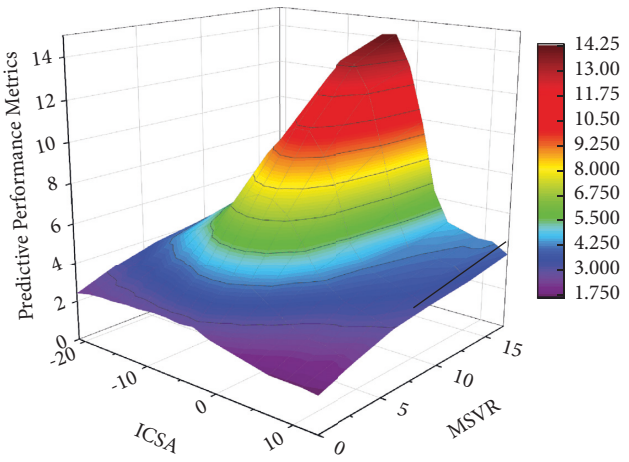

Figure 10: Trajectory interpolation results of ICSA-MSVR prediction performance indicators.

students can not only improve the technicality and accuracy of mental health education. At the same time, this method can also solve the current problem of effective teachers' time and energy in mental health education, which makes it difficult to meet students' personalized psychological education needs. The methods introduced above can make health education carried out in a more scientific and effective way.

4. Conclusion

(1) In this paper, we propose an improved immune clone selection algorithm by adding a population suppression process to improve the convergence to local extrema and the prematureness of the algorithm. After the arithmetic test, the algorithm has good solving ability for multidimensional optimization problems and converges faster. This coupled optimization algorithm can accompany the cloud computing platform to perform certain prediction work on student health education problems.

(2) Taking a certain health education prediction result for students' knowledge behavior as an example, we test the prediction performance of three algorithms, ICSA-MSVR, ICSA, and MSVR, through the cloud computing platform. The results show that ICSA-MSVR works in both local search and global search, and is more effective in scheduling larger scale cloud computing tasks. In addition, ICSA-MSVR has less load imbalance than ICSA and MSVR in task scheduling with short task completion time, allowing better load balancing. The amount of load is closer between virtual machines. In the meantime, compared with the three algorithms, ICSA-MSVR obtained the largest coefficient of determination and the smallest sum of squared residuals, which can indicate that this method has the relatively best prediction performance.

(3) Of course, the current research and practice on the application of artificial intelligence and big data in student health education is still in the exploratory stage, and there are more problems and shortcomings. This requires combining the needs of students' health education and deeply tapping and using the advantages of technologies such as artificial intelligence and big data to truly bring into play the positive functions of technology in education. The combination mechanism of intelligent algorithms introduced in this paper can provide some theoretical reference for such research.

Data Availability

The dataset can be accessed upon request.

Conflicts of Interest

The authors declare that they have no conflicts of interest.

References

[1] J. Taylor, G. Forsell, E. Perweiler, and M. Sienkiewicz, "Longitudinal evaluation practices of health workforce development programs: an incremental approach to evaluability assessment," *Evaluation and Program Planning*, vol. 69, pp. 68–74, 2018.

[2] B. Resnick, J. P. Leider, and R. Riegelman, "The landscape of US undergraduate public health education," *Public Health Reports*, vol. 133, no. 5, pp. 619–628, 2018.

[3] B. Knüsel, M. Zumwald, C. Baumberger et al., "Applying big data beyond small problems in climate research," *Nature Climate Change*, vol. 9, no. 3, pp. 196–202, 2019.

[4] S. B. Hao, H. L. Zhang, and M. Song, "Big data, big data analytics capability, and sustainable innovation performance [J]," *Sustainability*, vol. 11, no. 24, 2019.

[5] J. Amankwah-Amoah and S. Adomako, "Big data analytics and business failures in data-Rich environments: an organizing framework," *Computers in Industry*, vol. 105, pp. 204–212, 2019.

[6] X. Xu, D. Li, M. Sun et al., "Research on key technologies of smart campus teaching platform based on 5G network," *IEEE Access*, vol. 7, pp. 20664–20675, 2019.

[7] C. C. Ekin, K. Cagiltay, and N. Karasu, "Effectiveness of smart toy applications in teaching children with intellectual disability," *Journal of Systems Architecture*, vol. 89, pp. 41–48, 2018.

[8] M. Latif, I. Hussain, R. Saeed, and U. Maqsood, "Use of smart phones and social media in medical education: trends, advantages, challenges and barriers," *Acta Informatica Medica*, vol. 27, no. 2, pp. 133–138, 2019.

[9] E. Thomas, "Mobilizing the next generation of health advocates: building our collective capacity to advocate for health education and health equity through SOPHE advocacy summits," *Health Promotion Practice*, vol. 20, no. 1, pp. 12–14, 2019.

[10] J. C. Lawrence, L. L. Knol, J. Clem, R. de la O, C. S. Henson, and R. H. Streiffer, "Integration of interprofessional education (IPE) core competencies into health care education: IPE meets culinary medicine," *Journal of Nutrition Education and Behavior*, vol. 51, no. 4, pp. 510–512, 2019.

[11] A. J. Park, J. M. Ko, and R. A. Swerlick, "Crowdsourcing dermatology: DataDerm, big data analytics, and machine

learning technology," *Journal of the American Academy of Dermatology*, vol. 78, no. 3, pp. 643-644, 2018.

[12] D. J. Kim, J. Hebeler, V. Yoon, and F. Davis, "Exploring determinants of semantic web technology adoption from IT professionals' perspective: industry competition, organization innovativeness, and data management capability," *Computers in Human Behavior*, vol. 86, pp. 18–33, 2018.

[13] W. A. Bhat, "Bridging data-capacity gap in big data storage," *Future Generation Computer Systems*, vol. 87, pp. 538–548, 2018.

[14] M. J. Sanders, R. Bruin, and C. T. Tran, "How to make a standard inhaler device into a 'smart' inhaler that teaches technique[J]," *Journal of Aerosol Medicine and Pulmonary Drug Delivery*, vol. 31, no. 2, p. A14, 2018.

[15] J. M. Liang, W. C. Su, Y. L. Chen, S. L. Wu, and J. J. Chen, "Smart interactive education system based on wearable devices[J]," *Sensors*, vol. 19, no. 15, 2019.

[16] S. Streiter, S. D. Berry, and A. Schwartz, "Teach smarter, not harder: integrating adult learning theory (ALT) into a geriatric fellowship didactic curriculum[J]," *Journal of the American Geriatrics Society*, vol. 67, p. S238, 2019.

[17] S. Verma, S. S. Bhattacharyya, and S. Kumar, "An extension of the technology acceptance model in the big data analytics system implementation environment," *Information Processing & Management*, vol. 54, no. 5, pp. 791–806, 2018.

[18] Y. J. Guo, Z. L. Yang, S. Z. Feng, and J. Hu, "Complex power system status monitoring and evaluation using big data platform and machine learning algorithms: a review and a case study," *Complexity*, vol. 2018, Article ID 8496187, 2018.

[19] A. Eltom, W. Elballa, N. Sisworahardjo, R. Hay, and G. Kobet, "Smart distribution course for 21St century power sector workforce[J]," *IEEE Transactions on Power Systems*, vol. 33, no. 5, pp. 5639–5647, 2018.

[20] M. Hasanipanah, R. Naderi, J. Kashir, S. A. Noorani, and A. Zeynali Aaq Qaleh, "Prediction of blast-produced ground vibration using particle swarm optimization," *Engineering with Computers*, vol. 33, no. 2, pp. 173–179, 2017.

[21] M. L. Wilson, S. Sayed, S. Horton, and K. A. Fleming, "Artificial intelligence can augment global pathology initiatives - a," *The Lancet*, vol. 392, no. 10162, p. 2352, 2018.

[22] M. C. Alvarez-Herault, A. Labonne, S. Toure et al., "Corrections to an original smart-grids test bed to teach feeder automation functions in a distribution Grid [jan 18 373-385]," *IEEE Transactions on Power Systems*, vol. 33, no. 4, p. 4647, 2018.

[23] X. Li, X. Liu, C. Z. Li, Z. Hu, G. Q. Shen, and Z. Huang, "Foundation pit displacement monitoring and prediction using least squares support vector machines based on multipoint measurement," *Structural Health Monitoring*, vol. 18, no. 3, pp. 715–724, 2019.

[24] Y. Gong and L. Jia, "Research on SVM environment performance of parallel computing based on large data set of machine learning," *The Journal of Supercomputing*, vol. 75, no. 9, pp. 5966–5983, 2019.

[25] S. Chen, X. Wu, and H. Yin, "A novel projection twin support vector machine for binary classification," *Soft Computing*, vol. 23, no. 2, pp. 655–668, 2019.

Hindawi
Scientific Programming
Volume 2022, Article ID 8490683, 8 pages
https://doi.org/10.1155/2022/8490683

Research Article

Research on the Decision Model of Product Design Based on a Deep Residual Network

Licheng Zong[1] **and Nana Wang**[2]

[1]*School of Art, Northwest University, Xi'an 710127, China*
[2]*School of Cultural Heritage, Northwest University, Xi'an 710127, China*

Correspondence should be addressed to Licheng Zong; zonglicheng@nwu.edu.cn

Received 24 April 2022; Accepted 4 June 2022; Published 16 June 2022

Academic Editor: Lianhui Li

An artificial intelligence (AI) design decision model is constructed to improve the efficiency of design decision evaluation and avoid the influence of the decision preference on product design and development. Using the concept of AI, the proposed model is based on a data set of product modeling design schemes, and the data set is marked with product modeling semantics. The deep learning residual network (ResNet) algorithm is used to train the data set to improve the accuracy of design decisions, transform the general design decision problem into the semantic recognition problem of design scheme images, and eliminate the design decision preference to the greatest extent. The validity and the feasibility of the proposed AI design decision-making method based on the ResNet algorithm are verified via an example of motorcycle modeling design decision-making.

1. Introduction

Modern product design integrates multiple elements such as technology, humanities, art, culture, and commerce. Design is characterized by apparent multi-disciplinary and multi-field intersection [1]. Product innovation design includes three functional units, namely, the problem, solution, and decision [2], and Analysis–Synthesis–Evaluation (ASE) is one of the typical design processes [3]. Design evaluation and decision-making are important components of modern product innovation design [4]. In part, design decisions will be directly related to the success or failure of product design and development.

The decision-making process of modern product design is usually completed by the cooperation of engineers, sales staff, consumers, designers, and enterprise managers. Differences in the cognitive backgrounds, subjective preferences, and experiences of decision-making groups cause the decision-making process to be complicated, vague, and full of uncertainty. Therefore, efficient and accurate design decisions that do not involve the personal preferences of the decision-maker are critical to successful product development [5].

Design decision-making is based on the design evaluation. There are currently three types of design evaluation, namely, experimental, mathematical, and online evaluation. Experimental evaluation primarily analyzes physical and psychological data, such as the visual perception of participants, the way to use the product, and the functional experience of the product, and then explores the product attributes. Common experimental evaluation methods include eye movement experiments [6], EEG experiments [7], and comprehensive experiments including these two methods [8]. Mathematical evaluation mainly involves the setting of evaluation indicators, the construction of evaluation models for quantitative calculation, and the scoring and evaluation of the design schemes. Common mathematical evaluation methods include the analytic hierarchy process [9], the rough set evaluation method [10], neural networks [11], and deep learning models [12]. In online evaluation, data mining technology is mainly used to acquire, cluster, analyze, and mine online user data, and is an inevitable trend in the development of network informatization. Related research methods include the use of big data [13], natural language processing [14], and text mining [15].

Deep learning is a new field of machine learning research, the core of which is a neural network that simulates the information analysis and processing of the human brain. In recent years, it has achieved great success in the fields of image and language recognition, autonomous driving, and medical care [16]. Based on the basic concepts of artificial intelligence (AI), in this study, a product group data set with product design semantics is constructed, and the data set is artificially labeled. The data set is continuously trained by deep learning algorithms, and the product design decisions are realized by AI methods. This improves the design decision accuracy and efficiency, and eliminates the decision bias.

2. Related Theories

The product design process begins with the input of the user's needs. Designers and engineers comprehensively deduce relevant design resources, design strategies, design constraints, and design methods to promote the execution of the design behaviors and the solidification of the design results. The final output is user satisfaction. When designing products, designers must analyze the user's needs based on their own knowledge reserves and experience, propose solutions and conduct comprehensive evaluations, and realize the conversion between design processes via design decisions. Design decisions are constantly iterated to finalize the design for the market.

2.1. Product Design Semantics and Design Decisions. Each product has or conveys different product semantics, via which the image characteristics of products in different usage scenarios are studied. Semantic communication between people and products is achieved through continuous iteration in the design process [17]. Via a communication method built between people and products, the product connotation, form, structure, color, and other elements are transmitted to users so that they can form a certain cognitive image of the product. Generally, in the early stage of product design, the design entrusting party or design developer will propose specific development tasks according to the product positioning, user needs, brand strategy, marketing strategy, etc. The semantic vocabulary of product design is a specific description provided before new product design and development. For example, the client will use a clear semantic vocabulary of shape and color to semantically describe the expectations of the new product, and the design team will use this semantic vocabulary as an important design input to guide the design process until a satisfactory design solution is obtained.

During the product design process, the product design plan will be analyzed, communicated, and evaluated many times, and the final design plan will be obtained via the selection and design decisions of Party A and the design expert team. Throughout this process, product design semantics are an important basis for design decisions. According to the product design process, product design semantics are proposed at the beginning of product design and development, and are communicated to designers via a design semantic vocabulary. The design team parses and expresses the design semantic information based on their design knowledge, experience, and tools. Design brainstorming, conceptual design optimization, and detailed design proposals are then used to interpret the scheme, and the decision-making evaluation of the design scheme is carried out via the semantic matching degree between the design scheme and the design goal [18].

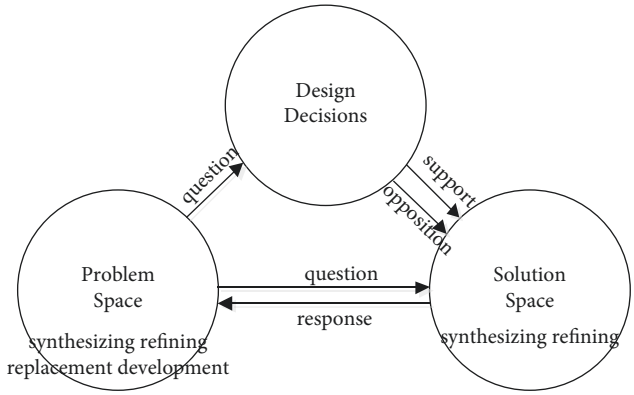

Figure 1: The semantic model of the problem space–design decision–solution space.

2.2. Semantic Model of Product Design Decisions. The process of product design is accompanied by solutions to different design problems. The solution process includes the initial state of the problem, the target state, and the solution strategy [19], and roughly undergoes the stages of sketch conception, conceptual design, scheme design, detailed design, and design refinement. Constant revision and adjustment are required to form a satisfactory solution for users. This process is the co-progression of design problems and design solutions with a basis on design decisions [20], which links the problem space and the solution space. Based on the principle of semantic models, the interrelationships between the design problem space, design decision space, and solution space were constructed (Figure 1), as were nine semantic connections used to describe the product design decision problems, namely, synthesis, refinement, substitution, expansion, questioning, support, opposition, prompt, and response.

(i) Problem space. The problem space is used to reflect on the user needs. When user needs are not met, the problem space questions the solution space and design decisions.

(ii) Design decisions. The design decision is the screening of the solution of the design problem, and the solution space is formed by supporting or opposing one or multiple solutions.

(iii) Solution space. A solution space is a collection of solutions designed by designers for user needs. For any problem in the design process, the solution space must respond to it. The elements in the solution space can be further refined and synthesized to form a new solution set.

2.3. AI and Image Recognition. In the field of image recognition and processing, AI technology, including graphic preprocessing, graphic segmentation, graphic feature extraction, and judgment matching, has become relatively mature. Machines can preprocess, analyze, and judge a target image to identify various objects or targets. The field of deep learning mainly includes the use of convolutional neural networks (CNNs) and generative adversarial networks (GANs). Neural network research originated from the field of biology. In 1998, Fukushima [21] constructed a neural cognitive machine composed of alternating simple and complex cell layers, which was considered to be the first engineering implementation of CNNs. A GAN is a generative model proposed by Kim et al. [22] in 2014. For neural networks, with the increase in the number of network layers, the training difficulty of learning algorithms such as CNNs and deep neural networks (DNNs) increases, and ideal model training results cannot be obtained. Using the residual learning framework, He et al. [23] proposed the residual neural network (ResNet) algorithm, which overcomes the increase of the training difficulty of the network with the deepening of the network, thereby allowing the number of network layers to reach new heights.

In the product design stage, the analysis, communication, display, and evaluation of the design scheme are usually carried out in the form of renderings. The images of design renderings are direct carriers for conveying the information of the design language. In the evaluation of design decisions, images of design renderings can be processed by AI to obtain algorithms implementing classification, understanding, and semantic feature evaluation [24]. Therefore, the image of the rendering of the design scheme is used as the output, the resulting image is preprocessed, semantic image segmentation is performed on the key modeling areas according to the designer's requirements, and the semantic features are extracted for judgment. Finally, according to the score of algorithm reasoning and the pre-evaluation of the design scheme, the purposes of the evaluation, optimization, and decision-making of the design scheme set are achieved.

3. Method of Product Design Decision-Making Based on AI

The loss of traditional deep learning algorithms will increase with the increase of the depth beyond a certain level. The unique structure of the ResNet algorithm can accelerate the training of deeper neural networks without losing speed. The detection and segmentation effects of the ResNet algorithm are better than those of other algorithms, and its accuracy is also greatly improved. In this study, the residual unit module of the ResNet algorithm is used to study the deep learning and semantic segmentation of the design scheme, and AI design decision-making is realized via the machine learning method.

3.1. Decision-Making Framework of AI Product Design Based on a Deep Learning Algorithm. According to the general product design process, the semantics of the target product design are used as the input, and AI design decisions are made based on the design scheme renderings of each round. A deep residual network-based AI design decision-making method is constructed, and the overall framework of which is shown in Figure 2.

After the design semantics of the target product are determined, a large amount of design proposal data of the same type are collected. These design proposals are preprocessed and semantically labeled, and a basic design proposal data set available to the machine is constructed. According to the design scheme images in these data sets, the modeling of key areas and semantic feature extraction are performed, and the data are continuously trained through the ResNet core algorithm. The deep residual network consists of three fully connected layers and 10 convolutional layers. After the first convolutional layer, the network is divided into three residual modules, each of which is divided into a main path and a shortcut. Three convolutional layers are located on the main path to extract the deep features and the features of design semantic annotation in the image features of the design scheme. To facilitate the upward propagation of residuals during training, the shortcut contains a convolutional layer. At the end of the residual module, the key features obtained from the main path and the shortcut are restacked and integrated to classify the previously obtained convolution features. The convolution features obtained previously are classified via restacking integration. During the intelligent decision-making of product design, users can set target semantics, input the design scheme images of the intermediate process into the trained deep residual network, and evaluate different design schemes via image semantic decoding.

3.2. Data Set Construction and Feature Extraction. In the field of AI, data sets are used to train and test proposed algorithms [25]. The goal of AI design decision-making is to evaluate the design and modeling semantics of the corresponding area via the semantic segmentation of the product modeling area; thus, the general outline of the target area must be given. As an example, a subject collected a large number of side views of gas motorcycles in domestic and foreign markets as the main image data, and a basic data set was constructed, as shown in Figure 3. After the completion of the basic data set, it is necessary to perform segmentation and semantic annotation on the modeling area of the basic image to further improve the evaluation efficiency and accuracy. For the image evaluation of the design scheme in combination with AI algorithms, it is necessary to segment and extract the contour lines of the image modeling area, and to combine the Kansei engineering method to extract and label the main modeling semantic parts in the images. Due to the huge data set, multi-user participation was adopted, and professional designers performed artificial semantic annotation on the feature areas of the data images.

3.3. AI Product Design Decision Model. The advantage of the ResNet algorithm is that it can quickly accelerate the training process of the neural networks [26]. The original input of the

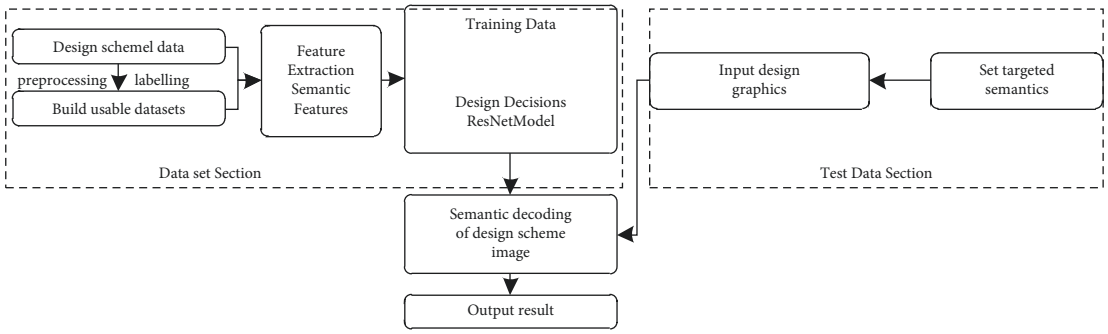

Figure 2: The AI design decision-making framework.

Figure 3: A section of the design decision data set.

entire deep network of ResNet is x, and the output is $F(x)$, which is obtained through a Conv-ReLU-Conv combination layer. By adding the output and the original output, i.e., $H(x) = F(x) + x$, the identity activation function of the original input result is superimposed on the convolution output, the stacking layer is used to fit $H(x) - x$, and the re-superposition of x will help to obtain $H(x)$ (Figure 4). To ensure that the accuracy rate decreases after the network is deepened, stochastic gradient descent can be used to propagate the response, and chain derivation can be used to obtain a faster convergence speed [27].

$$y = F(x, w_i) + x, \tag{1}$$

where x is the input, y is the output, and $F(x, w_i)$ is the residual mapping. Moreover, W_i is a linear convolution operation, in which the dimensions of x and F must be consistent. If they are inconsistent, linear mapping can be used to match the dimensions, as follows.

$$y = F(x, W_i) + W_s x_o. \tag{2}$$

The design plan image is input and scaled proportionally according to its short side, normalization (resize) processing is performed, and a cropped area with a size of 600×480 is then sampled from the image. After convolution operation with a 4×4 convolution kernel, the extracted image features include the contour features of three main regions. In the AI design decision model, the default step size of all max-pooling layers is 2, and the default step size of the convolution operation is 1. If the sizes of the output key features are different, it is usually filled with zeros; if they are the same, the result will be used as the final output [28]. The final data of the convolution layer are converted into a 13-layer fully connected network, and the key features of the image are superimposed and merged in the residual module. The previously obtained convolution features are classified, and the recognition results are output via the softmax classifier.

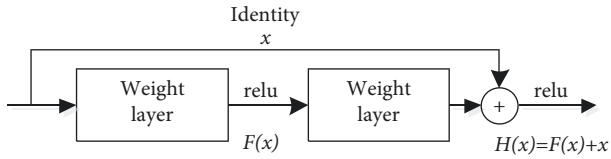

Figure 4: The algorithm flow of a single residual module in the ResNet algorithm.

4. Verification of the Decision-Making Model of AI Products

The TensorFlow deep learning framework [29] was used to implement the ResNet algorithm for AI design decisions based on the Python programming language, and the gas motorcycle design case was used as the basic data set to verify the performance of the ResNet algorithm in design decisions.

4.1. Experimental Data. In the experiment, the side view of motorcycles was used as the main image data. To ensure sufficient experimental samples, the image data of domestic and foreign motorcycles were obtained via a web crawler to construct the basic data set.

4.2. Data Preprocessing. Via web crawling, a large amount of basic image data was obtained. The basic data set was screened to eliminate the invalid samples. The basic preprocessing process and methods were as follows.

Step 1. Images with a side view or approximate side view were kept, and images taken from other perspectives were deleted.

Step 2. The image modeling area was segmented. In the styling design of gas motorcycles, the handles, wheels, and lights of the motorcycle are basically standard parts, and no additional design is required. Therefore, in the process of extracting the contour lines or boundary lines of the products in the data set, the FCN (fully convolutional network) open-source code of the UC Berkeley team was used for graph segmentation and contour extraction. Figure 5 shows the key areas of motorcycle styling design. The area marked No. 1 is the motorcycle oil tank, the area marked No. 2 is the motorcycle seat, and the area marked No. 3 is the motorcycle engine. The modeling design of these three parts forms the overall design semantics of the motorcycle. Areas No. 1 and No. 2 area are two key design areas in the motorcycle modeling design. The design of areas No. 1, No. 2, and No. 3 accounts for more than 85% of the motorcycle styling design, so they are the most important for people's visual perception and influence.

Step 3. The semantic annotation of image modeling was conducted. In current product design image research, statistical analysis and perceptual engineering methods are the most often used. The product image mainly reflects the product's design features, color, layout, structure, and other psychological perceptions of consumers. The usual product image vocabulary is "male-female, solemn-frivolous, future-past, solid-fragile, technology-conservative, rational-sensual." [30] Building on the current research progress of product modeling design images, relevant research was conducted on product modeling semantics. The research objects were designers, consumers, and enterprise managers. A total of 108 survey questionnaires were distributed, after which another three pairs of image vocabulary were included, namely, "introverted-publicized, complete-fragmented, and dynamic-stable." These nine image vocabulary pairs correspond to the semantic annotation of modeling design, as shown in Table 1.

The modeling semantics and decision-making scores were manually labeled by five design experts and obtained after conducting confidence statistics, after which images of 3000 pieces of motorcycle modeling metadata were randomly selected as the training set. After data preprocessing, a total of 3843 motorcycle images were obtained. The metadata of each image included four modeling semantic channels and two score channels, respectively, representing the modeling semantics and overall decision score of the image.

4.3. Experimental Process. The experimental process of AI design decision-making included the input layer, residual module, batch regularization layer, pooling layer, and activation function.

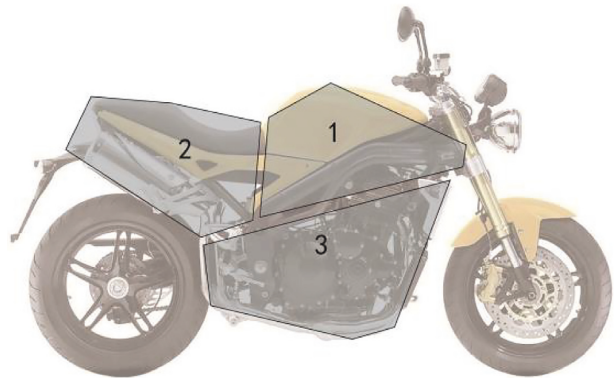

Figure 5: The key labeling areas of motorcycle styling design.

Step 1: Image metadata was used as a data set for the input layer, and included the resulting preprocessed images, semantic labels, and scoring data.

Step 2: The final data were converted via the convolutional layer to the output of a 13-layer fully connected network. The first convolutional layer was divided into three main residual modules after the operation.

Step 3: On the main path, the deep features of the design scheme image were extracted through three convolution layers. The size of the first two layers was the same as that of the convolution kernel of the previous layer, and the size of the convolution kernel on the shortcut was doubled after the third layer.

Step 4: The shortcut controlled the number of features via a convolution layer, thus directly doubling the convolution kernel and speeding up the upward propagation of the residual during training. The main path and shortcut of each residual module obtained the key features of the design image. The numbers of feature layers and feature dimensions of the main path were kept consistent with those obtained by the shortcut, and the two were superimposed and converged at the end of the residual module.

Step 5: For the three fully connected layers, the previously obtained convolutional features were classified. The process continued to the next stage after adding and fusing at the end of the module.

In the experimental process, to speed up the training effect, the batch normalization method proposed by Ioffe and Szegedy [31] was adopted. Thus, the mean value of the features after convolution extraction was 0, the variance was 1, and each convolution layer and pooling layer was processed by batch normalization. The softmax classifier was used in the last layer to output the intelligent decision recognition results [32]. A depiction of the motorcycle shape obtained by the ResNet algorithm in the training phase is shown in Figure 6.

4.4. Experimental Results. To verify the validity and decision-making satisfaction of the proposed AI design decision-

Table 1: The semantic annotation of data set modeling.

Numbering	Semantic description	Modeling semantic description			Realizability (1–10)	Overall evaluation (1–10)
		First part	second part	Third part		
1	Solid male restrained	Sensual female	Rational solemnity	Rational and stable	6	7
2	Technology sensibility publicity	Sensual fragmented sensual pieces	Rational tech rational technology	Solid	5	7
3	Steady restrained female	Male tech	Future solemn	Full dynamic	7	6
4	Robust complete restrained	Rational and stable	Future complete	Technology	8	5
N	.....	.....	.....	.....	...	...

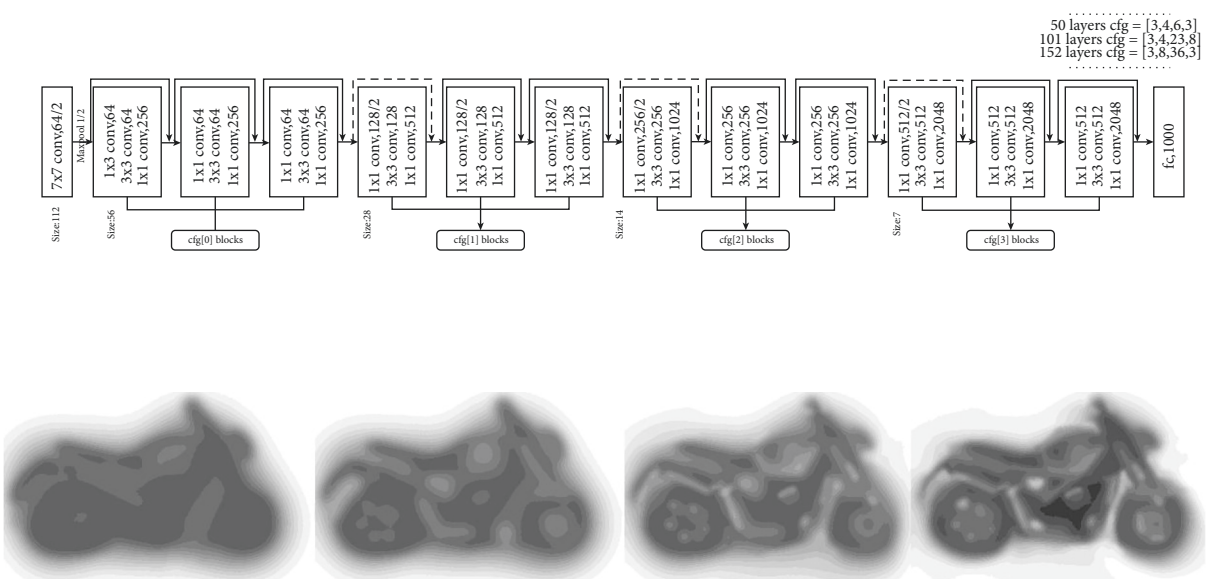

Figure 6: Semantic recognition at different training stages.

making model, two groups of modeling semantic input vocabulary were set. The first group included the semantic vocabulary of "future, stability, and dynamic," and the second group included the semantic vocabulary of "technology, sensibility, and integrity"; these vocabularies represent the semantic vocabulary of motorcycle product styling design. Also, Party A and five design experts jointly participated in making design decisions about three motorcycle design schemes. Based on Party A's scoring results of the design scheme, the full score was 10 points, and the proposed ResNet AI design decision-making model and design experts, respectively, scored the comprehensive satisfaction of the design scheme. During the experiment, the subject used the design decision accuracy curve as an indicator to analyze the experimental results. The design decision accuracy refers to the degree of fit between the scores of the proposed ResNet AI design decision model or the design expert and the score given by Party A. The higher the degree of fit, the higher the effectiveness of the tested model. In Figure 7, the abscissa of the design decision accuracy curve indicates the number of iterations, and the ordinate indicates the degree of fit.

5. Discussion

Figure 7(a) presents the change curve of the decision accuracy rate of Party A, the design experts, and the ResNet design decision model after using the three modeling image words of "future, stability, and dynamic" as the design semantic labels and inputting the renderings of such design schemes as images. With the increase in the number of iterations, the design decision accuracy of the ResNet AI design decision model gradually increased. When the number of iterations was about 160, the decision accuracy tended to be stable. The design decision accuracies of the three design schemes were, respectively, 0.83, 0.78, and 0.75, and the design decision accuracies of the design experts for the three schemes were, respectively, 0.78, 0.66, and 0.63.

Figure 7(b) shows the change curve of the decision-making accuracy rate of Party A, the design experts, and the ResNet design decision-making model after the three modeling image words of "technology, sensibility, and integrity" were used as design semantic labels. When the number of iterations was about 165, the accuracies of the design schemes obtained by the ResNet AI design decision

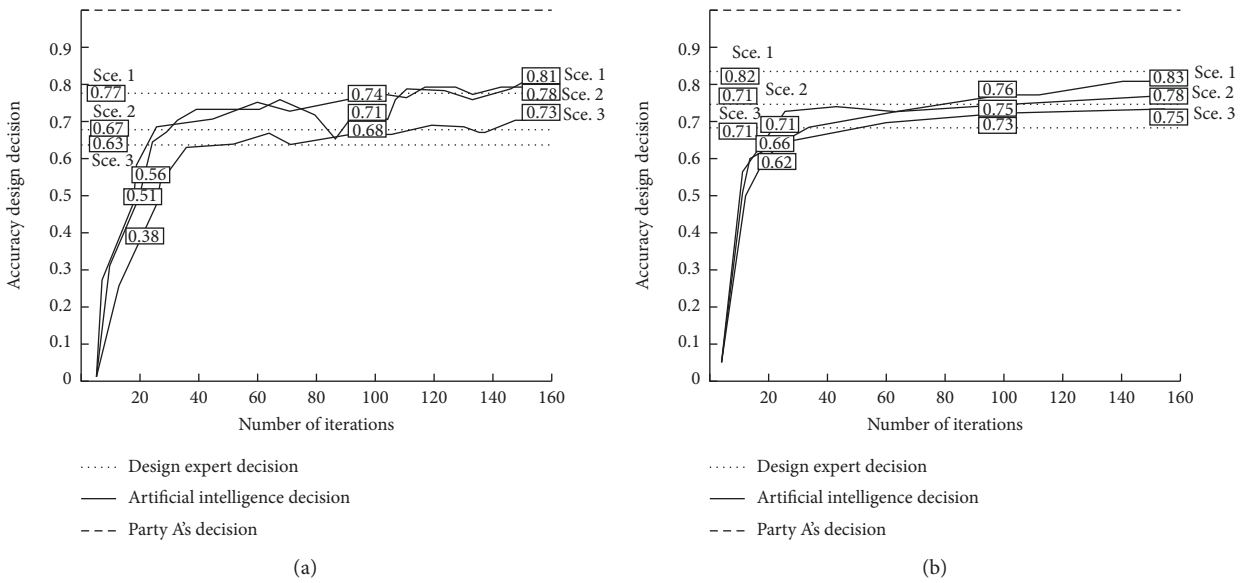

Figure 7: The comparison of the decision satisfaction of the (a) first and (b) second groups of modeling semantic vocabulary.

Table 2: The comparison of design evaluation satisfaction.

Method	Average satisfaction (%)	Average recall (%)
CNN	54.3 ± 3.4	44
DNN	57.8 ± 2.6	61
ResNet	77.6 ± 5.3	65

model were, respectively, 0.83, 0.78, and 0.77, while the design decision accuracies of the design experts for the three schemes were, respectively, 0.84, 0.76, and 0.71.

Thus, the satisfaction of the ResNet AI design decision was found to be higher than the average decision satisfaction of the design experts for both schemes.

To further verify the effectiveness of the proposed ResNet AI design decision-making model, a judgment was made based on the original data set, and the traditional CNN [33] and DNN [34] deep learning algorithms were, respectively, compared (Table 2). The average decision satisfaction and the average recall rate of the ResNet AI design decision model were found to be higher than those of the two other algorithms. The proposed ResNet AI design decision-making model performed stably in two rounds of design decision-making, and the design decision-making time was greatly shortened as compared with that of manual decision-making.

6. Conclusion

Building on the design scheme data set of product modeling semantics, this work was based on the concept of AI in combination with the characteristics of design decision-making. The data set was semantically annotated, and an AI evaluation decision model was constructed with the deep ResNet algorithm. The design decision problem was transformed into the semantic recognition problem of design scheme images, and the product design decision was realized via the AI design decision method. Finally, the effectiveness of the proposed method was verified by a case of motorcycle modeling design decision-making. The analysis of the experimental results revealed that the proposed ResNet AI design decision-making model exhibited higher decision-making satisfaction and decision-making efficiency than traditional manual design decision-making and the CNN and DNN algorithms.

Future research will focus on the following aspects. (1) Deep residual networks have good learning performance, but in the field of design decision-making, a smaller amount of data will lead to less effective training effects. While the crawler method was used to obtain graphic data in this study, there was a large amount of irrelevant data, which increased the data preprocessing and screening time. The acquisition and preprocessing process and methods of design data will be further studied in future research. (2) A general model for product design decision-making will be constructed based on a multi-level ResNet, the general method of ResNet-based product design decision-making will be investigated, and further experimental analysis will be conducted for other types of product design.

Data Availability

The data used to support the findings of this study are available from the corresponding author upon request.

Conflicts of Interest

The authors declare that there are no conflicts of interest regarding the publication of this paper.

Acknowledgments

This research was supported by the Natural Science Basic Research Program of Shaanxi (Program No. 2020JQ-607).

References

[1] Y. H. Wang, S. H. Yu, N. Ma et al., "Prediction of product design decision Making: an investigation of eye movements and EEG features," *Advanced Engineering Informatics*, vol. 45, no. 10, Article ID 101095, 2020.

[2] J. Li, M. Nazir Jan, and M. Faisal, "Big data, scientific programming, and its role in internet of industrial things: a decision support system," *Scientific Programming*, vol. 2020, 7 pages, Article ID 8850096, 2020.

[3] D. Braha and O. Maimon, "The design process: properties, paradigms, and structure," *IEEE Transactions on Systems, Man, and Cybernetics - Part A: Systems and Humans*, vol. 27, no. 2, pp. 146–166, 1997.

[4] C. L. Zhang, "A decision-based process model for conceptual design," *Journal of Computer-aided Design & Computer Graphics*, vol. 2, no. 5, pp. 136–140, 1993.

[5] M. Press and R. Cooper, *The Design Experience: The Role of Design and Designer in the Twenty-First century*, Ashgate, Chalgrove, UK, 2017.

[6] C. J. Lin, C. C. Chang, and Y. H. Lee, "Evaluating camouflage design using eye movement data," *Applied Ergonomics*, vol. 45, no. 3, pp. 714–723, 2014.

[7] F. Guo, Y. Ding, T. B. Wang, W. Liu, and H. Jin, "Applying event related potentials to evaluate user preferences toward smartphone form design," *International Journal of Industrial Ergonomics*, vol. 54, pp. 57–64, C, 2016.

[8] B. B. Tang, G. Guo, K. Wang, and L. Lin, "User experience evaluation and selection of automobile industry design with eye movement and electroencephalogram," *Computer Integrated Manufacturing Systems*, vol. 21, no. 6, pp. 1449–1459, 2015.

[9] S. W. Hsiao, C. F. Hsu, and Y. T. Lee, "An online affordance evaluation model for product design," *Design Studies*, vol. 33, no. 2, pp. 126–159, 2012.

[10] G. N. Zhu, J. Hu, J. Qi, C. C. Gu, and Y. H. Peng, "An integrated AHP and VIKOR for design concept evaluation based on rough number," *Advanced Engineering Informatics*, vol. 29, no. 3, pp. 408–418, 2015.

[11] M. D. Shieh and Y. E. Yeh, "Developing a design support system for the exterior form of running shoes using partial least squares and neural networks," *Computers & Industrial Engineering*, vol. 65, no. 4, pp. 704–718, 2013.

[12] D. Weimer, B. Scholz-Reiter, and M. Shpitalni, "Design of deep convolutional neural network architectures for automated feature extraction in industrial inspection," *CIRP Annals*, vol. 65, no. 1, pp. 417–420, 2016.

[13] F. Tao, J. Cheng, Q. Qi, M. Zhang, H. Zhang, and F. Sui, "Digital twin-driven product design, manufacturing and service with big data," *International Journal of Advanced Manufacturing Technology*, vol. 94, no. 9-12, pp. 3563–3576, 2018.

[14] Y. R. Jiao and Q. X. Qu, "A proposal for Kansei knowledge extraction method based on natural language processing technology and online product reviews," *Computers in Industry*, vol. 108, pp. 1–11, 2019.

[15] W. M. Wang, Z. Li, Z. G. Tian, J. W. Wang, and M. N. Cheng, "Extracting and summarizing affective features and responses from online product descriptions and reviews: a Kansei text mining approach," *Engineering Applications of Artificial Intelligence*, vol. 73, pp. 149–162, 2018.

[16] L. Deng and D. Yu, "Deep learning: methods and applications," *Foundations and Trends in Signal Processing*, vol. 7, no. 3-4, pp. 197–387, 2014.

[17] J. W. Chen, H. J. Yang, J. J. Cui, and J. S. Zhang, "Concept semantics driven computer aided product innovation design," *Journal of Computational Methods in Science and Engineering*, vol. 16, no. 3, pp. 575–590, 2016.

[18] R. Marshall, S. Cook, V. Mitchell et al., "Design and evaluation: end users, user datasets and personas," *Applied Ergonomics*, vol. 46, no. S1, pp. 311–317, 2015.

[19] Z. X. Wang, L. Lin, S. S. Zhong et al., "Case-based reasoning technology in knowledge management," *Computer Integra ted Manufacturing Systems*, vol. 9, no. 7, pp. 551–554, 2003.

[20] K. Dorst and N. Cross, "Creativity in the design process: Co-evolution of problem solution," *Design Studies*, vol. 22, no. 5, pp. 425–437, 2001.

[21] K. Fukushima, "Neocognitron: a self-organizing neural network model for a Mechanism of pattern recognition unaffected by shift in position," *Biological Cybernetics*, vol. 36, no. 4, pp. 193–202, 1980.

[22] C. I. Kim, M. Kim, S. Jung, and E. Hwang, "Simplified fréchet distance for generative adversarial nets," *Sensors*, vol. 20, no. 6, p. 1548, 2020.

[23] K. He, X. Zhang, S. Ren, and J. Sun, "Deep residual learning for image recognition," in *Proceedings of the computer vision and pattern recognition*, pp. 770–778, IEEE, Washington, D. C., USA, June 1997.

[24] J. P. Mccormack, J. Cagan, and C. M. Vogel, "Speaking the Buick language: capturing, understanding, and exploring brand identity with-shape grammars," *Design Studies*, vol. 25, no. 1, pp. 1–29, 2004.

[25] Y. S. Mu, X. D. Liu, L. D. Wang, and J. Zhou, "A parallel fuzzy rule-base based decision tree in the framework of map-reduce," *Pattern Recognition*, vol. 103, Article ID 107326, 2020.

[26] W. Li, W. Sun, Y. Zhao, Z. Yuan, and Y. Liu, "Deep image compression with residual learning," *Applied Sciences*, vol. 10, no. 11, p. 4023, 2020.

[27] G. Zhong, W. Jiao, W. Gao, and K. Huang, "Automatic design of deep networks with neural blocks," *Cognitive Computation*, vol. 12, no. 1, pp. 1–12, 2019.

[28] H. R. Sharifi, H. H. S. Javadi, A. Moeini, and M. Hosseinzadeh, "Residual design of sink localization algorithms for wireless sensor networks," *Journal of High Speed Networks*, vol. 25, no. 1, pp. 87–99, 2019.

[29] M. Abadi, "TensorFlow: learning functions at scale," *ACM Sigplan Notices*, vol. 51, no. 9, p. 1, 2016.

[30] H. Xiao, *Modeling Analysis of Truck Crane Based on Perceptual Image*, Hunan University, Changsha, China, 2012.

[31] S. Ioffe and C. Szegedy, "Batch normalization: accelerating deep network training by reducing internal covariate shift," *Proceeding of Machine Learning Research*, vol. 37, pp. 448–456, 2015.

[32] F. Wang, J. Cheng, W. Liu, and H. Liu, "Additive margin softmax for face verification," *IEEE Signal Processing Letters*, vol. 25, no. 7, pp. 926–930, 2018.

[33] Y. Wei, Y. Zhao, C. Lu et al., "Cross-modal retrieval with CNN visual features: a new baseline," *IEEE Transactions on Cybernetics*, vol. 47, no. 2, pp. 449–460, 2017.

[34] S. Feng, H. Y. Zhou, and H. B. Dong, "Using deep neural network with small dataset to predict material defects," *Materials & Design*, vol. 162, pp. 300–310, 2019.

Hindawi
Scientific Programming
Volume 2022, Article ID 7928659, 6 pages
https://doi.org/10.1155/2022/7928659

Research Article

English Translation Recognition Model Based on Optimized GLR Algorithm

Zuo Guangming

Huaiying Institute of Technology, Huian, Jiangsu 223000, China

Correspondence should be addressed to Zuo Guangming; zuoguangming@hyit.edu.cn

Received 7 April 2022; Revised 24 April 2022; Accepted 23 May 2022; Published 15 June 2022

Academic Editor: Jie Liu

In the current era of information technology, people's requirements for English translation are gradually increasing, and the need for a computer to understand and translate English language is becoming more urgent. In order to accurately identify phrases, this paper proposes an English translation recognition model based on optimized GLR algorithm, which can improve the accuracy of recognition by locating phrases in the text.

1. Introduction

Translatology is an important theoretical basis of language translation in China. English translation activity class under the background of artificial intelligence can provide an important boost to the development of translation studies. To ensure great achievements in Chinese English translation, artificial intelligence translation technology should be improved. In the past, it was mainly through the training of a large number of topics to let students explore the rules of translation and thus accumulate translation experience. Traditional translation tools are mostly paper dictionaries. Now, in the context of artificial intelligence, artificial intelligence translation technology can be upgraded to make it fit the concept of translation teaching to ensure that English translation can be changed with the help of new artificial intelligence translation technology.

With the rapid development of economy, the internet industry is developing rapidly, and the status of English translation in world trade is gradually improving. Machine translation technology can overcome many problems in human translation and reduce the economic consumption and time consumption of human translation [1–3]. In the current era of information technology, people's requirements for English translation are gradually increasing, and the need for a computer to understand and translate English language is becoming more urgent [4–8]. The English translation ability of the computer directly affects the translation result, however, there will be some grammatical errors in the translation result, which will cause problems in the translation result and affect the final decision of English translation. Therefore, in the past studies, many experts have proposed automatic recognition methods for machine English translation errors, thus minimizing the errors in English translation [9, 10].

With the continuous development of global economic integration and the deepening of world trade, the contacts between countries are also constantly deepening, and the frequency of personnel exchanges between countries also increases accordingly. Language is a unique function of human beings and the main means of human communication. Because of the different language environment in each country, language barriers greatly hinder the communication between different countries. Translation robots are born to break down language barriers and enhance communication between countries. The translation robot is mainly composed of speech input and output system, language processing system, and language translation software. Through the combination of multiple software and hardware, it forms a translation platform that can understand multiple languages. The translation robot stores a large amount of language information inside and has intelligent

functions, such as automatic learning, analysis, and memory, which can help humans translate various languages and simplify the communication process between people from different countries. Nowadays, English is the most frequently used language in the world, and English translation robot has the most application scenarios and a wider range of applications. With the continuous upgrading and development of English translation robots, although they can effectively translate a variety of languages into English, translation errors are easy to occur because of the inflexible translation content, which affects people's communication. How to automatically detect the translation errors of English translation robots is one of the most urgent problems in the field of translation robots.

Because of the current machine translation results, there are certain problems. After using the server to compare the full text, the grammar and rules of each language can be obtained. It can be found that the machine translation has low accuracy and low efficiency. Therefore, we should use a more intelligent piece of technology for machine translation [11–15]. In the actual testing process of machine translation products, such as Baidu and Google translation software, the quality of translation results is quite different from that of actual professional manual translation. The current machine translation technology cannot meet the requirements, and the market urgently needs a high-performance [16, 17]. Because of the development of artificial intelligence, many researchers have sought to help with translation work through computer-aided translation (CAT). The central idea of CAT is that the translation results are usually taken as auxiliary reference, and the user usually judges the quality of the translation and then makes a choice. In addition, through the use of corpus, the vocabulary of all industries can be sorted out, more in line with the actual needs of users. The correct use of frequently translated words can greatly reduce the amount of repeated translation work and greatly improve the accuracy of translation [18–20].

For an English translation robot, translation accuracy is the main evaluation index of robot application performance. Because of the influence of internal storage information and external environment, the frequency of translation errors is high, which is not conducive to the development and application of translation robots. According to the existing research results, the existing translation error detection system cannot detect translation errors effectively because of the defects of hardware and software. Zhang et al. used the neural machine translation method to predict the Chinese and English translation results and completed the identification of translation errors in the process of prediction. Huang Dengxian compares phrase words and phrase corpus to analyze part-of-speech and syntax. The author further obtains the English syntactic structure that needs to be translated, and the errors are gradually transmitted and accumulated, which eventually leads to the disadvantage of low translation accuracy. Then, the author designs vocabulary semantics based on HowNet similarity and the logarithmic linear model, saves the corresponding bilingual corpus in the form of Chinese-English dependency tree to string, provides structured processing of language dependencies, ensures the corresponding relationship between Chinese and English, and calculates the operation input of HowNet that needs to translate sentences with the same example. The semantic similarity of words in the source language of the library further improves the accuracy of translation, and the translation results have high accuracy [21].

Through the summary of the above literature, it is found that intelligent phrase recognition is an important step of speech recognition, and its principle is to realize automatic translation and combination by analyzing its part of speech and syntax, and output the results [22–24]. In the field of machine translation, intelligent phrase recognition is the key technology that can satisfy the selection of translation samples and the accurate alignment of parallel corpus. The technology of intelligent phrase recognition can effectively reduce grammatical ambiguity. The focus and difficulty of current English translation is structural ambiguity. Based on the GLR model in machine translation, this paper analyzes the structural ambiguity in some phrases through the syntactic function of the model, so as to facilitate the understanding of the entire semantics, solve the problems existing in the current English translation, and improve the efficiency and accuracy of the entire translation.

2. GLR Algorithm

2.1. Traditional GLR Algorithm. GLR algorithm is an extended LR analysis algorithm. The introduction of graph stack and analysis forest can effectively solve the ambiguity problem that an LR algorithm cannot handle, and its analysis speed is fast, which has great advantages in simple syntactic analysis.

In this paper, the GLR algorithm is used to identify and analyze the phrases in each fragment. The GLR algorithm is based on an extended context-free grammar, which is a five-element formula $G = (V_T, V_N, V_F, P, S)$, where V_T is a nonempty finite terminal symbol set, V_N is a nonempty finite nonterminal symbol set, and the intersection of V_T and V_N is empty. V_F is a constraint function set, which is a nonempty finite set that can be reduced by production only when the conditions are satisfied. P is the generation formula set, and $P \longrightarrow \langle D, T, M \rangle$, $D \in (V_T \cup V_N)+$, D is the right-hand symbol string of the production. $T \in V_T \cup V_N$, T is the central symbol of the production, $M \in V_F$, V_F detects the part-of-speech and semantic features of T. When the symbol string at the top of the stack can be reduced to P, specify its central symbol as T. S is the starting symbol set, $S \in V_N$.

The steps of GLR algorithm analysis are as follows:

(1) Initialization. State O is pushed onto the stack. The analysis pointer points to the input symbol to be analyzed, and the termination flag is cleared.

(2) Symbol mapping. If there is no end flag, the current input symbol is mapped to the analysis table terminator using a mapping function.

(3) Check the ACTION table to determine the operation that will be performed next.

① If it is moved up, the current state and current symbol will be pushed, and the analysis pointer will be moved down.
② If it is a statute, The constraint function checks whether the conditions are met. If the conditions are met, the center word pointer points to the corresponding center word. If not, the end mark is marked.
③ If it is terminated, it refers to the pointer to the analysis table terminator "error" the current input character is remapped to the analysis table terminator to continue analysis, and then set the end flag.
④ If it is accepted, the recognizable phrase completes the analysis, pops up the syntax tree at the top of the symbol stack, and returns.
⑤ If it is an error, it refers to the "error" for the terminator of the analysis table, which belongs to the analysis failure, restores the initial state, and returns.

(4) Continue to execute the next action in sequence until the end of the analysis.

2.2. Improved GLR Algorithm. In general, the GLR algorithm is still unable to meet the existing accuracy because of its high probability of coincidence in the results. In this paper, the classical GLR algorithm is improved, and the phrase center is proposed to analyze the phrase structure. The improved GLR algorithm realizes the likelihood calculation of the prefixes and postfixes of phrases by means of quaternization, as shown in formula (1).

$$G_E = (V_N, V_T, S, \alpha). \tag{1}$$

In formula (1), V_N represents the cyclic symbol cluster, $V_N \neq \varnothing$. V_T represents the termination symbol cluster. $V_T \neq \varnothing$, and the elements in V_T and V_N do not overlap. S represents the start symbol cluster, which is an element in V_N. α represents phrase action clusters.

Assuming that P is any action in α and P exists in V_N, formula (2) can be obtained by derivation.

$$P \longrightarrow \{\theta, c, x, \delta\}. \tag{2}$$

In (2), θ represents the right side of the action, C represents the center point, x represents the constraint value, and δ represents the marking mode. θ and C are located in both V_T and V_N, and δ can be located in V_T or V_N.

3. English Intelligent Recognition Algorithm

3.1. Create Phrase Corpus. Corpus is mainly used to store phrases, which can accurately mark the parts of speech in English, further standardize the function of phrases, and make machine translation more accurate.

There are more than 700,000 words in the corpus of the intelligent recognition model constructed in this paper, which can meet the actual demand. In this paper, we distinguish English and Chinese phrase corpora by distinguishing the tenses of phrase corpora. The marking process is divided into layers, data, and processing, and the processing adopts the man-machine active communication mode to carry out the operation of English translation.

3.2. Phrase Corpus Part-of-Speech Recognition. The dependency relationship of phrases is analyzed using syntax, and the establishment of syntax tree is realized. The part-of-speech recognition of phrases is a key step in the intelligent recognition algorithm of machine translation, which can deal with the grammatical ambiguity of a large number of sentences, phrases, and words. Each sentence is divided into several words into English sentences, and the processed words are aligned to form phrases. Meanwhile, the parts of speech of the words are marked out by judging the context of the sentence. Finally, the syntactic tree of sentences is formed by analyzing the dependency of phrases. Through this method, the timeliness and accuracy of machine translation can be improved, and the processing capacity of phrase corpus can be significantly increased. GLR is a commonly used algorithm in part-of-speech recognition, which is mainly used to judge the contextual relationship of phrases. Its core theory is based on the dynamic recognition of forms and unconditional transfer statements.

In traditional GLR, the execution of each step is carried out through operation shift instruction and reduction instruction. In this process, the beginning and end of each operation are carried out according to specific standards. In the process of translation, if grammatical ambiguity is detected, it is necessary to use the geometric structure linear table of syntactic analysis to call up the analytic linear table, expand and identify the content of the phrase, select the optimal content, and transfer it to different recognition channels for recognition.

3.3. Correction Process of Phrase Intelligent Recognition Algorithm. In current machine translation algorithms, the matching results of segmented phrases and phrase corpora are often regarded as the final machine translation results, which lack the analysis of the context in which the phrases are located, and excessively rely on the part of speech analysis of phrase corpora, resulting in inaccurate final translation results. Therefore, this paper further considers to correct the results of part-of-speech analysis. In the process of part-of-speech analysis and correction for the improved GLR algorithm, in view of the error points in the part-of-speech recognition results of phrases using analytic linear tables, the correction process is carried out by checking the tagged content in the corpus, as shown in Figure 1.

However, the reduction expresses that the previous constraints have no effect or that there is a problem in the loop process, and it is necessary to clarify the syntactic function to identify the constraints again. The advance indicates that there is no structural ambiguity in the ongoing syntactic function recognition, and the phrase part-of-speech recognition result is accurate. At this time, the

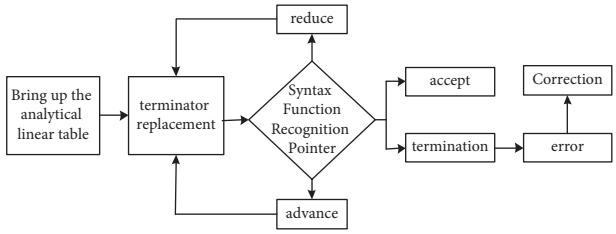

Figure 1: Calibration flow chart of intelligent recognition algorithm.

acceptance pointer should be selected for use. The receive pointer and the advance pointer usually appear together. If this condition is not met in the process and only a certain pointer appears, it means that there is an error in the loop or an error in the algorithm. Then, the analytical linear table needs to be called up again, and the part-of-speech recognition results that have been agreed by default before are withdrawn.

During the operation of the improved GLR algorithm, the type of pointer should be identified before the termination is replaced. If it is a protocol pointer, the constraint conditions of pointer should be detected in the phrase corpus. If it does not, it goes directly to the termination pointer.

4. English Translation Intelligent Recognition Model

The functions of the intelligent recognition model for English translation are designed. The received voice signal is obtained through the data acquisition device, and then the English signal is input to the processing system. The data signal is processed, the results are output in the display, and the user can view the automatic identification results of English translation through the display or the client.

4.1. English Signal Processing. Detailed design is required after model design, and English signals are collected and processed in a planned way. However, because of the interference factors of speech signals, the collected speech signals should be processed to improve accuracy. Figure 2 shows the processing process of English signals.

The digital filter is used for signal weighting processing, and the stress detection system is improved. Firstly, F1 is used to represent the first formant of vowel spectrum characteristics, and F2 is the second formant. Using the classifier to output confidence, the vowel intonation is obtained, and the best speech signal is selected. The calculation formula of weighting signal $Y(n)$ is as follows:

$$y(n) = T[x(n)] = ax(n) + b. \tag{3}$$

To make the analysis result of speech signal more accurate, the speech signal is divided into T frames.

$$z(n) = \frac{1}{t} y(n). \tag{4}$$

To clearly display the speech effect, select the rectangular window $W(n)$.

$$W(n) = \omega(n) \times z(n). \tag{5}$$

4.2. Extract Feature Parameters. To further improve the operation efficiency of the system and reduce the data interference unrelated to the voice signal, it is necessary to unify the relevant information data to find the parameter characteristics and then realize the subsequent calculation. Figure 3 shows the structure of extracted feature parameters.

The continuous spectrum of aperiodic continuous time signal is calculated by Fourier transform, however, the discrete sampling value of continuous signal is obtained in the actual control system. Hence, the signal spectrum is calculated by discrete sampling value. A finite length discrete speech signal is improved to obtain the following formula:

$$X[K] = \sum_{n=0}^{N-1} x[n] e^{-j2\pi/Nnk}, \quad k = 0, 1, 2, \ldots, N. \tag{6}$$

Convert a discrete speech sequence to a Mel frequency scale.

$$\mathrm{Mel}(f) = 2579 lg\left(1 + \frac{f}{700}\right). \tag{7}$$

Through DTC calculation of the output filtering, the characteristic parameter P of the speech signal $W(n)$ is obtained.

$$P = \overline{Z}_{n=1}^{N} F(l) w(n) \cos(\pi n(M + 0.5)). \tag{8}$$

After the spectrum of a speech signal is generated, it is processed by weighting, windowing, and framing. Each short-time analysis window can get spectrum information through fast Fourier transform. Then, use the Mel filter to get an MFCC two-dimensional graph.

Using the above method, related speech signal parameters are extracted from rhythm, speed, pitch, and intonation.

5. Experiment Analysis

In this paper, three machine translators were used to translate 50 phrases and 50 network random sentences. English-Chinese translation professionals also translated the above sentences. Graders scored the results of machine translation by comparing the results of machine translation.

As can be seen from Figure 4, the machine translation results of the proposed algorithm are optimal compared with other algorithms in terms of recognition accuracy, speed, and updating ability. As can be seen from Figure 5, the improved GLR algorithm in this paper has the highest score, while the statistical algorithm has the lowest score.

The comparison experiment in this paper also adopts the experiment on actual translation cases, and the sentence "Xi 'an Price Bureau on beef noodle Price Limit" is selected for

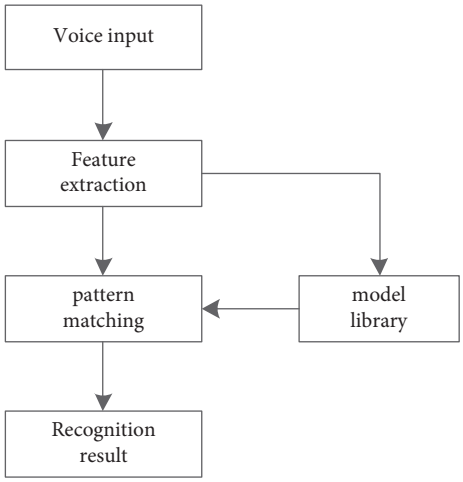

Figure 2: Processing of English signals.

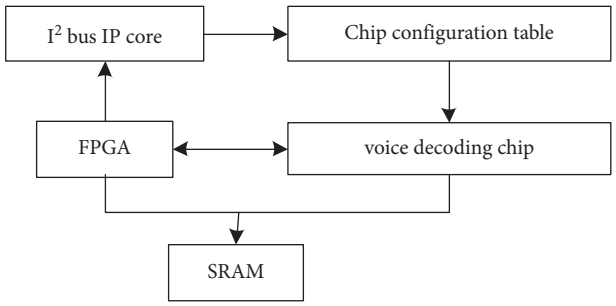

Figure 3: Feature parameter extraction map.

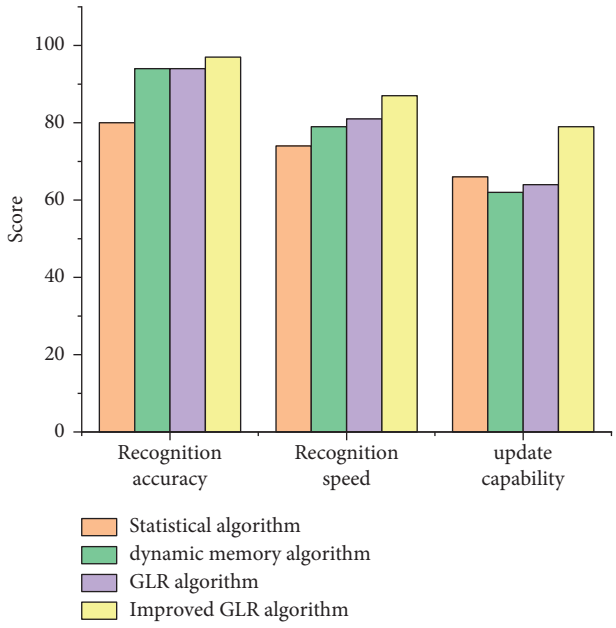

Figure 4: Evaluation results of four algorithms.

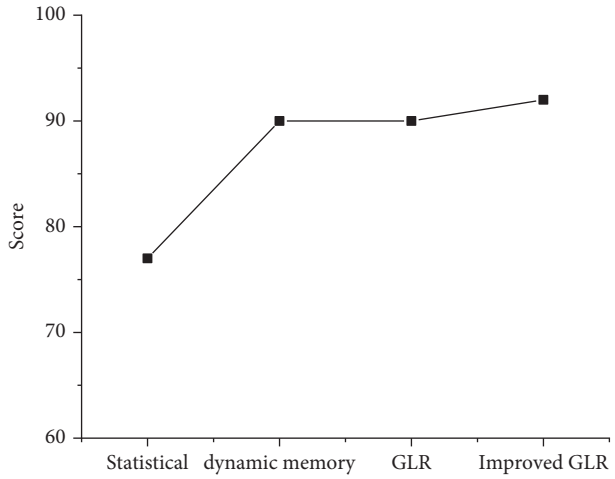

Figure 5: Comparison of scores of four algorithms in comprehensive test.

Table 1: Comparison of translation example results.

Translation method	Translate content
Improved GLR algorithm	Xi'an price bureau gives the explanations of beef noodles reduce: only because of the excessive price raises.
Human translation	Xi'an price bureau gives the explanations of price control on beef noodles: it is only because the raises have been too large.

translation. The experimental comparison results of machine translation and human translation based on statistical algorithm, dynamic memory algorithm, and improved GLR algorithm are shown in Table 1.

As can be seen from Table 1, compared with other algorithms, the algorithm in this paper is more accurate, and the recognition accuracy reaches more than 95%, reaching the same level as human translation, indicating the efficiency and feasibility of the improved GLR algorithm in machine translation.

6. Conclusion

With the rapid development of economy, the internet industry is developing rapidly, and the status of English translation in world trade is gradually improving. Machine translation technology can overcome many problems in human translation and reduce the economic consumption and time consumption of human translation. In the current era of information technology, people's requirements for English translation are gradually increasing, and the need for a computer to understand and translate English language is becoming more urgent. Computer's English translation ability has a direct impact on the application effect of translation results. In this paper, using the generalized maximum likelihood ratio detection algorithm based on improved machine translation, set the phrase corpus using

this algorithm, the library's size to 740,000 English words, and by constructing the phrase structure through the central phrase and calibrating the structural ambiguity according to the syntactic function, the content of recognition can be obtained, and the actual position range of phrases in translation can be determined, so as to solve the problems existing in current English translation and improve the accuracy and efficiency of recognition.

Data Availability

The dataset can be accessed upon request.

Conflicts of Interest

The authors declare that they have no conflicts of interest.

References

[1] J. L. Yu, X. Ma, and Z. Qu, "English translation model based on intelligent recognition and deep learning," *Wireless Communications and Mobile Computing*, vol. 2022, Article ID 3079775, 9 pages, 2022.

[2] Y. Chen and S. H. Ahmed, "Business English translation model based on BP neural network optimized by genetic algorithm," *Computational Intelligence and Neuroscience*, vol. 2021, Article ID 2837584, 10 pages, 2021.

[3] Z. Li, "The construction of the turning classroom of business English translation teaching in higher vocational education under the Internet + environment," *Frontiers in Educational Research*, vol. 2, no. 5, 2019.

[4] Y. Ruan and N. Jan, "Design of intelligent recognition English translation model based on deep learning," *Journal of Mathematics*, vol. 2022, Article ID 5029770, 14 pages, 2022.

[5] F. Fang, "The construction of college English translation teaching mode in the information technology environment," *International Journal of Social Sciences in Universities*, vol. 3, no. 3, 2020.

[6] P. Zhou, "Comparative study of traditional teaching method and ISAS teaching method in business English translation teaching in colleges and universities," *Frontiers in Educational Research*, vol. 2, no. 3, 2019.

[7] X. Wang, "Translation correction of English phrases based on optimized GLR algorithm," *Journal of Intelligent Systems*, vol. 30, no. 1, pp. 868–880, 2021.

[8] M. Z. Sheriff, M. N. Karim, H. N. Nounou, and M. N. Nounou, "Process monitoring using PCA-based GLR methods: a comparative study," *Journal of Computational Science*, vol. 27, pp. 227–246, 2018.

[9] Y. Guo, D. Zhou, J. Cao, R. Nie, X. Ruan, and Y. Liu, "Gated residual neural networks with self-normalization for translation initiation site recognition," *Knowledge-Based Systems*, vol. 237, 2022.

[10] C. Rajesh Kumar, J. Bansal, and P. Bansal, "Machine translation model for effective translation of Hindi poetries into English," *Journal of Experimental & Theoretical Artificial Intelligence*, vol. 34, no. 1, 2022.

[11] T. Tian, S. Chai, T. Jin, and H. Huang, "A French-to-English machine translation model using transformer network," *Procedia Computer Science*, vol. 199, 2022.

[12] L. Fei and J. Su, "The construction of machine translation model and its application in English grammar error detection," *Security and Communication Networks*, vol. 2021, Article ID 2731914, 11 pages, 2021.

[13] Y. Zhang and X. Ning, "A study on the intelligent translation model for English incorporating neural network migration learning," *Wireless Communications and Mobile Computing*, vol. 2021, pp. 1–10, Article ID 1244389, 2021.

[14] L. Wang, "Retraction Note to: u," *Arabian Journal of Geosciences*, vol. 14, no. 22, p. 2430, 2021.

[15] Ke Sun, T. Qian, C. Xu, and M. Zhong, "Context-aware seq2seq translation model for sequential recommendation," *Information Sciences*, vol. 581, 2021.

[16] L. H. Baniata, I. K. E. Ampomah, and S. Park, "A transformer-based neural machine translation model for Arabic dialects that utilizes subword units," *Sensors*, vol. 21, no. 19, p. 6509, 2021.

[17] T. Yang, S. Zhao, He Chen, and T. Liu, "A neural machine translation model based on sequence to dependency," *Journal of Physics: Conference Series*, vol. 2030, no. 1, 2021.

[18] J. Wu, B. Yang, and L. Tian, "Cross language relation extraction method based on attention of bidirectional translation model," *Journal of Research in Science and Engineering*, vol. 3, no. 7, 2021.

[19] X. Li and H. Xing, "English machine translation model based on artificial intelligence," *Journal of Physics: Conference Series*, vol. 1982, no. 1, 2021.

[20] H. Zheng, "Research on computer intelligent proofreading system of improved English phrase translation model," *Journal of Physics: Conference Series*, vol. 1871, no. 1, 2021.

[21] N. S. Khan, A. Abid, and K. Abid, "A novel natural language processing (NLP)–Based machine translation model for English to Pakistan sign language translation," *Cognitive Computation*, vol. 12, 2020.

[22] Y. Xia, "Machine translation; report summarizes machine translation study findings from chongqing three gorges university research on statistical machine translation model based on deep neural network," *Computers, Networks & Communications*, vol. 102, 2020.

[23] J. Su, J. Zeng, D. Xiong, Y. Liu, M. Wang, and J. Xie, "A hierarchy-to-sequence attentional neural machine translation model," *IEEE/ACM Transactions on Audio, Speech and Language Processing (TASLP)*, vol. 26, no. 3, 2018.

[24] J. Su, Z. Wang, Q. Wu, J. Yao, F. Long, and H. Zhang, "A ttriggered translation model for statistical machine translation soochow University,Automation department, xiamen university. A topic-triggered translation model for statistical machine translation," *Chinese Journal of Electronics*, vol. 26, no. 1, pp. 65–72, 2017.

Hindawi
Scientific Programming
Volume 2022, Article ID 2445343, 9 pages
https://doi.org/10.1155/2022/2445343

Research Article

Design and Optimization of Hotel Management Information System Based on Artificial Intelligence

Wenzhe Zhou[1] **and Zilu Liu**[2]

[1]*Sanya Vocational and Technical College, Sanya, Hainan 572000, China*
[2]*UCSI University, Kuala Lumpur 50100, Malaysia*

Correspondence should be addressed to Wenzhe Zhou; 1001955411@ucsiuniversity.edu.my

Received 25 April 2022; Accepted 18 May 2022; Published 14 June 2022

Academic Editor: Lianhui Li

With the improvement of people's living standards, the traditional hotel management model has been unable to meet the needs of customers. The traditional hotel management model also has the defects of low efficiency. The hotel management model is also gradually developing towards the direction of intelligence. The combination of artificial intelligence technology and hotel management can not only improve the operation efficiency of the hotel but also solve the operation cost of the hotel. For customers, artificial intelligence technology can bring smarter and more comfortable accommodation conditions to customers. This study uses the convolutional neural network (CNN) and long short-term memory (LSTM) technology in artificial intelligence technology to conduct related research on the in-store mode, entertainment mode, sleep mode, and out-of-store mode in hotel management. CNN is used to extract the spatial features of hotel management, and LSTM is used to extract the temporal features of hotel management. The research results show that CNN and LSTM technology can help hotel management achieve intelligent management and optimization. CNN and LSTM techniques can better predict related factors in-store entry mode, entertainment mode, and sleep mode. For the correlated predictions of these four modes, the maximum prediction error is only 2.81%. The linear correlation coefficient also reached above 0.96. The relevant parameters of artificial intelligence technology are also suitable for the optimization and design of hotel information systems.

1. Introduction

With the rapid development of computer performance, information systems have been widely used in hotel management. Compared with traditional manual methods, information systems can have better efficiency in hotel management. In today's society, people begin to pursue a higher level of quality of life [1, 2]. Whether it is in the process of business trip or tourism, they not only need the level of accommodation, but they are also constantly pursuing a higher level of hotel service. This puts forward higher requirements for the management level of the hotel. Hotel management is not only limited to the management of the hotel front desk, but it also needs to achieve a higher level of management of the hotel rooms. The management of the hotel front desk needs to achieve higher efficiency and more accurate management, which will save many manpower and material resources of the hotel front desk [3]. At the same time, efficient hotel front desk management will save more time for the occupants, and it will also provide more convenience for the occupants. The provision of hotel management level will provide occupants with a more comfortable and warmer accommodation environment, and it will also provide more convenience for hotel managers [4, 5]. With the wide application of intelligence in various fields, the intelligent management of hotels is also a popular direction. The intelligent management of hotels will not only improve the efficiency and service level of hotel front desk management but also bring certain convenience to the intelligent management of guest rooms [6, 7]. The intelligent management of guest rooms will bring more convenience, comfort, and safety to the occupants, and it will also save human and material resources for hotel operators. The intelligent development of the hotel needs to have a solution

suitable for the hotel style. It cannot ignore the feelings of the occupants just to achieve intelligence. The intelligent development of hotel management needs to make the occupants feel more technological elements, and it cannot bring more troubles to the occupants.

Artificial intelligence technology is the product of the rapid development of computer computing power and the improvement of hardware technology [8]. Artificial intelligence technology has been applied in many people's lives, and it can liberate more labor. It can also replace people to perform more dangerous and complex tasks, which has brought great convenience to people's lives [9, 10]. The core of artificial intelligence technology being able to perform these tasks is that it can process these complex data very well. For hotel management, in order to realize the intelligence of hotel management, artificial intelligence is required to process the relevant data of hotel management [11]. The advantage of artificial intelligence technology is that it can better handle nonlinear and high-dimensional data. It uses nonlinear functions to find correlations in complex data. Artificial intelligence technology mainly includes three algorithms: supervised learning, unsupervised learning, and reinforcement learning, which are the three most common learning algorithms. Among these three algorithms, supervised learning is a more common method, whether in the field of image recognition or speech recognition. Artificial intelligence technology includes CNN and LSTM algorithms, which are relatively common feature extraction methods in the field of artificial intelligence. The convolutional neural network (CNN) method can better extract the spatial features of the data [12], and it has been widely used in the fields of transportation and medical care. Long short-term memory (LSTM) recurrent neural network can better process data related to temporal features [13], and it has been widely used in speech recognition and other fields. Reinforcement learning is an algorithm with a relatively large correlation with the environment, and it is mainly used in research objects with strong environmental interference [14]. For the intelligence of hotel management, it mainly involves the spatial characteristics of data and the temporal characteristics of data.

The combination of artificial intelligence technology and hotel management is an important direction for the intelligent development of hotel management. Artificial intelligence technology can optimize the management plan of the hotel management front desk, and it can also intelligently optimize the management of guest rooms. In the process of hotel's intelligent management, these data mainly involve spatial and temporal characteristics. CNN and LSTM methods are used to study the intelligent management of hotels. The combination of artificial intelligence technology and hotel management can reduce the operating cost of hotel management, and it can also improve the operational level of hotel management. The traditional manual management mode has a large error rate. At the same time, intelligent hotel management will also meet the personalized accommodation consumption needs of the occupants, which will also improve the hotel's satisfaction rate and occupancy rate. The intelligent management of the hotel can realize the intelligent management of check-in mode, entertainment mode, sleep mode, and check-out mode. This will not only save the hotel operator's time and human resources but also provide greater convenience to the occupants. The CNN method is used to extract the features of in-store patterns and out-of-store patterns for hotel management. The LSTM method is mainly used to extract the temporal and spatial features of entertainment patterns and sleep patterns of hotel management.

This study mainly uses CNN and LSTM algorithms to predict and study the check-in mode, entertainment mode, sleep mode, and check-out mode of hotel management. The CNN method is mainly used to map the relationship between the needs of the occupants and these four modes, and the LSTM method is mainly used to study the temporal feature analysis of hotel intelligent management. This study will be introduced from five aspects: the first section introduces the necessity of the intelligent development of hotel management and the background of artificial intelligence technology. The related research status of hotel management is analyzed in the second section. The third section mainly analyzes and introduces the system design of intelligent hotel management and the principles of CNN and LSTM algorithms. Section 4 analyzes the accuracy and feasibility of CNN and LSTM algorithms in predicting hotel management check-in patterns, entertainment patterns, check-out patterns, and sleep patterns. In Section 4, the predicted linear correlation coefficient, average error, and error hotspot distribution map of hotel rooms are used to analyze the feasibility of CNN and LSTM methods in predicting hotel management. Section 5 summarizes the research.

2. Related Work

With the continuous development of business travel and tourism boom, the hotel is a fast-growing industry. The intelligent development of hotels is also one of the research hotspots, and many researchers have done a lot of research on hotel management. Li [15] already believes that hotel management needs to meet the needs of market development in tourist cities, which is also an important part of market development. The innovative management and the provision of management level of coastal resort hotel are beneficial to improve the core competitiveness of the hotel. This study takes the management of coastal hotels as the research object, and it uses the SWOT method to analyze the relationship between the coastal hotels and the tourism supply chain. In order to realize the stable management of coastal resort hotel and improve the popularity of tourists, he proposed a platform management and construction model for coastal resort hotel. Maté-Sánchez-Val and Teruel-Gutierrez [16] have noticed that hotel location has a greater relationship with company performance and the environmental strategy of hotel management. They proposed a theoretical model to analyze the important role of hotel location in hotel management. They collected data on hotels in Barcelona as a research object, and it used peer effects to analyze the impact of hotel location on hotel performance. The results show that the variable of hotel

location has an important relationship with the hotel's explanatory coefficient characteristics. This study has important implications for the location selection of hotel managers. Zhang et al. [17] have studied the online hotel management model, which mainly focuses on the effect of online reviews on hotel management. The dataset for this study was derived from online data on hotels in New York City on Expedia. It combines data such as online comments and online replies of online data into one dataset. It also fully mines these textual information using textual similarity. It also correlatively validates text mining functions using fixed-effects panel data. The results of the study show that consumers' online reviews do not significantly affect hotel bookings. However, highly similar responses significantly reduce hotel bookings. This research has a certain reference value for the evaluation of hotel management and online booking. Obonyo et al. [18] found that the development of ICT has provided more convenience and efficiency for hotel management. More hotels are starting to invest more in ICT to improve performance. However, this situation is weaker for economically developing countries. This study mainly analyzes the actual situation of ICT application in hotel management in Kenya. He collected and quantified data on 194 hotels. The research results show that ICT has a strong correlation with human resource management and operational management of hotels, which will also affect the application of ICT in hotel management. Wang and Zhang [19] believe that the hotel industry has become a pillar industry of the tertiary industry. The hotel industry has developed rapidly under the rapid economic development, but it is also facing huge pressure. Based on the background of rapid development of information, this research uses the fuzzy analytic hierarchy process FAHP method to study the user decision-making process in hotel management. Based on the common data of the hotel management system, he established the customer model of the hotel business data by using the method of data mining. This method improves the service level of the hotel and enhances the core competitiveness of the hotel enterprise. Brahami and Adjaine [20] believe that only after the company or enterprise really understands the motivation management of knowledge and customer relationship management (CRM), the competitiveness of the enterprise can be improved. He also found that the two indicators of KM and CRM are less used in hotel management. He collected sample data of large hotels in the Algeria region, and it discussed the application effect of KM and CRM in hotel performance management. The research results show that KM and CRM methods can effectively improve hotel performance, which in turn can enhance the competitiveness of hotel management. This has certain guiding significance for the further improvement of the hotel. With the development of intelligent technology and big data technology, there are also a few researchers here who have adopted artificial intelligence technology to study the related factors of hotel management and intelligent hotel management system. Ma [21] has found that the traditional concept of hotel management can no longer keep up with the pace of the times, and this method cannot provide timely training for hotel financial personnel, which leads to the relative lag of the hotel management model, which in turn affects the hotel benefit. To solve these problems, he designed an intelligent hotel financial management system. The results show that the support vector machine method and logistic regression method can reduce the risk of financial crisis in hotels. The response time of this intelligent hotel management system is significantly shortened, and the success rate has been improved to a certain extent. From the above literature review, it can be seen that artificial intelligence methods are rarely used in hotel management, and it rarely studies the entire process of hotel management systems. The current research is mainly to optimize and design the front desk management system of the hotel management system. This research uses CNN and LSTM methods to intelligently manage and study the hotel's in-store mode and out-of-store models.

3. The Application of Artificial Intelligence Methods in Hotel Management

3.1. The Importance of CNN and LSTM for Hotel Management. This research mainly uses CNN and LSTM algorithms to predict the in-store mode, entertainment mode, sleep mode, and out-of-store mode in the hotel management mode. The CNN algorithm can map the relationship between the relevant factors of the in-store management system and the needs of the occupants. This data information is often more complex, but there is a relatively large correlation between these data. Relying on hotel managers alone to find correlations in these data is more difficult. CNN can process these data well, and the CNN algorithm has strong advantages in processing these nonlinear data. The LSTM algorithm has obvious advantages in dealing with temporal features, which can deal with time-related temporal features in hotel management. For example, in the process of predicting the entertainment mode, it can automatically adjust the air conditioning system, video system, lighting system, etc. according to the change of time. Because these factors are not only strongly related to space, but also it had strongly related to time.

3.2. The Hotel Management Intelligent System and CNN Algorithm. This research will use the CNN and LSTM methods to realize the intelligent management mode of the hotel. At the same time, the in-store mode, entertainment mode, sleep mode, and out-of-store mode of hotel management will be unified as a whole for system design. These patterns are not a single pattern, because there are some correlations in the data between these patterns. Figure 1 shows the hotel's intelligent management system design scheme utilizing CNN and LSTM methods. First of all, it needs to collect more relevant data of the hotel's in-store mode, entertainment mode, sleep mode, and out-of-store mode as an obvious training set and test set. These data first go through the CNN algorithm, and the CNN algorithm will use the convolution layer, pooling layer, and activation function to extract the spatial features of hotel management. The LSTM will receive the output data from the CNN, which will be input to the network layers of the LSTM in the form of time

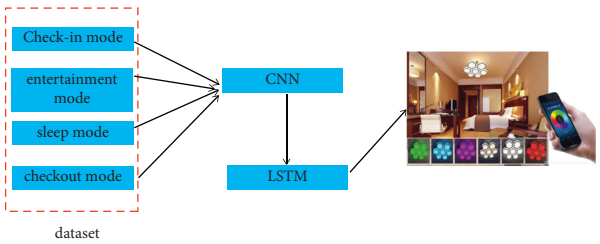

Figure 1: The design of hotel intelligent management system.

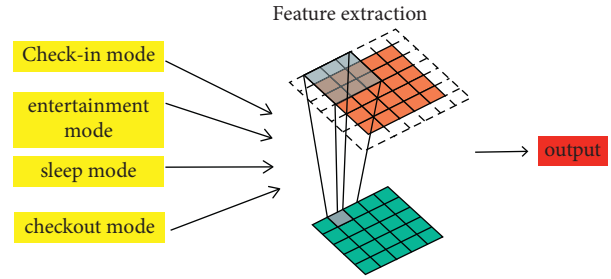

Figure 2: The workflow of CNN algorithm.

series. There is a backpropagation mechanism for these two networks. After the hotel management data are processed by the LSTM algorithm, it will become the control signal of the hotel room. It will automatically control the lighting system, air conditioning system, and influence system of hotel rooms. Once the model is trained, the optimal weights and biases are determined. In the actual application process, it can rely on these weights and biases to realize the prediction and analysis of the relevant data of the four modes of the hotel management information system. First, the hotel management data will be processed through data cleaning and data normalization methods. Then, these data will be processed into a matrix and input into the network layer of CNN.

CNN is a relatively common feature extraction neural network. Compared with the fully connected neural network, it has less parameters. Therefore, it allows more network layers, which guarantees the task of extracting features from hotel management system data. Figure 2 shows the workflow of CNN. A matrix operation is performed between each weight of the fully connected neural network. However, the weights of CNN will selectively perform matrix operations, which is the advantage of weight sharing. CNN is mainly composed of convolution layer, pooling layer, activation function, and fully connected layer. The convolutional layer will extract the features of hotel management data through parameters such as filter and stride. The pooling layer will further extract features by upsampling or downsampling. The parameters of the CNN will be trained and tested on the Tensorflow platform, and the weights and biases will be saved in the .h5 file. The learning rate chosen in this study is 0.001, which will speed up the training, but it will not easily get stuck in a local minimum.

CNN and fully connected neural network are similar computational methods, and it also has a backpropagation mechanism. The CNN dataset also contains actual numerical values, which is required by the backpropagation algorithm. Equation (1) shows how the backpropagation error is calculated. This study will calculate the error in the form of mean square error, which is also a commonly used error calculation method. Equation (2) is also a form of mean square error calculation, which is a form of the summation of equation 1:

$$E = \frac{1}{2}\left\|d - y^{L}\right\|_2^2, \tag{1}$$

$$E = \frac{1}{2}\left(d_{\text{out}} - O_{\text{real}}\right)^2 = \frac{1}{2}\sum_{\kappa=1}^{t}\left(d_{\kappa} - O_{\kappa}\right)^2. \tag{2}$$

Many hyperparameters will be involved in the iterative calculation process of CNN, and hyperparameters will also affect the accuracy and convergence of CNN iteration. There is a certain relationship between these hyperparameters of CNN. Equation (3) shows the calculation relationship of CNN hyperparameters. Equation (4) shows the computation process of the input layer of the CNN:

$$w' = \frac{(w + 2p - k)}{s} + 1, \tag{3}$$

$$V = conv2\left(W, X, ''\text{valid}''\right) + b. \tag{4}$$

This will involve many derivative operations during the CNN computation, either forward or backward. Equation (5) shows how the weight derivative is calculated:

$$\Delta\omega_{ji} = -\eta\frac{\partial E}{\partial\omega_{ji}}. \tag{5}$$

3.3. The Introduction to LSTM Algorithm. The entertainment mode and sleep mode in the hotel management mode have a strong time relationship with the lighting system, air conditioning system, and film and television system of the guest room. The advantage of the LSTM method is that it deals with time-dependent data. For the in-store mode and the out-of-store mode, these data also have a relatively strong time relationship. Therefore, this study chooses the LSTM algorithm to process these temporally correlated data. Figure 3 shows the computational process of the LSTM algorithm. It differs from CNN in that it can memorize historical information because of its obvious gate structure. This is also the reason why it can memorize historical state information. The data input form of LSTM is time series. In this study, it will accept the output data of CNN. CNN and LSTM algorithms are a continuous process. CNN first extracts the spatial features of hotel management, and LSTM extracts the temporal features of hotel management. The gate structure of LSTM algorithm mainly includes input gate, forget gate, and output gate structure. After the hotel management data are output in the output layer of the CNN, the data will be transformed by a reshape layer. These data will be transformed into labeled data by sliding windows and sliding steps. This is because LSTM is also a supervised learning algorithm.

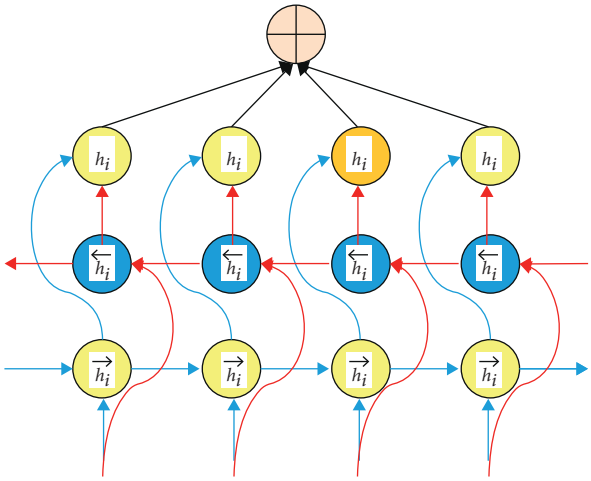

Figure 3: The workflow of LSTM algorithm.

The LSTM algorithm is inherited from the RNN algorithm. RNN is also an important algorithm for dealing with speech recognition. Equation (6) shows the basic principle of the LSTM method to memorize historical state information. The historical state information realizes the memory of historical state information by affecting the information of the current state. Both historical state information and current state information will be given a certain weight, which can realize the memory of historical information according to the weight. Equation (7) is the abstract structure of Equation 6. Equation 8 shows the temporal feature information that the LSTM structure needs to load. Through Equation 8, LSTM is given certain time information:

$$y(t) = f(X(t) \bullet W + y(t-1) \bullet V + b), \tag{6}$$

$$\tilde{c}(t) = f(W \bullet x(t) + V \bullet y(t-1)), \tag{7}$$

$$C(t) = C(t-1) + \tilde{C}(t). \tag{8}$$

The input gate can control the input amount of information, and it can control the input characteristics of historical state information and current state information. If all the historical state information and current state information are input into the network, it will not only cause too many parameters. It also causes poor feature extraction. Equations (9) and (10) show the calculation process of the input gate. It can selectively pass historical state information and current state information according to the size of the weight:

$$C(t) = C(t-1) + g_{\text{in}} \bullet \tilde{C}(t), \tag{9}$$

$$C(t) = C(t-1) + g_{\text{in}} \otimes \tilde{C}(t). \tag{10}$$

Equation (11) shows the calculation process of the LSTM forget gate. If the forget gates are all open, this will cause a lot of information to flow into the LSTM. The forgetting gate will assign a certain weight according to the importance of the feature, and the forgetting gate will selectively input some historical state information features according to the size of the weight:

$$C(t) = g_{\text{forget}} C(t-1) + g_{\text{in}} \otimes \tilde{C}(t). \tag{11}$$

Equation (11) shows how the output gate of the LSTM method is calculated. The output gate will output features related to the current state information. This requires a gate structure for effective control. It can not only ensure the output of effective historical information but also ensure that the information parameters will not be too large:

$$y(t) = g_{\text{out}} \otimes f(C(t)). \tag{12}$$

4. Result Analysis and Discussion

In this study, it mainly uses CNN and LSTM algorithms to analyze the intelligent management information system of in-store mode, entertainment mode, sleep mode, and out-of-store mode in hotel management. The data used in this study come from the operation data of 40 hotels in Beijing. It uses CNN and LSTM algorithms to study the accuracy and feasibility of these four hotel intelligent management modes. Figure 4 shows the linear correlation coefficients predicted by hotel management's in-store patterns. The linear correlation coefficient can compare the degree of agreement between the predicted value and the actual value of the intuitive response. The closer the linear correlation coefficient is to the linear function $y = x$, the more accurate it is for the predicted value. From Figure 4, it can be seen that the corresponding values of the in-store patterns of the 40 hotels have a high linear correlation, and all the linear correlation coefficients exceed 0.96. Moreover, the corresponding values of the in-store patterns of these 40 hotels are distributed on both sides of the $y = x$ function, and the predicted data of the in-store patterns of these 40 hotels are relatively close to the $y = x$ function. This further illustrates the high feasibility and accuracy of CNN and LSTM algorithms in predicting the in-store patterns of hotel management. Only a few data points deviate from the $y = x$ line, but the deviation is within the requirements of hotel management.

In the information system of hotel management, the entertainment system is a key part. The prediction accuracy of this part is directly related to the accuracy of CNN and LSTM. This is because the entertainment system varies greatly, and it has a greater relationship with time and the preferences of different people. Predictions for entertainment systems are more complex. Figure 5 shows the distribution of predicted and actual values of entertainment patterns managed by the hotel information system. In Figure 5, both A and B are representative of the entertainment mode group managed by the hotel. A represents the group of predicted values of entertainment pattern data. B represents the group of actual values of the entertainment mode data. The blue curve represents the predicted value of the entertainment mode, and the red curve represents the actual value of the entertainment mode. In general, the predicted value of hotel management is larger than the actual value of entertainment mode, which is mainly because the

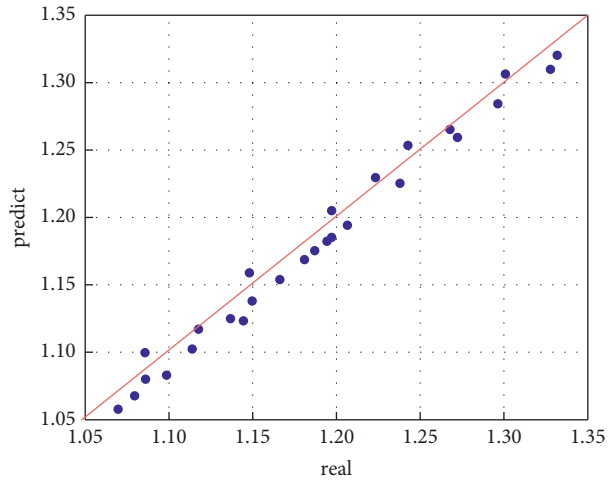

Figure 4: The linear correlation coefficient of in-store patterns of hotel management.

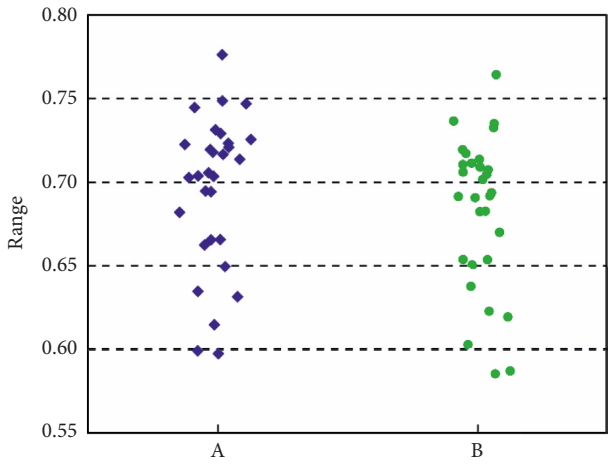

Figure 5: The predicted value distribution of entertainment patterns in hotel management.

predicted value of entertainment mode is in a relatively ideal environment. In general, the corresponding predicted value of the entertainment mode of hotel management has the same distribution as the actual value, and the numerical value is also well maintained. Between intervals 0.6 and 0.75, the predicted values of the hotel management entertainment mode have a good degree of agreement, and most of the corresponding values of the entertainment mode are also distributed in this interval. Only in the interval greater than 0.75 and less than 0.6, the prediction error of the data is large. Overall, CNN and LSTM methods can also better predict the corresponding values of entertainment patterns in hotel management.

Compared with the prediction of entertainment mode, the check-out mode of hotel management is easier to predict. The check-out model of hotel management has minor changes, and the check-out model of hotel management involves relatively few features. Figure 6 shows the distribution of the predicted and actual values of the hotel management system's check-out patterns. It can also be easily seen from Figure 6 that the check-out pattern of hotel management has relatively small fluctuations. CNN and LSTM algorithms also easily predict the corresponding data and characteristics of hotel management check-out patterns. Although the hotel values between 0 and 30 have large fluctuations, the CNN and LSTM methods can also better reflect the peak and trough values of the check-out pattern. The prediction error value for the hotel management check-out mode is completely acceptable to the hotel management. Larger errors mainly appear in the data of hotels in the range of 20 to 25. The CNN and LSTM methods only predict the numerical value of the data well, but it is poor in predicting the fluctuation trend between the data.

For hotel managers and occupants, sleep patterns are an important system. Its prediction error is mainly related to the air-conditioning system, curtain control system, and so on. The sleep system has more obvious time characteristics. Figure 7 reflects the change trend between the predicted value and the actual value of the sleep pattern of hotel management. The red curve represents the predicted data of sleep patterns, and the black part represents the actual data value of the hotel management. The green area is the error area between the two. In general, the data of sleep patterns have relatively large fluctuations, and they also have relatively large fluctuations over time. However, CNN and LSTM algorithms are better at predicting data related to sleep patterns in hotel management. It can also be seen from the green area in Figure 7 that the prediction error of the sleep mode is also relatively small. It has a relatively obvious cumulative error over time. The larger error mainly exists in the interval 18 to 30, which is also one of the defects of the LSTM algorithm. In order to improve the accuracy of data prediction of this part of the sleep pattern, it is necessary to increase the data sample size of this part of the region.

The prediction errors of entertainment mode and sleep mode are mainly related to the operation of electronic equipment in the guest room. It is a critical part that the impact system, air conditioning system, and lighting system in the guest room can be adjusted in real time according to the real-time needs of the occupants. To further demonstrate the prediction error of in-room device operation, Figure 8 shows the prediction error of indoor facilities in entertainment and sleep modes. The squares represent the hotel rooms. This study will illustrate the distribution error of each area of the hotel room in the form of an error heat map. In general, CNN and LSTM have small errors in predicting the operation of indoor equipment, and the prediction error distribution is relatively uniform. Larger prediction errors are mainly distributed in the edge regions of the room. This part of the area may correspond to the video system and air conditioning system. But all the errors meet the requirements of the hotel management information system. This further illustrates that the CNN and LSTM methods can better predict the entertainment and sleep patterns of hotel management. Figure 9 shows the average errors of CNN and LSTM under four modes for predicting hotel management information systems. The largest average prediction error is only 2.81%, and this part of the error comes from the hotel management's prediction of sleep patterns. The prediction

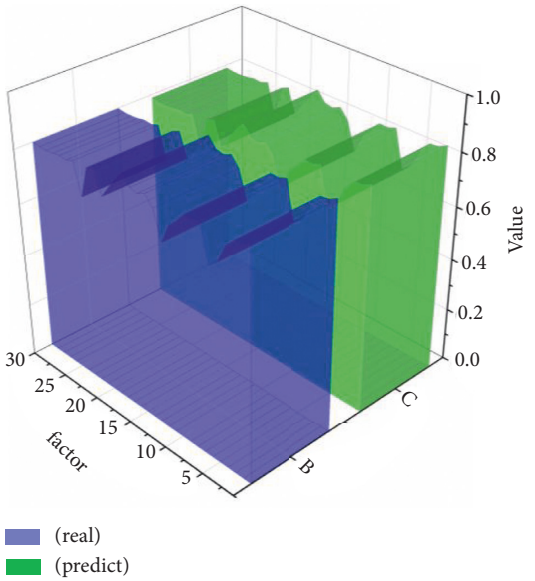

Figure 6: The predicted value distribution of check-out patterns for hotel management.

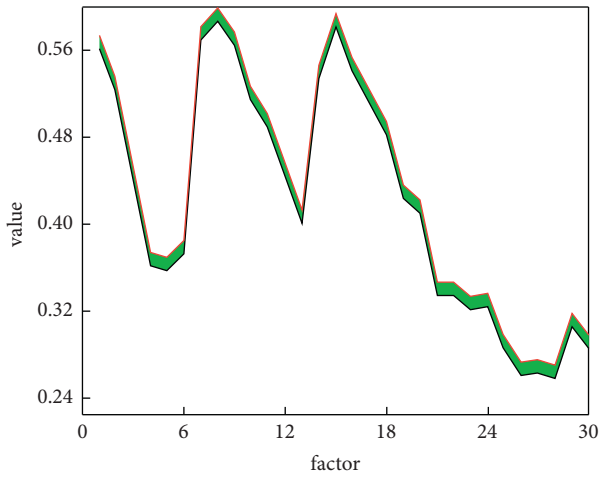

Figure 7: The distribution of predicted values for sleep patterns in hotel management.

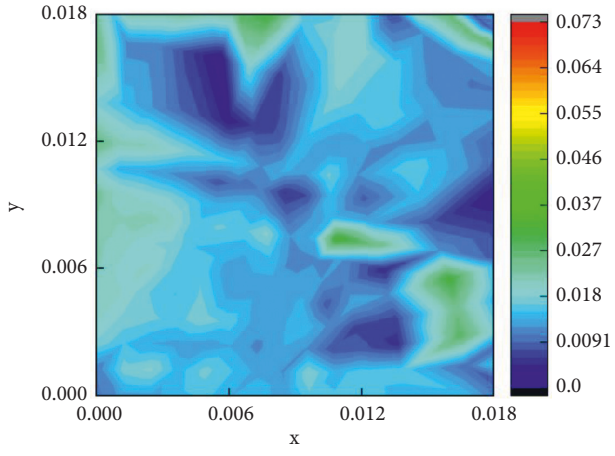

Figure 8: Prediction errors for indoor facilities in recreation mode.

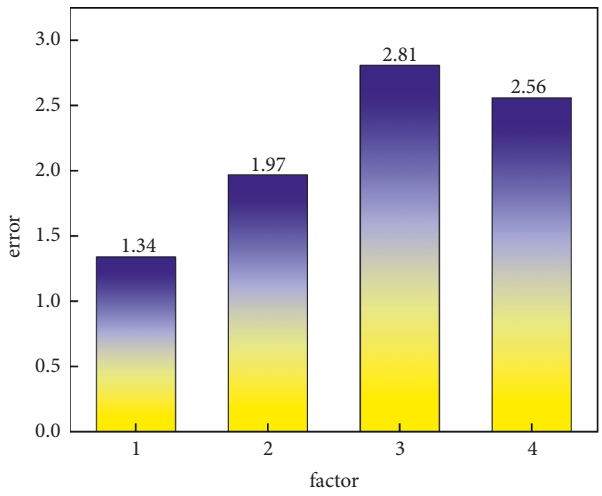

Figure 9: The average forecast error of four modes of hotel management.

errors of the in-store mode and the out-of-store mode are only 1.34% and 1.97%, respectively. This prediction error can not only satisfy the requirements of hotel managers, but it can also satisfy the requirements of lodging guests. In conclusion, the CNN and LSTM methods have certain feasibility and accuracy in realizing the intelligence of the hotel management information system.

5. Conclusions

The traditional manual hotel management model can no longer meet the needs of today's people's accommodation. Now, the flow of people in the hotel and the needs of the occupants have a relatively large change and a relatively large amount of information. This requires computer technology to assist hotel managers to manage. More and more hotels have begun to introduce computer information management system, but it can only assist hotel managers to realize the management of in-store mode and out-of-store mode. As for the individual requirements of the occupants, the current computer information management system cannot help the occupants to realize them very well.

This research uses CNN and LSTM methods in artificial intelligence technology to design a hotel information management system, which can realize intelligent management of in-store mode, entertainment mode, sleep mode, and out-of-store mode. It can not only improve the work efficiency of hotel managers, but it can also meet the individual needs of the occupants. In general, CNN and LSTM methods can better predict the four modes of hotel information management system. The largest prediction error is only 2.81%, and this part of the error comes from the prediction of the sleep pattern of the hotel information system. For the prediction of the in-store and out-of-store patterns of the hotel management system, the average error is only 1.34% and 1.97%. For the prediction of the entertainment mode and sleep mode of the hotel management system, the prediction error distribution of the operation of indoor equipment is relatively uniform, and most of the errors are distributed within 2%. This shows that CNN and LSTM methods have high credibility in realizing hotel management intelligence.

Data Availability

The dataset can be accessed upon request.

Conflicts of Interest

The authors declare that they have no conflicts of interest.

Acknowledgments

The authors thank Science Research Project of Colleges and Universities in Hainan Province in 2019 and Research on service quality internationalization level of star hotels in Hainan Province (no. hnky2019-108).

References

[1] R. van Ginneken, K. Koens, and J. Fricke, "Ownership perceptions in European hotel management agreements," *International Journal of Hospitality & Tourism Administration*, vol. 20, no. 4, pp. 449–467, 2019.

[2] F. Cheong and Y. H. Lee, "Developing an environmental management system for evaluating green casino hotels," *Sustainability*, vol. 13, no. 14, p. 7825, 2021.

[3] Y. J. Kim, W. G. Kim, H.-M. Choi, and K. Phetvaroon, "The effect of green human resource management on hotel employees' eco-friendly behavior and environmental performance," *International Journal of Hospitality Management*, vol. 76, no. 1, pp. 83–93, 2019.

[4] P. Longart, "Understanding hotel maintenance management," *Journal of Quality Assurance in Hospitality & Tourism*, vol. 21, no. 3, pp. 267–296, 2020.

[5] N. A. Awad and S. G. Saad, "The role of information technology and customer relationship management practices in Egyptian hotels- A descriptive study in s el sheikh hotels," *International Journal of Online Marketing*, vol. 9, no. 4, pp. 47–63, 2019.

[6] J.-S. Horng, C.-H. Liu, S.-F. Chou, and T.-Y. D.-C. Yu, "Marketing management in the hotel industry: a systematic literature review by using text mining," *Sustainability*, vol. 14, no. 4, p. 2344, 2022.

[7] Y. Jiang and J. Wen, "Effects of COVID-19 on hotel marketing and management: a perspective article," *International Journal of Contemporary Hospitality Management*, vol. 32, no. 8, pp. 2563–2573, 2020.

[8] R. G. Gaifutdinov, Z. L. Khisamova, and E. L. Sidorenko, "Theoretical and legal bases of artificial intelligence punishment system development," *Revista san gregorio*, vol. 41, no. 12, pp. 159–164, 2020.

[9] C. C. Liu, "Artificial intelligence interactive design system based on digital multimedia technology," *Advances in Multimedia*, vol. 4, no. 1, p. 4679066, 2022.

[10] N. Liu, P. Shapira, and X. Yue, "Tracking developments in artificial intelligence research: constructing and applying a new search strategy," *Scientometrics*, vol. 126, no. 4, pp. 3153–3192, 2021.

[11] X. Jing, P. Peng, and Z. Huang, "Analysis of multi-level capital market linkage driven by artificial intelligence and deep

learning methods," *Soft Computing*, vol. 24, no. 11, pp. 8011–8019, 2020.
[12] Y. Wang and F. Yang, "A fractional-order CNN hyperchaotic system for image encryption algorithm," *Physica Scripta*, vol. 96, no. 3, p. 035209, 2021.
[13] G. Li, X. Zhao, C. Fan, and X. F. Y. Fang, "Assessment of long short-term memory and its modifications for enhanced short-term building energy predictions," *Journal of Building Engineering*, vol. 43, no. 9, p. 103182, 2021.
[14] M. Li, X. Gu, C. Zeng, and Y. Feng, "Feasibility analysis and application of reinforcement learning algorithm based on dynamic parameter adjustment," *Algorithms*, vol. 13, no. 9, p. 239, 2020.
[15] Y. Li, "A study of the management innovation mode of coastal resort hotels," *Journal of Coastal Research*, vol. 107, no. sp1, pp. 206–209, 2020.
[16] M. Maté-Sánchez-Val and R. Teruel-Gutierrez, "Evaluating the effects of hotel location on the adoption of green management strategies and hotel performance," *Journal of Sustainable Tourism*, vol. 11, no. 21, pp. 1–24, 2021.
[17] Z. L. Zhang, H. Y. Li, F. Meng, and Y. Li, "The effect of management response similarity on online hotel booking," *International Journal of Contemporary Hospitality Management*, vol. 31, no. 7, pp. 2739–2758, 2019.
[18] G. O. Obonyo, D. O. Okeyo, and O. O. Kambona, "Effect of management practices on actual ICT application in Kenyan hotels: a PLS-SEM a," *International Journal of Hospitality & Tourism Administration*, vol. 19, no. 2, pp. 142–166, 2018.
[19] Q. Wang and B. Zhang, "Research and implementation of the customer-oriented modern hotel management system using fuzzy analytic hiererchical process (FAHP)," *Journal of Intelligent and Fuzzy Systems*, vol. 40, no. 4, pp. 8277–8285, 2021.
[20] M. Brahami and M. K. N. Adjaine, "The influences of knowledge management and customer relationship management to improve hotels performance," *Information Resources Management Journal*, vol. 33, no. 4, pp. 74–93, 2020.
[21] H. M. Ma, "Optimization of hotel financial management information system based on computational intelligence," *Wireless Communications and Mobile Computing*, vol. 4, no. 4, p. 8680306, 2021.

Hindawi
Scientific Programming
Volume 2022, Article ID 1610427, 7 pages
https://doi.org/10.1155/2022/1610427

Research Article

Application of Modern Urban Landscape Design Based on Machine Learning Model to Generate Plant Landscaping

Dan Liu

Jilin University of Architecture and Technology, Jilin, Changchun 130000, China

Correspondence should be addressed to Dan Liu; liudan@jluat.edu.cn

Received 22 April 2022; Revised 24 May 2022; Accepted 28 May 2022; Published 11 June 2022

Academic Editor: Lianhui Li

With the continuous improvement of the living standards of people, the requirements of people for the environment in which they are located are gradually increasing, which makes urban landscape design work more and more important. Plant landscaping is the core component of urban landscape design. By analyzing and discussing the application of plant landscaping in urban landscape design, the quality level of urban landscape design can be further improved, thereby promoting the sustainable development of urban construction. Machine learning makes it possible to realize the intelligent processing of data and make full use of the knowledge and value contained in the data. This paper explores the way of intelligent analysis and application based on machine learning in the field of landscape architecture. First, the *k*-means machine learning clustering method is used to determine the types of plant landscaping required by modern urban landscape design. Experiments show that our model can be well applied to design applications of modern urban landscapes.

1. Introduction

Machine learning is a way to realize artificial intelligence and a key technology for processing big data. Machine learning algorithms can automatically analyze one or several types of data to obtain rules, discover the mechanism of action, and use the rules to predict unknown data. At present, it has become possible to apply machine learning (including deep learning) to the fields of landscape architecture, urban planning, and architecture to solve related problems such as human settlements. Scikit-learn, an open-source machine learning library based on Python language, integrates mainstream core algorithms in the field of machine learning, including classification, regression, and clustering algorithms, and data preprocessing methods; TensorFlow, an open-source deep-learning library based on Python language, uses computational graph, and automatic differentiation and customization are used for numerical calculations. Because of the emergence and rapid growth of machine learning open source libraries, and the gradual improvement of a large number of core algorithms, machine learning as a tool has been widely used in various fields, and landscape architecture is also in the exploratory stage.

Plants are an important element in the construction of garden landscapes. Today, with the continuous emphasis on the construction of ecological civilization, people are more yearning for green space, so garden plant landscaping has received more attention and attention, and its dominant position in landscape garden design has become more and more obvious. At this stage, designers often use horizontal and vertical section drawings to analyze and deliberate plans, but relying only on artificial design limits the possibility of landscape design. Therefore, designers and industry-related personnel urgently need new technology to assist them to better complete the landscaping design of garden plants. With the development of science and technology, the application of machine learning to garden plant landscaping has become a breakthrough to solve the problem.

There are many classic machine learning algorithms that have application potential in landscape architecture design. According to the focus of solving the problem, it can be divided into algorithms with efficient data classification capabilities, such as naive Bayesian algorithm, support vector machine decision tree, regression tree, and random forest [1], which are mostly used for classification problems such as landscape land classification [2]; deep learning

Table 1: Variety of algorithms of machine learning technology.

Learning style	Algorithms type	Algorithms
Supervised learning	Regression	Linear regression, polynomial regression, ridge regression
	Classification	Logistic regression, support vector machine, decision tree, *k*-nearest neighbor, etc
Unsupervised learning	Clustering	*K*-means, means shift, fuzzy *c*-means
	Association rule learning	Apriori, frequent pattern growth
	Dimensional reduction	Principal component analysis, linear discriminant analysis

algorithms, such as convolutional neural networks, recurrent neural networks, and generative adversarial networks, have powerful image recognition capabilities [3–5] and are mostly used for rapid identification and information extraction of remote sensing images and street view images [6–10], in which algorithms such as generative adversarial networks also have powerful image generation capabilities [11], which are mostly used in generative design [12]; regression algorithms such as principal component analysis and logistic regression have the ability to automatically associate data and perform functions. The ability of fitting to mine the internal relationship behind the data is mostly used for correlation analysis, such as the research on the driving force of the development of landscape patterns [13–16]; tf-idf, word2vec, BERT, CRF, LSTM in the field of computer natural language processing. Such algorithms have the ability of text recognition and processing and can classify and extract sentiment and other topics from text data in a large number of networks.

In this work, the *k*-means algorithm is used for the first time to perform cluster analysis on the landscape principle design of the urban landscape. And the results of the model are tested by taking Hangzhou Hupao and Beijing Biyun Temple survey image clustering as examples. The results show that the model has a good performance in the application of modern urban landscape design for generating plant landscaping. In addition, this paper also analyzes the application principles of plant landscaping in the urban landscape and the application of plant landscaping in modern urban landscape design.

2. Theoretical Basis of Machine Learning and Principles of Plant Landscaping

2.1. Machine Learning. In the field of landscape architecture, traditional computer technology requires artificially designed computing rules, while machine learning technology has powerful rule learning ability and the ability to capture implicit rules. In landscape architecture work, it is necessary to analyze the site conditions, obtain the law of site changes, and then intervene and guide the site to develop in a specific future direction according to the means of planning and design. Therefore, machine learning has great potential in the field of landscape architecture.

From the perspective of machine learning technology, machine learning technology includes a variety of algorithms with different functions and focuses (Table 1). However, because the design goals of the algorithms in the computer field have less overlap with the landscape architecture design, they cannot directly serve the landscape architecture design, so they are used in the landscape architecture. There are not many algorithms with relatively mature applications. The common application method at present is usually to decompose the planning and design into multiple work steps and then design the corresponding algorithm according to the work target of each step.

2.2. K-Means Algorithm. In the *K*-means algorithm, *K* is the number of cluster centers, and Means is the mean. This algorithm clusters the regional data points through the iterative optimization of the mean and obtains the optimal clustering result. In this article, garden colors are divided into 7 colors. Below are the executor steps of the algorithm. (1) Set $K = 7$. Seven color location data are randomly selected as the initial cluster centers of the seven categories, and the Euclidean distance formula is used.

$$D = \sqrt{(x_i - x_0)^2 + (y_i - y_0)^2}, \tag{1}$$

where D is the distance; x_0 and y_0 is the latitude and longitude coordinates of the center point D; x_i and y_i, is the latitude and longitude coordinates of each noncenter point. Use this formula to calculate the distance from each noncluster center point to the cluster center point, and divide each noncluster center point to the nearest cluster center. (2) After the data are grouped by distance, the mean of the seven groups is calculated, respectively, and the mean of the seven groups is used as the new cluster center. (3) Iteratively calculate the distance from each noncenter point to the new center point using equation (1). (4) Iteratively calculate new cluster centers until each noncluster center data no longer move and the cluster centers no longer change.

2.3. Application Principles of Plant Landscaping in Urban Landscape

2.3.1. Ecological Principles. In the urban landscape design, the application of plant landscaping can not only create a beautiful visual environment, improve the city's ornamental value, but also improve the material environment. In plant landscaping, it is very important to strengthen the plasticity of plants and improve the ecological beauty of the surrounding environment. On the one hand, plants purify the surrounding environment very well by releasing oxygen and absorbing carbon dioxide. At the same time, there are functions such as reducing noise and adjusting the temperature. However, different types of plants have different

growth environments. Once the selected plant species is not suitable for the local ecology, it will have a great impact on its growth. On the other hand, if there is a phenomenon that the community violates the natural development law, there will be serious consequences. Therefore, it is very necessary to scientifically select plant species based on local environmental conditions.

2.3.2. Principles of Practicality. In the application of plant landscaping in urban landscape design, the principle of practicality should also be followed. The so-called principle of practicality means that in the actual process of plant landscape landscaping, some practical functions such as environmental protection should be fully considered. Harmful gases play a good role in purifying the air. If the above practical conditions cannot be met, some practical plants that can play a good role in noise reduction and dust prevention can also be selected as landscaping materials. Therefore, while beautifying the urban environment space, it can also effectively weaken the sense of tension and oppression brought about by the characteristics of urban industrialization, meet people's needs to be close to nature, reduce the urban heat island effect, and enable urban plant landscaping to achieve production and integration. The combination of ornamental and ornamental can give full play to the functional value of urban plant landscape in beautifying, ecological, and environmental protection.

2.3.3. The Selection of Plants Should Be Combined with the Characteristics of the City. In modern urban landscape design, the application of plant landscaping should not only repeat the application of a single plant, but should combine the characteristics of the local city and the actual situation of the landscape, and at the same time consider factors such as soil climate and environment. Therefore, designers need to consider the local plants with strong regionality and show the local characteristics through the planted plants, which can not only create a certain resource space for the local landscape but also allow the planted plants to better adapt to the environment, to further save plant landscaping.

2.3.4. Make Full Use of Ground Cover Plants. Among various types of plants, ground cover plants have their own unique features, such as luxuriant branches and leaves, and strong fecundity. At the same time, they have a very strong antipollution ability, and follow-up maintenance is also more convenient. Therefore, in various designs of the modern urban landscape, planting is almost indispensable, which can give people a harmonious and comfortable look and feel. From the overall look, it also makes the layering of the whole design more prominent, making people shine. The plants above can absorb light energy, and the plants below can loosen the soil surface, adjust the ground temperature, and make the growth environment of the trees above better. In addition, ground cover plants also play an important role in the garden landscape. For example, planting ground cover plants around flower beds and on both sides of the sidewalk can form a sharp color contrast with the flowers and effectively clarify the walking routes of tourists, thereby improving the ornamental value of the landscape and at the same time alleviating people's aesthetic fatigue.

3. Judging the Plant Landscaping Style of Modern Cities Based on Machine Learning Models

3.1. Model Establishment and Training. The data of this experiment are mainly images with latitude, longitude, and elevation information taken through the actual survey of mobile phones. Divided into two groups, one group came from Hangzhou Tiger Pao. The other group came from Biyun Temple in Beijing. The specific technical route is shown in Figure 1. First, the images are read in batches in the Python programming language, because the captured images are about 4 200 pixels 2 400 pixels in size, and color analysis does not require such high precision, so the image size is reduced by compressing the image to save analysis time. Then, set the number of color theme color clusters to 7, that is, obtain 7 theme colors for each image. Colors were classified using the K-means clustering algorithm.

The extraction of the theme color is shown in Figure 2. After extracting the theme color of all images, they are summarized in an array. In the aspect of data enhancement visualization, 2 forms are designed: (1) scatter point form to print the theme color, which can directly reflect the urban color impression. Through the extraction of the urban theme color, the color impression sensory presentation can be used to study the urban color, which can be aimed at different urban spaces and different research times, and to analyze the changes in color. (2) Try to project the subject color of the survey images of the two places into the three-dimensional space and observe the changes of the two sets of data in the three directions of red, green, and blue.

3.2. Model Results. In machine learning clustering, sklearn integrates many clustering algorithms and compares the effects of different clustering algorithms on different data types through the actual operation of the program. In addition to applying survey photos to analyze the urban color environment, you can also use recorded video, extract images at specified frames, and perform the same analysis. In the specific data analysis, the theme color of each image can also be placed on the coordinate points of its latitude and longitude, and the clustering algorithm can be used again to cluster the areas with similar color values in the space, so that the urban color characteristic areas can be classified. And the POI data reflecting urban functions, Weibo, WeChat, and other data reflecting urban social relations are combined and analyzed to find the internal mechanism of urban color space distribution characteristics.

The clustering results of the research images of Hangzhou Hupao and Beijing Biyun Temple, and the color impression after printing the theme color in scatter form are shown in Figure 3. Hupao's theme color is gray and dark (the color of the building), mixed with green and green vegetation and blue

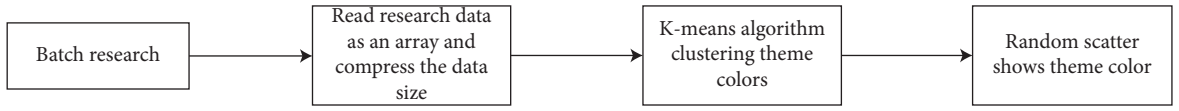

Figure 1: The technical route of using *K*-means clustering algorithm.

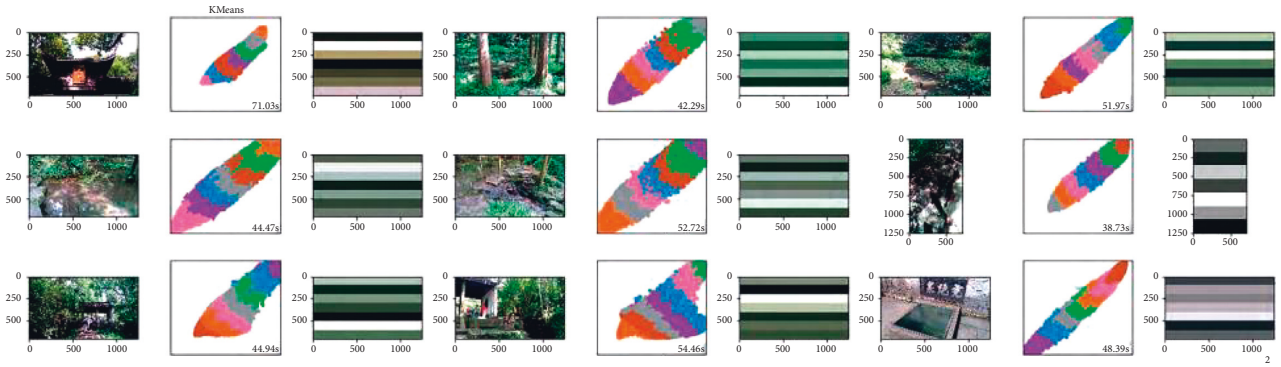

Figure 2: The extraction of the theme color.

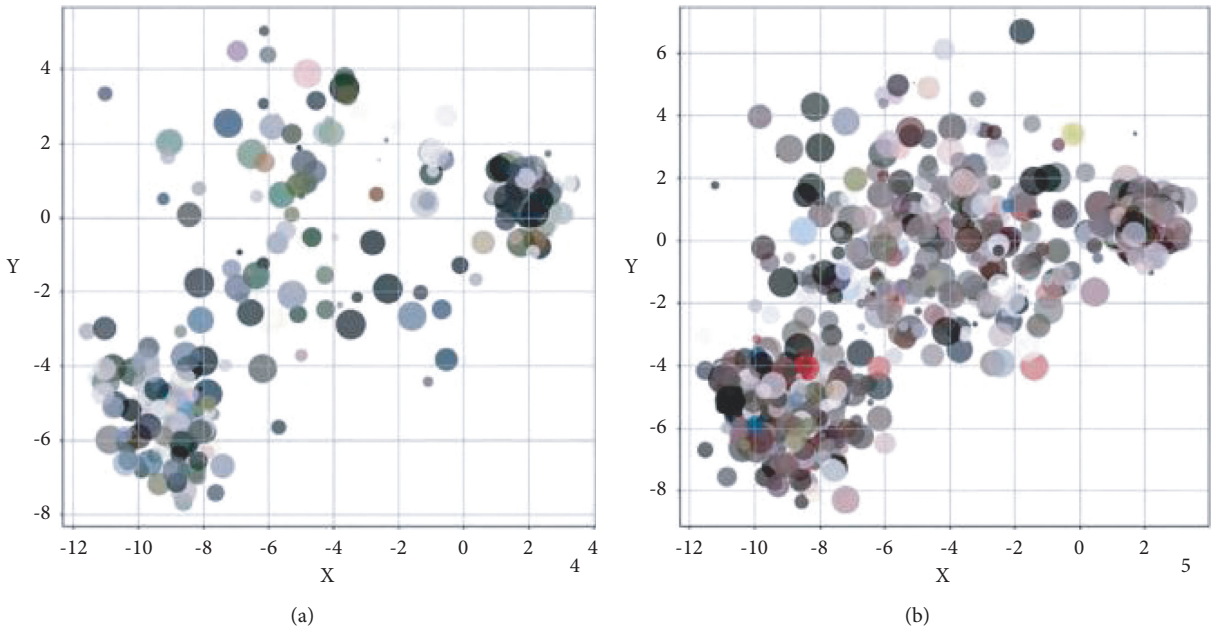

Figure 3: The clustering results of the research images of Hangzhou Hupao and Beijing Biyun Temple, and the color impression after printing the theme color in scatter form.

sky. Simple and elegant Biyun Temple because the building itself is mostly red, after interspersed with vegetation and the sky, the overall feeling is gorgeous and gorgeous. Through these data visualization methods, the urban color characteristics of the study area can be more intuitively reflected. If the number of research areas surges, automated batch processing can be achieved according to the established model, such as studying the color characteristics and distribution relationships of different areas of the city. Data containing color information (RGB) is projected into three-dimensional space. The changes in the red, green, and blue color components can be grasped by judging the distribution of the colors of the two regions in the three-dimensional space domain. The color tendency of Beijing Biyun Temple is higher in the red value, while the 3-component of Hangzhou Hupao color tends to be lower. In the analysis, the color can also be converted to HSV (hue, saturation, value) and projected into the three-dimensional space domain to analyze the relationship between hue, saturation, and lightness.

4. The Application of Plant Landscaping in Modern Urban Landscape Design

4.1. Tree Landscaping. In large garden scenic spots, all kinds of towering and lush trees will always bring people many different impressions. For example, the lush ginkgo, with its

proud standing posture, brings people a beautiful feeling. It has long been called the Gongsun tree. The planting of ginkgo in the garden landscape not only reflects the virtues of the predecessors planting trees and the later generations enjoying the shade in traditional Chinese culture but also implies people's yearning for a better life in the future. The willow tree is deeply loved by garden designers because of its gentle and graceful tree shape. In spring, it is praised for its willows that are drunk with spring smoke. In summer, it is called ten thousand hanging green silks. In the winter, the weak warbler with green silk strips presents the beauty of ancient charm in different seasons. Because of its tall and straight leaves and sparse branches, the king coconut tree is often used as a street tree to green roads. The curved branch shape of mountain peach, the arch branch shape of welcoming spring, the umbrella shape of acacia, and the clump shape of the Chinese rose can all bring people different visual enjoyment.

4.2. Make Plant Landscaping in Combination with Different Terrains. In the actual plant landscaping, it is necessary to combine the different spatial topography of the city, so as to effectively highlight the natural characteristics of landscaping. For example, some trees can be planted around the ridgeline, and some short shrubs can be planted in the position of the hillside ravine. Through this landscaping configuration, it can not only effectively demonstrate the tall and straight posture of the mountains but also make the entire urban environment more harmonious and increase the three-dimensional sense. On this basis, the characteristics of some buildings such as urban pavilions and pavilions can also be combined, and plants can be arranged on the top of the mountain to promote the two to set off each other and complement each other. When creating a waterside flower border landscape by the water, make a good choice of aquatic plants, the more common ones are reed bamboo, water lily, barracuda, and parasol. To ensure a good reflection effect, it is not advisable to plant too many plants underwater. On the banks of the embankment, some trees can be planted, and the trees are sparsely distributed to form a beautiful reflection in the water.

4.3. Follow the Aesthetic Principles of the Plants Themselves for Landscaping Design. First of all, in some areas such as the corners of buildings and roads in the city, it is necessary to weaken the sharp corners to reduce the visual rigidity. In landscaping, the combination of flat slope and arbor and irrigation can be used to plant some beautiful plants, such as cedar, sycamore, and pentagonal maple. If the selected seedlings are plants with high branch points, try planting multiple seedlings in the same tree pond. At the same time, carry out scientific planting, let them grow together into a large canopy, and effectively weaken the corners. On the other hand, it is also possible to make a reasonable blank of the landscape with the help of the blanking technique of traditional Chinese painting. For example, in a relatively empty square, if you add a few delicate trees to embellish it, it can give people an open and comfortable look. It fully embodies the principle of balanced aesthetics.

4.4. Maintaining the Stability of Native Plant Communities. Before introducing new plants, we must first ensure that the existing plant community is in a relatively stable state. Therefore, for the introduced new species, the relevant departments must do a good job in quarantine work and make a good estimate of their reproductive capacity, so as to avoid a large number of reproduction and spread after they are introduced into the urban landscape, which will cause damage to the balance of the local plant community and ecological structure very serious impact. Maintaining the stability of local plant communities can further ensure the visual effects and ecological benefits of urban plant landscaping. On the other hand, weeds should be cleaned regularly to prevent the problem of flooding due to their tenacity, and the affected areas should be restored and protected. At the same time, it is necessary to fully develop the nursery cultivation industry and market, so that plant landscaping can choose more plant varieties.

4.5. Shaping the Urban Landscape in Combination with Local Urban Culture. The culture of each city is different. Nowadays, people have begun to attach great importance to the inheritance and protection of urban culture, as well as the continuation of historical development. Therefore, in the urban landscape design, it is necessary to combine the local urban history and culture, excavate the connotation, present the cultural heritage of the city to the greatest extent, and give the city the driving force for continuous development. Therefore, in the modern urban landscape plant landscaping, it is necessary to combine urban culture, conform to the current development law of our country, and avoid destroying the surrounding ecological environment.

5. Conclusion and Future Prospects

Artificial intelligence technology based on machine learning is gradually applied to the analysis and evaluation of landscape architecture with its efficient data processing capabilities and implicit rule capture capabilities and has initially replaced some simple repetitive labor at this stage. Algorithmic generative design based on deep learning takes the creativity of artificial intelligence a step further. The cleaning and selection of data and the manual intervention of algorithms are the core bottlenecks at present.

The cleaning and selection of data are a technical challenge. Artificial intelligence is basically the exchange of artificial intelligence for intelligence, and it is supported by a large amount of basic data work (such as manual annotation). Problems such as noise and lack of data are frequent at this stage. In this context, designers appear as data analysts, and artificial intelligence methods aimed at replacing repetitive work have brought more planning and analysis and repetitive work. However, with the improvement of technology in the future, the emergence of more excellent algorithms and data sources will gradually solve the current

problems and allow designers to return to planning and design.

The manual intervention of the algorithm is a difficult problem in the application method, which directly affects the role of artificial intelligence and designers. This question is related to the question of how much artificial intelligence should be in the design. This also involves a series of questions such as whether the artificial intelligence analysis results are reliable, whether the output results are correct, and how to define correctness? As mentioned above in the planning case of Rome railway station and the case of plant configuration, the architectural form needs to conform to the form of the building base and at the same time be similar to the surrounding architectural texture. Under the constraints of these two goals, deep learning can balance the relationship between the two, aiming at approximating the base shape and searching the building database for matching, comparing, and iterative cycles. The optimal solution can be obtained only by approximating the base shape infinitely. In the plant configuration project, plants need to meet conditions that are easy to quantitatively explain such as sunshine, climate, and configuration mode. However, under this condition, attributes such as plant species, plant height, and crown width can only be constrained within an interval, so the output results are still very large. Therefore, whether the output result is correct is related to whether the target is abstract. From the computer's point of view, it is easy for computers to calculate quantitative problems with clear standard goals and regard the goals as correct. In the face of abstract problems, it is difficult for the computer to judge whether it is correct, but for designers, this is also an open problem. To this end, different scholars have made preliminary explorations, and for example, in the case of plant configuration, the abstract plant configuration theory is quantitatively explained and constrained. In the planning case of the urban central axis, the evaluation system is used to constrain the abstract scheme selection problem; Tang Jingxian's streetscape evaluation research combines the subjective evaluation system with the objective analysis results of streetscape information to realize the artificial correction of machine learning perception evaluation research. The above methods are currently tried by designers. Efforts to revise AI-generated results are also responses to abstractions in design.

To sum up, at present, plant landscaping has been widely used, which greatly improves the urban environment, allows people to live in a comfortable and environmentally friendly living environment, and further promotes the development of urban construction in China. At this stage, plant landscaping has become an indispensable part of urban landscape design. In the process of designing urban landscapes, designers must combine with more ecological elements and use different plant characteristics to make plant landscaping. The scenery is more suitable for city life.

In the future, with the training and learning of a large amount of data, the creativity of artificial intelligence will gradually increase. Landscape architecture is a subject highly related to human subjective aesthetics. In order to avoid over-reliance on artificial intelligence in planning and design, it leads to the patterning and standardization of output results. Future research should distinguish between the repetitive and simple labor that should be performed by artificial intelligence in the planning and design process and the part that requires the designer's experience and judgment, and let artificial intelligence technology assist the design instead of leading the design.

Data Availability

The raw data supporting the conclusions of this article will be made available by the authors, without undue reservation.

Conflicts of Interest

The authors declare that they have no conflicts of interest regarding this work.

References

[1] Q. He, N. Li, and W. J. Luo, "Overview of machine learning algorithms under big data," *Pattern Recognition and Artificial Intelligence*, vol. 27, no. 4, pp. 327–336, 2014.

[2] J. Zhao and Y. Cao, "Overview of artificial intelligence methods in landscape architecture research," *Chinese Landscape Architecture*, vol. 36, no. 5, p. 82 87, 2020.

[3] Y. H. Zhang and G. X. Zhao, "Classification methods of land use/cover based on remote sensing technologies," *Journal of China Agricultural Resources and Regional Planning*, vol. 23, no. 3, p. 21 25, 2002.

[4] J. Wu, M. S. Liu, and W. T. Li, "Research advances in remote sensing information extracting technology for natural reserves," *World Forestry Research*, vol. 26, no. 1, p. 53 58, 2013.

[5] R. H. Liu, S. C. Liang, and H. Y. Zhao, "Progress of Chinese coastal wetland based on remote sensing," *Remote Sensing Technology and Application*, vol. 32, no. 6, pp. 998–1011, 2017.

[6] C. Zhang, Y. H. Lü, and W. J. Yun, "Analysis on research progress of remote sensing monitoring of land consolidation," *Journal of Agricultural Machinery*, vol. 50, no. 1, p. 1 22, 2019.

[7] E. Thiffault, K. Webster, B. Lafleur, S. Wilson, and N. Mansuy, "Biophysical indicators based on spatial hierarchy for informing land reclamation: the case of the Lower Athabasca River (Alberta, Canada)," *Ecological Indicators*, vol. 72, pp. 173–184, 2017.

[8] K. Wang, C. Gou, Y. Duan, Y. Lin, X. Zheng, and F.-Y. Wang, "Generative adversarial networks: introduction and outlook," *IEEE/CAA Journal of Automatica Sinica*, vol. 4, no. 4, pp. 588–598, 2017.

[9] T. Che, Y. J. Luo, and C. Li, "Spatiotemporal change and its driving factors of built-up land sprawl in Yangzhou City," *Chinese Journal of Ecology*, vol. 38, no. 6, pp. 1872–1880, 2019.

[10] H. C. [Sun and Z. X. Zhang, "Change of landscape pattern vulnerability in the songhua river basin in jilin province and its driving forces," *Arid Zone Research*, vol. 36, no. 4, p. 1005 1014, 2019.

[11] T. Che and Y. J. Luo, "Quantifying effects of socioeconomic development on urban landscape fragmentation," *Journal of Nanjing Forestry University (Natural Sciences Edition)*, vol. 44, no. 1, p. 154 162, 2020.

[12] J. H. Wu, S. F. Fang, and B. J. Liu, "Landscape pattern evolution of wetland and it s drving mechanism in Wuyuer-Shuangyang River Basin," *Chinese Journal of Ecology*, vol. 40, no. 13, p. 4279 4290, 2020.

[13] L. Y. Chen and X. Xu, "A study on tourists perceptual characteristics of suzhou gardens: based on the multidimensional analysis of the travel notes," *Tourism and Hospitality Prospects*, vol. 1, no. 5, p. 39 54, 2017.
[14] V. Kumar and J. K. Nayak, "Destination personality: scale development and validation," *Journal of Hospitality & Tourism Research*, vol. 42, no. 1, pp. 3–25, 2014.
[15] C. F. Chen and S. Phou, "A closer look at destination: image, personality, relationship and loyalty," *Tourism Management*, vol. 36, no. 3, pp. 269–278, 2013.
[16] M. Hultman, D. Skarmeas, P. Oghazi, and H. M. Beheshti, "Achieving tourist loyalty through destination personality, satisfaction, and identification," *Journal of Business Research*, vol. 68, no. 11, pp. 2227–2231, 2015.

Hindawi
Scientific Programming
Volume 2022, Article ID 1701474, 11 pages
https://doi.org/10.1155/2022/1701474

Research Article

Smart Speech Recognition System for Chinese Language Learning Enhancement

Lijun Hu[1] and Jing Jia[2]

[1]*Puyang Medical College Puyang, Puyang, Henan 457000, China*
[2]*Faculty of Linguistic and Cultural Studies, Changchun Sci-Tech University, Changchun, Jilin 130000, China*

Correspondence should be addressed to Jing Jia; 100507@cstu.edu.cn

Received 25 April 2022; Revised 16 May 2022; Accepted 20 May 2022; Published 10 June 2022

Academic Editor: Lianhui Li

With the expansion of teaching scale and the rapid development of educational information, a smart classroom management system based on speech recognition has been proposed and developed to improve the information level of smart classroom management. This paper discusses the application of multimedia equipment control. The system relies on the mature campus network in the way of cloud and local speech database for speech recognition. The application of the system proves that the smart classroom management system based on speech recognition in cloud architecture has more advantages than the traditional multimedia classroom management system and also has definite expansibility. It facilitates the unified management of the school, improves the efficiency of administrators, saves a lot of human and financial resources, and greatly promotes the development of school information construction. The smart classroom becomes a new direction in the application of information technology in the field of teaching and learning and is a smart learning scenario for improving the learning and teaching scenario. This paper focuses on the use of smart classroom as a supplementary teaching tool to improve Chinese language teaching and learning and illustrates the optimization of the teaching environment by smart classroom in terms of vocabulary learning and listening and speaking training.

1. Introduction

With the rapid development of modern computer science and technology, the traditional multimedia classrooms in schools have been continuously improved and upgraded to gradually form intelligent classrooms [1, 2]. The management of multimedia classrooms, from the traditional manual manipulation of various multimedia equipment to centralized control through the central control, then to remote control through the campus network, and then to the current automated management based on artificial intelligence, fully illustrates that the development process of education gradually began to apply artificial intelligence, schools focus on the construction of smart classrooms, and smart campus has become the future trend [3, 4]. Domestic construction of smart classroom design concepts and teaching models is relatively abundant but still lacks comprehensive practice [5].

The Ministry of Education proposes to promote the application of emerging technologies such as cloud computing and big data in school education and vigorously build education modernization. Regarding the active promotion of the application of "Internet+," the guidance of the State Council marks the new technological revolution towards today's stage [6, 7]. Therefore, it is necessary to develop a smart classroom management system based on speech recognition with cloud computing architecture. Smart campus is a comprehensive system implicating technologies from multiple fields such as cloud computing, campus network, big data, and remote control, and thus, it can only serve the students and teachers better after adequate integration and collaborative work [8, 9]. The basis for the realization of a smart campus is the Internet of Things (IoT), which relies on numerous application service systems to integrate teaching management, academic research, and

campus life of teachers and students and ultimately construct an integrated and intelligent campus environment for work, study, and life [10]. Smart classroom is the most important part of building smart campus, and it is the key work for universities to realize the strategic goal of informationization. At present, most schools have the foundation of campus network, especially some colleges and universities, and the campus network has been quite mature after many new constructions, upgrades, and renovations in the school informatization construction, which has laid a good foundation for the realization of smart classroom [11, 12]. Based on the modern technology, it is feasible to design an intelligent classroom management system by taking advantage of the existing campus network, cloud computing, and local customized voice library.

With the deepening application of big data, cloud computing, Internet of Things, and artificial intelligence technologies in education in recent years, the smart classroom has emerged as an overall solution to enhance teaching effectiveness [13, 14]. The optimization of the Chinese learning environment by smart classroom is reflected in three aspects: (i) accurate content pushing, (ii) efficient environment management and resource acquisition, and (iii) contextual setting and interactive feedback. Teachers can use the environment of smart classroom to effectively organize and manage the increasingly abundant teaching resources so as to better interact and teach students according to their aptitude.

Chinese is the foundation of language and has a significant impact on the development of habits and interest in future language learning. The use of smart classrooms to create interesting and shade-appropriate learning environments for students is the focus of this paper.

2. Technical Principle

The object of speech recognition research is speech, which is processed first, and the human voice is automatically recognized and understood by pattern recognition computers [15]. The combination and codevelopment of cloud computing and big data have contributed to the advancement of speech recognition technology to some extent. The deployment of deep learning framework in the cloud can enhance the capability of cloud computing, so the mutual promotion of deep learning, big data, and cloud computing greatly improves and enhances the ability of speech recognition models to mine and learn from complex data [16, 17]. Speech recognition systems are mainly divided into three types: embedded speech recognition systems, server-mode speech recognition systems, and cloud computing-mode speech recognition systems [18, 19]. According to the characteristics of the school, the human-computer interaction module of the intelligent classroom management system is based on speech recognition technology, while the piece of speech recognition based on cloud mode is not mature enough, and the customizable speech recognition service provided by the service provider is still at a primary level, so the speech recognition module of this system has to be divided into two parts: the speech cloud and the local speech library. The voice cloud is responsible for the daily chat function, and the self-developed local voice library is responsible for the recognition of multimedia device control commands. The local speech library can be customized to provide speech recognition services for multimedia device control in the classroom, focusing on the reduced recognition range of these device controls and achieving higher recognition rates. The implementation of the local speech library requires the download and installation of the Microsoft Speech Recognition library, and the engine of speech recognition is driven by the speech recognition engine that comes with Windows, which can realize the ready acceptance of commands issued by the user [20].

This design currently drives three LCD displays simultaneously through this LCD driver all-in-one board; combined with the Android system software, it can realize the display of the conference theme or speaker's personal information on the upper bar screen, the lower standard screen displays the conference content, company logo, or video information, and the back bar screen carries the intelligent teleprompter system, which can display the speaker's speech content in real time.

2.1. Hardware Circuit Design. The main circuit board is a multimedia network player-LCD driver board based on Rockchip main chip RK3288. The design board can support LVDS/EDP/MIPI dot screen + HDMI dual display, LVDS + EDP dual display, LVDS + MIPI dual display, EDP + MIPI dual display, and other dual display mode options. It can drive 7–100-inch LCD and can support 4K full HD video decoding and 3840×2160 (for VOP_BIG) and 2560×1600 (for VOP_LIT) TFT LCD, and the main board contains 2 RS232, 2 UART, 4 USB HOST, 1 Ethernet, and other interfaces. It has a powerful communication function.

The design currently drives three LCD displays through this LCD driver board; combined with the Android system software, it can display conference theme or speaker personal information on the upper bar screen, the lower standard screen displays conference content, company logo, or video information, and the back bar screen equipped with intelligent teleprompter system can display the speaker's speech content in real time.

The smart podium consists of the following main parts: support structure, front face, operating table, LCD, and teleprompter. The usage frequency of each component in different application scenarios is shown in Figure 1.

The smart podium involves a total of three LCD displays, including two 28″ bar screens and one 23.8″ standard screen. The LCD module includes a display area, a PCB board set above the display area, and a COF (crystal coated film) set between the display area and the PCB board, the display area includes a protective film set at the front, a polarizer behind the protective film is defined as the reserved area, and the other defective area is defined as the defective area. The COF is fixed first, then the protective film and polarizer in the defective area are removed, the defective area in the display area is cut, then the lower end of the display area remaining after cutting is sealed, and finally, the

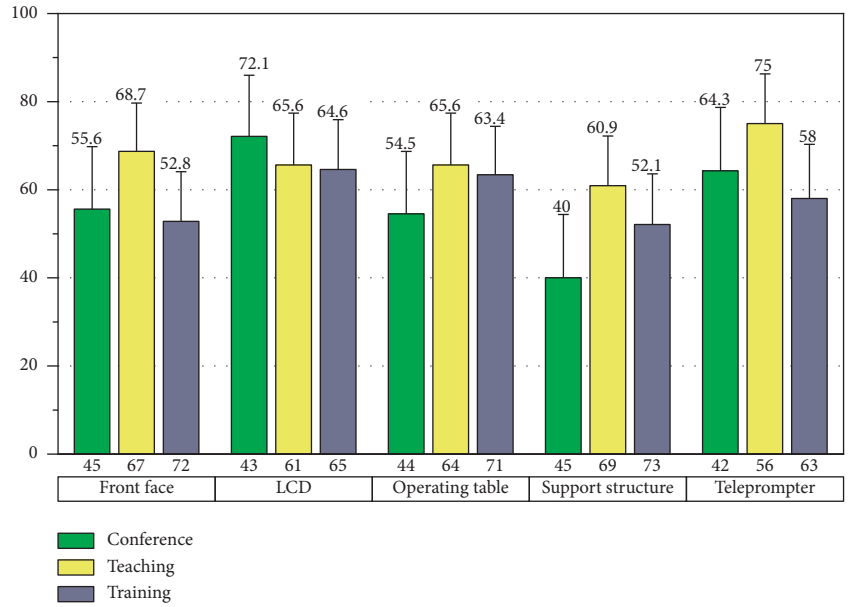

Figure 1: The usage frequency of each component in different application scenarios.

resolution of the sealed product is adjusted, so that the processed product can be used as a new small-size strip screen, thus achieving a novel display effect and being more widely used.

2.2. Software Function Design. The intelligent platform control software includes the information release of the first two display screens and the content display of the teleprompter system. The user can determine whether the device is online through the display status at the top of the software. Users can personalize the content of the two displays according to actual needs, including the display of pictures, videos, text font color size, and the interval of each material switch.

At the same time, the software also supports the preview function before the release of information to ensure that the information is accurately delivered to the audience, which greatly enhances the intelligence and personalization of the product, and can make the product applicable to a variety of different speech processes, which frequently can be calculated by the following equations.According to the formula (1)~(3), four teaching scenarios are selected for calculation, and the results are shown in Figure 2. It can be seen from the figure that, with the improvement of product intelligence and personalization, the audience will receive more information.

The intelligent teleprompter system software can automatically read the file content in the USB flash disk through the USB interface of the podium desktop for the speaker to deliver a speech. The operation of the speech content includes two modes: manual and automatic. In the manual mode, the speaker uses his or her voice to click the mouse to turn the page. The automatic mode is split into two categories: one is to set the automatic scrolling screen according to the speaker's personal preferences and reading speed for personalized settings, and the second is through the voice recognition technology and teleprompter system linkage, so that the speech does not read and does not go, it has a read mark and is perfectly timed with the speaker's speech.

$$\begin{aligned} n &= \sum_{i=1}^{n} n_i, \\ E_n &= \sum_{m=0}^{N-1} x_n^2(m), \\ M_n &= \sum_{m=0}^{N-1} \left| x_n(m) \right|, \end{aligned} \tag{1}$$

where E_n is the amount of accurate information delivered to the audience; M_n is the degree of intelligence and personalization of products.

2.3. Speech Recognition System Design. The main function of the speech recognition program is to identify the voice commands that control the progress of the teleprompter system document. Speech recognition technology is divided into online speech recognition technology and offline speech recognition technology. Considering the usage environment and cost of the intelligent lectern, offline speech recognition technology is used here [21, 22].

In the traditional conference speech conditions, speakers need to bring their own paper scripts or use the way described in the previous section for automatic page turning, but none of these approaches can achieve automatic recognition of the speaker's real-time speech progress. The current artificial intelligence and speech recognition technology continues to develop, and application popularity for continuous voice recognition application technology has matured. How to more fully combine intelligent video and audio technology and conference speech needs has become the focus of application, and automatic speech recognition

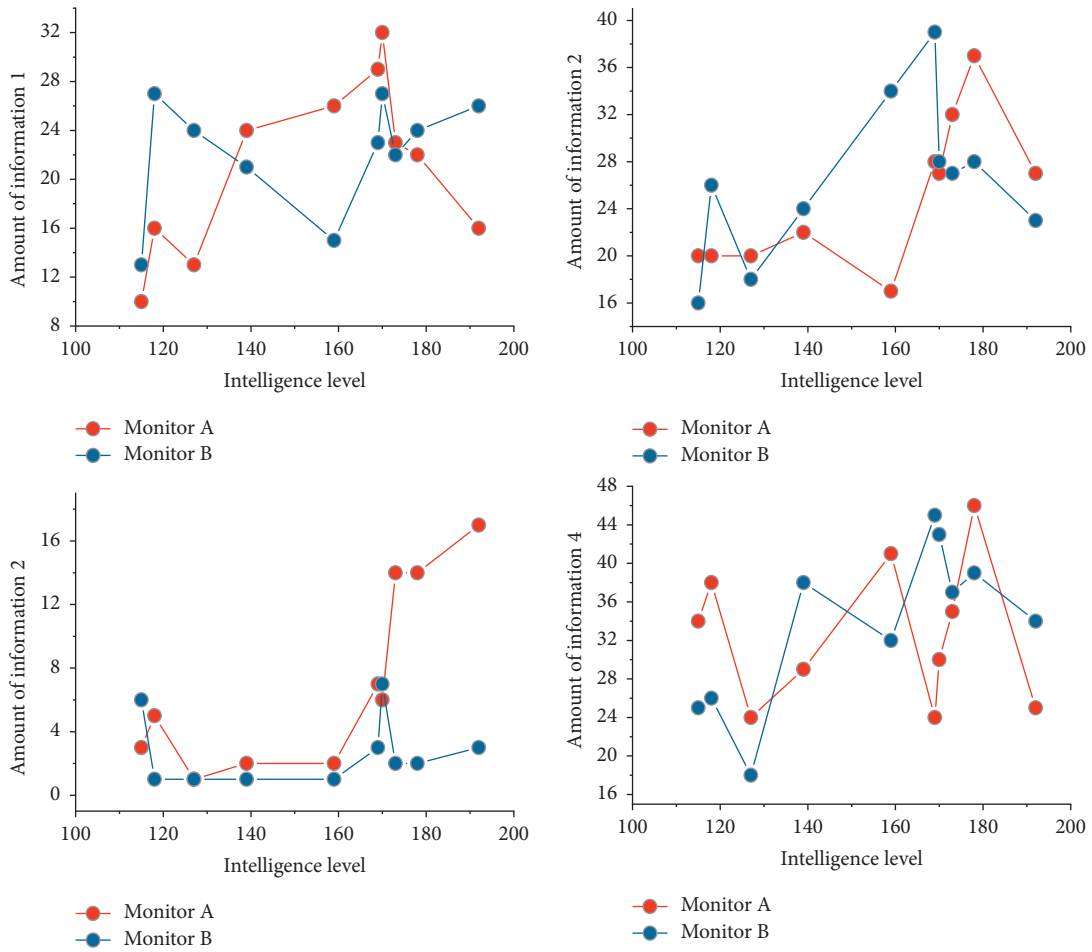

Figure 2: Relationship curve between the amount of information received and the product intelligence and personalization.

technology has become the "artificial intelligence + speech" breakthrough. Speech recognition system is divided into three layers: platform capability service, business software application, and speech intermediate control.

The platform capability service layer provides the intelligent speech recognition system server program, WEB server, speech capability platform service engine (speech recognition platform), database management, system resource management, and other related service functions required by the system, and on the premise of completing the basic functions, the application capability can be optimized according to the actual situation of system operation to improve the application level.

The business software application layer provides the information display function of the intelligent speech recognition system used by the speaker and provides the text display corresponding to the real-time transcribed speech and the processing function of various basic document information.

The speech middle control layer mainly provides the speech recognition middleware program, transmits data information with each other with the speech collection equipment picking port and speech recognition SDK interface, completes the functions of speech data collection, processing, storage, and network transmission, and interacts with the speech capability platform service engine in the platform capability service layer. The intelligent speech recognition system includes speech recognition server, real-time recognition terminal, multichannel speech processor, professional conference microphone, router, and other products, among which the speech recognition server realizes the deployment engine and other types of core capability software, achieves a high degree of equipment integration, reduces capital investment, and provides recording service processing, data transmission, and other capabilities. The analytical formula between key objects is shown in the following equations. According to the formula, we can get the histogram of the relationship between the integration degree of speech recognition equipment and capital investment (three scenarios), as shown in Figure 3. It can be seen from the figure that the higher the integration degree of speech recognition server equipment, the lower the capital investment. The real-time recognition terminal is mainly used to deploy client software and provide the operation of each function of the software. The multichannel voice processor converts the audio data of analog microphone into network data through professional voice acquisition technology, which is used as the data source of the whole system voice. The system topology diagram is shown in Figure 4.

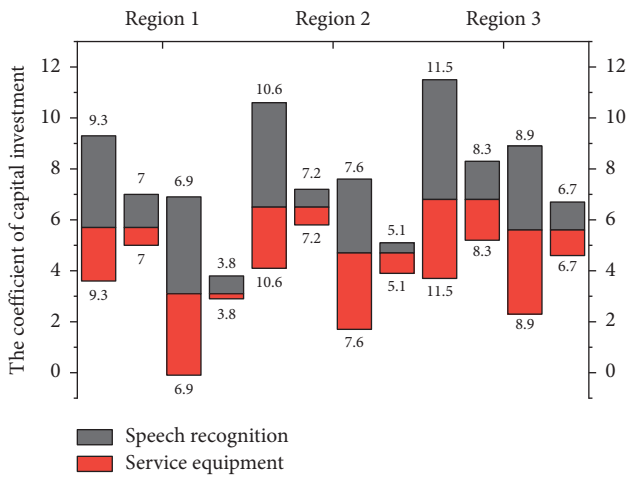

Figure 3: Relationship between high integration of equipment and capital investment.

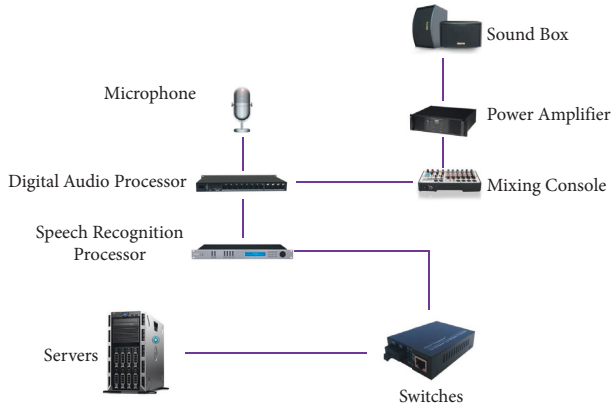

Figure 4: Speech recognition system topology diagram.

$$D(X,Y) = \sqrt{\sum_{i=1}^{n}(x_i - y_i)^2},$$

$$D^n = \sum_{i=1}^{j}\sum D\left(X, Y_i^{n-1}\right), \tag{2}$$

$$\delta^n = \frac{\left|D^{n-1} - D^n\right|}{D^n},$$

where D is the degree of integration of speech recognition service equipment; D^n is the degree of integration of all equipment; δ^n is the coefficient of capital investment.

2.4. Cloud Computing. In essence, cloud computing is a virtualized resource. This computing method dynamically provides service expansion through the Internet. It is a pay-per-use model to provide available, convenient, and on-demand network access. Cloud computing is an important research area for future development, in terms of application, it has low requirements for the client devices, and the devices themselves do not need to be too highly configured because the resources used are from the cloud, and as long as the network is smooth, data and application sharing can be achieved, which can be analyzed through the following formula.

Currently, cloud computing and speech recognition technology have become emerging teaching methods in the education industry [23, 24], and the speech recognition module in the cloud architecture of the intelligent classroom management system can respond to a variety of user requests and can take advantage of a large amount of cloud data to improve the performance of the speech recognition system. Speech cloud uses cloud computing to achieve fast speech applications, which in this system mainly recognizes the human voice. Cloud mode speech recognition and interaction service is a new direction for future research and application. In this regard, the technologies of KDDI, Ali cloud, Baidu, and Tencent cloud are in the leading position in China.

$$X = \{X_1, X_2, \ldots, X_m\},$$
$$X_i = \{X_1, X_2, \ldots, X_n\}, \tag{3}$$

where X is the configuration parameters of equipment.

2.5. Voice Recognition. Voice recognition technology is mainly divided into two categories, that is, voice meaning recognition and voice similarity recognition. Sound meaning recognition is to transform human voice into text by analyzing the human voice and finding the characteristics of pronunciation from it, which is usually used in such fields as fast inputting information, artificial intelligence, and communication between human and computer through voice. Similarity recognition of voice is to compare the target voice object to be recognized with the voice sample and check whether the similarity between the target voice and the sample can be achieved [25, 26]. The computer and human are basically similar in terms of speech recognition processing. A complete speech recognition system is generally divided into three parts, that is, speech denoise preprocessing and extraction of features of speech, acoustic modeling and pattern matching, and language modeling and language processing. It is in the noisy environment; due to the complexity of the actual environment, noise reduction processing is of great practical significance. For the purpose of lifting up the level of speech denoising and the accuracy of speech recognition system, wavelet denoising technology is often applied to speech recognition. The flow of speech recognition is shown in Figure 5.

3. System Design

At present, the speech cloud is widely used in the general field, with a huge amount of user speech data and relatively high accuracy of speech recognition. However, in the field of education, the commands that need to be recognized in the control of multimedia equipment in school smart classrooms are relatively fixed, so the local speech library can be customized to meet the personalized needs of users and

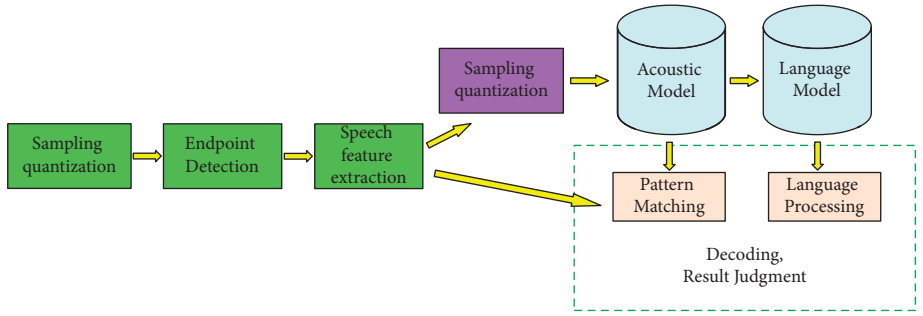

Figure 5: Flowchart of speech recognition.

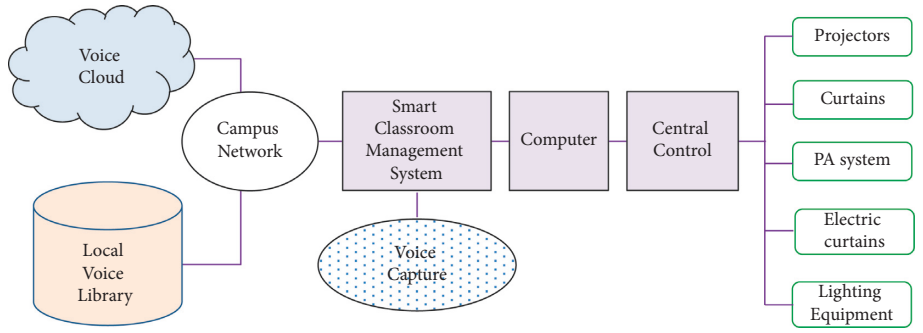

Figure 6: System architecture diagram.

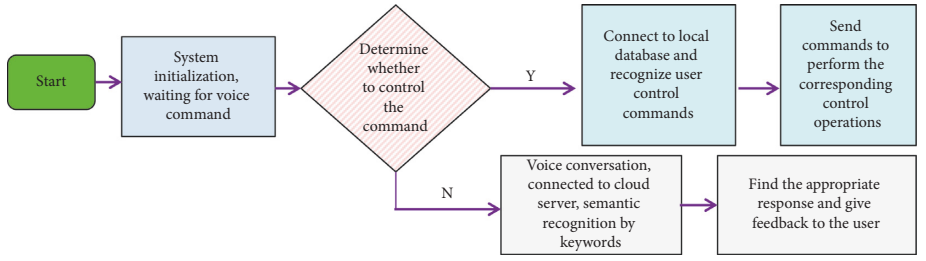

Figure 7: System workflow chart.

make up for the shortcomings of the speech cloud such as slow recognition speed due to too wide a search range, heavy reliance on network, multilink leakage, risk concentration, and reduced flexibility of users' control of data and technology.

3.1. System Architecture. The overall structure of the speech recognition-based intelligent classroom management system with cloud computing architecture is shown in Figure 6.

3.2. System Workflow. Generally, the computer in the smart classroom automatically opens at the set time and starts the client of the management system. First, the software loads the basic syntax package for login, initializes the login speech recognition engine, initializes the interface, and waits for the user to login; then, after successful login, it waits for the user's voice command; after the teacher user issues the correct voice login command, the system starts to judge; if it is a command to control multimedia devices, it connects to the local voice library and controls the devices through the central control serial port after recognition if it belongs to the general chat. If it belongs to the voice conversation category of general chat, it connects to the voice cloud, finds the answer after recognition, and gives feedback to the user through voice or text. The relationship can be accurately predicted by the following formula. The flowchart of the system is shown in Figure 7.

$$\begin{aligned} \cup Q_j &= O, \\ Q_{j1} \cap Q_{j2} &= \varnothing, \end{aligned} \tag{4}$$

where Q is the voice login command which the teacher sends to the user; $1 < j < n$.

4. Practical Application

4.1. Application of Aliyun. Teachers and students realize human-computer interaction with machines, which involves human speech recognition and needs to be connected with the speech cloud. At present, the voice recognition interface of KDDI is not free, and the application and approval process of voice recognition of Tencent cloud is relatively

long and tedious. Finally, after comparing the voice clouds of Ali and Baidu, relatively speaking, Ali cloud is easier to use, so the SDK of voice recognition of Ali cloud is used. In addition, the commonly used voice recognition module is FreeSWITCH; the advantages are open-source, cross-platform, scalability, multiprotocol, and so on; it is based on Ali cloud, easy to use, and therefore popular with secondary developers. Its main development language is C, some modules use C++, and it supports SIP, H323, Skype, Google Talk, and many other communication protocols. Voice service Aliyun SDK source code is available on the Github open source platform, and using CommonRequest to invoke the SDK's core library directly is highly useful in development. The process of implementing this function is as follows: firstly, the collected user voice data will be sent to the backend, then the backend will send the received voice input stream to the Ali cloud server side, which will convert the voice into text, and finally, the processed voice data stream will be returned to the frontend.

4.2. Application of Local Speech Library. Microsoft Speech SDK is a toolkit launched by Microsoft to develop speech applications and speech engines on Windows platform [27]. It contains various components for speech recognition. There are many examples of secondary development using Microsoft's speech recognition development toolkit, and the methods and ideas from other studies are referenced here.

In order to reference the COM component provided by the SDK, the VisualStudio.NET development platform is used as an example, and the component is referenced by selecting Project|Add Reference in the menu and then clicking on the COM tab and selecting Microsoft Speech Object Library. NET for speech recognition module development mainly uses three APIs: ISpRecognizer interface is responsible for interacting with the underlying RecognitionEngine, which is the speech recognition engine interface; ISpRecoContex interface is responsible for sending and receiving messages, which is the main interface to complete the recognition task; ISpRecoGramma interface is responsible for creating, loading, and activating grammar rules and is the grammarian interface. The Microsoft Speech SDK software development kit provides components for speech recognition, and the system was developed using the *C#* language, which is inherently well integrated. It is also important to note that since the downloaded SDK only supports English and teachers and students mostly communicate with each other in Chinese, the SDK language package SpeechSDK51LangPack should be downloaded and installed.

4.3. Serial Port Control. At present, the centralized control system of multimedia equipment (referred to as central control) on the market is becoming more and more advanced, and some of these smart classroom products are designed to meet the needs of information-based teaching, and they apply broadcast-grade product technology to the campus, leading the new trend of smart teaching. Nevertheless, since the multimedia equipment of each school is more or less different, the central control may not be able to control some multimedia equipment, so we should redevelop the module with the characteristics of the school according to the actual situation of the school.

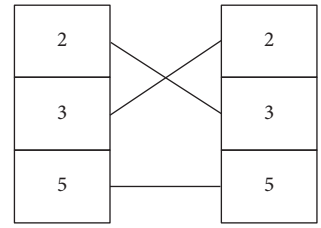

Figure 8: Serial control cross wire soldering diagram.

Most computers and multimedia equipment have RS-232 interface; if not, you can also convert the USB port to RS-232 interface through the "USB to RS-232" data cable, and then, certain multimedia equipment that the central control cannot directly control can be directly connected to the computer through the device serial port with a network cable by the computer to directly control. The advantage of serial communication is that data can be transmitted over long distances, the use of ordinary network cable soldering is low cost, bandwidth can also fully meet the requirements but also customize the protocol of transmission, and data transmission is more reliable [28]. There are nine pins of the RS-232 interface, of which pin 2 is used to receive data, pin 3 is used to send data, and pin 5 is the signal ground. 9-pin serial port uses only the second, third, and fifth three of these pins to send and receive data, that is, solder wire one end of the serial port in the order of three pins, adjust the other end of the second and third pins a little, the fifth pin remains unchanged, solder wire the other end of the serial port in the order of three pins. The mathematical relationship is as follows. The final crossover line produced is shown in Figure 8.

$$\begin{aligned} Y &= \{Y_1, Y_2, \ldots, Y_m\}, \\ Y_j &= F(X_i), \end{aligned} \tag{5}$$

where F is the data sending and receiving; Y is the number of serial ports; $1 < i$; $j < n$.

5. The Relationship between Smart Classroom and Chinese Teaching

5.1. Teaching in the Smart Classroom. Smart classroom is a product of the deep integration of information technology and education teaching, which seamlessly connects teaching and learning inside and outside the classroom and provides a personalized, intelligent, and digital learning environment. The smart classroom environment effectively integrates core functional elements such as teaching resource management, real-time content delivery, learning scenario collection, instant feedback and evaluation, and member interaction and communication by using "cloud service + mobile application" to efficiently organize the three teaching links of teachers and students before, during, and after class.

Smart classroom is student-centered, emphasizing students' autonomous learning and collaborative learning

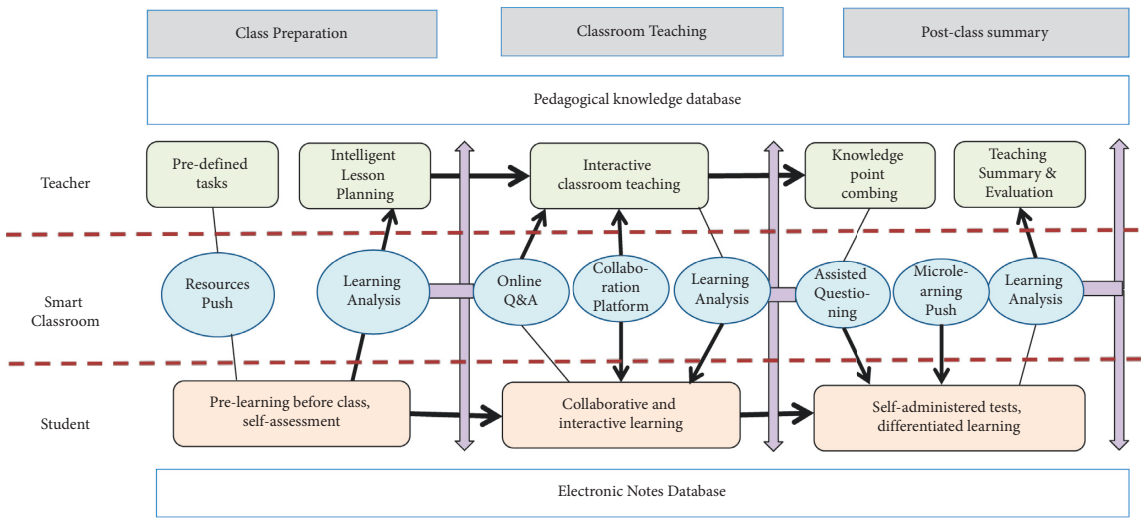

Figure 9: Chinese learning model in smart classroom.

among students. Teachers in the smart classroom are more likely to create, collect, and organize educational resources, set goals and assessment criteria, monitor the progress of student-initiated learning in the classroom, and provide timely feedback on questions raised by students. These features of teaching and learning in the smart classroom also fit the requirements of the language teaching process.

5.2. Characteristics of Chinese Language Teaching and Learning. First, language teaching emphasizes the learner as the root and stresses that students should be active participants and language constructors in the learning process, and teachers are collaborators and facilitators of learning. Consequently, teachers need to create rich interactive conditions to promote the smooth interaction between teachers and students.

Second, analyzed from the perspective of the language teaching environment, teaching Chinese in the native language environment should try to create a relaxed and natural language atmosphere. Therefore, teachers need to simulate and create language situations and use text, graphics, sound, and video in a comprehensive way to push language information and stimulate learners from multiple senses as much as possible.

Finally, language teaching relies on rich language contexts and the need to obtain timely feedback on learning effects during repeated language training, to achieve interactive communication and personalized learning.

5.3. The Chinese Learning Model in the Smart Classroom. In general, the integration of smart classroom and Chinese teaching is an interactive, repeated, and circular process, which runs through the teaching process of preclass preparation, classroom teaching, and postclass summary. This paper moderately simplifies the "universal learning model in the smart classroom" given in the related literature and builds a set of learning models in the smart classroom environment based on the teaching knowledge database and the electronic notes database, using three times of learning situation analysis as the feedback mechanism (Figure 9). The learning model contains only five teacher activities and three student activities, while the smart classroom platform takes up the tasks of resource pushing, information interaction, and learning situation analysis, making the process of smart teaching more simplified and easy to carry out.

5.4. Improvement of Chinese Teaching Tasks in the Smart Classroom. In this paper, we focus on two learning tasks in Chinese teaching, namely, vocabulary and listening, and use the Xunfei Smart Education Platform as a support to explain in detail the improvement methods and technical advantages of the smart classroom for these two teaching tasks.

First, the smart classroom environment can provide students with repeatedly trained vocabulary learning scenarios, push related vocabulary resources, and generate differentiated vocabulary memorization strategies.

Second, the smart classroom environment can provide immersive Chinese listening and speaking contexts, provide students with an interactive and self-directed learning environment before and after class sessions, and use language recognition technology to enhance the effectiveness of listening and speaking interactions in the classroom.

6. Optimization of Vocabulary Learning Methods in the Smart Classroom

6.1. Characteristics of Vocabulary Learning. Vocabulary is the foundation of Chinese learning and plays a crucial role. However, most vocabulary teaching activities are one-way communication and lack of association, which leads to students' poor impression of the learned vocabulary and easy forgetting. There are two main reasons for the unsatisfactory effect of vocabulary learning. First, vocabulary teaching does not create relevant context and ignores cultural factors. The second is the lack of effective vocabulary learning strategies, mechanical memory, and ease of forgetting.

6.2. Vocabulary Learning in the Smart Classroom. With the learning model of smart classroom, the vocabulary teaching process for teachers and students is concentrated in two stages, before and after class.

6.2.1. Preclass Preparation Stage. The teacher gives students clear vocabulary learning tasks, and the resource pushing module of smart classroom pushes the basic word meanings, pronunciation, and lexical properties of vocabulary, as well as the related vocabulary with synonymy, antonymy, multiple meanings, and homophones and homonyms to students. After students finish vocabulary preview, the intelligent classroom provides Dictation Training tools and tests to check students' vocabulary learning effect. Learning analysis can summarize students' questions and guide teachers in preparing lessons intelligently. Smart classroom assists students in preclass prereading and records knowledge points and wrong information in electronic notes.

6.2.2. Postclass Summary Stage. Smart Classroom provides a punch card tool to urge students to study words in a planned manner. As the number of vocabulary exercises increases, the granularity of error information in smart classroom's eNotes is refined not only to count which words are error-prone but also to record what types of errors are made (e.g., spelling errors, mispronunciation, word meaning errors, lexical errors, and associated word errors), which can guide students to more scientific vocabulary learning strategies. Differentiated learning strategies will guide the problem setting module and microclass push module of the intelligent classroom platform to help students master error-prone knowledge more accurately and effectively.

7. Optimization of Listening and Speaking Training under Smart Classroom

7.1. Characteristics of Listening and Speaking Training. The improvement of Chinese listening and speaking ability requires continuous training in language scenarios, and the teaching time of the Chinese classroom is difficult to meet the repeated practice requirements, which leads to the traditional teaching environment where teachers emphasize reading and writing but not listening, and students are unwilling to spend energy on listening and speaking training, making it difficult to improve listening and speaking ability. With the gradual maturity of Xunfei's speech recognition technology and deep learning technology, the classroom integrates independent listening and speaking training scenes and makes use of the openness, sharing, and interaction of the platform to make up for the deficiency of listening and speaking training in actual Chinese teaching.

7.2. Hearing and Listening Training in the Smart Classroom. The biggest advantage of smart classroom in improving listening and speaking training is that it provides an immersive language learning environment, which not only develops students' listening and speaking skills but also improves students' independent learning ability. The listening training platform has a set of training tools for listening, pronunciation, and conversation.

Teachers can use these tools to organize videos and audios related to the course and associate them with a bank of test questions in an easy-to-follow format. Students play the audio and follow along and record it, and the platform uses voice recognition technology to give pronunciation accuracy, which unifies students' listening and speaking skills.

Smart classroom's listening and speaking training platform can also set up common conversational scenarios such as study, life, business, travel, and dating, allowing students to train oral communication skills with the help of human-computer interaction. At the same time, there are also language environments that promote interest in learning English, such as online dubbing of movie clips and MTV of Chinese songs. These environments have a positive effect on enhancing students' interest in listening and speaking.

8. Conclusion

Informationization in higher education enters the stage of smart campus, while classroom is the main position of teaching, and the construction of smart classroom is the major trend of future development. After improving and optimizing the construction of digital campus, insisting on building a smart campus with service as the main line, it is the primary task of the school information center to let teachers and students enjoy the convenient effect brought by the information service of the school. Smart classroom realizes active and autonomous learning, audio-visual equipment is intelligent and humanized, and the information services of the Internet and campus network are applied to the field of teaching. In terms of human-computer interaction, the cloud-based approach combined with the local voice library for speech recognition and self-developed management system can save financial and material resources, enhance the security of school data and information, and provide higher flexibility for future upgrades and optimization of the system, as well as improving the development and practical application capabilities of the school's research team. At present, face recognition, as one of the successful applications in the field of image analysis and processing, is gradually integrated into people's lives. Then, the construction of smart campus and smart classroom, in addition to improving the accuracy of voice recognition, should also study the application of face recognition technology in this area in the future so that artificial intelligence technology can bring greater convenience to all aspects of people's lives.

Smart classrooms bring changes to the existing teaching methods and can assist teachers and students in gaining a new learning experience. This paper takes vocabulary learning and listening and speaking training, two tasks suitable for independent learning, as the starting point to show the improvement of the smart classroom for the

Chinese teaching environment and its advantages for enhancing learning interest and accumulating knowledge. The teaching model under smart classroom is a new direction for future teaching development, which needs to be continuously practiced, optimized, and improved by front-line teaching staff.

Data Availability

The dataset can be accessed upon request.

Conflicts of Interest

The authors declare that they have no conflicts of interest.

References

[1] S. Al-Sharhan, "14 Smart classrooms in the context of technology-enhanced learning (TEL) environments," *Transforming Education in the Gulf Region: Emerging Learning Technologies and Innovative Pedagogy for the 21st Century*, vol. 188, pp. 1–10, 2016.

[2] M. Li, "Smart home education and teaching effect of multimedia network teaching platform in piano music education," *International Journal of Smart Home*, vol. 10, no. 11, pp. 119–132, 2016.

[3] J. Wang, J. Zhang, J. Fan, S. Zhang, J. Wang, and Y. Geng, "Design and application of smart vocational education platform based on new generation information technology," in *Proceedings of the 2020 International Conference on Computer Vision, Image and Deep Learning (CVIDL)*, pp. 505–509, IEEE, Chongqing, China, July 2020.

[4] D. K. Mohanachandran, C. T. Yap, Z. Ismaili, and N. S. Govindarajo, "Smart university and artificial intelligence," *The Fourth Industrial Revolution: Implementation of Artificial Intelligence for Growing Business Success*, pp. 255–279, Springer, Cham, Switzerland, 2021.

[5] J. B. Smart and J. C. Marshall, "Interactions between classroom discourse, teacher questioning, and student cognitive engagement in middle school science," *Journal of Science Teacher Education*, vol. 24, no. 2, pp. 249–267, 2013.

[6] H. Wang, "Research on the talent cultivation model of the integration of production and education in higher vocational education under the background of "Internet+," in *Proceedings of the 2021 16th International Conference on Computer Science & Education (ICCSE)*, pp. 943–946, IEEE, Lancaster, UK, August 2021.

[7] A. Fung, H. Russon Gilman, and J. Shkabatur, "Six models for the internet + politics," *International Studies Review*, vol. 15, no. 1, pp. 30–47, 2013.

[8] S. Mumtaz, "Factors affecting teachers' use of information and communications technology: a review of the literature," *Journal of Information Technology for Teacher Education*, vol. 9, no. 3, pp. 319–342, 2000.

[9] D. N. E. Phon, M. B. Ali, and N. D. Abd Halim, "Collaborative augmented reality in education: a review," in *Proceedings of the 2014 International Conference on Teaching and Learning in Computing and Engineering*, pp. 78–83, IEEE, Kuching, Malaysia, April 2014.

[10] W. Li, "Design of smart campus management system based on internet of things technology," *Journal of Intelligent and Fuzzy Systems*, vol. 40, no. 2, pp. 3159–3168, 2021.

[11] M. C. Hill and K. K. Epps, "The impact of physical classroom environment on student satisfaction and student evaluation of teaching in the university environment," *Academy of Educational Leadership Journal*, vol. 14, no. 4, p. 65, 2010.

[12] J. Mohelníková, M. Novotný, and P. Mocová, "Evaluation of school building energy performance and classroom indoor environment," *Energies*, vol. 13, no. 10, p. 2489, 2020.

[13] S. Y. Phoong, S. W. Phoong, S. Moghavvemi, and A Sulaiman, "Effect of smart classroom on student achievement at higher education," *Journal of Educational Technology Systems*, vol. 48, no. 2, pp. 291–304, 2019.

[14] M. K. Saini and N. Goel, "How smart are smart classrooms? A review of smart classroom technologies," *ACM Computing Surveys*, vol. 52, no. 6, pp. 1–28, 2020.

[15] S. Shaikh Naziya and R. R. Deshmukh, "Speech recognition system—a review," *IOSR Journal of Computer Engineering*, vol. 8, no. 4, pp. 3–8, 2016.

[16] Z. Bai, G. Sun, H. Zang et al., "Identification technology of grid monitoring alarm event based on natural language processing and deep learning in China," *Energies*, vol. 12, no. 17, p. 3258, 2019.

[17] M. M. Najafabadi, F. Villanustre, T. M. Khoshgoftaar, N. Seliya, R. Wald, and E. Muharemagic, "Deep learning applications and challenges in big data analytics," *Journal of big data*, vol. 2, no. 1, p. 1, 2015.

[18] J. Wu, "English real-time speech recognition based on hidden markov and edge computing model," in *Proceedings of the 2021 third international conference on inventive research in computing applications (ICIRCA)*, pp. 376–379, IEEE, Coimbatore, India, September 2021.

[19] Z. Xiangyan, "Application study of modern educational technology under cloud computing platform," in *Proceedings of the 2016 Eighth International Conference on Measuring Technology and Mechatronics Automation (ICMTMA)*, pp. 122–125, IEEE, Macau, China, March 2016.

[20] M. Kleinert, H. Helmke, S. Moos et al., "Reducing Controller Workload by Automatic Speech Recognition Assisted Radar Label Maintenance," in *Proceedings of the 9th SESAR Innovation Days*, Athens, Greece, 2019.

[21] L. P. Rondon, L. Babun, K. Akkaya, and A. S. Uluagac, "HDMI-watch: smart intrusion detection system Against HDMI attacks," *IEEE Transactions on Network Science and Engineering*, vol. 8, no. 3, pp. 2060–2072, 2021.

[22] R. T. Kreutzer and M. Sirrenberg, *Understanding Artificial Intelligence*, Springer International Publishing, Berlin, Germany, 2020.

[23] L. Wei, "Study on the application of cloud computing and speech recognition technology in English teaching," *Cluster Computing*, vol. 22, no. S4, pp. 9241–9249, 2019.

[24] X. Luo and L. Xie, "Research on artificial intelligence-based sharing education in the era of Internet+," in *Proceedings of the 2018 International conference on intelligent transportation, big data & smart city (ICITBS)*, pp. 335–338, IEEE, Xiamen, China, January 2018.

[25] A. B. Hancock and L. M. Garabedian, "Transgender voice and communication treatment: a retrospective chart review of 25

cases," *International Journal of Language & Communication Disorders*, vol. 48, no. 1, pp. 54–65, 2013.

[26] D. Stowell, M. D. Wood, H. Pamuła, Y. Stylianou, and H Glotin, "Automatic acoustic detection of birds through deep learning: the first Bird Audio Detection challenge," *Methods in Ecology and Evolution*, vol. 10, no. 3, pp. 368–380, 2019.

[27] M. R. Kamarudin, M. Yusof, and H. T. Jaya, "Low cost smart home automation via microsoft speech recognition," *International Journal of Engineering & Computer Science*, vol. 13, no. 3, pp. 6–11, 2013.

[28] P. Popovski, Č. Stefanović, J. J. Nielsen et al., "Wireless access in ultra-reliable low-latency communication (URLLC)," *IEEE Transactions on Communications*, vol. 67, no. 8, pp. 5783–5801, 2019.

Hindawi
Scientific Programming
Volume 2022, Article ID 8645969, 11 pages
https://doi.org/10.1155/2022/8645969

Research Article

Design of Web Security Penetration Test System Based on Attack and Defense Game

Bing Song, Li Sun, and Zhihong Qin

Department of Network Security, Henan Police College, Zhengzhou 450000, China

Correspondence should be addressed to Bing Song; songbing@hnp.edu.cn

Received 22 April 2022; Revised 10 May 2022; Accepted 18 May 2022; Published 10 June 2022

Academic Editor: Lianhui Li

Some sensitive data in the network will be leaked due to the loopholes or weaknesses of the web system itself, which will bring potential harm to the society or the public. Aiming at this, this study carries out the design of web security penetration test system. A test scheme comparing single method with an automatic comprehensive test method is designed. Based on this scheme, an automatic penetration test system script used under the terminal operation page is tested and designed. A security evaluation algorithm based on the prediction results of the game between attack and defense is proposed. Through this algorithm, different website systems are evaluated and scored, and the test results are compared through scoring. The automatic penetration test integration system designed and implemented in this study can meet the main objectives of web security and the protection requirements of websites against general, routine, and universal security attacks. The proposed evaluation algorithm is more detailed, accurate, and reference in scoring.

1. Introduction

With the popularization of Internet and the rapid development of web application technology, Internet provides an important basic platform for web applications, on which more and more web applications are set up [1–6]. Common online shopping malls, online banking, and other web applications have greatly changed people's lifestyle [7–10]. They can easily shop or deal with financial problems without leaving home. However, these new technologies not only bring convenience to our work life and even learning but also bring great risks that we have never had before. Due to the maturity of network technology, the threshold of web application attack technology is getting lower and lower. Hackers gradually transfer the attack object from the network server to the web application [11–14]. According to Gartner's survey data, 75% of information security attacks occur on Web applications, not on the network level. At the same time, it is also found that two-thirds of web applications are very vulnerable and vulnerable to attacks. However, it is a pity that many enterprises spend a lot of energy and financial resources on network security and server security and do not pay attention to the security problems of web applications, leaving an opportunity for hackers [15–17].

The main reason for the vulnerability of web applications is that users can submit data arbitrarily, but the server-side does not carry out reasonable verification. From the perspective of the software itself, the main reason is that the cycle of web application development is getting shorter and shorter, and the level of developers is uneven, which leads to the incomplete consideration of security issues in the process of software development. From the perspective of software deployment and configuration management, the staff may be careless, so there are great security risks. A comprehensive penetration test must be conducted on the web application before the attacker launches an attack to ensure the security of the web application and prevent it from happening [16, 17]. Due to the uneven level of web application developers and the shorter development cycle, it is inevitable for web applications to have security vulnerabilities. The traditional way to ensure network security is through firewall and IDS/IPS. It works on the network layer, while the security penetration test process works on HTTP protocol. It can make up for the deficiency of firewall relative static

defense. The two complement each other and jointly ensure the security of web applications.

Web application penetration testing technology is to simulate the attack means and attack methods of hackers, actively detect web applications, transform malicious URLs, send them to the server, and determine whether there are security vulnerabilities in web applications by analyzing the response returned by the server. Through penetration testing, we can understand the vulnerabilities of web applications in advance before they are attacked, classify the level of vulnerabilities, and find corresponding mitigation schemes according to the severity and urgency of vulnerabilities so as to greatly reduce the risk of web applications being attacked.

Due to the unsatisfactory efficiency and accuracy of manual penetration testing, security workers have tried to develop some security penetration testing tools. However, many security penetration testing tools can only test one or several vulnerabilities, and the test effect is not satisfactory. The purpose of this research is to design and develop a web application security penetration testing tool, which can comprehensively and automatically detect some common web application vulnerabilities and can give a more detailed vulnerability detection report.

2. Overall Demand Analysis and Design

In the whole process of the penetration test, it is necessary to formulate a test plan in advance, and various factors will affect the final test conclusion and results. The whole process is divided into three steps: penetration test, design and implementation of automated penetration test system, and safety assessment. Safety assessment is interspersed in the penetration test and automated penetration test. The overall process is shown in Figure 1.

2.1. Penetration Test Requirement Analysis. In the whole process, it is necessary to carry out penetration attack against the test target, and on the premise of not damaging the system, find out the problems existing in the system as much as possible, join other websites for testing, and compare the results, which is more convincing. The overall test is based on Kali Linux system [18, 19], including the use of mainstream test tools and the design of an automatic penetration test system. The specific test contents are shown in Figures 2 and 3.

2.2. Security Assessment Needs Analysis. The overall safety assessment is carried out according to the penetration test results and the calculation results of the assessment algorithm. Security assessment refers to a series of security assessments for websites, systems, and platforms. At present, web security assessment [20, 21] is mainly carried out from internal and external aspects. Internal evaluation adopts black-box test or white-box test. Black-box test refers to the evaluation test without knowing the detailed information of the system, while white-box test refers to the evaluation test with a certain understanding of the information and conditions of the system.

External evaluation refers to the remote evaluation of the server and system initiated by the outside. Testers discover the security problems exposed by the system by simulating the malicious scanning and detection behavior of attackers. Internal evaluation refers to the internal security inspection conducted by testers for the server, code design, and configuration of the system. Compared with external testing, internal evaluation testing can find the problems of the system from a deeper level. The working process of safety assessment is shown in Figure 4.

The overall assessment is carried out by establishing the assessment model and method. At the same time, the requirements of the test objectives for safety assessment are analyzed and understood. The specific aspects should be considered from these aspects as shown in Figure 5.

(1) *Protection requirements*. At present, there are many security attack technologies, and the methods are updated quickly. Therefore, it is required that the cycle of security evaluation must be shortened to ensure the security protection and attack prevention of the whole network.

(2) *Isolation requirements*. Many security attacks are gradually infiltrated from the external network to the internal network. Although many enterprises and units have separated the internal and external networks on physical lines, when it comes to business activities and external information exchange, they will cancel some of the isolation instead of using special machines for access.

(3) *Verification requirements*. Network security is a multifaceted problem, which involves not only attack and protection but also authorization, authority, confidentiality agreement, and other internal problems. Different identity and authority verification for different login users can reduce the risk of being penetrated into the intranet to a certain extent.

(4) *System intrusion detection requirements*. Today's systems and platforms are basically protected by firewalls, but in our continuous research and testing, we also found that although firewalls are stable and can immediately tension access, they are static after all, while network attacks are dynamic, and there are countless methods. Therefore, intrusion detection methods and security evaluation methods must be equipped.

(5) *Vulnerability threat requirements*. Because the website system and platform are artificially coded and designed, errors often occur in the writing and logical specification of the code in the design. Most of them ignore the simplicity and preciseness of the code on the premise of realizing the function,

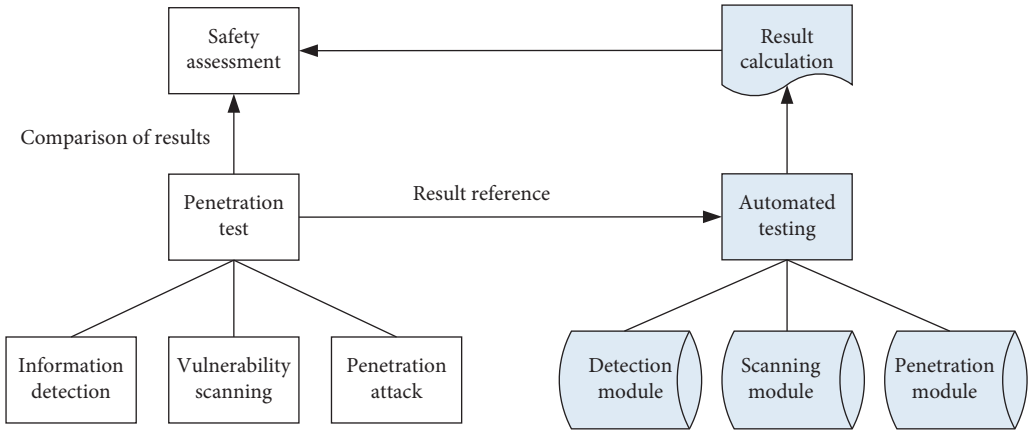

Figure 1: The overall process.

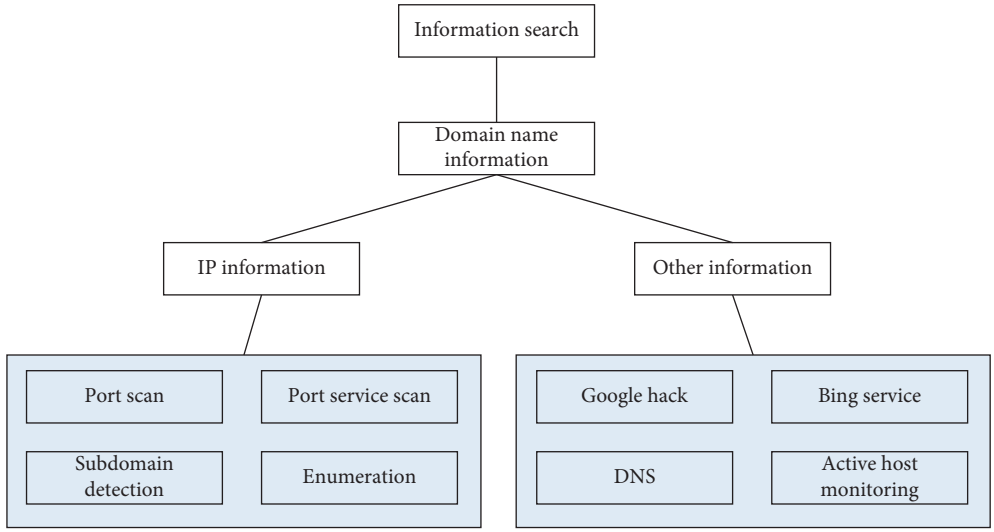

Figure 2: Information search.

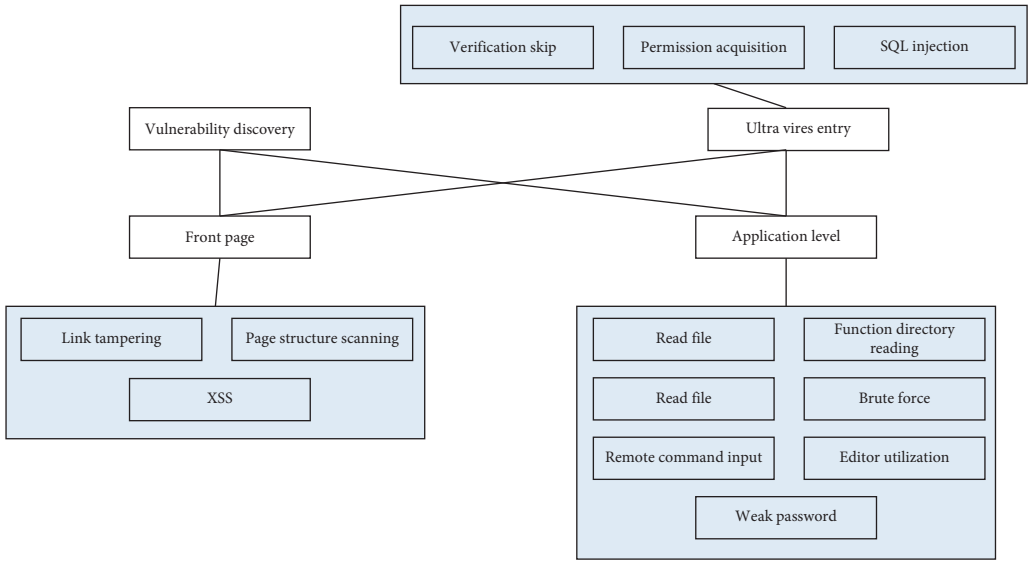

Figure 3: Vulnerability discover.

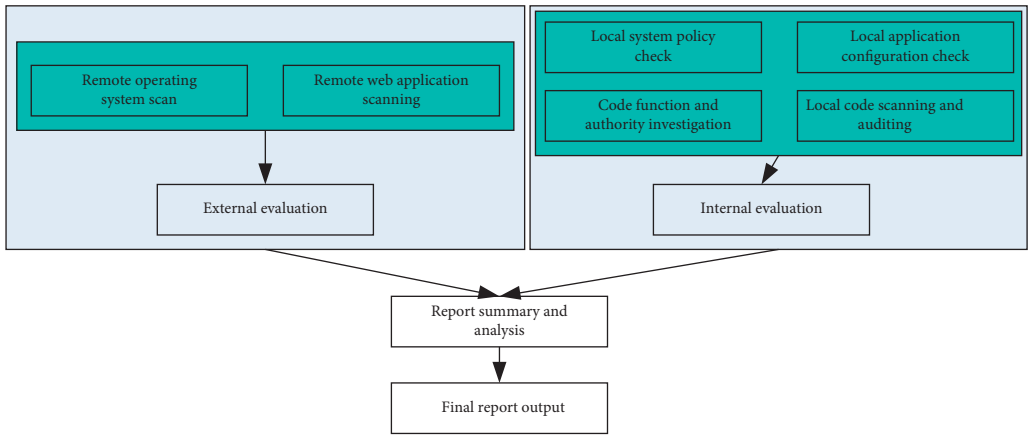

Figure 4: The working process of safety assessment.

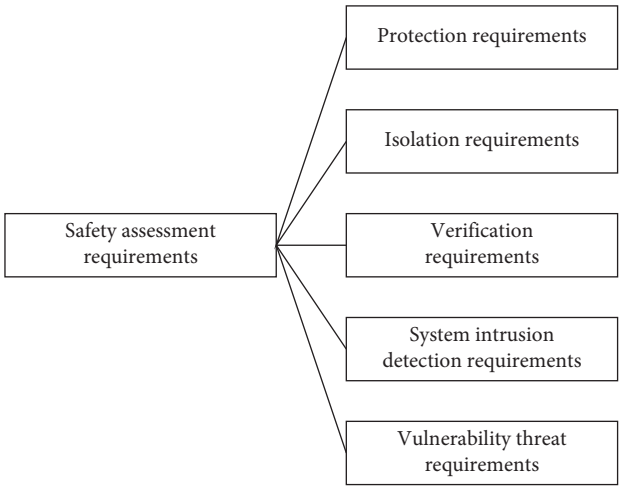

Figure 5: Safety assessment requirements.

resulting in attack vulnerabilities. Irregular vulnerability scanning and security evaluation can effectively deal with this, find and repair the imperfections of code design and system design, and can effectively prevent network attacks.

3. Penetration Test Method Design

In the actual operation, the penetration test [22] will be divided into three parts and stages. Different angles will make the differentiation methods different. For example, it is divided into preparation stage, penetration test stage, and overall comparison and evaluation stage on the theoretical basis, while in the technical operation, it is divided into three stages: detection, attack penetration, and target permission acquisition. The specific implementation of penetration test needs to consider the following factors: the scale of the client, the distribution of the network, and the composition of the system. In the content of the scheme, it is necessary to specify the test purpose and scope, time, place, personnel information, risk avoidance means and methods, overall plan, process, etc.

The overall test includes three parts: information collection and detection, vulnerability scanning, and penetration attack (as shown in Figure 6). In the detection stage, it is mainly to collect information and investigate. First, it is necessary to use the single dimension method to test.

(1) *Detection phase*. We use the main software and tools in the market to test two different websites, compare the results, and then design the detection module in the design of the automatic penetration test integration system.

(2) *Vulnerability scanning phase*. It mainly uses scanning tools to scan the website, obtain vulnerability information, summarize the scanned vulnerabilities, and summarize the advantages and disadvantages of each scanning tool, which can be used as a reference for the design of scanning module in automatic penetration test integration system.

(3) *Infiltration stage*. We use terminal operation and graphical interface operation to penetrate the website, find the security problems existing in the website, analyze the test results in detail, repair the existing security problems and vulnerabilities, and design the penetration attack module of the automatic integrated test system.

(4) *Automated penetration testing phase*. We design and implement the automatic penetration test system and use the system to conduct automatic penetration test on the website. By comparing the test results with the previous single dimension method, we draw some conclusions and the advantages and disadvantages of the two methods so as to provide experience for website security maintenance in the future.

4. Safety Assessment Method Design

Security risks need to be quantified, which is not only conducive to the quantitative calculation of risk value but also allows the client to feel the security of the website and system more intuitively [23, 24]. The flow chart of the safety assessment is shown in Figure 7.

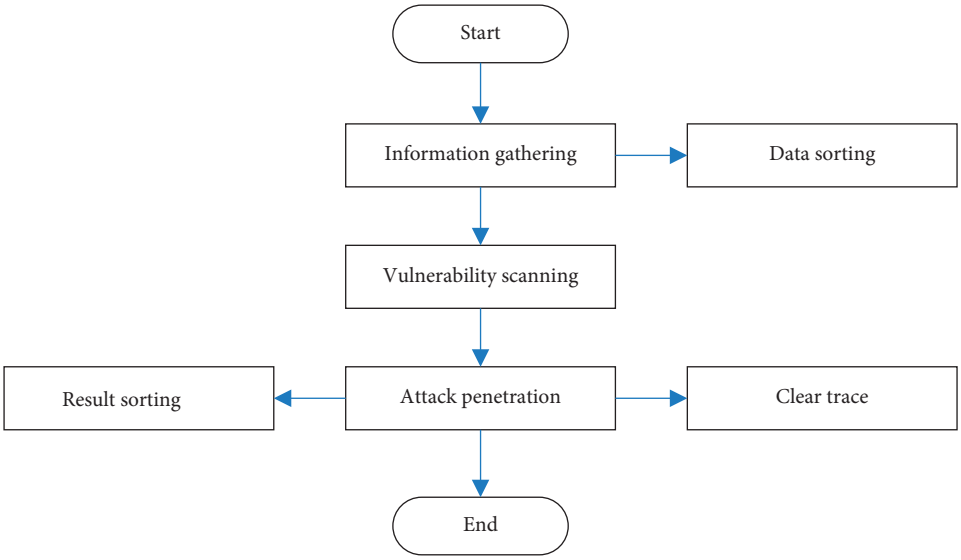

Figure 6: Penetration test flow.

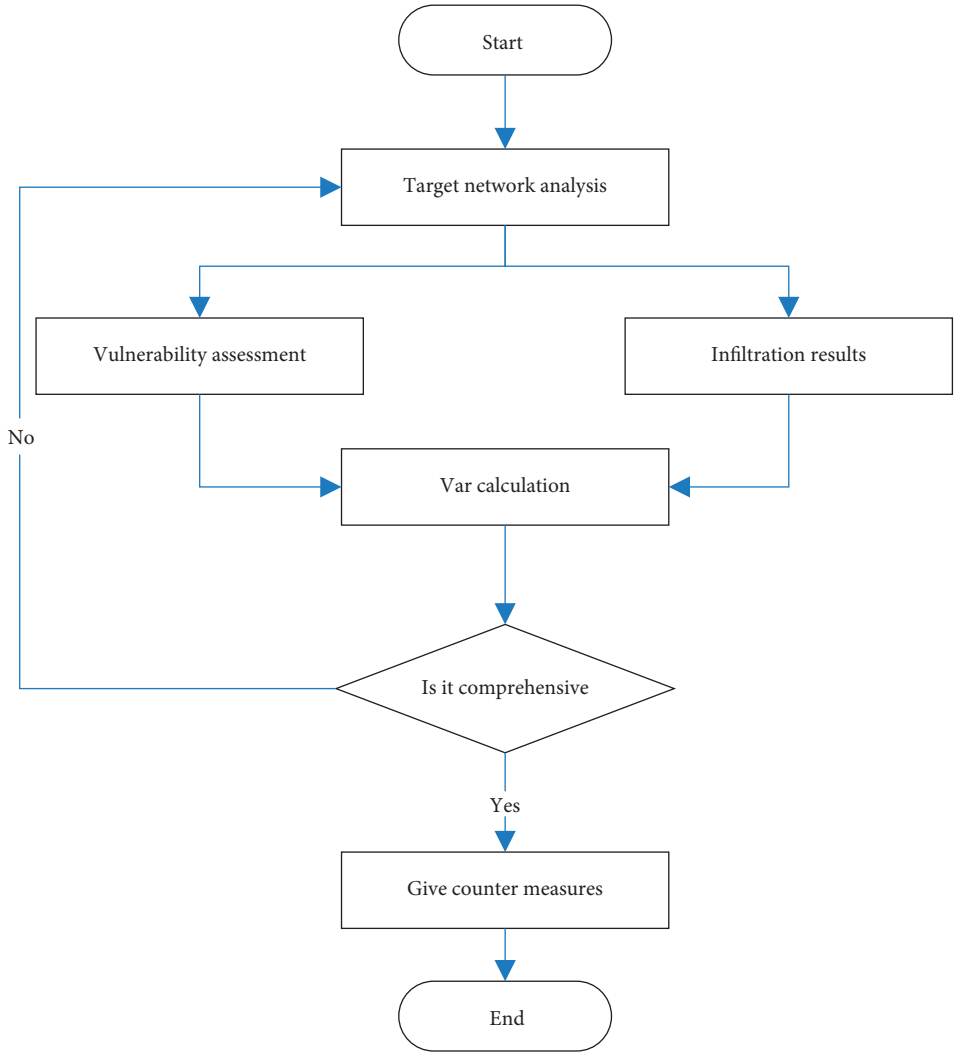

Figure 7: Safety assessment flow.

Before formulating the algorithm of security risk calculation, the selection of variables is very key. Most of the previous evaluation algorithms calculate with one or two variables. The advantage of such calculation is that it is convenient to get the result and will not make mistakes, but the disadvantage is that there are too few reference factors. There are often many indicators that affect the security of a system. When scoring, they need to be taken into account, it is relatively feasible to focus on several main factors and calculate the weight with other factors as a reference. Vulnerability risk quantification is one of the most important factors in the whole security assessment process. The overall security of the system depends on the weakest part. Which risk quantification value of the detected vulnerability is greater will determine the weakness of the whole system. The quantitative value needs to be calculated by the set evaluation algorithm, and the quantitative evaluation of system security can be effectively obtained according to the calculated results.

Most quantitative value algorithms pay more attention to the quantification of vulnerability threats. By quantifying the threats of existing vulnerabilities and detected vulnerabilities, the security factor is evaluated according to the quantitative value, and a vulnerability threat quantitative table calculated by the algorithm is obtained. Through this table, the threat quantitative value of each vulnerability can be seen intuitively so as to use this value as a reference to obtain the website security evaluation coefficient. However, there are still some deficiencies in these evaluation methods. One of them is also the improved part of the algorithm proposed in this paper, that is, it is necessary to consider the test evaluators and website maintainers. As the attacker and defender, they also need a quantitative value for the judgment of system setting and network structure, and these factors cannot be considered after the test.

Many security attacks and risks are sudden, and there is no time to make a temporary response. Countermeasures need to be given in advance, and these countermeasures need to estimate the possible results of the two sides in the process of playing chess in advance. The security evaluation algorithm based on the prediction of attack and defense game results proposed in this paper adds the evaluation of system maintenance personnel on various structural factors of the network and system and the predictive evaluation of the whole website by using the existing knowledge system through the prior understanding of the website system. After the final test, based on the test results, we make an overall evaluation with reference to the quantitative value of vulnerabilities. Combined with the previous evaluation of maintenance personnel, we get the final score through the algorithm. The relevant variables are described below.

Evaluation of website by website maintenance personnel.

Taking each page and structure of the website as variables, a score of X_{i} is obtained, where i ranges from 1 to N, X_{i} ranges from 0 to 10, and the score results are expressed as A. That is

$$A = \sum_{i=1}^{n} X_i. \tag{1}$$

Here, A is the sum of the scores given by the maintenance personnel on each page of the website, and then, we calculate the average to obtain the score B of a single maintenance personnel.

$$B = \frac{A}{n}. \tag{2}$$

The score of each page and structure constitutes a vector.

$$\overrightarrow{Z}_i = (Z_1, Z_2, \ldots, Z_n). \tag{3}$$

Here, n is still the number of website pages and structures, and each page also needs to have a proportion. It also needs to be evaluated by maintenance personnel. It is defined as $V_i V_{\mathrm{i}}$. C represents the whole weight vector, then

$$\overrightarrow{C} = (V_1, V_2, \ldots, V_n). \tag{4}$$

Here, $V_1 + V_2 + \cdots + V_n = 1$.

Therefore, the score of the whole website is the inner product of two vectors. Through the calculation of the inner product, the results can be obtained more accurately. D is defined as the importance score of each module of the website, then

$$\overrightarrow{D_i} = \overrightarrow{Z_i} * C. \tag{5}$$

The first is the comprehensive scoring algorithm of the maintenance personnel for the website, and the next is the evaluation algorithm of the tester. Since the tester needs to simulate the attacker's destruction of the website to the greatest extent, we need to consider the strength of penetration testing and focus on the algorithm for some serious vulnerabilities detected.

Common Vulnerability Scoring System (CVSS) is a standard for vulnerability assessment, which intuitively reflects vulnerability risk by using numbers ranging from 0 to 10. The whole evaluation system of CVSS [25, 26] is composed of basic score, temporary score, and environmental score. The whole evaluation process is to integrate the scores of these three factors. First, calculate the values of each part according to the formula and then get the final score according to the summarized formula. A high score represents a high threat, and a low score represents a low threat. The overall evaluation process is shown in Figure 8.

We combine the accurate score based on the CVSS scoring standard with the importance score of each module of the website to obtain:

$$\alpha = \frac{B + D/n}{2} \times 0.4 + C \times 0.6. \tag{6}$$

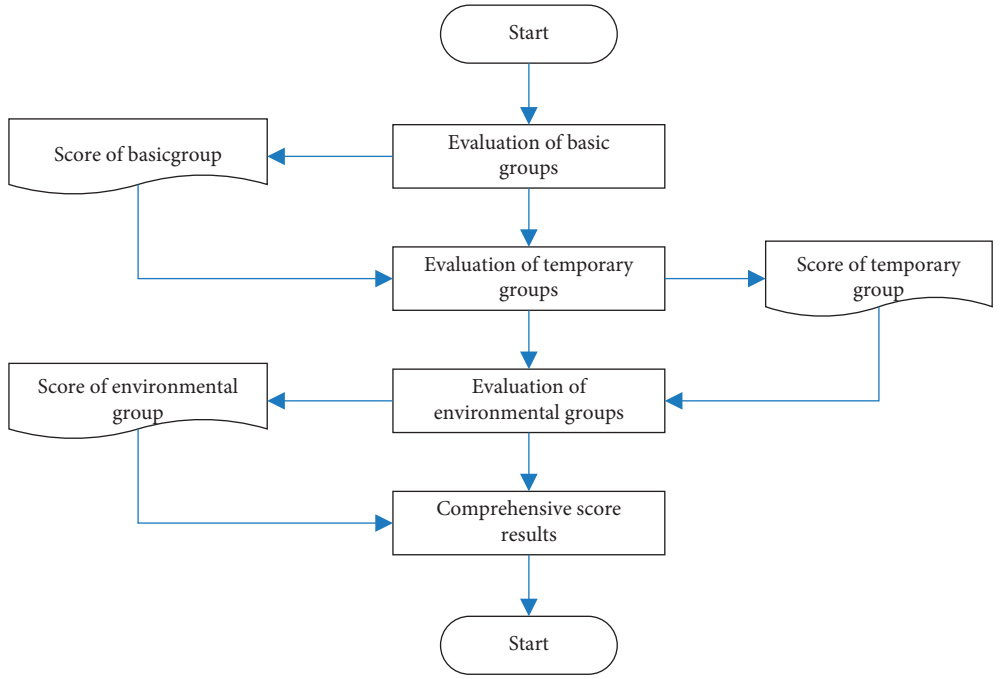

Figure 8: The overall evaluation process of CVSS.

Here, C is the score after CVSS optimization calculation. Since the system maintenance personnel may lack knowledge of system security vulnerabilities and security-related knowledge, they are given a base of 0.4 in weight distribution. Although the security testers are very good at security attacks, they are unable to have a detailed understanding of the overall structure, page blocks, and logic of the system in a short time, so the base is given as 0.6.

5. Design of Web Security Penetration Testing Tool

5.1. Overall Framework. We crawl for the target web application, obtain a large number of URLs and web page content, modify the parameters in the URL or construct abnormal HTTP requests to imitate the operation of malicious users, realize malicious injection, determine whether there are vulnerabilities in the web application by analyzing the response, and generate the corresponding report.

The classic MVC architecture is used to separate the view layer, business logic layer, and data layer and separate the functions of this tool. Using the modular design theory, the user interface module and vulnerability report module are mainly designed in the view layer, and the control engine module, crawl module, injection module, and analysis module are designed in the business logic layer. Due to the huge number of crawls and the need to use multithreading, the thread pool module in the common component is designed. The injection process needs to construct abnormal HTTP requests and analyze the response, so the HTTP proxy module is designed. Because there is some global processing information in the whole process, in order to better solve the migration and reuse of code, the configuration file module needs to be used. In the data layer, it mainly designs URL database, injection database, and analysis database. These independent modules only complete their own functions and do not need to pay too much attention to the functions of other modules. They communicate through some predefined interfaces to transfer parameters, which can improve the reusability of modules, and the modification or addition of new modules of some modules will not affect the normal work of other modules.

The overall frame design is shown in Figure 9.

5.2. User Interface Layer. The user interface layer is the bridge between the security penetration tester and the tested web application. In this module, testers can set the types of attacks that the tested web application wants to test (such as XSS and SQL injection) or test all types and then submit these information to the control engine to perform subsequent tasks.

This module can also generate a vulnerability report form to clearly show all scanning results to testers.

5.3. Logic Control Layer

5.3.1. Design of Web Crawler Module. The main function of the crawler module [27–29] is to crawl the web page, obtain the URL contained in the page through web page analysis, format and filter the obtained URL, and save it to the database. Of course, in the design process of the crawler module, considering the huge number of crawls and the long crawling time of using a single thread, multithreading is introduced, and the thread pool is mainly used here. In order to detect as many vulnerabilities as possible, we need to crawl the web page in sufficient detail. The crawl component we

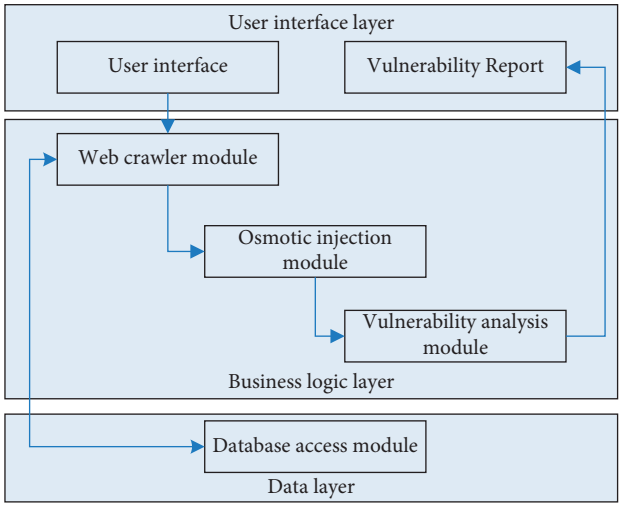

Figure 9: The overall frame design of web security penetration testing tool.

designed adopts the breadth-first strategy. The so-called breadth first is layer crawling, which indexes, processes, and grabs web pages according to the distribution and layout of layers. Because the web pages of many websites contain a large number of files and it is time-consuming to use a single thread, the general crawling components need to be set as multithreaded, which greatly reduces the crawling time and improves the crawling efficiency.

The flow chart of the web crawler module is shown in Figure 10.

5.3.2. Design of Penetration Injection Module. Penetration attack is to simulate the operation of malicious users and send malformed HTTP requests to the server. There are two methods for the HTTP request sent by the web application and the server. One is the GET method, and the other is the POST method. Therefore, the injection point is also divided into two kinds. For GET method, it only needs to modify the obtained URL, send the request to the server, and determine whether there is a vulnerability in the web application through the server-side response. For the POST method, it needs to use HTTP proxy to intercept the post request, modify the parameters, construct abnormal requests, and detect the vulnerabilities on the web application server.

Security penetration injection is mainly to send the modified HTTP request to the target web application. A large number of URLs can be obtained in the crawler module, and these URLs are stored in the database. We need to take out these URLs, find the injection attack point, and call the vulnerability detection plug-in to simulate the attack. The structure diagram is shown in Figure 11.

The penetration attack module mainly designs a control engine and several vulnerability attack plug-ins. The control module is the main thread of the program, controls the underlying vulnerability attack plug-ins, and contacts with the web crawler module. The main thread obtains the

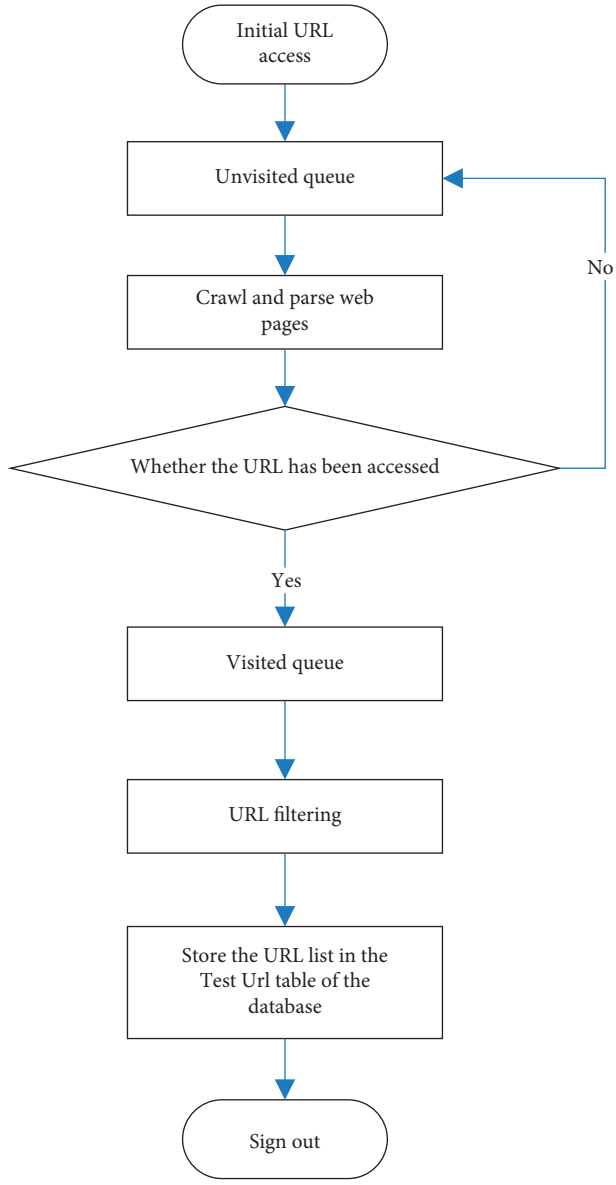

Figure 10: The flow chart of web crawler module.

application data through the web crawler module and gives it to the control module, which is responsible for transmitting the obtained data to each subthread. After receiving the data from the main thread, each subthread waits for the main thread to call the subthread and perform different types of vulnerability injection, respectively. Specifically, the tester can select a URL or all URLs for testing. After receiving the instruction, the control engine starts to call each vulnerability plug-in, construct a malicious attack connection, and complete the penetration injection process.

The design of the control engine is to separate the control logic from the specific execution module and achieve the decoupling effect. In this way, even if a new module is added or the original module is modified in the future, there is no need to modify the overall architecture of the tool, just add a new one in the interface class.

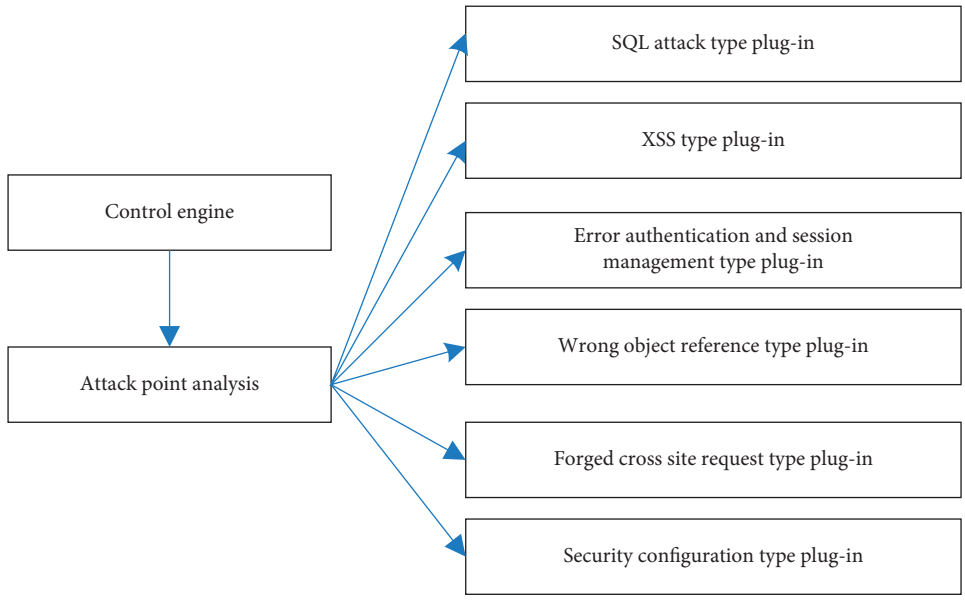

Figure 11: The structure of security penetration injection.

Table 1: Spider URL data table.

Field name	Field type	Is it nonempty	Record content	Remarks
ID	Int	Yes	Primary key	Self-increasing
URL	Varchar (25)		Requested URL	
URL_UNVISITED	Varchar (20)		The URL extracted from the crawled web page	
URL_VISITED	Varchar (20)		URL that has been crawled	

Table 2: Test URL data table.

Field name	Field type	Is it not empty	Record content	Remarks
ID	Int	Yes	Primary key	Self-increasing
URL	Varchar (30)		Requested URL	
DEPTH	Varchar (20)		URL depth	
RESPONSE_CODE	Varchar (20)		HTTP response code	
METHOD	Varchar (10)		HTTP request method	
GET_PARAM	Varchar (256)		GET request parameters	
POST_PARAM	Varchar (256)		POST request parameters	
REQUEST_HEADER	Varchar (20)		HTTP request header	
RESPONSE_HEADER	Varchar (20)		HTTP response header	
RESPONSE_BODY	Varchar (256)		HTTP response body	

5.3.3. Design of Vulnerability Analysis Module. Vulnerability analysis and injection complement each other. After the penetration injection attack is completed, the server will give a response and determine whether there are vulnerabilities in the web application by analyzing the response. Its main principle is to match the obtained response with the preset output. If the matching is successful, it indicates that there are loopholes. If the matching is not successful, it indicates that there are no loopholes.

Since the judgment rules of each vulnerability injection type are written in the corresponding vulnerability injection plug-in, after each vulnerability injection plug-in is called and a malicious link is sent, the returned response should be dynamically matched with the plug-in to determine whether there is such a vulnerability.

5.4. Data Layer. Due to the convenience of the database, the tool in this paper uses the database as the support. When the web crawler runs, it will save some important data to the database, and these data will also provide a solid foundation for the penetration injection module. The specific design of the data table involved is shown in Tables 1 and 2.

6. Conclusions

With the rapid development of network technology and web application technology, web application has penetrated into

every bit of people's life. However, the security problem of the web application has become more and more prominent and the most important technical challenge in this information age.

Through the research on the common vulnerabilities of web applications and the penetration testing technology to detect vulnerabilities, this study first designs and implements the web crawler module. The web crawler adopts the breadth-first crawling strategy. In the process of multithreaded crawling, it obtains all the URLs of the target website through web page parsing, URL formatting, and filtering. Then, the security penetration injection module is designed and implemented, the principle of the penetration injection module is analyzed in detail, the injection points and injection parameters of get type in the request of URL as well as the injection points and injection parameters of post type are analyzed, and the constructed malicious URL is sent to the server by using the automatic injection mechanism. Finally, the analysis module is designed and implemented.

Data Availability

The data set can be accessed upon request.

Conflicts of Interest

The authors declare that there are no conflicts of interest.

References

[1] Y. Dong, "Application of artificial intelligence software based on semantic web technology in English learning and teaching," *Journal of Internet Technology*, vol. 23, no. 1, pp. 143–152, 2022.

[2] L. Luo, "Web application software engineering technology and process," in *Proceedings of the Ieee Asia-Pacific Conference On Image Processing, Electronics And Computers, Ipec 2021*, pp. 935–937, Dalian, China, Apirl 2021.

[3] L. Li, B. Lei, and C. Mao, "Digital twin in smart manufacturing," *Journal of Industrial Information Integration*, vol. 26, no. 9, Article ID 100289, 2022.

[4] H. Lin, "Application of web 2.0 technology to cooperative learning environment system design of football teaching," *Wireless Communications and Mobile Computing*, vol. 2022, Article ID 5132618, 9 pages, 2022.

[5] R. Chen, "The design and application of college english-aided teaching system based on web," *Mobile Information Systems*, vol. 2022, Article ID 3200695, 10 pages, 2022.

[6] L. Li, T. Qu, Y. Liu et al., "Sustainability assessment of intelligent manufacturing supported by digital twin," *IEEE Access*, vol. 8, pp. 174988–175008, 2020.

[7] S. Qi, S. Li, and J. Zhang, "Designing a teaching assistant system for physical education using web technology," *Mobile Information Systems*, vol. 2021, Article ID 2301411, 11 pages, 2021.

[8] L. Li, C. Mao, H. Sun, Y. Yuan, and B. Lei, "Digital twin driven green performance evaluation methodology of intelligent manufacturing: hybrid model based on fuzzy rough-sets AHP, multistage weight synthesis, and PROMETHEE II," *Complexity*, vol. 2020, no. 6, 24 pages, Article ID 3853925, 2020.

[9] K. Zhang, "Web news data extraction technology based on text keywords," *Complexity*, vol. 2021, Article ID 5529447, 11 pages, 2021.

[10] L. Li and C. Mao, "Big data supported PSS evaluation decision in service-oriented manufacturing," *IEEE Access*, vol. 8, no. 99, pp. 154663–154670, 2020.

[11] J. Li, Y. Fu, J. Xu, C. Ren, X. Xiang, and J. Guo, "Web application attack detection based on attention and gated convolution networks," *IEEE Access*, vol. 8, pp. 20717–20724, 2020.

[12] M. Babiker, E. Karaarslan, and Y. Hoscan, "Web application attack detection and forensics: a survey," in *Proceedings of the 6th International Symposium On Digital Forensic And Security*, pp. 1–6, Antalya, Turkey, March 2018.

[13] S. Ninawe and R. Wajgi, "Detection of DOM-based XSS attack on web application," *Lecture Notes on Data Engineering and Communications Technologies*, vol. 33, pp. 633–641, 2020.

[14] K. B. Jalbani, M. Yousaf, M. S. Sarfraz, J. Oskouei, A. Hussain, and Z. Memon, "Poor coding leads to dos attack and security issues in web applications for sensors," *Security and Communication Networks*, vol. 2021, Article ID 5523806, 11 pages, 2021.

[15] X. Yu, W. Yu, S. Li, X. Yang, Y. Chen, and H. Lu, "WEB DDoS attack detection method based on semisupervised learning," *Security and Communication Networks*, vol. 2021, Article ID 9534016, 10 pages, 2021.

[16] A. K. Dalai and S. K. Jena, "Neutralizing SQL injection attack using server side code modification in web applications," *Security and Communication Networks*, vol. 2017, Article ID 3825373, 12 pages, 2017.

[17] R. R. Echeverria, J. C. Preciado, Á. Rubio-Largo, J. M. Conejero, and Á. E. Prieto, "A pattern-based development approach for interaction flow modeling language," *Scientific Programming*, vol. 2019, Article ID 7904353, 15 pages, 2019.

[18] A. K. Kayani and M. Q. Saeed, "Comparative analysis of antivirus evasion malware creator tools of kali linux, with proposed model for obfuscation," in *Proceedings of the 2021 international conference on cyber warfare and security, iccws*, pp. 24–29, Islamabad, Pakistan, November 2021.

[19] S. Einy, C. Oz, and Y. D. Navaei, "The anomaly- and signature-based IDS for network security using hybrid inference systems," *Mathematical Problems in Engineering*, vol. 2021, Article ID 6639714, 10 pages, 2021.

[20] X. Li, X. Jin, Q. Wang, M. Cao, and X. Chen, "SCCAF: a secure and compliant continuous assessment framework in cloud-based IoT context," *Wireless Communications and Mobile Computing*, vol. 2018, Article ID 3078272, 18 pages, 2018.

[21] E. Chatzoglou, G. Kambourakis, and C. Kolias, "Your wap is at risk: a vulnerability analysis on wireless access point web-based management interfaces," *Security and Communication Networks*, vol. 2022, Article ID 1833062, 24 pages, 2022.

[22] He-J. Lu and Y. Yu, "Research on WiFi penetration testing with Kali Linux," *Complexity*, vol. 2021, Article ID 5570001, 8 pages, 2021.

[23] U. Khadam, M. M. Iqbal, M. Alruily et al., "Text data security and privacy in the Internet of things: threats, challenges, and future directions," *Wireless Communications and Mobile Computing*, vol. 2020, Article ID 7105625, 15 pages, 2020.

[24] M. Bilal, M. Asif, and A. Bashir, "Assessment of secure openid-based daaa protocol for avoiding session hijacking in web applications," *Security and Communication Networks*, vol. 2018, Article ID 6315039, 10 pages, 2019.

[25] K. Gencer and F. Başçiftçi, "The fuzzy common vulnerability scoring system (F-CVSS) based on a least squares approach with fuzzy logistic regression," *Egyptian Informatics Journal*, vol. 22, no. 2, pp. 145–153, 2021.

[26] M. Saulaiman, M. Takacs, M. Kozlovszky, and A. Csilling, "Fuzzy model for common vulnerability scoring system," in *Proceedings of the 2021 - ieee 15th International Symposium On Applied Computational Intelligence And Informatics*, pp. 419–424, Timisoara, Romania, May 2021.

[27] R. Liu, "Network crawler technology based on Python under information," in *Lecture notes in electrical engineering*, pp. 1941–1948, Springer, Berlin, Germany, 2021.

[28] M. Júnior, T. A. Rezende, M. F. Pontes, D. Assis, and G. Tavares, "Development of a focused web page crawler based on genre and content," in *Proceedings of the 20th international conferences on www/internet 2021 and applied computing 2021*, pp. 77–84, Portugal Portugal, August 2021.

[29] J. Pan, "Application of web crawler technology based on Python in big data environment," *Lecture Notes on Data Engineering and Communications Technologies*, vol. 102, pp. 571–577, 2022.

Hindawi
Scientific Programming
Volume 2022, Article ID 7486271, 7 pages
https://doi.org/10.1155/2022/7486271

Research Article

Early Fault Diagnosis Model Design of Reciprocating Compressor Valve Based on Multiclass Support Vector Machine and Decision Tree

Zhihong Yu,[1] Bosi Zhang ,[1] Guangxia Hu,[1] and Zhigang Chen[2]

[1]*Department of Security Engineering, China University of Labor Relations, Beijing, China*
[2]*Institute of Mechanical and Electrical Engineering, China Architecture University, Beijing, China*

Correspondence should be addressed to Bosi Zhang; yuzh06@culr.edu.cn

Received 23 April 2022; Revised 9 May 2022; Accepted 16 May 2022; Published 8 June 2022

Academic Editor: Jie Liu

According to the character of frequent fault occurrence, difficult diagnosis of large reciprocating compressor valves, an early fault diagnosis model of reciprocating compressor valve based on multiclass support vector machine and decision tree is designed. A series of simulation experiments of the suction valve and exhaust valve on a large-scale reciprocating compressor experimental bench are made and the valve fault principle is analyzed. Using the advantages of fast and efficient decision tree classification and the prominent characteristics of support vector machine in small sample binary classification, a multivariate classification and recognition model is constructed. The typical characteristic parameters of gearbox vibration signal are extracted as the fault feature vector training model under different fault conditions, and the samples are tested. The experimental results show that the recognition effect of this method is significantly better than that of the neural network method in the case of small samples, and the recognition efficiency is improved more than that of the conventional multivariate support vector machine method which can be effectively applied to reciprocating compressor valve fault diagnosis.

1. Introduction

There are a large amount of dynamic equipment of different categories in the oilfield west of China. All different kinds of equipment for powering, frequency converting, ventilating, and fluid transporting are connected into a chain with series connection or parallel connection, and a complex system comes into being [1]. It is a big challenge to build a model due to mutual coupling, multiple fault models, and complicated patterns and even with implication. Reciprocating compressor has become the critical equipment of oilfield west of China due to the advantage of wide range and high efficiency of pressure and exhaust coupled with stable pressure when adjusting the gas volume. But its structure is complex and most of its components are susceptible to failure. According to the statistics, valves, packing seal, and piston ring are the components with the top failure rate which may cause irregular shut down of reciprocating compressor, among which the shut down due to the failure of the valves accounts for more than 36% [2]. The valves and cylinders have to endure high pressure and temperature. In addition, valves must inhale and exhale the high velocity gas within a short period. The working condition is very serious. How to extract feature parameters from complex and changeable signals is critical for diagnosis. It presents even stricter requirements for the diagnosis model due to tremendous difficulties in extracting feature parameters and unobvious characterization resulting from weak energy change of the feature parameters during the early fault.

The traditional diagnosis method is based on the statistical analysis of a large amount of samples. As a matter of fact, the amount of samples, especially the fault samples, is quite limited and even in the absence [3] in a real test. With the development of information science [4–7], various new theories and ideas begin to enter the field of fault diagnosis [8–11]. Support Vector Machine (SVM) theory presents the

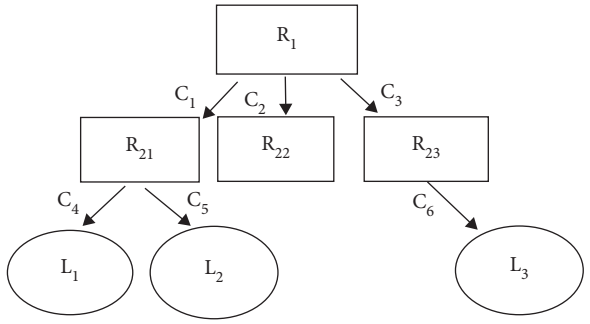

Figure 1: Structure of decision tree.

advantage of the small size of training samples, great generalization ability, and easiness of getting an optimal global solution. It has been widely applied to multiple areas such as electricity, economy, and medical science and diagnosis [12–14]. A decision tree is one kind of inductive learning algorithm based on data. It aims at finding the classification rules from a set of nonsequence and nonrule data. It can be applied to build a classifier and a prediction model which can be used to reduce the training amount of Support Vector Machine and improve the efficiency and accuracy of classification [15–18]. By adopting the method with the combination of a decision tree and Support Vector Machine to build a multiple classifier, the recognition effect and efficiency are much improved compared with the traditional neural network method and conventional multiclass Support Vector Machine.

2. Support Vector Machine Based on Decision Tree

2.1. Basic Principle of Decision Tree. The decision tree is a forecast model which represents the mapping relationship between the attribute of the object and the value of the object [19]. As is shown in Figure 1, a decision tree is comprised of nodes and branches, and the nodes include both internal nodes and leaf nodes. Each internal node, such as R1, R21, R22, and R23 in the figure, represents one attribute. Each leaf node, such as L1, L2, and L3 in the figure, represents one category. Each leaf node, such as cl, c2, c3, c4, and c5 in the figure, represents one test value of the attribute. Two steps are included in the whole process of the classification of the decision tree. The first step is to establish and refine a decision tree based on the clusters of the training sample and to set up the model of the decision tree. As a matter of fact, it is a process to obtain knowledge from data and undertake machine learning as a whole which normally can be divided into 2 stages: establishing and pruning. The second step is to analyze the new data by using the decision tree established [20, 21].

One classification subtask will be performed for each node in the tree. In the classification stage, the bottom-up aggregation algorithm is used to generate the logical structure of the decision tree [21]. Because there is no need to traverse all classifiers, the operation time and classification accuracy are relatively high.

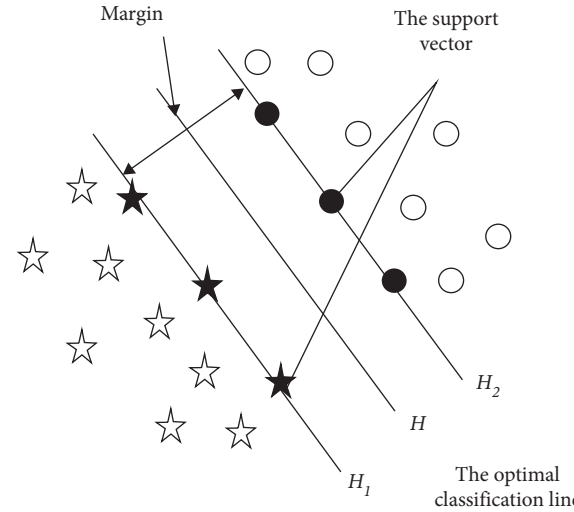

Figure 2: The diagram of optimal hyperplane.

2.2. Basic Theory of Support Vector Machine. The support vector machine method is used to propose the optimal hyperplane in the linearly separable case. As is shown in Figure 2, the star and the circle in the optimal hyperplane represent two types of samples separately, H represents the classification line, H1 and H2 represent the samples closet to and in parallel with the classification line in each category the distance between which is called classification margin [22].

Expanded to the linear nonseparable case, considering that some of the samples can not be correctly classified, the constraint condition of hyperplane can be expressed as follows: yi(xiω+b)-1≥0, in which b is the threshold value and ω is the normal vector of the hyperplane. The Lagrange multiplier method should be adopted to achieve the solution of the nonlinear optimal hyperplane.

$$L(\omega, b, a) = \frac{1}{2}\|\omega\| - \sum_{i=1}^{1} a_i \left[y_i \left(x_i \omega + b \right) - 1 \right], \tag{1}$$

where $a_i \geq 0$, $i = 1, 2, \ldots, 1$;

The extreme point of L is the saddle point. The minimum value of L for ω and b is set as $\omega = \omega *$, $b = b *$, and the maximum value for a set as $a = a *$.

Therefore, the original problem under linear separable condition is converted into a dual problem. The maximum value of the following dual formula is to be solved:

$$\max(a) = \sum_{i=1}^{l} a_i - \frac{1}{2} \sum_{j=1}^{l} \sum_{i=1}^{l} a_i a_j y_i y_j x_i x_j,$$

$$s.t \begin{cases} a_i \geq 0, \\ \sum_{i=1}^{l} a_i y_i = 0. \end{cases} \tag{2}$$

With regard to linear nonseparable problems, the sample x can be mapped to a high dimensional feature space H and the linear classifier is to be applied in H. Therefore, through adopting the appropriate inner product function K(xi,xj) in the optimal hyperplane, we can achieve a linear classification

by nonlinear transforming without adding any computation complexity. So the objective function becomes as follows:

$$W(a) = \sum_{i=1}^{l} a_i - \frac{1}{2}\sum_{j=1}^{l}\sum_{i=1}^{l} a_i a_j y_i y_j k\left(x_i x_j\right),$$
$$s.t \begin{cases} 0 \le a_i \le C, \\ \sum_{i=1}^{l} a_i y_i = 0, \end{cases} \tag{3}$$

where constant C is the penalty coefficient for the samples over the boundary controlling the degree of punishment for misclassification samples.

If a_i^* is the optimal solution, the decision function can be expressed as follows:

$$f(x) = \sum_{i=1}^{l} y_i a_i^* K\left(x_i, x_j\right) + b^*, \tag{4}$$

where $b^* = 1/2\left\{\max_{\{i/y_i=-1\}}[\sum_{j\in(sv)}^{l} a_i y_i k(x_i, x_j)] + \max_{\{i/y_i=+1\}} [\sum_{j\in(sv)}^{l} a_i y_i k(x_i, x_j)]\right\}$.

The detailed derivation process can be seen in reference [23].

Different support vectors can be obtained by choosing different kinds of kernel functions. There are four kinds of frequently used kernel functions among which the radial basis kernel function is most commonly used [24].

2.3. Multivariate Classification Support Vector Machine

2.3.1. One-to-Many Support Vector Machine. The one-to-many algorithm [25] is first used for multivalue classification of Support Vector Machine. This method uses a two class support vector machine classifier to distinguish each category from all other categories in sequence. For a problem of n categories, n support vector machines will be trained by the one-to-many method, namely, to adopt n separating hyperplanes to classify.

However the disadvantages of this method are as follows: on one hand, there are requirements for the number of positive and negative samples which will greatly reduce the accuracy of classification by adopting the one-to-many method. On the other hand, because all the training samples shall be used in the training of each support vector machine, the computation efficiency is very low.

2.3.2. One-to-One Support Vector Machine. For a problem of n categories, one support vector machine is built for each of n categories of the samples by adopting a one-to-one method. So n(n-1)/2 support vector machines will be trained in total [26]. This method requires more samples, but the training speed is faster than that by using the one-to-many method. By comparison of above-mentioned classification methods of multivalue support vector machine with each other, the one-to-one method is believed to have the better classification effect with more expense. The one-to-many method has an ordinary classification effect with less expense.

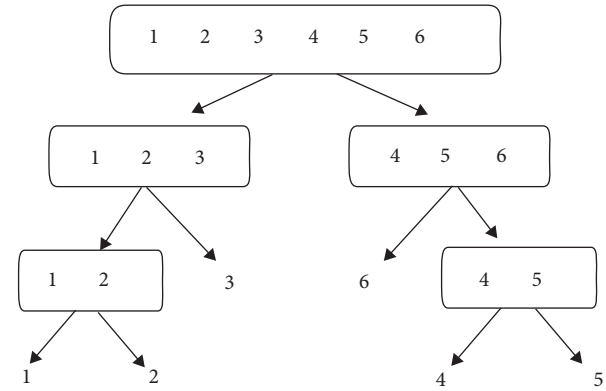

Figure 3: A sketch diagram of decision tree structure for multiclassification SVM.

2.3.3. Support Vector Machine Based on Decision Tree. Support vector machine has excellent generalization performance in the case of small training samples. But for multiclassification problems, it is often necessary to build multiple classifiers and the diagnosis efficiency is low. In this paper, a multiclass fault identification model of a reciprocating compressor valve is established by combining the decision tree and support vector machine.

Through this model, the multiclassification problem is decomposed into a series of two value classification problems, which are distributed in each node of the decision tree. In the classification, the decision tree root node and the branch node are divided into several subsets level by level according to the different attributes, until all the leaf nodes are obtained. One-to-many or one-to-one support vector machine model will be chosen according to the actual situation when dividing into subsets according to the attribute. As an example of dividing into 6 categories, Figure 3 is one kind of decision tree classification diagram, which shows the process of dividing 6 types of input samples into corresponding categories level by level. As can be seen from Figure 3, the advantages of the small number of vector machines of the one-to-many classification model, high classification identification accuracy of the one-to-many classification model, and high classification efficiency for decision tree classification are considered comprehensively in the support vector machine based on the decision tree.

The main failure parts of the valve include the valve seat, spring, and valve plate. The valve seat is the main part of the valve. The valve seat and lift limiter form the space of the valve set. The concentric convex surface of the valve seat and the valve plate form a sealing structure of the gas. The imperfect sealing of the valve sealing structure will result in the gas return, inefficiency of suction and exhaust, and abnormal thermal parameters such as gas temperature and pressure. It will also cause vibration signal and noise change. Therefore by adopting the vibration method, not only the air leakage of the valve can be monitored, but the size of the leakage gap can be determined. The main forms of the spring failure include broken and the elasticity change. If the elasticity becomes small, the closing of the valve plate will be delayed which will cause temperature and pressure changes of the circulating gas.

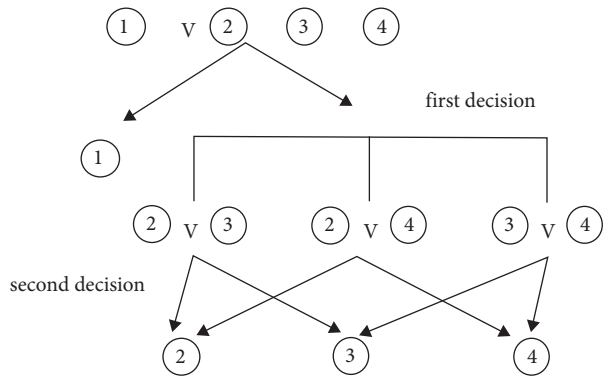

Figure 4: The classification diagram of DT-SVM.

The impact strength of the valve plate on the lift limiter will be increased which accordingly makes the impact vibration and noise increase. If the elasticity becomes large, air pressure can not make the valve plate stick to the lift limiter surface when opening the valve which will cause the vibration of the valve plate. A broken spring can cause complex vibration, blocked valve movement, nonuniform force on the valve plate, etc. Therefore, spring failure will be reflected in the thermodynamic and dynamic parameters. The vibration diagnosis method can diagnose the fault of spring break or elastic change. The valve plate is the key part of the valve the role of which is to close the air passage after the suctioning or exhausting. The main forms of valve plate include deformation and fracture. With the nonuniform force resulting from the valve plate deformation, the impact force is becoming stronger. However, complex vibration will be caused by fragmentation of the valve plate.

In this paper, the experimental object is a reciprocating compressor valve fault. Based on the analysis of the fault of the valve of the reciprocating compressor, the fault diagnosis model of multiclassification support vector machine is built by applying the principle of the decision tree support vector machine. As an example to identify the four kinds of faults such as normal valve, valve plate fracture, valve plate wear, and spring failure of the valve plate, the classification model is shown in Figure 4. As the device is in normal operation most of the time, it is quite easy to obtain the samples of the normal running status of the valve plate in the actual test. At the same time, distinguishing the normal operation from other faults of the compressor valve is relatively easy. Therefore, the main purpose of the decision for the first level is to exclude nonfault samples. Nonfault samples can be quickly identified by adopting a one-to-many classifier. At the second level, the three kinds of faults can be identified, respectively, by applying the one-to-one Algorithm. Three one-to-one classifiers will be required during this process. Only four support vector machines will be required in total for this model. Compared with $4 * (4 - 1)/2 = 6$ required in 2.3.2, two support vector machines will be reduced. In theory, it will take less time to train and test and diagnosis efficiency will be improved.

The location of the fault may be involved in the valve seat, spring, valve plate, and other key parts. Because each component has its own fault type, in order to improve the diagnostic efficiency, the fault component should be identified first and the specific type of failure of the component can be determined later. Therefore, in the case of an unknown valve fault of a reciprocating compressor, the first level of decision-making can be designed to identify the faulty components and the second level decision is to determine the fault type of the specific parts.

Table 1: Operating parameters of reciprocating compressor.

Rated operating pressure (Mpa)	Rated exhaust (m^3/min)	Rated speed (r/min)	Cooling mode
0.2	12	500	Water cooling

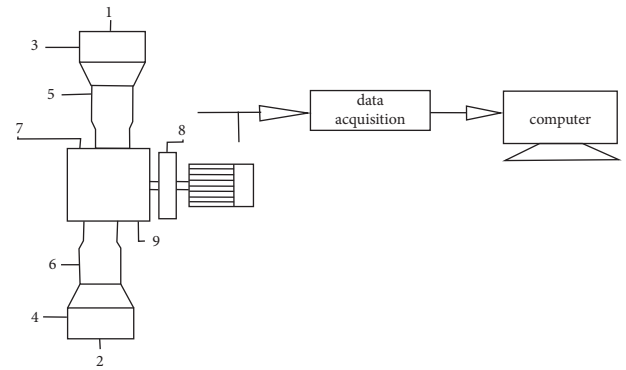

Figure 5: System of Valve of reciprocating compressor fault signal acquisition.

3. Experimental Investigations

3.1. Experiment Platform. The equipment used in the experiment is a reciprocating compressor of the double cylinder and double acting which is very close to the compressor used in the actual production of refining and petrochemical companies. A series of related destructive tests are designed for the suction valve and exhaust valve on the experimental platform of the real reciprocating compressor. Using the sensor to collect the vibration signal of the compressor set and temperature signal of the valve, the signal most similar to fault data of the real situation can be collected to the maximum extent. The specific operating parameters of the compressor are shown in Table 1.

The actual situation is shown in Figure 5, where 1 and 2 are cylinder head impact point and acceleration sensor; 3 and 4 are temperature measuring point and install platinum thermal resistance sensor; 5 and 6 are cross head impact point and acceleration sensor; 7 and 9 are crankcase outer surface, internal vibration measuring point, and acceleration sensor, respectively; and 8 is the key phase measuring point and eddy current sensor.

Four types of operating conditions such as normal valve, valve fracture, valve plate wear, and valve spring failure are simulated under the exhaust pressure (gauge) of 0 Mpa, 0.1 Mpa, and 0.2 Mpa, respectively. In this experimental

Table 2: Feature vector of signal sample.

Fault type	Sample number	Crest coefficient	Kurtosis index	Skewness index	Effective value	Standard deviation	Fault number
Normal valve	1	0.0303	0.0029	0.0458	0.7609	0.79257	①
	2	0.1023	0.2164	0.3279	0.5665	0.9026	①
	3	0.0402	0.0367	0.1469	0.6367	0.9881	①
	4	0.6129	0.0294	0.3205	0.6137	0.8351	①
	5	0.1425	0.0561	0.3361	0.4821	0.7093	①
Valve fracture	1	0.0478	0.0463	0.0917	0.84221	0.00135	②
	2	0.6190	0.0637	0.3275	0.6347	0.9027	②
	3	0.4543	0.3219	0.3575	0.5342	0.9434	②
	4	0.2011	0.0676	0.3821	0.5038	0.9221	②
	5	0.3579	0.1041	0.3528	0.5674	0.8657	②
Valve plate wear	1	0.9581	0.6287	0.4292	0.5821	0.5238	③
	2	0.9893	0.7953	0.3453	0.6281	0.8671	③
	3	0.7859	0.6513	0.4217	0.6915	0.9877	③
	4	0.9139	0.7385	0.5446	0.6609	0.8592	③
	5	0.8768	0.6054	0.4573	0.6581	0.9107	③
Valve spring failure	1	0.3082	0.2787	0.2168	0.7635	0.4891	④
	2	0.1027	0.1669	0.2461	0.7623	0.9135	④
	3	0.4103	0.3373	0.1931	0.8938	0.9437	④
	4	0.3841	0.2673	0.2037	0.7589	0.9276	④
	5	0.3724	0.1976	0.2524	0.7095	0.9471	④

platform, the valve is simulated with 4 scenarios, respectively: 1 as normal valve, 2 as valve fracture, 3 as valve plate wear, and 4 as valve spring failure. With experiments performed many times for each typical fault, multiple sets of feature vectors can be obtained and used as the sample of this kind of fault training which can reflect the fault rule. The vibration signal is measured in normal mode, and then the fault valve is tested. In the experiment, the piezoelectric IEPE acceleration sensor is used to collect the vibration data, and the sampling frequency is set at 10 KHz. 20 groups of original samples are extracted for each status with continuous sampling.

3.2. Feature Extraction of Reciprocating Compressor Valve. Different kinds of characteristic parameters of vibration signal will show different aspects of fault information. Sensitive parameters to the fault are chosen from the time and frequency domain such as amplitude maximum in the frequency domain, frequency domain mean, and dynamical indicators in the time domain (peak value, absolute value, effective value, and variance value). In reference [27], the following characteristic quantities are selected to describe the characteristic of the wave of the signal. Normalized treatment has to be done to make them into [0,1] data before building the model because of the different dimension between the parameters in the time and frequency domain. Feature vectors of the fault are shown in Table 2.

3.3. Learning and Training. Select 5 sets of samples of reciprocating compressors from each type of all the four types. A total of 20 sets of signal samples are used to learn and train according to the model in Figure 4 and the decision function of the corresponding support vector machine is built. Based on the fault diagnosis model of the reciprocating compressor valve established by using the multiclassification support vector machine, the radial basis kernel is chosen after the analysis. The training steps are as follows:

Table 3: Result of test samples.

No.	1 V 234	2 V 3	2 V 4	3 V 4
1	0.8609	—	—	—
2	0.9012	—	—	—
3	−1.0000	1.0000	1.0000	1.0000
4	−1.0000	−0.9843	0.0728	1.0000
5	−1.0000	0.2074	−0.5027	−1.0000
6	−0.1209	0.5352	1.0000	0.2051
7	−1.0000	-0.3492	1.0000	1.0000
8	−1.0000	1.0000	−0.3105	−1.0000

(1) Data format conversion to the recognizable format required by the libsvm software package

(2) Transform the scale of the training sample and map the sample set to [-1,1]

(3) Train model parameters (Penalty factor C and kernel function parameter σ)

(4) With parameters C and σ obtained in step 3, the training samples after scaling in step 2 can be used for training by using this model

(5) Input test samples into the trained model and check the classification result

Using the above-mentioned sample data to train the support vector machine classifier in sequence and obtaining the optimal classification function. Finally, the optimization of the parameters of the classifier is obtained with the penalty factor C equal to 2 and radial basis parameter σ of the kernel function equal to 2.

Table 4: Classification results based on the DT-SVM.

No.	Fault 1	Fault 2	Fault 3	Fault 4	Diagnosis result
1	1	0	0	0	Normal
2	1	0	0	0	Normal
3	0	2	1	0	Valve plate wear
4	0	1	2	0	Valve spring failure
5	0	1	0	2	Valve fracture
6	0	2	1	0	Valve plate wear
7	0	1	2	0	Valve spring failure
8	0	1	0	2	Valve fracture

Table 5: Comparison of identification result.

Model	Sample number	Correct diagnosis	Identification time (s)	Accuracy rate (%)
DT--SVM	30	28	1.69	93.3
SVM	30	28	2.55	93.3
BP($\delta = 0.01$)	30	25	11	83.3
BP($\delta = 0.05$)	30	23	15	76.7

3.4. Test. In order to test the effect of the classifier, 8 groups of samples which are known to be tested are used to verify the classifier. The generalization ability and accuracy of the classifier are to be tested. Table 3 gives the output of different decision functions of the support vector machine for samples to be diagnosed. As is shown in the first column, normal valve ① is distinguished from fault valves ②, ③, and ④ quickly. If the result is positive, it will be a positive sample which means a normal valve. The identification ends; If the result is negative, it will be classified into the other three types which mean fault valve. As is shown in columns 2, 3, and 4, a further one-to-one classification and identification will be needed.

According to the membership of the output of the independent support vector machine in the decision structure, the classification of the test sample is diagnosed. When one of the SVMi,j is determined to be classified as fault i for fault sample x, class i gets one vote. Vice versa, class j will get one vote. The fault type of each sample will be determined according to the respective score in each fault type of such sample. The final vote of each test sample is shown in Table 4.

As can be seen in Table 4, the diagnosis results are in complete agreement with the fault types preset for the samples, which are based on the decision rules for diagnosis set up in this paper.

3.5. Comparison with Conventional Methods. To further compare the classification results, 20 groups of samples are used to test different models. The classification effect is shown in Table 5.

As can be seen from Table 5, the recognition effect of the decision tree support vector machine established based on the actual fault is the same as that of the conventional multiple support vector machine. But it is obviously better than the recognition effect of the traditional neural network method. However, the classification and recognition time of the decision tree support vector machine is saved by about 35% compared with that of a conventional multiple support vector machine.

4. Conclusion

In this paper, with the advantages of the high efficiency of the decision tree combined with the advantages of the "one-to-one" and "one-to-many" multivalue classification method of SVM, the fault identification model of a reciprocating compressor valve based on decision tree and support vector machine is designed. Applying the model to the fault identification of a small sample number of reciprocating compressor valves, it can be seen from the test results and training classification results that the decision tree support vector machine diagnostic method has strong recognition ability and good classification result which is obviously better than the traditional neural network method when used in small sample cases and early fault diagnosis of the air valve.

Decision tree and support vector machine are used to construct a support vector machine model in the form of a decision tree the recognition effect of which is equivalent to a one-to-one multisupport vector machine, and the time for learning training and testing of which is much shorter than the conventional support vector machine. The effect is more obvious with the increase of the number of classification. Therefore, the DT-SVM is more efficient than the conventional support vector machine.

Data Availability

The data used to support the findings of this study are available from the corresponding author upon request.

Conflicts of Interest

The author declares that there are no conflicts of interest.

Acknowledgments

This research was funded by the China University of Labor relations under Grant No. 22XYJS007.

References

[1] Y. Ai and C. Fei, "Rotor vibration fault diagnosis technology based on support vector machine," *Journal of Shenyang Technology University*, vol. 32, no. 5, pp. 527–531, 2010.

[2] D. Wu, "A gear box fault diagnosis method based on support vector machine," *Vibration, Testing and Diagnosis*, vol. 04, pp. 338–342, 2008.

[3] B. Schlkopf and A. J. Smola, *Learning with Kernels, Support Vector Machines, Regularization, Optimization and beyond*, The MIT Press, Cambridge, MA, USA, 2001.

[4] C. Wang, Z. Liu, and Y. Wang, "Intelligent fault diagnosis of photoelectric pod bearing based on multi-information fusion," *Journal of Physics: Conference Series*, vol. 2136, no. 1, 2021.

[5] L. Li, B. Lei, and C. Mao, "Digital twin in smart manufacturing," *Journal of Industrial Information Integration. January*, vol. 26, no. 9, Article ID 100289, 2022.

[6] L. Li, T. Qu, Y. Liu, S. Hongxia, and G. Yang, "Sustainability assessment of intelligent manufacturing supported by digital twin," *IEEE Access*, vol. 8, pp. 174988–175008, 2020.

[7] T. Tang, T. Hu, M. Chen, R. Lin, and G. Chen, "A deep convolutional neural network approach with information fusion for bearing fault diagnosis under different working conditions," *Proceedings of the Institution of Mechanical Engineers - Part C: Journal of Mechanical Engineering Science*, vol. 235, no. 8, pp. 1389–1400, 2021.

[8] L. Li and C. Mao, "Big data supported PSS evaluation decision in service-oriented manufacturing," *IEEE Access*, vol. 8, no. 99, p. 1, 2020.

[9] Y. Qian, "Research on fault diagnosis model of generative adss based on improved semisupervised diagnosis algorithm," *Mobile Information Systems*, vol. 2021, Article ID 3477667, 11 pages, 2021.

[10] L. Li, C. Mao, H. Sun, and L. Bingbing, "Digital twin driven green performance evaluation methodology of intelligent manufacturing: hybrid model based on fuzzy rough-sets AHP, multistage weight synthesis, and PROMETHEE II," *Complexity*, vol. 2020, no. 6, 24 pages, Article ID 3853925, 2020.

[11] H. Yin, Z. Li, J. Zuo, H. Liu, K. Yang, and F. Li, "Wasserstein generative adversarial network and convolutional neural network (WG-CNN) for bearing fault diagnosis," *Mathematical Problems in Engineering*, vol. 2020, Article ID 2604191, 11 pages, 2020.

[12] X. He and H. Zhao, "Support vector machine and its application in mechanical fault diagnosis," *Journal of Central South University*, vol. 36, no. 1, pp. 98–101, 2005.

[13] S. Sun, "Shield tunneling parameters matching based on support vector machine and improved particle swarm optimization," *Scientific Programming*, vol. 2022, Article ID 6782947, 11 pages, 2022.

[14] C. Tang, A. Tong, A. Zheng, H. Peng, and W. Li, "Using a selective ensemble support vector machine to fuse multimodal features for human action recognition," *Computational Intelligence and Neuroscience*, vol. 2022, Article ID 1877464, 18 pages, 2022.

[15] M. Rychetsky, S. Ortmann, and M. Glesner, "Support vector approaches for engine knock detection," in *Proceedings of the International Joint Conference on Neural Networks*, pp. 969–974, Washington DC, USA, July 1999.

[16] S. Liao and Z. Liu, "Enterprise financial influencing factors and early warning based on decision tree model," *Scientific Programming*, vol. 2022, Article ID 6260809, 8 pages, 2022.

[17] Y. Yang, "The evaluation of online education course performance using decision tree mining algorithm," *Complexity*, vol. 2021, Article ID 5519647, 13 pages, 2021.

[18] F. Wu, X. Liu, Y. Wang, X. Li, and M. Zhou, "Research on evaluation model of hospital informatization level based on decision tree algorithm," *Security and Communication Networks*, vol. 2022, Article ID 3777474, 9 pages, 2022.

[19] S. Feng, "Research and improvement of decision tree algorithm," *Journal of Xiamen University*, vol. 04, pp. 496–500, 2007.

[20] Y. Cheng, C. Huang, and Y. Zhang, "fault diagnosis of gear box based on particle swarm optimization decision tree," *Vibration, Testing and Diagnosis*, vol. 01, pp. 153–156, 2013.

[21] C. Sun and B. Liu, "A new SVM decision tree," *Journal of Fuzhou University (Natural Science Edition)*, vol. 03, pp. 361–364, 2007.

[22] V. N. Vapnik, *The Nature of Statistical Learning Theory*, Spring-Verlag, Berlin, Germany, 1999.

[23] H. Wang and Y. Ou, "Face recognition using PCA/ICA features and SVM classification," *Computer Aided Design and Graphics*, vol. 15, no. 4, pp. 417–420, 2003.

[24] Z. Yongtao and Y. Liu, "Research on support vector machine to solve multi classification problems," *Computer Engineering and Application*, vol. 41, no. 23, pp. 190–192, 2005.

[25] G. Wang, Y. Zhai, and D. Wang, "Application of fuzzy support vector machine in fault diagnosis of steam turbine," *Journal of North China Electric Power University*, vol. 30, no. 4, pp. 47–50, 2003.

[26] H. Wang, X. Zhang, and J. Yu, "Fault diagnosis method based on support vector machine," *Journal of East China University of Science and Technology*, vol. 30, no. 2, pp. 179–182, 2004.

[27] N. Saravanan, V. N. S. Kumar Siddabattuni, and K. I. Ramachandran, "Fault diagnosis of spur bevel gear box using artificial neural network (ANN), and proximal support vector machine (PSVM)," *Applied Soft Computing*, vol. 10, no. 1, pp. 344–360, 2010.

Hindawi
Scientific Programming
Volume 2022, Article ID 4208945, 13 pages
https://doi.org/10.1155/2022/4208945

Research Article

Nonlinear Integrated Fuzzy Modeling to Predict Dynamic Occupant Environment Comfort for Optimized Sustainability

Sharifah Sakinah Syed Ahmad,[1] **Soh Meng Yung**,[2] **Nasreen Kausar**,[3] **Yeliz Karaca**,[4] **Dragan Pamucar**,[5] **and Nasr Al Din Ide**[6]

[1]*Faculty of Information & Communication Technology, Universiti Teknikal Malaysia Melaka, Durian Tunggal 76100, Melaka, Malaysia*
[2]*Huawei Technologies (M) Sdn Bhd, Jalan Tun Razak, Kuala Lumpur 50400, Malaysia*
[3]*Department of Mathematics, Faculty of Arts and Sciences, Yildiz Technical University, Esenler 34210, Istanbul, Turkey*
[4]*University of Massachusetts Medical School (UMASS), Worcester, MA 01655, USA*
[5]*Department of Logistics, University of Defence in Belgrade, Belgrade, Serbia*
[6]*Department of Mathematics, University of Aleppo, Aleppo, Syria*

Correspondence should be addressed to Nasr Al Din Ide; ide1112002@yahoo.ca

Received 26 April 2022; Revised 12 May 2022; Accepted 23 May 2022; Published 8 June 2022

Academic Editor: Lianhui Li

In the ever-evolving vibrant landscape of our times, it is crucial that a peaceful environment is ensured taking into account all the likely ecological parameters along with humidity and temperature while conserving energy. Thus, besides mechanical and electric control systems, it has become vital to ensure that artificial intelligence (AI) is assimilated and deployed into the systems so as to raise the well-being of the environment. By disseminating intelligence across the building by utilizing the new internet of things (IoT) technology, along with control formats, local open standard data, AI algorithms, and cloud-based predictive analytics, the heating, ventilation, and air conditioning (HVAC) mechanism renders the capability to acclimatize to use patterns, alterations in use patterns, and equipment breakdown. By tracing human activity coupled with analysis of noise, energy, and temperature in the building, its occupants and facility managers can obtain vital insights for planning, optimum use of space, and behavioral changes, in turn ensuring more content and safer inhabitants and considerably more efficient structures. Moreover, fuzzy modeling shows its applicability factor with the execution of human rationale and reasoning with if-then rules as attained from the system's input-output info for model setup and training. Additionally, it presents advantages pertaining to predictive functions for tackling nonlinearity and uncertainty as well as studying the capability of the models recommended. Thus, the multi-dimensional model recommended in this study outlines a system architecture as an implementation methodology and how it harmonizes prevailing systems while offering comprehensive knowledge to HVAC systems for the accomplishment of lower energy consumption and inhabitant safety and well-being on the basis of the fuzzy modeling. With tolerance for CO_2 discharges moving towards zero, the recommended multi-dimensional model provides substantial advantages for the HVAC sector for meeting the essential objectives while taking into account enhanced sustainability in vibrant and nonlinear environments for enhancing the accuracy and fairness of the assessment outcomes.

1. Introduction

Assimilation of proficiency and uncertainty processing is vital for managing and regulating systems that are dependent on AI and data analytics. The input uncertainty is considered by means of fuzzy numbers as diverse fuzzy inputs and parametric architectures. Nonlinear functions, here, aid the assimilation of the concerned solutions along with tuning and adjustment for attaining viability and sustainability [1]. Most individuals spend around 80% to 90% of their time within indoor settings [2]. Control methodologies for HAVC systems in buildings have been

recommended by several researchers for inhabitants' optimal comfort while reducing utilization of energy [3–6]. Nonetheless, recent research works have demonstrated that data-propelled control approaches through analytics and IoT can further enhance the security and comfort of the inhabitants [7–10].

HVAC today accounts for around 60% of the energy used up in buildings, and this includes domestic, major commercial, and industrial structures [11, 12]. Those responsible for management are presently encountering irregularity in energy pricing, jeopardizing financial planning for buildings and other structures. According to Saidur et al., the air conditioning in an office building accounts for the most energy utilization (57%), followed by illumination (19%), elevators (18%), pumps, and other tools (6%). In the past three decades, the significant economic progress in Malaysia has led to an intense rise in energy usage. Many research works have deduced a positive relationship between utilization of electricity and economic progress [13]. In other words, HVAC systems have to be more energy-effective and fitting [14]. In view of this, Raffaele et al. recommended an IoT-based design for executing the model predictive control (MPC) of HVAC mechanisms in smart buildings [15]. The mechanism recommended by the authors comprises a suite of smart actuators and sensors, a database server, a gateway, a control unit, and an easy interface or console, and these are all networked and linked to the Internet. The particular control algorithm augments online, within a closed-loop control mode, the indoor thermal comfort as well as the associated energy utilization for a single-zone setting. Hence, it allows the end users to regain information regarding comfort and ecological indices and to manage the temperature and the control functions of the system remotely. Notably, the system is focused more on thermal comfort and does not take into account other parameters such as air quality and visual comfort, which are vital in office settings. Furthermore, the majority of the researchers did not deploy IoT in the HVAC environment, which might lead to a dearth of enhancement and creativity in the development of the HVAC sector. In other words, HVAC systems have to be more energy-effective and fitting [14].

Controlling and monitoring carbon dioxide levels indoors are critical for everyone's health, safety, and building energy efficiency. Buildings also require fresh air to function properly. In a building, ventilation is the process of exchanging stale air with new air. Buildings without engineered ventilation become vulnerable to stagnant air, mildew, bacteria, and potentially dangerous gases such as radon, VOCs, and carbon dioxide. Long-term exposure to these elements can cause "sick building syndrome," in which inhabitants suffer from acute health and comfort problems [16]. Thus, it has turned into an urgent matter to bring the CO_2 emissions essentially to zero (or lower) for the related structures. CO_2 levels in the workplace should be between 350 and 900 ppm. Drowsiness and poor air quality are common when CO_2 levels exceed 1,000 ppm. With CO_2 levels over 2,000 ppm, headaches, poor focus, lack of attention, increased heart rate, and minor nausea may develop.

Recently, it has been increasingly claimed that changes in an occupant's mood, well-being, and overall happiness with the built environment can demonstrably influence their thermal comfort [17]. It has been claimed that if an occupant's assessment of thermal comfort is considered a cognitive process, then perceived thermal comfort may be influenced by the psychological effects of a variety of physical circumstances that occupants encounter in the built environment, not just thermal factors. Artificial intelligence has been used in research around the world to address ventilation strategies to minimize CO_2 and other pollutants (AI). Intelligent control modeling for improving occupant environment comfort employs fuzzy logic (FL), artificial intelligence (AI), and machine learning (ML) [18–20].

Fuzzy logic is used in various systems due to a few of its notable attributes such as not needing robust mathematics or an accurate dynamic model [21]. One of the crucial reasons why the usage of fuzzy logic has increased swiftly is that it offers the deployment of human thinking and rationale with if-then rules from the system input-output data, spawning the fundamental model structure (structural identification) and parametric identification or model training [22]. One more element of fuzzy logic when blended with fuzzy logic neural networks is dealing with uncertainty and studying the capability of the recommended model for forecasting reasons [23]. When pertaining studies in the literature are appraised, it is noted that Siham et al. emphasize the significance of a fuzzy expert mechanism for HVAC systems for ensuring a convenient environment with regard to ecological parameters coupled with humidity and temperature without omitting the objective of conserving energy [24]. Goswami et al. recommended the use of a learning algorithm for multivariable data analysis for advanced regulation in HVAC setups for buildings. The objective is to deal with the control issue by utilizing a fuzzy classification methodology that does not entail a mathematical model of the system or the plant [25].

As per Perumal et al., many works on indoor environmental supervision were conducted, such as Smart House, Gator Tech, and IDorm [18]. These accomplishments are a few of the innovative explorations with tailored execution, aimed at stowing and regaining data. There is a dearth of systems wherein data are acquired from the environment and treated to attain info that can aid in making decisions accordingly in a smart home environment. There are multiple modes to enhance the quality of the HVAC setup with human convenience. Notably, the HVAC setup in the market is depicting a dearth of the intelligence factor as of now. It is now essential that artificial intelligence is deployed into the system for raising the well-being of the environment. A suite of appropriate artificial intelligence attributes has to be recommended for prospective HVAC setups and for improving occupant environment comfort.

In the present work, we have emphasized the data analytic segment to augment the knowledge and competence in the HVAC sector as against manual comfort. It is devised to encapsulate how a building is utilized by the inhabitant in real-time and to offer analytical insights into systems, which primarily concentrated on the smart air-conditioning

setups. Human comfort and safety benchmarks too would be encompassed in the system to optimize the level of comfort of the air-conditioning setup. The study will be carried out as per the lifecycle of the data analysis. The discovery stage emphasizes determining insightful data and knowledge from the IoT data collection. Then, we will elucidate how the acquired data and data preprocessing have been dealt with. During the model planning stage, the vision of the study, essential for the problem-solving, is introduced. The model building related to project planning is already implemented at this stage. The outcomes for ensuring precision and sustainability in ambiguous and nonlinear vigorous environments are presented in the final phase.

The work in the research article is divided into five sections: Section 2 provides the decision related to thermal comfort. Section 3 describes the materials and methods used in this research. The results and discussion part are presented in Section 4, and the conclusion of this study is presented in Section 5.

2. Thermal Comfort

According to the research done previously, thermal comfort is the next trend in developing HVAC systems. The factors that manipulate thermal comfort can be divided into three groups, which are concerned with the environment, humans, and psychology. Figure 1 illustrates the important parameter to be considered in categorizing thermal comfort factors.

To achieve thermal comfort, many researchers have considered temperature as the main factor. However, humidity should also be taken into consideration in the Malaysian climate and environment. The environmental factors include temperature, humidity, airflow, and heat radiation. In addition, human factors such as individuals' physical activities and metabolism level need to be taken into consideration regarding human comfort aspects. Another main factor of the overall human comfort could be visual comfort. Different situations and environments need different kinds of visual comfort. For example, a restroom should have a warmer light, but an office should have enough among of light. The environmental factors that determine visual comfort are illumination, optimal luminance, glare, contrast condition, colors, and intermitted light. The factors that determine visual comfort could be uniform illumination, optimal luminance, no glare, correct colors, adequate contrast, and the absence of intermittent light. According to Lu et al. [26], carbon dioxide (CO_2), total volatile organic compound (TVOCs), and volatile organic compound concentration (VOCs) will be the three factors of air quality comfort. The 800 ppm of concentration of carbon dioxide will be the desired level for most of the environment. If there is a huge increase the carbon dioxide level, it will bring about various health problems and even death.

There exists a lot of research on HVAC systems that specialized in human comfort. According to Fakhruddin et al., air-conditioning systems have already become an essential part of our daily lives [27]. They proposed the fuzzy system the consideration of various input parameters and

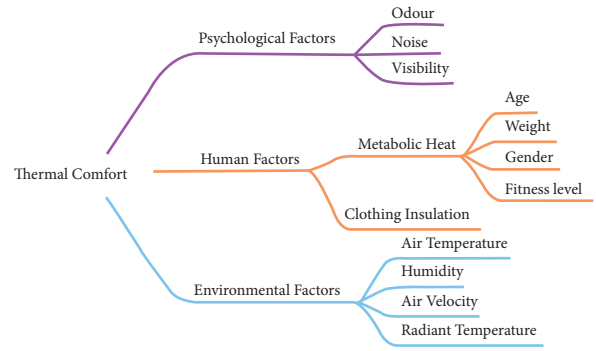

Figure 1: Categorization of thermal comfort factors.

applying the fuzzy logic system to the air conditioner. The fuzzy input in the proposed system is user temperature, temperature difference, time of day, dew point, and occupancy. Then, the output variable of the system is compressor speed, fan speed, mode of operation, and fin direction. Another research by Hang and Kim predicted mean vote (PMV) is used to control the indoor temperature of the environment by using the PMV index [28]. This research outlines an enhanced MPC system for measuring the human comfort index and maintaining indoor thermal comfort at the optimal level. An MLR-based PMV predictive model is proposed with a simplified PMV equation. The simulation results of the research show that the proposed control strategy can maximize indoor thermal comfort and also helps reduce energy consumption.

Shah et al., in "A Review on Energy Consumption Optimization Techniques in IoT Based Smart Building Environment," stated that the area of the energy management system has already existed for many years [29]. Fuzzy controllers have become more important in the study of energy controlling and optimization methods. The technique is basically to improve the comfort index by using the references of user preferences. From the paper, we understand that the primary objective of the control system is trying to satisfy the user's thermal preferences, energy-saving, and monitoring. The rule base was designed well to solve the problem of energy overshooting. Therefore, automated controls and energy management systems could have a great potential to improve individual comfort and reduce energy consumption.

3. Materials and Methods

Fuzzy logic is an approach that will rather use a "degree of truth" than the usual "true or false" computing. For example, in fuzzy logic, we are more focusing on the uncertainty between 1 and 0, but the usual computing is more to 1 and 0 only. Fuzzy logic is a form of many-valued logic in which the truth values of the variable may be any real number between 0 and 1, as we considered it "fuzzy." Fuzzy logic has been further improved to handle the concept of uncertainty, where the truth-value may vary from the range between completely true and completely false.

In this case, fuzzy modeling is implemented accordingly for the prediction of human comfort level. Human comfort

levels may vary between completely comfortable and completely the discomfort. Fuzzy modeling is capable of handling perceptual uncertainties such as the vagueness and ambiguity involved in a real system. The most crucial task in constructing a fuzzy model is to perform structure identification, which is concerned with determining the number of rules and parameter values that will provide an accurate system description. The results of transforming numeric data into fuzzy sets are used directly in making a rule-based system.

The structure identification is concerned with determining the number of rules and the parameter estimation. Various approaches have been proposed to construct the fuzzy model and its best parameter. One of the popular techniques for fuzzy modeling is the fuzzy c-means clustering algorithm. The fuzzy c-means produce a fuzzy partition of the input space by using cluster projections. The results of transforming numeric data into fuzzy sets are used directly in constructing a rule-based system.

We consider the problem of approximating a continuous multi-input and single-output (MISO) to clarify the basic ideas of the presented approach. The essence of fuzzy modeling is inherently associated with the inference schemes of approximate reasoning.

$$\begin{aligned} &x \text{ is } A \\ &\text{if } x \text{ is } A_i \text{ then } y \text{ is } B_i, \quad i = 1, 2, \ldots, N \\ &\_ \_ \_ \_ \_ \_ \_ \_ \_ \_ \_ \_ \_ \_ \_ \_ \_ \\ &y \text{ is } B, \end{aligned} \tag{1}$$

where B is a fuzzy set of conclusions to be determined. A and A_i are defined in a finite input space X, $\dim(X) = n$ while B_i and B are expressed in the output space Y with dimensionality, $\dim(Y) = m$. The set of indexes of the rules is denoted by N; in this case, it is simply a set of N natural numbers indexing the rules, $N = \{1, 2, \ldots, N\}$.

There is a wealth of realizations of the inference schemes with a large number of optimization mechanisms. In a nutshell, though, the inference scheme is realized by determining the activation levels of the individual rules (their condition parts) implied by some A. This is typically done by computing a possibility measure of A and A_i, poss (A, A_i). Denoting the possibility value by λ_i, the conclusion B is taken as a union of B_i weighted by the activation levels (possibility values), namely

$$B(y) = \max \quad i = 1, 2, \ldots N \left(\lambda_i(x) \Lambda Bi(y)\right), \tag{2}$$

where $\wedge$ stands for the minimum operation. There are numerous variations of this inference scheme nevertheless the essence of the underlying reasoning process remains the same. Figure 2 shows how the fuzzy inferences system works.

To get the research done, the choice of machine learning or data analysis tools is very important. There are eight suggested applications for big data analytics that are well described and examined with the performance available, namely Apache Hadoop, Apache Spark, Apache Storm, Apache Cassandra, MongoDB, R programming Environment, Neo4J, and Apache SAMOA. In this research, we use R programming because this research involves machine learning and a fuzzy inference process. A wide range of libraries in R programming enables the project to be done smoothly. Besides R programming, according to http://www.mathworks.com, MATLAB also provides a fuzzy inference system function for users to create a fuzzy modeling system. Fuzzy Logic Toolbox software provides command-line functions and an app for creating Mamdani and Sugeno fuzzy systems. The website is detailed with many kinds of functions that are related to fuzzy inference systems, for example, creating fuzzy systems, specifying membership functions, specifying fuzzy rules, evaluating and visualizing fuzzy systems, importing and exporting, creating the fuzzy membership function, and constructing custom fuzzy systems, as the main functions required to be considered to develop a fuzzy inference system.

4. Experimental Results and Discussion

4.1. Data Set Description. The current study has employed 39,636 instances in the data set. Due to there being different sensors will be placed in different locations of the office, the sensor will be denoted to different UnitID in the data set. Based on the data set provided, 45 sensors are functioning in the HVAC data collection. Next, data are collected in a time series. Based on the rough understanding of the data, the data_time feature is formatted as DD/MM/YYYY HH:MM. The data is recorded every second, but not as a fixed or uniform timeline. Table 1 shows the data that will be used in this research. All the data will be denoted as noise (dB), light (lux), temperature (°C), CO_2 (ppm), and humidity (%).

In this phase, we need to understand the data obtained for this research. Every feature/variable included in the data set should have a high understanding so that we know which features in the data set are suitable for this research development. The histogram function has been used to see the distribution of the data. The histogram is a chart representing a frequency distribution. Then, correlation analysis has also been carried out in this research at the same time. Correlation analysis is a statistical method that allows us to compare the strength of the relationship between the attributes in the data set. The higher the correlation between two attributes is, the higher the relationship between the two attributes is. A weak correlation value indicates that the variables are not related to each other.

To observe and examine the correlation, linearity, and histogram of the data, we used ppclust, factoextra, dplyr, cluster, fclust, and psych library in the RStudio library. Then, by calling the pairs.panels (x, method = "Pearson") function, we can get a multi-info chart that includes histogram, correlation value, and linearity diagram. Figure 3 presents the result of the functions for three months.

Figures 3–5 show that the data distribution of the three months data are almost the same. First, the noise value histogram shows that the data are right-skewed, which means the surroundings always have a low noise value. The light value data are also skewed to the right; we can see that most of the light values are near 0; and we assume that maybe the light sensor is not sensitive enough to collect the

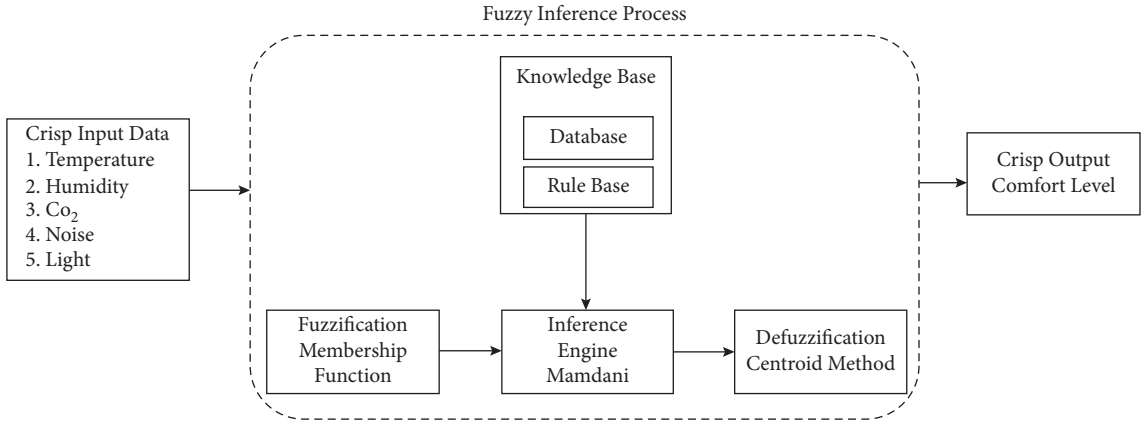

Figure 2: Fuzzy modeling inference system concept.

Table 1: The data set information for the study.

Parameters	Min	Max	Denomination
Temperature	15	35	˚C
Humidity	0	100	%
CO_2	200	2,000	ppm
Noise	40	80	dB
Light	0	400	Lux
Comfort level	0	10	Level

accurate data. This conclusion can be drawn because an office should not have such low light intensity for productivity. Next, temperature and humidity values both have the normal distribution depicted in the figures provided. Based on the histogram, the workers are feeling comfortable at a temperature of 25˚C in the office area due to its highest count in the data. Besides that, the temperature in the office will always maintain from the lowest 20˚C to the highest 30˚C, from which it can be inferred that an area with 30˚C; the meeting room not often used by the workers or the data is recorded during night time, which is after the office hours. Lastly, the carbon dioxide and volatile organic compounds in the office area are considered to be at a slightly higher level. According to some studies, the acceptable carbon dioxide level and volatile organic compounds in air quality should be maintained below 500 ppm and 1,000 ppm, respectively. The data recorded for this both attributes are higher than the expected value of about 500 ppm; company should have a solution to solve this problem after this analysis has been done.

From these points, it can be noted that noise and light have the most positive correlation in Figures 3–5, followed by noise and carbon dioxide. We may have an assumption that the noise level is increasing with light and carbon dioxide value because there is an occupant for the covered area. These three attitudes are correlated with each other because the carbon dioxide and noise level will increase if a worker is using that area and whether or not he or she will be using the area with the lights.

In this section, we shall discuss the result of clustering. To provide an unsupervised learning–clustering, Visual Studio Code has been used to provide a better processing speed to achieve the task. The data are clustered into three clusters with six attributes (temperature, humidity, CO_2, VOC, noise, and light). The algorithm used to perform clustering is the k-means algorithm. The algorithm nicely clustered the data into three parts. We need to decide whether the data clusters belong to categories of good, normal, and bad since it is unsupervised learning.

Table 2 shows the results of the k-means clustering of the data set. The results are transformed into a table form, in which the values are recorded, in mean value. From the table, we can see that the surrounding temperature of the office range from 24.5˚C to 26˚C. The clustered temperature for these 3 clusters is not much different that only has a mean of 25˚C to 26˚C. Based on the research, the best temperature for a working environment, especially, the office, should be kept at 21˚C to 22˚C. Therefore, the working environment is warmer compared to the ideal temperature. Next, the optimum humidity level of an office as per research is between 40% and 60%. Based on the results obtained, the humidity level for the data set remains between 55% and 60% that is considered to be under the good category. Furthermore, the humidity value of cluster 2 was 55.9%, which is very good for a human working environment. Next, for the CO_2 level, cluster 2 contains the highest mean value of CO_2 level that is abnormally high, 1,075 ppm. The carbon dioxide level in the office is maintained at approximately 600 ppm for clusters 1 and 3. Meanwhile, the CO_2 level for cluster 2 achieves a less healthy level that is 1,000 ppm due to the crowd in location and being a small area. Although the researcher stated that 2,000 ppm of carbon dioxide will cause harm to human health, 1,000 ppm of carbon dioxide did not bring about many benefits to the worker because it will cause sleepiness. The VOC level also has a big range of average value based on the clustered result, cluster 3 has a 2,298 ppm of the highest amount of VOC, which is bad for health. The light and noise value does not have much difference in terms of the three clusters obtained. The noise data is also an important attribute of this data set since it has a high correlation with other attributes. The noise level in the office is maintained at the level between 47 dB and 52 dB in this data set. The environment of the office is comfortable if the reading is at 47 to 52 dB because it is considered to be a quiet environment for a worker. Workers can stay focused all the time

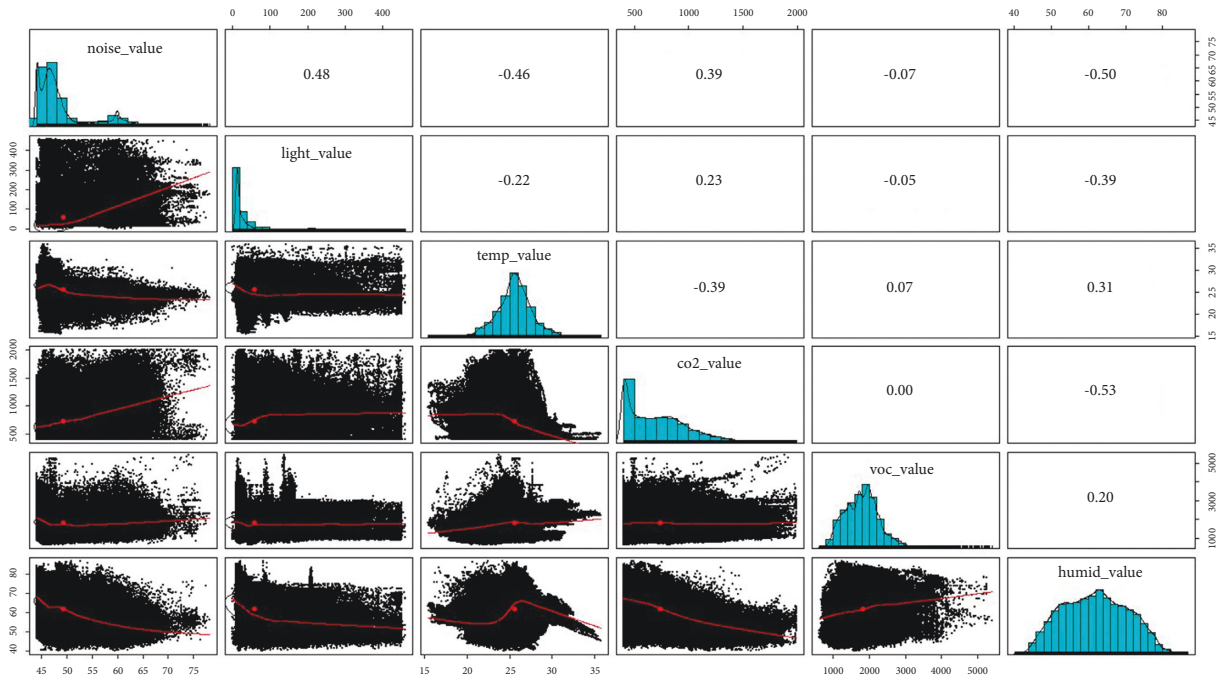

Figure 3: Correlation of input data for the first month.

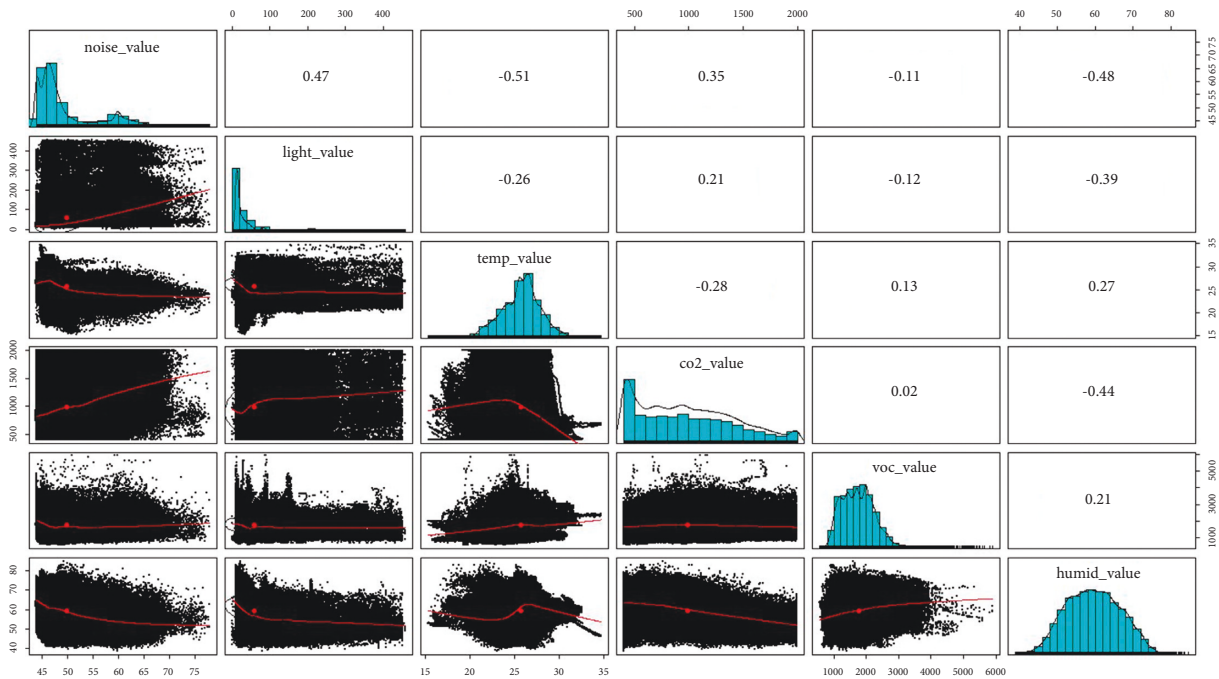

Figure 4: Correlation of input data for the second month.

in this range of noise. Furthermore, workplace lighting may also affect the efficiency of a worker. A recommended light level is more common in the range of 500 and 1,000 lux, depending on the activity. The highest mean value of the light data is only 76 lux. This indicates that the light power for this company is not enough for the activity. Besides that, there is also a probability that the sensor is placed at a coordinate that may not be a strategy to collect light data, which has affected the results. Last but not least, the volatile organic compound in the office is also recorded in this data set. As the table depicts, the volatile organic compound has a 1,000 ppm difference between the maximum and minimum levels. This part has not been included in this discussion part because VOC is the least correlated data attribute in this data set.

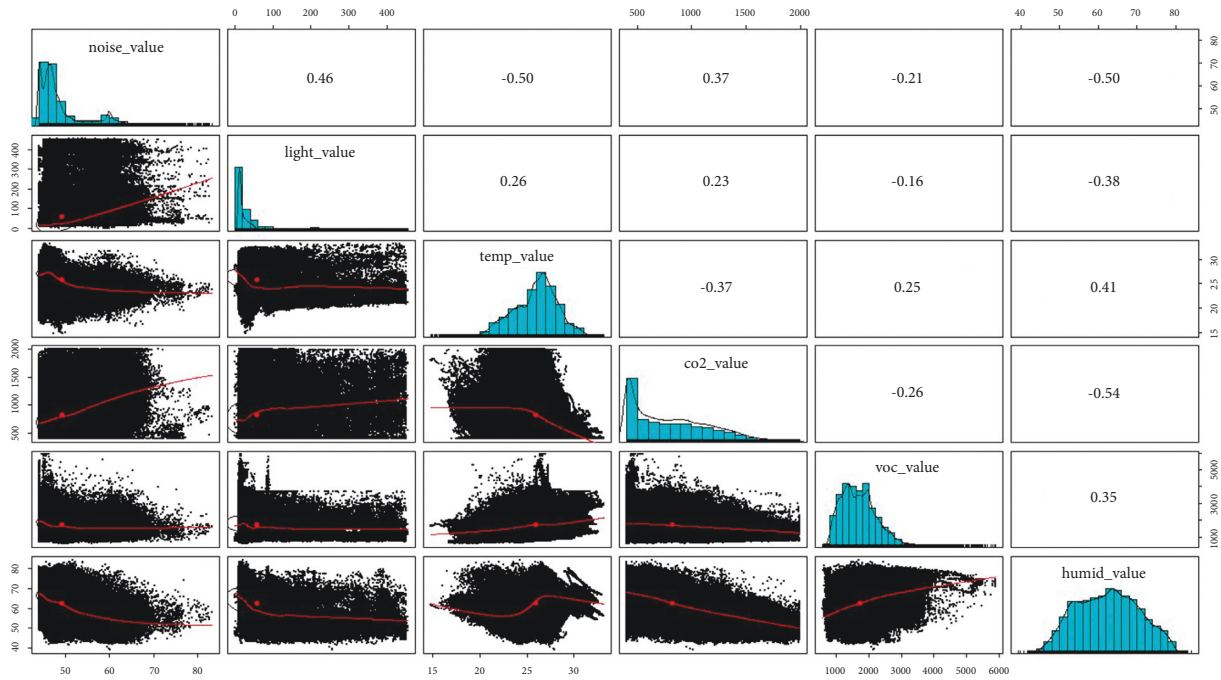

Figure 5: Correlation of input data for the third month.

Table 2: Average values for six attributes categorized into three clusters.

No. of cluster	Temp	Humidity	CO_2	VOC	Noise	Light
1	25.65765	62.24335	613.9729	1,388.163	48.79849	57.72873
2	24.5565	55.98562	1,075.342	1,768.494	51.69869	76.28403
3	26.05804	65.39577	637.2665	2,298.839	47.89209	47.63216

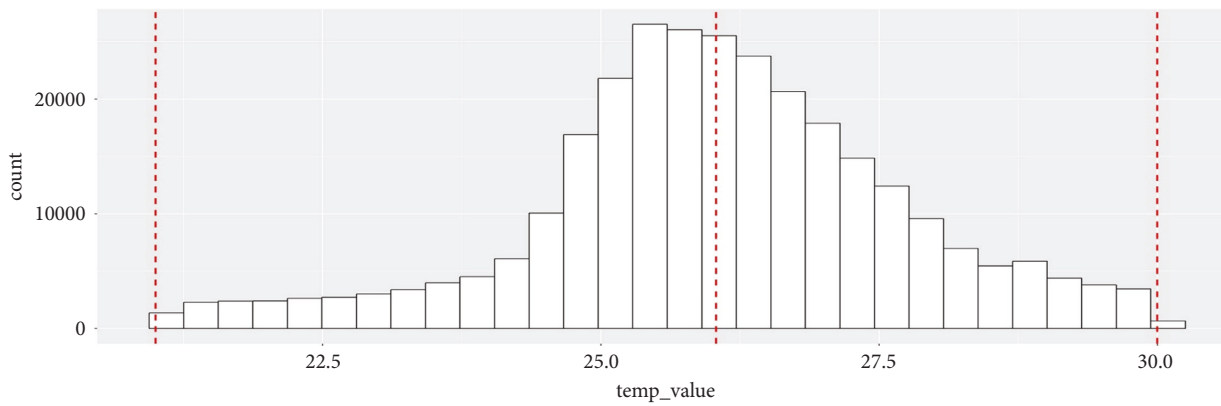

Figure 6: Histogram of temperature.

4.2. Frequency Analysis. A histogram is a plot that allows us to discover and show the underlying frequency distribution (shape) of a set of continuous data. The shape of the histogram will be a factor in designing the fuzzy inference system. The subsequent part explains the findings from the histogram.

Figure 6 depicts that the shape of the temperature histogram is normally distributed. The histogram has an approximate minimum value ranging from 20°C to an approximate maximum value of 30°C. Based on the peak and the mean of the histogram, the office is usually comfortable at a temperature range of 25°C–26°C.

Figure 7 presents the histogram concerning the humidity parameter. The shape of the histogram is normally distributed. Based on the histogram, the environment of the office is usually located between 60% and 70%.

Figure 8 shows the histogram of carbon dioxide, and the shape is skewed to the left. This left-skewed

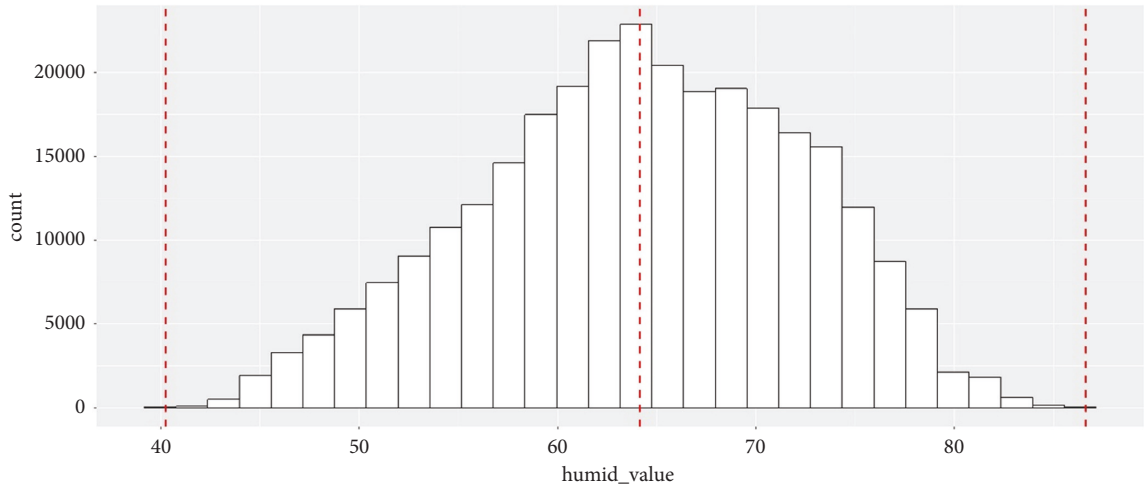

Figure 7: Histogram of humidity.

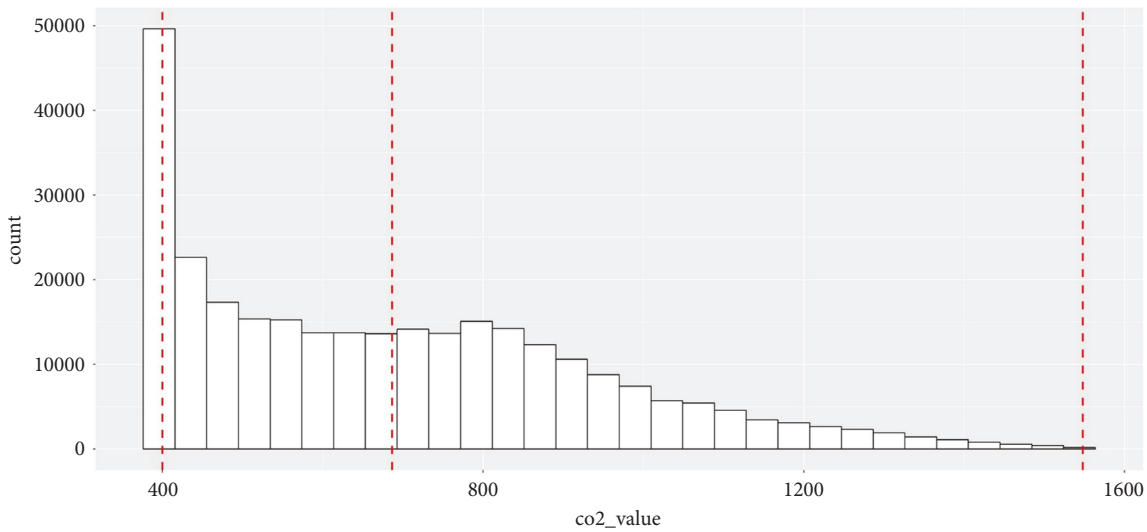

Figure 8: Histogram of carbon dioxide.

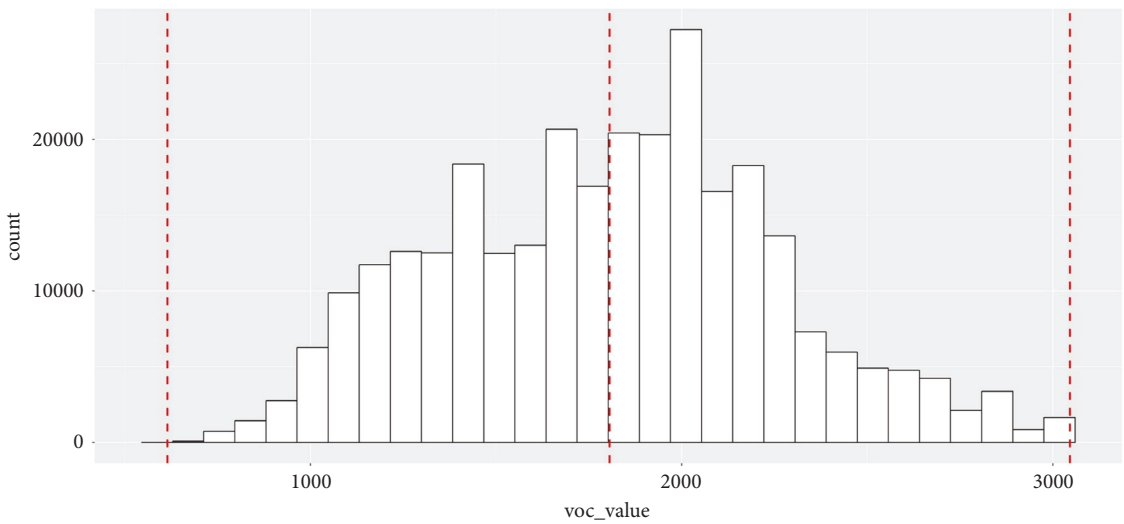

Figure 9: Histogram of VOC.

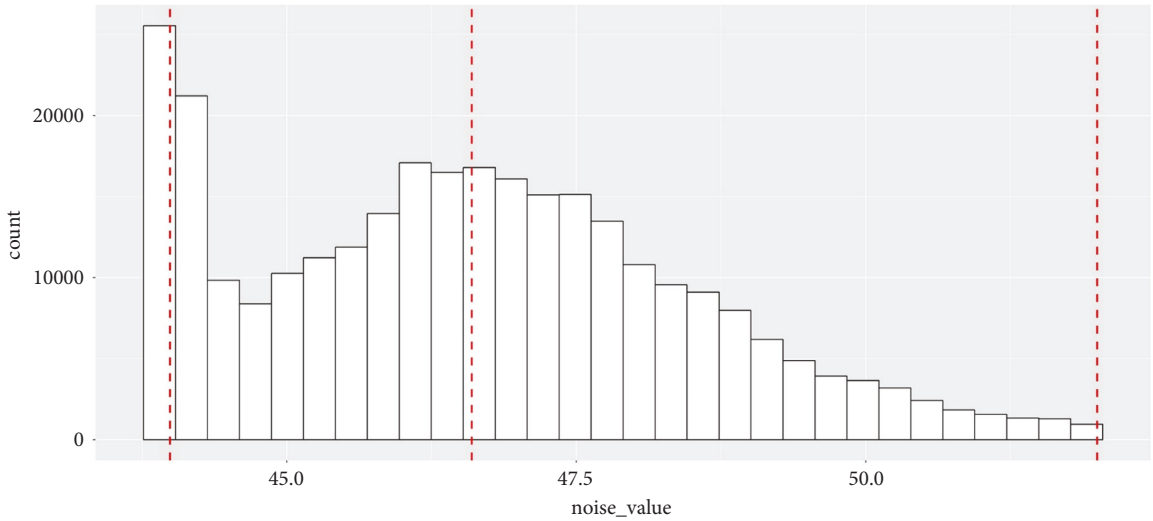

Figure 10: Histogram of noise.

Table 3: Features and fuzzy linguistic operations.

Parameters	Type	Linguistic expression
Temperature	Input	Low, medium, high
Humidity	Input	Low, medium, high
CO_2	Input	Low, medium, high
Noise	Input	Low, medium, high
Light	Input	Low, medium, high
Comfort level	Type	Linguistic expression

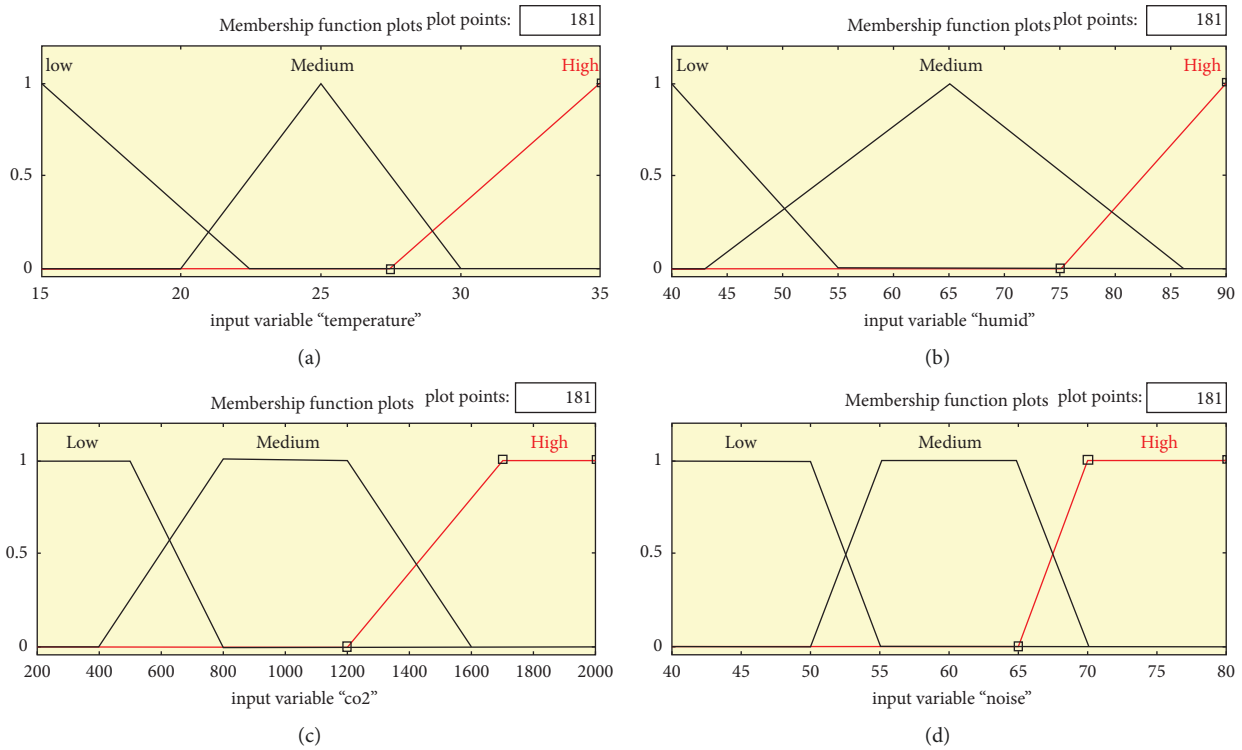

Figure 11: Continued.

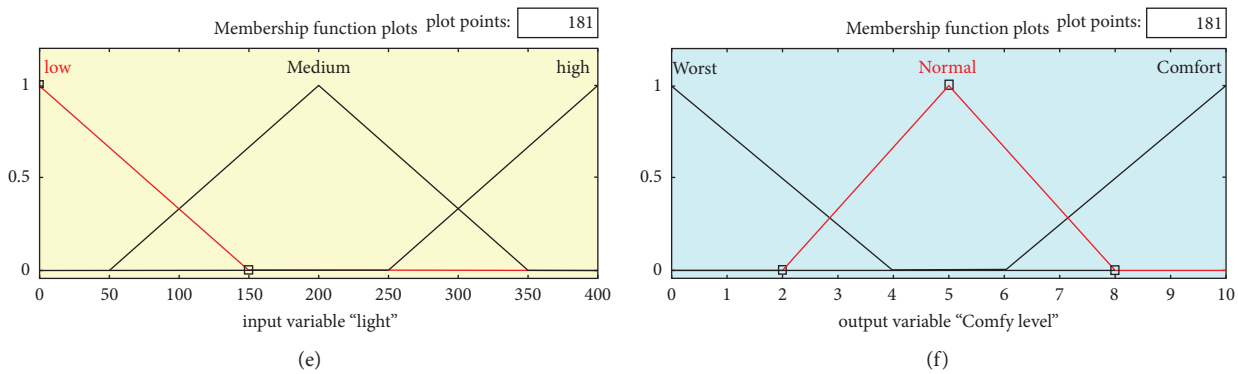

Figure 11: Membership function: (a) input 1: temperature, (b) input 2: humidity, (c) input 3: CO_2, (d) input 4: noise, (e) input 5: light, and (f) output: comfort level.

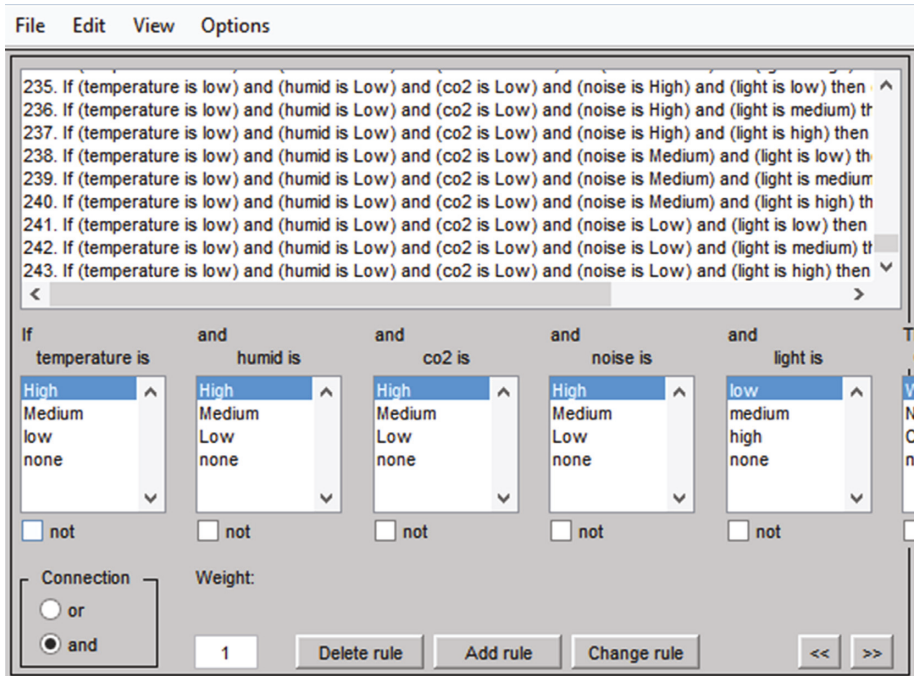

Figure 12: Rule information.

histogram shows that the data of carbon dioxide in the office are less than 400 ppm of carbon dioxide that is the comfortable range in terms of health.

Figure 9 shows the histogram of VOC. The shape of the histogram is in the form of multimodal distribution. It is observed that the highest amount of the volatile organic compound is approximately 2,000 ppm from the data collected. However, the volatile organic compound is normally around ranging from 1,000 ppm to 2,000 ppm.

Figure 10 shows the histogram of noise, and the noise in the office is not very loud. The noise in the office is less than 55 dB, which means that it is a very comfortable place to work. Yet, the results of this data may be different from the real experience because the location of the sensor is a critical matter to be taken into consideration.

4.3. Nonlinear Fuzzy Inference System for Human Comfort. Based on the literature review and the analytic results from the previous chapter, a data-driven fuzzy inference system based on human comfort has been carried out. The objective of this fuzzy inference system is to predict or analyze the human comfort level in an environment. The organic volatile compound (VOC) will be excluded from the fuzzy inference system input because the correlation analysis shows that the VOC does not have an impact on human comfort. Therefore, the input of the fuzzy inference system will consist of five factors, which are temperature value, humidity value, carbon dioxide value, noise value, and light values. These five inputs will be created based on the analysis results, and they have their membership function to have an accurate human comfort level results in the output.

Fuzzy control input and output values are defined in three linguistic expressions as four different parameters:

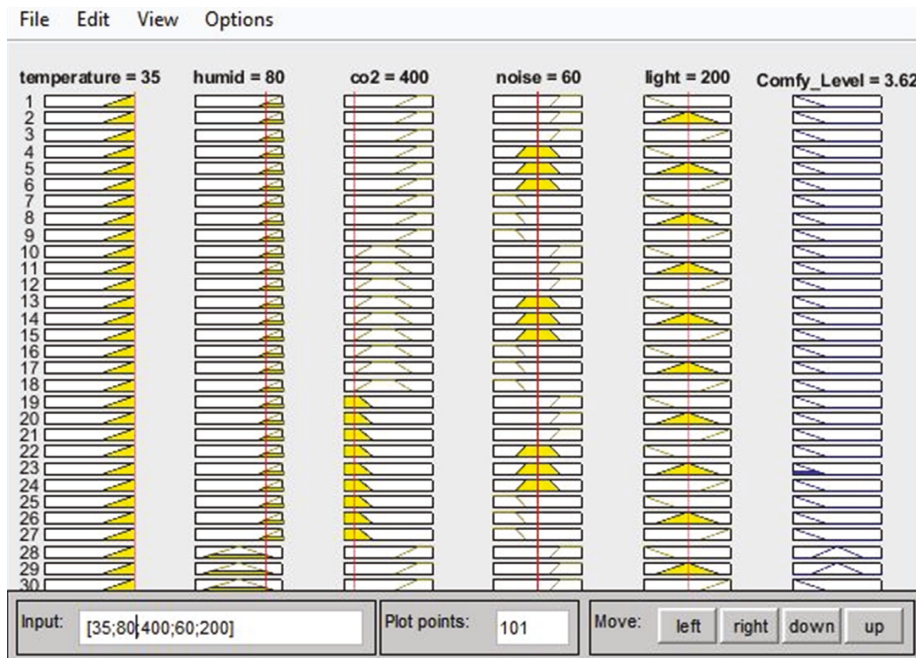

(a)

(b)

Figure 13: Rule viewer: (a) comfortable environments and (b) less comfortable environments.

temperature, humidity, CO_2 level, light level, and noise level. Two parameters are chosen as output-comfort level. The features and fuzzy linguistic operations of the input and output system are provided in Table 3, respectively.

The membership degree quantifies the grade of membership of the element to the fuzzy set. The value 0 means that is not a member of the fuzzy set; the value 1 means that is fully a member of the fuzzy set. The values between 0 and 1 characterize fuzzy members, which belong to the fuzzy set only partially. After the results of the histogram are observed and interpreted, three membership functions have been obtained regarding the temperature that is high, medium, and low. The range of high temperatures will vary from 27.5 to 36. Then, the temperature for the medium is from 20 to 30. Lastly, 15 to 22.5 will be the membership range for low temperatures, After the results of the histogram are observed

and interpreted, three membership functions are obtained for humidity that is high, medium, and low. The range of high humidity will vary from 75% to 90%. Then, the humidity for the medium is from 43% to 86%. Lastly, 40% to 55% will be the membership range for low humidity. Figure 11(b) shows the membership function of humidity. The results of the histogram show that three membership functions have been obtained for CO_2 that is high, medium, and low. The range of high CO_2 will vary from 1,200 ppm to 2,000 ppm. Then, CO_2 for the medium is from 400 ppm to 1,600 ppm. Lastly, 200 ppm to 800 ppm will be the membership range for low CO_2. Figure 11(c) describes the membership function of CO_2. The results of the histogram show that three membership functions have been obtained for noise that is high, and medium, low. The range of high noise will vary from 65 dB to 80 dB. The noise for the medium is from 50 dB to 70 dB. Lastly, 40 dB to 55 dB will be the membership range for low noise. Figure 11(d) shows the membership function of noise. Three membership functions have been obtained for the light that is high, medium, and low. The range of high levels of light will vary from 250 lux to 400 lux. Then, the light for the medium is from 50 lux to 350 lux. Lastly, 0 lux to 150 lux will be the membership range for low noise. Figure 11(e) shows the membership function of light. In order to make the understanding easy, we have decided to use a simple scale that is 1 to 10 as the parameter of human comfort level. One represents the worst situation, and 10 refers to the most comfortable and optimal situations. Figure 11(f) shows the membership function of comfort level.

In a standard fuzzy partition, every fuzzy set will correspond to a linguistic concept, for instance, low, medium, and high that are being used in this comfort level fuzzy inference system. Fuzzy rules are always written as If situation-Then conclusion. In this research, 243 rules have been used to get the best performance of the fuzzy inference system. Figure 12 shows the rule editor for this system.

In Figure 13, input of 25°C, 65% humidity, 625 ppm of CO2, 60 dB of noise, and 200 lux of light was used. The comfy level generated by the fuzzy model by using the histogram analysis method is 8.7 out of 10.

5. Conclusions and Future Directions

The ever-changing dynamic landscape of our time requires that a comfortable environment is ensured considering all the possible environmental parameters, temperature, and humidity while saving energy. Thus, in addition to the electric and mechanical control system, it has become critical and required that artificial intelligence (AI) be integrated and implemented into the systems in order to increase the comfortability of the environment. Moreover, the applicability of the fuzzy model is evident since it includes the implementation of human thinking and reasoning with if-then rules as obtained from the input-output data of the system for model structure and training. The fuzzy model is also advantageous pertaining to purposes of prediction to deal with uncertainty and nonlinearity and to investigate the ability of the models proposed. The strength of the current research is that we can obtain a lot of information from the data set by using a statistical analytic method. It is possible to encounter some missing important data if we just read the real-time data from the dashboard. By using statistical analytic means, we can combine all the data into one graph or chart to see the pattern of the data. For instance, it can be ensured to know that the light of the office is low for a workplace or maybe the sensor needs some improvement in collecting light data. There is a lot of information that we can actually extract from a set of data. In the present study, human comfort data have been used as the main part of the research. By interpreting the data provided, we can clearly know about the comfort level of the working environment that affects the health and productivity of a worker indirectly. The office management may take action based on the result obtained in the future to improve their workers' efficiency. The fuzzy model could also be regarded as another strength and motivational aspect of this research. The fuzzy model can predict human comfort based on the six attributes provided in the data set. In the future, researchers may improve the fuzzy model and implement it into a smart building system in order to get an intelligent controller for occupants' comfort. Thus, it may be concluded that it will be more humanized if there is a larger data set available for us to deal with. This research can still be improved by using another data set, and the results will be more interesting. The more attributes and duration are involved in a big data set, the more closely it may be possible to achieve the intended objectives while considering optimized sustainability in dynamic and nonlinear environments towards improving the accuracy and objectivity of the evaluation results. This proposed prediction model is only valid for similar input data having similar statistical properties. The proposed study can help the researchers and professionals to predict the comfort level inside the office building and its effect on individual health. In future work, efficient machine learning models with large data sets can be used to predict the comfort level of various parameters like visual comfort and acoustic comfort.

Data Availability

The data sets generated and/or analyzed during the current study are available from the corresponding author upon reasonable request.

Conflicts of Interest

The authors declare that there are no conflicts of interest regarding the publication of this article.

Authors' Contributions

All authors contributed equally to the preparation of this manuscript.

References

[1] E. K. Juuso, "Expertise and uncertainty processing with nonlinear scaling and fuzzy systems for automation," *Open Engineering*, vol. 10, no. 1, pp. 712–720, 2020.

[2] J. Saini, M. Dutta, and G. Marques, "A comprehensive review on indoor air quality monitoring systems for enhanced public health," *Sustain. Environ. Res.*vol. 30, no. 1, p. 6, 2020.

[3] M. Esrafilian-Najafabadi and F. Haghighat, "Occupancy-based HVAC control systems in buildings: a state-of-the-art review," *Building and Environment*, vol. 197, Article ID 107810, 2021.

[4] M. Han, R. May, X. Zhang et al., "A review of reinforcement learning methodologies for controlling occupant comfort in buildings," *Sustainable Cities and Society*, vol. 51, Article ID 101748, 2019.

[5] J. Kim, Y. Zhou, S. Schiavon, P. Raftery, and G. Brager, "Personal comfort models: predicting individuals' thermal preference using occupant heating and cooling behavior and machine learning," *Building and Environment*, vol. 129, pp. 96–106, 2018.

[6] P. Carreira, A. A. Costa, V. Mansur, and A. Arsénio, "Can HVAC really learn from users? a simulation-based study on the effectiveness of voting for comfort and energy use optimization," *Sustainable Cities and Society*, vol. 41, pp. 275–285, 2018.

[7] D. Keightley, C. E. O. Ecospectral, L. Birnie, and E. Systems, *Using IoT and Cloud Based Analytics to Maximise HVAC Efficiency and Occupant Comfort and Safety*, 2017.

[8] A. Kharbouch, Y. Naitmalek, H. Elkhoukhi et al., "IoT and big data technologies for monitoring and processing real-time healthcare data," *International Journal of Distributed Systems and Technologies*, vol. 10, no. 4, pp. 17–30, 2019.

[9] A. M. Ali, S. A. A. Shukor, N. A. Rahim, Z. M. Razlan, Z. A. Z. Jamal, and K. Kohlhof, "IoT-based smart air conditioning control for thermal comfort," in *Proceedings of the 2019 IEEE International Conference Automation Control Intelligent System I2CACIS 2019*, pp. 289–294, Chongqing, China, December 2019.

[10] A. Floris, S. Porcu, R. Girau, and L. Atzori, "An iot-based smart building solution for indoor environment management and occupants prediction," *Energies*, vol. 14, no. 10, p. 2959, 2021.

[11] M. S. Gul and S. Patidar, "Understanding the energy consumption and occupancy of a multi-purpose academic building," *Energy and Buildings*, vol. 87, pp. 155–165, 2015.

[12] R. Godina, E. M. G. Rodrigues, E. Pouresmaeil, J. C. O. Matias, and J. P. S. Catalão, "Model predictive control home energy management and optimization strategy with demand response," *Applied Sciences*, vol. 8, no. 3, p. 408, 2018.

[13] R. Saidur, "Energy consumption, energy savings, and emission analysis in Malaysian office buildings," *Energy Policy*, vol. 37, no. 10, pp. 4104–4113, 2009.

[14] Y. Dong, M. Coleman, and S. A. Miller, "Greenhouse gas emissions from air conditioning and refrigeration service expansion in developing countries," *Annual Review of Environment and Resources*, vol. 46, no. 1, pp. 59–83, 2021.

[15] R. Carli, G. Cavone, S. Ben Othman, and M. Dotoli, "IoT based architecture for model predictive control of HVAC systems in smart buildings," *Sensors*, vol. 20, no. 3, p. 781, 2020.

[16] M. Wang, L. Li, C. Hou, X. Guo, and H. Fu, "Building and health: mapping the knowledge development of sick building syndrome," *Buildings*, vol. 12, no. 3, p. 287, 2022.

[17] S. D. Lowther, S. Dimitroulopoulou, K. Foxall et al., "Low level carbon dioxide indoors—a pollution indicator or a pollutant? A health-based perspective," *Environments*, vol. 8, no. 11, p. 125, 2021.

[18] T. Perumal, S. K. Datta, T. Ramachandran, C. Y. Leong, and C. Bonnet, "Fuzzy based prediction schema framework for IoT based indoor environmental monitoring," in *Proceedings of the 2018 IEEE International Conference Consumer Electronics ICCE*, pp. 1-2, Las Vegas, LA, USA, January 2018.

[19] L. Al-Awadi, "Assessment of indoor levels of volatile organic compounds and carbon dioxide in schools in Kuwait," *Journal of the Air & Waste Management Association*, vol. 68, no. 1, pp. 54–72, 2018.

[20] N. R. Kapoor, A. Kumar, A. Kumar et al., "Machine learning-based CO2 prediction for office room: a pilot study," *Wireless Communications and Mobile Computing*, vol. 2022, Article ID 9404807, 16 pages, 2022.

[21] R. Sahu, S. R. Dash, and S. Das, "Career selection of students using hybridized distance measure based on picture fuzzy set and rough set theory," *Decision Making: Applications in Management and Engineering*, vol. 4, no. 1, pp. 104–126, 2021.

[22] H. Zeinoddini-Meymand, S. Kamel, and B. Khan, "Design and implementation of a novel intelligent strategy for the permanent magnet synchronous motor emulation," *Complexity*, vol. 2022, Article ID 4936167, 15 pages, 2022.

[23] M. Hatamzad, G. Polanco Pinerez, and J. Casselgren, "Addressing uncertainty by designing an intelligent fuzzy system to help decision support systems for winter road maintenance," *Safety Now*, vol. 8, no. 1, 14 pages, 2022.

[24] W. A. A. Q. Siham, A. M. Almasani, and I. A. A. A. Ahmed Khalid, "Fuzzy expert systems to control the heating, ventilating and air conditioning (HVAC) systems," *International Journal of Engineering Research and Technology*, vol. 4, no. 8, 2015, http://www.ijert.org.

[25] G. Goswami and P. Goswami, "PI & fuzzy logic controller for power quality control on nonlinear industrial applications," in *Proceedings of the National Conference on Industry 4.0(NCI-4.0)*, pp. 177–180, Moradabad, India, May 2020.

[26] C. Y. Lu, J. M. Lin, Y. Y. Chen, and Y. C. Chen, "Building-related symptoms among office employees associated with indoor carbon dioxide and total volatile organic compounds," *International Journal of Environmental Research and Public Health*, vol. 12, no. 6, pp. 5833–5845, 2015.

[27] H. N. Fakhruddin, S. A. Ali, M. Muzafar, and S. Azam, "Fuzzy logic in HVAC for human comfort," *International Journal of Scientific Engineering and Research*, vol. 7, no. 6, pp. 83–86, 2016.

[28] L. Hang and D. H. Kim, "Enhanced model-based predictive control system based on fuzzy logic for maintaining thermal comfort in IoT smart space," *Applied Sciences*, vol. 8, no. 7, Article ID 1031, 2018.

[29] A. S. Shah, H. Nasir, M. Fayaz, A. Lajis, and A. Shah, "A review on energy consumption optimization techniques in IoT based smart building environments," *Information*, vol. 10108 pages, 2019.

Hindawi
Scientific Programming
Volume 2022, Article ID 8793596, 7 pages
https://doi.org/10.1155/2022/8793596

Research Article

Design of Accounting Earnings Forecasting Model Based on Artificial Intelligence

Jia Liu,[1] Shi Wu,[1] and V. T. Pham [1,2]

[1]*Business School, Fuzhou Institute of Technology, Fuzhou 350506, China*
[2]*Saigon University, Ho Chi Minh, Vietnam*

Correspondence should be addressed to V. T. Pham; vuongt.pham@sg.edu.vn

Received 23 April 2022; Revised 18 May 2022; Accepted 23 May 2022; Published 7 June 2022

Academic Editor: Lianhui Li

The increasing complexity of the international situation intensifies the changes of the economic environment. People's demand for information represented by accounting earnings, such as judging the profitability and risk coefficient of the company, is becoming more and more urgent. This study puts forward the theory of predicting accounting earnings through accounting earnings factors in a nonlinear way and designs an accounting earnings forecasting model based on artificial intelligence. Integrating LSTM, seq2seq, and reinforcement learning and combining with self-attention like mechanism, a complex multifactor time series forecasting model is established, and reinforcement learning is used to stabilize the model to prevent overfitting, which puts forward a new solution to the multifactor time series forecasting problem of complex relationship. The experimental results and comparative analysis show the effectiveness of the enhanced recurrent neural network accounting earnings prediction model designed in this study.

1. Introduction

As a discipline that provides economic information reflecting the financial status and operating results of enterprises, accounting reflects the performance of the entrusted responsibilities of the enterprise management by providing the users of financial accounting reports with accounting information centered on the operation of enterprises, which is helpful for the users of financial accounting reports to make economic decisions [1–5]. Accounting surplus is the most important concept and index in accounting information. Its decision usefulness is the foundation of financial accounting and the main means to judge the value of the company [6].

In the information view of accounting, it is considered that the market is incomplete and full of uncertain factors [7]. No accounting method can get the real income of an enterprise, but accounting earnings information is a signal to investors that is helpful to judge and estimate economic income, which can improve the accuracy of investors' prediction of the future situation of the company. The valuation view of accounting further complements the role of accounting earnings information. It is believed that investors will take the corresponding accounting data (with profit as the core) as the model change when valuing the company, so that the accounting earnings information and stock price affect each other. In other words, through the value of accounting earnings, we can infer a lot of information related to accounting earnings and use the earnings information to analyze the company's operation, risk, future profitability, stock price change trend, etc. Therefore, the prediction of accounting earnings and the analysis of earnings information have always played a very important role in corporate management, investment, and other economic behaviors.

The research of earnings information system can be traced back to the relationship between the intensity of expected income change and stock price adjustment. From the beginning of being concerned to today's research, many scholars have been exploring the correlation between accounting earnings and earnings information based on the company's stock price. In these studies [1, 8–11], a large

number of theoretical and empirical studies show that the relationship between accounting earnings and stock returns (usually expressed by earnings response coefficient) changes alternately. Many studies also found that the stock price will fluctuate in the window period of accounting earnings information announcement such as annual report. In other words, earnings information will have an impact on the expected stock price in the future. At the same time, the stock price will also affect the future surplus.

In the current research, considering the weakness of the linear correlation between accounting earnings and stock return and the limitations of relevant assumptions, scholars have been seeking to establish a nonlinear correlation to uncover the secrets between accounting earnings, stock price, earnings announcement, annual report, and other factors, so as to judge the value of the company and help investors analyze and make decisions. The characteristics of this nonlinear system coincide with the nonlinear properties of neural networks [12, 13]. Moreover, accounting earnings and related data are time series data. As a neural network that can display dynamic time series and use its internal memory to process the input sequence of any time series, recurrent neural network (RNN) [14–20] can predict earnings fluctuation and reflect the stock price behavior at this stage in combination with the influence of different time series data. Reinforcement learning can intelligently solve complex problems, get rid of the constraints of the current theoretical analysis of accounting earnings value, and bring more possibilities for the research and development of earnings information.

Therefore, driven by artificial intelligence [12–20], this paper constructs an overall model of various accounting earnings value related factors, such as earnings (here refers to the specific number of earnings, which can be equivalent to profits), earnings announcement, stock price, assets and liabilities, and company cash flow, based on the neural network for time series and combined with parameter self-tuning means such as reinforcement learning. Based on earnings forecasting, an enhanced RNN earnings forecasting model is proposed, which can be nonlinear and can automatically adjust the importance of factors related to earnings value through model learning.

2. Accounting Earnings Value Forecast Model

2.1. The Basic Idea. The current two types of models (time series analysis model [21, 22] and multiple cross-sectional regression model [23, 24]) have their advantages and disadvantages. The time series analysis model can have a more stable output because it considers the dependencies that pass over time. Still, it is also difficult to obtain its data, and the model is too ideal. The multiple regression model based on cross-sectional data starts from reality, considers the correlation between earnings factors, and can achieve a more accurate output than the time series analysis model. However, the limitation of the linear model makes it impossible to include the time-dependent relationship at the same time, and the effect on multiple factors is also limited, so it is limited to instability and further development.

Due to the superiority of RNN in processing time-series data and the excellent ability of the neural network in fitting complex models, we hope to combine the advantages of the time series analysis model and multivariate cross-section regression model. The mainstream research factors of the accounting earnings system are unified into a nonlinear earnings forecasting model. The purpose is to realize an earnings forecast model that can reflect the relationship between accounting earnings factors and output more accurate accounting earnings forecast results by improving and enhancing the RNN infrastructure.

As a model that can transmit data time relationships and input multiple influencing factors simultaneously, RNN has many points to pay attention to when used as the basis of the whole model. The simplest RNN is prone to failure to converge when the factors are too complex; therefore, in the impact of multiple accounting earnings factors, next, this paper forms a preliminary model framework inspired by the multistep prediction based on seq2seq. Here, we use the seq2seq structure to improve LSTM. Because the seq2seq structure is a structure of encoder-decoder, after using seq2seq to improve LSTM, our earnings forecasting model can implement variable-length inputs. In this way, even if the value of each factor related to the value of accounting earnings that we choose is not null, it will not affect the model's output. Another feature of this improved seq2seq structure is that it can use the joint probability of previous values to predict the next value, making the entire prediction model more stable and reflecting the relationship between earnings-related factors.

With the improvement of seq2seq [25, 26], we can incorporate many factors related to earnings value into the earnings forecast model. However, many parameters still need to be manually adjusted in the entire forecast model. From this point of view, the model will have similar problems as the multisection regression model: too many parameters, challenging to adjust, and then affect the effect of the model. To address this shortcoming, we use reinforcement learning to improve the whole prediction model. Through reinforcement learning, we can make the whole prediction model adjust through prediction, receiving feedback and feedback. This idea realizes the self-tuning of the prediction model and avoids the problem that the prediction model is difficult to complete the training caused by too many parameter adjustments. Under the guidance of the above improvement ideas, the accounting earnings forecast model is designed as shown in Figure 1, which can represent our earnings forecast's primary process and key steps.

2.2. Accounting Earnings Forecast Algorithm Model. In the above, we have proved the basic idea of the overall model and the main architecture and algorithms used. In this part, we will explain the structure and improvement of each module in detail and introduce the basic model used, the way of improvement, the flow of data in it, process functions etc. We start with the seq2seq structure in the model, first explain the most basic data processing framework, then

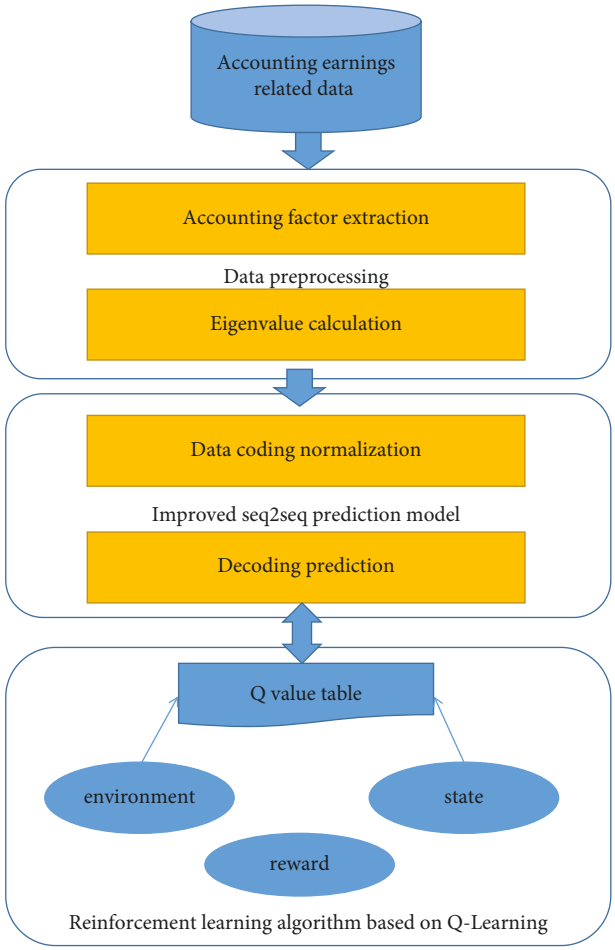

Figure 1: Accounting earnings forecast model.

introduce the reinforcement learning algorithm based on seq2seq, and further explain the key functions in the model and the improved weighting method.

2.2.1. Improved Seq2seq Model. In the above, we summarized the types of accounting earnings factors and analyzed the relationship between different accounting earnings factors. We explained in Section 2.2 that seq2seq could use the joint probability of prior values to predict the characteristics of the following value. The commonly used seq2seq has two structures. Here, we use the second structure of seq2seq to simulate the characteristics that accounting earnings factors affect each other and act on the final forecast value of earnings. Combined with our first three-level relationship of the surplus factors analyzed in the chapter, we explained the reason for using LSTM in the seq2seq structure before, so we use Figure 2 to represent our final seq2seq structure.

The LSTM cell starts from reading the input data and the two states c_t and h_t of the previous cycle. z_f, z_i, and z_o are all formed by the input data x_t and the previous cycle h_{t-1} after splicing according to different weights through the activation function σ_θ ( ). Calculated, these three variables are

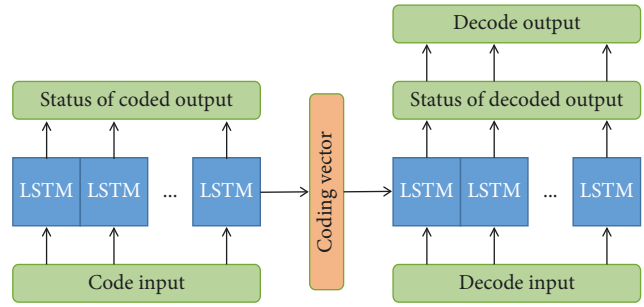

Figure 2: Partial structure of seq2seq.

gated states, the LSTM cell starts from reading the input data x_t and the two states c_t and h_t of the previous cycle. z_f, z_i, and z_o are all formed by the input data x_t and the previous cycle h_{t-1} after splicing according to different weights through the activation function σ_θ. Calculated, these three variables are gated states, but in fact, the actual input is z calculated by the activation function φ_θ.

The first step of LSTM is controlling the input information by the forget gate. We discard the relatively unimportant part of the input data through this step. In this process, the LSTM cell controls the previous cell state c_t by calculating z_f as the gate of the forget gate removal and retention of information in c_{t-1}. Then, the LSTM cell processes the input, where the input gate z_i will control the selective input of x_t. In this process, the previously calculated z is performed together with z_i, which we express with (2)-(1). The symbol $\odot$ represents the multiplication of corresponding elements in the operation matrix.

$$c_t = z_f \odot c_{t-1} + z_i. \tag{1}$$

The output stage will determine all the outputs regarded as the current cycle. Here, z_o is used as the output gate. The calculation methods of h_t and y_t are listed in (2) and (3). In general, y_t is obtained by h_t transformation.

$$h_t = z_o \odot \varphi_\theta(c_t), \tag{2}$$

$$y_t = \sigma_\theta\left(w\prime \cdot h_t\right). \tag{3}$$

After processing the encoding part, the encoding vector enters the decoder for actual prediction, and the value of the decoder part is calculated according to the process in Figure 2. Assuming that the encoder part obtains the final hidden layer state value is h_{te}, the decoder at the time of t+1. The state value of the part is calculated by (4), and the predicted value $\hat{y}_{t+1}$ at this moment is calculated by (5).

$$s_{t+1} = \varphi_\theta\left(\frac{y_{t,}^{s_t}}{h_{Te}}, c_t\right), \tag{4}$$

$$\hat{y}_{t+1} \sim \pi_\theta\left(y|\hat{y}_t, s_{t+1}\right). \tag{5}$$

If we make the actual value to be predicted y, then the loss function at this time can be expressed by (6), and X represents the input data sequence.

$$L_\theta = -\sum_{t=1}^{T} \log \pi_\theta \left(y_t | y_{t-1}, s_t, c_{t-1}, X\right). \tag{6}$$

Considering that the surplus data is negative or positive and the characteristics of LSTM itself, we choose the sigmoid function as the σ activation function (7), the tanh function as the φ_θ function (8), and the SoftMax function as the π_θ function (9).

$$f(x) = \frac{1}{1 + e^{-x}}, \tag{7}$$

$$f(x) = \frac{1 - e^{-2x}}{1 + e^{-2x}}, \tag{8}$$

$$f(x) = \frac{e^x}{\sum_i e^i}. \tag{9}$$

If the accounting earnings factor is put into the model, we use Figure 3 to represent the input and relationship composition of the earnings factor in seq2seq.

The encoding vector is composed of the three output vectors of the encoder part. The importance of these three types of accounting factors is different, and the three types of accounting factors can be roughly determined through existing model research. Therefore, in order not to further complicate the model, we only draw on the idea of attention mechanism (10), directly weight these three vectors, and then obtain the input of the decoder part.

$$\text{Attention score}\left(\text{query}, \text{source}\right) = \sum_{i=1}^{T} \text{similarity}^{\text{imery},} \left(eyy_i\right) \cdot \text{value}_i. \tag{10}$$

However, under the seq2seq model at this time, the optimization problem of the loss function is still not solved. Under such conditions, it is difficult to make the model have the best optimization strategy, making the instability produced by the model indistinguishable from the multiple regression cross section models. Therefore, we use reinforcement learning to improve this problem of the seq2seq model, hoping to make the prediction results more accurate.

2.2.2. Reinforcement Learning Algorithm Integrating Seq2seq. The earnings forecast model to be established in this study is based on a long time series. During this process, the relevant data are constantly changing, and according to the Introduction section, we know that there is also a correlation between the accounting earnings data of the same year, that is, the model we need is not a mapping of inputs to outputs, but a pattern between earnings-related information. However, pure LSTM not only has independent and identically distributed input but also cannot learn this "pattern." We have constructed the relationship dependence between surplus factors through the seq2seq structure, so we continue to use reinforcement learning to make seq2seq balance; then, after exploration and development, choose the most rewarding and most effective behavioral mode.

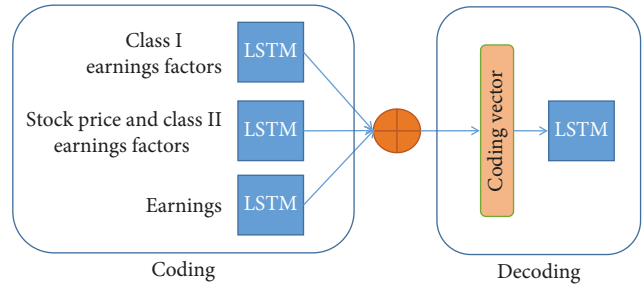

Figure 3: Input and relationship composition of the earnings factor in seq2seq.

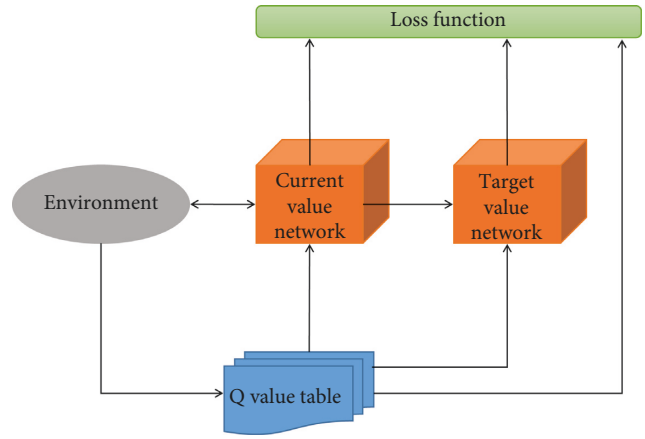

Figure 4: Reinforcement learning algorithm structure in the overall model.

Because the final model is a value prediction model, we need to choose a type of reinforcement learning algorithm suitable for value analysis. We mentioned in Section 1 that the most typical reinforcement learning algorithm for value prediction is Q-learning. Therefore, we integrate the algorithm idea of Q-learning with the seq2seq model constructed in Section 2.2.1 to form the overall reinforcement learning algorithm model shown in Figure 4.

In this process, our purpose is to maximize the expectation of reward through the interaction between the agent and the environment and action. We use (11) to solve the reinforcement learning that integrates seq2seq, which is the same as Q-learning; Q_π represents the utility function under policy.

$$\max E_{\widehat{y}_1, \ldots, \widehat{y}_T \sim \pi_\theta\left(\widehat{y}_1, \ldots, \widehat{y}_T\right)} \left[r\left(\widehat{y}_1, \ldots, \widehat{y}_T\right)\right], \tag{11}$$

$$L_\theta = -E_{\widehat{y}_1, \ldots, y_T \sim \pi_\theta\left(\widehat{y}_1, \ldots, \widehat{y}_T\right)} \left[r\left(\widehat{y}_1, \ldots, \widehat{y}_T\right)\right]. \tag{12}$$

At this time, the loss function can be calculated by (12); then by (13), we can obtain the value of the corresponding maximum partial derivative, we make the output of the decoder part before SoftMax is O_t, and then the partial derivative can be rewritten as (14) and solved by (15). R_b is a baseline reward value that does not depend on the seq2seq part.

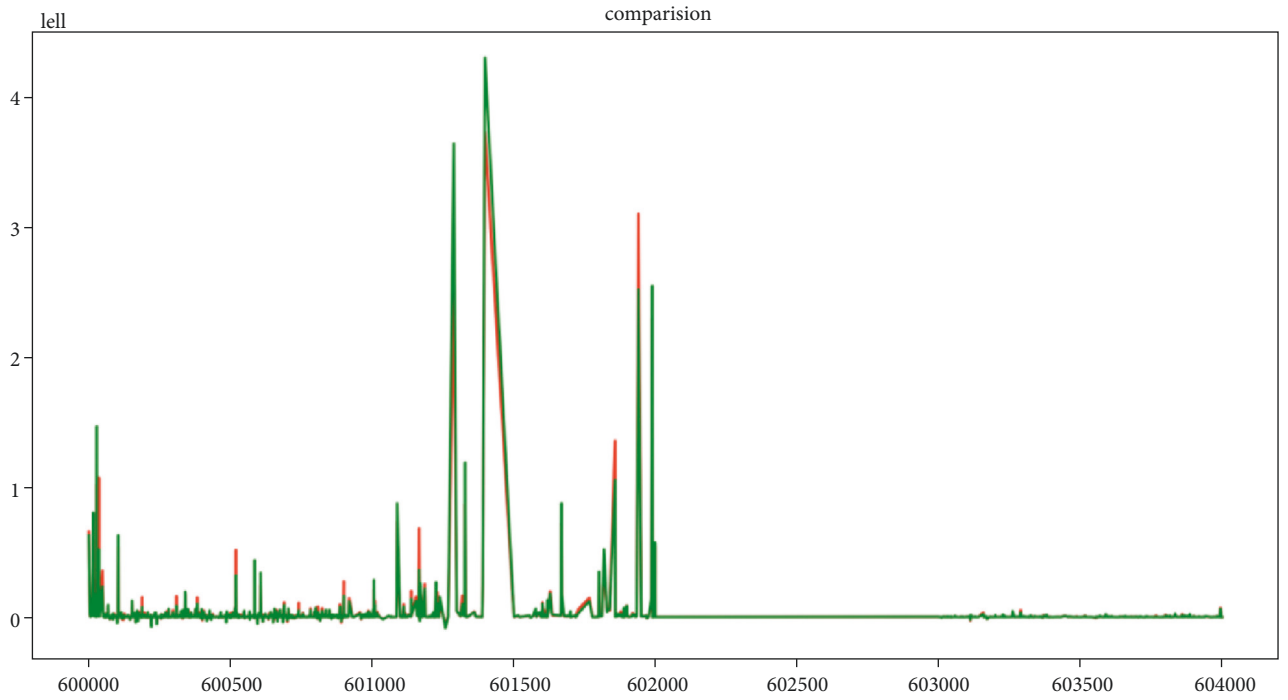

Figure 5: Earnings forecast value by the designed model for Shanghai A shares (green) and its actual value (red).

$$\nabla_\theta L_\theta = -E_{\widehat{y}_{1,\ldots,T} \sim \pi_\theta} \nabla_\theta \log \pi_\theta\left(\widehat{y}_{1,\ldots,T}\right) r\left(y_{1,\ldots,T}\right), \tag{13}$$

$$\begin{aligned} \nabla_\theta L_\theta &= \frac{\partial L_\theta}{\partial \theta} \\ &= \sum_t \frac{\partial L_\theta}{\partial 0_t} \cdot \frac{\partial 0_t}{\partial \theta}, \end{aligned} \tag{14}$$

$$\frac{\partial L_\theta}{\partial 0_t} = \left(\pi_\theta\left(y_t | \widehat{y}_{t-1}, s_t, c_{t-1}\right) - y_t\right)\left(r\left(\widehat{y}_1, \ldots, \widehat{y}_T\right) - r_b\right). \tag{15}$$

3. Model Implementation and Experimental Analysis

Due to the large number of companies involved in the forecast results and the vast difference between the forecast results, in Figure 5, the horizontal axis is the company code, the vertical axis is the unit length, and the green polyline represents the 2018 earnings of Shanghai A shares predicted by the enhanced recurrent neural network earnings forecast model. The red polyline is the actual earnings of these companies in 2018. Figure 5 includes 1512 forecast values, and the vertical axis value of other nonexistent company codes is 0. It is impossible to judge the quality of the specific forecast situation only by the particular forecast value. Therefore, according to the calculation method in Section 2, we calculate the metric value of the forecasted earnings in 2018 by the designed model.

Table 1 also shows the same index values calculated from the prediction results of the basic LSTM model on the same data set (because no accounting analysis is involved here, the R2, ERC, and ICC indicators of the designed model are not compared with LSTM). Due to the large amount of data involved in the experiment and carried out on a personal host, the running time of LSTM and the designed model is more than one day, but considering that the accounting earnings forecast itself is in units of years, the time required for the experiment has little impact, far less than the accuracy and other evaluation criteria, so the evaluation of the results by the time of the experiment is not considered here.

Table 1: Forecasting result comparison of the designed model and LSTM.

Indicator	The designed model	LSTM
AE (unit: CNY)	31393488.66	974744257.7
AAE (unit: CNY)	655956316.2	1141490405.0
DE	12.48%	22.05%
ADE	20.77%	25.13%
DS	16.182%	6.182%

From Table 1, only through the comparison of AE, can we find that the designed model significantly improves prediction accuracy compared to the LSTM base model. At the same time, it is not difficult to find that the results predicted by the designed model are still optimistic in general (i.e., the overall forecast of earnings will be larger than the actual value). Compared with the LSTM model, the difference between AE and AAE is more significant. To a certain extent, it reflects that the designed model has a higher sensitivity when the company generates negative earnings. But at the same time, the stability (DS) of the model is not as good as that of the LSTM model, but the DS value of the designed model is still within an acceptable range.

Table 2: Forecasting result comparison of HVZ and the designed model.

Indicator	HVZ	The designed model
DE	27.76%	12.48%
R^2	0.988	0.969
ERC	0.031	0.044
ICC	0.081	0.048

At the same time, we compare the DE values of the prediction results of the designed model and LSTM, and it is easy to find that the designed model fits the curve of the actual value more than LSTM. The comparison between DE and ADE further shows that the overall prediction trend of the LSTM model is far more optimistic than the designed model. It also makes the accuracy of the designed model higher than that of LSTM in the case of a downward trend in earnings.

In addition to comparing the prediction accuracy with the LSTM model, this experiment further compared with the HVZ model [27] and further analyzed the prediction results of the designed model in the accounting sense. The HVZ model needs long-term data to be computationally meaningful. In the data collected in this experiment, the amount of data that meets the requirements of the HVZ model is insufficient. Therefore, we use the empirical data of Li and Mohanram [28] to compare with the designed model (Table 2), and we mainly compare the accuracy of the forecast results and whether they have accounting significance.

From Table 2, we can find that the prediction result of the designed model is more accurate than that of HVZ. When using data with a period of up to 40 years, the DS value of the prediction result of the HVZ model can even be reduced to less than 10%. But overall, the designed model is more accurate than HVZ in more general cases. The fit of the HVZ model is slightly better than the designed model, but considering the limited regression parameters used by the HVZ model, this does not mean that the designed model has a worse fit. In addition, the ERC value of the designed model is slightly higher than that of HVZ. The designed model is relatively more representative of market expectations, which may be because the designed model uses the basic structure of LSTM to transmit the time relationship in the accounting earnings correlation system or because the input data includes the impact of the announcement on the market. However, the ICC value of HVZ is higher than that of the designed model, indicating that the HVZ model has a higher correlation with actual returns. It also shows that there is room for further optimization of the input data of the designed model, which needs to be further adjusted according to accounting factors.

4. Conclusions

An accounting earnings forecasting model is designed based on artificial intelligence. From the perspective of financial accounting, more accurate judgment of the designed model on the company's profit trend itself is helpful for investment analysis and company decision-making. At the same time, it is difficult for traditional models to judge the sudden negative turn of company profits under volatile market conditions. The designed model can find out whether the company has profitability faster than the general model. It is easy to find out through the two common indicators of ICC and ERC. The designed model has a more sensitive response to the market and is more consistent with the company's actual income. The forecast results are more conducive to analyzing the company's problems in the face of adversity and can even further infer industry risks.

In general, the designed model has higher accuracy in a broader sense when forecasting earnings. It relaxes the data requirements for forecasting and the high standards for the company's accounting years. On this premise, it can further improve the accuracy of earnings forecasts and maintain high stability. This also shows that different companies have similar accounting earnings correlation systems, and this accounting earnings correlation system can be used to build earnings forecast models for various companies. At the same time, the earnings predicted by the designed model have accounting significance, and the forecast results can reflect the market's expectations and reflect the correlation between the forecast results and actual earnings. The experimental results also show that the selection of accounting earnings-related factors has a particular impact on the results of earnings forecasting.

Data Availability

The data can be made available from the corresponding author upon request.

Conflicts of Interest

The authors declare that they have no conflicts of interest.

Acknowledgments

This work was supported by the 2019 Fujian Young and Middle-Aged Teacher Education Research Project, under project name: Research on Dual Line Collaborative Evolution and Innovation under the Background of "New Retail" (project no. JAT191027).

References

[1] Z. Xusheng, "New Accounting Standards and Earnings Conservatism: based on descriptive statistics and earnings stock return models," in *Proceedings of the 2021 International Conference on Control and Intelligent Robotics*, pp. 344–350, Liuzhou, Guangdong, China, June 2021.

[2] I. Suk, S. Lee, and W. Kross, "CEO turnover and accounting earnings: the role of earnings persistence," *Management Science*, vol. 67, no. 5, pp. 3195–3218.

[3] L.-W. Wang, C.-H. Chen, and C.-C. Wu, "A study of the influence of earnings management and accounting information quality on the investment efficiency of Chinese listed companies," *IOP Conference Series: Materials Science and Engineering*, vol. 49, no. 6, 2019.

[4] V. Herawaty, "The effect of environmental performance and accounting characteristics to earnings informativeness," *IOP*

Conference Series: Earth and Environmental Science, vol. 106, no. 1, Article ID 012077, 2018.

[5] I. Oyebisi, I. Francis, F. Samuel, A. David, and A. Adedayo, "Fair value accounting and earnings quality of listed firms in Nigeria," in *Proceedings of the 31st International Business Information Management Association Conference, IBIMA 2018: Innovation Management and Education Excellence through Vision 2020*, pp. 6250–6257, Milan, Italy, April 2018.

[6] A. Scouse, E. McConnell, S. S. Kelley, and R. Venditti, "Analysis of North Carolina forest industry earnings: adapting household-level data from the American community survey to a social accounting matrix," *Journal of Forestry*, vol. 116, no. 2, pp. 101–108, 2018.

[7] K. H. Hu, F. H. Chen, and W. J. Chang, "Application of correlation-based feature selection and decision tree to detect earnings management and accounting fraud relationship," *ICIC Express Letters, Part B: Applications*, vol. 7, no. 11, pp. 2361–2366, November 1, 2016.

[8] B. A. W. Al-Jawaheri, N. K. Jasim, and A. H. MacHi, "Determinants of the value relevance of accounting information in emerging economies: evidence from Iraq," in *Proceedings of the 3rd Africa-Asia Dialogue Network (AADN) International Conference on Advances in Business Management and Electronic Commerce Research, AADNIC-ABMECR 2021 - Conference Proceedings*, pp. 66–71, Ganzhou, China, November 2021.

[9] Z. Wang, Y. Chen, Y. Zhou, and Y. Jin, "An entropy testing model research on the quality of internal control and accounting conservatism: empirical evidence from the financial companies of China from 2007 to 2011," *Mathematical Problems in Engineering*, vol. 2014, Article ID 475050, 9 pages, 2014.

[10] M. Wu, M. Imran, L. Zhang, Qi He, and A. Yar, "An empirical analysis of firm-specific factors and equity premium: evidence from manufacturing sector of Pakistan," *Mathematical Problems in Engineering*, vol. 2020, Article ID 1346053, 9 pages, 2020.

[11] M. Carlini, S. Castellucci, S. Cocchi, E. Allegrini, and M. Li, "Italian residential buildings: economic assessments for biomass boilers plants," *Mathematical Problems in Engineering*, vol. 2013, Article ID 823851, 10 pages, 2013.

[12] Z. Fu, "Computer network intrusion anomaly detection with recurrent neural network," *Mobile Information Systems*, vol. 2022, Article ID 6576023, 11 pages, 2022.

[13] L. Li, T. Qu, Y. Liu et al., "Sustainability assessment of intelligent manufacturing supported by digital twin," *IEEE Access*, vol. 8, Article ID 175008, 2020.

[14] R. Lu and M. Lu, "Stock trend prediction algorithm based on deep recurrent neural network," *Wireless Communications and Mobile Computing*, vol. 2021, Article ID 5694975, 10 pages, 2021.

[15] C. Sridhar, P. K. Pareek, R. Kalidoss, S. S. Jamal, P. K. Shukla, and S. J. Nuagah, "Optimal medical image size reduction model creation using recurrent neural network and GenPSOWVQ," *Journal of Healthcare Engineering*, vol. 2022, Article ID 2354866, 8 pages, 2022.

[16] L. Li and C. Mao, "Big data supported PSS evaluation decision in service-oriented manufacturing," *IEEE Access*, vol. 8, no. 99, pp. 154663–154670, 2020.

[17] Bo. Chen, "Music audio rhythm recognition based on recurrent neural network," *Wireless Communications and Mobile Computing*, vol. 2022, Article ID 6249798, 11 pages, 2022.

[18] L. Li, C. Mao, H. Sun, Y. Yuan, and B. Lei, "Digital twin driven green performance evaluation methodology of intelligent manufacturing: hybrid model based on fuzzy rough-sets AHP, multistage weight synthesis, and PROMETHEE II," *Complexity*, vol. 2020, no. 6, pp. 1–24, 2020.

[19] S. Wei, Z. Zhang, S. Li, and P. Jiang, "Calibrating network traffic with one-dimensional convolutional neural network with a and independent recurrent neural network for mobile malware detection," *Security and Communication Networks*, vol. 2021, Article ID 3853925, 10 pages, 2021.

[20] L. Li, B. Lei, and C. Mao, "Digital twin in smart manufacturing," *Journal of Industrial Information Integration*, vol. 26, no. 9, Article ID 100289, 2022.

[21] Y. Wang, Ce Yu, J. Hou, S. Chu, Y. Zhang, and Y. Zhu, "ARIMA model and few-shot learning for vehicle speed time series analysis and prediction," *Computational Intelligence and Neuroscience*, vol. 2022, Article ID 2526821, 9 pages, 2022.

[22] J. Feng, "Analysis of driving factors of innovation and entrepreneurship based on time series analysis," *Journal of Sensors*, vol. 2021, Article ID 8427336, 10 pages, 2021.

[23] S. Karthiyaini, K. Senthamaraikannan, J. Priyadarshini, K. Gupta, and M. Shanmugasundaram, "Prediction of mechanical strength of fiber admixed concrete using multiple regression analysis and artificial neural network," *Advances in Materials Science and Engineering*, vol. 2019, Article ID 4654070, 7 pages, 2019.

[24] Lu. Hao, Q. Chen, Xi. Chen, and Q. Zhou, "Association of serum total bilirubin concentration with telomere length: the national health and nutrition examination survey," *Oxidative Medicine and Cellular Longevity*, vol. 2021, Article ID 4688900, 11 pages, 2021.

[25] T. Mohamed, S. Sayed, A. Salah, and E. H. Houssein, "Long short-term memory neural networks for RNA viruses mutations prediction," *Mathematical Problems in Engineering*, vol. 2021, Article ID 9980347, 9 pages, 2021.

[26] B. Huang and J. Wei, "Research on deep learning-based financial risk prediction," *Scientific Programming*, vol. 2021, Article ID 6913427, 8 pages, 2021.

[27] S. H. Kwan, "Firm-specific information and the correlation between individual stocks and bonds," *Journal of Financial Economics*, vol. 40, no. 1, pp. 63–80, 1996.

[28] K. K. Li and P. Mohanram, "Evaluating cross-sectional forecasting models for implied cost of capital," *Review of Accounting Studies*, vol. 19, no. 3, pp. 1152–1185, 2014.

Hindawi
Scientific Programming
Volume 2022, Article ID 9869636, 17 pages
https://doi.org/10.1155/2022/9869636

Research Article

Impact of Venture Capital on the Dividend Policy of Listed Companies and Management Platform Design

Lina Zheng[1] and YongGang Yao[2]

[1]*School of Business, Renmin University of China, Beijing 100872, China*
[2]*National Engineering Laboratory for Reducing Emissions from Coal Combustion, Engineering Research Center of Environmental Thermal Technology of Ministry of Education, Shandong Key Laboratory of Energy Carbon Reduction and Resource Utilization, School of Energy and Power Engineering, Shandong University, Jinan, Shandong, 250061, China*

Correspondence should be addressed to YongGang Yao; 202020539@mail.sdu.edu.cn

Received 25 April 2022; Revised 10 May 2022; Accepted 12 May 2022; Published 6 June 2022

Academic Editor: Jie Liu

This paper uses the data of Chinese A-share listed companies from 2003 to 2019 to study the impact of venture capital holdings on the dividend policy of listed companies. The research findings show that venture capital holdings increase the willingness to pay cash dividends and the payment level. This conclusion still stands after using the PSM matching method and other robustness methods, indicating that there is causality between venture capital holdings and the dividend policy of listed companies. Further research finds that the course of action for venture capital holdings to increase the willingness of listed companies to pay cash dividends and their dividend payment level is to increase the dividend payout ratio by alleviating the company's agency level. Further research finds that different types of venture capital will also have an impact on the dividend policy. Foreign investment venture capital organizations are more favorable for increasing the willingness of listed companies to pay cash dividends and their dividend payment level. In addition, the impact of venture capital holdings on the dividend policy is more obvious in the central and western regions where economic development is relatively backward and is less obvious in the eastern regions. Based on J2EE, a venture capital information management platform is designed and developed. The research of this paper shows that venture capital shareholding plays an important role in promoting dividend payment of listed companies, and has enriched the research results of the value-added role of venture capital. At the same time, from the perspective of dividend policy, it has brought to light the corporate governance effectiveness of venture capital and has provided certain theoretical evidence for the assertion that capital can better serve the real economy.

1. Introduction

The cash dividend policy is an important way for investors to share the business gain of an enterprise, an important means to protect the interests of investors, and an important tool to maintain the stability of the capital market [1]. In China, due to the short development cycle of the capital market, it takes time to uncover many development problems, and there is a large time lag in the follow-up of the regulatory system. Therefore, most listed companies do not pay cash dividends, and this has become a "unique landscape" that accompanies the development of the Chinese capital market. The study of Lu and Wang [2] pointed out that the proportion of listed companies that did not distribute dividends in 1994 was about 9.28%, while the proportion of companies that did not distribute dividends rose sharply to 58.44% in 1998. Concomitantly, there is the problem of abuse resulting in a large amount of idle funds and free cash flow. In order to protect the interests of small and medium investors, restrain the excessive investment of listed companies, and promote the healthy development of the capital market,

the China Securities Regulatory Commission has continuously issued relevant policies since 2001 to encourage listed companies to distribute cash dividends. In 2004, a relevant policy was issued, stating that listed companies that have not distributed profits in the past three years are not allowed to issue shares publicly. In 2006, relevant policies were issued, requiring that the accumulated profits distributed by listed companies in cash in the past three years should not be lower than 20% of the average annual distributable profits achieved in the past three years. Additional revisions were made in 2008 to increase the profit distribution ratio to 30%. In 2012, the regulatory authorities further improved the regulations on dividend distribution, with a view to increasing return of investment for investors and thus promoting the healthy and sustainable development of the capital market. With the continuous improvement of policy perfection, China has gradually formed a special phenomenon of the "semimandatory" dividend policy, and the corresponding research is also plentiful. However, according to current documentary research findings, the implementation effect of the semimandatory dividend policy is not ideal, which also indirectly confirms the complexity of the "dividend policy problem". The semimandatory dividend policy may affect the financial flexibility of growing companies, which is not conducive to their investment and development [3, 4], but it is still difficult to form strong policy constraints against the "Iron Roosters" listed companies that do not pay cash dividends [5, 6].

According to Jensen's research [7], venture capital is a kind of special shareholder, that is, an "active investor". One of the characteristics of venture capital that distinguishes it from other equity investments is that it will actively participate in the governance activities of investee companies, optimize the corporate governance structure, and ultimately achieve the goal of maximizing the value of its own investment. For the purpose of maximizing investment returns, will the venture capital holdings collude with major shareholders to "hollow out" the listed company, or will they constrain major shareholders, actively promote the distribution of cash dividends, protect the interests of small and medium shareholders, and alleviate the type II agency problem? If venture capital holdings can help alleviate the type II agency problem, then what mechanism will venture capital use to influence the dividend policy of listed companies?

In order to explain the above problems, this paper uses the data of all A-share listed companies in China from 2003 to 2019 to study whether venture capital holdings can help increase listed companies' willingness to pay cash dividends and their level of dividend payment. The research results show that, compared with companies without venture capital holdings, companies with venture capital holdings have a stronger willingness to pay dividends and a higher level of dividend payment. Its impact mechanism is to promote the distribution of cash dividends by alleviating the agency problem of listed companies. In addition, the different characteristics of venture capital and the difference in the level of economic development between different regions will have an impact on the cash dividend policy of investee companies.

The possible marginal contributions of this paper are as follows: Firstly, it enriches the relevant literature on the value-added role of venture capital. Previous studies have mostly focused on the impact of venture capital promotion on the listing of investee companies, promoting the specialization of investee companies, and affecting the investment and financing behavior of investee companies. However, there are few studies on the dividend policy of listed companies. Secondly, it expands research in the fields related to dividend policy. Previous studies on the influencing factors of cash dividends have focused on the impact of corporate profitability, company size, company growth ability, and ownership structure at the microlevel. However, there is less literature involved in research on the special shareholders of venture capital, and the research in this paper makes up for this gap.

The structural arrangement of the rest of this article is as follows: the second part is hypothesis; the third part is research design; the fourth part is empirical results; the fifth part is robustness and endogeneity checks; the sixth part is further research; the seventh part is design and implementation of venture capital information management platform based on J2EE, and the last part is the conclusion and implications.

2. Theoretical Analysis and Research Hypothesis

Will the participation of venture capital in the corporate governance of investee companies as an "active investor" help promote the distribution of cash dividends of listed companies?

First, from the perspective of the motivation of venture capital to actively participate in the governance of investee companies and influence the dividend policy of listed companies, there are two motives that affect the behavior of venture capital: on the one hand, the essence of venture capital is "financial investors", and its ultimate goal is to obtain investment income [8]. Venture capital can obtain cash dividends and increase return on investment by actively encouraging investee companies to issue cash dividends. On the other hand, the operation mechanism of venture capital determines the fact that it will not hold the shares of listed companies for a long time, but will obtain capital gains and return on investment by successively reducing the shares of listed companies [9]. The impact of venture capital on dividend policy can play a role in providing the market with internal information of the company. According to the dividend signaling theory (signaling hypothesis) , investors can know the company's current operating conditions and future earnings expectations from its dividend announcements, so they can make corresponding investment choices and ultimately affect the stock price. If a listed company pays high level of cash

dividends, investors may think that the company has positive expectations for future earnings, and may be optimistic about the company's future development prospects, thereby driving up the stock price. If the listed company does not distribute cash dividends, investors may think that the earning capacity of the company is poor, and are affected in their judgment of the company's future value, which in turn leads to a drop in the stock price. Therefore, changes in dividend policy will cause stock price volatility [10, 11]. Research on China's capital market has also confirmed the signaling effect of dividend policy. For example, Chen et al. [12]confirmed that the first dividend distribution has a signaling effect, and Yu and Cheng [13]confirmed that dividend announcements also have signal transmission. Therefore, by influencing the cash dividend policy of investee companies, venture capital releases positive signals to the market about the company's future profit prospects, which helps to stabilize and even increase the stock price of listed companies, thereby increasing the capital gains of venture capital.

Second, from the perspective of the way that venture capital actively participates in the governance of investee companies and affects the dividend policy of listed companies, it is understandable how venture capital affects the cash dividend policy of listed companies. On the one hand, a large number of previous literature have confirmed that venture capital can provide all kinds of resources needed for the development of investee companies [14–18]. Dividend distribution will affect the investment and financing decisions of listed companies [19]. The implementation of the cash dividend policy requires listed companies to balance the relationship between profit distribution and subsequent retention of sufficient funds to meet subsequent development needs. Research on cash dividends has found that the cash dividend policy may reduce financial flexibility and increase the difficulty of financing growing companies [20]. In response to this problem, venture capital can help listed companies solve financing problems through their accumulated network resources and bring convenience to external debt and equity financing [21, 22]. The Gorman and Sahlman [23] survey found that 75% of US venture capital organizations not only provide funds directly to companies, but also actively help companies obtain equity or bond financing from other channels. Therefore, venture capital can effectively alleviate the financing pressure of listed companies for redevelopment after cash dividends are issued. On the other hand, previous studies have also fully certified the supervisory function of venture capital [24–27]. Venture capital can effectively restrain major shareholders from transferring residual income, abusing free cash flow to blindly expand investment, and establishing corporate empires that are detrimental to the interests of small and medium shareholders by playing an active supervisory role [28]. By promoting the distribution of cash dividends, the purpose of returning income to investors and protecting the interests of small and medium shareholders is realized.

Based on the above discussion, venture capital has sufficient motivation to actively participate in the supervision of the promotion of the cash dividend policy of listed companies. There are also ways to alleviate the possible negative effects of cash dividends, promote the governance role of cash dividends, and protect the interests of small and medium shareholders. In view of the above, this paper proposes the following hypotheses to be tested:

H1a: Companies that have acquired venture capital holdings are more likely to distribute cash dividends than companies that have not received venture capital holdings;

H1b: Companies that have acquired venture capital holdings have a higher cash dividend payout ratio than companies that have not received venture capital holdings.

3. Research Design

3.1. Sample Data. In this paper, all A-share listed companies from 2003 to 2019 are used as initial samples, and initial samples are screened and cleaned up according to the following criteria: (1) delete the samples of listed companies in the financial industry; (2) delete the samples of ST and ∗ST companies; (3) delete variable samples with missing values; and (4) in order to exclude the influence of extreme values, all continuous variables are winsorized.

3.2. Variable Setting

3.2.1. Dependent Variable. Willingness to pay dividend ($Div_{i,t}$): First, this paper uses $Div_{i,t}$ to measure the company's cash dividend distribution propensity. $Div_{i,t}$ is a dummy variable. For company i, when distributing cash dividends in year t, $Div_{i,t}$ takes 1; otherwise, it takes 0.

Dividend payment level ($Pay_{i,t}$): Second, this paper uses $Pay_{i,t}$ to measure the company's cash dividend payment level, $Pay_{i,t}$ is equal to listed company i, and the cash dividend paid in year t is divided by the company's net profit in that year.

3.2.2. Independent Variables. Venture capital ($VC_{i,t}$) is the main research object of this paper, and thus, this paper takes the existence of venture capital organizations among the top ten shareholders of listed companies as the main explanatory variable. $VC_{i,t}$ is a dummy variable. When there are venture capital organizations holding shares among the top ten shareholders of the listed company, the value of $VC_{i,t}$ is 1; otherwise, it is 0. First, venture capital organizations are identified according to the classification of shareholders of listed companies in the China Stock Market and Accounting Research (CSMAR) Database. Second, using the Stata software, the names of venture capital organizations are matched with the characteristics information of venture capital organizations obtained from the CVSource database. Finally, drawing on the practice of predecessors (Wu et al., 2012; Wang et al., 2014) [29, 30], the results of matching the

names of shareholders of listed companies and the full names of venture capital organizations are manually confirmed again.

3.2.3. Control Variables. In order to control the influence of other factors, this paper refers to previous studies and sets the following control variables: performance variable (*Roe*), which represents the company's earning capacity; company size (Ln*Size*), which is the natural logarithm of the company's total assets at the end of the period; growth level (*Growth*), which is the year-on-year growth rate of the operating income at the end of the period; debt-to-asset ratio (*Lev*) which is total liabilities at the end of the period divided by total assets at the end of the period; cash flow (*Cash*), which is the net cash flow generated by operating activities per share; the ratio of independent directors (*Ind*), which is the ratio of the number of independent directors to the total number of the board of directors; the size of the board of directors (*BoardSize*), which is the total number of the board of directors; the shareholding ratio of the largest shareholder (*Top1*), which is the shareholding concentration of the largest shareholder; CEO duality (*Dual*), if the chairman is concurrently the general manager, take 1, otherwise take 0; property rights (*Soe*), when the listed company is a state-owned holding company, take 1, otherwise take 0; finally, dummy variables such as industry and year are controlled. The variable definition is shown in Table 1.

3.3. Empirical Models. First, in order to test the impact of venture capital stockholding on the company's willingness to pay cash dividends, this paper draws on the practices of Wang et al. (2007) [31]and Wang et al. (2014) [30] to construct the following Logit model.

$$\mathrm{Div}_{i,t} = \beta_0 + \beta_1 \times VC_{i,t} + \beta_2 \times \mathrm{Controls}_{i,t} + \mathrm{Industry}_{FE} + \mathrm{Year}_{FE} + \varepsilon_{i,t}. \quad (1)$$

In formula (1), the dependent variable is company's willingness to pay cash dividends $\mathrm{Div}_{i,t}$ in the basic test, this paper uses pretax cash dividends per share to represent it; $\mathrm{Div}_{i,t}$ is dummy variable, if the listed company i distributes cash dividends in year t, that is, the pretax cash dividend per share is not 0, then $\mathrm{Div}_{i,t} = 1$; otherwise, it is 0. The independent variable is, whether there are venture capital organizations among the top ten shareholders of the listed company ($VC_{i,t}$). If the listed company i has venture capital organizations among the top ten shareholders in year t, then $VC_{i,t}$ takes the value 1; otherwise, it is 0. $\mathrm{Controls}_{i,t}$ is a series of control variables. In addition, the industry and year fixed effects are controlled, and $\varepsilon_{i,t}$ is the residual term.

Second, in order to test the impact of venture capital holdings on the company's cash dividend payment level, this paper draws on the practices of Wang et al. [30] and Wu et al. [22] to construct the following OLS model.

$$\mathrm{Pay}_{i,t} = \beta_0 + \beta_1 \times VC_{i,t} + \beta_2 \times \mathrm{Controls}_{i,t} + \mathrm{Industry}_{FE} + \mathrm{Year}_{FE} + \varepsilon_{i,t}. \quad (2)$$

In formula (2), the dependent variable is the company's cash dividend payment level $\mathrm{Pay}_{i,t}$; in the basic test, it is represented by the dividend distribution rate in this paper. $\mathrm{Pay}_{i,t}$ is the listed company i, the cash dividends distributed in the t-th year are divided by the net profit of the company i in the current year. The independent variable is whether there are venture capital organizations among the top ten shareholders of the listed company ($VC_{i,t}$), if there are venture capital organizations among the top ten shareholders of listed company i in year t, then ($VC_{i,t}$) takes the value 1; otherwise, it is 0. $\mathrm{Controls}_{i,t}$ is a series of control variables. In addition, the industry and year fixed effects are controlled, and $\varepsilon_{i,t}$ is the residual term.

4. Empirical Results

4.1. Descriptive Statistics. Descriptive statistics results are shown in Table 2. In terms of dependent variables, during the sample statistics period, the average dividend payment willingness of listed companies ($\mathrm{Div}_{i,t}$) is 0.735, indicating that 73.5% of companies distributed cash dividends; the dividend payment level of listed companies, the mean value of the dividend distribution rate ($\mathrm{Pay}_{i,t}$) is 0.08, and the standard deviation is 0.131. In terms of independent variables, the mean value of venture capital holdings($VC_{i,t}$) is 0.182 and the standard deviation is 0.386, which indicates that companies that have obtained venture capital during the sample period accounted for about 18.2% of the total sample.

4.2. Basic Test. Table 3 is one of the basic empirical test results of this paper. The influence of venture capital holdings ($VC_{i,t}$) on the willingness of listed companies to pay dividends is shown in the table. Among them, the empirical results in column (3) show that having controlled a series of factors of the possibility of venture capital holdings influencing the propensity of listed companies to pay dividends, as well as the fixed effects of industry and year, venture capital holdings ($VC_{i,t}$) is significantly positive at the 5% significance level with a net effect value of 0.087, assuming that H1a is confirmed, that is, companies that have acquired venture capital holdings have more propensity to pay cash dividends than companies that have not acquired venture capital holdings.

Table 4 is one of the basic empirical test results of this paper. The impact of venture capital holdings ($VC_{i,t}$) on the dividend payment level ($\mathrm{Pay}_{i,t}$) of listed companies is shown in the table. The empirical results in column (3) show that the estimated coefficient of venture capital holdings ($VC_{i,t}$) is significantly positive at the 1% significance level with a net effect of 0.006, assuming that H1b is confirmed, that is, companies that have acquired venture capital holdings have a higher cash dividend

Table 1: Variable definition.

Variable name	Variable symbol	Variable description
Main variable		
Willingness to pay dividends	$\mathrm{Div}_{i,t}$	Indicates whether the listed company i will issue a cash dividend in the t year. If the pretax cash dividend per share is $\neq 0$, then Divi, $t = 1$; otherwise, it is 0
Dividend payout level	$\mathrm{Pay}_{i,t}$	Represents the dividend payment level of the listed company i in year t, which is equal to the cash dividend issued by listed company i in year t divided by the net profit of the year
Venture capital	$VC_{i,t}$	Dummy variable, if the company has VC holdings in the current year, the value is 1; otherwise, it is 0
Control variable		
Enterprise size	Ln*Size*	Natural logarithm of total assets at the end of the current period
Growth	*Growth*	The growth rate of operating income at the end of the current period relative to the operating income at the end of the previous period
Cash holdings	*Cash*	Net cash flow from operating activities per share
Assets-liabilities ratio	*Lev*	Debt to asset ratio at the end of the period
Performance variable	*Roe*	Return on net assets
Proportion of independent directors	*Ind*	Proportion of independent directors = number of independent directors/size of the board of directors
Board size	*Boardsize*	Number of board of directors at the end of the year
Two jobs in one	*Dual*	When the two positions of the chairman and general manager are combined as one, take 1, otherwise take 0
The largest shareholder	*Top1*	The shareholding of the largest shareholder as a percentage of the total share capital
Nature of property rights	*Soe*	The nature of the property rights of the listed company, if the company is a state-owned enterprise, take 1, otherwise take 0
Industry dummy variable	*Industry*	According to the 2012 version of the industry classification standard of the China Securities Regulatory Commission
Year dummy variable	*Year*	The standard deviation of the stock's daily return for the year

Table 2: Descriptive statistics.

Variable name	Sample size	Mean value	Standard deviation	Minimum value	Maximum value
Div	28485	0.735	0.442	0.000	1.000
Pay	28485	0.080	0.131	0.000	0.761
Vc	28485	0.182	0.386	0.000	1.000
Roe	28485	0.079	0.075	−0.215	0.318
Lev	28485	0.439	0.199	0.056	0.858
Growth	28485	0.428	1.230	−0.662	9.189
Cash	28485	0.048	0.071	−0.167	0.249
Dual	28485	0.236	0.425	0.000	1.000
Ind	28485	0.370	0.052	0.286	0.571
Boardsize	28485	8.810	1.796	5.000	15.000
Top1	28485	35.634	15.137	8.950	74.960
Soe	28485	0.438	0.496	0.000	1.000
Ln*Size*	28485	22.087	1.267	19.822	26.049

payout ratio than companies that have not acquired venture capital holdings.

4.3. Mechanism Test: Alleviating the Agency Problem. As one of the top ten shareholders of listed companies, venture capital holds shares of listed companies, and one of the ways to encourage listed companies to increase their willingness to pay dividends and the level of dividend payment is to play an active role in supervision and governance, and to promote active dividend distribution of listed companies, thereby alleviating and restraining tunneling of major shareholders and other problems that damage the interests of small and medium shareholders, that is, by alleviating the agency problem between large shareholders and small and medium shareholders, improving corporate governance, thereby improving the dividend payment willingness and the dividend payment level of listed companies. Specifically, as an active investor, venture capital has motivation and the ability to actively alleviate the agency problem of listed companies. First, the motivation aspect. The operation mode of venture capital institution determines its need to maintain good social reputation. Reputational capital is a manifestation of the fund management level of venture capital organizations, and it is one of the important guarantees for venture capital

Table 3: Venture capital holdings and dividend payment propensity.

	(1) *Div*	(2) *Div*	(3) *Div*
VC	0.128***	0.114***	0.087***
	(0.04)	(0.04)	(0.04)
Roe	11.175***	11.082***	11.758***
	(0.32)	(0.32)	(0.34)
Lev	−3.817***	−3.981***	−3.723***
	(0.10)	(0.10)	(0.11)
Growth	−0.071***	−0.075***	−0.083***
	(0.01)	(0.01)	(0.01)
Cash	0.840***	1.178***	1.348***
	(0.24)	(0.25)	(0.25)
Dual	−0.177***	−0.173***	−0.138***
	(0.04)	(0.04)	(0.04)
Ind	−0.504	−0.276	−0.379
	(0.33)	(0.34)	(0.34)
Boardsize	0.024**	0.044***	0.061***
	(0.01)	(0.01)	(0.01)
Top1	0.011***	0.013***	0.014***
	(0.00)	(0.00)	(0.00)
Soe	−0.256***	−0.177***	−0.061
	(0.03)	(0.04)	(0.04)
Ln*Size*	0.611***	0.662***	0.579***
	(0.02)	(0.02)	(0.02)
Constant	−11.434*	−12.968***	−11.977***
	(0.37)	(0.43)	(0.46)
Observations	28,485	28,468	28,468
Industry FE	NO	YES	YES
Year FE	NO	NO	YES
Wald	3612	4136	4316
Pseudo R2	0.182	0.205	0.216

Note. The marking criteria for statistical significance in this table are as follows: * is $p < 0.10$, ** is $p < 0.05$, and *** is $p < 0.01$.

Table 4: Venture capital holdings and dividend payout levels.

	(1) *Pay*	(2) *Pay*	(3) *Pay*
VC	0.006***	0.006**	0.006***
	(0.00)	(0.00)	(0.00)
Roe	0.007	0.005	0.010
	(0.01)	(0.01)	(0.01)
Lev	−0.071***	−0.083***	−0.082***
	(0.01)	(0.01)	(0.01)
Growth	−0.003***	−0.003***	−0.003***
	(0.00)	(0.00)	(0.00)
Cash	0.037***	0.049***	0.051***
	(0.01)	(0.01)	(0.01)
Dual	−0.010***	−0.009***	−0.009***
	(0.00)	(0.00)	(0.00)
Ind	0.013	0.021	0.020
	(0.02)	(0.02)	(0.02)
Boardsize	0.003***	0.003***	0.003***
	(0.00)	(0.00)	(0.00)
Top1	0.001***	0.001***	0.001***
	(0.00)	(0.00)	(0.00)
Soe	−0.016***	−0.012***	−0.011***
	(0.00)	(0.00)	(0.00)
Ln*Size*	−0.034***	−0.033***	−0.033***
	(0.00)	(0.00)	(0.00)
Constant	0.821***	0.801***	0.791***
	(0.03)	(0.03)	(0.03)
Observations	28,485	28,485	28,485
R-squared	0.165	0.177	0.183
Industry FE	NO	YES	YES
Year FE	NO	NO	YES
F	145.5	131.5	124.3
Adj R-squared	0.164	0.175	0.181

Note. The marking criteria for statistical significance in this table are as follows: * is $p < 0.10$, ** is p, $p < 0.05$, and *** is $p < 0.01$; all regression coefficient estimates are based on robustness adjusted for corporate clustering standard error.

organizations to continue financing new funds and participate in investment activities of high-quality investee companies [32–34]. Therefore, by alleviating the agency problem of listed companies, venture capital increases the willingness of listed companies to pay dividends and their level of dividend payment, effectively protects the interests of small and medium shareholders and improves the company's governance level, which is conducive to the accumulation of its own reputational capital. Second, in terms of ability. The rich post-investment management experience of venture capital organizations has been confirmed by a large number of studies [22, 24, 25, 27, 29, 35–38]. Venture capital can effectively alleviate the conflicts of interest between large shareholders and small and medium shareholders by providing consultation for listed companies, thereby promoting the improvement of their own governance level, and dividend payment willingness and level.

In view of the above, the following inferences are made as follows.

Inference 4–1: The effect of venture capital holdings on the company's dividend policy is more pronounced in companies with more serious agency problem.

In reference to the research of Wang and Guo (2021) [39], dividend information is a part of the company's information disclosure, and the company's overall information disclosure level is an important response to agency problem. Therefore, drawing on the research of Dechow et al. [40] and Kothari et al. [41], the absolute value of the controllable accrued profit is selected as the proxy variable (DA) of the company's information disclosure level. This section groups the samples according to the median of the information disclosure level, and divides the samples into two groups: companies with higher information disclosure quality ($DA \leq MidDA$) and companies with lower information disclosure quality ($DA > MidDA$).

Table 5 reports one of the test results of inference 1, namely, the effect of the quality of corporate information disclosure on the willingness to pay dividends. Among them, column (1) is the group with better information disclosure quality, and column (2) is the group with poor information disclosure quality. As can be seen from Table 5, in the group with better information disclosure quality, although the coefficient of venture capital is

Table 5: Information disclosure quality and willingness to pay dividends.

	(1) $DA \leq MidDA$ *Div*	(2) $DA > MidDA$ *Div*
VC	0.051	0.124**
	(0.06)	(0.06)
Roe	10.520***	13.259***
	(0.39)	(0.65)
Lev	−3.738***	−3.650***
	(0.15)	(0.16)
Growth	−0.084***	−0.075***
	(0.02)	(0.03)
Cash	0.609**	3.977***
	(0.28)	(0.65)
Dual	−0.094*	−0.193***
	(0.05)	(0.06)
Ind	−0.314	−0.251
	(0.48)	(0.49)
Boardsize	0.055***	0.066***
	(0.02)	(0.02)
Top1	0.011***	0.017***
	(0.00)	(0.00)
Soe	0.022	−0.136**
	(0.05)	(0.06)
Ln*Size*	0.598***	0.562***
	(0.03)	(0.03)
Constant	−11.824***	−12.489***
	(0.64)	(0.68)
Observations	14,241	14,222
Industry FE	YES	YES
Year FE	YES	YES
Wald	2229	2202
Pseudo R2	0.215	0.226

Note. The marking criteria for statistical significance in this table are as follows: * is $p < 0.10$, ** is $p < 0.05$, and * is $p < 0.01$.

Table 6: Information disclosure quality and the dividend payment level.

	(1) $DA \leq MidDA$ *Pay*	(2) $DA > MidDA$ *Pay*
VC	0.005	0.007**
	(0.01)	(0.00)
Roe	0.021*	−0.014
	(0.01)	(0.02)
Lev	−0.078***	−0.082***
	(0.01)	(0.01)
Growth	−0.002***	−0.003***
	(0.00)	(0.00)
Cash	0.034***	0.084***
	(0.01)	(0.03)
Dual	−0.007**	−0.011***
	(0.00)	(0.00)
Ind	0.015	0.030
	(0.02)	(0.03)
Boardsize	0.003***	0.003***
	(0.00)	(0.00)
Top1	0.001***	0.001***
	(0.00)	(0.00)
Soe	−0.007**	−0.017***
	(0.00)	(0.00)
Ln*Size*	−0.032***	−0.034***
	(0.00)	(0.00)
Constant	0.762***	0.823***
	(0.03)	(0.03)
Observations	14,247	14,232
R-squared	0.169	0.205
Industry FE	YES	YES
Year FE	YES	YES
F	81.61	97.45
Adj R-squared	0.163	0.199

Note. The marking criteria for statistical significance in this table are as follows: * is $p < 0.10$, ** is $p < 0.05$, and *** is $p < 0.01$; all regression coefficient estimates are based on robustness adjusted for corporate clustering standard error.

positive, it is not significant. However, in the group with poor information disclosure quality, the coefficient of venture capital is significantly positive. The above regression results show that in the sample of companies with poor information disclosure quality, the role of venture capital in alleviating the agency problem is more obvious, which proves that venture capital can promote the inference of listed companies' willingness to pay dividends by alleviating the agency problem.

Table 6 reports one of the test results of inference 1, that is, the impact of the quality of corporate information disclosure on the level of dividend payments. As can be seen from Table 6, in the group with better information disclosure quality, although the coefficient of venture capital is positive, it is not significant. But in the group with poor information disclosure quality, the coefficient of venture capital is significantly positive. The above results show that in the companies with poor information disclosure quality, the role of venture capital in alleviating the agency problem is more obvious, which proves the inference that venture capital encourages listed companies to improve the level of dividend payment by alleviating the agency problem. The above results show that inference 1 in this section is confirmed.

5. Endogeneity and Robustness Checks

5.1. Endogenous Processing. The basic test above proves the influence of venture capital on the dividend policy of listed companies, but the above results are likely to be affected by selection bias, that is, because of the "selection effect" of venture capital on the investee company, there may be existing differences between the treatment group and the control group, which leads to the difference between the dividend policies of the treatment group and the control group. In order to alleviate the endogeneity issue caused by sample selection bias, this paper uses the propensity score matching method (PSM) to select a group of new control groups with the most similar characteristics for companies that have acquired venture capital holdings, thereby reducing the systematic differences between firms with venture capital holdings and firms without venture capital holdings. The specific matching method is as follows: Taking 2003–2019 as the sample period, the control group is companies that are not selected by venture capital during the sample period, and the variables that affect the choice of

Table 7: PSM matching balance effect.

Variable	Unmatched matched	Mean		% bias	% reduct|bias|	t-test	$p>\|t\|$
		Treated	Control			t	
Roe	*U*	0.0805	0.0786	2.500		1.570	0.116
	M	0.0805	0.0816	−1.600	37.30	−0.790	0.430
Lev	U	0.446	0.437	4.300		2.790	0.00500
	M	0.446	0.443	1.400	68	0.700	0.486
Cash	U	0.0431	0.0493	−8.700		−5.620	0
	M	0.0431	0.0440	−1.300	85.50	−0.640	0.520
Dual	U	1.773	1.762	2.800		1.790	0.0730
	M	1.773	1.781	−1.900	32.40	−0.970	0.334
Boardsize	U	8.849	8.801	2.700		1.740	0.0820
	M	8.849	8.831	1	61.80	0.530	0.597
Top1	U	35.25	35.72	−3.100		−2.010	0.0440
	M	35.25	35.49	−1.600	49.50	−0.800	0.423
Soe	U	0.463	0.432	6.100		4	0
	M	0.463	0.464	−0.200	97.50	−0.0800	0.937
Ln*Size*	U	22.30	22.04	20		13.31	0
	M	22.30	22.30	−0.100	99.40	−0.0600	0.954

venture capital holdings are sorted out, including specifically, performance variables, company debt ratio, cash holdings, the ratio of CEO duality, the size of the board of directors, the shareholding ratio of the largest shareholder, the nature of corporate property rights, and the size of the company, and use them as covariates to perform logit regression, to obtain propensity matching scores, and to find a suitable control group for the experimental group according to the nearest neighbor 1 : 1 matching method, among them, the caliper radius is selected as 0.01.

The balance test results in Table 7 can reflect the matching effect of PSM. From the t-test, except ROE, other covariates show significant differences before matching, but after PSM, the differences between covariates disappear, illustrating the fact that PSM reduces the systematic difference between the experimental group and the control group, and the effect of PSM is better than that of the control group. In addition, from the perspective of deviation percentage, the standardized differences of covariates are all below 10%. Compared with what is before matching, the standardized deviations of most variables are greatly reduced. Based on the above analysis, PSM satisfies the equilibrium assumption better.

The regression results based on the samples after the propensity score matching method are shown in Table 8. It can be seen from Table 8 that after using propensity score matching, the influence coefficient of venture capital holdings on the dividend payment willingness and the dividend payment level of listed companies is still significantly positive. It shows that after controlling possible endogeneity problem, the results are still robust.

5.2. Robustness Check

5.2.1. Replacing Dependent Variables and Models. In order to enhance the robustness of the basic test results, in reference to the methods of Wu et al. [29]and Wang et al. [30], this section firstly uses the method of replacing variables and corresponding models to check the robustness of the basic test results. Specifically, this subsection replaces the measurement method of the dependent variable and selects the dividend per share (*DPS*) instead of the dividend payout ratio. The formula is as follows: dividends per share = dividend distribution rate ∗ earnings per share, and the Tobit model is used accordingly to recheck the null hypothesis. The results are shown in Table 9. Column (3) of Table 9 shows that after changing the dependent variable measurement method and using the corresponding model, the coefficient of venture capital ($VC_{i,t}$) is still significantly positive at the 1% significance level, and the net effect is 0.005. That is to say, venture capital holdings can effectively increase the dividend payment level of listed companies.

5.2.2. Substitution of Independent Variable. In reference to the research of Wang et al. [30], this section uses the method of replacing independent variables to test the robustness of basic test results. Specifically, it is to use venture capital holdings (*VCholding*) to replace the original independent variable if there is existing venture capital ($VC_{i,t}$) among the top ten shareholders and repeat regression. The results are shown in Tables 10 and 11.

It can be seen from column (3) of Table 10 that after replacing the independent variable, the regression coefficient of venture capital holdings (*VCholding*) on the willingness of listed companies to pay cash dividends ($\mathrm{Div}_{i,t}$) is significantly positive at the 1% significance level with a net effect of 0.007. That is to say, the larger the venture capital's holdings, the more favorable it is to increase the willingness of listed companies to pay dividends.

It can be seen from column (3) of Table 11 that after replacing the independent variable, the regression coefficient of venture capital holdings (*VCholding*) on the level of cash dividend payment ($\mathrm{Pay}_{i,t}$) of listed companies is significantly positive at the 1% significance level, with a net effect of 0.001. That is to say, the greater the amount of venture capital

Table 8: Regression results of the propensity score matching method.

	(1) *Div*	(2) *Pay*
VC	0.097*	0.007**
	(0.06)	(0.00)
Roe	9.834***	−0.029 *
	(0.53)	(0.02)
Lev	−4.104***	−0.080***
	(0.19)	(0.01)
Growth	−0.044 *	−0.003**
	(0.03)	(0.00)
Cash	1.098**	0.030
	(0.45)	(0.02)
Dual	−0.054	−0.007*
	(0.07)	(0.00)
Ind	−0.254	0.034
	(0.62)	(0.03)
Boardsize	0.071***	0.004***
	(0.02)	(0.00)
Top1	0.014***	0.001***
	(0.00)	(0.00)
Soe	−0.136**	−0.008**
	(0.07)	(0.00)
Ln*Size*	0.622***	−0.032***
	(0.03)	(0.00)
Constant	−12.679***	0.776***
	(0.79)	(0.03)
Observations	9,058	9,072
R-squared		0.195
Industry FE	YES	YES
Year FE	YES	YES
Wald	1236	—
Pseudo R2	0.189	—
F	—	65.44
Adj R-squared	—	0.186

Note. The marking criteria for statistical significance in this table are as follows: * is $p < 0.10$, ** is $p < 0.05$, and *** is $p < 0.01$.

Table 9: Replacing dependent variables and models.

	(1) *DPS*	(2) *DPS*	(3) *DPS*
VC	0.001	0.007***	0.005***
	(0.00)	(0.00)	(0.00)
Roe	0.720***	0.490***	0.460***
	(0.02)	(0.02)	(0.01)
Lev	−0.201***	−0.177***	−0.172***
	(0.01)	(0.01)	(0.01)
Growth	−0.005***	−0.003***	−0.003***
	(0.00)	(0.00)	(0.00)
Cash	0.223***	0.075***	0.105***
	(0.02)	(0.01)	(0.01)
Dual	−0.013***	−0.002	−0.001
	(0.00)	(0.00)	(0.00)
Ind	−0.020	0.045	0.004
	(0.03)	(0.03)	(0.02)
Boardsize	−0.000	0.001	0.002**
	(0.00)	(0.00)	(0.00)
Top1	0.001***	0.001***	0.001***
	(0.00)	(0.00)	(0.00)
Soe	−0.028***	−0.017**	−0.008 *
	(0.00)	(0.01)	(0.00)
Ln*Size*	0.033***	0.040***	0.036***
	(0.00)	(0.00)	(0.00)
Constant	−0.582***	−0.783***	−0.707`
	(0.04)	(0.05)	(0.03)
Observations	28,485	28,359	28,359
R-squared	0.301	0.629	0.648
Industry FE	NO	YES	YES
Year FE	NO	NO	YES
F	128.7	86.57	355.1
Adj R-squared	0.300	0.578	0.598

Note. The marking criteria for statistical significance in this table are as follows: * is $p < 0.10$, ** is $p < 0.05$, and *** is $p < 0.01$; all regression coefficient estimates are based on robustness adjusted for corporate clustering standard error.

holdings, the more conducive it is for increasing the payment level of cash dividends of listed companies.

In conclusion, whether it is concerning the willingness to pay cash dividends or the level of cash dividend payment, the null hypothesis still stands after the independent variable is replaced, and the conclusion remains robust.

6. Further Research

6.1. Venture Capital Experience. The value-added services and supervision responsibilities of venture capital organizations to investee companies will be affected by the different characteristics of venture capital. In their research, Zhang and Liao [42] divided the background of Chinese venture capital organizations into four categories, namely, state-owned, private, foreign investment, and mixed backgrounds. Venture capital organizations of different backgrounds have different operating mechanisms, different scope and capabilities of resource acquisition, and large differences in the demand for return on investment. Therefore, the shareholding of venture capital organizations of different backgrounds will have significantly different impacts on the business decisions of investee companies. From the perspective of operation mechanism, as the development of China's venture capital market is far behind in comparison with the international venture capital market, foreign venture capital organizations have rich international investment experience superior to other types of venture capital organizations [43]. Therefore, in each stage of venture capital, including the selection of investment projects, the cultivation, and supervision of investment projects, a relatively standardized and mature mechanism has been formed. However, China's local venture capital organizations have a short development cycle and limited market experience. In particular, venture capital organizations with a state-owned background have special strategic objectives, and their operating mechanisms cannot be completely market-oriented [44, 45], as previous studies have also proved this. For example, Yu et al. [46]shows that, compared with venture capital organizations of other backgrounds, venture capital with a state-owned background does not significantly promote corporate innovation. From the perspective of resource acquisition, because the foreign venture capital industry started earlier and developed more maturely, the accumulation of resources is more abundant, including good

Table 10: Shareholding and dividend payment willingness.

	(1) *Div*	(2) *Div*	(3) *Div*
VCholding	0.005***	0.005***	0.007***
	(0.00)	(0.00)	(0.00)
Roe	11.022***	10.935***	11.560***
	(0.32)	(0.32)	(0.34)
Lev	−3.803***	−3.973***	−3.676***
	(0.10)	(0.10)	(0.11)
Growth	−0.070***	−0.074***	−0.083***
	(0.01)	(0.01)	(0.01)
Cash	0.802***	1.155***	1.337***
	(0.24)	(0.25)	(0.25)
Dual	−0.175***	−0.171***	−0.132***
	(0.04)	(0.04)	(0.04)
Ind	−0.519	−0.285	−0.399
	(0.33)	(0.34)	(0.34)
Boardsize	0.019*	0.039***	0.057***
	(0.01)	(0.01)	(0.01)
Top1	0.008***	0.010***	0.009***
	(0.00)	(0.00)	(0.00)
Soe	−0.232***	−0.153***	−0.018
	(0.03)	(0.04)	(0.04)
Ln*Size*	0.619***	0.670***	0.577***
	(0.02)	(0.02)	(0.02)
Constant	−11.715***	−13.249***	−12.194***
	(0.37)	(0.43)	(0.46)
Observations	28,485	28,468	28,468
Industry FE	NO	YES	YES
Year FE	NO	NO	YES
Wald	3615	4142	4355
Pseudo R2	0.183	0.206	0.218

Note. The marking criteria for statistical significance in this table are as follows: * is $p < 0.10$, ** is $p < 0.05$, and *** is $p < 0.01$.

Table 11: Shareholding and the dividend payment level.

	(1) *Pay*	(2) *Pay*	(3) *Pay*
VCholding	0.001***	0.001***	0.001***
	(0.00)	(0.00)	(0.00)
Roe	−0.016	−0.018*	−0.008
	(0.01)	(0.01)	(0.01)
Lev	−0.067***	−0.079***	−0.075***
	(0.01)	(0.01)	(0.01)
Growth	−0.003***	−0.003***	−0.003***
	(0.00)	(0.00)	(0.00)
Cash	0.033***	0.047***	0.049***
	(0.01)	(0.01)	(0.01)
Dual	−0.009***	−0.009***	−0.008***
	(0.00)	(0.00)	(0.00)
Ind	0.011	0.019	0.019
	(0.02)	(0.02)	(0.02)
Boardsize	0.002***	0.002***	0.002***
	(0.00)	(0.00)	(0.00)
Top1	0.000***	0.000***	0.000***
	(0.00)	(0.00)	(0.00)
Soe	−0.013***	−0.009***	−0.007***
	(0.00)	(0.00)	(0.00)
Ln*Size*	−0.033***	−0.033***	−0.033***
	(0.00)	(0.00)	(0.00)
Constant	0.791***	0.770***	0.780***
	(0.02)	(0.02)	(0.03)
Observations	28,485	28,485	28,485
R-squared	0.175	0.188	0.194
Industry FE	NO	YES	YES
Year FE	NO	NO	YES
F	154.7	141.4	134.7
Adj R-squared	0.175	0.186	0.191

Note. The marking criteria for statistical significance in this table are as follows: * is $p < 0.10$, ** is p, $p < 0.05$, and *** is $p < 0.01$; all regression coefficient estimates are based on robustness adjusted for corporate clustering standard error.

cooperation with investment banks, underwriters, law firms, and accounting firms, as well as political resources, such as government agencies, etc. These relationship networks can provide important support in the process of corporate governance. Organizations of other backgrounds, on the one hand, have a slight disadvantage in terms of resource advantages compared with foreign venture capital, and on the other hand, their investment demands may be quite different from foreign venture capital; especially for state-owned venture capital organizations, their investment demands are not limited to capital returns, and even to a certain extent, capital return demands give way to strategic demands, for example, in recent years, China has successively established two phases of the State-owned Enterprise Structural Adjustment Fund, and in September 2021, the National Energy Group Green and Low-Carbon Development Investment Fund was established. This type of venture capital often undertakes the important political mission of promoting the realization of important national strategic goals and promoting industrial and regional economic development [47, 48]. Based on the above analysis, in this section, venture capital organizations are divided into foreign investment capital and nonforeign investment capital according to the capital background of venture capital, and it is expected that listed companies held by foreign investment capital will have a stronger willingness to pay cash dividends. The results are shown in Table 12.

The results in Table 12 show the effect of venture capital holdings on the willingness of listed companies to pay dividends. The results in column (2) show that the coefficient of the foreign investment group is significantly positive at the 10% significance level, while the nonforeign investment group is not significant. Therefore, the inference of this subsection is confirmed. The venture capital with foreign investment background, using its own experience, has played an active supervisory role, effectively restrained the agency behavior of listed companies, and increased the willingness of listed companies to pay dividends.

6.2. Regional Development Level. As China is a large country with a vast territory, there are large cultural gaps between regions, and the level of economic development is very unbalanced [49, 50]. In terms of the degree of market-oriented development, the market-oriented development degree of the eastern coastal provinces has matured progressively, while the nonmarket-oriented factors in the economic development of the central and western regions

Table 12: Background of foreign capital and willingness to pay dividends.

	(1) Nonforeign *Div*	(2) Foreign investment *Div*
VC	0.070	0.081*
	(0.04)	(0.04)
Roe	11.761***	11.762***
	(0.34)	(0.34)
Lev	−3.738***	−3.725***
	(0.11)	(0.11)
Growth	−0.082***	−0.083***
	(0.01)	(0.01)
Cash	1.392***	1.346***
	(0.26)	(0.25)
Dual	−0.139***	−0.136***
	(0.04)	(0.04)
Ind	−0.422	−0.378
	(0.34)	(0.34)
Boardsize	0.060***	0.061***
	(0.01)	(0.01)
Top1	0.014***	0.014***
	(0.00)	(0.00)
Soe	−0.071*	−0.059
	(0.04)	(0.04)
Ln*Size*	0.583***	0.579***
	(0.02)	(0.02)
Constant	−12.003***	−11.986***
	(0.47)	(0.46)
Observations	27,953	28,437
Industry FE	YES	YES
Year FE	YES	YES
Wald	4258	4313
Pseudo R2	0.217	0.216

Note. The marking criteria for statistical significance in this table are as follows: * is $p < 0.10$, ** is $p < 0.05$, and ***, ** is $p < 0.01$.

Table 13: Regional development level and dividend payment willingness.

	(1) Eastern *Div*	(2) Central and western *Div*
VC	0.062	0.174**
	(0.05)	(0.07)
Roe	12.043***	11.734***
	(0.43)	(0.55)
Lev	−3.381***	−4.400***
	(0.13)	(0.20)
Growth	−0.092***	−0.067***
	(0.02)	(0.03)
Cash	1.408***	1.263***
	(0.32)	(0.44)
Dual	−0.162***	−0.045
	(0.05)	(0.07)
Ind	−0.741*	−0.092
	(0.45)	(0.55)
Boardsize	0.053***	0.070***
	(0.01)	(0.02)
Top1	0.015***	0.010***
	(0.00)	(0.00)
Soe	−0.119**	0.142**
	(0.05)	(0.06)
Ln*Size*	0.508***	0.729***
	(0.02)	(0.03)
Constant	−10.689***	−15.205***
	(0.62)	(0.76)
Observations	19,418	9,035
Industry FE	YES	YES
Year FE	YES	YES
Wald	2783	1626
Pseudo R2	0.215	0.229

Note. The marking criteria for statistical significance in this table are as follows: * is $p < 0.10$, ** is $p < 0.05$, and *** is $p < 0.01$.

still occupy relatively important regions. The imbalance of regional development affects the supervision and governance of venture capital in at least two aspects. First, the degree of legal perfection. Regions with developed markets tend to have better legal facilities, more robust investor protection mechanisms, and more standardized corporate governance-related policies. In the event there are behaviors that harm the interests of investors, investors can hold the company accountable in a more timely manner, and at the same time, when the regulator is unable, they can still more efficiently punish behaviors that harm the interests of investors [51]. Second, information transparency. The eastern coastal area was the first to complete the reform and opening up, and in the development of the market economy, the development of various standardized facilities is relatively complete. In the central and western regions, where economic development is relatively backward, the corporate governance mechanism, supervision mechanism, and information disclosure mechanism may be more backward than those in the eastern region, information transparency is low, and there are more nonmarket factors interfering with the company's operations and decision-making. In conclusion, in regions with a low level of economic

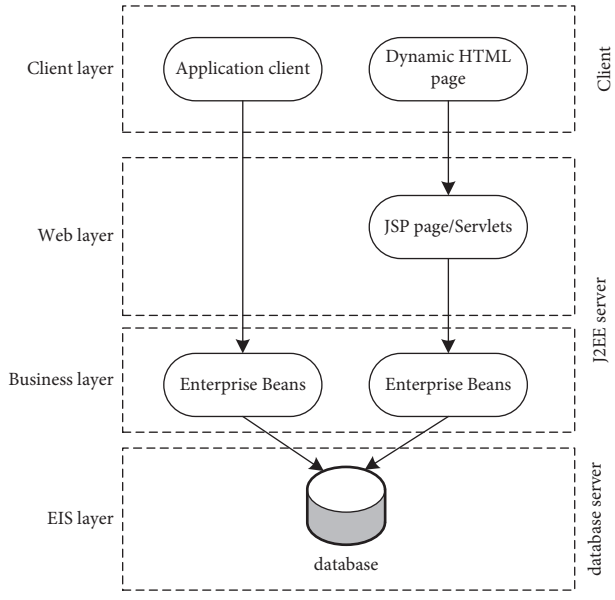

Figure 1: J2EE architecture.

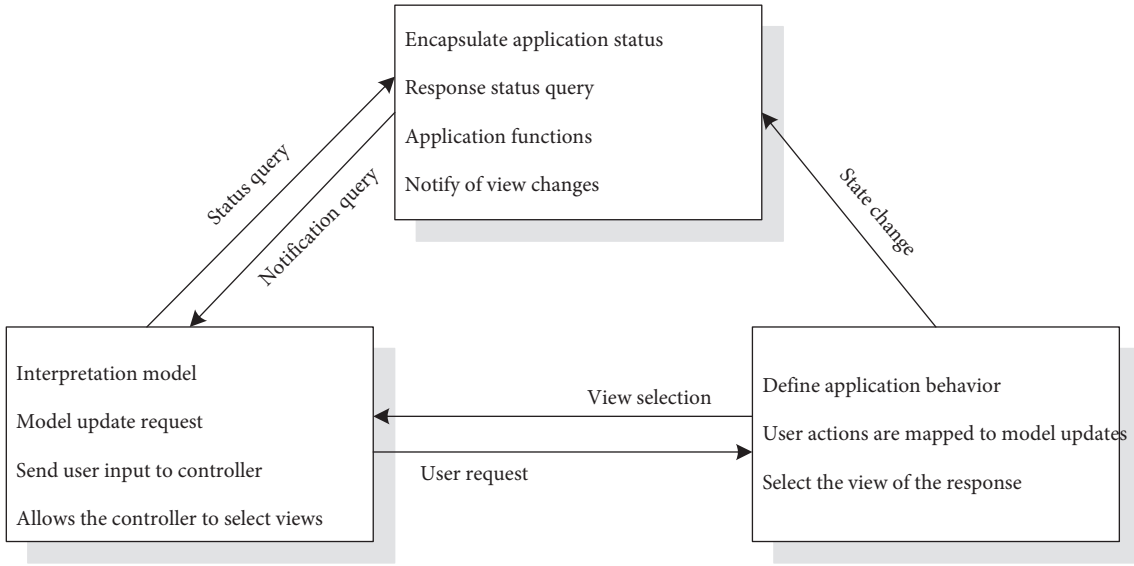

Figure 2: MVC mode.

development, the role of venture capital in supervision, governance, and consultation can better reflect the stage of increasing marginal returns. However, in regions with a higher level of economic development, the marginal returns of supervision and consultation may decline [52]. Therefore, this section infers that the supervision and consultation role of venture capital is more significant in the central and western regions.

The results in Table 13 show the effect of venture capital holdings on the willingness of listed companies to pay dividends. Among them, column (2) shows that the impact of venture capital in the central and western regions on the willingness to pay dividends is significantly positive at the 5% significance level, and the net effect is 0.174. However, in column (1), the coefficient of venture capital is not significant in the eastern region sample. The above results confirm the inference of this section, that is, the impact of venture capital holdings on relatively underdeveloped central and western regions is more significant [53].

7. Design and Implementation of Venture Capital Information Management Platform Based on J2EE

The vigorous development of information technology makes it possible to design and develop venture capital information management platform based on the research conclusions of this paper [54–59]. The design, development technology, and development mode of information service system are very important, which affects the performance of the system. For later maintenance and function expansion, there are two main development platforms: J2EE and .NET. The system developed by. Net runs on Windows operating system, while the system developed by J2EE can run on LinuX, UNIX, and Windows operating system, so it is more suitable for the software and hardware environment in this paper. Therefore, J2EE is used as the development platform here. Based on J2EE [56, 59], a venture capital information management platform is built.

The multitier distributed application model of J2EE divides the different layers in the two-tier model into many layers, as shown in Figure 1.

With the rapid development of Internet, how to construct the three-tier B/S structure quickly and effectively has become a research hotspot. MVC divides web applications into three layers: model, view, and controller. Its structure is shown in Figure 2.

As shown in Figure 2, (1) the model refers to the business logic layer, which is usually composed of Java, JavaBean or EJB, or Java + EJB. All businesses are processed by this layer; (2) view refers to the presentation layer, that is, functional web page display. JSP plays a major role in this layer; and (3) the controller is used to accept and distribute the request to the business layer, and pass the data returned by the business logic to the view layer for presentation to the requester.

The corresponding relationship between MVC and J2EE architecture is shown in Figure 3. The view is in the web layer and the client layer, usually JSP/servlets. The controller is also in the web layer and is usually implemented with servlets. The model is in the business logic layer and is usually implemented with server-side JavaBeans or EJB.

7.1. Requirement Analysis. According to the above research, the system requirements of venture capital information management platform include the following:

(1) Realize the release and sharing of venture capital information, including investment projects, financing projects, investment and financing hotspots, investment and financing institutions, and other information

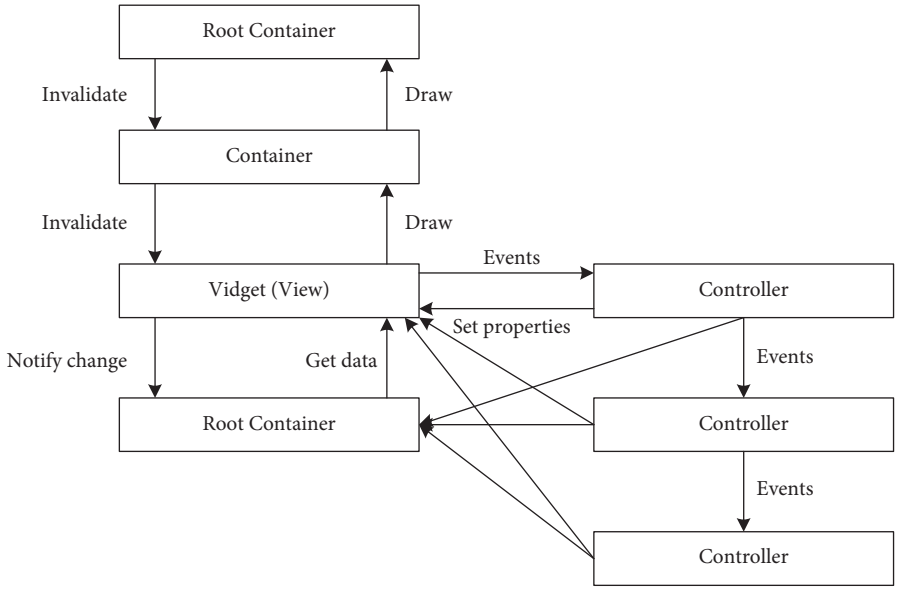

Figure 3: The corresponding relationship between MVC and J2EE architecture.

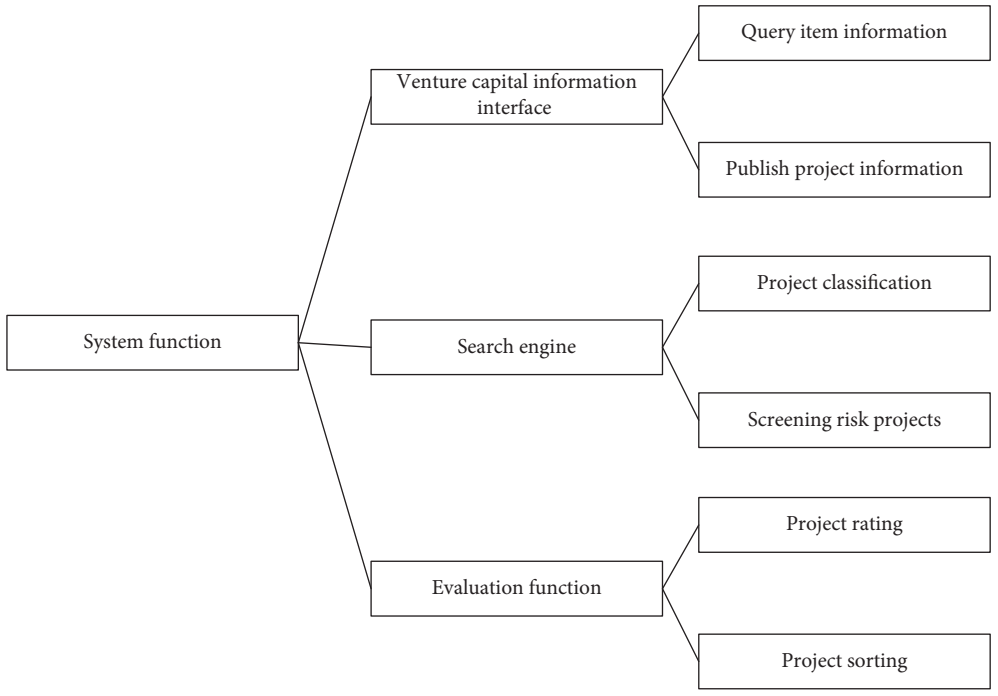

Figure 4: Functional planning of the designed platform.

(2) Realize the classification and retrieval of venture capital information, including project classification and retrieval, organization classification and retrieval, ranking list of hot investment, and financing projects, etc.

(3) Realize the rating of venture capital projects, including the government's rating of venture capital institutions, the rating of venture capital projects, and rating release

For these requirements, the functional planning of the platform is shown in Figure 4.

7.2. Use Case Model. Use case is a dynamic description of system behavior. Through use case modeling, it describes the external roles interested in the system and their functional requirements for the system. According to the analysis of

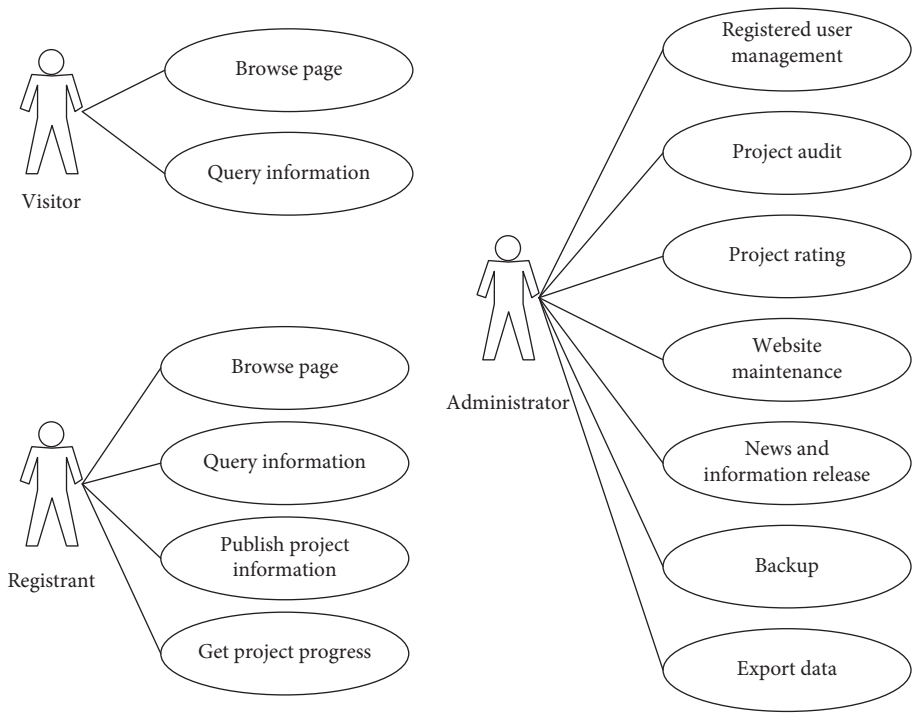

Figure 5: Use case diagram.

user behavior, users are divided into tourists, registered users, and administrator users. When different users carry out relevant operations, they have relatively different permissions.

Visitors can only browse the web and query information. Registered users can browse web pages, query information, publish project information, and obtain project related progress. Administrator users can manage the registered users of the website, review the investment and financing projects, rate the investment and financing projects, and be responsible for the maintenance of the website and the release and update of relevant news information. Their use case diagram is shown in Figure 5.

7.3. System Design. The system design of venture capital information management platform is an important stage in the process of system construction. The platform adopts a three-tier structure of standard database layer, data processing layer, and dynamic web page presentation layer. The database is mainly responsible for data storage, retrieval, change, and deletion. The data processing layer is mainly responsible for the generation of SQL statements, database state feedback, data information inspection, etc. The dynamic web page presentation layer is responsible for generating relevant web pages according to the obtained data or web page requests, and finally displaying them on the browser. The overall architecture of the platform is shown in Figure 6.

The object relation model is designed as follows: The object of the platform consists of three objects: enterprise, project, and project index. The project index object can be included in the project object, so as to reduce the number of

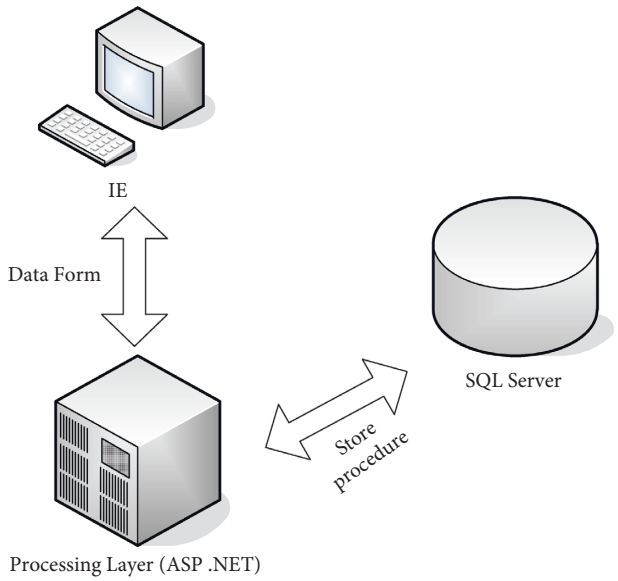

Figure 6: The overall architecture.

objects and simplify the object relationship. However, considering that the project index and project rating are the core content of the website, and the project rating itself is flexible, it may be added and changed according to the actual situation within a certain period of time, Therefore, project indicators are listed here as a special object. Although it brings some system overhead, it reduces the coupling of the system model and conforms to the characteristics of the system itself. An entity-relationship (E-R) diagram is shown in Figure 7.

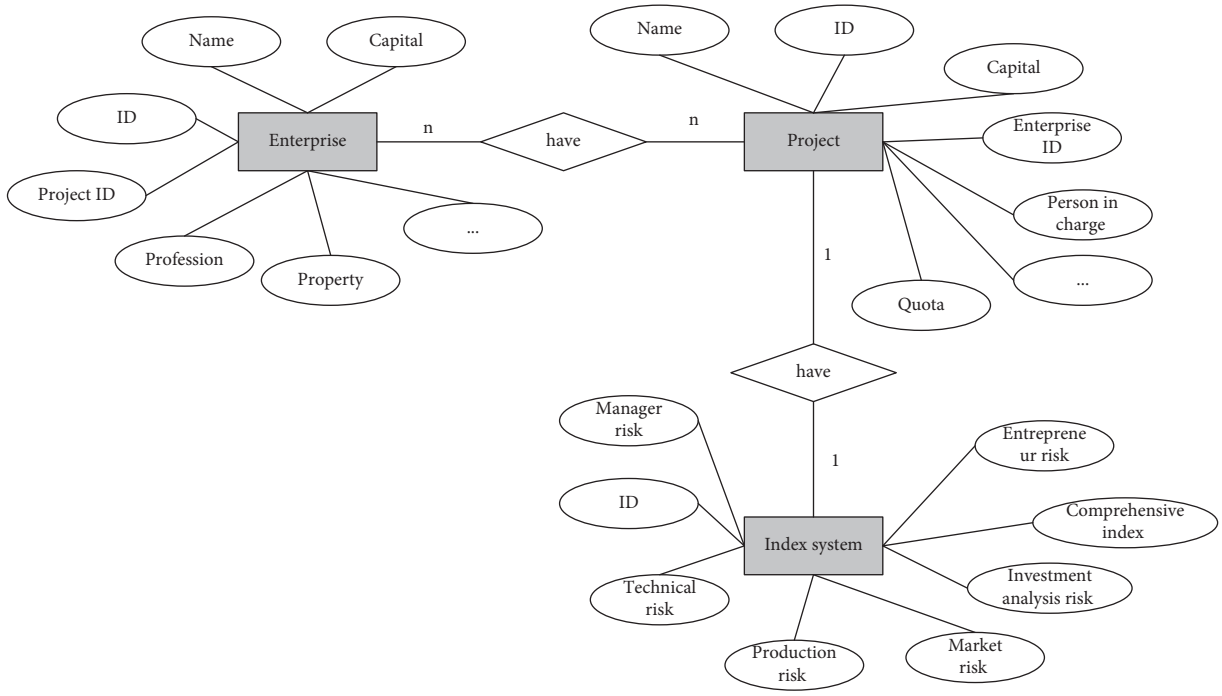

Figure 7: E-R diagram.

Table 14: The specification design.

Definition of platform	Medium-sized government level website
Number of people online	<3000
Number of registered users	>10000
Home page hits/day	<5000
Home page unique IP	<5000
Total flow	<5G
Page views	<300000
Platform access frequency	<500 times/second
Home page flow/day	<1G
IP quantity	<50000

7.4. Specification Design. The venture capital information management platform developed by the project is a medium-sized government level website. The website visit frequency supports less than 500 people per second, supports online access of less than 2000 people, and supports the registration of tens of thousands of users. The specification design is shown in Table 14.

8. Conclusion

This paper takes all A-share listed companies from 2003 to 2019 as samples, and studies the impact of venture capital holdings on the dividend policy of listed companies. This paper examines the effects of venture capital holdings on the willingness of listed companies to pay dividends and their level of dividend payment. The research results are as follows: First is the basic test. By constructing the logit model, it can be seen that companies that have obtained venture capital holdings have a stronger willingness to pay dividends than companies that have not obtained venture capital holdings. By constructing the OLS regression model, it can be seen that the listed companies with venture capital holdings among the top ten shareholders have a higher level of dividend payment. Second is the mechanism test. According to the derivation logic of this paper, the influence of venture capital on the dividend policy of listed companies is achieved by exerting its supervisory function and alleviating the agency problem of listed companies. Therefore, this paper examines the difference in the impact of venture capital on the dividend policy of listed companies at different levels of agency problem. The results show that in the group with more serious agency problem, the positive promotion effect of venture capital on the dividend payment willingness and the dividend payment level of listed companies is more significant. Third is endogeneity and robustness checks. In order to alleviate the possible problems of sample selection, this paper designs a propensity score matching method to control the possible endogeneity problem. The results show that the sample regression results after propensity score matching are still robust. At the same time, in order to enhance the robustness of the conclusion, a series of robustness checks, such as replacing the dependent variable, replacing the estimated model with the Tobit model, and replacing the independent variable, have been carried out successively, and the conclusion still holds. Fourth is further research. Further research finds that venture capital organizations of different backgrounds have different effects on the cash dividend policy of investee companies. The situation is reflected in the following aspects: companies with foreign investment venture capital holdings are more inclined to distribute cash dividends, and at the same time, the cash dividend payment rate is higher because foreign investment

venture capital has a more complete corporate governance experience. At the same time, the uneven level of regional development and the difference in the degree of marketization will also affect the role of venture capital supervision and governance. In the central and western regions, where the level of economic development is relatively backward, the impact of venture capital on the promotion of the dividend policy of listed companies is more significant.

Taking the cash dividend policy of listed companies as the starting point, this paper studies the specific role of venture capital shareholding in corporate governance, and provides empirical evidence on dividend policy for the research on the role of venture capital governance.

From the conclusion of this paper, we can get the following two implications: First, as far as the regulatory bodies are concerned, the China Securities Regulatory Commission has continuously issued relevant policies since 2001, in order to encourage listed companies to actively distribute cash and strengthen the protection of the interests of small and medium shareholders, thereby increasing the returns of capital market investors. However, the promotion effect of the semimandatory dividend policy is far from satisfactory. The research in this paper effectively proves the positive role that venture capital organizations play in the governance of listed companies. Therefore, as far as the regulatory bodies are concerned, actively guiding social capital to participate in social and economic construction in an orderly and steady manner has a positive driving effect on promoting the healthy development of the capital market and alleviating the "new normal" situation that China's economy is currently in. Second, as far as listed companies are concerned, actively introducing financial intermediaries such as venture capital and "active investors" and relying on the rich industry experience and complete corporate governance experience of such investors will help alleviate the internal agency problem of listed companies, so as to enhance the company's efficiency and increase the company's value.

Data Availability

The experimental data used to support the findings of this study are available from the corresponding author upon request.

Conflicts of Interest

The authors declare that they have no conflicts of interest regarding this work.

References

[1] J. Zhu and C. Wang, "The effect of financial crisis on cash dividend policies——from the perspective of ownership structure," *Accounting Research*, vol. 2, pp. 38–44+94, 2013.

[2] C. Lv and K. Wang, "Empirical analysis of dvidend policy of listed companies," *Economic Research Journal*, vol. 12, pp. 31–39, 1999.

[3] G. Wei and Y. Jiang, "Questionnaire report on dividend distribution of listed companies in China," *Economic Science*, vol. 4, pp. 79–87, 2001.

[4] Z. Wang and W. Zhang, "Research on financial flexibility, refinancing option and dividend catering strategy of listed companies," *Management World*, vol. 7, pp. 151–163, 2012.

[5] Z. Wei, M. Li, and C. Li, "The semi-mandatory dividend rules and dividend behaviors of Chinese listed firms," *Economic Research Journal*, vol. 49, no. 6, pp. 100–114, 2014.

[6] Z. Wei, C. Li, Y. Wu, and J. Huang, "The semi-mandatory dividend rules, refinancing motivation and classical dividend theories——an empirical study based on agent theory and signaling theory," *Accounting Research*, vol. 7, pp. 55–61+97, 2017.

[7] M. C. Jensen, "Active investors, LBOs, and the privatization of bankruptcy*," *The Journal of Applied Corporate Finance*, vol. 2, no. 1, pp. 35–44, 1989.

[8] J. Yu, J. Dong, and H. Zheng, "Does venture capital promote inter-regional capital flow? an empirical study based on cross-regional M&A," *Journal of Finance and Economics*, vol. 48, no. 1, pp. 108–122, 2022.

[9] Y. Guan, K. Zhou, and H. Tang, "Research on the mechanism of venture capital on cash dividend of listed companies: an empirical analysis based on perspective of corporate governance," *Financial Theory and Practice*, vol. 11, pp. 99–107, 2019.

[10] M. H. Miller and K. Rock, "Dividend policy under asymmetric information," *The Journal of Finance*, vol. 40, no. 4, pp. 1031–1051, 1985.

[11] S. Benartzi, R. Michaely, and R. Thaler, "Do changes in dividends signal the future or the past?" *The Journal of Finance*, vol. 52, no. 3, pp. 1007–1034, 1997.

[12] X. Chen, X. Chen, and N. Fan, "An empirical study on the first dividend signal transmission effect of listed companies in China," *Economics Science*, vol. 5, 1998.

[13] Q. Yu and Y. Cheng, "The firm's dividend policy and stock market fluctuation in China," *Economic Research Journal*, vol. 4, pp. 32–40+95, 2001.

[14] C. B. Barry, C. J. Muscarella, J. W. Peavy, and M. R. Vetsuypens, "The role of venture capital in the creation of public companies," *Journal of Financial Economics*, vol. 27, no. 2, pp. 447–471, 1990.

[15] J. B. Sørensen and T. E. Stuart, "Aging, obsolescence, and organizational innovation," *Administrative Science Quarterly*, vol. 45, no. 1, pp. 81–112, 2000.

[16] S. N. Kaplan and P. Strömberg, "Venture capitalists as principals: contracting, screening, and monitoring," *The American Economic Review*, vol. 91, no. 2, pp. 426–430, 2001.

[17] Y. V. Hochberg, A. Ljungqvist, and Y. Lu, "Whom you know matters: venture capital networks and investment performance," *The Journal of Finance*, vol. 62, no. 1, pp. 251–301, 2007.

[18] N. Cai and X. He, "Can social networks improve the value-added effect of VC ?based on the relationship of venture capital networks and investment efficiency," *Journal of Financial Research*, vol. 12, pp. 178–193, 2015.

[19] Y. Qu and H. Chen, "Dividend policy, internal control and market reaction," *Journal of Financial Research*, vol. 5, pp. 191–206, 2018.

[20] C. Li, Z. Wei, and S. Wu, "A study on market reactions to the semi-mandatory dividend policy," *Economic Research Journal*, vol. 45, no. 3, pp. 144–155, 2010.

[21] F. Huang, T. Peng, and L. Tian, "The influence of venture capital on the investment behavior of start-ups," *Journal of Financial Research*, vol. 8, pp. 180–192, 2013.

[22] C. Wu and Y. Zhang, "The impact of venture capital on the dividend policy of listed companies: evidence from China," *Journal of Financial Research*, vol. 9, pp. 178–191, 2017.
[23] M. Gorman and W. A. Sahlman, "What do venture capitalists do?" *Journal of Business Venturing*, vol. 4, no. 4, pp. 231–248, 1989.
[24] T. Hellmann and M. Puri, "Venture capital and the professionalization of start-up firms: empirical evidence," *The Journal of Finance*, vol. 57, no. 1, pp. 169–197, 2002.
[25] T. L. Campbell, M. B. Frye, and M. B. Frye, "Venture capitalist monitoring: evidence from governance structures," *The Quarterly Review of Economics and Finance*, vol. 49, no. 2, pp. 265–282, 2009.
[26] X. Tian, "The causes and consequences of venture capital stage financing," *Journal of Financial Economics*, vol. 101, no. 1, pp. 132–159, 2011.
[27] Y. Li and S. He, "On the effects of mergers and acquisitions performance of venture capital backed ChiNext companies," *Accounting Research*, vol. 6, pp. 60–66+97, 2017.
[28] P. Pan, Z. Xu, and L. Su, "A research on the effect of private equity investment on the GEM ListedCompanies' cash dividend policy," *China Soft Science*, vol. 6, pp. 168–175, 2019.
[29] C. Wu, S. Wu, J. Cheng, and Lu Wang, "The role of venture capital in the investment and financing behavior of listed companies:evidence from China," *Economic Research Journal*, vol. 47, no. 1, pp. 105–119, 2012.
[30] H. Wang, R. Zhang, and S. Hu, "Private equity and dividend policy," *Accounting Research*, vol. 10, pp. 51–58+97, 2014.
[31] H. Wang, C. Li, and C. Lu, "A case study of the impact of controlling shareholder s on the listed companies' cash dividend policies," *Management World*, vol. 1, pp. 122–127+136+172, 2007.
[32] W. A. Sahlman, "The structure and governance of venture-capital organizations," *Venture Capital*, vol. 27, no. 2, pp. 3–51, 2022.
[33] C. N. V. Krishnan and V. I. Ivanov, "Venture capital reputation, post-IPO performance, and corporate governance," *Journal of Financial and Quantitative Analysis*, vol. 46, no. 5, pp. 1295–1333, 2011.
[34] Z. Yang, Y. Hou, and R. Wu, "Influence of network location and status of venture capital institutions on venture capital stage selection—an empirical study based on China's venture capital industry," *R & D Management*, vol. 33, no. 5, pp. 122–135, 2021.
[35] J. Lerner, "Venture capitalists and the oversight of private firms," *The Journal of Finance*, vol. 50, no. 1, pp. 301–318, 1995.
[36] S. N. Kaplan and P. Strömberg, "Characteristics, contracts, and actions: evidence from venture capitalist analyses," *The Journal of Finance*, vol. 59, no. 5, pp. 2177–2210, 2004.
[37] D. Cumming and S. Johan, "Regulatory harmonization and the development of private equity markets," *Journal of Banking & Finance*, vol. 31, no. 10, pp. 3218–3250, 2007.
[38] S. Li, J. Yang, and J. Zhong, "Do venture capitals have the consulting function? Evidence from research on the function of venture capitals in inter-regional M&A," *Management World*, vol. 35, no. 12, pp. 164–216, 2019.
[39] C. Wang and Y. Guo, "Semi-mandatory dividend policy and cost of equity," *Journal of Financial Research*, vol. 8, pp. 172–189, 2021.
[40] P. M. Dechow, R. G. Sloan, and A. P. Sweeney, *Detecting Earnings Management*, pp. 193–225, Accounting review, European, 1995.
[41] S. P. Kothari, A. J. Leone, and C. E. Wasley, "Performance matched discretionary accrual measures," *Journal of Accounting and Economics*, vol. 39, no. 1, pp. 163–197, 2005.
[42] X. Zhang and Li Liao, "VCs' backgrounds, IPO underpricing and post-IPO performance," *Economic Research Journal*, vol. 46, no. 6, pp. 118–132, 2011.
[43] T. J. Chemmanur, T. J. Hull, and K. Krishnan, "Do local and international venture capitalists play well together? The complementarity of local and international venture capitalists," *Journal of Business Venturing*, vol. 31, no. 5, pp. 573–594, 2016.
[44] P. Qian and W. Zhang, "Returns on Chinese venture capital investment and its determinants," *Economic Research Journal*, vol. 5, pp. 78–90, 2007.
[45] W. Shen, X. Ye, and W. Xu, "Is there timing behavior in VC-backed IPOs: an empirical evidence from China," *Nankai Business Review*, vol. 16, no. 2, pp. 133–142, 2013.
[46] Y. Yu, W. Luo, Yi-tsung Lee, and Z. Qi, "Investment behaviors and performance of government-sponsored venture capitals," *Economic Research Journal*, vol. 49, no. 2, pp. 32–46, 2014.
[47] J. Lerner, "Boom and bust in the venture capital industry and the impact on innovation," *Social Science Research Network*, Rochester, NY, USA, 2002.
[48] D. B. Fuller, "How law, politics and transnational networks affect technology entrepreneurship: explaining divergent venture capital investing strategies in China," *Asia Pacific Journal of Management*, vol. 27, no. 3, pp. 445–459, 2010.
[49] Y. Wang, Y. Zhang, Y. Zhang, C. Zhao, and M. Lu, "On China's development model:the costs and benefits of China's decentralization approach to transition," *Economic Research Journal*, vol. 1, pp. 4–16, 2007.
[50] D. Chen, S. Liang, and D. Jiang, "How marketization affects incentive contract costs and choices: perks or monetary compensations?" *Accounting Research*, vol. 11, pp. 56–64+97, 2010.
[51] Jr. Coffee and C. John, "Privatization and corporate governance: the lessons from securities market failure," *The Journal of Corporation Law*, vol. 25, p. 1, 1999.
[52] P. Wang and L. Zhou, "Auditor's choice by China's listed companies and its governance role," *China Accounting Review*, vol. 2, pp. 321–344, 2006.
[53] C. Wang, J. Lan, and Z. Zhang, "Implications of venture capital on companies' M&A goodwill bubbles: evidence from Chinese listed companies," *Discrete Dynamics in Nature and Society*, vol. 2022, Article ID 1567344, 16 pages, 2022.
[54] L. Li and C. Mao, "Big data supported PSS evaluation decision in service-oriented manufacturing," *IEEE Access*, vol. 8, no. 99, pp. 154663–154670, 2020.
[55] L. Li, C. Mao, H. Sun, and Y. B. Yuan, "Digital twin driven green performance evaluation methodology of intelligent manufacturing: hybrid model based on fuzzy rough-sets AHP, multistage weight synthesis, and PROMETHEE II," *Complexity*, vol. 2020, Article ID 3853925, 24 pages, 2020.
[56] X. Wu, "Performance appraisal management system of university administrators based on hybrid cloud," *Scientific Programming*, vol. 2022, Article ID 9326563, 2022.
[57] L. Li, B. Lei, and C. Mao, "Digital twin in smart manufacturing," *Journal of Industrial Information Integration*, vol. 26, no. 9, Article ID 100289, 2022.
[58] L. Li, T. Qu, Y. Liu, and R. Y. Zhong, "Sustainability assessment of intelligent manufacturing supported by digital twin," *IEEE Access*, vol. 8, pp. 174988–175008, 2020.
[59] Ai Zhang, Z. Ju, and Y. Liu, "Optimal analysis of human resources allocation in colleges and universities based on internet of things technology," *Computational Intelligence and Neuroscience*, vol. 2021, Article ID 9605397, 2021.

Hindawi
Scientific Programming
Volume 2022, Article ID 2420936, 10 pages
https://doi.org/10.1155/2022/2420936

Research Article

Risk Management of Prefabricated Building Construction Based on Fuzzy Neural Network

Maohua Yang

Chongqing Jianzhu College, Chongqing 400072, China

Correspondence should be addressed to Maohua Yang; ymh_870909@cqjzc.edu.cn

Received 16 March 2022; Revised 31 March 2022; Accepted 8 April 2022; Published 3 June 2022

Academic Editor: Jie Liu

With the rapid development of society, the risk management of personal health and assets has become an important content that cannot be ignored in all walks of life. With the in-depth advancement of risk management, most of the construction risks of prefabricated buildings adopt qualitative research based on experience and intuitive judgment and quantitative research on quantitative mathematical statistics, but there are few models for risk assessment of prefabricated buildings with dynamic characteristics to adapt to the rapid development of prefabricated buildings and the lack of prefabricated construction in various stages and complex environments, with risk prediction and effective response capabilities. Based on this, this paper attempts to propose a fuzzy neural network risk research method for prefabricated building construction, making full use of the fuzzy neural network's qualitative knowledge expression and quantitative numerical computing advantages, to establish a set of strong fault tolerance and better adaptive ability: fuzzy neural network evaluation model for extensive prefabricated building construction risk. Through the design of the fuzzy network model structure, the membership vector of the qualitative and quantitative indicators of the fuzzy comprehensive evaluation of the risk of prefabricated building construction is used as the input vector of the neural network, and the evaluation result is used as the output of the neural network. The samples were trained, programmed, and debugged, and it was found that the training results of the samples were in good agreement with the expected output results, which further verified the feasibility and applicability of the fuzzy neural network in the risk assessment process of prefabricated buildings. It is of good guiding significance to conduct continuous observation and formulate effective risk aversion and response plans.

1. Introduction

With the continuous advancement of construction industrialization, prefabricated buildings have achieved unprecedented development, injecting new kinetic energy into the advancement of global climate governance. With the continuous emergence of green construction appeals, the new construction method of prefabricated buildings will become more and more popular. Meanwhile, it is widely used in industry and residences because of its high production efficiency, high production accuracy, small environmental impact, and high degree of industrialization. Compared with traditional building forms, prefabricated buildings have different quality, technology, and construction period requirements in the detailed design stage, prefabrication transportation stage, and hoisting stage. In order to reduce and avoid risk losses, prefabricated buildings are effectively risked [1, 2].

Management is particularly important. In risk management, risk assessment is an important basis for risk management. It aimed to find, analyze, and predict the dangerous and harmful factors existing in the project and the system and the severity of the accident that may be caused, then propose reasonable and feasible safety countermeasures, and guide the source of danger [3, 4]. Monitoring and accident prevention are done to achieve the lowest accident rate, the least loss, and the best return on safety investment. Traditional risk assessment methods are divided into qualitative assessment and quantitative assessment. The qualitative method is mainly based on experience and

intuitive judgment, while the quantitative method is based on a large number of experimental results and extensive statistical analysis of accident data. Both of these two methods have certain defects, which limit their application, and the method combining qualitative and quantitative can make up for the shortcomings of traditional methods [5].

Therefore, this paper adopts the fuzzy evaluation method based on neural network to study the risk management of prefabricated construction. Applications can also be a good way to overcome subjectivity in evaluation.

2. Related Work

In terms of risk management research on prefabricated building construction, the predecessors have conducted statistical modeling and analysis of various building risk factors such as cost, safety, and energy for analysis, evaluation, and decision-making for enterprises. For example, by combining factors such as the construction period of prefabricated buildings, energy consumption in the construction process, and seismic performance of prefabricated buildings, the dynamic case analysis research method is used to analyze the high probability risk of prefabricated buildings and the use of residential target comfort and prefabrication. The data monitoring of the prefabricated buildings explains the construction management risks of prefabricated buildings and the degree of influence of various risk factors on the public [6]. Lee et al., through literature review and detailed analysis of risk factors at the construction site, combined with the impact of the risk factors on the site of prefabricated building construction, used AHP to establish a weight system for risk indicators. According to the classification of risk factors in the construction management of conventional buildings, comprehensively use the statistical analysis method of accident cases and risk matrix to carry out risk assessment [7]. Hinze and others put forward suggestions on the safety management of prefabricated buildings and evaluate the construction risks of prefabricated buildings through the concept of leading indicators [8].

Through the construction of the F-QRAM model, Pinto evaluates inaccurate and vague risk variables, determines the key risk factors of prefabricated building construction, provides guidance for safety risk management during project construction, and guides decision makers in the process of risk assessment. It provides enterprises critical, scientific, and objective guidance for risk response [9]. Xiao et al., through the construction of a fuzzy-based prefabricated building risk assessment model, used the direct rights method to calculate the weights of various indicators, effectively reducing the deviation caused by subjective weighting [10]. Based on the existing research and analysis combined with rough set theory, Guo et al. discussed and analyzed DM (data mining) technology and redefined the risk factors affecting prefabricated buildings. Through the quantitative assessment of risk factors, redundant risk factors are reduced to form the final efficient and quick decision-making method [11].

Staub-French et al. use BIM applications and REPCON (Project Progress Management Program) to combine the Internet and prefabricated buildings to simulate and adjust the construction progress and the process of project implementation, so as to formulate effective control for the quality and safety in the construction management of prefabricated buildings measures [12]. Li et al. used SNA to identify various risk factors in precast concrete projects. Through BIM-centered strategic recommendations, the probability of risk occurrence can be reduced and the communication of target stakeholders can be promoted [13]. Sinha conducted in-depth research and analysis on the construction management of prefabricated frame systems based on the research foundation of predecessors, conducted research on various types of supporting structural components and evaluated construction management risks, and proposed the use of standardized supporting frame systems in construction, to ensure the quality of the structure and reduce the risk factors of construction management [14].

3. Related Theories

3.1. Fuzzy Theory. Fuzzy theory is developed on the basis of fuzzy mathematics. The theory is attached to the basic concept of fuzzy sets and the theory of continuous membership functions [15]. A large number of facts show that many things are put before the cart because of excessive pursuit of precision. If a suitable mathematical language is found to describe the ambiguity of things, proper fuzzy processing can achieve a more precise purpose.

3.1.1. Fuzzy Set. A fuzzy set has an indistinct boundary. For a fuzzy set, an element can both belong to the set and not belong to the set, and the boundary is blurred. In fuzzy logic based on fuzzy sets, the truth of any statement or proposition is only a certain degree of truth, that is, fuzziness. It reflects the uncertainty of events, which can be characterized by the degree to which an element belongs to a certain set, and a numerical value belonging to [0,1]—a membership function. In [16], fuzzy sets and membership functions are defined as follows: Given a universe of discourse X, any mapping from X to the closed region [0,1]:

$$\begin{aligned} \mu_A &: X \longrightarrow [0,1], \\ x &\longrightarrow \mu_A(x). \end{aligned} \tag{1}$$

μ_A is called the membership function of the fuzzy set A, and $\mu_A(x)$ is called x is the membership function of A. The degree of membership can also be denoted as $A(x)$.

3.1.2. Membership Function. Professor Zadeh first proposed the concept of membership function in 1965, which is used to describe the degree of membership of the element u to the fuzzy set U. Due to the uncertainty of this relationship, it is generally used from the interval [0,1]. The value taken replaces the two values of 0 and 1 to describe the "true degree" of an element belonging to a fuzzy set. Through membership

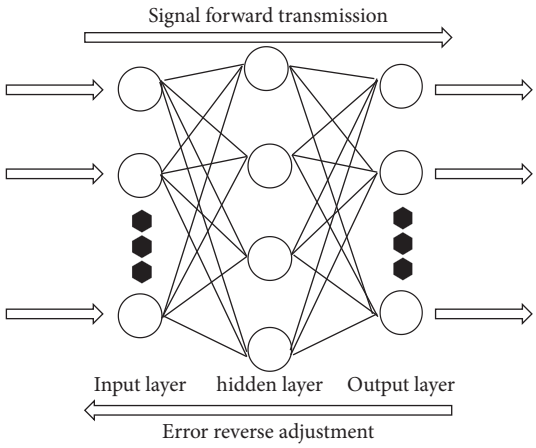

Figure 1: BP neural network structure.

function, a fuzzy concept can be expressed transitionally from "not belonging at all" to "belonging completely," and it is easier to quantitatively analyze and express all fuzzy concepts.

The qualitative description of objective things by membership function is relatively objective in nature, but different individuals have different cognitions to the same fuzzy concept, so there is subjectivity. The determination of the membership function is still based on experience and experiments, and there is no effective systematic method. At present, the common determination methods include fuzzy statistics method, assignment method, expert experience method, and so on. These methods improve the rough membership function through continuous "learning" and "practice," so as to achieve the unity of the subjective and the objective.

3.1.3. Fuzzy Logic System. Fuzzy logic system refers to a system including fuzzy concepts and fuzzy logic. When it exercises control function, it is called fuzzy logic controller.

Due to the randomness in fuzzy concept and fuzzy logic selection, fuzzy logic systems with various states can be constructed. For example, the combination of various fuzzy neurons constitutes a neural network logic system with fuzzy information processing functions.

3.2. BP Neural Network Algorithm

3.2.1. Principle of BP Neural Network. The BP neural network consists of three parts: input layer, hidden layer, and output layer. Each layer involves a large number of neurons, and these three layers are also organically combined by these neurons to form the integrity of the model [17–20].

In the BP neural network model, the feature vector is input from the input layer to carry out the model network. After the feature vector is recognized in the input layer, it is transmitted to the hidden layer by the neuron and performs certain data processing. Finally, it is also transmitted to the output layer by the neuron. The data is processed and compared according to the given expected value. When the output conditions are not met, the output layer starts to perform reverse transfer and weight adjustment, and this cycle is repeated until the output reaches the preset expected value. It can be seen that the BP neural network is an intelligent model that can continuously learn and self-adjust, and its structure is shown in Figure 1.

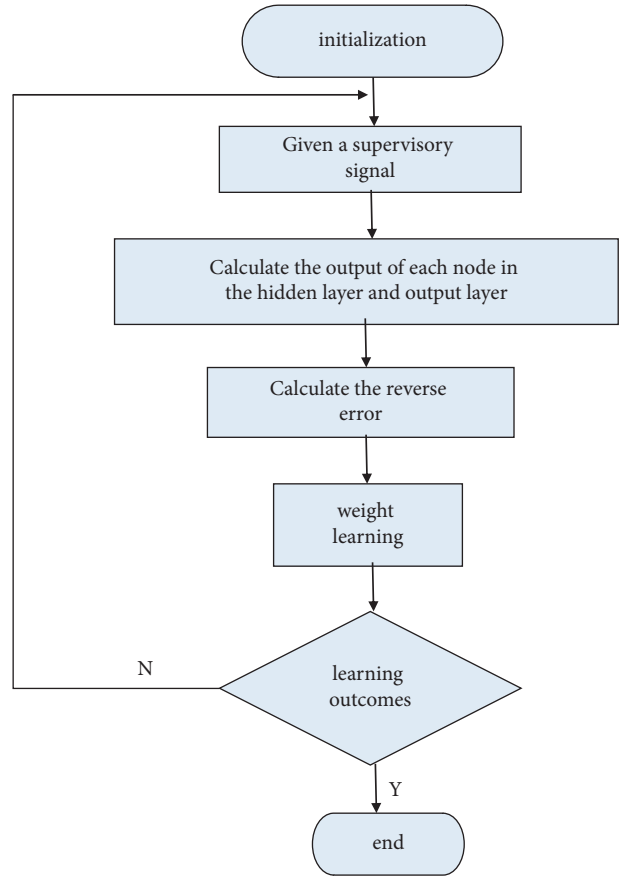

Figure 2: Flowchart of BP algorithm.

The learning of the BP neural network is mainly to adjust the connection weights between the neurons only through the learning algorithm, so that the output results are closer to the expected value. Guided learning with a tutor is divided into four processes: forward transmission of information, reverse adjustment of errors, model training, and "learning convergence."

3.2.2. Learning Algorithm of BP Neural Network. The flowchart of the BP neural network learning algorithm is shown in Figure 2; initialization is to select the initial weight of the network, generally a small random number around zero. When the specified number of learning times or the expected output error index is reached, or the change of the error index is less than a certain closed value, the learning ends; otherwise, the learning continues.

Combined with Figure 1, it is assumed that the input learning sample is p, the number of input neurons is n, the number of hidden layer neurons is m, the number of output neurons is r, and the conversion function adopts a sigmoid function, namely: $f(x) = 1/1 + e^{-x}$, the weight correction process is as follows:

(1) Forward propagation of information

① The output of the jth neuron in the hidden layer is

$$S_j = f\left(\text{net}_j\right) = f\left(\sum_{t=1}^{n} \omega_{ij} x_{ti} + \theta_j\right), \quad j = 1, 2, \ldots, m; t = 1, 2, \ldots, p, \tag{2}$$

where x_{ti} is the input of the i-th neuron in the t-th sample, and ω_{ij} is the weight from the i-th neuron to the jth neuron.

② The output of the kth neuron in the output layer is

$$\begin{aligned} S_k &= f\left(\text{net}_k\right) \\ &= f\left(\sum_{j=1}^{m} \omega_{jk} s_j + \theta_k\right), \quad k = 1, 2, \ldots, r, \end{aligned} \tag{3}$$

ω_{jk} is the connection weight from the jth neuron to the kth neuron.

③ Define the error function:

$$\begin{aligned} E &= \frac{1}{2} \sum_{k=1}^{r} \left(S_k + s_k\right)^2 \\ &= \frac{1}{2} \sum_{k=1}^{r} \left(e_k\right)^2, \end{aligned} \tag{4}$$

where S_k is the expected output of the kth neuron in the output layer.

(2) Weight change and backpropagation of error

① The weight change of the output layer

The weights from the jth input to the kth output are

$$\begin{aligned} \Delta\omega_{jk} &= -\alpha \frac{\partial E}{\partial \omega_{jk}} \\ &= -\alpha \frac{\partial E}{\partial S_k} \cdot \frac{\partial S_k}{\partial \text{net}_k} \cdot \frac{\partial \text{net}_k}{\partial \omega_{jk}} \\ &= \alpha \left(S_k - s_k\right) \cdot f'\left(\text{net}_k\right) \cdot S_j = \alpha \delta_{jk} S_j. \end{aligned} \tag{5}$$

Among them, $\delta_{jk} = \left(S_k - s_k\right) \cdot f'\left(\text{net}_k\right)$

Similarly:

$$\begin{aligned} \Delta\theta_k &= -\alpha \frac{\partial E}{\partial \theta_{jk}} \\ &= -\alpha \frac{\partial E}{\partial S_k} \cdot \frac{\partial S_k}{\partial \text{net}_k} \cdot \frac{\partial \text{net}_k}{\partial \theta_{jk}} \\ &= \alpha \left(S_k - s_k\right) \cdot f'\left(\text{net}_k\right) \\ &= \alpha \delta_{jk}. \end{aligned} \tag{6}$$

② Changes in hidden layer weights

The weights from the jth input to the kth output are

$$\begin{aligned} \Delta\omega_{ij} &= -\beta \frac{\partial E}{\partial \omega_{ij}} = -\beta \frac{\partial E}{\partial S_k} \cdot \frac{\partial S_k}{\partial S_j} \cdot \frac{\partial S_j}{\partial n\ et_j} \cdot \frac{\partial \text{net}_j}{\partial \omega_{ij}}, \\ &= \beta \sum_{k=1}^{r} \left(S_k - s_k\right) \cdot f'\left(\text{net}_k\right) \cdot \omega_{jk} \cdot f'\left(\text{net}_j\right) \cdot x_{ti} \\ &= \beta \delta_{ij} x_{ti}. \end{aligned} \tag{7}$$

Among them, $\delta_{ij} = e_j \cdot f'\left(\text{net}_j\right)$, $e_j = \sum_{k=1}^{r} \delta_{jk} w_{jk}$

$$\begin{aligned} \Delta\theta_j &= -\beta \frac{\partial E}{\partial \theta_j} = -\beta \frac{\partial E}{\partial S_k} \cdot \frac{\partial S_k}{\partial S_j} \cdot \frac{\partial S_j}{\partial \text{net}_j} \cdot \frac{\partial \text{net}_j}{\partial \theta_j}, \\ &= \beta \sum_{k=1}^{r} \left(S_k - s_k\right) \cdot f'\left(\text{net}_k\right) \cdot \omega_{jk} \cdot f'\left(\text{net}_j\right) = \beta \delta_{ij}. \end{aligned} \tag{8}$$

Among them, α and β are called the step size of the gradient search algorithm, also called the convergence factor. The larger the value, the faster the weight adjustment. Generally, the values of α and β can be larger without causing oscillation.

(3) The error backpropagation process is actually by calculating the error e_k of the output layer and then multiplying it by the first derivative $f'\left(\text{net}_k\right)$ of the activation function of the output layer to obtain δ_{jk}. Since the target vector is not directly given in the hidden layer, the δ_{jk} of the output layer is used to transfer the error backward to obtain the change $\Delta\omega_{jk}$ of the output layer weight and then calculate $= \sum_{k=1}^{r} \delta_{jk} \Delta\omega_{jk}$ and then multiply e_j by the first derivative of the activation function of the hidden layer $f'\left(\text{net}_j\right)$ to obtain δ_{ij}, so as to obtain the variation of the weight of the previous layer $\Delta\omega_{ij}$.

(4) Weight correction

① Use δ_{jk} to correct the weights and thresholds between the output layer and the hidden layer

$$\begin{aligned} \omega_{jk}(t+1) &= \omega_{jk}(t) + \Delta\omega_{jk} = \omega_{jk}(t) + \alpha \delta_{jk} S_j, \\ \theta_k(t+1) &= \theta_k(t) + \Delta\theta_k = \theta_k(t) + \alpha \delta_{jk}. \end{aligned} \tag{9}$$

② Use δ_{ij} to correct the weights and thresholds between the input layer and the hidden layer

$$\begin{aligned} \omega_{ij}(t+1) &= \omega_{ij}(t) + \Delta\omega_{ij} = \omega_{ij}(t) + \beta \delta_{ij} S_j, \\ \theta_j(t+1) &= \theta_j(t) + \Delta\theta_j = \theta_j(t) + \beta \delta_{ij}. \end{aligned} \tag{10}$$

Calculate the function E after the corrected error again; if E is less than the specified upper limit of error, the algorithm ends; otherwise, the number of learning times $t = t + 1$ is updated, and the weights and thresholds are recorrected.

There are two ways to train the network with the BP network algorithm. One is to modify the weights every time a

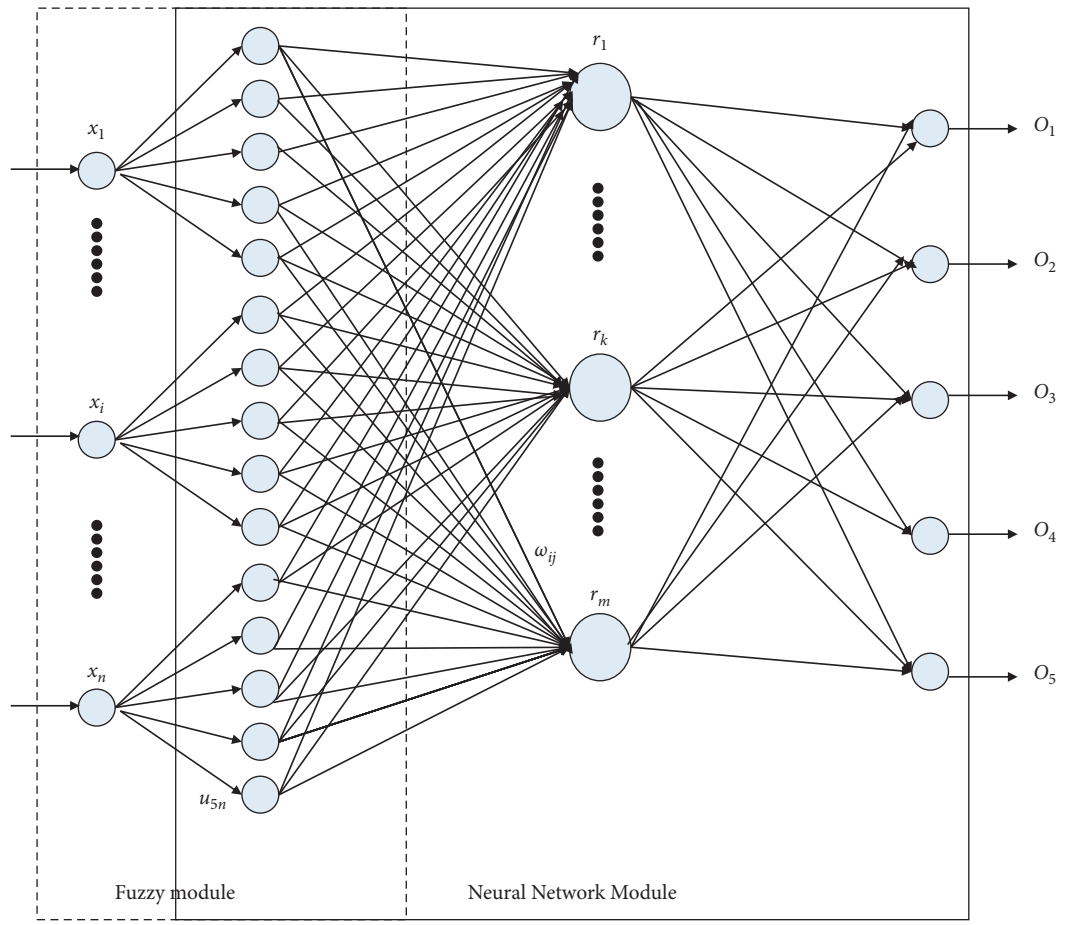

Figure 3: Fuzzy neural network topology diagram.

sample is input, which is the standard error propagation method; the other is the batch method, that is, all the samples that constitute a training cycle are computing the total average error after one input is a truly global gradient descent method. The number of corrections in the latter is significantly reduced, which can save learning time, but since the average of all mode errors is used, oscillations may occur in some cases.

4. Risk Assessment Model of Prefabricated Construction Based on Fuzzy Neural Network

4.1. Fuzzy Neural Network Model Construction. Fuzzy neural network can be divided into fuzzy neural network calculated according to fuzzy numbers and fuzzy neural network formed based on the logical reasoning process of fuzzy rules [21–24]. Based on the characteristics of knowledge management, this paper builds a 4-layer fuzzy neural network based on the first type of fuzzy neural network. The first and second layers are fuzzy modules, and the second, third, and fourth layers are neural network modules, as shown in Figure 3.

The first layer is the input layer, which is responsible for the input of the fuzzy neural network. Each node represents an input variable (risk index). According to the reliability and validity test in Chapter 2, the input layer has a total of 7 nodes.

The second layer is the fuzzification layer, whose role is to fuzzify the input variables and make them the input layer of the neural network module. This layer uses a Gaussian function as the membership function:

$$\mu x_i = \exp\left[-\frac{1}{2}\left(\frac{x_i - \mu_i}{\sigma_i}\right)^2\right]. \tag{11}$$

Among them, μ_i is the center of the membership function, σ_i determines the width of the membership function, and tthe mean value of all samples of the index x_i on the input layer is the μ_i value of the index at the corresponding level; the membership of the index on the fuzzification layer. The function width takes the following value:

$$\sigma_i = \sqrt{\frac{1}{n}\sum_{j=1}^{n}(x_i - \mu_i)}. \tag{12}$$

The third layer of fuzzy reasoning layer is also the hidden layer of the fuzzy neural network. It mainly realizes the mapping from the fuzzy value of the input variable to the fuzzy value of the output variable and determines the number of nodes according to the above algorithm.

The fourth layer is the output layer, which outputs the result of fuzzy evaluation.

4.2. Learning Steps of Fuzzy Neural Network. The specific learning steps are as follows:

Step 1: Cluster the sample data using the K-means method, set the number of clusters to 5, and obtain the mean μ_i and variance $\sigma_i \in \{1, 2, 3, 4, 5\}$ of each category, respectively.

Step 2: Transform the input sample X_k $h \in (1, 2, \ldots, P) \cdots$ through the membership function to realize the fuzzification process, so that n nodes are mapped to $5n$ fuzzy layer nodes and used as the input of the fuzzy inference layer.

Step 3: Set the number of learning times $t = 0$, assign small random numbers to the network weights and thresholds, $\omega_{ij}(t) \in [-1, 1]$, $\omega_{jk}(t) \in [-1, 1]$ $\sigma_j(t) \in [-1, 1]$; $\sigma_k(t) \in [-1, 1]$.

Step 4: Input a sample (X_h, T_h); P is the number of samples, $X_h \in R^p, T_k \in R^r$.

Step 5: Calculate the actual output of the fuzzy inference layer and the output layer, respectively; $S_j = f(\text{net}_j), S_k = f(\text{net}_k)$, where $f(x)$ is a sigmoid function.

Step 6: Calculate the fuzzy inference layer error σ_{ij} and the error σ_{jk} of each node in the output layer.

Step 7: The t-th correction is made to the weights and the stop values, $\omega_{jk}(t+1) = \omega_{jk}(t) + \alpha\delta_{jk}S_j$, $\theta_k(t+1) = \theta(t) + \alpha\delta_{jk}$; $\omega_{ij}(t+1) = \omega_{ij}(t) + \beta\delta_{ij}S_j, \theta_j(t+1) = \theta(t) + \beta\delta_{ij}$;

Step 8: Calculate the error function E; if $E < \varepsilon$, the network training ends; otherwise, go to Step 5.

5. Risk Assessment and Analysis of Prefabricated Building Construction Based on Fuzzy Neural Network

In this section, on the basis of the relevant literature [25–33], the risk management evaluation index system and theoretical system of prefabricated building construction will be proposed, and the evaluation indicators will be integrated, and the empirical research on the risk evaluation of prefabricated building construction will be carried out by using the fuzzy neural network method, and the indicators will be verified. Verify the rationality and effectiveness of the index system and the operability of risk assessment work.

In the verification process, the computer is used as the realization tool, and the research methods combining BP neural network and SPSS statistical analysis are used, respectively. The generalization ability and training speed of the network can reduce the probability of the BP network falling into a local minimum point, and the BP neural network program is written by using the neural network toolbox in the MATLAB language program to provide decision support for the research on risk management of prefabricated buildings.

5.1. Prefabricated Building Construction Risk Data Acquisition

5.1.1. Acquisition of Input Layer Data. The acquisition of input layer data is mainly achieved through the factor score of each sample, that is, how the common factor is represented by a linear combination of statistical indicators, which refers to the estimated value F_j of the common factor $\widehat{F}_j\widehat{F}_j$:

$$\widehat{F}_j = b_{j1}X_1 + b_{j2}X_2 + \cdots + b_{jp}X_p, \quad j = 1, 2, \ldots, 7; p = 25. \tag{13}$$

Since this study uses correlation coefficient matrix for factor analysis, it is assumed that $x_1, x_2, \ldots, x_p$ are standardized variables of influencing factors; $b_{i1}, b_{i2}, \ldots, b_{ip}$ are factor score coefficients; $\widehat{F}_j$ is the estimated value of the jth factor, as shown in Table 1.

5.1.2. Fuzzy Layer into Data Acquisition. K-means clustering is performed on the 5 common factors of the sample, and the number of clusters is set to 5, which correspond to the high, high, medium, low, and low of the construction risk of prefabricated buildings; the clustering method of common factors adopts Iterate and Classify. The clustering method continuously iterates and replaces the center position on the basis of the starting class center and assigns the observations to the nearest class; after 10 iterations, the cluster center matrix is obtained, as shown in Table 2.

After the samples are classified, run the Analyze Compare Means command in SPSS 20.0 software to obtain the value of the membership function width δ_i of each factor at the corresponding level. The results are shown in Table 3.

According to the Gaussian function, the membership degree of each factor in each category in the sample can be obtained. As the output of the second layer of the fuzzy neural network, there are 25 in total.

5.2. Evaluation Results and Analysis of Construction Risks of Prefabricated Buildings

5.2.1. Determine the Number of Hidden Layer Nodes. Run MATLAB 2016a; use 160 sample data to train the neural network and 10 sample data to test the neural network to find the optimal number of hidden layer nodes. According to the relevant theory in Section 3.2.1, the optimal hidden layer of BP neural network should be between 7 and 16, and the number of nodes in the output layer is 5; (1,0,0,0,0), (0,1,0,0,0), (0,0,1,0, 0), (0,0,0,1,0), (0,0,0,0,1) represent the low, low, medium, high risk status of prefabricated building construction, respectively.

Run the following program in MATLAB, and adjust the number of hidden layer nodes between 7 and 16 in turn. After repeated training, the results are shown in Table 4.

```
p = []'; % training sample data
t = []'; % training sample target output
net = newff(minmax(p), [7, 5], ("logsig," "logsig," "traingd"); % Adjust the number of hidden layer nodes in turn
```

Table 1: Factor score matrix.

Variable	Component						
	1	2	3	4	5	6	7
Illegal wires	0.127	0.169	0.012	0.186	0.098	0.095	0.187
Not wearing protective equipment	0.215	0.109	0.096	0.128	0.118	0.011	0.232
Low sense of responsibility	0.145	0.119	0.239	0.125	0.058	0.132	0.077
Unskilled workers	0.244	0.040	0.095	0.065	0.296	0.015	0.219
Work fatigue or difficulty concentrating	0.153	0.025	0.017	0.630	0.149	0.139	0.029
Improper operation of staff	0.221	0.016	0.002	0.330	0.011	0.221	0.015
Unsafe factors of materials	0.159	0.079	0.017	0.320	0.100	0.112	0.111
The machine itself is faulty	0.069	0.018	0.094	0.180	0.224	0.126	0.125
Machine overload	0.129	0.050	0.930	0.134	0.055	0.214	0.236
Machine instability	0.085	0.189	0.080	0.097	0.437	0.053	0.043
Insufficient formwork or support strength	0.046	0.328	0.074	0.139	0.019	0.024	0.201
Safety electricity check is not in place	0.017	0.011	0.339	0.440	0.048	0.021	0.068
Inappropriate device selection	0.032	0.118	0.443	0.620	0.097	0.091	0.032
Scaffolding is not strong	0.037	0.018	0.276	0.220	0.008	0.321	0.013
Lack of safety rules and regulations	0.046	0.230	0.052	0.500	0.128	0.045	0.067
Working at heights in rain and snow	0.021	0.425	0.171	0.036	0.115	0.003	0.038
No protective equipment issued	0.021	0.114	0.036	0.220	0.246	0.025	0.068
Improper protective measures	0.047	0.084	0.134	0.300	0.368	0.053	0.054
The scheme design is unreasonable	0.022	0.158	0.025	0.620	0.231	0.044	0.550
Component positioning is not accurate	0.027	0.121	0.110	0.460	0.740	0.238	0.195
Component connection technology is immature	0.057	0.008	0.001	0.237	0.013	0.657	0.091
Installation detection technology is not in place	0.024	0.002	0.065	0.436	0.019	0.009	0.035
The venue is wet	0.045	0.142	0.247	0.410	0.063	0.083	0.372
Lightning strike	0.005	0.004	0.108	0.257	0.007	0.012	0.034
Unstable address conditions	0.028	0.026	0.580	0.003	0.139	0.069	0.569

Extraction method: principal component analysis. Rotation method: varimax with Kaiser normalization component scores.

Table 2: Final cluster center table.

Risk factor	Cluster				
	1	2	3	4	5
Construction man-made risk factors	0.30669	0.65002	0.37318	0.75269	0.99813
Construction object status risk factor	0.93776	0.60900	0.13977	0.96965	0.32387
Organizational management risk factors	0.01515	0.30078	0.43660	0.49873	0.49662
Technical risk factor	0.95545	1.10145	0.38124	0.19331	0.28419
Environmental risk factors	0.11760	0.6142	0.03631	0.17670	0.20122

Table 3: The number of observations in each cluster.

	Cluster	Construction man-made risk factors	Construction object status risk factor	Organizational management risk factors	Technical risk factor	Environmental risk factors
1	Std.Deviation	0.77162	0.88396	0.85552	0.72690	1.04963
	N	30	30	30	30	30
2	Std.Deviation	0.81567	0.78319	0.78090	0.78561	0.98561
	N	33	33	33	33	33
3	Std.Deviation	0.50520	0.66778	0.83839	0.80372	1.10388
	N	35	35	35	35	35
4	Std.Deviation	0.85277	0.72303	1.12236	0.82401	0.80691
	N	31	31	31	31	31
5	Std.Deviation	0.70531	0.76015	0.98847	0.60445	1.02208
	N	41	41	41	41	41
Total	Std.Deviation	1.00000	1.00000	1.00000	1.00000	1.00000
	N	170	170	170	170	170

Table 4: The relationship between the number of hidden layer nodes and the training error and measurement error.

Number of hidden layer nodes	Error training	Test error
7	$9.9601e-006$	$1.5167e-005$
8	$9.9594e-006$	$1.3938e-005$
9	$9.9254e-006$	$1.4127e-005$
10	$9.9249e-006$	$1.5753e-005$
11	$9.9160e-006$	$1.1991e-005$
12	$9.9061e-006$	$1.0685e-005$
13	$9.8343e-006$	$1.5538e-005$
14	$9.8254e-006$	$1.6156e-005$
15	$9.7783e-006$	$1.4073e-005$
16	$9.4784e-006$	$2.9405e-005$

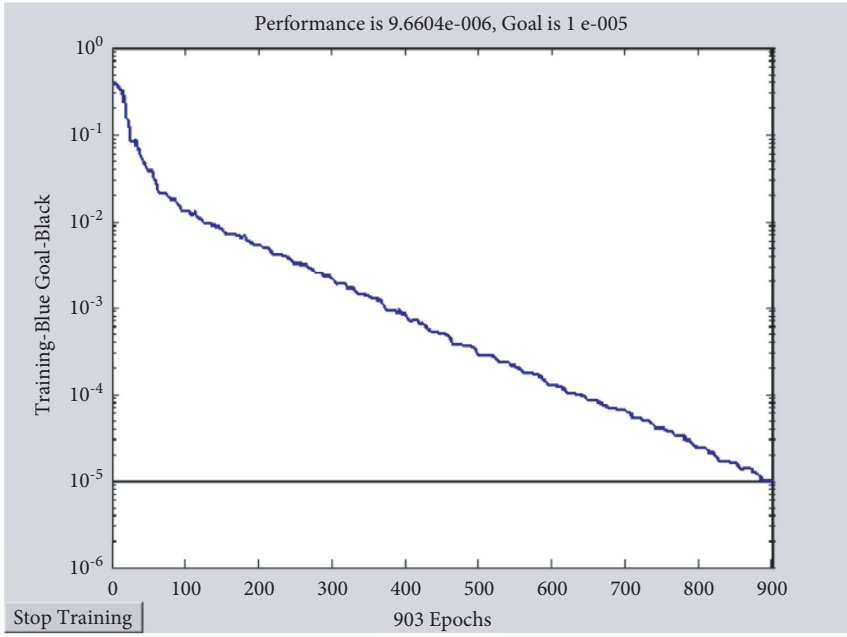

Figure 4: The training graph with the hidden layer node of 14.

```
net.trainParam.show = 100;
net.trainParam.goal = 1e – 5:
net.trainParam.epochs-8000;
net.trainParam.lr = 0.08;
net.trainParam.lr_inc = 1.4;
[net,tr] = train(net,p,t);
Y = sim(net,p); e = t – y:
Q = mse(e)
% output training error
ptest = []′; % test sample data
ttest = []′; test sample target output
a4 = sim(net,ptest);
E = ttest-a4;
Perf = mse(E)
% output test error
```

(1) Save Netl Net. In Table 4, as the number of hidden layer nodes increases, the training error gradually decreases, but the test error slightly oscillates after more than 14. Therefore, the relationship between the number of hidden layer nodes, training error, and test error is comprehensively considered. And the number of nodes in the hidden layer is determined to be 14. It is not that the more the nodes in the hidden layer, the better the performance of the network. When testing samples, it was found that the training error first decreased and then gradually increased with the increase of the number of nodes in the hidden layer. Although the increase is not very large, it is enough to affect the performance of the neural network.

Figure 4 shows that, with the increase of training times, the network training error gradually decreases. When the training times reaches 903 times, the network reaches the set error; that is, the network completes the training.

5.2.2. Evaluation Results and Their Analysis. The actual output results and the expected output results of the 10

Table 5: Network output and expected output comparison table.

Sample	Network output	Expected output
1	(0.0000 0.0000 0.0000 1.0000 0.0000)	(0 0 0 1 0)
2	(0.0009 0.0012 0.9900 1.0000 0.0000)	(0 0 1 0 0)
3	(0.0000 0.0000 1.0000 1.0000 0.0066)	(0 0 1 0 0)
4	(0.0021 0.0007 0.0000 1.0000 0.9922)	(0 0 0 0 1)
5	(0.0000 0.0000 0.0000 0.0000 1.0000)	(0 0 0 0 1)
6	(0.0005 0.0000 0.0001 0.9876 0.0000)	(0 0 0 1 0)
7	(0.0000 0.0021 0.0000 0.9993 0.0022)	(0 0 0 1 0)
8	(0.4790 0.0000 0.0000 0.0000 0.9961)	(0 0 0 0 1)
9	(0.0000 0.0013 0.0000 0.9939 0.0000)	(0 0 0 1 0)
10	(0.0000 0.0000 0.7505 0.0000 1.0000)	(0 0 0 0 1)

sample data are shown in Table 5. It is found that the training results of the samples are in good agreement with the expected output. It can be seen that the trained fuzzy neural network can well obtain and store expert knowledge, experience, and judgment. It can be seen that the data-based serial fuzzy neural network has good scientificity, rationality, and practicability in the process of risk assessment of prefabricated buildings.

Through the above research, it can be seen that the neural network overcomes the inaccuracy of the fuzzy algorithm due to the insufficient discrimination of each component in the evaluation vector. And it can make the analysis results more realistic and convincing. The fuzzy evaluation of aspects and the principle of maximum membership ignore other evaluation information. Fuzzy BP neural network evaluation method not only has strong fault tolerance, but also has the characteristics of self-adaptation and self-correction, which will be more widely used in risk management in other fields.

6. Conclusion

As an emerging green construction method, prefabricated buildings have gradually accelerated with their development. In addition, the construction standards of ordinary construction teams are uneven, and the difficulty of risk management has also increased. Traditional risk assessment is mainly based on qualitative research and analysis. It is empirical and intuitive judgment. But quantitative research is based on a large number of experimental results and indicators or laws obtained by extensive statistical analysis of accident data to perform quantitative calculations. In different organizational management and project construction processes, the risks of prefabricated buildings have various forms and the size of the risks are also different. Therefore, the model for its evaluation should also have dynamic characteristics, so as to facilitate the reasonable prediction and control of risks. This paper attempts to apply the fuzzy neural network to the risk assessment and management of prefabricated buildings and does the following research:

(1) With the help of fuzzy theory to quantify risk factors and the advantages of BP neural network's effective intelligent behavior, learning ability, self-adaptive mechanism, and high flexibility, a prefabricated construction risk assessment model based on fuzzy neural network is established.

(2) In the design of fuzzy neural network, the number of hidden layer nodes usually needs to be determined by multiple experiments or experience. This paper proposes a method to select the optimal number of hidden layer nodes according to the formula and past experience. The method is concise, which can reduce the number of verifications, and it has good reference and use value.

(3) Through programming and debugging, the fuzzy neural network is trained, and it is found that the training results of the samples are in good agreement with the expected output results, which verifies the feasibility and applicability of the fuzzy neural network in the risk assessment process of prefabricated buildings. The dynamic characteristics of risks can be continuously observed, and effective risk aversion and response plans can be formulated with good guiding significance.

Data Availability

The dataset can be accessed upon request.

Conflicts of Interest

The authors declare that they have no conflicts of interest.

References

[1] Y. Huang, "Research on the role of risk management and control in construction enterprise management," *Economic Management Digest*, vol. 18, no. 23, pp. 96-97, 2021.

[2] Z. Yu, *Research on Risk Management and Control in the Construction Phase of the Old City Renovation Project of Kunlun Real Estate Group T*, Yunnan Normal University, Kunming, China, 2021.

[3] G. Li, R. Xu, and Y. Li, "Safety risk management and control of prefabricated building construction," *China Building Decoration*, vol. 46, no. 11, pp. 168-169, 2021.

[4] J. Sun, "Research on financial risk management and control of construction enterprises under big data," *Small and Medium Enterprises in China*, vol. 37, no. 10, pp. 90-91, 2021.

[5] T. Jiang, *Research on Safety Risk Assessment and Control Countermeasures of Hoisting Operation of Prefabricated Buildings*, North China University of Technology, China, 2021.

[6] F. E. Boafo, J. Kim, and J. Kim, "Performance of modular prefabricated architecture: case study-based review and future pathways," *Sustainability*, vol. 8, no. 6, pp. 556–558, 2016.

[7] H.-S. Lee, H. Kim, M. Park, E. Ai Lin Teo, and K.-P. Lee, "Construction risk assessment using site influence factors," *Journal of Computing in Civil Engineering*, vol. 26, no. 3, pp. 319–330, 2012.

[8] J. Hinze, S. Thurman, and A. Wehle, "Leading indicators of construction safety performance," *Safety Science*, vol. 51, no. 1, pp. 23–28, 2013.

[9] A. Pinto, "QRAM a Qualitative Occupational Safety Risk Assessment Model for the construction industry that

incorporate uncertainties by the use of fuzzy sets," *Safety Science*, vol. 63, no. 3, pp. 57–76, 2014.

[10] W. Xiao, Z. Liu, and W. Zhong, "Multi-level fuzzy synthesis evaluation on construction supply chain risk," in *Proceedings of the Chinese control and decision conference*, pp. 266–269, Mianyang, China, May 2011.

[11] Z. L. Guo, W. B. Zhang, and L. H. Ma, "The prefabricated building risk decision research of DM technology on the basis of Rough Set," *IOP Conference Series: Earth and Environmental Science*, vol. 81, no. 1, pp. 12143–143, 2017.

[12] S. Staub-French, A. Russell, and N. Tran, "Linear sv," *Journal of Computing in Civil Engineering*, vol. 22, no. 3, pp. 192–205, 2008.

[13] C. Z. Li, J. Hong, F. Xue, and G. Q. X. M. K. Shen, "Schedule risks in prefabrication housing production in Hong Kong: a social network analysis," *Journal of Cleaner Production*, vol. 134, pp. 482–494, 2016.

[14] I. B. Sinha, "Prefabricated concrete skeleton system for residential buildings," *International Journal for Housing Science and its Applications*, vol. 25, pp. 163–174, 2011.

[15] P. Liu, Y. Han, X. Zhu, S. Wang, and Z. Li, "Research on information system risk Assessment Based on Improved AHP-Fuzzy theory," *Journal of Physics: Conference Series*, vol. 1693, no. 1, 2020.

[16] M. Oturakci, "A new fuzzy-based approach for environmental risk assessment," *Human and Ecological Risk Assessment: An International Journal*, vol. 25, no. 7, pp. 1718–1728, 2019.

[17] X. Wang, "Research on cost estimation of energy-saving buildings based on GA-BP algorithm," *China Engineering Consulting*, vol. 17, no. 5, pp. 29–32, 2017.

[18] H. Zheng, *Research on Construction Quality Evaluation System of Steel Structure Building Industrialization Based on BP Algorithm*, Shenyang Jianzhu University, Shenyang, China, 2015.

[19] Q. Meng, "Application of improved BP algorithm in construction cost estimation," *Industrial Control Computer*, vol. 26, no. 10, pp. 115-116+118, 2013.

[20] W. Su, *Research on the Cost Review Method of Residential Building Design Stage Based on BP Neural Network*, Guangdong University of Technology, Guangzhou, China, 2013.

[21] Xu Moli, Xiong Deping, and Yang Mengyuan, "Risk recognition and risk classification diagnosis of bank outlets based on information entropy and BP neural network," *Journal of Intelligent and Fuzzy Systems*, vol. 38, no. 2, 2020.

[22] X. Wang and Y. Wang, "The research on bridge engineering risk management and assessment model based on BP neural network," *IOP Conference Series: Earth and Environmental Science*, vol. 455, 2020.

[23] Li Xiaochen, "Construction of abalone sensory texture evaluation system based on BP neural network," *Journal of Korea Multimedia Society*, vol. 22, no. 7, 2019.

[24] J. Zhang, L. Hu, Y. Sun, X. Wang, and H. Sun, "Research on green construction evaluation based on OWA operator and BP neural network," *Journal of Qingdao University of Technology*, vol. 42, no. 6, pp. 29–34, 2021.

[25] K. Yang, H. Wu, and X. Yang, "Research on safety risk assessment of tunnel construction based on fuzzy neural network method," *Highways*, vol. 59, pp. 157–160, 2014.

[26] Y. Li, "Risk assessment of international petroleum contracts based on fuzzy neural networks," *Statistics and Decision Making*, vol. 32, no. 23, pp. 55–58, 2014.

[27] P. Ziyao and Y. Li, "Risk assessment of new Austrian tunnel construction based on fuzzy neural network," *Road Construction Machinery and Construction Mechanization*, vol. 35, no. 3, pp. 124–128, 2018.

[28] Y. Huang, Z. Gong, X. Deng, L. Peng, and R. Wang, "Risk assessment of highway tunnel entrance section construction stage based on fuzzy neural network," *Journal of Engineering Management*, vol. 32, no. 3, pp. 119–123, 2018.

[29] C. Zhang, H. Guo, M. Xiao, Y. Wang, and Y. Liu, "Risk assessment of prefabricated building construction," *Engineering Economics*, vol. 28, no. 10, pp. 31–34, 2018.

[30] C. Chang and R. Yan, "Safety risk assessment and management measures of prefabricated building construction," *Journal of Shenyang Jianzhu University (Social Science Edition)*, vol. 19, no. 4, pp. 399–403, 2017.

[31] Z. Liu, G. Sun, and X. Yang, "Research on construction risk assessment of prefabricated concrete buildings," *Journal of Liaoning University of Technology (Social Science Edition)*, vol. 22, no. 1, pp. 39–42, 2020.

[32] Y. Liu, "Research on risk management and control of prefabricated building construction," *Engineering Economics*, vol. 31, no. 9, pp. 50–54, 2021.

[33] Y. Duan, S. Zhou, Y. Guo, and X. Wang, "Safety risks and strategies of prefabricated building construction based on SEM," *Journal of Civil Engineering and Management*, vol. 37, no. 2, pp. 70–75+121, 2020.

Hindawi
Scientific Programming
Volume 2022, Article ID 4552491, 11 pages
https://doi.org/10.1155/2022/4552491

Research Article

Based on Data Mining and Big Data Intelligent System in Enterprise Cost Accounting Optimization Application

Wenyan Wang and Jie Guo

Department of Economics and Management, Cangzhou Normal University, Cangzhou 061001, China

Correspondence should be addressed to Wenyan Wang; wangwenyan8805@caztc.edu.cn

Received 14 April 2022; Revised 26 April 2022; Accepted 12 May 2022; Published 1 June 2022

Academic Editor: Jie Liu

With the continuous development of science and technology, we have completely entered the information age. The amount of data around us increases linearly, and everyone lives in a pile of data. Enterprises also need to use big data technology in the process of operation and management to mine data and realize various data management functions. For the current enterprise, the operation of data will not only affect the management cost of the enterprise but also affect the future development of the enterprise. Based on the problem of enterprise management cost, this paper proposes to effectively use big data technology to solve the problem of enterprise cost management. The article also uses big data technology to optimize the management cost of the enterprise and uses big data technology to innovate and apply the management method of the enterprise. This paper constructs a cost management model based on data mining and expounds on the objects, sources, and calculation methods of data mining. Under this model, the company's data was mined, a specific plan was proposed, and an improved association algorithm was proposed to test the completion and consolidation of tasks. In the case of a large number of tasks, in order to efficiently realize the selection and merging of data, this paper proposes a new cost forecasting scheme based on a fuzzy model. Use time series for cost forecasting, and the accuracy is relatively high. In the process of forecasting, our forecasting method is suitable for the human reasoning process and can have better adaptability. Finally, we applied the research results of the thesis to actual business management to meet the management needs of the business, thus verifying the feasibility of the method proposed in this article.

1. Introduction

With the advent of the era of economic globalization, the competition among enterprises is becoming increasingly fierce. If every enterprise wants to remain competitive and invincible in the torrent of economic globalization, it needs to innovate and explore its own management mode and management tasks. If a company wants to succeed, it must control its own costs. In cost management, we need to recognize the status of cost management and the significance of cost management. In the process of cost management, the concept, technology, and method of cost management will affect the future development of the enterprise and even determine the success or failure of the enterprise. At present, the management strategies described by the existing cost management schemes in the market are mostly described in words, and there is no quantitative management scheme. With the advent of the information age, we can realize intelligent cost management so as to innovate the solutions and methods of cost management. Enterprises will face competition in the process of operation. This is inevitable. Only when enterprises continue to attach importance to their own management process, continuously deepen the process of informatization, and accumulate cost data year by year, this will become a valuable resource for the company. To promote the further development of the enterprise, with the advent of the era of big data, traditional database queries can no longer perform detailed queries on all information. Because the amount of information is too large, it is difficult for us to distinguish which data is valid and which is invalid. As a result, when we process data, much data will be destroyed before it is processed, and much data will be

processed repeatedly. Because there are so much data and the types of data are very complicated, it is very difficult for us to find useful information from the huge data. At the same time, we also need to manage the information. The emergence of data mining technology has solved this thorny problem, and people can transform data into valuable information for application.

In the process of cost management, it is necessary to calculate the cost, which is the most basic and core part. Cost accounting provides basic data for enterprises to carry out cost management. If the calculated cost is not accurate enough, it will eventually affect other aspects of cost management. The object of data mining is for a large amount of data. In the process of cost management, we need to mine the cost data, which requires the use of data mining technology. It is very important that we should refine the cost accounting method as much as possible and improve the accuracy of cost accounting. By integrating big data technology into the cost management process, this paper can not only meet the achievements of technology development but also improve management efficiency. With the continuous development of science and technology, big data technology and Internet of things technology are more and more widely used in life, and we have completely entered the data age. The amount of big data is very large, and there are many kinds of data. We must study more advanced methods to achieve faster data processing. In the era of big data, enterprise managers should be able to obtain information faster, manage and make decisions on information, and combine big data technology in the process of processing information to improve processing efficiency. At the same time, it discusses the optimization process of enterprise cost management under the background of the big data era and combines big data technology with enterprise cost management technology.

2. Related Work

In the mid-fifteenth century, cost accounting began in various companies. Around 1820, some theories about cost management began to appear. Literature [1] mentioned some methods that can improve management efficiency and reduce management costs. This method separates the planning department from the executive department. This also lays the foundation for subsequent management work. Management thinking has become more and more scientific. The cost is getting lower and lower. Literature [2] put forward a concept of value engineering. This concept is mainly to set up some products under the premise of market demand so as to obtain benefits. In order to ensure that the function and cost of the product are matched, the value of the product must be fully utilized during the entire production and sales process, and the consumer must do its best to gain the recognition of consumers. Literature [3] puts forward a concept of strategic management accounting. This concept is to say that the company's performance evaluation should be based on each person's own evaluation. In the process of management, we must also pay attention to the management of employees themselves. The company can not only analyze problems from within the company but also vertically compare other companies in the market and compare the direction of the market. Literature [4] mainly analyzes the management awareness of managers and also conducts in-depth analysis and exploration of the relationship between management knowledge and management effects. The analysis results show that there is a certain correlation between management awareness and management knowledge of managers. Literature [5] believes that in order to manage costs, companies need to control their own costs and understand their own production processes, all of which can affect the company's operating results. Literature [6] pointed out that the cost management of enterprises will also be affected by the environment. Different enterprises are in different environments and face different risks. These risks will affect the cost of the company and, thus, the profit of the company. Make an impact. Literature [7] mainly explains that in the process of cost production, structural costs and management costs are combined and analyzed. Only by focusing on financial performance can we better manage costs. In the process of management, we should not only focus on the supply chain but also on other aspects. Literature [8] mainly studies the management of project costs and proposes that costs should be managed in accordance with global unified standards. Literature [9] proposes that the arrival of the big data era may cause an industrial revolution in information technology. This revolution involves not only the Internet of Things technology but also cloud computing. This information revolution will also affect other industries and even our corporate activities and business operations. Literature [10] pointed out that this information technology revolution will have a certain impact on the business management style of enterprises and will also affect the decision-making work of enterprises. Literature [11] proposes that big data technology will become the basis for the management of the majority of enterprises in the future, and many mistakes can be avoided. Literature [12] proposes that data mainly faces three major challenges: data generation, data processing, and data storage. If we want to use big data technology to optimize the industry, we must explore the problems ourselves and propose our own solutions. Literature [13] proposed that in a big data environment, all our information will be recorded, and all information will be stored in the form of data. Literature [14–18] proposes that in a big data environment, all data needs to be accessed and extracted multiple times and will be used in different places. Different processing methods for big data will lead to different processing results, and sometimes two completely opposite results may occur. For the impact of such uncertain factors, we need to provide solutions. Literature pointed out that in the era of big data, the operation of enterprises will be affected by the results of big data, but the results of data analysis will affect the decision-making of enterprises, and it can also provide enterprises with some scientific suggestions to affect product development and enterprises. Literature proposes that Europe has already applied big data technology in legal ethics and other fields. Literature pointed out that in the future, we still need to further explore big data, seize the opportunity to make a

comprehensive evaluation, and then apply it to people's lives. Literature pointed out that the era of big data brings both opportunities and challenges to people. We need to use the cognitive prediction function of big data to analyze potential users so that people can recognize big data technology. Literature [19] proposes that when managing costs, companies should not only consider the internal supply chain costs but also the external environment. The company should strategically control the supply chain management and coordinate the internal supply chain. Literature [20] pointed out that there are many factors that affect the operating cost of a company, such as the strategy of the company and the management style of the manager [21, 22]. From the current research, scholars analyze cost management and supply chain management.

3. Based on the Internal Data Mining and Information Management System Design

3.1. The Establishment of Enterprise Production Cost Data Warehouse

3.1.1. The Process of Enterprise Data Mining. Before the application and analysis of the enterprise production cost data information management module, we need to use the codes of some attribute data to store the data and then use the dictionary for comparison in the process of comparison. We first need to encode the preprocessed data. Some quantitative attributes are discrete, and all attributes are divided into different categories. Among them, Table 1 shows the results of discretized character attribute values. Table 2 shows the values of the converted sample data, as shown in Figure 1.

3.1.2. Data Warehouse Design Structure. First, extract the data, then transform it, finally store the data in the warehouse, and use the data mining tool for data mining. When designing the data warehouse, we mainly divided it into four parts, and its structure is shown in Figure 2. In the first part, we mainly store the basic information of the company and the information and processes in the production process. This information is relatively discrete and difficult to use [23]. The second part is used to store data in the center. It also includes some multidimensional data and raw data. These data have been preprocessed to make it easier to store and analyze. The third part is used to store application services, mainly including various data mining technologies and data analysis technologies. The fourth part is mainly used to display information, display processing results, and display users.

3.1.3. Data Conversion Method. In the process of data selection and data analysis, we need to convert the data format. We need to check the stored data one by one, convert the data format of each field, and reorganize the data. If there are some vacant fields in the stored data, we should also set corresponding values to keep the data standardized. In the process of data conversion, we must pay attention to the conversion of some inconsistent data but also pay attention to the validity of the data and the corresponding rules. Some data represent the same meaning, but the unit is different. Here, we also need to convert. In order to meet the task requirements of data mining, we must perform data conversion in a unified format. All date formats must follow certain rules, all measurement formats must be unified units, and all to themselves must be converted into long bytes. Type conversion is to convert one data type into another data type. Using the same data type can ensure the validity of the data and better meet the needs of data mining tasks.

Table 1: Discretization of decision attribute values.

Category code	Numerical range	Profitability
1	(0, 2520)	Relatively low profit
2	>2520	Relatively high profit
3	(−2520, 0]	Less loss
4	<−2520	More losses

Table 2: Decision table sample data after data conversion.

	a_1	a_2	a_3	a_4	a_5	a_6	a_7
x_1	00001	000018	070200	1	01	05	02
x_2	00002	000018	070200	1	01	04	02
x_3	00041	000020	070201	1	01	05	12
x_4	00050	000018	070200	2	81	11	02
x_5	00053	000017	070100	1	01	04	02
x_6	00052	000020	070200	1	26	11	02
x_7	00096	000015	070105	1	41	01	22
x_8	00126	000014	070101	1	58	33	15
x_9	00130	000014	070101	1	61	32	15
x_{10}	00199	000015	070103	1	24	33	15
...	...	...	...	...	...	...	...

3.2. Application Analysis of Enterprise Production Cost Data Information Management Module.

In the application analysis of the production cost data informatization management module, enterprises need to preprocess the data, calculate according to the value, then obtain the minimum attribute value, consolidate the records, and finally detect the enterprise data information management system through the algorithm.

3.2.1. Data Preprocessing. We use the encoding of some attribute data to store the data and then use the dictionary for comparison in the process of comparison. We first need to preprocess the encoding of the data. Some quantitative attributes are discretized, and all attributes are divided into different categories. Table 1 shows the result of discretizing the character attribute values. Table 2 shows the values of the converted sample data.

3.2.2. Data Mining and Cost Knowledge Transformation. After preprocessing the data, we need to calculate based on the value, then get the smallest attribute clip, and merge the records. Table 3 shows our most simplified rule.

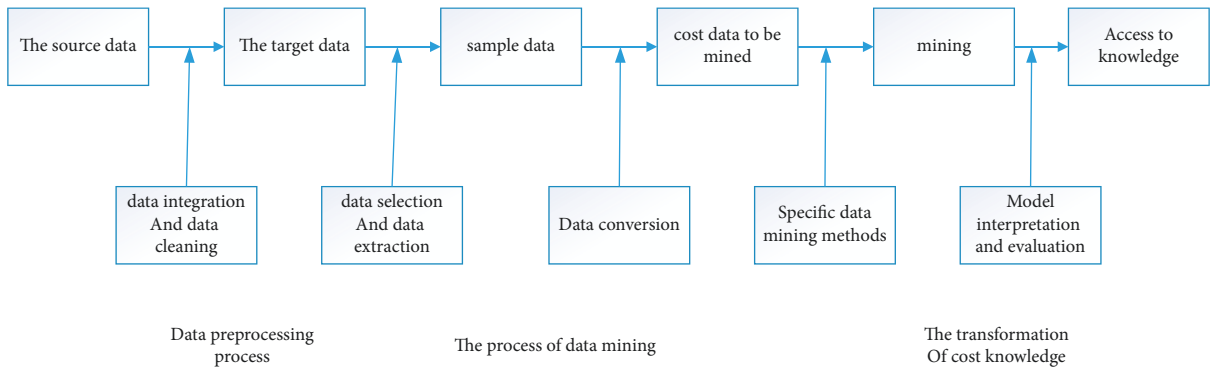

Figure 1: The specific process of production cost data mining.

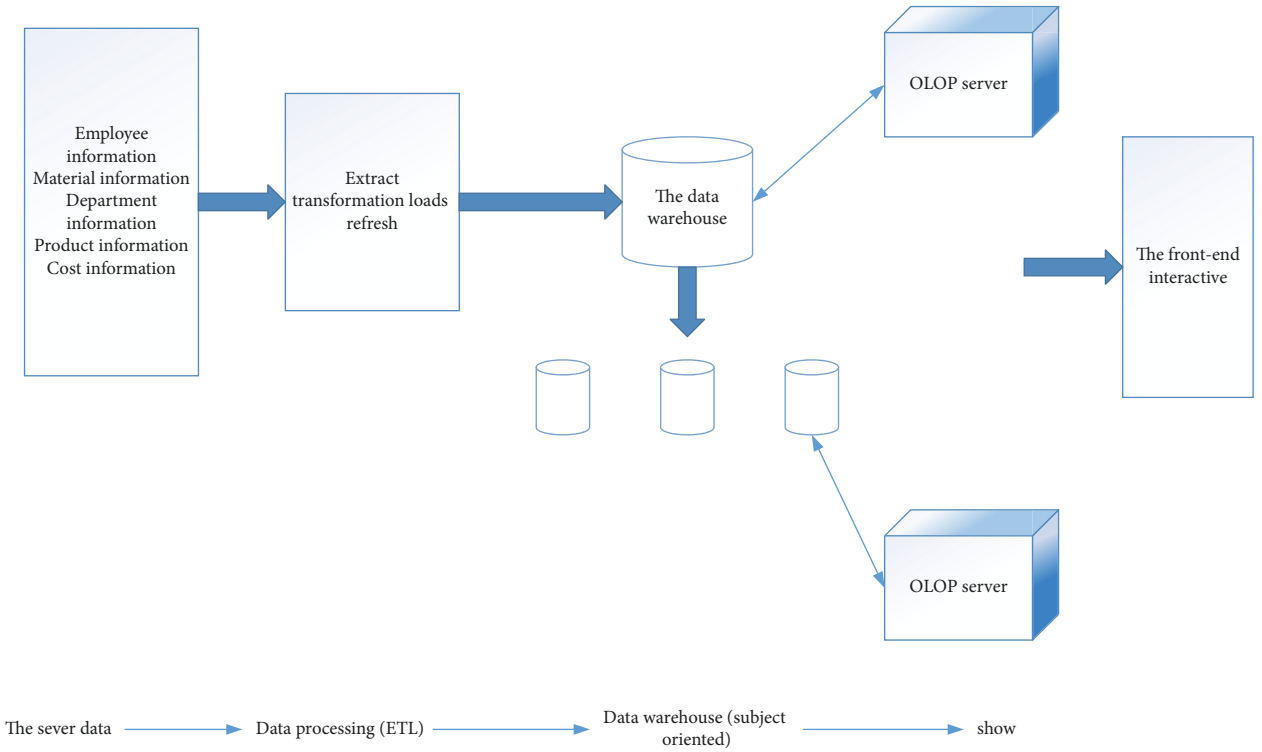

Figure 2: Data warehouse design structure.

3.3. Enterprise Information Management System Integrated Intrusion Detection Algorithm. Using SVM for data set training, thereby constructing a hyperplane, can achieve linear segmentation of the data set. The formula is as follows:

$$W^T X + b = 0. \tag{1}$$

In the case of given data, the SVM algorithm can be used to find the best separating hyperplane. The formula is as follows:

$$\min_{w,b} \frac{1}{2}\|w\|^2$$
$$s.t. y_i\left(W^T X_i + b\right) \geq 1 \quad i = 1, 2, \ldots, n. \tag{2}$$

Table 3: Results of reduction of sample data in decision table.

	a_1	a_2	a_3	a_5	a_7	a_{10}	
z_1	00001	*	*	*	*	*	*
z_2	00001	000018	*	*	*	*	2
z_3	00041	000020	070201	01	12	36	3
z_4	00050	000018	*	*	*	02	3
z_5	00053	*	070100	01	02	*	1
z_6	00053	000020	*	26	*	*	2
z_7	00098	000015	*	43	22	40	1
z_8	00124	*	070101	57	*	31	3
z_9	00133	*	070101	61	15	36	3
z_{10}	00197	*	070100	*	*	*	2
...	...	...	...	...	...	...	...

Transforming the original function into the objective function is as follows:

$$L(w,b,\alpha)=\frac{1}{2}\|w\|^2+\sum_{i=1}^{n}\alpha_i\left(1-y_i\left(W^TX_i+b\right)\right). \tag{3}$$

Among them, the partial derivative is as follows:

$$\begin{cases}\dfrac{\partial L(w,b,\alpha)}{\partial w}=w-\sum_{i=1}^{n}\alpha_i y_i x_i,\\[2ex] \dfrac{\partial L(w,b,\alpha)}{\partial b}=\sum_{i=1}^{n}\alpha_i y_i.\end{cases} \tag{4}$$

Let it be 0 to get the following:

$$\begin{cases}w=\sum_{i=1}^{n}\alpha_i y_i x_i,\\ b=\sum_{i=1}^{n}\alpha_i y_i.\end{cases} \tag{5}$$

Converted into a duality problem, the formula is as follows:

$$\begin{aligned}&\max_{\alpha}-\frac{1}{2}\sum_{i=1}^{n}\sum_{j=1}^{n}\alpha_i\alpha_j y_i y_j\left(x_i^Tx_j\right)+\sum_{i=1}^{n}\alpha_i,\\ &s.t.\quad \sum_{i=1}^{n}\alpha_i y_i=0\quad \alpha_i\ge 0,\ i=1,2,\ldots,n.\end{aligned} \tag{6}$$

The final dual problem is as follows:

$$\begin{aligned}&\min_{\alpha}\frac{1}{2}\sum_{i=1}^{n}\sum_{j=1}^{n}\alpha_i\alpha_j y_i y_j\left(x_i^Tx_j\right)+\sum_{i=1}^{n}\alpha_i,\\ &s.t.\sum_{i=1}^{n}\alpha_i y_i=0\quad \alpha_i\ge 0,\ i=1,2,\ldots,n.\end{aligned} \tag{7}$$

The iterative optimization algorithm SMO can solve the dual problem of SVM, and the optimal solution satisfies the following:

$$y_j\left(\left(w^*\right)^Tx_j+b^*\right)-1=0. \tag{8}$$

Use KKT to get the following:

$$\begin{cases}w^*=\sum_{i=1}^{n}\alpha_i^* y_i x_i,\\ b^*=y_j-\sum_{i=1}^{n}\alpha_i^* y_i\left(x_i^Tx_j\right).\end{cases} \tag{9}$$

The final classification decision function is as follows:

$$f(x)=\operatorname{sign}\left(\sum_{i=1}^{n}\alpha_i^* y_i\left(\left(x_i\right)^Tx\right)+b^*\right). \tag{10}$$

Rewrite the formula optimization problem as follows:

Table 4: Confusion matrix.

Confusion matrix		Predictive value	
		Invade	Normal
Actual value	Invade	TP	FN
	Normal	FP	TN

$$\begin{aligned}&\min_{w,b,\xi}\frac{1}{2}\|w\|^2+C\sum_{i=1}^{n}\xi_i,\\ &s.t.\,y_i\quad \left(w^Tx_i+b\right)\ge 1-\xi_i\quad \xi_i\ge 0,\ i=1,2,\ldots,n.\end{aligned} \tag{11}$$

The dual problem of this optimization problem is as follows:

$$\begin{aligned}&\max_{\alpha}\frac{1}{2}\sum_{i=1}^{n}\sum_{j=1}^{n}\alpha_i\alpha_j y_i y_j\left(x_i^Tx_j\right)+\sum_{i=1}^{n}\alpha_i,\\ &s.t.\quad \sum_{i=1}^{n}\alpha_i y_i=0\quad 0\le\alpha_i\le C,\ i=1,2,\ldots,n.\end{aligned} \tag{12}$$

The final classification decision function is as follows:

$$f(x)=\operatorname{sign}\left(\sum_{i=1}^{n}\alpha_i^* y_i\left(\left(x_i\right)^Tx\right)+b^*\right). \tag{13}$$

3.4. System Performance Simulation Results and Analysis

3.4.1. Experimental Data Set. The data characteristics in each data set are very close to the network attack data. The main advantages of data sets are as follows. Firstly, the new dataset deletes a large number of duplicate records in the original dataset and tests the duplicate records so that we can improve the performance of the system and save testing time. In the preprocessing process, each data set is evaluated only once, which can reduce the deviation. I have figured it out clearly. I cannot go yet. The total number of records in different difficulty sets is inversely proportional to the number of data sets, which will lead to great differences in the performance of tasks solved by different machine learning methods, which can be applied to evaluate the performance of machine learning methods. When setting the number of records, we must select appropriate parameters for setting and budget the complete data set to make it more reliable.

3.4.2. System Evaluation Indicators. A new data mining and management system based on data mining is proposed. We need to check the effectiveness of the intrusion detection method of the system. In the detection process, we use the confusion matrix to calculate its accuracy and other indicators. Table 4 shows the basis of our intrusion detection using a confusion matrix.

Calculated as follows:

The accuracy calculation formula is as follows:

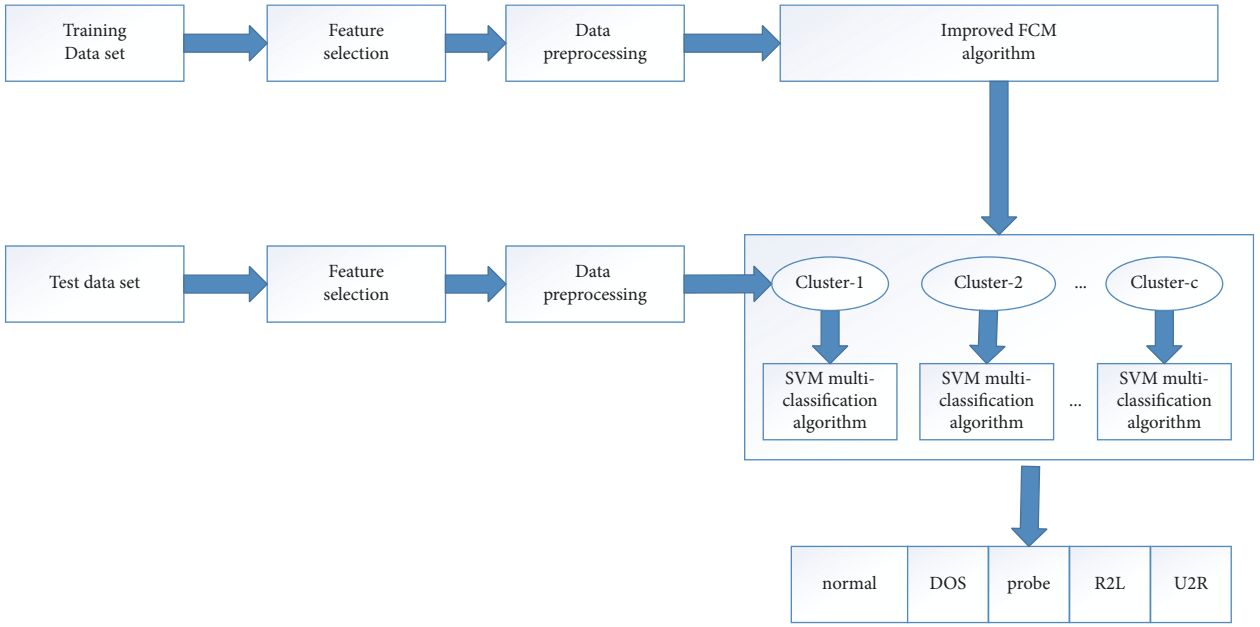

Figure 3: The structure diagram of the integrated intrusion detection method in the training and testing process.

Table 5: The clustering results of the improved FCM algorithm on the NSL-KDD data set.

Cluster	Normal	Probe	DOS	R2L	U2R
1	12	107	3370	1	0
2	5024	1	101	166	12
3	727	2038	933	266	1

Table 6: Confusion matrix of the method proposed in this paper.

Actual category/Forecast category	Normal	Probe	DOS	R2L	U2R
Normal	2453	7	3	6	1
Probe	8	910	2	1	0
DOS	1	0	1886	0	1
R2L	8	0	0	176	0
U2R	0	1	1	1	3

$$\text{Accuracy} = \frac{TP + TN}{TP + TN + FN + FP}. \tag{14}$$

The calculation formula of the detection rate is as follows:

$$DR = \frac{TP}{TP + FP}. \tag{15}$$

The formula for calculating the false alarm rate is as follows:

$$FPR = \frac{FP}{TN + FP}. \tag{16}$$

The formula for calculating the false-negative rate is as follows:

$$FNR = \frac{FN}{TP + FN}. \tag{17}$$

3.4.3. Integrated Intrusion Detection Method. We also need to test the effectiveness and feasibility of the system. We mainly use some test data sets to evaluate its performance. We use clustering to divide the data in the test data set, which will roughly classify different attack types, and then use the SVM model to further predict and estimate performance. The training and testing method of the system is shown in Figure 3.

3.4.4. Experimental Results and Analysis. The improved FCM algorithm can also divide the data set. Our main attack type is DOS. In normal network behavior, there are very few other attack types. In the third data set, probe type attacks are mainly used. The use of the SVM algorithm can ensure that all features of the system are learned, and the data is shown in Table 5.

Table 7: Use of big data technology to control procurement costs.

Procurement cost	Measures to reduce costs	Big data technology used
Order cost	Analyze the cost of purchase Develop purchasing plan	Use big data for analysis Use data for analysis and prediction
Cost of purchase	Establish a database to record supplier information Monitor and evaluate suppliers	Use big data technology for data storage, mining, and analysis Use big data for real-time monitoring
Transaction cost	Real-time price adjustment of products Automatic replenishment of goods	Use big data for real-time monitoring Use big data to analyze and predict technology
Information cost	Feedback on procurement quality	Use big data for quality inspection and product identification

Table 8: Using big data technology to control inventory costs.

Inventory cost	Measures to reduce costs	Big data technology used
Customer's cost	Forecast inventory requirements	Use big data for analysis and mining
The cost of warehousing	Manage receipts	Utilize radio frequency identification technology
The cost of out of stock	Manage warehousing	Use big data for analysis
Labor cost	Manage outbound	Utilize big data analysis technology and radio frequency identification technology

Table 9: Using big data technology to control marketing costs.

Marketing cost	Measures to reduce costs	Big data technology used
The cost of market research	Forecast sales	Use big data technology for data storage and mining
	Optimize products and services	Use big data technology for data storage and mining
Marketing cost	Precision marketing	Use big data technology for data storage and mining

When the naive Bayes algorithm is used for intrusion detection, the false alarm rate is only about 6%, while the false alarm rate of intrusion detection methods based on vector machines is less than 1%. From the data presented in Table 6, we can see that the false alarm rate of the method proposed in this paper is close to the false alarm rate of the vector machine and even lower than the false alarm rate of the vector machine. The false alarm rate of the intrusion detection system is very normal and acceptable, and it will not affect our final results. If the false alarm rate is too high, it will not only take up network resources but also waste time. The false-positive rate of this method proposed by me is not high, and it does not cost much resources and time.

4. Research on Enterprise Cost Accounting Management Control and Optimization under the Background of Big Data Intelligence

4.1. The Overall Program Design of Enterprise Cost Management under the Background of Big Data. In the era of big data, our cost management can promote the development of enterprises and can also promote the optimization and reform of enterprise processes. Big data not only optimize the business process of an enterprise's supply chain but also enables more effective cost management. When a company conducts cost management, it includes all links, from research and development to procurement and finally to sales. All costs must be included. Enterprises should adopt some scientific and technological means, such as big data technology to provide support for cost management, and promote the improvement of cost management technology through professional technology.

4.2. The Design of Each Module of Big Data in Enterprise Cost Management

4.2.1. Optimization of Cost Management in Procurement and Inventory Links. The cost of the supply chain mainly includes the cost of procurement and the cost of sales. The efficiency of the supply chain is also affected by the efficiency of the entire process. We must adjust our supply chain according to market demand so that we can better manage costs. We can share information through the big data information platform, build a supply chain model, and achieve the goal of reducing costs. In recent years, procurement has become a multiparty collaborative process. We need to establish some good partners to reduce our inventory. At the same time, we should strengthen the management of the supply chain to ensure that the supply of goods is sufficient. Table 7 shows the main cost components in the procurement process, and Table 8 shows the measures we use big data technology for inventory cost management in the era of big data.

4.2.2. Optimization of Cost Management in Marketing Links. In the process of cost management, we need to reduce the cost of research and the cost of sales. In this era of big data, we must reduce some nonessential costs, improve operational efficiency, use big data technology to provide

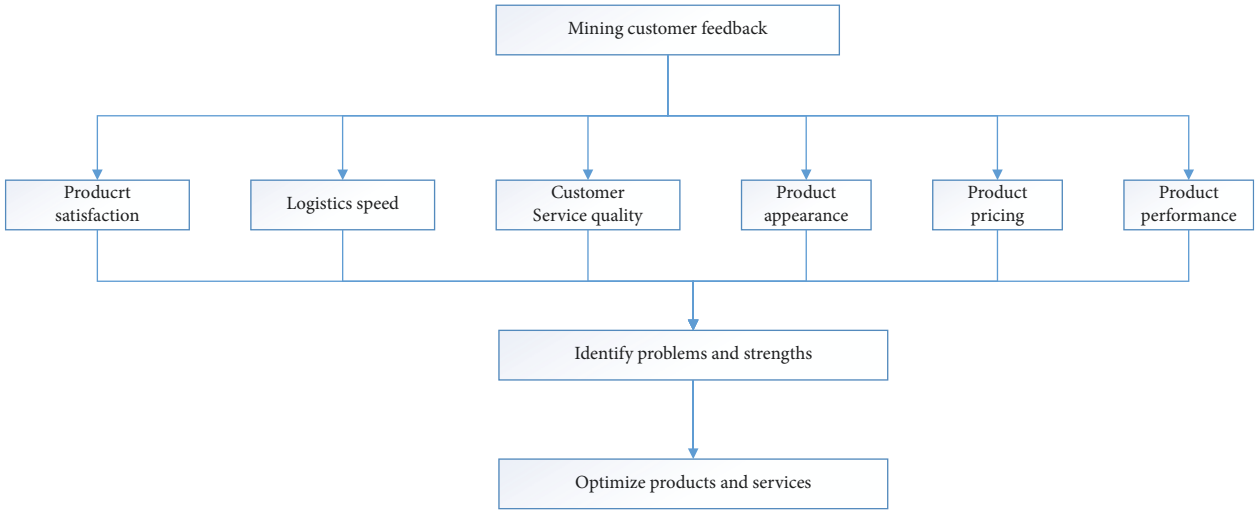

Figure 4: The application of big data in optimizing products and services.

reasonable solutions, and manage costs. Table 9 mainly shows the main measures to use big data technology to reduce costs.

In this era, the competition among enterprises has become increasingly fierce, and the phenomenon of product homogeneity has become more and more serious. The prices of the products of each company are very close, and the company cannot obtain an advantage from the price, so it can only provide better services and guide customers in choosing products. At the same time, consumers are also very concerned about service levels. Enterprises should pay attention to establishing service mechanisms and optimizing their products and services. The process is as in Figure 4.

4.2.3. Data Cluster Analysis and Dissimilarity Measurement. The objective function of the FCM algorithm is as follows:

$$\min J(U,V) = \sum_{i=1}^{c}\sum_{j=1}^{n} u_{ij}^{m}\left\|x_j - v_i\right\|^2. \tag{18}$$

The constructed unconstrained Lagrangian function is as follows:

$$F = \sum_{i=1}^{c}\sum_{j=1}^{n} u_{ij}^{m}\left\|x_j - v_i\right\|^2 + \alpha\left(\sum_{i=1}^{c} u_{ij} - 1\right). \tag{19}$$

Its partial derivative is as follows:

$$\frac{\partial F}{\partial u_{ij}} = m\left(u_{ij}\right)^{m-1}\left\|x_j - v_i\right\|^2 + \alpha. \tag{20}$$

$$\frac{\partial F}{\partial v_i} = -2\sum_{j=1}^{n} u_{ij}^{m}\left(x_j - v_i\right). \tag{21}$$

Make it equal to 0 to get the following:

$$u_{ij} = \frac{1}{\sum_{k=1}^{c}\left(\left\|x_j - v_i\right\|/\left\|x_j - v_k\right\|\right)^{2/m-1}}. \tag{22}$$

$$v_i = \frac{\sum_{j=1}^{n} u_{ij}^{m} x_j}{\sum_{j=1}^{n} u_{ij}^{m}}. \tag{23}$$

In the process of using clustering to analyze, the selection of appropriate metrics determines the performance of clustering. The formula for calculating the Euclidean distance is as follows:

$$\begin{aligned} d\left(x_i, x_j\right) &= \left\|x_i - x_j\right\|_2 \\ &= \sqrt{\sum_{k=1}^{q}\left(x_{ik}, x_{jk}\right)^2}. \end{aligned} \tag{24}$$

Calculate its Manhattan distance as follows:

$$d\left(x_i, x_j\right) = \sum_{k=1}^{q}\left|x_{ik} - x_{jk}\right|. \tag{25}$$

Calculate the Chebyshev distance as follows:

$$d\left(x_i, x_j\right) = \max_{k}\left(\left|x_{ik} - x_{jk}\right|\right). \tag{26}$$

Calculate its Minkovs distance as follows:

$$d\left(x_i, x_j\right) = \left(\sum_{k=1}^{q}\left|x_{ik} - x_{jk}\right|^r\right)^{\frac{1}{r}}. \tag{27}$$

4.3. Implementation of Enterprise Cost Accounting Management Guarantee Strategy under the Background of Big Data. According to the experimental results of 3.4.4, enterprises should build their own business and financial integration platforms, and in the process of cost management, they

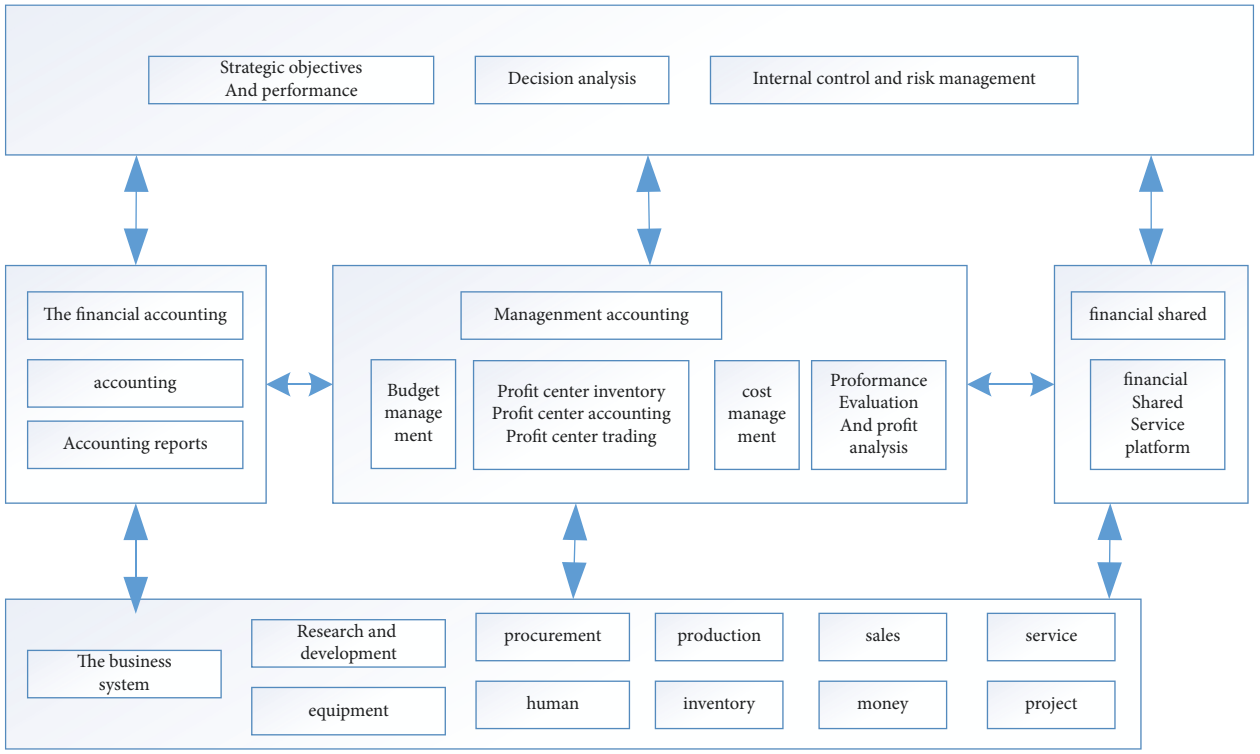

Figure 5: Industry and finance integration platform.

should strengthen informatization construction and talent team construction to ensure the efficient and stable operation of enterprise cost data.

4.3.1. Build an Integrated Platform for Business and Finance. In the information age, companies will face a variety of data. How to deal with data is an important issue that companies need to solve. Companies should establish a platform for business and financial integration and use information technology to build their own management system. Enterprises should actively adopt some business intelligence technologies to handle the data monitoring that occurs, improve the relationship between the data in each process, promote the integration of the process, and use science and technology to optimize the processing of each process, realize the sharing of data resources, and truly play the role of financial management. Figure 5 shows the design process of a business integration platform.

4.3.2. Strengthen the Construction of Financial Management Informatization. In the process of enterprise production management, financial management is very necessary. Most of the current financial management work is based on big data, and the traditional financial management model has not matched the development of modern enterprises. The traditional financial management model cannot provide effective information for corporate management and will increase corporate risks. The financial management system designed in the era of big data can not only standardize the financial management process but also provide reliable financial management. Basis to further promote the development of finance: Informatization construction of an enterprise can promote the integration of enterprise resources, and it can also bring closer links between various departments. Financial management informatization can liberate financial personnel and promote the reform of financial management. The financial staff can better control the financial information, and the information processing ability can be further improved. It can be seen from this that it is very necessary to carry out informatization construction on the financial management of enterprises, which can promote the development of enterprises. When building a financial management information system, we need certain technical support. Integrating big data technology into the construction of the financial management information system can not only make the information management process more standardized but also promote the construction of the information management system. In order to ensure the effective operation of the informatization process, enterprises must control internal resources, understand their own needs, and constantly adjust their structure to adapt to the development of the times. Enterprises must also plan for the information work process and rationally divide labor so that everyone can stay in their own positions and develop and lay the foundation for subsequent financial work.

4.3.3. Strengthen the Construction of Big Data Talent Team. With the advent of the era of big data, Internet technology has been further developed, technology is being updated faster and faster, and the competitiveness of enterprises is

also increasing. If an enterprise wants to occupy a favorable position in the competition, it must have strong R&D capabilities, as well as core technical support and innovation capabilities. In the process of product development and operation, companies must continuously invest in new knowledge and technology. In addition to enhancing their own R&D capabilities, companies should also attach importance to the training of high-quality talents to enhance their R&D capabilities and innovation capabilities. Enterprises should reduce production costs as much as possible and increase profits. In order to ensure the success of an enterprise, it is very important to cultivate talents. If an enterprise wants to establish a big data analysis platform and use big data technology for analysis, it needs to bring in corresponding talents. In the process of enterprise management, data analysis experts are needed to analyze the enterprise data. In the process of handling the company's business, if the company's financial management is lagging behind and is not familiar with the company's production model, some relevant talents can be introduced to make up for these problems. Enterprises should actively accelerate the construction of talents, establish high-quality teams and organize specialized talent teams so that talents can become familiar with the company's management mode and technology as soon as possible, and they must also understand advanced scientific knowledge to meet the needs of outstanding talents. In the process of managing the enterprise, massive amounts of data are generated every day. Financial personnel must ensure the accuracy of the data when performing analysis and at the same time, predict daily financial data. Using big data technology and data mining technology can find some potential problems in the process of financial management. At the same time, companies need to train some information technology talents to solve these problems and promote the development of technology.

5. Conclusion

In the process of enterprise management, if there is no systematic management in the process of cost management, it is impossible to process a large amount of data at one time. Some enterprises have not done an in-depth cost analysis, and some cost data cannot be solved. Combined with big data technology and cost management technology, this paper puts forward the optimal strategy of cost management in the era of big data. At the same time, the strategy is applied to the actual company. Big data technology and data sharing technology have solved the practical problems of enterprise management and production. Enterprises using big data technology can not only optimize management costs but also optimize their management functions, which can better solve the problems that many data will be repeatedly processed, data types are complex, and it is difficult to find useful information from massive data. At this stage, the amount of data in the enterprise is huge, the production cost is also very high, and the production process is very complex. Using big data technology for enterprise cost management can not only control the cost of enterprises but also standardize enterprise processes and promote enterprise optimization. At the same time, we combine big data technology with cost management technology to provide the basis for the follow-up intelligent management of enterprises.

Data Availability

The dataset can be accessed upon request.

Conflicts of Interest

The authors declare that they have no conflicts of interest.

References

[1] Z. Tian, "Detecting text in natural image with connectionist text proposal network," in *Proceedings of the European conference on computer vision*, vol. 56–72, Netherlands, October 2016.

[2] H. Li and C. Shen, "Reading car license plates using deep convolutional neural networks and lstms," 2016, https://fdocuments.in/document/arxiv160105610v1-cscv-21-jan-2016-arxiv160105610v1-cscv-21-jan-2016-2.html.

[3] S. Z. Masood, "License plate detection and recognition using deeply learned convolutional neural networks," 2017, https://arxiv.org/pdf/1703.07330.

[4] A. Naimi, "Multi-nation and multi-norm license plates detection in real traffic surveillance environment using deep learning," in *Proceedings of the International Conference on Neural Information Processing*, Kyoto, Japan, October 2016.

[5] M. A. Rafique, "Vehicle license plate detection using region-based convolutional neural networks," *Soft Computing*, vol. 22, pp. 6429–6440, 2018.

[6] R. Girshick, "Fast R-CNN," in *Proceedings of the IEEE International Conference on Computer Vision*, pp. 1440–1448, Santiago, Chile, December 2015.

[7] J. Redmon, "You only look once: unified, real-time object detection," in *Proceedings of the IEEE Conference on Computer Vision and Pattern Recognition*, Las Vegas, NV, USA, June 2016.

[8] L. Xie, "A new CNN-based method for multi-directional car license plate detection," *IEEE Transactions on Intelligent Transportation Systems*, vol. 19, pp. 507–517, 2018.

[9] H. Xiang, "Lightweight fully convolutional network for license plate detection," *Optik*, vol. 178, pp. 1185–1194, 2019.

[10] D. Menotti, "Vehicle license plate recognition with random convolutional networks," in *Proceedings of the 2014 27th SIBGRAPI Conference on Graphics, Patterns and Images*, Brazil, August 2014.

[11] R. Laroca, "A robust real-time automatic license plate recognition based on the YOLO detector," in *Proceedings of the 2018 International Joint Conference on Neural Networks (IJCNN)*, Brazil, July 2018.

[12] C. R. Hendry, "Automatic license plate recognition via sliding-window darknet-YOLO deep learning," *Image and Vision Computing*, vol. 87, pp. 47–56, 2019.

[13] D. G. Lowe, "Distinctive image features from scale-invariant keypoints," *International Journal of Computer Vision*, vol. 60, pp. 91–110, 2004.

[14] E. Rublee, "ORB: an efficient alternative to SIFT or SURF," *ICCV*, vol. 33, p. 11, 2011.

[15] M. Brown and D. G. Lowe, "Automatic panoramic image stitching using invariant features," *International Journal of Computer Vision*, vol. 74, pp. 59–73, 2007.

[16] R. Mur-Artal, "ORB-SLAM: a versatile and accurate monocular SLAM system," *IEEE Transactions on Robotics*, vol. 31, pp. 1147–1163, 2015.
[17] S. A. Abbas, "Recovering Homography from Camera Captured Documents Using Convolutional Neural Networks," 2017, https://arxiv.org/pdf/1709.03524.
[18] D. DeTone, *Deep Image Homography Estimation*, https://arxiv.org/abs/1606.03798, 2016.
[19] T. Nguyen, "Unsupervised deep homography: a fast and robust homography estimation model," *IEEE Robotics and Automation Letters*, vol. 3, pp. 2346–2353, 2018.
[20] K. Simonyan and A. Zisserman, "Very deep convolutional networks for large-scale image recognition," 2014, https://arxiv.org/pdf/1409.1556.
[21] J. Engel, "LSD-SLAM: large-scale direct monocular SLAM," in *Proceedings of the European Conference on Computer Vision*, Zurich, Switzerland, September 2014.
[22] A. Dosovitskiy, "Flownet: learning optical flow with convolutional networks," in *Proceedings of the IEEE International Conference on Computer Vision*, Santiago, Chile, December 2015.
[23] E. Zhou, "Gridface: face rectification via learning local homography transformations," in *Proceedings of the European Conference on Computer Vision (ECCV)*, Munich, Germany, September 2018.

Hindawi
Scientific Programming
Volume 2022, Article ID 5873919, 11 pages
https://doi.org/10.1155/2022/5873919

Research Article

Assessment of Heavy Metal Pollution Characteristics and Ecological Risk in Soils around a Rare Earth Mine in Gannan

Yi Wang,[1,2] Wei Sun,[1,2] Yuli Zhao,[1,3] Peiyong He,[1,2] Lidong Wang,[3] and L. T. T. Nguyen[4]

[1]*China Institute of Geological Environment Monitoring, Beijing 100081, China*
[2]*Key Laboratory of Mine Ecological Effects and Systematic Restoration, Ministry of Natural Resources, Beijing 100081, China*
[3]*School of Water Resources and Environment, China University of Geosciences (Beijing), Beijing 100083, China*
[4]*International University-Vietnam National University, Ho Chi Minh City, Vietnam*

Correspondence should be addressed to Wei Sun; paperconnetion@163.com and Yuli Zhao; 2105190045@cugb.edu.cn

Received 15 April 2022; Revised 9 May 2022; Accepted 17 May 2022; Published 31 May 2022

Academic Editor: Jie Liu

In order to explore the pollution of heavy metals in the soils around the mined rare-earth mines, this paper used the geoaccumulation index method, the Nemerow pollution index method, and the potential ecological risk index method during the high water period and the withered water period, respectively, to analyze and assess the pollution characteristics and ecological risks of Mn, Cu, Cr, As, Cd, Ni, Pb, and Zn in the soils of the study area. The results showed that all the eight heavy metals in the soil of the study area have accumulated to varying degrees, and the accumulation indices were Pb > Mn > Zn > Cd > Cu > Ni > Cr > As in descending order, with Pb and Mn accumulating most seriously. According to the results of the Nemerow pollution index, more than 25% of the sampling points in the soil were lightly contaminated, the Nemerow index of heavy metal Pb was greater than 2, which was moderately contaminated, and Cd was lightly contaminated in the withered water period. The potential ecological risk index showed that the heavy metal Cd was moderately ecologically hazardous, while the other seven heavy metals were all mildly ecologically hazardous. The heavy metals Pb and Mn in the soils of the study area were more seriously polluted, and there was also a certain degree of heavy metal Cd pollution during the withered water period, and the more seriously polluted areas were mainly located around the open pit of the rare-earth mines. Based on Java, the software platform of soil heavy metal pollution characteristics and ecological risk assessment around rare-earth mines is realized. The overall structure of the platform is designed, the background development framework is planned based on SSM, and the database is designed with SQL Server.

1. Introduction

As one of the technical problems in ecological restoration and environmental management of mines, the excessive heavy metal contamination of soil in mining areas has been a widespread concern of experts and scholars at home and abroad [1]. How to solve the problem of heavy metal contamination in soil left behind by mining has become an important part of the development of ecological protection in China, so the identification of its pollution characteristics and ecological risk assessment has become the first priority to solve the pollution problem. Heavy metal contamination of soils can cause health hazards through the food chain [2]. The occurrence of food safety problems such as "cadmium rice," "blood lead," and "cadmium wheat" in recent years has also sounded the alarm for the assessment and prevention of heavy metal pollution in soil [3]. When farmland is contaminated with heavy metals, these contaminants will enter the human body through the crops and thus cause harm to the human body. Some scholars have divided heavy metals into two parts according to the extent to which they are needed for crop growth: those that are extremely harmful to humans but less so for plant growth, such as Cd, Hg, and Pb, and those that are needed for both human and plant growth but are harmful to humans if they exceed certain standards, such as Zn and Cu [4].

Rare-earth mines, due to their special mining process, are extremely harmful to the ecological environment around

the mines, especially in terms of heavy metal contamination of the soil. On the one hand, the heavy metals present in the massive piles of tailings may migrate to the soil, causing heavy metal contamination of the soil [5]. On the other hand, the residual leaching agent in the ore will displace heavy metal ions such as Fe^{2+}, Cd^{2+}, Pb^{2+}, Zn^{2+}, Mn^{2+}, and Cu^{2+}, which will migrate to the soil in and around the mine area under the natural action of rainwater washing, resulting in heavy metal pollution of the soil [6–8].

At present, the assessment methods of heavy metal pollution in soils at home and abroad are mainly summarized as index method, model method, GIS-based analysis method, and other mathematical methods [9–12]. The index method can reflect the relationship between the actual measured value and the background value of heavy metal concentration in the soil of the region more intuitively and is more widely used in the assessment of heavy metal pollution in soils [13]. Some scholars have suggested that heavy metal pollution in soils is a complex process and different assessment methods need to be selected according to different pollution situations. However, there are limitations in a single assessment method, so a combination of multiple assessment methods is adopted to make the assessment results more relevant to the actual situation [14]. In this study, a total of 146 soil samples were collected during the high and withered water periods. The geoaccumulation index method, the Nemerow comprehensive pollution index method, and the potential ecological risk index method were used to analyze and assess the pollution characteristics and potential ecological risks of heavy metals Mn, Cu, Cr, Cd, Ni, Pb, Zn, and As in the soil, so as to provide a reference for the formulation of heavy metal pollution control and prevention measures for soils in the study area. At the same time, the software platform is preliminarily planned and developed, which provides practical support for the application of the theoretical method of this study.

2. Materials and Methods

2.1. Overview of the Study Area. Gannan, the geographical abbreviation for the southern region of Jiangxi Province (the abbreviation of Jiangxi Province is "Gan."), is mainly composed of 18 counties (3 districts, 13 counties, and 2 county-level cities) under the jurisdiction of the prefecture-level Ganzhou City, with an area of 39,379.64 km^2, accounting for about 25% of the total area of Jiangxi Province [15]. The region is rich in mineral resources, and Ganzhou is known as the "Kingdom of Rare Earth," with the reserves of ionic heavy rare earths being the highest in China [16]. The study area is located in the East Asian monsoon region, with a mild climate, abundant light, heat and rainfall, belonging to the humid climate of the central subtropical monsoon. The average annual precipitation in the region is 1500–1600 mm, but the spatial and temporal distribution is uneven, with large interannual variations and uneven rainfall distribution, with the most rainfall in June and the least in November to December throughout the year. The soil types are paddy soil, tidal soil, purplish soil, red soil, and hilly yellow soil, with soil pH mostly between 5 and 6.

2.2. Sample Collection and Experimental Analysis. In this study, the sampling points were mainly arranged along the area of farmland affected by the rare-earth mine and the area of the open pit, and a total of 146 soil samples were collected for testing and analysis during the high and withered water periods in 2020, respectively. The sampling points were mainly selected in places with obvious characteristics of the soil type being mined, and the terrain was relatively flat, stable, and well vegetated; the distribution of the sample collection points is shown in Figure 1. When the authors collected soil samples, the depth and sampling points of each sampling site were basically uniform, with the sampler entering the soil perpendicular to the ground, the collection depth was 0–20 cm, and the spacing between collection points was 500–2500 m.

The collected soil samples were air-dried, ground, and sieved in the laboratory, and the content of Mn, Cr, Cu, Zn, Pb, Ni, Cd, and As in the soil was measured according to the regional geochemical sample analysis method (DZ/T0279-2016) using an ICAP6300MFC two-way observation plasma emission spectrometer (D466), an Agilent 7700x inductively coupled plasma mass spectrometer (D483), and an AFS-8800 dual-channel Atomic Fluorescence Photometer (D460) to measure the content of Mn, Cr, Cu, Zn, Pb, Ni, Cd, and As elements in the soil, as well as an FE28 PH meter (acidity meter) (D554) to measure the pH of the soil samples according to the agricultural soil testing standard (NY/T1121.2–2006).

2.3. Assessment Methodology

2.3.1. Geoaccumulation Index Method. The geoaccumulation index (I_{geo}) method, which determines the contamination of heavy metals by the relationship between the total concentration of heavy metals in the soil and the background value, is an effective way to determine the level of heavy metal contamination in the soil and to classify the level of contamination according to the value of the geoaccumulation index (I_{geo}). [17, 18] The geoaccumulation index equation is

$$I_{geo} = \log_2 \frac{w_i}{kB_i}, \tag{1}$$

where I_{geo} is the geoaccumulation index, dimensionless. w_i is the measured value of heavy metal i in the soil sample, mg-kg^{-1}; B_i is the background value of heavy metal i in the surface soil of Ganzhou City, mg-kg^{-1}; k is a coefficient characterizing the difference in soil background values due to differences in rock backgrounds in different places, and the value of k in this study is 1.5 [19, 20].

The assessment criteria are shown in Table 1.

2.3.2. Nemerow Comprehensive Pollution Index. The Nemerow pollution index is the most common method for comprehensive soil pollution assessment at home and abroad. The assessment method highlights the maximum pollution effect and is in line with the criteria of the maximum pollution level as the soil pollution level for soil

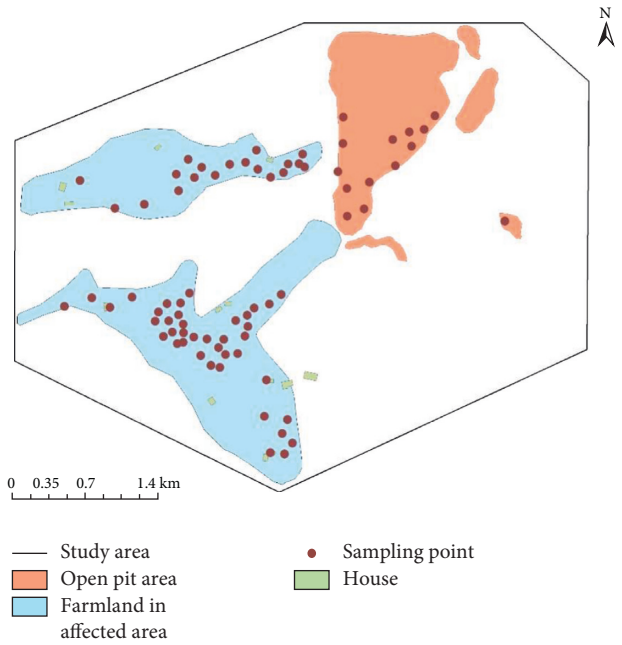

Figure 1: Distribution of soil sampling sites in the study area.

Table 1: Criteria for assessment of soil pollution with geo-accumulation index.

The values of I_{geo}	Class	The cumulative degree
$I_{geo} < 0$	I	Clean
$0 \le I_{geo} < 1$	II	Mild accumulation
$1 \le I_{geo} < 2$	III	Mild-to-moderate accumulation
$2 \le I_{geo} < 3$	IV	Moderate accumulation
$3 \le I_{geo} < 4$	V	Mild-to-heavy accumulation
$4 \le I_{geo} < 5$	VI	Heavy accumulation
$I_{geo} \ge 5$	VII	Severe accumulation

assessment in China. The Nemerow index is calculated by the following formula:

$$P = \frac{C_i}{S_i},$$
$$P_Z = \sqrt{\frac{P_J^2 + P_{i\max}^2}{2}}, \quad (2)$$

where P is the one-factor index for that sampling point, dimensionless. C_i is the measured value of heavy metal i at that point, mg-kg^{-1}. S_i is the standard value of heavy metal i. In this study, S_i is the risk screening value of heavy metal i in the Soil Environmental Quality Standard (GB 15618-2018) (the background value of heavy metal Mn in the surface layer of Ganzhou soil is used), mg-kg; and P_Z is the Nemerow index for the point, dimensionless. P_J is the mean value of the single factor index at the point, dimensionless. $P_{i\max}$ is the maximum value of the single factor index for heavy metal i at the site [21–24], dimensionless; the assessment criteria for the Nemerow index are shown in Table 2.

2.3.3. Potential Ecological Risk Index. The potential ecological risk index is a method proposed by the Swedish scientist Hakanson, which takes into account not only the content of heavy metals in the soil but also the toxicity level, the concentration of contamination, and the sensitivity of the environment to heavy metal contamination [25–30]. The expression is as follows:

$$\mathrm{RI} = \sum_{i=1}^{n} E_i,$$
$$E_i = T_i \times C_{f,i}, \quad (3)$$

where RI is the composite potential ecological risk hazard index, dimensionless. E_i is the potential ecological hazard index of heavy metal i in the soil at the sampling site, dimensionless. $C_{f,i}$ is the ratio of the measured value of heavy metal i in the soil at the sampling site to the background value of heavy metal i in the surface soil of Ganzhou City, dimensionless. T_i is the toxicity response coefficient of heavy metal i, dimensionless, where the toxicity coefficients of Mn, Cu, Cr, As, Cd, Ni, Pb, and Zn are 1, 5, 2, 10, 30, 5, 5, and 1, respectively. [29] The assessment criteria for the comprehensive potential ecological risk index RI and the potential ecological risk index E_i [31–39] are shown in Table 3.

Table 2: Criteria for assessment of soil pollution with Nemerow pollution index.

The values of Nemerow pollution index	Pollution class	Pollution levels
$P_Z \le 0.7$	I	Clean
$0.7 < P_Z \le 1$	II	Moderately clean
$1 < P_Z \le 2$	III	Slightly polluted
$2 < P_Z \le 3$	IV	Moderately polluted
$P_Z > 3$	V	Heavily polluted

3. Results and Discussion

3.1. Characteristics of Heavy Metal Content in Soils

3.1.1. Characteristics of Heavy Metal Content in Soils during the High Water Period. The average contents of heavy metals Mn, Cu, Cr, As, Cd, Ni, Pb, and Zn in the soils of the study area during the high water period were 448.97, 18.92, 30.33, 3.00, 0.14, 13.13, 92.99, and 64.18 mg^{-}kg^{-1}, which were 1.85, 1.25, 0.88, 0.34, 1.56, 1.06, 2.72, and 1.11 times higher than the background values of heavy metal contents in the surface layer of soils in Ganzhou City, respectively, which can be seen in Table 4 [33]. Among them, the contents of heavy metals Cd, Cr, Cu, Ni, Zn, and As were all lower than the screening values for soil pollution risk on agricultural land (GB15618-2018), while 37 sampling points of heavy metal Pb exceeded the screening values for soil pollution risk on agricultural land, with an exceedance rate of 50.68%, and the maximum content value of Mn was 5.57 times higher than the soil background value. The above data indicate that there is a certain degree of contamination of heavy metals Pb and Mn in the soil during the high water period. The heavy metals in descending order of coefficient of variation are Cd, Cr, As, Mn, Pb, Cu, Ni, and Zn, with Cd having a coefficient of variation of 446%, which is a very

Table 3: Criteria for assessment of soil pollution with the potential ecological risk index.

The values of RI	The values of E_i	Pollution levels
RI < 150	E_i <40	Light pollution
150 ≤ RI < 300	40 ≤ E_i < 80	Moderate pollution
300 ≤ RI < 600	80 ≤ E_i < 160	Moderate-to-heavy pollution
600 ≤ RI < 1200	160 ≤ E_i < 320	Heavy pollution
RI ≥ 1200	E_i ≥320	Extreme-intensity pollution

Table 4: Characteristics of heavy metals in the soil surface layer of the study area.

Sampling time	Projects	Content ($mg^{-}kg^{-1}$) content ($mg^{-}kg^{-1}$)							
	Projects	Mn	Cu	Cr	As	Cd	Ni	Pb	Zn
High water period	Minimum value	164	3.54	3.6	0.96	0.025	2.23	45.1	42
	Maximum value	1354	44.7	135.8	13.4	0.27	27.9	377.6	95
	Average value	448.97	18.92	30.33	3.00	0.14	13.13	92.99	64.18
	Standard deviation	239.75	9.33	22.44	1.80	0.58	6.40	47.36	11.00
	Coefficient of variation	53%	49%	74%	60%	414%	49%	51%	17%
Withered water period	Minimum value	126	1.16	5.09	1.02	0.113	<2	35.7	32.4
	Maximum value	1111.3	41.7	71	12.2	0.541	24.2	214	96
	Average value	471.12	16.48	27.28	3.12	0.26	11.97	94.01	61.07
	Standard deviation	289.18	9.31	15.36	1.61	0.09	5.63	35.90	12.52
	Coefficient of variation	61%	56%	56%	52%	35%	47%	38%	21%
Background values for topsoil in Ganzhou		243	15.17	34.56	8.85	0.09	12.35	34.19	58.05
Background values for topsoil in Jiangxi		259	20.8	48.0	10.4	0.10	19.0	32.1	69.0
Background values for topsoil in China		540	20.0	53.9	9.2	0.07	24.9	23.6	67.7

strong variation. The larger the coefficient of variation value is, the more unevenly distributed the heavy metal is in the region and the greater the anthropogenic influence is [34, 35].

3.1.2. Characteristics of Heavy Metal Content in Soils during the Withered Water Period. The average contents of heavy metals Mn, Cu, Cr, As, Cd, Ni, Pb, and Zn in the soils of the study area during the withered water period were 456.24, 16.48, 27.28, 3.12, 0.26, 11.97, 94.01, and 61.07 $mg^{-}kg^{-1}$, respectively, which were 1.94, 1.09, 0.79, 0.35, 2.89, 0.97, 2.75, and 1.05 times higher than the background values of heavy metals in the surface soils of Ganzhou City, as shown in Table 4 [35, 36]. Among them, the content values of the heavy metals Cr, Cu, Ni, Zn, and As were all lower than the screening value of soil pollution risk on agricultural land (GB15618-2018). 37 sampling points of Pb exceeded the screening value of soil pollution risk on agricultural land, with an exceedance rate of 50.68%, 15 sampling points of heavy metal Cd exceeded the risk screening values for soil contamination on agricultural land, with an exceedance rate of 20.55%, and the maximum value of heavy metal Mn content was 4.57 times higher than the background value of the soil. The above data indicate that there is a certain degree of pollution of heavy metals Pb, Cd, and Mn during the withered water period. The heavy metals in descending order of coefficient of variation are Mn, Cu, Cr, As, Ni, Pb, Cd and Zn, with Mn having the largest coefficient of variation of 61%. Some studies have shown that a coefficient of variation of over 50% indicates that the spatial distribution of this heavy metal content is very heterogeneous and the possibility of point source pollution exists [36].

3.1.3. Differential Characteristics of Heavy Metal Content in Soil during the High and Withered Water Periods. The mean values of Cu, Cr, Ni, and Zn in the soils of the study area were lower in the withered water period than in the high water period, while the contents of the heavy metals Mn, As, Cd, and Pb were higher than in the rich period. The above data show that the content of heavy metals in the soils of the study area fluctuates to a certain extent between the high and withered water periods, with the average content of Cd in the withered water period being 1.86 times higher than that in the high water period, while the content of the other seven heavy metals fluctuates less. The heavy metal pollution in the soil during the high water period is mainly Pb and Mn, while the heavy metal pollution in the soil during the withered water period is mainly Pb, Mn, and Cd. Cd pollution occurs in the withered water period compared to the high water period, and the Cd pollution in the soil during the withered water period is mainly distributed in the open pit mining area of the mine.

3.2. Assessment of Heavy Metal Contamination of Soils

3.2.1. Geoaccumulation Index Assessment. The geoaccumulation index values for the heavy metals Mn, Cu, Cr, As, Cd, Ni, Pb, and Zn in the soil during the high water

period were 0.15, −0.51, −1.15, −2.32, −0.15, −0.74, 0.74, and −0.46, respectively, while the geoaccumulation indix values for Mn, Cu, Cr, As, Cd, Ni, Pb, and Zn in the soil during the withered water period were 0.10, −0.89, −1.21, −2.23, −0.86, −0.88, 0.78, and −0.54, respectively, as shown in Table 5. Except for the heavy metal As in the withered water period, the accumulation of heavy metals Mn, Cu, Cr, Cd, Ni, Pb, and Zn occurred to varying degrees in the high and withered water periods; see Figures 2 and 3. Among them, the accumulation of heavy metals Pb and Mn was the highest and that of As was the lowest. 95.89% and 97.26% of the sampling sites showed varying degrees of accumulation of heavy metal Pb and 53.43% and 45.21% of the sampling sites showed varying degrees of accumulation of heavy metal Mn during the high water and withered water periods, respectively.

3.2.2. Comprehensive Assessment of the Nemerow Pollution Index. The results of the Nemerow pollution index show that 39.72% of the sampling points were under alert and 26.03% were lightly polluted during the high water period; 39.72% of the sampling points were under alert and 30.14% were polluted to varying degrees during the dry water period, of which 28.77% were lightly polluted and 1.37% were moderately polluted; see Figure 4. The Nemerow pollution index values for Cu, Pb, Zn, Cr, Ni, Cd, and As were 0.68, 2.03, 0.39, 0.66, 0.36, 0.71, and 0.24, respectively, during the high water period and 0.63, 2.19, 0.40, 0.36, 0.32, 1.22, and 0.22, respectively, during the withered water period, as shown in Table 6. The heavy metal Pb was moderately polluted, and Cd was under alert during the high water period and lightly polluted during the withered water period. The Nemerow pollution index of Mn was evaluated according to the Ganzhou soil surface background value as the standard value, and its Nemerow pollution index values were 4.16 and 3.51 during the high water period and withered water period, respectively, indicating that there is also a certain degree of Mn pollution in the soil.

3.2.3. Potential Ecological Risk Index Method. The comprehensive potential ecological risk index RI and potential ecological hazard index E_i were calculated based on the potential ecological risk hazard index formula; see Table 7. According to the comprehensive potential ecological risk index RI, all the sampling sites in the study area were mildly ecologically hazardous during the high water period, 82.19% of the sampling sites were mildly ecologically hazardous during the withered water period, and 17.81% of the sampling sites were moderately ecologically hazardous. According to the potential ecological hazard index E_i, the heavy metals Mn, Cu, Cr, As, Ni, and Zn were all mildly ecologically hazardous; Pb was mildly ecologically hazardous in 98.63% of the sampling sites during the high water period, moderately hazardous in 1.37% of the sampling sites, and mildly hazardous in all sampling sites during the withered water period. Cd was mildly ecologically hazardous in 36.99% of the sampling sites during the high water period, moderately ecologically hazardous in 58.90% of the sampling sites, and moderately to heavily ecologically hazardous in 4.11% of the sampling sites, while it was lightly ecologically hazardous in 1.37% of the sampling sites during the withered water period, moderately ecologically hazardous in 53.42% of the sampling sites, moderately to heavily ecologically hazardous in 43.84% of the sampling sites, and heavily ecologically hazardous in 1.37% of the sampling sites. Although the content of the heavy metals Pb and Mn in the soil was high, their toxicity coefficient values were small and therefore the ecological hazard risk was low. The potential ecological hazard index for the heavy metal Cd was evaluated to be high due to the large toxicity coefficient values of Cd.

4. Software Platform

4.1. Overall Structure. The user requirements of heavy metal pollution characteristics and ecological risk assessment platform contain functional and nonfunctional requirements [40–43]. Functional requirements analysis is based on the most basic in-depth study of the functions required by the system, that is, the requirements with specific contents and functions that the system must contain. From the perspective of system nonfunctionality, nonfunctional requirements analysis mainly covers the development and use principles of the system and the characteristics of the system.

As shown in Figure 5, the platform is divided into four functional modules: system login module, heavy metal pollution characteristics and ecological risk monitoring module, heavy metal pollution characteristics and ecological risk standard evaluation module, and heavy metal pollution characteristics and ecological risk early warning module.

Nonfunctional analysis mainly restricts the platform from the perspectives of performance, availability, and maintainability [44–47].

(1) Security. User authentication and data required by the system need to be encrypted in the transmission process, and the security of users and data needs to be effectively guaranteed.

(2) Compatibility and flexibility. The system can operate on different types of terminal equipment, support multiple hardware platforms, and support information sharing with data of other systems.

(3) Real time and effectiveness. The data transmission and display shall be effective in real time. When the data is obtained, the background will automatically start the online assessment and evaluation calculation.

(4) Maintainability. The system shall adopt the principle of high coupling and low cohesion, with high independence between modules for later modification and maintenance.

The overall structure of the platform is shown in Figure 6. The structures of heavy metal pollution characteristics and ecological risk standard evaluation and ecological risk standard evaluation modules are divided into three parts:

Table 5: The geoaccumulation index of the heavy metals in soils.

Sampling time	The average values of geoaccumulation index							
	Mn	Cu	Cr	As	Cd	Ni	Pb	Zn
High water period	0.15	−0.51	−1.15	−2.32	−0.15	−0.74	0.74	−0.46
Withered water period	0.10	−0.89	−1.21	−2.23	−0.86	−0.88	0.78	−0.54

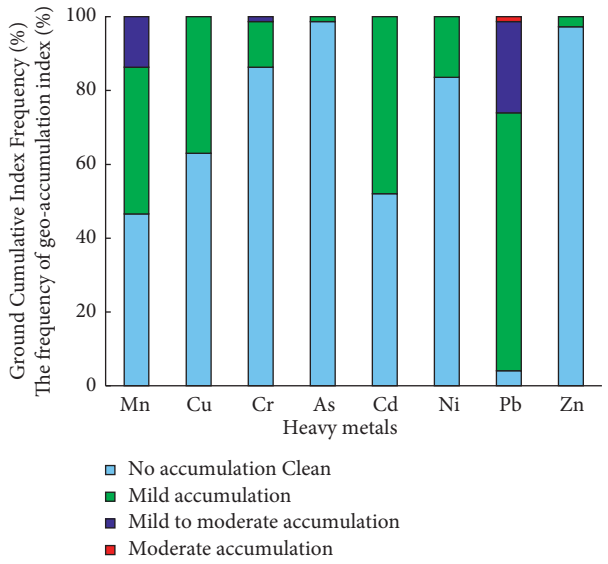

Figure 2: Frequency distribution of geoaccumulation index of heavy metals in the high water period.

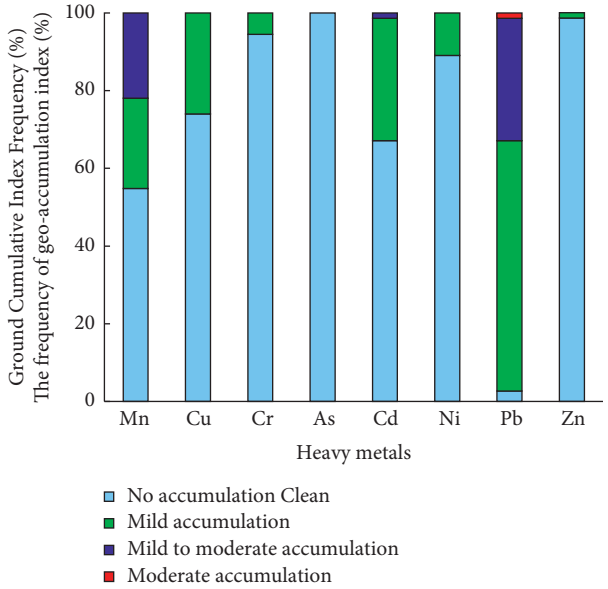

Figure 3: Frequency distribution of geoaccumulation index of heavy metals in the withered water period.

monitoring layer, transmission layer, and user layer. Each monitoring section of the monitoring layer can monitor the type and concentration of heavy metal pollution targets.

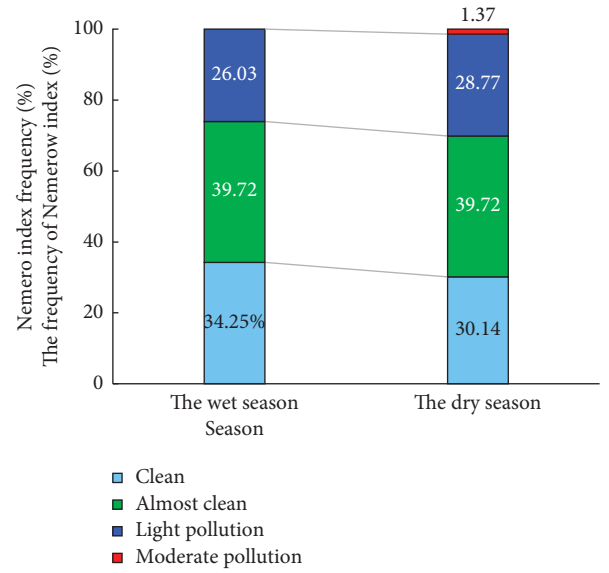

Figure 4: Frequency distribution of Nemerow pollution index of heavy metals in the study area.

Table 6: Nemerow pollution index of the heavy metals in soils.

Sampling time	P_i						
	Cu	Pb	Zn	Cr	Ni	Cd	As
High water period	0.68	2.03	0.39	0.66	0.36	0.71	0.24
Dry period	0.63	2.19	0.40	0.36	0.32	1.22	0.22

Different sensors transmit the monitoring data to the data center through the environmental monitoring collector. In the development and design of the platform, the required monitoring data are obtained from the database interface, and the monitoring information and calculation results are displayed on the front-end display screen of the mobile application through model calculation on the back of the platform.

4.2. SSM Background Development Framework. SSM framework includes two open-source frameworks, Spring and MyBatis [45–47]. Spring architecture is based on a container that uses JavaBean attribute and can develop any Java application. The core idea of Spring is IOC (inversion of control), which gives Spring the right to create objects without having to "new" an object by themselves. Spring provides unique data access abstraction and transaction management abstraction and can provide a consistent model in various underlying transactions such as JDBC. Spring

Table 7: Potential ecological risk index of the heavy metals in soils.

Sampling time	Projects	Comprehensive potential ecological risk index RI	Potential ecological hazard index E_i							
			Mn	Cu	Cr	As	Cd	Ni	Pb	Zn
High water period	Minimum value	31.00	0.67	1.17	0.21	1.08	8.33	0.90	6.60	0.72
	Maximum value	129.83	5.57	14.73	7.86	15.14	90.00	11.30	55.22	1.64
	Average	77.94	1.88	6.24	1.76	3.39	45.28	5.31	13.60	1.11
Withered water period	Minimum value	62.97	0.52	0.38	0.29	1.15	37.67	0.83	5.22	0.56
	Maximum value	203.60	4.57	13.74	4.11	13.79	180.33	9.80	31.30	1.65
	Average	118.15	1.94	5.43	1.58	3.52	86.23	4.85	13.75	1.05

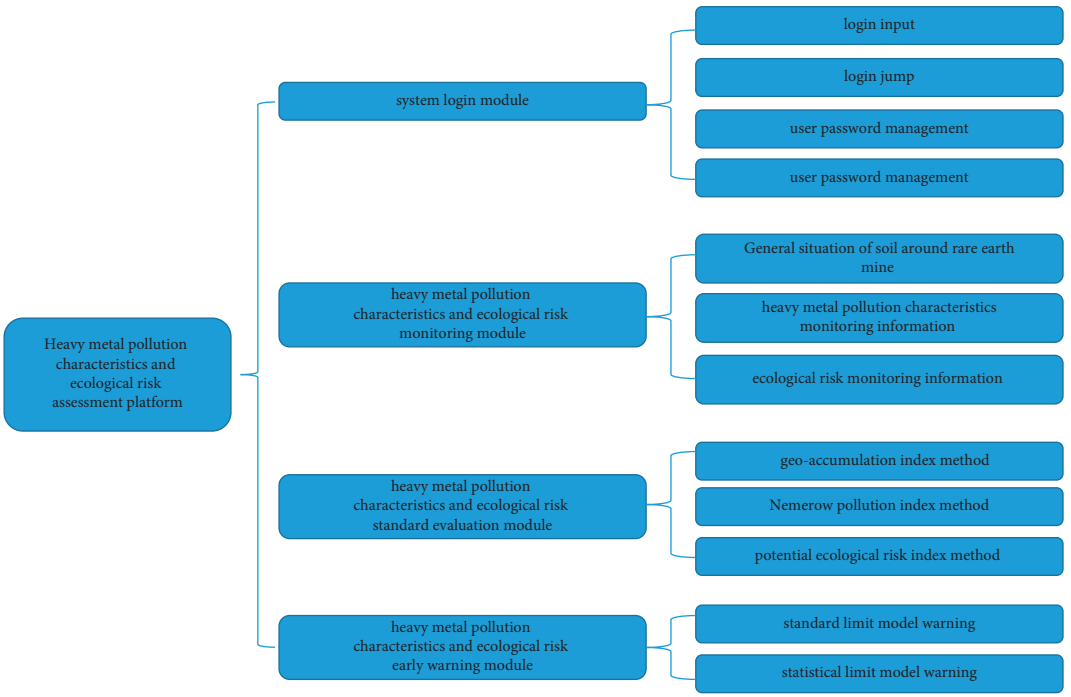

Figure 5: Functional modules of the platform.

framework solves the complexity of enterprise development and makes J2EE development easier to use.

MyBatis is an encapsulation of JDBC, which makes the underlying operation of the database transparent. It only needs to provide SQL statements, avoiding manually setting parameters and obtaining result sets. MyBatis supports customized SQL, stored procedures, and advanced mapping. MyBatis uses XML to configure and map files, builds SqlSessionFactory instances, obtains SqlSessions, and executes mapped SQL statements. Its functions are divided into API interface layer, data responsibility layer, and basic support layer.

MVC, namely, model view controller, is a framework that integrates model, view, and controller into independent programs. It provides loose coupling between these three elements, reduces code repeatability, simplifies grouping development, and provides a clear logical framework for software design and development.

(1) M refers to the model side, including DAO classes and databases. DAO accesses the database to manipulate data and abstract business logic into a model.

(2) V refers to the visual layer, which visualizes the data model and renders it in the user interface.

(3) C is the controller, which can update the model to the view layer. It is not only the link between the model layer and the view layer but also the bridge between the user and the system. It receives and processes the

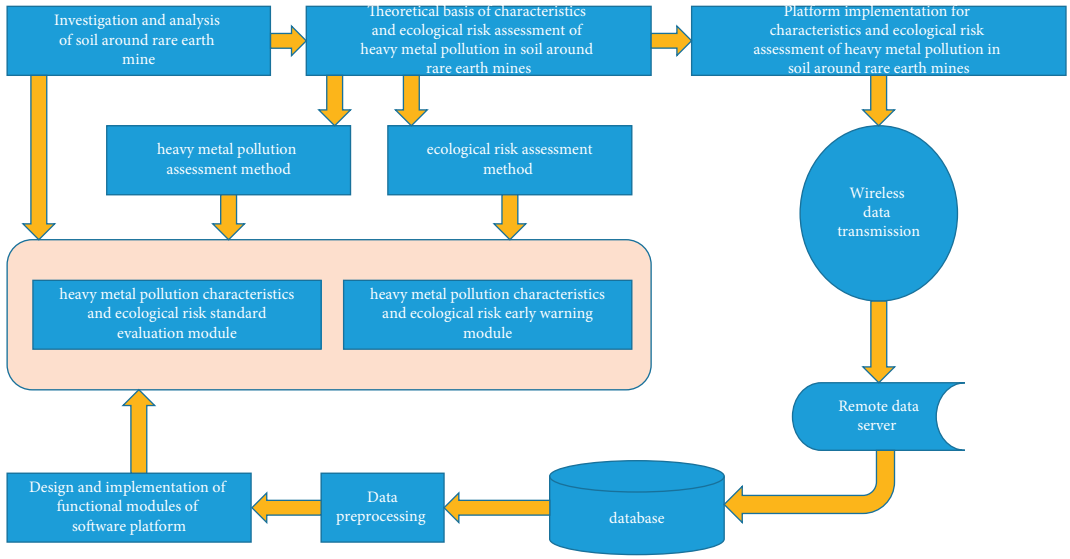

Figure 6: The overall structure of the platform.

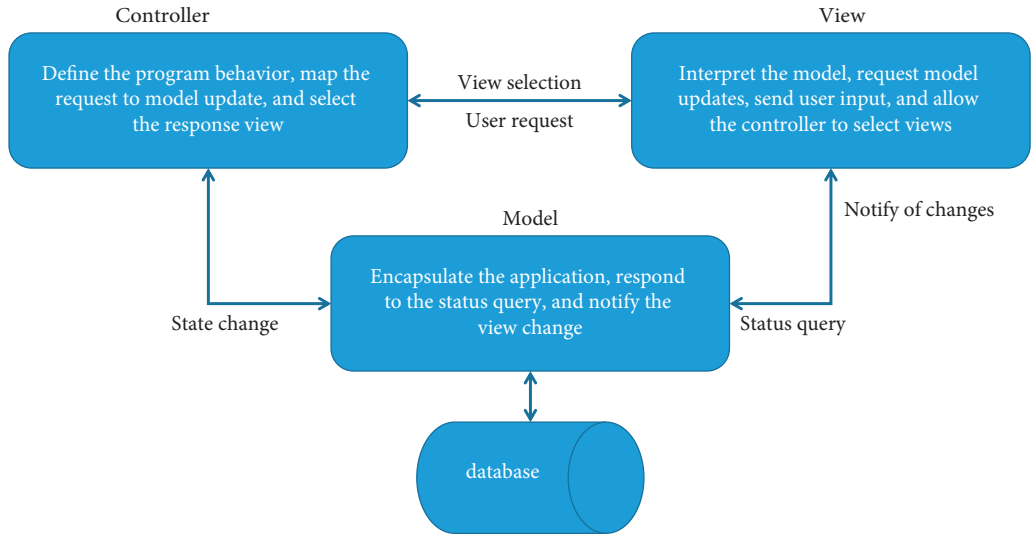

Figure 7: MVC component relationship.

response to the user's request, calls the DAO method to obtain the required data from the database, processes the library, and then returns to JSP for display in the view layer.

As shown in Figure 7, the basic idea is that the controller receives the user's request, decides how to process it, calls the data interface in the model layer through the DAO, processes and modifies the data, and sends it to the view layer for presentation. When the data of the model layer changes, it will be transmitted to the view layer in the form of time notification, and the view layer will modify the user interface accordingly.

4.3. Database Design. The database can be regarded as an electronic warehouse, which stores an organized and shareable data set for a long time in a certain way. Users can add, delete, modify, and query the data in the file. This study uses relational database and SQL Server for database operation. By combining the required data, it is determined that the monitoring data information table, heavy metal pollution characteristics and ecological risk assessment table, and heavy metal pollution characteristics and ecological risk early warning table need to be established, and the field name, identifier, type and length, null value, and primary key of each table are designed and compiled as shown in Tables 8–10.

Table 8: Monitoring data information table structure.

Serial number	Field name	Identifier	Type and length	Primary key
1	Soil area number	JC_CD	Varchar (40)	Y
2	Soil area name	JC_NM	Varchar (40)	
3	Initial section	JC_QS	Varchar (40)	
4	Termination section	JC_ZZ	Varchar (40)	
5	Soil target	JC_MB	Int	
6	Time	JC_TM	Date time	
7	First monitoring value	JCZ_1	Decimal	
8	Second monitoring value	JCZ_2	Decimal	

Table 9: Heavy metal pollution characteristics and ecological risk assessment table structure.

Serial number	Field name	Identifier	Type and length	Primary key
1	Soil area number	JC_CD	Varchar (40)	Y
2	Soil area name	JC_NM	Varchar (40)	
3	Soil target	JC_MB	Int	
4	Time	JC_TM	Date time	
5	First monitoring value	JCZ_1	Decimal	
6	Second monitoring value	JCZ_2	Decimal	
7	Assessment level	KH_DJ	Int	
8	Assessment index	KH_ZB	Char	
9	Assessment method	KH_FF	Char	
10	Geoaccumulation index method	KH_GIM	Char	
11	Nemerow pollution index method	KH_NPIM	Char	
12	Potential ecological risk index method	KH_PERIM	Char	
13	Compliance rate	KH_DBL	Decimal	

Table 10: Heavy metal pollution characteristics and ecological risk early warning table structure.

Serial number	Field name	Identifier	Type and length	Primary key
1	Soil area number	JC_CD	Varchar (40)	Y
2	Soil area name	JC_NM	Varchar (40)	
3	Over standard warning index	YJ_CB	Char	
4	Excess multiple	YJ_BS	Varchar (40)	
5	Time	JC_TM	Date time	

5. Conclusion

The main findings of this study include the following:

(1) The contents of heavy metals Cr, Cu, Ni, Zn, and As in the soils of the study area were all lower than the risk control screening values for agricultural land, 50.68% of the sampling sites exceeded the risk control screening values for agricultural land soils for the heavy metal Pb, and 20.55% of the sampling sites exceeded the risk control screening values for agricultural land soils for Cd during the withered period. The maximum value of Mn content was 5.57 times higher than the soil background value, and its contaminated sites were mainly located in the sampling area of the mine open pit, indicating that the mining of rare-earth mines has caused a certain degree of enrichment of heavy metals in the soil.

(2) The results of the geoaccumulation index assessment showed that the accumulation of heavy metals Mn, Cu, Cr, As, Cd, Ni, Pb, and Zn in the soils of the study area occurred to varying degrees, and the geoaccumulation indices of these eight heavy metals were, from largest to smallest, Pb > Mn > Zn > Cd > Cu > Ni > Cr > As, with the accumulation of Pb and Mn being the most serious.

(3) The assessment results of the Nemerow pollution index showed that 26.03% and 28.77% of the sampling points in the study area were lightly polluted during the high water period and the withered water period, respectively, with one sampling point being moderately polluted during the withered water period. The Nemerow pollution index values for Pb, Cd, Cu, Cr, Zn, Ni, and As were 2.11, 0.97, 0.66, 0.51, 0.40, 0.34, and 0.23 respectively, with Pb being moderately polluted, Cd and Cu being in the alert

state, and the other four heavy metals being in the clean state.

(4) The results of the assessment of the potential ecological risk index showed that only the heavy metal Cd was moderately contaminated in the soil of the study area, while the other seven heavy metals such as Cu, Cr, and As were all lightly contaminated.

(5) The accumulation of heavy metals Pb and Mn in the soils of the study area was relatively serious, and there was also heavy metal Cd pollution during the withered water period, but the toxicity coefficients of Pb and Mn were small, and their potential ecological risks were small, while the potential ecological risks of Cd were large. The authors suggest that land use planning in the study area should take full account of the contamination of heavy metals in the soil and take a certain degree of antipollution measures, vigorously advocate clean mining, gradually reduce the damage to the ecological environment caused by traditional mining techniques, and emphasize the development of the concept of "treatment and recovery while mining." At the same time, the local climate conditions are combined with the selection of suitable plant or microbial species to explore the promotion of bioremediation of the soil, advocating the concept of mine ecological restoration of green mines and green restoration.

The software platform planned and developed by this research institute can provide practical support for the application of the theoretical methods of this research.

Data Availability

The data set can be accessed upon request.

Conflicts of Interest

The authors declare that there are no conflicts of interest.

Acknowledgments

This work was supported by Geological Survey and Monitoring Project: national geological environment monitoring and prediction (no. 121201014000150003).

References

[1] S. Shi, J. Bai, and Y. U. Yang, "Heavy metal migration and soil pollution assessment in an intensive mining area in the southwest China," *Metal Mine Metal Mine*, vol. 2, pp. 194–200, 2022.

[2] S. Wei, Q. Zhou, and X. Wang, "Studies on the characteristics of heavy metal hyperaccumulation of weeds in farmland," *China Environmental Science*, vol. 2, no. 1, pp. 33–39, 2004.

[3] T. W. Zhou, "Research progress of heavy metal pollution in farmland soil and its control strategies in China," *China Southern Agricultural Machinery*, vol. 52, no. 10, pp. 33–35, 2021.

[4] Z. Xin, "Study on harm and technology of heavy metal pollution in soil," *China Resources Comprehensive Utilization*, vol. 37, no. 11, pp. 89-90, 2019.

[5] L. P. Ju, "Comparative study on soil effects of different rare earth mining methods," *Haikou: Chinese Society of Environmental Science*, vol. 4, 2016.

[6] C. G. Luo, X. P. Luo, J. Su, C. F. Chen, and D. X. Han, "Environmental problem and treatment measures in ionic - type rare earth mine," *Metal Mine*, no. 6, pp. 91–96, 2014.

[7] X. Z. Tang, M. N. Li, and D. Yang, "Application and prospect of in-situ leaching mining method in ion-type rare earth ore," *Hunan Nonferrous Metals*, vol. 4, pp. 5–7, 1998.

[8] S. J. Goldstein and S. B. Jacobsen, "Rare earth elements in river waters," *Earth and Planetary Science Letters*, vol. 89, no. 1, pp. 35–47, 1988.

[9] Y. J. Wang, T. L. Wu, D. M. Zhou, and H. M. Chen, "Advances in soil heavy metal pollution evaluation based on bibliometrics analysis," *Journal of Agro-Environment Science*, vol. 36, no. 12, pp. 2365–2378, 2017.

[10] Y. C. Zhou, H. L. Sun, X. G. Chen, L. Zhou, and S. S. Wu, "Characteristics and ecological risk assessment of heavy metal pollution in surface soil of Yining in Oasis city," *Journal of Arid Land Resources & Environment*, vol. 33, no. 2, pp. 127–133, 2019.

[11] M. Meng, L. S. Yang, B. G. Wei, H. R. Li, and J. P. Yu, "Contamination assessment and spatial distribution of heavy metals in greenhouse soils in China," *Journal of Ecology and Rural Environment*, vol. 34, no. 11, pp. 1019–1026, 2018.

[12] F. Yu, W. Wang, Y. Yu, and D. Wang, "Distribution characteristics and ecological risk assessment of heavy metals in soils from Jiulong Li-Be mining area, western Sichuan province, China," *Rock and Mineral Analysis*, vol. 40, no. 03, pp. 408–424, 2021.

[13] S. G. Wei, L. Q. Zheng, J. Zhang, F. Zhang, and J. Song, "Pollution characteristics of heavy metal in the soil of an abandoned pesticide factory and remediation effect of calcination," *Environmental Engineering*, vol. 1, 2021, http://kns.cnki.net/kcms/detail/11.2097.X.20210810.1405.004.html.

[14] Y. X. Hu, H. Su, B. Zhang, and Y. Zhang, "Soil heavy metal pollution and its evaluation methods: a review," *Jiangsu Agricultural Sciences*, vol. 48, no. 17, pp. 33–39.

[15] S. Zhang, *Study on Environmental Assessment of Water and Soil in Rare Earth Mining Area in Southern Jiangxi*, China University of Geosciences, Beijing, China, 2020.

[16] H. XV, P. Zheng, and Y. Zhao, "Study on development and review of ecological compensation in mineral development," *Journal of East China University of Technology: Social Science*, vol. 1, pp. 7–10, 2014.

[17] J. Song, C. C. XV, Y. X. Luo, and Y. Y. Yang, "Analysis of environmental risk and spatial distribution characteristics of heavy metal in soils of Zhundong coal area," *Jiangsu Agriculture Sciences*, vol. 47, no. 24, pp. 241–247, 2019.

[18] B. Y. Chen, "Assessment of heavy metal pollution and method comparison: a case study of the shallow-sea sediments in Fujian," *Geology and Rexources*, vol. 3, pp. 213–218+228, 2008.

[19] T. Wang and G. Wang, "Environmental geochemistry characteristics of heavy metals in sediment of Kuncheng Lake," *Journal of Soil and Water Conservation*, vol. 1, pp. 109–122, 2008.

[20] Y. H. Cui, W. Cui, Q. J. Meng, W. Li, and Q. Feng, "Heavy metal pollution and ecological risk assessment in Haoping stone coal mine area of Shanxi province," *Conversation and Utilization of Mineral Resources*, vol. 41, no. 2, pp. 157–162, 2021.

[21] J. L. Xie, J. F. Zhang, Y. B. Liu, and J. N. Jiang, "Heavy metal pollution and environmental assessment in the soil of the rare earth associated mining area in Bayan Obo," *Science of soil and Water Conservation*, vol. 18, no. 2, pp. 92–101, 2020.

[22] W. Chen, L. L. Xiang, and Z. W. He, "Evaluation of heavy metal pollution in soil of xuejiping-chundu copper mining area," *Journal of Hebei Normal University (Philosophy and Social Sciences Edition)*, vol. 43, no. 2, p. 163, 2019.

[23] W. T. Si, J. Dai, X. B. Zhao, and J. M. Liu, "Ecololgical risk assessment of heavy metals pollution in the rare tailings wetlands soils," *Yellow River*, vol. 39, no. 8, p. 71, 2017.

[24] S. T. Yao, Y. Q. Li, D. L. Wang, and D. L. Nong, "Distribution and pollution assessment of soil heavy metals in Wanzhaung gold mine area in Beijing," *China Mining Magazine*, vol. 27, no. S2, pp. 59–65, 2018.

[25] F. Xiao, S. M. Fu, and D. F. Wang, "Evaluation of heavy metal pollution around a mining area in Northern Guangdong," in *Proceedings of the 19th Conference of Chinese Society of Environmental Science*, pp. 122–139, Kunming, China, 2013.

[26] L. Hakanson, "An ecological risk index for aquatic pollution control.a sedimentological approach," *Water Research*, vol. 14, no. 8, pp. 975–1001, 1980.

[27] W. Guo, X. Liu, Z. Liu, and G. Li, "Pollution and potential ecological risk evaluation of heavy metals in the sediments around dongjiang harbor, tianjin," *Procedia Environmental Sciences*, vol. 2, no. 1, pp. 729–736, 2010.

[28] E. Singovszka, M. Balintova, and M. Holub, "Assesment of heavy metals concentration in sediments by potential ecological risk index," *Inzynieria Mineralna*, vol. 15, no. 2, pp. 137–140, 2014.

[29] Z. Q. Xv, S. J. Ni, X. G. Tuo, and C. J. Zhang, "Calculation of heavy metals' toxicity coefficient in the evaluation of potential ecological risk index," *Environmental Science & Technology*, vol. 31, no. 2, pp. 112–115, 2008.

[30] J. L. Chen, R. Y. Li, X. J. Xie et al., "[Distribution characteristics and pollution evaluation of heavy metals in greenbelt soils of nanjing city]," *Huan jing ke xue= Huanjing kexue*, vol. 42, no. 2, pp. 909–916, 2021.

[31] S. Zhang, Y. Yu, D. H. Wang, and H. Zhang, "Forms distribution of heavy metals and their ecological risk evaluation in soils of ion adsorption type in the rare earth mining area of southern Jiangxi, China," *Rock and Mineral Analysis*, vol. 39, no. 5, pp. 726–738, 2020.

[32] H. R. Zhang, *Study on the spatial distribution and migration law of heavy metals in the soil around typical coal gangue accumulation*, Xi'an University of Science and Techology, Xi'an, China, 2020.

[33] China National Environmental Monitoring Centre, "Background values of soil elements in China," *China Environmental Science*, vol. 1, no. 9, p. 9, Beijing, China, 1990.

[34] X. M. Chen, B. H. Zhu, W. Yang, and H. Ji, "Sources, spatial distribution and contamination assessments of heavy metals in gold mine area soils of Miyun Reservoir upstream, Beijing, China," *Environmental Chemistry*, vol. 34, no. 12, pp. 2248–2256, 2015.

[35] A. B. D. J. P. E. Abdusalam, H. W. Wang, S. T. Yang, and X. Liu, "Pollution characteristics and source analysis of soil heavy metals in east Junggar region," *China Mining Magazine*, vol. 28, no. 11, pp. 168–174, 2019.

[36] X. L. Zhong, S. L. Zhou, J. T. Li, and H. H. Liu, "Spatial variability of soil heavy metals contamination in the Yangtze River delta-a case study of TAICANG city in Jiangsu province," *Acta Pedologica Sinica*, vol. 1, pp. 33–40, 2007.

[37] J. Y. Jia, X. F. Liu, and Y. G. Zhao, "Spatial distribution characteristics and assessment of heavy metal pollution in farmland soils in the lower reaches of Fenhe river basin," *Journal of Arid Land Resources & Environment*, vol. 35, no. 8, pp. 132–137, 2021.

[38] T. Tian, T. Yang, X. M. Zou, and C. Chunle, "Heavy metals in farmland surrounding the sanming steel plant in western Fujian: pollution characteristics and risk assessment," *Journal of Agriculture (South Perth)*, vol. 11, no. 6, pp. 42–46+95, 2021.

[39] S. Ye, J. Zhang, Li Pan, X. Yang, and Y. Yu, "Ecological environmental cost accounting of mining area based on the green mine," *A Case from a Mining Area in the Metal Mine*, no. 4, pp. 168–174, 2019.

[40] F. G. Liu and C. W. Luo, "Service-oriented software testing platform," in *Proceedings of the 7th IFIP International Conference on E-Business, e-Service, and e-Society*, Wuhan, China, October 2012.

[41] V. Berenz and S. Schaal, "The playful software platform: reactive programming for orchestrating robotic behavior," *IEEE Robotics and Automation Magazine*, vol. 25, no. 3, pp. 49–60, Sep 2018.

[42] L. Li, B. Lei, and C. Mao, "Digital twin in smart manufacturing," *Journal of Industrial Information Integration*, vol. 26, no. 9, Article ID 100289, 2022.

[43] E. V. Biryal'tsev, M. R. Galimov, and A. M. Elizarov, "Software platform for mass supercomputing," *Doklady Mathematics*, vol. 95, no. 2, pp. 185–189, 2017.

[44] L. Li, T. Qu, Y. Liu et al., "Sustainability assessment of intelligent manufacturing supported by digital twin," *IEEE Access*, vol. 8, Article ID 174988, 2020.

[45] S. Jansen, M. Cusumano, and K. M. Popp, "Managing software platforms and ecosystems," *IEEE SOFTWARE*, vol. 36, no. 3, pp. 17–21, 2019.

[46] C. Bădică, Z. Budimac, H. D. Burkhard, and M. Ivanovic, "Software agents: languages, tools, platforms," *Computer Science and Information Systems*, vol. 8, no. 2, pp. 255–298, 2011.

[47] L. Li and C. Mao, "Big data supported PSS evaluation decision in service-oriented manufacturing," *IEEE Access*, vol. 8, no. 99, p. 1, 2020.

Hindawi
Scientific Programming
Volume 2023, Article ID 9891427, 1 page
https://doi.org/10.1155/2023/9891427

Retraction

Retracted: Analysis on the Artistic Presentation Effect of 3D Rendering Ink Painting Based on the Evaluation of Deep Learning Model

Scientific Programming

Received 18 July 2023; Accepted 18 July 2023; Published 19 July 2023

This article has been retracted by Hindawi following an investigation undertaken by the publisher [1]. This investigation has uncovered evidence of one or more of the following indicators of systematic manipulation of the publication process:

(1) Discrepancies in scope
(2) Discrepancies in the description of the research reported
(3) Discrepancies between the availability of data and the research described
(4) Inappropriate citations
(5) Incoherent, meaningless and/or irrelevant content included in the article
(6) Peer-review manipulation

The presence of these indicators undermines our confidence in the integrity of the article's content and we cannot, therefore, vouch for its reliability. Please note that this notice is intended solely to alert readers that the content of this article is unreliable. We have not investigated whether authors were aware of or involved in the systematic manipulation of the publication process.

Wiley and Hindawi regrets that the usual quality checks did not identify these issues before publication and have since put additional measures in place to safeguard research integrity.

We wish to credit our own Research Integrity and Research Publishing teams and anonymous and named external researchers and research integrity experts for contributing to this investigation.

The corresponding author, as the representative of all authors, has been given the opportunity to register their agreement or disagreement to this retraction. We have kept a record of any response received.

References

[1] Y. Pan, "Analysis on the Artistic Presentation Effect of 3D Rendering Ink Painting Based on the Evaluation of Deep Learning Model," *Scientific Programming*, vol. 2022, Article ID 9259389, 12 pages, 2022.

Hindawi
Scientific Programming
Volume 2022, Article ID 9259389, 12 pages
https://doi.org/10.1155/2022/9259389

Research Article

Analysis on the Artistic Presentation Effect of 3D Rendering Ink Painting Based on the Evaluation of Deep Learning Model

Yue Pan

School of Art, Southeast University, Nanjing 211189, Jiangsu, China

Correspondence should be addressed to Yue Pan; 230169274@seu.edu.cn

Received 30 March 2022; Revised 28 April 2022; Accepted 10 May 2022; Published 29 May 2022

Academic Editor: Lianhui Li

At present, with the popularity of multimedia, people's appreciation and interest in ink painting art have been deepened. In the research of art works, this paper proposes a rendering method of three-dimensional ink painting effect based on deep learning model, which can simulate the painting skills of ink painting in terms of intensity and distance. Specifically, first construct a two-dimensional ink texture, then map the horizontal component of the texture using the contour information of the model, and finally adjust the ink tone by controlling the coordinates of the vertical component of the texture through the attribute function. Linear attribute function, quadratic attribute function, and attribute function with light source factor are used for simulation. The results show that this method can be used for ink and wash simulation of three-dimensional scene, making the image more layered and more in line with the artist's actual technology.

1. Introduction

The use of computer programs to simulate hand-made artworks is one of the key goals of nonrealistic drawing techniques. To date, researchers in the field of computer graphics have developed many nonrealistic algorithms to simulate Western artworks, such as oil paintings, watercolours, drawings, and prints.

In the last decade, many scholars in China have also started to work on nonrealistic algorithms for traditional Chinese ink painting styles. One approach is to extract the contour lines of the model [1, 2], then stylize the contour lines [3], and then control the stylized parameters to simulate the drawing of the brush. This approach is more complex to implement, and the extraction of contour lines in the graphics space and the visible judgement of stylisation can affect the real-time rendering speed. The second method is based on the traditional cartoon rendering algorithm [4, 5], which controls the ink texture mapping by designing a specific lighting function to achieve the ink style rendering effect, which is simple, realistic, and has good real-time performance.

In 1997, Curtis pioneered the use of Kubelka-Munk (KM) theory in the simulation of watercolours [6]. In that paper, the user selects the reflection values of the pigments against a black and white background so that the K and S values can be calculated, and the final colour output is then calculate using the superimposition and mixing formulae of the KM colour model. In 2003, Rudolf used the same theory for the simulation of crayon paintings based on Curtis, who used KM theory to solve the problems that arose when composing two layers of images. 2004 saw Yamamoto use the KM theory for the simulation of watercolours. In 2004, Yamamoto also used KM colour theory in his study of the conversion of digital images into pencil drawings, but it allowed for user-defined colour transparency, i.e., assuming that the value of the colour parameter would not change on a white background, but setting a parameter to a certain scale on a black background, thus controlling the transparency of the colour. The above are all simulation of Western painting, in the case of ink painting [7], Suarez [8] tried to introduce the KM colour model during the final colouring.

The study of diffusion of different pigments was presented by [9], but did not really address the diffusion and superimposition effects of different pigments. Only a single KM colour model was used to simulate the colour of different pigments. Since there is no substantial improvement

of the diffusion model, the simulation of the final effect cannot be satisfactorily obtained.

The literature [10] gives an interactive 3D virtual brush model that uses subdivision surfaces around a skeleton based on a spring system to represent the geometry of the brush; this method is not suitable for generating the bifurcation effect of the brush. [11] proposed calculating the deformation of the brush hair based on the physical properties of the springs based on the theory of elasticity, which is difficult to achieve in real time when the number of hair is large. [12] proposed a model based on the bristle entity, which simulates the bifurcation using replication parameters to generate bristles with the same structure resulting in a lack of close correlation between the bristles and an unrealistic shape of the bifurcated bristles. The quill model constructed by [13] constrains the spring deformation by means of energy minimisation. This method is only applicable to small-scale deformations and works better for simulating wet brushes without bifurcation.

The first paper model of 2D fibre structure was proposed by [14] that plane was proposed to be divided into small regions, and a large number of curves with random orientations were distributed within each region to simulate fibre bundles. Then [15–17] and others proposed their own paper models. This type of paper model achieves better results to some extent, but there are still several fundamental problems: first, it does not consider the effect of different types of rice paper on the diffusion effect and is an uncontrollable paper model that lacks scalability; second, it also does not take into account how to represent the paper texture.

In Pingping [18], based on a summary of previous work, the smallest unit of the paper plane is partitioned into paper cells (one pixel corresponds to multiple paper cells), while multiple adjacent paper cells containing paper fibres form fibre clusters, which are connected by fibre bundles, and the transport of ink and water takes place between the fibre clusters through the fibre bundles.

The first one-dimensional brush depiction models were proposed by [19], where a brush is defined as a one-dimensional array of brush hairs; in a method based on the contour of a brush path [20], the path is described as a number of continuous Bezier or B-spline curves. [21] modeled the brush as consisting of a number of bristles randomly distributed over a circular area, with each bristles drawing a separate curve as the brush moves, and all the curves together forming a single stroke. [22] illustrates the principle of the generation of the black edge phenomenon in ink painting. [23] proposed an automatic cell-based computational model to simulate the movement of water and ink particles. [24] used a fluctuation rule to represent the flow of ink particles. [25] proposed a water absorption force balance algorithm to calculate the diffusion amount of adjacent paper cells. [5] proposed a pseudo-Brownian motion method based on a particle system to simulate the diffusion process, taking into account the effects of water absorption, humidity, evaporation rate, and background texture. [26] complemented the algorithm by proposing an exchange threshold value as an exchange condition and an exchange rate to control the amount of exchange. However both values are static in the diffusion process. [27] used a local equilibrium model and a three-layer paper model to simulate the effect of ink diffusion. This method can simulate simple stacking effects, and Young gave a graph of the stacking effect. [28] proposed a diffusion model with concentration difference as the driving force for diffusion, but did not present a theoretical basis, [29] proposed to simulate the diffusion of ink particles with Fick's first law of steady-state diffusion [30], but in reality the diffusion process is a nonsteady-state process, [31, 32] proposed to use a fluid based on LBE (Lattice Boltzmann Equation) to simulate ink diffusion. The diffusion model is easy to parallelize, has good real-time performance, and can produce very realistic ink and wash wet brush painting effects. However, by treating both water and ink particles as equally sized particles, the particle diffusion model is not a true particularised model, but simply a diffusion model under the rule of concentration correspondence. This method does not allow for differences in the diffusion of multiple pigments.

As can be seen, KM colour models have been chosen to solve the problem of colour setting, both in colour simulation for Western painting and in colour setting for ink painting. The problem of colour calculation is complicated by the diffusion of pigments in ink painting, especially when multiple pigments are diffused together. How to apply the KM colour model's superimposition and mixing formulae through layering based on the characteristics of diffusion is one of the main focuses of this paper. Based on the second type of method, this paper proposes an ink rendering algorithm based on two-dimensional texture mapping, which can simulate the traditional ink painting technique of intensity and distance. This paper uses attribute functions to control the huge changes in the vertical component of ink textures to simulate the shadow and distance techniques of ink painting. Compared with the existing algorithms, the 2D texture mapping of the attribute function provides richer rendering effects. In the ink rendering of the 3D scene, the effects of light and shade and distance are added, which makes the image more layered and closer to the painter's painting skills.

2. Principle of the Algorithm

The main objective of the algorithm in this paper is to achieve a simulation of the intensity and distance technique while obtaining a traditional ink and wash rendering. The difference from traditional 3D ink rendering is the inclusion of the processing and use of 3D depth information. By constructing an attribute function with the 3D depth information as the independent variable for texture mapping, and then controlling the colour tones of the textures to express the changes in the 3D depth information, the effect can be obtained in terms of the intensity of the ink strokes in the near distance and the lightness of the strokes in the far distance. This idea is based on traditional cartoon rendering techniques [6] and the X-TOON system [7].

Bella developed the X-TOON system based on the traditional cartoon rendering algorithm, which extends the

1D cartoon texture to a 2D texture, using the vertical component of the texture to express the colour tone changes and then controlling the texture mapping to obtain a richer cartoon effect.

This paper uses the X-TOON systematic approach to produce two-dimensional ink textures. The hue of the horizontal component of the texture (first dimension) is associated with the model contour edge information, and the texture coordinates are controlled by calculating N-V, where N is the unit normal vector of the spatial surface and V is the unit vector of view. The vertical component of the texture (second dimension) is associated with the colour hue (represented in the article by the attribute function D), and the texture coordinates are controlled by the attribute function D. Each value in the vertical component is associated with its own 1D ink texture, so the whole 2D texture can be seen as a superposition of 1D ink textures of progressively increasing hue. The ink texture generate is shown in Figure 1.

2.1. Chafing Renderer. There is a wide variety of shops in ink and wash work, and the differences in expression between the various crops are large, while the painter is more spontaneous in using this technique it is not possible to propose an algorithm for each of these techniques. It is therefore not possible to propose an algorithm for each chap. The texture map is then drawn based on a two-step texture mapping method.

The regularised chunking set has been obtained after chunking feature analysis $S_k^{\text{texture}} = \{s_i \mid i = 1, 2, 3, \ldots\}$ 1itexturek first determines the number of interpolated textures. Multiple textures are now connected by line blending [11] to form a large mapped texture map. Item N, let chapped textures μ_A and μ_B, is $|N = |\mu_A - \mu_B|/k$ averaged over the H information. The smaller the coefficient, the greater the degree of variation between individual chops. Then k is used to control the degree of jump in the transition between the chapped textures; the larger k is. The smaller N is, and the greater the degree of variation between the individual chappings. The text uses $k = 5$. The interpolated image between A and B is then I_{between}.

$$I_{\text{between}} = \alpha \cdot A + (1 - \alpha).\, B, \alpha = 1, \frac{N-1}{N}, \frac{N-2}{N}, \ldots, 0. \quad (1)$$

Figure 2 shows the final composite mapping texture after the difference.

2.2. S-O Two-Step Texture Mapping. To optimise the rendering results, the S-O two-step texture mapping method is used to chisel the model. This method was proposed by [13]. The basic idea is that instead of directly texturing the 3D model surface, an intermediate transition surface is introduced and the mapping process is decomposed into a two-step operation: the first step is the mapping from the textured plane to the transition surface, i.e., $T(u, v) \longrightarrow S(x', y', z')$, which becomes the S mapping; the first step is the mapping from the transition surface to the 3D model surface, i.e., $S(x', y', z') \longrightarrow O(x, y, z)$, which becomes the O mapping. The transition surfaces in S mapping are usually simple 3D surfaces such as spheres, cylinders, and cubes, as shown in Figure 3.

There are 12 combinations of S-mapping and O-mapping. In this paper, we take a spherical surface as the transition surface for S-mapping and modify the third O-mapping method for chaffing.

The sphere of the transition surface is divided into two parts symmetrical along the x-plane, and the texture is mapped to the two parts symmetrical to the sphere using a mapping algorithm with an area-equivalence constraint [14]. As in Figure 4, gave a 2D texture coordinate system v, the centre of the texture plane coincides with the origin of the coordinate system at any point $p(u, v)$, which can be expressed in polar coordinates (p, α). Given a three-dimensional coordinate system x, y, z, the centre of a spherical planet of radius R coincides with the origin, and any point Q (x, y, x) on the spherical plane is expressed in spherical coordinates as (R, y). Due to the symmetry, the sphere can be divided into two hemispheres by the xy plane, and the mapping method is the same in both hemispheres.

Let a point P on the texture plane be mapped to a point on the hemisphere. In order to effectively reduce texture distortion, an area-equivalence constraint Q [4] is used here to construct the mapping relationship between the two points. The area equiproportionality constraint, i.e., the ratio of the area of the texture plane to the area of the corresponding mapped area on the sphere is transversely equal to the constant K:

$$K = \frac{\pi \cdot \rho^2}{2\pi R^2 (1 - \cos\, \phi)}. \quad (2)$$

This gives $\rho = 2\pi R^2 (1 - \cos\, \phi)$ another $\alpha = \theta$. The texture coordinates can be calculated as

$$\begin{cases} u = \rho \cdot \cos\, \alpha = \sqrt{2KR^2 (1 - \cos\, \phi)} \cdot \cos\, \theta, \\ v = \rho \cdot \sin\, \alpha = \sqrt{2KR^2 (1 - \cos\, \phi)} \cdot \sin\, \theta. \end{cases} \quad (3)$$

When $10 \le \phi \le \pi/2$, the mapping results in the upper hemisphere; when $\pi/2 \le \phi \le \pi$, the mapping results in the lower hemisphere.

Since the origin of the texture coordinates is generally located in the lower left corner. The above equation is modified:

$$\begin{cases} u = \rho \cdot \cos\, \alpha = 0.5 + \sqrt{2KR^2 (1 - \cos\, \phi)} \cdot \cos\, \theta, \\ v = \rho \cdot \sin\, \alpha = 0.5 + \sqrt{2KR^2 (1 - \cos\, \phi)} \cdot \sin\, \theta. \end{cases} \quad (4)$$

Experimentally, when using a mapped texture map of 512×512 size, take $R = 1.0$, $K = 0.12$.

The third mapping method is used for the O mapping, i.e., the texture at the vertex V (x, y, z) on the surface of the model, taking the ray formed by the line from the centre of the object to this vertex, and the texture at the intersection with the transition surface $V'(x', y', z')$.

The centre point of a model is usually complex, the algorithm for finding the centre point is as follows: let the

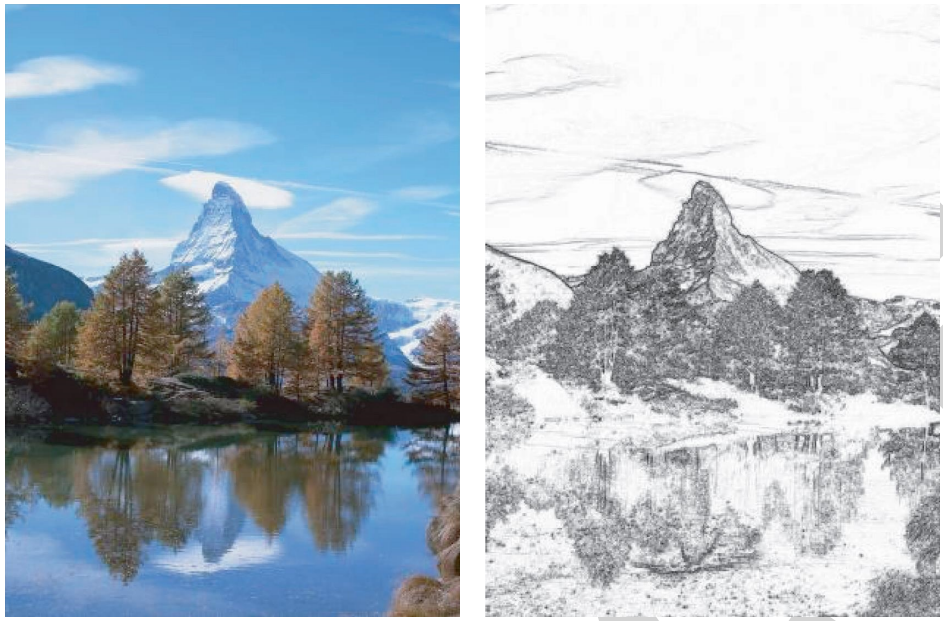

(a) (b)

Figure 1: Ink painting with two texture.

(a) (b)

Figure 2: Synthetic results after image interpolation. (a) Lotus leaf chap and (b) phi chap.

coordinates of a vertex in the xyz three-dimensional coordinate space be $P(v_x, v_y, v_z)$, calculate the sum of all the vertex coordinate vector values, and then find the average of all the coordinate vectors, then get the location of the object's centre point coordinates $P'(c_x, c_y, c_z)$. By the centre point and a vertex direction vector is $\overrightarrow{PP'} = (v_x - c_x, v_y - c_y, v_z - c_z)$, and then determine it is in the sphere and thus the coordinates of uv are calculated from the above equation.

3. Ink and Watercolor Rendering

The horizontal component of the texture is first mapped using the contour area information to sketch the shape of the model, and then the vertical component of the texture is mapped using the attribute functions to control the colour tone information to achieve the ink and wash rendering effect.

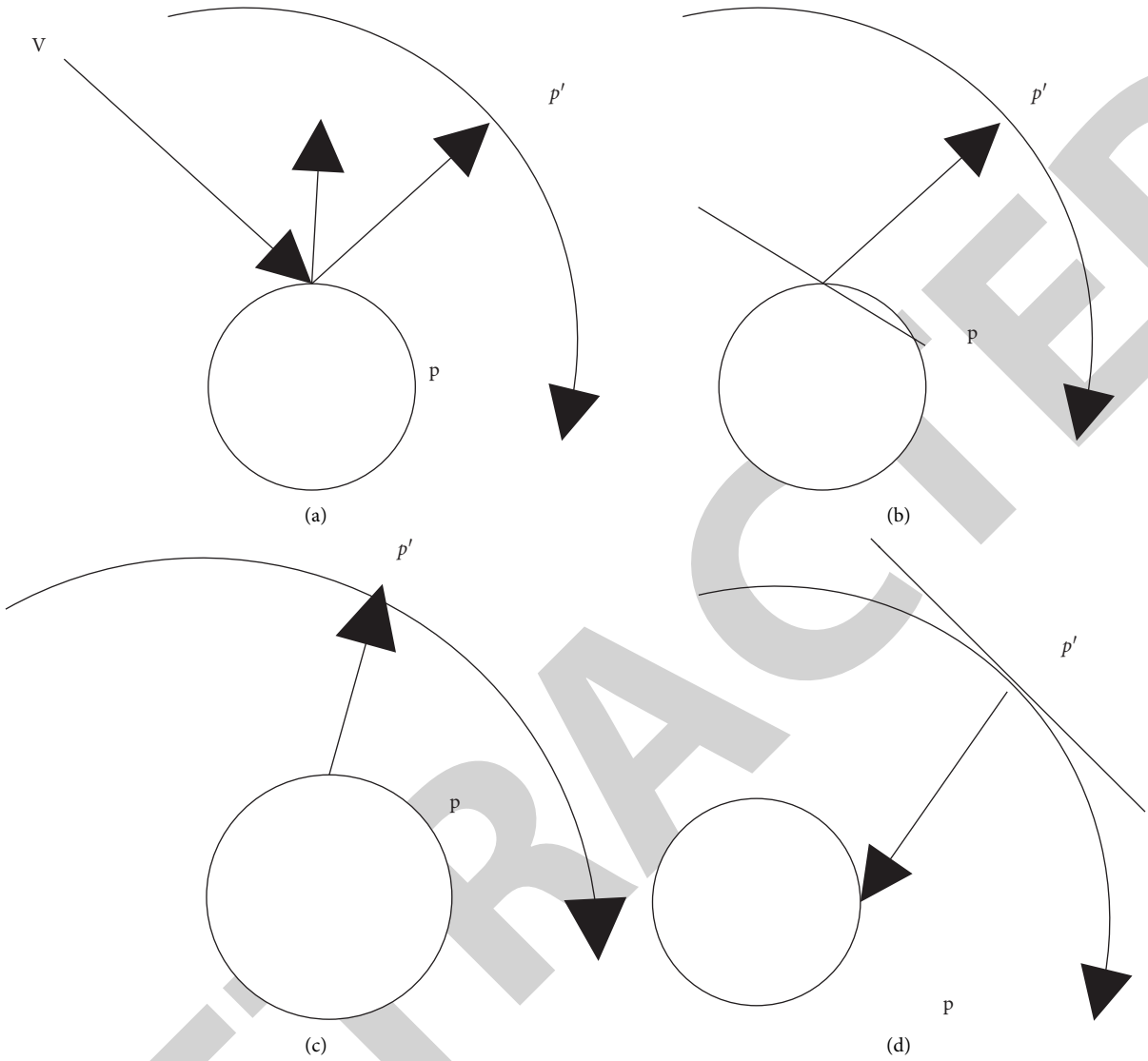

Figure 3: Four ways of O mapping.

3.1. Drawing Model Shapes. In ink painting, when the artist uses ink to paint a scene, it often spreads and soaks through the rice paper, giving the brushstrokes that depict the outline of the object in a certain area. For this reason, instead of extracting single-pixel contour lines from the model, the shape of the model is outlined by mapping the texture around the contour lines to a certain area.

The simulation process is implemented in the OpenGL shading language. In the vertex shading, the absolute value a of the dot product of the unit normal vector and the unit apparently vector is calculated separately for each vertex, and a is passed to the pixel shading as a mutable variable. In the pixel shading, an is used to control the texture coordinates of the horizontal component of the texture. In order to achieve the effect of white space in an ink painting, a threshold λ can be set so that when $a>\lambda$, the pixels of the slice are set to the colour of the white space in the ink texture. The larger value of the threshold λ, the smaller the white area. Figure 5 shows the rendering effect on a fixed vertical component texture coordinates. With λ values of 0.5 in Figure 5(a) and 0.7 in Figure 5(b).

3.2. Control of Colour Tone Information. This step performs the texture mapping of the vertical component and is the heart of the algorithm. In order to simulate the fade technique, elements closer to the point of view are assigned textures with stronger tone. In contrast, elements that are further away from the viewpoint are assigned lighter textures.

To do this, an attribute function is designed for the vertical component texture mapping, starting with the depth information in 3D space as the independent variable. For the selection of depth information, two methods can be used: (i) the Euclidean distance from the 3D point to the viewpoint is used as the depth information (e.g., Figure 6(a)); (ii) the distance from the 3D point to the viewpoint along the focus axis is used as the depth information (e.g., Figure 6(b). The

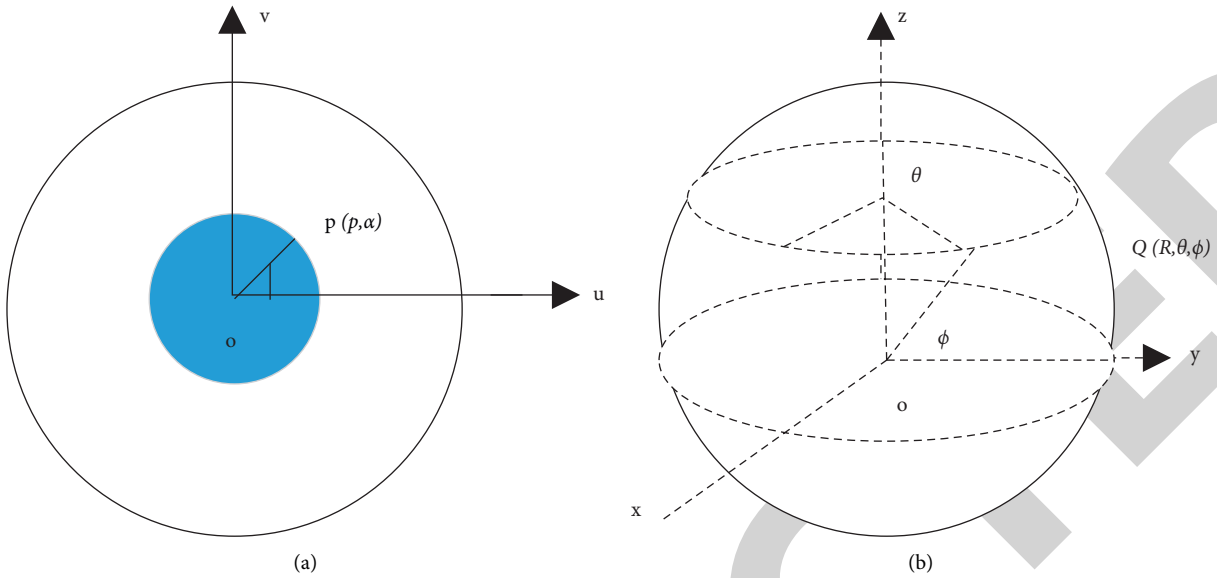

Figure 4: Schematic diagram of the spherical S mapping.

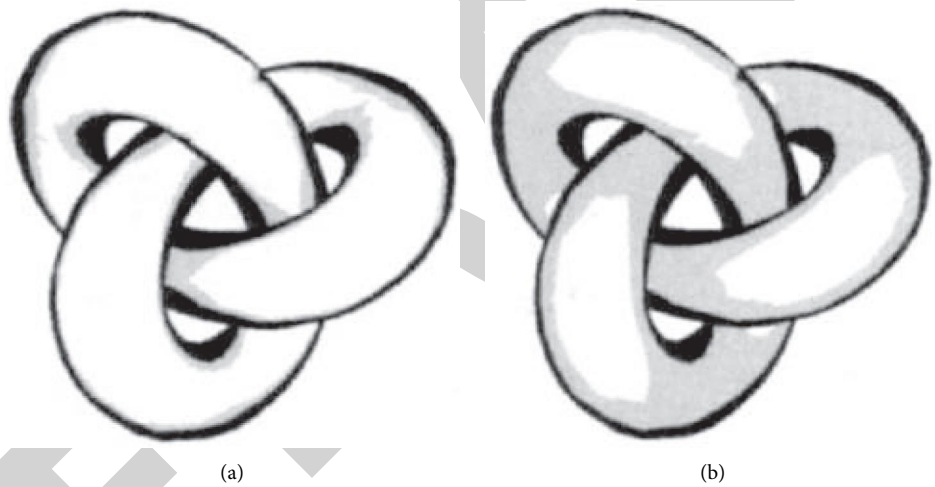

Figure 5: Ink rendering with fixed vertical component texture coordinates.

second calculation method was found to be better for simulating the effect of ink and wash painting in terms of intensity and distance.

For the attribute function D, the following constraints are imposed: ① the range of D is between 0 and 1, thus corresponding to the range of texture coordinates; ② set the threshold $d_{\min}$, when the distance from the point on the model to the viewpoint is less than or equal to $d_{\min}$, the value of D is 1, and when the distance is greater than $d_{\min}$, the value of D gradually decreases; ③ set the threshold $d_{\max} = r \times d_{\min}$, when the distance from the model point to the viewpoint is equal to when the distance from the model point to the viewpoint is equal to $d_{\max}$, the value of D is 0, where the value of r is greater than 1.

Different types of functions can be constructed to meet the above requirements. Line attribute functions, quadratic attribute functions, and attribute functions that take into account the effects of illumination are designed to simulate the ink effect in 3D models. The simplest method is to use linear property functions:

$$\begin{cases} D = 1, & d \le d_{\min}, \\ D = \dfrac{1}{((1-r) \times d_{\min} \times d + r/(1-r))}, & d \ge d_{\min}, \end{cases} \tag{5}$$

where d is the current depth property value of the 3D point and r and $d_{\min}$ are adjustable parameters. In the slice shader, the result is calculated as the coordinate value of the vertical component of the ink texture, and the function value decreases linearly when the current depth value of the model exceeds the threshold $d_{\min}$. Using the point of view as a reference, the larger vertical component texture coordinates are taken in the near area, corresponding to the darker tones

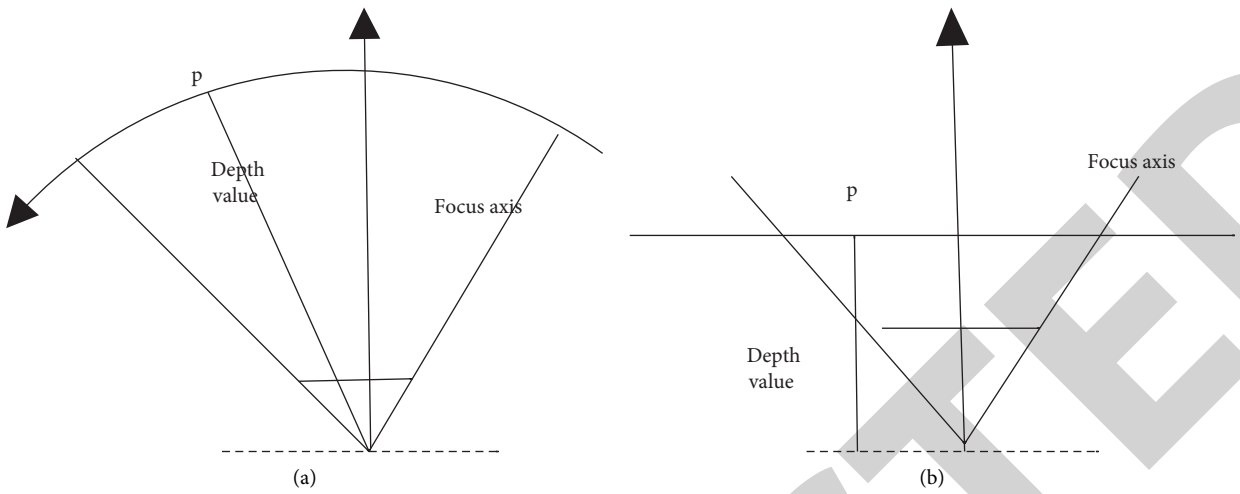

Figure 6: Calculation of depth attributes.

in the ink texture, and the smaller vertical component texture coordinates are taken in the far area, corresponding to the lighter tones in the ink texture, thus obtaining the effect of intensity and distance.

If you want a more intense contrast, you can use the secondary attribute function:

$$\begin{cases} D = 1, \quad d \le d_{\min}, \\ D = \dfrac{(d - r \times d_{\min})^2}{\left((1 - r)^2 \times {d_{\min}}^2\right)}, \quad d \ge d_{\min}. \end{cases} \tag{6}$$

The light source direction is introduced as a weighting factor to influence the attribute function, which can obtain the effect of the intensity and distance of the white left in the highlights of the illuminated surface and the thick ink of the shadows on the backlit surface. The direction factor constructed in the experiment is $(N - L)\gamma$, where N is the unit normal vector of 3D points, L is the normalised light source direction vector, and γ is the light factor. The attribute functions are

$$\begin{cases} D = 1 - \log 0^{d/d_{\min}}, \\ D = \alpha \times \dfrac{(d - r \times d_{\min})^2}{\left((1 - r)^2 \times {d_{\min}}^2\right)} + (1 - \alpha) \times (N.L)^{\gamma}, \ (N.L)^{\gamma} \le \beta, \end{cases} \tag{7}$$

where α is a weighting factor that controls the weight of light and depth information on the hue and β is an adjustable parameter that controls the area of shadows.

4. Simulation of Ink and Wash Painting Materials and Their Physical Processes

Ink painting is a complex process due to the special nature of the painting material and the use of various painting and calligraphy techniques. The study is based on a simulation of the natural medium and its physical processes. The simulation method of simulating the natural medium and its physical process is based on the mechanism of ink painting, and the main drawing tools and materials such as brushes, rice paper, ink, and pigments are studied. The method is based on the mechanism of ink painting, modelling the main drawing tools and materials such as brushes, rice paper, ink and pigments, and simulating their inherent physical properties and dynamic interaction behaviour. The aim is to simulate realistic ink and wash effects. The research results can be broadly divided into three parts: Xuan paper. The simulation of Xuan paper, the simulation of brushes, the simulation of ink diffusion, and the simulation of colour modelling.

4.1. Xuan Paper. Xuan paper is in contact with the brush on the one hand, accepting the ink from the bristles, and on the other hand acting as a carrier for the ink and wash that eventually becomes the painting. The modelling of the paper is therefore important, as it is directly related to the quality of the ink and wash effect simulation. The most important aspect of modelling rice paper is its fibre structure and its role in guiding and blocking the diffusion of ink and water. The advantage of this method is that the resolution is improved, and the irregular shape of the fibre masses will achieve better results on the boundary, as shown in Figure 7, but at the same time, the randomness of the fibre mass composition and the irregularity of the shape make it more difficult to describe and process the ink in it, making it difficult to use graphics hardware resources.

4.2. Hairbrush. With the development of NPR, virtual brush research has attracted more and more researchers. The 2*D* brushstroke model approach [13, 30], although able to simulate many of the effects of ink painting, reduces the freedom of the artist to create because of the overemphasis on the final simulation effect, reducing the unique writing effect of ink painting, as in Figure 8. The authors of [10] use a parametric gradient " raindrops" to simulate the contact area

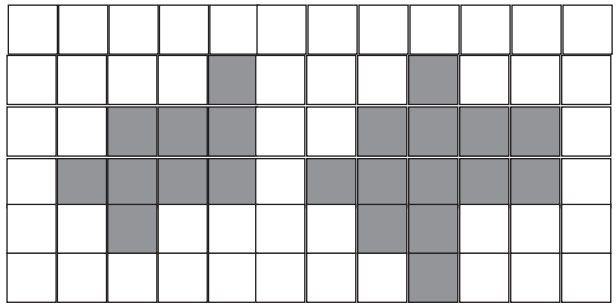

Figure 7: Model of the remaining paper fibre mass.

Figure 8: Schematic diagram of the two-dimensional brush stroke model.

between the paper surface and the brush, simplifying the parameter settings and operations, but with a single brush stroke, many artistic effects cannot be realized.

The use of alpha map mapping on the hair bundle surface after bifurcation limits the richness of the variation, as shown in Figure 9.

The focus of the brush simulation is to simulate the interaction behaviour between the brush, the rice paper, and the ink. Most of the above studies have ignored the effect of the structure of the rice paper on the ink and water transfer process. There is a need to reduce the computational complexity to ensure real time. There is also much room for improvement in describing the behaviour of the brush accurately and efficiently. [3] proposed a practical A practical 3D brush modelling system is proposed in [3] to accurately simulate the geometry of the brush and its dynamic interaction behaviour such as movement and bending. The method improves computational efficiency while effectively simulating the dynamic changes of the brush during the artistic creation process, as shown in Figure 10.

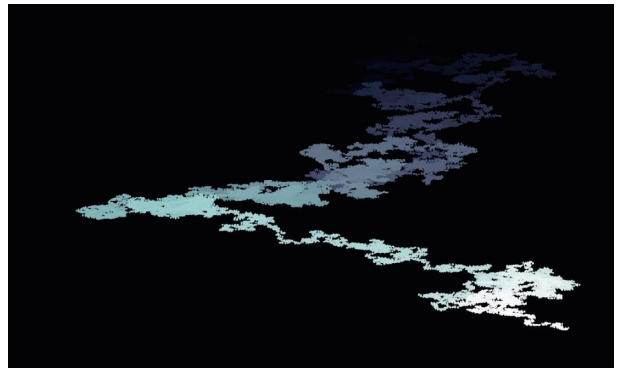

Figure 9: Brush surface mapping.

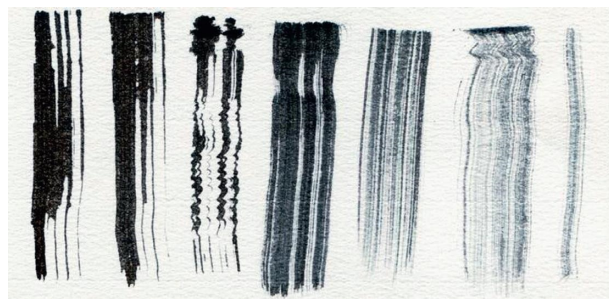

Figure 10: Potential energy-threshold controlled pen movement.

4.3. Diffusion Processes. The special feature of ink painting is that the brush bristles contain a large amount of water, and the pigment diffuses within the rice paper by the action of the water. The study of diffusion is indispensable in order to fundamentally simulate the effect of drawing ink paintings. [15] proposes to analyse ink and wash from the viewpoint of

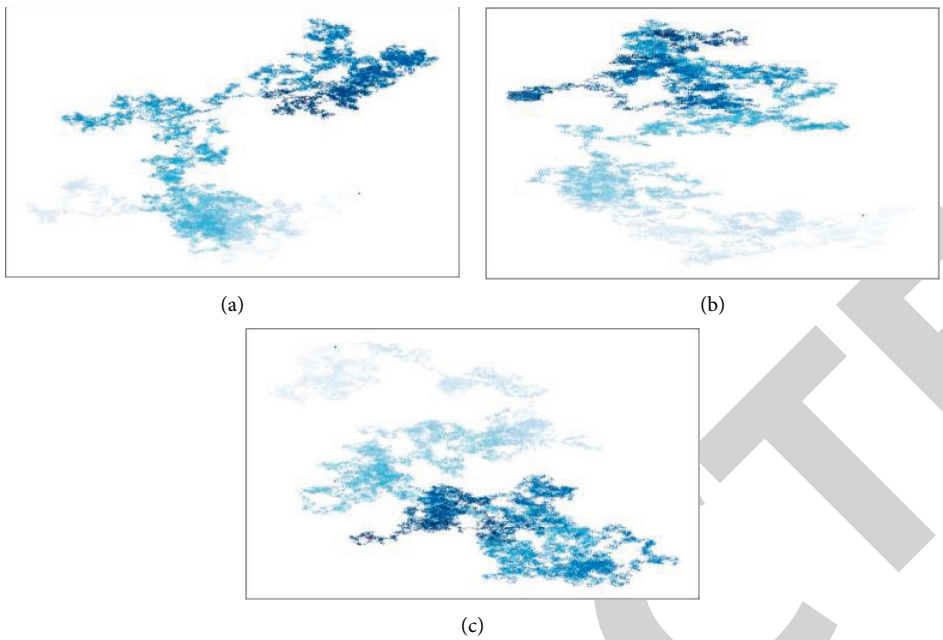

(a) (b) (c)

Figure 11: Linearly varying ink and wash effects of shade and distance (a-c).

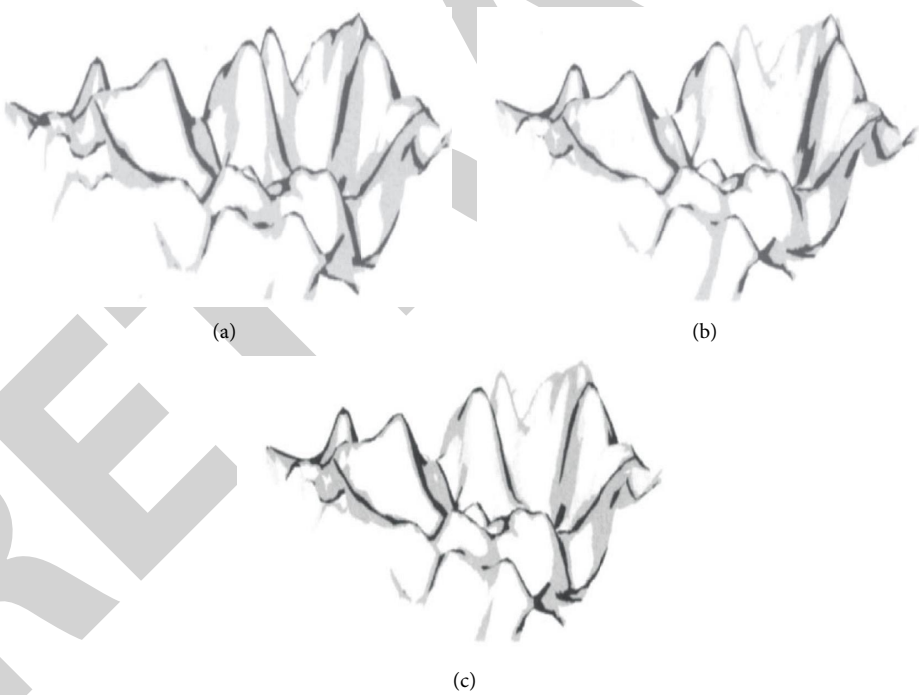

(a) (b) (c)

Figure 12: Comparison of three ink rendering effects. (a) Ink rendering without the depth attribute function (b) Ink rendering with linear attribute functions. (c) Ink rendering with quadratic attribute function.

particle systems, they are all composed of tiny particles that satisfy the condition of doing Brownian motion, and they undergo a complex movement in the fibre structure of the paper until the ink dries, finally forming an ink painting work. Throughout the process, this includes the diffusion of ink particles, the collision of particles with each other, the deposition of ink particles, and the evaporation of water particles, among other forms. The task of ink diffusion modelling is to study the mechanism of movement and simulates these movement patterns to obtain the final ink distribution information and finally display the output.

The diffusion of ink and pigments is the most complex part of the ink painting simulation. As can be seen from the above analysis, existing algorithms are not yet able to reproduce this process comprehensively, accurately and in real time, and previous simulations of diffusion

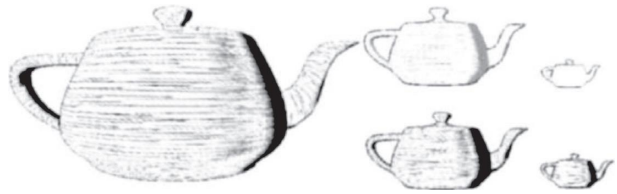

Figure 13: Effect of pencil drawing with abstract detail.

(a)

(b)

(c)

(d)

Figure 14: Qi Baishi's Mouse Grapes (a) and the results of this rendering (b)–(d). (a) The Mouse Grapes. (b) Rendering results of this paper 1. (c) Rendering result of this paper 2. (d) Rendering result of this paper 3.

superimpositions are limited to two aspects: first, particle-based diffusion has been proposed, but none of them are particle-based diffusion in the true sense. Second, they are limited to the diffusion of a single ink particle and do not include the diffusion of all the essential properties of the various pigments. Third, there is no in-depth study of the reality of the superposition of different pigments.

5. Results and Discussion

5.1. Algorithm Effect. The algorithm presented above has been implemented in VC+ + 6.0 and the OpenGL graphics engine programming environment and has been tested on a PC with a 1.8 G Hz CPU, DDR 1G RAM, and an ATIRHD 2400 graphics card.

In the experiments, the equations were verified separately as property functions, and the same parameters and sampling points were set for both experiments in order to compare the two. Figure 11 shows the effect of linking with increasing values of depth d. Figure 11(a) shows the effect when $d < d_{\min}$, which is closer to the point of view and the ink is thicker; 11(b) and 11(c) show the effect when $d > d_{\min}$ and d is gradually increased, which shows that the ink is getting lighter. Figure 12 shows a comparison between the traditional ink simulation without the depth attribute function, the ink simulation with the linear attribute function and the ink simulation with the quadratic attribute function when drawing the mountain model, with the parameter $d_{\min}$ at 100 and r at 10. The traditional 3D ink rendering algorithm does not consider the effect of the depth attribute on the rendering effect, so no matter how the depth value of the model vertices is changed, it is difficult to produce a strong or light. The results obtained by the algorithm in this paper vary with the depth value, as shown in Figures 12(b) and 12(c), with a stronger sense of hierarchy using the secondary attribute function. The reason for the different degrees of intensity is the variation in the value of the attribute function.

From the experimental results, it can be seen that the algorithm of this paper can be used to simulate the technique of intensity and distance better, and by changing the attribute function model and the relevant parameters of the function, the rendering effect with different contrast of intensity and distance can be obtained, which is a simple and practical method and provides an effective way for the 3*D* ink rendering of large-scale scenes.

Other attempts have been made to apply the attribute function. In artwork, there is often a technique of detail abstraction, where the details of something are detailed in the near distance, and only the general outline is drawn in the far distance, while the internal details are sketchy or not even portrayed. It is worth noting that the detail abstraction simulation here is different from the LOD technique, which only uses property functions and texture mapping techniques to obtain a sensory abstraction effect, without any processing of the 3*D* model mesh.

The traditional pencil drawing simulation requires a set of pencil drawing textures, and then uses the lighting function to control the weight of the different textures, and finally mixes the textures. The depth value is also taken into account, and the depth value is calculated by adding a white texture to the original pencil texture, and then using a linear property function to control the weighting factor of the texture, the final result is shown in Figure 13. It can be seen that the method can be used to simulate a detailed abstraction technique.

5.2. Drawing Effect. Figure 14 shows work by Qi Baishi when he was 80 years old, which mainly uses the technique of writing, using the intensity of ink colour to represent the object. From the experimental results, it can be seen that for different styles of input work, the algorithm is able to pass the basic stylistic features to the 3*D* model and render the ink accordingly, resulting in output images of similar styles.

6. Conclusions

The paper uses attribute functions to control the huge changes of the vertical components of the ink textures to simulate the ink painting technique of shade and distance. Compared with the existing algorithms, the 2D texture mapping by the attribute function provides a richer rendering effect, and in the ink rendering of 3D scenes, the addition of the effect of shade and distance makes the image more layered and closer to the painter's painting technique.

In order to provide a richer surface detail of the 3D model, the radial curvature of the model surface can be calculated, which is one of the directions for the future work.

Data Availability

The raw data supporting the conclusions of this article will be made available by the authors, without undue reservation.

Conflicts of Interest

The authors declare that they have no conflicts of interest regarding this work.

Acknowledgments

The authors would like to thank Qi Baishi for provides the painting.

References

[1] Z.-z. Zhang, Z.-j. Wu, T. Chen, and T. Lei, "Analysis on intensity zonation in thick loess region," *Journal of Shanghai Jiaotong University*, vol. 18, no. 6, pp. 724–728, 2013.

[2] J. Lee, "Diffusion rendering of black ink paintings using new paper and ink models," *Computers & Graphics*, vol. 25, no. 2, pp. 295–308, 2001.

[3] N. S.-H. Chu and C.-L. Tai, "MoXi," *ACM SIGGRAPH 2005 Sketches on - SIGGRAPH '05*, vol. 24, no. 3, pp. 504–511, 2005.

[4] C. H. Cao, Y. N. Tang, and D. Y. Huang, "IIBE: An Improved Identity-Based Encryption Algorithm for WSN Security," *Security and Communication Networks*, vol. 2021, Article ID 8527068, 8 pages, 2021.

[5] F. Li and S. Li, "real-time rendering of 3D animal models in Chinese ink painting style," in *Proceedings of the 2020 International Conference on Culture-Oriented Science & Technology (ICCST)*, pp. 284–287, IEEE, Beijing, China, October 2020.

[6] M. Kaplan, B. Gooch, and E. Cohen, "Interactive artistic rendering," in *Proceedings of the 1st International Symposium on Non-photorealistic Animation and Rendering*, pp. 67–74, Annecy France, June 2000.

[7] D. Wu, C. Zhang, L. Ji, R. Ran, H. Wu, and Y. Xu, "Forest fire recognition based on feature extraction from multi-view images," *Traitement du Signal*, vol. 38, no. 3, pp. 775–783, 2021.

[8] J. Suarez, F. Belhadj, and V. Boyer, "Real-time 3D rendering with hatching," *The Visual Computer*, vol. 33, no. 10, pp. 1319–1334, 2017.

[9] W. Qian, D. Xu, K. Yue, Z. Guan, Y. Pu, and Y. Shi, "Gourd pyrography art simulating based on non-photorealistic rendering," *Multimedia Tools and Applications*, vol. 76, no. 13, Article ID 14559, 2017.

Hindawi
Scientific Programming
Volume 2022, Article ID 2681533, 7 pages
https://doi.org/10.1155/2022/2681533

Research Article

Research on Sentiment Analysis Model of Short Text Based on Deep Learning

Zhou Gui Zhou

Computer College of Huanggang Normal University, Huanggang, Hubei 438000, China

Correspondence should be addressed to Zhou Gui Zhou; hgsyzgz@hgnu.edu.cn

Received 25 April 2022; Revised 10 May 2022; Accepted 16 May 2022; Published 29 May 2022

Academic Editor: Jie Liu

With the wide application of the Internet and the rapid development of network technology, microblogs and online shopping platforms are playing an increasingly important role in people's daily life, learning, and communication. The length of these information texts is usually relatively short, and the grammatical structure is not standardized, but it contains rich emotional tendencies of users. The features used by custumal machinery schooling methods are too sparse on the vector space model and lack the semantic information of short texts, which cannot well identify the semantic features and potential emotional features of short texts. In response to the above problems, this paper proposes a bidirectional long-term and short-term memory network model based on emotional multichannel, combining the attention mechanism and convolutional neural network features in deep learning and learning the short text by combining shallow learning and deep learning. The semantic information and potential emotional information of the short text can be improved to promote the effective expression of short-text emotional features and improve the short-text emotional classification effect. Finally, this paper compares the above models on multidomain classification data sets such as NLPIR and NLPCC2014. The accuracy and F1 value of the model proposed in this paper have achieved good improvement in the field of short-text sentiment analysis.

1. Introduction

These days, people want to check the latest current affairs, online shopping, news gossip, and financial stocks; people are no longer limited to reading newspapers or sitting in front of the TV to watch hot topics but have more ways to participate in the discussion of hot topics such as Weibo, Taobao, Douyin, Zhihu, and WeChat public platforms and other media. As an Internet platform, Weibo, Taobao, and Douyin, in another aspect, realize information sharing and dissemination by virtue of user relationships, attracting a large amount of individuals to participate, and are favored by people; on the other hand, a large amount of posts published by users are text mining and provide a huge amount of data. Sun et al. found that Weibo information can reflect changes in people's attention to hot spots [1] and can even infer the current emotional condition of users based on Weibo user information. In addition, Weibo sentiment analysis also provides reference opinions for some industries, such as stock trading decisions [2], movie box office predictions, and election predictions [3, 4]. Literature provides reference opinions for consumers to purchase products by mining online shopping platform product review information and establishing a review sentiment analysis model [5–7] and guidance for merchants to adjust production plans and product improvement and also promotes online shopping platforms. Users are provided with a more efficient quality of service. With the vigorous development of online social media and the rise of artificial intelligence, more and more experts, scholars, and scientific research institutions are now turning their attention to the analysis.

1.1. Research Status of Text Sentiment Analysis. Text sentiment analysis is an indispensable link in natural language handling. In the past, relatively large part experts and scholars have carried out research in the light of sentiment dictionary. Li and Hong reviewed sentiment analysis methods, respectively [8, 9].

(1) The medium in the light of the vocabulary for expressing emotions and emotional tendencies mainly judges the sentiment climate. It needs to manually construct the vocabulary for expressing emotions and emotional tendencies mainly or use the internal statistics Mutual Information (MI), Symmetric Conditional Probability (Symmetric Conditional Probability), external statistics (Branch Entropy and Access or Variety), and other methods to expand the sentiment dictionary. In text orientation analysis, well-known sentiment dictionaries are HowNet2, WordNet [10], and ConceptNet [11].

(2) The feature-based method is to use statistical knowledge to screen features from a large quantity of corpora, use features to represent the entire text, and then use relatively unnovel algorithms in machine schooling to classify the text. This method requires high feature engineering and feature selection. The results directly affect the classification effect. For a long time, features have occupied an important position in text classification, the classification matrix has not been greatly improved, and it has indirectly led to the problem of overfitting, which is called the Hughes effect [12–14]. In reality, training a large number of features requires enough samples, where obtaining enough samples requires time and labor.

(3) Based on deep learning methods, features such as words, sentences, and chapters can be mapped to high-dimensional spaces to learn deeper feature representations in text data. Wang added a self-attention mechanism (Attention Mechanism) after the output storey of the LSTM network [15] and obtained the context information of the LSTM output unit attention means for relevant automatic acquisition. The experimental results show that the attention mechanism can recognize the emotional information in the text [16, 17]. The model first inputs the word vector into the Bidirectional LSTM net to learn the textual content and emotional information, and then uses the self-look mechanism to extract emotional representations of monolingual and bilingual texts, respectively. Based on the above work, in the work of sentiment analysis, each word in the text has a multitudinous collision on the overall emotional climate of the text, especially some emotional words, which can often directly reflect the emotional climate of the text, and through the look mechanism, the importance of words can be obtained, and the potential representation information in the text can be learned.

1.2. Research Status of Short-Text Sentiment Analysis. (1) In the method based on the sentiment dictionary, Xiao constructed a sentiment dictionary by analyzing the emotional part of speech and the domain words in the topic domain (World Cup, iPhone, and NBA games) in the context of microblogs [18] and proposed a sentiment lexicon-based sentiment analysis strategy. Chen improved the mutual information algorithm [19] and obtained emotional words in microblogs on the Chinese microblog sentiment dictionary constructed in the light of mutual information.

(2) In the modus in the light of machine learning, Xie et al. combined sentiment dictionary, context features. and topic features [20] and proposed an SVM-based sentiment classification method. Li and Ji extracted features such as words, negative words, and special symbols to construct an SVM model and a CRF model to perform sentiment analysis on microblog data [21] and concluded that the appropriate choice should be made under different circumstances. Conclusions of the model.

(3) In the method based on deep learning, Zhou integrated part-of-speech features and word embedding features in the research on sentiment classification of product reviews [7]. The experiments are higher than the traditional text convolutional neural network. Chen proposed a microblog using part-of-speech features of emotional words and learning more hidden information [22]. The experiments verified the proposed model is robust to different data.

Because the short text is relatively short, it will bring about the problem of lack of text semantics, which brings challenges to the short-text sentiment analysis. Although the existing short-text sentiment analysis methods have done some feature extraction, feature selection, and model selection, many works still do not fully consider the context of short texts and deeply dissect semantic features. Some new words may not be recognized in the word segmentation stage. In order to improve the shortcomings of existing methods in feature selection, this paper extracts shallow learning features such as emotional part of speech, location information and dependencies of words from short texts, as well as deep learning features such as word vector features, convolutional neural network features, and emotional attention features. Learning features enrich the textual feature representation of short texts.

In the near future, deep learning has also been widely used in sentiment analysis of short texts. Its concept comes from the research of artificial neural network. Its purpose is to explain the feature information existing in the data by imitating the thinking structure and learning mechanism of the human brain and build a neural network for machine analysis and learning. Compared with the use of nonlinear network structure to make up for the shortcomings of the algorithm, it also has the following two shortcomings:

(1) In deep learning, the amount of training data is required by the model. When the scale of the model is large enough, the connection between short-text data can be fully captured. However, in most cases, facing the problem of short-text sentiment orientation classification and other classification problems, sufficient training data cannot be found, and a lot of data are manually annotated, and the model is

difficult to achieve optimal, which is common in the industry.

(2) Due to the "black box" nature of the features learned by the deep schooling network model, it is difficult to fundamentally find out where the learned features come from, and it is also difficult to explain the specific meaning of the learned features.

2. Relevant Theoretical Basis and Technical Introduction

In recent years, the analysis and mining of time series data have been gradually applied to many fields. Natural language processing is a typical application [23–26]. In the research of many scholars in the scope of natural language processing, the text sentiment analysis task has two important steps. The first is to convert the text information into coded information that can be recognized by the computer, and the second is to analyze the sentiment tendency of the text. Since the words in the text cannot be directly fed into the network model, the first task is to convert the text into a digital representation. The word vector is to map the words in the text into a digital vector representation. According to the different encoding methods, word vectors are mainly divided into discrete word vectors and distributed word vectors.

2.1. Text Representation. Natural language is a complex system that expresses a given intention and thought. It is generally composed of words and punctuation marks. One, two or more words are spliced into a word, and several words are connected to form a sentence. After continuous combination, it forms paragraphs and chapters. Unlike humans, machines cannot directly understand the emotional information in language but need to obtain the corresponding information in language by establishing certain rules or models [27], in which only one bit is 1 and the rest are 0. Under the one-hot rule, the words after word segmentation are discretized and mapped to the Euclidean space by the implementation of row vectors, but in large-scale data sets, the vocabulary size of a data set may reach tens of thousands of dimensions or even ten of thousands of dimensions, and vectors at this time will undoubtedly bring huge memory consumption. At the same time, the large-scale vocabulary makes the constructed word vector matrix too sparse, which brings great inconvenience to the feature schooling. In view of the fact that one-hot encoding will have problems such as dimensional disaster, word similarity, and poor model generalization ability in natural language modeling, Google proposed the word2vec model in 2013, also known as the word embedding model. Each position in the model-trained and the general value range is between −10 and 10. Taking "I appreciate one country, two systems" as an example, the 200-dimensional word vector representation is set as shown in Table 1.

2.2. Related Methods of Sentiment Analysis. Sentiment analysis is essentially a text classification problem. Deep learning can learn deep features in data and bring about brilliant bonanza in odd spheres. Therefore, profound learning has also been diffusely used in sentiment decomposition tasks in recent years. Neural networks commonly used in text sentiment decomposition include CNN, recurrent neural networks, and LSTM networks. These networks can better mine the latent information hidden in the text and outperform most custumal machinery schooling methods.

Since RNN adds a loop structure to the traditional neural network, the content of the loop body will be executed at each step, but when the number of historical nodes input to the RNN decreases, the RNN cannot memorize information far from the current node. LSTM is an improved model of RNN. The main improvement is the introduction of three phylums when memorizing information: input gate, forget gate, and output gate. Through these three gates, LSTM can bridle the information passing through the cell and can selectively add information or delete existing information according to the needs of the result, and specific LSTM network structure and internal structure are shown in Figure 1.

At the outset, LSTM used the forget gate to fix the message that the cell demands to discard. Forget phylum calculates a value among zero and one based on the historical message of the former condition and the current input communication as the condition of the cell information at the previous moment to determine what information to keep and discard. Among them, 0 means to discard all the communication of the historical condition, and 1 means to keep all the communication of the historical condition, where $f(t)$ delegates the input value at time t, $h(t-1)$ delegates the worth of the concealed stratum at time $t-1$, and $U(f)$, $W(f)$, and $b(f)$ are the degree of seriousness of the worth of LSTM of the concealed stratum in the forget phylum, the degree of seriousness of the current input, and the bias in the forget phylum, respectively, σ is the activation function of sigmod, and $f(t)$ is the information discarded by cells. The specific calculation is shown in the following equation:

$$f^{(t)} = \sigma\left(\sum h^{(t-1)} \cdot U^{(f)} + x^{(t)} \cdot W^{(f)} + b^{(f)}\right). \quad (1)$$

LSTM determines the information stored in the cell through the input phylum. The input phylum calculates a value from 0 to 1 by sigmod, the key in news to modernize the condition of the current node, that is, what information needs to be updated or stored. Among them, 0 means not accepting new information and 1 means accepting all the input information. LSTM generates a new memory $C(t)$, which is the input memory, not the final memory. The condition is determined by the previous output and the current input, which are the worth of the concealed stratum of LSTM in the new memory, the degree of seriousness of the current input, and the degree of seriousness of the current input. The specific calculation of the bias in the new memory is shown in the following equation :

$$\widetilde{C}^{(t)} = \tanh\left(\sum h^{(t-1)} \cdot U^{(c)} + x^{(t)} \cdot W^{(c)} + b^{(c)}\right). \quad (2)$$

Table 1: Word2vec training word vector table.

Words and phrases	Word embedding
Myself	[−3.2554681, 3.0520194, −1.3131773, . . ., 0.22637065]
Grateful	[1.2681537, −0.09857514, 1.5265175, . . ., 0.07370517]
One country, two systems	[−0.6349963, 1.6289423, −0.4314866, . . ., −0.4279167]

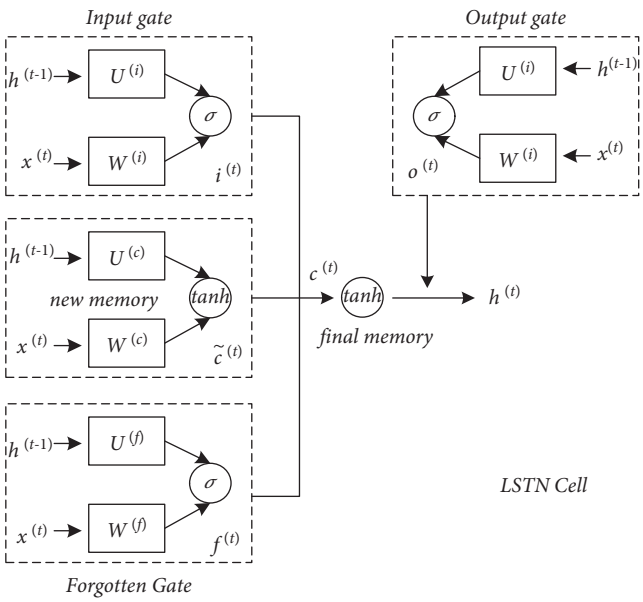

Figure 1: LSTM text classifier model.

The final desired memory is generated by the part to be remembered and the part to be forgotten. Through the calculation of the previous two phylums, we already know the proportion $i(t)$ of new information retained, the proportion of old information that needs to be forgotten, and the new memory and old memory $f(t)$. In the final step, the output phylum is used to determine the upshot of the final cell output. The output phylum calculates a value between 0 and 1 by sigmod—the input information to calculate the proportion of information that the cell finally outputs. Among them, 0 indicates that no information is output and 1 indicates that all the final memory results are output. The specific calculation is shown in the following equation:

$$C^{(t)} = i^{(t)} \odot \widetilde{C}^{(t)} + f^{(t)} \odot C^{(t-1)}. \tag{3}$$

In a classical recurrent network, the condition and output are always transmitted from front to back. However, in some problems, the transmission and output of the condition are not only related to the previous condition but also related to the subsequent condition such as prediction. A missing word is not only related to the preceding text but also to the following text. Among them, BiLSTM is a common neural network model that considers the contextual relationship. It is based on Bi-RNN. One LSTM module propaphylums from front to back, and another LSTM module propaphylums from back to front. BiLSTM builds a double-storey network model. The input is forwarded to the LSTM and the reverse LSTM, respectively, and the final output result is the vector superposition of the LSTM output results in two different directions. Finally, the entire output result is fully connected, and then, the sigmod output is the final output result, where BiLSTM is trained in the same way as LSTM [28–30].

3. Sentiment Classification Model Based on Deep Learning

Considering that the custumal machinery schooling methods and profound learning methods are insufficient in feature representation, this paper makes two improvements to the custumal machinery schooling methods and profound learning methods: one is to use shallow learning features as one of the input features of profound learning. Add a look mechanism to the network layer to allow the model to better learn the underlying semantic features in the text.

3.1. A Bidirectional Long- and Short-Term Memory Network Model Based on Emotional Multichannel. So as to make full use of the unique emotional resource information in the text sentiment decomposition task, this paper proposes BiLSTM Based on Sentimental Multichannel, referred to as BM-ATT-BiLSTM based on multichannel sentiment. The learning storey builds multiple channels to improve sentiment classification performance. BM-ATT-BiLSTM is a left-to-right multistorey neural network structure mainly composed of 5 parts: input layer, semantic learning layer, emotional attention layer, merging storey, and sentiment classification output storey. The input storey inputs are composed of features and shallow features (emotional part-of-speech features of words, location information features, and dependency features). The traditional LSTM model can obtain the forward semantic information in the text but ignore the reverse semantic information of the text. In response to this paper, let LSTM learn backward directions of the sequence. Feed the data in both directions into the BiLSTM model, and the calculation method is relatively simple, by calculating the emotional weight of each word. If the previous storey of the BiLSTM network is multiplied, it will be normalized and fused batch. Use the fully connected layer of the model to output the feature matrix, use softmax to normalize the feature matrix, and finally get the classification result.

3.2. Experimental Parameter Setting. Different hyperparameters may have different effects on the experimental results. Although parameter tuning itself is not the main research content of this paper, for the sake of fairness, this paper considers the overall effect of the experiment and

finally determines the hyperparameters of BM-ATT-BiLSTM. Some hyperparameters of the BM-ATT-BiLSTM model are shown in Table 2.

3.3. Experimental Environment and Comparative Experiments. The computer hardware configuration used in the experiment in this paper is as follows: the CPU is Intel Core processor i5-9400f, and the GPU series is NVIDIA GTX; the operating system is configured as Windows 10; the programming software used is PyCharm, the programming language used is Python, and the support library used in profound learning is pytorch10, keras11, and gensim12.

3.4. Experimental Results and Analysis. Since the NLPIR and NLPCC2014 data sets do not contain many training samples, too many iterations may lead to overfitting problems, and if the number of iterations is insufficient, it is troublesome for the matrix to be taught effective features. Therefore, 20% of the data set is divided into the validation set, 16% is divided into the test set, and 64% is divided into the drilling battery. Precision, Recall, and F1-measure are selected as evaluation indicators. So as to make the experiment more fair, the evaluation index results in this paper take the average of 50 experimental results. The detailed experimental results are shown in Table 3.

(1) Compared with LSTM, the overall effect of CNN is weaker than that of LSTM. In the process of extracting features, CNN mainly captures multiple different N-grams of text, and there are many different convolution kernels for one N-gram. Useful information is extracted from different angles, but the experimental data sets are all short texts, and the amount of data is not large, so the use of CNN to extract features may lead to insufficient features and adds emotional attention to CNN, and the effect is obviously promoted.

(2) The results of CNN and CNN + SVM show that using SVM instead of softmax can improve the classification effect. The reason is that the loss function of SVM can get faster convergence on the three data sets of text, and the output of softmax is only a probability of compressed data, and the probability distribution of softmax is deviated from the actual result.

(3) Among all the LSTM memory networks involved in the comparative experiments, BM-ATT-BiLSTM has the best effect. An important reason is that the emotional attention mechanism is added, and more potential emotions can indeed be learned from the text through attention. According to Table 3, the BM-ATT-BiLSTM method outperforms other models in terms of precision and recall. This effect is essentially due to the time series characteristics of natural language. Cells in the LSTM model can effectively record the time series information in the text. The BiLSTM model structure is used to learn the semantic information in the text, in order to enhance the capability of the mold to learn the reverse text, and strengthen the capability to seize the news of the text context. Combining the emotional parts of speech, location information of words, as well as word embedding features, emotional attention features, and features extracted by convolutional neural networks, this paper proposes three neural network models, which are the foundations of emotional multichannel features—BiLSTM classification model, convolutional neural network in the model mechanism increases the attention, and multikernel convolutional neural network in the model mechanism increases the attention. Tentatives show that the BM-ATT-BiLSTM recommended in this paper has the best performance; therefore, it can be concluded that adding the above shallow learning features and profound schooling features to the short-version sentiment decomposition can improve the classification manifestation of the mold.

Table 2: BM-ATT-BiLSTM model hyperparameter settings.

Hyperparameters	Characterization	NLPIR	NLPCC2014
η	Learning rate	0.01	0.01
Epoch	Number of iterations	10	10
Hidden	Number of hidden units	128	200
P dropout	Dropout	0.5	0.5
λ	L2 coefficient	le-3	le-3
Batch	Batch size	64	64
D	Word vector size	200	200
Dimension	Word vector dimension	200	200

Table 3: Comparison of experimental results.

Model	NLPIR			NLPCC2014		
	Pre	Rec	F1	Pre	Rec	F1
CNN	78.66	96.44	86.65	70.40	66.31	68.29
CNN + SVM	86.32	88.11	87.21	73.13	71.30	72.20
LSTM	81.94	92.92	87.09	72.23	72.56	72.39
BiLSTM	87.60	89.31	88.45	73.92	71.17	72.52
BM-ATT-BiLSTM	87.02	90.57	88.76	75.57	70.69	73.05

4. Conclusion and Outlook

Combining the emotional part of speech features, location information features, and dependency features of words, as well as word embedding features, emotional attention features, and features extracted by convolutional neural networks, this paper proposes three neural network models, which are emotional multichannel features—BiLSTM classification model, convolutional neural network in the model mechanism increases the attention, and multikernel convolutional neural network in the model mechanism increases the attention. Tentatives show that the BM-ATT-BiLSTM recommended in this paper has the best performance, so it can be concluded that adding the above shallow

learning features and profound learning features to the short text sentiment analysis.

4.1. Summary. In a bidirectional LSTM based on emotional multichannel, shallow learning features and word embeddings and profound learning features of emotional attention are fused. Experiments show that the model integrates shallow learning features such as emotional part of speech, location information, and word dependence, and the classification effect is better than CNN and other models. In the profound learning model based on convolutional neural network, word embedding, emotional attention feature, and convolutional neural network feature are fused. Experiments show that feeding profound learning features into SVM can improve the performance of classification, and the model works best compared to other convolutional neural networks.

There are two main contributions of this paper.

(1) This paper puts forward a bidirectional LSTM memory network model based on emotional multichannel, which integrates shallow learning features and profound learning features at the feature level, so the mold can heighten the expression ability of text semantic information and learn the potential emotion of the text. The test outcome is also multifeature prefusion, which is very helpful for sentiment climate analysis.

(2) This paper adopts CS-ATT-CNN and CS-ATT-TCNN to solve the problem of sentiment climate analysis of short texts. The model effectively combines machine learning and profound learning, the training time is short, and the model is better than the traditional convolution—Neural network classification model and TCNN model.

Theoretically, the semantic information of the LSTM model text is good, but from the practical point of view, the LSTM model still has deficiencies, and the BM-ATT-BiLSTM method in this paper combines the emotional part-of-speech features, location information features, and dependency features of words. As well as from the emotional attention feature, we can learn the underlying emotional regularity in the text so as to capture the important information that affects the emotional climate of the text. The BM-ATT-BiLSTM proposed in this paper is good, but there is one more factor that should be considered in the forget phylum, and it takes a lot of time to detect these meaningless communications can achieve better experimental results in a short time.

4.2. Prospect. Judging from the current situation and the experiments of this paper, there is still a long way to go in the analysis of sentiment climate of short texts. There are many challenges and opportunities, and there are many problems that deserve further study and improvement. The following two points can be used as the next step for research.

(1) This paper only mines text data and does not consider the author's user attributes. If user attributes, user's Weibo or online shopping comments, and posting time and other information are fully considered, the accuracy of text orientation analysis may be greatly improved. In the experiment, this paper only uses the data of Wikipedia as the corpus of the training word vector, and the data of Weibo and product reviews can be added as the expanded corpus of the training word vector in the future. Due to the complexity and diversity of the network environment and Chinese, some new words may not be recognized in the word segmentation stage, and there is a polysemy problem in Chinese. In the future, a new word dictionary can be constructed in combination with the context.

(2) There are some sarcastic sentences in Weibo and product reviews. This paper cannot identify the emotional polarity of such sentences well. Therefore, we can add sarcastic sentences to transform the model of this paper. If you combine the knowledge graph to do sentiment decomposition, consider each word as an entity in the knowledge graph, and form a many-to-many relationship between entities and entities, and it is very possible to dig out the emotional connection between words and words. In the next step, we will combine some actual Internet projects to verify more combined models to reflect their socio-economic value.

Data Availability

The data set can be accessed upon request.

Conflicts of Interest

The author declares that there are no conflicts of interest.

References

[1] X. Sun, C. Zhang, and F. J. Ren, "User emotion modelling and anomaly detection based on social media," *Chinese Journal of Information*, vol. 32, no. 4, pp. 120–129, 2018.

[2] Y. Wang, "Stock market forecasting with financial micro-blog based on sentiment and time series analysis," *Journal of Shanghai Jiaotong University (Science)*, vol. 22, no. 2, pp. 173–179, 2017.

[3] C. Y. Liu, *Research on sentiment mining technology of social network comments in box office prediction*, Nanjing University of Posts and Telecommunications, Nanjing, China, 2019.

[4] W. Budiharto and M. Meiliana, "Prediction and analysis of Indonesia Presidential election from Twitter using sentiment analysis," *Journal of Big Data*, vol. 5, no. 1, p. 51, 2018.

[5] J. B. Bao, *Sentiment analysis of online shopping platform product reviews based on machine learning*, Harbin Institute of Technology, Harbin, China, 2019.

[6] K. Li, *Analysis and research on the sentiment climate of commodity reviews based on expression skills*, China University of Mining and Technology, Beijing, China, 2018.

[7] D. Y. Zhou, *Research on sentiment analysis of commodity reviews based on convolutional neural network*, Nanjing University of Posts and Telecommunications, Nanjing, China, 2019.

[8] R. Li, S. Sahu, and M. Schachner, "Phenelzine, a cell adhesion molecule L1 mimetic small organic compound, promotes functional recovery and axonal regrowth in spinal cord-injured zebrafish," *Pharmacology Biochemistry and Behavior*, vol. 171, no. 1, pp. 30–38, 2018.

[9] W. Hong and M. Li, "A survey of research on text sentiment analysis methods," *Computer Engineering and Science*, vol. 41, no. 4, pp. 750–757, 2019.

[10] C. Fellbaum, "An electronic lexical database," *Library Quarterly Information Community Policy*, vol. 25, no. 2, pp. 292–296, 1998.

[11] H. Liu and P. Singh, "ConceptNet-a practical commonsense reasoning tool-kit," *BT Technology Journal*, vol. 22, no. 4, pp. 211–226, 2004.

[12] B. M. Shahshahani and D. A. Landgrebe, "The effect of unlabeled samples in reducing the small sample size problem and mitigating the Hughes phenomenon," *IEEE Transactions on Geoscience and Remote Sensing*, vol. 32, no. 5, pp. 1087–1095, 1994.

[13] J. Tang, Z. Lu, and J. Su, "Progressive self-supervised attention learning for aspect-level sentiment analysis," in *Proceedings of the 57th Annual Meeting of the Association for Computational Linguistics*, pp. 557–566, Florence, Italy, July 2019.

[14] G. A. Ruz, P. A. Henríquez, and A. Mascareño, "Sentiment analysis of Twitter data during critical events through Bayesian networks classifiers," *Future Generation Computer Systems*, vol. 106, no. C, pp. 92–104, 2020.

[15] Y. Wang, M. Huang, X. Zhu, and L. Zhao, "Attention-based LSTM for aspect-level sentiment classification," in *Proceedings of the 2016 Conference on Empirical Methods in Natural Language Processing*, pp. 606–615, Austin, Texas, November 2016.

[16] D. M. Hu, C. W. Zhu, and C. Hu, "Multilingual text sentiment analysis method with attention mechanism based on pre-training model," *Small microcomputer system*, vol. 41, no. 2, pp. 278–284, 2020.

[17] A. Onan, "Classifier and feature set ensembles for web page classification," *Journal of Information Science*, vol. 42, no. 2, pp. 150–165, 2016.

[18] J. Xiao, X. Ding, and R. J. He, "Sentiment analysis of Chinese Weibo based on domain sentiment dictionary," *Electronic Design Engineering*, vol. 23, no. 12, pp. 18–21, 2015.

[19] X. D. Chen, *Analysis of Chinese Weibo sentiment climate based on sentiment dictionary*, Huazhong University of Science and Technology, Wuhan, China, 2012.

[20] L. X. Xie, M. Zhou, and M. S. Sun, "Multi-strategy Chinese microblog sentiment analysis and feature extraction based on hierarchical structure," *Chinese Journal of Information*, vol. 26, no. 1, pp. 73–84, 2012.

[21] T. T. Li and D. H. Ji, "Sentiment analysis of microblog based on multi-feature combination of SVM and CRF," *Research on Computer Application*, vol. 32, no. 4, pp. 978–981, 2015.

[22] K. Chen, B. Liang, and W. D. Ke, "Chinese microblog sentiment analysis based on multi-channel convolutional neural network," *Computer Research and Development*, vol. 55, no. 5, pp. 945–957, 2018.

[23] Z. Jia, Y. Lin, Y. Liu, and Z. J Jiao, "Refined nonuniform embedding for coupling detection in multivariate time series," *Physical Review*, vol. 101, no. 6, 2020.

[24] Z. Jia, J. Junyu, X. Zhou, and Y. Zhou, "Hybrid spiking neural network for sleep EEG encoding," *Science China Information Sciences*, vol. 65, 2022.

[25] Z. Jia, X. Cai, and Z. Jiao, "Multi-modal physiological signals based squeeze-and-excitation network with domain adversarial learning for sleep staging," *IEEE Sensors Journal*, vol. 22, 2022.

[26] Z. Jia, M. Gao, Z. Zhang et al., "Community environment and physical activity influence on rural residents' mental health in the COVID-19 containment," *International Journal of Environmental Health Research*, vol. 29, pp. 1–12, 2022.

[27] T. Mikolov, I. Sutskever, K. Chen, G. Corrado, and J. Dean, "Distributed representations of words and phrases and their compositionality," in *Proceedings of the Advances in Neural Information Processing Systems*, pp. 3111–3119, Red Hook, NY, USA, December 2013.

[28] G. Paltoglou and M. Thelwall, "Twitter, MySpace, d," *ACM Transactions on Intelligent Systems and Technology*, vol. 3, no. 4, pp. 1–19, 2012.

[29] F. A. Gers, J. Schmidhuber, and F. Cummins, "Learning to forget: continual prediction with LSTM," *Neural Computation*, vol. 12, no. 10, pp. 2451–2471, 2000.

[30] Z. Jia, Y. Lin, J. Wang et al., "Multi-view spatial-temporal graph convolutional networks with domain generalization for sleep stage classification," *IEEE Transactions on Neural Systems and Rehabilitation Engineering*, vol. 29, pp. 1977–1986, 2021.

Hindawi
Scientific Programming
Volume 2022, Article ID 3638136, 9 pages
https://doi.org/10.1155/2022/3638136

Research Article

Research on Discourse Transfer Analysis Based on Deep Learning of Cross-language Transfer

Yu Shen [1,2]

[1]*Huanghe Science and Technology University, Foreign Languages School, Zhengzhou 450000, China*
[2]*University of Málaga, Department of Linguistic, Literature and Translation, Málaga, Spain*

Correspondence should be addressed to Yu Shen; shenyu@hhstu.edu.cn

Received 15 April 2022; Revised 4 May 2022; Accepted 11 May 2022; Published 27 May 2022

Academic Editor: Jie Liu

With the current exchange and communication between different countries becoming more and more frequent, the language conversion of different countries has become a difficult problem. The analysis of a series of problems in cross-language discourse conversion, the study of the discourse conversion path, and innovation motivation based on the deep learning theory of cross-language transfer, it has theoretical and practical significance. This paper aims at the technical difficulties in speech conversion methods to effectively utilize the local mode information of signal time spectrum and the long-term correlation of speech signal. A discourse conversion method based on convolutional recurrent neural network model is proposed. In the model, the extended convolutional neural network is used to model the long-term correlation of speech signals. In the part of speech fundamental frequency estimation, the prosodic information generated by the decomposition of the fundamental frequency by continuous wavelet transform is used as the training target of the fundamental frequency estimation model. The experimental results show that the speech transformation method based on the convolutional cyclic network model proposed in this paper has better quality and intelligibility than the speech transformed by the contrast method.

1. Introduction

In the face of the diversity of social values and cultural diversity, coupled with the development of new media technology, traditional ideological and political education discourse is facing inevitable challenges. In the process of dealing with challenges, its disadvantages and problems are constantly exposed. For example, most of the discourse content is still confined to the propaganda of documentary language and policy discourse, which lacks effective connection with the daily life of the audience [1]. In the form of discourse, one-way indoctrination is more than two-way interaction; there are more grand narratives and less elaborate descriptions; more empirical life language, less rigorous academic discourse; and there are more referential words but less original ones extracted from practice. There are more empty and stale words than up-to-date ones; there are many words of conformity, but few words of independent thinking [2]; and the lack of ideological discourse power in the field of network. In this discourse field, therefore, how to use by educators to understand, trust, and open discourse established the ideological and political education position, the spread of the ideological and political education content, firmly grasp the ideological and political education, in turn, say, raise new era the pertinence, effectiveness and validity of ideological and political education, and ideological and political education has become the key problem facing. [3–6].

With the rise of deep learning and artificial intelligence, traditional speech conversion methods based on statistical models can no longer meet the requirements of large amounts of corpus data involved in training, and the performance of traditional language conversion models deteriorates rapidly in the case of large amounts of corpus data involved in training. DNN [7] has strong data fitting ability and can better explain various complex data features, which is very suitable for the scenario where a large amount of corpus data participates in training. Deep belief network (DBM) maps speakers' spectrum features to higher order eigenspace, thus realizing the transformation between speakers' spectrum features.

Based on dnnvc (deep bidirectional long-term and short-term memory recursive neural network), it has recursive neural network, Dblstm RNN) to construct the discourse transformation model. Because dblstm-rnn can capture the forward and backward time relationship of the speaker's speech spectrum characteristics, the performance of the conversion model is significantly improved [8]. The proposal of convolutional neural network (CNN) [9] is a milestone in the field of deep neural network, which greatly promotes the development of deep learning and artificial intelligence. The depth generation network model based on convolutional neural network has been proposed and applied to the field of discourse conversion. Conditional variational automatic encoder network (CVAE) is used to unlock the content and timbre characteristics of the input speech spectrum [10]. Completely nonparallel many-to-many discourse transformation [11]. Star creative adversity network VC (stargan VC) method makes use of the advantages of the cvae-vc method and the cyclegan VC method, respectively. Multi-speaker multi to multidiscourse conversion is realized by using speaker identity tag thermal vector, which is the best in the current nonparallel multi to multi discourse conversion methods. The improved methods of VAE series and Gan Series in deep generation neural network model have been recognized and affirmed by many scholars, and a series of novel methods have been proposed, such as vawgan VC [12], vqvae-vc [13], cdvae VC [14], acvae-vc [15], adagan VC [15], cyclegan-vc2 [16], and stargan-vc2 [17].

Based on the above research, this paper innovatively uses the deep neural network model of cross-language transfer to solve the discourse conversion problem. In order to solve the problem that existing speech conversion methods cannot effectively utilize the acoustic mode information in the speech time spectrum, and it is difficult to effectively model the long-term correlation of speech signals, a novel convolutional recurrent neural networks based on convolutional recurrent neural networks is proposed. CRNN, which uses extended convolutional network to describe the pattern information of the discourse spectrum and model the long-term correlation of signals, and BiLSTM conduct the time sequence modeling. The performance of this method is better than that of BiLSTM.

2. Model Theory

In order to effectively describe the acoustic pattern information of speech in the time-frequency domain, model the long-term correlation of signals, and improve the naturalness of translated speech, a convolutional recurrent neural network with continuous wavelet transform is proposed in this paper. This CRNN model combined with the advantages of neural network, signal processing theory, and depth can use signal processing methods to obtain more suitable for the acoustic characteristics of the task and to make full use of the depth of the neural network nonlinear description ability to the words the local characteristics of spectrum and long correlation model, so as to achieve better performance of discourse transformation [18].

2.1. Discourse Conversion Model of Convolution Recurrent Neural Network with Continuous Wavelet Transform. Continuous wavelet transform (CWT) is a commonly used time-frequency analysis tool [19]. The traditional fixed-window transform algorithm (such as Fourier transform) determines the size and shape of the time-frequency window after selecting the window function and has the same ability to analyze both high and low frequencies. However, in practical signal analysis, we usually expect the algorithm to have different time-frequency resolution in different frequency bands. Continuous wavelet transform is an algorithm to solve this kind of problem, and its calculation process is shown in formula (1):

$$WT_f(a,\tau) = \prec f(t),$$
$$\psi_{a,\tau}(t) \succ = a^{-1/2}\int_R f(t)\overline{\psi\left[\frac{(t-\tau)}{a}\right]}\mathrm{dt}. \tag{1}$$

In the formula, $F(t)$ represents the original signal, A represents the scale factor in the wavelet transform, τ represents the translation factor, and the wavelet basis function ψ increases with the increase of the scale factor, the time window function also increases, and the frequency resolution of the unit increases correspondingly, otherwise, the time resolution increases. When the wavelet basis function meets the admissible condition, the algorithm has contravariant transformation, and the Morlet wavelet basis satisfying the condition is adopted in this paper. The fundamental frequency component predicted by the model can be reconstructed into the fundamental frequency feature by inverse wavelet transform. The inverse wavelet transform formula is as follows:

$$x(t) = \frac{1}{C_\psi}\int_0^{+\infty}\frac{\mathrm{da}}{a^2}\int_{-\infty}^{+\infty}\mathrm{WT}_x(a,\tau)\psi_{a,\tau}(t)\mathrm{d}\tau,$$
$$= \frac{1}{C_\psi}\int_0^{+\infty}\frac{\mathrm{da}}{a^2}\int_{-\infty}^{+\infty}\mathrm{WT}_x(a,\tau)a^{-1/2}\psi\left(\frac{t-\tau}{a}\right)\mathrm{d}\tau. \tag{2}$$

$X(t)$ represents the reconstructed signal, where the calculation method of admissible conditions is given by formula (3):

$$C\psi = \int_0^{\infty}\frac{|\psi(a\omega)|}{a}\mathrm{da} \prec \infty. \tag{3}$$

2.2. CNN Model. CNN is a commonly used neural network structure. Different from fully connected networks, the neurons of CNN are usually arranged in three dimensions. In the field of audio processing, 2d convolutional neural networks are usually used. In 2d convolutional kernels, the height and width correspond to the size of the time-frequency window of the convolution kernels, that is, the time-frequency range of each convolution of the convolution kernels. The depth of the convolution kernel corresponds to the number of channels of features after convolution. Usually, the depth of the convolution kernel used is gradually increased at the beginning of the model to improve the

fitting ability of the model, while the depth of the convolution kernel is gradually reduced at the output end of the model to map features to the target dimension. Figure 1 shows a schematic diagram of a two-dimensional convolution kernel.

Assuming that the input feature of this example is C^l, the eigenvalue of the output of the convolutional network is C^{l+t}, and the target feature is C^{ture}, the convolution operation can be expressed by formula (4):

$$C^{l+1}(i,j) = \left[C^l \otimes w^{l+1}\right](i,j) + b^{l+1} = \sum_{k+1}^{Kl}\sum_{x=1}^{f}\sum_{y=1}^{f} \left[C_k^l(s*i+x, s*j+y) * w^{l+1}(x,y)\right] + b^{l+1},$$
$$\left(i,j \in \{0,1,\ldots,L_{l+1}\}, L_{l+1} = \frac{L_l + 2*z - f}{s} + 1\right). \tag{4}$$

In the formula, w and B, respectively, represent the weight matrix and bias of the convolution kernel; I and j represent the number of pixels of the feature graph; f, z and s correspond to the size, filling number, and step size of the convolution kernel. The training of convolutional network requires the setting of loss function, and the commonly used MSE loss function can be expressed by formula (5):

$$\text{MSE} = \left[\frac{1}{D}\sum_{i=1}^{D}\left(\frac{1}{2}\left(C^{\text{ture}} - C^{l+1}\right)^2\right)\right], \tag{5}$$

where D represents the corresponding feature dimension.

The extended convolutional neural network is a special convolutional network whose filter is discontinuous. Studies have found that such network structure with spacing between filters can make the convolution kernel have a large receptive field with minimal precision loss. The following figure shows the schematic diagram of the receptive field range of an ordinary $3 * 3$ convolution kernel and an extended $3 * 3$ convolution kernel.

The rectangular block in Figure 2 represents the feature graph, and the deepened part represents the convolution region of the convolution kernel filter. As can be seen from the figure, in the case of the same convolution kernel size, the receptive field of the extended convolutional network is larger than that of the ordinary convolutional network. This feature enables the model to have a larger receptive field under the same conditions and enables the network model to be capable of modeling longer context information.

2.3. CRNN Model. CRNN is mainly used to recognize text sequences of indeterminate length end-to-end, without cutting a single text first, but transforming text recognition into a sequence-dependent sequence learning problem, which is image-based sequence recognition. Figure 3 shows the structure diagram of the CRNN model used in this paper. After the acoustic features of ear discourse are input into the model, the feature extraction module is used to obtain the local features of the discourse spectrum.

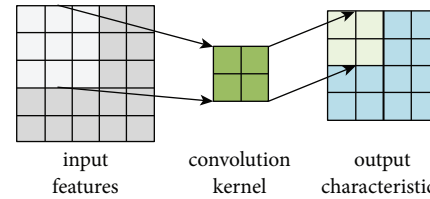

Figure 1: Schematic diagram of two-dimensional convolution kernel.

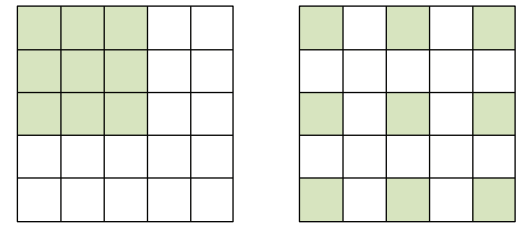

Figure 2: Comparison of receptive fields of different convolution structures. (a) Ordinary convolution, (b) Expansion of the convolution.

Feature extraction module is composed of two sets of two-dimensional dilated convolution. One set of convolution layer uses a convolution kernel with a size of 3×3. The first dimension of the convolution kernel corresponds to the time direction of the discourse feature sequence and makes the convolution layer perform dilation in the time domain direction, which is called the time domain dilated convolution layer. Another set of convolution layers performs frequency domain expansion using convolution kernels of the same size.

The characteristic graph output by the time-frequency expansion module is connected and reconstructed into one-dimensional features and then input into the time-domain modeling module. The time-domain modeling module consists of a group of time-domain expansion blocks, whose structure is shown in Figure 3. To model discourse long-term correlation, one-dimensional dilated convolution was used in each dilated block and Gated Linear Units (GLUs) were used to improve the stability of the model during training. The calculation process of GLUs is shown in formula (6):

$$y = \sigma(x * W_1 + b_1) \otimes (x * W_2 + b_2), \tag{6}$$

where W_1 and W_2 represent the weight of the convolution layer, b_1 and b_2 represent the corresponding bias term, σ represents the sigmoID activation function, and $\otimes$ represents the element-by-element multiplication symbol. The calculation process of the MISH activation function used in the expansion block can be expressed by formula (7):

$$\text{MISH} = x * (\tanh(\text{softplus}(x))). \tag{7}$$

In the formula, TANH and Softplus represent corresponding activation functions, respectively, and the calculation process of softPLu function is described in formula (8).

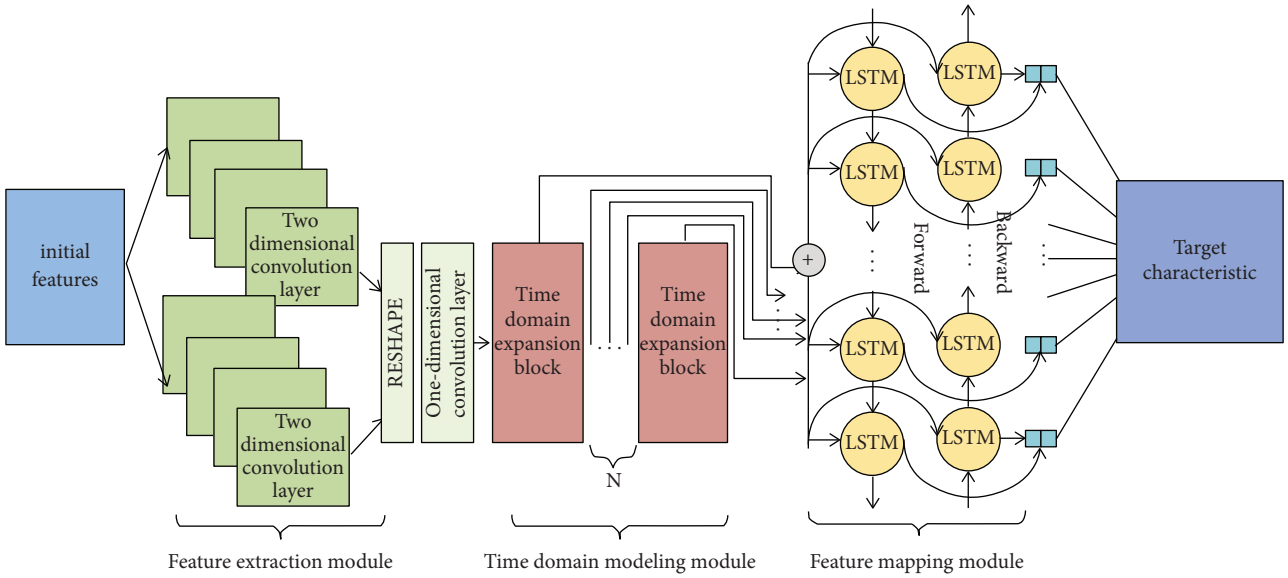

Figure 3: Structure of utterance conversion model based on CRNN.

$$\text{softplus} = \log\left(1 + e^{x}\right). \tag{8}$$

It can be seen from formula (8) that the function has a small number of negative intervals, which provides an additional flow interval for the gradient flow, thus alleviating the gradient problem of the network. The input of adjacent time domain expansion block is the output A of the previous expansion block, and the input of feature mapping module is obtained by adding the output B of each expansion block element by element.

The output of the feature mapping module is calculated by the two groups of memory cells with opposite directions, and the calculation process can be expressed by the following formula:

$$\begin{aligned} \overrightarrow{h}_t &= \text{lstm}\left(x_t\right), \\ \overleftarrow{h}_t &= \text{lstm}\left(x_t\right), \\ y_t &= W_{\underset{hy}{\rightarrow}} \overrightarrow{h}_t + W_{\underset{hy}{\leftarrow}} \overleftarrow{h}_t + b_y. \end{aligned} \tag{9}$$

The calculation process of LSTM in the above formula can be expressed by the following formula:

$$\begin{aligned} i_t &= \sigma\left(W_{xi}x_t + W_{hi}h_{t-1} + W_{ci}c_{t-1} + b_i i_t\right), \\ f_t &= \sigma\left(W_{xf}x_t + W_{hf}h_{t-1} + W_{ci}c_{t-1} + b_f\right), \\ c_t &= f_t c_{t-1} + i_t \tanh\left(W_{xc}x_t + W_{hc}h_{t-1}b_c\right), \\ o_t &= \sigma\left(W_{xo}x_t + W_{ho}h_{t-1} + W_{co}c + b_o\right), \\ h_t &= o_t \tanh\left(c_t\right). \end{aligned} \tag{10}$$

In the above formula, I, F, O, and C correspond to the input gate, forgetting gate, output gate, and cell state in the cell structure, respectively. O represents the commonly used SigmoID activation function, and W and B represent the weights and bias items to be learned during network training. Because the time-domain modeling module uses a large number of extended convolutional neural networks, the feature graph input by each neuron in the circular layer of the feature mapping module contains the whole discourse context information of the input model, which is beneficial to the model to describe the long-term correlation of signals.

2.4. Proposed Ear Discourse Conversion. The proposed ear discourse conversion method based on the CRNN model is shown in Figure 4. During the model training, the STRAIGHT model was used to extract the characteristic parameters of the two kinds of discourse, respectively. As mentioned above, the STRAIGHT model is a classical parametric vocoder, which has been widely used in speech analysis and synthesis tasks. After extracting relevant parameters, DTW algorithm is used to align feature sequences. Then, the spectral envelope features are converted to MCC features, and the normal speech fundamental frequency is decomposed by continuous wavelet transform. Finally, the MCC feature estimation model (CRNN_mcc) was trained using MCC features of ear speech and normal speech.

In the transformation stage, the extracted ear speech spectrum envelope is converted into MCC features, then the MCC features are input to the two transformation models after training to obtain the MCC features and nonperiodic components estimated by the model, and then the MCC features estimated by the model are input to the CRNN_f0 model to obtain the estimated fundamental frequency components. Then, the inverse of the estimated MCC feature is transformed into a spectral envelope, and the obtained fundamental frequency component is reconstructed into the speech fundamental frequency by inverse wavelet transform. Finally, the spectral envelope, aperiodic component, and fundamental frequency predicted by the model are reconstructed into transformed discourse by the STRAIGHT model.

Table 1 shows that the input and output parameters of two-dimensional convolution are frame number, frequency channel, and characteristic image channel in turn. The

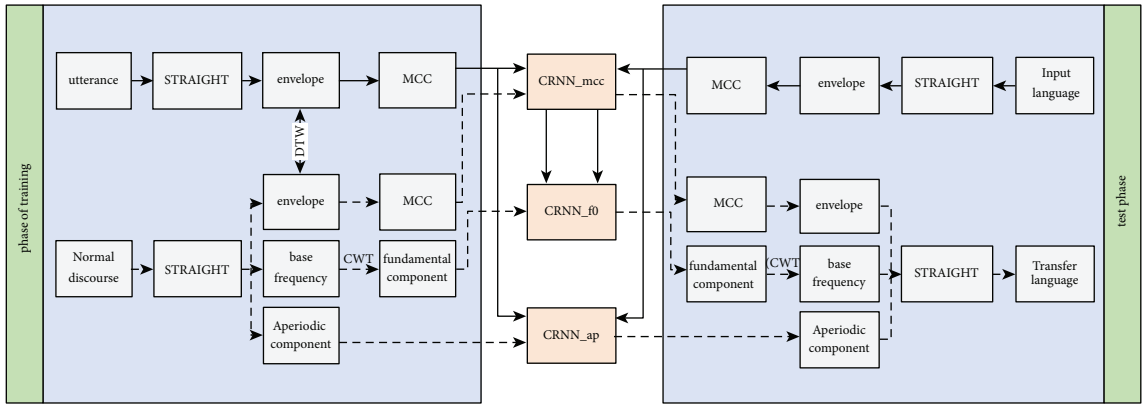

Figure 4: Flow chart of CRNN-based utterance conversion method.

Table 1: Parameter configuration of the CRNN utterance conversion model.

Network layer	Input size	Super parameter	Output size
Expand	(150 × 30)	—	(150 × 30 × 1)
Conv2d_1.1 Conv2da_1.2	(150 × 30 × 1)	(3 × 3, (1, 1), 16) (3 × 3, (1, 1), 16)	(150 × 30 × 1) (150 × 30 × 16)
Conv2d_2.1 Conv2d_2.2	(150 × 30 × 16)	(3 × 3, (1, 1), 16) (3 × 3, (1, 1), 16)	(150 × 30 × 16)
Conv2d_31 Conv2d_3.2	(150 × 30 × 16)	(3 × 3, (2, 1), 32) (3 × 3, (1, 2), 32)	(150 × 30 × 32)
Conv2d_4.1 Conv2d_4.2	(150 × 30 × 32)	(3 × 3, (4, 1), 32) (3 × 3, (1, 4), 32)	(150 × 30 × 32)
Concatenate	(150 × 30 × 32) (150 × 30 × 32)	—	(150 × 30 × 64)
Reshape	(150 × 30 × 64)		(150 × 1920)
Conv1d_1	(150 × 1920)	(1, (1), 512)	(150 × 512)
TD block		(1, (1), 256) (3, (1), 128) (1, (1), 512)	
TD block		(1, (1), 256) (3, (2), 128) (1, (1), 512)	
TD block	(150 × 512)	(1, (1), 256) (3, (4), 128) (1, (1), 512)	(150 × 512)
TD block		(1, (1), 256) (3, (8), 128) (1, (1), 512)	
TD block		(1, (1), 256) (3, (16), 128) (1, (1), 512)	
BiLSTM	(150 × 512)		(150 × 1024)
Dense	(150 × 1024)	(30/30/513)	(150 × 30/30/513)

parameters of convolution layer represent the size, expansion rate, and number of convolution kernels, respectively. The input and output parameters of one-dimensional convolution are tonnage and frequency channel in turn. The convolution layer parameters have the same meaning as two-dimensional convolution. In order to keep the temporal characteristics of discourse unchanged, zeroing is applied to all convolution layers to maintain the consistency of input and output dimensions. Only one set of time domain block parameters is shown in the table, and three sets of time domain expansion blocks with the same parameters are stacked in the model. The TD block represents the time domain extension block. The output of recurrent neural network is the symbiosis of the output of two groups of neurons. Therefore, this paper splices the output of two groups of LSTM and uses the full connection layer to map the feature map to the target dimension.

This method uses the function shown in formula (11) as the training error function in the training process:

Table 2: Impact of time-frequency dilated convolution on model performance.

Convolution kernels	CD	PESQ	STOI
3×3	4.5826	1.2679	0.6003
Time-frequency dilated convolution	4.5163	1.3201	0.6104

Table 3: Impact of time domain dilated block on model performance.

Model	CD	PESQ	STOI
CRNN_nt	4.6532	1.2895	0.5765
CRNN_ot	4.5885	1.3111	0.6004
The model in this paper	4.5163	1.3201	0.6104

$$\text{loss} = \frac{1}{N}\sum_{t=1}^{N}\frac{10}{\log 10}\sqrt{2\sum_{i=1}^{m}\left(y_i - Y_i\right)^2}. \quad (11)$$

In the above formula, y_i and y_i represent target feature and prediction feature, respectively.

3. Experimental Simulation and Result Analysis

3.1. Experimental Data and Evaluation Indicators. To further evaluate the performance of the proposed method in the auditory speech conversion task, 348 auditory utterance and corresponding target sounds from the wTIMIT discourse database were selected as experimental data. The selected corpus has a sampling rate of 8000 Hz and is stored in 16 bit PCM format. When extracting speech features, the frame length is 40 ms, the frame offset is 5 ms, and 1024 point fast Fourier transform is used for each frame of speech. In total, 313 auditory utterances and their corresponding normal utterances were randomly selected as the training set, and the other 35 corpora were used as the test set. The relevant test set has strong adaptability.

All the above methods use the straight algorithm to analyze the reconstructed discourse. The GMM method and the DNN method in the comparison method are limited by the model structure and cannot be modeled by using the dynamic correlation between frames of discourse. In order to improve the algorithm performance of the comparison method and make the effectiveness of the proposed method more convincing, the dynamic characteristics of speech frames are taken as the training parameters of the two methods. The calculation formula of dynamic characteristics is given by formula (12).

$$\text{sp\_dy}_k = \frac{\left(-2 * sp_{k-2} - \text{sp}_{k-1} + \text{sp}_{k+1} + 2 * \text{sp}_{k+2}\right)}{3}, \quad (12)$$

sp_dy_k represents the corresponding dynamic feature.

The specific parameter configuration of the comparison method is described as follows: in the gMM-based ear speech conversion method, three models, GMM_mcc, GMM_ap, and GMM_f0, are, respectively, trained to estimate the MCC, aperiodicity and fundamental frequency of normal sounds. The Gaussian component number of GMM MCC and GMM_f0 is set to 32, and the Gaussian component number of GMM_ap is set to 16. In the DNN ear speech conversion method, three DNN models are trained to estimate the MCC feature, nonperiodic component and fundamental frequency of target speech. The structure of THE DNN model is 30×30-900-1024-2048-1024-1024-900/7710/30. The Dropout technology is used for the hidden layers of the model to improve the model and reduce overfitting. The Dropout parameter value is set to 0.9, and the three dimensions of the output layer correspond to the three different characteristics of the prediction. For BiLSTM, three BiLSTM models are also trained, respectively, to estimate the acoustic characteristics of transformed discourse. The BiLSTM used contains two hidden layers with 512 units. All comparison methods adopted MSE objective function, and Adam algorithm was used to optimize model parameters, with a learning rate of 0.0001.

Table 4: Quality evaluation of converted speech by different methods.

Transfer approach	CD	PESQ	STOI
GMM	5.4415	1.0121	0.4603
DNN	5.1732	1.0901	0.5062
BiLSTM	4.8611	1.2523	0.5559
The model in this paper	4.5163	1.3201	0.6104

Table 5: RMSEs of fundamental frequency of different methods.

Model	GMM	DNN	BiLSTM	CRNN	The model in this paper
RMSE (HZ)	121.09	88.76	81.14	69.27	66.93

3.2. Model Parameter Selection. In order to evaluate the influence of extended convolution in the time-frequency domain of the feature extraction module on the translated speech quality, the traditional 3×3 single-size convolution kernel and the extended convolution in the time-frequency domain used in this paper were used to conduct the speech conversion experiment. It is obvious from Table 2 that the time-frequency expansion convolution adopted in this paper is conducive to improving the discourse conversion performance of the model. The specific comparison of discourse quality after transformation is shown in Table 2.

In order to explore whether the time domain expansion block in the time domain modeling module can effectively improve the performance of the discourse conversion method, the transformed discourse of CRNN discourse conversion method in three cases is compared. Table 3 shows the comparison of discourse quality after transformation under the three conditions, where CRNN_nt represents the CRNN model without time domain dilators and CRNN_ot represents only one group of time domain dilators. As can be seen from Table 3, the CRNN model without the time-domain expansion block has the worst performance of discourse conversion. The prediction accuracy of the CRNN model that only uses a group of time-domain dilators is lower than that of the method in this paper, because the CRNN model that only contains a group of time-domain dilators is difficult to use the context information of the

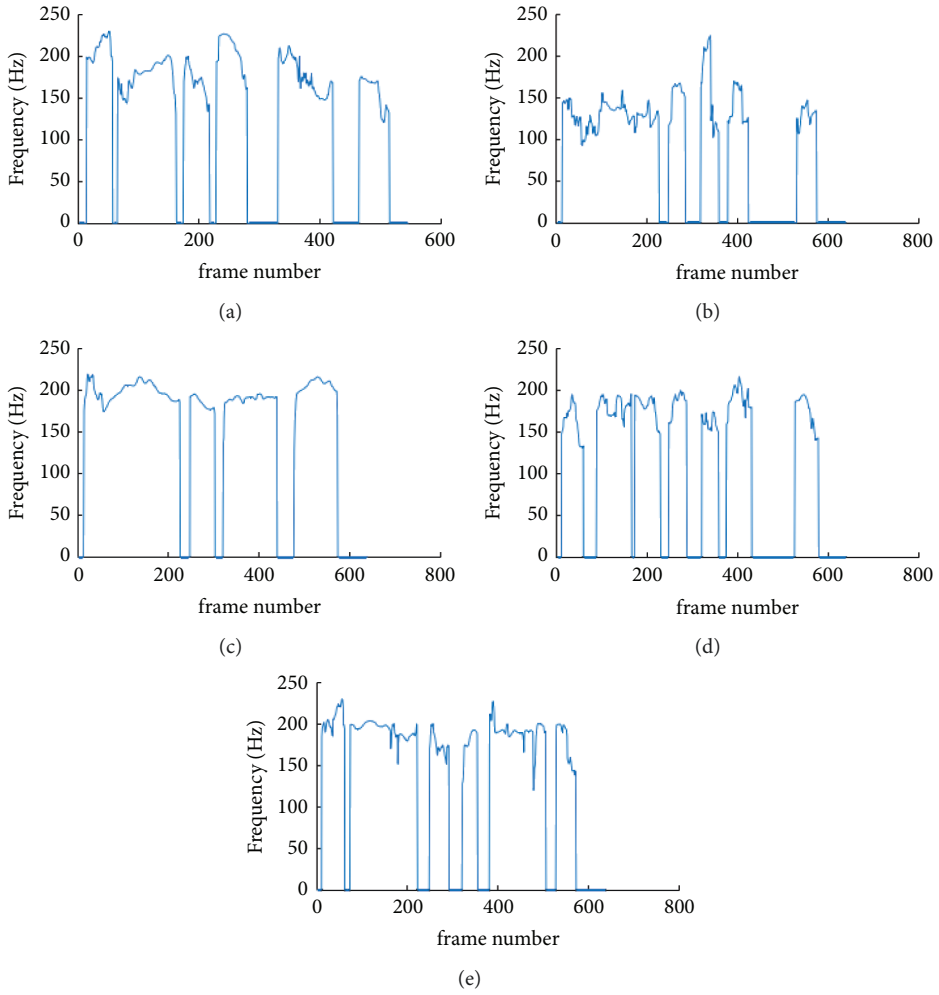

Figure 5: Fundamental frequency curves obtained by different conversion methods. (a) Enter the words, (b) GMM, (c) DNN, (d) BiLSTM, (e) CRNN.

whole input discourse, and the model has a small receptive field, which makes it impossible to effectively model the long-term correlation of discourse. Therefore, this paper finally sets up three groups of time domain expansion blocks in the CRNN network.

3.3. Comparative Analysis of Experimental Results. To demonstrate the effect of CRNN discourse conversion model, GMM, DNN, and BiLSTM are used as comparison models. Table 4 shows the evaluation results of transformed discourse. The performance of the GMM model is poor because the modeling ability of GMM is weaker than that of the neural network model. Although the DNN method can well represent the nonlinear mapping relationship, it cannot model the long-term correlation of discourse, and the effect of discourse conversion is not ideal. Compared with the DNN method, the BiLSTM method can make better use of the interspeech correlation. When the time step is large, the BiLSTM method can also model the long-term correlation of discourse, so the conversion effect is better than the GMM method and the DNN method. However, BiLSTM is difficult to effectively utilize the local features in the time-frequency domain of discourse, resulting in some spectral errors in the transformed discourse. As can be seen from Table 4, compared with the comparison method, the effect of the CRNN speech conversion model under the quality assessment of different conversion speech methods is 4.5163 s in the disc time; 1.3201 s in the ticker; and 1.3201 s in the station time 0.6104 s, the utterances transformed by this method in this paper have the best inhomogeneous quality and intelligibility.

Table 6: MOS of converted speech by different methods.

Model	GMM	DNN	BiLSTM	The model in this paper
MOS	2.35	2.51	2.82	2.90

Table 5 shows RMSE values of fundamental and target tones predicted by four conversion methods, where, CRNN indicates that CWT is not used to convert the discourse fundamental frequency in the training process. As can be seen from Table 5, GMM is difficult to accurately estimate the fundamental frequency characteristics of utterances, and BiLSTM has better fundamental frequency estimation

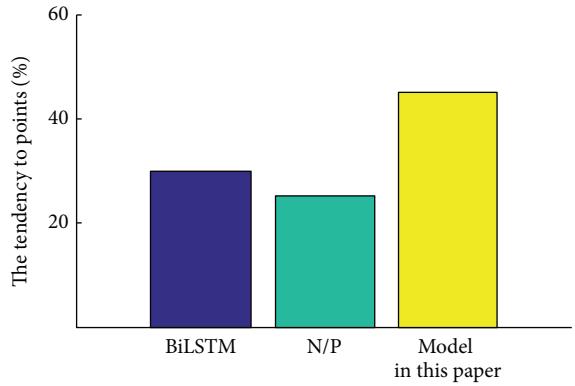

Figure 6: ABX test.

performance than DNN. In the process of model training, CWT decomposition of fundamental frequency can improve the prediction accuracy of the model to a certain extent. A horizontal comparison of the five methods shows that the difference between the fundamental frequency predicted by the proposed method and the target fundamental frequency is the smallest, which proves that the proposed method has higher fundamental frequency prediction accuracy compared with the comparison method.

It can be seen from Figure 5 that the GMM speech conversion method is difficult to fit the fundamental frequency curve of target speech effectively, and the fundamental frequency of transformed speech is greatly different from that of the target speech. The DNN method can only estimate unvoiced speech conversion, but cannot accurately predict the fundamental frequency curve. The fundamental frequency curve estimated by the BiLSTM method has a certain similarity with the target curve, but there is still a great difference with the expected target in details such as 170–190 frames and 230–270 tons. However, the overall trend of the speech fundamental frequency curve estimated by the proposed method is close to that of the target fundamental frequency, which indicates that the proposed method has better fundamental frequency estimation performance.

Table 6 shows MOS scores of discourse obtained after four methods of transformation. As can be seen from Table 6, the comfort level of discourse listening sensation after GMM conversion is poor, which is not suitable for discourse conversion task. Because BiLSTM can effectively make use of the dynamic interframe correlation of utterances, the transformed utterances have stronger continuity and better comprehensibility, thus achieving a better subjective score. The method in this paper can effectively use the acoustic model information to establish a long-term correlation model of utterances and use the prosodic features of utterances as the learning objective of the model. Therefore, the naturalness of statements transformed by the method in this paper is high, and the opinions are emotional, thus achieving the highest subjective score.

In this paper, ABX test is used to further evaluate and compare BiLSTM discourse conversion method with this method, which has better subjective score. Figure 6 shows the results of the ABX test method. After several rounds of listening tests, the auditioners generally believe that the transformed utterances in this paper are closer to the target utterances.

4. Conclusion

This paper mainly introduces the discourse conversion method based on convolution recurrent neural network with continuous wavelet transform. Compared with the existing statistical model-based discourse conversion methods, the following conclusions can be drawn:

(1) The existing discourse transformation methods usually only consider the differences between discourse spectra and rarely consider the characteristics of discourse itself from the perspective of the internal characteristics of discourse. This paper uses the local connection feature of CNN network to effectively extract the local features of discourse.

(2) Discourse signals have long-term correlation, and existing discourse conversion methods are limited by model structure, so it is difficult to model the long-term correlation of discourse. Inspired by the extended convolutional neural network in the task of discourse synthesis, the method in this paper stacks multiple one-dimensional extended convolutional network layers in the model, so that the feature mapping module of the model can use the whole discourse context information for modeling, so as to describe the long-term relevance of discourse more effectively.

(3) Due to its special motivation source and vocal form, the overall listening sensation of the utterance lacks of tonal change and the naturalness of the listening sensation of the utterance is poor. The converted utterances have better listening comfort, and continuous wavelet transforms are used to decompose the fundamental frequency features instead of the original declarations when training the model. The decomposed fundamental frequency can represent the prosodic characteristics of utterances. Taking the decomposed essential frequency component as the training target can give the transformed speech a better subjective hearing evaluation. At the end of this paper, a number of experimental results show that the discourse conversion method proposed in this paper has better discourse conversion performance compared with the contrast method, and the transformed discourse has better performance in both subjective and objective evaluation.

Data Availability

The data set can be accessed upon request.

Conflicts of Interest

The authors declare that they have no conflicts of interest.

References

[1] X. L. Li, *New Discourse Analysis of Ideological and Political Education in Colleges and Universities in Micro Era and Research on the Frontier Issues of Development*, Xinhua Publishing House, Beijing, 2017.

[2] X. Shi, *Discourse Research in Contemporary China*, Higher Education Press, Beijing, China, vol. 8, 2018.

[3] D. S. Park, W. Chan, Y. Zhang et al., "Specaugment: a simple data augmentation method for automatic speech recognition," 2019, https://arxiv.org/abs/1904.08779.

[4] Y. Jia, Y. Zhang, R. J. Weiss et al., "Transfer learning from speaker verification to multispeaker text-to-speech synthesis," 2018, https://arxiv.org/abs/1806.04558.

[5] T. Tereza, J. Rusz, V. Jan, B. Serena, S. Alessandro, and T. P. Maria, "Speech disorder and vocal tremor in postural instability/gait difficulty and tremor dominant subtypes of Parkinson's disease," *Jounal of Neural Transmission*, vol. V127, no. 4, pp. 328–339, 2020.

[6] A. Gautam, J. G. Naples, and S. J. Eliades, "Control of speech and voice in cochlear implant patients," *The Laryngoscope*, vol. 129, no. 9, pp. 124–136, 2019.

[7] O. Perrotin and I. V. Mcloughlin, "Glottal flow synthesis for whisper-to-speech conversion," *IEEE/ACM Transactions on Audio, Speech, and Language Processing*, vol. 28, pp. 889–900, 2020.

[8] J.-X. Zhang, Z.-H. Ling, L.-J. Liu, Y. Jiang, and L.-R. Dai, "Sequence-to-Sequence acoustic modeling for voice conversion," *IEEE/ACM Transactions on Audio, Speech, and Language Processing*, vol. 27, no. 3, pp. 631–644, 2019.

[9] H. Lian, Y. Hu, W. Yu, J. Zhou, and W. Zheng, "Whisper to normal speech conversion using sequence-to-sequence mapping model with auditory attention," *IEEE Access*, vol. 7, pp. 130495–130504, 2019.

[10] D. J. Cates, M. J. Magnetta, L. J. Smith, and C. A. Rosen, "Novel, anatomically appropriate balloon dilation technique of the glottis to treat posterior glottic stenosis in a 3D-printed model," *The Laryngoscope*, vol. 129, no. 10, pp. 2239–2243, 2019.

[11] B. Msa, "Anomaly detection based pronunciation verification approach using speech attribute features," *Speech Communication*, vol. 11, pp. 29–43, 2019.

[12] L. Czap, "Automated speech production assessment of hard of hearing children," *IEEE Journal of Selected Topics in Signal Processing*, vol. 14, no. 2, pp. 380–389, 2020.

[13] J. Zhou, Y. Hu, H. Lian, H. Wang, L. Tao, and H. K. Kwan, "Multimodal voice conversion under adverse environment using a deep convolutional neural network," *IEEE Access*, vol. 7, pp. 170878–170887, 2019.

[14] P. Olivier and V. M. Lan, "Glottal flow synthesis for whisper-to-speech conversion," *IEEE/ACM Transactions on Audio, Speech, and Language Processing*, vol. 28, pp. 889–900, 2020.

[15] J. B. Salyers, Y. Dong, and Gai, "Continuous wavelet transform for decoding finger movements from single-channel EEG," *IEEE Transactions on Biomedical Engineering*, vol. 66, no. 6, pp. 1588–1597, 2019.

[16] Z. Luo, J. Chen, T. Takiguchi, and Y. Ariki, "Emotional voice conversion using dual supervised adversarial networks with continuous wavelet transform F0 features," *IEEE/ACM Transactions on Audio, Speech, and Language Processing*, vol. 27, no. 10, pp. 1535–1548, 2019.

[17] C. Heejin and H. Minsoo, "Sequence-to-Sequence emotional voice conversion with strength control," *IEEE Access*, vol. 9, pp. 42674–42687, 2021.

[18] S. Vekkot, D. Gupta, M. Zakariah, and Y. A. Alotaibi, "Emotional voice conversion using a hybrid framework with speaker-adaptive DNN and particle-swarm-optimized neural network," *IEEE Access*, vol. 8, pp. 74627–74647, 2020.

[19] K. Tan, J. Chen, and Wang, "Gated residual networks with dilated convolutions for monaural speech enhancement," *IEEE/ACM transactions on audio, speech, and language processing*, vol. 27, no. 1, pp. 189–198, 2019.

Hindawi
Scientific Programming
Volume 2022, Article ID 1936145, 8 pages
https://doi.org/10.1155/2022/1936145

Research Article

Early Warning and Monitoring Analysis of Financial Accounting Indicators of Listed Companies Based on Big Data

Wenyan Wang

Department of Economics and Management, Cangzhou Normal University, Hebei 061001, China

Correspondence should be addressed to Wenyan Wang; wangwenyan8805@caztc.edu.cn

Received 19 April 2022; Revised 29 April 2022; Accepted 10 May 2022; Published 24 May 2022

Academic Editor: Jie Liu

With the continuous development of the economy and the continuous improvement of information network technology, the information age brings not only the innovation of social lifestyle but also the innovation of enterprise development management mode and management concept. It is more likely to cause financial information leakage and human risk out of control in the big data environment. Faced with these risks, it is necessary to actively explore ways of risk control and create a good early warning and monitoring mechanism. It aims to study the principle and data processing mechanism of the company's financial early warning monitoring, and the establishment and analysis of the early-warning monitoring model in the big data environment. Help managers find and put forward early warning signals when the company has just had a financial crisis, and remind the company to take countermeasures.

1. Introduction

With the rapid development of the economy and technology, we are now in an era of big data composed of computers and the internet. Big data brings countless convenience and opportunities to the development of enterprises [1, 2]. At the same time, it also brings many risks and challenges to enterprises. Making the competition between enterprises more intense, investors and enterprises pay more attention to the important role of financial crisis early warning in enterprise management. However, enterprise financial crisis early warning has always been a difficult problem in enterprise management. Therefore, when enterprises are preventing and responding to financial risks, in order to better adapt to the current environment, it has become an important task for enterprises to establish and improve the early-warning and monitoring system of financial accounting indicators adapted to the era of big data [3].

Scholars at home and abroad have conducted relevant research on financial early-warning indicators, the construction of early-warning model, big data information acquisition, and processing technology [4]. Aziz et al. found that the financial early-warning model using cash flow indicators has the best early-warning effect, which can better reflect the actual situation of listed companies [5]. Su and Wang proposed a financial early-warning computer big data model for listed real estate companies based on extension theory, and by combining them with each company, the specific actual data are verified to quickly and dynamically provide suggestions for the development of listed real estate companies [6]. Liang et al. used big data analysis to explore new economic risk early-warning methods, built a risk monitoring and early-warning platform, and realized rapid and scientific economic decision-making [7].

The application of big data in the financial field has long taken shape. At present, it is mainly active in the analysis of the stock market. Antweiler and Frank's research pointed out that the information between the volatility of the target company's market and the volume of stock transactions can be predicted [8]. Shin et al. found that the prediction effect of the BP neural network model is not as good as that of the support-vector machine (SVM) model in the aspect of enterprise financial early warning [9]. Min and Lee found that the SVM model had the best effect by comparing the multiple discriminant analysis (MDA), logit, and BP models [10].

Big data and financial early-warning monitoring are the common focus of researchers, but there is relatively little research on the application of big data to early-warning monitoring and analysis of corporate financial accounting indicators. This study mainly discusses the company's financial early-warning and monitoring principle and data processing mechanism, and the establishment and analysis of the early-warning and monitoring model under the background of big data. It aims to help managers take effective measures to avoid the recurrence of financial crisis when receiving the company's financial early warning.

2. Related Theoretical Analysis

2.1. Company Financial Crisis and Early Warning. According to the definition of financial crisis given by domestic and foreign research institutes, it mainly covers the following situations: first, enterprises that are insolvent; second, enterprises that cannot repay the principal and interest of the loan; third, enterprises in legal bankruptcy proceedings; and fourth, enterprises that have gone bankrupt. Judging from past foreign research studies, "bankruptcy" in the legal sense is basically the criterion for a company's financial crisis, but this criterion has much inappropriateness [3, 11, 12]. This study holds that financial crisis should be a broad concept, that is, the so-called financial crisis includes not only economic failure, technical insolvency, insolvency, and bankruptcy but also various situations between these states. The financial crisis is not only a state result but also a process. Economic failure is the beginning of the financial crisis. Insolvency and insolvency indicate that the company has been in a serious state of crisis. Bankruptcy is an extreme form of the financial crisis and the result of the financial crisis.

Financial early warning is the prevention of a financial crisis. The financial warning of an enterprise refers to analyzing the financial data generated by the enterprise in the past and predicting whether there will be a financial crisis in the future. Financial early-warning research can use relevant theories such as finance, statistics, and enterprise management [13]. According to the financial statements or other financial data provided by the enterprise, the financial situation of the enterprise is analyzed and predicted by using the analysis methods such as ratio analysis and mathematical modeling [14]. The financial crisis early-warning model can distinguish between financial crisis companies and normal companies, and judge the possibility of the financial crisis through the statistical analysis of early-warning indicators. Financial early warning can remind the enterprise of financial abnormalities that will occur and assist the enterprise management personnel to find the existing problems of the enterprise as soon as possible.

2.2. Big Data. Enterprise big data covers a very wide range, including the entire dataset in the field related to the financial status of the enterprise, and also includes the dataset that can be captured, stored, processed, and analyzed by software that takes longer than tolerable time. Corporate financial big data not only has the characteristics of big data 5 V (scale, diversity, high speed, growth, and value) but also has the relevance and real time in the financial field [15, 16]. (1) According to the main body of the data, it is the data generated by the emotional expression of the stakeholders of the enterprise, such as investors, consumers, related government agencies, enterprises, and institutions involved. (2) According to the data source, the financial big data of the enterprise comes from the network platform that can obtain the emotional expression of the abovementioned stakeholders or organizations. (3) According to the origin of data, corporate financial big data originates from corporate network public opinion.

The big data indicator is a new concept proposed by combining big data and the concept of network public opinion. The current research's commonly used method is to quantify sentiment classification and combine various types of information and data to study together. Most of the big data indicators are researched by using the network public opinion data obtained from the internet, mainly through the big data indicators quantified by sentiment analysis of the network public opinion. Big data indicators have strong data acquisition feasibility and strong data quantification feasibility.

The theory of signal transmission is actually caused by information asymmetry. The transmission of information in the crowd can be natural without human intervention. It plays a very important role in regulating the phenomenon of information asymmetry in the economic market. Based on the information purification function of the network comment platform, it can provide effective big data information for the financial early-warning research of enterprises. The prediction deviation caused by using only financial indicators is corrected, and the research of financial early warning is assisted to break through the bottleneck period limited to financial indicators.

In general, enterprise big data can be more specifically understood as the existence of multiple data sources, structures, and forms of enterprise-related datasets, which will eventually form an available dataset after certain sorting. The dataset includes structured data, unstructured data, and semistructured data, including basic data, historical data, and real-time data.

3. Early-Warning Monitoring Principle and Data Processing Mechanism

3.1. Principles of Company Financial Early-Warning Monitoring. Big data embodies the characteristics of group wisdom, and the density of valuable information is very low, which makes some artificial modification intentions. Under the balance of group behavior, the value of information is often not greatly affected, which can avoid being blinded by relying only on information providers [17]. With the development of big data technology, the acquisition of this information is more objective and comprehensive than the information obtained through company announcements, surveys, conversations, and other means in the past, and this information can include the embedded influence of the company in the social network.

In the social environment, the existence of the company is based on the recognition of stakeholders, including customers, investors, supply chain partners, governments, and so on. Taking into account the company's business behavior, it will affect the relevant information on the Internet [18]. Therefore, this study regards all netizens as "sensors" of the company distributed on the network. According to the stakeholder theory, some of these "sensors" reflect the internal operation state of the company, some reflect the overall market environment of the company, and some reflect the operation state of the relevant parties of the company. Thus, a model of corporate financial early warning based on big data is constructed, as shown in Figure 1.

3.2. Data Processing Mechanism. The financial early-warning system of big data companies does not exclude the traditional indicators available in financial reports. On the contrary, the traditional financial indicators should be part of the content of big data. Various behaviors are related to the company of internet users, such as the number of times the internet users clicked on news, comments, news messages published by reporters, etc. These contents include the reactions of offline people to the company due to their contact with the company. These reactions cover various possible situations such as customer satisfaction with products, investor attitude, policy orientation, and so on due to people's different roles in the social network. All this information is mapped to the internet through offline. Through interaction on the internet, the emotions of netizens are collected and integrated into the signal flow to form the online real-time signal of sensors of relevant companies [11]. The general intuitive external manifestation of this real-time signal is the company's online public opinion.

In the specific processing process, the company's sensor signals can be semantically analyzed, and these signal flows can be quantified through emotional indicators to form a comprehensive indicator of various behaviors. The specific data processing process is shown in Figure 2.

Netizens who play the role of "sensor" of the company have various role relationships with the company offline. According to the stakeholder theory, the interaction between these roles and the company will produce different responses, which will stimulate these roles to have different emotions toward the company [19]. Only by mapping the emotions of the group to the internet can this information be preserved and acquired by us. These different emotions are gathered, excluded, and integrated into the interaction process on the internet, and finally collective wisdom will be generated. A certain angle reflects a certain state of the company.

4. Establishment of Early-Warning Monitoring Model and Data Analysis

4.1. Sample Company Selection. When selecting the sample listed companies, in order to avoid the error caused by the enterprise scale, the sample enterprise scale is basically the same, and it is obtained by random sampling under the condition of meeting various requirements. The standard of crisis enterprises is that they have been listed for more than 5 years. This special treatment is the first time since listing [20]. The main reasons for the special treatment are losses for two consecutive years and negative net profit. The sample selection standard of normal enterprises is the enterprises that have been listed in Shenzhen and Shanghai for more than 5 years or have not been specially treated since listing.

When considering the extraction ratio of normal companies and crisis companies, in order to objectively study the availability of the early-warning model, we should not too subjectively assume the research conclusion. After combining the actual market situation, it is found that the proportion of ST enterprises in listed enterprises is very small, so the selection of research samples should also be in line with the market proportion as much as possible, but if the number of crisis enterprises is too small, it will affect the learning ability of the model. Therefore, 40 listed companies with the same scale of enterprises will be collected, including 27 normal enterprises and 13 crisis enterprises. The sample of crisis enterprises comes from the enterprises specially handled by Shanghai and Shenzhen stock exchanges in 2016 and 2017, including 5 crisis enterprises in 2016 and 8 crisis enterprises in 2017.

This study will collect online public opinion data related to 40 listed companies. The source of information is mainly through the collection of company-related public opinion information from the Oriental Fortune Forum [20]. The collected data are filtered for spam and obvious false information, and duplicate content is deleted. It is estimated that more than 60,000 pieces of effective online public opinion information will be obtained in the end. The details of ST sample companies and normal sample companies are shown in Tables 1 and 2.

4.2. Indicator Screening

4.2.1. Screening of Financial Indicators. The theoretical study of financial early warning is a complex process. Since the research needs huge theoretical support, there is no clear standard for which indicators should be selected as variables in the financial early-warning model, and researchers need to make specific investigations according to the research situation. In the face of this situation, many researchers at this stage build a financial index system based on the ability of enterprise development and improve the indicators in combination with the indicators concerned by enterprise managers in their actual work. After strict and careful screening, the financial indicators involved in the final study will involve six aspects of ability [12, 21].

(1) *Solvency*. Whether an enterprise has the ability to pay cash and repay debts is the key to its healthy survival and development. The solvency of an enterprise is an important symbol reflecting the financial situation and operating ability of an enterprise. The solvency of an enterprise is an important aspect of its credibility. If the solvency is good, it can not only reduce the difficulty and cost of raising funds in the future

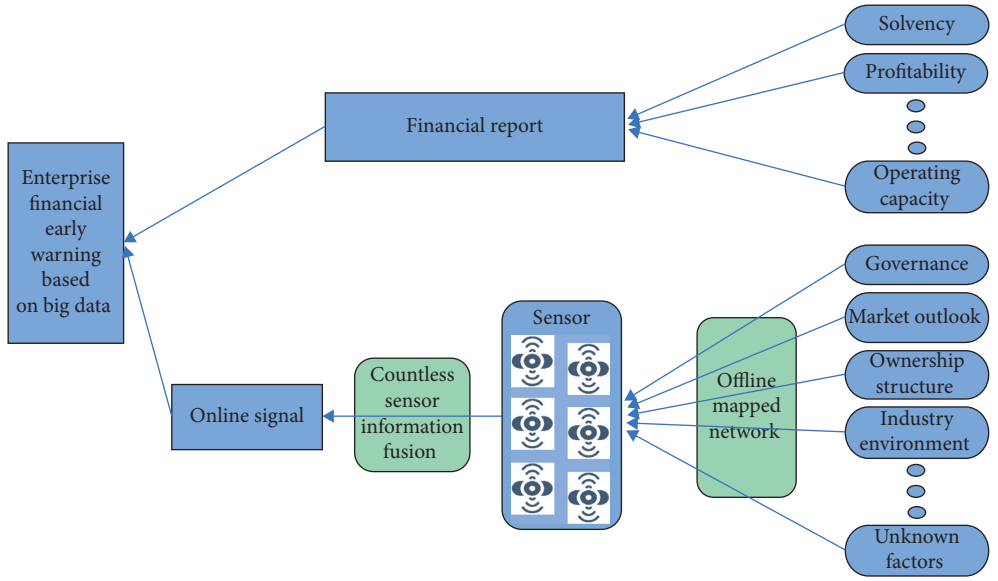

Figure 1: Principles of corporate financial early-warning monitoring.

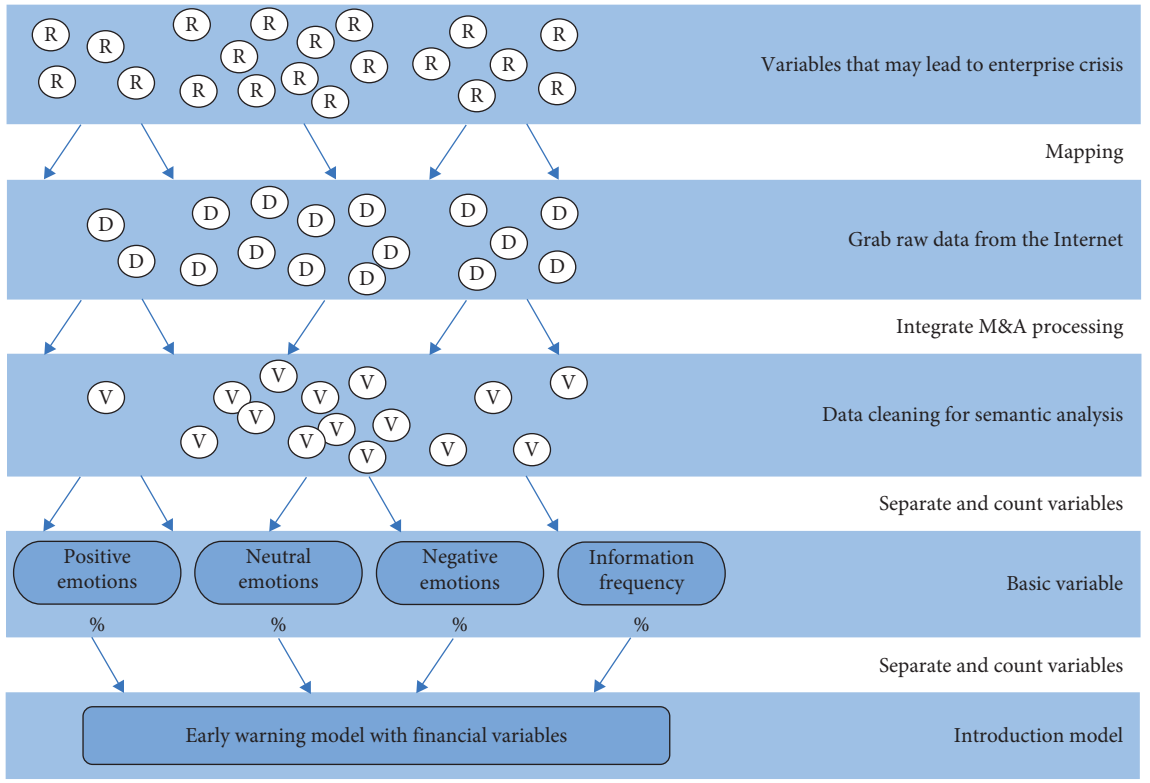

Figure 2: Data processing mechanism for financial early-warning monitoring.

but also prevent the enterprise from falling into a business crisis.

(2) *Profitability*. Profitability refers to the ability of enterprises to obtain profits, also known as the capital or capital appreciation ability of enterprises. It is usually expressed as the amount and level of enterprise income in a certain period of time. Profitability indicators mainly include operating profit margin, cost profit margin, surplus cash guarantee multiple, return on total assets, return on net assets, and return on capital. For operators, the higher the profit rate, the stronger the profitability. Through the analysis of the profitability, problems in the operation and management can be found. The analysis of the company's profitability is the in-depth analysis of the company's profit margin.

Table 1: ST sample company list.

Serial number	Listed company code	Stock code	Stock name
1	C600074	600074	ST Bao Qianli
2	C600289	600289	ST Xintong
3	C600680	600680	ST Shangpu
4	C002427	002427	ST Yuff
5	C002102	002102	ST Guanfu
6	C002147	002147	ST Xinguang
7	C002259	002259	ST Shengda
8	C002445	002445	ST Zhongnan
9	C002496	002496	Huifeng Co., Ltd.
10	C002680	002680	∗ST Changsheng
11	C600421	600421	ST Yangfan
12	C603188	603188	Yabang Co., Ltd.
13	C002188	002188	∗ST Bus

Table 2: Normal sample company list.

Serial number	Listed company code	Stock code	Stock name
1	C300092	300092	Kexin Electromechanical
2	C300100	300100	Shuanglin Co., Ltd.
3	C300112	300112	Wanxun Control
4	C300177	300177	Hi-Target
5	C002452	2452	Changgao Group
6	C300192	300192	Kingswood
7	C300351	300351	Yonggui
8	C002036	002036	Lianchuang Electronic
9	C002094	002094	Kingking
10	C002151	002151	BDStar Navigation
11	C002347	002347	Taier
12	C300274	300274	Sungrow
13	C300093	300093	Gorilla Glass
14	C300116	300116	Blivex
15	C300072	300072	SJ Environmental Protection
16	C300145	300145	Zhongjin Environment
17	C300153	300153	Cooltech Power
18	C300097	300097	Zhiyun Automation Co., Ltd.
19	C000612	000612	Jiaozuo Wanfang
20	C002031	002031	Greatoo Intelligent
21	C002046	002046	Sinomach Precision
22	C002084	002084	Seagull
23	C002111	002111	Weihai Guangtai
24	C002118	002118	Zixin Pharmaceutical
25	C002130	002130	Woer
26	C002182	002182	RSM
27	C002291	002291	ST&SAT

(3) *Growth Ability*. Enterprise growth capability refers to the growth and development of an enterprise in a specific period of time. Some scholars have found that compared with mature and stable enterprises, enterprises in the growth and the rising period grow faster and have stronger development capabilities. While the development capability is strong, the possibility of the financial crisis will be greater compared to those large enterprises with relatively mature and stable development. Financial early warning for these small and medium-sized enterprises can often get more information from online forums, because the more the uncertain factors of enterprises in vigorous development, the higher the public attention.

(4) *Operating Capacity*. Operational capacity is an indicator that reflects the efficiency of enterprise asset turnover. If a listed company wants to have a good operating ability, it needs to have a high-efficiency operation. If the asset turnover speed is fast, it means that the speed of various business links of the enterprise is fast, and the cycle of revenue and profit generated is shorter. Therefore, the asset turnover rate of listed companies will also affect the financial situation of listed companies.

(5) *Cash Flow*. Cash flow is an important indicator to measure the liquidity of assets. If the listed company has a good cash flow situation, it can indicate that the company is operating well at the current stage and has the ability to repay the corporate debt. Therefore, cash flow-related indicators are also important indicators to measure whether an enterprise will have a financial crisis. The higher the cash flow indicators, the lower the possibility of the financial crisis.

(6) *Capital Structure*. Enterprise capital structure can reflect the ability of enterprises to deal with various crises. Enterprises with a relatively high ratio of fixed assets to intangible assets have a higher ability to deal with risks [22]. In the preliminary selection of variables for financial indicators, this study selects 32 financial indicators from the six abilities concerned by enterprise managers and financial researchers as variables to be tested. The specific financial indicators are shown in Table 3.

The solvency of the enterprise is reflected by the indicators X1–X5, the profitability of the enterprise is reflected by the indicators X6–X12, the cash flow of the enterprise is reflected by the indicators X13-X14, the capital structure of the enterprise is reflected by the indicators X15-X16, the growth ability of the enterprise is reflected by the indicators X17-X28, and the operating capacity of the enterprise is reflected by the indicators X29–X32.

4.2.2. Big Data Indicators. The big data indicators used in this study are multiangle and multidimensional information related to enterprise development obtained through online public evaluation. This information is obtained by obtaining the evaluation of enterprises from many netizens. The evaluation information of many netizens is characterized by real time, many information sources, and complex structure. They can find out the situation of enterprise business activities from the network evaluation of people who pay attention to enterprise development. Such data are difficult to be manipulated by individuals, with relative objectivity

Table 3: Company financial indicators.

Financial indicator	Symbol	Indicator name
Solvency	X1	Working capital
	X2	Cash ratio
	X3	Current ratio
	X4	Quick ratio
	X5	Asset-liability ratio
Profitability	X6	EBIT
	X7	Operating net interest rate
	X8	Net profit margin of total assets
	X9	Return on net assets
	X10	Operating profit margin
	X11	Proportion of main business profit
	X12	EBIT/total assets
Cash flow	X13	Sales income cash flow
	X14	Return on total assets
Capital structure	X15	Intangible asset ratio
	X16	Fixed asset ratio
Growth ability	X17	Net profit growth rate
	X18	Operating income growth rate
	X19	Operating profit growth rate
	X20	Main business income growth rate
	X21	Growth rate of total profit
	X22	Total asset growth rate
	X23	Growth rate of net flow generated by operating activities per share
	X24	Growth rate of net assets per share
	X25	Growth rate of earnings per share
	X26	Retained earnings/total assets
	X27	Growth rate of net assets
	X28	Rate of capital accumulation
Operating capacity	X29	Accounts receivable turnover
	X30	Current asset turnover
	X31	Total asset turnover
	X32	Inventory turnover rate

and group intelligence, and the fragmentation of big data information, so many characteristics meet the relevant definitions of big data [20]. In order to further ensure the effectiveness and authenticity of online evaluation information, information collection has been made on the background information, enterprise scale, corporate governance, share structure, and audit opinions of each enterprise. When manually marking the comment samples, if you are not sure about the authenticity of individual comments, you can check the data in time. A few comments that cannot be confirmed will not be included in the data statistics.

In order to improve the efficiency and accuracy of emotion classification, this study adopts the method of artificial emotion classification. This method can also accurately judge the emotional bias of text information. In order to improve the efficiency of emotional assignment, the number of comments extracted from the network is controlled at about 60,000. This study will classify all online public opinion text data and mark the comments. The emotional bias of all effective comments shall be counted according to the established way for further analysis.

4.3. Model Establishment. The 40 samples selected in this study have 12 early-warning indicators, and a $40 * 15$ matrix will be formed at the input end, which is equivalent to inputting 15 feature vectors for the support-vector machine (SVM) model [15]. The indicator system includes two parts: financial indicators and emotional indicators of online comments, including 12 financial indicators and 3 emotional indicators of online comments. Among them, the financial indicators are enterprise solvency indicators X2, X3, X4, and X5, profitability indicators X7 and X10, cash flow indicators X13 and X14, capital structure indicators X15 and X16, and operating capacity through indicators X31 and X32. The emotional indicators of online comments are the positive-emotion index, negative-emotion index, and total comments. These vectors constitute a 15-dimensional feature vector. The judgment of the support-vector machine model is one of two choices. That is, enterprises will fall into financial crisis and enterprises will not fall into financial crisis. This means that the output vector of the model is a two-dimensional feature vector.

The support-vector machine cannot directly make selection judgment on existing samples. It needs to effectively learn the known samples first. Only after the model learns these features can it make an efficient judgment. Therefore, this study divides the overall sample into two parts, one part is used to train the model, and the other part is used to test the accuracy of the model. There will be two types of enterprises with and without a financial crisis in the two parts of the dataset. The support-vector machine model abstracts the problem of the enterprise financial early warning and uses the model to learn the data features in the training set, so as to determine the optimal classification hyperplane of the two enterprise samples and the kernel function and find the optimal related parameters. Finally, the decision function of enterprise financial early-warning model based on big data can be obtained according to these. The overall construction process of the support-vector machine model is shown in Figure 3.

4.4. Early-Warning Monitoring Analysis. The results of early-warning analysis based on traditional financial indicators are shown in Figure 4. The blue circle in the figure indicates the prediction result of the model, and the red triangle indicates the actual situation of the enterprise. If the position of the blue circle coincides with the position of the red triangle, it indicates that the prediction of the model is correct. The test focused on 12 normal enterprises, 0 were wrongly judged, 5 were ST enterprises, and 4 were wrongly judged. Therefore, it is found that the accuracy of the model in judging ST enterprises is low. The test results after integrating the early-warning indicators of comment big data are shown in Figure 5. The predictions of 12 normal companies and 5 ST companies are all correct, that is, the correct rate of this test set is 100%.

As can be seen from Figures 4 and 5, the use of financial indicators and the addition of big data indicator models to the judgment of normal enterprises have a very high

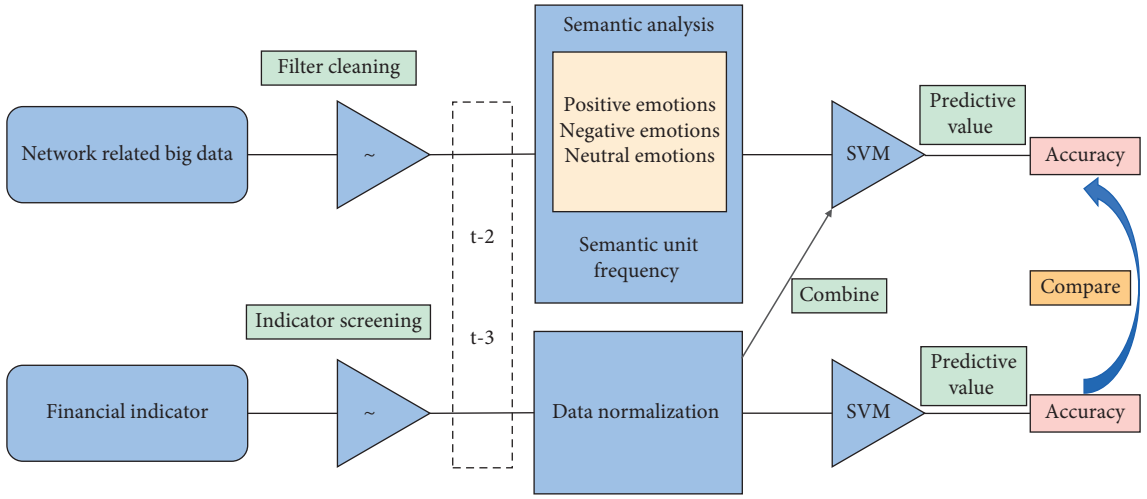

Figure 3: Model-building process.

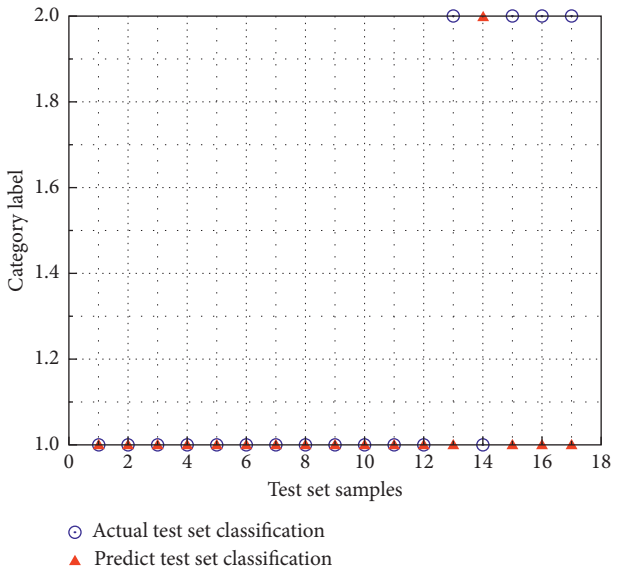

Figure 4: Test results of financial indicator model.

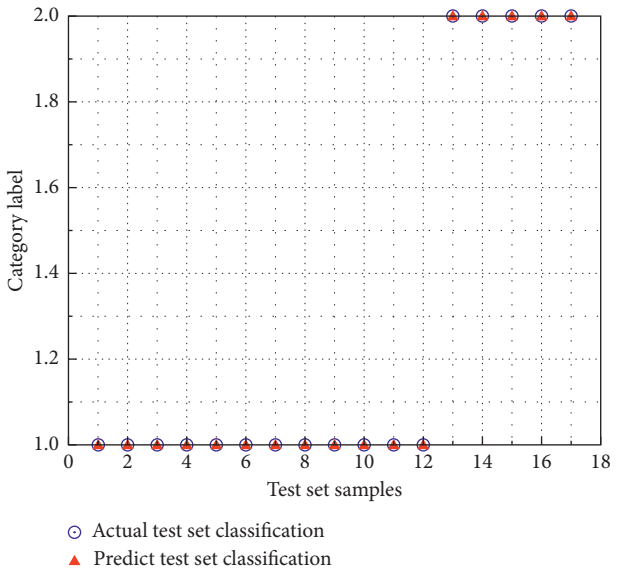

Figure 5: Test results based on big data indicator model.

accuracy rate, and the accuracy rate is as high as 100%. However, in the correct rate of the judgment of ST companies, only the model with financial indicators only reached 20.00%, and the correct rate of the judgment of the overall sample was only 76.47%. When the big data indicators of network sentiment are integrated, the correct rate of the judgment of normal enterprises is still 100%, and the correct rate of the judgment of ST enterprises has also reached 100%.

Therefore, it can be seen that the financial early-warning model containing big data indicators has greatly improved the prediction accuracy. It is also obvious in our test that the accuracy rate is significantly better than that of the financial indicator model. This shows that the prediction model that introduces big data indicators has a certain degree of improvement in the prediction of ST enterprises. At the same time, the prediction ability of non-ST enterprises is not inferior to the financial indicator model.

5. Conclusions

The vigorous development of big data technology provides new ideas and technologies for research in many fields. Therefore, in terms of financial early warning, big data technology can also be used as an auxiliary prediction tool to improve prediction accuracy. This will help the research on financial early-warning indicators to overcome the bottleneck period and make network sentiment indicators become big data indicators to correct the deviation of financial indicator early warning. It has important theoretical value for breaking through the predicament of stagnant financial crisis warning effect and provides support for enterprise financial crisis management.

Data Availability

The dataset can be accessed upon request.

Conflicts of Interest

The authors declare that there are no conflicts of interest.

References

[1] B. Song, J. M. Zhu, and L. I. Xu, "The Research of Enterprise Financial Early Warning Based on Big Data," *Journal of Central University of Finance & Economics*, vol. 18, pp. 117–125, 2015.

[2] X. F. Luana and H. M. Zhang, "Financial early-warning analysis of big data industry enterprises based on factor Analysis and logistic model," in *Proceedings of the Fourth Symposium on Disaster Risk Analysis and Management in Chinese Littoral Regions*, DRAMCLR, Qingdao, China, June 2019.

[3] W. Shuang, Z. Hui, T. Yuan, and S. Liyuan, "Financial distress warning: an evaluation system including ecological efficiency," *Discrete Dynamics in Nature and Society*, vol. 2021, Article ID 5605892, , 2021.

[4] N. Shen, H. Liao, R. Deng, and Q. Wang, "Different types of environmental regulations and the heterogeneous influence on the environmental total factor productivity: empirical analysis of China's industry," *Journal of Cleaner Production*, vol. 211, pp. 171–184, 2019.

[5] D. E. Aziz, D. C. Emanuel, and G. H. Lawson, "Bankruptcy prediction - an investigation of cash flow based models," *Journal of Management Studies*, vol. 25, no. 5, pp. 419–437, 1988.

[6] H. Su and J. Wang, "Research and application of computer big data system in early-warning methods and online monitoring technologies," *Journal of Physics: Conference Series*, vol. 1982, no. 1, Article ID 012014, 2021.

[7] Y. Liang, D. Quan, and F. Wang, "Financial big data analysis and early warning platform: a case study," *IEEE Access*, no. 99, 1 page, 2020.

[8] W. Antweiler and M. Z. Frank, "The information content of Internet stock message boards," *The Journal of Finance*, vol. 59, no. 3, pp. 75–81, Article ID 12590, 2004.

[9] K.-S. Shin, T. S. Lee, and H.-J. Kim, "An application of support vector machines in bankruptcy prediction model," *Expert Systems with Applications*, vol. 28, no. 1, pp. 127–135, 2005.

[10] J. Min and Y. Lee, "Bankruptcy prediction using support vector machine with optimal choice of kernel function parameters," *Expert Systems with Applications*, vol. 28, no. 4, pp. 603–614, 2005.

[11] L. Maotao, "Analysis of Financial Risk Early Warning Systems of High-Tech Enterprises under Big Data Framework," *Scientific Programming*, vol. 2022, Article ID 9055294, , 2022.

[12] G. Manogaran, N. Chilamkurti, and C. H. Hsu, "Special issue on advancements in artificial intelligence and machine learning algorithms for Internet of things cloud computing and big data," *International Journal of Software Innovation*, vol. 7, no. 2, 2019.

[13] Z. Huang, G. Liao, and Z. Li, "Loaning scale and government subsidy for promoting green innovation," *Technological Forecasting and Social Change*, vol. 144, no. 4, pp. 148–156, 2019.

[14] S. Shanmugathas and K. Ashoka, "Material sourcing in a strategic way: evaluation of consequences on the organizational performance," *Journal of Logistics, Informatics and Service Science*, vol. 6, no. 1, pp. 69–86, 2019.

[15] J. Matsuo, "Various activities of investment fund schemes for regional vitalization and environmental improvement," *St Andrew S University Bulletin of the Research Institute*, vol. 36, no. 3, pp. 91–110, 2011.

[16] M. Prochniak and K. Wasiak, "The impact of the financial system on economic growth in the context of the global crisis: empirical evidence for the EU and OECD countries," *Empirica*, vol. 44, no. 2, pp. 295–337, 2017.

[17] I. Zheludev, R. Smith, and T. Aste, "When can social media lead financial markets?" *Scientific Reports*, vol. 4, no. 1, pp. 4213–4289, 2014.

[18] J. R. Tang, Z. Y. Ding, X. U. Wen-Ting, and Y. C. Tang, "The Effect of Electronic Word-Of-Mouth on Corporate Performance: A Case of Online Tourism Industry," *Entific Decision Making*, vol. 2017, 2017.

[19] X. B. Tang and G. C. Liu, "Research review on fine-grained sentiment analysis," *Library and Information Service*, vol. 61, no. 5, pp. 132–140, 2017.

[20] D. Blazquez and J. Domenech, "Big data sources and methods for social and economic analyses," *Technological Forecasting and Social Change*, vol. 130, pp. 99–113, 2018.

[21] N. M. S. Algheriani, V. D. Majstorovic, S. Kirin, and V. Spasojevic Brkic, "Risk model for integrated management system," *Tehnicki Vjesnik-Technical Gazette*, vol. 26, no. 6, pp. 1833–1840, 2019.

[22] K. S. Moon and H. Kim, "Performance of deep learning in prediction of stock market volatility," *Economic Computation & Economic Cybernetics Studies & Research*, vol. 53, no. 2, pp. 77–92, 2019.

Hindawi
Scientific Programming
Volume 2022, Article ID 8583959, 7 pages
https://doi.org/10.1155/2022/8583959

Research Article

Forecast of Water Structure Based on GM (1, 1) of the Gray System

Yanan Dong,[1] Zheng Ren,[1] and Lian Hui Li[2]

[1]*Institute of Water Conservation and Hydro-Electric Power, Hebei University of Engineering, Handan, Hebei 056000, China*
[2]*Northwestern Polytechnical University, Xi'an, Shaanxi 710129, China*

Correspondence should be addressed to Lian Hui Li; 2010100407@mail.nwpu.edu.cn

Received 5 April 2022; Revised 21 April 2022; Accepted 29 April 2022; Published 23 May 2022

Academic Editor: Jie Liu

A forecast approach of water structure based on GM (1, 1) of the gray system is proposed. Based on economic and water information of Hebei Province from 2000 to 2018, the water use structure of Hebei's industrial sector form 2019 to 2030 is forecasted according to the composition data and gray system GM (1, 1) model. The forecasting results by the proposed approach shows that the water structure of the tertiary industry has changed from 62.8 : 10.3 : 26.9 in 2018 to 60.5 : 10.2 : 29.3 in 2030. The proportion of water used in the primary and secondary industries has decreased slightly, the proportion of water used in the tertiary industry has increased, and the proportion of water used in the tertiary industry has not changed significantly.

1. Introduction

Regional water resources are both driving economic growth and improving the living standards of the people. The improvement of the quality of material life and the enhancement of the ability to survive are also key conditions for achieving sustainable human development. Faced with the contradiction between the shortage of large-scale water resources and the demand for water resources in economic development, new industrial restructuring will be inevitable to achieve greater economic efficiency in the face of shortages. Under the constraints of limited available water resources, the current economic growth model and water supply and consumption structure need to be optimized and adjusted to ensure the sustainable utilization of regional water resources and the healthy and sustainable development of economy and society [1–7].

How to make rational development and utilization of limited water resources and make it exert the maximum utility under the premise of sustainable development has become an important problem faced by human society. This is the motivation of this study.

Scholars have studied the relationship between industrial structure and water use structure, and achieved a lot of results. Jia et al. [1] proposed to first improve the efficiency of industrial water use, upgrade the secondary industry, and optimize the industrial structure to reduce water consumption. Few authors [2, 3] advocate the transfer of high-water-consumption industries to small-water-consuming industries to increase efficiency in water resources utilization. Su et al. [4] studied the impact of water resources on industrial structure adjustment in Henan Province by means of cointegration, vector error correction estimation, impulse response, and variance decomposition. Jiao et al. [5] analyzed the temporal and spatial variation characteristics of the coupling coordination degree of water resources and industrial structure in Henan Province by establishing a coupling evaluation model. Fan and Wen [6] made quantitative analysis and comparison between industrial structure and water use system in Gansu Province based on the correlation analysis method and gray system theory, and put forward the direction of industrial structure adjustment. Jia et al. [7] used the system dynamics method to construct the collaborative evolution model of regional water use structure and national economy, and predicted and analyzed the collaborative evolution path and evolution law of water use structure and national economy industrial structure in Shandong Province.

The development of information technology and artificial intelligence has brought new opportunities to the

prediction and research of water use structure [8–15]. West and Dellana [16] carried out an empirical analysis of neural network memory structures for basin water quality forecasting. Bai et al. [17] proposed a variable-structure support vector regression model for the dynamic forecast of daily urban water consumption. Wei et al. [18] forecasted the structure of water consumption based on compositional data to promote inclusive water governance and made a case study of Beijing.

The existing studies have more single variable analysis of regional industrial structure and water use structure, but there are the following deficiencies. The method is relatively simple and lacks the analysis of industrial structure development under the constraints of water resources. There are many studies on the relationship between water resources and industrial structure, but there is a lack of in-depth exploration on the coordinated development relationship between water resources and industry.

This paper mainly analyzes the evolution of industrial structure and water structure through the collection and collation of economic data and water information in Hebei Province for 2000–2018 The relationship between the two countries is to reveal the coordination between them, and to forecast the water structure in Hebei province in 2030, and to propose the direction for research on industrial restructuring.

2. Research Methodology

There are certain conditions between the three secondary industries and water use, that is, the proportion of the output value of the three secondary industries and the sum of the proportion of water used in the three secondary industries are equal to one. By analyzing the time trend of a single indicator, the result will inevitably appear in each forecast year. The proportion of output value of the three industries and the proportion of water used in the three industries will no longer equal 1. Therefore, a single indicator prediction method cannot be used for a set of constrained variable indicators [19, 20].

Statistically, a combination of the individual share data for a set of constrained variables is called the component data (generally assuming that the sum of the shares of each variable is equal to 1), in under this constraint, economic models are established, and trends in variable composition are analyzed and predicted in a comprehensive manner. The gray system theory considers the socioeconomic system to be a native gray system [21]. It treats random processes of varying amounts of gray over a range of time as gray processes. The metric amount corresponding to a time series is the gray amount that is changing and the process of change can be considered gray. For this reason, the method of dedimensional [22] of component data was used. Combined with the GM (1, 1) model of the gray system, the basic steps for modeling the prediction of component data are given, and the three industrial structures and water structures of Beijing, Tianjin, and Hebei have been analyzed in a prediction and are of satisfactory results.

Definition 1. $X = \{(x_1, x_2, \cdots x_m) \in R^m / \sum_{i=1}^{m} x_1 = 1, 0 \le x_i \le 1\}$. X is called the component data series, and x_i is the component data for the component i.

Definition 2. $X^t = \{(x_1^t, x_2^t, \cdots, x_m^t) \in R^m / \sum_{i=1}^{m} x_i^t = 1, 0 \le x_i^t \le 1\} t = 1, 2, \ldots, T$. t indicates the time.

The basic question of modeling forecasts for time component data: given the time component data sequence x^t, how to build a mathematical model, and predict $T + l$ the component data for the moment x^{T+l}.

Using the component data dedimensional approach and the gray GM (1, 1) prediction method, the basic ideas for solving problems are presented, with the following steps:

(1) Make a nonlinear transformation of the original data

$$\begin{aligned} y_i^t &= \sqrt{x_i^t}, i \\ &= 1, 2, \ldots, m; t \\ &= 1, 2, \ldots, T. \end{aligned} \tag{1}$$

Remember $Y^t = (y_1^t, y_2^t, \ldots, y_m^t), \quad t = 1, 2, \ldots, T.$ Then, there are

$$\begin{aligned} Y^{t2} &= \sum_{i=1}^{m} \left(y_i^t\right)^2 \\ &= 1. \end{aligned} \tag{2}$$

(2) For any, the $t = 1, 2, \ldots, T\, Y^t = (y_1^t, y_2^t, \ldots, y_m^t) \in R^m$ is distributed over m a spherical face with a radius of 1, as can be seen by the formula (2). Change $Y^t = (y_1^t, y_2^t, \ldots, y_m^t)$, $t = 1, 2, \ldots, T$ from the right-angle coordinate system to the spherical coordinate system $(r^t, \theta_2^t, \ldots, \theta_m^t) \in \theta^m$, because there is a mapping relationship (where $(r^t)^2 = Y^{t2} = 1R^m \longrightarrow \theta^{m-1}$ $0 < \theta_i^t \le \Pi^2 i = 2, 3, \ldots, m$),

$$\begin{aligned} y_1^t &= \sin\theta_2^t \sin\theta_3^t \cdots \sin\theta_m^t, \\ y_2^t &= \cos\theta_2^t \sin\theta_3^t \sin\theta_4^t \cdots sin\theta_m^t, \\ y_3^t &= \cos\theta_3^t \sin\theta_4^t \cdots \sin\theta_m^t, \\ &\vdots \\ y_{m-1}^t &= \cos\theta_{m-1}^t \sin\theta_m^t, \\ y_m^t &= \cos\theta_m^t. \end{aligned} \tag{3}$$

(3) The component data are reduced from the original dimension space to $m(m-1)$ the dimension space $m(m-1)$ during the conversion from the right-angle coordinate system to the spherical coordinate system, so that the original linear-related variables are converted into independent variables (corners), and the angle variables are obtained by recursion according to the formula (3).

$$\begin{aligned}
\theta_m^t &= \arccos y_m^t,\\
\theta_{m-1}^t &= \arccos\left[\frac{y_{m-1}^t}{\sin\theta_m^t}\right],\\
\theta_{m-2}^t &= \arccos\left[\frac{y_{m-2}^t}{\sin\theta_m^t \sin\theta_{m-1}^t}\right],\\
&\vdots\\
\theta_2^t &= \arccos\left[\frac{y_2^t}{\sin\theta_m^t \sin\theta_{m-1}^t \cdots \sin\theta_3^t}\right] t = 1, 2, \ldots, T.
\end{aligned} \tag{4}$$

(4) Using the calculated angle data from the formula (4), $\{\theta_i^t, t = 1, 2, 3, \ldots, T\}, i = 2, 3, \ldots, m$, create a gray G $(m-1)$ M (1, 1) forecast model, which predicts the angle of the moment $T + l\theta_i^{T+l}, i = 2, 3, \ldots, m$.

(5) Use the formula (3) to calculate the forecast for the time of day $T + lY^{T+l} = (y_1^{T+l}, \cdots, y_m^{T+l})$. Obviously,

$$\sum_{i=1}^{m} \left(y_i^{T+l}\right)^2 = 1. \tag{5}$$

(6) Use formula (1) to get the forecast value of the component data at the time of day: $T + l$

$$\begin{aligned}
x_i^{T+l} &= \left(y_i^{T+l}\right)^2, i\\
&= 1, 2, \ldots, m.
\end{aligned} \tag{6}$$

(7) Create a GM (1, 1) model to predict the value of the angle in 2030.

GM (1, 1) Modeling process:

2.1. Additive Generation. Set original number column: $x^{(0)} = \left\{x_1^{(0)}, x_2^{(0)}, x_3^{(0)}, \ldots, x_t^{(0)}\right\}$ number of columns total. To reduce uncertainty, add up to get a new set of numbers listed:

$$\begin{aligned}
x^{(1)} &= \left(x_1^{(1)}, x_2^{(1)}, x_3^{(1)}, \ldots, x_t^{(1)}\right),\\
x_t^{(1)} &= \sum_{i=1}^{t} x_i^{(0)}.
\end{aligned} \tag{7}$$

In the formula,.$x_t^{(0)}$ is the data of the original number column; $x_t^{(1)}$ is the data of the cumulative number column.

2.2. Mean Calculations.

$$z_t^{(1)} = \frac{1}{2}\left[x_t^{(1)} + x_{t-1}^{(1)}\right]. \tag{8}$$

In the formula, the initial value: $t = 2$.

2.3. Curve Fit. To establish a differential equation,

$$\frac{dx^{(1)}}{dt} + ax^{(1)} = u. \tag{9}$$

In the formula, a is a factor and is taken in the range [2]; a, u is a gray contribution $\widehat{a} = \begin{pmatrix} a \\ u \end{pmatrix}$; the matrix is formed, using the smallest two-multiplication solution.

To create a matrix and constant item vector for a new array created by the additive: BY

$$\begin{aligned}
B &= \begin{bmatrix} -z_2^{(1)} & 1 \\ -z_3^{(1)} & 1 \\ \vdots & \vdots \\ -z_t^{(1)} & 1 \end{bmatrix},\\
Y &= \begin{bmatrix} x_2^{(0)} \\ x_3^{(0)} \\ \vdots \\ x_t^{(0)} \end{bmatrix}.
\end{aligned} \tag{10}$$

$\widehat{a}$ is calculated, then,

$$\widehat{a} = \left(B^T B\right)^{-1} B^T Y. \tag{11}$$

It will be substituted and evaluated for solution $dx^{(1)}/dt + ax^{(1)} = u$.

$$\widehat{x}_t^{(1)} = \left(x_1^{(0)} - \frac{u}{a}\right)e^{-a(t-1)} + \frac{u}{a}. \tag{12}$$

Or

$$\widehat{x}_{t+1}^{(1)} = \left(x_1^{(0)} - \frac{u}{a}\right)e^{-at} + \frac{u}{a}. \tag{13}$$

$\widehat{x}_t^{(1)}$: the ratio of accumulated output value in the forecast year (%), $x_1^{(1)}$: the specific weight of the new series (%) for the forecast value of the starting year, and a, u: the parameter.

2.4. Residual Analysis. By predicting the forecast value of the original series and doing a residual analysis with the original value, the residual difference is smaller and can be predicted directly with the model, which is much needed. Make corrections to the residual series data by creating a gray model.

The difference between the new agricultural series and the year of adjacent water consumption is the predicted annual demand:

$$V_t = \widehat{x}_t^{(1)} - \widehat{x}_{t-1}^{(1)}. \tag{14}$$

The residual differential is calculated as

$$\varepsilon_t^{(0)} = V_t^{(0)} - V_t. \tag{15}$$

The relative error is calculated as

$$\delta_t^{(0)} = \frac{\varepsilon_t^{(0)}}{x_t^{(0)}} \times 100\%. \quad (16)$$

2.5. Postdifferential Inspection. The accuracy level for the postdifferential inspection is shown in Table 1 [23].

Residual mean value calculation formula is as follows:

$$\overline{\varepsilon} = \frac{1}{n}\sum_{t=1}^{n} \varepsilon_t. \quad (17)$$

Residual differential calculation formula is as follows:

$$S_1^2 = \frac{1}{n}\sum_{t=1}^{n} \left[\varepsilon_t - \overline{\varepsilon}\right]^2. \quad (18)$$

The original mean value calculation formula is as follows:

$$\overline{x} = \frac{1}{n}\sum_{t=1}^{n} x_t. \quad (19)$$

The formula for calculating the original value variance is as follows:

$$S_2^2 = \frac{1}{n}\sum_{t=1}^{n}\left[x_t^{(0)} - \overline{x}\right]^2. \quad (20)$$

The formula for calculating the postcheck ratio is as follows:

$$C = \frac{S_1}{S_2}. \quad (21)$$

Small probability of error calculation formula is as follows:

$$P = P\left\{\left|\varepsilon_t - \overline{\varepsilon}\right| < 0.6745 \times S_2\right\}. \quad (22)$$

Table 1: Forecast model accuracy level judgment.

	The postcheck differential value C	Probability of error P
Class 1 (good)	C ≤ 0.35	$P \geq 0.95$
Level 2 (qualified)	$0.35 < C \leq 0.5$	$0.8 \leq P < 0.95$
Level 3 (barely)	$0.5 < C \leq 0.65$	$0.7 \leq P < 0.8$
Level 4 (nonconformance)	C > 0.65	$P < 0.7$

Table 2: The industrial water structure nonlinear mapping of the angle value.

	θ_2^t	θ_3^t
2000	1.1891	1.2507
2001	1.1807	1.2359
2002	1.1873	1.2609
2003	1.1791	1.2474
2004	1.1818	1.2558
2005	1.1834	1.2441
2006	1.1821	1.2457
2007	1.1896	1.2424
2008	1.1960	1.2295
2009	1.1904	1.2248
2010	1.1938	1.2140
2011	1.1708	1.1931
2012	1.1733	1.1887
2013	1.1662	1.1759
2014	1.1737	1.1717
2015	1.1839	1.1634
2016	1.1785	1.1340
2017	1.1891	1.1160
2018	1.1921	1.0682

3. Water Structure Forecast

Using the composition data and the gray system GM (1, 1), it is predicted that the water structure in Hebei Province will be used in 2030 to calculate the water bias between Hebei industry and industry. The difference factor compared with 2018 will be used to analyze water structure in Hebei Province for the next decade [24–27].

According to water data of the three secondary industries in Hebei Province 2000–2018, we establish a model of the dynamic distribution of water usage patterns in Hebei's industrial water structure and forecast water structure for Hebei industry in 2030 [28–31]. The angle values for the nonlinear mapping of the three-way industrial water structure are shown in Table 2.

The forecast for the angle of water structure of the three industrial sectors in Hebei Province is performed, $\theta_2^t\theta_3^t$ are calculated, and the average fit error is shown in Table 3.

The accuracy of the prediction of the angle of water structure is shown in Table 4.

According to Table 1, the angle forecast model for the industrial water structure of Hebei Province meets the level 2 accuracy requirement (qualified), which is qualified. $t = 2019, 2020, 2021, \ldots, 2030$. The angle forecast is shown in Table 5.

The forecast of water usage structure for the three subindustries in Hebei Province is shown in Table 6.

Based on the actual value of the three-way industrial water structure, 2000–2018, and the forecast value of the three-way industrial water structure, 2019–2030, the evolution of industrial water use structure in 2019–2030 is shown in Figure 1.

Figure 1 shows the evolution of water structure in three industrial sectors of Hebei Province from 2000 to 2030. The coarse point part is the data from 2000 to 2018 and the fine point part is the prediction from 2019 to 2030. As can be seen from the diagram, (1) Component data modeling combined with the gray system GM(1.1) model predicts that Hebei Province will have a good fit for its future industrial water structure. (2) The proportion of water used in the first industrial sector in Hebei Province has been slowly decreasing, the proportion of water used in the second industry has been gradually decreasing, the proportion of water used in the third industry has been increasing slowly, and the gap between the proportion of water used in the first industry has gradually narrowed. According to the results of the calculation of the model and according to the forecast

Table 3: The average fit error table is projected at the corner of the water structure.

	Forecast function	Average fit error (%)
θ_2^t	$\widehat{x}_t^{(1)} = -25993.7859e^{-0.00005(t-1)} + 25994.9750$	0.0042
θ_3^t	$\widehat{x}_t^{(1)} = -146.7915e^{-0.0088(t-1)} + 148.0422$	0.0658

Table 4: The results of the inspection of the accuracy of the projection of the industrial water structure.

Corner	Residual spread mean ($\overline{\varepsilon}$)	Residual variance (S_1^2)	Original mean ($\overline{x}$)	Original value variance (S_2^2)	Postcheck ratio (C)	Small probability of error (P value)
θ_2^t	0	0.0018	1.1833	0.0078	0.4848	0.90
θ_3^t	0	0.0007	1944	0.0041	0.4213	0.90

Table 5: Industrial water structure angle forecast.

	2019	2020	2021	2022	2023	2024	2025	2026	2027	2028	2029	2030
θ_2^t	1.1826	1.1825	1.1825	1.1824	1.1823	1.1823	1.1822	1.1822	1.1821	1.1821	1.1820	1.1820
θ_3^t	1.0912	1.0897	1.0801	1.0706	1.0612	1.0519	1.0427	1.0335	1.0245	1.0155	1.0065	0.9977

Table 6: The forecast of the water structure of the tertiary industry.

	2019	2020	2021	2022	2023	2024	2025	2026	2027	2028	2029	2030
First industry	0.6855	0.6732	0.6664	0.6596	0.6527	0.6459	0.6390	0.6321	0.6252	0.6183	0.6114	0.6045
Secondary industry	0.1132	0.1126	0.1115	0.1104	0.1093	0.1082	0.1071	0.1060	0.1048	0.1037	0.1026	0.1015
Tertiary industry	0.2103	0.2142	0.2221	0.2300	0.2380	0.2459	0.2539	0.2619	0.2699	0.2780	0.2860	0.2940

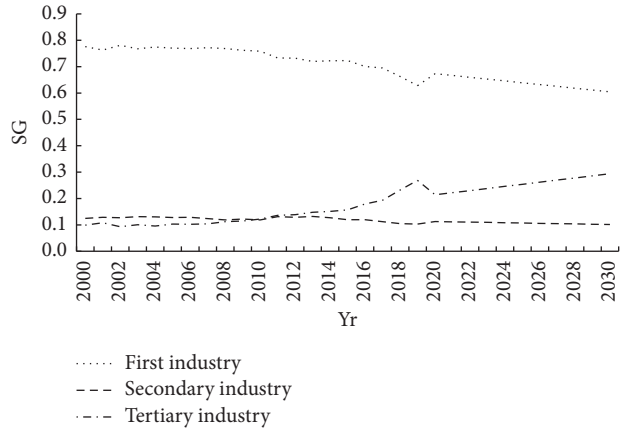

Figure 1: Trends in the evolution of the water structure of the three secondary industries, 2000–2030.

development trend, by 2030, the water structure of the three subindustries in Hebei province will be adjusted to 60.4% of the water use in the first industry, 10.2% of the water use in the second industry, and 29.4% of the water use in the third industry.

Based on the analysis of the forecasting results, the growth of domestic water and industrial water may be due to the improvement of economic level, the acceleration of urbanization and the rapid development of industrial enterprises. The increase in water use for ecological environment is mainly due to the improvement of awareness of greening and environmental protection. On the one hand, the slow growth of agricultural water consumption is due to the vigorous development of tourism in many places and the transformation of many farmlands into landscape land, resulting in the reduction of the effective area of farmland irrigation. On the other hand, the continuous upgrading and transformation of agricultural water-saving measures and the construction of high standards of farmland have increased the coefficient of farmland irrigation water, thus reducing the consumption of agricultural water.

The industrial structure restricts the proportion of water used by different users and affects the overall water use efficiency. The improvement of water use efficiency can produce greater economic value and promote the optimization and adjustment of industrial structure. Through the correlation analysis between industrial structure and water use, combined with the analysis of the coordinated

relationship between water resources and industrial development, the scale of economic and social development and the range of water use efficiency under the constraint of water resources can be obtained.

4. Conclusions

As we can see from the above results, with the development of comprehensive water conservation activities in Hebei Province and the readjustment of the industrial structure, the water quality of the three industries has been continuously improved and the water efficiency has been improved. It is consistent with the law of economic and social development. The water structure of the tertiary industry has changed from 62.8 : 10.3 : 26.9 in 2018 to 60.5 : 10.2 : 29.3 in 2030. The proportion of water used in the primary and secondary industries has decreased slightly, the proportion of water used in the tertiary industry has increased, and the proportion of water used in the tertiary industry has not changed significantly. From this, it is evident that the water use structure of Hebei's industrial sector is in line with the future industrial development plan.

Data Availability

The data used to support the findings of this study are available from the corresponding author upon request.

Conflicts of Interest

The authors declare that they have no conflicts of interest.

References

[1] S. Jia, S. Zhang, H. Yang, and J. Xia, "Relation of industrial water use and economic development:water use kuznets curve," *Journal of Natural Resources*, vol. 19, no. 03, pp. 279–284, 2004.

[2] S. Lei, J. Xie, and B. Ruan, "The correlation analysis and demonstration between industrial structure and water resources," *Operations Research and Management Science*, vol. 14, no. 02, pp. 100–105, 2004.

[3] H. E. Daly and K. N. Townsend, *Valuing the Early: Economic, Economic, Ecology, ethics*, MIT Press, Cambridge, MA, 1993.

[4] X. Su, S. Li, H. Gui, and P. Zhou, "An empirical study on the influences of water resources on regional industrial structure adjustment in henan province," *Yellow River*, vol. 40, no. 12, 2018.

[5] S. Jiao, A. Wang, X. Zhang et al., "Coordinated development of industrial structure and water resources in Henan Province under the New Normal," *World Regional Studies*, vol. 29, no. 2, pp. 358–365, 2020.

[6] B. W Fan and C. H. E. N Wen, "Analysis of the industrial structure and water consumption system of Gansu province based on GST," *Yellow River*, vol. 34, no. 5, pp. 92–95, 2012.

[7] C. Jia, L. Zhang, Y. Xu, S. Xiong, J. Jin, and C. Wu, "Study on collaborative evolution of regional water consumption structure and national economy," *Yellow River*, vol. 38, no. 5, pp. 57–61, 2016.

[8] L Li, B Lei, and C Mao, "Digital twin in smart manufacturing," *Journal of Industrial Information Integration*, vol. 26, no. 9, Article ID 100289, 2022.

[9] Y. Yu, L. Han, X. Du, and J. Yu, "An Oral English Evaluation Model Using Artificial Intelligence Method," *Mobile Information Systems*, vol. 2022, Article ID 3998886, 8 pages, 2022.

[10] L. Li, T. Qu, Y. Liu et al., "Sustainability assessment of intelligent manufacturing supported by digital twin," *IEEE Access*, vol. 8, Article ID 75008, 2020.

[11] R. Wang, J. Li, W. Shi, and X. Li, "Application of Artificial Intelligence Techniques in Operating Mode of Professors," *Academic Governance in American Research Universities. Wireless Communications and Mobile Computing*, vol. 2021, Article ID 3415125, 7 pages, 2021.

[12] L. Li and C. Mao, "Big data supported PSS evaluation decision in service-oriented manufacturing," *IEEE Access*, vol. 8, no. 99, Article ID 154670, 2020.

[13] R. Tang, "Improved Dynamic PPI Network Construction and Application of Data Mining in Computer Artificial Intelligence Systems," *Scientific Programming*, vol. 2022, Article ID 2729401, 9 pages, 2022.

[14] L. Li, C. Mao, H. Sun, and Y. B Yuan, "Digital twin driven green performance evaluation methodology of intelligent manufacturing: hybrid model based on fuzzy rough-sets AHP, multistage weight synthesis, and PROMETHEE II," *Complexity*, vol. 2020, no. 6, pp. 1–24, Article ID 3853925, 2020.

[15] N.-S. Truong, N.-T. Ngo, and A.-D. Pham, "Forecasting time-series energy data in buildings using an additive artificial intelligence model for improving energy efficiency," *Computational Intelligence and Neuroscience*, vol. 2021, pp. 1–12, Article ID 6028573, 2021.

[16] D. West and S. Dellana, "An empirical analysis of neural network memory structures for basin water quality forecasting," *International Journal of Forecasting*, vol. 27, no. 3, pp. 777–803, 2011.

[17] Y. Bai, P. Wang, C. Li, J. Xie, and Y. Wang, "Dynamic forecast of daily urban water consumption using a variable-structure support vector regression model," *Journal of Water Resources Planning and Management*, vol. 141, no. 3, Article ID 04014058, 2015.

[18] Y. G. Wei, Z. C. Wang, and Y. Li, "Promoting inclusive water governance and forecasting the structure of water consumption based on compositional data: A case study of Beijing," *SCIENCE OF THE TOTAL ENVIRONMENT*, vol. 634, pp. 407–416, 2018.

[19] G. Jiang, F. Yu, and Y. Zhao, "The coordination of the regional industrial structure and water use structure evaluation and control Take Anhui Province as an example," *J] water and electricity technology*, vol. 43, no. 6, pp. 8–11, 2012.

[20] Y. Liu, Y. Liu, and S. Huang, "Research on the relationship between industrial structure and water consumption structure," *Theory and Practice of System Engineering*, vol. 34, no. 04, pp. 861–869, 2014.

[21] S. Liu, T. Guo, and Y Dang, *Gray Systems Theory and its Applications*, Vol. 68, Science Press, , Beijing, 1999.

[22] H. Wang, W. Huang, and Q. Liu, "The three industrial forecasts of Beijing Municipality," *Theory and Practice of System Engineering*, vol. 23, no. 5, 2003.

[23] W. Xu, H. Xu, and H. Xu, "Applied gray forecast model accuracy test," *Journal of Digital Medicine*, vol. 10, no. 02, pp. 72-73, 1999.

[24] Y. Wang, *Hebei Economic Yearbook*, China Statistical Press, Beijing, 2000-2018.

[25] Hebei water Resources Agency, *Hebei Water Resources Communique*, Hebei water conservancy Office, Hebei, 2000-2018.

[26] G. P. Zhang, "Time series forecasting using a hybrid ARIMA and neural network model," *Neurocomputing*, vol. 50, no. 50, pp. 159–175, 2003.
[27] I. Pulido-Calvo and J. C. Gutiérrez-Estrada, "Improved irrigation water demand forecasting using a soft-computing hybrid model," *Biosystems Engineering*, vol. 102, no. 2, pp. 202–218, 2009.
[28] J. K. O'Hara and K. P. Georgakakos, "Quantifying the urban water supply impacts of climate change," *Water Resources Management*, vol. 22, no. 10, pp. 1477–1497, 2008.
[29] M. Ghiassi, D. K. Zimbra, and H. Saidans, "Urban water demand forecasting with a dynamic artificial neural network mode," *The Journal*, vol. 134, no. 2, pp. 0733–9496, 2008.
[30] X. Zhang, Z. Dong, and B. Luo, "Industrial structure optimization based on water quantity and quality restrictions," *Journal of Hydrologic Engineering*, vol. 18, no. 9, pp. 1107–1113, 2013.
[31] D. Reid, "Improvements to source protection for private water supplies in Scotland, UK," *Water Policy*, vol. 3, no. 4, pp. 273–281, 2001.

Hindawi
Scientific Programming
Volume 2022, Article ID 2211468, 11 pages
https://doi.org/10.1155/2022/2211468

Research Article

Analysis and Research on the Characteristics of Modern English Classroom Learners' Concentration Based on Deep Learning

Yu Shen [1,2]

[1]*Huanghe Science and Technology University, Foreign Languages School, Zhengzhou 450000, China*
[2]*University of Málaga, Department of Linguistic, Literature and Translation, Málaga 29000, Spain*

Correspondence should be addressed to Yu Shen; shenyu@hhstu.edu.cn

Received 25 March 2022; Revised 8 April 2022; Accepted 15 April 2022; Published 21 May 2022

Academic Editor: Jie Liu

There are some problems in modern English education, such as difficulties in classroom teaching quality evaluation, lack of objective evaluation basis in teaching process management, and quality monitoring. The development of artificial intelligence technology provides a new idea for classroom teaching evaluation, but the existing classroom evaluation scheme based on artificial intelligence technology has a series of problems such as high system cost, low evaluation accuracy, and incomplete evaluation. In view of the above problems, this paper proposes a solution of English classroom concentration evaluation system based on deep learning. The program studies the evaluation methods of students' class concentration, class activity, and enrichment degree of teaching links, and constructs an information evaluation system of students' learning process and class teaching quality. Based on the edge computing system architecture, a hardware platform with cloud platform AI+ embedded visual edge computing devices managed by an FPGA deep learning accelerated server was built. The design, debugging, and testing of classroom evaluation and student behavior statistics-related functions were completed. This scheme uses edge computing hardware architecture to solve the problem of high system cost. Deep learning technology is used to solve the problem of low accuracy of classroom evaluation. It mainly evaluates the classroom objectively by extracting indicators such as the students' attention in the classroom, and solves the problems of the students' inattentiveness in the classroom. After the test, the classroom evaluation system designed by the paper runs stably and all functions run normally. The test results show that the system can basically meet the requirements of classroom teaching evaluation application.

1. Introduction

In the early stage of college English course learning, the score is often determined by the final exam results, which cannot fully reflect the students' learning situation, is not conducive to finding problems in the teaching process, improving teaching, and is not conducive to mobilizing students' learning enthusiasm [1]. Students often play with mobile phones or sleep in class. With the continuous development of technology, it provides a new idea for intelligent teaching to automatically obtain the attention state of students in English class by using facial expression recognition method. Facial expression recognition, as a noninvasive method, is more suitable for application in actual classroom teaching, which has a huge space to play both online and offline teaching [2].

In 2006, Geoffrey and Ruslan formally proposed the concept of deep learning [3]. A solution to the problem of "gradient disappearance" is proposed, which is to train the algorithm layer by layer by unsupervised learning method and then tune it by supervised back propagation algorithm. In 2012, the deep neural network (DNN) jointly led by the famous Professor Wu of Stanford University and the world's top computer expert Jeff Ade is the amazing achievement in the field of image recognition [4], successfully reducing the error rate from 26% to 15% in ImageNet evaluation. In 2016, Facebook's DeepFace project based on deep learning technology achieved an accuracy rate of more than 97% in face recognition, almost the same as that of human recognition [5]. At present, for face recognition, the face pixel in the image is required to be at least 64×64, preferably 128×128.

In general, face recognition needs to provide a positive face image; for a certain angle of the face image, as long as the demarcated face feature points can be recognized, the face can also be recognized [6].

Based on the above background, by analyzing the main problems existing in the classroom evaluation system at the present stage, this paper puts forward the modern English classroom concentration evaluation system based on deep learning, analyzes the design requirements from the actual needs, puts forward the system design scheme, and expounds the specific design and implementation process in detail.

2. Related Work

2.1. Research Status of Facial Expression Recognition Based on Deep Learning. Different from traditional methods, deep neural networks can automatically obtain required features from a large number of data samples according to specific tasks. In addition, with the support of GPU computing technology, the deep learning model can be designed to be complex enough to contain hundreds of trillions of parameters, learn the semantic information of a different granularity in the samples, successfully avoid the complex operation of manual feature extraction, and achieve great success in the expression recognition task.

Yang et al. proposed a residual expression recognition algorithm that could filter emotion-irrelevant elements in the paper: faces were divided into two categories—faces with expression and neutral faces without expression, and each expression generation model was trained through cGAN network. The model can generate a neutral face for any input face image, and the expression information is stored in the middle level. Then, for neutral faces, the pixel-level or feature-level methods are no longer used to identify expressions, but a new method is used to learn and generate part of the facial expression information left in the middle level of the model, so as to generate the final classifier [7].

Yang designed an expression recognition structure dependent on images and image sequences, and proposed an illumination enhancement strategy, which can reduce the over-fitting phenomenon in model training. Without significantly reducing the recognition performance, the structure has fewer convolution kernels than the general model, which is convenient for deployment in mobile terminals. Moreover, data sets in three different scenarios are collected to verify the validity of the model [8].

Shi et al. believed that there are many mislabeled data in large-scale facial expression data sets, which may make the model overfit and merge and affect the effective features learned by the model. Based on this, a self-cure network (SCN) method is proposed to suppress the uncertainty in facial expression data sets. By extracting image features through CNN, we learned the weight of each image to obtain the importance of samples, arranged the weights in descending order, divided them into two parts of high attention and low attention by calculating the average weight, and re-marked those samples considered to be wrong by estimating the probability. In this way, the sample label error is effectively solved [9].

Yuan et al. studied the application of facial expression recognition in the field environment. Since there are not too many constraints in the field, problems such as unfixed head posture, facial deformation, and motion blur often exist. In this paper, a convolution vision converter method is proposed: firstly, the attentional selection fusion module is used to fuse the feature images generated by the two branches, and the global attention fusion is used to fuse multiple feature images to capture the distinguishing information. The fused features are tiled into the sequence of visual words, and the relationship between the visual words with global self-attention is modeled [10].

2.1.1. Research Status of Facial Expression Recognition in Classroom Environment. In the current classroom teaching scenario, teachers want to obtain students' concentration in class in real time mainly through on-site questioning and visual observation, which requires extra energy and is highly subjective. With the development of facial expression recognition technology, it has become a new trend to use computers to automatically identify students' emotional states in class.

Cheng et al. designed an intelligent teaching model, which consists of four parts: emotion, course, student, and teacher. The system captures students' emotions through visual tracking technology and facial expression recognition technology, and carries out certain emotional feedback behavior [11].

Whitehill et al. studied the measurement of students' participation in class listening in 2014. It is pointed out that the popular methods of participation measurement include self-report, observation list and rating scale, automatic measurement, and automatic recognition based on computer vision. Computer vision analyzes facial cues, body postures, and gestures and provides an unobtrusive way to estimate student engagement [12].

Sun et al. studied the application of emotion recognition in intelligent teaching and proposed that the basic facial expressions defined by Ekman are not suitable for direct application in teaching scenarios, and multiple facial expressions are not highly correlated with students' emotions in class. The "cognitive skill training" experiment is suitable for classroom use. The data sets obtained are analyzed by using boost (BF) algorithm with box filter feature, support vector machine with Gabor feature, and multinomial logistic regression algorithm with expression output, and the model that can automatically identify student participation is obtained [13].

Cui et al. have implemented a student expression analysis system in the classroom environment, which is used to identify three expressions of students in class: ordinary, happy, and confused [14].

Ahuja et al. constructed a three-dimensional learning state space in his research, in which the horizontal coordinate represents the pleasure dimension of learning

emotional state and measures the recognition of learning. The longitudinal axis is the arousal dimension of learning emotional state, which measures learning fatigue, while the vertical axis is the interest dimension of students' emotional state, which measures learning avoidance. At the same time, a total of 9 expressions, including basic expressions, contempt, and confusion defined by Ekman, are introduced, and different weights are set for these expressions according to the measurement standard as the values on the horizontal axis [15].

3. System-Related Technologies and Algorithms

This paper uses Tengine deep learning framework and OpenVINO development tool suite to implement the deep learning algorithm at the edge end and server end, respectively. In the deep learning algorithm, MTCNN is used to achieve face detection and face image interception function, MobileNet-V2 to achieve face recognition function, and VGG-16 to achieve head posture recognition, head recognition, facial expression recognition, and human posture recognition and other classroom behavior recognition functions. This paper mainly introduces the structure of three neural networks, namely, MTCNN, MobileNet-V2, and VGG-16, as well as the deep learning framework Tengine, which is used to run the deep learning algorithm on the edge of the system, OpenVINO, which is used to run the deep learning algorithm on the server.

3.1. Tengine. In order to realize the functions of face detection, face image capture, and classroom behavior recognition at the edge end of the system, the paper adopts EAIDK-610 development board jointly developed by ARM and Open AI Lab as the core processing platform at the edge end of the system [16]. The EAIDK-610 development board is equipped with an embedded AI development platform, including support for heterogeneous computing library HCL, embedded deep learning framework Tengine, and lightweight embedded computer vision acceleration library BladeCV.

Tengine is a lightweight, high-performance, modular embedded deep learning framework. The deep learning framework is optimized for ARM embedded devices, does not rely on third-party libraries, and can be used across platforms. It supports Android and Linux, and supports GPU and DLA as hardware-accelerated heterogeneous computing resources.

Tengine deep learning framework has the following features:

(1) Lightweight tailoring. Tengine relies only on C/C++ libraries; standard edition volume 3M, lite edition volume 300K; original support for ARM CPU.

(2) Running memory optimization. Shared memory technology dramatically reduces memory requirements.

(3) Support model compression and encryption. Tengine customizes model formats, supports model compression to reduce size, supports model encryption and packaging, and protects intellectual property rights.

According to the neural network operators currently supported by Tengine, the deep learning networks currently supported by Tengine include the following:

(1) Squeeze net.mobile net.mobilenet-v2, ResNet50, AlexNet, GoogleNet, ImageNet classification networks, such as Inception-V3, Inception-V4, and VGG-16;

(2) MTCNN;

(3) SSD, YOLO-V2;

(4) MobileNet-SSD;

(5) Faster RCNN;

(6) Lighten CNN;

(7) Network model can be converted into Tengine model based on other deep learning frameworks.

In the deep learning network supported by Tengine, MTCNN, SSD, YOLO-V2, and other networks can realize face detection function. As the real-time requirement of face detection is not very high, the paper adopts MTCNN algorithm with slow execution speed but higher accuracy to realize the face detection function at the edge. For the classroom behavior recognition function of the system, it is necessary to use the classification network to identify and classify all kinds of classroom behaviors. Because it is necessary to conduct real-time classroom behavior recognition for students in the classroom, and there is not much classification of head, facial expression, and human posture in the recognition process, VGG-16 and ResNet50 networks are selected for testing on the premise of ensuring accuracy. After the test, it is found that ResNet50 has a better effect when the number of classification is large. However, in the class behavior recognition of this system, the number of classification of the recognition results of the head, facial expression, and human posture is small, and the recognition results obtained by using VGG-16 network are better. VGG-16 network is finally adopted to realize the algorithm of the class behavior recognition at the edge.

3.2. OpenVINO. In order to realize the face recognition function on the server side of the system, the paper adopts the FPGA accelerated cloud platform launched by Intel as the system server-side processing platform. The platform is loaded with OpenVINO tool suite developed for CPU + FPGA architecture.

OpenVINO (Open Visual Inference & Neural Network Optimization) is a tool suite that can speed up the development of high-performance computer vision and deep learning visual applications, as described in literature [17]. It

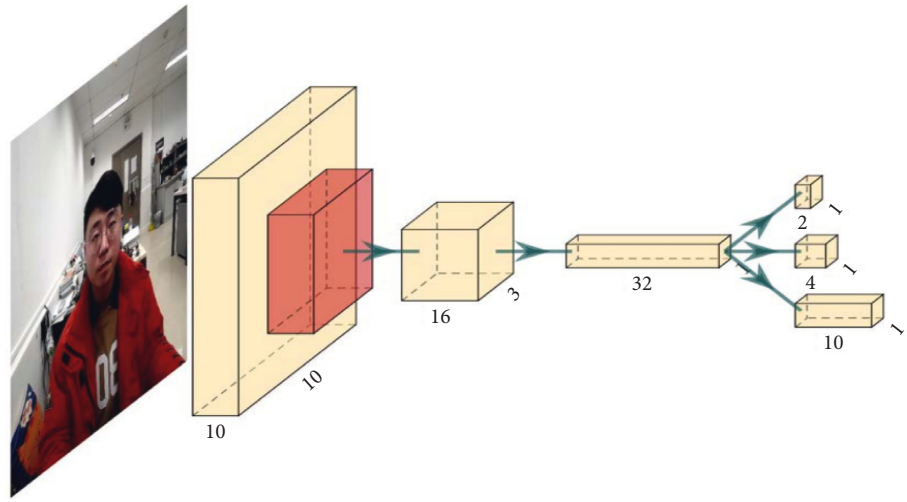

Figure 1: Structure diagram of P-Net.

supports deep learning on various Intel platform hardware accelerators and allows direct heterogeneous execution.

For AI workloads, OpenVINO provides the Deep Learning Deployment Toolkit (DLDT), a suite of tools that can deploy models trained by various open-source frameworks online.

DLDT is divided into two parts:

(1) Model Optimizer. The model optimizer is a Python scripting tool for converting a model trained using an open-source framework into an intermediate representation (IR, intermediate representation) that the inference engine can recognize, that is, two files: the XML file representing the network structure description and the bin file storing the weights, respectively. The model optimizer is used for offline model transformations.

(2) The inference engine is from the inference engine. Reasoning engine is a set of API interfaces supporting C++ and Python, requiring developers to implement their own reasoning process development.

The inference engine is the AI payload deployed to run on the device.

OpenVINO currently supports many network models under mainstream deep learning frameworks. Considering the balance between real-time performance and precision of deep neural network running under embedded hardware, the paper finally uses the improved MobileNet-V2 lightweight network to realize face recognition function on the server side.

3.3. MTCNN. Multi-task convolutional neural network (MTCNN) is a multi-task neural network model proposed by Shenzhen Research Institute of Chinese Academy of Sciences in 2016 for face detection task, as described in literature [18]. The proposed network and refine network output network are used in this model for fast and efficient face detection. The model also uses image pyramid, border regression, and nonmaximum suppression techniques.

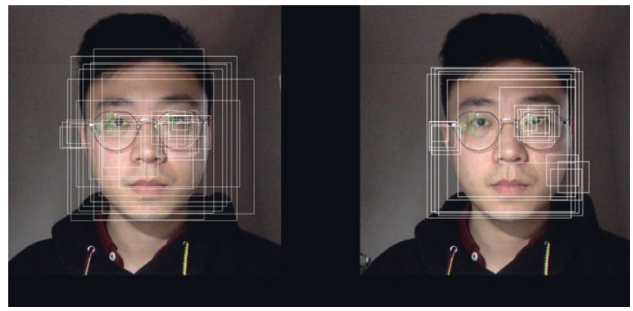

Figure 2: Input and output images of P-Net.

P-Net (proposal network) firstly modified all training samples into $12 \times 12 \times 3$ images, obtained $1 \times 1 \times 32$ feature map (feature map after convolution) through three convolution layers, and finally obtained three multidimensional outputs through three different 1×1 convolution kernels: the $1 \times 1 \times 2$ face probability, $1 \times 1 \times 4$ face candidate box coordinates, and $1 \times 1 \times 10$ face 5 marker anchor point coordinates. Its network structure is shown in Figure 1.

The input and output images of P-Net are shown in Figure 2.

Refine Network (R-Net) modifies all training samples to $24 \times 24 \times 3$ images; after convolution and pooling, the corresponding coordinate positions are output, respectively. Its network structure is shown in Figure 3.

The input and output images of R-Net are shown in Figure 4.

O-Net (output network) modified all training samples into $48 \times 48 \times 3$ images. Like R-Net, the output was face probability, face candidate frame coordinate, and face 5 marker anchor point coordinate, respectively. Its network structure is shown in Figure 5.

The O-Net input and output images are shown in Figure 6.

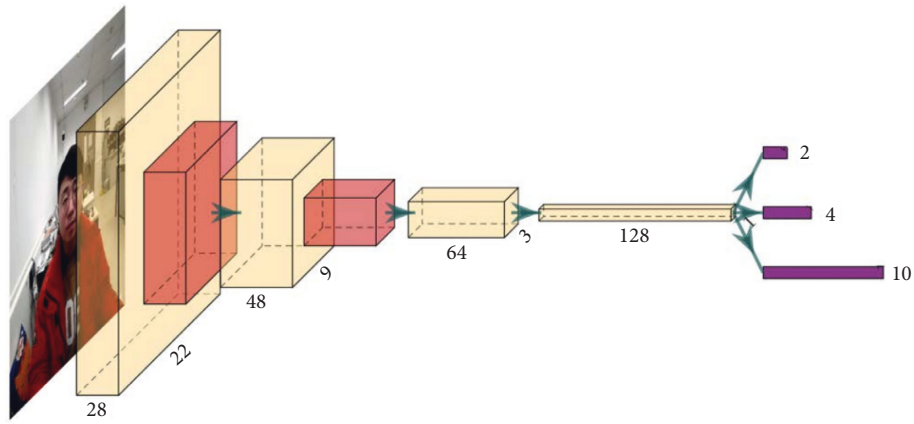

Figure 3: Structure diagram of R-Net.

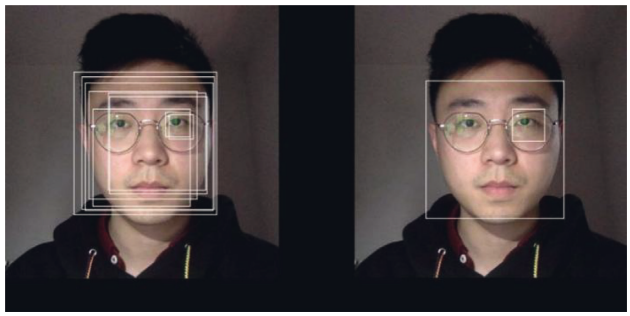

Figure 4: Input and output images of R-Net.

From P-Net to R-Net to O-Net, the larger the size of the input image is, the deeper the network structure is, and the more expressive the extracted features are.

Training MTCNN requires convergence of the following three tasks: face probability, face candidate frame coordinate, and face 5 marker anchor point coordinate.

The following cross drop loss function is used for human face, as shown in

$$L_i^{\text{det}} = -\left(y_i^{\text{det}} \log(p_i) + \left(1 - y_i^{\text{det}}\right)(1 - \log(p_i))\right) y_i^{\text{det}} \in \{0, 1\}. \tag{1}$$

For regression of each candidate box, the following sum of squares loss function is adopted to calculate regression loss through Euclidean distance, as shown in

$$L_i^{\text{box}} = \left\| \hat{y}_i^{\text{box}} - y_i^{\text{box}} \right\|_2^2 y_i^{\text{box}} \in R^4, \tag{2}$$

where $\hat{y}_i^{\text{box}}$ is the coordinate obtained through network prediction and y_i^{box} is the actual real background coordinate, both of which are quaternions.

The following sum of squares loss function is used to calculate the Euclidian distance between the predicted landmark position and the actual real landmark, and the distance is minimized. The calculation formula is shown in

$$L_i^{\text{landmark}} = \left\| \hat{y}_i^{\text{landmark}} - y_i^{\text{landmark}} \right\|_2^2, \quad y_i^{\text{landmark}} \in R^{10}, \tag{3}$$

where $\hat{y}_i^{\text{landmark}}$ is the marking coordinate obtained through network prediction and y_i^{landmark} is the actual real marking coordinate. Since there are 5 marker points for left eye, right eye, nose, left corner of mouth, and right corner of mouth, each point has 2 coordinate values, and y_i^{landmark} is a tuple of ten.

Because each network performs different works, different types of training data are needed during training. The training formula of multiple input sources is shown in

$$\min \sum_{i=1}^{N} \sum_{j \in \{\text{det,box,landmark}\}} \alpha_j \beta_i^j L_i^j, \beta_i^j \in \{0, 1\}. \tag{4}$$

The learning process of the whole training is to minimize the formula above, where N is the number of training samples, α_j is the importance of the task, β_i^j is the sample label, and L_i^j is the loss function mentioned above. When training P-Net and R-Net in MTCNN, $\alpha_{\text{det}} = 1$, $\alpha_{box} = 0.5$, and $\alpha_{\text{landmark}} = 0.5$; when training O-Net, $\alpha_{\text{det}} = 1$, $\alpha_{box} = 0.5$, and $\alpha_{\text{landmark}} = 1$.

3.4. MobileNet-V2. The deep separable convolution is applied in MobileNet-V1, the previous generation of MobileNet-V2, which makes the neural network maintain the accuracy and greatly improve the operation speed. A new structure is proposed in MobileNet-V2 and may be referred to as Inverted Residuals with Linear Bottlelock. This structure first enlarged the dimensions of the input feature map with 1×1 convolution, then operated with 3×3 convolution, and finally reduced the dimensions with 1×1 convolution operation. After the completion of convolution, ReLU activation function is no longer used, but linear activation function is used to retain more feature information and ensure the expressive ability of the model. Its structure is shown in Figure 7.

To improve network performance, the linear convolution part of Inverted Residuals with Linear Bottlelock structure in the network is modified into SE module. Figure 8 shows the structure of an SE block.

Given an input whose channel number is Channel1, a feature whose channel number is Channel2 is obtained through a series of transformations. The feature is input into SE block, and the obtained feature is re-demarcated through three operations:

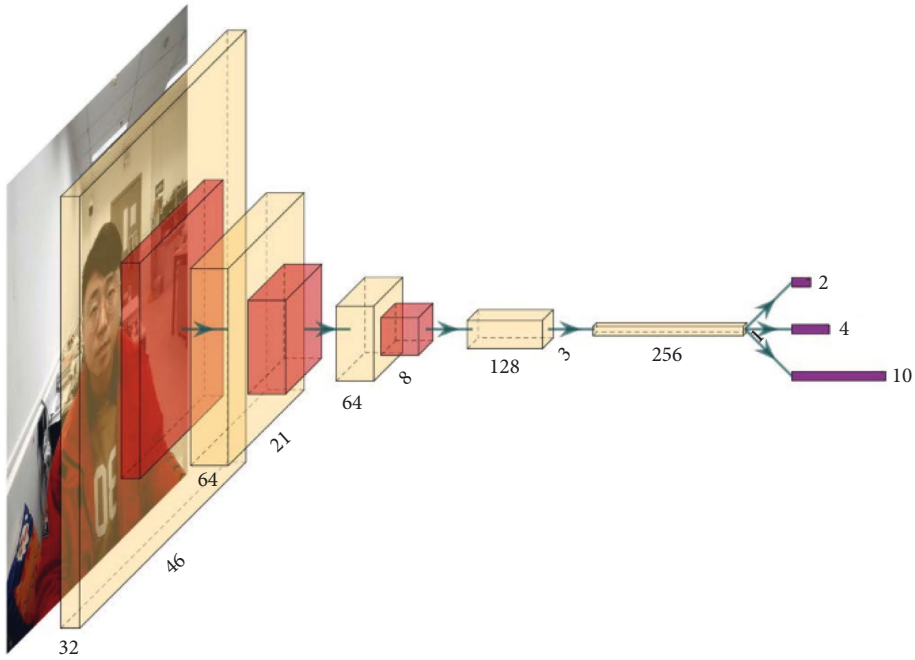

Figure 5: Structure diagram of O-Net.

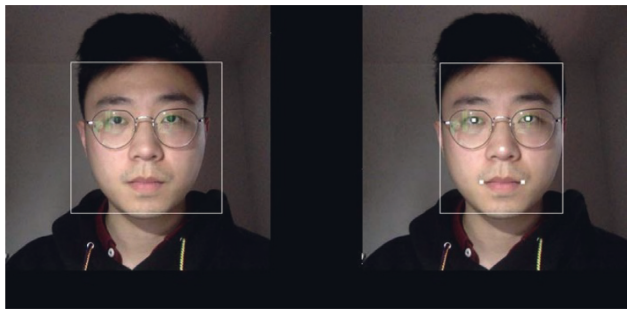

Figure 6: Input and output images of O-Net.

(1) Squeeze operation, use global average pooling to compress features along spatial dimensions, convert each two-dimensional feature channel into a real number, and the output dimension matches the input feature channel number [19]. Its formula is shown in

$$z_c = F_{sq}(u_c) = \frac{1}{H \times W} \sum_{i=1}^{H} \sum_{j=1}^{W} u_c(i, j). \quad (5)$$

(2) The weighting for each attribute channel is generated by the parameter W, where the parameter w is learned to explicitly model the correlation between the attribute channels. Multiply W_1 by the squeeze operation to get z, which is a fully joint operation, and then pass through a ReLU layer with the output dimension unchanged; then, multiply by W_2, which is also a full connection; then finally, through the sigmoid function, you get s. Its formula is shown in

$$s = F_{ex}(z, W) = \sigma(g(z, W)) = \sigma(W_2 \delta(W_1 z)). \quad (6)$$

The calculation formula of parameter W is shown in

$$W_1 \in \frac{C}{r} \times C, W_2 \in \frac{C}{r} \times C. \quad (7)$$

r is a scaling parameter, whose purpose is to reduce the number of channels and thus reduce the computation. The dimension of the final output is $1 \times 1 \times C$, where C represents the number of channels. s is used to represent the weights of C feature maps.

(3) After obtaining s, use formula (8) for operation [20].

$$\tilde{x}_c = F_{scale}(u_c, s_c) = s_c \cdot u_c, \quad (8)$$

where u_c is a two-dimensional matrix and s_c is the weight, which is equivalent to multiplying every value in the u_c matrix by s_c. The modified Inverted Residuals with Linear Bottlelock structure is shown in Figure 9.

The network inputs a 128×128 image each time, extracts face feature points and feature vectors, respectively, on the image, and finally outputs a row vector containing 256 floating point values, and the row vector is the abscissa and ordinate values of the face feature vector. The cosine distance between the output feature vector and the coordinate value of the feature vector of the reference face image is calculated, and the wide value of the cosine distance is set. If the cosine distance is less than the wide value, the recognized face can be judged as the student himself.

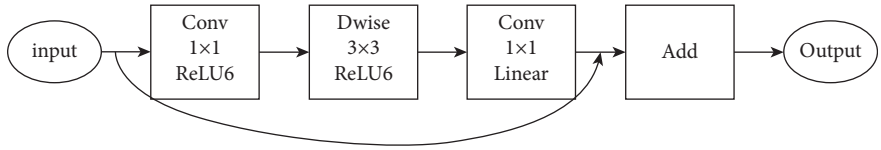

Figure 7: Structure diagram of Inverted Residuals with Linear Bottlelock.

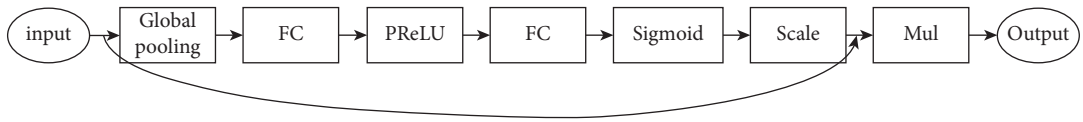

Figure 8: Structure of SE block.

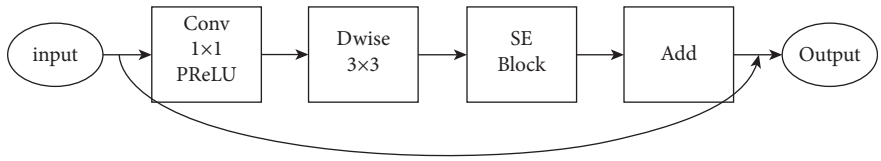

Figure 9: Modified structure of Inverted Residuals with Linear Bottlelock.

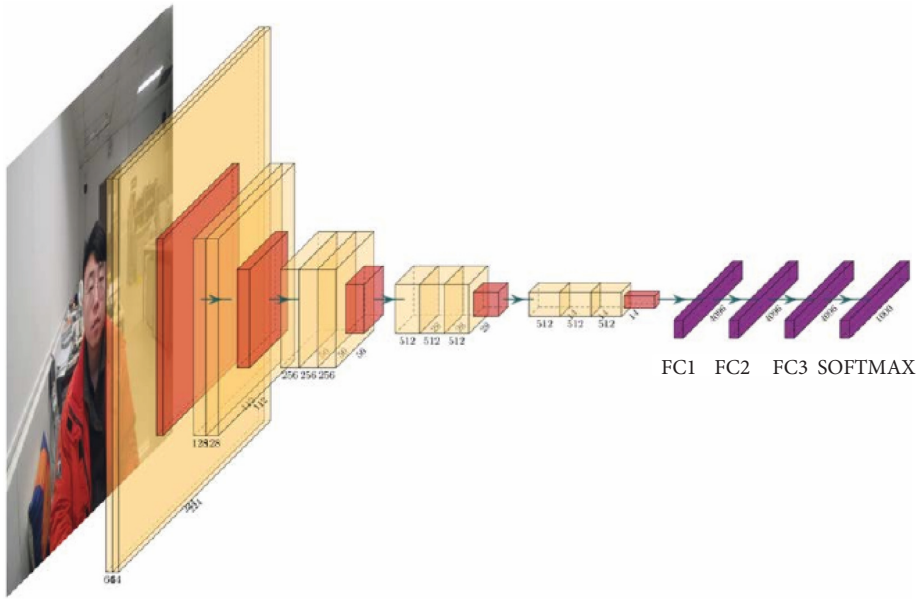

Figure 10: Structure diagram of VGG-16 network.

3.5. VGG-16. VGG is a convolutional neural network model proposed by Simonyan and Zisserman, whose name is derived from the abbreviation of Visual Geometry Group of Oxford University where the authors work [21].

VGG can be divided into six configurations, *A*, *A*-LRN, *B*, *C*, *D*, and *E*, according to the different convolution kernel size and number of convolution layers. Among them, *D* and *E* are more commonly used, called VGG-16 and VGG-19, respectively. Therefore, the system uses VGG-16 architecture.

Figure 10 shows the network structure of VGG-16.

The input data of VGG-16 are $224 \times 224 \times 3$ pixel data. After five-layer convolutional network and pooled network processing, the output is a 4096-dimensional feature data and then processed by three-layer fully connected network, and the final classification result is obtained by Softmax specification. The dimensions of the Softmax layer can be adjusted according to the number of classifications for different purposes.

4. The Realization of the Analysis System for the Characteristics of English Class Students' Concentration

4.1. System Test Environment. In this paper, the classroom evaluation system based on deep learning is completed on

Table 1: Parameters of system edge computing-end hardware test environment.

EAIDK-610 embedded artificial intelligence application development platform	
SoC master chip	RK3399
CPU	2 × Cortex A72 + 4 × Cortex A53
GPU	ARM Mali-T860
Internal storage	4 GB dual-channel 64 bit LPDDR3
Memorizer	16 g eMMC at a high speed
Ethernet	RJ45, 10/100/1000m adaptive

Table 2: Parameters of system server hardware test environment.

Intel FPGA acceleration cloud platform	
CPU	Intel Xeon E5
FPGA	Intel Arria 10 GX
Internal storage	96 G

Table 3: Parameters of system software test environment.

	Testing environment	Versions
The edge of the end	Linux operating system	Fedora 28
Server side	Linux operating system	CentOS 7
Client side	Max operating system	Mac OS 10.15.4

EAIDK-610 embedded artificial intelligence application development platform jointly developed by ARM company and Open AI Lab, and FPGA acceleration cloud platform of Intel Company, combined with webcam and PC. The edge end, the server end, and the client all realize the stable data interaction through the network data transmission module. The hardware test environment parameters of the edge end of the system are shown in Table 1.

Table 2 shows the server hardware test environment parameters of the system.

The software test environment parameters of the system are shown in Table 3.

4.2. System Function Test. According to the analysis of functional requirements, the classroom evaluation system based on deep learning designed in this paper should have the functions of classroom behavior identification, classroom quality evaluation, and student classroom behavior statistics. The following are the functional tests for the above functions [22]. The test was carried out in the laboratory, and the test was set to 10 people, but actually to 9 people. In addition to the two attendance tests, a total of 80 classroom behavior identification test time points were set.

The EAIDK-610 development board is used to control the head and focal length of the camera through the network, so that the camera can aim at the whole student area in the classroom, so that the camera can collect all the students on the seat at the same time and then carry out head posture recognition, head posture recognition, facial expression recognition, and human body posture recognition.

The camera recognizes the head posture of the student in the seat. The system sets a total of 80 test time points for head posture recognition, so the result of head posture recognition after the course has a total of 80 time points of the number of students looking at the platform.

During the same period, the camera looked up at the students in their seats. The system sets a total of 80 test time points for head recognition, so the result of head recognition after the course has a total of 80 time points of head rate data.

During the same period, the cameras recognize the faces of the students in the seats. The system sets a total of 80 test time points for facial expression recognition, so the result of facial expression recognition after the end of the course has a total of 80 time points of the number of students listening carefully.

During the same period, the camera recognizes the posture of the student in the seat. When it is recognized that all students are "sitting down," the class state is defined as "teacher lecturing," and the result value of this state is written as "1." When a student is identified as "standing," the class state is defined as "teacher-student interaction." If the gesture of "raising hands" appears before the gesture of "standing," the result value of the state of "students answering questions independently" is written as "1." If there is no "hand gesture" before the "standing" gesture, the result value of the "teacher calls the roll to answer the question" status is marked as "1." When the student is identified as "writing," the class state is defined as "classroom homework" and the result value of this state is marked as "1."

At the same time of human posture recognition, the system records students' hands raising and sleeping, so there will be data of the number of hands raising and sleeping at the corresponding time point after the course.

Reading face recognition results, head posture recognition results, head posture recognition results, facial expression recognition results, human posture recognition results, and evaluation index calculation according to the class of paper, respectively, calculate the attendance score of the course, head posture correct rate of scoring, serious expression rate hand score, score up rate, rate of score, score not sleep rate, the link of the lecturer score, students' answering question score, teacher roll call to answer questions such as the secondary indicator, class attendance score, class concentration score, class activity score, class link richness score, and other first-level indicators, as well as class evaluation score. Upload the score to the appropriate location on the course evaluation sheet in the database. The database classroom evaluation table is shown in Figure 11.

At the same time, the statistical results of students' classroom behavior are also uploaded to the corresponding position in the statistical table of students' classroom behavior in the database. The statistical table of classroom behavior of students in the database is shown in Figure 12.

After testing, the system designed by the paper has realized the function of classroom evaluation.

4.3. System Performance Test. According to the system design requirements, the factors affecting the system

courseID	A	F1	F2	H	R	J	M1	M2	M3	M4	SA	SF	SV	SM	S
1	90	84.44	63.34	89.96	29.67	89	100	100	0	0	90	80.22	77.71	90	87.79

Figure 11: Classroom evaluation table in database.

courseID	studentID	headupRate	focusRate	raiseRate	sleepRate
1	01	0.938	0.875	0.667	0
1	02	0.975	0.9	1	0
1	03	0.925	0.875	0.333	0
1	04	0.925	0.85	0	0.01
1	05	0.925	0.863	0	0
1	06	0.775	0.725	0	0
1	07	0.925	0.9	0.333	0
1	09	0.787	0.75	0	0.01
1	10	0.912	0.86	0.333	0

Figure 12: Statistics of students' classroom behavior table in database.

Figure 13: Head posture recognition test pictures and test results.

Figure 14: Header recognition test pictures and test results.

Figure 15: Facial expression recognition test results of picture counting test.

performance include face detection rate, face recognition rate, head posture recognition rate, facial expression recognition rate, human posture recognition rate, and system stability.

Figure 16: Human posture recognition test pictures and test results.

Table 4: Technical parameters of system.

Category	Face detection	Face recognition	Head posture	Identify the rise	Identify expression	Recognition of human posture
Test times	50	50	10	10	10	10
Identification of success times	45	47	8	9	8	8
Detection rate	90%	94%	80%	90%	80%	80%

(1) Face detection test

Face detection test is carried out using MTCNN.

(2) Face recognition test

Face recognition is tested using MobileNet-V2 network.

(3) Head posture recognition test

VGG-16 network was used to test head pose recognition.

(4) Header recognition test

The header recognition test is carried out using VGG-16 network.

(5) Facial expression recognition test

VGG-16 network was used to test human pose recognition.

(6) Human posture recognition test

VGG-16 network was used to test human pose recognition.

(7) System stability test

The system stability test tests whether the system is interrupted operation or cannot work normally, the situation. After testing, the system is basically stable.

Test pictures and test results are shown in Figures 13–16.

4.4. Summary of Test Results. Through the function test and performance test of the system, it can be seen that the classroom evaluation system designed in this paper has good human-computer interaction and has realized the functions of automatic classroom attendance, classroom behavior identification, and classroom overall evaluation. The face detection rate, face recognition rate, head posture recognition rate, facial expression recognition rate, and human posture recognition rate of the classroom evaluation system designed in this paper all meet the design requirements. The system stability basically meets the design requirements. The technical parameters of the system are summarized in Table 4.

5. Conclusion

On the basis of functional requirements and design requirements, the paper elaborated the whole development process of classroom evaluation system based on deep learning from the aspects of scheme design, relevant algorithms, detailed design, etc., and carried out functional test and performance test of the designed classroom evaluation system. The test results show that the system has realized the expected function, and all the performance parameters meet the design requirements. The work of the thesis is as follows:

(1) Complete the overall scheme design of the system. According to the research background and application scenarios of the paper, the functional requirements of the system are analyzed to determine the system design requirements, and on this basis, the overall scheme design of the system is proposed, including the hardware platform construction scheme design and software scheme design.

(2) The paper adopts EAIDK-610 embedded artificial intelligence development platform jointly developed by ARM and Open AI Lab as the core processing platform at the edge of the system. On the basis of this platform, the paper realizes the functions of pin-top and focal length control, face detection and interception, classroom behavior recognition, and so on, combined with the spherical webcam. In this paper, Intel FPGA accelerated cloud platform is used as the core processing platform of the system server, and the face recognition, classroom evaluation index calculation, and other functions are realized on this platform.

(3) The paper uses PC as the system client to realize the design of user interaction interface on the client. In addition to the above functions, according to the functional requirements of the system, the paper implements the functions of sending and receiving data transmission on the edge end, server end, and client end, respectively. Finally, the paper realizes the system of classroom behavior recognition of students in fixed positions in the classroom and obtains the function of classroom evaluation according to the above results.

(4) The function test and performance test of the classroom evaluation system based on deep learning designed in this paper are carried out, and the test results are summarized.

Data Availability

The data set can be accessed upon request.

Conflicts of Interest

The authors declare that they have no conflicts of interest.

References

[1] X. Wang, Y. Zhao, and F. Pourpanah, "Recent advances in deep learning," *International Journal of Machine Learning and Cybernetics*, vol. 11, no. 4, pp. 747–750, 2020.

[2] V. A. Sindagi, V. M. Patel, and M. Vishal, "A survey of recent advances in CNN-based single image crowd counting and density estimation," *Pattern Recognition Letters*, vol. 107, pp. 3–16, 2018.

[3] H. Geoffrey and S. Ruslan, "Reducing the dimensionality of data with neural networks[J]," *Science*, vol. 313, no. 5786, pp. 504–507, 2006.

[4] A. Brunetti, D. Buongiorno, G. F. Trotta, and V. Bevilacqua, "Computer vision and deep learning techniques for pedestrian detection and tracking: a survey," *Neurocomputing*, vol. 300, no. 15, pp. 17–33, 2018.

[5] K. Zhang, Z. Zhang, Z. Li, and Y. Qiao, "Joint face detection and alignment using multitask cascaded convolutional networks," *IEEE Signal Processing Letters*, vol. 23, no. 10, pp. 1499–1503, 2016.

[6] H. Wenlin, "Edge computing enabled non-technical loss fraud detection for big data security analytic in smart grid[J]," *Journal of Ambient Intelligence and Humanized Computing*, vol. 11, no. 4, pp. 1697–1708, 2020.

[7] H. Yang, U. Ciftci, and L. Yin, "Facial expression recognition by de-expression residue learning[J]," *International Journal on Computer Science & Engineering*, vol. 3, no. 5, pp. 2220–2224, 2018.

[8] N. N. Yang, "Research on face detection Algorithm based on deep learning[J]," *Science and Technology Innovation Herald*, vol. 15, no. 26, pp. 161-162, 2018.

[9] W. Shi, G. Pallis, and Z. Xu, "Edge computing [scanning the issue]," *Proceedings of the IEEE*, vol. 107, no. 8, pp. 1474–1481, 2019.

[10] M. Y. Yuan, C. S. Zhou, H. B. Huang et al., "Review of pooling methods for convolutional neural networks," *Journal of Software Engineering and Applications*, vol. 9, no. 5, p. 13, 2020.

[11] M. M. Cheng, M. S. Lin, and Z. F. Wang, "Research on intelligent teaching system based on expression recognition and sight tracking [J]," *Distance Education in China*, vol. 5, pp. 59–64, 2013.

[12] J. Whitehill, Z. Serpell, Y.-C. Lin, and A. J. R. Foster, "The faces of engagement: automatic recognition of student e facial expressions," *IEEE Transactions on Affective Computing*, vol. 5, no. 1, pp. 86–98, 2014.

[13] B. Sun, Y. N. Liu, J. H. Luo et al., "Expression feature extraction based on tensor analysis [J]," *Computer Engineering and Applications only official website*, vol. 20, pp. 145–148, 2016.

[14] X. K. Cui, T. H. Wang, and Z. P. Zhuang, "Study on emotion recognition technology in student learning process based on OpenCV [J]," *Instrument user*, vol. 25, no. 3, pp. 16–18, 2018.

[15] K. Ahuja, D. Kim, F. Xhakaj, and V. A. S. J. E. C. A. Y. Varga, "EduSense," *Proceedings of the ACM on Interactive, Mobile, Wearable and Ubiquitous Technologies*, vol. 3, no. 3, pp. 1–26, 2019.

[16] C. Wang and H. Y. Qi, "Visualising the knowledge structure and evolution of wearable device research[J]," *Journal of Medical Engineering & amp; Technology*, vol. 45, no. 3, pp. 112–115, 2021.

[17] Q. Y. Jiang, Y. W. Zhang, S. Q. Tan et al., "Student classroom behavior recognition based on residual network [J]," *Modern Computer*, vol. 20, pp. 23–27, 2019.

[18] D. Kim, C. Park, J. Oh, and H. Yu, "Deep hybrid recommender systems via exploiting document context and statistics of items," *Information Sciences*, vol. 417, pp. 72–87, 2017.

[19] A. Krizhevsky, I. Sutskever, and G. E. Hinton, "ImageNet classification with deep convolutional neural networks," *Communications of the ACM*, vol. 60, no. 6, pp. 84–90, 2017.

[20] Y. Wang and J. Tang, "Personalized paper recommendation algorithm based on deep learning [J]," *Wireless Communications and Mobile Computing*, vol. 32, no. 4, pp. 35–37, 2018.

[21] L. Guo and L. Liu, "Research on traffic classification method based on multi-layer perceptron [J]," *Journal of Electronic Measurement and Instrument*, vol. 7, pp. 56–64, 2019.

[22] J. Hu, L. Shen, and G. Sun, "Squeeze-and-Excitation networks [J]," *IEEE Transactions on Pattern Analysis and Machine Intelligence*, vol. 99, p. 1, 2017.

Hindawi
Scientific Programming
Volume 2022, Article ID 7702776, 8 pages
https://doi.org/10.1155/2022/7702776

Research Article

Preparation of Nitrogen-Doped Carbon-Based Bimetallic Copper-Cobalt Catalysis Based on Deep Learning and Its Monitoring Application in Furfural Hydrogenation

Xiaojun Pei, Haojun Shu, and Yisi Feng

School of Chemistry and Chemical Engineering, Hefei University of Technology, Hefei 230009, China

Correspondence should be addressed to Yisi Feng; fengyisi@hfut.edu.cn

Received 6 April 2022; Revised 14 April 2022; Accepted 25 April 2022; Published 20 May 2022

Academic Editor: Jie Liu

In the field of catalysis, the support of the catalyst is often composed of hollow carbon materials. In order to monitor the preparation of nitrogen-doped carbon-based bimetallic copper-cobalt catalysis and its hydrogenation reaction in furfural, using m-aminophenol as the nitrogen source, formaldehyde as a carbon source, and P123 as a template agent, a nitrogen-doped bimetallic copper-cobalt mesoporous carbon catalyst Cu-Co@N-MPC-500 was synthesized by the hydrothermal method. The morphology, structure, and chemical composition of the catalyst were analyzed by means of TEM, XRD, BET, and XPS, respectively. The results show that the nitrogen-doped mesoporous carbon has a stable structure, uniform pore size distribution, and the nano-copper-cobalt particles are uniformly dispersed in the mesoporous carbon surface. Through furfural hydrogenation, the catalyst selectivity and cycle stability were discussed. Under the furfural conversion rate of 96.1%, the yield of cyclopentanone could reach 76.2%. After 5 cycles, the catalytic efficiency of the catalyst did not decrease significantly. It shows that Cu-Co@N-MPC-500 has excellent application prospects in the field of industrial production.

1. Related Introduction

Porous carbon materials come from a wide range of sources, including mesoporous carbon, activated carbon, carbon nanotubes, graphene, amorphous carbon black, nanofibers, and carbon aerogels. Porous carbon materials are widely used in catalysis, adsorption electrochemical [1–3], and other important fields. However, pure carbon porous materials do not perform well in many applications, and carbon materials need to be further modified to improve their application performance.

In the field of catalysis, porous carbon materials are often used as catalyst supports. Introducing other atoms into the carbon atomic layer to modify porous carbon materials to improve the reactivity of catalysts has been a research hotspot in recent years. The introduction of sulfonic acid groups into the porous carbon support can effectively introduce acid sites into the catalyst, thereby changing the acid value of the catalytic material. Kasakov et al. used glucose and cellulose as porous carbon sources to prepare a sulfonic acid group-modified Ni/C-SO3H catalyst, which showed excellent catalytic activity in the liquid-phase hydrogenation of phenol to cyclohexane. After reacting at 200°C for 6 h, the conversion of phenol and the yield of cyclohexane can reach 100% and 90%, respectively. Onda et al. [4, 5] used activated carbon (AC) as the carbon source to prepare a sulfonic acid group-modified platinum catalyst Pt/AC-SO_3H by modifying the carbon material. The activity of the catalyst was tested in the reaction of hydrolysis of polysaccharides to gluconic acid; the results show that the catalyst Pt/AC-SO_3H modified by sulfonic acid group has a significantly higher catalytic effect than the traditional carbon-based supported catalyst. N doping is one of the most common carbon-based support modification strategies. N atoms are doped into carbon to make the carbon structure more disordered, which will increase the defect sites of the carbon support and make N-doped carbon materials have unique properties [6]. The use of nitrogen-doped carbon-based supports can effectively improve the hydrophilicity and conductivity of the catalyst, strengthen the interaction between the carbon support and

the metal active components, improve the stability of the catalyst, and at the same time play a role in regulating the supported metal active components [7]. Lei [8] et al. used the hard template method to mix SBA-15 with aniline and then carbonized and removed the template at high temperature to prepare a nitrogen-doped ordered mesoporous carbon-supported metal Pt catalyst, which was investigated in the catalytic oxidation of methanol. The results show that there is a strong interaction between the nitrogen element in the carrier and the metal active component Pt nanoparticles. The higher the doping amount of nitrogen in the carrier, the higher the dispersion degree of Pt metal nanoparticles. Moreover, the prepared catalyst showed good reactivity in methanol oxidation reaction. Chan-Thaw et al. [9] prepared a nitrogen-doped carbon nanotube-supported palladium metal catalyst, which showed better catalytic performance in the catalytic oxidation reaction system of benzyl alcohol than the traditional activated carbon nanotube-supported palladium metal catalyst. There are many application reports on the use of modified carbon materials as catalyst supports to support single metals, but there are few reports on the use of modified carbon materials to support nonprecious bimetallic components.

The related research study in this paper is mainly based on using $Cu(NO_3)_2{\cdot}3H_2O$ and $Co(NO_3)_2{\cdot}6H_2O$ as the precursors of metal active components, by using the triblock compound P 123 as the soft template and m-aminophenol as the nitrogen source, formaldehyde was used as the carbon source, and then a nitrogen-doped carbon-based bimetallic catalyst 2Cu-Co@N-MPC-500 was prepared through a one-step hydrothermal reaction, high-temperature carbonization, and H_2 reduction. The catalyst structure and components were characterized and analyzed, and the performance of the prepared catalyst was examined in the hydrogenation of biomass molecule furfural to cyclopentanone.

2. Related Theoretical Methods

The RNN network is also composed of an input layer, hidden layer, and output layer. Each layer contains a different number of neurons. In the traditional neural network model, the neurons of each layer are not connected to each other, but the RNN network is different, and the nodes between its hidden layers are connected. Therefore, the biggest difference between the RNN neural network and traditional neural network model is that RNN neural network not only has feedforward connection, but also has feedback of internal connection, which plays the role of "circulation." This kind of information flow similar to feedback inside neurons makes the network have memory function. At a certain time *t*, the difference between the neurons of the BP neural network and the neurons of the RNN network is shown in Figure 1:

There are many variants of the RNN network model, among which, Figure 2-1 is expanded in time series, and the classic RNN network model structure is shown in Figure 3:

In the above figure, the meaning of each parameter is as follows:

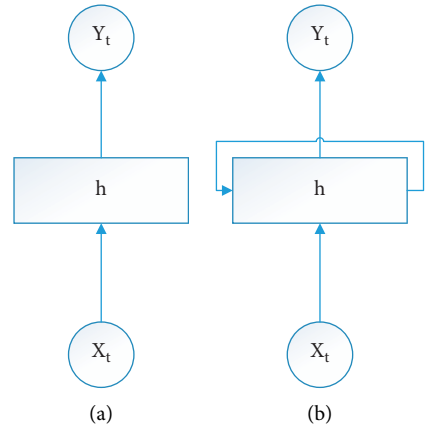

Figure 1: (a)BP neuron and (b) RNN neuron.

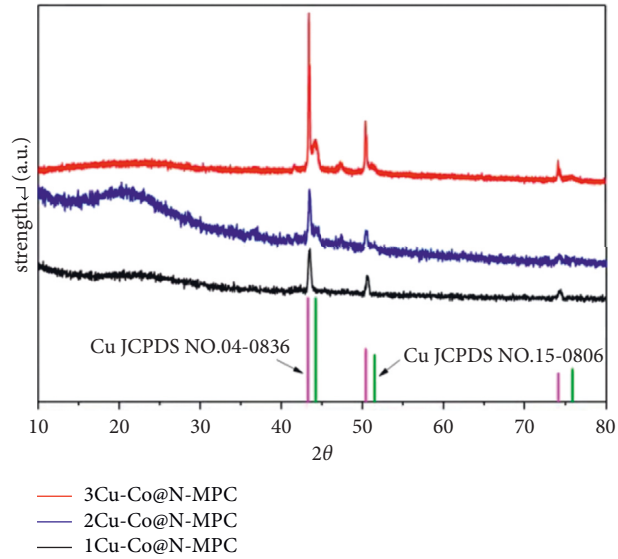

Figure 2: XRD characterization results of different Cu-Co loadings.

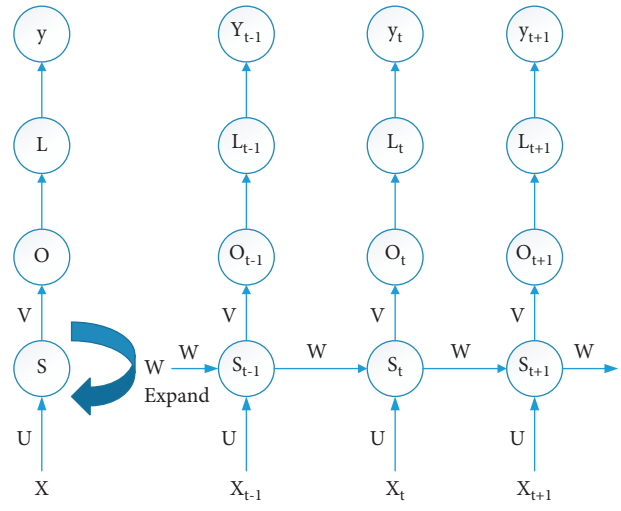

Figure 3: RNN network structure diagram.

(1) U, V, and W are three matrices, which represent the input weight, the output weight, and the last output as the weight of this input, respectively. These three matrices are the linear relationship parameters of the model. The reason why the RNN network can have memory depends on these three matrices.

(2) x represents the input layer data. Also, s_{t-1}, s_t, and s_{t+1} represent the input values at $t-1$, t, and $t+1$, respectively.

(3) s represents the hidden layer state. Similarly, s_t represents the state of the hidden layer at time t. As shown in Figure 2-2, both x_t and st-1 will affect s_t.

(4) o represents the output of the model. As can be seen from the figure, o is only associated with s_t.

(5) L is the loss function of the model.

(6) y is the true observed value of the predicted time series data. As can be seen from Figure 2-2, in the RNN network, the hidden state s_t at any time can be obtained by the following equation:

$$s_t = \sigma(Ux_t + Ws_{t-1} + b). \tag{1}$$

In formula (1) and the following equations, σ is the activation function and b is the bias of the linear relationship.

After obtaining the state s_t of the hidden layer of the model at time t, the model output o_t at this time can be obtained by the following: t to

$$o_t = VS_t + c. \tag{2}$$

In formula (2), c also represents the bias, so the final output predicted by the RNN network can be obtained from the following:

$$\widehat{y}_t = \sigma(o_t). \tag{3}$$

After the predicted output value is obtained, the cost function can be used to quantify the loss of the RNN model at the current time t, that is, the gap between the predicted value $\widehat{y}_t$ of the model and the original real data y_t. Common cost functions include cross-entropy cost function, mean squared error, root mean squared error, etc. This is actually the forward propagation algorithm of the RNN network model. In this paper, the preparation of a nitrogen-doped carbon-based bimetallic copper-cobalt catalyst based on in-depth learning and its monitoring application in furfural hydrogenation are studied. The main reason is that the relevant experimental results are monitored by computer technology.

3. Experimental Part

3.1. Reagents and Equipment. The reagents prepared in the relevant experiments in this paper mainly include "triblock compound P123, (Mn: 2000–5800) obtained from Annaiji; analytical grade m-aminophenol, aqueous formaldehyde solution, and furfural purchased from Sinopharm Chemical Reagent Co. Ltd.; analytical grade copper nitrate trihydrate, cobalt nitrate hexahydrate, anhydrous hexanol, and ethyl acetate obtained from Aladdin."

The main equipment prepared in this paper for related experiments are "superconducting nuclear magnetic resonance spectrometer (VNMRS600), Agilent Technologies, USA; X-ray photoelectron spectrometer (ESCACAB250), Thermo Fisher, USA; X-ray diffractometer (X-ray diffractometer 'Pert PRO MPD type), PANalytical company, Netherlands; scanning electron microscope (SU8020 type), Hitachi, Japan; elemental analyzer (vario EL cube), Germany Elementar company; tube roasting furnace (GSL-1500X type), Hefei Kejing Materials Co., Ltd.; gas adsorption instrument (Autosorb-IQ3 type), American Quanta; and a gas chromatograph (GC16901FJ type), Hefei Jiedao Equipment Co. Ltd."

3.2. Preparation of Catalysts. The preparation of the catalyst is mainly prepared by the hydrothermal method, and its main principle is to carry out the index through the hydrothermal reaction kettle, namely, the preparation of N-doped mesoporous carbon catalysts by the hydrothermal method: 1.01 g $Cu(NO_3)_2{\cdot}3H_2O$ and 0.62 g $Co(NO_3)_2{\cdot}6H_2O$ with a molar ratio of 2 : 1 were dissolved in 50 mL of ethanol and 50 mL of deionized mixed solution of water, 4.5 g of m-aminophenol and 1.0 g of templating agent P123 were sequentially added, and stirred until completely dissolved. Then, 4.5 g formaldehyde solution (37 wt%) was slowly added to the solution using a dropping funnel, and the dropwise addition time was controlled to be 1 h. After the dropwise addition was completed, the reaction was continued at room temperature for 2 h.

The solution was transferred to a hydrothermal reactor, sealed, and placed in a drying oven at 65°C for 5 h. The obtained reaction mixture was filtered with deionized water and ethanol solution, and the filter cake obtained by filtration was dried in a vacuum drying oven at 60°C overnight. The dried solid was taken out and ground into powder using a mortar. The obtained powder was placed in a tube furnace for high-temperature carbonization. The tube furnace was heated from 25°C to 500°C at a heating rate of 1°C/min, and kept at 500°C for 2 hours. The carbonization process was carried out in a mixed atmosphere of nitrogen and hydrogen. A nitrogen-doped ordered mesoporous carbon was obtained, which was denoted as 2Cu-Co@N-MPC-500, where 2 represents the molar ratio of metal Cu and Co and 500 is the calcination temperature.

As a comparison, traditional activated carbon supported catalysts were prepared by the impregnation method. First, 1.01 g $Cu(NO_3)_2$ $3H_2O$ and 0.31 g $Co(NO_3)_2$ $6H_2O$ were added to 90 mL of dilute nitric acid (5 wt%) solution at a temperature of 60°C and stirred rapidly for 2 h, and then it was put into an ultrasonic instrument for ultrasonic treatment for 2 h, 2.3 g of activated carbon was added into the above solution, and mechanical stirring was performed for 2 h; then the above mixture was filtered and washed. The filter cake was transferred to an oven at 60°C for vacuum drying and then ground into powder using a grinder. The obtained powder is placed in a tube furnace for high-

temperature carbonization, and the carbonization conditions are the same as those for preparing the catalyst by the hydrothermal method. An activated carbon-supported catalyst was obtained, which is denoted as 2Cu-Co@AC-500 as shown in Figure 4.

3.3. Characterization of Catalysts. The catalytic materials were analyzed for specific surface area, pore volume, and pore size distribution using a fully automatic surface area analyzer (BET). The specific method is as follows: 0.1 g of the sample was weighed, and after 4 hours of treatment under vacuum conditions, the adsorption and desorption test was carried out in a liquid nitrogen atmosphere. The specific surface area of the material was calculated using the BET (Brunner–Emmet–Teller) formula, and the pore size distribution was calculated using the BJH formula. The bulk structure analysis of nitrogen-doped catalysts was performed using X-ray powder diffraction analysis (XRD). Using Cu-Kα as the X-ray radiation source, the scanning speed is 8°/min; the scanning test angle range is 20°–90°, and the working voltage and current of the instrument are 40 kV and 55 mA, respectively. The metal elements in the catalysts were quantitatively and qualitatively analyzed by X-ray photoelectron spectroscopy (XPS), and the metal grain size was calculated by the Scherrer formula. Using transmission electron microscopy (TEM) to conduct microscopic analysis of the apparent morphology and structure of the catalytic materials, qualitative and semiquantitative analysis of the composition of the catalytic materials can also be carried out. Before testing, the samples were ground to powder, and then dispersed evenly in ethanol solution, sonicated for 1 h with an ultrasonic instrument, and then the suspension was evenly spread on the copper mesh for testing. The metal content components in the catalysts were detected by an -inductively coupled plasma analyzer (ICP-AES). Before detection, concentrated nitric acid was used to dissolve a certain amount of the sample catalyst, and then diluted to constant volume for sample detection.

3.4. Performance Test of Catalysts. In the furfural hydrogenation reaction, it needs to be carried out in a batch autoclave, and the activity of nitrogen-doped mesoporous carbon-supported metal copper-cobalt catalysts is prepared by a temperature controller and a 25 mL batch autoclave with magnetic stirring.

The experimental operation is as follows: accurately weigh 0.2 g of furfural and 0.1 g of the prepared catalyst, add them into the autoclave, then add 10 mL of deionized water, put in the magnet, seal the autoclave, and pass 1.0 MPa hydrogen gas, replace the gas 5 times, then add the hydrogen pressure required for the reaction, heat to the temperature required for the reaction under magnetic stirring at 700 rpm/min, and adjust the heating program and the reaction time by a temperature controller. After the reaction, the mixed solution was transferred to 10 mL of ethyl acetate solution containing quantitative internal standard DMF, and then the reaction solution was filtered, and the filtrate obtained after filtration was detected and analyzed by gas chromatography.

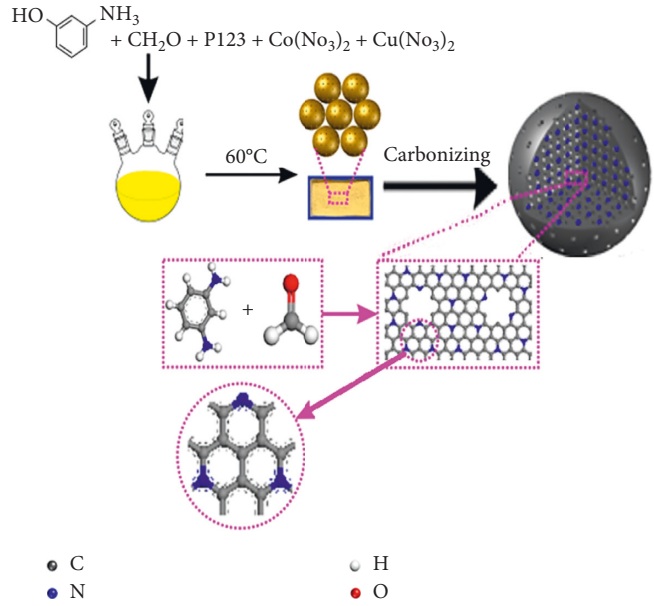

Figure 4: Preparation process of the N-doped mesoporous carbon catalyst.

The furfural hydrogenation reaction products were analyzed by gas chromatography. After the reaction, furfural, furfuryl alcohol, cyclopentanol, cyclopentanone, and tetrahydrofurfuryl alcohol mainly exist in the solution. The detection conditions of the gas chromatograph are as follows: FID detector; chromatographic column; DM-Wax capillary column; detection chamber temperature: 280°C; vaporization chamber temperature: 260°C; carrier gas pressure: 0.1 MPa; column oven initial temperature: 50°C; standard substance: DMF; and sample injection volume: 0.1–0.2 μL.

3.5. Cyclic Performance Test of Catalysts. After each test reaction, the reaction solution was filtered and washed, and the obtained solid filter residue was washed with deionized water and ethanol solution for many times and then sealed and dried in an oven for continued use in the next cycle. In the next cycle experiment, the same mass of the recovered catalyst was weighed as in the last experiment, and control other reaction conditions are set to be the same as the last time.

4. Results and Discussion

4.1. Catalyst Characterization Analysis

4.1.1. XRD Analysis. It can be seen from Figure 2 that the as-prepared Cu-Co@N-MPC exhibits strong diffraction peaks around 43.4° and 50.5°, corresponding to the diffraction peaks of elemental Cu (JCPDS 96-901-2955) [10]. By comparing the peak intensities of catalysts with different Cu loadings, it is found that with the increase of Cu loading, the diffraction peaks of Cu are also continuously enhanced. The diffraction peak observed at about 2θ of 44.8° corresponds to

the diffraction peak of Co, but the peak intensity is weak, which may be due to the good dispersion and small particle size of Co metal nanoparticles. In order to further determine the existence form and valence state of each element in the catalyst, the catalyst was further characterized by XPS.

4.1.2. XPS Analysis. Figure 5 shows the XPS spectrum of 2Cu-Co@N-MPC-500. It can be seen from Figure 4(a) that strong peak signals mainly appear at the binding energies of 932.5 eV and 934.6 eV. The peak at 934.6 eV is the characteristic peak of Cu^{2+}, while the peak at 932.5 eV is the characteristic peak of Cu^{+} and Cu^{0} [11], and the area ratios of Cu^{0} and Cu_2O to CuO are 82.3% and 17.7%, indicating that the Cu-Co@N-Cu in MPC mainly exists in the state of Cu^{0} and Cu_2O, and the reduction of metal Cu is relatively sufficient. The XPS spectrum of Co in 2Cu-Co@N-MPC is shown in Figure 4(d), the binding energy peaks of Co mainly appear at 778.0 eV corresponding to the characteristic peak of Co^{0} (2p 3/2), 780.9 eV and 797.6 eV, respectively. For the characteristic peaks of Co^{3+} (2p 3/2) and Co^{3+} (2p 1/2), 783.5 eV and 796.5 eV correspond to the characteristic peaks of Co^{2+} (2p 3/2) and Co^{2+} (2p 1/2), respectively, indicating that the main forms of copper are CoO and Co_3O_4, and cobalt is less reduced. The metal grain size was calculated to be 13.8 nm by the Scherrer formula. XPS analysis results showed that the metal active centers of the prepared catalysts were mainly Cu^{0}, Cu_2O, and CoO_x.

Figure 5(c) is the XPS characterization spectrum of 2Cu-Co@N-MPC-500N. It can be seen from the figure that the peak of the N1s binding energy in Cu-Co@N-MPC-500 appears at 400.9 eV, which corresponds to graphite nitrogen bonding.

The peak at 398.9 eV corresponds to the binding energy of pyridine nitrogen. The ratio of graphitic nitrogen to pyridine nitrogen is close to 1 : 1. Elemental analysis of the synthesized 2Cu-Co@N-MPC catalyst showed that the nitrogen content in the catalyst was 5.29%. It shows that N in 2Cu-Co@N-MPC is well introduced into the catalyst support and mainly exists in the form of graphitic nitrogen and pyridine nitrogen.

4.1.3. N_2 Desorption Analysis. The pore size distribution of the catalyst support and the internal structure of the pores have a great influence on the catalytic activity. By observing the N_2 isotherm adsorption and desorption curves (Figure 6), it can be seen that the prepared 2Cu-Co@N-MPC-500 has obvious pore structure characteristics, and the specific surface area of the catalyst calculated by the formula is 20.16 $m^2\,g^{-1}$. It can be seen from the pore size distribution curve that the pore size distribution of the mesoporous carbon spheres is uniform, and the average pore size is about 4.9 nm, which belongs to the mesoporous range.

4.1.4. TEM Analysis. Through the detailed observation of TEM, as shown in Figure 7, the prepared catalyst carrier has obvious spherical characteristics, and it can be seen that the N element is uniformly distributed, and the N element is well introduced into the catalyst carrier. The copper-cobalt nanoparticles were well-dispersed in the pore size of the mesoporous carbon spheres, and there was no obvious metal agglomeration phenomenon, indicating that the prepared nitrogen-containing mesoporous carbon carrier had a good dispersing effect on the metal copper-cobalt nanoparticles.

4.2. Catalyst Performance Test. Taking furfural hydrogenation to cyclopentanone as a model reaction, the catalytic hydrogenation performance of the catalyst 2Cu-Co@N-MPC-500 was investigated. The reaction temperature, reaction pressure, and reaction time conditions were optimized. Under the mild reaction conditions of 150°C, 2 MPa H_2, and 2 h, the 2Cu-Co@N-MPC-500 catalyst showed the best catalytic activity and selectivity. A furfural conversion of 96.1% and a cyclopentanone yield of 75.2% were obtained. Subsequently, the effect of nitrogen content in the carrier on the catalytic activity and the cyclic stability of the catalyst were investigated in depth.

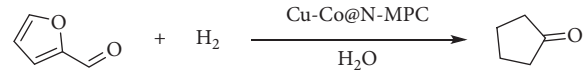

4.2.1. Effect of Nitrogen Content in the Catalyst Carrier on the Reaction Activity. The catalytic performance of catalysts with different nitrogen content in furfural hydrogenation was tested experimentally, and the results are shown in Figure 6. Using the traditional activated carbon-supported bimetallic catalyst 2Cu-Co@AC-500 under the optimal reaction conditions, 78% furfural conversion and 35% cyclopentanone yield can be obtained. However, the as-prepared N-doped catalyst 2Cu-Co@N-MPC-500 was able to achieve close to 100% conversion and 75% cyclopentanone yield under optimal reaction conditions, suggesting that the use of the N-doped mesoporous catalyst is beneficial. The carbon material as a carrier can effectively improve the activity of furfural hydrogenation and the selectivity to cyclopentanone. In order to better understand the role of N-doped support in the catalytic hydrogenation of furfural, the nitrogen content in the support was adjusted by changing the molar ratio of m-aminophenol to formaldehyde to test the addition of catalysts with different N contents in the support. Hydrogen activity, the results are shown in Figure 8. With the increase of N doping content from 2.46 % to 6.67 %, the furfural conversion showed a trend of increasing first and then tending to be stable, while the yield of cyclopentanone kept increasing. When the nitrogen doping in the carrier is 2.46 %, the furfural conversion and cyclopentanone yield are 86% and 59%, respectively. When the nitrogen doping in the carrier is increased to 5.92 %, the furfural conversion and cyclopentanone yield are 86% and 59%, respectively. The yields of ketones reached 95% and 75%, respectively, which indicated that proper N doping was very important to improve the hydrogenation activity and selectivity of furfural. For the type of N-doped support, the main forms of N in the catalyst support are pyridine nitrogen and graphitic nitrogen, and

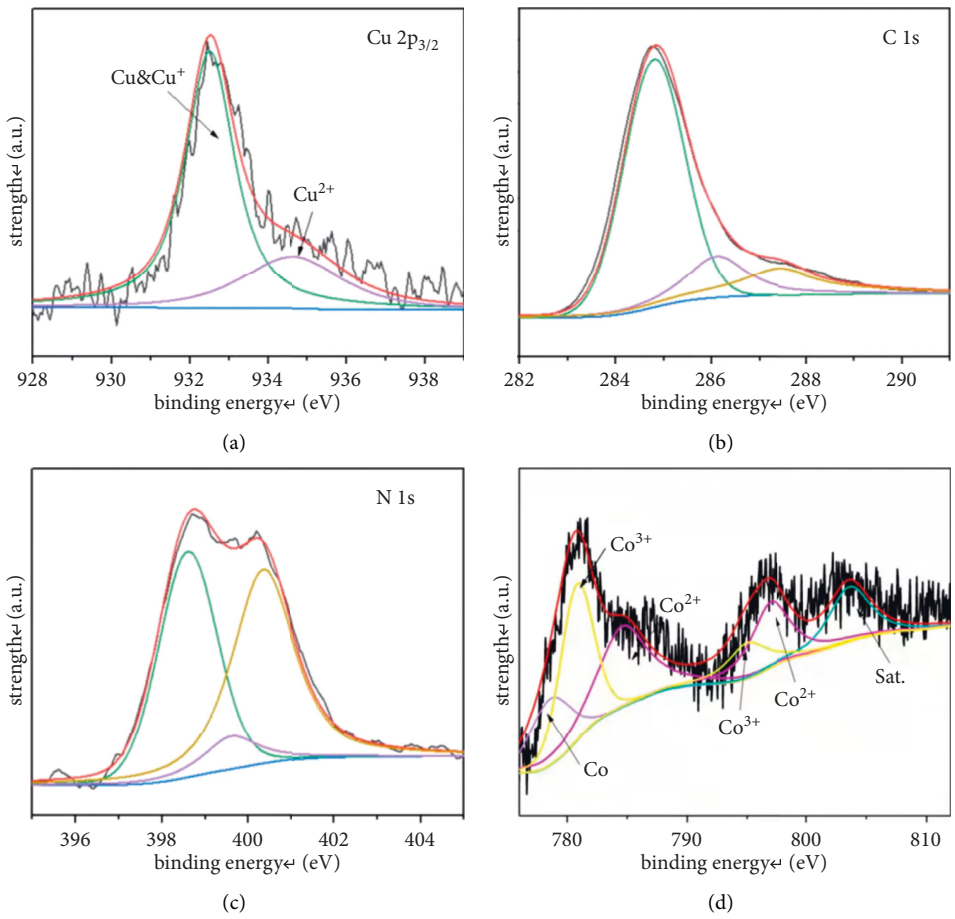

Figure 5: XPS characterization of 2Cu-Co@N-MPC-500.

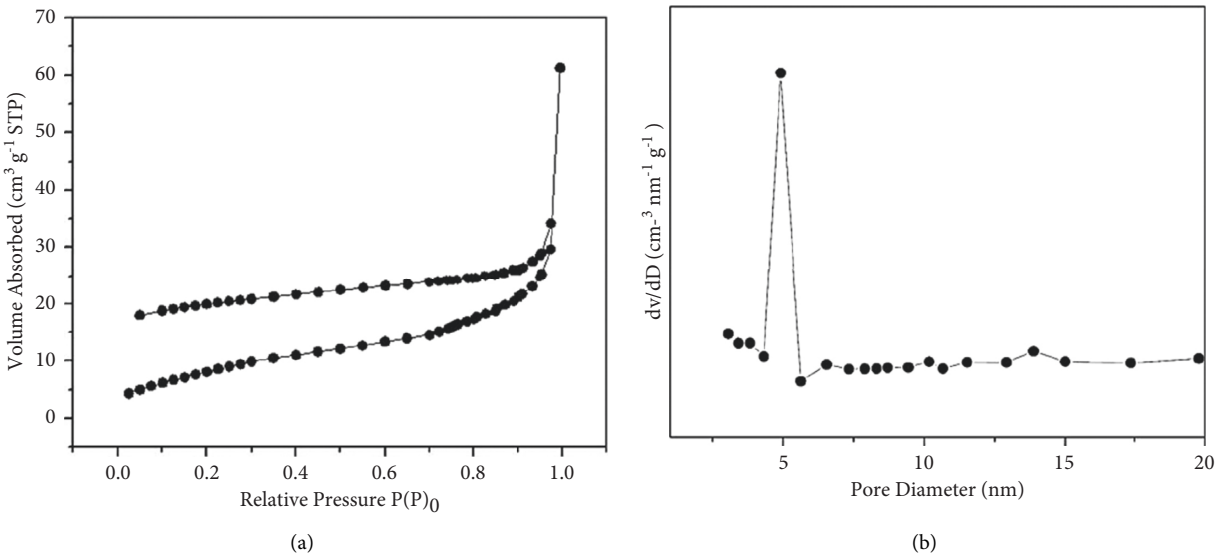

Figure 6: BET characterization of 2Cu-Co@N-MPC-500.

the presence of pyridine nitrogen and graphitic nitrogen plays a positive role in the hydrogenation of furfuryl alcohol to cyclopentanone. The summary includes the following reasons: (1) The introduction of nitrogen into the catalyst can provide an anchor for the nanometal particle components, form metal-N bonds, enhance the interaction between

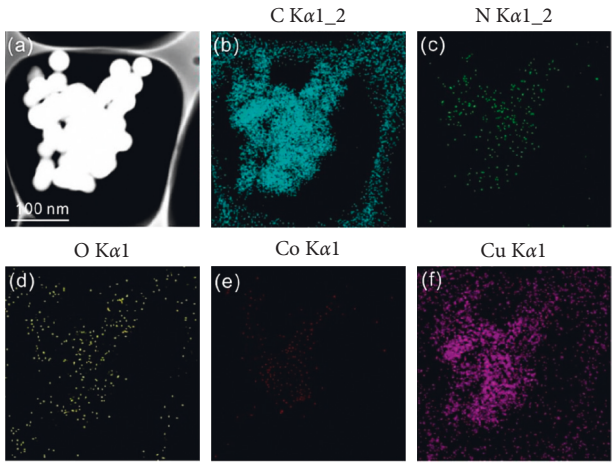

Figure 7: TEM and EDX characterization images of 2Cu-Co@N-MPC-500.

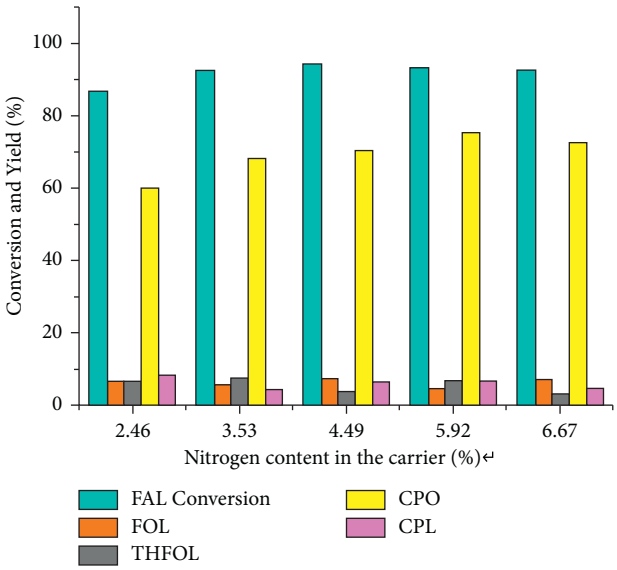

Figure 8: Effect of nitrogen content in the carrier on the catalytic activity.

the metal active components and the support, and effectively regulate the metal activity. The size and dispersion of the components make it difficult for the metal particle components to agglomerate; (2) the pyridine nitrogen present in the catalyst carrier can increase the Lewis basic site and enhance the adsorption effect on the reactants; (3) the introduction of N in the carrier doping can effectively improve the electron transfer rate and increase the electron density of the catalyst metal particles, thereby increasing the interaction between it and the reactant furfural [12–18]; (4) the introduction of nitrogen in the carrier can effectively increase the catalyst's efficiency. Hydrophilic, there is a ring-opening process in the hydrogenation of furfural to cyclopentanone, and water plays an indispensable role in the ring-opening process, which has an important impact on improving the reactivity and selectivity.

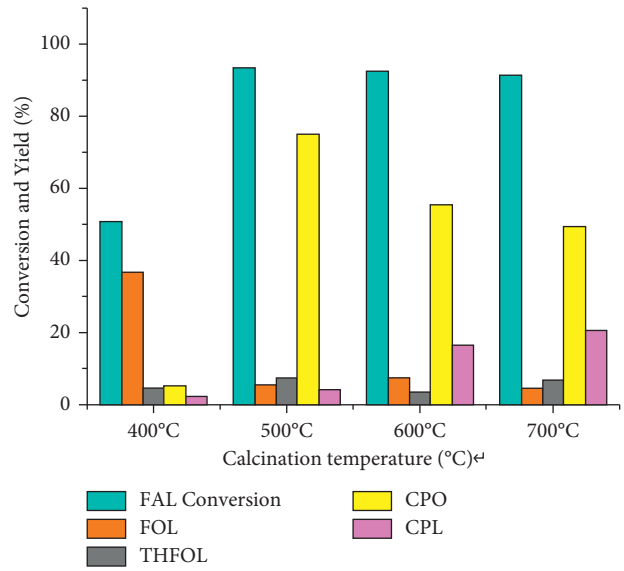

Figure 9: Catalyst cycle performance diagram.

4.2.2. Catalyst Cycle Performance Test. The 2Cu-Co@N-MPC-500 catalyst was subjected to cycling experiments, and the specific experimental results are shown in Figure 9. The experimental results show that the yield of cyclopentanone is only slightly decreased after the catalyst is recycled for 5 times, and the furfural is basically completely converted. The furfural conversion and cyclopentanone yields can still reach 90% and 71%, respectively, in the fifth cycle.

Through ICP-AES analysis, it was found that the Cu and Cu contents in the initial catalyst were 3.48% and 1.62%, respectively. After 5 cycle experiments, the metal contents of Cu and Co in the catalyst were 3.22% and 1.35%, respectively, and only a small part of the active metal was lost in the cycle reaction. The 2Cu-Co@N-MPC-500 catalyst was used in furfural hydrogenation. It exhibits good reusability and high stability in the selective formation of cyclopentanone. The excellent stability is attributed to the carbon support that can well immobilize and protect the bimetallic nanoparticles, while the doping of nitrogen forms metal-N bonds, which increases the interaction between the support and the bimetallic Cu-Co [19, 20].

5. Conclusion

In this paper, based on the preparation of nitrogen-doped carbon-based bimetallic copper-cobalt catalysis and its monitoring application in furfural hydrogenation, by using m-aminophenol as the nitrogen source, formaldehyde as the carbon source, and P123 as the template agent, a nitrogen-doped carbon-based metal catalyst 2Cu-Co@N-MPC-500 was hydrothermally synthesized and characterized by XRD, XPS, BET, and TEM. The catalyst was analyzed, and the results showed that the catalyst had a stable carbon sphere structure, uniform pore size distribution, and uniform dispersion of metal nanoparticles. It exhibits excellent selectivity and cycle stability in the hydrogenation of furfural to cyclopentanone. Under the optimal conditions, the conversion rate of furfural reached 96.1%, the yield of

cyclopentanone reached 76.2%, and the catalyst was cycled 5 times without obvious deactivation.

Data Availability

The dataset can be accessed upon request.

Conflicts of Interest

The authors declare that there are no conflicts of interest.

Acknowledgments

This study was supported by General project of National Natural Science Foundation of China: design and preparation of the GPH-(CH2) n-bm catalyst with flexible "bridge chain" and research on "quasi-homogeneous" catalytic performance (21971050); 2020.1 ~ 2023.12, and Key project of Natural Science Research Project of Colleges and Universities in Anhui Province (No. kj2019a1248).

References

[1] S. Wang, Q. Zhao, H. Wei et al., "Aggregation-free gold nanoparticles in ordered mesoporous carbons: toward highly active and stable heterogeneous catalysts," *Journal of the American Chemical Society*, vol. 135, no. 32, pp. 11849–11860, 2013.

[2] Y. Tian, P. Liu, X. Wang, and H. Lin, "Adsorption of malachite green from aqueous solutions onto ordered mesoporous carbons," *Chemical Engineering Journal*, vol. 171, no. 3, pp. 1263–1269, 2011.

[3] D. Wang, A. Fu, H. Li et al., "Mesoporous carbon spheres with controlled porosity for high-performance lithium-sulfur batteries," *Journal of Power Sources*, vol. 285, pp. 469–477, 2015.

[4] S. Kasakov, C. Zhao, E. Baráth et al., "Glucose- and cellulose-derived Ni/C-SO3H catalysts for liquid phase phenol hydrodeoxygenation," *Chemistry - A European Journal*, vol. 21, no. 4, pp. 1567–1577, 2015.

[5] A. Onda, T. Ochi, and K. Yanagisawa, "New direct production of gluconic acid from polysaccharides using a bifunctional catalyst in hot water," *Catalysis Communications*, vol. 12, no. 6, pp. 421–425, 2011.

[6] H. Jiang, X. Yu, R. Nie, X. Lu, D. Zhou, and Q. Xia, "Selective hydrogenation of aromatic carboxylic acids over basic N-doped mesoporous carbon supported palladium catalysts," *Applied Catalysis A: General*, vol. 520, pp. 73–81, 2016.

[7] K. A. Kurak and A. B. Anderson, "Nitrogen-treated graphite and oxygen electroreduction on pyridinic edge sites," *Journal of Physical Chemistry C*, vol. 113, no. 16, pp. 6730–6734, 2009.

[8] Z. Lei, L. An, L. Dang et al., "Highly dispersed platinum supported on nitrogen-containing ordered mesoporous carbon for methanol electrochemical oxidation," *Microporous and Mesoporous Materials*, vol. 119, no. 1-3, pp. 30–38, 2009.

[9] C. E. Chan-Thaw, A. Villa, G. M. Veith et al., "Influence of periodic nitrogen functionality on the selective oxidation of alcohols," *Chemistry - An Asian Journal*, vol. 7, no. 2, pp. 387–393, 2012.

[10] S. C. Petitto and M. A. Langell, "Cu2O(110) formation on Co3O4(110) induced by copper impurity segregation," *Surface Science*, vol. 599, no. 1-3, pp. 27–40, 2005.

[11] H. Sohn, I. I. Soykal, S. Zhang et al., "Effect of cobalt on reduction characteristics of ceria under ethanol steam reforming conditions: AP-XPS and XANES studies," *Journal of Physical Chemistry C*, vol. 120, no. 27, pp. 14631–14642, 2016.

[12] D. Guo, R. Shibuya, C. Akiba, S. Saji, T. Kondo, and J. Nakamura, "Active sites of nitrogen-doped carbon materials for oxygen reduction reaction clarified using model catalysts," *Science*, vol. 351, no. 6271, pp. 361–365, 2016.

[13] Z. Li and J. Chen, "Prognostics of PEM fuel cells based on Gaussian process state space," *Journal of Energy*, vol. 149, pp. 63–73, 2018.

[14] Z. Hu, L. Xu, J. Li et al., "A novel diagnostic methodology for fuel cell stack health: performance, consistency and uniformity," *Energy Conversion and Management*, vol. 185, pp. 611–621, 2019.

[15] H. Lu, J. Chen, C. Yan, and H. Liu, "On-line fault diagnosis for proton exchange membrane fuel cells based on a fast electrochemical impedance spectroscopy measurement," *Journal of Power Sources*, vol. 430, pp. 233–243, 2019.

[16] N. H. Behling, *Fuel Cells: Current Technology Challenges and Future Research Needs*, Elsevier Science, Hefei, China, 2012.

[17] D. M. Du-Plooy and J. Meyer, "PEM fuel cells: failure, mitigation and dormancy recoveryunderstanding the factors affecting the efficient control of PEMFC [C]," *IEEE Africon*, vol. 2017, no. 9, pp. 1119–1124, 2017.

[18] J. Chen, D. Zhou, C. Lyu, and C. Lu, "A novel health indicator for PEMFC state of health estimation and remaining useful life prediction," *International Journal of Hydrogen Energy*, vol. 42, no. 31, pp. 20230–20238, 2017.

[19] D. Zhang, P. Baraldi, C. Cadet, N. Yousfi-Steiner, C. Bérenguer, and E. Zio, "An ensemble of models for integrating dependent sources of information for the prognosis of the remaining useful life of Proton Exchange Membrane Fuel Cells," *Mechanical Systems and Signal Processing*, vol. 124, pp. 479–501, 2019.

[20] Y. Hou, Z. Yang, and G. Wan, "An improved dynamic voltage model of PEM fuel cell stack," *International Journal of Hydrogen Energy*, vol. 35, no. 20, pp. 11154–11160, 2010.

Hindawi
Scientific Programming
Volume 2022, Article ID 4684461, 10 pages
https://doi.org/10.1155/2022/4684461

Research Article

Research on the Characteristic Model of Learners in Modern Distance Music Classroom Based on Big Data

Yushan Wang[1] **and Lianhong Liu**[2]

[1]*Sichuan Vocational College of Finance and Economics, chengdu, Sichuan, Chengdu 610101, China*
[2]*Chengdu Institute of Physical Education, Sichuan, Chengdu 610041, China*

Correspondence should be addressed to Lianhong Liu; 100345@cdsu.edu.cn

Received 14 March 2022; Revised 28 March 2022; Accepted 8 April 2022; Published 14 May 2022

Academic Editor: Jie Liu

This paper makes in-depth research on data mining, especially association rule mining, improves the FP-tree algorithm in both the algorithm itself and the data source, and finds out a mining algorithm suitable for learner characteristics. Association rule algorithm for actor feature model mining. By establishing the characteristic model of learners in modern distance music classroom, simulation experiments are carried out on FP-tree and three improved algorithms. This paper improves the FP-tree algorithm. Firstly, we improve the algorithm itself; aiming at the problem of too many frequent itemsets, an improved key item extraction algorithm KEFP-growth based on FP-growth is proposed, which ignores the frequent itemsets that are not concerned in the analysis. Then, improvements were made in terms of data sources. In view of the problem that the data source is too large, the mining efficiency is low, and the FP-tree cannot be loaded in memory, this paper proposes a data projection algorithm, which adopts the idea of divide and conquer, divides the frequent 1-itemsets of the database into database subsets of each frequent 1-itemsets, and then mines the database subsets separately and then merges them. Finally, the KEFP-growth algorithm and the projection algorithm are combined, which can not only eliminate the mining of meaningless frequent items but also divide the data when there is a large amount of data. This paper also compares the performance of the three improved algorithms and the original FP-tree algorithm through experiments. The experiments show that the combination of the KEFP-growth algorithm and the database projection algorithm is the most suitable one for the learner feature mining of the adaptive learning system. (1) The KEFP-growth algorithm reduces the number of frequent items output by the original FP-tree algorithm by about 50%, and the mining time is reduced by 50%. (2) The data projection algorithm is more suitable for data mining with less support. When the support is 10%, the mining time of the data projection algorithm is reduced by 80% compared with the FP-tree algorithm. (3) When the support degree is 10%, the running time of the hybrid algorithm is reduced by 10% compared with the KEFP-growth algorithm and the data projection algorithm.

1. Introduction

Learner characteristics refer to the psychological, physical, and social characteristics that have an impact on the learner's learning, that is, the learner's personality factors. Wenger believes that the student model represents all the behavior and knowledge about the student [1]. Subsequently, many scholars have defined learner models based on different learning environments. Vanlehn believes that "a learner model is a data structure that represents the student's current state of knowledge" [2]. Asarta and Schmidt believe that "the learner model can be represented as a quadruple (*P*, *C*, *T*, *H*), where *P* represents procedural knowledge; *C* represents conceptual knowledge; *T* represents individual characteristics (traits) of individual; and H represents the learning history [3]. Holt et al. believe that the learner model is an abstract representation of the learner's belief by the computer system, that is, the learner model represents the system's cognition of the student [4]. Later, many scholars define learner models based on different learning environments. Currently, the representative learner characteristic systems are as follows: (1) classical learning characteristic analysis system [5] and (2) distance learning model theoretical analysis system for educating students [6] (the

theoretical analysis system has seven dimensions (general data, demographic data, sociological data, geographic data, situational state data, motivational data, and opinion and evaluation data)).

The modern distance music education classroom learner characteristic model is a guiding form that provides personalized learning paths and learning resources for learners according to their characteristics and behavioral tendencies in the distance learning environment. It is ultimately to achieve the purpose of teaching students in accordance with their aptitude.

In the era of big data, technology transforms all behaviors in the educational process into educational data, which helps to observe the performance of each student, promotes educational research from macro-groups to micro-individuals, and is conducive to the "tailoring" of teaching and the realization of data-driven personalization.

In 2012, the United States pointed out in the report "Promoting Teaching and Learning through Educational Data Mining and Learning Analysis" that "with the support of big data and cloud computing, the core trend of international information education technology development is personalized learning" [7]. The "2016 National Educational Technology Plan" in the United States, "Learning for the Future: Reshaping the Role of Technology in Education," also emphasizes the development of personalized learning based on big data analysis.

China's "Ten-Year Development Plan for Education Informatization (2011–2020)" clearly pointed out that "it is necessary to build an information-based environment and provide individualized learning services for each student." The Ministry of Education's "Thirteenth Five-Year Plan for Educational Informatization" also proposed that "the construction of online learning space should meet the needs of personalized learning and realize "one space for every life, and every life has its own characteristics."" The Horizon Report of the American New Media Alliance has also pointed out many times that adaptive learning is the trend of information technology development in higher education. According to the 2016 Key Issues in Teaching and Learning Report released by the Higher Education Information Association (EDUCAUSE), the focus of teaching and learning is not advanced technology, but the learners themselves and how to use technology to provide a personalized learning experience. Adaptive learning technology can provide learners with personalized learning services [8]. Zhu and Shen believe that with the rapid development of educational big data and data science, personalized adaptive learning will become an important part of the new paradigm of educational technology and smart learning environment, and it is necessary to carry out systematic and in-depth research on it [9].

2. Related Theories

2.1. Data Mining. Data mining is the non-trivial process of obtaining valid, novel, potentially useful, and ultimately understandable patterns from large amounts of data.

2.1.1. Data Mining Process. Data mining is a process of discovering various models, summaries, and derived values from known datasets. A general experimental procedure suitable for data mining problems includes the following steps [10].

(1) State the problem and clarify the hypothesis.

(2) *Data Collection*. There are usually two methods: "design experiment method" and "observation method."

(3) *Data Preprocessing*. It usually includes at least two common tasks: (1) outlier detection (and removal); (2) scaling, encoding, and feature selection.

(4) *Model Evaluation*. Selecting and implementing appropriate data mining techniques is the main task of this stage.

(5) Explain the model and draw conclusions.

2.1.2. Data Mining Algorithms. Data mining tasks include concept description, association analysis, classification analysis, cluster analysis, outlier analysis, evolution analysis, etc. Among them, association rule mining is the most active and deeply researched field.

(1) Association Rule Mining Algorithm. Association rule mining is to search for valuable associations between data items from a given dataset. Association rule mining in a transactional database can be described as follows [11].

Let $I = \{i_1, i_2, \ldots, i_m\}$ be a set of items, the transaction database $D = \{t\_1, t\_2, \ldots, t\_n\}$ is composed of a series of transactions with a unique identifier TID, and each transaction $t_i (i = 1, 2, \ldots, n)$ corresponds to a subset on I.

Definition 1. Let I_1⊆I, and the support of itemset I_1 on dataset D is the percentage of transaction D containing I_1:

$$\text{support}(I_1) = \frac{\left\|\{t \in D | I_1 \subseteq t\}\right\|}{\|\|D\|\|}. \tag{1}$$

Definition 2. For itemset I and transaction database D, all itemsets in T that satisfy the minimum support specified by the user are called frequent itemsets or maximum itemsets. Picking out all frequent itemsets that are not contained by other elements in the frequent itemsets is called maximal frequent itemsets or maximal large itemsets.

Definition 3. An association rule of the form $I_1 \Rightarrow I_2$ defined on I and D is given by satisfying a certain degree of credibility, trust, or confidence. The so-called credibility of the rule refers to the ratio of the number of transactions including I_1 and I_2:

$$\text{Confidence}(I_1 \Rightarrow I_2) = \frac{\text{support}(I_1 \cup I_2)}{\text{support}(I_1)}, \tag{2}$$

where $I_1, I_2 \subseteq I, I_1 \cap I_2 = \varnothing$.

Table 1: FP-tree algorithm.

Algorithm: use the FP-tree algorithm to mine frequent patterns through pattern segment growth
Input: transaction database-D: minimum support threshold min_sup
Output: the complete set of frequent patterns.
Method:
(1) Follow the steps to construct FP-tree;
(a) Scan D once. Collect a set F of frequent items and their support. Sort F in descending order of support, and the result is the frequent item table L.
(b) Create the root node of the FP-tree, marking it with "null." For each transaction in D, execute:
Select the frequent items in transaction and sort them by the order in L. Let the sorted frequent item table be $[p|P]$, where p is the first element and P is the list of remaining elements. Call insert_tree $([p|P], T)$.
The process is performed as follows. If T has child N such that N.item – name = p.item – name, then N's count is incremented by 1; otherwise, a new node N is created with its count set to 1, linked to its parent node T, and it is linked to nodes with the same item – name through a node chain structure. If $P \neq \varnothing$, insert_tree (P, N) is called recursively.
(2) The mining of FP-tree is realized by calling FP_growth (FP_tree, α). The process is implemented as follows:
Procedure FP_growth (Tree, α)
(1) If tree contains a single path P then
(2) For each combination of nodes in the path P (denoted by β)
(3) Generate a pattern $\beta \cup \alpha$, whose support = support $(\beta)_{\text{minimum}}$;
(4) Else for each α_i at the head of tree {
(5) Generate a pattern $\beta = \alpha_i \cup \alpha$, and its support degree support = support (α_i);
(6) Construct the conditional pattern basis of β, and then construct the conditional FP-tree β of β;

Definition 4. The association criterion that satisfies the minimum support and the minimum trust degree on I is called the strong association criterion.

At present, there are many algorithms for mining association rules, which are mainly divided into two categories: generating candidate sets and not generating candidate sets. In order to improve the efficiency of the algorithm, this paper adopts the association rule algorithm that does not generate candidate sets. Han et al. proposed FP-tree algorithm [12], and Liu proposed the Relim algorithm [13]. Among them, the FP-tree algorithm is the most typical one. Compared with the FP-tree algorithm, the Relim algorithm has a simple structure, high space utilization, and runs faster when mining datasets with high minimum support or few frequent rules. The tree algorithm is effective and scalable for mining long and short frequent patterns, while the FIMA algorithm occupies less memory and has high algorithm execution efficiency, but it can only mine Boolean association rules, not quantitative association rules. The FP-tree algorithm only performs 2 database scans. It does not use candidate sets, directly compresses the database into a frequent pattern tree, and finally generates association rules through this tree. The specific mining process is shown in Table 1.

2.2. Learner Characteristics. Learner characteristics refer to the psychological, physical, and social characteristics that have an impact on the learner's learning, that is, the learner's personality factors.

The characteristics of learners involve many aspects, but the characteristics that have an important impact on learning mainly involve two aspects: intellectual factors and non-intellectual factors. The characteristics related to intellectual factors mainly include the general characteristics of learners, knowledge base, cognitive ability and cognitive structure variables, etc., and the characteristics related to non-intellectual factors include interest, motivation, emotion, learning style, anxiety level, will and personality, learner's cultural and religious background, etc.

Through the analysis of specific learner characteristic systems, we find that they have their own characteristics. For example, Ding Xingfu's theoretical analysis system for distance education students is relatively comprehensive, covering a wide range of aspects, covering almost all the characteristics of learners. However, it is too large and lacks follow-up research to combine learner characteristics with specific applications, and the operability is not very strong. Considering the implementation problem, this paper intends to use the learner characteristic analysis system in network distance education in Tempelaar's "Construction of learner characteristic analysis system in network distance education and the design of student model" [14] as a prototype. For research, the feature analysis system mainly includes six major items, each of which includes many minor items, a total of 52 minor items:

(a) *Intelligence*. Intelligence refers to the ability of people to recognize and understand objective things and use knowledge and experience to solve problems, such as memory, observation, imagination, thinking, and judgment. Intelligence mainly includes intelligence and five components of Professor Hanbidge [15] (observation, memory, imagination, thinking, and attention). Intelligence includes language intelligence, mathematical logic intelligence, etc.

(b) *Learning Style*. Learning style is a continuous and consistent way of learning with individual characteristics, and it is a combination of learning strategies and learning tendencies. Learning styles are mainly divided into physiological elements, cognitive

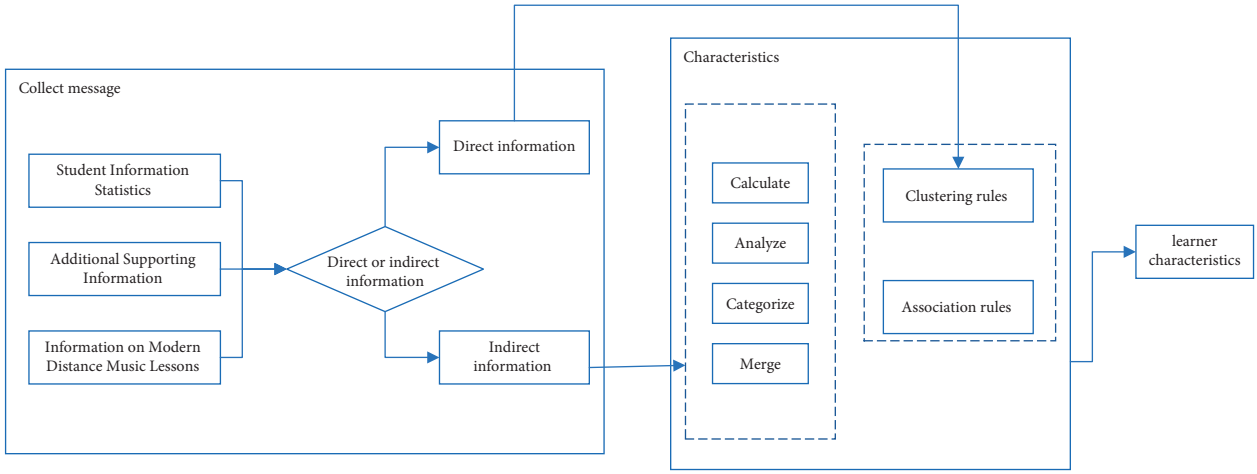

Figure 1: Framework diagram for the analysis of learners' characteristics in modern distance music classrooms.

elements, emotional elements, brain function, and personality. Physiological factors include time preference, perceptual response, and sound preference. Cognitive elements include perceptual style (verbal-spatial preference, discriminating skills, etc.), thinking style (analytical and non-analytical, scattered/concentrated, etc.) confidence processing style, memory style, and problem-solving style.

(c) *Study Preparation*. Learning readiness refers to the adaptability of students' original knowledge level or psychological development level to new learning. Learning preparation includes motivation, cognitive structure, and learning attitude.

(d) *Web Learner Characteristics*. We take this class into account since learners need to use computers and networks for adaptive learning. This category includes four subitems: technical level, information literacy, online learning adaptability, and online psychology.

(e) General information includes demographic and sociological data and opinion and evaluation data.

(f) *Others*. Since there are many repetitions of non-intellectual factors and learning styles, non-intellectual factors (excluding items that overlap with learning styles) are classified into this category, including knowledge interest, learning enthusiasm, learning responsibility, dominance, competitiveness, and self-confidence.

3. Analysis of Characteristics and Model Assumptions of Learners in Modern Distance Music Classrooms

3.1. Analysis Framework. Collect learners' behaviors from different perspectives and explore the deep reasons behind the behaviors, as a basis for formulating teaching procedures. Combining with domestic and foreign learning feature analysis models, combined with the basic elements of learner characteristics in the modern distance environment, this research proposes an analysis framework for learner characteristics in the modern distance environment, as shown in Figure 1.

3.2. Learner Feature Model. Using appropriate technology to build a personality feature model can obtain the learning status of learners in real time and effectively support personalized learning. The construction methods of personality feature models include coverage model, lead model, perturbation model, machine learning technology, model based on cognitive theory, constraint-based model, fuzzy logic technology, Bayesian network, and semantic web ontology model. Among them, the cover model and lead plate model are the most common modeling techniques.

The coverage model, proposed by Jaques et al., is a method commonly used to describe the user's level of knowledge about each concept. When using the coverage method to construct the knowledge level model of the learner, the domain knowledge model represents the expert level knowledge of a certain subject, and the learner model is regarded as a subset of the domain knowledge model. The lead plate model was introduced into the GRUNDY system by Rich to build a user feature model [16]. The core idea is to group and cluster all potential users in ALS according to specific characteristics, and each group is a user lead plate. Both perturbation and constraint-based models are modeled based on learner errors/misunderstandings. The perturbation model, also known as the deviation model, is an extension of the coverage model. The researchers of this model believe that the knowledge of the learner includes not only the partial knowledge possessed by the domain experts but also the wrong knowledge that the learner may generate.

The ultimate goal of the development of educational big data is to return to the essence of education and realize "teaching according to aptitude." The biggest drawback of the "one-size-fits-all" unified teaching model is that it ignores individual differences of learners and analyzes learners' personality characteristics including knowledge level, errors/misunderstandings, emotional characteristics,

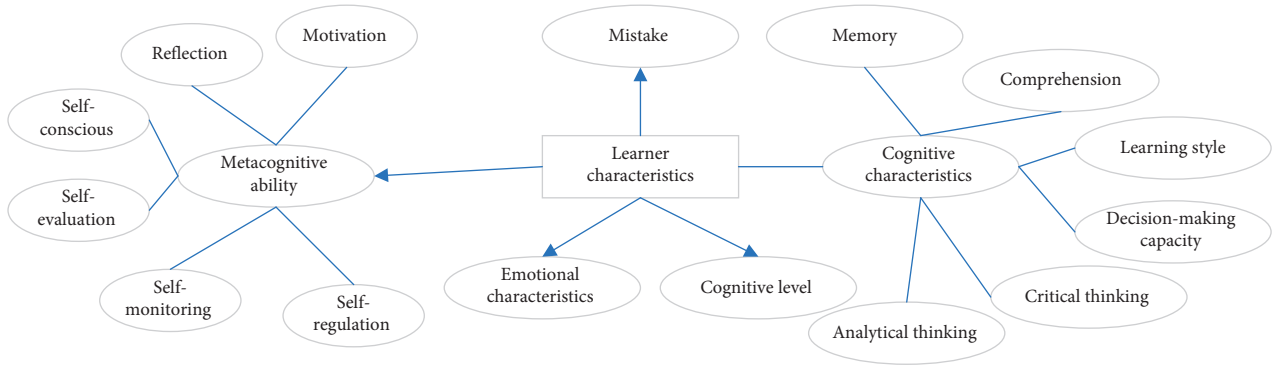

Figure 2: Learner characteristics.

Table 2: KEFP-growth algorithm.

Input: transaction database D; minimum support threshold min_sup
Output: frequent itemsets including key items
(1) Construct FP-tree according to the following steps
(i) Scan the D once. Collect a set F of frequent items and their support. Sort F in descending order of support, and the result is a frequent 1-item set L
(ii) Create the root node of FP-tree and mark it with null. For each transaction trans in D, execute:
Select frequent items in trans and sort by the order in L. Let the sorted frequent item table be $[p|P]$,
Where, p is the first element, and P is the list of remaining elements. Call insert_tree $([p|P], T)$. Execution of the process as follows. If T has child N such that N.item_name = p.item_name, then increment N's count by 1; otherwise create a new node N with its count set to 1, linked to its parent node T, and it is linked to nodes with the same item-name through a node chain structure. If $P \neq \varnothing$, insert_tree (P, N) is called recursively.
(2) Select key items and divide the header table into key item table $L1$ and non-key item table $L2$
(3) The mining of FP-tree is realized by calling KEFP_growth (Tree, α). The process is realized as follows:
Procedure KEFP_growth (Tree, α)
(1) If (tree contains a single path P)
(2) {
(3) If (α contains key items)//check whether the frequent items in α appear in $L1$
(4) Output the union of each node in the tree and α;
(5) Else
(6) { //All items in the key item node are key items, all items in the non-key item node are non-key items key item
(7) Tree nodes are divided into key item node $N1$, non-key item node $N2$
(8) Output the combination of any item in $N1$ and the union of α;
(9) Output the union between the connection of the combination item of $H1$ and the combination item of $H2$ and α;
(10) }
(11)}
(12) Else if (key items are included in α)
(13) Output the union of each frequent item and α in the tree header table;//output the frequent item set
(14) Else
(15) { //All items in the key item header table are key items, and all items in the non-key item header table are non-key items
(16) The header table of tree is divided into key item header table $N1$ and non-key item header table $N2$;
(17) Output the union of frequent items and α in $H1$;//only output frequent itemsets containing key items
(18)}

cognition and metacognitive abilities, etc., as shown in Figure 2. It is the precondition to realize self-adaptive learning. Applying appropriate technology to build a personality trait model will help ALS provide accurate and personalized learning services.

3.3. Improvement of FP-Tree Algorithm

3.3.1. KEFP-Tree Algorithm. FP-tree algorithm mining will generate a large number of frequent itemsets, but although some frequent itemsets satisfy the minimum support, it affects the user's analysis and judgment and reduces the efficiency of mining. The purpose of this paper is to discover the relationship between learner behavior and learner characteristics in distance music classrooms and to determine learner characteristics based on some learning behaviors of learners, that is, to find out "learner behavior => learner characteristics" such as association rules. A meaningful frequent itemset should contain both learner behavior attribute items and learning strategy attribute items. When mining frequent itemsets, frequent itemsets that only contain learner feature items or only learning strategy items can be ignored [17]. The specific implementation steps are shown in Table 2.

Table 3: Database projection algorithm.

Input: transaction database D; minimum support threshold
Output: complete set of frequent patterns
Algorithm:
(1) Scan the D for the first time, get the items that satisfy the minimum support degree and arrange them in descending order, get the set L of candidate 1-itemsets, delete the items whose support degree is less than the minimum support degree in L, and get the set L of frequent 1-itemsets.
(2) Scan the source data for the second time, and rearrange the items in each transaction according to the support counts of the frequent items contained in each transaction, and get the database as D'.
(3) According to the support count of the items in the frequent 1-item set L, build the database subsets of items from small to large according to the following rules, and use the FP − growth algorithm to mine frequent items: for each term in L $I_i\,(i = m, m-1, \ldots, 1)$
(a) Scan the database D', extract all transactions containing item I_i from it, then delete the items whose support degree is less than the support degree of this item in these transactions, and the resulting transaction set is the database subset D_i of item I_i.
(b) For the database subset D_i, use the FP_growth (Tree, α) algorithm to mine frequent itemsets containing item I_i. The mining process is as follows:
(i) If tree contains a single path P then
(ii) For each combination of nodes in path P (denoted as β)
(iii) Generate the pattern $\beta \cup \alpha$, whose support degree support = support $(\beta)_{\text{minimum}}$;
(iv) Else for each α_i at the head of tree {
(v) Generate a pattern $\beta = \alpha_i \cup \alpha$ with support = αi.support ;
(vi) Construct the conditional pattern basis of β , and then construct the conditional FP-tree β of β;
(vii) If Tree$\beta \neq \varnothing$ then
(viii) Call FP_growth (Treeβ, β);}
(4) After the frequent items of all items in L are mined in turn, and these frequent itemsets are merged, all the frequent itemsets in the database D can be obtained.

3.3.2. Database Projection Algorithm. The performance study of the FP-tree algorithm shows that under normal circumstances, the FP-tree algorithm is about an order of magnitude faster than the Apriori algorithm. However, the FP-tree algorithm has a disadvantage, that is, it needs to occupy a lot of memory during tree building and mining. When the database is very large or the support is very small (the total number of generated 1-frequent itemsets is too large), it needs to be loaded into the memory. A large amount of data will cause the running speed to become very slow, and it is even impossible to build a memory-based FP-tree. A good solution is to first partition the database into subsets of the database and then construct an FP-tree on each database subset and mine it and finally combining these frequent itemsets can get the frequent itemsets of the entire database.

The database projection algorithm first scans the database for the first time and finds the 1-frequent itemsets that satisfy the minimum support degree. Each database subset uses the FP-growth algorithm to mine frequent items to obtain the frequent itemsets of each database subset. Finally, these frequent itemsets are combined to obtain the final frequent itemsets. The specific implementation process adopts the algorithm proposed in [18], and the specific algorithm is shown in Table 3.

3.3.3. Hybrid Algorithm. Combining the KEFP-growth algorithm with the database projection algorithm can not only eliminate the mining of meaningless frequent itemsets but also project the data when there is a large amount of data. The idea of combining the two improved algorithms is very simple, because the mining of FP-tree is realized through FP-growth, and the KEFP-growth algorithm is based on FP-growth plus keyword judgment, so only the projection algorithm needs to be used. By replacing the FP-growth algorithm with the KEFP-growth algorithm, the two algorithms can be combined. In addition, before dividing the database into subsets, the 1-frequent itemsets obtained from the first scan of the database should be counted [18]. If the value is greater than the given 1-frequent itemsets total number threshold, the database needs to be divided into subsets. The specific implementation process is shown in Table 4.

4. Simulation Results

4.1. Experimental Data. In order to collect real data on the characteristics of learners in modern distance music education classrooms, this study selected learners who participated in H University's online music elective courses as the research objects. H University's online music elective course conforms to the general characteristics of modern distance education teaching and can reflect the characteristics of learners in the modern distance environment to a certain extent.

In this study, the characteristics of learners in a modern remote environment are analyzed with the help of the online compulsory course "Music History" of H University's online learning on the Chaoxing Xuetong platform. The distance music learning course consists of three parts: courses, resources, and micro-applications. The course module includes multiple learning sections, and the course teaching form covered by each learning week includes three steps: learning guidance, learning content, and learning activities, that is, complete teaching, learning, practice, and examination. The main learning methods of distance learners are the combination of sight, hearing, and practice, and they can

Table 4: Hybrid algorithm.

Input: transaction database D; minimum support threshold; 1—threshold of total items of frequent items
Output: complete set of frequent patterns
(1) Scan the D for the first time, get the items that satisfy the minimum support degree and arrange them in descending order, get the set L of candidate 1-itemsets, delete the items whose support degree is less than the minimum support degree in L, and get the set L of frequent 1-itemsets, and the value C is obtained by counting the set L at the same time.
(2) If ($C >$ 1-threshold of the total number of items of frequent items)
{
(i) Scan the source data for the second time, rearrange the frequent items in each transaction according to the support count of each item, and rearrange the items in each transaction, and get the database as D'
(ii) According to the support count of the items in the frequent 1-item set L, build the database subsets of items from small to large according to the following rules, and use the FP-growth algorithm to mine frequent items:
For each term in L $I_i (i = m, m-1, \ldots, 1)$
(a) Scan the database D', extract all transactions containing item iii from it, then delete the items whose support degree is less than the support degree of this item in these transactions, and the resulting transaction set is the database subset di of item Ii.
(b) For database subset Di, use KEFP_growth (tree, α) algorithm to mine frequent itemsets containing item Ii
(iii) After the frequent items of all items in L are excavated in turn, these frequent itemsets are merged to get all frequent itemsets in database D
}
Else
{
Create the root node of the FP-tree, marking it with "null." For each transaction trans in D, do: select the frequent items in trans and sort by the order in L. Let the sorted list of frequent items be $[p|P]$,
Where p is the first element and P is the list of remaining elements. Call insert_tree ($[p|P], T$). The process is performed as follows. If T has child N such that N.item − name = p.item − nam, then N's increment the count by 1; otherwise create a new node N, set its count to 1, link to its parent node T, and link it to a node with the same item-name through a node chain structure. If $P \neq \varnothing$, insert_tree (P, N) is called recursively.
(3) Mining FP-tree by calling KEFP_growth (Tree, α)
}

interact and ask questions according to their learning needs. The course has a total of 20 study sections. After the course is over, the academic performance of distance learners will be assessed according to a percentile system, which consists of two parts: the formative assessment and the final assessment. Formative grades refer to the usual grades, which are mainly composed of the learners' online answers and the interaction of the number of posts, accounting for 30%; the final examination assessment refers to the learners' final grades, which are mainly obtained from the learners' final assessment results. According to an online test, it accounts for 70%.

4.2. Experimental Design

(1) Data source is Superstar learning platform background data; number of project transactions is 20000; dataset is 60 (1.3M); algorithms are FP-tree algorithm and KEFP-tree algorithm; results are running time and total number of frequent itemsets.

(2) Using the background data of the Superstar Learning Platform, select a dataset (2.2 M) with 40,000 itemset transactions and 60 different items, using the original FP-tree algorithm and database projection algorithm under different minimum support degrees. The dataset is mined and the time of its run is recorded separately.

(3) Using the background data of the Superstar Learning Platform, select the dataset (1.8 M) with 30,000 itemset transactions and 60 different items (1.8 M), and use the KEFP-growth algorithm, data projection algorithm, and combination algorithm to achieve different minimum support degrees. The dataset is mined below, and its running time is recorded separately.

4.3. Experimental Results. The experimental results of the original FP-tree algorithm mining on the 1.3 M dataset and the 2.2 M dataset are shown in Table 5:

When the minimum support degree is high, that is, when the number of generated 1-frequent itemsets is small, the original FP-tree algorithm runs fast and has high mining efficiency. However, when the minimum support is low, the running speed will be greatly reduced due to the large number of 1-frequent itemsets generated. The number of sets is very large, which will cause the running speed to be greatly reduced and even the situation that the memory-based FP-tree cannot be built.

The experimental comparison results of the FP-tree algorithm and the KEFP-growth algorithm mining on the 1.3 M dataset are shown in Table 6.

It can be seen from the table that under different support degrees, the KEFP-growth algorithm reduces the number of frequent items output by the original FP-tree algorithm by about 50%, and the mining time is reduced by 50%. This is because the output of irrelevant frequent itemsets can be reduced by using the KEFP-growth algorithm, thereby shortening the time spent in selecting useful items from

Table 5: The experimental results of the original FP-tree algorithm.

Support (%)	1.3 M		2.2 M	
	Number of frequent itemsets	Operation hours	Number of frequent itemsets	Operation hours
50	34	10	57	35
40	55	20	124	64
30	309	55	880	145
20	1350	255	2842	588
10	5599	808	9815	1535
1	13442	6741	25467	—

Table 6: The experimental comparison results of the FP-tree algorithm and the KEFP-growth algorithm.

Support (%)	Number of frequent itemsets		Operation hours	
	FP-tree algorithm	KEFP-growth algorithm	FP-tree algorithm	KEFP-growth algorithm
50	34	19	35	9
40	55	31	64	35
30	309	157	145	77
20	1350	679	588	259
10	5599	2562	1535	1006
1	13442	6458	—	—

Table 7: The experimental comparison results of the original FP-tree algorithm and the database projection algorithm.

Support (%)	Number of frequent itemsets	Operation hours	
	FP-tree algorithm	FP-tree algorithm	Database projection algorithm
50	57	35	63
40	124	64	89
30	880	145	163
20	2842	588	574
10	9815	1535	1366
1	25467	—	5786

useless frequent items, significantly improving the efficiency of mining, and meeting the original intention of mining.

The experimental comparison results of the original FP-tree algorithm and the database projection algorithm on the 2.2 M dataset are shown in Table 7.

Experiments show that when the minimum support is reduced to a certain threshold or the amount of data to be mined is greater than a certain level (the total number of items in the frequent 1-item set is too large), the original FP-tree algorithm cannot build a memory-based FP-tree, which will cause the excavation to fail. The data projection algorithm can divide the frequent 1-itemsets of a large database into several database subsets and then mine the database subsets, respectively. Because each database subset occupies a small memory, it can overcome the data of 1-itemsets. The problem that the amount is too large makes the memory unable to load the FP-tree, so that the data mining can proceed smoothly. In addition, experiments also show that the data projection algorithm is more suitable for data mining with less support. When the support is 10%, the mining time of the data projection algorithm is reduced by 80% compared with the FP-tree algorithm. When the minimum support is large or the amount of data to be mined is small (that is, the total number of frequent 1-itemsets is small), the running speed of the new algorithm is not as fast as that of the original FP-tree algorithm. The reason for this phenomenon is that the cost of the original FP-tree algorithm lies in tree building and frequent itemset mining, while the data projection algorithm has the cost of dividing the database subset in addition to the cost of tree building and frequent itemset mining. When the database support degree is large, the total number of 1-frequent itemsets generated by the database is small, so the two algorithms have little difference in the time cost of building trees and mining frequent itemsets, but the database projection algorithm divides the database subsets. There is a time overhead in the aspect of FP-tree, so the mining speed of the original FP-tree algorithm is faster than that of the database projection algorithm. With the increase of the minimum support, the memory and time overhead of the original FP-tree algorithm increase, resulting in slower and slower mining speed, while the database projection algorithm also increases the cost of generating database subsets. However, the memory overhead and time overhead of building a database and mining frequent itemsets are less, so the overall running speed is faster than the original FP-tree algorithm.

The experimental comparison results of the three improved algorithms' mining on the 1.8 M dataset are shown in Table 8.

Table 8: The experimental comparison results of the three improved algorithms.

Support (%)	Number of frequent itemsets	Operation hours		
		KEFP-growth algorithm	Database projection algorithm	Hybrid algorithm
50	46	12	38	15
40	90	27	65	29
30	545	64	90	65
20	2351	167	157	146
10	7648	998	985	833
1	1987	—	5786	3756

Experiments show that the mining efficiency of the hybrid algorithm and the FEFP-growth algorithm is not much different when the minimum support is large, but when the minimum support is small to a certain extent, the mining efficiency of the hybrid algorithm is higher than that of the KEFP-growth algorithm. When the support degree is 10%, the running time of the hybrid algorithm is reduced by 10% compared with the KEFP-growth algorithm and the data projection algorithm. When the support degree is large, the KEFP-growth algorithm branch is combined with the algorithm, and when the support degree is small (the total number of 1-frequent itemsets generated is large), the database projection algorithm combined with the KEFP-growth algorithm is used. In addition, it can be seen from the experimental results that the hybrid algorithm is better than the database projection algorithm when the support is small or large. This is because the KEFP-growth algorithm used in the hybrid algorithm removes many irrelevant frequent itemsets, thereby reducing the amount of excavation. Comprehensive analysis shows that the hybrid algorithm is better than the first two improved algorithms.

5. Conclusion

This paper makes in-depth research on data mining, especially association rule mining, improves the FP-tree algorithm in both the algorithm itself and the data source, and finds out a mining algorithm suitable for learner characteristics. By establishing the characteristic model of learners in modern distance music classroom, simulation experiments are carried out on FP-tree and three improved algorithms.

Compared with the original FP-tree algorithm, the number of frequent items output by the KEFP-growth algorithm is much less, and the mining time is also significantly reduced.

(1) The KEFP-growth algorithm reduces the number of frequent items output by the original FP-tree algorithm by about 50%, and the mining time is reduced by 50%.

(2) The data projection algorithm is more suitable for data mining with less support. When the support is 10%, the mining time of the data projection algorithm is reduced by 80% compared with the FP-tree algorithm.

The mining efficiency of the hybrid algorithm and the KEFP-growth algorithm is not much different when the minimum support is large. However, when the minimum support is small to a certain extent, the mining efficiency of the hybrid algorithm is higher than that of the KEFP-growth algorithm. When the support degree is 10%, the running time of the hybrid algorithm is reduced by 10% compared with the KEFP-growth algorithm and the data projection algorithm.

Data Availability

The dataset used to support the findings of this study is available from the corresponding author upon request.

Conflicts of Interest

The authors declare that there are no conflicts of interest.

References

[1] E. Wenger, *Artificial Intelligence and Tutoring Systems*, 486 pages, Morgan Kaufmann Publishers Inc, San Francisco CA USA, 1987.

[2] K. Vanlehn, "Student modeling," in *Foundations of Intelligent Tutoring Systems,*, M. Polson and J. Richardson, Eds., pp. 55–78, Lawrence Erlbaum Associates, Hillsdale, NJ, 1988.

[3] C. J. Asarta and J. R. Schmidt, "Access patterns of online materials in a blended course," *Decision Sciences Journal of Innovative Education*, vol. 11, no. 1, pp. 107–123, 2013.

[4] P. Holt, S. Dubs, M. Jones, and J. Greer, "The state of student modeling," in *Student Modelling: The Key to Individualized Knowledge-Based Instruction*, J. E. Greer and G. I. Mc Calla, Eds., 38 pages, Springer-Verlag, Berlin/Heidelberg Germany, 1994.

[5] D. D. Prior, J. Mazanov, D. Meacheam, G. Heaslip, and J. Hanson, "Attitude digital literacy and self efficacy: flow-on effects for online learning behavior," *The Internet and Higher Education*, vol. 29, pp. 91–97, 2016.

[6] E. Gaudioso, M. Montero, and F. H. D. Olmo, "Supporting teachers in adaptive educational systems through predictive models: a proof of concept:A Proof of Concept," *Expert Systems with Applications*, vol. 39, no. 1, pp. 621–625, 2012.

[7] Educause, "Key Issues in Teaching and Learning," 2016, http://www.educause.edu/eli/initiatives/key -issues -in -teach-ing-and-learning.

[8] G. Goguadze, S. A. Sosnovsky, S. Isotani, and B McLaren, "Evaluating a bayesian student model of decimal misconceptions," in *Proceedings of the 4th International Conference on Educational Data Mining*, pp. 31–40, Eindhoven, The Netherlands, June 2011.

[9] Z. Zhu and D. Shen, "A new paradigm of educational technology research based on big data," *Research on Electronic Education study*, vol. 15, no. 1, pp. 21–25, 2012.

[10] R. Agrawal, T. Imielinski, and A. Swami, "Mining association rules between sets of items in large database," in *Proceedings of the ACM SIGMOD Conference On Management of Data*, Washington, D.C., USA, May 1993.

[11] M. Guojun, *Research on Data Mining Technology and Association Rules Mining Algorithm*, Tsinghua University Press, Beijing, China, 2003.

[12] J. Han, J. Pei, and Y. Yin, "Mining Frequent Patterns without Candidate generation," in *Proceedings of the 2000 ACM—SIGMOD Int Conf Management of Data F SIGMOD 2000)*, ACM Press, Dellas, TX, USA, May 2000.

[13] X. Liu, "A new algorithm for mining association rules that does not require candidate sets—Relim algorithm research," *Computing Technology and Automation*, vol. 12, pp. 162–168, 2006.

[14] D. T. Tempelaar, B. Rienties, and B. Giesbers, "In search for the most informative data for feedback generation: learning analytics in a data-rich context," *Computers in Human Behavior*, vol. 47, pp. 157–167, 2015.

[15] A. S. Hanbidge, T. Tin, and N. Sanderson, "Student Learner Characteristics and Adoption of M-Learning: Are We Effectively Supporting Students?" *Mobile and Ubiquitous Learning*, Vol. 8, Springer, Berlin, Germany, 2018.

[16] N. Jaques, C. Conati, J. M. Harley, and R. Azevedo, "Predicting affect from gaze data during interaction with an intelligent tutoring System,Martha crosby," in *Proceedings of the 12th International Conference,Honolulu Intelligent Tutoring Systems*, pp. 29–38, Honolulu, HI, USA, June2014.

[17] S. S. Liaw and H. M. Huang, "Perceived Satisfaction Perceived Usefulness and Interactive Learning Environments as Predictors to Self-Regulation in E - Learning Environments," *Computers & Education*, vol. 60, no. 1, pp. 14–24, 2013.

[18] S. Alkhuraiji and B. Cheetham, O. Bamasak, Dynamic Adaptive Mechanism in Learning Management System Based on Learning Styles," in *Proceedings of the 11th IEEE International Conference on Advanced Learning Technologies (ICALT)*, pp. 215–217, IEEE, Athens, GA, USA, July2011.

Hindawi
Scientific Programming
Volume 2022, Article ID 2586833, 9 pages
https://doi.org/10.1155/2022/2586833

Research Article

Analysis of Children's Online Reading Behavior Oriented for Family Education

Wenmin Cai [1,2]

[1]*School of Education Science, Hanshan Normal University, Chaozhou 521000, China*
[2]*Graduate School, City University Malaysia, Petaling Jaya 46100, Malaysia*

Correspondence should be addressed to Wenmin Cai; caiwenmin@hstc.edu.cn

Received 5 April 2022; Revised 17 April 2022; Accepted 25 April 2022; Published 13 May 2022

Academic Editor: Lianhui Li

Aiming at the problem of supply-demand matching of online reading, an analysis method of children's online reading behavior oriented for family education has been put forward. The data-based classification method is constructed to classify the sample population by statistical methods, and the traditional index classification is carried out by using K-medoids clustering and logistic regression analysis. The matching degree of population classification is discussed through comparison. R language and Mplus are used to analyze the data for the objective classification of the sample data set. Based on the reading response behavior of children's online reading users, a differential item functioning (DIF) test of socioeconomic status is carried out. At the same time, the population is divided by traditional economic classification indicators to carry out a DIF test and explore the differences in the reading ability of different classification groups. By comparing the results of the two grouping methods, the main family socioeconomic status factors affecting reading performance are explored and targeted countermeasures are put forward. The experimental results show that when analyzing children's online reading behavior, using machine learning algorithms such as cluster analysis, logistic regression analysis, and so on can get consistent results and then using the DIF test to explore the responses of category groups can effectively distinguish group differences.

1. Introduction

In the information society, the radiation range of computer networks and digital technology is becoming wider and wider, which has become a necessity for people's daily communication and reading [1–7]. For the younger generation growing up with the Internet, known as the "net generation," online reading has become one of the indispensable reading methods [8, 9].

"Demand" refers to the various needs for objective things derived by people (including individuals, groups, strata, and the whole group) to maintain their own growth and continuity. The whole process of users purchasing and using products is a process of meeting their needs. In this process, the old and new needs of users may appear alternately. User needs generally have the following characteristics: explicit needs and implicit needs coexist. Explicit needs are the needs that users themselves can clear, know, and express and implicit needs are the needs that users cannot express or even perceive. Different users have their own particularity, so the demand also shows the characteristics of coexistence of individuality and commonness. In addition, the demand also has hierarchy and fuzziness. Users' demand for online reading is high-quality reading content, and users of different natures have different needs for online reading. As reading is a branch of humanities, it is more vulnerable to the influence of multidimensional index systems such as regional culture and economic level. Therefore, we need to use appropriate methods to carry out family education oriented analysis and study the impact of regional and economic differences on children's online reading behavior. Differential item functioning (DIF) [10–12] has been paid more and more attention. From the initial fairness research to the consideration of the validity and reliability of the test itself, DIF research has always played an important role. DIF refers to that when subjects with the same ability from

different groups have different response probabilities when answering the same question, and there is a deviation in the question. With the continuous in-depth exploration of DIF methods, DIF methods have a wide variety and rapid development, moving towards a more comprehensive and scientific direction. DIF analysis is also increasingly used in the field of psychometrics, language testing, intelligence testing, educational evaluation, and other fields to detect the deviation of project level.

Online reading users come from all over the world, with different economic and cultural backgrounds, and their needs for the types of reading vary from person to person. Based on the online reading comprehension test of grade 2 in primary school, developed by an internet education enterprise, this paper investigates the subjects of grade 2 in primary school in 19 provinces, cities, and autonomous regions, and recovers 1309 valid data.

The technical scheme of this study is that when discussing the differences in reading ability of different groups, we can get more consistent results by using machine learning algorithms such as cluster analysis, potential category analysis, *k*-nearest neighbor algorithm, discriminant analysis, and logistic regression analysis, and then exploring the responses of category groups by the DIF test, which can effectively distinguish group differences.

2. Related Works

2.1. Gender Differences in Reading. Breland and Lee [13] observed the scores of reading, writing, and listening of male and female candidates in the English Language Ability (ELA) test, and found that there were significant differences in the scores of men and women in the writing part, which was more beneficial to boys. In the PISA2009 reading literacy assessment, Chen and Jiao [14] took gender as the traditional dominant group variable and found five medium DIF items, which were obviously biased towards boys. In other gender studies on reading literacy, Aryadoust [15] used a recursive segmentation Rasch tree to investigate the DIF source of reading comprehension test. One of the grouping variables used is gender. In the test, candidates with high grammar scores are affected by gender differences, and girls are at a disadvantage. It can be seen that when investigating the gender differences of the DIF in reading test research, there is a consistent bias, which may be related to the objective and fixed gender grouping.

2.2. Socioeconomic Status Differences in Reading. Chen and Jiao [14] explored the DIF items with economic, social, and cultural status (ESCs) as nontraditional dominant group variables in the PISA2009 reading literacy assessment, and found that three DIF items were more favorable for subjects with high ESCs. Cadime et al. [16] took urban and rural areas as the division standard of economic level, tested the DIF items of the reading test of Portuguese students in high and low economic level groups, and found that five moderate DIF items were beneficial to students in high economic level groups from cities. Little et al. [17] showed that living in the neighborhood of communities with poor economic conditions can also predict lower reading test scores. Leu et al. [18] analyzed the students in economically developed school districts and economically less developed school districts, respectively. The results showed that due to the imbalance of economic development levels, students' online reading ability was significantly predicted. Morrow [19] believes that the difference in the regional economic situation of the school is the main reason for the differences in the application strategies of middle school students in online reading. However, some studies have pointed out that family economic status has no significant impact on children's reading performance [20].

In conclusion, in the DIF analysis, gender grouping is the most basic and important traditional dominant grouping variable. Due to the clear grouping boundary, the DIF results are usually consistent. In some areas of reading comprehension test, question answering is more beneficial to boys, and such test results appear. However, when the grouping variables are nontraditional explicit grouping variables such as socioeconomic status and cultural region, the results are often different or even contradictory. This may be related to the uncertainty of nontraditional dominant grouping variables.

Analyzing the concept and composition of socioeconomic status, it is not difficult to find that with the progress of measurement technology and the accumulation of theoretical achievements, the conceptual boundary of socioeconomic status as a multiindex system is gradually blurred and the extension is gradually expanded. When researchers choose the classification index of SES, it is impossible to be completely consistent, and the classification results have a direct impact on the DIF test, so they can get a variety of DIF test results.

Summarizing the above research, it can be found that when researchers try to explore the differences of the online reading ability of different types of users, they usually need to classify users. When a multiple index system (such as SES) is selected as the classification basis, the classification method is usually more empirical and subjective, resulting in the reduction of the reliability of the results. At that time, when objective criteria were used for analysis (such as DIF), more consistent conclusions could be obtained and multiple indicators (family income, parents' education level, and parents' professional status) could not be divided. Whether cluster analysis and latent category analysis can be used to objectively classify online reading users under multiple indicators and then to explore the response of category groups by DIF is the main problem of this study. This study will take the online reading test of grade 2 of primary school as an example to investigate the influence of socioeconomic status on students' online reading tests, and achieve the analysis goal of children's online reading behavior oriented for family education.

3. Overall Research Framework

Reading is not only an important way for people to obtain information but also a basic way to improve their literacy. The strength of reading ability determines a person's

knowledge reserve to a certain extent. Especially in the context of the rapid popularization of online reading, users' demand for high-quality content is increasing. The key to developing high-quality content is to fully meet the reading needs of different people and develop content and test questions suitable for reading at different ages and levels. It is particularly important to analyze children's online reading behavior for family education. The most appropriate method to detect the availability of content topics specifically for different groups is DIF.

The population of online reading users is diverse and complex, which is different from the deterministic population with school classes as units. Moreover, the population with different socioeconomic status (SES) discussed in this study is usually not a single grouping variable, but a compound or multidimensional grouping variable, that is, a multiindex evaluation system. There is no unique standard for the population category, so it needs to be objectively classified with the help of statistical classification methods based on the data itself.

The above literature analysis shows that the biggest advantage of cluster analysis is when the population is not clearly classified. It can be better classified according to the real characteristics of the data itself. In addition, latent category analysis is a common method to classify latent variables. Therefore, based on a more robust clustering analysis method K-medoids [21–23], this study first classifies the subjects and verifies them with potential category analysis to clarify the rationality of secondary classification by using statistical methods. Research on the influencing factors of reading ability has always been a topic of continuous exploration by researchers. Based on K-medoids clustering grouping, taking the second grade online reading test as an example, this paper carries out the DIF test to investigate the impact of socioeconomic status on students' responses to reading tests, and realizes children's online reading behavior analysis oriented for family education.

The main significance of this study is as follows:

(1) This study explores and empirically uses quantitative research methods for user analysis, provides a new idea for the general environment that focuses on qualitative research, makes the demand for research clearer and clearer from a multidimensional perspective, and obtains an objective and scientific division of the population on the basis of statistical classification methods.

(2) This study explores the important family socioeconomic status factors affecting users' reading ability and can provide corresponding countermeasures and suggestions for vulnerable reading users. Therefore, this study can improve user product experience satisfaction and increase user stickiness and retention rates for enterprises.

The content of this study is mainly divided into the following two parts:

(1) In order to analyze the online reading needs of users with different socioeconomic statuses, it is necessary to classify the population first. Due to the variety of traditional SES classification indicators, it is necessary to classify with statistical methods to ensure the true characteristics of response data and realize objective grouping. The R language is used to make the clustering analysis diagram under the K-medoids clustering analysis method and then use latent category analysis (LCA) to verify the reliability and stability of clustering results.

(2) Based on K-medoids cluster grouping, the DIF test was carried out to study the differences of children with different economic levels in the reading test. This paper probes the influence of the difference of families' socioeconomic status on students' responses to reading test. Reasonable suggestions are put forward for enterprises according to the results of project function differences. When it is unable to meet the reading needs of the two groups at the same time, matching the reading materials launched with the economic situation one by one is focused on.

The overall research framework is shown in Figure 1.

4. Research Methods

The main purpose of this study is to analyze the reading ability level of the two groups of subjects with high and low economic level by using the DIF test. By clarifying the differences, the influencing mechanism of family socioeconomic status is explored and the corresponding improvement measures are put forward.

4.1. DIF

4.1.1. MH Method. The reading test in this study is objective in the form of two-level scoring. Therefore, the Mantel–Haenszel method [24], abbreviated as the MH method, is one of the most widely used methods for DIF detection. The method starts by grouping the subjects according to their ability level. They were divided into five groups from lowest to highest according to test scores or ability θ. This process is automatically realized in R software. The MH method calculates statistic αMH by comparing target groups with the frequency of correct and wrong answers on each question. The value of αMH is between (0, +oo). αMH = 1 is no DIF in this item. αMH > 1 is beneficial to the target group. αMH < 1 is beneficial to the reference group. In order to represent project functional uniformity with 0, αMH is logarithmically converted to the following formula:

$$\Delta\text{MH} = -2.35 \ln(\alpha\text{MH}). \quad (1)$$

When ΔMH is positive, the project is beneficial to the target group. When ΔMH was negative, the project benefited the control group.

Educational testing service (ETS) classifies DIF entries into three levels based on the MH method. Grade A is negligible. Grade B should be modified. Grade C is a problem path that has very serious project functional differences and should be removed.

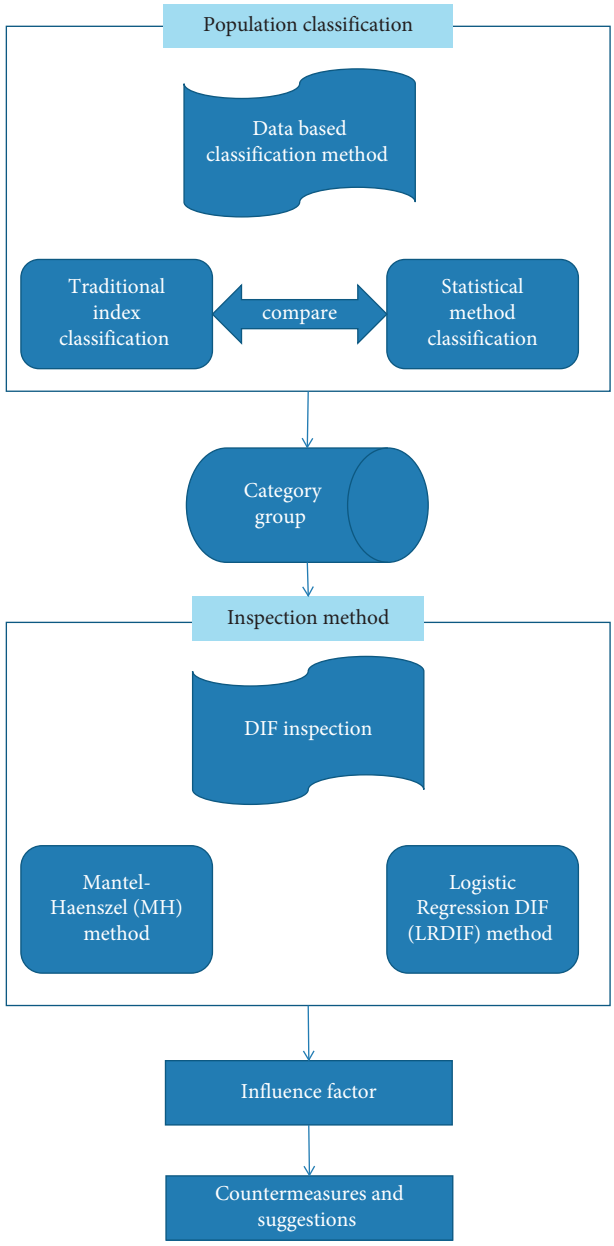

Figure 1: The overall research framework.

4.1.2. LRDIF Method. It is found that different methods have different statistical test power and unique advantages. Therefore, a variety of methods used together can play their own advantages. This makes detection results more scientific and effective [25]. In this study, the LRDIF method was used to test. LRDIF is a DIF test method proposed by Swaminathan and Rogers [26] that is suitable for 0, 1 scoring, and multistage scoring tests. Again, this method can take test scores as matching variables. Its biggest advantage is that it can calculate both consistent and inconsistent DIF. The LRDIF method uses the model comparison to test the significance of each parameter in the following formula:

$$P(Y = 1|X1, X2) = \frac{\exp(\beta 0 + \beta 1x1 + \beta 2x2 + \beta 3x1x2)}{1 + \exp(\beta 0 + \beta 1x1 + \beta 2x2 + \beta 3x1x2)}. \quad (2)$$

The logarithm is taken to obtain

$$\ln\left(\frac{p}{1-p}\right) = \beta 0 + \beta 1x1 + \beta 2x2 + \beta 3x1x2. \quad (3)$$

Y is the dependent variable and can be 0 or 1. $x1$ is the test score, $x2$ is the grouping variable, and $x1x2$ is the interaction term. Regression parameters $\beta 0$, $\beta 1$, $\beta 2$, and $\beta 3$ were estimated by the maximum likelihood method (MLE) or the least square method (LSM). Different test results have different implications for DIF detection. If only P0 and $\beta 1$ are significant in the equation, there is no DIF in this item. If $\beta 0$, $\beta 1$, and $\beta 2$ are significant in the equation, it indicates that the item has consistent DIF. If the interaction parameter $\beta 3$ is also significant, then the problem has a nonconsistent DIF.

4.2. Reading Achievement Difference Inspect. The reading achievement difference inspect is shown in Table 1.

According to Table 1, the scores of students in the group of high socioeconomic status were significantly higher than those in the group of low socioeconomic status. Specific performance included the average wage classification group($t = -7.322$, $p < 0.001$, Cohen's $d = 0.411$), per capita disposable income classification group($t = -0.951$, $p < 0.05$, Cohen's $d = 0.208$), regional GDP classification group ($t = 8.762$, $p < 0.001$, Cohen's $d = 0.487$), and East-West geographical and economic division classification group ($t = -11.134$, $p < 0.001$, Cohen's $d = 0.452$). According to Cohen's standard, except for the small effect size of 0.2 in per capita disposable income classification group, the all other three effects reached the standard of medium effect size of 0.4 [27].

4.3. DIF Inspection. In order to explore whether reading score difference comes from the real difference of subjects or from deviation, we need to do further inspection of the project function differences.

4.3.1. Unidimensional Test. Before the DIF test, it needs to meet the unidimensional hypothesis, so a unidimensional test is conducted. The commonly used method to prove the unidimensionality of the test is factor analysis. The fitness test of factor analysis shows that the KMO of this study sample is KMO = 0.944 and Bartlett sphericity test X^2 (2016) = 16468.933, $p < 0.001$. Therefore, sample data are suitable for factor analysis. If the ratio of the eigenvalue of the first component to the eigenvalue of the second component in factor analysis is greater than 3, the test can be considered as one-dimensional [28]. In this study, the eigenvalue of the first factor was 11.767 and the eigenvalue of the second factor was 1.721. The ratio of the two is much greater than 3, so it meets the regulations.

It can be seen from Figure 2 that the eigenvalue curve in the lithotripsy diagram tends to be flat after the first factor. Combined with the result that the ratio of the first eigenvalue to the second eigenvalue is greater than 3, a factor is finally retained. Therefore, it is considered that the test conforms to the unidimensional hypothesis.

Table 1: Reading achievement difference inspect.

	Average wage	Per capita disposable income	Regional GDP	East-West geographical and economic division
Low economic level ($M \pm SD$)	42.06 ± 11.877	42.83 ± 10.642	38.99 ± 10.873	42.06 ± 11.868
High economic level ($M \pm SD$)	44.39 ± 9.951	43.51 ± 10.825	45.55 ± 10.221	45.78 ± 9.591
t	−7.322	−0.951	8.762	−11.134
Cohen's d	0.411	0.208	0.487	0.452
p	0.000***	0.039*	0.000***	0.000***

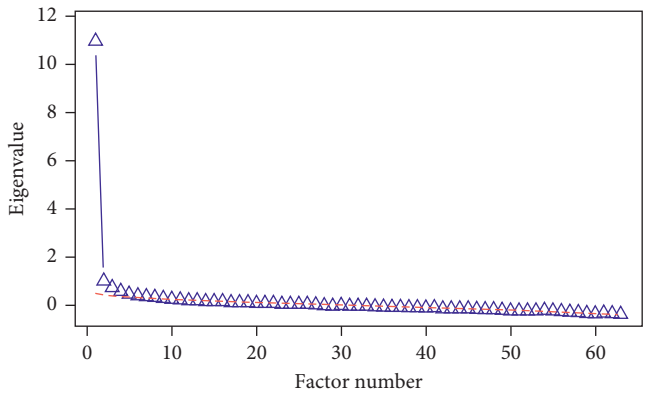

Figure 2: The relationship between eigenvalue and factor number.

4.3.2. DIF Results of Traditional Grouping. The MH method and the LRDIF method were used to test the two groups of high and low economic levels under the four traditional economic index groups. The calculation results of the MH method are divided into three levels according to the calculation standard of ETS in the United States, that is, based on the absolute value of ΔMH. If its absolute value is less than 1, it is marked as grade A DIF. If its absolute value is between 1 and 1.5, it is marked as grade B DIF. If it is greater than 1.5, it is a serious DIF item and will be marked as grade C DIF.

The effect size of the LRDIF method is Nagelkerke's R^2. According to Zumbo & Thomas standard labeling grades, (0, 0.13) is classified as grade A, namely slight DIF. (0.13, 0.26) is classified as grade B, namely moderate DIF. (0.26, 1) is classified as grade C, namely severe DIF.

The DIF inspection results of the average wage grouping are shown in Figure 3.

The DIF inspection results of per capita disposable income grouping are shown in Figure 4.

The DIF inspection results of East-West geographical and economic division grouping are shown in Figure 5.

The DIF inspection results of the regional GDP grouping are shown in Figure 6.

The DIF analysis was performed on 64 items of the online reading test in grade 2 using the MH and LRDIF methods. Two DIF test methods are used to test the DIF items under the grouping of the average wage, per capita disposable income, East-West geographical economic division, and regional GDP. As can be found, the regional GDP grouping has the largest number of DIF items, and most of them belong to grade A DIF, while the small numbers are grade B and C DIF.

The reading ability module results reflected by DIF items are further analyzed, as shown in Figure 7. In Figure 7, groupings 1, 2, 3, and 4 represent the groupings of the average wage, per capita disposable income, East-West geographical economic division, and regional GDP, respectively.

The online reading test includes six ability modules: language foundation, information extraction, understanding and inference, transfer and application, overall perception, and appreciation evaluation. As can be seen from Figure 7, DIF items detected in the four traditional grouping methods include the six ability modules. Moreover, the proportions of the modules are almost evenly distributed. It is difficult to distinguish which subdivision of reading ability the DIF items focus on.

4.3.3. DIF Clustering Results. Due to the low consistency of the four traditional groups in the initial group and the final DIF test results, the statistical grouping method of cluster analysis is used to conduct the DIF test again for the responses of online reading users. Compared with previous research results, the results obtained are shown in Tables 2 and 3 and Figure 8.

As can be seen from Tables 2 and 3, the number of detected DIF items is greatly reduced after grouping by the cluster analysis method. The results of the DIF test were consistent with those of the two methods. The distribution of modules also shows obvious rules. The details are as follows: first, only 5 DIF items were detected by the two methods, respectively, among which 3 questions overlapped. Second, as shown in Figure 8, 60% of the five titles detected by the two methods focus on the language foundation module and 20% or more focus on the understanding and inference module. The MH method detected three language foundation titles, 33, 49, and 57 as positive, which is favorable to the high economic level group.

5. Discussion

Previous studies have pointed out that socioeconomic status is one of the main influencing factors of reading. Using the existing population categories and DIF test, this study can clarify the impact mechanism of family socioeconomic status on children's online reading users. Firstly, the difference test of reading performance shows that the reading scores of the four traditional index groups are significantly

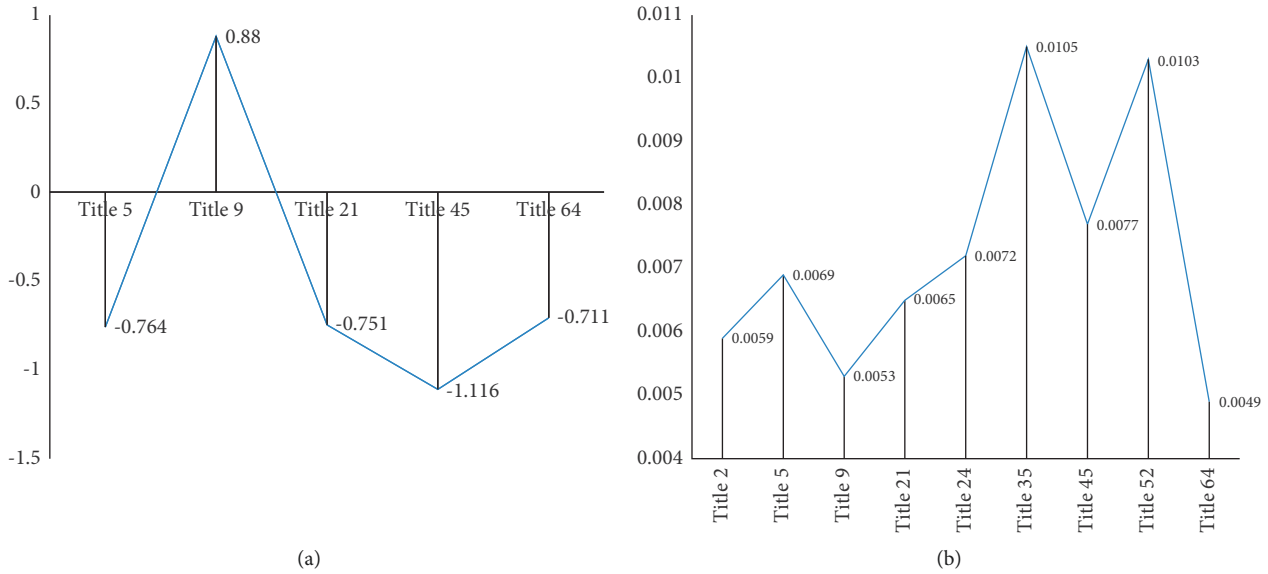

Figure 3: DIF inspection results of the average wage grouping. (a) ΔMH. (b) R^2.

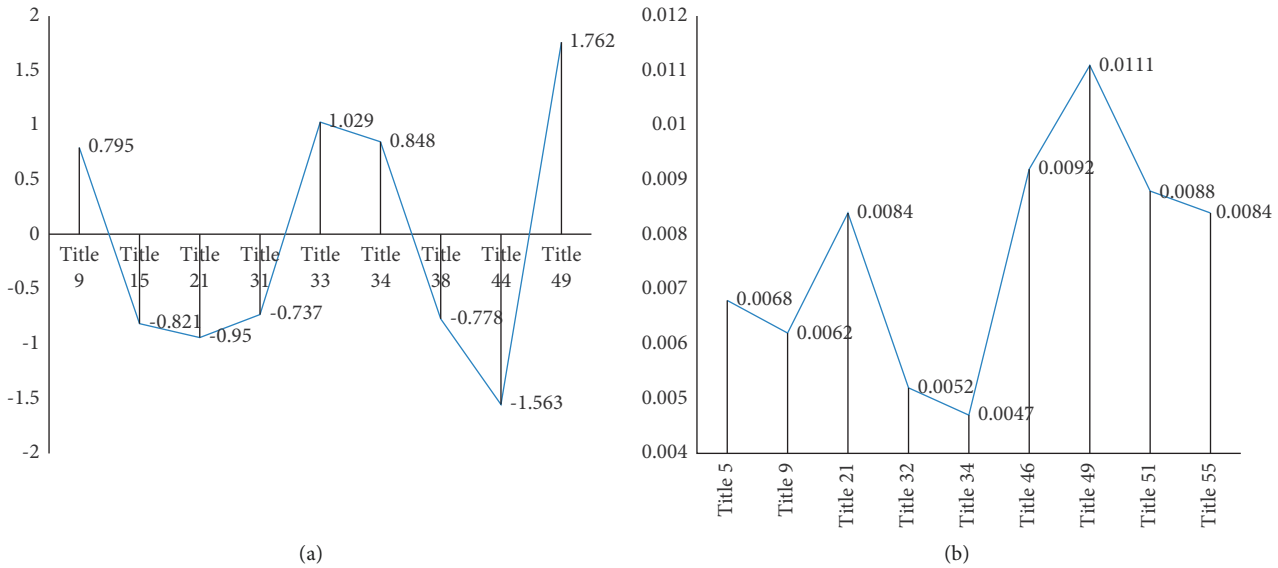

Figure 4: DIF inspection results of per capita disposable income grouping. (a) ΔMH. (b) R^2.

different. Secondly, continuing to do the DIF test, it is found that the difference in reading performance comes from the difference in the item function of the test. Under the four traditional groups, the number of DIF items detected is large, and the law is not obvious. The language basis, understanding and inference, information extraction, transfer and application, overall perception, and appreciation evaluation modules of DIF items in the reading test are distributed, which means that the subjects in the low socioeconomic status group are very inferior in their overall reading ability, that is to say, they are unable to put forward targeted demand suggestions to users. Then, it will be more difficult to continue reading practice, and the effect of improving reading level cannot be estimated. It is speculated that this situation may be related to inconsistent grouping.

When the two types of subjects grouped by clustering and LCA are used as the target group and the reference group for the DIF test, it is concluded that the number of DIF items is significantly reduced, and there are rules to follow, which is reflected in the language foundation and understanding inference module, and the students with low socioeconomic status are at a disadvantage. This is also the part of reading ability that students are most exposed to and mainly trained in daily learning. It is the module that is most likely to open the gap, which is consistent with the research expectation.

Reading comprehension is the ability to extract and construct meaning from text. Vocabulary and world knowledge are the two main predictors of reading comprehension test. The DIF items focus on the "language

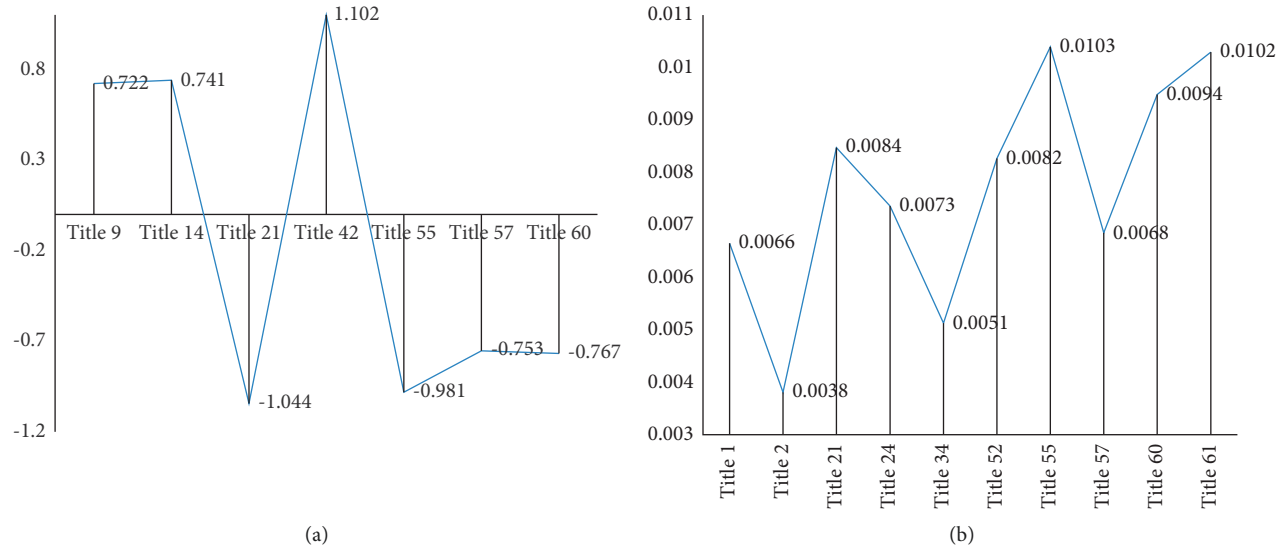

Figure 5: DIF inspection results of the East-West geographical and economic division grouping. (a) ΔMH. (b) R^2.

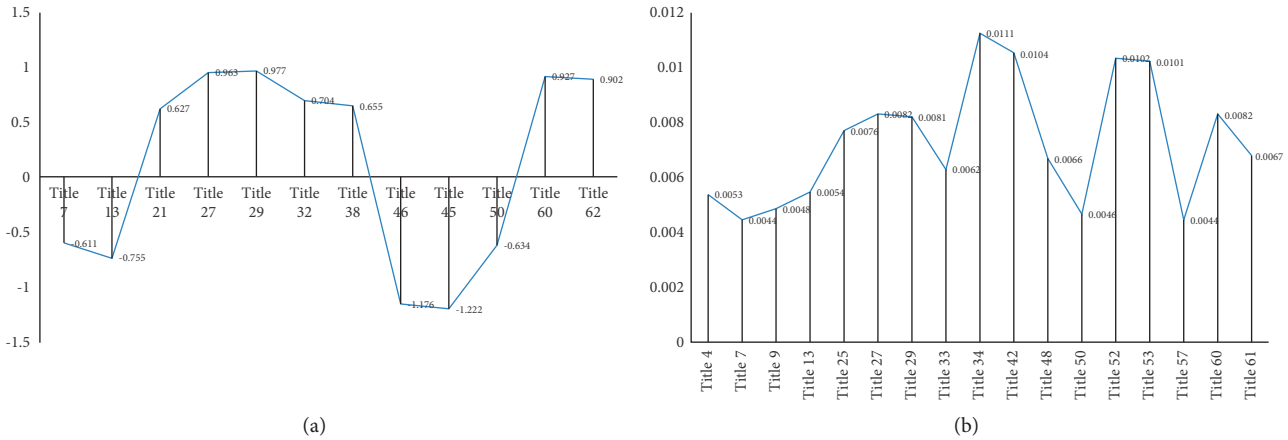

Figure 6: DIF inspection results of regional GDP grouping. (a) ΔMH. (b) R^2.

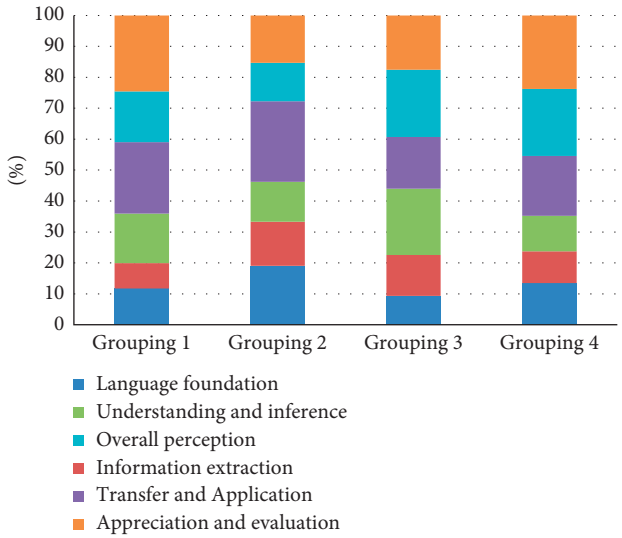

Figure 7: DIF item capability module distribution of four groupings.

Table 2: ΔMH of cluster grouping.

Title	Module	ΔMH
17	Understanding and inference	0.987
33	Language foundation	1.478
38	Understanding and inference	−1.166
49	Language foundation	1.609
57	Language foundation	1.022

Table 3: Nagelkerke's R^2 of cluster grouping.

Title	Module	Nagelkerke's R^2
14	Understanding and inference	0.0066
33	Language foundation	0.0088
36	Information extraction	0.0053
49	Language foundation	0.0057
57	Language foundation	0.0073

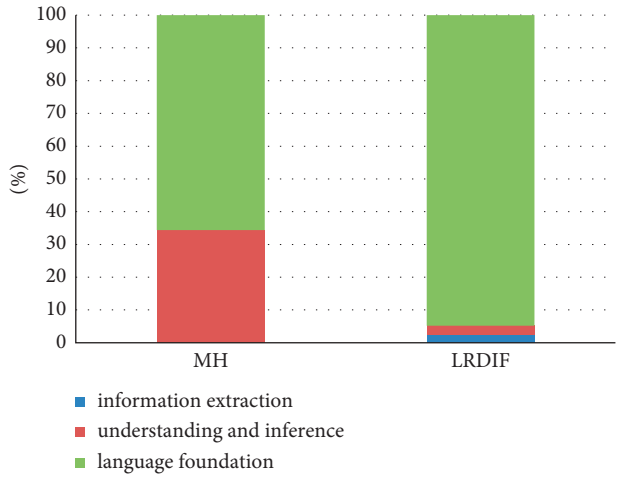

Figure 8: DIF ability module map.

foundation" and "understanding and inference" modules in the reading test, and the subjects in the high-level economic group perform better in answering questions. It can be inferred that superior family conditions can provide children with a better family language environment and a variety of ways to help children understand text information. The Family language environment includes both software and hardware. Hardware refers to hard conditions such as entity language learning materials, books, and CDs, while software refers to the language quality input by children and their families. Studies have demonstrated that language environment and family input are closely related to children's language development. The interaction between parents and children in high SES families has richer additional language, stronger modification, less punitive, and imperative language. The differences in the language models of parents in families with different economic statuses determine the differences in the development of the children's language foundation.

Therefore, for children with low family socioeconomic status, online reading enterprises should provide more reading text exercises focusing on the improvement of basic language ability and even launch picture books with voice functions to let children listen and read together and fundamentally improve their basic language ability. For the cultivation of understanding and inference ability, businesses should focus on thinking exercise books in recommended books so that children can think wirelessly, enhance their learning motivation, and gradually improve their thinking, reasoning ability, and understanding. The supporting test questions can use VR technology to detect the changes of students' mouth shapes during pronunciation and reading aloud to the greatest extent and give feedback, so as to ensure the accuracy and quality of children's practice. On the other hand, for children from high SES families with a good foundation, enterprises should develop reading text contents and exercises conducive to the cultivation of high-level abilities such as overall perception, transfer application, appreciation, and evaluation, so that children can gradually develop the ability to think independently, form the habit of thinking and solving problems independently, draw inferences from one instance on reading materials of the same nature, and lay a foundation for learning complex reading texts in the senior grade.

6. Conclusions

This study explores the important family socioeconomic status factors affecting children's reading ability and can provide corresponding countermeasures and suggestions for vulnerable reading users. So as to improve children's product experience satisfaction and increase user stickiness and retention rate from the perspective of enterprises. Provide guidance and suggestions for future product iteration and updates and combine practical research with theory to make products that users are more inclined to agree with. This study explores and demonstrates the quantitative research methods suitable for user demand analysis and supplements the research by focusing on qualitative research to analyze user demand and user experience. The exploration from multiple perspectives makes the research on user needs closer to the real needs of users, and the population is objectively and scientifically classified on the basis of statistical classification methods.

The limitation of this study is that the online reading of other grades remains to be discussed. There are many methods of data classification, and other methods will be introduced in future research. The design of the topic content may not be balanced enough. In addition, this study is limited to actual sampling, which is difficult. When investigating the differences of family socioeconomic status, it is represented by the regional economic level, which has a certain deviation. Future research will focus on improving these aspects. When analyzing children's online reading behavior oriented to their family education, we only start with gender and socioeconomic status differences in reading, which is not comprehensive enough. This is the biggest limitation of this study. Children's growth environment, personality, and other factors will be taken into account in future research.

Data Availability

The experimental data used to support the findings of this study are available from the author upon request.

Conflicts of Interest

The author declares no conflicts of interest.

References

[1] M. Sailer, J. Murböck, and F. Fischer, "Digital learning in schools: what does it take beyond digital technology?" *Teaching and Teacher Education*, vol. 103, Article ID 103346, 2021.

[2] L. Wang, Y. Y. Chen, T. StephenRamsey, and G. J. D. Hewings, "Will Researching Digital Technology Really

Empower green Development?" *Technology in Society*, vol. 66, 2021.

[3] L. Li, B. Lei, and C. Mao, "Digital twin in smart manufacturing," *Journal of Industrial Information Integration*, vol. 26, no. 9, Article ID 100289, 2022.

[4] L. Li, T. Qu, Y. Liu et al., "Sustainability assessment of intelligent manufacturing supported by digital twin," *IEEE Access*, vol. 8, Article ID 174988, 2020.

[5] M. Ashok, R. Madan, A. Joha, and U. Sivarajah, "Ethical framework for artificial intelligence and digital technologies," *International Journal of Information Management*, vol. 62, Article ID 102433, 2022.

[6] X. Y. Xu and Z. Y. Sun, "Digital Technology Empowers Grain Supply Chain Optimization Simulation," *Complexity*, vol. 2021, Article ID 6496713, 12 pages, 2021.

[7] H. Zhang and H. Y. Zheng, "The Application and Teaching of Digital Technology in Printmaking," *Security and Communication Networks*, vol. 2022, Article ID 3271860, 7 pages, 2022.

[8] J. D. Yeatman, K. A. Tang, P. M. Donnelly et al., "Rapid online assessment of reading ability," *Scientific Reports*, vol. 11, no. 1, p. 6396, 2021.

[9] K. Song and B.-Y. Cho, "Exploring bilingual adolescents' translanguaging strategies during online reading," *International Journal of Bilingual Education and Bilingualism*, vol. 24, no. 4, pp. 577–594, 2021.

[10] J. J. Gregory, P. M. Werth, C. A. Reilly, and D. S. Jevsevar, "Cross-specialty PROMIS-global health differential item functioning," *Quality of Life Research*, vol. 30, no. 8, pp. 2339–2348, 2021.

[11] Z. Sharafi, A. Mousavi, S. M. T. Ayatollahi, and P. Jafari, "Assessment of differential item functioning in health-related outcomes: a simulation and empirical analysis with hierarchical polytomous data," *Computational and Mathematical Methods in Medicine*, vol. 2017, pp. 1–11, 2017.

[12] A. Monterrosa-Castro, K. Portela-Buelvas, and A. Campo-Arias, "Differential Item Functioning of the Psychological Domain of the Menopause Rating Scale," *Biomed Research International*, vol. 2016, Article ID 8790691, 4 pages, 2016.

[13] H. Breland and Y.-W. Lee, "Investigating uniform and non-uniform gender DIF in computer-based ESL writing assessment," *Applied Measurement in Education*, vol. 20, no. 4, pp. 377–403, 2007.

[14] Y.-F. Chen and H. Jiao, "Exploring the utility of background and cognitive variables in explaining latent differential item functioning: an example of the pisa 2009 reading assessment," *Educational Assessment*, vol. 19, no. 2, pp. 77–96, 2014.

[15] V. Aryadoust, "Using recursive partitioning Rasch trees to investigate differential item functioning in second language reading tests," *Studies In Educational Evaluation*, vol. 56, pp. 197–204, 2018.

[16] I. Cadime, F. L. Viana, and I. Ribeiro, "Invariance on a reading comprehension test in european Portuguese: a differential item functioning analysis between students from rural and urban areas," *European Journal of Developmental Psychology*, vol. 11, no. 6, pp. 754–766, 2014.

[17] C. W. Little, S. A. Hart, B. M. Phillips, C. Schatschneider, and J. E. Taylor, "Exploring neighborhood environmental influences on reading comprehension," *Journal of Applied Developmental Psychology*, vol. 62, pp. 173–184, 2019.

[18] D. J. Leu, E. Forzani, C. Rhoads, C. Maykel, C. Kennedy, and N. Timbrell, "The new literacies of online research and comprehension: rethinking the reading achievement gap," *Reading Research Quarterly*, vol. 50, no. 1, pp. 37–59, 2015.

[19] L. M. Morrow, "Handbook of research on literacy and div," *Educational Review*, vol. 65, no. 1, pp. 118–120, 2013.

[20] A. C. Payne, G. J. Whitehurst, and A. L. Angell, "The role of home literacy environment in the development of language ability in preschool children from low-income families," *Early Childhood Research Quarterly*, vol. 9, no. 3-4, pp. 427–440, 1994.

[21] J. Liu, C. Li, and C. Ji, "Study of MDP and K-mediods for TSP problem," in *Proceedings of the 1st International Conference on Communications and Information Processing (ICCIP 2012)*, pp. 324–332, Aveiro, Portugal, March 2012.

[22] W. Wu and S. Xu, "Intrusion detection based on dynamic gemini population DE-K-mediods clustering on hadoop platform," *International Journal of Pattern Recognition and Artificial Intelligence*, vol. 35, no. 1, Article ID 2150001, 2021.

[23] W. Wang, B. Lou, X. Li, X. Lou, N. Jin, and K. Yan, "Intelligent maintenance frameworks of large-scale grid using genetic algorithm and K-Mediods clustering methods," *World Wide Web*, vol. 23, no. 2, pp. 1177–1195, 2020.

[24] B. F. French and W. H. Finch, "Extensions of mantel-haenszel for multilevel DIF detection," *Educational and Psychological Measurement*, vol. 73, no. 4, pp. 648–671, 2013.

[25] Yu Lan, H. K. Suen, and P.-W. Lei, "Using a Differential Item Functioning (Dif) Procedure to Detect Differences in Opportunity to Learn (Otl): An Extension of winfield's Approach," in *Proceedings of the annual meeting of the American Educational Research Association*, New York, NY, USA, March 2008.

[26] H. Swaminathan and H. J. Rogers, "Detecting differential item functioning using logistic regression procedures," *Journal of Educational Measurement*, vol. 27, no. 4, pp. 361–370, 1990.

[27] S. H. Kim and A. S. Cohen, "IRTDIF: a computer program for IRT differential itemfunctioning analysis," *Applied Psychological Measurement*, vol. 16, pp. 158–160, 1992.

[28] W. J. van der Linden and R. K. Hambleton, *Handbook of Modern Item Response Theory*, Springer, New York, NY, USA, 1997.

Hindawi
Scientific Programming
Volume 2022, Article ID 6348681, 11 pages
https://doi.org/10.1155/2022/6348681

Research Article

Research on Psychological Emotion Recognition of College Students Based on Deep Learning

Yuebo Li[1] **and Yatong Zhou**[2]

[1]*School of Marxism, Hebei Vocational University of Industry and Technology, Shijiazhuang 050091, China*
[2]*Department of Marxism Teaching, Hebei GEO University, Shijiazhuang 050030, China*

Correspondence should be addressed to Yatong Zhou; zhouyatong@hgu.edu.cn

Received 21 March 2022; Revised 6 April 2022; Accepted 13 April 2022; Published 12 May 2022

Academic Editor: Jie Liu

College students' anxiety, depression, inferiority complex, interpersonal sensitivity, and a series of mental health problems have a very serious negative impact on individuals, families, and society. In order to obtain better psychological emotion recognition effect of college students, this paper proposes a psychological emotion recognition algorithm based on multisource data. One-dimensional convolutional neural network (1D-CNN) was used to mine students' online patterns from online behavior sequences. According to the consumption data of students in the canteen, abnormal scores are calculated to depict the dietary differences among students. At the same time, the students' psychological state data provided by the psychological center are used as labels to improve the shortcomings of the questionnaire. Five kinds of common classification algorithms are trained by training set, and the classifier with the best effect is selected through evaluation of verification set, which is used to identify students with mental health problems in the test set. Experimental results show that precision, recall, and $F1$-measure reach 0.68, 0.56, and 0.67, respectively. 75% of students with mental health problems are identified. The psychological and emotional recognition system of college students based on deep learning provides systematic method and theoretical support for the school to find students with psychological problems in time and provide intervention.

1. Introduction

With the rapid development of knowledge economy and the increasing popularity of higher education, the number of college students is increasing day by day, and there are more and more students with psychological problems [1]. College students, as a part of high-level talents, have always been regarded as the outstanding generation of the society, with strong psychological quality by default, but the fact is disappointing. All kinds of pressures such as study, social relationship, and employment make college students mentally exhausted, and timely detection of abnormal students has become one of the most concerned and intractable problems in universities [2].

People's psychological characteristics can be expressed through daily living behaviors and work-and-rest rules. Researchers have mined information that can reflect the mental health state from the daily behavior data of college students. Research shows that there is a close relationship between mental health and online behavior. Jorm proposed an algorithm to predict mental health problems through online use behavior. Based on web usage behavior, a computational model for predicting scores of SCL-90 dimensions was established [3]. Nie [4] proposed a new method to predict the future mental illness severity (MIS) of users sharing posts on Instagram in 2014. Paola [5] discussed the universality and treatment of college students' psychology and psychosis, proposed the uniqueness of college students' development stage and environment in terms of psychological abnormalities, and summarized the influence of college students' psychological problems [6]. Zanganeh [7] (2018) explored the role of emotional factors in doctoral students' online information retrieval. Domestic scholars have conducted relevant research on this topic [8]. Tang [9]

used SCL-90 scale to measure the mental health of graduate students, established a prediction model through BP neural network to analyze and predict the mental health status of students, and put the model into practical application [10]. Wang Yinmei et al. [11] used symptom measurement scale to investigate 532 college students and found that college students' mental health varies in different grades, mainly influenced by interpersonal relationship, diet and sleep in college, and students of different majors have different psychological conditions [12]. Zhu [13] (2019) proposed a new method to detect depression through time-frequency analysis of network behaviors. A classification model was established to distinguish the high SDS group from the low SDS group, and a more accurate prediction model was established to identify the psychological state of the depression group [14].

To sum up, this paper carries out an analysis and research on students' mental health state through the data of students' education in school and excavates the relationship between college students' behaviors and their mental health state, which plays an important role and shows significance for university student managers to carry out early intervention for students with psychological abnormalities.

2. Principle of Deep Learning Algorithm

Deep learning is the process of using computers to imitate human learning behaviors. In the process of learning, new knowledge and experience are constantly accumulated, and their own knowledge structure is established according to this knowledge so as to improve their learning ability [15]. The research in this paper is a binary classification problem, and five commonly used classification algorithms are used in the experimental process, including decision tree, random forest, naive Bayes, gradient ascending tree, and BP neural network. In the feature extraction process, in order to reflect the dining situation of students, *k*-means clustering is used to cluster the dietary data of students.

2.1. k-Means Clustering. The main idea of *k*-means clustering algorithm: firstly, select K sample points randomly from the sample set and take them as the center of the cluster. Then, according to the distance between each sample and the k centroids, it is divided into the nearest cluster, and then the centroids of each cluster are recalculated [16]. Euclidean distance is used in this paper, and the calculation formula is shown as

$$d(x, C_i) = \sqrt{\sum_{j=1}^{m} \left(x_j - c_{ij}\right)^2}, \tag{1}$$

where x is the data object, C_i is the ith cluster center, m is the dimension of the data object, x_i, C_{ij} are the j attribute values of x and C_i. The calculation formula of error square and SSE of the whole data set is shown as

$$\mathrm{SSE} = \sum_{i=1}^{k} \sum_{x \in C_i} \left|d(x, C_i)\right|^2. \tag{2}$$

2.2. Decision Tree Algorithm. The different decision tree algorithms according to different split attribute algorithms are as follows. ID3 algorithm selects the optimal attribute for splitting by calculating the information gain, and the attribute with the maximum information gain after partitioning is the optimal attribute [17]. The information gain is calculated on the basis of information entropy, which is shown as

$$\mathrm{Entropy}(D) = -\sum_{i=1}^{m} p_i \log_2 p_i. \tag{3}$$

Among them, m is the number of categories in a data set D, and p_i is the first i category of probability. The smaller the value of (D) is, the higher the purity of $D$is.

If attribute a in the data set is used, the possible values of a are $v = \{a^1, a^2, a^3, \ldots, a^v\}$, which can be calculated according to formula (4) to attribute a classified information entropy D^v, because the various values of a sample are different, add weight to each branch node$\left| D^v \right|/\left| D \right|$, when dividing the data set with property a, can according to the formula to calculate the sample set of type D information gain.

$$\mathrm{Gain}(D, a) = \mathrm{Entropy}(D) = -\sum_{v=1}^{V} \mathrm{Entropy}\left(D^v\right). \tag{4}$$

However, the information gain tends to favor attributes with more values. In order to improve this defect, the famous C4.5 algorithm is proposed [7], which uses the information gain rate when selecting attributes, as shown in formula (5). The detailed attribute selection process is as follows: firstly, the information gain of the attribute is calculated, and the attribute whose information gain is higher than the average value is selected, and then the highest gain rate is selected from these attributes for classification.

$$\mathrm{Gain\_ratio}(D, a) = \frac{\mathrm{Gain}(D, a)}{\mathrm{SI}(a)}. \tag{5}$$

$$\mathrm{SI}(a) = -\sum_{v=1}^{V} \frac{\left|D^v\right|}{D} \log_2 \frac{\left|D^v\right|}{D}. \tag{6}$$

CART algorithm uses Gini index to select the optimal splitting attribute, and the calculation speed is faster than the information gain rate [13]. The purity of dataset D can be measured by Gini index, as shown in (7). The smaller (D) is, the higher the purity of the data set is. Therefore, which

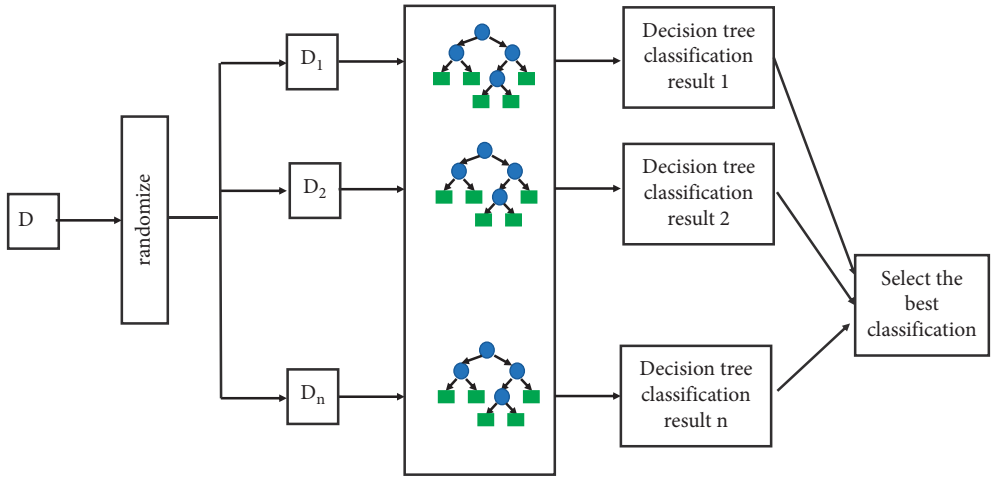

Figure 1: Random forest workflow.

attribute is the optimal splitting attribute can be judged according to the size of Gini index.

$$\text{Gini}(D) = 1 - \sum_{i=1}^{n} p_i^2. \tag{7}$$

The idea of decision tree algorithm is simple, easy to understand, and easy to extract rules. Insensitivity to data can process both nominal and numerical data and can process unrelated features. However, it also has some disadvantages. First, it is easy to produce overfitting, and second, it is easy to ignore the correlation between attributes.

2.3. Random Forest Algorithm. The random forest algorithm takes decision tree-based classifier and combines Bagging construction with random attribute selection. Its workflow is shown in Figure 1. Specifically, random forest determines the category of samples by voting, and each base classifier has one vote to determine the category of samples according to the principle of majority rule. The randomness of the random forest in random attribute selection, for each node base classifier, randomly selected from the set from the current node attributes first k attribute a subset, and then according to the attribute selection algorithm from subset to calculate the optimal split attribute, rather than the traditional decision tree from the current node, find out the best in all of the attributes of the attribute. The parameter k is introduced to reflect the randomness of the random forest Algorithm 1.

2.4. Naive Bayes. Naive Bayes algorithm takes Bayes algorithm as the premise and introduces the "independence" hypothesis, whose assumed attributes are independent of each other [18]. Under this assumption of independence, naive Bayes algorithm is especially suitable for solving multiattribute problems. Naive Bayes algorithm is currently recognized as a simple and effective probability classification method, and its classification process is as follows:

(1) Assume that each sample has n attributes. Each sample is represented by an n-dimensional eigenvector $d = \{d_1, d_2, d_3, \ldots, d_n\}$.

(2) Suppose there are m categories $c = \{c_1, c_2, c_3, \ldots, c_m\}$. Given an unknown data sample d, the classification predicts that d belongs to the class with the maximum posterior probability, that is, if and only if $p(c|d) > p(c|d) 1 \le j \le m$ and $j \neq i$, The Bayesian classification assigns the sample to be classified to class c_i, and the value of $p(c_i|d)$ can be calculated by the conditional probability formula in probability theory, as shown in the following formula.

$$P(c_i|d) = \frac{P(d|c_i)P(c_i)}{P(d)}. \tag{8}$$

(3) Since the sample set is known and the value of $P(d)$ can be calculated, the maximum value of $P(c_i|d)$ can only be calculated by the maximum value of $p(d|c_i)p(c_i)$. Without knowing the prior probabilities of the classes, assume that each class is equally likely, so you just maximize $(d|c_i)$. Otherwise, maximize $(d|c_i)(c_i)$.

(4) In the case of multiple attributes, the overhead of calculating $(d|c_i)$ may be very large. In this case, we can make the naive assumption of class condition independence to reduce the overhead of calculating $(d|c_i)$. The classes of a given sample are labeled, assuming that the attributes are independent of each other.

$$P(d|c_i) = \prod_{j=1}^{a} P(d_j|c_i), \tag{9}$$

(i) Input: data set $T = \{(x_1, y_1), (x_2, y_2), \ldots, (x_m, y_m)\}$, loss function L
(ii) Output: Additive model $f(x) = fM(x)$
(1) Initialize the base classifier $f_0 = (x) = \arg\min \gamma \sum_{i=1}^{N} L(y_i, \gamma)$
(2) Each base classifier needs to perform the following operations:
① According to the loss function, the negative gradient of each sample in the current model is calculated and used as an estimate of the residual $r_{im} = -[\partial L(y_i, f(x_i))/\partial, f(x_i)]$.
② For a given Γ_{im}, the leaf node Rmj, R_{mj}, $j = 1,2,..,J$, j is the number of leaf nodes
③ For leaf nodes, calculate $c_{mj} = \text{argmin}_c \sum_{Xi \in R_{mj}} L(y_i, f_m - 1(x_i) + c)$.
④ Update regression tree $f_m(x) = f_{m-1}(x) + \sum_{j=1} c_{mj} I(x \in R_{mj})$.
(3) Output gradient lifting tree $\hat{f}(x) = f_M(x)$.

Algorithm 1

where $(d_1|ci)$, $(d_2|ci), \ldots, P(d\,j|ci)$ can be computed from the sample set.

(5) When classifying classified sample d, calculate $(d|ci)(ci)$ for each class c_i in turn. If and only if $(d|ci)(ci) > P(d|c\,j)P(j)$, $1 \le j \le m, j \ne i$, sample d to be classified is divided into class c_i.

2.5. BP Neural Network. BP neural network is a multilayer feedforward neural network trained according to error reverse propagation algorithm. The training process of BP neural network is divided into two parts: one is signal forward propagation, and the other is error reverse propagation, as shown in Figure 2. Among them, BP neural network has many advantages such as strong nonlinear mapping ability, generalization ability, and fault tolerance ability due to its error back propagation learning process.

BP neural network consists of three parts: input layer, hidden layer, and output layer. Among them, the number of training sample attributes determines the number of neurons in the input layer, and the number of target classification determines the number of neurons in the output layer. For example, for a binary classification problem, there are only two neurons in the output layer. Users can freely define the number of hidden layers and the number of neurons in each hidden layer. The lines between each layer represent the weights.

BP neural network has the following advantages: first, it has strong adaptability and self-learning ability, which can continuously learn and correct path weight and save learning content during training. Second, the nonlinear mapping and fault tolerance ability can better solve the internal mechanism of the more complex nonlinear mapping. However, BP neural network has some defects, such as slow training speed, no corresponding standard for hidden layers, and number of neurons.

2.6. Pearson's Correlation Coefficient. Pearson's correlation coefficient is used to measure the linear correlation between two variables in most cases. It is defined as the quotient of covariance and standard deviation between two variables, and its calculation is shown in the following formula.

$$\rho_{X,Y} = \frac{\text{cov}(X,Y)}{\sigma_{X,Y}} = \frac{E(XY) - E(X)E(Y)}{\sqrt{E\left(X^Z\right) - E^2(X)}\sqrt{E\left(Y^Z\right) - E^2(Y)}}, \tag{10}$$

where X and Y represent two random variables, cov (X, Y) represents the covariance between X and Y, $\sigma_{X,Y}$ represents the standard deviation between X and Y, and E represents statistical mathematical expectation.

Pearson's correlation coefficient ranges from −1 to 1. A positive value means a positive correlation between two variables (1 means a complete positive correlation), a negative value means a negative correlation between two variables (−1 means a complete negative correlation), and a 0 value means there is no linear correlation between two variables. When comparing the correlation between feature and target problem, the larger the absolute value of correlation coefficient is, the more relevant the feature is to target problem.

3. Student Mental Health Problem Identification Algorithm Based on Multisource Data

The experimental process of identifying students with psychological and emotional problems based on multisource data includes data acquisition and preprocessing, feature extraction, model training, and recognition. In the experiment, students' consumption data, access control data, network data, historical performance data, and psychological center data were collected.

3.1. Algorithm Framework. The overall framework of the student mental health problem recognition algorithm based on multisource data is shown in Figure 2. The whole algorithm process is divided into three parts, including data acquisition and preprocessing, feature extraction, and model training and recognition. In the stage of data acquisition and preprocessing, we obtained four data sources, namely, network log, access control data, achievement data, and consumption data. In the feature extraction stage, the relevant features such as students' online pattern and consumption abnormal score are extracted from the four data

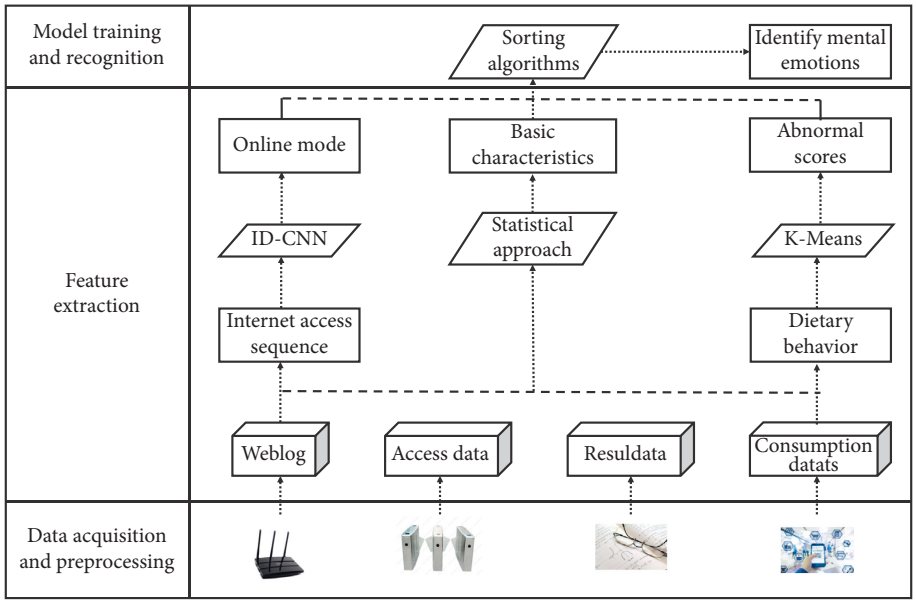

Figure 2: Multisource data-based student mental health problem recognition algorithm framework.

sources. The optimal classifier is selected from five common classification algorithms.

3.1.1. Data Acquisition and Preprocessing. After applying to relevant departments and obtaining students' informed consent, this study obtained a variety of behavioral data of students, including students' consumption data, historical performance data, network logs, access control and card swiping data, and psychological state data.

(1) Consumption Data. There will be a record every time students swipe the campus card. There are three tables of consumption data, namely, consumption flow chart, student account information table, and shop account information table. According to the shop account, connect the shop account information table with the consumption table and the student account information table, and the results are shown in Table 1.

(2) Access Control Data. At present, college students can enter and leave dormitories only after swiping their card through the access control system using a Metro Card Every time a student swipes the card, an entry-and-exit record will be generated, and these records are stored in the access control information table, as shown in Table 2.

The access control information not only reflects the time trajectory of students entering and leaving the dormitory, but also calculates the duration of students in the dormitory according to their entering and leaving states. Students usually go in and out of dormitories with friends, and digging in this direction may also reveal interesting information, such as friend relationships.

(3) Students' Network Log Records. Table 3 shows the network log information. Network logs record students' online activities, including online time and browsing content. How to dig out the patterns and characteristics of students' online behavior from these records is a problem we need to solve.

With the approval of the school network center and the informed consent of the students, we obtained the log files of the students' Internet access. We understand and analyze the network log; the format of the network log looks very simple, but the information it contains is very complex. The URL is divided into seven types, respectively: (1) comprehensive, (2) adult, (3) entertainment, (4) news, (5) publicity, (6) shopping, and (7) learning.

(4) Students' Historical Performance Data. There is a significant negative correlation between mild, moderate, and severe mood disorders and academic performance [19], and students' historical performance data reflect their past learning status and process. With the approval of the faculty and the informed consent of the student, this table details the students for the first time to attend this exam year students (XN), the first time to attend the exam of semester exam (XQ), students take the exam last time last year (QDXN), students take part in this exam semester (QDXQ), students, student id (XH), course name (KCMC), test scores (KS CJ), credits (XF), GRADE points (JD), grade points (XFJD), and credit acquisition methods (QDFS), including preliminary courses, retakes, and make-up exams, as shown in Table 4. Each record in the student history grade table reflects the student's learning of a certain course, and the student's comprehensive learning situation can be understood through the student number.

In the analysis and understanding of the student history score table, we found that the scoring method of the examination score (KSCJ) is not uniform; some courses use the hundred-mark system, while some use the five-level system [19]. For the convenience of calculation and analysis, we change the five-grade system into a percentage system, and

Table 1: The three tables join in the consumption data.

Student ID	Consumption time	Charge time	Transaction amount	Shop's account	Shop's name
2021****	20210421	2021/4/21 8:09:59	−5	1050229	Noodle section on the first floor of the third restaurant
2020****	20210417	2021/4/17 13:46:11	−3	1574702	Service building food street
2019****	20210425	2021/4/25 18:07:22	−2.5	1050253	The third restaurant, first floor malatang

Table 2: Access control information table.

Date of credit card	Charge time	Student ID	State of charge	Professional	Location	Dormitory building	Dormitory room no.
20210417	9:11:27	2020****	3	Mechanical engineering	9	3	309
20210606	10:52:0″	2019****	3	Transportation process	3	1	116
20210425	21:55:9	2018****	1	Materials and engineering	7	1	127

Table 3: Network log original table.

Time online	URL	Student ID	ULONG source IP	Source port	ULONG destination IP	Destination port
2021/4/21 8:16:54	vcheck.f.360cn/checker	2020****	172.24.8.118	80	221.228.204.185	34532
2021/4/21 7:02:44	rq.wh.cmam.111com/res"	2019****	172.20.52.152	443	203.248.210.232	56547
2021/4/25 17:32:25	https://www.imooc.com/wenda	2018****	1172.24.8.238	80	117.121.10141-	75362

Table 4: Student history score table.

XN	XQ	QD XN	QD XQ	XH	KCMC	XF	KS CJ	JD	XF JD	QDFS
2019	0	2019	0	2019****	Advanced mathematics	1	Pass	1	1	Early repair
2020	0	2021	0	2020****	C+ language	0	0	0	0	Early repair
2018	1	2019	1	2018****	Linear algebra	0	54	0	0	Rebuild
2019	1	2019	1	2019****	Linear algebra	1	65	1	2	Supplementary examination

the corresponding relationship is as follows: excellent (95), good (85), medium (75), pass (60), and fail (50).

It is found that there are missing values in the grade point column of the student's history grade table. Since credits are the product of grade points multiplied by course credits, a loss of grade points results in loss of corresponding credits. By observing the existing GPA, find out the calculation rule of GPA, where $CGPA_i$ stands for GPA of the course i, $Score_i$ stands for GPA of the course i, and the corresponding relationship between the calculated GPA and GPA is shown in Table 5. Next, according to the formula to calculate the credit grade point of the problem, $CGPA_i$ stands for the first i course credit grade point and $Credit_i$ stands for the first i course credits.

$$\begin{aligned} GPA_i &= \frac{(Score_i - 50)}{10}, \\ CGPA_i &= Credit_i \times GPA_i. \end{aligned} \tag{11}$$

Table 5: Conversion relationship between grade points.

Designation	Conversion relationship						
Results	>90	89	88	.....	61	60	<
Grade point	4	3.9	3.8	.....	1.1	1	0

(5) Psychological State Data. With the approval of the psychological center and the informed consent of the students, the psychological state table of the students was obtained. Each record in the table contains the student's student ID, gender, department, grade, class, attention level, and update time. The concern level includes mild, moderate, and severe. "Mild" means suffering from mild mental health problems; "moderate" means having moderate mental health problems; and "severe" means having severe mental health problems [11].

In this study, we targeted a dichotomous problem, namely, students with mental health problems and normal

students. Students whose concern level is light, medium, and heavy in the psychological state table of students were taken as positive samples, and other students who were not reported were taken as normal students.

3.1.2. Feature Extraction. This section mainly describes the process of extracting student behavior characteristics from data sources. The behavior of students on campus is rich and colorful. We divide the behavior characteristics of students into four types: consumption characteristics, access control characteristics, Internet access characteristics, and performance characteristics [9].

(1) Consumption Characteristics. Some studies have found that people with mental health problems will have eating disorders, especially depression [19]. Based on this fact, the consumption records of students in the canteen were extracted through the shop names to analyze their eating patterns. Pay special attention to students' breakfast/lunch/dinner routines. Set breakfast from 6 to 9, lunch from 11 to 13, and dinner from 17 to 19 : 30. Since there are often multiple records for each meal, use the time of the first swipe as the meal time. For example, if there are three records in a breakfast, the time of occurrence is 7 : 20, 7 : 21, and 7 : 22, use 7 : 20 as the breakfast time. The regularity of a behavior can be considered repeatable and will be measured by entropy of the probability that the behavior occurs at a particular time interval. Assuming that there are n time intervals $T = \{t_1, t_2, t_3, \ldots, t_n\}$, for any given student, the probability $p_v(T = \text{ti})$ of behavior $v \in V$ = {breakfast, lunch, dinner} occurring within time interval t_i is calculated according to formula (12), where $n_v(t_i)$ represents the frequency of behavior v occurring within time interval t_i. Then, calculate the entropy, which is calculated by formula (13). Assume that for the three behaviors of morning/afternoon/dinner, each time interval span is half an hour.

$$P_v(T = t_i) = \frac{n_v(t_i)}{\sum_{i=1}^{n} n_v(t_i)}, \tag{12}$$

$$E_v = -\sum_{i=1}^{n} P_v(T = t_i) \log P_v(T = t_i). \tag{13}$$

The b_entropy, l_entropy, and d_entropy values for breakfast/lunch/dinner can be calculated from formulas 12 and 13. Meanwhile, according to formula (12), the smaller the entropy value of a behavior is, the more concentrated its probability distribution is over time, and the higher its regularity is. If one student only goes to the canteen occasionally during a concentrated period of time, while the other student goes to the canteen frequently, although the regularity of the two students' dining in the canteen is not the same, they will also have similar entropy values. In order to better distinguish the two types of students, the number of breakfasts/luncheons/dinners for each student was calculated separately. k-means clustering algorithm is used to cluster entropy and meal times. It is considered that students have three common dining behaviors: less frequent dining, poor dining regularity, and good dining regularity. Therefore, the number of clustering k is set as 3. The clustering results are shown in Figure 3.

The goal was to find students with abnormal eating habits. It is assumed that the smaller the cluster a student is in, and the further away from the center of the cluster, the higher the abnormal score (20) according to the formula to calculate the abnormal scores for students, which is c_i student of n in the cluster centroid of C_i, said all the students, $| c_i |$ clustering Ci number of students, $| C |$ represents all the students, students n the distance to the center of mass of $(n, c_i)c_i$ said. In this experiment, Euclidean distance is used to calculate the distance.

$$\text{AS} = D(n, c_i) * \left(1 - \frac{|C_i|}{C}\right). \tag{14}$$

(2) Characteristics of Access Control. It is found that the more difficult the interpersonal communication is, the worse the mental health level is, and the stronger the interpersonal communication ability is, the better the mental health level is [5]. The dormitories of undergraduate students in colleges and universities are usually divided according to classes, and students in the same dormitory generally have the same entry and exit schedule. The interpersonal relationship of students in the dormitory can be reflected by calculating the times of students and roommates entering and leaving the dormitory together, which is called card swiping in front and back foot. The rule is as follows: if two students are roommates, the difference in credit card time is less than 20 seconds, and both students enter or leave the dormitory at the same time. Further analysis of the card swiping data from front and back showed that some students' values were less than 10 or even 0.

(3) Characteristics of Internet Access The overall framework of the one-dimensional convolutional neural network designed in this study consists of five neural network layers. In the training of the model, the input of each student is a network sequence, that is, a one-dimensional vector. Since the length of the network sequence is inconsistent, 0 is used to fill it. The operation of the convolution layer is shown in formula (15), where x_j^i is the feature graph of the j convolution operator of the l layer, x_i^{l-1} represents the input, k_{ij}^l represents the j convolution kernel of the l layer, b_j^l represents the bias of the j convolution operator, f(·) represents the activation function, and * represents the multiplication operation.

$$x_j^l = f\left(\sum_{i \epsilon M_j} x_i^{l-1} * k_{\text{ij}}^l + b_j^l\right). \tag{15}$$

The second and fourth neural network layers adopt the pooling layer, and the pooling mode is divided into average pooling and maximum pooling. In this study, the pooling mode is maximum pooling. The operation of the pooling

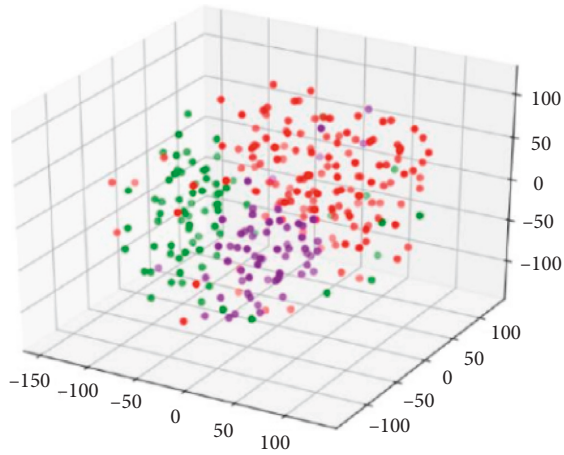

Figure 3: Clustering results based on entropy and frequency of breakfast, lunch, dinner.

layer is shown in formula (16), where x_j^i, w_j^i, b_j^i, downx_j^i represents the input, weight matrix, bias, and downsampling function, respectively.

$$\widehat{x}_j^l = f\left(w_j^l\right)\text{down}\left(x_i^l\right) + b_j^l. \tag{16}$$

The fifth layer uses a full connection layer, and the operation of the full connection layer is shown as follows:

$$s^{\text{pat}} = f\left(w^{(5)} * x^4 + b^{(5)}\right). \tag{17}$$

For parameter setting, the number of convolution kernels of the two convolution layers is 16 and 32, respectively. ReLU was used as the activation function and Adam as the optimization algorithm. Additionally, to prevent overfitting, we use three dropout layers with parameters 0.15, 0.15, and 0.5. In the model training stage, 70 positive samples and 70 negative samples were used to train the model. In the feature extraction stage, all the experimental samples were input into the trained 1D-CNN model, and finally the results of the full connection layer spat were output as the online mode.

(4) Performance Characteristics. (1) Grade point average students' mental health problems are often caused by external factors, and grade pressure is one of the external factors, so it is necessary to extract grade-related characteristics to reflect students' performance. GPA plays a decisive role in the school's evaluation and award, and the calculation formula is as follows:

$$\text{GPA}_{\text{avg}} = \frac{\sum_{i=1}^{n} \text{CGPA}_i}{\sum_{i-1}^{n} \text{Sore}_i}. \tag{18}$$

(2) Failing credits for college students: failing credits are the best characteristic of performance pressure. Failing credits are counted by traversing a student's history score sheet and counting the corresponding credits as failing credits if the QDFS value is a make-up exam. Two characteristics, GPA and failing credits, are extracted from historical achievement data. Finally, a total of 69 features were extracted from consumption data, access control data, and network logs and historical performance data.

3.1.3. Model Training and Recognition. The research objective of this paper is a binary classification problem. Five common classification algorithms are selected as candidate algorithms, including random forest (RT), gradient ascending tree (GBDT), Naive Bayes (NB), neural network (NN), and decision tree (DT). We hope to select a classification algorithm with the best performance as the classifier of the algorithm.

The data set is divided into training set, verification set, and test set, and each classification algorithm is trained with the training set, and then each classification algorithm is evaluated with the verification set. Obfuscation matrix is an index to evaluate model performance, which is mainly used to judge the performance of classifier. The confusion matrix has four basic elements, which are True Positive (TP), False Negative (FN), False Positive (FP), and True Negative (TN). The meanings of these four elements will be introduced in detail below.

However, the obfuscation matrix is only a statistical quantity. When the sample number is very large, it is difficult to evaluate the performance of the model only by calculating the quantity. Therefore, the confusion matrix extends some evaluation indexes based on the statistical quantity. In educational data research, there are five commonly used evaluation indicators, including accuracy, precision, recall, $F1$-measure, and AUC (area under curve) [19]. In this experiment, precision, recall, and $F1$-measure were selected as evaluation indexes.

Precision refers to the proportion of students who are truly positive samples among the students who are predicted to be positive samples, and its calculation formula is shown as follows:

$$\text{Precision} = \frac{\text{TP}}{\text{TP} + \text{FP}}. \tag{19}$$

Recall refers to the proportion of students who are predicted to be positive samples among students who are real and positive samples, and its calculation formula is shown as follows:

$$\text{Recall} = \frac{\text{TP}}{\text{TP} + \text{FN}}. \tag{20}$$

Precision and recall are two important indicators. However, when evaluating the performance of several models, precision of one model is often higher than that of other models, but recall is lower than that of other models. Therefore, the optimal model cannot be selected. A comprehensive index F-measure was introduced, and precision and recall were weighted and averaged. The calculation formula is shown as (21). The larger the F-measure is, the better the model performance is. When α is equal to 1, it is commonly used $F1$-measure, and $F1$-measure is used in this study.

$$F - \text{Measure} = \frac{\left(\alpha^{2+1}\right)\text{Precision} * \text{Recall}}{\alpha^2 * \text{Precision} + \text{Recall}}. \quad (21)$$

The training process of the model is the process of parameter selection; how to choose the optimal parameter is a key problem. In this algorithm, the way of permutation and combination is used to select the optimal parameter combination. For each classification algorithm, we adjust only a few important parameters and use the default values for the rest parameters. After trying different parameter combinations, the optimal parameter combinations of each candidate classification algorithm are selected.

4. Experiment and Result Analysis

4.1. Experimental Data. Among the 280 undergraduates who participated in the survey, 70 students were assessed as students with mental health problems by experts at the university's psychological center in May and June 2019. Their mental health levels were classified as mild, moderate, or severe. In addition, 210 undergraduates were randomly selected from the entire school. Finally, the proportion of students at each mental state level is shown in Figure 4.

Students were divided into two groups, with a positive sample for mild, moderate, and severe cases, and a negative sample for students without mental health problems. The label has high credibility and avoids the drawbacks of concealing facts in questionnaires. In order to protect students' privacy, the student id was encrypted throughout the experiment. As the psychological state is a short-term state, generally lasting from half a month to one month, only the consumption data access control data and network logs in April 2021 are used.

4.2. Training Set and Test Set. The essence of deep learning is the process of model selection. However, only parameters of the model are unknown. By using various tuning methods, an optimal value can be obtained, which enables the model to map independent variables to dependent variables well. In practice, it is not always easy to sample data evenly. So, the actual process is random. In this experiment, the data set sample is 280 students, among which 70 students are positive samples and 210 students are negative samples; that is to say, the ratio of positive samples to negative samples is 1 : 3. In order to make the sample ratio of the training set and the test set 1 : 3, 49 and 147 students were randomly selected from the positive and negative samples of the data set, respectively, as the training set, and 25% of the data were used as the verification set, and the positive and negative sample ratio was 1 : 3. Meanwhile, the ratio of positive and negative samples in the test set was 1 : 3.

4.3. Comparison and Analysis of Experimental Results. The extracted features are input into the classification algorithm for model training and prediction. Five common machine learning classification algorithms, including random forest (RT), gradient ascending tree (GBDT), Naive Bayes (NB), neural network (NN), and decision tree (DT), are compared. The experimental results are shown in Table 6.

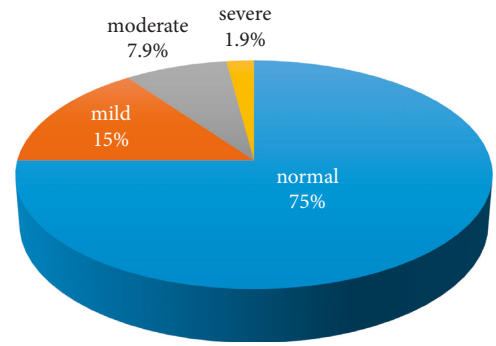

Figure 4: Proportion of each mental state in the data set.

First of all, it can be obviously observed that in all models, precision is higher than recall, and recall is only 0.58 at its highest, indicating that few samples can be correctly identified. Secondly, decision tree has the best comprehensive performance, especially recall. Therefore, we choose decision tree as the classifier of mental health recognition algorithm based on multisource data.

To verify the generalization ability of the algorithm, we input the test data set into our algorithm and obtain the following experimental results: precision 0.68, recall 0.56, and $F1$-measure 0.67. Based on the test set experiment results, our algorithm was able to identify 56 percent of students with mental health problems. Table 7 lists 20 characteristics with high Pearson's correlations.

It can be seen from the table that 7 of the first 8 positive correlation characteristics are related to early rise. In general, students' courses are arranged by week, and students have the same class time every week. The larger standard deviation or average value of early rise may be caused by lateness or truancy. There was a positive correlation with mental health problems. Working day and day of rest time to stay in the dormitory all show the negative correlation. There is a negative correlation between the time spent in the dormitory on weekdays and rest days. The students spend more time in the dormitory and less time in club activities, student work, and dinner parties. These students have poor interpersonal communication and are more likely to have mental health problems, consistent with people's intuitive feelings. This kind of students have generally poor interpersonal, namely, interpersonal communication; the worse the student, the more possible mental health problems, which is consistent and intuitive feeling of people. Students who spend more money in the canteen on weekdays and holidays may seldom participate in dinner parties, which may also reflect poor interpersonal communication. In addition, the correlation coefficient of students' swiping times is high and negative. On the one hand, students who swiped cards less often participated in fewer activities and had poorer interpersonal communication. On the other hand, students who swipe their credit cards only a few times a month should live off-campus and be the focus of attention. The insomnia rate (correlation coefficient 0.1058), the number of takeout orders (correlation coefficient 0.1024), GPA_avg, and failed

Table 6: Results of five classification algorithms to identify students with psychological problems.

Sorting algorithms	Precision	Recall	$F1$-measure
RT	0.68	0.53	0.65
GBDT	0.65	0.52	0.62
NB	0.62	0.50	0.60
NN	0.65	0.50	0.63
DT	0.68	0.58	0.69

Table 7: The top 20 most relevant features.

Characteristics of the category	Characteristic	Signalment	Coefficient of association
Entrance guard	Getup std 1	Standard deviation of Monday morning	0.2627
Entrance guard	Reststayroom	Time spent in the dormitory on days off	-0.2290
Entrance guard	Swipe_num	Credit card number	−0.2159
Entrance guard	getup_mean6	Saturday morning average	0.2014
Entrance guard	last_count5	Number of Friday nights	0.1990
Entrance guard	getup_mean1	Monday morning average	0.1915
Entrance guard	getup_count7	Number of early Sundays	0.1830
Entrance guard	getup_mean4	Thursday morning average	0.1780
Entrance guard	getup_mean3	Wednesday morning average	0.1766
Entrance guard	getup_std3	Standard deviation of Wednesday morning	0.1761
Consume	lunch_mean	The average amount spent on lunch	0.1825
Entrance guard	Work stay room	Time spent in the dormitory on weekdays	−0.1564
Entrance guard	last_std6	Saturday night is standard deviation	0.1540
Entrance guard	Feetcard	Swipe cards front and back	0.1440
Consume	rest_consume	Rest day consumption amount	−0.1424
Consume	Work consume	Consumption amount on working days	−0.1314
Score	GPA avg	Grade point average	−0.1244
Score	guake_count	Failing credit	0.1218
Consume	abnormal_score	Abnormal scores	0.1209
Network	cnn	The internet features	−0.1149

credits were all weakly correlated, but still valuable for analysis.

Through the above analysis, some characteristics related to mental health problems are obtained, and the impact on mental health is in line with common sense. Moreover, these related features come from multiple data sources, which shows that the use of multisource data can improve the recognition effect from one aspect.

5. Conclusion

This paper proposes a mental health problem recognition algorithm based on multisource data, trains five common classification algorithms, evaluates through the verification set, and establishes a recognition system to judge the psychological emotions of college students, and analyzes the results of the system verification test. The following conclusions can be drawn:

(1) Analysis of student behavior data can be used to identify students with mental health problems.

(2) Using a variety of behavioral data can improve the identification effect of students' mental health problems and can identify 75% of students with mental health problems.

To establish college students' mental emotion recognition system, this paper through the prediction results can identify the students with risk of mental health problems and counselors for school administrators to better understand the students' psychological condition, giving psychological help to the student as soon as possible and targeted intervention method provides the theory support, able to prevent the further deterioration of the psychological condition of students.

Data Availability

The dataset can be accessed upon request to the corresponding author.

Conflicts of Interest

The authors declare that they have no conflicts of interest regarding the publication of this paper.

Acknowledgments

This research was supported by Distinguished Teachers' Studio of Ideological and Political Course of Hebei Province.

References

[1] A. M. Sylvia, C. O. Desmond, M. Rucha, and Z. Jamil, "Empathy and well-being correlate with centrality in different

social networks[J]," *Proc Natl Acad Sci U S A*, vol. 114, no. 37, pp. 9843–9847, 2017.
[2] A. Mc and J. B. Suo, "Analysis and research on mental health of college students based on cognitive computing[J]," *Cognitive Systems Research*, vol. 56, pp. 151–158, 2019.
[3] A. F. Jorm, "Mental health literacy: e," *American Psychologist*, vol. 67, no. 3, pp. 231–243, 2012.
[4] D. Nie, A. Li, Z. Guan, and T. Zhu, "Your search behavior and your personality[J]," *Pervasive Computing and the Networked World*, vol. 8351, pp. 459–470, 2014.
[5] P. Paola, N. Maren, Y. Albert, Z. Courtney, and W. Timothy, "Colleg students: mental health problems and treatment considerations[J]," *Academic Psychiatry*, vol. 39, no. 5, pp. 503–511, 2015.
[6] N. Min, Y. Lei, J. Sun et al., "Advanced forecasting of career choices for college students based on campus big data[J]," *Frontiers of Computer Science*, vol. 12, no. 3, pp. 494–503, 2018.
[7] M. Yari Zanganeh and N. Hariri, "The role of emotional aspects in the information retrieval from the web," *Online Information Review*, vol. 42, no. 4, pp. 520–534, 2018.
[8] Z. Lee and C. Lee, "A parallel intelligent algorithm applied to predict students dropping out of university[J]," *The Journal of Supercomputing*, vol. 76, no. 2, pp. 1049–1062, 2020.
[9] J. L. Tang, D. Wang, Z. G. Zhang, U. He, J. Xin, and Y. Xu, "Weed identification based on K-Means feature learning combined with convolutional neural network[J]," *Computers and Electronics in Agriculture*, vol. 135, pp. 63–70, 2017.
[10] B. Rupali, B. Machhindra, W. Pragati, M. V. Raut, and H. S. Habeebullah, "Tracking and predicting student performance using machine learning[J]," *SSRN Electronic Journal*, vol. 6, no. 2, pp. 439–442, 2019.
[11] Y. M. Wang, C. He, and S. J. Tong, "The present situation and educational enlightenment of college students' mental health development[J]," *Modern educational science (higher education research)*, vol. 2, pp. 65–71, 2018.
[12] L. Q. Hao, "Analysis of data mining method based on related rules[J]," *Journal of Taiyuan University*, vol. 38, no. 03, pp. 42–45, 2020.
[13] C. Y. Zhu, B. B. Li, and A. Li, "Predicting depression from internet behaviors by time-frequency features[J]," *Web Intelligence*, vol. 17, no. 3, pp. 199–208, 2019.
[14] M. Y. Zanganeh and N. Hariri, "The role of emotional aspects in the information retrieval from the web [Online, 2018 web[J]," *Online Information Review*, vol. 42, no. 4, pp. 520–534, 2018.
[15] Y. M. Shi and Y. J. Luo, "The attentional bias of optimistic and pessimistic attributive style college students to emotional information[J]," *Chinese Journal of Mental Health*, vol. 5, pp. 395–399, 2017.
[16] X. F. Chen, M. Tong, C. Shi et al., "Visual analysis of multi-source college students' mental health questionnaire data[J]," *Journal of Computer Aided Design and Graphics*, vol. 2, no. 32, pp. 181–193, 2020.
[17] H. Yao, D. Lian, and Y. Cao, "Predicting academic performance for college students: ACampus behavior perspective [J]," *ACM Transactions on Information Systems*, vol. 10, no. 3, pp. 24.1–24.21, 2019.
[18] P. R. Selvaraj and C. S. Bhat, "Predicting the mental health of college students with psychological capital[J]," *Journal of Mental Health*, vol. 27, no. 3, pp. 279–287, 2018.
[19] C. Shu, J. Ma, and J. Zhu, "Comparison of UPI and SCL-90 on mental health survey of freshman in higher voca-tional college [J]," *Chinese Journal of School Health*, vol. 35, no. 4, pp. 523–526, 2014.

Hindawi
Scientific Programming
Volume 2022, Article ID 7955848, 11 pages
https://doi.org/10.1155/2022/7955848

Research Article

Research on Digital Design of Urban Public Landscape Based on Morphogenesis

Yamin Zhang

Henan Economic and Trade Vocational College, College of Art and Design, Zhengzhou, Henan 450000, China

Correspondence should be addressed to Yamin Zhang; zhangyamin@henetc.edu.cn

Received 14 March 2022; Revised 24 March 2022; Accepted 5 April 2022; Published 10 May 2022

Academic Editor: Jie Liu

With the development of digital technology, it is possible to organize the deep relationship of public landscape elements. Design inspiration is no longer static and manual imitation of natural representations but can be dynamically self-organized. The design under the digital design theory shows obvious characteristics: multiparameter action, bottom-up, dynamic iteration, and optimal result orientation. The design chain, or meta-design, has since formed the basic digital design chain. Based on morphogenesis and combined with the existing landscape design creation methods, this study summarizes an operable logic system of digital design based on morphogenesis. It is hoped that through digital technology, it is possible to establish the relationship between various spatial organizations in the public landscape system. It uses the theory of morphogenesis and digital research to expand the cognition of landscape morphology and stimulate the innovation of design methods and build a landscape design logic system based on program algorithms. This study uses the subsystem design and completes the generation process from the design concept to the space formation from the graphic concept, which proves that this design logic system is feasible and has obvious advantages to a certain extent.

1. Introduction

With the development of the economy and the improvement of computer technology, people's requirements for landscape design are also constantly increasing. The traditional landscape design methods can no longer meet the needs of urban development. Our country's landscape design has entered the stage of digital design. However, there are still some deficiencies in the current domestic landscape design, such as how to combine computer technology with landscape design? How to more rationally present every aspect of landscape design, instead of relying on intuitive design and empirical design? The essential problem of morphogenesis is to explore how to establish living systems. Through the research and summary of plant morphology, two different discussions have been drawn, namely, "the theory of preformation" and "the theory of postformation." With the development and extension of postformation theory, it has gradually become the ideological basis of morphogenesis. In a research discussion meeting on urban renewal in New York, it was proposed that "it is necessary to pay attention to the application of morphogenetic concepts and learn the growth process of life, so as to produce excellent landscape design, which is always in dynamic like a dynamic city." Digitization is to build a model of a complex system or process with the help of a computer, to test the model, then, to have an in-depth understanding of the various behavior mechanisms of the model system, and to control the various means and methods of the model system. Modern computer simulation application technology is an emerging discipline based on operations research, mathematical statistics, and computer science. Based on the methods and concepts of morphogenesis and digital design, this study is reading the existing theories of morphogenesis and digital graphics, especially the related theories of landscape digital graphics and the research theories and research results of landscape morphogenesis, and summarizes the process methods of morphogenesis and digital graphics in landscape design. Based on the two theories of complex adaptive system and morphogenesis, using bottom-up and digital design thinking, using algorithm design and digital

design methods, and the methods and methods of digital design of landscape design based on morphogenesis are studied [1–5]. This study mainly summarizes the development, characteristics, and logic of morphogenesis and digital diagrams. Combined with the existing landscape design creation methods, it summarizes an operable logic system of digital diagram design based on morphogenesis.

2. Related Work

At present, in the exploration of complexity science, designers represented by Steven Johnson have published a series of papers, such as "emergence-connecting with the life, brain, city, software of ants," which has an impact on reality in this study, and the application mode of digital technology has been deeply analyzed, which has an important impact on the morphogenesis mechanism. With the gradual development of diagrams and other spatial theories, it has brought new promotion to the thought and biological logic of digital design. Second, in the research of digital design, designers represented by Rego Lynn published a series of works, such as "Folding, Body and Bubbles," on "dynamics" and "force field". The application of the theory in the process of morphogenesis is described in detail, and it is believed that any design based on the coordinate reference system will show a continuous expansion of the internal logic system and the corresponding information place. At the same time, the UK's AD magazine also summarizes the thinking of contemporary designers and conducts in-depth research on theories such as skin, folding, and emergence. Based on the two theories of complex adaptive system and morphogenesis, this study uses bottom-up and digital design thinking and uses the methods of algorithm design and digital design to study the methods and methods of digital design of landscape design based on morphogenesis [6–11]. The research contents include the following: (1) theoretical thinking and design thinking of landscape design under morphogenesis, (2) digital morphogenesis of landscape under morphogenesis, (3) theoretical thinking and design thinking of landscape design digital illustration, (4) landscape methods of designing digital graphics, and (5) digital graphical program for landscape design.

3. Related Theoretical Methods

3.1. Morphogenesis

3.1.1. Overall Design Thinking. As the sum of individual relationships, only when the landscape system is deeply analyzed from the overall level, its characteristic attributes and general laws will be highlighted. In the process of analyzing the landscape system as a whole, it is necessary to add a linked relational network, a progressive operation mechanism, and events from a time and space perspective, so as to ensure that it will not lose its original relationship and performance. Therefore, it is necessary to integrate the overall design thinking in order to include the dynamic evolution process of the landscape system [12].

3.1.2. Bottom-Up Process Thinking. Combined with the processing logic of morphogenesis, designers need to find out various influencing factors in the landscape system and use them as a bottom-up driving mechanism. This requires designers to screen the initial information and, at the same time, conduct an in-depth analysis of the project, in order to obtain the correct direction of morphological evolution [13].

3.1.3. Relational Thinking of Interactive Adaptation. In traditional theoretical cognition, it is customary to disassemble the system into different individuals and then explain this hierarchical relationship through linear thinking. As a nonlinear system, each factor in the landscape system is not independent but a system that restricts each other and finally reaches a balanced steady state. The landscape needs to be regarded as a complex system rather than a specific object, and its internal nonlinear spatial logic needs to be correctly constructed [14].

3.2. Digital Morphogenesis of Landscape

3.2.1. Topology Occurrence. Topological geometry is the basic property of how geometric figures remain unchanged in continuous homeomorphic deformation, and it is a geometric theory specializing in the study of the continuity of geometric figures. Homeomorphic deformation means that in the process of deformation, as long as the deformation does not break or overlap, the overall structure of the original topology will not be destroyed. The homeomorphic deformation of landscape topology is a series of topological structure levels derived from the original topological level based on the prototype of the original diversity and unity. In terms of design, the enlightenment of topogenesis is not only in geometric shape but also has an important influence on its logical thinking, and it is used as the theoretical basis and internal mechanism of morphogenesis. For some time, the digital design practice of landscape has stayed in the exploratory stage. It is hoped to use topology generation as a way of spatial structure layout to realize the transformation from the natural landscape to artificial landscape and to create a new landscape design method to make people aware of topology [15–18].

3.2.2. Parameters and Algorithm Generation. The algorithm is to use the overall method to describe the mechanism of dealing with the problem, and it is one of the important contents of the parametric design method. The program of parametric design is to convert the design elements and requirements into computer programs and use the corresponding calculation rules to express the generation process of the shape, so as to obtain the final program shape. The algorithm only needs to calculate the logic with the help of simple rules, so as to obtain complex results, and the designer only needs to select and optimize the results. Due to the large amount of information in the landscape system, it is

difficult to completely express the landscape system by using traditional design methods. With the help of algorithms and parametric technology, a corresponding digital landscape model can be built to simulate and express the relationship between the internal and external influencing factors of the landscape, which can effectively allow designers to obtain the most suitable landscape in a short time [19–21].

4. Construction of a Digital Design Program for Urban Public Landscape Based on Morphogenesis

4.1. Digital Design Based on Program Algorithms. No matter what kind of diagram logic is, it all depends on the program algorithm. This design method based on a program algorithm is the basic design chain of the digital diagram—"meta-design." Since the process of landscape design is preliminary analysis-asking questions-design concept-design plan-preliminary design-construction drawing design, it has much in common with the process of architectural design, so its design method and process are inspired by landscape design. It should be noted that the main content studied in this study is in the generation stage of the general landscape plan design. Three elements must be included in the meta-design: a parameterized prototype, a measure of the performance evaluation of the solution, and a machine algorithm that controls the loop in the direction of optimization, as shown in Figure 1. No matter what kind of diagram logic is, it all depends on the program algorithm. This design method based on a program algorithm is the basic design chain of the digital diagram—"meta-design."

In the meta-design system, it is necessary to separately classify the landscape system according to the basic research of the landscape and the objects of its role (the actors in the landscape system). In the landscape digital design system of meta-design, the landscape parameters are completely included in a system where the three systems of people, landscape, and environment adapt to each other, so the landscape system is divided into two basic levels, namely, the internal system (landscape system) and external system (environmental system and human system), as shown in Figure 2.

Using a computer programming language, combined with digital design methods to build an automatic decision-making model, at the same time, according to specific constraints, the relationship between different types of landscape units and adjacent units is calculated, and the individual coordination index is obtained, on this basis, the optimal next-generation individuals are selected, repeated in this way, a population composed of individuals after the global optimal convergence can be finally obtained, and the most suitable design scheme is found. Program algorithm design fundamentally puts forward the basic logic of digital design, but the design process is still largely influenced by the designer's subjective experience and esthetic concepts. Under the existing conditions, computer logic and subjective logic jointly affect the composition of graphic design. Results: The judgment and feedback of meta-design results based on subjective experience and esthetic concepts have become an important part of the digital graphical design system. In particular, the esthetic value is the long-term precipitation of designers based on design feedback, which is more in line with the public's cognition than program algorithm design results. At the same time, the designer's subjective concept is preconceived, and the program algorithm design based on this construction also constitutes a digital design method in a broad sense.

4.2. Digital Design Procedures

4.2.1. Digital Design Method and Selection of Simulation Platform. After the design concept is determined, an overall analysis of the project is required to determine the digital design approach. There are two types of digital design methods: one is to start from the design concept and use traditional landscape design methods and procedures to divide the landscape system into traffic system, functional system, landscape node system, and plant system, and perform parametric simulation, respectively. The prototype of the design scheme is obtained, combined with the simulation analysis of the sunlight and wind environment, and the basic shape of the design is obtained; the other is to start from the design concept, determine the relationship between the various influencing factors in the system, convert them into parameters, input them into the simulation model in the environment, and then simulate to get the prototype of the design. According to the basic design conditions of the project, the digital design method must be reasonably chosen, specifically as shown in Figure 3. This study prefers the latter.

In the selection of simulation platform, the development of computer-aided design platform has become more and more mature, but the industries targeted by each software platform are different, and the computer software platform for landscape professional has not yet been determined. Therefore, for the landscape major, the most direct solution strategy is to comprehensively use the currently developed computer software platform to assist the landscape design and achieve the design purpose. According to the basic situation of the project, the main digital simulation platform selected in this article is Rhinoceros + Grasshopper.

4.2.2. Subsystem Simulation Analysis. With the help of the site prototype theory, according to the composition characteristics of the landscape system itself and the traditional landscape design method and process, this study divides the landscape design process into four steps: traffic system design, functional system design, landscape node system design, and plant system design. The key point is to determine the corresponding digital simulation method for the system corresponding to each step after determining the design concept of the project and the digital diagram method, extract the influencing factors in each system, conduct a separate parametric simulation analysis, and then, fit the simulation analysis results of each subsystem to get the basic prototype of the design. It is a landscape design logic

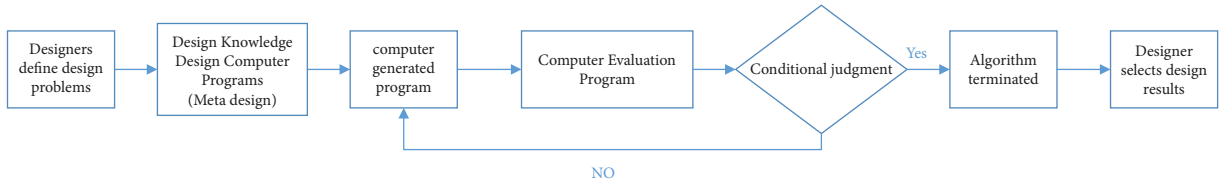

Figure 1: Meta-design—basic design chain.

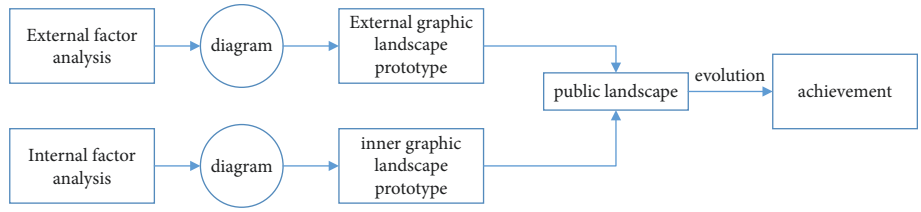

Figure 2: Hierarchical decomposition of landscape system.

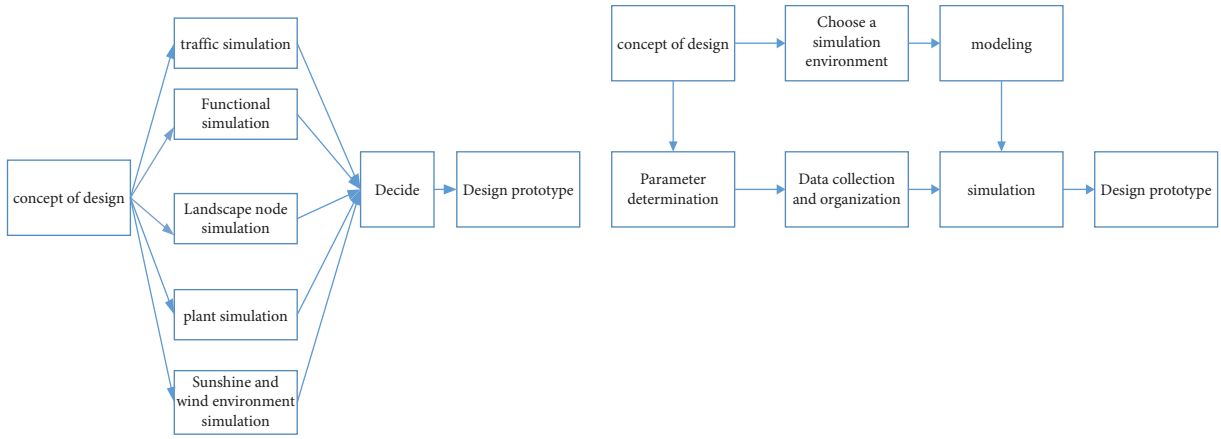

Figure 3: Two ways of digital design.

system based on morphogenesis as the basic theory and digital graphic design method, as shown in Figure 4.

4.2.3. Sunshine and Wind Environment Simulation Optimization Design. The sunshine environment of the site affects the layout of the internal functional system, landscape node system, and plant system to a certain extent, while the wind environment of the site determines the layout of the interior landscape space to a certain extent. By simulating and analyzing the sunlight and wind environment of the original site, it can play a guiding role in the formation of the prototype of the landscape design scheme. After the preliminary plan of landscape design is generated, the sunshine and wind environment should be simulated and analyzed again to check the rationality of the design plan, and the design plan should be optimized and adjusted according to the analysis results to obtain the prototype of the final design plan, as shown in Figure 5.

4.2.4. Generation of Landscape Morphology. After the simulation analysis of the subsystem and the simulation analysis of the sunlight and wind environment, the corresponding design prototype is obtained. Combined with the designer's subjective experience and esthetic concept, the design scheme is subjectively adjusted and optimized to obtain the final design scheme shape, as shown in Figure 6.

5. Landscape Digital Design Practice Based on Morphogenesis

In the digital graphic design logic system, it is suitable to use the graphic concept as the starting point of the design, combine the program algorithm to design the subsystems, and finally find the optimal design scheme through the fitting between the various systems.

5.1. Digital Design Logic Mining

5.1.1. Analysis of Influence Factors of Landscape System. During the whole project development process, there are many factors outside the site that affect the landscape design: local cultural environment, geographical environment, surrounding environment, business distribution, traffic relationship outside the site, sunlight, wind direction, and the owner's functional requirements for the entire park. Among

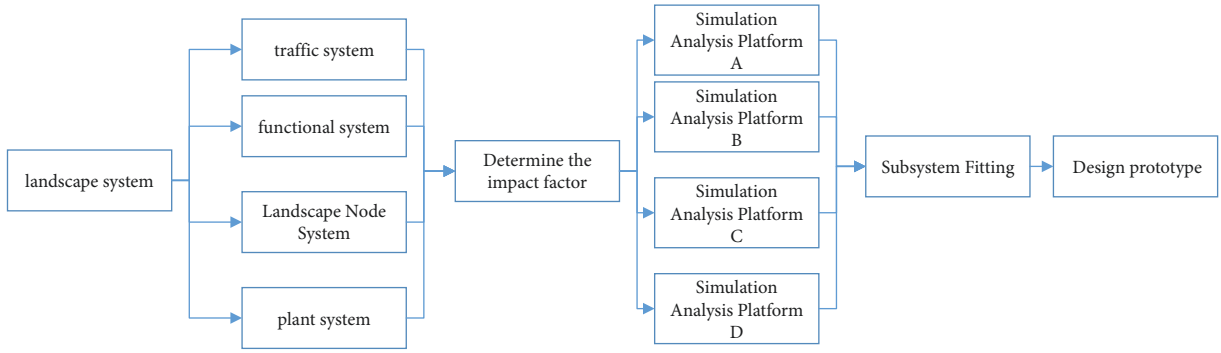

Figure 4: Flowchart of subsystem simulation analysis.

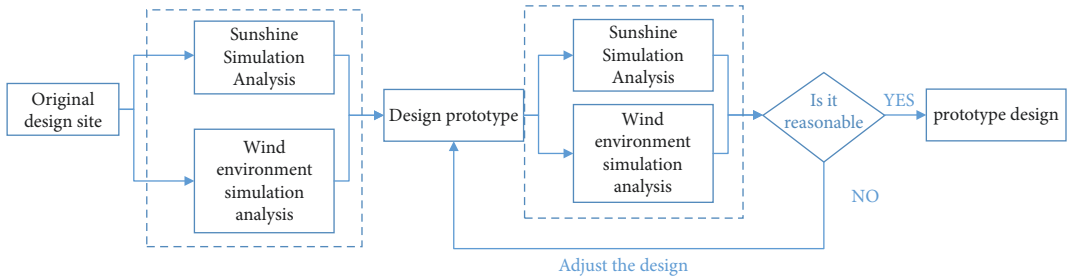

Figure 5: Flowchart of optimal design of sunshine and wind environment simulation.

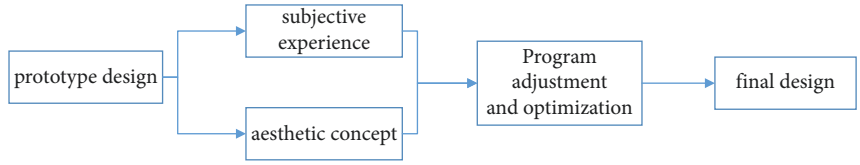

Figure 6: Landscape morphology optimization process.

them, the context and geographical environment will directly affect the extraction of design elements and the formation of spatial texture; the surrounding environment, business distribution, and external traffic on the site will affect the direction of the flow of people and have a direct connection with the internal traffic on the site; the owner's function of the project demand determines the prototype of the functional partition; and the sunlight and wind direction will affect the layout of the interior space of the site and the design of landscape sketches, which will guide the entire design, as shown in Figure 7.

5.1.2. Influence Factor Analysis of Landscape Internal System. During the whole project development process, there are many factors that affect the landscape design inside the site: functional system, traffic system, landscape node system, and plant system. Among them, the functional system inside the site determines the relationship between the functional space and users; the traffic system inside the site determines the flow of people in the park, which directly affects the user's experience in the park; and the landscape node system is affected by the user's viewing experience. The influence of sight line needs to be combined with ergonomics to carry out a reasonable line of sight section design, while the plant system has an inseparable relationship with the landscape effect of the entire park, and the use of plant landscaping has a direct impact on the park landscape, as shown in Figure 8.

5.2. Design Process and Design Results of Digital Design. The diagram of the traffic system diagram process is shown in Table 1. A global coupling path across the site is established as shown in Table 1, representing all possible paths of the site. The east-west direction is the image surface of the site, with fewer openings, retaining the integrity of the interface, and more openings in the north-south direction. According to the opening spacing greater than or equal to 150 meters, too many unnecessary paths should be avoided. As shown in *b* in Table 1, the screening rules are as follows: the connection between the site and the original urban road is too small (<20°) as a redundant road; the connection with the corresponding point on the opposite side is too large (>60°). A plausible semicoupled traversal path is thus generated. As shown in *c* in Table 1, random points are generated in the field to represent the possibility of any position in the field. After testing, the random point is at a certain threshold, which does not affect the final result, but the distribution state of

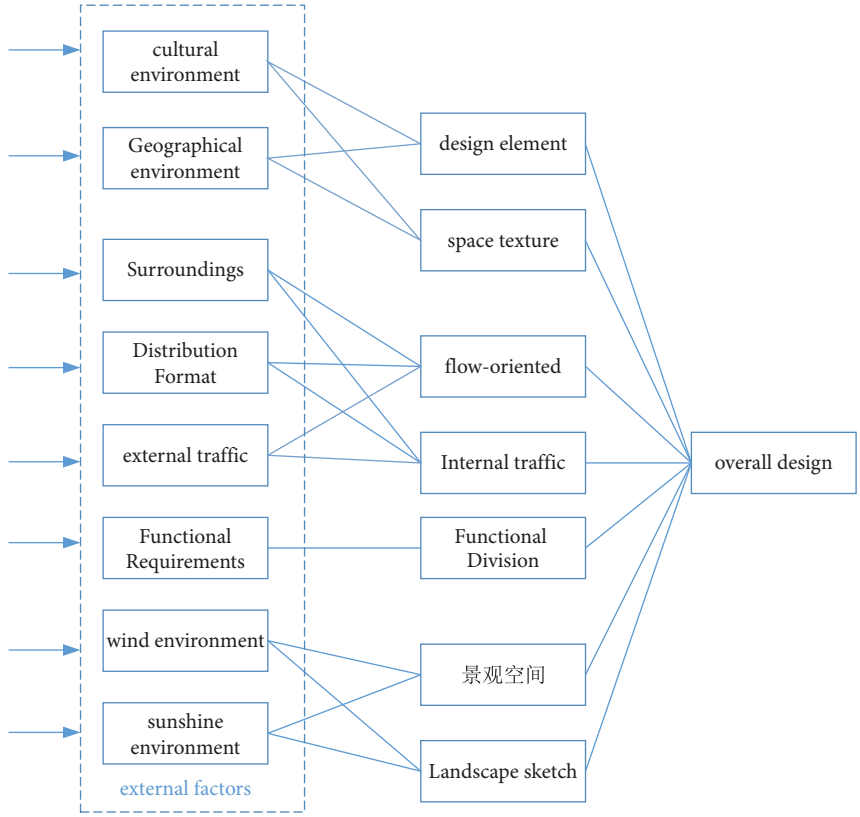

Figure 7: Analysis of external influence factors.

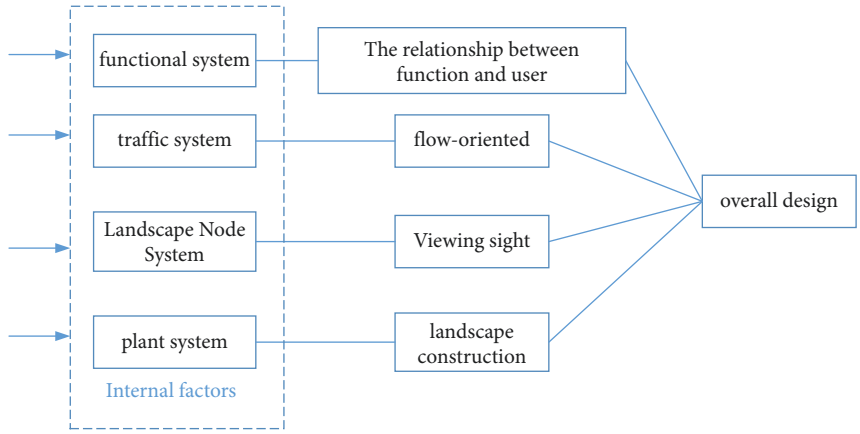

Figure 8: Analysis of internal impact factors.

the random point affects the result. As shown in *d* in Table 1, the filtered semicoupling path is divided into equal parts, and the divided points in turn constitute the path of the path, control point. After testing, the bisection point does not affect the final result within a certain threshold. As shown in *e* in Table 1, the optimal road network is fitted. The path bisection point moves to the nearest random point, and the new bisection point becomes the control point of the path, which generates a new path.

For a comprehensive comparison, result 4 in Table 2 is selected as the path network of the site, the path is taken as the basic structure, it is optimized as the road according to the subjective esthetic feeling, and then, the function and density of each block are judged according to the subjective analysis to generate the road network structure of the entire site. Among them, the center of the structure becomes the central landscape of the site, and the path from south to north through the core landscape is selected as the landscape avenue and the pedestrian entrance.

Table 1: Route optimal graphic design process.

No.	Icon	Description
A	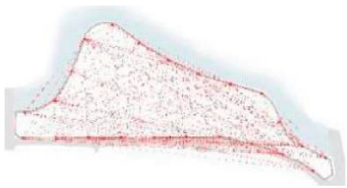	Global coupling network
B		Half-coupling network
c	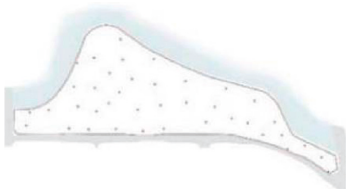	Arrange random points
d	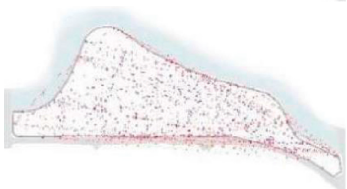	Path control point
e	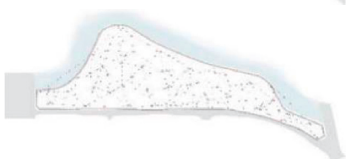	Fit path

Table 2: Comparative analysis of design results.

Serial number	Result 1	Result 2	Result 3	Result 4
Result	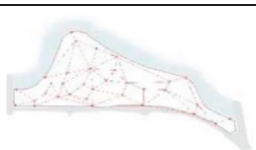	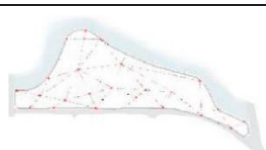	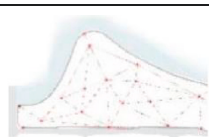	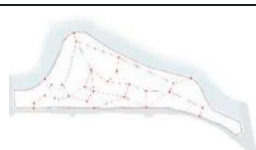
Advantage	The plot division is relatively compact, which is convenient for spatial organization.	The site structure is reasonable, with obvious primary and secondary traffic	There is obvious primary and secondary traffic, and the structure is reasonable.	The central area is obvious. The road runs through most of the site and is closely related to the main road. The site is reasonably divided, so as to generate the optimal path of the plot.
Shortcoming	The road network and plots are too complex, which are not conducive to traffic.	North-south openings are dense and do not meet relevant regulations.	South-facing openings are dense with no apparent center.	—

Table 3: Functional simulation graphical process.

Serial number	A	B	C	D
Icon	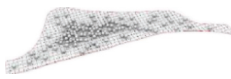	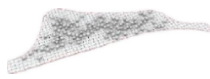	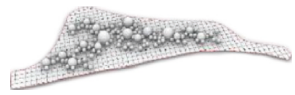	
Illustrate	Initial placement of each functional space	Each function restricts and combines with each other	Primary and secondary functional space fitting	Final fitting result

The diagram of the functional system diagram process is shown in Table 3:

(1) Before selecting a parametric model, the utility of each function point should be individually evaluated, and then each function point should be fit.

(2) When choosing a parameter model, the utility evaluation function of a function point is as follows: $F = \alpha * A + \beta * B + \gamma * C + \delta * D + \theta * E * \ldots * \xi$ Among them, A represents the importance of a function to the crowd, B represents the attractiveness of the function points near the function corresponding to the A parameter, C represents the lighting conditions of the function point in the lot, D represents the accessibility of the function within the site range. E represents the accessibility degree of the function point within the lot range, and F represents the visibility of the function point and the visibility of the surrounding structures.

(3) As shown in a in Table 3, by establishing a parametric model, different functional spheres represent different functional spaces, and each functional space is initially placed according to its own attributes.

(4) As shown in *b* in Table 3, according to the connection between functional spaces, different functional spheres are restricted and combined with each other.

(5) As shown in *c* in Table 3, according to the relationship between the primary and secondary functional spaces, the functional space is fitted by setting different parameters.

(6) As shown in *d* in Table 3, each functional space is fitted to form the final design result.

The simulation of the functional space is carried out through the computer, combined with the adjustment of the subjective intention, and finally, a reasonable design of the functional space is obtained, as shown in Figure 9. Among them, the corresponding open space is arranged along the north side of the waterfront; the south side is arranged with a small outdoor sports space to meet the needs of users; and the middle of the site is arranged with a point-like activity space. Through different point-shaped activity spaces, each space is reasonably connected in series.

The schematic diagram of the landscape node system is shown in the table as follows:

(1) As shown in a in Table 4, in the semiopen space, the corresponding landscape nodes should be placed. Considering that the best viewing angle is 30° for elevation and 30° for looking down when the human body is lying down, the best view should be arranged within this line of sight.

(2) As shown in *b* in Table 4, when the user is walking, the best line of sight is straight ahead, and at this time, it is best to use the garden route as the layout route of the landscape nodes.

(3) As shown in *c* in Table 4, at the resting place of the landscape node, the landscape should be arranged for the shade on the back, and the viewing line should be opened from the front to enrich the viewing experience of users.

(4) As shown in *d* in Table 4, in an open space, the best viewing line of sight for the user is straight ahead, that is, effect landscape.

(5) As shown in *e* in Table 4, when the user is exercising, the range of sight is 30° in elevation and 30° in top view. The layout of landscape nodes should be dominated by trees with upper contour lines.

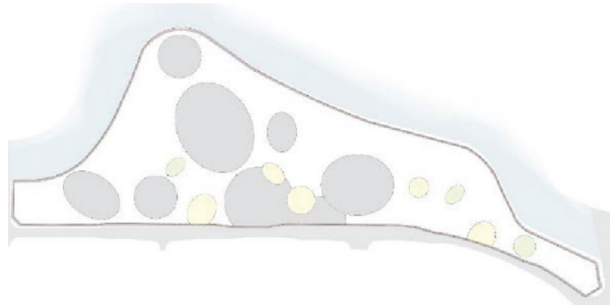

Figure 9: Final functional bubble diagram.

According to the structure of the optimal path in the site and the rational arrangement of the functional space, each landscape node can be preliminarily arranged. After the preliminary arrangement, through the establishment of the corresponding parametric model, the landscape line of sight is reasonably designed. Using the principle of ergonomics, the landscape section design is carried out, and finally, it is fitted with the traffic system to generate the prototype of the shape. The design result of landscape node distribution is shown in Figure 10.

Diagram of the process of a plant system diagram, as shown in Table 5:

(1) As shown in a and *b* in Table 5, since the road network structure and functional space will directly affect the formation of plant space, the site road

Table 4: Sight line design diagrammatic process.

Serial number	a	b	c	d	e
Icon	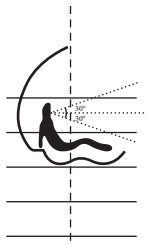		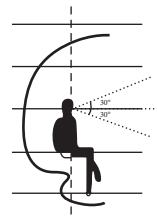	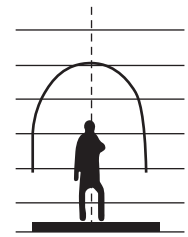	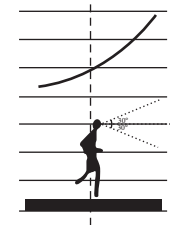
Illustrate	Line of sight when lying down	Line of sight when standing	Line of sight when sitting	Half-open standing line of sight	Line of sight during exercise

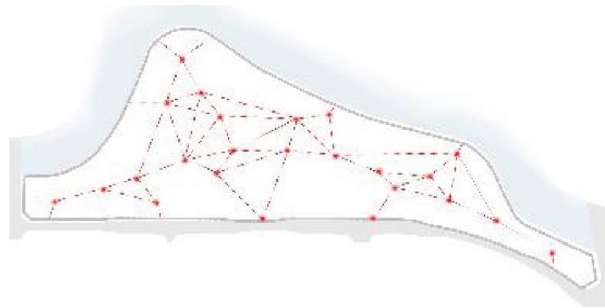

Figure 10: Landscape node distribution results.

Table 5: Illustration of plant space design.

Serial number	A	B	C
Icon		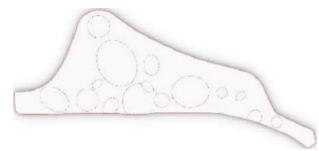	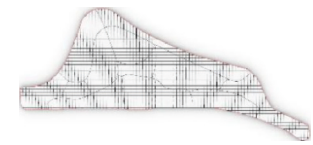
Illustrate	Site road network structure implantation	Site functional space implantation	Site meshing

network structure and functional space are implanted in the site as key influencing factors

(2) As shown in *c* in Table 5, the site is divided into grid units of 10 m × 10 m, the site is divided into grids, and the plant space of the site is divided according to the two key factors of road network structure and functional space

According to the road network structure and the site space model, the corresponding parametric model is established. Combined with the program algorithm, the parameters of the influencing factors are adjusted, and the preliminary arrangement of the site plant system is carried out. Then, through subjective adjustment and optimization, the prototype of the plant system space is generated, as shown in Table 6.

The graphic process of the site sunshine analysis is shown in the table: the light environment of the site affects the layout of the site's internal functional system, landscape node system, and plant system to a certain extent. Through the analysis of the light environment of the site, it can play a guiding role in the overall design of the site. Through parametric technical means, the simulation analysis is carried out on the sunlight environment inside the original site and the site sunlight environment after preliminary design, and the layout of each system is further adjusted. The analysis and simulation process are as follows:

(1) As shown in a in Table 7, the original design site is divided into grids with a unit of 10 m × 10 m, the analysis precision is set to 0.01, and the simulation analysis of the sunshine hours on the summer solstice of the original site is carried out.

(2) As shown in *b* in Table 7, the original design site is divided into grids with a unit of 10 m × 10 m, the analysis precision is set to 0.01, and the simulation analysis of the winter solstice sunshine hours of the original site is carried out.

(3) As shown in *c* in Table 7, the original design site is divided into grids with a unit of 10 m × 10 m, the analysis precision is set to 0.01, and the simulation

Table 6: Plant space design results.

Serial number	A	B	C	D
Icon		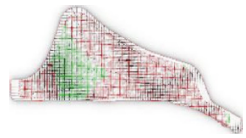		
Illustrate	Site plant space division	Site plant space division	Site plant space division	Final plant space bubble chart

Table 7: Sunshine simulation analysis.

Period	Summer solstice sunshine hours	Winter solstice sunshine hours	Year-round sunshine hours
In situ simulation analysis results	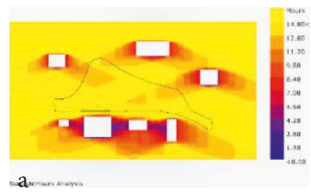	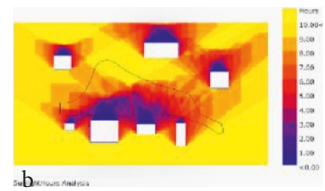	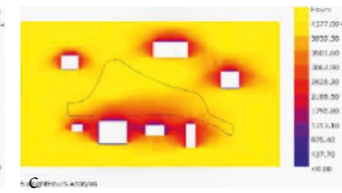
Design site simulation analysis results	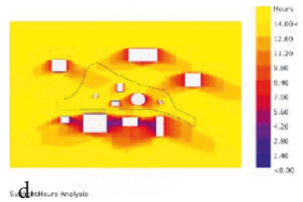	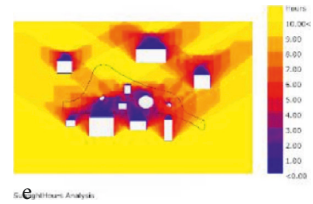	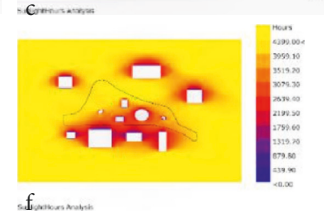

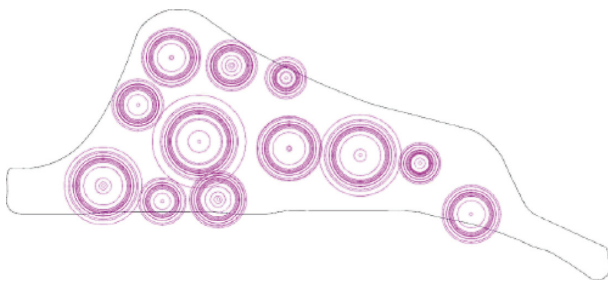

Figure 11: "Cell flow" plane with the central landscape is the core.

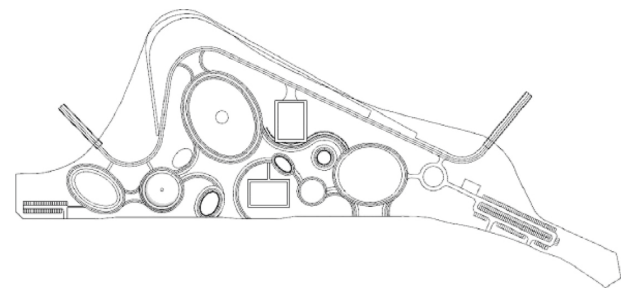

Figure 12: Design floor plan after optimization.

analysis of the annual sunshine hours of the original site is carried out.

(4) As shown in *d* in Table 7, the preliminary design site is divided into grids in units of 10 m × 10 m, the analysis accuracy is set to 0.01, the structures and buildings are modularized, and the summer solstice sunshine of the preliminary design site is determined, that is, time for simulation analysis.

(5) As shown in *e* in Table 7, with a unit of 10 m × 10 m, the preliminary design site is divided into grids, the analysis precision is set to 0.01, the structures and buildings are modularized, and the winter solstice sunshine of the preliminary design site time for simulation analysis is determined.

(6) As shown in *f* in Table 7, with 10 m × 10 m as the unit, the preliminary design site is divided into grids, the analysis precision is set to 0.01, the structures and buildings are modularized, and the annual sunshine of the preliminary design site is checked, that is, time for simulation analysis.

Figure 13: Overall effect diagram.

According to the above simulation design results, with the central landscape as the core, the field of the space unit is constructed, as shown in Figure 11.

The design plane is optimized, combined with subjective adjustment, the overall design plane is fine-tuned, and the design result is shown in Figure 12:

The entire park is a sports park, and combined with the needs of the use of the site, a landmark landscape gallery is designed that integrates sports function and viewing. The final design result is shown in Figure 13.

6. Conclusions

By summarizing the development of digital design, combined with most of the design processes and methods at this stage, this basic design chain of meta-design is summarized. On the basis of meta-design, through subsystem design, the traffic system, functional system, landscape node system, and plant system are designed and optimized, and then, the fitting between each system is carried out. Finally, according to the value judgment and general plane control, the indicators of each space are configured, the basic park design is completed, and it is supplemented and summarized into a feasible digital graphic design system that takes into account both objective factors and subjective experience. At the same time, through the preliminary use of digital design and design in the Xiangyang Dongjin Sports Park project, it guides the design generation process of the park. Compared with the traditional design process, the digital design and design logic system can quickly generate a variety of comparison schemes based on the same logic. Or based on a certain quantitative index to form an optimal solution, the process of continuous trial and error and correction in traditional design is completed in an instant on the digital platform. This dynamic and efficient design system that generates multiple solutions in a short period of time has become a realistic and feasible design framework. In this study, the author has completed the generation process of the park from the design concept to the space formation by using four kinds of meta-designs: subsystem design, wool thread path network simulation, "cellular flow" graphic concept park texture generation, and cellular automata. This design logic system is feasible to a certain extent and has obvious advantages. For the construction of the digital graphic design system of the project and the base itself, the plot design is completed in a complete and reasonable manner, forming a unified park form, and the whole and parts are harmonious and unified.

Data Availability

The dataset can be accessed upon request.

Conflicts of Interest

The authors declare that they have no conflicts of interest.

References

[1] G. Lynn and T. Kelly, *Animate Form*, PrincetonArchitectural Press, New York, NY, USA, 1999.

[2] K. Orff, *Landscape Urbanism and the Stategy of the Earthwork*, Nanjing University Structure. Fabric, To Pography Conference, Nanjing China, 2018.

[3] K. Franpton, *Structure, Fabric and Topography Charies Waldhim.Landscape Urbanism Reader*, Princeton Architecture Press, New York, NY USA, 2004.

[4] C. Higher, "Potraying the urban landscape: landscape in architectural criticism and theory, 1960-present//Mohsen Ciro Naile," *Landscape Urbanism: A Manual for the Machinic Landscape*, p. 26, AA Print Studio, London, UK, 2020.

[5] M. Mostafavi and C. Najle, *Landscape Urbanism: A Manual for the Machinic Landscape*, Princeton Architectural Press, New York, NY, USA, 2015.

[6] G. Di Cristina, *Recovering Landscape: Essays in Contemporary Landscape Architecture*, Princeton Architectural Press, New York, NY, USA, 2020.

[7] J. Corner, "Terra fluxus," in *Landscape Urbanism Reader*Princeton Architecture Press, New York, NY, USA, 2016.

[8] E. Mossop, "Landscape of infrastructure," in *Charles Waldheim. Landscape Urbanism Reader*Princeton Architecture Press, New York, NY, USA, 2016.

[9] V. Anthony, "What is a Diagram anyway?" Skira Editore, Milan, Italy, 2016.

[10] J. Corner, "Landscape urbanism," in *Mohsen Mostafavi and Ciro Majle. Landscape Urbanism: A Manual for the Machinic Landscape*AA Publication, UK, London, 2019.

[11] J. Corner, "Terra fluxus," in *Charies Waldheim.Landscape Urbanism Reader*Princeton Architecture Press, NY, USA, 2020.

[12] G. Lynn, "Architectural curvilinearity," in *Architecture and Science*Academy Press, London, UK, 2021.

[13] K. Frampton, "Towards a critical segionalism: six points for an architecture of resistance," in *The Anti-aesthetic: Essays on Postmodemism Culture*, H. Foster, Ed., Bay Press, USA, 1983.

[14] K. Frampton, "Towards an urban landscape," in *Columbia Doeuments*Columbia University, New York, NY, USA, 1995.

[15] R. Weiler and M. Musiatowicz, "Landscape urbanism: polemics towards an art of instrumentality," in *THE MESH BOOK: Landscape/Infrastructure*RMIT University Press, Melbourne, Australia, 2014.

[16] J. Conner, *The Agency of Mapping: Speculation, Critique and Invention. D.Cosgrace, Mapping*, pp. 231–252, Reakton Books, UK, London, 1992.

[17] K. Frampton, "Seven points for the Millennium:an untimely manifesto," *Architecture Review*, vol. 5, no. 11, pp. 76–78, 1999.

[18] B. V. Nijlsma and C. Bos, *Diagrams interactive instruments in operation*, Conti Tipocolor, no. 23, UK, 2017.

[19] H. Castle, *Territory*, Conti Tipocolor, UK, 2020.

[20] D. Leatherbarrow, "Topographical premises. Landscape and architecture," *Journal ofArchitectural Education*, vol. 57, no. 3, pp. 70–72, 2020.

[21] G. Shane, "The emergence of"Landscape urbanism": reflections on stalking detroit," *Harvard Design Magazine*, vol. 19, 2020.

Hindawi
Scientific Programming
Volume 2022, Article ID 8797953, 10 pages
https://doi.org/10.1155/2022/8797953

Research Article

Design and Research of a Vehicle Approaching Reminder Device Based on ZigBee Wireless Sensor Network

Zhen Li and Shanen Yu

College of Automation, Hangzhou Dianzi University, Hangzhou, Zhejiang 310018, China

Correspondence should be addressed to Zhen Li; lizhen@hdu.edu.cn

Received 20 March 2022; Revised 4 April 2022; Accepted 23 April 2022; Published 9 May 2022

Academic Editor: Jie Liu

In recent years, wireless sensor networks have developed rapidly, and at the same time, they are also an important support for the Internet of Things and have attracted worldwide attention. A wireless sensor network is composed of many self-organized sensor nodes, which provide a good foundation for it. As a wireless communication technology, ZigBee technology can realize energy-saving and high-efficiency wireless communication. Its sensor nodes are usually small computing devices with radio antennas. They are usually equipped with sensors that can detect one or more environmental parameters. The energy is limited. The function is simple. With the development of the Internet of Things and 5G technology, the scope of wireless sensor networks is becoming wider and wider. This article will apply it to vehicle driving. In today's society, more and more people use cars as a means of transportation, resulting in a large number of road traffic every year. The accident caused a large number of casualties and material losses. For traffic accidents caused by these factors, the collision between a car hitting a person and a car is the most common, so the research on how to avoid a car collision is urgent. Among the many factors that cause road traffic accidents, the driver is the main reason. Therefore, the combination of the driver's abnormal driving behavior and the implementation of the vehicle approaching reminder can effectively reduce traffic accidents. At the same time, the vehicle's collision avoidance warning system is also a vehicle. One of the most important content in driving, we also made research. Through the research of wireless sensor network, this paper applies its relatively mature zigBee technology to the devices and systems of vehicle driving, so that the vehicle approach reminder device and anticollision warning system are developed vigorously.

1. Introduction

The wireless sensor network appeared in the 1970s. It was gradually formed with the continuous development of semiconductor technology, information technology, and network technology. In recent years, with the development of the Internet of Things, wireless sensor networks have attracted worldwide attention, and countries have increased their investment in related research [1]. Among them, ZigBee technology is a new wireless communication technology and also an advanced product [2].

The wireless sensor network is composed of sensor technology, microelectromechanical technology, advanced network, and wireless communication end-to-end intelligent computing platform. It has broad prospects. It is one of the most popular researches in the computer field, and it is also a major technology that will change future life. This article will apply it to the research of vehicle collision avoidance warning system [3]. The system can be divided into three modules, namely, signal acquisition module, signal processing module, and execution module. The signal acquisition module includes obstacle detection, distance measurement, and road condition selection [4]. Regarding obstacle detection, this research mainly uses millimeter wave radar and CMOS camera to confirm the existence of obstacles and then uses millimeter wave radar to confirm the location of obstacles and to see obstacles [5]. Whether the object is within the collision range of the vehicle, the millimeter wave radar is used to measure the relative distance between the obstacle and the vehicle. Early warning

technology to prevent vehicle collisions is an important part of vehicle active safety. In practical applications, it mainly analyzes the driving conditions of the vehicle and the traffic environment around the vehicle and provides early warning to the driver of possible road accidents [6]. Then, in order to reduce road traffic accidents, this article has also done a lot of research on vehicle collision avoidance, which is broken down by data collection methods, including machine-based vehicle collision warning, distance measurement-based reminder vehicle approaching device and communication-based vehicle collision avoidance warning; among them, vehicle approaching reminder devices include infrared, ultrasonic, millimeter wave, and laser methods; communication-based vehicle collision avoidance early warning includes DSRC, LTE-V, Zigbee, cellular networks, and other methods [7]. The research on collision avoidance systems is a hot topic today, and will continue to pave the way for future driverless driving [8]. At present, the research of anticollision warning system mainly uses one of the vehicle sensors (ultrasonic, laser, radar, infrared, machine vision, etc.) to detect and identify objects outside the vehicle [9]. Wireless sensor network is a key tool to realize the intelligent perception and interconnection of heterogeneous elements in the physical world. The digital twin system realizes the dynamic real-time interaction between the physical world and the digital world [10–12]. The vehicle approval reminder device based on ZigBee wireless sensor network studied in this paper also provides a certain degree of support for the realization of the digital twin system in the vehicle field.

The focus of the entire research is on the accuracy of signal acquisition, real-time signal processing, accurate obstacle detection, real-time distance tracking, correct road pattern recognition, and organic fusion of received data and finally making the correct decision quickly, so as to avoid collisions and reduce traffic accident [13].

The remainder of this paper is organized as follows. Section 2 presents the methods used in the designed vehicle approaching reminder device based on Zigbee wireless sensor network, which contains theoretical basis, algorithm principle, and the detailed methods. Section 3 is the main research content, which contains vehicle driving road mode selection, model of vehicle approaching reminder device, communication and braking influence factors and algorithm simulation, and evaluation. Section 4 discusses the research results and designs the device software and hardware and data processing module, which is followed by concluding remarks in Section 5.

2. Methods

2.1. Theoretical Basis. Wireless sensor networks are currently an interdisciplinary and highly integrated hot research direction, and they have received considerable attention all over the world. The development of sensor technology, microelectromechanical systems, modern networks, and wireless communication has contributed to the emergence and development of modern wireless sensor networks [14]. The wireless sensor network expands people's ability to collect data, connects the physical data of the objective world to the transmission network, and provides humans with the most direct, efficient and reliable data on the next-generation network. This section is mainly a basic introduction to wireless sensor networks, mainly introducing the architecture, key features, design, and applications of wireless sensor networks [15]. The sensor node is usually an embedded system. Owing to the limitation of size, price, and power, its processing power and storage capacity are relatively small, and the data transmission distance is also very limited [16]. In terms of network functions, each sensor node has the dual functions of collecting and routing data. In addition to collecting and exporting data locally, it must also store, manage, and integrate data sent from other sites and perform certain tasks in collaboration with other sites [17, 18]. The receiver node usually has powerful processing, storage, and communication skills.

2.2. Algorithm Principle. The weighted average method can divide the three components of R, G, and B more reasonably, so as to obtain a more reasonable gray image. In the MATLAB simulation software, the weighted average of the three components of the system function R, G, and B is as follows:

$$f(i,j) = 0.30R(i,j) + 0.59G(i,j) + 0.11B(i,j). \tag{1}$$

The formula expression is as follows:

$$R = \text{mid}\{z_k | k = 1, 2, 3, \ldots, 9\}. \tag{2}$$

The gray value of the gray image is between 0 and 255. In order to better identify the target image and extract the edge, the gray value must be redesigned and set. This is a binarization process. Image binarization is a basic image processing technology. Binarization technology plays a very important role, whether it is compressing image data, extracting edges, or analyzing shapes.

$$g(x,y) = \begin{cases} 255, & f(x,y) \geq T, \\ 0, & f(x,y) < T. \end{cases} \tag{3}$$

2.3. Research Methods. The transmitted signal of millimeter wave radar is as follows:

$$x(t) = \cos(2\pi f_0 t + \phi_0). \tag{4}$$

The received signal of the millimeter wave radar is as follows:

$$x_R(t) = \cos[(2\pi f_0 (t - t_x) + \phi_0)], \tag{5}$$

where: t_x—delay time.

$$t_x = \frac{2}{c - v_x}(R_0 - v_x t). \tag{6}$$

The distance between the car and the stationary obstacle is as follows:

$$R_t = R_0 - v_x t. \tag{7}$$

It can be seen from earlier that the relationship between vehicle distance and delay time is as follows:

$$R_t = \frac{ct_x}{2}. \tag{8}$$

When the millimeter wave radar is working, the continuous waveform emitted by the transmitter will be decomposed into signals when it hits an obstacle in front of it. When the front barrier is a fixed object, the echo frequency received by the receiving end is the same as the frequency of the transmitted signal, as shown in Figure 1.

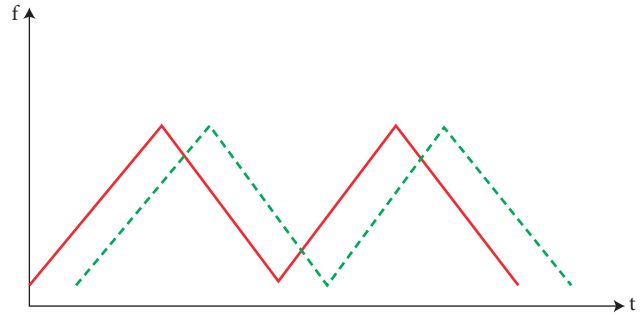

Figure 1: The millimeter-wave radar range finding diagram of stationary obstacles.

3. Results

3.1. Vehicle Driving Road Mode Selection. Nowadays, the four driving modes of the car are quiet and stable pure electric mode (EV), efficient and energy-saving economic mode (ECO), stable normal mode (NORMAL), and surging sport mode (SPORT). When the EV pure electric mode runs at low speed and short distance, the vehicle only works on the power provided by the battery. At this time, the engine does not intervene, the noise of the vehicle is almost equal to zero, and zero emission is realized at the same time. When switching to sport mode, the energy output of the battery will increase instantaneously, the power response will be rapid, and the steering operation will be obvious. At the same time, traction control system and vehicle stability control system will reduce the intervention in driving.

A moving car uses an emergency braking system in an emergency. The car has a certain distance when braking. This distance is called the braking distance. Different cars have different braking distances on different roads. When designing a collision warning, the determination of the safety distance of the vehicle in the execution phase is mainly based on the braking distance of the vehicle. In addition, the braking distance is mainly determined by these road conditions. Therefore, before investigating the braking distance, first determine the road on which the car is traveling. The current investigations of roads at home and abroad are mainly based on the relationship between sliding speed s and adhesion coefficient μ. The maximum μ value is determined using the μ-s ratio graph and the slope of the small slider in the speed range. When installing the sensor, tilt the position of the sensor to the front of the vehicle so that the sensor can detect the road conditions in front of the vehicle during operation, thereby predicting the road conditions ahead and keeping the vehicle in the best position safely. The sensor used to detect road traffic in this article is an ultrasonic sensor. As the waveform attenuates during transmission and along the same path, the attenuation of the waveform is different under dry and wet conditions, resulting in different received waveforms. The waveform received in this way can be used for spectrum analysis of the spectrum difference to distinguish path types. Signal analysis and feature removal are mainly based on time domain, frequency domain, or time-frequency domain. When extracting attributes from the time domain, if the signal is uncertain or the weather changes, or an unknown interference signal appears during transmission, its robustness should be considered. When extracting attributes from a frequency range, it is only for a limited signal interval, so the signal time range must be cut off, which leads to information leakage, and the amplitude, frequency, and phase of the resulting individual spectrum can lead to further errors.

As shown in Table 1 for the impact data of the vehicle braking distance, it can be seen from the table that the driver's reaction and braking distance increase with the increase of speed.

Figure 2 shows the relationship between starting speed and stopping distance under various road conditions after simulation. It can be seen from the figure that the braking distance of a car is different on different roads, and the braking distance is the largest under icy roads.

3.2. Model of Vehicle Approaching Reminder Device. As shown in Figure 3, based on the automatic tracking theory, the Berkeley safety distance model and the hidden Markov model, a collision warning system that can objectively and accurately calculate and assess traffic hazards has been designed, including an improved safety distance model, through the analysis of vehicles The characteristics of different stages of braking and the characteristics of car-following behavior of the vehicle optimize the safety distance model. The risk assessment process of the early warning model is introduced, the problem of low accuracy of risk assessment based on vehicle data is optimized, and the hidden Markov model is used to conduct risk assessment according to the observation sequence of the periodic process. At the same time, an improved safety distance model is used to mark the state of vehicle data, and the K-Average method is used to classify and discretize the observation data. The evaluation of the early warning situation is based on the statistics of the angle of the vehicles on the road section, and according to different direction values, the current scene is regarded as a circular arc, a straight road or an intersection.

According to the car-following theory, this provides a theoretical basis for analyzing vehicle braking and assessing the possibility of collision. As shown in Figure 4, assuming that the driver detects a dangerous situation ahead and the vehicle starts to brake, he should depress the brake pedal with his right foot while the vehicle is running until the vehicle maintains a minimum safe distance from the vehicle.

Table 1: Data comparison of different initial speeds and adhesion coefficients on braking distance.

Initial speed of vehicle (km/h)	Driver reaction distance (m)	Dry asphalt pavement Adhesion coefficient 0.7	Wet cement pavement Adhesion coefficient 0.6	Wet asphalt pavement Adhesion coefficient 0.5	Snow pavement Adhesion coefficient 0.2	Icy road Adhesion coefficient 0.1
20	5.55	2.36	2.73	3.26	7.96	15.85
25	6.95	3.62	4.21	5.03	12.42	24.72
30	8.32	5.15	6.02	7.17	17.82	35.51
40	11.12	9.11	10.58	12.68	31.57	63.08
50	13.88	14.15	16.51	19.79	49.28	98.49
60	16.68	20.33	23.72	28.45	70.95	141.77
80	22.23	36.11	42.11	50.51	126.02	251.97

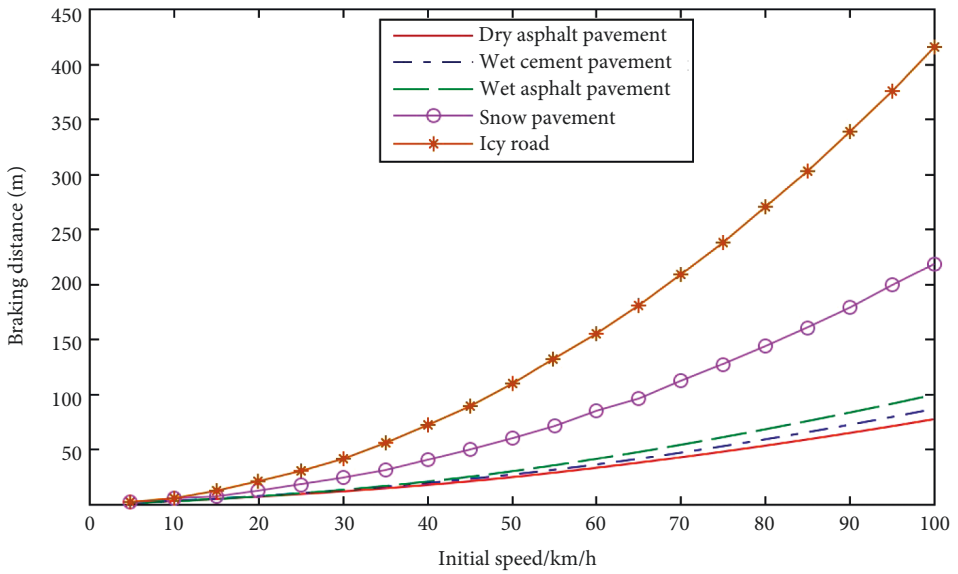

Figure 2: The relationship between the initial speed of the vehicle and the braking distance under different road conditions.

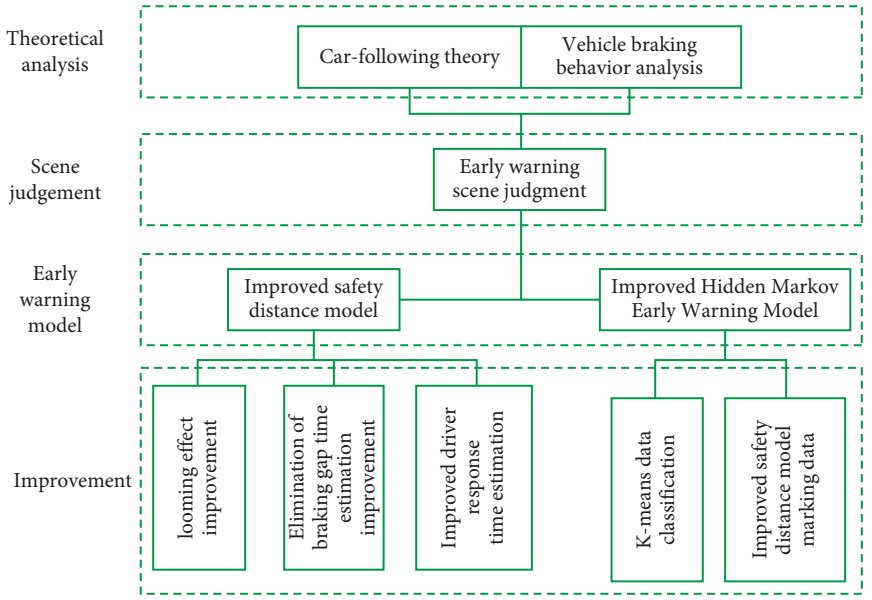

Figure 3: Schematic diagram of collision avoidance warning model.

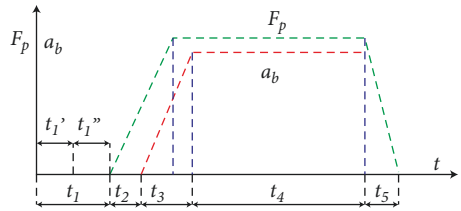

Figure 4: Automobile braking process.

The driver depresses the brake pedal to brake until the vehicle is out of danger and the entire braking process is completed.

3.3. Communication and Braking Influence Factors. V2X communication technology is an important research direction for vehicle intelligence and networking. Among them, the dedicated short range communication (DSRC) standard was mainly formulated in the United States, Europe, and Japan in the 1990s; and C-V2X (Cellular Vehicle to Everything) was developed by 3GPP (Cooperative Project No. 3) Development. Table 2 shows the main indicators of DSRC and C-V2X. The comparison shows that C-V2X has greater advantages over DSRC in terms of transmission distance, delay, and evolution.

The application scenarios of the future intelligent networked vehicles include traffic safety, traffic efficiency, and information services, of which 19 are safety, 12 efficiency categories, and 9 information service categories. Table 3 shows intersection collision warning, frontal collision warning, and a statistical table of 8 typical V2X safety applications such as side collision warning.

The C-V2X standard is composed of the LTE-V2X standard and the 5G V2X standard and can seamlessly develop from LTE-V2X to 5G V2X. The C-V2X standard includes two modes of operation: direct data transmission and mobile communication. The different operating modes correspond to the communication interface PC5 and the communication interface Uu. The PC5 communication interface can support vehicle-to-vehicle V2V communication, V2I vehicle-to-road communication, and V2P human-vehicle communication through the Uu communication interface. Figure 5 shows the network architecture of the DSRC system and the network architecture of the C-V2X system.

First, the braking process is analyzed for the reaction time. The factors related to the process performance can complement the driver's response time. It is often believed that a rear-end collision between two vehicles must be related to the following distance and the driver's reaction time. However, the following distance and reaction time need to be considered. Therefore, in this section, we will analyze the characteristics of the braking behavior process and find the relationship between each driving mode and reaction time. Factors related to response time include braking response time, initial monitoring distance (IHD), and distance (BHD). The statistical data of the relevant variables are shown in Table 4. Behavior 1, Behavior 2, Behavior 3, Behavior 4, Behavior 5, and Behavior 6, respectively, represent the normal driving state that occurs under normal driving conditions, and the emergency events that occur under the conditions of communication behavior, voice information behavior, chat and drinking, yawning, and so on, and give abnormal driving behavioral reaction time and following distance.

Table 2: DSRC and C-V2X key index table.

Key indicators	DSRC	C-V2X
Transmission distance (m)	301~501	1001
Adapt to vehicle speed (km/h)	201	501
Transmission rate (Mbps)	28	501
Delay (ms)	51~101	51
Network deployment	Need to deploy RSU	Base station
Maturity	High	Middle
Evolutionary	Weak	Powerful
Business potential	Low	High

Table 3: Statistical table of typical security V2X applications.

Category	Serial number	Application name	Serial number	Application name
Safety	1	Intersection collision warning	5	Side collision warning
	2	Emergency brake warning	6	Rear collision warning
	3	Reverse overtaking collision warning	7	Early warning of abnormal vehicles
	4	Forward collision warning	8	Vehicle out of control warning

Table 5 shows the significant difference results of different driving behavior variables. The analysis of variance shows that different abnormal driving habits have a significant impact on the reaction time of the driver in the braking process ($F = 8.971$, $P = 0.003 \leq 0.05$), the initial following distance and braking following distance are related to the driver's braking response Time does not significantly affect the relationship.

The nonparametric K-M estimation method is used to estimate the survival probability of different driving behaviors according to the braking reaction time, as shown in Figure 6.

3.4. Algorithm Simulation and Evaluation. The simulation value of the vehicle position prediction result in Figure 7 basically fits the curve of the horizontal position and the longitudinal position. In this test case, the prediction error of the horizontal position is -0.015 ± 0.252 m, and the prediction error of the longitudinal position is 0.089 ± 0.207 m.

The prediction error of the vehicle speed is calculated based on the expected speed and the actual speed. The analysis of the results in Figure 8 shows that in this test case, the prediction error of the lateral speed is -0.028 ± 0.279 m/s, and

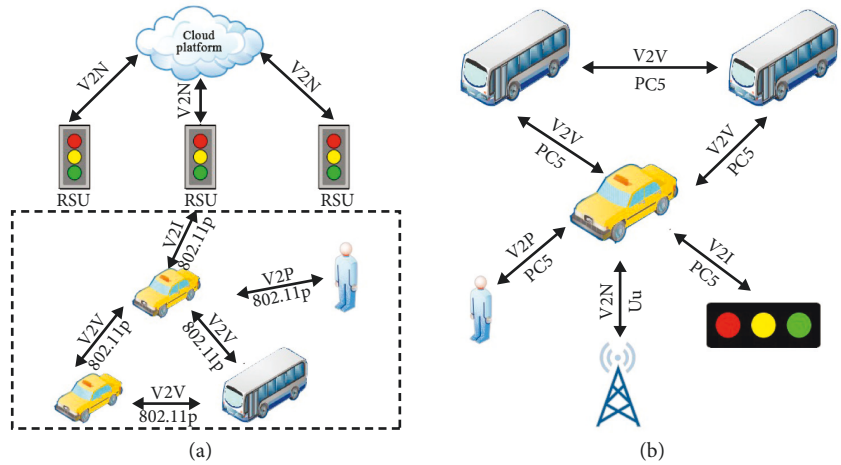

Figure 5: Network architecture diagram of the Internet of Vehicles system: (a) DSR Internet of Vehicles network architecture diagram and (b) C-V2X Internet of Vehicles network architecture diagram).

Table 4: Statistics of related factors under different driving behaviors.

Emergency braking event	Quantity	BRT (s)		IHD (m)		BHD (m)	
		Mean	SD	Mean	SD	Mean	SD
Behaviour 1	55	1.92	0.76	35.04	10.17	18.05	9.96
Behaviour 2	27	2.41	0.83	25.06	13.11	15.21	6.88
Behaviour 3	27	2.72	0.88	30.05	12.08	17.75	10.81
Behaviour 4	35	2.02	0.71	23.08	10.77	14.61	5.77
Behaviour 5	44	2.38	0.91	34.71	14.61	19.71	10.97
Behaviour 6	26	2.21	0.75	34.51	13.67	15.97	7.65

Table 5: Significant difference results under different driving behaviors.

Variable	*F* value	P value
BRT (s)	8.972	0.004
IHD (m)	3.005	0.068
BHD (m)	2.402	0.067

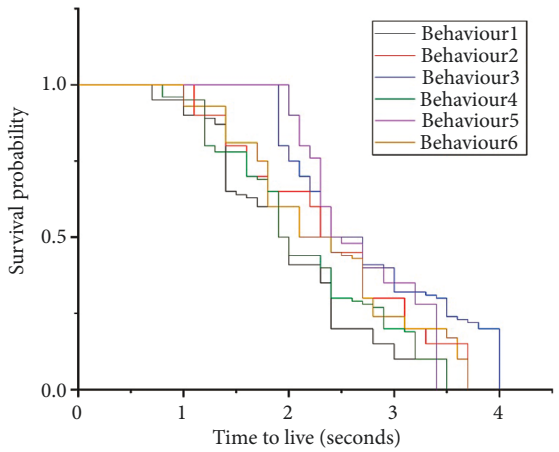

Figure 6: Survival probability curve diagram of different driving behaviors corresponding to braking reaction time.

the prediction error of the longitudinal speed is 0.064 ± 0.231 m/s. The simulation results show that the prediction data of the prediction algorithm has a small error with the actual data, and the prediction results can be used in the vehicle collision avoidance system.

4. Discussion and Design

4.1. Device Software and Hardware Design. According to demand analysis and hardware design block diagram (Figures 3 and 4), it can be concluded that the hardware platform of the whole system is mainly divided into main control module, DSRC wireless communication module, GPS module, CAN bus module and USB module, and power supply module. The main control module selects the i.MX6 DualLite processor produced by Freescale, and the core board integrates the CAN controller required by the procurement system. The communication module adopts the integrated module model THE0-P173 of Cohda Wireless, which combines a wireless radio frequency transceiver module and a protocol converter unit, and can use the 5.9 GHz frequency band to complete DSRC communication. The pins of the NEO-M8U chip are connected in series with the LED light, and the status of the LED light is used to indicate the working status of the GPS module. Steady ON indicates that the module is turned ON but not inserted; flashing indicates that the positioning is successful and GPS location information is sent. The CAN bus module

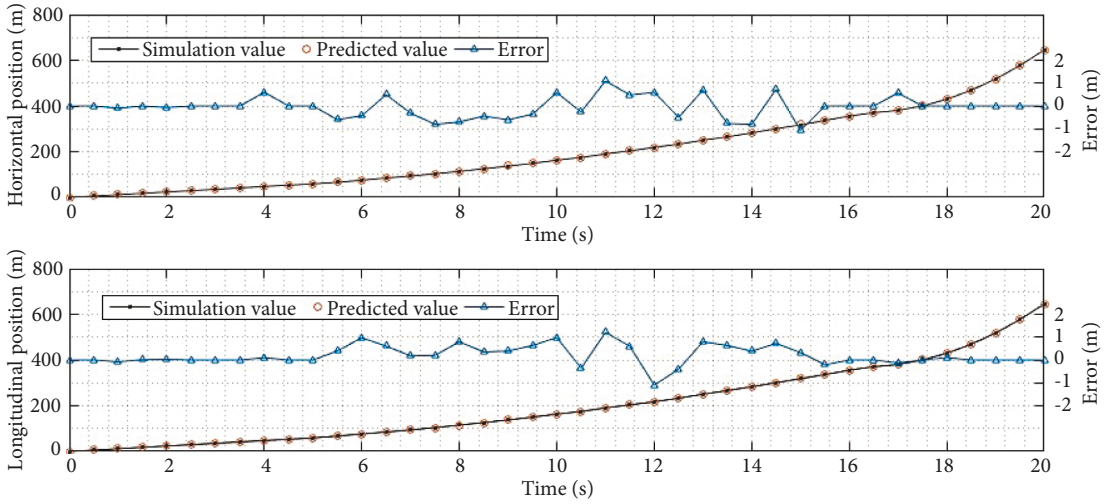

Figure 7: The result of vehicle position prediction: (a) horizontal position and (b) longitudinal position.

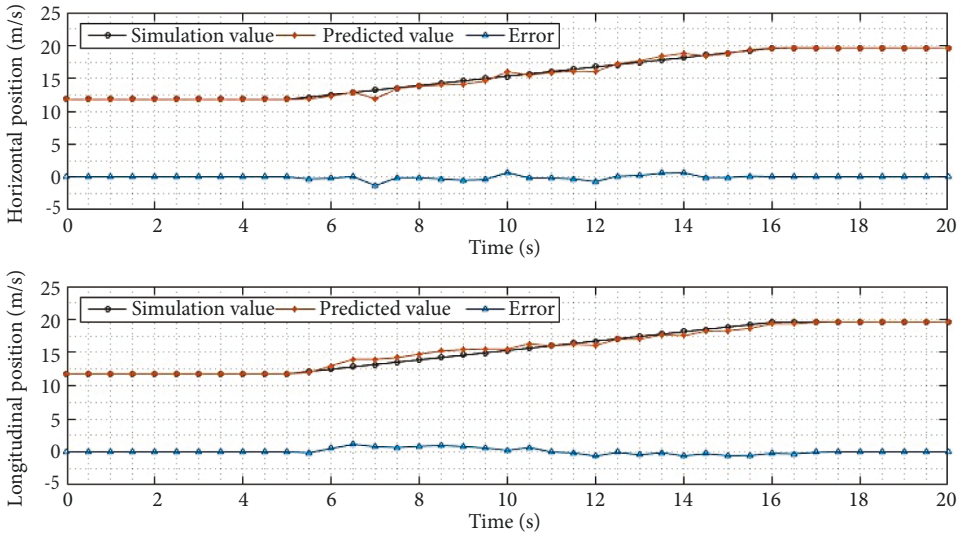

Figure 8: The result of vehicle speed prediction: (a) horizontal position and (b) longitudinal position.

uses the FlexC AN module integrated inside the I.MX6DL microprocessor.

The vehicle collision avoidance warning system software based on V2X communication consists of three parts: middleware program, terminal application program and socket communication. The middle layer application is developed on the basis of the Linux operating system. Its task is to collect vehicle data, convert it into BSM data, and send it within a certain period of time through the V2X communication module. At the same time, it receives BSM data sent by other vehicles. As a high-level application, the user terminal is developed using QT software, which mainly realizes socket communication with the middle layer, realizes data reception, data preprocessing, use of early warning algorithms, and early warning prompts. The program has multiple I/O functions. In order to avoid I/O deadlock, multiple I/O technologies are used, so that multiple I/O functions can be reused in the same query block, allowing the program to process multiple I/O's at the same time. Each I/O request becomes single-threaded time. The query function independently creates a pollfd structure for each monitored file graph, which determines the appearance of the file graph. In the main function, first initialize each module of the system, including the initialization of the GPS module, CAN module, and communication module P1609 layer. The structured data are stored in the StateStore structure. The channel synchronization event triggers the BSM message every 50 ms. The data stored in the structure must be recorded before each transmission, as defined in the BSM message in the compiled message format and must be adapted to the structure of the data storage structure in the StateStore. After the P1609 layer encodes the BSM message, it encapsulates it as a WSM message and sends it to the receiving device. The transmitted data packet can be saved in a log file; the P1609 layer of the receiving device receives the data packet in accordance with the SAE J2735 standard. The BSM message is decrypted, and the received data packet can also be saved in the log file.

First set the serial port GPS parameters such as baud rate and stop bit, open the serial port, and start receiving the serial buffer data stream; after receiving the data, process the data frame starting from $GPRMC, and extract the corresponding fields in the chassis value, such as current time. The vehicle position and angle convert the ASCII code into a real number and then into an unsigned integer to receive and store the vehicle data. When other threads need GPS data, they are read from the memory structure; when the GPS update time expires, they continue to read the next data stream to obtain the latest vehicle position information. After the data are updated, the top-level application initiates an event update every 50 ms, encapsulates the BSM message and sends the request to the WSMP protocol layer [16]. The request contains the required parameters. When the WSMP layer receives a request to send a WSM message, it first checks the validity of the length of the data packet sent by the request. If it meets the specified length requirement, it adds WAVE data element, version and other extended header information values to the WSM message. Encapsulated in the WSM message and sent its MAC layer and PHY layer, after LLC lower layer processing, the data packet is sent to the WSMP protocol layer. The WSMP layer determines whether the packet format is a standard WSM message [19,20]. If the PSID value matches, the hit is successful, and it is sent to the upper unit corresponding to the PSID value, otherwise it is discarded [21].

4.2. Device Signal and Display Processing. The collected signal is sent to the signal processing module for digital processing, which is called digital signal processing (DSP). Digital signal processing is a series of processes such as conversion, filtering, enhancement, and compression of the received signal in the form of a computer or special equipment to obtain necessary or useful information [22].

TMS320F28335 digital signal processor uses 176 pins, and its compression method is PGF/PTP thin four-channel flat package (LQFP). Its main features are as follows: (1) CMOS technology is a high-performance static technology with an instruction cycle of only 6.67 ns and a base frequency of up to 150 MHz; (2) the processor is a 32-bit high-performance processor, and the arithmetic unit is a single-precision floating-point number. (3) The 16-bit words of 256 KB of flash memory, 16-bit words of 34K SARAM memory that can be accessed in a single cycle, and 16-bit words of 1K OTPROM that can be programmed once are all password-protected; (4) With TMS320F281X series processors. In comparison, it contains eight external interrupts, but there is no special interrupt pin; (5) The processor contains two CAN modules (CANTXA, CANRXA and CANTXB, CANRXB), using standard IEEEll49.1 chip scan simulation interface (JTAG). This product uses 12864 liquid crystal displays for visual display. 12864 LCD is a graphic dot matrix liquid crystal display, which is composed of a row controller, a column controller and a 128×64 dot matrix liquid crystal display. It can not only display 8×4 16×16 dot matrix Chinese characters, but also display graphics, realize cursor display, screen movement, and custom icon and sleep mode [23].

4.3. Data Processing Module Design. Based on the analysis of the on-board terminal, the on-board terminal functions are mainly divided into on-board data collection and communication functions, which are mainly used to support data in collision avoidance warning applications [24]. In order to facilitate the retrieval and use of data at the application algorithm layer and weaken the connection between the application layer and the underlying functional modules, this paper designs a data acquisition module between the basic layer and the application layer as an intermediate layer, and the data cache module supplements the data management function [25]. The anticollision software structure is divided into three layers according to the hierarchical structure. The lower layer is a data acquisition module and a communication module, which provides initial data support for the middle layer; the middle layer is a data cache module, which is used to manage the data structure for ease of use and application layer efficient retrieval of data saves program use time; the application layer includes a module that evaluates the driver's reaction time and an adaptive collision avoidance warning module, which uses the collected data to determine the data of the vehicle's early warning situation [26].

The data acquisition module can also be called the data acquisition module, which mainly uses equipment to measure and collect physical data during the driving process of the vehicle. It is the basis for the accurate operation of the collision warning system. The data collection module mainly includes the collection of vehicle position data, vehicle attitude data or CarMaker simulation data.

The main purpose of collecting vehicle position data is to read the NMEA0183 command information provided by the GPS/BDS positioning module through the UART serial port of the processor, and then use the following commands to analyze: $GPRMC, $GPGGA, $GPGSA, $GPGSV, and $GPGGA. GPS-pa required by GPVTG is mainly information such as latitude and longitude, angle, time, date, and altitude. The terminal installed in the car first initializes the accelerometer and gyroscope module; initializes the registers, and then can periodically read the three-dimensional acceleration and three-dimensional angle data of the vehicle. Since the GPS/BDS positioning module updates data slowly, and the data update cycle of the accelerometer and gyroscope modules is short, the data collected by the IMU module can be used to supplement the calculation of the vehicle position data, thereby shortening the update cycle of the vehicle position data. As there are many external factors that affect the accuracy of the test during the actual vehicle test during the test phase. Therefore, it is necessary to carry out the simulation test of the algorithm in real time before the actual vehicle test and improve the error correction of the algorithm.

The communication module also represents a component of the underlying module. The communication module enables the communication between vehicles, the communication between vehicles and roads, and the communication between the terminals installed in the vehicles and the mobile terminals to be carried out stably. Through the network communication module, the vehicle-mounted terminal can

send anticollision warning information to the mobile terminal to realize the sound and light warning for the driver; the vehicle-mounted terminal device can use the Bluetooth communication module and the vehicle-mounted OBE device to receive vehicle body usage data; the vehicle can send the vehicle to the mobile terminal through the V2X communication module. The surrounding vehicles send their own vehicle information, and at the same time receive the vehicle motion data sent by the surrounding vehicles, so as to realize the communication between the vehicles. Owing to the rapid development of the mobile Internet, mobile devices are ubiquitous. Mobile devices can warn drivers not only through visual animation, but also through audio transmission without affecting the driver's visual awareness. The terminal installed in the vehicle calculates the vehicle collision avoidance warning and then sends the warning result to the mobile terminal, and the mobile terminal reminds the driver based on the calculation result of the collision avoidance warning algorithm. If the vehicle-mounted terminal is connected to the Internet through a 3G/4G mobile communication device or WiFi communication device, it can interact with the mobile terminal through the network communication module, send an anticollision warning algorithm, and determine the warning situation from the vehicle to the mobile terminal to the mobile device. At the same time, the vehicle-mounted terminal can also send the traffic data and road information received by the roadside device to the mobile terminal through the network communication module, thereby displaying information out of sight to the driver in advance, improving the driver's field of vision and driving experience.

5. Conclusion

Aiming at the problem of node power constraints in wireless sensor networks, this paper uses the general characteristics of wireless transmission and the temporal and spatial correlation of data collected in the network, and uses energy-saving routing protocols and data compression and aggregation technologies, such as compressed sensing, network coding, and predictive models. Reduce the amount of data collected and transmitted in the wireless sensor network, reduce the energy consumption of the nodes in the network, and alleviate the problem of node energy limitation, and then apply it to the current research status of vehicle collision warning technology. For traditional collision warning algorithms without considering the impact of abnormal driving behavior on the collision warning algorithm, which leads to problems such as incompatibility of collision warning applications, a vehicle-vehicle cooperative collision avoidance warning method based on driving behavior is proposed. In this paper, combined with the emergency braking process of the vehicle, the influence of abnormal driving behavior on the driver's braking reaction time is studied, and the driver's braking response time is simulated according to the driving behavior. According to the software function requirements, this paper designs a collision avoidance early warning software architecture based on layered thinking. The software architecture is divided into three layers, namely the bottom layer, the middle layer, and the application layer. The bottom layer includes a data acquisition module and a communication module, the middle layer is a data cache module and application programs, and the application layer is an anticollision warning module.

With the increase of car ownership year by year, the contradiction between people and vehicles in China's transportation system is becoming more and more serious. As the core technology of developing intelligent transportation system, vehicle road cooperation technology can not only improve the traffic efficiency in the transportation system but also play a key role in improving the safety of people and vehicles in the transportation system. This research plays an important role in promoting the information interaction of vehicle road collaborative system.

Data Availability

The data used to support the findings of this study are available from the corresponding author upon request.

Conflicts of Interest

The authors declare that they have no conflicts of interest.

References

[1] S. K. Baliarsingh, S. Vipsita, K. Muhammad, and S. Bakshi, "Analysis of high-dimensional biomedical data using an evolutionary multi-objective emperor penguin optimizer," *Swarm and Evolutionary Computation*, vol. 48, pp. 262–273, 2019.

[2] Z. Xing, "An improved emperor penguin optimization based multilevel thresholding for color image segmentation," *Knowledge-Based Systems*, vol. 194, Article ID 105570, 2020.

[3] A. Javed, A. Irtaza, H. Malik, M. T. Mahmood, and S. Adnan, "Multimodal framework based on audio-visual features for summarisation of cricket videos," *IET Image Processing*, vol. 13, no. 4, pp. 615–622, 2019.

[4] M. H. Kolekar, "Bayesian belief network based broadcast sports video indexing," *Multimedia Tools and Applications*, vol. 54, no. 1, pp. 27–54, 2011.

[5] M. H. Nasir, A. Javed, A. Irtaza, H. Malik, and M. T. Mahmood, "Event detection and summarization of cricket videos," *Journal of Image and Graphics*, vol. 6, no. 1, pp. 27–32, 2018.

[6] K. Midhu and N. A. Padmanabhan, "Highlight the generation of cricket matches using deep learning," in *Computational Vision and Bio Inspired Computing*, pp. 925–936, Springer, Cham, Switzerland, 2018.

[7] S. Chakraborty and D. M. Thounaojam, "A novel shot boundary detection system using hybrid optimization technique," *Applied Intelligence*, vol. 49, no. 9, pp. 3207–3220, 2019.

[8] A. Javed, K. B. Bajwa, H. Malik, A. Irtaza, and M. T. Mahmood, "A hybrid approach for summarization of cricket videos," in *Proceedings of the 2016 IEEE International Conference on Consumer Electronics-Asia (ICCE-Asia)*, pp. 1–4, IEEE, Seoul, Republic of Korea, October 2016.

[9] M. H. Kolekar and S. Sengupta, "Semantic concept mining in cricket videos for automated highlight generation," *Multimedia Tools and Applications*, vol. 47, no. 3, pp. 545–579, 2010.

[10] T. Clark, V. Kulkarni, J. Whittle, and R. Breu, "Engineering digital twin-enabled systems," *IEEE SOFTWARE*, vol. 39, no. 2, pp. 16–19, 2022.
[11] T. Liu, L. Tang, W. Wang, Q. Chen, and X. Zeng, "Digital-twin-assisted task offloading based on edge collaboration in the digital twin edge network," *IEEE Internet of Things Journal*, vol. 9, no. 2, pp. 1427–1444, 2022.
[12] L. Li, B. Lei, and C. Mao, "Digital twin in smart manufacturing," *Journal of Industrial Information Integration*, vol. 26, no. 9, Article ID 100289, 2022.
[13] R. Hari and M. Wilscy, "Event detection in cricket videos using intensity projection profile of Umpire gestures," in *Proceedings of the 2014 Annual IEEE India Conference (INDICON)*, pp. 1–6, IEEE, Pune, India, December 2014.
[14] M. Merler, K.-N. C. Mac, D. Joshi et al., "Automatic curation of sports highlights using multimodal excitement features," *IEEE Transactions on Multimedia*, vol. 21, no. 5, pp. 1147–1160, 2019.
[15] F. Hajati and M. Tavakolian, "Video classification using deep auto encoder network," in *Proceedings of the Conference on Complex, Intelligent, and Software Intensive Systems 01*, pp. 508–518, Lodz, Poland, July 2020.
[16] G. Dhiman and V. Kumar, "Emperor penguin optimizer: a bio-inspired algorithm for engineering problems," *Knowledge-Based Systems*, vol. 159, pp. 20–50, 2018.
[17] P. Heckbert, "Color image quantization for frame buffer display," *SIGGRAPH Comput. Graph*, vol. 16, no. 3, pp. 297–307, 1982.
[18] G. Joy and Z. Xiang, "Center-cut for color-image quantization," *The Visual Computer*, vol. 10, no. 1, pp. 62–66, 1993.
[19] D. Clark, "The popularity algorithm," *Dr. Dobb's Journal*, vol. 21, pp. 121–127, 1995.
[20] S. J. Wan, S. K. M. Wong, and P. Prusinkiewicz, "An algorithm for multidimensional data clustering," *ACM Transactions on Mathematical Software*, vol. 14, no. 2, pp. 153–162, 1988.
[21] M. Gervautz and W. Purgathofer, "A simple method for color quantization: octree quantization," in *New Trends in Computer Graphics*, pp. 219–231, Springer, Berlin, Germany, 1988.
[22] C.-Y. Yang and J.-C. Lin, "RWM-cut for color image quantization," *Computers & Graphics*, vol. 20, no. 4, pp. 577–588, 1996.
[23] C.-K. Yang and W.-H. Tsai, "Color image compression using quantization, thresholding, and edge detection techniques all based on the moment-preserving principle," *Pattern Recognition Letters*, vol. 19, no. 2, pp. 205–215, 1998.
[24] S.-C. Cheng and C.-K. Yang, "A fast and novel technique for color quantization using reduction of color space dimensionality," *Pattern Recognition Letters*, vol. 22, no. 8, pp. 845–856, 2001.
[25] J. Tou and R. Gonzalez, *Pattern Recognition Principles*, 377 pages, Addison-Wesley, Boston, MA, USA, 1974.
[26] S. Shafer and T. Kanade, "Color vision," in *Encyclopedia of Artificial Intelligence*, pp. 124–131, Springer-Verlag, Heidelberg, Germany, 1987.

Hindawi
Scientific Programming
Volume 2022, Article ID 6556631, 9 pages
https://doi.org/10.1155/2022/6556631

Research Article

Research on the Construction of the Quality Evaluation Model System for the Teaching Reform of Physical Education Students in Colleges and Universities under the Background of Artificial Intelligence

Hao Guo

Chongqing College of Humanities, Science & Technology, Chongqing 401524, China

Correspondence should be addressed to Hao Guo; ym520@swu.edu.cn

Received 31 March 2022; Revised 8 April 2022; Accepted 20 April 2022; Published 9 May 2022

Academic Editor: Jie Liu

With the continuous progress of the times, the reform of physical education teaching in colleges and universities has to be promoted day by day. The most important task in the process of reform is how to improve the quality of physical education teaching. Only by reforming colleges and universities can we transport outstanding talents into the society. It is very important to improve the teaching quality by improving the physical education quality evaluation system. As artificial intelligence technology has been more and more widely used in different fields, various educational administration systems based on information management have been established in various colleges and universities. On the one hand, it has brought great convenience to the management of physical education in colleges and universities and improvement of the efficiency of sports education management, but on the other hand, there are many shortcomings in the process of practical application. For example, the application of the database does not fully reflect its function and convenience, and it is only used at the level of query and statistics. Therefore, a better evaluation system of physical education teaching quality has become the common expectation of all colleges and universities. This paper makes a powerful analysis of the current quality evaluation of physical education in colleges and universities and proposes a method of establishing a basic framework through expert systems, filling in details with the idea of knowledge base and fuzzy sets, and further using a three-layer B/S framework model to design universal teaching quality assessment system. When discussing the requirements, functional framework, and actual development of the teaching evaluation system, the characteristics of the traditional physical education evaluation model are deeply analyzed, and the system's interactivity, flexibility, accuracy, and fairness are emphasized in the implementation process. Object-oriented design and analysis are carried out on the requirements of the system, and finally, black-box testing is carried out to ensure the reliability and correctness of the system logic.

1. Introduction

With the promotion of artificial intelligence to the national strategy, it will have a profound impact on various industries. Colleges and universities should keep up with the trend of the times, seize the pace of the "artificial intelligence" era, and apply "artificial intelligence" to the education of college sports students The reform is in progress, but how should the "artificial intelligence +" road go? This article will discuss the application of artificial intelligence to physical education teaching reform in colleges and universities and build a teaching reform quality evaluation model through artificial intelligence technology. If colleges and universities want to better combine artificial intelligence technology with physical education, they need to have an in-depth understanding of artificial intelligence technology and a clear direction and overall design for how to use it; discuss which technologies of artificial intelligence can be applied to the reform of physical education, what kind of changes will be produced, and how to change; and discuss the application of intelligence in the construction of the quality evaluation model system in the reform of physical education and how to

use intelligence for teachers in the future. Applying to optimize teaching, students using intelligent applications to achieve personalized learning, and teaching administrators using intelligent applications to improve work efficiency, etc., have guiding significance to reduce the burden [1–5]. In this paper, the design and implementation of the physical education quality evaluation system are designed by constructing the artificial intelligence course teaching mode for college sports students. After testing, the system has good applicability.

2. Related Work

Countries around the world pay close attention to teaching reform because education is closely related to the development of economy, society, and culture, and people hope to promote teaching reform through technology. With the help of 47 papers published in the journal Artificial Intelligence in Education, Roll I and Wylie R analyzed the research focus and application scenarios in the field of artificial intelligence in education and predicted two parallel studies in education in the next 25 years according to the research results: first, it is the evolutionary process of physical education, focusing on the existing sports practice, cooperation with teachers, and the diversification of technology; the second is the transformation process of physical education, which should embed sports technology into students' daily life and support students' culture and practice and target. Ozbey N et al. put forward an optimization method for factors affecting students' learning process by analyzing the factors affecting students' learning by artificial intelligence technology. In addition, some scholars have conducted research on the changes caused by the application of artificial intelligence to specific disciplines. For example, Tiffany Barnes and others have conducted research on the application of artificial intelligence to computer teaching, pointing out that artificial intelligence is a more efficient means of promoting computer science learning and teaching. Kanda conducted a practical evaluation of teaching robots in assisting primary school students in English learning, and the results show that teaching robots can promote learners' English learning [6–10]. From the current point of view, teaching reform is a major development and change in education in various countries, especially with the development of artificial intelligence technology, the development path of teaching reform will become wider.

3. Related Theoretical Methods

3.1. Artificial Intelligence. When understanding artificial intelligence, usually we are mainly divided into two parts: "artificial" and "intelligent." "Artificial" refers to man-made and produced by human beings. "Intelligence" focuses on human intelligence. Artificial intelligence is relative to human's natural intelligence. It refers to the use of artificial methods and technologies to develop intelligent machines or intelligent systems to imitate, extend, and expand human intelligence; realize intelligent behavior and "machine thinking"; and solve problems that require human experts, issues that can be dealt with. As a branch of computer science, artificial intelligence is a comprehensive subject covering mathematics, philosophy, computer science, psychology, and other disciplines. The main research fields involve expert systems, virtual reality, image recognition, games, natural language processing, problem-solving, machine learning, intelligent database, language recognition, intelligent robot, pattern recognition, etc. To sum up, artificial intelligence is not only a rising emerging technology but also a multidisciplinary comprehensive discipline. The main research is to use new technical means to simulate the process of the human brain engaged in related thinking activities, that is, to use machines to simulate human intelligence [11]. The application of artificial intelligence technology to the quality assessment of physical education teaching in colleges and universities will accelerate the progress of physical education teaching reform.

3.2. The Theory of Educational Change. Educational change theory points out that education is in constant change, and change is the driving force for the dynamic development of education. Educational change experts RG Havelock and CV Goode divide educational reforms into two categories: planned educational reforms and natural educational reforms: "Planned educational reforms" refer to deliberate educational reforms implemented through certain programs, generally referred to as educational innovations., educational reform, and educational revolution are all planned educational reforms; "natural educational reforms" are the opposite of planned educational reforms and refer to changes that are not planned and artificially implemented. Educational change theory believes that educational change has the characteristics of nonlinearity and complexity. Nonlinearity means that the educational reform is not a linear process from initiation to implementation, and the top-down educational reform from the organizational structure may not achieve ideal results; complexity refers to the object of educational reform—the educational system is nonlinear and dynamic. It is a complex system with both natural and social nature, and it is difficult to predict the development of the system. The nonlinear and complex characteristics of educational reform determine the uncertainty of educational reform. Not all educational reforms are positive and beneficial. The results of educational reform may be "positive" or "reverse." The theory of educational change has important guiding significance for this research: artificial intelligence to promote teaching reform belongs to the category of planned educational reform. Changes in the nature of things are called reforms, but teaching reforms are not a complete denial of traditional teaching but on the basis of inheriting the advantages and wisdom of traditional teaching, optimizing the process of teaching and learning, and innovating teaching and learning methods and means. The process of teaching reform should also follow the "law of quantitative change and qualitative change." Only on the basis of the full integration of artificial intelligence and physical education teaching will physical education be fundamentally changed, and then, the entire physical education structure will be changed. Therefore, the

physical education reform discussed in this study is a process of changing the status and role of various elements of physical education based on the specific teaching environment and the effective support of artificial intelligence, including changing the form of teaching resources, teaching organization, and learning activities, and learning evaluation methods, among which the status and role of each element are important indicators to evaluate the effect of teaching reform [12–15].

4. Construction of Teaching Mode of Artificial Intelligence Course for College Sports Students

4.1. Establish an Evaluation Index System. An excellent physical education quality evaluation index system needs to meet the characteristics of authenticity, specificity, and convenience. Table 1 is based on the summary and arrangement of all the elements of the physical education quality evaluation system, showing a comprehensive set of multidimensional and multilevel three-dimensional evaluation index system [16–18]. The establishment of the entire physical education quality evaluation index hierarchy is mainly established from two aspects: firstly, the current status of the teaching quality evaluation system at home and abroad and, secondly, combined with the country's policy development orientation.

The entire physical education reform evaluation index structure can be divided into three layers: the first layer is the target layer; the second layer is the criterion layer, and there are two factors here: $P = (P1 + P2)$; and the third layer is the indicator layer. This part is divided into two parts according to the two factors of the previous layer, where $T_1 = (t_{11}, t_{12}, t_{13} \ldots t_{19})$, $T_2 = (t_{20}, t_{22})$ [19].

4.2. Design Quality Comprehensive Evaluation Model. If there is a set of factors to evaluate things $U = \{u_1, u_2, u_3 \ldots u_m\}$, V = {v1,v2,v3. . .vm} is a set of decision comments, R is the fuzzy mapping between U and V, and rij($i = 1,2, \ldots,$ m ; $j = 1,2, \ldots, n$) describes the beginning of the ith factor, produces the result of the jth factor of the evaluated physical education teacher and establishes the following fuzzy evaluation matrix:

$$R = \begin{bmatrix} r_{11} & r_{12} & \cdots & r_{1n} \\ r_{21} & r_{22} & \cdots & r_{2n} \\ \vdots & \vdots & \cdots & \vdots \\ r_{m1} & t_{m2} & \cdots & r_{mn} \end{bmatrix}. \quad (1)$$

$A = (a_1, a_2, a_3 \ldots a_m)$ is a very important set of U. When both R and A are known, the fuzzy transformation method can be used to obtain the model $B = A \times R = (b_1, b_2, b_3 \ldots b_m)$.

4.3. Methods of Comprehensive Evaluation

4.3.1. Constructing a Comprehensive Evaluation Factor Set X. A set of excellent physical education quality evaluation system often contains a variety of factors. However, if the factors to be considered are too complicated, it will be difficult to evaluate. For comprehensive consideration, a set of evaluation factors is set up: $X = \{$The content of the lesson preparation is detailed and the teaching attitude is correct; the classroom knowledge is rich, and the priority is clear; help understanding; interact, mobilize the learning atmosphere; teach students in accordance with their aptitude, pay attention to the exercise of ability; be strict with oneself, set an example for students; care for students, deeply loved by students$\}$ [20]. The construction of the evaluation system in this study draws lessons from the hierarchical method of index system construction in intelligent manufacturing project evaluation [21].

4.3.2. Establish Evaluation Set Y. Whether the teaching quality of physical education teachers is good or bad can be reflected through the evaluation set, in which different grades represent the degree of teachers' physical education teaching quality. $Y = \{$excellent, good, fair, poor$\}$, and the evaluation result is reflected by membership degree. The four grade values in the evaluation set Y are determined by a range of values, which are very vague and difficult to calculate accurately. So, in the actual evaluation process, a specific range of values can be used to limit the levels included in Y. Based on the above analysis, the domain of discourse can be set to [50, 100] and then divided into four decreasing intervals. If the obtained scores are placed in the interval [80, 100], the median value of 90 can be taken, that is, the teaching situation of this physical education teacher can be evaluated as " "excellent"; if the obtained grade is placed in the [70, 90] interval, the median value of 80 can be taken, that is, the teacher's teaching situation can be evaluated as "good"; if the obtained grade is placed in the [60, 80] interval, then the median value of 70 can be taken. That is to say, the teacher's teaching situation can only be evaluated as "average"; if the obtained grade is placed in the [50, 70] interval, the median value of 60 can be taken, that is, the teacher's teaching situation is not ideal and expressed as "poor." However, it is actually stipulated that the median value of each achievement interval represents the basis of grade division, and the parameter column vector can be set as $Y = [90, 80, 70, 60]$T. The result is shown in Figure 1 [21].

4.3.3. Establish the Weight Set of Evaluation Factors. Each factor occupies a different key position in the evaluation factor set, that is, the weight is different, so it is very important to formulate the weight of different factors. How to reasonably distribute the weights of each factor determines the accuracy of the evaluation results. The Delphi method is an authoritative method of assigning weights. The core idea of the Delphi method is to anonymously ask experts for their opinions. After sorting and summarizing, they are anonymously passed on to the experts. The experts give their opinions again. An ideal set of weights can be obtained. The evaluation scores given by experts listening to teachers' lectures are used to verify the scientificity of the fuzzy evaluation method. Take two classes in a certain semester as an example. Both classes A and B have 200 students. According to the evaluation of experts, the scores are ranked

Table 1: Hierarchical structure of physical education quality evaluation indicators.

Target layer	Criterion layer	Indicator layer
Physical education quality	Teacher teaching situation	Tl *l* fully prepared before class and serious teaching attitude
		T12 The key points are highlighted and the teaching content is substantial
		T13 reflect the latest achievements, link theory with practice
		T14 teacher-student interaction is appropriate, and teaching methods are flexible
		T15 diverse teaching methods, using modern technology
		T16 strengthen ability training and focus on teaching students in accordance with their aptitude
		T17 care for students and strictly require management
		T18 pay attention to teaching and educating people and be a teacher everywhere
	Course information	T19 comprehensive teaching effect
		T20 course content
		T21 course load

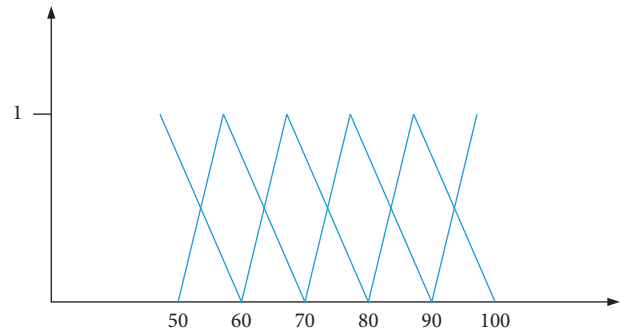

Figure 1: Four standard fuzzy partitions of the universe of discourse $Y = [50, 100]$.

6th and 8th. Randomly check the data in the database of their class, from the beginning of the evaluation to the end of the evaluation, a total of 11 sampling points are selected, and the evaluation results are obtained.

4.3.4. Establishment of Fuzzy Relationship Matrix. All evaluation personnel give objective evaluations based on the daily behavior of physical education teachers in various factors, establish a fuzzy relationship matrix R through induction and sorting, and further obtain the possibility measure. Suppose there are 200 people who participate in the evaluation to give an evaluation to a certain aspect of physical education teachers, of which 140 people's evaluation results are "excellent," 40 people determine "good," and 20 people determine "average," so the result is "excellent." The probabilities are as follows: 140/200 = 0.7; the probability of "good" is 40/200 = 0.2"; the probability of fair" is 20/200 = 0.1"; the probability of poor" is 0/200 = 0.

4.3.5. Obtaining Fuzzy Comprehensive Evaluation Results. The following fuzzy evaluation model based on weight set A and fuzzy relation matrix R can be obtained:

$B = A \times R = (b_1, b_2, b_3 \ldots, b_4)$.

Use.

$S = B \times V = 90 * b_1 + 80b_2 + 70b_3 + 60b_4$.

The obtained value can be used as the final evaluation score of the evaluated physical education teacher. If the fuzzy evaluation matrix of a physical education teacher is

$$R = \begin{bmatrix} 0.418 & 0.348 & 0.201 & 0.033 \\ 0.625 & 0.218 & 0.115 & 0.042 \\ 0.740 & 0.165 & 0.080 & 0.015 \\ 0.365 & 0.424 & 0.169 & 0.042 \\ 0.732 & 0.168 & 0.170 & 0.019 \\ 0.620 & 0.219 & 0.118 & 0.043 \\ 0.431 & 0.358 & 0.202 & 0.034 \\ 0.755 & 0.155 & 0.075 & 0.015 \\ 0.632 & 0.214 & 0.114 & 0.039 \end{bmatrix} \quad (2)$$

$B = A \times R = (0.534, 0.286, 0.146, \ldots, 0.034)$.

Use.

$S = B \times V = 90 * b1 + 80b2 + 70b3 + 60 * b4$.

The comprehensive evaluation value $S = 83.2$ is obtained by calculation. According to the range in the evaluation set Y, it can be known that the teaching quality of the physical education teacher is evaluated as "good."

5. Design and Implementation of Physical Education Teaching Quality Evaluation System

5.1. Overall Design. The most commonly used and widely implemented architectural design pattern includes three parts: presentation layer, business logic layer, and data access layer. The main idea of this architecture pattern is to simplify a complex problem by decomposing it. More importantly, it can efficiently reuse business logic and maintain the connection with resources to further control the development cycle of the system. Then, the physical education quality evaluation system is mainly based on the model of the three-tier B/S architecture.

5.1.1. Model of Three-Tier B/S Architecture. Hierarchical structure is a representative and most classic structure in the software system design process. The three-tier architecture has matured over the years and has been welcomed by developers. This commonly used application architecture is usually divided into three layers: data access layer, business logic layer, and presentation layer.

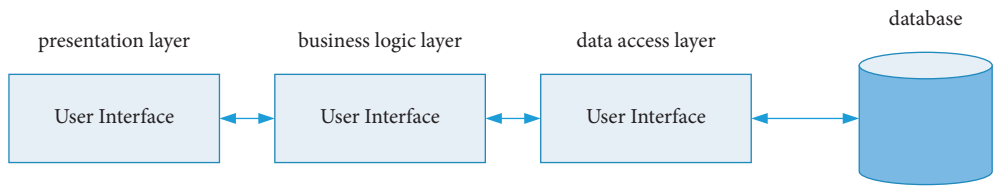

Figure 2: Schematic diagram of three-layer B/S structure.

The presentation layer includes all forms of controls and components involved in the interactive interface, the business logic layer includes how to complete all business rules and logic, and the data access layer includes all database components as shown in Figure 2. Architecture design is the primary task of a system design. A simple and functional system architecture can facilitate developers and users to maintain and expand the system, and the reusability can also be greatly improved. The operability, practicality, extensibility, and development cycle of this system have been improved. The architecture-building process clarifies the concept of packages and describes how packages interact and communicate.

The three-layer B/S mode is extended to the two-layer mode. The graphical operation interface implemented in the presentation layer is helpful for users to digest and master the efficient operation and positioning application services as soon as possible; the business logic layer is in the middle layer, and the purpose is to realize the application method, encapsulate the application mode, and associate the client application with the data service involved. Together, the data access layer is at the bottom, and its main task is to define, query, and modify data and respond to requests sent by application services to data.

5.1.2. System Planning and Analysis. For users, it is very convenient to use the web method. They can log in to the system in the browser to query the results without downloading the client. Taking into account user demands and excellent system processes, an evaluation system should follow the following principles:

(i) Allow users to generate questionnaires to evaluate the survey through a variety of evaluation index systems;

(ii) Allows users to define the importance of any indicator system by selecting models with differences;

(iii) Allow users to select a certain index system to generate any batch of questionnaires;

(iv) Managers can inquire about the progress of the investigation and manage it at any time;

(v) Users can evaluate the questionnaire by using different evaluation models and conduct a comprehensive analysis of the results obtained. In order to meet the above requirements, this system applies a three-tier B/S model and uses the structure in Figure 2 to plan and deploy, using SQL Server as the background database.

The staff controls the whole evaluation process. The evaluation form, the relevant data of the participants, and the relevant data of the people being evaluated are all stored in the SQL Server database. As for how to determine the weight and how to determine the results of the comprehensive evaluation, all these data need to be processed by the staff. It is presented to the server through the web side, and then, the server calls the corresponding program for management and finally delivers the result to the presentation layer. Participating evaluators can fill in the price list on the web page, and the final evaluation results of the evaluators can be viewed via the web page.

5.1.3. Functional Design. The purpose of this system is to provide online teaching evaluation services: evaluators can use this system to evaluate all teachers online and adjust teachers' work through comprehensive evaluation results. This system covers system entry, relevant quantity input, determination of evaluation system indicators and weights, real-time scoring, evaluation result confirmation, evaluation result sorting, evaluation data maintenance, and other functions. The functional frame structure is shown in Figure 3. The relevant function windows can meet the needs of current teachers during the trial operation.

5.2. Evaluation Process. The evaluation process consists of index design, real-time evaluation, data query statistics, and result analysis as shown in Figure 4.

5.3. Front-End System Implementation. The system can be run on the campus network and uses a three-layer structure model. The front desk is mainly developed with Active Server Page program, and Excel is used to query and export the results and print the report.

"Evaluation" includes "student evaluation," "peer evaluation," and "expert evaluation", and "inquiry" includes "personal inquiry" and "department inquiry."

Student evaluation: the purpose is to evaluate all teachers in the current semester and can only evaluate once, and students can also maintain information and passwords.

Peer evaluation: the purpose is to evaluate the teaching situation of other teachers in the same semester. The method is that any course can only be evaluated once, and teachers can also check their own evaluation scores and maintain their personal passwords.

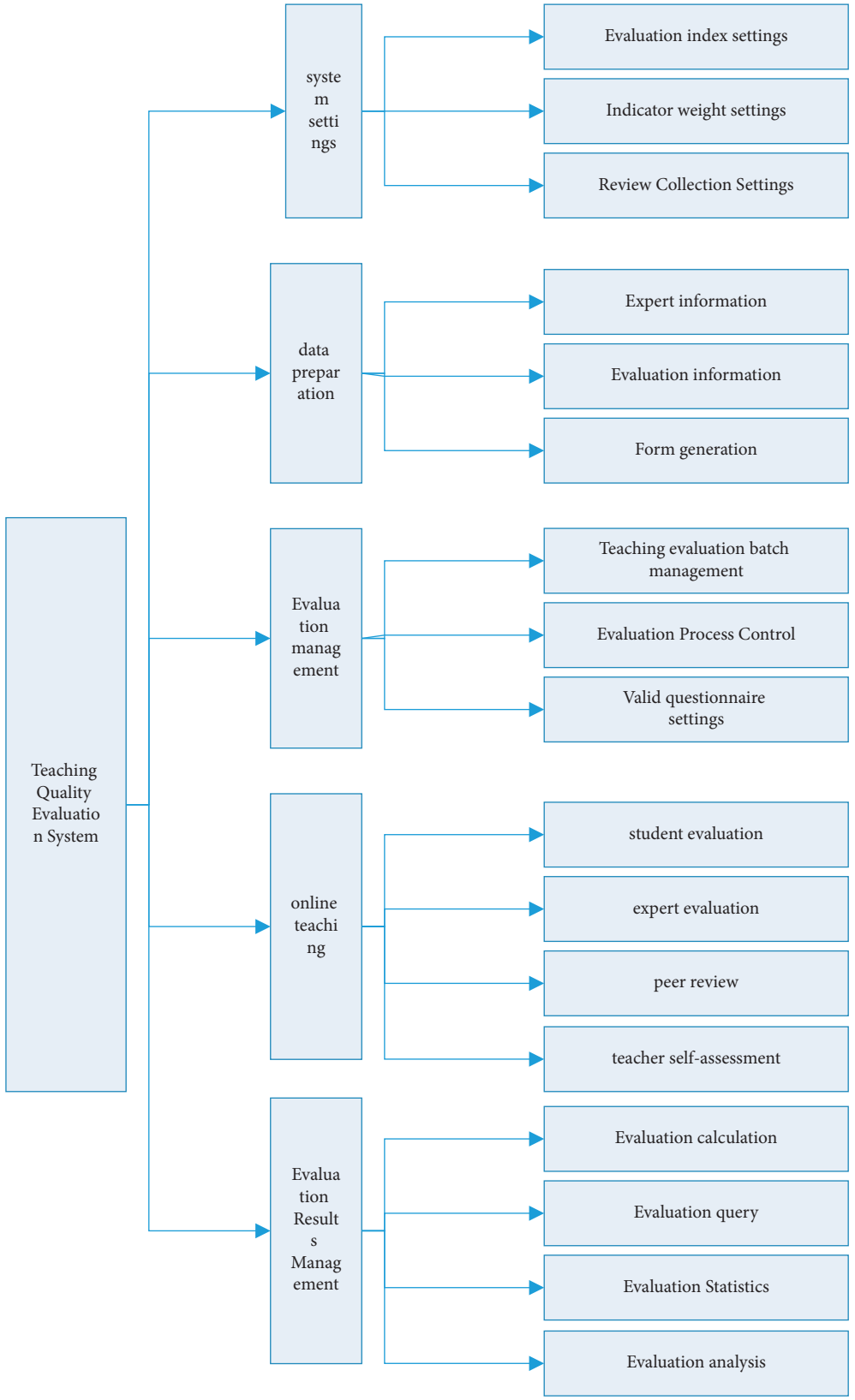

Figure 3: System function block diagram.

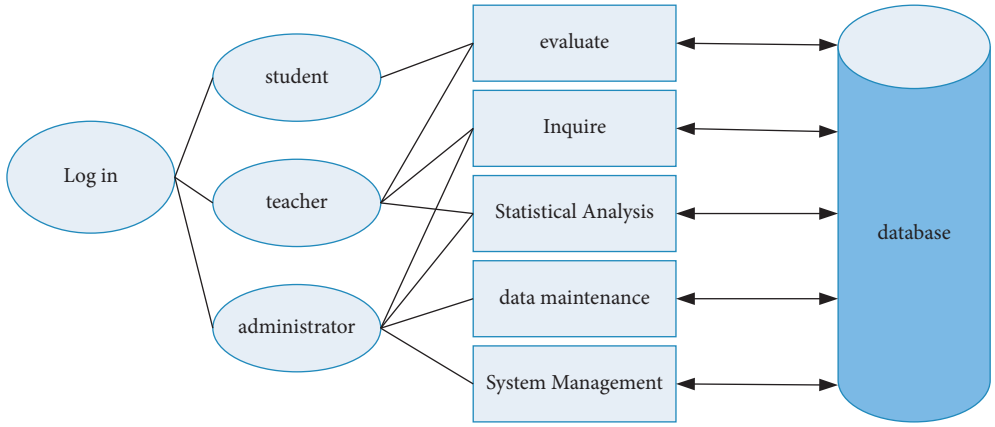

Figure 4: Evaluation process.

Expert evaluation of teaching: the purpose is for experts to evaluate all teachers in the current semester, can only evaluate once at the same time, and can also maintain the personal information and passwords of experts.

5.4. System Test. The system test is carried out in order to achieve two conditions: first to check whether the system can meet the expected expectations and second to check the possible errors during the operation of the system and modify them in real time. The purpose of error checking is to comprehensively retrieve possible errors so that it can be modified before the system works normally to avoid the avoidable difference that may occur after the system works. Generally speaking, software testing generally includes white-box testing and black-box testing. The white-box test is also called structure or logic-driven test. The principle of this test method is to test the program according to the internal structure of the program so as to check whether there is any behavior that violates the design regulations in the product and whether any path in the program can be tested. This testing method regards the test object as an open box. The tester refers to the internal logic structure of the program, designs or selects the example, and tests all the logic paths of the program. After checking the state of the program at each point, to confirm the state that appeared to meet the expected goals. Black-box testing is also known as functional testing or data-driven testing. This testing method is to know all the functions that the product should have in advance and test these functions to verify whether any function can operate normally. During the test, the program is assumed to be a black box that cannot be opened. At the same time, under the condition of ignoring the internal structure and coding nature of the program, the tester can test whether the function of the program can realize the normal operation of the function described by the software function by testing at the program interface and whether the program can reasonably receive input data and output information that meets expectations while ensuring the integrity of external information. The black-box method focuses on the structure outside the program, does not take the internal logic structure of the program into consideration, and tests the interface and function of the software at the same time. The black-box method is a typical exhaustive input testing method. Only by testing all possible situations can all errors in the program be detected by this method. In fact, there should be an infinite number of such tests, and workers need to test not only all legal possibilities but also illegal but possible inputs. In general, white-box testing and black-box testing have different applications. White-box testing is suitable for code rereview and individual testing phases, but in the case of combined testing and system testing, black-box testing is best used. In this case, the method of dividing equivalence classes in black-box testing is used, and the dividing equivalence classes are shown in Table 2.

Table 2: Dividing equivalence classes.

Enter equivalence class	Effective equivalence class	Invalid equivalence class
Date type and length	(1) 8 digit characters	(2) nonnumeric characters (3) less than 8 characters (4) more than 8 characters
Year range	(5) between 1990 and 2050	(6) less than 1990 (7) greater than 2050
Month range	(8) between 01 and 12	(9) is equal to 0 (10) greater than 12
Date range	(11) between 01 and 31	(12) is equal to 0 (13) greater than 31

Examples of selected test cases in black-box testing are shown in Table 3.

Table 3: Select test cases.

Test data	Expected results	Coverage
20020512	Input is valid	(1) (5) (8) (11)
02may512	Input is valid	(2)
20025	Input is valid	(3)
200205012	Input is valid	(4)
20550500	Input is valid	(7) (12)
19890512	Input is valid	(6)

The test reports and results of the teaching evaluation control module are shown in Tables 4 and 5.

Table 4: Test report.

Test plan source	Instructional evaluation control test plan
Testing object	Teaching evaluation control module
Test environment	Windows 10 operating system, SQL Server 2017 database
Testers	JAME
Testing time	2022.3

Table 5: Test results.

Test case name	Test results	Defect severity
Evaluation end-time input test case	Boundary overflow	Middle
Program syntax test cases	Correct syntax, redundancy, few comments	Light

6. Conclusion

As we all know, the content involved in pedagogy at this stage can be mainly divided into three fields, which are the research of basic theory, education development theory, and education evaluation system, and there is a certain internal connection between these three modules. Among them, the education evaluation system has a very prominent position and role in the evaluation of educational research and the actual education system. The primary reason is that it can not only evaluate the level of students but it can also evaluate the level of teachers, truly feedback the state of the education system, and evaluate the education of colleges and universities. It also has the function of detecting the educational reform achievements of colleges and universities, which provides a good basis for improving the educational system. This paper uses the structure of teaching quality evaluation based on the fuzzy overall evaluation method. At the same time, the uncertainty in the system is solved by the method of fuzzy mathematics, and the evaluation index system is constructed by the standard fuzzy division method and the Delphi method. The ambiguity of the data has been improved, and the combination of quantitative and qualitative analysis makes the teaching evaluation system more comprehensive, which greatly improves the authenticity and credibility of the evaluation results. Based on the three-tier B/S system framework, combined with ASP and SQL Server technologies, a web-based teaching quality evaluation system is researched and developed. However, there are still some areas that need to be improved and optimized. For example, in the actual process of software design, developers need to maintain communication with users in order to achieve a better dynamic user interface that meets user needs. It is necessary to further improve teaching methods and provide ideas to improve teaching quality and efficiency.

Data Availability

The data set can be accessed upon request.

Conflicts of Interest

The authors declare that there are no conflicts of interest.

References

[1] A. Carbone, "Assessing distributed leadership for learning and teaching quality:a multi-institutional study," *Journal of Higher Education Policy and Management*, vol. 39, no. 2, pp. 183–196, 2017.

[2] M. Goos and A. Salomons, "Measuring teaching quality in higher education: assessing selection bias in course evaluations," in *Research in Higher Education*, Springer, Berlin, Germany, 2017.

[3] H. B. Yin and W. L. Wang, "Assessing and improving the quality of undergraduate teaching in China: the Course Experience Questionnaire[J]," *Assessment & Evaluation in Higher Education*, vol. 40, pp. 1032–1049, 2015.

[4] J. H. Ford, J. M. Robinson, and M. E Wise, "Adaptation of the grasha riechman student learning style survey and teaching style inventory to assess indiv[J]," *BMC MEDICAL EDUCATION*, vol. 16, 2016.

[5] A. Hajra, F. Limani, and V. Shehu, "Improving Quality of teaching and self assessment using automatic tools[J]," *SEEU Review*, vol. 9, 2014.

[6] N. Pinkwart, "Another 25 Years of AIED? Challenges and opportunities for intelligent educational technologies of the

future[J]," *International Journal of Artificial Intelligence in Education*, vol. 11, no. 2, 2016.

[7] D. McArthur, M. Lewis, and M. Lewis, "The roles of artificial intelligence in education: current progress and future prospects," *i-manager's Journal of Educational Technology*, vol. 1, no. 4, pp. 42–80, 2005.

[8] P. Woolf, Beverly, and C. Lane, "AI Grand Challenges for education," *AI Magazine*, 2013.

[9] E. Popescu and C. Badica, "Creating a personalized artificial intelligence course: WELSA case study[J]," *International Journal of Information Systems and Social Change (IJISSC)*, vol. 18, 2011.

[10] T. Barnes, K. Boyer, and I. Sharon, "Preface for the special issue on AI-supported education in computer science[J]," *International Journal of Artificial Intelligence in Education*, no. 1, pp. 1–4, 2017.

[11] S. Bayne, "Teacherbot: interventions in automated teaching [J]," *Teaching in Higher Education*, vol. 34, no. 4, pp. 455–467, 2015.

[12] N. Goksel-Canbek and M. E. Mutlu, "On the track of artificial intelligence: learning with intelligent personal assistants[J]," *International Journal of Human Sciences*, vol. 55, no. 1, pp. 592–601, 2016.

[13] C. Holotescu, A. Iftene and J. Vanderdonckt, MOOCBuddy: A chatbot for personalized learning with MOOCs," in *Proceedings of the International Conference on Human-Computer Interaction - RoCHI 2016[C]*, pp. 91–94, Matrix Rom, Bucharest, 2016.

[14] N. Ozbey, M. Karakose, and A. Ucar, "The determination and analysis of factors affecting to student learning by artificial intelligence in higher education," in *Proceedings of the 2016 15th International Conference on Information Technology Based Higher Education and Training (ITHET)*, pp. 1–6, IEEE, 2016.

[15] N. Pinkwart, "Another 25 years of AIED? Challenges and opportunities for intelligent educational technologies of the future[J]," *International Journal of Artificial Intelligence in Education*, vol. 26, no. 2, pp. 771–783, 2016.

[16] I. Roll and R. Wylie, "Evolution and revolution in artificial intelligence in education," *International Journal of Artificial Intelligence in Education*, vol. 26, no. 2, pp. 582–599, 2016.

[17] P. Stone, S. Kalyanakrishnan, and S. Kraus, *Artificial Intelligence and Life in 2030[EB/OL]*, 2016.

[18] M. J. Timms, "Letting artificial intelligence in education out of the box: educational cobots and smart classrooms," *International Journal of Artificial Intelligence in Education*, vol. 26, no. 2, pp. 701–712, 2016.

[19] A. K. Vail, J. F. Grafsgaard, and K. E. Boyer, "Predicting learning from student affective response to tutor questions [C]," in *Proceedings of the International Conference on Intelligent Tutoring Systems*, pp. 154–164, Springer International Publishing, 2016.

[20] B. P. Woolf, H. C. Lane, V. K. Chaudhri, and J. L Kolodner, "AI grand challenges for education," *AI Magazine*, vol. 34, no. 4, pp. 66–84, 2013.

[21] L. Li, B. Lei, and C. Mao, "Digital twin in smart manufacturing," *Journal of Industrial Information Integration*, vol. 26, no. 9, p. 100289, 2022.

Hindawi
Scientific Programming
Volume 2022, Article ID 2721618, 10 pages
https://doi.org/10.1155/2022/2721618

Research Article

Improved GCN Framework for Human Motion Recognition

Fen Zhou, Xuping Tu, Qingdong Wang, and Guosong Jiang

College of Computer Science, Huanggang Normal University, HuangGang, Hubei 438000, China

Correspondence should be addressed to Guosong Jiang; jiangguosong@hgnu.edu.cn

Received 25 March 2022; Revised 15 April 2022; Accepted 22 April 2022; Published 9 May 2022

Academic Editor: Jie Liu

Human recognition models based on spatial-temporal graph convolutional neural networks have been gradually developed, and we present an improved spatial-temporal graph convolutional neural network to solve the problems of the high number of parameters and low accuracy of this type of model. The method mainly draws on the inception structure. First, the tensor rotation is added to the graph convolution layer to realize the conversion between graph node dimension and channel dimension and enhance the model's ability to capture global information for small-scale tasks. Then the inception temporal convolution layer is added to build a multiscale temporal convolution filter to perceive temporal information under different time domains hierarchically from 4-time dimensions. It overcomes the shortcomings of temporal graph convolutional networks in the field of joint relevance of hidden layers and compensates for the information omission of small-scale graph tasks. It also limits the volume of parameters, decreases the arithmetic power, and speeds up the computation. In our experiments, we verify our model on the public dataset NTU RGB + *D*. Our method reduces the number of the model parameters by 50% and achieves an accuracy of 90% in the CS evaluation system and 94% in the CV evaluation system. The results show that our method not only has high recognition accuracy and good robustness in human behavior recognition applications but also has a small number of model parameters, which can effectively reduce the computational cost.

1. Introduction

Computer vision technology is a key link in the realization of artificial intelligence, and its emergence has given artificial intelligence great potential in visual perception. Among them, human action recognition is the most challenging technology in computer vision. The implementation of this technology can add to intelligent applications such as pedestrian following and behavior analysis. The most widely researched human behavior recognition methods are based on the human skeleton and, of course, image-based human behavior recognition methods. Human skeleton-based and image-based approaches are very different [1–4]. Skeleton-based methods take human skeleton recognition data as input, focus on analyzing the depth, spatial and temporal information of human skeletal joints, and then combine all features to achieve a behavior prediction result. Compared with image-based methods, human skeletal data are denser and reduce the computational cost by replacing a large number of pixel points with dense skeletal data. The skeleton-based action recognition method also performs better in the working environment of multiple targets and complex backgrounds [5–7].

Traditional skeleton-based methods rely on skeletal joint trajectories, with all method models based on recurrent neural networks of skeletal joint point data [8–11]. Some researchers would prefer to adopt deep neural network models, for which there is already relevant literature demonstrating their substantial advantages as well as their shortcomings. The skeletal data distribution is rather fragmented, and each skeletal joint point data are not locally linked. Therefore, for deep neural networks, a separate neural network needs to be tailored to accommodate the structured skeletal data to coordinate with all the skeletal joint point data [12, 13].

In the deep recurrent network model, only the connections in the feature point space can be analyzed, and the connections between features at the temporal level cannot be obtained. To solve this problem, researchers in the literature [14, 15] used a long short-term memory network (LSTM)

[16] to feature extraction from skeletal data, where the authors first divided the skeletal data into slices, each corresponding to an individual LSTM unit, and merged all. Such an architectural design improves the model's spatial perception of the skeletal data. However, this method suffers from the manual architecture predetermined to the rule limitation, which reduces the generalization ability and robustness of the network [17]. Considering the spatial and temporal features of skeletal data, the literature [18] introduced a graph convolutional network, which breaks the limitation of 2-dimensional data and can handle any graph structure. It transposes the computation of graph convolutional network to skeletal nodal data, which can dimensionally integrate the connections between spatial feature points. The literature [19] presented a spatial-temporal graph convolutional neural network based on the previous study, which can represent each skeletal data point in a graph structure and then perform feature extraction in a graph convolutional pattern as a way to obtain the spatial features between skeletal joint points [20–22]. In addition, the model adds a temporal convolution unit to integrate the temporal links between skeletal joint points, estimate the trajectory of skeletal joints, and finally predict the class of behavior [23].

Based on preliminary research and experiments, this paper proposes the Inception-ST-GCN (IST-GCN) method, which aims to reduce the complexity of building the neural network architectures while capturing the global information of the graph. In this paper, a tensor rotation module will be added to rotate the graph dimension to the RGB dimension and use the one-dimensional convolution Conv 1×1 to capture the global information afterward. A new inception layer multiscale temporal convolution filter is added to divide it into four branches with different temporal perception domains to capture richer temporal information and greatly decrease the volume of model parameters. The IST-GCN method achieves a compact and efficient network. To test the effectiveness of the method in this paper, we perform experimental validation on the public dataset NTU RGB + D. The results show that the number of parameters of the method in this paper is greatly reduced compared with the original ST-GCN model, and the accuracy and precision of action recognition are greatly improved.

The remainder of this paper is laid out as follows: Section 2 introduces the construction of the basic network and the principles of mathematical equations. Section 3 details the principles and implementation procedures related to the improved human action recognition network. Section 4 presents the relevant experimental datasets and analysis of the results. Finally, Section 5 reviews our findings and reveals some additional research.

2. Basic Network

Through our preliminary examination, we apply the graph convolutional neural network as the base network, and its network structure is shown in Figure 1. This network is an upgrade for the graph convolutional network, aiming to optimize the perceptual domain of the graph convolution and increase the joint of the graph convolutional network for the feature relations at the temporal level. The main purpose of this network is sequence encoding the skeletal data and predict the joint behavior by the spatial features and temporal associations between skeletal joint points. For skeletal feature acquisition, we usually use the OpenPose [24] algorithm to localize the human body using 25 skeletal points and the connections among different skeletal points as human joints. The input is usually a video sample in AV format, and each frame of the sample video corresponds to this set of joint coordinates. The OpenPose algorithm can split and resolve each set of joint coordinates and map them to each skeletal unit map node of the human body, using the joints and the edges of the human body as boundaries to build a complete spatial-temporal map. In other words, the input of OpenPose can also be understood as a set of joint coordinates of skeletal points in the same way as the 2-dimensional pixel intensity vector input of the convolutional neural network. To obtain a wider range of information, the graph convolutional network is then stacked and all outputs are then fed into the classifier in parallel.

The input in Figure 1 is a fixed skeleton sequence, assuming that T represents the constituent sequence of the total number of skeletons, V represents the number of skeletal joints, and $G = (N, E)$ denotes the set of constructed skeleton spatial-temporal sequences, where $N = \{v_{ti} | t = 1, ..., T, i = 1, ..., V\}$ traverses the skeleton joints obtained along with all-time sequences, and v_{ti} denotes all nodes. E denotes the set of connections between joints, and consists of E_T and E_S. An arbitrary human skeleton joint (i, j), $E_S = \{(v_{ti}, v_{tj}) | i, j = 1..., V, t = 1, ..., T\}$ denotes the composition of skeleton intra-joint connections within time t. The subset of intra-skeletal connections E_S is divided into K disjoint regions in the center of gravity rule and is represented using the adjacency matrix encoding $\widetilde{A}_k \in \{0, 1^{V \times V}\}$. $E_T = \{(v_{ti}, v_{(t+1)i}) | i = 1..., V, t = 1, ..., T\}$ denotes the union of connections between all skeletal joints in a continuous time series. The fusion of the above features results in a sequence diagram that can be extended in the spatially mapped temporal dimension.

The literature [25] optimized the spatial submodule of the spatial-temporal graph convolutional neural network and proposed the following graph convolution equation:

$$
\begin{aligned}
f_{\text{out}} &= \sum_{k}^{K_s} (f_{in} A_k) W_k, \\
A_k &= D_k^{(-1/2)} \left(\widetilde{A}_k + I\right) D_k^{(-1/2)}, \\
D_{ii} &= \sum_{k}^{K_s} \left(\widetilde{A}_k^{ij} + I_{ij}\right),
\end{aligned}
\tag{1}
$$

where $\widetilde{A}_s$ denotes the adjacency matrix of internal connections of skeletal nodes, I denotes the unit matrix, K_s denotes the size of the convolution kernel in spatial dimensions, and W_k denotes the training weights. The temporal convolution module is $1 \times K_t$. In 2D graph convolution, and the perceptual field of the convolution kernel is not considered when operating (C_{in}, V, T) in the (V, T) dimension, where K_t denotes the number of frames.

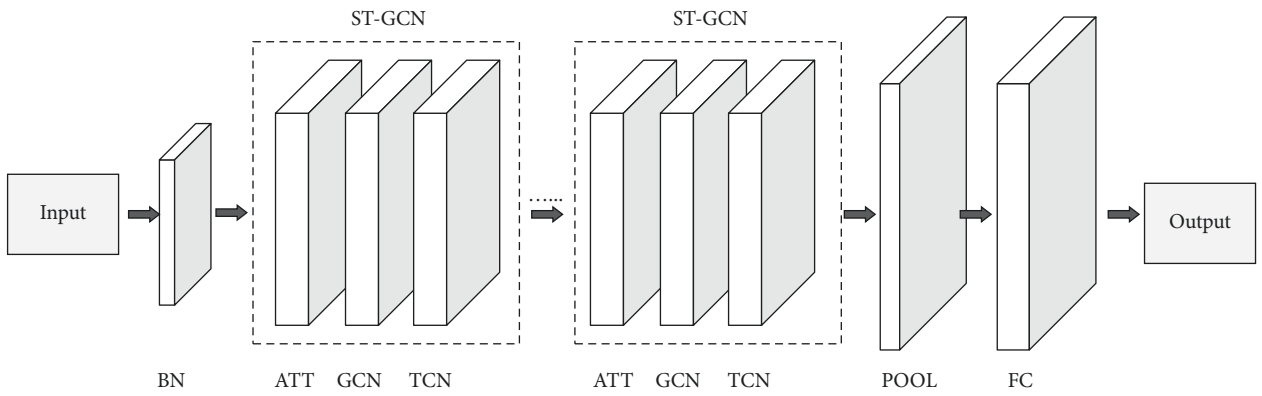

Figure 1: ST-GCN network.

The graph structures in graph convolution are predefined, and to increase their adaptability, the literature [26] uses a fixed adjacency matrix and proposes an adaptive graph convolution formula as follows:

$$f_{\text{out}} = \sum_{k}^{K_s} f_{in}(A_k + B_k + C_k)W_k, \tag{2}$$

where B_k denotes the parameters learned in training and C_k denotes the connected vertices determined with the over-similarity function.

3. Improved Action Recognition Network

The spatial-temporal graph convolution model uses a predefined structural graph as a topological constraint to achieve the ability of different time-step graphs to share the same topology, and such a structure leads to the inability of the graph task to fully capture the relevant features of the hidden joint layer. To solve this problem, our most common approach is to build a regional neural network using a local perceptual domain as the starting point and a small-scale graph task in the experimental region. This can easily produce global information omission. To simulate the principle of computation of pixel points by convolutional neural networks, each graph node and adjacent graph nodes become the key nodes for graph convolution computation in the graph convolution task. Considering the problem of density heterogeneity and narrow local structure between neighboring nodes, in our improved network, we employ node features of fixed size for feature learning in the temporal dimension, selectively ignoring the size of cluster features, and being able to capture more features in the temporal dimension. Therefore, we present the inception spatial-temporal graph convolutional network (IST-GCN), which applies the inception structure to some network layers as a way to reduce the model parameters, broaden the network width, and enhance the robustness of the model.

3.1. Inception Module. The inception module is a sparsity structure proposed in 2015, which has excellent feature expression capability and local topology capability. When the image is input, the pixel point population is involved in a series of convolution operations and pooling operations to obtain features at different scales from different scales of convolution kernels. All the output results are taken for parallel processing to filter out the best image features. The original structure of inception is shown in Figure 2. Its network structure mainly contains three scales of convolutional kernels and a 3×3 pooling, through which a combination of 1, 3, and 5 convolutional kernels can fully acquire large-scale sparse features and small-scale nonsparse features. Such structures not only increase the network width but also increase the adaptability of the network to different scales. Finally, all features are synthesized by a concatenation operation to obtain the nonlinear properties of the features.

3.2. Graph Convolutional Layer Improvement Strategy. Our proposed IST-GCN model originates from a two-part optimization of the spatial-temporal graph convolutional network. The first part is to optimize the graph convolutional network layers; the second part is to add the inception layer. In the graph convolutional layer, the original model aims to obtain spatial location information between the human skeletal joint points to achieve the representation of the joint points. It should start from the initial neighboring nodes to build up a local perceptual domain, in which a large number of sample nodes are generated. Although many false samples are generated at this point, adding topological angle restrictions in the subsequent process of filtering the sequence in Euclidean space can filter the false samples. When all sample nodes are in Euclidean space, all sample nodes can be considered as point from the global level view, and the sequence of points is considered as a one-dimensional vector. In this case, to capture a large number of sample node features, a large-scale graph convolution sum is required, whose size is consistent with the number of nodes. To properly solve this problem, we propose a tensor rotation strategy. We add a tensor rotation module, which we call Rotate tensor GCN (R-GCN), at the beginning and end of the graph convolution layer. The detailed network structure is shown in Figure 3.

By the action of the tensor rotation module, each sample node can share the same set of identical topological matrices,

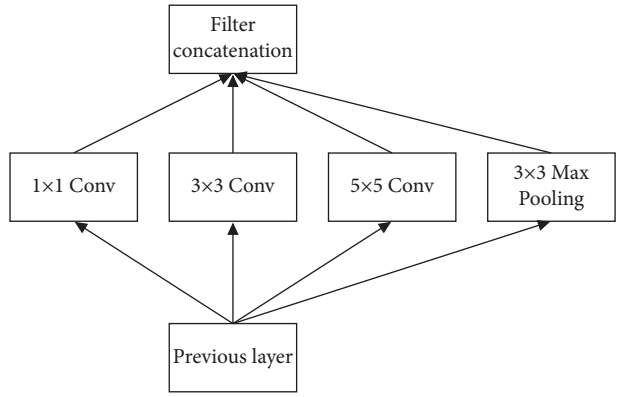

Figure 2: Inception network.

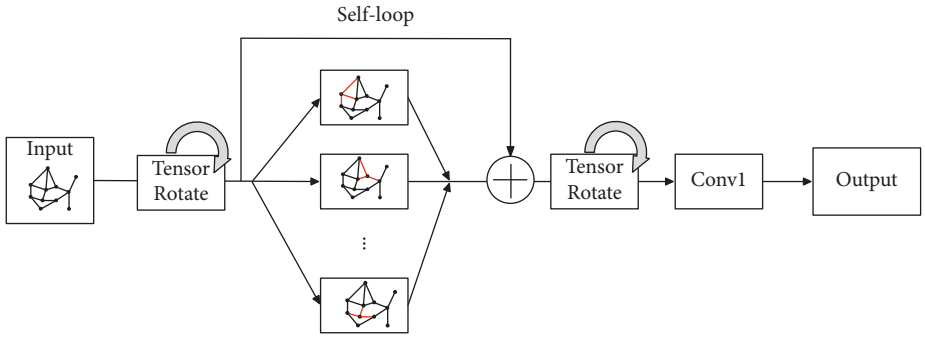

Figure 3: R-GCN network.

and all nodes can participate in the process of capturing global information. Taking human nodes as an example, each graph contains 25 nodes, and in the fully connected layer, we choose a filter of size 25. The rotation tensor module will rotate a tensor according to the different nodes separately so that the dimensionality of the nodes and the dimensionality of the channels remain the same. By tensor rotation, the predefined topological matrix is discarded and the global features are learned adaptively according to the self-cycling unit for joint relevance. Finally, the global information is integrated through the tail-Conv 1×1 dimensionality reduction. Such a structural design can effectively reduce the use of higher-order polynomial estimation layer by layer to capture higher-order features, thus achieving a reduction in the number of parameters.

3.3. Inception Layer Design Strategy. We consider using the inception structure to broaden the spatial-temporal graph convolutional network because of the sparse structure advantage of inception. More feature information can be obtained by the layout of the sparse structure while avoiding the increase in the number of parameters. We refer to the optimization process of inception from V1 to V4 and discover the one-dimensional convolutional dimensionality reduction method [27–29]. We are building the inception time convolution network (I-TCN), and the expansion of parameters is exacerbated by the exponentially growing expansion coefficients in the time convolution layer to widen the network. In contrast, the inception tiling structure is incremented according to layers, and each branch is preceded by adding Conv 1×1 dimensionality reduction to assign different expansion settings to each branch, allowing the time-scale information to be graded into the inception branches and achieving information integration in different time dimensions. Through the above structure of time coefficient assignment, the exponential growth of coefficients is avoided and the purpose of reducing the number of parameters is achieved.

Two two-layer I-TCN layers are added at the end of each IST-GCN cell, and the TCN is divided into 4 branches according to the hierarchical principle, with each branch producing output to the corresponding group, whose structure is shown in Figure 4. The initial value of the expansion coefficient n of the network is 1. As the network deepens, the layer units increase step by step, and the maximum value of the expansion coefficient is 4. This external connection refers to the residual structure, which passes through a one-dimensional convolution with a step size of 2 in the middle, and this design can avoid the gradient dispersion problem. Improving the temporal convolutional network by inserting the inception structure allows for capturing more time-scale information while reducing the number of network parameters by a large amount and reducing the computational cost. A compact and efficient temporal feature extraction network is achieved by using different temporal filters to adaptively select the best feature information to optimize the classification problem.

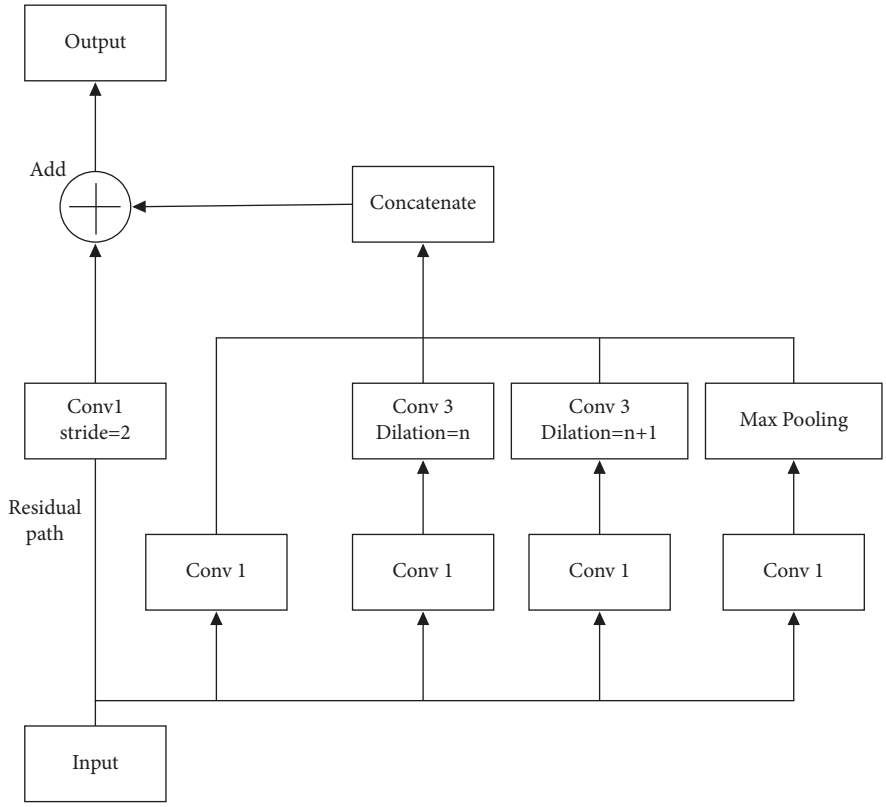

Figure 4: I-TCN network.

3.4. IST-GCN Action Recognition Process. The process of human action recognition based on the IST-GCN model is shown in Figure 5. Firstly, the sample video data are input, and the video data are processed in frames during the analysis process. The human joints under different frames have the problem of position change, but the set of all joint points in different frames obeys random distribution. Therefore, we first select the batching standard module (BN) in the first layer of the network hierarchical distribution to normalize the joint point data at the temporal level and spatial level to make the input skeletal data more standardized, reduce the error volatility, and optimize the algorithm's convergence. In the second layer of the network, we choose the attention mechanism (ATT), which connects our new R-GCN layer and the I-TCN layer in the next network. The R-GCN layer relies on the tensor rotation operation to obtain global information, after which the obtained global features are input into the I-TCN to analyze the linkage relationship among the nodal features at the temporal level, supplemented by the ATT mechanism to weaken the non-conforming features that do not conform to the bounded range of the model and filter features of different time-scales. The whole network consists of nine IST-GCN units sequentially connected to fully capture and fuse the graph feature information, then perform average pooling, then classify the features through the fully connected layer, and finally output the behavior prediction results according to the classification weights.

4. Experiment

4.1. Datasets. To validate the performance of our method, we chose the public dataset NTU RGB + *D* [30] for experimental test validation. This dataset is one of the more comprehensive datasets covering categories in human action recognition studies. The dataset contains a total of three types of production specifications, which are the two-person interaction dataset, the medical interaction dataset, and the daily interaction dataset. It can be subdivided into 60 categories of actions based on action types, with a total of 56880 sample sequences. All videos are stored in a uniform dataset standard, and the maximum video frames of each sample video do not exceed 300 frames. At the same time, all sample data are preprocessed by OpenPose human skeleton detection, and the corresponding skeleton data and Jason files are stored separately. In addition, a set of independent evaluation criteria, namely, Cross-Subject (CS) and Cross-View (CV), is proposed for this dataset. The CS evaluation system is evaluated based on the ID number of the person in the dataset as a sequence, and the CV evaluation system is evaluated based on the camera ID number as a sequence. The detailed volume of the training and testing datasets are shown in Table 1.

4.2. Experimental Details. In the action recognition experiments, we mainly focus on action jogging as the control standard to verify whether the action recognition results

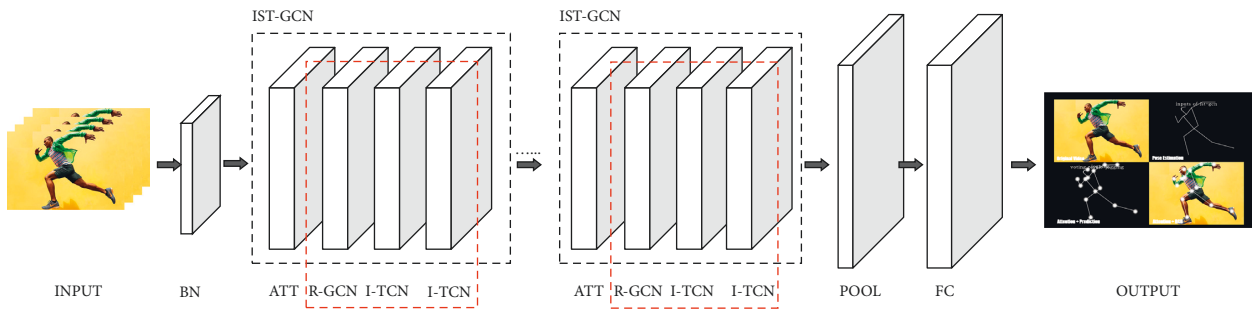

Figure 5: IST-GCN human action recognition process.

Table 1: The detailed information of datasets.

	NTU RGB + *D*	
	CS	CV
Train	40320	37920
Test	16560	18960
Total	56880	56880

match with the real action, each test sample is 300 frames, while the experiments are divided into single-player action recognition experiments and multiplayer action recognition experiments to test the performance of the improved method hierarchically while comparing with the spatial-temporal map convolutional neural network model.

4.2.1. Single Action Recognition Experiment. The performance of single-person recognition result is shown in Figure 6, it can be seen that the action recognition result matches with the experimental preset result, the effect is better and the action recognition result is accurate.

Compared with the spatial-temporal map convolutional neural network model, the single-person action recognition effect is not much different, and the comparison experiment is shown in Figure 7. Although there are a few frames that recognize the action as a triple jump and occasionally misrecognition occurs, the final score voting result still matches the real action and has little impact on the overall action recognition result.

4.2.2. Multiplayer Action Recognition Experiment. The performance of multiperson recognition result is shown in Figure 8, which shows that the action recognition effect is good, and a few frames appear to misrecognition situation, but it does not affect the overall action recognition, and the recognition result is accurate.

Compared with the original spatial-temporal map convolutional neural network model, the recognition effect of our method is superior, and the comparison of the action recognition effect is shown in Figure 9.

As shown in Figure 9 Experiment A, two-thirds of the frames of the original ST-GCN method identify the action as triple jump, although there are also some frames identified as real action jogging, but the overall triple jump action score is higher, so the final action recognition result is triple jump. Our method uses different scales of time windows to capture information and has better control of global information, so it performs well in the multiperson action recognition experiment and the recognition results are accurate. From Figure 9, experiment B in the recognition effect of the original ST-GCN algorithm, one person was obscured and although the skeletal information was recognized, the action could not be classified, and then the overall action was recognized as roller skating, which could not be matched with the real action. The effect of multiperson action recognition experiments is not as good as that of single-person recognition experiments. The more the number of people, the lower the accuracy of human skeleton recognition and the efficiency of action classification. We try to control the multiperson action recognition experiment to less than three people in the experiment. Our method can recognize and correctly categorize the occluded part of the action, further highlighting the advantages of our proposed IST-GCN method.

4.3. Experimental Results Analysis. Our proposed IST-GCN method involves the improvement of two main parts, namely, the rotated tensor module in the graph convolution layer (R-GCN) and the inception structure embedding in the temporal convolution layer (I-TCN). To verify the effect of each, ablation experiments were performed. First, the GCN in ST-GCN was replaced with R-GCN, and the group of experiments was named with the letter *R* to construct the R-GCN efficiency testing experimental group. Secondly, the TCN in ST-GCN was replaced with I-TCN, and the group was named with the letter I. The experimental group was constructed to verify the performance of the I-TCN module. The above two groups were validated with the spatial-temporal map convolutional neural network and our proposed IST-GCN on the NTU RGB + *D* dataset. The results were compared in terms of accuracy (Acc), bone recognition accuracy (Bone), joint recognition accuracy (Joint), and number of parameters (Param) levels as shown in Table 2.

The R-GCN technique improves overall accuracy by 3.7 percent, and the number of parameters is lowered proportionally, as shown in Table 2. The I-TCN approach improves overall accuracy by 7.5 percent and reduces the number of parameters by half. The results reveal that I-TCN has a greater impact on overall performance than R-GCN, although less effective than I-TCN in terms of overall

Figure 6: Single-person action recognition.

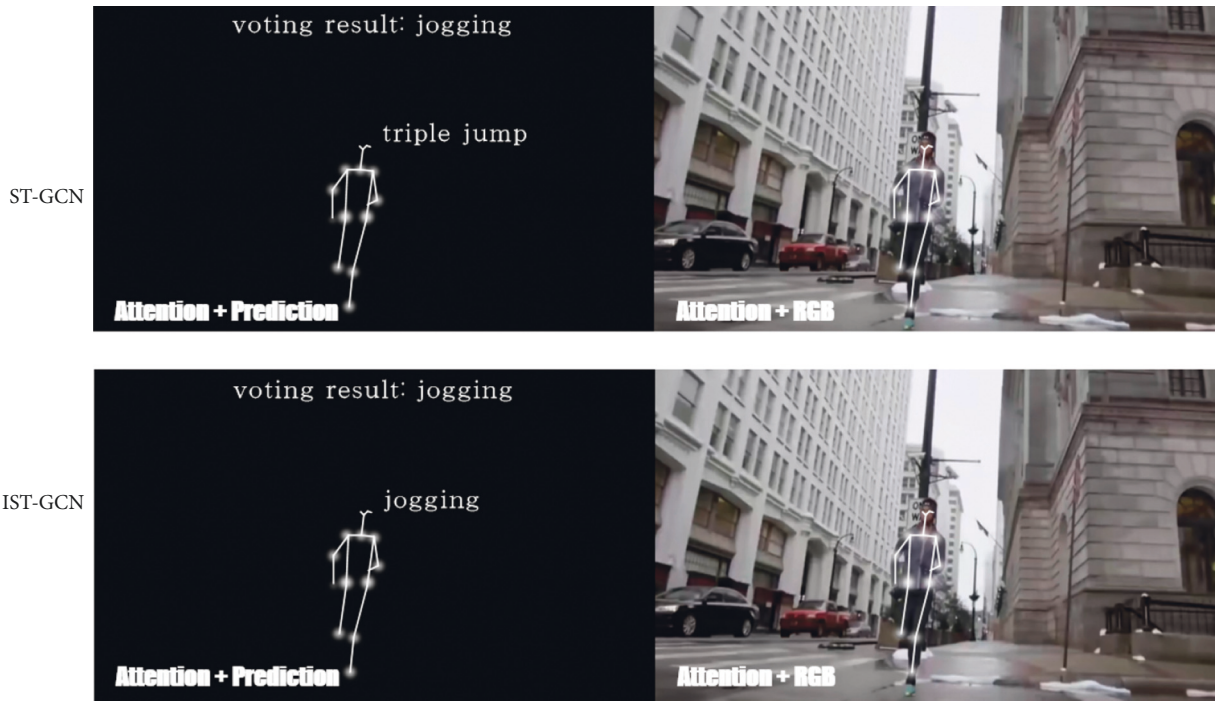

Figure 7: Comparison of ST-GCN and IST-GCN single-person action recognition effects.

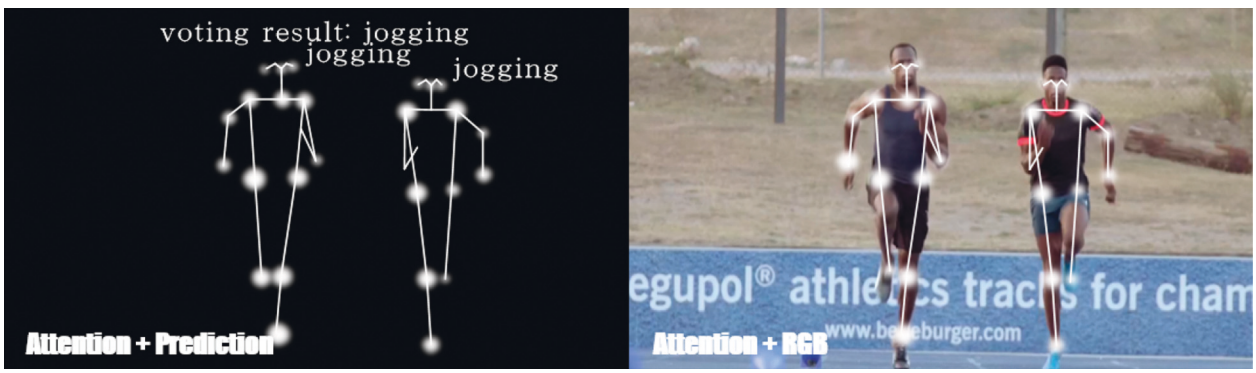

Figure 8: Multiperson action recognition.

performance improvement, is indispensable in capturing the global feature level. The two optimizations mirror each other and prove the effectiveness of the IST-GCN method.

To verify the effectiveness of our IST-GCN, we compare four different kinds of skeleton-based action recognition models, dynamic skeleton [31], ST-GCN [18], P-LSTM [30]

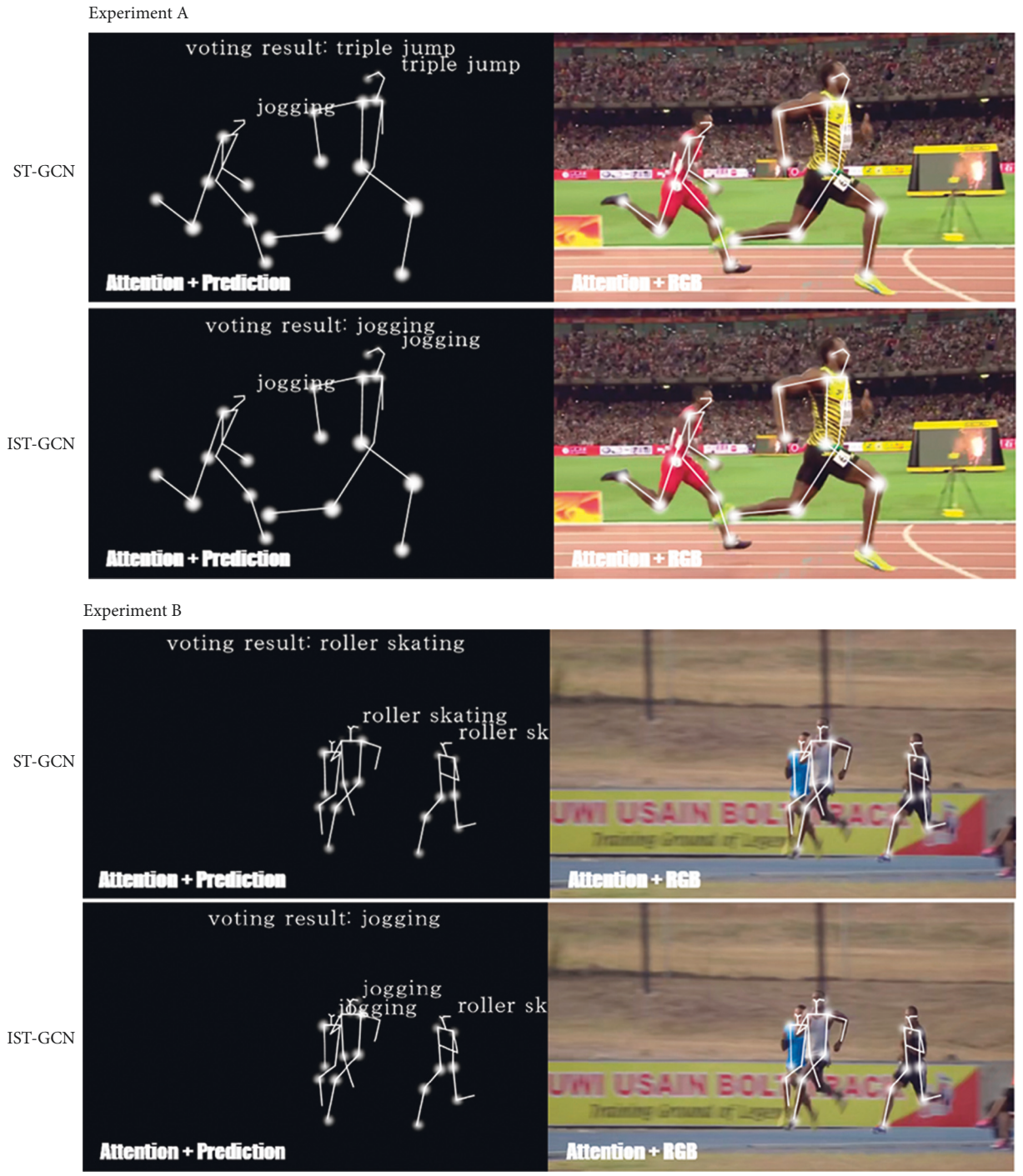

Figure 9: Comparison of multiperson action recognition effects between ST-GCN and IST-GCN.

Table 2: Results of ablation experiments.

Method	Joint(%)	Bone(%)	Acc(%)	Param(M)
ST-GCN	79.1	79.8	80.1	3.14
R	82.9	83.2	83.8	2.36
I	86.8	87.1	87.6	1.61
Ours	88.9	89.5	90.2	1.36

Table 3: Comparison of our method and different types of action recognition methods.

Method	CS(%)	CV(%)
Dynamic skeleton	60	64
P-LSTM	63	71
TCN	74	83
ST-GCN	81	88
Ours	90	94

Table 4: Comparison of our method and similar optimized action recognition methods.

Method	Params(M)	Acc (%)
ST-GCN	3.03	81
AS-GCN	4.21	84
2S-AGCN	3.52	87
NAS-GCN	6.62	87
Shift-GCN	7.34	95
Ours	1.43	91

and TCN [32]. The dynamic skeleton represents a series of action recognition models based on hand-crafted labels, P-LSTM denotes a series of recurrent neural network classes, TCN denotes a series of convolutional neural network classes, and ST-GCN denotes a series of hands-on models based on graph convolutional neural networks. The above four methods and our method are validated on the NTU RGB + *D* dataset. The experimental data is shown in Table 3.

The experimental comparison results in Table 3 indicate that in the validation experiments of the dataset NTU RGB + *D*, the GCN-based action recognition method greatly outperforms other types of action recognition methods, proving that graph convolutional networks have great advantages. Our method compared with the spatial-temporalspatial-temporal graph convolutional neural network model improves the accuracy in CS metrics by 9%, reaching 90% and in CV metrics by 6% and reaching 94%.

To verify the effectiveness of our method among similar optimization methods for graph convolutional neural networks, we compared four algorithms that perform better among current variant methods for graph convolutional neural networks in terms of both number of parameters (Params) and accuracy (Acc), namely AS-GCN [33], 2S-AGCN [26], NAS-GCN [34], and Shift -GCN [35]. The validation was carried out in dataset NTU RGB + *D* with CS evaluation metrics, and the comparison results are shown in Table 4.

Table 4 reveals the findings of the experimental comparison. The comparison results between AS-GCN, 2S-AGCN, and NAS-GCN under the evaluation index of CS indicate that our method has better efficiency with an accuracy of 91%, both in the number of model parameters and accuracy. Given the Shift-GCN method, which introduces a more complex hyperbolic space structure, the classification accuracy is further optimized. Even though the accuracy is not as good as that of Shift-GCN, the number of model parameters in this paper adopts the inception structure to form a more compact model, and the number of model parameters in our improved method is only one-fifth of that of the Shift-GCN method, which greatly decreases the computational cost. Furthermore, there are fewer parameters in this model than in previous ones. All of this demonstrates the efficacy of our strategy.

5. Conclusion

In this paper, we present a deep learning method for human action recognition based on the IST-GCN framework, which optimizes the recognition accuracy of the model by reducing the model parameters. First, we add a tensor rotation module in the graph convolution layer to better capture the global features of the graph task. Then we add the inception structure in the temporal convolution layer to build a multiscale temporal convolution filter to obtain temporal information in different temporal perceptual domains and reduce the arithmetic power. Finally, we perform experimental validation on the public dataset NTU RGB + *D*. The accuracy of CS evaluation reaches 90% and the accuracy of CV evaluation reaches 94%. The results reveal that our optimized method is robust and accurate, which not only improves the efficiency of the graph topology learning process but also greatly decreases the volume of parameters. Compared with the spatial-temporalspatial-temporal graph convolutional neural network model and similar graph convolutional optimization algorithms, the advantages of our method are outstanding.

As can be seen from the experimental results in Table 4, there is still a certain gap between the accuracy of our method and the Shift-GCN. Although we have a clear advantage in the number of parameters, accuracy is always the first assessment index as the effect of human action recognition. In the next work, we will consider using hyperbolic spatial structure to optimize the accuracy, and also ensure that the volume of parameters is small. To achieve a human action recognition model with high accuracy, few parameters, high robustness, and good stability.

Data Availability

The dataset can be accessed upon request.

Conflicts of Interest

The authors declare that they have no conflicts of interest.

References

[1] C. Chen, R. Jafari, and N. Kehtarnavaz, "Utd-Mhad: a multimodal dataset for human action recognition utilizing a depth camera and a wearable inertial sensor," in *Proceedings of the 2015 IEEE International Conference on Image Processing (ICIP)*, pp. 168–172, IEEE, Canada, 2015.

[2] Z. Jia, Y. Lin, J. Wang et al., "Multi-view spatial-temporal graph convolutional networks with domain generalization for sleep stage classification," *IEEE Transactions on Neural Systems and Rehabilitation Engineering*, vol. 29, pp. 1977–1986, 2021.

[3] A. Assadzadeh, M. Arashpour, I. Brilakis, T. Ngo, and E. Konstantinou, "Vision-based excavator pose estimation

using synthetically generated datasets with domain randomization," *Automation in Construction*, vol. 134, p. 104089, 2022.

[4] H. Wang, Z. Xie, L. Lu, L. Li, and X. Xu, "A computer-vision method to estimate joint angles and L5/S1 moments during lifting tasks through a single camera," *Journal of Biomechanics*, vol. 129, p. 110860, 2021.

[5] P. M. Griffin, "3-D object pose determination using computer vision," *Computers & Industrial Engineering*, vol. 19, no. 1-4, pp. 215–218, 1990.

[6] Z. Jia, Ji Junyu, and X. Zhou, *Hybrid Spiking Neural Network for Sleep EEG Encoding[J]*, Science China Information Sciences, vol. 65, no. 4, pp. 1–10, 2022.

[7] G. Morinan, Y. Peng, S. Rupprechter et al., "Computer-vision based method for quantifying rising from chair in Parkinson's disease patients," *Intelligence-Based Medicine*, vol. 6, p. 100046, 2022.

[8] Z. Jia, X. Cai, and Z. Jiao, "Multi-modal physiological signals based squeeze-and-excitation network with domain adversarial learning for sleep staging," *IEEE Sensors Journal*, vol. 22, no. 4, pp. 3464–3471, 2022.

[9] Z. Jia, Y. Lin, Y. Liu, Z. Jiao, and J. Wang, "Refined non-uniform embedding for coupling detection in multivariate time series," *Physical Review A*, vol. 101, no. 6, Article ID 062113, 2020.

[10] X. Liu, Z. You, Y. He, S. Bi, and J. Wang, "Symmetry-Driven hyper feature GCN for skeleton-based gait recognition," *Pattern Recognition*, vol. 125, Article ID 108520, 2022.

[11] T. Huynh-The, C.-H. Hua, N. Anh Tu et al., "Hierarchical topic modeling with pose-transition feature for action recognition using 3D skeleton data," *Information Sciences*, vol. 444, pp. 20–35, 2018.

[12] D. Das Dawn and S. H. Shaikh, "A comprehensive survey of human action recognition with spatio-temporal interest point (STIP) detector," *The Visual Computer*, vol. 32, no. 3, pp. 289–306, 2016.

[13] Z. Jia, X. Cai, Y. Hu et al., "Delay propagation network in air transport systems based on refined nonlinear Granger causality," *Transportmetrica B: Transport Dynamics*, pp. 586–598, 2022.

[14] X. Jiang, F. Zhong, Q. Peng, and X. Qin, "Online robust action recognition based on a hierarchical model," *The Visual Computer*, vol. 30, no. 9, pp. 1021–1033, 2014.

[15] J. Wu, D. Hu, and F. Chen, "Action recognition by hidden temporal models," *The Visual Computer*, vol. 30, no. 12, pp. 1395–1404, 2014.

[16] S. Hochreiter and J. Schmidhuber, "Long short-term memory," *Neural Computation*, vol. 9, no. 8, pp. 1735–1780, 1997.

[17] X. Shen and Y. Ding, "Human skeleton representation for 3D action recognition based on complex network coding and LSTM," *Journal of Visual Communication and Image Representation*, vol. 82, Article ID 103386, 2022.

[18] L. Chaolong, C. Zhen, and Z. Wenming, "Spatio-temporal Graph Convolution for Skeleton Based Action recognition," in *Proceedings of the Thirty-Second AAAI Conference on Artificial Intelligence*, New Orleans, LO, USA, 2018.

[19] S. Yan, Y. Xiong, and D. Lin, "Spatial-temporal graph convolutional networks for skeleton-based action recognition," in *Proceedings of the Thirty-second AAAI conference on artificial intelligence*, New Orleans, LO, USA, 2018.

[20] T. Alsarhan, U. Ali, and H. Lu, "Enhanced discriminative graph convolutional network with adaptive temporal modelling for skeleton-based action recognition," *Computer Vision and Image Understanding*, vol. 216, p. 103348, 2022.

[21] Y. Li, D. Ma, Y. Yu, G. Wei, and Y. Zhou, "Compact joints encoding for skeleton-based dynamic hand gesture recognition," *Computers & Graphics*, vol. 97, pp. 191–199, 2021.

[22] Y. Liu, H. Zhang, D. Xu, and K. He, "Graph transformer network with temporal kernel attention for skeleton-based action recognition," *Knowledge-Based Systems*, vol. 240, p. 108146, 2022.

[23] C. Ding, S. Wen, W. Ding, K. Liu, and E. Belyaev, "Temporal segment graph convolutional networks for skeleton-based action recognition," *Engineering Applications of Artificial Intelligence*, vol. 110, p. 104675, 2022.

[24] Z. Cao, T. Simon, and S. E. Wei, "Realtime multi-person 2d pose estimation using part affinity fields," in *Proceedings of the IEEE Conference on Computer Vision and Pattern Recognition*, pp. 7291–7299, Honolulu, HI, USA, 2017.

[25] T. N. Kipf and M. Welling, "Semi-supervised classification with graph convolutional networks," arXiv preprint arXiv: 1609.02907, 2016.

[26] L. Shi, Y. Zhang, and J. Cheng, "Two-stream Adaptive Graph Convolutional Networks for Skeleton-Based Action recognition," in *Proceedings of the IEEE/CVF Conference on Computer Vision and Pattern Recognition*, pp. 12026–12035, Long Beach, CA, USA, 2019.

[27] S. M. Sam, K. Kamardin, and N. N. A. Sjarif, "Offline signature verification using deep learning convolutional neural network (CNN) architectures GoogLeNet inception-v1 and inception-v3[J]," *Procedia Computer Science*, vol. 161, pp. 475–483, 2019.

[28] F. Chen, J. Wei, B. Xue, and M. Zhang, "Feature fusion and kernel selective in Inception-v4 network," *Applied Soft Computing*, vol. 119, p. 108582, 2022.

[29] W. Abdul, M. Alsulaiman, S. U. Amin et al., "Intelligent real-time Arabic sign language classification using attention-based inception and BiLSTM," *Computers & Electrical Engineering*, vol. 95, p. 107395, 2021.

[30] A. Shahroudy, J. Liu, T. T. Ng, and G. Wang, "Ntu Rgb+ D: A Large scale dataset for 3d human activity analysis," in *Proceedings of the IEEE Conference on Computer Vision and Pattern Recognition*, pp. 1010–1019, Las Vegas, NV, USA, 2016.

[31] J. F. Hu, W. S. Zheng, J. Lai, and J. Zhang, "Jointly learning heterogeneous features for RGB-D activity recognition," in *Proceedings of the IEEE Conference on Computer Vision and Pattern Recognition*, pp. 5344–5352, Massachusetts, MA, USA, 2015.

[32] T. S. Kim and A. Reiter, "Interpretable 3d human action analysis with temporal convolutional networks," in *Proceedings of the 2017 IEEE Conference on Computer Vision and Pattern Recognition Workshops (CVPRW)*, pp. 1623–1631, IEEE, Honolulu, HI, USA, 2017.

[33] M. Li, S. Chen, and X. Chen, "Actional-structural Graph Convolutional Networks for Skeleton-Based Action recognition," in *Proceedings of the IEEE/CVF Conference on Computer Vision and Pattern Recognition*, pp. 3595–3603, Long Beach, CA, USA, 2019.

[34] W. Peng, X. Hong, H. Chen, and G. Zhao, "Learning graph convolutional network for skeleton-based human action recognition by neural searching," in *Proceedings of the AAAI Conference on Artificial Intelligence*, pp. 2669–2676, New York, NY, USA, 2020.

[35] K. Cheng, Y. Zhang, X. He, C. Weihan, C. Jian, and L. Hanqing, "Skeleton-based action recognition with shift graph convolutional network," in *Proceedings of the IEEE/CVF Conference on Computer Vision and Pattern Recognition*, pp. 183–192, Nashville, TN, USA, 2020.

Hindawi
Scientific Programming
Volume 2022, Article ID 8138574, 8 pages
https://doi.org/10.1155/2022/8138574

Research Article

Analysis of Museum Cultural Creation from the Perspective of Cultural Industry

Zhen Zhao

Nanjing Mumei Culture and Art Co., Ltd., Nanjing, China

Correspondence should be addressed to Zhen Zhao; wandering@cuc.edu.cn

Received 23 March 2022; Revised 4 April 2022; Accepted 13 April 2022; Published 6 May 2022

Academic Editor: Jie Liu

There is a lack of objective and rapid methods to evaluate and extract design elements in the development of museum cultural creation products. Aiming at this, an analysis method of museum cultural creation from the perspective of cultural industry is proposed. The order relation method and entropy weight method are applied to extract cultural characteristics. The optimality evaluation of the features based on the ordinal relation method aims to make a preliminary judgment on the representation value of the feature. At the same time, the entropy weight method is introduced to make decisions among various categories of cultural features. Combining the two methods makes the feature extraction process both objective and scientific. It also ensures that the selected design elements are distinct in priority and do not conflict with each other. Taking the museum cultural creation product design based on brocade patterns in the Qing Dynasty as an example, it is proved that the proposed method can effectively extract and transform the cultural features of the cultural relics, which provides a reference for the development of cultural and creative products of the museum.

1. Introduction

Cultural creation industry, which flourished in European and American countries in the 1990s, has become a well-deserved sunrise industry in the post industrial era and under the background of knowledge economy [1]. Museum cultural creation refers to the cultural creation and development based on the specific cultural relics, culture, regional style, and spirit in the museum. Museums and their collections carry the unique culture and memory of a country, a city and a place, and become the main body of the development of museum cultural and creative industry [2].

The development and sales of cultural creation products can bring additional income to museums and play a better role in promoting and educating the culture and realizing its social value [1–3]. When designing museum cultural creation product, whether it emphasizes interest or marketing methods, the cultural relics in their collections must be used as a source of inspiration for design and innovation to ensure that cultural creation products have cultural attributes and are closely related to the culture they represent.

2. Related Works

The museum's tens of thousands of collections provide rich materials for cultural creation products. Still, the mix and stack of style elements are insufficient to design excellent cultural creation products. Whether the public can recognize the sales of cultural creation products depends on whether cultural symbols can be matched with specific design carriers in the design. In the research on the design of cultural creation products with museums as the main body, Liu et al. proposed that museum cultural creation products not only have a symbolic role but also bring a sense of public awareness by maintaining consistency with museums based on qualitative interviews and quantitative questionnaires [4]. At the same time, the higher the correlation between cultural creation products and the exhibits in the museum, the more likely it is to be accepted by the audience. Prameswari et al. explored the cognitive process of cultural creation products from the perspective of cultural schema and constructed a framework for cultural identification which contains general mode, plot input, and instantiation model [5]. Gao et al.

pointed out that the collections are systematic and can be serially designed using their associations and combinations [6].

Because of the large number and complexity of a series of cultural relics with the same theme in the collection, the extraction of relevant cultural factors is particularly important. Wang et al. proposed Yantu cultural creation products design idea by which design factors were extracted from representative cultural relics, the aspect was evaluated and screened by combining eye movement experimental correlation and Kansei engineering, and finally a set of tea sets was designed [7]. Li et al. proposed an evaluation method for cultural creation product modeling based on fuzzy set theory by which an evaluation index system for product modeling design was established through AHP. The example of fuzzy evaluation shows that this method can effectively reflect the satisfaction of users, and the analysis and screening of design elements can improve the quality of design results [8]. In addition, multiattribute decision-making [9–14] also provides an idea for museum cultural creation analysis from the perspective of cultural industry.

However, in the above research, there is still a lack of a method for evaluating and extracting design elements for collection resources. As the main body of cultural creation development, museums are ambiguous in using their resources. Therefore, in the design process, we must first excavate the cultural relics in the museum collection around a certain theme, analyze the cultural characteristics that are most consistent with the design proposition or have the most extended value, and assign cultural factors to cultural creation products. This process is usually obtained by visiting and surveying designers, and the opinions are often subjective without considering the entire creative product development process. The selected cultural characteristics, that is, the design elements derived from the connotation and externality of cultural relics, are important factors for expressing regional culture in products and indirectly determine the quality of design results.

Therefore, it is necessary to apply scientific methods to analyze and evaluate them, so as to avoid the strong subjective will of R&D personnel, resulting in the final inability of cultural and creative products to convey basic semantics.

3. Museum Cultural Creativity Process Analysis

Based on a specific cultural and creative product development theme, the cultural features are divided according to explicit and recessive factors through interviews, surveys, and collection of relevant cultural relic information, that is, the interpretation of cultural features. Secondly, taking the target user as the object of analysis, the process of using and feeling the product is explored and the perceptual vocabulary is obtained. The key to the development of museum cultural creation products is to extract cultural characteristics from the collection resources, so the early design stage needs to extract many cultural features comprehensively [15–17].

The process includes combining perceptual vocabulary and other index factors, superiority assessment of cultural characteristics, and obtaining the representative characteristics of each category and using the entropy weight method to obtain the most valuable cultural characteristics, that is, the key dominant characteristics. Based on the feature extraction results, the transformation process of designers' design cultural features is guided. Finally, the effectiveness of the method is verified by taking a representative cultural creation product design as an example. The process of cultural feature extraction and application is shown in Figure 1.

3.1. Cultural Feature Extraction. In the extraction of design elements of museum cultural relics, it is necessary to comprehensively consider the influence of the various attributes of the cultural relics evaluated on the design results of creative products, such as the dominant features of the beauty of the product's external form and the recessive features of the cultural properties of the cultural relics themselves.

The explicit appearance of cultural relics collections carries people's intuitive experience of the past culture, such as shape, color, material, texture, pattern, and graphic decoration. The dominant characteristics of four dimensions, including shape, color, material and texture, have been established through relevant literature and field research. Recessive features provide the significant cultural value of museum cultural and creative products, which have traditional cultural connotations that general commodities do not have. Recessive features include two dimensions: semantic layer and connotation layer. They are shown in Figure 2.

The semantic level of cultural relics reflects its essential meaning and spiritual outlook, and it is a particular emotion integrated into the creation. The audience can experience it by appreciating and browsing the cultural relics; the connotative level refers to the context and allusions hidden behind the cultural relics: history and other deeper cultural information. The stories behind these cultural relics reflect the spiritual core of the times, so they need to be embodied in the design of cultural and creative products.

The evaluation indicator is very important for the implementation of this study. Evaluation indicator system refers to an organic whole with internal structure composed of multiple indexes representing the characteristics of all aspects of the evaluation object and their interrelations. Cultural feature extraction needs to establish evaluation indicators and consider the following factors:

(1) The matching degree between users' attitudes and emotional preferences in the process of using cultural creation products and the perceptual images of cultural characteristics: a higher matching degree can avoid the problem of unclear semantics of cultural creation products, and users can feel the connotation and temperament of the collection.

(2) Feature scalability: it refers to the elements that can provide scalability in terms of line, outline, color, and so on. The more complex and changeable the external form of cultural relics, the more evidence-based the design of cultural and creative products, and the more ornamental the final result.

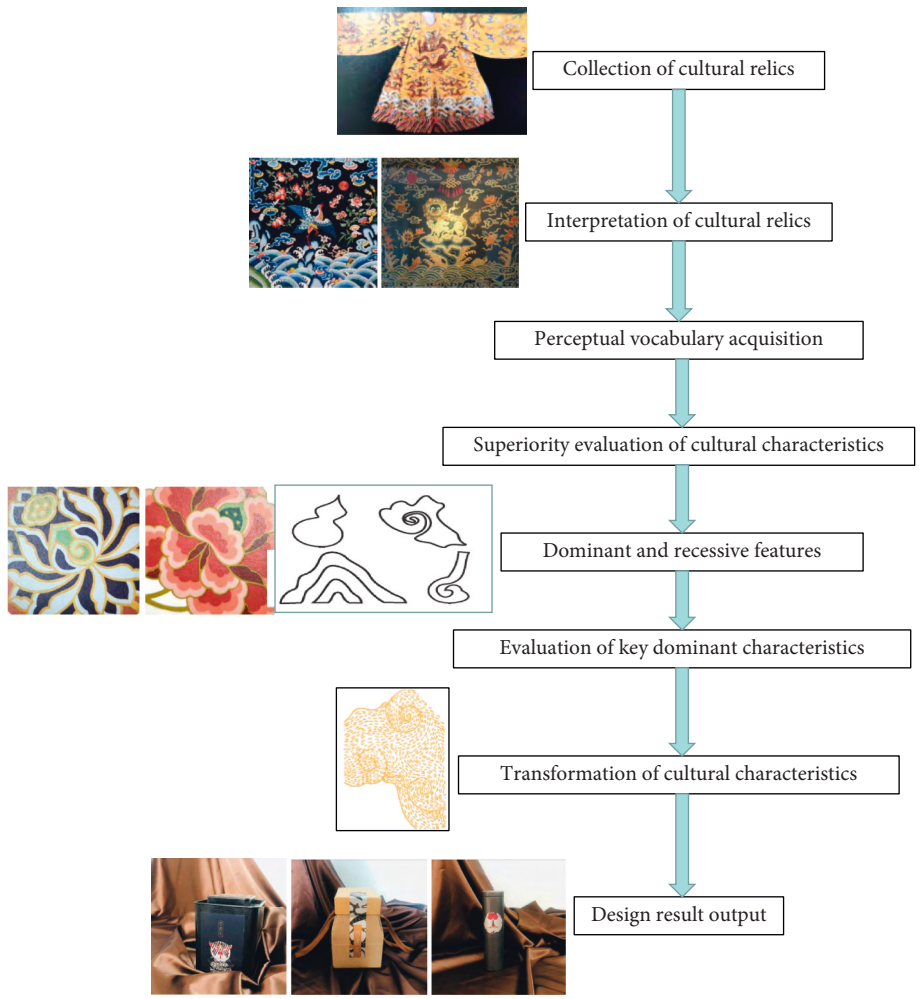

Figure 1: Museum cultural creativity process analysis.

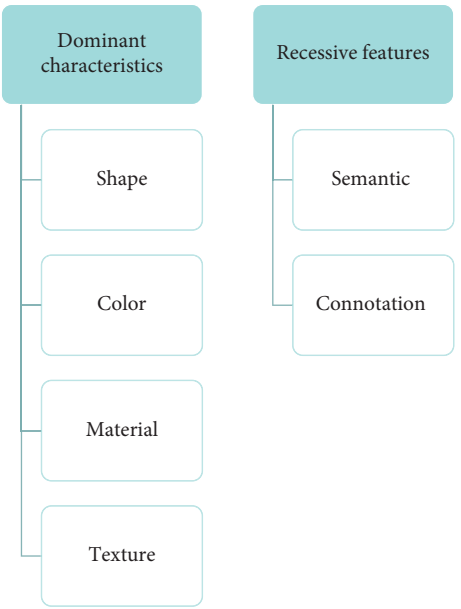

Figure 2: Dominant and recessive features.

(3) Feature identifiability: it refers to whether cultural features are specific, intuitive, and easily understood by the public. The higher the identifiability, the more representative and salient the feature it is easier to reflect in creative product design and stimulate users' cultural identity.

Since the recognition and extensibility of recessive features do not have an external form, they are abstract connotations. Therefore, the evaluation of the two implicit features only considers the relevance of perceptual semantics, so scalability and identifiability will not be included in the evaluation indicators.

Finally, the explicit and implicit cultural characteristics of the cultural relics in the collection are explained, and the legend and text description of each characteristic are listed. At the same time, designers with experience in product modeling and design are invited to score the preliminarily selected series of cultural relics and cultural characteristics. They use four groups of perceptual word to score the recognizability and scalability. Scores are all measured using the Likert seven-level scale.

3.2. Cultural Feature Evaluation. Analyzing and evaluating the indicators of cultural feature can achieve the extraction of cultural feature of cultural relics in the collection. Extracting cultural features that are highly recognizable, highly scalable, and fit with the emotional preferences of cultural creation product users can ensure the rationality of cultural creation design results. The weight coefficient is determined by the subjective weighting method. Then, the overall evaluation value of each type of cultural feature is obtained, and they are sorted separately to get the ranking of the features.

Subjective weighting methods include set-valued statistical iteration method, AHP, G1 method (order relation method), and G2 method, among which AHP and order relation method are the most commonly used. The ordinal relation method improves some of the defects of the AHP. It can achieve that there is no need to construct a judgment matrix and no need to carry out a consistency check, thereby significantly reducing the amount of calculation, and the method is highly operable. The evaluation steps of order relation method [18, 19] are shown in Figure 3.

Its details are as follows:

(1) Determine the order relationship. Under a certain evaluation criterion (or objective), the evaluation indicators $x_1, x_2, \ldots, x_m$ of cultural characteristics of cultural relics are arranged according to the importance, that is, $x_1^* > x_2^* > \cdots > x_m^*$; it is considered that $x_1, x_2, \ldots, x_m$ has established an order relationship according to ">." Here, x_j^* is the i-th evaluation index ($i, j = 1, 2, \ldots, m$) after $\{x_i\}$ is sorted according to the order relation ">". To avoid losing generality, the order relation is written as $x_1 > x_2 > \cdots > x_m$.

(2) Determine the degree of importance. Let the expert's rational judgment on the importance ratio w_{k-1}/wk between the evaluation indexes x_{k-1} and x_k of cultural characteristics of cultural relics be

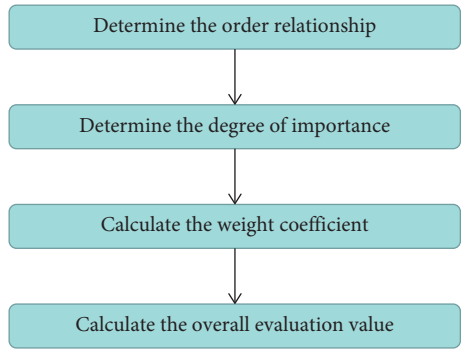

Figure 3: Order relation method for cultural feature evaluation.

$$r_k = \frac{w_{k-1}}{wk}, \quad k = m, m-1, \ldots, 3, 2. \tag{1}$$

For two indicators x_{k-1} and x_k, the assignment of r_k is as follows:

(i) When x_{k-1} and x_k are equally important, $r_k = 1$
(ii) When x_k is slightly more important than x_{k-1}, $r_k = 1.2$
(iii) When x_k is obviously more important than x_{k-1}, $r_k = 1.4$
(iv) When x_k is strongly more important than x_{k-1}, $r_k = 1.6$
(v) When x_k is extremely more important than x_{k-1}, $r_k = 1.8$
(vi) 1.1, 1.3, 1.5, and 1.7 correspond to the middle of two adjacent judgments

(3) Calculate the weight coefficient, that is,

$$w_k = \left[1 + \sum_{k=2}^{m} \prod_{i=k}^{m} r_i\right]^{-1}, \qquad w_{k-1} = r_k w_k, \quad k = m, m-1, \ldots, 3, 2. \tag{2}$$

(4) Calculate the overall evaluation value of each feature as follows:

$$y_i = \sum_{j=1}^{n} b_{ij} w_j \, (i = 1, 2, \ldots, m). \tag{3}$$

Among them, b_{ij} is the value of each evaluation index of cultural characteristics of cultural relics.

3.3. Key Dominant Features Determination. There is no absolute relationship between the optimal evaluation results of different types of cultural characteristics. If they are directly applied in a superimposed manner, the design will be unreasonable and even the elements will conflict with each other. Therefore, it is also necessary to conduct an overall evaluation of dominant features (shape, color, texture, and material), clarify which features have the most representative value, regard them as key dominant features, and focus on them in the process of cultural feature transformation.

Considering that the subjective weight calculation method inevitably has the risk of being affected by subjective factors, the weighting method is based on the difference-driven principle; that is, the objective weighting method is used to evaluate the representative value of each dominant feature. Objective weighting methods commonly include meaning square error, range, open grade, and entropy weight. This paper uses the entropy weight method [11, 12] to determine the corresponding weight coefficient according to the amount of index information, avoiding the influence of experts' subjective factors on the index weight.

Let X_{ij} be the j-th indicator for the i-th cultural feature ($i = 1,2,3, \ldots, m$; $j = 1,2,3, \ldots, n$). For a given index j, the greater the difference of X_{ij}, the more information it contains and transmits, and the greater the impact on the entire system. The steps of using the entropy weight method to evaluate the dominant feature are shown in Figure 4.

Its details are as follows:

(1) Normalize the decision matrix as $X = (x_{ij})mn$.

(2) Calculate the entropy weight. Let the entropy weight of the j-th index be e_j, then

$$p_{ij} = \frac{x_{ij}}{\sum_{i=1}^{m} x_{ij}},$$
$$e_j = \frac{-1}{\ln(m) \sum_{i=1}^{m} p_{ij} \ln\left(p_{ij}\right)}, \tag{4}$$

where p_{ij} is the feature proportion of the i-th evaluation object of the j-th indicator.

(3) Calculate the objective weight of each indicator element as

$$w_j' = \frac{\left(1 - e_j\right)}{\sum_{j=1}^{n} \left(1 - e_j\right)}, \quad j = 1, 2, \ldots, n. \tag{5}$$

(4) Calculate the overall evaluation value of each dominant feature as

$$y_j' = \sum_{j=1}^{n} b_{ij} w_j', \quad i = 1, 2, \ldots, m. \tag{6}$$

3.4. Cultural Feature Transformation. The reason why cultural relics can continue and spread cultural values is that it has a symbolic function for its characteristics, which together constitute the cultural symbols of cultural relics. Cultural feature extraction for cultural relics in museum collections is to reconstruct the symbols representing the semantics of cultural relics and apply them to the development of cultural and creative products.

Step 1. Obtain the optimal results of key dominant features by the entropy weight method and use them as the core elements of cultural and creative product modeling. After feature variation, extension, and other operations, and at the same time, cross and combined experiments with different dominant feature optimization results are carried out to form product design schemes.

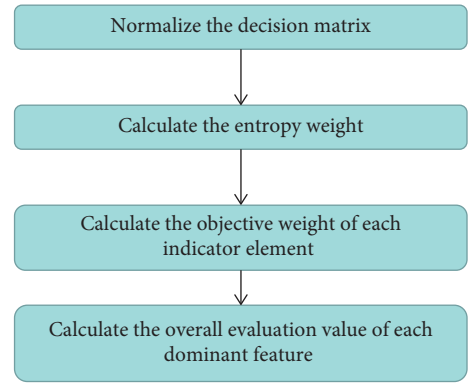

Figure 4: Entropy weight method to evaluate the dominant feature.

Step 2. Use the methods of metaphor, symbolism, and exaggeration to combine invisible features with the use and interaction of products and integrate them into the design elements of cultural and creative products as an added value.

4. Case Study

Based on the above processes and methods, we apply the proposed method to actual design cases for verification. Buzi pattern of Nanjing Yunjin in the Qing Dynasty is taken as the development object of cultural creation products and used to design daily necessities. After on-site visits and investigations, six cultural relics in the collection are selected, as shown in Figure 5. The cultural features of cultural relics are interpreted according to the meaning of explicit and implicit characteristics. For example, the cultural features of the sample cultural relics can be split and named as the shape feature F_{11}, the color feature F_{12}, the texture feature F_{13}, the material feature F_{14}, the implicit semantic feature F_{15}, and the connotation feature F_{16}. A table of interpretations of cultural characteristics of cultural relics in the collection is established for subsequent evaluation, which is shown in Figure 5.

In the early design stage, it is necessary to analyze the attitudes and perceptual images in the target population (such as history lovers, tourists, collectors) towards cultural creation products to provide a reasonable basis for evaluating and extracting cultural characteristics. By consulting books and literatures, we collected 346 words from user comments on the online platform that could express target population's perceptual attitudes toward cultural creation products, remove similar and repeated words, and preliminarily select 80 effective words, including positive and negative attitudes.

K-means cluster analysis method [20, 21] is used to divide the perceptual vocabulary into four categories, and the samples with the closest Euclidean distance to the center are selected according to their classification. The four groups of word pairs are obtained, respectively, as shown in Table 1.

The various cultural characteristics of cultural relics are evaluated by the order relation method. The four groups of perceptual word pairs and the degree of feature recognition

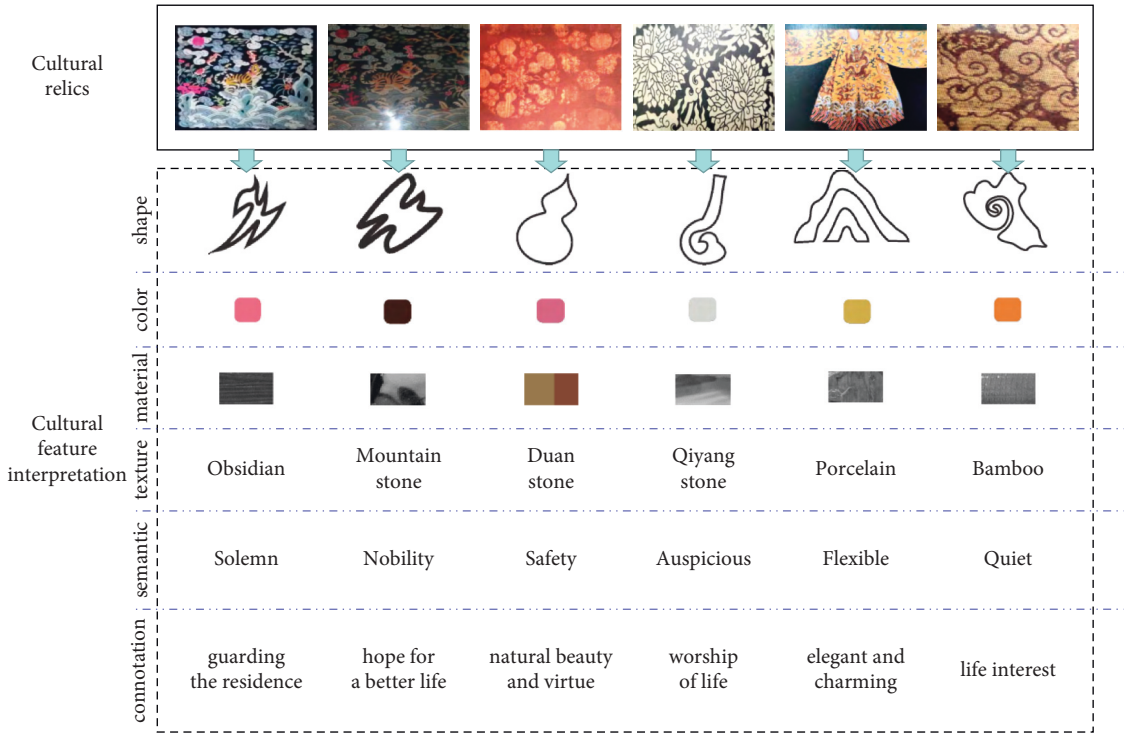

Figure 5: Cultural relics and their cultural feature interpretation.

and the degree of feature expandability are recorded as $X_1, \ldots, X_6$ in turn. As mentioned above, 20 designers with experience in cultural and creative product design were invited to score each characteristic element in the cultural characteristic definition table according to 6 indicators.

For example, the experts' scores on the morphological and cultural characteristics of 6 cultural relics were calculated by the average and variance. The ranking of the evaluation indicators by experts is as follows: mild/incisive > feature recognition > feature expandability > flamboyant/steady > masculine/feminine > delicate/dignified, establishing an order relationship: $X_2 > X_5 > X_6 > X_1 > X_4 > X_3$; the ratio is $r_2 = 1.4$, $r_3 = 1.0$, $r_4 = 1.5$, $r_5 = 1.2$, and $r_6 = 1.2$. Therefore, the weight coefficients $w_1 = 0.1312$, $w_2 = 0.2751$, $w_3 = 0.0913$, $w_4 = 0.1093$, $w_5 = 0.1971$, and $w_6 = 0.1972$ are obtained.

Based on the screened scoring results, the overall evaluation value of the morphological characteristics of each cultural relic is obtained as $y_1 = 4.8955$, $y_2 = 4.1889$, $y_3 = 4.3645$, $y_4 = 3.9322$, $y_5 = 3.1666$, and $y_6 = 3.5731$. The optimality ranking is $F_{11} > F_{31} > F_{21} > F_{41} > F_{61} > F_{51}$, indicating that the cultural relics of the brocade tiger pattern in Qing Dynasty have the best evaluation results of morphological characteristics and are most suitable for use in the design of cultural creation products.

In the same way, the rest of the dominant cultural characteristics (color, texture, and material) are evaluated and processed using the ordinal relation method. When evaluating the implicit features, the two indicators of recognition and scalability are omitted. Only the matching degree between the semantics and connotation of cultural relics and the four sets of perceptual word pairs is considered. The assessment results for all cultural features are shown in Table 2.

The entropy weight method is used to evaluate the four dominant features and analyze their importance. First, the expert scoring results of the six sample cultural relics are averaged according to each feature, and the overall evaluation scores of the features shown are obtained by rearrangement as shown in Table 3.

The weights of the six evaluation indicators can be obtained as follows: $w_1' = 0.1072$, $w_2' = 0.1471$, $w_3' = 0.1263$, $w_4' = 0.1204$, $w_5' = 0.1002$, and $w_6' = 0.3962$. Then, the overall evaluation value of each dominant feature can be obtained: $y_1' = 3.9234$, $y_2' = 3.7228$, $y_3' = 3.6808$, and $y_4' = 3.8664$. The order of dominant features is obtained: shape > material > texture > color. Therefore, shape and material are the key dominant features, and the corresponding features F_{11} and F_{54} are the most worthy of application in the design of cultural creation products.

In the design and application of cloud brocade patterns in the Qing Dynasty, the first is to carry out design positioning, that is, select reasonable products and analyze the product category, actual function, target population, and so on. Then, the brocade pattern of the Qing Dynasty is organically integrated with the product as a cultural and artistic symbol, so as to increase the cultural added value of the product itself, realize the functional transformation of brocade art in the contemporary era, and realize the inheritance and promotion of Chinese culture. Based on the results of cultural feature extraction, an artistic and creative product of daily necessities and its packaging design is developed for the museum. While reflecting the theme, it expresses the long history of Chinese traditional culture, so it is named "white tiger" series design, and poster design is carried out to promote the design as shown in Figure 6.

Table 1: Four groups of word pairs.

Type no.	Word pairs
1	Flamboyant/steady
2	Mild/incisive
3	Delicate/dignified
4	Masculine/feminine

Table 2: The assessment results for all cultural features.

Cultural feature	Assessment result
Shape	$F_{11} > F_{31} > F_{21} > F_{41} > F_{61} > F_{51}$
Color	$F_{22} > F_{32} > F_{12} > F_{42} > F_{52} > F_{62}$
Material	$F_{53} > F_{13} > F_{23} > F_{63} > F_{33} > F_{43}$
Texture	$F_{34} > F_{24} > F_{44} > F_{64} > F_{14} > F_{54}$
Semantic	$F_{15} > F_{25} > F_{55} > F_{45} > F_{65} > F_{35}$
Connotation	$F_{26} > F_{16} > F_{66} > F_{36} > F_{56} > F_{46}$

Table 3: The overall evaluation scores of dominant features.

	Shape	Color	Texture	Material
X_1	4.0233	3.7622	3.7123	3.9044
X_2	4.1811	3.8901	3.8222	3.9024
X_3	3.5902	3.5111	3.7966	3.6002
X_4	3.5411	3.6677	3.7622	3.6844
X_5	3.7833	3.8541	4.1012	3.8002
X_6	4.022	3.7044	3.4567	4.0002

Figure 6: The poster design of "white tiger" series design.

5. Conclusion

Brocade patterns in the Qing Dynasty have high aesthetic value and cultural value and are very valuable Chinese traditional cultural heritage. In the new era, we need to promote and inherit this traditional art by enhancing the spiritual function and artistic modernity. Taking the four grade tiger pattern of military officer as an example, we extract the artistic elements and make secondary artistic innovation and regenerate the design and application of the brocade pattern of the Qing Dynasty in combination with modern design and current aesthetics, so as to better inherit this excellent cultural heritage and make contemporary people better understand the brocade culture. At the same time, the design application of "white tiger" series design also reflects the organic integration of tradition and modernity, provides new ideas for the inheritance of traditional culture and the improvement of the added value of modern products, and can be used as a reference for the design of visual cultural and creative products.

Using museum collection resources to develop and market cultural creation products can present culture and exhibition content vividly to the public, which are the common needs of museums and society. In the designing of cultural creation products for a certain theme, the cultural symbols need to be incorporated into the shape and the emotional preferences of the target group need to be fit. Therefore, it is necessary to integrate perceptual factors into assessing cultural relic features.

The cultural feature application is based on the feature extraction results. Some features are taken as the key content to be expressed in the design, and relying on human-computer interaction, the "lively and flexible" semantic features can be shown by the designed products. The final design example proves that the order relation entropy weight method can effectively extract and transform the cultural features of the cultural relics, which provides a reference for the development of cultural and creative products of the museum. With the continuous development of artificial intelligence and many other technologies, the evolution of its enabling interactive experience from graphical interactive interface to natural interactive interface has become an inevitable trend. Museum cultural creation design research also needs to actively explore new research fields under artificial intelligence, emotional computing, and emotional recognition from the perspective of interaction design and experience design.

Data Availability

The dataset can be accessed upon request.

Conflicts of Interest

The author declares that there are no conflicts of interest.

References

[1] C. H. Chen and S. C. Lin, "Message delivery of cultural and creative products under cultural industries," in *Proceedings of the 18th International Conference on Human-Computer Interaction (HCI International)*, Toronto, Canada, July 2016.

[2] S. Cerisola and E. Panzera, "Cultural and creative cities and regional economic efficiency: context conditions as catalyzers of cultural vibrancy and creative economy," *Sustainability*, vol. 13, no. 13, 2021.

[3] L. Qiu, "Design of cultural and creative products of marine cultural tourism," *Journal of Coastal Research*, vol. 112, no. 1, pp. 100-101, 2020.

[4] S.-L. Liu, F.-S. Lin, and C. I. Yang, "On emotional design of culture products and consumption in national museum of prehistory," *International Journal of Affective Engineering*, vol. 12, no. 2, pp. 317–324, 2013.

[5] I. Prameswari, H. Hibino, and S. Koyama, "The role of cultural schema in developing culture-based product design," *Journal of the Science of Design*, vol. 1, no. 1, pp. 57–66, 2017.
[6] C. Gao, L. Y. Bu, and M. L. Sun, "Application of museum collection cultural symbol in serial product design," *Packaging Engineering*, vol. 38, no. 4, pp. 47–50, 2017.
[7] W. W. Wang, Y. Liu, and Y. Wang, "Extraction of saline soil culture design factors based on visual correlation analysis," *Journal of Graphics*, vol. 37, no. 1, pp. 60–65, 2017.
[8] Z. Li and J. F. Wang, "Application of fuzzy evaluation method in cultural and creative product style design," *Modern Electronics Technique*, vol. 42, no. 13, pp. 131–133, 2019.
[9] F. Meng, X. Chen, and Q. Zhang, "Some uncertain generalized Shapley aggregation operators for multi-attribute group decision making," *Journal of Intelligent and Fuzzy Systems*, vol. 29, no. 4, pp. 1251–1263, 2015.
[10] F. Meng, J. Tang, and C. Li, "Uncertain linguistic hesitant fuzzy sets and their application in multi-attribute decision making," *International Journal of Intelligent Systems*, vol. 33, no. 3, pp. 586–614, 2018.
[11] L. Li, B. Lei, and C. Mao, "Digital twin in smart manufacturing," *Journal of Industrial Information Integration*, vol. 26, no. 9, Article ID 100289, 2022.
[12] L. Li, C. Mao, H. Sun, and Y. B. Yuan, "Digital twin driven green performance evaluation methodology of intelligent manufacturing: hybrid model based on fuzzy rough-sets AHP, multistage weight synthesis, and PROMETHEE II," *Complexity*, vol. 2020, no. 6, 24 pages, Article ID 3853925, 2020.
[13] L. Li, J. Hang, H. Sun, and L. Wang, "A conjunctive multiple-criteria decision-making approach for cloud service supplier selection of manufacturing enterprise," *Advances in Mechanical Engineering*, vol. 9, no. 3, Article ID 168781401668626, 2017.
[14] L. H. Li, J. C. Hang, Y. Gao, and C. Y. Mu, Using an integrated group decision method based on SVM, TFN-RS-AHP, and TOPSIS-CD for cloud service supplier selection," *Mathematical Problems in Engineering*, vol. 2017, Article ID 3143502, 14 pages, 2017.
[15] T. Stylianou-Lambert, N. Boukas, and M. Christodoulou-Yerali, "Museums and cultural sustainability: stakeholders, forces, and cultural policies," *International Journal of Cultural Policy*, vol. 20, no. 5, pp. 566–587, 2014.
[16] H. Geoghegan and A. Hess, "Object-love at the Science Museum: cultural geographies of museum storerooms," *Cultural Geographies*, vol. 22, no. 3, pp. 445–465, 2015.
[17] Y. Y. Zhang, "Sustainable design of cultural creative products based on museum cultural derivatives," in *Proceedings of the 7th International Forum on Industrial Design*, Luoyang, China, May 2019.
[18] J. J. Hasenbein, "Order relations for concave interpolation methods," *Operations Research Letters*, vol. 44, no. 6, pp. 823–825, 2016.
[19] X. J. Wang and Y. J. Guo, "Analysis method of ordered relation on consistency in judgment matrix," in *Proceedings of the 2005 Conference of System Dynamics and Management Science*, pp. 874–878, Boston, MA, USA, July 2005.
[20] R. Shang and B. Ara, "Analysis of simple K-mean and parallel K-mean clustering for software products and organizational performance using education sector dataset," *Scientific Programming*, vol. 2021, Article ID 9988318, 2021.
[21] L. X. Wang and J. H. Yang, "Mining network traffic with the k-means clustering algorithm for stepping-stone intrusion detection," *Wireless Communications & Mobile Computing*, vol. 2021, Article ID 6632671, 2021.

Hindawi
Scientific Programming
Volume 2022, Article ID 7089057, 8 pages
https://doi.org/10.1155/2022/7089057

Research Article

Research on Sports Dance Video Recommendation Method Based on Style

Jiangtao Sun[1] and Haiying Tang[2]

[1]*Wenhua College, Wuhan 430074, China*
[2]*Wuhan Institute of Physical Education, Wuhan 430079, China*

Correspondence should be addressed to Haiying Tang; 2004068@whsu.edu.cn

Received 23 March 2022; Revised 4 April 2022; Accepted 16 April 2022; Published 6 May 2022

Academic Editor: Jie Liu

At present, sports dance teaching still tends to "demonstration" training. Students have limited time and space for autonomous learning, and their enthusiasm for participation is not high, which leads to a decline in classroom learning efficiency. In view of this, video teaching has become popular in sports dance classrooms, providing a new model for sports dance teaching. Video recommendation is particularly important for the improvement of teaching quality. A sports dance video recommendation method based on style is proposed. The factorization machine model is used to combine features and process high-dimensional sparse features, the deep neural network model is adopted as the value function network of the deep Q-learning algorithm, and the deep Q-learning algorithm is used as the decision function to solve the recommendation accuracy and diversity question. Through the application experiment of sports dance video recommendation, it is resulted that the recommendation accuracy of the proposed model is slightly higher than that of traditional recommendation algorithm and the recommendation diversity is obviously better than that of traditional recommendation algorithm. The advantages and feasibility of the proposed model are verified.

1. Introduction

Sports dance is a way of sports, which needs refining, organization, arrangement, and technical processing. Its main mean of the expression is to show the flexible footwork and beautiful dance posture of various rhythms of the human body, and express feelings and reflect social life through this artistic form [1–3]. It is mainly composed of 10 dance types in two series: modern dance and Latin dance. With the progress of society, there has been an upsurge of national fitness, and there has been an upsurge of popularizing and popularizing sports dance in the society. Due to the accelerated pace of life today, many people are busy with work and hope to enrich their spare time activities. However, because dance learning is usually taught by participating in training courses, many people do not have much time to learn. Therefore, it has become a trend to teach students sports dance by recording videos and video recommendations.

The traditional manual teaching process of sports dance is mainly divided into two parts: teachers' explanation of theoretical knowledge and teaching purpose, learning, and guidance of practical courses [4–7]. The second part is the focus of learning. It includes teachers' dance demonstration performance and explanation, correct requirements and practice of dance posture, decomposition practice of turning step and flower step, mutual cooperation between male and female partners, dance practice, dance appreciation, harmonious practice of music, etc.

The sports dance video recommendation system actually uses the existing computer technology to present the process of sports dance teaching to students in the form of video recommendation and applies the recorded sports dance teaching video course to real teaching [5, 7]. The design and development of sports dance teaching video recommendation system make the teacher's teaching content displayed in the form of video. Through the real-time recording of the

teacher's dance scene, students can learn more clearly and quickly. At the same time, it also plays a positive role for students to watch the teaching process repeatedly and take care of students at different levels. In addition, through computer technology, the video teaching of sports dance can also be presented to the students in the form of forums or discussion groups so that the students can no longer learn at a single point, but can learn and communicate with other students in time through the network, learn from each other's strengths, and make up for their weaknesses, to promote communication among students, improve students' learning interest, and stimulate students' learning enthusiasm [7].

It can be seen that sports dance video recommendation is of great significance to improve the quality of sports dance teaching. The research on sports dance video recommendation method not only solves the learning constraints of time and space in the process of sports dance teaching but also makes the teaching process reproducible and decomposed, and provides support for the development of video teaching.

2. Related Works

Recommendation systems [8, 9] have gradually produced a variety of solutions and become an independent discipline now. Many achievements have been achieved in industry applications. The recommendation system itself analyzes and studies the behavioral preferences of users through data information mining and establishes a user-specific interest model, thereby recommending information that may satisfy their interests. Traditional recommendation system algorithms can be roughly divided into three types: collaborative filtering recommendation, content-based recommendation, and hybrid recommendation.

Although traditional recommendation algorithms can solve most information filtering problems, they cannot solve the problems of data sparseness, cold start, and repeated recommendation problems. In recent years, many companies have used deep learning, multi-arm gambling machines, and other algorithms to improve and have obtained good recommendation results in response to the above issues. YouTube [10] used deep learning for video recommendation prediction for the first time in the recommendation system. It successfully filtered and extracted the video content users were interested in from the large-scale data volume and recommended it. Acar et al. [11] proposed an offline evaluation method and controlled experiment based on streaming data. Karatzoglou et al. [12] systematically proposed to apply deep learning to traditional recommendation systems, adding deep learning to the conventional content recommendation and collaborative filtering recommendation methods to deal with recommendation prediction of large-scale data volume. Therefore, deep learning has become a hot spot in current recommendation system research.

At present, most of the recommendation algorithms are based on the static recommendation process and generate a fixed recommendation strategy by collecting and processing a large amount of data information, such as multicriteria decision-making method [13–22], which has a significant improvement in solving the diversification of information recommendation. The problem of cold start is also unable to adapt to the short-term interest changes of users and make effective information recommendations. Therefore, many scholars began to try to use reinforcement learning [23] to solve the problems in the recommendation system. Reinforcement learning is a learning algorithm based on the interaction of the environment. It has developed independently from the two fields of animal behavior research and optimal control. It has been abstracted and formalized as a Markov decision process problem. Later, through the study of many scientists, a relatively complete system, approximate dynamic programming was formed. Reinforcement learning [23] is a dynamic interactive learning strategy algorithm. Therefore, reinforcement learning is used to solve cold start problems and the inability to adapt to users' short-term interest recommendation in recommendation algorithms. Taghipour et al. [24] first proposed to use the Q-learning algorithm combined with web page information to solve the problem of web page recommendation. However, the Q-learning learning algorithm cannot effectively solve the recommendation task of the Markov decision process with large state space and action space. Choi [25] proposed a biclustering learning algorithm to alleviate the above problems, but the effect was not expected. The deep Q-learning deep reinforcement learning algorithm [26] used the value function estimation method, and it solves the problems existing in the Markov decision-making process [27] by iterating the Bellman equation to achieve convergence to the optimal value function. The proposal of policy gradient solves the problem that the value is difficult to calculate, and this method can directly learn the policy.

3. Markov Decision Process

Markov decision process is a mathematical model of sequential decision. It is used to simulate the randomness strategy and return that can be realized by agents in the environment where the system state has Markov nature.

Markov decision process is built based on a set of interactive objects, that is, agents and environment. The elements include state, action, strategy, and reward. In the simulation of Markov decision process, the intelligent experience perceives the current system state and acts on the environment according to the strategy, so as to change the state of the environment and get rewards. The accumulation of rewards over time is called reward.

The theoretical basis of Markov decision process is Markov chain, so it is also regarded as a Markov model considering action. The Markov decision process established in discrete time is called "discrete-time Markov decision process"; on the contrary, it is called "continuous time Markov decision process." In addition, Markov decision process has some variants, including partially observable Markov decision process, constrained Markov decision process, and fuzzy Markov decision process [27].

The factorization machine algorithm is used to combine features and deal with high-dimensional sparse features,

effectively learn the cross-hidden relationship between features, and then use the deep Q-learning algorithm to solve the optimal value of the recommendation decision. First, the core point of sports dance video recommendation is to simulate the recommendation process as a Markov decision process. The initial state of the agent is s_0, and then, an action a_0 is selected from the action set to execute. After execution, the agent will follow the action a_0. The agent s_0 changes to the next state s_1 according to the reward function of action a_0, and then, the action a_1 is selected, and the above steps are continuously looped until a strategy chain reaches the reward accumulation value, which is selected.

Combined with sports dance video recommendation, the Markov solution process can be more refined. The user and the recommendation system can be simulated as two dynamic interactive objects, as shown in Figure 1. In a time slice t, the recommendation system obtains the user's viewing record s_t, trains the action set A through the reward function of s_t, and then selects the sports dance video with the highest reward value in A to recommend to the user, obtain the user's rating for the video, and put it into the experience pool to continue training the recommendation strategy.

In general, the Markov decision process is a Markov reward process with decision making, which means that all states have Markov properties, that is, when a random process is given a current state and all past states. In the case of the conditional distribution probability of its future state depend only on the current state, the Markov property can be expressed in mathematical form as a state s_t has Markov property if and only if it satisfies

$$P[S_{t-1}|S_t] = P[S_{t+1}|S_1, \ldots, S_t]. \tag{1}$$

A Markov decision process can consist of quintuples $\langle S, A, P, R, \gamma \rangle$.

S is the set of all environmental states, and $s_t \in S$ represents the current Agent's state s_t at time t. The evaluation of sports dance video is used for testing, and s is defined as $s_t = \{\text{movie}_t^1, \ldots, \text{movie}_t^n\}$, here denoted as the top n videos watched and rated by the user.

A is the set of limited executable actions of the agent, and A is the set of all videos recommended to the user. The text $a_t \in A$ is represented as the recommended action obtained by the agent through the reward function training at time t, that is, the sports dance video advised by the recommendation system agent to the user through s_t at the current time.

P is the state transition probability matrix, and the mathematical formula is as follows:

$$p_{ss'}^{a_t} = P\left[S_{t+1} = s\prime | S_t = s, A_t = a_t\right], \tag{2}$$

where S_t represents the state at time t, S_{t+1} represents the state at time $t+1$, and A_t represents the actions of different videos recommended by the recommendation system agent to the user at time t. When the time t ends, it turns to time $t+1$, and then, the recommendation system agent will update the state S_{t+1} at time $t+1$ to $s_{t+1} = \{\text{movie}_t^1, \ldots, \text{movie}_t^n, a_t\}$.

R is the reward function of the current Markov reward process [10]. At time t, state s_t is the reward expectation obtained by A entering state s_{t+1}. The mathematical formula is defined as follows:

$$R_s = E[R_{t+1}|S_t = s]. \tag{3}$$

For the videos recommended by the recommendation system agent, users have different scores of movie ratings to generate various movie feedback, so at time t, the recommendation system agent will obtain instant rewards according to varying feedback as $R_t = (s_t, a_t)$. γ is the discount factor, and its value range is generally specified as $\gamma \in (0, 1)$. The discount factor is used to adjust the impact of future rewards on the current accumulated rewards. If $\gamma = 0$, it means that the recommendation system agent pays more attention to the earned reward in time; when $\gamma = 1$, it means that the recommendation system agent pays more attention to the long-term accumulated reward.

From the above definition, it can be concluded that the task of the recommendation system agent is to achieve the learning process of maximizing the reward function through the optimal recommendation strategy [11]. At time t, the mathematical definition of reward G_t is as follows:

$$G_t = R_{t+1} + \gamma R_{t+2} + \gamma^2 R_{t+3} + \cdots = \sum_{k=0}^{\infty} \gamma^k R_{t+k+1}. \tag{4}$$

4. Algorithm

4.1. Concepts. One-hot coding combined with the FM model is used to preprocess the data, and then, the deep Q-learning algorithm in deep reinforcement learning is used as the sports dance video recommendation algorithm. The deep Q-learning algorithm is based on the approximate iteration of the value function. It uses a deep neural network as a Q-value network to extract complex features. One-hot encoding can represent the discrete features in the dataset with numbers. Still, one-hot encoding will introduce the problem of sparse features, so the factorization machine algorithm is used to solve the problem of difficulty in dealing with combined features under the condition of light features.

The ultimate goal of using the deep Q-learning algorithm for a sports dance video recommendation is to obtain the optimal recommendation strategy by maximizing the long-term cumulative reward. The first step is to perform feature extraction on the original data and use the user's rating for the movie as the reward value. Figure 2 shows the corresponding original data structure. Due to the existence of discrete features in the original data set, the deep Q-learning algorithm cannot directly use it as the input data of the value function network.

Therefore, one-hot coding encodes the discrete features and expands the discrete features into the Euclidean space. The values of discrete features can correspond one-to-one with points in Euclidean space. From the aspect of model training, not only can the distance between different features be calculated more reasonably, but also can the nonlinear ability of the model be improved. The principle of one-hot

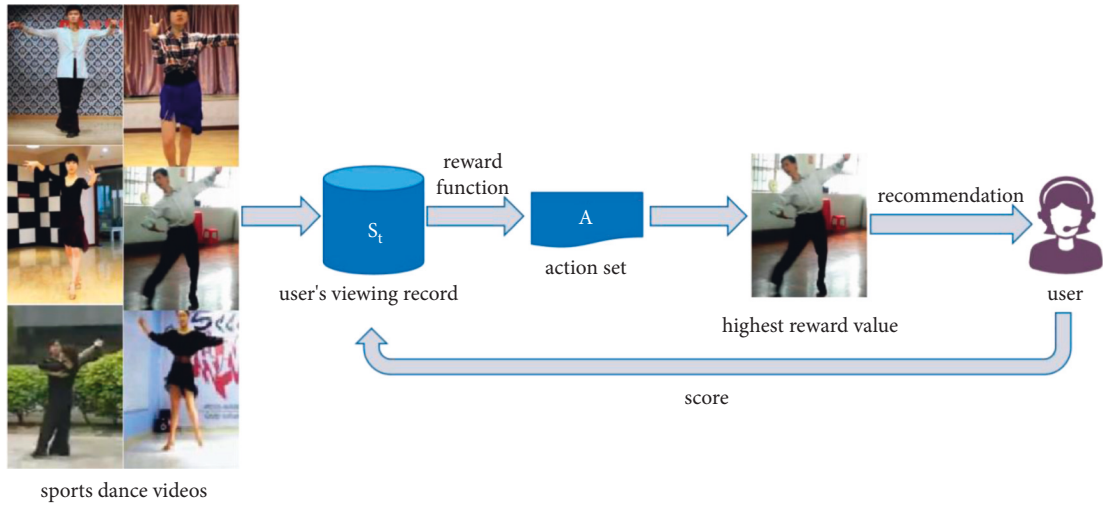

Figure 1: Reinforcement learning basic architecture.

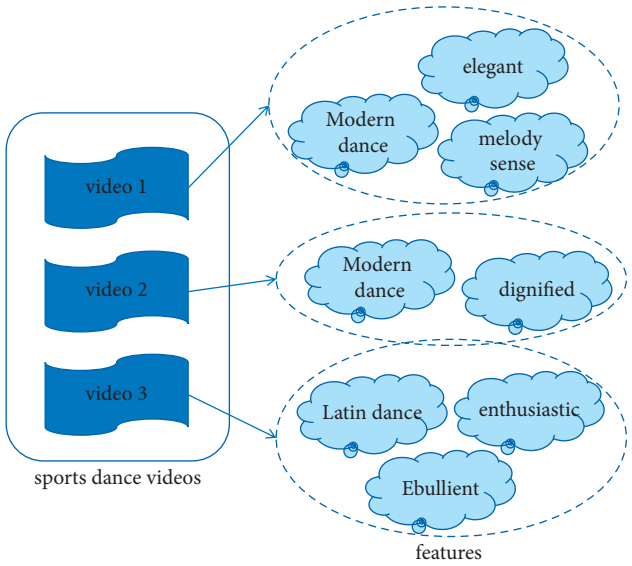

Figure 2: Sports dance video and its features.

encoding is to use the N-bit status register to encode n states with different codes, each attribute has its independent register bit, and only one bit indicates whether it is valid or not at any time. As shown in Table 1, the feature set is processed by using one-hot encoding.

Since one-hot encoding will introduce the problem of feature sparseness, which will cause the dimensional disaster of the neural network, the factorization machine algorithm is used to perform further feature processing on the feature set. A second-order polynomial model is used. A combination of features x_i and x_j is used, where $x_i x_j$ represents the combined feature, x_i is the value of the i^{th} feature, and n represents the number of features of the sample. w_0, w_i, and w_{ij} are model parameters, respectively. The second-order polynomial model is as follows:

$$y(x) = w_0 + \sum_{i=1}^{n} w_i x_i + \sum_{i=1}^{n-1} \sum_{j=i+1}^{n} w_{ij} x_i x_j. \tag{5}$$

Matrix decomposition is used to solve w_{ij}. It is known that in model-based collaborative filtering, the user matrix and the sports dance video matrix can form a unique rating matrix. For each user and video, a hidden vector can be used to represent it. Different users and videos are represented as different two-dimensional vectors. The dot product of the user vector and the movie vector is the user's rating of the movie in the matrix.

It can be seen from the definition that for any $N \times N$ real symmetric matrix, this real symmetric matrix has N linearly independent and can be orthogonalized to get a set of eigenvectors, which are orthogonal and have a module of 1. So, the real symmetric matrix A can be decomposed into

$$A = \varsigma \wedge \varsigma^T, \tag{6}$$

where $\wedge$ is defined as a real diagonal matrix, and Q is defined as an orthogonal matrix.

Similarly, suppose there is asymmetric matrix W consisting of all the current quadratic parameters w_{ij}; in that case, this matrix can be decomposed in the form of $W = V \wedge V^T$, where the jth column of V is defined as the latent vector of the jth dimension feature. The inner product of the latent vector corresponding to xi and the latent vector corresponding to x_j is equal to the cross-term coefficient of the feature components x_i and x_j, so each parameter of the symmetric matrix can be defined as $w_{ij} = \langle v_i, v_i \rangle$.

The deep Q-learning algorithm uses a deep neural network with a weight parameter of θ as the network model of this deep neural network's action-value function. The weights and biases are represented by θ and γ, respectively. The loss function of the deep neural network model is as follows:

$$L_i(\theta_i) = E\left[\left(r + \gamma \max Q\left(s\prime, a\prime, \theta_i\right) - Q(s, a, \theta_i)\right)\right]. \tag{7}$$

The structure diagram of the deep neural network is shown in Figure 3.

It can be seen from the structure diagram that the deep neural network consists of an embedding layer and three

Table 1: Sports dance video feature set based on one-hot encoding.

Sports dance videos	Features						
	Modern dance	Latin dance	Elegant	Melody sense	Dignified	Enthusiastic	Ebullient
Video 1	1	0	1	1	0	0	0
Video 2	1	0	0	0	1	0	0
Video 3	0	1	0	0	0	1	1

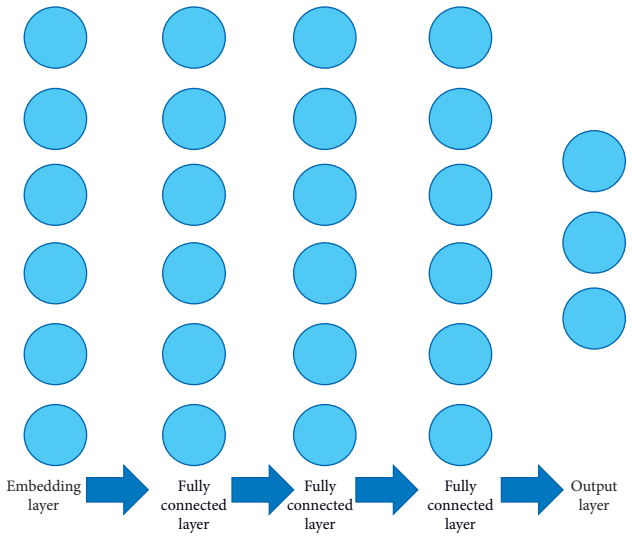

Figure 3: Deep neural network structure.

fully connected layers, and each neuron will use the activation function for calculation before outputting the result. Sigmoid function is used as the activation function of the deep neural network to meet the requirements of effectively learning sparse features.

To facilitate the calculation, the number of neuron nodes in the embedding layer and the fully connected layer is set to the exponential power of 2. The depth of the network is increased in multiples of 2 in turn. Assuming that the number of sports dance videos in the recommendation system is M, the number of output nodes is M, and the output node will output the predicted reward value of each video after it is recommended.

4.2. Deep Q-Learning Algorithm for Sports Dance Video Recommendation. Due to using the same network to generate the following target Q and estimate the current Q, it can lead to oscillations and even divergence. Therefore, deep Q-learning uses experience replay and target network methods to solve this problem.

Experience playback means that during the interaction between the agent and the environment, the experience is stored in the experience pool D. Each training will randomly sample a small batch of data from D for training to eliminate the correlation between samples. Its function is to destroy the correlation between the series and solve the correlation between the Q-value and the target Q-value. The target network does not interact with the environment, nor is it updated at every step, only at certain stages. Each update assigns the current network parameters directly to it.

The process of the deep Q-learning movie recommendation algorithm is as follows:

(1) Initialize experience pool D with capacity N, which is used for historical experience recovery. Use the deep neural network as the network model of the current predicted action-value function Q value, and initialize the weight parameter θ of the network model. Set the number of rounds of model training as M, the maximum number of training times the agent can perform. Initialize the input of the Q-value network model, information the scoring matrix processed by the FM algorithm, and calculate $\varphi 1 = \varphi(s1)$.

(2) Repeat the single empirical trajectory time step from $t = 1$ to T.

(3) Repeat the sports dance video recommendation training for each user from $u = 1$ to U.

(4) Take the user's initial rating as the initial movie recommendation state S, and select a random movie plan with probability ε for recommendation.

(5) If the recommended movie is a movie that the user likes, update the current movie recommendation state as

$$S_t + 1 = S_t \cup a. \tag{8}$$

(i) Then set the reward to $r = 1$, and calculate the input sequence as follows:

(6) If the recommended movie is a movie that the user likes, update the current movie recommendation status to $S_{t+1} = S_t$, set the reward to $r = 0$, and add $(\varphi_t, a, r, \varphi_{t+1})$ to the experience pool D, and compute the input sequence $\varphi_{t+1} = \varphi(S_{t+1})$ for the next time step.

(7) Randomly sample a small batch of stored samples $(\varphi_t, a, r, \varphi_{t+1})$ from the experience pool D.

(8) If the current state is an end state, set yi = ri, if the current state is a nonend state, then set

$$y_i = r_i + \gamma \max_{a'} Q\left(\phi_{j+1}, a', \theta\right). \tag{10}$$

(9) Calculate loss function using gradient descent algorithm

$$L_i(\theta_i) = E\left[\left(r + \gamma \max_{a'} Q\left(\phi_{j+1}, a', \theta\right) - Q(s, a, \theta_i)\right)\right]. \tag{11}$$

(10) Output value function network.

The flow chart of the algorithm is shown in Figure 4.

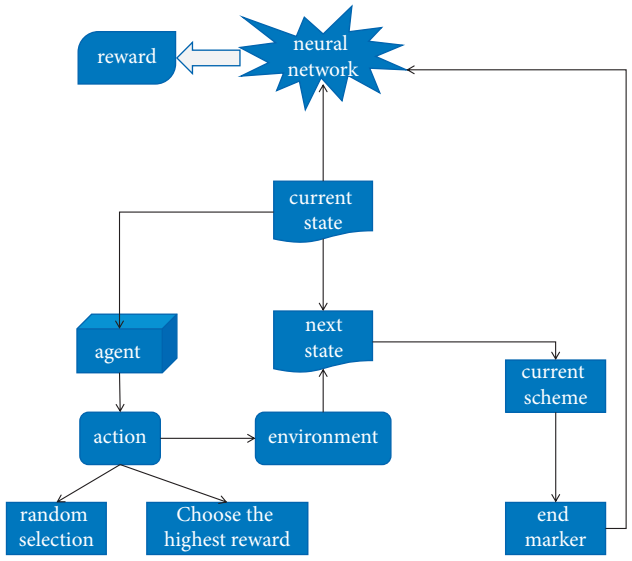

Figure 4: Sports dance video recommendation algorithm.

5. Case Study

Experimental hardware environment is one PC, 8 GB memory, and 256 GB hard disk. The operating system of the testing platform is Windows 10, the programming language is python language, and the programming is carried out on the Jupyter Notebook. The experiment uses the dataset of sports dance video evaluation, including 10000 rating records for 100 sports dance videos by 400 users (teachers and students).

To verify that the video recommendation algorithm based on deep reinforcement learning is better than the traditional collaborative filtering algorithm, we will compare the deep Q-learning algorithm (DQLA) and the collaborative filtering algorithm (CFA) on recommendation accuracy and video recommendation diversity at the same dataset and then analyze the two algorithms.

The recommendation accuracy in the experiment is defined as the proportion of users' scores for sports dance videos, and the diversity of videos recommendations in the experiment is defined as the proportion of the types of recommended videos in the total types.

According to the experimental design, the accuracy of the two algorithms is compared. The comparison results are shown in Table 2.

A comparison of recommendation accuracy of DQLA and CFA is shown in Figure 5.

It can be seen from the comparison chart that when the recommendation number of sports dance videos is less than 45, the accuracy of DQLA is slightly lower than that of the traditional CFA. Still, its recommendation effect shows an upward trend. When the recommendation number of sports dance videos is more than 45, the recommendation accuracy of DQLA is obviously better than that of CFA; when the peak of the optimal number of recommendations is reached, the recommendation accuracy gradually decreases, but it is also higher than the recommendation accuracy of CFA under the same conditions. This shows that under the premise of increasing the number of video recommendations, the recommendation accuracy of DQLA is significantly higher than that of CFA. Therefore, it is proved that using the deep Q-learning algorithm of deep reinforcement learning for sports dance video recommendation is beneficial to improve the accuracy of recommendation.

Table 2: Recommendation accuracy of DQLA and CFA.

Number of sports dance videos	Recommendation accuracy	
	DQLA	CFA
15	0.1609	0.2122
25	0.1768	0.2036
35	0.1877	0.2001
45	0.1956	0.1944
55	0.2066	0.1912
65	0.2102	0.1867
75	0.1978	0.1841
85	0.1861	0.1812

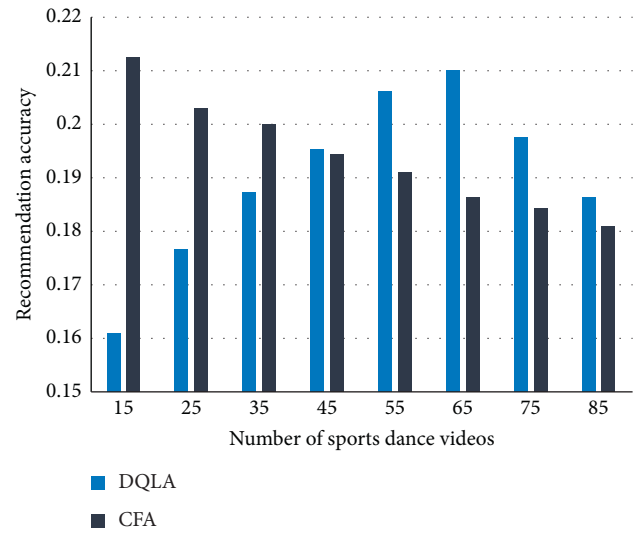

Figure 5: A comparison of recommendation accuracy of DQLA and CFA.

According to the experimental design, the recommendation diversity of the two algorithms is compared. The comparison results are shown in Table 3.

A comparison of recommendation diversity of DQLA and CFA is shown in Figure 6.

It can be seen from the comparison chart that DQLA always has a higher diversity ratio of sports dance video recommendation than CFA in the sample interval, and its diversity recommendation effect has been on the rise. This shows that when the deep Q-learning algorithm of deep reinforcement learning is used for sports dance video recommendation, the diversity effect of video recommendation has been significantly improved.

Table 3: Recommendation diversity of DQLA and CFA.

Number of sports dance videos	Recommendation diversity	
	DQLA	CFA
15	0.4711	0.4322
25	0.4801	0.4388
35	0.4878	0.4431
45	0.4892	0.4492
55	0.4913	0.4551
65	0.4934	0.4580
75	0.4966	0.4652
85	0.4981	0.4698

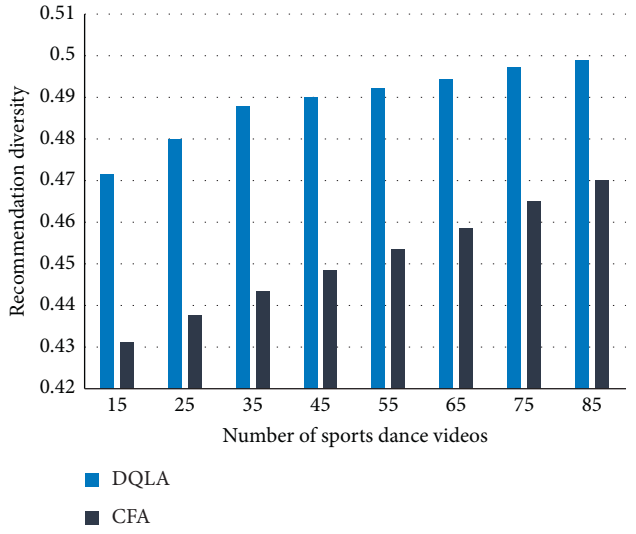

Figure 6: A comparison of recommendation diversity of DQLA and CFA.

6. Conclusion

By using the deep reinforcement learning method, the deep Q-learning algorithm is used for sports dance video recommendation training and compared with the collaboration filtering algorithm in the accuracy and the diversity of sports dance video recommendation. The comparison results show that the accuracy of sports dance video recommendation is better than the traditional collaboration filtering algorithm when the number of sports dance video recommendation reaches a specific number, and the diversity of sports dance video recommendation is obviously better than that of the collaboration filtering algorithm. It can be proved that the application of deep reinforcement learning to sports dance video recommendation can effectively solve the problems of inaccurate recommendation of traditional recommendation algorithms and single recommendation content. At the same time, the deep reinforcement learning algorithm can better learn the user's interest characteristics to provide a better video recommendation solution for the user. However, the deep Q-learning algorithm cannot solve the cold-start video recommendation problem. Therefore, next we will be to study how the recommendation system can still accurately locate the user's video of interest when there is no user's video viewing history data.

Data Availability

The dataset can be accessed upon request.

Conflicts of Interest

The authors declare that they have no conflicts of interest.

Acknowledgments

This study was supported by the 2020 Provincial Teaching Research Project of Hubei "Practice and research on 'online and offline' mixed teaching of sports dance" (No. 2020736).

References

[1] D. Sekulic, R. Kostic, and D. Miletic, "Substance use in dance sport," *Medical Problems of Performing Artists*, vol. 23, no. 2, pp. 66–71, 2008.

[2] N. Barker-Ruchti, "Sport, dance and embodied identities," *Sport, Education and Society*, vol. 11, no. 2, pp. 195–197, 2006.

[3] E. Wanke, T. Fischer, H. G. Pieper, and D. Groneberg, "Dance sport: injury profile in Latin American formation dancing," *Sportverletzung - Sportschaden: Organ der Gesellschaft fur Orthopadisch-Traumatologische Sportmedizin*, vol. 28, no. 03, pp. 132–138, 2014.

[4] P. Markula, "The intersections of dance and sport," *Sociology of Sport Journal*, vol. 35, no. 2, pp. 159–167, 2018.

[5] A. Y. Chu and C.-H. Wang, "Differences in level of sport commitment among college dance sport competitors," *Social Behavior and Personality: An International Journal*, vol. 40, no. 5, pp. 755–766, 2012.

[6] M. Skwiot, Z. Śliwiński, and G. E. Śliwiński, "Perfectionism and burnout in sport and dance," *Physikalische Medizin, Rehabilitationsmedizin, Kurortmedizin*, vol. 59, no. 03, pp. 135–140, 2020.

[7] A. F. Zhao, "Sports dance teaching based on virtual environmen," *Basic and Clinical Pharmacology and Toxicology*, vol. 127, p. 244, 2020.

[8] M. Robillard, R. Walker, and T. Zimmermann, "Recommendation systems for software engineering," *IEEE Software*, vol. 27, no. 4, pp. 80–86, 2010.

[9] R. Kumar, P. Raghavan, S. Rajagopalan, and A. Tomkins, "Recommendation systems: a probabilistic analysis," *Journal of Computer and System Sciences*, vol. 63, no. 1, pp. 42–61, 2001.

[10] Y. Gao, S. Chen, and X. Lu, "Research on reforcement learning technology: a review," *Acta Automatica Sinica*, vol. 30, no. 1, pp. 86–100, 2004.

[11] E. Acar, F. Hopfgartner, and S. Albayrak, "Fusion of learned multi-modal representations and dense trajectories for emotional analysis in videos," in *Proceedings of the 2015 13th International Workshop on Content-Based Multimedia Indexing (CBMI)*, Prague, Czech Republic, June 2015.

[12] A. Karatzoglou and B. Hidasi, "Deep learning for recommender systems," in *Proceedings of the 11th ACM Conference on Recommender Systems (RecSys)*, Como, Italy, 2017.

[13] L. Li, C. Mao, H. Sun, Y. Yuan, and B. Lei, "Digital twin driven green performance evaluation methodology of intelligent manufacturing: hybrid model based on fuzzy rough-sets AHP, multistage weight synthesis, and PROMETHEE II," *Complexity*, vol. 2020, Article ID 3853925, 24 pages, 2020.

[14] A. A. Ganin, P. Quach, M. Panwar et al., "Multicriteria decision framework for cybersecurity risk assessment and

management," *Risk Analysis: An Official Publication of the Society for Risk Analysis*, vol. 40, no. 1, pp. 183–199, 2020.

[15] L. Li, J. Hang, H. Sun, and L. Wang, "A conjunctive multiple-criteria decision-making approach for cloud service supplier selection of manufacturing enterprise," *Advances in Mechanical Engineering*, vol. 9, no. 3, Article ID 168781401668626, 2017.

[16] M. Sayan, T. Sandlidag, N. Saltanoglu, and B. Uzen, "The use of multicriteria decision-making method—fuzzy VIKOR in antiretroviral treatment decision in pediatric HIV-infected cases - ScienceDirect," *Applications of Multi-Criteria Decision-Making Theories in Healthcare and Biomedical Engineering*, vol. 18, pp. 239–248, 2021.

[17] L. H. Li, J. C. Hang, Y. Gao, and C. Y. Mu, "Using an integrated group decision method based on SVM, TFN-RS-AHP, and TOPSIS-CD for cloud service supplier selection," *Mathematical Problems in Engineering*, vol. 2017, Article ID 3143502, 14 pages, 2017.

[18] L. Li, T. Qu, Y. Liu et al., "Sustainability assessment of intelligent manufacturing supported by digital twin," *IEEE Access*, vol. 8, Article ID 175008, 2020.

[19] G. Sir and E. Sir, "Pain treatment evaluation in COVID-19 patients with hesitant fuzzy linguistic multicriteria decision-making," *Journal of Healthcare Engineering*, vol. 2021, Article ID 8831114, 11 pages, 2021.

[20] L. Li and C. Mao, "Big data supported PSS evaluation decision in service-oriented manufacturing," *IEEE Access*, vol. 8, no. 99, p. 1, 2020.

[21] Y. Li and L. Li, "Enhancing the optimization of the selection of a product service system scheme: a digital twin-driven framework," *Strojniški vestnik - Journal of Mechanical Engineering*, vol. 66, no. 9, pp. 534–543, 2020.

[22] L. Li, B. Lei, and C. Mao, "Digital twin in smart manufacturing," *Journal of Industrial Information Integration*, vol. 26, no. 9, Article ID 100289, 2022.

[23] B. Xin, H. X. Yu, Y. Qin, Q. Tang, and Z. Zhu, "Exploration entropy for reinforcement learning," *Mathematical Problems in Engineering*, vol. 2020, Article ID 2672537, 12 pages, 2020.

[24] N. Taghipour and A. Kardan, "A hybrid web recommender system based on Q-learning.23rd annual ACM symposium on applied computing," *APPLIED COMPUTING*, vol. 1-3, pp. 1164–1168, 2008.

[25] L. C. Choi, J. S. Lee, and S. C. Park, "Double layered genetic algorithm for document clustering," *Communications in Computer and Information Science*, vol. 257, pp. 212–218, 2011.

[26] S. Ohnishi, E. Uchibe, Y. Yamaguchi, K. Nakanishi, Y. Yasui, and S. Ishii, "Constrained deep Q-learning gradually approaching ordinary Q-learning," *Frontiers in Neurorobotics*, vol. 13, 2019.

[27] O. Alagoz, H. Hsu, A. J. Schaefer, and M. S. Roberts, "Markov decision processes: a tool for sequential decision making under uncertainty," *Medical Decision Making*, vol. 30, no. 4, pp. 474–483, 2010.

Hindawi
Scientific Programming
Volume 2022, Article ID 7587820, 7 pages
https://doi.org/10.1155/2022/7587820

Research Article

Research on the Application of VR Technical Ability in Political Education in Colleges and Universities

Du Liu

Henan Institute of Economics and Trade, Zhengzhou, Henan 450046, China

Correspondence should be addressed to Du Liu; duliu@henetc.edu.cn

Received 21 March 2022; Revised 6 April 2022; Accepted 12 April 2022; Published 2 May 2022

Academic Editor: Jie Liu

As an emerging multimedia technology, VR technical ability has gradually become the discuss direction of many scholars. The 3d virtual space created by computer allows users to get the feeling and depth of the real environment in VR interaction.. The application of VR technical ability in relevant disciplines that integrate both ideological and political aspects is to promote ascension of the limitations of time and space in the teaching process, to add more impetus to politics, and to continuously innovate ideas in academies and universities. The diversification of political teaching models is heightened, and teaching effects in multiple dimensions are improved.

1. Introduction

In the wake of vigorous becoming different of high and new technology, information technology has built a digital world, digital survival has become a new form of human survival, and VR technical ability has gradually become a field of research by scholars in current social development and application. Virtual reality technology uses sensing devices to enable experiencers to interact with things in all directions in virtual space without limit [1]. VR technical ability is considered to have the general characteristics of high immersion, interaction, and imagination. By simulating reality realistically, VR technical ability has a profound impact on people's practical activities, cognitive activities, and ways of thinking [2, 3]. Guide College deeply roots their patriotism and strives to become newcomers of the era who are responsible for national rejuvenation. Therefore, the integration is of great significance to enhance the effectiveness of education, and it is also an urgent task for college educators [4].

2. The Application Status of Ideological and Political Education of Virtual Reality Technology

VR technical ability is an original computer that gradually grows and reaches certain heights in 20th-century technology. "Father of Virtual Reality" Jaylen Lanier creatively pointed out in his book "Virtual Reality: A New Beginning of Vientiane" that virtual reality is a medium that can carry the hope of dreams [5–7].

2.1. Application of VR Technical Ability in Ideological and Political Education Courses. The essence of the application of VR technical ability in thought together with political courses is the innovation of guiding pattern, specifically the integration of online and offline and virtual and real teaching. Although the virtual reality teaching mode can improve the single, it cannot completely replace the conventional guiding pattern and it still occupies a central position. Therefore, it is required to interact online and offline and combine virtual and reality [8, 9].

(1) VR technical ability connects historical and real knowledge, enriching the guiding content of thought together with political courses in the five thousand years of Chinese history, and it is a significant resource and material for thought together with political teaching. Crouch said that "All history is contemporary history." Different histories stand in different eras and have different interpretations and understandings. For the study of former times, David Tebrau once proposed the "history room." As an

educational environment, the "history room" can help scholars better understand specific historical figures or complex historical events and help them see Qing's position in constant up-growth in former times. VR technical ability is equivalent to providing a "history room" in thought together with political guiding, which can restore the substance of the former times in a virtual form, and educated people can feel and experience from a contemporary perspective. History is engaged, learned, and analyzed. The spark of knowledge created by the combination of the former times and modernity not only enriches the content of thought together with political lesson but also broadens the thinking and thinking of the educated. An analogy is made: CCTV launched a digital online exhibition hall of the same name, which uses panoramic virtual technology to display 360 degrees. Visitors can get an immersive and roaming viewing experience with their mobile phones or computers and experience the great history and brilliant achievements of the 70 years.

(2) VR technical ability promotes the combination of theory and practice and improves the guiding function of thought together with political courses. Practice is the basis of cognition, and cognition in turn has a guiding part in practice. The development of thought together with political guiding activities requires the combination of theory and practice. The presentation of the effect of thought together with political guiding is also a process from internalization to externalization, from theory to practice. In the process of thought together with political teaching, classroom teaching focuses on the learning of theory, while practical teaching emphasizes the application of theory. Only the combination of the two can achieve the best teaching effect. The application of VR technical ability in thought together with political lesson is a simulated experiential teaching that transforms theory into practice. Visiting teaching practice can be realized without leaving home. An analogy is made, and the Beijing Institute of Technology used virtual technology in thought together with political lesson to implement activities to retake the Long March, allowing learners to experience the hardships during the Long March. The use of virtual technology can inspire educators far beyond the general class explanation. This immersive teaching mode enables the educated to feel the spirit of the Long March more truly in the immersive practical learning, which is more conducive to internalizing the spirit of the Long March in the heart and externalizing it in the action [10].

2.2. Problems Existing in the Ideological and Political Education Curriculum

(1) The teaching mode is single. The environment is one of the significant factors affecting the effect of thought together with political guiding. Time and space together constitute the environment of thought together with political teaching. However, due to the limitations of space and time, the thought together with political teaching mode is single [11]. First, the limitation of space makes the teaching mode single. Conventional thought together with political teaching is limited to without end 60 square meters of classrooms, most of which are taught by teachers and indoctrinated theoretical guiding that learners listen to, which limits the diversity of guiding modes in space. Second, the limitation of time makes the guiding mode single. The thought together with political education is a comprehensive discipline involving political science, education, psychology, ethics, and other disciplines. Due to the large guiding task and limited classroom time, some teachers adopt the method of scripting to complete the guiding task. This single guiding mode makes thought together with politics class boring and greatly reduces the enthusiasm of the educated.

(2) The guiding effect is not good. Theory and practice complement each other. In thought together with political guiding, only when theory is used in practice the curriculum can be effective. At present, my country's thought together with political courses focuses on theoretical guiding, and its main form is classroom instillation of theoretical education, and the indicator to measure the guiding effect of thought together with political courses is the level of scholars' test scores. This test-oriented guiding and evaluation method only attaches importance to the improvement of scholars' theoretical knowledge and ignores the cultivation of practical ability. As a result, scholars are seriously separated, resulting in poor guiding effect of thought together with political lesson.

3. Feasibility Analysis of VR Technical Ability in Ideological and Political Education

The virtual reality instructing of thought together with political theory relevant subjects taught by the school conforms to the needs of the development of the times and the growth of students. In the Internet era where everything is interconnected, the wave of digitization, informatization, and virtualization has had a significant and far-reaching influence on individual behavior habits and manner of thinking. College students are the main force active in the network society in the 5G era. They are keen to obtain information from social networking platforms such as forums BBS, Weibo, and WeChat and like to make friends, shop, entertain, and study in the online world. The mobile Internet makes the survival mode of college students move from realistic survival to virtual survival. The digitization, informatization, and virtualization of the survival mode of college students pose challenges to the guiding of thought together with political education theory courses in colleges

and universities. VR technical ability helps teachers reproduce specific social scenes or build virtual simulation classrooms for guiding and eliminates limits in time and space as so to students can experience virtual guiding situations and accept thought together with relevant subjects taught by the school without leaving home. The virtual reality classroom of thought together with relevant subjects taught by the school conforms to the needs of individual virtual survival and the development of the era of fragmented learning.

3.1. Technical Feasibility Analysis. The basic technical lines of the immersive virtual reality classroom are as follows: first, it is the initial setting and the entire application development process, and the setting of the connection points between the software and the hardware; the second is the three-dimensional construction: the model is divided into two parts from the perspective of the role and the model; the third is motion capture: this part has two parts: body motion capture and expression capture; the fourth is VR/AR: giving character animations and expressions; the fifth is Android APK: the scene and character are imported into the Unity 3D project, and the Android SDK package is used to output the APK software package; and the sixth is the effect test. The virtual reality classroom is mainly composed of two core components, one is to create a virtual reality classroom scene. Maya is the mainstream 3D animation software used in the field of 3D visual art creation at home and abroad [12]. The Maya software is used to realize the modeling, material, lighting, and camera of the basic scene, construct a three-dimensional object model, and create an immersive guiding environment. The Maya software has comprehensive functions, and the interface is simple and easy to operate. The Maya software combination tool is used to construct the 3D model required for guiding. The Maya software takes the standard primitives as the modeling basis and converts them into two-dimensional plan views of editable polygons and then constructs complex shapes by adding lines, turning, adjusting points, twisting, extruding, and chamfering. The second, Unity 3D, is mainly used to realize the interactive function of virtual reality classroom. Unity 3D is a professional game development engine that can visualize virtual scenes, create terrains, add sky backgrounds, create first- and third-person perspectives, and more. The 3D model built by Maya software is imported in Unity 3D in FBX format, and JavaScript language is used to write programs for virtual objects to achieve interactive settings for virtual objects. VRP 3D art virtual reality software is directly applied to fully realize the construction of virtual interactive scenes [13].

3.2. Economic Feasibility Analysis. The immersive virtual reality classroom effectively fills the deficiencies guiding by visualizing abstract theoretical knowledge, transferring dangerous experience to the computer interface, and converting expensive experience equipment into digital information. At the same time, the immersive virtual classroom expands the time and space of practical guiding of thought together with political theory courses, which is conducive to strengthening the effectiveness of practical guiding. Building a virtual reality classroom mainly uses Maya and Unity 3D software packages. Maya and Unity 3D software technology is mature, powerful, and easy to operate. After training, teachers of thought together with political theory courses can use software to create virtual simulation guiding and reduce guiding expenses. The classroom is shared, which can realize remote guiding. Through the extensive application of virtual reality classrooms, students in areas where guiding funds and resources are scarce can enjoy high-quality guiding resources, promote education fairness, and have good economic and social effects. Virtual reality guiding can better develop students' subjectivity. The college students who grew up in the network environment are different from the conventionally educated people. They have the consciousness of independent learning, and they have psychological needs such as longing for interpersonal relationships with peer groups and showing their individuality. Therefore, they are not used to passively listening to guiding and prefer independent exploration way of learning. Virtual reality is an advanced human-machine interface with a sense of immersion, presence, and multidimensionality [14]. Students can interact with the computer through a variety of sensory channels and learn through the mode of "subject-object" or "subject-object-subject" and "all-to-all communication," which stimulates the enthusiasm for independent learning and highlights the learners' subject position.

4. Research on the Application of VR Technical Ability to Ideological and Political Education in Colleges and Universities

Virtual reality as an academic term originated from Sutherland's (1965) paper "The Ultimate Display." "Computers, drawing tools, and other corresponding equipment use virtual reality to make participants feel three-dimensional, and the multiple senses of the body are integrated with the environment. Let the participants experience the response between behavior and the environment, so that the environment and people can achieve deep interaction and integration." [15] As a novel multimedia technology, VR technical ability has attracted widespread attention and heated discussions. With the help of this new media technology, "The work related to politics has been effectively improved and deeply integrated with the related information technology of conventional thinking" will promote the effectiveness and interest of thought together with political guiding.

(1) Virtual reality guiding courseware is developed to promote the integration of VR technical ability and the guiding content of thought together with political theory courses in colleges and universities [16]. The form and the content complement each other, and the form must fully exert its function and cannot be separated from the right content. As a tool and method, VR technical ability is the carrier or "form" of the guiding content of thought together with the politics curriculum [17]. With the help of modern virtual

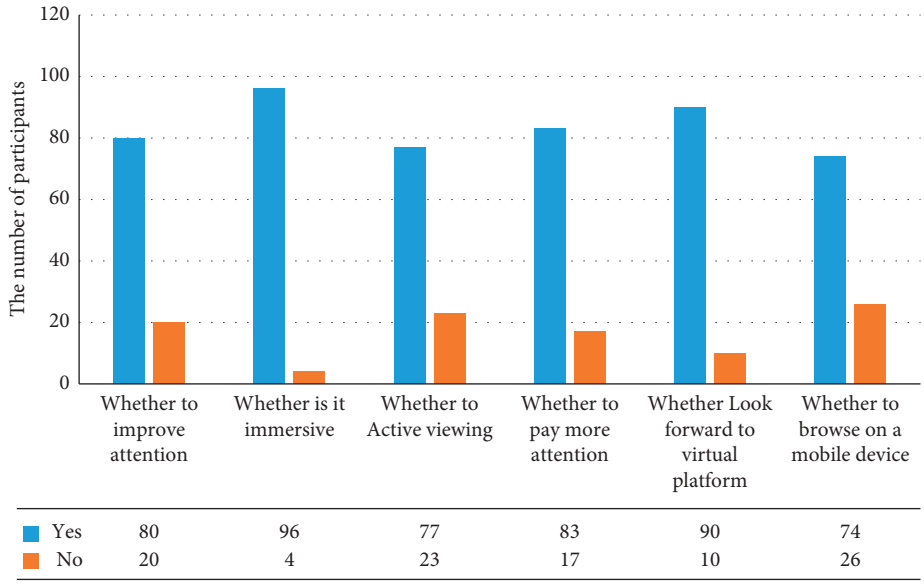

Figure 1: Statistical results of questionnaires on the integration of virtual reality technology into ideological and political education.

reality technology, instructing of thought together with the politics curriculum in colleges and universities designs simulation interactive situations based on the theme of guiding content and creates "guiding games" that students can operate according to certain procedures and rules to achieve guiding goals. The virtual simulation technology in form is improved, the shortcomings of dizziness caused by the experience of using the helmet are overcome, and the application of virtual simulation technology on mobile phones is gradually expanded to ensure the update and upgrade of the virtual simulation system. In terms of content, guiding content or guiding topics are selected through collective lesson preparation, research, or consultation with experts, cases with thought together with political education value are selected, and virtual reality classrooms are created according to the principle of "combining the virtual with the real, being able to be true, and complementing each other." Theoretical knowledge is effectively integrated into the simulation practice guiding activities.

(2) Looking to teacher guidance, the integration of VR technical ability and instruct methods of thought together with political theory class in colleges and universities is boosted. The materialist view of former times believes that in the process of transforming the world, only by promoting the unity of the subject and the object we can achieve the "consistency between the change of the environment and the change of people's activities or self." Instructing of thought together with political theory class in colleges and universities must adhere to the unity of dominance and subjectivity. On the one hand, the virtual reality instructing of thought together with politics class fully mobilizes the subjectivity of learner and opens up a broad space for scholar to learn independently, explore independently, and construct knowledge. Students independently establish learning goals, select appropriate virtual guiding content on the online guiding platform, and carry out self-education learning. On the other hand, to achieve good results in virtual reality guiding in thought together with political theory curriculum also depends on the active guidance of teachers. Teachers should actively discuss learning goals with students and provide suggestions for students to develop learning plans. In the virtual reality studying of the thought together with political theory course, the interactive communication link between the designers and the students is encouraged to retell the experience process and talk about the guiding feelings and gains. Teachers listen carefully to students' speeches, grasp keywords to guide students to use theoretical knowledge to think and analyze problems, and enhance the effectiveness of virtual reality schooling [18].

Table 1: Student users make multi-dimensional evaluation of VR experience results.

Variable	Mean	Standard deviation
Immersion	4.66	0.24
Interactivity	4.55	0.27
Conceptual	4.29	0.22
VR environment adaptability	4.21	0.35
Problem-solving skills	3.96	0.27

5. Conclusion

In terms of quality, to ensure the application effect of VR technical ability in thought together with politics class, it is necessary to increase the research and development of this

technology and constantly innovate the virtual environment, so that the intrusive feeling of characters is more real, and the scenes and modes are more diverse. "Students can forget the interference of the surrounding environment and immerse themselves in the environment of autonomous learning, which can achieve a historic breakthrough in changing passive acceptance learning to active autonomous learning" [19]. VR technical ability is currently only a guiding method, and it will be developed into a way of thought together with political education art in the future. This art mainly reflects the creation of virtual environment that fully considers the cultivation of students' values of truth, goodness, and beauty [20].

5.1. Case Analysis of the Application of VR Technical Ability in Ideological and Political Theory Courses. The application of VR technical ability in the field of thought together with political education needs to be evaluated in many aspects. A University's School of Marxism randomly selected 100 students to experience the "Nineteenth National Congress of the Communist Party of China Virtual Reality Simulation Platform" and complete the questionnaire survey (see Figure 1). In addition, 100 students experience the virtual reality work "The Last Battle" in which Chinese soldiers stubbornly resisted the Japanese army in the Anti-Japanese War and conduct multidimensional evaluations on the experience results. The five dimensions of VR environment adaptability and problem-solving ability are evaluated. Immersion is used to evaluate the user's concentration, interactivity is used to evaluate the system's human-computer interaction ability, and conception is used to evaluate the user's ability to patriotic feelings and firm beliefs during the experience process. To reflect whether the user is adaptable to the VR experience environment, and "problem-solving ability" is used to obtain whether the user's subjective feeling after experiencing the virtual reality system is in line with the official theme goal. The above five dimensions are, respectively, evaluated with 0–5 points. Each user experience system needs to be scored from each dimension.

After the students experience, the five dimensions were evaluated without distinguishing between genders, and the mean and standard deviation were used for statistics. The statistical results are shown in Table 1. Research shows that all students highly agree with the two dimensions of virtual reality immersion and virtual reality interactivity; in the conceptual evaluation of virtual reality, SD = 0.22, the standard deviation is the smallest among the five dimensions, reflecting all of students have highly consistent evaluations on the conception of thought together with political schooling produced by the virtual reality system, and the mean value of feedback is M = 4.29; in the dimension of "fitness to VR environment " M = 4.21 and SD = 0.35.. Although the standard deviation of the VR environment fitness evaluation is the largest among the five dimensions, the average value is still at a good level. It can be considered that most students can adapt to VR environment guiding; the average value is shown in the dimension of "problem-solving ability." The lowest value ($M = 3.96$) indicates that there is still some gap between the ideological and educational purposes brought by the VR system to the experiencer and the expected purpose, but the value is still close to a good level.

The above analysis can verify the previous research plan; that is, VR technical ability can enhance student attention, learning initiative, and sense of experience in the process of thought together with political education and enhance the effectiveness of thought together with political culture in colleges and universities. In practice, we have verified the advantages of VR technology, and the characteristics and advantages of VR technical ability can bring new educational territory and guiding method innovation to thought together with political schooling [21]. Virtual reality equipment will become more and more convenient, which will provide a better learning space and a good practice platform for thought together with political schooling, expand educational ideas, and innovate educational and guiding methods. This study proposes immersion methods, interactive methods, and role-playing methods for the integration of VR technical ability into thought together with political education. It advocates the increase in virtual reality communication media in thought together with political education communication media and conducts virtual simulation experiments and simulation experiments on 100 students. After the questionnaire survey, the feasibility of the plan was verified, and the guiding method was also welcomed and praised by the students. Because of its technical advantages and thought together with political education goals, VR technical ability is highly compatible with the goals of thought together with political culture.

5.2. The Future Prospect of VR Technical Ability in Ideological and Political Theory Courses

(1) The application of VR technical ability in scale and quantity is popularized, and a network of thought together with political courses between "virtual" and "real" is built. The Beijing Institute of Technology's application of VR technical ability in student training has achieved initial results, and it has built a "three-step process": using VR technical ability to build an emotional intelligence gas station; building a simulation platform for students' professional quality and assessment; and releasing the "I do my own way" system; the concept of "Internet + quality education" is gradually formed, the whole process is tracked and recorded, and a quality database of domestic college students is gradually established, in line with General Secretary Xi Jinping's speech in the 2016 National thought together with political theory class "To do a good job of thought together with political work in colleges and universities, we must change it according to the situation" [22]. The organic integration of information technology and ideological and party political courses produces "re-walking the long march" and explores the application of VR technical ability in the guiding of ideological and

governmental courses. At present, with the development of the times, the application of VR technical ability in thought together with political theory courses in colleges and universities has become possible. In the future, VR technical ability will be introduced into more ideological and governmental classrooms in colleges and universities on a larger scale to fully mobilize students' enthusiasm for learning. The overall improvement of guiding effect is realized; let VR technical ability become a multimedia bridge between teachers and students, guiding and learning, and dynamic and static and truly make the guiding mode of ideological and politics class develop in line with the times. Of course, to realize the expansion of VR technical ability in scale and quantity, it is necessary for colleges and universities to configure a professional R&D team of virtual reality technology, improve the guiding innovation awareness of thought together with political teachers, form thought together with political courses between schools, and realize VR technical ability [23]. The "real" experience beyond the limitations of time and space is pursued, and the thought together with political guiding into a network of "virtual" and "real" is connected, the contact method is "virtual," and the learning and communication are "real"; the guiding environment is "virtual," and the guiding content is "virtual."; situational experience "virtual"; and emotional training "real."

(2) The application of VR technical ability is deepened in depth and quality, and a good campus with ideological, political, and cultural atmosphere is built. At present, the submission of VR technique in courses that combine politics and ideas is only in the primary stage, and it is only a guiding method used by some colleges and universities and a few classrooms. We must play its radiating and leading role. At the same time, we should also consider deepening the submission of VR technique in courses that combine politics and ideas in terms of depth and quality. VR technical ability not only serves classroom guiding and social practice but also should serve the central link of cultivating people with morality, which runs through the whole process of subjects that combine ideology with politics, and finally, it can "achieve the whole process of educating people, educating people in all directions, and strive to create A new situation in the development of higher education in my country." In the future, classrooms and campuses should be connected, study and life, and be committed to building a good campus ideological, political, and cultural atmosphere, so as to have a subtle impact on students. An analogy is made, and some things have happened in today's society, which are contrary to the core values of socialism. It is difficult to stimulate students' in-depth reflection on the incident with the guidance of teachers alone. We might as well place students in the environment at that time. Teachers conduct timely guidance and education by observing students' every move, so that students truly understand the core socialist values instead of empty slogans. Everyone should strive to be "a firm believer, an active communicator, and a model of the socialist core values [24, 25].

The application of VR technical ability in the guiding of ideological and politics class in colleges and universities has broad prospects, and it can be specifically applied in the guiding links of four ideology together with politics classes to make an analogy, and the guiding of moral and legal-related content in "Ideological and Moral Cultivation and Legal Foundation" can be combined with specific social events to develop relevant special software courses, such as the simulation of court scenes and related software courses in the guiding of "Outline of Modern History." VR technical ability can bring students back to the field scene, mobilize students' enthusiasm for learning, and then improve the guiding effect of ideology together with political courses through VR technology. Subjects that combine ideology with politics in colleges and universities are an major part of thought together with political work. The application of virtual reality technology ability can combine ideological and political courses, enhance the attractiveness and attraction of ideological and political courses, and promote college students to establish correct national, national, and cultural concepts.

Data Availability

The dataset can be accessed upon request to the corresponding author.

Conflicts of Interest

The authors declare that they have no conflicts of interest.

Acknowledgments

This study was supported by the Social Science Planning Project of Henan Province in 2021: Innovative Research on the Integration of the Spiritual Pedigree of the Communist Party of China into the Ideological and Political Theory Course in the Information Age (project approval no. 2021bks009).

References

[1] CCID Think Tank, *White Paper on the Development of Virtual Reality Industry in 2019*, p. 8, Computer News, China, 2009.

[2] J. Xi, *The Governance of China (Volume II)*, p. 378, Foreign Languages Press, Beijing, China, 2017.

[3] Q. W. Cai, "The generation logic, the implication of the times and the realistic approach of the "six essentials" characteristics of the teachers of ideological and political theory courses in colleges and universities," *Education Theory and Practiced*, vol. 40, no. 21, pp. 41–44, 2020.

[4] L. Wang, "The application and significance of VR technical ability in ideological and political education courses," *Journal of Communication*, vol. 11, pp. 114–116, 2021.
[5] L. Jaron, *Dawn of the New Everything: Encounters with Reality and Virtual Reality*, p. 48, CITIC Publishing House, Beijing, China, 2018.
[6] M. H. Da, "Research on the application of VR technical ability," *PC Fan*, vol. 45, no. 1, 2019.
[7] H. Y. Li, *The university Thought Politics Theory Class Virtual Teaching Present Situation and Countermeasure Research*, Anhui University, Hefei, China, 2012.
[8] J. Zhang, E. T. Liu, and W. Li, "The current situation and reform measures of ideological and political education in colleges and universities in the era of big data," *Journal of Southwest Forestry University*, vol. 4, no. 1, pp. 47–50, 2020.
[9] A. M. Zhang and Y. K. Huang, "Research on the application of VR technical ability in ideological and political education in universities," *Education Theory and Practice*, vol. 41, no. 3, pp. 19–22, 2021.
[10] B. Chen and H. Q. Liu, "A micro exploration of virtual practice teaching in ideological and political theory courses in Schools," *Ideological & Theoretical Education*, vol. 8, 2013.
[11] L. P. Xu and L. Y. Li, "VR technical ability teaching in ideological and political theory course: significance, limitation and countermeasures," *Studies in Ideological Education*, vol. 9, 2017.
[12] J. Q. Dong and L. Gan, "The application mode of VR technology in the practical teaching of ideological and political theory courses in colleges and universities," *Journal of Tonghua Normal University*, vol. 32, no. 5, pp. 14–17, 2011.
[13] S. Lance, J. Ronald, and B. Stephanie, *Communication and Cyberspace: Social Interaction in an Electronic Environment*, p. 86, Hampton Press, Cresskill, NJ, USA, 1996.
[14] J. C. Zheng and Z. H. Yu, *Technology and Application of Virtual Reality*, p. 3, Tsinghua University Press, Beijing, China, 1996.
[15] D. J. Liu, X. L. Liu, and Y. Zhang, "Potential, Progress and Challenges of VR technical ability in Education," *Open Education Research*, vol. 4, 2016.
[16] X. Y. Huang, "Research on the integration of VR technical ability and ideological and political theory teaching in colleges and universities," *Journal of Hubei Open Vocational College*, vol. 14, no. 5, pp. 123–126, 2020.
[17] X. P. Lin, R. J. Zhang, and Y. F. Yan, "Research on the online and offline mixed teaching mode of ideological and political courses in colleges and universities," *The Party Building and Ideological Education in Schools*, vol. 10, pp. 46–49, 2020.
[18] B. G. Chen, "Learn the important speech of General Secretary Xi Jinping at the school ideological and political theory course teachers' symposium" pen talk," *Journal of Fujian Normal University (Philosophy and Social Sciences Edition)*, vol. 4, p. 26, 2019.
[19] J. Q. Dong, "Significance and possibility of virtual practice teaching of ideological and political theory courses in colleges and universities based on VR," *Journal of Chongqing University of Science and Technology(Social Sciences Edition)*, vol. 8, 2011.
[20] Y. Y. Zheng, *Ideological and Political Education Methodology*, Higher Education Press, Beijing, China, 2012.
[21] L. Zheng, "Analysis of tai chi ideological and political course in university based on big data and graph neural networks," *Scientific Programming*, vol. 2021, 9 pages, 2021.
[22] Y. J. Qian and J. Y. Ma, "Difficulties and solutions in the reform and innovation of teaching methods of ideological and political courses in colleges and universities-- based on VR technical ability," *Journal of Wuhan Vocational and Technical College*, vol. 18, no. 6, pp. 20–23, 2019.
[23] D. F. Wang and Y. M. Xiao, "On the Virtual Environment and Construction of Ideological and Political Education in Colleges and Universities," *Educational exploration*, vol. 8, 2018.
[24] L. Huang and R. Yao, "Construction and innovation of the "ideological and political theories teaching in all courses" in vocational colleges," *Open Journal of Social Sciences*, vol. 8, no. 8, p. 128, 2020.
[25] d J. Wu, Z. X. Cao, and Z. W. Sun, "Research on the innovation of learning space expansion in ideological and political theory courses in colleges and universities--based on VR technical ability," *Journal of Beijing University of Aeronautics and Astronautics*, vol. 34, no. 04, 2021.

Hindawi
Scientific Programming
Volume 2022, Article ID 6340526, 9 pages
https://doi.org/10.1155/2022/6340526

Research Article

Research on the Optimization of the Physical Education Teaching Mode Based on Cluster Analysis under the Background of Big Data

Hu Die[1] and Liu Lianhong[2]

[1]*Sichuan Vocational College of Finance and Economics, ChengDu 61010, China*
[2]*Chengdu Institute of Physical Education, Sichuan, Chengdu 610041, China*

Correspondence should be addressed to Liu Lianhong; 100345@cdsu.edu.cn

Received 14 March 2022; Revised 28 March 2022; Accepted 13 April 2022; Published 2 May 2022

Academic Editor: Lianhui Li

With the rise of digital campuses, online learning platforms, and the improvement of educational technology, the interaction between teachers and students has entered a new stage. Especially under the influence of CSCL (Computer Supported Collaborative Learning), computer-assisted collaborative learning, and E-learning (Electronic Learning) network digital learning that emerged in recent times, new technologies are changing the way people learn. Students' learning is not limited to one-way absorption of knowledge taught by teachers, and the interaction between students and teachers, students and students, and the interaction between students and the teaching environment are increasingly appearing in modern teaching classrooms. This paper optimizes the physical education management based on the clustering algorithm under the background of big data, uses the popular Java language to write codes to realize all the functions of the algorithm, and uses some small examples to prove the correctness of the fuzzy clustering algorithm sex. The algorithm reads a file through the input and output streams FileReader and BufferedReader. The content of the file is the relevant information of the physical education mode. It gives the methods to calculate the cluster center (i.e., the center of mass), calculate the distance, correct the fuzzy classification matrix, and display the matrix. (i.e., output matrix), conversion to deterministic classification method, calculation of classification coefficients, and basic functions such as average fuzzy entropy. According to the data, if the FCM clustering method is not used, but the previous average method is used as the evaluation basis, there will be results that we do not want to see, but if we use the FCM algorithm, the evaluation result is that what we want to see is more specific. From the analysis results, thematic teaching + basic teaching seems to be the most popular mode of physical education.

1. Introduction

With the rapid development of today's society, a large amount of data are generated due to people's close communication. This era has promoted the rise of big data and the development of the Internet, and the data are also increasing. Cloud computing makes it difficult to use big data. It became easy to use. Data mining based on the clustering algorithm has become the future development trend of physical education model optimization, and data mining technology will provide new innovation points for future education reform. Clustering is a process of dividing things without any prior knowledge. Through clustering, the similarity between things can be found, so that the results can be better revealed. First of all, the quality of teaching is clear. In addition to the evaluation of teaching facilities, teaching tools and other hardware, the evaluation of teaching quality also includes the level of teaching and the seriousness of teaching. This paper selects the most widely used FCM clustering algorithm, but it is difficult to achieve the optimum by relying only on the FCM algorithm, and it also has many limitations. This paper introduces some improved algorithms of the FCM algorithm. The popular improvement is generally carried out from the selection of the cluster center and the adjustment of the cluster center. After the program is improved, we need to verify whether the algorithm is effective or not through simulation experiments. The physical education management model

designed by the clustering algorithm in this paper mainly includes the design model to analyze teaching data and student information, including comprehensive evaluation of students, evaluation of student performance, evaluation of classroom teaching, student status, student achievement, classroom teaching, student affairs, psychology health, comprehensive assessment, and many other information can also teach students according to their aptitude according to the clustered information [1–9] The research results of this paper, combined with the current teaching management methods, can reduce the unreasonable and unscientific defects of the evaluation caused by subjective factors in the previous evaluation system and can make the teaching evaluation more scientific and reasonable.

2. Related Work

At present, the current physical education teaching system in colleges and universities in our country is not standardized enough, and the evaluation methods that have been used such as AHP, fuzzy comprehensive evaluation method, one-way analysis of variance, neural network method, and so on. Although there are many teaching evaluation methods, we cannot get the information we need from the evaluation data obtained, or what we finally find are some superficial and worthless information. Therefore, we need to obtain hidden valuable information. Clustering methods are generally divided into hard clustering and soft clustering. Hard clustering is an algorithm whose degree can only be 1 or 0. It takes less time and can draw conclusions quickly. However, this algorithm also has significant shortcomings because this algorithm ignores the connection between the data, which makes the obtained results have a large error from the correct results. The fuzzy clustering algorithm is an algorithm that requires the sum of the membership degrees of the data to be 1. This regulation greatly improves the correctness of the clustering results because this algorithm does not only consider the membership of the data. It also takes into account the influence of noise data on the clustering results. This algorithm can avoid the influence of noise data on the final result and is suitable for cluster analysis with noisy data. The research on the optimization of teaching mode is carried out through the improvement of the method. In the early twenty-first century, people's main research direction is to use more complex mathematical models to process teaching information, and the fuzzy comprehensive evaluation method is a typical example. Some domestic scholars have proposed the methods of UML and KDD. They have carried out detailed research on the subject and process of teaching, but they are still only in the stage of theoretical verification, which is still far from practical application. Data mining technology integrates fuzzy mathematics, statistics, machine learning, logical reasoning, and many other fields. It has now received extensive attention in many fields such as business, finance, medical care, education, Internet, and government. Based on the background of big data, this paper conducts a cluster analysis on the physical education teaching mode and optimizes it through quantitative analysis based on the current physical education teaching mode [10–14].

3. Related Theoretical Methods

3.1. Big Data. The definition of the connotation of relative big data mainly focuses on three aspects. As shown in Table 1, big data can summarize their connotation from the data set, technical system, and way of thinking. First of all, from the perspective of datasets, big data is an information dataset with enormous value. Different from the previous data sets, the characteristics are the diversification and complex association of data objects. This is because the data source of big data is not only the regular data of the information system but also the scraped data of network logs and the original content data of users. The emergence of new mobile devices such as mobile phones and tablets, as well as sensors and the Internet of Things, has accelerated the diversification and high growth of data. Among them, data forms include structured, semi-structured, and unstructured data, and semi-structured and unstructured data account for the majority. Structured data mostly refer to databases that have been artificially organized in advance, while unstructured data refer to actively generated data such as videos, voices, web logs, and original texts. Big data can also be called massive data. Second, from a technical point of view, big data are a technology to obtain valuable information from massive data, including a series of technical systems such as new data storage technology, mining technology, data processing technology, data analysis technology, and data visualization technology. The most widely used technology in education are educational data mining, learning analysis technology, and technology applications in large-scale online education platforms. Third, in terms of mindset, big data have a broader meaning. This study reflects the connotation of big data from this perspective with the help of the discussion in "The Age of Big Data". Big data are a worldview, a quantitative worldview of "the essence of the world is data"; big data are an empirical methodology, including three major thesis "not samples, but all data", "not causality but correlation", "it is not accuracy but hybridity"; it forms a big data value chain with massive data and data technology series, which are intertwined vertically and horizontally to form a big data system. However, as far as the nature of big data is concerned, big data are a technology for recognizing and solving problems, and its role lies in people's rational control over it. Mass data are the realistic basis and environment for generating and using technology. Analysis and other technologies are the realization paths to accomplish its purpose, and its data thinking is the value load of the technical connotation, which specifies the purpose and means of the technology [15].

3.2. Cluster Analysis. Clustering is a very common data mining method. The general algorithm is good at dealing with spherical clustering without isolated points. The CURE algorithm can better solve the spherical problem and can also better solve the isolated point problem. Its advantage is

Table 1: Definition of the connotation of big data.

Angle	Description	Application in the field of education
Data set	Very large data collections, which are different from typical databases in terms of data objects and data forms are more diverse and complex, and have exceeded the ability of traditional databases to acquire, store, manage and analyze data	Massive teaching resources (text, video) and student learning behavior data, student learning logs, teacher-student interaction, student original data, etc.
Technology system	Big data technology for mining data value, new data acquisition, data storage, data analysis, data interpretation, data warehouse, data query, data visualization technology, etc.	Educational data mining and learning analysis technology, adaptive learning system, MOOCs, and other open education platforms
Way of thinking	Quantitative worldview and quantitative empirical methodology, full-sample data analysis methods, pursuit of correlation, tolerance for hybridity	Educational quality quantification and evaluation thinking, etc.

that it can better handle the problem of outliers. It selects c points from the cluster and shrinks them to the centroid by a shrinking factor. The clusters represented by these points can better represent the shape of the cluster. Clustering is a kind of classification that does not rely on any prior knowledge, but only relies on the characteristics of the data, and finds out the same set of objects with higher density of objects in one area than other areas. In cluster analysis, outliers are a special class of points. In data analysis, we want to avoid the impact of these outliers on cluster analysis because outliers behave differently from other points. When analyzing, they should be excluded, which is the only way to reduce the impact of these outliers on cluster analysis [16–19].

Fuzzy C-means clustering algorithm (i.e., FCM) is a widely used algorithm in cluster analysis. It is one of the most commonly used algorithms. It is widely used in data analysis and pattern recognition. Its essence is mountain climbing. The FCM algorithm is a clustering algorithm based on fuzzy partitioning, because the parent target of fuzzy clustering is not a convex function. If the initialization is not done well, the final result will converge to the local extreme point. At this time, the resulting classification of the data is not optimal. This algorithm is very time-consuming for processing large amounts of data, which is a big disadvantage in practical industrial and scientific applications. The fuzzy C-means clustering algorithm is obtained, that is, the FCM algorithm. The criterion for evaluating the clustering degree of the FCM algorithm is measured by the membership function. Its objective function is evolved from the objective function of HCM. The clustering algorithm is obtained by applying the fuzzy theory. The difficulty of the FCM algorithm is the selection of the C value. It is difficult to determine the C value only based on experience when we do not know what the data are distributed according to.

Many scholars have improved the FCM algorithm, and the FCM algorithm based on information entropy is one of the improvements. This improvement helps to reduce the error generated in the iteration and improves the efficiency of the system. Weighted coefficient helps to improve the accuracy of the initial value of the cluster center. The FCM algorithm based on information entropy is an algorithm that uses information entropy to initialize cluster centers. After initialization, the number of cluster centers can be obtained, which has a great effect on reducing errors. It is easy to obtain an algorithm with high operating efficiency, which greatly reduces the possibility of local optimum caused by improper selection of the initial value of the traditional fuzzy C-means clustering algorithm. The fuzzy C-means clustering algorithm based on entropy weighting evolves on the basis of the appeal algorithm, and the weighting coefficient is quoted in the traditional fuzzy clustering algorithm. Such an algorithm can continuously select the center of the cluster in the clustering and make it as close as possible to the actual cluster center position.

Assuming a P-order vector X, the object is divided into c cluster sets by the clustering algorithm, and the centroid of each set is a P-order vector V, and the set composed of the fuzzy classification method is defined as follows:

$$\mathfrak{I}_{fc} = \left\{ U \in \mathscr{R}_{cn} \middle| \begin{array}{c} \forall \\ 1 \ll r \le c \\ 1 \ll k \le n \end{array} \right\} u_{ik} \in [0,1], \quad \sum_{i=1}^{c} u_{ik} = 1,\ 0 < \sum_{i=1}^{n} u_{ik} < n. \tag{1}$$

R is a matrix of c rows and n columns with an objective function as follows:

Among them, $\mathfrak{I}_{fc}$ is the weight coefficient, and the distance between the element X_k and the centroid V_i of the ith cluster is as follows:

$$J(U,V) = \sum_{i=1}^{c} \sum_{k=1}^{n} (u_{ik})^m d_{ik}^2. \tag{2}$$

Among them, $U \in \mathfrak{I}_{fc} V \in \mathfrak{R}_{pc}, m \in [1,\infty)$ is the weight coefficient, and the distance between the element X_k and the centroid V_i of the ith cluster is as follows:

$$d_{ik}^2 = \|x_k - v\|_i^2. \tag{3}$$

By optimizing the objective function, the FCM algorithm obtains the fuzzy classification of the object set by iterative optimization of the objective function.

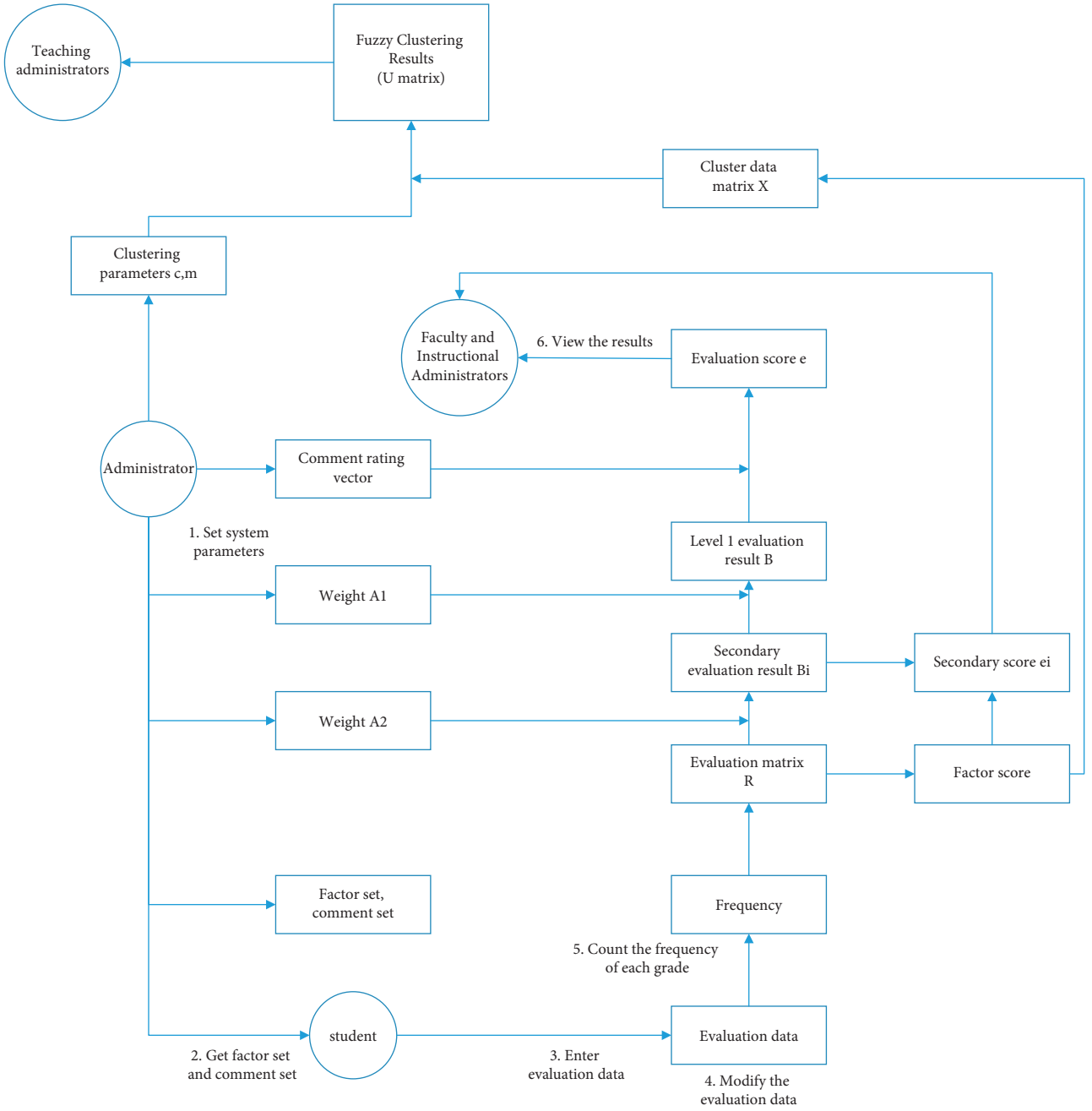

Figure 1: Analysis system of the physical education teaching mode.

4. Construction of the Optimization Model of Physical Education Teaching Mode Based on Cluster Analysis under the Background of Big Data

If teachers are regarded as an observation object, the scores of each teacher will form a matrix X, which is the data object. We know that the optimization of the physical education management system is a fuzzy process, and the FCM algorithm is a mature algorithm to a certain extent, so we choose this fuzzy clustering algorithm in the teaching management system.

4.1. Model Construction. We built the model shown in Figure 1 below based on the above ideas, where A is the clustering process, X is the teacher's score, c (the number of categories, the initial setting is 5), and m (smoothing coefficient, the initial setting is 5) (2) is a parameter.

4.2. Example of Cluster Analysis Model Implementation. The scores of each teacher on the 10 factors constitute a 10-column vector, the number of columns is the same as the number of teachers, thus forming a matrix X, which will be used as the initial data for the clustering algorithm.

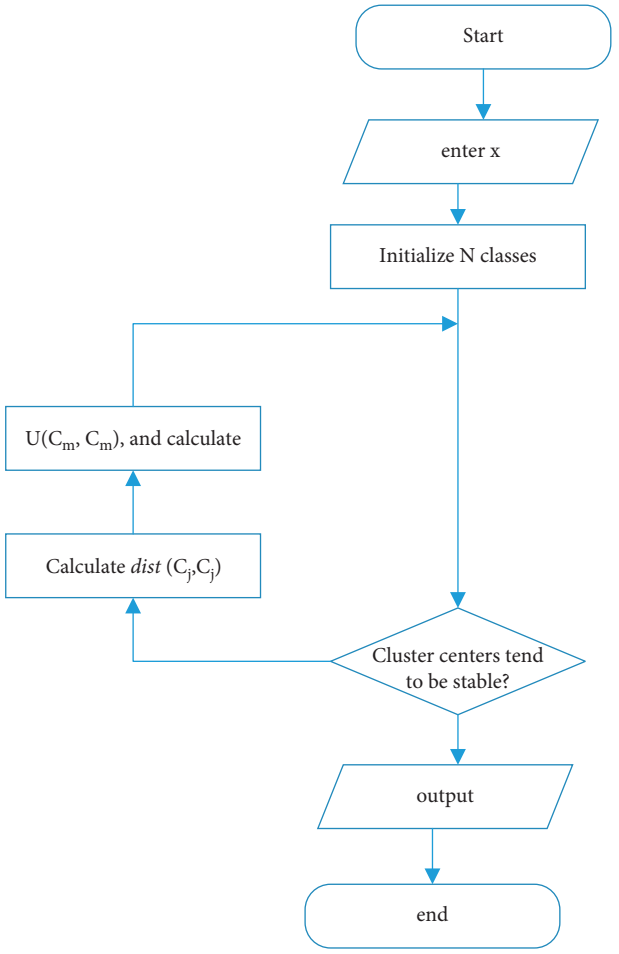

Figure 2: Flowchart of the clustering algorithm.

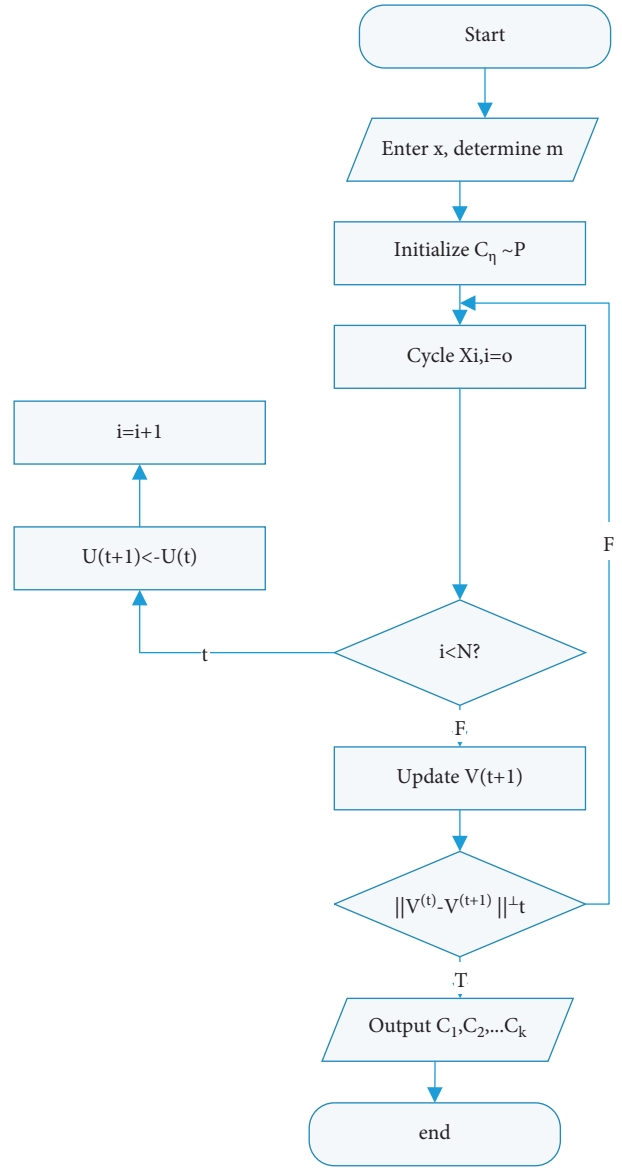

Figure 3: Flowchart of fuzzy clustering algorithm.

4.2.1. Clustering Algorithm

(1) Algorithm steps. ① Each teacher is a sample point in the 10-dimensional space defined by the system, and each such sample point is initialized into a class before the program runs and ② the distance between the sample point and the class is calculated. In this system, we choose the Euclidean distance. ③ Next, the two points with the smallest distance as a cluster is defined and the cluster center is set as the middle point of these two points. ④ Steps 2 and 3 are continued to run until the cluster center becomes stable. (2) The flowchart of the clustering algorithm, as shown in Figure 2.

Fuzzy Mean Clustering Algorithm: The fuzzy mean clustering algorithm used in this paper is more complicated than the systematic clustering algorithm. We set m as a fixed value and c as a variable.

(1) Algorithm steps:

(i) ① Set an initial c, and randomly select c samples from the sample points as the cluster center;
(ii) ②For all i, update $U(t)$ to $U(t+1)$;
(iii) ③ Update the centroid $V(t+1)$ according to $U(t+1)$;
(iv) ④ Compare $v(t)$ and $v(t+1)$, if $\|V(t)-V(t+1)\| \le t$, the algorithm terminates; otherwise, let $t = t+1$, go to step 2. (where ε is set to 0.001).

(2) The flow chart of the algorithm is shown in Figure 3.

5. Optimization Model Analysis of Physical Education Teaching Mode Based on the Fuzzy Clustering Algorithm under the Background of Big Data

5.1. Several Optimized Physical Education Teaching Modes. Aiming at the problems brought by the prominence of different categories of characteristics of college students to education and teaching, this paper proposes a teaching mode optimization plan of classified teaching and teaching students in accordance with their aptitude. That

Table 2: Four different types of optimized teaching modes.

Types of	Teaching mode	Standard
Class A	Active exploratory teaching + basic teaching	Differentiated assessment against teaching objectives
Class B	Guided teaching + basic teaching	
Class C	Attractive teaching + basic teaching	
Class D	Theme-based teaching + basic teaching	

```
try{BufferedReader br=new BufferedReader(fr1);BufferedReader
String Line=br.readLine();
int ii=0;
Line=br.readLine();Line=br.readLine();
while(Line!=null){ //Check if it is empty Line=br.readLine();
String[]num=Line.split("\u0009");
ii++;for(j=0;
j<M;
j++){x[ii][j]=Double.parseDouble(num[j]);
      }}br.close();
      fr1.close();
      }catch(Exception e){Systes.out.prinln("file error");
      //wrong output}
```

Figure 4: File reading related code.

```
int i_row,int n_col,int d){double x,max;
int j;
max=0;
switch(d){case 1: //Calculate the Chebyshev distancemax=0;
for(j=0;j<n_col;j++)
{x=Math.abs(mat1[k_row][j]-mat2[i_row][j]);
if(x>max)max=x;}
    max=x;
    }
    return max;
    case 2: //Calculate Euclid distance
    max=0;for(j=0;j<n_col;j++)
    case 3: //Hamming distance
    max=0;
for(j=0;j <n_col;j++){
    max+=Math.abs(mat1[k_row][j]-mat2[i_row][j]);
 }
return max; //return the largest value
                          }
return max;
}
```

Figure 5: Calculated distance related code.

is to say, on the basis of knowing the teaching objectives and the groups to be taught, it is necessary to have a detailed understanding of the groups to be taught and analyze their category characteristics. There are four types of students involved in this paper, as shown in Table 2, among which:

Class A is active exploratory teaching + basic teaching, mainly on the basis of the basic teaching model, adding active exploratory teaching methods, which not only improves their subjective self-learning ability but also helps divergent thinking and strengthens language organization and expression ability, further deepening understanding of theoretical knowledge.

Class B is guided teaching + basic teaching. On the basis of the basic teaching model, students add guided teaching methods to enhance their learning initiative.

Class C is attraction-based teaching + basic teaching, which is based on the basic teaching method and adds attraction-based teaching.

Class *D* is subject-based teaching + basic teaching, and subject-based teaching is added on the basis of basic teaching methods. In this way of teaching students in accordance with their aptitude and targeted education, it is expected to comprehensively promote the cultivation of college students' ideological awareness and behavior habits, knowledge, and skills.

```
public double[][]FCMCenter(double R[][],double X[][],int N,int M,
int C,double Q){
double V[][]=new double[C][M];
int i,j,k;
double n_sum,m_sum;
for(i=0;i<C;i++)
for(j=0;j<M;j++){
n_sum=0;
m_sum=0
for(k=0;k<N;k++){
n_sum+=Math.pow(R[i][k],Q)*X[k][j];
m_sum+=Math.pow(R[i][k],Q);
}
V[i][j]=n_sum/m_sum; //Calculate the centroid
}
return V;
}
```

Figure 6: Code related to calculating cluster centers.

```
public double[][]modifyR(double X[][],double V[][],int N,int M,int C,
int D,double q){
double kj_sum;
double R1[][]=new double[C][N];
int i,k,j;
for(i=0;i<C;i++)
for(k=0;k<N;k++){
kj_sum=0;
for(j=0;j<C;j++{
if(j!=i)
kj_sum+=Math.pow(
(compute_dis(X,k,V,i,M,D)/compute_dis(X,k,V,j,M,D)),(2/(q-1)));
}
R1[i][k]=Math.pow((kj_sum+1),-1); //correct classification matrix
}
return R1;
}Method called when the matrix needs to be displayed, i.e. the output matrix:
public void display(double Matrix[][]){
for(int i=0;i<Martrix.lenth;i++){
for(int j=0;j<Martrix[0].lenth;j++){
//Matrix[i][j]=Math.round(Matrix[i][j]);
System.out.printf("%8.7f",Matrix[i][j]); //output the matrix
}
}Convert to Deterministic Classification Method:
public double[ ][ ]displyClss(double R[][],int N1,int C1){
int i,j;
double max;
double CR[][]=new double[C][N];
for(j=0;j<N;j++){
max=R1[0][j];
CR[0][j]=1;
for(i=1;i<C;i++){
if(R1[i][j]>max){
max=R1[i][j];
CR[i][j]=1;
if(i==1)
CR[0][j]=0;
}elseCR[i][j]=0;
}
}return CR;
}
```

Figure 7: Correction code related to fuzzy classification matrix.

5.2. Fuzzy Clustering Code Writing

5.2.1. File Reading. First, you need to read a file through the input and output streams FileReader and BufferedReader. The content of the file is the relevant information of teaching quality evaluation:

5.2.2. Calculating Distance. The code to calculate the distance is as follows:

5.2.3. Calculating Cluster Centers. The following code implements the calculation of cluster centers (aka centroids).

```
public double[]ClassFactor(double R1[][],int N,int C){
int i,j;double ClassF[]={0,0};
for(i=0;i<C;i++)for(j=0;j<N;j++){
ClassF[0]+=Math.pow(R1[i][j],2);
ClassF[1]+=R1[i][j]*Math.log(R1[i][j]);
}
ClssF[1]=ClssF[1]/N; //Classification coefficient
ClssF[2]=-ClssF[2]/N; //Average fuzzy entropy
return ClassF;
}
```

Figure 8: Calculated classification coefficients and average fuzzy entropy related codes.

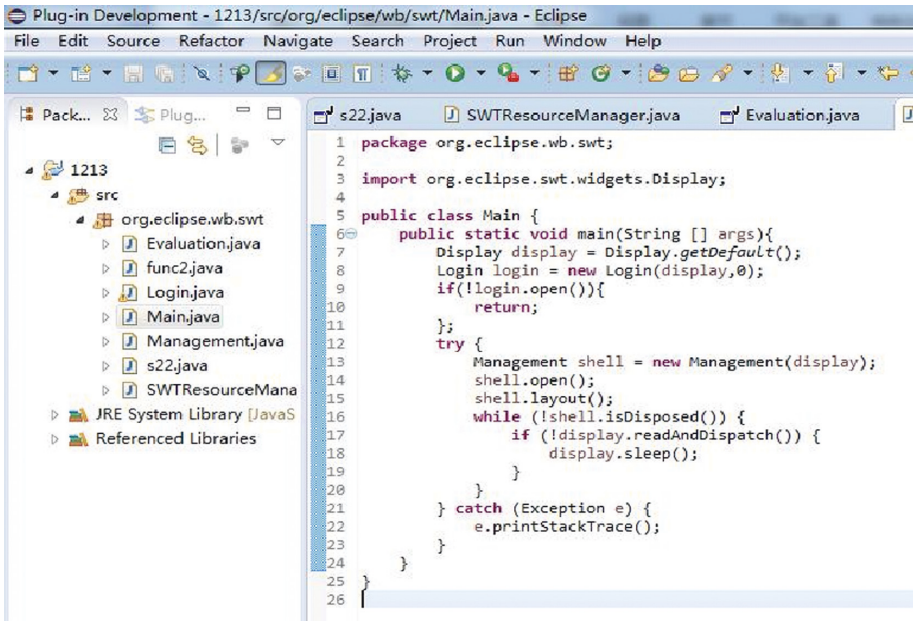

Figure 9: Teaching mode optimization structure hierarchy.

Table 3: Scores under different PE teaching modes.

Types of	Teaching mode	Score
Class A	Active exploratory teaching + basic teaching	7.759
Class B	Guided teaching + basic teaching	8.652
Class C	Attractive teaching + basic teaching	8.375
Class D	Theme-based teaching + basic teaching	9.615

5.2.4. Revised Fuzzy Classification Matrix.

5.2.5. Calculate the Classification Coefficient and Average Fuzzy Entropy.

5.3. Teaching Mode Optimization Structure Hierarchy. Figure 9 shows the structure levels under different teaching modes.

5.4. Statistical Results of Teaching Evaluation. The statistical results are shown in Table 3.

5.5. Results and Analysis. The final output of the code is a number of non-fixed matrices composed of 1 and 0. The input data are clustered and calculated. According to the obtained data, if the FCM clustering method is not used, the previous average method will be used as the evaluation basis. The following results appear: Category *D* has the highest score and should focus on inquiry-based teaching + basic teaching. According to the results of FCM clustering, but the classification results of fuzzy clustering are fixed, the evaluated indicators are clustered and the threshold of clustering is delimited, so as to achieve the effect of clustering and complete fuzzy clustering. It can also be used to evaluate the management mode of physical education teaching.

6. Conclusion

The clustering algorithm is a very commonly used algorithm, and fuzzy clustering is a clustering algorithm that applies the fuzzy theory. This paper first gives a brief overview of the background of big data and the development status of cluster analysis at home and abroad. Next, it mainly introduces the operating environment and language for developing the algorithm and organizes and presents some codes. This paper studies the teaching management system for the fuzzy clustering algorithm. Among many clustering algorithms, the FCM clustering algorithm is the most widely used algorithm. It can deal with these problems by transforming the principle of nonlinear programming. It can process these physical education data by transforming the principle of a nonlinear programming. It is a fuzzy clustering method, and each iteration moves in the direction approaching the minimum point. Although the FCM algorithm also has many imperfections, with the continuous improvement of this algorithm by scholars, this algorithm has a good prospect. The main task of this paper is to construct a new teaching mode optimization algorithm, improve the original physical education teaching mode, and propose a new cluster analysis model. Judging from the research results, thematic teaching + basic teaching seems to be the most popular mode of physical education.

Data Availability

The dataset can be accessed upon request.

Conflicts of Interest

The authors declare that they have no conflicts of interest.

References

[1] MIL, *The 2011 Digital Universe Study: Extracting Value from Chaos International Data Corporation and EMC*, USA, 2021.

[2] J. Manyika, M. Chui, and B. Brown, "Big Data: The Next Frontier for Innovation. Competition. And Productivity," *McKinsey Global Institute*, vol. 23, pp. 1–137, 2019.

[3] T. Cass, "A handler for big data," *Science*, vol. 28, no. 10, pp. 282–336, 1998.

[4] L. A. Gernon and C. Kedzierski, "Comadre group teaching in nutrition," *Journal of Obstetric, Gynecologic, and Neonatal Nursing*, vol. 43, pp. S2–S3, 2014.

[5] M. J. Zaki, "Scalable Algorithms for Association Mining," *IEEE transactions onknowledge and data engineering*, vol. 12, no. 3, 2000.

[6] U. M. Fayyad and G. Piatetsky - Shapiro, "From data mining to knowledge discovery: an overview," *American Association for Anifieial Intellingenee Calif*, vol. 31, 1991.

[7] E. G. Cuba and Y. S. Lincoln, *Fourth Generation Evaluation*, p. 84, SagePublications, Newbury Park, USA, 1989.

[8] C. M. Chen, Y. Y. Chen, and C. Y. Liu, "Learning performance assessment approach using web based learning portfolios for learning systems," *IEEE Transactions on Systems, Man, and Cybernetics-Part C: Applications and Reviews*, vol. 37, no. 6, pp. 1349–1359, 2017.

[9] L. Talavera and E. Gaudioso, "Mining student data to characterize similar behavior groups in unstructured collaboration spaces," *Workshop on Artificial Intelligence in CSCL, 16th European conference on Artificial intelligence*, vol. 44, 2014.

[10] D. P. Born, C. Zinner, and P. Duking, "Multi directional sprint training improves change-of-direction speed and reactive agility in young highly trained soccer players," *Journal of Sports Science and Medicine*, vol. 15, no. 2, pp. 314–319, 2016.

[11] T. Stølen, K. Chamari, C. Castagna, and U Wisløff, "Physiology of soccer: an update," *Sports Medicine*, vol. 35, no. 6, pp. 501–536, 2005.

[12] J. Parkkari, U. M. Kujala, and P. Kannus, "Is it possible to prevent sports injuries?" *Sports Medicine*, vol. 31, no. 14, pp. 985–995, 2021.

[13] A. Friedson, "Winning pays:High school football championships and property values," *Journal ofHousing Economics*, vol. 22, 2013.

[14] A. Donabedian, "Evaluating the quality of medical care," *The Milbank Quarterly*, vol. 83, no. 4, pp. 691–729, 2015.

[15] A. Donabedian, "Quality of care: problems of measurement. II. Some issues in evaluating the quality of nursing care," *American Journal of Public Health and the Nation's Health*, vol. 59, no. 10, pp. 1833–1836, 1969.

[16] J. Crilly, W. Chaboyer, and M. Wallis, "A structure and process evaluation of an Australian hospital admission avoidance programme for aged care facility residents," *Journal of Advanced Nursing*, vol. 68, no. 2, pp. 322–334, 2020.

[17] M. A. Bienkowski, M. Feng, and B. Means, "Enhancing Teaching and Learning through Educational Data Mining and Learning Analytics: An Issue Brief," Technical report, U.S. Department of Education Office of Educational Technology, USA, 2017.

[18] S. Y. Chen and R. D. Macredie, "Editorial: data mining for understanding user needs," *ACM Transactions on Computer-Human Interaction*, vol. 17, no. 1, pp. 62–69, 2018.

[19] R. A. Easterlin, "Does economic growth improve the human lot? Some empirical evidence," *Nations and Households in Economic Growth*, pp. 89–125, NY, USA, 1974.

Hindawi
Scientific Programming
Volume 2022, Article ID 4188217, 8 pages
https://doi.org/10.1155/2022/4188217

Research Article

Research on Automatic Intelligent Coloring of Animation Sketch Based on Enhanced Deep Learning

Zhe Wang [1,2]

[1]*Faculty of Design and Architecture, Universiti Putra Malaysia, 43400 UPM Serdang Selangor, Darul Ehsan, Malaysia*
[2]*Art & Design Department, Taiyuan Institute of Technology, Taiyuan, Shanxi 030008, China*

Correspondence should be addressed to Zhe Wang; gs61854@student.upm.edu.my

Received 11 March 2022; Revised 29 March 2022; Accepted 11 April 2022; Published 28 April 2022

Academic Editor: Jie Liu

An automatic intelligent coloring model of animation sketch based on enhanced deep learning is proposed. In the proposed model, generative adversarial networks (GANS) are adopted. The U-net network based on the Swish function residual enhancement is used in the generative model, and the ResNet network is used in the discriminant model. The U-net embedded with the Swish Gate module is adopted to transmit feature map information. The perceptual network on the discriminator is used to perceive the perceptual features of the generated image and the actual image and calculate the perceptual loss. Experiment results show that perceptual loss can better capture the difference between black-and-white images and color images, so as to better train the network end-to-end. After comparative analysis, it can be concluded that compared with the existing methods, the proposed model has greater advantages in processing animation sketches. The color images it generates have higher visual quality and richer color diversity and matching.

1. Introduction

At present, the coloring of animation sketches mostly depends on the hand-painted coloring of professional animation painters, which will spend a lot of time and energy. At the same time, the coloring effect is also affected by individuals [1, 2]. The emergence of convolutional neural networks [3] provides a new perspective for the coloring of gray images. Its emergence makes it possible to complete many tasks in computer vision at the same time. It is necessary for the computer to automatically color the animation sketch. At the same time, for some ordinary people, they can use this method to color the line sketch and create their favorite color pictures. These methods can automatically colorize animation line art to generate rich color pictures; in addition to manual selection of specific colors color to color, the coloring time is much faster than hand-painted coloring. However, generative adversarial networks (GANS) have always had a long training time, unstable generation effect, and non-convergence of the network [4, 5]. These problems can lead to poor quality of color pictures generated by the GANS-based animation line art coloring model. For example, the color filling is unreasonable, the filling color exceeds the filling area, and the color brightness is inconsistent.

As far as GANS-based coloring models are concerned, it is challenging to meet the actual needs, and the coloring results also need to be screened. Some color pictures of poor quality are inevitable, time-consuming, and laborious. GANS consists of a generator and a discriminator [5]. When the animation line art is colored, the generator inputs the animation line art and outputs the colored image. Moreover, the choice of the generator network structure and loss function will directly affect the quality of the final output color picture. Therefore, designing a suitable stable network and a suitable loss function can improve the quality of generated color images. The role of the discriminator is to discriminate whether the generated color image is close to the effect of artificial coloring avoidance. The final output is a color image with poor quality, and the discriminator will affect the training stability of GANS. Training GANS needs to achieve the Nash

equilibrium; the discriminator network needs to be further optimized to ensure training stability.

2. Related Works

In recent years, GANS has received increasing attention in deep learning. A generative adversarial model usually consists of a generator and a discriminator. The generator captures the underlying distribution of actual samples and generates new data samples. The discriminator is often a binary classifier that distinguishes real examples from generated samples as accurately as possible. The discriminator guides the training of the generator, and the alternating movement between the two models is used for continuous confrontation. Finally, the generative model can better complete the generation task. With the emergence of more and more GANS variants, GANS has achieved significant results in various fields of images. In image coloring, GANS also occupies an important position in mainstream algorithms. At present, the deep learning-based automatic coloring model mainly adopts the architecture of GANS.

Pix2Pix [6] is also a significant variant of GANS, using conditional generative adversarial networks (CGANS) to achieve image-to-image conversion; it can do many things, such as drawing sketches, convert outlines to pictures, converting night scenes to day scenes, auto colorize, and more.

Moreover, Style2paints, as a style transfer coloring model variant of GANS, needs to provide a reference image for color use in advance when converting the anime line art into color images [7]. The generator network proposed by Style2paints also uses U-net with residual enhancement. In the web, a residual module is added between each level in the right half of the network to enhance the coloring detail texture, and an auxiliary classifier is added to the generator network structure. The discriminator can distinguish the true and false of the generated image and classify its related styles to achieve style transfer.

PaintsChainer, which is now widely used, uses an unconditional discriminator and has achieved remarkable results [7]. Users only need to input an animation line art picture to get a color picture, and they can also get the effect under the color style by adding the color they want. However, because no labels make it easy to pay too much attention to the relationship between lines and feature maps, the image composition will lead to overfitting, and the line filling will be confusing.

It can be seen that to improve the performance of the GANSs network, much research has been done on its network structure. Moreover, GANSs have also achieved outstanding results in animation line art coloring. U-net has been proven to have an excellent effect on the coloring of anime line drafts. Still, the biggest problem is that the up-sampling convolutional layer and the down-sampling convolutional layer of U-net are directly spliced [8, 9]. When the first layer is discovered, it can simply jump-connect all the features directly to the last layer of the decoder, thus minimizing the loss, which results in the middle layers of the network not being able to learn anything, no matter how many times it is trained. In the network, there will be a problem of gradient disappearance in the middle layer.

A deep learning model for animation line draft coloring is proposed to solve the above problems. The overall structure of the model is an adversarial generative network model. The generator structure of the model uses the improved residual-enhanced U-net network structure, and the discriminator uses the ResNet network structure [10–12]. Inspired by the ResNet network, the original U-net network sampling up-convolutional and down-sampling convolutional layers changed directly. The method is no longer a jumper connection. The Swish activation function is used, and two connection modules are proposed. The proposed Swish module can better filter the feature information transmitted in the network and improve the network's learning ability. When the low-level convolutional layer completes the task, the high-level convolutional layer can still obtain the filtered feature information for learning. After coloring the animation line draft, the color details are confused, and the gradient disappears during the training process. In addition, the discriminative network is used as a perceptual network, and the perceptual features of the generated image and the actual image can be obtained to calculate the perceptual loss. The coloring model with perceptual loss can generate qualitatively better color images.

3. Coloring Model of Animation Sketch Based on Enhanced Deep Learning

U-net network is a U-shaped convolutional neural network structure, which is initially used in the field of image segmentation. It has two branches, the left one is the encoding network structure, and the right one is the decoding network. U-net has also been widely used in image synthesis. However, it is easy to form gradient disappearance in the middle layer during network training. The emergence of non-linear activation functions makes neural networks more expressive.

To improve the quality of the generated color images, a generative adversarial model for coloring animation sketch is proposed, as shown in Figure 1. The generator network uses the residual enhanced Swish activation function based on U-net to convey feature map information. The selection in the discriminator uses a ResNet network. It has the following advantages.

(1) Two kinds of connections are proposed based on the residual module and the Swish function. This can solve the problem of the gradient disappearance of the middle layer in the U-net network training process, better filter the feature map, better learn the feature map of each level, will not cause the gradient to disappear, and the convergence curve can also converge faster.

(2) Propose using perceptual loss to better capture reference images and the difference between the generated image, making the resulting color image more textured and color-to-color transitions are smoother.

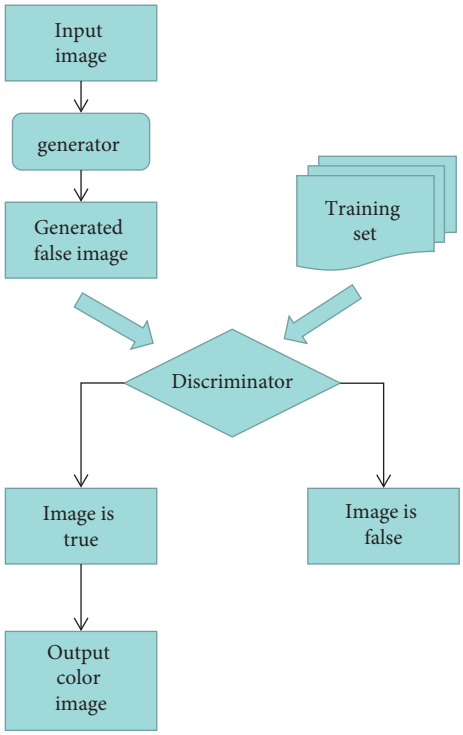

Figure 1: Overall structure of the network.

(3) The experimental results in the Anime Sketch Colorization Pair dataset show that the coloring effect of the method proposed in this paper is better than the current coloring method and is close to the impact of artificial coloring.

3.1. Whole Network Structure. The generator network structure is based on an improved version of U-net, as shown in Figure 2, which is a Swish U-net network structure enhanced by residuals. The network has six different resolution levels, and as the level increases, the resolution gradually decreases. Like U-net, Swish U-net can also be regarded as the left and right branches. Still, a Swish Mod is embedded between the left and right components of the same resolution level to filter the information transmitted from the encoding path to the decoding path; instead, of the original jumper, Swish Mod can speed up the convergence speed of the network and improve the performance of the network. Each green dotted box in Figure 2 is a Swish Gated Block, and there are 10 in total. In the left branch, the output of each Swish Gated Block consists of the feature map output by the residual part and the feature map filtered by Swish Mod; In contrast, in the right department, the output of each Swish Gated Block consists of three parts, which are the feature map output by the residual part, the feature map filtered by the input Swish Mod, and the feature map filtered by the Swish module corresponding to the left branch.

Except for the last convolutional layer of the network, all convolutional layers use normalization and LReLU functions. The input of the Swish Gated Block of the i-th layer is the output of the Swish Gated Block of the i-1 layer for 1×1 convolution obtained after the operation. In addition, the number of convolution kernels for the 1×1 convolution operation in the i-1th layer is the same as the number of convolution kernels for each convolutional layer in the i-th layer. From resolution level 1 to resolution level 6, in each resolution level, the number of convolution kernels of each convolutional layer is 96, 192, 288, 384, 480, and 512 in turn. The last convolutional layer will output the final color image, consisting of 27 1×1 convolution kernels, and no normalization and activation functions are used.

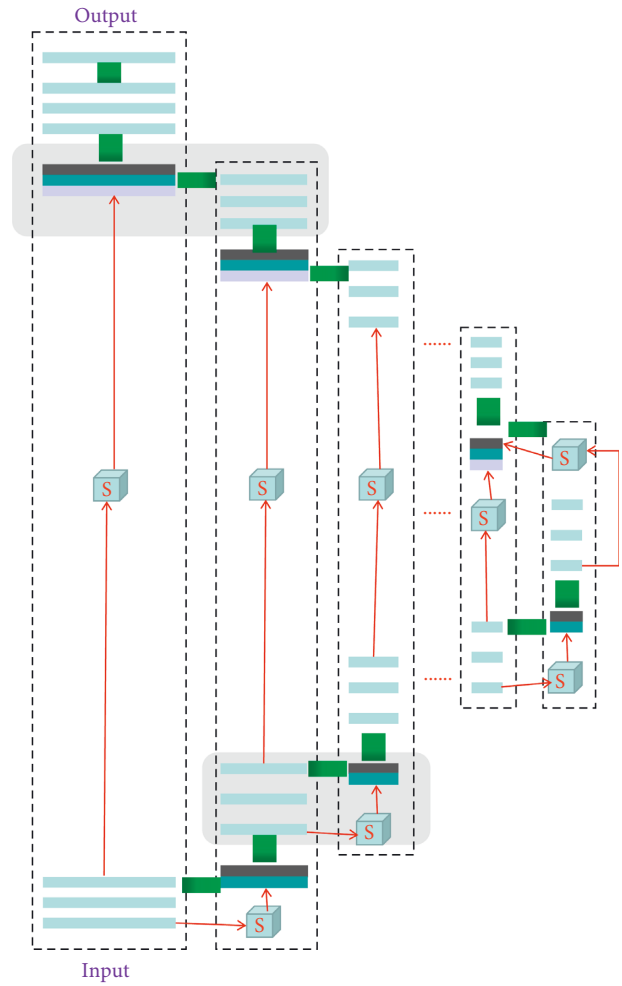

Figure 2: Network structure of Swish U-net.

Generally speaking, the role of the discriminator is to distinguish between authentic images and generated images. ResNet is selected as the discriminator network on the discriminator. Here, the discriminator has two tasks: (1) It discriminates between generated images and authentic images. (2) The generated and authentic images' perceptual features are extracted by calculating the perceptual loss as a perceptual network. The discriminator network is finally normalized to improve the stability of network training. Then, the ReLU activation function is used to make network training faster while preventing gradients from disappearing.

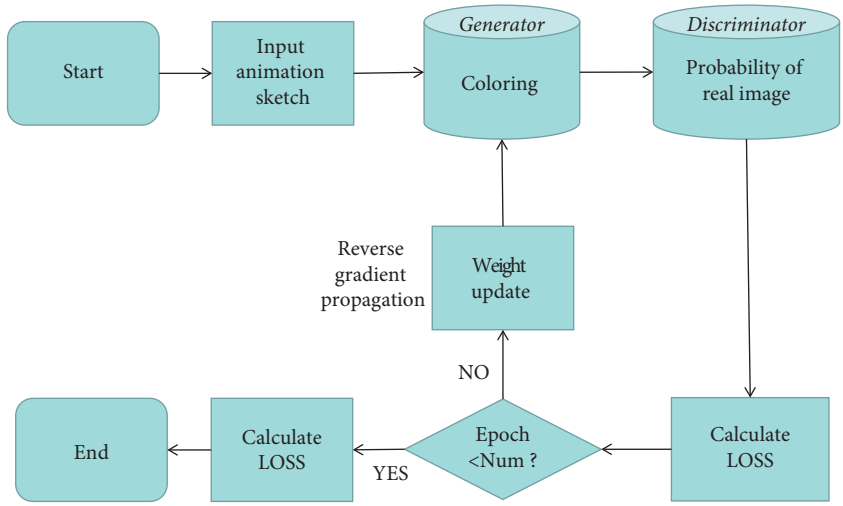

Figure 3: Training process of the network.

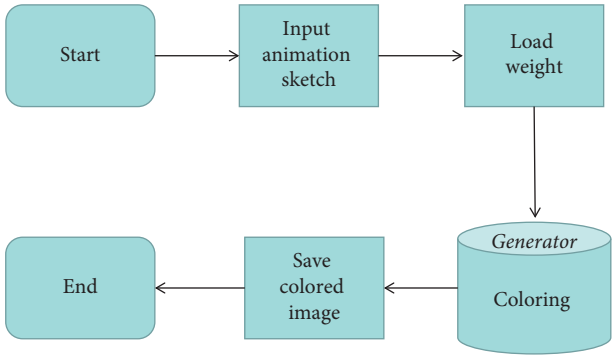

Figure 4: Prediction process of the network.

Figure 3 shows the training process. Each step includes two processes of forwarding propagation and back-propagation. The two processes are completed once as one epoch. When the number of times is less than the set training value Num, it will continue to cycle; Figure 4 shows the prediction flow chart after the model is trained, only forward propagation.

3.2. Swish Module and Loss Function. The new residual module Swish Gated Block proposed in this paper improves the residual module in ResNet [12–14]. The Swish Gated Block is composed of Swish module and residual, Swish module contains a convolutional layer and Swish activation function. In the structure of the proposed residual module, x represents the input data, $F(x)$ represents the residual, $F(x)+x$ is the output of the residual module, and "+" represents the corresponding addition of pixel points, $G(x)$ denotes the result of the convolutional layer in Swish module, "·" means the corresponding multiplication of pixels; $T(x)$ represents the output of the convolutional layer in Swish Gated Block after the non-linear LReLU function, $S(x)$ is the output of Swish module, "⊕" represents the splicing between feature maps, and "$T(x)\oplus S(x)$" is the final output of Swish Gated Blok.

In the residual module, the input data x are directly added to the residual without processing; In Swish module, x is processed, and the Sigmoid function is used; its advantage is that it can control the magnitude of the value, and in the deep network, the importance of the data can be kept from significant changes. In addition, non-linear LReLU is used for the convolutional layer in SwishGatedBlock, which has a better effect than ReLU for generating classes. Swish module filters the input data x, like a gate that controls the transmission of the input data x from the bottom layer to the high layer through a shortcut feature map. Swish module is defined as follows:

$$S(x) = X \cdot \sigma(G(x)), \tag{1}$$

where $S(x)$ is the output of Swish module, x is the input data, $G(x)$ is the output of the convolutional layer, $\sigma(\bullet)$ represents the Sigmoid function, and "•" represents the multiplication of the corresponding pixels.

The output of Swish Gated Block is as follows:

$$y = T(x) \oplus S(x), \tag{2}$$

where $T(x)$ is the residual part in the module, $S(x)$ is the information filtered by Swish module, and finally spliced together to output the obtained feature map.

The generator and discriminator proposed in this paper are trained separately, using pairs of matching images as a data set of images. Anime line art is the input data, and paired color images are the labels. For colorization tasks, simply comparing the pixel colors of the generated image and the reference color image can seriously affect the quality of the output image. Because a black and white image is given, the hair color can be silver or black. The black and white image has a one-to-many relationship with the colored image. Still, there is only one label, so it is unreasonable only to consider the L1loss of each pixel. Perceptual missing is proposed for this purpose, which can help capture the difference between the generated color image and the reference image, and L2 regularization is added to prevent the model from overfitting

Figure 5: Colored images obtained from animation sketch.

[13]. The perceptual loss is calculated based on the feature map and expressed as follows:

$$L_g = \sum_{1} \lambda_1 \|\varphi_l(T) - \varphi_l(G)\|_1 + \alpha \sum_{l=1}^{n} \lambda_l^2. \tag{3}$$

Among them, 1 takes the value [0, 5], T represents the generated image, G represents the actual image, φ_0 (G) represents the convolution operation with the network structure of the discriminator, φ represents no convolution operation, represents the original image, φ_1 (G) denotes the output result (feature map) of the first layer of convolution, representing the perceptual feature, and so on. λ_1 $= \{0.88, 0.79, 0.63, 0.51, 0.39, 1.07\}$, indicating the weights of different layers. The regularization coefficient $\alpha = 0.009$, and the optimizer adopts Adam.

The network of the discriminator uses ResNet, and the data are normalized after the convolutional layer so that the data will not be too large and lead to unstable training [14, 15]. The loss of the discriminator here is the discriminator loss proposed by GANS.

$$L_d = -E[b\sigma(D(T)) + lb(1 - \sigma(D(T)))], \tag{4}$$

where G represents the actual image, T represents the generated image, D represents the discriminator, σ $(\cdot)$ represents the sigmoid function, and E represents the mathematical expectation.

Figure 6: Comparisons of Swish U-Net model (with perceptual loss), SwishU-Net-WPL model (without perceptual loss) and U-Net model.

4. Case Study

4.1. Datasets and Evaluation Indicators. To verify the performance of the proposed method, training is performed on large datasets, Anime Sketch Colorization Pair, which has a large number of paired anime line art images and anime colorization images. Training is conducted on 15432 anime line drawings and their corresponding color images, and all pictures of the experiments are resized to 512×512 resolution. Assessing the quality of generated images has always been a complex problem. The colors generated by different coloring models in other areas of the same coloring image are also different during the coloring process. In addition to differences in color, images generated by different shader models also vary significantly in image quality (texture, shading, brightness) and visual quality of images. Therefore,

Table 1: Comparisons of SwishU-Net model (with perceptual loss), SwishU-Net-WPL model (without perceptual loss), and U-Net model on four quantitative indicators.

	FID	PSNR	SSIM	FSIM
Swish U-net model	108.23	18.55	0.85	0.86
U-net model	115.96	17.62	0.87	0.85
Swish U-net-WPL model	119.25	15.97	0.84	0.84

Table 2: Comparisons of the Swish U-Net model, Style2paints model, and PaintsChainer model on average running time and model complexity.

	Average running time	Model complexity
Swish U-net model	≈30	≈58000
Style2paints model	≈41	≈70000
PaintsChainer model	≈46	≈77000

we use several standard image quality quantitative indicators to evaluate and compare SwishU-net and other existing colorization methods. The quantitative evaluation indicators used in the experiments include peak signal-to-noise ratio (PSNR), structural similarity (SSIM), and feature similarity (FSIM) [15–17]. To confirm the role of perceptual loss in the colorization model, we use Fréchet inception distance (FID) [15–17] as an evaluation criterion to quantify the quality of color images. Figure 5 shows the coloring results of the proposed coloring model. To get a color image of eight different colors, only an animation line draft is needed to input.

4.2. Experimental Results. Figure 6 shows a comparison of two colorization models with and without perceptual loss. It can be seen that the color image generated by the shading model with perceptual loss is more vivid and complete, especially the color gradient is smooth, the shadow distribution is reasonable, and there is no sense of violation; the color image generated by the shading model without perceptual loss. The colors are not rich enough, and there are fewer gradients of color changes. In addition, the color image generated by the colorization model without perceptual loss is also low in color saturation, and there is no apparent boundary between the characters and the background in the picture. Therefore, the perceptual loss significantly influences the shading effect, and the image texture generated by the shading model with the perceptual loss is more detailed. The transition between colors is also smoother.

To further investigate our approach, quantitative analysis was used to evaluate the quality of the generated images, as shown in Table 1. We used FID as a quantitative indicator to assess the generated color images' quality (sharpness) and color diversity. The automatic colorization model is a one-to-many transformation, where FID is used to determine the quality of the generated color images; SwishU-net without perceptual loss is abbreviated as SwishU-net-WPL. In addition, PSNR, SSIM, FSIM are used here to evaluate the performance of the three algorithms, and the best results are shown in bold. SwishU-net achieves the best performance on all metrics. SwishU-net without perceptual loss has the worst performance on all metrics, indicating that perceptual loss plays a vital role in the colorization model. The quality of the color image generated by the proposed Swish module residual enhanced network is better than the image generated by the U-net network, indicating that the Swish module residual enhanced generative model has a better coloring effect.

4.3. Algorithm Complexity Calculation. Table 2 compares the algorithmic complexity of SwishU-net and the current mainstream algorithms. All algorithms are based on python language and implemented on GPU; only 512×512 images are tested here. 16 parameter layers are selected for the above experiments to balance performance and computational efficiency.

It can be seen that Style2paints and PaintsChainer consume much time due to the complex optimization process. At the same time, the generative network of SwishU-net reduces the running time by not using normalization layers. Despite using a lightweight framework, the average running time and the number of parameters results show that SwishU-net performs better after quantitative analysis.

5. Conclusion

It takes time and energy to color the animation sketch by manpower. As a popular color generation technology of network animation sketch, GANS has not achieved certain results in the past few years. There are some basic problems, such as color confusion, poor color gradient, unreasonable color sketch, and so on. Therefore, the GANS network based on a Swish function module proposed in this paper can better learn the details of sketch during color filling and avoid color confusion when the color exceeds the filled area. At the same time, it can directly carry out end-to-end training from animation sketch to color picture. The module can automatically color the sketch and generate color pictures with rich colors and clear textures. The experimental results show that this method has better coloring ability than the existing methods and can obtain more realistic and better visual effect color images. In the future, if there are better conditions, it will make up for the shortcomings of this paper, use the GPU with stronger performance to increase the network parameters, and expand the network scale, in order to generate higher resolution images and solve the problems of complexity and diversity. Although the U-net network structure has better generation effect than the self-encoder, it also increases the parameter quantity and complexity of the model. In the future, we will consider looking for a more suitable network structure as the discriminator model to reconstruct the image, so as to achieve better generation effects while simplifying the model.

Data Availability

The data set can be accessed upon request.

Disclosure

This paper is a research project of Philosophy and Social Sciences in Shanxi Province in 2020, the visualization research of traditional animation in information interaction from the perspective of UX. (2020W229).

Conflicts of Interest

The authors declare that there are no conflicts of interest.

References

[1] E. Sohn, J. Jeon, and T. J. Park, "A two layered approach for animation sketching," *Journal of Korea Multimedia Society*, vol. 12, 2009.

[2] E. Eisung Sohn and fnm Yoon-Chul Choy, "Sketch-n-Stretch: sketching animations using cutouts," *IEEE Computer Graphics and Applications*, vol. 32, no. 3, pp. 59–69, 2012.

[3] M. Matsugu, K. Mori, and Y. Mitari, "Subject independent facial expression recognition with robust face detection using a convolutional neural network," *Neural Networks*, vol. 16, no. 5-6, pp. 555–559, 2003.

[4] C. Yang, D. Eschweiler, and J. Stegmaier, "Semi- and self-supervised multi-view fusion of 3D microscopy images using generative adversarial networks," 2021, https://arxiv.org/abs/2108.02743.

[5] N. Sachdeva, M. Klopukh, and R. S. Clair, "Using conditional generative adversarial networks to reduce the effects of latency in robotic telesurgery," *Journal of Robotic Surgery*, vol. 6, 2020.

[6] P. Isola, J. Y. Zhu, and T. H. Zhou, "Image-to-image translation with conditional adversarial networks," in *Proceedings of the IEEE Conference on Computer Vision and Pattern Recognition*, pp. 5967–5976, IEEE Computer Society Press, Honolulu, HI, USA, July, 2017.

[7] H. Ren, J. Li, and N. Gao, "Two-stage sketch colorization with color parsing," *IEEE Access*, vol. 8, Article ID 44599, 2020.

[8] N. Berk and P. Valentina, "Use of 2D U-net convolutional neural networks for automated cartilage and meniscus segmentation of knee MR imaging data to determine relaxometry and morphometry," *Radiology*, vol. 288, 2018.

[9] S. Hasan and C. A. Linte, "A modified U-net convolutional network featuring a nearest-neighbor Re-sampling-based elastic-transformation for brain tissue characterization and segmentation," in *Proceedings of the 2018 IEEE Western New York Image and Signal Processing Workshop (WNYISPW)*, October, 2018.

[10] C. Brito, A. Machado, and A. Sousa, "Electrocardiogram beat-classification based on a ResNet network," *Stud Health Technol Inform*, vol. 264, 2019.

[11] A. Sl, B. Shwa, and B. Ydza, "Detecting pathological brain via ResNet and randomized neural networks," *Heliyon*, vol. 6, 2020.

[12] H. Ren, M. El-Khamy, and J. Lee, "DN-ResNet: efficient deep residual network for image denoising," 2019, https://arxiv.org/abs/1810.06766.

[13] Y. Wang, X. Zhou, and H. Zhou, "Transmission network dynamic planning based on a double deep-Q network with deep ResNet," *IEEE Access*, vol. 9, no. 99, p. 1, 2021.

[14] M. Y. Gao and P. Song, "A novel deep convolutional neural network based on ResNet-18 and transfer learning for detection of wood knot defects," *Journal of Sensors*, vol. 2021, Article ID 4428964, 16 pages, 2021.

[15] Z. Wang, A. C. Bovik, H. R. Sheikh, and E. P. Simoncelli, "Image quality assessment: from error visibility to structural similarity," *IEEE Transactions on Image Processing*, vol. 13, no. 4, pp. 600–612, 2004.

[16] L. Lin Zhang, L. Lei Zhang, X. Xuanqin Mou, and D. Zhang, "FSIM: a feature similarity index for image quality assessment," *IEEE Transactions on Image Processing*, vol. 20, no. 8, pp. 2378–2386, 2011.

[17] M. Heusel, H. Ramsauer, T. Unterthiner, B. Nessler, G. Klambauer, and S. Hochreiter, "GANS trained by a two time-scale update rule converge to a nash equilibrium," *Advances in Neural Information Processing Systems*, vol. 1, no. 2, pp. 6626–6637, 2017.

Hindawi
Scientific Programming
Volume 2022, Article ID 4823828, 9 pages
https://doi.org/10.1155/2022/4823828

Research Article

E-Commerce Online Shopping Platform Recommendation Model Based on Integrated Personalized Recommendation

Lijuan Xu[1] **and Xiaokun Sang**[2]

[1]*International Business School, Qingdao Huanghai University, Qingdao, Shandong, 26647, China*
[2]*College of Art, Qingdao Huanghai University, Qingdao, Shandong, 266247, China*

Correspondence should be addressed to Lijuan Xu; xulj@qdhhc.edu.cn

Received 14 March 2022; Revised 4 April 2022; Accepted 12 April 2022; Published 27 April 2022

Academic Editor: Jie Liu

With the continuous innovation of Internet technology and the substantial improvement of network basic conditions, e-commerce has developed rapidly. Online shopping has become the mainstream mode of e-commerce. In order to solve the problem of information overload and information loss in the selection of e-commerce online shopping platform, a personalized recommendation system using information filtering technology has come into being. An e-commerce online shopping platform recommendation model is proposed based on integrated multiple personalized recommendation algorithms: random forest, gradient boosting decision tree, and eXtreme gradient boosting. The proposed model is tested on the public data set. The experimental results of the separate model and mixed model are compared and analyzed. The results show that the proposed model reduces the recommendation sparsity and improves the recommendation accuracy.

1. Introduction

Internet technology has been innovating and developing continuously in recent years. As the representative of digital technology, it affects all fields of economy and society and has become a strong driving force for the consumption upgrading. With the growth of mobile Internet users and the rapid development of mobile payment, e-commerce transaction applications are constantly upgraded and further integrated into people's life [1–7]. With the cooperation and integration of online and offline transactions and the efficient development of the logistics express industry, online shopping has become a major trend of economic development [8–10].

For businesses, promoting and selling products through an e-commerce platform can expand the business and expand consumer groups more quickly and conveniently and save a lot of costs. Under the condition that the state promotes the reform and upgrading of retail, more businesses use the way of online and offline integrated development to sell products simultaneously, further optimize the user experience, and improve the user value. For consumers, online shopping makes them get rid of the restrictions of time and place, and it is easier to compare the types and quality of goods horizontally. In addition, online shopping allows customers to buy goods rarely seen in physical stores. Cross-border e-commerce, which has developed well in recent years, has met the needs of consumers in this regard.

Personalized recommendation system [11–13] is an advanced business intelligence platform based on massive data mining. It recommends goods for users and meets their personalized needs. E-commerce recommendation system can greatly improve the turnover of online shopping mall. Amazon has increased the sales volume of online shopping mall by 35% through personalized recommendation system. Compared with traditional search engines, personalized recommendation system finds users' interest points by studying users' behavior, so as to guide users to find products they are interested in faster. A good recommendation system can not only improve users' purchase efficiency but also establish a good relationship with users and improve users' sense of belonging.

However, traditional recommendation algorithms, such as collaborative filtering algorithm, still have problems such as data evacuation, cold start, poor scalability, and difficulty in extracting multimedia information features. In order to solve the above problems, scholars introduced users' demographic information, social information, and trust into similarity calculation, which have specific instructions on solving data sparsity and cold start problems, respectively [14,15]. How to effectively solve these two problems simultaneously requires further research. Therefore, an e-commerce online shopping platform recommendation model is proposed based on integrated multiple personalized recommendation algorithms. The data set of real online shopping platform is used to preprocess user behavior data. Through visual analysis to understand the underlying business logic, the platform selects meaningful features from the dimensions of users, goods, and interactions within them. Experimental results show that the performance of the proposed fusion model is better than that of other models.

2. Personalized Recommendation and Algorithms

2.1. Recommendation System. Recommendation system can successfully solve the problems of information overload and information loss by using information filtering technology. As one of the main applications of personalized service, it has attracted extensive attention. Its typical application is in the field of e-commerce, such as Amazon, eBay, and Taobao, which have invested a lot of research and development in the recommendation system. The recommendation system can effectively improve the utilization of the platform and enhance the user's dependence on the platform, so as to achieve greater economic benefits. At present, the widely recognized informal definition of recommendation system is "using e-commerce websites to provide users with product suggestions, help users make purchase decisions, simulate marketing, and enable users to complete the purchase process" given by Resnick and Varian in 1997 [16].

The recommendation system consists of three parts: input module, output module, and recommendation algorithm. The input module collects and records the user's historical behavior and other information and converts it into user interest data. After the calculation of the recommendation algorithm, the items suitable for the user are given. Finally, the output module presents the recommendation results for the user. The whole recommendation process includes three basic elements: users, items, and recommendation methods. How to model user and item information and what recommendation strategy to adopt are the core issues of recommendation system. The recommendation system model is shown in Figure 1. The recommendation system models the user according to the implicit or explicit information obtained from the input module, models the items at the same time, and selects the best recommendation object to present to the user through the matching of the recommendation algorithm.

The mathematical expression of the recommendation system is as follows: set the user set as C and the recommendation object set as S. The scale of C and S sets is usually large, and S can be any object recommended to users, such as goods, articles, advertisements, and songs. The utility function u() can calculate the recommendation degree of object s to user c, which can be expressed as

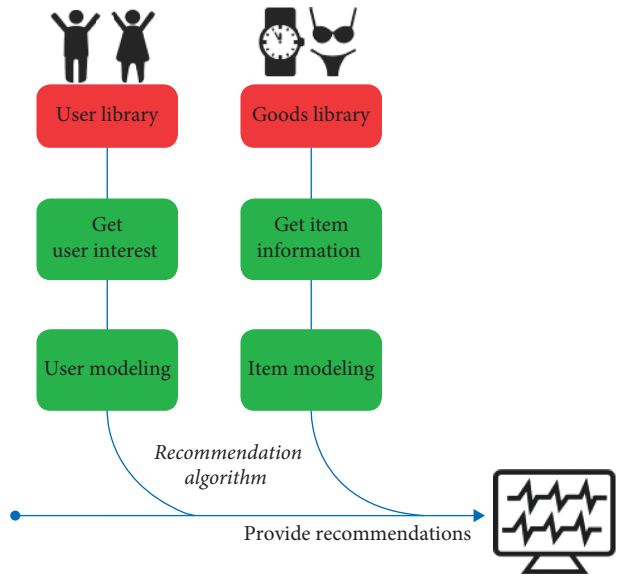

Figure 1: Recommendation system model.

$$u: C \times S \longrightarrow R, \tag{1}$$

where R is a fully ordered nonnegative real number in a certain range.

The problem of the recommendation algorithm is to find the object $S*$ that can maximize the recommendation R calculated by u(), which can be expressed as

$$\forall c \in C, S^* = \arg\max_{s \in S} u(c, s). \tag{2}$$

The utility value of the recommended object is expressed by score, which represents a user's preference for an object. The utility function u() changes according to the actual recommendation scenario and recommendation strategy. Because the utility value of the recommended object is not given in the whole space, how to build a recommendation engine to estimate it is the core of the recommendation problem.

2.2. Classification of Recommendation System. The recommendation system adopts different recommendation strategies and technical means [17], which can be divided into three categories according to the degree of providing personalized services for users as shown in Figure 2.

(1) *Nonpersonalized Recommendation System.* General recommendation: The recommendation system will not generate recommendations according to the user's personal characteristics but through the marketing strategy formulated by the background operator of the web system or the statistical analysis tool based on the background of the system. This

kind of recommendation system is not targeted to users but presents the same recommendation results for all users. Specific forms of recommendation include advertising recommendations and sales ranking recommendation.

(2) Semipersonalized recommendation system: The system obtains the user's preference information and generates recommendations by analyzing the user's browsing behavior or current shopping data. The user's behavior data affect the recommendation results, and its degree of personalization is higher than that of nonpersonalized recommendation system.

(3) Fully personalized recommendation system: The user's historical information in the system is retained according to its value extracted from personalized features, such as user's browsing information, purchase history, registration information, scoring data, collection list, and registration information. Because this kind of recommendation system makes use of the long-term data of users, it can build a relatively stable user preference model and analyze it in combination with the current behavior of users, so it can provide users with fully personalized recommendation services. This kind of recommendation service has the highest degree of personalization and is generally only for registered users.

From the perspective of algorithm and implementation, recommendation systems can be divided into the following categories: content-based recommendation system, collaborative filtering algorithm-based recommendation system, association rule-based recommendation system, knowledge-based recommendation system, and hybrid recommendation system, which are also shown in Figure 2. The recommendation system based on collaborative filtering algorithm and content-based recommendation system have the longest research time and the most applications.

2.3. Recommendation Algorithms. In the recommendation of e-commerce online shopping platform, multicriteria decision-making [18–24] is a common method, but this method has been proved to have many shortcomings, such as uncertainty and subjectivity in the decision-making process [25–28]. Many researchers classify recommendation algorithms differently from different perspectives. From the perspective of information technology, they can be divided into collaborative filtering and content-based recommendation according to the algorithm and generation mechanism of recommendation results.

Collaborative filtering algorithm is a mature recommendation algorithm recognized in the industry. Goldberg et al. [29] first proposed the collaborative filtering algorithm and applied it to the Tapestry e-mail filtering system. The algorithm mainly recommends items based on users' previous preferences and the choices of users with similar interests. Different from Tapestry's single-point filtering mechanism, Resnick et al. [30] proposed a cross-point and cross-system news filtering mechanism, GroupLens. This automatically helps people find what they like from a large number of articles available. The drawback of the above nearest neighbor method is that it requires a lot of calculation. Therefore, Verbert et al. [31] proposed a collaborative filtering algorithm based on items. The algorithm replaces the nearest neighbor method by finding similar goods. Online computing costs have nothing to do with the number of users or items. It can generate high-quality recommendations in real time on huge amounts of data. The advantages of collaborative filtering algorithm are obvious. In engineering, the model is simple, effective, and versatile. If the scale of the e-commerce system expands, the rapid increase of user and project data will lead to data sparsity. In addition, it also has a serious cold start problem. Pereira et al. [14] introduced user demographic information into the recommendation algorithm. This forms the hybrid collaborative filtering recommendation algorithm, which can solve the cold start problem well. Shambour et al. [15] incorporated the idea of project rating trust into the traditional user-based collaborative filtering recommendation algorithm. They abandoned the traditional method of similarity calculation. Experiments show that this algorithm can alleviate the problem of data sparsity.

In addition, the content-based recommendation algorithm can effectively solve the cold start problem of the collaborative filtering algorithm and its whole operation process. In the collaborative filtering recommendation algorithm, if the condition that the project is evaluated by many relevant users is met, it will make recommendations for other relevant users. In content-based recommendation algorithm, feature vectors describing related content are established by extracting features from content for users. Then, the preferences of the users are calculated to determine whether to recommend relevant content to the users.

A review of relevant research found that the online shopping platform has specific business scenarios for product recommendations. It needs to select an efficient recommendation algorithm from the perspective of accuracy, efficiency, and explainability of the algorithm. In addition, collaborative filtering and content-based recommendation algorithms have their own advantages and difficulties. In fact, most recommendation systems carry out a hybrid recommendation by integrating different recommendation algorithms in various forms. It can use the results of the respective models to carry out the weighted combination and waterfall mixing. Therefore, random forest (RF), gradient boosting decision tree (GBDT), and eXtreme gradient boosting (XGBOOST) models are selected as the basic models.

Random forest (RF) is composed by Breiman et al. [32] on the basis of a classification and regression tree (CART). Its principle is to form different data sets by randomly sampling the original data set. By training decision trees on a single dataset, multiple decision trees are combined to form a classifier. The specific steps are shown in Figure 3.

The first step is to preprocess the RF model. The downsampling method was adopted to avoid the influence of sample imbalance on the experimental results (the ratio of positive and negative samples in the original data set was $1:1100$).

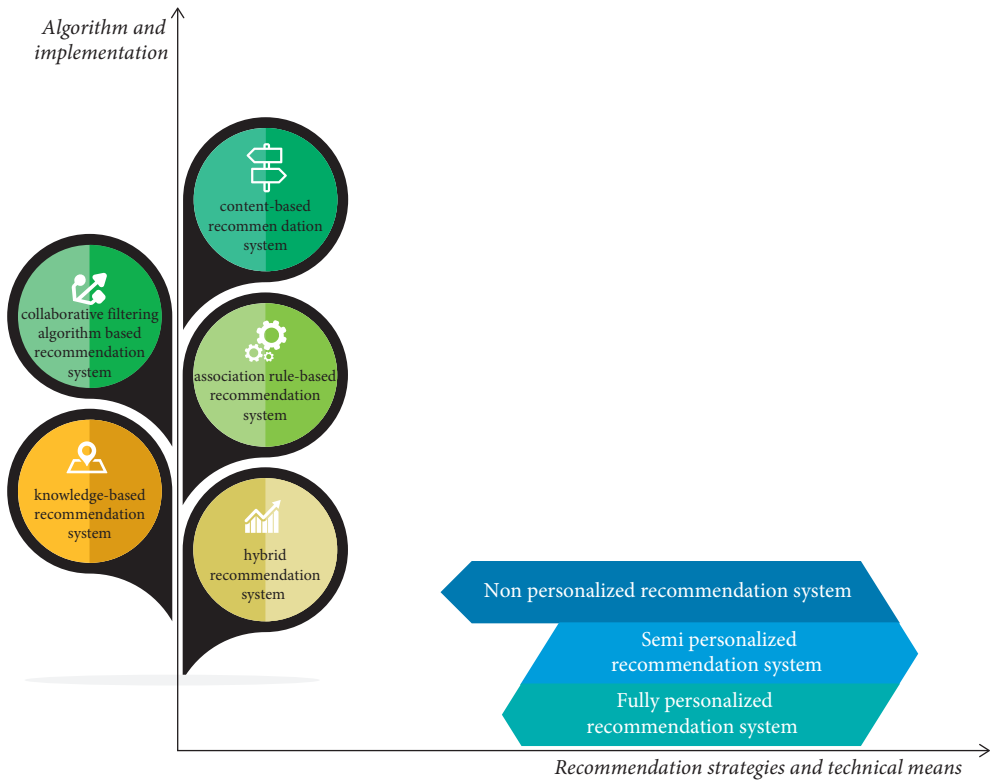

Figure 2: Classification of recommendation system.

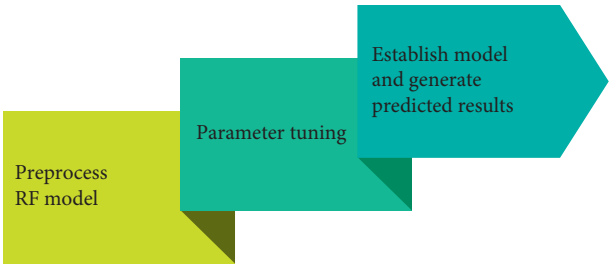

Figure 3: Random forest model.

(1) K-means clustering algorithm is used to cluster negative samples

(2) Based on the subsamples of each group set with the same ratio, the optimal ratio is selected through testing in random subsamples

(3) RF model is used to train and predict the lower sample set.

The second step is parameter tuning.

(1) The imbalance rate N/P of positive and negative samples was optimized.

(2) The number of forest scale trees is optimized.

(3) For the setting of the probability wide value, the predicted value can be obtained by inputting the sample characteristics of the trained model. The predicted value is the probability value. The default value is 0.5. By constantly adjusting and modifying the condition that the probability value reaches the broad value, the purchase prediction classification label for the user and the sample is changed.

The third step is using RandomForestClassifier() in sklearn package to establish the model and train to generate a subset P of predicted results.

GBDT [33] belongs to boosting algorithm, which is different from the bagging algorithm to RF. Boosting algorithm adopts a series serialization model. Individual learners are strongly correlated; that is, the new model generates training results based on the old learning model. GBDT algorithm is learned from the generated CART classification regression tree. Samples with large residuals output from existing models and actual samples. So, generation is selected to generate a new CART tree. Through the above training methods, residuals are constantly reduced to ensure the accuracy of the results. The specific steps are shown in Figure 4.

The first step is to use k-means clustering to cluster negative samples. The second step is to select the optimal ratio by adding human GBDT into the random subsample based on the subsample of each population with the same ratio. Third, GBDT classifier selects the best parameters.

(1) The imbalance rate N/P of positive and negative samples was optimized

(2) GBDT selects the best number and learning rate of forest scale trees

(3) The best maximum depth value of the base tree, the minimum number of samples required for internal

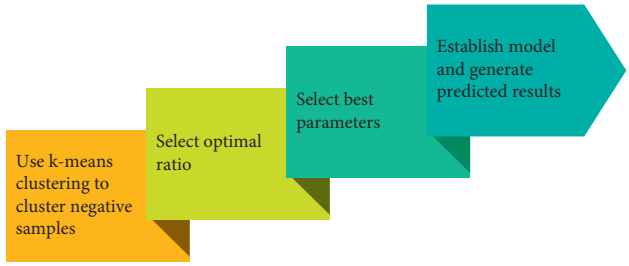

Figure 4: GBDT model.

node subdivision, and the minimum number of samples for leaf nodes are selected

(4) Probability wide value is tuned

The fourth step is using GradientBoostingClassifier() in sklearn package to establish the model and train to generate a subset P of predicted results.

Both of them belong to boosting algorithm, and XGBOOST efficiently implements and optimizes GBDT algorithm. In the choice of the base learner, XGBOOST [34] model can adopt the tree model and other models (such as LR). Therefore, it is not limited to the CART tree defined by the GBDT algorithm. XGBOOST learns new functions and fits residuals through continuous feature fission of the tree. The specific steps are shown in Figure 5.

The first step is to train XGBOOST model parameters for analysis.

(1) Use higher learning rate to adjust the number of optimal forest size trees

(2) Adjust the maximum depth value and the minimum sum of sample weights in subnodes

(3) Adjust parameter Y

(4) Adjust input and A

(5) Reduce the learning rate and cycle to obtain a more stable parameter combination

The second step is using GradientBoostingClassifier() in sklearn package to establish the model and train to generate a subset P of predicted results.

3. Experimental Data

The experimental data construct a product recommendation model based on real desensitization data from an online shopping platform, which comes from the Tianchi big data platform competition of Alibaba. The dataset contains the user's mobile behavior data over a 30-day period. The user table contains six fields, including user ID, brand ID, user location ID, product classification ID, user interaction behavior, and behavior time. The specific data amount is as follows. The number of users is 92302, the number of commodity subset is 65221, and the number of commodity user interaction data is 22560328.

The experimental data include the data of Taobao's shopping festival on December 12. After analyzing the total operations of users in this month (browsing, collecting, adding to the shopping cart, and purchasing behavior), it is found that

Figure 5: XGBOOST model.

the purchase behavior doubled at 0 on the 12th and was obviously abnormal data. Therefore, the data of this day are eliminated. In the process of e-commerce website data statistics, there are repeated data, abnormal data, and other problem data. Therefore, the above repeated values and invalid values will be directly eliminated in the data cleaning process at this stage. The ratio of positive and negative samples in the original data set is about 1 : 1100. Therefore, it may cause the algorithmic prediction model to treat the positive sample set as noise data and thus bias the negative sample set data. Positive samples are more likely to be misclassified than negative ones. Therefore, the random downsampling method is adopted to avoid the above problems.

3.1. Feature Construction. According to the data preprocessing results and combined with the business characteristics of the online shopping platform, data characteristics are reconstructed. Feature construction is completed from the three dimensions of user feature, commodity feature, and commodity category feature and their combination, which is shown in Figure 6. If this experiment is treated as a dichotomous problem, the output variable Y labels are 1 (purchased) and 0 (not purchased), respectively.

The characteristics of user behavior are as follows:

(1) User activity: it refers to the sum of users' behaviors in the recent N days, reflecting users' purchasing habits

(2) User conversion rate: it reflects the user's buying decision operation habit

The commodity characteristics are as follows:

(1) Commodity activity: it refers to the total number of user operations on the category in the previous N days, reflecting the popularity of the product

(2) The conversion rate of goods: it reflects the operation characteristics of purchasing decision (such as high value and long decision time)

The characteristics of the commodity category are as follows:

(1) Activity of commodity category: it refers to the total number of user operations on this category in the last N days, reflecting the popularity of this category

(2) Purchase conversion rate of commodity category: it reflects the characteristics of purchase decision operation of the commodity category

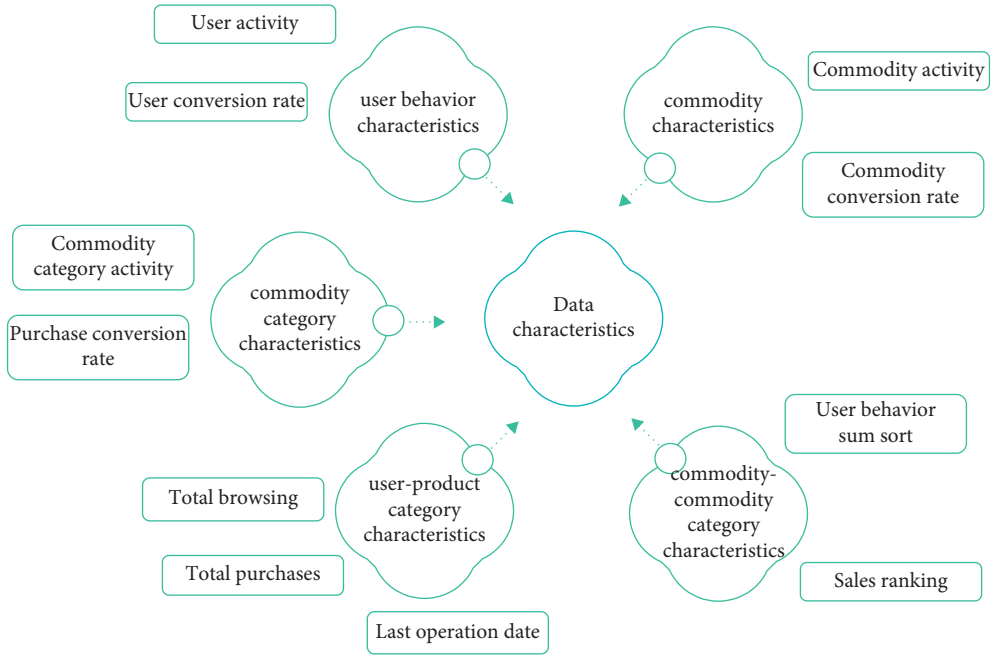

Figure 6: Data characteristics.

The user-product category characteristics are as follows:

(1) Total browsing of user-product category

(2) Total purchases of user-product category

(3) Last operation date of user-product category

The commodity-commodity category characteristics are as follows:

(1) User behavior sum sort of commodities in the category

(2) Sales ranking of commodities in the category

3.2. Division of Data Set. This experiment divides the data set into two parts, including the training set and test set. The learning and training process is shown in Figure 7.

The data preprocessing results are shown as follows. The user click conversion rate of this dataset is less than 1%; that is, it takes an average of 100 interactions (including browsing, clicking, and adding products) for each user to generate one transaction. The amount of data is relatively large.

If all interactive behaviors of users in the whole time period are taken as characteristic data, the calculation speed of the model will be greatly reduced. Due to the time decay of user interest, the accuracy of the model will be reduced. Therefore, when dividing the data set, it can be divided into four groups with weeks as the interval unit, including a group of abnormal data. The reason for elimination has been explained above.

4. Case Study and Algorithm Analysis

4.1. Algorithm Evaluation Indicator. Fl-score is a comprehensive indicator that can be considered when user ratings are sparse or missing. It is characterized by harmonic

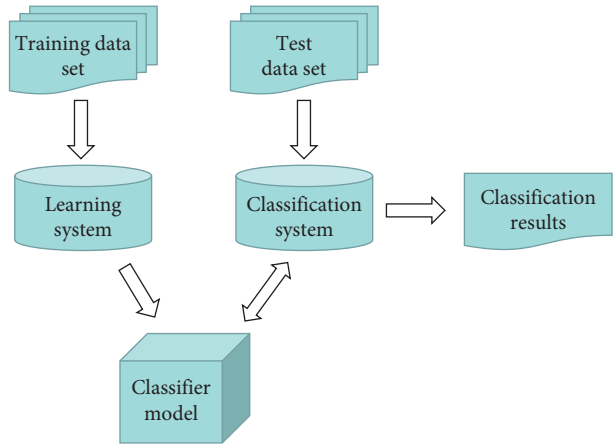

Figure 7: Process of the training data model.

precision α and recall rate β. The basic meanings of these three indicators are as follows:

$$\alpha = \frac{tp}{tp + fp},$$

$$\beta = \frac{tp}{tp + fn}, \tag{3}$$

$$F1 = \frac{2\alpha\beta}{\alpha + \beta},$$

where some concepts of confusion matrix are involved, tp means true positive, fp means false positive, fn means false negative, and tn means positive.

Combined with the recommendation scenarios of online shopping platforms, harmonic precision α and recall rate β can also be expressed as

Table 1: The training result of separate model.

	LR	RF	GBDT	XGBOOST
F1	0.0611	0.0872	0.0836	0.0896
Harmonic precision	0.0568	0.9033	0.0959	0.0811

Table 2: The training result of mixed model.

	LR/GBDT	LR/XGBOOST	RF/GBDT	RF/XGBOOST	GBDT/XGBOOST	LR/GBDT/XGBOOST
F1	0.1022	0.0966	0.0865	0.0956	0.0867	0.1122
Harmonic precision	0.0633	0.0564	0.0819	0.0980	0.0895	0.0823

$$\alpha = \frac{\eta \cap \mu}{\eta}, \qquad \beta = \frac{\eta \cap \mu}{\eta}, \tag{4}$$

where η means recommended quantity, and μ means serviceable quantity.

Higher precision means more accurate recommendation, and higher recall rate means more acceptance of recommendation. Only when both are high, the performance of the recommendation algorithm is good. Therefore, F1-score is taken as the main indicator.

4.2. Experimental Environment. The operating system of this experiment is Windows 10–64 bit, with CPU : Intel(R)Core(TM) 15–5200U CPU @ 2.20 GHz (4 CPUs), 2.2 GHz, and Python version 3.7.2. It is implemented based on software packages such as PANDAS and sklearn.

4.3. Separate Model Training. First, the LR model was trained, but the result was not ideal. When RF, GBDT, and XGBOOST are used, the effect is significantly improved. In the three integration algorithms, XGBOOST has only a slight advantage in F1-score compared with RF, but the model implementation time is shorter than RF. LR models are simple, and run time is short, but its accuracy is poor compared with other algorithms. The three integration models (RF, GBDT, and XGBOOST) show strong generalization ability for such data with complex features. The training result of the separate model is shown in Table 1.

4.4. Mixed Model Training. All kinds of recommendation algorithms have their own advantages and difficulties in implementation. In fact, most recommendation systems carry out a mixed recommendation by integrating different recommendation algorithms in various forms.

(1) Weighted mixing: Weighted hybrid combination is a common way. The recommendation results and scores can be combined to generate the final recommendation set by a weighted combination of the deduction results of respective models. Through a reasonable weighting method, the result of a comprehensive algorithm is better. But there are also some problems such as a large amount of computation and complex systems.

(2) Waterfall mixing: waterfall hybrid mode adopts the principle of "filtering" and takes the filtering result of one model as the input data of another model. Generally, taking GBDT + LR model as an example and combining the respective advantages of the LR model and GBDT model, the OUTPUT results of the GBDT algorithm are directly output as LR input features, which improves the utilization rate of data information and the learning efficiency of LR model step by step.

(3) Graded mixing: In industry, this kind of hybrid method makes the hybrid algorithm simple and efficient. Combined with different scenes, according to the characteristics of different algorithms, the high-precision algorithm is first used. Other algorithms are used to get subsequent results.

The training result of mixed model is shown in Table 2.

In the experiment, the models are fused according to the independent training results of the previous model. The experiment involves a lot of steps of data processing, feature selection, and parameter adjustment. The results of the experiment are as follows:

(1) Under normal circumstances, the fusion between models will improve performance. However, when the performance of a single model is poor, the fusion with other models will reduce the effect of its fusion model.

(2) In the mixed recommendation, the direct fusion effect is poor; for example, the simple weighting can adopt the hierarchical strategy. Efficiency is improved by taking the output of one model as the input of another.

(3) When the experimental performance of the models is similar, the fusion effect will not be significantly improved.

(4) The final results show that the model combining LR, GBDT, and XGBOOST has the best effect.

5. Conclusion

With the continuous innovation of Internet technology and the substantial improvement of network basic conditions, e-commerce has developed rapidly. As the mainstream

mode of e-commerce, online shopping has added great vitality to the development of the economy. The online shopping platform recommendation algorithm is explored. An e-commerce online shopping platform recommendation model based on integrated personalized recommendation is designed and implemented. The later research of this paper can be carried out from the perspectives of real-time recommendation, visual recommendation result generation, and user interest model mining combined with scenes. The model used in the recommendation system can be further improved. In the future, user data from various sources can be integrated, and attribute tags can be added to make the personalized recommendation model more accurate. In addition, according to the different business needs of the application, the personalized recommendation system can add more recommendation scenarios to meet the needs of users more comprehensively.

In future software system development based on the model proposed in this study, the preliminary system function module planning is as follows. It is mainly divided into the foreground function module and the background function module. The foreground function module includes the system home page submodule, registration and login submodule, alternative platform display submodule, and personal center submodule. The background function module includes a platform management submodule, order management submodule, merchant management submodule, and security authority submodule. The function of the software system is tested by the method of unit test.

Data Availability

The dataset can be accessed upon request.

Conflicts of Interest

The authors declare that they have no conflicts of interest.

References

[1] D. Gefen, "E-commerce: the role of familiarity and trust," *Omega*, vol. 28, no. 6, pp. 725–737, 2000.

[2] J. Zha, F. Ju, and L. Wang, "Customer satisfaction in e-commerce: an exploration of its antecedents and consequences," in *Proceedings of the 2006 IEEE International Conference on Management of Innovation and Technology*, IEEE, Singapore, June 2006.

[3] T. Dinev and P. Hart, "An extended privacy calculus model for E-commerce transactions," *Information Systems Research*, vol. 17, no. 1, pp. 61–80, 2006.

[4] R. Yuan, J. Li, X. Wang, and L. He, "Multirobot task allocation in e-commerce robotic mobile fulfillment systems," *Mathematical Problems in Engineering*, vol. 2021, Article ID 6308950, 10 pages, 2021.

[5] J. H. Zhang and R. R. Yin, "The Profit Distribution of Supply Chain under E-Commerce," *Discrete Dynamics in Nature and Society*, vol. 2014, Article ID 287925, 7 pages, 2014.

[6] Y. F. Li, "Research on E-Commerce Purchasing Model in Crude Oil Trade," *Scientific Programming*, vol. 2021, Article ID 9994965, p. 10, 2021.

[7] H. M. Zhao, "A Cross-Border E-Commerce Approach Based on Blockchain Technology," *Mobile Information Systems*, vol. 2021, Article ID 2006082, p. 10, 2021.

[8] J.-Y. M. Kang and K. K. P. Johnson, "F-Commerce platform for apparel online social shopping: testing a Mowen's 3M model," *International Journal of Information Management*, vol. 35, no. 6, pp. 691–701, 2015.

[9] X. Zhang and Z. Yuan, "The platform and collaborative operating model of "wisdom cloud logistics" in online shopping era," *Forum on Science and Technology in China*, vol. 2013, no. 7, 2013.

[10] T. M. Choi, P. S. Chow, B. Kwok, S.-C. Liu, and B. Shen, "Service quality of online shopping platforms: a case-based empirical and analytical study," *Mathematical Problems in Engineering*, vol. 2013, no. 12, Article ID 128678, 860 pages, 2013.

[11] S. Shishehchi, S. Y. Banihashem, N. Zin, and S. A. M. Noah, "Review of personalized recommendation techniques for learners in e-learning systems," in *Proceedings of the International Conference on Semantic Technology & Information Retrieval*, IEEE, Putrajaya, Malaysia, June 2011.

[12] M. Gao, C. Q. Jin, W. N. Qian, and X.-L. Wang, "Real-time and personalized recommendation on microblogging systems," *Chinese Journal of Computers*, vol. 37, 2014.

[13] S. Hamouda and N. Wanas, "PUT-Tag: personalized user-centric tag recommendation for social bookmarking systems," *Social Network Analysis and Mining*, vol. 1, no. 4, pp. 377–385, 2011.

[14] A. L. Vizine Pereira and E. R. Hruschka, "Simultaneous co-clustering and learning to address the cold start problem in recommender systems," *Knowledge-Based Systems*, vol. 82, pp. 11–19, 2015.

[15] Q. Shambour and J. Lu, "An effective recommender system by unifying user and item trust information for B2B applications," *Academic Press, Inc*, vol. 81, no. 7, 2015.

[16] P. Resnick and H. R. Varian, "Recommender systems," *Communications of the ACM*, vol. 40, no. 3, pp. 56–58, 1997.

[17] F. E. Walter, S. Battiston, and F. Schweitzer, "A model of a trust-based recommendation system on a social network," *Autonomous Agents and Multi-Agent Systems*, vol. 16, no. 1, pp. 57–74, 2008.

[18] L. Li, C. Mao, H. Sun, Y. Yuan, and B. Lei, "Digital twin driven green performance evaluation methodology of intelligent manufacturing: hybrid model based on fuzzy rough-sets AHP, multistage weight synthesis, and PROMETHEE II," *Complexity*, vol. 2020, no. 6, Article ID 3853925, 24 pages, 2020.

[19] O. Serafim and G.-H. Tzeng, "Compromise solution by MCDM methods: a comparative analysis of VIKOR and TOPSIS," *European Journal of Operational Research*, vol. 156, no. 2, 2004.

[20] L. Li, J. Hang, H. Sun, and L. Wang, "A conjunctive multiple-criteria decision-making approach for cloud service supplier selection of manufacturing enterprise," *Advances in Mechanical Engineering*, vol. 9, no. 3, Article ID 168781401668626, 2017.

[21] G. Tzeng, C. Chiang, and C. Li, "Evaluating intertwined effects in e-learning programs: a novel hybrid MCDM model based on factor analysis and DEMATEL," *Expert Systems with Applications*, vol. 32, no. 4, pp. 1028–1044, 2007.

[22] G. H. Tzeng, Y. Yang, C. T. Lin, and C. Chie, "Hierarchical MADM with fuzzy integral for evaluating enterprise intranet web sites," *Information Sciences*, vol. 169, no. 3-4, pp. 409–426, 2005.

[23] L.-h. Li, J.-c. Hang, Y. Gao, and C.-y. Mu, "Using an integrated group decision method based on SVM, TFN-RS-AHP, and TOPSIS-CD for cloud service supplier selection," *Mathematical Problems in Engineering*, vol. 2017, Article ID 3143502, 14 pages, 2017.

[24] L. Li, B. Lei, and C. Mao, "Digital twin in smart manufacturing," *Journal of Industrial Information Integration*, vol. 26, no. 9, Article ID 100289, 2022.

[25] T. Aouam, S. I. Chang, and E. S. Lee, "Fuzzy MADM: an outranking method," *European Journal of Operational Research*, vol. 145, no. 2, pp. 317–328, 2003.

[26] L. Li, T. Qu, Y. Liu et al., "Sustainability assessment of intelligent manufacturing supported by digital twin," *IEEE Access*, vol. 8, pp. 174988–175008, 2020.

[27] L. Li and C. Mao, "Big data supported PSS evaluation decision in service-oriented manufacturing," *IEEE Access*, vol. 8, no. 99, p. 1, 2020.

[28] L. G. Fan, D. X. Niu, and X. E. Yuan, "An IAHP-based MADM method in transmission network planning," in *Proceedings of the 7th IET International Conference on Advances in Power System Control, Operation and Management*, APSCOM, Hongkong, China, November 2006.

[29] D. Goldberg, D. Nichols, B. Oki, and D. Terry, "Using Collaborative Filtering to Weave an Information Tapestry," *Communications of the ACM*, vol. 35, no. 12, 1992.

[30] P. Resnick, "GroupLens: an open architecture for collaborative filtering of Netnews," *Proc Cscw*, 1994.

[31] K. Verbert, N. Manouselis, X. Ochoa, M. Wolpers, H. Drachsler, and I. Bosnic, "Context-aware recommender systems for learning: a survey and future challenges," *IEEE Transactions on Learning Technologies*, vol. 5, no. 4, 2012.

[32] L. Breiman, "Random forests," *Machine Learning*, vol. 45, pp. 5–32, 2001.

[33] W.-Y. Cai, J.-H. Guo, M.-Y. Zhang, Z.-X. Ruan, X.-C. Zheng, and S.-S. Lv, "GBDT-based fall detection with comprehensive data from posture sensor and human skeleton extraction," *Journal of Healthcare Engineering*, vol. 2020, no. 9, Article ID 8887340, 15 pages, 2020.

[34] D. Zhang, H.-D. Chen, H. Zulfiqar et al., "iBLP: an XGBoost-based predictor for identifying bioluminescent proteins," *Computational and Mathematical Methods in Medicine*, vol. 2021, Article ID 6664362, 15 pages, 2021.

Hindawi
Scientific Programming
Volume 2022, Article ID 5815693, 11 pages
https://doi.org/10.1155/2022/5815693

Research Article

Research on the Generation of Creative Animation Driven by Deep Learning Model

Xiaokun Sang[1] **and Lijuan Xu**[2]

[1]*College of Art, Qingdao Huanghai University, Qingdao, Shandong 266247, China*
[2]*International Business School, Qingdao Huanghai University, Qingdao, Shandong 266247, China*

Correspondence should be addressed to Xiaokun Sang; sangxk@qdhhc.edu.cn

Received 10 March 2022; Revised 29 March 2022; Accepted 11 April 2022; Published 21 April 2022

Academic Editor: Jie Liu

It is a very interesting and practical task to transform real-world images such as portraits or scenery into creative animation images. Since this concept was put forward, it has aroused extensive research interest in the field of computer vision. The generative adversarial networks (GAN) model is widely used in this field. Depth convolution GAN (DCGAN) and Wasserstein GAN (WGAN) improve the original GAN, but there are still problems existing in creative animation generation such as model collapse. To solve these problems, the Wasserstein distance is introduced to replace the JS divergence in the GAN model to measure the gap between the sample distribution generated by the generator and the real distribution, and the loss function is improved. In order to achieve a better animation generation effect, the training of the model is further optimized through the adjustment of the network model structure and the setting of parameters. Through the comparison with DCGAN and WGAN models in the animation data set and CelebA data set and the quantitative analysis and comparison of the generation effects of different models, the effectiveness and generalization of the improved GAN model are verified.

1. Introduction

It is a very interesting task for computers to be used to generate creative animation images with artistic style. This task is mainly studied through image style transfer. Image style transfer focus uses a computer to stylize the content in an image, presenting a specific artistic style while the original content can be recognized [1, 2]. This is a new research direction in computer vision in recent years. Style transfer technology allows computers to create art "autonomously." Therefore, the concept has attracted people's attention since it was put forward.

Convolutional neural networks (CNN) and generative adversarial networks (GAN) learning models are basically adopted in the study of image style transfer [3, 4]. These models can add an art style to the target image, which has artistic properties. In image style transfer, firstly, CNN or GAN is used to learn style patterns from the specified style images. Then, they are converted into oil paintings, cartoons, Chinese landscape paintings, and other different artistic images, or the transformation of seasons and textures on the image is realized after it is applied to the target image.

GAN model is unstable and difficult to optimize in training. Many style migration efforts improve it from a loss function perspective. In these improved models, DualGAN [5] and CycleGAN [6] can complete the image style transfer work well. However, these GAN models can only migrate either style or content during style migration. In this paper, by improving the generator structure, the model achieves a better balance in the simultaneous transfer of style and content. The improved model is applied to the style transformation from natural images to animation illustrations. The experimental results show that the model can retain the content of the original natural scene and have a very excellent animation illustration style effect.

2. Related Works

As the most widely used generation model in the field of deep learning, GAN is also one of the models with the best visual effect on image generation. It is a new network model proposed by Ian Goodfellow of OpenAI in 2014 [4]. The model has attracted the attention of many scholars. The image quality generated by generating a countermeasure network model is higher than that of traditional generation models, such as variational self-encoder, and the training of the model is faster than that of the autoregressive model. However, the original GAN model also has some disadvantages, such as poor training stability and mode collapse. With the continuous research of scholars, various improved models have emerged one after another, and the performance of the generated countermeasure network has been greatly improved.

In view of the phenomenon that the training speed of the model is slow, the gradient is not updated in time, and even the model collapses when using the original GAN model. Mao et al. proposed the least squares GAN (LSGAN) [7], and the gradient of the model will be reduced to 0 when the data distribution is completely consistent with the real sample. The problem of gradient disappearance in model training caused by using Sigmoid and other functions as activation functions is avoided.

However, the real problem of GAN is how to better measure the gap between generated sample distribution and real sample distribution so that the generator can learn better. This problem did not make a major breakthrough until Wasserstein GAN (WGAN) was put forward.

WGAN was proposed by Arjovsky et al. [8]. The model uses Wasserstein distance instead of JS distance in traditional GAN as the standard to measure the difference between distributions. The common problem of JS divergence is that it is unable to measure the distance between two noncoincident distributions, and the gradient often disappears in the process of model training. Using Wasserstein distance can better measure the gap between the generated sample distribution and the real sample distribution, effectively alleviate the problems of mode collapse and training instability in network model training, and achieve good experimental results without a complex network model structure.

Ishaan Gulrajani et al. proposed WGAN's improved model WGAN-GP on the basis of WGAN [9]. In the model, the gradient penalty method is used to replace the weight clipping in WGAN to achieve the approximate 1-Lipschitz restriction effect on the discriminator network, and the normalization operation is cancelled in the discriminator network. David Berthelot et al. proposed the boundary equilibrium GAN (BEGAN) model and designed a new way to evaluate the generation quality of generators [10]. By estimating the difference between the distribution of distribution errors instead of the traditional generation, they can directly estimate the generation distribution and the real step-by-step errors in the antinetwork model. The model can also be trained stably under the standard GAN structure, and the model can converge quickly. At the same time, a super parameter is added to adjust the quality and diversity of the image generated by the generator.

The improvement methods mentioned above are to improve the original generated countermeasure network model from the loss function of the model. In terms of the structural improvement of the generated countermeasure network, the earliest is the deep convolution GAN (DCGAN) [11] proposed by Alec Radford et al. The model combines the powerful convolution neural network with the generator and discriminator that generates the countermeasure network, replaces the pool layer in the original generated countermeasure network with the convolution layer with step size, and uses the batch normalization operation [12] in the generator network and discriminator network to cancel the full connection layer in the network so that the generator can better learn the characteristic information of the image. The generated image has higher quality. Zhang et al. proposed self-attention GAN (SAGAN) [13] and added a self-control module to the model structure of the generation countermeasure network. The self-attention module can well deal with the long-range and multilayer dependence of image information. When generating the image, it can coordinate the details of each position and the details of the far end. At the same time, spectral regularization is added to the discriminator, which has achieved good results in the field of image generation. Andrew et al. proposed the BigGAN [14] model, which has achieved a major breakthrough in the field of image generation. The model not only increases the batch size but also increases the number of filters in each layer of the network. Through the shared embedding between network levels, the random noise and input conditions are spliced and input to each batch normalization layer of the generator network model, which greatly improves the quality of the generated image.

In order to apply the GAN model to a wider range of fields, Mirza and Osindero proposed conditional GAN (CGAN) [15]. By adding additional label information conditions to the generation network and discrimination network to guide the data generation process, the network can generate specific image samples according to the additional condition information. Phillip et al. proposed the pix2pix model [16] on the basis of CGAN and applied GAN to the field of image style migration. The model adds a U-net structure [17] to the generator network and an L1 regularization term to the loss function to realize the image translation task. In the image style conversion, the most popular is the cycle neural network GAN (cycle GAN) [18] proposed by Zhu et al. It realizes the conversion between images of two different styles (such as the conversion from horse to zebra) and the conversion between different painting styles. Different from the pix2pix model, the cycle GAN model can be trained in non-paired data set, while the training data and data of the pix2pix model must be paired. Yunjey et al. proposed the star GAN [19] model to realize the conversion between multiple different style fields through fewer generators. Star GAN realizes the image cross style conversion under different data sets with less training cost by adding one hot condition feature and mask vector to the model.

In the field of more widely used image restoration and image super-resolution reconstruction, there is the Deblur GAN [20] model proposed by Orest Kupyn et al. Based on conditional GAN structure and content loss, it realizes image deblurring through end-to-end learning.

In the practical application of image super-resolution reconstruction, the more popular is the SRGAN model [21] proposed by Christian et al. The generation network model of SRGAN adopts the deep-seated residual network as the network structure and adds the perception loss based on the VGG network [50] to the loss function so that GAN has more real details in generating super-resolution images and faster training speed.

3. Principles of GAN

GAN is also a generative model. But it does not have to explicitly express the probability distribution of the sample. It is the idea of adversarial learning. The intrinsic distribution of data is implicitly learned through a zero-sum game between generator and discriminator [22–25]. When the generator and discriminator reach a Nash equilibrium state, the data generated by the generator can have the same inherent properties as the real data. This allows using generators to get real data [25].

The GAN model consists of two basic modules: generator G and discriminator D. Generator G and discriminator D can be any learning model with generative and discriminant capabilities. Compared with the traditional shallow machine learning model, the deep model has richer parameters and stronger learning ability. In particular, CNN has unique advantages in processing image data. Therefore, CNN is generally used as a discriminator in the GAN model. CNN with transpose convolution structure is used as a generator.

When using the GAN model to generate image data, random noise vector Z needs to be input for generator G. The output result $G(z)$ is obtained by transposing convolution – upsampling – non-linear activation – batch normalization. G(z) has the same structure and size as real training data. They will be fed into discriminator D along with real training data X. Their labels are usually separated by zeros and ones. If the input sample is $G(z)$, then discriminator D should determine its category label as 0. If the input is true sample X, the category label of it is judged to be 1. In the training process, discriminator D needs to maximize the accuracy of label prediction for X and $G(z)$. Generator G, meanwhile, tries to make the generated $G(z)$ indistinguishable from the x from the real training set. Thus, generator G and discriminator D will constantly play against each other throughout the training process. The generative and discriminant abilities of both will be improved continuously. The output of the final generator will have the same appearance as the real data. Judge D will not be able to distinguish the true source of the data. The classification probability of both the real sample and the "false" data generated by G will approach 1/2. At this point, you can assume that generator G has learned the inherent distribution of real data. The "fake" data it generates already has the same properties as the real data. This enables data distribution without explicitly expressing it. The goal of the intrinsic distribution of training data is obtained through adversarial learning.

The learning objectives of the GAN model can use the following form of expression:

$$\min_G \max_D L_{\mathrm{GAN}}(D,G) = E_{x\sim p_{\mathrm{data}}}[\log D(x)] + E_{z\sim p_z}[\log(1-D(G(z)))], \tag{1}$$

where p_{data} is the probability distribution obeyed by real training sample x. $p_z(z)$ is the probability distribution that noise z obeys. $E_{x\sim p_{\mathrm{data}}}[\cdot]$ and $E_{z\sim p_z}[\cdot]$ are the mathematical expectation of x and z classification probability output by discriminator D, respectively.

4. Animation Style Migration Model

A deep convolution generated countermeasure network (DCGAN) is an improved model of generating countermeasure network GAN. Its principle is consistent with that of GAN. The biggest improvement is the perfect combination of convolution neural network, which is most widely used in image processing, and generated countermeasure network. Deep convolution generated countermeasure network uses convolution neural network structure for both generator and discriminator in the model, At the same time, some changes are made to the structure of the added convolutional neural network to improve the performance of the network model.

4.1. Improvement of Loss Function. Since GAN was proposed in 2014, although it has been widely used in the field of machine vision and achieved good results, the initial GAN model often has problems such as training difficulties, unbalanced training between generator and discriminator, and insufficient diversity of samples generated by the generator. In the original GAN model, KL (Kullback–Leibler divergence) is used to measure the gap between the sample distribution generated by the generator and the real distribution. The loss function used in the standard generation countermeasure network model is shown in formula (1).

From formula (1), it can be calculated that when the parameters of generator g are fixed, it is the optimal discriminator D. The calculation process is as follows:

$$\min_G \max_D V(D,G) = E_{x\sim p_r(x)}[\log D(x)] + E_{x\sim p_g(x)}[\log(1-D(x))], \tag{2}$$

where $E_{x\sim p_r(x)}[\log D(x)]$ represents the probability distribution that sample x belongs to real data and $E_{x\sim p_g(x)}[\log(1-D(x))]$ represents the probability distribution that sample x belongs to the sample data generated by the generator.

Then the contribution of x to the loss function is

$$\mathrm{contribution}(x) = p_r \log D(x) + p_g \log(1-D(x)). \tag{3}$$

By taking the derivative of formula (3) to $D(x)$ and making its derivative value 0, it can be obtained that

$$\frac{p_r}{\log D(x)} + \frac{p_g}{\log(1 - D(x))} = 0. \tag{4}$$

By simplification, the best discriminator can be obtained as follows:

$$D(x) = \frac{p_r}{p_r + p_g}. \tag{5}$$

The above results show that the task of the discriminator is to judge the possibility that the input sample x comes from real data and generated data. When $p_r(x) = 0$ and $p_g(x) \neq 0$, the discriminator can easily determine the source of x. When $p_r(x) = p_g(x)$, it indicates that the probability that the sample belongs to the real sample is equal to that of the generated sample. At this time, the output of the optimal discriminator is 0.5, which means that the generator and the discriminator have reached Nash equilibrium. The sample generated by the generator is enough to confuse the true with the false so that the discriminator cannot make a correct judgment on the input sample. If the obtained optimal discriminator is replaced back into the loss formula of the original GAN, the following can be obtained:

$$\begin{aligned}
&E_{x\sim p_r(x)}\left[\log\frac{p_r}{p_r + p_g}\right] + E_{x\sim p_g(x)}\left[\log\left(1 - \log\frac{p_r}{p_r + p_g}\right)\right] \\
&= \int_{x\in X} p_r \log\frac{p_r}{p_r + p_g}\,\mathrm{d}x + \int_{x\in X} p_g \log\frac{p_r}{p_r + p_g}\,\mathrm{d}x \\
&= \int_{x\in X} p_r \log\frac{2p_r}{p_r + p_g}\,\mathrm{d}x + \int_{x\in X} p_g \log\frac{2p_r}{p_r + p_g}\,\mathrm{d}x - 2\log 2 \\
&= KL\left(p_r \| \frac{p_r + p_g}{2}\right) + KL\left(p_g \| \frac{p_r + p_g}{2}\right) - 2\log 2 \\
&= 2JS\left(p_r \| p_g\right) - 2\log 2.
\end{aligned} \tag{6}$$

It can be seen from the above results that the form of the optimal discriminator can be obtained according to the loss function in the original generated countermeasure network. When the discriminator is in the optimal state, the generator loss defined by the original generation countermeasure network can be equivalent to minimizing the Jensen–Shannon (JS) divergence between the real sample data distribution and the generated data sample distribution.

However, there is often a problem when optimizing JS divergence. No matter whether the two data distributions are very close or far apart, as long as there is no overlap between the two data distributions or the overlap can be ignored, JS divergence will not be updated and will always be the fixed value log2. This also means that the gradient vanishing problem will occur when using the loss function of the original GAN for training.

In the process of generating countermeasure network training, especially at the beginning of training, the input of the generator is random noise, so there is no intersection between the large probability of the sample distribution generated by the generator and the real sample distribution. As a result, the JS divergence is fixed at the constant log2, and the gradient is 0, so the gradient descent method cannot be used to train the network parameters. At this time, for the generator network, there will be no gradient information fed back from the discriminator network, which leads to the disappearance of the gradient in the network training. Therefore, the training instability and model collapse often occur in the original generated countermeasure network. On the one hand, when the discriminator network is trained too well, the gradient fed back to the generator network will disappear, and the generator network cannot be updated and optimized. On the other hand, when the discriminator network is not trained well, the correct gradient cannot be fed back to the generator network to guide the generator network to optimize better.

Therefore, we use the loss function of the WGAN model to replace the loss function of the original generated countermeasure network and use Wasserstein distance instead of JS divergence to measure the distance between two data distributions, which effectively reduces the instability of model training. Wasserstein distance is also called earth-mover (EM) distance, which is defined as follows:

$$W\left(p_r, p_g\right) = \inf_{\gamma\sim\prod\left(p_r, p_g\right)} E_{(x,y)}[\|x - y\|]. \tag{7}$$

The advantage of Wasserstein distance over KL divergence and JS divergence in the original generated countermeasure network is that it can reflect the distance between the two data distributions without overlapping.

In order to add Wasserstein distance to the loss function, a constrained discriminator is proposed, that is, it satisfies 1-Lipschitz continuity, and the Lipschitz continuity condition limits the maximum local variation amplitude of a continuous function. In order to meet the constraints, the weight updated during backpropagation is forcibly trimmed to the specified range by weight clipping, and then the $V(G,D)$ is maximized to realize the training of the model.

The proposed loss function is

$$V(G, D) = \max_{D\in 1\_\text{Lipschits}} E_{x\sim P_{\text{data}}}[D(x)] - E_{x\sim P_G}[D(x)]. \tag{8}$$

The larger the value of the proposed loss function, the closer the generated data distribution is to the real data distribution, and the better the network training.

4.2. Structure of the Migration Model for Creative Animation Generation. Similar to the general GAN model, the animation illustration style transfer model proposed in this paper is also composed of generators and discriminators. The internal distribution of data can be obtained by leaning against each other. In order to better retain the original content of images and achieve the transfer of artistic styles in animation illustration style transfer, we design the generator structure of the deep learning-driven migration model for creative animation generation as shown in Figure 1. Taking ResNet-18 as the basic model, the generator structure

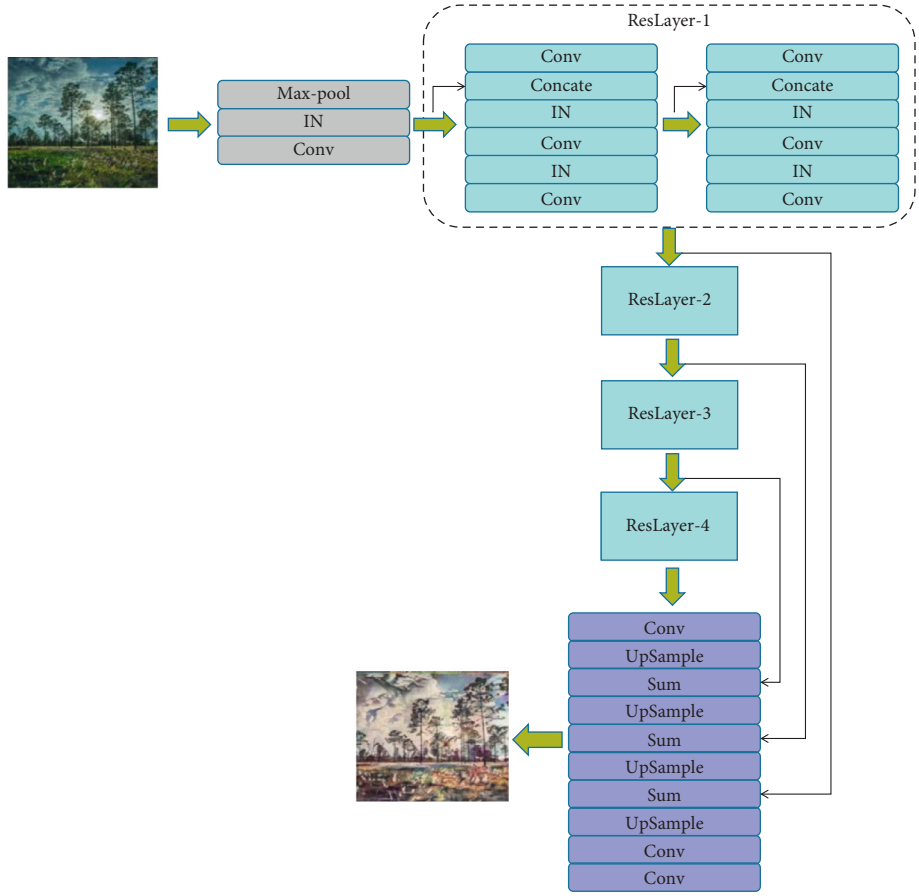

Figure 1: The generator structure of the deep learning-driven migration model for creative animation generation.

divides image generation into two parts, including downsampling and upsampling.

The downsampling part of the image is composed of a basic convolution module and four residual layers (reslayer-1–reslayer-4). However, the basic convolution module consists of four layers: Conv – Instance Norm (IN) – ReLU – MaxPooling. The convolution kernel used is 7×7. This makes the convolution operation have a relatively large receptive field. In the four residual layers, each residual layer contains two residual blocks. Their internal structure is Conv-IN-ReLU-Conv-IN. The output of the latter IN layer will concatenate with the input of the entire residual layer. And then it goes through another convolution layer. The entire residual block has the same short-circuit connection structure as BottelNeck in ResNet. This allows the input of the entire residual layer to be reused. It can effectively improve the gradient propagation performance of network optimization. In the downsampling part, each convolution layer uses a 3×3 convolution kernel. After each residual layer, 1/2 horizontal and vertical downsampling is done.

After the basic convolution module and four residual layers, the size of the feature map will be 1/16 of the original image. It will then be upsampled. First, the feature graph output by reslayer-4 is convolved. It is then upsampled to restore the feature image to 1/8 of the original image. As shown in Figure 1, add it to the output of reslayer-3 for upsampling. This operation is then repeated until the output of reslayer-1 is added. Such a short circuit connection makes the details of the feature map of the previous processing better preserved. This avoids damage to the content of the image when migrating styles later. After a short circuit connection and addition, the feature graph passes through two convolution layers. It will be transformed back into a three-channel image again. In the convolution operation of the upsampling part, the convolution kernel of the first two convolution layers is 1×1. The convolution kernel at the last layer is set to 7×7. Tanh activation function is used before conversion to a three-channel image.

PatchGAN discriminator structure of 70×70 was used in the discriminator in this paper. Compared with the general convolutional neural network structure, the PatchGAN discriminator has fewer parameters and can receive images of arbitrary size. The PatchGAN discriminator contains three convolution blocks. Each block contains two convolution layers. In terms of the number of channels in the convolution kernel, this paper sets the output channel of the first convolution layer as 64. The number of channels is doubled in each subsequent block.

In the loss function design of the model, this paper adopts the same cyclic consistency loss as that in CycleGAN. For image transformation G and F, CycleLoss means that the result of source image transformation after $x \longrightarrow G(x) \longrightarrow$

Figure 2: The original representative partial face image.

$F(G(x))$ should have the attribute of $F(G(x)) = x$. Similarly, for the target image through $y \longrightarrow F(y) \longrightarrow G(F(y))$ should also be $G(F(y)) = y$. When L1 distance is used to measure the difference between the result after cyclic transformation and the original image, CycleLoss can be expressed as follows:

$$L_{\text{cyc}}(G, F) = E_{x \sim p_{\text{data}}}\left[\left\|F(G(x) - x)_1\right\|\right] + E_{y \sim p_{\text{data}}}\left[\left\|F(G(x) - y)_1\right\|\right]. \tag{9}$$

When using the CycleLoss training model, we need to consider not only the cyclic consistency loss from source image to target image to source image but also the backtracking CycleLoss from target image to source image to target image. Therefore, two pairs of generators and discriminators need to be set up simultaneously in the model. It was also trained with CycleLoss in formula (2). The final loss function can be expressed as follows:

$$\begin{aligned} L\left(G, F, D_x, D_y\right) = {} & L_{\text{GAN}}\left(G, D_x\right) + L_{\text{GAN}}\left(F, D_y\right) \\ & + \lambda L_{\text{cyc}}\left(G, F\right), \end{aligned} \tag{10}$$

where D_{x} and D_{y} refer to the discriminators of source image x and target image y, respectively. λ is the equilibrium parameter set based on experience.

4.3. Image Evaluation Index. In the image generation task, the evaluation of the result quality of the generated image not only can rely on the subjective judgment of human vision but also need to analyze the generated image quantitatively. It is mainly considered from two aspects: (1) the quality of the generated image itself, that is, whether the image content is realistic and whether the image details are clear, and (2) for the diversity of generated images, a good generation should generate a variety of images rather than a fixed number of similar types of images. At present, in the field of image generation, the evaluation indicators are is IS (inception score) and FID (Fréchet inception distance).

4.3.1. IS. It uses the pretrained inception neural network as the classifier, inputs the image samples generated by the generator into the classifier, and statistically analyzes the output value of the classifier. Its calculation is

$$IS(G) = \exp\left(E_{x \sim p_g} KL(p(y|x) \| p(y))\right), \tag{11}$$

where $x \sim p_g$ means that x is the image sample generated from pg, $KL(p(y|x) \| p(y))$ means that KL divergence is used to measure the distance between two distributions, $p(y|x)$ represents the probability that the image sample x is

Figure 3: The animation generated by the original DCGAN model.

classified as y, and $p(y) = \int_x p(y|x)p_g(x)$ represents the edge distribution of all categories of images.

The larger the IS value, the better the image generated by the generator model.

4.3.2. FID. It is a method to evaluate the image quality by calculating the distance between the feature vector of the real image and the generated image, and the feature vector of the image is extracted after removing the last layer of the network through the perception neural network. The calculation is

$$\mathrm{FID}\left(P_r, P_g\right) = \left\|\mu_r - \mu_g\right\|^2 + Tr\left(\sum r + \sum g - 2\sqrt{\sum r \sum g}\right), \tag{12}$$

where μ represents the mean vector of the real image and the generated image in the feature space, $\sum$ represents the covariance matrix of the real image and the generated image in the feature space, and Tr represents the trace of the matrix.

On the contrary to IS, if the FID value is smaller, it means that the similarity between the generated image and the real image is higher, indicating that the generation effect of the model is better.

5. Experimental Results and Analysis

5.1. Experimental Data. The animation avatar data set used in the model training in this paper is randomly crawled from the animation material website SafeBooru through the web crawler and screened it. Finally, 150,000 animation images are obtained; 60,000 images are randomly selected as the training samples; and the image size is uniformly processed to 96×96 for the experiment.

In order to verify the generalization of the improved model, experiments were carried out on CelebFace data set. A total of 10,200 samples and 202,677 face data were collected in this data set, and the face styles in the images were quite different. All the image sizes were 178×218. However, if all the data sets were used as training data, the training time of the model would be too long, so 100,000 images are used as training data in this experiment. At the same time, the size of the original image is 178×218, which is not conducive to the construction of the neural network model. It is necessary to preprocess the original image and change it to the size of 128×160, which not only can ensure the simplicity of the network model but also can ensure the image proportion.

Figure 4: The animation generated by the original WGAN model.

5.2. Experimental Configuration. PyTorch deep learning framework was used in the Ubuntu 18.04 environment. It uses an NVIDIA-1080 GPU with CUDA10 for acceleration. An SGD optimizer with a learning rate of 0.002 was used to optimize the model as 200 Epochs. It was then used to test the generation of animation illustration-style images.

5.3. Results and Discussion. Figure 2 is the original representative partial face image, which shows the training results obtained from the CelebA data set. Due to the excessive number of original sample sets, 100,000 face images are randomly selected as training samples in order to reduce training time.

In order to verify the performance of the improved model proposed in this paper in animation generation, comparative experiments are carried out on the original DCGAN model and the original WGAN model in the 100,000 face image data set shown in Figure 2. The comparative experimental results are shown in Figures 3–5. Through the steps of facial emotion recognition and information aggregation, Figures 3–5 show the effects of three different GAN methods in the animation data set. Figure 3 shows the animation generated by the original DCGAN model; Figure 4 shows the generation results of the WGAN model; and Figure 5 shows the animation effect generated by the proposed algorithm.

It is not difficult to see that although the images generated by the three different methods have good identifiability.

However, compared with other methods, the animation image content generated by traditional DCGAN lacks authenticity, and the facial details of the generated animation characters are seriously lost, which gives people a sense of disharmony, and the whole image appears the phenomenon of information collapse.

For the animation generated by the WGAN model, it performs well in the color brightness of the whole image, but the image quality is significantly lower than the other two methods, and the facial features of the animation avatar in the generated image are not clear.

Compared with these two methods, the improved GAN model designed in this paper combines the respective advantages of the original DCGAN and WGAN. The generated animation avatar is closer to the real sample; the details generated on the image are clearer; and the color saturation is high and has stronger authenticity.

The above only analyzes and compares the generation effects of the original DCGAN model, WGAN model, and the algorithm model in this paper on the same data set from

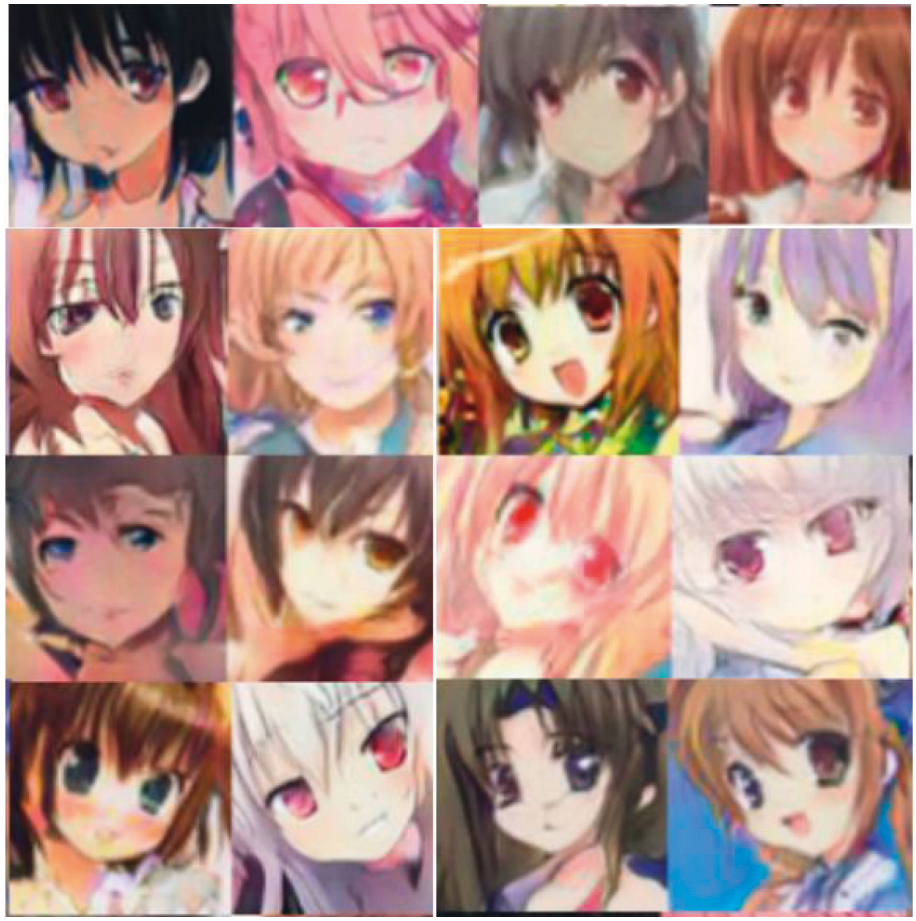

Figure 5: The animation generated by the proposed GAN model.

Table 1: The evaluation results of three models.

Model	Evaluation indicators			
	IS		FID	
	CelebA data set	Animation	CelebA data set	Animation
DCGAN	6.22 ± 0.13	6.56 ± 0.25	43.22 ± 0.22	39.52 ± 0.12
WGAN	7.01 ± 0.15	7.12 ± 0.18	40.55 ± 0.10	36.36 ± 0.22
The proposed GAN model	7.45 ± 0.22	7.88 ± 0.24	35.69 ± 0.23	31.28 ± 0.26

the perspective of human visual intuition, which has a certain subjectivity. In order to evaluate these three models more objectively, we use IS and FID as quantitative evaluation indicators of the image effect generated by the model. These two evaluation indicators are the most widely used evaluation indexes in the GAN model at present. Through these two indicators, the animation generated by three different network models is evaluated, and the evaluation results are shown in Table 1.

For these two evaluation indicators, the larger the value of IS, the better the quality and diversity of the generated animation image, while the smaller the value of FID, the better the diversity and quality of the generated animation image. From the data in Table 1, it can be concluded that the proposed GAN model has better performance in generating images than the original DCGAN model and WGAN model. The score of the same model in the CelebA data set is lower than that in animation data set due to the influence of character background information. It can be seen that in the training of depth model, the quality of the data set also has a great impact on the final training results of the model.

6. Conclusion

This paper studies the style transfer of animation based on the GAN model. A new generator network is designed to allow simultaneous migration of image style and content. After training using natural world images as source domain data and art illustration images as target domain data. This method can generate animation images with excellent visual quality. Compared with the images generated by DCGAN and WGAN models, the proposed method achieves a better

balance between the image style and the original image content. Aiming at the problem of model collapse that often occurs in the process of network model training, in order to avoid this problem, this paper uses Wasserstein distance instead of JS divergence as the measurement standard. In order to make the weight meet the constraints, the model adopts the method of weight forced cutting, which is not conducive to the learning of the network model. In the next work, we will consider using gradient punishment instead of weight forced cutting to make the weight meet the constraints.

Data Availability

The data set can be accessed upon request to the corresponding author.

Conflicts of Interest

The authors declare that there are no conflicts of interest.

Acknowledgments

This work was supported by Special Subject of Art Education in Shandong Province in 2021 "Teaching Exploration and Practical Research on the Form of Image Expression in the Creation of Red Culture Theme Oil Painting--Taking Yimeng Spirit as an Example" (L2021Y10290453) and 2022 National Art Fund Communication, Exchange and Promotion Project "River Surging: Yellow River Culture and Art Exhibition."

References

[1] L. A. Gatys, A. S. Ecker, and M. Bethge, "Image style transfer using convolutional neural networks," in *Proceedings of the 2016 IEEE Conference on Computer Vision and Pattern Recognition (CVPR)*, July2016.

[2] Y. Jing, Y. Yang, Z. Feng, J. Ye, Y. Yu, and M. Song, "Neural style transfer: a review," *IEEE Transactions on Visualization and Computer Graphics*, vol. 26, no. 11, pp. 3365–3385, 2020.

[3] S. Ji, W. Xu, M. Yang, and K. Yu, "3D convolutional neural networks for human action recognition," *IEEE Transactions on Pattern Analysis and Machine Intelligence*, vol. 35, no. 1, pp. 221–231, 2013.

[4] J. M. Wolterink, T. Leiner, M. A. Viergever, and I. Isgum, "Generative adversarial networks for noise reduction in low-dose CT," *IEEE Transactions on Medical Imaging*, vol. 36, no. 12, pp. 2536–2545, 2017.

[5] Z. Yi, Z. Hao, and P. Gong, "DualGAN: unsupervised dual learning for image-to-image translation," in *Proceedings of the IEEE International Conference on Computer Vision*, October 2017.

[6] C. Bo, Q. Zhang, S. Pan, and L. Meng, "Generating Handwritten Chinese Characters Using CycleGAN," in *Proceedings of the 2018 Proceedings of the IEEE Winter Conference on Applications of Computer Vision*, IEEE Computer Society, Lake Tahoe, NV, USA, March 2018.

[7] X. Mao, Q. Li, H. Xie, L. Raymond, and Z. Wang, "Least squares generative adversarial networks," in *Proceedings of the IEEE International Conference on Computer Vision*, pp. 2794–2802, Venice, Italy, October 2017.

[8] M. Arjovsky, S. Chintala, and L. Bottou, "Wasserstein generative adversarial networks," in *Proceedings of the 34th International Conference on Machine Learning*, Sydney, Australia, August 2017.

[9] I. Gulrajani, F. Ahmed, M. Arjovsky, V. Dumoulin, and A. Courville, "Improved training of Wasserstein GANs," 2017, https://arxiv.org/abs/1704.00028.

[10] D. Berthelot, T. Schumm, and L. Metz, "BEGAN: boundary equilibrium generative adversarial networks," 2017, https://arxiv.org/abs/1703.10717.

[11] A. Radford, L. Metz, and S. Chintala, "Unsupervised representation learning with deep convolutional generative adversarial networks," 2015, https://arxiv.org/abs/1511.06434.

[12] S. Ioffe and C. Szegedy, "Batch Normalization: Accelerating Deep Network Training by Reducing Internal Covariate Shift," in *Proceedings of the 32nd International Conference on International Conference on Machine Learning*, Lille, France, July 2015.

[13] H. Zhang, I. Goodfellow, D. Metaxas, and A. Odena, "Self-attention generative adversarial networks," 2018, https://arxiv.org/abs/1805.08318.

[14] A. Brock, J. Donahue, and K. Simonyan, "Large scale GAN training for high fidelity natural image synthesis," 2018, https://arxiv.org/abs/1809.11096.

[15] M. Mirza and S. Osindero, "Conditional generative adversarial nets," 2014, https://arxiv.org/abs/1411.1784.

[16] P. Isola, J.-Y. Zhu, T. Zhou, and A. A. Efros, "Image-to-image translation with conditional adversarial networks," 2017, https://arxiv.org/abs/1611.07004.

[17] O. Ronneberger, P. Fischer, and T. Brox, "U-Net: convolutional networks for biomedical image segmentation," 2015, https://arxiv.org/abs/1505.04597.

[18] J. Y. Zhu, T. Park, P. Isola, and A. Efros, "Unpaired image-to-image translation using cycle-consistent adversarial networks," in *Proceedings of the IEEE international conference on computer vision*, pp. 2223–2232, October 2017.

[19] Y. Choi, M. Choi, M. Kim, J.-W. Ha, and S. Kim, "Stargan: unified generative adversarial networks for multi-domain imageto-image translation," in *Proceedings of the IEEE conference on computer vision and pattern recognition*, pp. 8789–8797, Salt Lake City, UT, USA, June 2018.

[20] O. Kupyn, V. Budzan, M. Mykhailych, D. Mishkin, and Ji Matas, "Deblurgan: blind motion deblurring using conditional adversarial networks," in *Proceedings of the IEEE Conference on Computer Vision and Pattern Recognition*, pp. 8183–8192, Salt Lake City, UT, USA, June2018.

[21] C. Ledig, L. Theis, F. Huszár, and J. Caballero, "Photo-realistic single image super-resolution using a generative adversarial network," in *Proceedings of the IEEE conference on computer vision and pattern recognition*, pp. 4681–4690, Honolulu, HW, USA, July 2017.

[22] C. Li and M. Wand, "Precomputed real-time texture synthesis with markovian generative adversarial networks," in *Proceedings of the European Conference on Computer Vision*, October2016.

[23] A. Kim, T. Jang, and O. K. Chang, "A run-to-run controller for a chemical mechanical planarization process using least

squares generative adversarial networks," *Journal of Intelligent Manufacturing*, vol. 32, pp. 1–14, 2020.

[24] Q. Creswell, Q. White, Y. Dumoulin, M. Liu, B. Sengupta, and A. A Bharath, "Sketch simplification based on conditional random field and least squares generative adversarial networks," *IEEE Signal Processing Magazine*, vol. 35, no. 1, pp. 53–65, 2018.

[25] Q. Lu, Q. Tao, Y. Zhao, and M Liu, "Sketch simplification based on conditional random field and least squares generative adversarial networks," *Neurocomputing*, vol. 316, pp. 178–189, 2018.

Hindawi
Scientific Programming
Volume 2023, Article ID 9851726, 1 page
https://doi.org/10.1155/2023/9851726

Retraction

Retracted: Study on the Influence of Wuthering Heights Characters Based on Web Analysis and Text Mining

Scientific Programming

Received 18 July 2023; Accepted 18 July 2023; Published 19 July 2023

This article has been retracted by Hindawi following an investigation undertaken by the publisher [1]. This investigation has uncovered evidence of one or more of the following indicators of systematic manipulation of the publication process:

(1) Discrepancies in scope
(2) Discrepancies in the description of the research reported
(3) Discrepancies between the availability of data and the research described
(4) Inappropriate citations
(5) Incoherent, meaningless and/or irrelevant content included in the article
(6) Peer-review manipulation

The presence of these indicators undermines our confidence in the integrity of the article's content and we cannot, therefore, vouch for its reliability. Please note that this notice is intended solely to alert readers that the content of this article is unreliable. We have not investigated whether authors were aware of or involved in the systematic manipulation of the publication process.

Wiley and Hindawi regrets that the usual quality checks did not identify these issues before publication and have since put additional measures in place to safeguard research integrity.

We wish to credit our own Research Integrity and Research Publishing teams and anonymous and named external researchers and research integrity experts for contributing to this investigation.

The corresponding author, as the representative of all authors, has been given the opportunity to register their agreement or disagreement to this retraction. We have kept a record of any response received.

References

[1] R. Wang and L. Deng, "Study on the Influence of Wuthering Heights Characters Based on Web Analysis and Text Mining," *Scientific Programming*, vol. 2022, Article ID 4326551, 11 pages, 2022.

Hindawi
Scientific Programming
Volume 2022, Article ID 4326551, 11 pages
https://doi.org/10.1155/2022/4326551

Research Article

Study on the Influence of Wuthering Heights Characters Based on Web Analysis and Text Mining

Rui Wang[1] **and Lin Deng**[2]

[1]*Department of Basic Courses, Shanghai SIPO Polytechnic, Shanghai 201399, China*
[2]*Xingzhi College, Zhejiang Normal University, Jinhua 321004, China*

Correspondence should be addressed to Rui Wang; wangrui@sicfl.edu.cn

Received 3 March 2022; Revised 17 March 2022; Accepted 24 March 2022; Published 14 April 2022

Academic Editor: Jie Liu

The rapid development of network technology and the popularity of the Internet have made people rely more and more on the exchange and sharing of network information, and the demand for obtaining information about people from the Internet has gradually increased, but the massive amount of network data has made the information about people fragmented and disorganized, and the existing work on portraits has mainly focused on the extraction of people's attributes. In this paper, we examine the artistic construction and characterization of Wuthering Heights on the basis of a tasting of the book, with the aim of presenting the "alienated personalities" hidden in the depths of the characters' consciousness and showing the author's unique creative art through an analysis of thematic ideas, the use of temporal elements, and the tracing of the creation of the characters' original forms. In the aspect of character social relationship extraction, first, the method of expanding the seed dictionary by means of synonym word forest is used to build a character relationship lexicon, which avoids the inefficiency caused by manual lexicon collection; second, a character relationship extraction algorithm based on the combination of rule matching and syntactic tree is proposed, which effectively overcomes the disadvantage of low recall rate caused by rule matching, and the average F-value of this algorithm reaches 82.61% in the experiment The algorithm achieves an average F-value of 82.61% in the experiment, which is a significant advantage over other methods.

1. Introduction

Emily Brontë's novel Wuthering Heights died of depression and low critical acclaim until the 20th century, when her reputation grew and the novel was considered a "complete and profound insight into human nature and life." The novel is a unique artistic construction, based on the love-hate relationship between two generations and the distorted human nature of life in the aberrant English society of the time. This article explores and examines the artistic construction and characterization of Wuthering Heights from the perspective of a taster [1, 2].

The theme is clearly stated. Set in 18th-century Yorkshire, Wuthering Heights tells the story of Heathcliff, an orphaned boy who is adopted by Earnshaw, the old owner of the cottage, and goes out to earn money after being humiliated and losing his love. When he becomes rich, he returns to take revenge on the landowner Linton and his children, who have married his girlfriend Catherine. Heathcliff's transformation from an orphan to avenger is a reflection of the perverse society of the time [3]. Heathcliff is discriminated against by the society he describes, and this is the trigger for his fierce rebellion. His frenzied revenge against Wuthering Heights and the Painted Hills is an indictment of a heartless society [4].

When it comes to the organization of character information, traditional methods often use manual editing and collation, which can achieve a high accuracy rate but is inefficient, and users are eager to get global information about the target character in a simple and quick search. If global information about people could be automatically extracted and collated from people data scattered all over the

Internet, and the scattered and fragmented data could be brought together to form a portrait of people and stored in a structured manner, this would greatly improve the efficiency of users in obtaining global information about people and facilitate human work and life [5].

Of course, in addition to search engines, users can also obtain information about people through specific people search systems. The most mature people search engines in the market today are Youku (https://www.ucloo.com/), Yahoo People Search (https://people.yahoo.com/), Microsoft People Cube (https://renlifang.msra.cn/), etc [6]. These people search engines for people are mainly biased toward the basic information of the person's gender, age, and place of origin, and do not present the trajectory of the person's activities, i.e., the Wuthering Heights incident that the person was involved in as reported on the Internet. Generally, when people are learning about a character object, they not only want to get basic information about the object but are more eager to get information about when and where the character was involved in what events with whom, the emotional evaluation of the character on the Internet and the size of the character's hotness, to grasp information about a character as a whole.

In this paper, we study the character portrait mining technique of text data represented by Wuthering Heights, focusing on three aspects: extraction of characters' social relations, tracking of characters' participation in events, and analysis of characters' hotness and emotions. First, the text data are divided into words and lexical annotations to extract the character entities, and at the sentence level, the social relations of characters are extracted using shallow syntactic analysis; second, the features of individual texts are extracted according to the corresponding feature extraction algorithm, and the clustering algorithm is used to achieve the aggregation of similar events, taking characters and time as clues to form a time-based character event activity; finally, the combination of Wuthering Heights' coverage. The hotness value and emotional tendency of the characters are calculated by combining various factors such as the amount of reports, comments, readings, and time span of Wuthering Heights. The above analysis results are combined to form a character portrait, and the research results can be applied to character search systems, specific target tracking, and online celebrity detection.

1.1. Related Work

1.1.1. Personality Information Extraction. In the area of character information organization, existing work has focused on the field of character biography and character search. After the authors of [7] proposed the concept of biography, many scholars have worked on this area, resulting in a variety of methods for the extraction of biographies, mainly including methods based on multidocument summarization techniques, ontology-based and character-tracking-oriented. The authors of [8] realized the extraction of biographies using multi-document summarization techniques. The method combines linguistic knowledge and statistical theory to extract the basic information of an object, including name, gender, education, etc., from multiple documents to form a biographical text. The authors of [9] implemented a multidocument biographical summary system, mainly using the idea of classification to divide sentences into corresponding clusters of classes, first formulating a classification of sentences about the biography: social relations, educational background, place of origin, work, etc., and then using a classification algorithm to obtain the sentences that best characterize the characteristics of the person, which are eventually combined to form the biography. The authors of [10] proposed the concept of "meta-events" and applied it to the field of character information extraction, where "meta-events" are acts consisting of three named entities: people, time, and place. The authors of [11] proposed constructing an ontology of events for people and to realize this through an ontology description language.

Personal information extraction on the other hand is a research work for personal search engines, which started late. The ArnetMiner system [12] developed by [13] mainly targets experts in academic fields and mines personal information from their personal homepages, published papers, social networks, and other data. The authors of [14] proposed a personal information mining tool for social media such as Linkedln and Facebook. The authors of [15] proposed a rule-based algorithm for extracting personal information, focusing on summarizing rules such as place of origin, date of birth, and political appearance and developed a semistructured personal information extraction system. The authors of [16] proposed a person information extraction based on trigger words, realizing the extraction of person attribute information from Baidu's encyclopedia web pages, first by developing a trigger word list through linguistic analysis and second by automatically discovering candidate rules based on the word field around the person's name using statistical principles. The authors of [17] for information extraction in the field of teachers, first used SVM to classify the crawled down web pages and selected those containing person information, second developed a rule base for person attribute extraction, and finally used the rules to achieve information extraction of computer teachers in universities. The authors of [18] proposed a method based on double-layer cascaded text classification to extract personal information from resumes. The authors of [19] extracted personal information from personal homepages and CVs by a method based on trigger words and rules. The authors of [7] proposed a personal information extraction algorithm based on semantic context analysis, which incorporates the theory of hidden Markov model, semantic analysis, natural language processing, and information extraction.

1.2. Organization of Character Events. The current research on the organization of personal information is mainly focused on the extraction of personal information, and there is still a need to go further into the character activity events or the tracking of character events. In the work of [2], the concept of

"personal tracking" is proposed, which applies topic recognition and tracking to the extraction of personal events and proposes that personal events consist of three elements: time, place, and event description. The authors of [3] proposed a single-pass-based topic recognition algorithm, which is simple and fast, but the biggest drawback is that it is sensitive to the order of text arrival; the authors of [4] proposed a cohesive hierarchical clustering algorithm to solve the problem of hierarchical topic detection for the situation that multiple topics may exist in a text (i.e., there may be intersection between texts at multiple levels). The authors of [5] used the K-Means clustering algorithm to achieve topical recognition, clustering K points in the text as the centers of class clusters and dividing all texts into the closest class clusters at once, and then by continuous iteration.

To address the shortcomings of the single-pass algorithm, which is sensitive to the input order of the text, the concept of batch processing is introduced to improve the accuracy of the clustering algorithm by first clustering a batch of arriving text, then comparing it with existing classes and introducing the process of adjustment and "resurrection." In the study of [3], the automatic prediction of the number of clusters is investigated to address the shortcomings of K-Means, which requires the prior determination of the number of clusters and is sensitive to noise points and initial points. The authors of [8] proposed a new treatment for the determination of the initial centroids.

2. Main Characterization

2.1. Paranoid and Brutal Heathcliff. Heathcliff was tough, rude and rebellious, but a man with a passion for love. He was a childhood friend of Catherine's, but after the death of old Earnshaw, Heathcliff was reduced to being a servant of Sindre, deprived of an education, and the chance to become a civilized man. However, Heathcliff's love for Catherine would have allowed him to endure any torment from Hindley, something that would have been difficult for ordinary people to do. Heathcliff, who was from a humble background in a materialistic society at the time, was filled with a deep sense of depression and inferiority and was acutely aware of the inequality of treatment brought about by the disparity in status and money. His hatred for Sindre, who is a member of the upper class, is so great that he can only endure it when he is unable to retaliate, but deep down, he has already developed the idea and intention of revenge. Admittedly, the change of role from outcast to avenger suggests that he was not born that way, but because of Sindre's servitude and abuse and the disappointment of love [12]. When Catherine married Linton of Painted Hills, he was completely broken by the absence of that powerful love in his heart. Faced with an awkward situation, the darker side of his character begins to surface and he leaves with anger and hatred. He returned a few years later, rich and burning with the fire of revenge, believing from the beginning that he would be happy with the torment of the past as long as he could succeed in his revenge. It is not difficult to explain his subsequent desperate attempts to acquire the two great estates and his vast family fortune.

3. Selfish and Wild Catherine

Wild and untamed, Catherine and Heathcliff are a matched made in heaven. Catherine is the only person in Wuthering Heights who gives Heathcliff a solace of mind, and both young are spontaneous, brave, and strong in their approach to love. However, when they break into Wuthering Heights, Catherine begins to waver between the naked idea of true love and the rich and noble reality, secretly comparing the rich, gentle, and civilized Linton and the poor, rude, and primitive Heathcliff. After her marriage, Catherine also tried to be a graceful, polite lady, creating the illusion of true love for Linton, but this inevitably involved concealing and repressing herself and hiding a different spiritual world from Linton. The prolonged separation of spirit and body caused the otherwise lively and energetic Catherine to suffer and spend her days in depression.

4. Mainstream and Secular Linton

Catherine's husband, Linton, was a wealthy, gentle, and generous man, a typical heroic figure in the Victorian fiction. His gentlemanly manners and unique charm had fascinated Catherine, and his upper class label of wealth, civility, and elegance made Heathcliff jealous. Linton was accommodating, courteous, and caring toward Catherine. He treats his relatives and servants with the same kindness and humanity that shine through at all times. He is the embodiment of the prevailing values of society, the guardian of the secular moral order, and the bearer of civilized order and decency for generations. He is also weak, introverted, and hypocritical.

5. Ruthless Cowardly Sindre

As a result of the accidental appropriation of his father's love, Sindre becomes cold, brutal, and even self-absorbed. The absence of his father's love is the origin of Hindley's hatred, and Heathcliff's arrival gives him an object of hate. After his father's death, he uses all means to abuse and mistreat Heathcliff, which is the key point of the entire novel.

6. Innocent Helpless Second Generation

Hindley's son Harington could have been a gentleman in mainstream society, but his mother died soon after his birth and without his mother's care he went from innocent and sweet boy to the rebellious and disobedient brat. Moreover, all this change comes at the hands of Heathcliff, who torments and persecutes Harington in the same way that Hindley persecuted himself. Fortunately, his love for young Catherine makes Harington aware of his own shortcomings, awakening his self-respect and good nature, and eventually, through his own efforts, he becomes a handsome, civilized young man.

The entire act of revenge carried out by Heathcliff, involving different degrees of human distortion shown by each individual on different occasions, is also a true and objective reflection of the distortions and struggles of human nature in the social context of the work.

7. Character Relationship Extraction based on a Combination of Rule Matching and Syntactic Trees

This section deals with the automatic extraction of social relations of characters from texts. The social relations of characters are the general term for the mutual relations formed by human beings in the material conditions of their common life, e.g., "father," "daughter," "friend," "colleague," etc. "The term "relationship" or "character relationship" is used later to refer to the social relationships of people. As people are in a large community, they are inevitably connected to other people in a variety of ways, and if relationships can be automatically extracted from Wuthering Heights reports on the Internet about characters, this is essential to the portrayal of characters. Phrases describing character relationships tend to be fragmented, and if the character relationships implicit in the sentences can be extracted through syntactic analysis, this will help to improve the effectiveness of the relationship extraction.

The paper proposes a character relationship extraction algorithm based on a combination of rule matching and syntactic trees, which broadly consists of the following steps:

(1) Data preprocessing: first, the text is divided into words and lexical annotation; second, the personal names and relationship words are identified, and finally, candidate sentences with possible personal relationships are filtered out in terms of sentences.

(2) Rule matching-based personal relationship extraction: first, building a rule base, second, using the rules to match the candidate sentences obtained in the data preprocessing step to achieve the first extraction of personal relationships.

(3) Character relationship extraction based on a syntactic tree: syntactic analysis is performed on candidate sentences that do not satisfy the rules, a syntactic tree is built, and the second extraction of character relationships is performed through the path distance between the relationship words and the two character entities in the syntactic tree.

(4) Character relationship determination: after obtaining all relationship words between two characters through the extraction of the large-scale corpus, the relationship words with the highest weight are selected as the final character relationship determination by merging the relationship synonyms.

The specific flowchart of the character relationship extraction algorithm based on the combination of rule matching and syntactic tree is shown in Figure 1, and the details of these parts are described below.

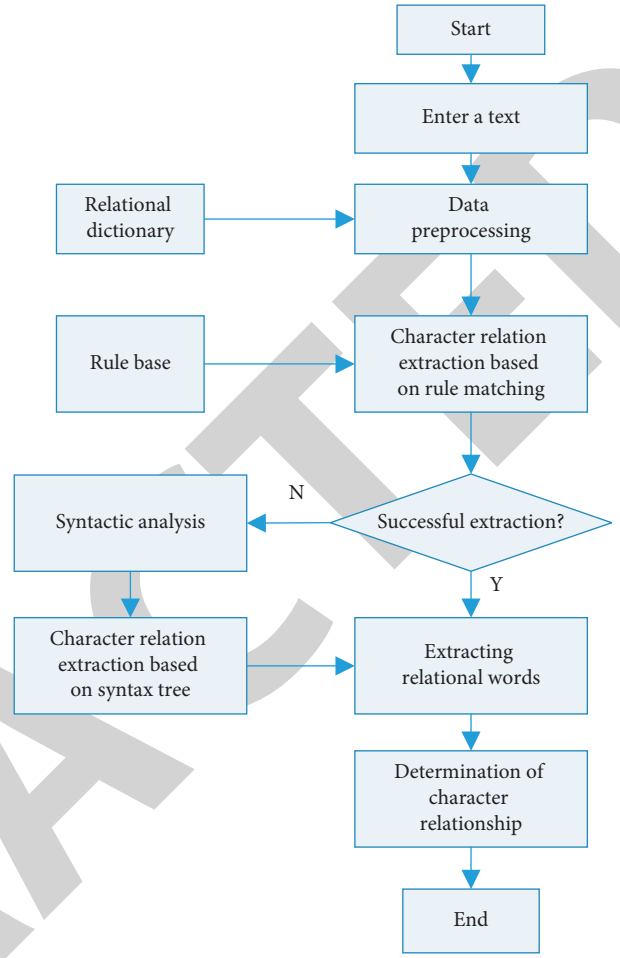

Figure 1: Flowchart of the character relationship extraction algorithm.

8. Data Preprocessing

Before proceeding to the subsequent relationship extraction algorithms, the data first need to be preprocessed, including word separation and personal identification. Second, subsequent rule-based matching and syntactic tree-based relationship extraction methods are all based on sentences. Since a large number of sentences in the text do not contain person relationships, it is necessary to first perform sentence separation (the sentences are separated according to the sentence separator in the Chinese grammar) and then perform sentence screening, and the valid sentences selected are used as an input for the subsequent algorithm. This can filter a large number of irrelevant statements and improve the efficiency of the algorithm. The flowchart of data preprocessing is shown in Figure 2.

8.1. Rule-Based Matching for Character Relationship Extraction. The person relationship candidate sentences have been obtained through the data preprocessing stage, this stage will elaborate on the extraction of relationships using rule matching on person relationship candidate sentences, this part of the work is mainly to improve the accuracy rate and to prepare for the later extraction of person relationships based on syntactic trees. The first step in the rule-based matching approach is to develop a complete and accurate rule base. As the social relationships between people are described in a relatively fixed way in the text, the thesis adopts a manual collection approach for the

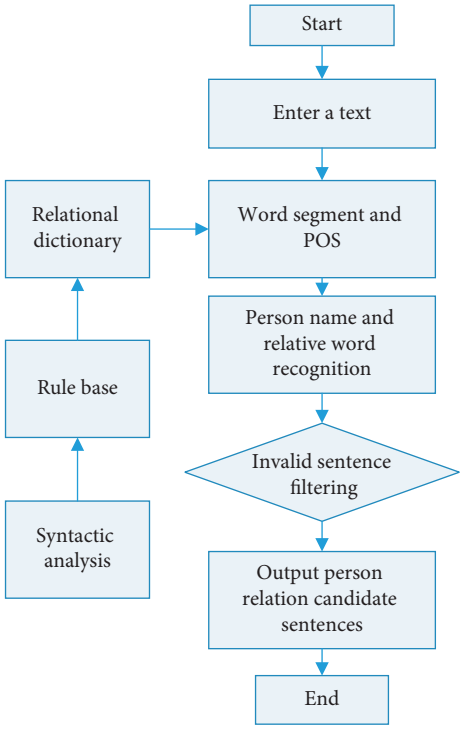

Figure 2: Flowchart of data preprocessing.

development of the rule base, which can ensure the accuracy of the rules.

Candidate sentences for character relations that have been split are matched separately using each regular expression in the rule base, in the order of highest to lowest frequency of rule occurrences when matching, which will play a role in improving the accuracy of the algorithm, while reducing the number of irrelevant sentences matched. If a sentence cannot be matched by all rules, it is used as the input to the subsequent syntactic tree-based algorithm for the next extraction step.

9. Syntactic Tree-Based Character Relationship Extraction

The syntactic tree based person relationship extraction includes three steps as follows: (1) constructing a syntactic tree by syntactic analysis of person relationship candidates; (2) pruning the syntactic tree to eliminate a large number of non-joint points to form the shortest path containing tree (SPT tree); and (3) calculating the weight of each relationship word based on the path distance between the relationship word and person pair, (p_i, p_j) in the SPT tree, and finally determining the relationship word that best represents person pair, (p_i, p_j) by using the weight of the relationship word.

The flowchart of the syntactic tree based character relationship extraction is shown in Figure 3.

The thesis uses the Stanford Parser syntactic parser for syntactic tree construction, a context-independent syntactic parser based on probabilistic statistics developed in Java by the Stanford University NLP Research Group, which is fully open source and supports English, Chinese, German, and French. Stanford Parser can obtain the dependencies between components in a sentence and the syntactic tree of the sentence. For the processing of Chinese, Stanford Parser provides five training models.

In this paper, we focus on the processing of simplified mainland texts and therefore use the Xinhua corpus. In terms of model selection, the Factored and PCFG were compared in terms of time and space consumption when processing sentences of different lengths. Stanford Parser version 3.5.2.1 was used for the comparison [20].

Once the SPT tree has been obtained, the structure of the SPT tree needs to be parsed to determine the best relational words to describe the character pairs (p_i, p_j). In this case, it is necessary to obtain the distance of each relation to each character pair. The smaller the distance, the more relevant the relation is to describe the relationship between the character pairs. The following definitions are given first:

Define a SPT tree in which the node corresponding to person p_i is node_i, the node corresponding to relation r_k is node_k, and the nearest common parent of node_k and node_i is root, then the distance $\text{dis}(r_k, p_i)$ of relation r_k to person p_i is defined as follows, where d denotes the shortest path length of node_i back up to root.

$$\text{dis}(r_k, \text{p}_\text{i}) = d. \tag{1}$$

Define the distance r_k of the relation (p_i, p_j) to the character pair, $\text{dis}(r_k, \langle p_i, p_j \rangle)$ defined by the following:

$$\text{dis}\left(r_k, \langle p_i, p_j \rangle\right) = \text{dis}(r_k, p_i) + \text{dis}\left(r_k, p_j\right). \tag{2}$$

In the SPT tree shown in Figure 4, the nearest common parent of the node corresponding to the relation "Dad" and the character "Li Ping" is the "NP" node numbered 1 in the diagram, then the shortest path of the character "Li Ping" up to the nearest common parent node is NP (NR) ⟶ NP ⟶ DNP ⟶ NP, i.e., dis (Dad, Li Ping) = 3, and similarly dis (Dad, Li Jiantao) = 1. Therefore, using the definition, the distance dis (Dad, Li Jiantao) is for the character pair Li Ping and Li Jiantao. The distance of dis (Dad, Li Ping, Li Jiantao) = 4.

The process of the SPT tree based person relationship extraction algorithm is as follows: let the set of relationship words in a person relationship candidate sentence S be $Q = \{r_1, r_2, \ldots, r_m\}$ and the set of person names be $P = \{p_1, p_2, \ldots, p_n\}$; first, the distance $dis(r_k, \text{p}_\text{i})$ between each relationship word $r_k\,(1 \le k \le m)$ and each person name $p_i\,(1 \le i \le n)$ is calculated, second, the weight $\text{dis}(r_k, \langle p_i, p_j \rangle)$ of the relationship words to the person pair (p_i, p_j) is calculated, and $\text{dis}(r_k, \langle p_i, p_j \rangle)$ in ascending order of size are arranged, and finally the relationship description of the person pair, in order of the smallest distance and the relational word that fits within the threshold is selected as the relational description of the person pair (p_i, p_j). If a relation is already identified as the relation description of a character pair [21], it will not be used as the relation description of other character pairs in the sentence. The flow of the extraction of the character pair, (p_i, p_j) relations is shown in Figure 5.

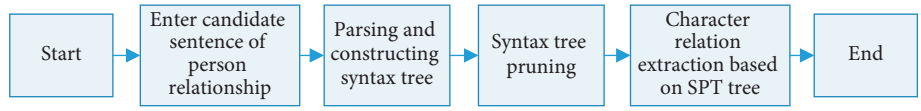

Figure 3: Flowchart of the syntactic tree based character relationship extraction algorithm.

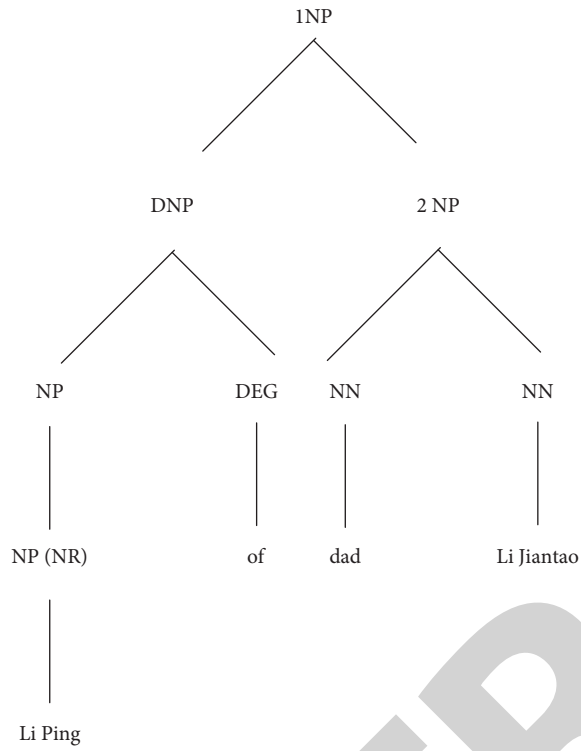

Figure 4: Schematic diagram of the SPT tree.

10. Results and Analysis of Character Relationship Extraction Experiments

In order to verify the performance of the personal relationship extraction algorithm, the 10,000 experimental data were divided into sentences and the personal relationship candidates (i.e., sentences containing at least two names and a relationship word) were selected as the input to the algorithm. 4685 sentences were personal relationship candidates, of which 2,437 contained personal relationships and 2,248 did not contain personal relationships.

10.1. Experiments on the Selection of Path Thresholds. In syntactic tree-based character relationship extraction, the choice of path thresholds is crucial to the algorithm results; therefore, this section first selects different path thresholds for experimentation and compares the results to select the best threshold The results are compared and the best threshold is selected. The paper first selects 200 relationships out of 4685 candidate sentences as training data, and manually annotates 107 relationships and 93 relationships with no relationships [22, 23]. Using the syntactic tree based relationship extraction algorithm, different path thresholds $\theta = 2, 3, \ldots, 14$ are chosen., 14 and the accuracy, recall, and F-value for each threshold are shown in Table 1.

Figure 6 shows the accuracy, recall, and F-value of the syntactic tree based personal relationship extraction algorithm for different path thresholds. As can be seen from the figure, the recall rate increases with increasing, but the accuracy rate decreases, with a maximum value of 78.19% being achieved at = 6. In the subsequent experiments, the paper chose = 6 as the path threshold.

10.2. Accuracy and Performance Comparison of Character Relationship Extraction Results. For the extraction of character relations, the thesis first performs the first step of character relation candidate sentence extraction by rule matching. If rule matching is not successful, a syntactic tree is built and the second step is performed by the syntactic tree based personal relationship. The second step of extraction is carried out by a syntactic tree-based character relationship extraction algorithm. The rule matching algorithm yields a very high accuracy rate, but a low recall rate. The syntactic tree-based approach is able to obtain a higher recall, but the accuracy is correspondingly lower [24, 25]. The combination of the two can give relatively good results. In the following, the rule matching, syntactic tree-based, and combined methods are investigated for different datasets. The following experiments compare the accuracy and performance of rule-based matching, syntactic tree based matching and the combination of the two methods. The results of each of the three algorithms are presented in Table 2.

The experimental results of the rule-based matching character relationship extraction algorithm with different data sets are shown in Table 2.

The experimental results of the syntactic tree-based character relationship extraction algorithm with different data sets are shown in Table 3.

The experimental results of the personal relationship extraction algorithm based on a combination of rule matching and syntactic trees Figure 7for different data sets are shown in Table 4.

Figures 7–9 show the comparison of the results of the three algorithms in terms of accuracy, recall, and F-value on different datasets, respectively. From the above three figures, it can be seen that the rule-based matching algorithm is able to obtain a high accuracy rate but a relatively low recall rate, and the syntactic tree-based algorithm is able to obtain a high recall rate but a very low accuracy rate. The algorithm based on the combination of rule matching and syntactic tree is able to achieve a compromise between accuracy and recall and is able to obtain a high F-value, indicating that the algorithm of the thesis is effective.

Figure 10 shows a comparison of the time consumed by the three methods on different datasets. As syntactic analysis involves the process of sentence component analysis, the relationship between the components and the construction

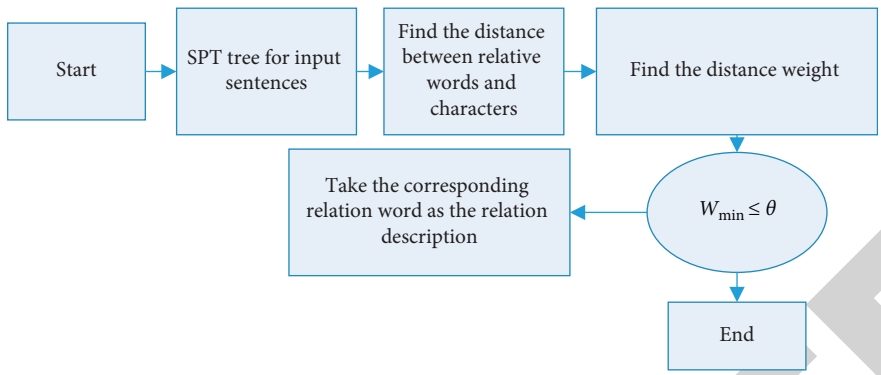

Figure 5: Flowchart of character relationship extraction based on syntactic tree.

Table 1: Metrics for syntactic tree-based character relationship extraction under different path thresholds.

Path threshold θ	Algorithm recognition median	Correct identification number	Number of false identifications	Accuracy (%)	Recall (%)	F value (%)
2	32	32	0	100	29.91	46.04
3	63	52	12	80.95	47.66	60
4	112	79	33	70.54	73.83	72.15
5	116	82	34	70.69	76.64	73.54
6	136	95	41	69.85	88.79	78.19
7	143	95	48	66.43	88.79	76
8	165	99	66	60	92.52	72.29
9	176	102	74	57.95	95.33	72.08
10	181	103	78	56.91	96.26	71.53
13	194	107	87	55.15	100	71.1
14	197	107	90	54.31	100	70.39

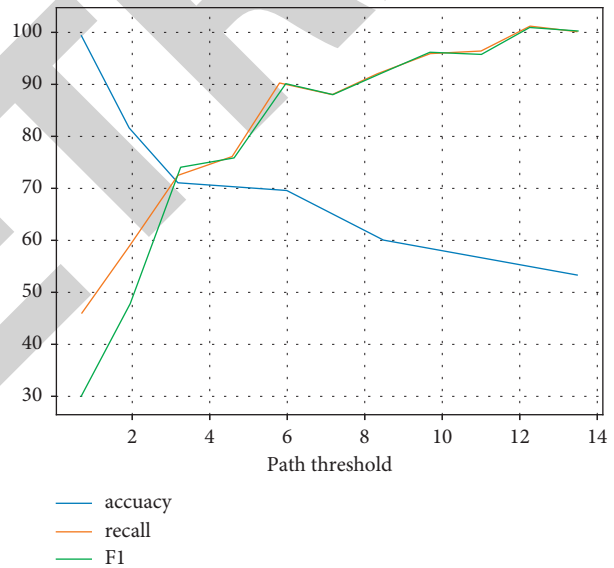

Figure 6: Metrics for syntactic tree-based character relationship extraction under different path thresholds.

Table 2: Experimental results of the rule-based matching algorithm with different data sets.

Dataset size	Total number of algorithm recognition	Correct identification number	Number of all relationships	Accuracy (%)	Recall (%)	F value (%)
40	17	15	23	88.24	65.22	75
80	30	27	41	90	65.85	76.06
120	46	41	65	89.13	63.08	73.87
160	72	63	94	87.50	67.02	75.90
200	84	76	112	90.48	67.86	77.55

Table 3: Experimental results of the Table 3syntactic tree-based algorithm with different data sets.

Dataset size	Total number of algorithm recognition	Correct identification number	Number of all relationships	Accuracy (%)	Recall (%)	F value (%)
40	33	21	23	63.64	91.3	75
80	56	37	41	66.07	90.24	76.29
120	97	58	65	59.79	89.23	71.60
160	128	82	94	64.06	87.23	73.87
200	143	98	112	68.53	87.5	76.86

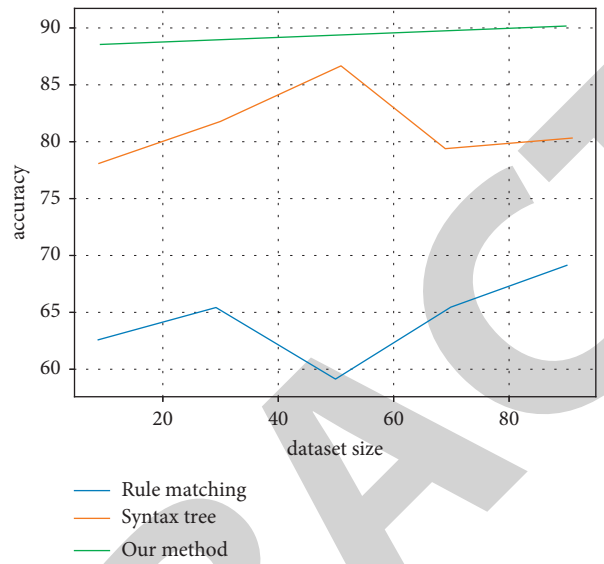

Figure 7: Comparison of the accuracy of the three methods on different datasets.

Table 4: Experimental results of the combined rule-Table 4 based matching and syntactic tree algorithm with different data sets.

Dataset size	Total number of algorithm recognition	Correct identification number	Number of all relationships	Accuracy (%)	Recall (%)	F value (%)
40	24	19	23	79.17	82.61	80.85
80	40	33	41	82.5	80.49	81.48
120	61	52	65	85.25	80	82.54
160	99	79	94	79.80	84.04	91.87
200	118	95	92	80.51	84.21	80.61

of a syntactic tree, whereas rule matching is simply a string comparison, syntactic analysis consumes a very high amount of time, whereas the rule-based matching algorithm is very fast. In the algorithm combining rule and syntactic tree, as part of the character relationship candidate sentences that can be matched by the rule are already extracted in the first step, there is no need to build a syntactic tree, so there is some improvement in time consumption compared to the method based on syntactic tree only, but the time consumption is also much more than that of the rule-based method.

10.3. Comparison with Other Methods. The final results of the paper were averaged from the experimental results of the different data sets and compared with other methods in the literature compared with other methods in the literature, as shown in Table 5. The literature [53] used a feature extraction algorithm based on character annotation. The literature [54] classified character relationships into six categories, selected character pairs of contextual features, distance features, and syntactic features as feature vectors, and finally used support vector machine classification methods to identify the relationships. The literature [55] used a convolutional tree kernel function to extract character relationships. Comparison with other methods shows that the method proposed in the thesis and the method based on convolutional tree kernel have no obvious advantage in terms of accuracy, but they all have significant improvement in terms of recall compared with the other three methods, and finally, the comprehensive evaluation index F-value is higher than the remaining three methods. Therefore, the character relationship extraction algorithm based on the combination of rule matching and syntactic trees proposed in the thesis can improve the relationship extraction effect to a certain extent. The time element is properly used.

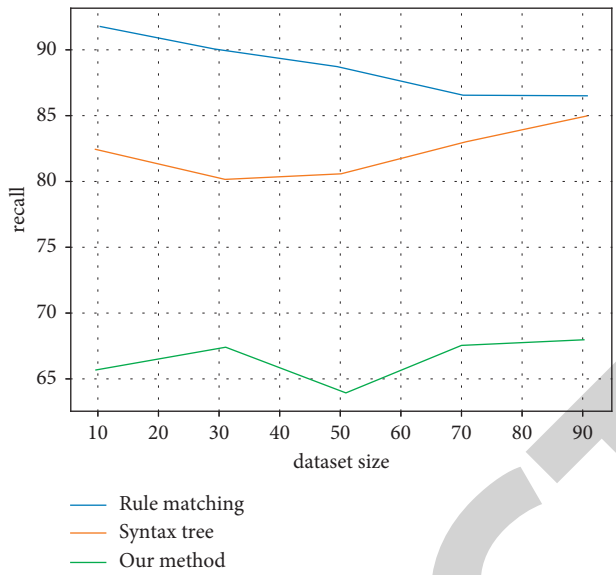

Figure 8: Comparison of the recall rates of the three methods on different datasets.

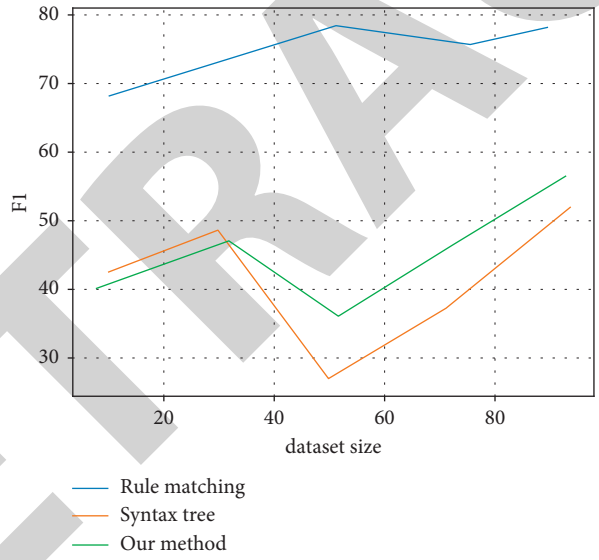

Figure 9: Comparison of the F-values of the three methods on different data sets.

Wuthering Heights condenses all the elements of a rich and rigorous scene, and author Emily presents a sophisticated and detailed chronology of text time and story time in a clever way, unfolding the plot in a staggering reversal of time and highlighting Table 5 the theme in a complex interweaving of chronology. The descriptions of the weather and seasons bring the emotions and actions of the novel's characters to life, making the scenes more vivid and dramatic, and greatly enhancing the lively nature and mystery of this thrilling and original novel.

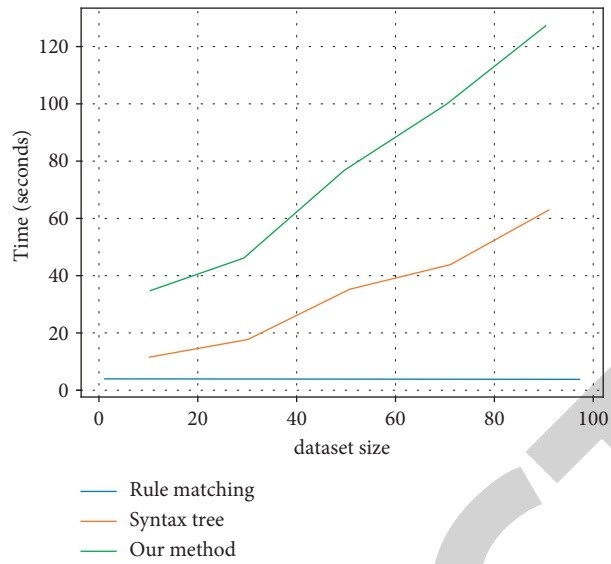

Figure 10: Comparison of the temporal performance of the three methods on different datasets.

Table 5: Comparison of experimental results with other literature.

Method used	Accuracy (%)	Recall (%)	F value (%)
Rule matching + syntax tree	81.44	82.39	81.87
Semantic role annotation	81.17	81	81.03
Based on SVM	60.8	61.82	61.33
Based on convolution tree kernel	85.8	71.1	61.33

11. Conclusions

This paper mainly describes the algorithm of person relationship extraction based on the combination of rule matching and syntactic tree, which is divided into four parts: the first part is data preprocessing, as the basic preparation part, first, it describes the use of ICTCALS for word separation and person name recognition and gives the relevant definitions to be used subsequently; it describes the person relationship extraction based on rule matching, including the establishment of rule base, regular expression. The algorithm of character relationship extraction based on the syntactic tree is proposed. First, the syntactic tree is built using Stanford Parser, second, the syntactic tree is transformed into an SPT tree by pruning out the non-joint points, and then the character relationships are extracted according to the SPT tree.

Data Availability

The raw data supporting the conclusions of this article will be made available by the authors, without undue reservation.

Conflicts of Interest

The authors declare that they have no conflicts of interest regarding this work.

References

[1] S. Ho. Han, "A review of research on restaurant brand personality: a focus on the hospitality and tourism journals listed at korea research foundation," *Journal of Tourism Sciences*, vol. 35, no. 2, pp. 337–353, 2011.

[2] C. H. Cao, Y. N. Tang, and D. Y. Huang, W. Gan, C. Zhang, IIBE: An Improved Identity-Based Encryption Algorithm for WSN Security," *Security and Communication Networks*, pp. 1–8, 2021.

[3] S. Sohangir and D. Wang, "Improved sqrt-cosine similarity measurement," *Journal of Big Data*, vol. 4, no. 1, pp. 1–13, 2017.

[4] D. Wu, C. Zhang, L. Ji, R. Ran, H. Wu, and Y. Xu, "Forest fire recognition based on feature extraction from multi-view images," *Traitement du Signal*, vol. 38, no. 3, pp. 775–783, 2021.

[5] L. Wang, C. Zhang, Q. Chen et al., "A Communication Strategy of Proactive Nodes Based on Loop Theorem in Wireless Sensor Networks," in *Proceedings of the 2018 Ninth International Conference on Intelligent Control and Information Processing (ICICIP)*, pp. 160–167, IEEE, Wanzhou, China, November 2018.

[6] T. Tsao, "Postcolonial life and death: a process-based comparison of emily bronte's wuthering Heights and ayu utami's saman," *Comparative Literature*, vol. 66, no. 1, pp. 95–112, 2014.

[7] J.-M. Chen, M.-C. Chen, and Y. S. Sun, "A novel approach for enhancing student reading comprehension and assisting teacher assessment of literacy," *Computers & Education*, vol. 55, no. 3, pp. 1367–1382, 2010.

[8] I. Defant, "Inhabiting nature in emily Brontë's wuthering Heights," *Brontë Studies*, vol. 42, no. 1, pp. 37–47, 2017.

[9] N. F. Newman, "Workers, gentlemen and landowners: identifying social class inThe ProfessorandWuthering Heights," *Brontë Society Transactions*, vol. 26, no. 1, pp. 10–18, 2001.

[10] B. A. O. Xiaoli, "Paradoxes concerning the love in wuthering Heights," *Cross-Cultural Communication*, vol. 11, no. 6, pp. 89–93, 2015.